PO Box 2345, Beijing 100023, China
www.wjgnet.com
wjg@wjgnet.com

ELSEVIER

World J Gastroenterol 2005;11(33):5095-5102
World Journal of Gastroenterology ISSN 1007-9327
© 2005 The WJG Press and Elsevier Inc. All rights reserved.

• *REVIEW* •

Structural and functional aspects of the liver and liver sinusoidal cells in relation to colon carcinoma metastasis

Katrien Vekemans, Filip Braet

Katrien Vekemans, Centre of Experimental Surgery and Anaesthesia, Abdominal Transplant Surgery Department, Catholic University of Leuven (KUL), Herestraat 49, 3000 Leuven, Belgium
Filip Braet, Australian Key Centre for Microscopy and Microanalysis, Electron Microscopy Unit, The University of Sydney, Sydney 2006, NSW, Australia
Supported by the Fund for Scientific Research-Flanders, No. 1.5.001.04N [F.B.]
Correspondence to: Katrien Vekemans, Centre of Experimental Surgery and Anaesthesia, Abdominal Transplant Surgery Department, Catholic University of Leuven, Herestraat 49, Leuven 3000, Belgium. katrien.vekemans@med.kuleuven.ac.be
Telephone: +32-16-34-58-45 Fax: +32-16-34-87-43
Received: 2004-09-26 Accepted: 2004-10-18

Abstract

Nowadays, liver metastasis remains difficult to cure. When tumor cells escape and arrive in the liver sinusoids, they encounter the local defense mechanism specific to the liver. The sinusoidal cells have been widely described in physiologic conditions and in relation to metastasis during the past 30 years. This paper provides an "overview" of how these cells function in health and in diseases such as liver metastasis.

© 2005 The WJG Press and Elsevier Inc. All rights reserved.

Key words: Metastasis; Liver; Colon carcinoma; Sinusoidal cells; Kupffer cells; Liver sinusoidal endothelial cells; Hepatic NK cells

Vekemans K, Braet F. Structural and functional aspects of the liver and liver sinusoidal cells in relation to colon carcinoma metastasis. *World J Gastroenterol* 2005; 11(33): 5095-5102
http://www.wjgnet.com/1007-9327/11/5095.asp

LIVER ARCHITECTURE

The liver is the largest organ of the body, constituting 2-5% of the adult body weight. It receives blood supply from two major blood vessels. The hepatic artery supplies oxygenated blood, whereas the portal vein, which provides 80% of the total blood supply, supplies nutrient-rich deoxygenated blood. The liver thus acts as a guard between the digestive tract and the rest of the body[1], transforming, detoxifying, and accumulating metabolites. The liver also produces different types of plasma proteins, such as albumin, which are delivered into the blood, as well as metabolites that are constituents of the bile[2,3].

The liver is surrounded by connective tissue, designated as Glisson's capsule. It is composed of polygonal lobules separated by connective tissue. At the periphery of the lobule, are regions that consist of bile ducts, lymphatics, nerves and branches of the hepatic artery and the portal vein. At the center of the lobule is the central vein. Hepatocytes (parenchymal cells) are the basic structural component of the liver, representing 60% of the total cell number and 80% of the total liver volume. They are arranged radially within the lobule to form cellular plates, between which the liver capillaries and the sinusoids are located.

Blood arriving through branches of the portal vein and the hepatic artery pass through the sinusoids, towards the central vein[1,4,5]. The liver sinusoids are lined with a discontinuous layer of fenestrated endothelial cells. Between the endothelial cells and the hepatocytes, is a discontinuous basal lamina and a subendothelial space named the space of Disse, through which exchange between the blood and the hepatocytes take place.

Various liver sinusoidal cells can be recognized within the sinusoids. These include, in addition to the sinusoidal endothelial cells, Kupffer cells, hepatic NK cells and stellate cells, which complement one another in performing their specialized functions.

LIVER SINUSOIDAL CELLS

The sinusoidal cells are the predominant non-parenchymal cells, comprising about 35% of the total cell number and about 17% of the total volume of the liver. These cells are divided into sinusoidal endothelial cells (44%), Kupffer cells (33%), stellate cells (10-25%) and hepatic NK cells (5%)[3,6-8].

Liver sinusoidal endothelial cells

The cells forming the sinusoidal wall (endothelium), the liver sinusoidal endothelial cells (LSECs), were first described at the electron microscopic level by Wisse[9]. They can be visualized by injection with fluorescent acetylated LDL (AcLDL)[15], latex beads of Ø 20 nm[16], or formaldehyde modified serum albumin (FSA)[17]. Katz *et al*.[18], mentioned that dendritic cells are also able to take up AcLDL; however, this cannot interfere upon injection of AcLDL in the blood, as dendritic cells are to be found within the tissue and not in the blood. The liver sieve plates are a group of open pores or fenestrae lacking a diaphragm and a basal lamina underneath the endothelium. They can be visualized by perfusion fixation of the liver. These fenestrae measured 150-175 nm in transmission electron microscopy[10]. It is assumed that the transport and exchange of fluid, solutes and particles between the space of Disse and the sinusoidal

blood occur through these open fenestrae[10,11].

A typical feature of endothelial cells is their high endocytic capacity[10]. This function is reflected in the presence of numerous endocytotic vesicles and in the effective uptake of a variety of substances from the blood by receptor-mediated endocytosis[10-13].

The typical LSECs phenotype, open fenestrae in sieve plates and lack of the basement membrane are maintained by paracrine and autocrine regulation[19]. CD31 has been mentioned as a de-differentiation and non-fenestration marker. In *in vitro* CD31 appears after 1 d monoculture; however, when co-culture with hepatocytes or stellate cells is performed, CD31 expression is prevented. This can be abolished by the addition of anti-VEGF. In accordance, VEGF stimulates the production of nitric oxide (NO)[19].

Kupffer cells

Kupffer cells are categorized as tissue macrophages and represent the largest population of their kind in the body[11]. Kupffer cells lay preferentially anchored to the periportal zone of the liver lobule[20].

Kupffer cells have irregular shapes with many cytoplasmic extensions and contain a large number of phagosomes and lysosomes that are associated with their endocytic function. Peculiarities of the ultrastructural morphology of Kupffer cells are fuzzy coat, worm-like structures, annulate lamellae and fuzzy-coated vacuoles[9,21]. Kupffer cells are scavengers that move along the sinusoids[22,23] and phagocytose foreign material present in the bloodstream; fusion of the phagosome with a lysosome leads to digestion of the ingested material. Different techniques are used to visualize these cells, such as staining for acid phosphatase activity[24] or peroxidase activity[25], and immunostaining for Fc receptors[26]. Due to their phagocytic activity, they can also be stained *in vivo* by injection with latex beads. Another option is staining for ED1, ED2, and ED3[27,28].

Hepatic NK cells

In 1976, 100 years after Kupffer cells were discovered, Wisse *et al*., described a new sinusoidal cell type[29]. These cells, designated as "Pit cells", are nowadays consideredas liver-specific natural killer cells[30] with a large granular morphology[31], and can be visualized using mAb 3.2.3 against NKR-P1A[32].

Hepatic NK cells are always in contact with LSECs, and frequently in contact with Kupffer cells[10]. There is an average of 1 NK cell per 10 Kupffer cells. Hepatic NK cells can be separated into low-density and high-density cells. The two subpopulations differ morphologically, immunophenotypically and functionally from each other and from blood NK cells, particularly in the higher toxicity of high-density Kupffer cells[10,33,34]. Morphologically, NK cells can be recognized by their electron-dense, azurophilic granules and rod-cored vesicles. Rod-cored vesicles are small inclusions found exclusively in NK cells. Each vesicle contains a straight rod structure that bridges its entire diameter[10]. Hepatic NK cells have the capacity to kill incoming malignant cells[35].

Stellate cells

Ito discovered the true function of stellate cells in 1952[36], followed by Wake[37,38]. These cells are located within the space of Disse. They contain lipid droplets rich in vitamin A, and they synthesize and secrete a variety of extra-cellular matrix proteins. The activation of stellate cells from a quiescent vitamin A storing cells to a proliferating, fibrogenic 'myofibroblast-like' phenotype is a main event following liver injury[39,40].

COLON CARCINOMA METASTASIS

The liver is the predominant site of recurrence of the disease following initial therapeutic colon surgery, mainly due to two factors. First, viable tumor cells can escape into the portal blood stream during surgical manipulation and invade the liver[41]. Second, major surgery causes a transient postoperative weakening of the immune system[42-44]. The temporary immunosuppression induced by surgery is therefore associated with enhanced risk of metastasis. When colon cancer spreads to the liver, ablation of metastasis by surgical resection, cryotherapy or radiofrequency is the only curative treatment[45]. Moreover, the vast majority of patients are not amenable to surgical resection, due to existence of multiple metastases. In order to develop new strategies aimed at preventing metastasis, it is crucial to understand the cellular defense mechanisms against tumor cells and the tumor escape mechanisms.

Cytotoxicity of sinusoidal cells towards tumor cells

When the tumor cells invade the vascular bed and metastasize into the liver, they encounter the defense mechanisms specific to the liver. Kupffer cells and hepatic NK cells are the main resident cells of immune surveillance, but sinusoidal endothelial cells also participate in this process.

Kupffer cells The most important function of Kupffer cells is defense against infections and tumor cells. Kupffer cells act as antigen presenting cells and as effector cells that act directly by phagocytosis, or indirectly by activation of other cells, e.g. NK cells[46,47]. Though Kupffer cells are constantly acting as scavengers, they can be activated through different pathways. Firstly, soluble mediators can trigger their activation. IFN-γ is the prototypical macrophage activating factor. It is central to the development of Th1-dominated immune responses, and it affects not only macrophages in an autocrine fashion, but other immune cells as well.

One of the key events during innate immune reactions is the production of IL-12, mainly by macrophages[48]. IL-12 induces NK cells to rapidly secrete IFN-γ, which then in turn activates macrophages early in the immune response. It also induces IFN-γ production by T cells. IL-18, which is produced by Kupffer cells and other cell types, is also involved in enhancing IFN-γ production by T cells[49,50]. Macrophages also secrete IFN-γ upon stimulation with IL-12 and IL-18 together. It is known that IFN-γ is a possible reducer of metastasis of colon cancer in the liver[51].

Macrophages can also be activated by direct interaction with micro-organisms or bacterial products such as lipopoly-saccharide, glucan, muramyl dipeptide and lipid A[52]. A pivotal role for IFN-γ in the clearance of various intracellular pathogens has been amply demonstrated[53,54]. It has been described that macrophages release the cytotoxic radical, NO[55,56]. *In vitro* studies suggested that NO induces mitochondrial dysfunction in tumor cells

followed by membrane barrier dysfunction in the liver sinusoid[57,58]. Another important cytotoxic factor released by activated macrophages is tumor necrosis factor alpha (TNF-α), which is produced in both soluble and membrane-bound forms. After binding to its receptor, apoptosis can be induced in the target cell[59].

Cytotoxicity of macrophages can be classified into antibody-dependent and antibody-independent cell-mediated cytotoxicity. Both pathways are contact dependent and induce tumor cell death after a number of hours. Antibody-dependent cell-mediated cytotoxicity is based on the recognition of an antibody-coated target by Fc receptors on the effector cells[60-62]. Upon cross-linking of the Fc receptor, secretion of cytotoxic mediators occurs. Secretion of reactive oxygen species, IL-1 and TNF-α are probably involved[63]. Antibody-independent cell-mediated cytotoxicity involves binding to the macrophage followed by translocation of the lysosomal organelles to the target[47]. Moreover, cytotoxicity towards tumor targets involves cytolysis and phagocytosis[64].

In certain pathophysiologic conditions, apoptosis is chaotic and non-selective, may be massive and occurs persistently over an extended period of time[65]. A large number of apoptotic bodies produced are phagocytosed by Kupffer cells. It has recently been reported that engulfment of apoptotic bodies results in the generation of death ligands, such as FasL and TNF-α on the membrane of the Kupffer cells, but engulfment of latex beads does not produce a similar response[59]. This means that uptake of apoptotic bodies induces an additional immunologic response involving liver inflammation and fibrosis[59,66].

Hepatic NK cells Cytotoxic lymphocytes (CTL) and NK cells induce target cell death by means of granules and by death receptor-mediated pathways. Apoptosis refers to orchestrated cell death that is indispensable for maintenance of homeostasis. Characteristics of apoptosis are chromatin condensation, nuclear fragmentation, membrane blebbing, cell shrinkage, protein degradation and internucleosomal DNA fragmentation. Most of the morphological changes are caused by a set of cysteine proteases that are activated specifically in apoptotic cells. These death proteases are homologous to each other and are members of a large protein family known as caspases[67]. Over a dozen caspases have been identified in humans, and it has been suggested that about two-thirds of them function in apoptosis[68,69]. Different pathways can induce apoptosis, of which the Fas/FasL pathway is the best known. This pathway is frequently used by cytotoxic T cells and other immunocompetent cells. Stimulation of the Fas receptor (CD95) with Fas ligand recruits the proform of the initiator caspase 8, by interaction with the adapter molecule Fas-associated death domain through death domains and death effector domains. This leads to the formation of a complex called the death inducing signaling complex. Subsequently, procaspase 8 is cleaved autocatalytically to yield the active initiator caspase 8. The consequences of the activation of caspase 8 depend on the cell type. In type 1 cells, the other members of the caspase family (such as caspase 3) are activated directly[70]. In type 2 cells, caspase 8 activation results in the cleavage of the pro-apoptotic Bcl-2 family member Bid. Subsequently Bid and Bax are translocated to the mitochondria to cause release of cytochrome *c*. This results in the activation of caspase 9 through interaction with the adapter molecule apoptotic protease-activating factor. Caspase 9 activates caspase 3, which can then perform its function[71,72].

The granules of CTL contain various proteins, some of which are known to be involved in target cell death, such as perforin and granzyme. Various isoforms of the granzymes have been described. After granzyme B enters the target cell, it can directly cleave procaspase 3, Bid and inhibitor of caspase-activated DNase, thereby inducing apoptosis[71,73-75]. Death induced by granzyme A appears to be independent of the pathways used by granzyme B[75,76]. Granzyme A does not activate caspases in target cells, nor does it induce cleavage of other granzyme B substrates. The functions of the other granzyme isoforms remain unclear[76]. Perforin forms transmembrane pores and is an essential enabler of granzyme-mediated apoptosis[77].

Liver sinusoidal endothelial cells LSECs, like Kupffer cells, express an Fc receptor that may be involved in immunological defense. FcR-mediated uptake of IgG-immune complex has been shown to enhance presentation of antigens by MHC class II[78]. This process might take place in a compartment reminiscent of the multi-vesicular compartments observed in the LSECs. It is therefore conceivable that these organelles are involved in processing and presentation of antigenic peptides. In contrast to Kupffer cells, however, the multi-vesicular compartments observed in LSECs are not rich in MHC class II, which might indicate that LSECs are not involved in antigen presentation[79-81]. Nevertheless, Knolle *et al*.[82,83], demonstrated that both Kupffer cells and LSEC have MHC class II, and that both of these cells are involved in antigen presentation. However, LSECs failed to induce differentiation towards inflammatory Th1[82]. Furthermore, antigen presentation of soluble blood-borne antigens leads primarily to tolerance, instead of immunosurveillance. LSECs are known to express CD80 and CD86, molecules that are present on professional antigen-presenting cells, such as dendritic cells[14]. In addition, LSECs play a key role in receptor-mediated uptake, in degradation of macromolecules from the sinusoidal blood[84-86] and in the clearance of circulating apoptotic bodies[83,84]. Katz *et al*.[18], reported about some conflicting data, low or absent MHC class II, CD86 and CD11c. However, they mentioned a high capacity for AG uptake *in vivo* and *in vitro*. According to Knolle *et al*.[14,83], LSECs were unable to stimulate allogeneic T cells.

LSECs are known to secrete NO and can induce apoptosis in different types of cancer cells, such as lymphoma and colorectal carcinoma[87,88]. NO has also been reported to function as a cytolytic factor in macrophage-mediated cancer cell cytotoxicity[89].

Seventeen days after injection of colon carcinoma cells CC531s into the mesenteric vein, metastases are observed as nodules of 1-3 mm diameter on the surface of the liver lobes. When the liver sinusoidal cells are stained *in vivo* with FSA, no staining can be detected in the center of the metastasis nodule (Figure 1). On the border of the tumor some positive staining can be seen, but of lower intensity than in normal tissue. It is known that nodules of 1-2 mm diameter have no internal vascularization, and that the cells

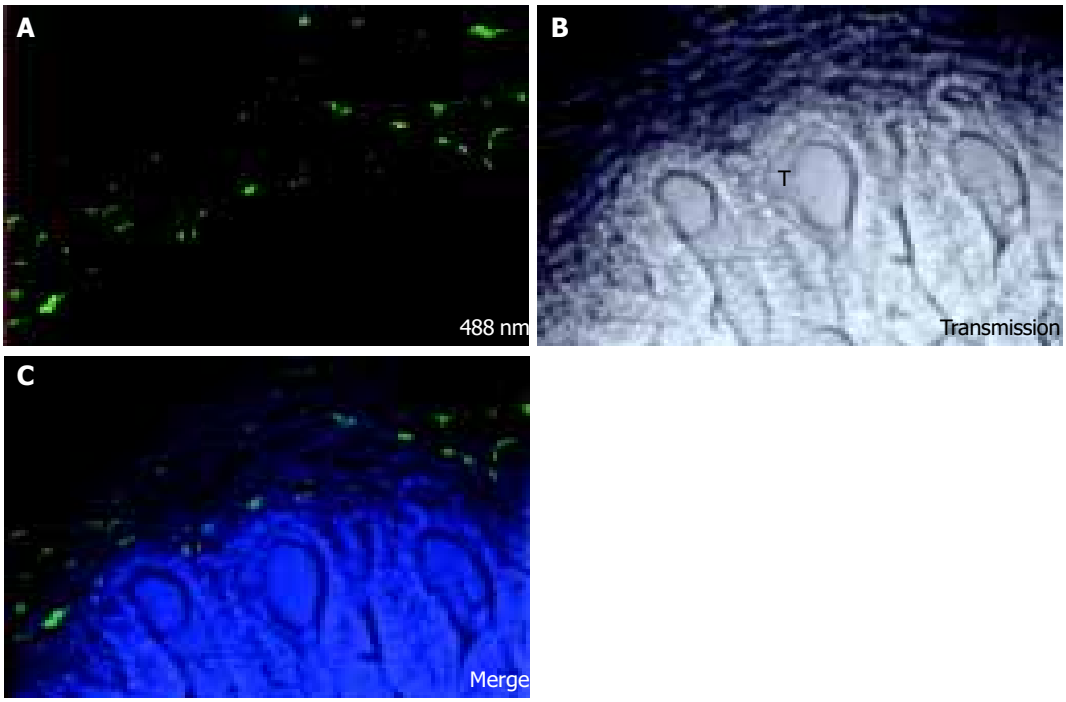


Figure 1 CC531s cells were injected into the mesenteric vein and were left in circulation for 17 d. One hour before perfusion fixation, FSA was injected into the penile vein. FSA stains only LSECs. Confocal microscopy was conducted and images were named after corresponding laser lines. **A**: FSA staining was measured with CLSM; fluorescence was observed only in part of the scanned field; **B**: Transmission image of the same field, with the tumor region in the lower part of the field. Formation of cryptae of the tumor (T) can be observed; **C**: After merging the two images, no staining was observed inside the tumor region. Image size: 500 μm×500 μm.

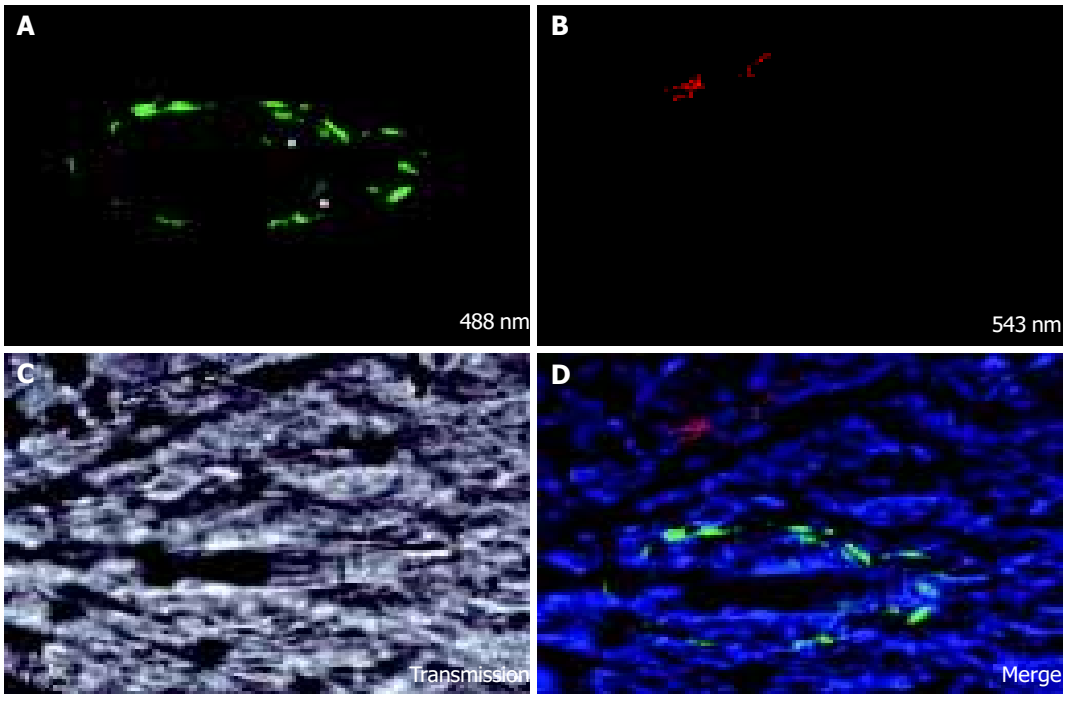


Figure 2 CC531s were labeled with DiO, injected into the mesenteric vein. After 24 h, Kupffer cells (KC) were stained *in vivo* with TRITC-labeled latex beads, and the liver was fixed by perfusion. Confocal microscopy was conducted and images were named after corresponding laser lines. **A**: Group of CC531s was visualized; **B**: KC was visualized by the up-take of fluorescent latex beads; **C**: The rest of the field was examined with the transmission function; **D**: CC531s proliferating inside the liver parenchyma and inside the group of CC531s cells, a vessel was seen. The vessel is much straighter than the normal liver sinusoids, indicating a newly formed vessel. Image size: 158.7 μm×158.7 μm.

receive nutrients and oxygen simply by diffusion (prevascular phase)[90]. Vessel formation, however, was observed with confocal microscopy in a cell cluster of 12 CC531s cells 24 h after injection of CC531s cells (Figure 2) and it is

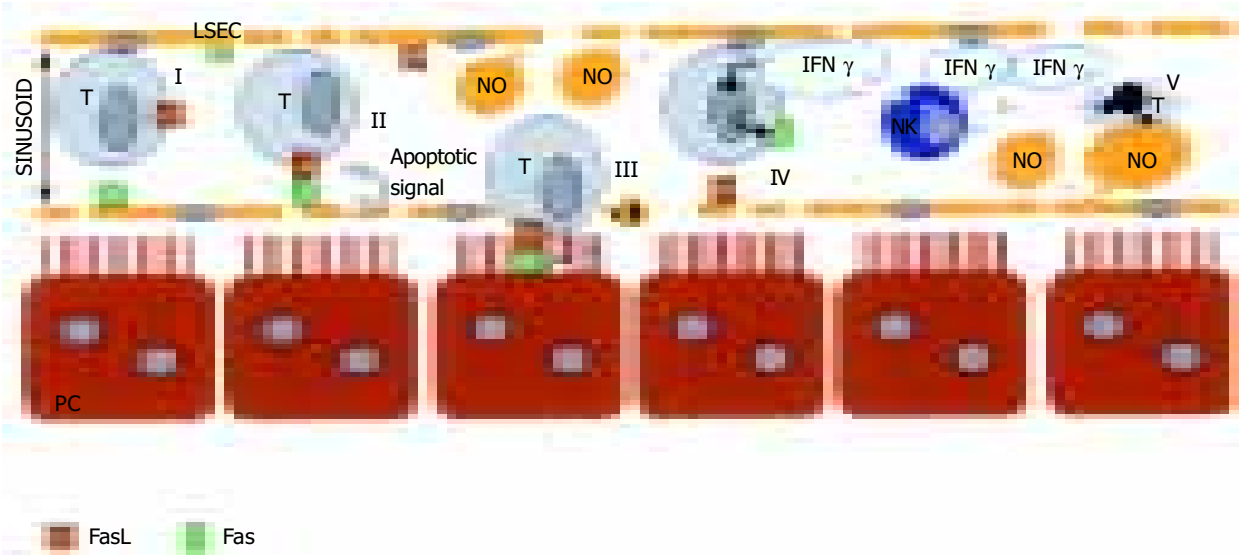


Figure 3 Schematic overview of the early metastatic events occurring along the liver sinusoid in which the LSECs and CC531s colon carcinoma cells (T) play a central role. Fas expressing LSECs (I) undergo apoptosis by FasL expressing CC531s (I and II). By doing so, the colon cancer cells provide themselves a gateway towards the liver parenchyma, as the LSECs retract and gaps are induced in the liver sinusoidal lining (III). Subsequently, the CC531s cells have free access to the hepatocytes, which expresses Fas (III). By this means, CC531s are able to invade in the liver parenchyma. LSECs express FasL and CC531s express Fas (IV). When IFN-γ is present in the sinusoid, Fas becomes active. NO produced by the LSECs induces apoptosis in CC531s cells only when IFN-γ is present (V). As a result the IFN-γ-activated pathway supports the immune system by killing tumor cells. Note: Parenchymal cell (PC). This figure is a compilation of the data reported in Refs. [93,94,96,97].

known that colon carcinoma cells produce angiogenic factors such as VEGF[91]. However, even though angiogenic factors permit formation of vessels in micro-metastases as shown in Figure 2, these vessels are incapable of extending to provide a blood supply within macro-metastasis nodules as shown in Figure 1.

CONCLUSION

In conclusion, with our published studies, we add these results that most of the CC531s cells trapped in the sinusoids get phagocytosed by the Kupffer cells and only 6% of the cells are living in the sinusoid or in the space of Disse[92]. Hepatic NK cells help in the removal of the CC531s. In NK cells, depleted rates up to 33% of the CC531s are free of interactions with Kupffer cells[92]. In order to understand the pathways involved, *in vitro* studies were conducted and the following conclusions were made. CC531s, colon carcinoma cells, are able to kill LSECs by usage of Fas/FasL pathway[94] (Figure 3). *In vivo*, destruction of the sinusoidal lining can be observed and is also confirmed by others[93-95]. However, when CC531s are pre-treated with IFN-γ, the outcome of apoptosis in cocultures is inversed. Then, LSECs are able to induce apoptosis in pre-treated CC531s by NO pathway[96,97] (Figure 3). Generally we state that Kupffer cells, NK cells, and LSECs orchestrate together in the removal of CC531s.

ACKNOWLEDGMENTS

We want to thank Mrs. C. Seynaeve, M. Baekeland, D. Blijweert, and Mrs. Chris Derom for excellent technical assistance. Also thanks to Dr. B. Smedsrød for giving the FSA. The members of the "Australian Key Center for Microscopy and Microanalysis" of The University of Sydney are gratefully acknowledged for excellent administrative, technical, and practical support.

REFERENCES

1 **Junqueira LC,** Carneiro J. *Basic Histology* 10th edition Lange international edition. 332-343
2 **Arias IM,** jakoby WB, Popper H, Scachter D, Schafritz DA: Section 4 the organ: The hepatic microvascular system. *The liver: Biology and Pathobiology*, 3rd Ed. Lippincott Williams & Wilkins, 1997. Available from: URL: http://liver.med.tufts.edu/
3 **Sasse D,** Spronitz UM, Mally IP, *Liver architecture. Enzyme* 1992; **46**: 8-32
4 **Lautt WW,** Greenway CV. Conceptual review of the hepatic vascular bed. *Hepatology* 1987; **7**: 952-963
5 **Muto M.** A scanning electron microscopic study on endothelial cells and Kupffer cells in rat liver sinusoids. *Arch Histol Jap* 1975; **37**: 369-386
6 **Knook DL,** Sleyster EC. Isolated parenchymal, Kupffer and endothelial cells characterised by their lysomal enzyme content. *Biochem Biophys Res Commun* 1980; **96**: 250-257
7 **Blouin A,** Bolender RP, Weibel ER. Distribution of organelles and membranes between hepatocytes and nonhepatocytes in the rat liver parenchyma. *J Cell Biol* 1977; **72**: 441-455
8 **Weibel ER,** Staubi W, Gnagi HR, Hess FA. Correlated morphometric and biochemical studies on the liver cell: I. Morphometric model, stereological methods and normal morphometric data for rat liver. *J Cell Biol* 1969; **42**: 68-91
9 **Wisse E.** An electron microscopic study of fenestrated endothelial lining of rat liver sinusoids. *J Ultrastruct Res* 1970; **31**: 125-150
10 **Braet F,** Luo D, Spector I, Vermijlen D, Wisse E. Endothelial and pit cells. In: Arias IM, Boyer JL, Chisari FV, Fausto N, Jakoby WB, Scachter D, Shafritz DA, eds. *The liver: Biology and pathobiology*, 4 ed. *Philadelphia: Lippincott Williams Wilkins* 2001: 437-453
11 **Smedsrod B,** De Bleser PJ, Braet F, Lovisetti P, Vanderkerken K, Wisse E, Geerts A. Cell biology of liver endothelial and

Kupffer cells. *Gut* 1994; **35**: 1509-1516
12 **Eskild W,** Smedsrod B, Berg T. Receptor mediated endocytosis of formaldehyde treated albumin, yeast invertase and chondroitin sulfate in suspensions of rat liver endothelial cells. *Int J Biochem* 1986; **18**: 647-651
13 **Eskild W,** Kindberg GM, Smedsrod B, Blomhoff R, Norum KR, Berg T. Intracellular transport of formaldehyde-treated serum albumin in liver endothelial cells after uptake via scavenger receptors. *Biochem J* 1989; **258**: 511-520
14 **Knolle PA,** Limmer A. Neighborhood politics: the immunoregulatory function of organ-resident liver endothelial cells. *Trends Immunol* 2001; **22**: 432-437
15 **Pitas RE,** Boyles J, Mahley RW, Bissell DM. Uptake of chemically modified low density lipoproteins *in vivo* is mediated by specific endothelial cells. *J Cell Biol* 1985; **100**: 103-117
16 **Shiratori Y,** Tananka M, Kawase T, Shiina S, Komatsu Y, Omata M. Quantification of sinusoidal cell function *in vivo*. *Semin Liver Dis* 1993; **13**: 39-49
17 **Yoshioka T,** Yamamoto K, Kobashi H, Tomita M, Tsuji T. Receptor-mediated endocytosis of chemically modified albumins by sinusoidal endothelial cells and Kupffer cells in rat and human liver. *Liver* 1994; **14**: 129-137
18 **Katz SC,** Pillarisetty VG, Bleier JI, Shah AB, DeMatteo RP. Liver sinusoidal endothelial cells are insufficient to activate T cells. *J Immunol* 2004; **173**: 230-235
19 **DeLeve LD,** Wang X, Hu L, McCuskey MK, McCuskey RS. Rat liver sinusoidal endothelial cell phenotype is maintained by paracrine and autocrine regulation. *Am J Physiol Gastrointest Liver Physiol* 2004; **287**: G757-763
20 **Bouwens L,** Baekeland M, De Zanger R, Wisse E. Quantitation, tissue distribution and proliferation kinetics of the Kupffer cells in normal rat liver. *Hepatology* 1986; **6**: 718-722
21 **Wisse E.** An ultrastructural characterization of the endothelial cell in the rat liver sinusoid under normal and various experimental conditions, as a contribution to the distinction between endothelial and Kupffer cells. *J Ultrastruct Res* 1972; **38**: 528-562
22 **Kan Z,** Ivancev K, Lunderquist A, McCuskey PA, McCuskey RS, Wallace S. *In vivo* microscopy of hepatic metastases: dynamic observation of tumor cell invasion and interaction with Kupffer cells. *Hepatology* 1995; **21**: 487-494
23 **MacPhee PJ,** Schmidt EE, Groom AC. Evidence for Kupffer cell migration along liver sinusoids, from high-resolution *in vivo* microscopy. *Am J Physiol* 1992; **263**: G17-23
24 **Matsubara S.** Glucose-6-phosphate dehydrogenase and mouse Kupffer cell activation: an ultrastructural dual staining enzyme-cytochemical study. *Histochem Cell Biol* 2002; **118**: 345-350
25 **Albegger KW.** Structure and function of the mononuclear phagocytic system (MPS) in chronic rhinosinusitis. A light and electron microscopic investigation. *Arch Otorhinolaryngol* 1976; **214**: 27-48
26 **Wood GW,** Gollahon KA. T-lymphocytes and macrophages in primary murine fibrosarcomas at different stages in their progression. *Cancer Res* 1978; **38**: 1857-1865
27 **Dijkstra CD,** Dopp EA, Joling P, Kraal G. The heterogeneity of mononuclear phagocytes in lymphoid organs: distinct macrophage subpopulations in the rat recognized by monoclonal antibodies ED1, ED2 and ED3. *Immunology* 1985; **54**: 589-599
28 **Ukai K,** Terashima K, Imai Y, Shinzawa H, Okuyama Y, Takahashi T, Ishikawa M. Proliferation kinetics of rat Kupffer cells after partial hepatectomy. Immunohistochemical and ultrastructural analysis. *Acta Pathol Jpn* 1990; **40**: 623-634
29 **Wisse E,** van't Noordende JM, van der Meulen J, Daems WT. The pit cell: description of a new type of cell occurring in rat liver sinusoids and peripheral blood. *Cell Tissue Res* 1976; **173**: 423-435
30 **Bouwens L,** Wisse E. Immuno-electron microscopic characterization of large granular lymphocytes (natural killer cells) from rat liver. *Eur J Immunol* 1987; **17**: 1423-1428
31 **Nakatani K,** Kaneda K, Seki S, Nakajima Y. Pit cells as liver-associated natural killer cells: morphology and function. *Med Electron Microsc* 2004; **37**: 29-36
32 **Van den Brink MRM,** Hunt LE, Hiserodt JC. *In vivo* treatment with monoclonal antibody 3.2.3 selectively eliminates natural killer cells in rats. *J Exp Med* 1990; **171**: 197-210
33 **Vanderkerken K,** Bouwens L, Wisse E. Characterization of a phenotypically and functionally distinct subset of large granular lymphocytes (pit cells) in rat liver sinusoids. *Hepatology* 1990; **12**: 70-75
34 **Luo D,** Vanderkerken K, Bouwens L, Kuppen PJ, Baekeland M, Seynaeve C, Wisse E. The role of adhesion molecules in the recruitment of hepatic natural killer cells (pit cells) in rat liver. *Hepatology* 1996; **24**: 1475-1480
35 **Vermijlen D,** Luo D, Robaye B, Seynaeve C, Baekeland M, Wisse E. Pit cells (Hepatic natural killer cells) of the rat induce apoptosis in colon carcinoma cells by the perforin / granzyme pathway. *Hepatology* 1999; **29**: 51-56
36 **Ito T,** Nemoto M. Uber die Kupffershen sternzellen und die fettspeicherungszellen in der blutkapillarwand der menschlichen leber. *Okajimas Folia Anat Jpn* 1952; **24**: 243-258
37 **Wake K.** "Sternzellen" in the liver: perisinusoidal cells with special reference to storage of vitamin A. *Am J Anat* 1971; **132**: 429-462
38 **Wake K.** Perisinusoidal stellate cells (fat-storing cells, interstitial cells, lipocytes), their related structure in and around the liver sinusoids, and vitamin A-storing cells in extrahepatic organs. *Int Rev Cytol* 1980; **66**: 303-353
39 **Sato M,** Suzuki S, Senoo H. Hepatic stellate cells: unique characteristics in cell biology and phenotype. *Cell Struct Funct* 2003; **28**: 105-112
40 **Li D,** Friedman SC: hepatic stellate cells: morphology, function, and regulation. In: Arias IM, Boyer JL, Fausto N, Jakoby WB, Schachter DA, Shafritz DA, eds. *The liver: biology and pathobiology*, 4 ed. *Philadelphia: Lippincott Williams Wilkins* 2001: 455-468
41 **Roberts S,** Long L, Jonasson O, McGrath R, McGrew E, Cole WH. The isolation of cancer cells from the blood stream during uterine curettage. *Surg Gynecol Obstet* 1960; **111**: 3-11
42 **Faist E,** Schinkel C, Zimmer S. Update on the mechanisms of immune suppression of injury and immune modulation. *World J Surg* 1996; **20**: 454-459
43 **Faist E,** Mewes A, Strasser T, Walz A, Alkan S, Baker C, Ertel W, Heberer G. Alteration of monocyte function following major injury. *Arch Surg* 1988; **123**: 287-292
44 **Sasson AR,** Sigurdson ER. Surgical treatment of liver metastasis. *Semin Oncol* 2002; **29**: 107-118
45 **Lennard TW,** Shenton BK, Borzotta A, Donnelly PK, White M, Gerrie LM, Proud G, Taylor RM. The influence of surgical operations on components of the human immune system. *Br J Surg* 1985; **72**: 771-776
46 **Unanue ER,** Allen PM. The basis for the immunoregulatory role of macrophages and other accessory cells. *Science* 1987; **236**: 551-557
47 **Adams DO,** Hamilton TA. The cell biology of macrophage activation. *Annu Rev Immunol* 1984; **2**: 283-318
48 **Trinchieri G.** Interleukin-12: a proinflammatory cytokine with immunoregulatory functions that bridge innate resistance and antigen-specific adaptive immunity. *Annu Rev Immunol* 1995; **13**: 251-276
49 **Boehm U,** Klamp T, Groot M, Howard JC. Cellular responses to interferon-gamma. *Annu Rev Immunol* 1997; **15**: 749-795
50 **Micallef MJ,** Ohtsuki T, Kohno K, Tanabe F, Ushio S, Namba M, Tanimoto T, Torigoe K, Fujii M, Ikeda M, Fukuda S, Kurimoto M. Interferon-gamma-inducing factor enhances T helper 1 cytokine production by stimulated human T cells: synergism with interleukin-12 for interferon-gamma production.

Eur J Immunol 1996; **26**: 1647-1651
51 **Robinson D,** Shibuya K, Mui A, Zonin F, Murphy E, Sana T, Hartley SB, Menon S, Kastelein R, Bazan F, O'Garra A. IGIF does not drive Th1 development but synergizes with IL-12 for interferon-gamma production and activates IRAK and NFkappaB. *Immunity* 1997; **7**: 571-581
52 **Rushfeldt C,** Sveinbjornsson B, Seljelid R, Smedsrod B. Early events of hepatic metastasis formation in mice: role of Kupffer and NK-cells in natural and interferon-gamma-stimulated defense. *J Surg Res* 1999; **82**: 209-215
53 **Schultz RM,** Chirigos MA. Macrophage activation for non-specific tumor cytotoxicity. *Adv Pharmacol Chemother* 1980; **17**: 157-193
54 **Munder M,** Mallo M, Eichmann K, Modolell M. Murine macrophages secrete interferon gamma upon combined stimulation with interleukin (IL)-12 and IL-18: A novel pathway of autocrine macrophage activation. *J Exp Med* 1998; **187**: 2103-2108
55 **Gaillard T,** Mulsch A, Busse R, Klein H, Decker K. Regulation of nitric oxide production by stimulated rat Kupffer cells. *Pathobiology* 1991; **59**: 280-283
56 **Yonei Y,** Kurose I, Fukumura D, Saito H, Miura S, Tsukada N, Oda M, Tsuchiya M. Evidence of direct interaction between Kupffer cells and colon cancer cells: an ultrastructural study of the co-culture. *Liver* 1994; **14**: 37-44
57 **Kurose I,** Miura S, Higuchi H, Watanabe N, Kamegaya Y, Takaishi M, Tomita K, Fukumura D, Kato S, Ishii H. Increased nitric oxide synthase activity as a cause of mitochondrial dysfunction in rat hepatocytes: roles for tumor necrosis factor alpha. *Hepatology* 1996; **24**: 1185-1192
58 **Fukumura D,** Yonei Y, Kurose I, Saito H, Ohishi T, Higuchi H, Miura S, Kato S, Kimura H, Ebinuma H, Ishi H. Role in nitric oxide in Kupffer cell-mediated hepatoma cell cytotoxicity *in vitro* and *ex vivo*. *Hepatology* 1996; **24**: 141-149
59 **Canbay A,** Feldstein AE, Higuchi H, Werneburg N, Grambihler A, Bronk SF, Gores GJ. Kupffer cell engulfment of apoptotic bodies stimulates death ligand and cytokine expression. *Hepatology* 2003; **38**: 1188-1198
60 **Fanger MW,** Shen L, Graziano RF, Guyre PM. Cytotoxicity mediated by human Fc receptors for IgG. *Immunol Today* 1989; **10**: 92-99
61 **Van de Winkel JG,** Anderson CL. Biology of human immunoglobulin G Fc receptors. *J Leukoc Biol* 1991; **49**: 511-524
62 **Lovdal T,** Andersen E, Brech A, Berg T. Fc receptor mediated endocytosis of small soluble immunoglobulin G immune complexes in Kupffer and endothelial cells from rat liver. *J Cell Sci* 2000; **113**: 3255-3266
63 **Loegering DJ,** Lennartz MR. Differential effect of Fc gamma receptor ligation on LPS-stimulated TNF-alpha secretion by hepatic, splenic, and peritoneal macrophages. *Inflammation* 2002; **26**: 305-310
64 **Gardner CR,** Wasserman AJ, Laskin DL. Differential sensitivity of tumor targets to liver macrophage-mediated cytotoxicity. *Cancer Res* 1987; **47**: 6686-6691
65 **Patel T,** Roberts LR, Jones BA, Gores GJ. Dysregulation of apoptosis as a mechanism of liver disease: an overview. *Semin Liver Dis* 1998; **18**: 105-114
66 **Jaeschke H.** Inflammation in response to hepatocellular apoptosis. *Hepatology* 2002; **35**: 964-966
67 **Alnemri ES,** Livingston DJ, Nicholson DW, Salvesen G, Thornberry NA, Wong WW, Yuan J. Human ICE/CED-3 protease nomenclature. *Cell* 1996; **87**: 171
68 **Earnshaw WC,** Martins LM, Kaufmann SH. Mammalian caspases: structure, activation, substrates, and functions during apoptosis. *Annu Rev Biochem* 1999; **68**: 383-424
69 **Thornberry NA,** Lazebnik Y. Caspases: enemies within. *Science* 1998; **281**: 1312-1316
70 **Scaffidi C,** Fulda S, Srinivasan A, Friesen C, Li F, Tomaselli KJ, Debatin KM, Krammer PH, Peter ME. Two CD95 (APO-1/Fas) signaling pathways. *EMBO J* 1998; **17**: 1675-1687
71 **Barry M,** Bleackley RC. Cytotoxic T lymphocytes: all roads lead to death. *Nat Rev Immunol* 2002; **2**: 401-409
72 **Krammer PH.** CD95's deadly mission in the immune system. *Nature* 2000; **407**: 789-795
73 **Yang X,** Stennicke HR, Wang B, Green DR, Janicke RU, Srinivasan A, Seth P, Salvesen GS, Froelich CJ. Granzyme B mimics apical caspases. Description of a unified pathway for trans-activation of executioner caspase-3 and -7. *J Biol Chem* 1998; **273**: 34278-34283
74 **Thomas DA,** Du C, Xu M, Wang X, Ley TJ. DFF45/ICAD can be directly processed by granzyme B during the induction of apoptosis. *Immunity* 2000; **12**: 621-632
75 **Russell JH,** Ley TJ. Lymphocyte-mediated cytotoxicity. *Annu Rev Immunol* 2002; **20**: 323-370
76 **Beresford PJ,** Xia Z, Greenberg AH, Lieberman J. Granzyme A loading induces rapid cytolysis and a novel form of DNA damage independently of caspase activation. *Immunity* 1999; **10**: 585-594
77 **Trapani JA,** Smyth MJ. Functional significance of the perforin/granzyme cell death pathway. *Nat Rev Immunol* 2002; **2**: 735-747
78 **Manca F,** Fenoglio D, Li Pira G, Kunkl A, Celada F. Effect of antigen/antibody ratio on macrophage uptake, processing, and presentation to T cells of antigen complexed with polyclonal antibodies. *J Exp Med* 1991; **173**: 37-48
79 **Pulford K,** Souhami RL. The surface properties and antigen-presenting function of hepatic non-parenchymal cells. *Clin Exp Immunol* 1981; **46**: 581-588
80 **Smedsrod B,** Pertoft H, Eggertsen G, Sundstrom C. Functional and morphological characterization of cultures of Kupffer cells and liver endothelial cells prepared by means of density separation in Percoll, and selective substrate adherence. *Cell Tissue Res* 1985; **241**: 639-649
81 **Lovdal T,** Andersen E, Brech A, Berg T. Fc receptor mediated endocytosis of small soluble immunoglobulin G immune complexes in Kupffer and endothelial cells from rat liver. *J Cell Sci* 2000; **113**: 3255-3266
82 **Knolle PA,** Germann T, Treichel U, Uhrig A, Schmitt E, Hegenbarth S, Lohse AW, Gerken G. Endotoxin down-regulates T cell activation by antigen-presenting liver sinusoidal endothelial cells. *J Immunol* 1999; **162**: 1401-1407
83 **Knolle PA,** Schmitt E, Jin S, Germann T, Duchmann R, Hegenbarth S, Gerken G, Lohse AW. Induction of cytokine production in naive CD4(+) T cells by antigen-presenting murine liver sinusoidal endothelial cells but failure to induce differentiation toward Th1 cells. *Gastroenterology* 1999; **116**: 1428-1440
84 **Hansen B,** Melkko J, Smedsrod B. Serum is a rich source of ligands for the scavenger receptor of hepatic sinusoidal endothelial cells. *Mol Cell Biochem* 2002; **229**: 63-72
85 **Dini L,** Lentini A, Diez GD, Rocha M, Falasca L, Serafino L, Vidal-Vanaclocha F. Phagocytosis of apoptotic bodies by liver endothelial cells. *J Cell Sci* 1995; **108**: 967-973
86 **Bogers WM,** Stad RK, Janssen DJ, van Rooijen N, van Es LA, Daha MR. Kupffer cell depletion in vivo results in preferential elimination of IgG aggregates and immune complexes via specific Fc receptors on rat liver endothelial cells. *Clin Exp Immunol* 1991; **86**: 328-333
87 **Edmiston KH,** Shoji Y, Mizoi T, Ford R, Nachman A, Jessup JM. Role of nitric oxide and superoxide anion in elimination of low metastatic human colorectal carcinomas by unstimulated hepatic sinusoidal endothelial cells. *Cancer Res* 1998; **58**: 1524-1531
88 **Rocha M,** Kruger A, Van Rooijen N, Schirrmacher V, Umansky V. Liver endothelial cells participate in T-cell-dependent host resistance to lymphoma metastasis by production of nitric oxide *in vivo*. *Int J Cancer* 1995; **63**: 405-411
89 **Kurose I,** Miura S, Fukumura D, Yonei Y, Saito H, Tada S, Suematsu M, Tsuchiya M. Nitric oxide mediates Kupffer cell-induced reduction of mitochondrial energization in hepatoma cells: a comparison with oxidative burst. *Cancer Res* 1993; **53**: 2676-2682
90 **Strohmeyer D.** Pathophysiology of tumor angiogenesis and

its relevance in renal cell cancer. *Anticancer Res* 1999; **19**: 1557-1561

91 **Carmeliet P,** Jain RK. Angiogenesis in cancer and other diseases. *Nature* 2000; **407**: 249-257

92 **Timmers M,** Vekemans K, Vermijlen D, Asosingh K, Kuppen PJK, Bouwens L, Wisse E, Braet F. Interactions between liver metastasizing rat colon carcinoma cells and Kupffer cells during the onset of metastasis. *Int J Cancer* 2004; **112**: 793-802

93 **Vekemans K,** Braet F, Vermijlen D, Timmers M, Wisse E. CC531s colon carcinoma cells induce apoptosis in hepatic endothelial cells by the Fas/FasL mediated pathway. *Liver International* 2003: **23**: 283-293

94 **Vekemans K,** Braet F, Wisse E. CC531S-induced damage of the rat liver sinusoidal endothelial lining is mediated by the Fas/FasL pathway. *Hepatology* 2003; **38**: 1314

95 **Mook OR,** Van Marle J, Vreeling-Sindelarova H, Jonges R, Frederiks WM, Van Noorden CJ. Visualization of early events in tumor formation of eGFP-transfected rat colon cancer cells in liver. *Hepatology* 2003; **38**: 295-304

96 **Vekemans K,** Braet F, Muyllaert D, Wisse E. Nitric oxide derived from rat liver sinusoidal endothelial cells induces apoptosis in IFNg - sensitized CC531s colon carcinoma cells. *J Hepatol* 2004; **41**: 11-18

97 **Vekemans K,** Braet F, Wisse E. DiO-labeled CCC531s colon carcinoma cells traverse the rat hepatic sinusoidal endothelium via the Fas/FasL pathway. *J Gastrointest Surg* 2004; **8**: 371-372

Science Editor Wang XL and Guo SY **Language Editor** Elsevier HK

PO Box 2345, Beijing 100023, China
www.wjgnet.com
wjg@wjgnet.com

ELSEVIER

World J Gastroenterol 2005;11(33):5103-5108
World Journal of Gastroenterology ISSN 1007-9327
© 2005 The WJG Press and Elsevier Inc. All rights reserved.

• *ESOPHAGEAL CANCER* •

Relationship between genetic polymorphisms of alcohol and aldehyde dehydrogenases and esophageal squamous cell carcinoma risk in males

Chia-Fang Wu, Deng-Chyang Wu, Hon-Ki Hsu, Ein-Long Kao, Jang-Ming Lee, Cheng-Chieh Lin, Ming-Tsang Wu

Chia-Fang Wu, Ming-Tsang Wu, Graduate Institute of Occupational Safety and Health and Department of Occupational Medicine, Kaohsiung Medical University, Kaohsiung, Taiwan, China
Hon-Ki Hsu, Department of Chest Surgery, Kaohsiung Veterans General Hospital, Kaohsiung, Taiwan, China
Ein-Long Kao, Department of Chest Surgery, Kaohsiung Medical University Hospital, Kaohsiung, Taiwan, China
Jang-Ming Lee, Department of Surgery, National Taiwan University Hospital, Taipei, Taiwan, China
Cheng-Chieh Lin, Ming-Tsang Wu, Department of Family Medicine, China Medical University and Hospital, Taichung 404, Taiwan, China
Supported by the Taiwan National Science Council, No. NSC 90-2320-B-037-040 and NSC 90-2320-B-037-052 and the Taiwan National Health Research Institute, No. NHRI-CN-IN-9007P and NHRI-EX949428PI
Correspondence to: Dr. Ming-Tsang Wu, Graduate Institute of Occupational Safety and Health, Kaohsiung Medical University, 100, Shih-Chuan 1st Road, Kaohsiung, Taiwan, China. mingtsangwu@yahoo.com
Telephone: +886-7-312-1101-2315 Fax: +886-7-3221806
Received: 2004-12-22 Accepted: 2005-02-18

Abstract

AIM: To investigate the association between the genetic polymorphisms of ADH2 and ALDH2, lifetime alcohol consumption and esophageal cancer risk in the Taiwanese men.

METHODS: Between August 2000 and June 2003, 134 pathologically-proven esophageal squamous cell carcinoma male patients and 237 male controls were recruited from Kaohsiung Medical University Hospital and Kaohsiung Veterans General Hospital in southern Taiwan. ADH2 and ALDH2 polymorphisms were genotyped using PCR-RFLP.

RESULTS: Compared to those with ADH2*2/*2, individuals with ADH2*1/*2 and ADH2*1/*1 had 2.28- and 7.14-fold, respectively, increased risk of developing esophageal cancer (95%CI = 1.11-4.68 and 2.76-18.46) after adjusting for alcohol consumption and other covariates. The significant increased risk was also noted among subjects with ALDH2*1/*2 (adjusted OR (AOR) = 5.25, 95%CI = 2.47-11.19), when compared to those with ALDH2*1/*1. The increased risk of esophageal cancer was made greater, when subjects carried both ADH2*1/*1 and ALDH2*1/*2, compared to those with ADH2*1/*2 or ADH2*2/*2 and ALDH2*1/*1 (AOR = 36.79, 95%CI = 9.36-144.65). Furthermore, we found a multiplicative effect of lifetime alcoholic consumption and genotypes (ADH2 and ALDH2) on esophageal cancer risk.

CONCLUSION: Our findings suggest that polymorphisms of ADH2 and ALDH2 can modify the influence of alcoholic consumption on esophageal cancer risk.

© 2005 The WJG Press and Elsevier Inc. All rights reserved.

Key words: Esophageal cancer; Alcohol; Alcohol dehydrogenase; Aldehyde dehydrogenase; Genetic polymorphisms

Wu CF, Wu DC, Hsu HK, Kao EL, Lee JM, Lin CC, Wu MT. Relationship between genetic polymorphisms of alcohol and aldehyde dehydrogenases and esophageal squamous cell carcinoma risk in males. *World J Gastroenterol* 2005; 11(33): 5103-5108

http://www.wjgnet.com/1007-9327/11/5103.asp

INTRODUCTION

Epidemiologic studies have demonstrated that drinking alcoholic beverages is associated with the development of cancers in the oral cavity, pharynx, larynx, and esophagus[1]. Our previous study also reported that, in addition to cigarette smoking and areca chewing, alcohol consumption is one of the leading risk factors for esophageal cancer in Taiwan[2]. In that study, we found that subjects who consumed more than 1 220 g/year of alcohol (about 4 cans of beer per day for 20 years) in a lifetime were found to have a 9.7-fold higher risk for esophageal cancer than those who did not drink (95%CI = 4.3-22.0).

When ethanol is consumed through drinking, it is metabolized primarily by class I alcohol dehydrogenase (ADH2) into acetaldehyde, an intermediate metabolite, and then it is metabolized by aldehyde dehydrogenase (ALDH2) into acetic acid in humans[3]. Acetaldehyde, a well-known carcinogen in animals, plays an important role in alcohol toxicity in humans[4].

Genetic variation in the ability to metabolize alcohol might be associated with esophageal cancer risk. ADH2 and ALDH2 genes are located on chromosomes 4q22 and 12q24, respectively. One amino acid has been found to change from arginine (CGC) (ADH2*1) to histidine (CAC) (ADH2*2) in ADH2 gene at codon 47 of exon 3[5]. Bosron and Li[3] has found ADH2*2/*2 to have about 40 times

higher V_{max} than ADH2*1/*1, because ADH2*2/*2 encodes a superactive subunit of ADH2 in the oxidation of ethanol, causing acetaldehyde to accumulate in the circulation. For ALDH2, a single nucleotide transition from glutamic acid to lysine (G→A) at codon 487 of exon 12 has also been reported[6]. The mutant allele of ALDH2*2 (A/A) has relatively lower ALDH2 activity than ALDH2*1 allele (G/G)[7] in the metabolization of acetaldehyde into acetic acid, leading to the accumulation of circulatory acetaldehyde[8].

Many studies from Japan have reported that subjects with ADH2*1/*1 or ALDH2*1/*2 genotypes were much more susceptible to esophageal cancer than those with the genotypes[9-15]. In Taiwan, however, only one study has reported the relationship between genetic polymorphisms of ADH2 and ALDH2 and esophageal cancer risk[16]. In that study, Chao and his colleagues[16], studying 59 esophageal cancer patients who were also alcoholics and 222 alcoholic controls, found the allele frequencies of ADH2*1 and ALDH2*2 in alcoholic cancer patients to be 51% and 31%, respectively, much higher frequencies than those found in alcoholics without cancer (39%; $P<0.025$ and 8%; $P<0.001$). In this study, we further investigated the independent or combined effects of the ADH2 and ALDH2 gene polymorphisms on esophageal cancer risks in the Taiwanese men. We also evaluated interaction of ADH2 and ALDH2 with alcohol consumption and study the interaction's relationship to esophageal cancer risk.

MATERIALS AND METHODS

Patients and controls

In this hospital-based case-control study, we recruited male case patients with new histological diagnosis of esophageal squamous cell carcinoma from Kaohsiung Medical University Hospital and Kaohsiung Veterans General Hospital in the southern Taiwan from August 2000 to June 2003. The Department of Preventive Medicine at each hospital chose 1-2 age-matched (±4 years) healthy male controls who had no malignancies to give blood specimens at the time as the cases. In total, 134 cases and 237 controls were interviewed and genotyped from peripheral blood specimens.

Using a standardized questionnaire, trained interviewers collected demographic characteristics and information about cigarette, alcohol and areca consumption from study subjects[2]. Information on habitual substance use included whether the subject had been a habitual areca chewer, cigarette smoker, or an alcoholic in his or her lifetime, what year the subject started and quitted, the duration of consumption and the daily amount consumed, and type of alcoholic beverage consumed. This study was approved by Kaohsiung Medical University Hospital's IRB. Informed consent was obtained from all subjects.

Genotyping

ADH2 polymorphisms at codon 47 were determined by polymerase chain reaction-restriction fragment length polymorphism (PCR-RFLP)[17,18]. The two primers were 5'-AAT CTT TTC TGA ATC TGA ACA G-3' (upstream) and 5'-GAA GGG GGG TCA CCA GGT TGC-3' (downstream). The PCR was carried out with 100 ng/μL genomic DNA, 10× buffer, 2.5 mmol/L dNTP, 20 pmol/L of each primer, 50 mmol/L $MgCl_2$ and 5 U Taq polymerase in a 25 μL reaction mixture. The PCR condition was performed by initial denaturation at 95 ℃ for 5 min, followed by 40 cycles at 95 ℃ for 1 min, 55 ℃ for 57.5 s, 72 ℃ for 45 s and a final extension at 72 ℃ for 10 min. The final PCR product was digested with *Mae*III for 4 h at 55 ℃ and electrophoresed and viewed on a 3% agarose gel. When a *Mae*III restriction site was presented, the 94-bp fragment was digested into two fragments: lengths of 59 and 35 bp. Individuals with ADH2*2/*2 and ADH2*1/*2 had 59- and 35-bp fragments and 94-, 59- and 35-bp fragments, respectively, whereas those with ADH2*1/*1 had only a 94-bp fragment (Figure 1).

ALDH2 polymorphisms at codon 487 were also determined by PCR-RFLP[11,19]. The DNA sample was amplified with two primers: 5'-CAA ATT ACA GGG TCA ACT GCT-3' (upstream) and 5'-CCA CAC TCA CAG TTT TCT CTT-3' (downstream). The PCR was carried out with 100 ng/μL genomic DNA, 10× buffer, 2.5 mmol/L dNTP, 20 pmol/L of each primer, 50 mmol/L $MgCl_2$ and 5 U Taq polymerase in a 25 μL reaction mixture. The PCR condition was performed by initial denaturation at 95 ℃ for 5 min, followed by 35 cycles at 94 ℃ for 15 s, 58 ℃ for 1 min 30 s, 72 ℃ for 30 s and a final extension at 72 ℃ for 10 min. The final PCR product was digested with *Mbo*II for 16 h at 37 ℃ and electrophoresed and viewed on a 12% polyacrylamide gel. When a *Mbo*II restriction site was presented, the 135-bp fragment was digested into two fragments: lengths of 126 and 9 bp. Individuals with ALDH2*1/*1 and ALDH2*1/*2 had 126- and 9-bp fragments and 135-, 126- and 9-bp fragments, respectively, whereas those with ALDH2*2/*2 had only a 135-bp fragment (Figure 2).

In addition, 20 case patients provided paired samples of tumors and peripheral blood for genotyping. We found that the evidence for both genotypes for ADH2 and ALDH2 were exactly the same in each case patient.

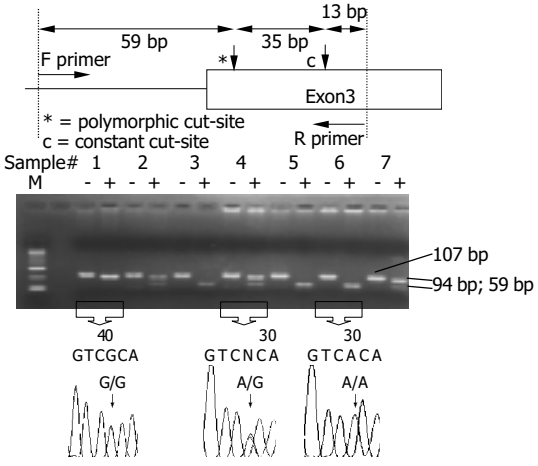


Figure 1 PCR-RFLP analyses of exon 3, codon 47 polymorphism of ADH2. M represents a size marker. Sample 1 is ADH2*1/*1; samples 2, 4, and 7 are ADH2*1/*2; samples 3, 5, and 6 are ADH2*2/*2. + and - represent the PCR product with and without restriction enzyme *Mae*III.

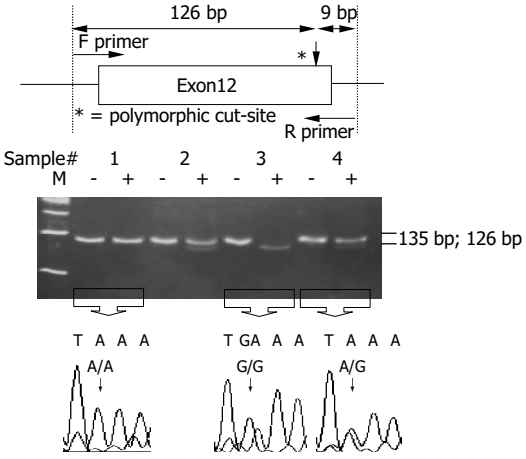


Figure 2 PCR-RFLP analyses of exon 12, codon 487 polymorphism of ALDH2. M represents a size marker. Sample 1 is ALDH2*2/*2; sample 3 is ALDH2*1/*1; samples 2 and 4 are ALDH2*1/*2. + and - represent the PCR product with and without restriction enzyme *Mbo*II.

Laboratory QA/QC

Three different genotypes of each ADH2 and ALDH2 were first sequenced to confirm the findings, then in each genotyping set (~10 samples), we included one positive control and one negative control sample. The positive control sample was included to ensure complete digestion of the PCR product by restriction enzymes. The negative control was placed with the same reagents as those used with actual samples, with the exception of DNA templates. In addition, about 3% of subjects (n = 12/378) were randomly selected for re-genotyping (the results were the same).

Statistical analysis

Hardy-Weinberg equilibrium statistic was calculated first. Genotype frequencies, demographic characteristics, and substance use (cigarette, alcohol, and areca) in cases and controls were compared by Student's t, χ^2, or Fisher's exact tests.

For substance use, subjects who reported smoking more than 10 cigarettes/week for at least 6 mo were defined as cigarette smokers, those who reported regularly chewing betel quid for at least 6 mo were defined as betel chewers, and those who reported drinking beer, wine, or distilled spirits more than one time per week for at least 6 mo were defined as alcoholics.

Using multiple logistic regression models, we determined the relationship of ADH2 and ALDH2 polymorphisms with esophageal cancer risk after adjusting for other covariates, including age (continuous variable), educational level (>high school, high school, and <high school), cigarette smoking (yes *vs* no), alcohol consumption (yes *vs* no) and areca chewing (yes *vs* no). Since the interactive effect between lifetime alcohol consumption and ADH2 and ALDH2 polymorphisms on esophageal cancer risk was also examined in this study, lifetime consumption of alcoholic beverage was calculated by multiplying the concentration of alcohol in the consumed beverage by the amount consumed per day by the number of years consumed, resulting in number designated as grams per year. The median cut-off point for lifetime alcohol consumption was 1 500 g/year, which equaled an average of five 300-350 cm^3 cans of beer (5% alcohol) per day for 20 consecutive years. Subjects were also classified as non-drinkers if they consumed ≤1 500 g/year, and those who consumed >1 500 g/year were used for the subsequent interaction analysis. The data were analyzed using the SAS 8.1 statistical package; all P-values were two-sided.

RESULTS

We found 231 pathology-proven cases of esophageal squamous cell carcinoma at Kaohsiung Medical University Hospital and Kaohsiung Veterans General Hospital between August 2000 and June 2003. Mean ages (±SD) of the recruited patients (n = 134) and non-recruited patients (n = 97) were 58.9±12.6 and 59.0±13.6 years, respectively, with no significant difference (P = 0.81).

Mean ages (range) of the 134 cases and 237 controls were 58.9 years (34-82 years) and 57.8 years (34-82 years), respectively, with no significant difference (Table 1). Educational level (P<0.0001) and the habitual use of cigarettes (P<0.0001), alcohol (P<0.0001), and areca (P<0.0001) were most significant predictors of esophageal cancer risk. We found cigarette smokers, alcoholics, and areca chewers had a 13.61-, 9.90-, and 13.33-fold higher risk, respectively, for developing esophageal cancer than non-smokers, non-drinkers, and non-chewers (95%CI = 6.81-27.21, 5.89-16.64, and 7.33-24.26, respectively) (data not shown).

The prevalence (number) of ADH2*1/*1, ADH2*1/*2, and ADH2*2/*2 in the controls was 6.8% (16/237), 38.4% (91/237), and 54.9% (130/237), respectively. The gene frequency of the ADH2*1 allele was 25.9%. The distribution of the different genotypes among the 237 controls closely conformed to expected Hardy-Weinberg frequencies (χ^2 = 0.00; df = 2; P = 1.00). The prevalence (number) of ALDH2*1/*1, ALDH2*1/*2, and ALDH2*2/*2 in the controls was 50.6% (120/237), 44.3% (105/237), and 5.1% (12/237), respectively. The gene frequency of the ALDH2*2 allele was 27.2%. The distribution of the different genotypes among the 237 controls also closely

Table 1 Demographic characteristics among 134 cases and 237 controls

Variables	Cases (%) n = 134	Controls (%) n = 237	Crude OR (95%CI)	P
Age (yr)				
Mean±SD	58.9±12.6	57.8±11.8	–	0.41
Education (%)				
<High school	107 (76.1)	86 (36.3)	1	
High school	23 (17.1)	94 (39.7)	0.20 (0.11–0.34)	
>High school	4 (3.0)	57 (24.1)	0.06 (0.06–0.16)	<0.0001
Ethnicity (%)				
Mainlander	102 (76.1)	186 (78.5)	1	
Fukienese	25 (18.7)	33 (13.9)	1.38 (0.78–2.45)	
Others	7 (5.2)	18 (7.6)	0.71 (0.29–1.75)	0.37
Cigarette smoking (%)				
No	10 (7.5)	124 (52.3)	1	
Yes	124 (92.5)	113 (47.7)	13.61 (6.81–27.21)	<0.0001
Alcohol consumption (%)				
No	24 (17.9)	162 (68.4)	1	
Yes	110 (82.1)	75 (31.6)	9.9 (5.89–16.64)	<0.0001
Areca chewing (%)				
No	66 (49.3)	220 (92.8)	1	
Yes	68 (50.8)	17 (7.2)	13.33 (7.33–24.26)	<0.0001

conformed to expected Hardy-Weinberg frequencies (χ^2 = 1.95; df = 2; P = 0.38).

Table 2 shows the association of ADH2 and ALDH2 genotypes with esophageal cancer risk before and after adjusting for other covariates. Subjects with ADH2*1/*2 and ADH2*1/*1 had 2.28 (95%CI = 1.11-4.68)- and 7.14 (95%CI = 2.76-18.46)-fold, respectively, greater risk of developing esophageal cancer than the subjects with ADH2*2/*2, after adjusting for age, educational level, cigarette smoking, alcohol consumption, areca chewing, and ALDH2 polymorphism. In addition, the effect of ADH2*1/*1 was still significantly elevated (adjusted OR (AOR) = 4.80; 95%CI = 2.02-11.44), when compared to the combined ADH2*1/*2 and ADH2*2/*2 (data not shown).

For ALDH2 genotypes, subjects with ALDH2*1/*2 (AOR = 5.25, 95%CI = 2.47-11.19) were found to have a significantly more increased risk of esophageal cancer compared to those with ALDH2*1/*1 (Table 2). The risk for subjects with ALDH2*2/*2 was slight, but not significantly higher than those with ALDH2*1/*1 (AOR = 2.44; 95%CI = 0.44-13.55). However, compared to ALDH2*1/*1, the combined risk effect of ALDH2*1/*2 and ALDH2*2/*2 was significantly elevated (AOR = 5.20; 95%CI = 2.46-11.00) (data not shown).

Table 3 shows the joint effect of ADH2 and ALDH2 genotypes on esophageal cancer risk. The significantly increased trend for esophageal cancer risk was noted in subjects with ADH2*1/*2 or *2/*2 and ALDH2*1/*1, ADH2*1/*1 and ALDH2*1/*1, ADH2*1/*2 or *2/*2 and ALDH2*1/*2, to ADH2*1/*1 and ALDH2*1/*2. However, the increased risk was not pronounced in a group of ALDH2*2/*2, possibly because of small sample size.

Table 4 shows the effect of a lifetime interaction between alcohol consumption and ADH2 and ALDH2 genotypes on esophageal cancer risk. Using non-drinkers with ADH2*1/*2 or *2/*2 and ALDH2*1/*1 as a baseline, we found that the higher the lifetime consumption of alcohol, the greater the risk for esophageal cancer in each category of ADH2 and ALDH2 genotypes, except for a group of ALDH2*2/*2. When categorizing the subjects into amount of alcohol consumed in a lifetime (non-drinkers, drinkers with ≤1 500 g/year, or drinkers with >1 500 g/year), we found an increased trend for esophageal cancer risk in the more highly susceptible ADH2 and ALDH2 genotypes. Compared to baseline, the risk for developing esophageal cancer increased in subjects carrying ADH2*1/*1 and ALDH2*1/*2 and consuming more than 1 500 g/year of alcohol in a multiplicative fashion (AOR = 139.35, 95%CI = 10.05-∞, Table 5).

Table 2 Association of ADH2 and ALDH2 genotypes with esophageal cancer risk before and after adjusting for other covariates

Genotypes	Cases (%) n = 134	Controls (%) n = 237	OR (95%CI)	AOR (95%CI)[1]
ADH2				
*2/*2	46 (34.3)	130 (54.9)	1	1
*1/*2	49 (36.6)	91 (38.4)	1.52 (0.94–2.47)	2.28 (1.11–4.68)
*1/*1	39 (29.1)	16 (6.8)	6.89 (3.52–13.49)	7.14 (2.76–18.46)
P for HW[2]		1.00		
ALDH2				
*1/*1	32 (23.9)	120 (50.6)	1	1
*1/*2	99 (73.9)	105 (44.3)	3.54 (2.19–5.70)	5.25 (2.47–11.19)
*2/*2	3 (2.2)	12 (5.1)	0.94 (0.25–3.52)	2.44 (0.44–13.55)
P for HW[2]		0.38		

[1]Adjusting for age (continuous variable), educational levels (high school *vs* <high school; >high school *vs* <high school), cigarette smoking (yes *vs* no), alcohol consumption (yes *vs* no), areca chewing (yes *vs* no), and ADH2 (*1/*1 *vs* *2/*2 and *1/*2 *vs* *2/*2) or ALDH2 (*2/*2 *vs* *1/*1 and *1/*2 *vs* *1/*1). [2]P value for deviation from Hardy–Weinberg equilibrium.

DISCUSSION

The present study finds alcohol consumption to be the major risk of esophageal cancer in the Taiwanese men. However, ethanol *per se* is not carcinogenic[1]. Researchers have paid much more attention to the relationship between acetaldehyde, the first metabolite of alcohol, and cancer risk, even though the detailed mechanisms of alcohol-associated cancers, such as esophageal cancer are still puzzling. Ethanol is metabolized mainly by ADH2 to become acetaldehyde and then further metabolized by ALDH2 to form acetic acid. Acetaldehyde is a very active intermediate able to attack DNA or protein to form adducts[20,21]. In addition, Yin and his colleagues[22] have reported the ADH activity in the 15 specimens of esophageal mucosa from the Chinese men to be about four-fold greater than that of gastric mucosa in the same population (n = 7). In contrast, the esophageal ALDH activity is only 20% of that in the stomach, suggesting that the concentration of acetaldehyde in esophagus is possibly much higher than that in the stomach after consuming the beverages.

Since the major metabolic pathway for ethanol is determined by ADH2 and ALDH2, polymorphisms on these two genes may affect the formation of acetaldehyde. For ALDH2 genotypes, Enomoto and his colleagues[23] reported that subjects with ALDH2*1/*2 had an average increase in peak blood acetaldehyde level that was five-fold higher than those with ALDH2*1/*1 after drinking a small amount of ethanol (0.1 g/kg of body weight), though this study did not investigate the effect of ADH2 genotypes on

Table 3 Joint effect of ADH2 and ALDH2 genotypes on esophageal cancer risk

ADH2	ALDH2	Cases (%) n = 134	Controls (%) n = 237	OR (95%CI)	AOR (95%CI)[1]
*1/*2 or *2/*2	*1/*1	23 (17.2)	112 (47.3)	1	1
*1/*1		9 (6.7)	8 (3.4)	4.20 (1.49–11.81)	3.54 (0.93–13.53)
*1/*2 or *2/*2	*1/*2	69 (51.5)	98 (41.4)	2.63 (1.58–4.37)	4.81 (2.17–10.70)
*1/*1		30 (22.4)	7 (3.0)	16.00 (6.40–39.99)	36.79 (9.36–144.65)
*1/*2 or *2/*2	*2/*2	3 (2.2)	11 (4.6)	1.02 (0.27–3.88)	3.40 (0.63–18.33)
*1/*1		0	1 (0.4)	–	–

[1]Adjusting for variables in Table 2.

Table 4 Interactive effect between lifetime alcohol consumption and ADH2 and ALDH2 genotypes on esophageal cancer risk

ADH2	ALDH2	Alcohol consumption (g/yr)	Cases (%) *n* = 134	Controls (%) *n* = 237	OR (95%CI)	AOR (95%CI)[1]
*1/*2 or *2/*2	*1/*1	Non-drinker	3 (2.2)	66 (27.9)	1	1
		≤1 500	5 (3.7)	19 (8.0)	5.79 (1.27–26.46)	3.76 (0.65–21.69)
		>1 500	15 (11.2)	27 (11.4)	12.22 (3.27–45.66)	6.07 (1.46–25.26)
*1/*1	*1/*1	Non-drinker	0	2 (0.8)	–	–
		≤1 500	4 (3.0)	4 (1.7)	22.00 (3.62–133.81)	14.91 (1.92–115.95)
		>1 500	5 (3.7)	2 (0.8)	55.00 (7.39–409.22)	33.54 (3.52–319.89)
*1/*2 or *2/*2	*1/*2	Non-drinker	13 (9.7)	76 (32.1)	3.76 (1.03–13.78)	2.92 (0.73–11.63)
		≤1 500	31 (23.1)	15 (6.3)	45.47 (12.26–168.68)	26.67 (6.05–117.57)
		>1 500	25 (18.7)	7 (3.0)	78.57 (18.83–327.89)	39.26 (7.05–218.68)
*1/*1	*1/*2	Non-drinker	5 (3.7)	6 (2.5)	18.33 (3.50–96.18)	18.60 (2.69–128.77)
		≤1 500	14 (10.5)	1 (0.4)	308 (29.80–3 183.05)	139.35 (10.05–∞)
		>1 500	11 (8.2)	0	–	–
*1/*2 or *2/*2	*2/*2	Non-drinker	3 (2.2)	11 (4.6)	6 (1.07–33.60)	2.20 (0.33–14.47)
		≤1 500	0	0	–	–
		>1 500	0	0	–	–
*1/*1	*2/*2	Non-drinker	0	1 (0.4)	–	–
		≤1 500	0	0	–	–
		>1 500	0	0	–	–

[1]Adjusting for age, educational levels, cigarette smoking, and areca chewing in Table 2.

Table 5 Allele frequencies of ADH2 and ALDH2 genotypes among different racial groups

Populations	ADH2		ALDH2	
	n	*1/*2 (%)	*n*	*1/*2 (%)
Germans[1]	233	0.96/0.04	193	1/0
Indians[1]	167	0.90/0.10	179	0.98/0.02
Chinese[1]	86	0.32/0.68	132	0.84/0.16
Japanese[2]	461	0.07/0.93	461	0.58/0.42
Taiwanese[3]	47	0.27/0.73	47	0.70/0.30
Our study	237	0.26/0.74	237	0.73/0.27

[1]Data from Goedde *et al*.[27]. [2]Data from Higuchi *et al*. [28]. [3]Data from Thomasson *et al*.[25].

acetaldehyde level. Another study done by Mizoi and his colleagues[24] found that, after consuming beverages, the blood acetaldehyde concentrations in those with ALDH2*2/*2 and ALDH2*1/*2 were 19- and 6-fold higher than in those with ALDH2*1/*1, respectively. The results of these studies suggest that subjects with ALDH2*2/*2 and ALDH2*1/*2 may have a higher risk of developing esophageal cancer than those with ALDH2*1/*1, which is consistent with our findings.

However, our study found no subjects with the highest susceptible genotype of ALDH2, ALDH2*2/*2, to be drinkers. Crabb *et al*.[8], and Thomasson *et al*.[25], found that individuals deficient in ALDH2 activity (ALDH2*2/*2 genotype) can develop intense facial flushing responses, because of high blood acetaldehyde levels, after drinking alcohol. This unpleasant discomfort may prevent people from consuming beverages and may keep them from developing alcoholism, which can explain our findings in this study.

In this study, we found subjects with ADH2*1 allele had a higher risk of developing esophageal cancer than those with ADH2*2 allele. Previous epidemiological studies from Japan also reported a significantly higher risk for esophageal cancer among Japanese drinkers with ADH2*1 allele, compared to those with ADH2*2 allele[10,15], which were consistent to our findings. In contrast, Mizoi and his colleagues[24] did not find any significant differences of blood acetaldehyde levels among the three ADH2 genotype groups. However, in an *in vitro* study done by Yin and his colleagues[26], the enzyme activity in ADH2*2 allele was reported to be much higher that that of ADH2*1, suggesting that ethanol is much easily metabolized by ADH2*2 allele to become acetaldehyde. This finding conflicts with the observations from epidemiological studies[10,12,13,15,16] and our study as well. Thus, the detailed mechanism of this ADH2 polymorphism, which may be involved in another metabolic pathway of ethanol or closely linked with other functional polymorphisms, on esophageal cancer risk deserves further examination.

The frequency of ADH2 and ALDH2 genotypes varies across different racial groups (Table 5). ADH2*1 allele is found to be predominant in Caucasians (~90%)[27], whereas most of the Asian people carry the ADH2*2 allele[25,28]. In addition, the frequency of ALDH2*1 allele is higher in Caucasian populations than in Asian populations. These differences in gene distributions, which affect the metabolism of ethanol, may explain why the Asian people experience facial flushing and other marked adverse reactions to drinking alcoholic beverages more easily than Caucasians[29].

Our study found 20 case patients with the paired DNA specimens of tumors and peripheral blood to have exactly the same genotypes of ADH2 and ALDH2 between them. Although the sample size is relatively small, it can be speculated that ADH2 and ALDH2 genes might be involved in an early rather than an advanced stage of esophageal tumorigenesis. This is a hospital-based case-control study, but it is unlikely that individuals carrying one particular genotype were recruited differently in the cases and controls. In addition, in this study, the genotype distribution among the controls closely conformed to Hardy-Weinberg expected frequencies. Information about the consumption of alcoholic beverages was collected from questionnaires, which may randomly misclassify the interest of exposure between the cases and controls and result in the underestimation of

our findings.

In conclusion, the present study found ADH2 and ALDH2 genotypes to be independently associated with esophageal cancer risk in the Taiwanese men. In addition, we have reported the interaction between the combined effect gene and environment on esophageal cancer risk. Subjects who consumed alcoholic beverages and carried susceptible genotypes of ADH2 and ALDH2 experienced a multiplicative increase in risk of developing esophageal cancer, much higher than those who were non-drinkers and did not carry susceptible genotypes of ADH2 and ALDH2. Our present findings can provide additional information about the role of alcohol on esophageal cancer risk in Taiwan.

REFERENCES

1 Alcohol drinking biological data relevant to the evaluation of carcinogenic risk to humans. *IARC Monogr Eval Carcinog Risks Hum* 1988; **44**: 101-152

2 **Wu MT,** Lee YC, Yang PW, Lee CJ, Wu DC, Hsu HK, Ho CK, Kao EL, Lee JM. Risk of betel chewing for oesophageal cancer in Taiwan. *Br J Cancer* 2001; **85**: 658-660

3 **Bosron WF,** Li TK. Genetic polymorphism of human liver alcohol and aldehyde dehydrogenases, and their relationship to alcohol metabolism and alcoholism. *Hepatology* 1986; **6**: 502-510

4 International Agency for Research on Cancer. Allyl compounds, aldehydes, epoxides and peroxides. *IARC Monogr Eval Carcinoge Risk Chemi Hum* 1985; **36**: 101-132

5 **Matsou Y,** Yokoyama Y, Yokoyama S. The genes for human alcohol dehydrogenases β_1 and β_2 differ by only one nucleotide. *Eur J Bilchem* 1989; **183**: 317-320

6 **Hsu LC,** Bendel RE, Yoshida A. Direct detection of usual and atypical alleles on the human aldehyde dehydrogenase-2 (ALDH2) locus. *Am J Hum Genet* 1987; **41**: 996-1001

7 **Farres J,** Wang X, Takahashi K, Cunningham SJ, Wang TT, Weiner H. Effects of changing glutamate 487 to lysine in rat and human liver mitochondrial aldehyde dehydrogenase. A model to study human (Oriental type) class 2 aldehyde dehydrogenase. *J Biol Chem* 1994; **269**: 13854-13860

8 **Crabb DW,** Edenberg HJ, Bosron WF, Li TK. Genotypes for aldehyde dehydrogenase deficiency and alcohol sensitivity: The inactive ALDH2^2 allele is dominant. *J Clin Invest* 1989; **83**: 314-316

9 **Yokoyama A,** Muramatsu T, Ohmori T, Higuchi S, Hayashida M, Ishii H. Esophageal cancer and aldehyde dehydrogenase-2 genotypes in Japanese males. *Cancer Epidemic Biomark Prev* 1996; **5**: 99-102

10 **Hori H,** Kawano T, Endo M, Yuasa Y. Genetic polymorphisms of tobacco- and alcohol-related metabolizing enzymes and human esophageal squamous cell carcinoma susceptibility. *J Clin Gastroenterol* 1997; **25**: 568-575

11 **Yokoyama A,** Muramatsu T, Ohmori T, Yokoyama T, Okuyama K, Takahashi H, Hasegawa Y, Higuchi S, Maruyama K, Shirakura K, Ishii H. Alcohol-related cancers and aldehyde dehydrogenase-2 in Japanese alcoholics. *Carcinogenesis* 1998; **19**: 1383-1387

12 **Yokoyama A,** Muramatsu T, Omori T, Matsushita S, Yoshimizu H, Higuchi S, Yokoyama T, Maruyama K, Ishii H. Alcohol and aldehyde dehydrogenase gene polymorphisms influence susceptibility to esophageal cancer in Japanese alcoholics. *Alcohol Clin Exp Res* 1999; **23**: 1705-1710

13 **Yokoyama A,** Muramatsu T, Omori T, Yokoyama T, Matsushita S, Higuchi S, Maruyama K, Ishii H. Alcohol and aldehyde dehydrogenase gene polymorphisms and oropharyngolaryngeal, esophageal and stomach cancers in Japanese alcoholics. *Carcinogenesis* 2001; **22**: 433-439

14 **Matsuo K,** Hamajima N, Shinoda M, Hatooka S, Inoue M, Takezaki T, Tajima K. Gene-environment interaction between an aldehyde dehydrogenase-2 (ALDH2) polymorphism and alcohol consumption for the risk of esophageal cancer. *Carcinogenesis* 2001; **22**: 913-916

15 **Yokoyama A,** Kato H, Yokoyama T, Tsujinaka T, Muto M, Omori T, Haneda T, Kumagai Y, Igaki H, Yokoyama M, Watanabe H, Fukuda H, Yoshimizu H. Genetic polymorphisms of alcohol and aldehyde dehydrogenases and glutathione S-transferase M1 and drinking, smoking, and diet in Japanese men with esophageal squamous cell carcinoma. *Carcinogenesis* 2002; **23**: 1851-1859

16 **Chao YC,** Wang LS, Hsieh TY, Chu CW, Chang FY, Chu HC. Chinese alcoholic patients with esophageal cancer are genetically different from alcoholics with acute pancreatitis and liver cirrhosis. *Am J Gastroenterol* 2000; **95**: 2958-2964

17 **Xu Y,** Carr LG, Bosron WF, Li TK, Edenberg J. Genotyping of human alcohol dehydrogenases at the ADH2 and ADH3 loci following DNA sequence amplification. *Genomics* 1988; **2**: 209-214

18 **Chen WJ,** Loh EW, Hsu YP, Chen CC, Yu JM, Cheng AT. Alcohol-metabolising genes and alcoholism among Taiwanese Han men: Independent effect of ADH2, ADH3 and ALDH2. *Br J Psychiatry* 1996; **168**: 762-767

19 **Harada S,** Zhang S. New strategy for detection of ALDH2 mutant. *Alcohol Alcohol* 1993; **28**: 11-13

20 **Fang JL,** Vaca CE. Detection of DNA adducts of acetaldehyde in peripheral white blood cells of alcohol abusers. *Carcinogenesis* 1997; **18**: 627-632

21 **Takeshita T,** Kawai T, Morimoto K. Elevated levels of hemoglobin-associated acetaldehyde related to alcohol drinking in the atypical genotype of low Km aldehyde dehydrogenase. *Cancer Res* 1997; **57**: 1241-1243

22 **Yin SJ,** Chou FJ, Chao SF, Tsai SF, Liao CS, Wang SL, Wu CW, Lee SC. Alcohol and aldehyde dehydrogenases in human esophagus: comparison with the stomach enzyme activities. *Alcohol Clin Exp Res* 1993; **17**: 376-381

23 **Enomoto N,** Takase S, Yasuhara M, Takada A. Acetaldehyde metabolism in different aldehyde dehydrogenase-2 genotypes. *Alcohol Clin Exp Res* 1991; **15**: 141-144

24 **Mizoi Y,** Yamamoto K, Ueno Y, Fukunaga T, Harada S. Involvement of genetic polymorphism of alcohol and aldehyde dehydrogenases in individual variation of alcohol metabolism. *Alcohol Alcohol* 1994; **29**: 707-710

25 **Thomasson HR,** Edenberg HJ, Crabb DW, Mai XL, Jerome RE, Li TK, Wang SP, Lin YT, Lu RB, Yin SJ. Alcohol and Aldehyde dehydrogenase genotypes and alcoholism in Chinese men. *Am J Hum Genet* 1991; **48**: 677-681

26 **Yin SJ,** Bosron WF, Magnes LJ, Li TK. Human liver alcohol dehydrogenase: Purification and kinetic characterization of the $\beta_2\beta_2$, $\beta_2\beta_1$, $\alpha\beta_2$ and $\beta_2\gamma_1$ 'Oriental' isozymes. *Biochemistry* 1984; **23**: 5847-5853

27 **Goedde HW,** Agarwal DP, Fritze G, Meier-Tackmann D, Singh S, Beckmann G, Bhatia K, Chen LZ, Fang B, Lisker R, Paik YK, Rothhammer F, Saha N, Segal B, Srivastava LM, Czeizel A. Distribution of ADH2 and ALDH2 genotypes in different population. *Hum Genet* 1992; **88**: 344-346

28 **Higuchi S,** Matsushita S, Muramatsu T, Takagi S, Hayashida M. Alcohol and aldehyde dehydrogenase polymorphisms and the risk for alcoholism. *Am J Psychiatry* 1995; **152**: 1219-1221

29 **Wolff PH.** Ethnic differences in alcohol sensitivity. *Science* 1972; **175**: 449-450

Science Editor Guo SY **Language Editor** Elsevier HK

PO Box 2345, Beijing 100023, China
www.wjgnet.com
wjg@wjgnet.com

ELSEVIER

World J Gastroenterol 2005;11(33):5109-5116
World Journal of Gastroenterology ISSN 1007-9327
© 2005 The WJG Press and Elsevier Inc. All rights reserved.

Bile salts inhibit growth and induce apoptosis of human esophageal cancer cell line

Ru Zhang, Jun Gong, Hui Wang, Li Wang

Ru Zhang, Jun Gong, Li Wang, Digestive Department of the Second Hospital, Xi'an Jiaotong University, Xi'an 710004, Shaanxi Province, China
Hui Wang, Department of Anesthesia, Provincial People's Hospital, Xi'an 710068, Shaanxi Province, China
Supported by the Clinical Key Program of Ministry of Public Health of China, No. 20012130
Co-first-authors: Ru Zhang and Jun Gong
Co-correspondents: Ru Zhang
Correspondence to: Dr. Jun Gong, Digestive Department of the Second Hospital, Xi'an Jiaotong University, Xi'an 710004, Shaanxi Province, China. jungong2003@hotmail.com
Telephone: +86-29-88083495 Fax: +86-29-87678758
Received: 2004-12-02 Accepted: 2005-02-18

Abstract

AIM: To explore the effect of six bile salts, including glycocholate (GC), glycochenodeoxycholate (GCDC), glycodeoxycholate (GDC), taurocholate (TC), taurochenodeoxycholate (TCDC), taurodeoxycholate (TDC), and two bile acids including cholic acid (CA) and deoxycholic acid (DCA) on esophageal cancer Eca109 cell line.

METHODS: Eca109 cells were exposed to six bile salts, two bile acids and the mixed bile salts at different concentrations for 24-72 h. 3-[4,5-Dimethylthiazol-2-yl]-2,5-diphenyltetrazolium bromide (MTT) assay was used to detect the cell proliferation. Apoptotic morphology was observed by phase-contrast video microscopy and deoxynucleotidyl transferase-mediated dUTP nick end labeling (TUNEL) assay. Sub-G1 DNA fragmentations and early apoptosis cells were assayed by flow cytometry (FCM) with propidium iodide (PI) staining and annexin V-FITC conjugated with PI staining. Apoptosis DNA ladders on agarose were observed. Activation of caspase-3 was assayed by FCM with FITC-conjugated monoclonal rabbit anti-active caspase-3 antibody and expressions of Bcl-2 and Bax proteins were examined immunocytochemically in 500 μmol/L-TC-induced apoptosis cells.

RESULTS: Five bile salts except for GC, and two bile acids and the mixed bile salts could initiate growth inhibition of Eca109 cells in a dose- and time-dependent manner. TUNEL, FCM, and DNA ladder assays all demonstrated apoptosis induced by bile salts and bile acids at 500 μmol/L, except for GC. Early apoptosis cell percentages in Eca109 cells treated with GCDC, GDC, TC, TCDC, TDC, CA at 500 μmol/L for 12 h, DCA at 500 μmol/L for 6 h, and mixed bile salts at 1 000 μmol/L for 12 h were 7.5%, 8.7%, 14.8%, 8.9%, 7.8%, 9.3%, 22.6% and 12.5%, respectively, all were significantly higher than that in control (1.9%). About 22% of the cell population treated with TC at 500 μmol/L for 24 h had detectable active caspase-3, and were higher than that in the control (1%). Immunocytochemical assay suggested that TC down-regulated Bcl-2 protein level and up-regulated Bax protein level.

CONCLUSION: GCDC, GDC, TC, TCDC, TDC, CA and DCA, except for GC, can inhibit growth and induce apoptosis of esophageal cancer Eca109 cells. Activation of caspase-3, decreased Bcl-2 protein and increased Bax protein are involved in TC-induced apoptosis of Eca109 cells.

© 2005 The WJG Press and Elsevier Inc. All rights reserved.

Key words: Bile salts; Esophageal cancer cells; Proliferation; Apoptosis

Zhang R, Gong J, Wang H, Wang L. Bile salts inhibit growth and induce apoptosis of human esophageal cancer cell line. *World J Gastroenterol* 2005; 11(33): 5109-5116
http://www.wjgnet.com/1007-9327/11/5109.asp

INTRODUCTION

Duodeno-gastro-esophageal reflux or bile reflux is involved in the pathogenesis of reflux esophagitis, Barrett's esophagus (BE), and esophageal adenocarcinoma. Recent studies have shown that bile acids and bile salts present frequently in the refluxate of BE patients, and influence the development and persistence of metaplasia[1-3]. Bile salts can enter mucosal cells in their non-ionized lipophilic form, cause injuries to cell membranes and tight junctions, and cell necrosis[4]. However, studies have shown that different bile salts induce cell apoptosis[5-7]. Whether different bile salts induce apoptosis of esophageal cancer cells remains unknown. Therefore, it is necessary to identify the effect of bile salts on esophageal cancer cells.

Glycine-conjugated bile acids such as glycocholic (GC) and glycochenodeoxycholic acids (GCDC) induce hepatocyte apoptosis *in vitro*[8], whereas taurine-conjugated bile acids such as taurocholic (TC) and taurochenodeoxycholic acids (TCDC) are well tolerated by hepatocytes[9,10]. Cell apoptosis is specifically induced by hydrophobic bile salts such as deoxycholate (DC) and dihydroxy bile salt, whereas conjugated bile salt glycodeoxycholate (GDC) and trihydroxy bile salt (TDC) and its conjugate glycocholate (GC) do not induce apoptosis in colorectal cancer cell lines[6]. Caspase cleavage and activation occur as early as 30 min after the

addition of DC to cells[6]. In a recent report, direct oligomerization of the Fas receptor (CD95/Apo-1) has been suggested as the primary causative mechanism of bile salt-mediated hepatocyte apoptosis[11-13]. However, CD95 is not involved in DC-induced apoptosis, but bile salt-mediated induction of mitochondrial permeability transition has been seen in colorectal cancer cell lines[6,14].

In the present study, we observed whether six bile salts and two bile acids could inhibit cell proliferation and induce apoptosis of human esophageal cancer Eca109 cells. We characterized the kinetics of bile salt-induced apoptosis of esophageal cancer cells. The difference in effects of different bile salts and bile acids on esophageal cancer cells was demonstrated. Activation of caspase-3 and expression of Bcl-2 and Bax proteins, as the key components in mitochondrial apoptosis "death-signal transduction" pathway[15-18], were described in bile salt-mediated apoptotic esophageal cancer cells.

MATERIALS AND METHODS

Materials

DMEM was purchased from Hyclone and trypsin was from Sigma. Fetal bovine serum (FBS) was from Hangzhou Jiangbin Biotechnology Co., Ltd. GC, GCDC, GDC, TC, TCDC, TDC, CA, and DCA were from Sigma. SP Histostain™-Plus kits and deoxynucleotidyl transferase-mediated dUTP nick end labeling (TUNEL) kits were purchased from Beijing Zhongshan Golden Bridge Biotechnology Co., Ltd. Mouse mAbs to Bcl-2 and Bax were from Antibody Diagnostica Inc. Annexin V-FITC apoptosis detection kit I and FITC-conjugated monoclonal active caspase-3 antibody apoptosis kit I were from BD Biosciences.

Cell lines

Eca109 cell lines were obtained from the Fourth Military Medical University. Cells were cultured in DMEM plus 10% FBS. All cell lines were cultured under standard tissue culture conditions.

Methods

Assessment of cell proliferation MTT assay was conducted to determine the cell proliferation[19]. Eight bile salts at concentrations of 500, 250, and 50 μmol/L, and mixed bile salts at concentrations of 1 500, 1 000, 500, and 250 μmol/L, including GC, GCDC, GDC, TC, TCDC, and TDC at the ratio of 2:2:1:2:2:1, were observed in MTT assay.

Eca109 cells were seeded in a 96-well plate (4 to 6×10^4 cells/well). After 24 h of post seeding, cells were treated with different bile salts for 3 d, and untreated cells served as a control. Prior to the determination, 10 μL of the 2.5 g/L stock solution of MTT was added to each well. After 4 h of incubation, the culture media were discarded, and then 100 mL of DMSO was added to each well and vibrated for 10 min. The absorbance (*A*) was measured at 492 nm with a microplate reader. The percentage of viable cells was calculated as follows: (*A* of experimental group/*A* of control group)×100%.

TUNEL assay

Cell apoptosis was analyzed using *in situ* cell death detection kit based on the terminal TUNEL technique. Cells were grown on chamber glass culture slides and treated with bile salts. To avoid disadherence of apoptotic cells, the slides were coated with poly-lysine. In brief, after the cells were treated with or without bile salts for the indicated time, they were fixed overnight in 100 g/L formaldehyde, and then treated with proteinase K and H_2O_2, labeled with dUTP in a humid box at 37 ℃ for 1 h. The cells without addition of TdT enzyme were used as negative control.

Flow cytometry by PI staining

Cells from the medium supernatant and adherent cells treated with bile salts were collected and pelleted at 1 200 U/min. The harvested cells were fixed with 1 mL of 75% cold ethanol at -20 ℃ for a night, and then washed with PBS. Cell pellets were incubated with 10 μg/mL RNase and stained with 50 μg/mL propidium iodide (PI) for 30 min in the dark. Samples were analyzed by FACSCalibur FCM at excitation wavelength of 488 nm. In the assay, 10 000 cells were detected by FCM. The resulting histograms were analyzed by the program CELLQuest.

Flow cytometry by annexin V-FITC conjugated with PI staining[20]

Cells from the medium supernatant and adherent cells treated with bile salts were collected and pelleted at 1 200 U/min. Pellets were washed twice with cold PBS and then resuspended in a binding buffer at a concentration of 1×10^6 cells/mL, and 100 μL of the solution (1×10^5 cells) was transferred to each of two 5-mL culture tubes. Five microliters of annexin V-FITC and 5 μL of PI were added into each 100 μL solution, the cells were gently vortexed and incubated for 15 min at RT in the dark. Four hundred microliters of 1´binding buffer was added to the sample and analyzed by FACSCalibur FCM within 1 h.

DNA fragmentation

A total of 10^6-10^7 cells treated with bile salts were collected and low molecular weight DNA was extracted using cell apoptosis DNA ladder extraction kit (Beijing Dingguo Biotechnology Co., Ltd). Standard loading buffer was added, 20 μL DNA samples was run on an 1% agarose gel containing 0.1% ethidium bromide in TAE buffer (Tris 40 mmol/L, sodium acetate 20 mmol/L, and 1 mmol/L EDTA, pH 8.0).

Caspase-3 assay

Caspase-3 was analyzed by FCM using FITC-conjugated monoclonal active caspase-3 antibody apoptosis kit I. Cells were collected and washed with cold PBS, then resuspended in Cytofix/Cytoperm™ solution at a concentration of 1×10^6 cells/0.5 mL and incubated for 20 min on ice. Samples were washed twice with Perm/wash™ buffer, and then FITC-conjugated monoclonal rabbit anti-active caspase-3 antibody was added and incubated for 30 min at room temperature. The marked samples were analyzed by FACSCalibur FCM.

Immunocytochemical assay of Bcl-2 and Bax

Cells were grown on chamber glass culture slides and treated with TC at 500 μmol/L. To avoid disadherence of apoptotic cells, the slides were coated with poly-lysine. Slides with cells

were fixed in 65% cold acetone for 20 min. Bcl-2 and Bax were stained with the mAb using standard immunocytochemical techniques. Positive-staining-area percentages were calculated using a cell image analysis system (Qwin550CW). A mean of 20 adjacent fields, at a magnification of ×400, was analyzed for each section[21].

Statistical analysis

All values were expressed as mean±SD. Statistical differences between means were calculated by Student's *t*-test and χ^2 test. $P<0.05$ was considered statistically significant.

RESULTS

Morphological changes

The influence of different bile salts on the apoptosis of Eca109 cells was established. Morphological criteria of cell apoptosis, such as membrane blebbing, cell shrinkage, nuclear conden-sation and fragmentation, were assessed by phase-contrast video microscopy. Morphological changes were observed 3 h after the addition of DCA at 500 μmol/L, and 24 h after the addition of the other bile salts at 500 μmol/L, except for GC.

Inhibition of Eca109 cell proliferation by some bile salts

The experimental Eca109 cells were treated with eight kinds of bile salts and mixed bile salts at different concentrations as described above. The cell viability was determined by MTT assay (Figure 1). Except for GC, the other bile salts or bile acids inhibited the growth of esophageal cancer cells in a dose- and time-dependent manner. Cell growth was suppressed by 85% after 24 h treatment with DCA at 500 μmol/L, higher than that after treatment with other bile salts and bile acid at the same concentration ($P<0.01$). Cell growth was suppressed by 65% and 95% after 24- and 72-h treatment with mixed bile salts at 1 000 μmol/L, by 59% and 94% after 24- and 72-h treatment with TC at 500 μmol/L, which were higher than those after treatment with the other five kinds of bile salts.

TUNEL assay

TUNEL assay revealed that bile salts, except for GC, induced apoptosis of Eca109 cells. When treated with GC, GCDC, GDC, TC, TCDC, TDC, CA at 500 μmol/L for 24 h, DCA at 500 μmol/L for 12 h, and mixed bile salts at 100 μmol/L for 24 h, the positive-cell percentages were 2%, 11%, 9%, 25%, 11%, 12%, 15%, 43% and 30%, respectively. Compared to 2% in control, the percentages were higher in the cells treated with bile salts ($P<0.05$) except for GC. Figure 2 shows the image of cells treated with 500 μmol/L TC for 24 h.

FCM by PI staining

Eca109 cells treated with bile salts and bile acids at 500 μmol/L and mixed bile salts at 1 000 μmol/L were stained with PI and analyzed by FCM. Except for GC, the bile salts induced cell apoptosis in a time-dependent manner (Figure 3A). When treated with DCA at 500 μmol/L, the apoptotic cell percentage reached 44.9% after 12 h and 80.5% after 24 h (Figure 3B). After 24 and 72 h, the percentages were 27.7% and 72.4% after being treated with mixed bile salts at 1 000 μmol/L, and 19.7% and 75.5% after being treated with TC at 500 μmol/L, respectively.

FCM by annexin V-FITC conjugated with PI staining

Early apoptotic cells were annexin V-FITC-positive and PI-negative[20]. Early apoptotic cells increased in the cells treated with bile salts except for GC. The percentages of early apoptotic cells of Eca109 cells treated with GC, GCDC, GDC, TC, TCDC, TDC, CA at 500 μmol/L for 12 h, DCA at 500 μmol/L for 6 h, and mixed bile salts at 100 μmol/L for 12 h were 1.9%, 7.5%, 8.7%, 14.8%, 8.9%, 7.8%, 9.3%, 22.6%, and 12.5%, respectively. Some of them are shown in Figure 4. Compared to 1.9% in control, the percentages were higher in the cells treated with bile salts ($P<0.05$) except for GC.

DNA fragmentation

In this study, we observed DNA ladder formation in cells treated with GC, TC, and DCA at 500 μmol/L for 24 h, and mixed bile salts at 1 000 μmol/L for 24 and 48 h (Figure 5).

Caspase-3 assay

We analyzed active caspase-3 in Eca109 cells treated with TC and GC at 500 μmol/L for 24 h by FCM with FITC-conjugated monoclonal active caspase-3 antibody (Figure 6). In control and cells treated with GC at 500 μmol/L, 1% was found to be primarily active caspase-3 cells, and there was no difference between the two groups ($P>0.05$). But about 22% of the cells treated with TC at 500 μmol/L for 24 h had detectable active caspase-3, being higher than that in the control ($P<0.01$).

Expressions of Bcl-2 and Bax proteins

Figure 7 shows the morphologic images of cells with immunocytochemical staining of Bcl-2 and Bax proteins. Bcl-2 protein staining was weaker than Bax because the positive staining was weaker. Expression of Bcl-2 protein was reduced in 500-μmol/L-TC-treated Eca109 cells, while expression of Bax protein was increased (Table 1), suggesting that TC could down regulate Bcl-2 protein level and up-regulate Bax protein level.

Table 1 TC's effects on the expression of Bcl-2 and Bax in Eca109 cells (mean±SD)

Positive-area-percentage (%)	Bcl-2	Bax
Control	45±3	22±4
500 μmol/L TC, 24 h	26±4[a]	47±6[b]
500 μmol/L TC, 48 h	24±5[a]	71±4[b]

[a]$P<0.05$, [b]$P<0.01$ *vs* control.

DISCUSSION

Bile salts and bile acids are likely to influence the development and persistence of esophageal mucosal cell metaplasia[1-3]. It is necessary to investigate the effect of bile salts on esophageal mucosal cancer cells. In our studies, we have demonstrated

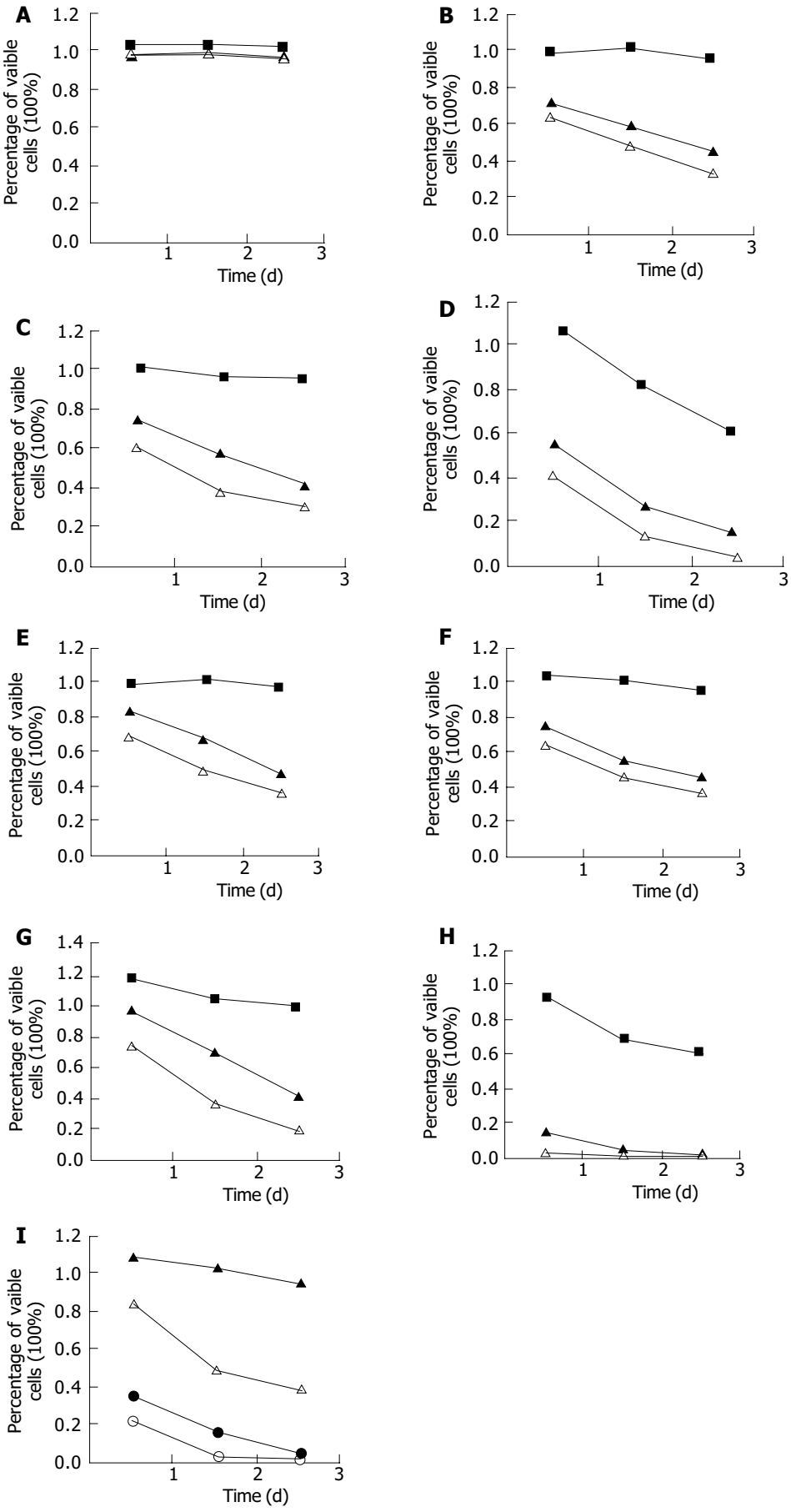


Figure 1 Effect of bile salts on Eca109 cell growth. ■ (at 50 μmol/L), ▲ (at 250 μmol/L), △ (at 500 μmol/L), ● (1 000 μmol/L), ○ (1 500 μmol/L). **A**: Glycocholate; **B**: Glycochenodeoxycholate; **C**: Glycodeoxycholate; **D**: Taurocholate; **E**: Taurochenodeoxychoate; **F**: Taurodeoxycholate; **G**: Cholic acid; **H**: Deoxycholic acid; **I**: Mixed bile salts.

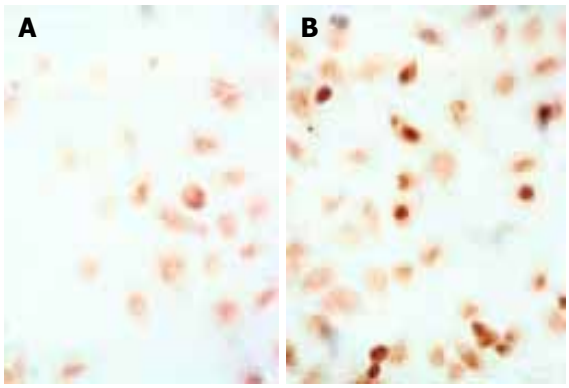


Figure 2 TC-induced apoptosis of control (**A**) and cells treated with TC (**B**) ×400.

that specific bile salts and bile acids at 50-500 μmol/L could inhibit growth and induce apoptosis of Eca109 cells.

Bile acids constitute 67% of normal bile, and are conjugated with glycine or taurine in normal human bile. Bile acids consisted of 40% CA, 40% CDCA, and 20% DCA. Lithocholic acid (LCA) and ursodeoxycholic acid (UDCA) is less than 5% respectively[22]. We selected GC, GCDC, GDC, TC, TCDC, and TDC, and CA and DCA in this study. The concentrations of bile salts in our study were from 25 to 500 μmol/L and those of mixed bile salts were 50 to 1 500 μmol/L, because the total bile acid concentration in esophagus of patients suffering from bile reflux is 0.89 mg/mL[23]. Six bile salts at concentration of less than 500 μmol/L are all water-soluble sodium salts in pH 7.1-7.5. Because of its hydrophobicity, the largest portion of DCA is not soluble in water, but a considerable amount of 700 μmol/L DCA is detectable in fecal water[24,25]. As this portion, at least theoretically, can get into contact with colonic epithelial cells, we selected the concentration at 25-500 μmol/L to investigate the effect of DCA on esophageal cancer cells. Our study demonstrated that less than 500 μmol/L DCA and CA could be dissolved thoroughly

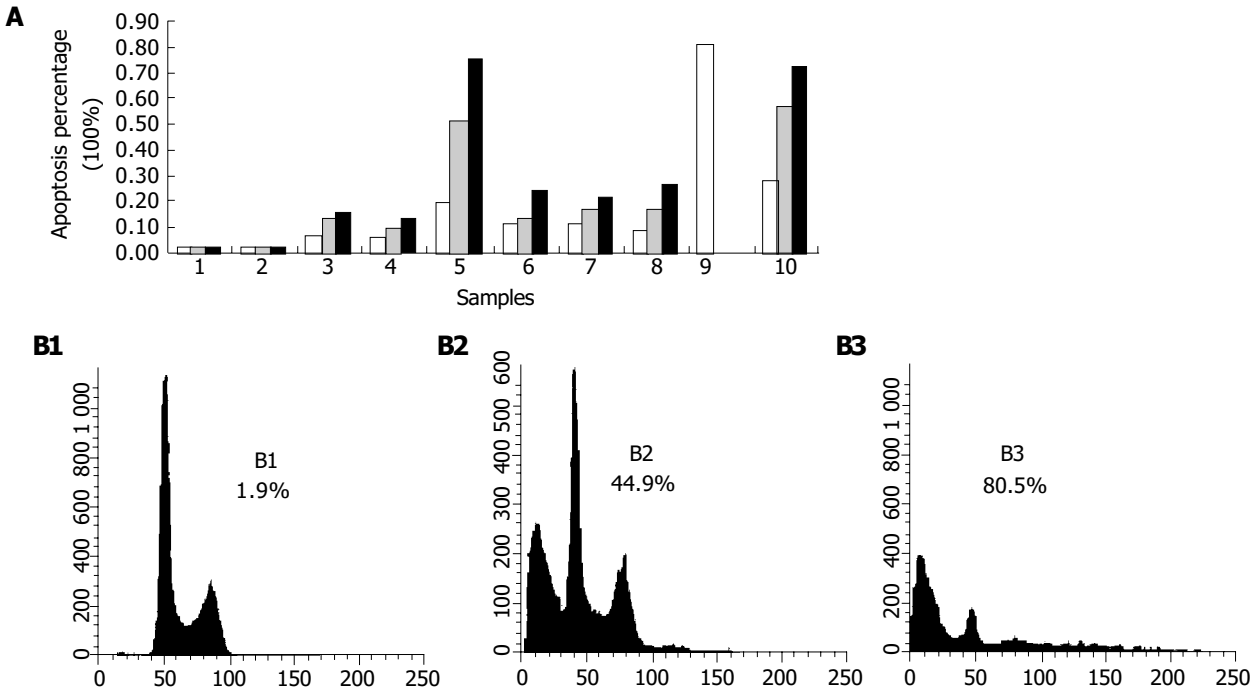


Figure 3 Time-dependent apoptosis of Eca109 cells induced by bile salts or bile acids (**A**) and DCA (**B**1-3). 1: Control; 2: GC; 3: GCDC; 4: GDC; 5: TC; 6: TCDC; 7: TDC; 8: CA; 9: DCA; 10: mixed bile salts. ■ (after 24 h), ▒ (after 48 h), □ (after 72 h).

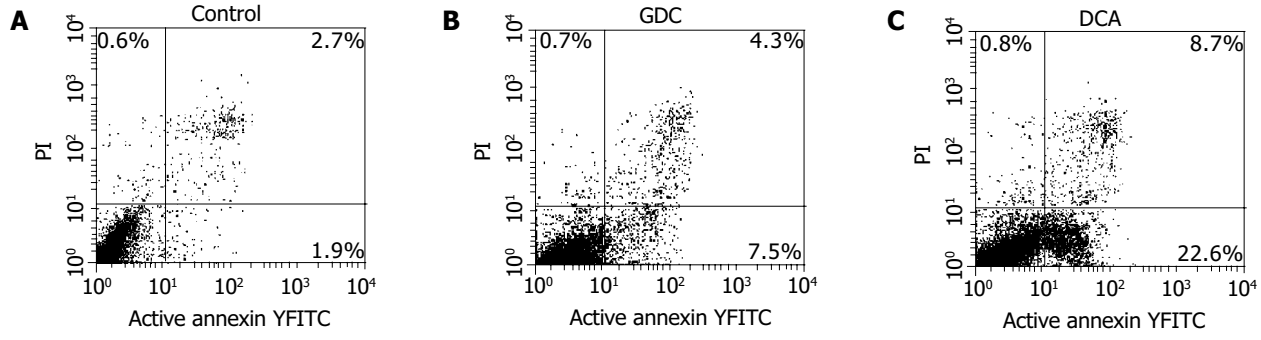


Figure 4 Apoptosis of control (**A**) and cells treated with GCDC (**B**) and DCA (**C**).

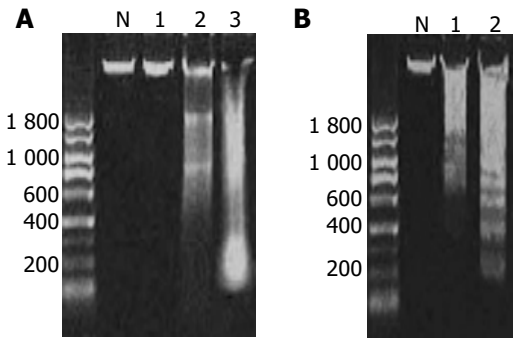


Figure 5 DNA ladder formation in cells treated with TC (**A**, Lane 2) and DCA (**A**, Lane 3) and mixed bile salts (**B**, Lane 1 and 2).

in the media. Based on the components of normal bile, the mixed bile salts in our study comprised GC, GCDC, GDC, TC, TCDC, and TDC at 2:2:1:2:2:1.

The present study demonstrated that five bile salts, two bile acids and the mixed bile salts except for GC, could inhibit the growth of human esophageal cancer Eca109 cells in a dose- and time-dependent manner. Our results also showed that the induced-cell death was a major reason for the cell growth inhibition. Necrosis is the major effect of bile salts on esophageal mucosal cells, by entering mucosal cells and causing injuries to cell membranes and tight junctions[4]. However, the effects of five bile salts, two bile acids and the mixed bile salts except for GC, on apoptosis-inducing activity in esophageal cancer cells were examined in our study. They caused typical apoptotic alterations including morphological changes assessed by phase-contrast video microscopy and TUNEL assay, positive annexin V staining by FCM, apoptotic sub-G_1 peak by FCM with PI staining, and DNA fragmentation by gel electrophoresis.

Seven bile salts or acids and mixed bile salts have different effects between Eca109 cells and hepatocytes[8-10] and colon cancer cell lines[6]. They could induce apoptosis of esophageal cancer cells in a dose- and time-dependent manner. Conversely, hepatocyte-cytotoxic glycine-conjugated bile acids such as GC induce hepatocyte apoptosis *in vitro*[8], but not apoptosis of esophageal cancer cells, whereas hepatocyte-tolerated TC and TCDC[9] induce apoptosis of esophageal cancer cells. Our results also showed that TC was more toxic to esophageal cancer cells than other bile salts, suggesting that apoptosis-induced effect is correlative with the conjugated forms or structures of bile acids in esophageal cancer cells. In hepatocytes, the effect of bile salts is based on the glycine- or taurine-conjugated structure. It was reported that some hydrophobic bile acids such as TC activate PI3K-dependent survival pathways, which prevent their inherent toxicity[5]. But it seemed that PI3K was not activated by TC in esophageal cancer cells. The different mechanism of different bile salts needs to be defined by further studies.

The apoptosis "death-signal transduction" pathway is currently classified into the Fas/FasL pathway[26-28], the

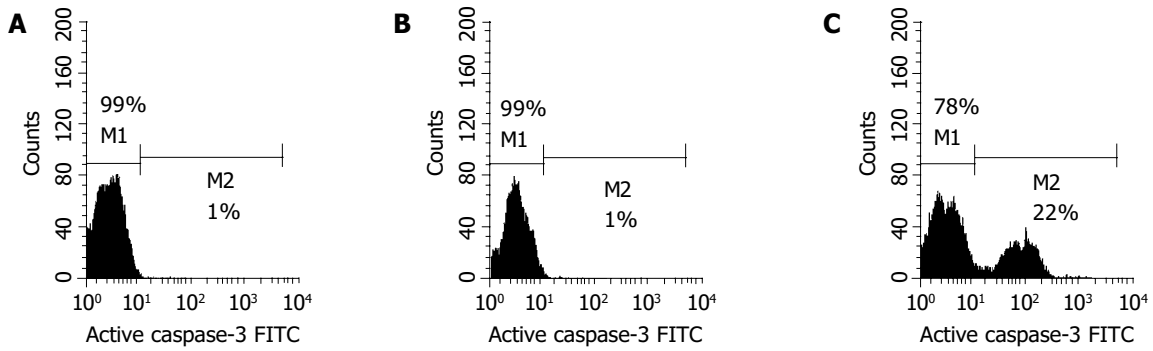


Figure 6 Active caspase-3 in the control (**A**) and cells treated with GC (**B**) and TC (**C**).

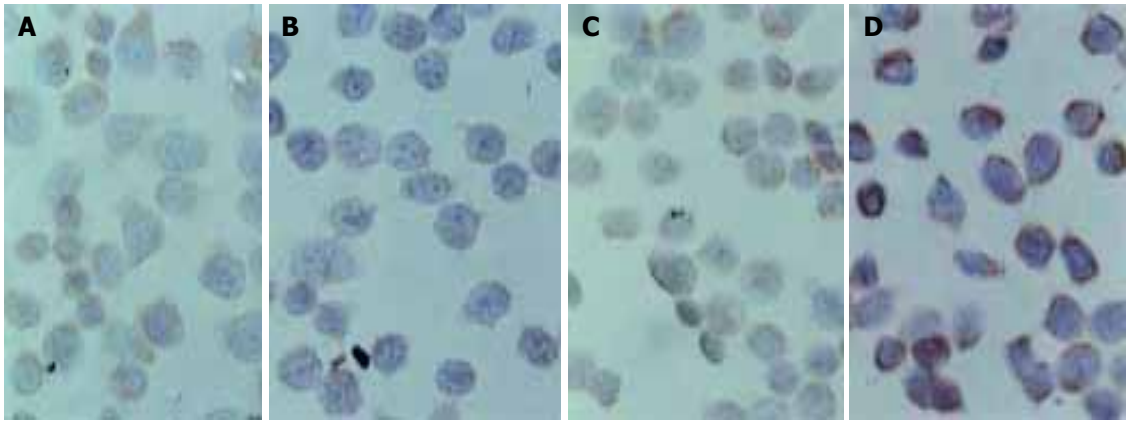


Figure 7 Expression of Bcl-2 (**B**) and Bax proteins (**D**) and controls (**A:** Bcl-2 and **C:** Bax) ×400.

mitochondrial pathway[16,29], and the endoplasmic reticulum-stress activated pathway[30,31]. It was reported that direct oligomerization of the Fas receptor is the primary causative mechanism of bile salt-mediated hepatocyte apoptosis[11-13]. The signal transduction of bile salt-mediated apoptosis of esophageal cancer cells was also investigated in our study. The data demonstrate that caspase-3 is activated in TC-induced cells. Activation of caspase-3 occurs as a consequence of TC-induced apoptosis. However, caspase-3 plays a pivotal role in the three apoptosis pathways[32-34]. We further observed the expression of Bcl-2 and Bax protein. Members of the Bcl-2 family, as the key components in the mitochondrial apoptosis "death-signal transduction" pathway, are important regulators in the apoptotic pathway[15,16]. As an oncogene-derived protein, Bcl-2 confers a negative control in the pathway of cellular suicide, whereas Bax, a Bcl-2-homologous protein, promotes cell death by competing with Bcl-2[17,18]. Reduced expression of Bcl-2 protein and increased expression of Bax protein in Eca109 cells treated with TC demonstrated in this study, suggest that TC-induced apoptosis is relative with the mitochondrial death-signal pathway in Eca109 cells. As opposed to hepatocyte death mediated by bile acids, CD95 is not involved in deoxycholate-induced apoptosis of colon cancer cell lines[6]. Because the changes of CD95 were not observed in our study, our results cannot prove that Fas receptor (CD95) is not involved in TC-induced esophageal cancer cell apoptosis. Toxic bile acids may be capable of stimulating multiple pathways to initiate cell death, but further studies are needed.

In conclusion, GCDC, GDC, TC, TCDC, TDC, CA, and DCA, except for GC, inhibit growth and induce apoptosis of Eca109 cells in a dose- and time-dependent manner *in vitro*. Activation of caspase-3, decreased Bcl-2 protein, and increased Bax protein are involved in TC-induced apoptosis of esophageal cancer cells.

ACKNOWLEDGMENTS

We thank Drs. Bing-Heng Zhang and Xiao-Ge Zhao in Central Laboratory for Biomedical Research of Xi'an Jiaotong University Medical School, for their help on FCM assays.

REFERENCES

1 **Jankowski JA,** Anderson M. Review article: management of oesophageal adenocarcinoma-control of acid, bile and inflammation in intervention strategies for Barrett's oesophagus. *Aliment Pharmacol Ther* 2004; **20** (Suppl 5): 71-80
2 **Kondo K,** Kojima H, Akiyama S, Ito K, Takagi H. Pathogenesis of adenocarcinoma induced by gastrojejunostomy in Wistar rats: role of duodenogastric reflux. *Carcinogenesis* 1995; **16**: 1747-1751
3 **Miwa K,** Miyashita T, Hattori T. Reflux of duodenal or gastroduodenal contents induces esophageal carcinoma in rats. *Nippon Rinsho* 2004; **62**: 1433-1438
4 **Stein HJ,** Kauer WK, Feussner H, Siewert JR. Bile acids as components of the duodenogastric refluxate: detection, relationship to bilirubin, mechanism of injury, and clinical relevance. *Hepatogastroenterology* 1999; **46**: 66-73
5 **Torchia EC,** Stolz A, Agellon LB. Differential modulation of cellular death and survival pathways by conjugated bile acids. *BMC Biochem* 2001; **2**: 11
6 **Schlottman K,** Wachs FP, Krieg RC, Kullmann F, Scholmerich J, Rogler G. Characterization of bile salt-induced apoptosis in colon cancer cell lines. *Cancer Res* 2000; **60**: 4270-4276
7 **Milovic V,** Teller IC, Faust D, Caspary WF, Stein J. Effects of deoxycholate on human colon cancer cells: apoptosis or proliferation. *Eur J Clin Invest* 2002; **32**: 29-34
8 **Agellon LB,** Torchia EC. Intracellular transport of bile acids. *Biochim Biophys Acta* 2000; **1486**: 198-209
9 **Torchia EC,** Agellon LB. Bile acid-induced morphological changes in hepatoma cells with elevated sodium-dependent bile acid uptake capacity. *Eur J Cell Biol* 1997; **74**: 190-196
10 **Roberts LR,** Kurosawa H, Bronk SF, Fesmier PJ, Agellon LB, Leung WY, Mao F, Gores GJ. Cathepsin B contributes to bile salt-induced apoptosis of rat hepatocytes. *Gastroenterology* 1997; **113**: 1714-1726
11 **Faubion WA,** Guicciardi ME, Miyoshi H, Bronk SF, Roberts PJ, Svingen PA, Kaufmann SH, Gores GJ. Toxic bile salts induce rodent hepatocyte apoptosis via direct activation of Fas. *J Clin Invest* 1999; **103**: 137-145
12 **Sodeman T,** Bronk SF, Roberts PJ, Miyoshi H, Gores GJ. Bile salts mediate hepatocyte apoptosis by increasing cell surface trafficking of Fas. *Am J Physiol Gastrointest Liver Physiol* 2000; **278**: G992-999
13 **Qiao L,** Studer E, Leach K, McKinstry R, Gupta S, Decker R, Kukreja R, Valerie K, Nagarkatti P, El Deiry W, Molkentin J, Schmidt-Ullrich R, Fisher PB, Grant S, Hylemon PB, Dent P. Deoxycholic acid (DCA) causes ligand-independent activation of epidermal growth factor receptor (EGFR) and FAS receptor in primary hepatocytes: inhibition of EGFR/mitogen-activated protein kinase-signaling module enhances DCA-induced apoptosis. *Mol Biol Cell* 2001; **12**: 2629-2645
14 **Wachs FP,** Krieg RC, Rodrigues CM, Messmann H, Kullmann F, Knuchel-Clarke R, Scholmerich J, Rogler G, Schlottmann K. Bile salt-induced apoptosis in human colon cancer cell lines involves the mitochondrial transmembrane potential but not the CD95 (Fas/Apo-1) receptor. *Int J Colorectal Dis* 2005; **20**: 103-113
15 **Tsujimoto Y,** Shimizu S. Bcl-2 family: life-or-death switch. *FEBS Lett* 2000; **466**: 6-10
16 **Rupniewska Z,** Bojarska-Junak A. Apoptosis: mitochondrial membrane permeabilization and the role played by Bcl-2 family proteins. *Postepy Hig Med Dosw* 2004; **58**: 538-547
17 **Merto GR,** Cella N, Hynes NE. Apoptosis is accompanied by changes in Bcl-2 and Bax expression, induced by loss of attachment, and inhibited by specific extracellular matrix proteins in mammary epithelial cells. *Cell Growth Differ* 1997; **8**: 251-260
18 **Lei K,** Nimnual A, Zong WX, Kennedy NJ, Flavell RA, Thompson CB, Bar-Sagi D, Davis RJ. The Bax subfamily of Bcl2-related proteins is essential for apoptotic signal transduction by c-Jun NH(2)-terminal kinase. *Mol Cell Biol* 2002; **22**: 4929-4942
19 **Saikawa Y,** Kubota T, Furukawa T, Suto A, Watanabe M, Kumai K, Ishibiki K, Kitajima M. Single-cell suspension assay with an MTT end point is useful for evaluating the optimal adjuvant chemotherapy for advanced gastric cancer. *Jpn J Cancer Res* 1994; **85**: 762-765
20 **Lecoeur H,** Prevost MC, Gougeon ML. Oncosis is associated with exposure of phosphatidylserine residues on the outside layer of the plasma membrane: a reconsideration of the specificity of the annexin V/propidium iodide assay. *Cytometry* 2001; **44**: 65-72
21 **Coppola D,** Schreiber RH, Mora L, Dalton W, Karl RC. Significance of Fas and retinoblastoma protein expression during the progression of Barrett's metaplasia to adenocarcinoma. *Ann Surg Oncol* 1999; **6**: 298-304
22 **Guoming X,** Meiyun K, Jinyan L. Bile acid reflux related disease. 1st ed. Shanghai. *Shanghai Sci Technol Pub* 2002: 24
23 **Stein HJ,** Feussner H, Kauer W, DeMeester TR, Siewert JR. Alkaline gastroesophageal reflux: assessment by ambulatory esophageal aspiration and pH monitoring. *Am J Surg* 1994; **167**: 163-168
24 **Van Munster IP,** Tangerman A, Nagengast FM. Effect of resistant starch on colonic fermentation, bile acid metabolism,

and mucosal proliferation. *Dig Dis Sci* 1994; **39**: 834-842
25 **Kishida T,** Taguchi F, Feng L, Tatsuguchi A, Sato J, Fujimori S, Tachikawa H, Tamagawa Y, Yoshida Y, Kobayashi M. Analysis of bile acids in colon residual liquid or fecal material in patients with colorectal neoplasia and control subjects. *J Gastroenterol* 1997; **32**: 306-311
26 **Pinkoski MJ,** Green DR. Fas ligand, death gene. *Cell Death Differ* 1999; **6**: 1174-1181
27 **Kavurma MM,** Khachigian LM. Signaling and transcriptional control of Fas ligand gene expression. *Cell Death Differ* 2003; **10**: 36-44
28 **Curtin JF,** Cotter TG. Live and let die: regulatory mechanisms in Fas-mediated apoptosis. *Cell Signal* 2003; **15**: 983-992
29 **Tournier C,** Hess P, Yang DD, Xu J, Turner TK, Nimnual A, Bar-Sagi D, Jones SN, Flavell RA, Davis RJ. Requirement of JNK for stress-induced activation of the cytochrome c-mediated death pathway. *Science* 2000; **288**: 870-874
30 **Breckenridge DG,** Germain M, Mathai JP, Nguyen M, Shore GC. Regulation of apoptosis by endoplasmic reticulum pathways. *Oncogene* 2003; **22**: 8608-8618
31 **Adams JM.** Ways of dying: multiple pathways to apoptosis. *Genes Dev* 2003; **17**: 2481-2495
32 **Aouad SM,** Cohen LY, Sharif-Askari E, Haddad EK, Alam A, Sekaly RP. Caspase-3 is a component of Fas death-inducing signaling complex in lipid rafts and its activity is required for complete caspase-8 activation during Fas-mediated cell death. *J Immunol* 2004; **172**: 2316-2323
33 **Yun YG,** Oh H, Oh GS, Pae HO, Choi BM, Kwon JW, Kwon TO, Jang SI, Chung HT. *In vitro* cytotoxicity of Mokko lactone in human leukemia HL-60 cells: induction of apoptotic cell death by mitochondrial membrane potential collapse. *Immunopharmacol Immunotoxicol* 2004; **26**: 343-353
34 **Bustamante J,** Di Libero E, Fernandez-Cobo M, Monti N, Cadenas E, Boveris A. Kinetic analysis of thapsigargin-induced thymocyte apoptosis. *Free Radic Biol Med* 2004; **37**: 1490-1498

Science Editor Wang XL and Guo SY **Language Editor** Elsevier HK

PO Box 2345, Beijing 100023, China
www.wjgnet.com
wjg@wjgnet.com

ELSEVIER

World J Gastroenterol 2005;11(33):5117-5122
World Journal of Gastroenterology ISSN 1007-9327
© 2005 The WJG Press and Elsevier Inc. All rights reserved.

• *ESOPHAGEAL CANCER* •

Gene expression in rats with Barrett's esophagus and esophageal adenocarcinoma induced by gastroduodenoesophageal reflux

Peng Cheng, Jun Gong, Tao Wang, Jie Chen, Gui-Sheng Liu, Ru Zhang

Peng Cheng, Jun Gong, Tao Wang, Jie Chen, Gui-Sheng Liu, Ru Zhang, Department of Gastroenterology, the Second Hospital, Xi'an Jiaotong University, Xi'an 710004, Shaanxi Province, China
Supported by the Major Program of Clinical Medicine of Ministry of Public Health, No. 20012130
Correspondence to: Dr. Peng Cheng, Department of Gastroenterology, Second Hospital of Xi'an Jiaotong University, Xi'an 710004, Shaanxi Province, China. cpzxczzc2004@yahoo.com.cn
Telephone: +86-29-88083495 Fax: +86-29-87231758
Received: 2004-11-23 Accepted: 2005-01-26

Abstract

AIM: To study the different gene expression profiles in rats with Barrett's esophagus (BE) and esophageal adenocarcinoma (EA) induced by gastro-duodeno-esophageal reflux.

METHODS: Esophagoduodenostomy was performed in 8-wk old Sprague-Dawley rats to induce gastro-duodeno-esophageal reflux, and a group of rats that received sham operation served as control. Esophageal epithelial pathological tissues were dissected and frozen in liquid nitrogen immediately. The expression profiles of 4 096 genes in EA and BE tissues were compared to normal esophagus epithelium in normal control (NC) by cDNA microarray.

RESULTS: Four hundred and forty-eight genes in BE were more than three times different from those in NC, including 312 upregulated and 136 downregulated genes. Three hundred and seventy-seven genes in EA were more than three times different from those in NC, including 255 upregulated and 142 downregulated genes. Compared to BE, there were 122 upregulated and 156 downregulated genes in EA. In the present study, the interested genes were those involved in carcinogenesis. Among them, the upregulated genes included cathepsin C, aminopeptidase M, arachidonic acid epoxygenase, tryptophan-2,3-dioxygenase, ubiquitin-conjugating enzyme, cyclic GMP-stimulated phosphodiesterase, tissue inhibitor of metalloproteinase-1, betaine-homocysteine methyltransferase, lysozyme, complement 4b binding protein, complement 9 protein, insulin-like growth factor binding protein, UDP-glucuronosyltransferase, tissue inhibitor of metalloproteinase-3, aldolase B, retinoid X receptor gamma, carboxylesterase and testicular cell adhesion molecule 1. The downregulated genes included glutathione synthetase, lecithin-cholesterol acyltransferase, p55CDC, heart fatty acid binding protein, cell adhesion regulator and endothelial cell selectin ligand.

CONCLUSION: Esophageal epithelium exposed excessively to harmful ingredients of duodenal and gastric reflux may develop into BE and even EA gradually. The gene expression level is different between EA and BE, and may be related to the occurrence and progression of EA.

© 2005 The WJG Press and Elsevier Inc. All rights reserved.

Key words: Gastroduodenoesophageal reflux; Barrett's esophagus; Esophageal adenocarcinoma; Gene expression

Cheng P, Gong J, Wang T, Chen J, Liu GS, Zhang R. Gene expression in rats with Barrett's esophagus and esophageal adenocarcinoma induced by gastroduodenoesophageal reflux. *World J Gastroenterol* 2005; 11(33): 5117-5122
http://www.wjgnet.com/1007-9327/11/5117.asp

INTRODUCTION

The incidence of esophageal adenocarcinoma (EA) has increased considerably in the past few years and has already exceeded any other kind of malignant tumor in USA and the incidence of EA in Caucasians has exceeded squamous carcinoma[1]. A Dundee inquisition discovered that the incidence of EA has increased 49% in the last few years[2]. No detailed clinical epidemiological data in this respect can be acquired in Asia. However, some gastroenterology specialists also thought that the incidence of EA has increased in their country[3]. This may be related to the increasing incidence of gastro-esophageal reflux diseases, especially Barrett's esophagus (BE)[4,5]. Gastro-esophageal reflux diseases are caused by mucosa exposed excessively to harmful ingredients of duodenal and gastric reflux. It is usually considered that gastro-esophageal reflux can lead to esophagitis, BE and even EA. However, the exact mechanism especially the molecular biological mechanism of EA is unknown. In the present study, the same surgical procedures were performed in Sprague-Dawley rats to induce gastro-duodeno-esophageal reflux and the difference in gene expression profiles between BE and EA was investigated by cDNA microarray.

MATERIALS AND METHODS

Experimental animal and animal model

One hundred and twenty healthy Sprague-Dawley rats weighing 200-250 g were purchased from the Experimental Animal Center of Xi'an Jiaotong University. The rats were housed in rat cages at 22-25 ℃ with free access to standard

rat pellet food and water for 40 wk. Rats were treated following the Guidelines for the Care and Use of Laboratory Animals of National Animal Welfare Committee. The male pairing female rats were divided into two groups. Esophago-duodenostomy was performed on 90 rats to produce gastro-duodeno-esophageal reflux, and sham operation was performed on 30 rats[6]. The animals were fed with a standard chow.

Tissues and specimens

All the tissue specimens including BE and EA were taken from animals 40 wk after esophago-duodenostomy, by which gastro-duodeno-esophageal reflux animal model was induced. Normal esophageal epithelium at the same anatomical site served as normal control (NC). Inner part of each sample was cut, frozen in liquid nitrogen immediately after surgical resection, at the same time about 0.2 cm×0.2 cm×0.2 cm tissue of outer marginal part was used for histopathological examination to ensure all the frozen tissue specimens and their corresponding histological morphology.

Chip preparation

Four thousand and ninety-six target cDNA clones were used in cDNA microarray (United Gene Ltd). These genes were amplified by PCR, using universal primers and then purified by standard method. The quality of PCR was monitored by agarose gel electrophoresis. The obtained genes were dissolved in 3×SSC spotting solution and then spotted on silylated slides (Telechem Inc.) by Cartesian 7500 spotting robotics (Cartesian, Inc.). Each target gene was dotted twice. After spotting, the slides were hydrated (2 h) and dried (0.5 h, room temperature). The samples were cross-linked with UV light and treated with 0.2% SDS, H_2O and 0.2% NaNBH4 for 10 min respectively. Then the slides were dried in cold condition for use.

Probe preparation

Total sample RNA was extracted by single step method. Briefly, after being taken out from liquid nitrogen, specimens were ground completely into tiny powders, while liquid nitrogen was added in ceramic mortar and then the powders were homogenized in D solution plus 1% mercaptoethanol. After centrifugation, the supernatant was extracted with phenol:chloroform (1∶1), NaAC and acidic phenol: chloroform (5∶1), respectively. The aqueous phase was precipitated by an equal volume of isopropanol and centrifuged. The precipitates were dissolved with Millie-Q H_2O. After further purification by LiCl precipitating method, RNA was obtained by UV analysis and electrophoresis. mRNA was isolated and purified with Oligotex mRNA Midi kit (Qiagen, Inc.). The fluorescent-labeled cDNA probe was prepared through retro-transcription as previously described[7]. The probes from NC were labeled with Cy3-dUTP, while those from BE and EA with Cy5-dUTP respectively. The probes were mixed (Cy3-dUTP NC+Cy5-dUTP BE and Cy3-dUTP NC+ Cy5-dUTP EA respectively) and precipitated by ethanol, and then resolved in 20 mL hybridization solution (5×SSC+0.2% SDS).

Hybridization and washing

Probes and the chip were denatured respectively in 95 ℃ bath for 5 min, and then the probes were added onto the chip. They were hybridized in a sealed chamber at 60 ℃ for 15-17 h and washed in turn with solutions of 2×SSC+0.2% SDS, 0.1×SSC+0.2% SDS and 0.1% SSC for 10 min each, then dried at room temperature.

Fluorescent scanning and result analysis

The chip was read by a Scan Array 3000 Scanner (General Scanning Inc.). The overall intensities of Cy3 and Cy5 were normalized and corrected by a coefficient, according to the ratios of the located 40 h keeping genes. Cy3 was normalized as Cy3*. The acquired image was further analyzed by Gene Pix Pro 3.0 software with digital computer to obtain the intensities of fluorescent signals and the Cy5/Cy3* ratio. The data were an average of the two repeated spots. The differentially expressed genes were defined as the absolute value of the Cy5/Cy3* natural logarithm being more than 1.10 (the variation of gene expression was more than threefold); either Cy3 or Cy5 signal value required being more than 800, or both signal values being more than 200, or else being thought as an ineffective gene dot; PCR results being satisfactory.

RESULTS

Features of esophagus pathological changes

Sixty-nine rats survived in animal model group in the end and all animals that had undergone sham operation survived. Incidences of BE and EA in esophago-duodenostomy animal group were 37.5% and 2.8% respectively, significantly higher than that in the sham operation group.

Total sample RNA extraction

Total sample RNA from normal esophagus epithelium, BE and EA was extracted and the A_{260}/A_{280} was 2-2.6, indicating that pure mRNA was acquired.

Scatter spots of hybridization signals on gene chip

The scatter spots plotted with Cy3 and Cy5 fluorescent signal values displayed quite a disperse pattern in distribution. Most spots gathered around a 45 angle diagonal line, in which blue spots represented the area, where the signal intensities ranged 0.33-3-folds compared to those of the control. Some yellow spots distributed beyond or far from 45 angle diagonal line, indicating the existence of abnormal gene expression in BE or EA and their signal intensities were three times more or less than those in NC (Figures 1A and B).

Results and gene expression pattern by scanning analysis

In BE epithelia, 448 genes exhibited expression variations more than three times compared to the control, the up- and down-regulated genes were 312 and 136 respectively. In EA, 377 genes showed expression variations more than three times compared to NC, the up- and down-regulated genes were 255 and 122 respectively. Difference in gene expression between EA and BE was acquired by subtracting genes in common from total genes expressed differently in EA and BE compared to NC (any ineffective dot of hybridization was excluded from analysis). A total of 268 genes expressed

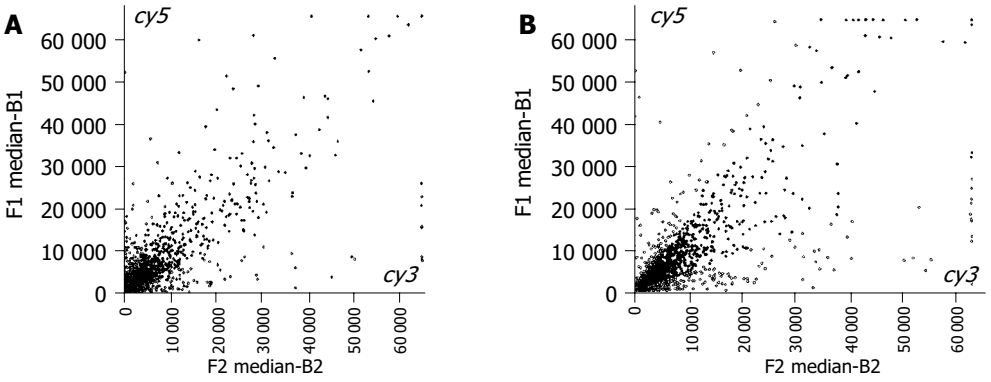


Figure 1 Scatter spots of hybridization signals on gene chip. **A**: Esophagus adenocarcinoma and normal control; **B**: Barrett's esophagus and normal control.

differently in BE compared to those in EA, the up- and down-regulated genes were 112 and 156 respectively. These genes might be divided into 12 groups (Table 1) according to their functions. Some genes involved in carcinogenesis are listed in Table 2.

Table 1 Different expressions of functional genes in BE and EA

Functional genes	Number	Upregulated	Downregulated
Oncogenes and tumor suppression genes	23	13	10
Ion channel and transporters	26	13	13
Cell cycle proteins	13	4	9
Extra-pressure reaction proteins	20	8	12
Cell regulatory proteins	15	5	10
Cell apoptosis-related proteins	19	11	8
DNA synthesis, repair, recombinant factors	20	6	14
DNA binding, transcription factors	23	7	16
Cell receptors	23	7	16
Immunity-related proteins	29	12	17
Cell signal transducing proteins	28	9	19
Metabolism-related proteins	29	17	12
Total	268	112	156

Table 2 Different expressions of some genes in BE and EA

Upregulated	Downregulated
Cathepsin C	Glutathione synthetase
Aminopeptidase M	Lecithin-cholesterol acyltransferase
Arachidonic acid epoxygenase	p55CDC
Tryptophan-2,3-dioxygenase	Heart fatty acid binding protein
Ubiquitin conjugating enzyme	Cell adhesion regulator
Cyclic GMP-stimulated phosphodiesterase	Selectin, endothelial cell, ligand
Tissue inhibitor of metalloproteinase 1	
Betaine-homocysteine methyltransferase	
Lysozyme	
Complement 4 binding protein, alpha	
Insulin-like growth factor binding protein	
UDP-glucuronosyltransferase	
Tissue inhibitor of metalloproteinase 3	
Rat liver aldolase B	
Retinoid X receptor gamma	
Complement component 9	
Rat liver carboxylesterase	
Testicular cell adhesion molecule 1	

DISCUSSION

Research has confirmed that BE is closely related to EA, every year the danger of BE developing into EA increases by 0.5% and the former is regarded as precancerous of the latter[5]. However, adenocarcinoma in the gastro-esophageal junction is thought as EA and its diagnosis can be made according to the fact that more than 50% carcinomas are situated in the esophageal lateral, mixing up the tissue origin of EA. Some clinical epidemiologic data on cardiac adenocarcinoma and EA indicate that the two diseases are similar in respects of age, sex, clinical, and pathological characteristics so that the origin of the two diseases is thought as the same tissue[8] and the two diseases are known as adenocarcinoma at the gastro-esophageal junction[9].

Miwa *et al*.[6], reported that EA arises from BE, which is induced by the contents of gastro-duodeno-esophageal reflux. The role of single genes in esophageal adenocarcinogenesis is reported[10]. However, the exact mechanism especially the molecular biological mechanism of EA is unknown. The carcinogenesis involved in more steps and more factors is caused by abnormal expression of tumor-associated genes including activation of oncogenes or inactivation of tumor suppression genes or both. Elucidation of the gene expression differences in malignant, precancerous and normal tissue is a crucial procedure for cancer control study. It is generally accepted that although the number of genes with mutation is limited in cancer, a large number of genes in related pathways may be affected at the expression level, and this aberrant gene transcriptional expression network plays an essential role in the initiation/maintenance of the malignant phenotype. With the advances in molecular biological techniques, cDNA microarray has been used to detect gene expression difference in various specimens by parallel analysis on a large scale[11]. In this research, animal model of gastro-duodeno-esophageal reflux was made and the difference in gene expression profiles between BE and EA was investigated by cDNA microarray. In the present study, we were interested in a group of genes involved in carcinogenesis.

Among the upregulated genes in EA, 18 genes were involved in carcinogenesis and carcinomatous progression including cathepsin C, aminopeptidase M, arachidonic acid epoxygenase, tryptophan-2,3-dioxygenase, ubiquitin-conjugating enzyme, cyclic GMP-stimulated phosphodiesterase,

tissue inhibitor of metalloproteinase-1, tissue inhibitor of metalloproteinase-3, betaine-homocysteine methyltransferase, lysozyme, complement 4b binding protein, complement 9 protein, insulin-like growth factor (IGF) binding protein, UDP-glucuronosyltransferase, aldolase B, retinoid X receptor gamma, carboxylesterase and testicular cell adhesion molecule-1. These genes might participate in carcinogenesis and carcinomatous progression of EA by various mechanisms.

Cathepsin C is a kind of cysteine protease. Cysteine proteases are negatively correlated with those inhibitors in effect and there is a balance in effect between them in normal tissues. However, in tumor tissue, genes expressing cysteine proteases are upregulated and inhibitors of cysteine protease are downregulated, thus breaking the balance in normal tissue and leading to extracellular matrix proteins decompounding, which might be related to invasion and metastasis of tumor[12]. Aminopeptidase M causes conversion of angiotensin III into angiotensin IV[13], which might be related to lesions of gastrointestinal tract mucosa[14]. The 5×-upstream region of the arachidonic acid epoxygenase gene was isolated by amplification of a 2 341-bp fragment and putative regulatory elements that resembled activator protein-1-like sequences were identified. Activator protein-1 as a nucleolus transcription factor, combined DNA by leucine zipper, is a pivotal factor of cellular malignant transformation in various oncogene signal-transducing pathways[15]. T lymphocytes undergo proliferation arrest when exposed to tryptophan shortage, which can be provoked by tryptophan 2,3-dioxygenase, an enzyme that catalyzes tryptophan degradation and is expressed in most human tumors and normal placenta[16]. Ubiquitin-conjugating enzyme is a key component of ubiquitin-proteasome-proteolytic pathway that is associated with tumorous cachexia and upregulated expression in some tumor tissues[17]. The cGMP phosphodiesterase decreases cGMP in SW480 and HT29 colon tumor cells, which inhibit apoptosis[18]. Tissue inhibitor of metalloproteinase inhibits the activity of metalloprotease and the latter is associated with tumor invasion and metastasis. In common, the former is downregulated and the latter is upregulated in tumor tissue. However, some researches indicate that some tissue inhibitor of metalloproteinase can also stimulate cell proliferation and angiogenesis, thus leading to tumorigenesis[19]. For example, overexpression of tissue inhibitor of metalloproteinase-1 is associated with poor prognosis and relapse in patients with tumor[19]. New data suggest that high levels of tissue inhibitor of metalloproteinase-3 mRNA in human breast tumors are associated with successful adjuvant endocrine therapy[20]. Betaine-homocysteine-methyltransferases catalyze synthesis of methionine from homocysteine, which provides methyl for DNA synthesis. Methionine, obtained in the diet and synthesized by several reactions in the body, is the sole precursor of *S*-adenosylmethionine, the primary methyl donor in the body. Enzymatic DNA methylation is an important component of gene control and may serve as a silencing mechanism for gene function. Disruption in methionine metabolism and methylation reactions may be involved in cancer process[21]. Lysozyme is an innate non-immunologic antibacterial enzyme produced by the Paneth cells of the upper intestinal tract. Lysozyme is not normally secreted in the alimentary tract without Paneth cells, where intense lysozyme production might herald a possible dysplastic evolution and even neoplasia[22]. Complement 4b binding protein and complement 9 are crucial ingredients of complement immune system and multi-complement 9 unites into a polymer as formation of the membrane attack complex, which mediates tumor cell lysis[23]. IGF-I and its main binding protein modulate cell growth and survival, and are important in tumor development and progression. Circulating concentrations of IGF and its binding protein are associated with an increased risk for common cancers, but the association is modest and varies between sites[24]. Uridine diphospho-glucuronosyltransferases are a family of drug metabolizing enzymes contributing to hepatic drug metabolism and protection against environmental toxins. They are involved in catalyzing estrogen, which may be associated with an increased risk for breast cancer[25]. Aldolase B is a kind of glycolytic enzyme. There is a direct relationship between the proliferation of tumor cells and the activities of glycolytic and gluconeogenic enzymes. A significant rise in glycolytic enzyme activities and a simultaneous fall in gluconeogenic enzyme activities are found in mammary carcinoma[26]. Retinoids are natural and synthetic compounds related to retinoic acid, that act through interaction with two basic types of nuclear receptors: retinoic acid receptors and retinoid X receptors (RXR alpha, RXR beta, and RXR gamma) as retinoid-inducible transcription factors. Thus, retinoid receptors are considered to be ligand-activated, DNA-binding, trans-acting, transcription-modulating proteins involved in a general molecular mechanism responsible for transcriptional responses in target genes. They exert both beneficial and detrimental activity related to the selective receptors[27]. Haugen *et al*.[28], reported that differential tumor expression of RAR beta and RXR gamma and lack of the RXR gamma isoform are found in normal thyroid tissue. Cell lines expressing both RAR beta and RXR gamma demonstrate significant growth suppression when treated with retinoids, whereas cell lines lacking these isoforms are unaffected. Carboxylesterase isoenzyme RL2 shows hydrolyzing activity towards activators of protein kinase C. Since protein kinase C is involved in carcinogenesis and cell proliferation, up-regulated carboxylesterase in adenocarcinoma might be involved in carcinogenesis[29]. Testicular cellular adhesion molecule is a cellular adhesion molecule expressed normally in testicle, which plays a role in cancer angiogenesis, progression, and metastasis[30].

Among the downregulated genes in EA, the downregulated genes involved in carcinogenesis include glutathione synthetase, lecithin-cholesterol acyltransferase, p55CDC, heart fatty acid binding protein, cell adhesion regulator and endothelial cell selectin ligand. The cellular defense system (including glutathione and glutathione-related enzymes) plays a crucial role in cell survival and growth. Glutathione and glutathione synthetase are associated with tumorigenesis and apoptosis[31]. An important factor that determines the movement of cholesterol in and out of the cells is the free cholesterol/esterified cholesterol ratio in plasma. The ratio

increases in several types of malignancies both in humans and in experimental animals, which might be related to decreased activity of lecithin-cholesterol acyltransferase[32]. p55CDC, a mitotic checkpoint protein, plays a crucial role in carcinogenesis and decreased expression of the proteins is associated with progression of some cancers[33]. Heart fatty acid binding protein is also known as a mammary-derived growth inhibitor, which is a tumor growth suppressor gene capable of inhibiting tumor cell proliferation[34]. Cell adhesion regulator can inhibit tumor cellular growth and regulate tumor angiogenesis. Its expression in some tumor tissues is downregulated and associated with progression of tumor[35]. Endothelial cell selectin ligand mediates lymphocytes interacting with endothelial cells or tumor cells and plays an important role in the metastasis of carcinoma[36], indicating that the ability to protect against esophagus tumorigenesis, decreases with the development of normal esophageal epithelium into BE, by overexposure to contents of gastric and duodenal reflux.

Many up- or down-regulated genes in EA compared to BE indicate that many genes in related pathways may affect development of BE into carcinoma and its molecular mechanism is very complex. The difference in gene expression between BE and EA indicates the molecular characteristics of the onset and promotion of BE and its progression into EA. The exact pathogenesis of EA and the relationship between EA and differently expressed genes need further study.

REFERENCES

1 Barret MT, Yeung KY, Ruzzo WL, Hsu L, Blount PL, Sullivan R, Zarbl H, Delrow J, Rabinovitch PS, Reid BJ. Transcriptional analyses of Barret's metaplasia and normal upper GI mucosae. *Neoplasia* 2002; **4**: 121-128

2 **Rana PS,** Johnston DA. Incidence of adenocarcinoma and mortality with Barrett's esophagus diagnosed between 1976 and 1986. Implications for endoscopic surveillance. *Dig Esophagus* 2000; **13**: 28-31

3 **Zhang J,** Chen XL, Wang KM, Guo XD, Zuo AL, Gong J. Barrett's esophagus and its correlation with gastroesophageal reflux in Chinese. *World J Gastroenterol* 2004; **10**: 1065-1068

4 **O'Connor JB,** Falk GW, Richter JE. The incidence of adenocarcinoma and dysplasia in Barrett's esophagus: report on the Cleveland Barrett's Esophagus Registry. *Am J Gastroenterol* 1999; **94**: 2037-2042

5 **Geboes K.** Barrett's esophagus: the metaplasia-dysplasia-carcinoma sequence: morphological aspects. *Acta Gastroenterol Belg* 2000; **63**: 13-17

6 **Miwa K,** Sahara H, Segawa M, Kinami S, Sato T, Miyazaki I, Hattori T. Reflux of duodenal or gastro-duodenal contents induces esophageal adenocarcinoma in rats. *Int J Cancer* 1996; **67**: 269-274

7 **Schena M,** Shalon D, Heller R, Chai A, Brown PO, Davis RW. Parallel human genome analysis: microarray-based expression monitoring of 1000 genes. *Proc Natl Acad Sci USA* 1996; **93**: 10614-10619

8 **Ruol A,** Parenti A, Zaninotto G, Merigliano S, Costantini M, Cagol M, Alfieri R, Bonavina L, Peracchia A, Ancona E. Intestinal metaplasia is probable common precursor of in barretts esophagus and adenocarcinoma of the gastric cardia. *Cancer* 2000; **88**: 2520-2526

9 **Byrne JP,** Mathers JM, Parry JM, Attwood SE, Bancewicz J, Woodman CB. Site distribution of oesophagogastric cancer. *Clin Pathol* 2002; **55**: 191-194

10 **Bektas N,** Donner A, Wirtz C, Heep H, Gabbert HE, Sarbia M. Allelic loss involving the tumor suppressor genes APC and MCC and expression of the APC protein in the development of dysplasia and carcinoma in Barrett esophagus. *Am J Clin Pathol* 2000; **114**: 890-895

11 **Huang GS,** Yang SM, Hong MY, Yang PC, Liu YC. Differential gene expression of livers from ApoE deficient mice. *Life Sci* 2000; **68**: 19-28

12 **Krepela E,** Prochazka J, Karova B, Cermak J, Roubkova H. Cysteine proteases and cysteine protease inhibitors in non-small cell lung cancer. *Neoplasma* 1998; **45**: 318-331

13 **Prieto I,** Hermoso F, Gasparo M, Vargas F, Alba F, Segarra AB, Banegas I, Ramirez M. Angiotensinase activities in the kidney of renovascular hypertensive rats. *Peptides* 2003; **24**: 755-760

14 **Sanchez S,** Alarcon de la Lastra C, Ortiz P, Motilva V, Martin MJ. Gastrointestinal tolerability of metamizol, acetaminophen, and diclofenac in subchronic treatment in rats. *Dig Dis Sci* 2002; **47**: 2791-2798

15 **Marden NY,** Fiala-Beer E, Xiang SH, Murray M. Role of activator protein-1 in the down-regulation of the human CYP2J2 gene in hypoxia. *Biochem J* 2003; **373**(Pt 3): 669-680

16 **Ishio T,** Goto S, Tahara K, Tone S, Kawano K, Kitano S. Immunoactivative role of indoleamine 2,3-dioxygenase in human hepatocellular carcinoma. *J Gastroenterol Hepatol* 2004; **19**: 319-326

17 **El-Nady GM,** Ling R, Harrison TJ. Gene expression in HCV-associated hepatocellular carcinoma-upregulation of a gene encoding a protein related to the ubiquitin-conjugating enzyme. *Liver Int* 2003; **23**: 329-337

18 **Liu L,** Li H, Underwood T, Lloyd M, David M, Sperl G, Pamukcu R, Thompson WJ. Cyclic GMP-dependent protein kinase activation and induction by exisulind and CP461 in colon tumor cells. *J Pharmacol Exp Ther* 2001; **299**: 583-592

19 **Miyata Y,** Kanda S, Nomata K, Hayashida Y, Kanetake H. Expression of metalloproteinase-2, metalloproteinase-9, and tissue inhibitor of metalloproteinase-1 in transitional cell carcinoma of upper urinary tract: correlation with tumor stage and survival. *Urology* 2004; **63**: 602-608

20 **Edwards DR.** TIMP-3 and endocrine therapy of breast cancer: an apoptosis connection emerges. *J Pathol* 2004; **202**: 391-394

21 **Shimizu K,** Abe M, Tsukada K. Deficiency of methionine synthesis enzyme activity in ascites tumor cells. *Biochem Int* 1990; **20**: 1105-1110

22 **Rubio CA.** Colorectal adenomas produce lysozyme. *Anticancer Res* 2003; **23**: 5165-5171

23 **Bomstein Y,** Fishelson Z. Enhanced sensitivity of P-glycoprotein-positive multidrug resistant tumor cells to complement-mediated lysis. *Eur J Immunol* 1997; **27**: 2204-2211

24 **Renehan AG,** Zwahlen M, Minder C, O'Dwyer ST, Shalet SM, Egger M. Insulin-like growth factor (IGF)-I, IGF binding protein-3, and cancer risk: systematic review and meta-regression analysis. *Lancet* 2004; **363**: 1346-1353

25 **Adegoke OJ,** Shu XO, Gao YT, Cai Q, Breyer J, Smith J, Zheng W. Genetic polymorphisms in uridine diphosphoglucuronosyltransferase 1A1 (UGT1A1) and risk of breast cancer. *Breast Cancer Res Treat* 2004; **85**: 239-245

26 **Sujatha V,** Sachdanandam P. Recuperative effect of Semecarpus anacardium linn. nut milk extract on carbohydrate metabolizing enzymes in experimental mammary carcinoma-bearing rats. *Phytother Res* 2002; **16**(Suppl 1): S14-18

27 **Brtko J,** Thalhamer J. Renaissance of the biologically active vitamin A derivatives: established and novel directed therapies for cancer and chemoprevention. *Curr Pharm Des* 2003; **9**: 2067-2077

28 **Haugen BR,** Larson LL, Pugazhenthi U, Hays WR, Klopper JP, Kramer CA, Sharma V. Retinoic acid and retinoid X receptors are differentially expressed in thyroid cancer and thyroid carcinoma cell lines and predict response to treatment with retinoids. *J Clin Endocrinol Metab* 2004; **89**: 272-280

29 **Maki T,** Hosokawa M, Satoh T, Sato K. Changes in carboxylesterase isoenzymes of rat liver microsomes during

hepatocarcinogenesis. *Jpn J Cancer Res* 1991; **82**: 800-806

30 **Perabo F,** Sharma S, Gierer R, Wirger A, Fimmers R, Steiner G, Adam M, Schultze-Seemann W. Circulating intercellular adhesion molecule-1 (ICAM-1), vascular cell adhesion molecule-1 (VCAM-1) and E-selectin in urological malignancies. *Indian J Cancer* 2001; **38**: 1-7

31 **Lee YY,** Kim HG, Jung HI, Shin YH, Hong SM, Park EH, Sa JH, Lim CJ. Activities of antioxidant and redox enzymes in human normal hepatic and hepatoma cell lines. *Mol Cells* 2002; **14**: 305-311

32 **Subbaiah PV,** Liu M, Witt TR. Impaired cholesterol esterification in the plasma in patients with breast cancer. *Lipids* 1997; **32**: 157-162

33 **Xu K,** Wang X, Xue W, Wang X, Hou S. Expressions of MAD2 and p55CDC in prostate cancer and their correlations with the prostate cancer grading. *Beijing Daxue Xuebao* 2003; **35**: 586-590

34 **Tang MK,** Kindler PM, Cai DQ, Chow PH, Li M, Lee KK. Heart-type fatty acid binding proteins are upregulated during terminal differentiation of mouse cardiomyocytes, as revealed by proteomic analysis. *Cell Tissue Res* 2004; **316**: 339-347

35 **Liu Y,** Jovanovic B, Pins M, Lee C, Bergan RC. Over expression of endoglin in human prostate cancer suppresses cell detachment, migration and invasion. *Oncogene* 2002; **21**: 8272-8281

36 **Mathieu S,** Prorok M, Benoliel AM, Uch R, Langlet C, Bongrand P, Gerolami R, El-Battari A. Transgene expression of alpha(1,2)-fucosyltransferase-I (FUT1) in tumor cells selectively inhibits sialyl-Lewis x expression and binding to E-selectin without affecting synthesis of sialyl-Lewis a or binding to P-selectin. *Am J Pathol* 2004; **164**: 371-383

Science Editor Wang XL and Guo SY **Language Editor** Elsevier HK

PO Box 2345, Beijing 100023, China
www.wjgnet.com
wjg@wjgnet.com

ELSEVIER

World J Gastroenterol 2005;11(33):5123-5128
World Journal of Gastroenterology ISSN 1007-9327
© 2005 The WJG Press and Elsevier Inc. All rights reserved.

• *GASTRIC CANCER* •

Adenocarcinoma of gastric cardia in the elderly: Surgical problems and prognostic factors

Natale Di Martino, Giuseppe Izzo, Angelo Cosenza, Guido Cerullo, Francesco Torelli, Antonio Brillantino, Alberto del Genio

Natale Di Martino, Giuseppe Izzo, Angelo Cosenza, Francesco Torelli, Antonio Brillantino, VIII Service of General Surgery and Gastroenterological Physiopathology, Second University of Study of Naples, Italy
Guido Cerullo, Department of General Surgery and Surgical Oncology, UO Surgical Oncology, University of Siena, Italy
Alberto del Genio, I Division of General and Gastroenterological Surgery, Second University of Study of Naples, Italy
Supported by the Second University of Study of Naples
Co-first-authors: Natale Di Martino and Guido Cerullo
Correspondence to: Professor Natale Di Martino, c/o VIII Servizio di Chirurgia Generale e Fisiopatologia Gastroenterologica, Seconda Università degli Studi di Napoli, Piazza Miraglia, 2-80135, Napoli, Italy. natale.dimartino@unina2.it
Telephone: +39-81-5665055 Fax: +39-81-5665055
Received: 2005-01-03 Accepted: 2005-01-26

Abstract

AIM: To analyze retrospectively, our results about patients who underwent surgical treatment for adenocarcinoma of the cardia in relation to age, in order to evaluate surgical problems and prognostic factors.

METHODS: From January 1987 to March 2003, 140 patients with adenocarcinoma of the cardia underwent resection in the authors' institution. They were divided into three groups with regard to age. Patients <70 and > 60 year old (31) were excluded; we also excluded 18 out of 109 patients with poor general status or systemic metastases. So, we compared 51 elderly ($\geqslant$ 70 year old) and 58 younger patients ($\leqslant$ 60 year old). The treatment was esophagectomy for type I tumors, and extended gastrectomy and distal esophagectomy for type II and III lesions.

RESULTS: Laparotomy was carried out in 91 patients (83.4%), 38 in the elderly (74.5%) and 53 in younger patients (91.3%, P<0.05). Primary resection was performed in 81 cases (89%) without significant differences between the two groups. Postoperative death was higher in the elderly (12.1%) than the other group (4.1%, P<0.05), while morbidity was similar in both groups. A curative resection (R0) was performed in 59 patients (72.8%), 69.6% in the elderly and 75% in the younger group (P>0.05). The overall 3- and 5-year survival rates were 26.7% and 17.8% respectively for the elderly and 40.7% and 35.1% respectively for younger patients (P = 0.1544). Survival rates were significantly associated with R0 resection, pathological node-positive category and tumor differentiation in both groups.

CONCLUSION: As the age of the general population increases, more elderly patients with gastric cardia cancer will be candidates for surgical resection. Age alone should not preclude surgical treatment in elderly patients with gastric cardia cancer and a tumor resection can be carried out safely. Certainly, we should take care in defining the surgical treatment in elderly patients, particularly as regarding the surgical approach; although the surgical approach does not influence the survival rate, the transhiatal way still remains the best one due, to the lower incidence of respiratory morbidity and thoracic pain.

© 2005 The WJG Press and Elsevier Inc. All rights reserved.

Key words: Gastric cardia carcinoma; Esophagogastric junction carcinoma; Elderly; Surgery

Di Martino N, Izzo G, Cosenza A, Cerullo G, Torelli F, Brillantino A, del Genio A. Adenocarcinoma of gastric cardia in the elderly: Surgical problems and prognostic factors. *World J Gastroenterol* 2005; 11(33): 5123-5128
http://www.wjgnet.com/1007-9327/11/5123.asp

INTRODUCTION

In the Western world, we observe a lower incidence of gastric and esophageal cancer in contrast with the annual increase in the adenocarcinoma of the esophagogastric junction (EGJ) equal to 5-10%[1-10]. Both for gastric adenocarcinoma and cardia cancer, we notice an increasing number of elderly patients[11-14]. Anyway, with regard to clinicopathological features of the adenocarcinoma of the EGJ in the elderly and its surgical problems in relation to age, few data have been published in the international literature. Adenocarcinoma of the EGJ has been defined as a tumor whose center is within 5 cm proximal and distal of the anatomical cardia, and today this tumor is considered as a separate neoplasm because of its distinctive prognostic and pathological features[4-6]. However, the surgical treatment of the cardia is still controversial, mainly regarding the extent of gastric and esophageal resection, the limphadenectomy, the surgical approach and the importance of adjuvant chemotherapy[4,5,15-17]. These themes are very important in order to define the treatment of old patients, especially for the increasing number of over 70 year old suffering from this neoplasm as well as from other comorbidities peculiar to old age.

The aim of this study is to analyze retrospectively, our results about patients who underwent surgical treatment for adenocarcinoma of the EGJ in relation to age, in order to

evaluate surgical problems and prognostic factors, in particular in patients over 70 year old.

MATERIALS AND METHODS

Between January 1987 and February 2003, in our Institute, we observed 140 patients with adenocarcinoma of the EGJ. They were divided retrospectively into three groups with regard to age: (1) Group A: age $\geqslant$ 70 years old; (2) Group B: age $\leqslant$ 60 years old; (3) Group C: age < 70- and > 60-years old.

The 31 patients of group C were excluded in order to characterize better the other two groups. Group A consists of 51 patients (44 male, 7 female), and group B 58 patients (50 male, 8 female, Table 1). A retrospective study was done on these two groups of patients.

The surgical risk has been evaluated preoperatively with ASA score[18]. Eighteen out of 109 patients were excluded, 10 for poor general status with ASA score >3 (nine in group A, one in group B) and 8 for systemic metastases on preoperative staging (four in group A, four in group B). So, a total of 91 patients with gastric cardia cancer underwent laparotomy and only 81 underwent surgical resection. The surgical procedure was considered curative (R0), if gross tumor tissue including the metastatic lymph nodes were removed completely and the microscopic examination revealed no cancer cells at both proximal and distal margins. The procedure was considered palliative (R1), if microscopic disease was left behind. Resection specimens were assessed by an experienced pathologist. Staging is reported according to the most recent version of the UICC/AJCC guidelines for esophageal cancer (type I tumors) or gastric cancer (type II and III tumors)[19,20].

A particular effort has been made to identify areas with intestinal metaplasia in the distal esophagus and in the region of the cardia in all resection specimens. The retrospectively collected data included demographic parameters, histomorphologic tumor characteristics, the presence of associated intestinal metaplasia in the distal esophagus (Barrett's esophagus), the type of resection, post-operative 30-d death rate, morbidity, the depth of tumor invasion (pT), the pN category, the presence of residual disease on intraoperative assessment and histopathologic analysis of the removed specimen.

Surgical approach

The choice of surgical approach was based on the tumor type and on the goal of achieving a complete macroscopic and microscopic tumor resection, both in elderly and younger patients. Regardless of the surgical approach, we have recently believed in the transhiatal approach according to Pinotti's technique as a more valid alternative than the transthoracic approach. In general, a radical transmediastinal or transthoracic en bloc esophagectomy with resection of the proximal stomach has been the procedure of choice in 14 patients with type I tumors (seven in group A, seven in group B). Radical transmediastinal esophagectomy and resection of the proximal stomach was performed by a laparotomy and wide exposure of the lower posterior mediastinum by anterior splitting of the diaphragmatic hiatus and a left cervical incision. Extended esophagectomy was associated with proximal gastric resection in nine patients and with total gastrectomy in 5 cases. An extended total gastrectomy with transhiatal resection of the distal esophagus according to Pinotti's technique was performed in 42 patients with type III tumors. In 25 patients with type II tumors, an attempt was usually made to achieve a complete tumor resection by means of an extended gastrectomy with transhiatal resection of the distal esophagus according to Pinotti's technique. Lymphadenectomy comprised an en bloc removal of all lymphatic tissue in the lower posterior mediastinum, along the cardia, proximal two-thirds of the lesser curvature, and the fundus, and along the common hepatic and splenic artery toward the celiac axis. A transthoracic en bloc esophagectomy with resection of the proximal stomach was performed using a right posterolateral thoracotomy and laparotomy and included an extended en bloc mediastinal lymphadenectomy and an abdominal lymphadenectomy (two-field lymphadenectomy), as described above. The reconstruction after transmediastinal or transthoracic esophagectomy was performed with a narrow gastric tube or colon interposition and a cervical or high intrathoracic anastomosis. The extended total gastrectomy has always included a wide splitting of the diaphragmatic hiatus, transhiatal resection of the distal esophagus, and en bloc lymphadenectomy of the lower posterior mediastinum, in addition to a formal D2 lymphadenectomy (i.e., lymph node stations 1-11 of the Japanese classification)[21]. A mediastinal Roux-en-Y end-to-side esophago-jejunostomy performed with a circular stapler, was the reconstruction procedure of choice, after extended total gastrectomy and distal esophagectomy.

Statistical analysis

The survival status of our patients was ascertained between January and February 2003 and the follow-up was completed.

Data are shown as prevalence or mean±SD. Continuous data were compared by the Mann-Whitney test, ordinal data by the χ^2-test. Survival rate was analyzed by the Kaplan-Meier method and log-rank test. Prognostic factors were assessed by means of Cox regression analyses. $P<0.05$ was considered significant.

RESULTS

Regarding demographic data, both groups showed a preponderance of the male sex (Group A: M/F 4.8:1; Group B: M/F 6.2:1), but the male to female ratio was higher in the younger group than in the older group ($P<0.05$). Median age was 75.4±3.1; (range 70-84) for over 70 year old patients and 53.7±5.6; (range 32-60) in the other group (Table 1). The most common comorbidities in both groups were diabetes mellitus, coronary artery disease, hypertension and chronic obstructive pulmonary disease. Patients were divided into three types of tumor according to Siewert's classification (Figure 1). Laparotomy was carried out in 91 patients (83.4%), 38 in group A (74.5%) and 53 in group B (91.3%) ($P<0.05$). Primary resection was performed in 81 cases (89%), 33 in group A (86.8%) and 48 in group B (90.5%) (Table 1). There were no differences between the two groups regarding tumor stage.

Table 1 Demographic and surgical data in 109 patients with adenocarcinoma of the EGJ

	Group A (51)[1]	Group B (58)[1]	*P*	Total (109)
Median age (±SD)	75.4±3.1	53.7±5.6	*P*<0.05	62.6±13.8
Sex ratio (M / F)	4.8 / 1	6.2 / 1	*P*<0.05	5.5 / 1
Operability (%)	38 (74.5)	53 (91.3)	*P*<0.05	91 (83.4)
Primary resection (%)	33 (86.8)	48 (90.5)	NS	81 (89)
Postoperative death (%)	4 (12.1)	2 (4.1)	*P*<0.05	6 (7.4)
Morbidity (%)	16 (48.4)	16 (33.3)	NS	32 (39.5)
Mean hospital stay (±SD)	19.3±7.1 d	18.1±6.3 d	NS	19±6.9 d

[1]Group A: ⩾70 years old; group B: ⩽60 years old.

In type I tumor, we observed a prevalence (71.4%) of associated intestinal metaplasia in the distal esophagus (Barrett's esophagus) of elderly patients; rarely it was noticed in type II (10% *vs* 13.3%; *P*>0.05) or in type III (11.7% *vs* 3.8%; *P*>0.05, Table 2). In types II and III, there was a prevalence of grading G2 (*P*<0.05) compared to type I, independent of the age.

A curative resection (R0) was performed in 59 patients (72.8%), 69.6% in group A and 75% in group B respectively (Table 2). Three out of 59 patients treated with resection of the distal esophagus had tumor infiltration of resection margins. Fifty patients (61.7%) had positive lymph nodes, 20 in group A (60.6%) and 30 (62.5%) in group B, respectively (Table 3). Analysis of the pattern of lymphatic spread showed a most important metastatic involvement of lower posterior mediastinum and paracardial stations for type I and abdominal lymph node stations for types II and III, without significant differences between the two groups (A *vs* B: *P*>0.05). A greater percentage of positive lymph nodes was noticed in elderly patients (25% *vs* 17.6%), but it was statistically insignificant.

Postoperative death was 12.1% (4/33) in elderly patients and 4.1% (2/48) in the other group (*P*<0.05), without any correlation with sex, type of tumor, extent of resection and stage. Regardless of morbidity, there are no significant differences between the two groups. The most frequent complications were respiratory insufficiency and anastomotic leakage. The mean hospital stay (SD) was 19.3±7.1 d for group A and 18.1±6.3 d for group B (*P*>0.05, Table 1).

The overall 3- and 5-year survival rates were 26.7% and 17.8% respectively for group A and 40.7% and 35.1% respectively for group B (*P* = 0.1544, Figure 2). The worst results were observed for type I in both groups (Figures 3A and B). We noticed a difference in survival rate for types I and II between group A and B, but not significantly. As regards the type III survival rates were similar in both groups (Figures 4A-C).

Analysis of prognostic factors showed significant differences in both groups regarding: (1) tumor resection (R0 *vs* R1-2, *P*<0.05); (2) lymph node involvement (N0 *vs* N+, *P*<0.05); (3) pT categories (*P*<0.05);

Statistical analysis showed that elderly patients had lower

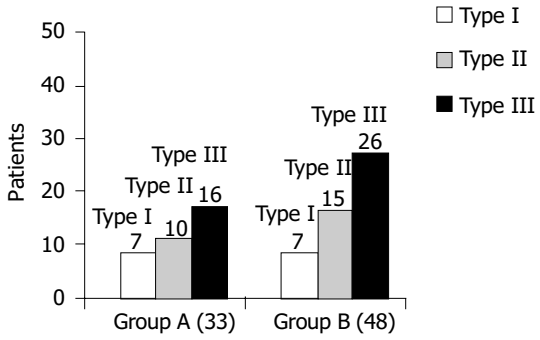


Figure 1 Subdivision of the 81 patients with adenocarcinoma of the EGJ, according to Siewert' Classification. Group A: ⩾70 years old; group B: ⩽ 60 years old. Type I A *vs* Type I B *P*>0.05; Type II A *vs* Type II B *P*>0.05; Type III A *vs* Type III B *P*>0.05.

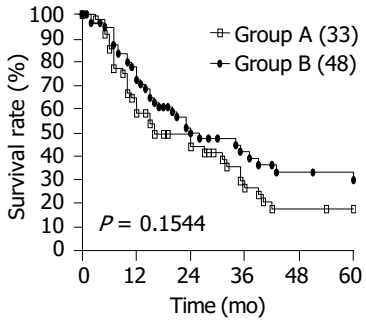


Figure 2 The 5-year survival rates of 113 patients with adenocarcinoma of the EGJ. The younger patients showed a better survival rate than the elderly (*P* = 0.1544). Group A: ⩾70 years old; group B: ⩽60 years old. Kaplan-Meier and log-rank test.

Table 2 Histopathologic data in 81 patients that underwent surgical resection for adenocarcinoma of the EGJ

	Group A (33, %)[1]	Group B (48, %)[1]	*P*
Intestinal metaplasia	71.4	71.4	NS
Curative resection (R0)	69.6	75	NS
Tumor involvement of resection margin	3	4.1	NS
Lymph nodes involvement (N+)	60.6	62.5	NS

[1]Group A: ⩾70-years old; group B: ⩽60-years old.

Table 3 Histopathologic data regarding pN category in 81 patients that underwent surgical resection for adenocarcinoma of the EGJ

pN category	Group A (33)[1]	Group B (48)[1]	*P*
Patients N0	13 (39.3)[2]	18 (37.5)[2]	NS
Patients N+	20 (60.6)[2]	30 (62.5)[2]	NS
Assessed lymph nodes	436	511	NS
Positive lymph nodes	109 (25)[2]	90 (17.6)[2]	NS

[1]Group A: ⩾70 years old; group B: ⩽60 years old. [2]Percentage in parenthesis.

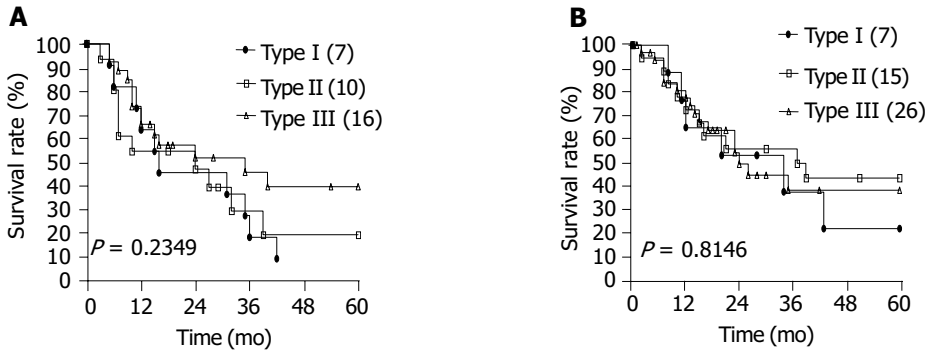


Figure 3 Survival curves according to Siewert's classification in the elderly (**A**) and in the younger group (**B**). In both groups the worst survival rate regarding type I. Group A: ⩾70 years old; group B: ⩽60 years old. Kaplan-Meier and log-rank test.

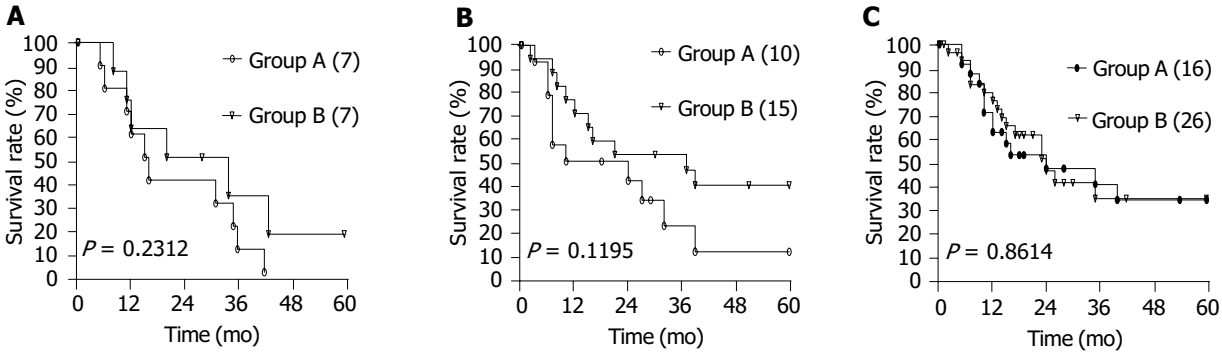


Figure 4 Survival curves according to Siewert's classification for type I (**A**), type II (**B**) and type III (**C**), respectively. There is a difference in survival rate only for types I and II between groups A and B, but not of much significance. Group A: ⩾70 years old; group B: ⩽60 years old. Kaplan-Meier and log-rank test.

5-year survival rate both into R0 (21% *vs* 49.9%) and N0 (24.1% *vs* 70%) category ($P<0.0001$) (Figures 5A and B). Differently, surgical approach and extent of esophago-gastric resection does not influence significantly the survival rates, both in the elderly and in the other group. The extent of esophago-gastric resection for type II tumor still remains a subject of controversy and debate. Regarding this type of tumor, we did not observe any significant improvement in patients that underwent total esophagectomy (Figure 6).

DISCUSSION

There are no major controversies in the surgical therapy of patients with esophageal and gastric cancer, but the management of patients with adenocarcinoma of the EGJ continues to be a matter of debate. Despite their rising incidence, there are marked discrepancies in the definition of such tumors, the selection of the surgical approach, and the outcome of surgical therapy[4,6,7,15]. The classification of Siewert, based purely on anatomical/topographic parameters, is needed for a valid comparison of data from various centers and assessment of different diagnostic and therapeutic approaches[4-6].

Anyway, the evaluation of our surgical results in relation with age was very difficult because not much information was available in the international literature. By comparison of two groups of patients that underwent surgical resection for adenocarc-inoma of the EGJ, we did not observe significant differences as regarding demographic data and survival rates. Younger patients showed a better but not a significant overall survival rate than the elderly people. In our study, this result is independent of the type of tumors, but the worst survival rate regarding type I, probably due to the inefficacious endoscopic screening in patients with EG chronic reflux disease. In elderly patients, we also observed that operability was significantly lower ($P<0.05$) while post-operative death was higher ($P<0.05$) than in the other group. Probably, both operability and primary

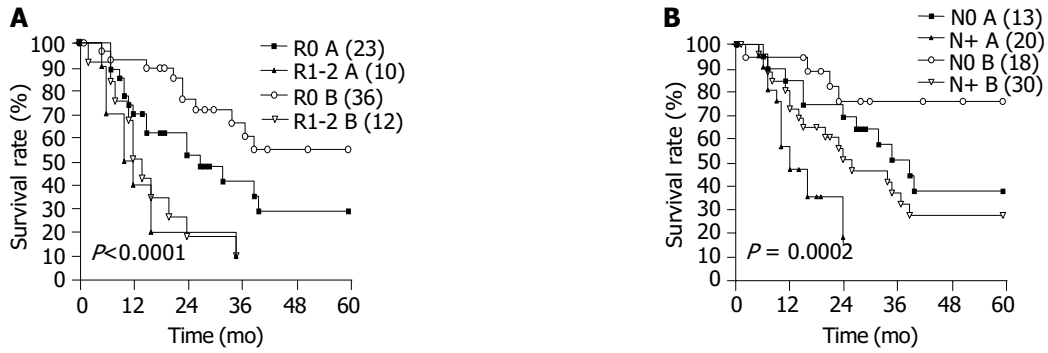


Figure 5 Overall 5-year survival rates of 81 patients with resected adenocarcinoma of the EGJ regarding type of resection (R0 *vs* R1-2) (**A**) and pN category (**B**). Elderly patients showed a lower 5-year survival rate than that of younger patients, both for pN0 category and curative resection (R0). Group A: ⩾70 years old; group B: ⩽60 years old. Kaplan-Meier and log-rank test.

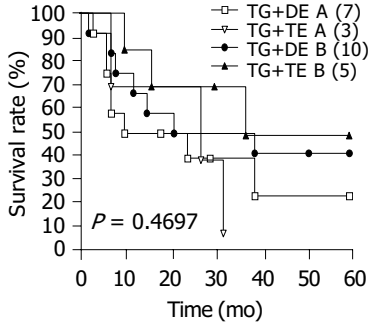


Figure 6 Survival rates of elderly and younger patients regarding the extent of esophagogastric resection for type II tumor: total gastrectomy with distal esophagectomy (TG+DE) *vs* total gastrectomy with total esophagectomy (TG+TE) (P = 0.4697). Both in the elderly and younger patients with type II tumor, total esophagectomy did not improve survival rates significantly. Group A: ⩾70 years old; group B: ⩽60 years old. Kaplan-Meier and log-rank test.

resection are lower in elderly patients due to their age-related comorbidity. Morbidity was higher but not significant in elderly patients[11,22]. Unlike other authors[11], R0 and N0 categories had significantly lower survival rates in the elderly group. It is very difficult to interpret these results, so further studies are needed. There were no differences between the two groups regarding other parameters. Moreover, in patients with type II tumor total esophagectomy did not improve survival rates[4,5].

A radical surgery is also necessary in distal esophagectomy through a safety margin of 3 cm according to some authors or 10 cm according to others[4,5,9,23-25]. In our experience, it is enough to have a safety distance of 5 cm from the upper margin of the tumor to ensure R0 resection. Therefore, the aim of the surgical treatment of the adenocarcinoma of the EGJ is to get a radical oncological resection, taking care of achieving R0 resection.

In conclusion, gastric cardia cancer is usually diagnosed in an advanced stage and is still associated with poor prognosis, particularly in elderly patients. As the age of the general population increases, more elderly patients with gastric cardia cancer will be candidates for surgical resection. In our study, as also observed by other authors for gastric cancer[26], the overall survival data were similar in both groups. Survival rate is strongly linked to curative resection (R0), lymph nodes involvement and stage of disease, which is advanced in more than half of patients. In our experience, unlike other authors, worst results regarding type I, is due to the inefficacious endoscopic screening in patients with EG chronic reflux disease which is correlated to intestinal metaplasia, independent of age. However, just like other authors[3], we observed a high percentage of Barrett's esophagus in elderly patients over 70 years. So, endoscopic secondary prevention should be enhanced in patients with EG reflux disease and particularly in the elderly.

Other authors just observed that an oncologically correct surgical procedure can safely be prosecuted, because age alone should not preclude gastric resection in elderly patients suffering from gastric cancer[26,27]. Regarding the adenocarcinoma of the EGJ, the extent of distal esophagectomy for type II tumor does not influence survival rates on the condition that it achieves a curative resection (R0). The role of lymphadenectomy continues to be a matter of debate. We agree with the necessity of extended lymphadenectomy by transthoracic[28,29] approach but, its potential benefits may be nullified by an associated increase in post-operative morbidity, particularly in over 70-year-old patients. However, we believe that the transhiatal approach according to Pinotti's technique is a more valid alternative than the transthoracic approach, due to the lower incidence of respiratory morbidity and thoracic pain[7,9,30-32]. According to some authors, in selected cases, it is also possible to perform a distal esophagectomy entirely by laparoscopy, without the need for any thoracic or cervical access[33].

In conclusion, age alone should not preclude surgical treatment in elderly patients with gastric cardia cancer and a tumor resection can be carried out safely. Certainly, further studies are needed to confirm the peculiarities observed in elderly patients, just like lower operability and survival rates for type I-II tumors and R0-N0 categories, higher post-operative death and morbidity after thoracotomy. If these data should be confirmed, we should take care in defining the surgical treatment in elderly patients, particularly as regarding the surgical approach.

REFERENCES

1 **Cai L,** Zheng ZL, Zhang ZF. Risk factors for the gastric cardia cancer: a case-control study in Fujian Province. *World*

J Gastroenterol 2003; **9**: 214-218
2 **Mueller JD,** Stein HJ, Oyang T, Natsugoe S, Feith M, Werner M, Siewert JR. Frequency and clinical impact of lymph node micrometastasis and tumor cell microinvolvement in patients with adenocarcinoma of the esophagogastric junction. *Cancer* 2000; **89**: 1874–1882
3 **Pera M.** Trends in incidence and prevalence of specialized intestinal metaplasia, barrett's esophagus, and adenocarcinoma of the gastresophageal junction. *World J Surg* 2003; **27**: 999-1008
4 **Siewert JR**, Feith M, Werner M, Stein HJ. Adenocarcinoma of the esophagogastric junction. Result of surgical therapy based on anatomical/topographic classification in 1002 consecutive patients. *Ann Surg* 2000; **232**: 353-361
5 **Mariette C,** Castel B, Toursel H, Fabre S, Balon JM, Triboulet JP. Surgical management of long-term survival after adenocarcinoma of the cardia. *Br J Surg* 2002; **89**: 1156-1163
6 **Ichikura T,** Ogawa T, Kawabata T, Chochi K, Sugasawa H, Mochizuki H. Is adenocarcinoma of the gastric cardia a distinct entity indipendent of subcardial carcinoma? *World J Surg* 2003; **27**: 334-338
7 **Hansson LE,** Ekstrom AM, Bergstrom R, Nyrén O. Carcinoma of the gastric cardia: surgical practices and short-term operative results in a defined Swedish population. *World J Surg* 2000; **24**: 473-478
8 **Graham AJ,** Finley RJ, Clifton JC, Evans KG, Fradet G. Surgical management of adenocarcinoma of the cardia. *Am J Surg* 1998; **175**: 418-421
9 **Wayman J,** Dresner SM, Raimes SA, Griffin SM. Transhiatal approach to total gastrectomy for adenocarcinoma of the gastric cardia. *Br J Surg* 1999; **86**: 536-540
10 **Bruno L,** Nesi G, Montinaro F, Carassale G, Lassig R, Boddi V, Bechi P, Cortesini C. Clinicopathologic findings and results of surgical treatment in cardiac adenocarcinoma. *J Surg Oncol* 2000; **74**: 33-35
11 **Rabuñal RR,** Pita SF, Rigueiro MTV, Casariego EV, Pértega SD, García-Rodeja E, Abraira V. Presentation and prognosis of gastric cancer in patients aged 80 years and older. *World J Surg* 2004; **28**: 155-159
12 **Borch K,** Jönsson B, Tarpala E, Franzen T, Berglund J, Kullman E, Franzen L. Changing pattern of histological type, location, stage and outcome of surgical treatment of gastric carcinoma. *Br J Surg* 2000; **87**: 618-626
13 **Kitamura K,** Yamaguchi T, Taniguchi H, Hagiwara A, Yamane T, Sawai K, Takahashi T. "Clinico-pathological characteristics of gastric cancer in the elderly". *Br J Cancer* 1996; **73**: 798-802
14 **Gillison EW**, Powell J, Conkey CCM, Spychal RT. Surgical workload and outcome after resection for carcinoma of the esophagus and cardia. *Br J Surg* 2002, **89**: 344-348
15 **Kodera Y,** Yamamura Y, Shimizu Y, Torii A, Hirai T, Yasui K, Morimoto T, Kato T. Adenocarcinoma of the gastresophageal junction in Japan: relevance of Siewert's classification applied to 177 cases resected at a single institution. *J Am Coll Surg* 1999; **189**: 594-601
16 **Bumm R,** Feussner H, Bartels H, Stein H, Dittler HJ, Hofler H. Radical transhiatal esophagectomy with two-field lymphadenectomy and endodissection for distal esophageal adenocarcinoma. *World J Surg* 1997; **21**: 822-831
17 **Wijnhoven BP,** Siersema PD, Hop WC, van Dekken H, Tilanus HW. Adenocarcinomas of the distal esophagus and gastric cardia are one clinical entity. Rotterdam Esophageal Tumour Study Group. *Br J Surg* 1999; **86**: 529-535
18 American Society of Anesthesiologist. New classification of physical status. *Anesthesiology* 1963; **24**: 111
19 **Tnm U**. Classification of Malignant Tumours; 6th Edition. *New York: Wiley Liss* 2002
20 Cancer Staging Handbook; 6th Edition. *New York: Springer* 2002
21 Japanese Gastric Cancer Association. Japanese classification of gastric carcinoma-2nd English Edition. *Gastric Cancer* 1998; **1**: 10-24
22 **Dhar DK,** Kubota H, Tachibana M, Kotoh T, Tabara H, Watanabe R, Kohno H, Nagasue N. Long-term survival of transmural advanced gastric carcinoma following curative resection: multivariate analysis of prognostic factors. *World J Surg* 2000; **24**: 588-593
23 **Stipa S,** Di Giorgio A, Ferri M. Surgical treatment of adenocarcinoma of the cardia. *Surgery* 1992; **111**: 386-393
24 **Siewert JR,** Bottcher K, Stein HJ, Roder JD. Relevant prognostic factors in gastric cancer: ten-year result of the German Gastric Cancer Study. *Ann Surg* 1998; **228**: 449-461
25 **Stark SP,** Romberg MS, Pierce GE, Hermreck AS, Jewell WR, Moran JF. Transhiatal versus transthoracic esophagectomy for adenocarcinoma of the distal esophagus and cardia. *Am J Surg* 1996; **172**: 478-481
26 **Coniglio A,** Tiberio GA, Busti M, Gaverini G, Baiocchi L, Piardi T, Ronconi M, Giulini SM. Surgical treatment for gastric carcinoma in the elderly. *J Surg Oncol* 2004; **88**: 201-205
27 **Saidi RF,** Bell JL, Dudrick PS. Surgical resection for gastric cancer in elderly patients: is there a difference in outcome? *J Surg Res* 2004; **118**: 15-20
28 **Chu KM,** Law SY, Fok M, Wong J. A prospective randomised comparison of transhiatal and transthoracic resection for lower-third esophageal carcinoma. *Am J Surg* 1997; **174**: 320-324
29 **Hulscher JB,** Tijssen JG, Obertop H, van Lanschot JJ. Transthoracic versus transhiatal resection for carcinoma of the esophagus: a meta-analysis. *Ann Thorac Surg* 2001; **72**: 306-313
30 **Hulscher JB,** van Sandick JW, Tijssen JG, Obertop H, van Lanschot JJ. The reccurrence pattern of esophageal carcinoma after transhiatal resection. *J Am Coll Surg* 2000; **191**: 143-148
31 **Orringer MB,** Marshall B, Stirling MC. Transhiatal esophagectomy for benign and malignant disease. *J Thorac Cardiovasc Surg* 1993; **105**: 265-276
32 **Orringer MB,** Marshall B, Iannettoni MD. Transhiatal esophagectomy for treatment of benign and malignant esophageal disease. *World J Surg* 2001; **25**: 196-203
33 **Costi R,** Himpens J, Bruyns J, Cadiere GB. Totally laparoscopic transhiatal esophago-gastrectomy without thoracic or cervical access. The least invasive surgery for adenocarcinoma of the cardia? *Surg Endosc* 2004; **18**: 629-632

Science Editor Guo SY **Language Editor** Elsevier HK

PO Box 2345, Beijing 100023, China
www.wjgnet.com
wjg@wjgnet.com

ELSEVIER

World J Gastroenterol 2005;11(33):5129-5135
World Journal of Gastroenterology ISSN 1007-9327
© 2005 The WJG Press and Elsevier Inc. All rights reserved.

• *GASTRIC CANCER* •

Recurrent chromosomal rearrangements at bands 8q24 and 11q13 in gastric cancer as detected by multicolor spectral karyotyping

Yasuhide Yamashita, Kazuhiro Nishida, Takashi Okuda, Kenichi Nomura, Yosuke Matsumoto, Shoji Mitsufuji, Shigeo Horiike, Hiroyuki Hata, Chohei Sakakura, Akio Hagiwara, Hisakazu Yamagishi, Masafumi Taniwaki

Yasuhide Yamashita, Takashi Okuda, Shoji Mitsufuji, Department of Gastroenterology and Hepatology, Kyoto Prefectural University of Medicine, Kyoto 602-8566, Japan
Kazuhiro Nishida, Kenichi Nomura, Yosuke Matsumoto, Shigeo Horiike, Masafumi Taniwaki, Department of Hematology and Oncology, Kyoto Prefectural University of Medicine, Kyoto 602-8566, Japan
Hiroyuki Hata, Second Department of Internal Medicine, Kumamoto University School of Medicine, Kumamoto 860-8555, Japan
Chohei Sakakura, Akio Hagiwara, Hisakazu Yamagishi, Department of Digestive Surgery, Kyoto Prefectural University of Medicine, Kyoto 602-8566, Japan
Masafumi Taniwaki, Department of Clinical Molecular Genetics and Laboratory Medicine, Kyoto Prefectural University of Medicine, Kyoto 602-8566, Japan
Correspondence to: Masafumi Taniwaki, MD, PhD, Department of Hematology and Oncology, Department of Clinical Molecular Genetics and Laboratory Medicine, Kyoto Prefectural University of Medicine, Kawaramachi-Hirokoji, Kamigyo-ku, Kyoto 602-8566, Japan. taniwaki@koto.kpu-m.ac.jp
Telephone: +81-75-251-5651 Fax: +81-75-251-5687
Received: 2005-01-19 Accepted: 2005-02-18

Abstract

AIM: To identify chromosomal translocations specific to gastric cancer (GC), spectral karyotyping (SKY) analysis was performed on established cell lines and cancerous ascitic fluids.

METHODS: SKY analysis of 10 established cell lines and seven cancerous ascitic fluid samples identified recurrent chromosomal breakpoints and translocations in GC, several of which involved chromosomal loci of oncogenes or tumor suppressor genes.

RESULTS: A total of 630 chromosomal breaks were identified. Chromosome no.8 was the most frequently involved in rearrangements (65 breaks), followed by chromosomes no.11 (53), no. 1 (49), no. 7 (46), no. 13 (37), no. 3 (36), no. 17 (33), and no. 20 (29). Frequent breakpoints were detected in 8q24.1 (30 breaks), 11q13 (29), 13q14 (16), 20q11.2 (14), 7q32 (13), 17q11.2 (13), 18q21 (12), 17q23 (9), 18q11.2 (9). SKY analysis identified a total of 242 chromosomal rearrangements including 190 reciprocal and non-reciprocal translocations. The recurrent combinations of chromosomal bands involved in translocations were 8q24.1 and 13q14 (3 cases), 8q24.1 and 11q13 (3), 11q13 and 17q11.2 (2), and 18q11.2 and 20q11.2 (2). Our study validated the ability of SKY to characterize in detail the chromosomal rearrangements in solid tumors and derived cell lines. Moreover, fluorescence *in situ* hybridization helped to identify the insertions, translocations, and homogeneously staining regions of *MYC* and *CCND1* gene loci.

CONCLUSION: The non-random co-localization of certain cytogenetic bands suggests the importance of chromosomal translocations in gastric carcinogenesis, by serving as landmarks for the cloning of GC causing genes.

© 2005 The WJG Press and Elsevier Inc. All rights reserved.

Key words: Gastric cancer; SKY; FISH; Chromosomal translocation

Yamashita Y, Nishida K, Okuda T, Nomura K, Matsumoto Y, Mitsufuji S, Horiike S, Hata H, Sakakura C, Hagiwara A, Yamagishi H, Taniwaki M. Recurrent chromosomal rearrangements at bands 8q24 and 11q13 in gastric cancer as detected by multicolor spectral karyotyping. *World J Gastroenterol* 2005; 11(33): 5129-5135
http://www.wjgnet.com/1007-9327/11/5129.asp

INTRODUCTION

Chromosomal aberrations are fundamental to cancer formation because they interfere with the function of oncogenes and tumor suppressor genes. Identification of recurrent chromosomal translocation may thus contribute to the cloning of cancer causing genes. Several genetic alterations associated with gastric cancer (GC) have been reported: (1) amplifications of *MYC, HST1/FGF4*, *INT2/FGF3*, *ERBB2*, *MET*, and *KSAM/FGFR2* genes[1-3], and (2) mutations of *APC*, *KRAS*, *TP53*, E-cadherin (*CDH1*), β-catenin (*CTNNB1*) and *RUNX3/PEBP2* genes[3-5]. These specific alterations have been implicated in multi-stage carcinogenesis of GC.

At the same time, previous cytogenetic studies of GC have demonstrated frequent aberrations of chromosome nos. 1, 3, 6, 7, 8, 13, 17, 20 and Y[6-9], while other chromosomes have also been found to be repeatedly involved in cytogenetic aberrations as demonstrated by recent comparative genomic hybridization (CGH) studies[10-13]. The chromosomal breakpoints identified were 1p22, 3p21, 3q23, 11p13-15, and 19p13 on primary gastric tumors[6,7,14], and 1q32, 5q11-22, 14q22, and 15q15 on human GC cell lines[15]. However, specific chromosomal translocations have not yet been identified in GC, because complete karyotypic analysis

was precluded by the complicated and cryptic nature of the rearrangements as well as the poor banding of condensed chromosomes. To overcome these limitations, multiplex fluorescence *in situ* hybridization (FISH) has been successfully used for two patients with GC[16].

To identify chromosomal translocations specific to human GC, we used multicolor spectral karyotyping (SKY) to analyze established cell lines and cancerous ascitic fluid samples and were able to identify and characterize recurrent chromosomal breakpoints and translocations in GC, several of which involved chromosomal loci of oncogenes or tumor suppressor genes.

MATERIALS AND METHODS

Cell lines and patient samples

Ten GC cell lines (KMK2, KHM14K, MKN1, MKN28, MKN45, MKN74, GT3TKB, SNU1, SNU5, and SNU16) and seven cancerous ascitic fluid samples from advanced GC (patient nos. 1-7) were the subjects of our study. SNU1, SNU5, and SNU16 were obtained from the Korean Research Institute of Bioscience and Biotechnology (Taejon, South Korea), and MKN1, MKN28, MKN45, MKN74, and GT3TKB from the RIKEN Cell Bank (Tsukuba, Japan). Two cell lines, KMK2 and KHM14K, were established at the Kumamoto University School of Medicine (Kumamoto, Japan) and their clinico-pathological features are summarized in Tables 1 and 2. Six cell lines were derived from poorly differentiated adenocarcinoma (MKN45, SNU1, SNU5, SNU16, KMK2, and KHM14K), two from moderately differentiated adenocarcinoma (MKN28 and MKN74), one from undifferentiated mucin-producing adenocarcinoma (GT3TKB), and one from adenosquamous cell carcinoma (MKN1). According to Lauren's classifications[17], seven cell lines (MKN45, SNU1, SNU5, SNU16, KMK2, KHM14K, and GT3TKB) were categorized as diffuse type, and two cell lines (MKN28 and MKN74) as intestinal type.

Primary tumors associated with carcinomatous peritonitis were histopathologically diagnosed as poorly differentiated adenocarcinoma in three patients, signet-ring cell carcinoma in two, and coexisting poorly differentiated adenocarcinoma and signet-ring cell carcinoma in two. These diagnoses indicated that all these tumors were diffuse type GC according to Lauren's classification. Ascitic fluid was aspirated with a syringe and the addition of heparin from the peritoneal cavities of seven patients with carcinomatous peritonitis. Informed consent in accordance with the institutional guidelines was obtained, for using the diagnostic material for research purposes.

Cell cultures and chromosome preparations

G-banding studies were performed as described previously[18]. Briefly, ascitic fluid was diluted in 10 mL of RPMI 1640 medium supplemented with 10% fetal calf serum at a final concentration of 1×10^6 cells/mL. The cells were cultured at 37 ℃ for 24-48 h in humidified air with 50 mL/L CO_2, exposed to colcemid (0.05 μg/mL) for 60 min, processed in 0.075 mol/L potassium chloride for 20 min, and fixed with methanol/glacial acetate (3:1). Chromosomes were stained with a Giemsa solution pretreated with trypsin, and karyotyped according to the International System for Human Cytogenetic Nomenclature (ISCN 1995)[19]. The remaining chromosome pellets were stored at -20 ℃ for SKY and FISH analyses.

SKY studies

Chromosomes prepared on a slide glass were denatured and hybridized with a cocktail probe mixture for 2 d at 37 ℃. The SKY probe mixture and hybridization reagents were purchased from Applied Spectral Imaging Inc. (Carlsbad, CA, USA) and signal detection was performed according to the manufacturer's protocol. Chromosomes were counterstained with 4', 6-diaminido-2-phenylindole dihydrochloride (DAPI) combined with an anti-fade solution (Vectaschield; Vector Laboratories, Burlingame, CA, USA). Images were acquired by means of an SD200 Spectracube (Applied Spectral Imaging) mounted on an Olympus BX50-RF (Olympus, Tokyo, Japan) using a custom-designed optical filter (SKY-1; Chroma Technology, Brattleboro, VT). With another special optical filter, the inverted DAPI images were captured in conjunction with spectral classifications as QFH band patterns for the identification of chromosomal breakpoints[20,21]. For each case, 10-20 metaphase spreads were analyzed, and karyotypes were described according to the ISCN 1995.

Double-color fluorescence in situ hybridization (DC-FISH)

Two cell lines, SNU16 and KMK2, were studied by means of DC-FISH using an oncogene and whole chromosome painting (WCP) probes. DC-FISH was performed as described previously[18]. The oncogene probe consisted of an I2 yeast artificial chromosome (YAC) clone containing *MYC* on 8q24.1 and a CPP29 cosmid containing *CCND1* on 11q13.3[22,23]. Human-specific DNA sequences were amplified from YAC by means of Alu-polymerase chain reaction[24], DNA probes were labeled by biotin-16-dUTP and digoxigenin-16-dUTP (Boehringer Mannheim Biochemicals, Mannheim, Germany). Metaphase spreads were counterstained with 0.04 μg/mL of DAPI, mounted in an anti-fade solution (Vectaschield), and observed with a BX40-RF fluorescence microscope (Olympus). Images were captured with a CCD camera (SenSys0400-G1; Photometrics Ltd, Tucson, AZ, USA).

RESULTS

Cytogenetic and SKY analysis

All established cell lines and patients with GC showed clonal karyotypic abnormalities. The modal chromosome number varied from 39 to 89. SKY detected chromosomal deletions, translocations (mainly unbalanced), inversions, insertions, dicentrics, duplication, ring chromosomes, isochromosomes, double minute chromosomes (DMs), and homogeneously staining regions (HSRs). Complex rearrangements involving more than three chromosomes were frequently encountered (Figure 1). Polysomy of chromosomes no. 16 (8 cases), no. 20 (8), no. 11 (7), and no. 9, no. 15, and no. 22 (5 each), and monosomy of chromosomes no. 5 (5 cases), and no. 4, no. 6, no. 13, no. 14, no. 15, no. 21, and no. 22 (4 each) were frequently observed. Structural rearrangements most

frequently involved chromosome no.8 (65 breaks), followed by chromosomes no. 11 (53), no. 1 (49), no. 7 (46), no. 13 (37), no. 3 (36), no. 17 (33), and no. 20 (29) (Figure 2). Chromosomal segments and bands were identified by combining SKY with DAPI banding (Figure 1). Representative karyotypes are listed in Tables 1 and 2.

A total of 630 chromosomal breaks that occurred in 177 breakpoints were identified by means of SKY analysis as shown in Figure 2 with several breakpoints highlighted: 8q24.1 (30 breaks), 11q13 (29), 13q14 (16), 20q11.2 (14), 7q32 (13), 17q11.2 (13), 18q21 (12), 17q23 (9), 18q11.2 (9), 1p22 (8), 1q32 (8), 7q22 (8), 8p11.2 (8), 8q22 (8), 9q22 (8), 10q22 (8), 20q13 (8), Xq22 (8), 7q11.2 (7), 11q23 (7), 22q11.2 (7), 3p13 (6), 3p21 (6), 3q21 (6), 4q12 (6), 9q13 (6), 13q12 (6), and 14p11.2 (6).

DC-FISH using YAC I2 and applied to two cell lines (SNU16 and KMK2) demonstrated that the chromosomal locus of the *MYC* gene (8q24.1) was involved in various types of chromosomal rearrangements including translocation, HSRs, and frequent insertion, thus resulting in gain and amplification of the gene (Figure 3). FISH using the MYC probe showed a periodic staining pattern, although we initially defined HSRs as abnormalities of chromosome no. 2 based on its SKY staining property as shown in Figure 3.

In KMK2, DC FISH with WCP 11 and cosmid CPP29 demonstrated that the chromosomal locus of the *CCND1* gene (11q13) was involved in translocations, resulting in increased copy number of the gene (Figure 4).

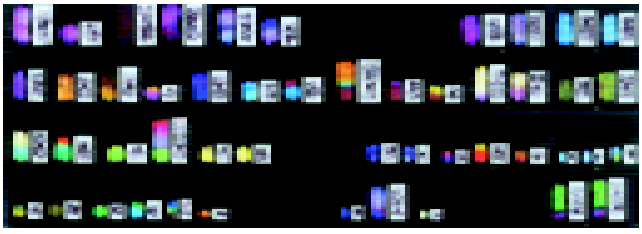


Figure 1 SKY analysis in GT3TKB. Color images are shown alongside inverted DAPI banding images.

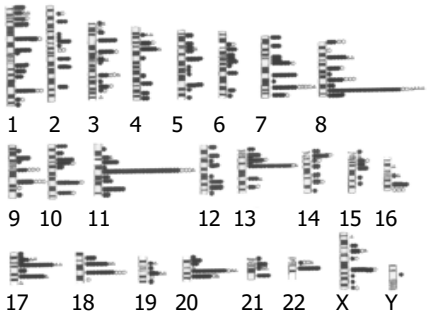


Figure 2 Assignment of breaks in 7 patients with GC and 10 established cell lines. A total of 630 breaks were identified by SKY. Closed and open circles represent diffuse type and intestinal type, respectively. Open triangle represents the breakpoints obtained from one cell line MKN1 established from a GC patient with adenosquamous cell carcinoma. Mapping analysis of breaks to the ideograms delineated two outstanding loci, 8q24.1 and 11q13. The other breakpoints highlighted are 13q14, 17q11.2, 18q21, and 20q11.2.

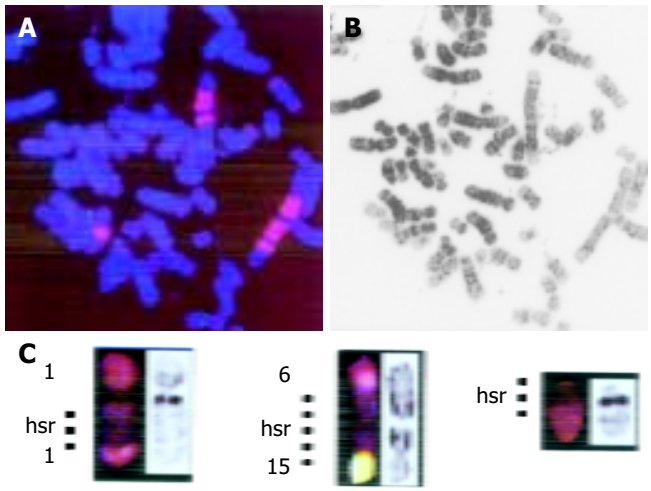


Figure 3 FISH and SKY analysis on SNU16. **A**: DC-FISH using YAC probe I2 (8q24.1, red) and cosmid probe CPP29 (11q13.3, green). I2 probe shows periodic staining pattern on HSRs, indicating amplification of *MYC* gene on HSRs but not double minute chromosomes (DMs). Three copies of *CCDN1* gene are detected; **B**: Inverted DAPI band image of the same metaphase plate shown in A; **C**: SKY findings of HSRs found in SNU16. Three HSRs were initially identified as originating from chromosome no. 2 based on their fluorescence color.

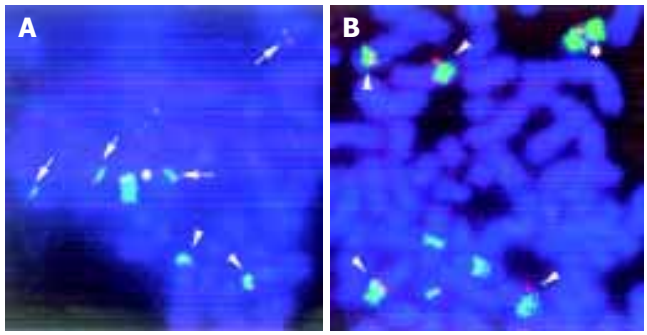


Figure 4 FISH analysis on KMK2. **A**: DC-FISH using YAC probe I2 (8q24.1, red) and WCP probe for chromosome 8 (green) demonstrates multiple insertions (arrows) and translocations (arrowheads) of *MYC* locus. Asterisk indicates a normal chromosome 8. **B**: DC-FISH using cosmid probe CPP29 (red) and WCP probe for chromosome 11 (green) demonstrates multiple translocations (arrowheads) at *CCND1* locus. Asterisk indicates a normal chromosome 11.

Identification of recurrent chromosomal translocations

A total of 242 chromosomal rearrangements including 190 translocations were identified. The four combinations of chromosomal bands repeatedly involved in translocations comprised 8q24.1 and 13q14 (SNU5, KMK2, and patient no. 6), 8q24.1 and 11q13 (SNU16, KMK2, and patient no. 1), 11q13 and 17q11.2 (KMK2 and MKN1), and 18q11.2 and 20q11.2 (GT3TKB and patient no. 7) as shown in Figure 5. Table 3 shows common translocation partners,

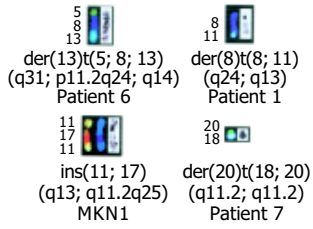


Figure 5 Partial karyotypes of recurrent translocations.

Table 1 Karyotypes according to SKY analysis on 10 cell lines derived from advanced gastric cancers

Cell line	Histologic grade[1]	Site[2]	Representative karyotype[3]
MKN45	Poor	LT	85,XX,del (1) (q32), del (1) (q32), +der (1) t (1;2) (p34;q21), +der (1) t (1;2) (p34;q21), der (2) t (2;22) (p23;q11.2), +del (2) (q23), +der (3) t (3;8) (p21.3;q24.1), +der (4) H (9qter→9q22::4p12→4q35::11p11.2→11pter), +der (4) (9qter→9 q22::4p12→4q35::11p11.2→11pter), +der (5) t (5;8) (q31;q22), +der (5) t (5;8) (q31;q22), der (6) t (1;6) (q25;q27), +der (7) t (7;12) (q32;q21), +der (7) t (7;11) (q11.1;q13), +der (7) t (7;11) (q11.1;q13), +der (7) t (7;11) (q11.1;q13), +der (7) t (7;9) (q11.2;q34),-8,-8, +9, +10, +der (10) t (8;10) (q23;p15), +der (10) t (8;10) (q23;p15), +del (11) (p11.2), +der (12) t (9;12) (p22;q24.1), +der (12) t (10;12) (q11.2;q12), +13, +13, +der (14) t (13;14) (q22;p11.2), +der (14) t (13;14) (q22;p11.2), +16, +16, +16, +der (17) t (12;17) (q22;p13), +i (17) (p11.1), +der (19) (19pter→19q13.4::7? →7?::11q23→11qter), +der (19) (19pter→19q11::8q21.2→8q24.1::20q13.1→20qter), +20, +20, +der (20) t (7;20) (q11.2;p12), +der (20) t (7;20) (q11.2;p12), +der (20) t (8;20) (p11.2;q11.2), +der (21) t (20;21) (p11.2;q11.2), +der (21) t (12;21) (p11.2;q22.3), +22, +22, +mar (6pter→6q21::20p13→20q11.2::7p11.2→7p15::8q22?8q24.1::18q21→18qter)
SNU1	Poor	AS	85,XXYY, +del (1) (p22), +del (1) (p22), -4, -5,-5, -11,-11, -13, -14, -17, -18, +20, +20, +20, +mar
SNU5	Poor	AS	74,XX,der (1) t (1;8) (p36.3;q24.1),der (1) t (X;1) (p11.4;p32), +der (1) t (X;1) (p11.4;p32), +der (2) t (2;11) (p21;q13), +der (2) t (2;11) (p21;q13), +2,-3,der (4) t (4;17) (q33;q23), +der (4) t (4;13) (q31;q32), +der (4) (4pter→4q12::13q14 →13q22::10q24→10qter), +del (5) (q15), +del (5) (p12), +5, +6, der (7) t (7;11) (q36;q13), +del (7) (q32), +del (7) (q32), +der (7) (7pter→7q22::11q13→11q23::13q12→13qter), +der (7) t (7;8) (q36;q24.1), +der (8) t (8;13) (q24.1;q14), + der (8) t (8;13) (q24.1;q14), +9, +10, +der (10) t (2;10) (p21;q24), +der (10) t (10;15) (q22;q15), +11, +11, +11, +12, der (13) (14qter→14q13::13p13→13q32::17q23→17qter), +14, +14, +der (15) t (15;22) (p13;q11.2), +16, +i (17q) (p10), +19, +20, +20, +21,-22, +hsr, +dmin
SNU16	Poor	AS	74,XX,del (1) (p13), +hsr (1) (pter→q21::hsr::q21→qter), +2, +3, +6, +6, +6, +del (7) (q22), +del (7) (q22), del (7) (q32), der (7) t (7;8) (q22;q24.1), +der (8) t (8;11) (q24.1;q13), +9,del (10) (q22), +11, +der (11) (5pter→5p13::11p11.2→11q25::17q23→17qter), + 12, +12, +13, +14, +der (15) (6pter→6p11.2→::hsr::15p11→15qter), +16, +17, +17, +18, +18, +19, +20, +20, +22, 30-50dmin
KMK2	Poor	AS	66,X,del (X) (p11.2) (q22),der (1) (20qter→20q13.1::1p36.1→1q23::8q22→8qter), der (1) (17qter→17q21::1p32→1q42::8q24.1→8qter), +der (1) (4qter→4q33::5q35→5q11.2::1p13?→q21::8q 13→8qter), +der (1) t (1;5) (q21;q32), +der (2) t (2;3) (q33;q25),t (3;5) (q25-26.2;q31), +der (3) (3pter→3q24::11q13→11q14::4p12→4pter), der (5) del (5) (p12) del (5) (q21), +der (5) (12qter→12q24.1::5p15.1→5q22::13q12→13qter), +der (5) t (5;7) (q13;q32), del (6) (q12), del (6) (q12), +del (6) (q25), +der (6) t (6;14) (q21;q22), del (7) (q22), der (7) t (7;15) (p22;q13), +der (7) t (6;7) (q15;p15), +der (7) t (7;20) (p11.2;q13), der (8) t (8;17) (p23;q11.2), der (9) (Xpter→Xp11.2::8q24.3→8q24.1::9p13→9qter), +der (9) t (3;9) (?;?), del (10) (q22), +der (10) (14q?ter→14q?24::10p13→10q21::1p13→1p34::8q24.1→8q24.3::11q13.1→11q13.5 ::7p15→7p22::15q13→15qter),der (12) (12pter→12q22::11q13.3→11q21::3q21→3qter), +der (12) (3pter→ 3p21::12p13→12q24.3::Xq13→Xq22::6p21.3→6pter), +der (12) (17qter→17q11.2::12p11.2→12q24.1::13q12 → 13qter),-13,der (13) (13pter→13q14::8q24.1→8q24.3::11q13.3→11q23::12q24.1→12qter),del (14) (q22), del (15) (q15), der (16) t (1;16) (p36.1;q22),der (17) (17pter→17q11.2:: 11q13.3→11q21::3q26.2→3qter), +der (17) t (16;17) (q22;q11.2), der (18) (22qter→22q11.2::11q21→11q13.3:: 8q24.1→8q22::18p11.2→18qter), +der (18) t (14;18) (q24;q21.3), +der (20) t (12;20) (q22;q13.1), +der (20) (20pter→20q11.2::13q12→13q14::8q24.1→8q24.3::11q13.3→11qter), +der (20) (20pter→20q11.2::13q12→13q14::8q24.1→8q24.3::11q13.3→11qter), +21, +der (22) t (5;22) (p13;q11.2)
KHM14K	Poor	LN	56,X,-Y, +1, +der (3) del (3) (p?) del (3) (q?), +der (3) (9qter?9q13::3q21→3p11::22q11.2→22qter), +der (5) (5qter →5p15::3?→3?::22q11.2→22qter),i (5p) (q10), +der (6) (6pter→6q11::5?→5?::17q23→17qter), t (8;16) (p23;q22), +der (8) t (8;20) (p11.2;q13.1), der (9) t (9;16) (p13;q12.1), +der (9) t (3;9) (q25;q13), +11, der (12) t (5;12) (q13;p13),der (13) t (3;13) (p13;q14), (14;15) (q32;q15), -15, del (15) (q24), +der (18) t (3;18) (p21.3;q21.1), +20, +20, +20,der (21) t (15;21) (q11.2-q13;p11.1),-22
GT3TKBU	Ndiffer. mucin-producing	AS	49,der (X) (Xpter→Xq28::HSR::1q32→1qter), +der (X) (Xpter→Xq28::HSR::1q32→1qter),-Y,-1, der (1) t (1;8) (p32-36.1;q24.1),der (2) t (2;4) (p12;q12-21),del (3) (p13),del (6) (q25),der (7) t (2;7) (q23;q11.2),-8,i (8q), der (9) t (9;10) (p13;q22), der (7;10) (7qter→7p22::13q13→13q11:: 10p11.2→10qter), der (10) t (8;10) (q24;p13), +der (10) t (10;15) (q11.2;q22),der (11) t (4;11) (q27;q23),der (11) t (1;11) (p13;q13),der (13) t (11;13) (q13;p11.2), der (13) t (13;17) (p11.2;p12),der (14) (14qter→14q11.2::3p11→3p26::17q11.2→17q23::3p21→3p23::17q21 →17qter), der (17) t (8;17) (q24;q11.2), der (17) t (17;19) (p11.2;q13.1), der (17) t (17;19), +del (18) (q21), +der (18) t (18;19) (q11.2;q13.1), -19,der (19) t (19;20) (p13.1;p12), +der (20) t (18;20) (q11.2;q11.2), +der (20) (8qter→8q24::20p11.2→20q11.2::2q33→2qter), +der (20) t (7;20) (q32;q11.2), der (21) t (4;21) (q12;p11.2),-22
MKN28	Moderate	LN	47, X, -X, del (1) (p22), +der (1) t (X;1) (q22-24;q32), del (2) (q13), del (2) (q13), +der (2) t (2;18) (p23;q21.3), der (3) del (3) (p13p25) del (3) (q21q25), +der (3) del (3) (p12) del (3) (q21q26.2), -4, -5, -5, -7, der (7) t (7;8) (q36;q22), -8, der (8) t (8;10) (p23;q11.2), -10, -13, der (14) t (7;14) (q11.2;q11.2), der (14) t (1;14) (q42;q24), +15, +der (16) t (13;16) (q12;q23-24), +der (19) t (11;19) (q13;q13.3), der (20) (20pter→20q13.1::8q13→8q24::7q32→7qter), +der (20) t (18;20) (q21.1;q11.2), +21, +21

MKN74	Moderate	LT	39, X, +der (X) (15qter→15q11.2::Xp11.2→Xq28::8q24.1→8qter), +der (X) t (X;7) (q13;q32), -Y, der (1) (9qter→9q32::1p34→1q32::18q21→18qter), +2, -3, der (4) t (4;6) (p12;p21.3), -5, der (7) (7pter→7q32::8q22→8q24.1::9q22→9qter), der (7) t (7;8) (q32;q22), der (8) t (8;10) (p23;q22), der (9) t (9;11) (q22;q13), -9, -10, +del (11) (q13), -12, -13, der (14) t (9;14) (q13;p11.2), -14, -15, der (16) t (9;16) (q13;q24), +der (16) t (9;16) (q13;q24) del (9) (q22), der (18) t (2;18) (?;q23), der (20) t (13;20) (q32;q11.1), -20, -21, -21, der (22) t (10;22) (q24;p11.2), +der (22) t (13;22) (q14;p11.2)
MKN1	Adenosqu amous carcinoma	LN	56, X, +inv (X) (p11.2p22.1), -Y, +der (1) t (1;8) (p36.1;q24.1), +der (1) t (1;8) (p36.1;q24.1), der (3) t (3;5) (p11;p12), der (3) t (3;20) (q27;q13.1), +der (3) t (3;7) (p26;q32.1), -5, -5, -6, +7, +7, +7, +7, del (8) (q24.1), +del (8) (q24.1), +del (8) (p11.2), +del (8) (p11.2), -9, -9, +ins (11;17) (q13;q11.2q25), -12, +del (13) (q14q22), der (15) t (4;15) (q12;p11.2), -15, +del (16) (q12.1), +del (16) (p11.2), +16, der (17) t (4;17) (p15.2;p11.2), der (17) t (4;17) (p15.2;p11.2), del (17) (q11.2), +der (18) t (3;18) (q21;q11.2), del (18) (q11.2), del (19) (p13.1), der (19) t (19;21) (q13.1;q11.2), +der (19) t (19;21) (q13.1;q11.2), +del (20) (q11.2), +der (20) t (17;20) (q23;q11.2), der (22) t (11;22) (p13;p11.2)

[1]Poor: poorly differentiated adenocarcinoma; Moderate, moderately differentiated adenocarcinoma. [2]ST: stomach; LT: metastatic liver tumor; AS: ascitic fluid; LN: lymph node. [3]Representative karyotypes are defined based on G-banding and SKY findings, and described according to ISCN1995.

Table 2 Karyotypes according to SKY analysis on 7 patients with advanced gastric cancer and carcinomatous peritonitis

Case number.	Age / Sex	Origin[1]	Histologic grade[2]	G-banding and SKY
1	52 / M	AS	Poor	89, XX, der (1) t (1;13) (q44;q14), t (1;2) (p36.3;p11.1), +der (1) t (1;2), +der (1) t (1;8) (p22;q24), +der (1) t (1;8) (p22;q24), +der (1) t (1;12) (q32;q13) del (1) (p32), +2, +2, +3, +4, +4, +del (5) (q13), +6, +6, +6, +7, +7, +7, der (8;8) (8pter→8q24.1::8p23→8q24.1::17q23→17qter), +der (8) t (8;11) (q24.1;q13), +del (8) (p11.2), +del (8) (p11.2), +9, +9, +i (9q), del (10) (q24), +der (10) t (8;10) (q24.1;q11.2), +der (10) t (8;10) (q24.1;q11.2), +inv (10) (p15.1q21), +11, +11, +12, +14, i (15q), i (15q), +16, +16, +17, del (18) (q11.2), +der (18) t (10;18) (p11.2;p11.2), +der (18) t (10;18) (p11.2;p11.2), +der (18) t (10;18) (q22;q21), +der (18) t (10;18) (q22;q21), +19, +19, +20, +20, +20, +20, +20, +20, -21, -21, +22
2	72 / M	AS	Poor	47, XY, +X, -3, del (13) (q14), +mar
3	63 / M	AS	Poor	54, der (X) t (X;3) (q24;q21), Y, +2, +del (4) (q21), +der (4) (4p15→4q12::17q11.2→17qter), +del (5) (q13), der (6) t (Y;6) (q11.2;p21.1), t (7;16) (q36;q22), der (11) t (9;11) (q13;q13), +del (11) (q13), +11, del (12) (p11.2), der (13) t (8;13) (q13;q14), +15, +16, -21, -21, +22, +22
4	56 / M	AS	Signet	46, X, -Y, +der (1) t (?;1;?) (?::1p13→1q21::?), t (2;20;8) (p11.2;q11.2;q24.1), t (2;20;8) (p11.2;q11.2;q24.1), +2, +2, der (3) (3qter→3p13::7?→7?::11q13→11qter), del (3) (p23) (q25), -4, -4, +del (5) (q13), +del (5) (q11.2), del (6) (q11), +der (6) (6p21.1→6q21::18q11.2→18qter), dic (7;11) (q11.2;p15), del (9) (p11), del (10) (p11.2), del (10) (p11.2), +10, der (11) t (?;11;?) (?::11p13→11q23::?), der (11) (2pter→2p11.2::11q12→11p11.2::7q11.2→7q32::17q23→17qter), der (11;20) (20pter→20q11.2::11p13→11q23::11q13→11q14::7q31→7q36::13q14→13qter), del (12) (q13), del (12) (q22), der (13) t (X;13) (p11.2;p11.2), der (13) (3pter→3p13::13p13→13q14::18q21→18qter), -14, -15, del (16) (q22), add (17) (p11.2), add (18) (q21.3), -18, -19, +20, der (21) t (17;21) (q23;q22), der (21) (7pter→7p11.2::21p13→21q22.1::hsr::21q22.1→21qter), -22
5	55 / M	AS	Signet	50, add (X) (p22.3), Y, +8, +9, +16, +18
6	37 / M	AS	Poor	69, der (X) (Xpter→Xq22::18q11.2→18q21::4q31.1→4qter),
			Signet	der (X) (Xpter→Xq22::18q11.2→18q21::4q31.1→4qter), -Y, +der (1) t (1;12) (q25;q13), +del (1) (p22), del (2) (q23), del (2) (q23), +der (2) t (1;2) (q23;q21), +der (2) t (1;2) (q23;q21), del (3) (p21), +del (3) (p13), +del (3) (q11.2), +5, +5, der (6) t (6;18) (q12;q11.2), -6, +7, +7, +der (8) (5qter→5q31::8p11.2→8q24.1::13q14→13qter), +der (8) (5qter→5q31::8p11.2→8q24.1::13q14→13qter), +der (10) t (4;10) (q12;q22), +der (10) t (4;10) (q12;q22), +der (11) t (7;11) (q22;q23), +der (11) t (11;17) (q25;q11.2), +12, der (13) t (6;13) (p21.1;p11.2), -13, der (14) t (14;17) (p11.2;q11.2), der (14) t (14;17) (p11.2;q11.2), +15, +15, +16, +16, der (17) t (X;17) (q22;q11.2), der (17) t (X;17) (q22;q11.2), +18, +18, +20, +21, +der (21) t (X;21) (q22;p11.2)
7	73 / F	AS	Poor	67, X, del (X) (q26), der (1) (1qter→1p22::11?→11?::8?→8?::22q11.2→22qter), der (1) (1?→1?::15?
			Signet	→15?::1?→1qter), der (1) (9pter→9p13::1p12→1q32::9q22→9qter), -2, -5, +der (7) t (7;9) (q32;q22), +der (7) t (7;9) (q32;q22), +der (7) t (7;20) (q22;q11.2), +der (7) t (7;20) (q22;q11.2), t (8;14) (q13;p13), +der (8) t (8;14), t (6;8) (p11.2;p21), +8, -9, +der (10) t (2;10) (p13;q24), +11, -12, +der (14) (20qter→20q13.1::14p11.2→14q24::11q13→11qter), +der (14) t (3;14) (p21;q13), +14, +15, +16, +17, +18, +18, +18, +18, +der (18) t (18;20) (q11.2;q11.2), +19, +20, +21, +21, +22, +der (22) t (1;22) (p22;p11.2)

[1]AS: ascitic fluid. [2]Poor: Poorly differentiated adenocarcinoma; Signet: signet ring cell carcinoma.

Table 3 Recurrent breakpoints and partners in gastric cancer cells defined by SKY analysis

Translocation breakpont	Number of breakpoints	Candidate genes	Partner breakpoints involved in chromsomal translocations or deletions[1]	
			Common	Single
8q24.1	30	MYC	11q13 [3], 13q14 [4]	1p22, 1p32-36.1, 1p34, 1p36.1, 1p36.3, 1q42, 2p11.2, 3p21.3, 7q22, 7q32, 7q36, 8p23, 9p13, 9q22, 10p13, 10q11.2, 17q11.2, 17q23, 18q21, 20p11.2, 20q11.2, 20q13.1, Xq28, deletion
11q13	26	FGFR4	8q24.1 [3], 8q24.3 [3],	1p13, 2p21, 7p15, 7q11.1, 7q22, 7q36, 7?, 9q13, 9q22, 11q23, 12q22, 13p11.2, 14q24, 17q25, 19q13.3
		FGF3 CCND1	3q24-25 [2], 17q11.2 [2], deletion [2]	
20q11.2	14	Unknown	18q11.2 [2]	2p11.2, 2q33, 7p11.2, 7q22, 7q32, 8p11.2, 8q24, 11p13, 13q12, 17q23, 18q21.1, deletion
1p32-36.3	12	RUNX3	8q24 [4]	2p11.1, 2q21, 9q32, 16q22, 17q21, 20q13.1, Xp11.4, deletion
13q14	12	RB	8q24.1 [3]	1q44, 3p13, 4q12, 7q36, 8q13, 13q22, 18q21, 22p11.2, deletion
17q11.2	12	ERBB2	11q13 [2]	3p26, 4q12, 8p23, 8q24, 11q25, 12p11.2, 14p11.2, 16q22, Xq22, deletion
7q32	11	MET	deletion [2]	3p26, 5q13, 8q22, 8q24, 9q22, 12q21, 17q23, 20q11.2, Xq13
18q21	11	BCL2	None	1q32, 2p23, 3p21.3, 4q31.1, 8q24.1, 10q22, 13q14, 14q24, 20q11.2, deletion
17q23	10	Unknown	11q25 [2]	3p21, 4q33, 5?, 7q32, 8q24.1, 13q32, 20q11.2, 21q22
10q22	9	KSAM	deletion [2]	4q12, 6p25, 8p23, 9p13, 15q15, 15q22, 18q21
18q11.2	9	Unknown	20q11.2 [2], deletion [2]	3q21, 6q12, 6q21, 19q13.1, Xq22

[1]The number of breaks are indicated.

some of which were previously undetectable because of the structurally complicated chromosomal rearrangements. The same der(20)t(18;20)(q11.2;q11.2) was found in two cases (GT3TKB and patient no. 7; Figure 3), and chromosome deletions of del(7)(q32), del(10)(q22), del(11)(q13), and del (18)(q11.2) were detected in two cases each.

DISCUSSION

SKY analysis proved to be capable of identifying 630 breaks and 242 rearrangements of chromosomes in 10 established cell lines and seven cancerous ascitic fluid samples of GC, as well as of identifying recurrent breakpoints. Chromosomal rearrangements frequently involved well-known oncogene and tumor suppressor gene loci that may be associated with gastric carcinogenesis, such as 8q24.1 (*MYC*), 11q13 (*HST1/FGF4, INT2/FGF3, and CCND1*), 7q32 (*MET*), 13q14 (*RB*), 17q11.2 (adjacent to the *ERBB2* locus), 18q21 (*DCC* and *BCL2*), 7q22 (*MET*), 3p21 (*CTNNB1*), and 16q22 (*CDH1*). The other breakpoints that were detected more than eight times were 20q11.2 (14 breaks), 17q23 (9), 18q11.2 (9), 1p22 (8), 1q32 (8), 8p11.2 (8), 8q22 (8), 9q22 (8), 10q22 (8), 20q13 (8), and Xq22 (8). However, it is not clear which breakpoints represent key genes during the earlier stages of tumorigenesis in this lineage, because when the entire tumor was examined in our study, it was already highly progressed and in the case of cell lines, they were further selected for liver culture conditions.

Two distinct breakpoints, which were not noted as unique occurrences by G-banding, 8q24.1 (30 breaks, 4.8% of 630 breaks) and 11q13 (29, 4.6%), were identified by a combination of SKY and DAPI banding analysis. The currently most likely candidate at 8q24 is the *MYC* gene, because it was frequently amplified and overexpressed in advanced GC, particularly in patients with carcinomatous peritonitis or distant metastasis[25,26]. The DC-FISH analysis used in our study showed that the *MYC* locus was involved in amplification resulting from the HSR as well as in multiple chromosomal translocations, insertions, and duplications in KMK2 (Figures 3 and 4). However, in SNU16, the *MYC* locus was amplified in HSRs but not on DMs, suggesting that other genes, for example the *K-sam* gene, may be involved in DMs (Figure 3)[27].

The second common breakpoint of 11q13 contains a variety of genes associated with cell proliferation and differentiation such as *HST1/FGF4, INT2/FGF3, CCND1, SEA, MYEOV*, and *SPA1*[28,29]. It has been demonstrated that *HST1/FGF4* is co-amplified with *INT2/FGF3* in human GC, although amplification of *FGF4* and *FGF3* does not correlate with mRNA overexpression[30], while high-level amplification of 11q13 has been frequently detected in CGH analysis[12,13]. All these genes are assigned to band 11q13.3. Band 11q13 may thus span a region approximately 25 Mb in size as estimated from both the physical length of 11q (86 Mb) and the number and size of the bands, which are divided into five sub-bands including three light bands (q13.1, q13.3, and q13.5). Since it is difficult to distinguish these subregions in a karyotype of 400 bands, 11q13.1 and 11q13.5 also warrant molecular dissection for the identification of target genes.

Combining SKY and DAPI banding analysis led to the identification of recurrent co-localization of the chromosomal bands involved in translocations: 8q24.1 and 13q14 (3 cases), 8q24.1 and 11q13 (3), 11q13 and 17q11.2 (2), and 18q11.2 and 20q11.2 (2). These translocations used to be frequently undetectable because of the complicated rearrangements of chromosomes. In most cases, each co-localized breakpoint contains chromosomal segments to which oncogenes or tumor suppressor genes have been assigned.

In conclusion, SKY analysis identified the frequently occurring breakpoints 8q24.1, 11q13, 20q11.1-13.1, and 13q14 and the recurrent translocations 8q24.1 and 13q14, 8q24.1 and 11q13, 11q13 and 17q11.2, and 18q11.2 and 20q11.2. SKY thus proved to be extremely useful for a comprehensive analysis of chromosomal translocations in GC and derived cell lines. The chromosomal breakpoints defined in our study may well contain critical genes which are involved in multistage carcinogenesis of GC and thus can serve as landmarks for crucial regions that warrant molecular dissection.

ACKNOWLEDGMENTS

We are grateful to Professor Carlo M. Croce (Kimmel Cancer Center, Thomas Jefferson University, Philadelphia, PA) for providing DNA probes I2 and P72 (*MYC*) and to Dr. Masao Seto (Aichi Cancer Center Research Institute, Nagoya) for providing CPP29 (*CCND1*). We also wish to thank Professor Takeshi Okanoue (Department of Gastroenterology and Hepatology, Kyoto Prefectural University of Medicine, Kyoto) for critical reading of the manuscript.

REFERENCES

1 **Kameda T,** Yasui W, Yoshida K, Tsujino T, Nakayama H, Ito M, Ito H, Tahara E. Expression of ERBB2 in human gastric carcinomas: relationship between p185ERBB2 expression and the gene amplification. *Cancer Res* 1990; **50**: 8002-8009

2 **Kuniyasu H,** Yasui W, Kitadai Y, Yokozaki H, Ito H, Tahara E. Frequent amplification of the c-met gene in scirrhous type stomach cancer. *Biochem Biophys Res Commun* 1992; **189**: 227-232

3 **Grady WM.** Genetics of gastric cancer. In: Cowell JK, editor. Molecular Genetics of Cancer. *San Diego: Bios Scientific Publishers* 2001: 115-148

4 **Becker KF,** Atkinson MJ, Reich U, Becker I, Nekarda H, Siewert JR, Hofler H. E-cadherin gene mutations provide clues to diffuse type gastric carcinomas. *Cancer Res* 1994; **54**: 3845-3852

5 **Li QL,** Ito K, Sakakura C, Fukamachi H, Inoue K, Chi XZ, Lee KY, Nomura S, Lee CW, Han SB, Kim HM, Kim WJ, Yamamoto H, Yamashita N, Yano T, Ikeda T, Itohara S, Inazawa J, Abe T, Hagiwara A, Yamagishi H, Ooe A, Kaneda A, Sugimura T, Ushijima T, Bae SC, Ito Y. Causal relationship between the loss of RUNX3 expression and gastric cancer. *Cell* 2002; **109**: 113-124

6 **Ochi H,** Douglass HO Jr, Sandberg AA. Cytogenetic studies in primary gastric cancer. *Cancer Genet Cytogenet* 1986; **22**: 295-307

7 **Misawa S,** Horiike S, Taniwaki M, Tsuda S, Okuda T, Kashima K, Abe T, Sugihara H, Noriki S, Fukuda M. Chromosome abnormalities of gastric cancer detected in cancerous effusions. *Jpn J Cancer Res* 1990; **81**: 148-152

8 **Seruca R,** Castedo S, Correia C, Gomes P, Carneiro F, Soares P, de Jong B, Sobrinho-Simoes M. Cytogenetic findings in eleven gastric carcinomas. *Cancer Genet Cytogenet* 1993; **68**: 42-48

9 **Panani AD,** Ferti A, Malliaros S, Raptis S. Cytogenetic study of 11 gastric adenocarcinomas. *Cancer Genet Cytogenet* 1995; **81**: 169-172

10 **Kokkola A,** Monni O, Puolakkainen P, Larramendy ML, Victorzon M, Nordling S, Haapiainen R, Kivilaakso E, Knuutila S. 17q12-21 amplicon, a novel recurrent genetic change in intestinal type of gastric carcinoma: a comparative genomic hybridization study. *Genes Chromosomes Cancer* 1997; **20**: 38-43

11 **Kokkola A,** Monni O, Puolakkainen P, Nordling S, Haapiainen R, Kivilaakso E, Knuutila S. Presence of high-level DNA copy number gains in gastric carcinoma and severely dysplastic adenomas but not in moderately dysplastic adenomas. *Cancer Genet Cytogenet* 1998; **107**: 32-36

12 **Nessling M,** Solinas-Toldo S, Wilgenbus KK, Borchard F, Lichter P. Mapping of chromosomal imbalances in gastric adenocarcinoma revealed amplified protooncogenes MYCN, MET, WNT2, and ERBB2. *Genes Chromosomes Cancer* 1998; **23**: 307-316

13 **Sakakura C,** Mori T, Sakabe T, Ariyama Y, Shinomiya T, Date K, Hagiwara A, Yamaguchi T, Takahashi T, Nakamura Y, Abe T, Inazawa J. Gains, losses, and amplifications of genomic materials in primary gastric cancers analyzed by comparative genomic hybridization. *Genes Chromosomes Cancer* 1999; **24**: 299-305

14 **Rodriguez E,** Rao PH, Ladanyi M, Altorki N, Albino AP, Kelsen DP, Jhanwar SC, Chaganti RS. 11p13-15 is a specific region of chromosomal rearrangement in gastric and esophageal adenocarcinomas. *Cancer Res* 1990; **50**: 6410-6416

15 **Chun YH,** Kil JI, Suh YS, Kim SH, Kim H, Park SH. Characterization of chromosomal aberrations in human gastric carcinoma cell lines using chromosome painting. *Cancer Genet Cytogenet* 2000; **119**: 18-25

16 **Stamouli MI,** Ferti AD, Panani AD, Raftakis J, Consoli C, Raptis SA, Young BD. Application of multiplex fluorescence in situ hybridization in the cytogenetic analysis of primary gastric carcinoma. *Cancer Genet Cytogenet* 2002; **135**: 23-27

17 **Lauren P.** The two histological main types of gastric carcinoma: diffuse and so-called intestinal-type carcinoma. an attempt at a histo-clinical classification. *Acta Pathol Microbiol Scand* 1965; **64**: 31-49

18 **Taniwaki M,** Nishida K, Ueda Y, Misawa S, Nagai M, Tagawa S, Yamagami T, Sugiyama H, Abe M, Fukuhara S. Interphase and metaphase detection of the breakpoint of 14q32 translocations in B-cell malignancies by double-color fluorescence in situ hybridization. *Blood* 1995; **85**: 3223-3228

19 International Standing Committee on Human Cytogenetic Nomenclature. In: Mittelman F, ed. *An International System for Human Cytogenetic Nomenclature.* Basel, Switzerland: S. Karger AG; 1995

20 **Schröck E,** du Manoir S, Veldman T, Schöell B, Weinberg J, Ferguson-Smith MA, Ning Y, Ledbetter DH, Bar-Am I, Söenksen D, Garini Y, Reid T. Multicolor spectral karyotyping of human chromosomes. *Science* 1996; **273**: 494-497

21 **Kakazu N,** Taniwaki M, Horiike S, Nishida K, Tatekawa T, Nagai M, Takahashi T, Akaogi T, Inazawa J, Ohki M, Abe T. Combined spectral karyotyping and DAPI banding analysis of chromosome abnormalities in myelodysplastic syndrome. *Genes Chromosomes Cancer* 1999; **26**: 336-345

22 **Veronese ML,** Ohta M, Finan J, Nowell PC, Croce CM. Detection of myc translocations in lymphoma cells by fluorescence in situ hybridization with yeast artificial chromosomes. *Blood* 1995; **85**: 2132-2138

23 **Takashima T,** Itoh M, Ueda Y, Nishida K, Tamaki T, Misawa S, Abe T, Seto M, Machii T, Taniwaki M. Detection of 14q32. 33 translocation and t(11;14) in interphase nuclei of chronic B-cell leukemia/lymphomas by in situ hybridization. *Int J Cancer* 1997; **72**: 31-38

24 **Taniwaki M,** Matsuda F, Jauch A, Nishida K, Takashima T, Tagawa S, Sugiyama H, Misawa S, Abe T, Kashima K. Detection of 14q32 translocations in B-cell malignancies by in situ hybridization with yeast artificial chromosome clones containing the human IgH gene locus. *Blood* 1994; **83**: 2962-2969

25 **Ninomiya I,** Yonemura Y, Matsumoto H, Sugiyama K, Kamata T, Miwa K, Miyazaki I, Shiku H. Expression of c-myc gene product in gastric carcinoma. *Oncology* 1991; **48**: 149-153

26 **Hajdu J,** Kozma L, Kiss I, Szentkereszty Z, Szakall S, Ember I. Is the presence of distant metastasis associated with c-myc amplification in gastric cancer? *Acta Chir Hung* 1997; **36**: 119-121

27 **Hara T,** Ooi A, Kobayashi M, Mai M, Yanagihara K, Nakanishi I. Amplification of c-myc, K-sam, and c-met in gastric cancers: detection by fluorescence *in situ* hybridization. *Lab Invest* 1998; **78**: 1143-1153

28 **Wada Y,** Kubota H, Maeda M, Taniwaki M, Hattori M, Imamura S, Iwai K, Minato N. Mitogen-inducible SIPA1 is mapped to the conserved syntenic groups of chromosome 19 in mouse and chromosome 11q13.3 centromeric to BCL1 in human. *Genomics* 1997; **39**: 66-73

29 **Katoh M,** Katoh M. FLJ10261 gene, located within the CCND1-EMS1 locus on human chromosome 11q13, encodes the eight-transmembrane protein homologous to C12orf3, C11orf25 and FLJ34272 gene products. *Int J Oncol* 2003; **22**: 1375-1381

30 **Yoshida MC,** Wada M, Satoh H, Yoshida T, Sakamoto H, Miyagawa K, Yokota J, Koda T, Kakinuma M, Sugimura T, Terada M. Human HST1 (HSTF1) gene maps to chromosome band 11q13 and coamplifies with the INT2 gene in human cancer. *Proc Natl Acad Sci USA* 1988; **85**: 4861-4864

Science Editor Guo SY **Language Editor** Elsevier HK

PO Box 2345, Beijing 100023, China
www.wjgnet.com
wjg@wjgnet.com

ELSEVIER

World J Gastroenterol 2005;11(33):5136-5141
World Journal of Gastroenterology ISSN 1007-9327
© 2005 The WJG Press and Elsevier Inc. All rights reserved.

In vitro effects of chitosan nanoparticles on proliferation of human gastric carcinoma cell line MGC803 cells

Li-Feng Qi, Zi-Rong Xu, Yan Li, Xia Jiang, Xin-Yan Han

Li-Feng Qi, Zi-Rong Xu, Yan Li, Xia Jiang, Xin-Yan Han, Nano-biology Laboratory of Animal Science College, Zhejiang University, Hangzhou 310029, Zhejiang Province, China
Co-first-authors: Li-Feng Qi and Zi-Rong Xu
Correspondence to: Dr. Li-Feng Qi, Nano-biology Laboratory of Animal Science College, Zhejiang University, Hangzhou 310029, Zhejiang Province, China. lifengqi01@hotmail.com
Telephone: +86-571-86971075 Fax: +86-571-86994963
Received: 2004-12-06 Accepted: 2005-01-26

Abstract

AIM: To investigate the effects of chitosan nanoparticles on proliferation of human gastric carcinoma cell line MGC803 *in vitro* and the possible mechanisms involved.

METHODS: Chitosan nanoparticles were characterized by particle size, zeta potential, and morphology. After treatment with various concentrations of chitosan nanoparticles (25, 50, 75, 100 μg/mL) at various time intervals, cell proliferation, ultrastructural changes, DNA fragmentation, mitochondrial membrane potential (MMP), cell cycle phase distribution and apoptotic peaks of MGC803 cells were analyzed by MTT assay, electron microscopy, DNA agarose gel electrophoresis, and flow cytometry.

RESULTS: Chitosan nanoparticles exhibited a small particle size as 65 nm and a high surface charge as 52 mV. Chitosan nanoparticles markedly inhibited cell proliferation of MGC803 cells with an IC_{50} value of 5.3 μg/mL 48 h after treatment. After treatment with chitosan nanoparticles, the typical necrotic cell morphology was observed by electron microscopy, a typical DNA degradation associated with necrosis was determined by DNA agarose electrophoresis. Flow cytometry showed the loss of MMP and occurrence of apoptosis in chitosan nanoparticles-treated cells.

CONCLUSION: Chitosan nanoparticles effectively inhibit the proliferation of human gastric carcinoma cell line MGC803 *in vitro* through multiple mechanisms, and may be a beneficial agent against human carcinoma.

© 2005 The WJG Press and Elsevier Inc. All rights reserved.

Key words: Chitosan nanoparticles; Gastric carcinoma; Necrosis; Apoptosis

Qi LF, Xu ZR, Li Y, Jiang X, Han XY. *In vitro* effects of chitosan nanoparticles on proliferation of human gastric carcinoma cell line MGC803 cells. *World J Gastroenterol* 2005; 11(33): 5136-5141
http://www.wjgnet.com/1007-9327/11/5136.asp

INTRODUCTION

Chitosan, the deacetylated derivative of chitin, is one of the abundant, renewable, nontoxic and biodegradable carbohydrate polymers, and available largely in the exoskeletons of shellfish and insects. Chitosan has been widely applied as a functional biopolymer in food and pharmaceutics. Chitosan is known to have various biological activities including immuno-enhancing effects, antitumoral, antifungal, and antimicrobial activities[1-3]. Chitosan nanoparticles have been previously synthesized as drug carriers[4-6]. In our previous reports, chitosan nanoparticles are prepared and characterized to investigate their heavy metal sorption, antibacterial, and antitumor activities[7-9]. The unique characteristics of chitosan nanoparticles could provide a higher affinity for negatively charged biological membranes and site-specific targeting *in vivo*[7]. Chitosan nanoparticles could elicit dose-dependent inhibitory effects on the proliferation of various tumor cell lines, while low toxicity against normal human liver cells[9].

In this paper, *in vitro* effects of chitosan nanoparticles on the proliferation of human gastric carcinoma (MGC803) cells were studied to illustrate the possible mechanisms involved. Cell viability was determined by MTT assay, necrotic cell morphology and DNA fragmentation were observed by electron microscopy and DNA agarose electrophoresis. Changes of mitochondrial membrane potential (MMP), cell cycle, and apoptotic peaks were analyzed by flow cytometry.

MATERIALS AND METHODS

Characterization of chitosan nanoparticles

Chitosan nanoparticles were prepared as described previously[7,8]. Particle size distribution and zeta potential of chitosan nanoparticles were determined using Zetasizer Nano-ZS90 (Malvern Instruments). The analysis was performed at a scattering angle of 90° at 25 ℃ using samples diluted to different intensity concentrations with de-ionized distilled water. Transmission electron microscopy (TEM, JEM-1200EX) was used to determine the morphology of chitosan nanoparticles.

Cell line and cell culture

Human gastric carcinoma MGC803 cell line was obtained from the Cell Bank of the Chinese Academy of Sciences, Shanghai, China. The cell line was cultured in RPMI-1640 supplemented with 10% heat-inactivated fetal bovine serum (GIBCO). The cell cultures were maintained at 37 ℃ in a humidified incubator in an atmosphere of 95% air and 50 mL/L CO_2.

Cell viability assay

In the case of floating MGC803 cells, 100 μL aliquot of

cell suspension containing 10^6 cells was added to each well of a 96-well plate (Corning, USA). After being cultured for 24 h, the cells were immediately treated with various doses (25, 50, 75, 100 μg/mL) of chitosan nanoparticles for another 24 or 48 h. The effect of different treatments on cell viability was assessed by the tetrazolium dye assay[10].

Scanning electron microscopy (SEM)

MGC803 cells grown on glass coverslips were incubated with 100 μg/mL chitosan nanoparticles at intervals from 30 min to 4 h. The appropriate solvent was added to the control. Chitosan nanoparticles-treated and untreated cells were fixed in glutaraldehyde/paraformaldehyde solution and prepared for SEM by the triple-fixation GTGO methods. Briefly, the glutaraldehyde/paraformaldehyde-fixed cell monolayer was post-fixed by 2% osmium tetraoxide (OsO_4) and the final fixation step was performed by 2% tannic acid/guanidine hydrochloride. Thereafter, the cells were dehydrated in graded ethanol solutions, ethanol was exchanged by graded solutions of Freon 113, and the cells were air-dried and gold-coated using a Polaron sputter coater. The surface morphology of cells was examined by a XL30-ESEM scanning electron microscope.

Transmission electron microscopy (TEM)

MGC803 cells grown on glass coverslips were incubated with 100 μg/mL chitosan nanoparticles for 24 h. The appropriate solvent was added to the controls. Chitosan nanoparticles-treated and untreated cells were fixed in glutaraldehyde/paraformaldehyde solution and prepared for TEM as previously described[11]. Observations and micrographs were made under a JEM-1200EX TEM.

DNA fragmentation

After treatment with 100 μg/mL chitosan nanoparticles for 6 or 24 h, cells were collected, washed with PBS, and lysed with a solution containing 10 mmol/L Tris-HCl pH 7.4, 10 mmol/L EDTA and 0.5% Triton X-100. The lysates were incubated with 200 mg/mL RNase A (Sigma) for 1 h followed by 200 mg/mL proteinase K (GIBCO) for 1 h at 37 ℃. These samples were then extracted with phenol/chloroform/isoamyl alcohol (25:24:1, v/v/v) followed by chloroform. DNA was precipitated in two volumes of ethanol in the presence of 0.3 mol/L sodium acetate. The DNA samples thus obtained were run on 1.5% agarose gel at 50 V and visualized by ethidium bromide staining under UV light.

Determination of mitochondrial membrane potential

To study the MMP, MGC803 cells were treated with various concentrations of chitosan nanoparticles (25, 50, 75, 100 μg/mL) for 4 h, and then stained with 10 μg/mL rhodamine 123 (Sigma) for 30 min, which is easily sequestered by the mitochondrial membrane[12]. Once the MMP was lost, rhodamine 123 was subsequently washed out of the cells. The MMP was determined using a FACSCalibur flow cytometer (Becton Dickinson, San Jose, CA) and analyzed by a CellQuest software program (BD PharMingen, Franklin Lakes, USA).

Cell cycle analysis

Flow cytometry was employed to determine the DNA content and the apoptotic peaks of the cells. MGC803 cells were seeded on 100-mm dishes and grown in RPMI-1640 supplemented with 10% fetal bovine serum. After being treated with various concentrations of chitosan nanoparticles (25, 50, 75, 100 μg/mL) for 24 h, the cells were harvested, trypsinized, washed with PBS, fixed by adding slowly 2 mL of cold 70% ethanol into the tube and then stored at 4 ℃. After fixation, the cells were washed, centrifuged, and resuspended in 0.05 mg/mL propidium iodide (Sigma, USA), 100 U/mL RNase (Sigma, USA) in PBS. The sample was incubated for 30 min at room temperature in the dark, and analyzed on a FACSCalibur flow cytometer. Cell cycle data originally obtained with CellQuest software were re-analyzed using ModFit software (Verity Software House, Topsham, USA). At the same time negative controls were constructed.

RESULTS

Size, zeta potential, and morphology of chitosan nanoparticles

The average particle size of chitosan nanoparticles was 65 nm and the size distribution ranged from 46 to 83 nm (Figure 1). Zeta potential, i.e., surface charge greatly influenced the particle stability in suspension through the electrostatic repulsion between the particles. It could also determine the interaction of nanoparticles *in vivo* with the tumor cell membrane, which was usually negatively charged. Chitosan nanoparticles had a positive charge about 52 mV (Figure 2A), much higher than that of chitosan in 0.25% acetic acid solution (Figure 2B). A solid dense structure and a round shape of chitosan nanoparticles were shown under TEM (Figure 3).

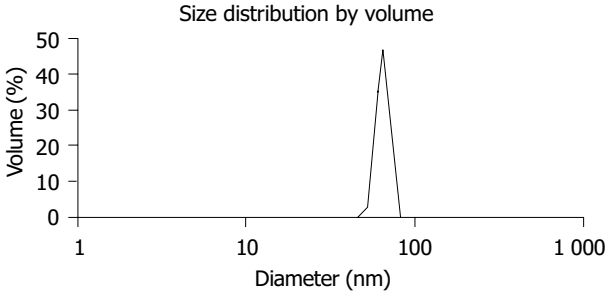


Figure 1 Size distribution of chitosan nanoparticles.

Cell viability assay

In this study, the exponentially grown gastric carcinoma MGC803 cells were treated with various concentrations of chitosan nanoparticles ranging from 25 to 100 μg/mL, and the cell viability was measured by the MTT assay. The inhibition of cell viability by chitosan nanoparticles was clearly observed in a dose- and time-dependent manner (Figure 4). The median lethal concentration of chitosan nanoparticles was 16.2 and 5.3 μg/mL for MGC803 cells at 24 and 48 h, respectively.

Necrotic cell morphology

Necrosis is known to occur due to the disruption of cellular and nuclear membranes under extreme physiological stimuli.

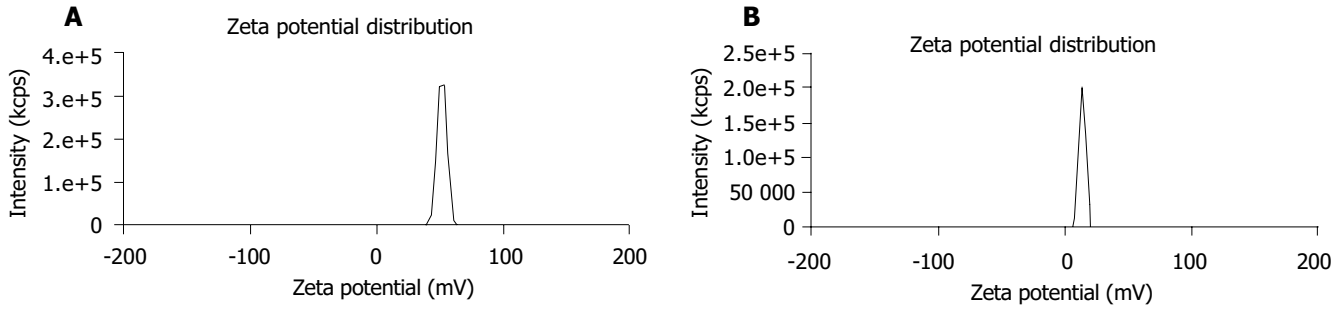


Figure 2 Zeta potential distribution of chitosan nanoparticles (**A**) and chitosan (**B**) in 0.25% acetic acid solution.

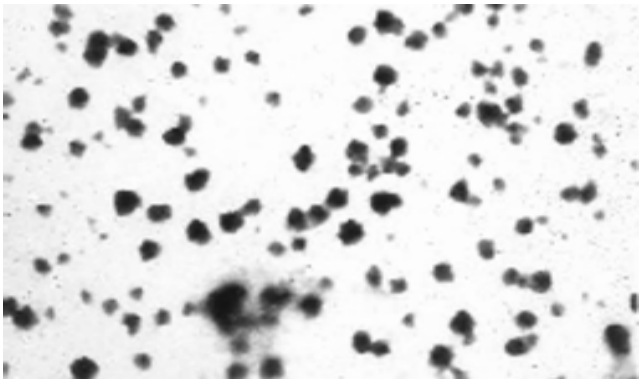


Figure 3 TEM photograph of chitosan nanoparticles. The bar stands for 100 nm.

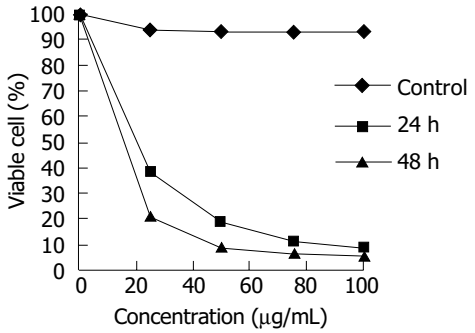


Figure 4 Inhibition of chitosan nanoparticles on MGC803 cell proliferation.

Rupture of the cellular membrane is one of the crucial criteria used to distinguish necrosis from apoptosis[12]. The ultrastructural alterations of MGC803 cells treated with chitosan nanoparticles were observed under scanning electron microscope and transmission electron microscope. MGC803 cells treated with chitosan nanoparticles displayed typical morphological features of necrosis. Control MGC803 cells showed their normal shape and surface morphology under SEM (Figure 5). The cell surface showed the presence of numerous, randomly distributed microvilli. Cell death induced by chitosan nanoparticles showed the features of necrosis as evidenced by an early membrane leakage and the microvilli reduction after 30-min treatment. Microvilli disappeared and irregular tiny holes appeared on the cells' surface when treated for 2 h, with fracturing membrane solubilization. MGC803 cells appeared extensively damaged. The cells that broke into pieces were observed as honeycomb shape after 4-h treatment. The loss of membrane integrity and pore forming surface morphology suggested a necrotic type of cell death and the unique mechanism of interaction between chitosan nanoparticles and plasma membrane.

Necrotic morphological features of MGC803 cells treated with chitosan nanoparticles such as disruption of the cytoplasm and appearance of remnants of swollen organelles were also revealed under TEM (Figure 6). Untreated cells showed integral membrane distributed with microvilli and normal organelle. While treated with chitosan nanoparticles for 24 h, cells became vacuolated, the plasma membrane was disrupted completely, and the content in the cells leaked out.

DNA fragmentation

DNA was extracted from cultured MGC803 cells treated with 100 μg/mL chitosan nanoparticles for 6 or 24 h, the occurrence of necrosis was detected by agarose gel electrophoresis. Specific DNA degradative smearing typical of necrotic degeneration[13] was prominent in cells incubated with chitosan nanoparticles for 6 h, and the fragmented DNA increased greatly in cells treated for 24 h (Figure 7).

Alterations of mitochondrial membrane potential (MMP)

One possible mechanism involved in the necrosis of MGC803 cells induced by chitosan nanoparticles is mitochondrial damage. In this study, chitosan nanoparticles caused a dose-dependent decrease of MMP in MGC803 cells treated for 4 h (Figure 8). The percentage of cells with the loss of MMP increased significantly with the increase of chitosan nanoparticles concentration, and reached 74% when treated with 100 μg/mL chitosan nanoparticles. The strong dissipation in MMP suggested a possible disruption of cell mitochondrial membrane after chitosan nanoparticle treatment.

Cell cycle effects

The effects of chitosan nanoparticles on cell cycle progression, population distribution and apoptotic incidence in MGC803 cells were determined by flow cytometry. Chitosan nanoparticles-induced effects were detected by comparing the cell cycle profiles between nanoparticles-treated and untreated cells. Results demonstrated a significant decrease of cells in the G_0/G_1 phase (Table 1). Apoptotic peaks were observed

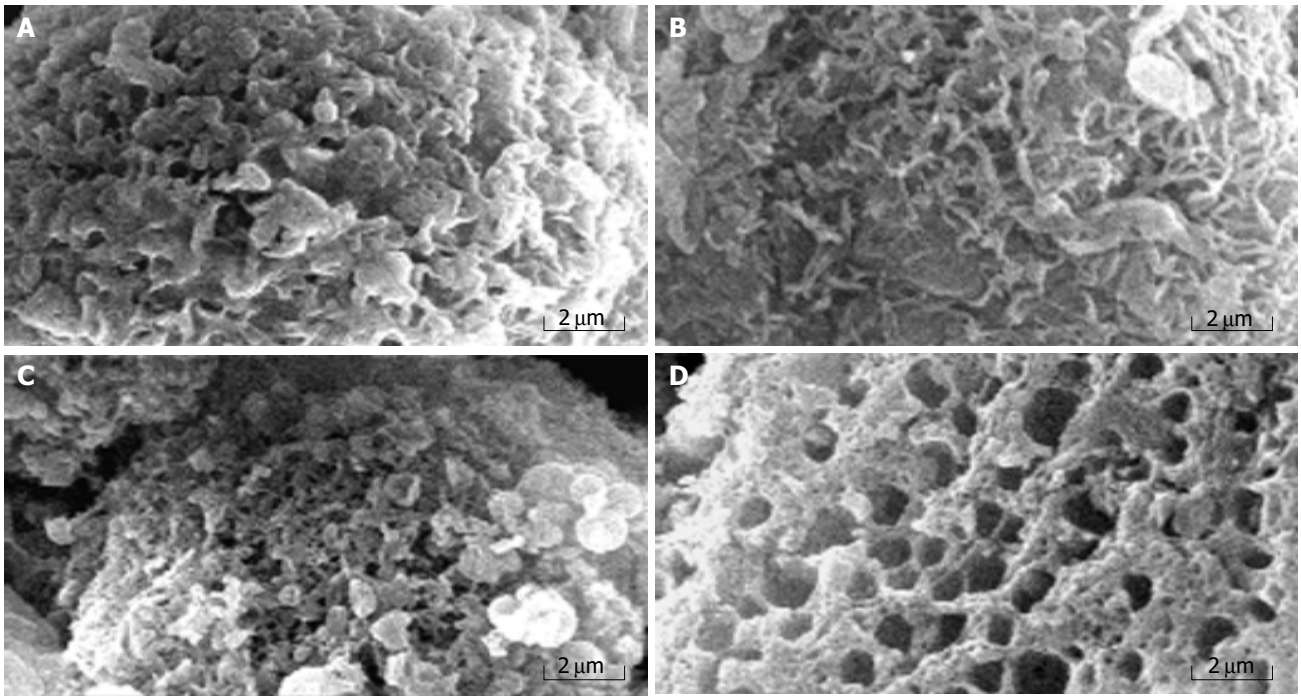


Figure 5 Surface morphology of control cells (**A**) and MGC803 cells treated with 100 μg/mL chitosan nanoparticles for 30 min (**B**), 2 h (**C**), and 4 h (**D**).

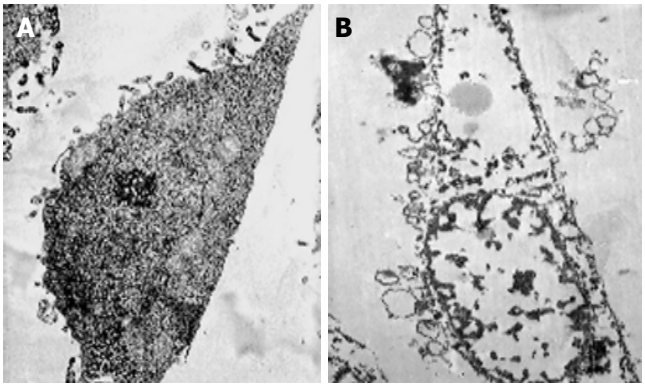


Figure 6 Transmission electron microscopic photographs of MGC803 cells cultured for 24 h in the absence (**A**) or presence of 100 μg/mL chitosan nanoparticles (**B**) *in vitro* (TEM, ×5 000).

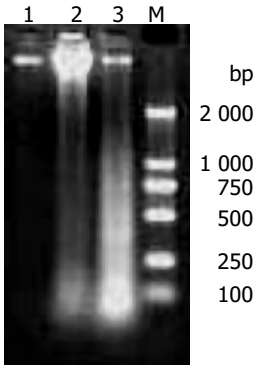


Figure 7 Agarose gel electrophoretic analysis of DNA isolated from MGC803 cells incubated with 100 μg/mL chitosan nanoparticles for 6 h (lane 2) and 24 h (lane 3) or without treatment (lane 1). M: a DNA marker.

and cell apoptotic incidence increased in a dose-dependent manner after chitosan nanoparticle treatment. The apoptotic incidence increased to 9.9% after being treated with 100 μg/mL chitosan nanoparticles (Figure 9).

DISCUSSION

Due to its reported biocompatibility and biodegradability[14], chitosan has been applied in drug delivery systems to prepare microspheres or nanospheres for encapsulation of drugs, enzymes, proteins, and DNA[15-17]. Chitosans could be developed as sole drugs for its biological activities. Soluble chitosan and chitosan microspheres are reported to show some degree of toxicity towards a murine melanoma cell line, B16F10, chitosan hydrochloride is most toxic having an IC_{50} of 0.21±0.04 mg/mL[18]. Amino-derivatized cationic chitosan derivatives show dose-dependent inhibitory effects on the proliferation of several tumor cell lines, with a lowest IC_{50} of 22±4 μg/mL towards liver cancer[19].

Positively charged chitosan nanoparticles prepared by our laboratory exhibit a higher cytotoxicity than other chitosan derivatives against various tumor cell lines, and a low toxicity against normal human liver cells[9]. The present study demonstrated that chitosan nanoparticles could exert a high cytotoxicity against human gastric carcinoma MGC803 cell line. The gastric carcinoma cell line has been proved to be sensitive to chitosan nanoparticles with an IC_{50} value of 5.3 μg/mL after 48-h treatment, suggesting that chitosan nanoparticles may be a good candidate for antitumoral drugs. Particle size of nanoparticles plays a crucial role in their antitumor activity and *in vivo* distribution[20,21]. Smaller nanoparticles show a higher accumulation at tumor sites and prolong *in vivo* half-life due to their avoidable capture by the reticuloendothelial system[22,23]. Here, the particle size

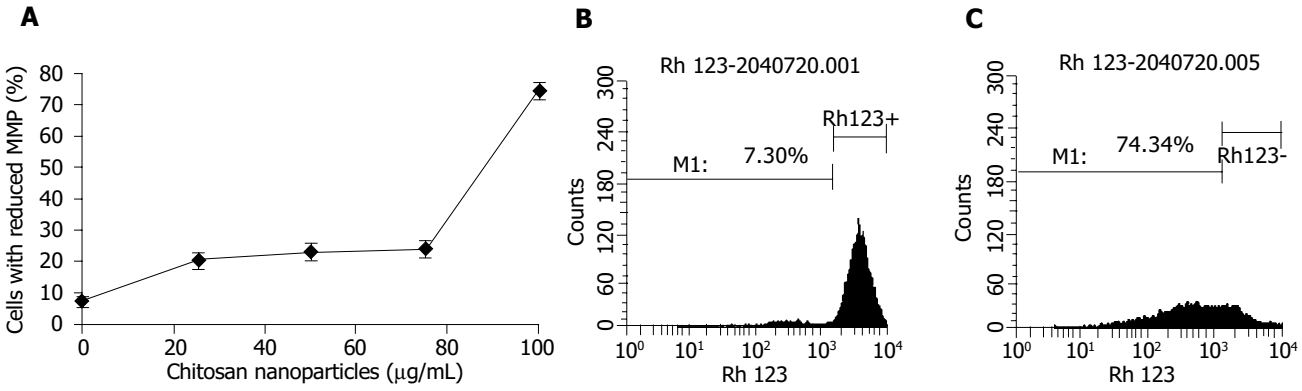


Figure 8 Chitosan nanoparticles-induced changes of MMP. **A:** Loss of MMP; **B:** histogram of untreated cells; **C:** histogram of cells treated with 100 μg/mL chitosan nanoparticles.

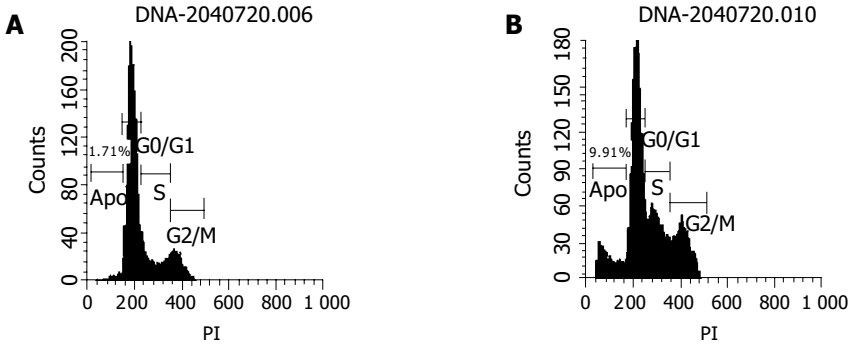


Figure 9 Effect of chitosan nanoparticles on cell cycle (**A**) and apoptotic incidence (**B**) of MGC803 cells.

Table 1 Effect of chitosan nanoparticles on cell cycle of MGC803 cells (mean±SD)

Concentration (μg / mL)	Cell cycle phase distribution (%)			AI
	G_0/G_1	S	G_2 / M	
0	71.8±1.3	17.3±0.9	9.5±0.2	1.7±0.2
25	70.5±0.8[b]	16.7±1.1	8.3±2.1	3.9±0.6[b]
50	69.4±0.6[b]	15.9±0.6	7.4±0.3	6.8±0.3[b]
75	67.3±0.4[b]	13.2±2.3	12.3±0.5	7.6±0.4[b]
100	51.5±1.3[b]	23.5±1.1	15.2±3.1	9.9±0.5[b]

AI: apoptotic incidence; [b]$P<0.01$ *vs* control.

of chitosan nanoparticles could be controlled only to 65 nm, which is in favor of the antitumor activity and prolongs efficacy of chitosan nanoparticles. Polymers with high cationic charge densities have higher cytotoxic effects than those with low charge densities[24]. As a kind of cationic polymers, the surface charge of chitosan derivatives is the major factor affecting its cytotoxic activity due to the electrostatic ionic interaction between the negatively charged groups of tumor cells and the positively charged amino groups of chitosans[19]. Therefore, the high surface charge about 52 mV of chitosan nanoparticles is responsible for its higher cytotoxic activity.

Morphologically, necrosis is quite different from apoptosis. During necrosis, cells first swell, then the plasma membrane collapses and cells are rapidly lysed, while apoptotic cells disintegrate into well-enclosed apoptotic bodies without loss of membrane integrity[25]. The ultrastructural alterations of MGC803 cells observed by electron microscopy displayed typical morphological features of necrosis due to the treatment of chitosan nanoparticles, suggesting that chitosan nanoparticles induce necrotic tumor cell death and can be used as a membrane-active drug. Chitosan nanoparticles are positively charged due to the cationic characteristics of chitosan[26]. Chitosan nanoparticles could be first adsorbed onto the negatively charged tumor cell membrane by electron interaction, then exhibit antitumoral effects by damaging membrane and disrupting organelle, and finally lead to cell death with the structure breakdown.

Fragmented DNA during apoptosis appears as a series of bands, which are described as "DNA ladders" on agarose gels, representing formation of oligonucleosomes with the characteristics of apoptosis[27,28]. In contrast, fragmented DNA during necrosis appears as a continuous spectrum of sizes[29]. In this study, chitosan nanoparticles-treated tumor

cells also yielded a continuous spectrum of DNA fragments of low molecular mass, indicating that necrosis is induced by chitosan nanoparticles.

It was reported that mitochondria play a crucial role in regulation of cell death[30]. Under extreme conditions (e.g., high Ca^{2+}, oxidative stress) mitochondria undergo drastic changes, accompanied with decrease of the mitochondrial potential, de-energization, swelling, and permeabilization of the inner membrane[31]. Furthermore, the occurrence of mitochondrial dysfunction is rapidly followed by or nearly coincident with the loss of plasma membrane integrity[32], thus leading to necrotic cell death at last. In this study, a drastic decrease of MMP was observed in chitosan nanoparticles-treated human gastric carcinoma cells, indicating that the mitochondrial membrane is damaged.

Cell cycle analysis showed a significant decrease of cells in the G_0/G_1 phase and the dose-dependent apoptosis in chitosan nanoparticles-treated cells, suggesting that apoptosis is also involved in the cell death induced by chitosan nanoparticles.

In summary, chitosan nanoparticles with a small particle size of about 65 nm and a positive surface charge of about 50 mV exhibit a high cytotoxicity towards human gastric carcinoma cell line MGC803 and induce cell death with predominant necrotic features. The antitumor mechanism of chitosan nanoparticles is related to their membrane-disrupting and apoptosis-inducing activities.

REFERENCES

1 **Qin CQ,** Du YM, Xiao L, Li Z, Gao XH. Enzymic preparation of water-soluble chitosan and their antitumor activity. *Int J Biol Macromol* 2002; **31**: 111-117

2 **Roller S,** Covill N. The antifungal properties of chitosan in laboratory media and apple juice. *Int J Food Microbiol* 1999; **47**: 67-77

3 **Zheng LY,** Zhu JF. Study on antimicrobial activity of chitosan with different molecular weights. *Carbohyd Polym* 2003; **54**: 527-530

4 **Janes KA,** Fresneau MP, Marazuela A, Fabra A, Alonso MJ. Chitosan nanoparticles as delivery systems for doxorubicin. *J Control Rel* 2001; **73**: 255-267

5 **Pan Y,** Li YJ, Zhao HY, Zheng JM, Xu H, Wei G, Hao JS, Cui FD. Bioadhesive polysaccharide in protein delivery system: chitosan nanoparticles improve the intestinal absorption of insulin *in vivo*. *Int J Pharm* 2002; **249**: 139-147

6 **Xu YM,** Du YM. Effect of molecular structure of chitosan on protein delivery properties of chitosan nanoparticles. *Int J Pharm* 2003; **250**: 215-226

7 **Qi LF,** Xu ZR, Jiang X, Hu CH, Zou XF. Preparation and antibacterial activity of chitosan nanoparticles. *Carbohyd Res* 2004; **339**: 2693-2700

8 **Qi LF,** Xu ZR. Lead sorption from aqueous solutions on chitosan nanoparticles. *Colloid Surface A* 2004; **251**: 183-190

9 **Qi LF,** Xu ZR, Jiang X, Li Y, Wang MQ. Cytotoxic activities of chitosan nanoparticles and copper-loaded nanoparticles. *Bioorg Med Chem Lett* 2005; **15**: 1397-1399

10 **Truter EJ,** Santos AS, Els WJ. Assessment of the antitumor activity of targeted immunospecific albumin microspheres loaded with cisplatin and 5-fluorouracil: toxicity against a rodent ovarian carcinoma *in vitro*. *Cell Biol Int* 2001; **25**: 51-59

11 **Luxo C,** Jurado AS, Madeira VMC, Silva MT. Tamoxifen induces ultrastructural alterations in membranes of *Bacillus Stearothermophilus*. *Toxicol In Vitro* 2003; **17**: 623-628

12 **Kim H,** You S, Kong BW, Foster LK, Farris J, Foster DN. Necrotic cell death by hydrogen peroxide in immortal DF-1 chicken embryo fibroblast cells expressing deregulated MnSOD and catalase. *Biochim Bioph Acta* 2001; **1540**: 137-146

13 **Kok YJ,** Swe M, Sit KH. Necrosis has orderly DNA fragmentations. *Biochem Bioph Res Commun* 2002; **294**: 934-939

14 **Mi FL,** Tan YC, Liang HF, Sung HW. *In vivo* biocompatibility and degradability of a novel injectable-chitosan-based implant. *Biomaterials* 2002; **23**: 181-191

15 **Kim TH,** Park IK, Nah JW, Choi YJ, Cho CS. Galactosylated chitosan/DNA nanoparticles prepared using water-soluble chitosan as a gene carrier. *Biomaterials* 2004; **25**: 3783-3792

16 **Bivas-Benita M,** Laloup M, Versteyhe S, Dewit J, Braekeleer JD, Jongert E, Borchard G. Generation of *Toxoplasma gondii* GRA1 protein and DNA vaccine loaded chitosan particles: preparation, characterization, and preliminary *in vivo* studies. *Int J Pharm* 2003; **266**: 17-27

17 **Mao HQ,** Roy K, Troung-Le VL, Janes KA, Lin KY, Wang Y, August JT, Leong KW. Chitosan-DNA nanoparticles as gene carriers: synthesis, characterization and transfection efficiency. *J Control Rel* 2001; **70**: 399-421

18 **Carreno-Gomez B,** Duncan R. Evaluation of the biological properties of soluble chitosan and chitosan microspheres. *Int J Pharm* 1997; **148**: 231-240

19 **Lee JK,** Lim HS, Kim JH. Cytotoxic activity of aminoderivatized cationic chitosan derivatives. *Bioorg Med Chem Lett* 2002; **12**: 2949-2951

20 **Yokoyama M,** Satoh A, Sakurai Y, Okano T, Matsumura Y, Kakizoe T, Kataoka K. Incorporation of water-insoluble anticancer drug into polymeric micelles and control of their particle size. *J Control Rel* 1998; **55**: 219-229

21 **Zhang LY,** Hu Y, Jiang XQ, Yang CZ, Lu W, Yang YH. Camptothecin derivative-loaded poly(caprolactone-co-lactide)-b-PEG-b-poly (caprolactone-co-lactide) nanoparticles and their biodistribution in mice. *J Control Rel* 2004; **96**: 135-148

22 **Jinno H,** Ikeda T, Matsui A, Kitagawa Y, Kitajima M, Fujii H, Nakamura K, Kubo A. Section 5. Breast Sentinel lymph node biopsy in breast cancer using technetium-99m tin colloids of different sizes. *Biomed Pharmacother* 2002; **56** (Suppl 1): 213s-216s

23 **Takenaga M.** Application of lipid microspheres for the treatment of cancer. *Adv Drug Deliver Rev* 1996; **20**: 209-219

24 **Fischer D,** Li YX, Ahlemeyer B, Krieglstein J, Kissel T. Cytotoxicity testing of polycations: influence of polymer structure on cell viability and hemolysis. *Biomaterials* 2003; **24**: 1121-1131

25 **Proskuryakov SY,** Konoplyannikov AG, Gabai VL. Necrosis: a specific form of programmed cell death? *Exp Cell Res* 2003; **283**: 1-16

26 **Hu Y,** Jiang XQ, Ding Y, Ge HX, Yuan YY, Yang CZ. Synthesis and characterization of chitosan-poly(acrylic acid) nanoparticles. *Biomaterials* 2002; **23**: 3193-3201

27 **Zhao Y,** Cao J, Ma H, Liu JW. Apoptosis induced by tea polyphenols in HL-60 cells. *Cancer Lett* 1997; **121**: 163-167

28 **Kono T,** Watanabe M, Koyama K, Kishimoto T, Fukushima S, Sugimura T, Wakabayashi K. Cytotoxic activity of pierisin, from the cabbage butterfly, Pieris rapae, in various human cancer cell lines. *Cancer Lett* 1999; **137**: 75-81

29 **Bicknell GR,** Cohen GM. Cleavage of DNA to large kilobase pair fragments occurs in some forms of necrosis as well as apoptosis. *Biochem Bioph Res Commun* 1995; **207**: 40-47

30 **Monti MG,** Ghiaroni S, Marverti G, Montanari M, Moruzzi MS. Polyamine depletion switches the form of 2-deoxy-d-riboseinduced cell death from apoptosis to necrosis in HL-60 cells. *Int J Biochem Cell B* 2004; **36**: 1238-1248

31 **Lemasters JJ,** Qian T, Bradham CA, Brenner DA, Cascio WE, Trost LC, Nishimura Y, Nieminen AL, Herman B. Mitochondrial dysfunction in the pathogenesis of necrotic and apoptotic cell death. *J Bioenerg Biomembr* 1999; **31**: 305-319

32 **Bonneau MJ**, Poulin R. Spermine oxidation leads to necrosis with plasma membrane phosphatidylserine redistribution in mouse leukemia cells. *Exp Cell Res* 2004; **259**: 23-34

Science Editor Wang XL and Guo SY **Language Editor** Elsevier HK

PO Box 2345, Beijing 100023, China
www.wjgnet.com
wjg@wjgnet.com

ELSEVIER

World J Gastroenterol 2005;11(33):5142-5150
World Journal of Gastroenterology ISSN 1007-9327
© 2005 The WJG Press and Elsevier Inc. All rights reserved.

• *COLORECTAL CANCER* •

Trans-10,*cis*-12, not *cis*-9,*trans*-11, conjugated linoleic acid decreases ErbB3 expression in HT-29 human colon cancer cells

Han Jin Cho, Woo Kyoung Kim, Jae In Jung, Eun Ji Kim, Soon Sung Lim, Dae Young Kwon, Jung Han Yoon Park

Han Jin Cho, Jae In Jung, Jung Han Yoon Park, Department of Food Science and Nutrition, Hallym University, Chuncheon 200-702, Korea
Eun Ji Kim, Soon Sung Lim, Silver Biotechnology Research Center, Hallym University, Chuncheon 200-702, Korea
Woo Kyoung Kim, Department of Food Science and Nutrition, Dankook University, Seoul 140-714, Korea
Dae Young Kwon, Korea Food Research Institute, Songnam 463-746, Korea
Supported by a grant of the Korea Health 21 R and D Project, Ministry of Heath and Welfare, Republic of Korea, No. 02-PJ1-PG10-22003-0001
Correspondence to: Jung Han Yoon Park, Department of Food Science and Nutrition, Hallym University, 1 Okchon Dong, Chuncheon 200-702, Korea. jyoon@hallym.ac.kr
Telephone: +82-33-248-2134 Fax: +82-33-256-0199
Received: 2005-01-12 Accepted: 2005-04-18

Abstract

AIM: To examine whether *trans*-10,*cis*-12 CLA (*t*10*c*12) or *cis*-9,*trans*-11 CLA (*c*9*t*11) inhibits heregulin (HRG)-β-stimulated cell growth and HRG-β-ErbB3 signaling in HT-29 cells.

METHODS: We cultured HT-29 cells in the absence or presence of the CLA isomers and/or the ErbB3 ligand HRG-β. MTT assay, [^{3}H]thymidine incorporation, Annexin V staining, RT-PCR, Western blotting, immunoprecipitation, and *in vitro* kinase assay were performed.

RESULTS: HRG-β increased cell growth, but did not prevent *t*10*c*12-induced growth inhibition. *T*10*c*12 inhibited DNA synthesis and induced apoptosis of HT-29 cells, whereas *c*9*t*11 had no effect. *T*10*c*12 decreased the levels of ErbB1, ErbB2, and ErbB3 proteins and transcripts in a dose-dependent manner, whereas *c*9*t*11 had no effect. Immunoprecipitation/Western blot studies revealed that *t*10*c*12 inhibited HRG-β-stimulated phosphorylation of ErbB3, recruitment of the p85 subunit of phosphoinositide 3-kinase (PI3K) to ErbB3, ErbB3-associated PI3K activities, and phosphorylation of Akt. However, *c*9*t*11 had no effect on phospho Akt levels. Neither *t*10*c*12 nor *c*9*t*11 had any effect on HRG-β-induced phosphorylation of ERK-1/2.

CONCLUSION: These results indicate that the inhibition of HT-29 cell growth by *t*10*c*12 may be induced via its modulation of ErbB3 signaling leading to inhibition of Akt activation.

© 2005 The WJG Press and Elsevier Inc. All rights reserved.

Key words: Akt; Phosphoinositide 3-kinase; DNA synthesis; Apoptosis; ERK-1/2

Cho HJ, Kim WK, Jung JI, Kim EJ, Lim SS, Kwon DY, Park JHY. *Trans*-10,*cis*-12, not *cis*-9,*trans*-11, conjugated linoleic acid decreases ErbB3 expression in HT-29 human colon cancer cells. *World J Gastroenterol* 2005; 11(33): 5142-5150
http://www.wjgnet.com/1007-9327/11/5142.asp

INTRODUCTION

Conjugated linoleic acid (CLA) is a mixture of positional and geometric isomers of octadecadienoic acid found naturally in beef, cheese, and butter fat. During the past few years, CLA has attracted considerable attention as one of the most promising cancer chemopreventive agents[1]. Previously, we have shown that dietary CLA inhibited colon tumor incidence in rats treated with 1,2-dimethylhydrazine[2,3]. In addition to animal studies, *in vitro* studies have shown that CLA inhibits the growth of human colon cancer cells, SW 480[4] and HT-29 cells[5-7]. In contrast to these observations, other studies reported results that dietary treatment with CLA had no effect on tumor number or size in the $APC^{min/+}$ mouse, a genetic model of intestinal tumorigenesis[8]. Most of the experimental and *in vitro* studies on CLA have utilized synthetic CLA mixtures containing the two principal isomers, *cis*-9,*trans*-11 CLA (c9*t*11) and *trans*-10,*cis*-12 CLA (*t*10*c*12)[9]. Recently, Rajakangas *et al*.[10], reported that *t*10*c*12 increased the size of adenoma in the distal part of the small intestine in the multiple intestinal neoplasia (Min) mouse model. The reason for these conflicting results can be resolved, if we understand the mechanisms by which CLA regulates colon cancer cell growth.

The ErbB family of receptor tyrosine kinases currently includes four members: epidermal growth factor receptor (EGFR)/ErbB1, ErbB2, ErbB3, and ErbB4. Polypeptides in the EGF family individually bind to and activate one or more ErbB family members[11,12]. Ligand-induced receptor homo- and hetero-dimerization stimulates ErbB receptor activation and subsequent transphosphorylation between the dimerization partners.[13] Although ErbB3 is devoid of intrinsic kinase activity[14], heregulin (HRG) binds to ErbB3 and facilitates the formation of heterodimers with ErbB2, the most mitogenic family member[15,16].

The activated ErbB family receptors interact with diverse signaling pathways that ultimately may lead to cell division, differentiation, and chemotaxis. Two representative intracellular effectors of ErbB2/ErbB3 HRG coreceptor complex are mitogen-activated protein (MAP) kinase and phosphoinositide 3-kinase (PI3K). ErbB3, which incorporates multiple PI3K

binding sites, has been shown to be a major recruiter of PI3K. PI3Ks phosphorylate inositol phospholipids at position 3 of the inositol ring and PI3K lipid products interact with certain proteins and modulate their localization and/or activity[17]. Protein kinase B (PKB) or Akt is known as an important downstream target for PI3K, which can be activated by a variety of growth factors and cytokines via phosphorylation on serine and threonine residues[18-20] and may participate in growth factor stimulated cell cycle[21,22] and inhibition of apoptosis[23]. Disturbance of normal PKB/Akt signaling has been reported in several human cancers[24,25] and Akt is a focal point for deregulation in cancer[26].

Overexpression of the ErbB family of receptor tyrosine kinases has been implicated in a variety of tumors including breast, lung, prostate, colon and brain. Most solid tumors express one or more of these receptors, which can often be related to tumor aggressiveness and poor patient prognosis. Several agents that target one or more members of the ErbB family of receptor tyrosine kinases are currently undergoing clinical investigation[27]. Ciardiello and coworkers reported that ErbB3 mRNA transcripts were expressed in a majority of human colon cancer cell lines and in primary and metastatic human colorectal tumors[28]. In colorectal cancer, an increase in ErbB3 expression is frequently associated with an increase in ErbB2 expression. However, no difference in ErbB1 protein levels was apparent between normal colon and cancer[29]. In addition, HRG is co-expressed with ErbB2 proteins in human colon cancer specimens and autocrine activation of ErbB2 occurs through heterodimerization with ErbB3 in GEO colon cancer cells[30]. These results suggest that the HRG/ErbB2/ErbB3 pathway may be an important modulator of aberrant growth in colon cancer[31,32], and therefore, agents that inhibit the ErbB3 receptor activation may be useful for the prevention and/or treatment of human colon cancer.

We have previously observed that the *t*10*c*12 isomer inhibited HT-29 cell growth, whereas the *c*9*t*11 isomer had no effect[7]. Therefore, in this study, we assessed whether the growth inhibitory effect of *t*10*c*12 is related to changes in HRG-ErbB3 signaling and the Akt pathway.

MATERIALS AND METHODS

Materials

We purchased the following reagents from the indicated suppliers: HT-29 cells (the American Type Culture Collection, Rockville, MD, USA); Dulbecco's Modified Eagle's Medium/Ham's F-12 nutrient mixture (DMEM/F12), essentially fatty acid-free, bovine serum albumin (BSA), ascorbic acid, α-tocopherol phosphate, and 3-[4,5-dimethylthiazol-2-yl]-2,5-diphenyltetrazolium bromide (MTT) [Sigma Chemical Co., St. Louis, MO, USA]; fetal bovine serum (FBS) and transferrin (Gibco BRL, Gaithersburg, MD); rainbow molecular weight markers, [methyl-^{3}H]thymidine (5 Ci/mmol), horseradish peroxidase (HRP)-conjugated anti-rabbit and anti-mouse Ig, protein A-Sepharose beads (Amersham, Arlington Heights, IL, USA); *c*9*t*11 and *t*10*c*12 (Cayman Chemical Company, Ann Arbor, MI, USA); anti-PI3K p85 antibody (Upstate Biotechnology, Inc., Charlottesville, VA, USA); [γ-^{32}P]ATP (PerkinElmer Life and Analytical Sciences, Inc., Boston, MA, USA); anti-phosphotyrosine-RC20 antibody linked to HRP (PY20-HRP; Transduction Laboratories, San Diego, CA, USA); recombinant human HRG-β EGF domain (R & D Systems, Minneapolis, MN, USA); antibodies against Akt (29752), phospho-Akt (p-Akt, 473), extracellular signal-regulated kinase (ERK-1/2), and phospho-ERK-1/2 (p-ERK-1/2, Thr202/Tyr203) [New England Biolabs, Beverly, MA, USA]; antibodies against ErbB1 (1005), ErbB2 (C-18), ErbB3 (C-17), and HRG (C-20) [Santa Cruz Biotechnology, Inc., Santa Cruz, CA, USA].

Cell culture

We used HT-29 cells between the 135th and 145th passage for these experiments. The complete medium for cell maintenance consisted of DMEM/F12 supplemented with 10% FBS, 100 U/mL penicillin, and 100 μg/mL streptomycin. To examine the effects of the CLA isomers and HRG-β, cells in the monolayer culture were serum starved in DMEM/F12 supplemented with 5 μg/mL transferrin, 5 ng/mL selenium, 0.1 mg/mL BSA, 50 ng/mL ascorbic acid, and 20 ng/mL α-tocopherol phosphate (serum-free medium). After serum starvation, cells were incubated in serum-free medium in the presence or absence of 4 μmol/L *t*10*c*12 or *c*9*t*11 and/or 20 ng/mL HRG-β. Fatty acids were complexed to essentially fatty acid-free BSA, with the molar ratio of fatty acid to BSA being 4:1, as described previously[33]. Media were changed every 2 d. Viable cell numbers were estimated by the MTT assay[34]. To examine DNA synthesis, [^{3}H]thymidine incorporation assay was performed as previously described[35].

Fluorescence-activated cell sorting (FACS) analysis

The cells were plated in 24-well plates, serum starved, and incubated for 3 d in the absence or presence of 4 μmol/L *t*10*c*12 or *c*9*t*11 with or without 20 ng/mL HRG-β as described above. To estimate apoptotic cell number, the cells were trypsinized and incubated with phycoerythrin (PE)-conjugated Annexin V (Annexin V-PE) and 7-amino-actinomycin D (7-AAD) (BD Pharmingen, Franklin Lakes, NJ, USA) for 15 min at room temperature in the dark. Apoptotic cells were analyzed by flow cytometry within 1 h utilizing FACScan™ (Becton Dickinson, Franklin Lake, NJ, USA). The data were analyzed using ModFit V.1.2. software.

Immunoprecipitation and immunoblotting analyses

We treated HT-29 cells with various concentrations of *t*10*c*12 or *c*9*t*11 and/or 20 ng/mL HRG-β. Cell lysates (0.75 mg protein) were prepared and immunoprecipitated by using anti-ErbB3 antibody and protein A-Sepharose beads as previously described[35]. The immunoprecipitates or total cell lysates (50 μg protein) were resolved on a sodium dodecyl sulfate (SDS) - 4-20% polyacrylamide gel and transferred onto polyvinylidene fluoride membrane (Millipore, Bedford, MA, USA). The blots were blocked for 1 h in 1% BSA in TBS-T (20 mmol/L Tris-Cl, pH 7.5, 150 mmol/L NaCl, 0.1% Tween 20) or 5% milk TBS-T and incubated for 1 h with either anti-phospho-Tyr (1:5000), ErbB1 (1:250), ErbB2 (1:500), ErbB3 (1:1000), p85 (1:1000), Akt (1:1000), p-Akt (1:1000), ERK-1/2 (1:1000), p-ERK-1/2 (1:1000), or HRG (1:500) antibody. The blots were then

incubated with anti-mouse or anti-rabbit horseradish peroxidase-conjugated antibody. Signals were detected by using the enhanced chemiluminescence method using SuperSignal® West Dura Extended Duration Substrate (Pierce, Rockford, IL, USA). Immunoblots were probed with an antibody for β-actin (1:2000) as a control for protein loading. Protein expression levels are normalized to β-actin, and the levels in the untreated samples are always set at 100%.

Reverse transcriptase-polymerase chain reaction (RT-PCR)

HT-29 cells were seeded at the density of 1×10^6 cells/dish in 100-mm dishes and treated with various concentrations of *t*10*c*12 or *c*9*t*11 as described above. Total RNA was isolated using the guanidium isothiocyanate-phenol-chloroform method and RT-PCR was performed as previously described[35]. Sequences for PCR primer sets, annealing temperatures, and numbers of cycles used for PCR amplification were previously described[35]. The levels of mRNA were corrected as a ratio to the corresponding β-actin level and the levels in the untreated samples were always set at 100%.

PI3K assay

We estimated PI3K activity as previously described[36]. Seven hundred and fifty micrograms of cell lysate was immunoprecipitated with ErbB3 antibody followed by incubation with protein A-Sepharose beads. The immunoprecipitates were washed twice with 1% NP-40-PBS, twice with 100 mmol/L Tris-HCl (pH 7.5) containing 500 mmol/L LiCl and 1 mmol/L Na_3VO_3, and twice with 50 mmol/L Tris-HCl (pH 7.2) containing 150 mmol/L NaCl. After the last wash, the beads were resuspended in 20 μL kinase buffer (20 mmol/L Hepes, pH 7.2, 50 mmol/L NaCl, 1 mmol/L EGTA) containing 4 μg of phosphatidylinositol (Sigma), 10 μmol/L ATP, 5 mmol/L $MnCl_2$, and 10 μCi of [γ^{32}]ATP and incubated for 20 min at 30 ℃. The resulting ^{32}P-labeled phosphatidylinositol 3-phosphate (PIP) lipids were separated from other reaction products by thin layer chromatography and visualized by autoradiography. The PIP signals were quantitated by densitometry using the Bio-profile Bio-1D application (Vilber-Lourmat, France).

Statistical analysis

For all studies, 3-6 independent experiments were performed with separate batches of cells. We expressed the results as the mean±SE and analyzed by one-way, two-way, or two-factor repeated measurements analysis of variance (ANOVA). Differences between treatment groups were analyzed by Duncan's multiple range test or *t* test. Means were considered significantly different at $P<0.05$. All statistical analyses were done using the SAS System for Windows V8.1 (SAS Institute, Cary, NC, USA).

RESULTS

T10c12 abrogates the growth stimulatory effects of HRG-β in HT-29 cells

Previously, we have observed that *t*10*c*12 (0-4 μmol/L) inhibited HT-29 cell growth in a dose-dependent manner, whereas *c*9*t*11 had no effect. We observed a 66±2% decrease in cell number within 96 h after the addition of 4 μmol/L *t*10*c*12[7]. In the present study, we first assessed whether HRG-β stimulates HT-29 cell growth and inhibits the growth inhibitory effect of *t*10*c*12. We cultured HT-29 cells in the absence or presence of 20 ng/mL HRG-β with or without 4 μmol/L *t*10*c*12 or *c*9*t*11. HRG-β significantly increased viable HT-29 cell numbers. *T*10*c*12 CLA decreased viable cell numbers, which was not prevented by the addition of HRG-β. In fact, viable cell numbers were even lower in the presence of both HRG and *t*10*c*12 compared to those in the presence of *t*10*c*12 alone (Figure 1A). By contrast *c*9*t*11 had no effect on viable cell numbers in either the presence or absence of HRG-β (Figure 1B).

To examine whether *t*10*c*12 inhibits DNA synthesis of HT-29 cells, we treated the cells with 4 μmol/L *t*10*c*12 in the absence or presence of HRG-β for 2 d and estimated [^{3}H]thymidine incorporation. As illustrated in Figure 2A, *t*10*c*12 decreased the incorporation of [^{3}H]thymidine into DNA of HT-29 cells. HRG-β increased [^{3}H]thymidine incorporation but did not abrogate the effect of the *t*10*c*12 isomer. The incorporation of [^{3}H]thymidine further decreased in the presence of both HRG-β and *t*10*c*12 compared to that in the presence of *t*10*c*12 alone. *C*9*t*11 CLA had no effect on [^{3}H]thymidine incorporation (data not shown).

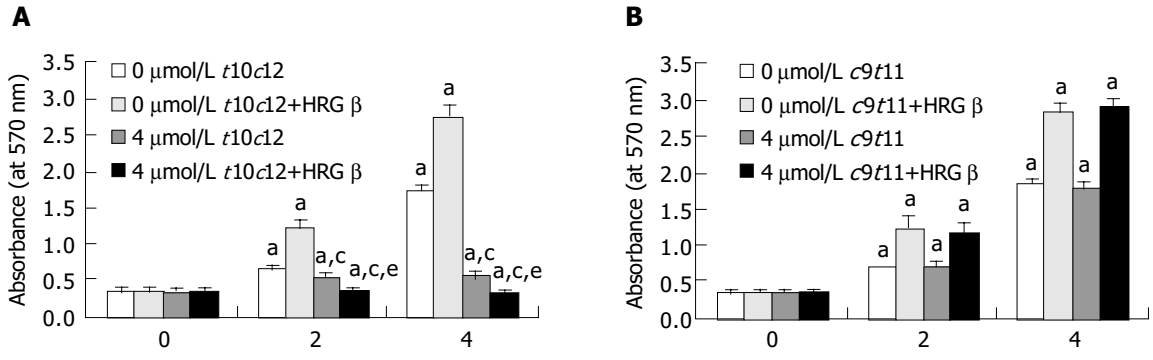


Figure 1 *Trans*-10,*cis*-12 (*t*10*c*12) CLA abrogates the growth stimulatory effect of heregulin (HRG)-β. HT-29 cells were plated in 24-well plates at 50000 cells/well in DMEM/F12 supplemented with 10% fetal bovine serum. A day later, the monolayers were serum-starved with serum-free DMEM/F12 supplemented with 5 μg/mL transferrin, 0.1 mg/mL BSA, and 5 ng/mL selenium for 24 h. After serum-starvation, cells were incubated in serum-free medium in the absence or presence of 4 μmol/L *t*10*c*12 (**A**) or *c*9*t*11 (**B**) with or without 20 ng/mL HRG-β. Cell numbers were estimated by the MTT assay. Each bar represents the mean±SE ($n = 6$). Comparisons between groups that yielded significant differences are indicated by different letters above each bar. For example, [a]$P<0.05$ *vs* 0 μmol/L *t*10*c*12, [c]$P<0.05$ *vs* 0 μmol/L *t*10*c*12 + HRGβ, [e]$P<0.05$ *vs* 4 μmol/L *t*10*c*12.

To examine whether HRG-β inhibits *t*10*c*12-induced apoptosis, we estimated the fractions of HT-29 cells undergoing apoptosis after treatment with *t*10*c*12 and/or HRG-β using Annexin-V staining followed by flow cytometry. As shown in Figure 2B, we observed an increase in apoptotic cell numbers after treatment with 4 μmol/L *t*10*c*12. HRG-β inhibited apoptosis in the absence and presence of *t*10*c*12 but did not completely abrogate *t*10*c*12-induced apoptosis. C9*t*11 did not induce apoptosis (data not shown).

T10c12 CL in italics A isomer inhibits HRG-b-ErbB3 signaling

We previously reported that HT-29 cells express ErbB1, ErbB2, and ErbB3 and ErbB3 was expressed at relatively higher levels than ErbB1 and ErbB2[35]. Because HRG-β increased DNA synthesis but did not abrogate the inhibitory effect of *t*10*c*12, we next wished to examine whether *t*10*c*12 inhibited ErbB3 signaling. We immunoblotted total cell lysates with antibodies specific for ErbB1, ErbB2, and ErbB3 to investigate whether *t*10*c*12 influences ErbB receptor expression in HT-29 cells. Treatment of HT-29 cells with increasing concentrations of *t*10*c*12 led to decreased ErbB1, ErbB2, and ErbB3 levels (Figure 3), whereas *c*9*t*11 had no effect (Figure 4). Neither *t*10*c*12 nor *c*9*t*11 affected levels of HRG or the p85 regulatory subunit of PI3K (Figures 3 and 4).

To determine whether *t*10*c*12 regulates the expression of ErbB1, ErbB2, and ErbB3 at an mRNA level, we similarly treated cells with the CLA isomer, isolated total RNA and determined mRNA levels using RT-PCR analysis. As shown in Figure 5, *t*10*c*12 decreased ErbB1, ErbB2, and ErbB3 transcripts in a concentration-dependent manner, whereas the same concentrations of *c*9*t*11 did not alter ErbB transcripts (Figure 6).

The tyrosine kinase subunits of the ErbB3 intracellular domain become tyrosine phosphorylated following activation by HRG-β. To determine whether *t*10*c*12 inhibits ErbB3 tyrosine phosphorylation, we treated cells with or without 4 μmol/L *t*10*c*12 for 3 d and prepared lysates after 0, 1, 5, or 60 min of stimulation with HRG-β. Using immunoprecipitation followed by immunoblotting, we measured levels of ErbB3 receptor expression and phosphorylation. Following the addition of HRG-β alone, ErbB3 levels remained invariable and increased ErbB3 phosphorylation was detected at 1 and 5 min, indicating that the receptor was being stimulated by the ligand (Figure 7A). Tyrosine phosphorylation of ErbB3 was drastically decreased and ErbB3 protein levels were decreased by approximately 35% in cells treated with

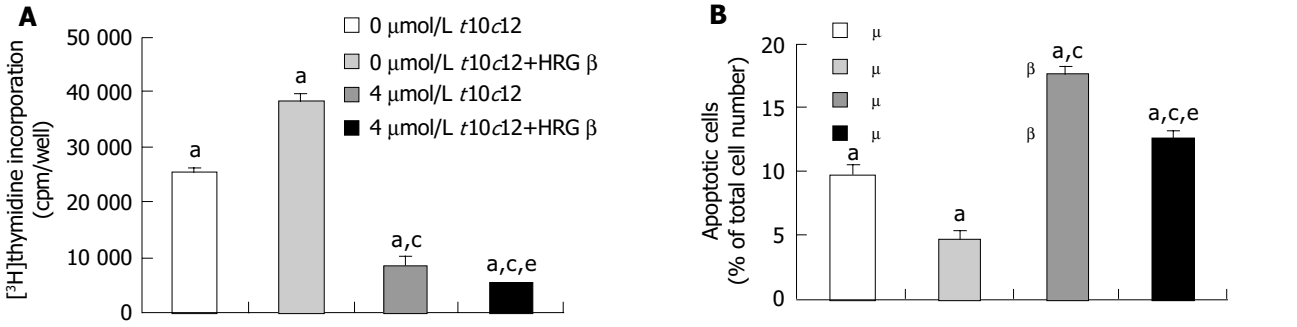


Figure 2 Effect of HRG-β and/or *t*10*c*12 on DNA synthesis and apoptosis of HT-29 cells. HT-29 cells were cultured and treated with 4 μmol/L *t*10*c*12 in the absence or presence of 20 ng/mL HRG-β. **A:** To estimate DNA synthesis, [^{3}H] thymidine incorporation into DNA was measured. **B:** To measure apoptosis, the cells were stained with 7-amino-actinomycin D (7-AAD) and Annexin V, and then analyzed by flow cytometry. The number of early apoptotic cells is expressed as a percentage of total cell number. Each bar represents the mean±SE from six independent experiments. Comparisons between groups that yielded significant differences are indicated by different letters above each bar. For example, $^aP<0.05$ *vs* 0 μmol/L *t*10*c*12, $^cP<0.05$ *vs* 0 μmol/L *t*10*c*12 + HRGβ, $^eP<0.05$ *vs* 4 μmol/L *t*10*c*12.

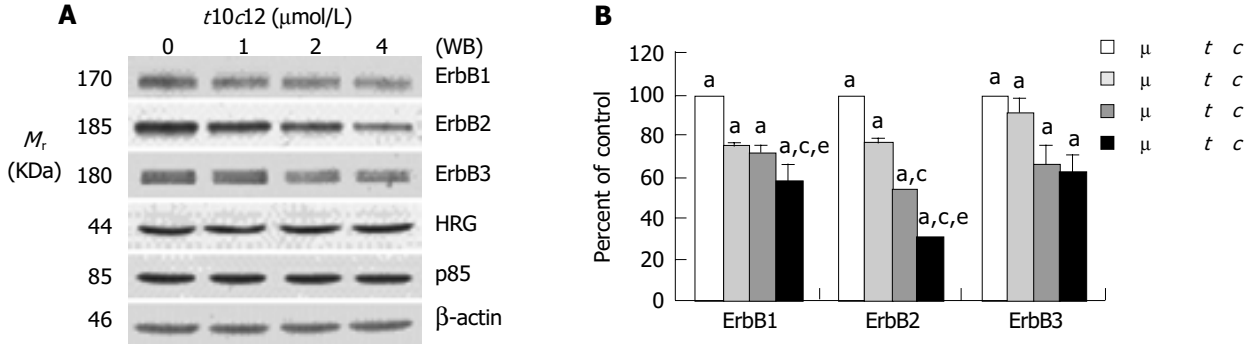


Figure 3 Effect of *t*10*c*12 on the protein expression of ErbB1, ErbB2, ErbB3, HRG, and the p85 subunit of PI3K. HT-29 cells were treated with various concentrations of *t*10*c*12 for 3 d. Cell lysates were subjected to immunoblotting with an antibody against ErbB1, ErbB2, ErbB3, p85 subunit of PI3K, HRG, or β-actin. **A:** Photographs of chemiluminescent detection of the blots, which were representative of three independent experiments, are shown; **B:** Quantitative analysis of immunoblots. The relative abundance of each band was estimated by densitometric scanning of the exposed films. Each bar represents the mean±SE (n = 3). Comparisons between groups that yielded significant differences are indicated by different letters above each bar. For example, $^aP<0.05$ *vs* 0 μmol/L *t*10*c*12, $^cP<0.05$ *vs* 1 μmol/L *t*10*c*12, $^eP<0.05$ *vs* 2 μmol/L *t*10*c*12.

4 μmol/L *t*10*c*12. The phosphotyrosine levels of ErbB3 were normalized to corresponding ErbB3 protein levels to distinguish whether the reduced tyrosine phosphorylation is a result of decreased ErbB3 protein levels or inhibition of phosphorylation of the signaling protein. After normalization, the reduced phosphorylation after *t*10*c*12 is still obvious (Figure 7B) indicating that the reduction is a result of both decreased ErbB3 levels and the inhibition of phosphorylation. These results are consistent with the finding that *t*10*c*12 prevented the effect of exogenous HRG-β on HT-29 cell growth.

T10 in italics c12 inhibits HRG-β-induced activation of PI3K and Akt

Activation of ErbB3 receptor signaling leads to activation

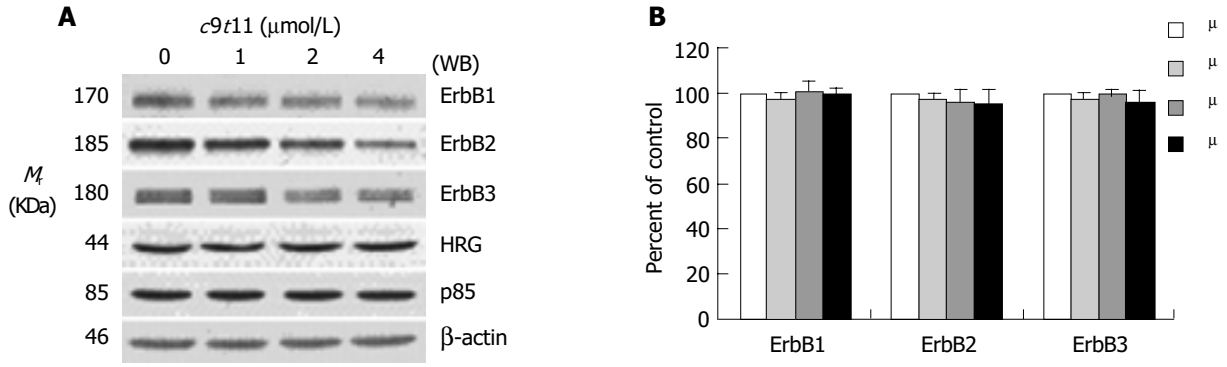


Figure 4 Effect of *c*9*t*11 on the protein expression of ErbB1, ErbB2, ErbB3, HRG, and the p85 subunit of PI3K. HT-29 cells were treated with various concentrations of *c*9*t*11 for 3 d. Cell lysates were subjected to immunoblotting with an antibody against ErbB1, ErbB2, ErbB3, p85 subunit of PI3K, HRG, or β-actin. **A:** Photographs of chemiluminescent detection of the blots, which were representative of three independent experiments, are shown. **B:** Quantitative analysis of immunoblots. The relative abundance of each band was estimated by densitometric scanning of the exposed films. Each bar represents the mean±SE (*n* = 3).

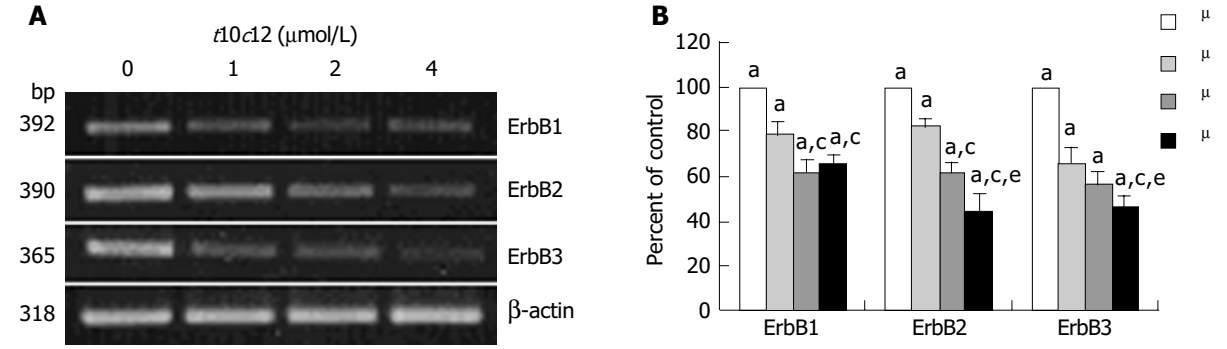


Figure 5 Effect of *t*10*c*12 on ErbB1, ErbB2, and ErbB3 transcripts. HT-29 cells were treated with various concentrations of *t*10*c*12 for 3 d. Total RNA was isolated and RT-PCR was performed as described in Materials and methods. **A:** Photographs of the ethidium bromide-stained gel, which were representative of three independent experiments, are shown; **B:** Quantitative analysis of mRNAs. The relative abundance of each band was estimated by densitometric scanning of the exposed films. Each bar represents the mean±SE (*n* = 3). Comparisons between groups that yielded significant differences are indicated by different letters above each bar. For example, $^{a}P<0.05$ *vs* 0 μmol/L *t*10*c*12, $^{c}P<0.05$ *vs* 1 μmol/L *t*10*c*12, $^{e}P<0.05$ *vs* 2 μmol/L *t*10*c*12.

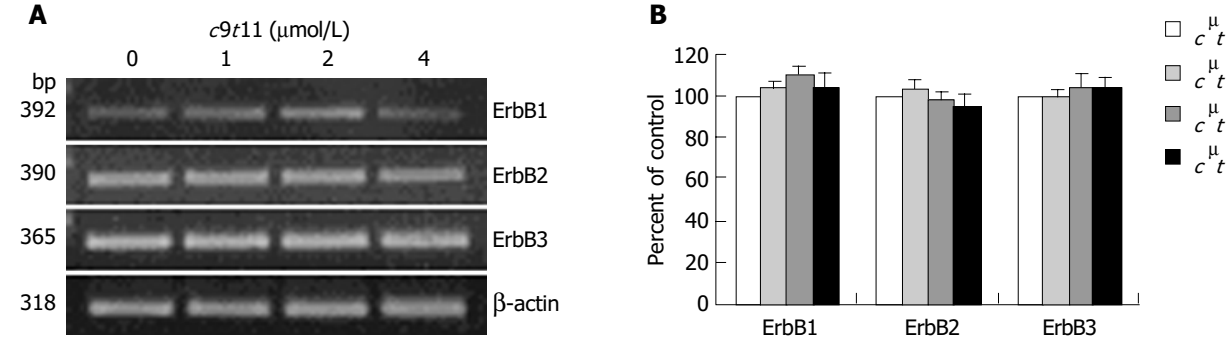


Figure 6 Effect of *c*9*t*11 on ErbB1, ErbB2, and ErbB3 transcripts. HT-29 cells were treated with various concentrations of *c*9*t*11. Total RNA was isolated and RT-PCR was performed as described in Materials and methods. **A:** Photographs of the ethidium bromide-stained gel, which were representative of three independent experiments, are shown; **B:** Quantitative analysis of mRNAs. The relative abundance of each band was estimated by densitometric scanning of the exposed films. Each bar represents the mean±SE (*n* = 3).

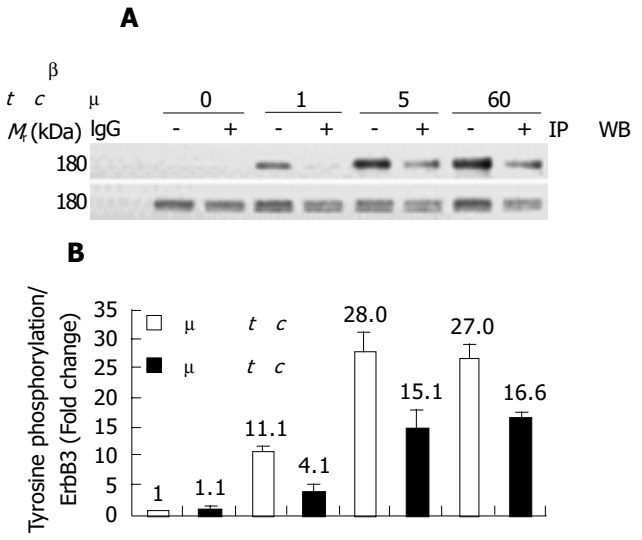


Figure 7 Effect of *t*10*c*12 on HRG-β-induced tyrosine phosphorylation of ErbB3 in HT-29 cells. Cells were treated in the absence or presence of 4 μmol/L *t10c12* for 3 d and lysed without stimulation (0) or after 1, 5, or 60 min of stimulation with HRG-β. Cell lysates were incubated with an anti-ErbB3 antibody and the immune complexes were precipitated with protein A-Sepharose. The immunoprecipitated proteins were analyzed by Western blotting with antibodies against phosphotyrosine or ErbB3. **A:** Photographs of chemiluminescent detection of the blots, which were representative of three independent experiments, are shown; **B:** The relative abundance of each band was estimated by densitometric scanning of the exposed films. Each bar represents the mean±SE (*n* = 3).

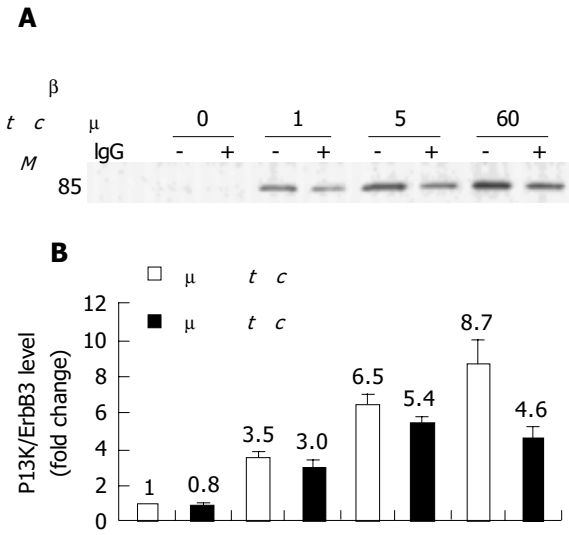


Figure 8 Effect of *t*10*c*12 on HRG-β-induced recruitment of the p85 subunit of PI3K to ErbB3 in HT-29 cells. Immunoprecipitation was performed with an anti-ErbB3 antibody and protein A-Sepharose as described above. The immunoprecipitated proteins were analyzed by Western blotting with an antibody against the p85 PI3K subunit. **A:** A photograph of chemiluminescent detection of the blot, which was representative of three independent experiments, is shown. **B:** The relative fold change in p85 to its own ErbB3 band on Western blots. Each bar represents the mean±SE (*n* = 3).

of PI3K. We examined the expression of the p85 regulatory subunit of PI3K in HT-29 cells treated with increasing amounts of *t*10*c*12 using Western blot analysis. We detected decreased levels of ErbB receptors without any change in p85 expression after the addition of *t*10*c*12 (Figure 3). We investigated whether *t*10*c*12 influences HRG-β-induced association of ErbB3 and p85. We performed immunoprecipitation with an anti-ErbB3 antibody followed by Western blotting with the p85 antibody. HRG-β stimulated association of p85 with ErbB3, and the association was reduced in *t*10*c*12-treated cells (Figure 8A). The levels of p85 associated with ErbB3 was normalized to ErbB3 expression levels to differentiate whether the reduced association after *t*10*c*12 treatment is a result of decreased ErbB3 levels or that of an inhibition of p85 recruitment. After normalization, the differences in p85 association between control and *t*10*c*12 are significant at 5 and 60 min after HRG-β addition (Figure 8B) indicating that both decreased ErbB3 levels and an inhibition of p85 recruitment are responsible for the decreased p85 association to ErbB3.

We analyzed PI3K activity in the anti-ErbB3 immunoprecipitates by *in vitro* kinase assays, wherein the PIP product was separated by thin layer chromatography. The spots of ^{32}P-labeled PIP on thin-layer chromatography plates are shown in Figure 9A with their activities plotted in Figure 9B. Similar to p85 Western blot analysis (Figure 8A), HT-29 cells incubated with HRG-β showed time-dependent changes in PI3K activity of their anti-ErbB3 immunoprecipitates. The PI3K activities increased 6-fold at 1 min after the HRG-β treatment and further increased at 5 min, and 4 μmol/L *t*10*c*12 decreased these changes.

It is well known that ErbB3 receptor activation of PI3K

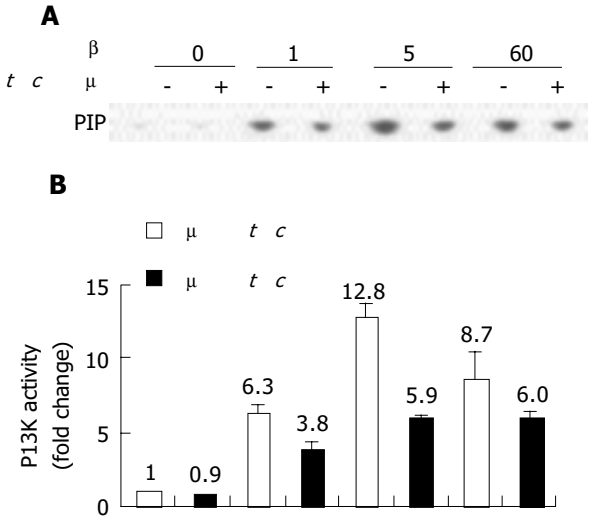


Figure 9 Effect of *t*10*c*12 and/or HRG-β on ErbB3-associated PI3K activity. Cells were treated, and lysates were prepared and immunoprecipitated with an anti-ErbB3 antibody as described in Figure 8. The immune complexes were incubated with phosphatidylinositol and [g-^{32}P]ATP. Phosphatidylinositol 3-phosphate (PIP) generated by immunoprecipitated PI3K was separated by thin-layer chromatography (TLC). **A:** An autoradiograph of the TLC plate, which was representative of three independent experiments, is shown; **B:** Relative fold changes in PIP. The radioactive PIP signals were quantitated by densitometry. Each bar represents the mean±SE (*n* = 3).

leads to movement of Akt to the membrane and its subsequent activation[20,37]. We immunoblotted total cell lysates using anti-p-Akt and whole Akt protein antibodies and quantitated the relative fold change in p-Akt to its own total Akt signal by densitometry. The time-dependent increase in Akt phosphorylation (p-Akt) by HRG-β is depicted in Figure 10. HRG-β induced phosphorylation of

AKT within 5 min, and the increase in p-Akt after HRG-β treatment was coherent with the increase in PI3K activity and ErbB3-associated p85 protein levels seen at 5 min after HRG-β treatment. We observed no changes in Akt protein levels during the 60-min HRG-β stimulation. However, p-Akt levels were substantially decreased in cells treated with *t*10*c*12, whereas the total Akt protein levels were only slightly decreased by *t*10*c*12 treatment. *C*9*t*11 did not cause any changes in HRG-β-induced Akt activation in HT-29 cells (data not shown).

T10c12 does not inhibit HRG-β-induced activation of ERK-1/2

Activation of ERK-1/2 has also been implicated in mitogenic signaling by the HRG-induced activation of ErbB3[38]. To examine the effect of *t*10*c*12 on HRG-β-induced activation of ERK-1/2, we performed Western blotting using antibodies raised against ERK-1/2 and p-ERK-1/2. HRG-β activation of ErbB3 receptor signaling resulted in an increase in phosphorylation of ERK-1/2 in HT-29 cells. Phosphorylated ERK-1/2 levels were increased at 5 min after HRG-β stimulation but HRG-induced ERK-1/2 phosphorylation was not changed by 4 μmol/L *t*10*c*12. Total ERK-1/2 levels did not change after *t*10*c*12 treatment (Figure 11). Neither phosphorylated nor total ERK-1/2 levels were altered by treatment with the same concentration of *c*9*t*10 (data not shown).

DISCUSSION

We previously reported that the *t*10*c*12, not the *c*9*t*11, isomer of CLA inhibited HT-29 colon cancer cell growth[7]. In the present study, the *t*10*c*12 isomer, which decreased viable HT-29 cell numbers, decreased the protein levels of ErbB1, ErbB2, and ErbB3. However, the *c*9*t*11 isomer, which did not alter viable HT-29 cell number, had no effect on ErbB protein levels. In addition, exogenous HRG-β stimulated cell growth in the absence of *t*10*c*12 but did not mitigate the growth inhibitory effect of *t*10*c*12. These results indicate that the decreased ErbB levels by the *t*10*c*12 isomer may be, at least in part, responsible for the decreased cell growth in HT-29 cells.

It has been observed in numerous types of cancers that cell proliferation and survival increased when control of the ErbB pathways is lost, leading to the malignant phenotype[39]. HRG is a potent mitogen for colon cancer cells and autocrine HRG generates growth factor independence and prevents apoptosis[30,40]. In order to study the mechanisms by which *t*10*c*12 decreases colon cancer cell growth, the present study examined the influence of *t*10*c*12 on ErbB3 signaling. In the present study, we provide the first evidence that *t*10*c*12 reduces ErbB2 and ErbB3 protein expression and ErbB3-mediated signaling. When HT-29 cells were incubated with HRG-β in serum-free medium, the cells reacted to HRG-β by increasing cell number. However, HRG-β was unable to increase the viable cell number in the presence of *t*10*c*12 suggesting that *t*10*c*12 downregulates the HRG-receptor signaling pathway. In fact, we observed decreased levels of the HRG receptor ErbB3 at 72 h after treatment with *t*10*c*12. However, the expression of HRG in HT-29 cells was not affected by *t*10*c*12. Previous studies have reported that HRG is expressed in gastrointestinal tissues[32,41] and human colon cancer samples, and is an autocrine growth regulator of GEO human colon cancer cells[30]. Because HT-29 cells express HRG and its receptor ErbB3, HRG may also be an autocrine growth regulator of HT-29 cells. Our present results indicate that *t*10*c*12 decreases cell's ability to respond to HRG without altering the production of this growth factor in HT-29 cells.

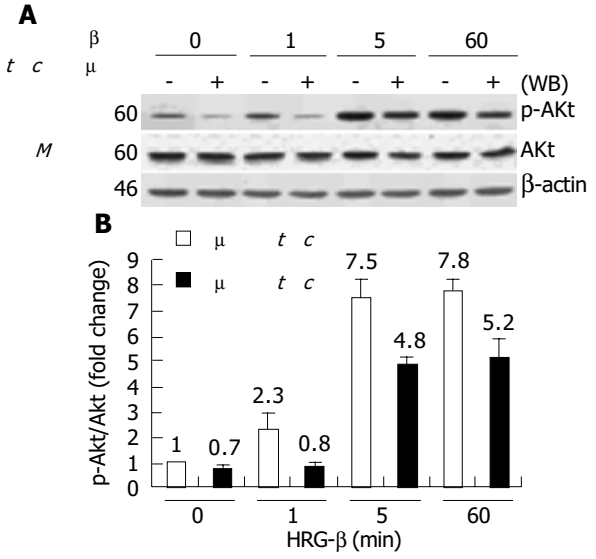


Figure 10 Effect of *t*10*c*12 on HRG-β-induced Akt activation. Similar protein samples as those in Figure 8 were analyzed by immunoblotting with anti-phospho-Ser473 Akt (p-Akt) or whole Akt protein antibodies. **A:** Photographs of chemiluminescent detection of the blots, which were representative of three independent experiments, are shown; **B:** Quantitative analysis of immunoblots. The relative fold change in p-Akt to its own Akt control band on Western blots was quantitated by densitometric analysis. Each bar represents the mean±SE (*n* = 3).

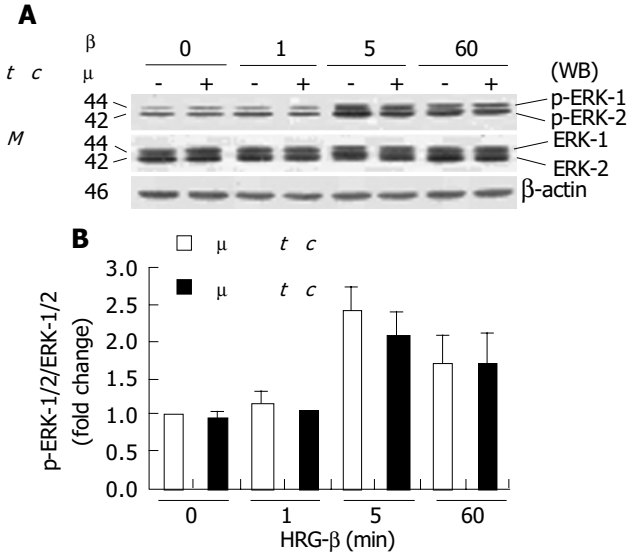


Figure 11 Effect of *t*10*c*12 on HRG-β-induced ERK-1/2 activation in HT-29 cells. Similar protein samples as those in Figure 8 were analyzed by immunoblotting with p-ERK-1/2 or whole ERK-1/2 antibodies. **A:** Photographs of chemiluminescent detection of the blots, which were representative of three independent experiments, are shown; **B:** Quantitative analysis of immunoblots. The relative fold change in p-ERK-1/2 to its own ERK-1/2 control band on Western blots was quantitated by densitometric analysis. Each bar represents the mean±SE (*n* = 3).

The present results indicate that the decrease in ErbB levels by *t*10*c*12 treatment was due to at least in part, to the decrease in mRNA expression. In this study, we did not examine the mechanisms by which the *t*10*c*12 isomer regulates ErbB genes. CLA has been reported to be an activator of the peroxisomal proliferators-activated receptor (PPAR) γ[42]. Ligands for PPARγ induce apoptosis and exert antiproliferative effects on several carcinoma cell lines[43,44]. Houseknecht *et al*.[45], have shown that mRNA levels of aP2, a PPAR responsive gene in the adipose tissue of fatty Zucker diabetic rats, were increased as a result of PPARγ activation by CLA. Other studies utilizing MCF-7 breast cancer cells have shown that the activation of PPARγ through the 15-deoxy-△-12,14-prostaglandin J2 ligand causes a dramatic inhibition of ErbB2 and ErbB3 tyrosine phosphorylation induced by HRG-α and HRG-β[46]. We speculate that *t*10*c*12 or its metabolites may activate the PPAR transcription factor family. It remains to be determined whether *t*10*c*12 inhibits ErbB gene expression by activating PPARγ and/or by other mechanisms.

Activation of tyrosine kinase receptors requires tyrosine phosphorylation of their intracellular subunits. *T*10*c*12 decreases HRG-β-induced tyrosine phosphorylation of ErbB3 when the data was normalized with ErbB3 protein levels indicating that *t*10*c*12 inhibits activation of this receptor in addition to decreasing the receptor protein levels. ErbB3 has been described as a key mediator of HRG-dependent activation of the PI3K pathway[47,48]. ErbB3 is especially well suited to mediate PI3K signaling because it contains six YXXM consensus-binding sites for p85[49]. We observed that HRG-β stimulated the recruitment of p85 to ErbB3 in HT-29 cells, and *t*10*c*12 decreased ErbB3-associated p85 protein levels and PI3K activities. These decreases do not appear to be due to changes in the p85 protein expression, but to the decrease in ErbB3 protein levels.

PKB/Akt is a downstream target of PI3K and plays a central role in PI3K-mediated protection against apoptosis[50]. The present results show that *t*10*c*12 inhibited HRG-β-induced activation of Akt, which could be attributed to both decreased ErbB3 levels and decreased ErbB3 activation. We speculate that *t*10*c*12 inhibits DNA synthesis and induces apoptosis of HT-29 cells by inhibiting the Akt signaling pathway. Increased expression and/or activity of ErbB receptors and downstream signaling proteins such as Akt are frequent events in cancer. Future studies are needed to study the effect of Akt on HT-29 cell growth.

The ERK/MAP kinase family of serine/threonine kinases comprises a cascade of three kinases; ERK-1/2, c-jun N-terminus kinase (JNK), and p38 MAP kinase. It is generally accepted that the balance between growth-factor-activated ERK-1/2 and stress-activated JNK and p38 pathways determines whether the cell lives or dies[51]. In the present experiment, *t*10*c*12 had no effect on either basal or HRG-β-induced phosphorylation of ERK-/2. It remains to be determined whether *t*10*c*12 alters stress activated JNK and p38 pathways in cancer cells.

In summary, *t*10*c*12 decreases viable HT-29 cell numbers, which was due to decreased DNA synthesis and induction of apoptosis. However, *c*9*t*11 had no effect on apoptosis or DNA synthesis. HRG-β stimulates DNA synthesis and inhibits apoptosis but did not abrogate the effects of the *t*10*c*12 isomer. In addition, the *t*10*c*12 isomer negatively regulates levels of ErbB receptors and subsequent activation of Akt but not activation of ERK-1/2 in HT-29 cells. These results suggest that the growth inhibitory effects of the *t*10*c*12 isomer may, at least in part, be mediated by decreasing HRG/ErbB3 signaling and the PI3K/Akt pathway. The ability of the *t*10*c*12 isomer to inhibit the PI3K/Akt pathway is especially important because aberrant activation of ErbB receptors and Akt signaling play a role in the development of many types of cancer. To date much attention has been focused on developing inhibitors of Akt for cancer therapy. However, in view of the recent study reporting that the *t*10*c*12 isomer increased the size of the adenoma in the small intestine of Min mouse[10], further animal studies are necessary to determine the effects of the *t*10*c*12 isomer on colon carcinogenesis.

REFERENCES

1 **Belury MA.** Inhibition of carcinogenesis by conjugated linoleic acid: potential mechanisms of action. *J Nutr* 2002; **132**: 2995-2998

2 **Park HS,** Ryu JH, Ha YL, Park JH. Dietary conjugated linoleic acid (CLA) induces apoptosis of colonic mucosa in 1,2-dimethylhydrazine-treated rats: a possible mechanism of the anticarcinogenic effect by CLA. *Br J Nutr* 2001; **86**: 549-555

3 **Park HS,** Cho HY, Ha YL, Park JH. Dietary conjugated linoleic acid increases the mRNA ratio of Bax/Bcl-2 in the colonic mucosa of rats. *J Nutr Biochem* 2004; **15**: 229-235

4 **O'Shea M,** Stanton C, Devery R. Antioxidant enzyme defence responses of human MCF-7 and SW480 cancer cells to conjugated linoleic acid. *Anticancer Res* 1999; **19**: 1953-1959

5 **Palombo JD,** Ganguly A, Bistrian BR, Menard MP. The antiproliferative effects of biologically active isomers of conjugated linoleic acid on human colorectal and prostatic cancer cells. *Cancer Lett* 2002; **177**: 163-172

6 **Shultz TD,** Chew BP, Seaman WR, Luedecke LO. Inhibitory effect of conjugated dienoic derivatives of linoleic acid and beta-carotene on the in vitro growth of human cancer cells. *Cancer Lett* 1992; **63**: 125-133

7 **Kim EJ,** Cho HJ, Kim SJ, Kang YH, Ha YL, Park JHY. Effect of conjugated linoleic acid on the proliferation of the human colon cancer cell line, HT-29. *Korean J Nutr* 2001; **34**: 896-904

8 **Petrik MB,** McEntee MF, Johnson BT, Obukowicz MG, Whelan J. Highly unsaturated (n-3) fatty acids, but not alpha-linolenic, conjugated linoleic or gamma-linolenic acids, reduce tumorigenesis in Apc(Min/+) mice. *J Nutr* 2000; **130**: 2434-2443

9 **Pariza MW,** Ha YL, Benjamin H, Sword JT, Gruter A, Chin SF, Storkson J, Faith N, Albright K. Formation and action of anticarcinogenic fatty acids. *Adv Exp Med Biol* 1991; **289**: 269-272

10 **Rajakangas J,** Basu S, Salminen I, Mutanen M. Adenoma growth stimulation by the trans-10, cis-12 isomer of conjugated linoleic acid (CLA) is associated with changes in mucosal NF-kappaB and cyclin D1 protein levels in the Min mouse. *J Nutr* 2003; **133**: 1943-1948

11 **Lemke G.** Neuregulins in development. *Mol Cell Neurosci* 1996; **7**: 247-262

12 **Riese DJ 2nd,** Stern DF. Specificity within the EGF family/ErbB receptor family signaling network. *Bioessays* 1998; **20**: 41-48

13 **Pinkas-Kramarski R,** Soussan L, Waterman H, Levkowitz G, Alroy I, Klapper L, Lavi S, Seger R, Ratzkin BJ, Sela M, Yarden Y. Diversification of Neu differentiation factor and epidermal growth factor signaling by combinatorial receptor interactions. *Embo J* 1996; **15**: 2452-2467

14 **Guy PM,** Platko JV, Cantley LC, Cerione RA, Carraway KL 3rd. Insect cell-expressed p180erbB3 possesses an impaired tyrosine

kinase activity. *Proc Natl Acad Sci USA* 1994; **91**: 8132-8136
15 **Carraway KL 3rd,** Sliwkowski MX, Akita R, Platko JV, Guy PM, Nuijens A, Diamonti AJ, Vandlen RL, Cantley LC, Cerione RA. The erbB3 gene product is a receptor for heregulin. *J Biol Chem* 1994; **269**: 14303-14306
16 **Tzahar E,** Waterman H, Chen X, Levkowitz G, Karunagaran D, Lavi S, Ratzkin BJ, Yarden Y. A hierarchical network of interreceptor interactions determines signal transduction by Neu differentiation factor/neuregulin and epidermal growth factor. *Mol Cell Biol* 1996; **16**: 5276-5287
17 **Vanhaesebroeck B,** Leevers SJ, Panayotou G, Waterfield MD. Phosphoinositide 3-kinases: a conserved family of signal transducers. *Trends Biochem Sci* 1997; **22**: 267-272
18 **Datta SR,** Brunet A, Greenberg ME. Cellular survival: a play in three Akts. *Genes Dev* 1999; **13**: 2905-2927
19 **Hemmings BA.** Akt signaling: linking membrane events to life and death decisions. *Science* 1997; **275**: 628-630
20 **Klippel A,** Kavanaugh WM, Pot D, Williams LT. A specific product of phosphatidylinositol 3-kinase directly activates the protein kinase Akt through its pleckstrin homology domain. *Mol Cell Biol* 1997; **17**: 338-344
21 **Muise-Helmericks RC,** Grimes HL, Bellacosa A, Malstrom SE, Tsichlis PN, Rosen N. Cyclin D expression is controlled post-transcriptionally via a phosphatidylinositol 3-kinase/Akt-dependent pathway. *J Biol Chem* 1998; **273**: 29864-29872
22 **Gille H,** Downward J. Multiple ras effector pathways contribute to G(1) cell cycle progression. *J Biol Chem* 1999; **274**: 22033-22040
23 **Kulik G,** Klippel A, Weber MJ. Antiapoptotic signalling by the insulin-like growth factor I receptor, phosphatidylinositol 3-kinase, and Akt. *Mol Cell Biol* 1997; **17**: 1595-1606
24 **Kandel ES,** Hay N. The regulation and activities of the multifunctional serine/threonine kinase Akt/PKB. *Exp Cell Res* 1999; **253**: 210-229
25 **Nicholson KM,** Anderson NG. The protein kinase B/Akt signalling pathway in human malignancy. *Cell Signal* 2002; **14**: 381-395
26 **Fresno Vara JA,** Casado E, de Castro J, Cejas P, Belda-Iniesta C, Gonzalez-Baron M. PI3K/Akt signalling pathway and cancer. *Cancer Treat Rev* 2004; **30**: 193-204
27 **Slichenmyer WJ,** Fry DW. Anticancer therapy targeting the erbB family of receptor tyrosine kinases. *Semin Oncol* 2001; **28**: 67-79
28 **Ciardiello F,** Kim N, Saeki T, Dono R, Persico MG, Plowman GD, Garrigues J, Radke S, Todaro GJ, Salomon DS. Differential expression of epidermal growth factor-related proteins in human colorectal tumors. *Proc Natl Acad Sci USA* 1991; **88**: 7792-7796
29 **Maurer CA,** Friess H, Kretschmann B, Zimmermann A, Stauffer A, Baer HU, Korc M, Buchler MW. Increased expression of erbB3 in colorectal cancer is associated with concomitant increase in the level of erbB2. *Hum Pathol* 1998; **29**: 771-777
30 **Venkateswarlu S,** Dawson DM, St Clair P, Gupta A, Willson JK, Brattain MG. Autocrine heregulin generates growth factor independence and blocks apoptosis in colon cancer cells. *Oncogene* 2002; **21**: 78-86
31 **Kapitanovic S,** Radosevic S, Kapitanovic M, Andelinovic S, Ferencic Z, Tavassoli M, Primorac D, Sonicki Z, Spaventi S, Pavelic K, Spaventi R. The expression of p185(HER-2/neu) correlates with the stage of disease and survival in colorectal cancer. *Gastroenterology* 1997; **112**: 1103-1113
32 **Noguchi H,** Sakamoto C, Wada K, Akamatsu T, Uchida T, Tatsuguchi A, Matsui H, Fukui H, Fujimori T, Kasuga M. Expression of heregulin alpha, erbB2, and erbB3 and their influences on proliferation of gastric epithelial cells. *Gastroenterology* 1999; **117**: 1119-1127
33 **Kim EJ,** Kim WY, Kang YH, Ha YL, Bach L, Park JHY. inhibition of Caco-2 cell proliferation by (n-3) fatty acids: possible mediation by increased secretion of insulin-like growth factor binding protein-6. *Nutr Res* 2000; **20**: 1409-1421
34 **Kim EJ,** Kang YH, Schaffer BS, Bach LA, MacDonald RG, Park JH. Inhibition of Caco-2 cell proliferation by all-trans retinoic acid: role of insulin-like growth factor binding protein-6. *J Cell Physiol* 2002; **190**: 92-100
35 **Cho HJ,** Kim WK, Kim EJ, Jung KC, Park S, Lee HS, Tyner AL, Park JH. Conjugated linoleic acid inhibits cell proliferation and ErbB3 signaling in HT-29 human colon cell line. *Am J Physiol Gastrointest Liver Physiol* 2003; **284**: G996-1005
36 **Gu C,** Park S. The EphA8 receptor regulates integrin activity through p110gamma phosphatidylinositol-3 kinase in a tyrosine kinase activity-independent manner. *Mol Cell Biol* 2001; **21**: 4579-4597
37 **Andjelkovic M,** Jakubowicz T, Cron P, Ming XF, Han JW, Hemmings BA. Activation and phosphorylation of a pleckstrin homology domain containing protein kinase (RAC-PK/PKB) promoted by serum and protein phosphatase inhibitors. *Proc Natl Acad Sci USA* 1996; **93**: 5699-5704
38 **Vijapurkar U,** Cheng K, Koland JG. Mutation of a Shc binding site tyrosine residue in ErbB3/HER3 blocks heregulin-dependent activation of mitogen-activated protein kinase. *J Biol Chem* 1998; **273**: 20996-21002
39 **Olayioye MA,** Neve RM, Lane HA, Hynes NE. The ErbB signaling network: receptor heterodimerization in development and cancer. *Embo J* 2000; **19**: 3159-3167
40 **Jackson JG,** St Clair P, Sliwkowski MX, Brattain MG. Blockade of epidermal growth factor- or heregulin-dependent ErbB2 activation with the anti-ErbB2 monoclonal antibody 2C4 has divergent downstream signaling and growth effects. *Cancer Res* 2004; **64**: 2601-2609
41 **Kataoka H,** Joh T, Kasugai K, Okayama N, Moriyama A, Asai K, Kato T. Expression of mRNA for heregulin and its receptor, ErbB-3 and ErbB-4, in human upper gastrointestinal mucosa. *Life Sci* 1998; **63**: 553-564
42 **Yu Y**, Correll PH, Vanden Heuvel JP. Conjugated linoleic acid decreases production of pro-inflammatory products in macrophages: evidence for a PPAR gamma-dependent mechanism. *Biochim Biophys Acta* 2002; **1581**: 89-99
43 **Elstner E,** Muller C, Koshizuka K, Williamson EA, Park D, Asou H, Shintaku P, Said JW, Heber D, Koeffler HP. Ligands for peroxisome proliferator-activated receptorgamma and retinoic acid receptor inhibit growth and induce apoptosis of human breast cancer cells *in vitro* and in BNX mice. *Proc Natl Acad Sci USA* 1998; **95**: 8806-8811
44 **Kubota T,** Koshizuka K, Williamson EA, Asou H, Said JW, Holden S, Miyoshi I, Koeffler HP. Ligand for peroxisome proliferator-activated receptor gamma (troglitazone) has potent antitumor effect against human prostate cancer both *in vitro* and *in vivo*. *Cancer Res* 1998; **58**: 3344-3352
45 **Houseknecht KL,** Vanden Heuvel JP, Moya-Camarena SY, Portocarrero CP, Peck LW, Nickel KP, Belury MA. Dietary conjugated linoleic acid normalizes impaired glucose tolerance in the Zucker diabetic fatty fa/fa rat. *Biochem Biophys Res Commun* 1998; **244**: 678-682
46 **Pignatelli M,** Cortes-Canteli M, Lai C, Santos A, Perez-Castillo A. The peroxisome proliferator-activated receptor gamma is an inhibitor of ErbBs activity in human breast cancer cells. *J Cell Sci* 2001; **114**: 4117-4126
47 **Carraway KL 3rd,** Soltoff SP, Diamonti AJ, Cantley LC. Heregulin stimulates mitogenesis and phosphatidylinositol 3-kinase in mouse fibroblasts transfected with erbB2/neu and erbB3. *J Biol Chem* 1995; **270**: 7111-7116
48 **Soltoff SP,** Carraway KL 3rd, Prigent SA, Gullick WG, Cantley LC. ErbB3 is involved in activation of phosphatidylinositol 3-kinase by epidermal growth factor. *Mol Cell Biol* 1994; **14**: 3550-3558
49 **Hellyer NJ,** Kim MS, Koland JG. Heregulin-dependent activation of phosphoinositide 3-kinase and Akt via the ErbB2/ErbB3 co-receptor. *J Biol Chem* 2001; **276**: 42153-42161
50 **Franke TF,** Kaplan DR, Cantley LC. PI3K: downstream AKTion blocks apoptosis. *Cell* 1997; **88**: 435-437
51 **Makin G,** Dive C. Apoptosis and cancer chemotherapy. *Trends Cell Biol* 2001; **11**: S22-26

Science Editor Guo SY **Language Editor** Elsevier HK

PO Box 2345, Beijing 100023, China
www.wjgnet.com
wjg@wjgnet.com

ELSEVIER

World J Gastroenterol 2005;11(33):5151-5155
World Journal of Gastroenterology ISSN 1007-9327
© 2005 The WJG Press and Elsevier Inc. All rights reserved.

• *COLORECTAL CANCER* •

Persistence of gene expression changes in noninflamed and inflamed colonic mucosa in ulcerative colitis and their presence in colonic carcinoma

Yuji Toiyama, Akira Mizoguchi, Kazushi Kimura, Toshimitsu Araki, Shigeyuki Yoshiyama, Kouhei Sakaguchi, Chikao Miki, Masato Kusunoki

Yuji Toiyama, Toshimitsu Araki, Shigeyuki Yoshiyama, Chikao Miki, Masato Kusunoki, The Second Department of Surgery, Mie University School of Medicine, 2-174 Edobashi, Tsu, Mie 514-8507, Japan
Akira Mizoguchi, Kazushi Kimura, Kouhei Sakaguchi, the Department of Anatomy, Faculty of Medicine, Mie University, Edobashi, Tsu Mie 514-8507, Japan
Correspondence to: Masato Kusunoki, the Second Department of Surgery, Mie University School of Medicine, 2-174 Edobashi, Tsu, Mie 514-8507, Japan. kusunoki@clin.medic.mie-u.ac.jp.
Telephone: +81-59-231-5294 Fax: +81-59-232-6968
Received: 2005-01-24 Accepted: 2005-02-18

© 2005 The WJG Press and Elsevier Inc. All rights reserved.

Key words: Ulcerative colitis; Oligonucleotide array; Gene expression

Toiyama Y, Mizoguchi A, Kimura K, Araki T, Yoshiyama S, Sakaguchi K, Miki C, Kusunoki M. Persistence of gene expression changes in noninflamed and inflamed colonic mucosa in ulcerative colitis and their presence in colonic carcinoma. *World J Gastroenterol* 2005; 11(33): 5151-5155
http://www.wjgnet.com/1007-9327/11/5151.asp

Abstract

AIM: A few studies have applied genomic-wide gene expression analysis in inflamed colon tissue sample in ulcerative colitis (UC). We reported the first study of non-inflamed mucosal gene expression in UC and explored its clinical implication.

METHODS: Non-inflamed mucosa was obtained from 6 UC patients who received total colectomy. The gene expression of UC in noninflamed mucosa was monitored with a microarray. For a selected gene, RT-PCR was performed to verify array results and to further examine expression pattern in inflamed mucosa of UC, colorectal cancer tissue and normal mucosa using additional matched pairs.

RESULTS: Two genes showing 2.5-fold decreased expression with significance set at in UC samples were homeo box a4 (HOXa4) and mads box transcription enhancer factor 2, polypeptide B (MEF2b). RT-PCR showed that MEF2b expression in non-inflamed mucosa was significantly downregulated, whereas the expression of MEF2b increased in accordance with the severity of mucosal inflammation. HOXa4 expression both in inflamed and non-inflamed mucosa in UC was consistently downregulated, and the downregulation of HOXa4 was also found in colorectal carcinoma.

CONCLUSION: It is suggested that the MEF2b expression in UC which increase in accordance with inflammation may be induced by the inflammatory mediator. In contrast the downregulation of HOXa4 may be partly involved in the pathogenesis of disease including UC and UC-related carcinogenesis.

INTRODUCTION

Ulcerative colitis (UC) and Crohn's disease (CD), two common inflammatory bowel diseases (IBDs) with shared clinical and demographic characteristics, harbor key differences in tissue damage and prognosis that suggest distinctive etiopathogeneic processes. In UC, inflammation with crypt abscess formation is limited to mucosa, while in CD, transmural granulomatous inflammation leads to fibrostenotic lesions and fistula formation[1]. Furthermore, these diseases have complicated clinical manifestations in which genetic, environmental, and microbial factors interact to determine the susceptibility response of immune and nonimmune cellular systems mediating inflammation[2].

In many murine models of colitis recently generated by gene targeting, bacterial flora in the gut appears to be a prerequisite for the development of acute and chronic inflammation[3]. Of great interest, although normal intestinal epithelial cell are hypo-responsive to normal flora *in vivo*, pathogenic bacteria and bacterial components can initiate an inflammatory response in colitis[4]. These reports suggest that UC mucosa is already a different gene expression compared to normal mucosa without inflammatory change.

Genome-wide gene expression analysis of tissue samples from affected and normal individuals can illuminate important events involved in disease pathogenesis. Recently, several research articles on IBD using cDNA or oligonucleotide array-based technology have been published[5-8]. But previous studies of genomic alteration of IBD-related genes using microarray were directed to inflamed and non-inflamed UC mucosa.

In this study, we first applied this approach of comparing gene expression in non-inflamed UC mucosa to normal human colonic mucosa and searched for these specific

changes in gene expression pattern of inflamed UC mucosa and colorectal carcinoma.

MATERIALS AND METHODS

Tissue specimens for oligoneucleotide array

This study included 6 UC patients who received total proctocolectomy with ileal J pouch anal anastomosis because of severe distal colitis. The ages of the patients ranged from 20 to 58 years (average 36.1 years). Classic clinical, radiologic, endoscopic, and histopathological criteria were used to confirm all diagnoses[9]. For UC sample, specimens of macroscopically noninflamed proximal colonic mucosa such as cecum or ascending colon was obtained.

Histologically normal samples (six colonic mucosa) were obtained from 6 patients ranging from 40 to 68 years of age (average 53 years) undergoing bowel resection for adenocarcinoma (n = 4), diverticulitis (n = 1), mucosal prolapse syndrome (n = 1). Tissues used for control RNA extraction were obtained from at least 10 cm of the area of pathology and all were histologically normal. Use of patient material was in accordance with Institutional Review Board guidelines and protocol.

Total RNA isolation

All mucosa were dissected from underlying tissue and homogenized in Physcotron (NITI-ON, Japan) for the isolation of total RNA. Total RNA was extracted with Sepasol-RNA (Nacalai Tesque, Tokyo, Japan) and RNA quality was confirmed by agarose gel electrophoresis.

Preparation of fluorescent-labeled cDNA targets for microarray

cDNA targets for hybridizations were synthesized by RT from 20 μg/slide of UC- and normal colonic mucosa - total RNA samples with Superscript II RT (Invitrogen) according to the manufacturer's instructions. AA-dUTP labeled cDNA purified using QIAquick PCR purification Kit (28014: Qiagen). Each AA-dUTP labeled cDNA was coupled with either monoreactiveCy3 (PA23001 Amersham Bioscience) or Cy5 (PA25001 Amersham Bioscience) and incubated for 1 h at 40 ℃. Free dye was removed using P30 column (732-6223 BioRad). The separately synthesized Cy3- and Cy5-labeled targets was mixed with 15 μL of Human Cot-1 DNA (15279: Invitrogen), 1 μL of poly A (POLYA GF Invitrogen) and 0.5 μL of t RNA, Yeast (15401-011: Invitrogen) and the mixture was applied to Microcon-YM30 (43409 Millipore) and concentrated to 5-10 μL.

Hybridization

Diluted dye-labeled, 12.5 μL of 20×SSC, 2.5 μL of 10% SDS, 4 μL of 50× Denhardt's solution, 10 μL of hybridization solution (supplied with AceGene®: Hitachi Software Engineering Co., Ltd) and adequate sterile distilled water were added and concentrated to 44.5 μL. This solution was incubated for 2 min at 95 ℃, and cooled on ice, and 0.5 μL of salmon sperm DNA and 5 μL of formamide was added to the solution, and incubated for 5 min at 42 ℃. The target cDNA solution was applied directly to the AceGene® Human Oligo Chip (Hitachi Software Engineering Co., Ltd), and coverglass (24 mm×60 mm) was set. Hybridization was performed for 16 h at 42 ℃. After hybridization, the slides were washed and rinsed. Finally they were dried with air-spray.

Data analysis

Fluorescent signals were detected on a confocal laser scanner (HB GeneArray Scanner, Affymetrix) and analyzed with the DenasisArray (Hitachi Software Engineering) and Excel (Microsoft Redmond, CA). To eliminate data with low reliability, genes with each hybridization intensity = 0 and each average intensity {(Cy3-Cy3 background)+(Cy5-Cy5 background)<2000} were excluded from all data sets. In addition, genes with average intensity ratio that showed a >2- or 0.5-fold change were selected. In the remaining genes, 2-fold average intensity ratio genes with each intensity ratio <1 on array tests and 0.5-fold average intensity ratio genes with each intensity ratio >1 were excluded. Finally, selected genes were further analyzed for statistical comparison. Mann-Whitney U-test was used, with significance set at P<0.05.

RT-PCR

Total RNA was extracted from an additional 6 UC patients' paired non-inflamed mucosa and inflamed mucosa as well as 9 patients' paired colon cancer and histological normal colonic mucosa with Sepasol-RNAI. For cDNA synthesis, 2 μg of total RNA was reverse transcribed with Superscript II. RT-PCR was done using specific primers for the array-selected gene. Primers are described in Table 1. Optimum cycling parameters, in the linear range of amplification, consisted of 30 s of denaturation at 94 ℃, 30 s of annealing at 58 ℃, and 2 min of elongation at 72 ℃, and 28 cycles were performed for the selected gene. A control PCR was also done for G3PDH which served as a standard for sample normalization for 25 cycles. Amplified products were separated electrophoretically, visualized, and photographed under UV light after ethidium bromide staining. Gel density was calculated with Sicon image (downloaded sicon's web site: www.siconcorp.com) and gene expressions were quantified. For statistical comparison Mann-Whitney U-test was used, with significance set at P<0.05 to compare differences in the level of gene expression.

RESULTS

To investigate gene expression profiles of the colon in UC

Table 1 Primer sets for reverse transcription-PCR

Gene	5'-Forward	3'-Reverse
Homeo box a4	ATGACCATGAGCTCGTTTTTGAT	TATGGAGGAGGGAACGGGTG
Mads box transcription factor 2b	ATGGGGAGGAAAAAAATCCAGA	CTGTTGGGTCTTCTCTGAAGA
G3PDH	ACCACAGTCCATGCCATCAC	TCCACCACCCTGTTGCTGTA

Table 2 Gene transcripts displaying a two fold or higher increase or decrease in expression level that was significant at the $P<0.05$ level

Accession number	Gene name	AI in controls	AI in UC	Control / UC	*P*
NM_002141	Homeo box a4 (Hoxa4)	356 193.4	144 705.0	2.46	0.005
NM_005919	Mads box transcription enhancer factor 2, polypeptide b (MEF2b)	283 291.9	113 174.8	2.50	0.009
XM_001566	Calcium activated chloride channel 3 precursor (CLCA3)	5 308.8	1 188.9	4.46	0.01
NM_032946	Nuclear rna export factor 5 (NXF5)	4 416.7	1 681.3	2.63	0.014
NM_022061	Ribosomal protein l17 isolog (RPL7)	299 317.9	143 755.9	2.08	0.027
NM_016638	Srp25 nuclear protein (SRP25)	2 872.1	6 576.4	0.43	0.043

AI: average intensity.

patients, we used AceGene® Human Oligo Chip arrays containing probes for approximately 20 000 human genes. Low reliability data was eliminated by performing data trimming as described in Materials and methods section. After data trimming, the remaining genes were analyzed for statistical comparison between the average intensity of non-inflamed UC group and normal control.

Table 2 lists the gene transcripts displaying a two fold or higher increase or decrease in expression level that was significant at the $P<0.05$ level. Five gene transcripts displayed a 2.1-4.4-fold lower expression in the non-inflamed UC samples compared with the normal colon samples, whereas only one transcript displayed a 2.3-fold higher expression in the non-inflamed UC samples (Figure 1). Among the six genes, the difference in the expression of the two genes *homeo box a4* (NM_002141) and *mads box transcription enhancer factor 2* (NM_005919) were statistically significant ($P<0.01$).

To verify array results, expression of two genes at the $P<0.01$ as differentially expressed by oligonucleotide array analysis was examined by RT-PCR using six additional pairs (noninflamed UC mucosa and normal control).

As a result, the expression of HOXa4 and MEF2b in non-inflamed UC mucosa was significantly reduced compared to that in the normal mucosa ($P = 0.0490$ and $P = 0.0253$, respectively), which gave results consistent with those by oligonucleotide array analysis (Figures 2 and 3).

Gene expression patterns of both these genes obtained from inflamed UC mucosa were examined comparing them with the non-inflamed UC mucosa and normal mucosa using RT-PCR. MEF2b expression in inflamed UC mucosa was significantly upregulated compared to that in non-inflamed UC mucosa ($P = 0.0209$; Figure 3). But there is no difference in MEF2b expression between normal control and inflamed UC mucosa (Figure 3). In contrast, no difference in the expression pattern of HOXa4 was found between those with and without colonic inflammation ($P = 0.2603$; Figure 2). Furthermore, the expression of HOXa4 in inflamed mucosa was significantly downregulated compared to that in normal mucosa ($P = 0.0172$; Figure 2). RT-PCR on eight samples of matched colon cancer and normal mucosa showed that the expression of HOXa4 in colon cancer tissue was significantly downregulated in 8 of 8 (100%). But the expression of MEF2b had no difference between colorectal carcinoma and normal mucosa (Figure 4).

DISCUSSION

Our present study is the first trial which draws a comparison between genomic alternation in non-inflamed UC mucosa and normal human colonic mucosa. This approach has allowed us to examine whether non-inflamed UC mucosa shows a different gene expression compared to normal control mucosa. We showed the intensities of the two genes HOXa4 and MEF2b to be reduced in the non-inflamed mucosa in patients with UC using the cDNA microarray. In addition, we compared the levels of the expression of

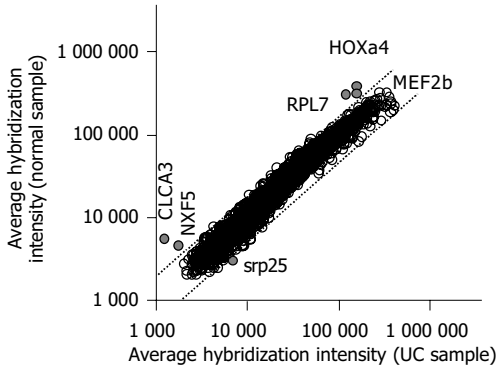


Figure 1 Comparison of expression of genes in non-inflamed mucosa of ulcerative colitis (UC) and normal control mucosa. The upper and lower boundaries represent a 2- and 0.5-fold difference in the mean of the expression of each gene between noninflamed UC mucosa and control, respectively. Axis scales are logarithmic.

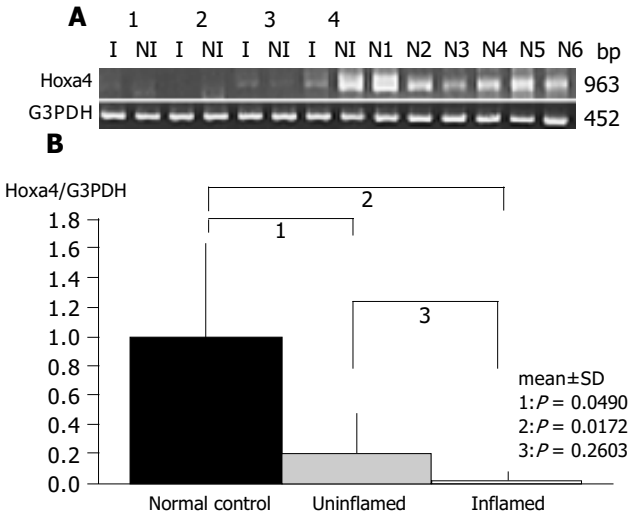


Figure 2 RT-PCR analysis of HOXa4 gene expression in normal colonic mucosa and UC mucosa (inflamed, non-inflamed). **A**: Showed RT-PCR was performed on four paired inflamed mucosa (I) and non-inflamed mucosa (NI) samples in UC as well as six normal control mucosa (N1-N6) G3PDH was used as a control for cDNA synthesis; **B**: Semiquantification of HOXa4 gene expression (HOXa4/G3PDH) was performed in six paired UC mucosa and six normal control mucosa using NIH image software.

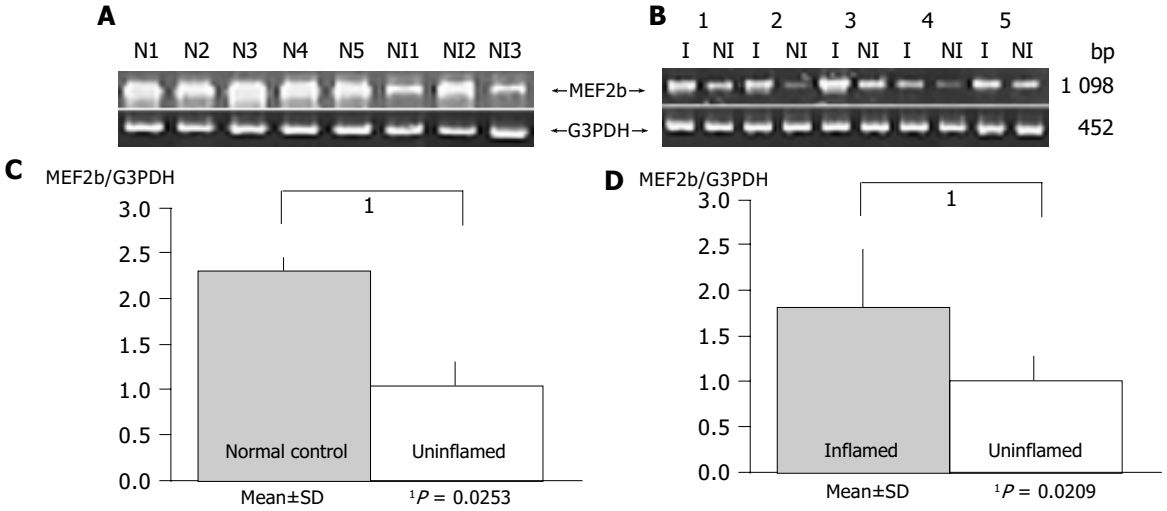


Figure 3 RT-PCR analysis of MEF2b gene expression in normal colonic mucosa and UC mucosa (inflamed, non-inflamed). **A**: Analysis was performed on five normal control mucosa (N1-N5) and three non-inflamed UC mucosa (NI) was performed on four paired inflamed mucosa (I) and non-inflamed mucosa (NI); **B**: Analysis was performed on four paired inflamed mucosa (I) and non-inflamed mucosa (NI). G3PDH was used as a control for cDNA synthesis; **C** and **D**: Semiquantification of MEF2b gene expression (MEF2b/G3PDH) was performed in six paired UC mucosa and six normal control mucosa using NIH image software.

mRNA of these two genes among control, non-inflamed and inflamed mucosa in UC, and colonic cancer tissues by RT-PCR.

HOXa4 includes the homeo box (HOX) family genes that are functionally homologous to the drosophila HOM-C gene. There are 39 HOX genes in the human genome that are arranged in four clusters on four different chromosomes. They are expressed at the beginning of gastrulation and define the body's axis formation. In adults, HOX B8 is involved in leukomorphogenesis[10]. Other HOX genes play a role in malignant transformation, through the regulation of cell-cycle checkpoints (e.g. P53) or protooncogenes (e.g. ras[11]). In cancer cells, HOX is either over-expressed (e.g. HOX C4 and HOX C6, in non-Hodgkin's lymphoma[10]) or downregulated (e.g. HOX B6, C8, C9 in adenocarcinoma and colon cells[12]). In our experiments, HOXa4 gene expression was downregulated in UC mucosa compared to normal mucosa whether colonic inflammation exists or not and this gene expression in colon cancer tissue was also significantly lower than normal mucosa with additional RT-PCR.

Earlier studies showed that HOX A4 is regulated both by retinoic acid and the ras oncogene[13]. Retinoic acid increased HOX A4 expression and guided the cells toward differentiation, while the ras oncogene decreased HOX A4 expression and guided the cells toward proliferation. Burmer previously reported that UC-associated neoplasia has a low incidence of *K-ras* mutations[14], but Ierardi *et al*., showed that the persistently increased epithelial proliferation associated with ras p21 expression in UC may be due to the action of an abnormal, mutated ras gene that could play a role in UC-related tumorigenesis[15]. Steingart *et al*.[16], previously reported that SNH (a lipophilic analog of vasoactive intestinal peptide (VIP)) increased the expression of HOX A4 and reduced Oct-3 mRNA level and demonstrated inhibition of HT 29 colon cancer cell line

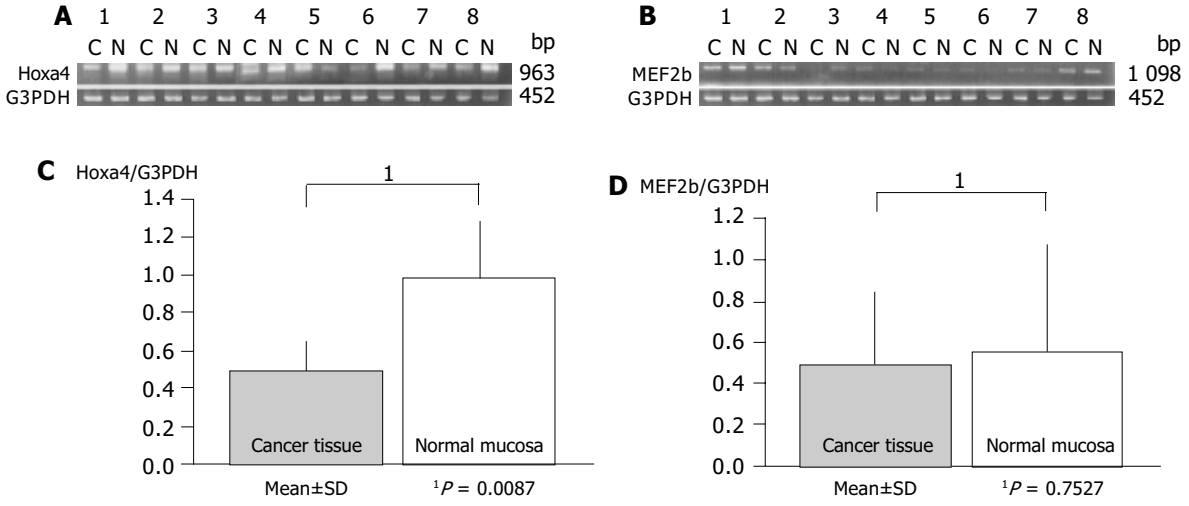


Figure 4 (**A** and **B**) RT-PCR analysis of *HOXa4* and *MEF2b* gene expression in eight paired colon cancer (**C**) and normal colonic mucosa (N). G3PDH was used as a control for cDNA synthesis. (**C** and **D**) Semiquantification of *HOXa4* and *MEF2b* gene expression (HOXa4, MEF2b/G3PDH) was performed in eight paired colon cancer and normal colonic mucosa using NIH image software.

proliferation by SNH.

This may suggest that decreased HOXa4 gene expression partly explains the pathogenesis of UC and UC-related carcinogenesis without ras protein participation and SNH might serve as a lead compound to prevent colitic cancer for UC patients who have received long-term medical therapy.

MEF2 (myocyte enhancer factor-2) was first described as a muscle-enriched transcription factor that bound to an A/T-rich DNA sequence in the control regions of numerous muscle-specific genes[17]. There are four human MEF2 genes, MEF2A, MEF2B, MEF2C and MEF2D, which are expressed in distinct, but overlapping patterns during embryogenesis and in adult tissues[18]. Recent studies have revealed a central role for MEF2 family of transcription factors in linking calcium-dependent signaling pathways to the genes responsible for cell division, differentiation and apoptosis[19]. In regulation of cell proliferation, it was made with the discovery that MEF2 regulates serum-inducible expression of c-jun, which positively regulates cell-cycle progression[20]. MEF2 has since been shown to play a role in the induction of the c-jun promoter in response to signals emanating from multiple cell surface receptors, including G-protein-coupled receptors[21], the epidermal growth factor receptor[22], the lipopolysaccharide receptor[23], and the CD28 co-stimulatory receptor in T lymphocytes[24]. It is therefore, conceivable that constant decreased expression of MEF2 might regulate epithelial cell proliferation and cell-cycle progression and result in difficulty of epithelial cell regeneration in noninflamed UC mucosa.

Interestingly, the present study demonstrated that MEF2 was overexpressed in inflamed UC mucosa compared to non-inflamed UC mucosa using RT-PCR. MEF2 stimulates the expression of the gene encoding the orphan nuclear hormone receptor Nur77[25], which is a potent activator of cytochrome *c*-mediated apoptosis. The present results suggest that ulceration of mucosa might be related to epithelial cell apoptosis induced by MEF2 overexpression in inflamed UC mucosa.

In conclusion, the present study indicates that UC mucosa already has a different gene expression compared to normal mucosa without inflammatory change. Downregulated HOXa4 expression pattern in UC mucosa consistently as well as in colorectal carcinoma may play an important role for carcinogenesis in UC mucosa. Since MEF2 expression pattern correlated to inflammation, it is a key molecule for colonic epithelial cell apoptosis in inflamed mucosa and cell remodeling difficulty in non-inflamed UC mucosa. In a subsequent research, we hope to study further to identify the function of selected UC-related gene.

REFERENCES

1 **Kinsner J,** Shorter R. Infalmmatory Bowel disease, 5th edn. *Lea&Febiger, Philadelphia, PA* 1999

2 **Fiocchi C.** Inflammatory bowel disease: etiology and pathogenesis. *Gastroenterology* 1998; **115**: 182-205

3 **Hibi T,** Ogata H, Sakuraba A. Animal models of inflammatory bowel disease. *J Gastroenterol* 2002; **37**: 409-417

4 **Savkovic SD,** Koutosouris A, Hecht G. Activation of NF-κB in the intestinal epithelial cells by enteropathogenic Escherichia Coli. *Am J Physiol Cell Physiol* 1997; **273**: 1160-1167

5 **Dieckgraefe BK,** Stenson WF, Korzenik JR, Swanson PE, Harrington CA. Analysis of mucosal gene expression in inflammatory bowel disease by parallel oligonucleotide arrays. *Physiol Genomics* 2000; **4**: 1-11

6 **Lawrance IC,** Fiocchi C, Chakravarti S. Ulcerative colitis and Crohn's disease: distinctive gene expression profiles and novel susceptibility candidate genes. *Hum Mol Genet* 2001; **10**: 445-456

7 **Uthoff SM,** Eichenberger MR, Lewis RK, Fox MP, Hamilton CJ, McAuliffe TL, Grimes HL, Galandiuk S. Identification of candidate genes in ulcerative colitis and Crohn's disease using cDNA array technology. *Int J Oncol* 2001; **19**: 803-810

8 **Masuda H,** Takahashi Y, Asai S, Takayama T. Distinct gene expression of osteopontin in patients with ulcerative colitis. *J Surg Res* 2003; **111**: 85-90

9 **Truelove SC,** Witts LJ. Cortisone in ulcerative colitis; final report on a therapeutic trial. *Br Med J* 1955; **4947**: 1041-1048

10 **Cillo C,** Faiella A, Cantile M, Boncinelli E. Homeobox genes and cancer. *Exp Cell Res* 1999; **248**: 1-9

11 **Cillo C,** Cantile M, Faiella A, Boncinelli E. Homeobox genes in normal and malignant cells. *J Cell Physiol* 2001; **188**: 161–169

12 **Vider BZ,** Zimber A, Chastre E, Gespach C, Halperin M, Mashiah P, Yaniv A, Gazit A. Deregulated expression of homeobox-containing genes, HOXB6, B8, C8, C9, and Cdx-1, in human colon cancer cell lines. *Biochem Biophys Res Commun* 2000; **272**: 513–518

13 **Doerksen LF,** Bhattacharya A, Kannan P, Pratt D, Tainsky MA. Functional interaction between RARE and an AP-2 binding site in the regulation of the human HOX A4 gene promotor. *Nucleic Acids Res* 1996; **24**: 2849–2857

14 **Burmer GC,** Levine DS, Kulander BG, Haggitt RC, Rubin CE, Rabinovitch PS. c-Ki-ras mutations in chronic ulcerative colitis and sporadic colon carcinoma. *Gastroenterology* 1990; **99**: 416-420

15 **Ierardi E,** Principi M, Francavilla R, Passaro S, Noviello F, Burattini O, Francavilla A. Epithelial proliferation and ras p21 oncoprotein expression in rectal mucosa of patients with ulcerative colitis. *Dig Dis Sci* 2001; **46**: 1083-1087

16 **Steingart RA,** Heldenberg E, Pinhasov A, Brenneman DE, Fridkin M, Gozes I. A vasoactive intestinal peptide receptor analog alters the expression of homeobox genes. *Life Sci* 2002; **71**: 2543–2552

17 **Black BL,** Olson EN. Transcriptional control of muscle development by myocyte enhancer factor-2 (MEF2) proteins. *Annu Rev Cell Dev Biol* 1998; **14**: 167–196

18 **Breitbart RE,** Liang CS, Smoot LB, Laheru DA, Mahdavi V, Nadal-Ginard B. A fourth human MEF2 transcription factor, hMEF2D, is an early marker of the myogenic lineage. *Development* 1993; **118**: 1095-1106

19 **Blaeser F,** Ho N, Prywes R, Chatila TA. Ca(2+)-dependent gene expression mediated by MEF2 transcription factors. *J Biol Chem* 2000; **275**: 197-209

20 **Han TH,** Prywes R. Regulatory role of MEF2D in serum induction of the c-jun promoter. *Mol Cell Biol* 1995; **15**: 2907-2915

21 **Coso OA,** Montaner S, Fromm C, Lacal JC, Prywes R, Teramoto H, Gutkind JS. Signaling from G protein-coupled receptors to the c-jun promoter involves the MEF2 transcription factor. Evidence for a novel c-jun amino-terminal kinase-independent pathway. *J Biol Chem* 1997; **272**: 20691-20697

22 **Clarke N,** Arenzana N, Hai T, Minden A, Prywes R. Epidermal growth factor induction of the c-jun promoter by a Rac pathway. *Mol Cell Biol* 1998; **18**: 1065-1073

23 **Han J,** Jiang Y, Li Z, Kravchenko VV, Ulevitch RJ. Activation of the transcription factor MEF2C by the MAP kinase p38 in inflammation. *Nature* 1997; **386**: 296-299

24 **Shin HM,** Han TH. CD28-mediated regulation of the c-jun promoter involves the MEF2 transcription factor in Jurkat T cells. *Mol Immunol* 1999; **36**: 197-203

25 **Woronicz JD,** Lina A, Calnan BJ, Szychowski S, Cheng L, Winoto A. Regulation of the Nur77 orphan steroid receptor in activation-induced apoptosis. *Mol Cell Biol* 1995; **15**: 6364-6376

Science Editor Guo SY **Language Editor** Elsevier HK

PO Box 2345, Beijing 100023, China
www.wjgnet.com
wjg@wjgnet.com

ELSEVIER

World J Gastroenterol 2005;11(33):5156-5161
World Journal of Gastroenterology ISSN 1007-9327
© 2005 The WJG Press and Elsevier Inc. All rights reserved.

• *COLORECTAL CANCER* •

Amygdalin inhibits genes related to cell cycle in SNU-C4 human colon cancer cells

Hae-Jeong Park, Seo-Hyun Yoon, Long-Shan Han, Long-Tai Zheng, Kyung-Hee Jung, Yoon-Kyung Uhm, Je-Hyun Lee, Ji-Seon Jeong, Woo-Sang Joo, Sung-Vin Yim, Joo-Ho Chung, Seon-Pyo Hong

Hae-Jeong Park, Seo-Hyun Yoon, Long-Shan Han, Long-Tai Zheng, Kyung-Hee Jung, Yoon-Kyung Uhm, Sung-Vin Yim, Joo-Ho Chung, Department of Pharmacology, Kohwang Medical Research Institute, College of Medicine, Kyung Hee University, Seoul 130-701, South Korea
Je-Hyun Lee, Ji-Seon Jeong, Woo-Sang Joo, Seon-Pyo Hong, Department of Oriental Pharmaceutical Sciences, College of Pharmacy, Kyung Hee University, Seoul 130-701, South Korea
Supported by a grant of the Oriental Medicine R&D Project, Ministry of Health and Welfare, Republic of Korea, No. 03-PJ9-PG3-21600-0014 and No. 0405-OM00-0815-0001 and Korea Institute of Oriental Medicine
Correspondence to: Seon-Pyo Hong, Department of Oriental Pharmaceutical Sciences, College of Pharmacy, Kyung Hee University, Seoul 130-701, South Korea. seonhong@khu.ac.kr
Telephone: +822-961-9207 Fax: +822-966-3885
Received: 2005-03-28 Accepted: 2005-04-09

Abstract

AIM: The genes were divided into seven categories according to biological function; apoptosis-related, immune response-related, signal transduction-related, cell cycle-related, cell growth-related, stress response-related and transcription-related genes.

METHODS: We compared the gene expression profiles of SNU-C4 cells between amygdalin-treated (5 mg/mL, 24 h) and non-treated groups using cDNA microarray analysis. We selected genes downregulated in cDNA microarray and investigated mRNA levels of the genes by RT-PCR.

RESULTS: Microarray showed that amygdalin downregulated especially genes belonging to cell cycle category: exonuclease 1 (*EXO1*), ATP-binding cassette, sub-family F, member 2 (*ABCF2*), MRE11 meiotic recombination 11 homolog A (*MRE11A*), topoisomerase (DNA) I (*TOP1*), and FK506 binding protein 12-rapamycin-associated protein 1 (*FRAP1*). RT-PCR analysis revealed that mRNA levels of these genes were also decreased by amygdalin treatment in SNU-C4 human colon cancer cells.

CONCLUSION: These results suggest that amygdalin have an anticancer effect via downregulation of cell cycle-related genes in SNU-C4 human colon cancer cells, and might be used for therapeutic anticancer drug.

© 2005 The WJG Press and Elsevier Inc. All rights reserved.

Key words: Amygdalin; SNU-C4; cDNA microarray; Cell cycle

Park HJ, Yoon SH, Han LS, Zheng LT, Jung KH, Uhm YK, Lee JH, Jeong JS, Joo WS, Yim SV, Chung JH, Hong SP. Amygdalin inhibits genes related to cell cycle in SNU-C4 human colon cancer cells. *World J Gastroenterol* 2005; 11 (33): 5156-5161
http://www.wjgnet.com/1007-9327/11/5156.asp

INTRODUCTION

The incidence of colorectal cancer has been increasing rapidly since 1975[1] with about 300 000 new cases and 200 000 deaths in Europe and USA every year[2,3]. Death from colorectal cancer is the second commonest cause of any cancer in men in the European Union[4]. The stage of the disease is an important effect to long-term survival of colorectal cancer. If detected early, it may be curable by surgery. But once metastases develop the prognosis becomes poor. At least 40% of patients with colorectal cancer develop metastases during their illness[5]. Although various therapies as surgery, radiotherapy, and chemotherapy are used on advanced cancer, the most effective approach is yet to be discovered.

Amygdalin is ingredient of *Prunus persica* Batsch (Persicae semen, Rosaceae), *Prunus armeniaca* L. var. *ansu* Max (Armenicae semen, Rosaceae) and *Prunus amygdalus* Batsch var. *amara* (Amygdali semen amara, Rosaceae), and these are abundant in the seeds of bitter almond and apricots[6]. The evidence for effect of amygdalin has been reviewed as prevention and control of cancers. Due to cyanide toxicity, there has been controversy for amygdalin as cancer drug[7-9]. However, Moertel *et al*., demonstrated that, in human, intravenous infusion of amygdalin produced neither cyanidemia nor signs of toxicity but that oral administration resulted in significant blood cyanide levels and that, in one case, oral amygdalin plus almond extract produced transient symptoms of cyanide intoxication and further increase of blood cyanide[9]. Additionally, Fukuda *et al*.[10], reported anti-tumor effect of amygdalin and other components of *Prunus persica* seeds. Kwon *et al*.[13], reported that controversy on anticancer effect of amygdalin was due to its conversion to inactivate isoform, and Persicae semen extract induced apoptosis. Although taking a growing interest and reports for amygdalin as cancer drug, anti-cancer mechanism of amygdalin has not been reported.

In this study, we determined whether amygdalin-treated SNU-C4 cells were susceptible to cell death, and compared the expression profiles of SNU-C4 cells between amygdalin-treated group and non-treated group using cDNA

microarray analysis. We also performed RT-PCR for genes selected by cDNA microarray analysis.

MATERIALS AND METHODS

Preparation of amygdalin

Both 500 g of Armeniacae semen hatched from the shell and 10 L of 4% citric acid solution were refluxed for 2 h. Filtered when it was still hot, the filtrate was passed through the column packed with HP-20. The substance absorbed within the column was concentrated after it had been eluted by ethanol. 4.2 g of amygdalin (with the yield rate of 0.84%) was obtained by recrystallizing the extract with ethanol. The amygdalin was used after it had been determined to be over 95.0% of purity, by means of high-pressure liquid chromatography (HPLC) to measure its purity (Figure 1).

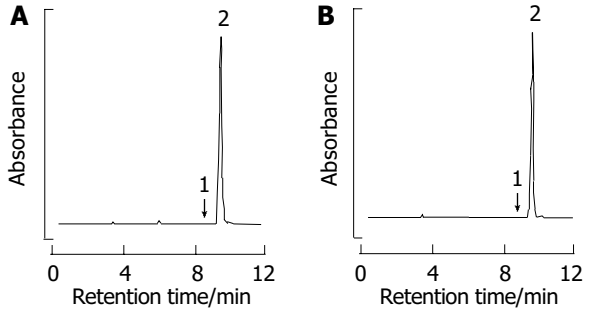


Figure 1 Reverse-phase HPLC separation of amygdalin by phosphate buffer. (**A**) D-amygdalin standard. (**B**) D-amygdalin obtained by our method; peaks: 1, neoamygdalin; 2, D-amygdalin.

Cell culture

The SNU-C4 cell line was obtained from the Korean Cell Line Bank (KCLB, Seoul, South Korea). Cells were cultured in RPMI-1640 medium (Gibco, NY, USA) supplemented with 10% heat-inactivated FBS (Gibco). Cultures were maintained in a humidified incubator at 37 ℃ in an atmosphere of 50 mL/L CO_2, 95% air, and the medium was changed every 2 d.

MTT assay

Cell viability was determined by 3-(4,5-dimethylthiazol-2-yl) -2,5-diphenyltetrazolium bromide (MTT) assay. Cells were seeded in triplicate at a concentration of 1×10^5 cells/well on a 96-well plate. SNU-C4 cells were treated with amygdalin at concentrations of 0.25, 0.5, 2.5, and 5 mg/mL for 24 h. After MTT (Sigma, MO, USA) was added to each group, the cells were incubated for 4 h. Then, they were further incubated for 1 h, including the solution in which MTT was dissolved. The viability was measured with a microtiter plate reader (Bio-Tek, VT, USA) at a test wavelength of 595 nm with a reference wavelength of 690 nm. The optical density (A) was calculated as the difference between the reference wavelength and the test wavelength. Percent viability was calculated as (A of drug-treated sample/A of untreated sample)×100.

cDNA synthesis

Total RNA was extracted using RNAzol™ B (TEL-TEST, TX, USA) as per the manufacturer's protocol. cDNA synthesis was performed with 3DNA™ Array 50™ detection method (Genisphere, PA, USA) as per the manufacturer's protocols. In the control and amygdalin treatment (5 mg/mL, 24 h), cDNA was synthesized from total RNA as follows: 3 μL of RT primer, total RNA and additional nuclease-free water were mixed to form a 29 μL RNA-RT primer mix, which was microfuged briefly, heated to 80 ℃ for 10 min, and immediately transferred to ice. One microliter of the RNase inhibitor Superase-In™ was added to the RNA-RT primer mix. Eight microliters of 5× SuperScript II First Strand Buffer (Gibco), 2 μL of dNTP mix (10 mmol/L each of dATP, dCTP, dGTP, dTTP), 4 μL of 0.1 mol/L dithiothreitol, 2 μL of Superscript II enzyme (400 units), and 3 μL of RNase-free water were mixed in each microtube, and the RNA-RT primer mix was then added. The tubes were then incubated at 42 ℃ for 2 h, and the reaction was heated by adding 7 μL of 0.5 mol/L NaOH/50 mmol/L EDTA. The microtubes were then incubated for denaturation at 65 ℃ for 10 min, and neutralization was carried out by adding 10 μL of 1 mol/L Tris-HCl at pH 7.5. The contents of two tubes were combined to yield a 130 μL cDNA solution in one single tube. The original tubes were rinsed with 16 μL of 10 mmol/L Tris at pH 8.0/1 mmol/L EDTA.

Upon completion of the synthesis procedure, the cDNA solution was concentrated by ethanol precipitation. Three microliters of thoroughly vortexed 5 mg/mL linear acrylamide solution was added to the cDNA solution. Six microliters of NaCl and 540 μL of 95-100% ethanol was then added and moderately vortexed. The mixture was then incubated at -20 ℃ for 30 min, centrifuged at >10 000 *g* for 15 min, and the supernatant was aspirated. The cDNA pellet was washed with 300 μL of 70% ethanol. After centrifuging again at >10 000 *g* for 5 min, the supernatant was aspirated, and the cDNA pellet was completely dried at 65 ℃ over a period of 10-30 min.

Microarray hybridization

A cDNA chip of TwinChip™ Human 8K (Digital Genomics, Seoul, South Korea) was used. The concentrated cDNA and 3DNA™ were hybridized on two identical arrays in a slide for a duplicate experiment. Two times formamide-based hybridization buffer was thawed and responded by heating at 55 ℃ for 10 min with intermittent inversions, and then microfuged for 1 min. Ten microliters of nuclease-free water was added to the cDNA pellet, and the cDNA was completely resuspended by heating at 55 ℃ for 10 min with intermittent inversions, and then microfuged for 1 min. Ten microliters of nuclease-free water was added to the cDNA pellet, and the cDNA was completely resuspended by heating at 65 ℃ for 10-15 min and vortexing for 5 min. Thirty microliters of hybridization mixture was prepared from 10 μL of cDNA, 15 μL of 2× hybridization buffer, 2 μL of Array50 dT Blocker, and 3 μL of nuclease-free water. The hybridization mixture was incubated at 80 ℃ for 10 min and then at 50 ℃ for 30-60 min. The hybridization mix was then added to the pre-warmed chip. After a disposable coverslip was applied, the chip was incubated

overnight in a dark humidified chamber at 50 ℃. After serial washing, the array was incubated for 2 min at room temperature with 95% ethanol. The slide was immediately transferred to a dry 50-mL centrifuge tube and dried by centrifugation for 2 min at 800-1 000 r/min. Array50 capture reagent was then thawed in the dark at room temperature over a period of 20 min and vortexed for 3 s. Thirty microliters of hybridization mixture was prepared from 15 μL of 2× hybridization buffer, 2.5 μL of 3DNA TM capture reagent #1 (Cy3), 2.5 μL of 3DNA TM capture reagent #2 (Cy5), and 10 μL of nuclease-free water. Following gentle vortexing and brief microfuging, the hybridization mixture was incubated at 80 ℃ for 10 min and then at 50 ℃ for 20 min. The hybridization mixture was applied to the pre-warmed chip after it was removed from the incubator. After a disposable coverslip was applied, the microarray was incubated in a dark humidified chamber at 50 ℃ for 2-3 h. After serial washing, the slide was immediately transferred to a dry 50-mL centrifuge tube and dried by centrifugation for 2 min at 800-1 000 r/min, and then transferred to a dark slide box.

Scanning and data analysis

The hybridized microarray was scanned with a confocal laser scanning microscope (ScanArray 5000; Packard Inc., CT, USA) at 532 nm for Cy3 and 635 nm for Cy5. Image analysis using GenePix (Axon Inc., CA, USA) produced quantitative values for each microarray spot. Pixel intensity of the background was subtracted from those of microarray spots. Spot intensities were normalized using the intensities generated by intensity/location dependent method[11]. Normalized spot intensities were calculated into gene expression ratios between the control and treatment groups. Mean data acquired from two identical arrays in a single slide of TwinChip™ were analyzed.

RT-PCR

Two micrograms of sample of RNA isolated from SNU-C4 cells using RNAzol™ B (TEL-TEST) and 2 μL of random hexamers (Promega, WI, USA) were added together, and the mixture was heated at 65 ℃ for 10 min. AMV reverse transcriptase (Promega) of 1 μL, 5 μL of 10 mmol/L dNTP (Promega), 1 μL of RNasin (Promega) and 5 μL of 10× AMV RT buffer (Promega) were then added to the mixture, and the final volume was brought up to 50 μL with diethyl pyrocarbonate-treated water. Subsequent PCR amplification was performed in a reaction volume of 40 μL containing 1 μL of the appropriate cDNA, 1 μL of each set of primers at a concentration of 10 pmol/L, 4 μL of 10× reaction buffer, 1 μL of 2.5 mmol/L dNTP and 2 U of *Taq* DNA polymerase (TaKaRa Bio Inc., Shiga, Japan). We selected five genes, exonuclease 1 (*EXO1*), ATP-binding cassette (ABC), sub-family F, member 2 (*ABCF2*), MRE11 meiotic recombination 11 homolog A (*MRE11A*), topoisomerase (DNA) I (*TOP1*), and FK506 binding protein 12-rapamycin associated protein 1 (*FRAP1*) downregulated in microarray analysis by treatment of amygdalin and performed PCR. Primer sequences, annealing temperatures and products size of genes are summarized in Table 1. The RT-PCR products were electrophoresed on a 1.5% agarose gel and visualized by staining with ethidium bromide.

Statistical analysis

Results were expressed as mean±SE. The data were analyzed by one-way ANOVA following the Dunnett's post hoc analysis, using SPSS. Differences were considered significant at $P<0.05$.

RESULTS

Cytotoxicity of amygdalin in SNU-C4 cells

When treated with amygdalin of 0.25, 0.5, 2.5, and 5 mg/mL concentrations for 24 h, viabilities of SNU-C4 cells were 96.1±7.4%, 87.8±2.4%, 82.9±5.5%, and 63.7±8.3%, respectively, compared with those of non-treated cells (Figure 2), and MTT assay showed dose-dependent cytotoxicity of amygdalin on SNU-C4 cells. Therefore, to compare the precise effect of amygdalin, further experiments were carried out, using 5 mg/mL amygdalin.

Table 1 Sequences of the primers used in RT-PCR analysis

Primer name	Primer sequence (sense / anti-sense)	Fragment length (bp)	Annealing temperature (℃)
EXO1	5'-CTCTTTTGAGAGCAGCAAAT-3'	400	58
	5'-GGTCTGGTCACTTTGACTGTC-3'		
ABCF2	5'-TGCACAACAAGAAACTGAAG-3'	523	58
	5'-TGCTCTTGTAAATGCTGATGGT-3'		
MRE11A	5'-GAAGGTACGTCGTTTCAGAGAA-3'	456	58
	5'-CGATCTTGACTCTGGGACATGATT-3'		
TOP1	5'-CTGTGAAGAGGAACAGTGTGGT-3'	561	58
	5'-GAACAGGTGTCTGAACCAAAAC-3'		
FRAP1	5'-GCTCGTAGTTGGGATAACAG-3'	426	58
	5'-GTTGCCAGGACATTATTGAT-3'		
EGFR	5'-ATGAAGAAGACATGGACGAC-3'	522	56
	5'-AGAAGTCCTGCTGGTAGTCA-3'		
CYCLOPHILIN	5'-ACCCCACCGTGTTCTTCGAC-3'	300	56
	5'-CATTTGCCATGGACAAGATG-3'		

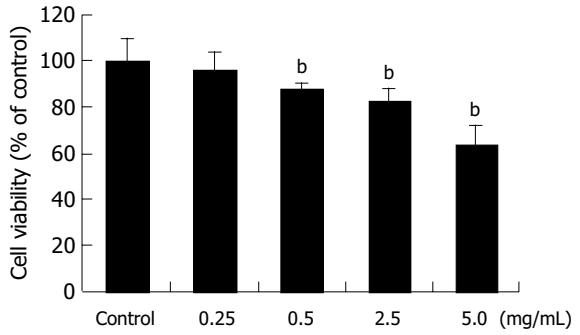


Figure 2 Cytotoxicity of amygdalin. SNU-C4 human colon cancer cells were treated with various concentrations (0.25, 0.5, 2.5, and 5 mg/mL) of amygdalin for 24 h prior to the determination of cellular viability through 3-(4,5-dimethylthiazol-2-yl)-2,5-diphenyltetrazolium bromide (MTT) assay. Independent experiment was repeated thrice. Results are presented as mean±SE (^bP<0.01 *vs* control group).

Analysis of microarray expression data

In order to assess the expression profiles in SNU-C4 cells treated with amygdalin (5 mg/mL, 24 h), cDNA microarray that contained duplicate cDNA probes from 8k human clones was performed to be screened at a time. Figure 3 showed the image of 8k human cDNA microarray. The green spots represented genes of control group that was labeled by Cy3-captured reagent and overexpressed than amygdalin group. In contrast, the red spots represented genes of amygdalin group that was labeled by Cy5-captured reagent and were overexpressed than control. The yellow spots represented genes that showed no difference in expression level between control and amygdalin group.



Figure 3 Expression pattern in a 8k human cDNA microarray.

To normalize intensity ratio of each gene expression pattern, global M method was used in this study. First, the primary data were normalized by the total spots of intensity between two groups, and then normalized by the intensity ratio of reference genes, such as housekeeping genes in both groups. Finally, the expression ratio of control and amygdalin group was converted to $\log_2$ ratio of each gene, and was represented by a scattered plot in Figure 4.

After normalizing the data, a difference in the normalized intensity ratio was selected. The genes of expression ratio were observed to be lower than -1 for which the observed expression was downregulated by amygdalin (Table 2). The genes downregulated by amygdalin were divided into seven categories by biological function; apoptosis-related gene, response to immune-related gene, signal transduction-related gene, cell cycle-related gene, cell growth-related gene, response to stress-related gene and transcription-related gene. We paid attention to genes belonging to cell cycle category. *EXO1*, *ABCF2*, *MRE11A*, *TOP1* and *FRAP1* cannot belong to category of cell cycle but category of cell growth, stress response, and transcription.

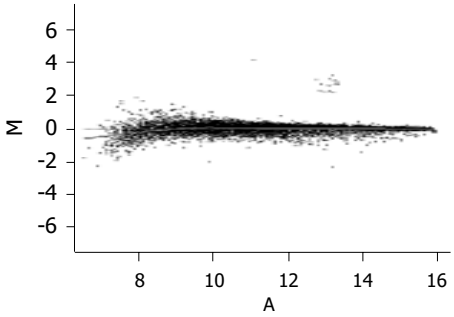


Figure 4 Scattered plot of the normalization results by global M method.

Confirmation of cDNA microarray findings by RT-PCR

We selected *EXO1*, *ABCF2*, *MRE11A*, *TOP1*, and *FRAP1* among the downregulated genes by amygdalin treatment, and observed mRNA expressions of *EXO1*, *ABCF2*, *MRE11A*, *TOP1*, and *FRAP1* using RT-PCR that reproduced the results of cDNA microarray. The efficiency of the reaction was adjusted by *CYCLOPHILIN* amplification. As shown in Figure 5, the expressions of *EXO1*, *ABCF2*, *MRE11A*, *TOP1*, and *FRAP1* were decreased by amygdalin treatment (5 mg/mL, 24 h).

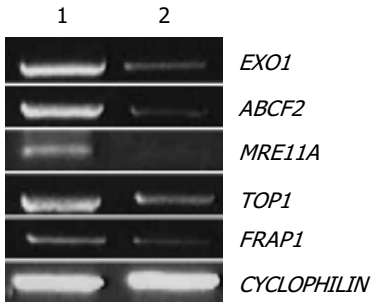


Figure 5 Confirmation of cDNA microarray results of downregulated genes by RT-PCR. Five genes, exonuclease 1 (*EXO1*), ABC, sub-family F (GCN20), member 2 (*ABCF2*), MRE11 meiotic recombination 11 homolog A (*MRE11A*), topoisomerase (DNA) I (*TOP1*), and FK506 binding protein 12-rapamycin associated protein 1 (*FRAP1*), were analyzed by RT-PCR with total RNA from control and amygdalin (5 mg/mL, 24 h)-treated human colon cancer cells. As an internal control, *CYCLOPHILN* was amplified.

DISCUSSION

Amygdalin belongs to a family of compounds called cyanogenic glycosides. Cyanide is believed to be the active cancer-killing ingredient in amygdalin. Amygdalin would be broken down by an enzyme in cancerous tissue, and toxic

Table 2 List of genes downregulated by amygdalin treatment

Gene	Chromosome	Title	Global M
Cell cycle			
FRAP1	1p36.2	FK506 binding protein 12-rapamycin associated protein 1	–1.029
TOP1	20q12–q13.1	Topoisomerase (DNA) I	–1.118
MRE11A	11q21	MRE11 meiotic recombination 11 homolog A (*S. cerevisiae*)	–1.235
EXO1	1q42–q43	Exonuclease 1	–1.740
ABCF2	7q36	ABC, sub-family F (GCN20), member 2	–1.993
Cell growth			
FRAP1	1p36.2	FK506 binding protein 12-rapamycin associated protein 1	–1.029
TIEG2	2p25	TGFB inducible early growth response 2	–1.082
NR3C2	4q31.1	Nuclear receptor subfamily 3, group C, member 2	–1.099
IGF2R	6q26	Insulin-like growth factor 2 receptor	–1.011
TOP1	20q12–q13.1	Topoisomerase (DNA) I	–1.118
MS4A2	11q13	Membrane-spanning 4-domains, subfamily A, member 2 (Fc fragment of IgE, high affinity I, receptor for; beta polypeptide)	–1.175
MRE11A	11q21	MRE11 meiotic recombination 11 homolog A (*S. cerevisiae*)	–1.235
COPA	1q23–q25	Coatomer protein complex, subunit alpha	–1.304
SORL1	11q23.2–q24.2	Sortilin-related receptor, L (DLR class) A repeats-containing	–1.360
NPC1	18q11–q12	Niemann-Pick disease, type C1	–1.405
FGD1	Xp11.21	FYVE, RhoGEF and PH domain containing 1 (faciogenital dysplasia)	–1.518
ABCF2	7q36	ABC, sub-family F (GCN20), member 2	–1.993
EXO1	1q42–q43	Exonuclease 1	–1.740
PLA2G1B	12q23–q24.1	Phospholipase A2, group IB (pancreas)	–2.293
Stress response			
IGF2R	6q26	Insulin-like growth factor 2 receptor	–1.011
FRAP1	1p36.2	FK506 binding protein 12-rapamycin associated protein 1	–1.029
TIEG2	2p25	TGFB inducible early growth response 2	–1.082
NR3C2	4q31.1	Nuclear receptor subfamily 3, group C, member 2	–1.099
TOP1	20q12–q13.1	Topoisomerase (DNA) I	–1.118
MS4A2	11q13	Membrane-spanning 4-domains, subfamily A, member 2 (Fc fragment of IgE, high affinity I, receptor for; beta polypeptide)	–1.175
MRE11A	11q21	MRE11 meiotic recombination 11 homolog A (*S. cerevisiae*)	–1.235
COPA	1q23-q25	Coatomer protein complex, subunit alpha	–1.304
SORL1	11q23.2–q24.2	Sortilin-related receptor, L(DLR class) A repeats-containing	–1.360
NPC1	18q11–q12	Niemann-Pick disease, type C1	–1.405
FGD1	Xp11.21	FYVE, RhoGEF and PH domain containing 1 (faciogenital dysplasia)	–1.518
EXO1	1q42–q43	Exonuclease 1	–1.740
ABCF2	7q36	ABC, sub-family F (GCN20), member 2	–1.993
PLA2G1B	12q23–q24.1	Phospholipase A2, group IB (pancreas)	–2.293
Transcription			
IGF2R	6q26	Insulin-like growth factor 2 receptor	–1.011
FRAP1	1p36.2	FK506 binding protein 12-rapamycin associated protein 1	–1.029
TIEG2	2p25	TGFB inducible early growth response 2	–1.082
NR3C2	4q31.1	Nuclear receptor subfamily 3, group C, member 2	–1.099
MS4A2	11q13	Membrane-spanning 4-domains, subfamily A, member 2 (Fc fragment of IgE, high affinity I, receptor for; beta polypeptide)	–1.175
TOP1	20q12–q13.1	Topoisomerase (DNA) I	–1.118
MRE11A	11q21	MRE11 meiotic recombination 11 homolog A (*S. cerevisiae*)	–1.235
COPA	1q23–q25	Coatomer protein complex, subunit alpha	–1.304
SORL1	11q23.2–q24.2	Sortilin-related receptor, L (DLR class) A repeats-containing	–1.360
NPC1	18q11–q12	Niemann-Pick disease, type C1	–1.405
FGD1	Xp11.21	FYVE, RhoGEF, and PH domain containing 1 (faciogenital dysplasia)	–1.518
ABCF2	7q36	ABC, sub-family F (GCN20), member 2	–1.993
EXO1	1q42–q43	Exonuclease 1	–1.740
PLA2G1B	12q23–q24.1	Phospholipase A2, group IB (pancreas)	–2.293

cyanide to release from broken amygdalin would kill the cancer. It is further hypothesized that another enzyme, rhodanese, which has the ability to detoxify cyanide, is present in normal tissues but deficient in cancer cells. These two factors supposedly combine to effect a selective poisoning of cancer cells by the cyanide, while normal cells remain undamaged[6,12]. However, amygdalin is not approved by the Food and Drug Administration (FDA) for use in USA, and the anticancer effect of amygdalin has admitted controversy. Kwon *et al*., demonstrated that the controversy on amygdalin was due to its conversion to inactivate isoform, and Persicae Semen extract induced apoptosis in human promyelocytic leukemia (HL-60) cells with IC50 of 6.4 mg/mL in the presence of 250 nmol/L of β-galactosidase[13].

One of the advantages of cDNA microarray is the possibility to observe the expression pattern of the whole

genes and compare with different conditions. This study is the first work of comparison of the gene expression profiles of SNU-C4 human colon cancer cells after amygdalin treatment. cDNA microarray analysis showed that amygdalin treatment downregulated genes belong to categories of cell cycle-related gene, and related to cell growth, response to stress and transcription.

Anticancer agents targeting DNA and DNA-associated processes are widely used in the treatment of human cancers and produce significant increases in the survival of patients[14]. In general, four complex systems have evolved to respond to DNA damage: DNA repair, cell cycle checkpoint control, apoptosis, and damage tolerance[15]. *EXO1* is involved in mismatch repair and recombination, and has been considered as a candidate gene for colorectal susceptibility[16,17]. *ABCF2* is a member of the superfamily of ABC transporters. ABC proteins transport various molecules across extra- and intracellular membranes[18]. *MRE11A* encodes a nuclear protein involved in homologous recombination, telomere length maintenance, and DNA double-strand break repair[19,20]. *TOP1* acts as a swivel during replication, transcription, and recombination to relieve overwinding if duplex DNA[15,21]. DNA topoisomerase inhibitors represent a major class of anticancer agents (e.g. camptothecin; CPT) with documented activities against a broad spectrum of human malignancies[22]. *FRAP1* has been identified as the downstream target of the FKBP12-rapamycin complex, which inhibits progression through G_1 of the cell cycle[23], and mediates cellular responses to stresses such as DNA damage and nutrient deprivation[24,25]. *EXO1*, *ABCF2*, *MRE11A*, *TOP1*, and *FRAP1* particularly belong to categories of cell cycle-related gene and associated to DNA replication, repair or recombination. Thus, downregulation of these genes by amygdalin would induce DNA damage in SNU-C4 cells. In confirmation through RT-PCR, mRNA expressions of these five genes were also decreased by amygdalin treatment. Our results indicate that amygdalin induced DNA damage, involved in cell cycle on SNU-C4 human colon cancer cells and amygdalin might be used for therapeutic anticancer drug.

REFERENCES

1 **Singh P,** Dai B, Dhruva B, Widen SG. Episomal expression of sense and antisense insulin-like growth factor (IGF)-binding protein-4 complementary DNA alters the mitogenic response of a human colon cancer cell line (HT-29) by mechanisms that are independent of and dependent upon IGF-I. *Cancer Res* 1994; **54**: 6563-6570

2 **Midgley R,** Kerr D. Colorectal cancer. *Lancet* 1999; **353**: 391–399

3 **Kim EJ,** Schaffer BS, Kang YH, MacDonald RG, Park JH. Decreased production of insulin-like growth factor-binding protein (IGFBP)-6 by transfection of colon cancer cells with an antisense IGFBP-6 cDNA construct leads to stimulation of cell proliferation. *J Gastroenterol Hepatol* 2002; **17**: 563–570

4 **Boyle P,** Langman JS. ABC of colorectal cancer: epidemiology. *BMJ* 2000; **321**: 805-808

5 **Szepeshazi K,** Schally AV, Groot K, Armatis P, Halmos G, Herbert F, Szende B, Varga JL, Zarandi M. Antagonists of growth hormone-releasing hormone (GH-RH) inhibit IGF-II production and growth of HT-29 human colon cancers. *Br J Cancer* 2000; **82**: 1724-1731

6 **Cho CJ,** Yang HS, Kim TH, Chong SY, Lee IR, Kim JH, Leem JP, Chong MH, Lee MW, Lee KY, Pae KH, Kim JW, Han DR. Hyundae-Saengyak-Hak, 8th ed. *Hak Chang Press* 1998: 321-323

7 **Flora KP,** Cradock JC, Ames MM. A simple method for the estimation of amygdalin in the urine. *Res Commun Chem Pathol Pharmacol* 1978; **20**: 367-378

8 **Khandekar JD,** Edelman H. Studies of amygdalin (laetrile) toxicity in rodents. *JAMA* 1979; **242**: 169-171

9 **Moertel CG,** Ames MM, Kovach JS, Moyer TP, Rubin JR, Tinker JH. A pharmacologic and toxicological study of amygdalin. *JAMA* 1981; **245**: 591-594

10 **Fukuda T,** Ito H, Mukainaka T, Tokuda H, Nishino H, Yoshida T. Anti-tumor promoting effect of glycosides from Prunus persica seeds. *Biol Pharm Bull* 2003; **26**: 271-273

11 **Yang YH,** Dudoit S, Luu P, Lin DM, Peng V, Ngai J, Speed TP. Normalization for cDNA microarray data: a robust composite method addressing single and multiple slide systematic variation. *Nucleic Acids Res* 2002; **30**: e15

12 **Newmark J,** Brady RO, Grimley PM, Gal AE, Waller SG, Thistlethwaite JR. Amygdalin (Laetrile) and prunasin beta-glucosidases: distribution in germ-free rat and in human tumor tissue. *Proc Natl Acad Sci USA* 1981; **78**: 6513-6516

13 **Kwon HY,** Hong SP, Hahn DH, Kim JH. Apoptosis induction of Persicae Semen extract in human promyelocytic leukemia (HL-60) cells. *Arch Pharm Res* 2003; **26**: 157-161

14 **Capranico G,** Zagotto G, Palumbo M. Development of DNA topoisomerase-related therapeutics: a short perspective of new challenges. *Curr Med Chem Anti Canc Agents* 2004; **4**: 335-345

15 **Wang Z.** DNA damage-induced mutagenesis: a novel target for cancer prevention. *Mol Interv* 2001; **1**: 269-281

16 **Tishkoff DX,** Amin NS, Viars CS, Arden KC, Kolodner RD. Identification of a human gene encoding a homologue of *Saccharomyces cerevisiae* EXO1, an exonuclease implicated in mismatch repair and recombination. *Cancer Res* 1998; **58**: 5027-5031

17 **Wilson DM 3rd,** Carney JP, Coleman MA, Adamson AW, Christensen M, Lamerdin JE. Hex1: a new human Rad2 nuclease family member with homology to yeast exonuclease 1. *Nucleic Acids Res* 1998; **26**: 3762-3768

18 **Dean M,** Hamon Y, Chimini G. The human ATP-binding cassette (ABC) transporter superfamily. *J Lipid Res* 2001; **42**: 1007-1017

19 **Paull TT,** Gellert M. The 3' to 5' exonuclease activity of Mre 11 facilitates repair of DNA double-strand breaks. *Mol Cell* 1998; **1**: 969-979

20 **Trujillo KM,** Yuan SS, Lee EY, Sung P. Nuclease activities in a complex of human recombination and DNA repair factors Rad50, Mre11, and p95. *J Biol Chem* 1998; **273**: 21447-21450

21 **Champoux JJ.** DNA topoisomerases: structure, function, and mechanism. *Annu Rev Biochem* 2001; **70**: 369-413

22 **Liu LF.** DNA topoisomerase poison as antitumor drugs. *Annu Rev Biochem* 1989; **58**: 351-375

23 **Astier AL,** Xu R, Svoboda M, Hinds E, Munoz O, de Beaumont R, Crean CD, Gabig T, Freedman AS. Temporal gene expression profile of human precursor B leukemia cells induced by adhesion receptor: identification of pathways regulating B-cell survival. *Blood* 2003; **101**: 1118-1127

24 **Brown EJ,** Albers MW, Bum Shin T, Ichikawa K, Keith CT, Lane WS, Schreiber SL. Amammalian protein targeted by G1-arresting rapamycin-receptor complex. *Nature* 1994; **369**: 756-758

25 **Chiu MI,** Katz H, Berlin V. RAPT1, a mammalian homology of yeast Tor, interacts with the FKBP12/rapamycincomplex. *Proc Natl Acad Sci USA* 1994; **91**: 12547-12578

Science Editor Guo SY **Language Editor** Elsevier HK

PO Box 2345, Beijing 100023, China
www.wjgnet.com
wjg@wjgnet.com

ELSEVIER

World J Gastroenterol 2005;11(33):5162-5168
World Journal of Gastroenterology ISSN 1007-9327
© 2005 The WJG Press and Elsevier Inc. All rights reserved.

• *COLORECTAL CANCER* •

Novel rapid tissue lysis method to evaluate cancer proteins: Correlation between elevated Bcl-X_L expression and colorectal cancer cell proliferation

Wei-Shone Chen, Hong-Yi Chang, Jui-Ting Chang, Jacqueline Ming Liu, Chung-Pin Li, Li-Li Chen, Huei-Ling Chang, Chia-Chi Chen, Tze-Sing Huang

Wei-Shone Chen, Hong-Yi Chang, Jacqueline Ming Liu, Li-Li Chen, Huei-Ling Chang, Chia-Chi Chen, Tze-Sing Huang, National Cancer Research Center, National Health Research Institutes, Taipei, Taiwan, China
Wei-Shone Chen, Hong-Yi Chang, Jui-Ting Chang, Division of Colon and Rectal Surgery, Department of Surgery, Taipei Veterans General Hospital and National Yang-Ming University School of Medicine, Taipei, Taiwan, China
Chung-Pin Li, Division of Gastroenterology, Department of Medicine, Taipei Veterans General Hospital and National Yang-Ming University School of Medicine, Taipei, Taiwan, China
Correspondence to: Dr. Tze-Sing Huang, National Cancer Research Center, NHRI, No. 161, Min-Chuan East Road Sec. 6, Taipei 114, Taiwan, China. tshuang@nhri.org.tw
Telephone: +886-2-26534401-25138 Fax: +886-2-27929654
Received: 2005-02-06 Accepted: 2005-03-23

Abstract

AIM: We optimized a rapid and efficient tissue lysis method using the MagNA Lyser (Roche, Germany). Using this novel method combined with immunoblot analysis, we investigated the correlation between abnormal Bcl-X_L expression and clinicopathological characteristics in colorectal cancer.

METHODS: Tissue samples from Sprague-Dawley rats were tested to determine optimal lysis conditions for use with MagNA Lyser. We next used the new method to extract tissue proteins from the tumor tissue of a colorectal cancer patient. The availability of extractable tissue proteins for proteomic study was demonstrated by two-dimensional (2D) gel electrophoresis and subsequent matrix-assisted laser desorption/ionization time-of-flight (MALDI-TOF) mass spectrometry. In addition, we prepared tissue lysates from paired tumor tissues and adjacent nontumor tissues of 50 colorectal carcinoma patients. Ensuing immunoblot analyses were performed to detect the level of Bcl-X_L expression.

RESULTS: The optimal sample sizes processed were found to be around 200 mg, with oscillation frequency of 6 500 r/min for 80 s. Test of the first human tissue lysate confirmed that the MagNA Lyser method was adequate for protein extraction and subsequent identification by current proteomic protocols. The method was also applicable to immunoblot analysis. Thirty of 50 (60%) colorectal patients exhibited higher level of Bcl-X_L expression in their tumor tissues. Raised level of Bcl-X_L expression correlated with patients' gender and tumor cell proliferation index ($P = 0.037$ and $P<0.001$, respectively), but was independent of clinicopathological characteristics and overall survival.

CONCLUSION: We report a novel tissue lysis method applicable to proteomic and immunoblot analyses, which can facilitate the discovery and detection of cancer protein alterations.

© 2005 The WJG Press and Elsevier Inc. All rights reserved.

Key words: Tissue lysis; MagNA Lyser; Bcl-X_L; Colorectal cancer

Chen WS, Chang HY, Chang JT, Liu JM, Li CP, Chen LL, Chang HL, Chen CC, Huang TS. Novel rapid tissue lysis method to evaluate cancer proteins: Correlation between elevated Bcl-X_L expression and colorectal cancer cell proliferation. *World J Gastroenterol* 2005; 11(33): 5162-5168
http://www.wjgnet.com/1007-9327/11/5162.asp

INTRODUCTION

Cancer is a complicated and heterogeneous disease involving multiple molecular alterations. To globally explore protein alterations in cancer tissues, the first and most essential step is to rapidly and efficiently extract tissue proteins from the study specimens. Conventional methods for tissue lysis usually require grinding, homogenization and sonication to disrupt tissues and cells[1,2]. It is not only tedious, but also carries biohazard concerns for laboratory personnel. Recently, the Roche Company (Penzberg, Germany) developed a machine called the MagNA Lyser, and it could be combined with certain commercially available reagent kits to rapidly isolate DNA or RNA from tissue specimens[3,4]. The basic principle of tissue lysis centers on the ability of the machine to make fast and reciprocal oscillations, which produce collisions between tissue samples and ceramic beads provided in special centrifuge tubes. The whole procedure is simple and quick, and is therefore highly suitable for protein extraction from tissues, even though protein extraction had not been previously published, as a function of the MagNA Lyser. In this study, we have optimized a rapid tissue lysis protocol for use with the MagNA Lyser. The tissue proteins prepared by this new method can be resolved by two-dimensional (2D) gel electrophoresis and further identified by matrix-assisted laser

desorption/ionization time-of-flight (MALDI-TOF) mass spectrometry. In addition, this novel method is also applicable to immunoblot analysis. We prepared tissue lysates from the tumor tissues and adjacent non-tumor tissues of 50 colorectal carcinoma patients. The ensuing immunoblot analyses were performed to detect the level of Bcl-X_L expression. Bcl-X_L is an important member of the Bcl-2 family proteins, contributing to the anti-apoptotic characteristic during the progression of tumors[5-7]. Previously, 43-60% of colorectal cancer patients have been reported to exhibit elevated level of Bcl-X_L expression in their tumor tissues by immunohistochemical staining[8,9]. In this study, elevated Bcl-X_L expression in tumor tissues was observed in 60% of colorectal cancer patients using the new tissue lysis method and immunoblot analysis. Raised levels of Bcl-X_L expression correlated with patients' gender and tumor cell proliferation index ($P = 0.037$ and $P<0.001$, respectively), but were independent of patients' age, tumor site, tumor size, grade of tumor cell differentiation, depth of tumor invasion, nodal or distant metastasis, and 5-year overall survival rate.

MATERIALS AND METHODS

Rat tissues

Sprague-Dawley rats weighing approximately 250 g (obtained from National Animal Center, Taiwan) were used in our pilot studies and fed with standard laboratory chow and water *ad libitum*. All procedures were performed in accordance with the Taipei Veterans General Hospital Animal Committee's guidelines for animal care. The rats were killed under anesthesia, and their organs were surgically taken and rinsed with phosphate-buffered saline (PBS). All specimens were cut into pieces, snap-frozen immediately and stored at -80 ℃ until use.

Patients and tumor specimens

Tumor specimens were obtained from 50 patients who received surgical resection for colorectal cancer at Taipei Veterans General Hospital during the time period of 1994-2004. Informed consent was obtained from each patient. Tissue specimens, both tumor and non-tumor parts, were frozen in liquid nitrogen immediately after resection and PBS rinse. All were kept in a -80 ℃ freezer until retrieval for the study. The non-tumor parts, taken from a site at least 10 cm away from the tumor part, were pathologically certified to be free from tumor cells.

Conventional grinder method for tissue lysis

Tissue specimens were ground in mortars with liquid nitrogen. The tissue powder obtained was then incubated overnight at -20 ℃ with 10% trichloroacetic acid plus 0.3% dithiothreitol (DTT) in acetone, then spun down, washed with acetone, and air-dried, followed by the addition of TLysis buffer, which is made up of 30 mmol/L Tris-HCl, pH 9.0, 9 mol/L of urea, 4% of CHAPS, 1% of DTT, 1 mmol/L of phenylmethylsulfonyl fluoride, 10 μg/mL of aprotinin, 10 μg/mL of pepstatin A, and 10 μg/mL of leupeptin. The mixture underwent three 20-s duration of homogenization on ice before further sonication at 10% output for 20 pulses. The lysate was then centrifuged at 100 000 *g* for 1 h at 4 ℃, and the supernatant was saved and assayed for protein concentration by the Lowry method[10].

MagNA Lyser method for tissue lysis

Tissue pieces were put into ceramic beads-containing special centritubes (Roche, Penzberg, Germany), 1 mL of pre-chilled TLysis buffer was immediately added, and subjected to oscillation made by the MagNA Lyser machine at 6 500 r/min for time periods as indicated. The lysate was then centrifuged at 100 000 *g* for 1 h at 4 ℃, and the supernatant was saved and assayed for protein concentration (Lowry method).

Two-dimensional (2D) gel electrophoresis

Prior to 2D gel electrophoresis, 2% of Ampholines/pharmalytes pH 3-10 (Amersham Biosciences, Piscataway, NJ, USA) was added to the tissue lysates. Immobilized linear pH gradient (IPG) strips were rehydrated with tissue lysate samples in the dark at room temperature overnight[11]. Isoelectric focusing was performed using IPG phor apparatus (Amersham Biosciences) for a total of 17 500 Vh at 20 ℃. The strips were then equilibrated for 15 min in 50 mmol/L Tris-HCl, pH 8.8, 6 mol/L urea, 2% (w/v) sodium dodecyl sulfate (SDS), 64 mmol/L DTT, 300 mL/L glycerol, and a trace of Bromophenol blue. Equilibrated IPG strips were transferred onto 12% uniform polyacrylamide gels. Standard SDS-polyacrylamide gel electrophoresis was performed, and the 2D gels were then stained with Coomassie blue and scanned directly using AlphaImager 2000 (Alpha Innotech Co., Avery Dennison, CA, USA). The images were further analyzed using ImageMaster 2-D Elite v3.01 software (Amersham Biosciences).

Protein spot identification

Spots of interest were manually excised from the 2D gels. After washing twice in 25 mmol/L ammonium bicarbonate/50% acetonitrile and once in 100% acetonitrile, gel pieces were vacuum-dried and rehydrated with 10 μg/mL of trypsin (Promega, Madison, WI, USA) in 25 mmol/L ammonium bicarbonate, pH 8.0. Proteins were proteolysed for 16-24 h at 37 ℃. Supernatants were collected, and the peptides in gel pieces were further extracted with 5% trifluoroacetic acid (TFA)/50% acetonitrile. The peptide extracts were vacuum-dried and re-solubilized in 5 μL of 0.1% TFA. The peptide extracts (1 μL for each) were then spotted onto the target plate, and α-cyano-4-hydroxycinnamic acid was added as a matrix (1 μL for each). Matrix-assisted laser desorption/ionization time-of-flight (MALDI-TOF) mass spectrometry was performed using M@LDI *R*™ reflector time-of-flight mass spectrometer (Micromass, Manchester, UK). All mass spectra were internally calibrated with ACTH peptide and trypsinized alcohol dehydrogenase peaks. Peptide mass mapping was carried out using the MS-Fit program (Protein Prospector, University of California, San Francisco, CA).

Immunoblot analysis

The expression levels of Bcl-X_L and Ki-67 in human tissue lysates were detected by conventional immunoblot analysis[12]. In brief, 40 μg of protein samples were resolved in 10% SDS-polyacrylamide gels and then electrotransferred onto

polyvinylidene membranes (Amersham Biosciences). After blocking with PBST (PBS plus 0.1% Tween-20) plus 5% non-fat milk, the blots were incubated with anti-Bcl-X_L (Santa Cruz Biotechnology, Santa Cruz, CA, USA) or anti-Ki-67 (NeoMarkers, Fremont, CA, USA) antibody at 4 ℃ for 12 h. The blots were then washed thrice with PBST buffer, and incubated with horseradish peroxidase-conjugated secondary antibody for 1 h at room temperature. Blots were again washed thrice with PBST buffer, and the protein band signals were obtained by enhanced chemiluminescence (ECL, Amersham Biosciences). The levels of β-tubulin in the tissue lysates were also analyzed as internal control. The antibody against β-tubulin was obtained from Santa Cruz Biotechnology.

Statistical analyses

Statistical analyses were performed using the SPSS 11.0 software (SPSS, Chicago, IL, USA). χ^2 or Fisher's exact test was used to analyze the relationship between Bcl-X_L expression and patients' clinicopathological characteristics. Independent sample *t* test was used to compare the ages and tumor sizes between the patients with or without Bcl-X_L overexpression. Overall survival rates were calculated by the Kaplan-Meier method and the statistical comparison was made using the log rank test. The difference was considered significant if the *P* value was less than 0.05 (two-tailed test).

RESULTS

Determination of conditions for tissue lysis using the MagNA Lyser

Different organs derived from the Sprague-Dawley rats were utilized as test tissue materials for a series of pilot studies. First, we intended to determine the optimal tissue size for lysis by MagNA Lyser. For each organ, we used four pieces of tissue specimens ranging from 100 to 600 mg. Tissue lysis was performed by setting the oscillation rate to 6 500 r/min durations of 20, 40, 80, 120, or 180 s. Evaluation of the lysing efficiency was preliminarily based on protein recovery rates. From the data shown in Figure 1, we realized that there was a ceiling limit to the size of tissue specimen tested, because the larger tissue pieces usually resulted in a low protein recovery rate. The big tissue samples were probably

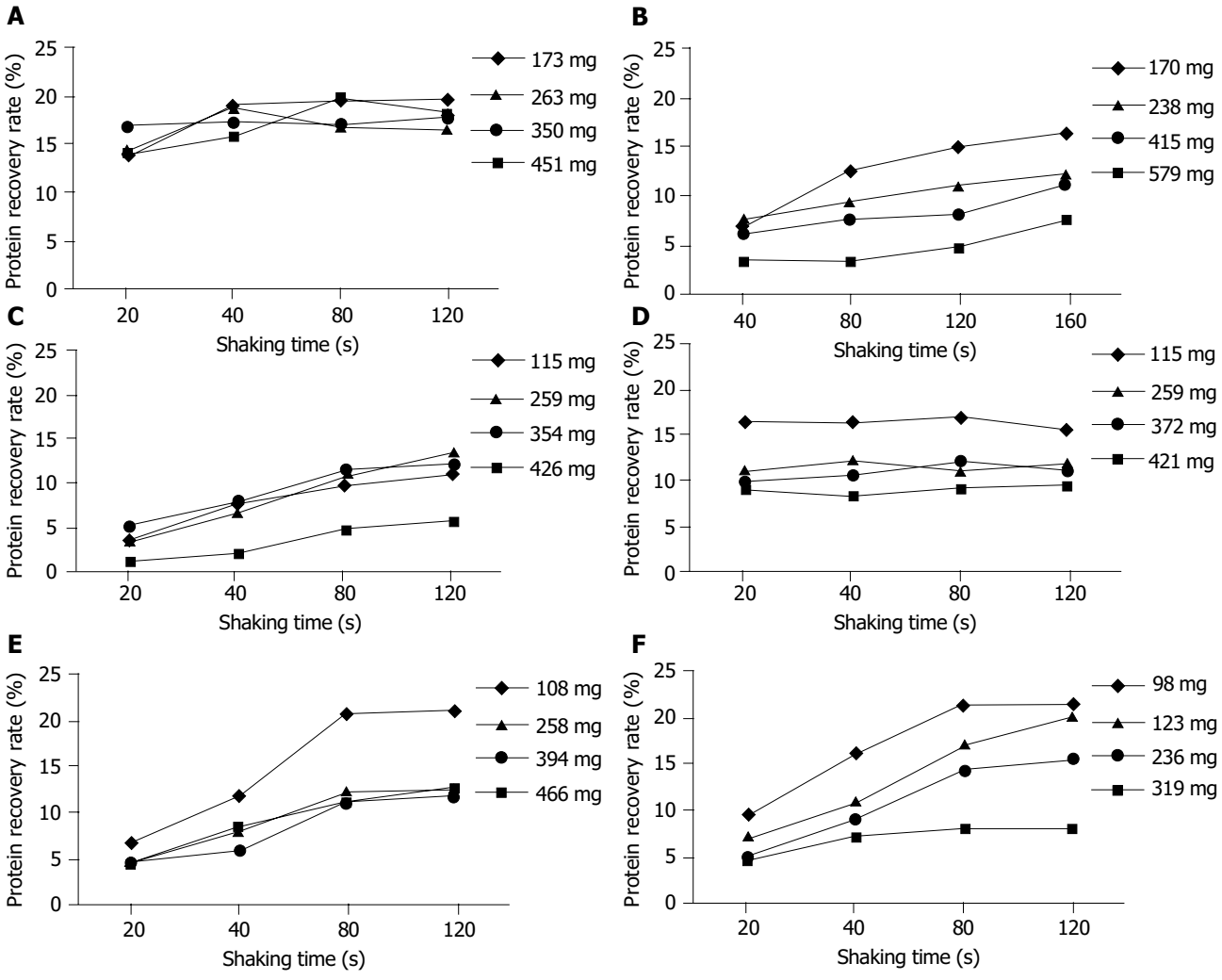


Figure 1 Determination of the optimal specimen size from different organs for tissue lysis by the MagNA Lyser. Four specimen sizes, ranging from 100 to 600 mg, of rat organs were tested for the protein recovery rates from the new tissue lysis method using the MagNA Lyser. The oscillation frequency and duration was set at 6 500 r/min for 20, 40, 80, 120, or 180 s as indicated. Protein concentrations of tissue lysates were assayed by the Lowry method. The protein recovery rate from tissue lysis was calculated as the amount of total protein obtained divided by the original weight of the specimen. **A**: Liver; **B**: Stomach; **C**: Colon; **D**: Kidney; **E**: Spleen; **F**: Heart.

subjected to incomplete lysis and thus were being wasted. Up to 350 mg of liver and colon tissues could be processed efficiently, but in general, the optimal tissue size of each organ for this study should not be more than 200 mg.

Next, the optimal shaking duration was determined. Tissue pieces in sizes ranging from 150 mg to 200 mg were oscillated in MagNA Lyser for different time periods. The protein recovery rate after each time period is shown in Figure 2A. Based on these data, optimal shaking time set at 80 s resulted in almost maximal protein recovery rates from the various organ tissues. When shaking time extends beyond 20 s, the lysates unavoidably became heated. To ascertain the impact of heat on tissue proteins, the tissue lysates prepared after different shaking periods in the MagNA Lyser were further analyzed by 2D gel electrophoresis. As shown in Figure 2B, the 2D profiles of tissue lysates prepared by 80-s oscillation seemed not worse than those prepared from shorter duration oscillations.

MagNA Lyser method vs conventional grinder method

According to the above test results, for optimal protein extraction from tissue samples using the MagNA Lyser, tissue size should be no more than 200 mg, and oscillation frequency should be set at 6 500 r/min for 80 s. Furthermore, in comparing tissue extraction efficiency using the MagNA Lyser or the conventional grinding method, protein recovery rates obtained through the MagNA Lyser were significantly superior at tissue specimens weighing between 150 and 200 mg (Figure 3A). The profiles from 2D gel electrophoresis were similar between tissue lysates prepared through either method (Figure 3B). Some protein spots appear to differ on two profiles, this could not be entirely attributed to the two different methods used for protein extraction, and quality variation during the 2D gel electrophoresis could also contribute to the differences. From our series of quality control pilot studies, we conclude that the MagNA Lyser method is indeed a convenient and efficient method for protein extraction from tissue samples.

MagNA Lyser method compatible with ensuing proteomic and immunoblot analyses

After the previous pilot studies using rat tissues as test material, we attempted protein extraction from human tumor specimen obtained from a colon cancer patient using the MagNA Lyser. The tissue lysate was resolved by 2D gel electrophoreses and several protein spots on the 2D profile were identified after standard procedure, including trypsin digestion, peptide extraction and MALDI-TOF mass spectrometric analyses (Figure 4). Our results confirmed that tissue lysate prepared using the MagNA Lyser method was entirely adequate for subsequent protein identification by the current proteomic protocols.

In order to ascertain whether the novel tissue lysis method is also applicable to immunoblot analysis, we used the MagNA Lyser to prepare tissue lysates from paired tumor and non-tumor tissues obtained from 50 colorectal cancer patients, followed by performing immunoblot analyses to compare the levels of Bcl-X_L expression in these patients. The results from six patients are shown in Figure 5 as representative examples. Only one of 50 colorectal cancer patients exhibited down regulation of Bcl-X_L expression in their tumor tissues, whereas 30 patients (60%) had raised levels of Bcl-X_L expression in the tumor tissues rather than their adjacent non-tumor tissues. Statistical analyses revealed that elevated Bcl-X_L expression correlated with patients' gender and elevated Ki-67 expression (P = 0.037 and P<0.001,

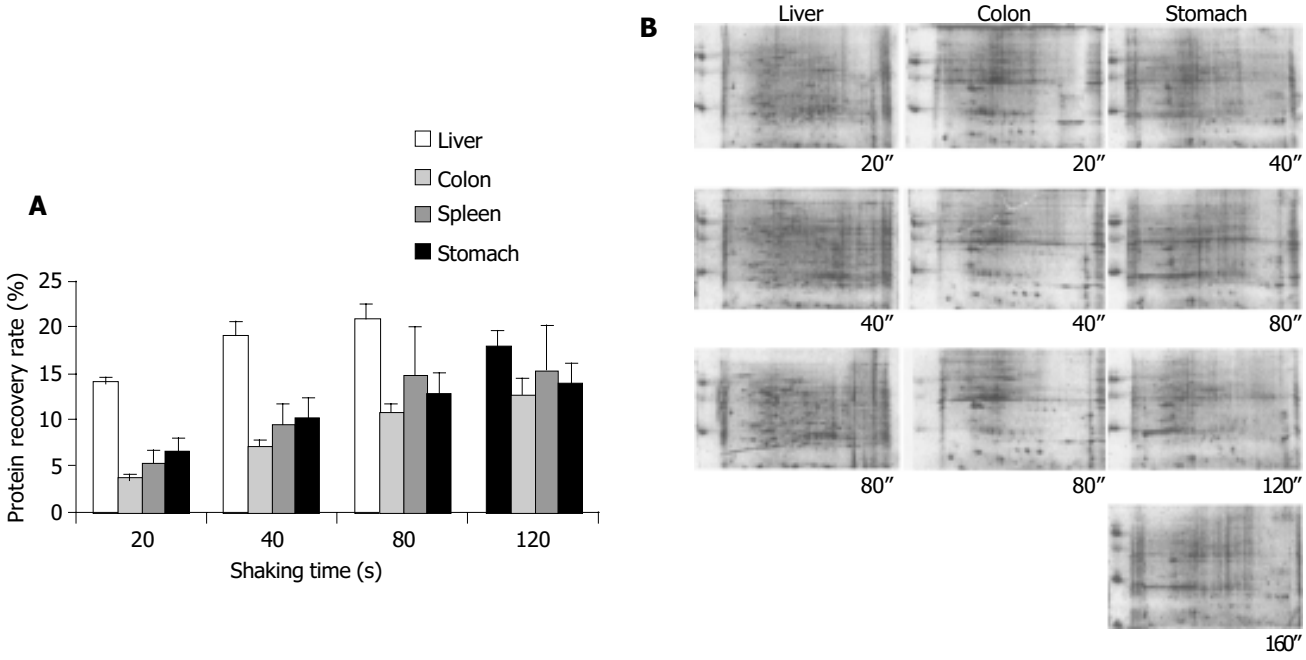


Figure 2 Determination of the optimal shaking time for tissue lysis by the MagNA Lyser. Tissue pieces in sizes ranging from 150 to 200 mg were subjected to reciprocal oscillation by the MagNA Lyser at 6 500 r/min for different time periods. Protein concentrations of tissue lysates were assayed, and protein recovery rates were calculated as above. Additionally, an aliquot (200 μg) of each tissue lysate was resolved on a 7-cm IPG strip, pH 3-10, then run in an 8×9-cm 12% SDS-polyacrylamide gel, and visualized by AlphaImager 2000 after staining with Coomassie blue dye. The optimal shaking time for tissue lysis by MagNA Lyser was determined according to both the protein recovery rates (**A**) and the protein profiling from 2D gel electrophoresis (**B**).

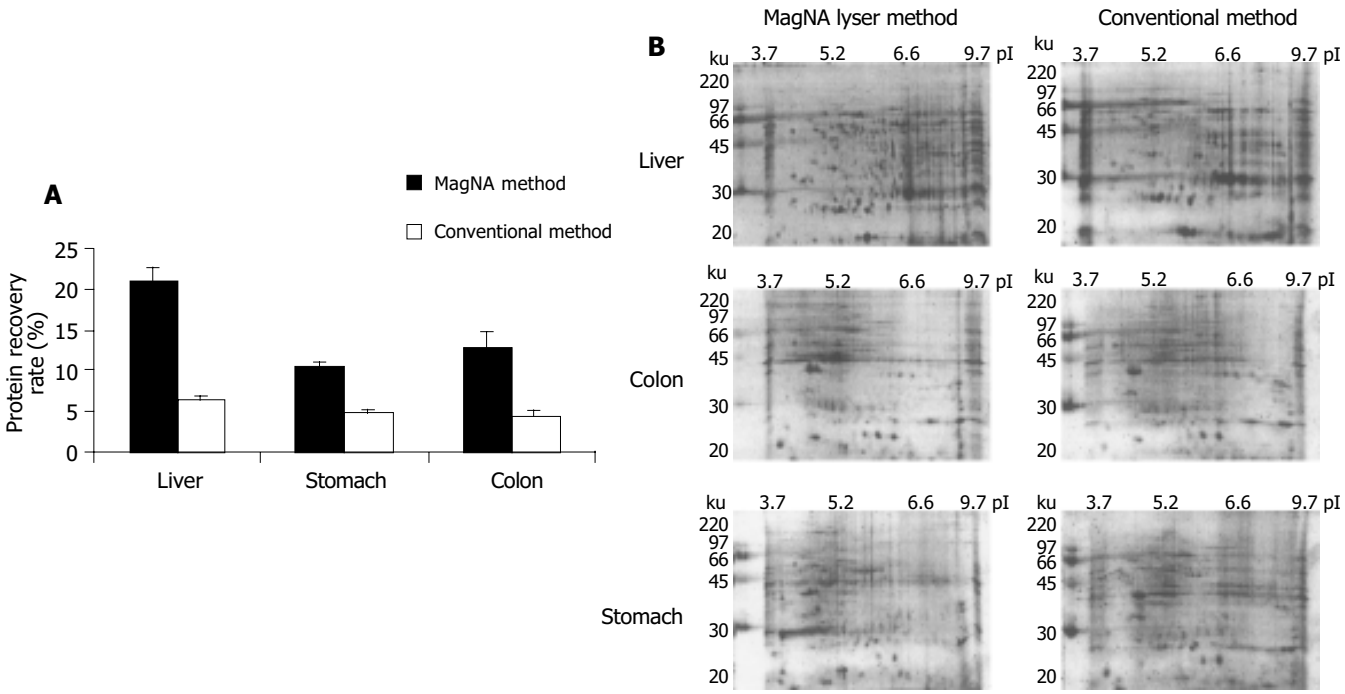


Figure 3 Comparison between conventional tissue lysis with the new method using MagNA Lyser. Tissue specimens ranging from 150 to 200 mg in size were processed using the conventional tissue lysis protocol and the new MagNA Lyser method. The protein recovery rates (**A**) and 2D gel profiling (**B**) were compared for the two methods.

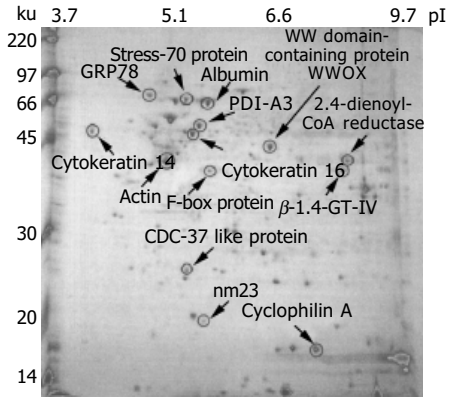


Figure 4 Proteomic analysis of the human colorectal cancer tissue lysate prepared by the MagNA Lyser. Approximately 150 mg of tumor specimen from a colon cancer patient was subjected to tissue lysis by the new MagNA Lyser method. One aliquot (600 μg) of tissue lysate was resolved on a 13-cm IPG strip, pH 3-10, and subsequently run in a 14 cm×15 cm 12% SDS-polyacrylamide gel, then visualized by staining with Coomassie blue dye. Protein spots were cut from the gel, after trypsin digestion and peptide extraction, the spots were identified through MALDI-TOF mass spectrometry, and have been labeled on the gel image.

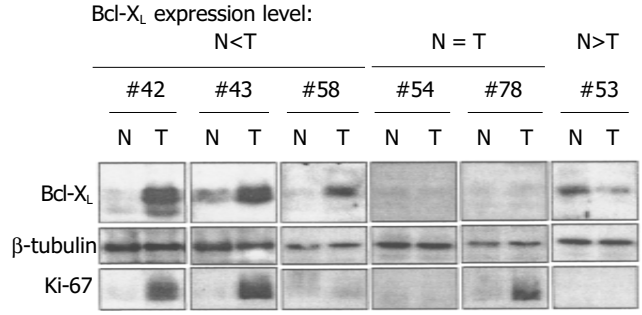


Figure 5 Differential expression levels of Bcl-X_L in colorectal cancer tissue specimens. Immunoblot analyses were performed to analyze the protein levels of Bcl-X_L in the lysates from nontumor tissues (N) and tumor tissues (T) of colorectal cancer patient #42, #43, #53, #54, #58, and #78. The levels of β-tubulin in the same-paired tissue lysates were analyzed as internal control.

respectively), but was not associated with patients' age, tumor site, tumor size, grade of tumor cell differentiation, depth of tumor invasion, lymph node or distant metastasis, and 5-year overall survival rate (Table 1).

DISCUSSION

Conventional methods for protein extraction usually require tedious grinding, homogenization and sonication steps to disrupt tissues and cells. A novel device, the MagNA Lyser (Roche, Germany) was recently designed and optimized to combine with different commercially available kits to facilitate the isolation of DNA and RNA from a variety of tissue samples, although without publication for protein extraction. In this study, we have firmly established the feasibility of using the MagNA Lyser to extract tissue proteins for subsequent proteomic and immunoblot analyses. Firstly, we exploited different organs of Sprague-Dawley rats as test samples in a series of pilot studies to determine the optimal tissue sizes for study as well as the time periods necessary for oscillation. The results suggest that the optimal tissue size should be no more than 200 mg, with oscillation frequency set at 6 500 r/min for 80 s. In addition, our data showed that protein recovery rates of the MagNA Lyser method were superior, when compared with those obtained through the conventional method, and visualization of the protein profiles provided by 2D electrophoreses showed both

	Elevated Bcl-X_L expression		
	Yes (n = 30, %)	No (n = 20, %)	P
Age (mean±SD, yr)	68.1±12.1	70.9±9.5	0.383
Gender (male / female)	21 / 9	19 / 1	0.037
Tumor size (mean±SD, cm)	4.8±1.8	5.1±2.5	0.631
Tumor site			0.347
Ascending colon	10.0	10.0	
Transverse colon	3.3	5.0	
Descending colon	10.0	5.0	
Sigmoid colon	13.3	40.0	
Rectum or rectosigmoid junction	60.0	35.0	
Multiple sites	3.3	5.0	
Elevated Ki-67 expression	66.7	15.0	0.000
Tumor cell differentiation			1.000
Well differentiated	6.7	5.0	
Moderate differentiation	93.3	95.0	
Poor differentiation	0.0	0.0	
TNM stage			0.640
I	10.0	5.0	
II	33.3	35.0	
III	40.0	30.0	
IV	16.7	30.0	
Tumor invasion depth			0.938
Submucosa	0.0	0.0	
Muscularis propria	13.3	10.0	
Subserosa	76.7	80.0	
Other organs or structures	10.0	10.0	
Lymph node or distant metastasis	56.7	60.0	0.815
Five-year overall survival rate	60.4	60.0	0.701

superior quality as well as quantity in protein extracted.

Completion of pilot studies in rats established preliminary conditions of study for human specimen. Study of the first colon cancer patient identified several proteins by 2D gel electrophoresis and MALDI-TOF mass spectrometry, suggesting that the MagNA Lyser method can foster clinical proteomic studies to assist us in the understanding of diverse processes of carcinogenesis, develop new biomarkers for diagnosis and early detection of cancer, and ultimately determine new therapeutic targets for future therapeutic manipulation. In addition, the MagNA Lyser method is adequate for large-scale tissue lysate preparation, which can be linked with ensuing immunoblot analyses to facilitate the rapid detection of cancer protein alterations in large-scale cancer tissues. As an example, we detected elevated Bcl-X_L expression in colorectal cancer patients. Further statistical analyses revealed that raised level of Bcl-X_L expression correlated with elevated Ki-67 expression (P<0.001), providing clinical evidence that abnormal Bcl-X_L expression contributed to tumor cell proliferation during colorectal cancer progression. The potency of tumor cell proliferation does not only depend on tumor cell growth, but also associates with tumor cell survival (e.g. anti-apoptosis) and cell cycle control[5-7]. However, the close correlation between elevated Bcl-X_L expression and tumor cell proliferation did not extend to enlargement of tumor size (P = 0.631), probably because the formation of tumor mass requires the involvement of other events like angiogenesis.

Bcl-2 family proteins comprise both pro-apoptotic members, e.g. Bax, Bak, BH3-only proteins, as well as anti-apoptotic molecules such as Bcl-2 and Bcl-X_L[5-7]. BH3-only proteins function as mediators of apoptotic response to elicit activation and translocation of Bax or Bak to the mitochondria, thereby facilitating Bax and Bak interaction with mitochondrial channels to release cytochrome *c*[13]. Bcl-2 and Bcl-X_L sequester Bax or BH3-only proteins and thus block this apoptotic process[14]. Much evidence indicates that induction of apoptosis is accompanied by an increase in Bax or Bak expression and/or a decrease in the expression of Bcl-2 or Bcl-X_L[15-18]. Overexpression of Bcl-2 or Bcl-X_L can prevent apoptotic cell death induced by diverse events including abnormal expression of p53 or c-Myc and exposure to chemotherapeutic agents[19-22]. In contrast, down-regulation of Bcl-2 or Bcl-X_L by antisense, siRNA or ribozymes sufficiently sensitize various types of cells destined for apoptosis[23-26]. Clinically, a characteristic feature of follicular lymphoma is the t(14;18) translocation, which brings *bcl-2* under the control of the immunoglobulin heavy chain gene locus leading to elevated Bcl-2 expression[27]. However, a survey of 30 colorectal carcinoma and 24 adenomatous polyps patients suggested that a transition from Bcl-2 to Bcl-X_L expression might occur during progression of colorectal tumors[8]. Only 10% of colon carcinoma patients had increased levels of Bcl-2 in tumor tissues rather than adjacent normal colonic mucosa, and in fact 83% of patients exhibited down regulation of Bcl-2 expression in their tumors[8]. But instead, the level of Bcl-X_L expression was increased in 18 (60%) of 30 colon carcinoma patients. Besides, there

was another study showing elevation of Bcl-X_L expression in 43% of 58 colorectal carcinoma patients[9]. These results were all obtained by immunohistochemical staining. In this study, we exploited the new tissue lysis method and immunoblot analysis to detect 30 (60%) of 50 colorectal carcinoma patients with elevated Bcl-X_L expression. This data compares well with previous immunohistochemical staining data.

Our study also suggests that elevated Bcl-X_L expression preferentially occurred in female colorectal cancer patients ($P = 0.037$). The underlying pathophysiological basis is unclear, but it could be partly attributed to the findings that Bcl-X_L expression can be regulated by female hormones estrogen and progesterone[28,29]. Further investigation is needed to elucidate the relationship between gender and elevated Bcl-X_L expression.

In conclusion, we report a rapid and efficient tissue lysis method compatible with subsequent proteomic and immunoblot analyses, which can facilitate the discovery or detection of cancer gene alterations at the protein level.

REFERENCES

1 **Chao Y,** Shih YL, Chiu JH, Chau GY, Lui WY, Yang WK, Lee SD, Huang TS. Overexpression of Cyclin A but not Skp 2 correlates with the tumor relapse of human hepatocellular carcinoma. *Cancer Res* 1998; **58**: 985-990

2 **Yuan CC,** Huang TS, Ng HT, Liu RS, Hung MW, Tsai LC. Elevated cytokeratin-19 expression associated with apoptotic resistance and malignant progression of human cervical carcinoma. *Apoptosis* 1998; **3**: 161-169

3 **Wittor H,** Aschenbrenner A, Thoenes U, Schnittger S, Leying H. Fully automated sample preparation: use for the detection of BCR-ABL fusion transcripts. *Biochemica* 2000; **3**: 5-8

4 **Noppen C,** Martinato I, Reischl U, Schaefer C. High-speed purification and detection of *Bordetella pertussis* -a straightforward application for MagNA Pure LC and the LightCycler System in microbiological research. *Biochemica* 2001; **1**: 17-19

5 **Fulda S,** Debatin KM. Exploiting death receptor signaling pathways for tumor therapy. *Biochim Biophys Acta* 2004; **1705**: 27-41

6 **Massague J.** G1 cell-cycle control and cancer. *Nature* 2004; **432**: 298-306

7 **Hajra KM,** Liu JR. Apoptosome dysfunction in human cancer. *Apoptosis* 2004; **9**: 691-704

8 **Krajewska M,** Moss SF, Krajewski S, Song K, Holt PR, Reed JC. Elevated expression of Bcl-X and reduced Bak in primary colorectal adenocarcinomas. *Cancer Res* 1996; **56**: 2422-2427

9 **Ogura E,** Senzaki H, Yamamoto D, Yoshida R, Takada H, Hioki K, Tsubura A. Prognostic significance of Bcl-2, Bcl-xL/S, Bax and Bak expressions in colorectal carcinomas. *Oncol Rep* 1999; **6**: 365-369

10 **Lowry OH,** Rosebrough NJ, Lewis Farr A, Randall RJ. Protein measurement with the folin phenol reagent. *J Biol Chem* 1951; **193**: 265-275

11 **Li CP,** Huang JH, Chang AC, Hung YM, Lin CH, Chao Y, Lee SD, Whang-Peng J, Huang TS. A G-quadruplex ligand 3,3'-diethyloxadicarbocyanine iodide induces mitochondrion-mediated apoptosis but not decrease of telomerase activity in nasopharyngeal carcinoma cells. *Pharm Res* 2004; **21**: 93-100

12 **Wu CW,** Chi CW, Huang TS. Elevated level of spindle checkprotein MAD2 correlates with cellular mitotic arrest, but not with aneuploidy and clinicopathological characteristics in gastric cancer. *World J Gastroenterol* 2004; **10**: 3240-3244

13 **Gross A,** McDonnell JM, Korsmeyer SJ. BCL-2 family members and mitochondria in apoptosis. *Genes Dev* 1999; **13**: 1899-1911

14 **Cheng EH,** Wei MC, Weiler S, Flavell RA, Mak TW, Lindsten T, Korsmeyer SJ. BCL-2, BCL-X(L) sequester BH3 domain-only molecules preventing BAX- and BAK-mediated mitochondrial apoptosis. *Mol Cell* 2001; **8**: 705-711

15 **Liu QY,** Stein CA. Taxol and estramustine-induced modulation of human prostate cancer cell apoptosis via alteration in bcl-xL and bak expression. *Clin Cancer Res* 1997; **3**: 2039-2046

16 **Jones NA,** Turner J, McIlwrath AJ, Brown R, Dive C. Cisplatin- and paclitaxel-induced apoptosis of ovarian carcinoma cells and the relationship between bax and bak up-regulation and the functional status of p53. *Mol Pharmacol* 1998; **53**: 819-826

17 **Po LS,** Wang TT, Chen ZY, Leung LK. Genistein-induced apoptosis in MCF-7 cells involves changes in Bak and Bcl-x without evidence of anti-oestrogenic effects. *Br J Nutr* 2002; **88**: 463-469

18 **Menzel T,** Schauber J, Kreth F, Kudlich T, Melcher R, Gostner A, Scheppach W, Luhrs H. Butyrate and aspirin in combination have an enhanced effect on apoptosis in human colorectal cancer cells. *Eur J Cancer Prev* 2002; **11**: 271-281

19 **Henry H,** Thomas A, Shen Y, White E. Regulation of the mitochondrial checkpoint in p53-mediated apoptosis confers resistance to cell death. *Oncogene* 2002; **21**: 748-760

20 **Hoang AT,** Cohen KJ, Barrett JF, Bergstrom DA, Dang CV. Participation of cyclin A in Myc-induced apoptosis. *Proc Natl Acad Sci USA* 1994; **91**: 6875-6879

21 **Panaretakis T,** Pokrovskaja K, Shoshan MC, Grander D. Activation of Bak, Bax, and BH3-only proteins in the apoptotic response to doxorubicin. *J Biol Chem* 2002; **277**: 44317-44326

22 **Lebedeva I,** Rando R, Ojwang J, Cossum P, Stein CA. Bcl-xL in prostate cancer cells: effects of overexpression and down-regulation on chemosensitivity. *Cancer Res* 2000; **60**: 6052-6060

23 **Keith FJ,** Bradbury DA, Zhu YM, Russell NH. Inhibition of bcl-2 with antisense oligonucleotides induces apoptosis and increases the sensitivity of AML blasts to Ara-C. *Leukemia* 1995; **9**: 131-138

24 **Xu Z,** Friess H, Solioz M, Aebi S, Korc M, Kleeff J, Buchler MW. Bcl-x(L) antisense oligonucleotides induce apoptosis and increase sensitivity of pancreatic cancer cells to gemcitabine. *Int J Cancer* 2001; **94**: 268-274

25 **Holle L,** Hicks L, Song W, Holle E, Wagner T, Yu X. Bcl-2 targeting siRNA expressed by a T7 vector system inhibits human tumor growth *in vitro*. *Int J Oncol* 2004; **24**: 615-621

26 **Dorai T,** Perlman H, Walsh K, Shabsigh A, Goluboff ET, Olsson CA, Buttyan R. A recombinant defective adenoviral agent expressing anti-bcl-2 ribozyme promotes apoptosis of bcl-2-expressing human prostate cancer cells. *Int J Cancer* 1999; **82**: 846-852

27 **Graninger WB,** Seto M, Boutain B, Goldman P, Korsmeyer SJ. Expression of Bcl-2 and Bcl-2-Ig fusion transcripts in normal and neoplastic cells. *J Clin Invest* 1987; **80**: 1512-1515

28 **Pike CJ.** Estrogen modulates neuronal Bcl-xL expression and beta-amyloid-induced apoptosis: relevance to Alzheimer's disease. *J Neurochem* 1999; **72**: 1552-1563

29 **Bagheri-Yarmand R,** Talukder AH, Wang RA, Vadlamudi RK, Kumar R. Metastasis-associated protein 1 deregulation causes inappropriate mammary gland development and tumorigenesis. *Development* 2004; **131**: 3469-3479

Science Editor Guo SY **Language Editor** Elsevier HK

PO Box 2345, Beijing 100023, China
www.wjgnet.com
wjg@wjgnet.com

ELSEVIER

World J Gastroenterol 2005;11(33):5169-5173
World Journal of Gastroenterology ISSN 1007-9327
© 2005 The WJG Press and Elsevier Inc. All rights reserved.

Novel genetic variations of the p53R2 gene in patients with colorectal adenoma and controls

Zong-Lin Deng, Da-Wen Xie, Roberd M Bostick, Xi-Jiang Miao, You-Ling Gong, Jin-Hui Zhang, Michael J Wargovich

Zong-Lin Deng, Da-Wen Xie, You-Ling Gong, Jin-Hui Zhang, Department of Epidemiology and Biostatistics, University of South Carolina School of Public Health and South Carolina Cancer Center, Columbia SC 29203, United States
Roberd M Bostick, Department of Epidemiology, Rollins School of Public Health, Emory University, Atlanta, GA 30322, United States
Xi-Jiang Miao, Department of Computer Science and Engineering, University of South Carolina, Columbia SC 29201, United States
You-Ling Gong, Tumor Center, West China Hospital, Sichuan University, Chengdu 610041, Sichuan Province, China
Michael J Wargovich, Department of Pathology, University of South Carolina School of Medicine and South Carolina Cancer Center, Columbia SC 29203, United States
Supported by the No. R03 CA92773-01A1 Grant to DX and No. R01 CA66539 Grant to RMB from the National Cancer Institute from National Institutes of Health, Department of Health and Human Services
Co-first-authors: Zong-Lin Deng and Da-Wen Xie
Correspondence to: Dr. Da-Wen Xie, University of South Carolina, 14 Richland Medical Park, Suite 500, Columbia, SC 29203, United States. dawen.xie@palmettohealth.org
Telephone: +1-803-434-3707 Fax: +1-803-434-3795
Received: 2005-01-12 Accepted: 2005-02-18

Abstract

AIM: p53-Inducible ribonucleotide reductase small subunit 2 (p53R2) encodes a 351-amino-acid peptide, which catalyzes conversion of ribonucleoside diphosphates to the corresponding deoxyribonucleotides required for DNA replication and repair. A recent study reported that a point mutation (G/T) in the p53 binding sequence in a colon cancer cell line completely impaired p53R2 protein activity.

METHODS: We screened the p53R2 gene coding regions and a regulatory region which contains a p53 binding sequence in 100 patients with colorectal adenoma and 100 control subjects using PCR, cold SSCP, and direct DNA sequencing.

RESULTS: Although we did not identify genetic variation in all nine exons, four regulatory-region variants were found, of which three were single nucleotide polymorphisms (SNPs) (nt 1 789 C/G, nt 1 928 A/G, 1 933 T/C), and one was 20 bp insertion which replaced a ATTTT between nt 1 831 and 1 835. Additionally, we determined the frequency of these p53R2 variants in a recently concluded case-control study of incident sporadic colorectal adenomas (163 cases and 210 controls).

CONCLUSION: Although more detailed functional characterizations of these polymorphisms remain to be undertaken, these polymorphic sites may be useful for identifying alleles associated with mis-splicing, additional transcript factors and, more generally, in cancer-susceptibility association studies.

© 2005 The WJG Press and Elsevier Inc. All rights reserved.

Key words: Genetic polymorphism; Colorectal neoplasia; p53R2; SSCP; PCR-RFLP

Deng ZL, Xie DW, Bostick RM, Miao XJ, Gong YL, Zhang JH, Wargovich MJ. Novel genetic variations of the p53R2 gene in patients with colorectal adenoma and controls. *World J Gastroenterol* 2005; 11(33): 5169-5173
http://www.wjgnet.com/1007-9327/11/5169.asp

INTRODUCTION

The p53 gene is a major target for genetic alterations or biochemical activations in human cancer. However, the mechanism by which p53 exerts its effects or alters other signaling systems is largely unknown. In recent years, a number of specific p53 target genes have been discovered that are likely to be involved in downstream target effects of altered p53 protein, including cell-cycle arrest, apoptosis, and tumor suppression. Recently, an important p53 downstream target gene, p53-inducible ribonucleotide reductase small subunit 2 (p53R2) consisting of nine exons and a p53-banding sequence in intron 1, was identified in cancer cell lines[1]. Human ribonucleotide reductase catalyzes the rate-limiting step in the production of deoxyribonucleotide triphosphate (dNTP), which is required for DNA replication and repair[2]. This enzyme is also regulated by the cell cycle[3]. The R2 subunit is made late in the G1 phase before DNA replication, and disappears in late S or early G2. p53R2 is a gene that is essential for DNA repair, and loss of function of this gene results in dysfunctional repair mechanisms[1]. Polymorphisms in either the regulatory or coding regions of the p53R2 gene may affect its expression and protein function, altering an individual's response to DNA damage, and thus affecting the risk of colorectal cancer. We screened the p53R2 gene coding regions and a regulatory region, which contains a p53 binding sequence, in 100 patients with colorectal adenoma and 100 control subjects for single-nucleotide polymorphisms and other mutations using PCR, cold SSCP, and direct DNA sequencing. Herein, we report several novel genetic variations designated as *Dde*I, *Nde*I, *Hha*I (according to restriction enzymes cut sites), and 20 bp insertion. Subsequently, we determined the allele frequencies

of the observed polymorphisms in 163 cases of incident sporadic colorectal adenoma and 216 colonoscopy negative controls.

MATERIALS AND METHODS

Study population

From 1994 to 1997, the Markers for Adenomatous Polyps (MAP) case-control study was conducted to assess the validity of colonic epithelial cell proliferation as a biomarker of risk for incident sporadic colorectal adenomatous polyps. Prior to the beginning of the study, MAP was approved by the Institutional Review Board of Wake Forest University School of Medicine in accordance with an assurance filed with and approved by the Department of Health and Human Services. Informed consent was obtained from each participant.

Eligibility criteria for study subjects consisted of English speaking adults from 30 to 74 years of age, of either sex, and of all races who were scheduled for elective outpatient colonoscopy by four large gastroenterology practices in Winston-Salem and Charlotte, North Carolina. Patients increased in number over a 24-mo period. Cases were identified as eligible colonoscopy patients who were determined to have a study index of pathologist-confirmed incident adenomatous polyps according to the criteria adapted from the National Polyp Study[4]. Controls consisted of all eligible colonoscopy patients with no previous history of adenomatous polyps and who were found to be free of adenomatous polyps. Persons with familial polyposis, Gardner's syndrome, ulcerative colitis, Crohn's disease, bowel resection, newly diagnosed recurrent adenomatous polyps, and incident colon cancer were excluded, as they had a history of cancer other than non-melanoma skin cancer. Blood was drawn and stored at -70 ℃ for possible later measurement of various genotypes.

Subjects

Among all three clinical sites, 2 246 colonoscopy patients were identified. Of these, 669 were eligible on initial screening (eligibility rate 29.8%), and of these 633 were willing to discuss the study, 617 of these were contacted, and 417 of these signed consent and had study colonoscopies (consent rate 63.1%). Of the 417 participants, 259 had some types of polyp, and of these, 179 had adenomatous polyps. Nine of the 417 total patients were subsequently determined ineligible for the study and 8 additional patients had incident colon cancer and were not eligible for the primary case-control analyses; thus, 400 patients were available for genotypic analysis. Of these 400 patients, viable DNA was isolated from 373 (163 cases and 210 controls) for genotyping.

Genomic DNA isolation

Genomic DNA was obtained from stored white blood cells (WBCs) digested in 500 μL of lysis buffer (50 mmol/L Tris-HCl, pH 8.5, 1 mmol/L EDTA, 0.2% SDS, 200 g/mL proteinase K) overnight at 55 ℃ with shaking. The digestion was precipitated directly with isopropanol and the pellets were washed with 70% ethanol. The genomic DNA pellets (50-100 μg) were dissolved in 300-800 μL of TE buffer, of which about 1 μL was used for each PCR reaction.

PCR amplification

The primers (Table 1) and PCR product sizes were designed following published genomic DNA sequences (GenBank accession no.: NC_000008). We designed primers that were 18-25 bases long with a 40-60% GC content and an annealing temperature (T_m) around 52-68 ℃. To obtain the optimal conditions for PCR amplification, we ran a set of PCRs with various concentrations of Mg^{++}, template DNA, dNTPs, and primers for each fragment.

Cold single-strand conformation polymorphism analysis

Five microliters of the PCR product was mixed with 15 μL denatured buffer [0.4 μL 1 mol/L MMH (methylmercury hydroxide), 12.6 μL 1.25×TBE, 2.0 μL 15% Ficoll containing 0.1% bromophenol blue, and 0.1% cyanol xylene blue], and then incubated for 10 min at room temperature, heated for 5 min at 95 ℃, and put on ice before being loaded on 20% TBE polyacrylamide gel and electrophoresed in a Novex Thermoflow system for 4-5 h at 10-15 ℃ at 300 V. The gel was stained in 1×TBE with 5 μg/mL ethidium bromide for 10 min and visualized on a UV lamp (Figure 1B). The shift bands were cut and re-amplified for direct sequencing.

DNA sequencing

For direct sequencing, the PCR products amplified from genomic DNA were purified and directly used for sequencing. DNA was sequenced with the Thermal Sequenase Cycle Sequencing Kit from Amersham Life Science (Cleveland, OH, USA) according to manufacturer's instructions. In cycle sequencing, the thermal cycle consisted of 2 min at 94 ℃, 45 cycles of 1 min at 94 ℃, 1 min at 60 ℃, and 1 min at 72 ℃. The reaction mixture was loaded on a 6% polyacrylamide sequencing gel made from Sequagel DNA Sequencing Solutions (National Diagnostics, GA, USA).

Restriction fragment length polymorphism

Since polymorphisms at the nt 1 789 G and nt 1 923 C alleles created *Dde*I and *Hha*I restriction enzyme cut sites, respectively, each PCR product was subjected to *Dde*I and *Hha*I restriction enzymes digestion prior to electrophoresis for determining genotype frequencies. The DNA fragments were then separated using 3% 2:1 Nusiev/SeaKern agarose gel. The allele types were determined for *Dde*I analysis as follows: three fragments of 6, 171, and 373 bp for the C allele, four fragments of 6, 97, 171, and 276 bp for the G allele; and five fragments of 6, 171, 276, and 373 bp for the C/G allele. The allele types were determined for *Hha*I analysis as follows: three fragments of 550 bp for the T allele, two fragments of 299 and 251 bp for the C allele; and three fragments of 550, 299, and 251 bp for the T/C allele nt 1 928 A/G, the polymorphism does not have a suitable restriction enzyme site. Therefore, we changed an A nucleotide to a T in the near 3' end of the forward primer. This change combines with the wild type allele (A) to create an *Nde*I cutting site, but does not do so with the variant allele (G). The PCR products (10 μL) were subjected to *Nde*I restriction enzyme. Bands for the wild-type (A/A) allele

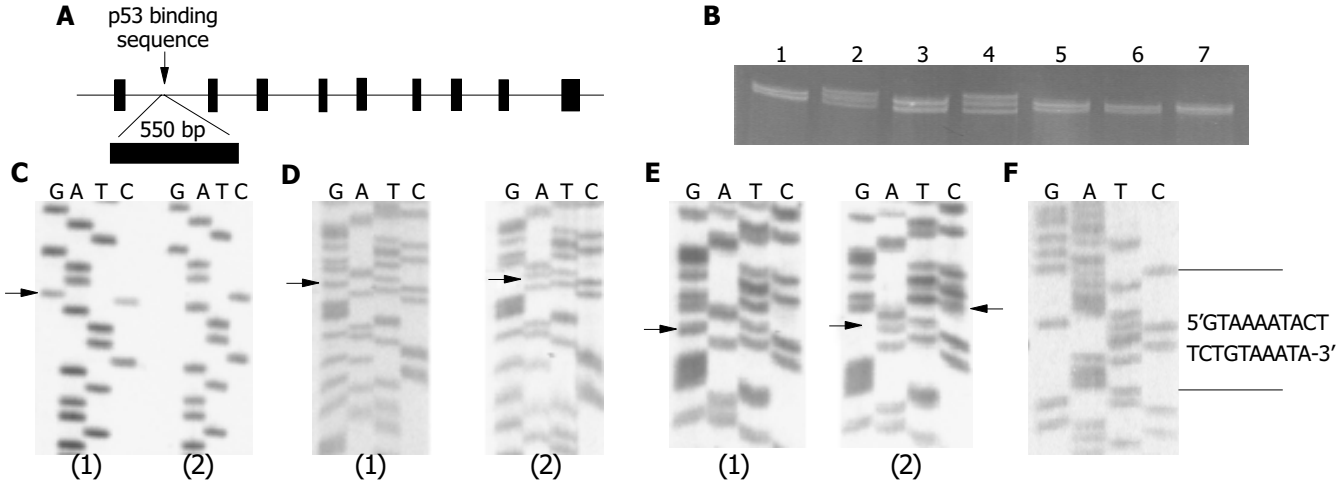


Figure 1 Structural feature and genetic variation analysis of p53R2. **A:** A representative p53R2 gene structure including a regulatory region with p53 binding sequence within intron 1; **B:** representative cold SSCP result. p53R2 Regulatory region was amplified, and PCR products were run on a 20% SSCP gel at 15 ℃. Lanes 2 and 4 are the heterozygous polymorphism pattern; **C:** alterations in regulatory region of p53R2 gene: (1) DdeI G/C, and (2) DdeI C/C genotypes; **D:** Alterations in regulatory region of p53R2 gene: (1) NdeI G/G and (2) A/A genotypes; **E:** Alterations in regulatory region of p53R2 gene: (1) NdeI G/G and HhaI T/T, and (2) NdeI A/A and HhaI T/C genotypes; **F:** Alterations in regulatory region of p53R2 gene: 20 bp insertion which replaced an ATTTT between nt 1 831 and nt 1 835.

were cut into 246 and 26 bp; the G/G variant allele showed at 272 bp; and the heterozygote (A/G) allele was cut into 272, 246, and 26 bp fragments (Figure 2).

Statistical analyses

All statistical inquiries were conducted using R language version 1.9.0 from http://www.R-project.org. Homogeneity test was used to check the non-dependency between genotypes and the frequencies of the p53R2 gene variants between the patients with colorectal adenoma and the control groups. Consistency of the genotype frequencies with the Hardy-Weinberg equilibrium was also tested by χ^2-analysis.

RESULTS

We screened nine exons and a regulatory region in first intron of p53R2 gene in 200 subjects including 100 patients with colorectal adenoma and 100 control subjects for mutation identification. No mutation was found in any of the nine exons; however, three SNP variations (nt 1 789 C/G, nt 1 928 A/G, and nt 1 933 T/C) were identified in the first intron of the p53R2 gene by cold SSCP (Figure 1B), and confirmed by direct DNA sequencing (Figures 1C-E and Table 2). A 20 bp variant, which is a short insertion variation that replaced 5 bp between nt 1 831 and nt 1 835 (Figure 1F and Table 2), was also found (Table 2). These polymorphisms are summarized in Figure 2.

Restriction enzyme mapping showed two restriction enzymes that could be used for population screening for nt 1 789 C/G (*Dde*I) and nt 1 933 T/C (*Hba*I) variations. We also designed a modified RFLP (*Nde*I) method for population screening for the nt 1 928 A/G alteration (Figure 2).

Table 1 Primers for PCR amplification, sequencing and RFLP (GenBank accession no. AC021004)

Number	Name	Sequence	PCR product (bp)
1	Exon 1 (F)	5’-GGAGAGTCACTCAATGGAC-3’	302
2	Exon 1 (R)	5’-CCTGCAACTTGCAATCTAAC-3’	
3	Exon 2 (F)	5’-GGAACACTGCACTATAGGATG-3’	291
4	Exon 2 (R)	5’-CCCTGACTTCCTTAGATG-3’	
5	Exon 3 (F)	5’-GCTAAAGGAGAACAAAAG-3’	218
6	Exon 3 (R)	5’-CCAAACACTTTGAGAAGAAC-3’	
7	Exon 4 (F)	5’-GCTCAGAAACTTCCATACTTG-3’	336
8	Exon 4 (R)	5’-CGATAATGCTGATGTCCAG-3’	
9	Exon 5 (F)	5’-CGTACTGGATAGTCACAC-3’	287
10	Exon 5 (R)	5’-CGAGATCGTGCCACTGCAC-3’	
11	Exon 6 (F)	5’-GGCACTAACTTGTGTATTTTG-3’	284
12	Exon 6 (R)	5’-CTAGAAAAACATTCCATTCC-3’	
13	Exon 7 (F)	5’-GGTACAAACATCAGAGAAAG-3’	224
14	Exon 7 (R)	5’-CCATCACCATATGCAAATAG-3’	
15	Exon 8 (F)	5’-GGTCCTTGCTTTCCTATA-3’	239
16	Exon 8 (R)	5’-CGAAAGTCCTCTTTCTA-3’	
17	Exon 9 (F)	5’-GCAGAGGAAAATAGACTAC-3’	317
18	Exon 9 (R)	5’-GGTTTTGAGAAACCTGAC-3’	
19	Intron 1 (F)	5’-CAGGACTCAGTAGAGGAGCT-3’	550
20	Intron 1 (R)	5’-CACAGGGTCAGTGACACTG-3’	

Table 2 Allele distributions at four polymorphic loci in the human p53R2 gene from a case-control study of incident sporadic colorectal adenoma

	Cases (n = 163)		Controls (n = 210)		P
	n	%	n	%	
*Dde*I					
CC	143	87.7	185	85.6	
GG	1	0.6	2	0.9	
CG	19	11.7	29	13.4	0.82
*Nde*I					
GG	131	80.4	178	82.4	
AA	1	0.6	6	2.8	
AG	30	18.4	31	14.4	0.25
*Hha*I					
TT	159	97.6	210	97.2	
CT	4	2.4	6	2.8	
CC	0	0	0	0	0.90
Insertion					
(+)	4	2.4	0	0	-

1 621 AATCTAATTC ATAGTCTATT GTCAAGGTAA AGTTTAGGCC AGAAAACATT AAATGGCATG
forward primer
1 681 **CCCAGGACTC AGTAGAGGAG CT**AAATTTAA AACCAAGTTC TTGCACCTGG GCGGGTATCC
DdeI
1 741 CATTGGTTCC GTCAGACTTT GTGGGAATAG AAGTGAAAAT AATACTTACA AGTAGTGTAT
G
1 801 GACTATGACA ACATACAGCT ATTTTACAGA AGTAGAAGAG ACATAAAGGC AAAGAAACGG
1 861 AAGTGGTGGA ATTGGGGCTG GATAGGAGGT AAGAGCCTGG TATGATGCCA GCCTAGATTG
*Nde*I *Hha*I
1 921 GGGCATCGTA AGTGCTTGCT GGGAAATCTT GACCTAAATT *GTTGTCCTGA CATGCCCAGG*
A C p53 binding sequence
1 981 CATGTCTTCC AACTGGGTGA CCAGAAATTG AGTCAGTCGG AAACTGGAAG TACCATTCTG
2 041 GAAAAAACAG CAGAATGTCA CTAAGGAATG CCTACTGCTA AACTTTATTT CAAATTCTCA
2 101 TCACTTTACA CCTGTGCGGC TATAATAATT TTGTTGTTTC TCTATCTCCT ATCTTACCTG
2 161 CCATTCAATC CTAATTACCA TTGCCAAGTT AATCCTTCAT TAGACCAGTG CC**TCAGTGTC**
2 221 ACTGACCCTG TGTCCCCCAA AAAACTCCCA AAAGAGTCTC AATTCCTACC AAAAAGCCTG
reverse primer
2 281 GCCAACACCT CAGGCTGGTG AAGTCTTGTT GAAGCTGCTT TTTTCATGCT AACTGCCACA
2 341 TCTTAATTCA AGTCCTCATT TCCATCTTTG AAATTGGTTC CTTAGTTGCT TGCAAAATCT

Figure 2 Representation of p53R2 intron 1. The human p53R2 partial intron 1, as enumerated in the original description of the p53R2 gene (GenBank accession no.: NC000008), is shown. The three variable loci are underlined, boxed 5 bp is replaced by 20 bp nucleotides (5'-GTAAAATACTTCTGTAAATA-3'), the p53 binding sequence is italicized, and forward and reverse primers set in bold.

Therefore, C/G, T/C, and A/G polymorphisms were designated *Dde*I, *Hba*I, and *Nde*I, respectively. Then, frequencies of these variations were determined in all of the 373 subjects (cases = 163, control = 210) from case-control study (Table 2). Since each of these four variations is close to the p53 binding sequence, they may play important roles in maintaining a three-dimensional structure with the p53 binding sequence. Of the four variations, the *Hba*I polymorphism occurred at a very low frequency (2.78%). The 20 bp variant was found in only 4 patients, all adenoma cases. The distribution of *Dde*I genotypes C/C, C/G, G/G, and G/G combined with C/G were 87.7%, 11.7%, 0.6% and 12.3% in cases, compared to 85.7%, 13.4%, 0.9% and 14.3% in controls, respectively. The distribution of *Nde*I genotypes G/G, G/A, A/A, and A/A combined with G/A were 80.0%, 18.4%, 1.23% and 19.6% in cases, compared with 82.8%, 14.4%, 2.79%, 17.2% in controls, respectively. All polymorphisms were in Hardy-Weinberg equilibrium in all populations, with the exception of the 20 bp variant, which was found in 4 patients only, all with colorectal adenoma. There is no statistical difference between the cases and control subjects (Table 2).

DISCUSSION

p53-Inducible ribonucleotide reductase small subunit 2 (p53R2) is an important p53 downstream target gene that is essential for DNA repair[1]. It has been demonstrated that p53R2 has an important role in delivering dNTP and maintaining the dNTP pool in response to DNA damage. Loss of function of this gene results in dysfunctional repair mechanisms.

Single-strand conformation polymorphism (SSCP) is a technique for detecting known and unknown genetic variation using PCR products[5]. Using this method about 70-90% of unknown mutations can be detected. Single strands assume a specific folded conformation, when double-stranded PCR product is denatured to single strand. These conformers

are separated by non-denaturing polyacrylamide gel electrophoresis. A single base mutation can cause a change in the folded conformation compared to the wild type and can change the separation pattern. This means that a change in separation pattern compared to that of the wild type indicates a mutation.

Using these methods, we here report mutation screening of the p53R2 gene, identification of four novel genetic variations in a regulatory region, their allele frequencies in both normal and colorectal adenoma populations, and the predicted functional impact of resulting transcriptional changes. Since each of these four mutations is close to the p53 binding sequence, these variations may play an important role in maintaining a three-dimensional structure with the p53 binding sequence. As of May 2004, only two polymorphisms of the p53R2 gene (-88 C/A and 8 bp insertion) have been reported[6,7]. We searched the available literature and the NCBI SNP database, and found no published information on these novel variants. To our knowledge, this is the first report of allele frequencies of novel p53R2 polymorphisms in a population consisting of patients with colorectal adenoma and controls.

Somatic mutation screening of p53R2 has been previously investigated in cancer. On the whole, two studies investigated the genetic variation of p53R2 in gastric and urothelial carcinoma[8,9]. Byun *et al*., did not detect any somatic variations in the p53R2 gene in 105 gastric carcinomas, including 15 cell lines[8]. One non-synonymous coding variant (Glu136/Asp) was identified in urothelial carcinoma; however, the frequency was rare (1/108)[9]. It was concluded that p53R2 is not a critical target of genetic inactivation in tumorigenesis.

Genetic polymorphisms have been identified in many genes related to DNA synthesis and repair, such as thymidylate synthase (TS)[10,11], MTHFR[11,12], and XRCC1[13,14]. Genetic polymorphisms could affect gene expression, enzyme function, or the protein's interaction with environmental and nutritional factors to modify the risk of neoplasia as we have demonstrated for other polymorphisms[15]. An 8 bp tandem repeat and a -88 C/A polymorphism were discovered in the 5'-untranslated region of the p53R2 gene[8,9]. Three polymorphisms in 3'-untranslated region of p53R2 gene were also identified[16]. Since we focused only on exons and the first intron regulatory regions, we did not investigate these polymorphisms.

As physical locations of these polymorphisms are so close to the p53 binding sequence as described above, it will be quite interesting to investigate their associations with cancer risk. Because polymorphic alleles at loci as close together as these are likely to be transmitted together, it will also be of interest to define haplotypes for the p53R2 gene.

In summary, we have reported newly identified polymorphisms in the p53R2 gene, and shown allele frequencies of the new variants in a case-control study population consisting of 163 patients with colorectal adenoma and 210 control subjects. Since p53R2 is important in response to DNA damage, and thus may also be in colon cancer prevention, genetic polymorphisms that may alter the expression of this gene are of interest. Further studies of the functional impact of these polymorphisms are needed. It would also be of great interest to investigate their possible association with colorectal cancer risk.

REFERENCES

1 **Tanaka H**, Arakawa H, Yamaguchi T, Shiraishi K, Fukuda S, Matsui K, Takei Y, Nakamura Y. A ribonucleotide reductase gene involved in a p53-dependent cell-cycle checkpoint for DNA damage. *Nature* 2000; **404**: 42-49

2 **Jordan A**, Reichard P. Ribonucleotide reductases. *Annu Rev Biochem* 1998; **67**: 71-98

3 **Bjorklund S**, Skog S, Tribukait B, Thelander L. S-phase-specific expression of mammalian ribonucleotide reductase R1 and R2 subunit mRNAs. *Biochemistry* 1990; **29**: 5452-5458

4 **O'Brien MJ**, Winawer SJ, Zauber AG, Gottlieb LS, Sternberg SS, Diaz B, Dickersin GR, Ewing S, Geller S, Kasimian D. The National Polyp Study. Patient and polyp characteristics associated with high-grade dysplasia in colorectal adenomas. *Gastroenterology* 1990; **98**: 371-379

5 **Hongyo T**, Buzard GS, Calvert RJ, Weghorst CM. 'Cold SSCP': a simple, rapid and non-radioactive method for optimized single-strand conformation polymorphism analyses. *Nucleic Acids Res* 1993; **21**: 3637-3642

6 **Smeds J**, Kumar R, Hemminki K. Polymorphic insertion of additional repeat within an area of direct 8 bp tandem repeats in the 5'-untranslated region of the p53R2 gene and cancer risk. *Mutagenesis* 2001; **16**: 547-550

7 **Smeds J**, Nava M, Kumar R, Hemminki K. A novel polymorphism (-88 C>A) in the 5' UTR of the p53R2 gene. *Hum Mutat* 2001; **17**: 82

8 **Byun DS**, Chae KS, Ryu BK, Lee MG, Chi SG. Expression and mutation analyses of P53R2, a newly identified p53 target for DNA repair in human gastric carcinoma. *Int J Cancer* 2002; **98**: 718-723

9 **Hayashi H**, Furihata M, Kuwahara M, Kagawa S, Shuin T, Ohtsuki Y. Pathobiology. Infrequent alteration in the p53R2 gene in human transitional cell carcinoma of the urinary tract. *Pathobiology* 2004; **71**: 103-106

10 **Horie N**, Aiba H, Oguro K, Hojo H, Takeishi K. Functional analysis and DNA polymorphism of the tandemly repeated sequences in the 5'-terminal regulatory region of the human gene for thymidylate synthase. *Cell Struct Funct* 1995; **20**: 191-197

11 **Chen J**, Giovannucci E, Kelsey K, Rimm EB, Stampfer MJ, Colditz GA, Spiegelman D, Willett WC, Hunter DJ. A methylenetetrahydrofolate reductase polymorphism and the risk of colorectal cancer. *Cancer Res* 1996; **56**: 4862-4864

12 **Ma J**, Stampfer MJ, Giovannucci E, Artigas C, Hunter DJ, Fuchs C, Willett WC, Selhub J, Hennekens CH, Rozen R. Methylenetetrahydrofolate reductase polymorphism, dietary interactions, and risk of colorectal cancer. *Cancer Res* 1997; **57**: 1098-1102

13 **Shen MR**, Jones IM, Mohrenweiser H. Nonconservative amino acid substitution variants exist at polymorphic frequency in DNA repair genes in healthy humans. *Cancer Res* 1998; **58**: 604-608

14 **Ratnasinghe DL**, Yao SX, Forman M, Qiao YL, Andersen MR, Giffen CA, Erozan Y, Tockman MS, Taylor PR. Gene-environment interactions between the codon 194 polymorphism of XRCC1 and antioxidants influence lung cancer risk. *Anticancer Res* 2003; **23**: 627-632

15 **Lewis RC**, Bostick RM, Xie D, Deng Z, Wargovich MJ, Fina MF, Roufail WM, Geisinger KR. Polymorphism of the cyclin D1 gene, CCND1, and risk for incident sporadic colorectal adenomas. *Cancer Res* 2003; **63**: 8549-8553

16 **Ye Z**, Parry JM. The discovery and confirmation of single nucleotide polymorphisms in the human p53R2 gene by EST database analysis. *Mutagenesis* 2002; **17**: 361-364

Science Editor Guo SY **Language Editor** Elsevier HK

PO Box 2345, Beijing 100023, China
www.wjgnet.com
wjg@wjgnet.com

ELSEVIER

World J Gastroenterol 2005;11(33):5174-5179
World Journal of Gastroenterology ISSN 1007-9327
© 2005 The WJG Press and Elsevier Inc. All rights reserved.

Helicobacter pylori infection in relation to *E-cadherin* gene promoter polymorphism and hypermethylation in sporadic gastric carcinomas

Yao-Chi Liu, Chen-Yang Shen, Hurng-Sheng Wu, De-Chuan Chan, Cheng-Jueng Chen, Jyh-Cherng Yu, Cheng-Ping Yu, Horng-Jyh Harn, Rong-Yaun Shyu, Yu-Lueng Shih, Chung-Bao Hsieh, Huan-Mieng Hsu

Yao-Chi Liu, De-Chuan Chan, Cheng-Jueng Chen, Jyh-Cherng Yu, Chung-Bao Hsieh, Huan-Mieng Hsu, Division of General Surgery, Department of Surgery, Tri-Service General Hospital, National Defense Medical Center, Taipei, Taiwan, China
Rong-Yaun Shyu, Yu-Lueng Shih, Division of Gastroenterology, Department of Internal Medicine, Tri-Service General Hospital, National Defense Medical Center, Taipei, Taiwan, China
Cheng-Ping Yu, Department of Pathology, Tri-Service General Hospital, National Defense Medical Center, Taipei, Taiwan, China
Horng-Jyh Harn, Department of Pathology, Buddhist Tzu-Chi General Hospital, Hualien, Taiwan, China
Hurng-Sheng Wu, Department of Surgery, Show Chwan Memorial Hospital, Changhua, Taiwan, China
Chen-Yang Shen, Institute of Biomedical Sciences, Academia Sinica, Taipei, Taiwan, China
Supported by Clinical Research Fund of the Tri-Service General Hospital and CY Foundation for Advancement of Education, Science and Medicine, Taipei, Taiwan, China
Correspondence to: Dr. Yao-Chi Liu, Division of General Surgery, Tri-Service General Hospital, No. 325, Sec. 2, Cheng-Kung Road, Neihu 114, Taipei, Taiwan, China. dlyaochi@yahoo.com.tw
Telephone: +886-2-87927191 Fax: +886-2-87927372
Received: 2004-12-30 Accepted: 2005-02-18

Abstract

AIM: To study *Helicobacter pylori* (*H pylori*) infection in relation to *E-cadherin* (*E-cad*) promoter polymorphism and hypermethylation in GCs.

METHODS: Specimens were taken from representative cancerous lesions and adjacent non-cancerous epithelia of 67 resected GCs. *H pylori* was detected by real-time PCR of the *cagA* gene from non-neoplastic epithelium. *E-cad* promoter polymorphism and hypermethylation were determined by restriction fragment length polymorphism analysis and methylation-specific PCR, respectively. Expression of *E-cad* protein was determined by immunohistochemistry.

RESULTS: *H pylori* was found in 57% of patients with GC. *H pylori* infection was more frequently found in tumors with the -160C/C genotype than those with the -160C/A and -160A/A genotypes (74% *vs* 47%, $P = 0.02$). *H pylori* infection was associated with *E-cad* methylation in non-neoplastic epithelium; however, no significant difference in *H pylori* was observed between methylated and unmethylated cancerous lesions.

CONCLUSION: Patients with the -160C/C genotype might require *H pylori* infection to promote the inactivation of *CDH1*, suggesting that *H pylori* infection might affect GC in an initial stage because polymorphism is germ line. Mechanism of hypermethylation of *CDH1* promoter in GC is complex, and *H pylori* infection might affect it in an initial stage.

© 2005 The WJG Press and Elsevier Inc. All rights reserved.

Key words: *H pylori*; *E-cadherin*; -160 C→A polymorphism; Hypermethylation; Gastric carcinoma

Liu YC, Shen CY, Wu HS, Chan DC, Chen CJ, Yu JC, Yu CP, Harn HJ, Shyu RY, Shih YL, Hsieh CB, Hsu HM. *Helicobacter pylori* infection in relation to *E-cadherin* gene promoter polymorphism and hypermethylation in sporadic gastric carcinomas. *World J Gastroenterol* 2005; 11(33): 5174-5179
http://www.wjgnet.com/1007-9327/11/5174.asp

INTRODUCTION

E-cadherin (E-cad, also known as CDH1) is a member of a family of transmembrane glycoproteins expressed on epithelial cells and is responsible for calcium-dependent cell-to-cell adhesion[1]. E-cad forms complexes and connects actin filaments with α-, β-, and γ-catenins[2,3], which is crucially involved in neoplastic transformation and metastasis[4,5]. Loss of cell adhesion may contribute to loss of contact inhibition of growth, which is an early step in the neoplastic process. Furthermore, loss of cadherin activity may result in cancer cell detachment and metastasis[6,7].

Gastric carcinogenesis is a multistep process with morphological progression involving multiple genetic and epigenetic events, whereas *CDH1* is an important putative tumor suppressor gene. In gastric carcinoma (GC), the percentage reduction in E-cad expression varies from 17% to 92%, and is more frequent in diffuse type carcinomas than in intestinal types[8-13]. Germ-line mutation of the *CDH1* gene is found in familial GCs[14,15]. Somatic mutations of *E-cad* are found in more than 50% of gastric carcinomas of the diffuse type[16-18]. In addition to the classic two-hit inactivation mechanism, *CDH1* can be silenced by cytosine-guanosine (CpG) sequence methylation in GC[17,18]. Moreover, Li *et al*., reported that -160C/A polymorphism has a direct effect on the transcriptional regulation of CDH1[19].

Helicobacter pylori (*H pylori*) is the single most important

etiological factor for gastric cancer development. The strongest evidence comes from three independent, nested case-control studies in which pre-existing infection markedly increased the risk of GC[20-22]. It is estimated that approximately 60% of all GC cases can be attributed to *H pylori* infection[20]. However, there are few data in the molecular profiles of E-cad of *H pylori*-positive and *H pylori*-negative GCs[23].

El-Omar *et al*.[24], reported that interleukin-1 polymorphisms that cause the up-regulation of interleukin-1β with *H pylori* infection are associated with an increased risk of GC. Moreover, Hmadcha *et al*.[25], found that interleukin-1β might induce gene methylation through the production of nitric oxide and the subsequent activation of DNA methyltransferase. It is possible that *H pylori* infection induces methylation through the production of interleukin-1β. In this study, we investigated the relationship between *H pylori* infection and *CDH1* methylation. Since -160C/A polymorphism is germ line, we also investigated the relationship between *H pylori* infection and polymorphism, to find if *H pylori* infection affects tumorigenesis in the initial stage.

MATERIALS AND METHODS

Patients and samples

The specimens were surgically obtained from 67 patients with GC between 2000 and 2002, at the Division of General Surgery, Department of Surgery, Tri-Service General Hospital, Taipei, Taiwan. None of the subjects received preoperative anti-cancer therapy. Clinical information was obtained from medical records. Samples were taken from representative cancerous lesions and the corresponding non-cancerous epithelia. All tumor DNA samples were obtained by microdissection from 5-μm-thick hematoxylin and eosin-stained paraffin-embedded tissue sections[26]. Non-cancerous DNA was extracted from tissues which were flash-frozen in liquid nitrogen and stored in -80 ℃. All 67 samples were classified according to the Lauren criteria[27]: 26 as intestinal, 41 as diffuse types. The tumors were staged at the time of surgery using the standard criteria for TNM staging, with the unified international gastric cancer staging classification[28].

H pylori detection with real-time PCR

Real time PCR amplification of the *cagA* gene was conducted by adding 62.5 ng of DNA from stomach normal tissues isolates to 20 μL reactions containing 10 μL of 2X QuantiTect SYBR Green PCR Master Mix (QIAGEN, Hilden, Germany), 0.5 μmol/L S1227 Sense Primer (nt 154-175: 5'-GATAACAGGCAAGCTTTTGAGG-3'), 0.5 μmol/L AS1576 Antisense Primer (nt 503-583:5'-CTGCAAA-AGATTGTTTGGCAG-3') and 0.4 U of Uracil-N-glycosylase (New England Biolabs, Boston, USA).

Real-time PCR amplification was carried out in a LightCycler™ (Roche, Basel, Switzerland). After a preincubation step at 50 ℃ for 2 min, 95 ℃ for 15 min in order to activate the Uracil-N-glycosylase and HotStar Taq DNA polymerase, amplification was performed during 65 cycles including denaturation (94 ℃, 15 s with a temperature transition rate of 20 ℃/s), annealing (60 ℃, 25 s, with a temperature transition rate of 20 ℃/s) and extension (72 ℃, 18 s with a temperature transition rate of 20 ℃/s). A single fluorescent signal was obtained once per cycle at the end of the extension step with detection channel F1. After amplification, melting curve analysis was performed on the products by heating to 95 ℃ for 0 s, cooling to 65 ℃ for 15 s, followed by a temperature increase to 95 ℃ with a temperature transition rate of 0.2 ℃/s while continuously collecting the fluorescent signal.

To analyze the data of the real-time PCR assay, the derivative melting curves were obtained with the LightCycler data analysis software, version 3.5 (Roche). The melting temperature (*T*m) of the melting curve in each sample was used to detect the *H pyloric cagA* gene.

Restriction-fragment length polymorphism analysis to identify nucleotide changes at -160 of the CDH1 promoter

The -160 polymorphic site contained either a C or a A residue. The tumor type was determined by *Bst*EII digestion of the PCR products amplified using the primer set 5'-TGATCCCAGGTCTTAGTGAG-3' (upstream) and 5'-AGTCTGAACTGACTT CCGCA-3' (downstream). The 318-bp PCR product was cut into two fragments (208 and 110 bp) it contained the A residue. To ensure that the observed polymorphism was specific and not an experimental artifact, the results were confirmed by direct DNA sequencing.

Methylation-specific PCR and bisulfite-modified genomic sequencing to detect promoter hypermethylation of CDH1

The bisulfite modification procedure was carried out by the Zymo's EZ DNA Methylation Kit (Zymo Research, USA). One microliter of bisulfite-modified DNA was amplified in a total volume of 25 μL containing 1×PCR Buffer II, 2 mmol/L $MgCl_2$, 0.25 mmol/L deoxynucleotide triphosphate (dNTPs), 0.2 μmol/L each primer, and 0.04 U of Ampli Taq Gold™ DNA polymerase (Applied Biosystems, USA) at 95 ℃ for 30 s, the specific annealing temperature for 30 s, and 72 ℃ for 45 s. Water was used as a negative control. Seven millimole per liter/L of PCR product was directly loaded onto 3% agarose gel stained with ethidium bromide and directly visualized under UV illumination. Samples were scored as methylation, when there was a clearly visible band on the gel with the methylation primers[29].

Immunohistochemical staining and evaluation of E-cad expression

In immunohistochemical studies, sections (5 μm thick) from fixed, paraffin-embedded tumors were reacted with monoclonal anti-E-cad antibody (Cappel, Aurora, OH, USA), then with secondary antibody, and the signal was detected using an avidin-biotin complex and diaminobenzidine (DAB) kit (Vector Laboratories, Burlingame, CA, USA). DAB produced a yellowish brown stain, if the sample was positive. If more than 90% of the tumor cells exhibited intense membranous staining similar to that of normal cells, the result was considered positive (++). If the staining intensity was demonstrably reduced in comparison with that of normal cells and/or the staining pattern was heterogeneous (10-90% positive), the result was deemed to be weakly

positive (+). If E-cad expression was completely lost or positive in less than 10% of cells, the result was defined as negative (-).

Statistical analysis

Analyses were performed using S-Plus®2000 for Windows Statistical Software (CANdiensten, Amsterdam, The Netherlands). The level of significance was set at $P<0.05$ for all tests. Continuous variables are expressed as mean±SD, and were tested using Student's *t* test; categorical variables were tested using Fisher's exact test.

RESULTS

Of these 67 patients, 45 were men, and 22 were women. Their median age was 68.56 years (range, 31-88 years). All patients underwent surgical resection of the primary tumor. Twenty-six and 41 tumors were of the intestinal and diffuse histotypes, respectively. Reduced E-cad expression was observed in 88% (36/41) of diffuse type tumors and in 50% (13/26) of intestinal type tumors ($P = 0.0015$). Representative examples of immunohistochemical staining for E-cad expression in non-cancerous epithelium (++) and diffuse type tumor (-) are shown in Figures 1A and B.

H pylori infection was detected by real-time PCR (iCycler iQ Real-Time Quantitative System) for *H pylori cagA* gene in non-cancerous gastric epithelial samples adjacent to tumors. *H pylori* was found in 57% of GC patients. No significant difference in *H pylori* infection was observed between intestinal and diffuse type tumors (23/41, 56% *vs* 15/26 58%). There was no significant difference in reduced E-cad expression between *H pylori*-positive tumors and *H pylori*-negative tumors (27/38, 71.1% *vs* 22/29, 76%).

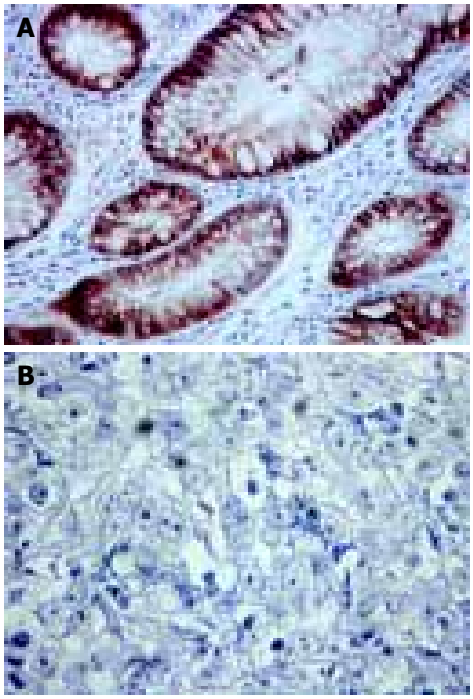


Figure 1 Immunohistochemical staining. **A**: Positive (++) immunohistochemical staining for E-cad expression in non-cancerous epithelium; **B**: Negative (-) immunohistochemical staining for E-cad expression in cancerous lesion in diffuse type tumor.

H pylori and -160C/A polymorphism

Among the 67 patients, 27 were genotype C/C (40%), 26 were genotype A/C (39%), and 14 were genotype A/A (21%) (Figure 2). There was no significant difference in the frequency of the C/A+A/A genotypes between tissues with normal and reduced E-cad expression (13/18, 72% *vs* 27/49, 55%). Interestingly, analyzing 67 available cases of *H pylori* infection and polymorphism status, *H pylori* infection was more frequently observed in tumors with C/C genotype of *CDH1* promoter than in C/A+A/A genotype tumors (20/27, 74% *vs* 18/40, 45%; $P = 0.02$, Table 1).

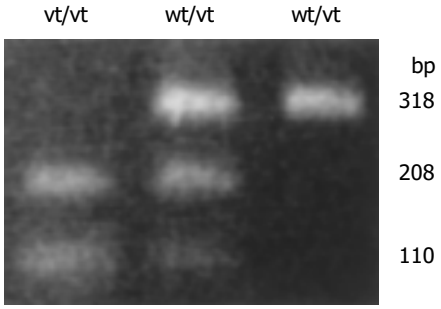


Figure 2 RFLP analysis of genetic polymorphism of the 160 site of the *E-cad* promoter. The C/A polymorphism was differentiated by *Bst*EII digestion of PCR products homozygous for the wild-type (high-activity) allele (wt/wt, CC genotype), heterozygous for the variant (low-activity) allele (wt/vt, CA genotype), and homozygous for the low-activity allele (vt/vt, AA genotype).

H pylori infection and hypermethylation in non-cancerous gastric epithelia

Promoter hypermethylation was found in 87% non-cancerous gastric epithelia of 67 GC patients (Figure 3A). Hypermethylation was frequently associated with *H pylori* positive than *H pylori* negative (36/38, 95% *vs* 22/29, 76%, $P = 0.025$, Table 1).

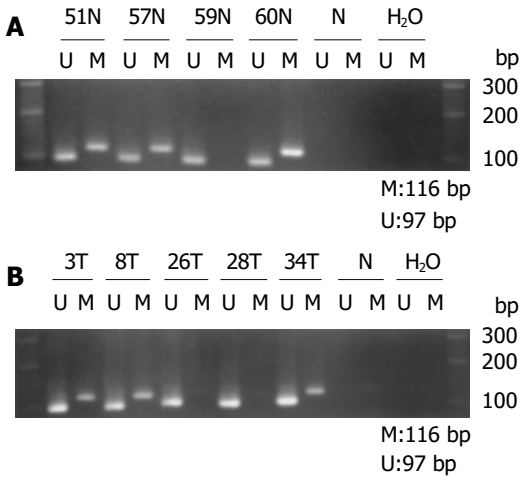


Figure 3 Gel electrophoresis picture demonstrating aberrant methylation in E-cad. Primer sets used for simple amplification are designed as unmethylated (U), methylated (M), unmodified DNA (N). Water is used as a negative control (H_2O). Molecular weight marker is 100-bp DNA ladder. **A**: Methylation in non-cancerous epithelium. Samples 51, 57, and 60 N are methylated. Sample 59 N is unmethylated; **B**: Methylation in cancerous lesion. Samples 3, 8, and 34 T are methylated. Samples 26 and 28 T are unmethylated.

H pylori infection and hypermethylation in cancerous lesions

Results from MSP indicated that the *CDH1* promoter was hypermethylated in 45 (67%) of 67 GCs (Figure 3B). Hypermethylation was more frequent in diffuse type tumors (76%, 31/41) than in intestinal type tumors (50%, 13/26; $P = 0.03$). Furthermore, hypermethylation was more frequent in GCs with reduced E-cad expression than normal expression (37/45, 82% *vs* 12/22, 55%, $P = 0.02$). No significant difference in *H pylori* infection was observed between methylated and unmethylated tumors (26/45, 58% *vs* 12/22, 55%, Table 1).

Table 1 *H pylori* infection in association with histotypes and E-cad expression profiles in GC

	H pylori (+) (%)	*H pylori* (–) (%)	*P*
Lauren's			
Intestinal type	23 (56.1)	18 (43.9)	
Diffuse type	15 (57.7)	11 (42.3)	NS
Promoter polymorphism			
C / C	20 (74.1)	7 (25.9)	
C / A+A / A	18 (45)	22 (55)	0.02
Methylation (noncancerous)			
Methylated	36 (94.7)	22 (75.9)	
Unmethylated	2 (5.3)	7 (24.1)	0.025
Methylation (cancerous)			
Methylated	26 (68.4)	19 (65.5)	
Unmethylated	12 (31.6)	10 (34.5)	NS
IHC			
Normal (++)	11 (28.9)	7 (24.1)	
Reduced (+, –)	27 (71.1)	22 (75.9)	NS

NS: not significant.

DISCUSSION

H pylori is responsible for the pathogenesis of atrophic gastritis and intestinal metaplasia[30,31]. Epidemiological studies have indicated that infection with *H pylori* is a risk factor for GC[20-22]. Moreover, Mongolian gerbils develop chronic gastritis, intestinal metaplasia, and adenocarcinoma after inoculation with *H pylori* into the stomach. However, the link between *H pylori* infection and the molecular mechanism of human gastric carcinoma remains to be investigated. Lim *et al*., reported that the increased expression of cell adhesion molecules (galectin 1, aldolase A, integrin α5, LMO7) and the decrease in E-cad expression induced by *H pylori* might contribute to cell adhesion, invasion, and possibly cell proliferation in gastric epithelial cells[32]. Kitadai *et al*., reported that coculture with *H pylori* increased the expression of interleukin-8, vascular endothelial growth factor (VEGF), angiogenin, uPA, and MMP-9 and increased angiogenic and collagenase activities in gastric carcinoma cells[33]. Sharma *et al*., reported that the activation of interleukin-8 gene expression by *H pylori* is regulated by the transcription factor, nuclear factor-kappa B, in gastric epithelial cells[34]. Akhtar *et al*., reported that promoter methylation regulates *H pylori*-stimulated cyclooxygenase-2 expression in gastric epithelial cells[35]. However, *in vivo* data on the differences in the molecular profile (ras, *MDM2*, c-erbB-2, cyclin D1, p53, *CDH1*) of *H pylori*-positive and *H pylori*-negative gastric carcinomas are almost non-existent[23].

In this study, *H pylori* was found in 57% of patients with GC. No significant difference in *H pylori* infection was observed between intestinal and diffuse type tumors (56% *vs* 58%). This is consistent with the current view that 60% of all GC cases are related to *H pylori* infection, irrespective of the histological tumor type[20,23].

H pylori and promoter polymorphism

Li *et al*., reported that the A allele of the -160C/A promoter polymorphism altered transcriptional binding, resulting in a reduction in transcriptional efficiency of 68% relative to that of the C allele[19]. In this study, *H pylori* was significantly more frequent in the C/C genotype of *CDH1* promoter than in the C/A+A/A genotypes. The C allele shows better transcriptional activity than the A allele, so patients with the C/C type may require *H pylori* infection to promote the inactivation of *CDH1*. Since -160C/A polymorphism is germ line, *H pylori* infection might affect *CDH1* inactivation in an early, possibly preneoplastic stage.

H pylori and promoter hypermethylation

In this study, hypermethylation of the *CDH1* promoter was present in 67% GCs, and was more frequent in diffuse type tumors (76%) than in intestinal type tumors (50%, $P = 0.03$). *CDH1* promoter hypermethylation was associated with decreased immunohistochemical expression of E-cad (82% *vs* 55%, $P = 0.02$). These data are similar to the results reported by Tamura *et al*., and Graziano *et al*.[37], which indicated that *CDH1* promoter methylation may play a major role, together with mutations or deletions, in causing inactivation of the *CDH1* gene in GC, especially in diffuse type tumors.

Chan *et al*.[18], investigated *CDH1* hypermethylation in the gastric mucosa of 35 patients with dyspepsia and found that hypermethylation was age-related and associated with *H pylori* infection. In our study, hypermethylation was found in 87% non-cancerous gastric epithelia of 67 GC patients and frequently associated with *H pylori* positive than *H pylori* negative epithelia. Therefore, our results of promoter hypermethylation of *E-cad* in non-cancerous gastric epithelia are compatible with hypothesis proposed by El-Omar *et al*.[24], and Hmadcha *et al*.[25]. However, we observed no association between *H pylori* infection and *CDH1* methylation in the gastric cancerous epithelia. It seems that *H pylori* is unrelated to *CDH1* methylation in GC. However, on the basis of current knowledge, *H pylori* should be considered as a factor facilitating the multifactorially determined process of gastric carcinogenesis, but by itself does not initiate or trigger the carcinogenic process (the "hypothesis of no return")[23,38]. Moreover, few *H pylori* are detected in cancerous epithelia in the human stomach. Under *in vivo* conditions, *H pylori* infects the non-cancerous epithelia surrounding the tumor and up-regulates methylation, and may indirectly stimulate hypermethylation in GCs at the tumor-normal tissue interface[33]. In addition, DNA methylation is catalyzed by DNA methyltransferase, and DNA CpG islands can be demethylated by MBD2[39]. *H pylori* infection might induce activation of DNA methyltransferase. However, Oue *et al*., reported that the mechanism of

CpG island hypermethylation is complex in the GC microenvironment and may not result from a simple transcriptional up-regulation of methyltransferase or down-regulation of *MBD2*[40]. Thus from the results of this study and the above statement, we conclude that the mechanism of hypermethylation of *CDH1* in GC is complex, and *H pylori* might affect hypermethylation in an initial stage.

In conclusion, patients with the -160C/C genotype might require *H pylori* infection to promote the inactivation of *CDH1*. *H pylori* infection might affect *E-cad* promoter hypermethylation of GC in an initial stage. Therefore, *H pylori* infection should be considered as a factor that facilitates a multifactorially determined process of gastric carcinogenesis in an initial stage.

ACKNOWLEDGMENTS

We are grateful to Ms. Pei-Ei Wu, Yi-Chien Mao and Chien-Shi Wang for their technical assistance.

REFERENCES

1 **Takeichi M.** Cadherin cell adhesion receptors as a morphogenetic regulator. *Science* 1991; **251**: 1451–1455
2 **Takeichi M.** Cadherins. A molecular family important in selective cell–cell adhesion. *Annu Rev Biochem* 1990; **59**: 237–252
3 **Grunwald G.** The structural and functional analysis of cadherin calcium-dependent cell adhesion molecules. *Curr Opin Cell Biol* 1993; **5**: 797–805
4 **Hirohashi S.** Inactivation of the E-cadherin-mediated cell adhesion system in human cancers. *Am J Pathol* 1998; **153**: 333–339
5 **Pignatelli M,** Vessey CJ. Adhesion molecules: novel molecular tools in tumor pathology. *Hum Pathol* 1994; **25**: 849–856
6 **Hashimoto M,** Niwa O, Nitta Y, Takeichi M, Yokoro K. Unstable expression of E-cadherin adhesion molecules in metastatic ovarian tumor cells. *Jpn Cancer Res* 1989; **80**: 459–463
7 **Bussemakers MJ,** van Moorselaar RJ, Giroldi LA, Ichikawa T, Isaacs JT, Takeichi M, Debruyne FM, Schalken JA. Decreased expression of E-cadherin in the progression of rat prostatic cancer. *Cancer Res* 1992; **52**: 2916–2922
8 **Shimoyama Y,** Hirohashi S. Expression of E- and P-cadherin in gastric carcinomas. *Cancer Res* 1991; **51**: 2185–2192
9 **Oka H,** Shiozaki H, Kobayashi K, Tahara H, Tamura S, Miyata M, Doki Y, Iihara K, Matsuyoshi N, Hirano S. Immunohistochemical evaluation of E-cadherin adhesion molecule expression in human gastric cancer. *Virchows Archiv* 1992; **421**: 149–156
10 **Matsuura K,** Kawanishi J, Fujii S, Imamura M, Hirano S, Takeichi M, Niitsu Y. Altered expression of E-cadherin in gastric cancer tissues and carcinomatous fluid. *Br J Cancer* 1992; **66**: 1122–1130
11 **Mayer B,** Johnson JP, Leitl F, Jauch KW, Heiss MM. Expression in primary and metastatic gastric cancer: Down-regulation correlates with cellular dedifferentiation and glandular disintegration. *Cancer Res* 1993: 1690–1695
12 **Gabbert HE.** Mechanisms in tumor invasion: evidence from *in vivo* observations. *Cancer Metastasis Rev* 1985; **4**: 293–309
13 **Shun CT,** Wu MS, Lin JT, Wang HP, Houng RL, Lee WJ, Wang TH, Chuang SM. An immunohistochemical study of E-cadherin expression with correlations to clinicopathological features in gastric cancer. *Hepatogastroenterology* 1998; **45**: 944–999
14 **Guilford P,** Hopkins J, Harraway J, McLeod M, McLeod N, Harawira P, Taite H, Scoular R, Miller A, Reeve AE. E-cadherin germline mutations in familial gastric cancer. *Nature* 1998; **392**: 402–405
15 **Gayther SA,** Gorringe KL, Ramus SJ, Huntsman D, Roviello F, Grehan N, Machado JC, Pinto E, Seruca R, Halling K, MacLeod P, Powell SM, Jackson CE, Ponder BA, Caldas C. Identification of germ-line E-cadherin mutations in gastric cancer families of European origin. *Cancer Res* 1998; **58**: 4086–4089
16 **Becker KF,** Atkinson MJ, Reich U, Becker I, Nekarda H, Siewert JR, Hofler H. E-cadherin gene mutations provide clues to diffuse type gastric carcinomas. *Cancer Res* 1994; **54**: 3845–3852
17 **Machado JC,** Oliveira C, Carvalho R, Soares P, Berx G, Caldas C, Seruca R, Carneiro F, Sobrinho-Simoes M. E-cadherin gene (*CDH1*) promoter methylation as the second hit in sporadic diffuse gastric carcinoma. *Oncogene* 2001; **20**: 1525–1528
18 **Chan AO,** Lam SK, Wong BC, Wong WM, Yuen MF, Yeung YH, Hui WM, Rashid A, Kwong YL. Promoter methylation of *E-cadherin* gene in gastric mucosa associated with *Helicobacter pylori* infection and in gastric cancer. *Gut* 2003; **52**: 502–506
19 **Li LC,** Chui RM, Sasaki M. A single nucleotide polymorphism in the E-cadherin gene promoter alters transcriptional activities. *Cancer Res* 2000; **60**: 873-876
20 **Forman D,** Newell DG, Fullerton F, Yarnell JW, Stacey AR, Wald N, Sitas F. Association between infection with *Helicobacter pylori* and risk of gastric cancer. *BMJ* 1991; **302**: 1302–1305
21 **Nomura A,** Stemmerman G, Chyou MJ, Kato I, Perez-Perez G, Blaser M. *Helicobacter pylori* infection and gastric carcinoma among Japanese Americans in Hawaii. *N Engl J Med* 1991; **325**: 1132–1136
22 **Parsonnet J,** Friedman GD, Vandersteen DP, Chang Y, Vogelman JH, Orentreich N, Sibley RK. *Helicobacter pylori* infection and the risk of gastric carcinoma. *N Engl J Med* 1991; **325**: 1170–1171
23 **Blok P,** Craanen ME, Offerhaus GJ, Dekker W, Kuipers EJ, Meuwissen SG, Tytgat GN. Molecular alterations in early gastric carcinomas. *Am J Clin Pathol* 1999; **111**: 241–247
24 **El-Omar EM,** Carrington M, Chow WH, McColl KE, Bream JH, Young HA, Herrera J, Lissowska J, Yuan CC, Rothman N, Lanyon G, Martin M, Fraumeni JF Jr, Rabkin CS. Interleukin-1 polymorphisms associated with increased risk of gastric cancer. *Nature* 2000; **404**: 398-402
25 **Hmadcha A,** Bedoya FJ, Sobrino F, Pintado E. Methylation-dependent gene silencing induced by interleukin 1β via nitric oxide production. *J Exp Med* 1999; **190**: 1595–1604
26 **Moskaluk CA,** Kern SE. Microdissection and polymerase chain reaction amplification of genomic DNA from histological tissue sections. *Am J Pathol* 1997; **150**: 1547-1552
27 **Lauren P.** The two main histological types of gastric carcinoma diffuse and so-called intestinal type of carcinoma. *Acta Pathol Microbiol Scand* 1965; **64**: 31–49
28 **Sobin LH,** Wittekind CH (editors). International union against cancers (UICC): TNM classification of malignant tumors. 5th ed. *New York: John Wiley* 1997
29 **Herman JG,** Graff JR, Myohanen S, Nelkin BD, Baylin SB. Methylation-specific PCR: a novel PCR assay for methylation status of CpG islands. *Proc Natl Acad Sci USA* 1996; **93**: 9821-9826
30 **Graff JR,** Herman JG, Myöhänen S, Baylin SB, Vertino PM. Mapping patterns of CpG island methylation in normal and neoplastic cells implicates both upstream and downstream regions in *de Novo* methylation. *J Biol Chem* 1997; **272**: 22322-22329
31 **Kawaguchi H,** Haruma K, Kohmoto K, Yoshihara M, Sumii K, Kajiyama G. *Helicobacter pylori* infection is the major risk factor for atrophic gastritis. *Am J Gastroenterol* 1996; **91**: 959–962
32 **Lim JW,** Kim H, Kim KH. Cell adhesion-related gene expression by *Helicobacter pylori* in gastric epithelial AGS cells. *Int J Biochem Cell Biol* 2003; **35**: 1284–1296
33 **Kitadai Y,** Sasaki A, Ito M, Tanaka S, Oue N, Yasui W, Aihara M, Imagawa K, Haruma K, Chayama K. *Helicobacter pylori* infection influences expression of genes related to

angiogenesis and invasion in human gastric carcinoma cells. *Biochem Biophys Res Commun* 2003; **311**: 809–814

34 **Sharma SA,** Tummuru MK, Blaser MJ, Kerr LD. Activation of IL-8 gene expression by *Helicobacter pylori* is regulated by transcription factor, nuclear factor-kappa B in gastric epithelial cells. *J Immunol* 1998; **160**: 2401–2407

35 **Akhtar M,** Cheng Y, Magno RM, Ashktorab H, Smoot DT, Meltzer SJ, Wilson KT. Promoter methylation regulates *Helicobacter pylori* stimulated cyclooxygenase-2 expression in gastric epithelial cells. *Cancer Res* 2001; **61**: 2399–2403

36 **Tamura G,** Yin J, Wang S, Fleisher AS, Zou T, Abraham JM, Kong D, Smolinski KN, Wilson KT, James SP, Silverberg SG, Nishizuka S, Terashima M, Motoyama T, Meltzer SJ. E-Cadherin gene promoter hypermethylation in primary human gastric carcinoma. *J Natl Cancer Inst* 2000; **92**: 569–573

37 **Graziano F,** Arduini F, Ruzzo A, Mandolesi A, Bearzi I, Silva R, Muretto P, Testa E, Mari D, Magnani M, Scartozzi M, Cascinu S. Combined analysis of E-cadherin gene (*CDH1*) promoter hypermethylation and E-cadherin protein expression in patients with gastric cancer: implication for treatment with demethylating drugs. *Ann Oncol* 2004; **15**: 489–492

38 **Wu MS,** Shun CT, Wang HP, Sheu JC, Lee WJ, Wang TH, Lin JT. Genetic alterations in gastric cancer: relation to histological subtypes, tumor stage and *Helicobacter pylori* infection. *Gastroenterology* 1997; **112**: 1457–1465

39 **Bhattacharya SK,** Ramchandani S, Cervoni N, Szyf M. A mammalian protein with specific demethylase activity for mCpG DNA. *Nature* 1999; **397**: 568–569

40 **Oue N,** Kuraoka K, Kuniyasu H, Yokozaki H, Wakikawa A, Matsusaki K, Yasui W. DNA methylation status of hMLH1, p16(INK4a), and CDH1 is not associated with mRNA expression levels of DNA methyltransferase and DNA demethylase in gastric carcinomas. *Oncol Rep* 2001; **8**: 1085-1089

Science Editor Guo SY **Language Editor** Elsevier HK

PO Box 2345, Beijing 100023, China
www.wjgnet.com
wjg@wjgnet.com

ELSEVIER

World J Gastroenterol 2005;11(33):5180-5184
World Journal of Gastroenterology ISSN 1007-9327
© 2005 The WJG Press and Elsevier Inc. All rights reserved.

• *BASIC RESEARCH* •

Gastroprotection induced by capsaicin in healthy human subjects

Gyula Mózsik, János Szolcsányi, István Rácz

Gyula Mózsik, First Department of Medicine, Medical and Health Center, University of Pécs, Hungary
János Szolcsányi, Department of Pharmacology and Pharmacotherapy, Medical and Health Center, University of Pécs, Hungary
István Rácz, First Department of Medicine, County Hospital of Gyõr, Hungary
Correspondence to: Professor Gyula Mózsik, MD, First Department of Medicine, Medical and Health Center, University of Pécs, Hungary. gyula.mozsik@aok.pte.hu
Telephone: +36-72-536-494 Fax: +36-72-536-495
Received: 2004-10-14 Accepted: 2004-12-23

Abstract

AIM: To evaluate the gastro-protective effect of capsaicin against the ethanol- and indomethacin (IND)-induced gastric mucosal damage in healthy human subjects.

METHODS: The effects of small doses (1-8 μg/mL, 100 mL) of capsaicin on the gastric acid secretion basal acid output (BAO) and its electrolyte concentration, gastric transmucosal potential difference (GTPD), ethanol- (5 mL 300 mL/L i.g.) and IND- (3×25 mg/d) induced gastric mucosal damage were tested in a randomized, prospective study of 84 healthy human subjects. The possible role of desensitization of capsaicin-sensitive afferents was tested by repeated exposures and during a prolonged treatment.

RESULTS: Intragastric application of capsaicin decreased the BAO and enhanced "non-parietal" component (GTPD) in a dose-dependent manner. The decrease of GTPD evoked by ethanol was inhibited by the capsaicin application, which was reproducible. Gastric microbleeding induced by IND was inhibited by co-administration with capsaicin, but was not influenced by two weeks pretreatment with a daily capsaicin dose of 3×400 μg i.g.

CONCLUSION: Capsaicin in low concentration range protects against gastric injuries induced by ethanol or IND, which is attributed to stimulation of the sensory nerve endings.

© 2005 The WJG Press and Elsevier Inc. All rights reserved.

Key words: Capsaicin; Ethanol; Indomethacin; Gastric transmucosal potential difference; Gastric microbleeding; Gastroprotection; Healthy human subjects

Mózsik G, Szolcsányi J, Rácz I. Gastroprotection induced by capsaicin in healthy human subjects. *World J Gastroenterol* 2005; 11(33): 5180-5184
http://www.wjgnet.com/1007-9327/11/5180.asp

INTRODUCTION

Spicy or hot foods are traditionally considered as dietary factors implicated in the causation of peptic ulcer[1,2]. Early and more recent studies[3-6] in human beings with pungent chilli powders and extracts have come to controversial conclusions about their injurious influence on gastric mucosa. Capsaicin is a hot topic in studies on gastro-protection[7-16]. In contrast, the effect of this pure ingredient of red peppers in defined concentrations on the human gastric mucosa seems not to be interesting for research. Capsaicin activates the TRPV1/VR1 capsaicin (vanilloid) receptor expressed by a subgroup of primary afferent nociceptive neurons. The TRPV1/VR1 receptor has been cloned[21] and turns out to be a cation channel. It is gated besides capsaicin and some vanilloids by low pH, noxious heat and various pain-producing endogenous and exogenous chemicals. Thus, these sensory nerve endings equipped with these ion channels are prone to be stimulated in gastric mucosa. The aim of the present study was to analyze the effect of capsaicin on mucosal injury induced by ethanol or the non-selective cyclooxygenase inhibitor, indomethacin (IND). Particular attention was paid to define whether the action of capsaicin was related to its acute stimulatory effect or to the sensory desensitization, a well known long lasting consequence of sensory stimulation in animal experiments[22,23].

MATERIALS AND METHODS

The observations were carried out in 84 healthy human subjects aged 25-65 years (40±10 years). The physical, laboratory, and iconographic examinations were normal and indicated normal.

The healthy persons were randomized into different groups to study the effect of intragastric application of capsaicin on their gastric mucosa and gastric acid secretion under different conditions.

The observations were carried out according to the good clinical practice. The studies were carried out from 1997 to 2002, which were permitted by the Regional Ethical Committee of Pécs, University of Pécs, Hungary. Written informed consent was obtained from all participants.

Identification of gastric basal acid output (BAO) without and with capsaicin

After an overnight fasting, a nasogastric tube was introduced at 8:00 a.m., and the total gastric content was completely suctioned.

Then the secreted gastric juice was suctioned every 15 min for 1 h (basal acid output, BAO). The healthy human subjects received intragastric capsaicin at the doses of 100, 200, 400, and 800 μg in 100 mL volume of saline solution. In

the control group, 100 mL of saline solution was given through the nasogastric tube and the same doses of capsaicin. Gastric acid secretion was measured by titration of gastric juice with 0.1 N NaOH to pH 7 (pH titrimeter, Radelkis, Budapest, Hungary). Gastric acid outputs were calculated and expressed in mEq/h after capsaicin administration. The values effective inhibitory dose of capsaicin (ED_{50}) was identified on the gastric BAO.

Chemical composition of gastric juice without and with capsaicin

The concentrations of Na^+, K^+, and Ca^{2+} in gastric juice were measured flamephotometrically. The concentration of Mg^{2+} was measured by atom absorption spectrometry, the chloride concentration by colorimetric method, the protein concentration by the method of biuret reaction.

The chloride linked to H^+ and sodium was calculated for the determination of "parietal" (chloride linked to H^+) and of "non-parietal" (liked to sodium) components of the gastric BAO[30].

Measurement of gastric transmucosal potential difference (GTPD)

GTPD was measured during endoscopy. The exploring mucosal electrode was passed through the biopsy force channel of gastroscope and the reference electrode was placed on the volar surface of the left forearm. The electrodes were connected to a digital voltmeter (Radelkis, Budapest, Hungary, OP 211/1). GTPD measurements were done at the greater curvature of the gastric body and the results were expressed in -mV (without and with intragastric application of different doses of capsaicin)[24-27]. Capsaicin in 5 mL saline solution was intragastrically applied and only saline solution was given to identify the baseline in GTPD.

The GTPD values were expressed in -mV, while -△PD max was calculated after intragastric application of capsaicin (n = 10).

Effect of capsaicin on ethanol-induced GTPD changes

The GTPD baseline was identified, and ethanol (5 mL 300 mL/L i.g.) was given intragastrically. The GTPD change was determined after the ethanol passed through the biopsy force channel of gastroscope without and with capsaicin (given in different doses in the same pathway after 1 min of ethanol administration) (n = 10).

Gastric microbleeding measurement during 1-d treatment with indomethacin (IND) and indomethacin plus capsaicin (n = 14)

Fourteen healthy human subjects were studied. They were randomly divided into different treatment groups.

Examinations were carried out before and after treatment after an overnight fasting. A plastic tube was inserted through his or her mouth until the intragastric end was 55 cm from the incisors. There were six openings in the intragastric part of the tube.

A test solution containing 100 mL of saline solution and 10 mL solution of concentrated phenol red (40 mg/100 mL), as a non-absorbable marker, was installed into the stomach without and with capsaicin (at doses of 200, 400, and 800 μg). The gastric content was recovered 10 min later[28-30]. The whole procedure was repeated thrice before and after the administration of IND (without and with application of capsaicin).

Gastric juice was aspirated. The strength of suction was adjusted to -50 mmHg.

The volume of each recovery sample was measured after homogenization for 10 min. Hemoglobin was determined as previously described[36,37]. The quantity of blood in the aspirated gastric samples was measured. Blue color developed (640 nm, pH 3.78, room temperature) and could be determined. Phenol red was measured spectrophotometrically[29,30]. The values of gastric microbleeding were expressed as milliliter per day.

Chronic capsaicin (3×400 μg i.g./d) treatment for 2 wk

Ten healthy human subjects were treated with capsaicin (3×400 μg orally) for 2 wk. Capsaicin substance (400 μg) was put into a gelatin capsule containing 0.23 g lactose.

The extent of IND-induced gastric mucosal bleeding and gastric mucosal preventive effect of capsaicin (200, 400 μg) were tested before and after capsaicin treatment. Prospective randomized studies were done for three consecutive days before and after capsaicin treatment.

Chemicals

Capsaicin was from Sigma, Budapest, Hungary. IND was from Sanofi-Synthelabo, Budapest, Hungary. Capsaicin solution was made by dilution with distilled water.

Statistical analysis

The results were calculated as mean±SE. The unpaired or paired Student's t-tests were used for the calculation of the results between the identical observations. $P<0.05$ was considered statistically significant.

RESULTS

The BAO decreased significantly and dose-dependently (Figure 1). The ED_{50} value of capsaicin was 400 μg.

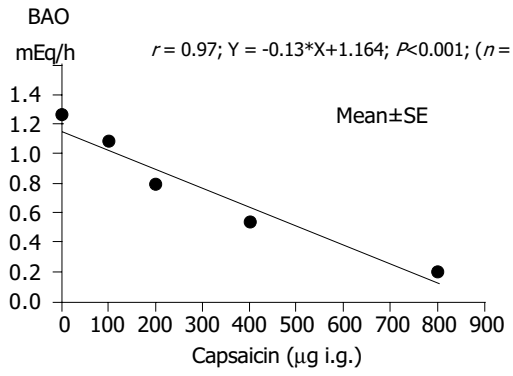


Figure 1 Inhibition of gastric acid output (BAO) by capsaicin in 16 healthy human subjects.

Electrolyte and albumin concentrations in gastric juice were measured in the healthy human subjects without and with capsaicin treatment. H^+, K^+, Ca^{2+}, and Mg^{2+} significantly

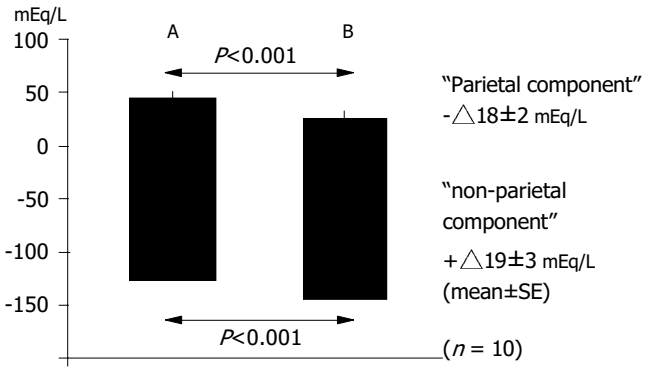


Figure 2 "Parietal" and "non-parietal" components before (A) and after (B) intragastric application of capsaicin in 10 healthy human subjects.

decreased (P<0.001), while Na^+ and its protein content increased (P<0.001) after capsaicin treatment (Table 1).

The "parietal" and "non-parietal" components of BAO were calculated by taking the H^+ output equivalent to Na^+ and Cl^- as gastric H^+, Na^+, and chloride in gastric juice without and with capsaicin treatment. The parietal component decreased (-△18 mmol/L) while the non-parietal component increased (+△19 mmol/L) in the BAO after capsaicin application (Figure 2).

Capsaicin increased the GTPD in a dose-dependent manner. The peak values reached within 3-5 min after capsaicin application (Figure 3A).

After intragastric application of ethanol (300 mL/L), the GTPD dropped from -33.4±2.7 to -10.5±2.4 mV (P<0.001) within 3 min (Figure 3C).

Capsaicin application (at doses of 400 and 800 μg) significantly prevented the ethanol-induced decrease in GTPD (Figure 3C).

The protective effect of capsaicin was reproducible before (Figure 3B) and after (Figure 3D) ethanol administration.

The gastric microbleeding was measured before and after IND (3×25 mg orally) application alone and in combination with 200, 400, and 800 μg capsaicin in 14 healthy human volunteers. The gastric microbleeding induced by IND increased (8; 25±0.5 mL/d from the basic level of 2.1±0.1; P<0.001) which was dose-dependently prevented by capsaicin at the dose of 200-800 μg (Y = 0.0071X+7.78; r = -0.98; P<0.001, Figure 4A).

In order to decide the potential role of desensitizing in the gastric protective effect of capsaicin, a daily dose of 3×400 μg capsaicin was applied for 2 wk in 14 healthy human subjects. Capsaicin protected gastric mucosal against IND-induced gastric microbleeding. There was no difference between the pretreated group and the central group (Figure 4B).

DISCUSSION

The present study provides evidence for the powerful gastroprotective potency of capsaicin. The threshold concentration of capsaicin in producing definite hot sensation is around 1-2 μg/mL and the capsaicinoid level in chilli sauce varies from 25 μg/mL to 0.5 mg/mL[22,24]. Therefore, the observed defensive responses using capsaicin have a clear dietary relevance.

Chronic peptic ulcer patients are warned to avoid spicy foods, although in the era of H_2-inhibitors this praxis is far less restrictive[2]. Nevertheless contradictory observations cannot decide whether spicy foods are harmful to or beneficial for gastric injury. In healthy subjects mucosal microbleeding with exfoliation and aggravation of aspirin-induced gastric bleeding are observed in response to chilli powder or red pepper "preparations"[3,4]. On the other hand, ingestion of "highly spiced" meals or chilli by normal individuals does not cause endoscopically gastric or duodenal mucosal damage[25] although gastric acid and pepsin secretion increases[31-33]. In other studies, red pepper sauce induces prolongation of gastric emptying[7] and chilli powder evokes protective effect against aspirin-induced gastric mucosal injury[6]. Improvement in dyspeptic symptoms of patients with and without gastro-esophageal reflux disease and irritable bowel syndrome after intake of red pepper powder in gelatin capsules has been reported[8,9]. In the latter case, the improvement of functional dyspepsia is attributed to desensitization of gastric nociceptive C-fibers induced by capsaicin although this conclusion is not supported by experimental evidence. In our earlier and present studies, pure capsaicin solution was injected into the stomach (1-8 μg/mL in 100 mL) of healthy subjects which inhibits the H^+ output and total secreted volume of gastric juice for about 1 h in a dose-dependent manner and increases its "non-parietal" component, gastric emptying[23].

The important role of capsaicin-sensitive peptidergic sensory fibers in maintaining of gastric mucosal integrity against injurious interventions has been well established in rats[10-13,15]. Capsaicin-sensitive primary afferent neurons and their nerve endings express the TRPV1/VR1 vanilloid receptor[14,21,23]. Stimulation of these chemoreceptive nerve terminals by H^+ or bradykinin, etc. is accompanied with release of CGRP, tachykinins, somatostatin, and NO from them. The arterial wall in stomach receives dense supply of these peptidergic fibers and capsaicin elicits neurogenic vasodilatation with enhanced mucosal blood flow. Clear evidence indicates that hyperemia is induced by sensory neuropeptides of CGRP neurokinin A with NO as well as somatostatin are involved in the sensory neuron-mediated gastroprotection[17-20].

Table 1 Chemical composition of gastric juice without (A) and with (B) application of capsaicin in healthy human subjects (mEq/L or in g/L) (mean±SE)

H^+		Na^+		K^+		Ca^{2+}		Mg^{2+}		"Parietal" component		"Non-parietal" component		Albumin (g/L)	
A	B	A	B	A	B	A	B	A	B	A	B	A	B	A	B
43±3	25±1	73±4	89±2	13±1	8±0.6	0.98±0.02	0.88±0.01	0.49±0.01	0.38±0.01	43±3	25±2	126±4	145±4	1.24±0.001	1 630 002
P<0.001		P<0.001		P<0.001		P<0.001		P<0.001		P<0.001		P<0.001		P<0.001	
100±7	58±2	100±5	122±3	100±8	62±5	100±2	90±1	100±2	78±2	100±7	58±5	100±3	115±3	100±1	131±2

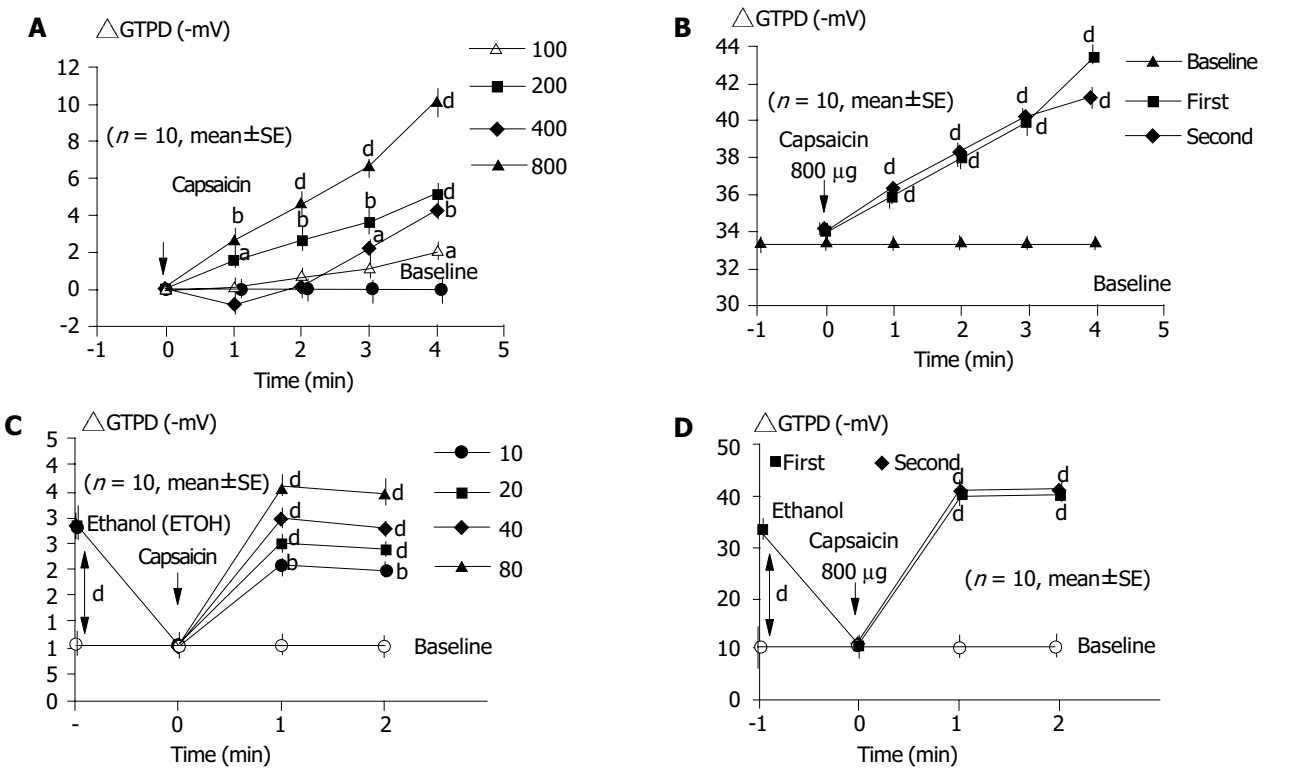


Figure 3 Dose-dependent gastric mucosal protective effect of capsaicin. **A:** Dose-response curve for capsaicin-induced changes in GTPD; **B:** effect of repeated capsaicin application on GTPD applied with 5-min time intervals; **C:** dose-response curves for capsaicin-induced gastric mucosal prevention on ethanol-produced decrease in GTPD; **D:** effects of repeated capsaicin application on ethanol-induced GTPD changes. [a]*P*<0.05, [b]*P*<0.01, [d]*P*<0.01 *vs* others.

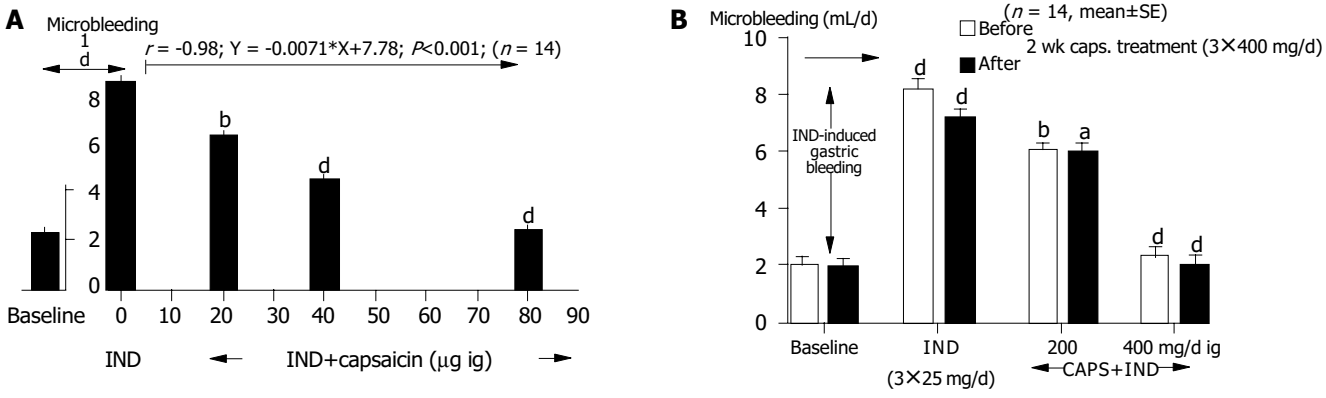


Figure 4 Gastric mucosal protection produced by capsaicin on IND-induced gastric mucosal damage before (**A**) and after (**B**) capsaicin treatment. [a]*P*<0.05, [b]*P*<0.01, [d]*P*<0.01 *vs* others.

Opposite effect has been observed in rats desensitized by capsaicin. Functional blockade of gastric sensory nerve endings elicited by systemic or intragastric capsaicin application results in impaired mucosal protection against various ulcer-provoking agents[10-14]. Repeated topical or systemic capsaicin application elicits reproducible effects at low concentrations and induces decreasing responses (desensitization) at high concentrations. In the rat's eye, 10 μg/mL concentration of capsaicin does not induce any desensitization[22]. On the human oral mucosa, this concentration of capsaicin induces some diminished sensation of irritation but only for a short time[28].

In the present study, the following evidence suggests that capsaicin-induced gastric mucosal protection against the injurious effects of ethanol or IND is due to the acute stimulatory effect of the compound. Microbleeding detected after IND administration does not differ from that in the controls. Enhanced GTPD evoked by the first and second capsaicin exposure in 1 h shows no sign of decrement. Counteraction of the ethanol-induced drop of gastric transmucosal potential is identical after the first and second capsaicin application.

The enhancement of gastric transmucosal potential is probably related to the mucosal hyperemia[32,34]. This response plays a significant role in capsaicin-induced gastroprotection. Furthermore, the present and earlier[27] findings reveal that intragastric administration of capsaicin in low concentration inhibits but does not increase[4,5,26] the acid output of stomach

and enhances the gastric emptying rate in healthy human subjects[29]. All these responses can be attributed to CGRP and NO released from the activated capsaicin-sensitive, TRPV1/VR1 expressing sensory nerve terminals. The present findings suggest that patients taking anti-inflammatory-analgesic agents regularly can decrease the incidence and severity of gastric ulceration, if they have moderate spicy foods[35-37].

REFERENCES

1 Anonymus, Diet and peptic ulcer. *Lancet* 1987; **2**: 80-81
2 **Marotta RB,** Floch MH. Diet and nutrition in ulcer disease. *Med Clin North Am* 1991; **75**: 967-979
3 **Desai HG,** Venugopalan K, Antia FP. Effect of red chilli powder on DNA content of gastric aspirates. *Gut* 1973; **14**: 974-976
4 **Myers BM,** Smith JL, Graham DY. Effect of red pepper and black pepper on the stomach. *Am J Gastroenterol* 1987; **82**: 211-214
5 **Graham DY,** Smith JL, Opekun AR. Spicy food and the stomach. Evaluation by videoendoscopy. *JAMA* 1988; **260**: 3473-3475
6 **Yeoh KG,** Kang JY, Yap J, Guan R, Tan CC, Wee A, Teng CH. Chilli protects against aspirin-induced gastroduodenal injury in humans. *Dig Dis Sci* 1997; **40**: 580-583
7 **Gonzales R,** Dunkel R, Koletzko B, Schsdziarra V, Allescher HD. Effect of capsaicin-containing red pepper sauce suspension on upper gastrointestinal motility in healthy volunteers. *Dig Dis Sci* 1998; **43**: 1165-1171
8 **Bortolotti M,** Coccia G, Grossi G. Red pepper and functional dyspepsia. *N Eng J Med* 2002; **346**: 947-948
9 **Bortolotti M,** Coccia G, Grossi G, Miglioli M. The treatment of functional dyspepsia with red pepper. *Alim Pharmacol Ther* 2002; **16**: 1075-1082
10 **Szolcsányi J,** Barthó L. Impaired defense mechanism to peptic ulcer in the capsaicin-desensitized rat In: Mózsik Gy, Hanninen O, Jávor T, eds. Advances in Physiological Science. Vol. 29. Gastrointestinal Defense Mechanisms; Oxford: Pergamon Press- *Budapest Akadémiai Kiadó* 1981: 39-51
11 **Szolcsanyi J,** Bartho L. Capsaicin-sensitive afference and their role in gastroprotection: an update. *J Physi Paris* 2001; **95**: 181-188
12 **Mózsik GY,** Abdel-Salam OME, Szolcsányi J. Capsaicin-sensitive afferent nerves in gastric mucosal damage and protection. *Budapest Akadémiai Kiadó* 1997: 1-125
13 **Mózsik GY,** Vincze Á, Szolcsányi J. Four responses of capsaicin-sensitive primary afferent neurons to capsaicin and its analog. Gastric acid secretion, gastric mucosal damage and protection. *J Gastroenterol Hepatol* 2001; **16**: 1093-1097
14 **Szállási Á,** Blumberg M. Vanilloid (Capsaicin) receptors and mechanisms. *Pharmacol Rev* 1991; **51**: 159-211
15 **Holzer P.** Neural emergency system in the stomach. *Gastroenterology* 1998; **114**: 823-839
16 **Maggi C.** Tachykinins and calcitonin gene-related peptides (CGRP) as contransmitters released from peripheral endings of sensory nerves. *Prog Neurobiol* 1995; **45**: 1-98
17 **Inui T,** Kinoshita J, Yamahuchi A, Yamatani T, Chiba T. Linkage between capsaicin-stimulated calcitonin gene-related peptide and somatostatin release in the rat stomach. *Am J Physiol* 1991; **261**: G770-774
18 **Li DS,** Raybould HE, Quintero E, Guth PH. Role of calcitonin gene-related peptide in gastric hyperemic response to intragastric capsaicin. *Am J Physiol* 1991; **261**: G657-661
19 **Kang JY,** Teng CH, Chen FC. Effect of capsaicin and chilli on ethanol induced gastric mucosal injury in the rat. *Gut* 1995; **36**: 664-669
20 **Chen RY,** Guth PH. Interaction of endgenous nitric oxide and CGRP in the sensory neuron-induced gastric vasodilatation. *Am J Phys* 1995; **268**: G791-796
21 **Caterina MJ,** Schumacher MA, Tominaga M, Rosen TA, Levine JD, Julius D. The capsaicin receptor: a heat-activated ion channel in the pain pathway. *Nature* 1997; **389**: 816-824
22 **Szolcsányi J.** Capsaicin type purgent agents producing pyrexia In: Milton ed. Handbook of Experimental Pharmacology. Pyretics and Antipyretcs Vol. 60. *Berlin Springer-Verlag* 1982: 437-478
23 **Hollander F.** The component of the gastric secretion. *Am J Dig Dis Sci* 1934; **1**: 319-329
24 **Andersson S,** Grossman M. Profile of pH, pressure and potential difference and gastroduodenal junction in man. *Gastroenterology* 1965; **49**: 364-369
25 **Hossenbocus A,** Fitzpatrick P, Colin-Jones DG. Measurement of gastric potential diference at endoscopy. *Gut* 1975; **14**: 410-415
26 **Rácz I.** Transmucosal potential diference. In: Cheli R, ed. Gastric protection. *New York: Raven Press* 1988: 65-86
27 **Rácz I.** Transmucosal potential difernce In: Parodi MC, Iaquinto G, Cheli R, eds. Gastroprotection Today. *Verona: Cortina International* 1995: 97-108
28 **Hunt JN,** Knox MT. The regulation of gastric emtying of meals containing citric acid and salt of citric acid. *J Physiol* 1962; **163**: 34-35
29 **Fisher MA,** Hunt JN. A sensitive method for measuring haemoglobin in the gastric juice. *Digestion* 1976; **14**: 409-414
30 **Nagy L,** Mozsik Gy, Feledi É, Ruzsa CS, Vezekényi Z, Jávor T. Gastric microbleeding measurements during one day treatment with indomethacin and indomethacin plus sodium salicylatecl (1:10): in patients. *Acta Physiol Hung* 1984; **64**: 373-377
31 **Edwards SJ,** Colquhoun EQ, Clark MG. Levels of pungent principles in chilli sauces and capsicum fruit in Australia. *Food Australia* 1990; **42**: 432-435
32 **Kang JY,** Yap I, Guan P, Lim TC. Chilli ingestion does not lead to macroscopic gastroduodenal mucosal damage in healthy subjects. *J Gastroenterol Hepatol* 1988; **3**: 573-576
33 **Solanke TF.** The effect of red pepper (capsicum frutescens) on gastric acid secretion. *J Surg Res* 1973; **15**: 385-390
34 **Debreceni A**, Abdel-Salam OM, Figler M, Juricskay I, Szolcsanyi J, Mozsik G. Capsaicin increase gastric emptying rate in healthy human subjects measured by ^{13}C-labeled octanoid acid breath test. *J Physiol Paris* 1999; **93**: 455-460
35 **Szolcsányi J.** Capsaicin receptors as target molecules on nociceptors for development of analgesic agents In: Kéri Gy, Tóth I. eds. Molecular Pathomechanisms and New Trends in Drug Research. London, *New York: Taylor and Francis* 2002: 319-333
36 **Green BG.** Rapid recovery from the capsaicin desensitation during recurrent stimulation. *Pain* 1966; **68**: 245-253
37 **Mózsik GY,** Debreceni A, Abdel-Salam OME, Szabó I, Figler M, Ludány A, Juricskay I, Szolcsányi J. Small doses of capsaicin given intragastrically inhibit gastric basal acid secretion in healthy human subjects. *J Physiol Paris* 1999; **93**: 433-436

Science Editor Wang XL and Guo SY **Language Editor** Elsevier HK

PO Box 2345, Beijing 100023, China
www.wjgnet.com
wjg@wjgnet.com

ELSEVIER

World J Gastroenterol 2005;11(33):5185-5192
World Journal of Gastroenterology ISSN 1007-9327
© 2005 The WJG Press and Elsevier Inc. All rights reserved.

• *BRIEF REPORTS* •

Preventative effects of a probiotic, *Lactobacillus salivarius ssp. salivarius*, in the TNBS model of rat colitis

Laura Peran, Desiree Camuesco, Monica Comalada, Ana Nieto, Angel Concha, Maria Paz Diaz-Ropero, Monica Olivares, Jordi Xaus, Antonio Zarzuelo, Julio Galvez

Laura Peran, Desiree Camuesco, Monica Comalada, Antonio Zarzuelo, Julio Galvez, Department of Pharmacology, School of Pharmacy, University of Granada, Spain
Ana Nieto, Health and Progress Foundation, Granada, Spain
Angel Concha, Department of Pathology, Hospital Universitario "Virgen de las Nieves", Granada, Spain
Maria Paz Diaz-Ropero, Monica Olivares, Jordi Xaus, Department of Immunology and Animal Sciences, Puleva Biotech, S.A. Granada, Spain
Supported by the Spanish Ministry of Science and Technology, No. SAF2002-02592 and by Instituto de Salud 'Carlos III', No. PI021732, with Funds from the European Union, and by Junta de Andalucia (CTS 164). Monica Comalada is a recipient of Juan de la Cierva Program from Spanish Ministry of Science and Technology. Laura Peran is a Recipient From Puleva Foundation Spain
Correspondence to: Julio Galvez, PhD, Department of Pharmacology, School of Pharmacy, University of Granada, Campus Universitario 'La Cartuja' s/n, Granada 18071, Spain. jgalvez@ugr.es
Telephone: +34-958-243889 Fax: +34-958-248964
Received: 2004-11-23 Accepted: 2005-02-28

Abstract

AIM: To investigate the intestinal anti-inflammatory effect and mechanism of a probiotic *Lactobacillus salivarius ssp. salivarius* CECT5713 in the TNBS model of rat colitis.

METHODS: Female Wistar rats (180-200 g) were used in this study. A group of rats were administered orally the probiotic *L. salivarius ssp. salivarius* (5×10^8 CFU suspended in 0.5 mL of skimmed milk) daily for 3 wk. Two additional groups were used for reference, a non-colitic and a control colitic without probiotic treatment, which received orally the vehicle used to administer the probiotic. Two weeks after starting the experiment, the rats were rendered colitic by intracolonic administration of 10 mg of TNBS dissolved in 0.25 mL of 500 mL/L ethanol. One week after colitis induction, all animals were killed and colonic damage was evaluated both histologically and biochemically. The biochemical studies performed in colonic homogenates include determination of myeloperoxidase (MPO) activity, glutathione (GSH) content, leukotriene B_4 (LTB_4) and tumor necrosis factor α (TNF-α) levels, as well as inducible nitric oxide synthase (iNOS) expression. In addition, the luminal contents obtained from colonic samples were used for microbiological studies, in order to determine Lactobacilli and Bifidobacteria counts.

RESULTS: Treatment of colitic rats with *L. salivarius ssp. salivarius* resulted in amelioration of the inflammatory response in colitic rats, when compared with the corresponding control group without probiotic treatment. This anti-inflammatory effect was evidenced macroscopically by a significant reduction in the extent of colonic necrosis and/or inflammation induced by the administration of TNBS/ethanol (2.3±0.4 cm *vs* 3.4±0.3 cm in control group, $P<0.01$) and histologically by improvement of the colonic architecture associated with a reduction in the neutrophil infiltrate in comparison with non-treated colitic rats. The latter was confirmed biochemically by a significant reduction of colonic MPO activity (105.3±26.0 U/g *vs* 180.6±21.9 U/g, $P<0.05$), a marker of neutrophil infiltration. The beneficial effect was associated with an increase of the colonic GSH content (1 252±42 nmol/g *vs* 1 087±51 nmol/g, $P<0.05$), which is depleted in colitic rats, as a consequence of the oxidative stress induced by the inflammatory process. In addition, the treatment of colitic rats with *L. salivarius* resulted in a significant reduction of colonic TNF-α levels (509.4±68.2 pg/g *vs* 782.9±60.1 pg/g, $P<0.01$) and in a lower colonic iNOS expression, when compared to TNBS control animals without probiotic administration. Finally, treated colitic rats showed higher counts of Lactobacilli species in colonic contents than control colitic rats, whereas no differences were observed in Bifidobacteria counts.

CONCLUSION: Administration of the probiotic *L. salivarius ssp. salivarius* CECT5713 facilitates the recovery of the inflamed tissue in the TNBS model of rat colitis, an effect associated with amelioration of the production of some of the mediators involved in the inflammatory response in the intestine, such as cytokines, including TNF-α and NO. This beneficial effect could be ascribed to its effect on the altered immune response that occurs in this inflammatory condition.

© 2005 The WJG Press and Elsevier Inc. All rights reserved.

Key words: *Lactobacillus salivarius ssp. salivarius*; TNBS rat colitis; Probiotic; Tumor necrosis factor α; Nitric oxide

Peran L, Camuesco D, Comalada M, Nieto A, Concha A, Diaz-Ropero MP, Olivares M, Xaus J, Zarzuelo A, Galvez J. Preventative effects of a probiotic, *Lactobacillus salivarius ssp. salivarius*, in the TNBS model of rat colitis. *World J Gastroenterol* 2005; 11(33): 5185-5192
http://www.wjgnet.com/1007-9327/11/5185.asp

INTRODUCTION

Inflammatory bowel disease (IBD) is a chronic disease of

the digestive tract, and usually refers to two related conditions, namely ulcerative colitis and Crohn's disease, characterized by chronic and spontaneously relapsing inflammation. Although the etiology of IBD remains unknown, there is increasing experimental evidence to support a role for luminal bacteria in the initiation and progression of these intestinal conditions; probably related to an imbalance in the intestinal microflora, relative predominance of aggressive bacteria and insufficient amount of protective species[1,2]. This could justify the remission achieved in intestinal inflammation, after treatment with antibiotics such as metronidazole or ciprofloxacin[3], or the fact that germ-free animals may fail to develop experimental intestinal inflammation[4]. In consequence, a possible therapeutic approach in IBD therapy is the administration to these patients of probiotic microorganisms, defined as viable nutritional agents conferring benefits to the health of the human host. In fact, it has been reported that administration of a mixture of *Bifidobacterium* and *Lactobacillus*[5] or of non-pathogenic viable *Escherichia coli*[6] prolongs remission in ulcerative colitis. Moreover, there are reports on successful induction and maintenance of remission of chronic pouchitis after oral bacteriotherapy[7,8]. However, treatments of Crohn's disease with probiotic preparations reported conflicting results[9-12].

Different mechanisms have been proposed to participate in the therapeutic effects exerted by probiotic microorganisms. First, probiotic microorganisms may exert their action through a modulation of the intestinal bowel flora, which may result from competitive metabolic interactions with potential pathogens, production of anti-microbial peptides, or inhibition of epithelial adherence and translocation by pathogens[5,13]; second, probiotics have been proposed to modulate the host defenses by influencing the intestinal immune system[14,15]; and third, these microorganisms have been reported to positively affect the intestinal barrier function[16,17]. However, the detailed mechanisms by which these bacteria mediate their effects are not fully understood.

Although the results obtained after probiotic treatment in both human IBD and experimental colitis are promising, new studies are required in order to further understand this new concept for the therapy of IBD, even if we consider the fact that many studies have shown that not all bacterial species have equal activities in reducing intestinal inflammation[18,19]. Hence, the selection of new probiotic strains for the treatment of IBD can be based on their ability to regulate the immune response of the intestinal mucosa. This can be the case of *Lactobacilli* strains, which were able to downregulate the production of tumor necrosis factor α (TNF-α). In fact, previous *ex vivo* experiments have reported the ability of *L. casei* and of *L. bulgaricus* to downregulate TNF-α production in colonic explants from patients with Crohn's disease[20], thus supporting their future development for IBD therapy. This may be of special relevance, since several studies have attributed a key role in the pathogenesis of IBD to this pro-inflammatory cytokine, as evidenced by the increased production of TNF-α in the intestinal mucosa from IBD patients[21,22] as well as by a number of clinical studies using anti-TNF-α mAb therapy that have clearly shown a beneficial effect in these patients[23].

The aim of the present study was to test the preventative effects of a *L. salivarius ssp. salivarius* strain in the trinitrobenzenesulfonic acid (TNBS) model of rat colitis, a well-established model of intestinal inflammation with some resemblance to human IBD[24]. The selection of this lactobacilli strain was based on previous *in vitro* studies that showed its ability to adhere to human intestinal cells, to inhibit pathogenic bacterial growth (unpublished results) and to reduce the production of inflammatory cytokines by immune cells. Special attention was paid to its effects on the production of some of the mediators involved in the inflammatory response, such as TNFα, leukotriene B_4 (LTB_4) and nitric oxide (NO). In addition, the correlation among the intestinal anti-inflammatory effect of *L. salivarius ssp. salivarius* and modifications on colonic flora induced by this probiotic was also studied.

MATERIALS AND METHODS

This study was carried out in accordance with the 'Guide for the Care and Use of Laboratory Animals' as promulgated by the National Institute of Health.

Reagents

All chemicals were obtained from Sigma Chemical (Madrid, Spain), unless otherwise stated. Glutathione (GSH) reductase was provided by Boehringer Mannheim (Barcelona, Spain).

In vitro modulation of cytokine production by bacteria

Puleva Biotech's lactic acid bacteria collection was screened for *Lactobacilli* bacteria with the ability to reduce the production of inflammatory cytokines by activated macrophages. For this purpose, rodent bone marrow-derived macrophages, obtained as previously described[25], were stimulated with 100 ng/mL LPS, in the presence or absence of 10^6 CFU/mL of each bacteria for 2 h. Then, cells were washed with culture media to eliminate non-attached bacteria, and cultured with new media for 12 h. TNF-α, IL-12, and IL-10 production was evaluated by ELISA in cell supernatants (CytoSets™, Biosource International, Nivelles, Belgium) following manufacturer's instructions.

Preparation and administration of the probiotic

L. salivarius ssp. salivarius CECT5713 was provided by Puleva Biotech (Granada, Spain) and it was normally grown in MRS media at 37 ℃ in anaerobic conditions using the AnaeroGen system (Oxoid, Basingstoke, UK). For probiotic treatment, bacteria was suspended in skimmed milk (10^9 CFU/mL) and stored at -80 ℃ until usage.

Experimental design

Female Wistar rats (180-200 g) were obtained from the Laboratory Animal Service of the University of Granada (Granada, Spain) and maintained in standard conditions. The rats were randomly assigned to three groups (n = 10); two of them (non-colitic and control groups) received no probiotic treatment and the other (treated group) received orally the probiotic (5×10^8 CFU suspended in 0.5 mL of skimmed milk) daily for 3 wk. Both non-colitic and control groups received orally the vehicle used to administer the probiotic (0.5 mL daily). Two weeks after starting the

experiment, the rats were fasted overnight and those from the control and treated groups were rendered colitic by the method originally described by Morris *et al*.[26]. Briefly, they were anesthetized with halothane and given 10 mg of TNBS dissolved in 0.25 mL of 500 mL/L ethanol by means of a Teflon cannula inserted 8 cm through the anus. Rats from the non-colitic group were administered intracolonically 0.25 mL of PBS instead of TNBS. All rats were killed with an overdose of halothane, 1 wk after induction of colitis.

Assessment of colonic damage

The body weight, water and food intake were recorded daily throughout the experiment. Once the rats were killed, the colon was removed aseptically and placed on an ice-cold plate, longitudinally opened and luminal contents were collected for the microbiological studies (see below). Afterwards, the colonic segment was cleaned of fat and mesentery, blotted on filter paper; each specimen was weighed and its length measured under a constant load (2 g). The colon was scored for macroscopically visible damage on a 0-10 scale by two observers unaware of the treatment, according to the criteria described by Bell *et al*.[27] (Table 1), which takes into account the extent as well as the severity of colonic damage. Representative whole gut specimens were taken from a region of the inflamed colon corresponding to the adjacent segment to the gross macroscopic damage and were fixed in 4% buffered formaldehyde. Cross-sections were selected and embedded in paraffin. Equivalent colonic segments were also obtained from the non-colitic group. Full-thickness sections of 5 μm were obtained at different levels and stained with hematoxylin and eosin. The histological damage was evaluated by two pathologist observers (AN and AC), who were blinded to the experimental groups, according to the criteria described previously by Stucchi *et al*.[28] (Table 2). The colon was subsequently divided into four segments for biochemical determinations. Two fragments were frozen at -80 ℃ for myeloperoxidase (MPO) activity and inducible nitric oxide synthase (iNOS) expression, and another sample was weighed and frozen in 1 mL of 50 g/L trichloroacetic acid for total GSH content determinations. The remaining sample was immediately processed for the measurement of TNF-α and LTB_4 levels. All biochemical measurements were completed within 1 wk from the time of sample collection and were performed in duplicate.

MPO activity was measured according to the technique described by Krawisz *et al*.[29]; the results were expressed as MPO units per gram of wet tissue; one unit of MPO activity was defined as that degrading 1 μmol hydrogen peroxide/min at 25 ℃. Total GSH content was quantified with the recycling assay described by Anderson[30], and the results were expressed as nanomole per gram of wet tissue. Colonic samples for TNF-α and LTB_4 determinations were immediately weighed, minced on an ice-cold plate and suspended in a tube with 10 mmol/L sodium phosphate buffer (pH 7.4) (1∶5 w/v). The tubes were placed in a shaking water bath (37 ℃) for 20 min and centrifuged at 9 000 r/min for 30 s at 4 ℃; the supernatants were frozen at -80 ℃ until assay. TNF-α was quantified by ELISA (Amersham Pharmacia Biotech, Buckinghamshire, UK) and the results were expressed as picogram per gram of wet tissue. LTB_4 was determined by enzyme immunoassay (Amersham Pharmacia Biotech, Buckinghamshire, UK) and the results expressed as nanogram per gram of wet tissue.

iNOS expression was analyzed by Western blotting as previously described[31]. Control of protein loading and transfer was conducted by detection of the β-actin levels.

Table 1 Criteria for assessment of macroscopic colonic damage

Score	Criteria
0	No damage
1	Hyperemia, no ulcers
2	Linear ulcer with no significant inflammation
3	Linear ulcer with inflammation at one site
4	Two or more sites of ulceration / inflammation
5	Two or more major sites of ulceration and inflammation or one site of ulceration / inflammation, extending >1 cm along the length of the colon
6-10	If damage covers >2 cm along the length of the colon, the score is increased by one, for each additional centimeter of involvement

Table 2 Criteria for assessment of microscopic colonic damage

Mucosal epithelium	
	Ulceration: none (0); mild - surface (1); moderate (2); extensive-full thickness (3)
Crypts	
	Mitotic activity: lower third (0); mild mid-third (1); moderate mid-third (2); upper third (3)
	Mucus depletion: none (0); mild (1); moderate (2); severe (3)
Lamina propria	
	Mononuclear infiltrate: none (0); mild (1); moderate (2); severe (3)
	Granulocyte infiltrate: none (0); mild (1); moderate (2); severe (3)
	Vascularity: none (0); mild (1); moderate (2); severe (3)
Submucosal	
	Mononuclear infiltrate: none (0); mild (1); moderate (2); severe (3)
	Granulocyte infiltrate: none (0); mild (1); moderate (2); severe (3)
	Edema: none (0); mild (1); moderate (2); severe (3)

Maximum score: 27. Modified from Stucchi *et al*.[28].

Microbiological studies

Luminal content samples were weighed, homogenized, and serially diluted in sterile peptone water. Serial 10-fold dilutions of homogenates were plated on specific media for *Lactobacillus* (MRS media, Oxoid) or *Bifidobacterium* (MRS media supplemented with 0.5 mg/L dicloxacillin, 1 g/L LiCl and 0.5 g/L L-cysteine hydrochloride) and incubated under anaerobic conditions in an anaerobic chamber for 24-48 h at 37 ℃. Coliforms and enterobacteria were also determined by using specific Count Plates Petrifilm (3M, St. Paul, MN). After incubation, the final count of colonies was reported as $\log_{10}$ colony forming units per gram of material.

Statistical analysis

All results are expressed as mean±SE. Differences between means were tested for statistical significance using a one-way analysis of variance (ANOVA) and post hoc least significance tests. Non-parametric data (score) are expressed as the median (range) and were analyzed using the Mann-Whitney *U*-test. Differences between proportions were analyzed with the χ^2 test. All statistical analyses were carried

out with the Statgraphics 5.0 software package (STSC, MD), with statistical significance set at $P<0.05$.

RESULTS

More than 30 lactic acid bacterial strains with the ability to adhere to human intestinal cell lines and to inhibit pathogenic bacterial growth *in vitro* belonging to the own Puleva Biotech collection were screened for their ability to modulate the production of inflammatory cytokines in LPS-stimulated macrophages. The results obtained were highly diverse, including bacteria with the ability to enhance or to reduce inflammatory cytokine production (TNF-α and IL-12) modifying or not the expression of the anti-inflammatory cytokine IL-10 (data not shown).

Among all the screened bacteria, *L. salivarius ssp. salivarius* (CECT5713) showed the best TNF-α/IL-10 and IL-12/IL-10 ratio (Figure 1), since it was able not only to reduce the LPS-induced TNF-α and IL-12 production, but also to increase the levels of IL-10. For these reasons, we decided to use this strain to test its ability to prevent the inflammatory response in the *in vivo* assay of experimental colitis.

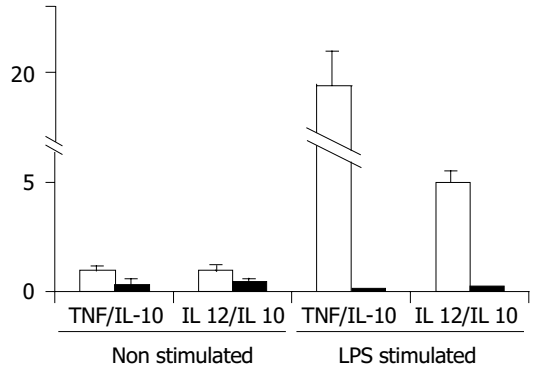


Figure 1 Production of inflammatory cytokines by bone marrow-derived macrophages (BMDM). TNF-α, IL-12, and IL-10 production was analyzed by ELISA in the supernatants of BMDM stimulated or not with LPS (100 ng/mL) and incubated with 10^6 CFU/mL of *L. salivarius ssp. salivarius* (CECT5713) (black bars) or in absence of bacteria (gray bars). The results are the mean of three assays±SE of the ratio between the pro-inflammatory cytokines (TNF-α and IL-12) and IL-10.

L. salivarius ssp. salivarius administration for 2 wk did not induce any symptoms of diarrhea or affected weight evolution. However, once the colitis was induced, the probiotic-treated rats showed an overall lower impact of TNBS-induced colonic damage compared to the TNBS control group. The anti-inflammatory effect was evidenced macroscopically by a significantly lower colonic damage score than that of control rats ($P<0.05$), with a significant reduction in the extent of colonic necrosis and/or inflammation induced by the administration of TNBS/ethanol (Table 3). This anti-inflammatory effect was also associated with a significant reduction in the colonic weight/length ratio between both colitic groups, an index of colonic edema, which increased significantly as a consequence of the inflammatory process (Table 3). The histological studies confirmed the intestinal anti-inflammatory effect exerted by *L. salivarius* (Figure 2). Histological assessment of colonic samples from the TNBS control group revealed severe transmural disruption of the normal architecture of the colon, extensive ulceration and inflammation involving all the intestinal layers of the colon, giving a score value of 18.9±1.1 (mean±SE). Colonic samples were characterized by severe edema, interstitial micro-hemorrhages and diffuse leukocyte infiltration, mainly composed of neutrophils in the mucosa layer and, to a lesser extent, lymphocytes in the submucosa. Most of the rats showed epithelial ulceration of the mucosa affecting over 75% of the surface. The inflammatory process was associated with crypt hyperplasia and dilation, and moderate goblet cell depletion. However, histological analysis of the colonic specimens from rats treated with the probiotic revealed a more pronounced recovery in the intestinal architecture than controls, with a score of 11.2±2.4 (mean±SE) ($P<0.01$ *vs* TNBS control group). Thus, most of the samples (7 of 10) showed almost complete restoration of the epithelial cell layer, in contrast to the extensive ulceration observed in non-treated animals; in fact, the zones with ulceration were surrounded by tissue in process of re-epithelization. Moreover, the transmural involvement of the lesions was reduced. The goblet cell depletion was less severe and thus they appeared replenished with their mucin content, and no dilated crypts were observed. The improvement in colonic histology was accompanied by a reduction in the inflammatory infiltrate, which was



Figure 2 Histological sections of colonic mucosa from colitic rats 1 wk after TNBS instillation stained with hematoxylin and eosin. **A**: Non-colitic group showing the normal histology of the rat colon (original magnification ×20); **B**: TNBS control group showing complete destruction of the mucosa, which has been substituted by inflammatory granulation tissue. There is evident edema and intense diffuse transmural inflammatory infiltrate (original magnification ×100); **C**: *L. salivarius ssp. salivarius* treated group showing amelioration of the inflammatory process and 'restoration' of the mucosal tissue with presence of mucin replenished goblet cells (original magnification ×100).

Table 3 Effects of *L. salivarius ssp. salivarius* (5×10^8 CFU/rat·d) treatment on macroscopic damage score, extent of the inflammatory lesion along the colon and changes in colon weight in TNBS experimental colitis in rats

Group (n = 10)	Damage score (0-10)	Extent of damage (cm)	Colon weight (mg/cm)
Non-colitic	0	0	63.3±2.5
TNBS control	6.5 (5-8)	3.4±0.3	209.7±17.0
TNBS probiotic	5 (3-7)[a]	2.3±0.4[b]	143.3±11.8[b]

Damage score for each rat was assigned according to the criteria described in Table 1 and data are expressed as median (range). Extent of damage and colon weight data are expressed as mean±SE. [a]P<0.05, [b]P<0.01 *vs* TNBS control. All colitic groups differ significantly from non-colitic group.

slight to moderate with a patchy distribution, although neutrophils were the predominant cell type.

The lower leukocyte infiltration was also assessed biochemically by the reduction in colonic MPO activity, a marker of neutrophil infiltration that was enhanced in the TNBS control group (Table 4). In addition, probiotic-treated colitic rats showed a significant increase in colonic GSH content, which is depleted in colitic rats as a consequence of the colonic oxidative stress induced by the inflammatory process, as previously reported in this model of experimental colitis[32] (Table 4). Finally, the colonic inflammation induced by TNBS was characterized by increased levels of colonic TNF-α and LTB_4 (Table 4) as well as by higher colonic iNOS expression (Figure 3) in comparison with non-colitic animals. Treatment of colitic rats with *L. salivarius* resulted in a significant reduction of colonic TNF-α levels (Table 4), that did not show any statistical differences with normal rats. No significant modification was observed on colonic LTB_4 levels. Finally, lower colonic iNOS expression was also seen in colitic animals that received the bacterial suspension, when compared to TNBS control animals (Figure 3).

Effects of L. salivarius administration on colonic bacterial profile

TNBS colitis resulted in a significant reduction in fecal lactobacilli count in comparison with normal rats (P<0.05). Probiotic-treated colitic rats showed higher counts of Lactobacilli species in colonic contents than control colitic rats, without showing statistical differences with both non-colitic and colitic control groups (Figure 4). No statistical differences were observed in Bifidobacteria counts among three groups (P>0.1, Figure 4) nor in the amount of other fecal potential pathogenic bacteria such as enterobacteria or coliform bacteria (data not shown).

DISCUSSION

The results obtained in the present study reveal the efficacy of probiotic therapy with a *L. salivarius ssp. salivarius* strain in intestinal inflammation, incorporating a new microorganism to the probiotics that have been reported to attenuate the development of colonic injury in experimental and human IBD[33]. Thus, oral administration of the probiotic facilitated recovery from TNBS-induced colonic damage, as it was evidenced histologically, with a significant reduction in the extent and severity of inflamed tissue. This beneficial effect was also stated biochemically by a decrease in colonic MPO activity, a marker of neutrophil infiltration that has been previously described to be upregulated in experimental colitis[29], and is widely used to detect and follow intestinal inflammatory processes. In consequence, a reduction in the activity of this enzyme can be interpreted as a manifestation of the anti-inflammatory activity of a given compound[34]. The ability of the probiotic to reduce granulocyte infiltration, showed by MPO activity reduction, was confirmed histologically, since the level of leukocyte infiltrate in the colonic mucosa was lower in treated colitic animals than in

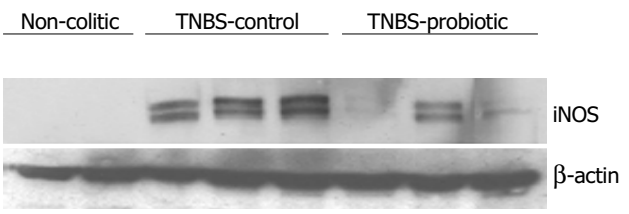


Figure 3 Effects of *L. salivarius ssp. salivarius* treatment (5×10^8 CFU/rat·d) on colonic nitric oxide synthase (NOS) expression in TNBS experimental colitis in rats.

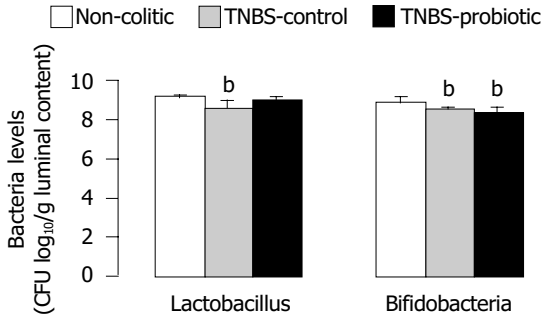


Figure 4 Effects of *L. salivarius ssp. salivarius* (5×10^8 CFU/rat·day) treatment on bacteria levels (Lactobacillus and Bifidobacteria) in TNBS experimental colitis in rats. [b]P<0.01 *vs* non-colitic group.

Table 4 Myeloperoxidase (MPO) activity, total GSH content, TNF-α and LTB_4 levels in colon specimens from non-colitic rats, TNBS control colitic rats and TNBS colitic rats treated with *L. salivarius ssp. salivarius* (5×10^8 CFU/rat·d)

Group (n = 10)	MPO activity (units MPO/g)	GSH (nmol/g)	LTB_4(ng/g)	TNF-α (pg/g)
Non-colitic	23.4±7.2	1 540±41	2.9±0.4	441.5±39.1
TNBS control	180.6±21.9[d]	1 087±51[d]	6.5±0.9[d]	782.9±60.1[d]
TNBS probiotic	105.3±26.0[a,d]	1 252±42[a,d]	6.9±0.8[d]	509.4±68.2[b]

Data are expressed as mean±SE. [a]P<0.05, [b]P<0.01 *vs* TNBS control group; [d]P<0.01 *vs* non-colitic group.

the corresponding TNBS control groups. The inhibitory effect on the infiltration of inflammatory cells into the colonic mucosa might account for the beneficial effect of this probiotic against tissue injury, because margination and extravasation of circulating granulocytes contribute markedly to the colonic injury in this model of IBD[35]. These results are in agreement with other studies, that describe the attenuation exerted by several probiotics in leukocyte-endothelial cell adhesion in this experimental model of rat colitis[36]. This effect can justify the inhibition of the synthesis and/or release of different mediators that participate in the inflammatory process, such as NO, since probiotic treatment of colitic rats was associated with a reduction in colonic iNOS expression. Moreover, this can also explain the improvement in the colonic oxidative stress in colitic rats after probiotic treatment, as evidenced by a partial restoration of the GSH depletion that took place as a consequence of the TNBS colonic damage.

During the last decade, it has become increasingly evident that chronic colonic inflammation, both in human IBD and in experimental colitis, is associated with enhanced NO production, mainly via iNOS activity[37-39], as well as with increased release of reactive oxygen metabolites, including superoxide[40-42]. The simultaneous overproduction of NO and superoxide can yield the highly toxic radical, peroxynitrite in the inflamed intestine[43], which have been demonstrated to produce widespread colonic injury[44]. It is important to note that neutrophils are thought to be important source of both NO[45,46] and reactive oxygen metabolites[47]. Considering the above, the effect exerted by *L. salivarius ssp. salivarius* in decreasing the neutrophil infiltration that occurs in response to TNBS, may preserve the colonic mucosa from oxidative insult. In fact, beneficial effects have previously been reported either after NOS inhibition[37,38] or by antioxidant therapy[31,42] in different experimental models of intestinal inflammation.

Probiotic treatment could attenuate neutrophil infiltration via inhibition of different mediators with chemotactic activity. The results obtained in the present study revealed that probiotic treatment did not significantly modify colonic LTB_4 levels, an eicosanoid with chemotactic activity involved in the pathogenesis of IBD[1]. In consequence, the inhibitory effect of leukocyte infiltration exerted by the probiotic should be related to the downregulation of other pro-inflammatory mediators, given the ability of this lactobacilli strain to modulate the immune response as demonstrated by the *in vitro* studies. In fact, the intestinal anti-inflammatory activity exerted by *L. salivarius ssp. salivarius* was also characterized by downregulation of colonic TNF-α. This may be relevant since TNF-α acts as a potent chemoattractant, thus contributing to the recruitment of neutrophil in the inflamed colonic mucosa and initiating the inflammatory pathogenic cascade that definitively perpetuates colonic inflammation[48]. The important role attributed to TNF-α in intestinal inflammation is strongly supported by the fact that different drugs capable of interfering with the activity of this mediator are being developed for IBD therapy[23]. The ability of probiotic bacteria to downregulate TNF-α production has been reported previously for other lactobacilli strains such as *L. casei* and of *L. bulgaricus*, when they were cultured with inflamed mucosa from patients with Crohn's disease[20]. This effect was attributed to the existence of a cross talk between bacteria and mucosal cells, being able to downregulate the degree of activation of intestinal immune cells[20]. This has also been demonstrated in the present study for *L. salivarius ssp. salivarius* since it was able to modify the cytokine profile in macrophages, reducing the amount of inflammatory cytokines (TNF-α and IL-12), while increasing the amount of the anti-inflammatory cytokine IL-10. The high diversity of immuno-modulatory action of probiotics observed in the screening of the bacteria are in concordance with previous works showing both the ability of some lactic bacteria to promote TNF-α production[49] while others such as *L. rhamnosus* GG (LGG) reduced it[50]. LGG, a probiotic that also reduces the ratio TNF-α/IL-10, has been reported to exert intestinal anti-inflammatory effects both in human[12] and in experimental intestinal inflammation[51]. This effect of some probiotics on the immune response may be of special relevance because it would promote a possible shift from a T_H1-mediated immune response toward a T_H2/T_H3 profile, similarly to that proposed to occur with Lactobacillus GG[15]. It is important to note that replacing the bacteria responsible for the constant antigenic drive leading to T_H1 cellular activation with probiotic species that preferentially induce protective immune responses may alter the normal course of these relapsing intestinal conditions. In addition, probiotics like *Bifidobacterium longum* or *L. bulgaricus* have been shown to inhibit the IL-8 secretion in intestinal epithelia, when stimulated by the pro-inflammatory cytokine TNF-α, thus reducing the activity of other pro-inflammatory cytokines with chemotactic activity[52].

However, the participation of the modification in the immune response in the intestinal anti-inflammatory effect exerted by this probiotic does not exclude mechanisms proposed for other probiotics, mainly due to a role in preventing the imbalance in the intestinal microflora, given the relative predominance of aggressive bacteria and insufficient amount of protective species that has been reported in these intestinal conditions[1,2]. Previous studies have suggested that in TNBS-induced colitis, specific strains from colonic microflora invades the colonic wall after disruption of the epithelium and the presence of bacteria within the wall participates in the transmural inflammation[53]. In fact, the present study reveals that the colonic damage induced by TNBS was associated with a significant reduction of lactobacilli count in the colonic lumen, which was counteracted after the probiotic treatment, since probiotic-treated rats showed no statistical differences from non-colitic rats in the lactobacilli content.

In conclusion, administration of the probiotic *L. salivarius ssp. salivarius* CECT5713 facilitates the recovery of the inflamed tissue in the TNBS model of rat colitis, an effect associated with amelioration of the production of some of the mediators involved in the inflammatory response of the intestine, such as cytokines, including TNF-α, and NO. This beneficial effect could be ascribed to its effect on the altered immune response characteristic of this inflammatory condition, which would attenuate the exacerbated immune response evoked by the colonic instillation of the hapten TNBS in the rats.

REFERENCES

1 **Fiocchi C.** Inflammatory bowel disease: aetiology and pathogenesis. *Gastroenterology* 1998; **115**: 182-205
2 **Shanahan F.** Probiotics and inflammatory bowel disease: is there a scientific rationale? *Inflammatory Bowel Dis* 2000; **6**: 107-115
3 **Chung PY,** Peppercorn MA. Antibiotics in inflammatory bowel disease. *Drugs Today* 1999; **35**: 89-103
4 **Taurog JD,** Richardson JA, Croft JT, Simmons WA, Zhou M, Fernandez-Sueiro JL, Balish E, Hammer RE. The germfree state prevents development of gut and joint inflammatory disease in HLA-B27 transgenic rats. *J Exp Med* 1994; **180**: 2359-2364
5 **Venturi A,** Gionchetti P, Rizzello F, Johansson R, Zucconi E, Brigidi P, Matteuzzi D, Campieri M. Impact on the composition of the faecal flora by a new probiotic preparation: preliminary data on maintenance treatment of patients with ulcerative colitis. *Aliment Pharmacol Ther* 1999; **13**: 1103-1108
6 **Rembacken BJ,** Snelling AM, Hawkey PM, Chalmers DM, Axon AT. Non-pathogenic Escherichia coli versus mesalazine for the treatment of ulcerative colitis: a randomised trial. *Lancet* 1999; **354**: 635-639
7 **Gionchetti P,** Rizzello F, Helwig U, Venturi A, Lammers KM, Brigidi P, Vitali B, Poggioli G, Miglioli M, Campieri M. Prophylaxis of pouchitis onset with probiotic therapy: a double-blind, placebo-controlled trial. *Gastroenterology* 2003; **124**: 1202-1209
8 **Gionchetti P,** Rizzello F, Venturi A, Brigidi P, Matteuzzi D, Bazzocchi G, Poggioli G, Miglioli M, Campieri M. Oral bacteriotherapy as maintenance treatment in patients with chronic pouchitis: a double-blind, placebo-controlled trial. *Gastroenterology* 2000; **119**: 305-309
9 **Malchow HA.** Crohn's disease and Escherichia coli. A new approach in therapy to maintain remission of colonic Crohn's disease? *J Clin Gastroenterol* 1997 **25**: 653-658
10 **Prantera C,** Scribano ML, Falasco G, Andreoli A, Luzi C. Ineffectiveness of probiotics in preventing recurrence after curative resection for Crohn's disease: a randomised controlled trial with Lactobacillus GG. *Gut* 2002; **51**: 405-409
11 **Gupta P,** Andrew H, Kirschner BS, Guandalini S. Is lactobacillus GG helpful in children with Crohn's disease? Results of a preliminary, open-label study. *J Pediatr Gastroenterol Nutr* 2000; **31**: 453-457
12 **Schultz M,** Timmer A, Herfarth HH, Sartor RB, Vanderhoof JA, Rath HC. Lactobacillus GG in inducing and maintaining remission of Crohn's disease. *BMC Gastroenterol* 2004; **4**: 5
13 **Tannock GW,** Munro K, Harmsen HJ, Welling GW, Smart J, Gopal PK. Analysis of the fecal microflora of human subjects consuming a probiotic product containing Lactobacillus rhamnosus DR20. *Appl Environ Microbiol* 2000; **66**: 2578-2588
14 **Ulisse S,** Gionchetti P, D'Alo S, Russo FP, Pesce I, Ricci G, Rizzello F, Helwig U, Cifone MG, Campieri M, De Simone C. Expression of cytokines, inducible nitric oxide synthase, and matrix metalloproteinases in pouchitis: effects of probiotic treatment. *Am J Gastroenterol* 2001; **96**: 2691-2699
15 **Schultz M,** Linde HJ, Lehn N, Zimmermann K, Grossmann J, Falk W, Scholmerich J. Immunomodulatory consequences of oral administration of Lactobacillus rhamnosus strain GG in healthy volunteers. *J Dairy Res* 2003; **70**: 165-173
16 **Madsen K,** Cornish A, Soper P, McKaigney C, Jijon H, Yachimec C, Doyle J, Jewell L, De Simone C. Probiotic bacteria enhance murine and human intestinal epithelial barrier function. *Gastroenterology* 2001; **121**: 580-591
17 **Otte JM,** Podolsky DK. Functional modulation of enterocytes by gram-positive and gram-negative microorganisms. *Am J Physiol* 2004; **286**: G613-626
18 **Shibolet O,** Karmeli F, Eliakim R, Swennen E, Brigidi P, Gionchetti P, Campieri M, Morgenstern S, Rachmilewitz D. Variable response to probiotics in two models of experimental colitis in rats. *Inflamm Bowel Dis* 2002; **8**: 399-406
19 **Kennedy RJ,** Hoper M, Deodhar K, Kirk SJ, Gardiner KR. Probiotic therapy fails to improve gut permeability in a hapten model of colitis. *Scand J Gastroenterol* 2000; **35**: 1266-1271
20 **Borruel N,** Carol M, Casellas F, Antolin M, de Lara F, Espin E, Naval J, Guarner F, Malagelada JR. Increased mucosal tumour necrosis factor alpha production in Crohn's disease can be downregulated ex vivo by probiotic bacteria. *Gut* 2002; **51**: 659-664
21 **Reinecker HC,** Steffen M, Witthoeft T, Pflueger I, Schreiber S, MacDermott RP, Raedler A. Enhanced secretion of tumour necrosis factor-alpha, IL-6, and IL-1 beta by isolated lamina propria mononuclear cells from patients with ulcerative colitis and Crohn's disease. *Clin Exp Immunol* 1993; **94**: 174-181
22 **Reimund JM,** Wittersheim C, Dumont S, Muller CD, Kenney JS, Baumann R, Poindron P, Duclos B. Increased production of tumour necrosis factor-alpha interleukin-1 beta, and interleukin-6 by morphologically normal intestinal biopsies from patients with Crohn's disease. *Gut* 1996; **39**: 684-689
23 **Rutgeerts P,** Van Assche G, Vermeire S. Optimizing anti-TNF treatment in inflammatory bowel disease. *Gastroenterology* 2004; **126**: 1593-1610
24 **Jurjus AR,** Khoury NN, Reimund JM. Animal models of inflammatory bowel disease. *J Pharmacol Toxicol Methods* 2004; **50**: 81-92
25 **Comalada M,** Xaus J, Valledor AF, Lopez-Lopez C, Pennington DJ, Celada A. PKC epsilon in involved in JNK activation that mediates LPS- induced TNF-alpha, which induces apoptosis in macrophages. *Am J Physiol* 2003; **285**: C1235-1245
26 **Morris GP,** Beck PL, Herridge W, Depew W, Szewczuk MR, Wallace JL. Hapten induced model of chronic inflammation and ulceration in rat colon. *Gastroenterology* 1989; **96**: 795-803
27 **Bell CJ,** Gall DG, Wallace JL. Disruption of colonic electrolyte transport in experimental colitis. *Am J Physiol* 1995; **268**: G622-630
28 **Stucchi AF,** Shofer S, Leeman S, Materne O, Beer E, McClung J, Shebani K, Moore F, O'Brien M, Becker JM. NK-1 antagonist reduces colonic inflammation and oxidative stress in dextran sulfate-induced colitis in rats. *Am J Physiol* 2000; **279**: G1298-1306
29 **Krawisz JE,** Sharon P, Stenson WF. Quantitative assay for acute intestinal inflammation based on myeloperoxidase activity. Assessment of inflammation in rat and hamster models. *Gastroenterology* 1984; **87**: 1344-1350
30 **Anderson ME.** Determination of glutathione and glutathione disulfide in biological samples. *Methods Enzymol* 1985; **113**: 548-555
31 **Camuesco D,** Comalada M, Rodríguez-Cabezas ME, Nieto A, Lorente MD, Concha A, Zarzuelo A, Gálvez J. The intestinal anti-inflammatory effect of quercitrin is associated with an inhibition in iNOS expression. *Br J Pharmacol* 2004; **143**: 908-918
32 **Galvez J,** Garrido M, Rodriguez-Cabezas ME, Ramis I, Sanchez de Medina F, Merlos M, Zarzuelo A. The intestinal anti-inflammatory activity of UR-12746S on reactivated experimental colitis is mediated through downregulation of cytokine production. *Inflamm Bowel Dis* 2003; **9**: 363-371
33 **Schultz M,** Sartor RB. Probiotics and inflammatory bowel diseases. *Am J Gastroenterol* 2000; **95**: S19-21
34 **Veljaca M,** Lesch CA, Pllana R, Sanchez B, Chan K, Guglietta A. BPC-15 reduces trinitrobenzene sulfonic-induced colonic damage in rats. *J Pharmacol Exp Ther* 1995; **272**: 417-422
35 **Ajuebor MN,** Zagorski J, Kunkel SL, Strieter RM, Hogaboam CM. Contrasting roles for CXCR2 during experimental colitis. *Exp Mol Pathol* 2004; **76**: 1-8
36 **Lamine F,** Fioramonti J, Bueno L, Nepveu F, Cauquil E, Lobysheva I, Eutamene H, Theodorou V. Nitric oxide released by Lactobacillus farciminis improves TNBS-induced colitis in rats. *Scand J Gastroenterol* 2004; **39**: 37-45
37 **Rachmilewitz D,** Karmeli F, Okon E, Bursztyn M. Experimental colitis is ameliorated by inhibition of nitric oxide synthase activity. *Gut* 1995; **37**: 247-255
38 **Hogaboam CM,** Jacobson K, Collins SM, Blennerhassett MG. The selective beneficial effects of nitric oxide inhibition in experimental colitis. *Am J Physiol* 1995; **268**: G673-684

39 **Kimura H,** Miura S, Shigematsu T, Ohkubo N, Tsuzuki Y, Kurose I, Higuchi H, Akiba Y, Hokari R, Hirokawa M, Serizawa H, Ishii H. Increased nitric oxide production and inducible nitric oxide synthase activity in colonic mucosa of patients with active ulcerative colitis and Crohn's disease. *Dig Dis Sci* 1997; **42**: 1047-1054

40 **Grisham MB.** Oxidants and free radicals in inflammatory bowel disease. *Lancet* 1994; **344**: 859-861

41 **McKenzie SJ,** Baker MS, Buffinton GD, Doe WF. Evidence of oxidant-induced injury to epithelial cells during inflammatory bowel disease. *J Clin Invest* 1996; **98**: 136-141

42 **Galvez J,** Coelho G, Crespo ME, Cruz T, Rodriguez-Cabezas ME, Concha A, Gonzalez M, Zarzuelo A. Intestinal anti-inflammatory activity of morin on chronic experimental colitis in the rat. *Aliment Pharmacol Ther* 2001; **15**: 2027-2039

43 **Pavlick KP,** Laroux FS, Fuseler J, Wolf RE, Gray L, Hoffman J, Grisham MB. Role of reactive metabolites of oxygen and nitrogen in inflammatory bowel disease. *Free Radic Biol Med* 2002; **33**: 311-322

44 **Rachmilewitz D,** Stamler JS, Karmeli F, Mullins ME, Singel DJ, Loscalzo J, Xavier RJ, Podolsky DK. Peroxynitrite-induced rat colitis-a new model of colonic inflammation. *Gastroenterology* 1993; **105**: 1681-1688

45 **Ikeda I,** Kasajima T, Ishiyama S, Shimojo T, Takeo Y, Nishikawa T, Kameoka S, Hiroe M, Mitsunaga A. Distribution of inducible nitric oxide synthase in ulcerative colitis. *Am J Gastroenterol* 1997; **92**: 1339-1341

46 **McCafferty DM,** Miampamba M, Sihota E, Sharkey KA, Kubes P. Role of inducible nitric oxide synthase in trinitrobenzene sulphonic acid induced colitis in mice. *Gut* 1999; **45**: 864-873

47 **Guo X,** Wang WP, Ko JK, Cho CH. Involvement of neutrophils and free radicals in the potentiating effects of passive cigarette smoking on inflammatory bowel disease in rats. *Gastroenterology* 1999; **117**: 884-892

48 **Stallmach A,** Giese T, Schmidt C, Ludwig B, Mueller-Molaian I, Meuer SC. Cytokine/chemokine transcript profiles reflect mucosal inflammation in Crohn's disease. *Int J Colorectal Dis* 2004; **19**: 308-315

49 **Miettinen M,** Vuopio-Varkila J, Varkila K. Production of human tumor necrosis factor alpha, interleukin-6, and interleukin-10 is induced by lactic acid bacteria. *Infect Immun* 1996; **64**: 5403-5405

50 **Pena JA,** Versalovic J. Lactobacillus rhamnosus GG decreases TNF-alpha production in lipopolysaccharide-activated murine macrophages by a contact-independent mechanism. *Cell Microbiol* 2003; **5**: 277-285

51 **Dieleman LA,** Goerres MS, Arends A, Sprengers D, Torrice C, Hoentjen F, Grenther WB, Sartor RB. Lactobacillus GG prevents recurrence of colitis in HLA-B27 transgenic rats after antibiotic treatment. *Gut* 2003; **52**: 370-376

52 **Bai AP,** Ouyang Q, Zhang W, Wang CH, Li SF. Probiotics inhibit TNF-α-induced interleukin-8 secretion of HT29 cells. *World J Gastroenterol* 2004; **10**: 455-457

53 **Garcia-Lafuente A,** Antolin M, Guarner F, Crespo E, Salas A, Forcada P, Laguarda M, Gavalda J, Baena JA, Vilaseca J, Malagelada JR. Incrimination of anaerobic bacteria in the induction of experimental colitis. *Am J Physiol* 1997; **272**: G10-15

Science Editor Li WZ **Language Editor** Elsevier HK

PO Box 2345, Beijing 100023, China
www.wjgnet.com
wjg@wjgnet.com

ELSEVIER

World J Gastroenterol 2005;11(33):5193-5198
World Journal of Gastroenterology ISSN 1007-9327
© 2005 The WJG Press and Elsevier Inc. All rights reserved.

• *BRIEF REPORTS*•

Hepatocellular carcinoma in Egypt: A single center study over a decade

Abdel-Rahman El-Zayadi, Hanaa M Badran, Eman MF Barakat, Mohy El-Deen Attia, Sherine Shawky, Mostafa K Mohamed, Osaima Selim, Ahmed Saeid

Abdel-Rahman El-Zayadi, Eman MF Barakat, Department of Tropical Medicine, Ain Shams University, Cairo, Egypt
Hanaa M Badran, Department of Hepatology, National Liver Institute, Menoufeya, Egypt
Mohy El-Deen Attia, Department of Hepatology and Gastroenterology, Theodor Bilharz Research Institute, Cairo, Egypt
Sherine Shawky, The Social Research Center, The American University in Cairo, Egypt
Mostafa K. Mohamed, Department of Community Medicine, Ain Shams University, Cairo, Egypt
Osaima Selim, Department of Clinical Pathology, Ain Shams University, Cairo, Egypt
Ahmed Saeid, Cairo Liver Center, Giza, Egypt
Correspondence to: Professor Abdel-Rahman El-Zayadi, MD, Hepatology and Gastroenterology, Ain Shams University and Director of Cairo Liver Center 5, El-Gergawy St. Dokki, Giza, Egypt. clcz@tedata.net.eg
Telephone: +202-7603002 Fax: +202-7481900
Received: 2004-09-16 Accepted: 2005-02-26

Abstract

AIM: To identify the trend, possible risk factors and any pattern change of hepatocellular carcinoma (HCC) in Egypt over a decade.

METHODS: All HCC patients attending Cairo Liver Center between January 1993 and December 2002, were enrolled in the study. Diagnosis of HCC was based on histopathological examination and/or detection of hepatic focal lesions by two imaging techniques plus α-fetoprotein level above 200 ng/mL. The duration of the study was divided into two periods of 5 years each; period I (1993-1997) and period II (1998-2002). Trend, demographic features of patients (age, gender, and residence), risk factors (HBsAg, HCV-Ab, schistosomiasis and others) and pattern of the focal lesions were compared between the two periods. Logistic regression model was fitted to calculate the adjusted odds ratios for the potential risk factors. The population attributable risk percentage was calculated to estimate the proportion of HCC attributed to hepatitis B and C viral infections.

RESULTS: Over a decade, 1 328 HCC patients out of 22 450 chronic liver disease (CLD) patients were diagnosed with an overall proportion of 5.9%. The annual proportion of HCC showed a significant rising trend from 4.0% in 1993 to 7.2% in 2002 (P = 0.000). A significant increase in male proportion from 82.5% to 87.6% (P = 0.009); M/F from 5:1 to 7:1 and a slight increase of the predominant age group (40-59 years) from 62.6% to 66.8% (P = 0.387) in periods I and II respectively, reflecting a shift to younger age group. In the bivariate analysis, HCC was significantly higher in rural residents, patients with history of schistosomiasis and/or blood transfusion. Yet, after adjustment, these variables did not have a significant risk for development of HCC. There was a significant decline of HBsAg from 38.6% to 20.5% (P = 0.000), and a slight increase of HCV-Ab from 85.6% to 87.9% in periods I and II respectively. HBV conferred a higher risk to develop HCC more than HCV in period I (OR 1.9 *vs* 1.6) and period II (OR 2.7 *vs* 2.0), but the relative contribution of HBV for development of HCC declined in period II compared to period I (PAR% 4.2%, 21.32%). At presentation, diagnostic α-fetoprotein level (⩾200 ng/mL) was demonstrated in 15.6% *vs* 28.9% and small HCC (⩽3 cm) represented 14.9% *vs* 22.7% (P = 0.0002) in periods I and II respectively.

CONCLUSION: Over a decade, there was nearly a twofold increase of the proportion of HCC among CLD patients in Egypt with a significant decline of HBV and slight increase of HCV as risk factors. α-Fetoprotein played a limited role in diagnosis of HCC, compared to imaging techniques. Increased detection of small lesions at presentation reflects increased awareness of the condition.

© 2005 The WJG Press and Elsevier Inc. All rights reserved.

Key words: Hepatocellular carcinoma; HCC prevalence; HCC risk factors; Pattern of HCC; HCV and HCC; HBV and HCC

El-Zayadi AR, Badran HM, Barakat EMF, Attia MED, Shawky S, Mohamed MK, Selim O, Saeid A. Hepatocellular carcinoma in Egypt: A single center study over a decade. *World J Gastroenterol* 2005; 11(33): 5193-5198
http://www.wjgnet.com/1007-9327/11/5193.asp

INTRODUCTION

Hepatocellular carcinoma (HCC) is the fifth most common malignancy in the world[1] complicating liver cirrhosis in most cases. Its incidence is increasing worldwide ranging between 3% and 9% annually[2]. In Egypt, HCC was reported to account for about 4.7% of chronic liver disease (CLD) patients[3]. The epidemiology of HCC is characterized by marked demographic and geographic variations.

HBV is considered as a major risk factor for the progression to liver cirrhosis and HCC[4]. The relative risk of developing HCC for HBV carriers may be 100-200-fold higher than

that for non-carriers[5]. Integration of the viral DNA into host genome was suggested to be the initiating event for HBV-induced carcinogenesis[6]. A recent study suggests that the HBx protein may inactivate p53 (tumor suppressor gene) leading to development of HCC[7]. However, the prevalence of HBV infection in Egypt has been declining over the last two decades[3].

The rising trend of HCC has been associated with increased prevalence of hepatitis C virus (HCV) infection[1]. In Egypt, the prevalence of HCV infection among general population has been estimated to be around 14%[8]. The fundamental mechanism by which HCV is related to HCC is not definitely known. Several lines of evidence indicate a strong causal association between HCV and HCC, as shown by the raised prevalence of anti-HCV[2,3] and/or HCV-RNA[9] in patients with HCC.

HCV mostly plays an indirect role in tumor development and appears to increase the risk of HCC by promoting fibrosis and cirrhosis. On the other hand, HCV may play a direct role in hepatic carcinogenesis through involvement of viral gene products in inducing liver cell proliferation[10]. However, it seems that cirrhosis is the common pathway by which several risk factors exert their carcinogenic effect[11].

Exposure to aflatoxin is an additional risk factor for the development of HCC, through damage of DNA in liver cells and mutation in p53 tumor suppressor gene[7]. A previous study showed that aflatoxin B1 has a considerable role in the development of HCC among Egyptians[3].

The aim of this study was to detect the trend of HCC in Egypt over the past decade, identify the possible risk factors and the proportion attributed to hepatitis B and C viral infections and changes in HCC pattern.

MATERIALS AND METHODS

The study was conducted at Cairo Liver Center (CLC), a private institute established to provide specialized care for patients with liver disease. The center receives patients from almost all regions of Egypt, besides patients from the neighboring Arab countries.

A specially designed database application was employed for collecting and managing data of the Egyptian patients attending the center during the period from January 1993 to December 2002. Patients were assigned unique records, which were presented through a designed form interface. The form consisted of three sections on socio-demographic characteristics (age, gender, occupation, and residence), history of exposure to known risk factors of viral hepatitis - blood transfusion and parenteral anti-schistosomal therapy, and laboratory findings (HBsAg status, HCV-Ab status, α-fetoprotein level). Another patient record-linked application was employed to record the imaging characteristics of HCC cases such as location, number, and size of hepatic focal lesions, as well as, portal vein status.

HCV-Ab was detected using second generation ELISA (Boehringer Mannheim Immunodiagnostics for ES-300). HBsAg was confirmed by ELISA test (ELISA-Abbot Laboratories), α-fetoprotein level was tested using Abbot Laboratories' method. No study in Egypt has stated the cut-off level of α-fetoprotein in Egypt yet; however, we considered a cut-off level of 200 ng/mL as reported internationally[12]. Ultrasonography was performed using Toshiba Sonolayer 600, with a convex linear probe using B mode.

Diagnosis of HCC was based on histopathological examination and/or detection of hepatic focal lesions by two imaging techniques (ultrasonography and dynamic CT) plus α-fetoprotein level above 200 ng/mL.

Statistical analysis

Data analysis was done using SPSS computer package. Trend of HCC among CLD patients was studied annually and χ^2 test for trend was used to detect significant annual differences. Also, the 10-year period was divided into period I from 1993 to 1997, and period 2 from 1998 to 2002. The differences in the characteristics of HCC patients between the two periods were compared. χ^2 test for association was used to detect significant associations between proportions.

Logistic regression model was fitted to identify the impact of the various risk factors on HCC. The dependent outcome was HCC (0 = absent, 1 = present) and the independent factors were age, sex, previous history of blood transfusion, schistosomiasis, HCV-Ab positivity and HBsAg positivity.

The population attributable risk percent (PAR%)[13] was calculated to express the proportion of HCC in the study population that was attributed to HCV-Ab or HBsAg positivity and thus can be eliminated, if exposure is prevented. PAR% was calculated as follows:

PAR% = Pe(OR-1)/Pe(OR-1)+1

Where Pe is the proportion of exposed individuals in the population and OR represents the adjusted odds ratio.

RESULTS

A total of 22 450 Egyptian patients with CLDs were registered at CLC between the year 1993 and 2002 (Table 1). Their ages ranged from 33 to 74 years (mean±SD = 53.3±11.67 years). 77.7% were males and 22.3% females and most of them (75.2%) resided in rural areas. Around 50% had history of parenteral anti-schistosomal therapy and 12.9% had history of blood transfusion. HCV-Ab accounted for 72.3% and HBsAg for 20.4%.

There were 1 328 HCC cases diagnosed over the 10-year period giving an overall proportion of 5.9%. HCC was diagnosed mainly among males between 40 and 59 years of age living in rural areas. Schistosomiasis, blood transfusion, HCV-Ab, and HBsAg were more prevalent among HCC-positive cases than HCC-negative cases (Table 1).

As shown in Table 2 and Figure 1, there was a significant annual increase (χ^2 = 29.9, df = 9, P = 0.000) in the proportion of patients with HCC attending CLC, during the study period ranging from 4.0% in 1993 to 7.2% in 2002.

Comparing the two periods (Table 3), there was a slight shift in age distribution to younger age group from age group ⩾60 years, to the most predominant age group 40-59 years, but the difference did not reach a statistical significance (P = 0.387). There were no significant changes as regards residence and history of schistosomiasis between the two periods. However, there was a significant increase in the proportion of males (χ^2 = 6.7, df = 1, P = 0.009) in period II (Table 3).

Table 1 Socio-demographic characteristics of CLD patients attending CLC during the period 1993-2002

	Total registered (n = 22 450)		HCC negative (n = 21 122)		HCC positive (n = 1 328)	
Age (P = 0.000)						
<40	5 670	25.3	5 591	26.5	79	5.9
40-59	13 717	61.1	12 858	60.9	859	64.7
60+	3 063	13.6	2 673	12.7	390	29.4
Sex (P = 0.000)						
Men	17 442	77.7	16 308	77.2	1 134	85.4
Women	5 008	22.3	4 814	22.8	194	14.6
Residence (P = 0.000)						
Rural	16 882	75.2	15 805	74.8	1 078	81.2
Urban	5 568	24.8	5 317	25.2	250	18.8
Blood transfusion (P = 0.004)						
No	19 548	87.1	18 426	87.2	1 122	84.5
Yes	2 902	12.9	2 696	12.8	206	15.5
Schistosomiasis (P = 0.000)						
No	10 126	45.1	9 617	45.5	509	38.3
Yes	12 324	54.9	11 505	54.5	819	61.7
HCV-Ab (P = 0.000)						
Negative	6 209	27.7	6 035	28.6	174	13.1
Positive	16 241	72.3	15 087	71.4	1 154	86.9
HBsAg (P = 0.000)						
Negative	17 864	79.6	16 913	80.1	951	71.6
Positive	4 586	20.4	4 209	19.9	377	28.4

Table 2 Annual number and proportion of HCC among chronic liver diseased patients attending CLC during the period 1993-2002

	Total registered	HCC	
	n	n	%
1993	2 636	106	4.0
1994	2 160	106	4.9
1995	2 054	109	5.3
1996	2 236	130	5.8
1997	2 154	127	5.9
1998	2 459	155	6.3
1999	2 448	162	6.6
2000	2 449	164	6.7
2001	2 064	140	6.8
2002	1 790	129	7.2
Total	22 450	1 328	5.9

χ^2 = 33.5, df = 9, P = 0.0000.

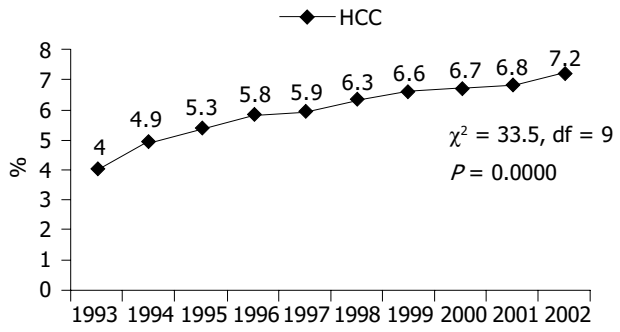


Figure 1 Annual number and proportion of HCC among chronic liver diseased patients attending CLC during the period 1993-2002.

Analysis of the major risk factors of HCC in period I compared to period II revealed appreciable changes (Table 3). There was a significant drop of HBsAg positivity from 38.6% to 20.5% (χ^2 = 52.3, df = 1, P = 0.000), in hepatitis C and B co-infection from 27.0% to 10.8% (χ^2 = 58.4, df = 1, P = 0.000) among HCC cases and decline in the proportion of patients with previous history of blood transfusion from 19.6% to 12.4% (χ^2 = 12.7, df = 1 , P = 0.000). There was a slight increase of HCV-Ab positivity from 85.6% to 87.9% (χ^2 = 1.42, df = 1, P = 0.23). Diagnostic α-fetoprotein level (⩾200 ng/mL) was reported in 15.6% of patients in period I and 28.9% in period II (χ^2 = 32.8, df = 1, P = 0.000, Table 3).

All HCC cases presented with focal hepatic lesions on imaging. The right lobe was affected in 65%, the left lobe in 13.4% and both lobes in 21.6%, most of which (54.9%) were diffusive or multinodular hepatic focal lesions. At presentation, the lesions tended to be multifocal (χ^2 = 7.65, df = 1, P = 0.006), more on the right side (χ^2 = 30.4, df = 1, P = 0.000) and large (>3 cm) in size (χ^2 = 86.1, df = 2, P = 0.000). However, there was a significant increase in the detection of small lesions in the second period more than in the first period (χ^2 = 12.7, df = 1, P = 0.000). Portal vein thrombosis was demonstrated in 18.0% of cases in period I and 17.9% in period II with no significant difference between the two periods (Table 3).

The adjusted odds ratios (Table 4) have shown that men were at higher risk to develop HCC than women (OR = 2.9) as well as patients of older age (age group 40-59 years, OR = 3.7 times and ⩾60 years, OR = 11.2, P = 0.000). HCV-Ab-positive cases were at double risk, while HBsAg were at nearly triple risk of developing HCC. Residents of rural areas, patients with previous history of schistosomiasis and/or blood transfusion were significantly related to HCC in the bivariate analysis. However, after adjustment for other risk factors in the logistic regression model, their impact on acquiring HCC did not reach statistical significance. Although HBsAg occurrence conferred a higher risk of HCC than HCV in both periods, HBsAg appears to have a less share in HCC development as the PAR% revealed that 42.0% of

Table 3 Comparison of the main risk factors and pattern of HCC between period I and II of the study among CLD patients attending CLC

	1993-1997 HCC (*n* = 578)		1998-2002 HCC (*n* = 750)		*P*
	n	%	*n*	%	
Age (yr)					0.387
<40	36	6.2	43	5.7	
40-59	362	62.6	497	66.3	
60+	180	31.1	210	28.0	
Sex					0.009
Male	477	82.5	657	87.6	
Female	101	17.5	93	12.4	
Residence					0.411
Rural	475	82.2	603	80.4	
Urban	103	17.8	147	19.6	
Schistosomiasis	371	64.2	448	59.7	0.098
Blood transfusion	113	19.6	93	12.4	0.000
HCV-Ab	495	85.6	659	87.9	0.233
HBsAg	223	38.6	154	20.5	0.000
Co-infection (HBV+HCV)	156	27	81	10.8	0.000
Non B Non C	16	2.8	18	2.4	0.673
α-Fetoprotein (≥200 ng / mL)	90	15.6	217	28.9	0.000
Number of lesions					0.006
Unifocal	264	45.7	286	38.1	
Multifocal	314	54.3	464	61.9	
Site of lesion					
Right lobe	339	58.7	524	69.9	0.000
Left lobe	73	12.6	105	14.0	
Both	166	28.7	121	16.1	
Size of lesion					0.000
[1]≤3.0 cm	86	14.9	170	22.7	
>3.0 cm	492	85.1	580	77.3	
PVT[2]	104	18.0	134	17.9	0.953

[1]May be eligible for intervention! [2]PVT; portal vein thrombosis.

Table 4 Logistic regression analysis of various HCC risk factors and PAR% among patients attending CLC during the period 1993-2002

	OR	95%CI	*P*	PAR%
Age (yr)			0.000	
<40	1.0	*Reference*		-
40-59	3.7	2.0-6.7		-
60+	11.2	5.7-21.9		-
Sex			0.000	
Men	2.9	1.7-4.8		-
Women	1.0	*Reference*		-
Residence			0.654	
Rural	1.0	*Reference*		-
Urban	0.9	0.6-1.4		-
Blood transfusion			0.908	
No	1.0	*Reference*		-
Yes	1.0	0.6-1.5		-
Schistosomiasis			0.906	
No	1.0	*Reference*		-
Yes	1.1	0.7-1.5		-
HCV-Ab			0.002	
Negative	1.0	*Reference*		-
Positive	2.0	1.3-3.0		42.0
HBsAg			0.001	
Negative	1.0	*Reference*		-
Positive	2.5	1.4-4.4		23.4

HCC cases were attributed to HCV positivity, while only 23.4% of them were attributed to HBV positivity. HBsAg has a lower contribution for development of HCC in period II (PAR% = 4.2%) than in period I (PAR% = 21.3%).

DISCUSSION

Worldwide, HCC is one of the most common malignancies associated with poor prognosis[14]. According to recent reports, the incidence of HCC has increased sharply in the last 5-10 years[1,2,15]. In USA, the rate of HCC has increased by 70% over the last two decades[16]. Registry data in Canada and Western Europe show similar trends[16]. So far, no enough attention has been paid to explore the magnitude of the problem of HCC in Egypt. In the current study, there has been a remarkable increase of the proportion

of HCC among CLD patients from 4.0% to 7.2% over a decade. This rising proportion may be explained by the increasing risk factors such as the emergence of HCV over the same period of time, the contribution of HBV infection, improvement of the screening programs and diagnostic tools of HCC[17], as well as the increased survival rate among patients with cirrhosis to allow time for some of them to develop HCC.

HCC is more prevalent in men than in women[18], which may be at least in part explained by differences in exposure to risk factors. However, sex hormones and other x-linked genetic factors may also be important[19]. It has been speculated that estrogens and androgens could modulate hepatocarcinogenesis and explain the higher incidence of HCC in men[20]. A significant increase in the proportion of HCC among males from 82.5% in periods I to 87.6% in period II ($P = 0.009$) was observed. The calculated risk of development of HCC was nearly three times higher in men than in women. This is consistent with the findings of Kasahara *et al*.[21], where men were at 4.35 times risk to develop HCC than women.

Analysis of age distribution among HCC patients revealed that the most predominant age group (40-59 years) showed a slight increase in period II compared to period I at the expense of older age group (⩾60 years) but the difference did not reach a statistical significance ($P = 0.387$). This shift to younger age group over the last two decades may be attributed to emergence of HCV infection[22,23], as well as to acquisition of both hepatitis B and C virus infection at younger age[2,24].

Velazquez *et al*.[2], found that cirrhotic patients older than 54 years are at four times greater risk to develop HCC. This is consistent with our findings, where patients of the age group 40-59 years were at 3.7 times and of age group ⩾60 years were at 11 times more risk to develop HCC.

Analysis of the risk factors of HCC in patients with CLD has been performed in several studies[25,26]. HBV and HCV infection are considered as the major risk factors that contribute to the development of HCC. During the entire study period, the proportions of HCV-Ab and HBsAg among HCC cases were 86.9% and 28.4% respectively. Surprisingly, there was a significant decline of HBsAg from 38.6% to 20.5% ($P = 0.000$) and slight increase in HCV-Ab from 85.6% to 87.9% ($P = 0.233$) in periods I and II respectively. Consequently, the proportion of co-infection of hepatitis C and B declined from 27% to 10.8%. The decline of HBsAg may be partially attributed to successful control measures of blood transfusion introduced in the mid-seventies and partially to the development of mutant or occult HBV infection, which requires costly assays for diagnosis. However, this decline could not be attributed to vaccination programs in children[27], which has been launched in Egypt about 10 years ago. It has been reported that the reduction of the incidence of HBV will be seen 30-40 years after the launch of the universal hepatitis B vaccination program[27]. Although HBV and HCV are both important causes of HCC, data do not suggest, neither do they conclusively refute, a super-additive interaction between the two infections in the development of HCC[28,29].

HBV conferred a higher risk to develop HCC more than HCV (OR 2.5 *vs* 2.0 respectively). Yet, the low prevalence of HBV render the relative contribution of HBV to HCC (PAR% = 23.4%) lower than HCV contribution (PAR% = 42%). Velazquez and his colleagues[2] in Spain, considered HBV as an insignificant risk factor for development of HCC due to the considerable small number of infected patients as well as low chronicity rate in acute HBV infection (10%) compared to high chronicity rate (50-80%) in acute HCV patients. Studies from earlier years indicated that the rise in the incidence of HCC was directly related to the increase in the prevalence of HCV infection[30]. The prevalence of HCV in Egypt is much more increased[31], which needs to intervene with the acquisition of acute HCV infection as a primary prevention measure. Hepatitis C vaccine is not available; therefore, the rising trend of HCC is most likely attributed to HCV infection[32].

The role of HBV infection in pathogenesis of HCC differs from that of HCV infection; HBV-DNA genome integrates in hepatocellular chromosomes[10], while HCV exerts its effect, most probably, through production of cirrhosis with severe liver damage[30]. The major part of the data shows that HCV plays an indirect role in hepatocarcinogenesis, and this may appear as a consequence of long-standing associated cirrhosis through the direct promotion of the chronic liver inflammation[33]. Recently, many reports point to a direct role of HCV in hepatocarcinogenesis, it is now believed that the core component of HCV may directly participate in the hepatocarcinogenesis[7].

In the current study, viral hepatitis markers were negative in 2.8% of HCC patients in period I and 2.4% of them in period II with no significant difference. A higher percent was reported by El-Serag[1], who found that 14.5% of patients with HCC remain without specific risk factors and diagnosed as non-specific cirrhosis. This could be explained by the development of mutant or occult viral infection or exposure to other risk factors such as aflatoxins, alcohol abuse, or heavy smoking.

A unique invisible risk factor for development of HCC in Egypt could be schistosomal infection and its parenteral therapy. Schistosomiasis induces immune suppression, which could result in increased persistence viremia, following acute infection of both hepatitis B and C[34]. Whereas, parenteral anti-schistosomal therapy had played a role in transmission of HBV and HCV through improperly sterilized glass syringes[35]. In spite that patients with history of schistosomiasis were at higher risk to develop HCC but the results did not reach a statistical significance, which could be attributed to the absence of direct causal effect of schistosomiasis in development of HCC[34].

According to the recommendations of a previous study[3], the awareness about HCC has been greatly improved, which subsequently led to better screening and earlier diagnosis of HCC. This is evidenced by increased rate of diagnosis of small lesions from 14.9% to 22.7% and decreased rate of diagnosis of large HCC lesions from 85.1% to 77.3% in periods I and II respectively.

α-Fetoprotein is the most widely used tumor marker, but has poor diagnostic accuracy and ethnic variability[12]. Diagnostic α-fetoprotein level (⩾200 ng/mL) was demonstrated only in 15.6% of cases in period I and 28.9%

in period II. The increased proportion of patients with diagnostic α-fetoprotein level may be attributed to the increasing adoption of HCC screening program as well as the use of more sensitive assay methods introduced over the recent years.

These results suggest a rising trend of HCC with increasing risk among HCV-infected men of older age groups; such patients should be carefully followed-up and screened for early detection of HCC.

REFERENCES

1 **El-Serag HB.** Hepatocellular carcinoma: an epidemiologic view. *J Clin Gastroenterol* 2002; **35** (Suppl 2): S72-78
2 **Velazquez RE,** Rodriguez M, Navascues CA, Linares A, Perez R, Sotorrios NG, Martinez I, Rodrigo L. Prospective analysis of risk factors for hepatocellular carcinoma in patients with liver cirrhosis. *Hepatology* 2003; **37**: 520-527
3 **Rahman El-Zayadi A,** Abaza H, Shawky S, Mohamed MK, Selim OE, Badran HM. Prevalence and epidemiological features of hepatocellular carcinoma in Egypt-a single center experience. *Hepatol Res* 2001; **19**: 170-179
4 **Ohata K,** Hamasaki K, Toriyama K, Ishikawa H, Nakao K, Eguchi K. High viral load is a risk factor for hepatocellular carcinoma in patients with chronic hepatitis B virus infection. *J Gastroenterol Hepatol* 2004; **19**: 670-675
5 **Xiong J,** Yao YC, Zi XY, Li JX, Wang XM, Ye XT, Zhao SM, Yan YB, Yu HY, Hu YP. Expression of hepatitis B virus X protein in transgenic mice. *World J Gastroenterol* 2003; **9**: 112-116
6 **Feitelson M.** Hepatitis B virus infection and primary hepatocellular carcinoma. *Clin Microbiol Rev* 1992; **5**: 275-301
7 **Szabó E,** Páska C, Kaposi Novák P, Schaff Z, Kiss A. Similarities and Differences in Hepatitis B and C Virus Induced Hepatocarcinogenesis. *Pathol Oncol Res* 2004; **1**: 5-11
8 **Heintges T,** Wands JR. Hepatitis C virus: epidemiology and transmission. *Hepatology* 1997; **26**: 521-526
9 **Liang TJ,** Rustgi V, Galun E, Blum HE. Viral pathogenesis of hepatocellular carcinoma in the United States. *Hepatology* 1993; **18**: 1326-1333
10 **El-Nady GM,** Ling R, Harrison TJ. Gene expression in HCV-associated hepatocellular carcinoma-upregulation of a gene encoding a protein related to the ubiquitin-conjugating enzyme. *Liver Int* 2003; **23**: 329-337
11 **Fattovich G.** Progression of hepatitis B and C to hepatocellular carcinoma in Western countries. *Hepatogastroenterology* 1998; **45** (Suppl 3): 1206-1213
12 **Nguyen MH,** Garcia RT, Simpson PW, Wright TL, Keeffe EB. Racial differences in effectiveness of alpha-fetoprotein for diagnosis of hepatocellular carcinoma in hepatitis C virus cirrhosis. *Hepatology* 2002; **36**: 410-417
13 **Hennekens CH,** Buring JE. Epidemiology in Medicine. Little, Brown and Company, Boston/Toronto
14 **Okano H,** Shiraki K, Inoue H, Deguchi M, Sugimoto K, Sakai T, Ohmori S, Murata K, Nakano T, Yamakado K, Takeda K. Treatment of hepatocellular carcinoma and the exacerbation of liver function. *Int J Oncol* 2001; **19**: 1279-1282
15 **Bruix J,** Sherman M, Llovet JM, Beaugrand M, Lencioni R, Burroughs AK, Christensen E, Pagliaro L, Colombo M, Rodes J. EASL Panel of Experts on HCC. Clinical management of hepatocellular carcinoma. Conclusions of the Barcelona-2000 EASL conference. *J Hepatol* 2001; **35**: 421-430
16 **Yu MC,** Yuan JM, Govindarajan S, Ross RK. Epidemiology of hepatocellular carcinoma. *Can J Gastroenterol* 2000; **14**: 703-709
17 **El-Serag HB.** Epidemiology of hepatocellular carcinoma. *Clin Liver Dis* 2001; **5**: 87-107
18 **Yu MW,** Chang HC, Chang SC, Liaw YF, Lin SM, Liu CJ, Lee SD, Lin CL, Chen PJ, Lin SC, Chen CJ. Role of reproductive factors in hepatocellular carcinoma: Impact on hepatitis B- and C-related risk. *Hepatology* 2003; **38**: 1393-1400
19 **Yu MC,** Tong MJ, Govindarajan S, Henderson BE. Nonviral risk factors for hepatocellular carcinoma in a low-risk population, the non-Asians of Los Angeles County, California. *J Natl Cancer Inst* 1991; **83**: 1820-1826
20 **Nagasue N,** Ogawa Y, Yukaka H, Ohta N, Ito A. Serum levels of estrogens and testosterone in cirrhotic men with and without hepatocellular carcinoma. *Gastroenterology* 1985: **88**: 768-772
21 **Kasahara A,** Hayashi N, Mochizuki K, Takayanagi M, Yoshioka K, Kakumu S, Iijima A, Urushihara A, Kiyosawa K, Okuda M, Hino K, Okita K. Risk factors for hepatocellular carcinoma and its incidence after interferon treatment in patients with chronic hepatitis C. Osaka Liver Disease Study Group. *Hepatology* 1998; **27**: 1394-1402
22 **Montalto G,** Cervello M, Giannitrapani L, Dantona F, Terranova A, Castagnetta LA. Epidemiology, risk factors and natural history of hepatocellular carcinoma. *Ann N Y Acad Sci* 2002; **963**: 13-20
23 **Hassan MM,** Frome A, Patt YZ, El-Serag HB. Rising prevalence of hepatitis C virus infection among patients recently diagnosed with hepatocellular carcinoma in the United States. *J Clin Gastroenterol* 2002; **35**: 266-269
24 **El-Serag H,** Mason AC. Rising incidence of hepatocellular carcinoma in the United States. *N Engl J Med* 1999; **340**: 745-750
25 **Colombo M,** de Franchis R, Del Ninno E, Sangiovanni A, De Fazio C, Tommasini M, Donato MF, Piva A, Di Carlo V, Dioguardi N. Hepatocellular carcinoma in Italian patients with cirrhosis. *N Engl J Med* 1991; **325**: 675-680
26 **Ganne-Carrie N,** Chastang C, Chapel F, Munz C, Pateron D, Sibony M, Deny P, Trinchet JC, Callard P, Guettier C, Beaugrand M. Predictive score for the development of hepatocellular carcinoma and additional value of liver large cell dysplasia in Western patients with cirrhosis. *Hepatology* 1996; **23**: 1112-1118
27 **Chang MH.** Decreasing incidence of hepatocellular carcinoma among children following universal hepatitis B immunization. *Liver Int* 2003; **23**: 309-314
28 **Kuper HE,** Tzonou A, Kaklamani E, Hadziyannis S, Tasopoulos N, Lagiou P, Trichopoulos D, Stuver S. Hepatitis B and C viruses in the etiology of hepatocellular carcinoma; a study in Greece using third-generation assays. *Cancer Causes Control* 2000; **11**: 171-175
29 **Donato F,** Boffetta P, Puoti M. A meta-analysis of epidemiological studies on the combined effect of hepatitis B and C virus infections in causing hepatocellular carcinoma. *Int J Cancer* 1998; **75**: 347-354
30 **Bosch FX,** Ribes J, Borras J. Epidemiology of primary liver cancer. *Semin Liver Dis* 1999; **19**: 271-285
31 **Habib M,** Mohamed MK, Abdel-Aziz F, Magder LS, Abdel-Hamid M, Gamil F, Madkour S, Mikhail NN, Anwar W, Strickland GT, Fix AD, Sallam I. Hepatitis C virus infection in a community in the Nile Delta: risk factors for seropositivity. *Hepatology* 2001; **33**: 248-253
32 **Teratani T,** Ishikawa T, Shiratori Y, Shiina S, Yoshida H, Imamura M, Obi S, Sato S, Hamamura K, Omata M. Hepatocellular carcinoma in elderly patients: beneficial therapeutic efficacy using percutaneous ethanol injection therapy. *Cancer* 2002; **95**: 816-823
33 **Colombo M.** Hepatitis C virus and hepatocellular carcinoma. *Semin Liver Dis* 1999; **19**: 263-269
34 **Ghaffar YA,** Fattah SA, Kamel M, Badr RM, Mahomed FF, Strickland GT. The impact of endemic schistosomiasis on acute viral hepatitis. *Am J Trop Med Hyg* 1991; **45**: 743-750
35 **Madwar MA,** El-Tahawy M, Strickland GT. The relationship between uncomplicated schistosomiasis and hepatitis B infection. *Trans R Soc Trop Med Hyg* 1989; **83**: 233-236

Science Editor Li WZ **Language Editor** Elsevier HK

PO Box 2345, Beijing 100023, China
www.wjgnet.com
wjg@wjgnet.com

ELSEVIER

World J Gastroenterol 2005;11(33):5199-5202
World Journal of Gastroenterology ISSN 1007-9327
© 2005 The WJG Press and Elsevier Inc. All rights reserved.

• *BRIEF REPORTS* •

Novel serum tumor marker, RCAS1, in pancreatic diseases

Koji Yamaguchi, Munechika Enjoji, Manabu Nakashima, Makoto Nakamuta, Takashi Watanabe, Masao Tanaka

Koji Yamaguchi, Masao Tanaka, Department of Surgery and Oncology, Graduate School of Medicine, Kyushu University, Japan
Munechika Enjoji, Makoto Nakamuta, Medicine Bioregulatory Sciences, Graduate School of Medical Sciences, Kyushu University, Japan
Manabu Nakashima, Takashi Watanabe, Department of Molecular Immunology, Medical Institute of Bioregulation, Faculty of Medicine, Kyushu University, Japan
Correspondence to: Koji Yamaguchi, MD, Department of Surgery and Oncology, Graduate School of Medical Sciences, Kyushu University, Fukuoka 812-8582, Japan
Telephone: +81-92-642-5438 Fax: +81-92-642-5457
Received: 2004-11-12 Accepted: 2005-02-18

Abstract

AIM: As tumor markers for pancreatic carcinoma, carcinoembryonic antigen (CEA) and carbohydrate antigen (CA) 19-9 have been used, but the sensitivity and specificity are not enough for the diagnosis of pancreatic carcinoma.

METHODS: A novel serum tumor marker, RCAS1, was compared with two conventional serum tumor markers, CEA (highly specific for pancreatic cancer) and CA 19-9 (highly sensitive for pancreatic cancer), in 48 patients with pancreatic exocrine tumors.

RESULTS: When the diagnosis of benign or malignant conditions was examined by one tumor marker, the sensitivity of RCAS1 alone (55%) was higher than that of CEA alone (27%) and the specificity of RCAS1 alone (92%) was greater than that of CA19-9 alone (78%). When examined by a combination of two markers, the sensitivity of a combination of RCAS1 and CA19-9 (95%) was superior to those of CA19-9 alone (78%), RCAS1 alone (55%, $P = 0.002$), CEA alone (27%) ($P<0.001$), RCAS1 and CEA (59%) and CA19-9 and CEA (82%).

CONCLUSION: These results suggest that the combination of RCAS1 and CA19-9 is highly sensitive for pancreatic carcinoma.

© 2005 The WJG Press and Elsevier Inc. All rights reserved.

Key words: RCAS1; CEA; CA19-9; Pancreatic diseases

Yamaguchi K, Enjoji M, Nakashima M, Nakamuta M, Watanabe T, Tanaka M. Novel serum tumor marker, RCAS1, in pancreatic diseases. *World J Gastroenterol* 2005; 11 (33): 5199-5202
http://www.wjgnet.com/1007-9327/11/5199.asp

INTRODUCTION

RCAS1 (receptor-binding cancer antigen expressed on SiSo cells) is a novel tumor-associated antigen expressed in malignant conditions of various organs. A human cancer cell line, SiSo, was established from a patient affected with uterine cervical adenocarcinoma[1]. The mAb 22-1-1 was manufactured from mice immunized with SiSo cells. Then a cDNA encoding the antigen 22-1-1 was isolated and named RCAS1[2]. The predicted amino acid sequences of RCAS1 (213 aa) possess an N-terminal transmembrane region and a coiled-coil structure in the C-terminal portion, indicating that RCAS1 is a type II membrane protein and is able to form oligomers through the coiled-coil structure.

RCAS1 was found to be identical to EBA G9 (estrogen receptor-binding fragment-associated gene), which was initially identified by cloning of CpG binding sites in the human genome as estrogen responsive gene and mapped to chromosome 8q23. RCAS1 expresses a pattern different from other known tumor-associated antigens, such as YH206, GA733, CA125, CEA, and sialyl Le molecules. Immunohistochemical studies have reported the presence of RCAS1 in malignant diseases of several organs including the uterus[3], endometrium[4], ovary, skin[5], breast[6,7], liver[8], gallbladder[9], stomach[10], lymphocytes[11], and lung[12] as well as pancreas[13]. Previous studies have also indicated that RCAS1 acts as a ligand for a putative receptor present on various human cells including T, B, and NK cells and RCAS1 inhibits *in vitro* growth of receptor-expressing cells and induces apoptosis[14]. It is suggested that tumor cells might evade host immune surveillance by expression of RCAS1. Recently, soluble RCAS1 was also detected by ELISA from the culture supernatant of a human cell line derived from bile duct carcinoma[15], suggesting a possible role of RCAS1 as a diagnostic or prognostic tumor marker. There are few reports on serum levels of RCAS1 in patients with pancreatic diseases. In this series, clinical implication of serum RCAS1 was examined by comparing with conventional tumor markers, carcinoembryonic antigen (CEA) and carbohydrate antigen (CA) 19-9, in 48 patients with pancreatic tumors.

MATERIALS AND METHODS

This series consisted of 48 patients with pancreatic exocrine neoplasms and 23 with benign inflammatory pancreato-biliary diseases (control group). Out of the 71 patients, 35 were men and 36 women, and their age ranged from 18 to 89 years with a mean of 61.9±12.5 years. The 23 patients in the control group consisted of 18 with benign inflammatory biliary diseases (four cholecystolithiasis, four cholangitis, four benign gallbladder polyp, three hepatolithiasis, two adenomyomatosis of the gallbladder and one choledocholithiasis) and five with

benign pancreatic diseases (four chronic pancreatitis, one pancreatolithiasis). The 48 patients with pancreatic neoplasms included 30 patients in the preoperative state of benign or malignant diseases (10 intraductal papillary-mucinous adenoma, 20 pancreatic carcinoma) and 18 patients in the postoperative state (3 intraductal papillary-mucinous adenoma, 4 intraductal papillary-mucinous adenocarcinoma and 11 pancreatic adenocarcinoma). Of the 15 postoperative patients with pancreatic carcinoma, 2 had unequivocal recurrence as judged by clinical findings including imagings, and the other 13 had no evidence of recurrence. In total, 22 patients were therefore considered to have pancreatic carcinoma. Serum levels of RCAS1, CEA, and CA19-9 were examined in all these 71 patients.

Peripheral blood was obtained in the early morning for the examination of RCAS1, CEA, and CA19-9. Serum RCAS1 level was measured using ELISA kit, which was kindly donated from Medical and Biological Laboratories Co., Ltd, Nagoya, Japan. The RCAS1 ELISA kit measures RCAS1 by sandwich ELISA. The assay used mAbs against RCAS1. The serum obtained was pre-treated with neuraminidase. Pretreated samples to be measured or standards were incubated in the cells coated with anti-human RCAS1 mAb; 22-1-1. After washing, a biotin-conjugated anti-human RCAS1 mAb was added into the microwell and incubated. After another washing, the streptavidin-peroxidase was added into the microwell and incubated. After another washing, the peroxidase substrate premixed with chromogen was added and allowed to incubate for an additional period of time. An acid solution was then added to each microwell to terminate the enzyme reaction and to stabilize the developed color. The optical density (*A*) of each microwell was then measured at 450 nm using a microplate reader. The concentration of RCAS1 was calibrated from a dose-response curve based on reference standards. Cut-off level was set at 20 U/mL by constructing a receiver operating characteristic curve (Figure 1). Serum CEA and CA19-9 levels were measured in Clinical Laboratory of Kyushu University Hospital. Their cut-off levels were 2.5 ng/mL and 37.4 IU/mL, respectively.

Clinical stages of malignant pancreatic diseases were determined by the Classification of Pancreatic Carcinoma from Japan Pancreas Society (First English Edition)[16]. Out of the 22 patients with primary or metastatic pancreatic adenocarcinoma, 1 was in stage I, 1 in stage III, 3 in stage IVa and the other 17 in stage IVb. Four of the twenty-two patients underwent pancreatic resection; three pylorus preserving pancreato-duodenectomy and another distal pancreatectomy.

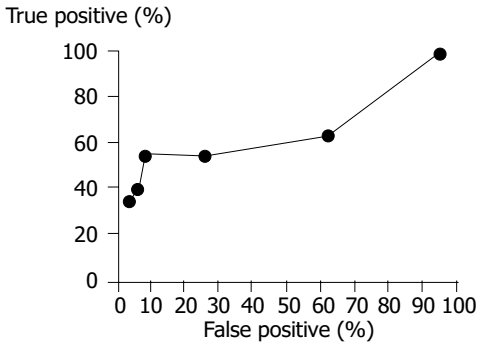


Figure 1 Receiver operating characteristic curve indicating test performance indicating pancreatic carcinoma for the following threshold values, 5, 10, 15, 20, 25, and 30 U/mL. ●–●, performance in distinguishing benign from malignant pancreatic disease.

Informed consent was obtained from each patient. The protocol was submitted to and was preapproved by the Senior Staff Committee of the Department.

Statistical analysis

Values were expressed as mean±SD. Mean values were measured by the Student's *t* test and the distribution of patients was measured by the χ^2 test. Sensitivity, specificity, positive predictive value, negative predictive value, and efficiency were measured. $P<0.05$ was considered as statistically significant.

RESULTS

RCAS1, CEA, and CA19-9 levels

Serum levels of RCAS1, CEA, CA19-9 in 26 patients with benign inflammatory bilio-pancreatic diseases were 12.1±1.1 U/mL, 1.1±0.1 ng/mL and 30.5±6.6 U/mL; 10 with adenoma of the pancreas (intraductal papillary-mucinous adenoma) 14.1±2.9, 1.2±0.2, and 13.5±4.4; and 22 with adenocarcinoma of the pancreas 113.0±70.8, 4.8±2.3, and 9 947.9±6 814.1, respectively. There were no statistically significant differences among the RCAS1, CEA, and CA19-9 values of the three conditions.

Diagnosis of benign and malignant conditions

Data concerning the diagnosis of benign and malignant conditions are shown in Table 1. When comparing by one

Table 1 Diagnosis of malignant and benign diseases by serum RCAS1, CEA and CA19-9

	RCAS1 (%)		CEA (%)		CA19-9 (%)		RCAS1+CEA (%)		RCAS1+CA19-9 (%)		CA19-9+CEA (%)	
	Pos	Neg	Pos	Neg	Pos	Neg	Pos	Neg	Pos	Neg	Pos	Neg
Malignant	12	10	6	16	16	6	13	9	21	1	18	4
Benign	3	33	2	34	8	28	5	31	11	25	9	27
Sensitivity	55[3]		27[b,2]		73[1]		59[2]		95[b,3]		82[d]	
Specificity	92		94		78		86		69		75	
Positive predictive value	80		75		67		72		66		67	
Negative predictive value	78		68		82		78		96		87	
Efficiency	78		69		76		76		79		78	

[b]$P<0.001$ *vs* RCAS1+CA19-9; [d]$P<0.001$ *vs* CA19-9+CEA; [1]$P = 0.003$ *vs* CA19-9; [2]$P = 0.033$ *vs* RCAS1+CEA; [3]$P = 0.002$ *vs* RCAS1+CA19-9.

tumor marker, the sensitivity was highest in CA19-9 (73%), while the specificity was highest in CEA (94%). The total efficacy was highest in RCAS1 (78%). When two tumor markers were joined, the sensitivity was highest by a combination of RCAS1 and CA19-9, the value being 95%, whereas the specificity was highest by a combination of RCAS1 and CEA (86%). The total efficiency was highest by a combination of RCAS1 and CA19-9 (79%).

Tumor stage of pancreatic carcinoma and three markers

The positivity of the three markers increased by the progression of tumors (Table 2).

Prediction of unresectability of pancreatic carcinoma by three markers

The sensitivity of prediction of unresectability was highest by CA19-9 alone (71%), while the specificity was highest by CEA alone (100%, Table 3). When combination assay was done, the sensitivity was highest by RCAS1 and CA19-9 (94%), while the specificity was highest by RCAS1 and CEA (80%).

Recurrence of pancreatic carcinoma after surgical resection

Data are present in Table 4. When examined by one tumor marker, RCAS1 alone and CA19-9 alone showed a high sensitivity and specificity. When two tumor markers were combined, a combination of RCAS1 and CA19-9 showed a high sensitivity (100%) and high specificity (92%).

DISCUSSION

CA19-9 (a highly sensitive marker for pancreatic carcinoma) and CEA (a highly specific marker for pancreatic carcinoma) have been used as serum tumor markers for pancreatic diseases. Usefulness of RCAS1, as a tumor marker, was studied in 48 patients with pancreatic tumors. The sensitivity of RCAS1 alone for pancreatic carcinoma was 55%, which was higher than 27% of CEA alone and lower than 73% of CA19-9 alone. When combination assay was done, the sensitivity of a combination of RCAS1 and CA19-9 was highest, the value being 95%. The specificity of RCAS1 alone for pancreatic carcinoma was 92%, which was lower than 94% of CEA alone and higher than 78% of CA19-9 alone. The specificity by a combination of RCAS1 and CA19-9 was 69%. Combination assay of RCAS1 and CA19-9 was the most powerful marker for the detection of pancreatic carcinoma.

Clinical differentiation of benign inflammatory disease and malignant disease is important as well as that of benign

Table 2 Tumor stage and serum RCAS1, CEA and CA19-9

Stage	RCAS1		CEA		CA19-9		RCAS1+CEA		RCAS1+CA19-9		CA19-9+CEA	
	Pos	Neg	Pos	Neg	Pos	Neg	Pos	Neg	Pos	Neg	Pos	Neg
1	1	0	0	1	0	1	1	0	1	0	0	1
3	0	1	0	1	1	0	0	1	1	0	1	0
4A	0	3	0	3	3	0	0	3	3	0	3	0
4B	11	6	6	11	12	5	12	5	16	1	14	3

Table 3 Unresectability and serum RCAS1, CEA and CA19-9

Unresectability	RCAS1 (%)		CEA (%)		CA19-9 (%)		RCAS1+CEA (%)		RCAS1+CA19-9 (%)		CA19-9+CEA (%)	
	Pos	Neg	Pos	Neg	Pos	Neg	Pos	Neg	Pos	Neg	Pos	Neg
Yes	11	6	6	11	12	5	12	5	16	1	14	3
No	1	4	0	5	4	1	1	4	5	0	4	1
Sensitivity	65		35[1,2,3]		71[2]		71[3]		94[b]		82[1]	
Specificity	80		100[4]		20		80		0		20	
Positive predictive value	92		100		75		92		76		78	
Negative predictive value	40		31		17		44		0		25	
Efficiency	68		50		59		73		73		68	

[1]$P = 0.005$ *vs* CA19-9+CEA; [b]$P<0.001$ *vs* RCAS1+CA19-9; [2]$P = 0.039$ *vs* CA19-9; [3]$P = 0.039$ *vs* RCAS1+CEA; [4]$P = 0.011$ *vs* RCAS1+CA19-9.

Table 4 Recurrence and serum RCAS1, CEA and CA19-9

Recurrence	RCAS1 (%)		CEA (%)		CA19-9 (%)		RCAS1+CEA (%)		RCAS1+CA19-9 (%)		CA19-9+CEA (%)	
	Pos	Neg	Pos	Neg	Pos	Neg	Pos	Neg	Pos	Neg	Pos	Neg
Yes	2	0	1	1	2	0	2	0	2	0	2	0
No	1	12	2	11	1	12	3	10	1	12	3	10
Sensitivity	100		50		100		100		100		100	
Specificity	92		85		92		77		92		77	
Positive predictive value	67		33		67		40		67		40	
Negative predictive value	100		92		100		100		100		100	
Efficiency	93		80		93		80		93		80	

neoplasm and malignant conditions. Mean serum levels of RCAS1, CEA, and CA19-9 in pancreatic carcinoma were higher than those of benign inflammatory diseases and pancreatic adenoma. The values in benign inflammatory diseases and adenoma were not different from each other. Therefore, although the differentiation of benign inflammatory diseases and adenoma was difficult by serum tumor markers alone, that of benign diseases and malignant conditions may be possible. Clinical diagnosis of pancreatic diseases should be made by clinical findings and imaging with the aid of serum tumor markers.

Originally, RCAS1 was suspected to be elevated only at advanced stage of pancreatic carcinoma, because RCAS1 is related with immune escape from the host immune and with carcinoma invasion. The specificity of RCAS1 for the presence of pancreatic carcinoma was expected to be high and the sensitivity was suspected to be low. The sensitivity of RCAS1 alone for malignant condition was 55%, which was higher than 27% by CEA alone, and the specificity of RCAS1 alone was 92%, higher than 78% of CA19-9 alone. Combination assay of RCAS1 and CA19-9 showed the highest sensitivity of 95%, although the specificity was 69%. The sensitivity of tumor marker is important to decrease the missing of pancreatic carcinoma and the specificity is also important to decrease the over diagnosis. Thus, combination assay of CA19-9 and RCAS1 is recommended for the detection of pancreatic carcinoma.

It is true that the surgical decision making is made on imaging or macroscopic findings, but the prediction of resectability by serum tumor marker is of great value for surgeons. The sensitivity of prediction of unresectability was 94% by a combination of RCAS1 and CA19-9 and the specificity was 80%. These findings indicate that elevation of serum RCAS1 and CA19-9 may be suggestive of unresectable pancreatic carcinoma, although the number of patients examined was so small, that the data obtained was not conclusive.

One of the purposes of serum tumor marker is to predict clinical outcome of patients with pancreatic carcinoma. Recent immunohistochemical reports suggest that RCAS1 expression is related to early stage of carcinogenesis[7], poor differentiation[4], progression of the disease[5,10], and poor prognosis of cancer[9,13,17]. In this series, clinical follow-up was so short that we could not yield data concerning the clinical outcome. Further examination using long-term follow-up is necessary to evaluate predictability of RCAS1.

Although this series is a preliminary report on serum RCAS1 in pancreatic diseases, combination assay of RCAS1 and CA19-9 showed 95% sensitivity for pancreatic carcinoma, suggesting usefulness of this combination as a checking-up marker for pancreatic carcinoma.

REFERENCES

1 **Sonoda K,** Nakashima M, Kaku T, Kamura T, Nakano H, Watanabe T. A novel tumor-associated antigen expressed in human uterine and ovarian carcinomas. *Cancer* 1996; **77**: 1501-1509

2 **Nakashima M,** Sonoda K, Watanabe T. Inhibition of cell growth and induction of apoptotic cell death by the human tumor-associated antigen RCAS1. *Nature Medicine* 1999; **5**: 938-542

3 **Kaku T,** Sonoda K, Kamura T, Hirakawa T, Sakai K, Amada S, Ogawa S, Kobayashi H, Nakashima M, Watanabe T, Nakano H. The prognostic significance of tumor-associated antigen 22-1-1 expression in adenocarcinoma of the uterine cervix. *Clinical Cancer Res* 1999; **5**: 1449-1453

4 **Sonoda K,** Kaku T, Hirakawa T, Kobayashi H, Amada S, Sakai K, Nakashima M, Watanabe T, Nakano H. The clinical significance of tumor-associated antigen RCAS1 expression in the normal, hyperplastic, and malignant uterine endometrium. *Gynecol Oncol* 2000; **79**: 424-429

5 **Takahashi H,** Iizuka H, Nakashima M, Wada T, Asano K, Ishida-Yamamoto A, Watanabe T. RCAS1 antigen is highly expressed in extramammary Paget's disease and in advanced stage squamous cell carcinoma of the skin. *J Dermatol Sci* 2001; **26**: 140-144

6 **Suzuki T,** Inoue S, Kawabata W, Akahira J, Moriya T, Tsuchiya F, Ogawa S, Muramatsu M, Sasano H. EBAG9/RCAS1 in human breast carcinoma: a possible factor in endocrine-immune interactions. *Br J Cancer* 2001; **85**: 1731-1737

7 **Tsuneizumi M,** Nagai H, Harada H, Kazui T, Emi M. A highly polymorphic CA repeat marker at the EBAG9/RCAS1 locus on 8q23 that detected frequent multiplication in breast cancer. *Ann Human Biol* 2002; **29**: 457-460

8 **Noguchi K,** Enjoji M, Nakamuta M, Nakashima M, Nishi H, Choi I, Taguchi K, Kotoh K, Shimada M, Sugimachi K, Tsuneyoshi M, Nawata H, Watanabe T. Expression of a tumor-associated antigen RCAS1 in hepatocellular carcinoma. *Cancer Lett* 2001; **168**: 197-202

9 **Oshikiri T,** Hida Y, Miyamoto M, Hashida H, Katoh K, Suzuoki M, Nakakubo Y, Hiraoka K, Shinohara T, Itoh T, Kondo S, Katoh H. RCAS1 as a tumour progression marker: an independent negative prognostic factor in gallbladder cancer. *Br J Cancer* 2001; **85**: 1922-1927

10 **Kubokawa M,** Nakashima M, Yao T, Ito KI, Harada N, Nawata H, Watanabe T. Aberrant intracellular localization of RCAS1 is associated with tumor progression of gastric cancer. *International J Oncol* 2001; **19**: 695-700

11 **Ohshima K,** Muta K, Nakashima M, Haraoka S, Tutiya T, Suzumiya J, Kawasaki C, Watanabe T, Kikuchi M. Expression of human tumor-associated antigen RCAS1 in Reed-Sternberg cells in association with Epstein-Barr virus infection: a potential mechanism of immune evasion. *International J Cancer* 2001; **93**: 91-96

12 **Izumi M,** Nakanishi Y, Yoshino I, Nakashima M, Watanabe T, Hara N. Expression of tumor-associated antigen RCAS1 correlates significantly with poor prognosis in nonsmall cell lung carcinoma. *Cancer* 2001; **92**: 446-451

13 **Hiraoka K,** Hida Y, Miyamoto M, Oshikiri T, Suzuoki M, Nakakubo Y, Shinohara T, Itoh T, Shichinohe T, Kondo S, Kasahara N, Katoh H. High expression of tumor-associated antigen RCAS1 in pancreatic ductal adenocarcinoma is an unfavorable prognostic marker. *International J Cancer* 2002; **99**: 418-423

14 **Matsushima T,** Nakashima M, Oshima K, Abe Y, Nishimura J, Nawata H, Watanabe T, Muta K. Receptor binding cancer antigen expressed on SiSo cells, a novel regulator of apoptosis of erythroid progenitor cells. *Blood* 2001; **98**: 313-321

15 **Enjoji M,** Nakamuta M, Noguchi K, Sugimoto R, Kotoh K, Nawata H, Nakashima M, Watanabe T. RCAS1 expression in immune-mediated liver diseases. *J Clinical Gastroenterol* 2002; **34**: 286-287

16 Japan Pancreas Society. Classification of pancreatic carcinoma. Kanahara & Co., Ltd, Tokyo, Japan 2002

17 **Suzuoki M,** Hida Y, Miyamoto M, Oshikiri T, Hiraoka K, Nakakubo Y, Shinohara T, Itoh T, Okushiba S, Kondo S, Katoh H. RCAS1 expression as a prognostic factor after curative surgery for extrahepatic bile duct carcinoma. *Annals Surgical Oncol* 2002; **9**: 388-393

Science Editor Wang XL and Guo SY **Language Editor** Elsevier HK

PO Box 2345, Beijing 100023, China
www.wjgnet.com
wjg@wjgnet.com

ELSEVIER

World J Gastroenterol 2005;11(33):5203-5208
World Journal of Gastroenterology ISSN 1007-9327
© 2005 The WJG Press and Elsevier Inc. All rights reserved.

• *BRIEF REPORTS* •

Flow cytometric detection of hepatitis C virus antigens in infected peripheral blood leukocytes: Binding and entry

Mostafa K El-Awady, Ashraf A Tabll, El-Rashdy M Redwan, Samar Youssef, Moataza H Omran, Fouad Thakeb, Maha El-Demellawy

Mostafa K El-Awady, Ashraf A Tabll, Samar Youssef, Moataza H Omran, Department of Biomedical Technology, National Research Center, Tahrir Street, Dokki, Cairo, Egypt
El-Rashdy M Redwan, Maha El-Demellawy, Genetic Engineering and Biotechnology Research Institute, New Borg El-Arab City, Alexandria, Egypt
Fouad Thakeb, Department of Gastroenterology-Hepatology, Faculty of Medicine Cairo University, Egypt
Co-first-authors: Mostafa K El-Awady and Ashraf A Tabll
Co-correspondents: Ashraf A Tabll
Correspondence to: Dr. Mostafa K El-Awady, Department of Biomedical Technology, National Research Center, Tahrir Street, PO 12622, Dokki, Cairo, Egypt. mkawady@yahoo.com
Telephone: +2-2-3362609 Fax: +2-2-3370931
Received: 2004-11-23 Accepted: 2004-12-08

Abstract

AIM: We designed two synthetic-core-specific peptides core 1 (C1) and core 2 (C2), and an E1-specific peptide (E1). We produced specific polyclonal antibodies against these peptides and used the antibodies for detection of HCV antigens on surface and within infected peripheral blood leukocytes.

METHODS: Peripheral blood from a healthy individual who tested negative for HCV RNA was incubated with HCV type 4 infected serum for 1 h and 24 h at 37 ℃. Cells were stained by direct and indirect immunofluorescence and measured by flow cytometry.

RESULTS: After 1 h of incubation, antibodies against C1, C2, and E1 detected HCV antigens on the surface of 27%, 26% and 73% of monocytes respectively, while 10%, 5% and 9% of lymphocytes were positive with anti-C1, anti-C2 and anti-E1 respectively. Only 1-3% of granulocytes showed positive staining with anti-C1, anti-C2 and anti E1 antibodies. After 24 h of incubation, we found no surface staining with anti-C1, anti-C2 or anti-E1. Direct immunostaining using anti-C2 could not detect intracellular HCV antigens, after 1 h of incubation with the virus, while after 24 h of incubation, 28% of infected cells showed positive staining. Only plus strand RNA was detectable intracellularly as early as 1 h after incubation, and remained detectable throughout 48 h post-infection. Interestingly, minus RNA strand could not be detected after 1 h, but became strongly detectable intracellularly after 24 h post-infection.

CONCLUSION: Monocytes and lymphocytes are the preferred target cells for HCV infection in peripheral blood leukocytes. Our specific anti-core and anti-E1 antibodies are valuable reagents for demonstration of HCV cell cycle. Also, HCV is capable of infecting and replicating in peripheral blood mononuclear cells as confirmed by detection of minus strand HCV RNA as well as intracellular staining of core HCV antigen.

© 2005 The WJG Press and Elsevier Inc. All rights reserved.

Key words: Flow cytometry; Hepatitis C virus; Envelope; Core; Antibodies; Indirect immunofluorescence; Minus and plus RNA strand; Peripheral blood mononuclear cells

El-Awady MK, Tabll AA, Redwan ERM, Youssef S, Omran MH, Thakeb F, El-Demellawy M. Flow cytometric detection of hepatitis C virus antigens in infected peripheral blood leukocytes: Binding and entry. *World J Gastroenterol* 2005; 11(33): 5203-5208
http://www.wjgnet.com/1007-9327/11/5203.asp

INTRODUCTION

Hepatitis C virus (HCV) is the major etiology of non-A, non-B hepatitis that infects 170 million people worldwide. Approximately 70-80% of HCV patients develop chronic hepatitis, 20-30% of which progress to liver cirrhosis[1]. At present, there is no vaccine available to prevent HCV infection, and current therapies are not optimal. The initial steps of HCV infection (binding and entry) that are critical for tissue tropism, and hence pathogenesis, are poorly understood. Studies to elucidate this process have been hampered by the lack of robust cell culture systems or convenient small animal models that can support HCV infection. HCV is an enveloped, positive-strand RNA virus that belongs to the *Flaviviridae* family. Based on the sequence heterogeneity of the genome, HCV is classified into six major genotypes and 100 subtypes[1]. The viral genome (~9.6 kb) is translated into a single polyprotein of ~3 000 amino acids (aa). A combination of host and viral proteases are involved in polyprotein processing to give at least nine different proteins[2]. The structural proteins of HCV are believed to comprise the core protein (~21 kDa) and two envelope glycoproteins: E1 (~31 kDa) and E2 (~70 kDa). Like other enveloped viruses, E1 and E2 proteins are most likely play a pivotal role in HCV life cycle: in the assembly of infectious particles and in the initiation of viral infection by binding to its cellular receptor(s). Since hepatocytes represent the

primary site of HCV replication *in vivo*, the HCV genome has also been found in lymphoid cells. Infection of the lymphoid cells has been implicated in extrahepatic manifestations of HCV infection such as mixed cryoglobulinemia and B-lymphocyte proliferative disorders[3-5]. Virus-cell interaction is a multistep process and frequently involves more than a single receptor. There are, at least, three ways employed by virus to bind its target cells. First, virus can harbor two receptor-binding sites that allow binding to alternative receptors expressed on different cell types (e.g., adenovirus type 37)[6]. Second, virus can bind to a "common" surface molecule that captures and concentrates virus at the cell surface, and this event is followed by binding to a high-affinity primary receptor (e.g., herpes simplex virus)[7]. Third, virus binds to a high-affinity receptor, and this event induces conformational changes leading to the exposure of binding sites for a co-receptor (e.g., HIV type 1)[8,9]. So far, little is known about which mechanism is adopted by HCV to bind and enter target cells. The association of CD81 and the LDL-R with E2 protein or HCV virion, respectively, have led to the assumption that either one may represent the cellular receptor for HCV[10-12]. Despite several reports demonstrating the E2 binding to CD81[13,14], the interaction between HCV virion with this molecule is less clear. CD81 molecule only inhibited the binding of truncated E2 protein, but not HCV virion, to Molt-4 cells[15], suggesting that the HCV virion may use other receptor(s) for entry into cells. Also, Triyanti *et al*.[16], demonstrated that HCV-LPs can be used as a valuable tool to study the mechanism of binding and entry of HCV infection. Further characterization of HCV-LP and its interaction with cells will help us understand the early steps of HCV infection and will facilitate studies to identify other candidate receptor(s) for HCV. In the present study, we aimed to use in-house polyclonal antibodies against HCV peptides from core and envelope regions for the detection of surface and intracellular HCV antigens in PBMCs infected with HCV type 4 positive serum, based on direct and indirect immunofluorescence labeling followed by flow cytometric analysis.

MATERIALS AND METHODS

Infected serum samples

For infection experiments, we utilized serum samples positive for HCV RNA as determined by nested RT-PCR and genotyped as genotype 4 using the method described by Ohno *et al*.[17].

Infection of peripheral blood with HCV type 4

Whole blood cells were obtained from a healthy volunteer (only a single subject was used for the sake of fixing the host factor throughout the experiment). Serum from this blood sample was tested negative for HCV RNA by using a standard nested RT-PCR. Whole blood was incubated at 37 ℃ for 1, 24 and 48 h with a serum sample that tested positive for HCV RNA (viral loads: 9 million copies/mL, G4 HCV RNA) at a ratio of 20 μL serum to 110 μL whole blood). After incubation, blood cells were thoroughly washed four times with PBS. Detection of HCV RNA strands in peripheral blood cells will be described later.

Design of HCV synthetic peptides

Sequence analysis of HCV quasispecies in local patients (results not shown) revealed several conserved regions within the core and the E1 proteins. We designed four synthetic-core-specific peptides and a E1-specific peptide, and results showed that all peptides detect HCV antibodies in infected sera to varying degrees. The relative sensitivities and specificities of these synthetic peptides in detecting circulating HCV antibodies in infected human sera were described[18]. In the present study, we raised HCV-specific polyclonal antibodies against two core peptides anti-C1 (DVKFPGGGQIVGGVYLLPRR), anti-C2 (IPKA-RRPEGRTWAQPGY) as well as a E1 peptide (anti-E1, GHRMAWDMM).

Production of polyclonal antibodies against core and envelope regions of HCV

New Zealand rabbits (2 rabbits per each peptide and 2 per control, injected only with KLH) were immunized independently with purified synthetic peptides coupled with KLH protein. Equal volume of diluted core 1 (C1), core 2 (C2) and E1 synthetic peptides and Freund's complete adjuvant were emulsified and injected subcutaneously into the rabbits in three different sites. On d 15 and 28, the rabbits were immunized again with the same protein emulsified with incomplete Freund's adjuvant. On d 32, the rabbits were killed and sera were separated and stored at -20 ℃. For direct immunofluorescence, immunized polyclonal antibodies were digested with pepsin A (porcine 1∶60 000 grade (sigma P-7012), St. Louis, MO, USA) at acidic pH and the $F(ab)_2$ portion was labeled with fluorescence isothiocyanate (FITC) according to Hudson and Hay[19].

Surface and intracellular staining of infected peripheral blood cells and flow cytometric analysis

After incubation of normal blood cells with HCV-infected serum positive for blood cells, they were washed four times with phosphate-buffered saline (PBS). Surface labeling was performed by direct and indirect immunofluorescence. Primary polyclonal antibodies (C1, C2 and E1) were incubated with cells for 30 min at 4 ℃. RBCs were ruptured by lysis buffer (83% ammonium chloride). Cells were centrifuged and supernatants were removed. Cell pellets were washed twice with PBS containing 1% normal goat serum, then incubated with anti-rabbit IgG labeled with FITC (1∶100 dilution, Sigma, St. Louis, MO, USA) for 30 min. Cells were washed once more, resuspended in PBS and kept at 4 ℃ until flow cytometric analysis. For intracellular staining, cells were incubated with 4% paraformaldehyde for 10 min and 0.1% Triton X-100 in Tris buffer (pH 7.4) for 6 min. After washing with PBS, cells were incubated with FITC-labeled $F(ab)_2$ portion of HCV core antibody (at 1∶2 000 dilution) for 30 min at 4 ℃. Cells were washed thrice with PBS containing 1% normal goat serum and cells were suspended in 500 μL and analyzed.

Isolation of PBMC and extraction of RNA

Infected peripheral blood cells were isolated, as reported by Lohr *et al*.[20]. Briefly, peripheral blood samples were

diluted with 5 volumes of a freshly prepared RBC lysis buffer (38.8 mmol/L NH_4Cl, 2.5 mmol/L K_2HCO_3, 1 mmol/L EDTA, pH 8.0), incubated at room temperature for 10 min and the nucleated cells were precipitated and washed in the same buffer to remove adherent viral particles before lysis in 4 mol/L guanidinium isothiocyanate containing 25 mmol/L sodium citrate, 0.5% sarcosyl and 0.1 mol/L β-mercaptoethanol. Cellular RNA was extracted using the single-step method described originally by Chomczynski and Sacchi[21].

PCR of genomic and anti-genomic RNA strands of HCV

Reverse transcription-nested PCR was carried out according to Lohr *et al*.[20], with few modifications. Retrotranscription was performed in 25 μL reaction mixture containing 20 U of AMV reverse transcriptase (Clontech, USA) with either 400 ng of total PBMCs RNA or 3 μL of purified RNA from serum samples as template, 40 U of RNAsin (Clontech, USA), a final concentration of 0.2 mmol/L from each dNTP (Promega, Madison, WI, USA) and 50 pmoL of the reverse primer 1CH (for plus strand) or 50 pmol of the forward primer 2CH (for minus strand). The reaction was incubated at 42 ℃ for 60 min and denatured at 98 ℃ for 10 min. Amplification of the highly conserved 5'-UTR sequences was done using two rounds of PCR with two pairs of nested primers. First round amplification was done in 50 μL reaction mixture, containing 50 pmol from each of 2CH forward primer and P2 reverse primer and P2 reverse primer, 0.2 mmol/L from each dNTP, 10 μL from RT reaction mixture as template and 2 U of Taq DNA polymerase (Promega, USA) in a 1× buffer supplied with the enzyme. The thermal cycling protocol was as follows: 1 min at 94 ℃, 1 min at 55 ℃ and 1 min at 72 ℃ for 30 cycles. The second round amplification was done similar to the first round, except for use of the nested reverse primer D2 and forward primer F2 at 50 pmol each. A fragment of 179 bp was identified in positive samples. Primer sequences were as follows:

1CH: 5'-ggtgcacggtctacgagacctc-3'
2CH: 5'-aactactgtcttcacgcagaa-3'
P2: 5'-tgctcatggtgcacggtcta-3'
D2: 5'-actcggctagcagtctcgcg-3'
F2: 5'-gtgcagcctccaggaccc-3'

To control false detection of negative-strand HCV RNA and known variations in PCR efficiency[22,23], specific control assays and rigorous standardization of the reaction were employed. Specific control assays were included: (1) cDNA synthesis without RNA templates to exclude product contamination; (2) cDNA synthesis without RTase to exclude Taq polymerase RTase activity; (3) cDNA synthesis and PCR step done with only the reverse or forward primer to confirm no contamination from mixed primers. These controls were consistently negative. In addition, cDNA synthesis was carried out using only one primer present followed by heat inactivation of RTase activity at 95 ℃ for 1 h, in an attempt to diminish false detection of negative-strand prior to the addition of the second primer.

RESULTS

Surface detection of HCV antigens by flow cytometry on infected blood leukocytes

The borders of the respective cell regions of lymphocytes, monocytes and granulocytes were clearly defined on the cytograms of flow cytometry based on the size and the granularity of cells (Figure 1). Using control healthy blood, no immunostained positive cells were found using any of the polyclonal antibodies (C1 or C 2 and anti-E1) compared with normal rabbit serum. After 1 h of incubation at 37 ℃ with HCV positive serum, indirect immunofluorescence-labeled anti-E1, antibody demonstrated positive staining in 9%, 73% and 1-2% of lymphocytes, monocytes and granulocyte respectively. Anti-C1 demonstrated positive staining in 10%, 27%, and 1% of lymphocytes, monocytes and granulocyte respectively. Staining with anti-C2 showed positive cells in 5%, 26% and 1% of lymphocytes, monocytes, and granulocyte respectively (Table 1 and Figure 1). Interestingly, after 24 h of incubation with HCV positive serum, no detectable viral antigens were demonstrated on the surface of any cell type.

Intracellular staining with direct immunofluorescence

Direct immunostaining of total peripheral mononuclear cells using FITC-F(ab)$_2$ portion of anti C2 antibody could not

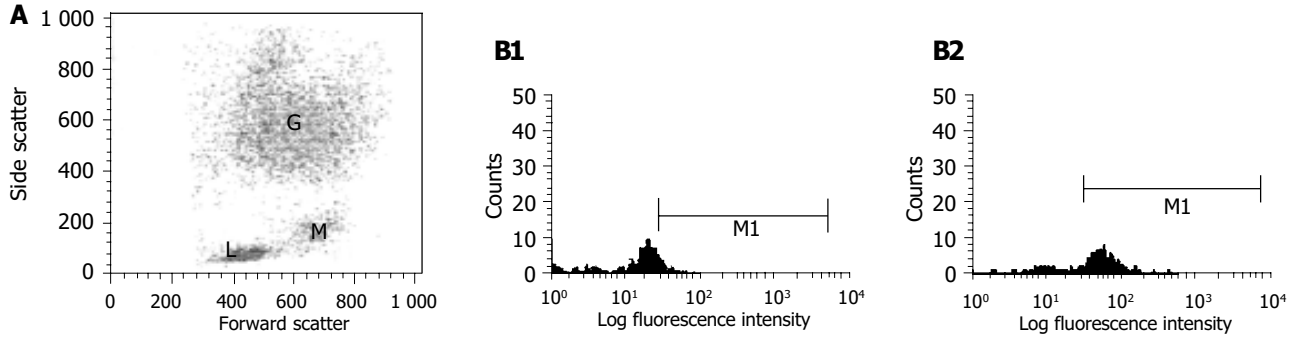


Figure 1 The borders of the respective cell regions of lymphocytes (L), monocytes (M) and granulocytes (G) were clearly defined on the cytograms of flow cytometry based on the size and the granularity (*x*-axis, forward scattered cells and *y*-axis, side scattered cells of cells after surface immunostaining) (**A**); Histograms from gated monocytes obtained from fluorescent activated cell sorter analysis of HCV-infected peripheral blood mononuclear leukocytes. Cells were stained with anti-E1 antibody against HCV E1 region. Histograms represent gated monocytes from (**B_1**) infected cells stained with normal rabbit serum as control or (**B_2**) infected cells stained with antibody against E1 after incubation of blood with serum sample after 1 h at 37 ℃ in which *x*-axis represents fluorescence intensity. M1 is marker for positive cell population.

detect intracellular viral antigens after 1 h of incubation with HCV-positive serum. However, after 24 h of incubation, 28% of infected cells stained positive for viral core antigen (Figure 2).

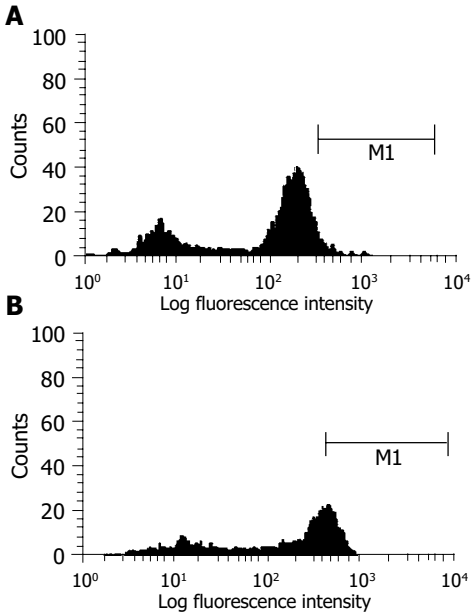


Figure 2 Histogram from gated leukocytes obtained from fluorescent activated cell sorter analysis of HCV-infected peripheral blood mononuclear leukocytes. Cells were stained intracellularly with anti-C2 antibody conjugated with FITC. Histogram represents gated leukocytes from (**A**) healthy uninfected cells or (**B**) infected cells stained with anti-C2 antibody conjugated with FITC after incubation of blood with serum sample after 24 h at 37 ℃ in which *x*-axis represents fluorescence intensity. M1 is marker for positive cell population.

RT-PCR for minus and plus RNA strand of HCV RNA in PBMCs

The genomic plus (+) strand was weakly detectable in PBMCs after 1 h of incubation, whereas antigenomic (-) strand was undetectable. After 24 and 48 h of incubation, both strands were detectable with stronger signal of the anti-genomic (-) strand (Figure 3).

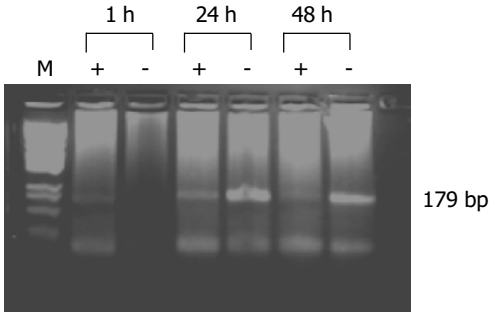


Figure 3 Analysis of HCV RNA plus strand and minus strand from infected PBMC. PCR amplification products of the genomic strand (+) and the replicative strand (-) of HCV from total cellular RNA of PBMC infected with HCV for 1, 24 and 48 h. Lane M represents the M.W. marker PGem.

DISCUSSION

Extrahepatic HCV replication has long been a controversial topic, since the finding of the high rate of re-infection of grafts after orthotopic liver transplantation in patients with the end-stage HCV-induced liver diseases. However, whether PBMCs are supportive for HCV replication is still uncertain. The detection of the minus strand HCV RNA is thought to be a reasonable marker for HCV replication, because the minus RNA strand is the replicative intermediate of HCV. In past decade, several reports on the detection of HCV RNA in PBMCs have been published[24-26]. Gribier *et al*.[27], incubated PBMCs from healthy donors with HCV positive sera, and detected HCV RNA plus and minus strands using RT-PCR and *in situ* hybridization. Results of Gong *et al*.[28], showed that HCV is capable of infecting and replicating in PBMCs, and HCV NS5 protein was clearly expressed in these cells. On a previous study by El-Awady *et al*.[29], we utilized PBMCs as a cellular component to assess viral replication in chronic HCV patients. This study demonstrated higher sensitivity of concomitant PCR amplification of plus and minus strands in PBMCs together with plus strand in serum samples over the traditional amplification of viral RNA in serum. Later, we employed this apparent intracellular amplification in PBMCs as a predictor for treatment relapse after interferon therapy[30]. After 1 h of incubation, in the present study, only plus RNA strand of the virus was weakly detectable. When incubation with positive serum was extended for 24 and 48 h, both plus and minus RNA strands have become strongly detectable (Figure 3). Flow cytometry is advantageous over RT-PCR in its ability to count directly the rate of infection into the cells. Furthermore, it is more specific than traditional immunocytochemical analyses via its ability to quantify the intensity of fluorescence per cell, thus facilitating clear distinction between specific and non-specific immunofluorescence. A greater number of cells are allowed to be counted, which is very important while considering that *in vitro* viral infections are variable biological phenomena. This gives us the possibility of testing several replicates simultaneously and elevating the accuracy in statistical analysis. In case of cells that are relatively less susceptible, such as PBML, it is desired to count large number of cells to obtain a significant number of positives, turning manual counting very laborious. Therefore, in our case, to gain a better understanding of the cell-specific tropism of HCV, we designed the experiments to detect HCV antigen on blood leukocyte subsets, lymphocytes, monocytes and granulocytes. Simultaneously, we planned to evaluate the usefulness of specific polyclonal anti-sera raised against synthetic core and envelope HCV peptides made from conserved sequences among several HCV isolates[18]. In a parallel investigation, the antibodies currently used

Table 1 Percentage of positive cells after 1-h incubation of peripheral blood with serum positive for HCV RNA

Antibody	Lymphocytes percentage of positive cells	Monocytes percentage of positive cells	Granulocytes percentage of positive cells
E1	5	73	1
C1	10	27	2
C2	9	26	3

Positive cells were determined by indirect immunofluorescence and flow cytometric analysis.

demonstrated 100% sensitivity and 100% specificity in detecting circulating viral antigens in HCV RNA-positive and HCV RNA-negative subjects, respectively (data not shown). Results presented here revealed that about 73% of infected monocytes were immunostained positive for envelope antigen. A well-defined HCV positive population in infected peripheral blood leukocytes showed that the monocytes are the preferred target for HCV. However, the results of previous studies have been conflicting; several investigators have reported inconsistent presence of HCV in B and T lymphocytes[26,31]. However, flow cytometry using specific monoclonal antibody could detect the presence of HCV core antigen that was demonstrated in monocytes but not in lymphocytes[32]. These reports demonstrated the presence of HCV RNA which was detected in peripheral blood mononuclear cells (PBMC) by PCR in 17 of 24 HCV-infected patients with chronic hepatitis with or without cirrhosis. In 29% of patients whose PBMC contained HCV RNA, flow cytometry with a murine monoclonal antibody to HCV core epitopes revealed cytoplasmic staining of peripheral blood monocytes, whereas cell surface of monocytes and lymphocytes did not stain for HCV core epitopes. The discrepancy between the current results and those of Bouffard *et al*.[32], may be related to either the difference between *in vivo* and *in vitro* infection of PBMCs or to the degree of the antibody specificity. In the present study, HCV tropism in peripheral leukocytes is not only limited to polymorphonuclear leukocytes, since granulocytes were also shown to stain positive with HCV antibodies after short incubation with positive sera. Since minus RNA strand of the HCV can hardly be detected in infected serum, its detection in PBMCs can be taken as a molecular indicator of intracellular genomic replication of HCV and ruling out false positive, due to contamination of cellular preparations with infected sera. In acute HCV infection, HCV RNA minus strand is rare in PBMCs, but in the chronic group, the minus strand HCV RNA is common in the PBMCs (14 of 35, 40%), which is similar to what Chang *et al*.[33], reported. The ratio of HCV RNA minus strand detected in chronic hepatitis C is much higher than that in acute hepatitis C, suggesting that the replication of HCV in PBMCs may play an important role in the processes of chronicity, and the mechanism could be that HCV in PBMCs escapes from host immunity, and makes the infection of HCV persistent. On one hand, the dysfunction of the HCV-infected PBMCs leads to immune function decline and this becomes more difficult for the host to clear intrahepatic HCV[34]. On the other hand, some authors are still arguing that the minus strand HCV RNA in the blood cells including PBMC may be artifacts from contamination or passive absorption by circulating virus[11] or self-priming/mis-priming during PCR reaction[35,36]. For this reason, the expression of HCV-related proteins in extrahepatic cells has become the key point for demonstrating intracellular HCV replication. HCV was repeatedly reported to replicate and express structural and non-structural proteins, primarily in PBMC[28,37,38]. In the present study, we utilized the combined results of nested RT-PCR of plus and minus RNA strands coupled with core and E1 protein expression to follow steps of viral binding, entry, replication and protein expression in human PBMCs. The detection of E1 and core antigens on cell surface as early as 1 h of incubation with virus, followed by disappearance of viral antigens after 24 h, suggests that viral entrance into cells occurs within 24 h. The concomitant intracellular appearance of E1 and core antigens suggests that binding, entry and expression of structural proteins occurs within 24 h. At the level of genomic replication, failure of minus strand detection after 1 h, followed by strong detection after 24 h supports the hypothesis that processing of HCV polyprotein and release of viral antigens with subsequent acceleration of genomic replication of viral RNA occurs within the first 24 h of infection. In conclusion, we suggest that the present method for detection of E1 and core antigens is useful in monitoring of HCV life cycle and can contribute to analysis of HCV infection more precisely. Therefore, the study of virus-host cell interaction may lead to interesting and probably non-expected concepts of HCV pathology.

REFERENCES

1 World Health Organization. Global surveillance and control of hepatitis C. Report of a W.H.O. Consultation organized in collaboration with the Viral Hepatitis Prevention Board, Antwerp. *Belgium J Viral Hepat* 1999; **6**: 35-47

2 **Bartenschlager R,** Lohmann V. Replication of hepatitis C virus. *J Gen Virol* 2000; **81**: 1631-1648

3 **Agnello V,** Chung RT, Kaplan LM. A role for hepatitis C virus infection in type II cryoglobulinemia. *N Engl J Med* 1992; **327**: 1490-1495

4 **Quinn ER,** Chan CH, Hadlock KG, Foung SH, Flint M. Levy S. The B cell-receptor of a hepatitis C virus (HCV)-associated non-Hodgkin lymphoma binds the viral E2 envelope protein, implicating HCV in lymphomagenesis. *Blood* 2001; **98**: 3745-3749

5 **Schmidt WN,** Stapleton JT, LaBrecque DR, Mitros FA, Kirby PA, Phillips MJ, Brashear DL. Hepatitis C virus (HCV) infection and cryoglobulinemia: analysis of whole blood and plasma HCV-RNA concentrations and correlation with liver histology. *Hepatol* 2000; **31**: 737-744

6 **Wu E,** Fernandez J, Fleck SK, Von Seggern DJ, Huang S. A 50-kDa membrane protein mediates sialic acid-independent binding and infection of conjunctival cells by adenovirus type 37. *Virol* 2001; **279**: 78-89

7 **Campadelli-Fiume G,** Cocchi F, Menotti L, Lopez M. The novel receptors that mediate the entry of herpes simplex viruses and animal alphaherpesviruses into cells. *Rev Med Virol* 2000; **10**: 305-319

8 **Finnegan CM,** Berg W, Lewis GK, DeVico AL. Antigenic properties of the human immunodeficiency virus envelope during cell-cell fusion. *J Virol* 2001; **75**: 11096-11105

9 **Klasse PJ,** Bron R, Marsh M. Mechanisms of enveloped virus entry into animal cells. Adv. *Drug Deliv Rev* 1998; **34**: 65-91

10 **Pileri P,** Uematsu Y, Campagnoli S, Galli G, Falugi F, Petracca R, Weiner AJ, Houghton M, Rosa D, Grandi G, Abrignani S. Binding of hepatitis C virus to CD81. *Science* 1998; **282**: 938-941

11 **Agnello V,** Abel G, Elfahal M, Knight GB, Zhang QX. Hepatitis C virus and other Flaviviridae viruses enter cells via low density lipoprotein receptor. *Proc Natl Acad Sci USA* 1999; **96**: 12766-12771

12 **Monazahian M,** Bohme I, Bonk S, Koch A, Scholz C, Grethe S, Thomssen R. Low density receptor as a candidate receptor for hepatitis C virus. *J Med Virol* 1999; **57**: 223-229

13 **Flint MC,** Maidens LD, Loomis-Price C, Shotton J, Dubuisson P, Monk A, Higginbottom S, McKeating JA. Characterization of hepatitis C virus E2 glycoprotein interaction with a putative cellular receptor, CD81. *J Virol* 1999; **73**: 6235-6244

14 **Higginbottom A,** Quinn ER, Kuo CC, Flint M, Wilson LH, Bianchi E, Nicosia A, Monk PN, McKeating JA, Levy S. Identification of amino acid residues in CD81 critical for interaction with hepatitis C virus envelope glycoprotein E2. *J Virol* 2000; **74**: 3642-3649

15 **Wünschmann S,** Medh JD, Klinzmann D, Schmidt WN, Stapleton JT. Characterization of hepatitis C virus (HCV) and HCV E2 interactions with CD81 and the low-density lipoprotein receptor. *J Virol* 2000; **74**: 10055-10062

16 **Triyanti M,** Saunier B, Maruvada P, Davis AR, Ulianich L . Interaction of hepatitis C virus-like particles and cells: a model system for studying viral binding and entry. *J Virol* 2002; **76**: 9335-9344

17 **Ohno O,** Mizokami M, Wu RR, Saleh MG, Ohba K, Orito E, Mukaide M, Williams R, Lau JY. New hepatitis C virus (HCV) genotyping system that allows for identification of HCV genotypes 1a, 1b, 2a, 2b, 3a, 3b, 4, 5a and 6a. *J Clinical Microbiol* 1997; **35**: 201-207

18 **El Awady MK,** El-Demellawy MA, Khalil SB, Galal D, Goueli SA. Synthetic peptide-based immunoassay as a supplemental test for HCV infection. *Clin Chim Acta* 2002; **325**: 39-46

19 **Hudson L,** Hay FC. Antibody as a probe. In: Practical Immunology, third edition, *Blackwell Scientific Publications Oxford London* 1989: 34-43

20 **Lohr HF,** Goergen B. Buschenfelde KHMZ and Gerken G HCV replication in mononuclear cells stimulates anti-HCV secreting B cells and reflects non responsiveness to interferon A. *J Med Virol* 1995; **46**: 314–320

21 **Chomczynski P,** Sacchi N. Single step method of RNA isolation by acid guanidinium thiocyanate-phenol-chloroform extraction. *Anal Biochem* 1987; **162**: 156–159

22 **Crotty PL,** Staggs RA, Porter PT, Killeen AA, McGlennen RC, Quantitative analysis in molecular diagnosis. *Hum Pathol* 1994; **25**: 572–579

23 **Reischl U,** Kochanowski B. Quantitative PCR. A survey of the present technology. *Mol Biotechnol* 1995; **3**: 55–71

24 **Wang JT,** Sheu JC, Lin JT, Wang TH, Chen DS. Detection of replication form of HCV RNA in peripheral blood mononuclear cells. *J Infect Dis* 1992; **166**: 1167-1169

25 **Taliani G,** Badolato MC, Lecce R, Poliandri G, Bozza A, Duca F, Pasquazzi C, Clementi C, Furlan C, Bac CD. HCV RNA in PBMC: relation with response to IFN treatment. *J Med Virol* 1995; **47**: 16-22

26 **Zignego AL,** De Carli M, Monti M, Careccia G, La Villa G, Giannini C, D'Elios MM, Del Prete G, Gentilini P. HCV infection of mononuclear cells from peripheral blood and liver infiltrates in chronically infected patients. *J Med Virol* 1995; **47**: 58-64

27 **Gribier B,** Schmitt C, Bingen A, Kirn A, Keller F. *In vitro* infection of peripheral blood mononuclear cells by HCV. *J Gen Virol* 1995; **76**: 2485-2491

28 **Gong GZ,** Lai LY, Jiang YF, He Y, Su XS. HCV replication in PBMC and its influence on interferon therapy. *World J Gastroenterol* 2003; **9**: 291-294

29 **El-Awady MK,** Ismail SM, El-Sagheer M, Sabour YA, Amr KS, Zaki EA. Assay for hepatitis C virus in peripheral blood mononuclear cells enhances sensitivity of diagnosis and monitoring of HCV-associated hepatitis. *Clin Chim Acta* 1999; **283**: 1-14

30 **El-Awady MK,** Abdel Rahman MM, Ismail SM, Amr KS, Omran M, Mohamed SA. Prediction of relapse after interferon therapy in hepatitis C virus-infected patients by the use of triple assay. *Gastroenterol Hepatol* 2003; **18**: 68-73

31 **Gabriellu A,** Manzin A, Candela M. Active HCV infection in bone marrow and peripheral blood mononuclear cells from patients with mixed cryoglobulinaemia. *Clin Exp Immunol* 1994; **97**: 87-93

32 **Bouffard P,** Hayashi PH, Acevedo R, Levy N, Zeldis JB. Hepatitis C virus is detected in a monocyte/macrophage subpopulation of peripheral blood mononuclear cells of infected patients. *J Infect Dis* 1992; **166**: 1276-1280

33 **Chang TT,** Yong KC, Yang YJ, Lei HY, Wu HL. Hepatitis C virus RNA in PBMC: comparing acute and chronic hepatitis C virus infection. *Hepatology* 1996; **23**: 977-981

34 **Muler HM,** Pfaff E, Goeser T, Kallinowski B, Solbach C. Peripheral blood leukocytes serve as a possible extrahepatic site for hepatitis C virus replication. *J Gen Virol* 1993; **74**: 669-676

35 **Mihm S,** Hartmann H, Ramadori G. A reevaluation of the association of hepatitis C virus replicative intermediates with peripheral blood cells including granulocytes by a tagged reverse transcriptase/polymerase chain reaction technique. *J Hepatol* 1996; **24**: 491-497

36 **Lerat H,** Berby F, Trabaud MA, Vidalin O, Major M, Trepo C, Inchauspe G. Specific detection of hepatitis C virus minus strand RNA in hematopoietic cells. *J Clin Invest* 1996; **97**: 845-851

37 **Sansonno D,** Lacobelli AR, Cornacchiulo V, Iodice G, Dammacco F. Detection of HCV proteins by immunofluorescence and HCVRNA genomic sequences by non-isotopic in situ hybridization in bone marrow cells and PBMC of chronically HCV infected patients. *Clin Exp Immunol* 1996; **103**: 414-421

38 **Chen LB,** Chen PL, Fan GR, Li L, Liu CY. Localization of hepatitis C virus core protein in the nucleus of PBMCs of hepatitis C patients. *Zhonghua Shiyan He Linchuangbin Duxue Zazhi* 2002; **16**: 37-39

Science Editor Guo SY **Language Editor** Elsevier HK

PO Box 2345, Beijing 100023, China
www.wjgnet.com
wjg@wjgnet.com

ELSEVIER

World J Gastroenterol 2005;11(33):5209-5212
World Journal of Gastroenterology ISSN 1007-9327
© 2005 The WJG Press and Elsevier Inc. All rights reserved.

• *BRIEF REPORTS* •

Complications of endoscopic retrograde cholangiography in the post-MRCP era: A tertiary center experience

Tze-Zen Ong, Jen-Lock Khor, Dede-Sutedja Selamat, Khay-Guan Yeoh, Khek-Yu Ho

Tze-Zen Ong, Jen-Lock Khor, Dede-Sutedja Selamat, Khay-Guan Yeoh, Khek-Yu Ho, Department of Gastroenterology and Hepatology, National University Hospital, Singapore
Correspondence to: Dr. Khek-Yu Ho, Department of Gastroenterology and Hepatology, National University Hospital, 5, Lower Kent Ridge Road, 119074 Singapore. mdchoky@nus.edu.sg
Telephone: +65-67724379 Fax: +65-67794112
Received: 2004-11-03 Accepted: 2004-12-20

Abstract

AIM: To evaluate our experience in endoscopic retrograde cholangio-pancreatography (ERCP) in terms of fulfilling the ASGE guidelines in indications, positive findings, and complications in the post-magnetic resonance cholangiopancreatography (MRCP) era.

METHODS: Between November 2001 and February 2003, consecutive ERCP cases were prospectively evaluated with regard to the indications, findings, cannulation techniques, devices used during the procedure, sedation given, duration of procedure, and complications. These data were entered in a database for subsequent processing and analysis.

RESULTS: Of 336 cases, 21.4% were diagnostic and 78.6% therapeutic ERCP. The indications for ERCP fulfilled the ASGE guidelines in 323 cases (96.1%). Suspected bile duct stone was the most frequent indication (26.8%), and this was followed by cholangitis (24.4%), dilated common bile duct (14.9%), and cholestatic jaundice (13.4%). Cannulation success rate was 94%. Biliary sphincterotomy was performed in 175 (52.1%) patients. Repeated ERCP was performed on 31.5% of the patients. Overall, the complication rate was 9.8% with 0.3% being procedure-related mortality. The complications were pancreatitis (5.4%), bleeding (0.8%), cholangitis (2.4%) and others (1.5%). No significant difference was observed between the complication rate and the type of ERCP performed.

CONCLUSION: Our study showed that post-ERCP complication rate was comparable with the other large prospective studies and there was no difference in the complication between the diagnostic and therapeutic ERCP.

© 2005 The WJG Press and Elsevier Inc. All rights reserved.

Key words: Endoscopic retrograde cholangiopancreatogram; Complication; Pancreatitis

Ong TZ, Khor JL, Selamat DS, Yeoh KG, Ho KY. Complications of endoscopic retrograde cholangiography in the post-MRCP era: A tertiary center experience. *World J Gastroenterol* 2005; 11(33): 5209-5212
http://www.wjgnet.com/1007-9327/11/5209.asp

INTRODUCTION

Endoscopic retrograde cholangio-pancreatography (ERCP) is the most complex endoscopic procedure. It is the preferred treatment for the majority of pancreatico-biliary diseases. Since its introduction in 1968[1], ERCP has evolved from a purely diagnostic to a therapeutic procedure because noninvasive imaging techniques such as magnetic resonance cholangio-pancreatography (MRCP) is increasingly being used for the diagnosis of conditions, otherwise previously diagnosed only by ERCP. Endobiliary sphincterotomy (ES) has become a common procedure in the era of endoscopic management of biliary and pancreatic diseases. However, these procedures carry certain mortality and morbidity[2-5] with acute pancreatitis, being the most common complication. The purpose of this study was to evaluate our experience in ERCP in terms of fulfilling acceptable ASGE guidelines[6] in indications, positive findings, and complications in the post-MRCP era.

MATERIALS AND METHODS

Study population

A prospective study was conducted at the National University Hospital, Singapore from November 2001 to February 2003. A total of 336 consecutive ERCPs were performed during the study period. All patients signed an informed consent for the procedures, after receiving an explanation on the risks, benefits and alternatives of ERCP and associated therapeutic procedures. Patients were given topical pharyngeal spray with 10% lignocaine spray, and sedated with midazolam and pethidine or fentanyl. All procedures were performed by Olympus duodenoscope JF200 or JF 240. Prophylactic antibiotics were routinely given to all patients.

Data on patients' characteristics, ERCP indications and findings, cannulation techniques, devices used during the procedure, sedation given, duration of procedure and complications were collected prospectively during the procedure, recovery period and hospitalization. These data were entered in a database for subsequent processing and analysis.

ERCP complications

Post-ERCP complications were defined as any adverse effect

related to the ERCP that prolonged hospitalization or required readmission for previously discharged patients. The complications were defined according to the previously published criteria[6]. Acute pancreatitis was defined as a new onset of abdominal pain with a rise in the level of amylase at least three times the upper limit of normal at more than 24 h after the procedure, requiring more than one night of hospitalization. Bleeding was defined as a clinical evidence of hemorrhage with decrease in hemoglobin greater than 2 g/dL or the need for a blood transfusion. Cholangitis was defined as a fever greater than 38 ℃ for more than 24 h that was thought to have biliary causes. Additional procedure-interrupting events such as hypoxia (decrease in oxygen saturation to below 90% for 2 min), duodenal tear and bradycardia (decrease in heart rate to less than 50 beats per minute for 2 min) were considered as post-ERCP complications. Any intensive care unit admission after procedure was graded as a severe complication.

ERCP was defined as therapeutic, where endoscopic sphincterotomy, precut, drainage, stricture dilatation, stent exchange, sphincter of Oddi manometry or biliary stone removal had been performed singularly or in combination.

Statistical analysis

Statistical analysis was performed using the Statistical Package for the Social Science (SPSS) version 10.0[9]. Comparison of diagnostic and therapeutic ERCP complications were evaluated using the χ^2- or Fisher's exact test. All tests of significance were two-tailed and a *P* value <0.05 was considered significant.

RESULTS

A total of 336 ERCPs were performed during the study period. Median age of the patients was 65 years (range 17-93 years). There were an equal number of males and females (167 men and 169 women). The ethnic distribution was Chinese in 78.3%, Malay in 11.3%, Indian in 5.7% and others in 4.8%. Indications of ERCP were suspected choledocholithiasis (26.8%), cholangitis (24.4%), dilated common bile duct (14.9%), cholestatic jaundice (13.4%), gallstone pancreatitis (7.7%), stent-related problems (6.3%) and others (6.5%, Figure 1). These indications fulfilled ASGE guidelines in 323 (96.1%) patients.

One hundred and seventy-three (51.5%) patients had co-morbidity such as diabetes mellitus with renal impairment, ischemic heart disease, heart failure, old stroke, atrial fibrillation, chronic renal failure and others. Twenty-seven (8%) patients were on anticoagulation or antiplatelet drugs for their underlying diseases. Anesthetist assistance (general anesthesia) was required in 8 patients (2.4%), whereas the endoscopic team assisted in sedation for all the remaining patients. Midazolam (dose 0.5-10 mg) was used in 97.6%, pethidine (dose 7-125 mg) in 97% and fentanyl (dose 20-75 μg) in 0.6% of all patients. Prophylactic antibiotics were routinely given to all patients.

ERCP failed in 20 patients (6%) because of unsuccessful cannulation and/or suboptimal ductal opacification whereas in 21 patients (6.3%), only shallow cannulation was achieved preventing further therapeutic procedure. Successful cannulation of the desired duct was obtained in 295 patients (87.7%).

Biliary sphincterotomy was performed in 175 patients (52.1%). Indications for sphincterotomy were common bile duct stones in 119 cases (68%), suspected passed biliary stone in 27 (15.4%), and biliary drainage in 11 (6.3%). Overall, therapeutic procedures were performed in 264 patients (78.6%). Sphincterotomy was the most common therapeutic procedure (66.5%) and this was followed by stenting (33.3%) and stone extraction (27.7%). Sphincter of Oddi manometry was performed in two (0.6%) patients (Table 1).

Of 336 patients undergoing ERCP, 33 complications (9.8%) were reported (Table 2). Eighteen cases were immediate and 16 cases were delayed complications. Post-ERCP pancreatitis was the most frequent complication and occurred in 18 patients (5.4%). Pancreatitis was mild in 15 patients (4.5%), moderate in 2 patients (0.6%) and severe in 1 patient (0.3%). Bleeding occurred in three patients (0.8%); two bled immediately after sphincterotomy (mild hemorrhage) and one had delayed hemorrhage (moderate hemorrhage), after dilatation and biopsy of malignant biliary stricture. All three of them were successfully treated with endoscopic therapy and only one required blood transfusion. Cholangitis occurred in eight patients (2.4%); mild cholangitis in four patients, moderate in three patients and severe in one patient. The cholangitis occurred after plastic stenting for biliary stricture or stones in three patients, after biliary stone extraction in another three, after biopsy of biliary stricture in one, and after diagnostic ERCP in the other. One patient had a duodenal tear (0.3%) sustained during intubation of a Bilroth 2 anatomy, one (0.3%) developed choledocho-duodenal fistula due to forceful cannulation, one (0.3%) had subcapsular liver perforation due to vigorous biliary stenting, one (0.3%) desaturated during the procedure, and one (0.3%) developed bradycardia. These patients were treated conservatively and recovered well with no ill sequelae. Six (1.8%) patients died within 1 mo of the procedure, but only one was deemed procedure-related (0.3%). This post-ERCP death was due to severe cholangitis 2 d after sphincterotomy and stone extraction for biliary stones. Four died of underlying severe cholangitis on presentation and one died of cardiac arrest 8 d after the procedure. No significant difference was observed between the complication rate and the type of ERCP performed (Table 2).

Table 1 Therapeutic procedure in 264 patients

Type of procedure	*n*	%
Sphincterotomy alone	40	11.9
Sphincterotomy+stone extraction	86	25.6
Sphincterotomy+biliary stenting	42	12.5
Stricture dilatation±sphincterotomy	3	0.9
Nasobiliary drainage±sphincterotomy	2	0.6
Biliary stenting/stent removal alone	73	21.7
Stone extraction alone	7	2.1
Dilatation and stenting	5	1.5
SOD manometry	2	0.6
Biopsy/cytology	4	1.2

Table 2 Major complications in 336 patients: comparison between diagnostic and therapeutic ERCP

Complication	Diagnostic ERCP *n* = 72 (%)	Therapeutic ERCP *n* = 264 (%)	*P*
Pancreatitis	5 (6.9)	13 (4.9)	0.50
Cholangitis	1 (1.4)	8 (3)	0.53
Hemorrhage	0	3 (1.1)	0.36
Other complications	2 (2.8)	3 (1.1)	0.31
Total	8 (11.1)	26 (9.8)	0.68

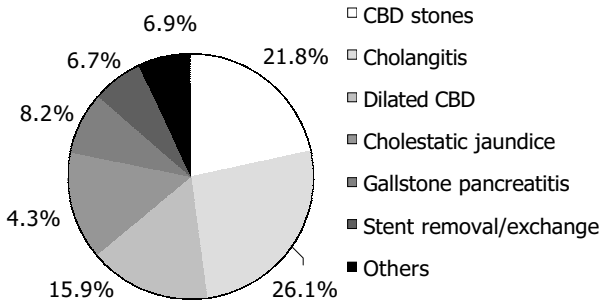


Figure 1 Indication of ERCP.

DISCUSSION

In recent years, ERCP had evolved from a purely diagnostic to a therapeutic procedure with the introduction of non-invasive investigative tools such as MRCP. Most of the ERCP procedures in the present series, were therapeutic (78.6%) compared to earlier studies[7-9] in which therapeutic ERCP only comprised 40-55% of the total number of procedures. The post-ERCP complication rate in the present series was no different compared to other studies[9-13]. The overall complication rate was 9.8%. There was no significant difference in the complication rate between diagnostic and therapeutic ERCP. This finding is consistent with that of a retrospective US survey by Male *et al*.[14], but was in contrast with those from a British survey[15] and an Italian study[16] in which therapeutic ERCP was associated with three- to four-fold higher complication rates.

The reported incidences of post-ERCP pancreatitis ranged 0-40%[17] but were commonly quoted as 2-7%[10,18,19]. The variation is likely due to the difference in definition of pancreatitis, method of data collection and indications for ERCP. In the present study, acute pancreatitis was the most common complication (5.4% of patients) and most cases were mild. This finding is comparable with those of two recently published large prospective studies by Freeman *et al*.[10], and Loperfido *et al*.[16]. In the former study, which only considered therapeutic procedure, the overall complication rate was 9.8%. Procedure-related pancreatitis occurred in 5.4% of patients; mild in 2.3%, moderate in 2.8% and severe in 0.4%. In the latter survey which also included diagnostic procedure (one-third of procedures), reported major complication rate was 4%, and pancreatitis (moderate and severe only) occurred in 1.3%. The risk of pancreatitis was similar for diagnostic and therapeutic ERCP in our study. This is similar to the finding from a prospective study from Boston[9] even though some studies[20,21] reported higher pancreatitis complication rates in therapeutic ERCP. Risk factors of procedure-related pancreatitis identified were factors related to patients' characteristics such as younger age[10,16,22], suspected dysfunction of sphincter of Oddi[10], history of ERCP-related pancreatitis[9], recurrent pancreatitis[9] and factors related to endoscopic technique such as pancreatic duct opacification[16,19], small bile duct[16,23], multiple cannulation attempt[9] or difficult cannulation[10], development of abdominal pain during the procedure[9], precut sphincterotomy[10,22] and pancreatic duct brushing for cytology[9]. ERCP-induced pancreatitis remains an important clinical problem even in diagnostic ERCP.

Incidence of post-ERCP hemorrhage varies between 0.65% and 4% in earlier retrospective studies[24,25]. In our study, procedure-related hemorrhage was only 0.8%. This low figure is similar to those from a few large prospective studies[9,10,16,22]. Cholangitis is an uncommon complication in ERCP, ranged 0.5-1.1%[9,10,16,22]. However, cholangitis seems to be slightly higher (2.3%) in our study, even though routine antibiotics were given before starting the procedure. Three patients with cholangitis had stent migration after plastic stenting for biliary stricture or stones (one required repeat ERCP), three had cholangitis after biliary stone extraction (one had incomplete stone removal and required the ERCP repeat for stones clearance and one who had severe cholangitis subsequently died), one developed cholangitis after biopsy of biliary stricture and one after diagnostic ERCP. Most of the patients with cholangitis resolved after one course of antibiotics.

Our study showed that post-ERCP complication rate was comparable with those of other large prospective studies and there was no difference in the complication rates between the diagnostic and therapeutic ERCP. In line with the current post-MRCP, most of our ERCPs were therapeutic (78.6%). Future research should focus on developing clinical pathways to guide clinicians in selecting patients who should undergo ERCP or MRCP as the initial investigation and those who would benefit from MRCP followed by ERCP.

REFERENCES

1 **McCune WS,** Shorb PE, Moscovitz H. Endoscopic cannulation of the ampulla of Vater: a preliminary report. *Ann Surg* 1968; **167**: 752-756
2 **Bilbao MK,** Dotter CT, Lee TG, Katon RM. Complications of endoscopic retrograde cholagiopancreatography (ERCP): A study of 10000 cases. *Gastroenterology* 1996; **70**: 314-320
3 **Sherman S,** Lehman GA. ERCP and endoscopic sphincterotomy-induced pancreatitis. *Pancreas* 1991; **6**: 350-367
4 **Roszler H,** Campbell WL. Post-ERCP pancreatitis: association with urographic visualization during ERCP. *Radiology* 1985; **157**: 595-598
5 **Reiertsen O,** Skjoto J, Jacobsen CD, Rosseland AR. Complications of fibreoptic gastrointestinal endoscopy-Five years experience in a central hospital. *Endoscopy* 1987; **19**: 1-6
6 **Vennes JA,** Ament M, Boyce HW Jr, Cotton PB, Jensen DM, Ravich WJ, Sugawa C, Wu WC, Sanowski RA, Ament M. Principals of training in gastrointestinal endoscopy American Society for Gastrointestinal Endoscopy. Standards of Training Committees. 1989-1990. *Gastrointestinal Endosc* 1992; **38**: 743-746
7 **Scheeres DE,** Simon I, Ponsky JL. Endoscopic retrograde cholangiopancreatography in a general surgery practice. *Am Surg* 1990; **56**: 185-191
8 **Farrell RJ,** Mahmud N, Noonan N, Kelleher D, Keeling PW.

Diagnostics and therapeutic ERCP: a large single centre's experience. *Ir J Med Sci* 2001; **170**: 176-180

9 **Vandervoort J,** Soetikno RM, Tham TC, Wong RC, Ferrari AP Jr, Montes H, Roston AD, Slivka A, Lichtenstein DR, Ruymann FW, Van Dam J, Hughes M, Carr-Locke DL. Risk factors for complications after performance of ERCP. *Gastrointest Endosc* 2002; **56**: 652-656

10 **Freeman ML,** Nelson DB, Sherman S, Haber GB, Herman ME, Dorsher PJ, Moore JP, Fennerty MB, Ryan ME, Shaw MJ, Lande JD, Pheley AM. Complication of endoscopic biliary sphincterotomy. *N Eng J Med* 1996; **335**: 909-918

11 **Safrany L.** Endoscopic treatment of biliary-tract diseases. An international study. *Lancet* 1978; **2**: 983-985

12 **Leese T,** Neoptolemos JP, Carr-Locke DL. Successes, failures, early complications and their management following endoscopic sphincterotomy: results in 394 consecutive patients from a single centre. *Br J Surg* 1985; **72**: 215-219

13 **Vaira D,** D'Anna L, Ainley C, Dowsett J, Williams S, Baillie J, Cairns S, Croker J, Salmon P, Cotton P. Endoscopic sphincterotomy in 1000 consecutive patients. *Lancet* 1989; **2**: 431-434

14 **Male R,** Lehman G, Sherman S. Severe and fatal complications of diagnostics and therapeutic ERCP [abstract]. *Gastrointest Endosc* 1996; **40**: P29

15 **Tanner AR.** ERCP: present practices in a single region. *Eur J Gastroenterol Hepatol* 1996; **8**: 145-148

16 **Loperfido S,** Angelini G, Benedetti G, Chilovi F, Costan F, De Berardinis F, De Bernardin M, Ederle A, Fina P, Fratton A. Major early complications from diagnostic and therapeutic ERCP: a prospective multicenter study. *Gastrointest Endosc* 1998; **48**: 1-10

17 **Aliperti G.** Complications related to diagnostic and therapeutic ERCP. *Gastrointest Endosc Clin N Am* 1996; **6**: 379-407

18 **Elfant AB,** Bourke MJ, Alhalel R, Kortan PP, Haber GB. A prospective study of endoscopic therapy for choledocholithiasis in an outpatient population. *Am J Gastroenterol* 1996; **91**: 1499-1502

19 **Cotton PB,** Baillie G, Leung J. Correlations with post-ERCP pancreatitis [abstract]. *Gastrointest Endoscopy* 1994; **40**: P29

20 **Catalano MF,** Geenen JE, Schmalz MJ. ERCP induced acute pancreatitis: risk assessment based on diagnostic and specific therapeutic cases [abstract]. *Gastrointest Endosc* 1996; **43**: 376

21 **Cohen SA,** Siegel JH, Kasmin FE. Complication of diagnostic and therapeutic ERCP. *Abdom Imaging* 1996; **21**: 385-394

22 **Masci E,** Toti G, Mariani A, Curioni S, Lomazzi A, Dinelli M, Minoli G, Crosta C, Comin U, Fertitta A, Prada A, Passoni GR, Testoni PA. Complications of diagnostic and therapeutic ERCP: a prospective multicenter study. *Am J Gastroenterol* 2001; **96**: 417-423

23 **Sherman S,** Ruffolo TA, Hawes RH, Lehman GA. Complications of endoscopic sphincterotomy. A prospective series with emphasis on increased risk associated with sphincter of Oddi dysfunction and nondilated bile ducts. *Gastroenterology* 1991; **101**: 1068-1075

24 **Boujaoude J,** Pelletier G, Fritsch J, Choury A, Lefebvre JF, Roche A, Frouge C, Liguory C, Etienne JP. Management of clinically relevant bleeding following endoscopic sphincterotomy. *Endoscopy* 1994; **26**: 217-221

25 **Cotton PB.** Towards safer endoscopic retrograde cholangiopancreatography. *Gut* 1993; **34**: 721-724

Science Editor Li WZ **Language Editor** Elsevier HK

PO Box 2345, Beijing 100023, China
www.wjgnet.com
wjg@wjgnet.com

ELSEVIER

World J Gastroenterol 2005;11(33):5213-5217
World Journal of Gastroenterology ISSN 1007-9327
© 2005 The WJG Press and Elsevier Inc. All rights reserved.

• *BRIEF REPORTS* •

Association of polymorphism of tumor necrosis factor-alpha gene promoter region with outcome of hepatitis B virus infection

Hong-Quan Li, Zhuo Li, Ying Liu, Jun-Hong Li, Jian-Qun Dong, Ji-Rong Gao, Chun-Yan Gou, Hui Li

Hong-Quan Li, Hui Li, Ying Liu, Jian-Qun Dong, Department of Epidemiology, Institute of Basic Medical Sciences, Chinese Academy of Medical Sciences; School of Basic Medicine, Peking Union Medical College, Beijing 100005, China
Zhuo Li, Jun-Hong Li, Ji-Rong Gao, Chun-Yan Gou, Institute of Hepatitis Research, Beijing You'an Hospital, Capital Medical University, Beijing 100005, China
Supported by the Beijing Municipal Government Commission for Science and Technology, No. H020920020590
Correspondence to: Hui Li, Department of Epidemiology, Institute of Basic Medical Sciences, Chinese Academy of Medical Sciences; School of Basic Medicine, Peking Union Medical College, 5 Dongdan Santiao, Beijing 100005, China. lihui99360@sohu.com
Telephone: +86-10-65296971 Fax: +86-10-65225752
Received: 2004-10-30 Accepted: 2004-12-21

Abstract

AIM: To determine whether -238G/A and -857C/T polymorphisms of tumor necrosis factor-alpha (TNF-α), gene promoter and hepatitis B (HB) viral genotypes were associated with outcomes of HBV infection.

METHODS: A total of 244 HBV self-limited infected subjects, 208 asymptomatic carriers, and 443 chronic HB patients were recruited to conduct a case-control study. TNF-α -238G/A and -857C/T gene promoter polymorphisms were examined by polymerase chain reaction-restriction fragment length polymorphism (PCR-RFLP), and HBV genotypes were examined by nested PCR.

RESULTS: The positive rate of HBV DNA in asymptomatic carrier group and chronic HB group was 46.6% and 49.9%, respectively. HBV genotype proportion among the asymptomatic carriers was 2.1% for genotype A, 25.8% for genotype B, 68.0% for genotype C, and 4.1% for genotype B+C mixed infection, and 0.9% for genotype A, 21.7% for genotype B, 71.5% for genotype C, 5.9% for genotype B+C mixed infection in chronic HB group. There was no significant difference in genotype distribution between the asymptomatic carrier group and chronic HB group ($\chi^2 = 1.66$, $P = 0.647$). The frequency of -238GG genotype in self-limited group was 95.1%, significantly higher than 90.7% in chronic HB group and 89.0% in asymptomatic carrier group ($P = 0.041$ and $P = 0.016$, respectively).The frequency of TNF-α-857 CC in chronic HB group was 79.7%, significantly higher than 64.4% in asymptomatic carrier group and 70.9% in self-limited group ($P<0.001$ and $P = 0.023$, respectively). A multiple logistic regression analysis revealed that TNF-α-238GA and -857CC were independently associated with chronic HB after gender and age were adjusted.

CONCLUSION: TNF-α promoter variants are likely to play a substantial role in the outcome of HBV infection.

© 2005 The WJG Press and Elsevier Inc. All rights reserved.

Key words: Hepatitis B; TNF-α gene; Single nucleotide polymorphism; Genotype; Haplotype

Li HQ, Li Z, Liu Y, Li JH, Dong JQ, Gao JR, Gou CY, Li H. Association of polymorphism of tumor necrosis factor-alpha gene promoter region with outcome of hepatitis B virus infection. *World J Gastroenterol* 2005; 11(33): 5213-5217
http://www.wjgnet.com/1007-9327/11/5213.asp

INTRODUCTION

It is estimated that HBV has infected more than 350 million people worldwide. HBV infection causes various clinical outcomes in patients. Ninety to ninety-five percent of adults infected with HBV can eliminate the virus and only 5-10% of them become chronic HBV carriers; 20-30% of chronic HBV carriers develop chronic hepatitis B (HB) and 5% of them develop liver cirrhosis and hepatocellular carcinoma in a long term of disease course. HB has become one of the severe public health problems.

The outcome of HBV infection may be associated with host genetic factors. Cytokines play an important role in defense against viral infection, indirectly through determination of the predominant pattern of the host response, and directly through inhibition of viral replication[1]. TNF-α is one of the important cytokines involved in noncytotoxic antiviral mechanism, and participates in the viral clearance and the host immune response to HBV[2]. It was found that individuals with acute HB have higher TNF-α plasma levels than controls[3]. The capacity for the cytokine production in individuals largely depends on promoter genetic polymorphisms[4]. At present, few studies corresponding to these results are reported in China.

The outcome of HBV infection is also associated with the genetic variability of virus, which influences the expression of viral antigens. In recent years, HBV genotypes A, B, C, and D have been reported in China, and genotypes B and C are the predominant genotypes[5].

In this case-control study, we analyzed TNF-α -238G/A and -857C/T promoter genetic polymorphisms among self-limited group, asymptomatic carrier group and chronic HB group, and HBV genotypes in asymptomatic carrier group and chronic HB group to elucidate whether host genetic and viral factors were associated with the outcome of HBV infection.

MATERIALS AND METHODS

Subjects

From November 2002 to March 2004, 244 self-limited HBV-infected subjects, 208 asymptomatic carriers, and 443 chronic HB patients were recruited at Beijing You'an Hospital. The diagnostic criteria used for three groups of subjects were determined, according to the protection and treatment protocol for viral hepatitis amended by Infectious Disease Branch and Liver Disease Branch of Chinese Medical Association in September 2000, and the diagnostic criteria and treatment principle of viral HB published by National Technical Supervision Bureau and Ministry of Public Health in January 1996 (GB15990-1995). All subjects enrolled in this study provided the informed consent. All subjects were Chinese Han people and not infected with other viral hepatitis.

Serological test

ELISA was used for detection of serum HBsAg, anti-HBs, and anti-HBc (IMX, Abbott Diagnostics, North Chicago, IL, USA).

Measurement of TNF-α gene promoter polymorphism

Genomic DNA was extracted from peripheral blood leukocytes collected in EDTA by standard phenol-chloroform extraction. Allelic polymorphisms in the TNF-α gene promoter at positions -238G/A[6] and -857C/T[7,8] were amplified into 152- and 131-bp fragments by PCR with the primers (for 152-bp fragment, sense 5'AGAAGACCCCCCTCGGAACC3' and antis-ense 5'ATCTGGAGGAAGCGGTAGTG3'; for 131-bp fragment, sense 5'AAGTCGAGTATGGGGACCCCCCGTTAA3' and anti-sense 5'CCCCAGTGTGTGGCCATATCTTCTT3'). Amplifications of the -238 and -857 fragments were performed in a volume of 25 μL containing 50 ng of genomic DNA, 20 pmol/L of each primer, 200 μmol/L dNTP, 1.5 mmol/L $MgCl_2$, buffer and 1 U *Taq* polymerase (Shanghai Biocolor). PCR conditions of -238 were as follows: pre-denaturation at 94 ℃ for 2 min, 30 cycles of denaturation at 94 ℃ for 30 s, annealing at 60 ℃ for 30 s, extension at 72 ℃ for 30 s, and a single final extension at 72 ℃ for 10 min in Perkin Elmer thermocycler (2700, Applied Biosystems, Foster City, CA, USA). For amplification of -857 polymorphism, annealing temperature was at 64 ℃ and other thermal cycling parameters were as the same as those for amplification of -238.

The PCR products of -238 and -857 were digested with *Msp*I and *Hinc*II restriction enzymes respectively. TNF-α -238 allele 1 was identified by 20- and 132-bp fragments and allele 2 by a single 152-bp fragment. TNF-α -857 allele 1 was identified by 25- and 106-bp fragments and allele 2 by a single 131-bp fragment.

HBV genotyping

Sequence data for the amplified region of HBV DNA were aligned from GenBank. Alignment of the sequences was performed with Vector NTI suite and Tree View software.

According to the comparisons of HBV DNA sequences and other papers[9,10], outer primers and inner primers specific for HBV genotypes are summarized in Table 1.

HBV genotypes were determined by PCR. Nested PCR primers amplified HBV DNA with two stages (Table 1). The first-stage amplification was performed in a volume of 30 μL containing 5 μL of genomic DNA, 0.1 mol/L of primers Ps1 and Ps2, 200 μmol/L dNTP, 1.5 mmol/L $MgCl_2$, buffer and 1 U *Taq* polymerase (Shanghai Biocolor). The procedure of amplification was as follows: pre-denaturation at 94 ℃ for 3 min, 35 cycles of denaturation at 94 ℃ for 40 s, annealing at 55 ℃ for 40 s, extension at 72 ℃ for 45 s. Two microliters of PCR products were required in the second-stage amplification, which involved two groups. The primers contained 0.1 μmol/L B2, 0.08 μmol/L BA1R, BB1R, and BC1R in group A. In group B, the primers contained 0.1 μmol/L B2R, 0.08 μmol/L BD1, BE1, and BF1. Thermal cycling parameters involved 94 ℃ for 3 min, 20 cycles of 94 ℃ for 40 s, 58 ℃ for 40 s, and 72 ℃ for 40 s, and 20 cycles of 94 ℃ for 40 s, 60 ℃ for 40 s, and 72 ℃ for 40 s. PCR products of the amplification were illuminated using ultraviolet rays, after electrophoresis on 6% acrylamide gel stained by EB.

Table 1 Nested PCR primer sequences for HBV genotype

Primer sequence	
Outer primers	
Ps1	5'TCACCATATTCTTGGGAACAAGA3'
Ps2	5'CGAACCACTGAACAAATGGC3'
Inner primers	
Group A	
B2	5'GGCTCCAGTTCCGGAACAGT3'
BA1R	5'CTCGCGGAGATTGACGAGATG3'
BB1R	5'CAGGTTGGTGAGTGACTGGAG3'
BC1R	5'GGTCCTAGGAATCCTGATGTTG3'
Group B	
BD1	5'GCCAACAAGGTAGGAGCT3'
BE1	5'CACCAGAAATCCAGATTGGGACCA3'
BF1	5'GCTACGGTCCAGGGTTACCA3'
B2R	5'GGAGGCGGATVTGCTGGCAA3'

Statistical analysis

Comparisons were performed using one-way ANOVA and χ^2 test. SAS version 6.12 software package was used to analyze data. All P values were two-tailed, and $P<0.05$ was considered statistically significant. Haplotypic analysis was performed using EH2.0 program.

RESULTS

Characteristics of subjects

The average age of chronic HB patients, asymptomatic carriers, and self-limited subjects was 33.37±12.67, 31.2±10.78, and 34.68±11.34 years, respectively. A significant difference was found in age of the three groups ($F = 4.985$, df = 2, $P = 0.008$).

The ratio of male to female patients (354/89) in the chronic HB group was significantly higher than those (136/108 and 113/95) of the self-limited group and the asymptomatic carrier group ($P<0.01$).

Association of HBV genotypes with outcomes of HBV infection

The positive rate of HBV DNA in the asymptomatic carrier group and the chronic HB group was 46.6% and 49.9%, respectively (Table 2).

The proportions of subjects with HBV genotypesA, B, C and mixed genotype B+C among the asymptomatic carriers were 2.1%, 25.8%, 68.0% and 4.1%. Among the chronic HB patients, the proportion of HBV genotypes was 0.9% for genotype A, 21.7% for genotype B, 71.5% for genotype C, 5.9% for mixed genotypes B+C. The difference in genotype distribution between the asymptomatic carrier group and chronic HB group was statistically significant ($\chi^2 = 1.66$, $P = 0.647$) (Table3).

Table 2 Positive rate of HBV DNA in asymptomatic carrier group and chronic HB group

Group	*n*	HBV DNA positive (%)
Carrier	208	97 (46.6)
Chronic HB	443	221 (49.9)

Table 3 Proportions of HBV genotype in asymptomatic carrier group and chronic HB group

Group	*n*	A	B	C	B+C
Carrier group	97	2 (2.1)	25 (25.8)	66 (68.0)	4 (4.1)
Chronic HB group	221	2 (0.9)	48 (21.7)	158 (71.5)	13 (5.9)

$\chi^2 = 1.66$, df = 3, $P = 0.647$.

Association of TNF-α -238G/A and -857C/T genotypes with outcomes of HBV infection

The frequency of -238GG genotype in the self-limited group was 95.1%, significantly higher than 90.7% in the chronic HB group and 89.0% in the asymptomatic carrier group ($P = 0.041$ and $P = 0.016$), respectively. No significant difference was found between chronic HB and carrier groups ($P = 0.496$). The frequency of -238G allele in the self-limited group was 97.5%, significantly lower than that in the other two groups ($\chi^2 = 3.99$, $P = 0.046$). There was no significant difference in Hardy-Weinberg among the three groups ($\chi^2 = 0.155$, $P = 0.69$, Table 4).

The frequency of TNF-α -857CC in chronic HB group was 79.7%, significantly higher than 64.4% of carrier group and 70.9% of self-limited group ($P<0.001$ and $P = 0.023$), respectively. The frequency of -857C allele in chronic HB group was 87.6%, significantly higher than those of the two groups ($\chi^2 = 17.953$, $P<0.001$). There is no significant difference in Hardy-Weinberg among the three groups ($\chi^2 = 3.54$, $P = 0.059$, Table 5).

The results of haplotype analysis are summarized in Table 6. The frequency of haplotype -238G/-857 C in asymptomatic carrier group was lower than that in the self-limited group ($P = 0.035$) and that of carrier group ($P = 0.04$). Frequency of haplotype -238G/-857T in carrier group was higher than that of chronic HB group ($P = 0.030$, Table 6).

Multivariate logistic regression analysis

Multivariate unconditional logistic regression model was

Table 4 TNF-238 polymorphism and allele frequencies in chronic HB, asymptomatic carrier and self-limited groups

Group	*n*	Genotype (%)					Alleles (%)[1]	
		GG	GA	AA	χ^2	*P*	G	A
Chronic HB group	433	402 (90.7)	41 (9.3)	0 (0.00)			845 (95.4)	41 (4.6)
Carrier group	208	187 (89.0)	23 (11.0)	0 (0.00)	0.464 (to patient)	0.496 (to patient)	397 (94.5)	23 (5.5)
Self-limited group	244	232 (95.1)	12 (4.9)	0 (0.00)	4.157 (to patient)	0.041 (to patient)	476 (97.5)	12 (2.5)
					5.776 (to carrier)	0.016 (to carrier)		

[1]$\chi^2 = 3.99$, $P = 0.046$. Hardy–Weinberg $\chi^2 = 0.155$, $P = 0.69$.

Table 5 TNF-857 polymorphism and allele frequencies in chronic HB, asymptomatic carrier and self-limited groups

Group	*n*	Genotype (%)					Alleles (%)[1]	
		CC	CT	TT	χ^2	*P*	C	T
Chronic HB	433	345 (79.7)	69 (15.9)	19 (4.4)			759 (87.6)	107 (12.4)
Carrier	208	134 (64.4)	59 (28.4)	15 (7.2)	17.358 (to patient)	<0.001 (to patient)	327 (78.6)	89 (21.4)
Self-limited	244	173 (70.9)	60 (24.6)	11 (4.5)	7.710 (to patient)	0.023 (to patient)	406 (83.2)	82 (16.8)
					2.728 (to carrier)	0.079 (to carrier)		

[1]$\chi^2 = 17.953$, $P<0.001$. Hardy-Weinberg $\chi^2 = 3.54$, $P = 0.059$.

Table 6 Frequencies of TNF-238/857 haplotype among chronic HB, carrier and self-limited groups

Number	Haplotype	Self-limited group (%)	Carrier group (%)	Chronic HB group (%)	*P* (1 to 2)	*P* (1 to 3)	*P* (2 to 3)
1	GC	0.8115	0.7297	0.8278	0.035	0.618	0.040
2	AC	0.0205	0.0554	0.0478	0.052	0.069	0.708
3	GT	0.1639	0.2148	0.1246	0.154	0.156	0.030
4	AT	0.0041	0.0002	0.0004	0.367	0.184	0.487

Table 7 Multivariate logistic regression analysis

Variable	Self-limited group to chronic HB group			Carrier group to chronic HB group			Self-limited group to carrier group		
	χ^2	*P*	OR	χ^2	*P*	OR	χ^2	*P*	OR
Intercept	11.05	0.0009	–	8.86	0.0029	–	11.43	0.0007	–
Sex (male = 1, female = 0)	46.74	0.0001	3.02	34.32	0.0001	3.67	0.6694	0.4133	1.18
Age (yr)	4.06	0.044	0.984	4.22	0.0399	0.903	11.41	0.0007	0.97
-238GA (GA = 1, GG = 0)	4.82	0.036	1.4	4.09	0.0427	1.927	8.91	0.0028	3.19
-857CC (CC = 1, TT+CT = 0)	8.54	0.0035	1.59	9.14	0.0001	2.41	0.664	0.415	1.19

used to analyze the association of the outcome of HBV infection with sex, age, TNF-α promoter polymorphisms. The results showed that, after confounding effects of gender and age were adjusted, TNF-α -238GA and -857CC were independently associated with chronic HB compared to self-limited group and asymptomatic carrier group. TNF-α -238GA was associated with asymptomatic carrier compared to self-limited group (Table 7).

DISCUSSION

HBV has eight different genotypes (A-H) according to the homogeneity of the viral sequence[11]. HBV genotypes have distinct geographical distribution. The results of several studies[12,13] indicated that HBV genotypes B, C, and mixed genotype are prevalent in China, and genotypes B and C are the major genotypes. The results of our study are in agreement with the studies conducted in other areas of China[12,13].

Some studies[13] indicated that there is a significant difference in HBV genotype distribution in different places of China. It was reported that the proportion of genotype C in northern cities is higher than that of southern cities of China[13]. In addition, infection with mixed genotypes has also been found in China.

We also found that there was no statistically significant difference in genotype distribution between the asymptomatic carrier group and chronic HB group, But another study[14] reported that the proportion of genotype C in the chronic HB group was higher than in the asymptomatic carrier group. The results are similar to another study[14].

Our findings suggest that both genotypes TNF-α -238GA and -857CC are positively associated with chronic HB. The frequency of -238GA genotype in self-limited group was significantly lower than that in the chronic HB group and asymptomatic carrier group, which is consistent with that in Caucasian[6] and Korean[15] population. The frequency of TNF-α -857CC in the chronic HB group was significantly higher than that in the self-limited group, which is consistent with another study[2]. TNF-α can suppress expression and replication of HBV. *In vitro* recombinant TNF-α inhibits HBV replication through a post-translational mechanism that accelerates the degradation of HBV messenger RNA[16]. Furthermore, HBV core promoter element is sensitive to TNF-α[17].

The results of multiple logistic regression analysis indicate that TNF-α -238GA and -857CC are independently associated with chronic HB, after adjustment for sex and age. Males seem more likely to develop chronic HB. The mechanism underlying the association remains unclear, but viral replication is sensitive to sex hormones[18].

In conclusion, HBV genotypes may play an important role in the outcome of HBV infection, and TNF-α promoter genetic polymorphisms may play an important role in the development of HBV infection.

REFERENCES

1 **Koziel MJ.** Cytokines in viral hepatitis. *Semin Liver Dis* 1999; **19**: 157-169

2 **Jung MC,** Pape GR. Immunology of hepatitis B infection. *Lancet Infect Dis* 2002; **2**: 43-50

3 **Koulentaki M,** Notas G, Petinaki E, Valatas V, Mouzas IA, Castanas E, Kouroumalis EA. Nitric oxide and pro-inflammatory cytokines in acute hepatitis B. *Eur J Intern Med* 2004; **15**: 35-38

4 **Jaber BL,** Rao M, Guo D, Balakrishnan VS, Perianayagam MC, Freeman RB, Pereira BJ. Cytokine gene promoter polymorphisms and mortality in acute renal failure. *Cytokine* 2004; **25**: 212-219

5 **Chu CJ,** Hussain M, Lok AS. Hepatitis B virus genotype B is associated with earlier HBeAg seroconversion compared with hepatitis B virus genotype C. *Gastroenterology* 2002; **122**: 1756-1762

6 **Hohler T,** Kruger A, Gerken G, Schneider PM, Meyer Z, Buschenefelde KH, Rittner C. A tumor necrosis factor-alpha(TNF-α) promoter polymorphism is associated with chronic hepatitis B infection. *Clin Exp Immunol* 1998; **111**: 579-582

7 **Soga Y,** Nishimura F, Ohyama H, Maeda H, Takashiba S, Murayama Y. Tumor necrosis factor-alpha gene (TNF-α) -1031/-863, -857 single-nucleotide polymorphisms (SNPs) are associated with severe adult periodontitis in Japanese. *J Clin Periodontol* 2003; **30**: 524-531

8 **Ma SL,** Tang NL, Lam LC, Chiu HF. Association between tumor necrosis factor-alpha promoter polymorphism and Alzheimer's disease. *Neurology* 2004; **62**: 307-309

9 **Naito H,** Hayashi S, Abe K. Rapid and specific genotyping system for hepatitis B virus corresponding to six major genotypes by PCR using type-specific primers. *J Clin Microbiol* 2001; **39**: 362-364

10 **Norder H,** Courouce AM, Magnius LO. Complete genomes, phylogenetic relatedness, and structural proteins of six strains of the hepatitis B virus, four of which represent two new genotypes. *Virology* 1994; **198**: 489-503

11 **Kato H,** Gish RG, Bzowej N, Newsom M, Sugauchi F, Tanaka Y, Kato T, Orito E, Usuda S, Ueda R, Miyakawa Y, Mizokami M. Eight genotypes (A-H) of hepatitis B virus infecting patients from San Francisco and their demographic, clinical, and virological characteristics. *J Med Virol* 2004; **73**: 516-521

12 **Xia G,** Nainan OV, Jia Z. Characterization and distribution of hepatitis B virus genotypes and subtypes in 4 prov-

inces of China. *Zhonghua Liuxingbingxue Zazhi* 2001; **22**: 348-351

13 **Xu J,** Wang QX, Fan CL, Jiang D, Li RB, Cong X, Fei R, Chen HS, Wei L, Wang Y. Comparison of hepatitis B virus serotypes among HBsAg positive hepatitis B patients in a northern and a southern city of China. *Zhonghua Shiyan He Linchuang Bingduxue Zazhi* 2003; **17**: 327-329

14 **Ge XM,** Li DY, Fang ZL, Huang GY, Jiang SQ, Pan HD, Du Y, Wang CY, Ding X, Masashi M. Distribution of hepatitis B virus genotypes and its clinical significance in Guangxi. *Zhonghua Shiyan He Linchuang Bingduxue Zazhi* 2003; **17**: 174-178

15 **Kim YJ,** Lee HS, Yoon JH, Kim CY, Park MH, Kim LH, Park BL, Shin HD. Association of TNF-α promoter polymorphisms with the clearance of hepatitis B virus infection. *Human Molecular Genetics* 2003; **12**: 2541-2546

16 **Tsui LV,** Guidotti LG, Ishikawa T, Chisari FV. Posttranscriptional clearance of hepatitis B virus RNA by cytotoxic T lymphocyte-activated hepatotytes. *Proc Natl Acad Sci USA* 1995; **92**: 12398-12402

17 **Romero R,** Lavine JE. Cytokine inhibition of the hepatitis B virus core promoter. *Hepatology* 1996; **23**: 17-23

18 **Almog Y,** Klein A, Adler R, Laub O, Tur-Kaspa R. Estrogen suppresses hepatitis B virus expression in male athymic mice transplanted with HBV transfected Hep G-2 cells. *Antiviral Res* 1992; **19**: 285-293

Science Editor Wang XL and Li WZ **Language Editor** Elsevier HK

PO Box 2345, Beijing 100023, China
www.wjgnet.com
wjg@wjgnet.com

ELSEVIER

World J Gastroenterol 2005;11(33):5218-5220
World Journal of Gastroenterology ISSN 1007-9327
© 2005 The WJG Press and Elsevier Inc. All rights reserved.

• *BRIEF REPORTS* •

Antitumor and synergistic effect of Chinese medicine "Bushen huayu jiedu recipe" and chemotherapy on transplanted animal hepatocarcinoma

Yong Cao, Qing-Hua Xia, Hua Meng, An-Pu Zhong

Yong Cao, Qing-Hua Xia, Hua Meng, An-Pu Zhong, Department of Traditional Chinese Medicine, Medical College, Jinan University, Guangzhou 510632, Guangdong Province, China
Supported by the Postdoctoral Science Foundation of China, No. [2001] 5
Correspondence to: Yong Cao, Associate Professor, Department of Traditional Chinese Medicine, Medical College, Jinan University, 601 West Huangpu Road, Guangzhou 510632, Guangdong Province, China. tcaoy@163.com
Telephone: +86-20-85223619 Fax: +86-20-85223619
Received: 2004-11-15 Accepted: 2004-12-09

Abstract

AIM: To investigate the antitumor and synergistic effect of Chinese medicine "Bushen huayu jiedu recipe" (recipe for invigorating the kidney, removing blood stasis and toxic substances) and chemotherapy on mice hepatocarcinoma.

METHODS: Bushen huayu jiedu recipe (BSHYJDR) consisting of Chinese Cassia Bark, Psoralea, Zedoary, Rhubarb, *etc.* is equal to 1.5 g/mL liquid of originated herbs after being decocted, filtered, and concentrated. Kunming mice, weighing 18-22 g, were injected with 0.2 mL ascitic hepatocarcinoma H_{22} containing 1×10^7 cells/mL into armpit of the right forelimb of mice. After 24 h, the mice were weighed and randomly divided into tumor-bearing model control group, cisplatin (DDP) group, BSHYJDR high dosage group, low dosage BSHYJDR group, DDP combined with high and low dosage BSHYJDR group, 10 mice in each group. DDP group received injection intraperitoneally (ip) at the dosage of 1 mg/kg (equal to 1/10 LD_{50}), once a day for 4 d. High and low dosage BSHYJDR groups received intragastric BSHYJDR at the dosages of 26.6 and 13.3 g/kg (20 and 10 times each of clinical adult dosage) respectively, while tumor-bearing model group received the equal volume of distilled water once a day for 10 d. On the 11th d, the mice were weighed and killed, then the tumor was dissected and weighed, the repression rate (RR) was calculated according to the mean weight of tumor (MWT).

RESULTS: Compared to the model group (MWT: 1.30±0.73), DDP group (MWT: 0.41±0.09, RR: 68.46%) had a significant difference in the inhibition of hepatocarcinoma H_{22} ($P<0.01$). High dosage BSHYJDR group (MWT: 0.69±0.29, RR: 46.92%) also had a significant difference in inhibition ($P<0.05$), while no difference was found in low dosage BSHYJDR group (MWT: 0.85±0.34, RR: 34.62%) ($P>0.05$). When DDP was combined with high dosage BSHYJDR (MWT: 0.29±0.17, RR: 77.69%) and low dosage BSHYJDR (MWT: 0.38±0.21, RR: 70.77%) respectively, we could see improvement of the inhibition effect of DDP on transplanted hepatocarcinoma H_{22}. DDP combined with high dosage BSHYJDR had a significant difference ($P<0.001$) compared to DDP, while DDP combined with low dosage BSHYJDR only had a little improvement that is not remarkable.

CONCLUSION: Chinese medicine BSHYJDR in combination with chemotherapy can inhibit transplanted hepatocarcinoma in mice.

© 2005 The WJG Press and Elsevier Inc. All rights reserved.

Key words: Bushen huayu jiedu recipe; Mice hepatocarcinoma H_{22}; Antitumor effects; Synergy

Cao Y, Xia QH, Meng H, Zhong AP. Antitumor and synergistic effect of Chinese medicine "Bushen huayu jiedu recipe" and chemotherapy on transplanted animal hepatocarcinoma. *World J Gastroenterol* 2005; 11(33): 5218-5220
http://www.wjgnet.com/1007-9327/11/5218.asp

INTRODUCTION

Bushen huayu jiedu recipe (BSHYJDR) is used in treatment of many kinds of cancer, especially digestive tract and respiratory system cancer. We have discovered that BSHYJDR could obviously improve clinical symptoms, quality of life and prolong the life span of cancer patients. BSHYJDR could restrain transplanted lung cancer cells, and has a synergistic effect, when combined with chemotherapy. After animals received intragastric BSHYJDR, it could inhibit the expression of drug-resistance gene, increase the level of DDP in drug-resistant cells, and regulate the activity of calcium channel of resistant cells. Meanwhile, BSHYJDR could also restrain transplanted Lewis lung cancer[1,2]. In order to investigate whether BSHYJDR in combination with chemotherapy could synergistically inhibit hepatocarcinoma, we selected transplanted mice hepatocarcinoma H_{22}, and investigated the inhibitory effect of BSHYJDR on transplanted hepatocarcinoma.

MATERIALS AND METHODS

Drugs

To prepare BSHYJDR decoction, Chinese Cassia Bark, Psoralea Fruit, Zedoary, Rhubarb, etc., were put into a container, cold water of about 5-7 times as the herbs was added. After being soaked for 1-2 h and boiled for 30 min, the decoction was filtered. Once again, water of about 3-5

times as the herbs was added, decocted and boiled for 20 min before the second filtration. The two decoctions were mixed. Then the mixture was concentrated into medical fluid (equals 1.5 g/mL originate herbs in water bath). The fluid was poured into a sterilized vial after cooling and stored at 4 ℃ for use. DDP was produced by Qilu Pharmacy Factory in Jinan, Shandong Province, China.

Animals

Kunming mice were supplied by Experimental Animal Center of Shandong University of traditional Chinese medicine.

Tumor strains

Hepatocarcinoma H_{22} was provided by Tumor Pharmacology Laboratory of Tumor Prevention and Treatment Center in Shandong University of traditional Chinese medicine.

Main instruments

Ultra-clean worktable was from Suzhou Yuhua Equipment Co. Electronic balance (Type FA2004) was purchased from Shanghai Balance Instrument Factory.

Inhibition of BSHYJDR on mice hepatocarcinoma H_{22}

Experimental animal model and grouping Ascites was drawn from hepatocarcinoma mice H_{22} under aseptic condition, and diluted in normal saline at 1:4. Concentration of tumor cells was 1×10^7 cells/mL. Then 40 healthy Kunming mice weighing 18-22 g were selected, 0.2 mL tumor cells was injected into the armpit of right forelimb of each mouse. After 24 h, they were weighed and randomly divided into model control group, high dosage BSHYJDR group, and low dosage BSHYJDR group and DDP group, 10 mice in each group.

Drug dosages and methods DDP group received intraperitoneal injection of DDP at the dosage of 1 mg/kg (equals to 1/10 LD50), once a day for 4 d. High and low dosage BSHYJDR groups received intragastric BSHYJDR decoction at the dosages of 26.6 and 13.3 g/kg (20 and 10 times each of clinical adult dosage) respectively, while tumor-bearing model group received the same dosage of distilled water, once a day for 10 d. On the 11th d, all the mice were weighed and killed, and then the tumor was dissected and weighed. The repression rate (RR) was calculated, according to the mean weight of tumor (MWT).

Synergistic effect of BSHYJDR and DDP on mice hepatocarcinoma H_{22}

Experimental animals model and grouping The mice were divided into tumor-bearing model control group, DDP group, DDP combined with high dosage BSHYJDR group, DDP combined with low dosage BSHYJDR group, 10 mice in each group.

Drug dosages and methods After grouping, DDP group received intraperitoneal injection DDP (1 mg/kg). DDP combined with high dosage BSHYJDR group received intraperitoneal injection of DDP (1 mg/kg) and intragastric BSHYJDR (26.6 g/kg). DDP combined with low dosage BSHYJDR group received intraperitoneal injection of DDP (1 mg/kg) and intragastric BSHYJDR (13.3 g/kg). Model control group received an equal volume of distilled water. DDP was injected once a day for 4 d, while Chinese medicine and distilled water were lavaged once a day for 10 d. Then on the 11th d, all the mice were weighed and killed, and then the tumor was dissected and weighed. The RR was calculated according to the MWT and the formula of calculating the RR. RR of the tumor (%) = tumor weight of the control group-tumor weight of the experimental group/tumor weight of the control group×100%.

Statistical analysis

The data were expressed as mean±SD. Student's *t*-test was used to assess the significant differences among groups. All statistical analyses were performed with the PEMS statistical software package.

RESULTS

Inhibition of BSHYJDR on mice hepatocarcinoma H_{22} (Table 1)

Table 1 shows that compared to the control group, significant inhibitory effect of BSHYJDR was found in DDP group ($P<0.01$) and high dosage BSHYJDR group ($P<0.05$). But no significant difference of inhibitory effect was found in low dosage BSHYJDR group ($P>0.05$). The inhibitory effect in high and low dosage BSHYJDR groups was lower than that in DDP group ($P<0.01$).

Table 1 Inhibition of BSHYJDR on hepatocarcinoma H_{22}

Group	Dose (mg/kg)	Mice (*n*) (before/after)	Tumor weight (g) (mean±SD)	RR (%)
Model	–	10/10	1.30±0.73	–
DDP	1×4	10/10	0.41±0.09[b]	68.46
BSHYJDR	26 600×10	10/10	0.69±0.29[a,d]	46.92
BSHYJDR	13 300×10	10/10	0.85±0.34[d]	34.62

[a]$P<0.05$, [b]$P<0.01$ *vs* control group, [d]$P<0.01$ *vs* DDP group.

Synergistic effect of BSHYJDR and DDP on mice hepatocarcinoma H_{22} (Table 2)

Table 2 shows that compared to control group, DDP exhibited significant inhibition on H_{22} ($P<0.01$). Both high and low dosage BSHYJDR could significantly improve the inhibition of DDP when used in combination with DDP ($P<0.001$). But low dosage BSHYJDR had no such effects compared to DDP ($P<0.05$).

Table 2 Synergistic effect of BSHYJDR and DDP on hepatocarcinoma H_{22}

Group	Doses (mg/kg)	Mice (*n*) (before/after)	Tumor weight (g) (mean±SD)	RR (%)
Model	–	10/10	1.30±0.73	–
DDP	1×4	10/10	0.41±0.09[b]	68.46
DDP+BSHYJDR	1×4+26 600×10	10/10	0.29±0.17[d]	77.69
DDP+BSHYJDR	1×4+13 300×10	10/10	0.38±0.21[b]	70.77

[b]$P<0.01$, [d]$P<0.001$ *vs* control group.

DISCUSSION

Hepatocarcinoma is one of the malignant tumors, and has high death rate in the world. Most patients in the middle or

late period are diagnosed of having the tumor. Therefore, it is very important to find a new therapy with Chinese medicine for middle and late hepatocarcinoma.

The present study has indicated that extractions from some herbs can restrain hepatocarcinoma. Alkaloids have cellulotoxic effect on hepatocarcinoma cells[3]. The herbal extractions of flavonoid and arsenic trioxide can not only restrain proliferation of hepatocarcinoma cells, but also induce apoptosis of hepatocarcinoma cells[4,5]. It was reported that Chinese medicine can induce cytodifferentiation of hepatocarcinoma[6].

Toxic side effect of chemotherapy is an important influencing factor in treatment of hepatocarcinoma. Chinese medicine combined with chemotherapy can reduce the toxic side effects and improve inhibition of chemotherapy on hepatocarcinoma cells, reduce the metastasis, enhance the quality of life and prolong the life span[7]. The use of Xuefu Zhuyu Tang (recipe for removing blood stasis in the vessels) combined with chemotherapy can enhance the effect of chemotherapy and prolong the life span of mice bearing hepatocarcinoma[8].

According to the theory of traditional Chinese medicine, the occurrence of tumor is closely related with stagnation of qi and blood and combination of blood stasis and poison, which are caused by deficiency of the kidney and invasion of poisonous pathogenic factors. BSHYJDR can reinforce the kidney and support yang, remove blood stasis and toxic substances.

It has been proved that cinnamic acid in Cassia Bark and its derivatives could induce apoptosis of cancer cells, promote the breakage of DNA, inhibit the proliferation of A549 cells in adenocarcinoma and promote its differentiation[9,10]. The psoralen in psoralea fruit has cellulotoxic effects on hepatocarcinoma cells, promotes the adherence and excursion of melanoma cells *in vitro*[11,12] by preventing cancer cells from metastasis. The extractions of Zedoary could improve immunogenicity of tumor cells and enhance the killer effect of the cells. Moreover, Zedoary could strengthen the antitumor effect of tumor necrosis factor. Zedoary preparation is mainly used to treat hepatocarcinoma. The main components of Rhubarb are Rhubarb substance and Rhubarb acid. Rhubarb substance could restrain proliferation of hepatocarcinoma cells, induce apoptosis, and promote gene expression of P53 and P21[13-16]. Rhubarb acid could restrain cell proliferation of various tumors, such as mastocarcinoma, lung cancer, hepatocarcinoma and colonocarcinoma, and has synergistic effects when used in combination with mutamycin. It could inhibit synthesis of DNA, promote apoptosis of cancer cells. It also has been found that the inhibitory effect of repression of Rhubarb on cancer cells is closely related with cell signal transduction[17].

Our research showed that BSHYJDR decoction could significantly restrain transplanted hepatocarcinoma H_{22} in mice, enhance the effect of DDP on transplanted hepatocarcinoma H_{22}, indicating that BSHYJDR restrains tumor and has synergistic effects when used in combination with chemotherapy. But the mechanisms still remain unknown and need further studies.

ACKNOWLEDGMENTS

The authors thank Professors Li-Ying Xia, and Guang-Juan Zheng, Dr. Dan Zhang and lecturer Jing Zhang, Tumor Pharmacology Laboratory in Shandong University of Traditional Chinese Medicine for their support and direction in the study.

REFERENCES

1 **Cao Y,** Zhang D, Zheng GJ, Yang Y, Zhang J. Study on drug resistance reversion and mechanism of Bushen Huyu Jiedu Recipe in drug resistance lung cancer cells. *Shandong Zhongyi Zazhi* 2004; **2**: 100-103
2 **Cao Y,** Zhang D, Zheng GJ, Zhang J. Study on effect of Bushen Huayu Jiedu Formula in mice lewis lung cancer. *Zhonghua Shiyong Zhongxiyi Zazhi* 2003; **11**: 1947-1949
3 **Hsieh TJ,** Chang FR, Chia YC, Chen CY, Lin HC, Chiu HF, Wu YC. The alkaloids of Artabotrys uncinatus. *J Nat Prod* 2001; **64**: 1157-1161
4 **Siu KP,** Chan JY, Fung KP. Effect of arsenic trioxide on human hepatocellular carcinoma HepG2 cells: inhibition of proliferation and induction of apoptosis. *Life Sci* 2002; **71**: 275-285
5 **Chang WH,** Chen CH, Lu FJ. Different effects of baicalein, baicalin and wogonin on mitochondrial function, glutathione content and cell cycle progression in human hepatoma cell lines. *Planta Med* 2002; **68**: 128-132
6 **Rui-Chuan C,** Jin-Hua S, Gao-Liang O, Ke-Xia C, Jin-Quan L, Xiao-Guang X. Induction of differentiation in human hepatocarcinoma cells by isoverbascoside. *Planta Med* 2002; **68**: 370-372
7 **Meng ZQ,** Xu YY, Liu LM, Song MZ, Huang WX. Clinical evaluation of integration of transcatheter arterial chemoembolization and traditional Chinese medicine in treating metastatic liver cancer. *Zhongxiyi Jiehe Xuebao* 2003; **3**: 187-188
8 **You JS,** Huang HF, Hau DM. Effects of Xuefu Zhuyu Tang and mitomycin C on liver tumors in mice. *Chang Gung Med J* 2003; **26**: 417-424
9 **Akao Y,** Maruyama H, Matsumoto K, Ohguchi K, Nishizawa K, Sakamoto T, Araki Y, Mishima S, Nozawa Y. Cell growth inhibitory effect of cinnamic acid derivatives from propolis on human tumor cell lines. *Biol Pharm Bull* 2003; **26**: 1057-1059
10 **Jin G,** Zhang T, Wang T, Yang LP. Inhibition of alpha-interferon and cinnamic acid on proliferation of human lung cancer cell. *Aizheng* 2002; **21**: 860-862
11 **Cho H,** Jun JY, Song EK, Kang KH, Baek HY, Ko YS, Kim YC. Bakuchiol: a hepatoprotective compound of Psoralea corylifolia on tacrine-induced cytotoxicity in Hep G2 cells. *Planta Med* 2001; **67**: 750-751
12 **Mou KH,** Zhang XQ, Yu B, Zhang ZL, Feng J. Promoting of melanocyte adhesion and migration by Malytea Scurfpea fruit *in vitro*. *Methods Find Exp Clin Pharmacol* 2004; **26**: 167-170
13 **Shieh DE,** Chen YY, Yen MH, Chiang LC, Lin CC. Emodin-induced apoptosis through p53-dependent pathway in human hepatoma cells. *Life Sci* 2004; **74**: 2279-2290
14 **Kuo PL,** Lin TC, Lin CC. The antiproliferative activity of aloe-emodin is through p53-dependent and p21-dependent apoptotic pathway in human hepatoma cell lines. *Life Scid* 2002; **71**: 1879-1892
15 **Jing X,** Ueki N, Cheng J, Imanishi H, Hada T. Induction of apoptosis in hepatocellular carcinoma cell lines by emodin. *Jpn J Cancer Res* 2002; **93**: 874-882
16 **Liu JB,** Gao XG, Lian T, Zhao AZ, Li KZ. Apoptosis of human hepatoma HepG2 cells induced by emodin *in vitro*. *Aizheng* 2003; **22**: 1280-1283
17 **Cichewicz RH,** Zhang Y, Seeram NP, Nair MG. Inhibition of human tumor cell proliferation by novel anthraquinones from daylilies. *Life Sci* 2004; **74**: 1791-1799

Science Editor Wang XL and Li WZ **Language Editor** Elsevier HK

PO Box 2345, Beijing 100023, China
www.wjgnet.com
wjg@wjgnet.com

ELSEVIER

World J Gastroenterol 2005;11(33):5221-5225
World Journal of Gastroenterology ISSN 1007-9327
© 2005 The WJG Press and Elsevier Inc. All rights reserved.

• *BRIEF REPORTS* •

Evaluation of HCPTd_1, d_{14}-double passaged intervening chemotherapy protocol for hepatocellular carcinoma

Zhi-Jian Yu, Jia-Wei Yu, Wei Cai, Hong-Xin Yuan, Xiao-Yan Li, Ye Yuan, Jian-Ping Chen, Xiao-Yin Wu, Deng-Fu Yao

Zhi-Jian Yu, Jia-Wei Yu, Wei Cai, Hong-Xin Yuan, Xiao-Yan Li, Ye Yuan, Center of Oncology, Affiliated Hospital of Nantong University, Nantong 226001, Jiangsu Province, China
Jian-Ping Chen, Xiao-Yin Wu, Department of Ultrasonography, Affiliated Hospital of Nantong University, Nantong 226001, Jiangsu Province, China
Deng-Fu Yao, Research Center of Clinical Molecular Biology, Affiliated Hospital of Nantong University, Nantong 226001, Jiangsu Province, China
Correspondence to: Professor Zhi-Jian Yu, MD, Center of Oncology, Affiliated Hospital of Nantong University, 20 Xisi Road, Nantong 226001, Jiangsu Province, China. yaodf@ahnmc.com
Telephone: +86-513-5052541 Fax: +86-513-5052523
Received: 2004-08-30 Accepted: 2004-12-08

Abstract

AIM: To establish a kind of standardization of the clinical chemotherapeutic prototypes for unresectable hepatocellular carcinomas (HCC).

METHODS: 10-Hydroxycamptothecin (HCPT) was applied through transcatheter arterial embolization (TAE) to HCC patients who were categorized into three groups: (1) test group: treatment with HCPT twice (HCPT d1 and 14) through TAE and portal venous embolization. (2) Control I: treatment with anticancer drugs without HCPT. (3) Control II: treatment with HCPT as a major component in anticancer drugs once (HCPT d1). A set of comparisons between test groups and control I and II groups were performed before and after the treatment to study the effectiveness of each treatment, in terms of tumor volumes, dynamic variations in serum alpha-fetoprotein (AFP), gamma-glutamyl transferase hepatoma-specific band (GGT-II), patient survival and adverse events.

RESULTS: The general effectiveness rate of the test group reached 62.1% (72/116), remarkably higher than that of control I (32.1%, 40/124) and control II (54.7%, 47/56), (P<0.01 and P<0.05, respectively). Especially, the reduction rate or disappearance of the portal vein tumor emboli was as high as 88.4% (61/69) in the test group, in contrast with 13.9% (10/72) in control I and 35.9% (18/51) in control II (P<0.01 and P<0.01, respectively). After treatment, AFP decreased or turned to negative levels at 52.3% (34/65) in control I, 67.3% (35/52) in control II, and 96.8% (60/62) in the test group. Also GGT-II declined or became negative at 37.8% (28/74) in control I, 69.5% (57/82) in control II, and 94.7% (89/94) in test group (P<0.01 and P<0.05, respectively).

CONCLUSION: We have designed a good protocol (test group) to treat HCC with excellent advantages of high efficiency, low cost, low toxicity and low adverse events and easy application. It could be recommended as one of the standardizations for HCC treatment in clinical practice.

© 2005 The WJG Press and Elsevier Inc. All rights reserved.

Key words: Hydroxycamptothecin; Transcatheter arterial embolization; Portal venous embolization; Hepatocellular carcinoma

Yu ZJ, Yu JW, Cai W, Yuan HX, Li XY, Yuan Y, Chen JP, Wu XY, Yao DF. Evaluation of HCPTd_1, d_{14}-double passaged intervening chemotherapy protocol for hepatocellular carcinoma. *World J Gastroenterol* 2005; 11(33): 5221-5225
http://www.wjgnet.com/1007-9327/11/5221.asp

INTRODUCTION

Hepatocellular carcinoma (HCC) is one of the most common and rapidly spreading fatal malignancies worldwide, and has been ranked as the 2nd cancer killer in China since the 1990s, particularly in the southeastern provinces, including the inshore area of the Yangtze river[1-3]. Major risk factors for HCC in these areas are exposure to aflatoxin B1 and infection by hepatitis viruses[4,5]. HCC prognosis is poor and early detection is of utmost importance[6]. Treatment options are severely limited by the frequent presence of metastases. Recent studies of DNA isomerase inhibitors for clinical use have made some progress[7,8]. The direct injection of 10-hydroxycamptothecin (HCPT) into tumor vessels in primary hepatic carcinoma has proved promising due to its high efficiency and low toxicity[9-11]. However, treatment protocols differ greatly in drug-application routes, methods, doses and final results[12-14].

Since October 2000, we have used HCPT as a major component in chemotherapy in combination with 5-fluorouracil (5-FU) and cisplatin (CDDP). Drugs were administered through transcatheter arterial embolization (TAE) and subsequent portal venous embolization (PVE) to treat hepatic cancer on d 1 and 14, respectively. We compared this method (called test group) with chemotherapy protocols with and without HCPT through TAE d1 and reported here the excellent results.

MATERIALS AND METHODS

Study populations

We evaluated 326 HCC patients treated at Affiliated Hospital

of Nantong University, China. Patients were divided into three groups: test group, control I, and control II. All patients were confirmed by alpha-fetoprotein (AFP), gamma-glutamyl transferase hepatoma-specific band (GGT-II) serological examination[7], and by ultrasonography (US), computed tomography (CT) or magnetic resonance imaging, partly by pathological checking. The diagnosis of HCC was based on the criteria stipulated in 2001 Chinese National Conference on HCC[15]. The test group consisted of 116 HCC patients (91 males and 25 females) aged 30-68 years with an average age of 46.2 years. Among them, 12 were in stage I, 86 in stage II, and 18 in stage III, respectively; and the liver function was categorized according to the Child-Pugh scale with 46 cases of level A, 61 cases of level B, and 9 cases of level C, respectively.

Control I had 124 HCC patients, who received chemotherapeutic agents such as 5-FU, doxorubicin (ADM), CDDP without HCPT through TAE and were hospitalized at the same time as test group or earlier. Control II had 86 patients, who received chemotherapeutic agents HCPT, 5-FU, CDDP through TAE only on d 1.

HCC patients in the three groups had similar general conditions. Actually, mostly patients were at mid-late stage, often some of them already had metastasized cancerous emboli in portal vein or hepatic vein, and some even had remote lymph nodes affected according to the UICC criteria, most HCC belonged to $T_{3-4}N_{0-1}M_{0-1}$.

Treatment drugs

HCPT was purchased from Hubei Lishizheng Pharmaceutical Co., Ltd. HCPT 40-50 mg, 5-FU 750-1 000 mg, CDDP 60-80 mg, ADM 40-50 mg, lipiodol (LP) 10-30 mL, and gelatin sponge 1-2 pieces were used for treatment (one dose).

Therapeutical methods

Arterial embolization was performed according to Seldinger's procedure via the femoral artery. After the catheter was sent into the hepatic artery and right or left hepatic artery, arteriography was carried out for further confirmation of the characteristics, location and size of the tumor. The types and doses of drugs varied with the Child-Pugh grades of hepatic functional reserve, clinical stages and the number, size and extent of tumors. Usually a combination of full dose of 5-FU, 4/5 of HCTP, and 2/3 of CDDP was infused to attack the tumor. Then 1/5 dose of HCPT, and 1/3 of CDDP were mixed with LP or gelfoam to embolize the blood-providing arteries.

We selected a puncture site using the portal vein branch which supplied blood for tumor foci, or proximal to cancerous emboli. The drugs used were the same but half of the dose 3-6 mL of LP was used. The operation was performed on d 14 after TAE.

Blood and urine analysis were routinely checked twice a week, and the liver function and serum tumor markers (AFP, GGT-II) were determined once in every 2 wk. US and CT were also checked on d 21-28, to observe LP precipitates and variations in volume of tumor foci.

Statistical analysis

Differences between groups were assessed by the χ^2 test. The survival time was calculated according to the Lifespan method. $P<0.05$ was considered to be significant.

RESULTS

The therapeutic effects were evaluated with regard to tumor-emboli volume alteration, changes of serum tumor markers (AFP, GGT-II) changes and survival time, based on the Criteria of Diagnosis and Treatment of HCC proposed at Chinese National Collaborative Cancer Research Group[15].

Tumor-emboli volume alteration

The overall effective rate of the test group was 62.1% (72/116), much higher than that of control I (TAE without HCPT, 32.1%, $P<0.01$) and control II (TAE with HCPT d1, 54.7%, $P<0.05$) as shown in Table 1. Six patients had survived for over 3-6 years, repeated follow-up with US and CT showed no occupied lesions. More importantly, color Doppler reported high frequency of arteries or veins around tumors with a resistance index >0.50, mostly more than 0.60-0.80 in 59 of 66 partial response patients. After treatment with TAE and PVE, 42 cases reported disappearance of the high blood flow frequency, and the rest showed remarkable reduction of blood supply. Fifteen patients acquired complete removal of tumor by surgery, among them six were reported as having pathologically complete necrosis in the tumors with large amount of lymphocytes encircling and infiltrating around the tumors.

In test group, the reduction rate of cancerous emboli in portal vein reached 88.4%, which was much higher than that in control I (13.9%, 10/72) or control II (35.3%, 18/51) with statistically significant difference ($P<0.01$). In the eight cases in which the main portal vein was affected, the tumor emboli showed no change or even progress, so the portal vein branch I or II in the other site had to be chosen for infusion of chemotherapeutic agents.

Dynamic changes of tumor markers

In test group, 62 cases showed AFP>400 ng/mL, with 53.4% positive. After treatment, the concentration of serum AFP decreased in 60 cases, accounting for 96.8%, which was much higher than that in control I (52.3%, 34/65) and control II

Table 1 Tumor-emboli volume after treatment

	Tumor volume Cases	CR	PR	NC	PD	Cases	Dis	Red	Un-ch	Prog
		Portal vein emboli								
Test	116	6	66	43	1	69	8	53	6	2
Control I	124	1	39	76	8	72	1	9	38	24
Control II	86	1	47	36	2	51	2	16	21	12

CR: complete response; PR: partial response; NC: no change; Dis: disappear; Red: reduction; PD: progressive disease; Un-ch: unchanged; Prog: progression.

(67.3%, 35/52) with significant difference ($P<0.05$). AFP was termed negative in 25.8% (16/62) of test group, in 1.5% (1/65) of control I, and in 9.6% (5/52) of control II, respectively. Significant difference ($P<0.01$) was found between test group and control groups.

The number of GGT-II positive cases in test group was 94, accounting for 81.0%. After treatment, 89 cases turned negative or its concentration decreased, accounting for 94.7%, much higher than that in control I (37.8%, 28/74) and control II (69.5%, 57/82) with striking differences ($P<0.01$ and $P<0.05$), respectively (Table 2).

Survival time

The survival time was calculated according to the Lifespan method. The survival rates of 1, 2 and 3 years in test group were 94.6%, 65.9% and 39.1% respectively, which were significantly different from those in control I (65.1%, 36.3%, and 20.5%, respectively) and control II (80.6%, 52.4%, and 31.5%), respectively ($P<0.05$).

Adverse events

Almost all patients had nausea, vomiting, fever and hepatic pain to some extent after TAE treatment, i.e., "post embolization syndrome". Fever was relatively higher and lasted longer in groups with HCPT as a chemotherapeutic agent. In all three groups, digestive responses such as nausea and vomiting were slight and transient. Hepatic pain varied with the embolization state and the amount of LP and gelfoam used in the operation. Generally, in control I (without HCPT), the patient's temperature would rise to 39 ℃ 1 or 2 d after TAE, began to decrease on d 3, and returned to normal on d 5-7. In the group with HCPT, the temperature would rise to 39 ℃, decrease on d 4. Sometimes, it took 2 wk for the patients to recover.

The adverse events after PVE on d 14 were slight. Only a few cases reported a little bloating pain in the operated area. Nausea and vomiting were seldom reported. Fever was moderate and lasted shorter than 1 wk. No serious complications such as pneumothorax, and bleeding in the abdominal cavity were found.

Regular check of blood and urine routine showed that only nine cases in the test group had slight decrease in the WBC or platelet counting, and no bleeding was found. In control I and control II, 7 and 11 cases respectively showed slight decrease of WBC and platelet count. Statistical analysis showed no difference among the three groups ($P>0.05$).

DISCUSSION

HCPT has been in use for more than 20 years. Recently, the American FDA has approved two drugs, irinotecan and topotecan, which are HCPT analogs with similar molecular structure. Cellular and molecular biology has proven that this class of drugs belongs to DNA topoisomerase I inhibitors, which have strong anti-cancer activities, and wide-spread antagonizing spectrum, low resistance, low toxicity and the ability to induce differentiation of tumor cells and apoptosis[16,17]. The combined use of this drug with other kinds of drugs may enhance efficacy[18-20]. It is the common interest of many basic and clinical scientists to know how to reasonably standardize the application and maximize the efficacy of the drugs[21-23]. Therefore, international standardization remains a common focus. Based on the treatment of 326 cases of HCC patients with or without HCPT in our hospital, we systematically studied the application of this drug, and proposed our own standardized protocol.

In vitro drug sensitivity tests of tumor cell line showed that at low dose, HCPT played double roles in human liver carcinoma cell lines (HepG2, Bel-7402, and Bel-7404): inducing differentiation and inhibiting cell growth slightly. The greater the dose, the stronger the inhibitory action was, and the effects became stronger with time[9].

For the unresectable hepatic carcinoma patients who had wide ranges of foci together with high rates of portal vein emboli[24-26], we adopted double-passaged intervening chemotherapy with HCPT in combination with other drugs for treatment[27-29]. We emphasized three aspects in the treatment: drug dose, treatment time and continuous treatment. For drug applying routes, we utilized both artery and portal vein for tumors. Under the guidance of digital subtraction angiography of tumor and US, the needle was directed into supplying artery and veins, exerting high dose for close attack on cancerous area, followed by chemical embolization to keep the drug-LP mixture in the suffered area for a longer time.

The drug action period is no longer than several hours or several days, but lasting for weeks or months[30]. This method keeps the local drug concentration high, hundred times more than that by systemic intravenous drip[12]. It has been reported that after tumor arteries were blocked through TAE, portal vein branches increased remarkably[31]. Therefore, to perform PVE, 2 wk after TAE not only accorded with blood dynamics but also increased drug administration frequency. And at the same time, it struck an attack with high drug dose on portal vein cancerous emboli. Drugs accumulated at low concentration in normal tissue areas or organs. It has been reported that HCPT is not affected by multi-drug resistance protein and multi-drug resistance related proteins, therefore, it seldom has drug resistance. With the development of diagnostic techniques

Table 2 Hepatic cancerous marker alterations before and after treatment

	Hepatic cancerous marker							
	AFP				GGT-II			
	P	N	D	I	P	N	D	I
Test	62	16	44	2	94	29	60	5
Control I	65	1	33	31	74	6	22	46
Control II	52	5	30	17	82	8	49	25

P: positive; N: negative; D: decrease; I: increase.

and agents, super-selection ability of drugs greatly enhanced. It is a common practice in clinic that the catheter head is directed to the closest area of tumor artery to achieve segment embolization, thus greatly enhancing effectiveness. Some patients were able to achieve partial regression or even complete regression, known as "chemical resection". In our test group, PR+complete response (CR) reached 62.1%, among them six were CR, with portal vein cancerous emboli disappearance or reduction rate of 88.4%. In eight cases, cancerous emboli disappeared completely. Such a high efficacy was probably related to the above-mentioned pharmacology (our HCPT protocol in d 1 and 14) and methodology (by TAE and PVE)[32]. The earliest and most frequent passages for hepatic carcinoma metastasis are portal veins. Therefore, treatment through/on portal venous emboli is the key step to control its metastasis across the liver.

Pharmacological study indicated that the effectiveness of application of topoisomerase I and II inhibitors rely on the sequence of drug application. Subsequent administration of topoisomerase I and II inhibitors exerted co-operative effect; while co-administration of them antagonized each other[9]. The method of TAE or PVE is a way to apply drugs to tumor feeding vessels (veins or arteries); therefore, here we considered to use combined application of HCPT (topoisomerase I inhibitor) as a major component in the chemotherapeutic agents with 5-FU and CDDP, which are highly liver-specific drugs and act during S phase and S, G_1 or G_2/M phase respectively. HCPT exerted its action on DNA topoisomerase inhibitor I to directly suppress the DNA and RNA synthesis, and induced sister chromatid exchanges, distortions and breaks, so that it selectively killed S phase cells and induced G_2 arrest. In addition, both HCPT and CDDP can induce apoptosis. Drug dose and concentration, infusing speed, and emboli-forming rate for HCC patients were most important in all detailed manipulations based on the above-mentioned pharmacological features[33]. During 5-FU full dose attack, two major points should be emphasized: injection time and injection route. When 5-FU concentration is more than effective concentration in the blood, higher dose would only increase its toxicity, while elongation of injection time can remarkably enhance the effectiveness. Therefore, it is better to slow down the injection time, usually to longer than 30-40 min.

The route was dependent upon the tumor location or cancer emboli location[28]. For example, if tumor was located in the right liver lobe, then the passage route would be: (1) superior mesentery artery→superior mesentery vein→right portal vein→tumor location; (2) common hepatic artery→right hepatic artery→tumor location. If tumor was located in the left lobe of the liver, then pass through: (1) celiac trunk→splenic artery→splenic vein→left portal vein→tumor location; (2) common hepatic artery→left hepatic artery→tumor location. Since the hepatic artery provides blood to tumor center, while the portal vein provides blood to tumor surroundings, our protocol not only the whole tumor (center and surrounding) made double attacks on through arteries and veins, but also elongated the drug action time. On d 14, through PVE, the tumor and the cancerous emboli would receive the 3rd attack, which greatly enhanced local drug concentration and drug-acting time.

HCPT was marketed and used widely in 1970s; the number of patients receiving HCPT had accumulated to more than a thousand[11,14]. However, due to various reasons no formal phase I and II pharmacodynamic studies have been carried out.

We report here the so-called HCPTd_1, d_{14}-TAE, PVE double passaged tumor intervening chemotherapy for hepatic carcinoma. The local concentration of HCPT reached as high as 40-50 mg in hepatic artery +20-25 mg in portal vein, without observing dose-limiting toxicities like drastic bone marrow inhibition and diarrhea. There was a slight decrease in WBC and platelet counting in nine cases. No dramatic hematuria, skin rashes, but only self-limiting tumor necrotic fever and transient digestive response were observed. For those who acquired chances to be operated on, there were widespread necroses around tumor and large amount of lymphocyte infiltration[34]. Our protocol exhibited high efficiency and low toxicity. HCPT does not induce drug resistance. It has anti-infection activity and the ability to increase body immunity. It is inexpensive and convenient to use. Thereby, we recommend the protocol as one of the standardizations in treating liver cancer with HCPT.

ACKNOWLEDGMENTS

We would like to express our sincere appreciation to Professor Sheng-Long Ye of the Liver Cancer Institute of Zhongshan Hospital, Fudan University for his guidance and help. We also thank Dr. Li Xu of Nantong University.

REFERENCES

1 **Pisani P,** Parkin DM, Bray F, Ferlay J. Estimates of the world-wide mortality from 25 cancers in 1990. *Int J Cancer* 1999; **83**: 18-29
2 **Thorgeirsson SS,** Grisham JW. Molecular pathogenesis of human hepatocellular carcinoma. *Nat Genet* 2002; **31**: 339-346
3 **Akriviadis EA,** Llovet JM, Efremidis SC, Shouval D, Canelo R, Ringes B, Meyers WC. Hepatocellualr carcinoma. *Br J Surg* 1998; **85**: 1319-1331
4 **Tang ZY.** Hepatocellular carcinoma-cause, treatment and metastasis. *World J Gastroenterol* 2001; **7**: 445-454
5 **Peto J.** Cancer epidemiology in the last century and the next decade. *Nature* 2001; **411**: 390-395
6 **Yao DF,** Jiang DR, Huang ZW, Lu JX, Tao QY, Yu ZJ, Meng XY. Abnormal expression of hepatoma specific γ-glutamyl transferase and alteration of γ-glutamyl transferase gene methylation status in patients with hepatocellular carcinoma. *Cancer* 2000; **88**: 761-769
7 **Hsiang YH,** Liu LF. Identification of mammalian DNA topoisomerase I as an intracellular target of the anticancer drug camptothecin. *Cancer Res* 1988; **48**: 1722-1726
8 **Zhang R,** Li Y, Cai Q, Liu T, Sun H, Chambless B. Preclinical Pharmacology of the natural product anticancer agent 10–hydroxycamptothecin, an inhibitor of topoisomerase I. *Cancer Chemother Pharmacol* 1998; **41**: 257-267
9 **Zhou YH,** Xu B. Advanced on CPT drugs in combined applications of anticancer. *Tumor* 1998; **18**: 302-304
10 **Yu ZJ,** Zheng YQ, Huang JF. Servey of treatment with transcatheter arterial embolization of late-stage hepatic carcinoma. *Nantong Yixueyuan Xuebao* 1991; **11**: 102-104
11 **Yu ZJ,** Meng XY, Xu KC, Ge ZJ. Hydroxycamptothecine and cantharidin combined with crsplatin and lipiodol through transcatheter arterial emobolization in hepatocellular carcinoma. *Zhongguo Zhongxiyi Zazhi* 1995; **1**: 175-178
12 **Yu ZJ,** Meng XY, Cheng JP, Liu YH, Zhou YQ, Huang JF, Wu

JX, Wu XY. Clinical observations on the sequencial TACE, TSAi, and PVE treatment in advanced hepatocellular carcinoma with portal vein tumor thrombius. *Zhonghua Xiaohua Zazhi* 1996; **16**: 32-35

13 **Yu ZJ,** Meng XY. Servey of treatment of hepatic carcinoma with HCPT, CDDP, 5 - FU through transcatheter arterial embolization. *Zhongguo Linchuang Zhongliu Zazhi* 1998; **25**: 73-75

14 **Guan ZZ.** Clinical study of 10-hydroxy-camptothecin in China: standardized reevaluation on necessary. *Aizheng* 2001; 20: 1333-1334

15 The liver cancer committee of Chinese anticancer association. Diagnostic criteria of primary hepatocellular carcinoma. *Zhonghua Ganzangbing Zazhi* 2000; **8**: 135

16 **El-Saadani MA.** A combination therapy with copper nicotinate complex reduces the adverse effects of 5-fluorouracil on patients with hepatocellular carcinoma. *J Exp Ther Oncol* 2004; **4**: 19-24

17 **Zhang L,** Li S, Liao H, Jiang WQ, Guqn ZZ. Phase 1 trial of pharmaco-kinetics and human tolerability to 10-hydroxycamptothecin in patients with advanced malignancy. *Aizheng* 2001; **20**: 1391-1395

18 **Patt YZ,** Hassan MM, Aguayo A, Nooka AK, Lozano RD, Curley SA, Vauthey JN, Ellis LM, Schnirer II, Wolff RA, Charnsangavej C, Brown TD. Oral capecitabine for the treatment of hepatocellular carcinoma, cholangio-carcinoma, and gallbladder carcinoma. *Cancer* 2004; **101**: 578-586

19 **Pourgholami MH,** Morris DL. 1,25-Dihydroxyvitamin D(3) in lipiodol for the treatment of hepatocellular carcinoma: cellular, animal and clinical studies. *J Steroid Biochem Mol Biol* 2004; **89-90**: 513-518

20 **Heinemann LA,** Thomas DB, Mohner M. MILTS Collaborative Study Team. Multicentre international liver tumour study protocol of the case-control study on hepatocellular cancer. *Pharmacoepidemiol Drug Saf* 1996; **5**: 173-186

21 **Date M,** Fukuchi K, Namiki Y, Okumura A, Morita S, Takahashi H, Ohura K. Therapeutic effect of photodynamic therapy using PAD-S31 and diode laser on human liver cancer cells. *Liver Int* 2004; **24**: 142-148

22 **Poon RT,** Ngan H, Lo CM, Liu CL, Fan ST, Wong J. Transarterial chemoembolization for inoperable hepatocellular carcinoma and postresection intrahepatic recurrence. *J Surg Oncol* 2000; **73**: 109-114

23 **Camma C,** Schepis F, Orlando A, Albanese M, Shahied L, Trevisani F, Andreone P, Craxi A, Cottone M. Transarterial chemoembolization for unresectable hepatocellular carcinoma: meta-analysis of randomized controlled trials. *Radiology* 2002; **224**: 47-54

24 **Lau WY,** Ho SK, Yu SC, Lai EC, Liew CT, Leung TW. Salvage Surgery Following Downstaging of Unresectable Hepatocellular Carcinoma. *Ann Surg* 2004; **240**: 299-305

25 **Goshima S,** Kanematsu M, Matsuo M, Kondo H, Kato H, Yokoyama R, Hoshi H, Moriyama N. Nodule-in-nodule appearance of hepatocellular carcinomas: Comparison of gadolinium-enhanced and ferumoxides-enhanced magnetic resonance imaging. *J Magn Reson Imaging* 2004; **20**: 250-255

26 **Acunas B,** Rozanes I. Hepatocellular carcinoma: treatment with transcatheter arterial chemoembolization. *Eur J Radiol* 1999; **32**: 86-89

27 **Huang HQ,** Jiang WQ, Hu XH, Lin XB, Liu KF, Li YH, Lin Z, Shen WX, Chen Q, He YJ, Guan ZZ. Preliminary study of lyophilized 10-hydroxycamptothecin in advanced or recurrent malignancies. *Aizheng* 2003; **22**: 1334-1338

28 **Zhou JJ,** Liu J, Xu B. Relationship between lactone ring forms of HCPT and their antitumor activities. *Acta Pharmacol Sin* 2001; **22**: 827-830

29 **Platzer P,** Thalhammer T, Reznicek G, Hamilton G, Zhang R, Jager W. Metabolism and biliary excretion of the novel anticancer agent 10-hydroxycamptothecin in the isolated perfused rat liver. *Int J Oncol* 2001; **19**: 1287-1293

30 **Zhang XW,** Qing C, Xu B. Apoptosis induction and cell cycle perturbation in human hepatoma hep G2 cells by 10-hydroxycamptothecin. *Anticancer Drugs* 1999; **10**: 569-576

31 **Zhang XW,** Jiang JF, Xu B. Differentiation-inducing action of 10-hydroxy-camptothecin on human hepatoma Hep G2 cells. *Acta Pharmacol Sin* 2000; **21**: 364-368

32 **Zangos S,** Gille T, Eichler K, Engelmann K, Woitaschek D, Balzer JO, Mack MG, Thalhammer A, Vogl TJ. Transarterial chemoembolization in hepato- cellular carcinomas: technique, indications, and results. *Radiologe* 2001; **41**: 906-914

33 **Livraghi T.** Treatment of hepatocellular carcinoma by interventional methods. *Eur Radiol* 2001; **11**: 2207-2219

34 **Loewe C,** Cejna M, Schoder M, Thurnher MM, Lammer J, Thurnher SA. Arterial embolization of unresectable hepatocellular carcinoma with use of cyanoacrylate and lipiodol. *J Vasc Interv Radiol* 2002; **13**: 61-69

Science Editor Zhu LH and Guo SY **Language Editor** Elsevier HK

PO Box 2345, Beijing 100023, China
www.wjgnet.com
wjg@wjgnet.com

ELSEVIER

World J Gastroenterol 2005;11(33):5226-5228
World Journal of Gastroenterology ISSN 1007-9327
© 2005 The WJG Press and Elsevier Inc. All rights reserved.

• *CASE REPORT* •

Localized intra-abdominal fibromatosis of the small bowel mimicking a gastrointestinal stromal tumor: A case report

Pierigiuseppe Colombo, Daoud Rahal, Fabio Grizzi, Vittorio Quagliuolo, Massimo Roncalli

Pierigiuseppe Colombo, Daoud Rahal, Massimo Roncalli, Department of Pathology, Istituto Clinico Humanitas, Rozzano, Milan, Italy
Fabio Grizzi, Scientific Direction, Istituto Clinico Humanitas, Rozzano, Milan, Italy
Vittorio Quagliuolo, Department of General Surgery, Istituto Clinico Humanitas, Rozzano, Milan, Italy
Massimo Roncalli, University of Milan School of Medicine, Milan, Italy
Correspondence to: Pierigiuseppe Colombo, MD, Department of Pathology, Istituto Clinico Humanitas, Via Manzoni 56, 20089 Rozzano MI, Italy. piergiuseppe.colombo@humanitas.it
Telephone: +39-2-82244712 Fax: +39-2-82244791
Received: 2004-10-13 Accepted: 2004-11-09

Abstract

Intra-abdominal fibromatosis (IAF) is a benign mesenchymal lesion that can occur throughout the gastrointestinal tract. Although rare, it is the most common primary tumor of the mesentery and can develop at any age. We describe a rare case of primary IAF involving the mesentery and small bowel which clinically, macroscopically and histologically mimicked malignant gastrointestinal stromal tumor (GIST). This report highlights the fact that benign IAF can be misdiagnosed as a malignant GIST localized in the mesentery or arising from the intestinal wall. Their diagnostic discrimination is essential because of their very different biological behaviors and the fact that the introduction of effective therapies involving tyrosine kinase inhibitor STI571 (imatinib mesylate) has greatly changed the clinical approach to intra-abdominal stromal spindle cell tumors.

© 2005 The WJG Press and Elsevier Inc. All rights reserved.

Key words: Intra-abdominal fibromatosis; Gastrointestinal tract; Gastrointestinal stromal tumor

Colombo P, Rahal D, Grizzi F, Quagliuolo V, Roncalli M. Localized intra-abdominal fibromatosis of the small bowel mimicking a gastrointestinal stromal tumor: A case report. *World J Gastroenterol* 2005; 11(33): 5226-5228
http://www.wjgnet.com/1007-9327/11/5226.asp

INTRODUCTION

Although rare in humans, intra-abdominal fibromatosis (IAF) is the most common primary mesenteric tumor with spindle cell morphology. It may occur at any age, can be solitary or multiple, and may involve the small bowel, omentum, mesocolon and/or retroperitoneum[1,2]. It can sometime mimic the clinical characteristics, radiological imaging and histopathological appearance of a gastrointestinal stromal tumor (GIST), thus leading to an incorrect diagnosis.

It has been clearly established that GISTs originate from gastrointestinal pacemaker Cajal cells, which are the primary effectors controlling gut motility[7,8]. Although they have been considered as a distinct tumoral entity for about 10 years, they can now be more precisely identified as a result of the widespread use of immunohistochemistry with *c-kit* (CD117, a protein synthesized in interstitial Cajal cells) for the diagnostic analysis of spindle cell lesions of the mesentery and gastrointestinal tract. This marker has emerged as their most important defining feature, and is probably the gold standard for GIST diagnosis[2]. *c-kit* gene mutations and *kit* protein overexpression also seem to be essential for the pathogenesis of GISTs[9].

We describe here a rare, localized variant of primary IAF involving the mesentery and small bowel, which mimicked a GIST by strongly expressing the *c-kit* protein. Because of the remarkably overlapping immunophenotype of the two lesions, the aim of this report is to highlight the need to discriminate them because of the introduction of specific therapeutic strategies and the fact that they have different biological behaviors: IAF is benign and exclusively locally aggressive, whereas GISTs are malignant and may lead to distant metastases.

CASE REPORT

A 50-year-old white man with recent weight loss was admitted to Istituto Clinico Humanitas (Rozzano, Milan, Italy) because of abdominal discomfort in the left iliac fossa and suprapubic region, and sub-occlusive symptoms. He had undergone a partial sigmoid resection to treat perforated diverticular disease, one year before.

During the instrumental evaluation of suspected recurrent diverticulitis, abdominal ultrasound analysis revealed a mass involving the small bowel loops, and computed tomography (CT) demonstrated the presence of a round, lobulated, suprapubic neoplasm in the mesenteric region near the small bowel, that was presumably its site of origin (Figure 1). On the basis of the available clinical data and radiological imaging, an initial hypothesis of malignant GIST was made.

After surgical exploration of the abdominal cavity, the ileal tract with the tumoral mass and the adjacent mesenteric adipose tissue were excised. No other signs of disease were found in the other abdominal organs.



Figure 1 Abdominal CT scan showing a round, lobulated mass in the mesenteric region, tightly related to the bowel wall.

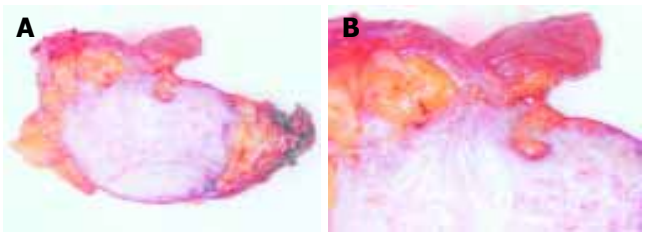


Figure 2 The resected small bowel with a well circumscribed firm mass in the mesenteric adipose tissue which exhibits an expanding growth pattern (**A**). The tumor has a tan-gray appearance on cut surface, and focally infiltrates the bowel wall (**B**).

Macroscopic examination of the specimen revealed a 7 cm×5 cm×5 cm encapsulated, well-circumscribed, firm, tan-gray mass infiltrating the adipose tissue and bowel wall (Figure 2).

Light microscopy showed a neoplasm with a prevalently hypocellular appearance consisting of spindle cells growing in long sweeping fascicles. At higher magnification, the neoplastic population was found to consist of uniformly shaped cells with abundant eosinophilic cytoplasm and delicate, sometimes plump, nuclei with clearly evident nucleoli (Figure 3A). The mitotic activity index ranged from 1 to 10 mitoses/50 high power fields in the hypercellular areas.

The presence of these hypercellular areas with partially circumscribed borders, and the infiltration spreading to the *muscularis propria* of the small bowel, consistently favored a microscopic diagnosis of GIST, thus supporting the clinical, radiological and macroscopic findings.

However, this hypothetical diagnosis was not supported by the generally hypocellular growth pattern, the digitiform infiltration margins inside the adjacent fat tissue, and the absence of foci of necrosis, hemorrhages or cysts. Immunohistochemistry showed that the cells making up the lesion were immunopositive for *c-kit* protein (Figure 3B), and some were positive for smooth muscle actin (Figure 3C) and desmin (Figure 3D); however, no CD34 or S100 expression was ever found.

The final diagnosis was localized IAF of the mesentery and small bowel. A control CT scan, 6 mo after surgery, showed no signs of recurrent disease.

DISCUSSION

Primary IAF of the mesentery is a rare variant of benign stromal neoplasms of fibroblast-myofibroblast origin that may arise *ex novo*, but is usually secondary to trauma or hormonal stimulation, or associated with familial polyposis coli or Gardner's syndrome[1-6]. This neoplastic disease most

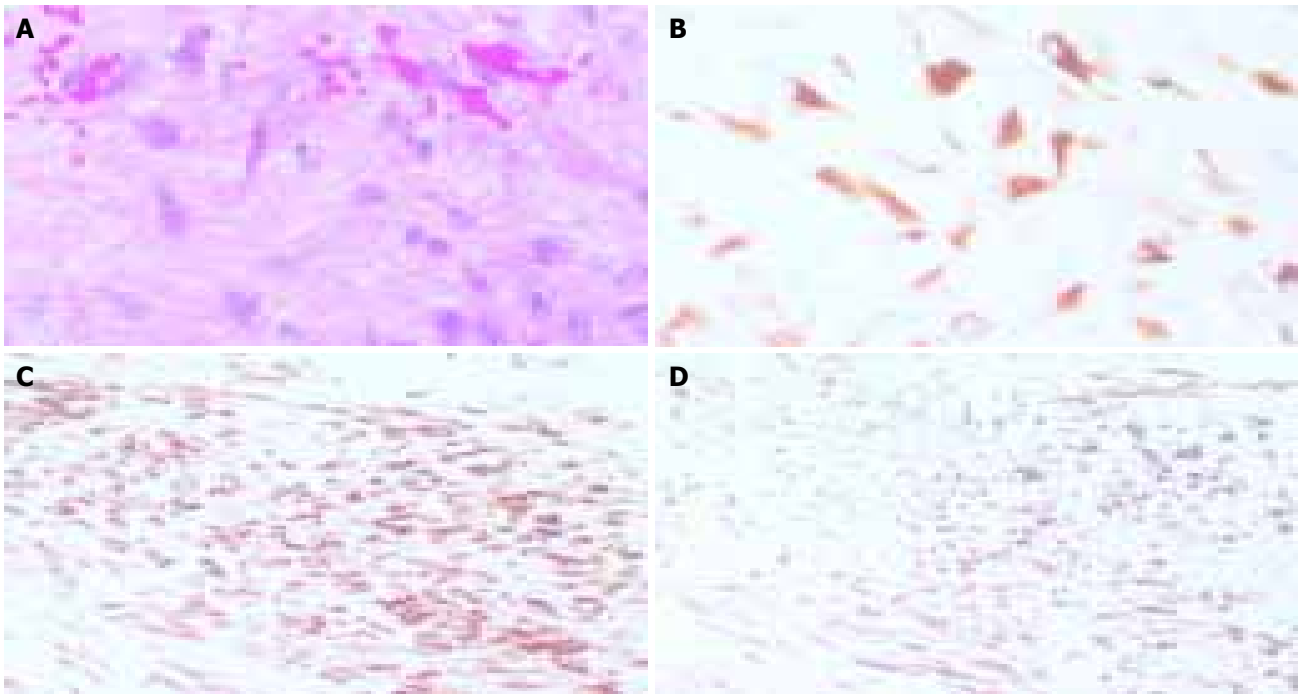


Figure 3 The tumoral lesion consisted of spindle cells growing in sweeping fascicles, with eosinophilic cytoplasm and sometimes plump nuclei (**A**, H&E 400×). Most of the tumor cells show immunoreactivity for *c-kit* (CD117) in their cytoplasm (**B**, IHC 400×). Immunohistochemical stain for smooth muscle actin (**C**, IHC 200×) and for desmin (**D**, IHC 200×) is also present in some hypercellular areas of the lesion.

frequently occurs in the anterior abdominal wall, and is usually treated exclusively by means of surgical excision with a wide margin of uninvolved tissue; however, local recurrences due to incomplete resection have been described in an estimated 16% of cases, leading to intestinal obstruction and death in 6%[2].

Although it is generally easy to diagnose primary IAF, the localized tumor growth and its apparent source in the bowel wall may lead to misinterpretations and clinical, radiological, macroscopic and microscopic hypotheses of a GIST (a mesenchymal tumor of the gastrointestinal tract).

The case presented here had a number of additional characteristics usually found in GISTs, such as *c-kit* cytoplasmic immunoreactivity, the fascicular arrangement of neoplastic cells with well-circumscribed borders, with many mitotic figures and cytological atypia with plump nuclei and prominent nucleoli.

However, light microscopy evaluation of the available tissue sections revealed the morphological features of fibromatosis, which can be summarized as: (a) spindle cells oriented along their long axis; (b) broad sweeping fascicles of varying cellularity with abundant collagenous stroma; (c) the absence of necrosis, hemorrhages, cysts and skenoid fibers deposits; and (d) the protrusion of the tumor into the lumen and ulceration of the overlying mucosa. Moreover, according to Monihan *et al*., the absence of CD34 and S100 expression supports the fibromatous nature of the lesion and highlight the fact that these proteins may be helpful in discriminating IAF from GIST[10].

Yantiss *et al*., have recently underlined the importance of making a more complete evaluation in order to distinguish these two very different neoplastic lesions, putting greater emphasis in their clinical, radiological, macroscopic, histological, immunophenotypical and ultrastructural features[11].

GISTs are potentially misdiagnosed as localized IAF arising within or involving the bowel wall, and their immunophenotypes may vary and overlap[1,2]. The overexpression of *c-kit* protein has been found in a large number of mesenchymal, epithelial and hematopoietic neoplasms, including fibromatosis, dermatofibrosarcoma protuberans, synovial sarcoma, anaplastic large cell lymphoma, glioma and germinoma[12]. These findings all confirm that *c-kit*, smooth muscle actin and desmin cannot help in differential diagnosis and their immunoreactivity must be interpreted in conjunction with the morphological analysis and clinical evaluation. In cases such as the one reported here, the clinical and histological differential diagnosis with GIST are mandatory, above all in the light of the current criteria predicting GIST outcomes (the number of mitoses and the size of the lesion), which classified our case as being at intermediate/high risk of sarcoma, which would require the consideration of a further therapeutic approach[13].

It is now well known that fibromatosis expresses *c-kit*, against which STI571 (imatinib mesylate) is a target-based molecule that has remarkable clinical effects and is well tolerated by patients with non-resectable GISTs or non-resectable extra-abdominal desmoid tumors[9]; however, the potential therapeutic role of this small molecule in IAF is still unclear.

In conclusion, although intra-abdominal lesions with spindle cell morphology are relatively rare, and similarities in their clinical data and radiological and histological appearances may lead to misdiagnoses, it is also true that tumor diagnoses based on immunohistochemical staining or traditional histological criteria alone are not specific enough[4].

Our report highlight the need for reliable new criteria for discriminating IAF and GIST because of the introduction of sophisticated therapeutic strategies (in order to select patients to be admitted to clinical trials) and their different biological behaviors: IAF is benign and exclusively locally aggressive, whereas GISTs are malignant and potentially capable of leading to distant metastases.

REFERENCES

1 **Burke AP,** Sobin LH, Shekitka KM, Federspiel BH, Helwig EB. Intra-abdominal fibromatosis. A pathologic analysis of 130 tumors with comparison of clinical subgroups. *Am J Surg Pathol* 1990; **14**: 335-341

2 **Al-Nafussi A,** Wong NA. Intra-abdominal spindle cell lesions: a review and practical aids to diagnosis. *Histopathology* 2001; **38**: 387-402

3 **Gardner EJ.** A genetic and clinical study of intestinal polyposis, a predisposing factor for carcinoma of the colon and rectum. *Am J Hum Genet* 1951; **3**: 167-176

4 **Kim DH,** Goldsmith HS, Quan HS, Huvos AG. Intra-abdominal desmoid tumor. *Cancer* 1971; **27**: 1041-1045

5 **Nichols RW.** Desmoid tumors: a report of 31 cases. *Arch Surg* 1923; **7**: 227-236

6 **Reitano JJ,** Scheinin TM, Hayry P. The desmoid syndrome: new aspects in the cause, pathogenesis and treatment of the desmoid tumor. *Am J Surg* 1986; **151**: 230-237

7 **Kindblom LG,** Remotti HE, Aldenborg F, Meis-Kindblom JM. Gastrointestinal stromal tumors show phenotypic characteristics of the interstitial cells of Cajal. *Am J Pathol* 1998; **152**: 1259-1269

8 **Robinson TL,** Sircar K, Hewlett BR, Chorneyko K, Riddell RH, Huizinga JD. Gastrointestinal stromal tumors may originate from a subset of CD34-positive interstitial cells of Cajal. *Am J Pathol* 2000; **156**: 1157-1163

9 **Lin SC,** Huang MJ, Zeng CY, Wang TI, Liu ZL, Shiay RK. Clinical manifestations and prognostic factors in patients with gastrointestinal stromal tumors. *World J Gastroenterol* 2003; **9**: 2809-2812

10 **Monihan JM,** Carr NJ, Sobin LH. CD34 immunoexpression in stromal tumors of the gastrointestinal tract and in mesenteric fibromatosis. *Histopathology* 1994; **25**: 469-473

11 **Yantiss RK,** Spiro IJ, Compton CC, Rosemberg AE. Gastrointestinal stromal tumor versus intra-abdominal fibromatosis of the bowel wall. *Am J Surg Pathol* 2000; **7**: 947-957

12 **Hurlimann J,** Gardiol D. Gastrointestinal stromal tumors: an immunohistochemical study of 165 cases. *Histopathology* 1991; **19**: 311-320

13 **Mace J,** Biermann JS, Sondak V. Response of extraabdominal desmoid tumors to therapy with imatinib mesylate. *Cancer* 2002; **11**: 2373-2379

Science Editor Zhu LH and Guo SY **Language Editor** Elsevier HK

PO Box 2345, Beijing 100023, China
www.wjgnet.com
wjg@wjgnet.com

ELSEVIER

World J Gastroenterol 2005;11(33):5229-5231
World Journal of Gastroenterology ISSN 1007-9327
© 2005 The WJG Press and Elsevier Inc. All rights reserved.

• *CASE REPORT* •

Hemobilia secondary to hepatic artery pseudoaneurysm: An unusual complication of bile leakage in a patient with a history of a resected IIIb Klatskin tumor

Dimitrios Siablis, Zafiria G. Papathanassiou, Dimitrios Karnabatidis, Nikolaos Christeas, Constantine Vagianos

Dimitrios Siablis, Zafiria G. Papathanassiou, Dimitrios Karnabatidis, Nikolaos Christeas, Department of Interventional Radiology, Medical School, University of Patras, Rio, Greece
Constantine Vagianos, Department of Surgery, Medical School, University of Patras, Rio, Greece
Correspondence to: Associate Professor, Dimitrios Siablis, MD, Department of Interventional Radiology, Medical School, University of Patras, Rio 26504 Patras, Greece. papaze@otenet.gr
Telephone: +30-2610-999213 Fax: +30-2610-993987
Received: 2004-12-19 Accepted: 2005-01-26

Abstract

We report a case of a 74-year-old woman with a 16-year history of a double bilo-enteric anastomosis due to resected hilar cholangiocarcinoma [Type IIIb Klatskin tumor]. The patient presented with cholangitis secondary to benign anastomotic stenosis which resulted in a large intrahepatic biloma. In order to restore the patency of the anastomosis and overcome cholangitis, several attempts took place, including endobiliary stenting, balloon-assisted biloplasty and transhepatic billiary drainage. Anastomotic patency was achieved, complicated, however, by persistent upper gastro-intestinal bleeding, presented as hemobilia. A biloma-induced pseudoaneurysm of the left hepatic artery was diagnosed. This had ruptured into the biliary tract, and presented the actual cause of the hemobilia. Selective embolism of the pseudoaneurysm resulted in control of the hemorrhage, and was successfully combined with transhepatic dilatation of the anastomosis and percutaneous drainage of the biloma. The patient was ultimately cured and seems to be in excellent condition, 5 mo after treatment.

© 2005 The WJG Press and Elsevier Inc. All rights reserved.

Key words: Hepatic artery pseudoaneurysm; Hemobilia; Embolization

Siablis D, Papathanassiou ZG, Karnabatidis D, Christeas N, Vagianos C. Hemobilia secondary to hepatic artery pseudoaneurysm: An unusual complication of bile leakage in a patient with a history of a resected IIIb Klatskin tumor. *World J Gastroenterol* 2005; 11(33): 5229-5231
http://www.wjgnet.com/1007-9327/11/5229.asp

INTRODUCTION

Bleeding into the biliary tree, either traumatic or iatrogenic, represents a rare cause of gastro-intestinal hemorrhage, which occurs in less than 3% of liver injuries[1]. Besides bleeding, typical signs of hemobilia include jaundice and pain[1,2]. Ten percent of hemobilia cases are reported to be secondary to ruptured hepatic artery aneurysms[3]. Apart from trauma and atherosclerosis, hepatic artery pseudoaneurysms may be created as a result of arterial wall erosion by local inflammation such as infected bilomas related to bile stasis and cholangitis[3].

In this case, we report an unusual pathological entity of an infected intrahepatic biloma secondary to a stenotic bilo-enteric anastomosis, complicated with a pseudoaneurysm of the left hepatic artery. This resulted in persistent hemobilia, which was ultimately treated by an aggressive combination of interventional radiological procedures.

CASE REPORT

Sixteen years ago, a 58 year-old woman, was operated on, due to malignant obstruction of the bile duct (Klatskin tumor, stage IIIb). At exploratory laparotomy, the tumor was resected (RO resection) and a double choledocho-jejunal anastomosis was performed (Roux-en-Y). She recovered well and was discharged 15 d later in good health. Histology of the resected specimen verified an adenocarcinoma of the bile ducts. Ever since, she has been in good condition, without evidence of tumor recurrence.

In October 2002, the patient was admitted to hospital, suffering from cholangitis. Transhepatic cholangiography demonstrated a longitudinal stenosis of the main left hepatic duct, at the area of the left bilio-enteric anastomosis, causing dilatation of the left bile ducts (Figure 1A). Considering the results of MRI as well as the long period after resection, the stenosis was finally attributed to benign postoperative fibrosis. Percutaneous balloon-assisted biliary decompression followed by transhepatic insertion of two expandable metallic stents through the bilo-enteric anastomosis resulted in clinical and radiological palliation of the cholangitis.

Two years later, a new severe episode of cholangitis led the patient to hospital again. Transhepatic cholangiography showed severe stenosis of the stent lumen that seemed to be secondary to endothelial hyperplasia. A nearby biloma was also depicted, due to bile leakage, probably related to bile stasis (Figure 1B). External drainage of the biloma and percutaneous transhepatic stent re-dilatation (Figures 2A and B) were performed. After receiving antibiotics for five days, the external drainage catheter was removed and the patient was discharged in acceptable clinical condition.

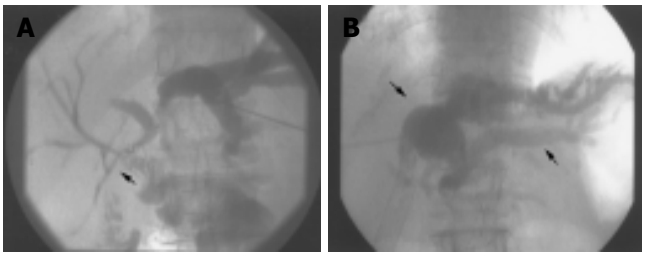


Figure 1 Percutaneous transhepatic cholangiography. **A:** A longitudinal stenosis affecting the area of the left bilio-enteric anastomosis is shown. The left bile ducts are markedly dilated; **B:** Percutaneous transhepatic cholangiography exhibits the extraductal bile collection in the form of a biloma (small arrow) and the dilatation of the left lobe bile ducts (big arrow).

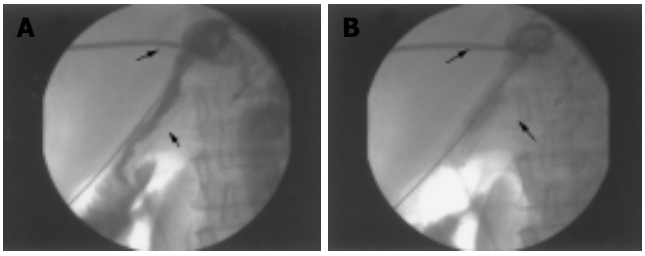


Figure 2 Bile stasis, secondary to stent lumen stenosis (small arrow, **A**), was managed with external drainage of the biloma (thin arrow, **A, B**) combined, in the same session, with transhepatic balloon-assisted stent re-dilatation (**B**).

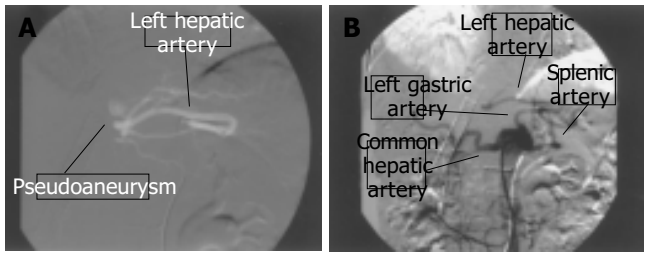


Figure 3 Catheter-directed, selective angiography demonstrates the presence of a pseudoaneurysm arising from the left hepatic artery. Note that the left hepatic artery originates from the left gastric artery (**A** and **B**).

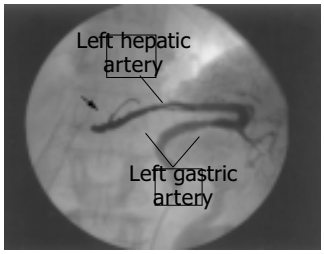


Figure 4 Trans catheter embolization. Detachment of adequate metallic coils (arrow) resulted in full occlusion of the aneurysmal sac.

Four weeks later, the patient returned to hospital due to weakness and anemia. She reported a 10-d history of melena. Urgent endoscopy disclosed no evidence of active gastro-duodenal bleeding. Computed tomography-assisted angiography displayed an aneurysmal sac located at the left hepatic arterial tract. A subsequent catheter-directed selective angiography detected precisely a pseudoaneurysm originating from a branch of the left hepatic artery. Technically, this was a particularly demanding procedure, due to an abnormal origin of the left hepatic artery from the left gastric artery (Type II variation, according to Hiatt's classification[4]) (Figures 3A and B). By means of super-selective catheterization, the neck of the pseudoaneurysm was approached and detachment of adequate metallic coils was performed resulting in full occlusion of the vascular lesion (Figure 4) and immediate control of the bleeding. The patient recovered well and was discharged a week later in good condition.

Five months later, the patient remained in good condition, without clinical or laboratory evidence of hemobilia or cholangitis.

DISCUSSION

Trauma (iatrogenic or accidental) and atherosclerosis consist of the most common causes of hepatic artery aneurysms[3,5], however, their formation may be less frequently encountered as a result of biliary inflammation. This is usually related to parasitic infection or stone impaction into the biliary tree[6]. The reported case suggests that other additional inflammatory factors such as infected, long lasting, intrahepatic bilomas may erode the arterial wall and lead to pseudoaneurysms.

Nonetheless, arterial injury is an unusual (2%), but possible complication of percutaneous transhepatic billiary drainaging (PTBD), which may also result in severe hemobilia[7]. The reported patient however, had been hospitalized for 5 d after PTBD and was discharged without any evidence of significant blood loss. This makes the scenario of a biloma-induced hepatic pseudoaneurysm that finally ruptures into a bile duct, more reasonable.

Hemobilia usually presents either with melena (90%) or hematemesis (72%)[1]. Other clinical manifestations include upper abdominal pain (71%) and obstructive jaundice (60%)[1]. The complete triad of bleeding, pain and jaundice is reported only in 22% of cases[1]. Hemobilia represents a potential life-threatening complication depending not only on the size of vessel wall deficit[7] but also on the fibrinolytic action of the bile that inhibits proper clot formation[1,8].

Liver angiography is the standard diagnostic method in cases of hemobilia especially, when endoscopic procedures fail to establish diagnosis[1,9]. This minimally invasive method detects precisely the bleeding site, also allowing simultaneous therapeutic intervention, by selective catheterization and embolization with the use of adequate embolic agents. Successful hemostasis rates exceed 95%[1] while procedure-associated morbidity and mortality are considerably lower than surgery[10]. The aforementioned advantages play a significant role especially in the management of patients with anatomic variations of the hepatic artery as well as for elderly patients with poor surgical prognosis, as in this case.

Apart from iatrogenic and accidental injury of the biliary tree, hemobilia may also occur under more complicated circumstances. The possibility of a biloma-induced hepatic pseudoaneurysm that finally erodes a bile duct should be taken into account, especially in patients with chronic obstructive jaundice, extra-ductal and encapsulated bile collections, repetitive episodes of cholangitis and hemobilia.

Transhepatic arterial embolization provides a safe and effective alternative in controlling patients with persistent hemobilia.

REFERENCES

1 **Forlee MV,** Krige JE, Welman CJ, Beningfield SJ. Haemobilia after penetrating and blunt liver injury: treatment with selective hepatic artery embolization. *Injury* 2004; **35**: 23-28

2 **Sandblom F,** Saegesser F, Mirkowitch V. Hepatic hemobilia: hemorrhage from the intrahepatic biliary tract. *World J Surg* 1984; **8**: 41-50

3 **Liu TT,** Hou MC, Lin HC, Chang FY, Lee SD. Life-threatening hemobilia caused by hepatic artery pseudoaneurysm: a rare complication of chronic cholangitis. *World J Gastroenterol* 2003; **9**: 2883-2884

4 **Koops A,** Wojciechowski B, Broering DC, Adam G, Krupski-Berdien G. Anatomic variations of the hepatic arteries in 604 selective celiac and superior mesenteric angiographies. *Surg Radiol Anat* 2004; **26**: 239-244

5 **Stauffer JT,** Weinman MD, Bynum TE. Hemobilia in a patient with multiple hepatic artery aneurysms: A case report and review of the literature. *Am J Gastroenterol* 1989; **84**: 59-62

6 **Bloechle C,** Izbicki JR, Rashed MY, el-Sefi T, Hosch SB, Knoefel WT, Rogiers X, Broelsch CE. Hemobilia: presentation, diagnosis, and management. *Am J Gastroenterol* 1994; **89**: 1537-1540

7 **L'Hermine C,** Ernst O, Delemazure O, Sergent G. Arterial complications of percutaneous transhepatic biliary drainage. *Cardiovasc Intervent Radiol* 1996; **19**: 160-164

8 **Vagianos C,** Karavias D, Dragotis C, Kalofonos H, Androulakis J. Obstructive jaundice due to intracholedochal blood clot: an unusual early presentation of primary hepatic carcinoma. *Br J Clin Pract* 1993; **47**: 222-223

9 **Moodley J,** Singh B, Lalloo S, Pershad S, Robbs JV. Non-operative management of haemobilia. *Br J Surg* 2001; **88**: 1073-1076

10 **Lygidakis NJ,** Okazaki M, Damtsios G. Iatrogenic hemobilia: how to approach it. *Hepatogastroenterology* 1991; **38**: 454-457

Science Editor Guo SY **Language Editor** Elsevier HK

PO Box 2345, Beijing 100023, China
www.wjgnet.com
wjg@wjgnet.com

ELSEVIER

World J Gastroenterol 2005;11(33):5232-5234
World Journal of Gastroenterology ISSN 1007-9327
© 2005 The WJG Press and Elsevier Inc. All rights reserved.

• *CASE REPORT* •

Laparoscopic cholecystectomy in situs inversus totalis with "inferior" cystic artery: A case report

Sumihiro Kamitani, Yosihiro Tsutamoto, Kazuyoshi Hanasawa, Tohru Tani

Sumihiro Kamitani, Yosihiro Tsutamoto, Kazuyoshi Hanasawa, Tohru Tani, First Department of Surgery, Shiga University of Medical Science, Japan
Correspondence to: Sumihiro Kamitani, First Department of Surgery, Shiga University of Medical Science, Ohtsu, Shiga 520-2192, Japan. sumihiro@belle.shiga-med.ac.jp
Telephone: +81-77-548-2238 Fax: +81-77-548-2240
Received: 2005-02-09 Accepted: 2005-03-23

Abstract

A 76-year-old man with known situs inversus totalis presented with left-sided discomfort. Abdominal ultrasonography and CT scan confirmed the diagnosis of a gallstone, as well as, situs inversus; the liver and gallbladder on the left side and the spleen on the right. The biliary system was thought to be left-right reversal, mirror image in the view of drip infusion cholangiogram and MRI. Laparoscopic cholecy stectomy was safely performed, despite of unexpected aberrant cystic artery running inferior to cystic duct of situs inversus. Laparoscopic surgeon should be careful for view of reversed relationships and also existence of other anomalies.

© 2005 The WJG Press and Elsevier Inc. All rights reserved.

Key words: Situs inversus totalis; Laparoscopic cholecystectomy; Inferior cystic artery

Kamitani S, Tsutamoto Y, Hanasawa K, Tani T. Laparoscopic cholecystectomy in situs inversus totalis with "inferior" cystic artery: A case report. *World J Gastroenterol* 2005; 11(33): 5232-5234
http://www.wjgnet.com/1007-9327/11/5232.asp

INTRODUCTION

Recently, laparoscopic cholecystectomy has become the standard technique for surgical removal of the gallbladder for symptomatic gallstones[1-3]. Situs inversus totalis is uncommon anatomic anomaly, with gallbladder on the left side. Some investigators reported that laparoscopic cholecystectomy was successfully applied in situs inversus totalis, but the patients of all these cases were without other additional anomaly. We recently encountered a patient in situs inversus, who had anomaly of the cystic artery with symptomatic gallstones and was managed by laparoscopic cholecystectomy.

CASE REPORT

A 76-year-old man, who was known to have situs inversus, was seen complaining of recurrent left-sided upper quadrant abdominal pain for 2 mo. Abdominal ultrasound and CT scan confirmed the solitary radiolucent gallstone and presence of chronic gallbladder wall inflammation as well as situs inversus with the liver and gallbladder on the left side and the spleen on the right. The cardiac shadow and stomach bubble were displayed on the right side of the chest roentgenogram. The endoscopic retrograde cholangiopancreatography (ERCP) was performed, but it was too difficult to perform cholangiography (Figure 1A). The ERCP revealed the right sided pancreatic duct. Three dimensional (3D) drip infusion cholangiogram (DIC)-CT and magnetic resonance cholangio-pancreatography (MRCP) revealed the right-left reversal biliary system (Figures 1B and C). We did not perform the abdominal angiography before operation. All the preoperative examinations we performed revealed the mirror image anatomy without additional anomaly. Unexpected aberrant cystic artery was encountered as predicted by preoperative ultrasonography, CT, and MRCP.

OPERATION

At first, small laparotomy was placed in the sub-umbilical portion, and a 10-mm trocar with a balloon was inserted into the abdominal cavity. A 10-mm trocar was placed in the sub-xiphoid locations, and two 5-mm trocars were placed in the left sub-costal and left lateral regions under the view of laparoscope (Figure 2). The surgeon mainly used the forceps inserted through the trocar of sub-xiphoid. By laparoscopic view of left upper abdomen, gallbladder was placed on the left side and hepatic round ligament on the right (Figure 3A). We grasped and tracted the fundus of gallbladder and the cord was revealed lying inferior to the cystic duct by dissection of Calot's triangle (Figures 3B and C). The whole of the cystic duct was revealed by the dissection of the surroundings of the cystic duct after the traction of the cord (Figure 3D). We performed clip ligature and cut the cystic duct (Figure 3E). After cystic duct had been ligated, more dissection of the neck of the gallbladder was done and it revealed that the cord lead only to the gallbladder (Figure 3F). We thought that the cord was the cystic artery that was not placed on the mirror image of normal position. We performed the clip ligature and cut the cord. Finally the gallbladder was dissected and removed as usual.

DISCUSSION

Situs inversus viscerum is a rare condition, occurring in 1:5 000-1:10 000 hospital admissions[4]. As reported by Sato *et al*., laparoscopic observations were performed in 1 802

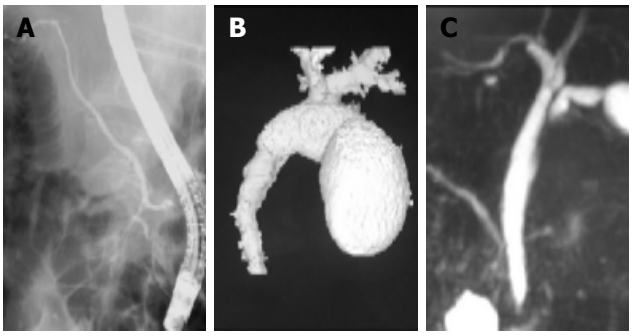


Figure 1 Reversed cholangiopancreatograms. **A:** ERCP; **B:** 3D-DIC CT; **C:** MRCP.

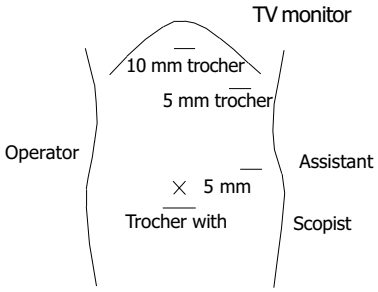


Figure 2 Arrangement around the operating table and positions of the trocars.

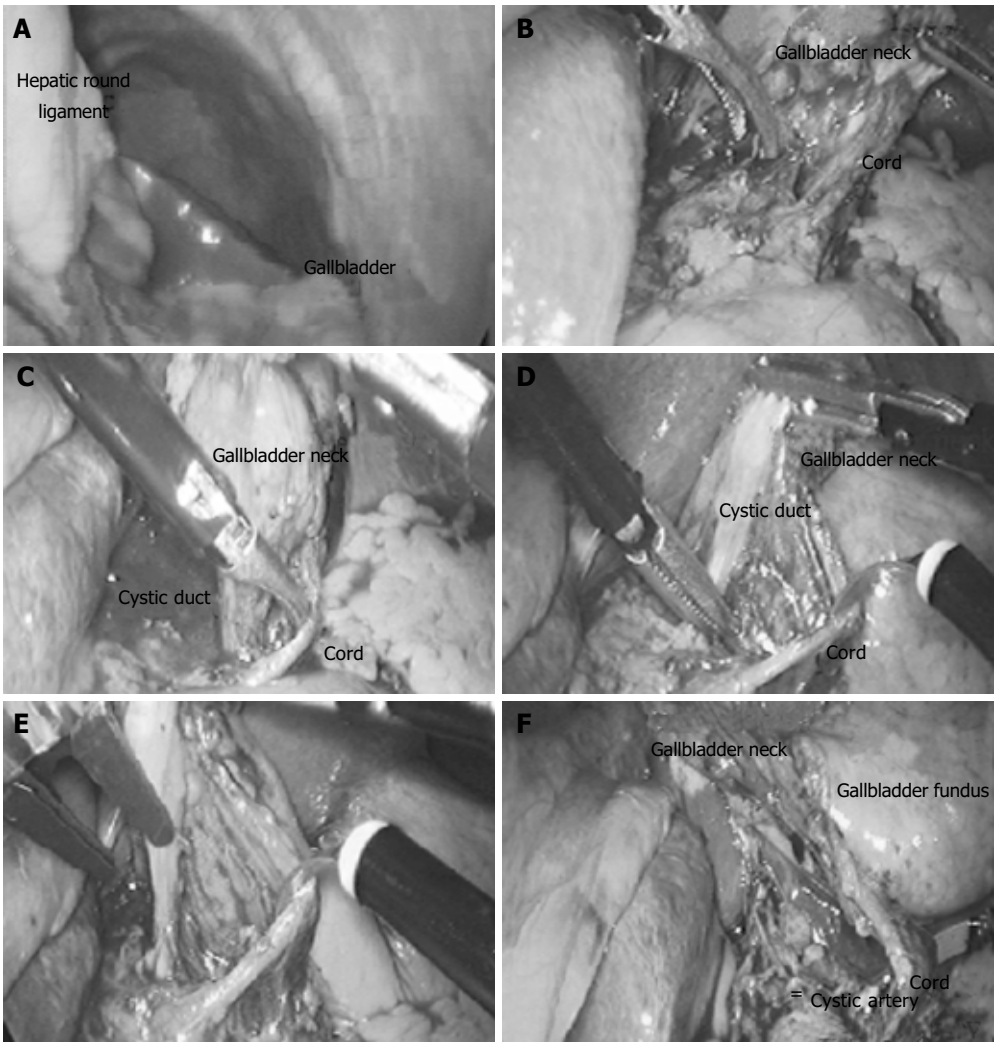


Figure 3 Laparoscopic view during cholecystectomy. **A:** Gallbladder was placed on the left side and hepatic round ligament on the right; **B:** the fundus of gallbladder was grasped and tracted; **C:** the cord was revealed lying inferior to the cystic duct; **D:** the surroundings of the cystic duct were dissected after the cord was tracted; **E:** the cystic duct was cut after the clip ligature; **F:** the cord lead only to the gallbladder.

consecutive patients and situs inversus was investigated in 0.2%[5]. Because the number of laparoscopic cholecystectomy recently becomes large, the reports of that of in situ inversus totalis have been increasing[6-15]. Ten cases of laparoscopic cholecystectomy in situs inversus totalis were reported.

In all reports, in which we can investigate about anatomy of cystic artery[6-10,12-15], it is reported that the cystic artery runs with the mirror image against normal patient. According to the report described by Hugh *et al*.[16], the cystic artery arises as a branch of the right hepatic artery within the hepato-biliary triangle and runs immediately cephalic to the cystic duct toward the gallbladder in 70-80% of patients without situs inversus totalis. It is also reported that "Inferior" cystic artery arises outside the hepatobiliary triangle, runs ventral to the bile duct and lies inferior to the cystic duct in 6% of the patients. We thought that the cystic

artery in our case is the mirror image of this anomaly. Because we did not perform the angiography, the anomalies of hepatic artery and cystic artery cannot be revealed indeed. However, we successfully and safely performed laparoscopic cholecystectomy in our case. According to consideration of our case, the angiography may be done in situs inversus totalis.

Since we carefully operated under the laparoscopic view and cut the cord recognized as the cystic artery, we have successfully carried out laparoscopic cholecystectomy in the patient with situs inversus totalis, despite the reversed anatomic relationships and other arterial anomaly. In the future, the frequency of anomalies of cystic artery detected in situs inversus totalis will increase under the laparoscopic cholecystectomy. In conclusion, we suggest that the experienced laparoscopic surgeons can successfully perform laparoscopic cholecystectomy in situs inversus totalis with care for the reversed relationships and possible existence of other anomalies.

REFERENCES

1 **Lüdtgke FE,** Lepsien G, Neufang T, Peiper HJ. Neue Tendenzen in der Gallenchirurgie. *Zentralbl Chir* 1994; **119**: 362-370
2 **Perissat JR.** Laparoscopic cholecystectomy: The europian experience. *Am J Surg* 1993; **165**: 444-449
3 **Siewert JR,** Feussner H. Minimalinvasive chirurgie-Zwishenbilanz 1994. *Langenbecks Arch Chir* 1994: 129-139
4 **Mayo CW,** Rice RG. Situs inversus totalis Statistical review of data on 76 cases with special reference to diseases of the biliary tract. *AMA Arch Surg* 1949; **58**: 724-730
5 **Sato S,** Watanabe M, Nagasawa S, Niigaki M, Sakai S, Akagi S. Laparoscopic observations of congenital anomalies of the liver. *Gastrointest Endosc* 1998; **47**: 136-140
6 **Campos L,** Sipes E. Laparoscopic cholecystectomy in a 39-year-old female with situs inversus. *J Laparoendosc Surg* 1991; **1**: 123-125
7 **Lipshutz JH,** Canal DF, Hawea RH, Ruffolo TA, Besold MA, Lehman GA. Laparoscopic cholecystectomy and ERCP with sphinctomy in an elderly patient with situs inversus. *Am J Gastroenterol* 1992; **87**: 218-220
8 **Drover JW,** Nguyan KT, Pace RF. Laparoscopic cholecystectomy in apatient with situs inversus viscerum: a case report. *Can J Surg* 1992; **35**: 65-66
9 **Takei HT,** Maxwell JG, Clancy TV, Tinslev EA. Laparoscopic cholecystectomy in situs inversus totalis. *J laparoendosc Surg* 1992; **2**: 171-176
10 **Goh P,** Tekani Y, Shang NS, Ngoi SS. Laparoscopic cholecystectomy in a patient with empyema of the gallbladder and situs inversus. *Endoscopy* 1992; **24**: 799-800
11 **Huang SM,** Chau GY, Lui WY. Laparoscopc cholecystectomy for cholelithiasis in a patient with situs inversus totalis. *Endoscopy* 1992; **24**: 802-803
12 **McDermott JP,** Caushai PF. ERCP and laparoscopic cholecystectomy for cholangitis in a 66-year-old male with situs inversus. *Surg Endosc* 1994; **8**: 1227-1229
13 **Crosher RF,** Harnarayan P, Bremner DN. Laparoscopic cholecystectomy in situs inversus totalis. *J R Coll Surg Edinb* 1996; **41**: 183-184
14 **Demetriades H,** Boisios D, Dervenis C, Evagelou J, Agelopoulos S, Dadoukis J. Laparoscopic cholecystectomy in two patients with symptomatic cholelithiasis and situs inversus totalis. *Dig Surg* 1999; **16**: 519-521
15 **Djohan RS,** Rodriguez HE, Wiesman IM, Unti JA, Podbleiski FJ. Laparoscopic cholecystectomy in situs inversus totalis. *JSLS* 2000; **4**: 251-254
16 **Hugh TB,** Kelly MD, Li B. Laparoscopic anatomy of the cystic artery. *Am J Surg* 1992; **163**: 593-595

Science Editor Guo SY **Language Editor** Elsevier HK

PO Box 2345, Beijing 100023, China
www.wjgnet.com
wjg@wjgnet.com

ELSEVIER

World J Gastroenterol 2005;11(33):5235-5238
World Journal of Gastroenterology ISSN 1007-9327
© 2005 The WJG Press and Elsevier Inc. All rights reserved.

• *CASE REPORT* •

Basket pattern blood flow signals discovered in a case of splenic hamartoma by power Doppler ultrasonography

Shigeo Nakanishi, Katsuya Shiraki, Kouji Yamamoto, Takeshi Nakano, Mutsumi Koyama, Takatsugu Yano, Takayuki Sanda, Hisao Tamaki, Tadanori Hirano, Kazuo Fukudome, Akinori Ishihara

Shigeo Nakanishi, Katsuya Shiraki, Kouji Yamamoto, Takeshi Nakano, First Department of Internal Medicine, Mie University School of Medicine, Tsu, Mie 514-8507, Japan
Shigeo Nakanishi, Mutsumi Koyama, Department of Internal Medicine, Matsusaka General Hospital, Matsusaka, Mie 102, Japan
Takatsugu Yano, Takayuki Sanda, Hisao Tamaki, Department of Surgery, Matsusaka General Hospital, Matsusaka, Mie 102, Japan
Tadanori Hirano, Department of Radiology, Matsusaka General Hospital, Matsusaka, Mie 102, Japan
Kazuo Fukudome, Akinori Ishihara, Department of Pathology, Matsusaka General Hospital, Matsusaka, Mie 102, Japan
Correspondence to: Katsuya Shiraki, MD, PhD, First Department of Internal Medicine, Mie University School of Medicine, 2-174 Edobashi, Tsu, Mie 514-8507, Japan. katsuyas@clin.medic.mie-u.ac.jp
Telephone: +81-59-231-5015 Fax: +81-59-231-5201
Received: 2004-09-10 Accepted: 2005-01-05

Abstract

We present the gray-scale ultrasonography (GSUS), power Doppler ultrasonography (PDUS), abdominal computed tomography (CT), and magnetic resonance imaging (MRI) findings for a case of splenic hamartoma in a 27-year-old man, showing a φ 50 mm homogeneous, iso- and hypo-echoic splenic mass with evidence of a small plural cystic lesion. This splenic hamartoma showed increased vascularity on power Doppler sonograms. PDUS showed multiple circular blood flow signals inside the mass (i.e. a basket pattern), which was consistent with the small plural cystic lesion shown by GSUS. Spectral analysis also confirmed arterial and venous flow. CT scans showed that the mass had low-density relative to the normal spleen and MRI showed that the mass was isodense, relative to the normal spleen. Therefore, CT and MRI are not useful for the diagnosis of splenic hamartoma. Ultrasonography can be used to diagnose splenic hamartoma without administration of a contrast material and therefore is an indispensable method for the diagnosis of splenic hamartoma.

© 2005 The WJG Press and Elsevier Inc. All rights reserved.

Key words: Splenic hamartoma; Ultrasonography; Basket pattern

Nakanishi S, Shiraki K, Yamamoto K, Nakano T, Koyama M, Yano T, Sanda T, Tamaki H, Hirano T, Fukudome K, Ishihara A. Basket pattern blood flow signals discovered in a case of splenic hamartoma by power Doppler ultrasonography. *World J Gastroenterol* 2005; 11(33): 5235-5238
http://www.wjgnet.com/1007-9327/11/5235.asp

INTRODUCTION

Splenic hamartoma is a rare benign tumor with a mortality rate of 0.13%[1]. Since the first description by Rokitansky in 1 861[2], more than 100 cases have been reported. However, hamartoma images have rarely been reported. On sonograms, most splenic hamartomas are a homogeneous and solid mass, with varying echogenicity relative to the normal splenic parenchyma[3-6]. Also, the power Doppler ultrasonography (PDUS) findings of splenic hamartomas show increased vascularity[7]. To our knowledge, PDUS findings, computed tomography (CT), magnetic resonance imaging (MRI) features, and pathologic findings of a splenic hamartoma have not been reported.

CASE REPORT

The patient was an asymptomatic 27-year-old man. Routine physical examination and blood test had no remarkable finding.

Sonographic examination of the patient's spleen was performed using the Aplio80 (Toshiba SSA-770A) equipped with a 4.5-MHz convex-array transducer. Gray-scale ultrasonography (GSUS) showed a φ 4.3 cm×4.7 cm hypo-echoic and iso-echoic (i.e. mixed pattern) solid mass (Figure 1A) at the middle pole of the spleen. The mass was homogeneous with evidence of cystic changes in the center, but without calcification. Sonography also showed a clear and smooth margin, and PDUS showed multiple circular blood flow signals inside the mass (i.e. basket pattern) (Figure 1B). Arterial and venous flow was confirmed by spectral analysis (Figure 1C) and the peak systolic velocity of the arterial flow noted in the mass was 16.4 cm/s with a resistance index of 0.38 and a pulsatility index of 0.52.

Abdominal CT scan before administration of a contrast material revealed a low-density mass (Figure 2). During the arterial phase of contrast-enhanced dynamic CT, the mass was enhanced earlier than the normal splenic parenchyma. During the delayed phase, the intensity of the mass was the same as that of the normal splenic parenchyma.

MRI showed that the mass in the spleen was iso-intense relative to the normal spleen on T1-weighed images and mild hyper-intense on T2-weighed images (Figure 3). During the arterial phase of contrast-enhanced dynamic MRI, the mass was enhanced earlier than the normal splenic parenchyma. During the delayed phase, the mass was mild hyperintense relative to the normal splenic parenchyma. These findings were suggestive of hemangioma, metastatic tumor, malignant lymphoma, angiosarcoma or hamartoma.

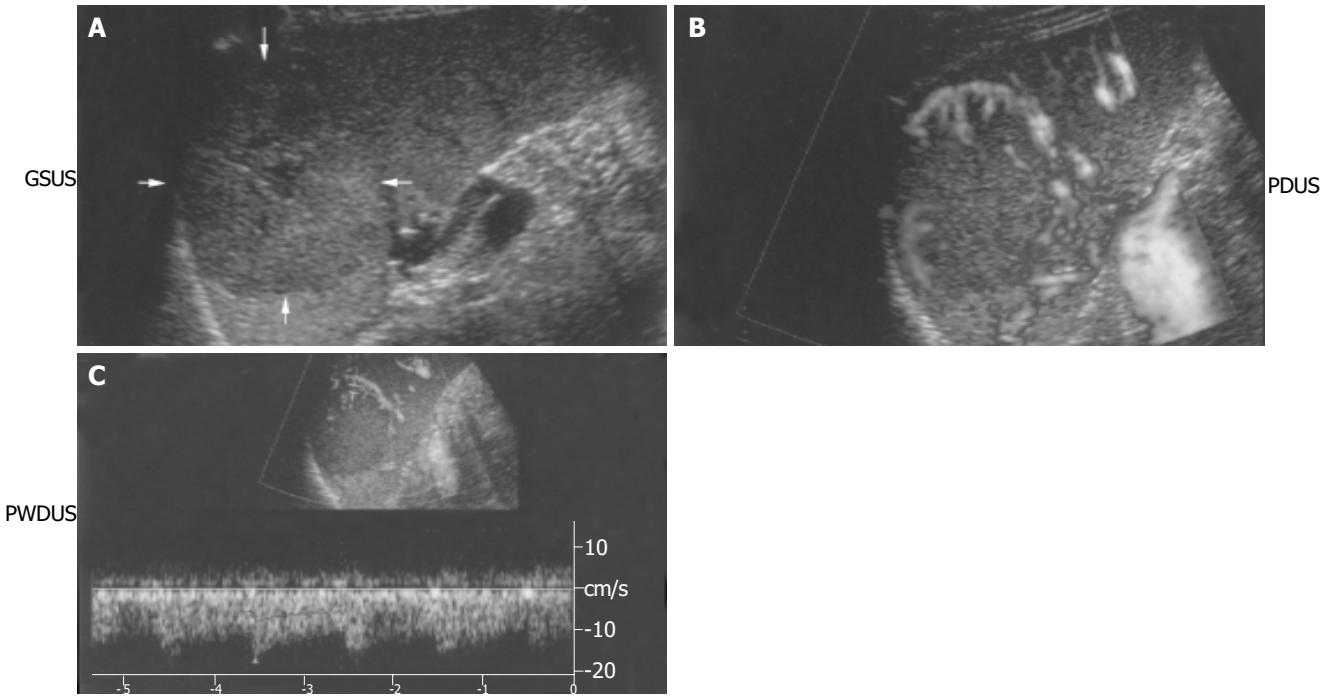


Figure 1 Splenic hamartoma on ultrasonogram. **A:** A homogeneous hamartoma on gray-scale sonogram with evidence of cystic changes in the mass (arrows); **B:** multiple circular blood flow signals within the mass on power Doppler sonogram (basket pattern); **C:** arterial and venous flow in the mass on duplex Doppler sonogram.

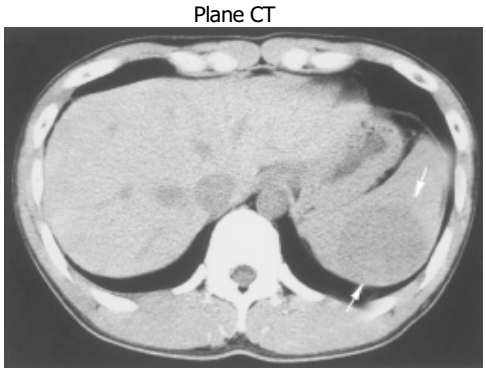


Figure 2 A low-density mass in the spleen shown by plane CT scan (arrows).

A splenectomy was performed because a malignant splenic neoplasm or metastasis could not be ruled out, as it could prevent the mass from spontaneous rupture. Histologic examination of the lesions revealed dilated vessels and congestion. The border of the mass and normal splenic parenchyma was smooth and clear (Figure 4A). The mass was composed of red pulp and lacked fibrous trabeculae and white pulp. The normal splenic parenchyma was compressed, and no capsule was found (Figure 4B).

The final pathologic diagnosis was a splenic hamartoma of the red pulp.

DISCUSSION

Splenic hamartoma is prevalent in either sex and has been reported in all age groups. However, it was reported that 50% of pediatric patients with a splenic hamartoma have clinical manifestations such as pancytopenia, anemia or thrombocytopenia[3]. Spontaneous rupture of the hamartoma with acute abdominal pain in adults has also been reported[2,8]. Here we present a case who was asymptomatic, and the splenic

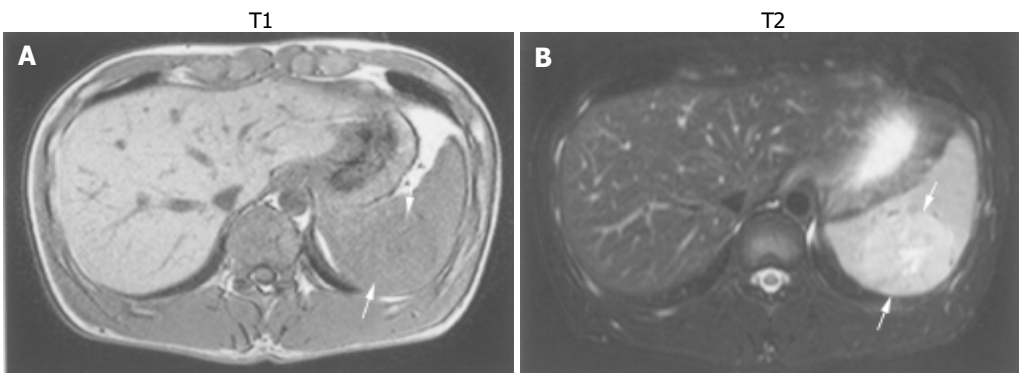


Figure 3 Isointense mass on standard T1-weighed MRI mass on (**A**) and mild hyperintense T2-weighed MRI (arrows **B**).

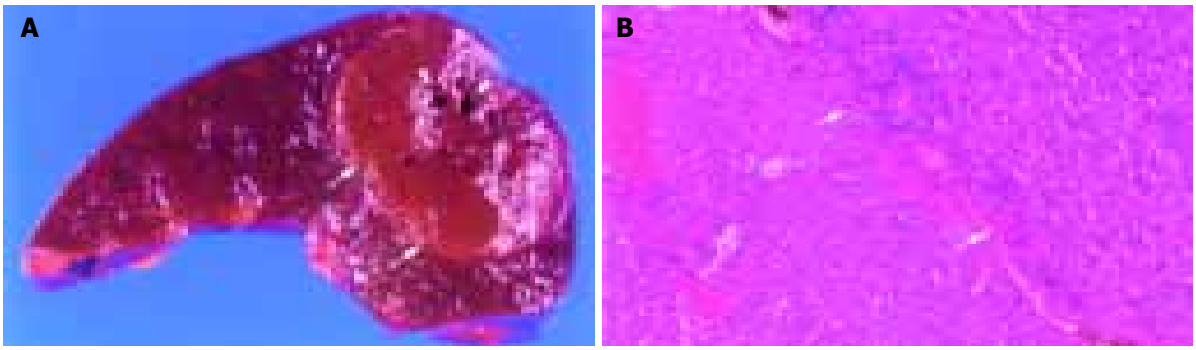


Figure 4 Dilated vessels (arrowheads) and border of the mass and normal splenic parenchyma (arrows) (**A**) and a mass consisting of red pulp **(B)** (HE×100).

tumor was coincidentally discovered, during a complete medical checkup.

Splenic hamartoma is a rare benign tumor. Wan *et al*.[9], have reported the sonographic findings in 53 cases of verified focal splenic lesions, such as cysts, infarcts, abscess, and hemangioma, spontaneous rupture, tuberculosis, lymphangioma, and hamartoma.

On gray-scale sonograms, most splenic hamartomas are solid and homogeneous masses with various echogenicities relative to the normal splenic parenchyma[3-6]. However, sonographic echogenicity indicates that splenic hamartoma is usually hypo-echoic[7,10], and occasionally heterogeneous and may exhibit cystic changes or calcification[4,11]. In our case, splenic hamartoma showed some solid and homogeneous characteristics via the gray-scale sonographic findings. However, internal echogenicity of the mass showed mixed pattern echoes containing a cystic area, but the posterior echo was only slightly enhanced. Gray-scale sonographic findings on tissue harmonic imaging (THI) have not been reported regarding the boundary echo of a splenic hamartoma. The gray scale of the boundary echoes shows a clear, smooth, and hyper-echoic rim. THI improves the resolution, because the high-condition wave beam is sharper than a standard wave beam. Also, THI is useful for improving the resolving power of the tumor. Splenic hamartomas are usually detected as hypo-echoic tumors, but in our case the echogenicity of the splenic hamartoma was iso-echoic and hypo-echoic (i.e. mixed pattern) on THI for gray-scale sonography. Splenic hamartomas are usually detected as hypervascular tumors by arteriography. Angiograms of the mass on power Doppler imaging (PDI) show tumor vessels with aneurysmal dilatation, arterio-venous shunts, vascular lakes, and tumor blush, presenting a typically malignant vascular pattern[12]. This is different from those on color Doppler image (CDI), because there is almost no dependence on the angle. Therefore, PDI exhibits excellent sensitivity compared to CDI. Tang *et al*.[7], have reported color Doppler sonographic findings in splenic hamartoma, and found that blood flow is concentrated around the mass as multiple radial blood flow signals. However, we found that blood flow was concentrated around the mass as surrounding blood flow signals coincident to the boundary echo and as multiple circular blood flow signals. Histologic analysis following splenectomy showed multiple vessels consistent with the PDUS findings.

Contrast-enhanced abdominal CT scans revealed that splenic hamartoma is iso-dense relative to the normal splenic parenchyma, before and after administration of intravenous contrast material[7,11]. The mass in our patient was iso-dense during the delay phase of contrast-enhanced dynamic CT, but had a low density relative to the normal splenic parenchyma, before administration of the intravenous contrast material. Also during the artery phase of contrast-enhanced dynamic CT, the mass had a high density relative to the normal splenic parenchyma.

Hamartomas of the spleen usually are iso-intense on T1-weighed MR images and hyper-intense on T2-weighed images[6,7] and the same was true for our case. However, Fernandez-Canton *et al*.[13], described that a histologically proven case presents a small (2.5 cm) focal mass, which is iso-intense to the splenic parenchyma on T1-weighed images and hypo-intense on turbo-spin-echo T2 and short T1 inversion recovery images. In addition, Chevallier *et al*.[10], reported that a fibrous-type splenic hamartoma measuring 7 cm in diameter that MRI showed is hyper-intense on T1-weighed MRI and hypo-intense on T2-weighed MRI.

Splenic hamartoma shows expansive growth and compresses the surrounding splenic tissue without a true capsule. Two histologic types of splenic hamartoma have been described[1]: the white-pulp (lymphoid) type and the red-pulp (pulposal) type. The white-pulp type is entirely composed of lymphoid tissue, whereas the red-pulp type defined by the Armed Forces Institute of Pathology as a hamartoma in 1995[14] is composed of sinuses and is histologically similar to that of normal splenic red pulp. Hamartomas are of the red-pulp type are the most reported cases, as was the case for our patient's splenic hamartoma.

Sonography permits differential diagnosis of tumor of the spleen. A splenic hemangioma is hyper-echoic on gray-scale sonograms[5,15] and color Doppler sonograms show few color echoes similar to the findings in hepatic hemangiomas. Color Doppler sonograms show an avascular pattern of metastatic tumors and malignant lymphoma of the spleen[5]. Sonograms of angiosarcomas show multiple hyper-echoic masses[16] and color Doppler sonograms show a fluctuating low-velocity flow pattern[17].

Since splenic hamartomas do not always exhibit hypervascularity[4], it should be included in the differential diagnosis of splenic tumors in which color Doppler sonograms show abundant blood flow. However, splenic

hamartomas are usually hypervascular tumors. The circular signals on power Doppler sonograms (basket pattern) in our case are consistent with the histologic findings.

In conclusion, abdominal CT and MRI require the administration of a contrast material to make an exact diagnosis. However, PDUS does not require the administration of a contrast material. Furthermore, PDUS does not affect the body. Therefore, the results of PDUS are equivalent to abdominal CT and MRI.

REFERENCES

1 **Silverman ML,** Livolsi VA. Splenic hamartoma. *Am J Clim Pathol* 1978; **70**: 224-229
2 **Morgenstern L,** Mccafferty L, Rosenberg J, Michel SL. Hamartomas of the spleen. *Arch Surg* 1984; **119**: 1291-1293
3 **Iozzo RV,** Haas JE, Chard RL. Symptomatic splenic hamartoma: a report of two cases and review of the literature. *Pediatrics* 1980; **66**: 261-265
4 **Komaki S,** Gombas OF. Angiographic demonstration of a calcified splenic hamartoma. *Radiology* 1976; **121**: 77-78
5 **Goerg C,** Schwerk WB. Color Doppler imaging of focal splenic masses. *Eur J Radiol* 1994; **18**: 214-219
6 **Ohtomo K,** Fukuda H, Mori K, Minami M, Itai Y, Inoue Y. CT and MR appearances of splenic hamartoma. *J Comput Assist Tomogr* 1992; **16**: 425-428
7 **Tang S,** Shimizu T, Kikuchi Y, Shinya S, Kishimoto R, Fujioka Y, Miyasaka K. Color Doppler sonographic findings in splenic hamartoma. *J Clin Ultrasound* 2000; **28**: 249-253
8 **Ferguson ER,** Sardi A, Beckman EN. Spontaneous rupture of splenic hamartoma. *J La State Med Soc* 1993; **145**: 48-52
9 **Wan YL,** Cheung YC, Lui KW, Tseng JH, Lee TY. Ultrasonographic findings and differentiation of benign and malignant focal splenic lesions. *Postgrad Med J* 2000; **76**: 488-493
10 **Chevallier P,** Guzman E, Fabiani P, Dib M, Oddo F, Padovani B. Fibrous splenic hamartoma: imaging features. *J Radiol* 1999; **80**: 1668-1671
11 **Zissin R,** Lishner M, Rathaus V. Case report: unusual presentation of splenic hamartoma; computed tomography and ultrasonic findings. *Clin Radiol* 1992; **45**: 410-411
12 **Kishikawa T,** Numaguchi Y, Watanabe K, Matsuura K. Angiographic diagnosis of benign and malignant splenic tumors. *Am J Roentgenol* 1978; **130**: 339-344
13 **Fernandez-Canton G,** Capelastegui A, Merino A, Astigarraga E, Larena JA, Diaz-Otazu R. Atypical MRI presentation of a small splenic hamartoma. *Eur Radiol* 1999; **9**: 883-885
14 **Warnke RA,** Weiss LM, Chan JK. Tumors of the lymph nodes and spleen. In: Rosai J, Sobin LH, editors. Atlas of tumor pathology. Series 3, Fascicle 14. Washington, DC: *Armed Forces Institute of Pathology* 1995
15 **Niizawa M,** Ishida H, Morikawa P, Naganuma H, Masamune O. Color Doppler sonography in a case of splenic hemangioma: value of compressing the tumor. *Am J Roentgenol* 1991; **157**: 965-966
16 **Ha HK,** Kim HH, Kim BK, Han JK, Choi BI. Primary angiosarcoma of the spleen. CT and MR imaging. *Acta Radiol* 1994; **35**: 455-458
17 **Aytac S,** Fitoz S, Atasoy C, Kuzu I, Cinar K, Erden I. Multimodality demonstration of primary splenic angiosarcoma. *J Clin Ultrasound* 1999; **27**: 92-95

Science Editor Wang XL and Guo SY **Language Editor** Elsevier HK

PO Box 2345, Beijing 100023, China
www.wjgnet.com
wjg@wjgnet.com

ELSEVIER

World J Gastroenterol 2005;11(33):5239-5240
World Journal of Gastroenterology ISSN 1007-9327
© 2005 The WJG Press and Elsevier Inc. All rights reserved.

• *CASE REPORT* •

Radiofrequency ablation for incidentally identified primary intrahepatic cholangiocarcinoma

Witold Zgodzinski, N. Joseph Espat

Witold Zgodzinski, Second Department of General Surgery, Skubiszewski Medical University of Lublin, Staszica 16, 20-081 Lublin, Poland
N. Joseph Espat, Department of Hepatobiliary Surgery, University of Illinois at Chicago, 840 South Wood Street, Chicago, IL 60612, United States
Correspondence to: Dr. N. Joseph Espat, MD, MS, FACS, Department of Surgery, UIC, 840 South Wood Street, Room 435E, Chicago, IL 60612, USA. jespat@uic.edu
Telephone: +1-312-355-1493 Fax: +1-312-355-1987
Received: 2004-12-14 Accepted: 2004-12-20

Abstract

Cholangiocarcinoma is the second most common primary hepato-biliary malignancy. The majority of patients with primary hepatic tumors are not suitable candidates for resection, due to advanced stage of the disease at presentation, anatomic limitations and medical co-morbidities. At present, radiofrequency ablation (RFA) may offer an alternative, feasible and safe therapy for selected patients with hepatic tumors, who are not otherwise candidates for hepatic resection. Herein, we present the case of successful RFA in a patient with a solitary, primary intrahepatic cholangiocarcinoma. The patient remained free of disease 24 mo after the procedure, and is still followed up. This is the first report of RFA application in the treatment of primary intrahepatic cholangiocarcinoma.

© 2005 The WJG Press and Elsevier Inc. All rights reserved.

Key words: Cholangiocarcinoma; Radiofrequency ablation; Hepatic tumor

Zgodzinski W, Espat NJ. Radiofrequency ablation for incidentally identified primary intrahepatic cholangiocarcinoma. *World J Gastroenterol* 2005; 11(33): 5239-5240
http://www.wjgnet.com/1007-9327/11/5239.asp

INTRODUCTION

Cholangiocarcinoma is a rare, malignant neoplasm arising from the biliary epithelium. The worldwide incidence of this malignancy is increasing and the annual incidence in USA is approximately 3 000-4 000 cases (0.85 per 100 000 rate)[1]. These cases are equally distributed between intrahepatic and extrahepatic lesions. The highest incidence rates of intrahepatic cholangiocarcinoma are noted in Northeast Thailand (96 per 100 000 for men and 38 per 100 000 for women). This variation in incidence is related to variations in the prevalence of risk factors. For example, in Thailand it is closely associated with liver fluke infestations[2]. The only potentially curative treatment for cholangiocarcinoma is surgical resection, but resectability of these tumors is determined by several factors including stage of the disease, anatomic conditions and patient's medical co-morbidities.

At present, RFA in selected cases of intrahepatic cholangiocarcinoma may be one alternative treatment approach, particularly for patients who are not candidates for major surgery. Herein, we present a case of successful RFA application in the patient with primary intrahepatic cholangiocarcinoma.

CASE REPORT

Subsequent to right upper abdominal discomfort, a 78-year-old man was found to have a solitary tumor in the right posterior hepatic lobe, by abdominal ultrasound examination. On physical examination, no significant findings were noted. Magnetic resonance scan confirmed the presence of an enhancing lesion located in segment VII, measuring approximately 4 cm×4 cm with enhancement on post-contrast images (Figure 1). No additional liver lesions or lymphadenopathy were identified. The patient's history was remarkable for radical right nephrectomy and partial left (upper-pole) nephrectomy for bilateral renal cell carcinoma, one year prior to the presentation. Given the history and radiographic findings, the most likely diagnosis was considered to be that of metastatic renal cell carcinoma. While the lesion was amenable to resection by proper posterior sectorectomy (segments VI, VII), the patient suffered from morbid obesity with BMI = 36, insulin-dependent diabetes, hypertension, renal insufficiency (baseline creatinine 1.8 mg/dL); placing him at significant risk for morbidity from major surgery. Treatment options inclusive of laparoscopic-guided RFA were presented to the patient and subsequently the patient underwent diagnostic laparoscopy with intent to perform RFA. At operation, no evidence of extrahepatic disease was identified. The lesion was observed to encompass the inferior-most aspect of the segment VI/VII interface with significant post right nephrectomy adhesions. To prevent inadvertent thermal injury to the colon at the hepatic flexure, the procedure was converted to open using a lateral sub-costal mini-laparotomy incision. A core needle biopsy of the lesion was performed and sent for permanent pathology review. Using the RITA 7-0 XLi device, and saline infusion, the lesion was targeted by intraoperative ultrasound, and the RFA system was deployed and placed at a 1.0 cm forward-throw distance from the deepest tumor margin. The system was initiated as per the manufacturer's instructions at 2 cm and subsequently advanced sequentially to 4-7 cm. The device needle was retracted in tract-ablation mode and the patient was awakened without complication. The post-operative period

was uneventful and the patient was discharged at d 4 with post-operative follow-up imaging at 1 mo (Figure 2).

Unexpectedly, the tumor biopsy pathology revealed primary bile duct adenocarcinoma with strong immunoreactivity for Cytokeratin 7, Cytokeratin CAM 5.2 and CEA. The tumor cells were negative for Cytokeratin 20 and Vimentin. The patient remained free of detectable disease after 24 mo (Figure 3) with stable normal liver function tests.

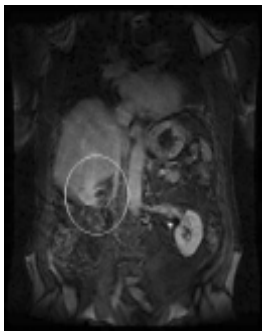


Figure 1 Magnetic resonance scan confirmed the presence of an enhancing lesion located in segment VII, measuring approximately 4 cm×4 cm with enhancement on post-contrast images.

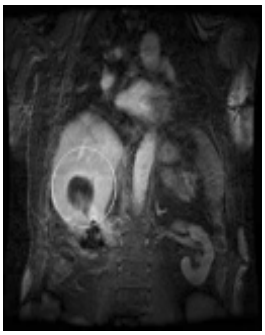


Figure 2 The post-operative period was uneventful and the patient was discharged at d 4 with post-operative follow-up imaging at 1 mo.

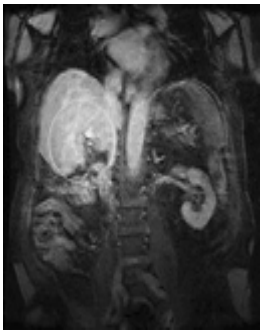


Figure 3 The patient remained free of detectable disease after 24 mo with stable normal liver function tests.

DISCUSSION

We have presented a case of successful ablation of incidentally found primary intrahepatic cholangiocarcinoma using the RFA technique. RFA has become a common treatment for patients otherwise not candidates for resection either as potentially curative or within the context of consolidation therapy in the multi-disciplinary management of patients with primary hepatic malignancy in the liver (including hepatocellular carcinoma) and hepatic metastasis from colon and rectum, lungs, breast, and numerous other sites[3-5]. RFA can be performed during an open intraoperative procedure, laparoscopically or percutaneously under ultrasound guidance. The tumor is destroyed by generating heat within the lesion which results in coagulative necrosis of the neoplastic tissue. Once tissue is heated above 48-50 ℃ for 4 min, mitochondrial death ensues, cell membranes melt and fuse, and with continued heating, protein denaturation and irreversible cell death occurs. A typical treatment results in local tissue temperatures that exceed 100 ℃. RFA has been reported to be relatively safe with acceptable rate of complications, when used by experienced surgeons. The combined overall early and late complication for this technique has been reported as 9.5% with higher risk in cirrhotic patients.

RFA has been previously reported as a salvage therapy for intrahepatic recurrent cholangiocarcinoma with a reported 10 mo survival after the procedure and ongoing follow-up. The present case report illustrates the potential expanding application of RFA technology in patients with primary cholangiocarcinoma, who are not otherwise surgical candidates. We emphasize that the selection criteria for RFA ablation should agree with the criteria used in selecting patients for potentially curative resection; i.e. tumor diagnosis that has demonstrated benefit from resection, no evidence of extrahepatic disease, capacity to encompass the entire lesion with a "margin", and recognition that ablation results in hepatic parenchymal destruction which is equivalent to resection volume loss, thus the underlying Child's status of the liver needs to be considered to prevent post-procedure hepatic failure. In the case presented, the diagnosis of cholangiocarcinoma was unknown and confirmed post procedure. The observed relatively long survival of this patient (24 mo) supports that, for selected patients, RFA may be a reasonable approach for effective therapy. However, until equivalence and/or survival data from appropriately designed clinical studies becomes available, the authors caution the judicious application of this technology.

REFERENCES

1 American cancer society. What are the key statistics for bile duct cancer? Available at: www.cancer.org
2 **Shaib Y,** El-Serag HB. The epidemiology of cholangiocarcinoma. *Semin Liver Dis* 2004; **24**: 115-125
3 **Curley SA,** Izzo F, Delrio P, Ellis LM, Granchi J, Vallone P, Fiore F, Pignata S, Daniele B, Cremona F. Radiofrequency ablation of unresectable primary and metastatic hepatic malignancies: results in 123 patients. *Ann Surg* 1999; **230**: 1-8
4 **Curley SA,** Izzo F, Ellis LM, Nicolas Vauthey J, Vallone P. Radiofrequency ablation of hepatocellular cancer in 110 patients with cirrhosis. *Ann Surg* 2000; **232**: 381-391
5 **Allgaier HP,** Deibert P, Zuber I, Olschewski M, Blum HE. Percutaneous radiofrequency interstitial thermal ablation of small hepatocellular carcinoma. *Lancet* 1999; **353**: 1676-1677

Science Editor Guo SY **Language Editor** Elsevier HK

PO Box 2345, Beijing 100023, China
www.wjgnet.com
wjg@wjgnet.com

ELSEVIER

World J Gastroenterol 2005;11(33):5241-5244
World Journal of Gastroenterology ISSN 1007-9327
© 2005 The WJG Press and Elsevier Inc. All rights reserved.

• *CASE REPORT* •

Refractory ulcerative colitis accompanied with cytomegalovirus colitis and multiple liver abscesses: A case report

Takuya Inoue, Ichiro Hirata, Yutaro Egashira, Kumi Ishida, Ken Kawakami, Eijiro Morita, Naoko Murano, Shingo Yasumoto, Mitsuyuki Murano, Ken Toshina, Takashi Nishikawa, Norihiro Hamamoto, Ken Nakagawa, Ken-Ichi Katsu

Takuya Inoue, Ichiro Hirata, Kumi Ishida, Ken Kawakami, Eijiro Morita, Naoko Murano, Shingo Yasumoto, Mitsuyuki Murano, Ken Toshina, Takashi Nishikawa, Norihiro Hamamoto, Ken Nakagawa, Ken-Ichi Katsu, The Second Department of Internal Medicine, Osaka Medical College, 2-7 Daigakucho, Takatsuki City, Osaka 569-8686, Japan
Yutaro Egashira, Department of Pathology, Osaka Medical College, Takatsuki City, Osaka 569-8686, Japan
Correspondence to: Dr. Ichiro Hirata, The Second Department of Internal Medicine, Osaka Medical College, 2-7 Daigakucho, Takatsuki City, Osaka 569-8686, Japan. hirata@poh.osaka-med.ac.jp
Telephone: +81-72-684-6532
Received: 2004-12-30 Accepted: 2005-01-26

© 2005 The WJG Press and Elsevier Inc. All rights reserved.

Key words: Liver abscess; Ulcerative colitis; Cytomegalovirus infection; Inflammatory bowel disease

Inoue T, Hirata I, Egashira Y, Ishida K, Kawakami K, Morita E, Murano N, Yasumoto S, Murano M, Toshina K, Nishikawa T, Hamamoto N, Nakagawa K, Katsu KI. Refractory ulcerative colitis accompanied with cytomegalovirus colitis and multiple liver abscesses: A case report. *World J Gastroenterol* 2005; 11(33): 5241-5244
http://www.wjgnet.com/1007-9327/11/5241.asp

Abstract

Various hepato-biliary complications are an increased incidence in patients with inflammatory bowel disease, and portal bacteremia is well documented in patients with ulcerative colitis (UC). However, few reports mention UC in association with liver abscesses. Recently, there are several reports describing cytomegalovirus (CMV) infection in association with disease exacerbation and steroid refractoriness in patients with UC. Here we present a case of refractory UC accompanied with multiple liver abscesses and CMV colitis. The patient, a 72-year-old male, with a five-year history of repeated admissions to our hospital for UC, presented with an exacerbation of his UC. Sigmoidoscopy performed on admission suggested that his UC was exacerbated, then he was given prednisolone and mesalazine orally, and betamethasone enemas. However, he had exacerbated symptoms. Repeat sigmoidoscopy revealed multiple longitudinal ulcers and pseudopolyps in the rectosigmoid colon. Although immunohistochemical staining of biopsy specimens and the serum testing for antigenemia were negative on admission and after the repeat sigmoidoscopy, they became histologically positive for CMV. Nonetheless, the patient developed spiking fevers, soon after ganciclovir was administered. Laboratory studies revealed an increased white cell count with left shift, and *Enterococcus fecalis* grew in blood cultures. An abdominal computed tomography (CT) scan was obtained and the diagnosis of liver abscesses associated with UC was made, based on CT results. The hepatic abscesses were successfully treated with intravenous meropenem for 6 wk, without further percutaneous drainage. To our knowledge, this is the first reported case of multiple liver abscesses that develop during UC exacerbation complicated by CMV colitis.

INTRODUCTION

Bacteremia involving the portal venous system is well documented in patients with inflammatory bowel disease (IBD)[1,2]. While studies of patients with ulcerative colitis (UC) suggest an increased incidence of portal bacteremia[1,2], the development of liver abscesses in these patients is relatively rare[3,4]. Only six such cases have been reported so far[5].

Cytomegalovirus (CMV) infection has been implicated in cases of refractory IBD[6,7], and can complicate severe steroid-resistant UC[8,9]. CMV infection characteristically forms discrete ulcers in the colon that can be seen during colonoscopy and may provide a clue to the diagnosis of this infection in UC patients[10]. The ulceration and loss of mucosal integrity that occur in CMV colitis are likely a predisposing factor for microbial invasion of the portal venous system. The subsequent development of any portal bacteremia might be related to the occurrence of liver abscesses in UC.

In this paper, we report a case of refractory UC accompanied with CMV colitis and multiple liver abscesses. To our knowledge, this is the first reported case of multiple liver abscesses that develop in the course of UC exacerbated by CMV colitis.

CASE REPORT

A 72-year-old male, with a 5-year history of repeated hospital admission for UC, was again admitted to our hospital with a month-long history of bloody diarrhea.

On admission, the patient with unremarkable vital signs complained of bloody diarrhea occurring six to ten times per day. On physical examination, his abdomen was slightly distended with normoactive bowel sounds but no tenderness, while his right upper quadrant was unremarkable. Initial

laboratory studies were remarkable for a slightly elevated white blood cell count of 8 640 per microliter (normal range 3 300-8 190/μL) with 66.5% neutrophils and an elevated C-reactive protein of 0.59 mg/dL (normal<0.25 mg/dL). All other laboratory values including liver function tests, were unremarkable. Additionally, the patient had no evidence in his serum of CMV antigen pp65, and stool cultures revealed no pathogenic organisms.

An abdominal X-ray revealed a normal bowel gas pattern, but no evidence of colonic dilatation. Abdominal computed tomography (CT) scan showed the presence of multiple liver cysts, bilateral renal cysts, and colonic inflammation extending from the distal sigmoid colon to the rectum. Sigmoidoscopy revealed diffuse mucosal edema, loss of normal vascular patterns, and friability without ulcerations in the rectum and distal sigmoid colon (Figure 1A).

Initially, the patient received 30 mg prednisolone orally in addition to 2 250 mg mesalazine orally and 3 mg betamethasone enema daily. Although, this treatment resulted in temporary resolution of the diarrhea, he subsequently developed bloody diarrhea, occurring as often as 14 times per day, accompanied with tenesmus, crampy lower abdominal pain, and elevated temperatures (Lichtiger's clinical activity index[11] was 17). Sigmoidoscopy on hospital d 18 revealed multiple longitudinal ulcers and pseudopolyps in the recto-sigmoid colon (Figure 1B). Although, colonoscopic findings suggested CMV infection in addition to UC, immunohistochemical CMV studies and serum testing for CMV antigenemia remained negative. Leukocytapheresis was initiated in addition to the other treatment; however, the patient's bloody and watery diarrhea persisted.

Repeat sigmoidoscopy performed in the hospital on d 29, revealed worsened progression of the previous findings. Biopsy specimens, obtained from the margin and base of the ulcers, showed CMV nuclear inclusion bodies in histiocytes (Figure 2A). Immunohistochemical staining revealed that these cells were indeed positive for CMV (Figure 2B). Moreover, the patient's serum also became positive for CMV antigenemia. These findings suggested that CMV infection was associated with the patient's UC exacerbation. His prednisolone was therefore gradually tapered, and ganciclovir (600 mg twice daily) was administered intravenously for 3 wk. Following the initiation of treatment with ganciclovir, his abdominal symptoms gradually resolved. After 3 wk of antiviral treatment, the Lichtiger's clinical activity index fell from 16 (on the day before ganciclovir was started) to 5.

Eight days after ganciclovir was started on, the patient had a spiking temperature of 38.5 ℃ associated with chills. Laboratory tests revealed an increase in his white blood cell count to 1 240 per microliter with 22.5% band forms, 73.0% polymorphonuclear leukocytes, and 4.5% lymphocytes. His C-reactive protein rose to 4.95 mg/dL. A CT scan demonstrated multiple, small hypo-dense lesions in the right lobe of the liver, suggesting multiple hepatic abscesses (Figure 3A). Blood cultures were positive for *Enterococcus fecalis*.

The patient was treated with intravenous human immunoglobulin (5 g daily) for 3 d, and 1.0 g meropenem intravenously every 12 h for 6 wk. Fever and diarrhea slowly resolved. Twenty-two days later, follow-up CT scan showed a decrease in the number of hypo-dense lesions in the liver. Another CT scan in the hospital on d 119, revealed no evidence of residual liver abscesses (Figure 3B). A colonoscopy performed in the hospital on d 120, demonstrated marked improvement in the appearance of the longitudinal ulcers. He was discharged from the hospital on the following day.

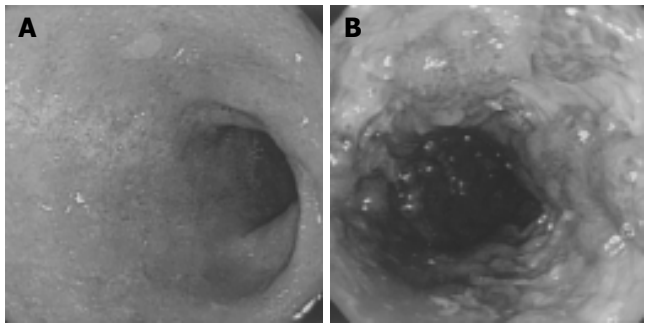


Figure 1 Diffuse mucosal edema, loss of vascular pattern, and friability without ulcerations in the rectum and distal sigmoid colon (**A**) and multiple longitudinal ulcers and pseudopolyps in the rectosigmoid colon (**B**).

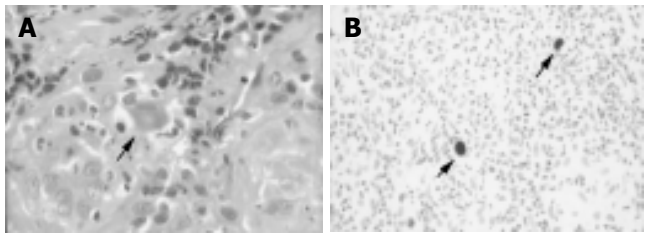


Figure 2 Enlarged histiocyte with Cowdry A type intranuclear inclusion body (**A**) and histiocytes positive for immunostaining of the CMV antigen (**B**).

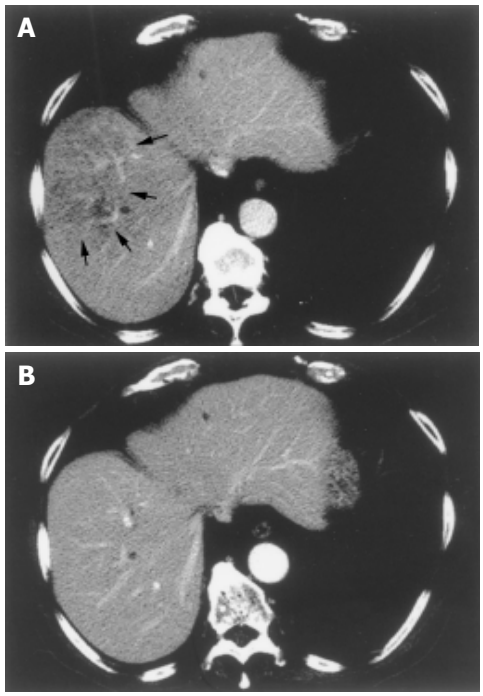


Figure 3 Small hypo-dense lesions in the right lobe of the liver, suggestive of multiple liver abscesses (**A**) and no evidence of residual hypo-dense lesions after treatment with meropenem (**B**).

DISCUSSION

Various hepato-biliary complications are known to have an increased incidence in patients with IBD[3]. These complications include fatty changes in the liver, cholelithiasis, pericholangitis, primary sclerosing cholangitis, cirrhosis, chronic active hepatitis, amyloidosis, and bile duct cancer[3]. Even though portal bacteremia is well documented in patients with IBD[1,2], liver abscess is a rare complication[3,4]. In an epidemiological study of 1 274 UC patients in Sweden over a 25-year period, Broome *et al*.[12], found only three cases of liver abscesses. To our knowledge, there are only six such case reports in the literature[5,12-17].

Recently, there are several reports that associate CMV infection with UC exacerbation and steroid refractoriness[6,18,19]. Several retrospective studies of UC patients undergoing proctocolectomy, document CMV anywhere from 4.6% to 13% of surgical specimens[20-22]. In a retrospective, case-control study of 80 patients, Kambham *et al*.[8], reported that immunohistochemistry detects CMV in 10 of 40 (25%) patients with refractory UC and one of 40 (2.5%) patients with non-refractory UC. Cottone *et al*.[9], looked at the prevalence and outcome of CMV infection in a prospective study and reported that CMV is detected in 5 out of 16 (31%) patients with refractory UC. Together, the data from these studies imply that untreated CMV infection is significantly associated with steroid-refractory UC.

Patients with IBD are at a higher risk of CMV infections, due to the following reasons: (1) the common use of immunosuppressive therapies including steroids, thiopurines, methotrexate, cyclosporine A, mycophenolate, tacrolimus, or other newer immunosuppressive agents; (2) suggested tropism for CMV at sites of inflammation and altered immunity in malnourished IBD patients[7]. Given the association of CMV infection with refractory UC, CMV infection should be ruled out with rectal biopsy and CMV serology, prior to initiating immunosuppressive therapy in UC patients presenting with exacerbation[7,8].

In the present case, we had difficulty in making a diagnosis of complicating CMV infection. Both admission immunologic testing for CMV antigen pp65 and finding from the first sigmoidoscopy did not present any evidence of a complicating CMV infection. After the patient failed to improve with initial therapy, although colonoscopic findings suggested CMV infection in addition to UC, immunohistochemical CMV studies and serum testing for CMV remained negative.

Papadakis *et al*.[7], suggested that CMV infection should be suspected in those with systemic symptoms and signs such as high fever, dyspnea, lymphadenopathy, or splenomegaly; and in those whose bowel disease is unresponsive to steroids; as well as in those who develop worsening clinical symptoms after an initial improvement while on immunosuppression. Though the patient had multiple negative results, we were highly suspicious of CMV colitis, and repeated rectal biopsies and serum antigen testing. Treatment with steroids might be a major predisposing factor for activation of CMV. Our experience suggests that discrete and longitudinal ulcers found during colonoscopy might be indicative of CMV infection in UC patients[10].

Although portal bacteremia does occur in UC patients, the incidence of portal vein bacteremia is unknown. Manousos *et al*.[23], and Brooke *et al*.[24], performed portal vein blood cultures at laparotomy and noted that portal bacteremia occurs in about 25% of patients with active UC. Nonetheless very few reports on liver abscess associated with IBD are available. Song *et al*.[5], reviewed six cases of UC reported until 2003. Approximately 30 cases of CD with liver abscess were reported until 1994[25]. Pylephlebitis, steroid administration, intra-abdominal abscesses related to the bowel, the presence of enteric fistula and perforation of the bowel are associated with the development of liver abscess[5,16,25,26]. However, the significance of these factors in UC patients remains undetermined.

Liver abscess is rare in UC patients. Treusch *et al*.[14], and Taylor[27], suggested that the rarity may be due to the fact that the infection is a chronic one in which the body has the opportunity to throw up local barriers and produce a certain amount of systemic immunity. Song *et al*.[5], described that considering portal bacteremia and pylephlebitis in UC patients, ulceration and loss of integrity of the normal mucosal barrier may predispose to microbial invasion of the portal venous system. The most common microorganisms that go on to cause liver abscesses are Gram-negative aerobes, such as *Escherichia coli*, *Streptococci*, *Proteus* species, *Klebsiella species*, and *Enterobacter* species[28]. In our patient, *Enterococcus* species grew in blood and stool cultures, suggesting that there might be an association between liver abscess and rectal ulcer. The time of the development of liver abscess, after steroid treatment and exacerbation of rectal ulcer, seems to indicate that CMV infection plays an important role in their development. Multiple abscesses have a higher mortality rate than single ones, probably in part related to the inability to effectively drain all sources of infection. However, in some cases, pharmacotherapy alone has produced good results[28,29]. Because of steroid treatment, we considered that he had an immunocompromised status, and then intravenous human immunoglobulin was administered. We believe that early diagnosis of CMV colitis complicating UC ultimately helps the resolution of liver abscesses. It should be considered that administration of ganciclovir and the gradual termination of steroid treatment result in remission of colitis and liver abscesses.

In conclusion, in cases of refractory UC, one should highly suspect underlying CMV infection, and early diagnosis of complicating CMV infection in UC patients may contribute to the resolution of liver abscesses and excellent clinical outcome.

REFERENCES

1 **Brooke BN,** Slaney G. Portal bacteremia in ulcerative colitis. *Lancet* 1958; **1**: 1206-1207
2 **Eade MN,** Brooke BN. Portal bacteraemia in cases of ulcerative colitis submitted to colectomy. *Lancet* 1969; **1**: 1008-1009
3 **Williams SM,** Harned RK. Hepatobiliary complications of inflammatory bowel disease. *Radiol Clin North Am* 1987; **25**: 175-188
4 **Greenstein AJ,** Janowitz HD, Sachar DB. The extra-intestinal complications of Crohn's disease and ulcerative colitis: a study of 700 patients. *Medicine* 1976; **55**: 401-412
5 **Song J,** Swekla M, Colorado P, Reddy R, Hoffmann S, Fine S. Liver abscess and diarrhea as initial manifestations of ulcer-

ative colitis: case report and review of the literature. *Dig Dis Sci* 2003; **48**: 417-421
6 **Berk T,** Gordon SJ, Choi HY, Cooper HS. Cytomegalovirus infection of the colon: a possible role in exacerbations of inflammatory bowel disease. *Am J Gastroenterol* 1985; **80**: 355-360
7 **Papadakis KA,** Tung JK, Binder SW, Kam LY, Abreu MT, Targan SR, Vasiliaukas EM. Outcome of cytomegalovirus infections in patients with inflammatory bowel disease. *Am J Gastroenterol* 2001; **96**: 2137-2142
8 **Kambham N,** Vij R, Cartwright CA, Longacre T. Cytomegalovirus infection in steroid-refractory ulcerative colitis: a case-control study. *Am J Surg Pathol* 2004; **28**: 365-373
9 **Cottone M,** Pietrosi G, Martorana G, Casa A, Pecoraro G, Oliva L, Orlando A, Rosselli M, Rizzo A, Pagliaro L. Prevalence of cytomegalovirus infection in severe refractory ulcerative and Crohn's colitis. *Am J Gastroenterol* 2001; **96**: 773-775
10 **Nishimoto Y,** Matsumoto T, Suekane H, Shimizu M, Mikami Y, Iida M. Cytomegalovirus infection in a patient with ulcerative colitis: colonoscopic findings. *Gastrointest Endosc* 2001; **53**: 816-818
11 **Lichtiger S,** Present DH, Kornbluth A, Gelernt I, Bauer J, Galler G, Michelassi F, Hanauer S. Cyclosporine in severe ulcerative colitis refractory to steroid therapy. *N Engl J Med* 1994; **330**: 1841-1845
12 **Broome U,** Glaumann H, Hellers G, Nilsson B, Sorstad J, Hultcrantz R. Liver disease in ulcerative colitis: an epidemiological and follow up study in the county of Stockholm. *Gut* 1994; **35**: 84-89
13 **Lansbury J,** Bargen JA. The association of multiple hepatic abscesses and chronic ulcerative colitis. *Med Clin North Am* 1933; **16**: 1427-1431
14 **Treusch JV.** Multiple liver abscesses complicating non-specific chronic ulcerative colitis: report of a case. *Gastroenterology* 1952; **20**: 166-173
15 **Davidson JS.** Solitary pyogenic liver abscess. *Br Med J* 1964; **2**: 613-615
16 **MacDonald PH,** Mercer CD. Hepatic abscess associated with subclinical ulcerative colitis. *Can J Gastroenterol* 1989; **3**: 123-125
17 **Dabrowski M,** Koc J, Kus J. Liver abscess in the course of ulcerative colitis. *Wiad Lek* 1997; **50**: 117-119
18 **Loftus EV Jr,** Alexander GL, Carpenter HA. Cytomegalovirus as an exacerbating factor in ulcerative colitis. *J Clin Gastroenterol* 1994; **19**: 306-309
19 **Streetz KL,** Buhr T, Wedemeyer H, Bleck J, Schedel I, Manns MP, Goke MN. Acute CMV-colitis in a patient with a history of ulcerative colitis. *Scand J Gastroenterol* 2003; **38**: 119-122
20 **Cooper HS,** Raffensperger EC, Jonas L, Fitts WT Jr. Cytomegalovirus inclusions in patients with ulcerative colitis and toxic dilation requiring colonic resection. *Gastroenterology* 1977; **72**: 1253-1256
21 **Eyre-Brook IA,** Dundas S. Incidence and clinical significance of colonic cytomegalovirus infection in idiopathic inflammatory bowel disease requiring colectomy. *Gut* 1986; **27**: 1419-1425
22 **Kaufman HS,** Kahn AC, Iacobuzio-Donahue C, Talamini MA, Lillemoe KD, Hamilton SR. Cytomegaloviral enterocolitis: clinical associations and outcome. *Dis Colon Rectum* 1999; **42**: 24-30
23 **Manousos ON,** Doxiades T. Colitis and liver disease. *Am J Proctol* 1966; **17**: 48-51
24 **Brooke BN,** Dykes PW, Walker FC. A study of liver disorder in ulcerative colitis. *Postgrad Med J* 1961; **37**: 245
25 **Vakil N,** Hayne G, Sharma A, Hardy DJ, Slutsky A. Liver abscess in Crohn's disease. *Am J Gastroenterol* 1994; **89**: 1090-1095
26 **Crass JR.** Liver abscess as a complication of regional enteritis: interventional considerations. *Am J Gastroenterol* 1983; **78**: 747-749
27 **Taylor FW.** Regional enteritis complicated by pyephlebitis and multiple liver abscess. *Am J Med* 1949; **7**: 838-840
28 **Brmbolic B.** Multiple abscesses of the liver caused by Campylobacter jejuni. *J Clin Gastroenterol* 1995; **20**: 307-309
29 **Zighelboim J,** Williams TW Jr, Bradshaw MW, Harris RL. Successful medical management of a patient with multiple hepatic abscesses due to Edwardsiella tarda. *Clin Infect Dis* 1992; **14**: 117-120

Science Editor Wang XL and Guo SY **Language Editor** Elsevier HK

PO Box 2345, Beijing 100023, China
www.wjgnet.com
wjg@wjgnet.com

ELSEVIER

World J Gastroenterol 2005;11(33):5245-5247
World Journal of Gastroenterology ISSN 1007-9327
© 2005 The WJG Press and Elsevier Inc. All rights reserved.

• *CASE REPORT* •

Endoscopic excision of a prolapsing malignant polyp which caused intermittent gastric outlet obstruction

Hugh J Freeman

Hugh J Freeman, Department of Medicine (Gastroenterology), University of British Columbia, Vancouver, BC, V6T 1W5, Canada
Correspondence to: Dr. Hugh J. Freeman, Gastroenterology, UBC Hospital, 2211 Wesbrook Mall, Vancouver, BC, V6T 1W5 Canada. hugfree@shaw.ca
Telephone: +1-604-822-7216 Fax: +1-604-822-7236
Received: 2004-12-30 Accepted: 2005-02-28

Abstract

A 69-year-old male with chronic lymphocytic leukemia presented with iron deficiency anemia and post-prandial abdominal fullness. Endoscopy showed a large polyp on a stalk, protruding through the pylorus into the duodenum causing intermittent gastric outlet obstruction. While prolapsing gastric antral polyps are usually benign and hyperplastic, inflammatory or regenerative in type, excisional snare polypectomy here led to complete resolution of his symptoms, but showed a malignant polyp.

© 2005 The WJG Press and Elsevier Inc. All rights reserved.

Key words: Gastric adenoma; Gastric carcinoma; Endoscopic polypectomy; Neoplastic gastric polyps

Freeman HJ. Endoscopic excision of a prolapsing malignant polyp which caused intermittent gastric outlet obstruction. *World J Gastroenterol* 2005; 11(33): 5245-5247
http://www.wjgnet.com/1007-9327/11/5245.asp

INTRODUCTION

Gastric epithelial polyps are uncommon, estimated to be present in less than 2% of all endoscopic examinations[1]. Up to 90% of all gastric polyps are benign, can usually be classified as inflammatory, regenerative or hyperplastic, and are often less than 1 cm in size[2,3]. Only 5-10% of all gastric polyps are adenomas. Malignant change occurs in less than 1%, usually only in those that are over 1 cm[4].

Since the vast majority of gastric polyps are not neoplastic, and have a very low risk of containing a carcinoma, some authorities have argued that polyp biopsy alone may be sufficient; indeed, most adenomas are reported to display a maximal degree of dysplastic change in the most superficial portion of the polyp permitting biopsy detection [5]. Polyps may also cause symptoms related to bleeding or intermittent outlet obstruction, and may be removed endoscopically or at surgical resection. However, in some centers, even larger asymptomatic polyps may be biopsied, rather than excised, especially in elderly patients[5]. It has been argued that polypectomy is not without significant risk, particularly from hemorrhage after gastric polypectomy where risk has been historically estimated to be as high as 4%[5,6].

Gastric adenomas are usually solitary and asymptomatic. They occur primarily in the antrum and their frequency increases with aging[4]. Logically, gastric adenomas are best completely excised, so that the malignant potential, although very low, is removed. If endoscopic removal is not possible, then surgical resection might be considered, but then the individual risk and benefits must be weighed compared to long-term endoscopic monitoring, since it has been estimated that about 11% of gastric adenomas develop carcinoma within 4 years[4]. Unless the polyps cause symptoms, however, some have advocated that it may be reasonable to do nothing[5].

The present case was unusual in that a prolapsing adenomatous gastric polyp, complicated by an adenocarcinoma, was responsible for gastric outlet obstructive symptoms and these were completely resolved with endoscopic excision of the gastric polyp.

CASE REPORT

A 69-years old Indo-Canadian male with chronic lymphocytic leukemia was referred by his hematologist for investigation of a progressively developing iron deficiency anemia over the prior year. He felt occasional fullness and nausea after meals. There were no other symptoms. He denied hematemesis, rectal bleeding, melena and occult blood testing was negative. Except for a single pea-sized cervical lymph node, there was no other lymphadenopathy. There was no hepatomegaly or splenomegaly. Laboratory studies revealed a hemoglobin of 109 g/L (normal, 135-175) and a white blood cell count of 13.4×A9/L (normal, 4.0-11.0), the majority being lymphocytes. Serum ferritin was 3.1 ug/L (normal, 20-300). INR and PTT were normal. Prior studies, including flow cytometry, had confirmed the typical immunophenotype of chronic lymphocytic leukemia. Upper endoscopic evaluation showed a large polyp with a stalk originating in the gastric antrum and prolapsing through the pylorus (Figure 1). After the polyp was maneuvered into the stomach, it was noted to be irregular with evidence of surface friability and ulceration (Figure 2). After the polyp was excised by snare polypectomy, pathological evaluation was reported to show an adenomatous polyp with high grade dysplasia along with foci of intramucosal carcinoma. Additional sections through the base of the polyp stalk, however, confirmed that polyp excision was

complete without evidence of invasion into the submucosa. No malignant cells were detected in the polyp stalk or cut margin. Other gastric biopsies were normal and stains for *Helicobacter pylori* were negative.



Figure 1 Polypoid lesion with long stalk protruding through the pylorus into the duodenum.



Figure 2 Slightly irregular gastric antral polyp with eroded surface. Polypectomy specimen showed adenoma with high-grade dysplasia and invasive intramucosal carcinoma. No invasion into stalk or submucosa.

DISCUSSION

This patient presented with a large gastric antral polyp that had prolapsed through the pylorus, causing symptoms due to a gastric outlet obstruction. The polyp was endoscopically excised and proved to be a large gastric adenoma complicated by adenocarcinoma. This is distinctly unusual. Endoscopic removal or excision of symptomatic and prolapsing gastric polyps have been occasionally reported in the literature, however, these have been, as might be anticipated, primarily large, sometimes pedunculated polyps with inflammatory, regenerative or hyperplastic histopathologic features, rather than adenomas or adenomas with superimposed carcinomas[7-12].

In the earlier endoscopic literature, endoscopic biopsy alone for most lesions was thought to be sufficient, and if the histopathologic changes in these biopsies were consistent with an adenoma, then endoscopic polypectomy, or surgical resection, could be considered[13-16]. Later, endoscopic excision, rather than biopsy alone, was recommended since the procedure could be done safely and since foci of *in situ* malignant change could be detected in some adenomas. Others have also demonstrated the detection of carcinoma or dysplastic change in hyperplastic gastric polyps[17-19]. Given the evolution of endoscopic accessories for control of post-polypectomy bleeding vessels (e.g., loops, clips), the excision of large, especially solitary, gastric polyps has clearly been facilitated.

An additional management issue for the future was also considered here. Gastric polyps that have been completely excised and contain invasive cancer may require additional evaluation. Data is currently very limited for gastric polyps on the role of a further local surgical resection to examine adjacent lymph nodes for metastases. It appears that the risk of lymph node metastases is exceedingly low, but it is not zero[20]. Previous studies of so-called early gastric cancer confined to the mucosa or submucosa may provide some guidance. For early gastric cancers of the polypoid subtype (type 1) treated with surgical resection, 1.8% of patients with intramucosal carcinoma had nodal metastases compared to 18.5% with submucosal involvement[5]. Thus, until more data is available, it would appear reasonable to treat all polyps with pathologically-defined intramucosal carcinoma alone with endoscopic resection alone, while an additional surgical resection should be considered, if submucosal infiltration is present.

REFERENCES

1 **Blackstone MO.** The endoscopic diagnosis of early gastric cancer. *Gastrointest Endosc* 1985; **31**: 225-226
2 **Tomasulo J.** Gastric polyps. HIstological types and their relationship to gastric carcinoma. *Cancer* 1971; **27**: 1346-1355
3 **Zea-Iriarte W,** Sekine I, Itsuno M, Makiyama K, Naito S, Nakayama T, Nishisawa-Takano JE, Hattori T. Carcinoma in gastric hyperplastic polyps. A phenotypic study. *Dig Dis Sci* 1996; **41**: 377-386
4 **Kamiya T,** Morishita T, Asakura H, Miura S, Munakata Y, Tsuchiya M. Long-term follow-up study on gastric adenoma and its relation to gastric protruded carcinoma. *Cancer* 1982; **50**: 2496-2503
5 **Lewin KJ,** Riddell RH, Weinstein WM. Gastric Polyps and Tumors. In: Gastrointestinal Pathology and Its Clinical Implications. Volume 1. *New York: Igaku Shoin* 1992: 588-623
6 **ReMine SG,** Hughes RW Jr, Weiland LH. Endoscopic gastric polypectomies. *Mayo Clin Proc* 1981; **56**: 371-375
7 **Vittal SB.** Endoscopic polypectomy of a symptomatic antral polyp. *Am J Gastroenterol* 1975; **64**: 55-58
8 **Kumar A,** Quick CR, Carr-Locke DL. Prolapsing gastric polyp, an ususual cause of gastric outlet obstruction: a review of the pathology and management of gastric polyps. *Endoscopy* 1996; **28**: 452-455
9 **Dean PG,** Davis PM, Nascimento AG, Farley DR. Hyperplastic gastric polyp causing progressive gastric outlet obstruction. *Mayo Clin Proc* 1998; **73**: 964-967
10 **Cerwenka H,** Bacher H, Mischinger HJ. Pyloric obstruction caused by prolapse of a hyperplastic gastric polyp. *Hepatogastroenterology* 2002; **49**: 958-960
11 **Alper M,** Akcan Y, Belenli O. Large pedunculated antral hyperplastic gastric polyp traversed to bulbus causing outlet obstruction and iron deficiency anemia: endoscopic removal. *World J Gastroenterol* 2003; **9**: 633-634
12 **Gencosmanoglu R,** Sen-Oran E, Kurtkaya-Yapicier O, Tozun N. Antral hyperplastic polyp causing intermittent gastric outlet obstruction: case report. *BMC Gastroenterol* 2003; **3**: 16

13 **Niv Y,** Bat L. Gastric polyps-a clinical study. *Isr J Med Sci* 1985; **21**: 841-844
14 **Chua CL.** Gastric polyps: the case for polypectomy and endoscopic surveillance. *J R Coll Surg Edinb* 1990; **35**: 163-165
15 **Seifert E,** Gail K, Weismuller J. Gastric polypectomy. Long-term results (survey of 23 centres in Germany). *Endoscopy* 1983; **15**: 8-11
16 **Archimandritis A,** Spiliadis C, Tzivras M, Vamvakousis B, Davaris P, Manika Z, Scandalis N. Gastric epithelial polyps: a retrospective endoscopic study of 12974 symptomatic patients. *Ital J Gastroenterol* 1996; **28**: 387-390
17 **Harju E.** Gastric polyposis and malignancy. *Br J Surg* 1986; **73**: 532-533
18 **Davaris P,** Petraki K, Archimandritis A, Haritopoulos N, Papcharalampous N. Mucosal hyperplastic polyps of the stomach. Do they have any potential to malignancy? *Pathol Res Pract* 1986; **181**: 385-389
19 **Daibo M,** Itabashi M, Hirota T. Malignant transformation of gastric hyperplastic polyps. *Am J Gastroenterol* 1987; **82**: 1016-1025
20 **Imaoka W,** Ida K, Katoh T, Okuda J, Kawai K. Is curative endoscopic treatment of early gastric cancer possible? *Endoscopy* 1987; **19**(Suppl 1): 7-11

Science Editor Guo SY **Language Editor** Elsevier HK

PO Box 2345, Beijing 100023, China
www.wjgnet.com
wjg@wjgnet.com

ELSEVIER

World J Gastroenterol 2005;11(33):5248-5250
World Journal of Gastroenterology ISSN 1007-9327
© 2005 The WJG Press and Elsevier Inc. All rights reserved.

• *CASE REPORT* •

Churg-Strauss syndrome complicated by colon erosion, acalculous cholecystitis and liver abscesses

Msahiro Suzuki, Kazuo Nabeshima, Mitsukazu Miyazaki, Hitoshi Yoshimura, Shinsei Tagawa, Katsuya Shiraki

Msahiro Suzuki, Kazuo Nabeshima, Mitsukazu Miyazaki, Hitoshi Yoshimura, Shinsei Tagawa, Internal Medicine, Mie Prefectual Shima Hospital, Japan
Katsuya Shiraki, First Department of Internal Medicine, University School of Medicine, Tsu 514-8507, Japan
Correspondence to: Katsuya Shiraki, MD, PhD, First Department of Internal Medicine, Mie University School of Medicine, 2-174 Edobashi, Tsu, Mie 514-8507, Japan. katsuyas@clin.medic.mie-u.ac.jp
Telephone: +81-592-31-5015 Fax: +81-592-31-5201
Received: 2004-12-17 Accepted: 2005-02-18

Abstract

We report on a case of Churg–Strauss syndrome (CSS) with colon erosion, cholecystitis and liver abscesses. A 21-year-old woman with a history of bronchial asthma for 3 years was admitted with a complaint of abdominal pain. Laboratory findings included remarkable leukocytosis and eosinophilia, and a colonoscopy revealed erosion from the rectum to the ileocecal region. In addition, a colonic biopsy specimen showed necrotizing vasculitis and marked eosinophilic infiltration. On the basis of the clinical features and histopathological findings, she was diagnosed with CSS and subsequently treated with oral prednisolone, after which the eosinophilia and abdominal pain disappeared. However, on the 15th d in hospital she developed cholecystitis and liver abscesses. She was therefore treated with antibiotics and as a result went into clinical remission.

© 2005 The WJG Press and Elsevier Inc. All rights reserved.

Key words: Churg-Strauss syndrome; Cholecystitis; Liver abscesses

Suzuki M, Nabeshima K, Miyazaki M, Yoshimura H, Tagawa S, Shiraki K. Churg-Strauss syndrome complicated by colon erosion, acalculous cholecystitis and liver abscesses. *World J Gastroenterol* 2005; 11(33): 5248-5250
http://www.wjgnet.com/1007-9327/11/5248.asp

INTRODUCTION

Churg and Straus[1] histopathologically investigated a group of 13 patients who first developed asthma, followed by fever, hypereosinophilia and systemic small vessel vasculitis noted that it was characterized by necrotizing vasculitis and extravascular granuloma with hypereosinophilia, which distinguished it from classic PAN. The following year, Zeek[2,3] referred to this vasculitis as allergic granulomatous angitis and distinguished it from hypersensitivity vasculitis as a type of necrotizing vasculitis. We have therefore referred to this as Churg-Strauss syndrome, a disease which is manifested as asthma, eosinophilia and vasculitis. When its biopsy specimen histopathologically shows hypereosinophilia or extravascular granuloma, we refer to it as allergic granulomatous angitis. Mononeuritis[4,5] multiplex and gastrointestinal involvement are common in CSS, but cholecystitis is less common. In the literature, six cases[6-11] of cholecystitis complicated with CSS have been reported, while for liver abscesses, only one[14] has been reported. We describe herein a case of CSS presented with colon erosion, cholecystitis and liver abscesses.

CASE REPORT

A 21-year-old woman was admitted on July 2, 2002, with a complaint of abdominal pain. The patient had a history of bronchial asthma and sinusitis 3 years prior to admission, and mentioned that her mother was an asthmatic. A year prior to admission, the patient had been diagnosed with eosinophilic infiltrating pneumonia and was treated with an oral corticosteroid, which had been tapered and continued until admission. On June 22, 2002 she felt severe pain in her left upper quadrant subsequently and on June 27, she consulted a doctor at our hospital and had her stomach examined. However, gastrofiberscopy showed no abnormalities. The patient was suspected to be constipated and thus administered a laxative. However, her abdominal pain had persisted, and so she went to the emergency department and was admitted for further evaluation and treatment. On physical examination, no rash or lymphadenopathy was found, no crackle was present over both lung fields, and no cardiac murmurs were heard, her abdomen was soft and flat, and there was no tenderness. In addition, her lower legs were not edematous. On neurologic examination, the patient was alert and oriented. Her cranial nerve functions, muscle strength, and deep-tendon reflexes were normal. Her hematologic findings showed a leukocyte count of 2.93×10^4 per microliter with 56.0% eosinophils, and a platelet count of 39.9×10^4 per microliter. Her C-reactive protein level was 2.5 mg/dL, but her lactate dehydrogenase was elevated to 398 IU/L. Her total protein was 7.7 g/dL with γ-globulin at 25.2%, serum alanine aminotransferase (ALT) level was 118 IU/L (normal range of 10-35 IU/L), aspartate aminotransferase (AST) level was 63 IU/L (normal range of 10-35 IU/L), and alkaline phosphatase level was 254 IU/L (normal range of 120-340 IU/L). In addition, the patient's and Leucine aminopeptidase level was 51 IU/L (normal range of 23-50 IU/L), and her γ-glutamyl-

transpeptidase level was 43 IU/L (normal range of 8-60 IU/L). Her total bilirubin and albumin levels were within normal limits and her immunoglobulin IgG and IgE levels were 1 980 mg/dL and 27 U/mL, respectively. A test for antinuclear antibody was borderline positive, rheumatoid factor was positive, but C-anti-neutrophil cytoplasmic antibodies (C-ANCA) and myeloperoxidase anti-neutrophil cytoplasmic antibodies (MPO-ANCA) were negative. The circulating levels immune complex CH50, C3 and C4 levels in the serum were all normal, renal function was almost normal, and there was no hematuria or sedimentation in the urine. Sputum bacteriology showed only normal flora and no tubercle bacilli and a worm egg test was negative, but the results of an occult blood test were positive. Radiographs of the chest showed a faintly nodular density in the left lower lung field, but radiographs of the abdomen were almost normal. A CT showed that her gallbladder had shrunk, but her liver and pancreas, GI tract and colon were normal. Ultrasonography (US) showed similar findings. Spontaneous pain emanating from her epigastrium to her left upper quadrant was so strong that the repeated use of analgesics had no effect. A colonoscopy showed multiple aphthous ulcers and erosion from the rectum to the ileocecal region (Figure 1). Furthermore, a colonic biopsy specimen showed marked eosinophilic infiltration from the muscular layer of the mucosa to the submucosa, and for the small vessels, lumen stenosis with thickening of the intima indicative of vasculitis was noted (Figure 2). On the basis of her clinical features such as bronchial asthma preceding vasculitis, the laboratory findings including remarkable leukocytosis and eosinophilia, and histopathological findings of eosinophilic vasculitis, a diagnosis of CSS was established. She was administered with oral prednisolone daily since her 10th d in hospital, so her eosinophil count gradually decreased and abdominal pain slowly disappeared. However, she was examined by abdominal CT because she developed a low grade fever, and laboratory findings showed increased liver function on the 15th d. CT showed that the gallbladder was distended and had a thickened wall (Figure 3). We could not detect stones in her gallbladder, but found low density areas, that were faintly enhanced at S6 and S8 of right lobe of the liver ,which we suspected to be abscesses (Figure 3). US showed similar findings. From these examinations, our diagnosis was cholecystitis and liver abscesses, and so intravenous antibiotic (IPM/CS) were administered. CT on the 38th d in hospital revealed low density areas at S6 and S8 that were fading, and that her gallbladder was becoming atrophic with simultaneous wall thickening. After 41 d in hospital, her prednisolone was gradually tapered. She continued to be asymptomatic without recurrence, and was discharged, on the 58th d. After discharge, US revealed a projection in her gallbladder 20 mm in diameter. We proposed its surgical removal because we could not distinguish it from a polyp. Therefore, a laparoscopic cholecystectomy was performed on October 15. No polyp was found, but debris was noted in the resected specimen. Histopathological findings of the resected gallbladder revealed necrotized vessels with occlusive intimal proliferation below the tunica serosa vesicae felleae, which had passed the peak of fibrinoid necrosis. We could not detect eosinophilic infiltration in the specimen (Figure 4), and a liver biopsy performed at the same time showed no remarkable abnormalities.



Figure 1 Colonoscopy showing multiple aphthous ulcers and erosion from the rectum to the ileocecal region.



Figure 2 A colonic biopsy specimen showing marked cellular infiltration from the muscular layer of the mucosa to the submucosa and small vessels, lumen stenosis with thickening of the intima, indicative of vasculitis. A H&E,×100.

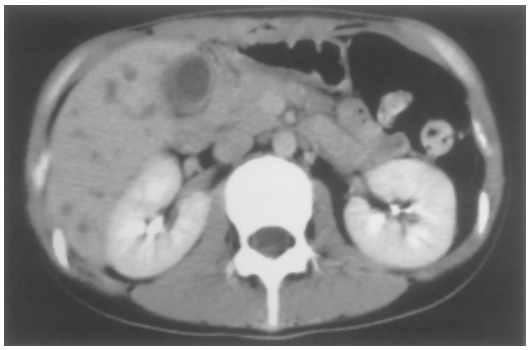


Figure 3 CT showing the gallbladder distended with a thickened wall. In addition, low density areas faintly enhanced at S6 and S8 in the right lobe of the liver suspected to be abscesses are seen.

DISCUSSION

Six criteria used for the classification of CSS were selected: (1) Bronchial asthma;(2) Eosinophilia >10% by differential WBC count; (3) Mononeuropathy or polyneuropathy, (4) Non-fixed pulmonary infiltrates on roentgenography, (5) Paranasal sinus abnormality, and (6) Biopsy containing a

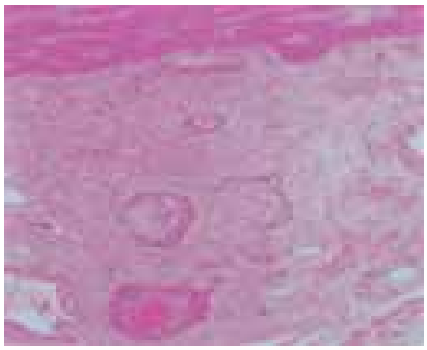


Figure 4 Histopathological findings of the resected gallbladder revealed necrotized vessels with occlusive intimal proliferation below the tunica serosa vesicae felleae, which had passed acute phase in the resected specimen. We could not detect eosinophilic infiltration in this specimen.

blood vessel with extravascular eosinophils[6,12]. Masi *et al*., reported that the existence of four or more of these six criteria yields a sensitivity of 85% and a specificity of 99.7%[12]. The present patient did not suffer from mononeuropathy or polyneuropathy, but fulfilled the other five criteria. Furthermore, she suffered from leukocytosis, an elevated RF level, thrombocytosis except an increased IgE level, and her histopathological findings showed necrosis with marked eosinophilic infiltration. Therefore, we diagnosed her condition as CSS. We can cite as differential diagnosis, eosinophilic leukocytosis, Wegener's granulomatosis, microscopic polyangitis, and PAN (polyarteritis nodosa). CSS is similar to eosinophilic leukocytosis in clinical manifestation, but we could distinguish it from the condition of this case as eosinophilic leukocytosis in thrombocytopenia was not observed and so many impaired internal organs were noted. We could distinguish this case from Wegener's granulomatosis in respect that she did not suffer from kidney trouble or exhibit positive reaction by the C-ANCA[13] test, supported by her histopathological findings. In addition, her past history of sinusitis was typical of one of the major features of CSS in America. She was not afflicted with microscopic polyangitis, because she did not exhibit any positive reaction for MPO-ANCA or the rapid progression of glomerulonephritis, and she did not have PAN because she did not have the various symptoms and showed remarkable eosinophilic infiltration as seen from her histopathological findings. We could only diagnose her with typical CSS judging from her initial course of asthma followed by systemic small vessel vasculitis after 4 years, and because she also had been suffering from eosinophilic infiltrating pneumonia before admission. Lanham *et al*., reported that for about 40% of case of CSS, such pneumonia with eosinophilic infiltration proceeds systemic small vessel vasculitis[5]. The present case developed cholecystitis and liver abscesses, and we could not detect stones in the resected GB. Therefore, we diagnosed her as having acalculous cholecystitis. There was no eosinophilic infiltration found in the resected specimen of the gallbladder because steroid treatment had been carried out. However, we detected necrotized vessels that had passed acute phase in that specimen. Therefore, we believed that her cholecystitis had been caused by CSS. Regarding her liver abscesses, since we could detect no remarkable abnormalities such as those found in the gallbladder among the pathological findings of her liver, we thought that the abscesses had been caused by infection via the blood circulation from cholecystitis or colitis. We report this case because the clinical manifestations of CSS usually include gastroenteritis and ischemic ulcerations of the stomach as well as the small and large bowel, but less often include cholecystitis and liver abscesses.

REFERENCES

1 **Churg J,** Strauss L. Allergic granulomatosis, allergic angitis, and periarteritis nodosa. *Am J Pathol* 1951; **27**: 277-301
2 **Zeek PM.** Periarteritis nodosa: A critical review. *Am J Clin Pathol* 1952; **22**: 777-790
3 **Zeek PM.** Periarteritis nodosa and other forms of necrotizing anditis. *N Engl J Med* 1953; **248**: 764-772
4 **Kimura K,** Nakaoka Y, Yoshida K, Sunami T, Murahashi Y, Hisatsune H, Kuriyama N, Sekikawa S, Kurihara N. Churg-strauss syndrome diagnosed and followed with gastrointestinal fiberscopic studies and electroneuromyography. *Internal Medicine* 1998; **37**: 646-650
5 **Lanham JG,** Elkon KB, Pusey CD, Hughes GR. Systematic vasculitis with asthma and eosinophilia: A clinical approach to the Churg-Strauss syndrome. *Medicine* 1984; **63**: 65-81
6 **Nishie M,** Tomiyama M, Kamijo M, Kannari K, Tanosaki M, Baba M, Matunaga M, Suda T. Acute cholecystitis and duodenitis associated with Churg-Strauss syndrome. *Hepatogastroenterology* 2003; **50**: 998-1002
7 **Lasser A,** Ghofrany S. Necrotizing granulomatous vasculitis (allergic gramulomatosis) of the gallbladder. *Gastroenterology* 1976; **71**: 660-662
8 **Boggi U,** Mosca M, Giulianotti PC, Naccarato AG, Bombardieri S, Mosca F. Surviving catastrophic gastrointestinal involvement due to Churg-Strauss syndrome: Report of a case. *Hepatogastroenterology* 1997; **44**: 1169-1171
9 **Imai H,** Nakamoto Y, Nakajima Y, Sugawara T, Miura A. Allergic gramulomatosis and angitis (Churg-Strauss syndrome) presenting as acute acalculous cholecystitis. *J Reumatol* 1990; **17**: 247-249
10 **Tatukawa H,** Nagano S, Umeno Y, Oribe M. Churg-Strauss syndrome with cholecystitis and renal involvement. *Internal Medicine* 2003; **42**: 893-896
11 **Ohwada S,** Yanagisawa A, Joshita T, Yanagisawa T, Iino Y, Izumi M, Inoue T, Komiya J, Morishita Y. Necrotizing granulomatous Vasculitis of transverse colon and gallbladder. *Hepatogastroenterology* 1997; **44**: 1090-1094
12 **Masi A,** Hunder G, Lie J, Mchel B, Bloch D, Areend W, Calabrese L, Edworthy S, Fauci A, Leavitt R, Lightfoot R Jr, Mcshane D, Millis J, Stevens M, Wallace S, Zvaifer N. The American college of rheumatology 1990 criteria for the classification of Churg-Strauss syndrome (allergic granulomatosis and angitis). *Arthritis Rheumatism* 1991; **33**: 1094-1100
13 **Bailey M,** Chapin W, Licht H, Reynolds J. The effects of vsculitis on the gastrointestinal tract and liver. *Gatroenterol Clinical North Am* 1998; **27**: 747-782
14 **Nakamura S,** Yokoi Y, Suzuki S, Sakaguchi S, Muro H, Maeda M, Kawasaki H. A case of melena caused by a hepatic aneurysm raptured into the intrahepatic bile duct in a patient with Allergic Granulomatous Angiitis. *Japanese J Surgery* 1991; **21**: 471-475

Science Editor Guo SY **Language Editor** Elsevier HK

PO Box 2345, Beijing 100023, China
www.wjgnet.com
wjg@wjgnet.com

ELSEVIER

World J Gastroenterol 2005;11(33):5251-5253
World Journal of Gastroenterology ISSN 1007-9327
© 2005 The WJG Press and Elsevier Inc. All rights reserved.

• *CASE REPORT* •

Squamous cell carcinoma arising from longstanding colocutaneous fistula: A case report

Yueh-Tsung Lee, Sheng-Der Hsu, Chien-Long Kuo, Dev-Aur Chou, Mao-Sheng Lin, Min-Ho Huang, Hurng-Sheng Wu

Yueh-Tsung Lee, Dev-Aur Chou, Min-Ho Huang, Hurng-Sheng Wu, Division of General Surgery, Department of Surgery, Show-Chwan Memorial Hospital, Changhua, Taiwan, China
Chien-Long Kuo, Department of Pathology, Show-Chwan Memorial Hospital, Changhua, Taiwan, China
Sheng-Der Hsu, Division of General Surgery, Department of Surgery, Tri-Service General Hospital, Taipei, Taiwan, China
Mao-Sheng Lin, Division of Urology, Department of Surgery, Show-Chwan Memorial Hospital, Changhua, Taiwan, China
Supported by the National Natural Science Foundation of China, No. 30224801
Correspondence to: Dr. Hurng-Sheng Wu, No 542 Sec.1, Chung-Shang Rd, Changhua 500, Taiwan, China. m0931m@yahoo.com.tw
Telephone: +886-4-7256166 Fax: +886-4-7227116
Received: 2005-01-05 Accepted: 2005-03-21

Abstract

A 60-year-old female patient suffered unhealed wounds over left flank for around 30 years after surgical removal of left renal stones. Fecal material spilled from the two small openings of the scar, bothered her all day long. During the course of the 30 years, she suffered from intermittent fever, diarrhea and wound pain and presented with malnourished condition. After serial examinations, tumor associated with iatrogenic colo-cutaneous fistula was impressed and she received en bloc resection. Pathology revealed squamous cell carcinoma arising from the fistula with colon and spleen invasion. To the best of our knowledge, no such case has been reported, as yet.

© 2005 The WJG Press and Elsevier Inc. All rights reserved.

Key words: Squamous cell carcinoma; Colo-cutaneous fistula

Lee YT, Hsu SD, Kuo CL, Chou DA, Lin MS, Huang MH, Wu HS. Squamous cell carcinoma arising from longstanding colocutaneous fistula: A case report. *World J Gastroenterol* 2005; 11(33): 5251-5253
http://www.wjgnet.com/1007-9327/11/5251.asp

INTRODUCTION

Malignant tumors arising from previously existing fistulas are rare. Squamous cell carcinoma arising from colocutaneous fistula has never been reported. Herein, we report a case of squamous cell carcinoma arising from previously existing longstanding colocutaneous fistula. The diagnosis made has been based on high suspicion, history, imaging and pathology.

CASE REPORT

A 60-year-old female patient was admitted due to general weakness, anorexia accompanied with fever and chills for 2 wk. She denied any other systemic disease. The patient originally was diagnosed with left renal stones and had left nephrectomy, at some other hospital three decades ago. She got stool spillage from surgical wound on left flank after that surgery. Despite wound treatment, two fistulous openings were left with intermittent fecal discharge. During this period, she received supportive treatment while infective symptoms such as fever, chills, diarrhea and local cellulites were present.

We noted that she was a cachectic, frail female with pale conjunctivae. The abdomen was palpated without tenderness and the bowels were normally peristaltic on auscultation. Two chronic unhealing wounds involving the left flank with fecal discharge were noted (Figure 1A). Local erythematous, swollen and tender to palpated were noted. No enlarged lymph nodes were palpated. Anemia (Hb 4.4 g/dL) and chronic renal insufficiency (Cr 2.3 mg/dL) were noted. Abdominal computed tomography discovered splenomegaly with soft tissue density adjacent to it and the splenic flexure of T-colon with air bubbles (Figure 1B). After infection had subsided, fistulograms revealed communication between skin and bowel tract (Figures 1C and D). Under a period of nutritional support, surgical intervention was performed. At laparotomy, the low pole of the spleen adhered to the splenic flexure of T-colon densely with irregular soft tissue beside the region (Figure 1E). Partial wall of the jejunum, 10 cm distal to Treitz's ligament, adhered to the distal T-colon was noted (Figure 1F). En bloc resection with splenectomy, segmental resection of colon with primary anastomosis and wedge resection of jejunum were performed (Figure 1G). Postoperative course was grossly smooth. She is being followed up at the outpatient department.

The pathologist reported moderately differentiated squamous cell carcinoma in virtually all specimens (Figure 2A). However, the microscopic photographs revealed the tumor cells arising from the fistulas (Figure 2B) with spleen (Figure 2C) and colon invasion (Figure 2D).

DISCUSSION

It is well-known that surgery is still the most common cause of entero-cutaneous fistula. The causes of persistent entero-cutaneous fistula include foreign body, radiation, infection, inflammation, epithelization, neoplasm and distal obstruction[1]. Squamous cell carcinoma can develop from chronic ulcers, scars, wounds, sinuses, and fistulas[2]. The latent periods are long and take around 37 years for patients

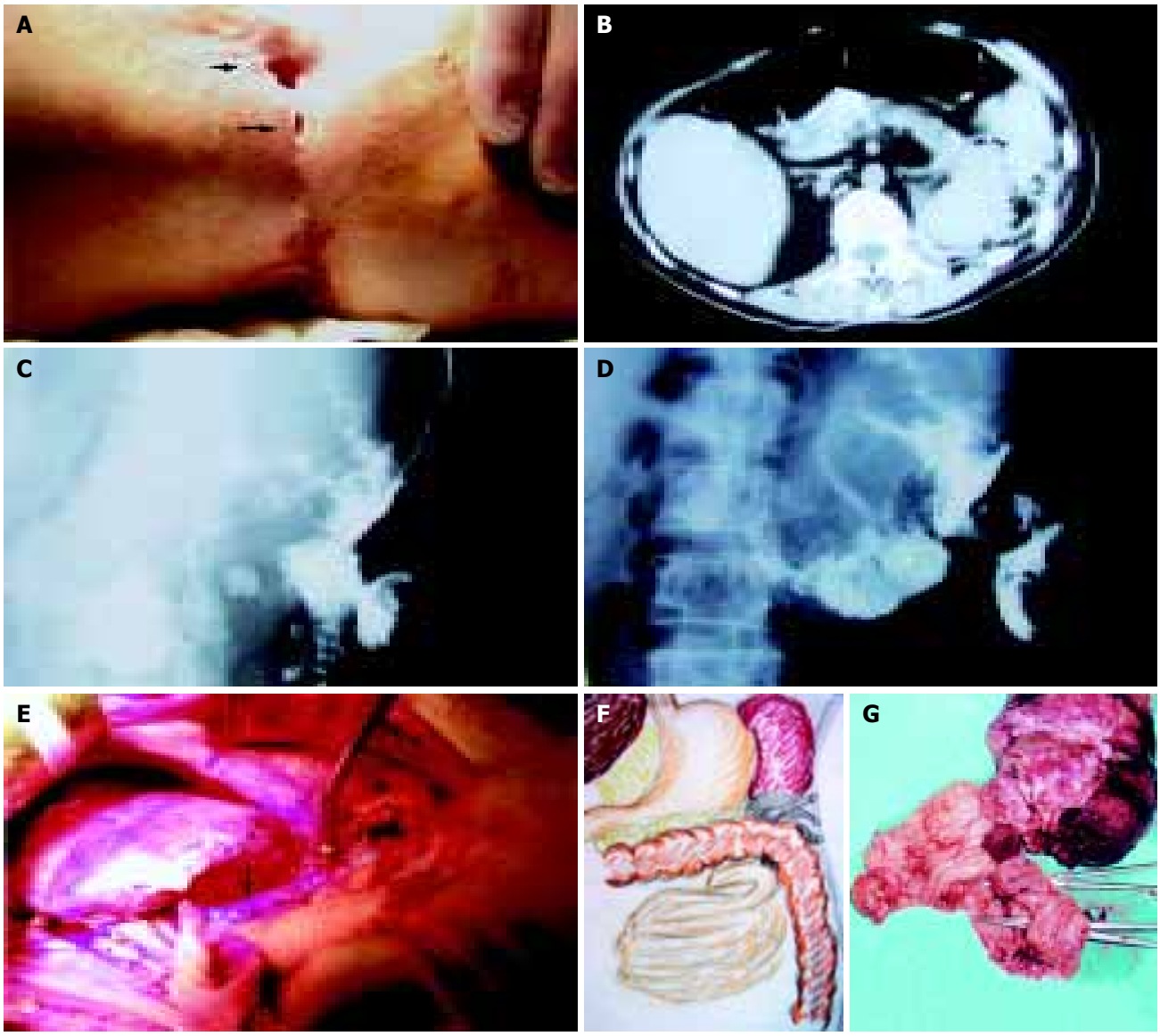


Figure 1 **A:** Surgical scar over left flank with two fistulous openings; **B:** Abdominal CT scan revealed irregular mass between the pancreatic tail, spleen and left lateral abdominal wall with air bubbles; **C:** The fistulogram revealed communication between the skin and sinus tract; **D:** The fistulogram revealed communication between the skin and intestinal tract; **E:** At laparotomy, splenomegaly and dense adhesion to the splenic flexure of colon (arrow) and the left abdominal wall were noted; **F:** The drawing revealed the relation between the fragile soft mass, the fistulas, the spleen and the bowels; **G:** The specimen was shown and these two openings in the colon communicating with skin were indexed with the instruments.

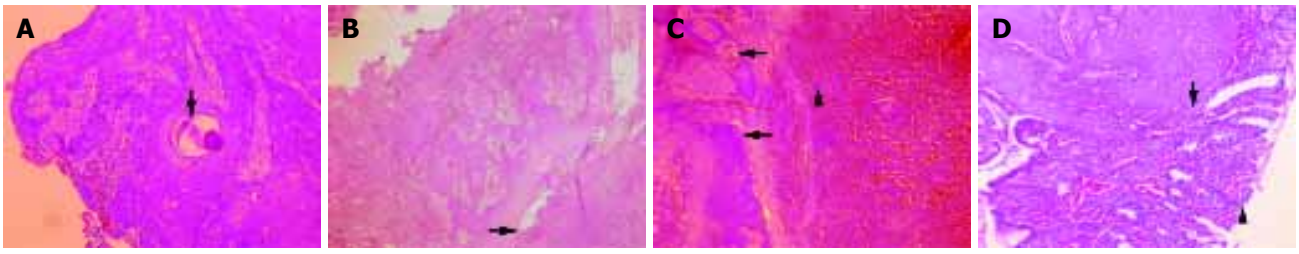


Figure 2 Microscopic photograph. **A:** The squamous cancer cells and keratin pearls (arrow) were shown on the microscopic photograph; **B:** The pathological photograph revealed fistulous tract (arrow) and the tumor cells arose from its epithelium; **C:** The microscopic photograph revealed the tumor cells (arrow) invading the spleen (triangular arrow); **D:** The microscopic photograph revealed the tumor cells (arrow) invading the colon (triangular arrow).

with burn scars except 1-7 years for immunocompromised patients[2,3]. The most significant factor reported in predicting the outcome for the squamous cell carcinoma from the pre-existing scar or sinus was the grade of the tumor[4]. Squamous cell carcinoma associated with prior renal stones have always been reported[5] and the median survival time was 3.6 mo[6]. It was dismal and was not compatible with the long-term history of the patients. We might consider

the development of squamous cell carcinoma as the result of chronic irritation and infection due to unhealed wounds[7]. The strong evidence was that the microscopic photographs revealed the origination of tumor cells from the epithelium of the fistulous tract. However, there are no prior reported articles available as this case. Because of its insidious course, the long-standing colo-cutaneous fistula should be examined carefully for tumor development. The early nutritional intervention is important for patients with entero-cutaneous fistula[8] and surgery is inevitable for long-term unhealed fistula.

REFERENCES

1 **Courtney M,** Townsend R Jr. Daniel Beauchamp B, Mark Evers, Kenneth L. Mattox. *Sabinston Textbook of Surgery* 16th ed 2001: 218-219

2 **Babak S**, Orkin BA. Squamous cell carcinoma arising in an unhealed wound in Crohn's disease. *South Med J* 1997; **90**: 940-942

3 **Edwards MJ,** Hirsch RM, Broadwater JR, Netscher DT, Ames FC. Squamous cell carcinoma arising in previously burned or irradiated skin. *Arch Surg* 1989; **124**: 115-117

4 **Lifeso RM,** Rooney RJ, el-Shaker M. Post-traumatic squamous-cell carcinoma. *J Bone Joint Surg Am* 1990; **72**: 12-18

5 **Ito H,** Oishi M, Murase T. A case of squamous cell carcinoma of the renal pelvis originating from a functional solitary kidney associated with renal stones. *Hinyokika Kiyo* 1988; **34**: 2171-2174

6 **Raghavendran M,** Rastogi A, Dubey D, Chaudhary H, Kumar A, Srivastava A, Mandhani A, Krishnani N, Kapoor R. Stones associated renal pelvic malignancies. *Indian J Cancer* 2003; **40**: 108-112

7 **Mosavy SH,** Tayebi SA. Carcinoma arising in a perianal sinus tract: report of a case. *Dis Colon Rectum* 1975; **18**: 416-417

8 **Wang XB,** Ren JA, Li TS. Sequential changes of body composition in patients with enterocutaneous fistula during the 10 days after admission. *World J Gastroenterol* 2002; **8**: 1149-1152

Science Editor Guo SY **Language Editor** Elsevier HK

PO Box 2345, Beijing 100023, China
www.wjgnet.com
wjg@wjgnet.com

ELSEVIER

World J Gastroenterol 2005;11(33):5254
World Journal of Gastroenterology ISSN 1007-9327
© 2005 The WJG Press and Elsevier Inc. All rights reserved.

Acknowledgments to Reviewers of *World Journal of Gastroenterology*

Many reviewers have contributed their expertise and time to the peer review, a critical process to ensure the quality of *World Journal of Gastroenterology*. The editors and authors of the articles submitted to the journal are grateful to the following reviewers for evaluating the articles (including those were published and those were rejected in this issue) during the last editing period of time.

Takafumi Ando, M.D.
Nagoya University Graduate School of Medicine, Therapeutic Medicine, 65 Tsurumai-cho, Showa-ku, Nagoya 466-8550, Japan

Gabrio Bassotti, M.D.
Department of Clinical and Experimental Medicine, University of Perugia, Via Enrico dal Pozzo, Padiglione W, Perugia 06100, Italy

Ramon Bataller, M.D.
Liver Unit, Hospital Clinic,Villarroel 170, Barcelona 08036, Spain

Josep M Bordas, M.D.
Department of Gastroenterology IMD, Hospital Clinic", Llusanes 11-13 at, Barcelona 08022, Spain

Pierre Brissot, Professor
Liver Disease Unit And Inserm U-522, University Hospital Pontchaillou, 2, Rue Henri Le Guilloux, Rennes 35033, France

Vincent Coghlan, Professor
Neurological Sciences Institute, 505 NW 185th Avenue, Beaverton, Oregon 97006, United States

Jacques Cosnes, Professor
Department of Gastroenterology, Hospital St. Antoine, Hospital St. Antoine, 184 rue du Faubourg St-Antoine, PARIS 75012, France

Radha K Dhiman, Associate Professor
Department of Hepatology, Postgraduate Institute of Medical Education and Research, Chandigarh 160012, India

Alfred Gangl, Professor
Department of Medicine 4, Medical University of Vienna, Allgemeines Krankenhaus, Waehringer Guertel 18-20, Vienna A-1090, Austria

Toru Ishikawa, M.D.
Department of Gastroenterology, Saiseikai Niigata Second Hospital, Teraji 280-7, Niigata, Niigata 950-1104, Japan

Michael A Kamm, Professor
Department of Gastroenterology, St Mark's Hospital, St Mark's Hospital, Watford Road, Harrow HA1 3UJ, United Kingdom

Seigo Kitano, Professor
Department of Surgery I, Oita University Faculty of Medicine, 1-1 Idaigaoka Hasama-machi, Oita 879-5593, Japan

Chris Jacob Johan Mulder, Professor
VUMC, PO Box 7057, Amsterdam 1007, Netherlands

Hiroki Nakamura, M.D.
Department of Gastroenterology and Hepatology, 1-1-1, Minami Kogushi, Ube, Yamaguchi 755-8505, Japan

Curtis T Okamoto, Associate Professor
Department of Pharmaceutical Sciences, University of Southern California, 1985 Zonal Ave. PSC 404A, Los Angeles CA 90089-9121, United States

Piero Portincasa, Professor
Internal Medicine - DIMIMP, University of Bari Medical School, Hospital Policlinico Piazza G. Cesare 11, Bari 70124, Italy

Bruno Stieger, Professor
Department of Medicine, Division of Clinical Pharmacology and Toxicology, University Hospital, Zurich 8091, Switzerland

Qin Su, Professor
Department of Pathology, Cancer Hospital and Cancer Institute, Chinese Academy of Medical Sciences and Peking Medical College, PO Box 2258, Beijing 100021, China

Koji Takeuchi, Professor
Department of Pharmacology and Experimental Therapeutics, Kyoto Pharmaceutical University, Misasagi, Yamashina, Kyoto 607-8414, Japan

Kam-Meng Tchou-Wong, Assistant Professor
Departments of Environmental Medicine and Medicine, NYU School of Medicine, 57 Old Forge Road, Tuxedo, New York 10987, United States

Anton Vavrecka, M.D.
Clinic Of Gastroenterology, SZU, NSP SV.CAM, Antolska 11, Bratislava 85107, Slovakia

Shinichi Wada, M.D.
Department of Gastroenterology, Jichi Medical School, Minamikawachi-machi, Kwachi-gun, Tochigi-ken, Tochigi 329-0498, Japan

Jia-Yu Xu, Professor
Shanghai Second Medical University, Rui Jin Hospital, 197 Rui Jin Er Road, Shanghai 200025, China

PO Box 2345, Beijing 100023, China
www.wjgnet.com
wjg@wjgnet.com

ELSEVIER

World J Gastroenterol 2005;11(33):5255
World Journal of Gastroenterology ISSN 1007-9327
© 2005 The WJG Press and Elsevier Inc. All rights reserved.

Meetings

MAJOR MEETINGS COMING UP

13th World Congress of Gastroenterology
September10-14, 2005
wcog2005@congrex.nl
www.wcog2005.org

APDW 2005 - Asia Pacific Digestive Week 2005
September 25-28, 2005
asiapdw@kornet.net
www.apdw2005.org

13th United European Gastroenterology Week
October 15-20, 2005
uegw@discongress.com
www.webasistent.cz / guarant / uegw2005 /

American College of Gastroenterology Annual Scientific Meeting
October 28 -November 2, 2005
annualmeeting@acg.gi.org
www.acg.gi.org

EVENTS AND MEETINGS IN THE UPCOMING 6 MONTHS

2005 World Congress of Gastroenterology
September 12-14, 2005
wcog2005@congrex.nl

15th World Congress of the International Association of Surgeons and Gastroenterologists
September 7-10, 2005
iasg2005@guarant.cz
www.iasg2005.cz

United European Gastroenterology Week
October 15-20, 2005
uegw@discongress.com
www.webasistent.cz / guarant / uegw2005 /

7th International Workshop on Therapeutic Endoscopy
September 10-12, 2005
alfa@alfamedical.com
www.alfamedical.com

ISGCON2005
November 11-15, 2005
isgcon2005@yahoo.co.in
isgcon2005.com

II Latvian Gastroenterology Congress
November 29, 2005
gec@stradini.lv
www.gastroenterologs.lv

70th ACG Annual Scientific Meeting and Postgraduate Course
October 28-November 2, 2005

Advanced Capsule Endoscopy Users Course
November 18-19, 2005
www.asge.org / education

2005 CCFA National Research and Clinical Conference - 4th Annual Advances in the Inflammatory Bowel Diseases
December 1-3, 2005
c.chase@imedex.com
www.imedex.com / calendars / therapeutic.htm

EVENTS AND MEETINGS IN 2005

XIII Argentine Hepatology Congress
XIII Congreso Argentino de HepatologÃa
June 10-13, 2005
mci@mcimeetings.com
www.hepatologia.org

9th Annual Coolum Update in Gastroenterology & Hepatology
June 11-13, 2005
info@e-Kiddna.com.au

Canadian Digestive Disease Week Conference
February 26-March 6, 2005
www.cag-acg.org

2005 World Congress of Gastroenterology
September 12-14, 2005
wcog2005@congrex.nl

International Colorectal Disease Symposium 2005
February 3-5, 2005
info@icds-hk.org

15th World Congress of the International Association of Surgeons and Gastroenterologists
September 7-10, 2005
iasg2005@guarant.cz
www.iasg2005.cz

7th International Workshop on Therapeutic Endoscopy
September 10-12, 2005
alfa@alfamedical.com
www.alfamedical.com

EASL 2005 the 40th annual meeting
April 13-17, 2005
www.easl.ch / easl2005 /

ISGCON2005
November 11-15, 2005
isgcon2005@yahoo.co.in
isgcon2005.com

Pediatric Gastroenterology, Hepatology and Nutrition
March 13, 2005

II Latvian Gastroenterology Congress
November 29, 2005
gec@stradini.lv
www.gastroenterologs.lv

21st annual international congress of Pakistan society of Gastroenterology & GI Endoscopy
March 25-27, 2005
psgc05@hotmail.com
www.psgc2005.com

8th Congress of the Asian Society of HepatoBiliary Pancreatic Surgery
February 10-13, 2005

1º Workshop de Gastrenterologia para Clí nica Geral
April 29, 2005
luis.m.lopes@sapo.pt

APDW 2005 - Asia Pacific Digestive Week 2005
September 25-28, 2005
asiapdw@kornet.net
www.apdw2005.org

World Congress on Gastrointestinal Cancer
June 15-18, 2005
meetings@imedex.com

British Society of Gastroenterology Conference
March 14-17, 2005
www.bsg.org.uk

Training Director's Workshop:Developing and Teaching Principles in the New Era of GI Training
February 4-6, 2005
www.asge.org / education

The Pharmacological, Surgical and Endoscopic Management of GERD
April 8-9, 2005
www.asge.org / education

Digestive Disease Week
DDW 106th Annual Meeting
May 15-18, 2005
ddwadmin@gastr.org
www.ddw.org

ASGE Advanced Endscopy Skills Hands-on Sessions
May 15, 2005
www.asge.org / education

ASGE GERD Hands-on Session
May 17, 2005
www.asge.org / education

Annual Postgraduate Course
May 18-19, 2005
www.asge.org / education

Advanced Capsule Endoscopy Users Course
June 4-5, 2005
www.asge.org / education

Advanced Capsule Endoscopy Users Course
August 12-13, 2005
www.asge.org / education

GI Practice Management Symposium: Solutions for a Successful Practice
August 18, 2005
www.asge.org / education

70th ACG Annual Scientific Meeting and Postgraduate Course
October 28-November 2, 2005

Advanced Capsule Endoscopy Users Course
November 18-19, 2005
www.asge.org / education

2005 CCFA National Research and Clinical Conference - 4th Annual Advances in the Inflammatory Bowel Diseases
December 1-3, 2005
c.chase@imedex.com
www.imedex.com / calendars / therapeutic.htm

EVENTS AND MEETINGS IN 2006

10th World Congress of the International Society for Diseases of the Esophagus
February 22-25, 2006
isde@sapmea.asn.au
www.isde.net

Easl 2006 - The 41st Annual Meeting
April 26-30, 2006

Canadian Digestive Disease Week Conference
March 4-12, 2006
www.cag-acg.org

XXX pan-american congress of digestive diseases
XXX congreso panamericano de anfermedades digestivas
November 25-December 1, 2006
amg@gastro.org.mx
www.gastro.org.mx

World Congress on Gastrointestinal Cancer
June 14-17, 2006
c.chase@imedex.com

7th World Congress of the International Hepato-Pancreato-Biliary Association
September 3-7, 2006
convention@edinburgh.org
www.edinburgh.org / conference

Annual Postgraduate Course
May 25-26, 2006
www.asge.org / education

71st ACG Annual Scientific Meeting and Postgraduate Course
October 20-25, 2006

PO Box 2345, Beijing 100023, China
www.wjgnet.com
wjg@wjgnet.com

ELSEVIER

World J Gastroenterol 2005;11(33):5256-5257
World Journal of Gastroenterology ISSN 1007-9327
© 2005 The WJG Press and Elsevier Inc. All rights reserved.

Instructions to authors

GENERAL INFORMATION

World Journal of Gastroenterology (*WJG*, ISSN 1007-9327 CN 14-1219/R) is a weekly journal of more than 48 000 circulation, published on the 7th, 14th, 21st and 28th of every month.

Original Research, Clinical Trials, Reviews, Comments, and Case Reports in esophageal cancer, gastric cancer, colon cancer, liver cancer, viral liver diseases, *etc*., from all over the world are welcome on the condition that they have not been published previously and have not been submitted simultaneously elsewhere.

Published jointly by

The WJG Press and Elsevier Inc.

SUBMISSION OF MANUSCRIPTS

Manuscripts should be typed double-spaced on A4 (297×210 mm) white paper with outer margins of 2.5 cm. Number all pages consecutively, and start each of the following sections on a new page: Title Page , Abstract, Introduction, Materials and Methods, Results, Discussion, Acknowledgements, References, Tables, Figures and Figure Legends. Neither the Editors nor the Publisher is responsible for the opinions expressed by contributors. Manuscripts formally accepted for publication become the permanent property of The WJG Press and Elsevier Inc., and may not be reproduced by any means, in whole or in part without the written permission of both the Authors and the Publisher. We reserve the right to put onto our website and copy-edit accepted manuscripts. Authors should also follow the guidelines for the care and use of laboratory animals of their institution or national animal welfare committee.

Authors should retain one copy of the text, tables, photographs and illustrations, as rejected manuscripts will not be returned to the author(s) and the editors will not be responsible for the loss or damage to photographs and illustrations.

Online submission

Online submission is strongly advised. Manuscripts should be submitted through the Online Submission System at: http://www.wjgnet.com/index.jsp. Authors are highly recommended to consult the ONLINE INSTRUCTIONS TO AUTHORS (http://www.wjgnet.com/wjg/help/instructions.jsp) before attempting to submit online. Authors encountering problems with the Online Submission System may send an email describing the problem to wjg@wjgnet.com for assistance. If you submit manuscript online, do not make a postal contribution. A repeated online submission for the same manuscript is strictly prohibited.

Postal submission

Send 3 duplicate hard copies of the full-text manuscript typed double-spaced on A4(297×210 mm) white paper together with any original photographs or illustrations and a 3.5 inch computer diskette or CD-ROM containing an electronic copy of the manuscript including all the figures, graphs and tables in native Microsoft Word format or *.rtf format to:

World Journal of Gastroenterology
Apartment 1066 Yishou Garden,
58 North Langxinzhuang Road,
PO Box 2345, Beijing 100023, China
E-mail: wjg@wjgnet.com
http: //www.wjgnet.com

MANUSCRIPT PREPARATION

All contributions should be written in English. All articles must be submitted using a word-processing software. All submissions must be typed in 1.5 line spacing and in word size 12 with ample margins. The letter font is Tahoma. For authors originating from China, one copy of the Chinese translation of the manuscript is also required (excluding references). Style should conform to our house format. Required information for each of the manuscript sections is as follows:

Title page

Full manuscript title, running title, all author(s) name(s), affiliations, institution(s) and/or department(s) where the work was accomplished, disclosure of any financial support for the research, and the name, full address, telephone and fax numbers and email address of the corresponding author should be involved. Titles should be concise and informative (removing all unnecessary words), emphasize what is NEW, and avoid abbreviations. A short running title of less than 40 letters should be provided. List the author(s)' name(s) as follows: initials and/or first name, middle name or initial(s) and full family name.

Abstract

An informative, structured abstract of no more than 250 words should accompany each manuscript. Abstracts for original contributions should be structured into the following sections: AIM: Only the purpose should be included. METHODS: The materials, techniques, instruments and equipments, and the experimental procedures should be included. RESULTS: The observatory and experimental results, including data, effects, outcome, *etc*. should be included. Authors should present *P* value where necessary, and the significant data should accompany. CONCLUSION: Accurate view and the value of the results should be included.

The format of structured abstracts is at: http://www.wjgnet.com/wjg/help/11.doc

Key words

Please list 3-10 key words that could reflect content of the study.

Text

For most article types, the main text should be structured into the following sections: INTRODUCTION, MATERIALS AND METHODS, RESULTS and DISCUSSION, and should include appropriate Figures and Tables. Data should be presented in the body text or Figures and Tables, not both.

Illustrations

Figures should be numbered as 1, 2, 3 and so on, and mentioned clearly in the main text. Provide a brief title for each figure on a separate page. No detailed legend should be involved under the figures. This part should add into the text where the figures are applicable. Digital images: black and white photographs should be scanned and saved in TIFF format at a resolution of 300 dpi; color images should be saved as CMYK (print files) and not RGB (screen-viewing files). Place each photograph in a separate file. Print images: supply images of size no smaller than 126×76 mm printed on smooth surface paper; label the image by writing the Figure number and orientation using an arrow. Photomicrographs: indicate the original magnification and stain in the legend. Digital Drawings: supply files in EPS if created by Freehand and Illustrator, or TIFF from Photoshop. EPS files must be accompanied by a version in native file format for editing purposes. Scans of existing line drawings should be scanned at a resolution of 1200 dpi and as close as possible to the size at which they will appear when printed, not smaller. Please use uniform legends for the same subjects. For example: Figure 1 Pathological changes of atrophic gastritis after treatment. A: ...; B: ...;C: ...; D: ...; E: ...; F: ...; G: ...

Tables

Three-line tables should be numbered as 1, 2, 3 and so on, and mentioned clearly in the main text. Provide a brief title for each table. No detailed legend should be involved under the tables. This part should add into the text where the tables are applicable. The information should complement but not duplicate that contained in the text. Use one horizontal line under the title, a second under the column heads, and a third below the Table, above any footnotes. Vertical and italic lines should be omitted.

Notes in tables and illustrations

Data which is not statistically significant should not be noted. $^{a}P<0.05$, $^{b}P<0.01$ ($P>0.05$ should not be noted). If there are other series of *P* values, $^{c}P<0.05$ and $^{d}P<0.01$ are used; Third series of *P* values can be expressed as $^{e}P<0.05$ and $^{f}P<0.01$. Other notes in tables or under

illustrations should be expressed as ^1F, ^2F, ^3F; or some other symbols with a superscript (Arabic numerals) in the upper left corner. In a multi-curve illustration, each curve should be labeled with ●, ○, ■, □, ▲, △, *etc*. in a certain sequence.

Acknowledgments

Brief acknowledgments of persons who have made genuine contributions to the manuscripts and who endorse the data and conclusions are included. Authors are responsible for obtaining written permission to use any copyrighted text and/or illustrations.

References

Cited references should mainly be drawn from journals covered in the Science Citation Index (http://www.isinet.com) and/or Index Medicus (http://www.ncbi.nlm.nih.gov/PubMed) databases. Mention all references in the text, tables and figure legends, and set off by consecutive, superscripted Arabic numerals. References should be numbered consecutively in the order in which they appear in the text. Abbreviate journal title names according to the Index Medicus style (http://www.ncbi.nlm.nih.gov/entrez/query.fcgi?db=journals). Unpublished observations and personal communications are not listed as references. The style and punctuation of the references conform to ISO standard and the Vancouver style (5th edition); see examples below. Reference lists not conforming to this style could lead to delayed or even rejected publication status. Examples:

Standard jounal article (list all authors and include the PubMed ID [PMID] where applicable)

1 **Das KM,** Farag SA. Current medical therapy of inflammatory bowel disease. *World J Gastroenterol* 2000; 6: 483-489 [PMID: 11819634]
2 **Pan BR**, Hodgson HJF, Kalsi J. Hyperglobulinemia in chronic liver disease: Relationships between *in vitro* immunoglobulin synthesis, short lived suppressor cell activity and serum immunoglobulin levels. *Clin Exp Immunol* 1984; 55: 546-551 [PMID: 6231144]
3 **Lin GZ,** Wang XZ, Wang P, Lin J, Yang FD. Immunologic effect of Jianpi Yishen decoction in treatment of Pixu-diarrhoea. *Shijie Huaren Xiaohua Zazhi* 1999; 7: 285-287 [CMFAID:1082371101835979]

Books and other monographs (list all authors)

4 **Sherlock S,** Dooley J. Diseases of the liver and billiary system. 9th ed. Oxford: Blackwell Sci Pub, 1993: 258-296

Chapter in a book (list all authors)

5 **Lam SK.** Academic investigator's perspectives of medical treatment for peptic ulcer. In: Swabb EA, Azabo S. Ulcer disease: investigation and basis for therapy. New York: Marcel Dekker, 1991: 431-450

Electronic journal (list all authors)

6 **Morse SS.** Factors in the emergence of infectious diseases. Emerg Infect Dis serial online, 1995-01-03, cited 1996-06-05; 1(1):24 screens. Available from: URL: http / / www.cdc.gov / ncidod / EID / eid.htm

PMID requirement

From the full reference list, please submit a separate list of those references embodied in PubMed, keeping the same order as in the full reference list, with the following information only: (1) abbreviated journal name and citation (e.g. *World J Gastroenterol* 2003;9(11): 2400-2403; (2) article title (e.g. Epidemiology of gastroenterologic cancer in Henan Province, China; (3) full author list (e.g. Lu JB, Sun XB, Dai DX, Zhu SK, Chang QL, Liu SZ, Duan WJ; (4) PMID (e.g. 14606064). Provide the full abstracts of these references, as quoted from PubMed on a 3.5 inch disk or CD-ROM in Microsoft Word format and send by post to The *WJG* Press. For those references taken from journals not indexed by *Index Medicus*, a printed copy of the first page of the full reference should be submitted. Attach these references to the end of the manuscript in their order of appearance in the text.

Inappropriate references

Authors should always cite references that are relevant to their article, and avoid any inappropriate references. Inappropriate references include those that are linked with a hyphen and the difference between the two numbers at two sides of the hyphen is more than 5. For example, [1-6], [2-14] and [1, 3, 4-10, 22] are all considered as inappropriate references. Authors should not cite their own unrelated published articles.

Statistical data

Present as mean±SD and mean±SE.

Statistical expression

Express *t* test as *t*(in italics), *F* test as *F*(in italics), chi square test as χ^2 (in Greek), related coefficient as *r*(in italics), degree of freedom as γ(in Greek), sample number as *n*(in italics), and probability as *P*(in italics).

Units

Use SI units. For example: body mass, m(B) = 78 kg; blood pressure, p (B)=16.2/12.3 kPa; incubation time, t(incubation)=96 h, blood glucose concentration, c(glucose) 6.4±2.1 mmol/L; blood CEA mass concentration, p(CEA) = 8.6 24.5 μg/L; CO_2 volume fraction, 50 mL/L CO_2 not 5% CO_2; likewise for 40 g/L formaldehyde, not 10% formalin; and mass fraction, 8 ng/g, *etc*. Arabic numerals such as 23,243,641 should be read 23 243 641.

The format about how to accurately write common units and quantum is at: http://www.wjgnet.com/wjg/help/15.doc

Abbreviations

Standard abbreviations should be defined in the abstract and on first mention in the text. In general, terms should not be abbreviated unless they are used repeatedly and the abbreviation is helpful to the reader. Permissible abbreviations are listed in Units, Symbols and Abbreviations: A Guide for Biological and Medical Editors and Authors (Ed. Baron DN, 1988) published by The Royal Society of Medicine, London. Certain commonly used abbreviations, such as DNA, RNA, HIV, LD50, PCR, HBV, ECG, WBC, RBC, CT, ESR, CSF, IgG, ELISA, PBS, ATP, EDTA, mAb, can be used directly without further mention.

Italicization

Quantities: *t* time or temperature, *c* concentration, *A* area, *l* length, *m* mass, *V* volume.
Genotypes: *gyr*A, *arg* 1, *c myc*, *c fos*, *etc*.
Restriction enzymes: *Eco*RI, *Hin*dI, *Bam*HI, *Kbo* I, *Kpn* I, *etc*.
Biology: *Helicobacter pylori*, *H pylori*, *E coli*, *etc*.

SUBMISSION OF THE REVISED MANUSCRIPTS AFTER ACCEPTED

Please revise your article according to the revision policies of *WJG*. The revised version including manuscript and high-resolution image figures (if any) should be copied on a floppy or compact disk. Author should send the revised manuscript, along with printed high-resolution color or black and white photos, copyright transfer letter, the final check list for authors, and responses to reviewers by a courier (such as EMS) (submission of revised manuscript by e-mail or on the WJG Editorial Office Online System is NOT available at present).

Language evaluation

The language of a manuscript will be graded before sending for revision. (1) Grade A: priority publishing; (2) Grade B: minor language polishing; (3) Grade C: a great deal of language polishing; (4) Grade D: rejected. The revised articles should be in grade B or grade A.

Copyright assignment form

It is the policy of WJG to acquire copyright in all contributions. Papers accepted for publication become the copyright of WJG and authors will be asked to sign a transfer of copyright form. All authors must read and agree to the conditions outlined in the Copyright Assignment Form (which can be downloaded from http://www.wjgnet.com/wjg/help/9.doc).

Final check list for authors

The format is at: http://www.wjgnet.com/wjg/help/13.doc

Responses to reviewers

Please revise your article according to the comments/suggestions of reviewers. The format for responses to the reviewers' comments is at: http://www.wjgnet.com/wjg/help/10.doc

Proof of financial support

For paper supported by a foundation, authors should provide a copy of the document and serial number of the foundation.

Publication fee

Authors of accepted articles must pay publication fee.

PO Box 2345, Beijing 100023, China
www.wjgnet.com
wjg@wjgnet.com

ELSEVIER

World J Gastroenterol 2005;11(33):5258
World Journal of Gastroenterology ISSN 1007-9327
© 2005 The WJG Press and Elsevier Inc. All rights reserved.

World Journal of Gastroenterology standard of quantities and units

Number	Nonstandard	Standard	Notice
1	4 days	4 d	In figures, tables and numerical narration
2	4 days	four days	In text narration
3	day	d	After Arabic numerals
4	Four d	Four days	At the beginning of a sentence
5	2 hours	2 h	After Arabic numerals
6	2 hs	2 h	After Arabic numerals
7	hr, hrs,	h	After Arabic numerals
8	10 seconds	10 s	After Arabic numerals
9	10 year	10 years	In text narration
10	Ten yr	Ten years	At the beginning of a sentence
11	0,1,2 years	0,1,2 yr	In figures and tables
12	0,1,2 year	0,1,2 yr	In figures and tables
13	4 weeks	4 wk	
14	Four wk	Four weeks	At the beginning of a sentence
15	2 months	2 mo	In figures and tables
16	Two mo	Two months	At the beginning of a sentence
17	10 minutes	10 min	
18	Ten min	Ten minutes	At the beginning of a sentence
19	50% (*V/V*)	500 mL/L	
20	50% (m/*V*)	500 g/L	
21	1 M	1 mol/L	
22	10 μM	10 μmol/L	
23	1N HCl	1 mol/L HCl	
24	1N H_2SO_4	0.5 mol/L H_2SO_4	
25	4rd edition	4th edition	
26	15 year experience	15- year experience	
27	18.5 kDa	18.5 ku,18 500u or M_r18 500	
28	25 g.kg^{-1}/d^{-1}	25 g/(kg·d) or 25 g/kg per day	
29	6900	6 900	
30	1000 rpm	1 000 r/min	
31	sec	s	After Arabic numerals
32	1 pg·L^{-1}	1 pg/L	
33	10 kilograms	10 kg	
34	13 000 rpm	13 000 *g*	High speed; *g* should be in italic and suitable conversion.
35	1000 *g*	1 000 r/min	Low speed. *g* cannot be used.
36	Gene bank	GenBank	International classified genetic materials collection bank
37	Ten L	Ten liters	At the beginning of a sentence
38	Ten mL	Ten milliliters	At the beginning of a sentence
39	umol	μmol	
40	30 sec	30 s	
41	1 g/dl	10 g/L	10-fold conversion
42	OD_{260}	A_{260}	"OD" has been abandoned.
43	One g/L	One microgram per liter	At the beginning of a sentence
44	*A*260 nm	A_{260} nm	*A* should be in italic.
	^{b}P<0.05	^{a}P<0.05	In Table, no note is needed if there is no significance in statistics: ^{a}P<0.05, ^{b}P<0.01 (no note if P>0.05). If there is a second set of P value in the same table, ^{c}P<0.05 and ^{d}P<0.01 are used for a third set: ^{e}P<0.05, ^{f}P<0.01.
45	$^{*}F$=9.87, $^{§}F$=25.9, $^{\#}F$=67.4	^{1}F=9.87,^{2}F=25.9, ^{3}F=67.4	Notices in or under a table
46	KM	km	kilometer
47	CM	cm	centimeter
48	MM	mm	millimeter
49	Kg, KG	kg	kilogram
50	Gm, gr	g	gram
51	nt	N	newton
52	l	L	liter
53	db	dB	decibel
54	rpm	r/min	rotation per minute
55	bq	Bq	becquerel, a unit symbol
56	amp	A	ampere
57	coul	C	coulomb
58	HZ	Hz	
59	w	W	watt
60	KPa	kPa	kilo-pascal
61	p	Pa	pascal
62	ev	EV	volt (electronic unit)
63	Jonle	J	joule
64	J/mmol	kJ/mol	kilojoule per mole
65	10×10×10cm^3	10 cm×10 cm×10 cm	
66	N·km	KN·m	moment
67	$\bar{x}$±s	mean±SD	In figures, tables or text narration
68	Mean±SEM	mean±SE	In figures, tables or text narration
69	*im*	im	intramuscular injection
70	*iv*	iv	intravenous injection
71	Wang et al	Wang *et al.*	
72	EcoRI	*Eco*RI	*Eco* in italic and RI in positive. Restriction endonuclease has its prescript form of writing.
73	Ecoli	*E.coli*	Bacteria and other biologic terms have their specific expression.
74	Hp	*H pylori*	
75	Iga	*Iga*	writing form of genes
76	*igA*	IgA	writing form of proteins
77	-70 kDa	~70 ku	

PO Box 2345, Beijing 100023, China
www.wjgnet.com
wjg@wjgnet.com

ELSEVIER

World J Gastroenterol 2005;11(34):5259-5265
World Journal of Gastroenterology ISSN 1007-9327
© 2005 The WJG Press and Elsevier Inc. All rights reserved.

• *REVIEW* •

Role of potassium in acid secretion

John P Geibel

John P Geibel, Professor of Surgery and Cellular and Molecular Physiology, Director of Surgical Research, Yale University School of Medicine, CT, United States
Correspondence to: Professor John P Geibel, Department of Surgery, Yale University School of Medicine, BML 265, New Haven, CT 06520, United States. john.geibel@yale.edu
Telephone: +1-203-737-4152 Fax: +1-203-737-1464
Received: 2004-12-18 Accepted: 2005-01-05

Abstract

Potassium (K^+) ions are critical for the activation and catalytic cycle of the gastric H^+,K^+-ATPase, resulting in the secretion of hydrochloric acid into the parietal cell canaliculus. As both symptom, severity and esophageal mucosal damage in gastro-esophageal reflux disease (GERD) are related to the degree of acid exposure, K^+ is a logical target for approaches to inhibit acid production. The probable K^+ binding site on the gastric H^+,K^+-ATPase has recently been described and studies are elucidating how K^+ activates the enzyme. K^+ channels in the apical membrane of the parietal cell are implicated in the recycling of K^+ and, to date, three potential K^+ channels (KCNQ1, Kir2.1 and Kir4.1) have been identified. The channels represent theoretical sites for agents to control acid secretion but it will be difficult to develop selective blockers. An alternative strategy is to prevent K^+ from activating gastric H^+,K^+-ATPase; the potassium-competitive acid blocker (P-CAB) class inhibits acid secretion by binding at or near the K^+ binding site. Ongoing research is further defining the role of K^+ in the functioning of the gastric H^+,K^+-ATPase, as well as determining the clinical utility of agents directed toward this important cation.

© 2005 The WJG Press and Elsevier Inc. All rights reserved.

Key words: Gastric H^+,K^+-ATPase; HCl; Parietal cell; Potassium; Potassium channel; Potassium channel blocker; Potassium-competitive acid blocker

Geibel JP. Role of potassium in acid secretion. *World J Gastroenterol* 2005; 11(34): 5259-5265
http://www.wjgnet.com/1007-9327/11/5259.asp

INTRODUCTION

Gastric acid is essential for the sterilization of food and water and for digestion. The very low pH of gastric juice (pH~1) is the result of H^+ and Cl^- ion secretion (hydrochloric acid [HCl] production) by parietal cells in the oxyntic mucosa of the stomach. Each day, these cells secrete 1-2 L of HCl to achieve a concentration of 150-160 mmol/L in the stomach lumen. This acid concentration, which represents a very high accumulation of H^+ in the lumen compared with parietal cell plasma, is facilitated by the activity of gastric H^+,K^+-ATPase in the apical membrane of the cell. K^+ has a critical role in the activation of gastric H^+,K^+-ATPase and is essential for the functioning of the enzyme[1-3]. This review examines the central role of K^+ in acid secretion and assesses how targeting this cation may provide novel ways of inhibiting gastric acid production.

GASTRIC H^+,K^+-ATPASE AND ACID SECRETION

Gastric H^+,K^+-ATPase is located in the apical membrane of the parietal cell and transports H^+ into the parietal cell canaliculus in exchange for K^+. The cations are exchanged in a 1:1 ratio, which maintains electroneutrality[4,5]. The enzyme is a member of the P-ATPase family that also includes Na^+,K^+-ATPase, Ca^{2+}-ATPase and colonic H^+,K^+-ATPase[6-8]. Gastric H^+, K^+-ATPase shares many features, including structure and enzymatic mechanism, with other members of the family. A central feature of the P-ATPase family is that the energy for the translocation of ions is provided by ATP.

The amount of energy released on hydrolysis of an ATP molecule effectively limits the concentration gradient that can be created by a P-ATPase enzyme. The transport of ions is also constrained if their exchange generates a charge. As the translocation of H^+ and K^+ is electroneutral, gastric H^+,K^+-ATPase achieves a 3-4 million-fold ion concentration gradient (the difference in H^+ concentration between plasma and parietal cell canaliculus), which is among the highest observed in the mammalian body.

The process of acid secretion also involves the movement of other ions into and out of the parietal cell[1,9,10]. In the classical model of gastric acid secretion, we find that for each H^+ ion that is transported into the canaliculus by the H^+,K^+-ATPase, the basolateral Cl^-/HCO_3^- exchanger delivers a HCO_3^- molecule into the plasma and a Cl^- ion into the cytosol (Figure 1)[11,12]. Cl^- is secreted into the canaliculus via Cl^- channels in the apical membrane of the parietal cell, and it is possible that more than one type of channel is involved, as is likely to be the case with K^+. However, so far there is only evidence for the ClC-2 channel[13]. These Cl^- channels allow Cl^- to act as a counter ion for the K^+ flux across the membrane, thereby balancing the charge and ensuring electroneutral HCl secretion.

In common with most other cells, the level of K^+ in the parietal cell is higher than that in the plasma. The higher intracellular K^+ level is dependent on the activity of the Na^+,

K^+-ATPase. This enzyme is located on the basolateral membrane of the cell where it exchanges intracellular Na^+ for extracellular K^+[14]. The level of K^+ within the cell is also regulated by K^+ channels that allow ion movement across the basolateral membrane. These channels have a particularly an important role in generating negative cell membrane potential.

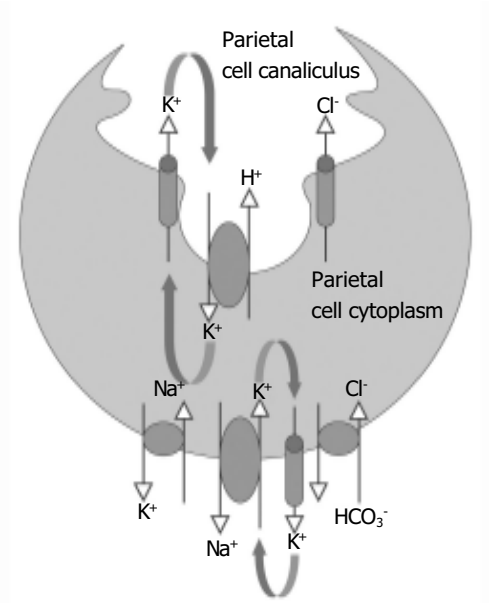


Figure 1 A simplified model for the secretion of gastric acid by the parietal cell. The H^+,K^+-ATPase located on the apical membrane of the parietal cell exchanges H^+ for K^+. K^+ is recycled from the canaliculus into the cytoplasm by K^+ channels in the apical membrane. The combined actions of K^+ channels and enzymes on the basolateral membrane regulate cytoplasmic K^+ levels. Cl^- enters the cell cytoplasm via a Cl^-/HCO_3^- exchanger and moves from the cytoplasm into the canaliculus via a Cl^- channel (most likely ClC-2).

ACTIVATION OF GASTRIC H^+,K^+-ATPASE BY K^+

When a parietal cell is in a resting state, H^+,K^+-ATPase is localized to tubulovesicular elements within the cell[15]. The concentration of K^+ in the tubulovesicular elements is low and their membranes are impermeable to K^+. Consequently, the enzyme cannot be activated and transport H^+ ions[1]. Stimulation of the parietal cell (e.g. by histamine) causes the tubulovesicular elements to fuse with the apical membrane of the cell[16,17]. The H^+,K^+-ATPase does not appear to undergo any chemical modification during activation of acid secretion but, as a result of the membrane fusion events, the enzyme is exposed to K^+-containing luminal fluid and can start to exchange H^+ for K^+.

This process of ion exchange involves several steps and conformational changes in the 3D structure of the H^+,K^+-ATPase (Figure 2)[5]. The enzyme exists in two important conformational states. In one of these states (referred to as E_1), the ionbinding site faces the parietal cell cytoplasm with high affinity for H^+ and low affinity for K^+; in the other state (E_2), the ion-binding site faces the extracellular canaliculus with low affinity for H^+ and high affinity for K^+. It is likely that the shape of the K^+ binding site or the path through which the ion accesses the binding site is different for the E_1 and E_2 forms[18], which may explain the relative affinity of the two forms for K^+.

In the E_1 form, the enzyme takes up H^+ and then converts into the E_2 form with the hydrolysis of ATP. As well as providing the energy for the shift between these conformational states, the hydrolysis of ATP also results in the phosphorylation of the enzyme (a state referred to as E_2P). The transformation to the E_2 form causes the translocation of H^+ from the parietal cell membrane into the canaliculus. Subsequently, the phosphorylated E_2 form binds K^+, which is required for the dephosphorylation of the H^+,K^+-ATPase.

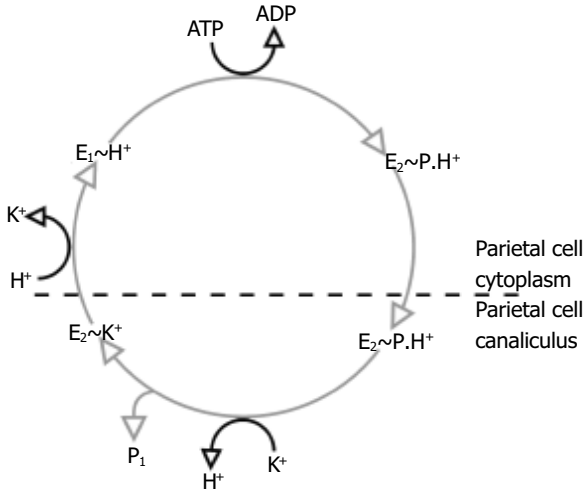


Figure 2 Post-Albers catalytic cycle of gastric H^+,K^+-ATPase.

During the cycling of the enzyme, K^+ becomes temporarily occluded within the transmembrane segments and the cations no longer have free access to the cytoplasm or canaliculus. It is in this state that the cation causes dephosphorylation of the H^+,K^+-ATPase[19]. The mechanism for this process is not fully elucidated. It is likely that K^+ does not stimulate dephosphorylation of the phosphorylated intermediate directly, but acts by neutralizing the inhibitory effect of a negative charge in the membrane[20]. After dephosphorylation, the enzyme returns to its E_1 form and releases K^+ into the parietal cell cytoplasm.

Some investigators have reported that one H^+ and one K^+ are exchanged for each ATP hydrolyzed[21], while others have found that there is reciprocal exchange of two pairs of ions per ATP hydrolysis[22,23]. The hypothesis that one H^+ is swapped for one K^+ ion is supported by recent modeling work, which demonstrated that gastric H^+,K^+-ATPase has a single K^+ binding site[24]. There are single ion binding sites in other P-type ATPases, such as yeast and plant H^+-ATPase[25], which provides support for the existence of a single cation binding site in gastric H^+,K^+-ATPase. Moreover, it has been proposed that one single binding site could more easily explain the ability of the H^+,K^+-ATPase to transport H^+ against a high concentration gradient[24].

K^+ BINDING SITE IN GASTRIC H^+,K^+-ATPASE

Much work has been directed at elucidating the identity of

the K^+ binding site (or sites) and potential sites have been located within the transmembrane segments M4, M5, M6 and possibly M8 of the α-subunit of the enzyme[26-29]. In accordance with the physiological role and location of K^+ (i.e. in the parietal cell canaliculus), the evidence suggests that the site is located towards the luminal face of the membrane domains[30]. When K^+ occupies this binding site, it appears to affect the conformation of a large intracellular loop in which phosphorylation occurs[20]. Moreover, K^+ is required for stabilization of a tight loop or 'hairpin' between M5 and M6[31]. This hairpin has a direct link with the phosphorylation domain on the intracellular loop that contains the ATP binding site, suggesting that it is involved in coupling ATP hydrolysis with cation transport[31].

As noted, recent work indicates that there is one high-affinity cation binding site in gastric H^+,K^+-ATPase[24]. The K^+ binding site is formed by amino acids from M4, M5 and M6, with the ion being held in place by six oxygen atoms provided by these domains[24]. The presence of a negative charge within the pocket (at residue 820) is thought to be important to the functioning of the enzyme[24].

This understanding of the likely structure of the K^+ site and its interaction with the phosphorylation domain has led to a theory on how K^+ activates the enzyme. The negative charge in the ion-binding pocket may exert an indirect inhibitory effect on the phosphorylated intermediate form of the enzyme, thereby preventing its hydrolysis[20]. When the cation-binding pocket is occupied by K^+, the negative charge is neutralized. A signal is then transferred to the nearby phosphorylation domain of the enzyme, possibly via a lysine amino acid residue, which results in enzyme dephosphorylation[32] and the subsequent translocation of K^+ from the parietal cell canaliculus to the cytoplasm.

K^+ SELECTIVITY OF THE H^+,K^+-ATPASE

The H^+,K^+-ATPase is highly selective for K^+, although it can also be activated *in vitro* by NH_4^+[33,34]. The cation selectivity of the enzyme appears to be generated through interactions with the residues of the transmembrane segments of the α-subunit and the flanking loops that connect these transmembrane domains[35]. The degree of K^+ affinity, along with the ATPase activity of the gastric H^+,K^+-ATPase, is also influenced by a salt bridge from M5 to M6 that exists only when the enzyme is in the E_2 form[24]. Importantly, this salt bridge only allows space for a single K^+ binding site and so prevents the formation of another K^+ binding site within the enzyme[24].

The β-subunit is also implicated in determining the K^+ affinity of gastric H^+,K^+-ATPase[36,37], as shown in a study comparing the pig and rat gastric H^+,K^+-ATPase. The different K^+ affinity of the enzymes from the two species was influenced by both the lipid matrix in which the enzymes were embedded and the identity of the β-subunit[37].

ROLE OF K^+ CHANNELS IN K^+ RECYCLING

At basal (i.e. unstimulated) levels of parietal cell activity, gastric juice consists mainly of NaCl, with only small amounts of K^+ and H^+. Stimulation of the parietal cell results in a sharp drop in pH. At a pH of approximately 1, the canaliculus of the parietal cell contains 150-160 mmol/L HCl[14]. Given the low concentration of K^+ ions in the unstimulated state, achieving such a low pH would appear to be difficult through 1:1 exchange of H^+ for K^+. However, stimulation actually elevates K^+ concentration (measured as KCl) in the gastric milieu (to 10-20 mmol/L KCl)[14]. Nevertheless, even at these levels there would be rapid K^+ depletion without a mechanism for replenishing of K^+ levels in the parietal cell canaliculus.

The K^+ ions that are exchanged with H^+ by the H^+,K^+-ATPase are provided by the parietal cell, while the Na^+,K^+-ATPase enzyme on the basolateral membrane accumulates K^+ within the parietal cell. Theoretically, a K–Cl co-transporterd could supply the H^+,K^+-ATPase enzyme with K^+, while also delivering Cl^- into the parietal cell canaliculus. This does not however appear to be the case, as Cl^- channels are present in the parietal cell apical membrane, and there is evidence that K^+ is recycled and enters the parietal cell canaliculus via specific K^+ channels[1].

To date, three different types of K^+ channels that may contribute to K^+ recycling have been identified in the apical membrane of the parietal cell. These K^+ channels belong to one of the largest and most diverse group of ion channels in the body[38]. There are over 60 K^+ channels, categorized according to whether they have 2, 4 or 6 transmembrane domains, and sharing a common feature of a pore-forming loop as part of the K^+ selective filter. Associated with these pore-forming subunits are additional regulatory units. Although the subunits are not essential for the formation of the ionic pore, they are responsible for membrane targeting and functional properties of the channel. The identity of the subunits in a cell, along with the type of K^+ channel they co-assemble with, determines the electrophysiological properties of that cell. In any given cell, there may be several types of channel and various subunits; some of the subunits may associate with more than one channel and so may result in channels with different functional attributes.

The K^+ channel KCNQ1 (formerly known as KvLQT1) was found to co-localize with gastric H^+,K^+-ATPase and to be abundantly expressed in human and mouse gastric mucosa[39,40]. Electrophysiological assessment of the KCNQ1 channel confirmed it had sustained activity at low pH[39,40]. This is an essential property of ion channels involved in acid secretion, as they must be capable of functioning at a low pH. The subunit KCNE2 (and possibly KCNE3) appears to co-assemble with KCNQ1 to form a functional K^+ channel in the apical membrane of parietal cells[40]. It is this subunit that is thought to determine the voltage dependence of KCNQ1 and its activation in response to extracellular acidification[40].

KCNQ1 has been proposed as an important K^+ channel in the apical membrane, as gastric acid secretion was inhibited by the 'specific' KCNQ1 channel inhibitor, chromanol 293B[40]. However, it has since been suggested that chromanol 293B has an alternative, unidentified target in the parietal cell[41]. Nevertheless, the contribution of this channel to acid secretion is further supported by the fact that KCNQ1 gene disruption leads to a loss of acid secretion in knockout mice[42].

Several members of another type of K^+ channel family,

the inward rectifying K^+ (Kir) family, have been shown to be expressed in rat gastric mucosa[43]. The Kir channels that were detected included Kir4.1, 4.2 and 7.1, although only Kir4.1 was found in parietal cells, where it was located at the apical region and appeared to co-localize with the β-subunit of H^+,K^+-ATPase.

Another member of the Kir family may also be involved in gastric acid secretion[41]. In rabbit gastric mucosa, high levels of Kir2.1 were detected along with lower levels of Kir4.1 and 7.1. Kir2.1 was found to be expressed in parietal cells from rabbit gastric mucosa and appeared to co-localize with H^+,K^+-ATPase and ClC-2 Cl^- channels. The K^+ channels were more likely to be open (i.e. allow K^+ transit) when they were obtained from stimulated stomach than from resting stomach. A reduction in pH also tended to increase the likelihood that the channels would be open, which suggests that these channels are regulated in a similar fashion to ClC-2 Cl^- channels. These findings, in a model that has been widely used to study the physiology of gastric acid secretion, suggest a role for Kir2.1 in K^+ recycling. However, as the electrophysiological properties of the channel were studied in gastric vesicles, caution must be applied when extrapolating the results to the native environment of the cell[41]. As with the Kir4.1 channel, the Kir2.1 channel associates with four subunits to form a functional K^+ channel.

Studies thus far have revealed a variety of potassium channels (i.e. KCNQ1, Kir2.1 and Kir4.1), albeit in different species, in the apical membrane of the parietal cell. All three channels have properties that are consistent with a role in K^+ recycling. However, it is uncertain which of these channels, if any, plays the major role in K^+ efflux and, as with the Cl^- channel(s), a complete understanding of the K^+ channel(s) involvement has yet to be achieved. Further study in both native tissues and transgenic animals may allow a more definite answer. A variety of K^+ channels have also been identified on the basolateral membrane of parietal cells, each with distinctive properties[44]. Thus, it is not unreasonable to assume that more than one type of K^+ channel in the apical membrane of the parietal cell may be involved in recycling the cation. Moreover, as noted previously, alongside this potential diversity of K^+ channels, different subunits may exist in the same cell, which may affect the properties of the channels[45,46]. This raises the possibility of a variety of functional channels with subtly different electrophysiological properties, making elucidation of the relative contribution of different K^+ channels extremely difficult. The present evidence indicates that more than one channel protein localizes to the apical region of the gland; as a result, the elimination of one channel may only lead to the upregulation of an alternative channel.

Caution must be applied in translating the findings in animal studies to man. For example, a single amino acid change can have a major influence on function. Thus, detailed studies need to determine the identity and composition of K^+ channels in humans before it can be confirmed which channel or channels are important in apical membrane K^+ flux. It also remains to be ascertained whether these channels are constitutively active or are regulated upon cell activation.

K^+ AS A TARGET FOR BLOCKING GASTRIC ACID PRODUCTION

The importance of K^+ in the production of gastric acid makes it a potential target for therapeutic intervention. One strategy is to block the K^+ channels that are responsible for the flow of the ion across the parietal cell apical membrane, while an alternative pharmacological approach is to compete with K^+ at the level of the gastric H^+,K^+-ATPase.

K^+ channel blockers

The K^+ channels in the apical membrane of the parietal cell represent a site for pharmacological modulation. The inhibition of gastric acid secretion by isolated gastric glands exposed to the 'specific' KCNQ1 K^+ channel blocker, chromanol 293B, indicates the potential of such an approach[40]. Even if a K^+ channel blocker did prevent H^+, K^+-ATPase activity, other challenges hinder the development of a therapeutic K^+ channel blocker. The identity of the channel(s) involved in K^+ recycling in the parietal cell will require further investigation, as will the possibility that more than one channel is involved in cation flux (which would require either several blockers or a drug that could inhibit a variety of channels). In addition to this potential problem, many of the identified ion channels can also be found in a variety of tissues (e.g. Kir4.1 is found on brain astrocytes[47] as well as in the apical membrane of parietal cells). This multi-organ distribution of channel proteins make organ-specific inhibitors a requirement, but a difficult target given the degree of cross-tissue homology exhibited by channel proteins.

Potassium-competitive acid blockers (P-CABs)

This group of mechanistically similar, developmental compounds has been identified as a potential therapeutic option for gastro-esophageal reflux disease (GERD) and other acid-related disorders[48]. They inhibit gastric H^+, K^+-ATPase by binding ionically to the enzyme and thus prevent activation by the K^+ cation. It is likely that P-CABs bind at or near the K^+ binding site and so prevent access of the cation to the site.

The early developmental compound, SCH28080, exemplifies the mechanism of action of P-CABs. This agent inhibited gastric acid production in healthy volunteers[49] and, although clinical development was not continued, it has been used extensively to explore the mechanisms of inhibition of gastric H^+,K^+-ATPase.

The large size of SCH28080 compared with K^+ ions suggests that the ion-binding site and inhibitor-binding site are not identical. Furthermore, mutational analysis of the gastric H^+,K^+-ATPase suggests that there are separate binding sites for SCH28080 and K^+. For example, mutations of several amino acid residues in the membrane domains reduce affinity for SCH28080 but have no effect on K^+ affinity[50,51]. Mutational analysis also indicates that the binding site of SCH28080 is closer to the luminal surface of the parietal cell than the ion-binding site[18].

SCH28080 gains access to its binding site and competes with K^+ when the gastric H^+,K^+-ATPase is in the phosphorylated E_2 form[52,53]. When the P-CAB binds to the H^+,K^+-ATPase, it stabilizes the enzyme in the E_2 conformation and, thereby,

prevents the movement of H^+ ions into the parietal cell canaliculus. Mutational data suggest that SCH28080 binds near the loop between M5 and M6, and at the luminal end of M6, about two helical turns away from the ion-binding site[18]. Homology modeling has suggested that SCH28080 interacts with residues in the M1–M6 domains[54], and, more specifically, it docks in a cavity formed by the M1, M4, M5, M6 and M8 transmembrane segments and by loops formed by M5/M6, M7/M8 and M9/M10[55]. This specificity was also demonstrated by another P-CAB, SPI447 in the same study[55]. A P-CAB molecule cannot occupy its binding pocket when the enzyme is in the E_1 form, due to rearrangement of the loop between M3 and M4, which alters the shape of the P-CAB binding cavity[55].

Inhibition of gastric acid production by P-CABs

The principle that P-CABs inhibit gastric H^+,K^+-ATPase was shown by studies with the experimental agents BY841[56], SCH28080[49], SK&F 96067[57], and SPI-447[58]. All P-CABs inhibit the gastric H^+,K^+-ATPase by competing with K^+[57-60], and their physico-chemical properties allow them to concentrate preferentially in highly acidic environments. Clinical develop-ment of the class is continuing with AZD0865, CS-526 (R-105266), revaprazan (YH1885) and soraprazan (BY359). Animal and early clinical studies have demonstrated that P-CABs are highly selective for gastric H^+,K^+-ATPase and inhibit gastric acid secretion with a fast onset of action[57,58,61-68]. Treatments that provide faster onset of effect and increased duration of action would offer improvement for patients with GERD and other acid-related disorders. An interesting observation is that the gastric isoform of the H^+,K^+-ATPase has been identified in only in two organs: the stomach and the kidney. Drugs targeted directly at this protein have shown no adverse effects on renal function, in either animal models or in humans following prolonged use. This is likely due to the relatively high pH in the kidney, which serves to preclude accumulation of these agents. Publication of ongoing studies investigating the efficacy of P-CABs in the treatment of GERD and other acid-related disorders are awaited.

CONCLUSION

In summary, we continue to gain insights into the role of K^+ in gastric H^+,K^+-ATPase function. This cation is not only the counterpart for H^+ that allows the generation of a highly acidic environment in the parietal cell canaliculus, but it is also an essential ion for the functioning of the enzyme itself. Investigations into the structure of the gastric H^+,K^+-ATPase indicate that the K^+ binding site is formed by amino acids from the M4, M5 and M6 domains of the enzyme. With the development of transgenic animals and new molecular markers, we are now only beginning to examine some of the subtle mechanisms by which K^+ induces the conformational changes that result in ion translocation.

The dependence of gastric H^+,K^+-ATPase on K^+ requires that relatively high levels of the cation are available in the parietal cell canaliculus. There is evidence that K^+ is recycled and enters the parietal cell canaliculus via specific K^+ channels. Three potential K^+ channels (KCNQ1, Kir2.1, and Kir4.1) that may contribute to K^+ recycling have been identified in the apical membrane of the parietal cell. The essential contribution of K^+ to gastric acid secretion makes K^+ channels attractive candidates for approaches to block acid production.

The specific KCNQ1 K^+ channel blocker, chromanol 293B, suggests the potential of such an approach. However, when the apical K^+ channels are inhibited by barium, the gastric H^+,K^+-ATPase continues to function. Despite the theoretical attractiveness of this approach, it is uncertain which of these channels, if any, plays the major part in cation recycling across the cell membrane and it is possible that more than one channel is involved. Moreover, homologous (or identical) K^+ channels can occur in different tissues, thereby making the development of an organ-specific channel blocker a challenging task. As research continues into the molecular identification of the apical K^+ channel(s) and their occurrence in other tissues, we will be able to assess whether these proteins are viable targets for inhibition of gastric acid secretion.

A group of mechanistically similar developmental compounds, the P-CAB class has been identified as a potential option for acid suppression therapy. P-CABs compete with K^+ at the level of the enzyme to inhibit acid production; the binding site of these agents appears distinct from the likely pocket that K^+ occupies. When the P-CAB occupies its binding site, it prevents K^+ from binding to and activating the enzyme. Animal and early clinical studies demonstrate that P-CABs are highly selective for gastric H^+,K^+-ATPase and inhibit gastric acid secretion with a fast onset of effect. Such treatments that offer the potential of a fast onset of effect and a long duration of action may provide significant benefits to patients with GERD and other acid-related disorders.

Clearly, by continuing to define the role of K^+ in gastric acid secretion, we will advance the development of novel approaches to regulate the production of gastric acid.

REFERENCES

1 **Reenstra WW,** Forte JG. Characterization of K+ and Cl- conductances in apical membrane vesicles from stimulated rabbit oxyntic cells. *Am J Physiol* 1990; **259**(5 Pt 1): G850-858

2 **Rabon E,** Chang H, Sachs G. Quantitation of hydrogen ion and potential gradients in gastric plasma membrane vesicles. *Biochemistry* 1978; **17**: 3345-3353

3 **Ganser AL,** Forte JG. K + -stimulated ATPase in purified microsomes of bullfrog oxyntic cells. *Biochim Biophys Acta* 1973; **307**: 169-180

4 **Sachs G,** Chang HH, Rabon E, Schackman R, Lewin M, Saccomani G. A nonelectrogenic H+ pump in plasma membranes of hog stomach. *J Biol Chem* 1976; **251**: 7690-7698

5 **Wallmark B,** Stewart HB, Rabon E, Saccomani G, Sachs G. The catalytic cycle of gastric (H+ + K+)-ATPase. *J Biol Chem* 1980; **255**: 5313-5319

6 **MacLennan DH,** Brandl CJ, Korczak B, Green NM. Amino-acid sequence of a Ca2+ + Mg2+-dependent ATPase from rabbit muscle sarcoplasmic reticulum, deduced from its complementary DNA sequence. *Nature* 1985; **316**: 696-700

7 **Shull GE,** Schwartz A, Lingrel JB. Amino-acid sequence of the catalytic subunit of the (Na+ + K+)ATPase deduced from a complementary DNA. *Nature* 1985; **316**: 691-695

8 **Crowson MS,** Shull GE. Isolation and characterization of a cDNA encoding the putative distal colon H+,K(+)-ATPase. Similarity of deduced amino acid sequence to gastric H+,K

(+)-ATPase and Na+,K(+)-ATPase and mRNA expression in distal colon, kidney, and uterus. *J Biol Chem* 1992; **267**: 13740-13748

9 **Cuppoletti J,** Sachs G. Regulation of gastric acid secretion via modulation of a chloride conductance. *J Biol Chem* 1984; **259**: 14952-14959

10 **Wolosin JM.** Ion transport studies with H+-K+-ATPase-rich vesicles: implications for HCl secretion and parietal cell physiology. *Am J Physiol* 1985; **248**(6 Pt 1): G595-607

11 **Muallem S,** Burnham C, Blissard D, Berglindh T, Sachs G. Electrolyte transport across the basolateral membrane of the parietal cells. *J Biol Chem* 1985; **260**: 6641-6653

12 **Paradiso AM,** Townsley MC, Wenzl E, Machen TE. Regulation of intracellular pH in resting and in stimulated parietal cells. *Am J Physiol* 1989; **257**(3 Pt 1): C554-561

13 **Malinowska DH,** Kupert EY, Bahinski A, Sherry AM, Cuppoletti J. Cloning, functional expression, and characterization of a PKA-activated gastric Cl- channel. *Am J Physiol* 1995; **268**(1 Pt 1): C191-200

14 **Sachs G,** Shin JM, Briving C, Wallmark B, Hersey S. The pharmacology of the gastric acid pump: the H+,K+ ATPase. *Annu Rev Pharmacol Toxicol* 1995; **35**: 277-305

15 **Smolka A,** Helander HF, Sachs G. Monoclonal antibodies against gastric H+ + K+ ATPase. *Am J Physiol* 1983; **245**: G589-596

16 **Kasbekar DK,** Forte GM, Forte JG. Phospholipid turnover and ultrastructural changes in resting and secreting bullfrog gastric mucosa. *Biochim Biophys Acta* 1968; **163**: 1-13

17 **Forte TM,** Machen TE, Forte JG. Ultrastructural changes in oxyntic cells associated with secretory function: a membrane-recycling hypothesis. *Gastroenterology* 1977; **73**: 941-955

18 **Vagin O,** Munson K, Denevich S, Sachs G. Inhibition kinetics of the gastric H,K-ATPase by K-competitive inhibitor SCH28080 as a tool for investigating the luminal ion pathway. *Ann N Y Acad Sci* 2003; **986**: 111-115

19 **Rabon EC,** Smillie K, Seru V, Rabon R. Rubidium occlusion within tryptic peptides of the H,K-ATPase. *J Biol Chem* 1993; **268**: 8012-8018

20 **Swarts HG,** Hermsen HP, Koenderink JB, Schuurmans Stekhoven FM, de Pont JJ. Constitutive activation of gastric H+, K+-ATPase by a single mutation. *Embo J* 1998; **17**: 3029-3035

21 **Reenstra WW,** Forte JG. H+/ATP stoichiometry for the gastric (K+ + H+)-ATPase. *J Membr Biol* 1981; **61**: 55-60

22 **Rabon EC,** McFall TL, Sachs G. The gastric [H,K]ATPase: H+/ATP stoichiometry. *J Biol Chem* 1982; **257**: 6296-6299

23 **Skrabanja AT,** de Pont JJ, Bonting SL. The H+/ATP transport ratio of the (K+ + H+)-ATPase of pig gastric membrane vesicles. *Biochim Biophys Acta* 1984; **774**: 91-95

24 **Koenderink JB,** Swarts HG, Willems PH, Krieger E, de Pont JJ. A conformation-specific interhelical salt bridge in the K+ binding site of gastric H,K-ATPase. *J Biol Chem* 2004; **279**: 16417-16424

25 **Bukrinsky JT,** Buch-Pedersen MJ, Larsen S, Palmgren MG. A putative proton binding site of plasma membrane H(+)-ATPase identified through homology modelling. *FEBS Lett* 2001; **494**: 6-10

26 **Munson KB,** Gutierrez C, Balaji VN, Ramnarayan K, Sachs G. Identification of an extracytoplasmic region of H+,K(+)-ATPase labeled by a K(+)-competitive photoaffinity inhibitor. *J Biol Chem* 1991; **266**: 18976-18988

27 **Swarts HG,** Klaassen CH, de Boer M, Fransen JA, de Pont JJ. Role of negatively charged residues in the fifth and sixth transmembrane domains of the catalytic subunit of gastric H+, K+-ATPase. *J Biol Chem* 1996; **271**: 29764-29772

28 **Vagin O,** Munson K, Lambrecht N, Karlish SJ, Sachs G. Mutational analysis of the K+-competitive inhibitor site of gastric H,K-ATPase. *Biochemistry* 2001; **40**: 7480-7490

29 **Asano S,** Tega Y, Konishi K, Fujioka M, Takeguchi N. Functional expression of gastric H+,K(+)-ATPase and site-directed mutagenesis of the putative cation binding site and catalytic center. *J Biol Chem* 1996; **271**: 2740-2745

30 **Munson K,** Lambrecht N, Shin JM, Sachs G. Analysis of the membrane domain of the gastric H(+)/K(+)-ATPase. *J Exp Biol* 2000; **203**(Pt 1): 161-170

31 **Gatto C,** Lutsenko S, Shin JM, Sachs G, Kaplan JH. Stabilization of the H,K-ATPase M5M6 membrane hairpin by K+ ions. Mechanistic significance for p2-type atpases. *J Biol Chem* 1999; **274**: 13737-13740

32 **de Pont JJ,** Swarts HG, Willems PH, Koenderink JB. The E1/E2-preference of gastric H,K-ATPase mutants. *Ann N Y Acad Sci* 2003; **986**: 175-182

33 **Lorentzon P,** Sachs G, Wallmark B. Inhibitory effects of cations on the gastric H+, K+ -ATPase. A potential-sensitive step in the K+ limb of the pump cycle. *J Biol Chem* 1988; **263**: 10705-10710

34 **Fryklund J,** Gedda K, Scott D, Sachs G, Wallmark B. Coupling of H(+)-K(+)-ATPase activity and glucose oxidation in gastric glands. *Am J Physiol* 1990; **258**(5 Pt 1): G719-727

35 **Mense M,** Rajendran V, Blostein R, Caplan MJ. Extracellular domains, transmembrane segments, and intracellular domains interact to determine the cation selectivity of Na,K- and gastric H,K-ATPase. *Biochemistry* 2002; **41**: 9803-9812

36 **Koenderink JB,** Swarts HG, Hermsen HP, de Pont JJ. The beta-subunits of Na+,K+-ATPase and gastric H+,K+-ATPase have a high preference for their own alpha-subunit and affect the K+ affinity of these enzymes. *J Biol Chem* 1999; **274**: 11604-11610

37 **Hermsen HP,** Swarts HG, Wassink L, Dijk FJ, Raijmakers MT, Klaassen CH, Koenderink JB, Maeda M, De Pant JJ. The K(+) affinity of gastric H(+),K(+)-ATPase is affected by both lipid composition and the beta-subunit. *Biochim Biophys Acta* 2000; **1480**: 182-190

38 **Coetzee WA,** Amarillo Y, Chiu J, Chow A, Lau D, McCormack T, Moreno H, Nadal MS, Ozaita A, Pountney D, Saganich M, Vega-Saenz de Miera E, Rudy B. Molecular diversity of K+ channels. *Ann N Y Acad Sci* 1999; **868**: 233-285

39 **Dedek K,** Waldegger S. Colocalization of KCNQ1/KCNE channel subunits in the mouse gastrointestinal tract. *Pflugers Arch* 2001; **442**: 896-902

40 **Grahammer F,** Herling AW, Lang HJ, Schmitt-Graff A, Wittekindt OH, Nitschke R, Bleich M, Barhanin J, Warth R. The cardiac K+ channel KCNQ1 is essential for gastric acid secretion. *Gastroenterology* 2001; **120**: 1363-1371

41 **Malinowska DH,** Sherry AM, Tewari KP, Cuppoletti J. Gastric parietal cell secretory membrane contains PKA- and acid-activated Kir2.1 K+ channels. *Am J Physiol Cell Physiol* 2004; **286**: C495-506

42 **Lee MP,** Ravenel JD, Hu RJ, Lustig LR, Tomaselli G, Berger RD, Brandenburg SA, Litzi TJ, Banton TE, Limb C, Francis H, Gorelikow M, Gu H, Washington K, Argani P, Goklenriny JR, Coffey RJ, Feinberg AP. Targeted disruption of the Kvlqt1 gene causes deafness and gastric hyperplasia in mice. *J Clin Invest* 2000; **106**: 1447-1455

43 **Fujita A,** Horio Y, Higashi K, Mouri T, Hata F, Takeguchi N, Kurachi Y. Specific localization of an inwardly rectifying K(+) channel, Kir4.1, at the apical membrane of rat gastric parietal cells; its possible involvement in K(+) recycling for the H(+)-K(+)-pump. *J Physiol* 2002; **540**: 85-92

44 **Supplisson S,** Loo DD, Sachs G. Diversity of K+ channels in the basolateral membrane of resting Necturus oxyntic cells. *J Membr Biol* 1991; **123**: 209-221

45 **Raap M,** Biedermann B, Braun P, Milenkovic I, Skatchkov SN, Bringmann A, Reichenbach A. Diversity of Kir channel subunit mRNA expressed by retinal glial cells of the guinea-pig. *Neurorepor* 2002; **13**: 1037-1040

46 **Wulfsen I,** Hauber HP, Schiemann D, Bauer CK, Schwarz JR. Expression of mRNA for voltage-dependent and inward-rectifying K channels in GH3/B6 cells and rat pituitary. *J Neuroendocrinol* 2000; **12**: 263-272

47 **Higashi K,** Fujita A, Inanobe A, Tanemoto M, Doi K, Kubo T, Kurachi Y. An inwardly rectifying K(+) channel, Kir4.1, expressed in astrocytes surrounds synapses and blood vessels in brain. *Am J Physiol Cell Physiol* 2001; **281**: C922-931

48 **Vakil N.** Review article: new pharmacological agents for the treatment of gastro-oesophageal reflux disease. *Aliment*

Pharmacol Ther 2004; **19**: 1041-1049
49 **Ene MD,** Khan-Daneshmend T, Roberts CJ. A study of the inhibitory effects of SCH 28080 on gastric secretion in man. *Br J Pharmacol* 1982; **76**: 389-391
50 **Lambrecht N,** Munson K, Vagin O, Sachs G. Comparison of covalent with reversible inhibitor binding sites of the gastric H,K-ATPase by site-directed mutagenesis. *J Biol Chem* 2000; **275**: 4041-4048
51 **Asano S,** Matsuda S, Hoshina S, Sakamoto S, Takeguchi N. A chimeric gastric H+,K+-ATPase inhibitable with both ouabain and SCH 28080. *J Biol Chem* 1999; **274**: 6848-6854
52 **Keeling DJ,** Taylor AG, Schudt C. The binding of a K+ competitive ligand, 2-methyl,8-(phenylmethoxy)imidazo(1,2-a) pyridine 3-acetonitrile, to the gastric (H+ + K+)-ATPase. *J Biol Chem* 1989; **264**: 5545-5551
53 **Mendlein J,** Sachs G. Interaction of a K(+)-competitive inhibitor, a substituted imidazo[1,2a] pyridine, with the phospho- and dephosphoenzyme forms of H+, K(+)-ATPase. *J Biol Chem* 1990; **265**: 5030-5036
54 **Yan D, Hu** YD, Li S, Cheng MS. A model of 3D-structure of H+, K+-ATPase catalytic subunit derived by homology modeling. *Acta Pharmacol Sin* 2004; **25**: 474-479
55 **Asano S,** Yoshida A, Yashiro H, Kobayashi Y, Morisato A, Ogawa H, Takeguchi N, Morii M. The cavity structure for docking the K(+)-competitive inhibitors in the gastric proton pump. *J Biol Chem* 2004; **279**: 13968-13975
56 **Martinek J,** Blum AL, Stolte M, Hartmann M, Verdu EF, Luhmann R, Dorta G, Wiesel P. Effects of pumaprazole (BY841), a novel reversible proton pump antagonist, and of omeprazole, on intragastric acidity before and after cure of *Helicobacter pylori* infection. *Aliment Pharmacol Ther* 1999; **13**: 27-34
57 **Keeling DJ,** Malcolm RC, Laing SM, Ife RJ, Leach CA. SK&F 96067 is a reversible, lumenally acting inhibitor of the gastric (H+ + K+)-ATPase. *Biochem Pharmacol* 1991; **42**: 123-130
58 **Tsukimi Y,** Ushiro T, Yamazaki T, Ishikawa H, Hirase J, Narita M, Nishigaito T, Banno K, Ichihara T, Tanaka H. Studies on the mechanism of action of the gastric H+,K(+)-ATPase inhibitor SPI-447. *Jpn J Pharmacol* 2000; **82**: 21-28
59 **Wallmark B,** Briving C, Fryklund J, Munson K, Jackson R, Mendlein J, Rabon E, Sachs G. Inhibition of gastric H+,K+-ATPase and acid secretion by SCH 28080, a substituted pyridyl(1,2a)imidazole. *J Biol Chem* 1987; **262**: 2077-2084
60 **Wurst W,** Hartmann M. Current status of acid pump antagonists (reversible PPIs). *Yale J Biol Med* 1996; **69**: 233-243
61 **Briving C,** Svensson K, Maxvall I, Andersson K. Mechanism of action of AZD0865, an H^+,K^+-ATPase selective, potassium-competitive acid blocker. *Gastroenterology* 2004; **126**: A333
62 **Holstein B,** Holmberg A, Florentzson M, Holmberg AA, Andersson M, Andersson K. AZD0865 - a new potassium-competitive acid blocker -exhibits maximal gastric antisecretory effects from first dose. *Gastroenterology* 2004; **126**: A334
63 **Andersson K,** Holmberg AA, Briving C, Holstein B. Preclinical profile of AZD0865, a novel, selective, potassium-competitive acid blocker. *Gastroenterology* 2004; **126**: A56
64 **Park S,** Ahn B, Lee B, Kang H, Song K. Pharmacokinetics of YH1885. *Gut* 2003: **52**(Suppl 6): A62
65 **Park S,** Lee S, Song K, Lee B, Kang H, Kang J. The pharmacological properties of a novel acid pump antagonist, YH1885. *Gut* 2003; **52**(Suppl 6): A62
66 **Yu KS,** Bae KS, Shon JH, Cho JY, Yi SY, Chung JY, Lim HS, Jang JJ, Shins G, Song KS, Moon BS. Pharmacokinetic and pharmacodynamic evaluation of a novel proton pump inhibitor, YH1885, in healthy volunteers. *J Clin Pharmacol* 2004; **44**: 73-82
67 **Kromer W,** Postius S, Riedel R. Animal pharmacology of reversible antagonism of the gastric acid pump, compared to standard antisecretory principles. *Pharmacology* 2000; **60**: 179-187
68 **Pope AJ,** Sachs G. Reversible inhibitors of the gastric (H+/K+)-ATPase as both potential therapeutic agents and probes of pump function. *Biochem Soc Trans* 1992; **20**: 566-572

Science Editor Guo SY **Language Editor** Elsevier HK

PO Box 2345, Beijing 100023, China
www.wjgnet.com
wjg@wjgnet.com

ELSEVIER

World J Gastroenterol 2005;11(34):5266-5272
World Journal of Gastroenterology ISSN 1007-9327
© 2005 The WJG Press and Elsevier Inc. All rights reserved.

Over-expression of fibroblast growth factor receptor 3 in human hepatocellular carcinoma

Wei-Hua Qiu, Bing-Sen Zhou, Peiguo G. Chu, Wen-Gang Chen, Christopher Chung, Jennifer Shih, Paul Hwu, Christopher Yeh, Richard Lopez, Yun Yen

Wei-Hua Qiu, Bing-Sen Zhou, Christopher Chung, Jennifer Shih, Paul Hwu, Christopher Yeh, Yun Yen, Department of Medical Oncology and Therapeutic Research, City of Hope National Medical Center, Duarte, CA 91010, United States
Peiguo G. Chu, Wen-Gang Chen, Department of Pathology, City of Hope National Medical Center, Duarte, CA 91010, United States
Richard Lopez, Department of Surgery, St. Vincent Hospital, LA, CA 90057, United States
Supported by Ralph M. Parsons Foundation and Shanghai Educational Commission Grant, No. 04BC32, and Sino American Cancer Foundation
Correspondence to: Yun Yen, MD, PhD, FACP, City of Hope National Medical Center, 1500 E. Duarte Road, Duarte, CA 91010, United States. yyen@coh.org
Telephone: +1-626-359-8111-62307 Fax: +1-626-301-8233
Received: 2004-10-16 Accepted: 2004-12-26

Abstract

AIM: To describe the significant over-expression of fibroblast growth factor receptor 3 (FGFR3), which is a signal transduction and cell proliferation related gene in hepatocellular carcinoma (HCC).

METHODS: Following DNA microarray, Northern blot and quantitative real-time PCR were employed to confirm FGFR3 expression difference in HCC tissues and surrounding non-neoplastic liver tissue. FGFR3 expression levels were further determined by immunohistochemical study in 43 cases of HCC.

RESULTS: Northern blot results showed the significant over-expression of FGFR3 in HCC tissues, which was consistent with that from DNA microarray. Quantitative real-time PCR demonstrated that the mean ratio of FGFR3 mRNA to glyceraldehyde-3-phosphate dehydrogenase (GADPH) mRNA in HCC tissue was 0.250, whereas the ratio in non-neoplastic liver tissue was 0.014. Statistical analyses of 43 cases of HCC revealed that HCC scored higher than the matched non-neoplastic liver tissues. Examination of clinicopathological features revealed a strong correlation of over-expression of FGFR3 with poor tumor differentiation and high nuclear grade.

CONCLUSION: Over-expression of FGFR3 may play an important role in liver carcinogenesis. FGFR3 may be an ideal candidate as a molecular marker in the diagnosis of HCC and a potential therapeutic target.

© 2005 The WJG Press and Elsevier Inc. All rights reserved.

Key words: Fibroblast growth factor receptor 3; Human hepatocellular carcinoma; Microarray

Qiu WH, Zhou BS, Chu PG, Chen WG, Chung C, Shih J, Hwu P, Yeh C, Lopez R, Yen Y. Over-expression of fibroblast growth factor receptor 3 in human hepatocellular carcinoma. *World J Gastroenterol* 2005; 11(34): 5266-5272
http://www.wjgnet.com/1007-9327/11/5266.asp

INTRODUCTION

Hepatocellular carcinoma (HCC) is one of the most common cancers in many parts of the world such as the Far East, Southern Sahara and Southern Europe, accounting for nearly half a million deaths worldwide[1]. Recent epidemiological data suggest that the incidence of HCC is increasing in USA, and the annual rate of new cases is 17 300[2]. Many risk factors, such as viral hepatitis, alcohol abuse, biliary disease, metabolic disorders, drugs, and toxins are related to carcinogenesis in HCC. These risk factors result in hepatocellular injury and replacement of normal acini by nodules. Regenerative hyperplasia of fibrous tissue and acini nodules profoundly disturbs the hepatic parenchymal structure and vascular network, which can directly or indirectly contribute to carcinogenesis, as a final stage of liver disease. Therefore, neoplastic transformation of HCC constitutes a long and complex course related to hepatocyte damage and the repair process, which involves multiple oncogenes and tumor suppressor genes.

With the development of the new molecular technology, DNA microarrays make it possible to study gene expression profiles in a global setting and screen thousands of genes rapidly and efficiently. Based on the panel of genes provided in the DNA microarray, further studies can be performed to determine the function of genes which have been identified to be significantly enriched or decreased, and these results can be used to discover new therapeutic target genes for the improvement of HCC prognosis[3]. This technology has been applied successfully in the identification of key genes in neoplastic transformation and as a diagnosis tool in molecular pathology[4,5].

In a previous study, a DNA microarray is used to compare the gene expression profile of HCC tissues with that of matched non-neoplastic tissue[6]. In this study, we focused on the expression change of transcription and translation-related genes in microarray gene profile. Among the 17 genes whose expression levels changed most significantly in this profile, 10 over-expressed genes and 7

under-expressed genes were identified in HCC. FGFR3 is a member of the FGFR family, which is involved in cell growth control, cell differentiation and migration. Based on the unclear role of amplification of these receptors in carcinogenesis in digestive tract carcinoma, we studied the role of FGFR3 in carcinogenesis in HCC. The expression of FGFR3 significantly increased in HCC tissue, which was confirmed by Northern blot. Quantitative real-time PCR study further demonstrated that the mean ratio of FGFR3 mRNA to GAPDH mRNA in HCC tissue was 0.250, whereas the ratio in non-neoplastic liver tissue was 0.014 (P<0.01). Immunohistochemical (IHC) studies of 43 cases of HCC proved the over-expression of FGFR3 in HCC and the extent of over-expression was associated with tumor differentiation and nuclear grade of HCC. Thus, over-expression of FGFR3 may play an important role in carcinogenesis in HCC.

MATERIALS AND METHODS

Patients and specimens

Four specimens of fresh HCC tissue, coupled with non-neoplastic liver tissue from each individual, were obtained from City of Hope National Medical Center and St. Vincent Hospital. All tissue specimens were submitted for routine pathological evaluation and diagnosis confirmation. Forty-three HCC tissue paraffin blocks were collected from surgical pathology files at the City of Hope National Medical Center with a highly controlled manner to ensure patient confidentiality. A section was stained with hematoxylin and eosin (H&E) and examined to confirm the diagnosis and tumor type.

DNA microarray and Northern blot analysis

All fresh tissue samples were cut into small pieces and snap-frozen in liquid nitrogen immediately. The tissues were confirmed by histopathologic examination to validate the adequate HCC cells in the tumor samples. No HCC cells were contaminated in non-neoplastic liver tissues which were reassured before further approach. RNA isolation, cRNA preparation and microarray hybridization were performed as described previously[6]. The microarray format, scanning and data analysis were performed at the Microarray Core Facility, Children's Hospital, Los Angeles,USA. For each sample, at least two hybridizations were carried out. The average of median ratios from replicates was calculated for each spot. We then used 2.0 SD as our cut-off for the determination of expression outlines.

Normal human embryonic liver cell line CL-48, and human HCC cell lines, HepG2 and Hep3B, were purchased from American Type Culture Collection (ATCC; Manassas, VA, USA) and cultured in high glucose Dulbecco's modified Eagle's medium (DMEM), 10% fetal bovine serum (FBS) and 1% P/S (100 U/mL penicillin and 100 μg/mL streptomycin) at 37 ℃ in 50 mL/L CO_2. Total RNA was isolated from the HCC and non-neoplastic liver tissues used for microarray analysis and from logarithmically growing CL-48, HepG2 and Hep3B cells using RNeasy Mini kit (Qiagen, Valencia, CA, USA). The RNA was electrophoresed in 1.2% formaldehyde-agarose gel, blotted to a Hybond-N membrane (Amersham, Arlington, IL) and UV-cross-linked. ^{32}P-labeled FGFR3 probe was prepared according to the protocol of the random priming probe kit from Roche (Indianapolis, IN, USA). The blots were hybridized for 1 h at 68 ℃, washed twice with 2×SSC/0.1% SDS at room temperature, and washed twice with 0.1×SSC/0.1% SDS at 60 ℃. After hybridization, membranes were exposed for 18-48 h to Kodak XAR-5 film (Eastman Kodak, Rochester, NY, USA) with intensifying screens and exposed to a phosphorimager screen for 18 h, then read by phosphorimager scanner. All experiments were repeated thrice for confirmation. The DNA probe for FGFR3 was generated by RT-PCR from CL-48 total RNA with the following primers: 5'-ATG GGC GCC CCT GCC TGC-3' (sense primer starting with FGFR3 cDNA nucleotide 40) and 5'-GTG GTG TGT TGG AGC TCA TG-3' (anti-sense primer starting with FGFR3 nucleotide 1 337). The PCR product included FGFR3 axons 2 and 3 sequence (according to the FGFR3 sequence NM_000142 in GenBank). The PCR conditions were as follows: 1 cycle at 95 ℃ for 15 min; 35 cycles at 94 ℃ for 40 s, at 60 ℃ for 40 s, at 72 ℃ for 2 min; and 1 cycle at 72 ℃ for 10 min. The products were purified and cleaned up using a gel extract and purification kit (Qiagen).

Quantitative real-time PCR

To further confirm and validate the microarray data, quantitative real-time PCR was employed to measure the FGFR3 messenger RNA expression in HCC tissue and matched non-neoplastic liver tissue. RNAs isolated from the fresh-frozen tissues for microarray were treated using RNA-free DNase I (Promega, Madison, WI, USA) according to the protocol to remove contaminated DNA. cDNA was reverse transcribed from total RNA using AMVRT and Oligo (dT) 12-18 primer. The forward primer 5'-TGC TGA ATG CCT CCC ACG -3', reverse primer 5'-CGT CTT CGT CAT CTC CCG AG-3', and probe 5'-FAM- TGT GCG GGT GAC AGA CGC TCC AT -TAMRA-3' were employed for the amplification of FGFR3. To avoid the genomic DNAs background, primers and TaqMan probes were designed to span axons 2 and 3. Pre-developed TaqMan assay reagent control kit (Perkin-Elmer Applied Biosystems, Foster City, CA, USA), including forward, reverse primer and VIK-probe of GAPDH, was used as internal control. FGFR-3-pCDNA3.1 plasmid and GAPDH-pT7T3D-PAC plasmid, containing the full-length FGFR3 and GAPDH structure genes respectively, were used to generate the standard curve. The PCR conditions were as follows: 1 cycle at 50 ℃ for 2 min, at 95 ℃ for 10 min; 40 cycles at 95 ℃ for 15 s, at 60 ℃ for 60 s. Each point of data was performed in duplicate.

Quantification of gene expression was performed using the ABI PRISM 7700 sequence detection system (Perkin-Elmer Applied Biosystems, Foster City, CA, USA) according to the Pre-developed TaqMan assay reagent gene expression quantification protocol. The normalized reporter signal was defined as the intensity of fluorescent reporter dye (FAM or VIK) relative to the passive reference dye TAMRA. The threshold line was determined as high as 10 times of the standard deviation of the baseline fluorescence signal. After reaching the threshold, the sample was designated positive and the threshold cycle (Ct) was

defined as the cycle number at this point. Standard curves for FGFR3 and GAPDH were generated by serial dilution of control plasmids and the amount of mRNA of FGFR3 and GAPDH in each test sample was calculated based on the standard curve. Values were expressed as the ratio of FGFR3 to GAPDH in each sample.

Immunohistochemical study

Paraffin sections were deparaffinized in xylene and rehydrated in a graded alcohol series. After retrieval in pH 8.0 EDTA for 20 min, the slides were blocked with DAKO protein block serum for 5 min (DAKO, Carpinteria, CA, USA). The primary rabbit anti-human polyclonal FGFR3 antibody (200 μg/mL, Santa Cruz Biotechnology, Santa Cruz, CA, USA) was used at an 1:100 dilution for 25 min and washed thrice (5 min each) with DAKO wash buffer. After 7 min of hydrogen peroxide treatment, the slides were incubated with labeled polymer HRP anti-rabbit antibody (DAKO, Carpinteria, CA, USA) for 30 min. Then, DAB (0.05 g DAB and 100 μL 30% H_2O_2 in 100 mL PBS) was applied for 5 and 10 min respectively. Each slide was counterstained with DAKO's hematoxylin. For all IHC studies, PBS was used as a negative control. Granular cytoplasmic staining was assessed as positive. The evaluation of staining intensity was performed by three independent observers.

Scoring and data analysis

The diagnosis of HCC, tumor cell differentiation, nuclear grade and growth pattern were assessed based on the examination of H&E-stained sections, according to the Edmondson's grade and nuclear grade criteria[7,8]. Briefly, well-differentiated HCC was composed of cells with minimal atypia and an increased nuclear/cytoplasmic ratio. In moderately-differentiated HCC, tumor cells were arranged in trabeculae of three or more cells in thickness and had abundant eosinophilic cytoplasm and round nuclei with distinct nucleoli. In poorly-differentiated HCC, tumor cells had an increased nuclear/cytoplasmic ratio, frequent pleomorphism and bizarre giant cells. Nuclear grade was classified in a four-tiered system. Nuclear grade I HCC comprised of adenoma-like cells that had abundant cytoplasm showing little variation in size and shape and was closely similar to benign hepatocyte nuclei, with an even distribution of chromatin. Nuclear grade II HCC contained cells with large and prominent nucleoli, some degree of nuclear membrane irregularity, and chromatin clumping, and were characterized by greater nuclear pleomorphism, angulated nuclei and occasionally multinucleated cells. Nuclear grade IV HCC was noted by its distinct pleomorphism, hyperchromatism, and anaplastic giant cells. Tumor growth pattern was also classified according to its trabecular, compact, pseudoglandular, cirrhotic and solid architecture. In cases that had several architectural patterns, the predominant one was captured for the statistics. The staining pattern of FGFR3 was classified in a subjective spectrum of 0 to ++: 0 as negative expression in tissue, + as weak staining, and ++ as strong staining. For each level of staining, the percentage of cells with the corresponding score was estimated visually. A combined weighed score, consisting of the sum of the percentage of cells at each staining intensity level, was calculated for each sample. In each case, staining of FGFR3 in matched surrounding non-neoplastic hepatocytes was evaluated at the same time. Statistical analysis of FGFR3 expression differences in HCC and surrounding non-neoplastic liver tissue was conducted using the Wilcoxon signed rank test. The association between the expression of FGFR3 and clinicopathologic parameters was examined by the non-parametric χ^2 tests. The relationship of the patients' demographic features, such as age, gender and hepatitis B status, to FGFR3 expression was examined with the *F*-statistic test for linear effects and non-parametric Kruskal-Wallis test for singly ordered tables. SPSS 10.0 statistical analysis software was used to calculate the statistics. $P<0.05$ was considered statistically significant.

RESULTS

Microarray and Northern blot analysis

The partial result of microarray has been published in our previous study[6]. Among the 59 genes whose expression levels were most significantly changed, 30 over-expressed genes and 29 under-expressed genes were identified in HCC. In this study, we focused on the expression change of transcription and translation-related genes in microarray gene profile. In this profile, a total of 10 genes including translational initiation factor EIF-2, GTP binding protein, CDC2-related protein kinase, FGFR3, elongation factor-1β, were over-expressed in HCC. Whereas, insulin-like growth factor, MAP2K5, cyclin D1 and other 4 genes were under-expressed (Table 1). Our results revealed that transcription and translation-related genes also played a very important role in hepatocarcinogenesis besides oncogenes and tumor suppressor genes. Based on the increasing importance of FGFR3 in carcinogenesis in digestive tract carcinoma, we studied the role of FGFR3 in carcinogenesis in HCC. Northern blot showed that the FGFR3 gene was strongly expressed in HCC tissue, HepG2 and Hep3B HCC cell

Table 1 Different expressions of transcription and translation-related gene in HCC

Gene name	Coding number
Most over-expressed genes in HCC	
Translational initiation factor EIF-2, alpha subunit	1 154
Homo sapiens GTP binding protein mRNA complete code	38 708
Human mRNA for elongation factor-1-β	35 748
Human CDC2-related protein kinase mRNA	1 793
Fibroblast growth factor receptor 3	36 165
Elongation factor-1-γ	1 676
mRNA for erythropoietin receptor	396
Human G protein-coupled receptor	1 097
Glutathione S-transferase	31 919
Homo sapiens NADH-ubiquinone oxidoreductase subunit CI-SGDH	32 232
Least expressed genes in HCC	
Human insulin-like growth factor binding protein gene	1 232
Homo sapiens mRNA for TGF-β IIR α	1 815
Heterogeneous nuclear ribonucleoprotein H	41 292
Polyubiquitin Ubc	32 334
Nucleic acid binding protein gene	32 841
MAP2K5	33 071
Cyclin D1	40 436

lines were opposed to match non-neoplastic liver tissue and CL-48 human normal embryonic liver cell lines (Figure 1). Under the image quantity measurement relative to the internal control by GAPDH, the expression of FGFR3 in HCC and HCC cell lines was as high as 4- or 2.5-folds in non-neoplastic liver tissue and CL-48, respectively. Therefore, our Northern blot analysis was consistent with the expression patterns generated by microarray data.

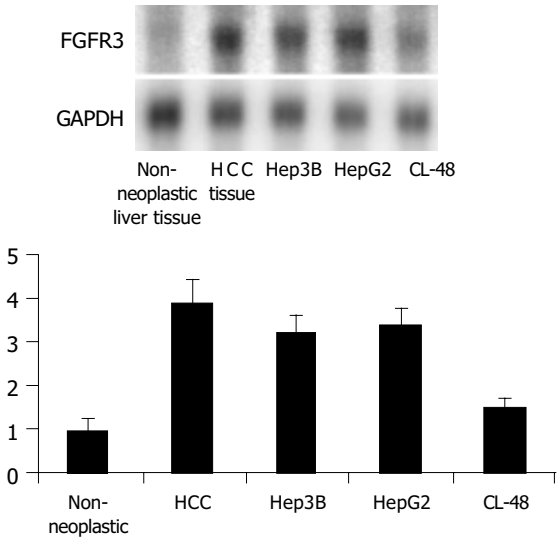


Figure 1 Northern blot validation of FGFR3 expression in matched HCC/non-neoplastic liver tissue and cell lines.

Quantitative analysis of mRNA expression in FGFR3 by real-time PCR

The standard curve formulas $Y = 45.01\text{-}3.86X$ ($r^2 = 0.994$) for FGFR3 and $Y = 38.38\text{-}3.31X$ ($r^2 = 0.991$) for GAPDH were derived from the lines of the calibration curves. The results from four liver cancer tissue and matched non-neoplastic liver tissue specimens were plotted on the standard curve. The mRNA expression in FGFR3 was calculated as mentioned above. The mean ratio of FGFR3 mRNA to GAPDH mRNA in HCC tissue was 0.250, and the ratio in non-neoplastic liver tissue was 0.014. The average mRNA expression in HCC tissue was significantly less than that in non-neoplastic liver tissue ($P<0.01$), compared to GAPDH. The typical analysis result is shown in Figure 2.

IHC study

To validate the specificity of DNA microarray and real-time PCR, IHC analysis was performed in paraffin sections of HCC tissue with surrounding non-neoplastic liver tissues (Figure 3). Immunostaining was performed under 10 high power fields (×400) in the most densely cellular areas. Areas having necrosis or fibrosis were excluded. Among the 43 HCC cases, 2 were cirrhotic, 24 trabecular, 6 psuedoglandular, 3 solid, 7 compact, and 1 sarcomatoid. H&E staining was examined first and used as a control. The positive staining of FGFR3 was diffuse brownish cytoplasmic staining. FGFR3 was predominantly localized in the tumor cells, with lower levels in the non-neoplastic hepatic cells. Among the 43 cases of HCC, only 2 cases of non-neoplastic tissues demonstrated very weak staining, and the difference in the distribution of FGFR3 staining in the HCC area and non-neoplastic liver tissue was noticeable ($P<0.01$) (Figure 3). Stromal cells, bile ductal epithelial cells, vascular epithelial cells and fibrotic tissue were negative for FGFR3. Less intense staining was observed in infiltrated lymphocytes, Kupffer's cells and smooth muscle cells.

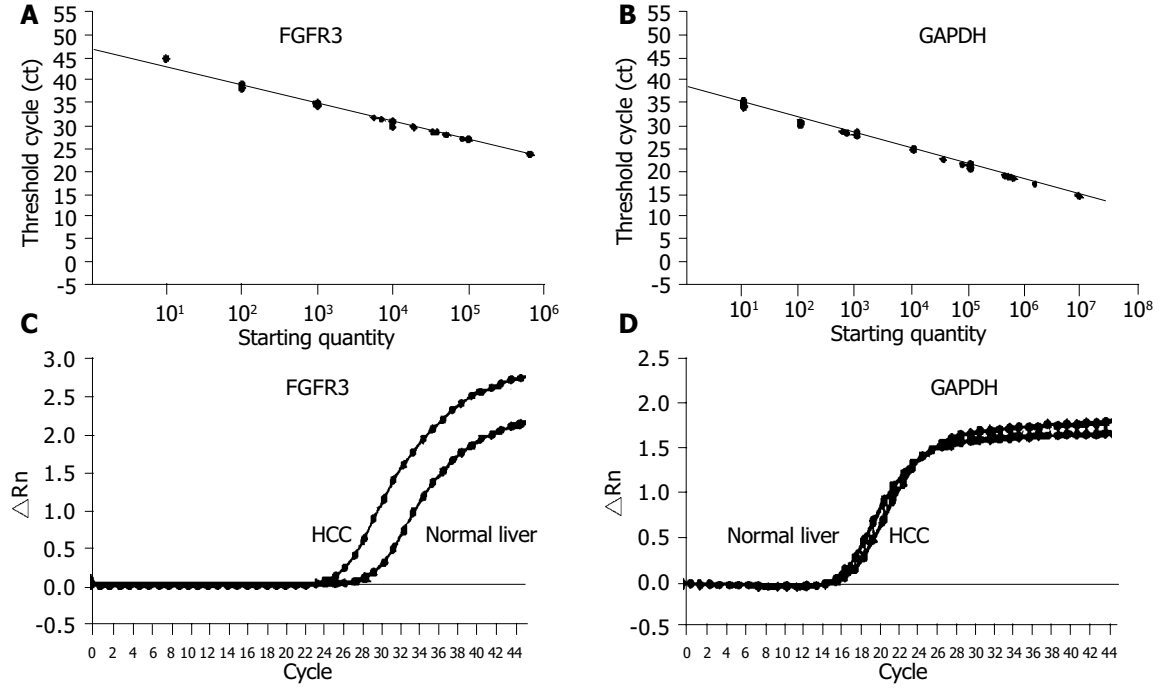


Figure 2 Standard curve and amplification plots of FGFR3 and GAPDH by quantitative real-time PCR. Starting quantity FGFR3 (A) and GAPDH (B); cycle FGFR3 (C) and GAPDH (D).

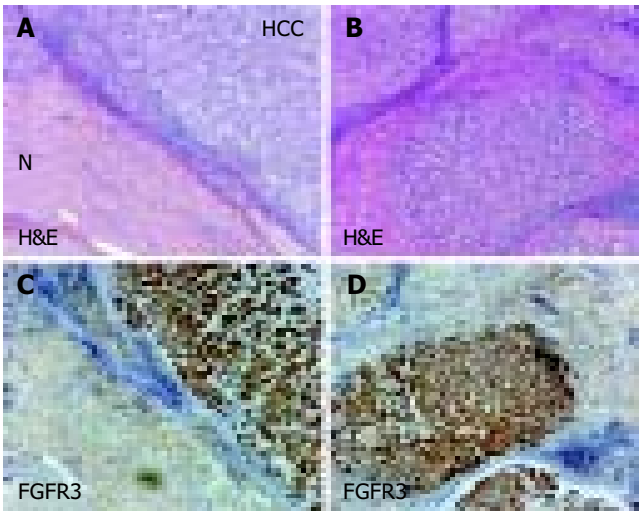


Figure 3 IHC of FGFR3 in HCC and matched non-neoplastic liver tissues. **A, B**: H and E; **C, D**: FGFR3.

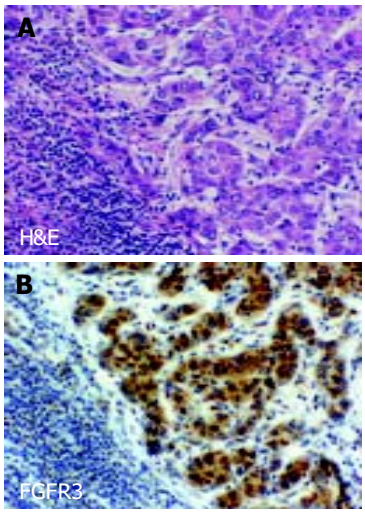


Figure 4 Association between FGFR3 staining, HCC differentiation and nuclear grade. **A**: H and E; **B**: FGFR3.

Clinicopathological features correlated with FGFR3 expression

We further examined the expression of FGFR3 in 43 cases of HCC tissue samples to confirm our above findings. As shown in Table 2, the age of the patients ranging from 26 to 82 years with a mean age of 59.79 years, 79% were men (34/43) and 21% were women (9/43). HBV positive patients accounted for 65.12% (28/43). Compared to the surrounding non-neoplastic liver tissue, 23.26% (10/43) of patients showed moderate staining for FGFR3 and 48.84% (21/43) of patients showed strong staining for FGFR3 in HCC tissue, indicating significant over-expression of FGFR3 in malignant tissues *vs* non-malignant tissues ($P<0.01$). Table 3 demonstrates the correlation between FGFR3 expression and clinicopathological features. Higher expression of FGFR3 was observed in most moderately- and poorly-differentiated HCC tissue samples. Nine of 20 cases with strong FGFR3 expression were poorly-differentiated. In 4 cases of well-differentiated HCC tissue samples, only 1 case showed very weak staining, whereas no FGFR3 staining was detectable in the other 3 cases. In the same manner, 11 of 20 cases with strong FGFR3 expression were nuclear grade 3, and 9 were nuclear grade 2. Only 1 of 3 HCC tissue samples with nuclear grade 1 showed very weak staining, whereas no FGFR3 staining was detectable in the other 2 cases. A significant correlation was observed between cancer differentiation ($P<0.05$) and nuclear grade ($P<0.05$) based on χ^2 test. These findings suggested that HCC could be distinguished by a significant increase of FGFR3, being compatible with the current clinical parameters. The association between FGFR3 staining and HCC differentiation and nuclear grade is illustrated in Figure 4. HCC with poor differentiation and nuclear grade 3 demonstrated very strong staining of FGFR3.

Table 2 Patients demographic features and FGFR3 expression ($n = 43$)

Demographic features	$n = 43$
Age (yr)	59.79
Gender	
Male	34
Female	9
Hepatitis B	
Positive	28
Negative	15
FGFR3 expression (%)	
0	3 (6.98)
+	20 (46.51)
++	20 (46.51)

DISCUSSION

To understand the characteristics of gene expression in HCC and the molecular processes involved in the cellular transformation from normal cells to neoplastic cells, global gene expression profiling with microarray was used to analyze the expression level change of 12 588 genes and oligos in HCC tissue and matched non-neoplastic liver tissue. Among the 17 transcription and translation-related genes whose expression levels changed most significantly, 10 over-

Table 3 Relationship between FGFR3 expression, HCC differentiation and nuclear grade ($n = 43$)

	Differentiation			Nuclear grade			
FGFR3 expression	Well	Moderate	Poor	1	2	3	4
0	3	0	0	3	0	0	0
1	1	17	2	0	16	4	0
2	0	11	9	0	9	11	0

expressed genes and 7 under-expressed genes were identified in HCC tissue. Due to the high false positive and false negative rates in microarray study, significant over-expression of FGFR3 in HCC tissue was validated by Northern blot and quantitative real-time PCR.

FGFR family has been reported to encode a set of transmembrane tyrosine kinase receptors, which are composed of an extracellular ligand-binding domain, a transmembrane domain, and a split intracellular kinase domain[9]. FGFR family can bind to a number of related mitogenic fibroblast growth factors, resulting in receptor dimerization, autophosphorylation, and downstream signal transduction[10]. Up to now, four members of the family have been identified with domains of similar constitution, namely extracellular immunoglobulin-like domain, transmembrane domain, and intracellular kinase domain[11]. Since the alternative mRNA splicing of FGFR1, FGFR2 and FGFR3, seven prototype receptors have been reported[12]. Each prototype receptor has a different ligand binding capacity and tissue distribution[13]. Given the multiple forms of the receptors, the enormous potential for diversity of FGFR family is involved in cell growth control, cell differentiation and migration. Recently a number of studies have provided increasing evidence that FGFR family may be involved in carcinogenesis[14,15]. However, the detailed mechanism still needs to be further elucidated.

Activation and dimerization of FGFR3 result in cell proliferation or differentiation via signal transduction pathways[10]. Point mutations in the transmembrane domain of FGFR3 have been identified as a causative factor for skeletal development disorders such as achondroplasia and hypochondroplasia[16,17]. Moreover, activating mutations of FGFR3 have been reported to be related with superficial low-grade non-invasive bladder tumors and primary urothelial cell carcinomas[18-21]. Recurrence of tumors with mutated FGFR3 often presents as solitary tumors in the same region of bladder and the presence of wild-type FGFR3 often precipitates multiple lesions in different regions of the bladder[22]. Several novel mutant transcripts caused by aberrant splicing and activation of cryptic splice sequences have been reported recently in digestive tract tumors, and high frequency of dysregulation of mRNA splicing is proposed to confer a selectable advantage on clones of cells in colorectal tumorigenesis[23]. More recently, two novel mutations of FGFR3 in colorectal carcinomas have also been identified[24]. All identified mutations occur at highly conserved sequences, not only in the FGFR family of molecules but also throughout evolution and are clustered in the immunoglobulin-like loop-III domain, highlighting the functional importance of this domain[24]. All the observations support that FGFR3 represents an important example of a single gene, causing different human developmental and tumoral diseases[25].

As malignant cells are characterized by uncontrolled growth genes that are over-expressed in malignant cells and not detectable in normal tissues, studies are conducted to elucidate the complicated process of carcinogenesis. In our study, IHC study of 43 clinical cases of HCC revealed that expression of FGFR3 increased significantly in HCC. More importantly, over-expression of FGFR3 was correlated with pathological factors including HCC differentiation and nuclear grade, suggesting that clinicopathologic index, morphologic grade, and molecular grade are consistent. Therefore, activation of FGFR3 may play an important role in hepatocarcinogenesis. The identification of FGFR3 somatic mutation in HCC is currently under investigation. However, the detailed mechanism needs to be further studied.

REFERENCES

1 **Parkin DM,** Pisani P, Ferlay J. Estimates of the worldwide incidence of 25 major cancers in 1990. *Int J Cancer* 1999; **80**: 827-841

2 **Jemal A,** Murray T, Samuels A, Ghafoor A, Ward E, Thun MJ. Cancer statistics, 2003. *CA Cancer J Clin* 2003; **53**: 5-26

3 **Moch H,** Kononen T, Kallioniemi OP, Sauter G. Tissue microarrays: what will they bring to molecular and anatomic pathology? *Adv Anat Pathol* 2001; **8**: 14-20

4 **Snijders AM,** Meijer GA, Brakenhoff RH, van den Brule AJ, van Diest PJ. Microarray techniques in pathology: tool or toy? *Mol Pathol* 2000; **53**: 289-294

5 **Graveel CR,** Jatkoe T, Madore SJ, Holt AL, Farnham PJ. Expression profiling and identification of novel genes in hepatocellular carcinomas. *Oncogene* 2001; **20**: 2704-2712

6 **Qiu W,** David D, Zhou B, Chu PG, Zhang B, Wu M, Xiao J, Han T, Zhu Z, Wang T, Liu X, Lopez R, Frankel P, Jong A, Yen Y. Down-regulation of growth arrest DNA damage-inducible gene 45 b expression is associated with human hepatocellular carcinoma. *Am J Path* 2003; **6**: 1961-1974

7 **Edmondson H,** Steiner P. Primary carcinoma of the liver: a study of 100 cases among 48 900 biopsies. *Cancer* 1954; **7**: 462-503

8 **Lauwers GY,** Terris B, Balis UJ, Batts KP, Regimbeau JM, Chang Y, Graeme-Cook F, Yamabe H, Ikai I, Cleary KR, Fujita S, Flejou JF, Zukerberg LR, Nagorney DM, Belghiti J, Yamaoka Y, Vauthey JN. International cooperative study group on hepatocellular carcinoma. The international cooperative study group on hepatocellular carcinoma. Prognostic histologic indicators of curatively resected hepatocellular carcinomas: a multi-institutional analysis of 425 patients with definition of a histologic prognostic index. *Am J Surg Pathol* 2002; **26**: 25-34

9 **Mason IJ.** The ins and outs of fibroblast growth factors. *Cell* 1994; **78**: 547–552

10 **Kanai M,** Göke M, Shoji Tsunekawa S, Podolsky DK. Signal transduction pathway of human fibroblast growth factor receptor 3. Identification of a novel 66-kDa phosphoprotein. *J Biol Chem* 1997; **272**: 6621-6628

11 **Johnson DE,** Williams LT. Structural and functional diversity in the FGF receptor multigene family. *Adv Cancer Res* 1993; **60**: 1-41

12 **McKeehan WL,** Wang F, Kan M. The heparan-sulfate fibroblast growth-factor family: diversity of structure and function. *Prog Nucleic Acid Res Mol Biol* 1998; **59**: 135–176

13 **Ornitz DM,** Xu J, Colvin JS, McEwen DG, MacArthur CA, Coulier F, Gao G, Goldfarb M. Receptor specificity of the fibro-blast growth-factor family. *J Biol Chem* 1996; **271**: 15292–15297

14 **Penault-Llorca F,** Bertucci F, Adelaide J, Parc P, Coulier F, Jacquemier J, Birnbaum D, deLapeyriere O. Expression of FGF and FGF receptor genes in human breastcancer. *Int J Cancer* 1995; **61**: 170–176

15 **Adnane J,** Gaudray P, Dionne CA, Crumley G, Jaye M, Schlessinger J, Jeanteur P, Birnbaum D, Theillet C. BEK and FLG, two receptors to members of the FGF family, are amplified in subsets of human breast cancers. *Oncogene* 1991; **6**: 659–663

16 **Naski MC,** Wang Q, Xu J, Ornitz DM. Graded activation of fibroblast growth factor receptor 3 by mutations causing achondroplasia and thanatophoric dysplasia. *Nat Genet* 1996; **13**:

233–237
17 **Webster MK,** Donoghue DJ. FGFR activation in skeletal disorders: too much of a good thing. *Trends Genet* 1997; **13**: 178–182
18 **Cappellen D,** De Oliveira C, Ricol D, de Medina S, Bourdin J, Sastre-Garau X, Chopin D, Thiery JP, Radvanyi F. Frequent activating mutations of FGFR3 in human bladder and cervix carcinomas. *Nat Genet* 1999; **23**: 18–20
19 **Billerey C,** Chopin D, Aubriot-Lorton MH, Ricol D, Gil Diez de Medina S, Van Rhijn B, Bralet MP, Lefrere-Belda MA, Lahaye JB, Abbou CC, Bonaventure J, Zafrani ES, van der Kwast T, Thiery JP, Radvanyi F. Frequent FGFR3 mutations in papillary non-invasive bladder (pTa) tumors. *Am J Pathol* 2001; **158**: 1955–1959
20 **Kimura T,** Suzuki H, Ohashi T, Asano K, Kiyota H, Eto Y. The incidence of thanatophoric dysplasia mutations in FGFR3 gene is higher in low-grade or superficial bladder carcinomas. *Cancer* 2001; **92**: 2555–2561
21 **van Rhijn BW,** van der Kwast TH, Vis AN, Kirkels WJ, Boeve ER, Jobsis AC, Zwarthoff EC. FGFR3 and P53 characterize alternative genetic pathways in the pathogenesis of urothelial cell carcinoma. *Cancer Res* 2004; **64**: 1911-1914
22 **van Rhijn BW,** Lurkin I, Radvanyi F, Kirkels WJ, van der Kwast TH, Zwarthoff EC. The fibroblast growth factor receptor 3 (FGFR3) mutation is a strong indicator of superficial bladder cancer with low recurrence rate. *Cancer Res* 2001; **61**: 1265-1268
23 **Jang JH,** Shin KH, Park YJ, Lee RJ, McKeehan WL, Park JG. Novel transcripts of fibroblast growth factor receptor 3 reveal aberrant splicing and activation of cryptic splice sequences in colorectal cancer. *Cancer Res* 2000; **60**: 4049-4052
24 **Jang JH,** Shin KH, Park JG. Mutations in fibroblast growth factor receptor 2 and fibroblast growth factor receptor 3 genes associated with human gastric and colorectal cancers. *Cancer Res* 2001; **61**: 3541-3543
25 **Intini D,** Baldini L, Fabris S, Lombardi L, Ciceri G, Maiolo AT, Neri A. Analysis of FGFR3 gene mutations in multiple myeloma patients with t(4;14). *Br J Haematol* 2001; **114**: 362-364

Science Editor Wang XL and Guo SY **Language Editor** Elsevier HK

PO Box 2345, Beijing 100023, China
www.wjgnet.com
wjg@wjgnet.com

ELSEVIER

World J Gastroenterol 2005;11(34):5273-5276
World Journal of Gastroenterology ISSN 1007-9327
© 2005 The WJG Press and Elsevier Inc. All rights reserved.

• *LIVER CANCER* •

Tea pigments induce cell-cycle arrest and apoptosis in HepG2 cells

Xu-Dong Jia, Chi Han, Jun-Shi Chen

Xu-Dong Jia, Chi Han, Jun-Shi Chen, Institute of Nutrition and Food Safety, Chinese Center for Disease Control and Prevention, 29 Nanwei Road, Beijing 100050, China
Supported by the National Natural Science Foundation of China, No. 39970639
Correspondence to: Dr. Jun-Shi Chen, Institute for Nutrition and Food Safety, Chinese Center for Disease Control and Prevention, 29 Nanwei Road, Beijing 100050 China. jshchen@ilsichina-fp.org
Telephone: +86-10-83132553 Fax: +86-10-83132021
Received: 2004-11-20 Accepted: 2004-12-21

Abstract

AIM: To investigate the molecular mechanisms by which tea pigments exert preventive effects on liver carcinogenesis.

METHODS: HepG2 cells were seeded at a density of 5×10^5/well in six-well culture dishes and incubated overnight. The cells then were treated with various concentrations of tea pigments over 3 d, harvested by trypsinization, and counted using a hemocytometer. Flow cytometric analysis was performed by a flow cytometer after propidium iodide labeling. Bcl-2 and $p21^{WAF1}$ proteins were determined by Western blotting. In addition, DNA laddering assay was performed on treated and untreated cultured HepG2 cells.

RESULTS: Tea pigments inhibited the growth of HepG2 cells in a dose-dependent manner. Flow-cytometric analysis showed that tea pigments arrested cell cycle progression at G_1 phase. DNA laddering was used to investigate apoptotic cell death, and the result showed that 100 mg/L of tea pigments caused typical DNA laddering. Our study also showed that tea pigments induced upregulation of $p21^{WAF1}$ protein and downregulation of Bcl-2 protein.

CONCLUSION: Tea pigments induce cell-cycle arrest and apoptosis. Tea pigments may be used as an ideal chemopreventive agent.

© 2005 The WJG Press and Elsevier Inc. All rights reserved.

Key words: Tea pigments; Cell cycle; Apoptosis

Jia XD, Han C, Chen JS. Tea pigments induce cell-cycle arrest and apoptosis in HepG2 cells. *World J Gastroenterol* 2005; 11(34): 5273-5276
http://www.wjgnet.com/1007-9327/11/5273.asp

INTRODUCTION

Liver cancer is the sixth most common cancer and the third most common cause of death from cancer in the world. In general, the disease is relatively uncommon in developed countries. In the developing world, however, liver cancer is very common, accounting for more than 80% of the global cases, with China alone accounting for 55% of the worldwide incidence. Liver cancer is almost always fatal and has no effective treatment. The survival rate is low, with only a 6% 5-year survival rate in the USA. In developing countries, the survival rate is even lower. Therefore, high prevalence, high death rate, and ineffective therapy have spurred the search of novel strategies in the prevention rather than treatment of liver cancer.

Nowadays, chemoprevention is gaining more attention. This approach aims to decrease overall cancer morbidity and mortality by using substances that are capable of preventing cancer progression. Several classes of compounds have been evaluated for this purpose. Tea is one of the most popular beverages consumed in the world. The two major types of tea consumed worldwide are black tea and green tea. Green tea polyphenols and extracts have been shown in a number of animal models to prevent against chemically-induced carcinogenesis in lung, forestomach, esophagus, duodenum, pancreas, breast, and colon[1-3]. Tea pigments, a major flavonol component in black tea, have strong antioxidant potency[4]. In our previous studies, we found tea pigments to be effective in preventing the occurrence and progression of precancerous liver lesions in rats[5]. However, studies on tea pigments are still limited, especially in terms of mechanism.

The purpose of this study was to investigate the molecular mechanisms by which tea pigments exert preventive effects on liver cancer cells and to provide the scientific rationale for using tea pigments as a chemopreventive agent against liver cancer.

MATERIALS AND METHODS

Tea pigments

Tea pigments were provided by the Institute of Tea Science and Research, Chinese Academy of Agricultural Sciences (Hangzhu, China).

Cell culture and growth inhibition studies

Human hepatoma cell line HepG2 was obtained from Beijing University Hospital (Beijing, China) and cultured in DMEM medium (Sigma, USA) supplemented with 10% fetal bovine serum and 1% penicillin-streptomycin in a 50 mL/L CO_2 atmosphere at 37 ℃. The cells were seeded at a density of 5×10^5/well in six-well culture dishes and incubated overnight. The cells then were treated with various concentrations of tea pigments over 3 d, harvested by trypsinization, and counted using a hemocytometer.

Flow-cytometric analysis

HepG2 cells were seeded at a density of 5×10^5/well in six-well culture dishes. To synchronize the cells at the G_0 phase, HepG2 cells were incubated in serum-free medium for 24 h before treatment with tea pigments. The cells were then treated with or without 100 mg/L tea pigments and harvested at one, or after 2 and 3 d by trypsinization. The cells were centrifuged at 2 000 r/min for 5 min, washed with phosphate-buffered saline (PBS), fixed with 70% ethanol, then subjected to flow cytometric analysis on a flow cytometer after propidium iodide labeling.

Protein extraction and Western blot analysis

Control cells, as well as cells treated with tea pigments, were harvested by scraping the cells from cultured dishes using a cell scraper and collected by centrifugation. Whole cell extracts were then prepared by lysing the cells using 4% sodium dodecyl sulfate (SDS) gel sample buffer. Cell extracts were boiled for 10 min and chilled on ice, subjected to 12% SDS-polyacrylamide gel electrophoresis, and transferred to a nitrocellulose membrane. Each membrane was cut into two pieces, one piece was incubated at 4 ℃ overnight with $p21^{WAF1}$ or Bcl-2 antibodies, and the other one with β-actin (used as a control for protein loading). All antibodies were obtained from Zymed Laboratories (USA). Then membranes were incubated at 37 ℃ for 1 h with secondary antibody conjugated with peroxidase, and the signal was detected using chemiluminescence detection reagent. The relative protein level was calculated as the ratio of the optical density of $p21^{WAF1}$ or Bcl-2 and that of β-actin.

DNA laddering assay

Treated and untreated cultured HepG2 cells were harvested and centrifuged at 2 000 r/min for 5 min. The cells were resuspended in lysis buffer and centrifuged for 15 min at 15 000 *g*. DNA was extracted with phenol, precipitated with 100% cold ethanol, resuspended in TE buffer, electrophoresed on 1.5% agarose gel, stained with ethidium bromide, detected by ultraviolet transillumination, and photographed.

RESULTS

Effect of tea pigments on cell growth

Treatment of HepG2 cells with tea pigments for 24-72 h resulted in a dose-dependent inhibition of cell proliferation. The effects of tea pigments on the proliferation of HepG2 cells are depicted in Figure 1. Tea pigments inhibited HepG2 cell growth at >25 mg/L over 3 d. The IC_{50}, as measured by the number of viable cells 72 h after the addition of tea pigments, was 50 mg/L.

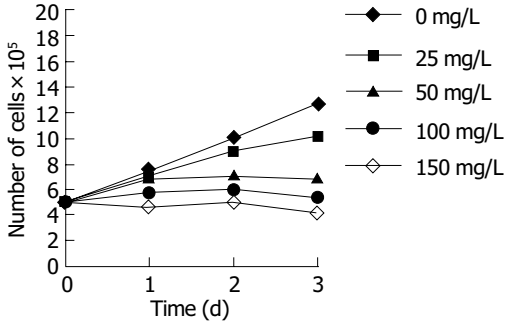


Figure 1 Effect of tea pigments on HepG2 cell growth.

Tea pigments induced G1 cell cycle arrest in HepG2 cells

Flow cytometric analysis of HepG2 cells treated with 100 mg/L tea pigments showed a G1 arrest. The percentage of cells in the G1 phase rose from a baseline of 38.0-55.2% after 24 h of treatment and increased from 37.5% to 76.7% after 72 h (Table 1).

Effect of tea pigments on $p21^{WAF1}$ expression

Western blot analysis of cell extracts from tea pigments-treated HepG2 cells showed upregulation of $p21^{WAF1}$, an inhibitory protein that could modulate cell growth and cell cycle. The result of a typical experiment is shown in Figure 2. To obtain a quantitative value for the protein expression of $p21^{WAF1}$, the optical density of $p21^{WAF1}$ was measured. The ratio of $p21^{WAF1}$ to β-actin was calculated, and the relative protein level of $p21^{WAF1}$ was measured as presented in Figure 2, which clearly shows the upregulation of $p21^{WAF1}$.

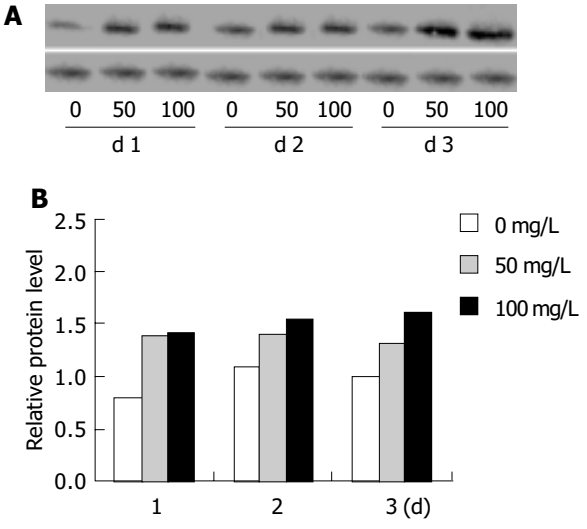


Figure 2 Upregulation of $p21^{WAF1}$ protein expression in HepG2 cell lines treated with tea pigments visualized by ECL detection system (**A**) and plotted as relative protein level (**B**).

Table 1 Flow cytometric analysis of HepG2 cells treated with 100 mg/L tea pigments

Tea pigments (mg/L)	D 1			D 2			D 3		
	G_1 (%)	S (%)	G_2/M (%)	G_1 (%)	S (%)	G_2/M (%)	G_1 (%)	S (%)	G_2/M (%)
0	38.0	48.0	14.0	47.1	39.5	13.4	37.5	50.3	12.2
100	55.2	27.8	17.0	68.7	22.0	9.3	76.7	10.3	13.0

Induction of apoptosis

Firstly, agarose gel electrophoresis was used to demonstrate low-molecular-weight DNA ladder formation. Nuclear DNA fragmentation, a classical feature of apoptotic cell death, was clearly shown in HepG2 cells with 100 mg/L tea pigments over 3 d (Figure 3). Then, we observed the expression of Bcl-2 protein, a known inhibitor of apoptosis. Western blot analysis showed downregulation of Bcl-2 protein. The result of a typical experiment is shown in Figure 4. The ratio of Bcl-2 to β-actin was calculated. The relative protein level of Bcl-2 was measured as presented in Figure 4.

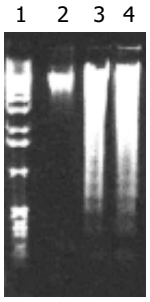


Figure 3 Induction of apoptosis by tea pigments in HepG2 cells. Lane 1: DNA molecular weight marker; lane 2 (control): DNA collected from untreated HepG2 cells after 3 d; lanes 3 and 4: DNA collected from HepG2 cells treated with 100 mg/L after 2 and 3 d.

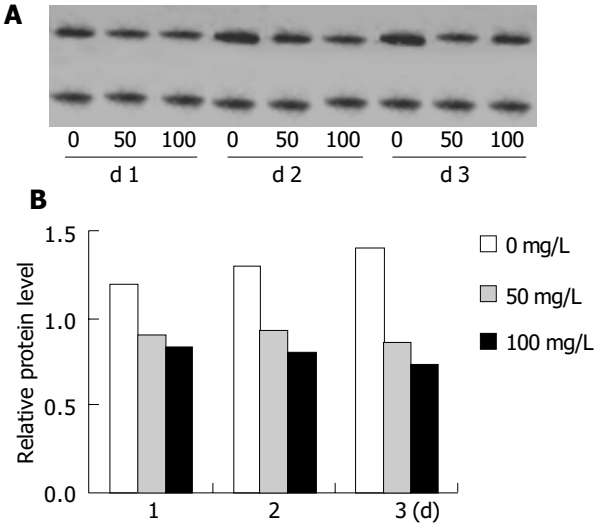


Figure 4 Downregulation of Bcl-2 protein expression in HepG2 cell lines treated with tea pigments visualized by ECL detection system (**A**) and plotted as relative protein level (**B**).

DISCUSSION

Green tea and its polyphenols have been demonstrated as chemopreventive agents in a number of experimental models[6]. However, the mechanism of chemoprevention by black tea compared with that of green tea is not quite clear. Tea pigments used in this study are the main constituents of black tea, mainly theaflavins and thearubigins. Morse *et al*.[7], demonstrated that theaflavins inhibit NMBA-induced esophageal tumorigenesis in rats. Another study showed that black tea constituents inhibit NNK-induced lung tumorigenesis in A/J mice[8]. Previously, we also found that tea pigments had an inhibitory effect on liver precancerous lesions in rats[5]. However, the exact mechanism is unclear.

Eukaryotic cell cycle is regulated by signal transduction pathways mediated by a series of cell-cycle regulators. Cyclins are positive regulators of cell-cycle progression and function by forming a complex with and activating cyclin-dependent kinases (CDKs). CDK inhibitors are negative regulators of cell cycle and bind to and inhibit the activity of cyclin-CDK complexes[9]. $p21^{WAF1}$ has gained much attention as a universal inhibitor of cyclin-dependent kinases, and overexpression of $p21^{WAF1}$ has been shown to induce tumor cell growth arrest and apoptosis[10]. In this study, we have demonstrated that the inhibition of HepG2 cell growth by tea pigments is accompanied with a G1 cell cycle arrest and upregulation of $p21^{WAF1}$ protein. The modulation of cell-cycle regulatory protein is thus a novel effect of tea pigments, suggesting the possible molecular mechanism by which tea pigments inhibit cell growth in HepG2 cells. Lee *et al*.[11], showed that doxorubicin, a commonly used anticancer drug, induces G_1 arrest and upregulation of $p21^{WAF1}$ in HepG2 cells. Qin *et al*.[12], also demonstrated that cisplatin induces a transient G_1 arrest and upregulation of $p21^{WAF1}$ expression in HepG2 cells. These results are similar to the effects of tea pigments in this study. Although we have recognized that tea pigments can modulate the expression of $p21^{WAF1}$, we do not fully understand how $p21^{WAF1}$ and cyclin-CDK complexes are working to elicit cell growth. Experiments are being conducted in our laboratory to elucidate the exact molecular mechanism by which tea pigments inhibit cell growth.

After treatment with tea pigments, the number of HepG2 cells decreased over time, suggesting the possibility of an increase in the rate of cell death. Agarose gel electrophoresis verified this suggestion. Nuclear DNA fragmentation, a classical feature of apoptotic cell death, was clearly shown in HepG2 cells with 100 mg/L tea pigments over 3 d. Additionally, we observed the expression of Bcl-2 protein. Modern molecular biological investigations indicate that apoptosis is regulated by many oncogenes, such as bcl-2, bax and p53[13]. Bcl-2 protein is an apoptosis-related protein and plays an important role in regulating apoptosis[14]. In our study, Western blot analysis showed that Bcl-2 protein expression was significantly downregulated in HepG2 cells after treatment with tea pigments. Bax is a homologous protein of Bcl-2, in the form of homopolymer (Bax/Bax) or isodipolymer (Bcl-2/Bax). Studies have demonstrated that the ratio of Bax and Bcl-2 protein influences the apoptotic rate of cells[15].

In conclusion, tea pigments inhibit cell growth and induce apoptosis in HepG2 cells, suggesting that tea pigments may be used as an ideal chemopreventive agent.

ACKNOWLEDGMENTS

The authors thank Professor Qi-Kun Chen (Institute of Tea Science, Chinese Academy of Agricultural Sciences) for providing tea pigments.

REFERENCES

1 **Jia XD,** Han C. Effects of green tea on colonic aberrant cryp+ foci and proliferative indexes in rats. *Nutr Cancer* 2001; **39**: 239-243
2 **Kim ES,** Hong WK, Khuri FR. Prevention of lung cancer. The new millennium. *Chest Surg Clin N Am* 2000; **10**: 663-690
3 **Katiyar SK,** Ahmad N, Mukhtar H. Green tea and skin. *Arch Dermatol* 2000; **136**: 989-994
4 **Leung LK,** Su Y, Chen R, Zhang Z, Huang Y, Chen ZY. Theaflavins in black tea and catechins in green tea are equally effective antioxidants. *J Nutr* 2001; **131**: 2248-2251
5 **Gong Y,** Han C, Chen J. Effect of tea polyphenols and tea pigments on the inhibition of precancerous liver lesions in rats. *Nutr Cancer* 2000; **38**: 81-86
6 **Chung FL.** The prevention of lung cancer induced by a tobacco-specific carcinogen in rodents by green and black tea. *Proc Soc Exp Biol Med* 1999; **220**: 244-248
7 **Morse MA,** Kresty LA, Steele VE, Kelloff GJ, Boone CW, Balentine DA, Harbowy ME, Stoner GD. Effects of theaflavins on N-nitrosomethylbenzylamine-induced esophageal tumorigenesis. *Nutr Cancer* 1997; **29**: 7-12
8 **Yang GY,** Liu Z, Seril DN, Liao J, Ding W, Kim S, Bondoc F, Yang CS. Black tea constituents, theaflavins, inhibit 4-(methylnitrosamino)-1-(3-pyridyl)-1-butanone (NNK)-induced lung tumorigenesis in A/J mice. *Carcinogenesis* 1997; **18**: 2361-2365
9 **Shah MA,** Schwartz GK. Cyclin-dependent kinases as targets for cancer therapy. *Cancer Chemother Biol Response Modif* 2003; **21**: 145-170
10 **Mandziuk S,** Dudzisz-Sledz M, Korszen-Pilecka I, Milanowski J, Wojcierowski J, Korobowicz E. Expression of p21 and bcl-2 proteins in paraffin-embedded preparations of non-small cell lung cancer in stage IIIA after Etoposide and Cisplatin induced chemotherapy. *Ann Univ Mariae Curie Sklodowska* 2003; **58**: 149-153
11 **Lee TK,** Lau TC, Ng IO. Doxorubicin-induced apoptosis and chemosensitivity in hepatoma cell lines. *Cancer Chemother Pharmacol* 2002; **49**: 78-86
12 **Qin LF,** Ng IO. Induction of apoptosis by cisplatin and its effect on cell cycle-related proteins and cell cycle changes in hepatoma cells. *Cancer Lett* 2002; **175**: 27-38
13 **Karczmarek-Borowska B,** Filip A, Zdunek M, Korobowicz E, Wojcierowski J, Korszen-Pilecka I, Furmanik F. The preliminary estination of bcl-2, bcl-X(L) and p53 genes expression in locally advanced non-small cell lung cancer. *Ann Univ Mariae Curie Sklodowska* 2003; **58**: 124-131
14 **Farczadi E,** Kaszas I, Baki M, Szende B. Changes in apoptotic and mitotic index, bcl-2, and p53 expression in rectum carcinomas after short-term cytostatic treatment. *Ann N Y Acad Sci* 2003; **1010**: 780-783
15 **Nakamura H,** Kumei Y, Morita S, Shimokawa H, Ohya K, Shinomiya K. Antagonism between apoptotic (Bax/Bcl-2) and anti-apoptotic (IAP) signals in human osteoblastic cells under vector-averaged gravity condition. *Ann N Y Acad Sci* 2003; **1010**: 143-147

Science Editor Wang XL and Guo SY **Language Editor** Elsevier HK

PO Box 2345, Beijing 100023, China
www.wjgnet.com
wjg@wjgnet.com

ELSEVIER

World J Gastroenterol 2005;11(34):5277-5282
World Journal of Gastroenterology ISSN 1007-9327
© 2005 The WJG Press and Elsevier Inc. All rights reserved.

Effects of *Pinus massoniana* bark extract on cell proliferation and apoptosis of human hepatoma BEL-7402 cells

Ying-Yu Cui, Heng Xie, Kang-Biao Qi, Yan-Ming He, Jin-Fa Wang

Ying-Yu Cui, Kang-Biao Qi, Yan-Ming He, Jin-Fa Wang, The State Key Laboratory for Biocontrol and The Key Laboratory of Gene Engineering of Ministry of Education, School of Life Sciences, Sun Yat-sen University, Guangzhou 510275, China
Heng Xie, Institute of Songzhen Nutritional Resource, Guangzhou 510645, Guangdong Province, China
Correspondence to: Professor Jin-Fa Wang, The State Key Laboratory for Biocontrol and The Key Laboratory of Gene Engineering of Ministry of Education, School of Life Sciences, Sun Yat-sen University, Guangzhou 510275, China. ls19@zsu.edu.cn
Telephone: +86-20-84039179 Fax: +86-20-84039179
Received: 2004-09-16 Accepted: 2004-11-19

Abstract

AIM: To study the effects of *Pinus massoniana* bark extract (PMBE) on cell proliferation and apoptosis of human hepatoma BEL-7402 cells and to elucidate its molecular mechanism.

METHODS: BEL-7402 cells were incubated with various concentrations (20-200 μg/mL) of PMBE for different periods of time. After 48 h, cell proliferation was determined by 3-(4,5-dimethyl-thiazolyl-2)-2,5-diphenyl tetrazolium bromide (MTT) assay. Apoptosis was evaluated by morphological observation, agarose gel electrophoresis, and flow cytometry analysis. Possible molecular mechanisms were primarily explored through immunohistochemical staining.

RESULTS: PMBE (20-200 μg/mL) significantly suppressed BEL-7402 cell proliferation in a time- and dose-dependent manner. After treatment of BEL-7402 cells with 160 μg/mL PMBE for 24, 48, or 72 h, a typical apoptotic "DNA ladder" was observed using agarose gel electrophoresis. Nuclear condensation and boundary aggregation or split, apoptotic bodies were seen by fluorescence and electron microscopy. Sub-G_1 curves were displayed by flow cytometry analysis. PMBE decreased the expression levels of Bcl-2 protein in a time-dependent manner after treatment of cells with 160 μg/mL PMBE.

CONCLUSION: PMBE suppresses proliferation of BEL-7402 cells in a time- and dose-dependent manner and induces cell apoptosis by possibly downregulating the expression of the *bcl-2* gene.

© 2005 The WJG Press and Elsevier Inc. All rights reserved.

Key words: *Pinus massoniana* bark extract; Procyanidins; Human hepatoma; BEL-7402 cell; Cell proliferation; Apoptosis; *bcl-2* gene

Cui YY, Xie H, Qi KB, He YM, Wang JF. Effects of *Pinus massoniana* bark extract on cell proliferation and apoptosis of human hepatoma BEL-7402 cells. *World J Gastroenterol* 2005; 11(34): 5277-5282
http://www.wjgnet.com/1007-9327/11/5277.asp

INTRODUCTION

Pinus massoniana needles and bark have been commonly used in diet therapies in eastern Asia (mainly China and Japan) for thousands of years, but until the last decade of the 20th century, bioactive substances from *P massoniana* bark have not been successfully extracted through crude sieving, centrifugation, or micro- and ultra-filtration with hollow fiber and coiled-spiral nanofiltration membranes[1]. Standard PMBE contains 26.0-28.3% flavonoids (mainly procyanidins) as important bioactive substances. The most important of these are included in the procyanidin B series, which only differ in the number and position of hydroxyl groups, as can be seen for procyanidin B_3 in Figure 1[2].

PMBE is well known for its antioxidant properties, which may result from its ability to scavenge free radicals[1]. It is this antioxidant activity that may be helpful in the prevention and therapy of diseases and degenerative processes associated with oxidative stress. The bark of *P massoniana* has been mentioned in the traditional Chinese pharmacopoeia, and has been mainly used to promote hemostasis and detoxification, and for the treatment of rheumatic arthralgia, hypertension, and chilblain in China and other countries of the Orient[3]. Our previous research results showed that PMBE can broadly inhibit the growth of eight different cancer cell lines *in vitro*[4]. Additionally, we found that PMBE can selectively inhibit the proliferation of human hepatoma BEL-7402 cells without impacting the growth of normal human liver L-02 cells at an effective concentration range similar to that of the chemotherapeutic agent, cisplatin[4]. It may play a role in cancer clinic as both antidote and potentiator of surgical therapy.

Considering that hepatoma is the most common malignant tumor occurring in both men and women in China, we wished to assess the processes by which PMBE inhibits growth and affects apoptosis of BEL-7402 cells and elucidate a possible molecular mechanism for these actions. It is reported that extracts from *P maritima* bark (*pycnogenol*)[5] and from *P radiata* bark (*enzogenol*)[6] have been used therapeutically in southwestern Europe (mainly France, Germany, and Spain), Australia, and New Zealand for nearly

10 years. Huynh and Teel[7] once reported that *pycnogenol* selectively induces apoptosis of human mammary cancer cells (MCF-7), but does not induce apoptosis of normal human mammary MCF-10 cells. It is reasonable to hypothesize that PMBE may also be helpful in therapies of human hepatoma, possibly through the regulation of cell proliferation and/or cell death. Therefore, this study aimed to assess the processes by which PMBE inhibits cancer cell growth, affects apoptosis of BEL-7402 cells, and the possible molecular mechanism for these actions.

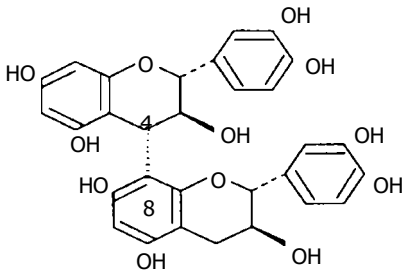


Figure 1 Chemical structure of procyanidin B_3.

MATERIALS AND METHODS

Preparation of PMBE

PMBE was provided by the Institute of Songzhen (Guangdong Province, China). A stock solution of 10 mg/mL PMBE was made in 100% dimethylsulfoxide (DMSO) and filtered via a 0.22 μm minipore membrane. The stock solution was aliquoted and stored at -20 ℃, thawed just before testing, and diluted with the culture medium. The final concentration of DMSO for all treatments was less than 0.25%.

Cell culture and treatment

Human hepatoma BEL-7402 cells were purchased from the Animal Cell Center, Medical College, Sun Yat-Sen University, China. BEL-7402 cells were incubated in RPMI 1640 medium (Sijiqing Co., Zhejiang, China) supplemented with 10% heat-inactivated fetal bovine serum (FBS), 100 U/mL penicillin, 100 μg/mL streptomycin, and 10 mmol/L HEPES, pH 7.4, and kept at 37 ℃ in a humidified 50 mL/L CO_2 incubator. For this study, cells were either incubated in the absence or presence of different concentrations of PMBE for 48 h or exposed to 160 μg/mL PMBE for different time periods.

Measurement of cell growth inhibition

Growth inhibition of BEL-7402 cells by PMBE was measured by 3-(4,5-dimethyl-thiazolyl-2)-2,5-diphenyl tetrazolium bromide (MTT) assay[8,9] with minor modifications. Briefly, cancer cells were seeded into 96-well microtiter plates at appropriate densities to maintain the cells in an exponential phase of growth during the experiment. BEL-7402 cells were exposed to PMBE either at 20, 40, 80, 160, or 200 μg/mL for 48 h or to 160 μg/mL PMBE for either 24, 48, or 72 h. Each concentration was tested in quadruplicate. At the end of the treatment, 20 μL of 5 mg/mL MTT (Sigma, St. Louis, MO, USA) was added to each well and the plates were incubated for 4 h at 37 ℃. DMSO (150 μL) was then added to each well and the plates were rotated for 10-20 min at 200 r/min by a shaker (THZ-C, Shenhua BioTech Co., Shenzhen, China). The optical absorbance was read on a plate reader (BIO-RAD Co., USA) at a wavelength of 570 nm. Media and DMSO controls were included for all experiments. The inhibitory rate of cell proliferation was calculated using the following formula: Growth inhibition (%) = $(A_{control}-A_{treated})/A_{control}\times100$. Results were measured in triplicate.

Cell morphology

Fluorescence microscopy BEL-7402 cells were seeded in sterile culture dishes on coverslips at a density of 10^5 cells/mL and cultured in 10% FBS-RPMI 1640 medium at 37 ℃ in a humidified atmosphere of 50 mL/L CO_2. Cells were grown to 80-90% confluence and synchronized by incubation in 0.5% FBS-RPMI 1640 for 56 h. The experiments were divided into test and control groups. Cells in the test group were incubated in 10% FBS-RPMI 1640 medium containing 160 μg/mL PMBE for 24 or 48 h. Cells in the control group were incubated in 10% FBS-RPMI 1640 alone for 24 h. The coverslips were washed with PBS (containing Ca^{2+}, Mg^{2+}) for 3-5 min, then a 1 000:1 mixture of methanol: DAPI was added and placed at 4 ℃ for 15-30 min, and then washed thrice with PBS for 3-5 min to reduce the background signal. Finally, the cells fixed on the coverslips were analyzed, and photographed under fluorescence microscope (BH-2, Olympus, Japan).

Electron microscopy BEL-7402 cells were incubated in 10% FBS-RPMI 1640 medium with or without 160 μg/mL PMBE at 37 ℃ in a humidified atmosphere of 50 mL/L CO_2 for 72 h. After treatment with 0.25% trypsin, 5×10^6 cells were collected, centrifuged at 10 000 *g* for 5 min and then washed twice with PBS for 5 min. Cell pellets were fixed in 2.5% glutaraldehyde in PBS at 4 ℃ overnight. After washing thrice (10 min each) in PBS, the pellets were incubated in 1% osmium tetroxide (Electron Microscopy Sciences) in PBS for 1 h at room temperature. After three more 10-min washes in PBS, the pellets were dehydrated using a successive ethanol series of 300, 500, 700, 800, and 950 mL/L in double distilled water (10 min each) at room temperature. The pellets were further dehydrated at room temperature in 100% acetone (3×10 min), incubated in 50% acetone/50% epoxy resin (Durcupan ACM, EMS) at room temperature for 1 h, and infiltrated with 100% epoxy resin (3×1 h) at room temperature. After the final incubation, the resin-infiltrated pellets plus excess resin were poured into capsules and polymerized at 70 ℃ overnight. Ultrathin (500 Å) sections were made using a heat-swelling ultramicrotome (LKB-NoVa-V, Switzerland). After being stained with uranium acetate and plumbum citrate, the sections were observed under a transmission electron microscope (JEM 100CX-II, Houghton, MI, USA) and electron micrographs were taken.

DNA fragmentation assay[10]

BEL-7402 cells were seeded in two 25-mL flasks at a density

of 10^5 cells/mL and incubated in 10% FBS-RPMI 1640 medium as previously described in the presence or absence of 160 μg/mL PMBE for 24 h. After harvesting the cells, samples were washed with PBS and centrifuged at 1 000 r/min. The cell pellets were resuspended in a 40-μL solution of 0.2 mol/L NaH_2PO_4/0.1 mol/L citric acid (192:8) and incubated at room temperature for 60 min. After centrifugation for 30 min at 480 r/min, the supernatant was transferred to a 1.5 mL microcentrifuge tube. Three microliters of NP-40 (2.5 mg/mL) and 3 μL RNase A (10 mg/mL) were added to the tube and incubated at 37 ℃ for 60 min. After the addition of 3 μL proteinase K (10 mg/mL), the tube was once again incubated at 50 ℃ for 50 min. At the end of the reaction, 5 μL loading buffer was added and samples were electrophoresed on a 10 g/L agarose gel containing 0.5 μg/mL ethidium bromide, at 7.5 V/cm in 1×TAE buffer for 1.5 h. Analyses and photography were performed with the gel imaging and analysis system (BIO-RAD Co., USA).

Flow cytometry

Cellular DNA content and cell distribution were quantified by flow cytometry using propidium iodide (PI)[11]. After treatment with PMBE, the cells were collected, washed in PBS, and fixed in 700 mL/L ethanol at 4 ℃ overnight. After fixation, the cells were washed in PBS and pellets obtained by centrifugation were stained with PI staining solution containing 50 μg/mL PI, 10 μg/mL RNase A, 5 mL/L Triton X-100, and 0.1% (w/v) trisodium citrate for 30 min at room temperature in the dark. DNA content was determined by flow cytometry (ELITE, BECKMAN Co., USA). Cell populations in the sub-G_1 area (the position where apoptotic cells located) were quantified from a standard count of 10^4 cells using MULTYCYCLE software (PHEONIX Co., USA).

Immunohistochemistry

BEL-7402 cells were seeded in sterile culture dishes on coverslips at a density of 10^5 cells/mL, and incubated as described previously. The experiments were divided into test and control groups. Cells in the test group were incubated with 10% FBS-RPMI 1640 medium containing 160 μg/mL PMBE for 24, 48, or 72 h. Cells in the control group were incubated with 10% FBS-RPMI 1640 alone for 24 h. Cells were first washed thrice (1 min each) with PBS, fixed in acetone for 10 min, immersed in 0.75% H_2O_2-PBS at 37 ℃ for 30 min to inactivate the peroxidase, and washed twice with PBS for 3 min. Normal goat serum was used to eliminate the unspecific staining. Fixed cells were incubated for 30 min at room temperature with mouse anti-human Bcl-2 mAb (primary antibody, Oncogene Research Products) and washed five times with PBS. Slides were then incubated at 37 ℃ for 30 min with biotinylated goat anti-mouse IgG (secondary antibody), washed twice with PBS, and visualized using the immunoperoxidase-based SABC kit (Boster Co.) under a phase contrast microscope. According to the kit protocol, BEL-7402 cells treated with 160 μg/mL of PMBE for 24 h without the addition of primary antibody were used as the negative control. Cells were regarded as positive, when the cell membrane was stained in a brown coffee color similar to the positive control provided by the kit manufacturer.

Statistical analysis

Data were expressed as mean±SD. All experiments were performed in triplicate, unless otherwise indicated. Statistical significance was evaluated either by Student's *t*-test or by one-way ANOVA using *SPSS10.0* software ($P<0.05$ was considered statistically significant, $P<0.01$ very statistically significant).

RESULTS

Dose- and time-dependent effects of PMBE on proliferation of BEL-7402 cells

Human hepatoma BEL-7402 cells were incubated with PMBE for different periods of time at concentrations ranging 20-200 μg/mL and analyzed by MTT assay. PMBE was shown to inhibit the proliferation of BEL-7402 cells in a dose- and time-dependent manner. After exposure of BEL-7402 cells to 20, 40, 80, 160, or 200 μg/mL of PMBE for 48 h, cell proliferation was inhibited by 16.97%, 25.20%, 30.64%, 36.64%, and 43.17%, respectively (Figure 2A). Treatment of BEL-7402 cells with 160 μg/mL PMBE for 24, 48, or 72 h, inhibited cell proliferation by 21.96%, 30.47%, and 34.36%, respectively (Figure 2B).

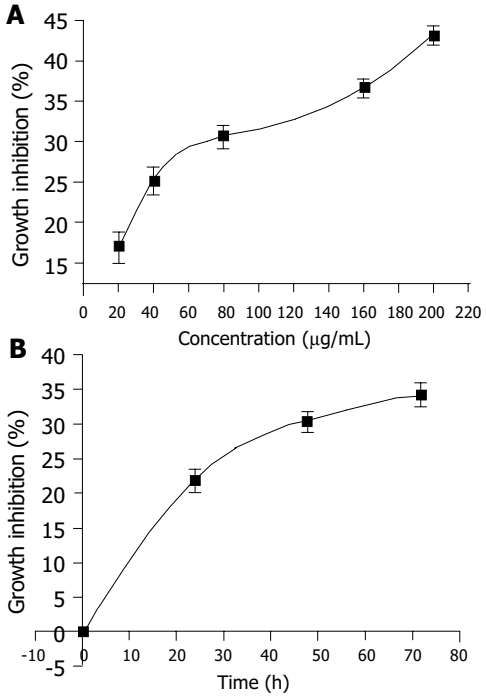


Figure 2 Dose-dependent effects (**A**) and time-dependent effects (**B**) of PMBE on inhibition of BEL-7402 cell growth.

Morphological changes

Under fluorescence microscope, untreated BEL-7402 cells displayed extended, flat cell bodies with uniform chromatin in the nuclei (Figure 3A). The nuclei of BEL-7402 cells, treated with 160 μg/mL PMBE for 24 h, showed the characteristic morphological changes of apoptosis, including nuclear condensation, boundary aggregation and split,

even DNA fragmentation (Figure 3B), which dramatically increased over time (Figure 3C). Under transmission electron microscope, apoptotic bodies were observed in cells treated with 160 μg/mL PMBE for 72 h (Figure 3D).

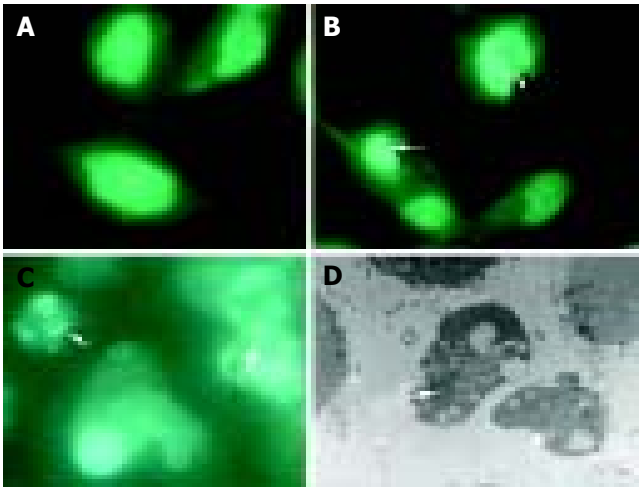


Figure 3 Morphological changes in BEL-7402 cells incubated without PMBE for 24 h (**A**), with 160 μg/mL PMBE for 24 (**B**), 48 (**C**) and 72 h (**D**). Arrows denote condensed, fragmented nuclei, apoptotic bodies.

Inter-nucleosomal DNA degradation induced by PMBE

In order to demonstrate that PMBE was able to induce an apoptotic response, we analyzed DNA degradation in PMBE-treated BEL-7402 cells by agarose gel electrophoresis. PMBE, at a concentration of 160 μg/mL, induced the typical inter-nucleosomal DNA fragmentation in multiples of 180-200 bp after 24 h, a hallmark of apoptosis (Figure 4). No chromosomal DNA cleavage was observed in the untreated control cells (Figure 4).

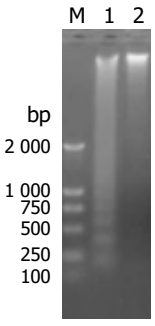


Figure 4 Apoptosis induced by PMBE. M: DNA marker DL2000; 1: Treatment with PMBE; 2: Untreated negative control.

Quantitative detection of apoptosis induced by PMBE

Apoptotic cells could be recognized by PI staining due to DNA degradation and subsequent leakage of stain from the cells. The hypodiploid population, formed by cells with a reduced DNA content in frequency histograms (sub-G_1 peak), could be quantified by flow cytometry and effects of PMBE on BEL-7402 cell distribution could be observed. Results showed that incubation with 160 μg/mL of PMBE for different time periods or with 140, 160, or 180 μg/mL of PMBE for 24 h resulted in accumulation of cells at G_1 or S phase (Figures 5A and B) and a blockade of cell proliferation. Arrest of the cell cycle at G_1 or S phase eventually led to cell death, as the prolonged incubation with 160 μg/mL PMBE induced an increasing apoptotic response, resulting in the rapid appearance of cells with a DNA content less than that at G_1 phase, characteristic of apoptotic cells (Figures 5C). In addition, PMBE induced apoptosis of BEL-7402 cells in a dose-dependent manner. In untreated BEL-7402 cells, the mean apoptotic population was 2.23%, which increased to 7.03%, 28.3%, and 8.43% after a 24-h treatment with 140, 160, and 180 μg/mL PMBE, respectively (Figure 5D). For the time-dependent relationship, the number of apoptotic cells increased with prolonged incubation in PMBE. The number of apoptotic cells increased from 2.23% to 25.1%, 70.6%, and 81.7% after 24, 48, and 72 h of exposure to 160 μg/mL PMBE, respectively (Figure 5E). Therefore, PMBE induced apoptosis of BEL-7402 cells in a dose- and time-dependent manner.

Role of Bcl-2 in PMBE-induced apoptosis

The involvement of the *bcl-2* gene in apoptosis was reported in several studies of anticancer drugs[12-14]. The role of Bcl-2 in PMBE-induced apoptosis of human hepatoma BEL-7402 cells was evaluated by immunohistochemical analysis. Three hundred cells were observed under a microscope and the positive cell ratio was calculated from three independent experiments. The results showed that cells in the control group had higher expression levels of Bcl-2, with a (21.3±1.5)% positive staining ratio, while Bcl-2 expression in test group cells decreased to (16.3±1.2)%, (9.3±0.9)%, and (9.7±1.4)% after treatment with 160 μg/mL PMBE for 24, 48, or 72 h, respectively (Figure 6). Compared with control, all test groups displayed significant differences ($P<0.05$). The positive staining ratio of Bcl-2 protein expression decreased with PMBE treatment time, suggesting that PMBE might play a role in inducing apoptosis of human hepatoma BEL-7402 cells by possibly down-regulating the expression of the *bcl-2* gene.

DISCUSSION

Hepatoma is one of the most common malignant tumors in China and Asia. Therefore, we chose the human hepatoma cell line BEL-7402, as an *in vitro* model to explore the effects of PMBE on cancer cell growth and apoptosis to evaluate the value of PMBE in cancer prevention and therapy.

Our results showed that PMBE at doses ranging 20-200 μg/mL, significantly suppressed cell proliferation in a time- and dose-dependent manner and induced characteristic morphological and biochemical changes associated with apoptosis of human hepatoma BEL-7402 cells. The inhibitory effect of PMBE on cancer cell growth may be attributed to its antioxidant function[1]. Additionally, PMBE appears to induce apoptosis via downregulation of the Bcl-2 protein. Moreover, we have observed that PMBE exhibits more potent effects on apoptosis than on growth inhibition at similar concentrations as described in the results. When exposed to 160 μg/mL of PMBE for 24, 48, and 72 h, the growth inhibition ratio and apoptosis ratio of

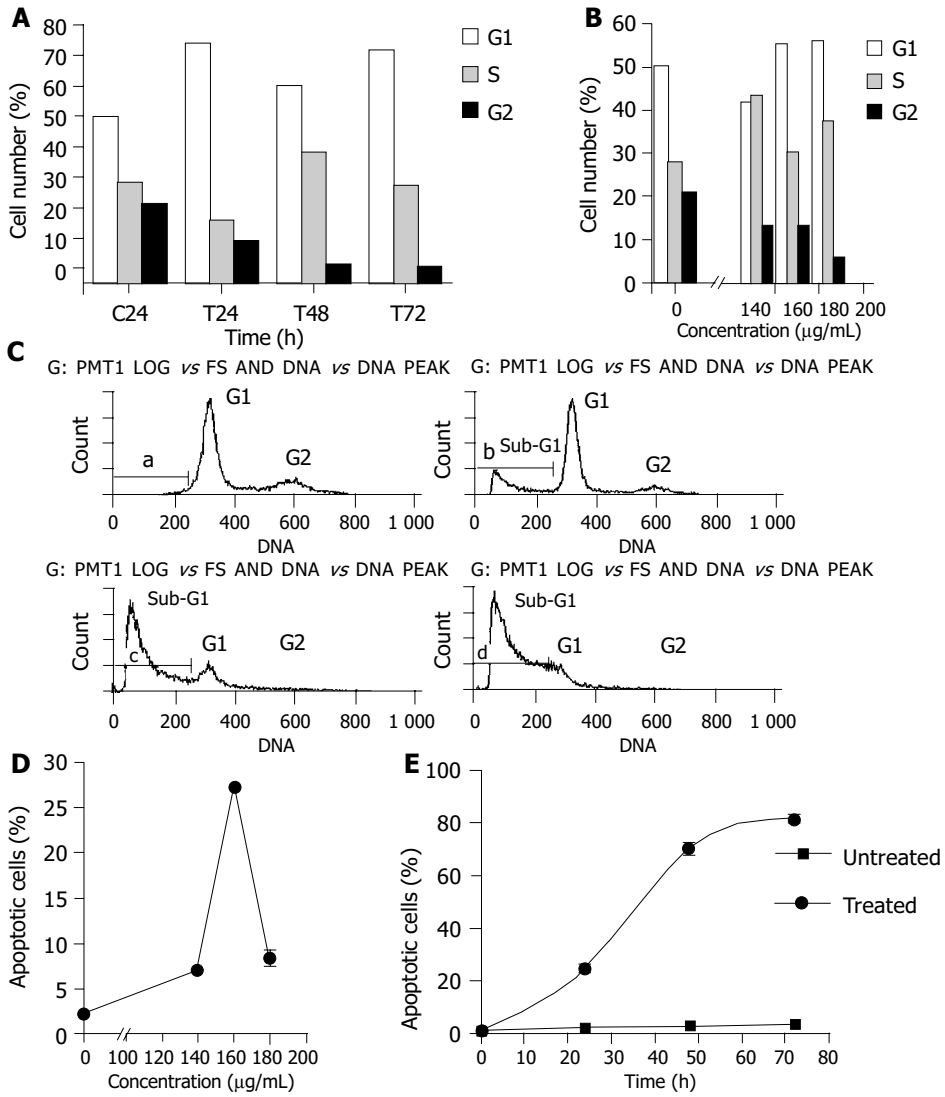


Figure 5 Time-course effects and dose–response effects of PMBE on cell cycle distribution (**A** and **B**) and apoptosis of BEL-7402 cells (**C**-**E**). a: control 24 h; b: 24 h; c: 48 h; d: 72 h.

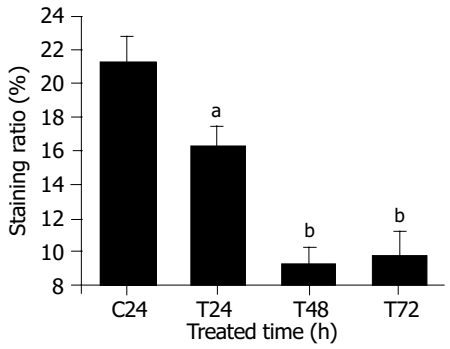


Figure 6 Expression of Bcl-2 protein in BEL-7402 cells treated with 160 μg/mL PMBE for different time periods. C: control; T: treatment with PMBE; $^{a}P<0.05$ as significant, $^{b}P<0.01$ very significant *vs* the control.

BEL-7402 cells were 21.96%, 30.47%, 34.36% and 25.1%, 70.6%, 81.7%, respectively. These distinct actions on cell cycle progression and apoptosis suggest that PMBE is able to trigger different signal transduction pathways, and to exert effects on two key processes during cancer treatment. Taken together, our data demonstrate PMBE has a high capacity of suppressing cell proliferation and triggering apoptosis of human hepatoma cells. Therefore, PMBE may have a therapeutic potential in human liver cancer and may find its use as an anticancer candidate.

The activities of PMBE may account for previously reported cytotoxic effects of this extract[4]. In this study, we showed compelling evidence for pro-apoptotic activity of PMBE using a combination of different techniques. Furthermore, these actions are time- and dose-dependent. We have also found that PMBE could induce accumulation of cells arrested at G_1 and S phases of the cell cycle. Therefore, the antitumor effects of PMBE may result from multiple mechanisms of action, such as interfering with cell cycle progression and inducing apoptosis, possibly by decreasing Bcl-2 protein expression. Oncogenes such as *bcl-2*, are often involved in the development of tumors, and may be related to tumor cell drug resistance[15]. Our results showed that PMBE not only induced BEL-7402 cell apoptosis, but also drastically decreased Bcl-2 protein expression concurrently. The identification of the genes involved and their related signal transduction pathways critical to tumorigenesis await further study.

In conclusion, PMBE is capable of inhibiting growth and inducing apoptosis of human hepatoma BEL-7402 cells in a dose- and time-dependent manner, indicating that PMBE may hold promise as an anticancer agent.

ACKNOWLEDGMENT

We thank the reviewers for their helpful comments.

REFERENCES

1 **Cui YY,** Xie H, Lai F, Wang JF. Preliminary study on antioxidative activities of *Pinus massoniana* bark extract (PMBE). *Shipin Kexue* 2004; **25**: 179-183
2 **Zhao JF,** Wang JN, Chen YJ, Agarwal R. Anti-tumor-promoting activity of a polyphenolic fraction isolated from grape seeds in the mouse skin two-stage initiation-promotion protocol and identification of procyanidin B5-3'-gallate as the most effective antioxidant constituent. *Carcinogenesis* 1999; **20**: 1737-1745
3 **Zhang HY,** Zhang ZY. *Pinus massoniana* Lamb In: Zeng MY, Zeng JF, eds. *Zhongguo Zhongyao Ziyuan Zhiyao. Beijing*: *Science Press* 1994: 146–147
4 **Cui YY,** Xie H, Wang JF. Broad-spectrum inhibition of *Pinus massoniana* bark extract (PMBE) to human cancer cells cultured *in vitro*. *Yaoxue Jinzhan* 2004; **28**: 418- 421
5 **Rohdewald P.** A review of the French maritime pine bark extract (Pycnogenol), a herbal medication with a diverse clinical pharmacology. *Int J Clin Pharmacol Ther* 2002; **40**: 158-168
6 **Shand B,** Strey C, Scott R, Morrison Z, Gieseg S. Pilot study on the clinical effects of dietary supplementation with Enzogenol, a flavonoid extract of pine bark and vitamin C. *Phytother Res* 2003; **17**: 490- 494
7 **Huynh HT,** Teel RW. Selective induction of apoptosis in human mammary cancer cells (MCF-7) by Pycnogenol. *Anticancer Res* 2000; **20**: 2417-2420
8 **Mosmman T.** Rapid colorimetric assay for cellular growth and survival: application to proliferation and cytotoxicity assays. *J Immunol Methods* 1983; **65**: 55-63
9 **Alley MC,** Scudiero DA, Monks A, Hursey ML, Czerwinski MJ, Fine DL, Abbott BJ, Mayo JG, Shoemaker RH, Boyd MR. Feasibility of drug screening with panels of human tumor cell lines using a microculture tetrazolium assay. *Cancer Res* 1988; **48**: 589-601
10 **Zhu XQ,** Wang GS, Zhang XJ, Zhao Q. Effects of sodium ferculate on the viability and apoptosis of human hepatoma BEL-7404 cells. *Shijie Huaren Xiaohua Zazhi* 1999; **7**: 715-716
11 **Darzynkiewicz Z,** Bruno S, Del Bino G, Gorczyca W, Hotz MA, Lassota P, Traganos F. Features of apoptotic cells measured by flow cytometry. *Cytometry* 1992; **13**: 795-808
12 **Yuan J,** Gu ZL, Zhou WH, Kwok CY. Elemene induces apoptosis and regulates expression of Bcl-2 protein in human leukemia K562 cells. *Zhongguo Yaoli Xuebao* 1999; **20**: 103-106
13 **Kuo ML,** Huang TS, Lin JK. Curcumin, an antioxidant and anti-tumor promoter, induces apoptosis in human leukemia cells. *Biochim Biophys Acta* 1996; **1317**: 95-100
14 **Gautam SC,** Xu YX, Pindolia KR, Janakiraman N, Chapman RA. Nonselective inhibition of proliferation of transformed and nontransformed cells by the anticancer agent curcumin (Diferuloylmethane). *Biochem Pharmacol* 1998; **55**: 1333-1337
15 **Hockenbery D.** Bcl-2 in cancer, development and apoptosis. *J Cell Sci (Suppl)* 1994; **18**: 51-55

Science Editor Wang XL and Guo SY **Language Editor** Elsevier HK

PO Box 2345, Beijing 100023, China
www.wjgnet.com
wjg@wjgnet.com

ELSEVIER

World J Gastroenterol 2005;11(34):5283-5288
World Journal of Gastroenterology ISSN 1007-9327
© 2005 The WJG Press and Elsevier Inc. All rights reserved.

Long-term hepatic consequences of chemotherapy-related HBV reactivation in lymphoma patients

Wen-Pin Su, Chi-Chung Wen, Chao A. Hsiung, Ih-Jen Su, Ann-Lii Cheng, Ming-Chih Chang, Chao-Jung Tsao, Woei-Yao Kao, Wu-Ching Uen, Chiun Hsu, Chih-Hung Hsu, Yen-Shen Lu, Hwei-Fan Tien, Tsu-Yi Chao, Li-Tzong Chen, Jacqueline Whang-Peng, Pei-Jer Chen

Wen-Pin Su, Ann-Lii Cheng, Chiun Hsu, Chih-Hung Hsu, Yen-Shen Lu, Department of Oncology, National Taiwan University Hospital, Taipei, Taiwan, China
Chi-Chung Wen, Chao A. Hsiung, Division of Biostatics and Bioinformatics, National Health Research Institutes, Taipei, Taiwan, China
Ih-Jen Su, Division of Clinical Research, National Health Research Institutes, Taipei, Taiwan, China
Ann-Lii Cheng, Hwei-Fan Tien, Pei-Jer Chen, Department of Internal Medicine, National Taiwan University Hospital, Taipei, Taiwan, China
Ming-Chih Chang, Department of Internal Medicine, Mackay Memorial Hospital, Taipei, Taiwan, China
Chao-Jung Tsao, Department of Internal Medicine, Chi-Mei Hospital, Tainan, Taiwan, China
Woei-Yao Kao, Tsu-Yi Chao, Department of Internal Medicine, Tri-Service General Hospital, Taipei, Taiwan, China
Wu-Ching Uen, Department of Internal Medicine, Shin Kong Memorial Hospital, Taipei, Taiwan, China
Li-Tzong Chen, Jacqueline Whang-Peng, Division of Cancer Research, National Health Research Institutes, Taipei, Taiwan, China
Pei-Jer Chen, Clinical Research Institute, National Taiwan University College of Medicine, Taipei, Taiwan, China
Supported by the National Health Research Institute, Taiwan, China
Co-correspondent: Pei-Jer Chen
Correspondence to: Ann-Lii Cheng, MD, PhD, Professor, Departments of Oncology and Internal Medicine, National Taiwan University Hospital, No. 7, Chung-Shan South Road, Taipei 10016, Taiwan, China. andrew@ha.mc.ntu.edu.tw
Telephone: +886-2-2312-3456-7251 Fax: +886-2-2371-1174
Received: 2005-02-22 Accepted: 2005-03-23

Abstract

AIM: To investigate the long-term consequences of chemotherapy-related HBV reactivation in patients with lymphoma.

METHODS: This study was based on the database of published prospective study evaluating HBV reactivation in HBV lymphoma patients during chemotherapy. Deteriorated liver reserve (DLR) was defined as development of either one of the following conditions during follow-up: (1) newly onset parenchyma liver disease, splenomegaly or ascites without evidence of lymphoma involvement; (2) decrease of the ratio (albumin/globulin ratio) to less than 0.8 or increase of the ratio of INR of prothrombin time to larger than 1.2 without evidence of malnutrition or infection. Liver cirrhosis was diagnosed by imaging studies.

RESULTS: A total of 49 patients were included. The median follow-up was 6.2 years (range, 3.9-8.1 years). There were 31 patients with and 18 patients without HBV reactivation. Although there was no difference of overall survival (OS) and chemotherapy response rate between the two groups, DLR developed more frequently in patients with HBV reactivation (48.4% *vs* 16.7%; $P = 0.0342$). Among the HBV reactivators, HBV genotype C was associated with a higher risk of developing DLR ($P = 0.0768$) and liver cirrhosis ($P = 0.003$). Four of five patients with sustained high titer of HBV DNA and two of three patients with multiple HBV reactivation developed DLR. Further, patients with a sustained high titer of HBV DNA had the shortest OS among the HBV reactivators ($P = 0.0000$). No patients in the non-HBV reactivation group developed hepatic failure or liver cirrhosis.

CONCLUSION: Chemotherapy-related HBV reactivation is associated with the long-term effect of deterioration of hepatic function.

© 2005 The WJG Press and Elsevier Inc. All rights reserved.

Key words: HBV reactivation; Liver function; Non-Hodgkin's lymphoma; Chemotherapy

Su WP, Wen CC, Hsiung CA, Su IJ, Cheng AL, Chang MC, Tsao CJ, Kao WY, Uen WC, Hsu C, Hsu CH, Lu YS, Tien HF, Chao TY, Chen LT, Wang-Peng J, Chen PJ. Long-term hepatic consequences of chemotherapy-related HBV reactivation in lymphoma patients. *World J Gastroenterol* 2005; 11(34): 5283-5288

http://www.wjgnet.com/1007-9327/11/5283.asp

INTRODUCTION

Reactivation of HBV is a well-recognized complication in patients with chronic HBV infection, who receive cytotoxic chemotherapy or immunotherapy management for cancers[1-16]. This complication is especially important in Taiwan, Hong Kong, Singapore and Mainland China, which have high HBV carrier rates of approximately 15-20% in the general population. Although the reported frequency of HBV reactivation in hepatitis B surface antigen (HBsAg)-positive non-Hodgkin's lymphoma (NHL) patients undergoing cancer chemotherapy has ranged widely from 14% to 72%[8-10], our recent prospective study indicated a HBV reactivation rate of around 70% in patients receiving

conventional glucocorticoids-containing systemic chemotherapy[17]. In the near-term, hepatitis flare-up in patients undergoing chemotherapy may jeopardize scheduled chemotherapy or cause severe hepatic damage and even lethal hepatic failure of the patients. However, for survivors of lymphoma who have HBV reactivation during chemotherapy, the long-term hepatic consequences have not been elucidated.

In this study, we analyzed the long-term hepatic consequence in HBV lymphoma patients with HBV reactivation during chemotherapy by using the database of the TCOG (Taiwan Cooperative Oncology Group)-1495, initiated in 1995 and a prospective multi-center randomized clinical study, to evaluate HBV reactivation in HBsAg (+)-lymphoma patients[17]. Most of the patients in this study were followed up for more than 6 years. Our results indicated that though there is no difference in overall survival (OS) in the patients with or without HBV reactivation, HBV reactivation during systemic chemotherapy may have long-term adverse effect on the livers of the lymphoma survivors.

MATERIALS AND METHODS

Patients

This retrospective study used data collected during the long-term follow-up of patients enrolled in a multi-center randomized clinical study conducted from November 1995 to February 2000, which compared steroid-containing and steroid-free chemotherapy in HBsAg (+)-lymphoma patients (T-1495)[17]. All 49 patients who participated in that prospective trial were included in this study. HBV DNA, hepatitis B e antigen (HBeAg) status, HBV genotype and biochemical data (albumin, globulin, bilirubin in total and direct forms, serum aspartate aminotransaminase, serum alanine aminotransaminase (ALT), and prothrombin time (PT)) were regularly examined before treatment and every 2 wk during chemotherapy. All these exams except HBV studies were regularly checked every 2 mo during follow-up. Imaging studies (i.e., abdominal ultrasonography and computed tomography) were performed every 3 mo during chemotherapy and annually during the long-term follow-up.

Hepatitis B virus serology and definition of HBV reactivation

Briefly, HBV DNA was tested in duplicate using the Chiron bDNA assay (VERSANT HBV DNA assay, Chiron Diagnostics, Emeryville, CA, USA). This assay has a sensitivity of 2.5 pg/mL. HBV genotypes were determined using PCR-restriction fragment length polymorphism (RFLP) of the surface gene of HBV[18]. Six genotypes (A-F) of HBV could be identified by the restriction patterns of DNA fragments.

Clinical hepatitis flare-up was defined as a threefold or greater increase in serum ALT level that exceeded 100 IU/L. The hepatitis or hepatitis flare-up was attributed to reactivation of chronic hepatitis B, when there was a five-fold or higher elevation of serum HBV DNA compared with the pre-chemotherapy baseline level or re-appearance of HBV DNA or HBeAg in the serum. Liver biopsy was electively performed to determine the etiology of hepatitis in this study. Only six patients received liver biopsy before or after chemotherapy. Three patients who developed HBV reactivation after early 1999 were treated with lamivudine.

Definition of subtype HBV reactivation during chemotherapy

The HBV reactivation pattern was categorized into three groups as transient, protracted and multiple reactivations[17]. Transient pattern was characterized by a rapid and transient surge of HBV DNA, which usually resolved in a few weeks. Protracted HBV reactivation was defined as a prolonged period of persistently high HBV DNA titer. Some patients with protracted HBV reactivation finally achieved resolution after several bouts of clinical hepatitis (protracted/resolved), while others maintained a high-titer of HBV DNA status throughout the entire period of chemotherapy (protracted/unresolved). Multiple HBV reactivations were characterized by repeated HBV increment after apparent resolution of previous episodes.

Definition of deteriorated liver reserve

In this retrospective study, hepatic images, albumin/globulin ratio (A/G ratio)[19-22] and international normalized ratio (INR) of PT[23-25] were used for the evaluation of liver status. Deteriorated liver reserve (DLR) was defined as the development of either one of the following conditions during the following period: (1) New onset of parenchyma liver disease, liver cirrhosis, splenomegaly or ascites[26] without evidence of lymphoma involvement of the liver; (2) Decrease of the ratio (A/G ratio) to less than 0.8 [(post-chemotherapy A/G ratio)/(pre-chemotherapy A/G ratio)] or increase of the ratio of INR of PT [(post-chemotherapy INR)/(pre-chemotherapy INR)] to larger than 1.2 without evidence of malnutrition or infection status.

Statistical analysis

All analyses were carried out according to the intent-to-treat principle. Survival curves were estimated by the Kaplan-Meier method. Chi-square test was used to compare variables between patients with and without HBV reactivation. A two-tailed P value less than 0.05 was considered statistically significant. SPSS statistical software (version 10.0) was used for the analysis in this study.

RESULTS

Baseline characteristics

The baseline characteristics of the NHL patients according to the occurrence HBV reactivation are shown in Table 1. The median follow-up of the patients was 6.2 years (range, 3.9-8.1 years). There were 31 patients (63.3%) in the HBV reactivation group and 18 patients (36.7%) in the non-HBV reactivation group. Among 31 patients with clinical HBV reactivation, only one patient had his liver biopsied to confirm the diagnosis. Patients who were more than 45 years old or those who had a lower pre-chemotherapy HBV DNA load (<100 copy numbers) had a significant tendency to develop HBV reactivation ($P = 0.019$ and $P = 0.010$, respectively). The likelihood of developing HBV reactivation was slightly higher in HBeAg (-) patients ($P = 0.0841$). Gender and HBV genotype did not contribute to HBV reactivation.

Table 1 Characteristics of the HBV carriers receiving chemotherapy for non-Hodgkin's lymphoma

	HBV reactivation (-)			HBV reactivation (+)		
	Total	*n*	%	*n*	%	*P*
Number of patients	49	18	36.7	31	63.3	
Median follow-up (yr)	6.2	5.4		6.7		
Age (yr)						
≤45	24	13	54.2	11	45.8	0.019
>45	25	5	20	20	80	
Sex						
Female	21	7	33.3	14	66.7	0.7689
Male	28	11	39.3	17	60.1	
HBeAg						
Positive	7	5	71.4	2	28.6	0.0841
Negative	42	13	31	29	69	
Pre-chemotherapy HBV DNA						
≥100 copy numbers	11	8	72.7	3	27.3	0.010
<100 copy numbers	38	10	26.3	28	73.7	
HBV genotype C						
Yes	12	5	41.7	7	58.3	0.7318
No	32	11	34.4	21	65.6	
Unknown or mixed type	5	2	40	3	60	
Tumor overall response (complete remission and partial remission)						
Yes	26	8	30.8	18	69.2	0.3897
No	23	10	43.5	13	56.5	

Long-term effect of HBV reactivation

None of the patients developed varices bleeding or hepatocellular carcinoma during the follow-up period. The median survival was 1 886 d in the HBV reactivation group (1 537±188 d, 95%CI as 1 168-1 907 d) and 828 d in the non-HBV reactivation group (1 255±217 d, 95%CI as 829-1 680 d) group. Although there was no difference in treatment response to chemotherapy (P = 0.3897) and OS between patients with and without HBV reactivation (P = 0.601, Figure 1A), DLR was developed more frequently in patients with HBV reactivation (48.4% *vs* 16.7%, P = 0.0342, Figure 1B).

Risk factors for developing deteriorated liver reserve

Among the HBV reactivators, those with HBV genotype C had a higher risk of developing DLR (P = 0.0768). No other factor including HBeAg status, age, gender, reactivation pattern and peak value of bilirubin, ALT and HBV DNA level was found to be associated with poor liver outcome (Table 2). Three of thirty-one patients who had viral genotype C had new onset of liver cirrhosis by imaging criteria with Child-Pugh classification A. Genotype C was associated with the development of liver cirrhosis after chemotherapy among lymphoma patients who had HBV reactivation during chemotherapy (P = 0.003, Figure 2).

The characteristics and outcome of patients who developed DLR with patterns of protracted/unresolved (A) and multiple reactivations (B) are listed in Table 3. Four of five patients with pattern A and two of three patients with pattern B developed DLR. All 3 of the 31 patients who died of hepatic failure had protracted/unresolved (A) or multiple reactivation (B) patterns. No cases of hepatic failure or new onset of liver cirrhosis developed in the non-HBV reactivation group.

Table 2 Risk factors for development of DLR among non-Hodgkin's lymphoma patients with HBV reactivation during chemotherapy

	DLR (–)			DLR (+)		
	Total	*n*	%	*n*	%	*P*
Number of patients	31	16	51.6	15	48.4	
Age (yr)						
≤45	11	4	36.4	7	65.6	0.2734
>45	20	12	60	8	40	
Sex						
Female	14	7	50	7	50	1
Male	17	9	52.9	8	47.1	
GPT>10X						
Yes	19	8	42.1	11	57.9	0.2734
No	12	8	66.7	4	33.4	
HBeAg						
Present	29	16	55.2	13	44.8	0.2258
Absent	2	0	0	2	100	
HBV genotype C						
No	21	13	61.9	8	38.1	0.0768
Yes	7	1	14.3	6	85.7	
Unknown or mixed type	3	2	66.7	1	33.3	
Total bilirubin >5						
Yes	5	1	20	4	80	0.1719
No	26	15	57.7	11	42.3	
Peak HBV DNA >100X						
Yes	18	9	50	9	50	1
No	13	7	53.8	6	46.2	
Patterns of reactivation						
Transient	16	10	62.5	6	37.5	0.508
Protracted / resolved	5	3	60	2	40	
Protracted / unresolved	5	1	20	4	80	
Multiple reactivation	3	1	33.3	2	66.7	
Unknown	2	1	50	1	50	

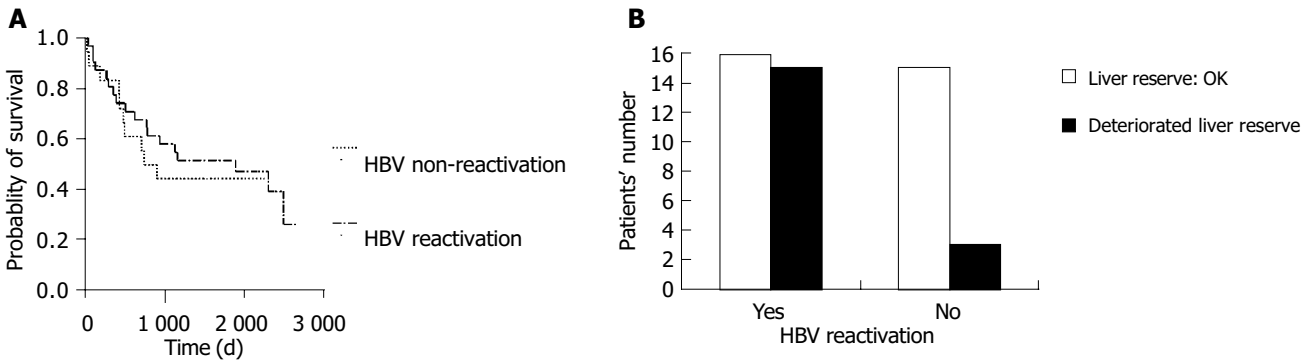


Figure 1 OS of total 49 HBV carriers' undergoing chemotherapy for non-Hodgkin's lymphoma, according to HBV reactivation status (P = 0.601) (**A**); comparison of liver reserve between HBV reactivators and HBV non-reactivators (P = 0.0342) (**B**).

Table 3 Characteristics of DLR of HBV reactivators with patterns of protracted/unresolved (A) and multiple reactivations (B)

Reactivation pattern	Outcome	Cause of death	Type of DLR	Ratio of A/G ratio	Ratio of INR of PT
A	Died	Hepatic failure	H	0.62	3.88
A	Died	Hepatic failure	H	1	1.27
A	Died	Cancer progression	N	0.86	NA
A	Died	Cancer progression	N	0.6	1.38
B	Alive	NA	N	NA	NA
B	Died	Hepatic failure/cancer progression	H	NA	1.36

H: HBV reactivation related hepatic failure; N: newly developed coarse liver echotexture; NA: not available.

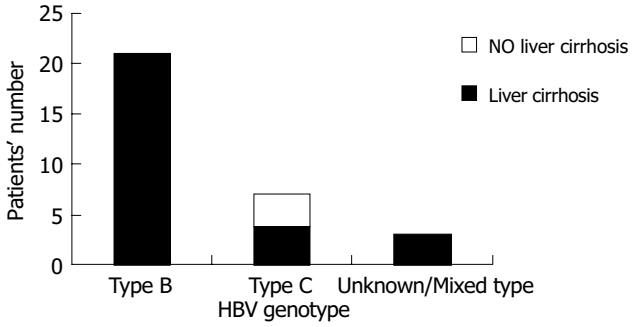


Figure 2 Relationship between genotype and liver cirrhosis in HBV reactivators (P = 0.003).

Treatment efficacy among HBV reactivators with different reactivation patterns

Response to chemotherapy (partial response or complete remission) occurred in 10 of 16 patients with transient reactivation, 4 of 5 patients with protracted/resolved reactivation, 2 of 5 patients with protracted/unresolved flare-up, 2 of 3 patients with multiple reactivation and none of 2 patients with unsure pattern. No correlation was found between reactivation pattern and treatment response (P = 0.325). However, patients with a protracted/unresolved reactivation pattern had shorter OS (189±41 d, 95%CI as 108-269 d, Figure 3, P = 0.000).

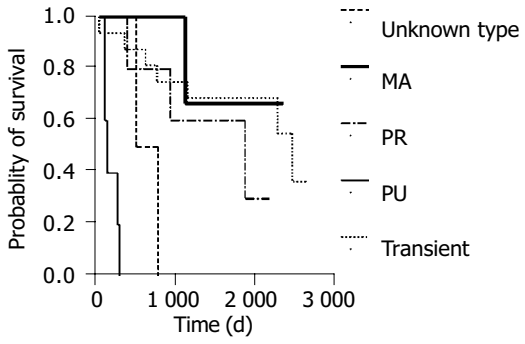


Figure 3 OS in HBV reactivation patients with different reactivation patterns (P = 0.000). (MA: multiple reactivations; PR: protracted/resolved; PU: protracted/unresolved.).

DISCUSSION

In this study, we demonstrated that though there is no survival difference between NHL patients with and without HBV reactivation during chemotherapy, the patients with HBV reactivation do have a long term effect on liver function or liver cirrhosis of the lymphoma survivors by biochemical tests or by imaging modality. HBV genotype C patients may have a higher risk of developing DLR and liver cirrhosis after chemotherapy. Moreover, patients with protracted/unresolved or multiple reactivations are associated with a higher risk of developing DLR and a high incidence of lethal hepatic failure. Furthermore, patients with sustained high titer of HBV DNA leads to poor OS duration compared to other HBV reactivators.

This study had several limitations. DLR after chemotherapy was defined by common biochemical tests with A/G and PT[19-25] and imaging modality because the condition of the patients (i.e. neutropenia and thrombocytopenia during chemotherapy) made routine performance of liver biopsy during lymphoma treatment problematic. The relatively short follow-up duration also limited this study. The longest follow-up duration was only 8.1 years and this might not have been long enough to observe the full clinical course of HBV infection, such as decompensated liver cirrhosis and hepatocellular carcinoma[27]. The small size was another limitation of this study; and in this study, only 31 patients were HBV reactivation patients. So genotype C of HBV only had a borderline of contribution to develop DLR (P = 0.0768). Therefore, further research is needed to establish the relationships among HBV, chemotherapy and host, and to determine the long-term effects of chemotherapy in lymphoma patients who are hepatitis B carriers.

Icteric hepatitis in HBV reactivation during chemotherapy may jeopardize the treatment schedule and thereby increase the risk of lymphoma progression and change the OS of patients with HBV reactivation. No difference was found in the treatment response rate and OS (Figure 1A) of between patients with and without HBV reactivation; however, as shown in Table 3 and Figure 3, patients with a protracted/unresolved reactivation pattern had a shorter OS. Protracted/unresolved reactivation was associated with a higher probability of subsequent hepatic failure or postponed chemotherapy schedule, both of which might contribute to shorter OS. However, in this study, only small proportion patients (4 of 31, 13%) was identified with protracted-unresolved pattern of HBV reactivation; so maybe we should enroll more patients to identify whether the reactivation patterns have influence on the survival.

The worldwide distribution of HBV genotype can be summarized as follows: genotype A is predominant in northern Europe; genotypes B and C are confined to

populations with origins in eastern Asia and the Far East; genotype D is found worldwide, but prevails in the Mediterranean area, the Near and Middle East and south Asia; genotype E is indigenous to western sub-Saharan areas; genotype F is likely to be present in populations with origins in the American continent and the newly identified genotype G is found in France and the USA[28]. In Taiwan, the major serotype of HBV is genotype B (about 81%)[29]. Generally speaking, genotype C is associated with more severe liver disease and hepatocellular carcinoma, which may be due to increased risk of HBeAg positivity, higher serum HBV DNA level, less frequent precore stop codon mutation, and a longer immune clearance phase[28].

In this study, patients with HBV genotype C contributed had a higher rate of impaired liver outcome including post-chemotherapy-related liver cirrhosis. However, among HBV re-activators, the proportion with genotype C who became HBeAg seropositive (1 of 7, 14.3%) was not significantly higher compared to those with genotype B (1 of 21, 4.8%) ($P = 0.4444$, Fisher's exact test). Besides, the pre-chemotherapy baseline HBV DNA copy numbers of all genotype C patients were not elevated, and all of them were within 100 copies. This suggests that the mechanism of DLR resulting from genotype C in HBV patients might not be fully explained by HBV DNA amount and HBeAg seropositivity. Host immune reaction response to hepatitis virus[19,30] and viral genomic factors[31,32] may be more predominant factors. Further studies are needed to test this hypothesis.

Antiviral drugs (i.e. lamivudine) are now commonly used for treatment and prevention of HBV reactivation in HBsAg seropositive patients undergoing cytotoxic chemotherapy[33,34]. They have shown a complete preventative effect of lamivudine, when used before chemotherapy in HBV carriers with lymphoma. However, there is a lack of data on the response to these antiviral drugs in treating or preventing chemotherapy-related HBV reactivation in cancer patients with different HBV genotypes. Further monitoring of the long-term consequences of HBV infection patients either treated or receiving prophylaxis with antiviral agents during chemotherapy and follow-up of the efficacy of these drugs in different HBV genotypes is needed.

ACKNOWLEDGMENT

We are very grateful to Lymphoma Committee of Taiwan Cooperative Oncology Group (TCOG) for their support.

REFERENCES

1 **Galbraith RM,** Eddleston AL, Williams R, Zuckerman AJ. Fulminant hepatic failure in leukaemia and choriocarcinoma related to withdrawal of cytotoxic drug therapy. *Lancet* 1975; **2**: 528-530
2 **Wands JR,** Chura CM, Roll FJ, Maddrey WC. Serial studies of hepatitis-associated antigen and antibody in patients receiving antitumor chemotherapy for myeloproliferative and lymphoproliferative disorders. *Gastroenterology* 1975; **68**: 105-112
3 **Hoofnagle JH,** Dusheiko GM, Schafer DF, Jones EA, Micetich KC, Young RC, Costa J. Reactivation of chronic hepatitis B virus infection by cancer chemotherapy. *Ann Intern Med* 1982; **96**: 447-449
4 **Thung SN,** Gerber MA, Klion F, Gilbert H. Massive hepatic necrosis after chemotherapy withdrawal in a hepatitis B virus carrier. *Arch Intern Med* 1985; **145**: 1313-1314
5 **Lau JY,** Lai CL, Lin HJ, Lok AS, Liang RH, Wu PC, Chan TK, Todd D. Fatal reactivation of chronic hepatitis B virus infection following withdrawal of chemotherapy in lymphoma patients. *Q J Med* 1989; **73**: 911-917
6 **Pariente EA,** Goudeau A, Dubois F, Degott C, Gluckman E, Devergie A, Brechot C, Schenmetzler C, Bernuau J. Fulminant hepatitis due to reactivation of chronic hepatitis B virus infection after allogeneic bone marrow transplantation. *Dig Dis Sci* 1988; **33**: 1185-1191
7 **Liang RH,** Lok AS, Lai CL, Chan TK, Tood D, Chiu EK. Hepatitis B infection in patients with lymphoma. *Hematol Oncol* 1990; **8**: 261-270
8 **Lok AS,** Liang RH, Chiu EK, Wong KL, Chan TK, Todd D. Reactivation of hepatitis B virus replication in patients receiving cytotoxic therapy. Report of a prospective study. *Gastroenterology* 1991; **100**: 182-188
9 **Liaw YF.** Hepatitis viruses under immunosuppressive agents. *J Gastroentrol Hepatol* 1998; **13**: 14-20
10 **Alexopoulos CG,** Vaslamatzis M, Hatzidimitriou G. Prevalence of hepatitis B virus marker positivity and evaluation of hepatitis B virus profile, during chemotherapy, in patients with solid tumors. *Br J Cancer* 1999; **81**: 69-74
11 **Markovic S,** Drozina G, Vovk M, Fidler-Jenko M. Reactivation of hepatitis B but not hepatits C in patients with malignant lymphoma and immunosuppressive therapy. A prospective study in 305 patients. *Hepatogastroenterology* 1999; **46**: 2925-2930
12 **Liang R,** Lau GK, Kwong YL. Chemotherapy and bone marrow transplantation for cancer patients who are also chronic hepatitis B carriers: a review of the problem. *J Clin Oncol* 1999; **17**: 394-398
13 **Cheng AL.** Steroid-free chemotherapy decreases the risk of hepatitis flare-up in hepatitis B virus carriers with non-Hodgkin's lymphoma. *Blood* 1996; **87**: 1202
14 **Kumagai K,** Takagi T, Nakamura S, Sawada U, Kura Y, Kodama F, Shimano S, Kudoh I, Nakamura H, Sawada K, Ohnoshi T. Hepatitis B virus carriers in the treatment of malignant lymphoma: an epidemiological study in Japan. *Ann Oncol* 1997: **8**(Suppl 1): 107-109
15 **Faggiolli P,** De Paschale M, Tocci A, Luoni M, Fava S, De Pali A, Tosi A, Cassi E. Acute hepatic toxicity during cyclic chemotherapy in non-Hodgkin's lymphoma. *Hematologica* 1997; **82**: 38-42
16 **Perrillo RP.** Acute flares in chronic hepatitis B: the natural and unnatural history of an immunologically mediated liver disease. *Gastroenterology* 2001; **120**: 1009-1022
17 **Cheng AL,** Hsiung CA, Su IJ, Chen PJ, Chang MC, Tsao CJ, Kao WY, Uen WC, Hsu CH, Tien HF, Chao TY, Chen LT, Wang-Peng J. Lymphoma Committee of Taiwan Cooperative Oncology Group. Steroid-free chemotherapy decreases risk of hepatitis B virus (HBV) reactivation in HBV-carriers with lymphoma. *Hepatology* 2003; **37**: 1320-1328
18 **Kao JH,** Chen PJ, Lai MY, Chen DS. Hepatitis B genotypes correlate with clinical outcomes in patients with chronic hepatitis B. *Gastroenterology* 2000; **118**: 554-559
19 **Triger DR,** Wright R. Hyperglobulinaemia in liver disease. *Lancet* 1973; **1**: 1494-1496
20 **Czaja AJ,** Wolf AM, Baggenstoss AH. Clinical assessment of cirrhosis in severe chronic active liver disease: specificity and sensitivity of physical and laboratory findings. *Mayo Clin Proc* 1980; **55**: 360-364
21 **Lin DY,** Liaw YF, Chu CM, Chang-Chien CS, Wu CS, Chen PC, Sheen IS. Hepatocellular carcinoma in noncirrhosis patients. A laparoscopic study of 92 cases in Taiwan. *Cancer* 1984; **54**: 1466-1468
22 **Luo JC,** Hwang SJ, Chang FY, Chu CW, Lai CR, Wang YJ, Lee PC, Tsay SH, Lee SD. Simple blood tests can predict compensated liver cirrhosis in patients with chronic hepatitis C. *Hepatogastroenterology* 2002; **49**: 478-481

23 **Schlichting P,** Christensen E, Andersen PK, Fauerholdt L, Juhl E, Poulsen H, Tygstrup N. Prognostic factors in cirrhosis identified by Cox's regression model. *Hepatology* 1983; **3**: 889-895

24 **Oberti F,** Valsesia E, Pilette C, Rousselet MC, Bedossa P, Aubé C, Gallois Y, Rifflet H, Maiga MY, Penneau-Fontbonne D, Cales P. Noninvasive Diagnosis of hepatic fibrosis or cirrhosis. *Gastroenterology* 1997; **113**: 1609-1616

25 **Nagamatsu H,** Kumashiro R, Itano S, Matsugaki S, Sata M. Investigation of associating factors in exacerbation of liver damage after chemotherapy in patients with HBV-related HCC. *Hepatol Res* 2003; **26**: 293-301

26 **Christensen E,** Schlichting P, Fauerholdt L, Gluud C, Andersen PK, Juhl E, Poulsen H, Tygstrup N. Prognostic value of Child-Turcotte criteria in medically treated cirrhosis. *Hepatology* 1984; **4**: 430-435

27 **Fattovich G.** Natural history and prognosis of hepatitis B. *Semin Liver Dis* 2003; **23**: 47-58

28 **Kao JH.** Hepatitis B viral genotypes: clinical relevance and molecular characteristics. *J Gastroenterol Hepatol* 2002; **17**: 643-650

29 **Liu CJ,** Kao JH, Chen PJ, Lai MY, Chen DS. Molecular epidemiology of hepatitis B viral serotypes and genotypes in Taiwan. *J Biomed Sci* 2002; **9**: 166-170

30 **Kao JH,** Chen PJ, Lai MY, Chen DS. Hepatitis B virus genotypes and spontaneous hepatitis B e antigen seroconversion in Taiwanese hepatitis B carriers. *J Med Virol* 2004; **72**: 363-369

31 **Grandjacques C,** Pradat P, Stuyver L, Chevallier M, Chevallier P, Pichoud C, Maisonnas M, Trepo C, Zoulim F. Rapid detection of genotypes and mutations in the pre-core promotor and the pre-core region of hepatitis B virus genome: correlation with viral persistence and disease severity. *J Hepatol* 2000; **33**: 430-439

32 **Rodriguez-Frias F,** Buti M, Jardi R, Cotrina M, Viladomiu L, Esteban R, Guardia J. Hepatitis B virus infection: precore mutants and its relation to viral genotypes and core mutations. *Hepatology* 1995; **22**: 1641-1647

33 **Lau GK,** Yiu HH, Fong DY, Cheng HC, Au WY, Lai LS, Cheung M, Zhang HY, Lie A, Ngan R, Liang R. Early is superior to deferred preemptive lamivudine therapy for hepatitis B patients undergoing chemotherapy. *Gastroenterology* 2003; **125**: 1742-1749

34 **Yeo W,** Chan PK, Ho WM, Zee B, Lam KC, Lei KI, Chan AT, Mok TS, Lee JJ, Leung TW, Zhong S, Johnson PJ. Lamivudine for the prevention of hepatitis B virus reactivation in hepatitis B s-antigen seropositive cancer patients undergoing cytotoxic chemotherapy. *J Clin Oncol* 2004; **22**: 927-934

Science Editor Guo SY **Language Editor** Elsevier HK

PO Box 2345, Beijing 100023, China
www.wjgnet.com
wjg@wjgnet.com

ELSEVIER

World J Gastroenterol 2005;11(34):5289-5294
World Journal of Gastroenterology ISSN 1007-9327
© 2005 The WJG Press and Elsevier Inc. All rights reserved.

Comparison of childhood hepatic malignancies in a hepatitis B hyper-endemic area

Jeng-Chang Chen, Ming-Ling Chang, Jer-Nan Lin, Hong-Shiee Lai, Chiu-Chiang Chen, Wei-Jao Chen, Wen-Tsung Hung

Jeng-Chang Chen, Jer-Nan Lin, Department of Surgery, Chang Gung Children's Hospital, Taoyuan, Taiwan, China
Ming-Ling Chang, Division of Gastroenterology, Department of Medicine, Chang Gung Memorial Hospital, Taoyuan, Taiwan, China
Hong-Shiee Lai, Chiu-Chiang Chen, Wei-Jao Chen, Wen-Tsung Hung, Department of Surgery, National Taiwan University Hospital, Taipei, Taiwan, China
Supported by Chang Gung Children's Hospital, Taoyuan, Taiwan, China, CMRPG 33063
Correspondence to: Jer-Nan Lin, Department of Surgery, Chang Gung Children's Hospital, 5 Fu-Shin Street, Kweishan, 333, Taoyuan, Taiwan, China. bx9619@cgmh.org.tw
Telephone: +886-3-3281200-8227 Fax: +886-3-3287261
Received: 2005-01-03 Accepted: 2005-02-18

Abstract

AIM: To examine the differences of clinical behaviors between hepatocellular carcinomas (HCC) and hepatoblastomas (HB) in children.

METHODS: From 1979 to 1997, we collected 73 HCC and 54 HB from two major medical centers in Taiwan. Demographic, laboratory and radiological data, and survival curves were statistically compared.

RESULTS: HCC clinically differed from HB in mean age (10.6 *vs* 2.5 years; $P<0.001$), status of hepatitis B infection (56/56 *vs* 4/35, $P<0.001$) and accompanying liver cirrhosis (26/40 *vs* 0/30, $P<0.001$), portal vein thrombi (22/56 *vs* 5/38, $P = 0.006$) and para-aortic lymphadenopathy (10/56 *vs* 1/38, $P = 0.026$). Due to a higher recurrence rate (7/12 *vs* 2/13, $P = 0.041$), stage I HCC compared poorly in survivals with stage I HB ($P = 0.0183$). Chemotherapy could only benefit HB as evidenced by 66.7% of resectability conversion and improve survivals for advanced HB, even with unsuccessful conversion. The survival difference between stage I HB and advanced HB with delayed complete resection was of borderline insignificance ($P = 0.0507$).

CONCLUSION: HCC and HB were preliminarily distinguishable by some clinical clues. Delayed resection after chemotherapy was only possible for HB. However, further studies are needed to strengthen our observation that appropriate reliance upon chemotherapy to subsequently resect advanced HB could achieve the comparable survival to that of stage I HB.

© 2005 The WJG Press and Elsevier Inc. All rights reserved.

Key words: Chemotherapy; Children; Hepatitis B; Hepatoblastoma; Hepatocellular carcinoma

Chen JC, Chang ML, Lin JN, Lai HS, Chen CC, Chen WJ, Hung WT. Comparison of childhood hepatic malignancies in a hepatitis B hyper-endemic area. *World J Gastroenterol* 2005; 11(34): 5289-5294
http://www.wjgnet.com/1007-9327/11/5289.asp

INTRODUCTION

Hepatocellular carcinomas (HCC) and hepatoblastomas (HB) are the most common primary hepatic malignancies in children. The two malignancies usually receive identical management. In the literature dealing with the two tumors, the main emphasis has often been on facilitating surgical management by more effective chemotherapy[1,2]. However, the two malignancies have lots of basic differences. Physicians should take these differences into consideration during the diagnostic work-up, before therapy is instituted. Because the tumors are rare, comparisons of their clinical behaviors have rarely been made in any detail. This study enrolled children with HCC or HB at Chang Gung Children's Hospital (CGCH) and National Taiwan University Hospital (NTUH), two major medical centers in northern Taiwan. Its purpose was to examine the differences of the clinical behaviors of these two malignancies.

MATERIALS AND METHODS

We collected the cases of children with HCC or HB at CGCH and NTUH from 1979 to 1997. A total of 127 children were eligible for inclusion in this study. Their diagnosis was confirmed by tissue obtained from laparotomy or needle biopsy. There were 73 cases of HCC and 54 cases of HB. Demographic data included gender and age at diagnosis. Laboratory investigations included alpha-fetoprotein (AFP), hepatitis B surface antigen (HBsAg), and Child's grading. Anti-hepatitis C antibody was checked after 1990 only in 13 cases (9 HCC and 4 HB) and all had negative results. The Child's classification employed was a modified classification (Table 1) based upon encephalopathy, the sonographic finding of ascites, and the levels of albumin, bilirubin and prothrombin time prolongation[3]. By evaluating the five parameters, 1, 2, or 3 points were scored for increasing severity of each parameter measured. Those whose score totaled 5 or 6 were categorized in good-risk grade A, 7-9 in moderate-risk grade B and 10-15 in poor-risk grade C. Radiological examinations included plain chest films, sonography, computed tomography (CT), magnetic resonance imaging (MRI), or angiography. They were evaluated to define tumor extent with special emphasis on distant metastasis,

Table 1 Points scored for clinical and laboratory parameters in Pugh modification of Child's classification of liver disease severity

Clinical and laboratory parameters	Points scored		
	1	2	3
Hepatic encephalopathy[1]	None	Grade 1 or 2	Grade 3 or 4
Ascites	Absent	Slight	Moderate
Bilirubin (mg / dL)	<2	2-3	>3
Albumin (g / dL)	>3.5	2.8-3.5	<2.8
Prothrombin time prolongation (s)	1-4	4-10	>10

[1]Grade 0: normal consciousness, personality, neurological examination; Grade 1: restless, sleep disturbed, irritable / agitated, tremor, impaired hand writing; Grade 2: lethargic, time-disoriented, inappropriate, asterixis, ataxia; Grade 3: somnolent, stuporous, place-disoriented, hyperactive reflexes, rigidity; Grade 4: unrousable coma, no personality / behavior, decerebrate.

portal vein (PV) or inferior vena cava (IVC) thrombi, para-aortic lymphadenopathy, and hilar involvement. Those made tumors inadvisable to attempt from primary tumor extirpation. Chemotherapy would be administered only in the case of consent from the family. Its regimens were the combination of vincristine, cyclophosphamide, doxorubicin and 5-fluouracil before 1991[4]. Cisplatin (or carboplatin) and doxorubicin (or epirubicin) were substituted for the former regimens after 1991[1,2]. The resected specimens indicating the surgical surface and the location of sections were taken for microscopic examination to identify the presence or absence of tumor at the section margins. Cirrhosis was examined in all cases if possible. The histologic subtype of HB was also investigated. The two liver malignancies were staged according to intergroup staging system raised by Children's Cancer Group (CCG) and the Pediatric Oncology Group (POG)[5], mainly based upon the initial operative findings and procedure, and the final pathologic examination. Stage I: Completely resected at initial surgery. Stage II: Resection with microscopic residual disease at margin. Stage III: Unresectable, tumor spillage or resection with gross residual disease but not metastatic. Stage IV: Metastatic disease, regardless of the status of primary tumor.

Chi-square test was used to compare the proportions. When the sample size in a 2×2 table was 20 or less, Fisher's exact test was calculated. Student's *t* test was used to compare the means. As for survival analysis, the survival time was defined by estimating the length of time from the date of initial diagnosis to the event of interest or the date of last follow-up. A patient who died was considered to have experienced an event. Otherwise, the patient was considered censored at last follow-up. Plots of survival time were constructed by Kaplan-Meier method. The log rank test was employed to compare survival curves. Differences were regarded as significant if $P<0.05$.

RESULTS

The demographic characteristics and clinical features in this group of patients are summarized in Figure 1 and Table 2. The mean age (10.6 years) of HCC patients was significantly older than that (2.5 years) of HB patients ($P<0.001$). Both tumors were male predominant with a male to female ratio of 3.3:1 in HCC and 2.4:1 in HB, but the difference between them was not statistically significant ($P = 0.420$).

The AFP level was elevated in 54 of 55 HCC patients

Table 2 Summary of clinical characteristics, laboratory investigations, cirrhosis, primary resectability, chemotherapeutic conversion and tumor recurrence in children with hepatic malignancies

	Hepatocellular carcinoma	Hepatoblastoma	*P*
Mean age in yr (SD)	10.6 (3.3)	2.5 (3.5)	<0.001[2]
Median age in yr	11.3	1.0	
Sex			0.420
Male	56	38	
Female	17	16	
Serum alpha fetoprotein			0.299[1]
≤20 ng / mL	1	3	
>20 ng / mL	54	34	
Hepatitis B carrier			<0.001
Yes	56	4	
No	0	31	
Child's classification			0.673
A	41	29	
B	14	8	
Liver cirrhosis			<0.001
Yes	26	0	
No	14	30	
Primary complete resection			0.285
Yes	12	13	
No	61	41	
Tumor recurrence after resection			0.041[1]
Yes	7	2	
No	5	11	
Complete resection after chemotherapy			<0.001
Yes	0	12	
No	14	6	

[1]Fisher's exact test and [2]Two samples, independent-groups *t* test.

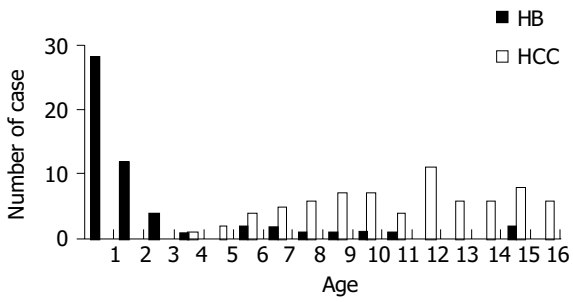


Figure 1 Age distribution of childhood hepatocellular carcinomas (HCC) and hepatoblastomas (HB).

and 34 of 37 HB patients ($P = 0.299$). Among them, 66.7% of those with HCC and 61.8% of those with HB had the AFP level of more than 35 000 ng/mL. HBsAg was tested in 56 HCC patients and 35 HB patients. There was a significantly higher rate of positivity for HBsAg in HCC patients (100% *vs* 11.4%; $P<0.001$). Among 55 HCC patients and 37 HB patients whose tumors could be completely graded by modified Child's classification, 41 HCC patients and 29 HB patients were in Child's group A, 14 HCC patients and 8 HB patients in Child's group B, and no patients in Child's group C. Both tumors appeared to have a Child's A predominance in an A to B ratio of 2.9:1 for HCC and 3.6:1 for HB without a statistically significant difference ($P = 0.673$).

There were 19 HCC patients and 11 HB patients with lung metastasis at diagnosis. Additional brain metastasis was found in 1 HCC patient and additional skin metastasis in 1 HB patient. Radiological images of 94 patients (56 with HCC and 38 with HB) were available for review of tumor extent and invasiveness. A summary of these findings that were compared between HCC and HB is listed in Table 3. The variables to reach statistical significance were PV invasion (39.3% *vs* 13.2%; $P = 0.006$) and para-aortic lymphadenopathy (17.9% *vs* 2.6%; $P = 0.026$).

Cumulative survival curves for patients with liver malignancies in each intergroup stage are shown in Figure 2. Resection with a histologically clear margin (stage I) could be achieved in 12 HCC patients and 13 HB patients, contributing to primary resectability rates of 16.4% and 24.1%, respectively (Table 2, $P = 0.285$). Adjuvant chemotherapy was administered postoperatively to 2 HCC patients and 11 HB patients. However, intrahepatic recurrence ensued in 7 HCC patients (1 with chemotherapy) and 2 HB patients (both with chemotherapy). Therefore, HCC posed a higher recurrence rate than HB after curative resection (Table 2, 58.3% *vs* 15.4%; $P = 0.041$). Repeated hepatectomy could only be performed in 2 HCC patients, one of whom remained alive at last follow-up exam (184 mo). Conclusively, stage I HB compared favorably in survival with stage I HCC with the 5-year survival rate of 32.4% for HCC and 82.5% for HB by the Kaplan-Meier survival curves ($P = 0.0183$). As for stage II tumor, there was none for HCC but 4 for HB. All the 4 HB patients died of recurrence, despite postoperative chemotherapy in one. Stage III disease was found in 42 HCC and 26 HB, which included 5 ruptured HCC and 1 ruptured HB on account of potential tumor spillage into the peritoneal cavity. Stage IV disease consisted of 19 HCC and 11 HB as evidenced by distant metastasis at diagnosis. Due to the heterogenous management for those advanced tumors (III and IV) ranging from no treatment, chemotherapy

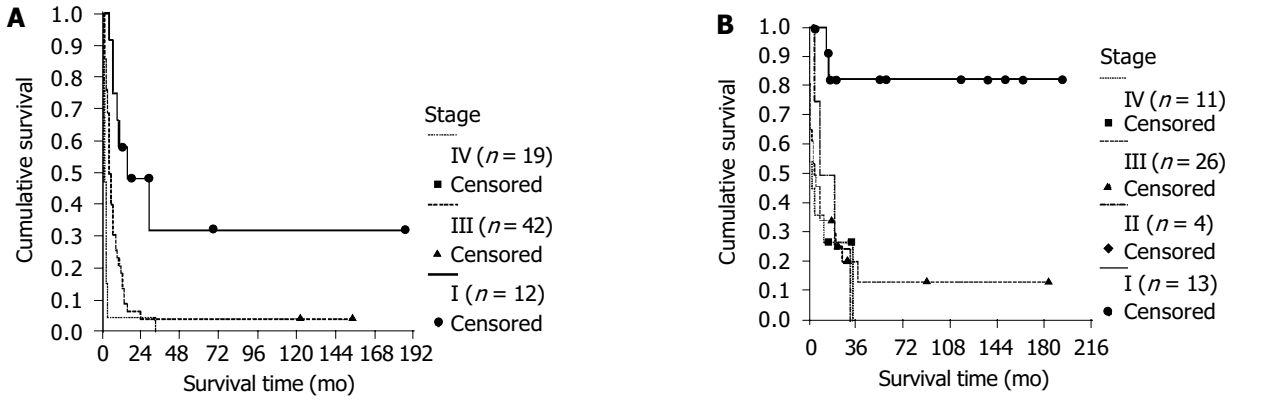


Figure 2 Cumulative survival curves for patients with liver malignancies in each intergroup stage. **A**: HCC (I *vs* III, $P = 0.0011$; III *vs* VI, $P = 0.0002$; log rank test); **B**: HB (I *vs* II, $P = 0.0019$; II *vs* III, $P = 0.8783$; III *vs* VI, $P = 0.5365$; log rank test).

Table 3 Summary of tumor extent and invasiveness on imaging studies of children with hepatic malignancies

	Hepatocellular carcinoma (%)	Hepatoblastoma (%)	*P*
Bilobar involvement	38/56 (67.9)	20/38 (52.6)	0.136
Portal vein invasion	22/56 (39.3)	5/38 (13.2)	0.006
Inferior vena cava invasion	8/56 (14.3)	3/38 (7.9)	0.516[1]
Para-aortic lymphadenopathy	10/56 (17.9)	1/38 (2.6)	0.026[1]
Hepatic hilum involvement	3/56 (5.4)	2/38 (5.3)	1.000[1]
Distant metastasis at diagnosis	19/73 (26.0)	11/54 (20.4)	0.458

[1]Fisher's exact test.

alone, resection after chemotherapeutic conversion to resection with adjuvant chemotherapy, the comparison of survivals between HCC and HB within the same stage could not be free from bias. However, in view of the survivals of HCC or HB patients in different stages shown in Figure 2, differences among the curves of stages I, III and IV HCC could reach statistical significance (I *vs* III, $P = 0.0011$; III *vs* VI, $P = 0.0002$). As regards HB, this difference of survival curves was only seen between stages I and II ($P = 0.0019$) but not among stages II, III and VI (II *vs* III, $P = 0.8783$; III *vs* VI, $P = 0.5365$).

In consideration of advanced tumors (III & IV), 38 HCC and 15 HB were left untreated. There were 14 HCC and 18 HB receiving intensive chemotherapy with the successful conversion into delayed complete resection in 12 of 18 HB but none of 14 HCC (Table 2, $P<0.001$). It contributed to the overall HB resectability of 46.3%, which compared favorably with that of HCC ($P<0.001$). Statistically, the survival difference between 13 stage I HB and 12 advanced HB with delayed complete resection after chemotherapy was of borderline insignificance ($P = 0.0507$). The remaining patients whose tumors failed to be chemotherapeutically converted (14 HCC and 6 HB) eventually succumbed to disease progression. It was found that advanced HB with unsuccessful conversion by chemotherapy had the significantly better survival than HB untreated (Figure 3, $P = 0.0015$) However, this beneficial effect of chemotherapy could not favor advanced HCC (Figure 3, $P = 0.0690$). HCC either with chemotherapy only or untreated had the better survival experience than HB untreated (Figure 3, $P = 0.0015$ and 0.0040, respectively). However, the differences of survivals could not reach statistical significance when compared with HB with chemotherapy only (Figure 3, $P = 0.8139$ and 0.0718, respectively).

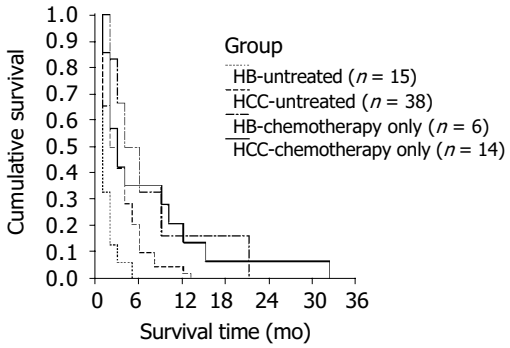


Figure 3 Cumulative survival curves for eventually unresected HCC and HB (stages III and IV). HB-untreated compared poorly in survival with HB-chemotherapy only, HCC-untreated and HCC-chemotherapy only ($P = 0.0015$, 0.0040 and 0.0015; log rank test).

Among 40 HCC specimens and 30 HB specimens available for pathologic evaluation, liver cirrhosis was demonstrated in 65.0% of HCC but none of HB (Table 2, $P<0.001$). It made no difference of sex ratio between cirrhotic and non-cirrhotic HCC ($P = 0.281$). There were 15 children whose HCC resection stayed margin-free (including 5 ruptured HCC). Of them, 6 had cirrhotic HCC and all succumbed to intrahepatic recurrence. HCC recurrence after complete resection was statistically associated with the presence of cirrhosis ($P = 0.007$). The survival of non-cirrhotic resected HCC was significantly better than cirrhotic resected HCC (Figure not shown, $P = 0.0209$). Among 22 resectable HB whose histologic subtypes could be traced, there were 13 with mixed epithelial-mesenchymal component and 9 with epithelial component, including mixed fetal and embryonal types in 3, pure fetal type in 2, embryonal type in 2 and macrotrabecular type in 2. Given the small number of HB patients in whom the histologic subtypes were known, comparisons of survivals between different histologic subtypes could not be done.

DISCUSSION

As shown in this study, childhood HCC and HB could be generally differentiated by some clinical data such as age, the status of hepatitis B virus (HBV) and the findings of imaging studies. HCC was mostly found in school age children, whereas HB was mainly diagnosed in infancy and rarely occurred after 3 years of age. The age distribution of HCC was somewhat skewing to the left with the peak age at around 12 years (Figure 1). It was in sharp contrast to the figure reported from Exelby *et al*., in which there are two age peaks, one below 4 years and a second peak between 12 and 15 years[6]. However, the age distribution of HB showed great resemblance to that of Exelby's series[6], looking rather asymmetric and skewing to the right (Figure 1). Imaging studies disclosed that HCC was more inclined to invade the PV and para-aortic lymph nodes than HB. As for AFP, its level was often extremely high, but not a reliable test to differentiate HCC from HB. However, it was a good marker for monitoring recurrence if its preoperative level was high.

In this series, HBV infection was found in 100% of the HCC patients who had been examined for HBsAg. A positive HBsAg status has long since been a critical marker for children with HCC in Taiwan[7]. As a hyper-endemic area of HBV infection, Taiwan launched a nationwide hepatitis B vaccination in 1984. After a 10-year universal immunization, evidence showed that this program has effectively reduced both the HBV carrier rate[8] and the incidence of HCC in children[9]. As for hepatitis C virus (HCV), it has also been etiologically linked with HCC development[10]. Since specific serologic tests for HCV became available in 1989[11], only 13 cases in this cohort study have been checked for HCV and all showed negative results. Based upon the limited data, it was hard to conclude a causal relationship between HCV and childhood hepatic malignancies. Despite a low seroprevalence of HCV infection in children, HCV can be transmitted to infants and children either perinatally or through blood transfusion[12]. However, the progression from chronic hepatitis to cirrhosis and sometimes to HCC is most commonly a slow and silent process. It may take about 30 and occasionally even more years to reach its end point[10,13]. Therefore, those infected by HCV in childhood may be at risk of developing HCC at their young adult age. This may explain why HCV-related HCC has never been reported in children in spite of overwhelming evidence indicating a strong correlation

between HCV and HCC in adults.

In the Western countries, childhood HCC does not differ from the adult counterpart in terms of gross and microscopic features, except in the lack of an association with cirrhosis in most childhood HCC[14]. We had found that liver cirrhosis occurred in 65% of HCC children, comparable to adult cases (70%) in Taiwan[15], while cirrhotic HB was never seen in this series. Undoubtedly, this strong association between childhood HCC and cirrhosis could be attributed to the preceding HBV infection. Cirrhosis represented as a pessimistic histologic feature with a worse outcome for resected HCC in adults[16] and children, as evidenced by inevitable intrahepatic recurrence. Although HCC in both adults and children are frequently associated with liver cirrhosis, it is well recognized that adult patients more frequently decompensate or develop liver failure, if an overaggressive resection for cirrhotic HCC is attempted[17]. Hence, it has been suggested that hepatectomy be performed in cirrhotic adult patients who have good-risk Child's A grading[18]. In considering the resection of childhood liver malignancies, liver function is rarely an unfavorable factor. Child's A group accounted for over 70% in both types of tumors but Child's C group was never observed in this series. Why liver function was better preserved in childhood liver malignancies was not well explained. However, it might have been due to a short duration of cirrhotic HCC[17] and low incidence of cirrhotic HB in children.

Complete resection of liver malignancies is the only therapeutic modality that could offer patients long-term survival or even a cure[6,19,20]. Primary resection could be achieved only in 16.4% of HCC and 24.1% of HB mainly because most liver malignancies presented with distant metastasis, PV thrombi, IVC thrombi, para-aortic lymphadenopathy, or hepatic hilar invasion at the time of diagnosis. Bilobar involvement was not always a hindrance to complete resection unless resection required compromise of critical vessels. Although HCC was more inclined to invade the PV and para-aortic lymph nodes in comparison with HB, this made no difference between the two tumors' primary resectabilities. Tumor recurrence is the major cause of unsatisfactory results in adults with resectable HCC, occurring in around 50% of cases[21]. A rather pessimistic background was observed in childhood HCC. Even with a successful resection, tumor recurrence in this series happened in over half of the HCC patients but only in 15% of the HB patients. Due to the higher intrahepatic recurrence of HCC, stage I HCC compared poorly in survival with stage I HB. Although repeated hepatectomy has been considered to remain the best treatment for tumor recurrence[21], it could only benefit two of 11 recurrent HCC in this series.

Our data were not sufficient to conclude the necessity of postoperative chemotherapy for stage I disease. However, HCC compared poorly with HB in response to chemotherapy. A better response of HB to chemotherapy might be attributed to the higher proliferation rate of HB[22]. This could, on the other hand, reflect a more ominous natural course of disease as evidenced by the fact that if untreated, advanced HB apparently had a worse survival experience than advanced HCC. It was reported that delayed resection for childhood HCC after combined chemotherapy was the rare exceptions[1,4,20]. We even never experienced any successful conversion of unresectable HCC by chemotherapy for these years despite the higher incidence of HCC in Taiwan. In contrast, we had 66.7% of successful rate to use chemotherapy as a detour leading to complete resection for initially unresectable HB. Even if chemotherapy failed to facilitate resection, it could substantially bring advanced HB to better survivals when compared with untreated HB.

The stage of tumors was reported as the most important criterion for determining the prognosis of HCC and HB in children[23]. In this study, stage I HCC or HB still represented the best prognosis. However, the differences among the survival curves of stages II-IV HB became indistinguishable from one another due to delayed complete resection of advanced HB, which had become an attainable goal since the advent of chemotherapy. Another important issue in dealing with an advanced HB was whether the survival of those tumors with delayed complete resection could catch up with that of stage I HB. As we knew, diagnostic imaging studies are important in assessing the resectability of hepatic malignancies. Although better imaging techniques have improved the accuracy, they do not provide an absolutely reliable evaluation of resectability. The error rate may reach 20% with a combination of sonography and either CT or MRI[24]. Whenever there is the indeterminable resectability of HB on imaging studies, pediatric surgeons will be in a dilemma as to whether they should show boundless enthusiasm for an aggressive surgical approach or rely upon preoperative chemotherapy to subsequently perform a delayed resection. We found that the survival difference between stage I HB and advanced HB resected after chemotherapy could only reach borderline insignificance with a P value of 0.0507. Although it was not solid enough in consideration of survival to support appropriate reliance upon chemotherapy in advance to deal with a potentially risky surgical problem for strategically located HB, this approach could render a delayed but safe hepatectomy with less blood loss, minimal operative complications and more substantial preservation of normal hepatic tissue[25]. There was also evidence showing that if an attempted primary resection for HB ended up as incompleteness and was then boosted by postoperative chemotherapy, such a therapeutic modality did not necessarily achieve a more favorable outcome than initial chemotherapy with delayed resection[26]. Thus, the therapeutic philosophy of "stage creep" from the enrollment of more stage III HB and then preoperative reliance upon chemotherapeutic cytoreduction can be justified in some aspects, but requires further investigations for its impact on survival. As for strategically located HCC, pediatric surgeons should show the enthusiasm for aggressive surgical intervention in view of their unresponsiveness to chemotherapy because primary resection of HCC is undoubtedly the only chance for a cure or long-term survival. Although liver transplantation can be an alternative for advanced HCC[27], it was rarely pursued in Taiwan due to unfavorable factors including large tumor size, nearly absolute HBV carrier status, nonfibrolamellar histology, and a high frequency of local and metastatic spread[17].

REFERENCES

1 **King DR,** Ortega J, Campbell J, Haas JE, Ablin AR, Lloyd D, Newman K, Quinn J, Krailo M, Feusner J, Hammond D. The

surgical management of children with incompletely resected hepatic cancer is facilitated by intensive chemotherapy. *J Pediatr Surg* 1991; **26**: 1074-1081

2 **Ortega JA,** Krailo MD, Haas JE, King DR, Ablin AR, Quinn JJ, Feusner J, Campbell JR, Lloyd DA, Cherlow J. Effective treatment of unresectable or metastatic hepatoblastoma with cisplatin and continuous infusion doxorubicin chemotherapy: a report from the Children's Cancer Study Group. *J Clin Oncol* 1991; **9**: 2167-2176

3 **Pugh RNH,** Murray-Lyon IM, Dawson JL, Pietroni MC, Williams R. Transection of the oesophagus for bleeding oesophageal varices. *Br J Surg* 1973; **60**: 646-649

4 **Evans AE,** Land VJ, Newton WA, Randolph JG, Sather HN, Tefft M. Combination chemotherapy (vincristine, adriamycin, cyclophosphamide, and 5-fluorouracil) in the treatment of children with malignant hepatoma. *Cancer* 1982; **50**: 821-826

5 Children's Cancer Group-8881. *Intergroup protocol for the treatment of childhood hepatoblastoma and hepatocellular carcinoma*, Arcadia, Calif, 1989, Children's Cancer Group

6 **Exelby PR,** Filler RM, Grosfeld JL. Liver tumors in children in the particular reference to hepatoblastoma and hepatocellular carcinoma: American Academy of Pediatrics Surgical Section Survey-1974. *J Pediatr Surg* 1975; **10**: 329-337

7 **Chen WJ,** Lee JC, Hung WT. Primary malignant tumor of liver in infants and children in Taiwan. *J Pediatr Surg* 1988; **23**: 457-461

8 **Chen HL,** Chang MH, Ni YH, Hsu HY, Lee PI, Lee CY, Chen DS. Seroepidemiology of hepatitis B virus infection in children: ten years of mass vaccination in Taiwan. *JAMA* 1996; **276**: 906-908

9 **Chang MH,** Chen CJ, Lai MS, Hsu HM, Wu TC, Kong MS, Liang DC, Shau WY, Chen DS. Universal hepatitis B vaccination in Taiwan and the incidence of hepatocellular carcinoma in children. *N Engl J Med* 1997; **336**: 1855-1859

10 **Kiyosawa K,** Sodeyama T, Tanaka E, Gibo Y, Yoshizawa K, Nakano Y, Furuta S, Akahane Y, Nishioka K, Purcell RH. Interrelationship of blood transfusion, non-A, non-B hepatitis and hepatocellular carcinoma: analysis by detection of antibody to hepatitis C virus. *Hepatology* 1990; **12**: 671-675

11 **Kuo G,** Choo QL, Alter HJ, Gitnick GL, Redeker AG, Purcell RH, Miyamura T, Dienstag JL, Alter MJ, Stevens CE. An assay for circulating antibodies to a major etiologic virus of human non-A, non-B hepatitis. *Science* 1989; **244**: 362-364

12 American Academy of Pediatrics. Committee on Infectious Diseases: Hepatitis C virus infection. *Pediatrics* 1998; **101**: 481-485

13 **Tong MJ,** El-Farra NS, Reikes AR, Co RL. Clinical outcomes after transfusion-associated hepatitis C. *N Engl J Med* 1995; **332**: 1463-1466

14 **Weinberg AG,** Finegold MJ. Primary hepatic tumors of childhood. *Hum Pathol* 1983; **14**: 512-537

15 **Beasley RP,** Hwang LY, Lin CC, Chien CS. Hepatocellular carcinoma and hepatitis B virus: a prospective study of 22, 707 men in Taiwan. *Lancet* 1981; **2**: 1129-1133

16 **Hsu HC,** Wu TT, Wu MZ, Sheu JC, Lee CS, Chen DS. Tumor invasiveness and prognosis in resected hepatocellular carcinoma: clinical and pathogenetic implications. *Cancer* 1988; **61**: 2095-2099

17 **Chen JC,** Chen CC, Chen WJ, Lai HS, Hung WT, Lee PH. Hepatocellular carcinoma in children: clinical review and comparison with adult cases. *J Pediatr Surg* 1998; **33**: 1350-1354

18 **Kubota K,** Makuuchi M, Kusaka K, Kobayashi T, Miki K, Hasegawa K, Harihara Y, Takayama T. Measurement of liver volume and hepatic function reserve as a guide to decision-making in resectional surgery for hepatic tumors. *Hepatology* 1997; **26**: 1176-1181

19 **Randolph JG,** Altman RP, Arensman RM, Matlak ME, Leikin SL. Liver resection in children with hepatic neoplasms. *Ann Surg* 1978; **187**: 599-605

20 **Pazdur R,** Bready B, Cangir A. Pediatric hepatic tumors: clinical trials conducted in the United States. *J Surg Oncol Suppl* 1993; **3**: 127-130

21 **Lee PH,** Lin WJ, Tsang YM, Hu RH, Sheu JC, Lai MY, Hsu HC, May W, Lee CS. Clinical management of recurrent hepatocellular carcinoma. *Ann Surg* 1995; **222**: 670-676

22 **Sakairi T,** Kobayashi K, Goto K, Okada M, Kusakabe M, Tsuchiya T, Sugimoto J, Sano F, Mutai M. Greater expression of transforming growth factor alpha and proliferating cell nuclear antigen staining in mouse hepatoblastomas and hepatocellular carcinomas induced by a diethylnitrosamine-sodium phenobarbital regimen. *Toxicol Pathol* 2001; **29**: 479-482

23 **Stocker JT.** An approach to handling pediatric liver tumors. *Am J Clin Pathol* 1998; **109**(Suppl 1): S67-72

24 **von Schweinitz D,** Burger D, Mildenberger H. Is laparotomy the first step in treatment of childhood liver tumors? The experience from the German Cooperative Pediatric Liver Tumor Study HB-89. *Eur J Pediatr Surg* 1994; **4**: 82-86

25 **Seo T,** Ando H, Watanabe Y, Harada T, Ito F, Kaneko K, Horibe K, Sugito T, Ito T. Treatment of hepatoblastoma: less extensive hepatectomy after effective preoperative chemotherapy with cisplatin and adriamycin. *Surgery* 1998; **123**: 407-414

26 **von Schweinitz D,** Hecker H, Harms D, Bode U, Weinel P, Burger D, Erttmann R, Mildenberger H. Complete resection before development of drug resistance is essential for survival from advanced hepatoblastoma-a report from the Germany Cooperative Pediatric Liver Tumor Study HB-89. *J Pediatr Surg* 1995; **30**: 845-852

27 **Tagge EP,** Tagge DU, Reyes J, Tzakis A, Iwatsuki S, Starzl TE, Wiener ES. Resection, including transplantation, for hepatoblastoma and hepatocellular carcinoma: impact on survival. *J Pediatr Surg* 1992; **27**: 292-297

Science Editor Guo SY **Language Editor** Elsevier HK

PO Box 2345, Beijing 100023, China
www.wjgnet.com
wjg@wjgnet.com

ELSEVIER

World J Gastroenterol 2005;11(34):5295-5302
World Journal of Gastroenterology ISSN 1007-9327
© 2005 The WJG Press and Elsevier Inc. All rights reserved.

• *BASIC RESEARCH* •

Liver-directed gene expression employing synthetic transcriptional control units

Marie-Luise Lemken, Wolfgang A. Wybranietz, Ulrike Schmidt, Florian Graepler, Sorin Armeanu, Michael Bitzer, Ulrich M. Lauer

Marie-Luise Lemken, Wolfgang A. Wybranietz, Ulrike Schmidt, Florian Graepler, Sorin Armeanu, Michael Bitzer, Ulrich M. Lauer, Department of Internal Medicine I, University Clinic Tübingen, D-72076 Tübingen, Germany
Supported by German Research Foundation (LA 649/11-1); Fortüne-program of the Medical Faculty of the Eberhard-Karls-University Tübingen (F.128101.1); Scholarship from the Pinguin Foundation (Henkel KGaA)
Correspondence to: Ulrich M. Lauer, Department of Internal Medicine I, Medical University Clinic Tübingen, Otfried-Müller-Str. 10, D-72076 Tübingen, Germany. ulrich.lauer@uni-tuebingen.de
Telephone: +49-7071-29-83189 Fax: +49-7071-29-5692
Received: 2004-09-29 Accepted: 2004-10-26

Abstract

AIM: To generate and characterize the synthetic transcriptional control units for transcriptional targeting of the liver, thereby compensating for the lack of specificity of currently available gene therapeutic vector systems.

METHODS: Synthetic transcriptional control unit constructs were generated and analyzed for transcriptional activities in different cell types by FACS quantification, semi-quantitative RT-PCR, and Western blotting.

RESULTS: A new bifunctionally-enhanced green fluorescent protein (EGFP)/neo^r fusion gene cassette was generated, and could flexibly be used both for transcript quantification and for selection of stable cell clones. Then, numerous synthetic transcriptional control units consisting of a minimal promoter linked to "naturally" derived composite enhancer elements from liver-specific expressed genes or binding sites of liver-specific transcription factors were inserted upstream of this reporter cassette. Following liposome-mediated transfection, EGFP reporter protein quantification by FACS analysis identified constructs encoding multimerized composite elements of the apolipoprotein B100 (ApoB) promoter or the ornithin transcarbamoylase (OTC) enhancer to exhibit maximum transcriptional activities in liver originating cell lines, but only background levels in non-liver originating cell lines. In contrast, constructs encoding only singular binding sites of liver-specific transcription factors, namely hepatocyte nuclear factor (HNF)1, HNF3, HNF4, HNF5, or CAAT/enhancer binding protein (C/EBP) only achieved background levels of EGFP expression. Finally, both semi-quantitative RT-PCR and Western blotting analysis of Hep3B cells demonstrated maximum transcriptional activities for a multimeric 4xApoB cassette construct, which fully complied with the data obtained by initial FACS analysis.

CONCLUSION: Synthetic transcriptional control unit constructs not only exhibit a superb degree of structural compactness, but also provide new means for liver-directed expression of therapeutic genes.

© 2005 The WJG Press and Elsevier Inc. All rights reserved.

Key words: Liver gene therapy; Hepatoma gene therapy; Liver-directed gene expression; Synthetic liver-specific promoters

Lemken ML, Wybranietz WA, Schmidt U, Graepler F, Armeanu S, Bitzer M, Lauer UM. Liver-directed gene expression employing synthetic transcriptional control units. *World J Gastroenterol* 2005; 11(34): 5295-5302
http://www.wjgnet.com/1007-9327/11/5295.asp

INTRODUCTION

One of the major challenges in liver gene therapy is the achievement of hepato-specific therapeutic gene expression[1,2]. In general, transcriptional targeting is highly desirable for all *in vivo* gene therapy applications as it can prevent expression of the transgene in non-target cells, thus mimicking physiological regulation[3-5].

For the liver, numerous approaches to incorporate house-keeping cellular promoters or organ-specific regulatory sequences into retroviral, lentiviral or adenoviral vectors have been reported so far[6-8], with variable and repeatedly disappointing results. On one hand, the level of expression does not approach that of strong viral promoters such as human cytomegalovirus immediate early gene (hCMV IE) promoter. On the other hand, a functional tissue specificity only rarely has been demonstrated. As a consequence, the search for effective liver-restricted promoters has been extended to intensive screening of liver-expressed sequence tag (EST)-libraries still awaiting breakthrough[9,10].

For these reasons, promoter units providing sufficient transcriptional activity and concomitantly also tissue specificity still are required. Such promoter units can be built up synthetically on so-called minimal promoters, providing a basic/minimal transcriptional activity, which are combined with enhancer elements of either natural or synthetic origin being composed of suitable transcription factor binding sites (TFBS). This alternative approach should enable both a high degree of structural compactness and a

high degree of liver specificity[11-13].

We here report the results of a comparative study addressing this issue. We employed a minimal core promoter derived from the Herpes simplex virus thymidine kinase promoter (HSV TK-37) which was combined in various arrangements with either "naturally" derived composite enhancer elements from liver-specific expressed house-keeping ally genes or binding sites for transcription factors guiding expression of liver-specific genes.

The enhancer elements of natural origin employed in this work were from the liver-specific human apolipoprotein B100 (ApoB) gene promoter which is located upstream at the region -109-55 of the transcription start site and exhibits binding sites for liver-specific transcription factors HNF1, HNF3, HNF5, CAAT/enhancer binding protein (C/EBP)[14-16] and from the liver-specific enhancer of the rat ornithine transcarbamoylase (OTC) gene promoter which is located 11 kbp upstream of the transcription start site and exhibits binding sites for liver-specific transcription factors HNF4 and C/EBP[17].

Sequences for single binding sites for liver-specific transcription factors were taken from the human albumin gene promoter (TFBS sequences for HNF1 and C/EBP[18]) and from the ApoB gene promoter (TFBS sequences for HNF3/4/5[14-16]).

All newly generated constructs were analyzed for transcriptional activity in different cell types in cell culture.

MATERIALS AND METHODS

Basic minimal HSV TK-37 core promoter construct

All synthetic transcriptional control unit constructs were based on a Herpes simplex virus thymidine kinase derived minimal core promoter (HSV TK-37), which only comprises the RNA initiation site and 37 upstream base pairs[19]. As a basic construct for the generation of new reporter plasmids, we used plasmid pTK-37CAT, in which the HSV TK-37 minimal core promoter drives expression of the chloramphenicol acetyltransferase (CAT) reporter gene[20].

Generation of a new fusion reporter gene EGFP/neo^r

Plasmid pEGFP-C1 (BD Biosciences Clontech, Heidelberg, Germany) facilitating the creation of protein fusions to the C-terminus of enhanced green fluorescent protein (EGFP), which constitutes a human codon-optimized cDNA of GFP[21, 22] was used to generate a new EGFP/neo^r fusion reporter gene. For this purpose, the neomycin aminoglycoside phosphotransferase coding sequence of transposon 5 (i.e., neomycin resistance - neo^r) was cut out of plasmid pNEO (Pharmacia, Freiburg, Germany) and inserted in frame downstream of the EGFP coding sequence. This EGFP/neo^r fusion gene was cut out and used for exchange with the CAT coding sequence in pTK-37CAT, thus a new reporter construct pGreeN (i.e., encoding the "GreeN(eo) fusion") was yielded. Since expression of EGFP in pEGFP-C1 is driven by the strong, constitutive hCMV IE promoter, this vector was used also as a simple transfection marker for all cell lines of interest.

Generation of synthetic transcriptional control unit constructs

Since pGreeN was designed to exhibit a multiple cloning site (MCS) upstream of the HSV TK-37 minimal core promoter, insertion of composite enhancer elements from liver-specifically expressed genes or TFBS sequences via *Bam*HI and *Bgl*II endonuclease restriction sites was facilitated. Insertion of complementary oligonucleotides encoding the binding sites of liver-specific transcription factors, namely hepatocyte nuclear factor 1 (HNF1; TFBS sequence originating from the human albumin gene promoter), hepatocyte nuclear factors 3/4/5 (HNF3/4/5; TFBS sequences all originating from the human apolipoprotein B100 gene promoter), C/EBP (TFBS sequence originating from the human albumin gene promoter) led to the generation of synthetic transcriptional control unit constructs p1×HNF1-GreeN, p3×HNF1-GreeN (exhibiting three consecutive HNF1 TFBS), p1×HNF3-GreeN, p1xHNF4-GreeN, p1×HNF5-GreeN, p1×C/EBP-GreeN, respectively. Insertion of "natural" composite enhancer elements being important for liver-specific expression of the ApoB gene (60 bp; encoding TFBS for HNF3, HNF4, HNF5, and C/EBP) or the OTC gene (52 bp; encoding TFBS for HNF4 and C/EBP) also was inserted upstream of the HSV TK-37 minimal core promoter giving rise to synthetic transcriptional control unit constructs p1×ApoB-GreeN and p1×OTC-GreeN (Figure 1; first lines of upper and middle panel). Finally, plasmids encoding up to 16 monotype ApoB cassettes (Figure 1; upper panel), up to 16 monotype OTC cassettes (Figure 1; middle panel), and mixed ApoB/OTC cassettes (Figure 1; lower panel; exhibiting up to 4 mixed ApoB and OTC units) were constructed. All PCR-derived segments/constructs were sequenced thereby confirming their predicted composition (More detailed information about the construction process is available from the authors upon request).

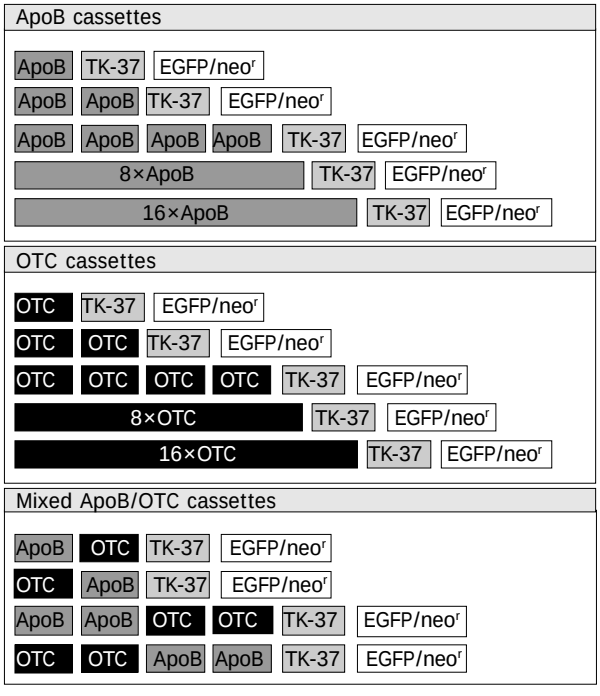


Figure 1 Schematic representation of synthetic transcriptional control unit constructs.

Cell culture

Cell lines HepG2 (human hepatocellular carcinoma), Hep3B (human hepatocellular carcinoma), HeLa (human cervix carcinoma), HEK293 (human embryonic kidney) all were purchased from the European Collection of Cell Cultures (ECACC). Cell line HuH7 (human hepatocellular carcinoma) was generated originally and provided by Nakabayashi[23]. All cell lines were grown in Dulbecco's modified Eagle's medium (DMEM) supplemented with 10% fetal calf serum (FCS) at 37 ¡æin 50 mL/L CO_2. No antibiotics were added.

Transfection experiments

Cells were plated at 3×10^5 cells/well into 6-well trays (Falcon-Becton Dickinson Labware, Franklin Lakes, NJ, USA) and transfected 24 h later with 2 µg DNA complexed with either the multi-component lipid-based FuGENE 6™ transfection reagent (Roche Diagnostics, Mannheim, Germany), the cationic lipid reagent Lipofectamine™ 2000 (Invitrogen, Karlsruhe, Germany), the 1:1 (w/w) DOTMA/DOPE liposome Lipofection™ reagent (Invitrogen), the polycationic DOSPER™ reagent (Boehringer, Mannheim, Germany), or the monocationic cholesterol DAC-30™ reagent (Eurogentec, Seraing, Belgium), according to the protocols of the manufacturers. To determine the transfection efficiencies, two separate transfections with samples were performed in triplicates, respectively.

Flow cytometry

Forty-eight hours after transfection, cells were washed with PBS, trypsinized and spun by centrifugation at 1200 r/min for 2 min. Cell pellets were resuspended in 500 µL PBS. The percentage of EGFP expressing cells was calculated by FACS analysis using the FL1-H profile employing a flow cytometer (FACS Calibur™, BD Biosystems, Heidelberg, Germany) with the CellQuest software according to the manufacturer's instructions. To standardize the transfection efficiencies, all cell lines obtained underwent triple transfections with hCMV IE-driven control plasmid pEGFP-C1. The resulting pEGFP-C1-mediated mean EGFP positive cells were set to 100%; EGFP positive cells obtained by transfection with synthetic transcriptional control unit constructs were set in relation to this EGFP standard level, thereby defining the ratio of relative EGFP expression. Data plotted represented the mean ± SD of two separate transfections performed in triplicates, respectively.

Reverse transcription and semi-quantitative PCR

Total RNA was extracted 48 h after transfection with the NucleoSpin RNA II kit (Macherey Nagel, Düren, Germany). Reverse transcription was performed using the SuperScript™ II RT kit (Invitrogen, Karlsruhe, Germany). Semi-quantitative PCR analysis was done using the Taq DNA polymerase kit (QIAGEN, Hilden, Germany). All protocols were performed according to the manufacturer's instructions. The sequences of primers for semi-quantitative PCR are as follows. The 5' primer for amplification of the EGFP gene is 5'-ATG GTG AGC AAG GGC GAG GAG CTG TTC-3' and the 3' primer is 5'-CTT GTA CAG CTC GTC CAT GCC GAG AGT-3', giving rise to a specific band of 717 bp; the 5' primer for amplification of the α-tubulin house-keeping gene (used as an internal standard) is 5'-ATG CCA AGC GTG CCT TTG TTC ACT GGT AC-3' and the 3' primer is 5'-GAA ATT CTG GGA GCA TGA CAT GCT GCA G -3', giving rise to a specific band of 208 bp.

Western blot

Forty-eight hours after transfection, cells were washed in PBS and trypsinized, proteins were extracted with 120 µL lysis buffer (50 mmol/L Tris-HCl, 150 mmol/L NaCl, 1% Nonidet P-40, 200 mmol/L PMSF). Then 50 µL of cell lysates was loaded onto a 10% SDS polyacrylamide gel and separated by electrophoresis and transferred to a polyvinylidene difluoride membrane (Amersham Pharmacia Biotech, Freiburg, Germany). After the non-specific binding sites were blocked with 5% non-fat milk in TBS-T (10 mmol/L Tris-HCl, 150 mmol/L NaCl with 0.05% Tween20) overnight at 4 ¡æ; the membrane was incubated for 3 h with monoclonal mouse anti-α-tubulin antibody (Sigma, Saint Louis, USA) and monoclonal mouse anti-GFP antibody (Roche Applied Science, Indianapolis, USA). Proteins were visualized using horseradish peroxidase-conjugated anti-mouse antibody (BioRad, Hercules, USA) diluted in TBS for 45 min at room temperature followed by enhanced chemoluminescence (ECL; Amersham Pharmacia Biotech, Freiburg, Germany).

RESULTS

Generation of a new EGFP/neo^r fusion reporter gene

To facilitate both the quantification of transcriptional activities of newly designed synthetic transcriptional control cassettes and the selection of stable cell clones transfected with such constructs, a new bifunctional EGFP/neo^r fusion gene cassette was generated. Employing plasmid pEGFP-C1, a neomycin aminoglycoside phosphotransferase coding sequence, was linked in frame downstream of the EGFP coding sequence. Subsequently, this EGFP/neo^r fusion gene was cut out and used for exchange with the CAT coding sequence encoded in reporter plasmid pTK-37CAT[20], yielding the new reporter construct pGreeN, which also exhibits a multiple cloning site (MCS) upstream of the HSV TK-37 minimal core promoter.

Generation of synthetic transcriptional control unit constructs

New reporter construct pGreeN was used to generate synthetic transcriptional control unit constructs. For this purpose, either composite enhancer elements from liver-specifically expressed genes or binding site sequences of transcription factors guiding expression of liver-specific genes were inserted into the MCS-located upstream of the HSV TK-37 minimal core promoter.

Insertion of "natural" composite enhancer elements which are important for liver-specific expression of the human apolipoprotein B100 (ApoB) or the rat ornithin transcarbamoylase (OTC), generated synthetic transcriptional control unit constructs pApoB-GreeN and pOTC-GreeN. In addition, plasmids encoding up to 16 monotype ApoB

cassettes, up to 16 monotype OTC cassettes, as well as mixed ApoB/OTC cassettes were constructed (Figure 1).

Insertion of complementary oligonucleotides encoding the binding sites of liver-specific transcription factors HNF1/3/4/5 or C/EBP led to the generation of synthetic transcriptional control unit constructs p1×HNF1-GreeN, p3×HNF1-GreeN (exhibiting three consecutive HNF1 TFBS), p1×HNF3-GreeN, p1×HNF4-GreeN, p1×HNF5-GreeN, p1×C/EBP-GreeN, respectively (constructs not depicted).

Comparison of transfection efficiencies of cell lines of liver and non-liver origin in correlation to different lipid-based transfection reagents

To evaluate the tissue-related transcriptional activities of pGreeN-based synthetic transcriptional control unit constructs, three human hepatoma cell lines (HepG2, Hep3B, HuH7) were chosen and compared with two carcinoma cell lines of cervix (HeLa) and human embryonic kidney (HEK293) origin, respectively. By mixing reporter plasmid pEGFP-C1 with five different commercially available lipid-based transfection reagents (FuGENE 6™, Lipofectamine 2000™, Lipofection™, DOSPER™, DAC-30™) followed by subsequent FACS quantitation of EGFP expressing cells, we identified the multi-component lipid-based FuGENE 6 transfection reagent and yielded the best overall transfection efficiencies considering all five cell lines tested (data not shown). In particular, the transfection efficiencies obtained by FuGENE 6 were in the range of 60-75% for four of five cell lines tested (Figure 2; cell lines Hep3B, HuH7, HeLa, HEK293). Only HepG2 cells yielded a significant lower transfection efficiency of nearly 20% (Figure 2; first bar). However, none of the other transfection reagents tested was found to be able to achieve a roughly equivalent transfection efficiency in HepG2 cells (data not shown). Therefore, all successive transfection experiments were performed using FuGENE 6. Cell line-dependent differences in transfection efficiencies were normalized by setting EGFP expression levels obtained with hCMV IE-driven control plasmid pEGFP-C1 to 100% for each cell line tested. EGFP expression levels obtained by transfection with synthetic transcriptional control unit constructs were related to this cell line-dependent EGFP standard level.

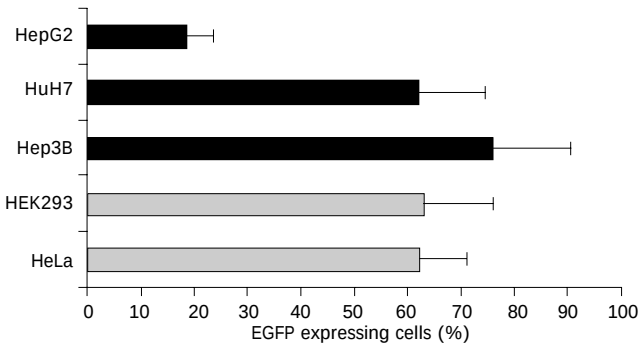


Figure 2 Transfection efficiencies of cell lines of human hepatoma and non-liver origin.

Transfection experiments for comparison of transcriptional activities of synthetic transcriptional control unit constructs

Following FuGENE 6-mediated transfection of cell lines HepG2, Hep3B, HuH7, HeLa, HEK293, with synthetic transcriptional control unit constructs, percentages of EGFP expressing cells were determined in a simplified first round of testing by FACS analysis, constituting a first rough correlation for the individual transcriptional activities of each construct.

As a result, constructs comprising monotype ApoB cassettes (Figure 3; upper panel) exhibited high EGFP levels of over 60% (Figure 3; Hep3B and HepG2 cells transfected with 4×ApoB cassette construct) only in human hepatoma derived cell lines. In contrast, EGFP expression of non-liver origin cell lines HeLa and HEK293 transfected with monotype ApoB cassette constructs only reached background levels below or around 10% of cell line-dependent EGFP standard levels (Figure 3; black and grey bars in upper panel).

Therefore, monotype ApoB cassette constructs (encoding TFBS for HNF3, HNF4, HNF5, and C/EBP) could provide a strong liver-directed gene expression. Interestingly, maximum hepatoma cell-based reporter gene expression was obtained with the 4×ApoB cassette construct (Figure 3). In contrast, constructs exhibiting 8 or 16 multimeric ApoB cassettes only demonstrated EGFP expression levels between 30% and 40% or just below 30%, respectively, a phenomenon which could be referred to excess presentation of TFBS encoded by these highly multimeric ApoB cassette constructs.

Constructs comprising monotype OTC cassettes (Figure 3; middle panel) exhibited high EGFP-levels of over 50% (Figure 3; Hep3B cells transfected with 4× or 8× OTC cassette constructs) only in human hepatoma derived cell lines. EGFP expression of non-liver origin cell lines HeLa and HEK293 transfected with monotype OTC cassette constructs only reached background levels below or around 10% of cell line-dependent EGFP standard levels (Figure 3; black and grey bars in middle panel).

Therefore, monotype OTC cassette constructs (encoding TFBS for HNF4 and C/EBP) could also provide a strong liver-directed gene expression in Hep3B and HepG2 hepatoma cells. On the contrary, HuH7 cells transfected with monotype OTC cassette constructs exhibited only EGFP expression levels of up to 16% (Figure 3; middle panel transfected with 8×OTC cassette construct). Again, all hepatoma cell lines (HepG2, Hep3B, HuH7) transfected with construct p16×OTC-GreeN exhibiting 16 multimeric OTC cassettes demonstrated lower EGFP expression levels in comparison to transfections with constructs p4×OTC-GreeN and p8×OTC-GreeN (Figure 3; middle panel), a phenomenon which again could be referred to excess presentation of TFBS encoded by this highly multimeric (16×) OTC cassette construct.

Transfection experiments with non-liver origin cell lines HeLa and HEK293 employing mixed ApoB/OTC cassette constructs (Figure 3; lower panel; exhibiting up to 4 ApoB/OTC units) exhibited EGFP expression levels being unexceptionally below the 5% margin of cell line-dependent EGFP standard levels. In contrast, maximum EGFP expression levels between 30% and nearly 50% were obtained in hepatoma cell lines HepG2, Hep3B, and HuH7

(Figure 3; yellow, orange and brown bars in lower panel).

Therefore, mixed ApoB/OTC cassette constructs (encoding TFBS for HNF3, HNF4, HNF5, C/EBP plus HNF4, C/EBP) could not only provide a strong liver-directed gene expression, but also exhibit a high ratio of liver cell to non-liver cell origin reporter gene expression. Furthermore, mixed ApoB/OTC cassette constructs did not exhibit any significant orientation effect related to the order of ApoB/OTC subcassettes (Figure 3; EGFP expression levels obtained with p1×ApoB/OTC-GreeN *vs* p1×OTC/ApoB-GreeN and p2×ApoB/OTC-GreeN *vs* p2×OTC/ApoB-GreeN).

In sharp contrast to all constructs made up of "natural" composite enhancer elements of the ApoB or the OTC gene, constructs encoding single TFBS of liver-specific transcription factors (p1×HNF1-GreeN, p3×HNF1-GreeN, p1×HNF3-GreeN, p1×HNF4-GreeN, p1×HNF5-GreeN, p1×C/EBP-GreeN) did not achieve EGFP expression levels much higher than background levels (data not shown). Therefore, neither liver-directed nor strong reporter gene expression could be obtained with such single TFBS encoding constructs, demonstrating the superiority of "natural" composite enhancer element constructs.

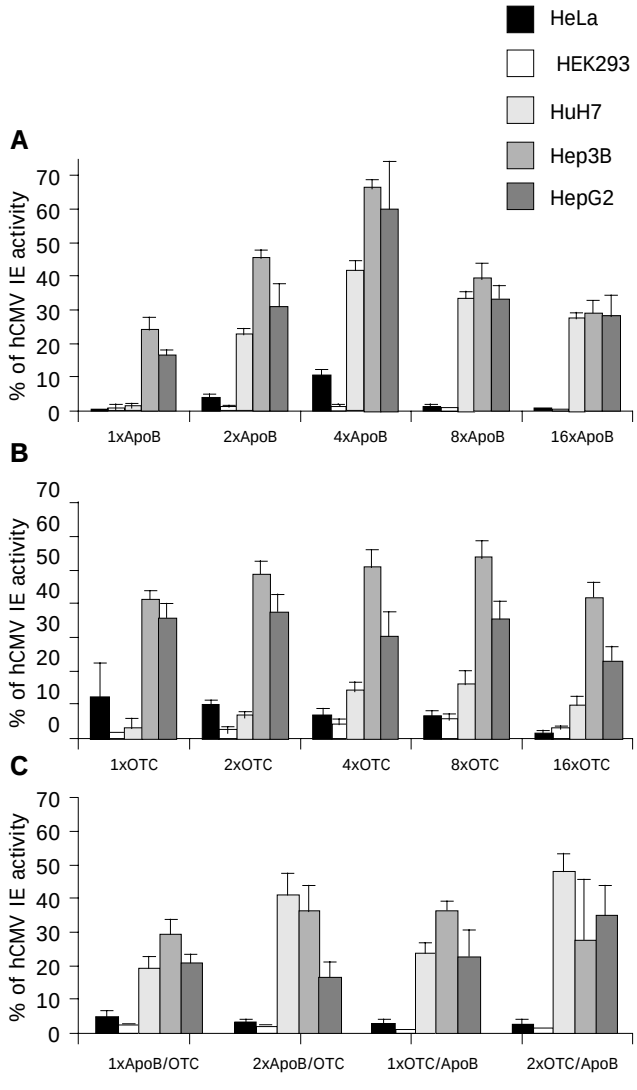


Figure 3 Transcriptional activities of synthetic transcriptional control unit constructs (A-C).

Semi-quantitative RT-PCR and Western blotting analysis of transcriptional activities of synthetic ApoB transcriptional control units

Since transcriptional control unit constructs encoding ApoB cassettes could exhibit high relative EGFP levels (in our first round of testing by FACS analysis: 4×ApoB construct reaching nearly up to 70% of expression obtained with the strong hCMV IE driven control plasmid pEGFP-C1; FACS analysis data is depicted in upper panel of Figure 3), we additionally performed a more precise second round testing and also analyzed synthetic ApoB transcriptional control unit transcriptional activities by semi-quantitative RT-PCR and Western blotting (Figures 4 and 5).

For this purpose, Hep3B cells were transiently transfected with enhancer module plasmids exhibiting single or multimeric ApoB cassettes. Following total RNA extraction and reverse transcription, EGFP expression was analyzed by semi-quantitative PCR analysis which showed a specific band of 717 bp (Figure 4; EGFP). As an internal standard, the α-tubulin house-keeping gene was amplified in parallel giving rise to a specific band of 208 bp (Figure 4; α-tubulin). As a result, a maximum EGFP signal was obtained with the p4×ApoB-GreeN construct (Figure 4; lanes 5, 6), which corresponded with the FACS analysis data and also exhibited the strongest EGFP expression level for Hep3B cells transfected with the p4×ApoB-GreeN construct (Figure 3; upper panel, 4×ApoB, orange bar).

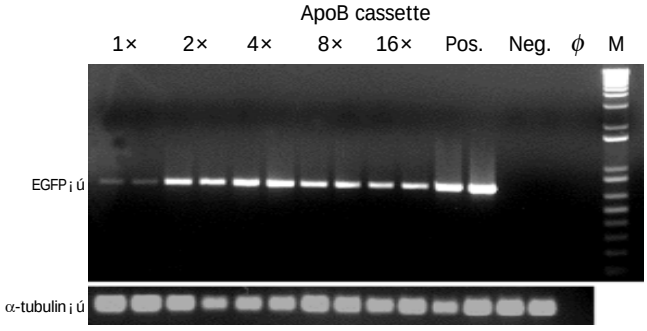


Figure 4 Transcriptional activities of synthetic ApoB transcriptional control units.

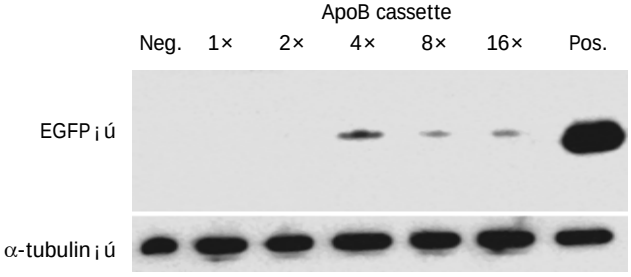


Figure 5 Western blot of EGFP expression driven by synthetic ApoB transcriptional control units. Lane 1: untransfected Hep3B cells used as a negative control (Neg.); lanes 2-6: detection of a 27 kDa band specific for EGFP expressing Hep3B cells transiently transfected with enhancer module plasmids exhibiting single (lane 2: 1×) or multimeric ApoB cassettes (lane 3: 2×; lane 4: 4×; lane5: 8×; lane 6: 16×); lane 7: Hep3B cells transfected with EGFP-encoding hCMV IE promoter plasmid pEGFP-C1 used as a positive control (Pos.), and Western blot detection of á-tubulin used as an internal standard.

Furthermore, EGFP protein contents obtained in cell lysates from Hep3B cells transiently transfected with enhancer module plasmids exhibiting single or multimeric ApoB cassettes were analyzed by Western blotting (Figure 5), using α-tubulin protein expression as an internal standard. As a result, a maximum EGFP signal was again obtained with the p4 × ApoB-GreeN construct (Figure 5; lane 4), which again corresponded with the FACS analysis data and also exhibited the strongest EGFP expression level for Hep3B cells transfected with the p4 × ApoB-GreeN construct (Figure 3; upper panel, 4 × ApoB, orange bar). Similar results were obtained under neomycin(G418)-selection of Hep3B cells transfected with the p4 × ApoB-GreeN construct, again demonstrating potent expression of the neo^r/neomycin aminoglycoside phosphotransferase coding sequence driven by the 4 × ApoB-TK-37 promoter cassette (data not shown).

Taken together, semi-quantitative RT-PCR, Western blotting analysis, and G418-selection of Hep3B cells demonstrated maximum transcriptional activities for the multimeric 4 × ApoB cassette construct (p4 × ApoB-GreeN), which fully complied with the data obtained by simple FACS analysis. Importantly, this finding could underline the possibility to first perform simple and quick FACS screening analysis based on our new EGFP/neo^r fusion reporter gene before doing any detailed analysis on a direct reporter mRNA or protein level.

DISCUSSION

Proper transcriptional regulation of therapeutic transgene expression constitutes a major requirement in liver-directed gene therapy. Gene regulatory elements used in liver gene therapy should meet several requirements. First, they should drive expression of the therapeutic gene at a sufficient high level. Second, they should restrict expression to the liver. Third, they should be well characterized and have suitable size to allow a most versatile usage in the context of a variety of different gene vector systems. Fourth, the well-known phenomenon of interaction of viral vector sequences with internal liver-specific promoters[24] should be kept at a minimum to avoid any interrelation with the expression of therapeutic transgenes.

Promoters of cellular genes expressed preferentially in the liver have been studied extensively and are used for hepatocyte/hepatoma-specific gene delivery[25-29]. However, the major shortcomings considering their widespread usage in liver gene therapy are the big size (contradictory to the restricted cloning space offered by many vector systems), the low transcriptional activity compared to hCMV or long terminal repeat (LTR) promoter sequences widely used in current gene therapy protocols[30-32], and/or interaction with viral vector sequences influencing expression of therapeutic transgenes[33].

Synthetic promoter/enhancer elements based on minimal promoters offer a promising alternative approach[34]. Combining DNA fragments encoding liver gene transcription factor binding sites potentially enables both a high degree of structural compactness and a high degree of liver specificity[12,13,35]. Also control elements derived from genes exhibiting a strict liver-restricted regulation like albumin, apolipoproteins, and alpha-1-antitrypsin can be used for this purpose[36,37]. In addition, this synthetic approach helps to exclude any repressor coding sequences preventing unwanted interactions of endogenous repressor factors with TFBS encoded in naturally originating promoter/enhancer elements.

In an attempt to construct promoters of high liver specificity and activity, we selected hepatospecific transcriptional sequences using the following criteria: short size, wellknown TFBS, expression independent of tight metabolic or hormonal control, and non-species-specificity. We first set out to evaluate both therapeutic efficiency and tissue specificity of this approach in our tissue culture model systems in order to subsequently pre-select liver-specific expression cassettes which could finally be tested within the context of different viral vectors (e.g., adenoviral or lentiviral vectors) both *in vitro* and *in vivo* as effective new liver gene transfer systems.

For this purpose, it worked out to be quite helpful to use a newly generated bifunctional EGFP/neo^r fusion gene cassette, which proved its flexible usage both for transcript quantification by simple FACS analysis (Figure 3) and for selection of stable cell clones (data not shown). Thereby, a proof of principle could be provided demonstrating the possiblity to first perform widespread simple and quick FACS screening analysis based on our new EGFP/neo^r fusion reporter gene before doing any detailed analysis on a direct reporter mRNA or protein level (Figures 4 and 5). This new approach is of great help in screening any of the numerous modifications of yet available or newly designed promoter cassette constructs.

As a leading result, our comparative analysis of transcriptional activities of synthetically generated promoter cassettes showed that it was not possible to achieve liver-directed gene expression fully approaching that of strong viral promoters such as the hCMV IE promoter. We chose the strong hCMV IE promoter as a reference promoter since it is believed to be similarly active in most tissues at least when used for short term expression. Of the different synthetic promoter cassette configurations tested, the most efficient construction was a multimeric 4 × ApoB cassette construct (p4 × ApoB-GreeN construct) as evidenced by FACS quantification (Figure 3), semi-quantitative RT-PCR (Figure 4), and Western blotting (Figure 5). These results clearly demonstrate that our multimeric 4 × ApoB cassette is a novel regulatory module that allows for an efficient and specific expression of therapeutic transgenes in liver cells. Of particular importance is the small size of this module, which makes it possible to accommodate this transcriptional control unit in any type of viral or non-viral vector, even in conjunction with large effector genes. Therefore, the 4 × ApoB cassette potentially represents a helpful new tool to explore the feasability of liver-directed gene therapy in further detail.

A further advantage of our synthetic minimal promoter based expression cassettes is the possibility to enable finely adjustable levels of therapeutic proteins (low to high) to be delivered/expressed by choosing a 1 × ApoB cassette or a 4 × ApoB cassette. Thereby, increasing or decreasing the number of multimeric monotypic or mixed TFBS-encoding cassettes can adjust the level of therapeutic transgene

expression.

In contrast to the good results obtained with "naturally" derived composite enhancer elements from liver-specifically expressed genes, our results with single binding sites of liver-specific transcription factors inserted upstream of the EGFP/neo^r fusion gene cassette are disappointing (data not shown). This might reflect the strict necessity for optimal spacing of TFBS, a feature that is neglected when single binding sites of liver-specific transcription factors are coupled together in a simple head-to-tail manner.

In comparison to promoters of viral origin, synthetic minimal promoter-based expression cassettes should not undergo *in vivo* shutdown as a result of DNA methylation processes or because of the presence of transcription factor binding sites at which cognate proteins are not expressed in the quiescent liver[38,39], thereby enabling long-term gene expression. Furthermore, usage of liver-specific promoters in the context of adenoviral vectors has been demonstrated to prevent the generation of antibodies against therapeutic transgenes[40], an eventuality that may occur when a ubiquitous promoter (e.g., hCMV IE) is used. Thus, our synthetic minimal promoter-based expression cassettes might also be helpful in focusing the therapeutic gene expression to the liver concurrently avoiding induction of any significant host immune response to the transgenic protein of choice, thereby prolonging transgene expression *in vivo* as demonstrated recently for liver-specific gutless adenoviral vectors[41].

In conclusion, we have identified a number of liver-specific promoter sequences that may be valuable tools for targeting heterologous genes to the liver when acceptable levels of therapeutic proteins need to be produced. For reasons of expression efficiency, vector security (especially in the context of suicide gene or other cytotoxic gene expression), and prevention of immune system-induced destruction of transduced cells, our synthetic liver-directed transcriptional control units seem to be a good choice for expression of potential therapeutic genes in the liver. Also clinical usage of non-viral constructs encoding these synthetically generated transcriptional cassettes might be facilitated. This view is based on the recent progress in techniques for delivery of naked DNA to the human liver as well as on their easier high-scale production and better acceptance by regulatory boards than the currently used viral vectors.

ACKNOWLEDGMENTS

The authors thank Drs. M. Spiegel, C.D. Groß, F. Prinz, U. Dau, and S. Lambrecht, former members of the Department of Internal Medicine I, Medical University Clinic Tübingen, for helpful discussions and excellent contributions.

REFERENCES

1 **Xia D,** Zhang MM, Yan LN. Recent advances in liver-directed gene transfer vectors. *Hepatobiliary Pancreat Dis Int* 2004; **3**: 332-336

2 **Prieto J,** Herraiz M, Sangro B, Qian C, Mazzolini G, Melero I, Ruiz J. The promise of gene therapy in gastrointestinal and liver diseases. *Gut* 2003; **52**(Suppl 2): 49-54

3 **Shiratori Y,** Kanai F, Ohashi M, Omata M. Strategy of liver-directed gene therapy: present status and future prospects. *Liver* 1999; **19**: 265-274

4 **Tenenbaum L,** Lehtonen E, Monahan PE. Evaluation of risks related to the use of adeno-associated virus-based vectors. *Curr Gene Ther* 2003; **3**: 545-565

5 **Schagen FH,** Ossevoort M, Toes RE, Hoeben RC. Immune responses against adenoviral vectors and their transgene products: a review of strategies for evasion. *Crit Rev Oncol Hematol* 2004; **50**: 51-70

6 **Ferry N,** Heard JM. Liver-directed gene transfer vectors. *Hum Gene Ther* 1998; **9**: 1975-1981

7 **Ghosh SS,** Takahashi M, Thummala NR, Parashar B, Chowdhury NR, Chowdhury JR. Liver-directed gene therapy: promises, problems and prospects at the turn of the century. *J Hepatol* 2000; **32**: 238-252

8 **Follenzi A,** Sabatino G, Lombardo A, Boccaccio C, Naldini L. Efficient gene delivery and targeted expression to hepatocytes in vivo by improved lentiviral vectors. *Hum Gene Ther* 2002; **13**: 243-260

9 **Kim JW,** Wang XW. Gene expression profiling of preneoplastic liver disease and liver cancer: a new era for improved early detection and treatment of these deadly diseases? *Carcinogenesis* 2003; **24**: 363-369

10 **Suriawinata A,** Xu R. An update on the molecular genetics of hepatocellular carcinoma. *Semin Liver Dis* 2004; **24**: 77-88

11 **Wu CH,** Sapozhnikov E, Wu GY. Evaluation of multicomponent non-viral vectors for liver directed gene delivery. *J Drug Target* 2002; **10**: 105-111

12 **Gehrke S,** Jerome V, Muller R. Chimeric transcriptional control units for improved liver-specific transgene expression. *Gene* 2003; **322**: 137-143

13 **Papadakis ED,** Nicklin SA, Baker AH, White SJ. Promoters and control elements: designing expression cassettes for gene therapy. *Curr Gene Ther* 2004; **4**: 89-113

14 **Paulweber B,** Sandhofer F, Levy-Wilson B. The mechanism by which the human apolipoprotein B gene reducer operates involves blocking of transcriptional activation by hepatocyte nuclear factor 3. *Mol Cell Biol* 1993; **13**: 1534-1546

15 **Metzger S,** Halaas J, Breslow J, Sladek FM. Orphan receptor HNF-4 and bZIP protein C/EBPa bind to overlapping regions of the apolipoprotein B gene promoter and synergistically activate transcription. *J Biol Chem* 1993; **268**: 16831-16838

16 **Shachter N,** Zhu Y, Walsh A, Breslow J, Smith J. Localisation of a liver-specific enhancer in the apolipoprotein E/C-I/C-II gene locus. *J Lipid Res* 1993; **34**: 1699-1707

17 **Nishiyori A,** Tashiro H, Kimura A, Akagi K, Yamamura K, Mori M, Takiguchi M. Determination of tissue specificity of the enhancer by combinatorial operation of tissue-enriched transcription factors. *J Biol Chem* 1994; **269**: 1323-1331

18 **Wu KJ,** Wilson DR, Shih C, Darlington GJ. The transcription factor HNF1 acts with C/EBPa to synergistically activate the human albumin promoter through a novel domain. *J Biol Chem* 1994; **269**: 1177-1182

19 **Baniahmad A,** Steiner C, Kohne AC, Renkawitz R. Modular structure of a chicken lysozyme silencer: involvement of an unusual thyroid hormone receptor binding site. *Cell* 1990; **61**: 505-514

20 **Kekule AS,** Lauer U, Weiss L, Luber B, Hofschneider PH. Hepatitis B virus transactivator HBx uses a tumour promoter signalling pathway. *Nature* 1993; **361**: 742-745

21 **Cormack BP,** Valdivia RH, Falkow S. FACS-optimized mutants of the green fluorescent protein (GFP). *Gene* 1996; **173**: 33-38

22 **Haas J,** Park EC, Seed B. Codon usage limitation in the expression of HIV-1 envelope glycoprotein. *Curr Biol* 1996; **6**: 315-324

23 **Nakabayashi H,** Taketa K, Miyano K, Yamane T, Sato J. Growth of human hepatoma cells lines with differentiated functions in chemically defined medium. *Cancer Res* 1982; **42**:

3858-3863

24 **Ye X,** Liang M, Meng X, Ren X, Chen H, Li ZY, Ni S, Lieber A, Hu F. Insulation from viral transcriptional regulatory elements enables improvement to hepatoma-specific gene expression from adenovirus vectors. *Biochem Biophys Res Commun* 2003; **307**: 759-764

25 **Kuriyama S,** Yoshikawa M, Ishizaka S, Tsujii T, Ikenaka K, Kagawa T, Morita N, Mikoshiba K. A potential approach for gene therapy targeting hepatoma using a liver-specific promoter on a retroviral vector. *Cell Struct Funct* 1991: **16**: 503–510

26 **Kistner A,** Gossen M, Zimmermann F, Jerecic J, Ullmer C, Lubbert H, Bujard H. Doxycycline-mediated quantitative and tissue-specific control of gene expression in transgenic mice. *Proc Natl Acad Sci USA* 1996; **93**: 10933–10938

27 **Tomizawa M,** Yu L, Wada A, Tamaoki T, Kadomatsu K, Muramatsu T, Matsubara S, Watanabe K, Ebara M, Saisho H, Sakiyama S, Tagawa M. A promoter region of the midkine gene that is frequently expressed in human hepatocellular carcinoma can activate a suicide gene as effectively as the alpha-fetoprotein promoter. *Br J Cancer* 2003; **89**: 1086-1090

28 **Lu SY,** Sui YF, Li ZS, Pan CE, Ye J, Wang WY. Construction of a regulable gene therapy vector targeting for hepatocellular carcinoma. *World J Gastroenterol* 2003; **9**: 688-691

29 **Shi YJ,** Gong JP, Liu CA, Li XH, Mei Y, Mi C, Huo YY. Construction of a targeting adenoviral vector carrying AFP promoter for expressing EGFP gene in AFP-producing hepatocarcinoma cell. *World J Gastroenterol* 2004; **10**: 186-189

30 **Ponder KP,** Dunbar RP, Wilson DR, Darlington GJ, Woo SL. Evaluation of relative promoter strength in primary hepatocytes using optimized lipofection. *Hum Gene Ther* 1991; **2**: 41-52

31 **Hafenrichter DG,** Wu X, Rettinger SD, Kennedy SC, Flye MW, Ponder KP. Quantitative evaluation of liver-specific promoters from retroviral vectors after in vivo transduction of hepatocytes. *Blood* 1994; **84**: 3394-3404

32 **Hafenrichter DG,** Ponder KP, Rettinger SD, Kennedy SC, Wu X, Saylors RS, Flye MW. Liver-directed gene therapy: evaluation of liver specific promoter elements. *J Surg Res* 1994; **56**: 510-517

33 **Wu X,** Holschen J, Kennedy SC, Ponder KP. Retroviral vector sequences may interact with some internal promoters and influence expression. *Hum Gene Ther* 1996; **7**: 159-171

34 **Xu ZL,** Mizuguchi H, Ishii-Watabe A, Uchida E, Mayumi T, Hayakawa T. Optimization of transcriptional regulatory elements for constructing plasmid vectors. *Gene* 2001; **272**: 149-156

35 **Kramer MG,** Barajas M, Razquin N, Berraondo P, Rodrigo M, Wu C, Qian C, Fortes P, Prieto J. *In vitro* and *in vivo* comparative study of chimeric liver-specific promoters. *Mol Ther* 2003; **7**: 375-385

36 **De Simone V,** Cortese R. Transcriptional regulation of liver-specific gene expression. *Curr Opin Cell Biol* 1991; **3**: 960-965

37 **Noda C,** Ichihara A. Regulation of liver-specific gene expression. *Cell Stru Funct* 1993; **18**: 189-194

38 **Kay MA,** Baley P, Rothenberg S, Leland F, Fleming L, Ponder KP, Liu T, Finegold M, Darlington G, Pokorny W. Expression of human alpha 1-antitrypsin in dogs after autologous transplantation of retroviral transduced hepatocytes. *Proc Natl Acad Sci USA* 1992; **89**: 89–93

39 **Loser P,** Jennings GS, Strauss M, Sandig V. Reactivation of the previously silenced cytomegalovirus major immediate-early promoter in the mouse liver: involvement of NFkappaB. *J Virol* 1998; **72**: 180–190

40 **Pastore L,** Morral N, Zhou H, Garcia R, Parks RJ, Kochanek S, Graham FL, Lee B, Beaudet AL. Use of a liver-specific promoter reduces immune response to the transgene in adenoviral vectors. *Hum Gene Ther* 1999; **10**: 1773–1781

41 **Wang L,** Hernandez-Alcoceba R, Shankar V, Zabala M, Kochanek S, Sangro B, Kramer MG, Prieto J, Qian C. Prolonged and inducible transgene expression in the liver using gutless adenovirus: a potential therapy for liver cancer. *Gastroenterology* 2004; **126**: 278-289

Science Editor Wang XL and Zhu LH, Guo SY **Language Editor** Elsevier HK

PO Box 2345, Beijing 100023, China
www.wjgnet.com
wjg@wjgnet.com

ELSEVIER

World J Gastroenterol 2005;11(34):5303-5308
World Journal of Gastroenterology ISSN 1007-9327
© 2005 The WJG Press and Elsevier Inc. All rights reserved.

• *CLINICAL RESEARCH* •

Persistence of high CD40 and CD40L expression after restorative proctocolectomy for ulcerative colitis

Lino Polese, Imerio Angriman, Giuseppe De Franchis, Attilio Cecchetto, Giacomo C. Sturniolo, Renata D'Incà, Marco Scarpa, Cesare Ruffolo, Lorenzo Norberto, Mauro Frego, Davide F D'Amico

Lino Polese, Imerio Angriman, Marco Scarpa, Cesare Ruffolo, Lorenzo Norberto, Mauro Frego, Davide F D'Amico, Department of Gastroenterological and Surgical Sciences. Surgical Unit, University of Padova, Italy
Giacomo C. Sturniolo, Renata D'Incà, Department of Gastroenterological and Surgical Sciences, Gastroenterological Unit, University of Padova, Italy
Giuseppe De Franchis, Department of Laboratory Medicine, University of Padova, Italy
Attilio Cecchetto, Department of Pathology, University of Padova, Italy
Correspondence to: Lino Polese, Clinica Chirurgica I, Policlinico Universitario, via Giustiniani 2, Padova 35128, Italy. linopolese@hotmail.com
Telephone: +39-3490587897 Fax: +39-049656145
Received: 2005-02-17 Accepted: 2005-03-09

Polese L, Angriman I, De Franchis G, Cecchetto A, Sturniolo GC, D'Incà R, Scarpa M, Ruffolo C, Norberto L, Frego M, D'Amico DF. Persistence of high CD40 and CD40L expression after restorative proctocolectomy for ulcerative colitis. *World J Gastroenterol* 2005; 11(34): 5303-5308
http://www.wjgnet.com/1007-9327/11/5303.asp

Abstract

AIM: To focus on the role of CD40 and CD40L in their pathogenesis.

METHODS: We analyzed by immunohistochemistry the CD40 and CD40L expression in the pouch mucosa of 28 patients who had undergone RPC for UC, in the terminal ileum of 6 patients with UC and 11 healthy subjects. We also examined by flow cytometry the expression of CD40 by B lymphocytes and monocytes in the peripheral blood of 20 pouch patients, 15 UC patients and 11 healthy controls.

RESULTS: Ileal pouch mucosa leukocytes presented a significantly higher expression of CD40 and CD40L as compared to controls. This alteration correlated with pouchitis, but was also present in the healthy pouch and in the terminal ileum of UC patients. CD40 expression of peripheral B lymphocytes was significantly higher in patients with UC and pouch, respect to controls. Increased CD40 levels in blood B cells of pouch patients correlated with the presence of spondyloarthropathy, but not with pouchitis, or inflammatory indices.

CONCLUSION: High CD40 expression in the ileal pouch mucosa could be implied in the pathogenesis of pouchitis following proctocolectomy for UC, whereas its increased levels on peripheral blood B lymphocytes are associated with the presence of extraintestinal manifestations.

© 2005 The WJG Press and Elsevier Inc. All rights reserved.

Key words: Ulcerative colitis; Pouchitis; Spondyloarthropathy; CD40; CD40L; Arthritis

INTRODUCTION

The etiology of ulcerative colitis (UC) is not clear, but abnormal immunological activity against normally tolerated antigens has been demonstrated[1,2]. This disease is usually treated by immunosuppressive or anti-inflammatory drugs, but, in the case of unresponsive or steroid-dependent patients, or dysplasia, surgical treatment is indicated.

The standard of care for elective surgical treatment of patients with UC is restorative proctocolectomy (RPC), with ileal pouch-anal anastomosis (IPAA). After RPC, over 90% patients have shown good long-term function and high satisfaction, with full continence at 5 years in 72% of subjects and a mean stool frequency of six bowel movements per day[3,4]. The health-related quality of life reported by these patients is similar to that in subjects with UC in remission and better than in patients with moderate-severe colitis[5]. However, these patients sometimes suffer from pouchitis and extraintestinal manifestations such as arthritis, uveitis, erythema nodosum or pyoderma gangrenosum.

Pouchitis, an inflammation of the ileal reservoir, can develop in up to 50% of the patients that undergo RPC for UC, but in less than 1% of those operated on RPC for familial adenomatous polyposis (FAP)[6-8]. Clinically it is characterized by bloody diarrhea, fever, abdominal cramps and urgent defecation, and, at times, the symptoms resemble those of UC. Fortunately excision of the pouch is required in only 1-2% of these patients in whom the disease becomes chronic[9,10]. Several different hypotheses have been made to explain the etiology of pouchitis, which might be caused by ischemia of the ileal reservoir, transformation of the microbial flora, or fecal stasis possibly causing bacterial overgrowth or by a recurrence of UC. The last postulation has been sustained by many studies demonstrating immunological aspects that are similar to those in UC. A comparable expression to what is seen in UC of interleukin (IL)-1β, IL6, IL8 and tumor necrosis factor (TNF)α in the gut[11], an increased concentration of IgG and the activation of CD4 T cells[12,13] are all patterns demonstrating immunologic over-activity.

CD40 and CD154 (CD40 ligand or CD40L), two surface molecules, both members of TNF receptor family, are co-stimulators, expressed respectively by the antigen presenting cell and the T cells. While their presence is necessary to activate the immune response toward the antigen during its presentation, their absence leads to tolerance[14]. It has been reported that the expression of CD40 and CD40L by gut leukocytes is elevated in patients with UC and Crohn's disease even during remission, as compared to healthy controls or to other inflammatory events[15-17]. Sawada-Hase *et al*., also found an increased expression of CD40 by the blood B cells of patients with active UC and by the blood monocytes of patients with active Crohn's disease[18]. Recent studies on inflammatory bowel diseases (IBD) have demonstrated that CD40/CD40L interaction plays a key role not only in setting off an immune reaction, but also in the late inflammatory stage. In fact, there is evidence that CD40L positive T cells can induce cell adhesion molecules and expression of soluble mediators by CD40-positive human intestinal fibroblasts and microvascular endothelial cells. This event recruits more T cells from the blood to the tissue, thus amplifying intestinal inflammation[19].

The aim of this study was to evaluate if CD40 and CD40L may have a role in the pathogenesis of pouchitis. It was with this interest that we analyzed CD40 and CD40L expression by leukocytes from the ileal pouch mucosa and from the blood of patients who underwent RPC for UC, comparing it to that in non-operated UC patients and normal controls. The correlation between elevated levels of these molecules and the presence of pouchitis or extra-intestinal manifestations was also evaluated.

MATERIALS AND METHODS

Immunohistochemistry

Patients In the first part of the study, histologic samples were obtained from the ileal pouch biopsies of 28 patients (16 males, 12 females) who had undergone RPC for UC. Patients' mean age was 36 years (range 22-52 years) and time interval after RPC was in mean 5±4 years. According to the pouchitis disease activity index (PDAI) classification[20], 14 of these patients presented pouchitis (score ⩾7), while the other 14 presented a healthy pouch (score <7). A total of 76 pouch biopsies (35 from pouchitis and 41 from healthy pouches) were analyzed. Histochemical analyses were also carried out on ileal biopsies taken during standard surveillance colonoscopy of 6 consecutive un-operated patients with UC without ileitis and of 11 healthy subjects (who underwent endoscopy for screening, and whose test result was normal).

Methods All the samples were kept in formalin and subsequently paraffin embedded. The expression of CD40 (clone MAB 89, mouse, Immunotech) and CD154 (clone H-125, rabbit, Santa Cruz Biotechnologies) were analyzed in the same sample by immunohistochemical staining. Staining was performed using avidin-biotin complex (ABC), as described elsewhere[15].

In order to quantify the number of CD40+ and CD154+ cells present, we counted the percentage of leukocytes stained by the ABC immediately below the epithelium. We examined 10 fields at ×60 magnification from each sample. The percentage of the molecular expression was determined in a "blind" way by a single pathologist, who did not know the sample's origin.

Blood flow cytometric analysis

Patients In the second part of the study, we collected blood for flow cytometric analysis from 20 patients (12 males and 8 females, mean age 47 years, range 31-70 years) who had undergone RPC for UC (10 of them also participated in the first part of the study performed with immunohistochemistry), 15 patients with UC (7 males, 8 females, mean age 47 years, range 23-59 years) and 11 healthy subjects (controls). Patients receiving immunosuppressive or steroid treatment were excluded. Of the 20 patients who had undergone IPAA, 7 presented diagnosis of pouchitis, according to the PDAI (score ⩾7) and 13 did not (score <7). Extraintestinal diseases were found in 7 (6 with spondyloarthropathy, 1 pyoderma gangrenosum), while 13 were asymptomatic. Presence of both pouchitis and extraintestinal manifestations was found in 3. The diagnosis of spondyloarthropathy was made according to the European Spondyloarthropathy Study Group criteria[21]. Of the 15 patients with UC, 10 were in remission, 5 were in activity according to clinical and endoscopic patterns[22,23]. Extraintestinal symptoms were reported in five patients (three with spondyloarthropathy, one uveitis, one arthritis and pyoderma gangrenosum).

ESR and CRP were also measured respectively by Westergren method and immunonephelometry. We considered 6 mg/L and 15 mm/h the cut-off points for CRP and ESR, respectively.

All sampling procedures for histology and flow cytometry were performed after informed consent was obtained from each patient.

Methods Blood samples were collected in heparinized tubes. A four flow cytometric analysis was performed, with the sequent associations:

- CD45, CD40, CD20, CD14
- CD45, CD3, CD154

Anti-CD20 and anti-CD45 mAb were obtained from Coulter Beckman (Coulter Inc., Fullerton, CA, USA), anti-CD14 mAb, anti-CD40 mAb and anti-CD154 (CD40L) from Becton Dickinson & Co., (San Jose, CA) (Table 1). Anti CD-3 mAb was obtained from Caltag Laboratories (Bayshore Burlingame, CA, USA) (Table 1). For flow cytometry, all mAbs were used at optimal saturating concentrations as recommended by the manufacturers.

Quadruple staining was performed for CD20 (FITC), CD45 (ECD), CD14 (PE), CD40 (PC5) on one hand and triple staining for CD45 (ECD), CD154 (PC5), CD3 (FITC) on the other hand. As for the quadruple staining the cells were washed in FACS buffer containing PBS, 5% FCS, 0.05% sodium azide and incubated with 10 mg of human IgG (Sigma Chemical Co., St. Louis, MO) for 30 min at 4-8 ℃ to block Fc receptors. Cells were washed to remove excess IgG and were quadruple-stained with either PC5-conjugated mAb against human CD40 or PC5-control IgG_1 mAb, PE-conjugated mAb against CD14, or PE-control IgG

Table 1 Antibodies and sources for flow cytometry

Cluster differentiation	Clone	Isotype	Fluorochromes	Excitation	Emission	Source
CD45	J.33	IgG1	ECD	486–575	610–635	Coulter
CD20	H299 (B1)	IgG2a	FITC	468–505	504–541	Coulter
CD14	M5E2	IgG2a	PE	486–575	568–590	Becton–Dickinson
CD40	5C3	IgG1	PC5	486–580	660–680	Becton–Dickinson
CD154	TRAP1	IgG1	PC5	486–580	660–680	Becton–Dickinson
CD3	UCHT1	IgG1	FITC	468–505	504–541	Caltag

mAb, FITC-conjugated mAb against CD20 or FITC-control IgG mAb and ECD-conjugated mAb against CD45 for 30 min at 4-8 ℃. Cells were washed twice, re-suspended in FACS buffer, fixed with 1% paraformaldehyde, and analyzed by flow cytometry using Coulter EPICS XL-MCL (Beckman Coulter Inc., Fullerton, CA, USA). PBMCs were gated according to their CD45 expression characteristics. Different subsets of cells (CD20, CD14) were gated further based on FL1 and FL2 staining. A similar procedure was utilized for the co-staining of CD154, CD45, and CD3. An immunologic gate on CD20+ and CD14+ cells to evidence CD40 and on CD3+ to reveal CD154+ were respectively performed. As CD40 is expressed by most of the peripheral blood-except terminally differentiated-B cells, but the number of molecules on the lymphocytes surface rises during UC activity[18], we arbitrarily regulated the FL3 photomultiplicator voltage, positioning the CD40 expression below the threshold, previously set by the negative isotypic control of the relative antibody. In this way, all the B cells with homogeneous CD40 expression were below, while those with high CD40 expression were above the cut-off. In the present manuscript, we have called these cells as "high fluorescence intensity (hfi) CD40+". This instrumental setting was performed utilizing blood samples from four healthy controls (not included in the study). After that, isotypic controls were used for all the samples, maintaining the voltage setting of the photomultiplicator at the new level. We considered the CD40 expression by B lymphocytes above the cut-off level a pattern of activated B cells[18]. The same methods were utilized to detect monocytes CD14+ with high CD40 expression.

Statistical analysis

The aim was to detect a 50% difference, since a 300% difference was found in previous studies on CD40 tissue and blood expression in UC patients with respect to controls[15,18]. So the minimum sample sizes were calculated at one-sided alpha of 5%, a power of 80% and an estimated standardized effect size of 100%.

Results are expressed as mean±SE. Statistical analysis was performed by multi-way ANOVA followed by least significant difference (LSD) test. When only two samples were compared, Mann-Whitney *U* test was utilized. Frequency analysis was performed with Fisher exact test. Correlations were assessed using Spearman's rank correlation test. Statistical significance was set at $P<0.05$.

RESULTS

Immunohistochemistry

Results of immunohistochemical analysis are presented in Table 2. In healthy controls, the percentage of leukocytes exposing CD40 on the cell surface in the ileal mucosa was 4.0±1.62%. They were located just below the epithelium, probably in response to stimuli of luminal origin, as previously found in the normal colon[15]. Higher CD40 expression was found in the ileal pouch mucosa (14.0±1.72%, $P<0.05$) and in the ileal mucosa of non-operated UC patients (9.60±2.73%, in this case, although Mann-Whitney *U* test gave a statistical significant difference ($P<0.05$), the comparison with healthy controls did not reach the full statistical significance with LSD test). In the mucosa of the ileal pouch, there were more CD40+ cells in patients with active pouchitis compared to subjects with a healthy pouch (19.7±2.75% *vs* 8.6±1.76%, $P<0.01$) and their percentage correlated with the PDAI score ($P<0.01$). Similarly, we found more CD40L+ cells in the ileal mucosa of the pouch (17.5±2%), rather than in healthy controls, in whom the expression of this molecule was hardly detectable (0.4±0.21%, $P<0.01$, Figure 1). CD40L+ cells percentage (26.0±6.12%, $P<0.01$) in the ileal mucosa of non-operated patients with UC was also high. During an episode of pouchitis, CD40L -just as CD40 - expression was increased (20.4±2.54% *vs* 12.3±2.64%, $P = 0.01$, Figure 2) and correlated with the PDAI score ($P<0.01$). The ileal tissue of healthy pouches had significantly more CD40L than negative controls ($P<0.01$). CD40 and CD40L expression was not influenced by the pouch age.

Table 2 CD40 and CD154 expression by lymphocytes in the intestinal mucosa

	Controls	Ileum UC	Pouch	Pouchitis	Healthy pouch
CD40 (%)	4.0±1.62	9.60±2.73	14.0±1.72[a]	19.7±2.75[a,c]	8.6±1.76[a]
CD40L (%)	0.4±0.21	26.0±6.12[a,c]	17.5±2[a]	20.4±2.54[a,c]	12.3±2.64[a]

[a]$P<0.05$ *vs* controls; [c]$P<0.05$ *vs* healthy pouch.

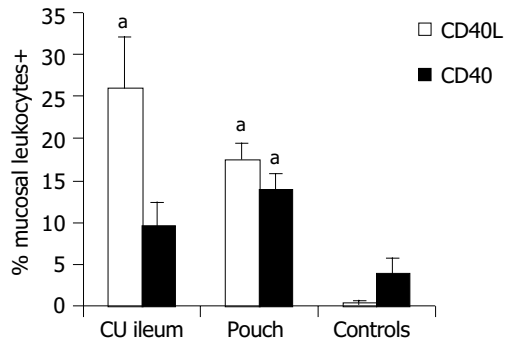


Figure 1 Mean percentages with standard error of CD40L+ and CD40+ leukocytes in the mucosa of UC ileum, ileal pouch, and controls. [a]*P*<0.05 *vs* controls.

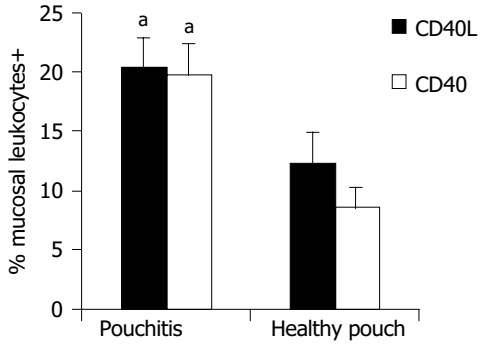


Figure 2 Comparison of CD40L and CD40 leukocytes' expression between pouchitis and healthy pouch mucosa. [a]*P*<0.05 *vs* healthy pouch.

Flow cytometric analysis

Results of flow cytometric analysis are presented in Table 3 There was a less homogeneous distribution of blood CD40+B cells in the flow cytometry diagram in samples presenting elevated CD40 expression, with respect to that in normal controls (Figure 3). Blood B cells of pouch and UC patients presented higher CD40 expression compared to controls (hfiCD40+/CD20+ cells percentage respectively 9.0±2.37% in patients with pouches, 9.7±1.34% in those with UC and 3.6±0.99% in controls, $P<0.05$, Figure 4). All except 1 control presented a percentage of hfiCD40+/CD20+ blood cells <7% (10/11, 91%), while 11/15 (73%) UC patients and 10/20 (50%) pouch patients presented a percentage ⩾7%. No significant increase in CD40 expression by CD14+ blood population (monocytes) was found in UC (0.38±0.13%) or pouch (0.16±0.06%) with respect to controls (0.09±0.06%). It was found that CD40L was not expressed in the CD3 population of the subjects analyzed.

No significant difference in CD40 expression by B cells was found between normal (hfiCD40+/CD20+ 11.00±3.6%) and inflamed pouches (6.40±2%). Moreover, no correlation was found with PDAI score or with pouch age. Enhanced CD40 expression in B lymphocytes of pouch population, instead, was correlated with extra-intestinal manifestations. Patients with extraintestinal manifestations (spondyloarthropathy, or pyoderma gangrenosum) showed a significant increase of CD40 expression (hfiCD40+CD20+ 16.86±5.25% *vs* 5.30±1.58% in patients without extraintestinal manifestations, $P<0.05$). The difference was statistically significant also considering only patients with spondyloarthropathy (Figure 5). The CD40 expression in blood monocytes was not correlated to extraintestinal manifestations. Patients with pouchitis did not present a higher incidence of extraintestinal manifestations.

CD40 expression in B lymphocytes or in monocytes did not correlate with the levels of ESR or CRP.

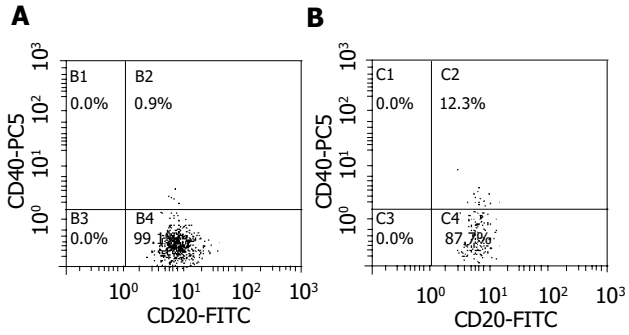


Figure 3 CD40 expression in B cells (CD20+) in controls (**A**) is homogeneously distributed under the cut-off. This expression is instead above the cut-off value, in several B cells in pouch patients with spondyloarthropathy (**B**), as in those with UC.

DISCUSSION

The pathogenesis of pouchitis after proctocolectomy remains to be elucidated. From our results, pouchitis does not seem to represent the manifestation of systemic disease. In fact we found activated peripheral B cells in the presence of arthritis, but not in the presence of pouchitis. Moreover, pouchitis was not related to extraintestinal manifestations. Our results are in disagreement with those reported by

Table 3 Flow cytometry results: CD40 expression on B cells and monocytes

	HfiCD40+CD20+ (%)	*P*	HfiCD40+CD14+ (%)	*P*
UC *vs* controls	9.7±1.34 *vs* 3.6±0.99	<0.05	0.38±0.13 *vs* 0.09±0.06	NS
Pouch *vs* controls	9.0±2.37 *vs* 3.6±0.99	<0.05	0.16±0.06 *vs* 0.09±0.06	NS
Extraint+ *vs* extraint-	16.86±5.25 *vs* 5.30±1.58	<0.05	0.1±0.03 *vs* 0.2±0.13	NS
PDAI ⩾7 *vs* PDAI<7	11.00±3.6 *vs* 6.40±2.0	NS	0.1±0.04 *vs* 0.2±0.08	NS
CRP+ *vs* CRP–	8.6±2.25 *vs* 10.7±2.0	NS	0.2±0.13 *vs* 0.7±0.4	NS
ESR+ *vs* ESR–	8.6±1.8 *vs* 10.4±2.8	NS	0.3±0.2 *vs* 0.7±0.4	NS

CRP, C reactive protein; ESR, erythrocyte sedimentation rate; extraint, extraintestinal diseases; Hfi, high fluorescence intensity; NS, non significant; PDAI, pouchitis disease activity index.

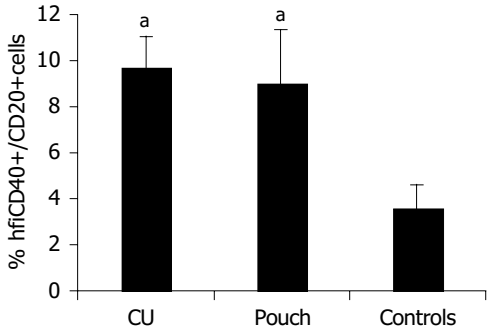


Figure 4 Flow cytometric analysis of CD40+/CD20+ cells in blood. [a]*P*<0.05 *vs* controls.

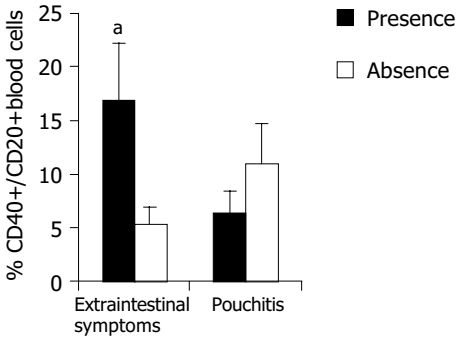


Figure 5 Blood B cells in pouch patients with extraintestinal manifestations, such as spondyloarthropathy or pyoderma gangrenosum, present a higher expression of CD40 with respect to the other pouch patients. Instead no difference is present during pouchitis. Hfi, high fluorescence intensity. [a]*P*<0.05 *vs* absence.

Lohmuller *et al*.[24], and Hata *et al*.[25], which found higher rates of pouchitis in patients with extraintestinal manifestations than in those without. Our findings were supported instead by Thomas *et al*.[26], who observed that histological scores of pouch inflammation were not different in patients with and without joints diseases.

Increased CD40 and CD40L expression was found in the terminal ileum of some patients with UC who had not undergone surgery. This finding is in agreement with the hypothesis that the ileal segment used for pouch construction, even if apparently regular, could nevertheless be abnormal with regard to its immunology and function[27]. Known underlying diseases in the terminal ileum could be Crohn's disease, indeterminate colitis, or backwash ileitis[6]. In a study by Battaglia *et al*.[17], the ileal tissue of patients with Crohn's disease presented higher levels of CD40L and CD40 on T and B lymphocytes, with respect to controls. Backwash ileitis has already been considered as a risk factor for pouchitis. Schmidt *et al*.[28], analyzed 67 preoperative terminal ileal and colonic resections in patients with UC who underwent proctocolectomy. In their study ileal inflammation or pancolitis were significant predictors of subsequent pouch inflammation. On the other hand, Gustavsson *et al*.[29], found a similar incidence of pouchitis in patients presenting backwash ileitis at surgery than in those without. The alteration we found in CD40 and CD40L expression in the terminal ileum of patients with UC is not associated with clear inflammatory patterns. Nevertheless it could yield a reduced tolerance status that becomes clinically evident only in certain conditions, such as, probably, the presence of fecal stasis, different bacterial flora or colonic metaplasia. Colonic metaplasia alone cannot cause pouchitis, since this histologic pattern has been found in 50% of pouch constructed for patients with FAP, which rarely becomes inflamed[30].

The analysis of CD40 and CD40L in the ileum of patients with UC who are possible candidates for RPC could represent a predictive marker for the future development of pouchitis or fistulas. Prospective studies are needed to clarify this hypothesis.

The analysis of soluble CD40L in the serum using ELISA could be easier than the research by flow cytometry of CD40 and CD40L on B lymphocytes' and monocytes' surface, but it was excluded from this study because it was mainly expressed by platelets[31]. The presence of increased CD40 expression in blood B lymphocytes of IBD patients has already been reported by others. Sawada-Hase *et al*.[18], found a higher CD40 expression in the CD19+ blood cells in patients with active UC and in the CD14+ blood cells in subjects with active Crohn's disease. CD40 expression in peripheral B cells has however never been analyzed in pouch patients. An increased CD40 expression in the blood B lymphocytes of subjects who have undergone RPC demonstrates that some systemic alterations persist following the surgical treatment of UC, suggesting that it is a systemic rather than just a colonic disease. Nevertheless, only half of the pouch patients presented an altered expression of this molecule on peripheral B-cells' surface. Extraintestinal manifestations of UC-such as spondyloarthropathy-seem to be related to CD40 levels on blood B cells, while other analyzed factors, like pouchitis, pouch age, ESR or CRP, do not.

The importance of CD40 and CD40L in arthritis has been previously demonstrated. In patients with rheumatoid arthritis (RA), in fact, increased expression of CD40 on synovial monocytes, fibroblasts and dendritic cells has been reported[32-34] and blocking CD40-CD154 interaction improved collagen-induced arthritis in a murine model of RA[35]. Thomas *et al*.[26], studied 97 UC patients with pouch for rheumatological diseases. Articular symptoms in joints were reported in 31% of the patients, but clinical and radiological findings were nearly normal. On the basis of our findings, increased CD40 expression by blood B cells seems to be a measurable marker of this disease.

In conclusion, pouchitis is characterized by an increased expression of CD40 and CD40L on mucosal leukocytes. This result, also found in the terminal ileum of some UC patients who were analyzed here, could represent a predisposing factor for pouchitis, activated in the presence of bacteria and feces following pouch construction or colonic metaplasia.

High levels of CD40 on the surface of blood B cells did not correlate with pouchitis, but with spondyloarthropathy. These findings suggest a different pathogenesis of the two diseases, with local events the first, systemic immunological alterations the second. Prospective studies, before and after

pouch construction and before and after symptoms, are mandatory to evaluate these analyses as prognostic markers for the development of pouchitis, if conducted in the ileal mucosa, and of spondyloarthropathy following RPC, if performed on blood samples.

REFERENCES

1 **Radford-Smith G.** Ulcerative colitis: an immunological disease? *Baillière's Clinical Gastroenterol* 1997; **11**: 35-52
2 **Fiocchi C.** Inflammatory bowel disease: etiology and pathogenesis. *Gastroenterology* 1998; **115**: 182-205
3 **Lavery IC,** Sirimarco MT, Ziv Y, Fazio VW. Anal canal inflammation after ileal pouch-anal anastomosis. The need for treatment. *Dis Colon Rectum* 1995; **38**: 803-806
4 **Michelassi F,** Lee J, Rubin M, Fichera A, Kasza K, Karrison T, Hurst RD. Long-term functional results after ileal pouch anal restorative proctocolectomy for ulcerative colitis A prospective observational study. *Ann Surg* 2003; **238**: 433–445
5 **Scarpa M,** Angriman I, Ruffolo C, Ferronato A, Polese L, Barollo M, Martin A, Sturniolo GC, D'Amico DF. Health related quality of life after restorative proctocolectomy for ulcerative colitis: long-term results. *World J Surg* 2004; **28**: 124-129
6 **Nicholls RJ,** Banerjee MS. Pouchitis: risk factors, etiology and treatment. *World J Surg* 1998; **22**: 347-351
7 **Stocchi L,** Pemberton JH. Pouch and pouchitis. *Gastroenterol Clin North Am* 2001; **30**: 223-241
8 **Simchuk EJ**, Thirlby RC. Risk factors and true incidence of pouchitis in patients after ileal pouch-anal anastomoses. *World J Surg* 2000; **24**: 851-856
9 **Stahlberg D,** Gullberg K, Liljeqvist L, Hellers G, Lofberg R. Pouchitis following pelvic pouch operation for ulcerative colitis: Incidence, cumulative risk, and risk factors. *Dis Colon Rectum* 1996; **39**: 1012
10 **Gramlich T,** Delaney CP, Lynch AC, Remzi FH, Fazio VW. Pathological subgroups may predict complications but not late failure after ileal pouch-anal anastomosis for indeterminate colitis. *Colorect Dis* 2003; **5**: 315-319
11 **Patel RT,** Bain I, Youngs D, Keighley MR. Cytokine production in pouchitis is similar to that in ulcerative colitis. *Dis Colon Rectum* 1995; **38**: 831-837
12 **Stallmach A,** Schafer F, Hoffmann S, Weber S, Muller-Molaian I, Schenider T, Kohne G, Ecker KW, Feifel G, Zeitz M. Increased state of activation of CD4 positive T cells and elevated interferon gamma production in pouchitis. *Gut* 1998; **43**: 499
13 **Stallmach A,** van Look M, Scheiffele F, Ecker KW, Feifel G, Duchmann R, Zeitz M. IgG, albumin, and sCD44 in whole-gut lavage fluid are useful clinical markers for assessing the presence and activity of pouchits. *Int J Colorect Dis* 1999; **14**: 35
14 **Van Kooten C,** Banchereau J. Functional role of CD40 and ist ligand. *Int Arch Allergy Immunol* 1997; **113**: 393-399
15 **Polese L,** Angriman I, Cecchetto A, Norberto L, Scarpa M, Ruffolo C, Barollo M, Sommariva A, D'Amico DF. The role of CD40 in ulcerative colitis: histochemical analysis and clinical correlation. *Eur J Gastroenterol Hepatol* 2002; **14**: 237-241
16 **Liu Z,** Colpaert S, D'Haens GR, Kasran A, de Boer M, Rutgeerts P, Geboes K, Ceuppens JL. Hyperexpression of CD40 ligand (CD154) in inflammatory bowel disease and its contribution to pathogenic cytokine production. *J Immunol* 1999; **163**: 4049-4057
17 **Battaglia E,** Biancone L, Resegotti A, Emanuelli G, Fronda GR, Camussi G. Expression of CD40 and its ligand, CD40L, in intestinal lesions of Crohn's disease. *Am J Gastroenterol* 1999; **94**: 3279-3284
18 **Sawada-Hase N,** Kiyohara T, Miyagawa J, Ueyama H, Nishibayashi H, Murayama Y, Kashihara T, Nakahara M, Miyazaki Y, Kanayama S, Nezu R, Shinomura Y, Matsuzawa Y. An increased number of CD40-high monocytes in patients with Crohn's disease. *Am J Gastroenterol* 2000; **95**: 1516-1523
19 **Vogel JD,** West GA, Danese S, De La Motte C, Philipps MH, Strong SA, Willis J, Fiocchi C. CD40 mediated immune-nonimmune cells interactions induce mucosal fibroblast chemokines leading to T-cell transmigration. *Gastroenterology* 2004; **126**: 63-80
20 **Sandborn WJ,** Tremaine WJ, Batts KP, Pemberton JH, Phillips SF. Pouchitis after ileal pouch-anal anastomosis: pouchitis activity index. *Mayo Clinic Proc* 1994; **69**: 409-415
21 **Dougados M,** Van der Linden S, Juhin R, Huitfeldt B, Amor B, Calin A, Cats A, Dijkmans B, Olivieri I, Pasero G. The European Spondyloarthropaty Study Group preliminary criteria for the classification of spondyloarthropathy. *Arthritis Rheum* 1991; **34**: 1218-1227
22 **Seo M,** Okada M, Yao T, Ueki M, Arima S, Okomura M. An index of disease activity in patients with ulcerative colitis. *Am J Gastroenterol* 1992; **87**: 971-976
23 **Baron JH,** Connel AM, Lennard-Jones JE. Variation between observers in describing mucosal appearances in proctocolitis. *Br Med J* 1964; **1**: 89-92
24 **Lohmuller JL,** Pemberton JH, Dozois RR, Ilstrup D, van Heerden J. Pouchitis and extraintestinal manifestations of inflammatory bowel disease after ilal pouch-anal anastomosis. *Ann Surg* 1990; **211**: 622-627
25 **Hata K,** Watanabe T, Shinozaki M, Nagawa H. Patients with extraintestinal manifestations have a higher risk of developing pouchitis in ulcerative colitis: multivariate analysis. *Scan J Gastroenterol* 2003; **38**: 1055-1058
26 **Thomas PD,** Keat AC, Forbes A, Ciclitira PJ, Nicholls RJ. Extraintestinal manifestations of ulcerative colitis following restorative proctocolectomy. *Eur J Gastroenterol Hepatol* 1999; **11**: 1001-1005
27 **Kuhbacher T,** Schreiber S, Runkel N. Pouchitis: pathophysiology and treatment. *Int J Colorect Dis* 1998; **13**: 196-207
28 **Schmidt CM,** Lanzeby AJ, Hendrickson RJ, Sitzmann JV. Preoperative terminal ileal and colonic resection histopathology predicts risk of pouchitis in patients after ileoanal pull-through procedure. *Ann Surg* 1998; **227**: 654-665
29 **Gustavsson S,** Weiland LH, Kelly KA. Relationship of backwash ileitis to ileal pouchitis after ileal pouch-anala anastomosis. *Dis Colon Rectum* 1987; **30**: 25-28
30 **Polese L,** Keighley MRB. Adenomas at resection margins do not influence the long-term development of pouch polyps after restorative proctocolectomy for familial adenomatous polyposis. *Am J Surg* 2003; **186**: 32-34
31 **Danese S,** Katz JA, Saibeni S, Papa A, Gasbarrini A, Vecchi M, Fiocchi C. Activated platelets are the source of elevated levels of soluble CD40 ligand in the circulation of inflammatory bowel disease patients. *Gut* 2003; **52**: 1435-1441
32 **Thomas R,** Davis LS, Lipsky PE. Rheumatoid synovium is enriched in mature antigen-presenting dendritic cells. *J Immunol* 1994; **152**: 2613-2623
33 **Rissoan MC,** Van Kooten C, Chomarat P, Galibert L, Durand I, Thivolet-Bejui F, Miossec P, Banchereau J. The functional CD40 antigen of fibroblast may contribute to proliferation of rheumatoid synovium. *Clin Exp Immunol* 1996; **104**: 481-490
34 **Sekine C,** Yagita H, Miyasaka N, Okomura K. Expression and function of CD40 in rheumatoid arthritis synovium. *J Rheumatoid* 1998; **25**: 1048-1053
35 **Kyburtz D,** Corr M, Brinson DC, Von Damm A, Tighe H, Carson DA. Human rheumatoid factor production is dependent on CD40 signaling and autoantigens. *J Immunol* 1999; **163**: 3116-3122

Science Editor Guo SY **Language Editor** Elsevier HK

PO Box 2345, Beijing 100023, China
www.wjgnet.com
wjg@wjgnet.com

ELSEVIER

World J Gastroenterol 2005;11(34):5309-5313
World Journal of Gastroenterology ISSN 1007-9327
© 2005 The WJG Press and Elsevier Inc. All rights reserved.

• *CLINICAL RESEARCH* •

Different profile of cytokine synthesis according to the severity of acute pancreatitis

Raquel Laveda, Juan Martínez, Carlos Muñoz, Juan Carlos Penalva, Jesus Sáez, Germán Belda, Salvador Navarro, Faust Feu, Anton Mas, José Ma Palazón, José Sánchez-Payá, José Such, Miguel Pérez-Mateo

Raquel Laveda, Juan Martínez, Carlos Muñoz, Juan Carlos Penalva, Jesus Sáez, German Belda, José Ma Palazón, José Sánchez-Payá, José Such, Miguel Pérez-Mateo, Gastroenterology Department and Liver Unit, Hospital General Universitario, Alicante, Spain
Salvador Navarro, Faust Feu, Anton Mas, Institut de Malalties Digestives, Hospital Clínic. Institut d'Investigacions Biomédiques August Pi I Sunyer, Barcelona, Spain
Supported by grants C03/02 and G03/156 from Instituto de Salud Carlos III (Madrid, Spain)
Co-first-authors: Raquel Laveda and Juan Martínez
Co-correspondents: Raquel Laveda
Correspondence to: Dr. Juan Martínez, Department of Gastroenterology, Hospital General Universitario de Alicante, Pintor Baeza s/n, Alicante 03010, Spain. jmsempere@coma.es
Telephone: +34-96-5938345 Fax: +34-96-5938355
Received: 2005-01-24 Accepted: 2005-02-18

Abstract

AIM: To evaluate the cellular synthetic ability of cytokines involved in pro- and anti-inflammatory reactions in patients with AP.

METHODS: Sixty-seven patients with AP (16 severe, 51 mild) and 10 controls were included in the study. Cultures of whole blood were performed in samples obtained within the first 72 h from the onset of pain. Serum levels of interleukins (IL) 6, 8, 10, and TNF-α were measured at baseline and in the supernatant of cultures with (functional reserve) or without stimulation with phytohemaglutinin.

RESULTS: Basal levels of cytokines were significantly higher in patients with severe AP. A significant increase of all pro-inflammatory cytokines *vs* basal levels was observed in the supernatant after 24 h of whole blood cultures in patients, but not in controls. In contrast, IL-10 increased significantly in the supernatant of cultures only in patients with mild AP. Cells showed a statistically significant functional reserve for all IL in patients with mild, but only for pro-inflammatory cytokines in patients with severe AP.

CONCLUSION: A marked activation of immune system may be observed in patients with AP, being balanced between pro- and anti-inflammatory cytokines in patients with mild but not severe AP. A reduced functional reserve for the synthesis of IL-10 may be observed in patients with severe AP, which might lead to a worst prognosis.

© 2005 The WJG Press and Elsevier Inc. All rights reserved.

Key words: Acute pancreatitis; Cytokines; Severity; Whole blood

Laveda R, Martínez J, Muñoz C, Penalva JC, Sáez J, Belda G, Navarro S, Feu F, Mas A, Palazón JM, Sánchez-Payá J, Such J, Pérez-Mateo M. Different profile of cytokine synthesis according to the severity of acute pancreatitis. *World J Gastroenterol* 2005; 11(34): 5309-5313
http://www.wjgnet.com/1007-9327/11/5309.asp

INTRODUCTION

Patients with acute pancreatitis (AP) show an exacerbated local inflammatory reaction, likely as the consequence of the pancreatic cellular injury[1,2], which may be followed by a generalization of the process, leading to a potentially severe systemic form of the disease with multiple organ failure and eventually death[3]. This clinical situation is at least partially mediated by a marked host's immune response and a prolonged or exacerbated synthesis of pro-inflammatory cytokines, such as tumor necrosis factor-α (TNF-α) and interleukins (IL) 1, 6 and 8[4-8]. In fact, recent findings have shown the existence of a significant correlation between the serum levels of the mentioned cytokines and the severity of AP[8-12].

The liberation of pro-inflammatory cytokines is followed by the synthesis of anti-inflammatory cytokines, such as IL-10, whose function is to counterbalance the hypothetical deleterious effects of an exacerbated immune response[7,13]. There is scarce and conflicting information regarding the possible effect of IL-10 in the control of the inflammatory process in patients with AP[14,15].

A main drawback in the study of cytokines in any clinical setting is its intermittent pattern of secretion and short half-life[16]. To overcome these complications, several approaches have been considered, such as the measurement of the more durable soluble cytokine receptors[9], or the measurement of the cytokine secretion patterns *in vitro* either by the culture of mononuclear cells[16] or whole blood with or without the addition of cellular stimulants.

The *in vitro* model has been utilized in different clinical settings[17,19], and it has revealed as simple, reproducible, and accurate method for evaluation of the cytokine secretion patterns, allowing the estimation of functional immune cellular reserve[20,21]. To our knowledge, no study has evaluated the usefulness of this method to investigate the inflammatory response in patients with AP. Then, the aims of this study

have been to investigate the *in vitro* secretion pattern of pro- and anti-inflammatory cytokines by whole blood cultures in patients with AP, and the estimation of the functional cellular reserve.

MATERIALS AND METHODS

Patients

A prospective series of patients with clinical diagnosis of AP and less than 48 h from the onset of symptoms admitted to the Gastroenterology Departments of two academic hospitals were consecutively included in a prospective study. The diagnosis of AP was defined as the presence of clinically compatible abdominal pain with an increase of serum amylase three times above the upper normal limit, evidence of pancreatic swelling by imaging techniques and exclusion of other possible causes of abdominal pain.

Patients with severe or mild forms of AP according to Atlanta's criteria[22] of severity were analyzed separately. A group of healthy subjects were considered as controls. The Hospital General Universitario Ethics Committee approved the study protocol, and all patients gave their informed consent for the inclusion in the study.

Methods

Blood was obtained for routine hematological, biochemical, and coagulation studies within 72 h from the onset of symptoms. Ten milliliters of blood was inoculated into two rubber-sealed pyrogen-free tubes (Endo Tube ET, Chromogenix AB, Vienna, Austria). One of the aliquots was centrifuged 10 min at 3 500 r/min and stored at -70 ℃ until analysis. Tubes were not exposed to free air.

Whole blood cultures Blood was distributed in a 24-well plate with or without the addition of 40 μL of phytohemaglutinin (PHA) at a concentration of 1 μg/mL for 24 h at 37 ℃ in a humidified atmosphere with 50 mL/L CO_2. Supernatants were obtained by centrifugation at 2 500 r/min for 5 min and stored at -80 ℃ until assay. The maximum period of time between being frozen and thawing was 3 mo, and none of the specimens was thawed and refrozen prior to analysis in the current study.

Measurement of TNF-α, IL-6, IL-8, and IL-10 Immunoenzymometric assays for the quantitative measurement of human TNF-α, IL-6, 8 and 10 in serum samples and in the supernatant of whole blood cultures were performed by handling Biosource IFN-γ EASIA Kit (Biosource Europe SA, Nivelles, Belgium), human TNF-α HS Quantikine®, and IL-6, IL-8 and IL-10 Quantikine® (R&D Systems, Minneapolis, MN, USA) according to manufacturer's instructions. All samples were tested in duplicate and read at 450 and 490 nm in a ThermoMax microplate reader (Molecular Devices, Sunnyvale, CA, USA). The lower levels of sensitivity for measurement of cytokines were 1.7 pg/mL for TNF-α, 5 pg/mL for IL-6, 2 pg/mL for IL-8 and 10 pg/mL for IL-10.

We consider the presence of a status of cellular pre-activation, when the levels of the different cytokines measured in the supernatant of non-stimulated whole blood cultures were significantly higher to that measured in basal samples. We considered that cellular functional reserve exists for the synthesis and secretion of cytokines, when the levels of the different parameters measured in the supernatant of whole blood cultures plus the addition of PHA were higher to those measured in the non-stimulated cultures, and conversely, no functional reserve was considered, when the levels obtained with cellular stimulants were similar to those obtained without PHA.

Statistical analysis

All the observations are reported as median and 25th and 75th percentiles. Statistical differences were analyzed using the Mann-Whitney *U* test for the comparison among different groups and the Wilcoxon test for the comparisons within each group at different times. A P value <0.05 indicated statistical significance. Analyses were performed with the SPSS Statistical package (SPSS Inc., version 11.0, Chicago, IL).

RESULTS

Sixty-seven patients diagnosed of AP were included in the study. AP was considered severe in 16 patients (6 male, mean age 66±16 years) and mild in 51 cases (23 male, mean age 61±16 years). Ten healthy subjects were studied as controls (6 male, mean age 45±19 years). The etiology of AP was biliary in 37 patients (55.3%), alcoholic in 8 patients (11.9%) and others (hypertriglyceridemia, post-endoscopic cholangiopancreatography (ERCP), drugs or idiopathic) in 22 cases (32.8%). We did not find statistically significant differences in sex, age, and etiology of AP among groups. Five patients developed respiratory insufficiency (7.5%) and one progressed to acute renal failure (1.5%). Regarding local complications, five patients developed a pseudocyst (7.5%), pancreatic necrosis was observed in five cases (7.5%), and infected pancreatic necrosis in one patient (1.5%). Overall, seven patients died during admission (10.4%), all being considered as severe AP.

Table 1 shows the levels observed in all parameters studied in basal conditions and in the supernatant of whole blood cultures with all recorded statistical significances. Basal levels of IL-6 in patients with SAP were significantly higher than that observed in controls and patients with mild AP ($P<0.05$). Basal IL-8 and TNF-α measured in patients with severe AP were significantly higher than those in patients with mild AP, but not *vs* healthy controls ($P<0.01$ in both cases). Quite opposite, statistically significant differences were observed when comparing IL-10 levels between patients with severe *vs* mild AP ($P<0.05$), but not *vs* controls (Figure 1).

When comparing basal values with those measured in the supernatant of non-stimulated cultures, significant differences were observed in all pro-inflammatory cytokines in patients with mild or severe AP, but not in controls. IL-10 increased significantly in these experimental conditions only in patients with mild AP (Figure 2).

When analyzing the cellular functional reserve (i.e., values measured in the supernatant of non-stimulated *vs* stimulated cultures), significant increases in pro-inflammatory cytokines were observed in all groups of patients (Figure 3).

Table 1 IL-6, IL-8, TNF-α and IL-10 levels in groups I–III

		IL-6 (pg / mL)	IL-8 (pg / mL)	TNF-α (pg / mL)	IL-10 (pg / mL)
SAP	Basal	105.6 (52.0–210)[a]	46.8 (26.2–95)[b]	15.8 (7.1–21.7)[b]	17.7 (7.5–29.4)[c]
	24 h	208.0 (140–476)[e]	872.0 (316–3 280)[e]	58.7 (52–132)[e]	12.5 (8.4–34.6)
	24 h+PHA	925.0 (303–1 219)[g]	2 715.0 (760–8 599)[g]	473.0 (308–518)[g]	7.2 (2.2–47.3)
MAP	Basal	15.0 (5.4–33.2)	18.5 (1.2–33.6)	7.9 (4.1–17.7)	7.3 (4.1–-1.6)
	24 h	133.0 (53.6–856)[e]	1 611.0 (484–4 336)[e]	62.4 (45.5–100.5)[e]	20.8 (6.5–44.1)[e]
	24 h+PHA	2 057.0 (605–4 189)[g]	8 045.0 (3 377–28 209)[g]	540.5 (422–824.7)[g]	51.9 (32.1–131.3)[g]
Controls	Basal	3.2 (0.9–6.7)	35.6 (17.9–93.7)	4.3 (2.2–6.1)	9.4 (6–14.4)
	24 h	7.1 (4.9–9.6)	46.9 (32.2–94.5)	7.1 (4.1–10.1)	21.3 (18.3–34.5)
	24 h+PHA	610.0 (404.7–1 026)[g]	1 396.0 (962–3 065.2)[g]	792.0 (573.2–1 064.7)[g]	53.0 (43.4–80.1)[g]

Data are shown as median (25th–75th percentiles). SAP: severe acute pancreatitis; MAP: mild acute pancreatitis; controls: healthy controls; basal: samples obtained within 72 h from the onset of symptoms; 24 h: supernatant of culture after 24 h without stimulation; 24 h+PHA: supernatant of culture after 24 h with addition of PHA to the culture media; IL-6, IL-8, and IL-10: interleukins 6, 8 and 10 respectively; TNF-α: tumor necrosis factor-α. [a]$P<0.05$ *vs* the corresponding values in groups II and III; [b]$P<0.01$ *vs* the corresponding value in group II; [c]$P<0.05$ *vs* the corresponding value in group II; [e]$P<0.05$ *vs* basal levels within each group; [g]$P<0.05$ *vs* 24 h levels within each group.

However, a significant functional reserve for IL-10 was observed only in controls and in patients with mild, but not severe AP (Figure 3).

For better measurement of functional reserve, we estimated the increase observed in each studied parameter with values obtained in non-stimulated *vs* stimulated cultures in all three groups, and observed that this increment is higher in patients with mild than in severe AP, although this reached significance only when measuring IL-6 and IL-10 (Figure 4).

DISCUSSION

Cytokines are soluble components of the inflammatory cascade that play a seminal role in the pathogenesis of the systemic response syndrome that usually takes place in patients with AP[4-8]. Different works have shown a relationship between the levels of different pro-inflammatory cytokines reached in serum and the severity of AP, and patients with highest levels of these factors in the early phases of the disease are those developing systemic complications[8-12].

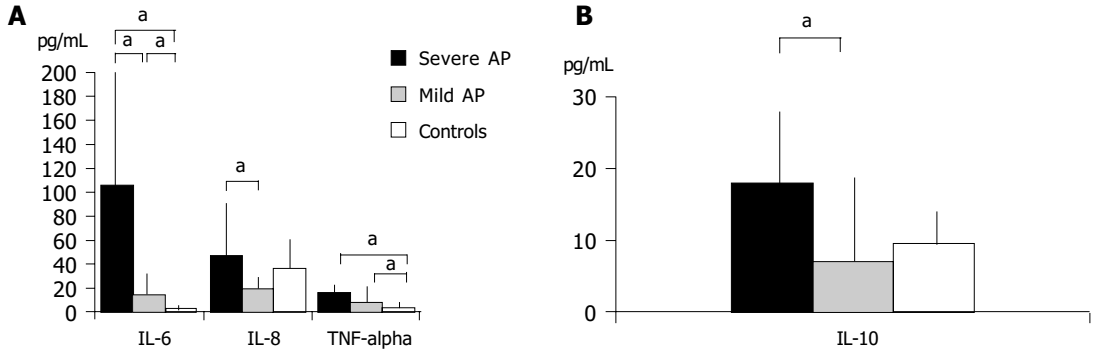


Figure 1 Basal levels of pro- (**A**) and anti-inflammatory cytokines (**B**) in patients and healthy controls. [a]$P<0.05$ *vs* others.

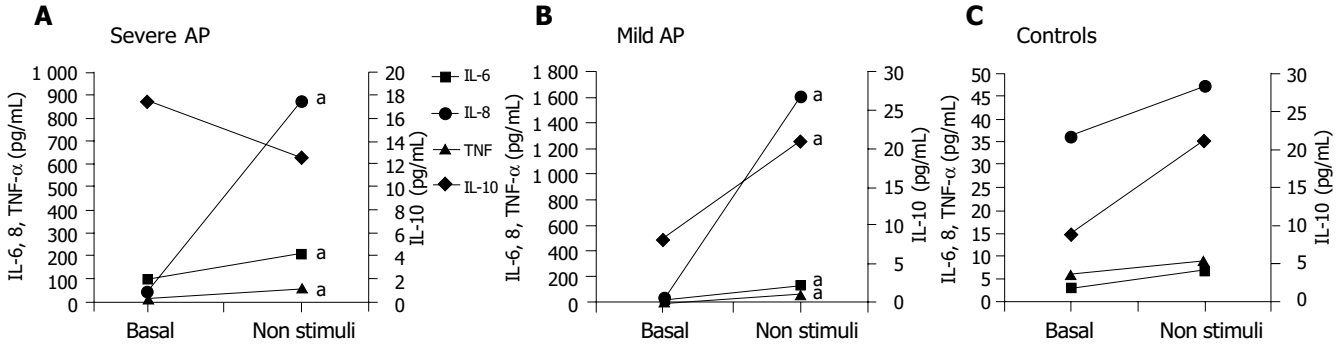


Figure 2 Cellular pre-activation status: comparison of basal levels of cytokines with those measured in the supernatant of non-stimulated cultures, in patients with severe (**A**) or mild AP (**B**), and healthy controls (**C**). [a]$P<0.05$ *vs* others.

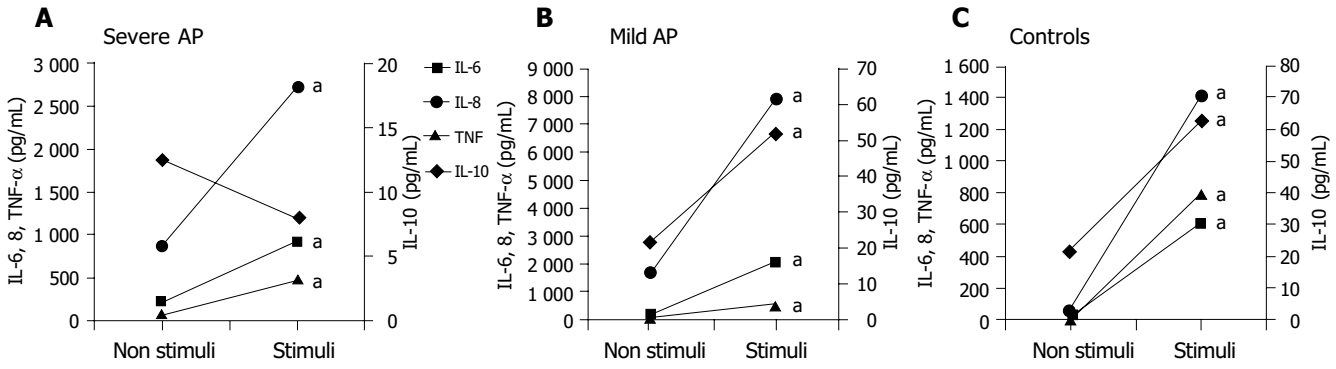


Figure 3 Cellular functional reserve: comparison of levels of cytokines measured in the supernatant of stimulated whole blood cultures with values obtained in non-stimulated cultures in patients with severe (**A**) or mild AP (**B**), and healthy controls (**C**). [a]*P*<0.05 *vs* others.

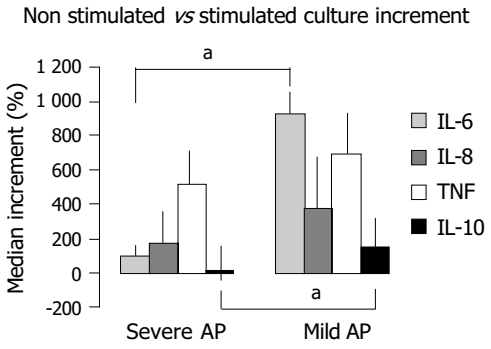


Figure 4 Cellular functional reserve represented as increments of all studied cytokines in patients. [a]*P*<0.05 *vs* others.

It has been recently described the anti-inflammatory role of certain cytokines, namely IL-10, and the most accepted hypothesis suggests that this is a mechanism devoted to compensate the systemic inflammatory response that precedes the development of multi-organ failure[7,13,23,24]. The existence of a misbalance between pro- and anti-inflammatory cytokines would participate in the genesis of the systemic complications that may develop in some patients with AP[25]. The information available regarding IL-10 levels in patients with AP is controversial, and the results obtained in the different studies show a great variability[13-15,23,24]. However, the experimental administration of IL-10 in animal models of induced AP has been shown to reduce cytokine release, the severity of AP and also mortality[26-28]. Similarly, the administration of this cytokine has been shown to reduce the incidence of AP in patients undergoing ERCP[29].

The discrepancies found when studying the cytokine profile in the clinical setting may be a reflection of several drawbacks inherent to the study of cytokines, such as the moment of obtaining the blood samples, its intermittent pattern of secretion, its autocrine or paracrine natural way of action[16], and short half-life. The culture of immunocompetent cells and measurement of cytokines and effector molecules in the supernatant has revealed that it is a useful method to investigate the inflammatory status and cellular functional reserve in different clinical settings[17-19]. Although early attempts with the culture of monocytes did not give satisfactory data, likely due to a different environmental situation to what is expected to find *in vivo*[16], the culture of whole blood and measurement of cytokines in the supernatant appears to be a simple, reproducible and accurate method in the evaluation of synthesis of components of the inflammatory cascade, since it closely approximates to what is expected to find *in vivo*. In addition, it allows the study not only of the basal status of cellular activation, but also of the cellular functional reserve, when comparing the spontaneous cellular ability to synthesize cytokines with that when the cells are further stimulated[20,21]. To our knowledge, this methodological approach has not been explored in patients with AP.

We have observed a spontaneous and significant increase in the synthesis of pro-inflammatory cytokines in patients, when compared to controls after 24 h of non-stimulated culture that represents the degree of cellular preactivation (Figure 2), which likely supports the contention of the existence of an inflammatory pre-activation status in patients with AP. The fact that IL-10 increases significantly in non-stimulated cultures with respect to basal values in patients with mild AP (Figure 2B) likely suggests that an anti-inflammatory response follows a parallel course to the inflammatory reaction, probably as a balancing mechanism in patients with mild AP. This situation is not found in patients with severe AP (Figure 2A), and it is similar to what is observed, when comparing the non-stimulated IL-10 synthetic ability with that after culture stimulation in this same subgroup of patients (Figure 3A), suggesting the absence of cellular functional reserve for this anti-inflammatory cytokine. The rest of the cytokines evaluated in both groups of patients show a significant increase when cultures are stimulated with PHA *vs* values obtained in the supernatant of cultures without stimulation (Figures 2 and 3). Then, cells obtained from patients with AP, either mild or severe, show a marked pre-activation status that is reflected in the amount of pro-inflammatory cytokines that spontaneously secrete in culture (Figure 2) and show a certain degree of cellular functional reserve when PHA is added to the culture medium (Figure 3). This is not, however, the case with respect to IL-10, as a key parameter of anti-inflammatory cytokines, since in both situations, i. e., in spontaneous culture, and after stimulation with PHA, the levels of this cytokine stabilize or even decrease (Figures 2 and 3). Figure 4 reinforces this concept when analyzing the increments of all parameters evaluated in different experimental situations.

We cannot exclude that a continuous status of inflammatory activation in patients with severe AP may lead to an early depletion of anti-inflammatory cytokines and incapacity to counterbalance the inflammatory cascade. Following this same line of thinking, it would be logical to hypothesize that an insufficient anti-inflammatory response might exert a causative effect in a subgroup of patients with AP, favoring a worse clinical evolution. The conserved cellular reserve in patients with mild AP (Figure 3B) likely supports our hypothesis.

In conclusion, the practice of whole blood cultures and measurement of cytokines either in non-stimulated *vs* stimulated conditions allows the estimation of the pre-activation status and the cellular functional reserve in patients with AP. In our series, the synthetic pattern of cytokines shows a different behavior in patients with mild or severe AP, and suggests that a reduced ability to synthesize anti-inflammatory cytokines in cases of severe AP may play a role in the clinical evolution of patients.

REFERENCES

1 **Weber CK,** Adler G. From acinar cell damage to systemic inflammatory response: current concepts in pancreatitis. *Pancreatology* 2001; **1**: 356-362
2 **Dominguez-Muñoz JE,** Viedma JA, Pérez-Mateo M, Carballo F, García Fe M. Inflammatory response in the initial phase of acute pancreatitis: Relationship to the onset and severity of the disease. *Rev Esp Enf Digest* 1995; **87**: 236-246
3 **De Beaux AC,** Palmer KR, Carter DC. Factors influencing morbidity and mortality in acute pancreatitis; an analysis of 279 cases. *Gut* 1995; **37**: 121-126
4 **Bhatia M,** Brady M, Shokuhi S, Christmas S, Neoptolemos JP, Slavin J. Inflammatory mediators in acute pancreatitis. *J Pathol* 2000; **190**: 117-125
5 **Kusske AM,** Rongione AJ, Reber HA. Cytokines and acute pancreatitis. *Gastroenterology* 1996; **110**: 639-642
6 **Schmid RM,** Adler G. Cytokines in acute pancreatitis: new pathophysiological concepts evolve. *Eur J Gastroenterol Hepatol* 1999; **11**: 125-127
7 **Schölmerich J.** Interleukins in acute pancreatitis. *Scand J Gastroenterol* 1996; **219**: 37-42
8 **Norman J.** The role of cytokines in the pathogenesis of acute pancreatitis. *Am J Surg* 1998; **175**: 76-83
9 **De Beaux AC,** Goldie AS, Ross JA, Carter DC, Fearon KC. Serum concentrations of inflammatory mediators related to organ failure in patients with acute pancreatitis. *Br J Surg* 1996; **83**: 349-353
10 **Berney T,** Gasche Y, Robert J, Jenny A, Mensi N, Gau G, Vermeulen B, Morel P. Serum profiles of interleukin-6, interleukin-8 and interleukin-10 in patients with severe and mild acute pancreatitis. *Pancreas* 1999; **18**: 371-377
11 **Chen CC,** Wang SS, Lee F, Lee FY, Chang FY, Lee SD. Proinflammatory cytokines in early assesment of the prognosis of acute pancreatitis. *Am J Gastroenterol* 1999; **94**: 213-218
12 **Hirota M,** Nozawa F, Okabe A, Shibata M, Beppu T, Shimada S, Egami H, Yamaguchi Y, Ikei S, Okajima T, Okamoto K, Ogawa M. Relationship between plasma cytokine concentration and multiple organ failure in patients with acute pancreatitis. *Pancreas* 2000; **21**: 141-146
13 **Simovic M,** Bonham M, Abu-Zidan F, Windsor JA. Anti-inflamatory cytokine response and clinical outcome in acute pancreatitis. *Crit Care Med* 1999; **27**: 2662-2665
14 **Pezzilli R,** Billi P, Miniero R, Barakat B. Serum interleukin-10 in human acute pancreatitis. *Dig Dis Sci* 1997; **42**: 1469-1472
15 **Chen CC,** Wang SS, Lu RH, Chang FY, Lee SD. Serum interleukin 10 and interleukin 11 in patients with acute pancreatitis. *Gut* 1999; **45**: 895-899
16 **McKay CJ,** Gallagher G, Brooks B. Increased monocyte production in association with systemic complications in acute pancreatitis. *Br J Surg* 1996; **83**: 919-923
17 **Beck J,** Rondot P, Catinot L, Falcoff E, Kirchner H, Wietzerbin J. Increased production of interferon gamma and tumor necrosis factor precedes clinical manifestation in multiple sclerosis: do cytokines trigger off exacerbations? *Acta Neurol Scand* 1988; **78**: 318-323
18 **Fahey JL.** Cytokines, plasma immune activation markers, and clinically relevant surrogate markers in human immunodeficiency virus infection. *Clin Diagn Lab Immunol* 1998; **5**: 597-603
19 **Katial RK,** Hershey J, Purohit-Seth T, Belisle JT, Brennan PJ, Spencer JS, Engler RJ. Cell-mediated immune response to tuberculosis antigens: comparison of skin testing and measurement of *in vitro* gamma interferon production in whole-blood culture. *Clin Diagn Lab Immunol* 2001; **8**: 339-345
20 **De Groote D,** Zangerle PF, Gevaert Y, Fassotte MF, Beguin Y, Noizat-Pirenne F, Pirenne J, Gathy R, López M, Dehart I. Direct stimulation of cytokines (IL-1 beta, TNF-alpha, IL-6, Il-2, INF-gamma and GM-csf) in whole blood. Comparison with isolated PBMC stimulation. *Cytokine* 1992; **4**: 239-248
21 **Van der Liden MW,** Huizinga TW, Stoeken DJ, Sturk A, Westendorp RG. Determination of tumour necrosis factor-alpha and interleukin-10 production in a whole blood stimulation system: assesment of labortory error and individual variation. *J Immunol Methods* 1998; **218**: 63-71
22 **Bradley E.** A clinically based classification system for acute pancreatitis: Summary of the international symposium on acute pancreatitis. *Arch Surg* 1993; **128**: 284-288
23 **Mayer J,** Rau B, Gansauge F, Beger HG. Inflammatory mediators in human acute pancreatitis: clinical and pathophysiological implications. *Gut* 2000; **47**: 546-552
24 **Brivet FG,** Emilie D, Galanaud P. Pro- and anti-inflammatory cytokines during acute severe pancreatitis: an early and sustained response, although unpredictable of death. Parisian Study Group on Acute Pancreatitis. *Crit Care Med* 1999; **27**: 749-755
25 **Bone RC.** Inmunologic dissonance: a continuing evolution in our understanding of the systemic immflamatory response síndrome (SIRS) and the multiple organ dysfunction syndrome (MODS). *Ann Intern Med* 1996; **125**: 680-687
26 **Rongione AJ,** Kusske AM, Kwan K, Ashley SW, Reber HA, McFadden DW. Interleukin 10 reduces the severity of acute pancreatitis in rats. *Gastroenterology* 1997; **112**: 960-967
27 **Kusske AM,** Rongione AJ, Ashley SW, McFadden DW, Reber HA. Interleukin-10 prevents death in lethal necrotizing pancreatitis in mice. *Surgery* 1996; **120**: 284-288
28 **Van Laethem JL,** Marchant A, Delvaux A, Goldman M, Robberecht P, Velu T, Deviere J. Interleukin 10 prevents necrosis in murine experimental acute pancreatitis. *Gastroenterology* 1995; **108**: 1917-1922
29 **Dumot JA,** Conwell DL, Zuccaro G, Vargo JJ, Shay SS, Easley KA, Ponsky JL. A randomized double blind study of interleukin 10 for he prevention of ERCP-induced pancreatitis. *Am J Gastroenterol* 2001; **96**: 2098-2102

Science Editor Guo SY **Language Editor** Elsevier HK

PO Box 2345, Beijing 100023, China
www.wjgnet.com
wjg@wjgnet.com

ELSEVIER

World J Gastroenterol 2005;11(34):5314-5321
World Journal of Gastroenterology ISSN 1007-9327
© 2005 The WJG Press and Elsevier Inc. All rights reserved.

• *CLINICAL RESEARCH* •

Severity of ultrasonographic liver steatosis and metabolic syndrome in Korean men and women

Hyeon Chang Kim, Sung Hee Choi, Hae Won Shin, Jae Youn Cheong, Kwan Woo Lee, Hyun Chul Lee, Kap Bum Huh, Dae Jung Kim

Hyeon Chang Kim, Department of Preventive Medicine, Yonsei University College of Medicine, Seoul, South Korea
Sung Hee Choi, Department of Internal Medicine, Seoul National University College of Medicine, Seongnam, South Korea
Hae Won Shin, Department of Public Health, Graduate School of Yonsei University, Seoul, South Korea
Jae Youn Cheong, Department of Gastroenterology, Ajou University School of Medicine, Suwon, South Korea
Kwan Woo Lee, Dae Jung Kim, Department of Endocrinology and Metabolism, Ajou University School of Medicine, Suwon, South Korea
Hyun Chul Lee, Department of Internal Medicine, Yonsei University College of Medicine, Seoul, South Korea
Kap Bum Huh, Huh's Diabetes Center and the 21st Century Diabetes and Vascular Research Institute, Seoul, South Korea
Correspondence to: Dae Jung Kim, MD, San-5 Wonchon-dong Youngtong-gu, Suwon 443-721, South Korea. djkim@ajou.ac.kr
Telephone: +82-31-219-5128 Fax: +82-31-219-4497
Received: 2005-03-16 Accepted: 2005-04-02

Abstract

AIM: To evaluate the association between the severity of liver steatosis and metabolic syndrome in apparently healthy Korean adults.

METHODS: We examined 1 022 men and women, aged 30-79 years, who participated in a health screening test. A standard interview, anthropometrics, biochemical studies, and abdominal ultrasonography were conducted for each participant. Metabolic syndrome was defined according to the National Cholesterol Education Program Adult Treatment Panel III, with a modification for the waist circumference cut-off level. The severity of liver steatosis was evaluated using liver ultrasonography, and serum aspartate aminotransferase (AST), alanine aminotransferase (ALT), and γ-glutamyl transferase (γ-GT) levels were determined.

RESULTS: Ultrasonographic liver steatosis was strongly associated with metabolic syndrome and common metabolic abnormalities. Compared with people without steatosis, people with mild, moderate, and severe steatosis had adjusted odds ratios for metabolic syndrome of 1.72 (95%CI, 1.01-2.94), 2.89 (1.75-4.76) and 3.53 (1.25-9.98) in men, and 2.86 (1.64-5.01), 3.19 (1.80-5.65) and 3.70 (0.82-16.73) in women, respectively. The serum AST level was not associated with metabolic syndrome. The serum ALT and γ-GT levels were significantly associated with metabolic syndrome in men but not in women.

CONCLUSION: The occurrence of metabolic syndrome shows a stronger association with the severity of ultrasonographic steatosis than with the serum liver enzyme levels. The degree of fatty infiltration detected on ultrasonography can be used as an indicator of liver dysfunction attributable to metabolic abnormalities.

© 2005 The WJG Press and Elsevier Inc. All rights reserved.

Key words: Metabolic syndrome; Liver steatosis; Non-alcoholic fatty liver disease; Ultrasonography

Kim HC, Choi SH, Shin HW, Cheong JY, Lee KW, Lee HC, Huh KB, Kim DJ. Severity of ultrasonographic liver steatosis and metabolic syndrome in Korean men and women. *World J Gastroenterol* 2005; 11(34): 5314-5321
http://www.wjgnet.com/1007-9327/11/5314.asp

INTRODUCTION

Non-viral non-alcoholic fatty liver disease (NAFLD) is an increasingly recognized condition that accompanies an increase in obesity[1-3]. NAFLD is known to be associated with various metabolic abnormalities including central obesity, type 2 diabetes, dyslipidemia, and high blood pressure[2,4-9], which are also well-established cardiovascular risk factors. Recently, it was suggested that fatty liver disease can be considered to be the hepatic consequence of metabolic syndrome or of a cluster of metabolic disorders[10-14]. In a previous report, we showed that NAFLD is closely associated with various metabolic abnormalities even in non-obese non-diabetic Korean people[15].

NAFLD has a wide clinical spectrum, and its severity can be measured by several methods. Liver biopsy represents the best diagnostic test for staging liver steatosis, inflammation, and fibrosis, but medical and ethical considerations limit its use in subjects with non-progressive fatty liver conditions[14,16]. The severity of fatty liver disease can also be evaluated based on the serum levels of liver enzymes such as aspartate aminotransferase (AST), alanine aminotransferase (ALT), and γ-glutamyl transferase (γ-GT)[1,2]. These enzymes are sensitive markers of liver cell damage, but they cannot provide information on the underlying causes of that damage. It has been shown that liver ultrasonography, although not sufficiently sensitive to detect liver inflammation and fibrosis, demonstrates a good correlation with histological findings of fatty infiltration, and international guidelines have been proposed for the diagnosis of different degrees of steatosis[17-19]. However, there are few data available on the

association of metabolic syndrome with the severity of liver steatosis assessed by ultrasonography.

Therefore, in the present study, we expanded our investigation to examine the sex-specific association between the severity of ultrasonographic liver steatosis and the presence of metabolic syndrome. In addition, we also examined the sex-specific association between the serum liver enzyme levels and metabolic syndrome.

MATERIALS AND METHODS

Subjects

This study was performed as part of the Korean metabolic syndrome study, which was undertaken to evaluate the role of metabolic syndrome as a risk factor for cardiovascular disease in Korean adults. We measured the metabolic profile, evaluated the cardiovascular risk factors, and performed abdominal ultrasonography scans on 1 244 men and women. The measurements were made over a 3-mo period (April-June, 2001) at a health screening center in Seoul, South Korea. All participants were healthy, independently functioning individuals who visited the health center for health-screening tests. From among the 1 244 initial volunteers, we selected 1 142 people who were between 30 and 79 years and who had completed anthropometric measurements, serum biochemistry profiles, and liver ultrasonography. We excluded 120 people who had a previous history of coronary heart disease or stroke and 35 people who tested positive for hepatitis B virus surface antigen (HBsAg). Ultimately 1 022 subjects (557 men and 465 women) were included in the analyses.

Measurements

Trained nurses interviewed all participants and obtained their medical history, family history of chronic disease, and information on life style factors, using a standardized questionnaire. The weight and height of each participant were measured while the participant was clothed only in a light gown, and the body mass index was calculated as body weight divided by height squared (kg/m^2). The waist circumference was measured midway between the lowest rib margin and the iliac crest in a standing position, by the same examiner. The percent body fat was measured by bioelectrical impedance analysis (Inbody 2.0, Biospace Co., South Korea). The participants were required to rest for at least 5 min prior to two repeated measurements of their blood pressure at an interval of at least 1 min. The mean value of these two measurements was used for the analyses. Blood samples were obtained from each participant after a fasting period of at least 8 h. The blood glucose level was measured using the glucose oxidase method. The serum insulin level was measured using a radioimmunoassay that had an interassay coefficient of variation of 4%. As an index of insulin resistance, we used the fasting insulin-glucose product. When divided by 22.5, this product is numerically equivalent to the homeostasis model assessment of insulin resistance (HOMA-IR)[20], which has been shown to correlate well with the results of the euglycemic hyper-insulinemic clamp in population-based studies[21]. Serum total cholesterol, high-density lipoprotein (HDL) cholesterol, and triglyceride levels were measured on an autoanalyzer using enzymatic colorimetry. Serum levels of AST, ALT, and γ-GT were also measured using enzymatic methods.

The carotid arteries were evaluated by the same examiner using high-resolution B-mode ultrasonography with a 7.5-MHz probe. The carotid intima-media thickness (IMT) was obtained by measuring the distance between the first and second echogenic lines using a caliper. For each common carotid artery, three measurements were performed and the maximum IMT of each common carotid artery was selected. All measurements were made by the same examiner. Liver ultrasound scans were performed to assess the presence and degree of liver steatosis. All ultrasound scans were performed by the same operator, who was unaware of the participants' medical histories and laboratory findings, using a high resolution B-mode scanner (SSD-5500, Aloka, Tokyo, Japan). Liver steatosis was assessed semi-quantitatively on a scale of 0-3 (0, absent; 1, mild; 2, moderate; 3, severe), on the basis of abnormally intense, high-level echoes arising from the hepatic parenchyma, liver-kidney difference in echo amplitude, echo penetration into the deep portion of the liver, and clarity of the blood vessel structure in the liver (Figure 1)[17].

Metabolic syndrome was defined according to the criteria established by the National Cholesterol Education Program Adult Treatment Panel III (ATP III), except for the determination of abdominal obesity by waist circumference[22]. We used a waist circumference cut-off level of >90 cm in men and >80 cm in women, based on the report by the International Diabetes Institute/Western Pacific World Health Organization/International Obesity Task Force[23]. Hence, in this study, participants having three or more of the following five criteria were defined as having metabolic syndrome: high blood pressure (≥130/85 mmHg), elevated fasting blood glucose (≥110 mg/dL or 6.05 mmol/L), hypertriglyceridemia (≥150 mg/dL or 1.65 mmol/L), low HDL-cholesterol (men, <40 mg/dL or 1.05 mmol/L; women, <50 mg/dL or 1.30 mmol/L), and abdominal obesity by waist circumference (men, >90 cm; women, >80 cm). Participants taking anti-hypertensive or anti-diabetic medications were included in the high blood pressure group and the high fasting blood glucose group, respectively.

Statistical analysis

We reported the clinical and biochemical characteristics of the participants according to the severity of the liver steatosis on ultrasound examination, separating the data for the men and women. For each variable, the linear trend with the severity of ultrasound liver steatosis was tested. The prevalence of abnormal metabolic conditions and metabolic syndrome were calculated for each level of severity of liver steatosis, and the linear trends were also tested. In order to assess the independent association between liver steatosis and metabolic syndrome, age- and multivariate-adjusted logistic regression models were used. First, we estimated the age-adjusted odds ratios of having metabolic syndrome for each level of severity of liver steatosis. In the multivariate model, we estimated the corresponding odds ratios after adjustments for age, menopause (women only), body mass index, cigarette smoking, and alcohol intake. We also estimated the adjusted

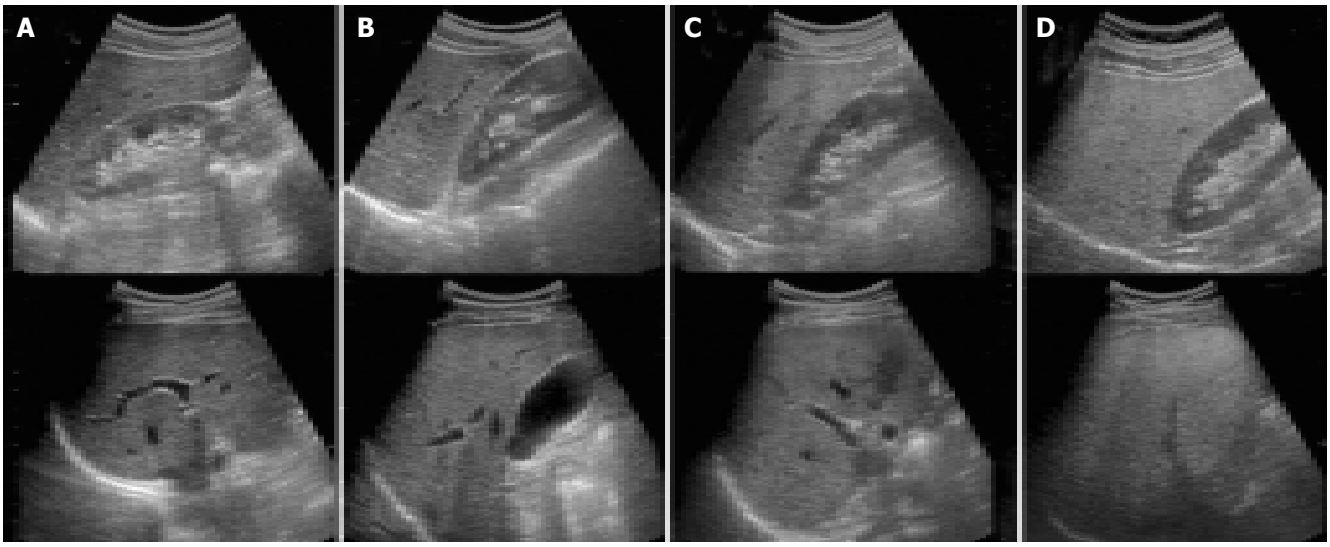


Figure 1 Ultrasonographic findings of liver according to the degree of steatosis. (**A**) Normal liver, (**B**) mild steatosis: a slight augmentation in liver echogenicity, a slight exaggeration of echogenic discrepancy between liver and kidney, and a relative preservation of echo line in the portal vein wall. (**C**) Moderate steatosis: a loss of echo line in the portal vein wall, particularly from the peripheral branches, resulting in a featureless appearance of the liver. (**D**) Severe steatosis: much greater reduction in echo penetration, a loss of echogenicity in most of the portal vein wall, including the main branches, and a large echo discrepancy between liver and kidney. Adapted from Saverymuttu *et al*.[17].

odds ratios of having metabolic syndrome for the different levels of the serum liver enzymes, AST, ALT, and γ-GT. For each enzyme, four categories were established using cut-off values determined by the level at which the number of individuals in each category was nearest to the number in the corresponding level of ultrasonographic severity. The SAS System version 8.01 (SAS Institute, Cary, NC, USA) was used to perform all statistical analyses. All statistical tests were two-sided, and *P*-values less than 0.05 were considered statistically significant.

RESULTS

Among the 557 men and 465 women examined, ultrasonographic scans revealed mild steatosis in 133 (23.9%) men and 87 (18.7%) women, moderate steatosis in 165 (29.6%) men and 93 (20.0%) women, and severe steatosis in 19 (3.4%) men and 10 (2.2%) women. The clinical characteristics and laboratory data of the participants with different degrees of steatosis as detected on ultrasonography are shown in Table 1. In men, the mean age was similar among the groups with different severities of steatosis, but in women there was a positive association between age and liver steatosis. With increasing severity of liver steatosis, there were statistically significant progressive increases in mean body mass index, waist circumference, body fat percent, blood pressure, total serum cholesterol, and serum triglycerides, and there was a statistically significant decrease in mean HDL-cholesterol. A statistically significant increase was also observed in the mean fasting glucose and insulin levels, and in insulin resistance, as assessed by mean HOMA values. The levels of liver enzymes (AST, ALT, and γ-GT) and carotid IMT were also positively associated with the degree of fatty infiltration. In contrast, cigarette smoking and alcohol intake were not associated with liver steatosis.

In both men and women, fatty liver detected by ultrasonography was strongly associated with metabolic syndrome and the five metabolic abnormalities, which are criteria for its clinical diagnosis. Among the 515 people without liver steatosis, only 19.6% (16.3% for men and 22.6% for women) had metabolic syndrome, whereas almost half (48.3%; 41.0% for men and 60.5% for women) of those with liver steatosis had metabolic syndrome. In addition, the prevalence of metabolic syndrome and of each of the five metabolic abnormalities progressively increased with the severity of liver steatosis (Table 2).

In the age-adjusted logistic regression model, the participant group with liver steatosis had a significantly higher odds ratio of having metabolic syndrome than did the group without steatosis. The odds ratio also increased with increasing severity of liver steatosis. When we adjusted for age, menopause, body mass index, cigarette smoking and alcohol intake, the association between liver steatosis and metabolic syndrome was attenuated but still was highly significant (Table 3). To assess the possible confounding effects of alcoholic hepatitis, we examined the association between liver steatosis and metabolic syndrome by frequency of alcohol intake and found similar results regardless of the frequency of alcohol consumption (data not shown).

The possible associations of serum levels of AST, ALT, and γ-GT with metabolic syndrome were also examined. The serum AST level was not significantly associated with metabolic syndrome in either sex. Serum ALT and γ-GT levels were significantly associated with metabolic syndrome in men but not in women (Table 4).

DISCUSSION

Metabolic syndrome is very common in Western countries and is also increasingly frequent in most developing countries. Fatty liver is a common condition increasingly detected by

Table 1 Clinical and biochemical characteristics of 557 men and 465 women with different severities of ultrasonographic liver steatosis

Characteristics	Ultrasonographic liver steatosis									
	Men				*P* for trend	Women				*P* for trend
	Absent (*n* = 240)	Mild (*n* = 133)	Moderate (*n* = 165)	Severe (*n* = 19)		Absent (*n* = 275)	Mild (*n* = 87)	Moderate (*n* = 93)	Severe (*n* = 10)	
Age (yr)	51.6±11.0	50.0±9.9	51.4±10.6	49.2±11.2	0.521	51.5±9.4	52.7±9.5	55.5±7.8	55.9±9.1	<0.001
Body mass index (kg / m^2)	23.1±2.5	24.7±2.3	25.3±2.6	26.5±2.1	<0.001	23.6±2.7	25.8±3.1	26.6±3.0	27.5±4.0	<0.001
Waist circumference (cm)	83.0±6.9	88.0±6.5	89.2±6.3	92.1±6.8	<0.001	79.0±7.0	85.2±7.7	88.0±7.4	88.5±8.5	<0.001
Body fat percent	20.0±4.4	23.0±4.2	23.4±4.1	24.1±3.5	<0.001	30.1±4.7	33.2±5.4	34.8±4.9	36.1±3.8	<0.001
Systolic BP (mmHg)	126.7±16.9	129.4±16.0	133.9±18.8	133.7±10.7	<0.001	128.4±20.2	131.7±17.3	136.5±19.1	138.5±10.6	<0.001
Diastolic BP (mmHg)	78.2±11.5	79.9±11.1	83.0±12.2	84.2±7.9	<0.001	78.2±13.2	80.7±12.0	82.7±11.9	82.0±7.9	0.002
Total cholesterol (mg / dL)	194.5±32.2	200.6±33.4	205.3±34.6	204.7±25.1	0.001	201.3±33.0	208.3±37.3	217.0±36.9	225.4±28.2	<0.001
Triglyceride (mg / dL)	149.4±104.9	200.2±119.5	230.1±161.8	230.6±111.7	<0.001	123.5±93.1	164.5±115.3	188.6±122.0	184.0±80.1	<0.001
HDL-cholesterol (mg / dL)	46.2±10.4	43.7±9.6	41.3±8.3	41.7±8.8	<0.001	52.9±13.4	47.3±12.8	47.0±12.1	47.0±7.6	<0.001
Fasting glucose (mg / dL)	97.5±23.3	101.7±19.6	108.3±29.4	117.2±36.0	<0.001	92.7±21.2	102.9±36.3	103.4±27.4	109.7±17.7	<0.001
Fasting insulin (IU / L)	9.8±11.4	11.9±6.9	12.6±7.1	13.2±5.1	0.002	9.1±4.9	13.9±8.6	15.1±9.7	16.9±6.2	<0.001
HOMA-IR	2.6±5.4	3.0±1.9	3.3±2.0	3.9±1.8	0.037	2.1±1.4	3.5±2.3	3.8±2.5	4.5±1.5	<0.001
AST (IU / L)	22.4±7.2	25.0±10.0	27.5±21.5	29.5±8.0	<0.001	21.0±7.8	21.4±11.3	23.0±11.2	28.2±6.3	0.013
ALT (IU / L)	23.4±11.8	31.5±18.3	38.3±35.9	50.8±19.0	<0.001	19.2±13.5	21.8±13.8	26.8±17.4	34.8±12.9	<0.001
γ-GT (IU / L)	45.1±50.6	67.1±63.4	69.4±148.8	69.4±42.6	0.009	23.7±22.8	31.6±37.7	32.8±21.3	38.7±11.1	<0.001
Carotid IMT (mm)	0.71±0.19	0.75±0.21	0.79±0.26	0.73±0.13	<0.001	0.70±0.21	0.77±0.23	0.79±0.23	0.81±0.31	<0.001
Menopause (%)						58.2	60.9	81.5	90.0	<0.001
Current smoking	47.9	46.6	42.4	42.1	0.269	5.1	5.8	1.1	10.0	0.345
Alcohol intake≥4 / wk	55.6	60.9	53.0	42.1	0.387	13.2	17.2	9.7	-	0.314
Carotid IMT≥1.0 (mm)	10.0	10.5	17.0	5.3	0.143	6.6	12.6	8.6	20.0	0.145

Table 2 Sex-specific prevalence of metabolic disorders by the severity of ultrasonographic liver steatosis

	Severity of ultrasonographic liver steatosis				*P*
	Absent	Mild	Moderate	Severe	
Men (%)	(*n* = 240)	(*n* = 133)	(*n* = 165)	(*n* = 19)	
Waist circumference >90 (cm)	14.6	33.1	44.2	57.9	<0.001
Blood pressure≥130 / 85 (mmHg)[1]	51.7	52.6	72.1	84.2	<0.001
Fasting glucose≥110 (mg / dL)[2]	11.3	12.0	21.8	15.8	0.008
Triglyceride≥150 (mg / dL)	33.8	63.2	67.3	73.7	<0.001
HDL-cholesterol <40 (mg / dL)	30.4	39.8	42.4	36.8	0.020
Metabolic syndrome (≥3 of the above)	16.3	31.6	46.7	57.9	<0.001
Number of metabolic abnormalities, mean±SD	1.4±1.1	2.0±1.2	2.5±1.1	2.7±1.1	<0.001
Women (%)	(*n* = 275)	(*n* = 87)	(*n* = 93)	(*n* = 10)	
Waist circumference >80 (cm)	42.9	81.6	87.1	90.0	<0.001
Blood pressure≥130 / 85 (mmHg)[1]	56.4	64.4	73.1	100.0	<0.001
Fasting glucose≥110 (mg / dL)[2]	2.2	14.9	16.1	40.0	<0.001
Triglyceride≥150 (mg / dL)	22.9	34.5	47.3	60.0	<0.001
HDL-cholesterol <50 (mg / dL)	41.8	62.1	62.4	70.0	<0.001
Metabolic syndrome (≥3 of the above)	22.5	54.0	65.6	70.0	<0.001
Number of metabolic abnormalities, mean±SD	1.7±1.1	2.6±1.1	2.9±1.1	3.6±1.3	<0.001

HDL: high density lipoprotein. [1]Including subjects taking anti-hypertensive medication. [2]Including subjects taking anti-diabetic medication.

routine abdominal ultrasonographic examination; however, the spectrum of fatty liver varies from mild NAFLD to progressive non-alcoholic steatohepatitis (NASH). NAFLD is a benign fatty liver disease, which accounts for the majority of elevated aminotransferase levels in asymptomatic patients[24]. In contrast, NASH is a more progressive form of fatty liver disease that can progress to liver fibrosis and even cirrhosis[1,14,25]. It has been suggested that fatty liver develops as the result of various metabolic conditions that promote fat accumulation and inflammation in the liver[10-14].

Liver biopsy is the only diagnostic test that is able to differentiate benign NAFLD from progressive NASH, but

Table 3 Sex-specific associations between the severity of ultrasonographic liver steatosis and metabolic syndrome

Ultrasound liver steatosis	Number of people	Number with metabolic syndrome (%)	Age-adjusted odds ratio (95%CI)	Multivariate-adjusted odds ratio (95%CI)[1]
Men				
Absent	240	39 (16.3)	1.00	1.00
Mild	133	42 (31.6)	2.43 (1.47-4.01)	1.72 (1.01-2.94)
Moderate	165	77 (46.7)	4.54 (2.87-7.20)	2.89 (1.75-4.76)
Severe	19	11 (57.9)	7.32 (2.76-19.44)	3.53 (1.25-9.98)
Total	557	169 (30.3)	*P*<0.001	*P*<0.001
Women				
Absent	275	62 (22.6)	1.00	1.00
Mild	87	47 (54.0)	4.06 (2.41-6.83)	2.86 (1.64-5.01)
Moderate	93	61 (65.6)	5.81 (3.45-9.80)	3.19 (1.80-5.65)
Severe	10	7 (70.0)	7.07 (1.73-28.89)	3.70 (0.82-16.73)
Total	465	177 (38.1)	*P*<0.001	*P*<0.001

[1]Adjusted for age, menopause (in women), body mass index, cigarette smoking, and alcohol intake.

Table 4 Sex-specific associations between liver enzyme levels and metabolic syndrome

	AST (IU/L)	Multivariate-adjusted odds ratio (95%CI)[1]	ALT (IU/L)	Multivariate-adjusted odds ratio (95%CI)[1]	γ-GT (IU/L)	Multivariate-adjusted odds ratio (95%CI)[1]
Men						
	9-21	1.00	4-22	1.00	9-35	1.00
	22-25	0.69 (0.42-1.16)	23-31	1.76 (1.04-2.99)	36-52	1.66 (0.95-2.90)
	26-46	0.89 (0.54-1.45)	32-77	2.57 (1.54-4.29)	53-180	3.20 (1.87-5.47)
	47-278	1.81 (0.62-5.28)	78-421	5.23 (1.69-16.18)	181-1 885	3.33 (1.09-10.16)
		P = 0.953		*P*<0.001		*P*<0.001
Women						
	9-21	1.00	4-19	1.00	8-22	1.00
	22-24	0.58 (0.32–1.06)	20-24	1.22 (0.70-2.12)	23-31	1.87 (1.06-3.30)
	25-42	0.96 (0.54–1.70)	25-61	1.44 (0.83-2.50)	32-100	1.25 (0.72-2.19)
	43-117	0.68 (0.16–2.93)	62-172	0.87 (0.20-3.73)	101-323	1.46 (0.33-6.37)
		P = 0.475		*P* = 0.271		*P* = 0.230

AST: aspartate aminotransferase; ALT: alanine aminotransferase; γ-GT: γ-glutamyl transferase. [1]Adjusted for age, menopause (in women), body mass index, cigarette smoking, and alcohol intake.

it should not be performed on the majority of patients with asymptomatic or mild fatty liver disease. Thus, the clinical evaluation of the severity of fatty liver disease in people with metabolic syndrome is usually based on a combination of ultrasonographic findings and laboratory tests. Liver ultrasonography is frequently used to assess fatty infiltration of the liver, but there is little information on the association between the metabolic diseases and the severity of fatty liver detected by ultrasonography. One previous study reported an association between common metabolic disorders and the severity of liver steatosis assessed by routine ultrasonography in 340 patients[14]. The present study showed that various metabolic abnormalities and metabolic syndrome were positively associated with the severity of ultrasonographic liver steatosis detected in 1 022 healthy people. Our findings suggest that liver ultrasonography can be used to monitor liver dysfunction that occurs in association with common metabolic abnormalities and metabolic syndrome.

Serum aminotransferase assays have also been widely used to detect and diagnose NAFLD[2,9], which is the most common cause of unexplained aminotransferase elevations in most Western populations and in some Asian populations. Thus, we assessed the associations between metabolic syndrome and the levels of several liver enzymes. In our data, metabolic syndrome showed a significant association with ALT and γ-GT levels only in men and showed no significant association with AST levels in either sex. For purposes of comparison, we categorized the enzyme levels so that the distribution of participants in the categories was similar to the distribution of subjects by ultrasonographic severity of steatosis; however, this type of categorization would not be relevant in clinical settings. Thus, we performed further analyses using different classification schemes and obtained similar findings.

The serum AST level is a sensitive marker of liver cell damage, but it has been less frequently used than ALT and γ-GT levels to monitor liver dysfunction because it is relatively non-specific for liver disease and correlates poorly with the clinical severity of liver disease[26]. Our findings support the use of serum ALT and γ-GT levels as indicators of the development of liver steatosis in men with metabolic syndrome. Recently, Jeong and colleagues reported that serum ALT levels were positively associated with metabolic disorders in a population, even when the levels were in the

normal range[27]. The results of that study differed from ours in that, the authors found a significant association in both sexes, although the association in women was weaker than that in men.

The sex-specific differences in the associations between liver enzyme levels and metabolic syndrome were not fully explained by the data. One contributing factor may be that, compared with men, women have relatively low ALT and γ-GT levels that fall within relatively narrow ranges[28,29]. Thus, serum enzyme levels in women might show a poor correlation with liver dysfunction. Another contributing factor to the sex-specific differences might be that the underlying causes of the enzyme elevation may differ by sex. For example, if central obesity is a major cause of enzyme elevation in men but not in women, the relationship between enzyme elevation and metabolic syndrome would likely differ by sex. Sakugawa *et al*., reported that serum γ-GT was correlated with the components of metabolic syndrome and its risk factors in the univariate analysis, but four variables were independently associated with γ-GT: age, hemoglobin, triglyceride, and diabetes[30]. The sex-specific differences shown by our analysis may also be attributable to chance observation. Thus, the association between the serum enzyme levels and metabolic syndrome in women requires further investigation.

The association between fatty liver disease and metabolic syndrome may be explained by several mechanisms. Type 2 diabetes (or insulin resistance) and central obesity have been frequently reported to be associated with both benign NAFLD and progressive NASH[2,4-9]. Insulin resistance is a key component of metabolic syndrome and is also a well-known risk factor for the development of NAFLD[31-33]. However, it is still controversial whether liver disease plays a primary role in the development of hyper-insulinemia and insulin resistance or is a consequence of insulin resistance. Recent studies have added evidence supporting the interpretation that insulin resistance is the primary phenomenon, by showing that hyper-insulinemia and insulin resistance do not stem from a reduction in hepatic insulin extraction, but from an enhancement in pancreatic insulin secretion that is compensatory to reduced insulin sensitivity[12,34-36].

Fatty liver disease has been reported to be closely related to indices of central obesity, such as waist circumference, waist-to-hip ratio, and visceral fat thickness[5,35,37]. Central obesity may contribute to insulin resistance, and increased visceral adiposity might be relevant in the pathogenesis of NAFLD[35,38]. Compared with adipose tissue in other sites, visceral adipose tissue is more resistant to insulin, exhibits greater lipolysis, and produces more free fatty acids[39]. The increased availability of substrates for lipogenesis and the relative hyperinsulinemia that accompany insulin resistance promote lipogenesis in the liver[40]. Visceral adipose tissue is also known to be a potent modulator of insulin action in hepatic glucose production and gene expression[41]. However, the significance of central obesity in the association between liver steatosis and metabolic syndrome may differ by ethnicity. It is well known that Asian people have lower body mass indices and waist circumferences than do Caucasians, but they have higher percent body fat and more cardiovascular risk factors for a given level of obesity[42,43]. In further analysis, we found that the association between liver steatosis and metabolic syndrome remained after additional adjustments were made for waist circumference; the odds ratios for mild, moderate, and severe steatosis were 1.37, 2.39, and 2.72 for men (P for trend <0.001), and 2.47, 2.57, and 3.27 for women (P for trend <0.001), respectively. Moreover, we have already reported that NAFLD was associated with various metabolic abnormalities in non-obese non-diabetic subjects[15]. Further studies will be required to investigate the ethnic and regional differences in the relationship between liver steatosis and metabolic syndrome.

Our study had several strengths. First, we showed an association between the degree of severity of liver steatosis detected by ultrasonography and the occurrence of metabolic syndrome in apparently healthy subjects. The progressive association between ultrasonographic liver steatosis and common metabolic diseases had previously been observed in data collected from patients, but had not yet been studied in the general population. Second, we were able to diminish the sources of inter-observer measurement error, for the liver ultrasonography in particular, because all of the measurements were performed by the same examiner in the same regulated setting, over a relatively short period (3 mo). Third, we were able to assess the association between metabolic syndrome and serum liver enzyme levels. Our data suggest that liver ultrasonography may be a better diagnostic tool than the determination of serum enzyme levels for monitoring liver function in people with metabolic syndrome.

We should point out some of the limitations of the present study. First, we could not assess the temporal relationship between fatty liver disease and metabolic syndrome because the study had a cross-sectional design. Although there is increasing evidence indicating that NAFLD is a hepatic consequence of metabolic syndrome[2,12,34,35], further prospective studies should be conducted to examine the temporal relationship between aminotransferase levels and metabolic syndrome in the general population. Second, we could not take into consideration any variation in the metabolic profile over time because we obtained only one measurement in each participant. Third, it is possible that we did not control entirely for confounding effects caused by viral and alcoholic liver diseases. We excluded subjects who were positive for HBsAg from the analyses because HBV infection is the most common liver disease in Korea, but we could not rule out the effects of other types of viral hepatitis. Alcoholic liver diseases are also common forms of chronic liver disease, but, in a further analysis, the association between liver steatosis and metabolic syndrome was not significantly affected by the level of alcohol intake. However, the possibility of residual confounding effects still exists because we measured alcohol intake with a simple questionnaire and did not use any objective index for alcohol intake. Finally, the study participants were apparently healthy members of the general population, but they were recruited from within a health screening center. Therefore, our study population was not necessarily representative of the general Korean population.

In conclusion, the present study showed a strong positive

association between the severity of ultrasonographic liver steatosis and the prevalence of metabolic syndrome in 1 022 apparently healthy Koreans. Our findings indicate that the degree of fatty infiltration detected on ultrasonography can be used as an indicator of liver dysfunction attributable to metabolic abnormalities. In addition, ultrasonography may be a better diagnostic tool than serum enzyme assays for monitoring liver function in people with metabolic syndrome.

REFERENCES

1 **James OF**, Day CP. Non-alcoholic steatohepatitis (NASH): a disease of emerging identity and importance. *J Hepatol* 1998; **29**: 495-501
2 **Angulo P**. Nonalcoholic fatty liver disease. *N Engl J Med* 2002; **346**: 1221-1231
3 **Marchesini G**, Bugianesi E, Forlani G, Cerrelli F, Lenzi M, Manini R, Natale S, Vanni E, Villanova N, Melchionda N, Rizzetto M. Nonalcoholic fatty liver, steatohepatitis, and the metabolic syndrome. *Hepatology* 2003; **37**: 917-923
4 **Wanless IS**, Lentz JS. Fatty liver hepatitis (steatohepatitis) and obesity: an autopsy study with analysis of risk factors. *Hepatology* 1990; **12**: 1106-1110
5 **Luyckx FH**, Lefebvre PJ, Scheen AJ. Non-alcoholic steatohepatitis: association with obesity and insulin resistance, and influence of weight loss. *Diabetes Metab* 2000; **26**: 98-106
6 **Bellentani S**, Saccoccio G, Masutti F, Croce LS, Brandi G, Sasso F, Cristanini G, Tiribelli C. Prevalence and risk factors for hepatic steatosis in northern Italy. *Ann Intern Med* 2000; **132**: 112-117
7 **Chitturi S**, Farrell GC. Etiopathogenesis of nonalcoholic steatohepatitis. *Semin Liver Dis* 2001; **21**: 27-41
8 **Loguercio C**, De Girolamo V, de Sio I, Tuccillo C, Ascione A, Baldi F, Budillon G, Cimino L, Di Carlo A, Di Marino MP, Morisco F, Picciotto F, Terracciano L, Vecchione R, Verde V, Del Vecchio Blanco C. Non-alcoholic fatty liver disease in an area of southern Italy: main clinical, histological and pathophysiological aspects. *J Hepatol* 2001; **35**: 568-574
9 **Dixon JB**, Bhathal PS, O'Brien PE. Nonalcoholic fatty liver disease: predictors of nonalcoholic steatohepatitis and liver fibrosis in the severely obese. *Gastroenterology* 2001; **121**: 91-100
10 **Cortez-Pinto H**, Camilo ME, Baptista A, De Oliveira AG, De Moura MC. Non-alcoholic fatty liver: another feature of the metabolic syndrome? *Clin Nutr* 1999; **18**: 353-358
11 **Marceau P**, Biron S, Hould FS, Marceau S, Simard S, Thung SN, Kral JG. Liver pathology and the metabolic syndrome X in severe obesity. *J Clin Endocrinol Metab* 1999; **84**: 1513-1517
12 **Pagano G**, Pacini G, Musso G, Gambino R, Mecca F, Depetris N, Cassader M, David E, Cavallo-Perin P, Rizzetto M. Nonalcoholic steatohepatitis, insulin resistance and metabolic syndrome: further evidence for an etiologic association. *Hepatology* 2002; **35**: 367-372
13 **Marchesini G**, Forlani G. NASH: from liver diseases to metabolic disorders and back to clinical hepatology. *Hepatology* 2002; **35**: 497-499
14 **Angelico F**, Del Ben M, Conti R, Francioso S, Feole K, Maccioni D, Antonini TM, Alessandri C. Non-alcoholic fatty liver syndrome: a hepatic consequence of common metabolic diseases. *J Gastroenterol Hepatol* 2003; **18**: 588-594
15 **Kim HJ**, Kim HJ, Lee KE, Kim DJ, Kim SK, Ahn CW, Lim SK, Kim KR, Lee HC, Huh KB, Cha BS. Metabolic significance of nonalcoholic fatty liver disease in nonobese, nondiabetic adults. *Arch Intern Med* 2004; **164**: 2169-2175
16 **`Brunt EM**, Janney CG, Di Bisceglie AM, Neuschwander-Tetri BA, Bacon BR. Nonalcoholic steatohepatitis: A proposal for grading and staging the histological lesions. *Am J Gastroenterol* 1999; **94**: 2467-2474
17 **Saverymuttu SH**, Joseph AE, Maxwell JD. Ultrasound scanning in the detection of hepatic fibrosis and steatosis. *BMJ* 1986; **292**: 13-15
18 **Osawa H**, Mori Y. Sonographic diagnosis of fatty liver using a histogram technique that compares liver and renal cortical echo amplitudes. *J Clin Ultrasound* 1996; **24**: 25-29
19 **Ricci C**, Longo R, Gioulis E, Bosco M, Pollesello P, Masutti F, Croce LS, Paoletti S, de Bernard B, Tiribelli C, Dalla Palma L. Noninvasive *in vivo* quantitative assessment of fat content in human liver. *J Hepatol* 1997; **27**: 108-113
20 **Matthews DR**, Hosker JP, Rudenski AS, Naylor BA, Treacher DF, Turner RC. Homeostasis model assessment: insulin resistance and beta-cell function from fasting plasma glucose and insulin concentrations in man. *Diabetologia* 1985; **28**: 412-419
21 **Dowse GK**, Qin H, Collins VR, Zimmet PZ, Alberti KG, Gareeboo H. Determinants of estimated insulin resistance and beta-cell function in Indian, Creole and Chinese Mauritians. The Mauritius NCD Study Group. *Diabetes Res Clin Pract* 1990; **10**: 265-279
22 Expert panel on detection, evaluation, and treatment of high blood cholesterol in adults. executive summary of the third report of the national cholesterol education program (NCEP) expert panel on detection, evaluation, and treatment of high blood cholesterol in adults (adult treatment panel III). *JAMA* 2001; **285**: 2486-2497
23 WHO/IASO/IOTF. *The Asia-Pacific perspective: redefining obesity and its treatment*. Health Communications Australia: *Melbourne* 2000
24 **Clark JM**, Brancati FL, Diehl AM. The prevalence and etiology of elevated aminotransferase levels in the United States. *Am J Gastroenterol* 2003; **98**: 960-967
25 **Matteoni CA**, Younossi ZM, Gramlich T, Boparai N, Liu YC, McCullough AJ. Nonalcoholic fatty liver disease: a spectrum of clinical and pathological severity. *Gastroenterology* 1999; **116**: 1413-1419
26 **Pratt DS**, Kaplan MM. Evaluation of abnormal liver-enzyme results in asymptomatic patients. *N Engl J Med* 2000; **342**: 1266-1271
27 **Jeong SK**, Nam HS, Rhee JA, Shin JH, Kim JM, Cho KH. Metabolic syndrome and ALT: a community study in adult Koreans. *Int J Obes Relat Metab Dis* 2004; **28**: 1033-1038
28 **Siest G**, Schiele F, Galteau M, Panek E, Steinmertz J, Fagnani F, Gueguen R. Aspartate aminotransferase and alanine aminotransferase activities in plasma: statistical distributions, individual variations, and reference values. *Clin Chem* 1975; **21**: 1077-1087
29 **Manolio TA**, Burke GL, Savage PJ, Jacobs DR Jr, Sidney S, Wagenknecht LE, Allman RM, Tracy RP. Sex-and race-related differences in liver-associated serum chemistry tests in young adults in the CARDIA study. *Clin Chem* 1992; **38**: 1853-1859
30 **Sakugawa H**, Nakayoshi T, Kobashigawa K, Nakasone H, Kawakami Y, Yamashiro T, Maeshiro T, Tomimori K, Miyagi S, Kinjo F, Saito A. Metabolic syndrome is directly associated with gamma glutamyl transpeptidase elevation in Japanese women. *World J Gastroenterol* 2004; **10**: 1052-1055
31 **Marchesini G**, Brizi M, Morselli-Labate AM, Bianchi G, Bugianesi E, McCullough AJ, Forlani G, Melchionda N. Association of nonalcoholic fatty liver disease with insulin resistance. *Am J Med* 1999; **107**: 450-455
32 **Knobler H**, Schattner A, Zhornicki T, Malnick SD, Keter D, Sokolovskaya N, Lurie Y, Bass DD. Fatty liver-an additional and treatable feature of the insulin resistance syndrome. *QJ Med* 1999; **92**: 73-79
33 **Kelley DE**, McKolanis TM, Hegazi RA, Kuller LH, Kalhan SC. Fatty liver in type 2 diabetes mellitus: relation to regional adiposity, fatty acids, and insulin resistance. *Am J Physiol Endocrinol Metab* 2003; **285**: E906-916
34 **Lee JH** , Rhee PL, Lee JK, Lee KT, Kim JJ, Koh KC, Paik SW, Rhee JC, Choi KW. Role of hyerinsulinemia and glucose intolerance in the pathogenesis of nonalcoholic fatty liver in

patients with normal body weight. *Korean J Intern Med* 1998; **13**: 12-14

35 **Marchesini G**, Brizi M, Bianchi G, Tomassetti S, Bugianesi E, Lenzi M, McCullough AJ, Natale S, Forlani G, Melchionda N. Nonalcoholic fatty liver disease: a feature of the metabolic syndrome. *Diabetes* 2001; **50**: 1844-1850

36 **Chitturi S**, Abeygunasekera S, Farrell G, Holmes-Walker J, Hui JM, Fung C, Karim R, Lin R, Samarasinghe D, Liddle C, Weltman M, George J. NASH and insulin resistance: Insulin hypersecretion and specific association with the insulin resistance syndrome. *Hepatology* 2002; **35**: 373-379

37 **Omagari K**, Kadokawa Y, Masuda J, Egawa I, Sawa T, Hazama H, Ohba K, Isomoto H, Mizuta Y, Hayashida K, Murase K, Kadota T, Murata I, Kohno S. Fatty liver in non-alcoholic non-overweight Japanese adults: incidence and clinical characteristics. *J Gastroenterol Hepatol* 2002; **17**: 1098-1105

38 **Farrell GC**. Non-alcoholic steatohepatitis: what is it, and why is it important in the Asia-Pacific region? *J Gastroenterol Hepatol* 2003; **18**: 124-138

39 **Kissebah AH**, Krakower GR. Regional adiposity and morbidity. *Physiol Rev* 1994; **74**: 761-811

40 **Haque M**, Sanyal AJ. The metabolic abnormalities associated with non-alcoholic fatty liver disease. *Best Pract Res Clin Gastroenterol* 2002; **16**: 709-731

41 **Barzilai N**, She L, Liu BQ, Vuguin P, Cohen P, Wang J, Rossetti L. Surgical removal of visceral fat reverses hepatic insulin resistance. *Diabetes* 1999; **48**: 94-98

42 **Wang J**, Thornton JC, Russell M, Burastero S, Heymsfield S, Pierson RN Jr. Asians have lower body mass index (BMI) but higher percent body fat than do whites: comparisons of anthropometric measurements. *Am J Clin Nutr* 1994; **60**: 23-28

43 **Deurenberg P**, Deurenberg-Yap M, Guricci S. Asians are different from Caucasians and from each other in their body mass index/body fat per cent relationship. *Obes Rev* 2002; **3**: 141-146

Science Editor Guo SY **Language Editor** Elsevier HK

PO Box 2345, Beijing 100023, China
www.wjgnet.com
wjg@wjgnet.com

ELSEVIER

World J Gastroenterol 2005;11(34):5322-5326
World Journal of Gastroenterology ISSN 1007-9327
© 2005 The WJG Press and Elsevier Inc. All rights reserved.

• *CLINICAL RESEARCH* •

Limited influences of chemotherapy on healthy and metastatic liver parenchyma

Nancy Van Damme, Pieter Demetter, Wouter De Bock, Marianne Rottiers, Marleen Praet, Bernard de Hemptinne, Marc Peeters

Nancy Van Damme, Wouter De Bock, Marc Peeters, Department of Gastroenterology, Ghent University Hospital, De Pintelaan 185, 1K12IE, Ghent 9000, Belgium
Pieter Demetter, Marianne Rottiers, Marleen Praet, Department of Pathology, Ghent University Hospital, De Pintelaan 185, Blok A, Ghent 9000, Belgium
Bernard de Hemptinne, Department of Surgery, Ghent University Hospital, De Pintelaan 185, 2K12IC, Ghent 9000, Belgium
Correspondence to: Nancy Van Damme, PhD, Department of Gastroenterology, Ghent University Hospital, De Pintelaan 185, 1K12IE, Ghent 9000, Belgium. nancy.vandamme@ugent.be
Telephone: +32-9-2405665 Fax: +32-9-2404984
Received: 2004-12-22 Accepted: 2005-01-05

Abstract

AIM: To examine the expression of E-cadherin, β-catenin, γ-catenin, VEGF, and p53 in 39 patients with hepatic metastasis from colorectal cancer immunohistochemically.

METHODS: The patients were divided into two groups: those (n = 16) who had no chemotherapy for at least 6 mo before the liver resections and those (n = 23) who were treated with chemotherapy before liver resections. A score from 0 to 3 was given for the number of positive cells and from 0 to 3 for the intensity of staining in these cells, in both healthy and metastatic liver parenchyma.

RESULTS: No significant differences in the expression of E-cadherin, β- and γ-catenin, VEGF and p53, could be observed between patients who received and did not receive chemotherapy, in both normal and metastatic liver parenchyma.

CONCLUSION: Despite the assumption that chemotherapy had an effect on liver metastasis, no influences were noticed immunohistochemically.

© 2005 The WJG Press and Elsevier Inc. All rights reserved.

Key words: Chemotherapy; Metastatic liver parenchyma; Cadherin; Catenin; VEGF

Van Damme N, Demetter P, De Bock W, Rottiers M, Praet M, de Hemptinne B, Peeters M. Limited influences of chemotherapy on healthy and metastatic liver parenchyma. *World J Gastroenterol* 2005; 11(34): 5322-5326
http://www.wjgnet.com/1007-9327/11/5322.asp

INTRODUCTION

Colorectal cancer is one of the most common solid tumors and is the second leading cause of cancer deaths in Western countries. Approximately half of all patients develop metastatic disease[1]. Lymph node or hematogenic metastasis (liver or lung metastasis) are thought to be most significant prognostic factors for patients with colorectal cancer.

Until recently, 5-fluorouracil (5-FU) and leucovorin (LV) were the standard of care, however without major impact on survival. Two new drugs, irinotecan and oxaliplatin have demonstrated survival improvement, when given either alone or in combination with 5-FU+LV, in first- or second-line therapy. Recently, Tournigand *et al*., described that FOLFIRI (irinotecan and 5-FU/LV) followed by FOLFOX6 (oxaliplatin and 5-FU/LV) or the reverse in advanced colorectal cancer achieved a prolonged survival with a median of 24 mo and similar efficacy[2].

The metastatic cascade of colorectal cancer starts with the infiltration of neoplastic cells through the basement membrane, which enables tumor cells to leave epithelial structures, to invade the surrounding stroma, to enter either blood or lymphatic vessels and create a metastasis in the appropriate target organs.

The cadherin-mediated cell-cell adhesion system plays a critical role in cancer invasion and metastasis[3,4]. Cadherins are calcium-dependent transmembrane adhesion molecules that connect cells homotypically. The cytoplasmic domain of E-cadherin interacts with intracellular proteins called α-, β- and γ-catenins, which are the major elements in the intracytoplasmic microfilament network[4,5]. Both β- and γ-catenin bind directly to E-cadherin; Alpha or-catenin links the bound β- or γ-catenin to the actin cytoskeleton, thereby forming complexes of either E-cadherin/β-catenin/α-catenin or E-cadherin/γ-catenin/α-catenin[5]. Loss of expression of E-cadherin and catenins is found to be associated with de-differentiation, invasion, and metastasis, and is, therefore, suggested as a potential prognostic factor in colorectal carcinoma[6,7]. β-catenin, apart from linking with E-cadherin, forms complexes with the tumor-suppressor protein - aden-omatous polyposis coli (APC) gene products, which are independent from the cadherin/catenin[8-10]. The APC gene is often mutated in colorectal cancer tissue. *In vitro* and *in vivo* data suggest a pivotal role of cadherins and catenins in various aspects of tumor progression.

Angiogenesis is required for tumor growth and metastasis of human solid tumors. This process is driven by a balance of stimulatory and inhibitory influences[11]. The potent angiogenic factor - vascular endothelial growth factor (VEGF)

is associated with metastasis in human colon cancer[12]. An association exists between VEGF expression, angiogenesis, and metastasis in colon cancer. Warren *et al*., demonstrated that antibodies to VEGF inhibit metastasis in a murine model of human colon cancer[13].

On the other hand, tumor progression is known to occur through the sequential deregulation of rearrangement of proto-oncogenes together with the inactivation of tumor suppressor genes[14]. *In vitro* studies demonstrated the important role of p53 tumor suppressor gene in controlling tumor angiogenesis[15,16].

Direct effect of treatment on the liver consisting of hepatocyte steatosis is a common response to liver injury and is characterized by macro- and microvesicular fatty infiltration of hepatocytes[17]. These fatty changes may be accompanied by hepatocyte ballooning, an inflammatory infiltrate, fibrosis and even cirrhosis[18,19].

Limited data are available about the effect of chemotherapy on healthy and malign liver parenchyma. One study described a small necrotic focus of hepatocytes on normal liver of Wistar rats who were treated with 5-FU[20]. Therefore, in the present study we analyzed by immunohistochemistry the expression of E-cadherin, β- and γ-catenin, VEGF and p53 in normal and metastatic liver parenchyma of colorectal cancer patients. The percentage of macro- and microvesicular steatosis was also analyzed. The patients were divided into two groups: those who received chemotherapy and those who did not.

MATERIALS AND METHODS

Patients

Paraffin-embedded tumor specimens from 39 patients with liver metastasis of colorectal carcinoma who had undergone surgery were retrieved from the archival material of the Department of Pathology of the Ghent University Hospital. The characteristics of primary tumors are listed in Table 1. The mean age of patients at the time of liver metastasis diagnosis was 60±12 years (range 28-81 years). The study population consisted of 27 males and 12 females. Sixteen patients received no chemotherapy for at least 6 mo before the liver resections. Twenty-three patients received chemotherapy for at least 6 mo before the liver resections (Table 2). The study was approved by the Ethical Committee of the Ghent University Hospital.

Table 1 Colorectal cancer patients' characteristics

	Number
Sex (M/F)	27/12
Location	
Sigmoid	12
Rectum	6
Rectosigmoid	4
Cecum	4
Colon ascendens	3
Colon descendens	1
Splenic feature	2
Bauhin's valve	1
Not specified	6

Table 2 Twenty-three patients received chemotherapy before the liver resection

Type of chemotherapy	Number
5-FU, LV, oxaliplatin	7
5-FU, LV, CPT-11	2
5-FU, LV	5
Cetuximab, FOLFIRI	1
Cetuximab, CPT-11	1
CPT-11	1
Oxaliplatin, capecitabine, CPT-11	1
Others	5

5-FU: 5-fluorouracil, LV: leucovorin.

Immunohistochemical staining

Monoclonal anti-E-cadherin, anti-β-catenin, and anti-γ-catenin antibodies (clones 36, 14, and 15, respectively) were obtained from BD Biosciences (San Diego, CA,USA). Monoclonal anti-VEGF antibody (C-1) was purchased from Santa Cruz Biotechnology, Inc. (Santa Cruz, CA,USA). Monoclonal anti-p53 antibody was obtained from Biogenex (San Ramon, CA, USA). Immunohistochemical staining was based on the labeled streptavidin-biotin method and carried out using a DAKO LSAB® +Kit (DAKO Corporation, Carpinteria, CA,USA). Tissue sections (5 μm) were deparaffinized with xylene and dehydrated in graded ethanol. For unmasking the antigens, the slides were heated in a microwave oven in citrate buffer (0.01 mol/L, pH 6) (except for anti-VEGF staining). Endogenous peroxidase activity was quenched by incubating in 0.3% hydrogen peroxidase for 20 min. Slides were then incubated with appropriately diluted antibodies for 30 min (anti-γ-antibody) and 1 h (for the other molecules). Immunostaining was visualized using diaminobenzidine tetrahydrochloride solution (for p53) or 3-amino-9-ethylcarbazole (for the other molecules); both products were obtained from DAKO. The sections were counterstained with hematoxylin. Isotype-specific irrelevant antibodies were used to control nonspecific binding of the primary antibodies.

Histology of liver parenchyma

Histology of the liver parenchyma was reviewed for the presence of macro- and microvesicular steatosis. The extent of steatosis was determined as the percentage of hepatocytes involved, in the range of 10%.

Evaluation and analysis

Sections were examined by light microscopy and the same scoring system was used for the hepatocytes and the metastatic cells. A score from 0 to 3 was given for the number of positive cells and from 0 to 3 for the intensity of staining in these cells. The sum of both scores, with a maximum of 6, was made[21]. The differences in the numerical data between the two groups (chemotherapy or no chemotherapy) were evaluated using the Mann-Whitney *U* test. Values are expressed as median and range. *P* values of less than 0.05 were considered statistically significant.

RESULTS

Expression of the adhesion molecules in normal and metastatic liver parenchyma

Table 3 summarizes the expression of E-cadherin, β- and

γ-catenin in normal and metastatic liver parenchyma. One patient was not evaluated in the metastatic liver parenchyma due to the low number of metastatic cells. E-cadherin was expressed in 100% in normal and in 97% of the cases in metastatic liver parenchyma (Figure 1). β-catenin was expressed in 90% of the cases in normal and in 95% of the cases in metastatic liver parenchyma. γ-catenin was expressed in 46% of the cases in normal and in 66% of the cases in metastatic liver parenchyma. VEGF was expressed in 100% in normal and in 84% of the cases in the metastatic liver parenchyma (Figure 2). No staining for p53 was found in normal liver parenchyma, and p53 staining was found in 66% of the tumors (Figure 3).

Table 3 Positive staining of the adhesion molecules in normal and metastatic liver parenchyma

	Normal (%)	Metastatic (%)
E-cadherin	39/39 (100)	37/38 (97.37)
β-catenin	35/39 (89.74)	36/38 (94.74)
γ-catenin	18/39 (46.15)	25/38 (65.79)
VEGF	39/39 (100)	32/38 (84.21)
p53	0/39 (0)	25/38 (65.79)

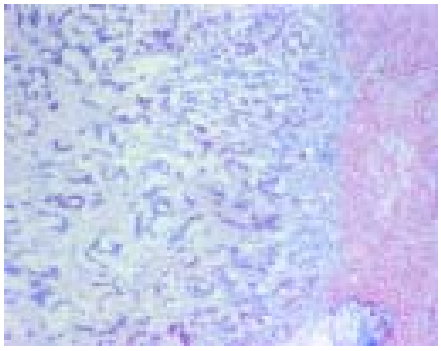


Figure 1 E-cadherin expression in a liver metastasis. Magnification x40.

Effect of chemotherapy on the expression of adhesion molecules and macro- and microvesicular steatosis

The patients were divided into two groups: those who received no chemotherapy (n = 16) and those who received chemotherapy (n = 23) for at least 6 mo before the liver resection. Both in normal and in metastatic liver parenchyma, no significant differences in the expression of adhesion molecules could be observed between the patients who received and who did not receive chemotherapy (Table 4).

Also, no significant differences were observed in macro- and microvesicular steatosis between patients receiving chemotherapy and no chemotherapy (Table 5).

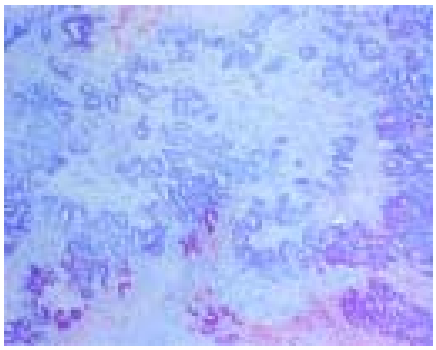


Figure 2 VEGF expression in a liver metastasis. Magnification x40.

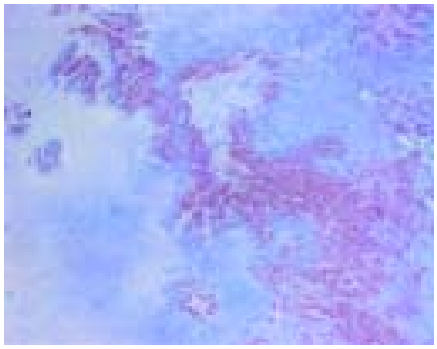


Figure 3 p53 expression in a liver metastasis. Magnification x40.

Table 5 Percentage of macro- and microvesicular steatosis (median and range)

	Chemotherapy (n = 23, %)	No chemotherapy (n = 16, %)
Macrovesicular	10 (0-40)	10 (0-30)
Microvesicular	0 (0-10)	0 (0-10)

DISCUSSION

Invasion and metastasis of tumor cells are the primary causes of fatal outcome of cancer. E-cadherin plays a major role in the cell-cell adhesion of normal epithelial cells. The reduced expression of E-cadherin has been correlated with de-differentiation, tumor invasion, and metastasis in various cancer tissues. Several immunohistochemical studies describe a reduced expression of the E-cadherin/α-catenin in primary

Table 4 Expression of the adhesion molecules in normal and metastatic liver parenchyma (median and range)

	Normal		Metastatic	
	Chemotherapy (n = 23)	No chemotherapy (n = 16)	Chemotherapy (n = 23)	No chemotherapy (n = 16)
E-cadherin	3 (2-4)	3 (2-6)	3 (0-6)	4 (2-6)
β-catenin	3 (0-5)	3 (0-5)	6 (0-6)	5 (0-6)
γ-catenin	0 (0-3)	1 (0-2)	2 (0-4)	2 (0-4)
VEGF	5 (3-5)	5 (3-5)	4 (0-5)	3 (0-4)
p53	0 (0-0)	0 (0-0)	3 (0-6)	2.5 (0-6)

colorectal carcinomas[6,7,22,23]. In contrast, the marked reduction in E-cadherin and α-catenin, β- and γ-catenin were seldom reduced[7]. Hugh *et al*., described that α-catenin expression was reduced or lost more frequently than either E-cadherin or β-catenin on 60 colorectal cancer specimens[24].

Little information is available about the expression of E-cadherin/catenin complex in colorectal cancer liver metastases. Ghadimi *et al*., found a reduced E-cadherin and α-catenin expression in 48% and 36% of the cases, respectively[7]. The expression of β- and γ-catenin was preserved in colorectal liver metastases in more than 85% and 96% of the cases, respectively. Gofuku *et al*., described a reduced expression of E-cadherin/α-catenin in metastatic liver tumors[6]. In contrast, Ikeguchi *et al*., described an increased expression of E-cadherin, α- and β-catenin in metastatic liver tumors[23].

In the present study, we analyzed by immunohistochemistry the expression of E-cadherin, β- and γ-catenin in normal and metastatic liver parenchyma of colorectal cancer patients. The expression of E-cadherin and β-catenin was preserved in 97% and 95% of the cases in metastatic liver parenchyma, respectively. γ-catenin expression was reduced in 34% of the cases. Re-expression of E-cadherin, α-catenin and β-catenin, but not of γ-catenin was found in metastatic tissue from breast cancer patients[25]. Mayer *et al*., reported that E-cadherin expression in the metastatic liver tumors was stronger than in the primary tumors in many cases of gastric cancer[26]. Another study in advanced gastric cancer showed a re-expression of the cadherin/catenin complex in lymph nodes with metastasis[27]. The mechanism behind this re-expression remains unclear. Mareel *et al*. showed that tumor cells re-express E-cadherin at the metastatic site[28]. Whether the same mechanism is true for catenins is not known. Re-expression of these adhesion molecules by tumor cells after release from the primary site may be important and perhaps necessary for tumor cells to adhere in remote organs.

Over the past decade, numerous studies have demonstrated that the neo-vascularity of tumors correlates with aggressiveness and metastatic potential[29-31]. VEGF is one of the critical factors in determining the angiogenic phenotype in a majority of human colon cancers. The overexpression of VEGF is correlated with liver metastasis and poor prognosis in colorectal cancer patients[32,33]. The most common genetic alteration in colorectal cancer is reported to be the loss of p53 tumor suppressor gene function[14]. Protein p53 has various important functions in cellular aggregation, including cell growth control, response to DNA damage, regulation of transcription and control of genetic stability.

In the present study we analyzed by immunohistochemistry the expression of VEGF and p53 in normal and metastatic liver parenchyma of colorectal cancer patients. The expression of VEGF and p53 was seen in 84% and 66% of the cases in metastatic liver parenchyma, respectively. VEGF and p53 expression status coincided in 19 of 39 tumors (48%). Kang *et al*., described that the incidence of liver metastasis was very high, 52% in patients whose primary colorectal tumors were both p53 and VEGF positive[34].

No data are available in the literature about the effect of chemotherapy on the expression of adhesion molecules. In the present study, 23 patients received chemotherapy for at least 6 mo before the liver resection. No significant differences in the expression of E-cadherin, β-, γ-catenin, VEGF and p53 could be observed between patients receiving and patients receiving no chemotherapy before the liver resection. We could not make a distinction in type of chemotherapy due to small groups of patients. Further investigation is necessary with greater number of patients in each type of chemotherapy.

Despite the assumption that chemotherapy had an effect on the liver metastasis, no significant differences were observed immunohistochemically on the expression of E-cadherin/catenin complex, VEGF and p53.

REFERENCES

1 **Landis SH,** Murray T, Bolden S, Wingo PA. Cancer statistics, 1999. *CA Cancer J Clin* 1999; **49**: 8-31

2 **Tournigand C,** André T, Achille E, Lledo G, Flesh M, Mery-Mignard D, Quinaux E, Couteau C, Buyse M, Ganem G, Landi B, Colin P, Louvet C, de Gramont A. FOLFIRI followed by FOLFOX6 or the reverse sequence in advanced colorectal cancer: a randomized GERCOR study. *J Clin Oncol* 2004; **22**: 229-237

3 **Pignatelli M,** Vessey CJ. Adhesion molecules: Novel molecular tools in tumour pathology. *Hum Pathol* 1994; **25**: 849-856

4 **Kemler R.** From cadherins to catenins: cytoplasmic protein interaction and regulation of cell adhesion. *Trends Genet* 1993; **9**: 317-321

5 **Takeichi M.** Cadherin cell adhesion receptors as a morphogenetic regulator. *Science* 1991; **251**: 1451-1455

6 **Gofuku J,** Shiozaki H, Tsujinaka T, Inoue M, Tamura S, Doki Y, Matsui S, Tsukita S, Kikkawa N, Monden M. Expression of E-cadherin and α-catenin in patients with colorectal carcinoma. Correlation with cancer invasion and metastasis. *Am J Clin Pathol* 1999; **111**: 29-37

7 **Ghadimi BM,** Behrens J, Hoffmann I, Haensch W, Birchmeier W, Schlag PM. Immunohistological analysis of E-cadherin, α-, β- and γ-catenin expression in colorectal cancer. Implications for cell adhesion and signaling. *Eur J Cancer* 1999; **35**: 60-65

8 **Rubinfeld B,** Souza B, Albert I, Muller O, Chamberlain SH, Masiarz FR, Munemitsu S, Polakis P. Association of the APC gene product with beta-catenin. *Science* 1993; **262**: 1731-1734

9 **Su LK,** Vogelstein B, Kinzler KW. Association of the APC tumour suppressor protein with catenins. *Science* 1993; **262**: 1734-1737

10 **Hülsken J,** Birchmeier W, Behrens J. E-cadherin and APC complex for the interaction with beta-catenin and the cytoskeleton. *J Cell Biol* 1994; **127**: 2061-2069

11 **Folkman J.** Angiogenesis in cancer, vascular, rheumatoid and other disease. *Nat Med* 1995; **1**: 27-31

12 **Takahashi Y,** Bucana CD, Cleary KR, Ellis LM. p53, vessel count, and vascular endothelial growth factor expression in human colon cancer. *Int J Cancer* 1998; **79**: 34-38

13 **Warren RS,** Yuan H, Matli MR, Gillet NA, Ferrara N. Regulation by vascular endothelial growth factor of human colon cancer tumorigenesis in a mouse model of experimental liver metastasis. *J Clin Invest* 1995; **95**: 1789-1797

14 **Fearon ER,** Vogelstein B. A genetic model for colorectal tumorigenesis. *Cell* 1990; **61**: 759-767

15 **Dameron KM,** Volpert OV, Tainsky MA, Bouck N. Control of angiogenesis in fibroblasts by p53 regulation of thrombospondin-1. *Science* 1994; **265**: 1582-1584

16 **Van Meir EG,** Polverini PJ, Chazin VR, Su Hang HJ, de Tribolet N, Cavenee WK. Release of an inhibitor of angiogenesis upon induction of wild type p53 expression in glioblastoma cells. *Nat Genet* 1994; **8**: 171-176

17 **Behrns KE,** Tsiotos GG, DeSouza NF, Krishna MK, Ludwig J, Nagorney DM. Hepatic steatosis as a potential risk factor for major hepatic resection. *J Gastrointest Surg* 1998; **2**: 292-298

18 **Ludwig J,** Viggiano TR, McGill DB, Oh BJ. Nonalcoholic

steatohepatitis: Mayo Clinic experiences with a hitherto unnamed disease. *Mayo Clin Proc* 1980; **55**: 434-438

19 **Schaffner F,** Thaler H. Nonalcoholic fatty liver disease. *Prog Liver Dis* 1986; **8**: 283-298

20 **Zafiriou G,** Grekou A, Stravoravdi P, Natsis K, Barich A. Histological and ultrastructural study of the effect of chemotherapy with 5-fluorouracil on normal liver of Wistar rats. *Chemotherapy* 2002; **48**: 298-302

21 **Coppola D,** Lu F, Fruehauf JP, Kyshtoobayeva A, Karl RC, Nicosia SV, Yeatman TJ. Analysis of p53, p21WAF1, and TGF-beta1 in human ductal adenocarcinoma of the pancreas: TGF-beta 1 protein expression predicts longer survival. *Am J Clin Pathol* 1998; **110**: 16-23

22 **Ropponen KM,** Eskelinen MJ, Lipponen PK, Alhava EM, Kosma VM. Reduced expression of α catenin is associated with poor prognosis in colorectal carcinoma. *J Clin Pathol* 1999; **52**: 10-16

23 **Ikeguchi M,** Makino M, Kaibara N. Clinical significance of E-cadherin-catenin complex expression in metastatic foci of colorectal carcinoma. *J Surg Oncol* 2001; **77**: 201-207

24 **Hugh TJ,** Dillon SA, O'Dowd G, Getty B, Pignatelli M, Poston GJ, Kinsella AR. beta-catenin expression in primary and metastatic colorectal carcinoma. *Int J Cancer* 1999; **82**: 504-511

25 **Bukholm IK,** Nesland JM, Boressen-Dale AL. Re-expression of E-cadherin, α-catenin and β-catenin, but not γ-catenin, in metastatic tissue from breast cancer patients. *J Pathol* 2000; **190**: 5-19

26 **Mayer B,** Johnson JP, Leitl F, Jauch KW, Heiss MM, Schildberg FW, Bichmeier W, Funke I. E-cadherin expression in primary and metastatic gastric cancer: down-regulation correlates with cellular dedifferentiation and glandular disintegration. *Cancer Res* 1993; **53**: 1690-1695

27 **Liu J,** Ikeguchi M, Nakamura S, Kaibara N. Re-expression of the cadherin-catenin complex in lymph nodes with metastasis in advanced gastric cancer: the relationship with patient survival. *J Exp Clin Cancer Res* 2002; **21**: 65-71

28 **Mareel M,** Bracke M, Van Roy F. Cancer metastasis: negative regulation by an invasion-suppressor complex. *Cancer Detect Prev* 1995; **19**: 451-464

29 **Takahashi Y,** Kitadai Y, Bucana CD, Cleary KR, Ellis LM. Expression of vascular endothelial growth factor and its receptor, KDR, correlates with vascularity, metastasis, and proliferation of human colon cancer. *Cancer Res* 1995; **55**: 3664-3968

30 **Takahashi Y,** Clearly KR, Mai M, Kitadai Y, Bucana CD, Ellis LM. Significance of vessel count and vascular endothelial growth factor and its receptor (KDR) in intestinal-type gastric cancer. *Clin Cancer Res* 1996; **2**: 1679-1684

31 **Weidner N,** Semple JP, Welch WR, Folkman J. Tumor angiogenesis and metastasis correlation in invasive breast carcinoma. *N Engl J Med* 1991; **324**: 1-8

32 **Ishigami SI,** Arii S, Furutani M, Niwano M, Harada T, Mizumoto M, Mori M, Onodera H, Imamura M. Predictive value of vascular endothelial growth factor (VEGF) in metastasis and prognosis of human colorectal cancer. *Br J Cancer* 1998; **78**: 1379-1384

33 **Tokunaga T,** Oshika Y, Abe Y, Ozeki Y, Sadahiro S, Kijima H, Tsuchida T, Yamazaki H, Ueyama Y, Tamaoki N, Nakamura M. Vascular endothelial growth factor (VEGF) mRNA isoform expression pattern is correlated with liver metastasis and poor prognosis in colon cancer. *Br J Cancer* 1998; **77**: 998-1002

34 **Kang SM,** Maeda K, Onoda N, Chung YS, Nakata B, Nishiguchi Y, Sowa M. Combined analysis of p53 and vascular endothelial growth factor expression in colorectal carcinoma for determination of tumor vascularity and liver metastasis. *Int J Cancer* 1997; **74**: 502-507

Science Editor Guo SY **Language Editor** Elsevier HK

PO Box 2345, Beijing 100023, China
www.wjgnet.com
wjg@wjgnet.com

ELSEVIER

World J Gastroenterol 2005;11(34):5327-5331
World Journal of Gastroenterology ISSN 1007-9327
© 2005 The WJG Press and Elsevier Inc. All rights reserved.

• *CLINICAL RESEARCH* •

American ginseng supplementation attenuates creatine kinase level induced by submaximal exercise in human beings

Cheng-Chen Hsu, Min-Chen Ho, Li-Chin Lin, Borcherng Su, Mei-Chich Hsu

Cheng-Chen Hsu, Graduate Institute of Physical Education, National College of Physical Education and Sports, Taoyuan County, and School of Medicine, Taipei Medical University, Taipei, Taiwan, China
Min-Chen Ho, Mei-Chich Hsu, Graduate Institute of Sports Science, National College of Physical Education and Sports, Taoyuan County, Taiwan, China
Li-Chin Lin, Taiwan Biotech Co., Ltd, Taiwan, China
Borcherng Su, Department of Anatomic Pathology, E-Da Hospital, I-Shou University, Kaoshiung County, Taiwan, Republic of China
Supported by the Taiwan Biotech Co., Taiwan, China
Co-first-authors: Cheng-Chen Hsu and Min-Chen Ho
Co-correspondents: Cheng-Chen Hsu
Correspondence to: Dr. Mei-Chich Hsu, Graduate Institute of Sports Science, National College of Physical Education and Sports, Taoyuan County, Taiwan, China. meichich@mail.ncpes.edu.tw
Telephone: +886-3-3374601 Fax: +886-3-3311843
Received: 2004-12-07 Accepted: 2005-02-18

Abstract

AIM: To investigate whether American ginseng (AG, *Panax quinquefolium*) supplementation was able to improve endurance exercise performance.

METHODS: Thirteen physically active male college students were divided into two groups (AG or placebo) and received supplementation for 4 wk, before the exhaustive running exercise. Treadmill speed was increased to a pace equivalent to 80% VO_{2max} of the subject. A 4-wk washout period followed before the subjects crossed over and received the alternate supplement for the next 4 wk. They then completed a second exhaustive running exercise. The physiological variables that were examined included time to exhaustion and oxygen pulse. Moreover, the plasma creatine kinase (CK) and lactate were measured prior to the exercise, at 15 and 30 min during exercise, immediately after exercise, and 20, 40, 60, and 120 min after exercise.

RESULTS: The major finding of this investigation was that the production plasma CK during the exercise significantly decreased for group AG than for group P. Secondary physiological finding was that 80% VO_{2max} running was not improved over a 4-wk AG supplementation regimen.

CONCLUSION: Supplementation with AG for 4 wk prior to an exhaustive aerobic treadmill running reduced the leakage of CK during exercise, but did not enhance aerobic work capacity. The reduction of plasma CK may be due to the fact that AG is effective for the decrease of skeletal muscle cell membrane damage, induced by exercise during the high-intensity treadmill run.

© 2005 The WJG Press and Elsevier Inc. All rights reserved.

Key words: *Panax quinquefolium*; American ginseng; Creatine kinase; Endurance exercise

Hsu CC, Ho MC, Lin LC, Su B, Hsu MC. American ginseng supplementation attenuates creatine kinase level induced by submaximal exercise in human beings. *World J Gastroenterol* 2005; 11(34): 5327-5331
http://www.wjgnet.com/1007-9327/11/5327.asp

INTRODUCTION

Traditional Chinese medicine plays a key role in the formation of integrative medicine[1]. Ginseng (*Genus Panax*) root has been a popular Chinese medicine with the belief of restoring *Qi* or life energy. It is also thought to be a tonic to stimulate appetite, counteract fatigue, boost the immune system, relieve pain and headaches, and improve mental function and physical stamina[2]. The mechanism of action of ginseng is not known, but it is thought to have effects on production of corticotropin and cortisol, immunomodulation, antioxidants and neuroendocrine activity, modulate carbohydrate and lipid metabolism, and stimulation of nitric oxidation production in cardiovascular system[3-6].

Adequate dietary supplements or nutritional ergogenic aids are an important means to optimize exercise performance and to ward off fatigue. Ergogenic aids are believed to increase performance by some of the following mechanisms: renewing or increasing energy stores in the body, facilitating the biochemical reactions that yield energy, reducing or neutralizing performance-inhibiting metabolic byproducts, and facilitating recovery[7,8]. Performance in aerobic-type events depends on the ability to maintain a high output per unit of time. There is a growing inclination among athletes to use herbs to improve endurance performance or increase recovery after exercise.

The most studied herb for human aerobic physical performance is ginseng. Although the mechanism underlying the alleged ergogenicity of ginseng on physical performance has not been defined, theories include stimulation of the hypothalamic-pituitary-adrenal cortex axis and increased resistance to the stress of exercise, enhanced myocardial metabolism, increased hemoglobin levels, vasodilatation, increased oxygen extraction by muscles, and improved mitochondrial metabolism in the muscle, all of which theoretically

could enhance aerobic exercise performance[9-13].

In the review studies of Bahrke and Morgan, administration of ginseng or its components enhanced exercise endurance by altering fuel homeostasis during exercise, increased free fatty acid utilization in preference over glucose for cellular energy demands in rats and mice[14,15]. However, the evidence for ginseng as an endurance aerobic exercise ergogenic supplementation in men is variable. As ginseng is touted as a dietary ergogenic aid, incomplete study on performance has yielded little proof to reinforce performance affirmations.

A number of chemically similar steroid glycosides or saponin chemicals, known as ginsenosides, have been identified as active ingredients in ginseng. The original medicinal species of ginseng is Chinese or Korean ginseng (Panax ginseng C.A. Meyer). American ginseng (*Panax quinquefolius*) contains many of the same compounds, although in slightly different proportions. It is the North American variety of ginseng, which grows in eastern and central USA and Canada.

There is relatively little research that shows a performance benefit of American ginseng (AG) in human beings. The purpose of the present study was to determine, whether 4 wk of oral supplementation with AG had any benefit on endurance exercise and/or recovery after exercise.

MATERIALS AND METHODS

Subjects and anthropometric measurements

Thirteen male volunteers completed this randomized, double blind, crossover experimental research study with a washout period of 4 wk. Both body height and body weight were measured by an auto-anthropometer, Nakamura KN-3000 (Nakamura, Tokyo, Japan). Body weight was measured to the nearest 0.1 kg with subjects not wearing shoes or outerwear. Body weight was recorded to the nearest 0.1 cm. Age, weight, and heights (mean±SD) were 23.0±1.6 years, 70.2±6.3 kg, and 172.5±5.2 cm, respectively. A medical examination was performed on each subject before entering the study. Written voluntary consent to participate was obtained from all subjects after informing them of the purpose of the experiment, the procedure, and the possible risks. This investigation received the approval of the National College of Physical Education and Sports (Taoyuan, Taiwan). All subjects were healthy, physically active, college students with normal dietary habits.

American ginseng supplementation

Each subject was instructed to ingest either 4 AG capsules (400 mg AG per capsule) daily or a hydroxymethylcellulose placebo in the same capsule form (both provided by Taiwan Biotech Co., Taiwan), and received his allotment of CS or placebo in 4 weekly portions.

The Panax-bearing ginsenosides content was determined from its degree of concentration in a hot water extract. The compositions of the AG that we used were, ginsenosides Rb1 (8.67%, w/w), Rc (0.99%, w/w), Rd (1.05%, w/w), and Re (5.08%, w/w). At an initial meeting, 4 wk prior to commencing any supplementation, subjects were asked to cease taking any dietary supplementations that contained ginsenosides and were instructed to maintain a consistent diet before and during the experimental period.

Procedures

VO_{2max} was determined in the pre-experimental period. Each subject came to the laboratory 7 d before the start of the actual study, and performed an incremental running test on a motor-driven treadmill (Quinton Instruments, Model 1 860, Washington, USA) according to the Bruce protocol until exhaustion. In order to determine the baseline endurance performance time, maximum oxygen consumption (VO_{2max}) was determined by the automated system (Model 29C, SensorMedics, Yorba Linda, CA,USA). The VO_{2max} was defined as the attainment of at least two of the three following criteria: (1) an increase of ≤140 mL VO_{2max} with an increasing workload; (2) heart rate within 10 beats of age-predicted maximum; and (3) rating of perceived exertion (RPE) greater than 17 using the Borg scale. Heart rate (HR) measured by the Sport Tester (PE 3 000, Polar Electro, Kempele, Finland) were monitored during the treadmill exercise. The RPE was recorded by using the modified Borg scale[16]. Endurance performance time was also recorded at the end of the test for each subject. On the day of the experiment, subjects reported to the laboratory at 7-9 a.m. following a 10-12 h overnight fast, and abstained from rigorous exercise for 48 h prior to the test. An antecubital vein connected to a three-way stopcock with a 10-cm extension tube for blood sampling was inserted in the subjects. The cannula was kept patent by periodic flushing with a sodium chloride solution (9 g/L) and remained in place throughout the experimental period. No heparin was used in the catheter.

Protocol

Baseline physiological data was collected, while subjects stood quietly on the treadmill (Quinton Instruments, Model 1 860, Washington, USA) for 3 min prior to commencing the running test. Subjects then commenced a 5 min warm-up at a running speed equivalent to 60% VO_{2max}, the treadmill speed was increased to a pace equivalent to 80% VO_{2max} of the subjects. The subjects ran until volitional fatigue. Volitional fatigue was defined as the point at which subjects could no longer maintain the required running speed. VO_{2max} and HR were monitored throughout the exercise and were recorded, and oxygen pulse was calculated from oxygen consumption and heart rate. In addition, oxygen pulse (mLO_2/beat) was calculated by dividing oxygen consumption (mLO_2/min) by heart rate (beat/min).

Blood sampling and analysis

Blood samples were taken prior to the exercise, at 15 and 30 min during exercise, immediately after exercise, and 20, 40, 60, and 120 min after exercise. At each sampling time, about 5 mL of venous blood was taken. Whole blood for determination of hematocrit and hemoglobin was collected in EDTA tubes cooled at -4 ℃ and examined within 4 h after venepuncture to correct relative changes in plasma volume by using hematocrit and hemoglobin values from each test, according to the methods described by Dill and Costill[17]. The other venous blood was to obtain EDTA-plasma and stored at -20 ℃ for later analysis. The plasma

creatine kinase (CK) and plasma lactate were measured by a spectrophotometer technique (Johnson & Johnson DT-60II, Orthoclinical Diagnostics, Rochester, NY,USA) by means of ultraviolet test kits (Orthoclinical Diagnostics, Rochester, NY,USA).

Statistical analyses

SPSS 11.0 for Windows statistical program was used to perform all analyses. The independent variables between the two supplements (AG *vs* placebo), including an endurance run time to exhaustion and VO_{2max} after supplements were compared using Student's *t*-test for paired data. Differences in oxygen pulse and plasma CK, and plasma lactate values between the two treatment levels were analyzed by factorial (two-way, time×treatment) ANOVA with repeated measures. A Tukey's *post hoc* test was used to locate any significant difference. Significance was accepted at the $P<0.05$ level. All data are presented as mean±SD.

RESULTS

Basic physical characteristics

There was no difference between groups in VO_{2max} and the run time to exhaustion (Table 1).

Table 1 Maximal oxygen consumption and run time to exhaustion[1,2]

Group	VO_{2max} (mL / min / kg)	Time to exhaustion (s)
AG	44.6±3.1	2 279.5±252.7
P	45.1±5.0	2 218.3±345.9

[1]AG: American ginseng supplement; P: placebo supplement. [2]Values are expressed as mean±SD (n = 13).

Oxygen pulse

Data of oxygen consumption were collected in the time period of 0-1, 14-15, and 29-30 min. The oxygen pulse had no significant difference between groups during these periods (Figure 1).

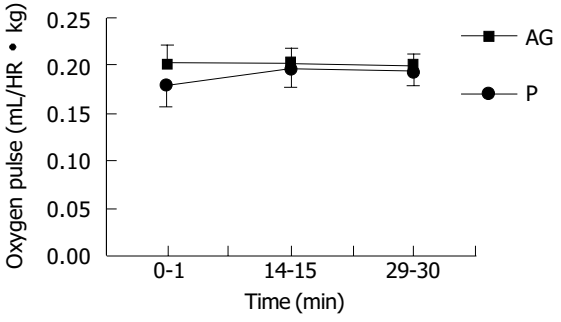


Figure 1 Oxygen pulse during exercise phase in group AG (—■—) and group P (—●—). Each point represents the mean±SD (n = 13).

Blood chemistry

In both placebo and AG groups, plasma CK and plasma lactate were significantly increased with the duration of exercise and reached a peak at exhaustive time (Figures 2 and 3). Blood lactate concentration at 15, 30 min of exercise, and 120 min after exercise in AG group (9.3±2.1, 11.4±2.7, and 2.2±0.4 mmol/L) were significantly lower than in the placebo group (10.6±2.4, 13.3±2.7, and 2.6±0.4 mmol/L), respectively (Figure 3). Moreover, plasma CK activity at 30 min of exercise, immediately, 20, 60, and 120 min after exercise in the AG group (181.2±78.0, 217.5±64.0, 167.5±56.2, 155.3±57.8, and 167.7±61.5 U/L) were significantly lower than in the placebo group (254.3±81.6, 280.2±90.0, 246.5±66.3, 227.8±58.4, and 231.9±67.8 U/L), respectively (Figure 2).

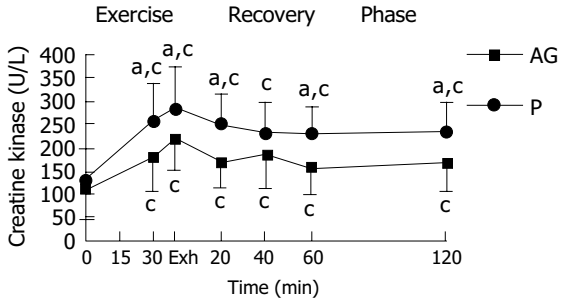


Figure 2 Plasma CK levels observed during exercise and recovery phases in group AG (—■—) and group P (—●—). Each point represents the mean±SD (n = 13). [a]$P<0.05$ *vs* P groups; [c]$P<0.05$ *vs* before exercise.

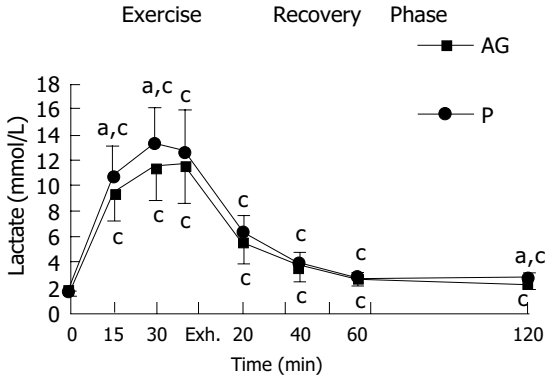


Figure 3 Plasma lactate levels observed during exercise and recovery phases in group AG (—■—) and group P (—●—). Each point represents the mean±SD (n = 13). [a]$P<0.05$ *vs* P groups; [c]$P<0.05$ *vs* before exercise.

DISCUSSION

The research was designed to determine whether or not supplementation with AG for 4 wk prior to 80% VO_{2max} run would increase the time to exhaustion and/or have any ergogenic benefit in healthy male college students. The variables that were examined included time to exhaustion, oxygen pulse, plasma CK, and plasma lactate. To our knowledge, this is the first study of AG in human clinical trials to determine endurance aerobic physical performance. The major finding of this investigation was that the production of plasma CK during exercise significantly decreased for

group AG over group P ($P<0.05$). Secondary physiological findings suggested that 80% VO_{2max} running was not improved over a 4-wk AG supplementation regimen.

The CK marker is used to determine muscle damage. The amount of plasma CK of healthy adults at rest is approximately 40-200 U/L for men[18]. In this study, the plasma CK concentrations before exercise are within the normal range in both groups and have no significant difference between groups (AG group, 108.1±62.4; P group, 138.6±94.6, respectively).

Although most studies indicate that muscle injury is assessed through prolonged endurance exercise, it is obvious that it can be caused during high intensity short-term exercise as well[19,20]. During running exercise, the extensor muscles of the lower limb performed eccentric actions as the foot touches the ground and the dorsiflexors of the ankle contract eccentrically. In eccentric exercise, the contracting muscle is forcibly lengthened as it develops tension, potentially causing damage. Therefore, endurance exercise, such as an exhaustive running exercise can induce damage and pathological alteration in skeletal muscle.

With high-intensity exercise, the high-force contractions cause muscle cell injury early in the exercise period[20]. Mechanical rupture of muscle fiber is one of the major mechanisms to explain how the muscle injury was induced by exercise. This stress on the cross bridges of the myofiber causes disruption of the muscle fibrils leading to Z-line in disintegration or Z-line streaming[21]. Moreover, strenuous exercise can also disrupt the sarcolemma and sarcoplasmic reticulum[22]. Mair *et al*., demonstrated a transient rise in the serum concentrations of muscle proteins such as CK, an indicator of muscle damage due to sarcolemma disruption, which cause a leakage of CK into the blood[23].

In this study, the total CK activity significantly increased in both groups during exhaustive running exercise. We assign this to plasma CK increasing in both groups of the subjects due to exercise-induced skeletal muscle damage. The increases in plasma CK in this study indicate that muscle damage had occurred during the exhaustive running in both groups.

Intense exercise may increase the production of free radicals or reactive oxygen species. A free radical prefers to steal electrons from the lipid membrane of a cell, initiating a free radical attack on the cell known as lipid peroxidation. Kanter *et al*., have demonstrated that post-exercise plasma CK elevations may be related to an exercise-induced lipid peroxidation[24]. The American ginseng *Panax quinquefolium* exhibits effective antioxidant, free radical scavenging activity, and inhibiting lipid peroxidation[25-29].

Lactate is an important indicator of muscle performance under stress. Lactate levels rise as intensity increases during exercise. The lower blood lactate concentration during running exercise presumably reflects a lower intramuscular lactate concentration and an increased relative contribution of anaerobic metabolism to ATP production. In this study, the AG group exhibited lower plasma levels of lactate at 15, 30 min of exercise than that in the placebo group. It seems unlikely to be due to amelioration of oxygen extraction from the blood by the working muscles as a consequence of AG supplementation, since VO_{2max} and oxygen pulse was unaffected by prior supplementation. Decreased blood lactate accumulation is not necessarily a result of muscle tissue anti-hypoxia. Factors other than an increased cellular PO_2, a decrease in intracellular calcium concentration, decreased activation of glycogen phosphorylase, or decreased intracellular pH can also cause a decrease in intramuscular lactate production[30]. Otherwise, the rate of efflux of lactate from the contractile muscle could be decreased due to the decreased muscle cell membrane permeability after exercise-induced damage[31].

In conclusion, a 4-wk AG supplementation reduced the leakage of CK from skeletal sarcoplasm into blood streaming during an exhaustive treadmill run, but did not enhance aerobic work capacity. The reduction of plasma CK level may be due to AG that is effective for the decrease of skeletal muscle cell membrane damage induced by exercise during the high intensity treadmill run. In the future, we will investigate if the reduction in CK efflux is simply an indication of increased sarcolemma stability or whether the muscles are in fact receiving less damage.

ACKNOWLEDGMENTS

We wish to extend our deep appreciation to all participating subjects for their dedication to this study.

REFERENCES

1 **Lu AP,** Jia HW, Xiao C, Lu QP. Theory of traditional Chinese medicine and therapeutic method of diseases. *World J Gastroenterol* 2004; **10**: 1854-1856
2 **Coleman CI,** Hebert JH, Reddy P. The effects of Panax ginseng on quality of life. *J Clin Pharm Ther* 2003; **28**: 5-15
3 **Tode T,** Kikuchi Y, Hirata J, Kita T, Nakata H, Nagata I. Effect of Korean red ginseng on psychological functions in patients with severe climacteric syndromes. *Int J Gynaecol Obstet* 1999; **67**: 169-174
4 **Yuan CS,** Attele AS, Wu JA, Lowell TK, Gu Z, Lin Y. Panax quinquefolium L. inhibits thrombin-induced endothelin release *in vitro*. *Am J Chin Med* 1999; **27**: 331-338
5 **Ji LL,** Peterson DM. Aging, exercise, and phytochemicals: promises and pitfalls. *Ann N Y Acad Sci* 2004; **1019**: 453-461
6 **Tan BK,** Vanitha J. Immunomodulatory and antimicrobial effects of some traditional chinese medicinal herbs: a review. *Curr Med Chem* 2004; **11**: 1423-1430
7 **Lawrence ME,** Kirby DF. Nutrition and sports supplements: fact or fiction. *J Clin Gastroenterol* 2002; **35**: 299-306
8 **Maughan RJ,** King DS, Lea T. Dietary supplements. *J Sports Sci* 2004; **22**: 95-113
9 **Kim DH,** Moon YS, Jung JS, Min SK, Son BK, Suh HW, Song DK. Effects of ginseng saponin administered intraperitoneally on the hypothalamo-pituitary-adrenal axis in mice. *Neurosci Lett* 2003; **343**: 62-66
10 **Zhang HG,** Li XH, Yang ZC. Effects of Panax notoginseng saponins on myocardial Gsalpha mRNA expression and ATPase activity after severe scald in rats. *Burns* 2003; **29**: 541-546
11 **Bae JW,** Lee MH. Effect and putative mechanism of action of ginseng on the formation of glycated hemoglobin *in vitro*. *J Ethnopharmacol* 2004; **91**: 137-140
12 **Li Z,** Chen X, Niwa Y, Sakamoto S, Nakaya Y. Involvement of Ca2+ -activated K+ channels in ginsenosides-induced aortic relaxation in rats. *J Cardiovasc Pharmacol* 2001; **37**: 41-47
13 **Wang BX,** Zhou QL, Yang M, Wang Y, Cui ZY, Liu YQ, Ikejima T. Hypoglycemic mechanism of ginseng glycopeptide. *Acta Pharmacol Sin* 2003; **24**: 61-66
14 **Bahrke MS,** Morgan WP. Evaluation of the ergogenic properties of ginseng. *Sports Med* 1994; **18**: 229-248

15 **Bahrke MS,** Morgan WR. Evaluation of the ergogenic properties of ginseng: an update. *Sports Med* 2000; **29**: 113-133
16 **Borg GA,** Perceived exertion: a note on "history" and methods. *Med Sci Sports Exerc* 1973; **5**: 90-93
17 **Dill DB,** Costill DL. Calculation of percentage changes in volumes of blood, plasma, and red cells in dehydration. *J Appl Physiol* 1974; **17**: 247-248
18 **Tietz NW.** Clinical guide to laboratory tests. 3rd ed. *Philadelphia: Saunders* 1995: 180
19 **Byrd SK.** Alterations in the sarcoplasmic reticulum: a possible link to exercise-induced muscle damage. *Med Sci Sports Exerc* 1992; **24**: 531-536
20 **Friden J,** Lieber RL. Structural and mechanical basis of exercise-induced muscle injury. *Med Sci Sports Exerc* 1992; **24**: 521-530
21 **MacIntyre DL,** Reid WD, McKenzie DC. Delayed muscle soreness. The inflammatory response to muscle injury and its clinical implications. *Sports Med* 1995; **20**: 24-40
22 **Clarkson PM,** Hubal MJ. Exercise-induced muscle damage in humans. *Am J Phys Med Rehabil* 2002; **81**(11 Pt 1): S52-S69
23 **Mair J,** Mayr M, Muller E, Koller A, Haid C, Artner-Dworzak E, Calzolari C, Larue C, Puschendorf B. Rapid adaptation to eccentric exercise-induced muscle damage. *Int J Sports Med* 1995; **16**: 352-356
24 **Kanter MM,** Lesmes GR, Kaminsky LA, La Ham-Saeger J, Nequin ND. Serum creatine kinase and lactate dehydrogenase changes following an eighty kilometer race. Relationship to lipid peroxidation. *Eur J Appl Physiol Occup Physiol* 1988; **57**: 60-63
25 **Li J,** Huang M, Teoh H, Man RY. Panax quinquefolium saponins protects low density lipoproteins from oxidation. *Life Sci* 1999; **64**: 53-62
26 **Li JP,** Huang M, Teoh H, Man RY. Interactions between Panax quinquefolium saponins and vitamin C are observed *in vitro*. *Mol Cell Biochem* 2000; **204**: 77-82
27 **Kitts DD,** Wijewickreme AN, Hu C. Antioxidant properties of a North American ginseng extract. *Mol Cell Biochem* 2000; **203**: 1-10
28 **Fu Y,** Ji LL. Chronic ginseng consumption attenuates age-associated oxidative stress in rats. *J Nutr* 2003; **133**: 3603-3609
29 **Ng TB,** Liu F, Wang HX. The antioxidant effects of aqueous and organic extracts of Panax quinquefolium, Panax notoginseng, Codonopsis pilosula, Pseudostellaria heterophylla and Glehnia littoralis. *J Ethnopharmacol* 2004; **93**: 285-288
30 **Connett RJ,** Honig CR, Gayeski TE, Brooks GA. Defining hypoxia: a systems view of VO_2, glycolysis, energetics, and intracellular PO_2. *J Appl Physiol* 1990; **68**: 833-842
31 **Newham DJ,** Jones DA, Edwards RH. Large delayed plasma creatine kinase changes after stepping exercise. *Muscle Nerve* 1983; **6**: 380-385

Science Editor Guo SY **Language Editor** Elsevier HK

PO Box 2345, Beijing 100023, China
www.wjgnet.com
wjg@wjgnet.com

ELSEVIER

World J Gastroenterol 2005;11(34):5332-5335
World Journal of Gastroenterology ISSN 1007-9327
© 2005 The WJG Press and Elsevier Inc. All rights reserved.

• *CLINICAL RESEARCH* •

Diagnosis and treatment of acute rejection in the first case of human living-related small bowel transplantation with a long-term survival in China

Wei-Liang Song, Wei-Zhong Wang, Guo-Sheng Wu, Meng-Bin Li, Ji-Peng Li, Gang Ji, Guang-Long Dond, Hong-Wei Zhang

Wei-Liang Song, Wei-Zhong Wang, Guo-Sheng Wu, Meng-Bin Li, Ji-Peng Li, Gang Ji, Guang-Long Dond, Hong-Wei Zhang, Department of Gastrointestinal Surgery, Xijing Hospital, Fourth Military Medical University, Xi'an 710032, Shaanxi Province, China
Supported by the National Natural Science Foundation of China, No. 30070742
Correspondence to: Wei-Liang Song, Department of Gastrointestinal Surgery, Xijing Hospital, Fourth Military Medical University, Xi'an 710032, Shaanxi Province, China. chenggong9999699@sohu.com
Received: 2004-12-08 Accepted: 2005-01-26

Abstract

AIM: To report the comprehensive diagnosis and treatment of acute rejection in the first case of living-related small bowel transplantation with a long-term survival in China.

METHODS: A 18-year-old boy with short gut syndrome underwent living-related small bowel transplantation, with the graft taken from his father (44-year old). A segment of 150-cm distal small bowel was resected from the donor. The ileo-colic artery and vein from the donor were anastomosed to the infrarenal aorta and vena cava of the recipient respectively. The intestinal continuity was restored with an end-to-end anastomosis between the recipient jejunum and donor ileum, and the distal end was fistulized. FK506, MMF and prednisone were initially used for post-transplant immunosuppression. Endoscopic observation and mucosal biopsies of the graft were carried out through the terminal ileum enterostomy; serum was collected to detect the levels of IL-2R, IL-4, IL-6 and IL-8. The change of the graft secretion and absorption was observed.

RESULTS: Acute rejection was diagnosed promptly and cured. The patient was in good health, 5 years after living-related small bowel transplantation.

CONCLUSION: The correct diagnosis and treatment of acute rejection are the key to the long-term survival after living-related small bowel transplantation.

© 2005 The WJG Press and Elsevier Inc. All rights reserved.

Key words: Rejection; Comprehensive diagnosis; Small bowel transplantation

Song WL, Wang WZ, Wu GS, Li MB, Li JP, Ji G, Dond GL, Zhang HW. Diagnosis and treatment of acute rejection in the first case of human living-related small bowel transplantation with a long-term survival in China. *World J Gastroenterol* 2005; 11(34): 5332-5335
http://www.wjgnet.com/1007-9327/11/5332.asp

INTRODUCTION

The first patient after small bowel transplantation in China has survived for more than 5 years. The prompt diagnosis and treatment of acute rejection following transplantation are essential for a successful transplantation and long survival. However, there is no conventional standard for acute rejection diagnosis following small bowel transplantation. The present paper describes its comprehensive diagnosis post-transplantation and control.

MATERIALS AND METHODS

Clinical data

The patient, a 18-year-old man, suffered from volvulus necrosis and underwent a partial enterectomy in September 1998, the remaining jejunum was only 40 cm long. He was diagnosed as having short bowel syndrome. He was 185 cm high and weighed only 35 kg. He received intravenous feeding for a rather long period of time following transplantation. On May 20, 1999, he underwent living-related small bowel transplantation with a 150 cm long terminal ileum from his father as the donor intestine. The superior mesenteric artery from the donor was anastomosed to the infrarenal aorta and the mesenteric vein from the donor superior was anastomosed to the recipient portal vein or inferior vena cava. The arteries and veins from the donor intestine were anastomosed to the recipient's abdominal aorta and inferior vena cava in an end-to-side fashion respectively. The recipient's intestine was cut at 10 cm prior to the ileum. The proximal end of intestine from the donor was anastomosed to the proximal end of the recipient's jejunum in an end-to-end fashion. The distal end of intestine from the donor was anastomosed to the distal end of the recipient's jejunum in a side-to-end fashion. An intestinal fistula was made at 10 cm prior to graft as a viewing fenestra[1-4]. The recipient was given anticoagulant and anti-infectious treatment and total parenteral nutrition. He was treated with FK506, MMF and hydroprednisone and their combinations. On the next day following transplantation, intravenous administration of FK506 was replaced by intra-intestinal

administration. The patient recovered after transplantation. He could take fluid food 2 d after transplantation. On d 31 after transplantation, the absorption rate of xylitol was 30.6%. A month after transplantation he could feed himself, and gained weight steadily. MMF was stopped and the dosage of hydroprednisone was reduced. Discharge increased at the site of the intestinal fistula, and reached more than 1 500 mL/d, 60 d after transplantation, which suggested acute rejection. On the basis of the graft absorptive functional changes in the immunological indexes, endoscopic and pathologic examination, he was diagnosed as acute rejection and administered an impact treatment with a large dosage of immunosuppressive agents. Three days later, the symptoms were alleviated and all the indexes returned to normal gradually. Acute rejection did not occur again. One year after transplantation, the intestinal fistula was closed. At present, the patient is still alive, weighing 56-58 kg[5-8].

Endoscopic examination

Olympus GIF-XQ230 electron gastroscope was used to observe the mucous membrane with the remaining jejunum as a control. Mucous membrane from different sites was taken for pathological and microbiological examination. When we closed the intestinal fistula, we could examine the graft through the anus. However, no abnormal symptom has occurred since then.

Monitoring immunological indexes

Substrate coloration with ABTS was carried out, standard curve was drawn according to the standard, and then the serum levels of SIL-2R, IL-6, and IL-8 were determined with antagonistic sandwich ELISA kit. The serum level of IL-4 was determined with the biosource cytoscreen solid-phase sandwich ELISA kit (USA) for IL-4 detection. The above-mentioned four indexes were re-examined every 3 mo.

D-xylitol absorption test

D-xylitol absorption test was done to detect the absorptive function of the graft. The discharge at the site of the graft fistula and its changes were observed. The stool was also observed after the fistula was closed. The test was done every 3 mo.

RESULTS

Endoscopic and pathological findings

The graft membrane was present with the edema. The membrane appeared as an intensified light reflection. Yellowish white mucus was attached to the graft membrane and there were hemorrhage, erosions and round ulcers (0.3-0.6 cm in diameter) and linear ulcers (Figures 1 and 2). Under endoscope, the graft membrane was encrusted with yellowish white thin mucus. The graft wall was brittle and apt to bleed when touched, and it bled a lot when biopsy specimen was taken. The graft canal had hypanakinesia. On the other hand, these symptoms were absent in the remaining jejunum. Erosion occurred where there were lesions, some epithelial cells appeared in an atrophic short column shape, goblet cells became smaller or even disappeared. There was a general edema in lamina propria. Neutrophilic granulocytes were present at the lamina propria and tunica muscularis. Infiltration occurred in plasma cells and lymphocyte, neutrophilic granulocytes in blood vessels increased. Microbiological examination was negative and pathological examination showed that the patient's remaining jejunum was almost normal. When the intestinal fistula was closed one year later, the patient had no abnormal symptoms.

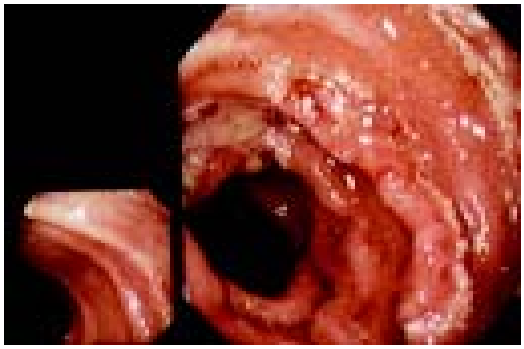


Figure 1 Mucous membrane at 70 cm of the graft fistula 67 d after transplantation.

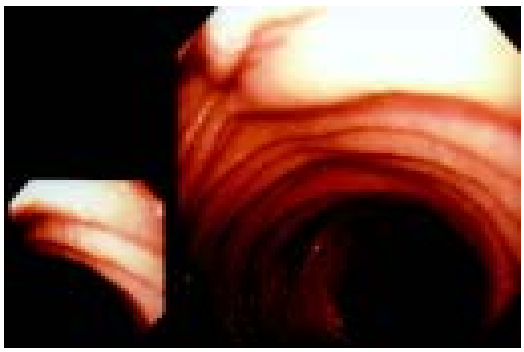


Figure 2 Normal mucous membrane of the recipient's remaining jejunum.

Absorptive function of the graft and discharge at the intestinal fistula

The absorptive function of the graft returned to normal 30 d after transplantation (the absorption rate of xylitol was 30.6%) and remained normal until the onset of rejection. Sixty-five days after transplantation, the absorption rate dropped to 24.6% and on 67th d, 19.6% increased gradually after treatment and returned to normal again 80 d after transplantation (Figure 3A). The discharge at the intestinal fistula remained normal just after transplantation. Sixty days after transplantation, the discharge began to increase and reached 1 520 mL, 61 d after transplantation. The discharge decreased after treatment and returned to normal, 80 d after transplantation (Figure 3B). Then, the absorptive function of the graft was examined every 3 mo and no change was found. After the intestinal fistula was closed, the patient's stool was solid and no loose and watery stool occurred.

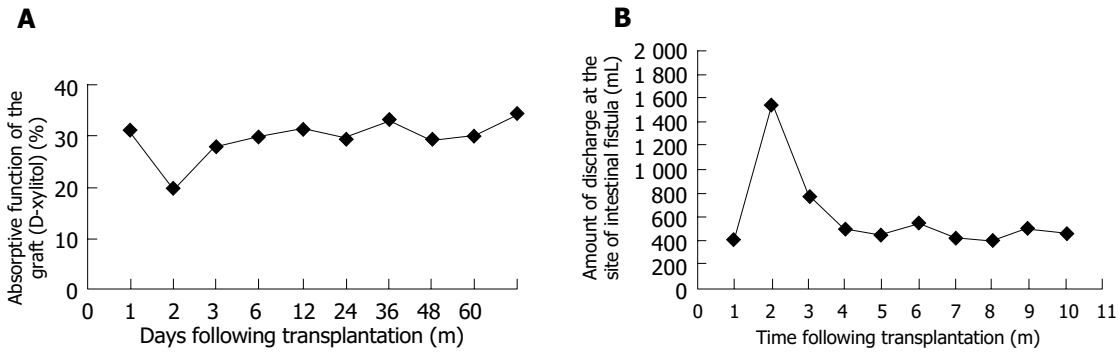


Figure 3 Changes in graft absorptive function (**A**) and discharge at the intestinal fistula (**B**).

Immunological indexes

The serum level of SIL-2R was 15.68 kU/L before transplantation, reached its first peak one day after transplantation, began to increase again 65 d after transplantation and reached its second peak 67 d after transplantation (243.98 kU/L). After treatment, its level decreased gradually and returned to normal, 80 d after transplantation (Figure 4A). The serum level of IL-8 was 0.26 μg/L before transplantation, reached its first peak one day after transplantation, began to increase again 65 d after transplantation, and reached its second peak 67 d after transplantation (1.47 μg/L). The level of IL-8 began to drop slowly when rejection was treated, and returned to the level before transplantation, 96 d after transplantation (Figure 4B). The serum level of IL-4 and IL-6 had no change before and after transplantation. Then, the four indexes were examined every 3 mo and no change was found.

DISCUSSION

Small bowel transplantation is the only therapy for end-stage intestinal diseases. However, since the small bowel is characterized by the existence of plenty of bacteria and a high immunogenicity, it is prone to rejection, which usually results in a transplantation failure. The incidence rate of acute rejection after small bowel transplantation is as high as 90% and acute rejection usually occurs 4-60 d after transplantation[9]. Prompt diagnosis and treatment of acute rejection after transplantation are crucial to a successful small bowel transplantation. However, the detecting indexes, which are instrumental in suggesting acute rejection of the graft, have not been identified yet. Based on the clinical symptoms, endoscopic and pathological findings and changes in absorptive function of the graft, acute rejection was diagnosed 67 d after transplantation. Following the control of immunological indexes and absorptive function of the graft, no significant changes were found and acute rejection did not recur.

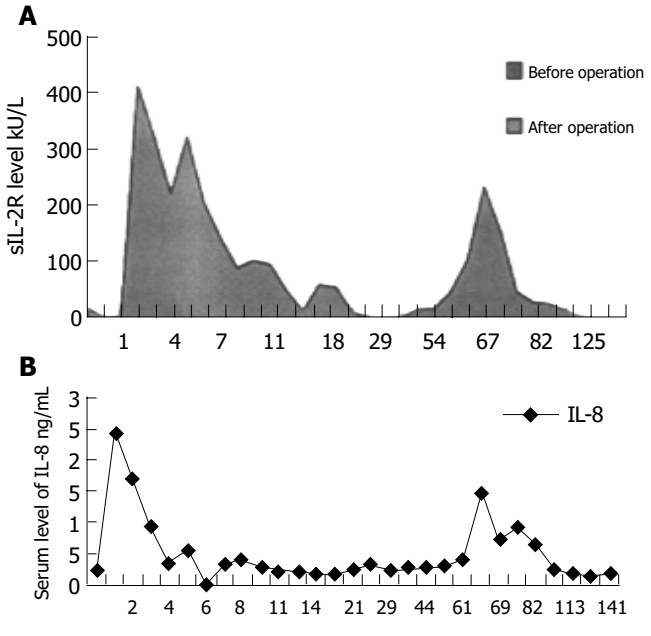


Figure 4 Serum level of sIL-2R (**A**) and IL-8 (**B**) before and after occurrence of acute rejection.

Endoscopic and pathological examinations

The first endoscopic examination was done 15 h following transplantation, once every day in the first 3 d, once every 2-3 d after 3 d, and once or twice every month after month. When there was evidence for acute rejection, endoscopic examination was performed more frequently. Since acute rejection of the graft is heterogeneous, biopsy specimens were taken at more than one site from the graft with the remaining jejunum as a control. Microbiological examination was done to exclude the risk for other intestinal pathological changes. The patient had an increased intestinal discharge and his immunological indexes were changed 2 mo after transplantation. Endoscopic examination and pathologic biopsy specimens suggested acute rejection, which accords with the findings of previous studies[9-12]. Treatment with intensive immunosuppressive drugs alleviated the symptoms. Endoscopic and pathological examinations are now essential for the control of acute rejection following transplantation[11]. When the intestinal fistula was closed one year later, no abnormal symptom was found.

Absorptive function of the graft and discharge at the intestinal fistula

The presence of congestion, edema, sporadic ulcer and necrosis on the graft at the early stage of acute rejection after transplantation, is theoretically followed by increased discharge and decreased absorptive function of the graft.

However, it has not been reported in any clinical case report. The present study showed that at the early stage of acute rejection after transplantation, increased discharge of the graft was the only clinical symptom. The absorptive rate of the graft decreased greatly and reached its lowest point when severe acute rejection occurred. After being treated with intensive immunosuppressive drugs, it returned to normal and then remained normal (30%) and no acute rejection occurred after the intestinal fistula was closed, suggesting that changes in the graft discharge and absorptive function are worth to consider in observing and identifying the presence of acute rejection of the graft.

Control of immunological indexes

The immunological indexes, which are instrumental in suggesting acute rejection of the graft, are still being studied. Rejection following homotransplantation is initiated by the T cell's recognition of the graft and antigen complex, which is compatible with the patient's own tissue with its specific T-cell antigen recognition receptor. Since the direct recognition pathway of $CD4^+$ T cells plays an essential role in the above process and in the presence of the first acute rejection[13], and $CD4^+$ T cells secrete such cell factors as IL-2, with which IL-2R can be combined and inhibit its mutual action with cells, the serum IL-2R level might be a sensitive immunological index of the presence of rejection following homotransplantations[13,14]. We detected many immunological indexes, which might be connected with rejection, and found that IL-2R increased one day after transplantation and then decreased gradually, but increased again and reached its second peak until acute rejection occurred, suggesting that there might be a close relationship between the serum level of IL-2R and the onset of acute rejection of the graft. Thus, the serum level of IL-2R can be used as an useful index for the onset of acute rejection following small bowel transplantation. When the graft rejection occurs, mononuclear leukocytes/macrophages, and T lymphocytes may be present with characteristic cellular infiltration, and these cells can secrete IL-8. It has been reported that the serum level of IL-8 increases in patients with acute rejection after transplantation of the liver or kidney and then decreases after being treated with intensive immunosuppressive drugs[15-17]. In the present study, the serum level of IL-8 reached its first peak one day after transplantation, which might be attributed to the long period of cold ischemia and lesions due to reperfusion. Since the serum level of IL-8 reached its second peak 67 d after transplantation, when acute rejection occurred no changes were observed after treatment with immunosuppressive drugs, there may be a close connection between the second peak of serum IL-8 and the onset of acute rejection. Therefore, it can be used as an important index for the diagnosis of acute rejection.

In addition, effective anti-infectious treatment and scientific nutrition arrangement may contribute to the survival rate of patients after the small bowel transplantation.

REFERENCES

1 **Wang WZ,** Wu GS, Song WL, Ling R, Zhang SH, Du JJ, Chen DL, Zhao JX, Li MB, Li JP, Liu XN, Ji G, Luo L. The case of the clinical living-related small bowel transplantation. *Zhonghua Waike Zazhi* 2000; **38**: 236-238

2 **Chen DL,** Wang WZ, Li MB, Wu GS. The irrigation and preserve of the living-Related small bowel transplantation. *Zhonghua Putong Waike Zazhi* 2000; **15**: 504-506

3 **Wang WZ,** Song WL, Ling R, Wu GS, Wang G, Zhu QS, Xue YJ, Chao ZN. The management of graft blood vessel in the living-related small bowel transplantation. *Zhonghua Putong Waike Zazhi* 2000; **15**: 491-494

4 **Wang WZ,** Ling R, Song WL, Zhang SH, Chen DL, Li MB, Ji G. Anagement of intestinal graft in living-related small bowel transplatation. *Disi Junyi Daxue Xuebao* 2000; **21**: 773-775

5 **Wang WZ,** Song WL, Wu GS, Ling R, Pu JS, Zhang SH, Du JJ, Chen DL, Zhao JX, Xue YJ, Dong GL, Zhang HW, Li MB, Li JP, Liu XN, Ji G, Luo L. The perioperative management of living-related small bowel transplantation. *Zhonghua Putong Waike Zazhi* 2000; **15**: 411-413

6 **Song WL,** Wang WZ, Ling R, Wu GS, Zhao JX, Ji G. The prevention of the infection in the living related small bowel transplantation. *Disi Junyi Daxue Xuebao* 2000; **21**: 2-10

7 **Dong GL,** Wang WZ, Wu GS, Song WL, Ji G, Luo L, Xu JL, Zhao CH. Strategy of nutritional support for a patient with partial live small bowel transplantation during perioperation. *Shijie Huaren Xiaohua Zazhi* 2000; **8**: 539-541

8 **Liu XN,** Wang WZ, Song WL, Wu GS. The diagnose and treatment of the virus in the small bowel transplantation. *Disi Junyi Daxue Xuebao* 2001; **22**: 343

9 **Abu-Elmagd KM,** Tzakis A, Todo S, Reyes J, Fung J, Nakamura K, Wright H, Furukawa H, Demetris J, Van Thiel DH, Starzl TE. Monitoring and Treatment of intestinal allograft rejection in humans. *Transplant Proc* 1993; **25**(1 Pt 2): 1202-1203

10 **Lee RG,** Nakamura K, Tsamandas AC, Abu-Elmagd K, Furukawa H, Hutson WR, Reyes J, Tabasco-Minguillan JS, Todo S, Demetris AJ. Pathology of human intestinal transplantation. *Gastroenterology* 1996; **110**: 1820-1834

11 **Su ZX,** Yu LX, Huang JF. Small bowel transplantation. Moder Transplantation. 1st ed. *Beijing: People's Health Publishing House* 1998: 616-652

12 **Hassanein T,** Schade R, Soldevilla-Pico C, Tabasco-Minguillan J, Abu-Elmagd K, Furukawa H, Kadry Z, Demetris A, Tzakis A, Todo S. Clinical and endoscopic features of rejection in small bowel transplant recipients. *Transplant Proc* 1994; **26**: 1413

13 **Shirwan H,** Leamer M, Wang HK, Makowka L, Cramer DV. Peptides derived from alpha-helices of allogeneic class I major histocompatibility complex antigens are potent inducers of $CD4^+$ and $CD8^+$ T cell and B cell responses after cardiac allograft rejection. *Transplantation* 1995; **59**: 401-410

14 **Shirwan H,** Barwari L, Cramer DV. Rejection of cardiac allografts by T cells expressing a restricted repertoire of T-cell receptor Vbeta genes. *Immunology* 1997; **90**: 572-578

15 **Yagihashi A,** Zou XM, Hirata K, Asanuma K, Tsuruma T, Matsuno T, Yamaguchi H, Yamashiro K, Koide S, Torimoto K, Sasaki K, Kurokawa I. Evaluation of serum IL-8 concentrations after orthotopic liver transplantation in rats. *Transplantation Proc* 1995; **27**: 1632-1633

16 **Boratynska M.** Monitoring of IL-8 in urine and in serum of patients after kidney transplantation. *Przeyl Lek* 1998; **55**: 576-580

17 **Tilg H,** Ceska M, Vogel W, Herold M, Margreiter R, Huber C. Ihterleukin-8 serum concentrations after liver transplantation. *Transplantation* 1992; **53**: 800-803

Science Editor Wang XL and Guo SY **Language Editor** Elsevier HK

PO Box 2345, Beijing 100023, China
www.wjgnet.com
wjg@wjgnet.com

ELSEVIER

World J Gastroenterol 2005;11(34):5336-5341
World Journal of Gastroenterology ISSN 1007-9327
© 2005 The WJG Press and Elsevier Inc. All rights reserved.

• *CLINICAL RESEARCH* •

Role of SPECT/CT in diagnosis of hepatic hemangiomas

Jian-Guo Zheng, Zhi-Ming Yao, Chong-Ye Shu, Ying Zhang, Xia Zhang

Jian-Guo Zheng, Zhi-Ming Yao, Department of Nuclear Medicine, Beijing Hospital, Beijing 100730, China
Chong-Ye Shu, Imaging Center, Central Hospital of Siping City, Siping 136000, Jilin Province, China
Ying Zhang, Department of Nuclear Medicine, People's Hospital in Liaocheng City, Liaocheng 252000, Shandong Province, China
Xia Zhang, Department of Anesthesiology, West China Hospital, Sichuan University, Chengdu 610041, Sichuan Province, China
Correspondence to: Xia Zhang, Department of Anesthesiology, West China Hospital, Sichuan University, Chengdu 610041, Sichuan Province, China. huaxizhangxia@hotmail.com
Telephone: +86-28-85422518 Fax: +86-28-85422518
Received: 2005-02-17 Accepted: 2005-04-02

Abstract

AIM: To investigate the role of SPECT/CT in the diagnosis of hepatic hemangiomas whose anatomical positions are not ideal, situated adjacent to the heart, the inferior cava, hepatic vessels or abdominal aorta, etc.

METHODS: The hepatic perfusion, blood pool, and fusion imaging were carried out using SPECT/CT in 54 patients, who were suspected for hepatic hemangiomas. When the anatomical positions were not ideal, the diagnosis was difficult by SPECT only. So the information of computed tomography (CT) was applied to help in diagnosing. The results were recorded as hemangiomas or not.

RESULTS: Of the 54 patients, 31 patients were diagnosed as suffering from hepatic hemangiomas. The anatomical positions of eight patients' hepatic hemangiomas (25.81%) were not ideal. Among these lesions of the eight patients, three patients' hepatic lesions were located near to the abdominal aorta, one to the heart, and four to the inferior cava. In addition, six abnormal radioactivity accumulation regions, adjacent to the heart and inferior cava, with the help of CT, were confirmed to be the imaging of inferior cava other than hepatic hemangiomas.

CONCLUSION: When the anatomical positions of hepatic hemangiomas are not good enough for diagnosis, the fusion imaging of SPECT/CT is a simple and efficient method for differential diagnosis.

© 2005 The WJG Press and Elsevier Inc. All rights reserved.

Key words: SPECT/CT; Hepatic hemangiomas; Scintigraphy

Zheng JG, Yao ZM, Shu CY, Zhang Y, Zhang X. Role of SPECT/CT in diagnosis of hepatic hemangiomas. *World J Gastroenterol* 2005; 11(34): 5336-5341
http://www.wjgnet.com/1007-9327/11/5336.asp

INTRODUCTION

The diagnosis of a number of atypical hepatic hemangiomas in cross-sectional images is also very difficult[1]. Moreover, when the tumor is present in staging or in the follow-up of oncological patients, the differentiation of hepatic hemangioma from hepatic metastatistic diseases is a common clinical question. Contrast-enhanced magnetic resonance imaging (MRI) and multiple helical computed tomography (CT) is also limited to distinguish focal hepatic lesions in some ways[2]. Contrast-enhanced ultrasonography (US) is helpful to confirm the characterization of the focal liver disease. However, the diagnosis is associated with the experience of the surgeon. As regards single-photon emission computed tomography (SPECT), when the anatomical positions of hepatic hemangiomas were not ideal, for example, close to the heart, inferior cava or main hepatic vessels, etc., it may cause some difficulty for diagnosis, because the radioactivity of the ^{99m}Tc-labeled RBC is centralized in the heart, inferior cava, abdominal aorta and main hepatic vessels, and the radioactivity of blood pool is existing from the start. Thus, it is difficult to detect hepatic hemangioma, which is close to the above-mentioned structure, especially tiny ones.

A method, SPECT/CT, which can localize the hepatic lesions accurately will be helpful to diagnose this kind of hepatic hemangioma. The imaging of ^{99m}Tc-labeled red blood cell scintigraphy through SPECT is non-invasive and highly specific, able to avoid invasive method or biopsy. Meanwhile, when the anatomical position is not ideal, close to heart, inferior cava, main hepatic vessels, abdominal aorta, upside of right kidney, the diagnosis accuracy is improved owing to the locating function of the CT.

MATERIALS AND METHODS

Objects

Fifty-four patients who were suspected for hepatic hemangiomas found by US, CT, and or MRI, and were examined by SPECT/CT from April 26, 2001 to July 15, 2004 in Beijing Hospital. Their average age was 49.15±13.78 years. Among them, 31 were men with an average age of 50.38±15.36 years; 23 were women with an average age of 47.36±11.22 years. The oldest was 91 years old and the youngest was 27 years old.

Acquisition methods

First, the patients were required to take 400 mg of perchlorate potassium. Thirty minutes later, 10 mg of pyrophosphate dissolved in 2 mL of water for injection was administered into one patient. Thirty minutes later again, 740 MBq of $Na^{99m}TcO_4$ was also administered intravenously by bolus injection. The imaging was obtained using the SPECT/CT (Hawkeye, General Electronic Medical System).

Hepatic blood perfusion imaging

The patients were laid on the table and the detector was placed at front-back imaging position or back-front one. The field of vision included parts of heart, abdominal aorta, liver, spleen, and kidney. The SPECT was equipped with low-energy parallel hole general collimator or high-resolution collimator. The energy peak was 140 keV, the width of the energy window was from 15% to 20%, and the matrix 128×128. When $Na^{99m}TcO_4$ was injected through elbow vein by bolus, the acquisition was carried out immediately at the speed of 2 s/frame, totally 30 frames.

Planar hepatic blood pool imaging

The static imaging was obtained at 5, 10, 15, and 20 min after intravenous injection. The delayed imaging was obtained from 1.5 to 2 h after injection, and 4-6 h if necessary.

Planar imaging: The patients were laid on the table. The detector was placed at the front-back and back-front position, or in the position where hepatic lesions were able to be shown clearly. The detectors were equipped with low-energy parallel hole general collimator or high-resolution collimator. The energy peak was 140 keV, the width of the window 20%, and the matrix 256×256. The count was set up 500 K/frame in advance.

Fusion imaging

The hepatic blood pool cross-sectional imaging was acquired and together with CT scanning after 40 min of bolus intravenous injection. The X-ray transmission scanning, which needed 0.8 min, was obtained firstly with the matrix of 384×800 to identify the liver position. Then X-CT acquisition, which needed 10.8 min, was followed with matrix of 256×256, zoom of 1.105, 10 mm per layer, totally 40 cross-sections. After transmission process, the detector automatically came back to the start position. Then SPECT acquisition over 360° was performed with the matrix of 128×128, zoom of 1.28, 20 s/frame, and 6°/frame. The technique of automatic human body contour was applied to making detector get closer to the patient's body.

Images reconstruction

The SPECT images were reconstructed from the raw data by filtered back projection using a HANN filter (filter parameter: 0.85). The CT data were reconstructed using nuclear medicine workstation (eNTEGRA, General Electronic Medical System). Then the matching emission and transmission were fused to form the fusion images.

Standard of diagnosis

The standard of diagnosis is that an increase of blood pool activity within a liver lesion is typical of hemangioma. And in the CT scanning, the density of the lesion is low and even. The images were read by experienced physicians, who have worked in the department of nuclear medicine for at least 5 years. The results were recorded as hepatic hemangioma or not.

RESULTS

Of the 54 patients, 31 (57.41%) were diagnosed as hepatic hemangioma patients by SPECT/CT and were not taken for further examination. The diameter of hepatic lesions was from 1 to 9 cm. Twenty-three patients (42.59%) were excluded from the hepatic hemangioma, because their hepatic lesions did not meet the characterization of the hepatic hemangioma. Among them, 9 patients lost contact with us, the 13 patients' were diagnosed as hepatic cancer, and one as hepatic cyst.

Of the 31 patients, the anatomical positions of the hepatic hemangiomas in 8 patients (25.81%) were not ideal. Among them, the hepatic lesions of three patients' were close to abdominal aorta (Figures 1A and B and 2A), that of four patients to inferior cava, that of one patient to heart (Figure 2B). Under these conditions, it was difficult to diagnose by only using SPECT. In SPECT/CT fusion imaging, CT was able to locate the position of focal radioactivity accumulation region, and at last diagnosed it as hepatic hemangioma.

In the research, there are six round-like regions with high radioactivity, close to the heart and inferior cava in six patients on the brim of the liver. The CT showed that they were in the inferior cava. Finally, hepatic hemangioma was excluded (Figure 2C).

DISCUSSION

As a benign tumor, the hepatic hemangioma most frequently appeared in the liver. The incidence of the disease is about from 2% to 7% of the liver lesions. The hepatic hemangioma is classified as capillary and cavernous hepatic hemangioma. The former is not common, and able to change to the other. Thus, the majority is cavernous hepatic hemangioma.

As a non-invasive and highly specific method for diagnosing hepatic hemangioma, the ^{99m}Tc-labeled RBC scintigraphy can avoid invasive imaging or biopsy. And thanks to the application of SPECT, the sensitivity of the method is improved obviously. However, when the diameter of hepatic lesion is less than 1.3 cm, the sensitivity of SPECT is quite low. When the diameter is less than 1 cm, false negative appeared. And when the larger hepatic lesions (diameter more than 2.5 cm) with the bad anatomical positions, close to the heart, inferior cava or main hepatic vessels, *etc*., the diagnosis is difficult in a way, especially tiny hepatic hemangiomas. As reported by Birnbaum *et al*.[3], the hepatic lesions of 18 patients, whose hepatic hemangiomas were adjacent to the above-mentioned positions, 6 of the patients were not able to find them out. As reported by Schillaci *et al*.[4], 24 patients were sceptical of suffering from hepatic hemangiomas. Of them, six patients' anatomical position were not ideal; three patients' were close to main hepatic vessel, and two close to inferior cava, one close to heart. When SPECT/CT was carried out, with the help of CT, four were diagnosed as hepatic hemangioma, two were excluded from the hepatic hemangioma. In this research, about 25.81% patients' anatomical position was not ideal. When SPECT/CT was applied, with the help of CT, finally hepatic hemangioma was diagnosed.

The functional information from the SPECT combining with the anatomical information from the CT is able to solve the problem that anatomical position of hepatic hemangioma is not ideal. CT can accurately locate the lesion of radioactivity concentration region. Several years ago, a new apparatus was discovered. It combined the rotatable double-detectors camera γ with low-dose X-rays tube. The

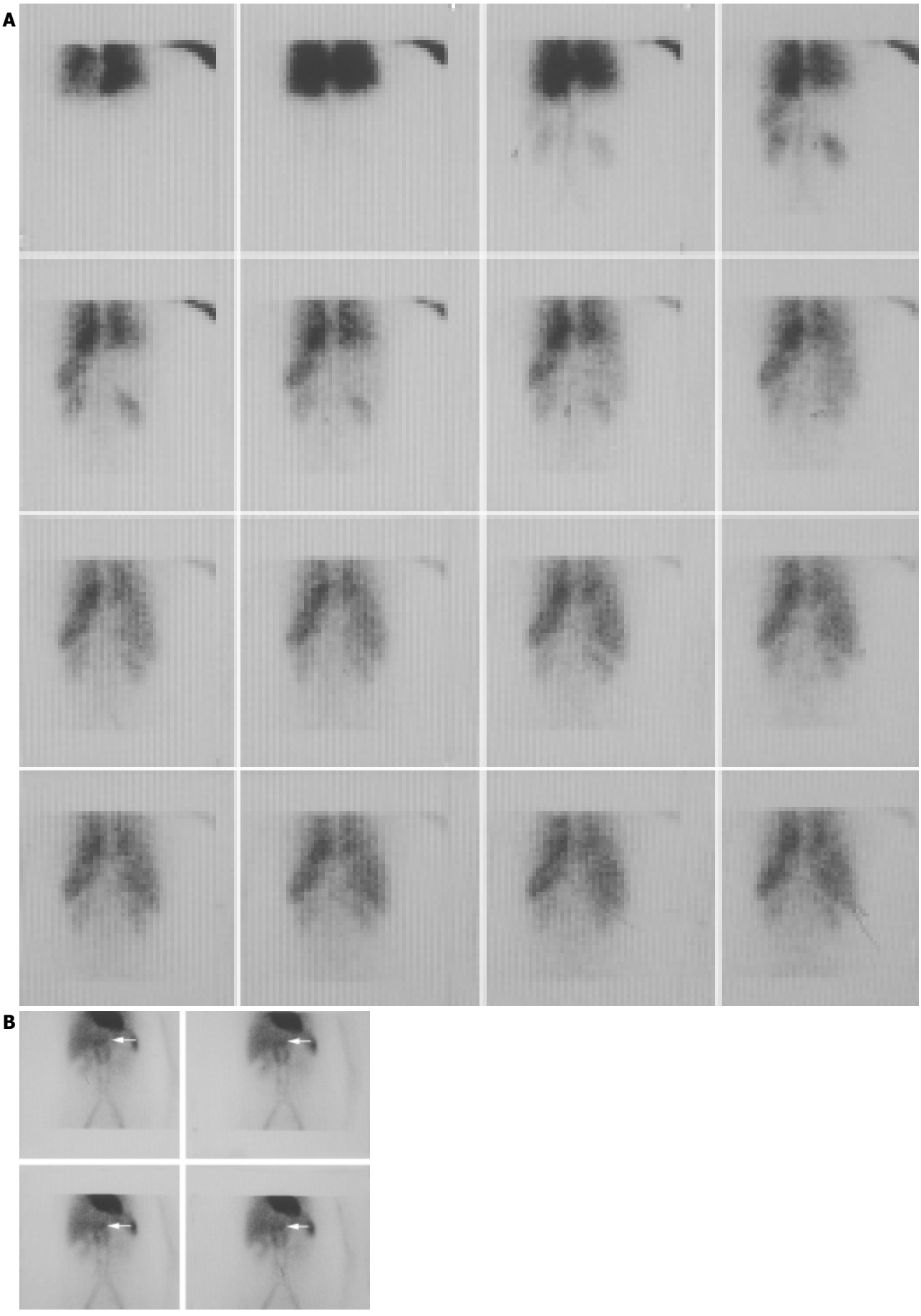
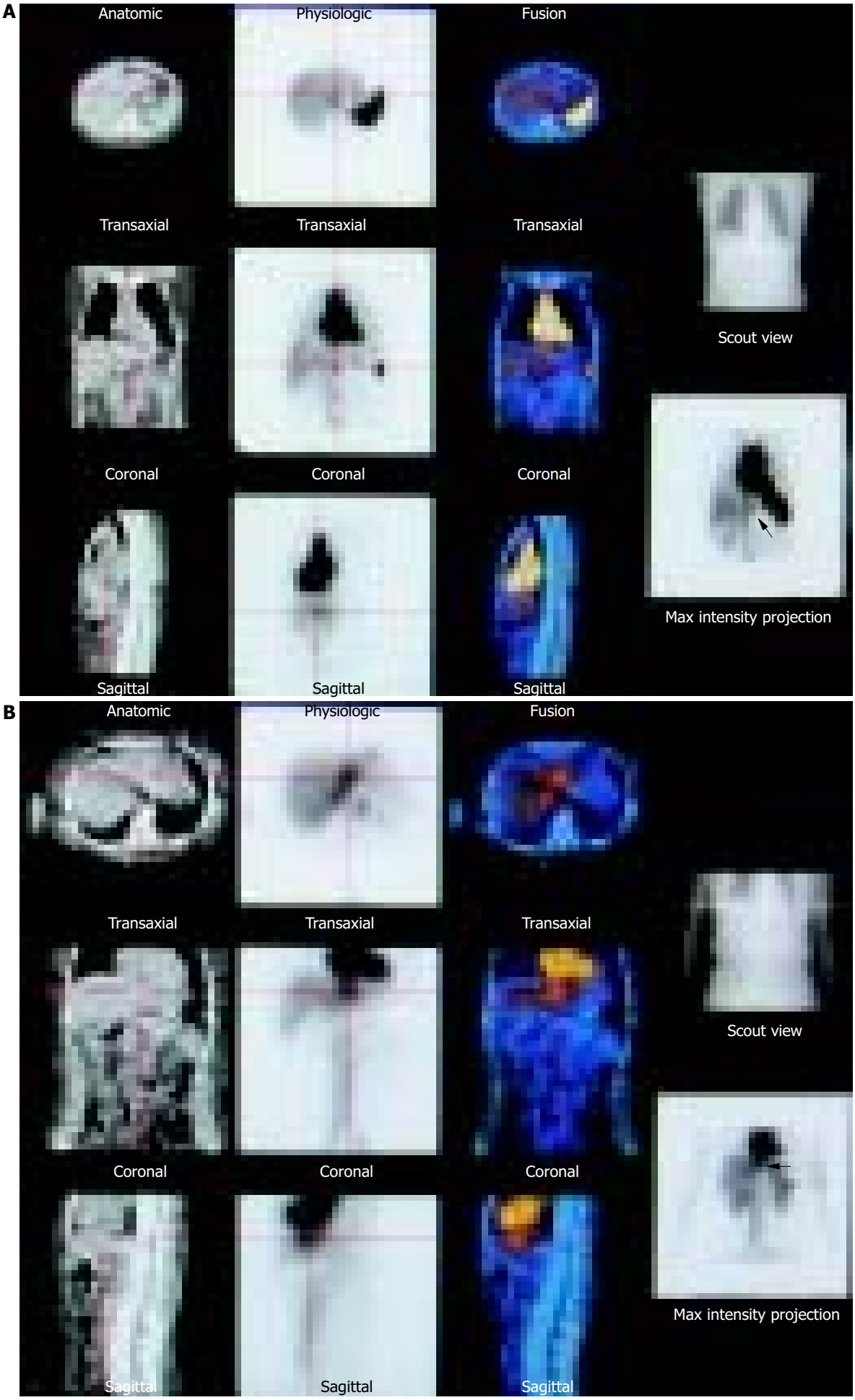


Figure 1 Female, 46 years old. US showed that there was a lesion in the left liver with the size 3.6×2.3 cm^2. The function of liver was normal. SPECT/CT test was carried out to exclude hepatic hemangioma. **A:** The hepatic blood perfusion imaging. The abnormal focal accumulation of the radioactivity was not shown obviously; **B:** The radioactivity accumulation of the focus (pointed by the red arrows) in the left liver was a little higher than the normal liver tissue.


A
Anatomic
Physiologic
Fusion
Transaxial
Transaxial
Transaxial
Scout view
Coronal
Coronal
Coronal
Max intensity projection
Sagittal
Sagittal
Sagittal
B
Anatomic
Physiologic
Fusion
Transaxial
Transaxial
Transaxial
Scout view
Coronal
Coronal
Coronal
Max intensity projection
Sagittal
Sagittal
Sagittal

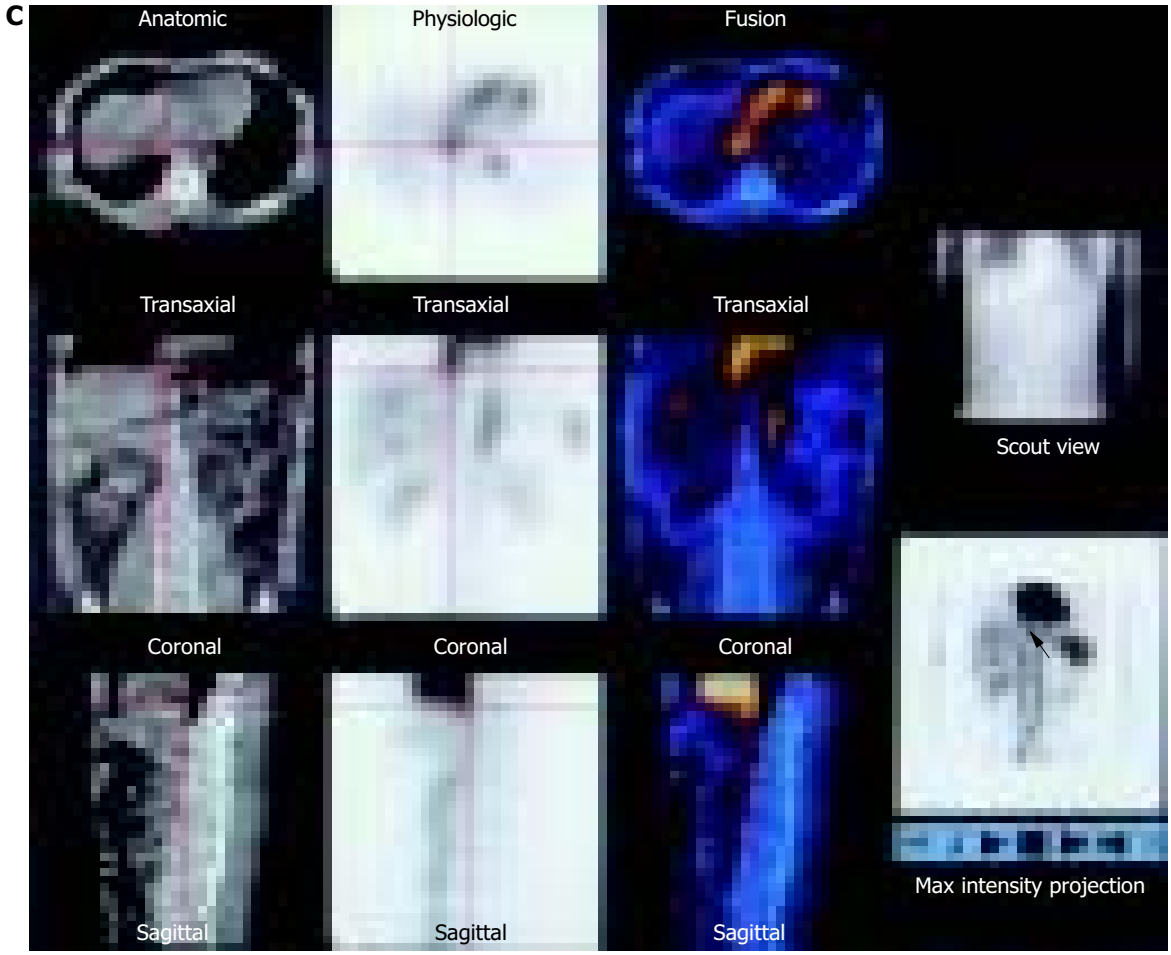


Figure 2 The round-like radioactive accumulation region (pointed by the red arrow) was just on the abdominal aorta. If fusion imaging was not obtained, then to decide whether it was abdominal aorta or hepatic hemangioma would have been difficult. As shown in the CT of fusion imaging, the focus (the red cross) was located in the left liver, but not in abdominal aorta, thus diagnosed as hepatic hemangioma. Female, 39 years old. A lesion in the liver with the diameter of 4 cm was found in the physical examination by US. It might be a hepatic hemangioma. SPECT/CT was performed for differentiation (**A**). The hepatic lesion (pointed by the red arrow) situated adjacent to the heart, whose abnormal radioactive concentration was a bit lower than the heart. The CT showed that the lesion (the red cross) was located in the left liver. The diagnosis was a left hepatic hemangioma. Male, 43 years old. The US showed a few lesions in the liver. They were sceptical of hepatic hemangiomas to go through SPECT/CT examination (**B**). The abnormal focal radioactive concentration region of left liver (pointed by the red arrow) was not only close to the heart, but also close to the inferior cava. The CT indicated that it was a part of the inferior cava (the red cross), and exclude the possibility of hepatic hemangioma. But other three round-like radioactive accumulation regions in the right liver were diagnosed as hepatic hemangiomas (**C**).

camera γ/CT machine would obtain SPECT and CT images respectively. The projection of X-ray was helpful to find the location of the radioactivity concentration focus. This was SPECT/CT fusion imaging. The SPECT/CT was used to diagnose hepatic hemangioma with the following advantages.

A. CT can accurately locate the position of radioactivity accumulating focus theoretically. However, the quality of the present CT in SPECT/CT is not very good. Under some conditions, it is very difficult to indicate the position accurately. But it is believed when multiple helical CT is used in fusion imaging in the future, the position of the hepatic lesions will be located accurately. Moreover, it may reach the function of diagnosis CT but not only in locating the position of the disease.

B. When hepatic lesions are detected by CT scanning, the hepatic colloid imaging may not be necessary. The colloid imaging is mainly used to find out the lesion of the liver. But CT is more superior to the hepatic colloid imaging in this respect. Its sensitivity is much higher than the hepatic colloid imaging. Therefore, when hepatic lesions are detected by CT scanning, the hepatic colloid imaging is not necessary.

C. Fusion imaging can be attenuation-corrected by X-ray. Therefore, the quality of the images would be improved. Because of the high quantity of information of X-ray, especially when the injected dose of ^{99m}Tc-labeled RBC is comparatively low and the patient is fat, the quality of the images will be improved obviously.

D. Improving the accuracy of diagnosis. Typical characterization of hepatic hemangioma is that its density is even and low by general CT scanning. The worth of common CT is limited. Usually it indicates the position of hepatic lesions, which is radioactive accumulation region. It provides anatomical information for hepatic hemangioma. SPECT can provide the functional information for pathological changes. Functional information coordinates with anatomical information, in this way the accuracy of diagnosis is improved.

Furthermore, it is worth paying attention to that, when

inferior cava passes by the liver, and enters right heart, a great majority can form a round-like radioactive accumulation region on the brim of the liver (Figure 2C). Under the condition, with the help of CT, the radioactive concentration region may be seen under the heart, link with the inferior cava and out of the liver. If it is, then hepatic hemangioma can be excluded. If it is not and the, the focus is in the liver, the diagnosis of hepatic hemangioma could be made.

REFERENCES

1 **Jang HJ,** Kim TK, Lim HK, Park SJ, Sim JS, Kim HY, Lee JH. Hepatic hemangioma: atypical appearances on CT, MR imaging, and sonography. *Am J Roentgenol* 2003; **180**: 135-141

2 **Zheng WW,** Zhou KR, Chen ZW, Shen JZ, Chen CZ, Zhang SJ. Characterization of focal hepatic lesions with SPIO-enhanced MRI. *World J Gastroenterol* 2002; **8**: 82-86

3 **Birnbaum BA,** Weinreb JC, Megibow AJ, Sanger JJ, Lubat E, Kanamuller H, Noz ME, Bosniak MA. Definitive dignosis of hepatic haemangiomas: MR imaging versus Tc-99m-labeled red blood cell SPECT. *Radiology* 1990; **176**: 95-101

4 **Schillaci O,** Danieli R, Manni C, Capoccetti F, Simonetti G. Technetium-99m-labelled red blood cell imaging in the diagnosis of hepatic haemangiomas: the role of SPECT/CT with a hybrid camera. *Eur J Nucl Med Mol Imaging* 2004; **31**: 1011-1015

Science Editor Guo SY **Language Editor** Elsevier HK

PO Box 2345, Beijing 100023, China
www.wjgnet.com
wjg@wjgnet.com

ELSEVIER

World J Gastroenterol 2005;11(34):5342-5346
World Journal of Gastroenterology ISSN 1007-9327
© 2005 The WJG Press and Elsevier Inc. All rights reserved.

• *BRIEF REPORTS* •

High-dose interferon-α2b induction therapy in combination with ribavirin for treatment of chronic hepatitis C in patients with non-response or relapse after interferon-α monotherapy

Holger G. Hass, Christian Kreysel, Johannes Fischinger, Josef Menzel, Stephan Kaiser

Holger G. Hass, Stephan Kaiser, Department of Gastroenterology and Hepatology, University of Tuebingen, Germany
Christian Kreysel, Department of Gastroenterology, Klinikum Krefeld, Germany
Johannes Fischinger, Department of Gastroenterology and Hepatology, University of Saarland, Germany
Josef Menzel, Department of Gastroenterology and Hepatology, University of Muenster, Germany
Correspondence to: Dr. Holger G. Hass, Department of Gastroenterology and Hepatology, University of Tuebingen, Otfried-Müller-Straße 10, 72076 Tübingen, Germany. holger.hass@med.uni-tuebingen.de
Telephone: +49-7071-2982712 Fax: +49-7071-293467
Received: 2004-12-22 Accepted: 2005-01-05

Abstract

AIM: To evaluate the daily high-dose induction therapy with interferon-α2b (IFN-α2b) in combination with ribavirin for the treatment of patients who failed with interferon monotherapy and had a relapse, based on the assumption that the viral burden would decline faster, thus increasing the likelihood of higher response rates in this difficult-to-treat patient group.

METHODS: Seventy patients were enrolled in this study. Treatment was started with 10 MU IFN-α2b daily for 3 wk, followed by IFN-α2b 5 MU/TIW in combination with ribavirin (1 000-1 200 mg/d) for 21 wk. In case of a negative HCV RNA PCR, treatment was continued until wk 48 (IFN-α2b 3 MU/TIW+1 000-1 200 mg ribavirin/daily).

RESULTS: The dose of IFN-α2b or ribavirin was reduced in 16% of patients because of hematologic side effects, and treatment was discontinued in 7% of patients. An early viral response (EVR) was achieved in 60% of patients. Fifty percent of all patients achieved an end-of-treatment response (EOT) and 40% obtained a sustained viral response (SVR). Patients with no response had a significantly lower response rate than those with a former relapse (SVR 30% *vs* 53%; $P = 0.049$). Furthermore, lower response rates were observed in patients infected with genotype 1a/b than in patients with non-1-genotype (SVR 28% *vs* 74%; $P = 0.001$). As a significant predictive factor for a sustained response, a rapid initial decline of HCV RNA could be identified. No patient achieving a negative HCV-RNA PCR at wk 18 or later eventually eliminated the virus.

CONCLUSION: Daily high-dose induction therapy with interferon-α2b is well tolerated and effective for the treatment of non-responders and relapsers, when interferon monotherapy fails. A fast decline of viral load during the first 12 wk is strongly associated with a sustained viral response.

© 2005 The WJG Press and Elsevier Inc. All rights reserved.

Key words: Chronic hepatitis C; High-dose interferon-α induction therapy; Ribavirin; Nonresponder; Relapse

Hass HG, Kreysel C, Fischinger J, Menzel J, Kaiser S. High-dose interferon-α2b induction therapy in combination with ribavirin for treatment of chronic hepatitis C in patients with non-response or relapse after interferon-α monotherapy. *World J Gastroenterol* 2005; 11(34): 5342-5346
http://www.wjgnet.com/1007-9327/11/5342.asp

INTRODUCTION

Chronic infection with hepatitis C virus (HCV) is the main cause of chronic hepatitis, liver cirrhosis and hepatocellular carcinoma worldwide, more than 2% of the world population are chronically infected with this virus[1,2]. Until introduction of the nucleoside analog ribavirin, standard therapy for chronic hepatitis C was the monotherapy with interferon-α (IFN-α). The initial data published on the efficacy of IFN-α monotherapy demonstrate that about 50% of patients who have achieved a biochemical end-of-treatment response (ETR) have a relapse within the first 6 mo after cessation of treatment[3], only about 6% of patients with genotype 1 and/or high viral load can achieve a sustained viral response (SVR)[4].

Antiviral combination therapy with IFN-α and ribavirin can lead to significant response rates in treatment-of naive patients with chronic hepatitis C; however, sustained response rates for patients with no former response after IFN-α monotherapy are still low (12-16%)[5,6]. Furthermore, recent introduction of pegylated interferons has not resulted in a substantial increase in response rates among non-responders with a SVR rate being 14-27% after IFN-α monotherapy[7-9]. In order to increase the sustained response rate, it is important to decline the viral load during the initial weeks of antiviral therapy because IFN-α dose administered is directly related with the decline of HCV RNA[10-13].

The aim of the present study was first to evaluate the efficacy as well as safety and tolerability of a high-dose IFN-α2b induction therapy in combination with ribavirin

in patients who failed with interferon monotherapy and had a relapse. Further, the data were analyzed for potential predictive factors for a viral response in this subgroup of patients.

MATERIALS AND METHODS

Patients

A total of 70 patients (49 males/21 females) with chronic hepatitis C (elevated ALT, HCV RNA positive) who failed IFN-α monotherapy (group A, $n = 44$) or had a relapse (group B, $n = 26$), were enrolled in the study. Other inclusion criteria included hemoglobin level >120 g/L, white blood cell count >2.5/nL, platelet count >80/nL, and normal bilirubin, albumin and creatinine levels. Written informed consent was obtained from all patients. Exclusion criteria were decompensated liver cirrhosis (Child-Pugh B or C), autoimmune hypo- or hyperthyroidism, neuropsychiatric disorders, cardiovascular disease, HIV infection or infection with other hepatitis virus or other causes of liver disease, and pregnancy.

Seventy percent of all patients were infected with genotype 1a/b, 7% with genotype 2a/c, 20% with genotype 3a and 3% with genotype 4. Pre-treatment quantitative HCV RNA levels were determined using the Roche Cobas Amplicor v2.0 test. In 71% of patients a liver biopsy was performed and the degree of inflammation and fibrosis was estimated according to the Ishak-Knodell score. More details are listed in Table 1.

Table 1 Baseline characteristics of patients

	All patients	Group A (non-responder)	Group B (relapser)
Male (%)	70	80.5	59
Mean age	40.4	39.6	41.8
Genotype 1 (%)	70	75	57
Serum ALT (U/L)	70±2	67±6	75±10
Viral load[1] (%)			
<2 Mio copies/mL	37	39	35
>2 Mio copies/mL	63	61	65
HAI score[2] (%)			
HAI score (0-1)	72	68	77
HAI score (3-4)	28	32	23

[1]Quantitative HCV-PCR was measured in 48 patients pre-treatment. [2]Liver biopsies of 50 patients (22 relapsers/28 non-responders) were analyzed.

Study design

This study was carried out as an open, randomized, multicenter study (three centers).

Patients were treated first with 10 MU IFN-α2b daily for 3 wk. After the induction phase, patients received 5 MU IFN-α2b TIW for 21 wk. If a negative HCV RNA PCR result was obtained, treatment was continued for the remaining 24 wk with 3 MU IFN-α2b TIW. Ribavirin was added at 1 000-1 200 mg (according to body weight of > or <75 kg) at treatment wk 4 until wk 48 (Figure 1). The concept of a delayed onset of ribavirin was based on the observation that in the initial phase of antiviral therapy ribavirin has no significant effects on viral kinetics[14,15]. Thus the drug was given at a later time point to ameliorate side effects during the IFN high dose induction period. For severe adverse events other than anemia, interferon dosage was decreased (10 MU>5 MU or 5 MU>3 MU) or stopped if the actual dose was 3 MU. For anemia (<100 g/L), ribavirin dose was lowered to 600 mg/d, and discontinued if hemoglobin concentrations fell to <85 g/L. If severe leuko- or thrombocytopenia (white blood cell count <1 500/μL, platelet count <40 000/μL) occurred, interferon medication was stopped.

During the IFN-α2b high-dose induction phase, all patients were evaluated for tolerance, safety and treatment response twice weekly, while for the further follow-up patients were seen at wk 4, 8, 12, 18, 24, 36 and 48. At each visit, hematological, biochemical and HCV RNA testing was done.

When the treatment was completed, all patients were followed up for 48 wk.

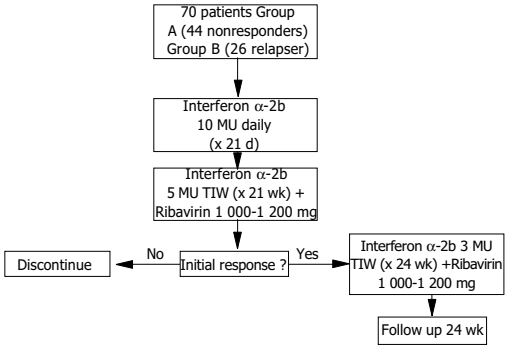


Figure 1 Trial profile of group A (non-responder) and group B (relapser).

Definition of response

Biochemical response was estimated after 12 wk of therapy and defined by a normalization of primary elevated ALT values. Undetectable serum HCV RNA at wk 24 during therapy was the criterion for an initial virological response. Virological end-of-treatment response was defined by a negative testing for HCV RNA at wk 48. If HCV RNA was still undetectable 24 wk after completion of the treatment, a virological sustained response was achieved.

Statistical analysis

The primary end point of the study was the comparison of virological response rates in relation to the prior response to the initial IFN-α monotherapy (non-responder *vs* relapser). Secondary parameters were differences in virological response rates in relation to genotype (genotype 1 *vs* non-1-genotypes) and viral kinetics (estimated after 12 wk of treatment). All safety and efficacy analyses were based on an intention-to-treat basis for all patients who received at least one dose of study medication. Statistical analysis was performed using χ^2 and Fisher's exact test (SPSS for Windows 10.0; SPSS, Inc., Chicago, IL).

Ethical aspects

According to the Declaration of Helsinki, a positive ethics

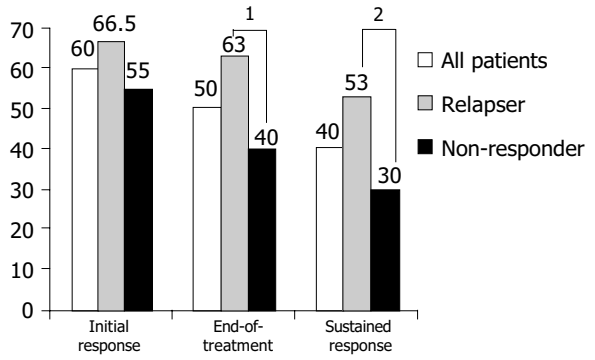


Figure 2 Response rates in relation to former response after IFN-α monotherapy. ^1P = 0.05; ^2P = 0.049; χ^2 test.

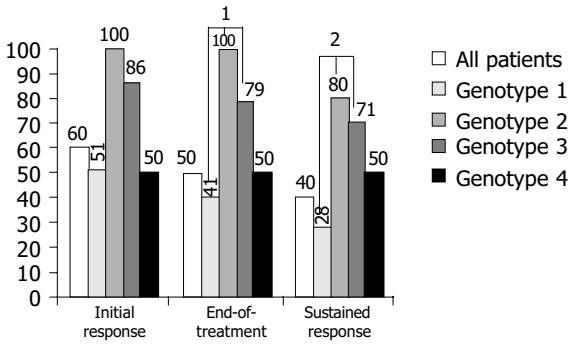


Figure 3 Response rates in relation to genotype (genotype 1 *vs* 2/3). ^1P = 0.005; ^2P = 0.001; χ^2 test.

committee approval was obtained. Patients were only included in this study after giving their written informed consent.

RESULTS

In 5 patients (7%), therapy was discontinued because of side effects such as insomnia, myalgia and fatigue (three patients) or because of a significant increase (>5×ULN) in alanine aminotransferase levels (two patients). The IFN-α dosage was reduced in seven patients (10%) because of severe neutropenia (<1 500/μL). Average IFN-α induced a mean neutropenia of 2 695±629/μL and a mean thrombopenia of 119.700±31.500/μL. Hemolytic anemia as a common side effect of ribavirin leads to a mean hemoglobin decrease of 3±14.8 g/L in all patients. In four patients (5.7%), ribavirin was reduced because the hemoglobin value was persistently lower than 100 g/L.

At wk 24, a biochemical response was observed in 85% and an initial virological response was achieved in 60% of all patients. Ten percent of patients had a break-through phenomenon after a previous negative HCV RNA PCR in serum in the first 24 wk of therapy. An end-of-treatment response (EOT) was achieved in 50% of all patients. During the follow-up, 10% of patients experienced a relapse. Accordingly, an overall sustained response (SR) of 40% was obtained. Patients with no primary response had a significant lower response rate than those with a former relapse (SVR 53% *vs* 30%; P = 0.049 (χ^2 test; Figure 2)). Likewise, genotype 1a/b showed a significantly lower response rate than other genotypes (28% *vs* 74% for genotypes 2 and 3; P = 0.001 χ^2 test; Figure 3).

To estimate the effect of a fast decline of viral load as a potential predictive factor for a viral response especially in former non-responders, HCV-RNA was analyzed after 12 wk of therapy in 40 patients. An early loss of HCV RNA level was significantly (P = 0.001; Fisher's exact test) associated with higher sustained response rates as all patients with a late negative HCV RNA testing (>12 wk of therapy), experienced a breakthrough or relapse during further follow-up. In contrast, 65% of all patients with a rapid drop of HCV RNA level and a negative PCR result at wk 12, finally experienced a sustained viral response (Table 2). No correlation between the observed decline of viral load and the result of previous treatment (relapse or non-response) or initial viral load could be demonstrated in this small subgroup in the present study.

DISCUSSION

Therapy of patients who failed with IFN-α monotherapy and had a relapse remains a difficult issue though the advances have been achieved with the introduction of ribavirin combination therapy as well as the introduction of pegylated interferons. Retreatment of this patient group with standard doses (TIW) of interferon plus ribavirin especially in non-responders or patients infected with genotype 1 was largely ineffective, resulting in SVR of 12-16%[5,6]. Even when treated with the pegylated interferons-α2a or -α2b, the sustained response rate was between 14% and 27%[7-9].

Many studies have shown the importance of a rapid initial decline of viral load in obtaining a better response rate[10,11]. Higher INF-α dosage is correlated with a faster decline of the viral load[12,13]. Based on these observations, this study using an induction therapy with 10 MU IFN-α daily was designed. To reduce the extent of expected side effects, ribavirin was subsequently added at the end of the IFN-α induction phase (end of wk 3).

The interferon induction phase with 10 MU IFN-α2b daily for over 3 wk was safe and at least moderately tolerated. Treatment was discontinued only in 7% of patients, interferon or ribavirin was reduced in 16% of patients, mainly because of hematological side effects. In comparison to other studies using high-dose interferon

Table 2 Response rates in relation to an early viral response in former non-responders after IFN-α monotherapy

Treatment week	"Fast responder" (HCV RNA negative at wk 12, n = 31)	"Slow responder" (HCV RNA negative after wk 12, n = 9)	P
48 (ETR, %)	25 patients PCR negative (81)	3 patients PCR negative (33)	0.012[1]
Follow-up (SR, %)	20 patients PCR negative (65)	0 patient PCR negative (0)	0.001[1]

[1]Fisher's exact test.

induction therapy in combination with non-pegylated interferons[16-19], the sustained response rate in the present study was higher (30% *vs* 6-27%) , perhaps as a result of the higher initial IFN dose or a longer induction period leading to a faster decline in serum HCV RNA level. Another reason for the relatively higher sustained response rate in the present trial may be due to the low dropout rate (7%) in comparison to other treatment schedules (15-21.9%) using a higher dose of INF-α.

The sustained response rate was significantly lower in patients with no former response than in relapsers (30% *vs* 53%; $P = 0.049$). Possible reasons for these observations might be the higher number of patients infected with genotype 1, male gender and a higher Ishak score of 3-4 in the non-responder group. These viral and host characteristics are known as negative predictive factors for the treatment of chronic hepatitis C[18,19]. Independent of these factors other studies have also shown higher response rates in patients with an earlier relapse than in non-responders after INF-α monotherapy[17,20].

All former non-responders with a sustained response had a negative serum HCV RNA at treatment wk 12, which underscores the importance of a fast decline in viral load and may serve as a rationale in using higher initial interferon doses especially in treating non-responders[21-23]. However, in patients with genotype 1, sustained response rates were significantly lower in those with other HCV types. These observations are due to multiple factors, including higher drug effectiveness, a faster free virion clearance rate and possibly an enhanced immunological response in patients infected with non-1 genotype[24].

As one explanation for the differences in viral kinetics between the HCV subgroups, it has been speculated that HCV genotype 1 is not as sensitive to IFN-α as other viral strains[25,26]. As described above and shown in the large registration trials for treatment of naive patients with pegylated interferons[27], an early therapeutic decision regarding the continuation of treatment at 12 wk appears also to be amenable in non-reponders.

At present, pegylated interferons in combination with ribavirin can improve the sustained response rate of about 50-56% in naive HCV positive patients. The subgroup of genotype 1/high viral load patients, however, did not show improved sustained response rates of 30-34% when treated with pegylated interferons. Furthermore, patients who failed the standard interferon and ribavirin therapy did not show significant sustained response rates when retreated with pegylated interferons (SVR 6-12%). Thus, the sustained response rate reported in this study together with good tolerability using a standard daily interferon dose makes this type of treatment a valuable alternative for this difficult-to-treat patient group. An even longer high-dose induction period for more than 3 wk may lead to an even higher sustained response rate, but this might be counterbalanced by a relatively lower tolerability. For a final evaluation of the optimal duration of induction, larger clinical trials are needed.

REFERENCES

1 **Purcell RH.** Hepatitis viruses: Changing patterns of human disease. *Proc Natl Acad Sci USA* 1994; **91**: 2401

2 **Detre KM,** Belle SH, Lombardero M. Liver transplantation for chronic viral hepatitis. *Viral Hepatitis Rev* 1996; **2**: 219-228

3 **Davis GL,** Balart LA, Schiff ER, Lindsay K, Bodenheimer HC Jr, Perrillo RP, Carey W, Jacobson IM, Payne J, Dienstag JL. Treatment of chronic hepatitis C with recombinant Interferon alfa. *N Engl J Med* 1989; **321**: 1501-1506

4 **McHutchinson JD,** Gordon SC, Schiff E, Shiffman ML, Lee WM, Rustgi VK, Goodman ZD, Ling MH, Cort S, Albrecht JK. Interferon alfa-2b alone or in combination with ribavirin as initial treatment for chronic hepatitis C. *N Engl J Med* 1998; **339**: 1485-1491

5 **Barbaro G,** Di Lorenzo G, Soldini M, Giancaspro G, Bellomo G, Belloni G, Grisorio B, Annese M, Bacca D, Francavilla R, Rizzo G, Barbarini G. Interferon-alfa-2B and ribavirin in combination for chronic hepatitis C patients not responding to interferon-alfa alone: An Italian multicenter, randomized, controlled, clinical study. *Am J Gastroenterol* 1998; **93**: 2445-2451

6 **Sostegni R,** Ghisetti V, Pittaluga F, Marchiaro G, Rocca G, Borghesio E, Rizzetto M, Saracco G. Sequential versus concomitant administration of ribavirin and interferon alfa-n3 in patients with chronic hepatitis C not responding to interferon alone: Results of a randomized, controlled trial. *Hepatology* 1998; **28**: 341-346

7 **Sulkowski M,** Rothstein K, Stein L, Godowsky E, Goodman R, Dieterich D. PEG-Interferon alfa-2B + Ribavirin for Treatment of patients with chronic Hepatitis C who have previously failed to achieve a sustained virologic response following Interferon alfa or Interferon alfa-2B + Ribavirin Therapy [abstract]. DDW (Orlando 2003)

8 **Jacobson IM,** Ahmed F, Russo MW, Brown RS, Lebovics E, Min A, Esposito S, Brau N, Tobias H, Klion F, Bini E, Brodsky N, Rovner D, Brass C. Pegylated Interferon alfa-2B plus Ribavirin in patients with chronic Hepatitis C: A trial in prior Nonresponders to Interferon Monotherapy or Combination Therapy and in Combination Therapy Relapsers: Final Results [abstract]. DDW (Orlando 2003)

9 **Lawitz EJ,** Bala NS, Becker S, Brown G, Davis M, Dhar R, Ganeshappa KP, Gordon S, Holtzmuller K, Jeffries M, Li J, Monsour H, Nader P, Rosenfield T, Tolman K, Kadakia S. Pegylated Interferon alfa 2B and Ribavirin for Hepatitis C Patients who were Nonresponders to previous Therapy [abstract]. DDW (Orlando 2003)

10 **Karino Y,** Toyota J, Sugawara M, Higashino K, Sato T, Ohmura T, Suga T, Okuuchi Y, Matsushima T. Early loss of serum hepatitis C virus RNA can predict a sustained response to interferon therapy in patients with chronic hepatitis C. *Am J Gastroenterol* 1997; **92**: 61

11 **Fried MW,** Shiffman M, Sterling RK, Weinstein J, Crippin J, Garcia G, Wright TL, Conjeevaram H, Reddy KR, Peter J, Cotsonis GA, Nolte FS. A multicenter, randomized trial of daily high-dose interferon-alfa 2b for the treatment of chronic hepatitis c: pretreatment stratification by viral burden and genotype. *Am J Gastroenterol* 2000; **95**: 3225-3229

12 **Neumann AU,** Lam NP, Dahari H, Gretch DR, Wiley TE, Layden TJ, Perelson AS. Hepatitis C viral dynamics *in vivo* and the antiviral efficancy of interferon-a therapy. *Science* 1998; **282**: 103-107

13 **Lam NP,** Neumann AU, Gretch DR, Wiley TE, Perelson AS, Layden TJ. Dose-dependent acute clearence of hepatitis C genotype 1 virus with interferon-alpha. *Hepatology* 1997; **26**: 226-231

14 **Dixit NM,** Layden-Almer JE, Layden TJ, Perelson AS. Modelling how ribavirin improves interferon response rates in hepatitis C virus infection. *Nature* 2004; **432**: 922-924

15 **Saab S,** Hu R, Ibrahim AB, Goldstein LI, Kunder G, Durazo F, Han S, Yersiz H, Ghobrial RM, Farmer DG, Busuttil RW, Lassman C. Discordance between ALT values and fibrosis in liver transplant recipients treated with ribavirin for recurrent hepatitis C. *Am J Transplant* 2003; **3**: 328-333

16 **Ferenci P,** Stauber R, Steindl M, Gschwantler M, Fickert P,

Datz C, Muller C, Hackl F, Rainer W, Watkins-Riedel T, Lin W. Interim analysis of a randomized controlled trial of combination of ribavirin and high dose interferon-alpha in interferon nonresponders with chronic hepatitis C. *J Viral Hepat* 1999; **6**: 153-158

17 **Min AD,** Jones JL, Esposito S, Lebovics E, Jacobson IM, Klion FM, Goldman IS, Geders JM, Tobias H, Bodian C, Bodenheimer HC Jr. Efficacy of high-dose interferon in combination with ribavirin in patients with chronic hepatitis C resistant to interferon alone. *Am J Gastroenterol* 2001; **96**: 1143-1149

18 **Poynard T,** Marcellin P, Lee SS, Niederau C, Minuk GS, Ideo G, Bain V, Heathcote J, Zeuzem S, Trepo C, Albrecht J. Randomized trial of interferon alfa-2b plus ribavirin for 48 wk or for 24 wk versus interferon alpha-2b plus placebo for 48 wk for the treatment of chronic infection with hepatitis C virus: International Hepatitis Interventional Therapy Group. *Lancet* 1998; **352**: 1426-1432

19 **Tong MJ,** Reddy KR, Lee WM, Pockros PJ, Hoefs JC, Keeffe EB, Hollinger FB, Hathcote EJ, White H, Foust RT, Jensen DM, Krawitt EL, Fromm H, Black M, Blatt LM, Klein M, Lubina J. Treatment of chronic hepatitis C with consensus interferon: a multicenter, randomized, controlled trial. *Hepatology* 1997; **26**: 747-754

20 **Marco VD,** Almasio P, Vaccaro A, Ferraro D, Parisi P, Cataldo MG, Di Stefano R, Craxi A. Combined treatment of relapse of chronic hepatitis C with high-dose alpha2b interferon plus ribavirin for 6 or 12 mo. *J Hepatol* 2000; **33**: 456-462

21 **Zeuzem S,** Feinman SV, Rasenack J, Heathcote EJ, Lai MY, Gane E, O'Grady J, Reichen J, Diago M, Lin A, Hoffman J, Brunda MJ. Peginterferon alfa-2a in patients with chronic hepatitis C. *N Engl J Med* 2000; **343**: 1666-1672

22 **Bekkering FC,** Brouwer JT, Leroux-Roels G, Van Vlierberghe H, Elewaut A, Schalm SW. Ultrarapid hepatitis C virus clearence by daily high-dose interferon in non-responders to standard therapy. *J Hepatol* 1998; **28**: 960-964

23 **Di Marco V,** Vaccaro A, Ferraro D, Alaimo G, Rodolico V, Parisi P, Peralta S, Di Stefano R, Almasio PL, Craxi A. High-dose prolonged combination therapy in non-responders to interferon monotherapy for chronic hepatitis C. *Aliment Pharmacol Ther* 2001; **15**: 953-958

24 **Neumann AU,** Lam NP, Dahari H, Davidian M, Wiley TE, Mika BP, Perelson AS, Layden TJ. Differences in Viral Dynamics between Genotypes 1 and 2 of Hepatitis C Virus. *J Inf Dis* 2000; **182**: 28-35

25 **Enemoto N,** Sakuma I, Asahina Y, Kurosaki M, Murakami T, Yamamoto C, Izumi N, Marumo F, Sato C. Comparison of full lenght sequences of interferon sensitive and resistant hepatitis C virus 1b. *J Clin invest* 1995; **96**: 224-230

26 **Gale MJ Jr,** Korth MJ, Katze MG. Repression of the PKR protein kinase by the hepatitis C virus NS5A protein: A potential mechanism of interferon resistance. *Clin Diagn Virol* 1998; **10**: 157-162

27 **Berg T,** Sarrazin C, Herrmann E, Hinrichsen H, Gerlach T, Zachoval R, Wiedenmann B, Hopf U, Zeuzem S. Prediction of treatment outcome in patients with chronic hepatitis C: significance of baseline parameters and viral dynamics during therapy. *Hepatology* 2003; **37**: 600-609

Science Editor Wang XL and Guo SY **Language Editor** Elsevier HK

PO Box 2345, Beijing 100023, China
www.wjgnet.com
wjg@wjgnet.com

ELSEVIER

World J Gastroenterol 2005;11(34):5347-5350
World Journal of Gastroenterology ISSN 1007-9327
© 2005 The WJG Press and Elsevier Inc. All rights reserved.

• *BRIEF REPORTS* •

Is osteoporosis a peculiar association with primary biliary cirrhosis?

Annarosa Floreani, Andrea Mega, Valentina Camozzi, Vincenzo Baldo, Mario Plebani, Patrizia Burra, Giovanni Luisetto

Annarosa Floreani, Andrea Mega, Patrizia Burra, Department of Surgical and Gastroenterological Sciences, University of Padova, Italy
Valentina Camozzi, Giovanni Luisetto, Department of Medical and Surgical Sciences, University of Padova, Italy
Vincenzo Baldo, Department of Public Health, University of Padova, Italy
Mario Plebani, Department of Clinical Chemistry, University of Padova, Italy
Supported by a University grant (MURST 60%)
Correspondence to: Professor Annarosa Floreani, Div. Gastroenterologia, Via Giustiniani, 2, Padova 35128, Italy. annarosa.floreani@unipd.it
Telephone: +39-49-8212894 Fax: +39-49-8760820
Received: 2004-04-15 Accepted: 2004-08-22

Abstract

AIM: (1) To compare the prevalence of osteoporosis (*t*-score ⩽-2.5 SD) between stage IV PBC patients, and two groups of age- and sex-matched controls: one with hepatitis C virus (HCV)-related cirrhosis, and the other one consisting of a group of healthy subjects from the general population; (2) to identify the main risk factors for the development of bone loss.

METHODS: Thirty-five stage IV PBC patients (mean age 52.5±10 years), 49 females with HCV-related cirrhosis (mean age 52.9±5.8 years) and 33 healthy females (mean age 51.8±2.22 years) were enrolled in the study. Bone metabolism was evaluated by measuring serum calcium corrected for serum albumin (Ca corr.), 25-hydroxy vitamin D (25-OH vit D), parathyroid hormone, osteocalcin. Bone mineral density (BMD) was assessed at the lumbar spine by dual-photon X-ray absorptiometry.

RESULTS: Osteoporosis was present in 5/35 PBC patients (14.2%) and in 7/49 HCV-related cirrhotic patients (14.3%), without any statistical difference between the two groups. Among healthy control subjects, none had osteoporosis. No difference was found between the three groups in serum parameters of bone metabolism. Univariate analysis showed that menopausal state and low BMI were significantly correlated with osteoporosis. Multivariate regression analysis showed that menopausal status, BMI <23, and old age were independent variables significantly correlated with osteoporosis.

CONCLUSION: PBC in itself has no negative influence on BMD. End-stage liver disease patients carry a disease-specific risk for osteoporosis, but have an effective risk of bone loss in relation to individual potential risk for each patient. A practical message should be taken into account, that is, every effort should be made to prevent osteoporosis when a patient has simple osteopenia, or if it is a woman in or near menopausal age.

© 2005 The WJG Press and Elsevier Inc. All rights reserved.

Key words: Osteoporosis; Primary biliary cirrhosis; HCV infection

Floreani A, Mega A, Camozzi V, Baldo V, Plebani M, Burra P, Luisetto G. Is osteoporosis a peculiar association with primary biliary cirrhosis? *World J Gastroenterol* 2005; 11 (34): 5347-5350
http://www.wjgnet.com/1007-9327/11/5347.asp

INTRODUCTION

Osteopenia is a major complication of end-stage liver disease and a real risk in liver transplant patients[1]. It is also a common clinical problem, however, in association with chronic cholestatic liver disease, particularly PBC, due to predominant female sex and older age[2]. Osteoporosis was recently found in 20% of 176 patients with PBC, occurring 32 times more frequently than expected[3]. Despite the wisdom that osteoporosis is common in PBC than in other types of liver disease, new data are emerging in the literature concerning this field.

In a previous study, including cirrhotic patients evaluated for liver transplantation, we failed to find any significant difference in bone mineral density (BMD) between patients with chronic cholestatic liver disease and cirrhotics of various etiology[4]. Newton *et al*., retrospectively reviewed a large group of PBC patients in Newcastle (UK) and found osteoporosis in 31.2% of cases; none of the patients went on to develop *de novo* osteoporosis during a mean follow-up of 10.1 years[5]. The authors concluded that osteoporosis is not a specific complication of PBC. They had not considered age- and sex-matched controls from the general population or control groups with different types of liver disease. It should also be stressed that PBC is a heterogeneous disease, and usually any PBC study population includes patients with different severity of liver damage ranging from early disease to cirrhotic stage.

The aims of the present study were therefore: (1) to compare the prevalence of osteoporosis between stage IV PBC patients and two groups of age- and sex-matched controls: one with hepatitis C virus (HCV)-related cirrhosis, and the other one consisting of healthy subjects from general population; (2) to identify the main risk factors for osteoporosis.

MATERIALS AND METHODS

Patients

Thirty-five consecutive female stage IV PBC patients (mean

age 52.5±10 years), 49 females with HCV-related cirrhosis (mean age 52.9±5.8 years) and 33 female healthy subjects (mean age 51.8±2.22 years) were enrolled in the study. The clinical characteristics of the three groups are summarized in Table 1. Body mass index was significantly lower in both PBC and HCV-related cirrhosis patients compared to healthy controls ($P<0.05$). All subjects were asymptomatic for bone loss, and none were taking calcium and/or vitamin D supplementation. None of the patients were treated with steroids. Patients with HCV-related cirrhosis have not been previously treated with interferon/ribavirin therapy. The patients were not given hormone replacement. PBC patients were treated with ursodeoxycholic acid [12-15 mg/(kg·d)] twice a day after meals.

The diagnosis of PBC was obtained according to clinical, immunological, and histological grounds. All the patients with PBC has histological stage IV, according to Scheuer's classification[6]. The diagnosis of HCV-related cirrhosis was obtained by clinical, histological, and virological methods, including serum positivity for HCV-RNA by means of PCR assay.

None of the patients were ingesting alcohol. Ethical approval was obtained from the hospital's ethics committee and informed consent was obtained from each patient, prior to their inclusion in the study.

Table 1 Clinical details of the patients

	PBC	HCV+	Control group
Number of patients	35	49	33
Age (mean±SD), yr	52.5±10	52.9±5.8	51.8±2.22
Age at menopause (mean±SD), yr	48.3±4.5	48.5±4.9	47±7.46
BMI (mean±SD)	22.8±3.2[a]	23.4±4.2[a]	25.9±4.29

[a]$P<0.05$ *vs* control group.

Bone density measurement

BMD was assessed by DEXA (Hologic QDR 4500 C, Walthom, MA, USA) at lumbar spine (L2-L4). The manufacturer's reference database was obtained by measuring more than 500 healthy male volunteers at the University of California (San Diego, CA) and at other QDR-1000 installations across the USA. Reference data collected on Hologic systems in Europe, including Italy, have demonstrated a close correlation with US values. In our hands, the long-term (1 year) coefficient of variation *in vitro* with a Hologic phantom is 0.44%; the short-term (1 wk) coefficient of variation *in vivo*, with five consecutive measurements performed in 10 healthy volunteers, is 1.2%. Osteoporosis was defined according to WHO in terms of *t*-score lower than -2.5 SD. The *t*-score was defined as the number of SD above or below the mean BMD for young adult mean value. The *z*-score for BMD was defined as the number of SD above or below the mean BMD for age- and sex-matched normal population.

Biochemical parameters

The following parameters were assessed in all subjects: serum calcium, parathyroid hormone (PTH), osteocalcin (BGP), 25-hydroxy vitamin D (25-OHD). Serum Ca was measured by common automated laboratory methods. Serum calcium corrected for albumin concentration was calculated using the following formula:

Ca corr (mg/dL) = Ca tot (mg/dL)+4-albumin (g/L)

The result was divided by 4 and expressed in mmol/L.

PTH was tested by IRMA (Allegro TM Intact, Nichols Institute, S. Juan Capistrano, CA, USA). This method detects the biologically intact 1-84 amino acid chain of PTH. The normal range is 10-55 ng/L. The coefficient of variation was 3.6% intra-assay and 5.8% inter-assay. BGP was assayed by IRMA (Cis Bio International, Italy). The normal range is 4-26 mg/L. The coefficient of variation was 3.1% intra-assay, and 5.7% inter-assay. 25-OHD was determined by RIA (Incstar Corp, Stillwater, MN, USA). The normal range is 25-150 nmol/L. The coefficient of variation was 5.1% intra-assay and 9.7% inter-assay.

Statistical analysis

Results were expressed as the mean±SD. Student's *t*-test for unpaired data and the linear regression test were used, as appropriate. Logistic regression analysis was used to establish in which characteristics were independently associated with osteoporosis (age, menopausal status, BMI, 25-OHD, PTH, BGP). A P value $\leqslant 0.05$ was considered significant. Analyses were performed with the EPI-Info 6.04 and the Statistical Package for the Social Sciences (SPSS 10.0).

RESULTS

Osteoporosis was present in 5/35 PBC patients (14.3%) and in 7/49 HCV-related cirrhotic patients (14.3%), without any statistical difference between the two groups. No subjects with osteoporosis were identified in healthy female controls. The mean age of patients with osteoporosis was 54.2±55 years, and the mean age of those without osteoporosis was 52.5±8.4 years (P = NS). No difference was found between the three groups in s-Ca. The mean BMD at lumbar spine was lower in both PBC and HCV-related cirrhosis groups compared to healthy controls, without any statistical significance (Table 2). However, *t*-score was significantly lower in PBC group compared to either HCV-related cirrhosis group or control group (-1.55±0.99 in PBC *vs* -0.39±2.65 in HCV+ *vs* -0.29±0.98 in healthy controls, $P<0.05$).

Table 2 Bone metabolism in PBC, in HCV+ patients and in healthy controls

	PBC	HCV+	Controls
BMD (lumbar spine)	0.810±0.130	0.860±0.140	0.972±0.128
t-score ⩽–2.5 SD	–1.55±0.99[a]	–0.39±2.65	–0.29±0.98
z-score	–0.94±1.10[c]	–0.52±1.23	–0.82±1.02
25-OHD (nmol/L)	103.48±58.85[e]	98.38±44.65[g]	49.66±19.72
BGP (mg/L)	8.80±8.7	6.43±11.14	9.56±2.92
Intact (1–84) PTH (ng/L)	39.8±26.3	35±29.78	33.60±11.77
Ca corr albumin (mg/dL)	2.27±0.26	2.32±0.13	2.31±0.14

[a]$P<0.05$ *vs* controls. [c]$P<0.05$ *vs* HCV+. [e]$P<0.05$ *vs* controls. [g]$P<0.05$ *vs* controls.

Serum 25-OH vit D was significantly higher in both PBC group and HCV+ group *vs* healthy controls (103.48±58.85 nmol/L in PBC *vs* 98.38±44.65 in HCV+ *vs* 49.66±19.72 in healthy controls, $P<0.005$). No significant differences in serum BGP and PTH were found between the three groups. Univariate analysis showed that menopausal state and low BMI were significantly correlated with osteoporosis (Table 3). Multivariate regression analysis showed that menopausal status, BMI <23, and advanced age were independent variables significantly correlated with osteoporosis (Table 4).

Table 3 Univariate analysis

Variable	*n*	Osteoporosis		*P*
		n	%	
Menopausal status				
Yes	46	10	(21.7)	
No	38	2	(5.2)	0.032
Disease				
HCV	49	7	(14.3)	
PBC	35	5	(14.3)	1.000
Normal 25-OH vit D				
Yes	67	10	(14.9)	
No	17	2	(11.8)	0.739
Normal BGP				
Yes	18	4	(22.2)	
No	66	8	(12.1)	0.278
Serum PTH				
Normal	48	5	(10.4)	
High	36	7	(19.4)	0.242
BMI >23				
Yes	56	4	(7.1)	
No	28	8	(25.8)	0.008

Table 4 Multivariate analysis

Variable	Adjusted OR	95.0%CI		*P*
		Low	Upper	
Disease (HCV *vs* PBC)	0.429	0.086	2.149	0.304
BGP	1.785	0.323	9.866	0.507
25-OH vit D	0.674	0.098	4.609	0.687
PTH	2.050	0.494	8.501	0.323
Menopausal status	23.102	1.524	350.186	0.024
BMI <23	5.703	1.228	26.488	0.026
Age (yr)	1.151	1.004	1.320	0.044

DISCUSSION

Our results indicate that female patients with end-stage PBC have a similar percentage of osteoporosis than sex- and age-matched controls with HCV-related cirrhosis. However, PBC patients had significantly lower *t*-score compared to age- and sex-matched controls from general population. All types of liver disease are acknowledged and some osteopenia risk factors are common, e.g. cirrhosis, female sex, old age, alcohol consumption, hypogonadism, steroid therapy, impaired conversion to 25-OH vit D, low BMI, vitamin D receptor (VDR) polymorphism, reduced BGP activity[7-14], but certain specific risk factors for osteoporosis exist in chronic cholestatic liver disease, i.e. calcium and vitamin D malabsorption, hyperbilirubinemia, and cholestyramine therapy[15,16]. In our patients, however, vit D status, evaluated by 25-OH vit D serum levels, was similar in the three groups of subjects, as well as serum Ca, and serum BGP. Furthermore, no secondary hyperparathyroidism was found in our cases, suggesting a normal intestinal calcium absorption.

In order to avoid confounding factors such as corticosteroids and alcohol consumption, we have chosen three groups of subjects with the same demographic characteristics (same geographical area, same prevalence of menopausal status, same age) without evidence of bone disease, and without calcium and/or vitamin D supplementation. Multivariate analysis showed that menopausal status, BMI <23, and old age were independent variables significantly correlated with osteoporosis. This finding apparently confirms previous results[4,11,17] in which chronic liver disease *per se*, and not a specific etiology, should be responsible for hepatic osteodystrophy. Osteoporosis has been shown to be significantly associated with postmenopausal status in several studies[18,19]; however, all PBC series include patients with different histological stages. In our study, we included only patients with advanced disease, namely cirrhotic patients.

As far as our results are concerned, the univariate analysis (which included the type of liver disease, menopausal status, 25-OHD, BGP, PTH, BMI >23) showed that both menopause and old age were associated to bone loss in both groups. We did not assay VDR gene polymorphism in these study groups, but there is evidence that VDR genotypes predict lower BMD in general population in different countries[20,21]. As far as VDR gene polymorphism in liver disease is concerned, there is evidence that similar results may be extended also in PBC[9,22]; however, in our knowledge, no other groups of liver disease patients have been tested for VDR gene polymorphism.

Nevertheless, the mean values of serum parameters of bone metabolism (25-OH vit D, BGP, PTH, and Ca corr) in both PBC and HCV-related cirrhosis patients did not show any difference compared to controls. These data suggest that osteodystrophy in end-stage liver disease patients is characterized by a low turnover osteoporosis.

BGP is a bone matrix protein synthesized by osteoblasts is vitamin K-dependent, but we failed to find any correlation between BGP and vitamin K activity measured by prothrombin activity (data not shown). Moreover, no difference was found in prothrombin activity between the two groups of cirrhotic patients.

PTH was assayed by RIA, using an antiserum directed against the mid-region of the hormone. When intact 1-84 PTH was assayed in cirrhotic patients, normal values of PTH levels were found.

In conclusion, PBC in itself has no negative influence on BMD. End-stage liver disease patients carry a disease-specific risk for osteoporosis, but have an effective risk of bone loss in relation to individual potential risk for each patient. A practical message should be taken into account, that is, every effort should be made to prevent osteoporosis when a patient has simple osteopenia, or if it is a woman in or near menopausal age.

REFERENCES

1 **Hay JE.** Osteoporosis in liver disease and after liver transplantation. *J Hepatol* 2003; **38**: 856-865
2 American gastroenterological association medical position statement: osteoporosis in hepatic disorders: *Gastroenterology* 2003; **125**: 937-940
3 **Menon KV,** Angulo P, Weston S, Dickson ER, Lindor KD. Bone disease in primary biliary cirrhosis: independent indicators and rate of progression. *J Hepatol* 2001; **35**: 316-323
4 **Floreani A,** Fries W, Luisetto G, Burra P, Fagiuoli S, Boccagni P, Della Rovere GR, Plebani M, Piccoli A, Naccarato R. Bone metabolism in orthotopic liver transplantation: a prospective study. *Liver Transpl Surg* 1998; **4**: 311-319
5 **Newton J,** Francis R, Prince M, James O, Bassendine M, Rawlings D, Jones D. Osteoporosis in primary biliary cirrhosis revisited. *Gut* 2001; **49**: 282-287
6 **Scheuer PJ.** Primary biliary cirrhosis. *Proc R Soc Med* 1967: **60**: 257-260
7 **McCaughan GW,** Feller RB. Osteoporosis in chronic liver disease: pathogenesis, risk factors, and management. *Dig Dis* 1994; **12**: 223-231
8 **Rosen H.** Primary biliary cirrhosis and bone disease. *Hepatology* 1995; **21**: 253-255
9 **Springer JE,** Cole DE, Rubin LA, Auch-Dudek K, Harewood L, Evroski J, Peltekova VD, Heathcote EJ. Vitamin D-receptor genotypes as independent genetic predictors of decreased bone mineral density in primary biliary cirrhosis. *Gastroenterology* 2000; **118**: 145-151
10 **Rouillard S,** Lane N. Hepatic osteodystrophy. *Hepatology* 2001; **33**: 301-307
11 **Ormarsdottir S,** Ljunggren O, Mallmin H, Brahm H, Loof L. Low body mass index and use of corticosteroids, but not cholestasis, are risk factors for osteoporosis in patients with chronic liver disease. *J Hepatol* 1999; **31**: 84-90
12 **Diamond T,** Stiel D, Lunzer M, Wilkinson M, Roche J, Posen S. Osteoporosis and skeletal fractures in chronic liver disease. *Gut* 1990; **31**: 82-87
13 **Krane SM,** Schiller AL. Metabolic bone disease: Introduction and classification. In: De Groote LJ ed. Endocrinology, ed 2. *Philadelphia, Saunders* 1989: 1151-1164
14 **Hodgson SF,** Dickson ER, Wahner HW, Johnson KA, Mann KG, Riggs BL. Bone loss and reduced osteoblast function in primary biliary cirrhosis. *Ann Int Med* 1985; **103**: 855-860
15 **Diamond T,** Stiel D, Mason R, Lissner D, Bilde D, Wilson S, Posen S. Serum vitamin D metabolites are not responsible for low turnover osteoporosis in chronic liver disease. *J Clin Endocrinol Metab* 1989; **69**: 1234-1239
16 **Janes CH,** Dickson ER, Okazaki R, Bonde S, McDonagh AF, Riggs BL. Role of hyperbilirubinemia in the impairment of osteoblast proliferation associated with cholestatic jaundice. *J Clin Invest* 1995; **95**: 2581-2586
17 **Linderthal B,** Leuschner MS, Ackerman H, Happ J, Leuschner UF. Is primary biliary cirrhosis (PBC) in itself a risk factor for osteoporosis? *Hepatology* 2000; **32**: 168A
18 **Le Gars L,** Grandpierre C, Chazouilleres O, Berenbaum F, Poupon R. Bone loss in primary biliary cirrhhosis : absence of association with severity of liver disease. *Joint Bone Spine* 2002; **69**: 195-200
19 **Solerio E,** Isaia G, Innarella R, Di Stefano M, Farina M, Borghesio E, Framarin L, Rizzetto M, Rosina F. Osteoporosis: still a typical complication of primari biliary cirrhosis? *Dig Liver Dis* 2003; **35**: 339-346
20 **Spector TD,** Keen RW, Arden NK, Morrison NA, Major PJ, Nguyen TV, Kelly PJ, Baker JR, Sambrook PN, Lanchbury JS, Eisman JA. Influence of vitamin D receptor genotype on bone mineral density in postmenopausal women: a twin study in Britain. *BMJ* 1995; **310**: 1357-1360
21 **Cooper GS,** Umbach DM. Are vitamin D receptor polymorphisms associated with bone mineral density? A meta-analysis. *J Bone Miner Res* 1996; **12**: 1841-1849
22 **Baragiotta A,** Floreani A, James O, Venturi C, Craggs A. Vitamin D receptor (VDR) TAQI polymorphism in primary biliary cirrhosis (PBC). *J Hepatol* 2001; **34**(Suppl 1): 209-370

Science Editor Zhu LH and Guo SY **Language Editor** Elsevier HK

PO Box 2345, Beijing 100023, China
www.wjgnet.com
wjg@wjgnet.com

ELSEVIER

World J Gastroenterol 2005;11(34):5351-5357
World Journal of Gastroenterology ISSN 1007-9327
© 2005 The WJG Press and Elsevier Inc. All rights reserved.

• *BRIEF REPORTS* •

Lack of specific association between gastric autoimmunity hallmarks and clinical presentations of atrophic body gastritis

Bruno Annibale, Edith Lahner, Riccardo Negrini, Flavia Baccini, Cesare Bordi, Bruno Monarca, Gianfranco Delle Fave

Bruno Annibale, Edith Lahner, Flavia Baccini, Gianfranco Delle Fave, Department of Digestive and Liver Disease, II School of Medicine, University "La Sapienza", Sant'Andrea Hospital, Rome, Italy
Riccardo Negrini, Microbiology Department, Spedali Civili, Brescia, Italy
Cesare Bordi, Pathology Department, University of Parma, Parma, Italy
Bruno Monarca, Hematology Department, University "La Sapienza", Sant'Andrea Hospital, Rome, Italy
Supported by Grants From the Italian Ministry for the University (MIUR), No. 02/12/01/10 1999-2002 and No. 8.111.126.5
Correspondence to: Bruno Annibale, MD, Department of Digestive and Liver Disease, University "La Sapienza", Ospedale Sant'Andrea, Via di Grottarossa 1035, Roma 00189, Italy. bruno.annibale@uniroma1.it
Telephone: +39-6-49972369 Fax: +39-6-4455292
Received: 2004-12-14 Accepted: 2005-01-15

Abstract

AIM: To investigate the possible relationships between gastric autoimmune phenomena and clinical presentations of this disorder, in consecutive atrophic body gastritis patients.

METHODS: A total of 140 atrophic body gastritis patients, diagnosed as consecutive outpatients presenting with macrocytic or iron deficiency anemia, or longstanding dyspepsia underwent gastroscopy with antral and body biopsies, assay of intrinsic factor, parietal cells and *Helicobacter pylori* (*H pylori*) antibodies. Gastritis was assessed according to Sydney System.

RESULTS: Parietal cell antibodies were equally distributed in all clinical presentations, whereas the positivity of intrinsic factor antibodies (49/140, 35%) was significantly higher in pernicious anemia patients (49.2%) than in iron deficiency (21.1%) and dyspeptic patients (27.8%). No specific pattern of autoantibodies was related to the clinical presentations of atrophic body gastritis. A positive correlation was obtained between the body atrophy score and the intrinsic factor antibody levels ($r = 0.2216$, $P = 0.0085$). Associated autoimmune diseases were present in 25/140 (17.9%) patients, but the prevalence of autoimmune diseases was comparable, irrespective of the clinical presentations.

CONCLUSION: The so-called hallmarks of gastric autoimmunity, particularly in intrinsic factor antibody cannot be usefully employed in defining an autoimmune pattern in the clinical presentations of ABG.

© 2005 The WJG Press and Elsevier Inc. All rights reserved.

Key words: Atrophic body gastritis; Intrinsic factor antibodies; *Helicobacter pylori*; Iron deficiency anemia; Pernicious anemia

Annibale B, Lahner E, Negrini R, Baccini F, Bordi C, Monarca B, Fave GD. Lack of specific association between gastric autoimmunity hallmarks and clinical presentations of atrophic body gastritis. *World J Gastroenterol* 2005; 11 (34): 5351-5357
http://www.wjgnet.com/1007-9327/11/5351.asp

INTRODUCTION

Atrophic body gastritis (ABG), particularly in association with pernicious anemia (PA), is believed to be an autoimmune disease, due to the presence of autoantibodies to the secretory elements of the gastric oxyntic mucosa and other associated autoimmune disorders[1,2]. Indeed, parietal cell antibodies (PCA) are detected in 60-90%, and intrinsic factor antibodies (IFA) are found in 50-70% of patients with PA[3-7]. In particular, IFA belonging to the IgG class of immunoglobulins, are considered highly specific to patients with PA, since they have rarely been found in the absence of this condition[8,9].

ABG is usually considered synonymous with the presence of PA, a disorder believed to be most common in individuals of north European descent[10]. However, macrocytic anemia is not the only hematological presentation of ABG. It has been reported, that iron deficiency anemia (IDA) should also be taken into consideration as a presentation symptom of ABG[11]. In fact, in 27% of IDA patients without gastrointestinal symptoms, ABG has been identified as the likely cause of IDA[12]. Furthermore, it is well known, that patients with ABG often complain of dyspepsia, even without hematological disorders[13].

It is now apparent that *Helicobacter pylori* (*H pylori*) is involved in the induction of ABG[14]. In fact, it has recently been reported that two-thirds of ABG patients and a large percentage of PA patients present evidence of *H pylori* infection[15,16]. At the same time, it is well established that *H pylori* infection can induce gastric autoimmunity, since the presence of the bacteria leads to the production of antibodies cross-reacting with human gastric mucosa[17,18]. Recently, it has been reported that the progression of the severity of gastric corporal atrophy is inversely correlated with circulating IgG to *H pylori* and positively with the titer of antibodies to parietal cells[15]. Indeed, most of the studies

regarding the role of IFA in ABG and PA date back to the early seventies[4,5,8,9], and were thus performed before a histological consensus classification of gastritis (e.g., Sydney System) was developed, and the role of *H pylori* infection in this condition was recognized. To our knowledge, studies that evaluate the pattern of gastric autoimmune autoantibodies in relation to *H pylori* status and presentation symptoms of atrophic body gastritis are scarce. Thus, the aim of the present study is to investigate the relationships between the main clinical presentations of ABG and gastric autoimmune phenomena in a consecutive series of patients with ABG.

MATERIALS AND METHODS

Patients

We included 140 patients with ABG diagnosed in consecutive outpatients referred to our Gastroenterology Department from the Hematology Department for evaluation of their anemia (n = 122, either macrocytic or iron-deficiency anemia) or attending our department for unexplained long-standing dyspepsia (n = 18), in application of previously reported screening programs[11,19]. The ABG patients with dyspepsia did not show any type of anemia. Patients taking anti-secretory drugs or with a history of previous gastric and/or intestinal surgery were carefully excluded. Other causes of anemia (e.g., myelodysplasia, neoplasia, blood loss, epistaxis, heavy menstrual loss, fecal occult blood positivity, cirrhosis) were also carefully excluded, as previously reported[12]. None of the patients were vegetarians and none presented with disorders associated with the small bowel.

All ABG patients had a detailed initial assessment including fasting gastrin, gastroscopy with gastric antrum and body mucosa biopsies as well as basal and peak acid output to pentagastrin (PAO). A serum sample was taken for detection of antibodies against intrinsic factor, parietal cells and *H pylori*. Anamnestic data were obtained from each patient by a scrupulously detailed clinical interview and, whenever possible by checking medical records, for the presence of associated autoimmune diseases. All patients gave informed consent to the study, which was approved by a local ethics committee.

Diagnosis of atrophic body gastritis The diagnosis of ABG was based on the following criteria: fasting hypergastrinemia, pentagastrin-resistant achlorhydria or hypochlorhydria (PAO lower than 13 mEq/h) and histological confirmation of gastric body mucosa atrophy (see section on histological procedure).

Diagnosis of pernicious anemia PA was defined as a hemoglobin concentration <14 g/dL for men (normal range 14-18 g/dL) and <12 g/dL for women (normal range 12-16 g/dL), mean corpuscular volume (MCV) ⩾100 fL, low level of vitamin B12 (n.v. 190-950 pg/mL), response to vitamin B_{12} therapy, and histological confirmation of gastric body mucosa atrophy, as described elsewhere[11,16].

Diagnosis of iron deficiency anemia Iron deficiency anemia was defined as hemoglobin concentration <14 g/dL for men (normal range 14-18 g/dL) and 12 g/dL for women (normal range 12-16 g/dL), MCV <80 fL (normal range 80-100 fL) and low serum ferritin (normal range 30-180 ng/mL), as previously described[11,12].

Diagnostic investigation

Gastric acid secretion studies PAO (6 μg subcutaneous, Peptavlon, ICI, UK) was determined as previously described[20]. The median reference value for PAO in our laboratory was 31.1 mEq/h (range 13-44.4 mEq/h).

Serological testing Fasting gastrin levels were evaluated by a specific radioimmunoassay using antibody no. 4562 (kindly provided by Professor JF Rehfeld Copenhagen, Denmark), as described elsewhere[20]. Normal values were ⩽40 pg/mL.

H pylori antibodies were detected by competitive ELISA based on a mAb against 64-ku *H pylori* antigen, as previously described[21]. Antibody concentration was expressed as U/mL. Negative values were <450 U/mL.

Pepsinogen I levels were measured using a commercial RIA kit (Pepsik, Sorin, Saluggia, Italy) as previously reported[22]. The normal reference values were 20-80 ng/mL.

Parietal cell antibodies (PCA) were determined on serum using a solid phase immunosorbent assay commercial kit (AUTOSTAT, Cogent Diagnostic Ltd., Edinburgh, UK), as described elsewhere[15,19]. Intrinsic factor antibody (IFA) IgG was determined by an indirect ELISA using highly purified porcine IF (Sigma-Aldrich, Saint Louis, USA) as a target. Microwells were overcoated with 10% normal rabbit serum to avoid nonspecific binding of human IgG. Antibody concentration was calculated by a calibration curve and expressed as arbitrary U/mL. Values >2 U/mL were considered positive for IFA[23].

Histological procedures

All patients underwent upper gastrointestinal endoscopy with three antral biopsy samples (smaller and greater curve, anterior or posterior) and three from the midbody along the greater curve, taken with a standard biopsy forceps[24]. The specimens were immediately fixed in Bouin's solution for 4-8 h, at room temperature, rinsed in 0.1 mol/L phosphate-buffered saline, pH 7.4 and routinely processed to wax. Serial paraffin sections (5 μm) were stained with hematoxylin and eosin for conventional histological evaluation and with Giemsa stain for *H pylori* determination.

Assessment of the degree of gastritis was performed according to the updated Sydney System[25]. The following scores were assigned to each graded variable: 0 for absence and 1, 2, 3, for mild, moderate or severe presence, respectively. Atrophy of gastric mucosa was defined as focal or complete replacement of oxyntic glands by metaplastic pyloric or intestinal glands.

The biopsies were examined independently by two histopathologists, unaware of the clinical data of the patients. In case of any disagreement, the relevant biopsies were re-examined simultaneously by both histopathologists, until an agreement was reached.

H pylori status in ABG patients

H pylori status of ABG patients was evaluated considering both tissue stain and serology, as described elsewhere[15]:

patients were defined as *H pylori* negative/negative (group I) when both histology and serology were negative for *H pylori*, as *H pylori* negative/positive (group II) when *H pylori* was not detected at histology but circulating antibodies to *H pylori* exceeded the reference value, and as *H pylori* positive/positive (group III) when they were found to be positive at histology and circulating antibodies to *H pylori* exceeded the reference values.

Statistical analysis

Data were expressed as mean±SE and/or median (range) and evaluated by appropriate statistical tests (Student *t*-test or Wilcoxon test). Subgroups (percentages) of the population were compared by Fisher's exact test. $P<0.05$ was considered statistically significant.

RESULTS

Clinical presentation of ABG and gastric autoimmunity

ABG patients presenting with PA, IDA, and dyspepsia were not homogeneous as far as gender, age, gastrin and pepsinogen I levels, and body atrophy score were concerned (Table 1). Whereas gender was equally distributed in ABG patients presenting with PA and dyspepsia, ABG patients with IDA were predominantly female. ABG patients with PA were significantly older and had higher levels of gastrin and lower levels of pepsinogen I, compared to those with IDA and dyspepsia. Moreover, ABG patients with PA also had a higher body atrophy score than those with IDA and dyspepsia. However, it is of interest that all ABG patients, regardless of the three clinical presentations, showed comparable stimulated acid secretion values. It is also worthwhile pointing out that the serological levels of vitamin B_{12} were as expected, significantly lower in ABG patients with PA, albeit also the patients presenting with IDA and dyspepsia had median levels of $B_{12,}$ close to the lower normal value. Finally, *H pylori* positivity was significantly lower in the PA group than in the IDA and dyspeptic patients.

Among the 140 ABG patients, associated autoimmune diseases were observed in only 25 (17.9%, 13 females, 12 males, median age 52 years, range 26-76 years), who presented autoimmune thyroid disease ($n = 10$), alopecia ($n = 6$), vitiligo ($n = 5$), psoriasis ($n = 2$), rheumatoid arthritis ($n = 1$) and type I diabetes mellitus ($n = 1$). However, the prevalence of autoimmune diseases was similar in ABG patients, irrespective of the clinical presentations.

As far as gastric autoimmune antibodies are concerned, the prevalence of PCA was equally distributed among the different clinical presentations, whereas the prevalence of IFA positive cases was significantly higher in ABG patients with PA than in those with IDA and dyspepsia ($P = 0.001$). Moreover, in order to establish whether gastric autoantibodies were specifically related to any of the clinical presentations, ABG patients were classified on the basis of their positivity for PCA alone, for IFA alone, and positivity and negativity for both antibodies. However, no specific pattern of autoantibodies was related to the clinical presentations of ABG (data not shown).

Nevertheless, the presence of the "spared" antrum, a typical histological aspect of autoimmune gastritis, was similar in ABG patients presenting with PA and IDA (46.1% and 43.8%, respectively), but lower (22.2%) in ABG patients presenting with dyspepsia, albeit statistical significance was not reached. Moreover, the positivity of PCA and IFA was equally distributed in ABG patients with the "spared" antrum and those with antral involvement (data not shown).

Table 1 Demographic, clinical, biochemical and histological findings and *H pylori* status in 140 patients with atrophic body gastritis (ABG)

	Pernicious anemia	Iron deficiency anemia	Dyspepsia
Demographic and clinical features			
Patients (%)	65 (46.5)	57 (40.7)	18 (12.8)
Gender (M/F)	34/31[a]	8/49[e]	7/11
Age, yr	63 (30–83)[a]	46 (22–78)	56 (31–81)
Associated autoimmune disease, *n* (%)	11 (16.9)	10 (17.5)	4 (22.2)
Biochemical features and gastric autoantibodies			
Gastrin, pg/mL	500 (55–2 700)[b]	375 (50–1 650)	370 (49–950)
Pepsinogen I, ng/mL	5 (0–68)[b]	10 (0–72)	10 (2–84)
PAO[1], mEq/h	0 (0–11.6)	0 (0–11.9)	0 (0–12.5)
PCA positive[2], *n* (%)	46 (70.7)	38 (66.6)	15 (83)
IFA positive[3], *n* (%)	32 (49.2)[a]	12 (21.1)	5 (27.8)
Vitamin B_{12}, pg/mL	80 (13-394)[a,d]	200 (80–701)	195 (100–760)
Histological features			
Body atrophy, *n* (%)	65 (100)	57 (100)	18 (100)
Body atrophy score	2.83±0.06[a,d]	2.1±0.10	1.94±1.7
Antral atrophy, *n* (%)	15 (23.1)	14 (24.6)	7 (38.9)
Antral atrophy score	1.47±0.13	1.29±0.13	1.29±0.18
Antrum spared, *n* (%)	30 (46.1)	25 (43.8)	4 (22.2)
H pylori positive[4], *n* (%)	40 (61.5)[a,c]	51 (89.5)	16 (88.9)

[a]$P<0.05$ iron deficiency anemia, [b]$P<0.001$ *vs* iron deficiency anemia, [c]$P<0.05$ *vs* dyspepsia, [d]$P<0.001$ *vs* dyspepsia, [e]$P<0.05$ iron deficiency anemia *vs* dyspepsia. Data are expressed as median (range) and mean±SE. [1]Peak acid output, [2]parietal cell antibodies, [3]intrinsic factor antibodies, [4]sum of *H pylori* positive patients at histology and at serology.

Characteristics of ABG patients with positive gastric autoimmune antibodies

Among the 140 ABG patients, 99 (70.7%, 32 males, 67 females, median age 54 years, range 22-83 years) had a positive PCA titer. However, no significant differences were observed between PCA positive and negative ABG patients in any of the following parameters: age, fasting gastrin and pepsinogen I levels, clinical presentation, stimulated acid secretion, and associated autoimmune diseases (data not shown).

In contrast, IFA were positive in 49 of the 140 ABG patients (35%, 18 males, 31 females, median age 58 years, range 26-83). The median level in IFA positive patients was 7.5 U/mL (range 2.1-40 U/mL) *vs* 0.8 U/mL (range 0-1.95 U/mL) in IFA negative patients ($P<0.0001$). Clinical, serological and histological features of IFA positive and negative patients are shown in Table 2. Male/female ratio, age, and the presence of associated autoimmune diseases were similar in IFA positive and negative patients. Among the 25 ABG patients with autoimmune diseases, only 10 (40%) had positive IFA levels: 5 of them with PA, 4 with IDA and 1 with dyspepsia.

Table 2 Demographic, clinical, biochemical and histological findings in 140 patients with atrophic body gastritis (ABG)

	IFA positive	IFA negative	*P*
Demographic and clinical features			
Patients (%)	49 (35)	91 (65)	
Gender (M / F)	18 / 31	31 / 60	NS
Age, yr, median (range)	58 (26–83)	55 (22–78)	NS
Pernicious anemia, *n* (%)	32 (65.3)	33 (36.3)	*P* = 0.0013
Iron deficiency anemia, *n* (%)	12 (24.5)	45 (49.4)	*P* = 0.0042
Dyspepsia, *n* (%)	5 (10.2)	13 (14.3)	NS
Associated autoimmune disease, *n* (%)	10 (20.4)	15 (16.5)	NS
Biochemical features and gastric autoantibodies			
PCA positive[1], *n* pts (%)	39 (80)	70 (77)	NS
Gastrin (pg / mL) median (range)	500 (55–2.500)	405 (49–2.700)	*P* = 0.0579
Pepsinogen I (ng / mlL median (range)	5 (0–72)	10 (0–84)	*P* = 0.0027
Histological features			
Body atrophy score (mean±SE)	2.67±0.09	2.28±0.08	*P* = 0.0028
Antral atrophy, *n* (%)	10 (20.4)	26 (28.6)	NS
Antral atrophy score (mean±SE)	1.2±0.13	1.42±0.1	NS
Antrum spared, *n* (%)	22 (44.9)	37 (40.7)	NS
H pylori positive[2], *n* (%)	37 (76)	70 (77)	NS

[1]Parietal cell antibodies, [2]sum of *H pylori* positive patients at histology and at serology. NS = not significant.

Moreover, IFA positive patients had a significantly higher body atrophy score than IFA negative patients (2.67±0.09 *vs* 2.28±0.08, $P = 0.0028$). As far as the antrum was concerned, the presence of antral atrophy and the "spared" antrum as well as its histological score and its presence did not differ between the two groups.

As expected, the median value of fasting gastrin was higher and the median value of pepsinogen I was lower in IFA positive than in IFA negative patients ($P = 0.05$ and $P = 0.002$, respectively). IFA positive patients were more likely to present with PA ($P = 0.0013$ *vs* IFA negative, Fisher's test), while IFA negative patients presented more frequently with IDA ($P = 0.0042$ *vs* IFA positive, Fisher's test), even though 24.5% of IDA patients and 10.2% of dyspeptic patients had positive IFA levels. It is of interest that the distribution of PCA positive patients was similar between the IFA positive and negative patients.

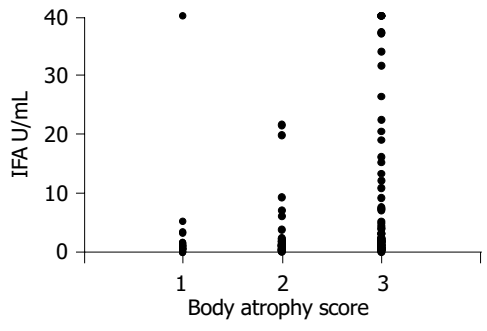


Figure 1 Correlation between histological score of body atrophy and level of intrinsic factor antibodies (IFA) in 140 patients with atrophic body gastritis ($r = 0.2216$, $P = 0.0085$, Spearman rank correlation).

Considering all the 140 ABG patients, there was a positive, statistically significant correlation between the histological score of body atrophy and the IFA levels ($r = 0.2216$, $P = 0.0085$, Spearman rank correlation), suggesting that the progression of oxyntic cell damage could lead to an increase in the production of IFA (Figure 1).

H pylori status and IFA

Among the 140 ABG patients, 33 (23.6%) were *H pylori* negative/negative (group I), 76 (54.3%) were *H pylori* negative/positive (group II) and 31 (22.1%) were *H pylori* positive/positive (group III).

IFA were found to be positive in 12 out of 33 (36.4%) group I patients, in 33 out of 76 (43.5%) group II patients, and in 4 out of 31 (12.9%) group III patients (Figure 2). The proportion of IFA positive patients were significantly higher in groups I and II than in group III (Fisher's test: $P = 0.043$ and $P = 0.003$, respectively). Also the mean level of IFA was significantly higher in groups I and II than in group III ($P = 0.01$ and $P = 0.004$, respectively).

The relationships between IFA positivity, *H pylori* status and clinical presentations observed in ABG patients are shown in Figure 3. The majority of IFA positive ABG

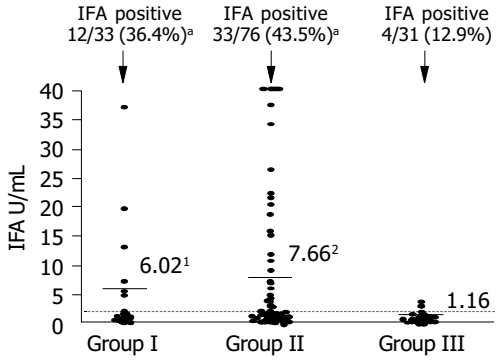


Figure 2 Intrinsic factor antibodies (IFA) in 140 patients with atrophic body gastritis. *H pylori* negative at histology and serology ($n = 33$), *H pylori* negative at histology and positive at serology ($n = 76$), *H pylori* positive at histology and serology ($n = 31$). Broken line indicates cut-off (>2 U/mL positive); bar indicates mean; [1]$P = 0.01$ *vs* group III; [2]$P = 0.004$ *vs* group III; [a]$P<0.05$ *vs* group III, Fisher's test.

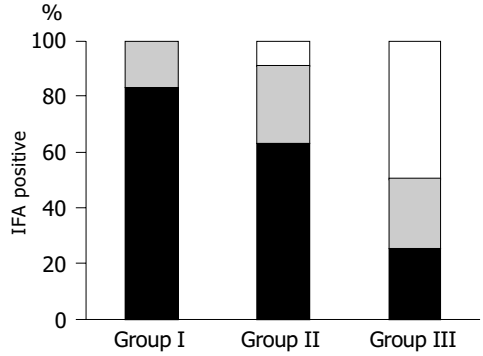


Figure 3 Distribution of clinical presentations of ABG with respect to positivity of IFA and *H pylori* status. *H pylori* negative at histology and serology ($n = 33$), *H pylori* negative at histology and positive at serology ($n = 76$), *H pylori* positive at histology and serology ($n = 31$). Diagonal lines = pernicious anemia; vertical lines = iron deficiency anemia; horizontal lines = dyspepsia.

patients had PA, and most of the PA patients were in the *H pylori* negative group. Albeit, at the same time, the positivity for IFA was not exclusive to PA patients, occurring in a considerable percentage of ABG patients presenting with IDA or even with dyspepsia. ABG patients with these two latter clinical presentations were mainly *H pylori* positive.

DISCUSSION

Two mechanisms are generally considered to induce body mucosa atrophy. On the one hand, the autoimmune pathogenesis of atrophic gastritis is well accepted, and PA is considered as its most characteristic clinical presentation[13,14]. On the other hand, it has been recognized that long-standing *H pylori* infection may induce atrophy of the oxyntic mucosa, which may clinically present with long-standing dyspepsia or IDA[11,15,26].

The main finding from this study is that gastric autoantibodies are present in ABG patients irrespective of the clinical presentations. In fact, the presence of gastric autoantibodies is not exclusive of pernicious anemia, but is also found in ABG patients with iron-deficiency anemia and dyspepsia. In particular, PCA are certainly present in the vast majority of ABG patients irrespective of the clinical presentations. In contrast, the presence of IFA is significantly higher in PA patients (50%), but is also detectable in >20% of IDA and dyspeptic ABG patients. In our opinion, the results obtained are due mainly to the original methodological approach to the diagnosis of ABG, which is based on a screening program for the early detection of this condition in patients with anemia and/or long-standing dyspepsia[11,12]. Thus, the study population comprises a wider clinical spectrum of this condition than in previous studies [8,9], thus avoiding a potential bias due to the *a priori*-selection of the patients. For example, in our study the prevalence of IFA, in all ABG patients, was relatively low (35%), but considering only those with PA, the positivity of IFA reached 50%, which is similar to that described in previous reports[3-7]. In the present study, the classification of ABG patients based on the absence and/or the co-existing positivity and negativity of IFA and PCA failed to identify any specific pattern of gastric autoantibodies related to the clinical presentations of ABG.

Another important finding from the present study was the positive correlation between IFA levels and the histological score of gastric body atrophy in ABG patients, suggesting that progression of the oxyntic mucosa damage leads to an increase in the production of IFA, as previously observed for PCA[15]. Thus, our findings suggest that the positivity of IFA and/or PCA may be an expression of the degree of oxyntic mucosa damage in each patient, rather than a specific hallmark of autoimmunity.

It is of interest, that one-third of the ABG patients with positivity for IFA do not have PA, but present with IDA and dyspepsia. In previous studies, IFA are considered highly specific for PA[8,9] and only appear once when PA develops, thus assigning them a pathogenetic role in this condition[27]. Furthermore, it has been recognized that in PA patients, the co-existence of iron deficiency can occur in up to 20% of patients at initial diagnosis and in another 20% of patients during a 2-year follow-up,[28], indicating that both cobalamin and iron deficiency may overlap during the failure of oxyntic function. On the other hand, in our ABG patients presenting with iron deficiency anemia or dyspepsia, the serum levels of vitamin B_{12} were relatively low (Table 1), suggesting the presence of "latent" pernicious anemia in a proportion of ABG patients. Thus, chronic oxyntic failure may be present with a variable spectrum of hematological disorders depending on the age at onset of the disease, and gender, as observed elsewhere[16,29].

The positivity of IFA, like the positivity of PCA in patients with ABG and PA, together with the association of autoimmune disorders, is considered to be a hallmark of the autoimmune origin of these conditions[1,2]. In our study, <20% of patients with ABG had associated autoimmune disease and <50% of patients with ABG and autoimmune disease were IFA positive, only half of them having associated PA. However, the presence of associated autoimmune disease was similarly distributed in ABG patients with PA, IDA, and dyspepsia. Thus, these findings further highlight that these characteristics, previously considered specific, are not reliable in defining a specific subgroup of patients with autoimmune ABG.

Furthermore, it is well known that autoimmune gastritis has no distinctive histological features[30]. The "spared" antrum is often considered to be associated with autoimmune gastritis, which in fact is generally body-restricted[31]. However, this histological finding is not peculiar to any of the clinical presentations of ABG (Table 1).

Taking *H pylori* infection into consideration, results of this study suggest a possible relationship between the positivity of IFA and the time course of *H pylori* infection (Figure 2). Indeed, at an earlier stage of *H pylori* infection, when the organism is still detectable by tissue staining, the proportion of IFA positive ABG patients and their median level of IFA are significantly lower than that of those patients presenting with a long-standing infection, in whom only immunological memory or even no sign of infection is detectable. These data show that there is a positive correlation between the progression of body atrophy and production of IFA, since it has been reported that evidence of *H pylori* infection disappears parallel to the progression of body mucosa damage[15,32].

In fact, in ABG patients, oxyntic mucosa damage may be triggered by *H pylori* infection[14,33], and may be, as a consequence, exposed to autoantigens on these damaged cells. In animal models, it has been shown that gastric autoimmunity could be the consequence of a local inflammatory response induced by the local expression of pro-inflammatory molecules[34,35]. This hypothesis is supported by the findings of Ma *et al*.[36], who have observed a positive correlation between PCA and *H pylori* antibodies in patients with PA. Furthermore, Claeys *et al*.[37], also showed a positive correlation between antibodies against H^+, K^+-ATPase and antibodies against *H pylori* in patients with PA, suggesting that mixed forms of bacterial and autoimmune gastritis might occur. Recently, it has also been reported that, in genetically susceptible individuals, *H pylori* infection may trigger the development of gastric autoimmunity via molecular mimicry[38]. Thus, these data suggest that the sole

autoimmune origin of ABG may be questionable, and that the role of *H pylori* infection, as an initial trigger of chronic damage to the oxyntic mucosa, should be taken into consideration, regardless of the clinical presentations of ABG.

In conclusion, the so-called hallmarks of gastric autoimmunity, particularly in IFA, cannot be usefully employed in defining an autoimmune pattern in the clinical presentations of ABG.

ACKNOWLEDGMENTS

The authors thank Mrs. Amelia Pasquali for skilled technical support and Mrs. Marian Shields for revision of English style and editorial assistance.

REFERENCES

1 **Toh BH,** Gleeson PA, Whittingham S, Van Driel IR. Autoimmune gastritis and pernicious anemia. In: Rose NR, Mackay IR, Eds. *The Autoimmune Diseases*, 3rd edition. San Diego, London, Boston, New York, Sydney, Tokyo, Toronto, *Academic Press* 1998: 459-476

2 **Babio BM.** Erythrocyte disorders: *Anemias related to disturbance of DNA synthesis (megaloblastic anaemias).* In: Williams WJ, Beutler E, Erslev AJ, Lichtman MA, eds. *Haematology, 4th edition. New York* 1998: 453-481

3 **Wintrobe MM,** Lee GR, Boggs DR, Bithell TC, Foerster J, Athens JW, Lukens JN. *Megaloblastic and nonmegaloblastic macrocytic anaemias*. In: Wintrobe MM, Lee GR, Boggs DR, Bithell TC, Foerster J, Athens JW, Lukens JN, eds. *Clinical Haematology, 8th edition, Philadelphia* 1981: 559-604

4 **Irvine WJ,** Cullen DR, Scarth L, Simpson JD. Intrinsic-factor secretion assessed by direct radioimmunoassay and by total-body counting in patients with achlorhydria and in acid secretors. *Lancet* 1968; **2**: 184-188

5 **Fisher JM,** Taylor KB. The significance of gastric antibodies. *Br J Haematol* 1971; **20**: 1-7

6 **Kapadia CR,** Donaldson RM. Disorders of cobalamin (vitamin B12) absorption and transport. *Annu Rev Med* 1985; **36**: 93-110

7 **Carmel R.** Reassessment of the relative prevalence of antibodies to gastric parietal cell and to intrinsic factor in patients with pernicious anaemia: influence of patient age and race. *Clin Exp Immunol* 1991; **89**: 74-77

8 **Hift W,** Moshal MG, Pillay K. Megaloblastic anaemia, achlorhydria, low intrinsic factor, and intrinsic factor antibodies in the absence of pernicious anaemia. *Lancet* 1973; **1**: 570-573

9 **Rose MS,** Doniach D, Chanarin I, Brostoff J, Ardeman S. Intrinsic factor antibodies in absence of pernicious anaemia. 3-7 year follow-up. *Lancet* 1970; **2**: 9-12

10 **Scheuner M,** Yang H, Rotter JI. Gastrointestinal manifestations of specific genetic disorders. In: Yamada T, Ed. *Textbook of Gastroenterology*, 2nd edition, Philadelphia: *JB Lippincott Company* 1995: 2380-2419

11 **Marignani M,** Delle Fave G, Mecarocci S, Bordi C, Angeletti S, D'Ambra G, Aprile MR, Corleto VD, Monarca B, Annibale B. High prevalence of atrophic body gastritis in patients with unexplained microcytic and macrocytic anaemia. *Am J Gastroenterol* 1999; **84**: 766-772

12 **Annibale B,** Capurso G, Chistolini A, D'Ambra G, Di Giulio E, Monarca B, Delle Fave G. Gastrointestinal causes of refractory iron deficiency anemia in patients without gastrointestinal symptoms. *Am J Med* 2001; **111**: 439-444

13 **Yardley JH,** Hendrix TR. Gastritis, gastropathy, duodenitis, and associated ulcerative lesions. In: Yamada T Ed. *Textobook of Gastroenterology*, 1st Edition Lippincott, Williams & Wilkins, Philadelphia, New York, *Baltimore* 1999: 1463-1499

14 **Peterson WL,** Graham DY. *Helicobacter pylori*. In: Feldman M, Friedman LS, Sleisenger MH Eds. Sleisenger & Fordtran's *Gastrointestinal and Liver Disease: pathophysiology, diagnosis, management*, 7th edition, Philadelphia, London, New York, St. *Louis, Sydney, Toronto* 2002: 732-746

15 **Annibale B**, Negrini R, Caruana P, Lahner E, Grossi C, Bordi C, Delle Fave G. Two-thirds of atrophic body gastritis patients have evidence of *Helicobacter pylori* infection. *Helicobacter* 2001; **6**: 225-233

16 **Annibale B,** Lahner E, Bordi C, Martino G, Caruana P, Grossi C, Negrini R, Delle Fave G. Role of *Helicobacter pylori* infection in pernicious anaemia. *Dig Liver Dis* 2000; **32**: 756-762

17 **Appelmelk BJ,** Faller G, Claeys D, Kirchner T, Vandenbroucke-Grauls CM. Bugs on trial: the case of *Helicobacter pylori* and autoimmunity. *Immunol Today* 1998; **19**: 296-299

18 **Negrini R,** Lisato L, Zanella I, Cavazzini L, Gullini S, Villanacci V, Poiesi C, Alberini A, Ghielmi S. *Helicobacter pylori* infection induces antibodies cross-reacting with human gastric mucosa. *Gastroenterology* 1991: **101**: 437-445

19 **Annibale B,** Marignani M, Azzoni C, D'Ambra G, Caruana P, D'Adda T, Delle Fave G, Bordi C. Atrophic body gastritis: distinct features associated with *Helicobacter pylori* infection. *Helicobacter* 1997; **2**: 57-64

20 **Delle Fave G**, Kohn A, de Magistris L, Annibale B, Bruzzone R, Sparsoli C, Severi C, Torsoli A. Effects of bombesin on gastrin and gastric acid secretion in patients with duodenal ulcer. *Gut* 1983; **24**: 231-235

21 **Negrini R,** Zanella I, Savio A, Poiesi C, Verardi R, Ghielmi S, Alberini A, Sangaletti O, Lazzaroni M, Bianchi Porro G. Serodiagnosis of *Helicobacter pylori*-associated gastritis with a monoclonal antibody competitive enzyme-linked immunosorbent assay. *Scand J Gastroenterol* 1992; **27**: 599-605

22 **Annibale B,** de Magistris L, Corleto V, D'Ambra G, Marignani M, Iannoni C, Delle Fave G. Zollinger-Ellison syndrome and antral G-cell hyperfunction in patients with resistant duodenal ulcer disease. *Aliment Pharmacol Ther* 1994; **8**: 87-93

23 **Negrini R,** Benedini S, Annibale B, Delle Fave G, Vaira D, Bertolat G, Savio A. Antibodies against intrinsic factor are induced by *Helicobacter pylori* infection. *Gut* 2000; **47**(Suppl 1): A87-88

24 **Bordi C,** Annibale B, Azzoni C, Marignani M, Ferraro G, Antonelli G, D'Adda T, D'Ambra G, Delle Fave G. Endocrine cell growths in atrophic body gastritis. Critical evaluation of a histological classification. *J Pathol* 1997; **182**: 339-346

25 **Dixon MF,** Genta RM, Yardley JH, Correa P. Classification and grading of gastritis. The updated Sydney system. *Am J Surg Pathol* 1996; **20**: 1161-1181

26 **Kuipers EJ,** Uyterlinde AM, Pena AS, Roosendaal R, Pals G, Nelis GF, Festen HP, Meuwissen SG. Long-term sequelae of *Helicobacter pylori* gastritis. *Lancet* 1995; **345**: 1525-1528

27 **Roitt IM,** Doniach D, Shapland C. Autoimmunity in pernicious anaemia and atrophic gastritis. *Ann NY Acad Sci* 1965; **124**: 644-656

28 **Carmel R,** Weiner JM, Johnson CS. Iron deficiency occurs frequently in patients with pernicious anaemia. *JAMA* 1987; **257**: 1081-1083

29 **Capurso G,** Marignani M, Delle Fave G, Annibale B. Iron deficiency anemia in premenopausal women: Why not consider atrophic body gastritis and *Helicobacter pylori* role? *Am J Gastroenterol* 1999; **94**: 3084-3085

30 **Capella C,** Fiocca R, Cornaggia M, Rindi G, Moratti R, Solcia E. Autoimmune Gastritis. In: *Gastritis*, Graham DY, Genta RM, Dixon MF (Eds), Philadelphia, *Lippincott Williams & Wilkins* 1999: 79-96

31 **Lee EL,** Feldman M. Gastritis and other gastropathies. In: Sleisenger & Fordtran's *Gastrointestinal and Liver Disease: pathophysiology, diagnosis, management*. Feldman M, Friedman LS, Sleisenger MH (eds). 7th edition. *Philadelphia; Saunders* 2002: 810-827

32 **Karnes WE,** Samloff IM, Siurala M, Kekki M, Sipponen P, Kim SWR, Walsh JH. Positive serum antibody and negative

tissue staining for *Helicobacter pylori* in subjects with atrophic body gastritis. *Gastroenterology* 1991; **101**: 167-174

33 **Lahner E,** Bordi C, Di Giulio E, Caruana P, D'Ambra G, Milione M, Grossi C, Delle Fave G, Annibale B. Role of *Helicobacter pylori* serology in atrophic body gastritis after eradication treatment. *Aliment Pharmacol Ther* 2002; **16**: 507-514

34 **Alderuccio F,** Sentry JW, Marshall ACJ, Biondo M, Toh BH. Animal models of human disease: experimental autoimmune gastritis–a model for autoimmune gastritis and pernicious anaemia. *Clin Immunol* 2002; **102**: 48-58

35 **Croinin TO,** Clyne M, Appelmelk BJ, Drumm B. Antigastric antibodies in ferrets naturally infected with *Helicobacter mustelae*. *Infec Immun* 2001; **69**: 2708-2713

36 **Ma JY,** Borch K, Sjöstrand SE, Janzon L, Mardh S. Positive correlation between H,K-Adenosine Triphosphatase autoantibodies and *Helicobacter pylori* antibodies in patients with pernicious anaemia. *Scand J Gastroenterol* 1994; **29**: 961-965

37 **Claeys D,** Faller G, Appelmelk BJ, Negrini R, Kirchner T. The gastric H+,K+-ATPase is a major autoantigen in chronic *Helicobacter pylori* gastritis with body mucosa atrophy. *Gastroenterology* 1998; **115**: 340-347

38 **Amedei A,** Bergman MP, Appelmelk BJ, Azzurri A, Benagiano M, Tamburini C, van der Zee R, Telford JL, Vandenbroucke-Grauls C, D'Elios MM, Del Prete G. Molecular mimicry between *Helicobacter pylori* antigens and H+, K+-Adenosine triphosphatase human gastric autoimmunity. *J Exp Med* 2003; **198**: 1147-1156

Science Editor Wang XL and Guo SY **Language Editor** Elsevier HK

PO Box 2345, Beijing 100023, China
www.wjgnet.com
wjg@wjgnet.com

ELSEVIER

World J Gastroenterol 2005;11(34):5358-5361
World Journal of Gastroenterology ISSN 1007-9327
© 2005 The WJG Press and Elsevier Inc. All rights reserved.

• *BRIEF REPORTS* •

Effect of indomethacin on electrical field stimulation-induced contractions of isolated transverse and longitudinal rat gastric fundus strips

Salimeh Afshin, Mansoor Keshavarz, Mahmood Salami, Fatemeh Mirershadi, Bijan Djahanguiri

Salimeh Afshin, Mansoor Keshavarz, Fatemeh Mirershadi, Department of Physiology, School of Medicine, Tehran University of Medical Sciences, Tehran, Iran
Mahmood Salami, Department of Physiology, School of Medicine, Kashan University of Medical Sciences, Kashan, Iran
Bijan Djahanguiri, Department of Pharmacology, School of Medicine, Tehran University of Medical Sciences, Tehran, Iran
Co-first-authors: Salimeh Afshin and Mansoor Keshavarz
Correspondence to: Dr. Mansoor Keshavarz, Department of Physiology, School of Medicine, Tehran University of Medical Sciences, Tehran, Iran. mkeshavarz@tums.ac.ir
Telephone: +98-21-641-9484 Fax: +98-21-641-9484
Received: 2004-12-14 Accepted: 2005-01-05

Abstract

AIM: To study the effects of indomethacin on the isolated transverse and longitudinal rat gastric fundus strips.

METHODS: The strips were suspended in an organ bath containing oxygenated Krebs solution, and contractile responses to electrical field stimulation were recorded on a physiograph in an isotonic manner after administration of cumulative concentrations of indomethacin. The effects of indomethacin on the strips pretreated with K_{ATP} channel modulators, diazoxide and glybenclamide were studied.

RESULTS: Treatment of the transverse strips with indomethacin resulted in a concentration-dependent inhibitory response. In longitudinal strips, biphasic responses were seen, which included a stimulatory response at low concentrations of indomethacin, followed by an inhibitory response at higher concentrations. Diazoxide pre-treatment inhibited the stimulatory response of longitudinal strips. Glybenclamide pre-treatment not only blocked inhibitory effect of the low concentrations of indomethacin on transverse strips, but also increased the amplitude of contractions. Moreover, the drug decreased the amplitude of contractions in longitudinal strips.

CONCLUSION: Responses of the isolated longitudinal and transverse rat gastric fundus strips to indomethacin are not similar, and are influenced by K_{ATP} channel modulators.

© 2005 The WJG Press and Elsevier Inc. All rights reserved.

Key words: Gastric fundus; K_{ATP} channel; Indomethacin; Diazoxide; Glybenclamide

Afshin S, Keshavarz M, Salami M, Mirershadi F, Djahanguiri B. Effect of indomethacin on electrical field stimulation-induced contractions of isolated transverse and longitudinal rat gastric fundus strips. *World J Gastroenterol* 2005; 11 (34): 5358-5361
http://www.wjgnet.com/1007-9327/11/5358.asp

INTRODUCTION

Hypermotility of the stomach is proposed to be one of the mechanisms of the ulcerogenic action of indomethacin in rats[1-3]. It has been suggested that the stomach hypermotility plays a key role in the onset of the lesions, and the other factors are involved in the later extension of damage induced by indomethacin[2,4-6]. Ueki *et al*.[3], demonstrated that administration of atropine and 16,16-dimethyl PGE_2 suppressed gastric hypermotility and reduced gastric ulcerations. On the other hand, the K_{ATP} channels have also been shown to play a part in the pathogenesis of indomethacin-induced gastric ulceration[7-10].

In the present work, since our preliminary studies showed that indomethacin has relaxatory effects on the strips, we have studied the effects of different concentrations of indomethacin on contractile response of the isolated longitudinal and transverse rat gastric fundus strips stimulated by the electrical field stimulation (EFS). The effects of diazoxide as K_{ATP} channel opener and glybenclamide as the channel antagonist on the contractile pattern of the stomach were studied as well.

MATERIALS AND METHODS

Male Sprague-Dawley rats (160-200 g) were used. They were fasted overnight and killed by a blow on the head, followed by removal of the stomach through abdominal incision. Longitudinal and transverse strips of the gastric fundus were prepared as previously described by Milenov and Kalfin[11]. The strips were 4-5 mm wide and 15-20 mm long. Not more than four strips were prepared from each stomach. The strips were suspended under 1 g preload in a 20 mL organ bath containing oxygenated Krebs solution (113 mmol/L NaCl, 2.5 mmol/L $CaCl_2$, 4.7 mmol/L KCl, 25 mmol/L $NaHCO_3$, 1.1 mmol/L $MgSO_4$, 1.1 mmol/L KH_2PO_4, and 11 mmol/L glucose at the pH of 7.2). Pre-warmed water (37 ℃) was circulated through the outer

jacket of the tissue bath via constant-temperature circulator pump. The temperature of the Krebs solution in the organ bath was maintained within 37±0.5 ℃. The strips were allowed to equilibrate for approximately 45 min by the change of bath solution every 15 min. After stabilization of the tissue, EFS was applied via two platinum electrodes through which the preparation was surrounded by. Electrical impulses (rectangular waves, 50 V, 20 Hz, 1 ms for 8 s train duration with 100-s intervals between the trains) were provided by a modified stimulator (Harvard 6002, USA). The stimulus resulted in uniform strip contractions which were recorded via isotonic transducer and Universal Oscillograph (Harvard Apparatus, USA).

Cumulative concentrations of indomethacin (3×10^{-7} -2×10^{-4} mol/L) were added to the organ bath for evaluation of effects of indomethacin. In a series of experiments, the strips were pretreated with diazoxide (10^{-4} mol/L) or glybenclamide (4×10^{-6} mol/L) followed, 15 min later, by the administration of cumulative concentrations of indomethacin.

Drugs

All drugs were purchased as pure powder except diazoxide (aqueous solution). Tween 20 was used for the preparation of drug suspensions (indomethacin and glybenclamide). Drug concentrations were adjusted so that the volume of the added drug to the organ bath exceeds not more than 0.2 mL.

Statistical analysis

Each tissue was used for one dose-response curve. This was repeated with eight different tissues. The contractile response of each intact tissue to the EFS was considered as control (100%), and amplitude of the responses to different concentrations of drugs were compared with it. The means and SE for response to each concentration were calculated. Student's *t*-test and two-way analysis of variance with Newman-Keuls post hoc were used to test the statistical significance between different groups. Data were expressed as mean±SE. $P<0.05$ was considered statistically significant.

RESULTS

EFS produced uniform contractile responses in both longitudinal and transverse strips, which lasted for more than 100 min and were abolished following atropine treatment. Vehicle had no effect on contractions.

Strips response to cumulative concentrations of indomethacin

In the transverse strips, administration of cumulative concentrations of indomethacin (3×10^{-7}-2×10^{-4} mol/L) produced concentration-dependent decrease in amplitude of contractile response. The inhibitory effect of indomethacin started from the concentration of 3×10^{-7} mol/L and its maximum effect was obtained at the concentration of 2×10^{-4} mol/L. In the longitudinal strips, indomethacin, at low concentrations (3×10^{-7}-6×10^{-6} mol/L), increased the amplitude of contractile responses. The peak of increase was 14.1±3.14%. With higher concentrations (10^{-5}-2×10^{-4} mol/L), a decrease in contractile response was observed (Figure 1).

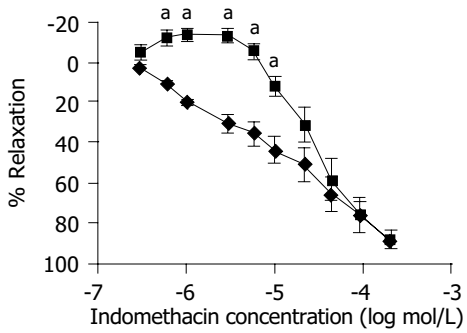


Figure 1 Cumulative concentration-response curves for the effect of indomethacin on EFS-induced contractions of transverse (◆) and longitudinal (■) rat gastric fundus strips. Each point represents the mean±SE of responses observed in eight strips. Relaxations are expressed as percentages of the amplitude of contractions induced in the same strip by EFS before drug treatment. The responses of transverse and longitudinal strips of rat gastric fundus for each concentration of indomethacin were compared. [a]$P<0.05$ *vs* EFS-induced contractions of transverse.

Effects of K_{ATP} channel modulators on responses to indomethacin

Pretreatment with diazoxide (10^{-4} mol/L), a K_{ATP} channel opener, 15 min before indomethacin administration showed no change in the response to indomethacin of transverse strip (Figure 2A). However, in longitudinal strips, "primary contractile response" was abolished and a continuous relaxation was seen following the administration of indomethacin. The concentration-response curve was shifted to the left and down and became similar to the transverse strip responses to indomethacin alone (Figure 2B).

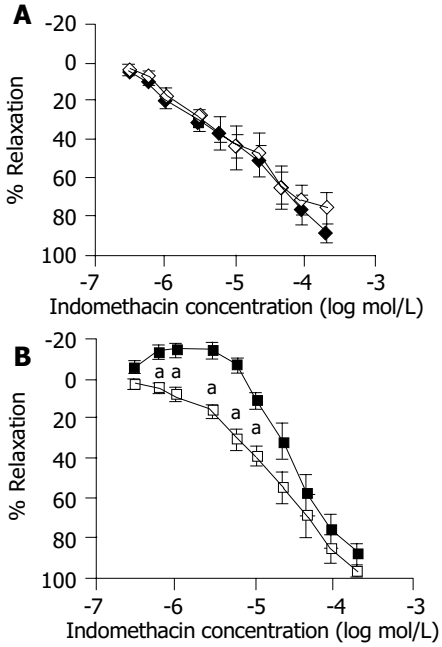


Figure 2 Effect of diazoxide (10^{-4} mol/L) on cumulative concentration-response curves for relaxant effect of indomethacin on EFS-induced contractions of transverse (**A**) and longitudinal (**B**) strips of rat gastric fundus. Each point represents the mean±SE of responses observed in eight strips. Relaxations or early contractions are expressed as percentages of the amplitude of contractions induced in the same strip by EFS before drug treatment. **A**: Responses of transverse strips of rat gastric fundus pretreated with diazoxide (◇) after administration of each concentration of indomethacin compared to saline-treated (◆) strips; **B**: responses of longitudinal strips of rat gastric fundus pretreated with diazoxide (□) after administration of each concentration of indomethacin compared to saline-treated (■) strips. [a]$P<0.05$ *vs* saline-treated strips.

Glybenclamide pre-treatment (4×10^{-6} mol/L) 15 min before indomethacin administration, not only prevented "acute inhibitory response" in transverse strips, but also increased the amplitude of contractile responses to indomethacin at concentrations of 3×10^{-7}-10^{-6} mol/L. The curve shifted to the right and up and became similar to longitudinal strip response to indomethacin alone (Figure 3A). Longitudinal strip responses to indomethacin decreased in the presence of glybenclamide, resulting in a shift to the left and down of the response curve and making the curve similar to the response curve of transverse strip to indomethacin alone (Figure 3B).

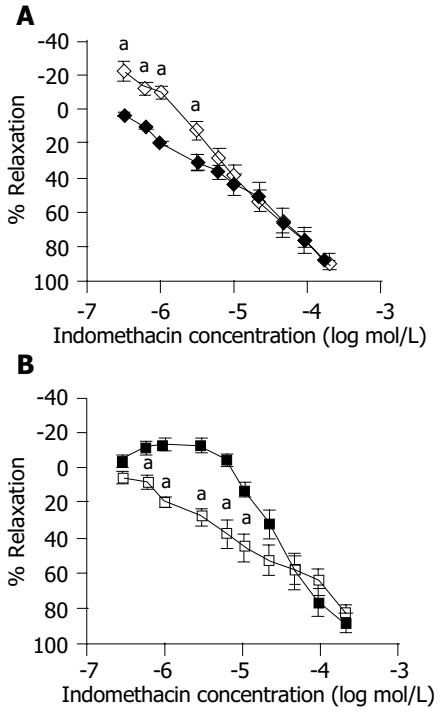


Figure 3 Effect of glybenclamide (4×10^{-6} mol/L) on cumulative concentration-response curves for relaxant effect of indomethacin on EFS-induced contractions of transverse (**A**) and longitudinal (**B**) strips of rat gastric fundus. Each point represents the mean±SE of responses observed in eight strips. Relaxations or early contractions are expressed as percentages of the amplitude of contractions induced in the same strip by EFS before drug treatment. **A**: Responses of transverse strips of rat gastric fundus pretreated with glybenclamide (◇) after administration of each concentration of indomethacin compared to saline-treated (◆) strips; **B**: responses of longitudinal strips of rat gastric fundus pretreated with glybenclamide (□) after administration of each concentration of indomethacin compared to saline-treated (■) strips. $^aP<0.05$ *vs* saline-treated strips.

DISCUSSION

Several mechanisms, including the hypermotility of the stomach, have been proposed to explain indomethacin-induced gastric ulceration[1-4]. Hypermotility may be due to the action of drugs on the CNS, or peripheral effects of indomethacin on the stomach nerves or muscles. In the present study, we have investigated the effects of indomethacin on the contractile responses of the isolated transverse and longitudinal strips of rat gastric fundus to myenteric plexus activation via EFS.

The fact that atropine prevented the EFS-induced strip contractions suggests that the contractions originate, at least in part, from the cholinergic system. According to the present results, the responses of transverse and longitudinal strips to indomethacin were not identical. In the transverse strips, the effect of indomethacin was inhibitory while in the longitudinal strips, the response to indomethacin was dependent on the concentrations of the drug. We observed an increase in the amplitude at the low concentrations, while a decrease in the amplitude at higher concentrations. Takeuchi *et al*.[1,2], and Ueki *et al*.[3], in *in vivo* studies, demonstrated that indomethacin administration resulted in a significant gastric hypermotility. In our experiments, contrary to the hypermotility reported by the aforementioned investigators, we observed relaxation of the strips after indomethacin administration. The reason for this discrepancy may be due to the fact that in the previous published reports, the effects of indomethacin have been studied in the intact animals (*in vivo*) while the present work is an *in vitro* study, independent of humoral and/or neural influences. It is possible that the reported results are the net effect of several different factors; some of them are not limited to the stomach and are systemic effects. Gastric motility is under the control of neural, humoral, and mechanical factors with stimulatory or inhibitory effects on the stomach contractility. The net results of these effects will determine the contractility of the stomach. The strip relaxation may be due to the inhibition of stimulatory prostaglandins (PGs)[12,13], L-type calcium channels[14] or phosphodiesterase 4[15].

The presence of the K_{ATP} channels has been demonstrated in the smooth muscles of the stomach[16]. The difference between the results obtained in transverse and longitudinal strips following indomethacin administration may be dependent on the state of K_{ATP} channels of the tissues. Opening of the channels by diazoxide, in the longitudinal strips, resulted in responses similar to that of transverse strips under indomethacin treatment. On the other hand, the administration of glybenclamide, a K_{ATP} channel antagonist, interestingly, changed the response of transverse strip to a response similar to that of longitudinal strips under indomethacin treatment. Altogether, these results are suggestive of the possible role played by K_{ATP} channels on the effects of indomethacin on the motility of the isolated rat gastric fundus strips.

The stomach is one of the sources of different types of PGs with stimulatory or inhibitory effects on contractility of the organ[17]. It has been known that indomethacin has inhibitory effects on the generation of PGs. On the other hand, the effects of PGs are known to be through their receptors[18]. Some PG receptors are only present in the longitudinal muscles[19]. This also may explain the difference between the results obtained in longitudinal and transverse strips as observed in our present study.

As shown in Figure 3, the stimulatory effect of indomethacin on the EFS-induced contraction of the longitudinal strip was abolished by both diazoxide and glybenclamide. These drugs have an opposing effect on K_{ATP} channels: diazoxide has an ability to open the channels while glybenclamide has an ability to inhibit the channels. Because K_{ATP} channel opener induces relaxation of smooth muscle through hyperpolarization, it is easy to understand the effect of diazoxide. However, glybenclamide causes depolarization through inhibition of K_{ATP} channels and results in activation

of the cell (contraction). Yet, this agent abolished the stimulatory effect of indomethacin on the EFS-induced contraction of the longitudinal smooth muscle. It seems that glybenclamide acts more than a K_{ATP} channel blocker, thus other possible mechanisms for this action of glybenclamide must be evaluated.

In conclusion, the pattern of response of transverse and longitudinal strips to indomethacin is not quite similar, which may be due to the involvement of K_{ATP} channels. However, the overall effect of indomethacin on EFS-induced contractions of the isolated strips of rat gastric fundus is an inhibitory action.

REFERENCES

1 **Takeuchi K,** Ueki S, Okabe S. Importance of gastric motility in the pathogenesis of indomethacin-induced gastric lesions in rats. *Dig Dis Sci* 1986; **31**: 1114-1122

2 **Takeuchi K,** Tanaka A, Hayashi Y, Kubo Y. Functional mechanism underlying COX-2 expression following administration of indomethacin in rat stomachs: importance of gastric hypermotility. *Dig Dis Sci* 2004; **49**: 180-187

3 **Ueki S,** Takeuchi K, Okabe S. Gastric motility is an important factor in the pathogenesis of indomethacin-induced gastric mucosal lesions in rats. *Dig Dis Sci* 1988; **33**: 209-216

4 **Takeuchi K,** Kato S, Nishiwaki H, Hirata T. Analysis of pathogenic elements involved in gastric lesions induced by non-steroidal anti-inflammatory drugs in rats. *J Gastroenterol Hepatol* 1997; **12**: 360-367

5 **Suzuki K,** Araki H, Komoike Y, Takeuchi K. Permissive role of neutrophils in pathogenesis of indomethacin-induced gastric lesions in rats. *Med Sci Monit* 2000; **6**: 908-914

6 **Okada M,** Niida H, Takeuchi K, Okabe S. Role of prostaglandin deficiency in pathogenic mechanism of gastric lesions induced by indomethacin in rats. *Dig Dis Sci* 1989; **34**: 694-702

7 **Toroudi HP,** Rahgozar M, Bakhtiarian A, Djahanguiri B. Potassium channel modulators and indomethacin-induced gastric ulceration in rats. *Scand J Gastroenterol* 1999; **34**: 962-966

8 **Rahgozar M,** Pazokitoroudi H, Bakhtiarian A, Djahanguiri B. Diazoxide, a K(ATP) opener, accelerates restitution of ethanol or indomethacin-induced gastric ulceration in rats independent of polyamines. *J Gastroenterol Hepatol* 2001; **16**: 290-296

9 **Akar F,** Uydes-Dogan BS, Buharalioglu CK, Abban G, Heinemann A, Holzer P, Van de Voorde J. Protective effect of cromakalim and diazoxide, and pro-ulcerogenic effect of glybenclamide on indomethacin-induced gastric injury. *Eur J Pharmacol* 1999; **374**: 461-470

10 **Peskar BM,** Ehrlich K, Peskar BA. Role of ATP-sensitive potassium channels in prostaglandin-mediated gastroprotection in the rat. *J Pharmacol Exp Ther* 2002; **301**: 969-974

11 **Milenov K,** Kalfin R. Cholinergic-nitrergic interactions in the guinea-pig gastric fundus. *Neuropeptides* 1996; **30**: 365-371

12 **Sanders KM,** Northrup TE. Prostaglandin synthesis by microsomes of transverse and longitudinal gastrointestinal muscles. *Am J Physiol* 1983; **244**: G442-G448

13 **Sanders KM.** Role of prostaglandins in regulating gastric motility. *Am J Physiol* 1984; **247**: G117-G126

14 **Northover BJ.** Indomethacin: a calcium antagonist. *Gen Pharmacol* 1977; **8**: 293-296

15 **Newcombe DS,** Thanassi NM, Ciosek CP Jr. Cartilage cyclic nucleotide phosphodiesterase: inhibition by anti-inflammatory agents. *Life Sci* 1974; **14**: 505-519

16 **Vogalis F.** Potassium channels in gastrointestinal smooth muscle. *J Auton Pharmacol* 2000; **20**: 207-219

17 **Atay S,** Tarnawski AS, Dubois A. Eicosanoids and the stomach. *Prostaglandins Other Lipid Mediat* 2000; **61**: 105-124

18 **Narumiya S,** Sugimoto Y, Ushikubi F. Prostanoid receptors: structures, properties, and functions. *Physiol Rev* 1999; **79**: 1193-1226

19 **Northey A,** Denis D, Cirino M, Metters KM, Nantel F. Cellular distribution of prostanoid EP receptors mRNA in the rat gastrointestinal tract. *Prostaglandins Other Lipid Mediat* 2000; **62**: 145-156

Science Editor Kumar M and Guo SY **Language Editor** Elsevier HK

PO Box 2345, Beijing 100023, China
www.wjgnet.com
wjg@wjgnet.com

ELSEVIER

World J Gastroenterol 2005;11(34):5362-5366
World Journal of Gastroenterology ISSN 1007-9327
© 2005 The WJG Press and Elsevier Inc. All rights reserved.

• *BRIEF REPORTS* •

Differing coping mechanisms, stress level and anorectal physiology in patients with functional constipation

Annie OO Chan, Cecilia Cheng, Wai Mo Hui, Wayne HC Hu, Nina YH Wong, KF Lam, Wai Man Wong, Kam Chuen Lai, Shiu Kum Lam, Benjamin CY Wong

Annie OO Chan, Wai Mo Hui, Wayne HC Hu, Nina YH Wong, KF Lam, Wai Man Wong, Kam Chuen Lai, Shiu Kum Lam, Benjamin CY Wong, Department of Medicine, the University of Hong Kong, Hong Kong, China
KF Lam, Department of Statistics, the University of Hong Kong, Hong Kong, China
Cecilia Cheng, Division of Social Science, the Hong Kong University of Science and Technology, Hong Kong, China
Correspondence to: Annie OO Chan, MD, PhD, Department of Medicine, University of Hong Kong, Queen Mary Hospital, Hong Kong, China. aoochan@hku.hk
Telephone: +852-2855-5414 Fax: +852-2855-5411
Received: 2004-12-18 Accepted: 2005-01-26

Abstract

AIM: To investigate coping mechanisms, constipation symptoms and anorectal physiology in 80 constipated subjects and 18 controls.

METHODS: Constipation was diagnosed by Rome II criteria. Coping ability and anxiety/depression were assessed by validated questionnaires. Transit time and balloon distension test were performed.

RESULTS: 34.5% patients were classified as slow transit type of constipation. The total colonic transit time (56 h *vs* 10 h, $P<0.0001$) and rectal sensation including urge sensation (79 mL *vs* 63 mL, $P = 0.019$) and maximum tolerable volume (110 mL *vs* 95 mL, $P = 0.03$) differed in patients and controls. Constipated subjects had significantly higher anxiety and depression scores and lower SF-36 scores in all categories. They also demonstrated higher scores of 'monitoring' coping strategy (14±6 *vs* 9±3, $P = 0.001$), which correlated with the rectal distension sensation ($P = 0.005$), urge sensation ($P=0.002$), and maximum tolerable volume ($P = 0.035$). The less use of blunting strategy predicted slow transit constipation in both univariate ($P = 0.01$) and multivariate analysis ($P = 0.03$).

CONCLUSION: Defective or ineffective use of coping strategies may be an important etiology in functional constipation and subsequently reflected in abnormal anorectal physiology.

© 2005 The WJG Press and Elsevier Inc. All rights reserved.

Key words: Constipation; Anorectal physiology; Coping mechanism

Chan AOO, Cheng C, Hui WM, Hu WHC, Wong NYH, Lam KF, Wong WM, Lai KC, Lam SK, Wong BCY. Differing coping mechanisms, stress level and anorectal physiology in patients with functional constipation. *World J Gastroenterol* 2005; 11(34): 5362-5366
http://www.wjgnet.com/1007-9327/11/5362.asp

INTRODUCTION

Functional constipation is a common problem in clinical practice. In the Western population, the prevalence was reported to be as high as 24% in elderly subjects and more commonly among women[1]. We observed a prevalence of 14% of constipation in Asian population[2].

There are growing interests in exploring the role of psychological factors on the pathogenesis of functional constipation. These patients report high levels of emotional distress[3-5]. Patients with functional constipation generally have a higher prevalence of anxiety, depression, and social dysfunction than do normal controls[6,7].

It has been reported that voluntary holding in healthy people can remarkably delay defecation and at the same time slow transit through the ascending colon and the recto-sigmoid tract[8]. This type of mechanism often produces constipation in children, which in some leads to constipation with megarectum-megacolon. This type of constipation can continue into adulthood as an acquired illness behavior[9]. In addition, a recent study[10] demonstrated that general psychosocial function, somatization, anxiety, depression, and feelings about the female role are impaired in women with constipation and are associated with altered rectal mucosal blood flow, which is an indirect measurement of the autonomic function. Furthermore, constipated subjects with slow bowel transit are associated with more psycho-social distress than those with normal bowel transit[11]. These findings suggest that behavior and psychological factors could lead to and be reflected by changes in anorectal physiology.

Drossman *et al*.[12], have proposed that life factors will later influence psycho-social experiences, physiological functioning or susceptibility to developing a functional gastrointestinal disorder, including functional constipation. These psycho-social factors include coping ability and social support and play a role in modulating the effect of stress[13,14]. Coping ability plays an important role in amelioration of the stressful events and behaviors[14]. Penley *et al*.[15], reported that coping ability was correlated with health outcomes.

Despite that psychological dysfunction in constipated patients is well reported, these patients have rarely been

subjected to systematic psychiatric and anorectal physiology study. In addition, their general coping ability has not been investigated. We hypothesized that stresses if not coped will be "internalized" and may lead to symptom expression and different clinical outcomes, as mediated through central nervous system/enteric nervous system pathways. Hence, patients with functional constipation have different coping mechanisms and stress levels from normal subjects, which might contribute to the pathogenesis of functional constipation. We examined this hypothesis by testing the stress level, coping strategies used and anorectal physiology in both constipated patients and healthy subjects.

MATERIALS AND METHODS

The 80 patients in this study were a consecutive group, referred for assessment of constipation. All 80 subjects had been assessed by a gastroenterologist and had chronic constipation, defined by the Rome II criteria as follows: At least 12 wk, which need not be consecutive, in the preceding 12 mo of two or more of: less than three bowel movements per week, straining at stool more than 25% of the time, passage of lumpy or hard stools more than 25% of the time, sensation of incomplete evacuation for more than 25% of the time, sensation of anorectal obstruction/blockage for more than 25% of the time and manual maneuvers to facilitate more than 25% of the time of defecation. In addition, loose stools are not present, and there were insufficient criteria for the diagnosis of irritable bowel syndrome[16]. Patients with associated medical conditions that might result in constipation (i.e. secondary causes) were excluded. In addition, patients with associated psychological illness and/or being followed up by a psychiatrist were also excluded from the present study. Eighteen healthy volunteers were recruited as controls.

The volunteers were recruited through advertisement. They were interviewed by the research nurse about their health status. They did not have any past chronic medical disease including gastrointestinal diseases. They were currently asymptomatic, did not attend any medical practitioners, and had not taken any sick leave or medication over the past 2 mo.

Assessment of bowel transit time

Normal and slow transit constipation were confirmed by X-ray and colonic motility studies performed in all 80 patients, who had been shown to have long-standing severe constipation. Colonic transit time was assessed through the use of radiopaque markers. In brief, four sets of distinctive radiopaque markers of different shapes and size (circle on d 1, semi-cylinder on d 2, dot on d 3 and cylinder on d 4) were ingested by the volunteers on 4 consecutive d. X-ray of the abdomen was taken on d 5 and 7 to assess the mouth to anal transit and segmental colon transit. Transit in the right, left, and recto-sigmoid colon was calculated by adding all markers seen in these regions on d 5 and 7. Slow total colonic transit was defined as >67 h, the mean transit plus 2SD averaged from published studies[17,18].

Rectal sensation

Balloon distension is used to detect the threshold for three common sensations, the first detectable sensation, the sensation of urgency to defecate and the sensation of pain. A commercially available anorectal catheter was connected with a terminal polyethylene balloon (Zinetics: Anorectal Replacement Balloons, one size). The rectal sensation was evaluated by sequentially inflating the rectal balloon with a hand-held syringe using the following volumes: 10, 20, 30, 40, 50, 60, 80, 100, 150, and 200 mL of air. Each inflation was maintained for 1 min after deflation, a rest period of 2 min was allowed before re-inflating the balloon. During this test, the volumes of air inflated were recorded at the following sensations: the first sensation, urge to defecate and the maximum tolerable volume[19].

Questionnaire measures

Psychological well being was assessed by anxiety and depression. The anxiety and depression were assessed by the multiple affect adjective check list (MAACL)[20]. A combined score of anxiety and depression (the MAACL score) was generated by adding anxiety and depression scores.

Coping questionnaire: The coping questionnaires were based on the extended version of Miller Behavioral Style Scale[21,22]. The questionnaire examined the frequency of use of different coping strategies with different controllable (C) and uncontrollable (U) situations. The coping strategies included monitoring, blunting, problem solving, distancing, ventilation, wishful thinking and social support. The questionnaire has been validated and demonstrated previously to have good internal consistency[22]. It was delivered by one investigator [NYHW] to allow consistency.

Outcome measurement: The outcome measurement was measured in terms of the quality of life. The quality of life was assessed by the Short Form 36 (SF-36) health survey questionnaire. The SF-36 is a 36 question survey, which is well tested, valid, and reliable self-report tool developed for use in the Medical Outcomes Study[23,24]. The SF-36 is scored so that higher scores represent better functioning on both the two summary measures and on all eight subscales.

This study was approved by the Ethics Committee of the University of Hong Kong.

Statistical analysis

Comparison between groups was made by Mann-Whitney *U* tests for the demographic, colonic transit and the anal rectal pressures, anxiety and depression scores and the coping scores. Scoring of the SF-36 was performed following the scoring algorithms found in the SF-36™ Health Survey Manual and Interpretation Guideline. The data from the SF-36 were expressed as mean±SE of the means. Spearman's rank correlation was used to assess for correlations between coping strategies, SF-36 and MAACL score. Regression analysis was performed for identifying independent predicting factors for anorectal physiology variables. A stepwise regression analysis was carried out. All statistical analysis was performed using SPSS software.

RESULTS

Demographic characteristics

There were 8 men and 72 women in the patient group and 8

Table 1 Transit time and anorectal physiological assessment in patients and controls (mean±SD)

	Control (n = 17)		Patient (n = 80)		P
Transit time					
Right segment	7.3	6.4	12.7	11.5	0.08
Left segment	5.8	6.3	17.8	6.8	<0.0001
Sigmoid-rectal segment	6.1	6.2	23.9	19.1	<0.0001
Total colon	10.4	7.6	56.2	29.1	<0.0001
Balloon measurements (*mL*)					
First sensation	33	9	39	17	0.2
Constant sensation / urge	63	20	79	30	0.019
Maximum tolerable volume	95	16	110	38	0.03

men and 10 women in the control group. The mean patient age was 42±16 years (range from 18 to 83 years) and that in the control group was 41±11 years (range from 25 to 64 years) (P = 0.7).

The mean duration of constipation in the patients was 7.2±8 years (range from 1 to 40 years). Sixty-five percent of the patients had straining for more than one quarter of the time, 57% had lumpy or hard stool, 82% had sensation of incomplete evacuation, 47% had anorectal blockade/ obstruction, 78% had fewer than three times of spontaneous opening per week, and 43% need digital evacuation. There were 34.5% patients classified as having slow colonic transit.

Anorectal physiology, anxiety, depression, coping strategies, and SF-36 scores in patients and controls

The readings of transit time and rectal sensation are summarized in Table 1. Transit time, including, left colon, sigmoid-rectal segment, and total colon, differed significantly in patients and controls (Table 1). Constipated patients also differed significantly from controls in the urge sensation and maximum tolerable volume in the assessment of rectal sensation (Table 2).

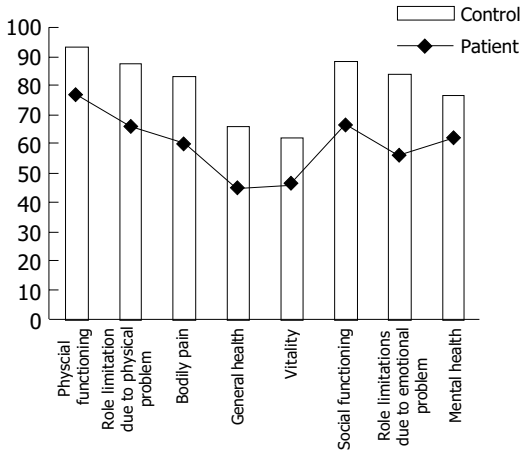


Figure 1 Self assessment of physical and mental health (SF-36) in patients and controls. Mean values of SF-36 scores for patients with constipation (line) compared with normal subjects (bar). Constipated patients differed from the normal subjects in all eight categories. They had decreased physical functioning scores (77 *vs* 93, P<0.0001), role-physical scores (66 *vs* 87, P = 0.009), bodily pain scores (60 *vs* 83, P = 0.001), general health scores (45 *vs* 68, P<0.0001), vitality scores (46 *vs* 62, P = 0.002), social functioning scores (67 *vs* 88, P<0.0001), role emotional scores (56 *vs* 84, P = 0.001), and mental health scores (61 *vs* 76, P = 0.003).

Table 2 Correlation between anxiety/depression (the MAACL score) and the scores of various coping strategies

Coping strategies	Correlation coefficient	P
Monitoring	0.2	0.9
Blunting	-0.05	0.6
Social support	-0.4	0.003
Controllable problem solving	-0.4	<0.0001
Uncontrollable problem solving	-0.3	0.03
Controllable catharsis	-0.3	0.009
Uncontrollable catharsis	-0.2	0.1
Controllable wishful thinking	-0.2	0.1
Uncontrollable wishful thinking	-0.2	0.3
Controllable distancing	0.1	0.7
Uncontrollable distancing	0.002	0.9

Anxiety and depression scores, and hence the MAACL score, differed significantly in patients and controls (34±8 *vs* 26±7 for anxiety score, P = 0.009; 32±7 *vs* 26±7 for depression score, P<0.0001; 66±14 *vs* 52±14 for MAACL score, P = 0.001). Constipated patients also differed significantly from the normal subjects in all eight categories of the SF-36 scores (Figure 1).

The correlation between the MAACL score and the scores of coping strategies are summarized in Table 2. Significant correlation was observed between the MAACL score and social support (P = 0.003), controllable problem solving (P<0.0001), uncontrollable problem solving (P = 0.03), and controllable catharsis (P = 0.009). The scores of coping strategies are summarized in Table 3. Patients with constipation had more frequent use (higher scores) of the 'monitoring' coping strategy than the controls, but no difference in the other coping strategies (14±6 *vs* 9±3, P = 0.001). When patients were stratified according to transit time, those with slow transit type of constipation had less frequent use (lower scores) of the 'blunting' coping strategy than other patients (7±3 *vs* 10±3, P = 0.01). When stratified according to rectal sensation, it was found that the use of the 'monitoring' coping strategy in constipated subjects correlated positively with the balloon volume at the first sensation (P = 0.005), the urge sensation (P =0.002), and the maximum tolerable volume (P = 0.035).

Multivariate analysis for predicting duration of constipation and anorectal physiology

Variables including sex, age, various coping strategies and

Table 3 Coping scores in patients and controls

Coping strategies	Patient (n = 80)		Control (n = 18)		P
	Median scores	Range	Median scores	Range	
Monitoring	14	3-27	9	2-15	0.001
Blunting	8	1-16	9	5-16	0.9
Social support	43	33-56	41	34-51	0.3
Controllable problem solving	6	1-11	6	1-12	0.3
Uncontrollable problem solving	5	1-11	5	1-9	0.8
Controllable catharsis	6	1-12	6	2-10	0.7
Uncontrollable catharsis	5	1-11	5	1-10	0.9
Controllable wishful thinking	5	1-12	5	1-12	0.6
Uncontrollable wishful thinking	4	1-12	5	1-12	0.3
Controllable distancing	4	1-10	3	1-7	0.4
Uncontrollable distancing	5	1-12	5	1-12	0.9

MAACL score were entered for the regression analysis for the prediction of symptoms of constipation. It was observed that female sex (P = 0.01) and age (P = 0.002) were the independent predictive variables for symptom of duration of constipation, despite that there were not enough men to comment on the predictive value of gender.

Variables including sex, age, various coping strategies and MAACL score were entered for the regression analysis for the prediction of anorectal physiology. We observed that the more often use of coping strategies of blunting (P = 0.03) predicted slow transit type of constipation. On the other hand, there was no significant independent predictive factor for rectal sensation.

DISCUSSION

High prevalence of emotional distress including anxiety, depression, and social dysfunction in patients with functional constipation has been well reported[6,7]. Our study further supported this observation and the observation was corroborated by objective evidence from anorectal physiology study. Emotional distress can cause physical problems but the reverse is also true: having a physical problem may cause distress. We examined the former link and at a higher level: by hypothesizing that defective coping mechanisms existed in patients with functional constipation and that defective coping mechanism subsequently led to internalization of stress and hence reflected as psycho-somatic disease such as functional constipation. Our study confirmed this hypothesis, showing that defective coping mechanisms existed in these patients and were independent factors for predicting abnormal anorectal physiology.

The present study demonstrated that coping strategies of monitoring and blunting were associated with anorectal physiology. Blunting (information avoiding coping style) has been shown to directly associate with the reporting of symptoms associated with infections like common colds and flu-like symptoms[25]. Similar finding was observed in the current study that blunting was directly associated with the slow transit type of constipation. "Monitoring" or information-gathering coping style was associated with more anticipatory anxiety[26]. Similar finding was observed in our present study that frequent use of monitoring coping strategy was found in constipation patients and associated with larger balloon volume at first sensation, urge sensation and maximum tolerable volume. These ineffective or less use of coping strategies are in accordance with the recent finding that constipated subjects have more social dysfunction and less satisfaction in their sexual life[6]. Testing for both controllable and uncontrollable situations, which were employed in the present study allowed for better assessment of the coping response because uncontrollable life events are better predictive of psychological distress over time[27]. Problem solving and catharsis are strategies that have been used to deal with a variety of stressful situations with different characteristics[15,28] and correlate with health outcomes[15]. Patients with functional dyspepsia have also been reported to have a non-discriminative, action-oriented coping style[29]. Hence we postulated that defective coping mechanism also exists and is an important etiology factor in patients with functional constipation. In addition, the defective coping strategy in the constipated subjects could not be explained by the associated anxiety and depression as there was no correlation observed in the current study between the MAACL score and the coping strategies of monitoring and blunting.

The current study again demonstrated significant anxiety and depression level in constipated patients, which has already been reported previously[2,4-7]. However, it is worth noting that the patients' anxiety and depression scores were relatively higher than individuals in the control group, rather than having absolute high levels in anxiety and depression. SF-36 scale, as a measurement of quality of life, has been demonstrated to be low in patients with functional constipation. This is again further confirmed in our study.

The limitation of our study was that the constipated patients were recruited in the hospital in the present study. Caution should be taken when attempting to generalize the present results to non-consulters. Another limitation was the small sample size of the normal controls. Taking into account the high prevalence of emotional and behavioral abnormalities in general population, a small control group could underestimate the real prevalence of psychological disorders in "healthy" volunteers. Nonetheless, our results suggested the role of defective coping mechanisms as another psychological factor in the pathogenesis of functional constipation. It is possible that failure to cope with stressful situation results in stress internalization and in turn leads to anxiety and other psychological distress. These are in accordance with the findings in this study that coping was associated with both physical and mental well being (SF-36)

as well as anxiety and depression. These distresses may act via the enteric nervous system to inhibit colonic motility and thus prolonged colonic transit, as demonstrated in the present study. This was supported by a recent study[10] demonstrating constipated subjects with psychological abnormality was associated with altered extrinsic gut innervation. Furthermore in cats, it has been demonstrated that stimulation of the pelvic nerves affects colonic contractions[30]. These findings suggest a link between central brain activity, enteric nervous system and gut dysfunction. The current study broadens our knowledge on the pathogenetic mechanisms of constipation and might provide clue to treatment, such as psychotherapy directing at the defective coping mechanisms.

REFERENCES

1 **Talley NJ,** O'Keefe EA, Zinsmeister AR, Melton LJ 3rd. Prevalence of gastrointestinal symptoms in the elderly: a population-based study. *Gastroenterology* 1992; **102**: 895-901
2 **Cheng C,** Chan AO, Hui WM, Lam SK. Coping strategies, illness perception, anxiety, and depression of patients with idiopathic constipation: Apopulation-based study. *Aliment Pharmacol Ther* 2003; **18**: 319-326
3 **Fisher SE,** Keighley MRB, Brecon K, Smart V, Andrews H. Do patients with disordered defecation have a primary personality disorder? *Gut* 1987; **28**: A1373
4 **Devroede G,** Girard G, Bouchoucha M, Roy T, Black R, Camerlain M, Pinard G, Schang JC, Arhan P. Idiopathic constipation by colonic dysfunction. Relationship with personality and anxiety. *Dig Dis Sci* 1989; **34**: 1428-1433
5 **Wald A,** Hinds JP, Caruana BJ. Psychological and physiological characteristics of patients with severe idiopathic constipation. *Gastroenterology* 1989; **97**: 932-937
6 **Mason HJ,** Serrano-Ikkos E, Kamm MA. Psychological morbidity in women with idiopathic constipation. *Am J Gastroenterol* 2000; **95**: 2852-2857
7 **Nehra V,** Bruce BK, Rath-Harvey DM, Pemberton JH, Camilleri M. Psychological disorders in patients with evacuation disorders and constipation in a tertiary practice. *Am J Gastroenterol* 2000; **95**: 1755-1758
8 **Klauser AG,** Voderholzer WA, Heinrich CA, Schindlbeck NE, Müller-Lissner SA. Behavioural modification of colonic function. Can constipation be learned? *Dig Dis Sci* 1990; **35**: 1271-1275
9 **Whitehead WE.** Illness behaviour. in Constipation, ed.: M Kamm & JE Lennard-Jones; *Wrightson Biomedical Publishing LTD Petersfield UK* 1994: 95-100
10 **Emmanuel AV,** Mason HJ, Kamm MA. Relationship between psychological state and level of activity of extrinsic gut innervation in patients with a functional gut disorder. *Gut* 2001; **49**: 209-213
11 **Dykes S,** Smilgin-Humpreys S, Bass C. Chronic idiopathic constipation: a psychological enquiry. *Euro J Gastroenterol Hepatol* 2001: **13**: 39-44
12 **Drossman DA,** Creed FH, Olden KW, Svedlund J, Toner BB, Witehead WE. Psychosocial aspects of the functional gastrointestinal disorders. In: The functional gastrointestinal disorders. Ed.: Drossman DA, Corazziari E, Talley N, Thompson WG, *Whitehead WE* 2000: 165-166
13 **Cobb S.** Social support as a moderator of life events. *Psychosom Med* 1976; **38**: 300-314
14 **Lazarus RS,** Folkman S. Stress, appraisal and coping. *New York: Springer* 1984
15 **Penley JA,** Tomaka J, Wiebe JS. The association of coping to physical and psychological health outcomes: a meta-analytic review. *J Behav Med* 2002; **25**: 551-603
16 **Drossman DA,** Thompson WG, Talley NJ, Funch-Jenesn P, Jansens J, Whitehead WE. Rome II. multinational consensus document on functional gastrointestinal disorders. *Gut* 1999; **45**(Suppl 2): II1-1181
17 **Chaussade S,** Khyari A, Roche H, Garret M, Gaudric M, Couturier D, Guerre J. Determination of total and segmental colonic transit time in constipated patients. Results in 91 patients with a new simplified method. *Dig Dis Sci* 1989; **34**: 1168-1172
18 **Metcalf AM,** Phillips SF, Zinsmeister AR, MacCarty RL, Beart RW, Wolff BG. Simplified assessment of segmental colonic transit. *Gastroenterology* 1987; **92**: 40-47
19 **Whitehead WE,** Schuster MM. Anorectal physiology and pathophysiology. *Am J Gastroenterol* 1987; **82**: 487-497
20 **Bloom PM,** Brady JP. An ipsative validation of the multiple affect adjective check list. *J Clin Psychol* 1968; **24**: 45-46
21 **Miller S,** Managan C. The interacting effects of information and coping style in adapting to gynecologic stress: should the doctors tell all? *J Pers Soc Psychol* 1983; **54**: 224-236
22 **Cheng C,** Hui W, Lam S. Perceptual style and behavioral pattern of individuals with functional gastrointestinal disorders. *Health Psychol* 2000; **19**: 146-154
23 **Ware E,** Sherbourne CD, The MOS 36-item Short-From Health Survey (SF-36). I. Conceptual Framework and item selection. Med Care 30 [1992], pp. 473-481
24 **Ware E.** SF-36 Health Survey Manual and interpretation guide, The Medical Outcomes Trust, Boston, 1993
25 **Davey GC,** Tallis F, Hodgson S. The relationship between information-seeking and information-avoiding coping styles and the reporting of psychological and physical symptoms. *J Psychosom Res* 1993; **37**: 333-344
26 **Lerman C,** Rimer B, Blumberg B, Cristinzio S, Engstrom PF, MacElwee N, O'Connor K, Seay J. Effects of coping style and relaxation on cancer chemotherapy side effects and emotional responses. *Cancer Nurs* 1990; **13**: 308-315
27 **McFarlane AH,** Norman GR, Streiner DL, Roy R, Scott DJ. A longitudinal study of the influence of the psychosocial environment on health status: a preliminary report. *J Health Soc Behav* 1980; **21**: 124-133
28 **Gellis ZD.** Coping with occupational stress in healthcare: A comparison of social workers and nurses. *Administration Social Work* 2002; **26**: 37-52
29 **Cheng C,** Hui WM, Lam SK. Coping style of individuals with functional dyspepsia. *Psychosom Med* 1999; **61**: 789-795
30 **Anderson PO,** Bloom SR, Jarhuet J. Colonic motor and vascular responses to pelvic nerve stimulation and their relation to local peptide release in the cat. *J Physiol* 1983: **334**: 293-307

Science Editor Guo SY **Language Editor** Elsevier HK

PO Box 2345, Beijing 100023, China
www.wjgnet.com
wjg@wjgnet.com

ELSEVIER

World J Gastroenterol 2005;11(34):5367-5372
World Journal of Gastroenterology ISSN 1007-9327
© 2005 The WJG Press and Elsevier Inc. All rights reserved.

• *BRIEF REPORTS* •

Esophagectomy for locally advanced esophageal cancer, followed by chemoradiotherapy and adjuvant chemotherapy

Hung-Chang Liu, Shih-Kai Hung, Charn-Jer Huang, Chung-Chu Chen, Ming-Jen Chen, Chun-Chao Chang, Cheng-Jeng Tai, Chi-Yuan Tzen, Li-Hua Lu, Yu-Jen Chen

Hung-Chang Liu, Shih-Kai Hung, Charn-Jer Huang, Chung-Chu Chen, Ming-Jen Chen, Chi-Yuan Tzen, Li-Hua Lu, Yu-Jen Chen, Departments of Thoracic Surgery, Radiation Oncology, Gastroenterology, and Pathology, Mackay Memorial Hospital, Taipei, Taiwan, China
Hung-Chang Liu, Chun-Chao Chang, Cheng-Jeng Tai, Taipei Medical University Hospital, Taipei, Taiwan, China
Hung-Chang Liu, Mackay Junior College of Nursing, Taipei, Taiwan
Correspondence to: Dr. Yu-Jen Chen, Department of Radiation Oncology, Mackay Memorial Hospital, 92 Chung San North Road, Section 2, Taipei 104, Taiwan, China. chenmdphd@yahoo.com
Telephone: +886-2-28094661 Fax: +886-2-28096180
Received: 2004-12-29 Accepted: 2005-02-28

Abstract

AIM: To compare the efficacy and toxicity of a three-step combination therapy with post-operative radiation alone for locally advanced esophageal cancer.

METHODS: Patients with T3-4 and N0-1 esophageal carcinoma from a number of institutions were non-randomly, prospectively enrolled in the study. All patients underwent single-stage curative en bloc esophagectomy. The patients were then assigned into one of two treatment groups based on treatment consisting of either post-operative concurrent chemoradiotherapy (CCRT) with weekly cisplatin 30 mg/m^2 followed by systemic adjuvant chemotherapy (four monthly cycles of cisplatin 20 mg/m^2 and 5-fluorouracil 1 000 mg/m^2 for five consecutive days), or, post-operative radiation alone. The radiotherapy dose was 55-60 Gy for all patients. Primary end-point of this study was to assess the per-protocol patients' improvement of overall survival benefit. Secondary end-point was designed to evaluate both the per-protocol and intent-to-treat patients' outcome of survival.

RESULTS: A total of 60 patients (n = 30 per group) were enrolled in this study. The two groups were generally comparable for demographic characteristics and hematological and non-hematological toxicities. The CCRT with weekly cisplatin was well tolerated, with significantly better overall survival (30.9 mo *vs* 20.7 mo; 95% CI, 27.5-36.4 *vs* 15.2-26.1) and 3-year survival (70.0% *vs* 33.7%; P = 0.003). Low histological grade of tumor (P<0.001) was associated with favorable survival in these locally advanced patients.

CONCLUSION: For locally advanced esophageal cancer, the combination of esophagectomy, post-operative CCRT with weekly cisplatin and systemic adjuvant chemotherapy is well tolerated and effective. A large-scale, prospective randomized trial of this regimen is in progress.

© 2005 The WJG Press and Elsevier Inc. All rights reserved.

Key words: Curative esophagectomy; Concurrent chemoradiotherapy; Cisplatin

Liu HC, Hung SK, Huang CJ, Chen CC, Chen MJ, Chang CC, Tai CJ, Tzen CY, Lu LH, Chen YJ. Esophagectomy for locally advanced esophageal cancer followed by chemoradiotherapy and adjuvant chemotherapy. *World J Gastroenterol* 2005; 11(34): 5367-5372
http://www.wjgnet.com/1007-9327/11/5367.asp

INTRODUCTION

Carcinoma of the esophagus often presents at a locally advanced stage. Even with aggressive surgical resection, however, the reported long-term survival rates remain sub-optimal[1]. From analysis of surgical specimens, it appears that a significant proportion of this disease involves regional lymph nodes[2]. In one inter-group comparison report, the local recurrence rate for complete resection was 31%, and the overall local failure rate was 61%[3]. Besides local recurrence, distant metastases of esophageal cancer are another common type of treatment failure.

Several studies have demonstrated that, compared with single modality treatment, a combination of chemotherapy and/or radiotherapy with surgery can improve local control and reduce distant metastases[4-9]. Although post-operative concurrent chemoradiotherapy (CCRT) is reportedly beneficial in terms of outcome in locally advanced diseases such as cervical[10], nasopharyngeal[11], gastric[12], and colorectal[13,14] cancer, by 1998, the role of this type of treatment in post-operative esophageal cancer remains controversial.

An important concern in multi-modal therapy is the greater prevalence of treatment-related complications. Previous CCRT trials for esophageal cancer were hospital-based and used moderate-high doses of cisplatin and 5-fluorouracil (5-FU) every 3-4 wk during the radiation course. This clinical experience shows that many people are unable to tolerate CCRT, especially after surgery[8,15]. It is important, therefore, to develop an effective but less-toxic CCRT regimen for these patients. In this study, we conducted a non-randomized, prospective, preliminary trial to evaluate the efficacy, toxicity and tolerance of a

postoperative CCRT regimen, using weekly cisplatin as a radiosensitizer. The subsequent systemic adjuvant chemotherapy was also included in this multi-modal treatment strategy to achieve systemic control.

MATERIALS AND METHODS

Study design and subjects

Between July 1999 and June 2002, patients with T3 to operable T4, N0/N1, and M0 thoracic esophageal cancer (TNM system[16]), were prospectively enrolled. Patients with adenocarcinoma of the esophagus were excluded from this study. Experienced pathologists diagnosed all the cancers as squamous cell carcinoma. None of the patients had any prior treatment for their cancer. Written informed consent was obtained from each subject, and the study protocol was reviewed and approved by the institutional review board of studying institutes.

Pre-treatment evaluation included a complete history, physical examination, assessment of ECOG performance status, serum chemistry profile and complete blood cell count, chest radiography, echocardiogram, endoscopy with biopsy, esophagogram with barium enhancement, endoscopic ultrasound, computer tomography, and abdominal ultrasonography. All patients were informed with respect to the differences between the two arms of treatment prior to surgery. This briefing included consideration of adjuvant therapy for the very probable advanced status, the benefits of adjuvant therapy, and unpredictable benefits or side effects from chemotherapy during CCRT. The patients were then non-randomly assigned to a treatment group by a central coordinated office composed with a multi-disciplinary team including chest surgeons, radiation oncologists, medical oncologists, gastroenterologists, and nutritionists after their eligibility was established. Patients were assigned to a treatment group. Grouping was done by cross-referencing.

Surgical intervention

The surgical procedures generally consisted of right-sided thoracotomy for en bloc esophagectomy followed by abdominal and left cervical approach for reconstruction of the esophagus using proximal gastrectomy and gastroesophagostomy via the extrapleural retrosternal route. En bloc resection defined sub-total resection of the esophagus along with bilateral 10-cm margin adjacent soft tissue, including all tissue behind superior vena cava, pericardium, and inferior vena cava, medial to aorta and azygous vein, and in front of the spine. For the upper third tumors, lowest 4-cm margin was accepted in order for later reconstruction. Abdominal dissection included removal of proximal one-third of the stomach, greater omentum, lymph nodes in the porta hepatic around the celiac axis, and retro-peritoneal lymph node-bearing tissue. Only sampling of cervical lymph nodes was done for all patients. All patients underwent remedial resection with a margin negative for malignant cells. Feeding jejunostomy and subclavian venous-access catheters were placed in all patients, as needed, for post-operative nutrition support and replacement of oral drug administration, respectively. All consenting patients were eligible for study if: ECOG performance status<2; serum albumin $\geqslant$30 g/L; serum creatinine level<15 mg/dL; absolute neutrophil count $\geqslant$2 000 cells/μL; and platelet count>10 000/μL. Patients who did not fulfill these criteria were excluded from the study.

Treatment protocol

Adjuvant therapy, consisting of either CCRT or radiotherapy (RT) alone, was begun 2-3 wk after surgery. RT for both groups was delivered by linear accelerator (Clinac® 1800; Varian Associates, Inc, CA) at 6 MV at 320 cGy/min. The initial 40 Gy dose was administered using a conventional appositional two-way technique, followed by a boost of 15-20 Gy using a 3D conformal treatment planning system (Clinac® 600C; Varian Associates Inc, CA). RT was delivered at 1.8 Gy/day for five consecutive days in a given week. Patients lay supine on a customized alpha cradle, with the tumor volume and surrounding nodes included within the RT field with longitudinal and lateral margins of 5 and 3 cm, respectively. The spinal cord dose was limited to 45 Gy.

In addition to RT, the CCRT group received concurrent chemotherapy consisting of six weekly doses of cisplatin (CDDP) (30 mg/m^2 intravenous injection over 2 h, with adequate hydration, mannitol and anti-emetic drugs) completed approximately 1 h prior to RT in the outpatient department. Adjuvant chemotherapy consisted of four monthly cycles of CDDP (20 mg/m^2 per d) plus 5-FU (1 000 mg/m^2 per d) for five consecutive days, beginning 3-4 wk after completion of CCRT. CDDP was administered as a bolus over 30 min, simultaneously started with the 5-FU continuously infused over 16 h, with adequate hydration and anti-emetic drugs.

Dose modification

Toxicity was evaluated using the common toxicity criteria published by the National Cancer Institute[17]. Both CDDP and 5-FU were held if the absolute neutrophil count was <1 500 cells/μL or the platelet count was <75 000 cells/μL. Both chemotherapeutic agents were given at 70% of the initial dose, if the neutrophils were 1 500-2 000 cells/μL or platelets were 75 000-100 000 cells/μL. RT was held only if the neutrophil level was <1 000 cells/μL or platelets were <50 000 cells/μL. For grades 3 and 4 oropharyngeal mucositis or diarrhea, the 5-FU was held until the symptoms improved. It was then restarted at 70% of the initial dose. For grades 3 and 4 renal toxicity, CDDP was held until the creatinine was <1.5 mg/dL. It was administered at 70% of the initial dose thereafter.

Patient follow-up and patterns of failure

Patients were assessed at 3, 6 and 12 mo, and then every 6-12 mo thereafter or more often, if clinically indicated. Evaluation included clinical examination, chest radiography, computed tomography, esophagography, abdominal sonography, bronchoscopy, and nuclear whole-body bone scan. Survival was calculated from the date of surgery to the most recent follow-up contact or to the date of death. The pattern of failure was defined according to the first site of failure evidenced by follow-up examination. Local failure included recurrence of the primary tumor or metastasis to regional lymph nodes. Distant failure included metastasis to any site beyond the primary tumor and regional

lymph nodes. After recurrence, the patients received any salvage therapy that was considered useful.

Statistical analysis

The two treatment groups were compared with respect to base-line characteristics, with the *t*-test and the χ^2 test used for continuous and categorical variables, respectively. Primary end-point was to assess the per-protocol patients' improvement of overall survival benefit. Secondary end-point was designed to evaluate both the per-protocol and intent-to-treat patients' outcome of survival. Estimation of sample size for each group was performed on the basis to detect an improvement in survival over a baseline survival rate (in literatures, about 10-15% in RT group) according to the investigation reported by Freedman[18]. The Kaplan-Meier method was used for the survival analysis[19]. Differences between survival curves were determined using the log-rank test[20]. The Cox multivariate proportional hazards model was utilized for simultaneous analysis to determine the effect of multiple factors on survival, with applying possible covariates from univariate analysis to the multivariate regression. Factors tested for univariate analysis included were performance status, tumor size, tumor location, disease stage, histological features and treatment group. SPSS 10.0 software (SPSS Inc., Chicago) was used for analysis of all the data. Statistical significance was assumed where $P<0.05$.

RESULTS

Patient characteristics

The sample population of 60 patients was evenly divided between the CCRT and RT groups. The most frequent symptom at diagnosis, present in over 90% of individuals, was dysphagia. Other common symptoms included weight loss, vomiting, choking with cough, and chest pain (demographic characteristics presented in Table 1). Both groups of patients received operation for resection of their tumor. Most of them were uneventful during the peri-operative course, except 7 patients had post-operative cervical anastomotic leakage, 4 in CCRT group and 3 in RT group.

Treatment outcome

Median patient follow-up at the commencement of the analysis was 18.0 mo (range 4-40). Patients in the CCRT arm received 5 580-5 940 cGy (mean 5 880 cGy). Of these 30 patients, 15 completed a full course of CDDP during the RT course, 10 had four weekly cycles of full dose CDDP, and 5 had less than four cycles of reduced-dose CDDP. All patients in the CCRT group received the planned dose of RT. After the CCRT, 15 of 30 patients completed the full course of adjuvant chemotherapy, while the others received less than four cycles at a reduced dose. The mean survival for these patients was 31.9 mo, with an estimated 3-year overall survival of 70.0%, and only nine deaths. Local regional failure occurred in 40% of the group and distant metastases in 27%.

Patients in the RT arm received 5 040-5 940 cGy of radiation (mean 5 832 cGy). Twenty-four of 30 patients received the full dose. Six patients went without full planned radiation due to poor tolerance (3/6), minor anastomotic leakage (2/6), and thoracotomy wound disruption (1/6). Mean survival time for the RT group was 20.7 mo, with a median of 11.0 mo for this arm, and 38.0 mo for those still alive at the end of the study period. The estimated 3-year overall survival was 33.7%. Local regional failure occurred in 60% of the group, and distant metastases in 57% (Table 2). The cause of death for all patients after surgery and the metastatic sites are presented in Table 3. A statistically significant difference was demonstrated comparing group survival times ($P = 0.003$, Figure 1).

Variance analysis

Multivariate factor analysis for overall survival revealed that CCRT treatment and tumor cell differentiation were significant predictors (Table 4). Significant and favorable factors for overall survival included CCRT treatment ($P = 0.003$, Figure 1A) and moderate-well differentiation ($P<0.001$, Figure 1B).

Complications and toxicity

The most prevalent treatment-related complications for the subjects were stricture over anastomosis (36%), chronic aspiration (33%), and pneumonia (20%). There were no CCRT-related deaths during treatment, or CT-related deaths during adjuvant chemotherapy administration. Six of the 30 CCRT patients had grade 3 hematological toxicity during

Table 1 Characteristics of patients

Characteristics	CCRT[1] *n* (%)	RT alone[1] *n* (%)
Gender		
Male	30 (100)	27 (90)
Female	0 (0)	3 (10)
Mean age±SD (yr)	59.9±10.0	62.2±6.7
ECOG performance status		
0	18 (60.0)	18 (60.0)
1	11 (36.7)	10 (33.3)
2	1 (3.3)	2 (6.7)
Tumor size±SD (cm)	3.7±1.0 (2.0–5.0)	4.5±0.96 (2.0–6.0)
Location of tumor		
Upper-third	7 (23.3)	2 (6.7)
Middle-third	19 (63.3)	22 (73.3)
Lower-third	4 (13.3)	6 (20.0)
Mean radiation dosage±SD (cGy)	5 880±98	5 832±274
Histologic classification		
Well differentiated	9 (30.0)	7 (23.3)
Moderately differentiated	9 (30.0)	10 (33.3)
Poorly differentiated	12 (40.0)	13 (43.3)
Pathological disease staging		
T3N0	11 (36.7)	11 (36.7)
T3N1	4 (13.3)	6 (20.0)
T4N0-1	15 (50.0)	13 (33.3)
T stage		
T3	15 (50.0)	17 (56.7)
T4	15 (50.0)	13 (43.3)
N stage		
N0	22 (73.3)	19 (63.3)
N1	8 (26.7)	11 (36.7)

[1]All items have been calculated with no significant difference between treatment groups with *t*-test for continuous variables and χ^2 test for categorical variables. CCRT: Surgery plus concurrent chemoradiotherapy. RT alone: Surgery plus radiotherapy alone.

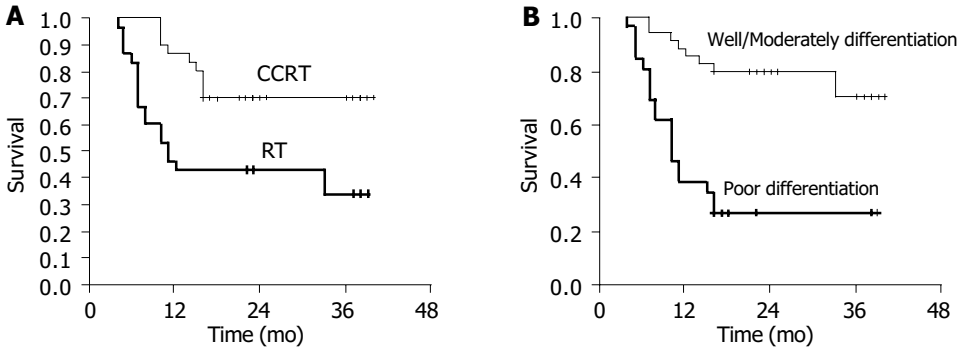


Figure 1 Kaplan–Meier curves for overall survival as a function of treatment group. *P* value is 0.003 (**A**); Kaplan-Meier curves for overall survival as a function of squamous cell differentiation state (**B**).

adjuvant chemotherapy, which required treatment modification. In the RT group, there were two treatment-related deaths secondary to upper gastrointestinal bleeding from ulcers. These two patients had grade 3 hematological toxicity, at the time of upper gastrointestinal bleeding. Renal toxicity was less than grade 2 in both groups. The most prevalent of the non-hematological toxic effects were nausea, dermatitis and esophagitis, with the rates comparable for the two groups (Table 5).

DISCUSSION

In comparison to surgery followed by RT alone, surgery with CCRT was associated with longer survival and higher 3-year survival rate. This not only corresponds with the findings of previous non-surgical randomized trials[7,8], but it is also in line with the outcome reported for post-operative combined modality treatment[4,5,15,21]. Most of our patients receiving CCRT had promising outcomes accompanied with acceptable and tolerable toxicity.

In the past, the overall 3-year reported survival rate for esophageal cancer remained below 35%, despite treatment with aggressive resection alone[15,22,23]. The outcome of locally advanced esophageal cancer is even less favorable, however, with no survivors from two samples of patients with either residual microscopic or macroscopic disease with single-modality treatment at 5 years[24-26]. In the study of

Table 2 Treatment outcome

	CCRT (*n* = 30, %)	RT alone (*n* = 30, %)
3-yr survival	70.0	33.7
Local recurrence	40.0	60.0
Distant metastasis	27.0	57.0

Table 3 Status after surgery and causes of death

	CCRT (*n* = 30)	RT alone (*n* = 30)
Alive at last follow-up	21	11
Metastasis		
Lymph nodes	14	13
Regional	12	7[1]
Distant	2	9
Lung	3	3
Liver	1	3
Bone	2	2
Causes of death	9	19
Esophageal cancer	7	12
Pneumonia	0	2
Cardiovascular disease	1	2
Gastrointestinal bleeding	1	2
Hepatic failure	0	1

[1]Three patients had both regional and distant nodal metastases.

Table 4 Cox multivariate analysis

Characteristics	Patient number	*P*	Hazard ratio (95% CI)
Adjuvant therapy			
RT *vs*	30	<0.001	5.83 (2.36–14.43)
CCRT	30		
Cell differentiation			
Poor *vs*	25	0.001	5.88 (2.08–16.93)
Well / moderate	35		
Tumor size			
≤4.1 cm *vs*	30	0.058	2.68 (0.97–7.43)
>4.1 cm	30		
Age (yr)			
≤61.7 yr *vs*	28	0.480	1.34 (0.60–2.99)
>61.7 yr	32		
Nodal status			
Yes *vs*	41	0.060	2.71 (1.00–7.38)
No	19		
T status			
T4 *vs*	28	0.532	1.47 (0.44–4.92)
T3	32		

CI: confidence interval.

Table 5 Toxicity assessment

	CTC grades CCRT / RT				
	0	1	2	3	4
Renal toxicity	21 / 26	9 / 4	0 / 0	0 / 0	0 / 0
Anemia	21 / 19	3 / 6	1 / 2	5 / 3	0 / 0
Leukopenia	20 / 23	5 / 5	5 / 2	0 / 0	0 / 0
Thrombocytopenia	25 / 26	0 / 0	4 / 2	1 / 2	0 / 0
Nausea, vomiting	3 / 6	14 / 14	12 / 10	0 / 0	0 / 0
Esophagitis / mucositis	10 / 15	15 / 8	5 / 7	0 / 0	0 / 0
Dermatitis	9 / 14	13 / 11	8 / 5	0 / 0	0 / 0
Pneumonitis	25 / 22	5 / 7	0 / 1	0 / 0	0 / 0
Stenosis	24 / 20	6 / 10	0 / 0	0 / 0	0 / 0

Sun *et al*., 44.5% of their patients had regional lymph-node involvement at the time of surgery. As to the treatment of esophageal cancer, a recent report with a systemic review and meta-analysis investigating the impact of neoadjuvant or adjuvant therapy on resectable thoracic esophageal cancer concluded that only surgery could remain the standard[23]. However, a few investigators have reported that adjuvant therapy may be beneficial after resection[4,5,15]. The role of chemotherapy and radiotherapy for locally advanced esophageal cancer still needs to be assessed. Teniere *et al*., have reported that post-operative RT improved local control in their sample, although it did not increase survival[27]. Rice[15] and Saito[21] have reported a significant survival advantage with adjuvant CCRT compared to adjuvant RT. This is in line with our results, where weekly CCRT followed by adjuvant chemotherapy resulted in a better 3-year survival than adjuvant RT alone.

The efficacy of adjuvant chemotherapy has been tested in this investigation because the principal cause of death from esophageal cancer is widespread dissemination. Although the Japanese Esophageal Oncology Group found no survival benefit from two cycles of adjuvant chemotherapy containing cisplatin and vindesine in their 1993 study[28], several years later they reported that two cycles of cisplatin and 5-FU after curative resection improved survival and decreased the incidence of distant and regional-node metastasis[29]. In the current study, four cycles of adjuvant chemotherapy were added to CDDP and 5-FU because the low weekly dose of CDDP during CCRT was included for its local radio-sensitizing effect rather than as systemic therapy. As only 27% of the patients in this arm of the study subsequently developed distant metastases compared to 57% in the RT arm, it seems reasonable to suggest that systemic adjuvant chemotherapy has a role in controlling distant metastasis. For the causes of death, it seemed a higher rate of non-cancer-related death in the RT groups, but most of the non-cancer-related causes were still from poor control of the tumor, local recurrence or distant metastasis. CCRT can get better control of the tumor and related death.

An important concern in CCRT is treatment toxicity. Although combined modality therapy improves outcome, it was reported to be associated with a higher incidence of toxicity. Coia *et al*., have reported a 56% incidence of moderate-severe acute toxicity with combined treatment[30]. Further, Herskovic *et al*., found that CCRT-treated patients had a higher incidence of acute grade 3 (44% *vs* 25%) and acute grade 4 toxicities (20% *vs* 3%) compared with RT alone[7], with only 50% of their sample completing all four cycles of chemotherapy. It may be that the concurrent use of 5-FU and RT in those studies caused significant mucositis and myelosuppression. To reduce toxicity while preserving the radiosensitizing effect of chemotherapy, we excluded 5-FU from the CCRT regimen and used low-dose cisplatin instead. Cisplatin is considered one of the agents most active against esophageal cancer, with single-agent response rate consistently 20% or more[31]. Most of our patients were able to tolerate this regimen during CCRT, with over 80% receiving more than four doses of weekly CDDP during radiotherapy and half tolerating a full course of adjuvant chemotherapy. The only grade 3 or 4 toxicity that occurred was hematological, however, it only affected relatively few patients (20% and 17% in the CCRT and RT group, respectively). Nausea, dermatitis and mucositis of the mouth, pharynx and esophagus were common, but tolerable and reversed after supportive care. Significant renal toxicity was not noted.

To our knowledge, there were no randomized reports that explored the effects and toxicity of post-operative CCRT. One pitfall of the current study is some of the patients receiving adjusted dosage of adjuvant therapy. However, it was for the safety of the patients. From the review of articles, we learned that uniform adjuvant treatments without individualized adjustment would sometimes do harm for patients[23]. Besides, another drawback of current study was non-randomized comparison. Some potential and unmeasured factors that might have influenced patient selection were subjective ones, such as vigor, mental status, ability to cooperate with and consent to treatment protocols, referral and physician bias, and the unblended nature of the treatments. During the process of grouping, our central office had attempted to assign patients through cross-referencing method to avoid selection bias as much as possible. In conclusion, this trial implies the result of superior outcome and reduced toxicity with this combination regimen. Another large-scale randomized, double-blinded clinical trial is in progress to verify the results of this study.

REFERENCES

1 **Salazar JD,** Doty JR, Lin JW, Dyke MC, Roberts J, Heitmiller ES, Heitmiller RF. Does cell type influence post esophagectomy survival in patients with esophageal cancer? *Dis Esophageal* 1998; **11**: 68–71

2 **Frunberger L,** Kraus B, Dworak O. Distribution of lymph nodes and lymph node metastasis in esophageal carcinoma. *Zentealbl Chir* 1996; **121**: 102–105

3 **Kelsen DP,** Ginsberg R, Pajak TF, Sheahan DG, Gunderson L, Mortimer J, Estes N, Haller DG, Ajani J, Kocha W, Minsky BD, Roth JA. Chemotherapy followed by surgery compared with surgery alone for localized esophageal cancer. *N Engl J Med* 1998; **339**: 1979–1984

4 **Ebie N,** Kang HJ, Millikan K, Murthy AK, Griem K, Hartsell W, Recine DC, Doolas A, Taylor S 4th. Integration of surgery in multimodality therapy for esophageal cancer. *Am J Clin Oncol* 1997; **20**: 11–15

5 **Bedard EL,** Inculet RI, Malthaner RA, Brecevic M, Dar R. The role of surgery and postoperative chemoradiation therapy in patients with lymph node positive esophageal carcinoma. *Cancer* 2001; **91**: 2423–2430

6 **Bosset JF,** Gignoux M, Triboulet JP, Tiret E, Mantion G, Elias D, Lozach P, Ollier JC, Pavy JJ, Mercier M, Sahmoud T. Chemoradiotherapy followed with surgery alone in squamous-cell cancer of the esophagus. *N Eng J Med* 1997; **337**: 161–167

7 **Herskovic A,** Martz K, Al-Sarraf M, Leichman L, Brindle J, Vaitkevicius V, Cooper J, Byhardt R, Davis L, Emami B. Combined chemotherapy and radiotherapy compared with radiotherapy alone in patients with cancer of the esophagus. *N Engl J Med* 1992; **326**: 1593–1598

8 **Al-Sarraf M,** Martz K, Herskovic A, Leichman L, Brindle J, Vaitkevicius V, Cooper J, Byhardt R, Davis L, Emami B. Progress report of combined chemoradiotherapy versus radiotherapy alone in patients with esophageal cancer. *J Clin Oncol* 1997; **15**: 277–284

9 **Kavanagh B,** Anscher M, Leopold K, Deutsch M, Gaydica E, Dodge R, Allen K, Allen D, Staub W, Montana G. Pattern of failure following combined modality therapy for esophageal

cancer. *Int J Radiat Oncol Biol Phys* 1992; **24**: 633–642
10 **Rose PG,** Bundy BN, Watkins EB, Thigpen JT, Deppe G, Maiman MA, Clarke-Pearson DL, Insalaco S. Concurrent cisplatin based radiotherapy and chemotherapy for locally advanced cervical cancer. *N Engl J Med* 1999; **340**: 1144–1153
11 **al-Sarraf M,** Pajak TF, Cooper JS, Mohiuddin M, Herskovic A, Ager PJ. Chemo-radiotherapy in patients with locally advanced nasopharyngeal carcinoma: a radiation therapy oncology group study. *J Clin Oncol* 1990; **8**: 1342–1351
12 **Macdonald JS,** Smalley SR, Benedetti J, Hundahl SA, Estes NC, Stemmermann GN, Haller DG, Ajani JA, Gunderson LL, Jessup JM, Martenson JA. Chemoradiotherapy after surgery compared with surgery alone for adenocarcinoma of the stomach or gastroesophageal junction. *N Eng J Med* 2001; **345**: 725–730
13 **Moertel CG,** Fleming TR, Macdonald JS, Haller DG, Laurie JA, Goodman PJ, Ungerleider JS, Emerson WA, Tormey DC, Glick JH. Levamisole and fluorouracil for adjuvant therapy resected colon carcinoma. *N Eng J Med* 1990; **322**: 352–358
14 **Fisher B,** Wolmark N, Rockette H, Redmond C, Deutsch M, Wickerham DL, Fisher ER, Jones J, Glass A, Lerner H, Lawrence W. Postoperative adjuvant chemotherapy or radiation therapy for rectal cancer: results from NSABP protocol R-01. *J Natl Cancer Inst* 1988; **80**: 21–29
15 **Rice TW,** Adelstein DJ, Chidel MA, Rybicki LA, DeCamp MM, Murthy SC, Blackstone EH. Benefit of postoperative adjuvant chemoradiotherapy in locoregionally advanced esophageal carcinoma. *J Thorac Cardiovasc Surg* 2003; **126**: 1590–1596
16 **Greene FL,** Page DL, Fleming ID, Fritz AG, Balch CM, Haller DG, Morrow N. AJCC Cancer Staging Manual (ed 6). *New York: Springer-Verlag* 2002
17 DCTD, NCI, NIH, DHHS. Cancer Therapy Evaluation Program Common Toxicity Criteria, *Version 2.0* 1999
18 **Freedman LS.** Tables of the number of patients required in clinical trialsusing the logrank test. *Stat Med* 1982; **1**: 121-129
19 **Kaplan EL,** Meier P. Nonparametric estimation for incomplete observation. *J Am Stat Assoc* 1958; **53**: 457–481
20 **Mantle N.** Evaluation of survival data and two new rank order statistics arising in its consideration. *Cancer Chem Rep* 1966; **5**: 163–170
21 **Saito T,** Shigemitsu Y, Kinoshita T, Shimoda K, Abe T, Nakamura A, Chikuba K, Kobayashi M. Cisplatin, vindesine, pepleomycin and concurrent radiation therapy following esophagectomy with lymphadenectomy for patients with an esophageal cancer. *Oncology* 1993; **50**: 293–297
22 **Ilson DH,** Minsky BD. Chemotherapy and radiotherapy as primary treatment of esophageal cancer. In: Pearson FG, Cooper JD, Deslauriers JD, Ginsberg RJ, Hiebert CA, Patterson GA. eds. Esophageal Surgery. *2nd ed, New York, Churchill Livingston* 2002: 751–772
23 **Malthaner RA,** Wong RK, Rumble RB, Zuraw L. Members of gastrointestinal cnacer disease site group of cnacer care ontario's program in evidence-based care. Neoadjuvant or adjuvant therapy for respectable esophageal cancer: a systemic review and meta-analysis. *BMC Med* 2004; **2**: 35
24 **Ellis FH Jr.** Standard resection for cancer of the esophagus and cardia. *Surg Oncol Clin North Am* 1999; **8**: 279–294
25 **Kitajima M,** Kitagawa Y. Surgical treatment of esophageal cancer-the advent of the era of individualization. *N Eng J Med* 2002; **347**: 1705–1709
26 **Sun K,** Zhang R, Zhang D, Huang G, Wang L. Prognostic significance of lymph node metastasis in surgical resection of esophageal cancer. *Chin Med J* 1996; **121**: 102–105
27 **Teniere P,** Hay JM, Fingerhut A, Fingerhut PL. Postoperative radiation therapy dose not increase survival after curative resection for squamous cell carcinoma of the middle and lower esophagus as shown by multicenter controlled trial. *Surg Gynecol Obstet* 1991; **173**: 123–130
28 A comparison of chemotherapy and radiotherapy as adjuvant treatment to surgery for esophageal carcinoma. Japanese Esophageal Oncology Group. *Chest* 1993; **104**: 203–207
29 **Ando N,** Iizuka T, Kakegawa T, Isono K, Watanabe H, Ide H, Tanaka O, Shinoda M, Takiyama W, Arimori M, Ishida K, Tsugane S. A randomized trial of surgery with and without chemotherapy for localized squamous carcinoma of the thoracic esophagus. The Japan Clinical Oncology Group Study. *J Thorac Cardiovasc Surg* 1997; **114**: 205–209
30 **Coia LR,** Engstrom PF, Paul AR, Stafford PM, Hanks GE. Long term results of infusional 5-FU, mitomycin C, and radiation as primary management of esophageal carcinoma. *Int J Radiat Oncol Biol Phys* 1991; **20**: 29–36
31 **Leichman L,** Berry BT. Experience with cisplatin in treatment regimens for esophageal cancer. *Semin Oncol* 1991; **18**: 64–72

Science Editor Guo SY **Language Editor** Elsevier HK

PO Box 2345, Beijing 100023, China
www.wjgnet.com
wjg@wjgnet.com

ELSEVIER

World J Gastroenterol 2005;11(34):5373-5376
World Journal of Gastroenterology ISSN 1007-9327
© 2005 The WJG Press and Elsevier Inc. All rights reserved.

• *BRIEF REPORTS* •

Effect of Gui Zhi decoction on enteric mucosal immune in mice with collagen-induced arthritis

Gui-Qin Zhou, Ning Zhao, Hao Zhang, Hong-Wei Jia, Wan-Dong Zhang, Lin-Hua Zhao, Cheng Lu, Ying-Hui He, Ai-Ping Lu

Gui-Qin Zhou, Ning Zhao, Hao Zhang, Hong-Wei Jia, Wan-Dong Zhang, Lin-Hua Zhao, Cheng Lu, Ying-Hui He, Ai-Ping Lu, Institute of Basic Theory, China Academy of Traditional Chinese Medicine, Beijing 100700, China
Ai-Ping Lu, National Pharmaceutical Engineering Centre for Herbal Preparations, 347 Fuzhou Road, Nanchang 330077, Jiangxi Province, China
Supported by the project of National Natural Science Foundation of China, No. 30171133 and 39870952
Correspondence to: Ai-Ping Lu, MD, Professor, Department of Cellular Pathology, Institute of Basic Theory, China Academy of Traditional Chinese Medicine, Dongzhimen, Beijing 100700, China. lap@jzjt.com
Telephone: +86-10-64067611 Fax: +86-10-64013896
Received: 2005-01-01 Accepted: 2005-02-18

Abstract

AIM: To explore the effect of Gui Zhi decoction on enteric mucosal immune in type II collagen-induced arthritis (CIA) in DBA mice.

METHODS: Eighty DBA/1, weighing 18-22 g, were randomly divided into four groups with 20 in each group: control group, CIA group, treatment groups at high dosage and low dosage (GZH and GZL). CIA was induced by immunization with type II collagen (CII) emulsified with equal complete adjuvant at 0.1 mg CII each mouse. Blood lymphocyte suspension was screened for CD4 and CD8 expression using a flow cytometry, the CD4 and CD8 and secretory IgA (sIgA)-positive cells in enteric lamina propria tested with immunohistochemical staining. Tumor necrosis factor-alpha (TNF-α), interleukin-1 (IL-1)-β, and IL-6 concentrations in serum were assayed with RIA.

RESULTS: Gui Zhi decoction can lower the arthritic scores and decrease the occurrence of arthritis. The CD4, CD8, and sIgA-positive cells in CIA mice are less than in control mice, and in Gui Zhi decoction at high dosage could restore the lowered CD4- and CD8-positive cells in lamina propria, and at both high and low dosages could increase the lowered sIgA-positive cells in lamina propria, even still lower than in normal mice. In periphery, the CD4 cells in periphery are higher in CIA mice than in control mice, and Gui Zhi decoction at high and low dosages could decrease the CD4 and CD8 cells. Also, Gui Zhi decoction at high dosage could decrease the IL-6 and TNF-α concentration in serum.

CONCLUSION: Gui Zhi decoction can lower the arthritic scores and decrease the incidence of CIA in mice, and the mechanism is in part regulating enteric mucosal immune.

© 2005 The WJG Press and Elsevier Inc. All rights reserved.

Key words: Gui Zhi decoction; Mucosal immune; Collagen-induced arthritis

Zhou GQ, Zhao N, Zhang H, Jia HW, Zhang WD, Zhao LH, Lu C, He YH, Lu AP. Effect of Gui Zhi decoction on enteric mucosal immune in mice with collagen-induced arthritis. *World J Gastroenterol* 2005; 11(34): 5373-5376
http://www.wjgnet.com/1007-9327/11/5373.asp

INTRODUCTION

Mucosal immune system is an integrated network of tissues, lymphoid and constitutive cells and effector molecules characterized by production of secretory IgA (sIgA), Th1- and Th2-type CD_4 T-lymphocytes responses and CD_8 CTL responses. It functions through protecting the host from infection of the mucous membrane surfaces, on the other hand, it can induct tolerance to the antigen in the food, and now it has become the focus of more and more scientists[1,2].

Gui Zhi decoction is a classical herbal preparation, and functions as regulating Ying and Wei in traditional Chinese medicine. It is commonly used as one of the therapies of rheumatic arthritis and rheumatoid arthritis[3]. While how the Gui Zhi decoction works in anti-rheumatic effect and how the enteric mucosal immune is involved in the mechanism is less clarified.

Collagen-induced arthritis (CIA) is a common animal model for auto-immune disease, special for the research on rheumatoid arthritis, since its pathology and immunology is similar to that in human rheumatoid arthritis[4]. In this paper, the effect of Gui Zhi decoction on enteric immune in CIA mice was explored.

MATERIALS AND METHODS

Animals

Total 80 DBA/1 mice, male, 8-10-wk old with a mean weight of 18-22 g were purchased from Research Institute of Experimental Animals, Chinese Academy of Medical Science. Mice were randomly divided into four groups in average: control group, CIA group, treatment groups at high dosage and low dosage (GZH and GZL). Mice were housed in a temperature-, humidity- and light-controlled environment with free access to rodent chow and water. The light-dark

cycle was 12:12 h with the light phase from 06:00 a.m. to 18:00 p.m. The rodent license of the laboratory (No. SCXK11-00-0006) was issued by National Science and Technology Ministry of China.

Induction of CIA and evaluation of arthritis

Soluble pure type II collagen (CII) was from Dr. Rikard Holmdahl (Lund University, Sweden) and complete adjuvant was purchased from Sigma Corporation, USA. CIA was induced by II collagen, dissolved in 0.1 mol/L acetic acid (2 mg in 1 mL) emulsified with equal complete adjuvant and 0.1 mol/L acetic acid. Each rat in CIA group and treatment group was immunized by injection of mixture (containing 0.15 mg CII) under fur skin at the left sole of the foot. Starting from 14th d after immunization, the degree of arthritis was examined every 2 d. The severity of arthritis was represented as mean arthritic index on a 0-4 scale according to the following criteria: 0 = no edema or swelling; 1 = slight edema and erythema limited to the foot and/or ankle; 2 = slight edema and erythema from the ankle to the tarsal bone; 3 = moderate edema and erythema from the ankle to the tarsal bone; and 4 = edema and erythema from the ankle to the entire leg. Each limb was graded, and thus the maximum possible score was 16 for each animal. A rat or mice with a score of 1 or more was regarded as arthritic.

Treatment of CIA with Gui Zhi decoction

Gui Zhi decoction recipe was a classical one, and consists of Ramulus Cinnamomi, Radix Paeoniae Alba, Rhizoma Zingiberis Recens, and Fructus Jujubae at the ratio of 10:10:7:10:10. The herbal mixtures were extracted by boiling water to the concentration at 1 g/mL. The dosage in GZH was at 30 g/kg (body weight) and in GZL at 8.75 g/kg. All the agents were orally administered in a volume of 0.8 mL/mouse. The animals in normal group and CIA group were administered with the same volume of saline. The admini-strations were conducted that started from 2 wk after the immunization, once a day and lasted for 4 wk.

Immunohistochemistry

The CD4-, CD8- and sIgA-positive cells in enteric lamina propria were tested by immunohistochemical staining method with the test kits. The staining process referred to the manuals for the products. Briefly, on d 36, animals were euthanized under anesthesia, and the mid-section of small intestine were removed and fixed in 10% paraformaline, embedded in paraffin, sectioned at 5 μm, then ice acetone fixed for 10 min. The first antibodies were rabbit anti-rat antibodies, and the second antibodies were goat anti-rabbit antibodies, and the samples were stained with DAB (Sigma, USA) and counterstained with hematoxylin. The positive granules can be observed. The positive granule averages of three samples (6 scopes in each sample) from Q-win DC100 image analysis were used for further statistical analysis.

Peripheral lymphocyte preparation and flow cytometry

The blood was sampled before the animals were killed, and suspended in tubes containing 25 μL heparin (5 000 IU/mL). The erythrocytes were lyzed in a buffer containing 0.84% NH_4Cl at pH 7.4 for 3-5 min. The remaining cells were then washed twice in saline. After washing in saline, the cells were resuspended and fixed in 500 μL saline. Blood lymphocyte suspension was screened for CD4 and CD8 expression using a flow cytometry. The mAbs used for CD4 staining were R-Phycoerythrin-conjugated OX-38 (BD Biosciences Pharmingen) and CD8a staining were Peridinin Chlorophyll-a Protein-conjugated OX-8 (BD Biosciences Pharmingen). Each sample of 0.1 mL peripheral lymphocyte or PP single-cell suspension was incubated for 30 min at 4 ℃ in the dark, with a solution consisting of 6 μL 0.01 mol/L PBS and an appropriate concentration of antibodies. After washing in saline, the cells were resuspended and fixed in 500 μL saline. The cells were then analyzed on a FACSort using the CellQuest software (Becton-Dickinson).

Radioimmune assay

Tumor necrosis factor-alpha (TNF-α), IL-1β, and IL-6 concentrations in serum were assayed using mouse cytokine RIA test kits (Wuhan Boster Biotech Inc., China). The assay was performed in duplicate according to the manufacturer's recommended procedures. The results of the radioactivity count were recorded by an automatic Gamma counter (SN-695B), and expressed as mean±SE of individual rat.

Statistical analysis

Using SPSS 10.0 software, ANOVA was used to determine significance in the data set. Student-Newman-Keuls test was employed for variables between both groups when equal variances assumed and Dunnett's *t*-test for equal variances not assumed.

RESULTS

Scores and incidence changes in different groups

Figure 1A shows the changes of arthritic scores in CIA group and Gui Zhi decoction-treated groups. Figure 1B shows the changes of arthritis incidence, and there is a significant difference in CIA group and Gui Zhi decoction-treated groups. These results demonstrate that Gui Zhi decoction can significantly lower the arthritic scores and decrease the occurrence of arthritis.

Expression of CD4-, CD8- and sIgA-positive cells in enteric lamina propria

The positive expression of CD4, CD8, and sIgA were shown as brown granules in the sections. Most of CD4-positive lymphocytes and sIgA-positive cells were located in lamina propria, and majority of CD8-positive lymphocytes were located in epithelial surfaces. Table 1 shows the positive-stained granules from six scopes under microscope, which represents the numbers of CD4- and CD8-positive cells. The results demonstrate that the CD4- and CD8-positive cells in lamina propria in CIA mice are less than in control mice, and in Gui Zhi-decoction-treated mice at high dosage and they are similar to that in the control mice. The results suggest that the enteric mucosal immunity to some extent was inhibited in CIA mice, and Gui Zhi decoction at high dosage could recover the mucosal immunity.

Table 2 shows that the sIgA-positive cells in lamina

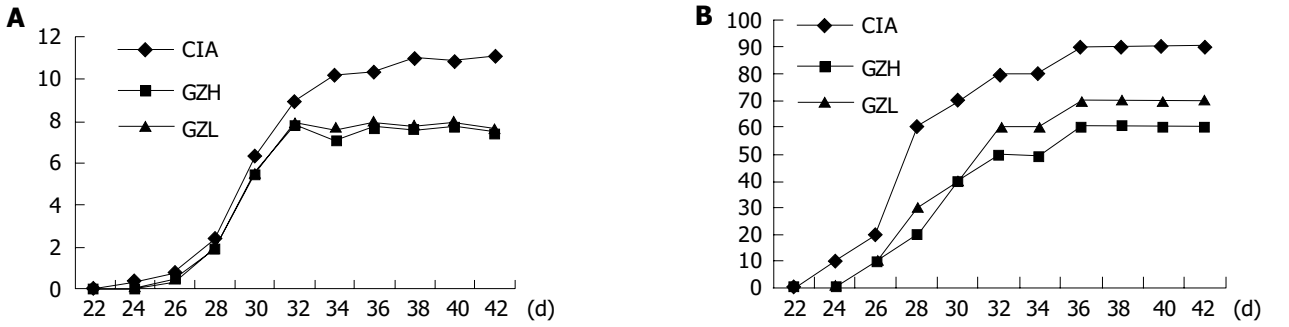


Figure 1 Arthritic scores in the different days after the immunization with CII. From the d 34 after the immunization, the arthritic scores were decreased in the mice treated with Gui Zhi decoction at both high dosage and low dosage (**A**); Incidence of CIA in different groups of mice. Gui Zhi decoction could lower the incidence of CIA (**B**).

Table 1 CD4 and CD8 cells in enteric lamina propria

Group	*n*	CD4 positive	CD8 positive
Control	20	492.7±156.7	446.5±122.5
CIA	20	337.5±101.6[a]	272.8±165.6[a]
GZH	20	491.8±58.6[c]	443.9±58.9[c]
GZL	20	410.1±131.4	338.4±131.4

[a]*P*<0.05 *vs* control; [c]*P*<0.05 *vs* CIA.

Table 2 sIgA-positive cells in lamina propria

Group	*n*	sIgA-positive cells
Control	20	607.4±203.45
CIA	20	261.5±50.29[c]
GZH	20	403.2±157.47[a,e]
GZL	20	367.8±103.4[a,e]

[a]*P*<0.05 *vs* control; [c]*P*<0.05 *vs* control; [e]*P*<0.05 *vs* CIA group.

propria in CIA mice are less than in control mice, and in Gui Zhi-decoction-treated mice they are similar to that in the control mice, but still lower than in control mice.

The results suggest that the enteric mucosal immunity was inhibited in CIA mice by showing decrease of the CD4 and CD8 cells in enteric lamina propria, and Gui Zhi decoction could recover to some extent the CD4-, CD8- and sIgA-positive cells in lamina propria, and further might recover the inhibition role of mucosal immunity.

CD4 and CD8 cells in periphery

Table 3 shows that the CD4 cells in periphery are higher in CIA mice than in control mice, the CD8 cells in CIA mice are similar to those in control mice. In the mice treated with Gui Zhi decoction at high and low dosages, CD4 and CD8 cells decrease.

Table 3 CD4 and CD8 cells in periphery

Group	*n*	CD4 (%)	CD8 (%)
Control	10	48.24±5.071	13.84±2.17
CIA	10	56.86±3.817[b]	12.59±1.74
GZH	10	41.11±3.886[d]	8.75±2.259[d]
GZL	10	43.33±6.046[d]	9.968±2.2

[b]*P*<0.01 *vs* control; [d]*P*<0.01 *vs* CIA group.

Changes of IL-6, IL-1β, and TNF-α in serum

Table 4 shows that the IL-6, IL-1β, and TNF-α concentrations are higher in CIA mice than in control mice, and after being treated with Gui Zhi decoction at high dosage, the IL-6 and TNF-α concentration decrease comparing to the concentrations in CIA mice.

Table 4 Changes of IL-6, IL-1β, and TNF-α in serum

Group	*n*	IL-6 (ng/mL)	IL-1β (ng/mL)	TNF-α (fmol/mL)
Control	10	0.331±0.027	0.133±0.048	6.528±0.991
CIA	10	0.432±0.064[b]	0.206±0.034[b]	7.835±0.992[b]
GZH	10	0.333±0.033[d]	0.150±0.027	6.383±1.301[d]
GZL	10	0.423±0.081	0.177±0.060	6.592±0.500

[b]*P*<0.01 *vs* control; [d]*P*<0.01 *vs* CIA.

DISCUSSION

Lymphoid tissue in the human body is associated with the mucosal system. Mucosa-associated lymphoid tissue includes gut-associated lymphoid tissue, bronchial/tracheal-associated lymphoid tissue, nose-associated lymphoid tissue, and vulvovaginal-associated lymphoid tissue, as the first barrier of the human body, protects the body from antigens entering along mucosal surfaces[5]. Functional disturbance of mucosal system may lead to autoimmune diseases or downregulation of immune function[6,7], which has some similarity with the function of "Ying and Wei" in traditional Chinese medicine.

The gastrointestinal mucosa is a vast interface between the body and the environment; it is the main entry site for many environmental antigens. The influx of multiple antigens through the gastrointestinal mucosa usually results in tolerance. High-dose tolerance is due to T cell deletion or anergy, whereas low-dose tolerance involves activation of TGF-β producing Th2 or Th3 cells. This intolerance effect has been used to try to induce oral tolerance. For instance, pre-treatment with oral bovine type II collagen has proved capable of modulating several models of experimental polyarthritis. Arthritis severity was considerably reduced[8]. Nasal admin istration of 10 μg of CII 15 times had the most prominent suppressive effects, reducing disease incidence by 50% and inhibiting both CII-specific IgG antibody and DTH responses[9].

The enteric immune cells could be considered to be the

effector cells in regarding to deal with food antigen, and also would be the inducer cells with regard to tolerance induction. However, what about the change of enteric immune in autoimmune is not well known. Our group reported a primary result on how Gui Zhi decoction affects on the numbers of enteric mucosal lamina propria CD4-, CD8- and sIgA-positive cells[10,11], and the results suggest that the enteric mucosal immune might involve the pathway of CIA in mice.

In this paper, the results show that Gui Zhi decoction can significantly lower the arthritic scores and decrease the occurrence of arthritis. The CD4 cells in periphery are higher in CIA mice than in control mice, and the results are similar to the previous study. In the mice treated with Gui Zhi decoction at high and low dosages, CD4 and CD8 cells in periphery decrease. The CD4- and CD8-positive cells in enteric lamina propria in CIA mice are less than in control mice, and in Gui Zhi-decoction-treated mice at high dosage they are similar to that in the control mice. The sIgA-positive cells in lamina propria in CIA mice are less than in control mice, and in Gui Zhi-decoction-treated mice they are similar to that in the control mice, but still lower than in control mice, suggesting that the enteric mucosal immunity to some extent was inhibited in CIA mice. The results suggest that the enteric mucosal immunity was inhibited in CIA mice by showing the decrease of the CD4 and CD8 cells in enteric lamina propria, and Gui Zhi decoction could recover to some extent the CD4-, CD8- and sIgA-positive cells in lamina propria, and further might recover the inhibition role of mucosal immunity.

The onset of arthritis in IL-6-/- mice was delayed for 2 wk compared with that in IL-6+/+ mice, and the severity of arthritis, as indicated by the arthritis score, remained significantly lower in IL-6-/- mice during the entire follow-up period (14 wk), although all IL-6-/- mice developed definite arthritis as did the IL-6+/+ mice. These findings suggest that blockade of IL-6 might be beneficial in the treatment of RA[12-14]. IL-1 and TNF-α play dominant roles in mediating the progression of many inflammatory joint diseases, including rheumatoid arthritis in humans, CIA in mice and rats, and adjuvant arthritis in rats. Treating autoimmune arthritic diseases with combinations of anti-IL-1 and anti-TNF molecules will achieve superior efficacy compared to the use of a single class of anti-cytokine agent and may allow for dose reductions that could prove useful in minimizing potential side effects[15]. In this paper, the results show that the IL-6, IL-1β, and TNF-α concentrations are higher in CIA mice than in control mice, and after being treated with Gui Zhi decoction at high dosage, the IL-6 and TNF-α concentration decrease comparing to the concentrations in CIA mice.

In conclusion, Gui Zhi decoction could lower the arthritic scores, and regulate the enteric mucosal immune, and the results indicate that the enteric mucosal immune might involve in the pathogenesis of CIA, and also it might be an important target for anti-rheumatic therapy. However, more detailed studies on how enteric mucosal immune are involved in the pathogenesis of CIA, and how the mucosal immune serves as a pathway for the treatment of CIA need further research works.

REFERENCES

1 **Didierlaurent A,** Sirard JC, Kraehenbuhl JP, Neutra MP. How the gut senses its content. *Cell Microbiol* 2002, **4**: 61-72
2 **Tlaskalova-Hogenova H,** Tuckova L, Lodinova-Zadnikova R, Stepankova R, Cukrowska B, Funda DP, Striz I, Kozakova H, Trebichavsky I, Sokol D, Rehakova Z, Sinkora J, Fundova P, Horakova D, Jelinkova L, Sanchez D. Mucosal immunity: it's role in defense and allergy. *Int Arch Allergy Immunol* 2002; **128**: 77-89
3 **Lu XF.** Experimental study on the immunosuppressive effects of gui zhi tang. *Zhongxiyi Jiehe Zazhi* 1989; **9**: 283-285
4 **Trentham DE,** Townes AS, Kang AH. Autoimmunity to type II collagen: an experimental model of arthritis. *J Exp Med* 1977; **146**: 857-868
5 **Mowat AM,** Viney JL. The anatomical basis of intestinal immunity. *J Immunol Rev* 1997; **156**: 145-166
6 **Yuan Q,** Walker WA. Innate immunity of the gut: mucosal defense in health and disease. *J Pediatr Gastroenterol Nutr* 2004; **38**: 463-473
7 **Tishler M,** Caspi D, Almog Y, Segal R, Yaron M. Increased incidence of urinary tract infection in patients with rheumatoid arthritis and secondary Sjogren's syndrome. *Ann Rheum Dis* 1992; **51**: 604-606
8 **Kim WU,** Lee WK, Ryoo JW, Kim SH, Kim J, Youn J, Min SY, Bae EY, Hwang SY, Park SH, Cho CS, Park JS, Kim HY. Suppression of collagen-induced arthritis by single administration of poly (lactic-co-glycolic acid) nanoparticles entrapping type II collagen: a novel treatment strategy for induction of oral tolerance. *Arthritis Rheum* 2002; **46**: 1109-1120
9 **Higuchi K,** Kweon MN, Fujihashi K, McGhee JR, Kiyono H. Comparison of nasal and oral tolerance for the prevention of collagen induced murine arthritis. *J Rheumatol* 2000; **27**: 1038-1044
10 **Zhou GQ,** Xiao C, Zhou J. Effect of guizhi decoction on CD4+, CD8+ T-lymphocytes and SIgA in mucosal immune system in intestine of mice with Bi syndrome (collagen induced immune arthritis). *Zhongguo Zhongxiyi Jiehe Zazhi* 2004; **24**: 336-338
11 **Heel KA,** McCauley RD, Papadimitriou JM, Hall JC. Review: Peyer's patches. *J Gastroenterol Hepatol* 1997; **12**: 122-136
12 **Sasai M,** Saeki Y, Ohshima S, Nishioka K, Mima T, Tanaka T, Katada Y, Yoshizaki K, Suemura M, Kishimoto T. Delayed onset and reduced severity of collagen-induced arthritis in interleukin-6-deficient mice. *Arthritis Rheum* 1999; **42**: 1635-1643
13 **Feige U,** Hu YL, Gasser J, Campagnuolo G, Munyakazi L, Bolon B. Anti-interleukin-1 and anti-tumor necrosis factor-alpha synergistically inhibit adjuvant arthritis in Lewis rats. *Cell Mol Life Sci* 2000; **57**: 1457-1470
14 **Beagley KW,** Eldridge GH, Kiyono H, Everson MP, Koopman WJ, Honjo T, McGhee JR. Recombinant murine IL- 5 induces high rate IgA synthesis in cycling IgA- positive Peyer' s patch B cells. *J Immunol* 1988; **141**: 2035-2042
15 **Beagley KW,** Eldridge JH, Lee F, Kiyono H, Everson MP, Koopman WJ, Hirano T, Kishimoto T, McGhee JR. Interleukins and IgA synthesis. Human and murine inter leukin-6 induce high rate IgA secretion in IgA- committed B cells. *J Exp Med* 1989; **169**: 2133-2148

Science Editor Wang XL and Guo SY **Language Editor** Elsevier HK

PO Box 2345, Beijing 100023, China
www.wjgnet.com
wjg@wjgnet.com

ELSEVIER

World J Gastroenterol 2005;11(34):5377-5380
World Journal of Gastroenterology ISSN 1007-9327
© 2005 The WJG Press and Elsevier Inc. All rights reserved.

• *BRIEF REPORTS* •

Relationship between entero-hepatic bile acid circulation and interdigestive migrating myoelectrical activity in rats

Ping Fang, Lei Dong, Wei-Jin Zhang, Jin-Yan Luo

Ping Fang, Lei Dong, Jin-Yan Luo, Department of Internal Medicine, Second Hospital of Xi'an Jiaotong University, Xi'an 710004, Shaanxi Province, China
Wei-Jin Zang, Division of Cardiovascular Physiology and Pharmacology, Medical School of Xi'an Jiaotong University, Xi'an 710061, Shaanxi Province, China
Supported by National Natural Science Foundation of China, No. 30170414
Correspondence to: Professor Lei Dong, Department of Internal Medicine, Second Hospital of Xi'an Jiaotong University, Xi'an 710004, Shaanxi Province, China. pingf7613@sina.com
Telephone: +86-29-87679368
Received: 2004-10-09 Accepted: 2004-11-19

Abstract

AIM: To investigate the effects of entero-hepatic bile acid circulation on the inter-digestive migrating myoelectrical complex (MMC) in rats.

METHODS: Thirty-two rats were divided into four groups. Three pairs of bipolar silver electrodes were chronically implanted in the antrum, duodenum and jejunum. Three groups of them were ligated around the upper part of common bile duct (CBD). The experiments were performed in conscious and fasting state. The gastrointestinal myoelectrical activity was recorded. Ursodeoxycholic acid (UDCA) and saline were then perfused into stomachs of two groups with CBD obstruction and the effects of them on the MMC were observed.

RESULTS: A typical pattern of MMC was observed in normal fasting rats. MMC of antral and duodenal origin disappeared temporarily in earlier stage of CBD obstruction. While MMC of jejunum origin appeared. increased MMC cycle duration was seen after 4 d in rats with CBD obstruction. The MMC after CBD obstruction was characterized by an increased duration of phase II-like activity and decreased duration of phase I & III activity. Perfusion into stomachs with UDCA resulted in a shorter MMC cycle duration and a longer duration of phase III of duodenal origin compared to the normal group.

CONCLUSION: Entero-hepatic bile acid circulation initiates inter-digestive MMC of duodenal origin.

© 2005 The WJG Press and Elsevier Inc. All rights reserved.

Key words: Migrating myoelectrical complex; Entero-hepatic Bile acid circulation; Ursodeoxycholic acid; Common bile duct obstruction

Fang P, Dong L, Zhang WJ, Luo JY. Relationship between entero-hepatic bile acid circulation and interdigestive migrating myoelectrical activity in rats. *World J Gastroenterol* 2005; 11(34): 5377-5380
http://www.wjgnet.com/1007-9327/11/5377.asp

INTRODUCTION

Inter-digestive motility has been physically studied intensively[1-3], but mechanism is still unclear. Inter-digestive motility of gastrointestinal tract is characterized by a typical cycling complex of myoelectric activity. The migrating myoelectrical complex (MMC) is a distinct pattern of electromechanical activity observed in gastrointestinal tract during fasting. It serves as a housekeeping role and sweeps residual undigested materials through the digestive tract. Phase III MMC originates at variable sites in the gut from the esophagus to the proximal ileum, especially from antrum and duodenum[2,3].

Previous studies showed that entero-hepatic bile acid circulation and inter-digestive motility should be associated with each other[4]. Bile flow increases during phase II activity and reaches peak just before start of the MMC in the duodenum. It has been thought to exert an important regulatory function on the MMC[5]. Furthermore, phase III MMC plays an important role in the transport of bile acids from the proximal duodenum to the distal small intestine, where bile acids are absorbed for transport back to the liver. But use of different animal species and different methods has led to conflicting results[4-6].

In this article, we describes a new model which was used to further elucidate the role of bile acids in regulating MMC in unrestrained rats without the bias of anesthesia and post-operative influence on gastrointestinal motility. Therefore, the present study aimed to investigate the effects of common bile duct obstruction and UDCA perfusion into stomachs on the inter-digestive myoelectrical activity.

MATERIALS AND METHODS

Animals

Thirty-two healthy Sprague-Dawley rats (20 males and 12 females) weighing 200-250 g were fed with a dry food, with free access to tap water. After fasting for one night, the rats were intraperitoneally anesthetized with sodium pentobarbital (30 mg/kg). The hair on the skull and abdomen was shaved. The surgery was done under strict aseptic conditions. The abdominal musculature and peritoneum were opened through the linea alba. Three bipolar insulated silver electrodes made of Teflon-coated wire (outer diameter 0.5 mm, length 20 cm)

were implanted into the muscular layer of the bowel with a needle as a trocar. One milliliter of the wire was exposed near the implanted end, and the distance between pairs of electrodes should be 2.0-3.0 mm. The electrodes were placed on the gastric antrum 5 mm proximal to the pylorus, the duodenum and jejunum respectively 1 cm and 15 cm distal to the pylorus. The bundled electrode wires were grasped by the clamp through a silastic tube (diameter 2.4 mm), which was then passed through the subcutaneous tunnel from the abdominal incision to the back of the shoulder exit. Furthermore, 24 of them were ligated around the upper part of common bile duct (CBD). During operation, the intestine was kept moist with 9 g/L sterile NaCl solution, and 4 mL of this solution was used intraperitoneally to compensate for intraoperative fluid loss before closure of the abdomen. The abdominal wall was closed in three layers with running Vicryl 4-0 sutures. The rats were kept in a humidified room at 37 ℃ for 2 to 4 h after operation. Then, they were individually housed with free access to water and food. Housing conditions were at 22 ℃, 60% humidity and a 12 h light/dark cycle for 1 wk before experiment.

Gastrointestinal motility recordings

The rats were fasted for 12 h with free access to water. The gastrointestinal myoelectrical activity in conscious rats was recorded by a computerized, multichannel recorder (RM-6280C, Chengdu, China). Myoelectrical activity was sampled at a frequency of 1 kHz. The signals were amplified and bandpass was filtered (above 0.3 Hz and below 100 Hz were cut off). The amplitudes of contractions were recorded as μV.

Experimental procedures

The rats were coded and randomly divided into four groups (groups A, B, C and D), 8 in each. Group A had implanted electrode; group B had implanted electrodes +CBD obstruction; group C had implanted electrodes +CBD obstruction+UDCA perfusion; group D had implanted electrodes +CBD obstruction+saline perfusion. Three days after operation, we started to measure the gastrointestinal motility every day for 3 d. During experiment, the gastrointestinal myoelectrical activity in each rat was recorded for 2 h at least. On the 4th d after operation, before the MMC of duodenal origin recovered, UDCA (Pharmaceutical Factory of Changzhou City) was dissolved immediately before use in 3 mL normal saline at a dose of 20 mg/kg and then perfused into stomachs of one group with implanted electrodes and CBD obstruction. After UDCA was used, the gastrointestinal myoelectrical activity in the rats was continuously recorded for more than 2 h. As a control, normal saline was given in another group with implanted electrodes and CBD obstruction. After the conversion from analog to digital, the signals were stored on optical disk for later analysis.

Statistical analysis

Data are shown for duodenum. All parameters such as MMC cycle duration, duration of phase III, mean amplitude and frequency of phase III were expressed as mean±SD unless otherwise stated. $P<0.05$ was considered statistically significant. One way analysis of variance was performed to compare the means of all variables among groups using software package SPSS 10.0. A comparison was made between two groups using LSD method. Variables could be transformed when they were not coincident with each other.

RESULTS

Inter-digestive and digestive gastrointestinal myoelectrical activity in rats with implanted electrodes

The gastrointestinal motility pattern in rats could mainly be divided into inter-digestive and digestive stage. The inter-digestive stage was characterized by cyclical phase III contractions of the migrating motor complex which occurred in the stomach and duodenum and migrated to the small intestine. The digestive state was characterized by sustained contractions in the gastric antrum and small intestine. In our experiments, a typical pattern of myoelectrical activity in the fasting state appeared gradually in all rats with implanted electrodes about 3 d after operation. The phases of the MMC were as follows: phase I, motor quiescence; phase II, a period of irregular contractile activity; and phase III, a period of rhythmic contractions. The migrating motor complex pattern was disrupted by feeding, and irregular contractions were sustained in the antrum, duodenum and jejunum for 30 min after feeding (Figures 1 and 2).

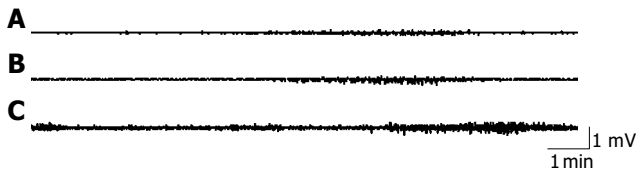


Figure 1 Inter-digestive gastrointestinal motility in antrum (**A**), duodenum (**B**), and jejunum (**C**) of rats with implanted electrodes.

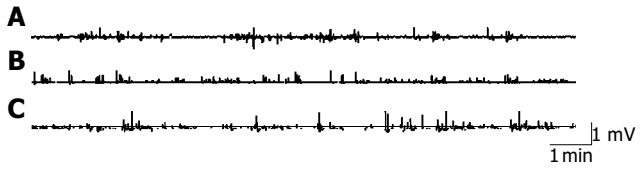


Figure 2 Digestive gastrointestinal motility shows sustained irregular contractions with relatively low amplitude in antrum (**A**), duodenum (**B**), and jejunum (**C**) of rats with implanted electrodes.

Interdigestive gastrointestinal myoelectrical activity in rats with CBD obstruction rats

Early after CBD obstruction regular MMC of duodenal origin disappeared, myoelectric activity was characterized by a continuous, irregular, low amplitude phase II-like activity without migrating activity fronts (Figure 3), while MMC of jejunum origin appeared. On the fourth day after CBD obstruction, MMC of duodenal origin started to recover gradually with a lower frequency. Five days after CBD obstruction, 74% of the MMC originated in the jejunum and 26% of the MMC originated in the duodenum. The MMC cycle duration of duodenal origin in CBD obstruction group was obviously longer than that in the group with implanted electrodes. The increased MMC duration was

mainly caused by increase of phase II-like activity. But the duration of phase III in CBD obstruction group was not significantly different from that of the group with implanted electrodes. There was no statistical difference between the MMC characteristics of jejunal origin in CBD obstruction group and the group with implanted electrodes.

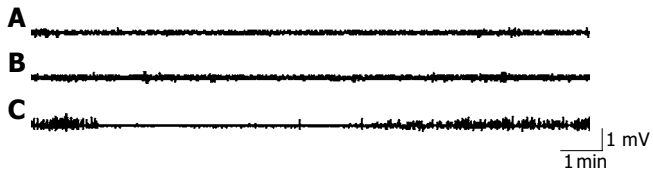


Figure 3 Inter-digestive gastrointestinal myoelectrical activity in antrum (**A**), duodenum (**B**), and jejunum (**C**) of rats with CBD obstruction.

Effects of UDCA on inter-digestive gastrointestinal myoelectrical activity in rats with CBD obstruction

Four days after control recordings were obtained in rats with CBD obstruction and no MMC of duodenal origin was observed. UDCA (20 mg/kg) was dissolved in 3 mL saline and perfused into stomachs of rats. The recording was continued for additional 2 h. The effects of UDCA on the inter-digestive gastrointestinal myoelectrical activity were established after the stomach was perfused with UDCA. Administration of UDCA led to a restart of duodenal MMC. The shorter MMC cycle duration and the longer duration of phase III of duodenal origin were observed. There was no significant difference in the other parameters of MMC of duodenum between the two groups (Figure 4, Table 1). Furthermore, there was no change in the interdigestive gastrointestinal myoelectrical activity of rats with CBD obstruction after normal saline treatment.

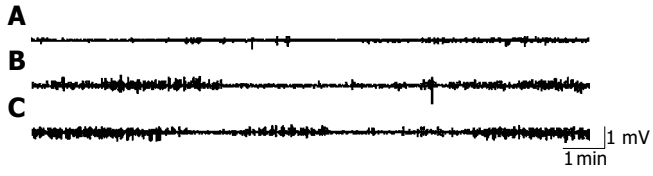


Figure 4 Effects of UDCA on inter-digestive gastrointestinal myoelectrical activity in antrum (**A**), duodenum (**B**), and jejunum (**C**) of rats with CBD obstruction.

Table 1 Effects of CBD obstruction and UDCA perfusion on interdigestive gastrointestinal myoelectrical activity in fasting rats. (n = 32, mean±SD)

Group	MMC cycle duration / s	Duration of phase III / s	Amplitude of phase III / μV	Frequency of phase III / (bursts / min)
A	730.5±44.71	163.5±19.1	288.4±21.9	11.2±1.6
B	1 680.9±89.5[a]	175.5±23.3	270.5±31.2	10.8±1.5
C	658.5±42.7[a,c]	228.8±36.5[a,c]	279.6±19.8	11.6±1.4
D	1 529.5±75.8[a,e]	172.5±20.5[e]	272.6±28.9	10.9±1.8

[a]P<0.05 *vs* A; [c]P<0.05 *vs* B; [e]P<0.05 *vs* C. Values are shown for duodenum.

DISCUSSION

The gastrointestinal motility pattern in rats can be divided into the inter-digestive and digestive states. The inter-digestive state is characterized by cyclical phase III contractions which occurs in antrum and duodenum and migrates to the small intestine. The digestive stage is characterized by sustained, irregular contractions in antrum and small intestine. These two phenomena were observed in our experiments. The migrating motor complex pattern could be disrupted by feeding.

The regulating mechanism of MMC is not completely understood[7-9]. Previous study showed that entero-hepatic bile acid circulation influences MMC and exerts an important regulatory function on MMC[10-12]. Our experiment showed that when entero-hepatic bile acid circulation was interrupted, spontaneous MMC in duodenum disappeared in early CBD obstruction. MMC originated mostly in the jejunum and migrated to the terminal ileum as a compensating mechanism. The duodenum showed continuous phase II-like activity. During the next 4 d after CBD obstruction, MMC of duodenal origin recovered gradually with a longer MMC cycle duration. The increased duration of MMC was mainly the result of an increase of phase II-like activity. UDCA perfusion into stomach resulted in a shorter MMC cycle duration and a longer duration of phase III of duodenal origin. But normal saline did not influence the MMC in rats with CBD obstruction. The underlying mechanisms for the absence of duodenal MMC during the interruption of entero-hepatic circulation are unknown. The possible explanation is that the development of MMC of duodenal origin is not autonomous but dependent on the stimulation of bile acids to the duodenum or the increased pressure in biliary tract[13]. Nieuwenhuijs *et al*.[14], thought that increased pressure in the biliary tract disrupts MMC early after CBD obstruction and the absence of bile in the duodenum and small intestine lengthens the MMC cycle. Ozeki *et al*.[15], thought that duodenum is not a spontaneous MMC oscillator which keeps resting below its oscillation threshold till a stimulus causes oscillation. However, the resting level of the duodenal MMC oscillator is close enough to its exciting threshold and sometimes may exhibit spontaneous oscillation. Artificial drainage of duodenal bile acids could also lead to increase of MMC cycle and phase II-like activity in healthy volunteers[16]. Thus, stimulation of higher bile acid concentration to the mucosa of duodenum in a short time is the prerequisite for the initiation of duodenal origin MMC[17].

Whether entero-hepatic bile acid circulation and intragastric bile salt infusion influence the MMC is still controversial. Some researchers supported the idea that there are no special effects of bile acids on inter-digestive MMC[18]. Luiking *et al*.[19], did not find any change of gallbladder emptying and small intestinal MMC when they perfused artificial bile into duodenum of healthy volunteers during inter-digestive stage. Van Felius *et al*.[20], found that prolongation of the MMC causes pancreatitis, and ligation of the proximal CBD near the bifurcation does not prolong the MMC, suggesting that pancreatitis influences the MMC cycle and hepatic biliary secretion alone does not play a primary role in the regulation of MMC. Some studies showed that initiation of MMC is closely related to the increasing

speed of bile acids in plasma. This may explain the conflicting results in the above researches[21,22].

Our model is suitable for studying the possible relationship between entero-hepatic bile acid circulation and inter-digestive gastrointestinal motility. At first, we ligated the CBD near the entrance to the duodenum. Almost all the rats died of pancreatitis. Ligation of the proximal CBD did not influence the function of pancreas. Post-operative gastrointestinal myoelectrical motility was measured in conscious state after the rats recovered from operation and could move freely. The advantages of this model are as follows. The surgical procedures are well tolerated by the animals. Experiments can be performed in unrestrained rats without the bias of sedative drugs, anesthesia and stress of operation. Ligation of the proximal CBD does not influence the function of the pancreas.

In conclusion, our model has made it easier and more precise to study the effects of CBD obstruction and UDCA on MMC in unrestrained rats without the bias of anesthetic agents or post-operative effects. Our findings indicate that that the entero-hepatic bile acid circulation initiates the inter-digestive MMC of duodenal origin, which provides a new therapy for patients with gut motility disorders.

REFERENCES

1 **Luiking YC,** Akkermans LM, van der Reijden AC, Peeters TL, van Berge-Henegouwen GP. Differential effects of motilin on interdigestive motility of the human gastric antrum, pylorus, small intestine and gallbladder. *Neurogastroenterol Motil* 2003; **15**: 103-111

2 **Wang L,** Zhou L, Tian R. Role of the area postrema of medulla oblongata in the regulation of canine interdigestive migrating motor complex. *Chin Med J* 2002; **115**: 384-388

3 **Tanaka T,** Kendrick ML, Zyromski NJ, Meile T, Sarr MG. Vagal innervation modulates motor pattern but not initiation of canine gastric migrating motor complex. *Am J Physiol Gastrointest Liver Physiol* 2001; **281**: G283-292

4 **Hellstrom PM,** Nilsson I, Svenberg T. Role of bile in regulation of gut motility. *J Intern Med* 1995; **237**: 395-402

5 **Romanski KW,** Salomon E, Borodulin-Nadzieja L, Janocha A. Fluctuations of gastrin, motilin and total bile acid levels in porcine blood before and after feeding. *Folia Med Cracov* 2002; **43**: 5-12

6 **Qvist N,** Oster-Jorgensen E, Pedersen SA, Rasmussen L, Hovendal C, Holst JJ. Increases in plasma motilin follow each episode of gallbladder emptying during the interdigestive period, and changes in serum bile acid concentration correlate to plasma motilin. *Scand J Gastroenterol* 1995; **30**: 122-127

7 **Suzui H,** Mochiki E, Haga N, Shimura T, Itoh Z, Kuwano H. Effect of duodenectomy on gastric motility and gastric hormones in dogs. *Ann Surg* 2001; **233**: 353-359

8 **Spencer NJ,** Bywater RA. Enteric nerve stimulation evokes a premature colonic migrating motor complex in mouse. *Neurogastroenterol Motil* 2002; **14**: 657-665

9 **Plaza MA.** 5-hydroxytryptamine and the gastrointestinal migrating motor complex. *Curr Opin Investig Drugs* 2001; **2**: 539-544

10 **Kajiyama Y,** Irie M, Enjoji A, Ozeki K, Ura K, Kanematsu T. Role of bile acids in duodenal migrating motor complexes in dogs. *Dig Dis Sci* 1998; **43**: 2278-2283

11 **Van Ooteghem NA,** Van Erpecum KJ, Van Berge-Henegouwen GP. Effects of ileal bile salts on fasting small intestinal and gallbladder motility. *Neurogastroenterol Motil* 2002; **14**: 527-533

12 **Einarsson C,** Ellis E, Abrahamsson A, Ericzon BG, Bjorkhem I, Axelson M. Bile acid formation in primary human hepatocytes. *World J Gastroenterol* 2000; **6**: 522-525

13 **Utsunomiya N,** Tanaka M, Ogawa Y, Konomi H, Takahata S, Nabae T, Yokohata K, Chijiiwa K. Pain associated with phase III of the duodenal migrating motor complex in patients with postcholecystectomy biliary dyskinesia. *Gastrointest Endosc* 2000; **51**: 528-534

14 **Nieuwenhuijs VB,** Luiking YC, Verheem A, van Berge-Henegouwen GP, Gooszen HG, Akkermans LM. Disrupted bile flow affects interdigestive small bowel motility in rats. *Surgery* 1997; **122**: 600-608

15 **Ozeki K,** Sarna SK, Condon RE, Chey WY, Koch TR. Enterohepatic circulation is essential for regular cycling of duodenal migrating motor complexes in dogs. *Gastroenterology* 1992; **103**: 759-767

16 **Nilsson I,** Svenberg T, Hedenborg G, Lordal M, Hellstrom PM. Inhibition of the migrating motor complex by duodenal drainage in man. *Neurogastroenterol Motil* 1995; **7**: 31-37

17 **Portincasa P,** Peeters TL, van Berge-Henegouwen GP, van Solinge WW, Palasciano G, van Erpecum KJ. Acute intraduodenal bile salt depletion leads to strong gallbladder contraction, altered antroduodenal motility and high plasma motilin levels in humans. *Neurogastroenterol Motil* 2000; **12**: 421-430

18 **Neubrand MW,** Dominguez-Munoz JE, Reichel C, Kampmann S, Eschmann K, von Falkenhausen M, Bregulla M, Malfertheiner P, Sauerbruch T. Effect of intraduodenal administration of ursodeoxycholic acid on interdigestive interaction between gallbladder motility, pancreatic secretion and endocrine activity. *Digestion* 2004; **69**: 149-157

19 **Luiking YC,** Kloppers NJ, Roelofs JM, Nieuwenhuijs VB, Peeters TL, Akkermans LM, van Berge-Henegouwen GP. Effects of intraduodenal bile on interdigestive gastrointestinal and gallbladder motility in healthy subjects. *Digestion* 2001; **63**: 195-202

20 **Van Felius ID,** Akkermans LM, Bosscha K, Verheem A, Harmsen W, Visser MR, Gooszen HG. Interdigestive small bowel motility and duodenal bacterial overgrowth in experimental acute pancreatitis. *Neurogastroenterol Motil* 2003; **15**: 267-276

21 **Van Ooteghem NA,** Moschetta A, Rehfeld JF, Samsom M, van Erpecum KJ, van Berge-Henegouwen GP. Intraduodenal conjugated bile salts exert negative feedback control on gall bladder emptying in the fasting state without affecting cholecystokinin release or antroduodenal motility. *Gut* 2002; **50**: 669-674

22 **Andersen PV,** Mortensen J, Oster-Jorgensen E, Rasmussen L, Pedersen SA, Qvist N. Cholecystectomy in patients with normal gallbladder function did not alter characteristics in duodenal motility which was not correlated to size of bile acid pool. *Dig Dis Sci* 1999; **44**: 2443-2448

Science Editor Wang XL and Guo SY **Language Editor** Elsevier HK

PO Box 2345, Beijing 100023, China
www.wjgnet.com
wjg@wjgnet.com

ELSEVIER

World J Gastroenterol 2005;11(34):5381-5384
World Journal of Gastroenterology ISSN 1007-9327
© 2005 The WJG Press and Elsevier Inc. All rights reserved.

• *BRIEF REPORTS* •

Studies on BN rats model to determine the potential allergenicity of proteins from genetically modified foods

Xu-Dong Jia, Ning Li, Yong-Ning Wu, Xiao-Guang Yang

Xu-Dong Jia, Ning Li, Yong-Ning Wu, Xiao-Guang Yang, National Institute for Nutrition and Food Safety, Chinese Center for Disease Control and Prevention, 29 Nanwei Road, Beijing 100050, China
Supported by the State 863 Projects, No. 2001AA212291 and 2002AA212041 and the State 973 Project, No. 001CB109007
Correspondence to: Dr. Ning Li, National Institute for Nutrition and Food Safety, Chinese Center for Disease Control and Prevention, 29 Nanwei Road, Beijing 100050, China. lining65@yahoo.com
Telephone: +86-10-83132553 Fax: +86-10-83132021
Received: 2004-12-17 Accepted: 2005-03-24

Abstract

AIM: To develop a Brown Norway (BN) rat model to determine the potential allergenicity of novel proteins in genetically modified food.

METHODS: The allergenicity of different proteins were compared, including ovalbumin (OVA), a potent respiratory and food allergen, bovine serum albumin (BSA), a protein that is considered to have a lesser allergenic potential, and potato acid phosphatase (PAP), a non-allergenic protein when administered to BN rats via different routes of exposure (intraperitoneally or by gavage). IgG and IgE antibody responses were determined by ELISA and PCA, respectively. An immunoassay kit was used to determine the plasma histamine level. In addition, possible systemic effect of allergens was investigated by monitoring blood pressure.

RESULTS: OVA provoked very vigorous protein-specific IgG and IgE responses, low grade protein-specific IgG and IgE responses were elicited by BSA, while by neither route did PAP elicit anything. In either routes of exposure, plasma histamine level in BN rats sensitized with OVA was higher than that of BSA or PAP. In addition, an oral challenge with BSA and PAP did not induce any effect on blood pressure, while a temporary drop in systolic blood pressure in few animals of each routes of exposure was found by an oral challenge with OVA.

CONCLUSION: BN rat model might be a useful and predictive animal model to study the potential allergenicity of novel food proteins.

© 2005 The WJG Press and Elsevier Inc. All rights reserved.

Key words: Animal model; Food protein; Allergenicity

Jia XD, Li N, Wu YN, Yang XG. Studies on BN rats model to determine the potential allergenicity of proteins from genetically modified foods. *World J Gastroenterol* 2005; 11 (34): 5381-5384
http://www.wjgnet.com/1007-9327/11/5381.asp

INTRODUCTION

Modern biotechnology has resulted in the introduction of a number of new proteins to foods, the potential allergenicity of these new proteins is a major concern in the safety assessment on genetically modified foods. The best known systematic approach for the assessment of the allergenic properties of novel proteins was called IFBC/ILSI decision tree, which was jointly developed by the International Food Biotechnology Council (IFBC) and the International Life Sciences Institute (ILSI)[1]. A universal, reliable and relevant *in vitro* or *in vivo* test to study the sensitizing potential of a new protein is, however, not available. Therefore, it is recommended that the development and validation of a widely accepted animal model should be the most direct approach to determine the sensitizing potential of a new protein. In 2001, FAO/WHO revised this decision tree and developed another one called FAO/WHO 2001 decision tree, in which animal models were included[2].

An ideal animal model should satisfy the following important criteria: sensitization and challenge should preferably be oral; preferably no use of adjuvants; the test animal should produce a significant amount of IgE antibody; the test animal should tolerate most food proteins; clinical reactions should be similar to those seen in humans; antibody responses should be directed to similar proteins as found in patient sera; and the model should be relatively easy to conduct and reproducible both in time and in different laboratories[3]. Several attempts have been made to develop animal models for food allergy research, mainly in mouse, guinea pig, and rats[4-6]. Some drawbacks limited the further use of the guinea pig in food allergy research, including significant differences in immunophysiology, limited knowledge of its immune system, and lack of tools to study its immune system. Studies in mice on oral protein administration without adjuvants readily resulted in tolerance induction[7]. For the rat, there are some advantages including the most commonly used species in toxicity testing, a reasonable amount of knowledge on its immune system, and many tools for immune-related studies. Studies have showed that the Brown Norway (BN) rat is a high-immunoglobulin (particularly IgE) responder strain[8,9].

There is some debate regarding the most appropriate route of administration. In theory, oral administration

appears to be the most attractive and relevant; however, it is well known that exposure of rats to proteins in this way can result in immunological tolerance. While parenteral administration of protein can avoid the development of oral tolerance but can provide a clear indication of inherent ability of proteins to induce IgE antibody responses. Therefore, FAO/WHO recommended that the results from two sensitization routes should be considered. FAO/WHO also suggested that the potential allergenicity of the expressed protein be ranked against well-known strong and weak food allergens and non-allergenic proteins in the animal models.

For these reasons, in the present study, the allergenicity of different proteins were compared, including ovalbumin (OVA), a potent respiratory and food allergen, bovine serum albumin (BSA), a protein that is considered to have a lesser allergenic potential, and potato acid phosphatase (PAP), a non-allergenic protein when administered to BN rats intraperitoneally or by gavage.

MATERIALS AND METHODS

Rats

Male BN rats, 4-6-wk old, were obtained from the Animal Center of the Chinese Academy of Medical Sciences (Beijing, China). The rats were housed in an animal room maintained at 24±1 ℃ and 50±10% relative humidity with the altering 12:12-h light-dark cycle. The animals were housed in stainless-steel wire cages in groups of five and had free access to milk and egg-free diet and water.

Allergens

OVA, a potent respiratory and food allergen, and BSA, a protein that is considered to have a lesser allergenic potential, were obtained from Sigma Chemicals, USA. PAP also purchased from Sigma was used as a non-allergenic protein.

Oral sensitization

Animals were randomly divided into three groups, 10 rats in each group. The rats were exposed by gavage to OVA, BSA, or PAP (1 mg protein/mL tap water; 1 mL/animal) respectively for 6 wk, without the use of an adjuvant. At weekly intervals, blood samples were obtained from the orbital plexus. Blood samples for IgG antibody and reagnic antibody analysis were centrifuged for 20 min at 2 000 r/min to obtain sera. Blood samples for plasma histamine level determination were collected into chilled tubes containing EDTA-K_2 to obtain plasma aliquots.

Intraperitoneal sensitization

Rats were randomly divided into three groups, 10 rats in each group. The animals were exposed intraperitoneally to OVA, BSA, or PAP (100 μg protein/mL tap water; 1 mL/animal) respectively on days 0 and 7. Animals were bled at weekly intervals from d 7 to 42. Blood samples for IgG antibody and reagnic antibody analysis were centrifuged for 20 min at 2 000 r/min to obtain sera. Blood samples for plasma histamine level determination were collected into chilled tubes containing EDTA-K_2 to obtain plasma aliquots.

IgG antibody analysis

Antigen-specific IgG was determined using an ELISA technique. Solution of OVA, BSA, or PAP (10 μg/mL) was bound to a 96-well microtiter plates (100 μL/well) overnight at 4 ℃. The plates were washed thrice with tap water containing 0.5% Tween 20. This was followed by the addition of 100 μL/well PBS containing 0.5% Tween 20 and 2% sheep serum albumin. After 1-h incubation at 37 ℃, the plates were washed and serial dilutions of rat serum were added to the wells and incubated for 1 h at 37 ℃. After washing, 100 μL/well peroxidase conjugated goat anti-rat IgG (H+L) (Zymed, USA) was added. After incubation for 1 h at 37 ℃, the plates were washed again and an enzyme-substrate solution of tetramethylbenzidine (Sigma, 100 μL/well) was added. The plates were developed at room temperature for 10 min. Finally, 100 μL/well of 1 mol/L H_2SO_4 was added. Optical densities were read at 450 nm with an ELISA plate reader. A pre-serum pool was used as negative control. The pooled pre-serum was measured at a 1:4 dilution. The average extinction in negative control wells, to which three times the standard deviation was added, provided the reference value taken to determine the titer in the test sera. Each test serum was titrated starting at a 1:4 dilution, and the reciprocal of the greatest serum dilution giving an extinction higher than the reference value was read as the titer. The titer $>2^5$ was considered as positive IgG antibody responses.

Reaginic antibody analysis

The presence of reaginic antibody was assessed by passive cutaneous anaphylaxis assay (PCA)[7]. Naïve BN rats were shaved on the back and flanks and injected intradermally with 0.1 mL of the test sera in serial dilutions followed 64 h later with an intravenous injection of 1 mL of 1:1 mixture of a solution of OVA, BSA, or PAP (5 mg/mL) and a solution of Evans blue (2% in sterile saline). After 20-30 min, the animals were examined for positive responses. The diameter of dye extravasation at the site of the serum injection was measured. The positive response was considered when a colored spot of at least 5 mm in diameter appeared.

Measurement of plasma histamine level

In order to evaluate the plasma histamine level, blood samples of rat were collected into chilled tubes containing 40 μL of 7.5% potassium ethylenediamine tetraacetic acid (EDTA-K_2) on d 7 after antigen injection or antigen exposure by gavage. After centrifugation, plasma aliquots were collected and frozen at -80 ℃ until use. Plasma histamine levels were determined using an immunoassay kit (IBL, Germany) following the manufacturer's instructions.

Measurement of blood pressure

Before challenge, individual baseline blood pressures were determined on two separate days. Prior to blood pressure measurements, the animals were placed under a heating light (30 ℃) for 20 min. Thereafter, an inflatable pressure cuff was put around the tail and a distal sensor was used to record the systolic blood pressure. The OVA, BSA, or PAP sensitized and control animals were challenged orally with 2 mL of a 5 mg/mL OVA, BSA, or PAP solution or 2 mL of tap water. Blood pressure was recorded at intervals for

over a period of 7 h.

Statistical analysis

Plasma histamine levels were compared among three groups by Student's *t*-test.

RESULTS

IgG antibody responses to antigen

During the whole study of either exposure routes, OVA and BSA provoked protein-specific IgG antibody responses, while PAP did not elicit protein-specific IgG antibody responses (Tables 1 and 2).

Table 1 IgG antibody responses to antigens exposed by oral gavage

Groups	Number of responders on day				
	14	21	28	35	42
OVA	10	10	10	10	10
BSA	5	7	8	8	6
PAP	0	0	0	0	0

Table 2 IgG antibody responses to antigens exposed by intraperitoneal injection

Groups	Number of responders on day				
	14	21	28	35	42
OVA	10	10	10	10	10
BSA	6	8	8	8	7
PAP	0	0	0	0	0

Reaginic antibody responses

Reaginic antibody responses determined by PCA were shown in Tables 3 and 4. Strong OVA-specific IgE antibody responses were provoked, only a limited BSA-specific IgE responders were observed and PAP did not elicit protein-specific IgE antibody responses.

Table 3 Reaginic antibody (IgE) responses to antigens exposed by oral gavage

Groups	Number of responders on day				
	14	21	28	35	42
OVA	8	8	9	9	8
BSA	2	3	3	3	2
PAP	0	0	0	0	0

Table 4 Reaginic antibody (IgE) responses to antigens exposed by intraperitoneal injection

Groups	Number of responders on day				
	14	21	28	35	42
OVA	8	9	9	9	8
BSA	3	4	4	4	3
PAP	0	0	0	0	0

Plasma histamine level

In either routes of exposure, plasma histamine level in BN rats sensitized with OVA was higher than that of BSA or PAP (Tables 5 and 6).

Table 5 Plasma histamine levels (oral sensitization)

Groups	Plasma histamine level (ng / mL)
OVA	44.4±12.5[a]
BSA	29.2±7.8
PAP	27.5±10.4

[a]$P<0.05$ *vs* BSA and PAP.

Table 6 Plasma histamine levels (intraperitoneal sensitization)

Groups	Plasma histamine level (ng / mL)
OVA	64.4±12.5[a]
BSA	36.2±9.6
PAP	30.0±6.9

[a]$P<0.05$ *vs* BSA and PAP.

Blood pressure determination

An oral challenge with BSA and PAP did not induce any effect on blood pressure, while a temporary drop in systolic blood pressure in three animals of each routes of exposure was found by an oral challenge with OVA. Representative results of blood pressure changes induced by OVA via oral sensitization or intraperitoneal sensitization are shown in Figure 1.

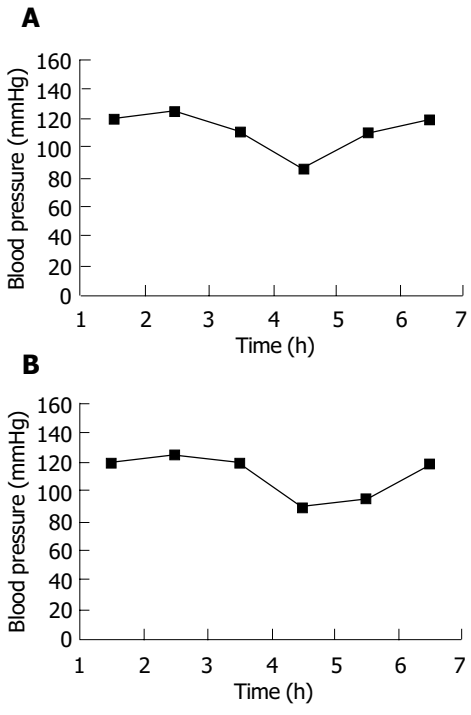


Figure 1 Changes of blood pressure in two representative rats. **A**: Oral sensitization; **B**: intraperitoneal sensitization.

DISCUSSION

Food allergy is an important health issue of growing interest. By definition, food allergy is an adverse reaction to a harmless food or food components that involves an abnormal response of the body's immune system to specific protein in foods. The most common type of food allergy is mediated by allergen-specific IgE[10]. Sensitization is induced by following exposure of the susceptible individual to the protein allergen sufficient to stimulate an IgE antibody response. If the now-sensitized individual is exposed subsequently to the same protein, then antigen cross-links specific membrane-bound IgE antibodies and this in turn causes mast cell degranulation and the release of inflammatory mediators such as histamine, cytokine, and so on, which together initiate the symptoms of food allergy[11,12].

Not all proteins display allergenic potential, despite being immunogenic (able to stimulate IgG antibody responses), proteins appear to differ markedly with respect to their ability to cause IgE-mediated allergic sensitization[13]. Therefore, in this study, IgG antibody response (antigen), IgE antibody response (allergen), histamine level (inflammatory mediators) and blood pressure (systemic challenge effects) were used as parameters to develop the BN rat model.

Collectively, our study has shown that BN rats, bred and raised on a diet free of the antigen to be tested, can be sensitized by daily dosing with the antigen via enteral route or intraperitoneal injection without use of adjuvants. However, there appears to be significant differences between the proteins examined with respect to IgE antibody response. By either route of exposure, OVA provoked very vigorous protein-specific IgG and IgE responses, low grade protein-specific IgG and IgE responses were elicited by BSA, while by neither route did PAP elicit anything. The same phenomenon was described in BN rats sensitized by daily intra-gastric administration of OVA, hen's egg white (HEW) and cow's milk (CM) proteins[14]. In that study, OVA provoked strong antigen-specific IgG as well as IgE responses in almost all rats, while only a limited number of IgE responders were observed in rats with HEW or CM. These results indicate that BN rats demonstrate IgE antibody responses to a comparable selection of proteins upon exposure of different proteins and support that the BN rat may provide a suitable animal model for assessing the allergenicity of novel food proteins and for research on the mechanisms of food allergy. For a more detailed characterization of the rat model developed, additional studies were performed to study the release of inflammatory mediators (histamine) and systemic immune-mediated effects (blood pressure).

Histamine is a potent mediator of numerous biological reactions. In the human organism, it is virtually ubiquitous in tissues and body fluids, being mainly stored in its inactive form in the metachromatic granula of mast cells and basophilic leucocytes. On release, histamine functions as a potent mediator of numerous physiological and pathophysiological processes in nearly all organs and tissues[11,12]. Histamine has been clearly implicated as a primary mediator of "immediate type" allergic reactions (IgE-mediated allergic sensitization). In this study, the plasma histamine level in rats sensitized by OVA was higher than that of BSA and PAP, which is consistent with the results of antigen-specific IgE responses. Also, other mediators such as platelet-activating factor, prostaglandins, leukotrienes and some newly formed cytokines release in anaphylactic reactions have been studied in experimental models.

The possible systemic effect was investigated by monitoring blood pressure. An oral challenge with BSA and PAP did not induce any effect on blood pressure, while a temporary drop in systolic blood pressure in some animals was found by an oral challenge with OVA. Although this effect was observed in only a few animals (around 30%), this low incidence is in agreement with observations from food allergic patients. The results indicate that systemic effects can be induced upon an oral challenge with allergens such as OVA.

In conclusion, although additional studies are needed with more purified strong and weak allergens, non-allergens, and allergenic whole foods, to further validate the developed BN rat model, the results obtained in this study indicate that BN rat model might be a useful and predictive animal model to study the potential allergenicity of novel food proteins.

REFERENCES

1 **Metcalfe DD,** Astwood JD, Townsend R, Sampson HA, Taylor SL, Fuchs RL. Assessment of the allergenic potential of foods derived from genetically engineered crop plants. *Crit Rev Fd Sci Nutr* 1996; **36**(Suppl): S165-186

2 **Kimber I,** Betts CJ, Dearman RJ. Assessment of the allergenic potential of proteins. *Toxicol Lett* 2003; **140-141**: 297-302

3 **Taylor SL,** Lehrer SB. Principles and characteristics of food allergens. *Crit Rev Fd Sci Nutr* 1996; **36**(Suppl): S91-118

4 **Dearman RJ,** Kimber I. Determination of protein allergenicity: studies in mice. *Toxicol Lett* 2001; **120**: 181-186

5 **Piacentini GL,** Vicentini L, Bodini A, Mazzi P, Peroni DG, Maffeis C, Boner AL. Allergenicity of a hydrolyzed rice infant formula in a guinea pig model. *Ann Allergy Asthma Immunol* 2003; **91**: 61-64

6 **Knippels LM,** Penninks AH, Spanhaak S, Houben GF. Oral sensitization to food proteins: a Brown Norway rat model. *Clin Exp Allergy* 1998; **28**: 368-375

7 **Penninks AH,** Knippels LM. Determination of protein allergenicity: studies in rats. *Toxicol Lett* 2001; **120**: 171-180

8 **Knippels LM,** Penninks AH, Smit JJ, Houben GF. Immune-mediated effects upon oral challenge of ovalbumin-sensitized Brown Norway rats: further characterization of a rat food allergy model. *Toxicol Appl Pharmacol* 1999; **156**: 161-169

9 **Knippels LM,** Houben GF, Spanhaak S, Penninks AH. An oral sensitization model in Brown Norway rats to screen for potential allergenicity of food proteins. *Methods* 1999; **19**: 78-82

10 **Taylor SL,** Hefle SL. Will genetically modified foods be allergenic? *J Allergy Clin Immunol* 2001; **107**: 765-771

11 **Koppelman SJ,** Wensing M, Ertmann M, Knulst AC, Knol EF. Relevance of Ara h1, Ara h2 and Ara h3 in peanut-allergic patients, as determined by immunoglobulin E Western blotting, basophil-histamine release and intracutaneous testing: Ara h2 is the most important peanut allergen. *Clin Exp Allergy* 2004; **34**: 583-590

12 **Jutel M,** Blaser K, Akdis CA. Histamine in allergic inflammation and immune modulation. *Int Arch Allergy Immunol* 2005; **137**: 82-92

13 **Kimber I,** Kerkvliet NI, Taylor SL, Astwood JD, Sarlo K, Dearman RJ. Toxicology of protein allergenicity: prediction and characterization. *Toxicol Sci* 1999; **48**: 157-162

14 **Knippels LM,** van der Kleij HP, Koppelman SJ, Houben GF, Penninks AH. Comparison of antibody responses to hen's egg and cow's milk proteins in orally sensitized rats and food-allergic patients. *Allergy* 2000; **55**: 251-258

Science Editor Guo SY **Language Editor** Elsevier HK

PO Box 2345, Beijing 100023, China
www.wjgnet.com
wjg@wjgnet.com

ELSEVIER

World J Gastroenterol 2005;11(34):5385-5389
World Journal of Gastroenterology ISSN 1007-9327
© 2005 The WJG Press and Elsevier Inc. All rights reserved.

• *BRIEF REPORTS* •

Rapid quantification of semen hepatitis B virus DNA by real-time polymerase chain reaction

Wei-Ping Qian, Yue-Qiu Tan, Ying Chen, Ying Peng, Zhi Li, Guang-Xiu Lu, Marie C. Lin, Hsiang-Fu Kung, Ming-Ling He, Li-Ka Shing

Wei-Ping Qian, Luofu Hospital, Shenzhen 518033, Guangdong Province, China
Wei-Ping Qian, Yue-Qiu Tan, Guang-Xiu Lu, Institute of Reproduction and Stem Cell Engineering, Xiangya School of Medicine, Central South University, Changsha 410008, Hunan Province, China
Zhi Li, Marie C. Lin, The Institute of Molecular Biology, The University of Hong Kong, Hong Kong Special Administrative Region, China
Ying Peng, Department of Neurology, The Second Affiliated Hospital, Sun Yat-Sen University, Guangzhou 510120, Guangdong Province, China
Ying Chen, Hsiang-Fu Kung, Ming-Ling He, Li-Ka Shing, The Center for Emerging Infectious Diseases, The Chinese University of Hong Kong, Hong Kong Special Administrative Region, China
Supported by Research Fund for the Control of Infectious Diseases and Research Grant Committee of Hong Kong Government
Co-first-authors: Wei-Ping Qian and Yue-Qiu Tan
Correspondence to: Dr. Ming-Liang He, The Center for Emerging Infectious Diseases, The Chinese University of Hong Kong, Hong Kong Special Administrative Region, China. mlhe@cuhk.edu.hk
Telephone: +852-2252-8813 Fax: +852-2635-4977
Received: 2004-09-14 Accepted: 2005-01-26

Abstract

AIM: To examine the sensitivity and accuracy of real-time polymerase chain reaction (PCR) for the quantification of hepatitis B virus (HBV) DNA in semen.

METHODS: Hepatitis B viral DNA was isolated from HBV carriers' semen and sera using phenol extraction method and QIAamp DNA blood mini kit (Qiagen, Germany). HBV DNA was detected by conventional PCR and quantified by TaqMan technology-based real-time PCR (quantitative polymerase chain reaction (qPCR)). The detection threshold was 200 copies of HBV DNA for conventional PCR and 10 copies of HBV DNA for real time PCR per reaction.

RESULTS: Both methods of phenol extraction and QIAamp DNA blood mini kit were suitable for isolating HBV DNA from semen. The value of the detection thresholds was 500 copies of HBV DNA per mL in the semen. The viral loads were 7.5×10^7 and 1.67×10^7 copies of HBV DNA per mL in two HBV infected patients' sera, while 2.14×10^5 and 3.02×10^5 copies of HBV DNA per mL in the semen.

CONCLUSION: Real-time PCR is a more sensitive and accurate method to detect and quantify HBV DNA in the semen.

© 2005 The WJG Press and Elsevier Inc. All rights reserved.

Key words: Hepatitis B virus; Semen; Real-time polymerase chain reaction; Viral load

Qian WP, Tan YQ, Chen Y, Peng Y, Li Z, Lu GX, Lin MC, Kung HF, He ML, Shing LK. Rapid quantification of semen hepatitis B virus DNA by real-time polymerase chain reaction. *World J Gastroenterol* 2005; 11(34): 5385-5389
http://www.wjgnet.com/1007-9327/11/5385.asp

INTRODUCTION

Human hepatitis B virus (HBV) is the major epidemiological agent of acute and chronic hepatitis, cirrhosis, and hepatocellular carcinoma[1-3]. At present, around 10-15% of individuals (estimated 200 million people) are chronically infected with HBV in China, and HBV-associated hepatocellular carcinoma (HCC) has become the country's second most lethal disease.

One of the major HBV transmission pathways is parenteral[4,5]. HBV is therefore in most cases transmitted to individuals at birth or in the postnatal period by infected mothers, less commonly through close contact with infected fathers, siblings, and relatives during early childhood[2]. In developed countries, sexual transmission plays a major role in infecting individuals[3]. Mother-to-baby vertical transmission gives a large number of HBV carriers in China and other eastern Asian countries. It has also been reported that fetuses become infected in the uterus by their fathers as a result of transmission through sexual contact, although the mothers are negative for any HBV marker[6]. Therefore, the viral load in the semen or vaginal secretions is a very important parameter for safe sex and human reproduction.

Few attempts have been made to monitor HBV viral load in semen or vaginal secretions. Many people, especially in conservative Asian cultures, are reluctant to disclose information on their sexual habits, and unwilling to provide semen or vaginal secretions for epidemiological studies. When semen or vaginal secretions become available for study, they are in far smaller volumes than typical blood samples, and their viral titers are much lower than those of blood samples. These factors have hindered the progress of virological studies of reproduction-related body fluids. Although several methods have been developed for the detection of HBV DNA in semen[7-10], and HBV is routinely monitored when semen is screened for artificial insemination[11-13], the quantitative data produced have been disappointingly small. Southern blot has been used to estimate HBV viral load in semen in a study conducted 15 years ago[7], but no follow-up was made, probably because the work involved would have been tedious, time-consuming,

and possibly of limited accuracy. At present, there are still insufficient virological data to enable the risk factors for HBV infection through semen to be evaluated.

The sensitive quantitative real-time PCR (qPCR) provides an opportunity to investigate the viral load in the semen of HBV patients or carriers seeking assisted reproduction. The qPCR technology has greatly improved the precision of DNA quantification[14-16]. In this paper, we compared two different methods for the preparation of HBV DNA from HBV carriers' semen, and presented a TaqMan technology-based assay to quantify HBV DNA in semen. Our assay is highly sensitive, and theoretically suitable for quantifying most HBV genotypes.

MATERIALS AND METHODS

Sera and semen samples

The study was conducted in patients who were seeking assisted reproduction in Luofu Hospital, Shenzhen, in 2003 and 2004. In accordance with the standard protocols, all patients who received assisted reproduction were systematically screened for serum hepatitis B virus surface antigen (HBsAg), hepatitis B surface antibody (HBsAb), hepatitis B e antigen (HBeAg), and hepatitis B e antibody (HBeAb) with commercially-available enzyme immunoassays (Abbott Laboratories, Chicago, IL, USA). The recommended viral markers including human immunodeficiency virus antibody (HIV Ab), and hepatitis C antibody (anti-HCV) were also detected. Hepatitis B core antibody (HBcAb) was also systematically tested by RIA (Corab; Abbott). Semen HBV DNA was detected by PCR. All patients were tested with liver function tests (including serum alanine aminotransferase, serum albumin and bilirubin) before assisted reproductions were carried out. Five patients were selected for this study. Two patients were positive for HBsAg, HBeAg and anti-HBc, and their serum ALT levels were normal over 6 mo. Two patients presented HBsAb only. One patient with all HBV markers negative (s, e, and c antibody negative; s and e antigene negative) was selected as a control (Table 1). HCV or HIV was not detected by RT-PCR in these patients' sera. Patients were asked not to ejaculate for five days before semen samples were collected. Informed consent was obtained from all patients. Study procedures were approved by the Ethics Committee of Luofu Hospital and the Chinese University of Hong Kong. Each ejaculation was liquefied for at least 30 min at 37 ℃. The sperm concentration and percentage of motile spermatozoa were evaluated by Makler chamber, under a phase-contrast microscope. The serum and semen samples were stored at -20 ℃ until use.

Table 1 HBV status in sera of HBV carriers

Sample	Antigen-antibody test[1]					ALT[2]	Bilirubin
	HBsAg	HBsAb	HBeAg	HBeAb	HBcAb		
1	+	–	+	–	+	39.8	11.7
2	+	–	+	–	+	18.7	7.5
3	–	+	–	–	–	71.7	19
4	–	+	–	–	–	33.8	4.6
5	–	–	–	–	–	18.7	6.2

[1]HBsAg: hepatitis B surface antigen; HBsAb: antibody to HBsAg; HBeAg: hepatitis B e antigen; anti-HBe: antibody to HBeAg; anti-HBc: antibody to hepatitis B core antigen (HBcAg). [2]ALT: alanine aminotransferase. +Represents positive; – represents negative.

Isolation of viral DNA

The spermatozoa in the semen were removed by centrifugation at 3 000 *g* at 4 ℃ for 10 min. Different amounts of each seminal plasma (10, 50, and 200 μL) were used to isolate viral DNA by two methods. Viral DNA was isolated with QIAamp Blood Mini Kit (Qiagen, Germany) following manufacturer's instructions. In the case of a small amount of semen, up to 200 μL of PBS was supplemented to avoid loss of viral DNA. In the phenol extraction experiments, an equal volume of saturated phenol (Sigma, St. Louis, USA) was added to the samples, and vortexed for 1 min. After centrifugation at 13 000 *g* for 10 min, upper layer was transferred to a fresh tube and repeated the extraction with phenol-chloroform (1∶1). Then 0.1 volume of 3 mol/L potassium acetate (pH 5.2), 1 μL glycogen (1 μg/μL, invitrogen), and 2.5 volume of absolute alcohol were added to the extract, and frozen at -80 ℃ for 20 min. The viral DNA was then precipitated by centrifugation at 13 000 *g* for 10 min, and finally resuspended in 20 μL TE buffer. As a control, 200 μL of each serum sample was used to isolate HBV DNA.

Standard HBV DNA

A plasmid containing Chinese HBV genome (pHBV-adr), kindly donated by Professor Yuan Wang[17], was isolated by CsCl purification. The DNA concentration was measured by A_{260} and verified by agarose gel electrophoresis. The copy number was determined by its molecule weight.

Oligonucleotide design

Previously, we used commercial detection kits to quantify HBV DNA in the sera[17]. To develop cheaper reagents and cover more HBV genotypes, we designed a set of primers and probes for this study. Various HBV genotypes undergo rapid mutagenesis because their reverse-transcriptase (RT) lacks proof-reading functions. To obtain specific PCR primers, we aligned over 150 sequences representing all the HBV genotypes, and designed a pair of primers for amplification of the S gene (conventional PCR) and core gene (quantitative PCR). Sequence alignments were carried out with the default settings using the BLAST algorithm (www.ncbi.nlm.nih.gov). Primers were chosen to facilitate amplification of most HBV genotypes. To achieve this goal, degenerated primers were designed. The primer pairs 5'-AGACTCGTGGTGGACTTCTCTC-3' (forward) and 5'-AAGCCA(A/T/C/G)ACA(A/G)TGGGGGAAAGC-3' (reverse) were used for amplification of the S gene in conventional PCR experiments while primers 5'-CCTGGGTGGGAAGTAATTTGG-3' (forward), 5'-TTTTA(A/G)GCCCATATTAACATTGACAT-3' (reverse), and TaqMan probe 5'-FAM-AGACCCA-GCATCCAGGGAATTAGTAGTCAGC-TAMRA-3' were used to amplify core gene fragments in real-time PCR experiments. These primers could target different regions, thereby providing an important cross-check for the results.

Conventional PCR

Conventional PCR was used to detect HBV DNA in sera

and semen. The PCR reactions were set in 20 μL volume containing 100 mmol/L Tris-HCl (pH 8.0), 2.5 mmol/L $MgCl_2$, 1 unit of Taq DNA polymerase (Premega, Wisconsin, USA), 200 μmol/L each of the deoxynucleotide, triphosphates (dNTP), 1 μmol/L each of primers, and 1 μL viral DNA as template in each reaction. Thermal cycling included an initiation step at 94 ℃ for 3 min, followed by 40 cycles at 94 ℃ for 30 s, at 60 ℃ for 30 s, and at 72 ℃ for 60 s. Products were visualized on agarose gels after electrophoresis.

Quantification of HBV viral DNA in serum and semen by real-time PCR

Each 20-μL reaction contained 2 μL of sample extracts (template), 250 nmol/L of the probe, 900 nmol/L of each PCR primer, and 10 μL Master Mix (Roche, New Jersey, USA). PCR was performed using the ABI 7900HT sequence detection system. PCR cycling program consisted of an initial background eliminating step at 50 ℃ for 5 min and a HotStart activation step at 95 ℃ for 10 min, followed by 40 amplification cycles at 95 ℃ for 15 s, and at 61 ℃ for 40 s. The PCR products were further confirmed by electrophoresis loaded in 2% agarose gels. The experiments were repeated twice.

RESULTS

Detection of HBV DNA in sera and semen by PCR

To detect hepatitis B viral DNA in the semen, HBV DNA was isloated from 200 μL of semen using QIAamp blood mini kit. Viral DNA was also isolated from the sera to serve as a control. Conventional PCR was carried out to amplify a 480-bp of DNA fragment. A specific fragment was amplified from viral DNA templates isolated from both sera and semen of HBV carriers (Patients 1 and 2), indicating that hepatitis B viruses existed in the semen of HBV carriers (Figure 1). The bands amplified from serum DNA (lanes 2 and 4) were much stronger than those amplified from semen DNA (lanes 3 and 5), indicating that the viral titers were much lower in semen than in sera. No DNA fragment was amplified from the samples (sera and semen) from the patient with HBsAb only or without any HBV markers (Patients 3-5, data not shown).

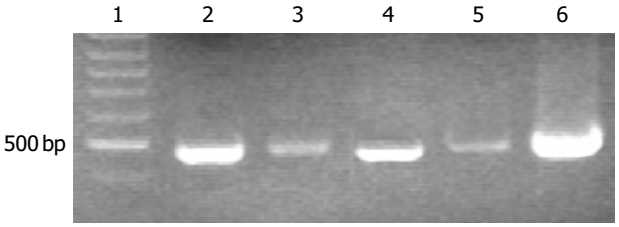


Figure 1 Detection of HBV DNA in sera and semen of HBV carriers by PCR. Lane 1: 100 bp DNA ladder; lanes 2 and 3: sera and semen of patient 1; lanes 4 and 5: sera and semen of patient 2; lane 6: positive control (pHBV plasmid).

Quantification of HBV DNA in sera and semen by real-time PCR

To test the performance of our primers and probes in real-time PCR, we used 10, 10^2, 10^3, 10^4, 10^5, 10^6, and 10^7 copies of HBV DNA[17]. Our results showed that amplification performance was good in all reactions (Figure 2A). A linear relationship was observed between 10 and 10^7 copies of HBV templates (Figure 2B). The viral titers in the sera and semen of patients were further quantified by real-time PCR. The consistent values of the qPCR were obtained by three independent qPCR (Table 2). We detected 7.56×10^7 copies of HBV per mL in the sera, but only 2.14×10^5 copies per mL in the semen of patient 1. Similar results were obtained from patient 2. We observed that the ratio of viral load in semen to sera was 0.3% in patient 1 and 1.8% in patient 2, respectively. The viral DNA isolations with different methods did not result in a statistically-significant difference (Student's *t*-test). As we expected, no viral DNA was detected in the samples from non-infected patients (patient 5) or from the patient with positive HBsAb only (patients 3 and 4).

To validate whether our methods could apply to low-volume semen samples, we isolated HBV DNA from 10, 50 and 200 μL of semen and quantified HBV DNA copies by real-time PCR. Again, all experiments produced consistent results (Table 3), indicating that our methods could indeed be used to quantify HBV DNA with low-volume semen samples.

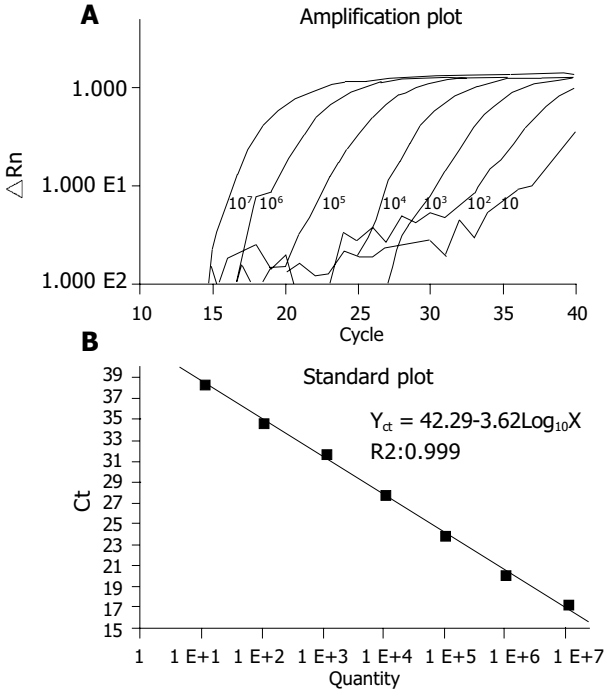


Figure 2 Real-time PCR profile. The amplification profile when 10-10^7 copies of HBV DNA were used (**A**) and standard curve (**B**).

DISCUSSION

In this study, we found that TaqMan technology-based real-time PCR assay could be used to quantify HBV DNA in semen. As this method is highly sensitive and reproducible, and has a wide dynamic linear range, it can be used to monitor HBV viral load in small samples of body fluids.

Table 2 Viral load in sera and semen of HBV carriers

Sample[1]	Method of HBV DNA Isolation	HBV DNA (copies / mL)[2]			Mean	SD[3]
		1	2	3		
Sera-1	Qiagen kit	6.73×10^6	7.14×10^6	8.8×10^6	7.56×10^7	1.11×10^7
Semen-1	Qiagen kit	2.18×10^5	2.34×10^5	1.69×10^5	2.14×10^5	4.31×10^4
Semen-1	Phenol	1.82×10^5	2.31×10^5	1.98×10^5	2.04×10^5	2.52×10^4
Sera-2	Qiagen kit	1.82×10^7	1.73×10^7	1.47×10^7	1.67×10^7	1.82×10^6
Semen-2	Qiagen kit	2.81×10^5	2.59×10^5	3.67×10^5	3.02×10^5	5.71×10^4
Semen-2	Phenol	3.58×10^5	2.62×10^5	2.41×10^5	2.87×10^5	5.22×10^5

[1]Sample from patient 1 or 2. [2]Data show the average of each independent experiment. [3]SD represents standard deviation.

Table 3 Viral load in different volumes of semen (copies/mL)

Sample	Method of HBV DNA isolation	10 μL	50 μL	200 μL
Semen-1	Qiagen kit	2.37×10^5	2.26×10^5	2.43×10^5
	Convention	2.25×10^5	3.04×10^5	1.80×10^5
Semen-2	Qiagen kit	2.76×10^5	2.92×10^5	2.87×10^5
	Convention	2.38×10^5	2.56×10^5	2.74×10^5

The detection threshold of this assay is 10 copies of HBV DNA per reaction.

Traditionally, HBV in sera is monitored by antigen/antibody test, Dot blot, Southern blot, branched DNA assay, or hybrid capture test[2,18,19]. The minimal template requirement for these assays on blood is at least 7×10^5 copies of HBV DNA per millilter. The threshold of Roche Cobas RT-PCR commercial kit is 400 copies and that of New England DNA kit is around 100 copies. Due to sensitivity limitations, these requirements often give rise to problems in clinical settings. A large portion of HBV patients with undetectable viral antigens or viral DNA often relapse after the cessation of anti-HBV treatments[19], and for this reason real-time PCR has been recently introduced to monitor HBV viral load in sera[18,21]. In this study, we introduced real-time PCR method to quantify HBV DNA in semen of HBV carriers. Possible PCR inhibitors in the seminal extracts may cause false results. To exclude this possibility, we measured viral load from a sample extracted by different methods, as well as by the same method but with a different amount of samples. Our assay produced consistent reproducible results (Tables 2 and 3). These results indicated that this method is highly accurate and reproducible.

Theoretically, our quantification method may be used to quantify HBV DNA with multiple genotypes or mutants. Since HBV genome undergoes fast mutagenesis, the designed PCR primers may not match to a special HBV template or a mutated HBV template with reduced sensitivity. To make our assay applicable to most HBV genotypes, we aligned multiple HBV genome sequences containing most genotypes, and then designed primers targeting the most conserved core region. In addition, we defined the hot spot mutation sites in the HBV genome and designed degenerated PCR primers that could match the natural HBV templates or accumulated HBV mutations during anti-HBV treatment.

The use of TaqMan probe-based real-time PCR to quantify HBV DNA in body fluids has a number of advantages. Firstly, it is highly sensitive and accurate. As shown in Figure 2, as few as 10 copies of HBV template (corresponding to 500 copies of HBV DNA/mL semen) were sufficient to produce a marked amplification profile in the PCR reaction, and a wide linear range from 10 to 10^7 copies of HBV DNA was obtained. Real-time PCR can therefore be used to monitor HBV DNA in small samples of body fluid. Secondly, it has a low background. We noticed that there was no detectable HBV DNA either in the sera of non-HBV-carriers or in the semen of patients 3-5. When reaction and detection are carried out in the same reaction tube, the chance of contamination is greatly reduced. Thirdly, it could produce a very small number of false positive results. Positive results can only be obtained when PCR primers and molecular probes work in a small genomic element simultaneously. The chance of three specific primers targeting any other templates is very low. In our experiment, HBV DNA was not detected in the samples from non-HBV-infected patients. Fourthly, no PCR inhibitors were found in the semen, because consistent results were obtained from different DNA isolation methods. Finally, the method is quick and easy, and has a high throughput. A large number of samples can be simultaneously tested on a 96-well plate within 2-3 h. This is a particularly important consideration in clinical settings. There are about 200 million HBV carriers in China, and doctors need to know the HBV status of patients before medical treatments such as assisted reproduction, surgery, transfusion, and transplantation. These advantages make a popular way of quantifying HBV DNA in body fluids in the near future.

In summary, quantitative real-time PCR is a simple, sensitive, specific, and reproducible assay for the measurement of HBV viral load in semen. The viral load in body fluids, including semen and vaginal secretions, is an important parameter for the estimation of risk factor for HBV transmission through sexual contact.

REFERENCES

1 **Llovet JM,** Burroughs A, Bruix J. Hepatocellular carcinoma. *Lancet* 2003; **362**: 1907-1917

2 **Lai CL,** Ratziu V, Yuen MF, Poynard T. Viral hepatitis B. *Lancet* 2003; **362**: 2089–2094

3 **Lee WM.** Hepatitis B virus infection. *N Engl J Med* 1997; **337**: 1733-1745

4 **Spada E,** Mele A, Ciccozzi M, Tosti ME, Bianco E, Szklo A, Ragni P, Gallo G, Balocchini E, Sangalli M, Lopalco PL, Moiraghi A, Stroffolini T. SEIEVA collaborating group. Changing epidemiology of parenterally transmitted viral hepatitis: results from the hepatitis surveillance system in Italy. *Dig Liver Dis* 2001; **33**: 778-784

5 **Judson FN**. Epidemiology of sexually transmitted hepatitis B infections in heterosexuals: a review. *Sex Transm Dis* 1981; **8** (4 Suppl): 336-343
6 **Wang S,** Peng G, Li M, Xiao H, Jiang P, Zeng N, Wang Z. Identification of hepatitis B virus vertical transmission from father to fetus by direct sequencing. *Southeast Asian J Trop Med Public Health* 2003; **34**: 106-113
7 **Jenison SA,** Lemon SM, Baker LN, Newbold JE. Quantitative analysis of hepatitis B virus DNA in saliva and semen of chronically infected homosexual men. *J Infect Dis* 1987; **156**: 299-307
8 **Davison F,** Alexander GJ, Trowbridge R, Fagan EA, Williams R. Detection of hepatitis B virus DNA in spermatozoa, urine, saliva and leucocytes, of chronic HBsAg carriers. A lack of relationship with serum markers of replication. *J Hepatol* 1987; **4**: 37-44
9 **Karayiannis P,** Novick DM, Lok AS, Fowler MJ, Monjardino J, Thomas HC. Hepatitis B virus DNA in saliva, urine, and seminal fluid of carriers of hepatitis B e antigen. *Br Med J* 1985; **290**: 1853-1855
10 **Scott RM,** Snitbhan R, Bancroft WH, Alter HJ, Tingpalapong M. Experimental transmission of hepatitis B virus by semen and saliva. *J Infect Dis* 1980; **142**: 67-71
11 **Eastlund T.** Infectious disease transmission through cell, tissue, and organ transplantation: reducing the risk through donor selection. *Cell Transplant* 1995; **4**: 455-477
12 **Berry WR,** Gottesfeld RL, Alter HJ, Vierling JM. Transmission of hepatitis B virus by artificial insemination. *JAMA* 1987; **257**: 1079-1081
13 **Mascola L,** Guinan ME. Screening to reduce transmission of sexually transmitted diseases in semen used for artificial insemination. *N Engl J Med* 1986; **314**: 1354-1359
14 **Abe A,** Inoue K, Tanaka T. Quantitation of hepatitis B virus genomic DNA by real-time detection PCR. *J Clin Microbiol* 1999; **37**: 2899-2903
15 **Heid CA,** Stevens J, Livak KJ, Williams PM. Real-time quantitative PCR. *Genome Res* 1996; **6**: 986-994
16 **Gibson UE,** Heid CA, Williams PM. A novel method for real time quantitative RT-PCR. *Genome Res* 1996; **6**: 995-1001
17 **He ML,** Wu J, Chen Y, Lin MC, Lau GK, Kung HF. A new and sensitive method for the quantification of HBV cccDNA by realtime PCR. *Biochem Biophys Res Commun* 2002; **295**: 1102-1107
18 **Xunrong L,** Yan AW, Liang R, Lau GK. Hepatitis B virus (HBV) reactivation after cytotoxic or immunosuppressive therapy-pathogenesis and management. *Rev Med Virol* 2001; **11**: 287-299
19 **Lau GK,** He ML, Fong DY, Bartholomeusz A, Au WY, Lie AK, Locarnini S, Liang R. Preemptive use of lamivudine reduces hepatitis B exacerbation after allogeneic hematopoietic cell transplantation. *Hepatology* 2002; **36**: 702-709
20 **Lewin SR,** Ribeiro RM, Walters T, Lau GK, Bowden S, Locarnini S, Perelson AS. Analysis of hepatitis B viral load decline under potent therapy: complex decay profiles observed. *Hepatology* 2001; **34**: 1012-1020

Science Editor Wang XL and Li WZ **Language Editor** Elsevier HK

PO Box 2345, Beijing 100023, China
www.wjgnet.com
wjg@wjgnet.com

ELSEVIER

World J Gastroenterol 2005;11(34):5390-5391
World Journal of Gastroenterology ISSN 1007-9327
© 2005 The WJG Press and Elsevier Inc. All rights reserved.

• *CASE REPORT* •

Withdrawing method of the stiffening tube incidentally inserted into the descending colon

Shinsaku Fukuda, Tatsuya Mikami, Tadashi Shimoyama, Norihiro Hanabata, Hideki Iwamura, Akihiro Munakata

Shinsaku Fukuda, Tatsuya Mikami, Tadashi Shimoyama, Norihiro Hanabata, Akihiro Munakata, First Department of Internal Medicine, Hirosaki University School of Medicine, Hirosaki, Japan
Hideki Iwamura, Tsugaru Center Hospital for Adult, Tsugaru, Japan
Correspondence to: Dr. Tatsuya Mikami, First Department of Internal Medicine, Hirosaki University School of Medicine, 5 Zaifu-cho, Hirosaki, Aomori 036-8562, Japan. tmika@cc.hirosaki-u.ac.jp
Telephone: +81-172-39-5053 Fax: +81-172-37-5946
Received: 2005-02-04 Accepted: 2005-03-23

Abstract

We experienced a very rare complication of colonoscopy, a migration of stiffening tube into the colorectum. We herein introduce a withdrawing method of migrating stiffening tube incidentally inserted into the colorectum. A 65-year-old Japanese woman underwent colonoscopy because of abdominal discomfort. We used stiffening tube to insert the scope to the proximal colon because of her redundant sigmoid colon. When withdrawing the scope, we realized that the tube was fully inside the colorectum. We could not remove the tube instantly, and it reached the splenic flexure, finally. We reinserted the scope through the migrating tube, straightened the scope, and withdrew it holding a slight angle of the scope over the proximal end of the tube. Then, we could safely remove the tube along with the scope through the anus.

© 2005 The WJG Press and Elsevier Inc. All rights reserved.

Key words: Colonoscopy; Complication; Migration; Stiffening tube

Fukuda S, Mikami T, Shimoyama T, Hanabata N, Iwamura H, Munakata A. Withdrawing method of the stiffening tube incidentally inserted into the descending colon. *World J Gastroenterol* 2005; 11(34): 5390-5391
http://www.wjgnet.com/1007-9327/11/5390.asp

INTRODUCTION

Colonoscopy is now performed as a screening exam or as a diagnosing procedure, when the patient has some clinical manifestations of colorectal diseases. Stiffening tube is a useful device sometimes used to facilitate the insertion of colonoscope into the proximal colon[1]. We experienced a very rare untoward event that stiffening tube was fully inserted incidentally into the descending colon, and then drawn out successfully through the anus. We herein introduce the safe and easy withdrawing method.

CASE REPORT

A 65-year-old Japanese woman visited our hospital because of abdominal discomfort. We performed colonoscopy (using the scope: Olympus PCF 240I) with the aid of fluoroscopy. Her sigmoid colon was very long and redundant and made a loop when inserting the scope into the descending colon. We removed the loop after reaching the splenic flexure, and then inserted the stiffening tube (Olympus ST-C6S; about 30 cm in length) over the scope gently. However, it was very difficult to advance the scope into the cecum, because her transverse colon was also long and ptotic.

When withdrawing the colonoscope from transverse colon to descending colon, we realized that the stiffening tube was fully inside the colorectum. The distal end of the tube was inside the rectum, so we removed the scope and firstly tried to grasp the tube by our digits through the anus, but failed. W then inserted the scope again and attempted to grasp by biopsy forceps or grasping forceps, but the stiffening tube migrated gradually into the splenic flexure finally (Figure 1A). We therefore reinserted another stiffening tube along with the scope and tried to connect with the migrated tube according to the previous report[2]. However, we could not connect the two tubes smoothly.

We reinserted the scope through the migrated tube until the proximal end of the tube (Figure 2). After we assured that the scope was straight by fluoroscopy, we made a slight angle of the scope over the proximal end of the tube (Figure 1B). We withdrew the scope very slowly holding the slight angle (Figure 3), and the stiffening tube was successfully removed together from the anus (Figure 1C). There were no mucosal damages after this procedure. She went home without abdominal pain or hematochezia after about 1-h rest.

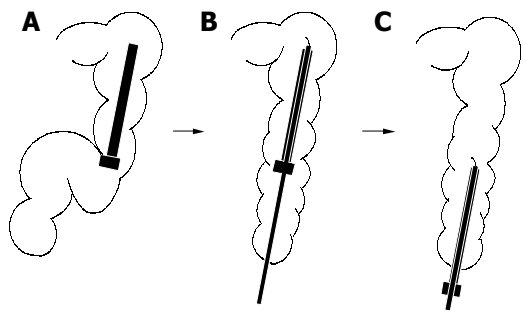


Figure 1 Schema shows our method briefly. **A**: The sliding tube was fully inserted into the descending colon incidentally; **B**: we reinserted the colonoscope through the migrating tube and made a slight angle; **C**: finally, we could remove the tube along with the scope by holding the angle of the scope.

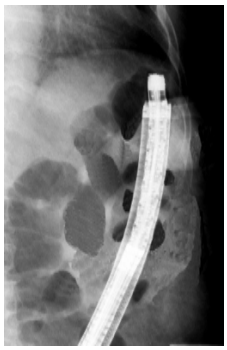


Figure 2 Abdominal X-ray shows that the oral edge of the stiffening tube reaches near the splenic flexure. We reinserted the endoscope through the tube.



Figure 3 We made a slight angle of the scope over the oral end of the stiffening tube and removed the scope gently.

DISCUSSION

Endoscopic examination has now been routinely performed for colorectal diseases or screening. The stiffening tube is an instrument to maintain the sigmoid colon straight, when endoscopists insert the scope into the proximal colon[1]. Colonoscopes have improved in design, and there are many scopes available including the variable stiffness colonoscope[3]. Although the stiffening tube is not necessary when using the variable stiffness scope, they have not spread yet all over the world.

We sometimes used stiffening tube when we have to use other scopes, especially for the patients who are thought to have long and redundant sigmoid colon. Some complications may arise by the insertion of the stiffening tube, for example, bleeding or perforation[4]. We experienced a very rare complication, migration of the stiffening tube into the colorectum. There was only one report of the migration of the tube so far[2]. They successfully drew it through the anus using a balloon-attached endoscope and another stiffening tube. We tried their method, but could not connect two tubes straight. There was also a risk that colonic mucosa was involved between two tubes by this method.

Anyway, straightening is necessary between descending colon and rectum when withdrawing the migrated stiffening tube. So we reinserted the colonoscope through the migrated tube, straightened the scope, and attempted to withdraw the migrated tube together with scope making a slight angle. It is necessary to make sure that there are no mucosal damages, after withdrawing the scope and stiffening tube.

When the stiffening tube was fully inserted into the colorectum, we recommended our method at first, before withdrawing the scope only and leaving the tube inside the colorectum.

Needless to say, it is most important that the distal edge of the tube is always grasped during colonoscopy to prevent complications like this.

REFERENCES

1 **Deyhle P.** A plastic tube for the maintenance of the straightening of the sigmoid colon during colonoscopy. *Endoscopy* 1972; **4**: 224-226

2 **Nakagawa T,** Kodama T, Watanabe Y, Suzuki M, Nakaya S, Inaba H, Yoneshima M, Kitajima S, Saito N, Akaishi O, Yamada K, Abiko R, Endo T, Kusakari K. The endoscopic method of drawing out a sliding tube which slipped into the descending colon: A case report. *Gastroenterol Endosc* 2000; **42**: 1864-1867

3 **Brooker JC,** Saunders BP, Shah SG, Williams CB. A new variable stiffness colonoscope makes colonoscopy easier: a randomised controlled trial. *Gut* 2000; **46**: 801-805

4 **Shinya H,** Wolff WI. Colonoscopy. *Surg Annu* 1976; **862**: 257-295

Science Editor Guo SY **Language Editor** Elsevier HK

PO Box 2345, Beijing 100023, China
www.wjgnet.com
wjg@wjgnet.com

ELSEVIER

World J Gastroenterol 2005;11(34):5392-5393
World Journal of Gastroenterology ISSN 1007-9327
© 2005 The WJG Press and Elsevier Inc. All rights reserved.

• *CASE REPORT* •

Acute sensorineural hearing loss associated with peginterferon and ribavirin combination therapy during hepatitis C treatment: Outcome after resumption of therapy

Victor K Wong, Cindy Cheong-Lee, Jo-Ann E Ford, Eric M Yoshida

Victor K Wong, Eric M Yoshida, Department of Medicine, Vancouver, BC, Canada
Cindy Cheong-Lee RN, Jo-Ann E Ford, Eric M Yoshida, University of British Columbia and the British Columbia Hepatitis Program, Vancouver, BC, Canada
Correspondence to: Dr. Eric M Yoshida, Division of Gastroenterology, Vancouver General Hospital, 100-2647 Willow Street, Vancouver, BC V5Z 3P1, Canada. eyoshida@interchange.ubc.ca
Telephone: +1-604-875-5371 Fax: +1-604-875-5371
Received: 2005-03-28 Accepted: 2005-04-18

Abstract

Peginterferon and ribavirin combination therapy for the treatment of hepatitis C virus (HCV) is well known to be associated with significant adverse effects. Sensorineural hearing loss, that in most cases is unilateral, has been reported as a consequence of therapy with both non-pegylated and pegylated interferon (pegIFN) but is not a well-known adverse effect. We report a 45-year-old Caucasian woman who developed acute sensorineural hearing loss 2 mo after starting therapy with pegIFN-α 2b and ribavirin for the treatment of chronic HCV, genotype 1a. She did not report the hearing loss to the hepatitis clinic until 1 mo, later whereupon therapy was promptly discontinued. Although her serum alanine aminotransferase (ALT) normalized and her HCV-RNA became undetectable after 12 wk of pegIFN and ribavirin therapy, after discontinuation, her HCV-RNA became detectable with significant elevations of serum ALT. Four months after initial discontinuation, the patient re-commenced pegIFN and ribavirin combination therapy. After 44 of 48 wk of therapy, the patient's liver biochemistry has normalized and the HCV-RNA is undetectable. She has not developed worsening of her hearing loss and hearing on the left-side is unaffected. Both patients and physicians should be aware that sensorineural hearing loss may occur with pegIFN therapy. Our experience suggests that re-institution of therapy is not always associated with further hearing impairment.

© 2005 The WJG Press and Elsevier Inc. All rights reserved.

Key words: Peginterferon; Hepatitis C; Sensorineural hearing loss

Wong VK, Cheong-Lee C, Ford JE, Yoshida EM. Acute sensorineural hearing loss associated with peginterferon and ribavirin combination therapy during hepatitis C treatment: Outcome after resumption of therapy. *World J Gastroenterol* 2005; 11(34): 5392-5393
http://www.wjgnet.com/1007-9327/11/5392.asp

INTRODUCTION

Chronic hepatitis C affects an estimated 300 million people worldwide, and within Canada, the prevalence is estimated between 0.75% and 1.0% of the general population[1]. Treatment of hepatitis C virus (HCV) with interferon alpha (IFN-α) 2b and ribavirin therapy has been shown to be effective for many years now, with 41-47% of patients achieving a sustained virologic response[2-4]. With the current pegylated interferons (pegIFN) and ribavirin combination, overall sustained virologic response rates are reported to be 54-56%[5-7].

In spite of the current popularity of pegIFN and ribavirin therapy, many reported side-effects with standard IFN-α ARE also seen with pegIFN combination therapy. Flu-like symptoms such as fever, chills, muscle ache, nausea, vomiting, and fatigue are common side effects of treatment. Depression and related symptoms, such as anxiety, irritability, insomnia, and mental confusion, are not rare and may be significant in patients with a previous history. Common hematologic side effects that require monitoring include neutropenia and thrombocytopenia. Withdrawal rates in IFN-based combination studies due to side effects have ranged from 6% to 7%[4,8].

Although IFN-based therapy has been reported to affect any organ system, there have been occasional reports of sudden hearing loss while on IFN therapy[9-14]. We report a case of sudden unilateral hearing loss in a patient with HCV being treated with pegIFN and ribavirin combination therapy. The interesting aspect of our case is that pegIFN combination therapy was re-commenced at the patient's request, despite the reservations of the hepatitis clinic staff.

CASE REPORT

A 45-year-old Caucasian woman with chronic hepatitis C (genotype 1a) acquired 25 years previously after the administration of Rh immune globulin, developed sudden onset of right sided hearing loss 2 mo after beginning therapy with pegIFN-α 2b at a dose of 1.5 μg/kg per week subcutaneously (100 μg/wk) and ribavirin 1 000 mg/d (Pegetron, Schering-Canada, Point-Clare QC, Canada). Before treatment, she had no evidence of decompensated liver disease and her serum alanine aminotransferase (ALT) was 132 U/L (upper limit of normal <36 U/L). At the time of her acute unilateral hearing loss, she had completed a course of antibiotics for an otis media in the left ear. The right-sided hearing loss was described as a sudden onset of deafness followed by marginal improvement such that the

patient could hear a telephone dial tone and low-pitched sounds associated with tinnitus. She was seen in consultation by an otolaryngologist who reported that both middle ears were normal on visual inspection. Audiometric testing performed approximately 1 mo after the acute hearing loss was consistent with severe unilateral right-sided sensorineural loss. The patient's pegIFN and ribavirin combination was discontinued immediately after the patient's disclosure, to the hepatitis clinic, of the unilateral hearing impairment 1 mo after onset and 3 mo after commencement of antiviral therapy. Although her liver enzymes normalized and her HCV-RNA was undetectable (qualitative Cobas Amplicor HCV Test, Roche-Diagnostics Canada, Laval QC, Canada; lower detection limit = 10-15 IU/mL) after 12 wk of therapy, within 2 mo after discontinuation, the HCV-RNA was again detectable and her serum ALT flared to 267 U/L. Symptomatically, her unilateral hearing impairment did not improve further and she was advised not to continue with further anti-HCV therapy. Despite medical advice to the contrary, she re-commenced pegIFN and ribavirin therapy 4 mo after the initial discontinuation. After 44 wk of continued pegIFN and ribavirin therapy, her serum liver biochemistry has remained persistently normal (serum ALT = 16 U/L at mo 9 of therapy) and her HCV-RNA was undetectable at wk 24 of therapy. She has not had any left-sided hearing impairment although her right-sided hearing remains significantly impaired.

DISCUSSION

Side effects of IFN therapy for HCV have been well documented. However, acute sensorineural hearing loss is relatively rarely reported and not well known amongst those who provide treatment for HCV. Several cases were reported of sudden hearing loss in patients with HCV being treated with the previous standard of non-pegylated IFN-α2 therapy[10–13], presumably on the basis of focal small vessel vasculitis. One prospective study of 73 patients reported tinnitus and/or hearing loss in 32 patients (43.8%) during IFN therapy, and audiometry-documented sensorineural hearing loss in 27 cases (36.9%)[14]. These investigators reported that auditory disability frequently developed in the later stages of treatment, but most patients in this report recovered 7-14 d after the discontinuation of therapy.

More recently, Formann *et al*.[9], reported six cases of hearing loss that was associated with the current standard treatment of pegIFN and ribavirin combination therapy. In contrast to the study by Kanda *et al*., these authors reported that hearing loss did not fully resolve after discontinuation of the therapy with pegIFN but also did not worsen on continued treatment. Our patient developed unilateral sensorineural hearing loss that was associated with pegIFN and ribavirin therapy. Therapy was discontinued but subsequently re-instituted at the patient's request. Although the unilateral hearing loss was persistent, it did not worsen on re-treatment and bilateral hearing loss has not occurred.

We believe that sudden hearing loss as a side effect should be discussed, along with the other more commonly known side effects, with patients prior to being treated with standard or pegIFN therapy. We recommend that patients on interferon-based therapies should be monitored during treatment for changes in hearing perception. It remains possible that those who do develop sudden hearing loss can be continued on IFN therapy, if the risk-benefit ratio of treatment dictates.

REFERENCES

1 **Patrick DM,** Buxton JA, Bigham M, Mathias RG. Public health and hepatitis C. *Can J Public Health* 2000; **91**(Suppl 1): S18-23
2 **McHutchison JG,** Manns M, Patel K, Poynard T, Lindsay KL, Trepo C, Dienstag J, Lee WM, Jak C, Garaud JJ, Albrecht JK. International Hepatitis Interventional Therapy Group. Adherence to combination therapy enhances sustained response in genotype-1-infected patients with chronic hepatitis C. *Gastroenterology* 2002; **123**: 1061-1069
3 **Poynard T,** Marcellin P, Lee SS, Niederau C, Minuk GS, Ideo G, Bain V, Heathcote J, Zeuzem S, Trepo C, Albrecht T. Randomized trial of interferon alpha2b plus ribavirin for 48 wk or for 24 wk versus interferon alpha 2b plus placebo for 48 wk for treatment of chronic infection with hepatitis C virus. International Hepatitis Interventional Therapy Group (IHIT). *Lancet* 1998; **352**: 1426-1432
4 **McHutchison JG,** Gordon SC, Schiff ER, Shiffman ML, Lee WM, Rustgi VK, Goodman ZD, Ling MH, Cort S, Albrecht JK. Interferon alfa-2b alone or in combination with ribavirin as initial treatment for chronic hepatitis C. Hepatitis Interventional Therapy Group. *N Engl J Med* 1998; **339**: 1485-1492
5 **Manns MP,** McHutchison JG, Gordon SC, Rustgi VK, Shiffman M, Reindollar R, Goodman ZD, Koury K, Ling M, Albrecht JK. Peginterferon alfa-2b plus ribavirin compared with interferon alfa-2b plus ribavirin for initial treatment of chronic hepatitis C: a randomised trial. *Lancet* 2001; **358**: 958-965
6 **Fried MW,** Schiffman ML, Reddy KR, Smith C, Marinos G, Goncales FL Jr, Haussinger D, Diago M, Carosi G, Dhumeaux D, Craxi A, Lin A, Hoffman J, Yu J. Peginterferon alfa-2a plus ribavirin for chronic hepatitis C virus infection. *N Engl J Med* 2002; **347**: 975-982
7 **Hadziyannis SJ,** Sette H Jr, Morgan TR, Balan V, Diago M, Marcellin P, Ramadori G, Bodenheimer H Jr, Bernstein D, Rizzetto M, Zeuzem S, Pockros PJ, Lin A, Ackrill AM. PEGASYS International Study Group. *Ann Intern Med* 2004; **140**: 346-355
8 **Reichard O,** Norkrans G, Fryden A, Braconier JH, Sonnerborg A, Weiland O. Randomized, double-blind , placebo-controlled trial of interferon alpha-2-b with and without ribavirin for chronic hepatitis C. *Lancet* 1998; **351**: 83-87
9 **Formann E,** Stauber R, Denk DM, Jessner W, Zollner G, Munda-Seinedl P, Gangl A, Ferenci P. Sudden hearing loss in patients with chronic hepatitis C treated with pegylated interferon/ribavirin. *Am J Gastroenterol* 2004; **99**: 873-877
10 **Obrebowski A,** Walczak M, Swidzinski P, Karlik M, Kurywczak-Grykiel K, Obrebowska-Karsznia Z. *Otolarngol Pol* 2003: **57**: 531-555
11 **Cadoni G,** Marinelli L, De Santis A, Romito A, Manna R, Ottaviani F. Sudden hearing loss in a patient hepatitis C virus (HCV) positive on therapy with alpha-interferon: a possible autoimmune-microvascular pathogenesis. *J Laryngol Otol* 1998; **112**: 962-963
12 **Bailly F,** Mattei A, Si Ahmed SN, Trepo C. Sudden deafness induced by interferon-alpha in viral hepatitis. *Gastroenterol Clin Biol* 1997; **21**: 157-158
13 **Okanoue T,** Sakamoto S, Itoh Y, Minami M, Yasui K, Sakamoto M, Nishioji K, Katagishi T, Nakagawa Y, Tada H, Sawa Y, Mizuno M, Kagawa K, Kashima K. Side effects of high-dose interferon therapy for chronic hepatitis C. *J Hepatol* 1996; **25**: 283-291
14 **Kanda Y,** Shigeno K, Matsuo H, Yano M, Yamada N, Kumagami H. Interferon-induced sudden hearing loss. *Audiology* 1995; **34**: 98-102

Science Editor Guo SY **Language Editor** Elsevier HK

PO Box 2345, Beijing 100023, China
www.wjgnet.com
wjg@wjgnet.com

ELSEVIER

World J Gastroenterol 2005;11(34):5394-5397
World Journal of Gastroenterology ISSN 1007-9327
© 2005 The WJG Press and Elsevier Inc. All rights reserved.

• *CASE REPORT* •

Liver cirrhosis induced by long-term administration of a daily low dose of amiodarone: A case report

Hiroki Oikawa, Chihaya Maesawa, Ryo Sato, Kanta Oikawa, Hiroyuki Yamada, Seizo Oriso, Sadahide Ono, Akiko Yashima-Abo, Koji Kotani, Kazuyuki Suzuki, Tomoyuki Masuda

Hiroki Oikawa, Chihaya Maesawa, Kanta Oikawa, Akiko Yashima-Abo, Koji Kotani, Tomoyuki Masuda, Department of Pathology, Iwate Medical University School of Medicine, Morioka, Japan
Ryo Sato, Kazuyuki Suzuki, Department of Internal Medicine I, Iwate Medical University School of Medicine, Morioka, Japan
Hiroyuki Yamada, Seizo Oriso, Department of Internal Medicine, Iwate Prefectural Ninohe Hospital, Ninohe, Japan
Sadahide Ono, Department of Pathology, Iwate Prefectural Central Hospital, Morioka, Japan
Supported by Grants-in-Aid No. 16590289, 16790211 and 16790212, and "Open Research Center" Project for Private Universities: Matching fund Subsidy (2004-2008), from Ministry of Education, Culture, Sports, Science and Technology, Japan
Correspondence to: Dr. Chihaya Maesawa, Department of Pathology, Iwate Medical University School of Medicine, Uchimaru 19-1, Morioka 020-8505, Japan. chihaya@iwate-med.ac.jp
Telephone: +81-19-651-5111 Fax: +81-19-629-9340
Received: 2005-01-18 Accepted: 2005-04-09

Abstract

The anti-arrhythmic agent amiodarone (AD) is associated with numerous adverse effects, but serious liver disease is rare. The improved safety of administration of daily low doses of AD has already been established and this regimen is used for long-term medication. Nevertheless, asymptomatic continuous liver injury by AD may increase the risk of step-wise progression of non-alcoholic fatty liver disease. We present an autopsy case of AD-induced liver cirrhosis in a patient who had been treated with a low dose of AD (200 mg/d) daily for 84 mo. The patient was a 85-year-old male with a history of ischemic heart disease. Seven years after initiation of treatment with AD, he was admitted with cardiac congestion. The total dose of AD was 528 g. Mild elevation of serum aminotransferase and hepatomegaly were present. Liver biopsy specimens revealed cirrhosis, and under electron microscopy numerous lysosomes with electron-dense, whorled, lamellar inclusions characteristic of a secondary phospholipidosis were observed. Initially, withdrawal of AD led to a slight improvement of serum aminotransferase levels, but unfortunately his general condition deteriorated and he died from complications of pneumonia and renal failure. Long-term administration of daily low doses of AD carries the risk of progression to irreversible liver injury. Therefore, periodic examination of liver function and/or liver biopsy is required for the management of patients receiving long-term treatment with AD.

© 2005 The WJG Press and Elsevier Inc. All rights reserved.

Key words: Amiodarone; Liver cirrhosis; NASH; NAFLD; Liver biopsy

Oikawa H, Maesawa C, Sato R, Oikawa K, Yamada H, Oriso S, Ono S, Yashima-Abo A, Kotani K, Suzuki K, Masuda T. Liver cirrhosis induced by long-term administration of a daily low dose of amiodarone: A case report. *World J Gastroenterol* 2005; 11(34): 5394-5397
http://www.wjgnet.com/1007-9327/11/5394.asp

INTRODUCTION

Amiodarone (AD) is a cationic, amphophilic, iodinated benzofuran derivative primarily used for the treatment of refractory ventricular tachyarrythmias[1]. Although AD has been used since 1962, it causes various side effects affecting the lung, thyroid gland, cornea, peripheral nerves, and liver[1-3]. In early clinical trials, higher maintenance doses of AD (300-800 mg/d) caused serious side effects in the first year of therapy, and these patients required drug withdrawal[1-6]. In the last two decades, several investigators have shown that daily lower doses of AD (<200 mg/d) are better tolerated but still possess appreciable efficacy in serious cardiac arrhythmias[4-6].

The hepatotoxicity associated with AD is manifested as an asymptomatic and transient elevation of serum aminotransferase[2,3,6-8]. Fortunately, the vast majority of these events are reversible after discontinuation of the medication[2,3,6]. The safer schedule of administration of low doses daily may contribute to reducing the incidence of serious hepatic adverse effects. The histologic appearance of AD-induced liver disease shares several features with that of alcoholic hepatitis. Asymptomatic continuous liver injury by AD may increase the risk of step-wise progression of non-alcoholic fatty liver disease (NAFLD)[7-19]. This implies that severe morphological alterations of the liver may coexist with very mild symptoms in patients receiving long-term treatment with daily low doses of AD. We present herein an autopsy case of AD-induced liver cirrhosis in a patient treated with a low dose of AD daily for 84 mo. We discuss the risk of progression to irreversible liver injury during administration of AD and the value of liver biopsy for patients receiving long-term treatment with a low dose of AD daily.

CASE REPORT

A 85-year-old male with a history of ischemic heart disease

was being treated with AD for continuing symptomatic ventricular arrhythmias. He was admitted with cardiac congestion in December 2001, 7 years after administration of AD had begun. There was no history of alcohol abuse, obesity or diabetes mellitus. Serological screening and PCR examination for hepatitis viruses were all negative. There were no signs of autoimmune hepatitis. His initial dose of AD was 400 mg daily for 17 d, which was then reduced to a maintenance dose of 200 mg daily. The patient had received continuous medication with AD for 84 mo. On physical examination, corneal opacities were found. No skin discoloration or neuronal symptoms were seen.

Serum total bilirubin was 1.2 mg/dL, aspartate aminotransferase 81 IU/L, alanine aminotransferase 35 IU/L, alkaline phosphatase 452 IU/L, gamma-glutamyl transpeptidase 210 IU/L, lactate dehydrogenase 848 IU/L, and prothrombin time activity 59%. Up to that time, no elevation of serum aminotransferase or signs suggesting liver dysfunction had been observed.

The chest radiograph revealed cardiac enlargement and bilateral pleural effusion without findings of interstitial fibrosis. Abdominal ultrasonography showed enlargement of the left lobe of the liver relative to atrophy of the right lobe, and an irregular liver surface. In addition, ascites and mild splenomegaly were seen. An unenhanced computed tomography (CT) scan of the upper abdomen showed an abnormally high density of liver tissue [111.8 Hounsfield units (HU); normal range 30-70 HU] (Figure 1). A percutaneous liver biopsy examination revealed micronodular cirrhosis accompanied by findings of alcoholic liver disease (Figure 2). Fibrous septa containing proliferating bile ductules and neutrophil polymorphs connected adjacent portal areas (Figure 2). Scattered foci of hepatocellular necrosis with neutrophilic infiltration were observed (Figure 2). Electron microscopic observations showed that hepatocytes contained numerous lysosomes with electron-dense, whorled, lamellar inclusions (LI), characteristic of a secondary phospholipidosis (Figure 3). The findings of the CT scan and the liver biopsy indicated that AD-induced liver cirrhosis was responsible for the hepatotoxicity and his poor general condition. Administration of AD was discontinued. The total dose of AD administered over the 84 mo was 528 g.

Initially, withdrawal of AD led to a slight improvement in the serum aminotransferase level and the ascites. The CT density of the liver decreased to 97.2 HU in February 2002, whereas no significant improvement was observed in the size of the liver. Unfortunately, his general condition deteriorated as a result of complications of pneumonia and renal failure. He died in April 2002.

Autopsy was performed on April 22nd, 2002. Microscopically, features affected by AD were observed in the follicular epithelial cells of the thyroid gland and in the liver. Notably, there were no histological findings suggesting AD-induced pulmonary toxicity, which is more common and often more serious than hepatotoxicity, whereas both his lungs revealed congestion with pneumonic foci.

We compared the light-microscopic and electron-microscopic findings for the biopsy (December 2001) and autopsy (April 2002) materials (Table 1). Light microscopy of the autopsy materials also revealed micronodular cirrhosis. The biopsy material showed both microvesicular and macrovesicular steatosis, but the autopsy material showed only microvesicular steatosis. The number of hepatocytes with Mallory bodies was similar to that of the biopsy specimen. We counted the number of lysosomes

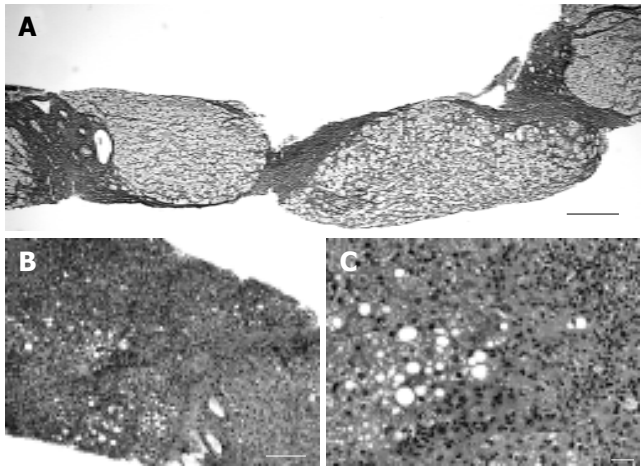


Figure 2 Microscopic features of the liver biopsy specimen. **A**: Micronodular cirrhosis has become established (silver impregnation, scale bar = 200 μm); **B**: Low power view of the liver biopsy specimen (hematoxylin and eosin stain, scale bar = 200 μm). Fatty degeneration and marked fibrosis with inflammatory cell infiltration were observed; **C**: High power view of the liver biopsy specimen (hematoxylin and eosin stain, scale bar = 20 μm). Foci of hepatocellular necrosis and dense fibrosis with neutrophilic infiltration were observed. Hepatocytes showed both the microvesicular and macrovesicular types of steatosis.

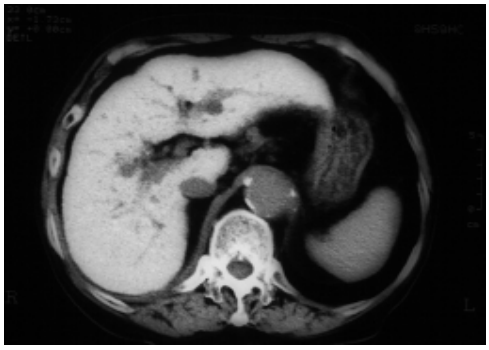


Figure 1 An unenhanced computed tomography (CT) scan of the upper abdomen. The liver has a greatly increased density (111.8 HU).

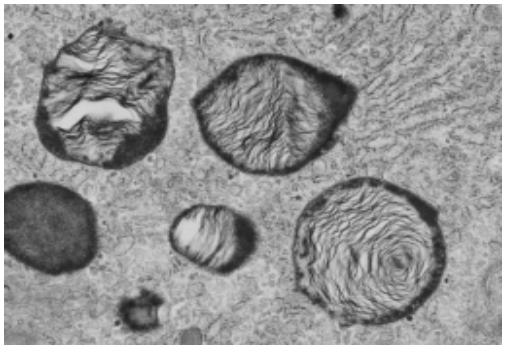


Figure 3 Transmission electron micrograph of the biopsy specimen with lamellated inclusions in the cytoplasm of the hepatocyte (original magnification ×20 000).

with LI relative to the total number of lysosomes in the liver. The incidence was relatively lower in the autopsy specimen compared with the biopsy specimen (Table 1). Unfortunately, we could not assess the tissue concentration of AD.

Table 1 Comparison of CT density and light and electron microscopic findings between biopsy and autopsy specimens of the liver

	Biopsy	Autopsy
CT density (HU)	111.8	97.2
Light microscopic findings		
Nodular formation	Micronodular	Micronodular
Fibrosis	Dense	Dense
Steatosis	Macro / microvesicular	Microvesicular
Infiltration of inflammatory cells	Moderate	Moderate
Electron microscopic findings		
Number of lysosomes with lamellar inclusion / total number of lysosomes (%)[1]	992 / 2 726 (36.4%)	862 / 2 578 (33.4%)

[1]Counts were performed of 10 fields (×18 000) of five blocks for each material.

DISCUSSION

The true incidence of AD-induced liver cirrhosis is obscure, since liver biopsy has not been performed routinely in AD-treated patients. Almost all cases of AD-induced liver cirrhosis have been reported in patients receiving higher maintenance doses[15,16], and only five cases arising from administration of daily low doses have been described in the literature (Table 2)[12-14,18,19]. Some investigators have speculated that the total cumulative dose might be more important in estimating the risk of irreversible liver injury[10,15,16]. The cumulative doses of the patients previously reported ranged from 165 to 213 g, with a duration of treatment of 12-48 mo. The present patient had been treated with 200 mg of AD daily for 84 mo, with a total cumulative dose of 528 g. Even though this dosage is greater than that in previous reports, hepatic abnormalities were not detected during the course of treatment. As asymptomatic progression of liver disease might occur more frequently in patients receiving long-term treatment with AD, periodic examination of liver function and/or biopsy should be performed to detect liver injury. Gilinsky *et al*.[9] described that drug withdrawal was insufficient to restore liver function, if irreversible liver damage had already occurred. Early histological examination for hepatic abnormalities is helpful to warn off irreversible liver changes.

Table 2 Summary of published cases of cirrhosis after long-term administration of daily low doses of AD

No	Reference	Age (yr)	Duration (mo)	Cumulative dose (g)	Outcome
1	Present case	85	84	528	Dead
2	12	76	48	Not described	Dead
3	13	68	13.5	165	Dead
4	14	77	12	202	Dead
5	18	79	33	200	Dead
6	19	83	35	213	Non-fatal

We suggest that genetic background might also be important in determining the risk of progression of NAFLD in patients receiving long-term treatment with AD. It is well known that steatosis and non-alcoholic steatohepatitis (NASH) can be induced by drugs such as tamoxifen, some anti-retroviral agents and AD[20-22]. These drugs inhibit the mitochondrial β-oxidation of fatty acids (causing steatosis) and respiration[20,23]. Inhibition of respiration decreases ATP and also increases the mitochondrial formation of reactive oxygen species (ROS). In hepatocytes, ROS and lipid peroxidation products further impair the respiratory chain, either directly or indirectly through oxidative damage to the mitochondrial genome. Mitochondrial dysfunction can also lead to apoptosis or necrosis, depending on the energy status of the cell. ROS and lipid peroxidation products also activate stellate cells, thus resulting in fibrosis. Finally, ROS and lipid peroxidation increase the generation of several cytokines (TNF-α, TGF-β, and Fas ligand) that play various roles in the pathogenesis of drug-induced NASH[20,23].

Some investigators have postulated that in insulin resistance the combination of elevated plasma concentrations of glucose and fatty acids promotes hepatic fatty acid synthesis and impairs oxidation, leading to hepatic steatosis[20,24,25]. Several polymorphisms in genes related to insulin resistance appear to be associated with the severity of steatosis[25-29]. We examined a few polymorphisms in the *TNF-α*, *HFE*, *CYP2E1*, and *IL-10* genes, but the susceptibility alleles were not present in the patient (data not shown). However, we are now undertaking a genome-wide single nucleotide polymorphism study in patients with drug-induced NASH[20]. Further, several experimental and clinical studies suggest that a number of drugs could be useful for the prevention and/or treatment of NASH. These genetic and clinical approaches may help increase the safety of the long-term administration of AD.

REFERENCES

1 **Mason JW.** Amiodarone. *N Engl J Med* 1987; **316**: 455-466
2 **Kowey PR,** Friehling TD, Marinchak RA, Sulpizi AM, Stohler JL. Safety and efficacy of amiodarone. The low-dose perspective. *Chest* 1988; **93**: 54-59
3 **Kerin NZ,** Aragon E, Faitel K, Frumin H, Rubenfire M. Long-term efficacy and toxicity of high- and low-dose amiodarone regimens. *J Clin Pharmacol* 1989; **29**: 418-423
4 **Nicklas JM,** McKenna WJ, Stewart RA, Mickelson JK, Das SK, Schork MA, Krikler SJ, Quain LA, Morady F, Pitt B. Prospective, double-blind, placebo-controlled trial of low-dose amiodarone in patients with severe heart failure and asymptomatic frequent ventricular ectopy. *Am Heart J* 1991; **122**: 1016-1021
5 **Singh SN,** Fletcher RD, Fisher SG, Singh BN, Lewis HD, Deedwania PC, Massie BM, Colling C, Lazzeri D. Amiodarone in patients with congestive heart failure and asymptomatic ventricular arrhythmia. Survival Trial of Antiarrhythmic Therapy in Congestive Heart Failure. *N Engl J Med* 1995; **333**: 77-82
6 **Vorperian VR,** Havighurst TC, Miller S, January CT. Adverse effects of low dose amiodarone: a meta-analysis. *J Am Coll Cardiol* 1997; **30**: 791-798
7 **Simon JB,** Manley PN, Brien JF, Armstrong PW. Amiodarone hepatotoxicity simulating alcoholic liver disease. *N Engl J Med* 1984; **311**: 167-172
8 **Poucell S,** Ireton J, Valencia-Mayoral P, Downar E, Larratt L, Patterson J, Blendis L, Phillips MJ. Amiodarone-associated

phospholipidosis and fibrosis of the liver. Light, immunohistochemical, and electron microscopic studies. *Gastroenterology* 1984; **86**: 926-936
9 **Gilinsky NH,** Briscoe GW, Kuo CS. Fatal amiodarone hepatoxicity. *Am J Gastroenterol* 1988; **83**: 161-163
10 **Bach N,** Schultz BL, Cohen LB, Squire A, Gordon R, Thung SN, Schaffner F. Amiodarone hepatotoxicity: progression from steatosis to cirrhosis. *Mt Sinai J Med* 1989; **56**: 293-296
11 **Harrison RF,** Elias E. Amiodarone-associated cirrhosis with hepatic and lymph node granulomas. *Histopathology* 1993; **22**: 80-82
12 **Tordjman K,** Katz I, Bursztyn M, Rosenthal T. Amiodarone and the liver. *Ann Intern Med* 1985; **102**: 411-412
13 **Rinder HM,** Love JC, Wexler R. Amiodarone hepatotoxicity. *N Engl J Med* 1986; **314**: 318-319
14 **Flaharty KK,** Chase SL, Yaghsezian HM, Rubin R. Hepatotoxicity associated with amiodarone therapy. *Pharmacotherapy* 1989; **9**: 39-44
15 **Lewis JH,** Ranard RC, Caruso A, Jackson LK, Mullick F, Ishak KG, Seeff LB, Zimmerman HJ. Amiodarone hepatotoxicity: prevalence and clinicopathologic correlations among 104 patients. *Hepatology* 1989; **9**: 679-685
16 **Lewis JH,** Mullick F, Ishak KG, Ranard RC, Ragsdale B, Perse RM, Rusnock EJ, Wolke A, Benjamin SB, Seeff LB. Histopathologic analysis of suspected amiodarone hepatotoxicity. *Hum Pathol* 1990; **21**: 59-67
17 **Babany G,** Mallat A, Zafrani ES, Saint-Marc Girardin MF, Carcone B, Dhumeaux D. Chronic liver disease after low daily doses of amiodarone. Report of three cases. *J Hepatol* 1986; **3**: 228-232
18 **Singhal A,** Ghosh P, Khan SA. Low dose amiodarone causing pseudo-alcoholic cirrhosis. *Age Ageing* 2003; **32**: 224-225
19 **Guigui B,** Perrot S, Berry JP, Fleury-Feith J, Martin N, Metreau JM, Dhumeaux D, Zafrani ES. Amiodarone-induced hepatic phospholipidosis: a morphological alteration independent of pseudoalcoholic liver disease. *Hepatology* 1988; **8**: 1063-1068
20 **Fromenty B,** Robin MA, Igoudjil A, Mansouri A, Pessayre D. The ins and outs of mitochondrial dysfunction in NASH. *Diabetes Metab* 2004; **30**: 121-138
21 **Fromenty B,** Fisch C, Labbe G, Degott C, Deschamps D, Berson A, Letteron P, Pessayre D. Amiodarone inhibits the mitochondrial beta-oxidation of fatty acids and produces microvesicular steatosis of the liver in mice. *J Pharmacol Exp Ther* 1990; **255**: 1371-1376
22 **Letteron P,** Sutton A, Mansouri A, Fromenty B, Pessayre D. Inhibition of microsomal triglyceride transfer protein: another mechanism for drug-induced steatosis in mice. *Hepatology* 2003; **38**: 133-140
23 **Samuel VT,** Liu ZX, Qu X, Elder BD, Bilz S, Befroy D, Romanelli AJ, Shulman GI. Mechanism of hepatic insulin resistance in non-alcoholic fatty liver disease. *J Biol Chem* 2004; **279**: 32345-32353
24 **Day CP.** The potential role of genes in nonalcoholic fatty liver disease. *Clin Liver Dis* 2004; **8**: 673-691
25 **Farrell GC.** Drugs and steatohepatitis. *Semin Liver Dis* 2002; **22**: 185-194
26 **Valenti L,** Fracanzani AL, Dongiovanni P, Santorelli G, Branchi A, Taioli E, Fiorelli G, Fargion S. Tumor necrosis factor alpha promoter polymorphisms and insulin resistance in nonalcoholic fatty liver disease. *Gastroenterology* 2002; **122**: 274-280
27 **George DK,** Goldwurm S, MacDonald GA, Cowley LL, Walker NI, Ward PJ, Jazwinska EC, Powell LW. Increased hepatic iron concentration in nonalcoholic steatohepatitis is associated with increased fibrosis. *Gastroenterology* 1998; **114**: 311-318
28 **Vidali M,** Stewart SF, Rolla R, Daly AK, Chen Y, Mottaran E, Jones DE, Leathart JB, Day CP, Albano E. Genetic and epigenetic factors in autoimmune reactions toward cytochrome P4502E1 in alcoholic liver disease. *Hepatology* 2003; **37**: 410-419
29 **Grove J,** Daly AK, Bassendine MF, Gilvarry E, Day CP. Interleukin 10 promoter region polymorphisms and susceptibility to advanced alcoholic liver disease. *Gut* 2000; **46**: 540-545

Science Editor Guo SY **Language Editor** Elsevier HK

PO Box 2345, Beijing 100023, China
www.wjgnet.com
wjg@wjgnet.com

ELSEVIER

World J Gastroenterol 2005;11(34):5398-5400
World Journal of Gastroenterology ISSN 1007-9327
© 2005 The WJG Press and Elsevier Inc. All rights reserved.

• *CASE REPORT* •

Asymptomatic early acute appendicitis initiated and diagnosed during colonoscopy: A case report

Michelle Petro, Anil Minocha

Michelle Petro, Anil Minocha, Division of Digestive Diseases, University of Mississippi Medical Center, Jackson, MS 39216, USA
Correspondence to: Anil Minocha, MD, Director, Division of Digestive Diseases, 2500 North State Street, Jackson, MS 39216, United States. aminocha@medicine.umsmed.edu
Telephone: +1-601-984-4545
Received: 2005-01-21 Accepted: 2005-02-18

Abstract

Colonoscopic diagnosis of asymptomatic early acute appendicitis is exceedingly rare. Although obstruction of the lumen due to various causes is believed to be the most common physiologic mechanism of acute appendicitis, all of the previously documented cases in the literature have only shown a patent appendiceal lumen with pus flowing into the cecum. We present the case of a patient undergoing colonoscopy for colorectal cancer evaluation with no abdominal symptoms. An obstructed, swollen appendix was seen. The process was probably initiated during the colonoscopy, documenting perhaps the earliest stage of acute appendicitis for the first time. Endoscopic, CT and microscopic documentation of the case is also presented.

© 2005 The WJG Press and Elsevier Inc. All rights reserved.

Key words: Colonoscopy; Appendicitis; Complications; Endoscopy

Petro M, Minocha A. Asymptomatic early acute appendicitis initiated and diagnosed during colonoscopy: A case report. *World J Gastroenterol* 2005; 11(34): 5398-5400
http://www.wjgnet.com/1007-9327/11/5398.asp

INTRODUCTION

Colonoscopic diagnosis of asymptomatic early acute appendicitis is exceedingly rare. Acute appendicitis has been described as a complication of colonoscopy[1-4]. Although obstruction of the appendiceal lumen due to various causes is believed to be the most common physiologic mechanism of acute appendicitis, the few endoscopically documented cases thus far have demonstrated a patent appendiceal lumen with pus flowing out. An obstructed appendix has not been documented earlier in the literature. We describe a case of a patient undergoing colonoscopy for evaluation of colorectal cancer that demonstrated an obstructed, swollen appendix, which is the earliest stage of acute appendicitis.

CASE REPORT

WT is a 53-year-old Caucasian gentleman who presented to our endoscopy suite for colonoscopic evaluation for colon cancer. Pre-colonoscopic evaluation did not reveal any abdominal pain, fever, chills, night sweats, nausea, vomiting, change of appetite, anorexia, hematemesis, diarrhea, constipation, hematochezia or melena. His past medical history was significant only for positive hepatitis C virus antibody. He had no past surgical history. His family history was negative for gastrointestinal cancer and polyps. His physical exam revealed a healthy Caucasian male in no acute distress with normal vital signs. Cardiovascular and pulmonary findings were within normal limits. Abdominal exam revealed normal active bowel sounds in all four quadrants. His abdomen was soft, without any evidence of tenderness or peritoneal signs.

He underwent an uneventful colonoscopy with one diminutive polyp removed with cold biopsy forceps in the ascending colon during the insertion phase. Once the cecum was reached, a mildly erythematous and markedly edematous appendiceal orifice was seen with the appendix bulging into the cecal lumen (Figure 1). The cecum was quickly deflated and the scope was withdrawn.



Figure 1 An obstructed and swollen appendix as seen during colonoscopy.

Surgical consultation was immediately requested. A complete blood count performed following the colonoscopy revealed a WBC count of 11.5 K with 70% segmented neutrophils and no bands.

The patient was admitted to the hospital. Although he felt well initially, later that afternoon he developed some tenderness at McBurney's point. A computed tomography scan of the abdomen revealed an enlarged appendix that was 1.6 cm in total diameter with a thickened appendiceal

wall measuring 6 mm (Figure 2). There were no fluid collections or strands around the appendix.

He underwent an uneventful open appendectomy post-colonoscopy and the intraoperative findings were consistent with mild, early acute appendicitis. Microscopy demonstrated very early, mild, acute appendicitis (Figure 3). There was acute mucosal inflammation with some necrosis, mild acute inflammation of the muscularis mucosa (less neutrophils than are typically seen with appendicitis), and mild acute serosal inflammation. The lumen had some pus in it. No perforation was seen. The patient did well and was discharged the next day.

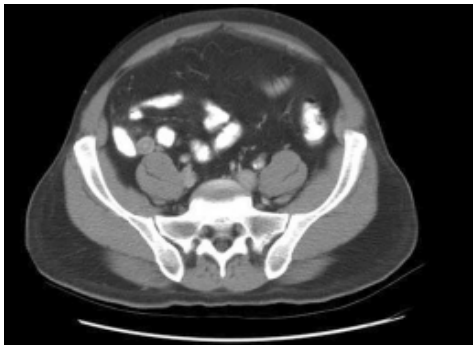


Figure 2 CT scan showing enlarged appendix (1.6 cm) with thickened appendiceal wall (6 mm).

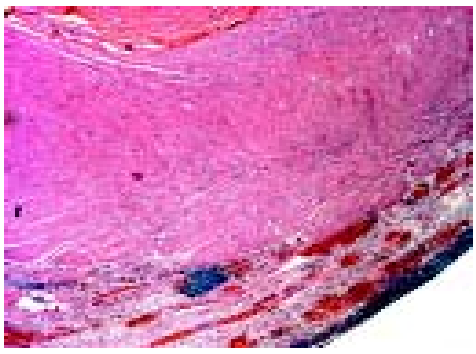


Figure 3 Histopathology of appendix.

DISCUSSION

Our case represents a unique situation of where appendicitis was diagnosed and probably initiated during the colonoscopy, thus documenting perhaps the earliest stage of the pathologic process.

Pathophysiology

Obstruction of the appendix is believed to be the inciting event for the development of acute appendicitis. In young patients, lymphoid follicular hyperplasia is the main cause. This process is either initiated or exacerbated by an infectious event. In elderly patients, obstruction is more likely to be caused by fibrosis, stool, or neoplasia. In endemic areas, parasites as benign as *Enterobius vermicularis* may be the culprit.

Since the only cases reported in literature have showed a patent lumen, it appears that the early obstructed appendix may follow either of the two courses. The appendix may continue to be obstructed which then leads to perforation and abscess formation or rather benign course occurs where the obstruction is relieved as the infection progresses resulting in pus flowing intraluminally into the cecum. This is consistent with the postulate advanced by some authors that some people with acute appendicitis may not have any symptoms, if the pus drains into the cecum and they do not develop serositis. These cases may be self-limiting or result in recurrent or chronic appendicitis[5].

In patients undergoing colonoscopy, the obstruction may occur in the preparation phase during aggressive catharsis or rarely even during the actual procedure. We believe the inciting event in our case may have been that the fecal material was forced into the appendix by the air insufflation, although we do not have any direct evidence. This is supported by the following facts: (1) the symptoms of appendicitis appeared after the colonoscopic diagnosis; (2) WBC count was borderline normal without any left shift; and (3) even though surgery occurred almost 12 h after the colonoscopic diagnosis, a mild acute appendicitis was noted during surgery as well as on histopathology. The other etiologic possibilities include *de novo* or coincidental infection or the irritation by cathartics used for colonic cleansing.

Appendicitis following colonoscopy

Development of acute appendicitis following colonoscopy has been described as a rare complication of this procedure[1-4]. One such case describes an appendiceal colic, due to probable inspissation of fecal material into the lumen of the appendix during insufflation of air in the cecum.

Diagnosis of appendicitis

The diagnosis is primarily clinical with supporting laboratory and CT findings. A false negative rate of about 10-15% still persists although it has declined somewhat with the advent of newer imaging modalities. The role of colonoscopy has been determined to be possibly useful in the diagnosis of appendicitis in patients with symptoms atypical for appendicitis and/or with nondiagnostic imaging studies[5].

There has also been a reported case of a patient presenting with atypical symptoms in whom appendicitis was both diagnosed and treated during colonoscopy by insertion of a catheter into the appendiceal orifice to drain the pus[6]. An elective appendectomy was then performed 5 mo later, after all the symptoms had resolved. The histopathology of the resected appendix showed fibrous thickening of the appendiceal wall correlating with an old inflammatory process, along with changes typical for acute ulcero-phlegmonous appendicitis.

Colonoscopic diagnosis of appendicitis

Colonoscopic diagnosis of acute appendicitis has been reported in the literature of patients with atypical symptoms associated with right lower quadrant pain, and/or non-diagnostic imaging. In one case, a mildly inflamed and erythematous cecum was seen with pus exuding from an edematous appendiceal orifice[7]. Another paper documented an appendix bulging into the cecum with frank pus flowing

from the orifice[8]. Histopathology revealed acute inflammation limited primarily to the lumen and mucosa, which was mostly ulcerated, with an inflammatory infiltrate in the lumen. Earlier, we had described an endoscopic view of appendicitis similar to others[9]. However, the appearance was different from the one we are demonstrating now, i.e., an obstructed/ impacted appendix not previously endoscopically documented in the literature.

Chronic appendicitis has also been diagnosed incidentally by colonoscopy[10,11]. The patient had right lower quadrant abdominal pain for 2 wk prior to colonoscopy. The colonoscopy revealed an inflamed appendiceal orifice. Neither pus nor obstruction was described and it was thought to be low grade appendicitis. She was treated conservatively with a course of metronidazole and discharged. Her symptoms persisted and she gradually became worse over the next 5 wk and an appendectomy was performed. Histology showed an abscess arising in an acquired appendiceal diverticulum and connecting with the lumen of the appendix. The appendix itself showed changes consistent with chronic appendicitis.

In conclusion, we have endoscopically documented for the first time an early obstructive phase of acute appendicitis. Endoscopists need to be aware of the potential for appendicitis during colonoscopy and its appearance, so that prompt appropriate management can be initiated.

REFERENCES

1 **Srivastava V,** Pink J, Swarnkar K, Feroz A, Stephenson BM. Colonoscopically induced appendicitis. *Colorectal Dis* 2004; **6**: 124-125

2 **Kapral C,** Wewalka F, Kopf C, Aufreiter M, Lenz K. Acute appendicitis after colonoscopy: causality or coincidence? *Z Gastroenterol* 2003; **41**: 999-1000

3 **Hirata K,** Noguchi J, Yoshikawa I, Tabaru A, Nagata N, Murata I, Itoh H. Acute appendicitis immediately after colonoscopy. *Am J Gastroenterol* 1996; **91**: 2239-2240

4 **Vender R,** Larson J, Garcia J, Topazian M, Ephraim P. Appendicitis as a complication of colonoscopy. *Gastrointest Endosc* 1995; **41**: 514-516

5 **Houghton A,** Aston N. Appendicitis complicating colonoscopy. *Gastrointest Endosc* 1988; **34**: 489

6 **Chang HS,** Yang SK, Myung SJ, Jung HY, Hong WS, Kim JH, Min Y, Ha HK, Kim JC, Yu CS, Kim HC, Kim JS. The role of colonoscopy in the diagnosis of appendicitis in patients with atypical presentations. *Gastrointest Endosc* 2002; **56**: 343-348

7 **Said M,** Ledochowski M, Dietze O, Simander H. Colonoscopic diagnosis and treatment of acute appendicitis. *Eur J Gastroenterol Hepatol* 1995; **7**: 569-571

8 **Triadafilopoulos G.** Acute Appendicitis. *Gastrointest Endosc* 2001; **54**: 624

9 **Kaushik N,** Krasinskas A, Slivka A, McGrath K. Acute appendicitis. *Gastrointest Endosc* 2004; **60**: 102-103

10 **Minocha A.** An endoscopic view of appendicitis. *N Engl J Med* 1998; **339**: 1481

11 **Courtney ED,** Melville D, Leicester RJ. Chronic appendicitis diagnosed incidentally by colonoscopy. *Hosp Med* 2003; **64**: 434-435

Science Editor Guo SY **Language Editor** Elsevier HK

PO Box 2345, Beijing 100023, China
www.wjgnet.com
wjg@wjgnet.com

ELSEVIER

World J Gastroenterol 2005;11(34):5401-5403
World Journal of Gastroenterology ISSN 1007-9327
© 2005 The WJG Press and Elsevier Inc. All rights reserved.

• *CASE REPORT* •

Successful treatment of advanced hepatocellular carcinoma by combined administration of 5-fluorouracil and pegylated interferon-α

Kazutaka Kurokohchi, Kouichi Takaguchi, Keiji Kita, Tsutomu Masaki, Shigeki Kuriyama

Kazutaka Kurokohchi, Tsutomu Masaki, Shigeki Kuriyama, Third Department of Internal Medicine, Kagawa University School of Medicine, 1750-1 Ikenobe, Miki-cho, Kita-gun, Kagawa 761-0793, Japan
Kouichi Takaguchi, Keiji Kita, Department of Internal Medicine, Kagawa Prefectural Central Hospital, 5-4-16 Ban-cho, Takamatsu, Kagawa 760-8557, Japan
Co-correspondents: Kazutaka Kurokohchi
Correspondence to: Dr. Shigeki Kuriyama, Third Department of Internal Medicine, Kagawa University School of Medicine, 1750-1 Ikenobe, Miki-cho, Kita-gun, Kagawa 761-0793, Japan. skuriyam@med.kagawa-u.ac.jp
Telephone: +81-87-891-2156 Fax: +81-87-891-2158
Received: 2005-03-19 Accepted: 2005-04-18

Abstract

We report a case of hepatocellular carcinoma (HCC) treated successfully by transarterial chemoembolization (TACE) followed by combination therapy of 5-fluorouracil (5-FU) and pegylated interferon-α (PEG-IFN-α). In the present case, the patient had massive and advanced HCC with a diameter of over 8 cm located in segment 7 (S7) of the liver. Furthermore, the tumor invaded into the major branch of the portal vein (Vp3). After TACE, combined administration of 5-FU and PEG-IFN-α was performed for 5 mo. HCC was totally eradicated and the serum levels of tumor markers were markedly decreased by the treatment. Although it has been reported that the combined use of conventional IFN-α and 5-FU showed striking effects on HCC in some cases, this case may suggest the more promising effect of PEG-IFN-α with a long-lasting effect, in the combined use with 5-FU for the treatment of massive advanced HCC.

© 2005 The WJG Press and Elsevier Inc. All rights reserved.

Key words: Hepatocellular carcinoma; 5-Fluorouracil; Pegylated interferon-α; Combination therapy

Kurokohchi K, Takaguchi K, Kita K, Masaki T, Kuriyama S. Successful treatment of advanced hepatocellular carcinoma by combined administration of 5-fluorouracil and pegylated interferon-α. *World J Gastroenterol* 2005; 11(34): 5401-5403
http://www.wjgnet.com/1007-9327/11/5401.asp

INTRODUCTION

Despite the recently innovated treatment modalities including radiofrequency ablation (RFA), hepatocellular carcinoma (HCC) is still one of the most progressive malignancies resistant to the local treatment or chemotherapy. Repeated recurrences often occur due to the multicentric carcinogenesis and intrahepatic metastasis. For the treatment of advanced HCC invading into the major branches of the portal tract, the effectiveness of the combination therapy of 5-fluorouracil (5-FU) and interferon-α (IFN-α) has been reported[1-4]. In the reports, conventional IFN-α has been used as a component of the combination therapy. In the present study, instead of conventional IFN-α, pegylated (PEG) IFN-α was used once a week with continuous infusion of 5-FU for the treatment of advanced HCC and its effectiveness was evaluated.

CASE REPORT

A 74-year-old female had been followed as a diabetes mellitus and chronic hepatitis (non-B and non-C) at Kagawa University Hospital since 1988. The first HCC emerged in S4, S5 and S6 of the liver in 1995. As her hepatic reserve was enough for surgical operation, partial hepatectomy was performed for the multiple HCC. Recurrence of HCC occurred in the middle of 2001, 6 years after the operation. The solitary tumor was detected in S7 of the liver. As it was a relatively small-sized tumor with a diameter of 1 cm, regional treatment by the combination of percutaneous ethanol injection and radiofrequency ablation (PEI-RFA), innovated at our department[5], was performed. The tumorous lesion was totally destroyed by PEI-RFA. Since then she was followed for her liver function and periodically checked for detection of new HCC by blood examination and computed tomography (CT). In January 2002, serum levels of AFP and AFP-L3, tumor markers for HCC, was 13 ng/mL and 4.1%, respectively. Both levels were kept within normal ranges until the end of 2003 and newly developed HCC was not detected by CT or ultrasonography during the period. Both tumor markers suddenly jumped up in March 2004. The levels of AFP reached 555 ng/mL in March and 2 888 ng/mL in June, and AFP-L3 reached 81.7% in April 2004. CT taken in March 2004 showed the development of massive HCC located in S6 and S7 of the liver, with the maximum diameter of over 8 cm. Moreover, HCC invaded into the main branch of the portal vein. The patient was admitted to Kagawa Prefectural Central Hospital for the treatment of HCC. The patient immediately underwent angiography. The angiography clearly showed the massive hypervascular tumor occupying the wide area of the right

hepatic artery (Figure 1A). Furthermore, tumor thrombus was present in the portal tract (Figure 1B). Therefore, in addition to transarterial chemoembolization (TACE) using Farmorubicin (Kyowa Hakko Co., Tokyo, Japan) and gelfoam (Figure 1C), a reservoir for intra-arterial infusion was inserted into the proper hepatic artery (Figure 1D) and the injection port was subcutaneously implanted. From early May 2004, combination therapy of IFN-α and 5-FU was initiated. The patient was treated with subcutaneous administration of PEG-IFN-α-2a (Pegasys, Chugai Pharmaceutical Co., Ltd, Tokyo) and continuous intra-arterial infusion of 5-FU (Kyowa Hakko Co., Tokyo, Japan). Continuous infusion of 5-FU (250 mg/d) was performed for 2 wk with an interval of 2 wk via the implanted reservoir port according to the regimen previously published[2]. PEG-IFN-α-2a (90 μg) was administrated on d 1 of every week. Between May and November, 6 repeated cycles of administration of continuous 5-FU and PEG-IFN-α were performed. No significant side effects were observed. A series of CT examination revealed the marked anti-tumor effect of the combination therapy. Massive HCC in the right hepatic lobe was gradually reduced and the portal tumor thrombus finally disappeared in October 2004, 5 mo after the initiation of the combination therapy. The level of AFP was also decreased to 38 ng/mL in October 2004. No recurrence of HCC has not been detected on enhanced dynamic CT and no elevation of the tumor markers has not been observed so far (Figures 2A-D).

DISCUSSION

HCC is one of the world's most common malignancies, especially in Asia. Despite the advances in diagnostic and therapeutic techniques, HCC often progress to an advance stage regardless of several treatment modalities. RFA technique is one of the promising treatment modalities recently innovated for the treatment of HCC and is used worldwide at present. This newly developed technique appears very effective to induce wider coagulated necrosis rather than percutaneous ethanol injection therapy without major complications, but the efficacy of RFA is limited to relatively small-sized HCC with the maximum diameter of 3 cm or less. Thus, we have developed the combination therapy of PEI-RFA for inducing wider coagulated necrosis[5,6] and for achieving safer treatment of HCC[7]. Nevertheless, recurrences of the tumor after the local treatment often occurs and some of the tumor progress to an advanced stage. For these advanced HCC, chemotherapy alone is not necessarily effective. Recently, combination therapy of some chemical reagents, such as 5-FU and cisplatin, and systemic administration of IFN-α was shown to be effective for the treatment of HCC[1-4]. Indeed, this newly developed therapy could increase the therapeutic effect on HCC that could not be treated by any other therapeutic modalities. However, according to the reports cited above, the response rate including the complete response (CR) and partial response are not necessarily high. Especially, the number of CR cases was extremely small. In the present case, not only the massive tumor but also the tumor thrombus in the major branch of the portal vein was eradicated completely by the combination therapy of 5-FU and PEG-IFN-α. The response to the combination therapy in this case is considered to be CR. Disappearance of massive large-sized HCC of more than 8 cm in diameter as shown in the present case has never been reported. To our knowledge, this case is the first descriptive report of the case with massive HCC

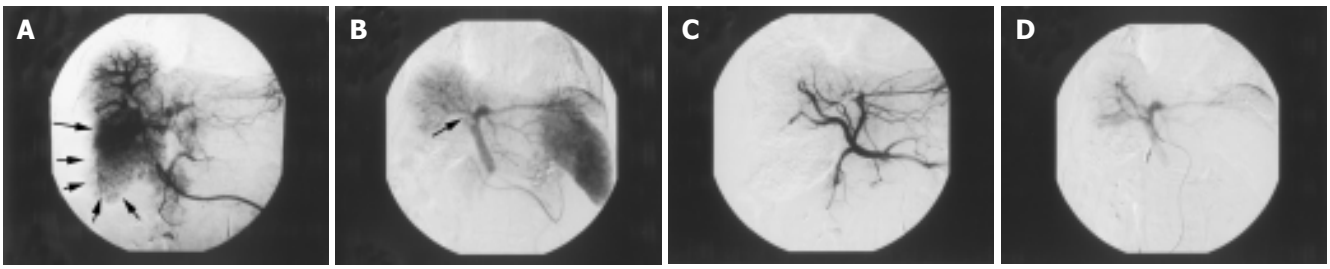


Figure 1 Angiography of the celiac artery before and after TACE was taken on April 15, 2004. Massive tumor stain (small arrow) was exhibited by the celiac arteriography (**A**). Large arterioportal shunt (big arrow) was exhibited above the massive tumor stain. The right branch of the portal vein was not exhibited by the portography (arrow) (**B**). The tumor stain disappeared after the TACE (**C**). The reservoir for intra-arterial infusion was inserted into the proper hepatic artery (**D**).

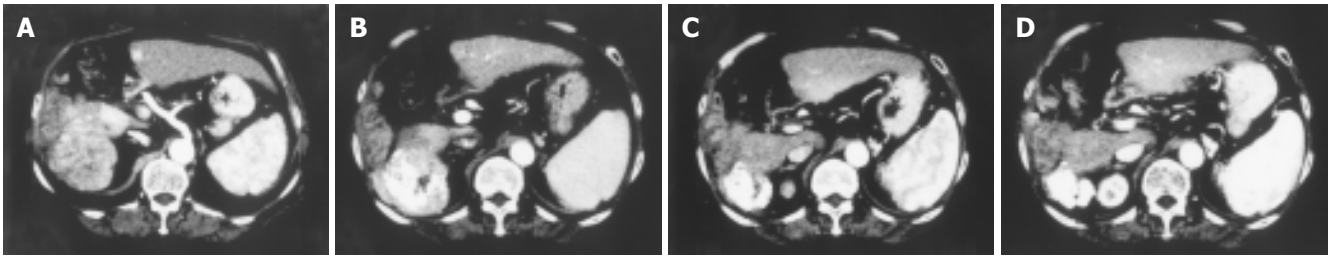


Figure 2 Photographs of enhanced dynamic CT in the time course of the combination therapy of PEG-IFN-α and 5-FU on March 29, 2004 (**A**), June 21, 2004 (**B**), August 27, 2004 (**C**) and October 8, 2004 (**D**). Massive tumor was rapidly reduced during the combination therapy. Only the accumulation of lipiodol remained in the final CT taken on October 8, 2004.

successfully treated with the new combination therapy of systemic administration of PEG-IFN-α and intra-arterial administration of 5-FU. The major difference between the PEG-IFN-α and conventional IFN-α is the retention time of the effect. High concentration of IFN-α in the blood is retained for a week by administration of PEG-IFN-α, whereas high and low concentrations of IFN-α are repeated by turns in the conventional IFN-α treatment. Thus, the present case showing CR to the combination therapy may give us an insight into the promising anti-tumor effects of the combined use of PEG-IFN-α and chemical agents such as 5-FU and cisplatin. Although the study including a large number of patients with advanced HCC is necessary, the combination therapy of PEG-IFN-α and chemical agents may open up a new avenue for the treatment of advanced HCC.

REFERENCES

1 **Chung YH,** Song IH, Lee GC, Koh MS, Yoon HK, Lee YS, Sung KB, Suh DJ. Combined therapy consisting of intraarterial cisplatin infusion and systemic interferon-α for hepatocellular carcinoma patients with major portal vein thrombosis or distant matastasis. *Cancer* 2000; **88**: 1986-1991

2 **Kaneko S,** Urabe T, Kobayashi K. Combination chemotherapy for advanced hepatocellular carcinoma complicated by major portal vein thrombosis. *Oncology* 2002; **62**: 69-73

3 **Sakon M,** Nagano H, Dono K, Nakamori S, Umeshita K, Yamada A, Kawata S, Imai Y, Iijima S, Monden M. Combined intraarterial 5-fluorouracil and subcutaneous interferon-a therapy for advanced hepatocellular carcinoma with tumor thrombi in the major portal branches. *Cancer* 2002; **94**: 435-442

4 **Patt YZ,** Hassen MM, Lozano RD, Brown TD, Vauthey JN, Curley SA, Elliis LM. Phase III trial of systemic continuous fluorouracil and subcutaneous recombinant interferon alfa-2b for treatment of hepatocellular carcinoma. *J Clin Oncol* 2003; **21**: 421-427

5 **Kurokohchi K,** Watanabe S, Masaki T, Hosomi N, Funaki T, Arima K, Yoshida S, Miyauchi Y, Kuriyama S. Combined use of percutaneous ethanol injection and radiofrequency ablation for the effective treatment of hepatocellular carcinoma. *Int J Oncol* 2002; **21**: 841-846

6 **Kurokohchi K,** Watanabe S, Masaki T, Hosomi N, Funaki T, Arima K, Yoshida S, Nakai S, Murota M, Miyauchi Y, Kuriyama S. Combination therapy of percutaneous ethanol injection and radiofrequency ablation against hepatocellular carcinomas difficult to treat. *Int J Oncol* 2002; **21**: 611-615

7 **Kurokohchi K,** Watanabe S, Masaki T, Hosomi N, Miyauchi Y, Himoto T, Kimura Y, Nakai S, Deguchi A, Yoneyama H, Yoshida S, Kuriyama S. Comparison between combination therapy of percutaneous ethanol injection and radiofrequency ablation and radiofrequency ablation alone for patiens with hepatocellular carcinoma. *World J Gastroenterol* 2005; **11**: 1426-1432

Science Editor Guo SY **Language Editor** Elsevier HK

PO Box 2345, Beijing 100023, China
www.wjgnet.com
wjg@wjgnet.com

ELSEVIER

World J Gastroenterol 2005;11(34):5404-5407
World Journal of Gastroenterology ISSN 1007-9327
© 2005 The WJG Press and Elsevier Inc. All rights reserved.

• *CASE REPORT* •

Cerebral sinus thrombosis in patients with inflammatory bowel disease: A case report

Hasan Umit, Talip Asil, Yahya Celik, Ahmet Tezel, Gulbin Dokmeci, Nermin Tuncbilek, Ufuk Utku, Ali Riza Soylu

Hasan Umit, Ahmet Tezel, Gulbin Dokmeci, Ali Riza Soylu, Department of Gastroenterology, Trakya University Faculty of Medicine, Edirne 22030, Turkey
Talip Asil, Yahya Celik, Ufuk Utku, Department of Neurology, Trakya University Faculty of Medicine, Edirne 22030, Turkey
Nermin Tuncbilek, Department of Radiology, Trakya University Faculty of Medicine, Edirne 22030, Turkey
Correspondence to: Dr. Hasan Umit, Trakya Üniversitesi Týp Fakültesi, Gastroenteroloji BD, Gullapoglu Yerleskesi, Edirne 22030, Turkey. hasanumit@ttnet.net.tr
Telephone: +90-284-235-56-35
Received: 2005-01-09 Accepted: 2005-01-26

Abstract

Inflammatory bowel disease (IBD) is an idiopathic inflammatory disease of the gastrointestinal tract. The pathophysiology of IBD is probably the result of the complex interaction of genetic susceptibility and environmental influences. There is a well-known risk of thrombosis in patients with IBD. We present the case of a 53-year-old man with ulcerative colitis, who spontaneously developed intracranial sinus thrombosis that was treated with low molecular weight heparin. Literature was searched to assess the frequency and characteristics of cerebral sinus thrombosis in IBD and the role of certain etiopathological factors in such thrombotic patients.

© 2005 The WJG Press and Elsevier Inc. All rights reserved.

Key words: Inflammatory bowel disease; Cerebrovascular thrombosis; Cerebral sinus thrombosis

Umit H, Asil T, Celik Y, Tezel A, Dokmeci G, Tuncbilek N, Utku U, Soylu AR. Cerebral sinus thrombosis in patients with inflammatory bowel disease: A case report. *World J Gastroenterol* 2005; 11(34): 5404-5407
http://www.wjgnet.com/1007-9327/11/5404.asp

INTRODUCTION

Inflammatory bowel disease (IBD) is an idiopathic inflammatory disease of the gastrointestinal tract. The pathophysiology of IBD is probably the result of the complex interaction of genetic susceptibility and environmental influences. The exact pathogenesis of IBD is unknown. There is a well-known risk of thrombosis in patients with IBD. This pro-thrombotic state seen in IBD has been proposed as a factor contributing to the pathogenesis of IBD, especially in Crohn's disease[1,2]. This conclusion is based on the presence of thrombi in the small vessels of mucosa and submucosa. Furthermore, some IBD patients have been successfully treated with heparin[3-6].

Thromboembolism is a serious complication of IBD patients. The yearly incidence of thromboembolic events in IBD is 13-64/1 000[7,8]. Corticosteroid usage to diminish inflammatory activity and concomitant abnormalities of coagulation cascade such as factor V mutations, protein C and S deficiency, prothrombin gene mutation, hyperhomocysteinemia could increase the risk of thromboembolic complications. On the other hand, some researchers found that the incidence (1.5/1 000 IBD patients per year) of venous thrombosis does not increase in IBD patients and that IBD patients have venous thrombosis earlier in life than non-IBD patients[9].

Deep venous thrombosis and pulmonary emboli are the most common thrombotic complications in IBD. However, cerebral vascular involvement is rare. It was reported that 92 of 7 199 IBD patients suffer from thrombotic complications, 9 of the 92 patients have cerebral vessel involvement[7].

CASE REPORT

A 53-year-old man suffering from abdominal pain, bloody diarrhea (8-10 stools per day) and weight loss (10 kg in the past 3 mo) was admitted to our hospital in April 2003. On admission, his body temperature was 38 ℃. His physical examination revealed no abnormalities except for mild sinusal tachycardia (100 pulses/min). Neurological examination revealed no paralysis and sensory motor disturbances. The blood and stool cultures obtained on his first day of admission did not yield any pathogens. Microscopic stool examination revealed abundant leukocytes and erythrocytes. The stool C. Difficile toxin A assay was negative. Laboratory data showed elevated C reactive protein (CRP) levels and ESR, mild elevations of aminotransferases with ALT/AST ratio >1, mild thrombocytosis (568 000/mm^3) and normochromic anemia with a hemoglobin value of 10 g/L. His colonoscopic evaluation revealed loss of mucosal vascular pattern, granularity and friability of the whole colonic mucosa and widespread pseudopolyps. Histopathological examination of the rectal mucosa showed an abundant infiltration of neutrophils, lymphocytes and plasma cells. Histopathology also revealed cryptitis and crypt abscess in some areas. The patient's ultrasonography and carcinoembryonic antigen (CEA) levels were normal. Hepatotrophic virus (Hepatitis B and C) and autoimmune markers (anti-nuclear, anti-smooth muscle and anti-neutrophilic cytoplasmic antibodies) were negative. Based on these findings, the patient was diagnosed with moderately active ulcerative pancolitis and

started on 4 g of sulfasalazine as anti-inflammatory therapy. Nutritional support was also provided. One week after treatment, his number of times of defecation decreased to 5 stools per day with no blood and the patient was afebrile. CRP levels decreased, thrombocytes were in normal limit but mild anemia persisted. During the second week of therapy the platelet count was 130 000/mm^3. Sulfasalazine was discontinued and 40 mg prednisolone was started. On the third day of corticosteroid treatment, the patient complained of weakness of the right arm and leg. His neurological examination revealed left sided hemiparesis. Motor strength was 2/5 and 4/5 in upper and lower left extremities, respectively. The patient had mild dysarthria. Deep tendon reflexes were brisk. Plantar response in left side was extensive. Cranial CT scan and T2 weighted magnetic resonance imaging showed bifrontal and right parietal infarction (Figure 1). Sagittal MRI venography revealed signal dropout in the superior sagittal sinus and right transverse sinus (Figure 2). We started low molecular weight heparin (LMWH) therapy immediately. The patient also developed focal motor seizures. He became unconscious (Glasgow coma score was 6) 3 d after the first neurological sign. He was on therapy of LMWH and control CT showed no additional abnormality. Laboratory tests for coagulation abnormalities revealed heterozygous factor V Leiden gene mutation. The patient died of pulmonary nosocomial infection and sepsis 2 wk after the onset of neurological findings.

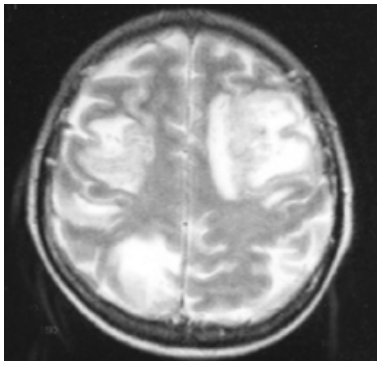


Figure 1 T2 weighted magnetic resonance image demonstrating bifrontal and right parietal lesions consistent with infarctions.

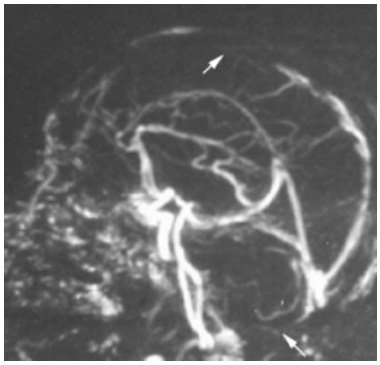


Figure 2 Sagittal MRI venographic image demonstrating signal dropout in superior sagittal sinus (arrow) and right transverse (arrowhead) sinus.

DISCUSSION

Extraintestinal manifestations are common in ulcerative colitis and Crohn's disease occurring in at least 25-40% of patients and can be classified as related to disease activity or not[10]. If secondary systemic effects of therapy on disease and complications are also included, almost all patients have extraintestinal manifestations.

Thromboembolism is a serious complication of IBD patients. Intravascular thrombosis in mucosal blood vessels may play a role in the pathogenesis of IBD. Some studies indicate that heparin may benefit the treatment of IBD[3-6]. There are some conflicting data about the incidence of thrombotic events in IBD patients. The risk factors, relationship between disease activity, corticosteroid use and thrombotic events, incidence of concomitant coagulation disorders and effect of corticosteroid on thrombosis in IBD patients are still not completely understood. Grip *et al.*[9], found that the incidence of venous thrombosis does not increase in IBD patients. However, studies showed that the incidence of thrombotic complications increases in IBD patients[7,8]. These contradictory data may be related to the changing management of IBD patients. Nowadays, IBD patients are less frequently hospitalized and immobilized. This may be the reason why the current incidence of thrombotic complications is lower in IBD patients[9].

Pro-thrombotic factors (anti-cardiolipin antibodies, hyperhomocysteinemia and changes in the lipid spectrum), IBD-induced alterations in plasma and mucosal hemostasis (increased endothelial activation and tissue factor expression, and impaired inhibition of coagulation in IBD), and changes secondary to inflammation have been suggested as the explanatory factors for the high prevalence of thromboembolism in IBD patients. The balance between pro-coagulant and pro-fibrinolytic factors seems to favor plasma hypercoagulability in IBD patients. Inflammation-induced changes in serum, endothelial cells and platelets induce plasma alterations resulting in coagulation activation, whereas coagulation activation induces pro-inflammatory effects, thus providing a looping chain of reactions[11].

van Bodegraven *et al.*[12], studied hemostatic imbalance in active and quiescent ulcerative colitis and found that coagulation and fibrinolytic cascades are activated in active ulcerative colitis and 20% of patients are in remission with a hemostatic imbalance in favor of coagulation. The clinical significance of these phenomena is unknown. Meanwhile previous studies have shown that activated plasma coagulation markers increase in clinically quiescent IBD[13]. Thus, clinical activity of the disease may increase the risk, but it is probably of minor importance.

Hyperhomocysteinemia and coagulation cascade abnormalities in IBD patients have been studied[14-16]. Hyperhomocysteinemia is common in IBD patients but elevated total homocysteine levels do not contribute to the development of thrombotic complications[17].

No correlation is found between hereditary conditions predisposing to thrombosis such as factor V mutation, prothrombin gene mutation, MTHFR mutation, proteins C and S, antithrombin III deficiencies and IBD[18]. Thus, higher prevalence of thrombosis in IBD patients is not due to genetic linkage. Taken together, existing data indicate that

thrombosis in IBD patients is due to multifactors.

Deep venous thrombosis and pulmonary emboli are the most common thrombotic complications in IBD patients, however, cerebral vascular involvement is rare. It was reported that IBD patients are relatively young and have no other relevant risk factors except for IBD[19].

Cerebral venous and dural sinus thrombosis in association with IBD is rare and few cases have been reported[20-24]. Some clinical characteristics of these patients are summarized in Table 1. The frequency of cerebral venous thromboembolic complications in ulcerative colitis patients appears to be greater than that in patients with Crohn's

Table 1 Clinical characteristics of ulcerative colitis patients with cerebral venous thrombosis

Reference	Sex	Age	IBD activity	IBD location	IBD duration	CNS circulation involved	Outcome	Coagulation studies	Miscellaneous
Gonera *et al*.[20]	F	30	Active	Pancolitis	-	SSS	Recovered	Functional APC resistance, hyperhomocysteinemia	Deep venous thrombosis
Tsujikawa *et al*.[21]	M	27	Active	Recto-sigmoid	9 yr	SSS	Recovered	-	-
Derdeyn *et al*.[22]	F	26	Remission	-	-	Isolated cortical vein (sylvian vein)	Residual	-	Deep venous thrombosis
Das *et al*.[23]	M	31	Active	Pancolitis	-	SSS	Death	-	Pulmonary emboli at autopsy
	M	20	Active	Pancolitis	2 yr	SSS and superficial cerebral veins	Death	-	Pulmonaryemboli at autopsy
Philips *et al*.[24]	F	35	-	-	-	SSS, TS, StS	Recovered	-	-
	F	14	-	-	-	SSS, vein of labbe	Recovered	-	-
Srivastava *et al*.[25]	M	29	Remission	-	6 mo	SSS, left sigmoid sinus	Recovered	No abnormality found	-
Papi *et al*.[26]	F	33	Active	-	First attack	Superior, inferior long. Sinuses	Residual	Lupus anticoagulant positive	Impending megacolon
Kao *et al*.[27]	-	14	-	-	3 yr	SSS, vein of labbe	Residual		ANCA positive
	-	7	-	-	4 mo	Transverse and sigmoid sinuses	Residual	Elevated anticardiolipin antibody	-
	-	20	-	-	6 yr	SSS and transverse sinuses	Recovered	Elevated anticardiolipin antibody	-
	-	13	-	-	18 mo	SSS, cortical veins, TS, SS	Recovered	Hyperhomocysteinemia, heterozygous for prothrombin gene	-
Kiff *et al*.[28]	F	26	Active	Pancolitis	First attack	Straight sinus and great cerebral vein of Galen	Death	-	In the postpartum period
Markowitz *et al*.[30]	M	14	Active	Pancolitis	9 mo	Left sigmoid and lateral sinuses	Residual	-	-
Borda *et al*.[31]	M	23	Active	-	-	All major venous sinuses	Death	-	Pulmonary emboli, renal vein thrombosis
Schneiderman *et al*.[32]	F	12	Active	-	-	Straight sinus, vein of galen	Death	-	-
Lam *et al*.[33]	F	28	-	Pancolitis	-	-	Residual	-	-
Averback *et al*.[34]	F	25	Remission	-	-	-	Death	-	-
Yerby *et al*.[35]	M	28	Remission	Pancolitis	-	-	Recovered	-	10 yr after proctocolectomy
Bewermeyer *et al*.[36]	F	35	Active	-	-	Inf. Sagittal sinus, StS	Death	-	-
Gil-Peralta *et al*.[37]	F	48	Active	-	-	Superficial cortical veins	Death	-	-
Musio *et al*.[29]	M	24	-	Pancolitis	2 yr	SSS	Recovered	-	-
Present study	M	53	Active	Pancolitis	First attack	SSS	Death	F V Leiden heterozygous mutant	Nosocomial pulmonary infection, sepsis
Total	F:11 M: 9	Mean: 25.6 yr	Active: 12 remission:4	Pancolitis: 10 RS: 1	-	-	-	-	-

M: male, F: female, SSS: superior sagittal sinus, TS: transverse sinus, SS: sigmoid sinus, StS: straight sinus, APC: activated protein C.

disease. The superior sagittal sinus and lateral sinuses are commonly involved[25-27]. Less frequently, isolated cortical venous thromboses have been reported[22]. Although one case that present with sagittal sinus thrombosis 10 years after proctocolectomy for ulcerative colitis has been reported, these cerebral venous thrombotic events occur more frequently in patients with active inflammatory bowel disease[28-32]. The most frequent symptoms and signs are headache, paresis, seizures, dysphasia and papilla edema. Approximately 1/3 of patients have some coagulation abnormalities such as FV Leiden mutation, hyperhomocysteinemia, positive anti-cardiolipin antibodies[20,26,27]. The clinical outcome is devastating[33-37].

In conclusion, cerebral venous thrombosis is a devastating complication of IBD, especially, ulcerative colitis. The diagnosis of these patients depends on the demonstration of the thrombus by neuroimaging.

REFERENCES

1 **Dhillon AP,** Anthony A, Sim R, Wakefield AJ, Sankey EA, Hudson M, Allison MC, Pounder RE. Mucosal capillary thrombi in rectal biopsies. *Histopathology* 1992; **21**: 127-133
2 **Wakefield AJ,** Sawyerr AM, Dhillon AP, Pittilo RM, Rowles PM, Lewis AA, Pounder RE. Pathogenesis of Crohn's disease: multifocal gastrointestinal infarction. *Lancet* 1989; **334**: 1057-1062
3 **Folwaczny C,** Wiebecke B, Loeschke K. Unfractioned heparin in the therapy of patients with highly active inflammatory bowel disease. *Am J Gastroenterol* 1999; **94**: 1551-1555
4 **Gaffney PR,** Doyle CT, Gaffney A, Hogan J, Hayes DP, Annis P. Paradoxical response to heparin in 10 patients with ulcerative colitis. *Am J Gastroenterol* 1995; **90**: 220-223
5 **Torkvist L,** Thorlacius H, Sjoqvist U, Bohman L, Lapidus A, Flood L, Agren B, Raud J, Lofberg R. Low molecular weight heparin as adjuvant therapy in active ulcerative colitis. *Aliment Pharmacol Ther* 1999; **13**: 1323-1328
6 **Papa A,** Danese S, Gasbarrini A, Gasbarrini G. Review article: potential therapeutic applications and mechanisms of action of heparin in inflammatory bowel disease. *Aliment Pharmacol Ther* 2000; **14**: 1403-1409
7 **Talbot RW,** Heppell J, Dozois RR, Beart RW Jr. Vascular complications of inflammatory bowel disease. *Mayo Clin Proc* 1986; **61**: 140-145
8 **Edwards FC,** Truelove SC. The course and prognosis of ulcerative colitis. III. Complications. *Gut* 1964; **32**: 1-22
9 **Grip O,** Svensson PJ, Lindgren S. Inflammatory bowel disease promotes venous thrombosis earlier in life. *Scand J Gastroenterol* 2000; **35**: 619-623
10 **Isaacs KL.** Extra-intestinal manifestations. In: Theodore M Bayless, Stephen B Hanauer ed. Advanced therapy of inflammatory bowel disease. Hamilton, London: B.C. *Decker Inc* 2001: 267-270
11 **van Bodegraven AA.** Haemostasis in inflammatory bowel diseases: clinical relevance. *Scand J Gastroenterol* 2003; **239**: 51-62
12 **van Bodegraven AA,** Schoorl M, Baak JP, Linskens RK, Bartels PC, Tuynman HA. Hemostatic imbalance in active and quiescent ulcerative colitis. *Am J Gastroenterol* 2001; **96**: 487-493
13 **Chiarantini E,** Valanzano R, Liotta AA, Cellai AP, Fedi S, Ilari I, Prisco D, Tonelli F, Abbate R. Hemostatic abnormalities in inflammatory bowel disease. *Thromb Res* 1996; **82**: 137-146
14 **Papa A,** De Stefano V, Danese S, Chiusolo P, Persichilli S, Casorelli I, Zappacosta B, Giardina B, Gasbarrini A, Leone G, Gasbarrini G. Hyperhomocysteinemia and prevalence of polymorphisms of homocysteine metabolism-related enzymes in patients with inflammatory bowel disease. *Am J Gastroenterol* 2001; **96**: 2677-2682
15 **Bjerregaard LT,** Nederby NJ, Fredholm L, Brandslund I, Munkholm P, Hey H. Hyperhomocysteinaemia, coagulation pathway activation and thrombophilia in patients with inflammatory bowel disease. *Scand J Gastroenterol* 2002; **37**: 62-67
16 **Romagnuolo J,** Fedorak RN, Dias VC, Bamforth F, Teltscher M. Hyperhomocysteinemia and inflammatory bowel disease: prevalence and predictors in a cross-sectional study. *Am J Gastroenterol* 2001; **96**: 2143-2149
17 **Oldenburg B,** Fijnheer R, van der Griend R, van Berge-Henegouwen GP, Koningsberger JC. Homocysteine in inflammatory bowel disease: a risk factor for thromboembolic complications? *Am J Gastroenterol* 2000; **95**: 2825-2830
18 **Vecchi M,** Sacchi E, Saibeni S, Meucci G, Tagliabue L, Duca F, De Franchis R. Inflammatory bowel diseases are not associated with major hereditary conditions predisposing to thrombosis. *Dig Dis Sci* 2000; **45**: 1465-1469
19 **Lossos A,** River Y, Eliakim A, Steiner I. Neurologic aspects of inflammatory bowel disease. *Neurology* 1995; **45**: 416-421
20 **Gonera RK,** Timmerhuis TP, Leyten AC, van der Heul C. Two thrombotic complications in a patient with active ulcerative colitis. *Neth J Med* 1997; **50**: 88-91
21 **Tsujikawa T,** Urabe M, Bamba H, Andoh A, Sasaki M, Koyama S, Fujiyama Y, Bamba T. Haemorrhagic cerebral sinus thrombosis associated with ulcerative colitis: a case report of successful treatment by anticoagulant therapy. *J Gastroenterol Hepatol* 2000; **15**: 688-692
22 **Derdeyn CP,** Powers WJ. Isolated cortical venous thrombosis and ulcerative colitis. *AJNR Am J Neuroradiol* 1998; **19**: 488-490
23 **Das R,** Vasishta RK, Banerjee AK. Aseptic cerebral venous thrombosis associated with idiopathic ulcerative colitis: a report of two cases. *Clin Neurol Neurosurg* 1996; **98**: 179-182
24 **Philips MF,** Bagley LJ, Sinson GP, Raps EC, Galetta SL, Zager EL, Hurst RW. Endovascular thrombolysis for symptomatic cerebral venous thrombosis. *J Neurosurg* 1999; **90**: 65-71
25 **Srivastava AK,** Khanna N, Sardana V, Gaekwad S, Prasad K, Behari M. Cerebral venous thrombosis in ulcerative colitis. *Neurol India* 2002; **50**: 215-217
26 **Papi C,** Ciaco A, Acierno G, Di Battista G, Talamanca LF, Lo Russo F, Natali G, Capurso L. Severe ulcerative colitis, dural sinus thrombosis, and the lupus anticoagulant. *Am J Gastroenterol* 1995; **90**: 1514-1517
27 **Kao A,** Dlugos D, Hunter JV, Mamula P, Thorarensen O. Anticoagulation therapy in cerebral sinovenous thrombosis and ulcerative colitis in children. *J Child Neurol* 2002; **17**: 479-482
28 **Kiff RS,** Denton GW. Fatal cerebral venous thrombosis complicating acute ulcerative colitis. *Am J Gastroenterol* 1989; **84**: 577-578
29 **Musio F,** Older SA, Jenkins T, Gregorie EM. Case report: cerebral venous thrombosis as a manifestation of acute ulcerative colitis. *Am J Med Sci* 1993; **305**: 28-35
30 **Markowitz RL,** Ment LR, Gryboski JD. Cerebral thromboembolic disease in pediatric and adult inflammatory bowel disease: case report and review of the literature. *J Pediatr Gastroenterol Nutr* 1989; **8**: 413-420
31 **Borda IT,** Southern RF, Brown WF. Cerebral venous thrombosis in ulcerative colitis. *Gastroenterology* 1973; **64**: 116-119
32 **Schneiderman JH,** Sharpe JA, Sutton DM. Cerebral and retinal vascular complications of inflammatory bowel disease. *Ann Neurol* 1979; **5**: 331-337
33 **Lam A,** Borda IT, Inwood MJ, Thomson S. Coagulation studies in ulcerative colitis and Crohn's disease. *Gastroenterology* 1975; **68**: 245-251
34 **Averback P.** Primary cerebral venous thrombosis in young adults: the diverse manifestations of an underrecognized disease. *Ann Neurol* 1978; **3**: 81-86
35 **Yerby MS,** Bailey GM. Superior sagittal sinus thrombosis 10 years after surgery for ulcerative colitis. *Stroke* 1980; **11**: 294-296
36 **Bewermeyer H,** Dreesbach HA, Krakamp B. Cerebral venous and sinus thrombosis in ulcerative colitis. *ROFO* 1985; **143**: 597-598
37 **Gil-Peralta A,** Salazar JA, Chinchon I, Alberca R. Cerebral venous thrombosis and ulcerative colitis. *Med Clin* 1982; **79**: 332-335

Science Editor Wang XL and Guo SY **Language Editor** Elsevier HK

PO Box 2345, Beijing 100023, China
www.wjgnet.com
wjg@wjgnet.com

ELSEVIER

World J Gastroenterol 2005;11(34):5408-5411
World Journal of Gastroenterology ISSN 1007-9327
© 2005 The WJG Press and Elsevier Inc. All rights reserved.

• *CASE REPORT* •

Gardner's syndrome: A case report and review of the literature

C Fotiadis, DK Tsekouras, P Antonakis, J Sfiniadakis, M Genetzakis, GC Zografos

C Fotiadis, 3rd University Department of General Surgery, Athens School of Medicine, Athens, Greece
GC Zografos, DK Tsekouras, P Antonakis, M Genetzakis, 1st University Department of General Surgery, Athens School of Medicine, Ippokration Hospital, Athens, Greece
J Sfiniadakis, Department of Pathology, Athens Naval Hospital, Athens, Greece
Correspondence to: Professor C Fotiadis, 8 Tripoleos Street, Melissia, Athens 15721, Greece. costfot@yahoo.gr
Telephone: +11-30210-5326431 Fax: +11-30210-8133184
Received: 2005-02-07 Accepted: 2005-03-09

Abstract

Gardner's syndrome is an autosomal dominant disease characterized by the presence of colonic polyposis, osteomas and a multitude of soft tissue tumors. The syndrome may present at any age from 2 mo to 70 years with a variety of symptoms, either colonic or extracolonic. We present a case of a 11-year-old female patient with Gardner's syndrome who presented with a lumbar area desmoid tumor and treated with resection of the desmoid, restorative proctocolectomy and ileal pouch anal anastomosis, A review of the current literature has been performed.

© 2005 The WJG Press and Elsevier Inc. All rights reserved.

Key words: Gardner's syndrome; Desmoid tumor; RPC; IPAA

Fotiadis C, Tsekouras DK, Antonakis P, Sfiniadakis J, Genetzakis M, Zografos GC. Gardner's syndrome: A case report and review of the literature. *World J Gastroenterol* 2005; 11 (34): 5408-5411
http://www.wjgnet.com/1007-9327/11/5408.asp

INTRODUCTION

Gardner's syndrome is a rare (1:1 000 000 population in USA) autosomal dominant inherited disorder with a high degree of penetrance characterized by the triad of colonic polyposis, multiple osteomas and mesenchymal tumors of the skin and soft tissues[1-3].

In 1951, Gardner reported the association between surface tumors and colonic polyps that are prone to malignant degeneration[4]. In 1952, Gardner and Plenk described the dominant hereditary pattern of multiple osteomas associated with colonic polyposis[5]. Later that year, Gardner and Richards reported the association of hereditary colonic polyposis and osteomatosis with multiple cutaneous and subcutaneous tumors describing the so-called Gardner's syndrome[6].

It is believed that Gardner's syndrome and familial adenomatous polyposis (FAP) are variants of the same disorder, since they share the same genetic alterations. The fact that Gardner's syndrome is associated with extracolonic manifestations may be explained by a variable penetrance of a common mutation. The disorder is linked to band 5q21-q22, the adenomatous polyposis coli locus (APC gene). More than 1 400 different mutations of this gene have been reported. The specific area of the APC gene that is mutated determines the extracolonic manifestations as well as the number, time frame and malignant potential of adenomatous polyps. Although most cases show familial clustering, one-third of cases occur due to spontaneous mutations. MYH (1p34.3-p32.1) is another gene associated with FAP. In general, the clinical picture of FAP patients with mutations in the MYH gene is milder than those with mutations in the APC gene. The presence of extracolonic manifestations is linked to the vast majority of cases, if not exclusively, to mutations of the APC gene. It is believed that in the pathogenesis of FAP and possibly Gardner's syndrome, environmental factors such as diet, exercise and smoking also play an important role[1,7-11].

The clinical spectrum of disease presentation is variable and often diagnosis is delayed, despite the presence of clues for a significant amount of time. We present the rare case of a 11-year-old girl with Gardner's syndrome that was diagnosed due to the finding of a desmoid tumor on the lumbar area.

CASE REPORT

A 11-year-old female patient presented with a small tumor in the right lumbar area. The patient was afebrile with normal vital signs. Giordano's sign was absent and she had a normal urinalysis, CBC and blood biochemistry. After careful clinical examination, the only abnormal finding was a 4-cm mass on the right lumbar area. The mass was fixed, non-tender and had a bony firm consistency. IVP was scheduled with insignificant findings. Follow up of the tumor growth was advocated for a year before further investigations should take place, but the rapid increase in tumor size lead to a CT scan evaluation of the abdomen and pelvis 3 mo later. A 6-cm tumor of indeterminate quality was revealed originating or adhering to the left latissimus dorsi muscle. After careful medical history was taken again, the patient recalled an episode of hematochezia that had been attributed to hemorrhoids. On colonoscopy, she was found to have numerous polyps carpeting the entire colon and rectum, which was consistent with FAP. The clinical suspicion of Gardner's syndrome was raised. No family history of FAP was evident. A fundoscopic examination was performed showing the typical hypertrophy of the pigmented layer of

the retina. An upper endoscopy was performed revealing normal findings. Subsequently resection of the lumbar tumor was performed via a posterior approach. The pathologist reported a firm tumor with a gritty sensation during transection. On cross section, a glistening white coarsely trabeculated surface was revealed resembling scar tissue (Figure 1A). On microscopic examination, the tumor consisted of eosinophilic or amphophilic spindle-shaped cells embedded within moderate amount of collagen. These cells did not show atypical or hyperchromatic nuclei but some pleomorphism was present (Figure 1B). The final report was that of a desmoid tumor. The next step was a restorative proctocolectomy with ileal pouch anal anastomosis (RPC/IPAA) and mucosectomy. Pathology of the specimen confirmed the diagnosis of FAP (Figure 1C). Colonic polyps proved to be tubular adenomas. The epithelial cells showed moderate differentiation into normal cells although scattered goblet cells could be found. Cellular atypia were manifested by tall cells with pseudostratified nuclei (Figure 1D). No malignant transformation was present.

On discharge, it was recommended that all family members must be evaluated for FAP. Still, the patient was lost to follow-up 2 mo later because of address change.

DISCUSSION

Gardner's syndrome represents a multisystemic disease. Symptoms are usually evident by the 20th year of age, but they may present anytime between 2 mo and 70 years. In general the cutaneous and bone abnormalities develop approximately 10 years prior to polyposis[1,3,12]. However, in our case the polyps were already symptomatic at the time of diagnosis, before the extracolonic manifestation of the disease became evident.

The gastrointestinal manifestations of Gardner's syndrome include colonic adenomatous polyps (tubular, villous, tubulovillous), gastric and small intestinal adenomatous polyps (12% of patients) and peri-ampullary carcinomas (2% of patients). Polyp formation starts at puberty but diagnosis is usually in the third decade, while malignant transformation approaches 100% by the fourth decade of life. The presenting symptoms are anemia, lower gastrointestinal bleeding, cramping abdominal pain, diarrhea, bowel obstruction and mucous discharge. Most of the polyps are small (<5 mm) and therefore difficult to demonstrate on imaging studies. The larger sized polypi may prolapse through the anus or may lead to intussusception or ileus. On colonoscopy, the rectum and whole large intestine appear carpeted by the polyps[1,3,12-14].

Osteomas appear in about half of Gardner's syndrome patients and manifest earlier than polyposis. They may be endosteal or exosteal and demonstrate sclerosis and deformity. The vast majority of osteomas are located on the skull. Since the most commonly affected bones are the mandible and maxilla, many patients present initially to dental surgeons. However, long bones and even phalanges may be affected. A finding of three or more osteomas has been proposed as a screening method for Gardner's syndrome[1,12,15].

The commonest skin manifestations of Gardner's syndrome are epidermoid or sebaceous cysts (66%) and are found on the face, scalp and extremities. They are usually asymptomatic although mild pruritus or signs of inflammation may be evident. Other skin manifestations are fibromas, neurofibromas, lipomas, leiomyomas, and pigmented skin lesions[1,16].

Desmoid tumors appear in 3.5-5.7% of patients and usually appear within 3 years following surgery although they can appear at anytime. Common locations are the incision sites, the abdominal cavity (especially the mesentery) or the retroperitoneum. They are considered as one of the

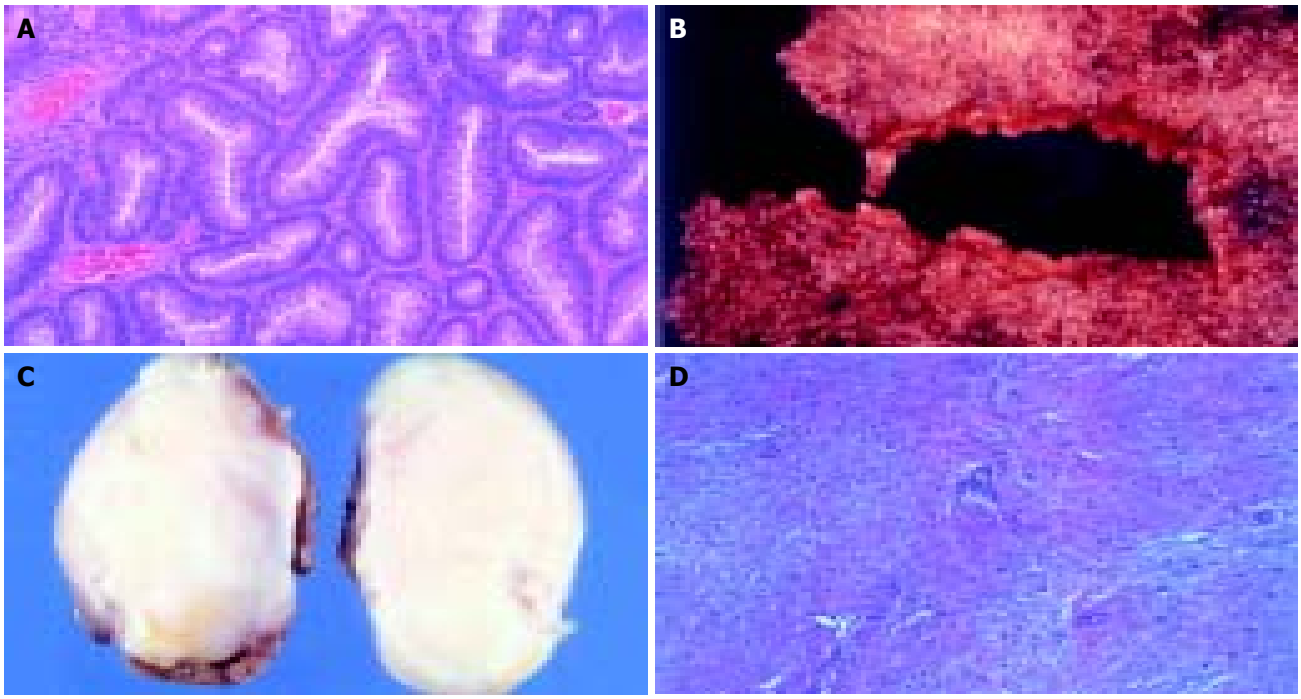


Figure 1 Desmoid tumor. Macroscopic appearance (**A**). Desmoid tumor. Microscopic appearance (HE ×40) (**B**). The resected colon specimen (opened) showing the characteristic carpeting of Gardner's syndrome (**C**). Microscopic appearance of an adenomatous colon polyp (HE ×40) (**D**).

most troublesome manifestations of Gardner's syndrome since they may cause life threatening complications and are usually resistant to treatment[1,17-22]. In our case, the desmoid tumor was the sole manifestation of the disease and with a misleading medical history, diseases of the left kidney and ureter were first considered.

In about 90% of population, hypertrophy of the retinal pigmented layer occurs. Other manifestations of Gardner's syndrome are papillary thyroid cancer (often multicentric), benign intracranial neoplasms such as meningiomas and epidermoid cysts, hepatoma, hepatoblastoma, fibromas, leiomyomas, lipomas, biliary and adrenal neoplasms, osteosarcoma, chondrosarcoma, and in 70% of patients dental disorders (congenitally missing teeth, hypercementosis, odontomas, dentigerous cysts, impacted teeth, supernumerary teeth, fused or unusually long roots and multiple caries)[1-9,12-16].

The diagnosis of FAP and Gardner's syndrome can be made by genetic testing for gene mutations or by the demonstration of multiple colonic polyps during colonoscopy. Genetic testing is the most effective method for demonstrating mutated APC gene in relatives of patients with FAP syndrome[1,23].

Owing to the increased risk of cancer in various organs, patients with FAP/Gardner's syndrome or their relatives should undergo surveillance programs. These include both large bowel and upper GIT surveillance, as well as thyroid and possibly hepatic surveillance too.

Large bowel surveillance is indicated in the following cases:

I Family history of FAP, but no demonstrable mutation

Annual flexible sigmoidoscopy starting from the age of 13-15 till the age of 30. Sigmoidoscopy every 3-5 years from 30 to 60 years.

II Known APC mutation, but patient refuse surgical treatment.

Flexible sigmoidoscopy every 6 mo and annual colonoscopy starting from the age of 10-12. Advise surgery at an age, earlier than 25 years.

III Known FAP following surgery

Annual rectoscopy following ileo-rectal anastomosis (IRA).

Annual proctoscopy following IPAA.

Today no widely accepted upper gastrointestinal tract surveillance program exists. However, all patients with known FAP should undergo an upper GIT surveillance program, due to higher risk of malignancy development in this area. A triennial upper gastrointestinal endoscopy utilizing both direct and side view endoscope has to be performed. In the case of multiple polyps, annual endoscopy is advised.

Annual clinical and ultrasonographic examination of the thyroid gland is mandatory. Hepatic surveillance by ultrasound and AFP level measurement is under investigation[1,23].

Treatment is advised at diagnosis considering the malignant potential of the polyps and due to the fact that 25% of cases presenting with symptoms have cancer. Treatment options include total proctocolectomy and permanent terminal ileostomy, RPC and construction of an IPAA, subtotal colectomy and IRA. Prophylactic resection should be performed before the 25th year of life, ideally between the age of 16 and 20 years. However, patients with a large number of polyps early in life may benefit from an operation at an earlier age, considering the relationship between polyp number and cancer risk. None of these options is ideal and the choice of operation is always a combination of the patient's preference and the surgeon's experience. The first operative option seems to be the safest, since no large intestinal epithelium remains, but the patient must learn to live with an ileostomy. The second option avoids an ileostomy, but is more technically demanding, is associated with greater morbidity and the need for lifetime follow-up, due to the possibility of residual mucosa. The third option should be reserved for those patients whose rectum is relatively disease free (less than 20 polyps). Once thought to result in spontaneous regression of the remaining rectal polyps, this procedure appears to be of questionable efficacy. In our case, we performed the more technically demanding RPC/IPAA after explaining to the patient (and her relatives) the possible choices[1,3,11,24,25].

Owing to the morbidity and mortality associated with the surgical treatment options, there is intensive investigation for drugs that could decrease the malignant potential of adenomatous polyps. In 1983, Waddell and Loughry reported that the rectal polyps of patients with FAP almost disappeared following sulindac administration. Sulindac and other NSAID's have been tested in subsequent clinical studies demonstrating a reduction in the number and size of polyps during the period of their administration. However, the appearance of new polyps as well as the malignant transformation of polyps has been demonstrated in patients on sulindac therapy. In order to avoid the side effects of long-term NSAID administration while maintaining efficacy, researchers have focused on the newer COX-2 inhibitors (celecoxib, rofecoxib) following the demonstration of COX-2 expression in colonic carcinomatous mucosa but not in normal GIT mucosa. A decrease in the polyp size was noted but at higher than usual doses. Currently celecoxib 400 mg/d has granted FDA approval for FAP patients by decreasing the polyps' size, but whether it reduces the malignant potential of them remains to be investigated[11,26].

Non-NSAID substances that have been tested for the prevention of malignant transformation of polyps in FAP patients seem to be of inferior efficacy. These include 5-FU, Vit C, Vit E, calcium, DHA and green tea extract[11].

Treatment options for the cutaneous cysts of Gardner's syndrome are the same as for ordinary cysts. Treatment is indicated for symptomatic cases or for cosmetic reasons. In the same manner, osteomas may require resection if they interfere with function or for cosmetic reasons[1,16].

Treatment of desmoids is generally considered to be a challenge for both the doctor and the patient. Operation is recommended only for symptomatic patients due to common recurrence (up to 80%). Medical treatment consists of sulindac, tamoxifen or toremifene, raloxifene alone or in combination. Doxorubicin, dacarbazine as well as carboplatin, vinblastine and methotrexate have been used in case of aggressive unresectable desmoids. Radiotherapy can also be tried. The treatment plan greatly depends on the location of the desmoid tumor. Mesenteric desmoids tend to involve the mesentery diffusely, altering gross anatomy and can

invade vessels or ureters. Often complex operative procedures have to be employed and recurrence is typical. So a less aggressive medical approach is preferred initially and surgery should be performed in case of failure. Abdominal wall desmoids should be treated surgically since they are easier to be excised and recurrence rates are lower, compared to their mesenteric counterparts[1,17-22]. In our case, we had an unusual occurrence of a desmoid tumor at the muscles of the back. The excisional biopsy raised the clinical suspicion and led to the final diagnosis and treatment. Still, there are no follow-up data to evaluate recurrence.

In conclusion, we presented a case of Gardner's syndrome with an unusual clinical presentation of a desmoid tumor in the left lumbar area that led to the final diagnosis after taking careful medical history. RPC/IPAA was the surgical modality of choice with excellent immediate post-operative results. Even though in our case the patient was lost to follow-up it cannot be over expressed that after the diagnosis of Gardner's syndrome, the patients must be aggressively followed-up, since there is a constant threat to their lives at any age.

REFERENCES

1 **Nandakumar G,** Morgan JA, Silverberg D, Steinhagen RM. Familial polyposis coli: clinical manifestations, evaluation, management and treatment. *Mt Sinai J Med* 2004; **71**: 384-391
2 **Leblanc R.** Familial adenomatous polyposis and benign intracranial tumors: a new variant of Gardner's syndrome. *Can J Neurol Sci* 2000; **27**: 341-346
3 **Cruz-Correa M,** Giardiello FM. Diagnosis and management of hereditary colon cancer. *Gastroenterol Clin North Am* 2002; **31**: 537-549
4 **Gardner EJ.** A genetic and clinical study of intestinal polyposis: a predisposing factor for carcinoma of the colon and rectum. *Am J Hum Genet* 1951; **3**: 167-176
5 **Gardner EJ,** Plenk HP. Hereditary pattern for multiple osteomas in a family group. *Am J Hum Genet* 1952; **4**: 31-69
6 **Gardner EJ,** Richards RC. Multiple cutaneous and sub-cutaneous lesions occurring simultaneously with hereditary polyposis and osteomatosis. *Am J Hum Genet* 1952; **5**: 139-147
7 **Groden J,** Thliveris A, Samowitz W. Identification and characterization of the familial adenomatous polyposis coli gene. *Cell* 1991; **66**: 589-600
8 **Kinzler KW,** Nilbert MC, Su LK. Identification of FAP locus genes from chromosome 5q21. *Science* 1991; **253**: 661-665
9 **Kinzler KW,** Vogelstein B. Lessons from hereditary colorectal cancer. *Cell* 1996; **87**: 159-170
10 **Baglioni S,** Genuardi M. Simple and complex genetics of colorectal cancer susceptibility. *Am J Med Genet C Semin Med Genet* 2004; **129**: 35-43
11 **Ishikawa H.** Chemoprevention of carcinogenesis in familial tumors. *Int J Clin Oncol* 2004; **9**: 299-303
12 **Newman CA,** Reuther WL 3rd, Wakabayashi MN, Payette MM, Plavsic BM. Gastrointestinal case of the day. Gardner syndrome. *Radiographics* 1999; **19**: 546-548
13 **Debinski HS,** Love S, Spigelman AD, Phillips RK. Colorectal polyp counts and cancer risk in familial adenomatous polyposis. *Gastroenterology* 1996; **110**: 1028-1030
14 **Luk GD.** Diagnosis and therapy of hereditary polyposis syndromes. *Gastroenterologist* 1995; **3**: 153-167
15 **Ida M,** Nakamura T, Utsunomiya J. Osteomatous changes and tooth abnormalities found in the jaw of patients with adenomatosis coli. *Oral Surg Oral Med Oral Pathol* 1981; **52**: 2-11
16 **Perniciaro C.** Gardner's syndrome. *Dermatol Clin* 1995; **13**: 51-56
17 **Clark SK,** Phillips RK. Desmoids in familial adenomatous polyposis. *Br J Surg* 1996; **83**: 1494-1504
18 **Soravia C,** Berk T, McLeod RS, Cohen Z. Desmoid disease in patients with familial adenomatous polyposis. *Dis Colon Rectum* 2000; **43**: 363-369
19 **Tonelli F,** Ficari F, Valanzano R, Brandi ML. Treatment of desmoids and mesenteric fibromatosis in familial adenomatous polyposis with raloxifene. *Tumori* 2003; **89**: 391-396
20 **Lynch HT,** Fitzgibbons R Jr, Chong S. Use of doxorubicin and dacarbazine for the management of unresectable intra-abdominal desmoid tumors in Gardner's syndrome. *Dis Colon Rectum* 1994; **37**: 260-267
21 **Kiel KD,** Suit HD. Radiation therapy in the treatment of aggressive fibromatoses (desmoid tumors). *Cancer* 1984; **54**: 2051-2055
22 **Chatzipetrou MA,** Tzakis AG, Pinna AD. Intestinal transplantation for the treatment of desmoid tumors associated with familial adenomatous polyposis. *Surgery* 2001; **129**: 277-281
23 **Dunlop MG.** Guidance on gastrointestinal surveillance for hereditary non-polyposis colorectal cancer, familial adenomatous polypolis, juvenile polyposis, and Peutz-Jeghers syndrome. *Gut* 2002; **51**(Suppl 5): V21-27
24 **Contessini-Avesani E,** Botti F, Negri C. Familial adenomatous polyposis. Surgical treatment: when and how. *Tech Coloproctol* 2004; **8**(Suppl 2): s309-314
25 **Vasen HF,** van Duijvendijk P, Buskens E. Decision analysis in the surgical treatment of patients with familial adenomatous polyposis: a Dutch-Scandinavian collaborative study including 659 patients. *Gut* 2001 **49**: 231-235
26 **Giardiello FM,** Yang VWW, Hylind LM. Primary chemoprevention of familial adenomatous polyposis with sulindac. *N Engl J Med* 2002; **346**: 1054-1059

Science Editor Guo SY **Language Editor** Elsevier HK

PO Box 2345, Beijing 100023, China
www.wjgnet.com
wjg@wjgnet.com

ELSEVIER

World J Gastroenterol 2005;11(34):5412-5413
World Journal of Gastroenterology ISSN 1007-9327
© 2005 The WJG Press and Elsevier Inc. All rights reserved.

• *CASE REPORT* •

Sclerosing encapsulating peritonitis in a liver transplant patient: A case report

Chien-Hua Lin, Jyh-Cherng Yu, Teng-Wei Chen, De-Chuan Chan, Cheng-Jueng Chen, Chung-Bao Hsieh

Chien-Hua Lin, Jyh-Cherng Yu, Teng-Wei Chen, De-Chuan Chan, Cheng-Jueng Chen, Chung-Bao Hsieh, Division of General Surgery, Department of Surgery, Tri-Service General Hospital, National Defense Medical Center, Taipei, Taiwan, China
Correspondence to: Dr. Chung-Bao Hsieh, Division of General Surgery, Department of Surgery, Tri-Service General Hospital, National Defense Medical Center, 325, Sec. 2, Cheng-Kung Road, Neihu 114, Taipei, Taiwan, China. albert0920@yahoo.com.tw
Telephone: +886-2-87927191 Fax: +886-2-87927273
Received: 2005-03-09 Accepted: 2005-04-18

Abstract

We report a patient with HBV-related hepatocellular carcinoma (HCC) and refractory ascites who had received a peritoneal-venous shunt (PVS) 1 year before liver transplantation. Urgent surgical intervention following bowel obstruction and failure of immunosuppression therapy. No intestinal obstruction was found during an initial PVS. However, intestinal obstruction developed 2 wk after liver transplantation; and a cocoon abdomen was found upon exploration. This is the first reported case of cocoon abdomen caused by PVS and exacerbated by liver transplantation.

© 2005 The WJG Press and Elsevier Inc. All rights reserved.

Key words: Sclerosing encapsulating peritonitis; Cocoon abdomen; Intestinal obstruction; Liver transplantation

Lin CH, Yu JC, Chen TW, Chan DC, Chen CJ, Hsieh CB. Sclerosing encapsulating peritonitis in a liver transplant patient: A case report. *World J Gastroenterol* 2005; 11(34): 5412-5413
http://www.wjgnet.com/1007-9327/11/5412.asp

INTRODUCTION

Cocoon abdomen or sclerosing encapsulating peritonitis (SEP) is a rare cause of small bowel obstruction. In this condition, the bowel is partially or totally encased or wrapped by a thick fibrous membrane forming several compartments (cocoons) containing loops of small bowel. SEP usually presents with symptoms of intestinal obstruction, and pre-operative diagnosis is difficult. The pathogenesis of this condition remains unclear; however, it is a form of chronic irritation and inflammation, and may be summarized as primary (idiopathic) or secondarily induced[1]. Here we report a patient with liver cirrhosis and massive ascites who had received a peritoneal-venous shunt (PVS) 1 year before liver transplantation. Thickened parietal peritoneum and fibrotic changes were found during the liver transplantation. After surgery, the patient received treatment with high-dose immunosuppressive agents. Intestinal obstruction developed 2 wk later and this was resolved by surgery.

CASE REPORT

A 64-year-old man received a liver transplantation on August 10, 2003, for decompensated end-stage liver disease caused by hepatitis B, with liver cirrhosis and hepatoma. His pre-transplant history included receiving transarterial embolization of the hepatocellular carcinoma, (HCC) 2 wk before transplantation and a PVS drainage, 1 year before liver transplantation for treating refractory ascites. After the PVS had been performed, the ascites was controlled and the patient was feeding well.

Before liver transplantation, the patient's laboratory data were albumin 3.4 g/dL, total bilirubin 1.9 mg/dL, and prothrombin time 12.3/11.2 s. His Child-Pugh classification was B (score, 8), and he had no history of hepatic encephalopathy. During the liver transplantation, the parietal peritoneum and most of the colonic wall and retroperitoneal liver were observed to be thickened and fibrotic. Hydrocortisone Sod. Succinate (Solu-cortef) (1 000 mg) was administered. After liver transplantation, the patient started to receive immunosuppressive treatment, including Prograf (1 mg twice daily), Solumedrol (40 mg four times daily), CellCept (500 mg twice daily), and we maintained the therapeutic level of Prograf at 10-12 ng/mL. The patient's oral feeding condition was poor; he could not even tolerate semi-liquid diet.

Two weeks after liver transplantation, colicky abdominal pain, vomiting and constipation developed, but no rebounding pain was found by physical examination. Contrasted abdominal computer tomography (CT) revealed a dilated C-shaped region of small intestine over the right lower pelvis, and an adhesion band was suspected to have caused a closed-loop obstruction (Figure 1). Conservative treatment was started, but little improvement occurred and the patient still could not tolerate oral feeding. The patient's abdominal distension increased; repeated plain abdominal radiography showed that the obstructed small bowel loops were enlarged, so we decided on emergency surgery.

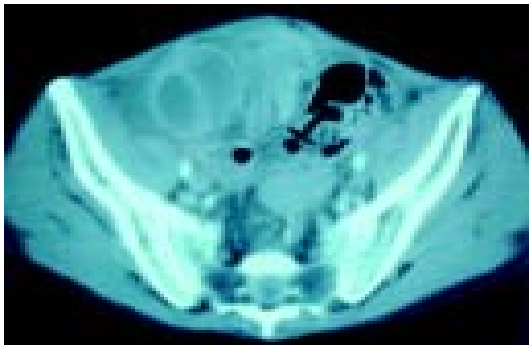


Figure 1 Contrasted abdominal CT revealed a cluster of intestinal loops sacculated in thin, membrane-like sac (black arrow).



Figure 2 Dense thick adhesive sheaths circumferentially wrapping loops of small bowel giving the shape of cocoons in the abdomen (**A**); we excised these fibrous tissues easily using finger dissection (**B**); the serosa was intact and there was no need for bowel resection (**C**).

At laparotomy, we found dense, thick, adhesive sheaths circumferentially wrapping loops of small bowel giving the shape of cocoons in the abdomen (Figure 2). The loops within each cocoon were normal and adherent to each other with avascular fine fibrous tissue; this was easily broken down with finger dissection. The serosa of the bowel was intact. The patient's post-operative recovery was uneventful, and he was discharged 2 wk later.

DISCUSSION

SEP involves entrapment of the intestine in a fibrous sac, resulting in complete intestinal obstruction. It was first described in 1907 by Owtschinnikow[2]. The real causes of SEP are unclear, but it can be classified as primary and secondary forms[1]. Primary (idiopathic) SEP occurs in young women living in warm climates, and is thought to be caused by retrograde menstruation or infection via the Fallopian tubes[3]. Secondary SEP can be classified as systemic caused by local irritants, or as local combined with systemic irritants. The major possible causes include long-term use of β-adrenergic blocking agents, chronic ambulatory peritoneal dialysis, and liver cirrhotic patients after PVS[1,4-6].

If diagnosed before obstruction occurs, the sclerotic membrane can frequently be separated from the small intestine. Successful separation is almost impossible when associated with complete obstruction. Thus, early diagnosis is important.

The clinical picture of cocoon abdomen usually includes recurrent episodes of intestinal obstruction caused by kinking and compression of the intestines within the constricting cocoon. The condition should be suspected in patients with bowel obstructive signs or soft, non-tender abdominal masses. Pre-operative diagnosis of abdominal cocoon is difficult. Plain radiographs and oral contrast studies may show a circumscribed mass of bowel loops with absent or delayed passage of contrast. Ultrasound examination may show a mass of tightly bound small bowel loops surrounded by a thick rim of echo-poor tissue. CT scans might also reveal a mass comprising an encapsulating cluster of dilated small bowel loops with failure of orally taken contrast medium to pass distally.

Beta-blockers, particularly propranolol, have been implicated in the etiology of this condition because they may lead to enhanced collagen production and subsequent fibrosis. Yamamoto *et al*., reported SEP in two patients with liver cirrhosis[5]. Cambria *et al*., and Greenlee *et al*., reported possible associations with the Le Veen shunt. Abul reported the first case of cocoon abdomen in a liver transplant patient[2], but that patient did not receive the Le Veen shunt.

Our patient suffered from liver cirrhosis with massive ascites and received PVS, but he presented with SEP following liver transplantation and developed intestinal obstruction 2 wk later. Although the actual pathogenesis of SEP is unclear, we believe that PVS may be one of the causes. Thus, ascites flow through the PVS and fibrin deposition in the peritoneum may lead to chronic inflammation. Hence, the cause of SEP in this patient may have been a combination of PVS with recurrent spontaneous bacterial peritonitis. Intraperitoneal bleeding may have helped induce this condition. Following liver transplantation, bleeding and manipulation irritation would have exacerbated it[5].

Definitive diagnosis of SEP can only be made at laparotomy. Yamamoto reported successful treatment with total enterolysis and the oral administration of prednisolone[5], and Junor and McMillan reported that immunosuppression has a beneficial effect on SEP in patients with or without a successful transplantation. However, in this patient, even large doses of immunosuppressants were ineffective. Hence, surgery was essential with lysis of the membranes and adhesions. Bowel resection was not necessary. We recommend that SEP should be cleared away during liver transplantation to prevent any following possible intestinal obstruction.

REFERENCES

1 **Cohen O**, Abrahamson J, Ben-Ari J, Frajewicky V, Eldar S. Sclerosing encapsulating peritonitis. *J Clin Gastroenterol* 1996; **22**: 54-57
2 **Abul S**, Al-Oazweni H, Zalat S, Al-Sumait B, Asfar S. Cocoon abdomen in a liver transplant patient. *J R Coll Surg Edinb* 2002; **47**: 579-581
3 **Narayana R**, Bhargava BN, Kabra SG, Sangal BC. Idiopathic sclerosing encapsulating peritonitis. *Lancet* 1989; **2**: 127-129
4 **Brown P**, Baddeley H, Read AE, Davies JD, McGarry J. Sclerosing peritonitis, an unusual reaction to a beta-adrenergic blocking drug (practolol). *Lancet* 1974; **2**: 1477-1481
5 **Yamamoto S**, Sato Y, Takeishi T, Kobayashi T, Hatakeyama K. Sclerosing encapsulating peritonitis in two patients with liver cirrhosis. *J Gastroenterol* 2004; **39**: 72-175
6 **Klimopoulos S**, Kalsoulis IE, Margellos V, Nikolopoulou N. Sclerosing encapsulating peritonitis secondary to CAPD: the effect of fibrotic debridement on further dialysis. *J R Coll Surg Edinb* 2002; **47**: 485-490

Science Editor Guo SY **Language Editor** Elsevier HK

PO Box 2345, Beijing 100023, China
www.wjgnet.com
wjg@wjgnet.com

ELSEVIER

World J Gastroenterol 2005;11(34):5414-5415
World Journal of Gastroenterology ISSN 1007-9327
© 2005 The WJG Press and Elsevier Inc. All rights reserved.

• *CASE REPORT* •

Intrauterine contraceptive device appendicitis: A case report

Hao-Ming Chang, Teng-Wei Chen, Chung-Bao Hsieh, Chung-Jueng Chen, Jyh-Cherng Yu, Yao-Chi Liu, Kuo-Liang Shen, De-Chuan Chan

Hao-Ming Chang, Teng-Wei Chen, Chung-Bao Hsieh, Chung-Jueng Chen, Jyh-Cherng Yu, Yao-Chi Liu, Kuo-Liang Shen, De-Chuan Chan, Division of General Surgery, Department of Surgery, Tri-Service General Hospital, National Defense Medical Center, Taipei, Taiwan, China
Correspondence to: Dr. De-Chuan Chan, Division of General Surgery, Department of Surgery, Tri-Service General Hospital, National Defense Medical Center, Taipei, Taiwan 325, Sec 2, Cheng-Kung Road, Taipei, Taiwan, China. chrischan1168@yahoo.com.tw
Telephone: +886-2-87927191 Fax: +886-2-87927273
Received: 2005-01-21 Accepted: 2005-03-09

Abstract

Uterine perforation is one of the serious complications associated with use of the intrauterine contraceptive device (IUD). Uterine perforation by IUD can involve several neighboring organs. A case of acute appendicitis was caused by a Multiload Cu 375 IUD inserted previously. This is a rare complication and only fourteen previous cases were recorded in the literature.

© 2005 The WJG Press and Elsevier Inc. All rights reserved.

Key words: Appendicitis; Intrauterine contraceptive device; Uterine perforation

Chang HM, Chen TW, Hsieh CB, Chen CJ, Yu JC, Liu YC, Shen KL, Chan DC. Intrauterine contraceptive device appendicitis: A case report. *World J Gastroenterol* 2005; 11(34): 5414-5415
http://www.wjgnet.com/1007-9327/11/5414.asp

INTRODUCTION

Intrauterine contraceptive device (IUD) has been widely used since 1965[1]. Perforation of the uterus by an IUD is a rare and serious complication, occurring in 1/350 to 1/2 500 insertions[2]. Perforation by IUD can involve several neighboring organs such as the bladder, and particularly the intestinal tract[3] resulting frequently in serious complications which require intensive treatment including intestinal surgery. Perforation can occur during insertion or later[4]. Perforation occurring at the time of insertion correlates directly with the skill of the clinician. Delayed onset of symptoms is mostly due to chronic inflammatory reaction of copper-containing IUD. We report a case of acute appendicitis in a 50-year-old woman caused by a Multiload Cu 375 IUD inserted 18 years previously.

CASE REPORT

The patient was a 50-year-old gravida 3 para 3 woman, admitted because of severe lower abdominal pain associated with fever, nausea and vomiting. A Multiload Cu 375 IUD had been inserted, 18 years prior to the present admission and she did not receive regular physical examination after insertion.

On physical examination, the abdomen had decreased bowel sounds and rebounding tenderness mostly in the right lower quadrant. Laboratory data revealed leukocytosis and plain abdominal film showed the IUD to be overlying the right iliac crest (Figure 1). The abdomen was opened through a McBurney incision under the impression of acute appendicitis. The operative finding was the IUD located in the abdominal cavity behind the ileocecal junction and its tip had penetrated the tip of appendix (Figure 2). The whole area was edematous and covered with omentum. No fecalith impaction in appendix was found. Appendectomy was performed and the IUD was retrieved. The patient recovered uneventfully.



Figure 1 KUB showed IUD migration.



Figure 2 Intraoperative photograph showing IUD penetrated the tip of appendix.

DISCUSSION

IUD is generally a safe modality for long-term contraception.

Associated complications are bleeding, infection, ectopic pregnancy and uterine perforation. Uterine perforation is one of the most serious but uncommon complications associated with an IUD[3]. The mechanism of perforation is thought to be the insertion procedure or chronic inflammatory reaction with gradual erosion through the uterine wall[1]. The incidence is influenced by several factors including the timing of insertion, parity, previous abortions, type of IUD inserted, experience of the operator and position of the uterus[4]. Most of the perforations take place at the time of insertion. Delayed onset of symptoms supports secondary migration[1]. The timing of IUD insertion is flexible. Previous studies showed IUD insertion 0-3 mo postpartum increased the risk of uterine perforation as did insertions at 3-6 mo postpartum[4].

In this case, we considered the mechanism of IUD perforation was secondary by gradual erosion through uterine wall due to inserted 18 years prior to the present admission. No fecalith impaction in the appendix was found during operation and we considered that the acute appendicitis was induced by chronic inflammatory reaction of the copper-containing IUD.

Patients with IUD should be alerted about the possibility of its migration. Regular self examination for "missing threads" is useful in the early detection of migration of the IUD. A plain radiograph of the abdomen is usually the initial examination of choice to verify the presence of the IUD in the pelvis. Once found, an ultrasound examination has to be done to determine the location of the IUD relative to the uterus. The treatment of a migrated IUD is surgical, either laparoscopy or laparotomy. Withdrawal of the migrated IUD is advisable even if its migration has not given rise to any clinical symptoms[5] and can avoid further complications like bowel perforation, bladder perforation, or fistula formation[6]. To our knowledge, this is the 15th case of a perforated IUD causing acute appendicitis[7-18].

REFERENCES

1 **Zakin D,** Stern WZ, Rosenblatt R. Complete and partial uterine perforation and embedding following insertion of intrauterine devices. *Obstet Gynaecol Surg* 1981; **36**: 335-353

2 **Ohana E,** Sheiner E, Leron E, Mazor M. Appendix perforation by an intrauterine contraceptive device. *Eur J Obstet Gynecol Reprod Biol* 2000; **88**: 129-131

3 **Key TC,** Kreutner AK. Gastrointestinal complications of modern intrauterine contraceptive device. *Obstet Gynecol* 1980; **55**: 239-244

4 **Heartwell S,** Schlesselman S. Risk of uterine perforation among users of intrauterine devices. *Obstet Gynecol* 1983; **61**: 31-36

5 **Treisser A,** Colau JC. Causes, diagnosis and treatment of uterine perforations by intrauterine devices. *J Gynecol Obstet Biol Reprod* 1978; **7**: 837-847

6 **Berman MC**, Cohen HL. Obstetrics and gynecology: A guide to clinical practice. Diagnostic Medical Sonography. *Lippincott* 1997: 569-571

7 **Carson SA,** Gatlin A, Mazur M. Appendiceal perforation by Copper-7 intrauterine contraceptive device. *Am J Obstet Gynecol* 1981; **141**: 586-587

8 **Gruchy MV.** Perforated appendix caused by an IUD. *Med J Aust* 1982; **2**: 116-117

9 **Goldman JA,** Peleg D, Feldberg D. IUD appendicitis. *Eur J Obstet Gynecol Reprod Biol* 1983; **15**: 181-183

10 **McWhinney NA,** Jarrett R. Uterine perforation by a Copper-7 intrauterine contraceptive device with subsequent penetration of the appendix. *Br J Obstet Gynecol* 1983; **90**: 774-776

11 **Serra I.** Appendicitis caused by an intrauterine contraceptive device. *Br J Surg* 1986; **73**: 927-928

12 **McLaughlin DI,** Bevins W, Karas BK, Sonnenberg L. IUD appendicitis during pregnancy. *West J Med* 1988; **149**: 601-602

13 **Abbey RK,** Gupta R, Sharma RK, Sood PC. Acute appendicitis-an unusual cause. *Indian J Med Sci* 1999; **53**: 108-110

14 **Rubinoff L.** IUD appendicitis. *JAMA* 1975; **231**: 67-68

15 **Chang TC,** Eden JA. Intra-uterine device appendicitis. *J Obstet Gynaecol* 1989; **9**: 257-258

16 **Cuillier F,** Ben Ghalem S, Haffaf Y. Intrauterine device appendicitis: an exceptional complication. *J Gynecol Obstet Biol Reprod* 2003; **32**: 55-57

17 **Khanna AK,** Khanna A. Perforation of the appendix caused by an IUD. *Med J Aust* 1986; **144**: 109

18 **Katara AN,** Chandiramani VA, Pandya SM, Nair NS. Migration of intrauterine contraceptive device into the appendix. *Indian J Surg* 2004; **66**: 179-180

Science Editor Guo SY **Language Editor** Elsevier HK

PO Box 2345, Beijing 100023, China
www.wjgnet.com
wjg@wjgnet.com

ELSEVIER

World J Gastroenterol 2005;11(34):5416-5417
World Journal of Gastroenterology ISSN 1007-9327
© 2005 The WJG Press and Elsevier Inc. All rights reserved.

• *CASE REPORT* •

Diverticulosis of the jejunum with intestinal obstruction: A case report

Chien-Hua Lin, Huan-Fa Hsieh, Chih-Yung Yu, Jyh-Cherng Yu, De-Chuan Chan, Teng-Wei Chen, Peng-Jen Chen, Yao-Chi Liu

Chien-Hua Lin, Jyh-Cherng Yu, De-Chuan Chan, Teng-Wei Chen, Yao-Chi Liu, Division of General Surgery, Department of Surgery, Tri-Service General Hospital, National Defense Medical Center, Taipei, Taiwan, China
Chih-Yung Yu, Department of Radiology, Tri-Service General Hospital, National Defense Medical Center, Taipei, Taiwan, China
Peng-Jen Chen, Division of Gastroenterology, Department of Internal Medicine, Tri-Service General Hospital, National Defense Medical Center, Taipei, Taiwan, China
Huan-Fa Hsieh, Department of Surgery, Yee-Zen General Hospital, Tauyan, Taiwan, China
Correspondence to: Dr. Yao-Chi Liu, Division of General Surgery, Department of Surgery, Tri-Service General Hospital, National Defense Medical Center, 325, Sec. 2, Cheng-Kung Road, Neihu 114, Taipei, Taiwan, China. linjh93@yahoo.com.tw
Telephone: +886-2-87927191 Fax: +886-2-87927273
Received: 2005-03-14 Accepted: 2005-04-02

Abstract

A diagnosis of intestinal diverticulosis is difficult to make pre-operatively because the clinical symptoms are usually non-specific. We report the case of a 70-year-old man who had suffered from three episodes of intestinal obstruction in 1 year. He experienced dull pain and a sensation of fullness over the whole abdomen. The symptoms did not improve after conservative treatment. The presumptive diagnosis was intestinal obstruction, and an exploratory laparotomy found diverticulosis of the proximal jejunum, with an adhesion band formed from the base of one diverticulum. Strangulation of a segment of the jejunum resulted from the internal herniation caused by the band. The band was removed and the proximal jejunum segmentally resected. His postoperative course was uneventful.

© 2005 The WJG Press and Elsevier Inc. All rights reserved.

Key words: Diverticulosis of jejunum; Intestinal obstruction

Lin CH, Hsieh HF, Yu CY, Yu JC, Chan DC, Chen TW, Chen PJ, Liu YC. Diverticulosis of the jejunum with intestinal obstruction: A case report. *World J Gastroenterol* 2005; 11(34): 5416-5417

http://www.wjgnet.com/1007-9327/11/5416.asp

INTRODUCTION

The incidence of acquired jejunal diverticulosis varies from 0.2% to 1.3% in autopsy studies to 2.3% when assessed on enteroclysis. The clinical presentation is normally asymptomatic and it is usually diagnosed incidentally on laparotomy. Complications may include perforation, hemorrhage, enterolith formation, diverticulitis, and intestinal obstruction. Enterolith formation is the most common complication and intestinal obstruction is rare. An adhesion band, arising from the base of one of the diverticula, may be formed after repeated diverticulitis, and may cause strangulation of the intestine. We report a rare case of diverticulosis of the jejunum with an adhesion band resulting in intestinal obstruction.

CASE REPORT

A 70-year-old male was admitted to our emergency department with dull abdominal pain and no passage of stools for 3 d. He reported a sensation of fullness over the whole abdomen and nausea. He had previously been admitted to our hospital thrice in 1 year with partial intestinal obstruction. An abdominal examination showed a diffuse tympanic sound, with percussion and tenderness over the whole abdomen. Laboratory tests indicated a white-cell count of 4 800/μL, and normal serum sodium (136 mmol/L) and potassium levels (3.8 mmol/L). A plain X-ray of the abdomen showed dilatation of the small intestine, especially in the proximal jejunum (Figure 1A). An upper gastrointestinal (GI) oral contrast study showed multiple diverticula in the proximal jejunum and a mechanical obstruction of the proximal jejunum (Figure 1B). The presumptive diagnosis was partial intestinal obstruction and the patient was admitted. After admission, nasogastric tube decompression was performed. The sensation of abdominal fullness was persistent 3 d later. An exploratory laparotomy revealed minimal clear ascites and diverticulosis of the proximal jejunum and an adhesion band with a dilated proximal jejunum (Figure 2). Segmental resection of the proximal jejunum (20 cm in length) with end-to-end jejuno-jejunostomy was performed. The final pathological diagnosis was diverticulosis of the jejunum with serosal fibrosis, hemorrhage, calcification, and inflammatory change.

The patient had an uneventful post-operative course and was discharged 8 days after the procedure.

DISCUSSION

Diverticulosis of the small bowel (excluding Meckel's diverticulosis) is uncommon, and is found in less than 5% of post-mortem examinations[1]. It is caused by herniation of the mucosa and submucosa through the muscular layer of the bowel wall (false diverticula). Diverticula are usually multiple and occur at the mesenteric border, in contrast to

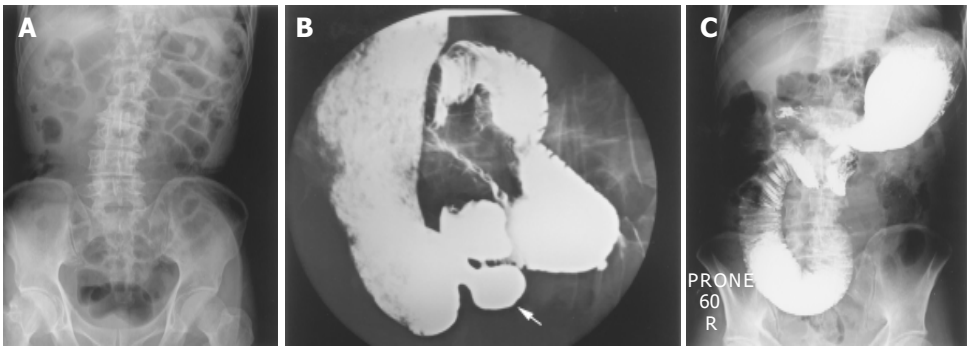


Figure 1 A plain X-ray of the abdomen showing dilatation of the small intestine, especially the proximal jejunum (**A**). **B** and **C:** An upper GI oral contrast study showing multiple diverticula in the duodenum and proximal jejunum (the white arrow, (**B**) and dilatation of the proximal jejunum (**C**).

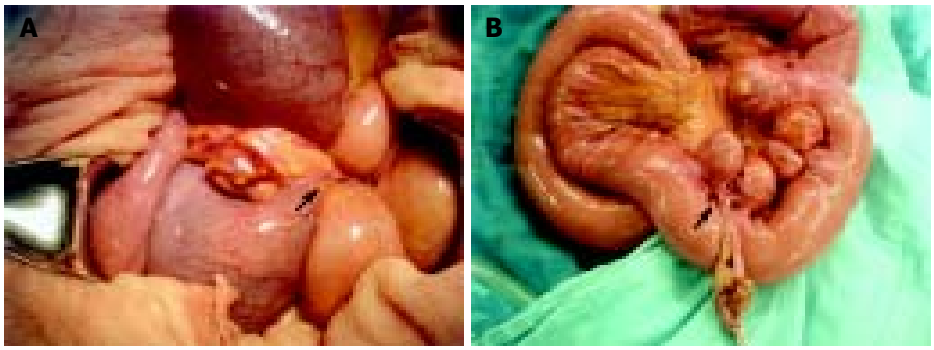


Figure 2 The photograph shows an adhesion band overriding the jejunum (the black arrow), with ischemic changes in the proximal jejunum (**A**). After surgical removal of the adhesion band, we found that the band was connected to one of the diverticula, arising from the mesentery side (the black arrow) (**B**).

the true congenital Meckel's diverticulum. The probable cause of diverticulosis of the small bowel is motor dysfunction of the smooth muscle or the myenteric plexus in the small bowel. If contraction of the affected small intestine is disordered, it may increase the intraluminal pressure, and the mucosa and submucosa would pass through the weakest mesenteric site in the bowel wall[3]. This condition is usually asymptomatic and is found incidentally. Most patients have chronic abdominal pain and a bloated sensation. Complications include hemorrhage, perforation, diverticulitis, and intestinal obstruction. Mechanical intestinal obstruction occurs in 2.3-4.6% of cases of jejuno-ileal diverticulosis, and is reported to be the most frequent complication of jejunal diverticula requiring surgery[3-6]. Previous cases of intestinal obstruction associated with intestinal diverticulosis include distended diverticula, inflammatory mass associated with diverticulitis, stricture or adhesions from recent or past diverticulitis, and intussusception at the site of the diverticulum, most of which are caused by enteroliths[3]. The obstruction is induced by adhesion band rarely, as it occurred in our case.

Lobo *et al*., reported that dynamic intestinal obstruction is the most frequent complication of jejunal diverticulosis necessitating surgery and may be due to enteroliths, adhesions secondary to diverticulitis, volvulus, or intussusception[2].

This is the first report of strangulation of the jejunum caused by a mesodiverticular band in the literature. The band may have formed during recurrent diverticulitis, because it arose from the mesodiverticulum. Although this phenomenon is rare, we should keep in mind that intestinal diverticulosis may induce intestinal obstructions of different kinds, repeat physical examinations and X-ray films are needed and enteroclysis studies or CT scan are helpful in diagnosis. Surgery is indicated for acute abdominal or repeated intestinal obstruction.

REFERENCES

1 **Hayee B,** Khan HN, Al-Mishlab T, McPartlin JF. A case of enterolith small bowel obstruction and jejunal diverticulosis. *World J Gastroenterol* 2003; **9**: 883–884
2 **Lobo DN,** Braithwaite BD, Fairbrother BJ. Enterolith ileus complicating jejunal diverticulosis. *J Clin Gastroenterol* 1999; **29**: 192–193
3 **Bree ED,** Grammatikakis J, Christodoulakis M, Tsiftsis D. The clinical significance of acquired jejunoileal diverticula. *Am J Gastroenterol* 1998; **93**: 2523–2528
4 **Fronticelli CM,** Bellora P, Ferrero A, Anselmetti GC, Passarino G, Burlo P. Complicated jejunal diverticulosis: report of a case. *Surg Today* 1996; **26**: 192–195
5 **Chiu KW,** Changchien CS, Chuah SK. Small-bowel diverticulum: is it a risk for small-bowel volvulus? *J Clin Gastroenterol* 1994; **19**: 176–177
6 **Palder SB,** Frey CB. Jejunal diverticulosis. *Arch Surg* 1988; **123**: 889–894

Science Editor Guo SY **Language Editor** Elsevier HK

PO Box 2345, Beijing 100023, China
www.wjgnet.com
wjg@wjgnet.com

ELSEVIER

World J Gastroenterol 2005;11(35):5423-5432
World Journal of Gastroenterology ISSN 1007-9327
© 2005 The WJG Press and Elsevier Inc. All rights reserved.

• *REVIEW* •

Treatment of Zollinger-Ellison Syndrome

Paola Tomassetti, Davide Campana, Lydia Piscitelli, Elena Mazzotta, Emilio Brocchi, Raffaele Pezzilli, Roberto Corinaldesi

Paola Tomassetti, Davide Campana, Lydia Piscitelli, Elena Mazzotta, Emilio Brocchi, Raffaele Pezzilli, Roberto Corinaldesi, Department of Internal Medicine and Gastroenterology, University of Bologna, Italy
Correspondence to: Professor Paola Tomassetti, Department of Internal Medicine and Gastroenterology, University of Bologna, Policlinico S.Orsola-Malpighi, Via Massarenti, 9, 40138, Bologna, Italy. paola.tomassetti@unibo.it
Telephone: +39-51-6364186 Fax: +39-51-6364186
Received: 2005-01-31 Accepted: 2005-03-09

Abstract

In this article, we have reviewed the main therapeutic measures for the treatment of Zollinger-Ellison syndrome (ZES). Review of the literature was based on computer searches (Pub-Med, Index Medicus) and personal experiences. We have evaluated all the measures now available for treating patients with sporadic gastrinomas or gastrinomas associated with Multiple Endocrine Neoplasia Type 1, (MEN 1) including medical therapy such as antisecretory drugs and somatostatin analogs (SST), chemotherapy and chemoembolization, and surgical procedures. In ZES patients, the best therapeutic procedure is surgery which, if radical, can be curative. Medical treatment can be the best palliative therapy and should be used, when possible, in association with surgery, in a multimodal therapeutic approach.

© 2005 The WJG Press and Elsevier Inc. All rights reserved.

Key words: Gastrinoma; Zollinger-Ellison Syndrome; MEN 1; Proton pump inhibitors; Somatostatin analogs; Chemoembolization

Tomassetti P, Campana D, Piscitelli L, Mazzotta E, Brocchi E, Pezzilli R, Corinaldesi R. Treatment of Zollinger-Ellison Syndrome. *World J Gastroenterol* 2005; 11(35): 5423-5432
http://www.wjgnet.com/1007-9327/11/5423.asp

INTRODUCTION

The Zollinger-Ellison Syndrome (ZES) represents a clinical, diagnostic and therapeutic challenge. In this paper, we have reviewed the recent advances on this fascinating syndrome. One MEDLINE (PubMed) search, was carried out using only MESH terms with the following strategy: Therapy AND (gastrinoma OR Multiple Endocrine Neoplasia Type 1 OR Zollinger-Ellison Syndrome). No limits were set and 4 369 papers were found. Only those papers *in-extenso* were considered. The authors reviewed all the papers and other papers or chapters in the published book were also manually searched in the references of the papers reviewed, if considered necessary for the present review.

CAUSES

The ZES, as described in 1955, is characterized by peptic ulcers of the upper gastrointestinal tract refractory to medical therapy, diarrhea and severe gastric acid hypersecretion associated with non-beta islet cell tumors of the pancreas[1]. It was later demonstrated that this pancreatic tumor, named gastrinoma, ectopically releases gastrin, which is responsible for the gastric hypersecretion. More than 80% of gastrinomas are localized in the anatomic area called the triangle of the gastrinomas. This triangle includes the convergence of the cystic duct and the common bile duct, the junction of the second and third portion of the duodenum, and the junction of the head and body of the pancreas[2-5]. Most gastrinomas arise from the duodenum (about 75%), whereas they are localized in the pancreas in 25% of cases[4]. Occasionally gastrinomas occur in the ovary, mesentery, liver, bile duct, gastric antrum/pyloric area, renal capsule, and in the jejunum[6,7]. Furthermore, extra-abdominal primary gastrinomas in the heart[8,9] and gastrin-releasing lung tumor causing ZES have recently been described[10].

The structure can be glandular or trabecular, and the cells are round with small nuclei and prominent nucleolus. The cells which produce gastrin are generally well-differentiated and contain the histological markers typical of neuroendocrine tumors, i.e., chromogranin A, neurospecific enolase and synaptophysin. These tumors are positive at immunohistochemistry not only for gastrin but, frequently, also for other peptides, including the pancreatic peptide (PP), somatostatin (SST), the adrenocorticotrophic hormone (ACTH) and the vasoactive intestinal peptide (VIP).

This tumor presents itself at various ages from 7 to 90 years, but the diagnosis is usually made between the ages of 30 and 50 years. There is no clear sex prevalence even if 60% of the patients affected are men[11-14].

Gastrinomas may behave in a benign or malignant manner, but usually, even when malignant, they can be slow growing. Numerous studies support the conclusion that gastrinomas pursue an aggressive growth pattern in 20-30% of cases and an indolent growth pattern in the rest; this seems to be independent of the presence or the absence of positive lymph nodes[3,15,16]. The most common site of metastases are the local lymph nodes, followed by the liver; these metastatic lesions, unlike those of adenocarcinomas, are vascular. Bone metastases are common in advanced disease, probably occurring in the majority of patients[17]. The percentage of patients presenting a malignant form of

sporadic ZES is not clear; some data in the literature report that about 65% of gastrinomas are malignant, but perhaps this is overestimated[18]. Furthermore, it has been suggested that a poor prognosis is associated with the development of ectopic Cushing's syndrome, reported in up to 5% of patients with ZES[19].

The gastrin secreting tumor responsible for ZES is the most common tumor in patients affected by Multiple Endocrine Neoplasia type 1 (MEN 1).

MULTIPLE ENDOCRINE NEOPLASIA TYPE 1

MEN 1 is an autosomal dominant inherited syndrome characterized mainly by the development of hyperplasia and/or multiple tumors in the parathyroid, endocrine pancreas, duodenum, anterior pituitary, foregut-derived neuroendocrine tissue, and adrenocortical glands. This syndrome, first described by Wermer in 1954, has a prevalence of 0.2-2/100 000 people/year, even if this is underestimated since, generally, the endocrinopathies which constitute this disease are not adequately classified[20,21]. MEN 1 is associated with inactivating mutations of a tumor suppressor gene (*MEN1*), mapped on chromosome 11q13 in 1988[22]. The MEN 1 gene was sequenced in 1997 and was found to encode for a transcriptional regulator, named "menin"[23]. In MEN 1 patients, one allele of the gene is inactivated by the germline mutation, and phenotype expression occurs with inactivation of the second allele by somatic cellular mutation. Somatic mutations of the MEN 1 gene have also been reported in sporadic forms of endocrine tumors with a variable incidence of 20-30% in the parathyroid, the endocrine pancreas (33% gastrinomas, 17% insulinomas), 25% in lung carcinoids, but less than 1% in pituitary and adrenocortical tumors[24-27].

In clinical practice, it is important to perform genetic analysis in order to diagnose MEN 1, but the diagnosis cannot be excluded with certainty, when a mutation is not found[28]. Therefore, the clinical screening of patients remains a prerequisite for genetic analysis. Screening for MEN 1 is a crucial step in the diagnosis and the management of neuroendocrine tumors, because prognosis and treatment may differ from the sporadic case.

Gastrinoma with ZES is found in 20-61% of patients with MEN 1[29,30]; conversely, MEN 1 is found in 30-38% of all patients with gastrinomas[30-32]. In MEN 1, gastrinomas are mainly localized in the duodenum, they are small and frequently multifocal and may therefore be difficult to detect either by traditional imaging methods or at surgery[33,34].

ZES-MEN 1 is associated with gastric carcinoids, also called ECL-omas (type 2 carcinoids), due to chronic effect of hypergastrinemia on ECL cells. These tumors seem to be found in 13-30% of patients with ZES-MEN 1 and in 0-0.6% of patients without MEN 1[35,36]. ECL-cell tumors in MEN 1 are often multicentric and are generally characterized by a low mitotic index; most of these tumors are less than 1 cm in diameter and are limited to the mucosa and submucosa[37]. The percentage of patients in whom these tumors are invasive is unknown; metastases to local lymph nodes can be observed, but patient survival is usually excellent with tumor persistence for more than 25 years and very few related deaths[38].

CLINICAL MANIFESTATIONS

The signs and symptoms of ZES are primarily due to gastric acid hypersecretion. The most common initial symptom is abdominal pain and 90-95% of patients develop peptic ulcers in the upper gastrointestinal tract. In 36% of cases, the ulcers are multiple or in an unusual site; however, there is a percentage of patients with ZES (from 18% to 25%) who do not have ulcers at diagnosis. The ulcer can appear as a common duodenal ulcer, but it is usually less responsive to therapy with respect to ulcers in patients without gastrinomas. The most common is a single ulcer of the duodenal bulb which can also appear in the second, third, or fourth portion of the duodenum or in the jejunum[39].

Gastroesophageal reflux, present in two-thirds of patients with ZES, can vary from light to severe forms and can be complicated by stenosis or Barrett's mucosa[39]. Diarrhea is the second most common symptom, developing in 50-65% of patients, and can precede, accompany or follow the ulcerous disease; in 7-35%, it may be the only initial symptom[39]. The diarrhea is due to massive acid hypersecretion which activates pepsinogens which are responsible for mucosal damage; in addition, acid inactivation of the pancreatic enzyme and acid damage to enterocytes also contribute to it. Steatorrhea is a result of inactivation of pancreatic lipase by intraluminal acid in the upper small intestine; the low pH also renders some primary bile acids insoluble, reducing the formation of micelles, which are needed for absorption of fatty acid and monoglycerides[3].

DIAGNOSIS

The diagnosis of ZES is based on the finding of elevated fasting serum gastrin associated with gastric acid hypersecretion. Other conditions exist in which gastrin levels can be elevated; these are hypochlorhydria in the course of chronic atrophic gastritis, the prolonged use of proton pump inhibitors or the presence of *Helicobacter pylori* (*H pylori*) infection. When the diagnosis is not completely clear, a reliable test is the measurement of basal acid secretion (BAO) or, alternatively, it can be useful to determine the pH of the gastric juice which can be obtained during endoscopy or through a nasogastric tube. If the gastric pH is >2 in the absence of antisecretory therapy, the patient is hypochlorhydric and, therefore, ZES can be excluded; if the pH is <2 and the plasma gastrin is higher than 1 000 pg/mL, the diagnosis of ZES is certain while, if the pH is <2 and the plasma gastrin concentration is between 100 and 1 000 pg/mL, a secretin test must be carried out[40]. The secretin test is performed by the administration of 2 IU/kg of secretin intravenously in 2 min, after having taken a blood sample in order to perform the basal gastrin concentration; after the injection, blood samples are taken after 2.5, 5, 10, 15 and 30 min. An increase of plasma gastrin >200 pg/mL is diagnostic of ZES. The test can give a false positive result in some patients with Type A chronic atrophic gastritis, but this is identified by measuring the gastric pH[41]. The secretin test can also give a false negative result in 10% of patients with ZES, and this is usually associated with a malignant course of the disease[42]. The calcium test might be of value in those patients in whom ZES is strongly suspected when

the secretin test is negative. There is agreement in the literature that calcium and meal tests are less useful than secretin for detecting ZES.

Imaging techniques

To localize and stage gastrinomas, conventional non-invasive and occasionally invasive diagnostic modalities may be required. At present, the most important study should be somatostatin receptor scintigraphy (SRS) using ^{111}In-pentetreotide with single photon emission tomography (SPECT) scanning[4]. Recent studies demonstrated that SRS allows total body localization study simultaneously at one time, thus allowing detection of liver and distant metastases and it is more sensitive in both localizing the primary gastrinoma and identifying patients with liver metastases than conventional methods such as CT, MRI, US[43]. Unfortunately, SRS detects 30-75% of gastrinomas measuring less than 1 cm, primarily duodenal gastrinomas; a negative scan in the presence of a visible tumor suggests either a poorly-differentiated neuroendocrine tumor or a pancreatic adenocarcinoma[44]. Ultrasonography can detect gastrinomas in 30% of cases and the detection rates are better for lesions greater than 3 cm in diameter and are poor for lesions smaller than 1 cm[45].

Using EUS, the sensitivities as high as 79-82% can be obtained[46,47]. A recent prospective study found a sensitivity of 93% and a specificity of 95% in the localization of intrapancreatic lesions[48]. EUS, in combination with SRS up to 69%, although it may still miss up to 50% of duodenal gastrinomas[49]. Therefore, when a gastrinoma is suspected, endoscopy or EUS should also be performed to identify duodenal as well as pancreatic gastrinomas, especially when multiple lesions are suspected as in MEN 1[33,34].

Regarding CT and MRI, the most recently published series showed that CT with bolus of contrast administration can achieve sensitivities ranging from 82% to 92%[50,51] and MRI, using T1-weighed fat suppression images, has a 91% sensitivity[52,53]. A comparative study demonstrated that MRI is equivalent to dynamic CT. Furthermore, MRI is considered the most sensitive technique for demonstrating liver and bone metastases in patients with neuroendocrine tumors and is recommended for monitoring the response to therapy. However, CT and MRI are both very sensitive and specific methods for demonstrating hepatic metastases and pancreatic tumors, and they show specific advantages in routine tumor staging and monitoring of therapy[54,55].

Functional studies, measuring hormonal gradients by transhepatic portal venous sampling, seem to be more sensitive; however, this method is invasive, and does not lead to the exact location and requires considerable expertise. A modification of the hormonal gradient during angiography has been developed; in brief, secretin is injected intra-arterially selectively into different vessels and hepatic venous samplings are collected and assayed for hormonal gradients. Selective angiography can identify the site of the tumor in up to 75% of cases, but has largely been supplanted by the combination of Octreoscan, EUS and CT[56,57].

In about 20% of patients, a gastrinoma cannot be identified by conventional imaging techniques and SRS[58]. In these cases, during laparotomy, operative techniques such as duodenal transillumination and intraoperative ultrasound can be used[4].

A suggested algorithm for the diagnosis of ZES is reported in Figure 1.

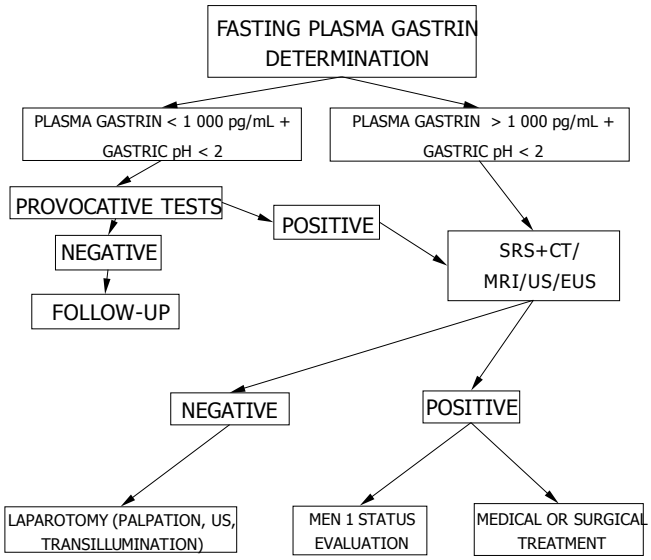


Figure 1 Diagnostic algorithm for Zollinger-Ellison Syndrome. SRS: somatostatin receptor scintigraphy; CT: computed tomography; MRI: magnetic resonance imaging; US: ultrasonography; EUS: endoscopic ultrasonography.

TREATMENT

In patients with ZES, the two main principal therapeutic objectives are to control the gastric acid hypersecretion which causes the most debilitating symptoms (ulcers, diarrhea and dehydration) and to control the growth of the tumor which, even if slow-growing, is able to produce early and diffuse hepatic metastases.

Until the end of the 1970s, the only effective therapy for controlling acid hypersecretion was total gastrectomy. Currently, after the introduction of potent antisecretory drugs, such as H_2 antagonists and proton pump inhibitors, the most important aspect for these patients is the growth of the neoplasm. In fact, half of the patients die from causes related to the tumoral mass and not from the effects of the massive gastric acid hypersecretion[59]. Thus, at present, a large number of treatment options are available for the therapy of patients with ZES: control of the gastric acid hypersecretion; control of the gastrin hypersecretion; surgical resection or cytoreduction of the tumor; control of the tumor size by using chemotherapy or interferon alfa; control of the hepatic metastases with chemoembolization and/or embolization.

Control of gastric acid hypersecretion

If ZES is suspected, it is important, while waiting for the conclusive results of the diagnostic tests, to prevent the complications which could arise. For this reason, it is advised to rapidly start an antisecretory therapy which is usually well-tolerated and without particular contraindications.

Histamine H_2 receptor antagonists

Since proton pump inhibitors have been available commercially,

H_2 receptor antagonists are no longer the drugs of choice for patients with ZES, even if they have actually been proven effective in alleviating the symptoms and healing ulcers in gastrinomas. Ranitidine is the drug of choice among the H_2 antagonists, due to its low side effects and its limited interaction with other drugs. However, despite the first excellent results, long-term studies have shown that the use of these drugs is limited by many factors such as poor control of the gastric acid hypersecretion and sometimes the need for high and frequent doses of the drug[60]. The pharmacological basis of these observations is unknown, even if various possibilities have been suggested, such as a diminished bioavailability due to reduced absorption, an altered metabolism of the drug with increased excretion, the development of tachyphlaxis and the hypersecretory state itself[61]. The poor effectiveness of H_2 antagonists is usually evident in ZES associated with severe gastroesophageal reflux, MEN 1 with hyperparathyroidism and partial gastric resection[62].

Proton pump inhibitors

Omeprazole, the first proton pump inhibitor available, belongs to a new class of drugs which has proven to be safe and effective in controlling gastric hypersecretion in patients with ZES and has completely substituted the use of H_2 antagonists. The PPIs commonly used are omeprazole, lansoprazole, pantoprazole, rabeprazole and esomeprazole[63]. These drugs show differences in pharmokinetics and pharmodynamics, but it is not always clear, if these fine variations have clinical importance[64].

Initial therapy

The goal of ZES therapy is to obtain improvement of the symptoms and healing of the ulcers by controlling the gastric hypersecretion. Various studies have shown that a reliable criterion for the control of the hypersecretion is the reduction of the BAO below 10 mEq/h in the hour preceding the next administration of the drug in cases of uncomplicated ZES and below 5 mEq/h in cases of ZES associated with MEN 1, gastro-esophageal reflux disease or in patients undergoing a partial gastrectomy[2,65].

Using the acute upward dose titration method, widely accepted for establishing the initial dosage of omeprazole, some studies have demonstrated that the average dosage of omeprazole capable of controlling gastric hypersecretion in the majority of patients is between 60 and 100 mg of the drug per day[66]. The only reliable parameter able to demonstrate the absence of damage to the mucosa is the level of acid inhibition when the "steady state" has been reached; therefore, the BAO must be measured every 3-4 wk and the patient should be evaluated by endoscopy and acid secretion analysis at intervals from 3 to 6 mo and, successively, from 6 to 12 mo. The objective of the therapy is not achlorhydria, but a BAO between 1 and 10 mmol/h; if complete inhibition of the acid hypersecretion is seen, the dosage of omeprazole should be reduced by 50% and the patient should be re-evaluated. If the BAO is greater than 10 mmol/h, the dosage of the PPI should be increased gradually and, for doses of omeprazole over 60 mg (or equivalent doses of another PPI), it would be advisable to administer the drug in two divided doses. The lack of control of gastric acid secretion could be a high risk for patients affected by ZES[66,67] and some data in the literature have demonstrated that an initial dose of 20 mg is not able to control the acid secretion and the symptoms linked to the disease[68].

PPI long-term treatment

Many data have been reported on the effectiveness and safety of the PPIs, when these drugs are administered on a long-term basis in patients with ZES. After having established the initial dosage and having monitored the gastric secretion, the long-term maintenance dosages can be reduced significantly in the majority of patients, when control of the gastric secretion is stabilized[69,70]. This can be easily explained by the fact that the effectiveness of omeprazole increases with time[70-72]. In fact, Metz *et al*., have shown that the maintenance dosages of omeprazole can be partially or completely reduced in all patients with ZES, above all in those who are not affected by MEN 1, serious gastro-esophageal reflux or those who have undergone a partial gastrectomy[70]. Some studies have shown that, in the long-term, it is not necessary to increase the dosage of omeprazole; if, however, during the first year, repeated increments in therapy are necessary, it means that the initial dose was inappropriate and there was no progressive development of pharmaceutical resistance[73]. While the H_2 antagonists have demonstrated the phenomenon of tachyphylaxis with prolonged use, only in 10% of patients is it necessary to increase the dose of the PPIs[74]. PPIs have been proven to be safe and effective in the maintenance therapy of patients with ZES for more than 10 years, without any effect of related toxicity[65]. It does not seem that treatment with PPIs in ZES has induced any significant increase in the concentration of plasma gastrin or alterations in the percentage of argyrophil cells[75].

Intravenous PPIs

Patients affected by ZES who are not able to take PPIs orally and who need a therapy which primarily suppresses gastric acid secretion; patients with active peptic ulcer, recent hemorrhage and endoscopic stigmata that puts them at high risk of rebleeding, are candidates to receive PPIs intravenously. Another possible means of administration of solutions prepared with oral PPIs is intragastric, which can be utilized as an alternative to the intravenous route in critically ill patients or in whom esophageal stenosis is present.

Vitamin B12 levels during prolonged treatment with PPIs

During prolonged treatment with proton pump inhibitors, reduced serum levels of vitamin B12, but not of folate, have occasionally been documented[76]. This phenomenon seems to be related to the achlorhydria induced by the drug which, moreover, is not common during therapy with PPIs.

Helicobacter pylori and ZES

Some studies have considered the interactions between ZES, *H pylori* and PPIs, pointing out how the *Helicobacter* infection does not constitute a risk factor for the onset of peptic ulcers in these patients. In fact, the prevalence of *H pylori* infection in these subjects is lower than in the overall population and

is much lower than in patients with common peptic ulcer disease. Indeed long term PPIs therapy in HP-positive patients with ZES may lead to the reduction of parietal cell mass[77].

Control of the hormonal secretion

Somatostatin analogs It is well-known that somatostatin and its analogs are able to reduce gastric acid and serum gastrin levels in patients with ZES, with both short-term and long-term administration[78]. In addition to immediate-release subcutaneous octreotide, other long-acting somatostatin analogs such as lanreotide, which can be administered every 10-14 d, and octreotide LAR, which can be administered every 28 d, are currently available on the market[79,80]. In 1993, Rusniewsky noted an average decrease in serum gastrin of 87% in patients with ZES treated with octreotide subcutaneously for a period of 9–12 mo. It was also seen that octreotide was capable of controlling gastric hypersecretion without an "escape phenomenon" and was able to reduce, and sometimes eliminate, the hyperplasia of the ECL cells when this was present before treatment[81]. In the same period, Bordi reported that prolonged treatment with octreotide is able to significantly decrease the fundic argyrophil cells in patients with a gastric pathology[82].

Thereafter, several studies have shown that treatment with somatostatin analogs has an inhibiting effect on tumoral growth in patients with malignant gastrointestinal neuroendocrine neoplasias, such as pancreatic tumors or carcinoids, and is able to stabilize the tumoral growth in 37-80% of patients; in only a few patients (0-17%), a reduction of the tumor dimensions has been observed[83,84].

Moreover, up to now, only one study on the effectiveness of octreotide in controlling tumoral growth in patients with metastatic gastrinomas has been carried out. In this study, performed on 15 patients, it was shown that, in 53% of these patients with malignant gastrinomas, the tumoral growth progressed, 47% of patients presented stabilization and 6% had a reduction of the tumor size[85]. In patients who responded to treatment, stabilization of the tumor was long lasting and the incidence of side-effects was lower in comparison to the group treated with chemotherapy. In this study, it was concluded that, in gastrinomas, somatostatin analogs are not the drugs of first choice in controlling gastric acid hypersecretion, but are very useful in controlling tumoral growth.

The most common side-effects of somatostatin analogs are gallstones, abdominal pain, diarrhea and pain in the injection site.

Receptor-mediated radiotherapy with ^{90}Y-DOTA-D-Phe1-Try3-octreotide for neuroendocrine tumors has recently been proposed as a palliative treatment; this modality of treatment can, however, cause myelotoxicity and nephrotoxicity[86]. In the past 3 years, several studies have been published on the use of this therapy in neuroendocrine tumors associated with syndromes, using not only ytrium but also lutetium which seems to be less toxic for the kidneys[87]. As regards the therapy for gastrinomas, a regression of metastases in 25% of the patients has been described[88].

As previously reported, long lasting somatostatin analogs have been shown to be capable of reducing the mass of gastric endocrine cells[89]; furthermore, it has been demonstrated that these drugs can inhibit growth in hypergastrinemic experimental models which develop gastric carcinoids[90,91]. This evidence supporting the use of octreotide can be utilized in patients with gastric carcinoids. These data have been confirmed in a recent study of our group which showed the regression of gastric carcinoids associated with ZES-MEN 1 after 1 year of treatment with long acting somatostatin analogs[92].

Control of neoplasia growth

Surgery The role of surgery in the treatment of ZES has evolved considerably from 1955 to now[1]. Initially, the surgical therapy proposed was total gastrectomy with the aim of removing the high levels of gastrin from the target organ[93]; in the past 20 years, improved pharmacological control of gastric acid hypersecretion has eliminated the role of surgery in containing the hypersecretion itself. The availability of PPIs allows us to adequately control the symptoms in all patients with ZES, making the natural history of gastrinomas, the only determining factor in long-term survival[94].

Since adequate medical therapy is able to eliminate the symptoms in all patients and, although it is hard to treat the neoplastic disease with chemotherapeutic drugs, some authors claim that the risks and complications of exeresis of the gastrinoma exceed the actual benefits of this procedure[58]. More recently, however, some others have reported that surgical excision of a gastrinoma has proven highly effective in order to prevent hepatic metastases[93,95]. At present, surgical exploration plays a key role in identifying and removing the primary tumor, and in preventing the onset of liver metastases.

The main objectives of surgery are to stage the tumor, improve survival by removing the malignant tumor and control the acid hypersecretion syndrome. Since the majority of patients with ZES present either with occult disease or with localized disease, the surgeon has to search for and remove the non-localized lesion laparotomically using imaging techniques. Furthermore, intra-operative techniques such as palpation, ultrasonography and transillumination of the duodenal wall can contribute to the identification of pancreatic and duodenal gastrinomas, including lymph nodes and hepatic metastases. It is important to consider that a large percentage of primary occult tumors are found inside the duodenum. Gastrinomas commonly metastasize in the lymph nodes and sometimes arise in this site; hence, the resection of all the lymph nodes in the peripancreatic region is important, even if they do not appear swollen. Exploration of the liver and the rest of the abdomen is also recommended in order to identify possible metastatic disease[96].

It has also been reported that more than 50% of patients are free from disease after surgery and the majority of them remain so for the following 5-10 years[93,95].

Gastric acid hypersecretion caused by hypertrophy of parietal cells can persist, after surgery, despite biochemical evidence of cure; for this reason it is very important for all patients to continue maintenance, antisecretory therapy until the BAO determination is less than 10 mEq/h[97]. In those patients in whom there is a persistence of neoplastic tissue or post-operative relapse, debulking the tumor often leads

to a proven benefit[95].

Liver transplant is characterized by a remarkable morbidity and, for the most part, post-operative immunosuppressive therapy stimulates the relapse of growth of the tumor[98]. A careful evaluation of the data found in the literature shows that a non-carcinoid histotype is present among the exclusion criteria for liver transplants in patients with hepatic metastases and neuroendocrine tumors. In this regard, French authors, in a retrospective study, have pointed out an unfavorable prognosis in patients with non-carcinoid endocrine tumors undergoing a liver transplant[99].

Surgery in ZES associated with MEN 1 The indications for surgery in patients with ZES-MEN 1 are controversial, since previous experience has shown that surgery rarely cures these patients[100,101]. Some authors have carried out an exploratory laparotomy on patients with ZES-MEN 1 in which the tumor, studied using imaging techniques, had a diameter greater than 2.5 cm. A direct relationship between the size of the tumor and the onset of hepatic metastases has been hypothesized and, as in other malignant solid tumors, the effectiveness of the cure is expected to be greater, if the tumors are resected, when they are still small[36,102].

In a recent study, a group of Swedish researchers established that the best surgical procedures include enucleation of the tumor in the head of the pancreas, excision of duodenal gastrinomas together with the removal of the metastasized lymph nodes and, as prophylaxis of tumoral relapse, the combination of these procedures with an 80% subtotal resection of the distal pancreas. It is thought that a more extensive resection of the tumor reduces the risk of the malignant evolution of pancreatic and duodenal tumors[101].

In patients with ZES-MEN 1, hyperparathyroidism is usually present at the moment of diagnosis[103]; therefore, in patients with hypercalcemia, a parathyroidectomy should be performed before any other surgical procedure in order to better control the pathological effects of hypercalcemia. It has been demonstrated that a parathyroidectomy is capable of reducing the fasting serum levels of gastrin and the BAO, and this, therefore, improves the response to the antisecretory therapy[32].

Control of tumor size

Systemic chemotherapy Therapeutic strategies for the management of patients with metastatic gastroenteropancreatic endocrine tumors have to take into consideration the fact that controlling the hormone-mediated symptoms often improves the quality of life, to the point that the patients feel well despite the extensive metastatic disease[104]. At best, chemotherapy has furnished only unclear results utilizing the classical anti-tumoral agents, such as 5-fluorouracil, in controlling metastatic endocrine tumors. Systemic chemotherapy reached a new therapeutic dimension immediately after the introduction of streptozotocin (STZ) into clinical use[105]; there have been several studies on the effects of this drug on metastatic islet-cell tumors which have confirmed the effectiveness of streptozotocin. Despite this, there are a number of acute and chronic side effects, such as serious renal or hematologic toxicity[106]. Various studies have standardized the dosage and administration schedule of streptozotocin and have suggested its combination with other cytotoxic drugs such as 5 fluorouracil (5-FU) and doxorubicin (adriamycin); the combination of STZ and doxorubicin has been superior to other regimens, mainly STZ and 5-FU, and seems to be associated with a 69% objective response lasting for 18 mo and overall median survival of 2.2 years[107].

In a detailed study conducted on 10 patients with metastatic gastrinomas and treated with streptozotocin, 5-fluorouracil and doxorubicin, 4 patients showed a partial response to the treatment, but the survival rate was the same both in the 4 responders and in the 6 non-responders[108]. Another type of chemotherapy proposed is monotherapy with chlorozotocin, a nitrosourea having a composition similar to streptozotocin characterized by less gastrointestinal toxicity but increased myelosuppression or monotherapy with dacarbazine[109].

In conclusion, chemotherapy is not the treatment of first choice in patients with gastrin secreting tumors, but seems to be indicated in rapidly evolving tumors in which the mass of the primary tumor increases more than 25% in a period of follow-up of 12 mo or in which the tumoral symptoms cannot be treated by other means[110].

Interferon In recent years, the validity of interferon has been sustained in neuroendocrine tumors, especially in the carcinoid syndrome. The data in the literature demonstrate that therapy with interferon-alpha leads to the stabilization of the tumor in 20-40% of patients with different gastrointestinal neuroendocrine tumors, including those with metastatic gastrinomas, but it did not result in an increase in the survival rate of these patients[111]. It has been proposed, therefore, that gastrinomas can be treated with chemotherapy and/or interferon when they grow and metastasize[111].

Role of chemoembolization or embolization Selective embolization of the hepatic arteries causes transient and complete ischemia with an objective, symptomatic and hormonal response of 65% and 81%, respectively; this treatment has been demonstrated to be useful in patients with liver metastases from neuroendocrine pancreatic tumors. Unfortunately, only a small number of gastrinomas have been treated with chemoembolization and there are no sufficient data on long-term survival after this procedure. Chemoembolization, which uses a combination of gelfoam and chemotherapeutic agents (streptozotocin or doxorubicin), may determine a notable improvement in the quality of life of the patient and is usually accompanied by a reduction in circulating peptide serum levels and the size of the tumor. However, it has not been clearly demonstrated that the inhibition of tumoral growth improves the survival rate[112-115].

Chemoembolization is an alternative to chemotherapy for progressive liver metastases in patients with gastrinomas.

A suggested algorithm for medical and surgical treatment of ZES is reported in Figure 2.

CONCLUSIONS

Proton pump inhibitors have been used to more drastically inhibit gastrin action on the parietal cells, thus allowing the patient to rapidly return to a normal clinical condition without the need for surgery. If it is possible to eliminate the morbidity

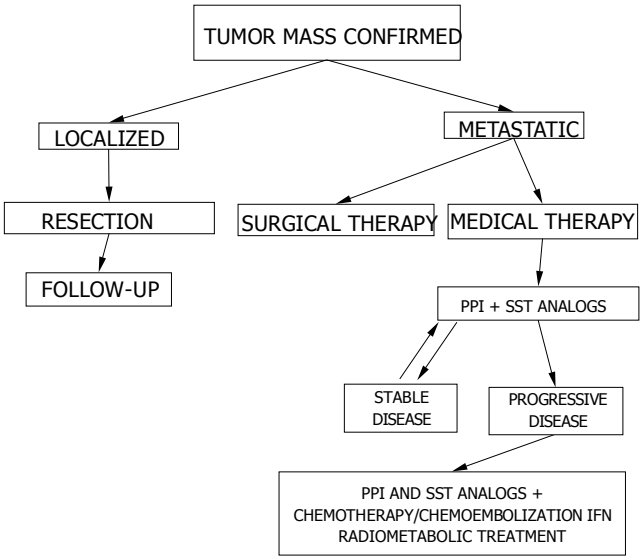


Figure 2 Therapeutic algorithm of Zollinger-Ellison Syndrome. PPI: proton pump inhibitors; SST: somatostatin analogs; IFN: interferon.

and mortality caused by acid hypersecretion, the majority of patients affected by ZES should be able to be maintained in good clinical condition, without symptoms. In ZES, antisecretory drugs have been proven to be safe and effective, without particular side effects over a long period of time, even 15 years or more.

Recent developments in surgical techniques, and pre- and intra-operatory imaging investigation, have permitted the identification and successive resection of more than 95% of gastrinomas. Therefore all localized gastrinomas should be excised, if possible. If hepatic metastases are also present, their enucleation may improve the symptoms and the survival rate as well as facilitate medical treatment. Another possibility is to carry out surgery, only when the tumor is greater than 2 cm in diameter, because these dimensions are associated with a greater risk of metastases in the liver. However, there is some controversy about the surgical approach to gastrinomas associated with MEN 1.

Somatostatin analogs can be useful in reducing gastric acid hypersecretion, serum gastrin and gastric ECL-cells, thus contributing to curing the disease more effectively. Furthermore, thanks to their antiproliferative effects, these drugs are used in treating patients with hepatic metastases and in those affected by ZES-MEN 1 with gastric carcinoids.

Chemotherapy may be particularly indicated in the malignant evolving form, but not in slow-growing tumors or as first choice therapy in gastrinomas.

Embolization and/or chemoembolization may be a palliative procedure for patients with hepatic metastases.

Finally, we would like to emphasize that the choice of treatment must involve a multidisciplinary approach.

REFERENCES

1 **Zollinger RM**, Ellison EH. Primary peptic ulcerations of the jejunum associated with islet cell tumors of the pancreas. 1955. *CA Cancer J Clin* 1989; **39**: 231-247

2 **Jensen RT**, Gardner JD, Raufman JP, Pandol SJ, Doppman JL, Collen MJ. Zollinger-Ellison syndrome: current concepts and management. *Ann Intern Med* 1983; **98**: 59-75

3 **Jensen RT**, Doppman JL, Gardner JD. Gastrinoma. In: Go V. LW, Brooks FA, DiMagno EP, Gardner JD, Lebenthal E, Scheele GA, eds. The exlocrine pancreas: biology, pathobiology and disease. *New York*: *Raven Press* 1986: 727-744

4 **Norton JA**, Jensen RT. Current surgical management of Zollinger-Ellison syndrome (ZES) in patients without multiple endocrine neoplasia-type 1 (MEN1). *Surg Oncol* 2003; **12**: 145-151

5 **Pipeleers-Marichal M**, Somers G, Willems G, Foulis A, Imrie C, Bishop AE, Polak JM, Hacki WH, Stamm B, Heitz PU. Gastrinomas in the duodenums of patients with multiple endocrine neoplasia type 1 and the Zollinger-Ellison syndrome. *N Engl J Med* 1990; **322**: 723-727

6 **Jensen RT**. Zollinger-Ellison syndrome. In: Doherty GM, Skogseid B, eds. Surgical endocrinology: clinical syndromes. *Philadelphia* 2001: 291-344

7 **Soga J**, Yakuwa Y. The gastrinoma/Zollinger-Ellison syndrome: statistical evaluation of a Japanese series of 359 cases. *J Hepatobiliary Pancreat Surg* 1998; **5**: 77-85

8 **Gibril F**, Curtis LT, Termanini B, Fritsch MK, Lubensky IA, Doppman JL, Jensen RT. Primary cardiac gastrinoma causing Zollinger-Ellison syndrome. *Gastroenterology* 1997; **112**: 567-574

9 **Noda S**, Norton JA, Jensen RT, Gay WA. Surgical resection of intracardiac gastrinoma. *Ann Thorac Surg* 1999; **67**: 532-533

10 **Abou-Saif A**, Lei J, McDonald TJ, Chakrabarti S, Waxman IF, Shojamanesh H, Schrump DS, Kleiner DE, Gibril F, Jensen RT. A new cause of Zollinger-Ellison syndrome: non-small cell lung cancer. *Gastroenterology* 2001; **120**: 1271-1278

11 **Zollinger RM**, Ayres HP. The Zollinger-Ellison syndrome. In: Nyhus LM, Wastell C, Donahue PhE, eds. *Surgery of the Esophagus, Stomach and Small Intestine* 1987: 491-513

12 **Isenberg JI**, Walsh JH, Grossman MI. Zollinger-Ellison syndrome. *Gastroenterology* 1973; **65**: 140-165

13 **Ellison EC**, Wilson SD. The Zollinger-Ellison syndrome: reappraisal and evaluation of 260 registered cases. *Ann Surg* 1964; **160**: 512-530

14 **Stage JG**, Stadil F. The clinical diagnosis of the Zollinger-Ellison syndrome. *Scand J Gastroenterol Suppl* 1979; **53**: 79-91

15 **Yu F**, Venzon DJ, Serrano J, Goebel SU, Doppman JL, Gibril F, Jensen RT. Prospective study of the clinical course, prognostic factors, causes of death, and survival in patients with long-standing Zollinger-Ellison syndrome. *J Clin Oncol* 1999; **17**: 615-630

16 **Weber HC**, Venzon DJ, Lin JT, Fishbein VA, Orbuch M, Strader DB, Gibril F, Metz DC, Fraker DL, Norton JA. Determinants of metastatic rate and survival in patients with Zollinger-Ellison syndrome: a prospective long-term study. *Gastroenterology* 1995; **108**: 1637-1649

17 **Durieux S**, Liote F, Timsit MA, Duet M, Valleur P, Lemaire V, Dryll A. Bone metastases in epidural invasion of gastrinoma. *Rev Rhum Ed Fr* 1994; **61**: 453-455

18 **Maton PN**. Gastrinoma and other hypergastrinemic syndrome. In: Walsh JH, Dockray GJ, eds. Gut Peptides. *New York*: *Raven Press* 1994: 675-700

19 **Ruszniewski P**, Girard F, Benamouzig R, Mignon M, Bonfils S. Long acting somatostatin treatment of paraneoplastic Cushing's syndrome in a case of Zollinger-Ellison syndrome. *Gut* 1988; **29**: 838-842

20 **Wermer P**. Genetic aspects of adenomatosis of endocrine glands. *Am J Med* 1954; **16**: 363-371

21 **Shepherd JJ**. The natural history of multiple endocrine neoplasia type 1. Highly uncommon or highly unrecognized? *Arch Surg* 1991; **126**: 935-952

22 **Larsson C**, Skogseid B, Oberg K, Nakamura Y, Nordenskjold M. Multiple endocrine neoplasia type 1 gene maps to chromosome 11 and is lost in insulinoma. *Nature* 1988; **332**: 85-87

23 **Chandrasekharappa SC**, Guru SC, Manickam P, Olufemi SE, Collins FS, Emmert-Buck MR, Debelenko LV, Zhuang Z, Lubensky IA, Liotta LA, Crabtree JS, Wang Y, Roe BA, Weisemann J, Boguski MS, Agarwal SK, Kester MB, Kim YS,

Heppner C, Dong Q, Spiegel AM, Burns AL, Marx SJ. Positional cloning of the gene for multiple endocrine neoplasia-type 1. *Science* 1997; **276**: 404-407

24 **Heppner C**, Kester MB, Agarwal SK, Debelenko LV, Emmert-Buck MR, Guru SC, Manickam P, Olufemi SE, Skarulis MC, Doppman JL, Alexander RH, Kim YS, Saggar SK, Lubensky IA, Zhuang Z, Liotta LA, Chandrasekharappa SC, Collins FS, Spiegel AM, Burns AL, Marx SJ. Somatic mutation of the MEN1 gene in parathyroid tumours. *Nat Genet* 1997; **16**: 375-378

25 **Zhuang Z**, Vortmeyer AO, Pack S, Huang S, Pham TA, Wang C, Park WS, Agarwal SK, Debelenko LV, Kester M, Guru SC, Manickam P, Olufemi SE, Yu F, Heppner C, Crabtree JS, Skarulis MC, Venzon DJ, Emmert-Buck MR, Spiegel AM, Chandrasekharappa SC, Collins FS, Burns AL, Marx SJ, Lubensky IA. Somatic mutations of the MEN1 tumor suppressor gene in sporadic gastrinomas and insulinomas. *Cancer Res* 1997; **57**: 4682-4686

26 **Debelenko LV**, Brambilla E, Agarwal SK, Swalwell JI, Kester MB, Lubensky IA, Zhuang Z, Guru SC, Manickam P, Olufemi SE, Chandrasekharappa SC, Crabtree JS, Kim YS, Heppner C, Burns AL, Spiegel AM, Marx SJ, Liotta LA, Collins FS, Travis WD, Emmert-Buck MR. Identification of MEN1 gene mutations in sporadic carcinoid tumors of the lung. *Hum Mol Genet* 1997; **6**: 2285-2290

27 **Rindi G**, Villanacci V, Ubiali A. Biological and molecular aspects of gastroenteropancreatic neuroendocrine tumors. *Digestion* 2000; **62** (Suppl 1): 19-26

28 **Calender A**. Molecular genetics of neuroendocrine tumors. *Digestion* 2000; **62** (Suppl 1): 3-18

29 **Norton JA**, Jensen RT. Multiple endocrine neoplasia. In: DeVita VT, Hellman S, Rosenberg SA, eds. Cancer Principies and practice of oncology. *Philadelphia*: *Lippincott Raven Publisher* 1997: 1723-1729

30 **Gibril F**, Schumann M, Pace A, Jensen RT. Multiple endocrine neoplasia type 1 and Zollinger-Ellison syndrome: a prospective study of 107 cases and comparison with 1009 cases from the literature. *Medicine* 2004; **83**: 43-83

31 **Benya RV**, Metz DC, Venzon DJ, Fishbeyn VA, Strader DB, Orbuch M, Jensen RT. Zollinger-Ellison syndrome can be the initial endocrine manifestation in patients with multiple endocrine neoplasia-type I. *Am J Med* 1994; **97**: 436-444

32 **Mignon M**, Cadiot G, Rigaud D, Ruszniewski PH, Jais P, Lehy T, Lewin MJM. Management of islet cell tumors in patients with multiple endocrine neoplasia type 1. In: Mignon M, Jensen RT eds. Endocrine tumors of the pancreas: Recent advances in research and management. *Karger[23]* 1995: 342-359

33 **Tomassetti P**, Migliori M, Lalli S, Campana D, Tomassetti V, Corinaldesi R. Epidemiology, clinical features and diagnosis of gastroenteropancreatic endocrine tumours. *Ann Oncol* 2001; **12** (Suppl 2): S95-99

34 **Jensen RT**. Gastrointestinal endocrine tumours. Gastrinoma. *Baillieres Clin Gastroenterol* 1996; **10**: 603-643

35 **Lehy T**, Cadiot G, Mignon M, Ruszniewski P, Bonfils S. Influence of multiple endocrine neoplasia type 1 on gastric endocrine cells in patients with the Zollinger-Ellison syndrome. *Gut* 1992; **33**: 1275-1279

36 **Jensen RT**. Management of the Zollinger-Ellison syndrome in patients with multiple endocrine neoplasia type 1. *J Intern Med* 1998; **243**: 477-488

37 **Rindi G**, Bordi C, Rappel S, La Rosa S, Stolte M, Solcia E. Gastric carcinoids and neuroendocrine carcinomas: pathogenesis, pathology, and behavior. *World J Surg* 1996; **20**: 168-172

38 **Solcia E**, Rindi G, Larosa S, Capella C. Morphological, molecular, and prognostic aspects of gastric endocrine tumors. *Microsc Res Tech* 2000; **48**: 339-348

39 **Roy PK**, Venzon DJ, Shojamanesh H, Abou-Saif A, Peghini P, Doppman JL, Gibril F, Jensen RT. Zollinger-Ellison syndrome. Clinical presentation in 261 patients. *Medicine* 2000; **79**: 379-411

40 **Roy PK**, Venzon DJ, Feigenbaum KM, Koviack PD, Bashir S, Ojeaburu JV, Gibril F, Jensen RT. Gastric secretion in Zollinger-Ellison syndrome. Correlation with clinical expression, tumor extent and role in diagnosis-a prospective NIH study of 235 patients and a review of 984 cases in the literature. *Medicine* 2001; **80**: 189-222

41 **Frucht H**, Howard JM, Slaff JI, Wank SA, McCarthy DM, Maton PN, Vinayek R, Gardner JD, Jensen RT. Secretin and calcium provocative tests in the Zollinger-Ellison syndrome. A prospective study. *Ann Intern Med* 1989; **111**: 713-722

42 **Tartaglia A**, Bianchini S, Vezzadini P. Biochemical diagnosis of gastroenteropancreatic endocrine tumors. *Minerva Med* 2003; **94**: 1-7

43 **Gibril F**, Reynolds JC, Doppman JL, Chen CC, Venzon DJ, Termanini B, Weber HC, Stewart CA, Jensen RT. Somatostatin receptor scintigraphy: its sensitivity compared with that of other imaging methods in detecting primary and metastatic gastrinomas. A prospective study. *Ann Intern Med* 1996; **125**: 26-34

44 **van Eijck CH**, Lamberts SW, Lemaire LC, Jeekel H, Bosman FT, Reubi JC, Bruining HA, Krenning EP. The use of somatostatin receptor scintigraphy in the differential diagnosis of pancreatic duct cancers and islet cell tumors. *Ann Surg* 1996; **224**: 119-124

45 **London JF**, Shawker TH, Doppman JL, Frucht HH, Vinayek R, Stark HA, Miller LS, Miller DL, Norton JA, Jensen RT. Zollinger-Ellison syndrome: prospective assessment of abdominal US in the localization of gastrinomas. *Radiology* 1991; **178**: 763-767

46 **Rosch T**, Lightdale CJ, Botet JF, Boyce GA, Sivak MV, Yasuda K, Heyder N, Palazzo L, Dancygier H, Schusdziarra V. Localization of pancreatic endocrine tumors by endoscopic ultrasonography. *N Engl J Med* 1992; **326**: 1721-1726

47 **Glover JR**, Shorvon PJ, Lees WR. Endoscopic ultrasound for localisation of islet cell tumours. *Gut* 1992; **33**: 108-110

48 **Anderson MA**, Carpenter S, Thompson NW, Nostrant TT, Elta GH, Scheiman JM. Endoscopic ultrasound is highly accurate and directs management in patients with neuroendocrine tumors of the pancreas. *Am J Gastroenterol* 2000; **95**: 2271-2277

49 **Ruszniewski P**, Amouyal P, Amouyal G, Grange JD, Mignon M, Bouche O, Bernades P. Localization of gastrinomas by endoscopic ultrasonography in patients with Zollinger-Ellison syndrome. *Surgery* 1995; **117**: 629-635

50 **Van Hoe L**, Gryspeerdt S, Marchal G, Baert AL, Mertens L. Helical CT for the preoperative localization of islet cell tumors of the pancreas: value of arterial and parenchymal phase images. *Am J Roentgenol* 1995; **165**: 1437-1439

51 **Legmann P**, Vignaux O, Dousset B, Baraza AJ, Palazzo L, Dumontier I, Coste J, Louvel A, Roseau G, Couturier D, Bonnin A. Pancreatic tumors: comparison of dual-phase helical CT and endoscopic sonography. *Am J Roentgenol* 1998; **170**: 1315-1322

52 **Semelka RC**, Cumming MJ, Shoenut JP, Magro CM, Yaffe CS, Kroeker MA, Greenberg HM. Islet cell tumors: comparison of dynamic contrast-enhanced CT and MR imaging with dynamic gadolinium enhancement and fat suppression. *Radiology* 1993; **186**: 799-802

53 **Debray MP**, Geoffroy O, Laissy JP, Lebtahi R, Silbermann-Hoffman O, Henry-Feugeas MC, Cadiot G, Mignon M, Schouman-Claeys E. Imaging appearances of metastases from neuroendocrine tumours of the pancreas. *Br J Radiol* 2001; **74**: 1065-1070

54 **Wiedenmann B**, Jensen RT, Mignon M, Modlin CI, Skogseid B, Doherty G, Oberg K. Preoperative diagnosis and surgical management of neuroendocrine gastroenteropancreatic tumors: general recommendations by a consensus workshop. *World J Surg* 1998; **22**: 309-318

55 **Ricke J**, Klose KJ, Mignon M, Oberg K, Wiedenmann B. Standardisation of imaging in neuroendocrine tumours: results of a European delphi process. *Eur J Radiol* 2001; **37**: 8-17

56 **Maton PN**, Miller DL, Doppman JL, Collen MJ, Norton JA, Vinayek R, Slaff JI, Wank SA, Gardner JD, Jensen RT. Role of selective angiography in the management of patients with Zollinger-Ellison syndrome. *Gastroenterology* 1987; **92**: 913-918

57 **Roche A**, Raisonnier A, Gillon-Savouret MC. Pancreatic venous sampling and arteriography in localizing insulinomas and gastrinomas: procedure and results in 55 cases. *Radiology* 1982; **145**: 621-627

58 **Norton JA**, Fraker DL, Alexander HR, Venzon DJ, Doppman JL, Serrano J, Goebel SU, Peghini PL, Roy PK, Gibril F, Jensen RT. Surgery to cure the Zollinger-Ellison syndrome. *N Engl J Med* 1999; **341**: 635-644

59 **Lew EA**, Pisegna JR, Starr JA, Soffer EF, Forsmark C, Modlin IM, Walsh JH, Beg M, Bochenek W, Metz DC. Intravenous pantoprazole rapidly controls gastric acid hypersecretion in patients with Zollinger-Ellison syndrome. *Gastroenterology* 2000; **118**: 696-704

60 **Howard JM**, Chremos AN, Collen MJ, McArthur KE, Cherner JA, Maton PN, Ciarleglio CA, Cornelius MJ, Gardner JD, Jensen RT. Famotidine, a new, potent, long-acting histamine H2-receptor antagonist: comparison with cimetidine and ranitidine in the treatment of Zollinger-Ellison syndrome. *Gastroenterology* 1985; **88**: 1026-1033

61 **Jensen RT**, Collen MJ, McArthur KE, Howard JM, Maton PN, Cherner JA, Gardner JD. Comparison of the effectiveness of ranitidine and cimetidine in inhibiting acid secretion in patients with gastric hypersecretory states. *Am J Med* 1984; **77**: 90-105

62 **Jensen RT**, Maton PN, Gardner JD. Current management of Zollinger-Ellison syndrome. *Drugs* 1986; **32**: 188-196

63 **Welage LS**, Berardi RR. Evaluation of omeprazole, lansoprazole, pantoprazole, and rabeprazole in the treatment of acid-related diseases. *J Am Pharm Assoc* 2000; **40**: 52-62

64 **Thomson AB**. Are the orally administered proton pump inhibitors equivalent? a comparison of lansoprazole, omeprazole, pantoprazole, and rabeprazole. *Curr Gastroenterol Rep* 2000; **2**: 482-493

65 **Metz DC**, Strader DB, Orbuch M, Koviack PD, Feigenbaum KM, Jensen RT. Use of omeprazole in Zollinger-Ellison syndrome: a prospective nine-year study of efficacy and safety. *Aliment Pharmacol Ther* 1993; **7**: 597-610

66 **Jensen RT**, Gardner JD. Zollinger-Ellison syndrome: clinical presentation, pathology, diagnosis and treatment. In: Zakim D, Dannenberg AJ, eds. Peptic ulcer disease and other acid-related disorder. *New York Accademic Research Associates* 1991: 117-246

67 **Metz MD**, Jensen RT. Advances in gastric antisecretory therapy in Zollinger-Ellison syndrome. Mignon M, Jensen RT, eds. Endocrine tumors of the pancreas: Recent advances in research and management. *Karger[23]* 1995: 240-257

68 **Termanini B**, Gibril F, Stewart CA, Weber HC, Jensen RT. A prospective study of the effectiveness of low dose omeprazole as initial therapy in Zollinger-Ellison syndrome. *Aliment Pharmacol Ther* 1996; **10**: 61-71

69 **Stadil F**, Stage JG. The Zollinger-Ellison syndrome. *Clin Endocrinol Metab* 1979; **8**: 433-446

70 **Metz DC**, Pisegna JR, Fishbeyn VA, Benya RV, Feigenbaum KM, Koviack PD, Jensen RT. Currently used doses of omeprazole in Zollinger-Ellison syndrome are too high. *Gastroenterology* 1992; **103**: 1498-1508

71 **Andersson T**, Bergstrand R, Cederberg C, Eriksson S, Lagerstrom PO, Skanberg I. Omeprazole treatment does not affect the metabolism of caffeine. *Gastroenterology* 1991; **101**: 943-947

72 **Jansen JB**, Lundborg P, Baak LC, Greve J, Ohman M, Stover C, Rohss K, Lamers CB. Effect of single and repeated intravenous doses of omeprazole on pentagastrin stimulated gastric acid secretion and pharmacokinetics in man. *Gut* 1988; **29**: 75-80

73 **Lloyd-Davies KA**, Rutgersson K, Solvell L. Omeprazole in the treatment of Zollinger-Ellison syndrome: a 4-year international study. *Aliment Pharmacol Ther* 1988; **2**: 13-32

74 **Wolfe MM**, Jensen RT. Zollinger-Ellison syndrome. Current concepts in diagnosis and management. *N Engl J Med* 1987; **317**: 1200-1209

75 **Maton PN**, Lack EE, Collen MJ, Cornelius MJ, David E, Gardner JD, Jensen RT. The effect of Zollinger-Ellison syndrome and omeprazole therapy on gastric oxyntic endocrine cells. *Gastroenterology* 1990; **99**: 943-950

76 **Howden CW**. Vitamin B12 levels during prolonged treatment with proton pump inhibitors. *J Clin Gastroenterol* 2000; **30**: 29-33

77 **Weber HC**, Venzon DJ, Jensen RT, Metz DC. Studies on the interrelation between Zollinger-Ellison syndrome, *Helicobacter pylori*, and proton pump inhibitor therapy. *Gastroenterology* 1997; **112**: 84-91

78 **Ruszniewski P**, Laucournet H, Elouaer-Blanc L, Mignon M, Bonfils S. Long-acting somatostatin (SMS 201-995) in the management of Zollinger-Ellison syndrome: evidence for sustained efficacy. *Pancreas* 1988; **3**: 145-152

79 **Tomassetti P**, Migliori M, Gullo L. Slow-release lanreotide treatment in endocrine gastrointestinal tumors. *Am J Gastroenterol* 1998; **93**: 1468-1471

80 **Tomassetti P**, Migliori M, Corinaldesi R, Gullo L. Treatment of gastroenteropancreatic neuroendocrine tumours with octreotide LAR. *Aliment Pharmacol Ther* 2000; **14**: 557-560

81 **Arnold R**, Simon B, Wied M. Treatment of neuroendocrine GEP tumours with somatostatin analogues: a review. *Digestion* 2000; **62** (Suppl 1): 84-91

82 **Bordi C**, Azzoni C, Pilato FP, Robutti F, D'Ambra G, Caruana P, Rindi G, Corleto VD, Annibale B, Delle FG. Morphometry of gastric endocrine cells in hypergastrinemic patients treated with the somatostatin analogue octreotide. *Regul Pept* 1993; **47**: 307-318

83 **Arnold R**, Trautmann ME, Creutzfeldt W, Benning R, Benning M, Neuhaus C, Jurgensen R, Stein K, Schafer H, Bruns C, Dennler HJ. Somatostatin analogue octreotide and inhibition of tumour growth in metastatic endocrine gastroenteropancreatic tumours. *Gut* 1996; **38**: 430-438

84 **Jensen RT**. Carcinoid and pancreatic endocrine tumors: recent advances in molecular pathogenesis, localization, and treatment. *Curr Opin Oncol* 2000; **12**: 368-377

85 **Shojamanesh H**, Gibril F, Louie A, Ojeaburu JV, Bashir S, Abou-Saif A, Jensen RT. Prospective study of the antitumor efficacy of long-term octreotide treatment in patients with progressive metastatic gastrinoma. *Cancer* 2002; **94**: 331-343

86 **Paganelli G**, Zoboli S, Cremonesi M, Bodei L, Ferrari M, Grana C, Bartolomei M, Orsi F, De Cicco C, Macke HR, Chinol M, de Braud F. Receptor-mediated radiotherapy with 90Y-DOTA-D-Phe1-Tyr3-octreotide. *Eur J Nucl Med* 2001; **28**: 426-434

87 **Waldherr C**, Pless M, Maecke HR, Haldemann A, Mueller-Brand J. The clinical value of [90Y-DOTA]-D-Phe1-Tyr3-octreotide (90Y-DOTATOC) in the treatment of neuroendocrine tumours: a clinical phase II study. *Ann Oncol* 2001; **12**: 941-945

88 **Leimer M**, Kurtaran A, Smith-Jones P, Raderer M, Havlik E, Angelberger P, Vorbeck F, Niederle B, Herold C, Virgolini I. Response to treatment with yttrium 90-DOTA-lanreotide of a patient with metastatic gastrinoma. *J Nucl Med* 1998; **39**: 2090-2094

89 **Peghini PL**, Annibale B, Azzoni C, Milione M, Corleto VD, Gibril F, Venzon DJ, Delle FG, Bordi C, Jensen RT. Effect of chronic hypergastrinemia on human enterochromaffin-like cells: insights from patients with sporadic gastrinomas. *Gastroenterology* 2002; **123**: 68-85

90 **Cadiot G**, Lehy T, Bonfils S. Action of somatostatin analogue (SMS 201-995) on the growth-promoting effect resulting from sustained achlorhydria in rat gastric mucosa, with special reference to endocrine cell behaviour. *Eur J Clin Invest* 1988; **18**: 360-368

91 **Modlin IM**, Kumar R, Nangia A, Soroka CJ, Pasikhov D, Goldenring JR. Gastrin-dependent inhibitory effects of octreotide on the genesis of gastric ECLomas. *Surgery* 1992; **112**: 1048-1056

92 **Tomassetti P**, Migliori M, Caletti GC, Fusaroli P, Corinaldesi R, Gullo L. Treatment of type II gastric carcinoid tumors with somatostatin analogues. *N Engl J Med* 2000; **343**: 551-554

93 **Fraker DL**, Norton JA, Alexander HR, Venzon DJ, Jensen RT. Surgery in Zollinger-Ellison syndrome alters the natural his-

tory of gastrinoma. *Ann Surg* 1994; **220**: 320-328
94 **Hirschowitz BI**. Clinical course of nonsurgically treated Zollinger-Ellison syndrome. Mignon M, Jensen RT, eds. Endocrine tumors of the pancreas: Recent advances in research and management. *Karger[23]* 1995: 360-371
95 **Thompson NW**, Bondeson AG, Bondeson L, Vinik A. The surgical treatment of gastrinoma in MEN I syndrome patients. *Surgery* 1989; **106**: 1081-1085
96 **Delcore R**, Cheung LY, Friesen SR. Outcome of lymph node involvement in patients with the Zollinger-Ellison syndrome. *Ann Surg* 1988; **208**: 291-298
97 **Fraker DL**, Norton JA, Saeed ZA, Maton PN, Gardner JD, Jensen RT. A prospective study of perioperative and postoperative control of acid hypersecretion in patients with Zollinger-Ellison syndrome undergoing gastrinoma resection. *Surgery* 1988; **104**: 1054-1063
98 **Azoulay D**, Bismuth H. Role of liver surgery and transplantation in patients with hepatic metastases from pancreatic endocrine tumors. Mignon M, Jensen RT, eds. Endocrine tumors of the pancreas: Recent advances in research and management. *Karger[23]* 1995: 461-476
99 **Le Treut YP**, Delpero JR, Dousset B, Cherqui D, Segol P, Mantion G, Hannoun L, Benhamou G, Launois B, Boillot O, Domergue J, Bismuth H. Results of liver transplantation in the treatment of metastatic neuroendocrine tumors. A 31-case French multicentric report. *Ann Surg* 1997; **225**: 355-364
100 **Thompson NW**. Current concepts in the surgical management of multiple endocrine neoplasia type 1 pancreatic-duodenal disease. Results in the treatment of 40 patients with Zollinger-Ellison syndrome, hypoglycaemia or both. *J Intern Med* 1998; **243**: 495-500
101 **Akerstrom G**, Hessman O, Skogseid B. Timing and extent of surgery in symptomatic and asymptomatic neuroendocrine tumors of the pancreas in MEN 1. *Langenbecks Arch Surg* 2002; **386**: 558-569
102 **Thompson NW**, Pasieka J, Fukuuchi A. Duodenal gastrinomas, duodenotomy, and duodenal exploration in the surgical management of Zollinger-Ellison syndrome. *World J Surg* 1993; **17**: 455-462
103 **Brandi ML**, Gagel RF, Angeli A, Bilezikian JP, Beck-Peccoz P, Bordi C, Conte-Devolx B, Falchetti A, Gheri RG, Libroia A, Lips CJ, Lombardi G, Mannelli M, Pacini F, Ponder BA, Raue F, Skogseid B, Tamburrano G, Thakker RV, Thompson NW, Tomassetti P, Tonelli F, Wells SA, Marx SJ. Guidelines for diagnosis and therapy of MEN type 1 and type 2. *J Clin Endocrinol Metab* 2001; **86**: 5658-5671
104 **Arnold R**, Frank M. Systemic chemotherapy for endocrine tunors of the pancreas. Mignon M, Jensen RT, eds. Endocrine tumors of the pancreas: Recent advances in research and management. *Karger[23]* 1995: 431-438
105 **Murray-Lyon IM**, Eddleston AL, Williams R, Brown M, Hogbin BM, Bennett A, Edwards JC, Taylor KW. Treatment of multiple-hormone-producing malignant islet-cell tumour with streptozotocin. *Lancet* 1968; **2**: 895-898
106 **Broder LE**, Carter SK. Pancreatic islet cell carcinoma. II. Results of therapy with streptozotocin in 52 patients. *Ann Intern Med* 1973; **79**: 108-118
107 **Moertel CG**, Lefkopoulo M, Lipsitz S, Hahn RG, Klaassen D. Streptozocin-doxorubicin, streptozocin-fluorouracil or chlorozotocin in the treatment of advanced islet-cell carcinoma. *N Engl J Med* 1992; **326**: 519-523
108 **von Schrenck T**, Howard JM, Doppman JL, Norton JA, Maton PN, Smith FP, Vinayek R, Frucht H, Wank SA, Gardner JD. Prospective study of chemotherapy in patients with metastatic gastrinoma. *Gastroenterology* 1988; **94**: 1326-1334
109 **Kvols LK**, Buck M. Chemotherapy of endocrine malignancies: a review. *Semin Oncol* 1987; **14**: 343-353
110 **Rougier P**, Mitry E. Chemotherapy in the treatment of neuroendocrine malignant tumors. *Digestion* 2000; **62** (Suppl 1): 73-78
111 **Oberg K**. Advances in chemotherapy and biotherapy of endocrine tumors. *Curr Opin Oncol* 1998; **10**: 58-65
112 **Clouse ME**, Perry L, Stuart K, Stokes KR. Hepatic arterial chemoembolization for metastatic neuroendocrine tumors. *Digestion* 1994; **55**(Suppl 3): 92-97
113 **Perry LJ**, Stuart K, Stokes KR, Clouse ME. Hepatic arterial chemoembolization for metastatic neuroendocrine tumors. *Surgery* 1994; **116**: 1111-1116
114 **Drougas JG**, Anthony LB, Blair TK, Lopez RR, Wright JK, Chapman WC, Webb L, Mazer M, Meranze S, Pinson CW. Hepatic artery chemoembolization for management of patients with advanced metastatic carcinoid tumors. *Am J Surg* 1998; **175**: 408-412
115 **Kress O**, Wagner HJ, Wied M, Klose KJ, Arnold R, Alfke H. Transarterial chemoembolization of advanced liver metastases of neuroendocrine tumors-a retrospective single-center analysis. *Digestion* 2003; **68**: 94-101

Science Editor Guo SY **Language Editor** Elsevier HK

PO Box 2345, Beijing 100023, China
www.wjgnet.com
wjg@wjgnet.com

ELSEVIER

World J Gastroenterol 2005;11(35):5433-5437
World Journal of Gastroenterology ISSN 1007-9327
© 2005 The WJG Press and Elsevier Inc. All rights reserved.

• *GASTRIC CANCER* •

Effects of allitridi on cell cycle arrest of human gastric cancer cells

Min-Wen Ha, Rui Ma, Li-Ping Shun, Yue-Hua Gong, Yuan Yuan

Min-Wen Ha, Rui Ma, Li-Ping Shun, Yue-Hua Gong, Yuan Yuan, Cancer Institute of the First Affiliated Hospital of China Medical University, Shenyang 110001, Liaoning Province, China
Supported by the China State Key Basic Research Program, No. G1998051203
Correspondence to: Professor Yuan Yuan, Cancer Institute of the First Affiliated Hospital of China Medical University, 155 Northern Nanjing Street, Heping District, Shenyang 110001, Liaoning Province, China. yyuan@mail.cmu.edu.cn
Telephone: +86-24-23256666-6153 Fax: +86-24-22703576
Received: 2004-07-20 Accepted: 2004-09-09

Abstract

AIM: To determine the effect of allitridi on cell cycle of human gastric cancer (HGC) cell lines MGC803 and SGC7901 and its possible mechanism.

METHODS: Trypan blue dye exclusion was used to evaluate the proliferation, inhibition of cells and damages of these cells were detected with electron microscope. Flow cytometry and cell mitotic index were used to analyze the change of cell cycle, immunohistochemistry, and RT-PCR was used to examine expression of the $p21^{WAF1}$ gene.

RESULTS: MGC803 cell growth was inhibited by allitridi with 24 h IC_{50} being 6.4 μg/mL. SGC7901 cell growth was also inhibited by allitridi with 24 h IC_{50} being 7.3 μg/mL. After being treated with allitridi at the concentration of 12 μg/mL for 24 h, cells were found to have direct cytotoxic effects, including broken cellular membrane, swollen and vesiculated mitochondria and rough endoplasmic reticula, and mass lipid droplet. When cells were treated with allitridi at the concentration of 3, 6, and 9 μg/mL for 24 h, the percentage of G_0/G_1 phase cells was decreased and that of G_2/M phase cells was significantly increased ($P = 0.002$) compared with those in the group. When cells were treated with allitridi at the concentration of 6 μg/mL, cell mitotic index was much higher ($P = 0.003$) than that of control group, indicating that allitridi could cause gastric cancer cell arrest in M phase. Besides, the expression levels of $p21^{WAF1}$ gene of MGC803 cells and $p21^{WAF1}$ gene of SGC7901 cells were remarkably upregulated after treatment.

CONCLUSION: Allitridi can cause gastric cancer cell arrest in M phase, and this may be one of the mechanisms for inhibiting cell proliferation. Effect of allitridi on cells in M phase may be associated with the upregulation of $p21^{WAF1}$ genes. This study provides experimental data for clinical use of allitridi in the treatment of gastric carcinoma.

© 2005 The WJG Press and Elsevier Inc. All rights reserved.

Key words: Allitridi; Gastric cancer cells; Cell cycle; $p21^{WAF1}$

Ha MW, Ma R, Shun LP, Gong YH, Yuan Y. Effects of allitridi on cell cycle arrest of human gastric cancer cells. *World J Gastroenterol* 2005; 11(35): 5433-5437
http://www.wjgnet.com/1007-9327/11/5433.asp

INTRODUCTION

Garlic has been used for over 3 000 years in traditional Chinese medicine and is widely used in preventing manifold diseases all over the world. Garlic is the bulb of onion genus lily family plants. Allitridi is a compound extracted from the garlic bulb. It is an important constituent of garlic oil containing diallyl trisulfide (DATS) and diallyl disulfide (DADS)[1,2].

Epidemiological studies indicate that garlic has remarkable antithrombotic, hypolipidemic, hypocholesterolemic and antineoplastic effects. Allitridi has been shown to have anticancer activities, such as inhibiting nitrate reductase, enhancing anticancer activity of macrophages, increasing sensitivity of anticancer drugs[3]. However, its definitive mechanism of anticancer activities has not been established. In this study, human gastric cells MGC803 and SGC7901 were treated with allitridi to study its effect on cell cycle arrest of human gastric cancer (HGC) cell lines MGC803 and SGC7901 and its possible mechanism.

MATERIALS AND METHODS

Cell line and culture

MGC803 was the human gastric mucinous adenocarcinoma cell line and SGC7901 was the human gastric carcinoma metastatic lymph node cell line. These cell lines were grown in RPMI 1640 supplemented with 10% heat-inactivated fetal calf serum, 50 U/mL penicillin and 50 μg/mL streptomycin. The cells were maintained at 37 ℃ in a humidified atmosphere containing 50 mL/L CO_2 and 95% air. Viability of the cells used in these experiments was consistently more than 95%, when evaluated by the trypan blue exclusion method.

Analysis of cell viability

The effect of allitridi on cell growth and viability was determined by counting the number of cells. The cells at a density of 2.5×10^5/mL were seeded onto 24-well plates, and treated with allitridi with different concentrations for 24 h. Cells in control group were also incubated simultaneously. Cell proliferation and inhibition curves were drawn and drug IC_{50} was detected.

Morphological analysis by electron microscope

Cells (1×10^6) were collected after being induced by allitridi at 12 μg/mL for 24 h, washed twice with PBS, centrifuged for 5 min at 1 500 r/min, fixed with 2% glutaral at 4 ℃ and dessicated, embedded in EPON-812. They were then double stained with uranium and plumbum, and observed under transmission electron microscope.

Cell cycle analysis

Flow cytometry was employed to determine the DNA content of these cells. The cells were seeded onto 100-mm dishes and grown in RPMI-1640 supplemented with 10% FCS. After being treated with allitridi at the concentration of 3, 6, and 9 μg/mL for 24 h respectively, the cells were harvested. The cells were trypsinized and washed with D-PBS. The sample was fixed by slowly dropping 2 mL of cold 70% ethanol into the tube and stored at 4 ℃. After fixation, the cells were washed, re-pelleted, and re-suspended in 0.05 mg/mL propidium iodide (Fluka Co.), 100 U/mL RNase (Fluka Co.) in PBS. The sample was incubated at room temperature for 30 min, and analyzed on a FACSCalibur (BD PharMingen). Cell cycle data originally obtained with CellQuest software (BD PharMingen) were re-analyzed using ModFit software (Verity Software House, Topsham, ME, USA). Next, 6 μg/mL allitridi was added to the cultured cells. The induced cells were collected after 24 h. At the same time the negative control was constructed. The cells were smeared and stained with Giemsa dye. The mitotic cells in 1 000 cells were counted under light microscope, and the mitotic index of the cells was calculated.

Analysis of immunohistochemistry

The p21 protein was detected by immunohistochemistry using specific mAb (Maxin Co.). After being treated with allitridi at concentrations of 3, 6, and 9 μg/mL for 24 h, the cells were harvested. At the same time, the negative contrast was constructed. The cells were made into smears and stained using normal S-P immunohistochemical method. Color was displayed with DAB reagent and stained again with hernatein. Results were observed under light microscope. The cells had brown nuclei and plasma was positive.

Semi-quantitative reverse transcription-PCR

The expression of p21 and p16 mRNA was tested by RT-PCR. An aliquot containing 5 μg/mL of RNA was used for the first-strand cDNA synthesis (TaKaRa). In each reaction, 100 μL solution contained 3 μmol/L of random hexamers, 25 mmol/L Tris-HCl, 37 mmol/L KCl, 1.5 mmol/L $MgCl_2$, 10 mmol/L DTT, 0.25 mmol/L dNTP, 40 units of RNAsin, 50 U/mL Super Taq DNA polymerase, and 200 units of reverse transcriptase. The annealing mixture was incubated at room temperature for 15 min, and then incubated in water bath at 41 ℃ for 60 min. The reverse transcriptase enzyme was inactivated by heating the solution to 95 ℃ for 5 min. Thirty cycles of PCR were carried out using the Perkin-Elmer PCR reaction kit and primers, each consisting of denaturation at 94 ℃ for 1 min, annealing at 57 ℃ for 1 min, and extension at 72 ℃ for 2 min. PCR products were separated on 2% agarose gel. Primers used for PCR were p21 sense (5'-GGG GAC AGC AGA GGA AGA C-3') and p21 antisense (5'-CGG CGT TTG GAG TGG TAG A-3'), β-actin sense (5'-GAT TGC CTC AGG ACA TTT CTG- 3') and β-actin antisense (5'-GAT TGC TCA GGA CAT TTC TG-3'). Gene primers were synthesized by Beijing Oake Co.

Statistical analysis

Student's *t*-test was used to compare the difference between control group and allitridi treatment group. The data of cell growth and mitotic index were presented as mean±SD. *P* value less than 0.05 was considered statistically significant.

RESULTS

Allitridi-inhibited proliferation of MGC803 and SGC7901 cells in a concentration-dependent manner

Figure 1 shows the proliferation curves of the cells treated with allitridi at various concentrations. The proliferation of MGC803 and SGC7901 cells inhibited by allitridi was clearly observed in a concentration-dependent manner during the 24-h period. MGC803 cell growth was inhibited by allitridi with 24 h IC_{50} being 6.4 μg/mL. SGC7901 cell growth was inhibited by allitridi with 24 h IC_{50} being 7.3 μg/mL.

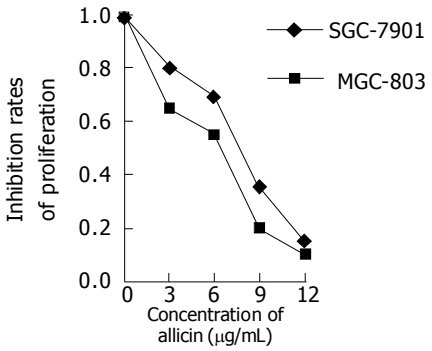


Figure 1 Inhibition of allitridi on MGC803 and SGC7901. Allitridi (3, 6, or 9 μg/mL) inhibited cell growth in a dose-dependent manner.

Morphological observation after allitridi treatment

After being treated with allitridi at the concentration of 12 μg/mL for 24 h, cell morphological change was observed under transmission electron microscope. The ultrastructure showed that the cells were directly killed and broken cellular membrane, swollen and vesiculated mitochondria and rough endoplasmic reticula and mass lipid droplet could be seen. The nuclei had no obvious morphological change or typical apoptosis (Figure 2).

Allitridi-induced cell cycle arrest of MGC803 and SGC7901 cells in M phase

To assess the effects of allitridi on cell cycle progression and population distribution, MGC803 and SGC7901 cells were studied using flow cytometry. A comparison of the cell cycle profiles of allitridi treatment and control cells confirmed the existence of allitridi-induced effects. It was found that 24-h allitridi treatment induced significant cell cycle arrest in G_2/M phase ($P<0.01$) in comparison to

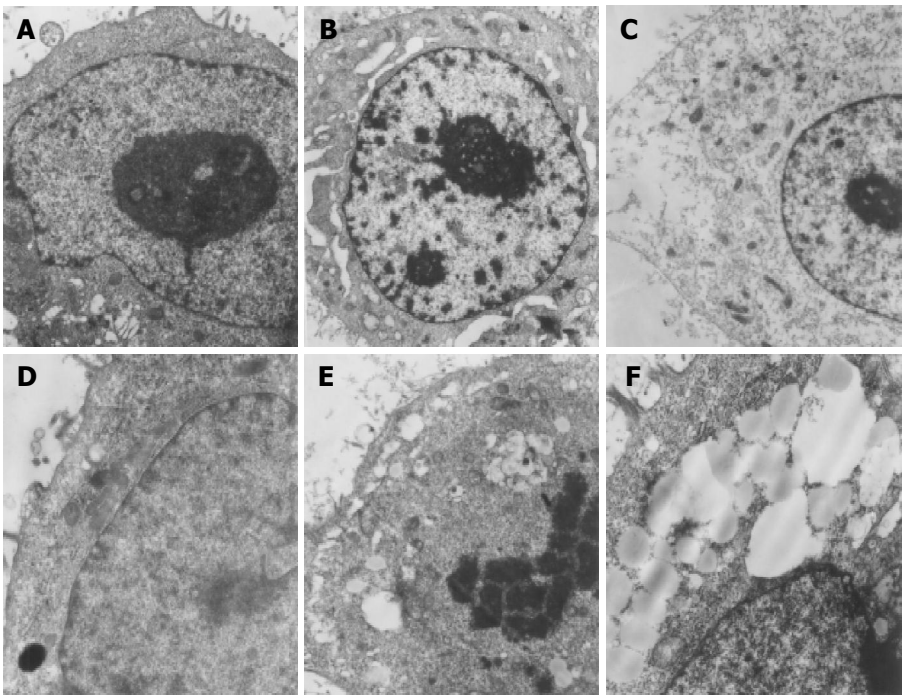


Figure 2 Morphological changes of allitridi-treated MGC803 and SGC7901 cells under electron microscope (×5 000). **A:** MGC803 control cells; **B** and **C:** 12 μg/mL allitridi-induced MGC803 cells; **D:** SGC7901 control cells; **E** and **F:** 12 μg/mL allitridi-induced SGC7901 cells.

untreated cells. Histograms are shown in Figure 3. The percentage of cells in the S phase, G_1, and G_2/M regions are shown in Table 1. After being treated with allitridi at the concentration of 6 μg/mL for 24 h, cell mitotic index was determined. The mitotic index of MGC803 was 316‰ after allitridi treatment, and 21‰ in control group. The mitotic index of SGC7901 was 207‰ after allitridi treatment, and 16‰ in control group. Compared with the control group, the cell mitotic index of allitridi treatment group was much higher (P<0.01), indicating that allitridi caused potential M phase blockage in gastric cancer cells.

Allitridi resulted in increase of p21 expression

The effect of allitridi on p21 protein levels was determined by immunohistochemistry analysis. p21 was not expressed in MGC803 and the SGC7901 cells. However, when MGC803 cells were treated with allitridi at the concentrations of 3, 6, and 9 μg/mL for 24 h, p21 was expressed in high levels, the positive rates of p21 were 28.2%, 29.1%, and 31.8% respe-ctively. Similarly when SGC7901 cells were treated under exactly same as above, p21 expressed in high levels too, the positive rates of p21 were 25.5%, 35.1%, or 39.6%. Figure 4 shows the levels of p21 in MGC803 and SGC7901 cells.

Allitridi upregulated p21^{WAF1} expression

p21^{WAF1} mRNA expressed little in MGC803 and SGC7901 cells. However, we demonstrated that treatment with 6 or 9 μg/mL allitridi did induce upregulation of p21^{WAF1} mRNA in MGC803 and SGC7901 cells. In this study, RT-PCR products of β-actin were used as an inter control. Figures 5A and B show that treatment of MGC803 and SGC7901 cells with allitridi induced an upregulation of p21^{WAF1}.

DISCUSSION

Allitridi containing DATS and DADS is widely used in cancer chemoprevention and anti-cardiovascular disease research[4-6]. Some scholars have reported its protective effects on HGC. DATS can significantly inhibit bacterial nitrosamines. The mechanism is that the constituent of garlic can diminish NO_2, thus preventing the formation of carcinogens[7]. Cellular immune response of patients treated with allitridi shows that the macrophage phagocytotic ability

Table 1 Effect of allitridi on cell cycle arrest of MGC-803 and SGC-7901 cells (mean±SD)

	MGC803				SGC7901			
	Control	Treated with allitridi			Control	Treated with allitridi		
		3 μg/mL	6 μg/mL	9 μg/mL		3 μg/mL	6 μg/mL	9 μg/mL
G_0/G_1 (%)	57.2±3.1	27.5±2.8[b]	12.4±1.7[b]	3.3±0.6[b]	62.1±2.4	27.7±1.0[b]	17.9±3.8[b]	13.2±1.7[b]
S (%)	14.4±1.6	13.6±1.4	12.4±2.2	11.2±1.3	10.1±0.5	12.3±0.1	13.7±2.1	12.1±0.4
G_2/M (%)	13.3±0.2	20.1±3.5[b]	36.5±1.4[b]	36.4±4.5[b]	13.2±1.2	21.7±2.3[b]	39.4±4.3[b]	37.4±3.3[b]

[b]P<0.01 *vs* control.

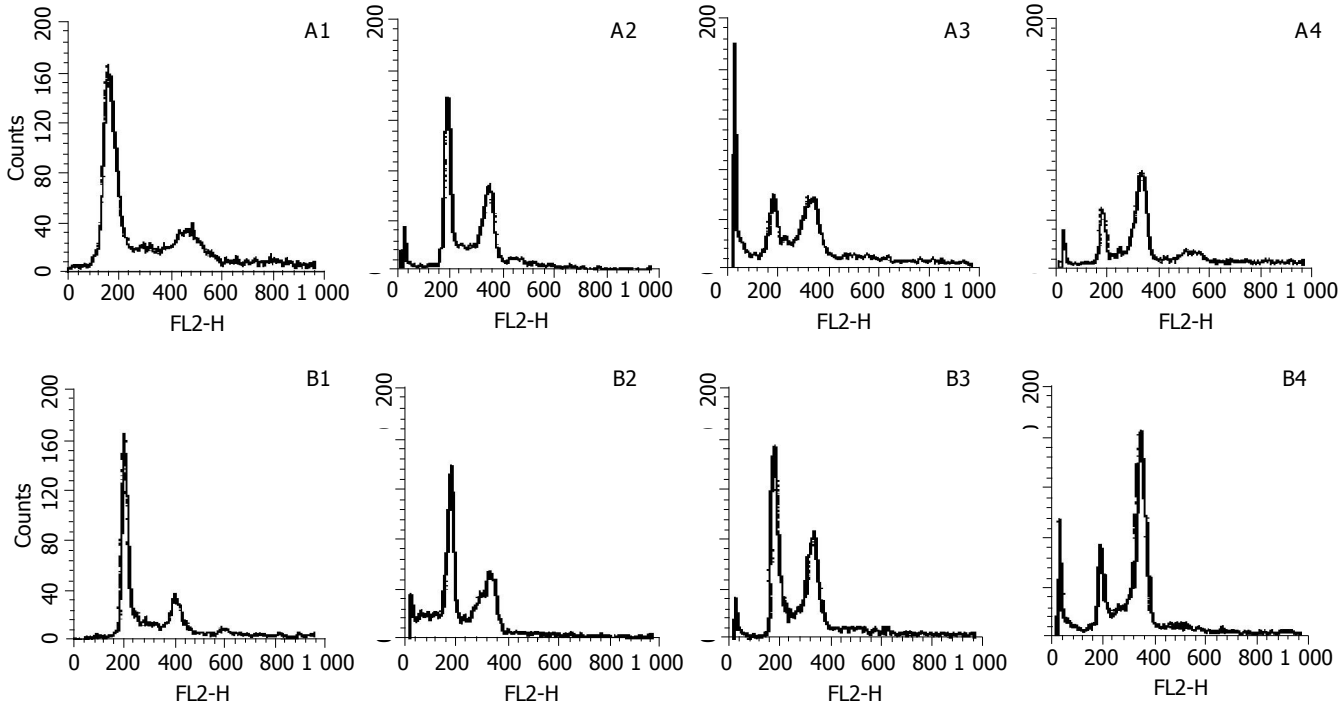


Figure 3 Cell cycle changes of MGC803 cells (**A1-4**) and SGC 7901 cells (**B1-4**) 24 h after allitridi treatment. **A1, B1:** Control cells; **A2, B2:** allitridi 3 μg/mL; **A3, B3:** allitridi 6 μg/mL; **A4, B4:** allitridi 9 μg/mL.

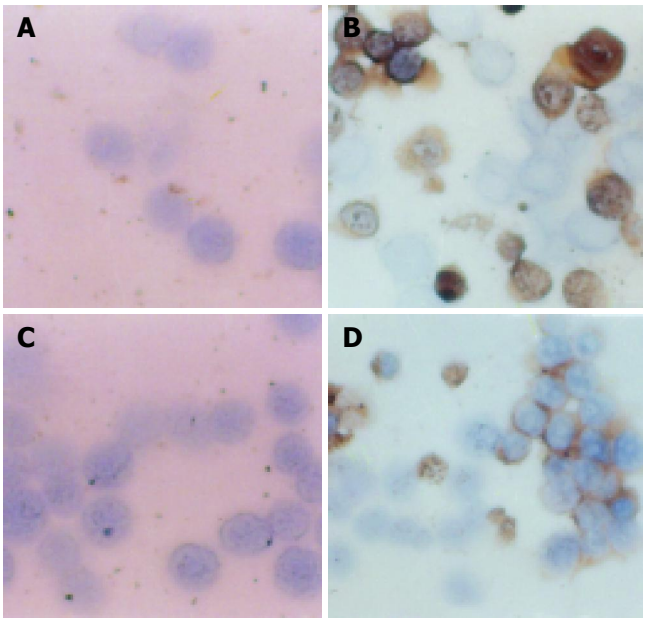


Figure 4 Expression of p21 in MGC803 and SGC7901 cells after being treated with allitridi (SP ×400). **A:** Control of MGC803 cells; **B:** treated MGC803 cells with 6 μg/mL allitridi; **C:** control of SGC7901 cells; **D:** treated SGC7901 cells with 6 μg/mL allitridi.

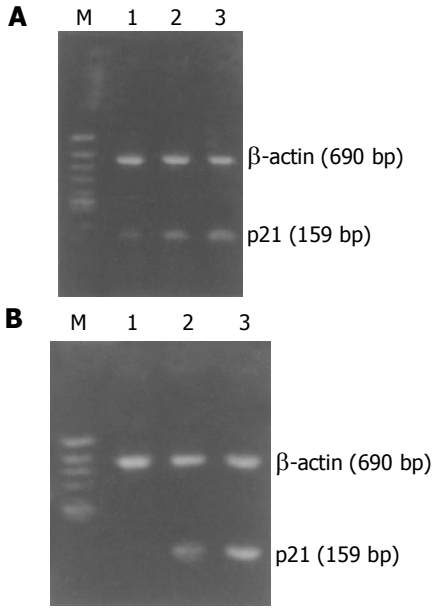


Figure 5 Effect of allitridi treatment on $p21^{WAF1}$ mRNA expression in MGC803 cells (**A**) and SGC7901 cells (**B**). M: DNA markers: 1: control cells; 2: 6 μg/mL allitridi; 3: 9 μg/mL allitridi.

and lymphocyte transformation percentage are obviously increased in most patients. Cell cycle plays an important role in the modulation of growth of tumor cell, and attention has been paid to preventing unlimited proliferation of tumor cells by cell cycle control[8]. In this study, the proliferation of human gastric cell lines MGC803 and SGC7901 was significantly inhibited after being treated with allitridi at different concentrations. Morphological analysis demonstrated direct cytotoxic effects of allitridi on tumor cells. The cells were detected using flow cytometer in order to examine the distribution of DNA content. The first peak (2C C = haploid DNA content) was produced by the cells in G_1 phase, the second (4C) was produced in G_2/M phase with or without cells in G_1 phase at higher DNA ploidy (tetraploidy, G_{1t}),

and the third (8C) was produced in G_2 phase at higher DNA ploidy (tetraploidy, G_{2t}). The results show that the cells are blocked in G_2/M phase. Furthermore, after allitridi treatment, cell mitotic index was much higher, the cell cycle was blocked just in M phase, indicating that allitridi makes damaged cells stagnate at mitosis phase of cell cycle, and inhibits the proliferation of cells. If this happens, cells re-enter the cycle, otherwise they undergo apoptosis or death. More importantly, allitridi affects M phase of these cells selectively and participates in the regulation of cell cycle, and the blocking effect of allitridi on cells in M phase could be the mechanism of its antitumor effect. Allitridi can be used as a chemotherapeutic agent. Thus, the goal in cancer therapy is to kill cancer cells. Cell cycle control offers a new set of potential target for chemotherapeutic compounds, many of these new agents may be biological modifiers, rather than nonselective cytotoxic agents. The results of the present study reveal that MGC803 and SGC7901 cells have low p21 expression, but allitridi increases the expression of $p21^{WAF1}$ of MGC803 and SGC7901 cells. Completion of the cell cycle requires the co-ordination of a variety of macromolecular syntheses, assemblies, and movements. Negative controls on cell cycle progression are exerted during cell development, differentiation, senescence, and death. These negative controls may play an important role in preventing tumorigenesis. $p21^{WAF1}$ has been implicated as a growth arrest mediator in cell terminal differentiation and apoptosis[9,10]. Regulation of cell cycle progression is orchestrated by CDKs.

$p21^{WAF1}$ is a downstream effector of p53 that mediates cell cycle arrest in G_1 and G_2/M phases. Mechanically, the $p21^{WAF1}$-mediated cell cycle arrest in the G_1 and G_2/M phases has been suggested to include $p21^{WAF1}$-CDK2 and $p21^{WAF1}$-PCNA protein interaction[11]. As we have known, p21 is the cell cycle profiling, when overexpressed it inhibits the CDK4/6-cyclinD complex, leading to cell growth arrest and apoptosis[12], suggesting that many such control points exist within the cell cycle and they play a major role in maintaining the integrity of genome. At least two checkpoints detect DNA damage, one at the G-S transition, the other at the G_2-M transition. In addition, there are mitotic checkpoints, altered expression of cyclins A, B, and CDC2. All potential targets of mitotic checkpoint controls occur in some cancers[13]. Allitridi can upregulate $p21^{WAF1}$. P21 can affect the growth of cells by repressing M phase, and may interact with Cdc2-cyclinB mitosis promoting complex and inhibit its kinase activity; at this point it needs to be further investigated.

In conclusion, allitridi can effectively inhibit the proliferation of HGC MGC803 and SGC7901 cells and upregulate the expression of $p21^{WAF1}$. This study provides experimental data for clinical use of allitridi in treatment of gastric carcinoma.

ACKNOWLEDGMENTS

We are deeply grateful to Dr. Yun-Peng Liu, Director of Department of Internal Oncology, First Affiliated Hospital of China Medical University for providing MGC803 and SGC7901 cells suggestions and reading of the manuscript. We also thank Kezuo Hou for skillful technical inst-ruction.

REFERENCES

1 **Fleischauer AT,** Poole C, Arab L. Garlic consumption and cancer prevention: meta-analyses of colorectal and stomach cancers. *Am J Clin Nutr* 2000; **72**: 1047-1052
2 **Singh SV,** Pan SS, Srivastava SK, Zaren HA, Xia H, Hu X, Orchard JL. Differential induction of NAD(P)H:quinone oxidoreductase by anti-carcinogenic organosulfides from garlic. *Biochem Biophys Res Commun* 1998; **244**: 917-920
3 **Balasenthil S,** Arivazhagan S, Ramachandran CR, Nagini S. Effects of garlic on 7,12-Dimethylbenz [a] anthracene-induced hamster buccal pouch carcinogenesis. *Cancer Detect Prev* 1999; **23**: 534-538
4 **Wartenberg M,** Fischer K, Hescheler J, Sauer H. Modulation of intrinsic P-glycoprotein expression in multicellular prostate tumor spheroids by cell cycle inhibitors. *Biochim Biophys Acta* 2002; **1589**: 49-62
5 **Zeng YX,** el-Deiry WS. Regulation of p21WAF1/CIP1 expression by p53-independent pathways. *Oncogene* 1996; **12**: 1557-1564
6 **Wu Q,** Kirschmeier P, Hockenberry T, Yang TY, Brassard DL, Wang L, McClanahan T, Black S, Rizzi G, Musco ML, Mirza A, Liu S. Transcriptional regulation during $p21^{WAF1/CIP1}$-induced apoptosis in human ovarian cancer cells. *J Biol Chem* 2002; **277**: 36329-36337
7 **Bertrand R,** Solary E, O'Connor P, Kohn KW, Pommier Y. Induction of a common pathway of apoptosis by staurosporine. *Exp Cell Res* 1994; **211**: 314-321
8 **Lin SY**, Liang YC, Ho YS, Tsai SH, Pan S, Lee WS. Involvement of both extracellular signal-regulated kinase and c-jun N-terminal kinase pathways in the 12-o-tetradcanoylphorbol-13-acetate-induced upregulation of $p21^{Cip1}$ in colon cancer cells. *Mol Carcinog* 2002; **35**: 21-28
9 **Prall OW**, Carroll JS, Sutherland RL. A low abundance pool of nascent $p21^{WAF1/Cip}$ is targeted by estrogen to activate cyclin E/Cdk2. *J Biol Chem* 2001; **276**: 45433-45442
10 **Javelaud D**, Besancon F. Inactivation of $p21^{WAF1}$ sensitizes cells to apoptosis via an increase of both $p14^{ARF}$ and p53 levels and an alteration of the Bax/Bcl-2 ratio. *J Biol Chem* 2002; **277**: 37949-37954
11 **Chen B,** He L, Savell VH, Jenkins JJ, Parham DM. Inhibition of the interferon-γ/signal transducers and activators of transcription (STAT) pathway by hypermethylation at a STAT-binding site in the $p21^{WAF1}$ promoter region. *Cancer Res* 2000; **60**: 3290-3298
12 **Richon VM**, Sandhoff TW, Rifkind RA, Marks PA. Histone deacetylase inhibitor selectively induces $p21^{WAF1}$ expressionand gene-associated histone acetylation. *Cell Biol* 2000; **97**: 10014-10019
13 **Kovalsky O,** Lung FD, Roller PP, Fornace AJ. Oligomerization of Human Gadd45a Protein. *J Biol Chem* 2001; **276**: 39330-39339

Science Editor Wang XL and Yu DH **Language Editor** Elsevier HK

PO Box 2345, Beijing 100023, China
www.wjgnet.com
wjg@wjgnet.com

ELSEVIER

World J Gastroenterol 2005;11(35):5438-5443
World Journal of Gastroenterology ISSN 1007-9327
© 2005 The WJG Press and Elsevier Inc. All rights reserved.

Study of transactivating effect of pre-S2 protein of hepatitis B virus and cloning of genes transactivated by pre-S2 protein with suppression subtractive hybridization

Dong Ji, Jun Cheng, Guo-Feng Chen, Yan Liu, Lin Wang, Jiang Guo

Dong Ji, Guo-Feng Chen, the 7th Department of Infectious Diseases, The 302 Hospital of PLA, Beijing 100039, China
Jun Cheng, Jiang Guo, Beijing Ditan Hospital, Beijing 100011, China
Yan Liu, Lin Wang, Center for Viral Hepatitis Research, Institute of Infectious Diseases, The 302 Hospital of PLA, Beijing 100039, China
Correspondence to: Dong Ji, the 7th Department of Infectious Diseases, The 302 Hospital of PLA, Beijing 100039, China. jd@genetherapy.com.cn
Telephone: +86-10-669332
Received: 2004-02-03 Accepted: 2005-02-03

Abstract

AIM: To investigate the transactivating effect of pre-S2 protein of hepatitis B virus (HBV) and construct a subtractive cDNA library of genes transactivated by pre-S2 protein with suppression subtractive hybridization (SSH) technique, and to pave the way for elucidating the pathogenesis of HBV infection.

METHODS: pcDNA3.1(-)-pre-S2 containing pre-S2 region of HBV genome was constructed by routine molecular methods. HepG2 cells were cotransfected with pcDNA3.1 (-)-pre-S2/pSV-lacZ and empty pcDNA3.1(-)/pSV-lacZ. After 48 h, cells were collected and detected for the expression of β-galactosidase (β-gal). SSH and bioinformatics techniques were used, the mRNA of HepG2 cells transfected with pcDNA3.1(-)-pre-S2 and pcDNA3.1(-) empty vector was isolated, respectively, cDNA was synthesized. After digestion with restriction enzyme *RsaI*, cDNA fragments were obtained. Tester cDNA was then divided into two groups and ligated to the specific adaptor 1 and adaptor 2, respectively. After tester cDNA was hybridized with driver cDNA twice and underwent two times of nested PCR, amplified cDNA fragments were subcloned into pGEM-Teasy vectors to set up the subtractive library. Amplification of the library was carried out with *E.coli* strain DH5α. The cDNA was sequenced and analyzed in GenBank with Blast search after PCR.

RESULTS: The pre-S2 mRNA could be detected in HepG2 cells transfected with pcDNA3.1(-)-pre-S2 plasmid. The activity of β-gal in HepG2 cells transfected with pcDNA3.1 (-)-pre-S2/pSV-lacZ was 7.0 times higher than that of control plasmid (P<0.01). The subtractive library of genes transactivated by HBV pre-S2 protein was constructed successfully. The amplified library contains 96 positive clones. Colony PCR showed that 86 clones contained 200-1 000 bp inserts. Sequence analysis was performed in 50 clones randomly, and the full length sequences were obtained with bioinformatics method and searched for homologous DNA sequence from GenBank, altogether 25 coding sequences were obtained, these cDNA sequences might be the target genes transactivated by pre-S2 protein.

CONCLUSION: The pre-S2 protein of HBV has transactivating effect on SV40 early promoter. The obtained sequences may be target genes transactivated by pre-S2 protein among which some genes coding proteins involved in cell cycle regulation, metabolism, immunity, signal transduction and cell apoptosis.This finding brings some new clues for studying the biological functions of pre-S2 protein and further understanding of HBV hepatocarcinogesis.

© 2005 The WJG Press and Elsevier Inc. All rights reserved.

Key words: HBV; pre-S2 surface protein; Transactivation

Ji D, Cheng J, Chen GF, Liu Y, Wang L, Guo J. Study of transactivating effect of pre-S2 protein of hepatitis B virus and cloning of genes transactivated by pre-S2 protein with suppression subtractive hybridization. *World J Gastroenterol* 2005; 11(35): 5438-5443
http://www.wjgnet.com/1007-9327/11/5438.asp

INTRODUCTION

Hepatitis B virus (HBV) causes acute and chronic infections of the liver. Acute infections may produce serious illness, and approximately 0.5% terminate with fatal, fulminant hepatitis. Chronic infections may also have serious consequences[1]. In addition to causing acute and chronic hepatitis, HBV is considered to be a major cliological factor in the development of human hepatocellular carcinoma (HCC), one of the most frequent fatal malignancies worldwide, and worldwide deaths from HCC caused by HBV infection probably exceed one million per year[2-4]. Epidemiological studies have demonstrated an approximately 10-fold increase in the relative risk of HCC among HBV carriers compared to noncarriers[5-8].

The precise role of HBV in the etiology of HCC is not well understood. Only occasionally, genes controlling the cell growth and differentiation are disturbed by HBV DNA sequences intergration, but since no common sites of viral DNA integration have been observed, the induction of cell

growth by HBV enhancer or promoter insertion cannot be regarded as a general mechanism of transformation in human HCC. An alternative mechanism of hepatocarcinogenesis could be the activation and/or repression, operated by HBV proteins, of the expression of genes crucial for cell growth regulation. Recent data have showed that some HBV proteins can exert a significant transactivational activity on both viral and cellular promoter[9]. Almost all HBV-associated HCCs studied so far harbor chromosomally integrated HBV DNA[10]. Integrated HBV DNA can encode two types of transcriptional transactivators: the already well studied HBx[11] and the pre-S2 transactivators: LHBs (large hepatitis B virus surface protein) and MHBs^t (C-terminally truncated middle surface protein)[12-14].

Although it is true the transactivator functions are preformed by the LHBs or MHBs^t, on closer inspection, one can easily see that this role is mostly performed by the pre-S region of the envelope protein. This observation naturally leads to the question, whether pre-S protein fragments alone might also have the transactivating role in the absence of the S region. Actually, *in vitro* studies with protease-treated HBV particles showed specific cleavage of pre-S fragments from LHBs, which indicate the presence of protease-sensitive sites within the junction of the pre-S and S proteins[15,16]. So, while the proteolytic cleavage and generation of the free pre-S fragments are quite evident, their biological meanings remain obscure[17-19]. Recently, we have studied the transactivator function of pre-S proteins. In the present study, we showed that pre-S2 protein functions as a transcriptional transactivator, and constructed the subtractive library of genes transactivated by HBV pre-S2 protein, successfully.

MATERIALS AND METHODS

Plasmid construction

The pre-S2 gene was amplified by PCR from the plasmid G376-7 (GenBank number: AF384371)[20-22] using sense (5'- GAT ATC ATG CAG TGG AAC TCC ACC -3') and antisene (5'- GGA TCC TTA GTT CGG TGC AGG GTC -3') primers (Shanghai BioAsia Biotechnology Co., Ltd). As these primers contain *Eco*RV and *Bam*HI (Takara) recognition sites on their respective 5'- ends, the amplified 180 bp PCR fragment was subcloned into the *Eco*RV/*Bam*HI sites of pcDNA3.1(-) vector (Invitrogen), the expression vector, pcDNA3.1(-)-pre-S2 which could direct expression of pre-S2 fusion protein was obtained, then identified by PCR and digested of *Eco*RV/*Bam*HI.

Cell culture and DNA transfection

HepG2 cells were cultured in Dulbecco's modified Eagle's medium (DMEM) containing 100 IU of penicillin and 100 μg of streptomycin per mL, supplemented with 10% (vol/vol) heat-inactivated fetal bovine serum (FBS), at 37 ℃ in a 50 mL/L CO_2 atmosphere. 1.5×10^6 cells were seeded in 35-mm plates 12 h prior to transfection and reached 50% confluence at the time of transfection. Cells were transfected with FuGENE6 Transfection Reagent (Roche), the transfection was carried out with 2.0 μg of pcDNA3.1 (-) empty and pcDNA3.1(-)-pre-S2 plasmid DNA according to the manufacture's protocol, respectively.

mRNA and cDNA isolation

The mRNA from HepG2 cells transfected with pcDNA3.1 (-)-pre-S2 and pcDNA3.1(-) empty vector was isolated by using a micro mRNA purification kit (Amersham Biosciences), respectively, cDNAs were reverse-transcribed from mRNA. Identification was done by PCR with pre-S2-specific primers.

Effect of pre-S2 protein on SV40 early promoter

HepG2 cells were transfected with various concentrations of pSV-lacZ (0.1-1.8 μg) (promega) plasmid DNA, expression of β-gal was detected by using a β-gal assay kit (promega). In pSV-LacZ plasmid, the LacZ gene is under the control of the SV40 early promoter element. The best concentration of pSV-lacZ was selected, HepG2 cells with pSV-lacZ (1.0 μg) and pcDNA3.1(-)-pre-S2 (2.0 μg) were cotransfected as a test group. At the same time, cotransfected with empty pcDNA3.1 (-) (2.0 μg) and pSV-lacZ (1.0 μg) was used as control as control group The cells were collected after 48 h, and the expression of β-gal was detected. Seven separate transfections were present in test and control groups, respectively, and Stata 7.0 program was used to analyze the experimental data.

Suppression subtractive hybridization (SSH)

Genome comparisons was done by suppression subtraction hybridization according to the manufacturer's instructions of PCR-select™ cDNA subtraction kit (Clontech). In brief, 2 μg of mRNA from the tester and the driver was subjected to cDNA synthesis. Tester and driver cDNAs were digested with *RsaI*. The tester cDNA was split into two groups, and each was ligated with a different cDNA adapter. In a first hybridization reaction, an excess of driver was added to each sample of tester. The samples were heat denaturated and allowed to anneal. Because of the second-order kinetics of hybridization, the concentration of high- and low-abundance sequences is equalized among the single-stranded tester molecules. At the same time, single-stranded tester molecules were significantly enriched for differentially expressed sequences. During a second hybridization, the two primary hybridization samples were mixed together without denaturation. Only the remaining equalized and subtracted single-stranded tester cDNAs can reassociate forming double-stranded tester molecules with different ends. After filling in the ends with DNA polymerase, the entire population of molecules was subjected to nested PCR with two adapter-specific primer pairs. After that, secondary PCR products were used as templates for PCR amplification of G3PDH (a housekeeping gene) at 18, 23, 28, 33 cycles to assure subtracted efficiency.

Cloning of subtracted cDNA libraries

Products of these amplified overhangs containing a subtracted cDNA library (6 μL) were ligated into a pGEM-Teasy vector (Promega). Subsequently, the plasmid was transformed into *E. coli* strain DH5α. Bacteria were taken up in 800 μL of LB medium and allowed to incubate for 45 min at 37 ℃ and 225 r/m. after incubation, Bacteria were plated onto agar plates containing ampicillin (100 μg/mL),

5-bromo-4-chloro-3-indolyl-β-D-galactoside (X-Gal, 20 μg/cm^2) and isopropyl-β-D-thiogalactoside (IPTG, 12.1 μg/cm^2) and incubated overnight at 37 ℃. White colonies were selected and identified by PCR. Primers were T7/SP6 primer of pGEM-Teasy vector. After sequencing the plasmids DNA of positive colonies (Shanghai BioAsia Biotechnology Co., Ltd), nucleic acid homology searches were performed using the BLAST (basic local alignment search tool) server at the National Center for Biotechnology Information.

RESULTS

Identification of expression vector

Restriction enzyme analysis of pcDNA3.1(-)-pre-S2 plasmid with *Eco*RV/*Bam*HI yielded two bands: 5 396 bp empty pcDNA3.1(-) and 172 bp HBV pre-S2, cleaved with *Pst*I got only one 5 568 bp band (5 396 bp+172 bp). The plasmid by PCR amplification with pre-S2-sepcific primers got a clear band of the expected size (180 bp, Figure 1). Sequencing the PCR products was correct.

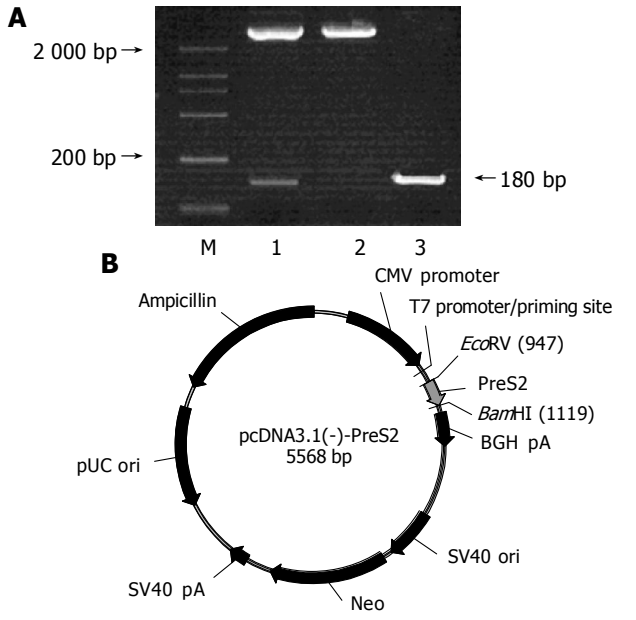


Figure 1 **A**: Products of pcDNA3.1(-)-pre-S2 PCR and restriction enzyme cleaved were eletrophoresed in 2.0% agarose gel. Lane 1: *Eco*RV/*Bam*HI cleaved, lane 2: *Pst*I cleaved, lane 3: production of plasmid PCR, M: DNA marker (2 000 bp). **B**: Structure of expression plasmid pcDNA3.1(-)-pre-S2.

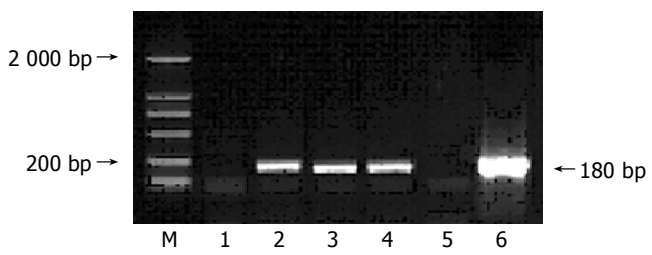


Figure 2 RT-PCR products were eletrophoresed in 0.9% agarose gel. Lane 1: negative control, lanes 2-4: mRNA was isolated from pcDNA3.1(-)-pre-S2 and RT-PCR was performed by three different Oligod T, lane 5: blank control, lane 6: positive control, M: DNA marker (2 000 bp).

Expression of HBV pre-S2 protein

Reverse-transcribed by three different Oligo dT, identification of cDNA by PCR yielded common 180 bp band (Figure 2).

Transactivation of HBV pre-S2 protein on early promoter of SV40

The *A* data about expression of β-gal of the test group (n = 7) was 0.238±0.007. In contrast, the *A* data about that of the control group (n = 7) was 0.034±0.009. Expression of β-gal were 7.0-fold higher when contransfected pcDNA3.1(-)-pre-S2 and pSV-lacZ than when contransfected empty pcDNA3.1(-) and pSV-lacZ. The significant increase of expression of β-gal (P<0.01) was attributed to the transactivating effect of HBV pre-S2 protein on early promoter of SV40, increasing the expression of downstream gene lacZ (Figure 3).

Analysis of the subtraction library

Subtraction efficiency analysis showed that the PCR products of G3PDH in unsubtracted library were visible after 18 cycles, however, 28 cycles were required in the subtracted one for G3PDH to be detected (Figure 4). The abundance of non-differentially expressed gene was effectively reduced, which indicated that the subtraction library had the high subtraction efficiency.

Using SSH technique, we obtained a total of 96 positive clones. These clones were prescreened by using PCR amplification to ensure that only clones with different inserts were subjected to sequencing (Figure 5). Among these clones,

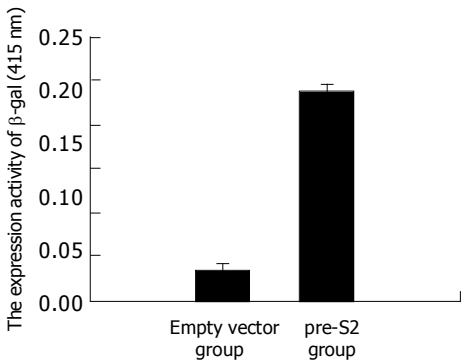


Figure 3 Result of β-galactosidase enzyme analysis. The numbers represent mean±SD of 7 separate transfections.

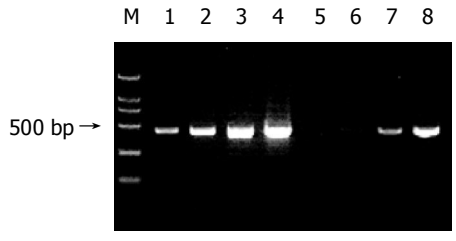


Figure 4 Reduction of G3PDH abundance by PCR-select subtraction. PCR was performed on unsubtracted (lanes1-4) or subtracted (lanes 5-8) secondary PCR products with the G3PDH 5' and 3' primers. Lanes 1, 5: 18 cycles; lanes 2, 6: 23 cycles; lanes 3, 7: 28 cycles; lanes 4, 8: 33 cycles. Lane M: DNA marker (2 000 bp).

eighty-six clones contained 200-1 000 bp inserts. A total of 50 clones from the cDNA library were randomly chosen and sequenced, altogether 25 coding sequences were obtained. Summary of the data is presented in Table 1.

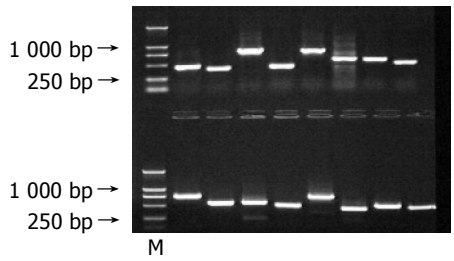


Figure 5 Results of PCR amplification of part clones (17-32). M: DNA marker (2 000 bp).

DISCUSSION

The sequence encoding the pre-S2 transactivators is localized in the HBV surface gene. The surface gene consists of a single open reading frame divided into three coding regions: pre-S1, pre-S2 and S, each starting with an in-frame ATG codon. Through alternate translational initiation at each of the three AUG codons, a large (LHBs, pre-S1+pre-S2+S), a middle (MHBs, pre-S2+S) and a small (SHBs, S) envelope glycoprotein can be synthesized[23-27]. The transactivator function of the surface protein requires the cytoplasmic orientation of the pre-S2 domain (the minimal functional unit) that occurs in the case of MHBs^t and in a fraction of LHBs[28,29]. In contrast, full-length MHBs displays no transcriptional activator function, here the pre-S2 domain directs into the lumen of the endoplasmic reticulum (ER). The generation of functional MHBs^t from MHBs requires deletion of the 3' end of the pre-S2/S gene encoding at least the last 70 amino acids corresponding to the hydrophobic region III of the S domain during the integration process[30]. Deletions of 3' sequences of the pre-S2/S gene generating functional MHBs^t transactivators were found in one-third of the integrates investigated so far[31,32]. This fact and the presence of complete pre-S/S genes in some other systematically studied integrates indicate the biological significance of the pre-S2 transactivators[33].

The transactivator function of the pre-S2 activators is based on the cytoplasmic orientation of the pre-S2 domain, and many reports have demonstrated that the pre-S2 region is sufficient for generation of the transcriptional transactivator function. The pre-S2 domain is PKC-dependent phosphorylated. Moreover, the pre-S2 domain binds of PKC α/β and triggers a PKC-dependent activation of the c-Raf-1/MAPKKK signal transduction cascade, resulting in an activation of transcription factors such as AP-1 and NF-κB. Furthermore, by activation of this signaling cascade, the pre-S2 activators cause an increased proliferation rate of hepatocytes. According to the two-step model of carcinogenesis (initiation/promotion), the pre-S2 activators could exert a tumor-promoter-like function by activation of the PKC/c-Raf-1/MAPKKK signaling cascade: cells harboring critical mutations (initiation) may be positively selected (promotion). Such a multistep process may account for the long latency period in HCC development, but it also leads to the hypothesis that each tumor reflects an individual case[34-37].

We cotransfected HepG2 cells with pcDNA3.1(-)-pre-

Table 1 Homolog searching of sequenced cDNA fragments from SSH library

High similarity proteins to known genes	GenBank No.	Number of similarity clones
Eukaryotic translation elongation factor1 alpha 1	BC018641	15
Ribosomal protein	BC004294	7
Fibronectin 1 (FN1)	BC016875	3
Mitochondrion	AY289054	2
Ferritin, heavy polypeptide 1	BC063514	2
Albumin	BC036003	2
Keratin 18	BC000698	1
Phospholipase A2	HUMPHPLA2	1
Pituitary tumor-transforming 1 interacting protein	BC034250	1
NADH dehydrogenase 2 (MTND2)	NM_173709	1
Cytochrome c oxidase II (MTCO2)	NM_173705	1
Laminin, beta 1	BC026018	1
Tumor rejection antigen (gp96)1 (TRA1)	NM_003299	1
Calmodulin 2 (phosphorylase kinase,delta)(CALM2)	NM_001743	1
M-phase phosphoprotein, mpp11	HSMPP11	1
Spermidine/spermine N1-acetyltransferase (SSAT)	HSU40369	1
Nucleophosmin	BC020467	1
Alpha-2-macroglobulin	HUMA2MGL	1
Tubulin	BC018948	1
Prostaglandin F synthase	AB032154S4	1
Methionine-tRNA synthetase (MARS)	NM_004990	1
Bile acid-binding protein	AB032151S1	1
Tyrosine 3-monooxygenase/tryptophan 5-monooxyge nase activation protein, zeta polypeptide	BC013265	1
Ras-related C3 botulinum toxin substrate 1 (rho family, small GTP binding protein Rac1) (RAC1)	NM_198829	1
Aldo-keto reductase family 1,member C3(3-alpha hydroxysteroid dehydrogenase, type II)	BC001479	1

S2 and pSV-lacZ and demonstrated that the HBV pre-S2 protein is successfully expressed in transfected HepG2 cells. Expression of β-gal were 7.0-fold higher when contransfected with pcDNA3.1(-)-pre-S2 and pSV-lacZ than when contransfected with empty pcDNA3.1(-) and pSV-lacZ. HBV pre-S2 protein has significant transactivating effect on early promoter of SV40, increasing the expression of downstream gene lacZ. This result indicates that the HBV pre-S2 protein expressed in HepG2 cells retains its biological activity in terms of transcriptional activation, which is consistent with the previous report[38,39].

To get insight into the transactivation mechanism of HBV pre-S2 protein, the SSH was used for identification of transactivating relative target genes of pre-S2 protein, and a subtractive library was set up successfully. Sequence analysis was performed in 50 clones, and 25 coding sequences were obtained. These genes can be divided into 4 groups: (1) The genes involving in cell structure and cell cycle. They possess the important ability to control cell growth, differentiation and adherence, such as ribosomal protein, mitochondrion, nucleophosmin, tubulin, keratin, M-phase phosphoprotein, eukaryotic translation elongation factor, and so on. (2) The genes relating to cell energy or substance metabolism, (i.e., ferritin, albumin, NADH dehydrogenase 2, cytochrome c oxidase II, spermidine/spermine N1-acetyltransferase, 3-alpha hydroxysteroid dehydrogenase, methionine-tRNA synthetase). Bile acids may be important regulators of gene expression in the liver and intestines. Bile acids have been shown to modulate a variety of cellular functions, such as secretion of lipoproteins from hepatocytes and translocation of bile acid transporters to the hepatocyte canalicular membrane[40-42]. Our results indicate that the HBV pre-S2 protein interact with the bile acid-binding protein, maybe it is a way that HBV affect cellular lipid metabolism. (3) The genes involving in the formation mechanism of hepatic fibrosis. alpha-2-macroglobulin (A2M) is a glycoprotein with high molecular weight, which can bind with different proteases, including interstitial collagenases and the other metalloproteases. A2M's proteinase inhibitor effect can inhibit the activity of collagenases, and participate the formation of hepatic fibrosis[43,44]. Laminin (LN) is a kind of serum fibrosis markers, during fibrogenesis LN continuously accumulate in liver tissues and form basement membrane resulting in sinusoidal capillaration[45], the stages of hepatic fibrosis are correlated with the serum levels of LN, so LN can be used in detecting the degree of hepatic fibrosis. The serum levels of LN were elevated from S1 to S4, because of the increase of hepatic fibrosis. Our data suggest that HBV pre-S2 protein may play a role in the progress of liver cirrhosis[46-48]. (4) The genes controlling cell signal transduction and apoptosis. Such as tyrosine 3-monooxygenase/tryptophan 5-monooxygenase activation protein, calmodulin 2, ras-related C3 botulinum toxin substrate 1 (rho family, small GTP binding protein Rac1) (RAC1), Phospholipase A2 (PLA2). PLA2 is a family of enzymes thought to play a key role in inflammation by releasing arachidonic acid for the synthesis of eicosanoids and lysophospholipid for the synthesis of platelet-activating factor and take part in different singaling pathways, including apoptosis and MAPKKK signaling cascade. CPLA2 (cytosolic phospholipase A2) is activated by MAP kinase due to a phosphorylation of serine residue 505[49].

Altogether, we testified the transactivator ability of HBV pre-S2 protein again, and obtained the subtractive cDNA library of genes transactivated by pre-S2 protein with SSH technique, successfully. Furthermore, we brought some new clues for studying the biological functions of HBV pre-S2 protein and and pave the way for elucidating the pathogenesis of HBV infection.

REFERENCES

1 **Shouval D**. Hepatitis B vaccines. *J Hepatol* 2003; **39**: S70-S76
2 **Humphries JC,** Dixon JS. Antivirals for the treatment of chronic hepatitis B: current and future options. *Intervirology* 2003; **46**: 413-420
3 **Colombo M,** Sangiovanni A. Etiology, natural history and treatment of hepatocellular carcinoma. *Antiviral Res* 2003; **60**: 145-150
4 **Gjorup IE,** Skinhoj P. New aspects on the natural history of chronic hepatitis B infection: implication for therapy. *Scand J Infect Dis* 2003; **35**: 808-813
5 **Dong J,** Cheng J, Wang Q, Shi S, Wang G, Si C. Cloning and analysis of the genomic DNA sequence of augmenter of liver regeneration from rat. *Chin Med Sci J* 2002; **17**: 63-67
6 **Fujioka S,** Shimomura H, Iwasaki Y, Fujio K, Nakagawa H, Onishi Y, Takagi S, Taniguchi H, Umeoka F, Nakajima H, Moriya A, Nanba K, Piao CY, Shinji T, Koide N, Shiratori Y. Hepatitis B virus gene in liver tissue promotes hepatocellular carcinoma development in chronic hepatitis C patients. *Dig Dis Sci* 2003; **48**: 1920-1924
7 **Dohmen K,** Shigematsu H, Irie K, Ishibashi H. Trends in clinical characteristics, treatment and prognosis of hepatocellular carcinoma. *Hepatogastroenterology* 2003; **50**: 1872-1877
8 **Blum HE.** Molecular therapy and prevention of hepatocellular carcinoma. *Hepatobiliary Pancreat Dis Int* 2003; **2**: 11-22
9 **Seeger C,** Mason WS. Hepatitis B virus biology. *Microbiol Mol Biol Rev* 2000; **64**: 51-68
10 **Beasley RP,** Hwang LY, Lin CC, Chien CS. Hepatocellular carcinoma and hepatitis B virus. A prospective study of 22 707 men in Taiwan. *Lancet* 1981; **2**: 1129-1133
11 **Murakami S.** Hepatitis B virus X protein: structure, function and biology. *Intervirology* 1999; **42**: 81-99
12 **Kekule AS,** Lauer U, Meyer M, Caselmann WH, Hofschneider PH, Koshy R. The preS2/S region of integrated hepatitis B virus DNA encodes a transcriptional transactivator. *Nature* 1990; **343**: 457-461
13 **Hildt E,** Saher G, Bruss V, Hofschneider PH. The hepatitis B virus large surface protein (LHBs) is a transcriptional activator. *Virology* 1996; **225**: 235-239
14 **Hildt E,** Urban S, Eckerskorn C, Hofschneider PH. Isolation of highly purified, functional carboxy-terminally truncated hepatitis B virus middle surface protein activators from eucaryotic expression systems. *Hepatology* 1996; **24**: 502-507
15 **Gerlich WH,** Lu X, Heermann KH. Studies on the attachment and penetration of hepatitis B virus. *J Hepatol* 1993; **17**: S10-S14
16 **Lu X,** Block TM, Gerlich WH. Protease-induced infectivity of hepatitis B virus for a human hepatoblastoma cell line. *J Virol* 1996; **70**: 2277-2285
17 **Cho EW,** Park JH, Yoo OJ, Kim KL. Translocation and accumulation of exogeneous hepatitis B virus preS surface proteins in the cell nucleus. *J Cell Sc* 2001; **114**: 1115-1123
18 **Sugauchi F,** Ohno T, Orito E, Sakugawa H, Ichida T, Komatsu M, Kuramitsu T, Ueda R, Miyakawa Y, Mizokami M. Influence of hepatitis B virus genotypes on the development of preS deletions and advanced liver disease. *J Med Virol* 2003; **70**: 537-544
19 **Kondo J,** Shimomura H, Fujioka S, Iwasaki Y, Takagi S,

Ohnishi Y, Tsuji H, Sakaguchi K, Yamamoto K, Tsuji T. Mutations in the hepatitis B virus preS2 region and abrogated receptor activity for polymerized human albumin. *Acta Med Okayama* 2002; **56**: 193-198

20 **Liu Y,** Cheng J, Shao DZ, Wang L, Zhong YW, Dong J, Li K, Li L. Synergetic transactivating effect of HCV core and HBV X proteins on SV40 early promoter/enhancer. *Zhonghua Shiyan He Linchuang Bingduxue Zazhi* 2003; **17**: 70-72

21 **Huangfu J,** Dong J, Deng H, Cheng J, Shi S, Hong Y, Ren X, Li L. A preliminary study on the heterogeneity of preS2 region in hepatitis B virus. *Zhonghua Neike Zazhi* 2002; **41**: 233-236

22 **Dong J,** Cheng J, Wang Q, Wang G, Shi S, Liu Y, Xia X, Si C. Cloning and sequence analysis of truncated S gene from circulation of patients with chronic hepatitis B virus infection. *Zhonghua Ganzangbing Zazhi* 2001; **9**: 163-165

23 **Borchani-Chabchoub I,** Mokdad-Gargouri R, Gargouri A. Glucose dependent [correction of dependant] negative translational control of the heterologous expression of the preS2 HBV antigen in yeast. *Gene* 2003; **311**: 165-170

24 **Soussan P,** Pol S, Garreau F, Brechot C, Kremsdorf D. Vaccination of chronic hepatitis B virus carriers with preS2/S envelope protein is not associated with the emergence of envelope escape mutants. *J Gen Virol* 2001; **82**: 367-371

25 **Park JH,** Lee MK, Kim HS, Kim KL, Cho EW. Targeted destruction of the polymerized human serum albumin binding site within the preS2 region of the HBV surface antigen while retaining full immunogenicity for this epitope. *J Viral Hepat* 2003; **10**: 70-79

26 **Borchani-Chabchoub I,** Gargouri A, Mokdad-Gargouri R. Genotyping of Tunisian hepatitis B virus isolates based on the sequencing of preS2 and S regions. *Microbes Infect* 2000; **2**: 607-612

27 **Tai PC,** Suk FM, Gerlich WH, Neurath AR, Shih C. Hypermodification and immune escape of an internally deleted middle-envelope (M) protein of frequent and predominant hepatitis B virus variants. *Virology* 2002; **292**: 44-58

28 **Hildt E,** Urban S, Hofschneider PH. Characterization of essential domains for the functionality of the MHBst transcriptional activator and identification of a minimal MHBst activator. *Oncogene* 1995; **11**: 2055-2066

29 **Bruss V,** Lu X, Thomssen R, Gerlich WH. Post-translational alterations in transmembrane topology of the hepatitis B virus large envelope protein. *EMBO J* 1994; **13**: 2273-2279

30 **Lauer U,** Weiss L, Hofschneider PH, Kekule AS. The hepatitis B virus pre-S/S(t) transactivator is generated by 3′ truncations within a defined region of the S gene. *J Virol* 1992; **66**: 5284-5289

31 **Schluter V,** Meyer M, Hofschneider PH, Koshy R, Caselmann WH. Integrated hepatitis B virus X and 3′ truncated preS/S sequences derived from human hepatomas encode functionally active transactivators. *Oncogene* 1994; **9**: 3335-3344

32 **Zhong S,** Chan JY, Yeo W, Tam JS, Johnson PJ. Hepatitis B envelope protein mutants in human hepatocellular carcinoma tissues. *J Viral Hepat* 1999; **6**: 195-202

33 **Hildt E,** Munz B, Saher G, Reifenberg K, Hofschneider PH. The PreS2 activator MHBs(t) of hepatitis B virus activates c-raf-1/Erk2 signaling in transgenic mice. *EMBO J* 2002; **21**: 525-535

34 **Hildt E,** Hofschneider PH. The PreS2 activators of the hepatitis B virus: activators of tumour promoter pathways. *Recent Results Cancer Res* 1998; **154**: 315-329

35 **Bock CT,** Tillmann HL, Manns MP, Trautwein C. The pre-S region determines the intracellular localization and appearance of hepatitis B virus. *Hepatology* 1999; **30**: 517-525

36 **Henkler F F,** Koshy R. Hepatitis B virus transcriptional activators: mechanisms and possible role in oncogenesis. *J Viral Hepat* 1996; **3**: 109-121

37 **Stockl L,** Berting A, Malkowski B, Foerste R, Hofschneider PH, Hildt E. Integrity of c-Raf-1/MEK signal transduction cascade is essential for hepatitis B virus gene expression. *Oncogene* 2003; **22**: 2604-2610

38 **Caselmann WH,** Meyer M, Kekule AS, Lauer U, Hofschneider PH, Koshy R. A trans-activator function is generated by integration of hepatitis B virus preS/S sequences in human hepatocellular carcinoma DNA. *Proc Natl Acad Sci USA* 1990; **87**: 2970-2974

39 **Su TS,** Hwang WL, Yauk YK. Characterization of hepatitis B virus integrant that results in chromosomal rearrangement. *DNA Cell Biol* 1998; **17**: 415-425

40 **Lin Y,** Havinga R, Schippers IJ, Verkade HJ, Vonk RJ, Kuipers F. Characterization of the inhibitory effects of bile acids on very-low-density lipoprotein secretion by rat hepatocytes in primary culture. *Biochem J* 1996; **316**: 531-538

41 **Lin Y,** Havinga R, Verkade HJ, Moshage H, Slooff MJ, Vonk RJ, Kuipers F. Bile acids suppress the secretion of very-low-density lipoprotein by human hepatocytes in primary culture. *Hepatology* 1996; **23**: 218-228

42 **Misra S,** Ujhazy P, Gatmaitan Z, Varticovski L, Arias IM. The role of phosphoinositide 3-kinase in taurocholate-induced trafficking of ATP-dependent canalicular transporters in rat liver. *J Biol Chem* 1998; **273**: 26638-26644

43 **Naveau S,** Poynard T, Benattar C, Bedossa P, Chaput JC. Alpha-2-macroglobulin and hepatic fibrosis. Diagnostic interest. *Dig Dis Sci* 1994; **39**: 2426-2432

44 **Lu LG,** Zeng MD, Wan MB, Li CZ, Mao YM, Li JQ, Qiu DK, Cao AP, Ye J, Cai X, Chen CW, Wang JY, Wu SM, Zhu JS, Zhou XQ. Grading and staging of hepatic fibrosis, and its relationship with noninvasive diagnostic parameters. *World J Gastroenterol* 2003; **9**: 2574-2578

45 **Xiao W,** Wang Y, Liu X. The coordinated expression of laminin and its integrin receptor in hepatic sinusoidal capillarization. *Zhonghua Neike Zazhi* 2001; **40**: 618-620

46 **Xu GG,** Luo CY, Wu SM, Wang CL. The relationship between staging of hepatic fibrosis and the levels of serum biochemistry. *Hepatobiliary Pancreat Dis Int* 2002; **1**: 246-248

47 **Castera L,** Hartmann DJ, Chapel F, Guettier C, Mall F, Lons T, Richardet JP, Grimbert S, Morassi O, Beaugrand M, Trinchet JC. Serum laminin and type IV collagen are accurate markers of histologically severe alcoholic hepatitis in patients with cirrhosis. *J Hepatol* 2000; **32**: 412-418

48 **Cai WM,** Tao J, Weng HL, Liu RH. Study on the influence factors of the serum fibrosis markers. *Zhonghua Ganzangbing Zazhi* 2003; **11**: 23-25

49 **Lindbom J,** Ljungman AG, Lindahl M, Tagesson C. Expression of members of the phospholipase A2 family of enzymes in human nasal mucosa. *Eur Respir J* 2001; **18**: 130-138

Science Editor Guo SY **Language Editor** Elsevier HK

PO Box 2345, Beijing 100023, China
www.wjgnet.com
wjg@wjgnet.com

ELSEVIER

World J Gastroenterol 2005;11(35):5444-5449
World Journal of Gastroenterology ISSN 1007-9327
© 2005 The WJG Press and Elsevier Inc. All rights reserved.

• *BASIC RESEARCH* •

Hepatic fibrosis in biliary-obstructed rats is prevented by *Ginkgo biloba* treatment

Göksel Şener, Levent Kabasakal, Meral Yüksel, Nursal Gedik, İnci Alican

Göksel Şener, Levent Kabasakal, Department of Pharmacology, Marmara University School of Pharmacy, Istanbul, Turkey
Meral Yüksel, Marmara University, Vocational School of Health Related Professions, Istanbul, Turkey
Nursal Gedik, Division of Biochemistry, Kasımpasa Military Hospital, Istanbul, Turkey
İnci Alican, Department of Physiology, School of Medicine, Marmara University, Istanbul, Turkey
Correspondence to: Göksel Şener, PhD, School of Pharmacy, Marmara University, Tıbbiye Cad. İstanbul 34668, Turkey. gokselsener@hotmail.com
Telephone: +90-216-41482962 Fax: +90-216-3452952
Received: 2005-01-15 Accepted: 2005-01-26

Abstract

AIM: To assess the antioxidant and antifibrotic effects of long-term *Ginkgo biloba* administration on liver fibrosis induced by biliary obstruction in rats.

METHODS: Liver fibrosis was induced in male Wistar albino rats by bile duct ligation and scission (BDL). *Ginkgo biloba* extract (EGb 761, 50 mg/kg·per d) or saline was administered for 28 d. At the end of the treatment period, all rats were killed. Serum aspartate aminotransferase (AST), alanine aminotransferase (ALT), and lactate dehydrogenase (LDH) levels were determined to assess liver functions and tissue damage, respectively. Tumor necrosis factor-α (TNF-α) was also assayed in serum samples. Liver tissues were taken for determination of the hepatic malondialdehyde (MDA) and glutathione (GSH) levels, myeloperoxidase (MPO) activity and collagen content. Production of reactive oxidants was monitored by chemiluminescence (CL) assay. Serum AST, ALT, LDH, and TNF-α levels were elevated in the BDL group as compared to control group and were significantly decreased by EGb treatment.

RESULTS: Hepatic GSH level, depressed by BDL, was elevated back to control level in EGb-treated BDL group. Increase in tissue MDA level, MPO activity and collagen content due to BDL were also attenuated by EGb treatment. Furthermore, luminol and lucigenin CL values in BDL group increased dramatically compared to control and reduced by EGb treatment.

CONCLUSION: Our results suggest that *Ginkgo biloba* protects the liver from oxidative damage following BDL in rats. This effect possibly involves the inhibition of neutrophil infiltration and lipid peroxidation; thus, restoration of oxidant and antioxidant status in the tissue.

© 2005 The WJG Press and Elsevier Inc. All rights reserved.

Key words: *Ginkgo biloba*; Bile duct ligation; Hepatic fibrosis; Oxidant

Şener G, Kabasakal L, Yüksel M, Gedik N, Alican İ. Hepatic fibrosis in biliary-obstructed rats is prevented by ginkgo biloba treatment. *World J Gastroenterol* 2005; 11(35): 5444-5449
http://www.wjgnet.com/1007-9327/11/5444.asp

INTRODUCTION

Hepatic fibrosis, which is usually initiated by hepatocyte damage, leads to recruitment of inflammatory cells and platelets, activation of Kupffer cells and subsequent release of cytokines and growth factors[1]. These factors probably link the inflammatory processes and oxygen free radicals, which are known to cause tissue fibrosis[2,3].

Accumulation of hydrophobic bile acids during cholestasis leads to generation of reactive oxygen free radicals in the liver[4,5]. Previous studies showed that hepatic mitochondria generate reactive oxygen species when isolated hepatocytes are exposed to hydrophobic bile acids[4,6]. Thus, mitochondrial free radical production may be an important mechanism of cholestatic liver injury and fibrosis[7-9]. Therapeutic attempts with anti-fibrotic drugs are still under investigation[10-12]. Disadvantages associated with anti-fibrotics are toxicity due to chronic administration and reduced therapeutic effect when used in clinical studies. Anti-fibrotics from natural sources may reduce the risk of toxicity and preserve therapeutic effectiveness in clinical usage[13-15].

An extract of the leaves of *Ginkgo biloba* L., a mixture mainly composed of flavonoid glycosides and terpenoides (ginkgolides and bilobalide), has been shown to exhibit a variety of pharmacological actions[16]. *Ginkgo biloba* extract has been reported to be a potent-free radical scavenger and an antioxidant. The leaf extract suppresses platelet aggregation induced by *tert*-butyl hydroperoxide and hydrogen peroxide through its antioxidant action[17]. Furthermore, the extract and its ingredients exhibit an antagonistic effect on platelet-activating factor[18], and inhibitory effect on the expression of inducible nitric oxide synthase and nitric oxide production[19]. They also provide protection in myocardial and brain ischemia/reperfusion injury[20,21].

In the light of these findings, in this study, we investigated the anti-fibrotic and antioxidant effects of *Ginkgo biloba* extract on oxidative damage and liver fibrosis in bile duct-ligated rats.

MATERIALS AND METHODS

Animals

Male Wistar albino rats (200-250 g) were housed in a room at a mean constant temperature of 22± 2 ℃ with a 12-h light-dark cycle, and free access to standard pellet chow and water. The study was approved by the Marmara University School of Medicine Animal Care and Use Committee.

Induction of liver fibrosis

Rats were anesthetized (100 mg/kg ketamine and 0.75 mg/kg chlorpromazine; ip) and the common bile duct was exposed and ligated by double ligatures with suture silk. The first ligature was made below the junction of the hepatic ducts and the second ligature was made above the entrance of the pancreatic ducts. Finally, the common bile duct was resected between the double ligatures[15]. In sham-operated rats, abdominal incision was made without a ligation.

Experimental groups

Ginkgo biloba extract was administered to control (EGb group) and bile duct ligated (BDL+EGb group) rats for 28 d at a daily dose of 50 mg/kg, ip. The sham-operated control (C) and BDL groups received equal amounts of saline for 28 d.

After 28 d of treatment, the rats were killed and trunk blood was collected. Serum samples were used for the measurement of aspartate aminotransferase (AST), alanine aminotransferase (ALT), lactic dehydrogenase (LDH), bilirubin and tumor necrosis factor (TNF)-α levels. Liver samples were taken and stored at -70 ℃ for the measurement of malondialdehyde (MDA) and glutathione (GSH) levels, myeloperoxidase (MPO) activity and collagen contents. Formation of reactive oxygen species in liver samples was monitored by using chemiluminescence (CL) method.

Determination of serum AST, ALT, LDH, bilirubin, and TNF-α levels

Serum AST and ALT levels - as indicators of liver function - and LDH activity - as a marker of tissue injury - were assessed by using commercial kits (Roche Diagnostics, GmbH, D-68298, Mannheim, Germany) in Roche-Hitachi Modular Autoanalyzer (Roche Diagnostics, GmbH, D-68298, Mannheim, Germany)[22]. Serum total bilirubin level was assayed on Bayer Opera Autoanalyzer according to a method described previously[23]. Serum TNF-α level was evaluated by a radioimmunoassay-immunoradiometricassay method by using a commercial kit (Biosource Europe S.A., Nivelles, Belgium). The activity of radioactive assays was measured by gamma counter (LKB WALLAC 1270 RACK Gamma Counter, Canada).

Measurement of liver MDA and GSH levels

Tissue samples were homogenized with ice-cold trichloroacetic acid (1 g tissue+10 mL 10% TCA) in an Ultra Turrax tissue homogenizer. The MDA levels were assayed for products of lipid peroxidation by monitoring thiobarbituric acid reactive substance formation as described previously[24]. Lipid peroxidation was expressed in terms of MDA equivalents using an extinction coefficient of 1.56×10^5 mol/(L·cm) and results were expressed as nanomole MDA per gram tissue. GSH was determined by a spectrophotometric method, which was based on the use of Ellman's reagent[25]. GSH levels were calculated using an extinction coefficient of 13 600 mol/(L·cm) and the results were expressed in micromole per gram tissue.

Measurement of liver myeloperoxidase (MPO) activity

Tissue samples (0.2-0.3 g) were homogenized in 10 volumes of ice-cold potassium phosphate buffer (50 mmol/L K_2HPO_4, pH 6.0) containing hexadecyltrimethylammonium bromide (HETAB, 5 g/L). The homogenate was centrifuged at 30 000 *g* for 10 min at 4 ℃, and the supernatant was discarded. The pellet was then rehomogenized with an equivalent volume of 50 mmol/L K_2HPO_4 containing 5 g/L HETAB and 10 mmol/L EDTA (Sigma). MPO activity was assessed by measuring the H_2O_2-dependent oxidation of *o*-dianizidine·2HCl. One unit of enzyme activity was defined as the amount of the MPO present per gram of tissue weight that caused a change in absorbance of 1.0 per min at 460 nm and 37 ℃[26].

Measurement of liver collagen content

Tissue samples were cut with a razor blade and immediately fixed in 40 g/L formaldehyde in 0.1 mol/L phosphate buffer (pH 7.2) in paraffin and sections of 15-μm thick were obtained. Collagen content was measured according to a method described by Lopez de Leon and Rojkind[27]. The method is based on selective binding of the dyes Sirius red and fast green FCF to collagen and noncollagenous components, respectively. Both dyes were eluted readily and simultaneously by using 0.1 N NaOH-methanol (1∶1, v/v). Finally, the absorbances at 540 and 605 nm were used to determine the amount of collagen and protein, respectively.

Chemiluminescence (CL) assay

Luminescence of the hepatic tissue samples was recorded at room temperature using Mini Lumat LB 9 506 luminometer (EG&G Berthold, Germany) in the presence of luminol or lucigenin, 0.2 mmol/L each. All counts were obtained at 15-s intervals for 5 min and the results were expressed as area under the curve of relative light unit (rlu) for 5 min/mg tissue[28].

Statistical analysis

Statistical analysis was carried out using GraphPad Prism 3.0 (GraphPad Software, San Diego, CA, USA). All data were expressed as mean±SE. Groups of data were compared with an analysis of variance (ANOVA) followed by Tukey's multiple comparison tests. Values of $P<0.05$ were regarded as significant.

RESULTS

As shown in Table 1, serum bilirubin, AST, ALT, and LDH levels were significantly higher in BDL rats compared to controls ($P<0.001$) and EGb administration to BDL group reduced these values ($P<0.001$). In untreated BDL group, serum TNF-α level showed a significant increase compared to that of the sham-operated control group ($P<0.001$). Similarly, BDL-induced rise in serum TNF-α level was significantly reduced by EGb treatment ($P<0.001$, Figure 1).

Table 1 Serum total bilirubin, AST, ALT, LDH and TNF-α levels in control (C), EGb, BDL and BDL+EGb groups

Groups	C (n = 8)	EGb (n = 8)	BDL (n = 8)	BDL+EGb (n = 8)
Total bilirubin (mg/dL)	0.36±0.3	0.35±0.6	10.1±0.6[d]	1.68±0.3[b,f]
AST (mg/dL)	148±16.6	150±12.4	300±18[d]	155±12[f]
ALT (mg/dL)	68±7.3	77±6.1	135±9.7[d]	67±5.7[f]
LDH (U/L)	1 672±240	1 499±219	5 082±225[d]	1 763±226[f]

[b]P<0.01, [d]P<0.001 *vs* control group. [f]P<0.001, *vs* untreated BDL group.

The liver MDA was found to be significantly higher in the BDL group (51.0±3.3 nmol/g; P<0.01) compared to that of the sham-operated control group (32.2±3.1 nmol/g). Treatment with EGb reversed the MDA level (33.8±2.6 nmol/g; P<0.01) back to control level (Figure 2).

The hepatic GSH level showed a marked reduction in the BDL group (0.88±0.07 μmol/g; P<0.001) compared to that of the sham-operated control group (2.1±0.15 μmol/g). Similarly, treatment with EGb reversed this effect (1.8±0.12 μmol/g; P<0.01) (Figure 3).

Liver MPO activity, which was observed to be higher in the BDL group (21.8±2.0 U/g; P<0.01) compared to sham-operated control group (13.8±1.3 U/g) was also attenuated by EGb treatment (13.3±0.7 U/g; P<0.01) (Figure 4).

Hepatic collagen content of the untreated BDL rats (21.3±2.1 μg/mg protein; P<0.01) was found to be significantly higher than that of the control group (12.8±1.4 μg/mg protein). EGb treatment significantly reduced the increase in hepatic collagen content (13.2±1.2 μg/mg protein; P<0.05) to the levels that were close to control values (Figure 5).

Luminol and lucigenin CL values of the liver samples of the BDL group (18.7±1.1 and 38.3±3.2 rlu/mg, respectively) were found to be significantly higher than those of the control group (11.1±1.0 and 14.8±1.1 rlu/mg; P<0.01 and P<0.001, respectively) and EGb treatment reversed these values (12.5±2.0 and 16.1±2.6 rlu/mg; P<0.05 and P<0.001, respectively) (Figures 6 and 7).

DISCUSSION

The present study demonstrates that EGb treatment improved BDL-induced impairment in liver functions and decreased BDL-induced elevations in serum LDH activity and TNF-α levels. Furthermore, increase in hepatic lipid peroxidation, MPO activity, oxidant production and collagen content, and

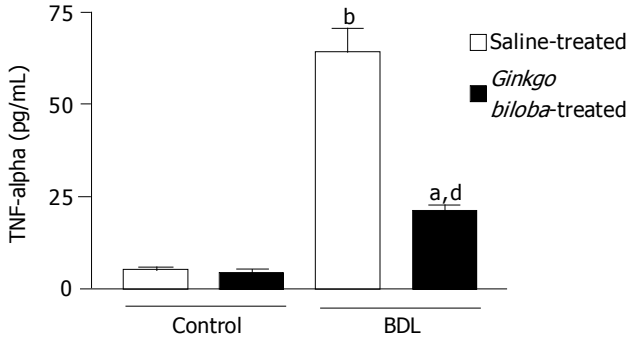


Figure 1 Serum TNF-α levels of the control, *Ginkgo-biloba*-treated, saline-treated BDL and *Ginkgo-biloba*-treated BDL groups. [a]P<0.05, [b]P<0.001 *vs* control; [d]P<0.001 *vs* saline-treated BDL group.

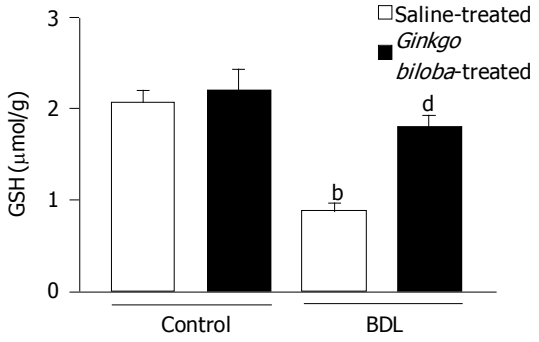


Figure 3 Liver GSH levels of the control, *Ginkgo-biloba*-treated, saline-treated-BDL, and *Ginkgo-biloba*-treated BDL groups. [b]P<0.001 *vs* control; [d]P<0.001 *vs* saline-treated BDL group.

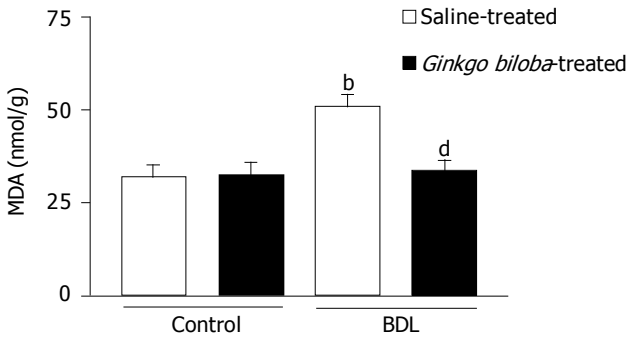


Figure 2 Liver MDA levels of the control, *Ginkgo-biloba*-treated, saline-treated-BDL, and *Ginkgo-biloba*-treated BDL groups. [b]P<0.01 *vs* control; [d]P<0.01 *vs* saline-treated BDL group.

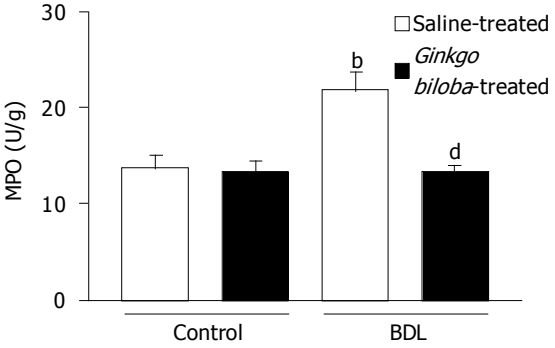


Figure 4 Liver MPO activities of the control, *Ginkgo-biloba*-treated, saline-treated BDL, and *Ginkgo-biloba*-treated BDL groups. [b]P<0.01 *vs* control; [d]P<0.01 *vs* saline-treated BDL group.

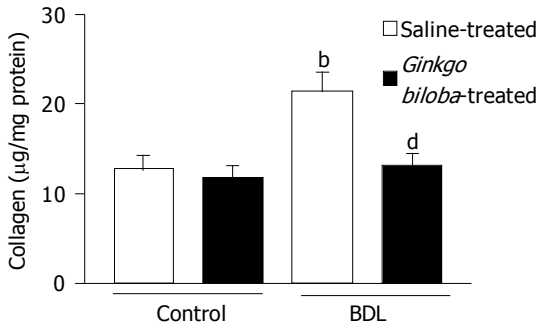


Figure 5 Liver collagen levels of the control, *Ginkgo-biloba*-treated, saline-treated-BDL, and *Ginkgo-biloba*-treated BDL groups. $^{b}P<0.01$ *vs* control; $^{d}P<0.01$ *vs* saline-treated BDL group.

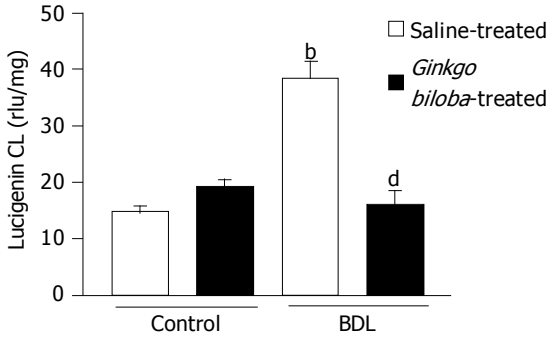


Figure 7 Liver lucigenin CL values of the control, *Ginkgo-biloba*-treated, saline-treated BDL, and *Ginkgo-biloba*-treated BDL groups. $^{b}P<0.001$ *vs* control; $^{d}P<0.001$ *vs* saline-treated BDL group.

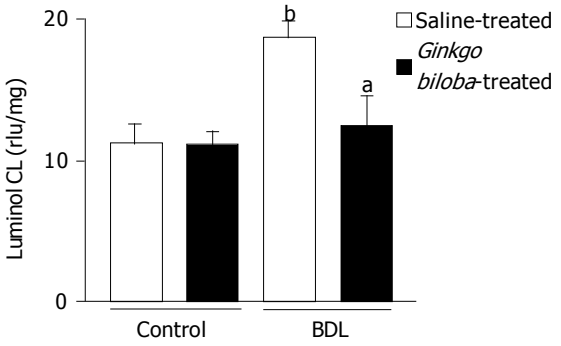


Figure 6 Liver luminol CL values of the control, *Ginkgo-biloba*-treated, saline-treated BDL, and *Ginkgo-biloba*-treated BDL groups. $^{a}P<0.05$ *vs* saline-treated BDL group; $^{b}P<0.01$ *vs* control.

decrease in GSH levels following BDL were reversed by EGb treatment.

Hepatic fibrosis, characterized by an increased production and deposition of extracellular matrix component accompanies most chronic liver disorders and its presence is a major factor contributing to hepatic failure[29,30]. Although the mechanism of liver fibrosis is not fully understood, activated hepatic stellate cells play an important role in connective tissue synthesis and deposition during fibrogenesis[12]. On the other hand, oxidative stress caused by accumulation of hydrophobic bile acids also have a critical role in fibrogenesis[3,31].

Bile duct ligation (BDL) induces a type of liver fibrosis, which etiologically and pathogenitically resembles the biliary fibrosis in the human beings. Injury to hepatocytes results in the generation of lipid peroxides, which may have a direct stimulatory effect on matrix production by activated stellate cells[8,32]. Liu *et al.*, demonstrated excessive production of superoxide radicals and hydroxyl radicals in blood and liver in rats with obstructive jaundice induced by common BDL[33]. In the present study, BDL caused significant increases in the hepatic MDA level -end product of lipid peroxidation - and EGb treatment prevented the increase in MDA, probably in part by scavenging the very reactive hydroxyl and peroxyl radicals. Moreover, attenuation of the increase in hepatic luminol- and lucigenin-enhanced CL levels by EGb treatment in BDL animals also supports the scavenging ability of the agent.

An extract of the leaves of *Ginkgo biloba L.*, a mixture mainly composed of flavonoid glycosides and terpenoides (ginkgolides and bilobalide), has been shown to exhibit a variety of pharmacological actions. The leaf extract acts as a scavenger of reactive oxygen species, that is, superoxide radical, peroxyl radical and nitric oxide[34-36]. It has been reported that the extract suppresses platelet aggregation induced by *tert*-butyl hydroperoxide and hydrogen peroxide through its antioxidant action[17]. Moreover, the extract and its ingredients (especially ginkgolide C) exhibit a potent antagonistic effect on platelet-activating factor and inhibitory effects on the expression of inducible nitric oxide synthase as well as nitric oxide production[18,19,37,38]. It decreased ethanol- or cold stress-induced gastric injury, protected against cerulein-induced acute pancreatitis and hepatic damage evoked by CCl_4 in the rat[39-42]. It has also been demonstrated that EGb has protective effects on aging liver. Thus, these effects suggest that EGb is beneficial in various cardiovascular, cerebrovascular, and neurological disorders in which oxidants are involved.

GSH, a key antioxidant, is an important constituent of intracellular protective mechanisms against various noxious stimuli, including oxidative stress. On the other hand, reduced GSH, which constitutes the main component of endogenous non-protein sulfhydryl pool, is known to be a major low molecular weight scavenger of free radicals in the cytoplasm[43]. Because of their exposed sulfhydryl groups, non-protein sulfhydryls bind a variety of electrophilic radicals and metabolites that may be damaging to the cells[44]. Huang *et al.*, studied the mitochondrial functions in bile duct-ligated rats and suggested that biochemical and molecular changes are related to oxidative stress in the liver[45]. In accordance with the previous reports, our results also support the notion that depletion of tissue GSH, as observed in the BDL-induced hepatic injury, is one of the major factors that permit lipid peroxidation and subsequent tissue damage. Since administration of *Ginkgo biloba* extract prevented the hepatic GSH depletion, it appears that the protective effect of the extract involves the maintenance of antioxidant capacity in protecting the hepatic tissue against oxidative stress.

Excessive production of hydroxyl radicals in blood and liver has previously been demonstrated by Liu *et al.*, in rats with obstructive jaundice induced by common BDL[33]. It has been demonstrated by various investigators that circulating

proinflammatory cytokines, such as TNF-α, interleukin-1-β (IL-1β) and IL-6, which trigger hepatic injury, were increased, at least in part, by a free radical-mediated apoptotic mechanism. Therefore, it seems reasonable to propose that antioxidants or free radical scavengers counteract the oxidant stress produced by cholestasis. In our study, increased TNF-α levels of BDL rats tended to decrease following the treatment by EGb, also supports the notion that EGb ameliorates oxidative liver injury caused by BDL through its antioxidant effect.

Observations suggest that reactive oxygen metabolites (ROM) play a role in the recruitment of neutrophils into damaged tissue, but activated neutrophils are also a potential source of ROM[46,47]. Although it is not certain whether neutrophil accumulation and activation are the causes or the results of injury, increasing evidence suggests that mesangial cells and neutrophils release chemotactic substances (e.g., IL-8), which further promote neutrophil migration and activation[48]. Several methods have been used to define the role of neutrophils in the tissue injury. MPO, which is an essential enzyme for normal neutrophil function, is released as a response to various stimulatory substances[49]. In the present study, increased hepatic MPO activity due to BDL, which indicates that tissue injury involves the contribution of neutrophil infiltration, was effectively reversed by EGb treatment. Moreover, BDL-induced increase in fibrotic activity, as assessed by hepatic collagen content, was also reduced by EGb treatment. These findings suggest that EGb has an additional protective effect on inflammation-induced production and deposition of extracellular matrix components, which result in hepatic fibrosis.

In conclusion, the findings of our present study demonstrate that *Ginkgo biloba* extract, with its potent free radical scavenging and antioxidant properties, seems to be a highly promising agent in protecting hepatic tissue against oxidative damage and in preventing hepatic fibrosis and dysfunction due to obstructive jaundice.

REFERENCES

1 **Kullak-Ublick GA,** Meier PJ. Mechanisms of cholestasis. *Clin Liver Dis* 2000; **4**: 357-385
2 **Bruck R,** Shirin H, Aeed H, Matas Z, Hochman A, Pines M, Avni Y. Prevention of hepatic cirrhosis in rats by hydroxyl radical scavengers. *J Hepatol* 2001; **35**: 457-464
3 **Zhong Z,** Froh M, Lehnert M, Schoonhoven R, Yang L, Lind H, Lemasters JJ, Thurman RG. Polyphenols from Camellia sinenesis attenuate experimental cholestasis-induced liver fibrosis in rats. *Am J Physiol Gastrointest Liver Physiol* 2003; **285**: G1004-1013
4 **Sokol RJ,** Winklhofer-Roob BM, Devereaux MW, McKim JM. Generation of hydroperoxides in isolated rat hepatocytes and hepatic mitochondria exposed to hydrophobic bile acids. *Gastroenterology* 1995; **109**: 1249-1256
5 **Orellana M,** Rodrigo R, Thielemann L, Guajardo V. Bile duct ligation and oxidative stress in the rat: effects in liver and kidney. *Comp Biochem Physiol C Toxicol Pharmacol* 2000; **126**: 105-111
6 **Pastor A,** Collado PS, Almar M, Gonzales-Gallego J. Antioxidant enzyme status in biliary obstructed rats:effects of N-acetylcysteine. *J Hepatol* 1997; **27**: 363-370
7 **Sokol RJ,** Devereaux MW, Khandwala R. Effect of oxypurinol, a xanthine oxidase inhibitor, on hepatic injury in the bile duct-ligated rat. *Pediatr Res* 1998; **44**: 397-401
8 **Serviddio G,** Pereda J, Pallardo FV, Carretero J, Borras C, Cutrin J, Vendemiale G, Poli G, Vina J, Sastre J. Ursodeoxycholic acid protects against secondary biliary cirrhosis in rats by preventing mitochondrial oxidative stress. *Hepatology* 2004; **39**: 711-720
9 **Yang S,** Tan TM, Wee A, Leow CK. Mitochondrial respiratory function and antioxidant capacity in normal and cirrhotic livers following partial hepatectomy. *Cell Mol Life Sci* 2004; **61**: 220-229
10 **Park EJ,** Ko G, Kim J, Sohn DH. Antifibrotic effects of a polysaccharide extracted from Ganoderma lucidum, glycyrrhizin, and pentoxifylline in rats with cirrhosis induced by biliary obstruction. *Biol Pharm Bull* 1997; **20**: 417-420
11 **Park EJ,** Nan JX, Kim JY, Kang HC, Choi JH, Lee SJ, Lee BH, Kim SJ, Lee JH, Kim YC, Sohn DH. The ethanol-soluble part of a hot-water extract from Artemisia iwayomogi inhibits liver fibrosis induced by carbon tetrachloride in rats. *J Pharm Pharmacol* 2000; **52**: 875-881
12 **Nan JX,** Park EJ, Kim HJ, Ko G, Sohn DH. Antifibrotic effects of the methanol extract of Polygonum aviculare in fibrotic rats induced by bile duct ligation and scission. *Biol Pharm Bull* 2000; **23**: 240-243
13 **Wasser S,** Ho JM, Ang HK, Tan CE. Salvia miltiorrhiza reduces experimentally-induced hepatic fibrosis in rats. *J Hepatol* 1998; **29**: 760-771
14 **Li D,** Friedman SL. Liver fibrogenesis and the role of hepatic stellate cells: new insights and prospects for therapy. *J Gastroenterol Hepatol* 1999; **14**: 618-633
15 **Shimizu I,** Ma YR, Mizobuchi Y, Liu F, Miura T, Nakai Y, Yasuda M, Shiba M, Horie T, Amagaya S, Kawada N, Hori H, Ito S. Effects of Sho-saiko-to, a Japanese herbal medicine, on hepatic fibrosis in rats. *Hepatology* 1999; **29**: 149-160
16 **van Beek TA.** Chemical analysis of Ginkgo biloba leaves and extracts. *J Chromatogr A* 2002; **967**: 21-55
17 **Akiba S,** Kawauchi T, Oka T, Hashizume T, Sato T. Inhibitory effect of the leaf extract of *Ginkgo biloba* L. on oxidative stress-induced platelet aggregation. *Biochem Mol Biol Int* 1998; **46**: 1243-1248
18 **Lamant V,** Mauco G, Braquet P, Chap H, Douste-Blazy L. Inhibition of the metabolism of platelet activating factor (PAF-acether) by three specific antagonists from Ginkgo biloba. *Biochem Pharmacol* 1987; **36**: 2749-2752
19 **Kobuchi H,** Droy-Lefaix MT, Christen Y, Packer L. Ginkgo biloba extract (EGb 761): inhibitory effect on nitric oxide production in the macrophage cell line RAW 264.7. *Biochem Pharmacol* 1997; **53**: 897-903
20 **Shen J,** Wang J, Zhao B, Hou J, Gao T, Xin W. Effects of EGb 761 on nitric oxide and oxygen free radicals, myocardial damage and arrhythmia in ischemia-reperfusion injury *in vivo*. *Biochim Biophys Acta* 1998; **1406**: 228-236
21 **Hu B,** Sun S, Mei G, Chen L, Tong E. Protective effects of Ginkgo biloba extract on rats during cerebral ischemia/reperfusion. *Chin Med J* 2002; **115**: 1316-1320
22 **Martinek RG.** A rapid ultraviolet spectrophotometric lactic dehydrogenase assay. *Clin Chim Acta* 1972; **40**: 91-99
23 **Winsten S,** Cehelyk B. A rapid micro diazo technique for measuring total bilirubin. *Clin Chim Acta* 1969; **25**: 441-446
24 **Buege JA,** Aust SD. Microsomal lipid peroxidation. *Methods Enzymol* 1978; **52**: 302-311
25 **Beutler E.** Glutathione in red blood cell metabolism. A Manual of Biochemical Methods, Grune & Stratton, *New York* 1975: 112-114
26 **Hillegass LM,** Griswold DE, Brickson B, Albrightson-Winslow C. Assessment of myeloperoxidase activity in whole rat kidney. *J Pharmacol Methods* 1990; **24**: 285-295
27 **Lopez De Leon A,** Rojkind M. A simple micromethod for collagen and total protein determination in formalin-fixed paraffin-embedded sections. *J Histochem Cytochem* 1985; **33**: 737-743
28 **Haklar G,** Özveri ES, Yüksel M, Aktan AÖ, Yalçin AS. Different kinds of reactive oxygen and nitrogen species were detected in colon and breast tumors. *Cancer Lett* 2001; **165**: 219-224
29 **Fort J,** Oberti F, Pilette C, Veal N, Gallois Y, Douay O, Rousselet MC, Resenbaum J, Cales P. Antifibrotic and he-

modynamic effects of the early and chronic administration of octreotide in two models of liver fibrosis in rats. *Hepatology* 1998; **28**: 1525-1531

30 **Friedman SL.** Liver fibrosis-from bench to bedside. *J Hepatol* 2003; **38**(Suppl 1): S38-S53

31 **Muriel P,** Moreno MG. Effects of silymarin and vitamins E and C on liver damage induced by prolonged biliary obstruction in the rat. *Basic Clin Pharmacol Toxicol* 2004; **94**: 99-104

32 **Lee KS,** Buck M, Houglum K, Chojkier M. Activation of hepatic stellate cells by TGF alpha and collagen type I is mediated by oxidative stress through c-myb expression. *J Clin Invest* 1995; **96**: 2461-2468

33 **Liu TZ,** Lee KT, Chern CL, Cheng JT, Stern A, Tsai LY. Free radical-triggered hepatic injury of experimental obstructive jaundice of rats involves overproduction of proinflammatory cytokines and enhanced activation of nuclear factor kappaB. *Ann Clin Lab Sci* 2001; **31**: 383-390

34 **Pincemail J,** Dupuis M, Nasr C, Hans P, Haag-Berrurier M, Anton R, Deby C. Superoxide anion scavenging effect and superoxide dismutase activity of Ginkgo biloba extract. *Experientia* 1989; **45**: 708-712

35 **Maitra I,** Marcocci L, Droy-Lefaix MT, Packer L. Peroxyl radical scavenging activity of Ginkgo biloba extract EGb 761. *Biochem Pharmacol* 1995; **49**: 1649-1655

36 **Marcocci L,** Maguire JJ, Droy-Lefaix MT, Packer L. The nitric oxide-scavenging properties of Ginkgo biloba extract EGb 761. *Biochem Biophys Res Commun* 1994; **201**: 748-755

37 **Cheung F,** Siow YL, Chen WZ, O K. Inhibitory effect of Ginkgo biloba extract on the expression of inducible nitric oxide synthase in endothelial cells. *Biochem Pharmacol* 1999; **58**: 1665-1673

38 **Cheung F,** Siow YL, O K. Inhibition by ginkgolides and bilobalide of the production of nitric oxide in macrophages (THP-1) but not in endothelial cells (HUVEC). *Biochem Pharmacol* 2001; **61**: 503-510

39 **Wang Q,** Zhao WZ, Ma CG. Protective effects of Ginkgo biloba extract on gastric mucosa. *Acta Pharmacol Sin* 2000; **21**: 1153-1156

40 **Soybir G,** Koksoy F, Ekiz F, Yalcin O, Fincan K, Haklar G, Yuksel M. The effects of free oxygen radical scavenger and platelet-activating factor antagonist agents in experimental acute pancreatitis. *Pancreas* 1999; **19**: 143-149

41 **Ozenirler S,** Dincer S, Akyol G, Ozogul C, Oz E. The protective effect of Ginkgo biloba extract on CCl4-induced hepatic damage. *Acta Physiol Hung* 1997-1998; **85**: 277-285

42 **Luo YJ,** Yu JP, Shi ZH, Wang L. Ginkgo biloba extract reverses CCl4-induced liver fibrosis in rats. *World J Gastroenterol* 2004; **10**: 1037-1042

43 **Ross D.** Glutathione, free radicals and chemotherapeutic agents. Mechanisms of free-radical induced toxicity and glutathione-dependent protection. *Pharmacol Ther* 1988; **37**: 231-249

44 **Szabo S,** Nagy L, Plebani M. Glutathione, protein sulfhydryls and cysteine proteases in gastric mucosal injury and protection. *Clin Chim Acta* 1992; **206**: 95-105

45 **Huang YT,** Hsu YC, Chen CJ, Liu CT, Wei YH. Oxidative-stress-related changes in the livers of bile-duct-ligated rats. *J Biomed Sci* 2003; **10**: 170-178

46 **Zimmerman BJ,** Grisham MB, Granger DN. Role of oxidants in ischemia-reperfusion induced granulocyte infiltration. *Am J Physiol* 1990; **258**: G185-G190

47 **Granger DN,** Korthuis RJ. Physiologic mechanisms of postischemic tissue injury. *Annu Rev Physiol* 1995; **57**: 311-332

48 **Donnahoo KK,** Meng X, Ayala A, Cain MP, Harken AH, Meldrum DR. Early kidney TNF-α expression mediates neutrophil infiltration and injury after renal ischemia-reperfusion. *Am J Physiol* 1999; **277**: R922-929

49 **Winterbourn CC,** Kettle AJ. Biomarkers of myeloperoxidase-derived hypochlorous acid. *Free Radic Biol Med* 2000; **29**: 403-409

Science Editor Guo SY **Language Editor** Elsevier HK

PO Box 2345, Beijing 100023, China
www.wjgnet.com
wjg@wjgnet.com

ELSEVIER

World J Gastroenterol 2005;11(35):5450-5454
World Journal of Gastroenterology ISSN 1007-9327
© 2005 The WJG Press and Elsevier Inc. All rights reserved.

• *BASIC RESEARCH* •

KL-6 mucin expression in carcinoma of the ampulla of Vater: Association with cancer progression

Wei Tang, Yoshinori Inagaki, Norihiro Kokudo, Qian Guo, Yasuji Seyama, Munehiro Nakata, Hiroshi Imamura, Keiji Sano, Yasuhiko Sugawara, Masatoshi Makuuchi

Wei Tang, Norihiro Kokudo, Qian Guo, Yasuji Seyama, Hiroshi Imamura, Keiji Sano, Yasuhiko Sugawara, Masatoshi Makuuchi, Hepato-Biliary-Pancreatic Surgery Division, Department of Surgery, Graduate School of Medicine, the University of Tokyo, 7-3-1 Hongo, Bunkyo-ku, Tokyo 113-8655, Japan
Yoshinori Inagaki, Department of Applied Biochemistry, Tokai University, Hiratsuka, Kanagawa 259-1292, Japan
Munehiro Nakata, Department of Applied Biochemistry and Institute of Glycotechnology, Tokai University, Hiratsuka, Kanagawa 259-1292, Japan
Supported by Grants-in-aid From the Ministry of Education, Science, Sports, and Culture of Japan and a grant for Hi-Tech Research from Tokai University
Correspondence to: Dr. Wei Tang, Hepato-Biliary-Pancreatic Surgery Division, Department of Surgery, Graduate School of Medicine, the University of Tokyo, 7-3-1 Hongo, Bunkyo-ku, Tokyo 113-8655, Japan. tang-sur@h.u-tokyo.ac.jp
Telephone: +81-3-5800-8654 Fax: +81-3-5684-3989
Received: 2005-03-01 Accepted: 2005-04-09

Abstract

AIM: To assess histochemical expression of KL-6 and its clinicopathological significance in carcinoma of the ampulla of Vater.

METHODS: Ampullary carcinoma tissues were collected from 38 patients who underwent pancreatoduodenectomy or local resection. Tissues were subjected to immunohistochemical analysis using KL-6 antibody.

RESULTS: Positive staining of ampullary carcinoma cells was observed in 26 (68.4%) cases. Staining was not found in the surrounding non-cancer regions of the ampullary tissues. Remarkable KL-6 expression was observed in invasive carcinoma cells in pancreatic and duodenal tissues and in metastatic carcinoma cells in lymph nodes. Positive KL-6 expression was related to lymph node metastasis (P = 0.020), pancreatic invasion (P = 0.016), duodenal invasion (P = 0.034), and advanced stage of TNM clinical classification (P = 0.010). Survival analysis showed that positive expression of KL-6 was related to a poorer prognosis (P = 0.029).

CONCLUSION: The aberrant expression of KL-6 mucin is significantly related to unfavorable behaviors of carcinoma of the ampulla of Vater.

© 2005 The WJG Press and Elsevier Inc. All rights reserved.

Key words: KL-6 mucin; Carcinoma of the ampulla of Vater; Invasion; Metastasis; Prognosis

Tang W, Inagaki Y, Kokudo N, Guo Q, Seyama Y, Nakata M, Imamura H, Sano K, Sugawara Y, Makuuchi M. KL-6 mucin expression in carcinoma of the ampulla of Vater: Association with cancer progression. *World J Gastroenterol* 2005; 11 (35): 5450-5454
http://www.wjgnet.com/1007-9327/11/5450.asp

INTRODUCTION

Carcinoma of the ampulla of Vater is a malignancy with a low incidence[1]. Although the prognosis for patients with this cancer is higher than that for patients with cancer arising within the pancreas or common bile duct, the 5-year survival rate after resection is less than 50%[2,3]. Therefore, the mechanism for development of this cancer must be understood to improve the patient's prognosis.

Cell surface sialylation changes dramatically during oncogenesis[4-6]. In several tumors, histochemical studies with sialic acid-binding lectins and antibodies against sialylated carbohydrate antigens showed that aberrant expression of sialylated glycoconjugates may play an important role in tumor progression[7-10]. However, the natures of these glycoconjugates and their clinical application are not yet known.

KL-6 is a type of MUC1 mucin, recognized by a murine mAb, KL-6 antibody, as obtained by Kohno *et al*., from a hybridoma established from the splenocytes of a BALB/c mouse immunized with a human pulmonary adenocarcinoma cell line, VMRC-LCR[11,12]. The epitope recognized by the KL-6 antibody exists in sialylated carbohydrate moieties of the mucin molecule, and this sialylation is essential to the recognition by the KL-6 antibody[12].

Histochemical expression of KL-6 has been observed in malignant tissues in several organs[11,12]. However, little is known about the expression profile and clinical significance of KL-6 in carcinoma of the ampulla of Vater. With due consideration to the importance of sialylation of glycoconjugates in tumor behavior, and that the epitope of KL-6 antibody is a sialylated carbohydrate, investigation of the expression profile of KL-6 in carcinoma of the ampulla of Vater will yield significant pointers in clarification of the mechanisms involved in the development of this cancer. In this study, we performed histochemical analysis of KL-6 in ampullary carcinoma tissues and examined the relationship between KL-6 expression and clinicopathological parameters in carcinoma of the ampulla of Vater.

MATERIALS AND METHODS

Patients

Ampullary carcinoma tissues were collected from 38 patients (22 males and 16 females; median age of 68 years; range of 54-85 years) surgically treated at the Hepato-Biliary-Pancreatic Surgery Division, Department of Surgery, Graduate School of Medicine, the University of Tokyo, between April 1976 and December 2002. All of the patients except one underwent pancreatoduodenectomy, whereas one patient underwent local resection. The size of the tumors varied from 1.0 to 7.5 cm (2.4±1.3 cm, mean±SD). Histopathological examination was performed according to the guidelines of the Japanese Society of Biliary Surgery[13]. The TNM staging system of the International Union Against Cancer was used for TNM classification[14].

Immunohistochemistry

Five-mircometer-thick sections were cut from archival formalin-fixed paraffin-embedded tissue blocks, deparaffinized, and dehydrated through a graded series of ethanol. Endogenous peroxidase activity was quenched with 0.3% hydrogen peroxide/methanol. The sections were incubated at 4 ℃ overnight with KL-6 antibody (Eisai, Tokyo, Japan) diluted to 1:150. The sections were then incubated with biotinylated anti-mouse antibody for 30 min at room temperature followed by development with the biotin-streptavidin-peroxidase complex method, using a commercial kit as per the manufacturer's instructions (Vectastain ABC Elite kit; Vector, Burlingame, CA, USA). 3,3'-Diaminobenzidine was used as the chromogen, and hematoxylin was used as a counterstain. Each tissue sample was microscopically analyzed over its entire area to determine histopathological characteristics. The percentage of cancer cells that were stained of the total number of cancer cells was determined in 10 random microscopic fields of each tissue sample, or using the entire area, if the tissue sample comprised less than 10 fields (magnification ×200). Cases in which more than 10% carcinoma cells were stained were defined as positive.

Statistical analysis

The χ^2 test was used to evaluate the relationship between KL-6 expression and clinicopathological parameters. Survival curves were calculated by the Kaplan-Meier method and compared with results of the log rank test. Differences of $P<0.05$ were considered significant. Statview 5.0J (Abacus Concepts, Berkeley, CA, USA) statistical software was used for data analysis.

RESULTS

Immunohistochemistry

Figure 1 shows immunohistochemical analysis of ampullary carcinoma tissues using KL-6 antibody. Positive staining was observed in 26 (68.4%) of 38 cases. The population of KL-6-positive tumor cells in the cancer regions varied among the samples (mean 49.2%, range 17.0-84.0%). The staining was localized in the tumor-cell cytoplasm and cell membrane in cancer regions (Figure 1A), whereas staining was not detected in the surrounding non-cancer regions of the ampullary tissues. In some cases, the stained materials were also detected along the inner surfaces of glands (Figure 1B). On the other hand, in 12 of 38 cases (31.6%), stained cells were scarce (Figure 1C).

Immunohistochemical analysis was focused on pancreatic and duodenal tissues showing pathological invasion of the ampullary carcinoma cells (Figure 2). Strongly stained carcinoma cells were frequently observed in the invaded areas of pancreatic tissues (Figure 2A), whereas only weak staining was sporadically observed in the surrounding normal pancreatic tissues (Figure 2B). Similarly, strongly stained carcinoma cells were frequently observed in the invaded areas of duodenal tissues (Figure 2C), whereas the surrounding normal duodenal epithelium was scarcely stained by KL-6 antibody (Figure 2D).

In all of the metastatic lymph node tissues tested, strong staining was found in carcinoma cells, whereas staining was not found in the surrounding normal tissues (Figure 3). Staining was not found in metastatic negative lymph node tissues (data not shown).

Clinicopathological and survival characteristics

The relationship between KL-6 expression and clinicopathological characteristics of tumors was examined. As shown in Table 1, positive KL-6 expression was significantly frequent in cases of lymph node metastasis than those without it ($P = 0.020$), in cases of pancreatic invasion than those without it ($P = 0.016$), in cases of duodenal invasion than

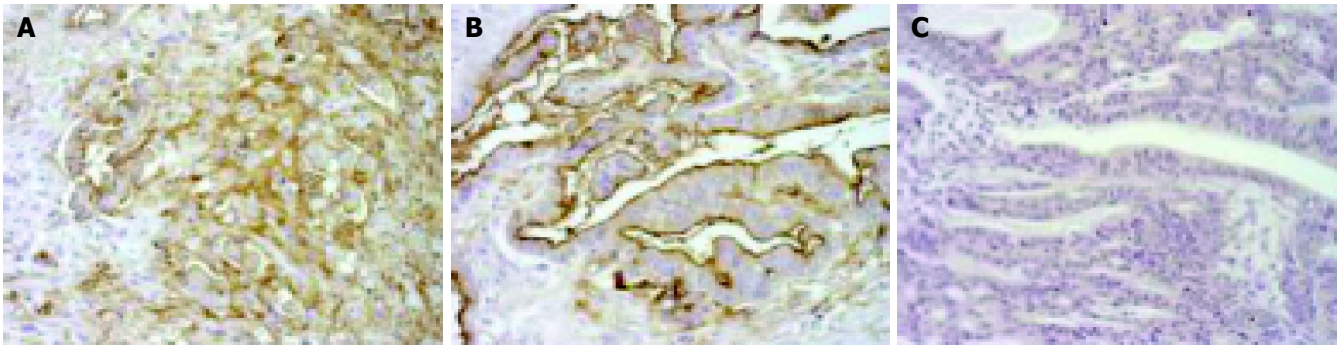


Figure 1 Immunohistochemical stain of the ampullary carcinoma tissues using KL-6 antibody. **A**: A typical example showing moderately positive staining; **B**: a typical example showing the moderately positive staining of inner surface of glands; **C**: a typical example in which stained cells are scarcely observed. Original magnification ×200.

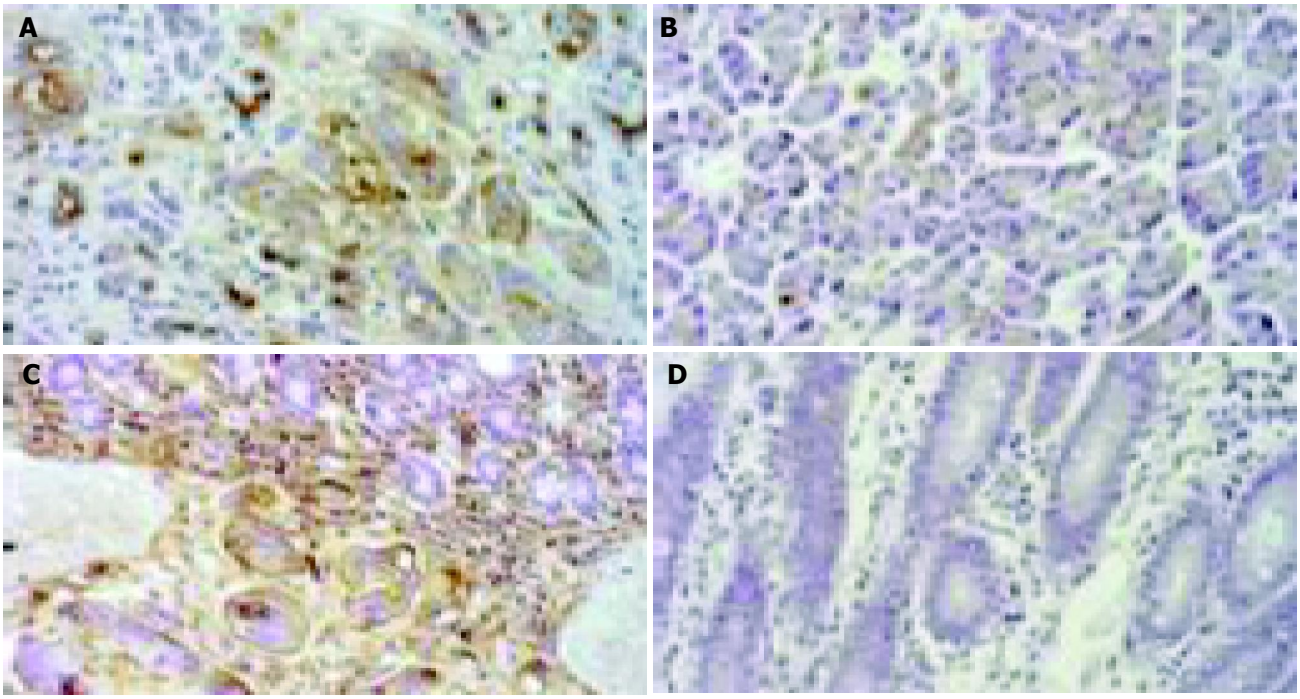


Figure 2 Immunohistochemical stain of KL-6 in invasive area of tumor. **A**: Area of pancreatic tissue invaded by carcinoma; **B**: normal pancreatic tissue; **C**: area of duodenal tissue invaded by carcinoma; **D**: normal duodenal tissue. Original magnification ×200.

Table 1 Relationship between KL-6 expression and clinicopathological parameters in patients with carcinoma of the ampulla of Vater

Parameters	*n*	Positive KL-6 expression (*n* = 26; %)	*P*
Age (yr)			
⩾65	24	14 (58.3)	
<65	14	12 (85.7)	0.080
Sex			
Male	22	16 (72.7)	
Female	16	10 (62.5)	0.503
Histological grade			
Well differentiated	31	22 (71.0)	
Moderately differentiated	4	3 (75.0)	
Poorly differentiated	3	1 (33.3)	0.390
Lymphatic vessel invasion			
Present	23	18 (78.3)	
Absent	15	8 (53.3)	0.106
Lymph node metastasis			
Present	23	19 (82.6)	
Absent	15	7 (46.7)	0.020
Venous invasion			
Present	17	14 (82.4)	
Absent	21	12 (57.1)	0.096
Pancreatic invasion			
Present	26	21 (80.8)	
Absent	12	5 (41.7)	0.016
Duodenal invasion			
Present	30	23 (76.7)	
Absent	8	3 (37.5)	0.034
TNM clinical classification			
III+IV	18	16 (88.9)	
I+II	20	10 (50.0)	0.010

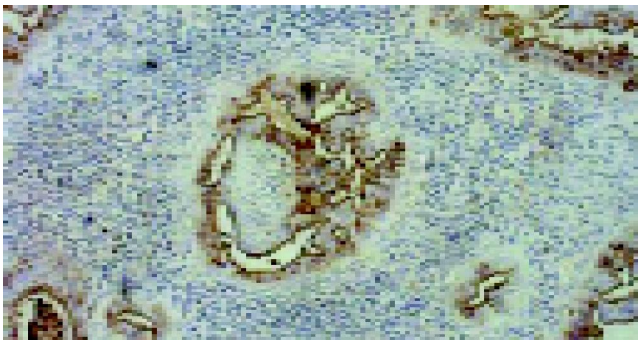


Figure 3 A typical example showing moderately positive staining of KL-6 in carcinoma cells in a metastatic lymph node tissue. Original magnification ×100.

those without it ($P = 0.034$), and in cases classified into III or IV by TNM clinical classification than those classified into I or II ($P = 0.010$). On the other hand, KL-6 expression was not associated with age, sex, histological grade, lymphatic vessel invasion, and venous invasion (Table 1).

The relationship between KL-6 expression and patient survival was then analyzed. As shown in Figure 4, patients showing positive KL-6 expression ($n = 26$) displayed a significantly poorer prognosis than those showing negative KL-6 expression ($n = 12$): 5-year survival rates were 30.8 and 75.0%, respectively, as determined by the Kaplan-Meier method ($P = 0.029$ by the log rank test).

DISCUSSION

Mucins are large extracellular glycoproteins with high carbohydrate content and marked diversity both in the apoprotein and in the oligosaccharide moieties[15]. It has been

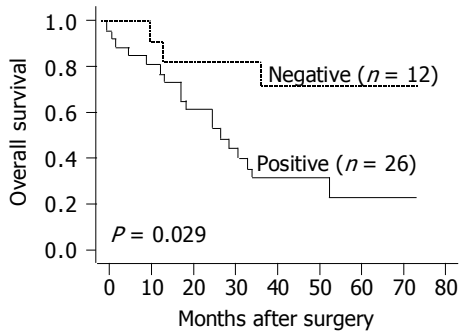


Figure 4 Kaplan-Meier curves for overall survival rates of patients with carcinoma of the ampulla of Vater. Patients with positive (solid line, *n* = 26) and negative (dotted line, *n* = 12) KL-6 expression were followed-up for over 70 mo.

noted that ampullary carcinoma have a heterogeneous mucin expression pattern[16,17] and that overexpression of MUC1 was associated with invasive and metastatic potency of several adenocarcinoma[18-20]. However, the studies on MUC1 expression were mostly done with different antibodies, which recognize different carbohydrate epitopes or the core peptide. This study addresses clinicopathological significance of histochemical expression of KL-6, MUC1 mucin-bearing sialylated carbohydrate epitope recognized by KL-6 antibody, in carcinoma of the ampulla of Vater. Sialylation of tumor cell surface glycoconjugate is thought to contribute to tumor progression and metastasis[7-10]. Furthermore, since sialylated oligosaccharide moieties are exposed on the mucin molecules, KL-6 antibody could effectively recognize the mucin without epitope masking as Cao and Karsten indicated with several antibodies against peptide epitopes of MUC1[21]. Therefore, immunohistochemical detection of KL-6 mucin seems to be a reasonable strategy.

The present data shows that aberrant expression of KL-6 mucin is related to unfavorable behaviors of the carcinoma, such as lymph node metastasis, pancreatic invasion, duodenal invasion, and the advanced stage of TNM clinical classification (Table 1), and poorer prognosis (P = 0.029, Figure 4). Furthermore, remarkable expression of KL-6 was found in invasive carcinoma cells in pancreatic and duodenal tissues and in metastatic carcinoma cells in lymph nodes (Figures 2 and 3). These results suggest that KL-6 mucin might play an important role in unfavorable tumor behaviors, such as invasions and metastasis of carcinoma of the ampulla of Vater.

Several tumor-associated carbohydrate antigens have been identified on mucins[22,23]. Aberrant forms of mucins expressed in cancer cells have been considered to arise as a consequence of the deregulation of expression of enzymes that modify them[15]. The epitope recognized by KL-6 antibody is sialylated carbohydrates included in MUC1 molecule[12], although the detailed structure of the epitope remains to be determined. Among the many types of carbohydrates, sialic acid is vital for cancer growth, since enhanced sialylation is thought to play a role in tumor progression and metastasis[5,24]. Carbohydrate moieties of glycoconjugates are constructed by complex interactions involving a series of glycosyltransferases[25,26]. In our previous study, the aberrant sialylation of glycoconjugates in carcinoma of the ampulla of Vater has been found in histochemical analyses using sialic acid-binding lectins such as *Maackia amurensis* leukoagglutinin and *Sambucus nigra* agglutinin[27]. Therefore, it is postulated that the aberrant expression of KL-6 stems from the aberrant expression of the glycosyltransferase (s) such as sialyltransferase, which participates in the construction of the epitope for KL-6 antibody. Relationship of KL-6 expression to invasions and metastasis has also been suggested in colorectal carcinoma[28,29].

Surgery is still the only option that provides a cure for patients with carcinoma of the ampulla of Vater. Patient outcome after surgery for carcinoma of the ampulla of Vater is better than that for pancreatic cancer or bile duct cancer. However, patients with lymph node metastasis or invasion of carcinoma to adjacent organs including the pancreas or duodenum display a poorer prognosis[30-32]. The present study revealed that positive KL-6 expression was significantly related to lymph node metastasis, pancreatic invasion, and duodenal invasion of ampullary carcinoma. These clinicopathological parameters are recognized as prognostic factors of ampullary carcinoma[30,31]. In particular, the presence of lymph node metastasis, pancreatic invasion, and duodenal invasion was found in 73% (19/26), 81% (21/26), and 88% (23/26), respectively, of KL-6-positive cases. Further, strong staining of KL-6 was frequently found in invasive carcinoma cells in pancreatic and neonatal tissues and in metastatic carcinoma cells in lymph nodes. Therefore, histochemical analyses of preoperatively biopsied tissues using anti-KL-6 antibody might be helpful for the assessment of the development of lymph node metastasis, pancreatic invasion, and duodenal invasion, which would increase a physician's ability to determine operative procedures or predict prognosis for individual patients. Examination with a larger population and a biochemical approach is needed to understand clinical significance of KL-6 expression and biochemical role of carbohydrate moiety of KL-6 mucin in carcinoma of ampulla of Vater.

REFERENCES

1 **Conlon KC**, Dougherty E, Klimstra DS, Coit DG, Turnbull AD, Brennan MF. The value of minimal access surgery in the staging of patients with potentially resectable peripancreatic malignancy. *Ann Surg* 1996; **223**: 134-140
2 **Klempnauer J**, Ridder GJ, Pichlmayr R. Prognostic factors after resection of ampullary carcinoma: multivariate survival analysis in comparison with ductal cancer of the pancreatic head. *Br J Surg* 1995; **82**: 1686-1691
3 **Nakao A**, Harada A, Nonami T, Kishimoto W, Takeda S, Ito K, Takagi H. Prognosis of cancer of the duodental papilla of Vater in relation to clinicopathological tumor extension. *Hepatogasteroenterology* 1994; **41**: 73-78
4 **Fogel M**, Altevogt P, Schirrmacher V. Metastatic potential severely altered by changes in tumor cell adhesiveness and cell-surface sialylation. *J Exp Med* 1983; **157**: 371-376
5 **Numahata K**, Satoh M, Handa K, Saito S, Ohyama C, Ito A, Takahashi T, Hoshi S, Orikasa S, Hakomori S. Sialosyl-Le^x expression defines invasive and metastatic properties of bladder carcinoma. *Cancer* 2002; **94**: 673-685
6 **Hakomori S**. Tumor malignancy defined by aberrant glycosylation and sphingo(glyco)lipid metabolism. *Cancer Res* 1996; **56**: 5309-5318
7 **Li XW**, Ding YQ, Cai JJ, Yang SQ, An LB, Qiao DF. Studies on mechanism of Sialy Lewis-X antigen in liver metastases of human colorectal carcinoma. *World J Gastroenterol* 2001; **7**:

425-430
8 **Ikeda Y**, Mori M, Kajiyama K, Haraguchi Y, Sasaki O, Sugimachi K. Immunohistochemical expression of sialyl Tn, sialyl Lewis^{a}, sialyl Lewis^{a-b-}, and sialyl Lewis^{x} in primary tumor and metastatic lymph nodes in human gastric cancer. *J Surg Oncol* 1996; **62**: 171-176
9 **Tang W**, Mafune K, Nakata M, Konishi T, Kojima N, Mizuochi T, Makuuchi M. Association of histochemical expression of *Maackia amurensis* leukoagglutinin-positive glycoconjugates with behaviour of human gastric cancer. *Histopathology* 2003; 42: 239-245
10 **Vierbuchen MJ**, Fruechtnicht W, Brackrock S, Krause KT, Zienkiewicz TJ. Quantitative lectin histochemical and immunohistochemical studies on the occurrence of alpha(2,3)- and alpha(2,6)-linked sialic acid residues in colorectal carcinomas. Relation to clinicopathologic features. *Cancer* 1995; **76**: 727-735
11 **Kohno N**. Serum marker KL-6/MUC1 for the diagnosis and management of interstitial pneumonitis. *J Med Invest* 1999; **46**: 151-158
12 **Kohno N**, Akiyama M, Kyoizumi S, Hakoda M, Kobuke K, Yamakido M. Detection of soluble tumor-associated antigens in sera and effusions using novel monoclonal antibodies, KL-3 and KL-6, against lung adenocarcinoma. *Jpn J Clin Oncol* 1988; **18**: 203-216
13 Japanese Society of Biliary Surgery. General rules for surgical and pathological studies on cancer of biliary tract, 5th ed. *Tokyo: Kanehara* 2003
14 **Sobin LH**, Wittekind C. TNM classification of malignant tumors, 5th ed. *New York: Wiley-Liss* 1997
15 **Hollingsworth MA**, Swanson BJ. Mucins in cancer: protection and control of the cell surface. *Nat Rev* 2004; **4**: 45-60
16 **Adsay NV**, Mrati K, Basturk O, Iacobuzio-Donahue C, Levi E, Cheng JD, Sarkar FH, Hruban RH, Klimstra DS. Pathologically and biologically distinct types of epithelium in intraductal papillary mucinous neoplasms. *Am J Surg Pathol* 2004; **28**: 839-848
17 **Gürbüz Y**, Klöppel G. Differentiation pathways in duodenal ampullary carcinomas: a comparative study on mucin and trefoil peptide expression, including gastric and colon carcinomas. *Virchows Arch* 2004; **444**: 536-541
18 **Kashiwagi H**, Kijima H, Dowaki S, Ohtani Y, Tobita K, Tsukui M, Tanaka Y, Matsubayasi H, Tsuchida T, Yamazaki H, Nakamura M, Ueyama Y, Tanaka M, Tajima T, Makuuchi H. DF3 expression in human gallbladder carcinoma: significance for lymphatic invasion. *Int J Oncol* 2000; 16: 455-459
19 **Luttges J**, Feyerabend B, Buchelt T, Pacena M, Kloppel G. The mucin profile of noninvasive and invasive mucinous cystic neoplasms of the pancreas. *Am J Surg Pathol* 2002; **26**: 466-471
20 **Nakamori S**, Ota DM, Cleary KR, Shirotani K, Irimura T. MUC1 mucin expression as a marker of progression and metastasis of human colorectal carcinoma. *Gastroenterology* 1994; **106**: 353-361
21 **Cao Y**, Karsten U. Binding patterns of 51 monoclonal antibodies to peptide and carbohydrate epitopes of the epithelial mucin (MUC1) on tissue sections of adenolymphomas of the parotid (Warthin's tumours): role of epitope masking by glycans. *Histochem Cell Biol* 2001; **115**: 349-356
22 **Kim YS**, Gum J, Brockhausen I. Mucin glycoproteins in neoplasia. *Glycoconj J* 1996; **13**: 693-707
23 **Lloyd KO**. The chemistry and immunohemistry of blood group A, B, H, and Lewis antigens: past, present and future. *Glycoconj J* 2000; **17**: 531-541
24 **Hakomori S**. Possible functions of tumor-associated carbohydrate antigens. *Curr Opin Immunol* 1991; **3**: 646-653
25 **Brockhausen I**. Pathways of O-glycan biosynthesis in cancer cells. *Biochim Biophys Acta* 1999; **1473**: 67-95
26 **Kornfeld R**, Kornfeld S. Assembly of asparagine-linked oligosaccharides. *Annu Rev Biochem* 1985; **54**: 631-664
27 **Tang W**, Guo Q, Usuda M, Kokudo N, Seyama Y, Minagawa M, Sugawara Y, Nakata M, Kojima N, Makuuchi M. Histochemical expression of sialoglycoconjugates in carcinoma of the papilla of Vater. *Hepato-gastroenterology* 2005; **52**: 67-71
28 **Hiraga Y**, Tanaka S, Haruma K, Yoshihara M, Sumii K, Kajiyama G, Shimamoto F, Kohno N. Immunoreactive MUC1 expression at the deepest invasive portion correlates with prognosis of colorectal cancer. *Oncology* 1998; **55**: 307-319
29 **Tanimoto T**, Tanaka S, Haruma K, Yoshihara M, Sumii K, Kajiyama G, Shimamoto F, Kohno N. MUC1 expression in intramucosal colorectal neoplasms. Possible involvement in histogenesis and progression. *Oncology* 1999; **56**: 223-231
30 **Roder JD**, Schneider PM, Stein HJ, Siewert JR. Number of lymph node metastases is significantly associated with survival in patients with radically resected carcinoma of the ampulla of Vater. *Br J Surg* 1995; **82**: 1693-1696
31 **Yoshida T**, Matsumoto T, Shibata K, Yokoyama H, Morii Y, Sasaki A, Kitano S. Patterns of lymph node metastasis in carcinoma of the ampulla of Vater. *Hepatogastroenterology* 2000; **47**: 880-883

Science Editor Guo SY **Language Editor** Elsevier HK

PO Box 2345, Beijing 100023, China
www.wjgnet.com
wjg@wjgnet.com

ELSEVIER

World J Gastroenterol 2005;11(35):5455-5459
World Journal of Gastroenterology ISSN 1007-9327
© 2005 The WJG Press and Elsevier Inc. All rights reserved.

• *BASIC RESEARCH* •

Cancer-derived VEGF plays no role in malignant ascites formation in the mouse

Bayasi Guleng, Keisuke Tateishi, Fumihiko Kanai, Amarsanaa Jazag, Miki Ohta, Yoshinari Asaoka, Hideaki Ijichi, Yasuo Tanaka, Jun Imamura, Tsuneo Ikenoue, Yasushi Fukushima, Keita Morikane, Makoto Miyagishi, Kazunari Taira, Takao Kawabe, Masao Omata

Bayasi Guleng, Keisuke Tateishi, Fumihiko Kanai, Amarsanaa Jazag, Miki Ohta, Yoshinari Asaoka, Hideaki Ijichi, Yasuo Tanaka, Jun Imamura, Tsuneo Ikenoue, Yasushi Fukushima, Takao Kawabe, Masao Omata, Department of Gastroenterology, Graduate School of Medicine, University of Tokyo, 7-3-1 Hongo, Bunkyo-ku, Tokyo 113-8655, Japan
Fumihiko Kanai, Masao Omata, Clinical Research Center, University of Tokyo Hospital, 7-3-1 Hongo, Bunkyo-ku, Tokyo 113-8655, Japan
Keita Morikane, Infectious Disease Surveillance Center, National Institute of Infectious Diseases, 1-23-1 Toyama, Shinjuku-ku, Tokyo 162-8640, Japan
Makoto Miyagishi, Kazunari Taira, Department of Chemistry and Biotechnology, Graduate School of Engineering, University of Tokyo, Tokyo 113-8656, Japan
Correspondence to: Keisuke Tateishi, MD, PhD, Department of Gastroenterology, Graduate School of Medicine, University of Tokyo Hospital, 7-3-1 Hongo, Bunkyo-ku, Tokyo 113-8655, Japan. tateishik-int@h.u-tokyo.ac.jp
Telephone: +81-3-3815-5411 Fax: +81-3-3814-0021
Received: 2004-11-08 Accepted: 2004-12-20

Abstract

AIM: Vascular endothelial growth factor (VEGF) is a potent mediator of peritoneal fluid accumulation following tumor progression. This study investigated the role of VEGF secreted by cancerous cells in the formation of malignant ascites.

METHODS: VEGF expression was eliminated by knockdown in the pancreas cancer cell-line PancO2 using vector-based short-hairpin type RNA interference (RNAi). Malignant ascites formation in the mouse was analyzed by intraperitoneal injection of PancO2 cells expressing VEGF or with expression knockdown.

RESULTS: The VEGF knockdown PancO2 cell was successfully established. Knockdown of VEGF did not affect cancer cell proliferation *in vitro* or *in vivo*. The volume of ascites following peritoneal expansion of the tumor in VEGF knockdown cells and control cells did not differ statistically in this *in vivo* study. Moreover, the VEGF concentration in the ascites did not differ statistically.

CONCLUSION: Malignant ascites formation might be mediated by VEGF production in noncancerous tissues, such as stromal compartments. An anti-VEGF strategy against malignant ascites could be applied to various tumors regardless of whether they secrete VEGF.

© 2005 The WJG Press and Elsevier Inc. All rights reserved.

Key words: VEGF; Ascites; RNAi

Guleng B, Tateishi K, Kanai F, Jazag A, Ohta M, Asaoka Y, Ijichi H, Tanaka Y, Imamura J, Ikenoue T, Fukushima Y, Morikane K, Miyagishi M, Taira K, Kawabe T, Omata M. Cancer-derived VEGF plays no role in malignant ascites formation in the mouse. *World J Gastroenterol* 2005; 11 (35): 5455-5459
http://www.wjgnet.com/1007-9327/11/5455.asp

INTRODUCTION

Ascites formation is a critical problem in patients with advanced pancreatic cancer. Vascular endothelial growth factor (VEGF), known as an angiogenic growth factor, is a potent mediator of peritoneal fluid accumulation in tumors. The accumulation of tumor ascites fluid may result from increased permeability of the blood vessels lining the peritoneal cavity. The hyperpermeability of vessels might be mediated by VEGF secreted from tumor cells[1,2]. VEGF antisense plasmid suppresses ascites formation in ovarian carcinoma[3]. VEGF is widely expressed in various normal tissues and many tumors[4,5]. VEGF expression has been detected in both cancer cells themselves and stromal compartments[6-8], raising the question of the relative role of each compartment in VEGF-mediated ascites formation. Recent studies using *RAS*-transformed VEGF-deficient adult dermal fibroblasts or fibrosarcomas generated from VEGF-null *RAS*-transformed mouse embryonic fibroblasts concluded that VEGF production in stromal compartments plays a critical role in tumor angiogenesis[9,10]. However, the role of VEGF in ascites formation in the stroma is poorly understood.

RNA interference (RNAi) is an evolutionarily conserved mechanism of gene silencing. Recently, 21- to 23-nucleotide double-stranded RNA (short interfering RNA, siRNA) molecules have been shown to exhibit specific RNAi characteristics. A plasmid vector expressing siRNA was reported to enable long-term persistence of the silencing effect; a phenomenon termed as 'stable RNAi'[11-13]. This system is a powerful tool for analyzing endogenous gene silencing.

To confirm whether VEGF secreted from cancer cells has a critical role in malignant ascites formation, we used the stable RNAi system to knockdown the VEGF gene in a mouse pancreatic cancer cell line.

MATERIALS AND METHODS

Plasmids

pcDNA-Flag-VEGF expressing vector was constructed as follows: The total RNA was extracted from mouse Colon26 cell using ISOGEN (Nippon Gene, Tokyo, Japan), then the cDNA templates were synthesized from 1 μg of total RNA using the ImProm-II™ Reverse Transcription System (Promega). PCR amplification of mouse VEGFA (191 amino acids) containing Flag sequence was performed using the following two primers: 5'-ATG GAC TAC AAG GAC GAC GAT GAC AAA GAT AAC TTT CTG CTC TCT TGG GTG-3' and 5'-TCA CCG CCT TGG CTT GTC ACA-3'. The PCR product was subcloned into the pCR4Blunt-TOPO vector (Invitrogen, USA), and then *Eco*RI-Flag-VEGF-*Eco*RI fragment was inserted into the *Eco*RI site of the pcDNA vector (Invitrogen, USA).

Plasmid carrying RNAi targeted to VEGF was constructed as previously described[12]. Five 21-nucleotide sequences of the mouse VEGF gene, which had no homology to genomic sequences in a BLAST search, were originally selected using the original algorithm[12]. We designed forward and reverse short-hairpin RNA (Table 1), and both oligonucleotides were annealed to each other (99 ℃ for 2 min, 72 to 4 ℃ for 2 h) and inserted into the *Bsp*MI site of the pcPUR+ U6icassette vector, thereby generating pcPUR+U6-VEGFi.

Cell culture

PancO2 cell line[14] was generated from pancreatic cancer cells derived from C57BL/6 mice, obtained from Dr. Michael A. Hollingsworth, Eppley Institute, University of Nebraska, Omaha, NE, USA. The cells were maintained in Dulbecco's modified Eagle's medium (Sigma, St. Louis, MO, USA) supplemented with 10% fetal bovine serum (Sigma) at 37 ℃ in a 50 mL/L CO_2 atmosphere.

Establishing VEGF knockdown pancreatic cancer cell lines

Stable knockdown cells were established as described[13]. Briefly, the targeting or control vectors were transfected into PancO2 cells using FuGene6 (Roche), and the puromycin-resistant clones or cell pools were selected as stable transfectants. We called stable clones transfected with pcPUR+U6-VEGFi or pcPUR+U6-iRenilla (control vector) as "VEGF-KD" or "VEGF-WT", respectively.

Western blot analysis

Western blot analysis was performed as described[15]. Briefly, cells were lysed in RIPA buffer (50 mmol/L Tris pH 8, 0.1% SDS, 0.5% deoxycholate, 1% NP-40, 150 mmol/L NaCl, 1 tablet complete mini protease inhibitor/10 mL, Roche Diagnostics GmbH, Germany). Next, equal amounts of total cell lysates were electrophoresed and transferred to Pall Fluoro Trans W membrane (Wako, Osaka, Japan). The membranes were incubated with anti-Flag (M2) antibody or anti-β-actin antibody. After washing, the membrane was incubated with horseradish peroxidase-conjugated secondary antibody and visualized using an enhanced chemiluminescence detection system (ECL Advance, Amersham Bioscience, UK).

VEGF measurement by ELISA

To analyze the VEGF production of VEGF-WT and VEGF-KD clones, they were grown in six-well plates with standard medium for 24 h. The medium was replaced with 1 mL of fetal bovine serum-free medium and cells were grown for another 24 h. Then, the VEGF content of the culture supernatants was measured using ELISA (SRL, Japan).

MTT assay

3×10^4 VEGF-KD7 and VEGF-WT cells were seeded in 24-well plates, and the numbers of viable cells were determined using the 3-(4,5-dimethylthiazol-2-yl)-2,5-diphenyltetrazolium bromide (MTT) assay (Sigma, St. Louis, MO, USA) at 24 and 48 h[16]. The absorbance at 570 nm was measured using a microplate reader.

In vivo animal study

C57BL/6 mice were purchased from CLEA (Japan). All procedures involving experimental animals were performed in accordance with protocols approved by the Committee for Animal Research of the University of Tokyo and complied with the Guide for the Care and Use of Laboratory Animals (NIH Publication No. 86-23, revised 1985). 1×10^6 VEGF-KD7 or VEGF-WT cells were injected intraperitoneally into C57BL/6 mice. Ascites accumulation and peritoneal dissemination occurred approximately 2 wk following inoculation of the cancer cells. In this model, the tumor-bearing mice survived for 30-40 d. We weighed the mice every 2-3 d. Twenty-four days after inoculation, some of the mice were anesthetized with pentobarbital sodium (120 mg/kg) and the ascites collected. After centrifuging to remove cancer cells, the volume of ascites was measured. The VEGF concentration was measured using ELISA (SRL, Japan).

Statistical analysis

The data are expressed as mean±SD. Groups were compared using Student's *t*-test. $P<0.05$ was considered statistically significant.

RESULTS

Establishing VEGF knockdown pancreatic cancer cell lines

To study whether VEGF secreted from cancer cells has a critical role in the formation of malignant ascites in pancreatic cancer, we attempted to knockdown the VEGF gene in the mouse pancreatic cancer cell line PancO2. We constructed five plasmids that expressed short hairpin RNAs (as shown in Table 1) targeting the non-isoform-specific common area of VEGF (GenBank locus: NM 009505) under the control of the U6 promoter (pcPUR+U6-VEGFi1-5)[12]. Next, we transiently transfected PancO2 cells with pcPUR+U6-VEGFi1-5 and the Flag-VEGF expression vector, and examined VEGF expression using Western blotting. As shown in Figure 1A, of the five different sites tested, RNAi1-3 proved to be effective for blocking VEGF protein expression, and site 1 was used in subsequent experiments.

To establish stable VEGF knockdown cells, PancO2 cells were transfected with pcPUR+U6-VEGFi1 or

Table 1 siRNAs targeting VEGF gene

Site 1	Sense 5′-caccgagatagagtatatctttaaggtgtgctgtcccttgaagatgtactctatctcttttt-3′
	Antisense 5′-gcataaaaagagatagagtacatcttcaagggacagcacaccttaaagatatactctatctc-3′
Site 2	Sense 5′-caccgagtatatcttcaagttgttcgtgtgctgtccggacggcttgaagatgtactctttttt-3′
	Antisense 5′-gcataaaaagagtacatcttcaagccgtccggacagcacacgaacaacttgaagatatactc-3′
Site 3	Sense 5′-caccattatgaactttctgttctctgtgtgctgtccagagagcagaaagttcatggttttttt-3′
	Antisense 5′-gcataaaaaaccatgaactttctgctctctggacagcacacagagaacagaaagttcataat-3′
Site 4	Sense 5′-caccatggatgtctattagtgaagcgtgtgctgtccgcttcgctggtagacgtccatttttt-3′
	Antisense 5′-gcataaaaaatggacgtctaccagcgaagcggacagcacacgcttcactaatagacatccat-3′
Site 5	Sense 5′-caccaagttactgttgtctaattgagtgtgctgtcctcaattggacggcagtagcttttttt-3′
	Antisense 5′-gcataaaaaaagctactgccgtccaattgaggacagcacactcaattagacaacagtaactt-3′

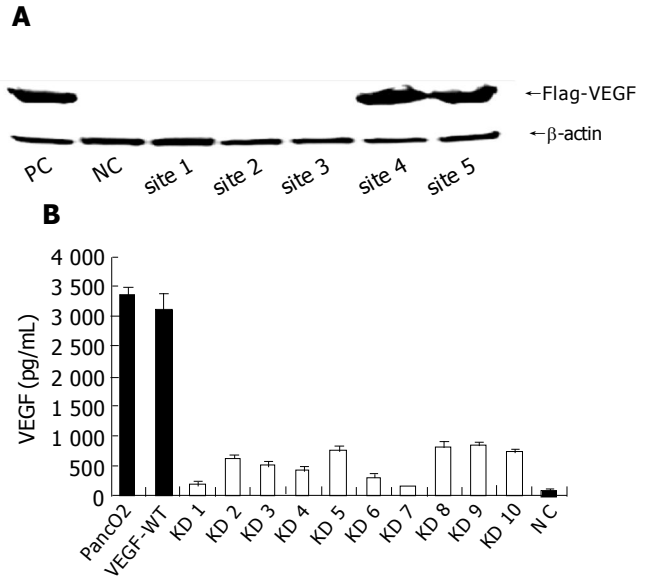


Figure 1 Establishment of VEGF knockdown pancreatic cancer cell lines. **A**: Western blot showing marked reduction of VEGF expression in knockdown cells. Screening of the most effective targeting site for the VEGF gene. **B**: VEGF production of stable knockdown PancO2 cell clones. VEGF-WT and VEGF-KD clones (KD 1-10) were grown in 6-well plates, and the VEGF concentration in culture supernatant was measured using ELISA in triplicates. The growth medium was used as negative control (NC).

pcPUR+U6-iRenilla (control), and incubated with 5 μg/mL puromycin (Wako, Osaka, Japan). Then, we selected puromycin-resistant clones. Parental PancO2 cells, VEGF-WT, and VEGF-KD clones were grown in 6-well plates and the VEGF content in the culture supernatant was measured in triplicates. As shown in Figure 1B, parental cells produced VEGF 3 340±151 pg/mL for 2×10^5 cells/24 h *vs* 3 102±285 pg/mL in VEGF-WT controls. VEGF production was significantly reduced in the pcPUR+U6-VEGFi1 stable clones. VEGF-KD7 produced VEGF (152±16 pg/mL) and was used in subsequent experiments.

Effect of VEGF knockdown on cancer cell growth

To investigate the effect of VEGF knockdown on the cell proliferation potential *in vitro*, 3×10^4 VEGF-KD7 and VEGF-WT cells were grown in 24-well plates. The numbers of viable cells were assessed using the MTT assay. As shown in Figure 2A, there was no statistical difference in cell proliferation between these two cell lines. To study the cell growth *in vivo*, 2×10^6 VEGF-KD7 or VEGF-WT cells were injected into C57BL/6 mice subcutaneously. Small tumors were typically observed, 1 wk after tumor implantation, measured, and the volume was calculated as [(length (mm) ×width (mm)²)]/2. As shown in Figure 2B, the growth of the VEGF knockdown cell line and control cells was not statistically different.

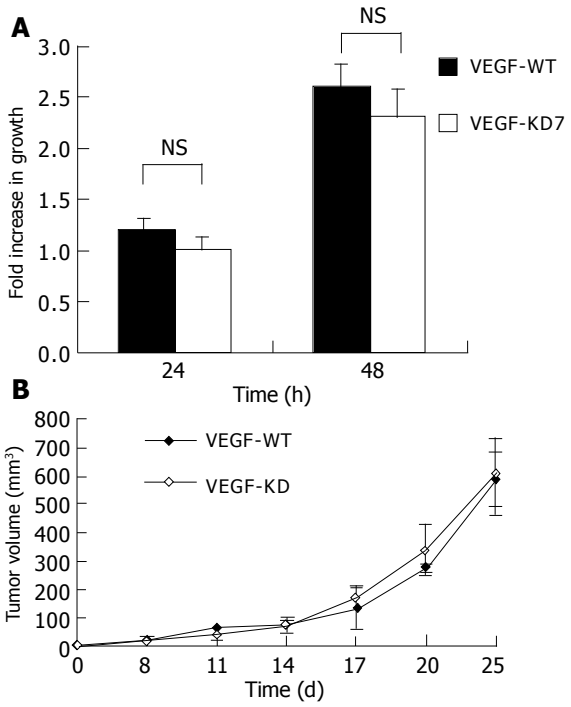


Figure 2 Effect of VEGF knockdown on cell proliferation. **A**: 3×10^4 VEGF-KD7 or VEGF-WT cells were grown in 24-well plates, and the numbers of viable cells were assessed using the MTT assay at 24 (P = 0.082) and 48 h (P = 0.078) (n = 4, mean±SD); **B**: 2×10^6 VEGF-KD7 or VEGF-WT cells were injected into C57BL/6 mice subicutaneous, the tumor size was measured, and the volume was calculated as [(length (mm)×width (mm)²)]/2 (n = 4, P = 0.18, mean±SD).

Effect of VEGF knockdown in the tumor grafted mouse ascites model

Ascites was induced by the intraperitoneal injection of 1×10^6 VEGF-KD7 or VEGF-WT cells into C57BL/6 mice. Ascites accumulation and peritoneal dissemination occurred about 2 wk after cancer cell inoculation. The ascites was bloody in both groups. As shown in Figure 3A, the volume of ascites did not differ between the VEGF-KD7 cell line and control VEGF-WT cells (1.9±0.22 *vs* 1.7±0.16 mL, P = 0.10). Next, we measured the concentration of VEGF in ascites. As shown in Figure 3B, the VEGF tended to be

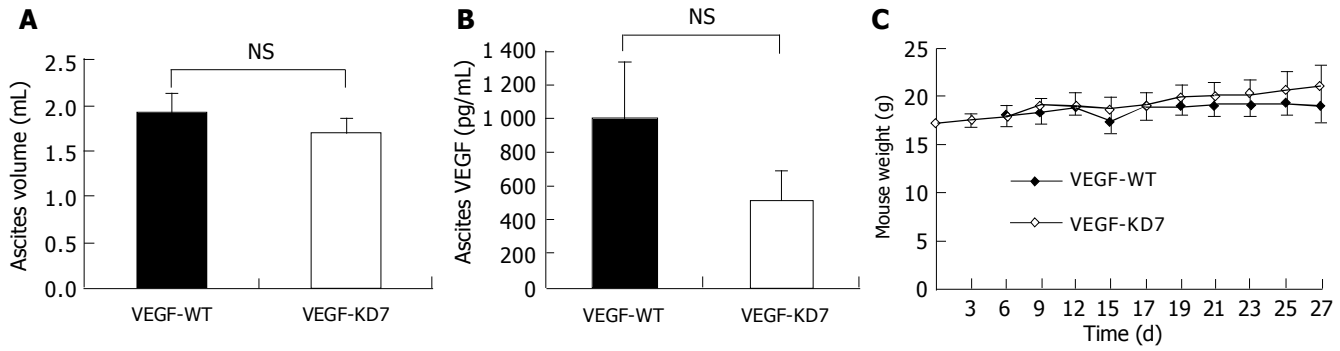


Figure 3 Effect of VEGF knockdown in a tumor grafted mouse ascites model. **A**: The ascites volume of mice inoculated with VEGF-KD7 or VEGF-WT cells (n = 5, P = 0.10, mean±SD); **B**: The VEGF concentration in ascites. VEGF in the ascites was measured using ELISA (n = 4, P = 0.054, mean±SD). **C**: 1×10^6 VEGF-KD7 or VEGF-WT cells were inoculated into mice intraperitoneally and the mice were weighed (n = 8, $P \geqslant 0.05$ in each data point).

lower in the VEGF-KD7 cell line (517±181) compared with VEGF-WT cells (1 001±331), but the difference was not significant (P = 0.054). Both study groups showed extensive macroscopic peritoneal dissemination, but there was no difference in tumor weight between VEGF-KD7 and VEGF-WT cells (0.63±0.15 g *vs* 0.56±0.16 g, P = 0.8). To analyze the systemic effect, the mice were weighed every 2 or 3 d. As shown in Figure 3C, no difference was observed between VEGF-KD7 and VEGF-WT cells. The survival of mice inoculated with VEGF-KD7 or VEGF-WT cells did not differ statistically (35±4.7 d *vs* 38.2±4.2 d, P = 0.29).

DISCUSSION

Pancreatic cancer progression is associated with the accumulation of ascites in the peritoneal cavity. At least three different pathological events cause ascites, i.e., reduced lymphatic drainage from the peritoneal cavity: the obstruction of lymphatic vessels by tumor cells; hyperpermeability of the microvessels lining the peritoneal cavity; and angiogenesis[17]. VEGF contributes to ascites formation by enhancing vascular permeability and promoting new vessel growth[4].

To investigate the role of VEGF secreted from cancer cells in ascites formation following pancreatic cancer progression, we established VEGF knockdown pancreatic cancer cell lines using the stable RNAi method. The stable RNAi system is a useful tool for analyzing endogenous gene silencing[11-13]. Using this system, we were the first to succeed in establishing a VEGF knockdown stable cell line, and to analyze its effect *in vivo*. Others have used VEGF knockdown cells, but their analyses involved *in vitro* experiments[18].

Recent studies using fibrosarcomas generated from VEGF-null *RAS*-transformed mouse embryonic fibroblasts concluded that VEGF production in stromal compartments plays a critical role in tumor angiogenesis[10]. It has also been reported that tumor-infiltrating lymphocytes produce a number of potent angiogenic growth factors, cytokines, and proteases[19]. In another study, we used mouse syngenic colon cancer cells, which do not express VEGF protein *in vitro*, but the levels of VEGF protein expression in the tumor tissues did not differ statistically from PancO2 tumors (data not shown). Although VEGF protein expression was significantly reduced in our VEGF-KD7 cell line *in vitro*, the VEGF concentration in the ascites fluid was not statistically different compared with VEGF-WT cells. During tumor progression, infiltrating cells to the stroma produce a number of potent angiogenic growth factors, cytokines, and proteases. These findings indicate that cancerous compartments, such as the stromal tissues of a tumor, can play a critical role as the scaffold in VEGF production, and VEGF production in tumor tissues is not solely dependent on tumor cells. The accumulation of tumor ascites maybe induced by VEGF-dependent increase of permeability in the blood vessels of the peritoneum, and stromal compartments of the tumor tissue and peritoneum plays a critical role in VEGF-mediated ascites formation.

VEGF is a key mediator of tumor angiogenesis. Recent reports indicate that blocking VEGF is an effective strategy for treating human cancer[20]. The VEGF-specific antibody bevacizumab has anti-vascular effects in human rectal cancer[21]. Malignant ascites formation might be mediated in a cancer cell-type independent manner, and anti-VEGF strategy could be applied to various tumors regardless of whether they secrete VEGF.

ACKNOWLEDGMENT

We thank Mitsuko Tsubouchi for technical assistance.

REFERENCES

1 **Yeo KT,** Wang HH, Nagy JA, Sioussat TM, Ledbetter SR, Hoogewerf AJ, Zhou Y, Masse EM, Senger DR, Dvorak HF. Vascular permeability factor (vascular endothelial growth factor) in guinea pig and human tumor and inflammatory effusions. *Cancer Res* 1993; **53**: 2912-2918

2 **Senger DR,** Galli SJ, Dvorak AM, Perruzzi CA, Harvey VS, Dvorak HF. Tumor cells secrete a vascular permeability factor that promotes accumulation of ascites fluid. *Science* 1983; **219**: 983-985

3 **Akutagawa N,** Nishikawa A, Iwasaki M, Fujimoto T, Teramoto M, Kitajima Y, Endo T, Shibuya M, Kudo R. Expression of vascular endothelial growth factor and E-cadherin in human ovarian cancer: association with ascites fluid accumulation and peritoneal dissemination in mouse ascites model. *Jpn J Cancer Res* 2002; **93**: 644-651

4 **Dvorak HF,** Brown LF, Detmar M, Dvorak AM. Vascular permeability factor/vascular endothelial growth factor, microvascular hyperpermeability, and angiogenesis. *Am J Pathol* 1995; **146**: 1029-1039

5 **Berse B,** Brown LF, Van de Water L, Dvorak HF, Senger DR. Vascular permeability factor (vascular endothelial growth

factor) gene is expressed differentially in normal tissues, macrophages, and tumors. *Mol Biol Cell* 1992; **3**: 211-220

6 **Hlatky L,** Tsionou C, Hahnfeldt P, Coleman CN. Mammary fibroblasts may influence breast tumor angiogenesis via hypoxia-induced vascular endothelial growth factor up-regulation and protein expression. *Cancer Res* 1994; **54**: 6083-6086

7 **Lewis JS,** Landers RJ, Underwood JC, Harris AL, Lewis CE. Expression of vascular endothelial growth factor by macrophages is up-regulated in poorly vascularized areas of breast carcinomas. *J Pathol* 2000; **192**: 150-158

8 **Pilch H,** Schlenger K, Steiner E, Brockerhoff P, Knapstein P, Vaupel P. Hypoxia-stimulated expression of angiogenic growth factors in cervical cancer cells and cervical cancer-derived fibroblasts. *Int J Gynecol Cancer* 2001; **11**: 137-142

9 **Viloria-Petit A,** Miquerol L, Yu JL, Gertsenstein M, Sheehan C, May L, Henkin J, Lobe C, Nagy A, Kerbel RS, Rak J. Contrasting effects of VEGF gene disruption in embryonic stem cell-derived versus oncogene-induced tumors. *Embo J* 2003; **22**: 4091-4102

10 **Dong J,** Grunstein J, Tejada M, Peale F, Frantz G, Liang WC, Bai W, Yu L, Kowalski J, Liang X, Fuh G, Gerber HP, Ferrara N. VEGF-null cells require PDGFR alpha signaling-mediated stromal fibroblast recruitment for tumorigenesis. *Embo J* 2004; **23**: 2800-2810

11 **Brummelkamp TR,** Bernards R, Agami R. Stable suppression of tumorigenicity by virus-mediated RNA interference. *Cancer Cell* 2002; **2**: 243-247

12 **Miyagishi M,** Taira K. U6 promoter-driven siRNAs with four uridine 3′ overhangs efficiently suppress targeted gene expression in mammalian cells. *Nat Biotechnol* 2002; **20**: 497-500

13 **Imamura T,** Kanai F, Kawakami T, Amarsanaa J, Ijichi H, Hoshida Y, Tanaka Y, Ikenoue T, Tateishi K, Kawabe T, Arakawa Y, Miyagishi M, Taira K, Yokosuka O, Omata M. Proteomic analysis of the TGF-beta signaling pathway in pancreatic carcinoma cells using stable RNA interference to silence Smad4 expression. *Biochem Biophys Res Commun* 2004; **318**: 289-296

14 **Morikane K,** Tempero RM, Sivinski CL, Nomoto M, Van Lith ML, Muto T, Hollingsworth MA. Organ-specific pancreatic tumor growth properties and tumor immunity. *Cancer Immunol Immunother* 1999; **47**: 287-296

15 **Kanai F,** Marignani PA, Sarbassova D, Yagi R, Hall RA, Donowitz M, Hisaminato A, Fujiwara T, Ito Y, Cantley LC, Yaffe MB. TAZ: a novel transcriptional co-activator regulated by interactions with 14-3-3 and PDZ domain proteins. *Embo J* 2000; **19**: 6778-6791

16 **Kanai F,** Kawakami T, Hamada H, Sadata A, Yoshida Y, Tanaka T, Ohashi M, Tateishi K, Shiratori Y, Omata M. Adenovirus-mediated transduction of Escherichia coli uracil phosphoribosyltransferase gene sensitizes cancer cells to low concentrations of 5-fluorouracil. *Cancer Res* 1998; **58**: 1946-1951

17 **Belotti D,** Paganoni P, Manenti L, Garofalo A, Marchini S, Taraboletti G, Giavazzi R. Matrix metalloproteinases (MMP9 and MMP2) induce the release of vascular endothelial growth factor (VEGF) by ovarian carcinoma cells: implications for ascites formation. *Cancer Res* 2003; **63**: 5224-5229

18 **Zhang L,** Yang N, Mohamed-Hadley A, Rubin SC, Coukos G. Vector-based RNAi, a novel tool for isoform-specific knockdown of VEGF and anti-angiogenesis gene therapy of cancer. *Biochem Biophys Res Commun* 2003; **303**: 1169-1178

19 **Coussens LM,** Werb Z. Inflammation and cancer. *Nature* 2002; **420**: 860-867

20 **Ferrara N,** Hillan KJ, Gerber HP, Novotny W. Discovery and development of bevacizumab, an anti-VEGF antibody for treating cancer. *Nat Rev Drug Dis* 2004; **3**: 391-400

21 **Willett CG,** Boucher Y, di Tomaso E, Duda DG, Munn LL, Tong RT, Chung DC, Sahani DV, Kalva SP, Kozin SV, Mino M, Cohen KS, Scadden DT, Hartford AC, Fischman AJ, Clark JW, Ryan DP, Zhu AX, Blaszkowsky LS, Chen HX, Shellito PC, Lauwers GY, Jain RK. Direct evidence that the VEGF-specific antibody bevacizumab has antivascular effects in human rectal cancer. *Nat Med* 2004; **10**: 145-147

Science Editor Guo SY **Language Editor** Elsevier HK

PO Box 2345, Beijing 100023, China
www.wjgnet.com
wjg@wjgnet.com

ELSEVIER

World J Gastroenterol 2005;11(35):5460-5467
World Journal of Gastroenterology ISSN 1007-9327
© 2005 The WJG Press and Elsevier Inc. All rights reserved.

• *BASIC RESEARCH* •

Changes of the intestinal endocrine cells in the C57BL/6 mouse after implantation of murine lung carcinoma (3LL): An immunohistochemical quantitative study

Sae-Kwang Ku, Seung-Kyoo Seong, Dae-Young Kim, Hyeung-Sik Lee, Jong-Dae Kim, Hae-Yun Choi, Bu-Il Seo, Jae-Hyun Lee

Sae-Kwang Ku, Seung-Kyoo Seong, Pharmacology and Toxicology Laboratory, Central Research Laboratories, Dong-Wha Pharmaceutical Industrial Co, Ltd, Anyang 430-017, Republic of Korea
Dae-Young Kim, Developmental Biology/Embryology, Division of Biological Science, Gachon Medical School, Kanghwha 417-840, Republic of Korea
Hyeung-Sik Lee, Department of Herbal Biotechnology, Daegu Haany University, Gyeongsan 712-715, Republic of Korea
Jong-Dae Kim, Hae-Yun Choi, Bu-Il Seo, College of Oriental Medicine, Daegu Haany University, Gyeongsan 712-715, Republic of Korea
Jae-Hyun Lee, Laboratory of Histology, College of Veterinary Medicine, Kyungpook National University, Taegu 702-701, Republic of Korea
Co-first-authors: Sae-Kwang Ku and Hyeung-Sik Lee
Correspondence to: Dr. Hyeung-Sik Lee, Department of Herbal Biotechnology, Daegu Haany University, Gyeongsan 712-715, Republic of Korea. endohist@dhu.ac.kr
Telephone: +82-53-819-1436 Fax: +82-53-819-1574
Received: 2005-03-07 Accepted: 2005-04-09

Abstract

AIM: To study the distributions and frequencies of intestinal endocrine cells in the C57BL/6 mouse with immunohistochemical method using seven types of specific antisera against chromogranin A (CGA), serotonin, somatostatin, glucagons, gastrin, cholecystokinin (CCK)-8 and human pancreatic polypeptide (hPP) after abdominal subcutaneous implantation of murine lung carcinoma (3LL).

METHODS: The experimental animals were divided into two groups, one is non-implanted Sham and the other is 3LL-implanted group. Samples were collected from six regions of intestinal tract at 28th d after implantation of 3LL cells (1×10^5 cell/mouse).

RESULTS: In this study, five types of immunoreactive (IR) cells were identified except for gastrin and hPP. The regional distributions of the intestinal endocrine cells in the 3LL-implanted group were similar to those of the non-implanted Sham. However, significant decreases of IR cells were detected in 3LL-implanted group compared to those of non-implanted Sham. CGA- and serotonin-IR cells significantly decreased in 3LL-implanted groups compared to that of non-implanted Sham. Somatostatin-IR cells in the jejunum and ileum and CCK-8-IR cells in the jejunum of 3LL-implanted groups significantly decreased compared to that of non-implanted Sham. In addition, glucagon-IR cells were restricted to the ileum and colon of non-implanted Sham.

CONCLUSION: Implantation of tumor cell mass (3LL) induced severe quantifiable changes of intestinal endocrine cell density and the abnormality in density of intestinal endocrine cells may contribute to the development of gastrointestinal symptoms such as anorexia and indigestion, frequently encountered in patients with cancer.

© 2005 The WJG Press and Elsevier Inc. All rights reserved.

Key words: Intestinal endocrine cell; Immunohistochemistry; C57BL/6 mouse; 3LL; Tumor

Ku SK, Seong SK, Kim DY, Lee HS, Kim JD, Choi HY, Seo BI, Lee JH. Changes of the intestinal endocrine cells in the C57BL/6 mouse after implantation of murine lung carcinoma (3LL): An immunohistochemical quantitative study. *World J Gastroenterol* 2005; 11(35): 5460-5467
http://www.wjgnet.com/1007-9327/11/5460.asp

INTRODUCTION

A system using the 3-Lewis lung carcinoma (3LL), a tumor which once arose spontaneously in C57BL/6 mice, is particularly useful because it metastasizes into the lungs. Now, 3LL is considered as one of the widely used type of tumor in the development and study of antitumoral agents[1,2]. C57BL/6 mouse is an inbred black mouse and is probably the most widely used of all inbred strains, though in many ways it seems to be atypical of inbred strains of laboratory mice. This strain of mice is resistant to chloroform toxicity[3], to induction of cleft palate by cortisone, to lethal effects of ozone[4] and to colon carcinogenesis by 1, 2-dimethylhydrazine[5]. In addition, it is also a recommended host for the following transplantable tumors: 3LL, mammary adenocarcinoma BW 10232, melanoma B16, myeloid leukemia C 1498 and preputial gland carcinoma ESR586 T.

Gastrointestinal endocrine cells dispersed in the epithelia and gastric glands of the digestive tract synthesize various kinds of gastrointestinal hormones and play an important role in the physiological functions of the alimentary tract. Until now, the investigation of gastrointestinal endocrine cells is considered to be an important part of a phylogenic study[6] and the endocrine cells are regarded as the anatomical units responsible for the production of gut hormones, and the change in their density would reflect a change in the capacity of producing these hormones[7]. Many studies have

elucidated the regional distribution and relative frequency of different endocrine cells in the gastrointestinal tract (GIT) of the various vertebrates and also the researches or data processing about gastrointestinal endocrine cells in the mouse strains have been widely executed including normal C57BL/6 mouse[8]. The changes of gastrointestinal endocrine cells in some diseases are also well demonstrated. An abnormal density of gastrointestinal endocrine cells was reported in patients with diabetes[7] and proliferation of endocrine cells in the epithelium was detected in pernicious anemia[9]. Some quantitative changes of endocrine cells were also demonstrated in celiac sprue[10] and in pancreatectomy[11]. In addition, changes of endocrine cells in colorectal carcinoma induced by chemicals were demonstrated[12].

In cancer patients, the most frequent and distressing symptoms are gastrointestinal disorder, and Komurcu *et al*.[13], reported that dry mouth, weight loss, early satiety, taste changes, constipation, anorexia, bloating, nausea, abdominal pain and vomiting were 10 most common gastrointestinal symptoms in patients with lung, breast and prostate cancer. In the change of the gastrointestinal endocrine cells with tumor, most of the reports were related to the induction of gastrointestinal endocrine tumor by some chemicals[14,15] or by some diseases[16]. In addition, the composition, number, and types of endocrine cells in the endocrine tumors located in the gastrointestinal tract are well recognized[17-19].

Although nearly one-half of the most frequently reported and most distressing symptoms in patients with cancer are gastrointestinal in nature[13], the study about changes of gastrointestinal endocrine cells was restricted to the region of endocrine carcinoid tissues or nonneoplastic mucosa around the carcinoids. In addition, there was no report dealing with changes of gastrointestinal endocrine cell profiles after subcutaneous implantation of tumor. The objective of this study was to clarify the changes of the endocrine cells in the intestinal regions of C57BL/6 mouse after subcutaneous implantation of 3LL by specific immunohistochemistry using seven types of antisera against chromogranin A (CGA), serotonin, somatostatin, glucagons, gastrin, cholecystokinin (CCK)-8 and human pancreatic polypeptide (hPP).

MATERIALS AND METHODS

Experimental animals

Twenty adult female C57BL/6 mice (6-wk old, 21-26 g of body weight upon receipt) were acquired from the Charles River Laboratories (Yokohama, Japan) and used in this study after acclimatization for 1 wk. Animals were allocated five per autoclaved filter-top cages (Nalgene, Rochester, NY, USA) in a temperature (20-25 ℃) and humidity (50-55%) controlled room during acclimatization periods. Light:dark cycle was 12:12 h and sterilized feed (Samyang, Korea) and autoclaved water were supplied, with free access. Animals were divided into two groups, 3LL-implanted group and non-implanted Sham group. Each of 10 mice was used in this study. All procedures in this study were in compliance with the Animal Welfare Act Regulations (9CFR Parts 1, 2 and 3) and with the Guide for the Care and Use of Laboratory Animals (Institute of Laboratory Animal Resources, 1996).

Implantation of Lewis lung carcinoma (3LL)

Lewis lung carcinoma was maintained as subcutaneous tumor mass. Maintained subcutaneous tumor mass was excised under sterile conditions and single cell suspensions were prepared by collagenase type IV and DNase I (Sigma, USA) in PBS and filtration of the resulting tumor cell suspension through cell strainer (Costar, USA). After counting and adjusting the cell number (1×10^5 cell/mouse), 3LL cell was subcutaneously implanted at abdominal skin with viable tumor cells.

Sampling

After 28 d of implantation, all experimental animals were anesthetized with diethyl ether. For inducing gastric and/or intestinal emptying, animals were fasted for about 24 h. After phlebotomization, samples from six regions of the intestinal tract, the duodenum, jejunum, ileum, cecum, colon and rectum were fixed in Bouin's solution.

Histology

After paraffin embedding, 3-4 μm serial sections were prepared. Representative sections of each tissue were stained with hematoxylin and eosin for light microscopic examination of the normal gastrointestinal architecture.

Immunohistochemistry

Each representative section was deparaffinized, rehydrated and immunostained with the peroxidase anti-peroxidase (PAP) method[20]. Blocking of nonspecific reaction was performed with normal goat serum, prior to incubation with the specific antisera (Table 1). After rinsing with phosphate buffered saline (PBS; 0.01 mol/L, pH 7.4), the sections were incubated in secondary antiserum. They were then washed in PBS buffer and finally the PAP complex was prepared. The peroxidase reaction was carried out in a 3, 3'-diaminobenzidine tetrahydrochloride solution containing 0.01% H_2O_2 in Tris-HCl buffer (0.05 mol/L, pH 7.6). After immunostaining, the sections were lightly counterstained with Mayer's hematoxylin and the immunoreactive (IR) cells were observed under light microscope.

The specificity of each immunohistochemical reaction was determined as recommended by Sternberger[20], including the replacement of specific antiserum by the same antiserum, which had been preincubated with its corresponding antigen.

Frequency

In the restricted view fields on a computer monitor using automated image analysis process (Soft Image System, Germany) attached to light microscopy, IR cells showing immunoreactivities against each antiserum were counted among 1 000 epithelial and intestinal acinar cells. The frequencies of IR cells were calculated as mean±SD of total 10 parts (one filed in each animal) of each intestinal region.

Statistical analysis

Mann-Whitney *U*-Wilcoxon rank sum *W* test (M-W test) was used to analyze the significance of data with SPSS for Windows (Release 6.1.3, SPSS Inc., USA) and the significant values were represented by a and b ($P<0.05$; $P<0.01$).

RESULTS

In this study, five kinds of the IR endocrine cells were detected against CGA, serotonin, somatostatin and CCK-8 in the intestine of C57BL/6 mice regardless of implantation (Tables 2 and 3). However, glucagon-IR cells were restricted to non-implanted Sham and no gastrin- and hPP-IR cells were demonstrated in this study. According to the location of the intestines, different regional distributions and frequencies of these IR cells were observed and these differences are shown in Table 2. Most of these IR cells in the epithelial regions were generally spherical or spindle in shape, while occasionally round in shape cells were also found in the intestinal gland regions. In addition, most of these IR cells showed significant ($P<0.01$ or $P<0.05$) decrease in 3LL-implantation group compared to that of non-implanted Sham group.

CGA-IR cells

CGA-IR cells were observed in the entire intestinal regions of both groups. They were mainly dispersed in the basal portions of intestinal mucosal regions rather than the surface epithelial regions and they were more numerously detected in the small intestine compared to that of the large intestine regardless of implantation of 3LL except for the colon in which CGA-IR cells were more numerously detected than that of the jejunum and ileum (Figures 1A-M). In addition, CGA-IR cells in the colon of 3LL-implanted group that were restricted to the surface epithelium differed from that of non-implanted Sham (Figures 1E, K and L). The frequency of CGA-IR cells in the entire intestinal regions of 3LL-implanted group significantly ($P<0.01$) decreased compared to that of non-implanted Sham (Tables 2 and 3). About 46.56%, 65.88%, 77.42%, 69.86%, 40.14% and 75.00% of CGA-IR cells in the duodenum, jejunum, ileum, cecum, colon and rectum of 3LL-implanted group decreased compared to that of non-implanted Sham, respectively.

Serotonin-IR cells

Serotonin-IR cells were observed in the entire intestinal regions of both groups. These IR cells were dispersed throughout whole gastric mucosa, mainly in the surface epithelium and the intestinal gland regardless of 3LL-implantation (Figures 2A-L). They showed the highest frequency in the rectum of non-implanted Sham and in the colon and duodenum of 3LL-implanted group. The frequency of serotonin-IR cells in the entire intestinal regions of 3LL-implanted group was significantly ($P<0.01$ or $P<0.05$) decreased compared to that of non-implanted Sham (Tables 2 and 3). About 51.32%, 25.41%, 32.79%, 42.28%, 59.86% and 95.24% of serotonin-IR cells in the duodenum, jejunum, ileum, cecum, colon and rectum of 3LL-implanted group were decreased compared to that of non-implanted Sham, respectively.

Table 1 Antisera used in this study

Antisera raised[1]	Code	Source	Dilution
CGA[2]	A430	DAKO Corp., Carpinteria, CA, USA	1:1 000
Serotonin	BO68082C	BioGenex Lab., San Ramon, CA, USA	1:20
Somatostatin	PUO421295	BioGenex Lab., San Ramon, CA, USA	1:20
Glucagon	927604	Dia Sorin, Stillwater, MN, USA	1:2 000
Gastrin	PUO190796	BioGenex Lab., San Ramon, CA, USA	1:20
CCK-8[2]	750257	Dia Sorin, Stillwater, MN, USA	1:500
HPP[2]	A610	DAKO Corp., Carpinteria, CA, USA	1:600

[1]All antisera were raised in rabbits. [2]CGA: chromogranin A, CCK-8: cholecystokinin-8, hPP: human pancreatic polypeptide.

Table 2 Regional distributions and frequencies of the endocrine cells in the small intestinal tract of the C57BL/6 mouse after implantation of 3LL

Antisera	Non-implanted Sham			3LL-implanted group		
	Duodenum	Jejunum	Ileum	Duodenum	Jejunum	Ileum
CGA[1]	24.70±4.11	21.10±3.70	9.30±1.95	13.20±3.79[b]	7.20±3.12[b]	2.10±1.29[b]
Serotonin	22.80±4.76	12.20±4.24	6.10±1.73	11.10±4.20[b]	9.10±1.60[a]	4.10±0.99[b]
Somatostatin	1.70±3.01	6.10±1.91	2.60±0.84	1.60±0.84	0.90±0.57[b]	1.40±0.70[b]
Glucagon	ND[2]	ND	1.40±0.52	ND	ND	ND
CCK-8[1]	8.30±2.71	3.40±1.35	ND	9.40±2.55	1.30±0.48[b]	ND

mean±SD, number of IR cells among 1 000 epithelial and intestinal acinar cells (1 field in each animal, total 10 fields); [1]CGA: chromogranin A, CCK-8: cholecystokinin-8; [2]ND: not detected; [a]$P<0.05$ *vs* non-implanted Sham by M–W test; [b]$P<0.01$ *vs* non-implanted Sham by M–W test.

Table 3 Regional distributions and frequencies of the endocrine cells in the large intestinal tract of the C57BL/6 mouse after implantation of 3LL

Antisera	Non-implanted Sham			3LL-implanted group		
	Cecum	Colon	Rectum	Cecum	Colon	Rectum
CGA[1]	7.30±2.45	14.70±4.85	3.20±1.14	2.20±1.14[b]	8.80±3.19[b]	0.80±0.63[b]
Serotonin	12.30±3.97	29.40±9.41	37.80±9.75	7.10±1.37[b]	11.80±3.74[b]	1.80±1.03[b]
Somatostatin	ND[2]	ND	ND	ND	ND	ND
Glucagon	ND	0.60±0.52	ND	ND	ND	ND
CCK-8[1]	ND	ND	ND	ND	ND	ND

mean±SD, number of IR cells among 1 000 epithelial and intestinal acinar cells (1 field in each animal, total 10 fields); [1]CGA: chromogranin A, CCK-8: cholecystokinin-8; [2]ND: not detected; [b]$P<0.01$ *vs* non-implanted Sham by M–W test.

Somatostatin-IR cells

Somatostatin-IR cells were restricted to the small intestine regions of non-implanted Sham and 3LL-implanted groups. These IR cells were dispersed in the surface epithelium and intestinal gland regions of the mucosa of both groups (Figures 3A-F). The frequency of somatostatin-IR cells in the duodenum of 3LL-implanted group was similar to that of non-implanted Sham (about 5.88% was decreased). However, cells in the jejunum and ileum of 3LL-implanted group significantly ($P<0.01$) decreased compared to that of non-implanted Sham (about 85.25% and 46.15% were decreased, respectively, Tables 2 and 3).

Glucagon-IR cells

A few glucagon-IR cells were restricted to the intestinal gland regions of ileum and colon of non-implanted Sham (Figures 4A and B). However, no glucagon-IR cells were observed in 3LL-implanted group (Tables 2 and 3).

Gastrin-IR cells

No gastrin-IR cells were demonstrated in the entire intestinal regions of non-implanted Sham and 3LL-implanted groups

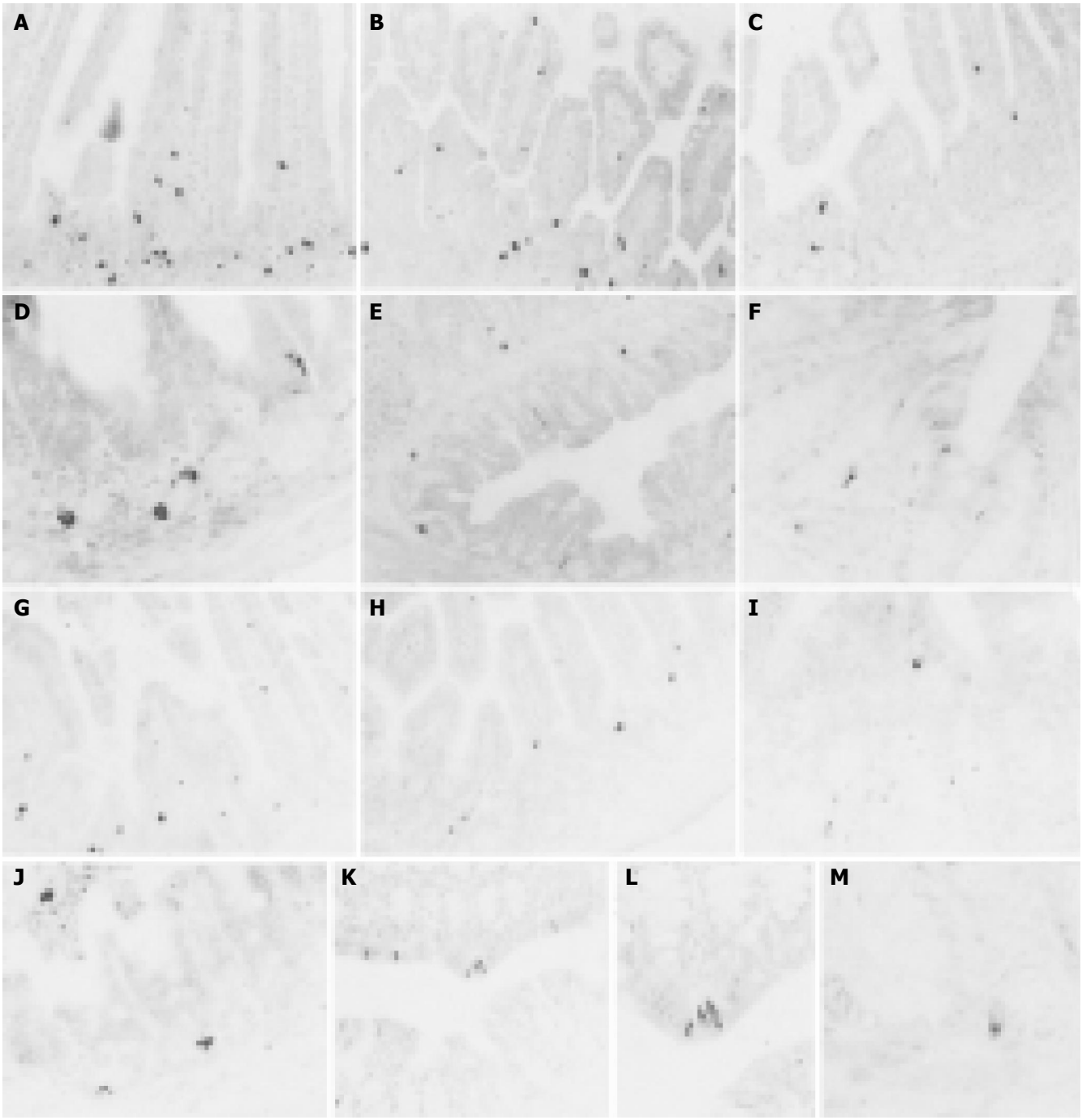


Figure 1 CGA-IR cells of the duodenum (**A**, **G**), jejunum (**B**, **H**), ileum (**C**, **I**), cecum (**D**, **J**), colon (**E**, **K**, **L**) and rectum (**F**, **M**) of non-implanted Sham (**A**-**F**) and 3LL-implanted group (**G**-**M**). In 3LL-implanted group, CGA-IR cells were dramatically decreased in the entire intestinal regions. **A**-**C**, **E**, **G**, **H** and **K**: ×120; **D**, **F**, **I**, **J** and **L**: ×240; **M**: ×480; PAP methods.

(Tables 2 and 3).

CCK-8-IR cells

CCK-8-IR cells were restricted to the duodenum and jejunum of both groups and most of these IR cells were dispersed in the surface epithelium and intestinal gland of the intestinal mucosa similar to that of other IR cells (Figures 5A-D). The frequency of CCK-8-IR cells in the duodenum of 3LL-implanted group was similar to that of non-implanted Sham (about 13.25% was increased). However, cells in the jejunum of 3LL-implanted group were significantly ($P<0.01$) decreased compared to that of non-implanted Sham (about 61.76% were decreased, Tables 2 and 3).

hPP-IR cells

No hPP-IR cells were demonstrated in this study, regardless of implantation of 3LL (Table 2).

DISCUSSION

In the present study, the changes of the endocrine cells in the intestinal regions of C57BL/6 mouse after subcutaneous implantation of 3LL were observed by specific immuno-

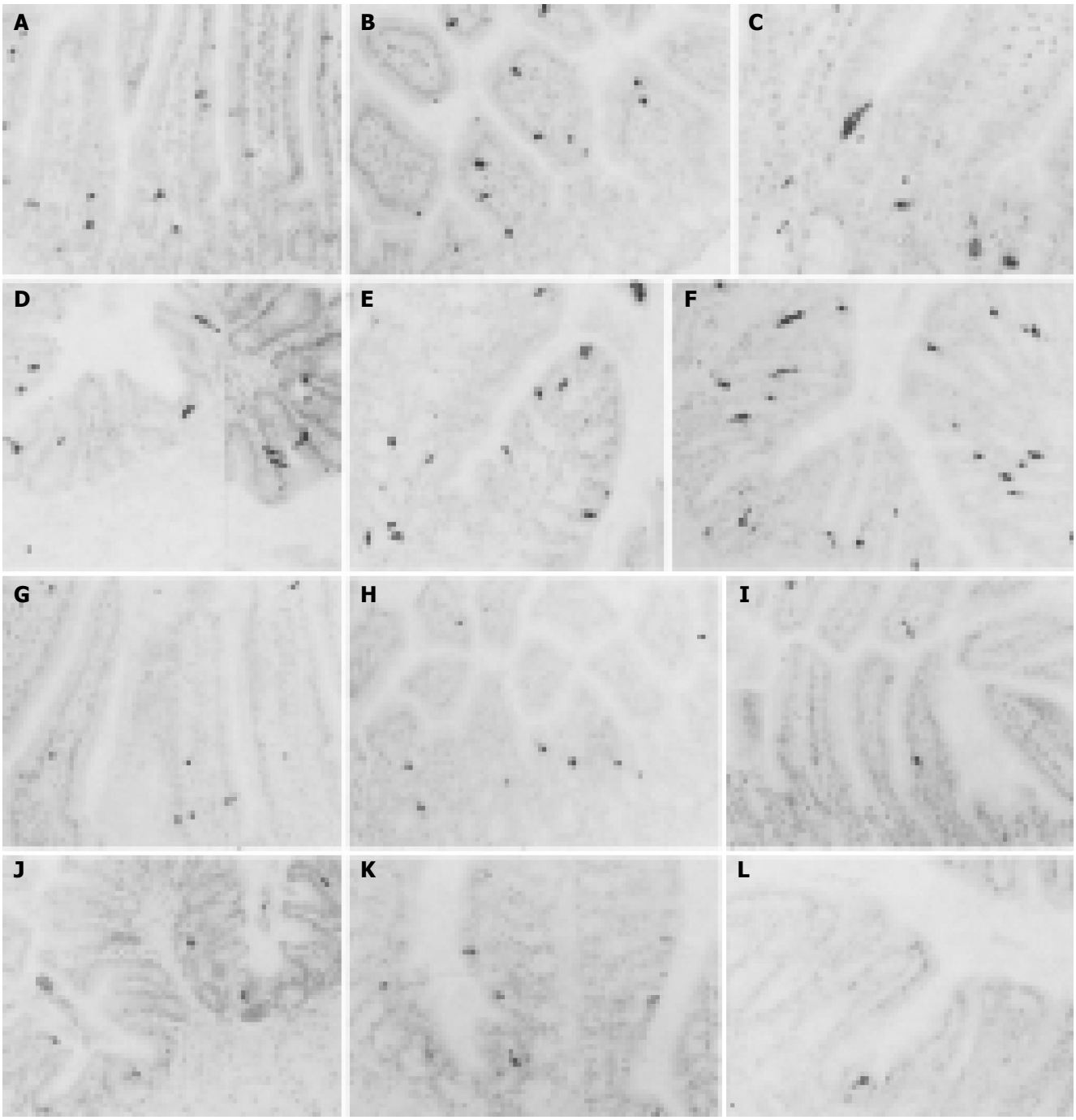


Figure 2 Serotonin-IR cells of the duodenum (**A**, **G**), jejunum (**B**, **H**), ileum (**C**, **I**), cecum (**D**, **J**), colon (**E**, **K**) and rectum (**F**, **L**) of non-implanted Sham (**A-F**) and 3LL-implanted group (**G-L**). In 3LL-implanted group, serotonin-IR cells were dramatically decreased in the entire intestinal regions. **A**, **B**, **D-L**: ×120; **C**: ×240; PAP methods.

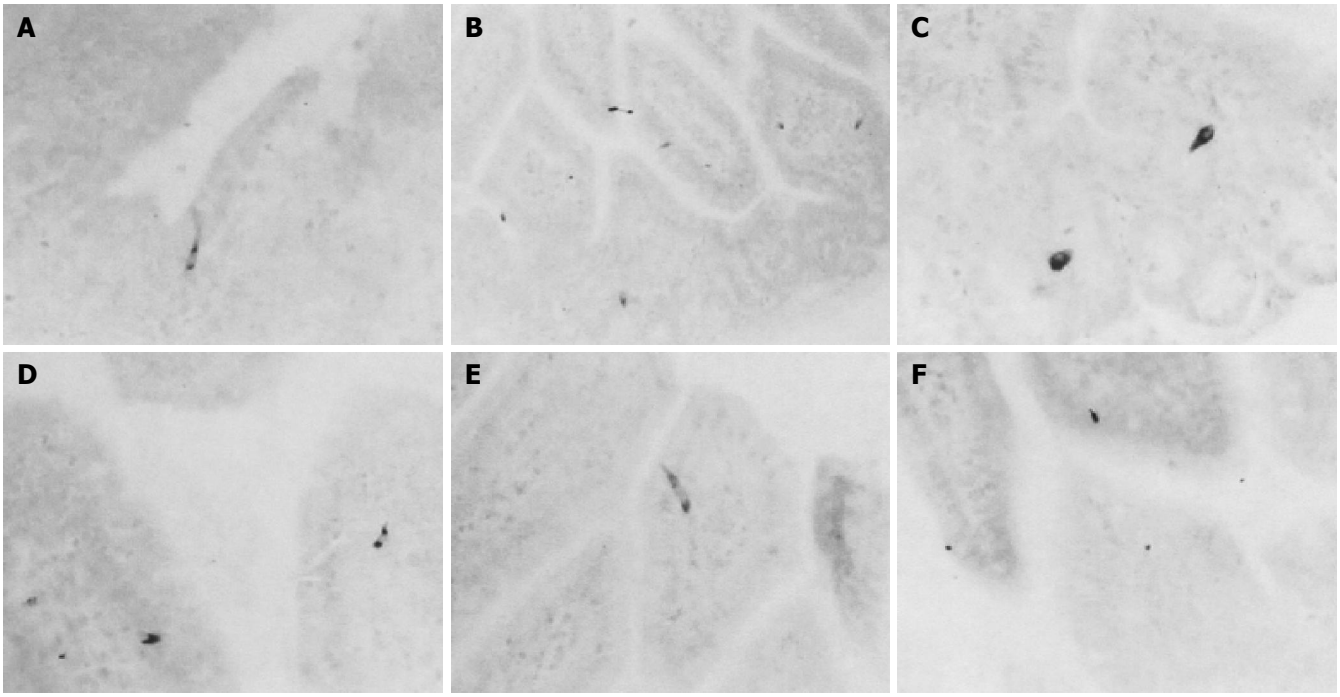


Figure 3 Somatostatin-IR cells of the duodenum (**A**, **D**), jejunum (**B**, **E**) and ileum (**C**, **F**) of non-implanted Sham (**A**-**C**) and 3LL-implanted group (**D**-**E**). In 3LL-implanted group, somatostatin-IR cells were slightly decreased in the jejunum and ileum. **A**, **C**-**F**: ×240; **B**: ×120; PAP methods.

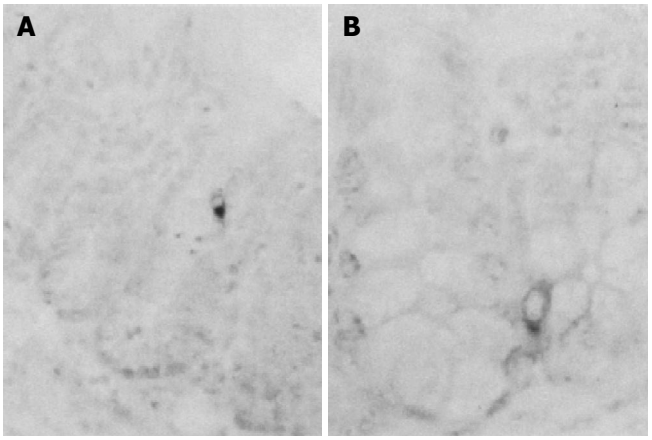


Figure 4 Glucagon-IR cells were restricted to the ileum (**A**) and colon (**B**) of non-implanted Sham. They were located in the intestinal gland regions. **A**: ×240; **B**: ×480; PAP methods.

histochemistry. As results of 3LL implantation, most of IR cells were significantly ($P<0.01$ or $P<0.05$) decreased in the entire intestinal tract except for somatostatin- and CCK-8-IR in the duodenum in which similar cell numbers were detected between non-implanted Sham and 3LL-implanted groups. In the rectum, the most dramatical changes were demonstrated and the most dramatical changes were demonstrated in serotonin-IR cells. These changes might be inducing a gastrointestinal disorder observed in patients with cancer[13].

Chromogranins have been found to occur in a large variety of endocrine organs and cells outside the adrenal medulla, and they have been claimed as common "markers" of all neuroendocrine cells[21]. Although, seldom there were changes of frequency of CGA-IR cells in the GIT of Rodentia, Qian *et al*.[22], reported that decrease of CG-IR cells was demonstrated in the intestine of unilateral cervical

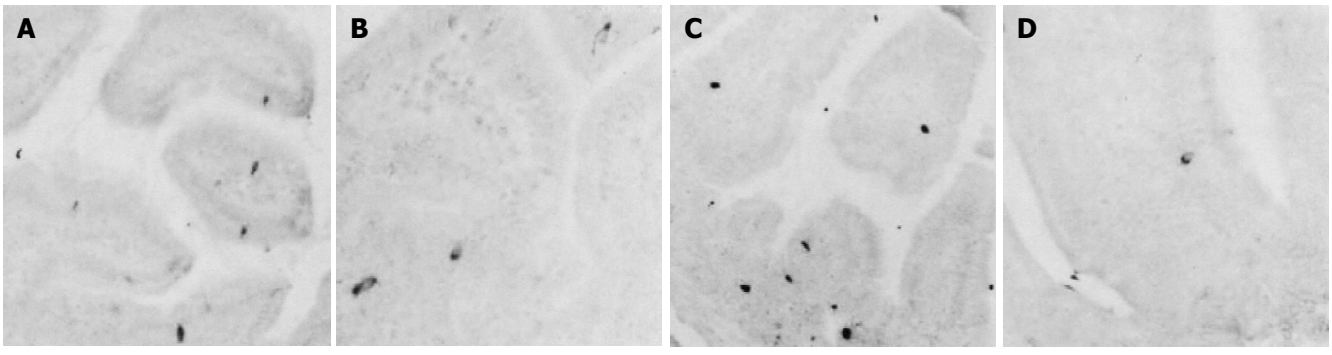


Figure 5 CCK-8-IR cells of the duodenum (**A**, **C**) and jejunum (**B**, **D**) of non-implanted Sham (**A**, **B**) and 3LL-implanted group (**C**, **D**). In 3LL-implanted group, CCK-8-IR cells were decreased in the jejunum. **A**, **C**: ×120; **B**, **D**: ×240; PAP methods.

vagotomized mouse. In addition, increase of CG-IR cells was also demonstrated in the intestine of proton pump inhibitor treated rat[23] and celiac children[24]. According to the previous reports, it is considered that changes of CG-IR cells were possible as a sign of disease and these changes were also considered as results of changes of other endocrine cells because CGs were regarded as a common marker of other endocrine cells[21]. In the present study, CGA-IR cells were remarkably decreased in the intestine of 3LL-implanted groups compared to that of non-implanted Sham.

Serotonin consisted of monoamines widely distributed in the nervous system and gastro-entero-pancreatic endocrine cells and the main functions of serotonin were inhibition of gastric acid secretion and contraction of smooth muscle in the GIT[25]. Serotonin-IR cells were dramatically decreased in the duodenum of diabetic mouse[26] and the number of these IR cells and occupied area were significantly decreased in the damaged gastroduodenal regions of mouse, induced by ethanol[27]. In the present study, among used antisera serotonin-IR cells were most significantly decreased in the entire regions of the intestine. These changes might induce gastrointestinal problems, especially some clinical signs related to gastric motility and gastric acid secretion.

Somatostatin consisting of 14 amino acids was isolated from hypothalamus of sheep for the first time and it could be divided into straight form and cyclic form[28]. This substance inhibits the secretion of the other neuroendocrine hormones[29]. It is known that somatostatin-IR cells show the widest distribution in the whole GIT except for the large intestine of all vertebrate species investigated, including the primitive agnathans with serotonin-IR cells[8]. Somatostatin-IR cells were significantly increased in the cancer adjacent mucosa compared to that of cancer distant mucosa of colorectal endocrine cancer patients[30] and decrease of these IR cells was demonstrated in the duodenal ulcer patients with *Helicobacter pylori*, but they were increased to normal after eradication of *H pylori*[31]. In the present study, somatostatin-IR cells were remarkably decreased in the jejunum and ileum of 3LL-implanted groups compared to that of non-implanted Sham. This decrease of somatostatin-IR cells is considered to have induced somewhat serious problems to gastrointestinal physiology, particularly their functions on the digestive tract.

Glucagon is synthesized in the A cells of the pancreas and regulates serum glucose levels. These IR cells have been demonstrated in various mammals. However, there were no reports dealing with the evidence of changes of glucagon-IR cells in any disease case or in any abnormality induced by any chemical or any manipulation. In the present study, corresponding to that of previous study[8], they were restricted to the ileum and colon of non-implanted Sham. However, no glucagon-IR cells were demonstrated in the intestine of 3LL-implanted group.

Gastrin secreted by intestinal G cell, promotes gastric acid secretion and CCK secreted by intestinal I cell stimulates the pancreatic enzyme secretion. However, gastrin-IR cells in the C57BL/6 mice were restricted to the stomach regions[8] and they were not detected in this study. Enteric CCK-8-IR cells significantly increased in celiac sprue[11]. In the present study, marked decrease of CCK-8-IR cells were demonstrated in the jejunum, after implantation of 3LL and these results induce some gastric disorders. Since PP was isolated from insulin extraction of pancreas at 1961, the regional distribution of PP-IR cells in the mouse strains was relatively well known, but strain-dependant differences existed among mice[8,32]. In the C57BL/6 mice, generally no hPP-IR cells were demonstrated in the GIT[8].

In conclusion, implantation of tumor cell mass (3LL) induce severe quantifiable changes of the intestinal endocrine cell density and the abnormality in density of endocrine cells may contribute to the development of gastrointestinal symptoms such as anorexia and indigestion, frequently encountered in patients with cancer. However, the overall hormone states such as amounts in blood in 3LL-implanted animals were not observed in this study, the exact meaning of the decrease of endocrine cells is unclear. Therefore, to understand the exact relationship between the decrease of GI endocrine cells and gastrointestinal disorder observed in patients with cancer, some quantified study of blood hormone states must be made.

REFERENCES

1 **DeWys WD.** A quantitative model for the study of the growth and treatment of a tumor and its metastases with correlation between proliferative state and sensitivity to cyclophosphamide. *Cancer Res* 1972; **32**: 367-373

2 **Moon EY,** Seong SK, Jung SH, Lee M, Lee DK, Rhee DK, Pyo S, Yoon SJ. Antitumor activity of 4-phenyl-1-arylsulfonylimidazolidinone, DW2143. *Cancer Lett* 1999; **140**: 177-187

3 **Deringer MK,** Dunn TB, Heston WE. Results of exposure of strain C3H mice to chloroform. *Proc Soc Exp Biol Med* 1953; **83**: 474-479

4 **Goldstein BD,** Lai LY, Ross SR, Cuzzi-Spada R. Susceptibility of inbred mouse strains to ozone. *Arch Environ Health* 1973; **27**: 412-413

5 **Evans JT,** Shows TB, Sproul EE, Paolini NS, Mittelman A, Hauschka TS. Genetics of colon carcinogenesis in mice treated with 1, 2-dimethylhydrazine. *Cancer Res* 1977; **37**: 134-136

6 **D'Este L,** Buffa R, Pelagi M, Siccardi AG, Renda T. Immunohistochemical localization of chromogranin A and B in the endocrine cells of the alimentary tract of the green frog, *Rana esculenta*. *Cell Tissue Res* 1994; **277**: 341-349

7 **El-Salhy M,** Sitohy B. Abnormal gastrointestinal endocrine cells in patients with diabetes type 1: relationship to gastric emptying and myoelectrical activity. *Scand J Gastroenterol* 2001; **36**: 1162-1169

8 **Ku SK,** Lee HS, Lee JH. An immunohistochemical study of the gastrointestinal endocrine cells in the C57BL/6 mice. *Anat Histol Embryol* 2003; **32**: 21-28

9 **Rode J,** Dhillon AP, Papadaki L, Stockbrugger R, Thompson RJ, Moss E, Cotton PB. Pernicious anaemia and mucosal endocrine cell proliferation of the non-antral stomach. *Gut* 1986; **27**: 789-798

10 **Buchan AM,** Grant S, Brown JC, Freeman HJ. A quantitative study of enteric endocrine cells in celiac sprue. *J Pediatr Gastroenterol Nutr* 1984; **3**: 665-671

11 **Ravazzola M,** Baetens D, Engerman R, Kovacevic N, Vranic M, Orci L. Endocrine cells in oxyntic mucosa of a dog 5 years after pancreatectomy. *Horm Metab Res* 1977; **9**: 480-483

12 **Sitohy B,** El-Salhy M. Colonic endocrine cells in rats with chemically induced colon carcinoma. *Histol Histopathol* 2001; **16**: 833-838

13 **Komurcu S,** Nelson KA, Walsh D, Ford RB, Rybicki LA.

Gastrointestinal symptoms among inpatients with advanced cancer. *Am J Hosp Palliat Care* 2002; **19**: 351-355
14 **Wangberg B,** Nilsson O, Theodorsson E, Modlin IM, Dahlstrom A, Ahlman H. Are enterochromaffin like cell tumours reversible? An experimental study on gastric carcinoids induced in Mastomys by histamine2-receptor blockade. *Regul Pept* 1995; **56**: 19-33
15 **Solcia E,** Fiocca R, Villani L, Luinetti O, Capella C. Hyperplastic, dysplastic, and neoplastic enterochromaffin-like-cell proliferations of the gastric mucosa. Classification and histogenesis. *Am J Surg Pathol* 1995; **19**(Suppl 1): S1-S7
16 **Sjoblom SM,** Sipponen P, Karonen SL, Jarvinen HJ. Mucosal argyrophil endocrine cells in pernicious anaemia and upper gastrointestinal carcinoid tumours. *J Clin Pathol* 1989; **42**: 371-377
17 **Iwafuchi M,** Watanabe H, Ishihara N, Shimoda T, Iwashita A, Ito S. Peptide YY immunoreactive cells in gastrointestinal carcinoids: immunohistochemical and ultrastructural studies of 60 tumors. *Hum Pathol* 1986; **17**: 291-296
18 **Yasui W,** Sumiyoshi H, Hata J, Mandai K, Tahara E. Gut endocrine cells in rat stomach carcinoma induced by N-methyl-N'-nitro-N-nitrosoguanidine. *J Cancer Res Clin Oncol* 1986; **111**: 87-92
19 **Shimamoto F,** Tahara E, Yanaihara N. Gut endocrine cells in rat intestinal-tract carcinoma induced by 1,2-dimethylhydrazine. *J Cancer Res Clin Oncol* 1983; **105**: 221-230
20 **Sternberger LA.** The unlabeled antibody peroxidase-antiperoxidase (PAP) method In: Sternberger LA, ed. Immunocytochemistry. *New York: John Wiley Sons* 1979: 104-169
21 **Cohn DV,** Elting JJ, Frick M, Elde R. Selective localization of the parathyroid secretory protein I/adrenal medulla chromogranin A protein family in a wide variety of endocrine cells of the rat. *Endocrinology* 1984; **114**: 1963-1974
22 **Qian BF,** El-Salhy M, Danielsson A, Shalaby A, Axelsson H. Effects of unilateral cervical vagotomy on antral endocrine cells in mouse. *Histol Histopathol* 1999; **14**: 705-709
23 **White SL,** Smith WC, Fisher LF, Gatlin CL, Hanasono GK, Jordan WH. Quantitation of glandular gastric changes in rats given a proton pump inhibitor for 3 mo with emphasis on sampling scheme selection. *Toxicol Pathol* 1998; **26**: 403-410
24 **Mariani P,** Pietroletti R, D'Alessandro MD, Castro M, Lucidi V, Ceccamea A, Lomanto D, Carlei F, Lezoche E. Changes in the prostanoid content and the population of endocrine cells in jejunal biopsies from celiac children. *Minerva Pediatr* 1990; **42**: 131-134
25 **Guyton AC.** Secretory functions of the alimentary tract In: Guyton AC, ed. Textbook of medical physiology. *Philadelphia: WB Saunders* 1988: 801-815
26 **Spangeus A,** Forsgren S, El-Salhy M. Effect of diabetic state on co-localization of substance P and serotonin in the gut in animal models. *Histol Histopathol* 2001; **16**: 393-398
27 **Penissi A,** Mariani L, Souto M, Guzman J, Piezzi R. Changes in gastroduodenal 5-hydroxytryptamine-containing cells induced by dehydroleucodine. *Cells Tissues Organs* 2000; **166**: 259-266
28 **Brazeau P,** Vale W, Burgus R, Ling N, Butcher M, Rivier J, Guillemin R. Hypothalamic polypeptide that inhibits the secretion of immunoreactive pituitary growth hormone. *Science* 1973; **179**: 77-79
29 **Kitamura N,** Yamada J, Calingasan NY, Yamashita T. Immunocytochemical distribution of endocrine cells in the gastrointestinal tract of the horse. *Equine Vet J* 1984; **16**: 103-107
30 **Zhao R,** Wang Y, Chen T. Somatostatin and its secretory cells in tumor surrounding mucosa in colorectal cancer patients and its significance. *Zhonghua Waike Zazhi* 1997; **35**: 268-270
31 **Queiroz DM,** Mendes EN, Rocha GA, Moura SB, Resende LM, Barbosa AJ, Coelho LG, Passos MC, Castro LP, Oliveira CA. Effect of *Helicobacter pylori* eradication on antral gastrin- and somatostatin-immunoreactive cell density and gastrin and somatostatin concentrations. *Scand J Gastroenterol* 1993; **28**: 858-864
32 **Ku SK,** Lee JH, Lee HS, Park KD. The regional distribution and relative frequency of gastrointestinal endocrine cells in SHK-1 hairless mice: an immunohistochemical study. *Anat Histol Embryol* 2002; **31**: 78-84

Science Editor Guo SY **Language Editor** Elsevier HK

PO Box 2345, Beijing 100023, China
www.wjgnet.com
wjg@wjgnet.com

ELSEVIER

World J Gastroenterol 2005;11(35):5468-5474
World Journal of Gastroenterology ISSN 1007-9327
© 2005 The WJG Press and Elsevier Inc. All rights reserved.

• *BASIC RESEARCH* •

Porcine acute liver failure model established by two-phase surgery and treated with hollow fiber bioartificial liver support system

Yi Gao, Ning Mu, Xiao-Ping Xu, Yan Wang

Yi Gao, Ning Mu, Xiao-Ping Xu, Yan Wang, Department of Hepatobiliary Surgery, Zhujiang Hospital, Southern Medical University, Guanzhou 510282, Guangdong Province, China
Supported by the Key Technologies R and D Program of Guangdong Province during the 10th Five-Year Plan Period, No. 2002A3020206
Correspondence to: Yi Gao, Department of Hepatobiliary Surgery, Zhujiang Hospital, Southern Medical University, Guangzhou 510282, Guangdong Province, China. mnwsq@163.com
Telephone: +86-20-85143210
Received: 2004-09-22 Accepted: 2004-12-09

Abstract

AIM: To establish a highly reproducible animal model of acute liver failure (ALF), for assessing the effect of bioartificial liver support system (BALSS).

METHODS: A two-phase complete liver devascularization procedure was performed in eight loco-hybrid pigs. Blood biochemical index and liver biopsy were studied every 2 h after surgery, and survival time was recorded. The BALSS constructed with high volume recirculating technique was a hollow fiber circulating system consisting of a hepatocyte reactor-hollow fiber module inoculated with microcarrier-adhering hepatocytes, and a double pump, heparinized, thermostabilized, micro-capsulized activated carbon-adsorbing plasmapheresis system. Twelve pigs undergoing two-phase surgery were randomized into: control group (perfused without hepatocytes, $n = 6$) and treatment group (perfused with hepatocytes, $n = 6$). Intergroup liver biochemical indexes, survival time, and liver pathological changes were analyzed at regular intervals.

RESULTS: Two-phase surgery was performed in all the experimental pigs, and there was no obvious difference between their biochemical indexes. After 3 h of phase II surgery, ammonia (Amm) increased to (269±37) μmol/L. After 5 h of the surgery, fibrinogen (Fib) decreased to (1.5±0.2) g/L. After 7 h of the surgery, ALT, AST, Tbil and PT were (7.6±1.8) nka/L, (40±5) nka/L, (55±8) μmol/L and (17.5±1.7) nka/L respectively. After 9 h of surgery, ALB and Cr were (27±4) g/L and (87±9) μmol/L. After 13 h of surgery, BUN was (3.5±0.9) μmol/L. All the above values were different from those determined before surgery. Survival time of pigs averaged 13.5±1.4 h. ALF pigs in the other group were treated with BALSS. The comparison analysis between the treated and control animals showed the changes of Tbil, PT, Alb, BUN, Cr, Fib, and Amm ($P<0.01$), but there was no change of ALT and AST. The survival time was statistically different ($P<0.01$), and there was no significant difference in histological changes.

CONCLUSION: The porcine ALF model established by two-phase devascularized surgery is valid and reproducible. The hollow fiber BALSS can meet the needs of life support and is effective in treating ALF.

© 2005 The WJG Press and Elsevier Inc. All rights reserved.

Key words: Acute liver failure; Animal model; Bioartificial liver; Micro-capsulized activated carbon adsorbing; Porcine hepatocyte

Gao Y, Mu N, Xu XP, Wang Y. Porcine acute liver failure model established by two-phase surgery and treated with hollow fiber bioartificial liver support system. *World J Gastroenterol* 2005; 11(35): 5468-5474
http://www.wjgnet.com/1007-9327/11/5468.asp

INTRODUCTION

A highly reproducible animal model of ALF is crucial for assessing the extracorporeal BAL support efficiency. In our investigation, when a two-phase complete liver devascularization surgery was performed, acute loss of compensation for liver functions occurred, and pigs died of acute liver failure (ALF) eventually. Blood samples were collected to analyze biochemical indexes and liver biopsy was obtained for pathologic examinations under light and electron microscope. The survival time of all experimental animals was recorded. Pigs with ALF were treated with the bioartificial liver support system (BALSS) consisting of a hepatocyte reactor-hollow fiber module inoculated with microcarrier-adhering hepatocytes, and a double pump, heparinized, thermostabilized, micro-capsulized activated carbon-adsorbing plasmapheresis system. Pigs with ALF in the other group were treated with BALSS. Compared to the control animals, Tbil, PT, Alb, BUN, Cr, Fib, and Amm in the treated animals changed ($P<0.01$), but ALT and AST did not change. Survival time was statistically different ($P<0.01$), but there was no difference in histological changes.

MATERIALS AND METHODS

Animals and reagents

Twenty 2-3 mo old healthy native hybrid pigs (15-20 kg) purchased from the Animal Center of Sun Yat-Sen University of Medical Sciences were used in the experiment. All the animals received humane care and the study protocols were in compliance with the animal care guidelines established by the First Military Medical University. Twelve grams per

liter alginic acid sodium reservoir, 13 g/L $CaCl_2$ solution, poly-lysine solution, and 0.6 g/L alginic acid sodium solution were kindly provided by the Institute of Molecular Immunology, The First Military Medical University. All other chemicals were purchased from Sigma Chemical Co. (St. Louis, MO, USA). Machines used included Fresenius hemodialysis machine (A2008C, Germany), UF5.5F6 dialyzer (Fresenius Polysulfone, Germany), YT-HP-160 hemoperfusion machine (Yatai Medical Instrumentation Co., Ltd, Ningbo, Zhejiang Province, China).

Animal surgery

Prior to surgery, animals were kept fasting for 12 h, with water available *ad libitum*. Anesthesia was induced with an intra-abdominal bolus of 30 mg/kg pentobarbital (30 g/L). A double lumen catheter was inserted into the right upper limb vein for drug and infusion delivery. Animals received oxygen through nasal catheter intubation. Laparotomy was performed in midline from xiphoideus down to the lower abdomen. After mobilization of the portal vein and right renal vein, 0.25 mg heparin was injected into the portal vein, which was clamped in the middle part with a hemostat, a 15 cm×0.8 cm silica-gel catheter containing 20 g/L heparin saline was introduced into the inferior caval vein with a depth of 2-3 cm from the far-forth end of the right renal vein, and secured. Another end of this catheter was placed in the portal vein toward the far-forth end with a depth of 1.5 cm, then the catheter was secured and opened. When there was no distinct bleeding, the abdominal wound was closed. Thus a portacaval shunt was established end to side. Phase II surgery was performed after 2 d. All the peri-hepatic ligaments were cut. The branches of hepatic artery were transfixed; hepatic artery and gastroduodenal artery were ligated completely. An 18-G catheter was inserted into the left femoral artery for direct blood pressure measurement. After 1, 4, and 7 h of complete liver devascularization, liver biopsies were taken for postoperative histology examination. The operative wound was closed in a single layer. During the surgery, 500 mL 0.9% NaCl and 800 000 U benzylpenicillin were infused. When the animal died, autopsy was practiced, and specimens of liver were taken for histology examination.

Biochemical index assessment During phase II surgery, blood sample was collected before the obstruction of blood liver (0 h) and at regular intervals (every 2 h after phase II surgery) to monitor AST, ALT, Alb, Tbil, Amm, BUN, Cr, PT, and Fib until the pigs died.

Histology examination Under light microscope, liver specimens were trimmed into 5-mm sections, fixed into 100 mL/L formalin, dehydrated with alcohol, embedded with paraffin and sliced up, then stained with HE for observation under light microscope. Under electronic microscope, liver specimens were doubly-fixed with 25 g/L glutaral and 10 g/L osmium acid, dehydrated with acetone, embedded with Epon-812 resin and sliced up by LKB-2088 ultramicrotome, then stained with acetic acid and citromalic acid lead for electronic microscopy with Hitachi-600 transmission electron microscope (Japan).

Survival time record Survival time (from phase II surgery to the death of animal) of all the animals was recorded.

Treatment with BALSS

Porcine hepatocyte preparation Hepatocytes of native hybrid pigs were isolated by the two-step collagenase digestion method[1]. The digested liver parenchyma was suspended in ice cold Hanks-Hepes medium and filtered with gauze and 500 μm of stainless steel mesh. Then, the cell pellet was collected by centrifugation at 50 r/min and washed several times with Hanks-Hepes balanced solution. Viability of the cells was always greater than 90%, as judged by trypan blue exclusion. Isolated liver cells were attached to hydrated microcarriers according to the methods of Demetriou *et al*.[2].

Construction of BAL circulatory system Micro-capsulization of activated carbon was conducted according to the method of Rozga *et al*.[3]. (Figure 1).

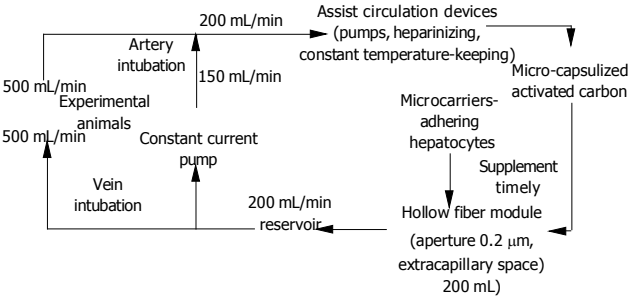


Figure 1 Pattern of BAL circulating system.

System parameters Blood was pumped out from the femoral catheter at a flow rate of 50 mL/min and into a high flux recirculation circuit, and then converged with the recircling blood at a flow rate of 150 mL/min, which was pumped out of the reservoir by constant current pump. The confluent blood was filtrated through the double pumps, heparinizing, thermostabilized, oxygenating, pressure monitoring and micro-capsulized charcoal adsorption devices in order, and then passed through the intracapillary space of the hollow fiber module at 200 mL/min. The extracapillary space of the device was filled with 200 mL of microcarrier-adhering hepatocytes and culture media system (containing 5×10^9 hepatocytes). Solute exchange occurred through the side pore of the fiber. Subsequently, 500 mL of the circling blood flowed into the reservoir and a majority of it (150 mL/min) turned into recirculation through the pump. The rest (50 mL/min of blood) was infused back into the pigs through the femoral vein catheter.

Treatment of ALF with BALSS Twelve experimental pigs were randomized into control group and treatment group (n = 6 in each group). When construction of BALSS was completed, the groups with ALF were treated with BALSS. The control animals were treated with BALSS containing no hepatocytes, but only 200 mL of culture medium, and the treatment group was treated with BALSS containing 5×10^9 hepatocytes in the same volume of culture medium. Analysis of liver biochemical indexes, survival time and morphological changes was carried out to judge the extracorporeal liver support efficiency of BALSS.

Statistical analysis

Results were expressed by mean±SD. Data were analyzed by the *t* test. $P<0.05$ was considered statistically significant.

RESULTS

Establishment of ALF models

Experimental ischemic ALF model was established successfully in eight pigs by two-phase complete liver devascularization surgery. After the obstruction, the average survival time was (13.5±1.4) h.

Biochemical assays After devascularization, Amm increased immediately, followed by a decrease after 9-11 h, and then increased progressively again. Levels of AST, ALT, Tbil, BUN, Cr, and PT increased. Alb and Fib decreased (Table 1).

Histology observation Light microscopy observation: Before the complete liver devascularization (0 h), structure of hepatic lobules was normal, Disse cavity did not dilate, hepatocytes did not swell, and arrayed radiatively around the central vein (Figure 2A). One hour later, structure of hepatic lobules was still normal, so was the linage of hepatocytes. Disse cavity dilated slightly, and hepatocytes were swollen and turbid, while nuclear membrane and nucleoli were still clear (Figure 2B). Four hours later, structure of hepatic lobules was still in existence, so was the frame of hepatic plates. While Disse cavity dilated obviously, central veins caved in and ballooning degeneration occurred in cytolymph. Pyknosis and vanishment of nucleoli occurred as well (Figure 2C). Seven hours after the obstruction, structure of hepatic lobules was in disorder, hepatic plate was dissociated and the arrangement of hepatocytes was disordered, Disse cavity dilated more, ballooning degeneration in cytolymph was more significant, so was the swelling of hepatocytes, chromatin gathered borderly, and there was evidence of lytic necrosis of hepatocytes (Figure 2D). When the experimental animals died of ALF, pathological examinations revealed that hepatic lobules were unrecognized, hepatocytes diminished, hepatic plate dissociated, and obvious extensive piecemeal necrosis of hepatocytes emerged (Figure 2E). Electronic microscopy observation: Before devascularization, the examination of hepatocyte ultrastructures showed that there was abundant glycogen granules in cytolymph, also plenty of endoplasmic reticulum with no dilation and no swelling mitochondria, and mitochondrial cristae were clear, so was mitochondrial membrane, chromatin was symmetrical, nucleoli and nuclear membrane were also legible (Figure 3A). Four hours later, it was obvious that glycogen granules in cytolymph were

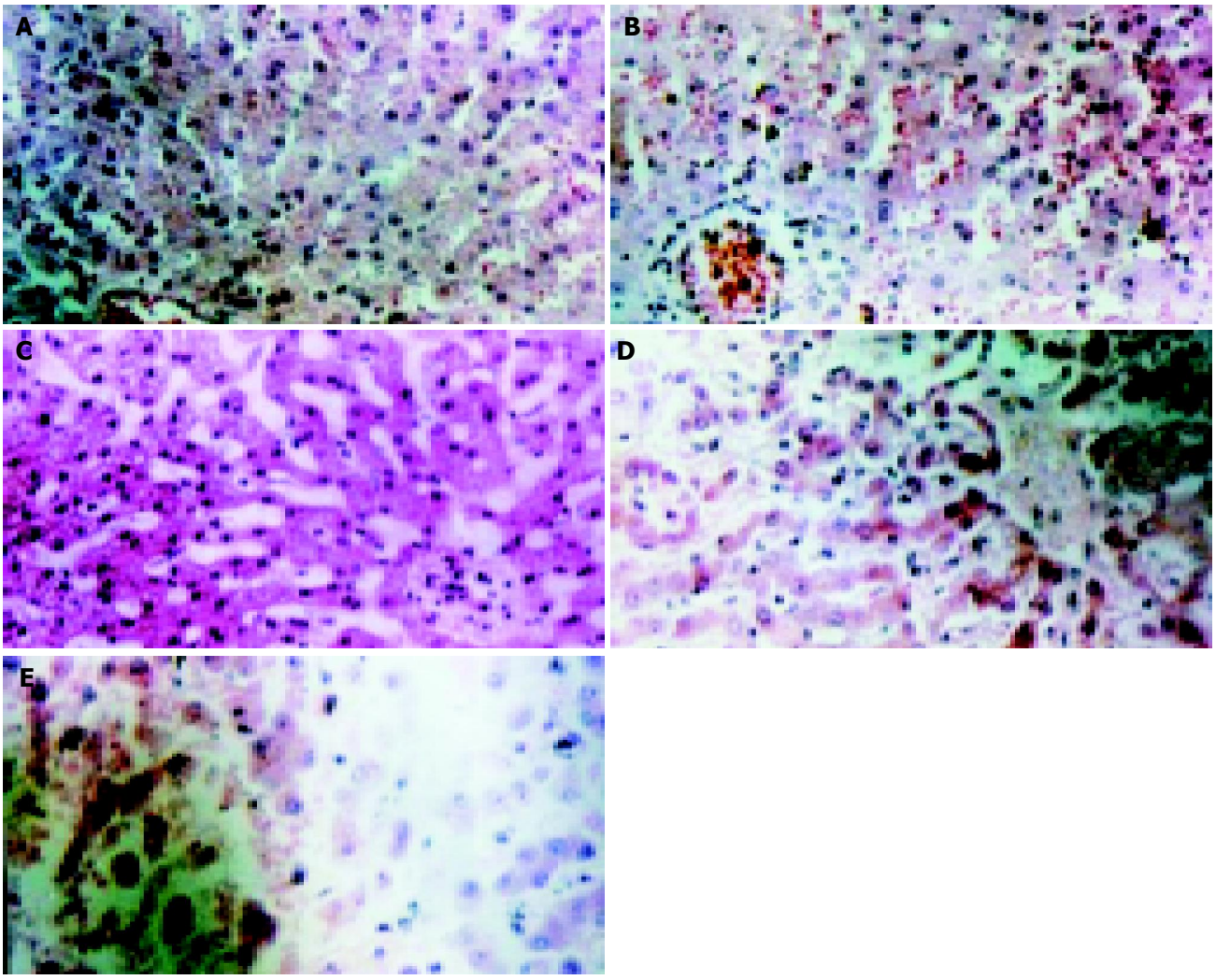


Figure 2 Liver histology observation at 0 h (**A**), 1 h (**B**), 4 h (**C**), 7 h (**D**) after liver devascularization, and death of pigs (**E**) under light microscope.

Table 1 Biochemical indexes of ALF pigs at different time points (mean±SD)

	0 h	1 h	3 h	5 h	7 h	9 h	11 h	13 h
ALT (nkat/L)	4.7±0.7	5.1±1.3	4.9±1.2	5.2±1.5	7.6±1.8[a]	8.2±2.1[a]	10.9±3.4[a]	16.2±1.2[a]
AST (nkat/L)	18±1	19±1	20±1	25±2	40±5[a]	113±22[a]	30±8[a]	10±4[a]
Tbil (μmol/L)	40±6	44±9	41±7	47±10	55±8[a]	49±8[a]	52±5[a]	59±10[a]
Alb (g/L)	36±5	33±4	31±4	30±4	28±3	27±4[a]	27±3[a]	25±4[a]
Amm (μmol/L)	117±18	215±29	269±37[a]	285±34[a]	275±30[a]	239±28[a]	216±19[a]	280±35[a]
BUN (mmol/L)	2.7±0.6	2.8±0.4	2.5±0.4	2.5±0.6	2.8±0.5	2.8±0.4	2.9±0.5	3.5±0.9[a]
Cr (μmol/L)	74±8	77±7	77±9	64±5	63±7	87±9[a]	102±17[a]	98±10[a]
PT (s)	12.8±1.0	13±1.1	14.4±1.4	15.4±1.8	17.5±1.7[a]	19.2±1.9[a]	21.3±1.9[a]	21.9±2[a]
Fib (g/L)	2.2±0.2	2.1±0.2	1.9±0.2	1.5±0.2[a]	1.2±0.2[a]	0.8±0.1[a]	0.8±0.1[a]	0.7±0.1[a]

[a]$P<0.05$ *vs* 0 h group.

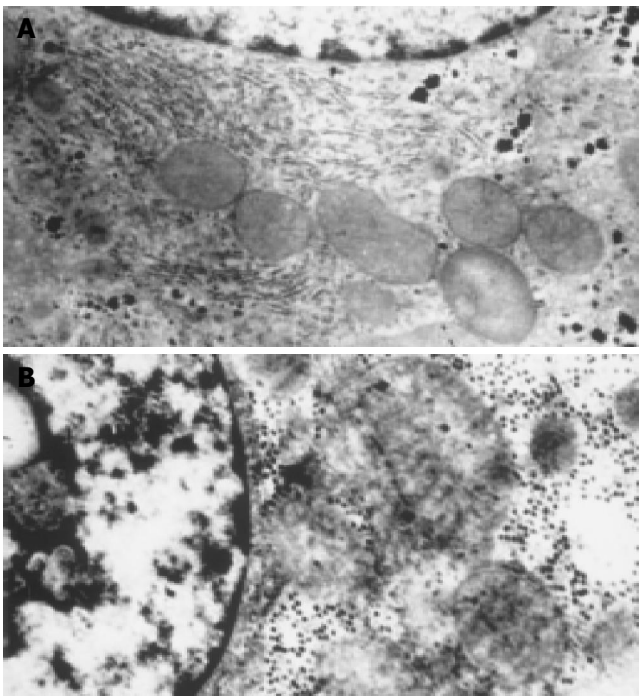


Figure 3 Electronic microscopy observation of hepatocytes at 0 h (**A**) and 4 h (**B**).

homogenized, rough endoplasmic reticulum de-grained, mitochondrion was swollen, and part of it was lysed, mitochondrial cristae blurred, cholangiole microvilli between the hepatocytes significantly diminished, chromatin centralized, nuclei deformed, and pseudo-inclusion bodies in nuclei appeared (Figure 3B).

Treatment with BALSS

Experimental ischemic ALF model was established successfully in 12 pigs by the two-phase complete liver devascularization surgery, and treatment of all the pigs with BALSS was accomplished successfully.

Determination of biochemical indexes Before the complete liver devascularization, the difference in ALT and AST had no statistical significance between the two groups; after the surgery, ALT and AST increased progressively and swiftly in both groups after the surgery, but there was no statistical significance between the two groups (Figures 4A and B). A significant difference in Tbil level emerged between the two groups after 7 h ($P<0.05$), this difference became more significant after 9 h ($P<0.01$, Figure 4C). The significant difference in Alb between the two groups emerged after 3 h ($P<0.05$) and became more significant 2 h later ($P<0.01$, Figure 4D). Amm level increased rapidly in the control animals, but slowly in the treated animals, the difference was significant ($P<0.01$, Figure 4E). The levels of BUN and Cr increased more slowly in both groups as compared to Amm; the difference between the two groups was observed after 5 h ($P<0.05$), and became more significant 7 h later ($P<0.01$, Figures 4F and G). There was no statistical significant difference in PT and Fib between the two groups after 3 h, but the difference in PT tended to be significant 5 h later ($P<0.05$), and difference in Fib was more significant ($P<0.01$, Figures 4H and I).

Morphology observation Liver pathological impairment in the two groups was analogous to the pathological images of ALF model.

Survival time Survival time of the control animals was 11.6-15.1 (averaged 13.17±1.47) h, and that of the treated animals was 18.1-24.4 (averaged 21.33±2.16) h. The difference was significant between the two groups ($P<0.01$).

DISCUSSION

Hepatotoxins, such as alcohol, anaflon, dimethyl-nitramine and D-galactosamine, are used as ALF chemical inducers. But the chemical ALF models induced by hepatotoxin can have much diversity in the changes of biochemical indexes, pathological examinations, mortality rate, and survival time. Thus, it is hard to evaluate the effects of treatments in those models. Also hepatotoxins often impair the internal organs such as kidneys and lungs, thus complicating the causes of death. Surgical ALF models are preferred, especially when a large animal model is established. Since devascularization method to induce canine ALF with two-phase surgery was reported by Rapaport and Gigesin, 1953, the procedure has been modified by the technique of hepatic artery ligation[4-6].

In our experiment, two-phase surgery was performed for liver devascularization. The pigs underwent portal-right renal venous shunt, and 2 d later, hepatic artery, gastroduodenal artery and peri-hepatic ligaments were cut to obstruct blood flowing into the liver. Acute loss of compensation for liver functions was then produced and the pigs died of ALF. We found that this model was simple and easy to operate. The choice of portal-right renal venous intubation shunt instead

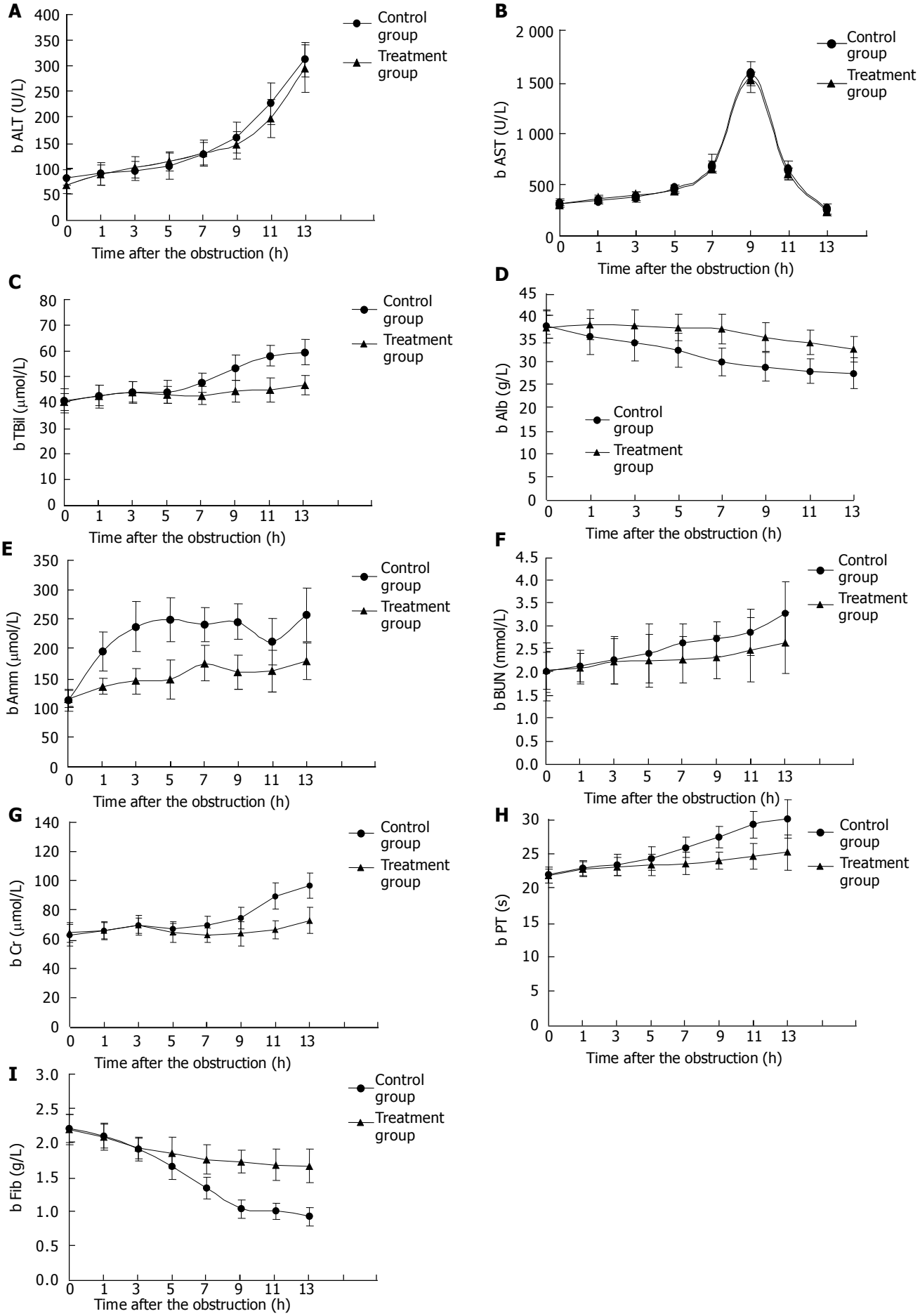


Figure 4 Changes of ALT (**A**), AST (**B**), Tbil (**C**), Alb (**D**), Amm (E), BUN (**F**), Cr (**G**), PT (**H**), and Fib (**I**).

of portal-cava anastomosis reduced the difficulty of the surgery greatly. The blood flowing into liver was obstructed in phase I surgery, which induced ischemia tolerance of the pig. Thus, all the experimental pigs could accept phase II surgery. The model was reproducible. Stable parameters like biochemical indexes and survival time could be obtained, and the success rate of surgery was high. The two-phase surgery could achieve devascularization of liver, while not abruptly diminishing the blood volume in heart, the function of other internal organ was not influenced greatly. The pathologic changes in this model were irreversible, just like the model of total hepatectomy. The key technical point of this ALF model is as follows: The liver rami of left gastric artery and diaphragm artery must be ligated thoroughly during phase II surgery. Because the anatomic structure of porcine liver is similar to that of human beings, the same procedures to obstruct liver rami of human peri-hepatic ligaments were adopted in this study. Portocaval anastomosis is advantageous over portocaval intubation shunt theoretically, but in practice, portocaval intubation shunt is simple and reliable. In the prophase experiments of our study, the metabolism indexes of normal pigs were compared to those of the pigs with their right renal vein ligated. The results indicated that there was no significant difference in Amm, BUN, Cr, and blood sugar fluctuation between the two groups. The time of portocaval intubation shunt was much shorter than that of portocaval anastomosis (just about 5 min). No interference with hemodynamics of portal vein was found in the cases of right renal venous cannulation. The color and luster of bowel were ruddy during phase II surgery, indicating that 0.8-cm caliber of the shunt catheter is advisable.

ALF is a clinical syndrome involving massive hepatocyte necrosis, and resulting in liver function failure and encephalopathy. The death rate of ALF can reach 80%, and there is no specific therapy for it. The introduction of liver transplantation into clinical practice has improved the survival time of patients. However, because of the deficiency in donor liver, about 50% of the ALF patients would die waiting for donors. Since liver has a powerful ability to regenerate, an effective artificial liver assembly has been established to replace the liver functions of ALF patients for a temporary period, till the liver itself regenerates and recovers from acute decompensation. Recently, with advances in cell engineering and material technology, various kinds of large-scale cell culture techniques are used for the study of bioartificial liver, such as microcarriers[7,8], microcapsule coating[9], gelatin embedding[10-12], hollow fiber module[13-15] and spheroid culture[16], *etc*. The BALSS of porcine hepatocyte reactor-hollow fiber module was established and has entered into phase I clinical trials. It has been proven that such a system can yield multifunctions of hepatocytes to support the patients with ALF passing over the crisis. The BALSS can serve as a bridge to liver transplantation[14-18].

The technical characteristics of BALSS are as follows: (1) The microcarrier-adhering hepatocytes and culture media system increase the adsorbing area of hepatocytes greatly. Sufficient contact of cell-matrix or cell-cell is ensured. It is quite helpful to maintain hepatocytes polarity, thus prolonging the stability of hepatocytes. (2) In the circulation loop, high volume recirculating technique is adopted, which facilitates liquor convection greatly, and improves the substrate-product exchange of hepatocytes and the efficiency of BAL circulation. (3) Before the blood is pumped into the hepatocyte reactor, hemoperfusion over charcoal is used to relieve the hepatocyte impairment induced by the toxic substances in blood, thus hepatocyte viability and function can be maintained longer[19,20]. In this study, after devascularization of the liver, ALT increased progressively and swiftly in both groups, but there was no statistical significance between the two groups, suggesting that the degree of hepatocyte impairment is similar in both groups. Since devascularization of the liver in this study was permanent, the impairment of liver function was irreversible. AST could not be determined in treated animals 15 h later. The reason is likely that hepatocyte mitochondria which could not endure hypoxia for a long time reach the peak of disruption about 9 h later, and AST is exhausted gradually. After the experimental pigs died, liver pathological impairment of the two groups was analogous to the pathological image of ALF models, suggesting that the model of ALF established in this study is stable.

During the treatment of BAL, the most impressive result was the fluctuation of Amm. Amm is mainly produced by intestinal bacteria and detoxificated through being synthesized into urea in liver. After the obstruction, Amm level in control animals increased rapidly from (110±17) μmol/L to (240±35) μmol/L 5 h later, while increased slowly from (112±14) μmol/L to (144±34) μmol/L in the treated animals ($P<0.01$), suggesting that the BALSS can detoxify and depress Amm. Similar results have been reported by Chen *et al*. The levels of Tbil, Alb, BUN, Cr, PT, and Fib were significantly different between the two groups 3-7 h later, suggesting that BALSS has some action on bilirubin metabolism.

In conclusion, the BALSS can be used in the treatment of ALF. The results achieved in this study of large animals may contribute to the clinical therapy of ALF with BALSS.

REFERENCES

1 **Seglen PO.** Preparation of rat liver cells. 3. Enzymatic repuirements for tissue dispersion. *Exp Cell Res* 1973; **82**: 391-398

2 **Demetriou AA,** Whiting JF, Feldman D, Levenson SM, Chowdhury NR, Moscioni AD, Kram M, Chowdhury JR. Replacement of liver function in rats by transplantation of microcarrier-attached hepatocytes. *Science* 1986; **233**: 1190-1192

3 **Rozga J,** Holzman MD, Ro MS, Griffin DW, Neuzil DF, Giorgio T, Moscioni AD, Demetriou AA. Development of a hybrid bioartificial liver. *Ann Surg* 1993; **217**: 502-509

4 **Rivas-Vetencourt PA,** Aranda ED, Sorio L, Quero Z, Martinez A, Vegas AM, Zerpa MJ. Xenotra-nsplantation of isolated encapsulated porcine hepatocytes in the treatment of a highly fulminant hepatic failure model. *Transplant Proc* 1997; **29**: 920-922

5 **Dixit V,** Gitnick G. The bioartificial liver: state of the art. *Eur J Surg* 1998; **582**(Suppl): 71-76

6 **Ryska M,** Kieslichova E, Pantoflicek T, Ryska O, Zazula R, Skibova J, Hajek M. Devascularization surgical model of acute liver failure in minipigs. *Eur Surg Res* 2004; **36**: 179-184

7 **Werner A,** Duvar S, Muthing J, Buntemeyer H, Lunsdorf H, Strauss M, Lehmann J. Cultivation of immortalized human hepatocytes HepZ on macroporous CultiSpher G microcarriers. *Biotechnol Bioeng* 2000; **68**: 59-70

8 **Morsiani E,** Pazzi P, Moscioni AD, Rozga J, Azzena G, Demetriou AA. *In vitro* morphological and functional characterization of isolated porcine hepatocytes for extracorporeal liver support: bile acid uptake and conjugation. *J Surg Res* 1998; **79**: 54-60
9 **Yin C,** Mien Chia S, Hoon Quek C, Yu H, Zhuo RX, Leong KW, Mao HQ. Microcapsules with improved mechanical stability for hepatocyte culture. *Biomaterials* 2003; **24**: 1771-1780
10 **Naka S,** Takeshita K, Yamamoto T, Tani T, Kodama M. Bioartificial liver support system using porcine hepatocytes entrapped in a three-dimensional hollow fiber module with collagen gel: An evalution in the swine acute liver failure model. *Artif Organs* 1999; **23**: 822-828
11 **Suh KS,** Lilja H, Kamohara Y, Eguchi S, Arkadopoulos N, Neuman T, Demetriou AA, Rozga J. Bioartificial liver treatment in rats with fulminant hepatic failure: effect on DNA-binding activity of liver-enriched and growth-associated transcription factors. *J Surg Res* 1999; **85**: 243-250
12 **Rivera DJ,** Gores GJ, Misra SP, Hardin JA, Nyberg SL. Apoptosis by gel-entrapped hepatocytes in a bioartificial liver. *Transplant Proc* 1999; **31**: 671-673
13 **Hay PD,** Veitch AR, Smith MD, Cousins RB, Gaylor JD. Oxygen transfer in a diffusion-limited hollow fiber bioartificial liver. *Artif Organs* 2000; **24**: 278-288
14 **Patzer JF 2,** Mazariegos GV, Lopez R, Molmenti E, Gerber D, Riddervold F, Khanna A, Yin WY, Chen Y, Scott VL, Aggarwal S, Kramer DJ, Wagner RA, Zhu Y, Fulmer ML, Block GD, Amiot BP. Novel bioartificial liver support system: preclinical evalution. *Ann N Y Acad Sci* 1999; **875**: 340-352
15 **Chung YJ,** Lee HJ, Koh YT, Kim SB, Kim SH, Choi SH, Yi NJ, Chang SH, Yang EL, Suh KS, Lee YS, Lee KU. Isolation and culture of pig hepatocyte in large scale for the application of bioartificial liver system. *Taehan Kan Hakhoe Chi* 2002; **8**: 249-255
16 **Maddrey WC.** Bioartificial liver in the treatment of hepatic failure. *Liver Transpl* 2000; **6**(4 Suppl 1): S27-30
17 **Nyberg SL,** Hay EJ, Ramin KD, Rosen CB. Successful pregnancy after porcine bioartificial liver treatment and liver transplantation for fulminant hepatic failure. *Liver Transpl* 2002; **8**: 169-170
18 **Tsiaoussis J,** Newsome PN, Nelson LJ, Hayes PC, Plevris JN. Which hepatocyte will it be? Hepatocyte choice for bioartificial liver support systems. *Liver Transpl* 2001; 7: 2-10
19 **Flendrig LM,** Chamuleau RA, Maas MA, Daalhuisen J, Hasset B, Kilty CG, Doyle S, Ladiges NC, Jorning GG, la Soe JW, Sommeijer D, te Velde AA. Evaluation of a novel bioartificial liver in rats with complete liver ischemia: treatment efficacy and species-specific alpha-GST detection to monitor hepatocyte viability. *J Hepatol* 1999; **30**: 311-320
20 **Baquerizo A,** Mhoyan A, Kearns-Jonker M, Arnaout WS, Shackleton C, Busuttil RW, Demetriou AA, Cramer DV. Characterization of human xenoreactive antibodies in liver failure patients exposed to pig hepatocytes after bioartificial liver treatment: an ex vivo model of pig to human xenotransplantation. *Transplantation* 1999; **67**: 5-18

Science Editor Wang XL and Guo SY **Language Editor** Elsevier HK

PO Box 2345, Beijing 100023, China
www.wjgnet.com
wjg@wjgnet.com

ELSEVIER

World J Gastroenterol 2005;11(35):5475-5479
World Journal of Gastroenterology ISSN 1007-9327
© 2005 The WJG Press and Elsevier Inc. All rights reserved.

• *BASIC RESEARCH* •

Establishment of a pig model with enteric and portal venous drainage of pancreatoduodenal transplantation

Zhao-Da Zhang, Fang-Hai Han, Ling-Xiang Meng

Zhao-Da Zhang, Fang-Hai Han, Ling-Xiang Meng, Third General Department, West China Hospital of Sichuan University, Chengdu 610041, Sichuan Province, China
Supported by the Doctorate Foundation of Ministry of Education of China, No. 20030610071; Foundation of China Medical Board of New York, No. 82412
Correspondence to: Zhao-Da Zhang, Third General Department, West China Hospital of Sichuan University, Chengdu 610041, Sichuan Province, China. zdzhang@wcums.edu.cn
Telephone: +86-28-85409176 Fax: +86-28-85502321
Received: 2004-06-11 Accepted: 2004-07-27

Abstract

AIM: To establish the pig model of pancreatoduodenal transplantation with enteric drainage (ED) and portal venous drainage (PVD).

METHODS: Forty-six hybrid Landrace pigs were divided into two groups (donors and recipients) randomly, and pancreatoduodenal allotransplantation was performed. Donors were perfused via abdominal aorta without clamping the portal venous outflow with UW solution at 80–100 cm H_2O after heparinization. Whole pancreatoduodenal grafts were harvested with segments of abdominal aorta and portal vein, and shaped under 4 ℃ UW solution. Then, end-to-end anastomosis was performed with the donor iliac artery bifurcation Y graft to the recipient superior mesenteric artery and celiac artery. Furthermore, type I diabetes model was made by removal of the recipient pancreas. The venous anastomosis was reconstructed between the donor portal vein and the recipient superior mesentery vein. Meanwhile, end-to-side anastomosis was performed with the donor common iliac artery bifurcation Y graft to the recipient abdominal aorta, and side-to-side intestinal anastomosis was performed between the donor duodenum and the recipient jejunum. External jugular vein was intubated for transfusion. Levels of plasma glucose, insulin and glucagon were measured during the operation and on the 1st, 3rd, 5th, and 7th d after operation.

RESULTS: Pancreatoduodenal allotransplantation was performed on 23 pigs of which 1 died of complication of anesthesia. The success rate of operation was 95.6%. Complications of operation occurred in two cases in which one was phlebothrombosis with an incidence of 4.6%, and the other was duodenojejunal anastomotic leak with an incidence of 4.6%. The level of plasma glucose decreased within 30 min, after removal of pancreas and recovered on the 2nd d after operation. The level of plasma insulin and glucagon increased within 30 min after removal of pancreas and recovered on the 2nd d after operation. Rejection occurred on the 1st d and reached the worst level on the 7th d after transplantation, without change of plasma insulin and glucagon or clinical symptoms of rejection.

CONCLUSION: Pancreatoduodenal transplantation in pigs can treat type I diabetes. ED and PVD can keep the function of endocrine in normal. The technique of pancreatoduodenal transplantation with ED and PVD may pave the way for the further application of pancreas transplantation in clinic.

© 2005 The WJG Press and Elsevier Inc. All rights reserved.

Key words: Pancreatoduodenal transplantation; Enteric drainage; Portal venous drainage

Zhang ZD, Han FH, Meng LX. Establishment of a pig model with enteric and portal venous drainage of pancreatoduodenal transplantation. *World J Gastroenterol* 2005; 11(35): 5475-5479
http://www.wjgnet.com/1007-9327/11/5475.asp

INTRODUCTION

Pancreas transplantation or combined pancreas-kidney transplantation is a radical therapy method for insulin-dependent diabetes mellitus and its complications. Though immune inhibitors and improvement of surgical technology have achieved obvious improvement of graft functional survival, surgical technology is still one of the important factors contributing to the failure of pancreas transplantation. The rate of it was 7-14% to simultaneous pancreas-kidney transplantation (SPK), 8-23% to pancreas after kidney transplantation (PAK), 10-23% to pancreas transplantation alone (PTA). Since 1995, over 1 000 cases of pancreas transplantation have been done[1]. Surgeons always want to decrease the failure caused by surgical technology, and to perform pancreas transplantation according to the status of anatomy and physiology. To pancreas transplantation, there are two types of exocrine drainage, one is bladder drainage (BD), the other is enteric drainage (ED). There are two types of endocrine drainage, one is systemic drainage (SVD), the other is portal venous drainage (PVD). BD could cause metabolic acidosis, uterine reflux pancreatitis, and urinary bladder stimulation that contributes to mucous erosion, bleeding, urinary tract stricture, etc.; so ED has to be performed after about 25% of BD operations[2]. In SVD cases, insulin and glucagon flow into systemic venous system,

not through the liver first; so it is not good in improving of microvascular lesions[3]. In PVD cases, pancreas glucagonoma can be avoided, and immune intolerance can be induced because the graft antigen goes into the liver directly. The combination of ED and PVD in pancreas transplantation is better to the status of anatomy and physiology. The pig anatomy structure is similar to that of human being, so it is very useful to set up an animal model with combined ED and PVD in pancreas transplantation.

MATERIALS AND METHODS

Experimental animals

Forty-six local Sichuan hybrid Landrace pigs, weighing 25-32 kg, were used as donors and recipients, and were provided by the Pig Institute of Sichuan Agriculture Science Academy. They were fasted for 12 h and forbidden drinking water for 6 h before operation.

Anesthesia and monitoring

Atropine (0.5 mg) and ketamine (15-20 mg/kg) were intramuscularly injected before anesthesia, 0.25% thiopental sodium was intravenously used, ventilation was provided by tracheal intubation. The anesthesia was maintained with 2% procaine and 0.15% succinylcholine chloride. During operation, ketamine, diazepam or fentanyl was sometimes used for better anesthesia; ECG, arterial pressure and SaO_2 were monitored. A trocar was placed in the auricular vein for fluid infusion.

Donor operation

We used anterior abdominal median incision. The stomach was removed, and the end of duodenum was blocked. The proper hepatic artery and common bile duct were ligated and divided. The portal vein was isolated. The superior mesentery artery and vein were isolated and ligated. The jejunum was divided at the site of 5 cm to the superior mesentery artery, the bilateral renal arteries and veins were isolated and ligated. The spleen artery and vein were ligated. Heparin (200 IU/kg) was intravenously injected to get systemic heparinization, 1 000 mL of normal solution (4 ℃) was poured into abdominal cavity. An abdominal aorta cannula was placed, the abdominal aorta was blocked at the site up to the celiac artery, and the in site flushing of fluctuating UW (4 ℃) fluid (about 2 000 mL) was made through the former cannula. The perfusion pressure was 80-100 cm water column. The portal vein was divided, and the end near the pancreas was open, the other end was ligated. The perfusion was stopped when the temperature was down, pancreas became pale, and effluent from the portal vein was clear (Figure 1). The head of pancreas was mobilized to the right of aorta, the tail of pancreas and spleen were mobilized. The aorta was divided above its fork, lumbar arteries derived from the proximal part of abdominal aorta were ligated and divided. The left or right common iliac artery and internal and external iliac arteries were removed.

Modification and storage of donor grafts

The pancreas and duodenum were stored in UW fluid (4 ℃) of a plastic bag, which was placed in a basin containing cold normal solution (Figure 2). The abdominal aorta was opened in the back wall, the peripheral of celiac artery and superior mesentery artery remained as elliptic Carrel patch, whose diameters were 0.5-0.8 cm. The celiac stem cannula and superior mesenteric artery cannula were placed for UW fluid perfusion. The portal vein was modified and 1.5-3.0 cm of it remained. The small blood and lymphatic vessels around the pancreas were ligated one by one. The fat tissue and lymph nodes were removed. The incision of anterior duodenum wall was made for the wash with metronidazole (0.5 g) and amikacin (0.4 g). The length of 20-30-cm duodenum was left for transplantation. An anastomosis was made for the opening of celiac stem and the distal end of external iliac artery, so did for the opening of superior mesenteric artery and the distal end of internal iliac artery. The modified graft was placed in UW fluid (4 ℃).



Figure 1 Pale pancreas after perfusion.



Figure 2 Modified graft for transplantation.

Recipient operation

After anesthesia worked, a cannula was placed in the external jugular vein, an anterior abdominal median incision (18-20 cm) was applied. Then the whole pancreas was removed. The superior mesentery vein and portal vein were exposed. After the anterior part of superior mesentery vein or portal vein was clamped with a vessel nip, whose caliber was similar to the diameter of the proximal end of the donor portal vein, was made. The lacuna was rinsed with normal saline containing heparin. The donor portal vein anastomosis was performed in an end-to-side fashion to the recipient superior mesenteric vein or portal vein

(Figure 3A). The abdominal aorta distal to the renal vein was freed. After the anterior part of abdominal aorta was clamped with a Satinski nip, an incision (1.0-1.5 cm) was made in corresponding part of the recipient anterior abdominal aorta wall. The donor common iliac artery anastomosis was performed in an end-to-side fashion to the recipient aorta (Figure 3B). The blood circulation to the graft was recovered after the former anastomoses were finished, the graft became pink, and its arteriopalmus and peristalsis were restored. The donor duodenum anastomosis was performed in a side-to-side fashion to the recipient jejunum 8-10 cm distal to the recipient Treitz ligament (Figure 3C). After the spleen was removed, the graft was placed in the right part of abdominal cavity.

Postoperation management

After autonomous respiration, steady blood pressure, and normal pulse were recovered, the tracheal intubate was removed. After operation, the recipient pig was forbidden drinking for 24 h, and eating for 2-4 d, and received 1 000-2 500 mL fluid infusion intravenously in those days. During the 1st d after operation, the recipient received the fluid at the ratio of glucose to insulin 1:4, 3 g ampicillin, 0.5 g of metronidazole, 40 mL danshen injection, 500 mL low molecular dextran, and heparin (1 mg/kg). To monitor the graft function status, the plasma glucose, insulin, and glucagon were measured, and pathology examination was performed. Plasma glucose, insulin, and glucagon were measured 30 min after the pancreas was removed, 30 min after blood circulation to the graft was recovered, and on each of the first 7 d after operation. The graft biopsy tissues were obtained on the 1st, 3rd, 5th and 7th d after transplantation. The biopsy tissues were observed by naked eyes and microscope after being stained with HE. The Nakhleh criteria[4] were used as follows:

Criteria for pancreas rejection The score was 0, if no rejection could be seen. The score was 1, if mild rejection could be seen (Lymph cells could be seen scattering in external secretion tissues, especially in tissues among pancreas lobules. The pancreas islet and pancreas duct were normal.). The score was 2, if moderate rejection could be seen (Diffused lymph cells and plasma cells can be seen in pancreas tissue, and local necrosis lesions or small pitch of wrecked granules could be seen. Lymph cells infiltrated in the area around pancreas duct. The structure of islet was normal, sometimes a few inflammation cells could be seen in islet.). The score was 3, if severe rejection could be seen (Much more lymph cells and plasma cells can be seen in pancreas tissue. Sweeping wreck of granules and sometimes pancreas fibrosis could be seen. Islets were wrecked and some or all of them disappeared. Vascular rejection, vessel endothelium inflammation, and fibroid necrosis could be seen.).

Criteria for vascular rejection The score was 1, if lymph cells infiltrated into the area under minority of venous endothelium cells. The score was 2, if lymph cells infiltrated into the area under majority of venous endothelium cells. The score was 3, if lymph cell infiltration and inflammation around the veins could be seen.

Statistical analysis

SPSS10.0 was used for analysis of data.

RESULTS

Success rate of operation

Of the 23 pigs that received pancreas transplantation, only one pig died from anesthesia accident. The survival rate was 95.65%. The longest survival time was 96 d. The operation time of donors was 73.84±6.86 min, and that of recipients was 143.25±18.14 min. There was no warm ischemia, the time of cold ischemia was 117.30±18.02 min. The portal vein anastomosis was 38.30±5.60 min, the time of artery anastomosis was 26.20±2.26 min. Two complications were observed, one was pancreas phlebothrombosis, the other was duodenojejunal anastomotic leak. There was no complication of vessel anastomosis, transplantational pancreatitis, or pancreatic ascites.

Survival of grafts

The graft biopsy tissues were obtained on the 1st, 3rd, 5th, and 7th d after transplantation. There was one case of pancreas infarction. Seventeen cases survived with good blood supply to pancreas.

Graft function after operation

Normal limosis plasma glucose of pigs was 5.22±0.92 mmol/L, plasma insulin was 8.34±2.43 mU/L, plasma glucagon was 177.73±12.11 pg/mL.

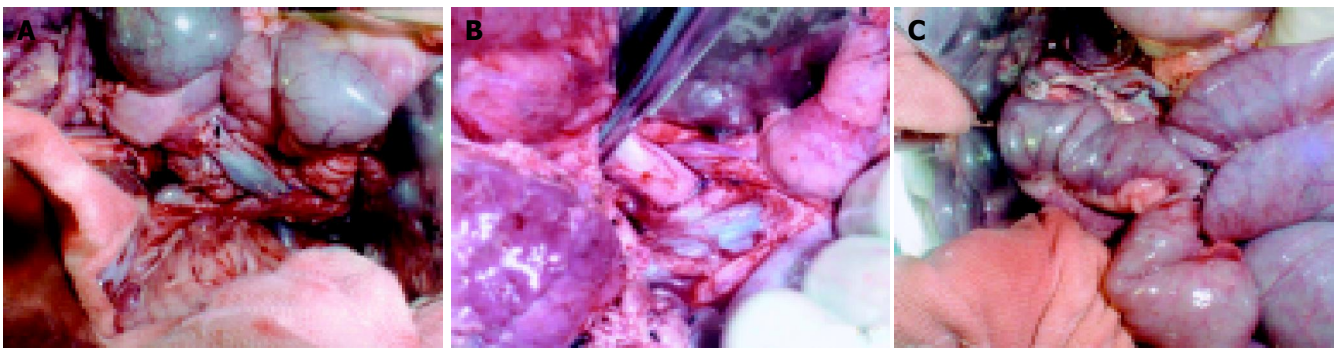


Figure 3 Anastomosis of donor portal vein to recipient superior mesenteric vein (**A**), donor common iliac artery to recipient aorta (**B**) in an end-to-side fashion, and donor duodenum to recipient jejunum (**C**) in a side-to-side fashion.

Pathology of rejection

During the first 3 d after transplantation, mild edema of pancreas could be seen. There were no exudation, congestion, or adhesion of pancreas. Under microscopy, lymph cells and monocytes could be seen in pancreas matrix, not in islet (Figure 4A). During the 5^{th}-7^{th} d, there were mild edema, congestion and adhesion of pancreas. Under microscopy, local or extensive infiltration of lymph cells and monocytes, apoptosis body could be seen (Figures 4B and C). There was separated or small pitch of necrosis of pancreas adrenal cells, extensive infiltration of lymph cells could be seen around small vessels, a few lymph cells could be seen around islets. During the 7^{th}-9^{th} d, the pancreas became more flexible, adhered to peripheral tissues, looked pale, and had good blood supply (Figure 4D). Under microscopy, extensive infiltration of lymph cells and monocytes could be seen in pancreas and around vessels. There were vessel endothelium inflammation and extensive fibrosis of pancreas (Figure 4E). During the 2^{nd}-4^{th} wk after operation, the pancreas glands and islets were replaced by connective tissues. Extensive lymphocyte infiltration could be seen in pancreas (Figure 4F).

DISCUSSION

Our data indicated that the plasma glucose arose 30 min after the pancreas was removed, became normal 2 d after transplantation, and arose again 15-21 d after transplantation. The half life of insulin or glucagon was only 5-10 min, indicating that the graft endocrine function was normal 2 d after transplantation. There was no host plasma insulin or glucagon after the recovery of grafts. It was different from SVD, the plasma insulin and glucagon levels were normal[5,6] indicating that the PVD in pancreas transplantation is better for the treatment of type I diabetes mellitus. To the rejection, our data indicated that mild rejection appeared on the 1^{st} d after operation, and became more serious with the time protracted. At the same time (2 wk after transplantation) plasma glucose, insulin, and glucagon were normal, indicating that we cannot know if there is rejection, or how serious the rejection is, after the operation. More sensitive criterion must be found for clinical work[7]. The length and diameter of pig portal vein are similar to those of human beings[8], setting up of a pig animal model is beneficial in clinical pancreas transplantation with ED+PVD. It was reported that primary ED was associated with a high incidence of early graft

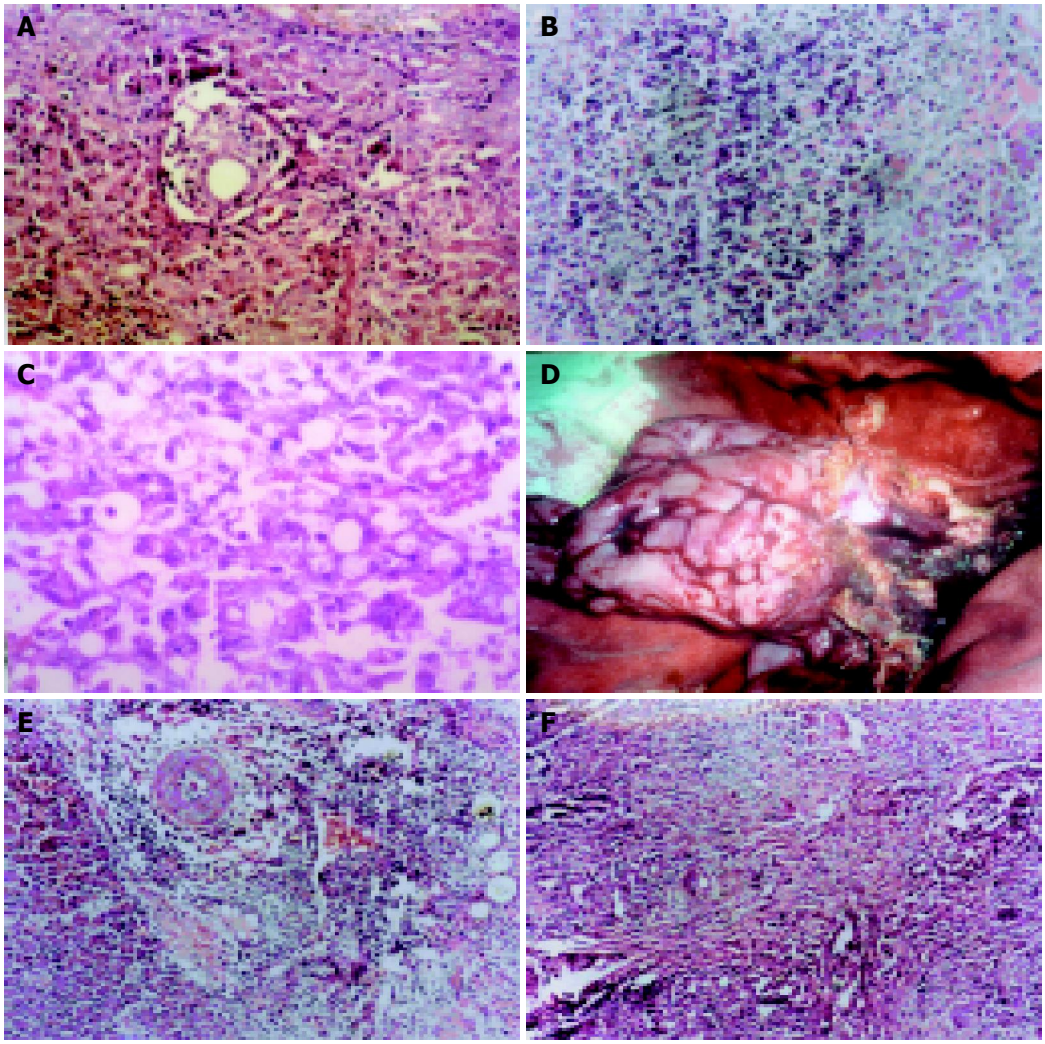


Figure 4 Mild rejection 3 d after operation (**A**) (HE ×200) and moderate rejection 5 d after operation (**B**) (HE ×100), apoptosis body and pancreatic edema 7 d after operation (**C**), pale pancreas with flexible mild edema 9 d after operation (**D**), severe rejection 10 d after operation (**E**), and infiltration of lymphocytes and hyperplasia of connective tissue 21 d after operation (**F**).

thrombosis, a complication that is the major cause of graft loss in PTA recipients[9]. Our data show that only 1/23 had thrombosis of pancreas, no complication of vessel anastomosis was found.

Our pig model of pancreas transplantation was improved on the following aspects[5,10,11]: (1) The outflow of the graft was performed through the anastomosis of donor portal vein to the recipient inferior vena cava. (2) The arterial inflow to the allograft was achieved by a single anastomosis of an aortic patch to the intended target in the recipient. (3) The pancreas exocrine drainage to the urinary bladder was performed through the duodenocystostomy. The present technique has the following advantages. (1) The outflow of the graft was performed through the anastomosis of donor portal vein to the recipient portal vein. It is better to the status of anatomy and physiology. (2) The Y-graft was anastomosed to the recipient abdominal aorta and the blood supply was achieved through it. It is a standard arterial reconstruction of clinical pancreas transplantation[12], because it is good for simultaneous liver procurrent[13]. The allograft was modified, and Y-graft was achieved under the protection of cold preservation solution. It did not prolong warm ischemia[14,15]. (3) The pancreas exocrine drainage to the jejunum was gained through an anastomosis of donor duodenum to the recipient jejunum. So there were no complications in duodenocystostomy, such as metabolic acidosis, uterine reflux pancreatitis, and urinary bladder stimulation that could contribute to mucous erosion, bleeding, urinary tract stricture, etc.[16]. (4) During the operation of blood vessel anastomosis, the abdominal aorta or inferior vena cava was not obstructed completely. Then, during the operation, the disadvantage effect on the recipient blood circulation was lesser.

In conclusion, our pig model is a model with ED and PVD. It is better to the status of anatomy and physiology. Now, more and more clinical pancreas transplantations with ED and PVD are performed[16,17], our pig model of pancreas transplantation can work better for the further study of pancreas transplantation.

REFERENCES

1 **Sutherland DE,** Cecka M, Gruessner AC. Report from the International Pancreas Transplant Registry-1998. *Transplant Proc* 1999; **31**: 597-601

2 **Weir GC,** Bonner-Weir S. Scientific and political impediments to successful islet transplantation. *Diabetes* 1997; **46**: 1247-1256

3 **West M,** Gruessner AC, Metrakos P, Sutherland DE, Gruessner RW. Conversion from bladder to enteric drainage after pancreaticoduodenal transplantations. *Surgery* 1998; **124**: 883-893

4 **Nakhleh RE,** Sutherland DE, Tzardis P, Schechner R, Gruessner RW. Correlation of rejection of the duodenum with rejection of the pancreas in a pig model of pancreatico-duodenal, transplantation. *Transplantation* 1993; **56**: 1353- 1356

5 **Xu ZK,** Liu XL, Zhang W, Miao Y, Du JH. Establishment of a pig model of combined pancreas-Kidney transplantation. *World J Gastroenterol* 1999; **5**: 172-174

6 **Katz H,** Homan M, Velosa J, Robertson P, Rizza R. Effects of pancreas transplantation on postprandial glucose metabolism. *N Engl J Med* 1991; **325**: 1278–1283

7 **Fernandez JA,** Claver MA, Llorente S, Gimeno L, Robles R, Ramirez P, Bueno FS, Rodriguez JM, Lujan JA, Munitiz V, Parrilla P. Clinical noninvasive evaluation of simultaneous pancreas-kidney transplants with the combined use of gamma graphy, Doppler ultrasound and serum markers. *Transplant Proc* 2002; **34**: 209-211

8 **Terajima H,** Shirakata Y, Yagi T, Mashima S, Shinohara H, Satoh S, Arima Y, Gomi T, Hirose T, Takahashi R, Ikai I, Morimoto T, Inamoto T, Yamamoto M, Yamaoka Y. Successful longterm xenoperfusion of the pig liver: continuous administration of prostaglandin EI and insulin. *Transplantation* 1997; **63**: 507-512

9 **Sutherland DE,** Gruessner A. Pancreas transplantation in the United States as reported to the United Network for Organ Sharing (UNOS) and analyzed by the International Pancreas Transplant Registry. *Clin Transpl* 1995; **9**: 49-67

10 **Ganger KH,** Mettler D, Boss HP, Ruchti C, Stoffel M, Schilt W. Experimental duodeno-pancreatico-renal composite transplantation: a new alternative to avoid vascular thrombosis. *Transplant Proc* 1987; **19**: 3960-3964

11 **Gruessner RW,** Nakhleh R, Tzardis P, Schechner R, Platt JL, Gruessner A, Tomadze G, Najarian JS, Sutherland DE. Differences in rejection grading after simultaneous pancreas and kidney transplantation in pigs. *Transplantation* 1994; **57**: 1021-1028

12 **Sollinger HW,** Odorico JS, Knechtle SJ, D'Alessandro AM, Kalayoglu M, Pirsch JD. Experience with 500 simultaneous pancreas-kidney transplants. *Ann Surg* 1998; **228**: 284-296

13 **Troppmann C,** Gruessner AC, Benedetti E, Papalois BE, Dunn DL, Najarian JS, Sutherland DE, Gruessner RW. Vascular graft thrombosis after pancreatic transplantation: univariate and multivariate operative and nonoperative risk factor analysis. *J Am Coll Surg* 1996; **182**: 285-316

14 **Johnson CP,** Roza AM, Adams MB. Simlutaneous liver and pancreas procurement: a simplified method. *Transplant Proc* 1990; **22**: 425-426

15 **Mizrahi S,** Boudreaux JP, Hayes DH, Hussey JL. Modified vascular trconstruction for pancreaticoduodenal allograft. *Surg Gynecol Obstet* 1993; **177**: 89-90

16 **Sutherland DE,** Gruessner RW, Dunn DL, Matas AJ, Humar A, Kandaswamy R, Mauer SM, Kennedy WR, Goetz FC, Robertson RP, Gruessner AC, Najarian JS. Lessons learned from more than 1000 pancreas transplans at a single institution. *Ann Surg* 2001; **233**: 463

17 **Gruessner AC,** Sutherland DE. Report for the international pancreas transplant registry. *Transplant Proc* 2001; **33**: 1643

Science Editor Wang XL and Li WZ **Language Editor** Elsevier HK

PO Box 2345, Beijing 100023, China
www.wjgnet.com
wjg@wjgnet.com

ELSEVIER

World J Gastroenterol 2005;11(35):5480-5484
World Journal of Gastroenterology ISSN 1007-9327
© 2005 The WJG Press and Elsevier Inc. All rights reserved.

• *BASIC RESEARCH* •

Effect of Jianweiyuyang granule on gastric ulcer recurrence and expression of VEGF mRNA in the healing process of gastric ulcer in rats

Xing-Ping Dai, Jia-Bang Li, Zhao-Qian Liu, Xiang Ding, Cheng-Hui Huang, Bing Zhou

Xing-Ping Dai, Jia-Bang Li, Cheng-Hui Huang, Bing Zhou, Institute of Integrated Traditional Chinese and Western Medicine, Central South University, Changsha 410078, Hunan Province, China
Zhao-Qian Liu, Institute of Clinical Pharmacology, Xiangya School of Medicine, Central South University, Changsha 410078, Hunan Province, China
Xiang Ding, Department of Gastroenterology, Xiangya Hospital Central South University, Changsha 410078, Hunan Province, China
Supported by the Foundation of Traditional Chinese Medicine of the Bureau of Health of Hunan Province, No. 202053
Correspondence to: Professor Jia-Bang Li, Institute of Integrated Traditional Chinese and Western Medicine, Central South University, Changsha 410078, Hunan Province, China. mwdlyy@sina.com
Telephone: +86-731-4327227
Received: 2004-11-23 Accepted: 2005-01-12

Abstract

AIM: To investigate the effect of Jianweiyuyang (JWYY) granule on gastric ulcer recurrence and its mechanism in the treatment of gastric ulcer in rats.

METHODS: Gastric ulcer in rats was induced according to Okeba's method with minor modification and the recurrence model was induced by IL-1β. The expression of vascular endothelial growth factor mRNA (VEGF mRNA) was examined by reverse transcription polymerase chain reaction in gastric ulcer and microvessel density (MVD) adjacent to the ulcer margin was examined by immunohistochemistry.

RESULTS: MVD was higher in the JWYY treatment group (14.0±2.62) compared with the normal, model and ranitidine treatment groups (2.2±0.84, 8.8±0.97, 10.4±0.97) in rats (P<0.01). The expression level of VEGF mRNA in gastric tissues during the healing process of JWYY treatment group rats significantly increased compared with other groups (normal group: 0.190±0.019, model group: 0.642±0.034, ranitidine group: 0.790±0.037, P<0.01).

CONCLUSION: JWYY granules can stimulate angiogenesis and enhance the expression of VEGF mRNA in gastric ulcer rats. This might be the mechanism for JWYY accelerating the ulcer healing, and preventing the recurrence of gastric ulcer.

© 2005 The WJG Press and Elsevier Inc. All rights reserved.

Key words: Jianweiyuyang granule; Gastric ulcer; VEGF mRNA

Dai XP, Li JB, Liu ZQ, Ding X, Huang CH, Zhou B. Effect of Jianweiyuyang granule on gastric ulcer recurrence and expression of VEGF mRNA in the healing process of gastric ulcer in rats. *World J Gastroenterol* 2005; 11(35): 5480-5484
http://www.wjgnet.com/1007-9327/11/5480.asp

INTRODUCTION

Peptic ulcer (PU) is one of the common clinical diseases. The incident rate of PU has been on the rise over the recent two decades[1]. Some latest studies showed that H_2 antagonists and the proton pump inhibitor omeprazole had about 80-100% of healing rate and produced a good therapeutic effect on gastroduodenal ulcer after a 4-8-wk administration. However, gastroduodenal ulcer has 40-80% of recurrent frequency, once the drug is withdrawn within a year. Moreover, *Helicobacter pylori* eradication ameliorates symptoms and improves the quality of lives of patients, but many of them still cannot avoid ulcer relapses[2-4].

The repair of gastric ulcers requires the reconstitution of epithelial structures and underlying connective tissue, including vessels and muscle layers. This complex sequence of events requires a high degree of coordination among different cell types, which is regulated by several factors. Of them, some growth factors, such as vascular endothelial growth factor (VEGF) and the platelet-derived growth factor (PDGF), have received much attention in recent years, because they play a pivotal role in gastric ulcer repair[5]. Previous studies indicated that the Chinese traditional medicine Jianweiyuyang granules (JWYY) can accelerate ulcer healing, improve scar quality, and prevent ulcer recurrence[6,7]. However, the mechanisms responsible for these actions are not fully elucidated. In this study, we examined the microvessel density (MVD) in the ulcer margin by immunohistochemistry and demonstrated the specific expression of VEGF mRNA at the gastric ulcer margin tissue using reverse transcription polymerase chain reaction (RT-PCR). The aim of this study was to determine whether JWYY accelerated ulcer healing by enhancing the expression of VEGF mRNA and angiogenesis.

MATERIALS AND METHODS

Medicine and reagents

JWYY granules were purchased from Hunan Xiangya Pharmaceutical Co., Ltd (No. Z10960018). Ranitidine capsule (purity 98%) was from Hangzhou Sanofi-Synthélabo

Minsheng Pharmaceutical Co., Ltd (No. H33021741). TRIzol reagent was from GIBCO BRL Co., Ltd (MRI, USA). Factor VIII antibody, revert Aid™ first strand cDNA synthesis kit and marker were provided by Fermentas Life Sciences Co. (MBI, Lithuania). DEPC was from Sigma Co. (St. Louis, USA). SABC kit and DAB kit were from Wuhan Boster Biotechnology Co., Ltd.

Animals and ulcer induction

Ninety Sprague-Dawley rats, half male and half female, weighing 180-220 g, were chosen for use in this study. All the rats were obtained from Experimental Animal Center of Xiangya Medical School of Central South University. The rats were kept individually in wire-bottom cages with free access to standard rat diet and water. The animal room was illuminated with a 12-h light-dark cycle. The room temperature was kept at 18-22 ℃ and the humidity at 60-70%. Rats underwent laparotomy under pentobarbital anesthesia.

Ninety rats were divided into six groups: normal group, sham operation group, ulcer model group, ulcer recurrence group, ranitidine group, and JWYY treatment group. Gastric ulcers were induced by a minor modification of the previously described method[8]. In control group, the operation procedures of rats were similar procedures except the application of acetic acid (sham operation).

Rats with healed ulcers were subjected to experiments of induction of ulcer recurrence. The rats in the ulcer model group were killed without treatment with interleukin 1β (IL-1β). The ulcer index, MVD and the expression of VEGF mRNA were measured. Recombinant human IL-1β (1 μg/kg) diluted to 1 mL with isotonic saline was injected intraperitoneally to the remaining animals to induce the ulcer recurrence model[9].

Drug treatment

Each of the rats in JWYY group were treated with a single dose of 0.162 g/(mL·100 g) JWYY granules daily; each rat in the ranitidine control group was treated with a single dose of 5.4 mg/(mL·100 g) of ranitidine daily. Other groups were treated with distilled water.

Tissues preparation

Rats were killed 7 or 92 d later after they received drug treatment or feed, then the gastric walls of rats were removed. A portion of the wall was put into 4% formaldehydum polymerisatum for 1 h to examine the ulcer index by the method designed by us. Another portion of the wall was embedded into the paraffin wax for HE staining. The gastric ulcer margin tissue was removed for MVD and VEGF mRNA expression measurement separately.

Measurement of ulcer index

The length, width, and depth of the ulcer were measured by a compass. The area of the ulcer equals to the width of the ulcer times the length of the ulcer. The ulcer was divided into two grades by its depth more than or less than 2 mm. The ulcer index was classified into 10 degrees[6] (Table 1).

Determination of MVD

The consecutive 5-μm sections were cut and mounted onto glass slides. Sections were stained with HE. The microvessel was examined using immunohistochemistry method with an anti-VIII mouse monoclonal antibody with a dilution of 1:80. Negative controls were detected by PBS substitution for the primary antibodies. All the procedures were carried out according to the manufacturer's instruction.

MVD was evaluated according to the previous method as described by Wang and Liao[10,11]. The stained sections were screened under low power, and five areas with the most intense neovascularization were selected. Microvessel counting of these areas was performed at the ulcer margin (×400). Any brown-stained endothelial cell or endothelial cell cluster was counted as a vessel. Vascular counts of each case were calculated. The mean microvessel count of the five richest vascular areas was taken as MVD.

Determination of expression of VEGF mRNA

Total RNA was isolated from gastric biopsy tissues by using TRIzol reagent according to the manufacturer's instruction.

RT-PCR was performed according to the manufacturer's instruction. RT-PCR reaction mixture containing 2 μL of total RNA, 1 μL oligo (dT)18 (0.5 μg/μL), 9 μL ddH_2O in a tube was mixed gently and then spinned down 3-5 s in a microcentrifuge. The mixture was incubated at 70 ℃ for 5 min and chilled on ice and the drops were collected by brief centrifugation. Four microliters of 5× buffer, 2 μL 10 mmol/L dNTP, and 1 μL (20 U) Rnasin were added to the above collected drops and then the mixture was incubated at 37 ℃ for 5 min. Then 1 μL (200 U/μL) M-MuLV reverse transcriptase was added to the above mixture and incubated at 42 ℃ for 60 min. The reaction was stopped by heating at 70 ℃ for 10 min. The first strand cDNA synthesized was chilled on ice and stored at -20 ℃ until next analysis.

The specific primers were designed by software primer premier 5.0 and purchased from Shanghai DNA Biotechnology Corporation Ltd. The primers for VEGF were 5'-CCTGGTGGACATCTTCCAGGAGTACC-3' (sense) and 5'-GAAGCTCATCTCTCCTATGTGCTGGC-3' (anti-sense), and the size of the amplified fragment conserved in all of the variant spliced forms was 104 bp. PCR products for β-actin were used as a positive control and internal standard. The primers for β-actin were 5'-

Table 1 Method of measuring the gastric ulcer index

Area (mm^2)	Depth	
	<2 mm	>2 mm
0	_	_ (ulcer healing)
1–4	1[1]	2
5–9	2	3
10–14	3	4
15–19	4	5
20–24	5	6
25–29	6	7
30–34	7	8
35–39	8	9
40	9	10

[1]1–10 = grade of the ulcer index.

GAGGGAAATCGTGCGTGAC-3' (sense) and 5'-CTGGAAGGTGGACAGTGAG-3' (anti-sense). The length was 445 bp. PCR was carried out in a final volume of 25 μL reaction mixture containing 9.5 μL ddH_2O, 2.5 μL 10× buffer, 1.5 μL $MgCl_2$, 0.5 μL 10 mmol/L dNTP, 4 μL VEGF primer, 4 μL β-actin primer, 0.5 μL Taq DNA polymerase (1.5 μL) and 2.5 μL cDNA. The final concentration of each primer was 0.1 μmol/L. Amplification conditions included an initial denaturation at 95 ℃ for 5 min, followed by 30 cycles of denaturation at 94 ℃ for 45 s, annealing at 63 ℃ for 45 s, and 1 min extending at 72 ℃, and a final extension at 72 ℃ for 10 min. Negative reaction mixture had no cDNA. PCR products were electrophoretically separated on 1.5% agarose gel in 1× TBE buffer, after which the gel was stained with ethidium bromide (0.5 μg/mL). The PCR instrument was purchased from Perkin Elmer Company.

For quantitative assessment of the PCR products, a computerized video analysis system was used. The results are expressed as the VEGF/β-actin ratio.

Statistical analysis

Results are expressed as the mean±SD. The Student's *t*-test was used to determine statistical significance of differences between two treatment groups. Comparisons of data between groups were performed with analysis of variance followed by *F*-test. $P<0.05$ was taken as significant. Statistical software SPSS10.0 was used in this study.

RESULTS

Effect of JWYY on gastric ulcer recurrence

After rats were induced by acetic acid, ulcers were detected in all rats by macroscopic examination except for the normal and sham operation groups (Figures 1 and 2). Moreover, after rats were induced by IL-1β, no ulcers in the normal and sham operation groups were detected by macroscopic examination (Figure 3). However, as shown in Figures 4-6 and Table 2, 9 of 10 rats in the model recurrence group had a gastric ulcer recurrence. In contrast, only 1 of 10 rats in the model group without IL-1β treatment was observed with ulcer recurrence. Moreover, 8 of 10 rats in the ranitidine group and 3 of 10 rats in the JWYY group with IL-1β treatment had gastric ulcer recurrence.

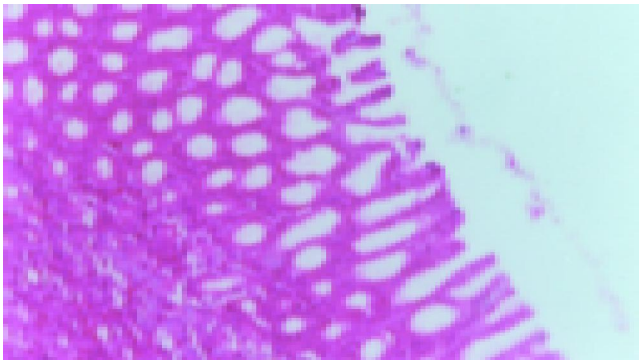


Figure 1 Normal gastric mucous (×200).

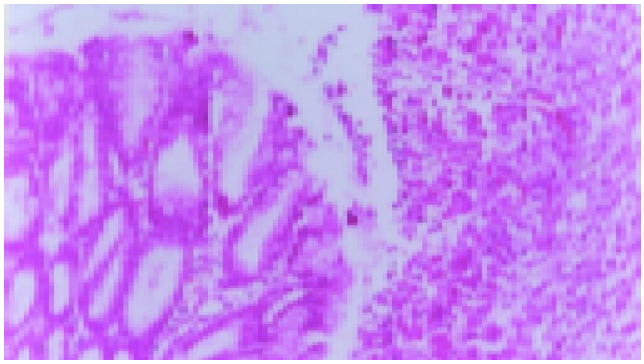


Figure 2 Model group ulcer formation (7 d, ×200).

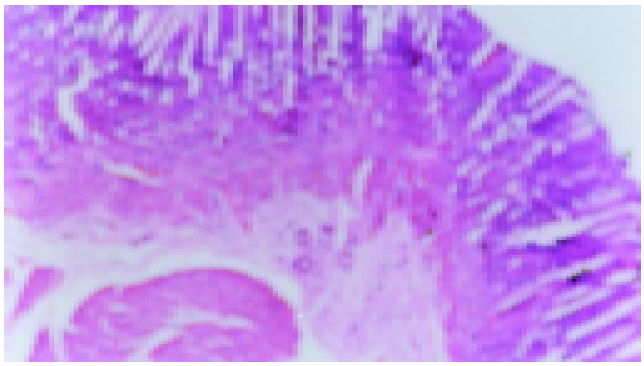


Figure 3 Model group without IL-β (92 d), scar tissue under the thinned gastric mucosa (×200).

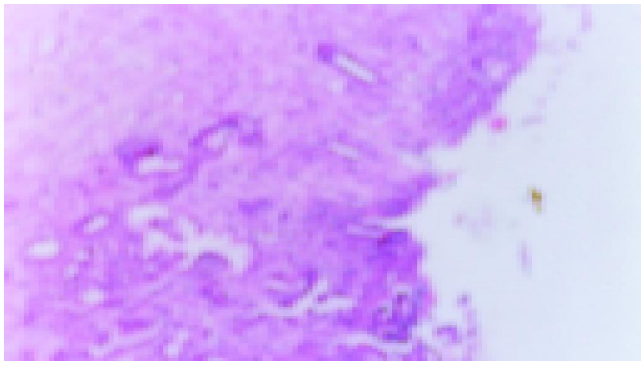


Figure 4 Ranitidine group with IL-β, small ulcer can be seen (×200).

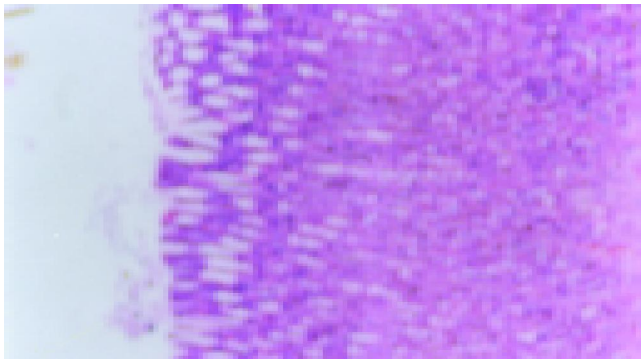


Figure 5 JWYY group, after ip IL-β, no ulcer recurrence (×200).

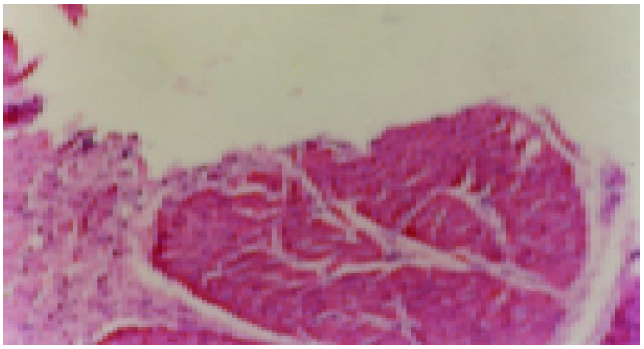


Figure 6 Model recurrence group, after ip IL-β, ulcer relapses (×200).

Table 2 Ulcer index and the rate of recurrence (mean±SD)

Group	*n* IL-1β	Recurrence rate	Ulcer index (7 d)	Ulcer index (92 d)
Normal	5	0	0	0
Sham operation	5	0	0	0
Model	10	10%	8.7±0.48	0.12±0.32
Model recurrence	10	90%[b]	8.7±0.48	6.8±0.48[b]
Ranitidine	10	80%[e]	6.3±0.57[a]	5.8±0.57[e]
JWYY	10	30%[f]	3.8±0.86[c,d]	0.82±0.84[f]

[a]P<0.05 *vs* the model group; [b]P<0 01 *vs* the model group; [c]P<0.05, [d]P<0 01 *vs* the ranitidine group; [e]P>0.05 *vs* the model recurrence group; [f]P<0.01 *vs* the ranitidine group.

Effect of JWYY on MVD

As shown in Figure 7 and Table 3, microvessel was stained brown. MVD in the normal and sham operation groups were relatively few. MVD in the model group was increased compared with normal group, and MVD in the JWYY group was significantly increased *vs* other groups.

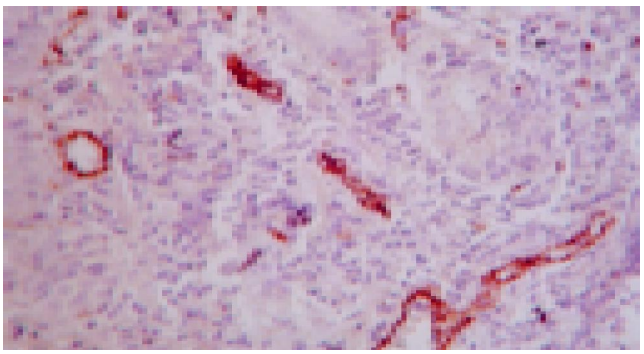


Figure 7 Microvessel of gastric ulcer margin in the rat stained by VIII factor (method of SABC ×400).

Table 3 Change of MVD in tissues 7 d later (mean±SD)

Group	*n*	MVD (7 d)
Normal	5	2.2±0.84
Sham operation	5	2.6±1.14
Model	10	8.8±0.97[b]
Ranitidine	10	10.4±0.97[b,a]
JWYY	10	14.0±2.62[a,d,f]

[a]P<0.05 *vs* the model group; [b]P<0.01 *vs* the normal and sham operation groups; [d]P<0.01 *vs* the model group; [f]P<0.01 *vs* ranitidine group.

Expression of VEGF mRNA

In this study, the extracted total RNAs were of high purity (a range of A_{260}/A_{280} of RNA is from 1.807 to 1.913).

The result showed that the expression level of VEGF mRNA in gastric tissues of rats was low in the normal and sham operation groups. However, the expression level of VEGF mRNA in model, model recurrence, ranitidine, and JWYY groups were significantly increased after 7 d of treatment.

As shown in Table 4, the same results of VEGF expression in gastric ulcer were observed in all groups except for the model group after treatment for 92 d. Taken together, JWYY could enhance the expression of VEGF mRNA in gastric ulcer rats.

The result in black figure is considered as the result of the model recurrence group as well as the model group.

Table 4 VEGF mRNA expression in each group (mean±SD)

Group	VEGF mRNA		
	n	7 d	92 d
Normal	5	0.190±0.019	0.186±0.028
Sham operation	5	0.188±0.019	0.184±0.028
Model	10	0.642±0.034[b]	0.188±0.012[h]
Model recurrence	10		0.794±0.02[g]
Ranitidine	10	0.790±0.037[b,d,f]	0.794±0.025[h]
JWYY	10	0.898±0.046[b,d]	0.899±0.043[h]

[b]P<0.01 *vs* the normal and sham operation groups; [d]P<0.01 *vs* the model group; [f]P<0.01 *vs* the ranitidine group; [h]P<0.01 *vs* itself on the 7th d; [g]P>0.01 *vs* itself on the 7th d.

DISCUSSION

IL-1β is secreted by monocytes, macrophages, and other inflammatory cells. It can cause acute damage of gastric mucosa[12]. Recently, Watanabe *et al*., have developed a rat model of gastric ulcer recurrence induced by IL-1β and the pathologic characterization is very similar to that of the human chronic gastric ulcer[9,13].

In this experiment, we observed gastric ulcer in all rats after they underwent operation by Okabe's method. Nine of ten healed ulcers in the group treated with IL-1β relapsed in the model recurrence group. In contrast, only 1 of 10 relapsed in the model group and no ulcer was observed in the normal and sham operation groups. Taken together, this model of ulcer recurrence was very successful.

The repair of gastric ulcers is a complicated process. It is associated with the reconstitution of epithelial structures and the underlying connective tissue, including vessels and muscle layers. It has been reported that the recurrence of ulcer is associated with the quality of ulcer healing (QOUH)[14], which is related to angiogenesis. Some studies have shown that several growth factors and their receptors are involved in ulcer healing process. Of those, VEGF has received considerable attention, since it is considered to be the only factor that specifically acts on endothelial cells. The delay of ulcer healing and the poor QOUH may result from the lower expression or absence of some growth factors and their receptors[15,16].

VEGF, previously described as a vascular permeability factor, is a growth factor that is involved in the mucosal protection and the angiogenic response taking place during ulcer healing. VEGF is a peptide which is secreted as dimeric glycoproteins containing characteristic regularly spaced eight-cysteine residues. Multiple isoforms can be generated by alternative splicing of a single gene transcript. VEGF has a variety of effects on vascular endothelium, including the ability to promote endothelial cell viability, mitogenesis, chemotaxis, and vascular permeability. Expression of VEGF and its receptors has been demonstrated in the ulcer margin of the human PU disease. In experimental models of acute gastric damage, the expression of VEGF increases during healing, while the pretreatment of rats with a single dose of oral VEGF may exert a protective effect against acute ethanol damage in the gastric mucosa[17]. Furthermore, the daily administration of VEGF has been found to promote the healing of cysteamine duodenal ulcer in rats by stimulation of angiogenesis and formation of granulation tissue. These data suggest that VEGF might play a dual role in mucosal protection and repair. On the one hand, it might improve mucosal resistance by an increase of vascular permeability that dilutes gastrotoxic agents and reduces the area of the hemorrhagic lesions. On the other hand, it might contribute to the development of the angiogenic response together with other growth factors[5,17]. The recent research findings indicate that the gene therapy with either VEGF or PDGF may be a rapid approach to achieve duodenal ulcer healing[18].

JWYY enhanced the expression of VEGF mRNA by stimulation of angiogenesis in the human gastric mucosa in our study. As a result, it improved the QOUH, accelerated the healing of ulcer and prevented its recurrence.

JWYY granules consist of Chinese thorowax root, pilose asiabell root, white peony root, corydalis tuber, common bletilla tuber, natural indigo, pearl powder and liquorice root. It can soothe the liver and strengthen the spleen, it has anti-spasm and pain relieving effect, stop bleeding, and regenerate muscle, and disperse the visceral heat. Previously, we demonstrated that JWYY accelerated the healing of acetic acid-induced gastric ulcer in rats and had good effect for the PU patients with stagnation of liver Qi and deficiency of spleen Qi syndrome or inharmonic liver and gastric syndrome. At the same time, it could prevent ulcer recurrence[6,7].

In conclusion, our results show that JWYY enhances the expression of VEGF mRNA in gastric ulcer in rats. This may be the mechanism by which JWYY improves the QOUH, and prevents its recurrence in the treatment of PU.

REFERENCES

1 **Szabo S,** Vincze Á. Growth factors in ulcer healing: lessons from recent studies. *J Physiol* Paris 2000; **94**: 77-81

2 **Verma S,** Giaffer MH. *Helicobacter pylori* eradication ameliorates symptoms and improves quality of life in patients on long-term acid suppression. A large prospective study in primary care. *Dig Dis Sci* 2002; **47**: 1567-1574

3 **Forrest EH,** MacKenzie JF, Stuart RC, Morris AJ. *Helicobacter pylori* eradication for peptic ulceration: an observational study in a Scottish primary care setting. *Scott Med J* 2002; **47**: 28-33

4 **Luo JC,** Shin VY, Liu ES, Ye YN, Wu WK, So WH, Chang FY, Cho CH. Dexamethasone delays ulcer healing by inhibition of angiogenesis in rat stomachs. *Eur J Pharmacol* 2004; **485**: 275-281

5 **Milani S,** Calabro A. Role of growth factors and their receptors in gastric ulcer healing. *Microsc Res Tech* 2001; **53**: 360-371

6 **Li JB,** Tian YL, Cheng WH, Xiong GL. Jian-Wei-Yu-Yang granules in treatment of experimental gastric ulcer in rats. *Shijie Huaren Xiaohua Zazhi* 2002; **10**: 1282-1287

7 **Li JB,** Jin YQ, Hu SY,YI ZJ, Cao GF, Zhou JH, Liu ZX. Curative effect of Chinese drugs for peptic ulcer is related to dosage form. *Shijie Huaren Xiaohua Zazhi* 1998; **6**: 310-312

8 **Pai R,** Ohta M, Itani RM, Sarfeh IJ, Tarnawski AS. Induction of mitogen-activated protein kinase signal transduction pathway during gastric ulcer healing in rats. *Gastroenterology* 1998; **114**: 706-713

9 **Watanabe T,** Arakawa T, Fukuda T, Higuchi K, Kobayashi K. Role of neutrophils in a rat model of gastric ulcer recurrence caused by interleukin 1β.*Am J Pathol* 1997; **150**: 971-979

10 **Wang J,** Dou KF. Expression of hPTTG1 and bFGF in gallbladder carcinoma tissue and their correlation with angiogenesis. *Shijie Huaren Xiaohua Zazhi* 2004; **12**: 680-684

11 **Liao XF,** Yi JL, Li XR, Deng W, Yang ZF, Tian G. Angiogenesis in rabbit hepatic tumor after transcatheter arterial embolization. *World J Gastroenterol* 2004: **10**: 1885-1889

12 **Mulligan MS,** Ward PA. Immune complex-induced lung and dermal vascular injury. Differing requirements for tumor necrosis factor-αand IL-1β. *J Immunol* 1992; **149**: 331-339

13 **Watanabe T,** Higuchi K, Tominaga K, Fujiwara Y, Arakawa T. Acid regulates inflammatory response in a rat model of induction of gastric ulcer recurrence by interleukin 1β. *Gut* 2001; **48**: 774–781

14 **Tarnawski A,** Stachura J, Krause WJ, Douglass TG, Gergely H. Quality of gastric ulcer healing: a new, emerging concept. *J Clin Gastroenterol* 1991; **13**(Suppl 1): S42-S47

15 **Baatar D,** Jones MK, Tsugawa K, Pai R, Moon WS, Koh GY, Kim I, Kitano S, Tarnawski AS. Esophageal ulceration triggers expression of hypoxia-inducible factor-1 and activates vascular endothelial growth factor gene: implications for angiogenesis and ulcer healing. *Am J Path* 2002; **161**: 1449-1457

16 **Takahashi M,** Kawabe T, Ogura K, Maeda S, Mikami Y, Kaneko N, Terano A, Omata M. Expression of vascular endothelial growth factor at the human gastric ulcer margin and in cultured gastric fibroblasts: a new angiogenic factor for gastric ulcer healing. *Biochem Biophys Res Commun* 1997; **234**: 493-498

17 **Szabo S,** Deng X, Khomenko T, Yoshida M, Jadus MR, Sandor Z, Gombos Z, Matsumoto H. Gene expression and gene therapy in experimental duodenal ulceration. *J Physiol Paris* 2001; **95**: 325-335

18 **Deng X,** Szabo S, Khomenko T, Jadus MR, Yoshida M. Gene therapy with adenoviral plasmids or naked DNA of VEGF and PDGF accelerates healing of duodenal ulcer in rats. *J Pharmacol Exp Ther* 2004; **311**: 982-988

Science Editor Zhu LH and Guo SY **Language Editor** Elsevier HK

PO Box 2345, Beijing 100023, China
www.wjgnet.com
wjg@wjgnet.com

ELSEVIER

World J Gastroenterol 2005;11(35):5485-5491
World Journal of Gastroenterology ISSN 1007-9327
© 2005 The WJG Press and Elsevier Inc. All rights reserved.

• *BASIC RESEARCH* •

Functional and morphological changes of the gut barrier during the restitution process after hemorrhagic shock

Jian-Xing Chang, Shuang Chen, Li-Ping Ma, Long-Yuan Jiang, Jian-Wen Chen, Rui-Ming Chang, Li-Qiang Wen, Wei Wu, Zhi-Peng Jiang, Zi-Tong Huang

Jian-Xing Chang, Shuang Chen, Li-Ping Ma, Long-Yuan Jiang, Jian-Wen Chen, Rui-Ming Chang, Li-Qiang Wen, Wei Wu, Zhi-Peng Jiang, Zi-Tong Huang, The Second Affiliated Hospital, Sun Yat-Sen University, Guangzhou 510120, Guangdong Province, China

Jian-Wen Chen, School of Pharmaceutical Science, Sun Yat-Sen University, Guangzhou 510080, Guangdong Province, China

Supported by the Grants from the Health Research Foundation (A2003189) and the Science Research Project (2004B30601001) of Guangdong Province, China

Correspondence to: Professor Zi-Tong Huang, The Second Affiliated Hospital, Sun Yat-Sen University, 107# West Yanjiang Road, Guangzhou, 510120, Guangdong Province, China. wang2it@163.net
Telephone: +86-20-81332469 Fax: +86-20-81332650

Received: 2004-12-31 Accepted: 2005-03-24

Abstract

AIM: To investigate the functional, morphological changes of the gut barrier during the restitution process after hemorrhagic shock, and the regional differences of the large intestine and small intestine in response to ischemia/reperfusion injury.

METHODS: Forty-seven Sprague-Dawley rats with body weight of 250-300 g were divided into two groups: control group (sham shock $n = 5$) and experimental group ($n = 42$). Experimental group was further divided into six groups ($n = 7$ each) according to different time points after the hemorrhagic shock, including 0th h group, 1st h group, 3rd h group, 6th h group, 12th h group and 24th h group. All the rats were gavaged with 2 mL of suspension of lactulose (L) (100 mg/2 mL) and mannitol (M) (50 mg/each) at the beginning and then an experimental rat model of hemorrhagic shock was set up. The specimens from jejunum, ileum and colon tissues and the blood samples from the portal vein were taken at 0, 1, 3, 6, 12 and 24 h after shock resuscitation, respectively. The morphological changes of the intestinal mucosa, including the histology of intestinal mucosa, the thickness of mucosa, the height of villi, the index of mucosal damage and the numbers of goblet cells, were determined by light microscope and/or electron microscope. The concentrations of the bacterial endotoxin lipopolysaccharides (LPS) from the portal vein blood, which reflected the gut barrier function, were examined by using Limulus test. At the same time point, to evaluate intestinal permeability, all urine was collected and the concentrations of the metabolically inactive markers such as L and M in urine were measured by using GC-9A gas chromatographic instrument.

RESULTS: After the hemorrhagic shock, the mucosal epithelial injury was obvious in small intestine even at the 0th h, and it became more serious at the 1st and the 3rd h. The tissue restitution was also found after 3 h, though the injury was still serious. Most of the injured mucosal restitution was established after 6 h and completed in 24 h. Two distinct models of cell death-apoptosis and necrosis-were involved in the destruction of rat intestinal epithelial cells. The number of goblet cells on intestinal mucosa was reduced significantly from 0 to 24 h (the number from 243±13 to 157±9 for ileum, 310±19 to 248±18 for colon; $r = -0.910$ and -0.437 respectively, all $P<0.001$), which was the same with the large intestine, but the grade of injury was lighter with the values of mucosal damage index in 3 h for jejunum, ileum, and colon being 2.8, 2.6, 1.2, respectively. The mucosal thickness and the height of villi in jejunum and ileum diminished in 1 h (the average height decreased from 309±24 to 204±23 μm and 271±31 to 231±28 μm, $r = -0.758$ and -0.659, all $P<0.001$; the thickness from 547±23 to 418±28 μm and 483±45 to 364±35 μm, $r = -0.898$ and -0.829, all $P<0.001$), but there was no statistical difference in the colon ($F = 0.296$, $P = 0.934$). Compared with control group, the urine L/M ratio and the blood LPS concentration in the experimental groups raised significantly, reaching the peak in 3-6 h (L/M: control *vs* 3 h *vs* 6 h was 0.029±0.09 *vs* 0.063±0.012 *vs* 0.078±0.021, $r = -0.786$, $P<0.001$; LPS: control *vs* 3 h *vs* 6 h was 0.09±0.021 *vs* 0.063±0.012 *vs* 0.25±0.023, $r = -0.623$, $P<0.001$), and it kept increasing in 24 h.

CONCLUSION: The gut barrier of the rats was seriously damaged at the early phase of ischemic reperfusion injury after hemorrhagic shock, which included the injury and atrophy in intestinal mucosa and the increasing of intestinal permeability. Simultaneously, the intestinal mucosa also showed its great repairing potentiality, such as the improvement of the intestinal permeability and the recovery of the morphology at different phases after ischemic reperfusion injury. The restitution of gut barrier function was obviously slower than that of the morphology and there was no direct correlation between them. Compared with the small intestine, the large intestine had stronger potentiality against injury. The reduction of the amount of intestinal goblet cells by injury did not influence the ability of intestinal mucosal restitution at a certain extent and it appeared to be intimately involved in the restitution of the epithelium.

© 2005 The WJG Press and Elsevier Inc. All rights reserved.

Key words: Gut barrier; Hemorrhagic shock; Restitution

Chang JX, Chen S, Ma LP, Jiang LY, Chen JW, Chang RM, Wen LQ, Wu W, Jiang ZP, Huang ZT. Functional and morphological changes of the gut barrier during the restitution process after hemorrhagic shock. *World J Gastroenterol* 2005; 11(35): 5485-5491
http://www.wjgnet.com/1007-9327/11/5485.asp

INTRODUCTION

In recent years, it has been made clear that the intestinal tract is one of the earliest organs involved in ischemia-reperfusion injury after hemorrhagic shock. Owing to the increased intestinal permeability with gut barrier injury, the bacteria and lipopolysaccharides (LPS) can enter the systemic circulation through the portal vein and the mesenteric lymph, and result in sepsis and multiple organ dysfunction syndrome (MODS)[1-3]. The intestinal tract, therefore, is regarded as "initiator" of MODS and its potential pathogenicity has been given more attention. Although the recent focus has been on the study of intestinal barrier function, there are a lot of problems to be solved and the exact mechanism about gut barrier function is uncertain[4,5]. The object of this study, based on the model of intestinal ischemia-reperfusion injury in the early phases after hemorrhagic shock, was to observe the intestinal mucosal changes in all process from injury to restitution after hemorrhagic shock and collect more evidences on the function of gut barrier and its influencing factors.

MATERIALS AND METHODS

Experimental animals and grouping

To begin with, 47 adult and healthy Sprague-Dawley rats with body weight of 250-300 g were used (supplied by Experimental Animal Center, Sun Yat-Sen Medical College, Sun Yat-Sen University) and were gavaged with suspension of lactulose (L) (100 mg/each) and mannitol (M) (50 mg/each) dissolved in 2 mL water (Sigma Chemical Company, USA). All rats were randomly divided into two groups: control group (sham shock n = 5) and experimental group (n = 42 each). According to the different time points of the shock resuscitation, the experimental group was further divided into six groups (n = 7 each), namely 0^{th} h group, 1^{st} h, 3^{rd} h, 6^{th} h, 12^{th} h and 24^{th} h group.

Experimental model

Animals were subjected to hemorrhagic shock as previously described[6]. Briefly, the rats were anesthetized with an intraperitoneal injection of 1 200 mg/kg of urethane. A 1.5 cm incision was made, and the common carotid artery and jugular vein were catheterized. The rats were bled to a mean arterial pressure of 40 mm Hg and kept for 60 min and the shock ended, when the initially shed blood volume and partes aequales of saline were reinfused. Following the termination of shock, the animals were killed at 0, 1, 3, 6, 12 and 24 h time points, respectively. Several segments were taken from jejunum, ileum and colon respectively and rinsed with ice-cold normal saline, fixed in 20% buffered formalin and 3% glutaraldehyde. Meanwhile, 1.5 mL of portal vein blood was drawn from each rat, centrifuged and stored at -80 ℃. All urine, except for that of 0^{th} h group, were collected and stored at -80 ℃. The control rats were only anesthetized and catheterized, not bled.

Light and electron microscopic preparations

Tissue samples were prepared for histological examination of lesions. The resected segments of small intestine and colon were opened lengthwise, embedded in paraffin, sectioned (6 μm), and stained with hematoxylin-eosin (H&E) and Alcian blue-safranin O (pH 0.4). The sections were analyzed with a light microscope (Nikon, Tokyo, Japan).

Mucosal specimens of ileum and colon sections were fixed with 3% glutaraldehyde in 0.1 mol/L cacodylate buffer (pH 7.2) for 2 h at 4 ℃. These samples were then washed several times with the same buffer and postfixed with osmium tetroxide for 2 h at 4 ℃. Specimens were washed with 0.1% sodium acetate, stained en bloc with 2% uranyl acetate, dehydrated through ethanol, and embedded in Spurr's low-viscosity resin. Representative areas were sectioned and stained with toluidine blue. The selected fields were trimmed further for ultrathin section and stained with 3% uranyl acetate in 3% ethanol, followed by treatment with Reynolds' lead citrate. Ultrathin sections were examined under a Hitachi H-600 transmission electron microscope.

Histological scoring

The H&E stained sections were coded and evaluated at 40× and 100× by an unbiased observer. Mucosal damage was classified as follows[7]: 0 (normal), 1 (surface epithelium damaged), 2 (<50% mucosa damaged), 3 (>50% mucosa damaged) and 4 (entire mucosa damaged). In each section, multiple readings of mucosal damage were obtained at 500 μm intervals. The mean of these 15-20 readings for each section provided a mucosal damage index for that section.

Quantitative morphometry of intestinal mucosal injury

Mucosal injury was quantitated under light microscope. Specimens were embedded in paraffin, section was cut and stained with H&E. Measurements of villous height in microns (measured from the villous tip to the muscularis mucosa) were made in the control and experimental groups with an objective micrometer. Average value was calculated and documented. All the calculation was done being unaware of the details by an experienced pathologist.

Gut mucosal goblet cell number

Goblet cells were identified by their classical morphology in each small intestine and colon section in all rats. Total goblet cell number was determined along the combined crypt-villi axis of 10 well-oriented crypt-villus units in each small bowel section and 10 well-oriented colonic crypt units, from the crypt base to the luminal surface[8]. To confirm goblet cell numbers identified by morphology, goblet cells in small intestine and colon sections from the same animals were localized using Alcian blue staining. Positive staining with Alcian blue indicates the presence of acid mucins within goblet cells and was quantitated as outlined for morphological assessment.

Permeability determination of small intestine with L/M assay

Urinary L and M concentrations and the L/M ratio were determined using GC-9A high performance gas chromatography with pulsed electrochemical detector. Increased intestinal permeability was defined by a L/M ratio >0.03. Markedly increased intestinal permeability was defined by a L/M ratio >0.10.

Determination of the LPS concentration in portal venous plasma

The LPS concentration in portal venous blood was determined using Limulus test kit II (Medical Science Research Institute, Shanghai); 0.05 mL of Limulus reagent was added to 0.1 mL of plasma pretreated with modified perchloric acid and mixed frequently, then it was water bathed for 25 min at 37 ℃. The solution was added with Limulus tripeptide 0.05 mL again and water bathed for 3 min at 37 ℃, then sodium nitrite, sulfamoyl ammonium and naphthyl ethylidene, each of which was 0.5 mL, were added one by one, and mixed frequently. Using 722-Spectrophotometer (Optical Instrument Station, Shanghai), an *A*-value of absorbance was obtained after shade selection, then the LPS concentration (EU/mL) was obtained from the standard curve.

Statistical analysis

All comparisons were made by analysis of variance with multiple comparison tests. All data were expressed as the mean±SD. Statistical significance was considered to be reached, when *P* value was 0.05 or less. The linear trends were measured by linear correlation coefficients and corresponding tests.

RESULTS

Light microscopic findings

The control specimens showed normal and typical leaf-like villi crypts. In contrast, the specimens from the experimental group after shock resuscitation showed different degrees of structural changes ranging from swelling and degeneration of villous epithelial cells to extensive denudation and collapse of the villi. The severity of the damage was clearly related to the time of resuscitation after ischemic shock. At the beginning after restoration of blood pressure, an increased degree of mucosal injury was observed. The major injury occurred at the 3rd h after shock resuscitation of the small intestine, which was heavily injured. Following tissue restitution, the denuded mucosal surface covered intensively by goblet cells was found at the 3rd h. But the injury was still serious and heavy inflammatory cell infiltration occurred at this time. Mucosal restitution was reestablished in most of the injured area after 6 h, totally completed at 12-24 h. Compared to the small intestine, the injury to the large intestine was less severe (Figure 1).

Electron microscopic findings

Electron microscopic examination of the intestinal mucosa revealed some changes as follows (Figure 2): the apoptosis and necrosis were major injury mode in the intestinal mucosa. There were a lot of enterocytes with the chromatins compacting and segregating against the nuclear envelope between normal appearing cells, and membranes enclosed with cytoplasmic blebs were observed. Some detached cells had characteristic features of apoptosis, but still preserved microvilli and intact mitochondria. The others showed the swelling of mitochondria and endoplasmic reticulum, scarce and lodging microvilli and opening of tight junction among the cells. No apoptotic features were found in control intestinal epithelium except at the tips of the villi.

Thickness of mucosa and height of villi

In the small intestine, experimental groups showed a progressive reduction of the mucosal thickness (jejunum and ileum: r = -0.898 and -0.829 respectively, all P<0.001) and the villous height (jejunum and ileum: r = -0.758 and -0.659 respectively, all P<0.001). The average height of villi significantly decreased from 309±24 μm in the control to 231±28 μm in the 24 h group in jejunum, from

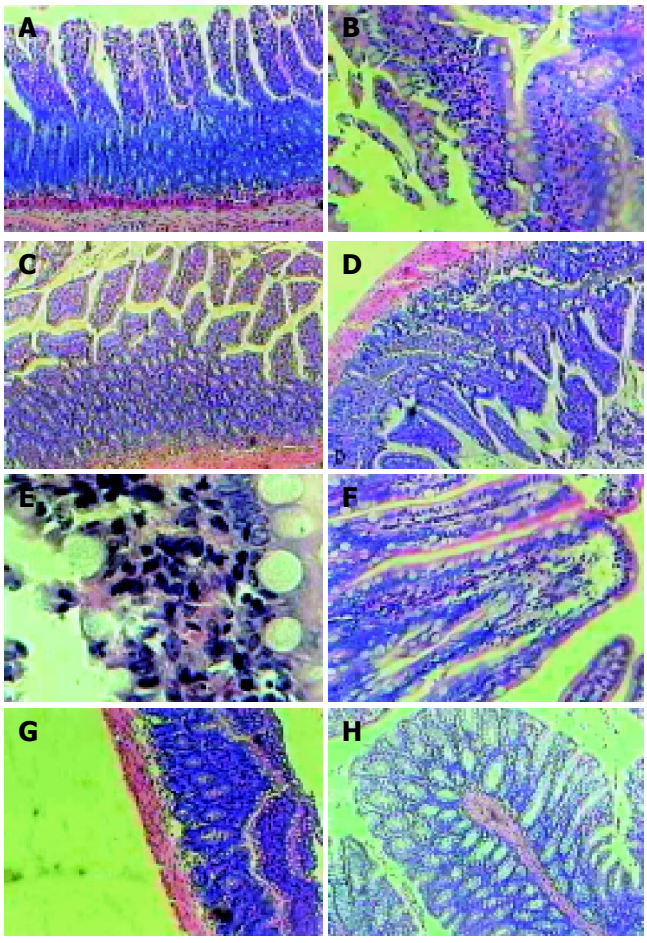


Figure 1 Sections of ileum following ischemia-reperfusion injury after resuscitation of hemorrhagic shock. **A**: Shedding of cell at the tip of the villi is apparent (1 h); **B**: Notes the sloughed epithelial cells detached from the villi and some regions of the villi are destroyed, goblet cells reside throughout the length of the villi (3 h); **C**, **D**: extensive denudation and collapse of the villi and the enterocytes in the upper of the villi had lifted and detached from the villi (3 h); **E**: the tip of the villi was denuded, but some of the goblet cells still remained on the surface (3 h); **F**: Restitution is nearly completed and the area of the villi covered by goblet cells and their number are decreased (6 h); **G**: The restitution of the villi is complete except for the shortening of the villous height and goblet cells cover the villi (12 h). Epithelial cells are lifted off the basement membrane after 1 h. Original magnification: ×40 (**A**), ×100 (**B**, **C**, **D**, **G**, **H**); ×200 (**E**).

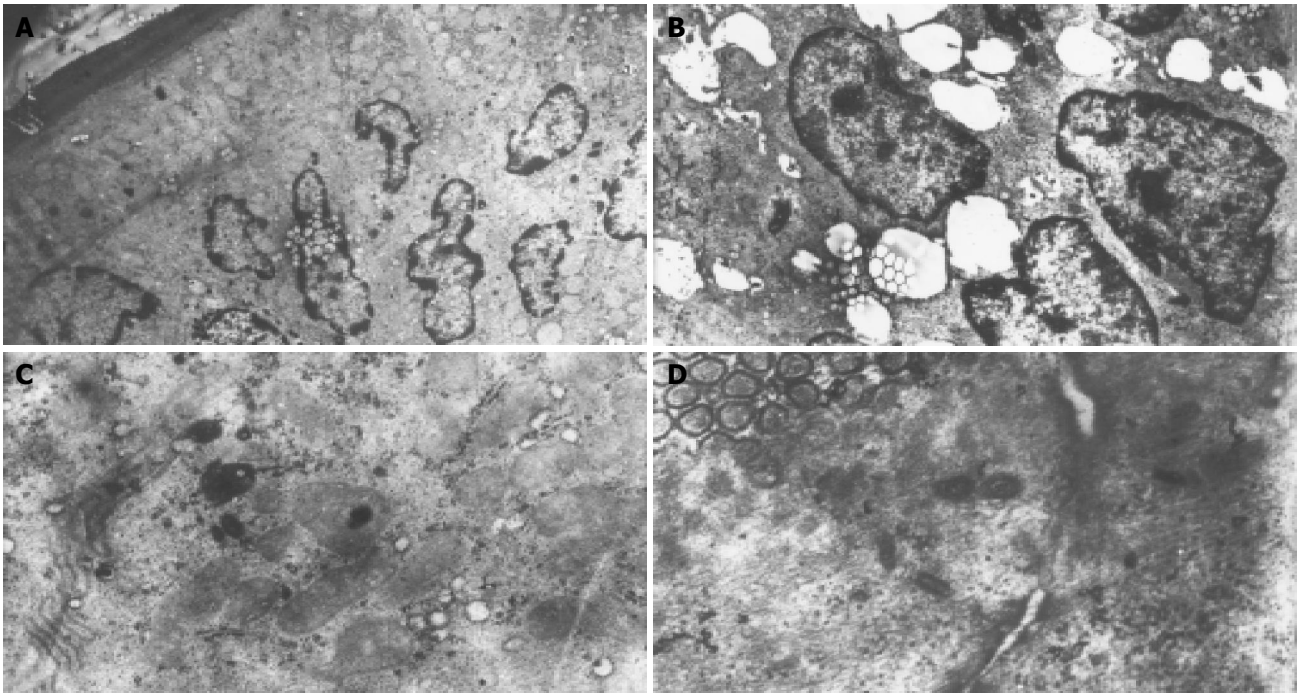


Figure 2 Electron microscopic examination of ileum following ischemia-reperfusion injury after resuscitation of hemorrhagic shock. The apoptosis and necrosis were main manifestation in the intestinal mucosal injury. **A**: Many enterocytes show compaction and segregation of chromatin against the nuclear envelope, but still preserve mcrovilli and intact mitochondria; **B**: Showing the appearance of membrane blebs which cause detachment from the basement membrane; **C**: Some enterocytes show the swelling of mitochondria and endoplasmic reticulum, scarce and lodging microvilli; **D**: the opening of tight junction among the cells. Original magnification: ×2 500 (**A**, **B**), ×4 000 (**C**,**D**).

271±31 μm in the control to 204±23 μm in the 24 h group in ileum. As compared to the control group, the mucosal thickness at 24 h diminished by 25.2%, 23.6%, 23.4% and 24.5% respectively, namely from 547±23 μm to 418±28 μm in jejunum, 483±45 μm to 364±35 μm in ileum. The mucosal thickness of colon was not markedly changed in each time point group ($F = 0.296$, $P = 0.936$, Table 1).

Table 1 Morphometric assessment of small Intestine and colon in different time points after shock resuscitation

Group		Villous height (μm)		Mucosal thickness (μm)		
		Jejunum	Ileum	Jejunum	Ileum	Colon
Con		310±30	270±22	545±13	482±19	633±58
Exp(h)	0	309±24	271±31	547±23	483±45	651±65
	1	297±29	244±25[a]	523±18[a]	445±26[a]	639±60
	3	278±24[a]	210±27[a]	501±27[a]	420±31[a]	674±58
	6	264±19[a]	228±32[a]	470±31[a]	394±27[a]	664±71
	12	252±25[a]	220±18[a]	433±19[a]	380±33[a]	652±69
	24	231±28[a]	204±23[a]	418±28[a]	364±35[a]	631±78

Values are mean±SE; $n = 5$ rats in control group, $n = 7$ in each experiment group. [a]$P<0.05$ *vs* control group.

Mucosal damage index in small intestine and colon

Control samples taken from small intestine and colon exhibited a minor grade of damage at each time point group. In the experimental group, the 0th h after shock resuscitation showed moderate damage with the values of the mucosal damage index being 1.4 in jejunum, 1.6 in ileum and 0.6 in colon. The value was significantly elevated in the 1st h group and the 3rd h group with their damage grade being 2.6 in jejunum, 2.8 in ileum and 1.2 in colon, then it dropped gradually at the 6th h (0.8, 1.0, and 0.6, respectively in the above three areas). In the 12th h, all mucosal damage and degradation were nearly closer to that in the control group. For the mucosal thickness change, the damage in colon was significantly less (Figure 3).

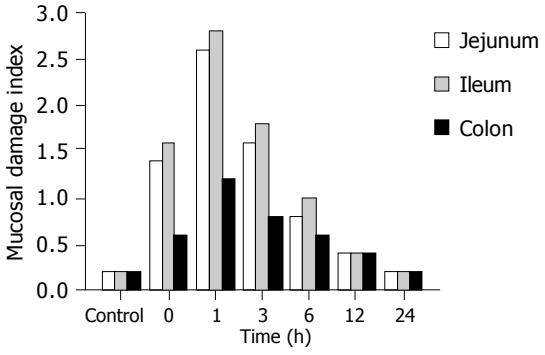


Figure 3 Mucosal damage index in small intestine and colon following resuscitation after hemorrhagic shock. Bars are mucosal damage index, the color represented different sites.

Effect of L/M and the LPS test

Intestinal permeability to macromolecules, as measured by the urinary concentration of L and M, was significantly increased in experimental group rats. The value of L/M was elevated following the time, and reached the peak from 3 to 6 h (0.063±0.012, 0.098±0.011 respectively, $P<0.001$),

then decreased significantly at the 12th h, but was still higher than that in the control group (0.049±0.016, $P<0.001$). The value of L/M was approximate to that of the control group in 24th h group (0.037±0.011, $P>0.05$). The increase and decrease trends of L/M, with 6 h as the turning point, are both of statistical significance (before 6 h: $r = -0.786$, $P<0.001$; after 6 h: $r = -0.767$, $P<0.001$). In general, the change of LPS concentration from portal venous plasma was similar to that of L and M in urine (Table 2 and Figure 4).

Table 2 Changes of L/M ratio and LPS at different time points after shock resuscitation

Group		L/M	LPS (EU/mL)
Con		0.029±0.009	0.09±0.021
Exp(h)	0		0.16±0.042[a]
	1	0.045±0.017[a]	0.14±0.012[a]
	3	0.063±0.012[c]	0.25±0.023[a]
	6	0.098±0.021[c]	0.25±0.028[a]
	12	0.049±0.016[a]	0.15±0.045[a]
	24	0.037±0.011	0.11±0.026

Values are mean±SE; $n = 5$ rats in control group, $n = 7$ in each experiment group. [a]$P<0.05$ *vs* control group; [c]$P<0.05$ *vs* 1 h, 12 h group.

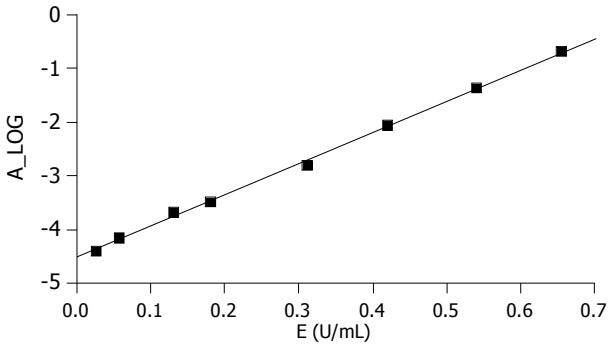


Figure 4 Linear fitness between the standard amount of LPS and absorbance A-value of LPS in portal vein plasma.

Determination of intestinal mucosal goblet cell number

In the experimental group, the number of goblet cells decreased gradually by 35.4% and 20.0% after shock resuscitation, from 243±13 of the control group to 157±9 of the 24th h group in the ileum ($r = -0.910$, $P<0.001$), 310±19 of the control group to 248±18 of 24th h group in the colon ($r = 0$-0.437, $P<0.001$). But the decrease degree in colon mucosa was less than that in the ileum (Table 3).

DISCUSSION

A major function of the gut is to prevent the absorption of toxins, antigens, protease and micro-organisms across the intestinal wall. Epithelial cells cover the surface of the gastrointestinal tract, serving as a barrier between the luminal and tissue compartments[9,10]. Hemorrhagic shock results in a condition of incomplete ischemia of the gut. The ischemia of the small intestine leads rapidly to an impairment of the protective barrier function of the mucosa, and thus the earliest restitution of the mesenteric blood flow is necessary. Although it is evident that circulatory re-establishment is vital in rescuing hypoxic tissues, it is well known that reperfusion would lead to a paradoxical injury. Ikeda *et al*., had reported that the characteristic feature of ischemia/reperfusion injury to the small mucosal epithelium is the detachment of enterocytes from the basement membrane and the apoptosis is regarded as major injury form[11-13]. In this study, two distinct models on cell death-apoptosis and necrosis were involved in the destruction of rat intestinal mucosal epithelium through electron microscopy.

Based on semiquantitative histological examination and the mucosal damage index, we found that the small intestine is more susceptible to ischemia/reperfusion injury than the colon (mucosal damage index: ileum *vs* colon in 3rd h group was 2.8 *vs* 1.2).These data provide probably an explanation for the clinical observation that patients with small intestinal ischemia tend to have worse outcomes than large intestine ischemia. This would also explain why there is a minor injury in the colon. Allopurinol, a competitive inhibitor of xanthine oxidase, is more effective in diminishing the exacerbation of injury in the small intestine after reperfusion because of the level of xanthine oxidase being much higher in the small intestine than that in the colon. However, the exact mechanism why the injury in colon was less severe than in the small intestine is not totally clear. Inherent anatomical structure and biological function of large intestine would be the principal factors against injury.

Repair of intestinal mucosa is called as restitution, where epithelial cells near the wound rapidly flatten, extend with lamellipodia and migrate to form an intact epithelial barrier[14]. The present study suggests that goblet cells were involved in the process of restitution of the small intestine subjected to superficial ischemia/reperfusion injury. Accumulation of goblet cells observed at villous tips by light microscopy in our study seems to be the mode of rapid mucosal repair as restitution. Masuda *et al*.[15], reported, in the recent study, that no incorporation of 5-bromodeoxyuridine (BrdU) was found in the goblet cells covering the villus tips indicating that the accumulation of goblet cells was not due to cell proliferation[16,17].

The decreased number of goblet cells could be an explanation for the reason they participate in the process of the intestinal mucosal restitution. Goblet cells reside throughout the length of intestine and are responsible for the production and maintenance of the mucous blanket by synthesizing and

Table 3 Goblet cell number in ileum and colonic mucosa in different time points after shock resuscitation

Group		Ileum	Colon
Con		243±13	310 ±19
Exp(h)	0	244±21	259±11[a]
	1	227±19[a]	215±9[c]
	3	203±14[c]	231±17[c]
	6	187±15[c]	243±21[c]
	12	166±12[c]	242±16[c]
	24	157±9[c]	248±18[c]

Values are mean±SE; $n = 5$ rats in the control group, $n = 7$ rats in each experiment group. [a]$P<0.05$ *vs* control group for colon; [c]$P<0.05$ *vs* control and the 0 h group for ileum.

secreting mucins which can protect the intestinal mucosal epithelium from damage by preventing bacteria and toxin from accessing the underlying mucosa[18-20]. Goblet cells can discharge mucins in response to reactive oxygen species, inflammatory mediators and LPS[21,22]. By means of increasing mucins production and secretion, goblet cells play a function against intestinal injury. A goblet cell has only a time of secretory course from its differentiation to death, so overexpression of mucins will result, when there is a decrease in number. The present study suggests that the mucins were upregulated at sites of gastric and intestinal mucosa injury[23]. On the other hand, intestinal mucosal atrophy would be associated with a reduction in the number of goblet cells.

Maintenance of the intestinal barrier function depends on the integrity of cellular plasma membrane, tight junctions as well as the elaboration of endothelial and epithelial secreting products[24]. Ischemia/reperfusion injury of the gut after hemorrhagic shock lead to epithelial injury and increased intestinal mucosal permeability LPS are the major outer surface membrane components containing in almost all Gram-negative bacteria and act as extremely strong stimulators of tissue damage[25]. LPS flowing across the basement membrane into the lamina propria and portal vein indicated loss of the gut barrier function, while it was difficult to detect LPS from portal vein clinically. The metabolically inactive tracers L and M used in this study can determine whether and when an increase of intestinal permeability occurred in severe stress and how the degree of permeability increase correlated with the severity of initial injury. In the hemorrhagic shock setting, an increase in the L/M ratio corresponding to increased intestinal permeability was observed in rats. The intestinal mucosal injury exactly induced a marked increase of intestinal permeability (L/M>0.10). At the same time, the degree of mucosal damage index and histological alteration in initial injury (in 3rd h group) correlated with the increase in intestinal permeability (including L/M ratio and concentration of LPS). But, there was no significant positive correlation between the morphometric alteration and the degree of increased intestinal permeability. The degree of intestinal mucosal injury did not appear to be consistent with the value of L/M and LPS in urine and plasma. After the restitution had been reestablished, the intestinal permeability was still increased (L/M = 0.039±0.016; LPS 0.15±0.045, $P<0.05$). It means that the developing of leakage of intraluminal markers was behind the morphological alteration. This also suggested that the restitution on the injury mucosa did not achieve its completely normal condition. Complete repair of injury mucosa takes several days because it concerns a process involving mitosis[26,27].

In conclusion, the gut barrier was subjected to ischemia/reperfusion injury after hemorrhagic shock. Damaged intestinal mucosal cells showed two distinct models of cell death-apoptosis and necrosis. The injury of gut barrier resulted in an increase in permeability to intraluminal substances. It is uncertain whether there is a correlation between the morphological alteration and the degree of increased intestinal permeability. The morphological alteration after intestinal mucosal injury cannot reflect the function of gut barrier. On the other hand, goblet cells appear to be intimately involved in restitution of the epithelium. The decreased number of goblet cells perhaps represent the increasing consumption of the goblet cell itself and its secreting products. Compared to the small intestine, the large intestine has stronger potentiality against injury.

REFERENCES

1 **Wilmore DW,** Smith RJ, O'Dwyer ST, Jacobs DO, Ziegler TR, Wang XD. The gut: a central organ after surgical stress. *Surgery* 1988; **104**: 917-923
2 **Deitch EA,** Forsythe R, Anjaria D, Livingston DH, Lu Q, Xu DZ, Redl H. The role of lymph factors in lung injury, bone marrow suppression, and endothelial cell dysfunction in a primate model of trauma-hemorrhagic shock. *Shock* 2004; **22**: 221-228
3 **Davidson MT,** Deitch EA, Lu Q, Osband A, Feketeova E, Nemeth ZH, Hasko G, Xu DZ. A study of the biologic activity of trauma-hemorrhagic shock mesenteric lymph over time and the relative role of cytokines. *Surgery* 2004; **136**: 32-41
4 **Ackland G,** Grocott MP, Mythen MG. Understanding gastrointestinal perfusion in critical care: so near, and yet so far. *Crit Care* 2000; **4**: 269-281
5 **Kanwar S,** Windsor AC, Welsh F, Barclay GR, Guillou PJ, Reynolds JV. Lack of correlation between failure of gut barrier function and septic complications after major upper gastrointestinal surgery. *Ann Surg* 2000; **231**: 88-95
6 **Chaudry IH.** Rat and mouse models of hypovolemic-traumatic shock. In: Schlag G, Redl H (Ed). Pathophysioloty of shock, sepsis and organ failure. *Berlin: Springer Verlag* 1993: 371
7 **Chiu CJ,** Mcardle AH, Brown R, Scott HJ, Gurd FN. Intestinal mucosal lesion in low flow states. I. A morphological, hemodynamic, and metabolic reappraisal. *Arch Surg* 1970; **101**: 478-483
8 **Fernandez-Estivariz C,** Gu LH, Gu L, Jonas CR, Wallace TM, Pascal RR, Devaney KL, Farrell CL, Jones DP, Podolsky DK, Ziegler TR. Trefoil peptide expression and goblet cell number in rat intestine: effects of KGF and fasting-refeeding. *Am J Physiol Regul Integr Comp Physiol* 2003; **284**: R564-573
9 **Baumgart DC,** Dignass AU. Intestinal barrier function. *Curr Opin Clin Nutr Metab Care* 2002; **5**: 685-694
10 **Gewirtz AT,** Liu Y, Sitaraman SV, Madara JL. Intestinal epithelial pathobiology: past, present and future. *Best Pract Res Clin Gastroenterol* 2002; **16**: 851-867
11 **Ikeda H,** Suzuki Y, Suzuki M, Koike M, Tamura J, Tong J, Nomura M, Itoh G. Apoptosis is a major mode of cell death caused by ischaemia and ischaemia/reperfusion injury to the rat intestinal epithelium. *Gut* 1998; **42**: 530-537
12 **Zhang C,** Sheng ZY, Hu S, Gao JC, Yu S, Liu Y. The influence of apoptosis of mucosal epithelial cells on intestinal barrier integrity after scald in rats. *Burns* 2002; **28**: 731-737
13 **Noda T,** Iwakiri R, Fujimoto K, Matsuo S, Aw TY. Programmed cell death induced by ischemia-reperfusion in rat intestinal mucosa. *Am J Physiol* 1998; **274**: G270-G276
14 **Ikeda H,** Yang CL, Tong J, Nishimaki H, Masuda K, Takeo T, Kasai K, Itoh G. Rat small intestinal goblet cell kinetics in the process of restitution of surface epithelium subjected to ischemia-reperfusion injury. *Dig Dis Sci* 2002; **47**: 590-601
15 **Masuda K,** Ikeda H, Kasai K, Fukuzawa Y, Nishimaki H, Takeo T, Itoh G. Diversity of restitution after deoxycholic acid-induced small intestinal mucosal injury in the rat. *Dig Dis Sci* 2003; **48**: 2108-2115
16 **Itoh H,** Yagi M, Fushida S, Tani T, Hashimoto T, Shimizu K, Miwa K. Activation of immediate early gene, c-fos, and c-jun in the rat small intestine after ischemia/reperfusion. *Transplantation* 2000; **69**: 598-604
17 **Itoh H,** Yagi M, Hasebe K, Fushida S, Tani T, Hashimoto T, Shimizu K, Miwa K. Regeneration of small intestinal mucosa after acute ischemia-reperfusion injury. *Dig Dis Sci* 2002; **47**:

2704-2710
18 **Kim KC,** McCracken K, Lee BC, Shin CY, Jo MJ, Lee CJ, Ko KH. Airway goblet cell mucin: its structure and regulation of secretion. *Eur Respir* J 1997; **10**: 2644-2649
19 **Belley A,** Keller K, Gottke M, Chadee K. Intestinal mucins in colonization and host defense against pathogens. *Am J Trop Med Hyg* 1999; **60**: 10-15
20 **Smirnova MG,** Guo L, Birchall JP, Pearson JP. LPS up-regulates mucin and cytokine mRNA expression and stimulates mucin and cytokine secretion in goblet cells. *Cell Immunol* 2003; **221**: 42-49
21 **Verburg M,** Renes IB, Van Nispen DJ, Ferdinandusse S, Jorritsma M, Buller HA, Einerhand AW, Dekker J. Specific responses in rat small intestinal epithelial mRNA expression and protein levels during chemotherapeutic damage and regeneration. *J Histochem Cytochem* 2002; **50**: 1525-1536
22 **Blanchard C,** Durual S, Estienne M, Bouzakri K, Heim MH, Blin N, Cuber JC. IL-4 and IL-13 up-regulate intestinal trefoil factor expression: requirement for STAT6 and de novo protein synthesis. *J Immunol* 2004; **172**: 3775-3783
23 **Itoh H,** Beck PL, Inoue N, Xavier R, Podolsky DK. A paradoxical reduction in susceptibility to colonic injury upon targeted transgenic ablation of goblet cells. *J Clin Invest* 1999; **104**: 1539-1547
24 **Nusrat A,** Turner JR, Madara JL. Molecular physiology and pathophysiology of tight junctions. IV. Regulation of tight junctions by extracellular stimuli: nutrients, cytokines, and immune cells. *Am J Physiol Gastrointest Liver Physiol* 2000; **279**: G851-G857
25 **Alexander C,** Rietschel ET. Bacterial lipopolysaccharides and innate immunity. *J Endotoxin Res* 2001; **7**: 167-202
26 **Renes IB,** Verburg M, Bulsing NP, Ferdinandusse S, Buller HA, Dekker J, Einerhand AW. Protection of the Peyer's patch-associated crypt and villus epithelium against methotrexate-induced damage is based on its distinct regulation of proliferation. *J Pathol* 2002; **198**: 60-68
27 **Prasad M,** Ito S, Silen W. Functional studies of in vitro rat distal colon before and after restitution. *Surgery* 1997; **121**: 430-439

Science Editor Guo SY **Language Editor** Elsevier HK

PO Box 2345, Beijing 100023, China
www.wjgnet.com
wjg@wjgnet.com

ELSEVIER

World J Gastroenterol 2005;11(35):5492-5497
World Journal of Gastroenterology ISSN 1007-9327
© 2005 The WJG Press and Elsevier Inc. All rights reserved.

• *BASIC RESEARCH* •

Protective effects of non-mitogenic human acidic fibroblast growth factor on hydrogen peroxide-induced damage to cardiomyocytes *in vitro*

Zhuo-Feng Lin, Xiao-Kun Li, Yuan Lin, Fan Wu, Li-Min Liang, Xiao-Bing Fu

Zhuo-Feng Lin, Department of Rheumatology, the Third Affiliated Hospital of Sun Yat-Sen University, Guangzhou 510630, Guangzhou Province, China
Zhuo-Feng Lin, Xiao-Kun Li, Li-Min Liang, Department of Biopharmacy, Pharmacy College, Jinan University, Guangzhou 510632, Guangdong Province, China
Xiao-Kun Li, Biopharmaceutical Research and Development Center, Jinan University, Guangzhou 510632, Guangdong Province, China
Yuan Lin, Department of Ophthalmology, the First Affiliated Hospital of Medical College, Jinan University, Guangzhou 510632, Guangdong Province, China
Fan Wu, Daan Gene Diagnosis Center of Sun Yat-Sen University, Guangzhou 510089, Guangdong Province, China
Xiao-Bing Fu, Wound Healing and Cell Biology Laboratory, Institution of Burns, 304 Hospital, Trauma Center of Postgraduate Medical College, Beijing 100037, China
Supported by the National 863 Project, No. 2001AA215131 and No. 2002AA2Z3318
Correspondence to: Xiao-Kun Li, MD, Biopharmaceutical Research and Development Center, Jinan University, Guangzhou 510632, Guangdong Province, China. zflwf@sohu.com
Telephone: +86-20-85565109-801
Received: 2004-09-18 Accepted: 2004-12-26

Abstract

AIM: To study the protective effect of non-mitogenic human acidic fibroblast growth factor (FGF) on cardiac oxidative injury *in vivo*.

METHODS: Ventricular cardiomyocytes were isolated from 1- to 3-d-old neonatal SD mice and cultured in Dulbecco's minimum essential medium supplemented with 15% fetal bovine serum under an atmosphere of 50 mL/L CO_2-95% air at 37 ℃, as well as assessed by immunocytochemical assay. We constructed the cardiomyocyte injury model by exposure to a certain concentration of H_2O_2. Cellular viability, superoxide dismutase (SOD) activity, leakage of maleic dialdehyde and anti-apoptosis effect were included to evaluate the cardiac protective effect of non-mitogenic human acidic FGF.

RESULTS: Over 50% of the cardiomyocytes beat spontaneously on the 2nd d of culture and synchronously beat after being cultured for 3 d. Forty-eight hours after plating was completed, the purity of such cultures was 95% myocytes, assessed by an immunocytochemical assay. Cellular viability dramatically decreased with the increasing of the concentration of H_2O_2. Non-mitogenic human acidic FGF showed significant resistance to the toxic effect of H_2O_2, significantly increased the cellular viability as well as the activity of SOD, and dramatically decreased the leakage of maleic dialdehyde as well as the cellular apoptosis rate.

CONCLUSION: Hydrogen peroxide shows strong cytotoxicity to the cultured cardiac myocytes, and non-mitogenic human acidic FGF shows strong cardio-protective effect when exposed to a certain concentration of H_2O_2.

© 2005 The WJG Press and Elsevier Inc. All rights reserved.

Key words: Non-mitogenic human acidic fibroblast growth factor; Cardioprotection; Cardiomyocytes; H_2O_2

Lin ZF, Li XK, Lin Y, Wu F, Liang LM, Fu XB. Protective effects of non-mitogenic human acidic fibroblast growth factor on hydrogen peroxide-induced damage to cardiomyocytes *in vitro*. *World J Gastroenterol* 2005; 11(35): 5492-5497
http://www.wjgnet.com/1007-9327/11/5492.asp

INTRODUCTION

Fibroblast growth factor (FGF) is a family of at least 21 structurally and functionally relevant polypeptides characterized by a high affinity of heparin[1]. Acidic FGF found mainly in the brain and retina as well as in the cardiac tissue is also a multifunctional protein, which has many effects including mitogenesis and non-mitogenesis effects.

Studies indicate that intracoronary, intrapericardial, or myocardial administration of FGFs in chronically ischemic canine and porcine hearts can stimulate angiogenesis, a process to minimize infarct size and improve cardiac function[2]. At the same time, though there are some promising results in animal model trials, it produces acute negative inotropic effects on adult cardiac myocytes resulting from alterations in intracellular Ca^{2+} homeostasis[3]. Many people wonder if there would be a potential danger of stimulating the growth of tumor, since NIH-3T3 fibroblasts transfected to express constitutively a secreted form of FGF-1 that becomes tumorigenic[4,5]. FGF-1 behaves as a tumorigenic factor in the NBT-II bladder carcinoma cell model[6].

According to the function and structure of human aFGF, by the method of gene engineering, we removed the part of gene related to mitogenesis, eliminated or reduced the power of mitogenesis, and found it was expressed in

Escherichia coli. We isolated the non-mitogenic human fibroblast growth factor (nm-haFGF) protein, and justified them by mAb of human FGF. Our relevant research results showed that, after modifying the structure of gene and protein, modified haFGF reduced its mitogenetic effect, and preserved its other bio-effects including anti-apoptosis effect, cardio-protective effect, etc.[7]. In this paper, we isolated and cultured the primary cardiomyocytes from 1- to 3-d neonatal SD mice, and observed the pharmacological cardio-protective effect *in vivo*.

MATERIALS AND METHODS

Drugs and reagents

Nm-haFGF was recombined in our experiment laboratory. DMEM, fetal bovine serum (FBS) and trypsin were purchased from Hyclone Co. (UT, USA). Cell death detection kit and immunocytochemical assay kit were purchased from Boster Co. (Wuhan, China). 3-[4,5-Dimethylthiazol-2-yl]-2, 5-diphenyltetrazolium bromide (MTT) was obtained from Sigma (St. Louis, MO, USA). Superoxide dismutase (SOD) and maleic dialdehyde (MDA) were purchased from Jiancheng Bioengineering Institute of Nanjing, China.

Animals

Sprague-Dawley (SD) rats (1-3 d old) were purchased from the Animal Center of Sun Yat-Sen University.

Neonatal mouse primary cardiomyocyte culture

The procedure of culturing ventricular cardiomyocytes from neonatal mice was established by modifications of the previously described methods[7-10]. One- to three-day-old neonatal mice were euthanized by cervical dislocation. Hearts were removed aseptically from the mice, the ventricles were retained, and kept in Hanks' balanced salt solution (HBSS) without Ca^{2+} and Mg^{2+} (in g/L: 0.4 KCl, 0.06 KH_2PO_4, 8.0 NaCl, 0.35 $NaHCO_3$ and 0.06 $Na_2HPO_4 \cdot 7H_2O_2$, pH 7.2) at 4 ℃. The ventricles were washed thrice with HBSS and minced into small fragments and washed twice again during mincing. The cells were dissociated at 37 ℃ for 8 min in enzyme solution (0.8 g/L trypsin in HBSS without Ca^{2+} and Mg^{2+}, pH 7.2), the ventricle tissue was churned by the magnetic stirring (100 r/min) during the digestion. The cells released after the first digestion were discarded, whereas the cells after subsequent digestion were added to an equal volume of cold HBSS with Ca^{2+} and Mg^{2+} (in g/L: 0.14 $CaCl_2$, 0.4 KCl, 0.06 KH_2PO_4, 0.047 $MgCl_2$, 0.049 $MgSO_4$, 8.0 NaCl, 0.35 $NaHCO_3$, 0.05 Na_2HPO_4, and 1.0 D-glucose, pH 7.4) until all cardiac cells were isolated (six times). The resulting mixture was centrifuged for 8 min at 200 r/min, and the cells were resuspended in the FBS-MEM (MEM supplemented with 150 mL/L FBS, 100 U/mL penicillin, and 100 μg/mL streptomycin). To exclude the nonmuscle cells, the isolated cells were first plated in tissue culture dishes at 37 ℃ for 1.5 h in a water-saturated atmosphere of 50 mL/L CO_2-95% air based on the observation that nonmuscle cells attached to the substratum more rapidly. The suspended cells were then collected and plated at a density of 1.0×10^5 cells/cm^2 and incubated under the same conditions as mentioned above.

Immunocytochemical staining

Cardiomyocytes and its purity were monitored by staining with antibody to cardiac α-sarcomeric actin according to the manufacturer's instructions (Boster). Briefly, myocytes were plated on plastic four-chamber culture slides at 1.0×10^5 cells/cm^2. The cells were fixed with 50% methanol and 50% acetone at 20 ℃ and then incubated with antigen-specific primary antibody (mouse multiclonal anti-α-sarcomeric-actin antibody diluted at 1:150). After a brief wash, the myocytes were incubated with biotinylated secondary antibody (goat anti-mouse IgM, μ-chain specific). At the addition of an extravidin peroxidase reagent, a stable avidin-biotin complex was formed with the bound biotinylated antibody. The sites of antibody deposition were visualized by the addition of freshly prepared substrate containing H_2O_2 and chromogen 3-amino-9-ethyl-carbazole. Nuclei were stained with Mayer's hematoxylin. Myocytes were visualized under a reverse microscope (Olympus).

Cytotoxicity of H_2O_2

The cytotoxicity of H_2O_2 was determined by observing cellular morphology, measuring cellular apoptosis and examining the cell viability. Observing the change of cellular morphology is a traditional method to determine the cellular injury. We observed the change of cellular morphology by reverse microscopy, when cardiomyocytes were exposed to different concentrations of H_2O_2. Cardiomyocytes were plated on six-well microplates at the density of 1×10^5 cells/well containing 1 000 μL FBS-DMEM, and cultured in a water-saturated atmosphere of 50 mL/L CO_2-95% air box for 48 h. The myocardium was treated with 0.625, 1.25, 2.5, 5, 10 mmol/L H_2O_2. A photo was taken to record the change of cardiomyocyte morphology after 3 h. The media were removed, the cells were collected and cell genome DNA were extracted, the change of genome DNA was analyzed and the process of cellular apoptosis was evaluated by electrophoresis on 1% agarose gels.

Cell viability was determined by short-term microculture MTT assay. On 96-well microplates, cardiac myocytes were plated at the density of 3×10^4 cells/well containing 150 μL FBS-DMEM. After being cultured for 48 h, the cells were exposed to different concentrations (0.075, 0.15, 0.3, 0.6 mmol/L) of H_2O_2 for 3 h, and then the media were replaced by 100 μL of DMEM and 20 μL of MTT solution (5 mg/mL). The cells were incubated for another 4 h. After being incubated for 4 h, the media and MTT solution were removed. The remaining formazan blue crystals were dissolved by MDSO. Absorbance at 570 nm was measured by Thermo Lab Systems (Multiskan MK3).

Cardioprotection of nm-haFGF

The cardio-protective effect of nm-haFGF was evaluated on the basis of its anti-oxidic effect of nm-haFGF including measuring the total activity of SOD, monitoring the injury of cells membrane, examining cell viability as well as monitoring cell apoptosis by terminal deoxynucleotidyl transferase-mediated dUTP nick-end labeling (TUNEL).

SOD and MDA were measured by respective assay kit (Jiancheng Bioengineering Co.). Cardiomyocytes were plated on 96-well microplates at the density of 3×10^4 cells/well

containing 100 μL FBS-DMEM, and cultured in a water-saturated atmosphere of 50 mL/L CO_2-95% air box for 48 h. The FBS-DMEM media were replaced by free-serum DMEM containing different concentrations of nm-haFGF (10, 20, 40, 80 ng/mL), and incubated in a water-saturated atmosphere of 50 mL/L CO_2-95% air for 24 h, then the cardiomyocytes were treated with 0.15 mmol/L H_2O_2. The leakage of MDA and the activity of SOD were measured after exposure to H_2O_2 for 3 h, and the cell viability of cardiomyocytes was measured by MTT.

TUNEL assay was performed. After being treated with nm-haFGF and H_2O_2, cardiomyocytes were fixed with 4% paraformaldehyde in PBS overnight at 4 ℃. The sample was washed with PBS and then permeabilized by 0.2% Triton X-100 in PBS for 5 min at room temperature. After being washed, cells were equilibrated at room temperature for 5-10 min in equilibration buffer (200 mmol/L potassium cacodylate, 0.2 mmol/L dithiothreitol, 0.25 g/L bovine serum albumin, and 2.5 mmol/L cobalt chloride in 25 mmol/L Tris-HCl, pH 6.6) and then incubated in the presence of biotinylated nucleotide mix and terminal deoxynucleotidyl transferase at 37 ℃ for 1 h in a humidified chamber. The tail reaction was terminated by 2× standard saline citrate (SSC). Then, 0.3% hydrogen peroxide was added to block the endogenous peroxidase. After being washed thrice in PBS, streptavidin HRP was added for 30 min at room temperature, and washed in PBS again. At last, DAB was added to stain the sample, until a suitable background occurred and the positive cells were mounted under a reverse microscope. At least 1 000 cells were counted, and the percentage of TUNEL-positive cells was determined.

Statistical analysis

Data were expressed as mean±SD. Statistical analysis was performed by Student's *t*-test to compare data in different groups. $P<0.05$ was considered statistically significant.

RESULTS

Neonatal mouse primary cardiomyocytes culture and identification

It was noted that the animal age should not be more than 3 d, because cardiomyocytes obtained from neonatal mice older than 3 d, did not attach to the dishes. After being separated from non-muscle cells by preculturing for 2 h, the cardiomyocytes were replated at a density of 1.0×10^5 cells/cm^2 and incubated under the condition described in Materials and methods. After being cultured for 24 h, almost all the cardiomyocytes attached to and spread on the substratum of the dishes and beat spontaneously. The culture media were changed at this time and then changed every 3 d. Forty-eight hours after culturing was completed, the myocytes were identified by the immunocytochemical assay. The cells isolated and cultured were cardiomyocytes, and the cellular morphological characteristics are shown in Figure 1. The myocyte purity averaged 94±2.25%.

Cytotoxicity of H_2O_2

Cardiomyocytes were exposed to different concentrations of H_2O_2. Morphological alteration, cardiomyocyte apoptosis and cell viability were measured as the cytotoxicity of this oxidant. As shown in Figure 2, a dramatic change of cellular morphology and a concentration-dependent injury effect could be observed. When exposed to 0.6125 mmol/L hydrogen peroxide for 3 h, there were no significant differences in cellular morphology. When the concentration increased, a dramatic change in cellular morphology was found. All the cells lost their characteristics of spontaneous beating, and cellular membrane became shrunk, cellular nuclei were contracted.

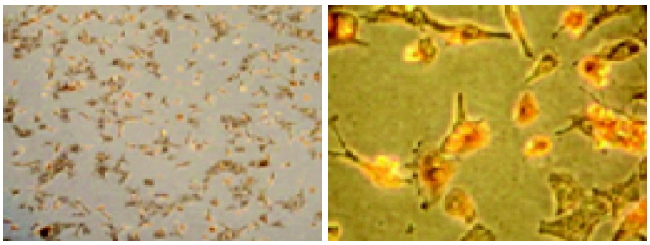


Figure 1 Cardiac myocytes identified by immunocytochemical assay.

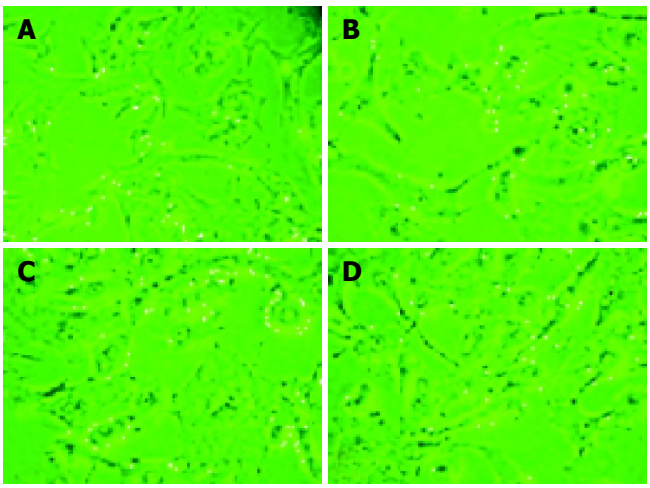


Figure 2 Cellular morphological change of cardiomyocytes after exposure to different concentrations of hydrogen peroxide for 4 h. **A:** Normal control group (magnification ×200); **B:** cardiomyocytes exposure to 1.25 mmol/L H_2O_2 (magnification ×200); **C:** cardiomyocytes exposure to 2.5 mmol/L H_2O_2 (magnification ×200); **D:** cardiomyocytes exposure to 5 mmol/L H_2O_2 (magnification ×200).

Genomic DNA was measured to indicate alterations in cardiomyocyte apoptosis, when cardiomyocytes were exposed to different concentrations of H_2O_2. As shown in Figure 3, genomic DNA remained intact after being exposed to 0.625 mmol/L H_2O_2 for 3 h; when H_2O_2 concentration was changed to 1.25 mmol/L, genomic DNA was divided into some small fragments; when H_2O_2 concentration increased to 5 and 10 mmol/L, all genomic DNAs were divided. There were electrophoresis stains, suggesting that apoptosis of cardiomyocytes occurred when they were exposed to H_2O_2.

MTT assay was used to monitor the cellular viability. There were significant differences in the cell viability at different concentrations of H_2O_2. The higher the concentration of H_2O_2, the lesser the viability of cardiomyocytes (Table 1).

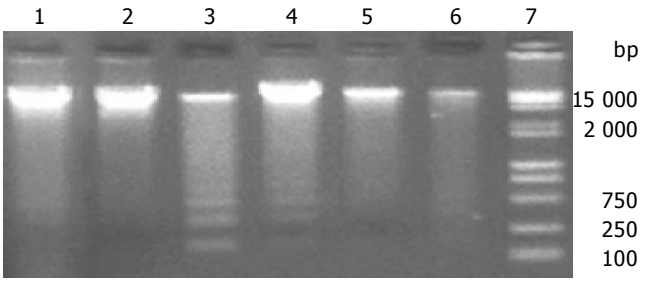


Figure 3 Electrophoresis analysis of DNA extracted from cultured myocytes. Lane 1: normal control group; lane 2: 0.625 mmol/L H_2O_2 for 3 h; lane 3: 1.25 mmol/L H_2O_2 for 3 h; lane 4: 2.5 mmol/L H_2O_2 for 3 h; lane 5: 5 mmol/L H_2O_2 for 3 h; lane 6: 10 mmol/L H_2O_2 for 3 h; lane 7: DNA marker.

Table 1 Viability of cardiomyocytes

Group (n=8)	Concentration of H_2O_2 (mmol/L)	$A_{570\,nm}$ (mean±SD)
Normal	0	0.162±0.007
1	0.075	0.153±0.016
2	0.15	0.121±0.017[a]
3	0.3	0.098±0.012[b]
4	0.6	0.0798±0.006[d]

[a]P<0.05, [b]P<0.01, [d]P<0.001 *vs* normal group.

Cardio-protective effect of nm-haFGF

Cardiomyocytes were exposed to a certain concentration of H_2O_2 and different concentrations of nm-haFGF. The total activity of SOD, MDA leakage, cellular viability and apoptosis were measured as the parameters for evaluating the protective effects of nm-haFGF. As shown in Table 2, the total activity of SOD dramatically increased with the concentration of nm-haFGF, the MDA leakages decreased with the concentration of nm-haFGF, and there was a significant difference between the control and experiment groups. As shown in Table 3, cellular viability increased with the increasing of concentration of nm-haFGF. All these showed that nm-haFGF had a significant cardiomyocytes protective effect on cardiomyocytes exposed to H_2O_2.

To examine the effect of H_2O_2 on apoptosis, myocytes were pretreated with different concentrations of H_2O_2. The initiating effect of H_2O_2 on cardiomyocytes apoptosis was confirmed by determining the change of DNA fragment (Figure 3). The cellular protective effect of nm-haFGF was confirmed by the same method (Figure 4). The rate of TUNEL-positive cells was 32.9±3.3% in the H_2O_2 group, and 1.1±0.26% in the normal group. But after being exposed to 0.15 mmol/L H_2O_2-DMEM, the rate of TUNEL-positive cells was 25.4±2.6% in 10 ng/mL nm-haFGF group, the cellular apoptosis rate in the 40 ng/mL nm-haFGF group was only 19.7±1.9%.

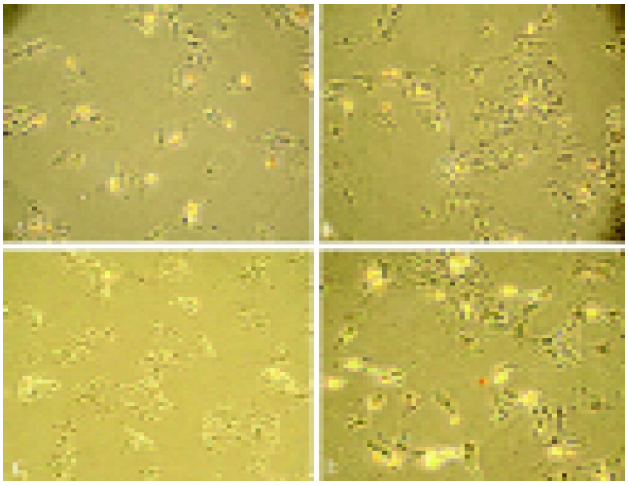


Figure 4 Anti-apoptosis effect of nm-haFGF on cardiomyocytes injured by H_2O_2.

Table 3 Influence of nm-haFGF on cardiomyocyte viability (mean±SD)

Group	H_2O_2 concentration (mmol/L)	Nm-haFGF concentration (ng/mL)	$A_{570\,nm}$
Normal			0.542±0.035[b]
Control	0.15		0.396±0.113
1	0.15	10	0.407±0.054
2	0.15	20	0.42±0.033
3	0.15	40	0.438±0.021[a]
4	0.15	80	0.456±0.058[a]

[a]P<0.05, [b]P<0.01 *vs* control group.

DISCUSSION

Studies indicate that intracoronary, intrapericardial or myocardial administration of FGFs, in chronically ischemic canine and porcine hearts, can stimulate angiogenesis, a process to minimize infarct size and improve cardiac function[11-13]. Although there are some promising results in the animal model trials, some questions, such as dose dependence[14], acute negative inotropic effects[10] still exist. Some investigators

Table 2 Protective effect of nm-haFGF on the cardiomyocytes exposed to H_2O_2 (mean±SD)

Group	H_2O_2 concentration (mmol/L)	Nm-haFGF (ng/mL)	MDA (nmol/L)	SOD (nU/mL)
Normal			0.388±0.145	0.948±0.034
Positive	0.15		0.602±0.122[b]	0.612±0.045[b]
1	0.15	10	0.583±0.052	0.651±0.055
2	0.15	20	0.510±0.026	0.690±0.049
3	0.15	40	0.452±0.073[a]	0.779±0.019[a]
4	0.15	80	0.426±0.085[a]	0.782±0.027[a]

[a]P<0.05 *vs* normal group, [b]P<0.01 *vs* positive group.

wondered if there would, be a potential danger of stimulating the growth of tumor for their strong power of mitogenesis[15]. In this study, we explored nm-haFGF responding to free radical-induced injury of primary cardiomyocytes when exposed to H_2O_2, which induces cardiac apoptosis[16,17]. As shown in Figure 2, when primary cultured neonatal SD mouse cardiac myocytes were exposed to different concentrations of hydrogen peroxide, a dramatic difference of morphological alteration was found, showing a concentration-dependent injury effect. The higher the concentration of H_2O_2, the more serious injury of the cardiomyocytes. As shown in Figure 3, at the lower concentration of H_2O_2, the cellular genomic DNA remained intact, when the concentration of H_2O_2 increased, cellular genomic DNA was divided into small fragments, suggesting that H_2O_2 has a strong cytotoxicity to primary cultured cardiac myocytes.

There is evidence that FGF family protein plays an important role in cardiac protection during hypoxia and reperfusion of ischemic myocardium[18-21]. It was reported that FGF should be considered as a protector rather than a promoter of myocardium regeneration in myocardium reperfusion injury[22-25].

In this study, we isolated and cultured the neonatal SD rat cardiomyocytes, built a cardiac myocyte injury model, and observed the cardio-protective effect of non-mitogenic human acidic FGF *in vitro*. We determined the cardiac myocytes injury by exposing it to different concentrations of H_2O_2, the cellular viability and the concentration of H_2O_2 showed a dose-dependent relationship. Cellular morphology and apoptosis examination showed that H_2O_2 had strong cytotoxicity to the cultured cardiomyocytes. nm-haFGF increased the total activity of SOD, protected the integrity of cellular membrane, and decreased the leakage of MDA as well as cell apoptosis, when cardiomyocytes were exposed to a certain concentration of H_2O_2. All these suggest that nm-haFGF can weaken the injury of cardiomyocytes in a dose-independent manner.

FGF has cardio-protective action on an isolated rat heart model[23,26,27]. Myocardial preconditioning can reduce infarct size, attenuate neutrophil infiltration, reduce calcium influx into cardiomyocytes, delay ultrastructural changes, and decrease programmed cell death (apoptosis)[23,28,29]. Therefore, one of the important mechanisms that can promote cardioprotection is by decreasing myocardial cell apoptosis identified in a wide variety of cardiovascular disorders, including myocardial infarction. As shown in Figure 3, when cardiomyocytes were exposed to a high concentration of H_2O_2, almost all the cells underwent apoptosis (Figure 2), and electrophoresis analysis showed the same results. When exposed to different concentrations of nm-haFGF, TUNEL assay showed that the rate of apoptosis dramatically decreased (Figure 4). All these indicate that nm-haFGF has the anti-apoptosis effect.

In conclusion, nm-haFGF has the anti-apoptosis effect at cell level.

ACKNOWLEDGMENT

The authors thank Dr. Tan Zhi (Physiological and Pathological Department, Sun Yat-Sen University) for his excellent technical support.

REFERENCES

1 **Nishimura T,** Nakatake Y, Konishi M, Itoh N. Identification of a novel FGF, FGF-21, preferentially expressed in the liver. *Biochim Biophys Acta* 2000; **1492**: 203-206
2 **Waltenberger J.** Modulation of growth factor action: implications for the treatment of cardiovascular diseases. *Circulation* 1997; **96**: 4083-4094
3 **Ishibashi Y,** Urabe Y, Tsutsui H, Kinugawa S, Sugimachi M, Takahashi M, Yamamoto S, Tagawa H, Sunagawa K, Takeshita A. Negative inotropic effect of basic fibroblast growth factor on adult rat cardiomyocytes. *Circulation* 1997; **96**: 2501-2504
4 **Forough R,** Xi Z, MacPhee M, Friedman S, Engleka KA, Sayers T, Wiltrout RH, Maciag T. Differential transforming abilities of non-secreted and secreted forms of human fibroblast growth factor factor-1. *J Biol Chem* 1993; **268**: 2960-2968
5 **Jouanneau J,** Plouet J, Moens G, Thiery JP. FGF-2 and FGF-1 expressed in rat bladder carcinoma cells have similar angiogenic potential but different tumorigenic properties *in vivo*. *Oncogene* 1997; **14**: 671-676
6 **Jouanneau J,** Moens G, Thiery JP. The community effect in FGF-1 mediated tumor progression of a rat bladder carcinoma does not involve a direct paracrine signaling. *Oncogene* 1999; **18**: 327-333
7 **Cao DG,** Li XK, Fu XB, Cheng B, Fang LJ. Effect of modified acidic fibroblast growth factor thymocyte apoptosis induced by dexamethasone in mouse. *J China Biotechnol* 2003; **23**: 80-84
8 **Goldspink PH,** Thomason DB, Russell B. Beating affects the posttranscriptional regulation of α-myosin mRNA in cardiac cultures. *Am J Physiol* 1996; **271**: H2584-2590
9 **Long X,** Boluyt MO, Hipolito ML, Lundberg MS, Zheng JS, O'Neill L, Cirielli C, Lakatta EG, Crow MT. p53 and the hypoxia-induced apoptosis of cultured neonatal rat cardiac myocytes. *J Clin Invest* 1997; **99**: 2635-2643
10 **Nakamura TY,** Goda K, OkamotoT, Kishi T, Nakamura T, Goshima K. Contractile and morphological impairment of cultured fetal mouse myocytes induced by oxygen radicals and oxidants. Correlation with intracellular Ca2+ concentration. *Circ Res* 1993; **73**: 758-770
11 **Wang GW,** Schuschke DA, Kang YJ. Schuschke, Metallothionein-overexpressing neonatal mouse cardiomyocytes are resistant to H_2O_2 toxicity. *Am J Physiol* 1999; **276**: H167-H175
12 **Waltenberger J.** Modulation of growth factor action. Implications for the treatment of cardiovascular diseases. *Circulation* 1997; **96**: 4083-4094
13 **Sellke FW,** Li J, Stamler A, Lopez JJ, Thomas KA, Simons M. Angiogenesis induced by acidic fibroblast growth factor as an alternative method of revascularization for chronic myocardial ischemia. *Surgery* 1996; **120**: 182-188
14 **Laham R,** Simons M, Tofukuji M, Hung D, Sellke FW. Modulation of myocardial perfusion and vascular reactivity by pericardial basic fibroblast growth factor: insight into ischemia-induced reduction in endothelium-dependent vasodilation. *J Theorac Cardiovasc Surg* 1998; **116**: 1022-1028
15 **Baffour R,** Berman J, Garb JL, Rhee SW, Kaufman J, Friedmann P. Enhanced angiogenesis and growth of collaterals by *in vivo* administration of recombinant basic fibroblast growth factor in a rabbit model of acute lower limb ischemic: dose-response effect of basic fibroblast growth factor. *J Vasc Surg* 1992; **16**: 181-191
16 **Aikawa R,** Komuro I, Yamazaki T, Zou Y, Kudoh S, Tanaka M, Shiojima I, Hiroi Y, Yazaki Y. Oxidative stress activates extracellular signal-regulated kinases through Src and Ras in cultured cardiac myocytes of neonatal rats. *J Clin Invest* 1997; **100**: 1813-1821
17 **Forrest VJ,** Kang YH, McClain DE, Robinson DH, Ramakrishnan N. Oxidant stress-induced apoptosis prevented by torolox. *Free Radic Biol Med* 1994; **16**: 675-684
18 **Adderley SR,** Fitzgerald DJ. Oxidative damage of cardiomyocytes is limited by extracellular regulated kinases 1/2-mediated induction of cyclooxygenase-2. *J Biol Chem* 1999; **274**: 5038-5046

19 **Jiang ZS,** Srisakuldee W, Soulet F, Bouche G, Kardami E. Non-angiogenic FGF-2 protects the ischemic heart from injury, in the presence or absence of reperfusion. *Cardiovasc Res* 2004; 62: 154-166
20 **Detillieux KA,** Cattini PA, Kardami E. Beyond angiogenesis: the cardioprotective potential of fibroblast growth factor-2. *Can J Physiol Pharmacol* 2004; **82**: 1044-1052
21 **Safi J,** DiPaula AF, Riccioni T, Kajstura J, Ambrosio G, Becker LC, Anversa P, Capogrossi MC. Adenovirus-mediated acidic fibroblast growth factor gene transfer induces angiogenesis in the nonischemic rabbit heart. *Microvasc Res* 1999; **58**: 238-249
22 **Horrigan MC,** MacIsaac AI, Nicolini FA, Vince DG, Lee P, Ellis SG, Topol EJ. Reduction in myocardial infarct size by basic fibroblast growth factor after temporary coronary occlusion in a canine model. *Circulation* 1996; **94**: 1927-1933
23 **Horrigan MC,** Malycky JL, Ellis SG, Topol EJ, Nicolini FA. Reduction in myocardial infarct size by basic fibroblast growth factor following coronary occlusion in a canine model. *Int J Cardiol* 1999; **68**(Suppl): S85-91
24 **Hampton TG,** Amende I, Fong J, Laubach VE, Li J, Metais C, Simons M. Basic FGF reduces stunning via a NOS2-dependent pathway in coronary-perfused mouse hearts. *Am J Physiol* 2000; **279**: H260-268
25 **Htun P,** Ito WD, Hoefer IE, Schaper J, Schaper W. Intramyocardial infusion of FGF-1 mimics ischemic preconditioning in pig myocardium. *J Mol Cell Cardiol* 1998; **30**: 867-877
26 **Padua RR,** Sethi R, Dhalla NS, Kardami E. Basic fibroblast growth factor is cardioprotective in ischemia-reperfusion injury. *Mol Cell Biochem* 1995; **143**: 129-135
27 **Murry CE,** Richard VJ, Reimer KA, Jennings RB. Ischemic preconditioning slows energy metabolism and delays ultrastructural damage during a sustained ischemic episode. *Circ Res* 1990; **66**: 913-931
28 **Bolli R,** Marbán R. Molecular and cellular mechanisms of myocardial stunning. *Physiol Rev* 1999; **79**: 609-634
29 **Saraste A,** Pulkki K, Kallajoki M, Henriksen K, Parvinen M, Voipio-Pulkki LM. Apoptosis in human acute myocardial infarction. *Circulation* 1997; **95**: 320-323

Science Editor Wang XL and Guo SY **Language Editor** Elsevier HK

PO Box 2345, Beijing 100023, China
www.wjgnet.com
wjg@wjgnet.com

ELSEVIER

World J Gastroenterol 2005;11(35):5498-5505
World Journal of Gastroenterology ISSN 1007-9327
© 2005 The WJG Press and Elsevier Inc. All rights reserved.

• *BASIC RESEARCH* •

Immunohistochemical study on gastrointestinal endocrine cells of four reptiles

Xu-Gen Huang, Xiao-Bing Wu

Xu-Gen Huang, Xiao-Bing Wu, Key Laboratories on Conservation and Use of Important Biological Resources of Anhui Province, College of Life Science, Anhui Normal University, Wuhu 241000, Anhui Province, China
Supported by Special Foundation for Anhui Young Leaders Fellowship, No. 04043049, Natural Science Foundation of Anhui Province, No. 01043501, Special Foundation on Key Laboratories on Conservation and Use of Important Biological Resources of Anhui Province and Nature Science Research Program for Young Teacher in University of Anhui Province, No. 2004jq0123
Correspondence to: Professor Xiao-Bing Wu, Key Laboratories on Conservation and Use of Important Biological Resources of Anhui Province, College of Life Science, Anhui Normal University, Wuhu 241000, Anhui Province, China. wuxb@mail.ahnu. edu.cn
Telephone: +86-553-3836873 Fax: +86-553-3869298
Received: 2004-11-20 Accepted: 2004-12-21

Abstract

AIM: To clarify the types, regional distributions and distribution densities as well as morphological features of gastrointestinal (GI) endocrine cells in various parts of the gastrointestinal track (GIT) of four reptiles, *Gekko japonicus*, *Eumeces chinensis*, *Sphenomorphus indicus* and *Eumeces elegans*.

METHODS: Paraffin-embedded sections (5 μm) of seven parts (cardia, fundus, pylorus, duodenum, jejunum, ileum, rectum) of GIT dissected from the four reptiles were prepared. GI endocrine cells were revealed by using immunohistochemical techniques of streptavidin-peroxidase (S-P) method. Seven types of antisera against 5-hydroxytryptamine (5-HT), somatostatin (SS), gastrin (GAS), glucagon (GLU), substance P (SP), insulin and pancreatic polypeptide were identified and then GI endocrine cells were photomicrographed and counted.

RESULTS: The GI endocrine system of four reptiles was a complex structure containing many endocrine cell types similar in morphology to those found in higher vertebrates. Five types of GI endocrine cells, namely 5-HT, SS, GAS, SP and GLU immunoreactive (IR) cells were identified in the GIT of *G. japonicus, E. chinensis* and *S. indicus*; while in the GIT of *E. elegans* only the former three types of endocrine cells were observed. No PP- and INS- IR cells were found in all four reptiles. 5-HT-IR cells, which were most commonly found in the pylorus or duodenum, distributed throughout the whole GIT of four reptiles. However, their distribution patterns varied from each other. SS-IR cells, which were mainly found in the stomach especially in the pylorus and/or fundus, were demonstrated in the whole GIT of *E. chinensis*, only showed restricted distribution in the other three species. GAS-IR cells, with a much restricted distribution, were mainly demonstrated in the pylorus and/or the proximal small intestine of four reptiles. GLU-IR cells exhibited a limited and species-dependent variant distribution in the GIT of four reptiles. SP-IR cells were found throughout the GIT except for jejunum in *E. elegans* and showed a restricted distribution in the GIT of *G. japonicus* and *S. indicus*. In the GIT of four reptiles the region with the highest degree of cell type heterogeneity was pylorus and most types of GI endocrine cells along the GIT showed the peak density in pylorus as well.

CONCLUSION: Some common and unique features of the distribution and morphology of different types of GI endocrine cells are found in four reptiles. This common trait may reflect the similarity in digestive physiology of various vertebrates.

© 2005 The WJG Press and Elsevier Inc. All rights reserved.

Key words: Immunohistochemistry; Gastrointestinal tract; Endocrine cells; Distribution patterns; Four reptiles

Huang XG, Wu XB. Immunohistochemical study on gastrointestinal endocrine cells of four reptiles. *World J Gastroenterol* 2005; 11(35): 5498-5505
http://www.wjgnet.com/1007-9327/11/5498.asp

INTRODUCTION

Today more than 30 GI hormone genes and a multitude of GI hormones have been recognized, thus making the GIT the largest endocrine organ in the body[1]. GI hormones as regulatory peptides appear to be the major components of body integration and have important regulatory actions on physiological function of the GIT[2-6]. In recent years, the field of GI hormones expanding at a dazzling speed has become an important domain in gastroenterology. Some GI dysfunctions are related to GI hormones[7]. Some GI hormones have synergistic expression in gastric carcinoma and take part in the occurrence of gastric carcinoma[8,9]. Furthermore, some GI hormones in combination with their peptide analogs are helpful in developing new diagnostic and therapeutic strategies[10]. The physiological role of hormonal messengers, peptide receptors and their potential involvement in disease are under investigation.

GI endocrine cells, dispersed in epithelia and gastric gland of the GIT, are the anatomical units responsible for the production of GI hormones. Since pathological changes

of GIT also correlate with the changes of GI endocrine cells[11-15], the investigation of GI endocrine cells has been considered as an important part of GI hormone studies and can provide baseline data for basic research in gastroenterology.

It is generally accepted that GI endocrine cells are remarkably different in regional distribution, relative frequency, cell types, and each regional part of the GIT. Many studies have elucidated the regional distribution and relative frequency of different endocrine cells in the GIT of other vertebrates, such as fishes, amphibians[16,17], especially mammals[18-22]. Some studies on regional distribution and relative frequency or distribution density of GI endocrine cells of reptilian species have also been carried out[23-28], because they are centrally placed on the vertebrate phylogenetic tree.

The present study was conducted to clarify the types, regional distribution, distribution densities and morphology of GI endocrine cells in the GIT of *G. japonicus*, *E. chinensis*, *S. indicus* and *E. elegans* by specific immunohistochemical methods, and to provide baseline data not only for further morphological studies but also for physiological and pathological research on the digestive system of reptilians.

MATERIALS AND METHODS

Specimens and sections

G. japonicus (n = 5, body length: 130±14 mm) in the campus of Anhui Normal University, *E. chinensis* (n = 3, body length: 180±20 mm) in the campus of the 9th Middle School in Wuhu City, *S. indicus* (n = 5, body length: 190±18 mm) and *E. elegans* (n = 5, body length: 150±10 mm) in Langya Mountain were collected in summer and autumn. The animals were lightly anesthetized with ether and decapitated with their cardia, fundus, pylorus, duodenum, jejunum, ileum and rectum dissected and fixed in Bouin's fluid for 24 h. After being dehydrated through an ethanol-xylene series the specimens were embedded in paraffin. Sections were cut at 5 μm thickness and mounted on gelatin-coated slides.

Antisera and reagents

The details of the seven antisera and main reagents used in this study are listed in Table 1.

Immunohistochemical staining

Each representative section was deparaffinized, rehydrated and immunostained with the S-P method. Endogenous peroxidase activity was blocked by incubating the sections with 0.3% H_2O_2 in methanol for 10 min. The non-specific reaction was blocked with normal goat serum prior to overnight incubation at 4 ℃ with the primary antiserum (Table 1). After being rinsed in phosphate-buffered saline (PBS; 0.01 mol/L, pH 7.4), the sections were incubated for 15 min at room temperature with biotinylated goat anti-rabbit IgG serum for all antisera, while biotinylated goat anti-mouse IgG serum was used for insulin. They were then washed in PBS and incubated for 15 min with S-P. Peroxidase reaction was carried out in a solution of DAB containing 0.01% H_2O_2 in Tris-HCl buffer (0.05 mol/L, pH 7.6). After the being lightly counterstained with Mayer's hematoxylin, the sections were dehydrated and cover-slipped.

Experiment control

To investigate the specificity of the reactions, negative and positive controls were used. By replacement of the primary antisera with normal goat serum and PBS, negative control was set. A positive control was also established using tissue sections from the GIT of tortoise containing the hormones being studied. The positive reaction cells were colored brown.

Observation, photomicrograph and cell count

All animals were used for each of the four reptiles studied, seven specimens of each reptile were observed and photomicrographed under the Olympus BX-51 photomicroscope. The dark-brown positive reaction cells on the sections were counted under 10×40 times field. The average number of positive reaction cells from the 10 fields selected randomly in each specimen was the number of IR cells in each reptile. Then the average number of all the reptiles was again quantified as distribution density of IR cells.

Statistical analysis

Data were expressed as mean±SD and variance analysis was performed using SPSS 11.0 software. One-way analysis of variance was used for multiple comparisons, and Duncan's test was used for intra-group comparisons. $P<0.05$ was considered statistically significant.

RESULTS

Types, distributional feature of GI endocrine cells in GIT of four reptiles

Table 1 Details of antisera and main reagents used

Antisera and reagent	Donor	Code number	Working dilution	Source
Human 5-HT	Rabbit	ZA-0231	1:100	ZYMED Lab. Inc., USA
Human GAS	Rabbit	ZA-0115	1:50	Same as above
Human SS	Rabbit	ZA-0232	1:50	Same as above
Human PP	Rabbit	ZA-0211	1:50	Same as above
Human SP	Rabbit	ZA-0235	Working solution	Same as above
Human GLU	Rabbit	ZA-0119	1:100	Same as above
Human INS	Mouse	ZM-0155	1:50	Same as above
S-P Kit		SP-9001	Working solution	Zhongshan Biotech Co. LTD., Beijing, China
S-P Kit		SP-9002	Working solution	Same as above
DAB		ZLI-9030	0.6 g/L	Same as above

SP-9002 was only used in detecting INS-IR cells.

Five types of endocrine cells namely 5-HT-, SS-, GAS-, SP- and GLU-IR cells were identified in the GIT of *G. japonicus*, *E. chinensis* and *S. indicus*. However, in the GIT of *E. elegans* only 5-HT-, SS-, GAS-IR cells were found. PP- and INS-IR cells were not detected in the GIT of the four reptiles. The regional distribution and distribution density of GI endocrine cells in the GIT of four reptiles are listed in Tables 2-5. No positive reactions were detected in the negative control sections.

5-HT-IR cells detected throughout the whole GIT of four reptiles were the most predominant GI endocrine cells. These cells showed the highest density in pylorus of four reptiles except for *G. japonicus* in which the most abundant cells were observed in the duodenum. However, the distribution pattern of 5-HT-IR cells in the GIT varied considerably in four reptiles (Figure 1). SS-IR cells were demonstrated in the whole GIT of *E. chinensis*, but only showed restricted distribution in the other three. They were found in stomach and duodenum of *G. japonicus* and only in stomach of *S. indicus* and *E. elegans*.

Table 2 Distribution and density of endocrine cells in GIT of *G. japonicus* (cells/400× field, mean±SD)

	5-HT	SS	GAS	GLU	SP	PP	INS
Cardia	4.8±0.8	5.5±1.9	0	4.3±1.2	3.6±1.1	0	0
Fundus	5.6±1.4	6.0±1.2	0	11.7±0.7	14.6±1.8	0	0
Pylorus	4.1±1.5	9.6±1.0	0	16.3±2.2	11.2±2.2	0	0
Duodenum	8.6±2.2	1.0±0.5	3.8±0.8	0	0	0	0
Jejunum	7.0±2.9	0	1.4±0.5	0	0	0	0
Ileum	7.8±1.2	0	0	0	0	0	0
Rectum	7.0±1.6	0	0	0	0	0	0

Table 3 Distribution and density of endocrine cells in GIT of *E. chinensis* (cells/400× field, mean±SD)

	5-HT	SS	GAS	GLU	SP	PP	INS
Cardia	9.9±2.0	4.0±0.6	0	0	6.1±1.7	0	0
Fundus	10.4±1.4	6.8±1.4	0	0.5±0.5	5.1±0.9	0	0
Pylorus	13.2±2.4	14.0±0.6	6.6±3.5	0	5.6±2.6	0	0
Duodenum	11.8±2.3	1.6±0.3	0	0	2.1±0.7	0	0
Jejunum	9.0±3.0	0.3±0.4	0	0	0	0	0
Ileum	7.3±0.8	7.5±0.9	0	7.9±1.7	8.0±0.8	0	0
Rectum	5±1.1	2.7±0.9	0	3.8±1.4	3.3±1.4	0	0

Table 4 Distribution and density of endocrine cells in GIT of *S. indicus* (cells/400× field, mean±SD)

	5-HT	SS	GAS	GLU	SP	PP	INS
Cardia	4.1±1.5	2.8±1.0	0	0	0	0	0
Fundus	3.2±1.7	1.8±0.8	0	0	0	0	0
Pylorus	11.3±2.7	3.7±1.2	4.6±4.1	0	0	0	0
Duodenum	3.0±0.9	0	1.7±1.4	0	0	0	0
Jejunum	1.6±1.0	0	0	0	0	0	0
Ileum	3.1±1.1	0	0	1.4±0.7	0	0	0
Rectum	7.0±2.4	0	0	6.5±1.7	7.5±2.3	0	0

Table 5 Distribution and density of endocrine cells in GIT of *E. elegans* (cells/400× field, mean±SD)

	5-HT	SS	GAS	GLU	SP	PP	INS
Cardia	1.6±1.1	1.1±1.2	0	0	0	0	0
Fundus	4.2±1.0	2.3±0.7	0	0	0	0	0
Pylorus	9.1±1.7	4.6±1.9	21.4±11.6	0	0	0	0
Duodenum	3.1±0.9	0	1.3±1.1	0	0	0	0
Jejunum	1.4±1.4	0	0	0	0	0	0
Ileum	3.4±1.6	0	0	0	0	0	0
Rectum	5.2±2.0	0	0	0	0	0	0

SS-IR cells were most predominant in pylorus of four reptiles except for *G. japonicus* in which most SS-IR cells were detected in fundus (Figure 2). GAS-IR cells showed limited distribution in the GIT of four reptiles and were confined to pylorus of *E. chinensis*, pylorus and duodenum of *S. indicus* and *E. elegans*, duodenum and jejunum of *G. japonicus*, respectively. In the pylorus of *E. elegans*, GAS-IR cells showed the highest density (Figure 3). GLU-IR cells were detected in the whole stomach of *G. japonicus*, in ileum and rectum of *S. indicus*, in ileum and rectum, and rarely in fundus of *E. chinensis* (Figure 4). SP-IR cells distributed throughout the GIT except for jejunum of *E. elegans*, and were found in stomach of *G. japonicus* and in rectum of *S. indicus* respectively (Figure 5). In the GIT of four reptiles, the region with the highest degree of cell type heterogeneity was the pylorus and most types of GI endocrine cells in the GIT showed the peak density in pylorus as well.

Morphological features and localization of GI endocrine cells in GIT of four reptiles

The GI endocrine system of four reptiles contained many endocrine cell types similar in morphology to those found in higher vertebrates. The endocrine cells showed the characteristic form of both open and close types. They appeared as close-type cells as they did not possess lamina contact with their apical cytoplasmic processes and as open-type cells with apical cytoplasmic processes that reached the glandular or intestinal lumen. The GI endocrine cells were round, oval, triangular, spindle-, shuttle- or flask-like in shape. They were mostly found in gastric glands and intestinal epithelium, and occasionally in gastric epithelia. In gastric glands, the GI endocrine cells were located between

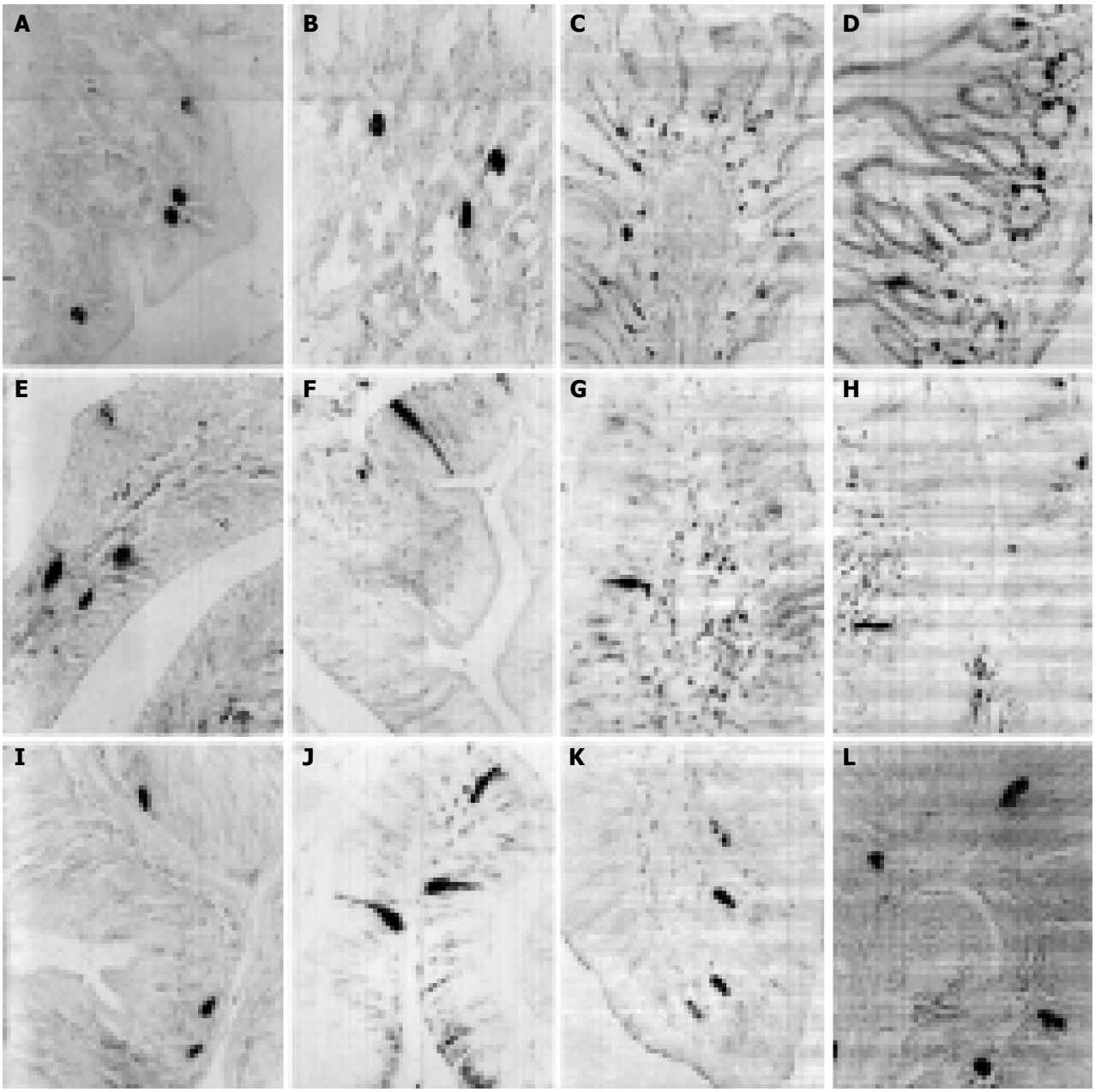


Figure 1 5-HT-IR cells in cardia of *E. chinensis* (**A**), fundus of *E. elegans* (**B**), pylorus of *S. indicus* (**C**) and *E. elegans* (**D**), duodenum of *G. japonicus* (**E**) and *S. indicus* (**F**), jejunum of *S. indicus* (**G**) and *E. elegans* (**H**), ileum of *S. indicus* (**I**) and *E. elegans* (**J**), rectum of *E. elegans* (**K**) and *E. chinensis* (**L**).

the glandular cells and the basement membrane at the basal portion of the glands. In the intestinal parts, most of these cells were situated in the basal portion of the epithelia.

DISCUSSION

The present study demonstrated that the GI endocrine system of four reptiles is a complex structure containing many endocrine cell types similar to those found in mammals except for PP-IR cells[19-22]. 5-HT-, SS-, GAS-, GLU-, SP-IR cells were identified in the GIT of four reptiles, except for *E. elegans*, in which only the former three types were found.

5-HT, a monoamine, which has a strong effect on regulation of digestive functions, is widely distributed in gastric epithelial endocrine cells, 5-HT-IR cells[4,23]. El-Salhy *et al*.[23], reported that 5-HT-IR cells are detected throughout the GIT of all species of vertebrates, suggesting that they have been established in the GIT at an early stage of vertebrate evolution. By using specific antiserum against 5-HT, these cells were detected throughout the GIT of four reptiles in the present study, further approving that 5-HT-IR cells have a wider distribution than other types of GI endocrine cells in GIT of vertebrates. Similarly to

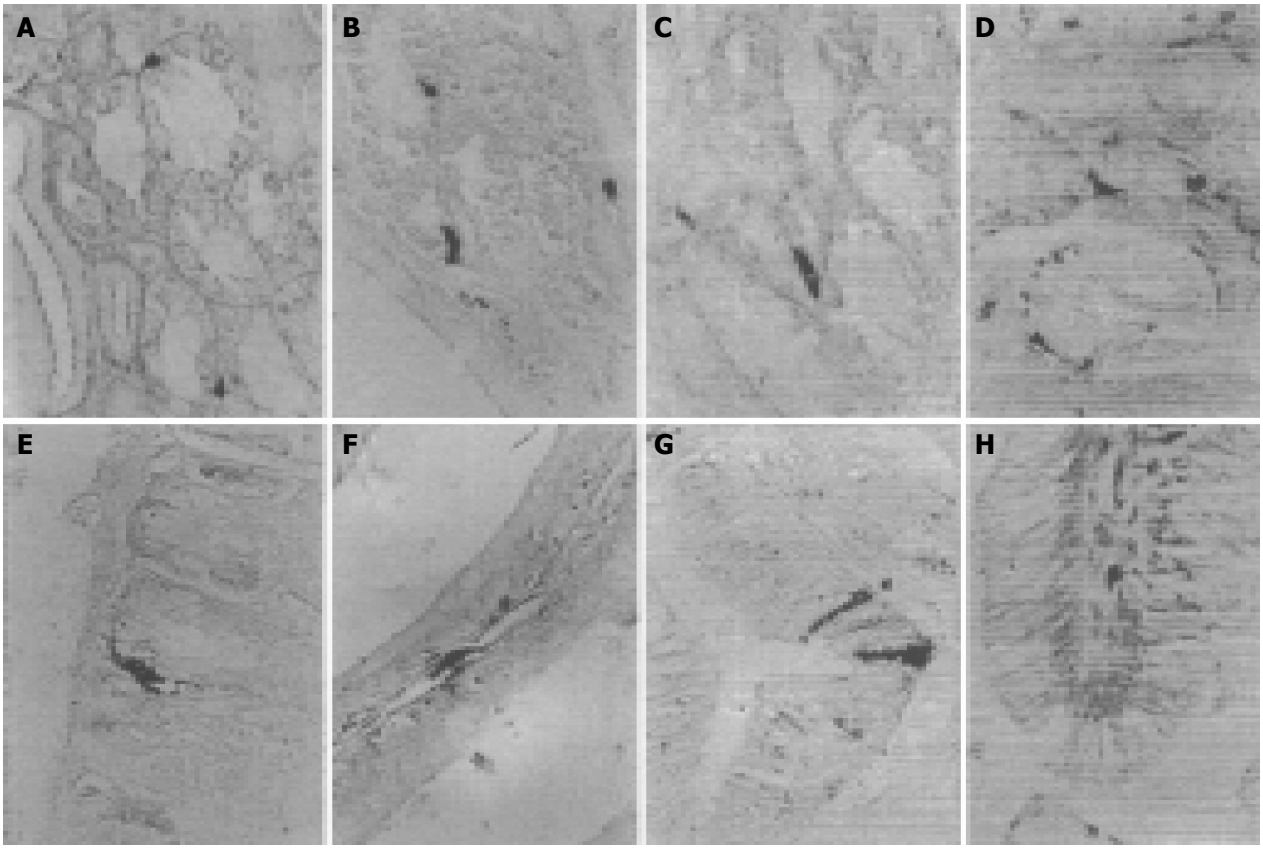


Figure 2 SS-IR cells in cardia of *S. indicus* (**A**) and *E. elegans* (**B**), fundus of *S. indicus* (**C**) and *G. japonicus* (**D**), pylorus of *G. japonicus* (**E**), duodenum of *G. japonicus* (**F**), ileum of *E. chinensis* (**G**), rectum of *E. chinensis* (**H**).

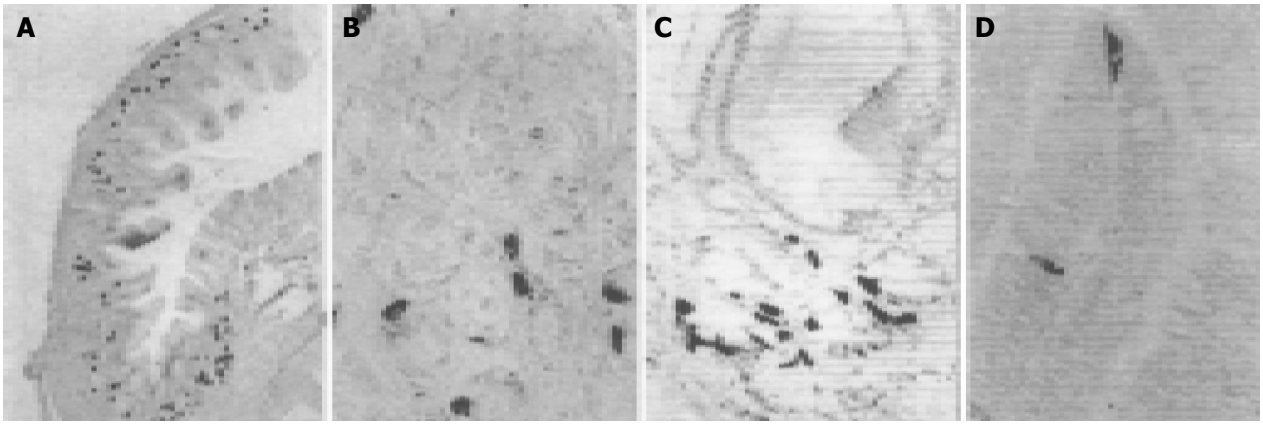


Figure 3 GAS-IR cells in pylorus of *E. elegans* (**A**) and *E. chinensis* (**B**) and *S. indicus* (**C**), duodenum of *G. japonicus* (**D**).

Ku *et al*.[29], and Arena *et al*.[30], 5-HT-IR cells are most predominant in pylorus of *E. chinensis*, *S. indicus* and *E. elegans*. In other studies[24,25,28,31,], the highest frequency of 5-HT-IR cells is in the duodenum and similar results are found in *G. japonicus*, suggesting that pylorus and/or duodenum are important parts in GIT for digestion and a great deal of 5-HT is needed to facilitate the digestive process. As for the distribution pattern (regional distribution and relative frequency or distribution density in GIT) of 5-HT-IR cells in the GIT of four reptiles, considerable variation was observed, and no one was similar to each other, suggesting that the distribution pattern of 5-HT-IR cells may vary from different species. In the present study, some 5-HT-IR cells in the stomach of four reptiles exhibited narrow apical cytoplasmic processes reaching adjacent cells or the gastric gland lumen, indicating that these cells can probably secrete 5-HT by paracrine pathway. In the intestines of four reptiles, 5-HT-IR cells with cytoplasmic processes reaching intestinal lumen were also observed, suggesting that 5-HT may be secreted by exocrine pathway to intestinal lumen.

In most mammals as well as some reptiles, SS-IR cells have a wide distribution in the GIT, except for the large intestine[29-33]. However, species-dependent variations in the distribution patterns of these IR cells have also been reported[24-28]. In the present study, SS-IR cells were demonstrated in the whole GIT of *E. chinensis*, which are in agreement with those reported in *Trimeresurus stejnegeri*, *Trionyx sinensis*, *Alligator mississippiensis* and *Caiman latirostris*[24-27]. In the other three reptiles, SS-IR cells showed restricted distribution. In the GIT of *G. japonicus*, SS-IR cells were demonstrated in stomach and duodenum, as in *Alligator sinensis*[28]. In the GIT of *S. indicus* and *E. elegans*, SS-IR cells are only restricted to the stomach, which differ from those of previous reports on other reptiles[29-33]. These studies suggest that the distribution pattern of SS-IR cells varies greatly in reptiles. On the other hand, common distribution features of SS-IR cells also exist. Studies show that in the GIT of other vertebrates especially mammals, SS-IR cells are found mainly in stomach[20,22], and this common place is also found in most reptiles[27-32]. In the present study SS-IR cells were most predominant in pylorus of *E. chinensis*, *S. indicus* and *E. elegans*. This finding is in line with those of most vertebrates[29,31]. Somewhat different from the above results, SS-IR cells were most abundant in fundus rather than in pylorus of *G. japonicus*, and this difference may be due to the different species. The results found in *G. japonicus* have also been reported in some mammals[18,19,22]. Larsson *et al*.[5], reported that in the stomach, SS-IR cells have cytoplasmic processes terminated on GAS-producing cells, and SS is secreted through cytoplasmic processes by paracrine pathway, inhibiting the secretion of GAS. In the present study, both SS- and GAS-IR cells showed the highest density in pylorus of four reptiles except for *G. japonicus*, suggesting that some relationships may exist between them. Some SS-IR cells with cytoplasmic processes extending to adjacent cells were also found, suggesting that SS-GAS paracrine regulation may exist in reptiles as in mammals.

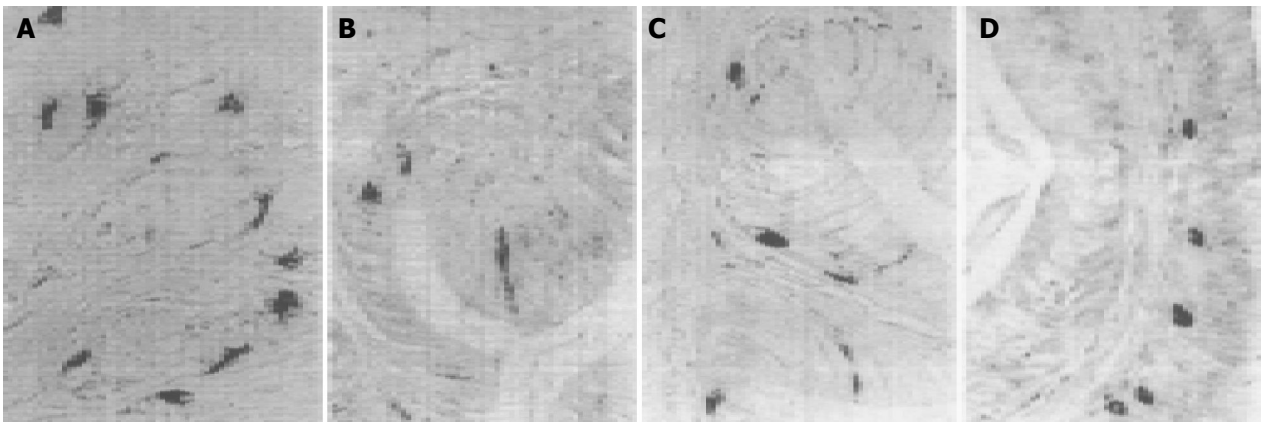


Figure 4 GLU-IR cells in fundus of *G. japonicus* (**A**), ileum of *E. chinensis* (**B**), rectum of *E. chinensis* (**C**) and *S. indicus* (**D**).

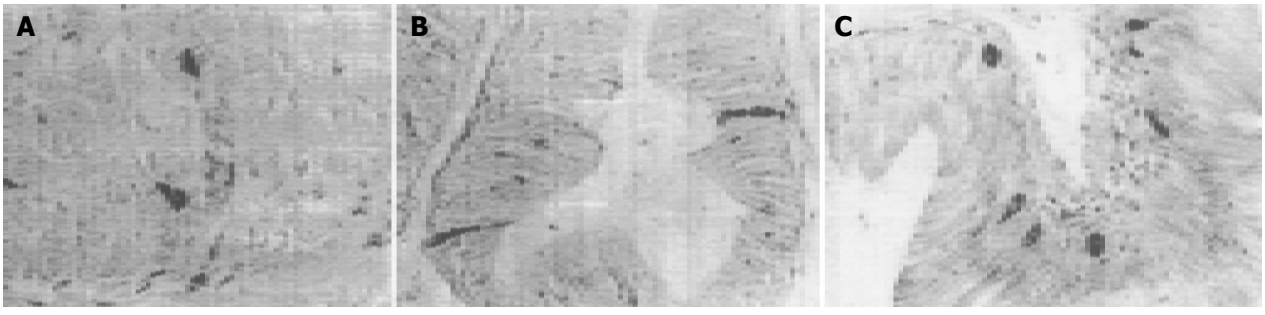


Figure 5 SP-IR cells in cardia of *G. japonicus* (**A**), ileum of *E. chinensis* (**B**), rectum of *S. indicus* (**C**).

In some reptiles, GAS-IR cells are observed in pylorus and whole small intestine of GIT[25,30-33], while in the present study, GAS-IR cells showed restricted distribution in the GIT of four reptiles and the results are similar to those reported in most mammals[18-22]. GAS-IR cells in pylorus and duodenum of *S. indicus* and *E. elegans* are reported in *Bubalus bubalis* and *Caiman latirostris*[20,27]. In the GIT of *E. chinensis*, GAS-IR cells are confined to the pylorus, corresponding to those found in C57BL/6 mice and SKH-1 hairless mice[18,19]. Interestingly, GAS-IR cells were not detected in the pylorus but in the duodenum and jejunum of *G. japonicus*, which differ from those of other three reptiles in which GAS-IR cells were numerous in the pylorus. However, this distribution is consistent with that in *Rana japonica japonica*[17]. In addition, GAS-IR cells are observed in the intestines of *Alligator sinensis* but not in the pylorus[28]. GAS secreted by GAS-IR cells, regulate gastric acid secretion[6]. In *E. chinensis*, *S. indicus* and *E. elegans*, like most vertebrates[30-32], the highest density of GAS-IR cells is found in the pylorus, and this distribution may be important for them to fulfill the regulation of digestive function. However, GAS-IR cells were detected in small intestine in *G. japonicus* but not in the pylorus. Gut hormones have been demonstrated to release into tissue spaces in a paracrine way, they can also release into the gut lumen in a partial exocrine manner or into the blood in an endocrine fashion[3]. In the present study, GAS-IR cells in the intestines of *G. japonicus* were often found with cytoplasmic processes either reaching intestinal lumen or extending to lamina propria, suggesting an exocrine or endocrine secretion of these cell types. Maybe in this way, GAS-IR cells in the intestine can regulate gastric acid secretion. Studies are required to elucidate the functional meaning of these findings.

GLU is synthesized in A cells of the pancreas and regulates serum glucose levels. GLU-IR cells have been demonstrated in various mammals and it is considered that the distribution pattern of these cells in GIT of mammals show species-dependent variation[18-22]. In the present study no GLU-IR cells were found in GIT of *E. elegans* and the findings are similar to those in *Trionyx sinensis*, *Alligator sinensis* and *Egernia kingii* and remarkably different from those in *Caiman latirostris* in which GLU-IR cells were detected throughout the GIT except for the cloaca[25,27,28,30]. In GIT of *G. japonicus*, GLU-IR cells are only found in the stomach, corresponding well with those in *Alligator mississippiensis*[26]. In GIT of *E. chinensis* and *S. indicus* GLU-IR cells are mainly localized in the ileum and rectum. The above studies suggest that the regional distribution of GLU-IR cells in the GIT varies in reptilians.

Up to date, reports on SP-IR cells in the GIT of reptiles are scarce[24,28,31,33,34]. The present study showed that SP-IR cells exhibited variant distribution patterns in GIT of four reptiles. In *E. chinensis* SP-IR cells were found throughout the GIT except for jejunum. Similar to *Lacerta lepida*[31], SP-IR cells are confined to the stomach in GIT of *G. japonicus*. The GIT of *E. elegans* is devoid of SP-IR cells, which is consistent with that in *Trimeresurus stejnegeri*, *Alligator sinensis*, *Testudo graeca* and *Mauremys caspica*[24,28,31]. In *S. indicus* SP-IR cells are only found in the rectum, which are quite different from those of previous studies[33,34].

In this study, the region with the highest degree of cell type heterogeneity was the pylorus. The distribution of most endocrine cell types in the GIT showed the peak density in the pylorus as well. The heterogeneity and concentration of endocrine cells in the pylorus may be attributed to the role of the cells in the feedback control of the function of the segment. In *G. japonicus* and *E. elegans* the spectrum of cell types in the intestine gradually narrowed. While in *E. chinensis* and *S. indicus* the spectrum gradually narrowed from duodenum to jejunum and then widened and got its minimum in jejunum and maximum in rectum.

In conclusion, some common features of the distribution and morphology of different types of GI endocrine cells are found in GIT of four reptiles. This common trait may reflect the similarity in digestive physiology of various vertebrates. Further physiological studies are required to elucidate the ways in which the distribution of GI endocrine cells may be related to the regulatory characteristics of the GIT of reptiles.

REFERENCES

1 **Ahlman H**. The gut as the largest endocrine organ in the body. *Ann Oncol* 2001; **12**(Suppl 2): S63-S68
2 **Solcia E**, Rindi G, Buffa R, Fiocca R, Capella C. Gastric endocrine cells: types, function and growth. *Regul Pept* 2000; **93**: 31-35
3 **Fujita T**. Gut hormone secreting cells- unsolved problems. *Hum Cell* 1990; **3**: 27-30
4 **Solcia E**, Capella C, Vassallo G, Buffa R. Endocrine cells of the gastric mucosa. *Int Rev Cytol* 1975; **42**: 223-286
5 **Larsson LI**, Goltermann N, de Magistris L, Rehfeld JF, Schwartz TW. Somatostatin cell processes as pathways for paracrine secretion. *Science* 1979; **205**: 1393-1395
6 **Larsson LI**. Developmental biology of gastrin and somatostatin cells in the antropyloric mucosa of the stomach. *Microsc Res Tech* 2000; **48**: 272-281
7 **Milutinovic AS**, Todorovic V, Milosavljevic T, Micev M, Spuran M, Drndarevic N. Somatostatin and D cells in patients with gastritis in the course of *Helicobacter pylori* eradication: a six-month, follow-up study. *Eur J Gastroenterol Hepatol* 2003; **15**: 755-766
8 **Henwood M**, Clarke PA, Smith AM, Watson SA. Expression of gastrin in developing gastric adenocarcinoma. *Br J Surg* 2001; **88**: 564-568
9 **Watson SA**, Morris TM, McWilliams DF, Harris J, Evans S, Smith A, Clarke PA. Potential role of endocrine gastrin in the colonic adenoma carcinoma sequence. *Br J Cancer* 2002; **87**: 567-573
10 **Grimberg A**. Somatostatin and cancer: applying endocrinology to oncology. *Cancer Biol Ther* 2004; **3**: 731-738
11 **El-Salhy M**, Sitohy B. Abnormal gastrointestinal endocrine cells in patients with diabetes type1: relationship to gastric emptying and myoelectrical activity. *Scand J Gastroenterol* 2001; **36**: 1162-1169
12 **Tzaneva MA**. Endocrine cells in gastric carcinoma and adjacent mucosa. An immunohistochemical and ultrastructural study. *Histochem J* 2002; **34**: 173-180
13 **Tzaneva M**. Effects of duodenogastric reflux on gastrin cells, somatostatin cells and serotonin cells in human antral gastric mucosa. *Pathol Res Pract* 2004; **200**: 431-438
14 **Zhao R**, Baig MK, Wexner SD, Chen W, Singh JJ, Nogueras JJ, Woodhouse S. Enterochromaffin and serotonin cells are abnormal for patients with colonic inertia. *Dis Colon Rectum* 2000; **43**: 858-863
15 **Tzaneva M**. Light and electron microscopic immunohistochemical investigation on G and D cells in antral mucosa in *Helicobacter pylori*-related gastritis. *Exp Toxicol Pathol* 2001; **52**: 523-528

16 **Zhang SZ**, Huang XG, Wu XB. Immunohistochemical studies on endocrine cells in the digestive tract of *Paa spinosa*. *Dongwu Xuebao* 2003; **49**: 858-864
17 **Huang XG**, Wu HL, Wu XB, Zhang SZ. Immunohistochemical studies on endocrine cells in the gastrointestinal tract of *Rana japonica japonica*. *Dongwuxue Zazhi* 2004; **39**: 19-25
18 **Ku SK**, Lee JH, Lee HS, Park KD. The regional distribution and relative frequency of gastrointestinal endocrine cells in SHK-1 hairless mice: an immunohistochemical study. *Anat Histol Embryol* 2002; **31**: 78-84
19 **Ku SK**, Lee HS, Lee JH. An immunohistochemical study of the gastrointestinal endocrine cells in the C57BL/6 mice. *Anat Histol Embryol* 2003; **32**: 21-28
20 **Baltazar ET**, Kitamura N, Hondo E, Yamada J, Maala CP, Simborio LT. Immunohistochemical study of endocrine cells in the gastrointestinal tract of the Philippine carabao *(Bubalus bubalis*). *Anat Histol Embryol* 1998; **27**: 407-411
21 **Eerdunchaolu DV**, Takehana K, Kobayashi A, Yamada J, Ueda H, Baiyin GF, Abe M. Immunohistochemical study of the distribution of endocrine cells in the gastrointestinal tract of the camel (*Camel bactrianus*). *Eur J Morphol* 2001; **39**: 57-63
22 **Agungpriyono S**, Macdonald AA, Leus KY, Kitamura N, Adnyane IK, Goodall GP, Hondo E, Yamada J. Immunohistochemical study on the distribution of endocrine cells in the gastrointestinal tract of the babirusa, *Babyrousa babyrussa* (Suidae). *Anat Histol Embryol* 2000; **29**: 173-178
23 **El-salhy M**, Wilander E, Lundqvist M. Comparative studies of serotonin-like immuno- reactive cells in the digestive tract of vertebrates. *Biomedical Res* 1985; **6**: 371-375
24 **Zhang ZQ**, Zhang SZ, Wu XB. Immunohistochemical localization of the endocrine cells in the digestive tract of *Trimeresurus stejnegeri*. *Dongwu Xuebao* 2001; **47**: 666-671
25 **Lin SG**, Huang ZJ, Wang SK. Localization and identification of endocrine cells in the Gastro-Entero-Pancreatic system of *Trionyx sinensis*. *Shuichan Xuebao* 2001; **25**: 328-333
26 **Buchan AM**, Lance V, Polak JM. Regulatory peptides in the gastrointestinal tract of Alligator mississipiensis. An immunocytochemical study. *Cell Tissue Res* 1983; **231**: 439-449
27 **Yamada J**, Campos VJ, Kitamura N, Pacheco AC, Yamashita T, Yanaihara N. An immunohistochemical study of the endocrine cells in the gastrointestinal mucosa of the *Caiman latirostris*. *Arch Histol Jpn* 1987; **50**: 229-241
28 **Wu XB**, Zhang SZ, Chen BH, Deng ZP, Zhou ZX, Wang CL, Nie JS, Xie WS. Immunohistochemical studies on endocrine cells in the digestive tract of *Alligator sinensis*. *Dongwu Xuebao* 1999; **45**: 155-161
29 **Ku SK**, Lee HS, Lee JH, Park KD. An immunohistochemical study on the endocrine cells in the alimentary tract of the red-eared slider (*Trachemys scripta elegans*). *Anat Histol Embryol* 2001; **30**: 33-39
30 **Arena PC**, Richardson KC, Yamada J. An immunohistochemical study of endocrine cells of the alimentary tract of the King's skink(*Egernia kingii*). *J Anat* 1990; **170**: 73-85
31 **Perez-Tomas R**, Ballesta J, Pastor LM, Madrid JF, Polak JM. Comparative immunohistochemical study of the gastroenteropancreatic endocrine system of three reptiles. *Gen Comp Endocrinol* 1989; **76**: 171-191
32 **El-Salhy M**, Grimelius L. The endocrine cells of the gastrointestinal mucosa of a squamate reptile, the grass lizard (*mabuya quinquetaeniata*.) A histological and immunohistochemical study. *Biomedical Res* 1981; **2**: 639-658
33 **Morescalchi AM**, Gaccioli M, Faraldi G, Tagliafierro G. The gastro-enteric- pancreatic neuroendocrine system in two reptilian species: *Chalcides chalcides* and *Zoonosaurus madascariensis* (Sauridae). *Eur J Histochem* 1997; **41**: 29-40
34 **Huang XG**, Wu XB, Zhang ZQ, Zhang SZ. Comparative immunohistochemical study of endocrine cells in the gastrointestinal tract of two reptiles. *Zhongguo Zuzhi Huaxue Yu Xibao Huaxue Zazhi* 2003; **12**: 433-440

Science Editor Wang XL and Guo SY **Language Editor** Elsevier HK

PO Box 2345, Beijing 100023, China
www.wjgnet.com
wjg@wjgnet.com

ELSEVIER

World J Gastroenterol 2005;11(35):5506-5511
World Journal of Gastroenterology ISSN 1007-9327
© 2005 The WJG Press and Elsevier Inc. All rights reserved.

• *BASIC RESEARCH* •

MR diffusion-weighed imaging of rabbit liver

You-Hong Yuan, En-Hua Xiao, Zhong He, Jun Xiang, Ke-Li Tang, Rong-Hua Yan, Ke Jin, Zi-Wen Peng

You-Hong Yuan, En-Hua Xiao, Zhong He, Jun Xiang, Ke-Li Tang, Rong-Hua Yan, Ke Jin, Zi-Wen Peng, Department of Radiology, the Second Xiangya Hospital, Central South University, Changsha 410011, Hunan Province, China
Supported by the National Natural Science Foundation of China, No. 30070235, 30470508; Science Foundation of Hunan Province, No. 202064, 04-SK-306-2
Correspondence to: Dr. En-Hua Xiao, Department of Radiology, the Second Xiangya Hospital, Central South University, Changsha 410011, Hunan Province, China. xiaogdk@sohu.com
Telephone: +86-731-5550355 Fax: +86-731-4510190
Received: 2004-07-26 Accepted: 2004-12-29

Abstract

AIM: To study the techniques of MR diffusion-weighed imaging (DWI) for normal rabbit liver.

METHODS: After 15 normal New Zealand white rabbits and one New Zealand white rabbit implanted with VX-2 tumor were anesthetized with 3% soluble pentobarbitone, DWI was performed respectively for different *b* values, repetition times (TR) or thicknesses, when other parameters were the same and magnetic resonance imaging (MRI) was performed respectively, or with different field of views (FOV) or coil when other parameters were the same. The distinction between groups was analyzed by SPSS10.0 with apparent diffusion coefficient (ADC), quality index (QI) or signal-noise ratio (SNR).

RESULTS: As *b* value increased, liver ADC, QI and SNR of DWI became smaller and simultaneously (F = 292.87, 156.1, 88.23, P<0.01). QI of DWI was high, when *b* value was 10, 50 or 100 respectively, but the distinction between them was insignificant; when *b* value was 800, QI and SNR of DWI were low. QI and SNR of DWI had no significant difference between TR = 4 000, 6 000 and 8 000. QI of DWI with 2 mm thickness was bigger than that with 5 mm thickness (t = 3.04, P<0.01), but SNR of DWI with 2 mm thickness was significantly smaller (t = -17.86, P<0.01). SNR of MRI with knee joint coil was obviously bigger than that with cranium coil [t = -5.77 (T1WI) or -4.02 (T2WI), P<0.01], but QI of MRI was smaller on the contrary [t = 7.10 (T1WI) or 3.97 (T2WI), P<0.01]. When FOV was enlarged gradually, SNR of MRI increased [F = 85.81 (T1WI) or 221.96 (T2WI), P<0.01], but QI firstly increased, then decreased [F = 68.67 (T1WI) or 69.46 (T2WI), P<0.01] and QI of MRI was the biggest when FOV was 20 cm×15 cm.

CONCLUSION: The scanning technique is very important in DWI of rabbit liver and the overall quality of DWI with *b* (100 s/mm^2), thickness (2 mm), cranium coils and FOV (20 cm×15 cm) was best in our study, when other parameters were the same.

© 2005 The WJG Press and Elsevier Inc. All rights reserved.

Key words: Liver; Rabbits; Magnetic resonance imaging; Diffusion-weighted imaging; Technology

Yuan YH, Xiao EH, He Z, Xiang J, Tang KL, Yan RH, Jin K, Peng ZW. MR diffusion-weighed imaging of rabbit liver. *World J Gastroenterol* 2005; 11(35): 5506-5511
http://www.wjgnet.com/1007-9327/11/5506.asp

INTRODUCTION

Hepatocellular carcinoma (HCC) is one of the most frequent malignant tumors[1]. Many researches on its computed tomography (CT)[2-6], ultrasonography (US)[4-8] and digital subtraction angiography (DSA)[7-9] have been performed in recent years and they have demonstrated their significant values in diagnosis or prognosis of HCC.

However, the application of MRI[10-14], especially diffusion-weighted imaging (DWI)[14-16], in diagnosing hepatic tumors and evaluating its progression is much less than that of CT and US. With the development of software and the scanning technology of MRI, common MRI, including T1WI, T2WI of the axial, the coronal or the sagittal and magnetic resonance cholangiopancreatography (MRCP), has been used widely in diagnosing and evaluating progression of hepatic tumors in recent years.

Diffusion is caused by random water molecular motion. The amount of diffusion is determined by diffusion coefficient. However, because the measurement of the diffusion coefficient (DC) *in vivo* may be affected by many factors, such as temperature, blood perfusion, magnetic susceptibility in the tissue, or other kinds of motion, more of apparent diffusion coefficient (ADC) rather than DC is used clinically[17-19]. DWI was initially used to evaluate early ischemic stages of the brain and its value has been accepted in recent years all over the world. Meanwhile, several research groups have concluded that DWI has great potential for understanding normal and pathological brain function[20-22]. But only a few researches, including that of Inoha *et al.*[23,24], and Geschwind *et al.*[14], on the value of DWI in diagnosing or evaluating the progression of hepatic lesions, especially VX-2 tumor of rabbit, have been reported.

The rabbit VX-2 tumor, today, is seen as the valued animal modality of HCC in researching its imaging characteristics, because most experiments have demonstrated that the blood supply of VX-2 tumor is similar to that of HCC and VX-2 tumor is implanted easily and grows quickly so that

the diameter of the tumor can reach 2 cm or more, 3 wk after implantation and it is able to transfer or metastasize to the liver, the lump, mediastina, etc. in the early stage, and VX-2 tumor animal models have been applied increasingly in the study of HCC[10-13,24]. Thus, it is important to study the characteristics of rabbit liver MR DWI. Geschwind *et al*.[14], have performed researches on the value of DWI in assessing VX-2 tumor cell apoptosis and histologic analysis after transcatheter arterial chemoembolization (TACE). However, the study on the characteristics of rabbit liver VX-2 tumor MR DWI has not been reported. The main reason is its poor quality of imaging which greatly limits its use in diagnosing or evaluating the progression of tumors[14-17].

The purpose of our experiment is to study the techniques of MR DWI of normal rabbit liver in order to improve its image quality and to prepare for the study of MR DWI of rabbit liver VX-2 tumor, which is an important part of the HCC study on MR DWI after TACE.

MATERIALS AND METHODS

Experimental animals

The animal studies were performed under the supervision of a veterinarian and were completely compliant with the National Institutes of Health (NIH) guidelines for the use of laboratory animals. All animals were provided by the Animal Department of the Second Xiangya Hospital and all protocols were approved by the Animal Use and Care Committee of the hospital.

Of 15 New Zealand normal white rabbits, seven were male rabbits and eight were female, their weights ranging from 1.5 kg to 2.0 kg and their ages ranging from 5 mo to 6 mo. One New Zealand white rabbit was transplanted with VX-2 tumor for 21 d, and four rabbits were for pre-experiment. All New Zealand white rabbits were healthy.

Magnetic resonance imaging protocol

After animals were anesthetized, by injecting 3% soluble pentobarbitone into auricular vein at a dose of 1 mL/kg or different dose based on different animal status in order to make sure that the breath of animals was slowest, other than for the dead ones, and stable, T1WI, T2WI or DWI was performed on a 1.5-Tesla Signa Twinspeed MR scanner (General Electron Medical Systems, USA). Our experiment was divided into seven steps.

Firstly, to clearly observe the effect of animal breathing on MRI quality and choose the most suitable dose of anesthesia, T1WI and T2WI were obtained repeatedly in pre-experiment after four rabbits (excluding 15 rabbits in formal experiment) were anesthetized with different dosage, from low to high, of 3% soluble pentobarbitone injected into auricular vein. Then we compared the quality of images with that of the images after the rabbits died from an overdose of anesthesia. From this, we concluded that the quality of the images was the best, when breathing of animals was slow and stable and this dose was the most suitable anesthetic dosage. Secondly, T1WI and T2WI of 15 rabbits were obtained respectively with the cranium coil and the knee joint coil, and the other similar parameters included fast reverse fast spin echo (FRFSE) series, T1WI [(TR) 400 ms/echo time (TE) 12.3 ms], T2WI (TR3000/TE80 ms), FOV 20 cm×15 cm, NEX 4, thickness of the layer 5 mm, spacing 0 mm, matrix 256×192 (T1WI) and 320×256 (T2WI). Thirdly, different FOVs included 24 cm×24 cm, 20 cm×15 cm, 16 cm×12 cm, while the other parameters were similar to those in step two; T1WI and T2WI of 15 rabbits were carried out respectively. Fourthly, DWIs of 15 rabbits were acquired respectively for different *b* values including 10, 50, 100, 300, 800 s/ mm^2 while other parameters remained the same (Table 1). Fifthly, DWIs of 15 rabbits were performed respectively with different TR values including 4 000, 6 000, and 8 000, while the other parameters remained the same (Table 1). Sixthly, DWIs of 15 rabbits were obtained respectively for different layer thicknesses including 2 and 5 mm, while other parameters remained the same (Table 1). Finally, DWI of VX-2 tumor rabbit was performed for a *b* value of 100 or 300 s/mm^2, TR 6 000, and a 2-mm thick cranium coil.

Data analysis

Based on the ADC value of the region of interest (ROI), QI and SNR, the distinction between different scanning parameter groups was respectively evaluated quantitatively. Of them, the ADC and SNR values were obtained through GE working station.

ADC values of 15 normal rabbit liver parenchyma were obtained by getting the ADC average value from five different ROIs at the central layer of the liver, of which each area was 50 mm^2, which was measured five times, with the help of the relative functional software in GE working station.

QI value was an image marker, which was obtained by combining SNR, the artifact and the liver anatomy manifestation of the image with the same weight after they were quantified respectively with five levels, which could reflect the image

Table 1 The parameters of normal rabbit MR DWI

Series	*b*	TR	TE	FOV	NEX	Thickness	Spacing	Matrix	Coils
SE-EPI	10	6 000	45	20×15	8	2	0.5	128×128	Cranium
SE-EPI	50	6 000	45	20×15	8	2	0.5	128×128	Cranium
SE-EPI	100	6 000	45	20×15	8	2	0.5	128×128	Cranium
SE-EPI	300	6 000	45	20×15	8	2	0.5	128×128	Cranium
SE-EPI	800	6 000	45	20×15	8	2	0.5	128×128	Cranium
SE-EPI	100	4 000	45	20×15	8	2	0.5	128×128	Cranium
SE-EPI	100	6 000	45	20×15	8	2	0.5	128×128	Cranium
SE-EPI	100	8 000	45	20×15	8	2	0.5	128×128	Cranium

SE-EPI: spin echo echo planar imaging.

quality collegiately. SNR is the contrast of SH to SD. SH was the average signal of the hepatic parenchyma from the average value of five different ROIs, each area of which was 50 mm^2 excluding biliary ducts and blood vessels. SD is standard deviation of background signal intensity in the direction of the phase coding. It was obtained by calculating the average value of five ROIs which were not only in front of the abdominal wall but in the field of the scanning as well. The values of "SNR<5", "5<SNR<10", "10<SNR <20", "20<SNR<30", "30<SNR<50" and "SNR>50" are thought of as 0, 1, 2, 3, 4 and 5 scores respectively. As far as the artifact of the images is concerned, when the artifact was the highest and the images could not be used for diagnosis, we considered it as 1 score and when the artifact was very high and it affected diagnosis seriously, we considered it as 2 scores. When the artifact of the images was general and it had some effects on manifestation and diagnosis of the lesions, we regarded it as 3 scores and when the artifact was not high and it did not affect diagnosis seriously, we regarded it as 4 scores. Then, when the artifact was little or none, we regarded it as 5 scores. As for the liver anatomy manifestation of the images, 1 score represented the poorest quality of the images which could not display, at all, the border of the organ or the intrahepatic vessels and 3 scores indicated the average quality of the images which could display the border of most organs, comparatively display the major intrahepatic vessels and vaguely display the border of stomach and bowel and, then, 5 scores showed the highest quality of the images which could distinctly display the border of most organs, clearly display the intrahepatic microvessels and that of the border of the stomach and bowel. When the quality of the images was between 1 and 3 scores, we regarded it as 2 scores and, when the quality of the images was between that of 3 scores and 5 scores, we regarded it as 4 scores.

All MR images were retrospectively analyzed by three experienced radiologists and evaluation of the images artifact and liver anatomy manifestations were obtained by average value statistical analysis, based on the above criteria.

The statistical significance was calculated using SPSS10.0 with analysis of variance (ANOVA) of the randomized block design or paired *t*-test.

RESULTS

Considering only the increase in *b* value and no other parameter, the mean ADC value of hepatic parenchyma was decreased and, at the same time, QI also decreased (Table 2). The distinction of ADC among *b* values of 100 and that of 10, 50, 300 or 800 was significant, respectively (Tukey HSD, $P<0.01$). The distinction of QI among groups of *b* values 10, 50 and 100 s/mm^2 was insignificant, and those among *b* values 100, 300 or 800 was significant (Tukey HSD, $P<0.01$), and was significant between groups of *b* values of 800 and 300 (Tukey HSD, $P<0.01$). With *b* value increase, SNR became smaller and, when *b* value was 800, SNR was no more than 10 (Table 2, Figures 1 and 2). The distinction of SNR between *b* values 100, 10, 300 or 800 was significant (Tukey HSD, $P<0.01$) and that between *b* values 100 and 50 was not significant.

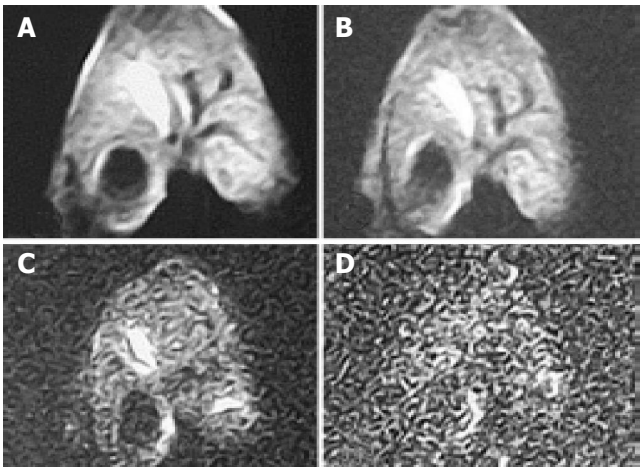


Figure 1 With *b* value, thickness, TR value, scanning coil and NEX were different, ADC value, the ability of liver anatomy manifestation or differentiation and SNR of rabbit liver on MR DWI were also different. b value were respectively 10,100, 300 and 800 s/mm^2 of the image (**A**), (**B**), (**C**) and (**D**). ADC value, SNR and the liver anatomy manifestation of the images became lower and lower with increasing b value. The distinction between b values 10 and 100 was insignificant and the diagnostic value of images at b value 800 was low.

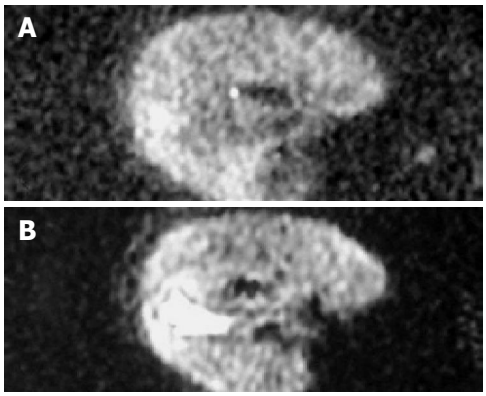


Figure 2 *b* value, the thickness and the NEX of image (**A**) were 300, 2 mm and 8 respectively while those of image (**B**) were 100, 2 mm and 1 respectively. The quality and SNR of the images were poorer than that of Figure 3.

When TR value was 4 000, 6 000 or 8 000, and other parameters were the same, ADC values of hepatic parenchyma

Table 2 DWI of normal rabbit liver with different *b* values (s/mm^2)

	b = 10	*b* = 50	*b* = 100	*b* = 300	*b* = 800	*F*	*P*
ADC[1]	3.23±0.41	2.92±0.43	2.58±0.41	1.73±0.37	0.93±0.56	292.87	<0.01
QI	12.74	12.07	11.80	7.87	3.98	156.1	<0.01
SNR	43.28	33.56	28.65	16.27	9.23	88.23	<0.01

[1](mean±SD)×10^{-3}mm^2/s.

were 2.48±0.52, 2.58±0.43 and 2.70±0.37 (F = 5.6, P<0.01) respectively, QI were 11.11, 11.80 and 10.83 (F = 3.15, P>0.05) respectively, and SNR were 26.61, 28.65 and 29.21 (F = 0.94, P>0.05) respectively, which indicates that QI and SNR did not change significantly. The distinction of ADC between TR 4 000 and 8 000 was significant (Tukey HSD, P<0.05) and that between TR 6 000 and 4 000 or 8 000 was not significant.

When the thickness was 2 or 5 mm and other parameters were the same, ADC values of hepatic parenchyma were 2.57±0.54 and 3.3±0.39 (t = -16.73, P<0.01) correspondingly, QI were 11.80 and 10.90 (t = 3.04, P<0.01) correspondingly and SNR were 28.65 and 71.56 (t = -17.86, P<0.01) correspondingly. The mean ADC value of the hepatic parenchyma and SNR of images were a great deal bigger, when the thickness was 5 mm than when the thickness was 2 mm, but QIs of images were smaller, when the thickness was 5 mm than when the thickness was 2 mm (Figure 3).

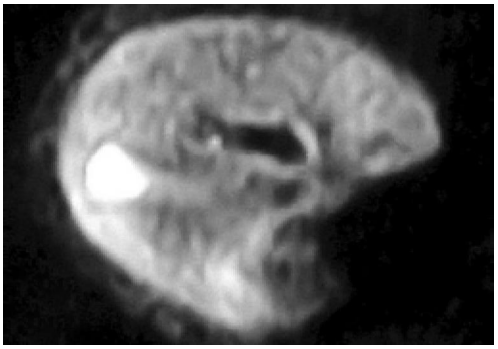


Figure 3 When *b* value was 100 and the thickness was 2 mm, SNR and the liver anatomy manifestation of the images were all good, while the artifact was low and the quality was high.

If rabbit liver was scanned with the cranium coil and the knee joint coil respectively while other parameters remained the same, QI of T1WI were 13.80 and 11.70 (t = 7.10, P<0.01) correspondingly and SNR of T1WI were 96.97 and 137.50 (t = -5.77, P<0.01) correspondingly while QI of T2WI were 11.23 and 9.71 (t = 3.97, P<0.01) correspondingly and SNR of T2WI were 36.41 and 43.63 (t = -4.02, P<0.01) correspondingly. SNR of the images was much bigger when the knee joint coil was used than when the cranium coil was used but QI of the images was smaller when the knee joint coil was used than when the cranium coil was used.

When FOV was 24 cm×24 cm, 20 cm×15 cm or 16 cm×12 cm while other parameters were the same, QI of T1WI were 12.87, 13.90 and 9.89 (F = 68.67, P<0.01) correspondingly and SNR of T1WI were 136.28, 96.97 and 52.03 (F = 85.81, P<0.01) respectively while QI of T2WI were 10.57, 11.23 and 7.45 (F = 69.46, P<0.01) correspondingly and SNR of T2WI were 47.86, 36.41 and 16.81 (F = 221.96, P<0.01) respectively. SNR of the images was the highest when FOV was 24 cm×24 cm and the smallest when FOV was 16 cm×12 cm and QI of the images was the highest when FOV was 20 cm×15 cm.

Based on 15 normal rabbit DWI with *b* value 100, TR 6 000 and thickness 2 mm, 13 images of the liver manifested average and high signals and the other two images of the liver did not manifest well due to the artifact. Eleven borders of the liver displayed well and the contrast between the liver and the neighboring organs was significant. The intrahepatic vessels of 10 cases manifested low signal and concentrated toward the first or the second porta hepatis. The intrahepatic bile ducts of four cases partly displayed high signal like the branches of a tree. All 15 cholecysts manifested high signal and part of them looked like "lamp bulbs". The VX-2 tumor manifested significantly high signal while surrounding hepatic parenchyma displayed low signal on DWI with a *b* value of 100, TR of 6 000 and a thickness of 2 mm. The distinction between VX-2 tumor and surrounding hepatic parenchyma was significant and the border of VX-2 tumor was clear (Figure 4).

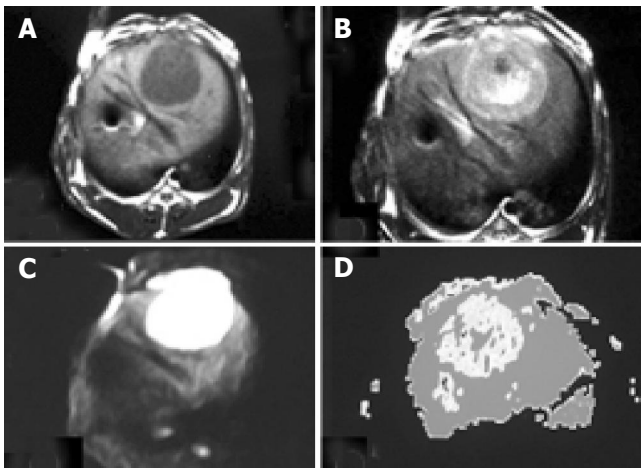


Figure 4 The VX-2 tumor manifests low signal on MR T1WI in image (A), while it displayed high signal on T2WI in image (B). The VX-2 tumor manifested significantly high signal while surrounding hepatic parenchyma displayed low signal on DWI in image (C) with b value 100, TR 6 000 and thickness 2 mm,the distinction between the VX-2 tumor and surrounding hepatic parenchyma was significant and the border of the VX-2 tumor was clear. The image (D) is the ADC map from VX-2 tumor DWI of the image (C).

DWI manifestation of rabbit liver

With *b* value, thickness, TR value, scanning coil and NEX were different, ADC value, the ability of liver anatomy manifestation or differentiation and SNR of rabbit liver on MR DWI were also different. In Figure 1, *b* values were respectively 10, 100, 300 and 800 s/mm^2 of the images (1), (2), (3) and (4). ADC value, SNR and the liver anatomy manifestation of the images became lower and lower with increasing *b* value. The distinction between *b* values 10 and 100 was insignificant and the diagnostic value of images at *b* value 800 was low. In Figure 2, *b* value, the thickness and the NEX of image (1) were 300, 2 mm and 8 respectively while those of image (2) were 100, 2 mm and 1 respectively. The quality and SNR of the images were poorer than that of Figure 3. In Figure 3, when *b* value was 100 and the thickness was 2 mm, SNR and the liver anatomy manifestation of the images were all good while the artifact was low and the quality was high. In Figure 4, the VX-2 tumor manifests low signal on MR T1WI in image (1), while it displayed high signal on T2WI in image (2). The VX-2 tumor manifested

significantly high signal while surrounding hepatic parenchyma displayed low signal on DWI in image (3) with *b* value 100, TR 6 000 and thickness 2 mm, the distinction between the VX-2 tumor and surrounding hepatic parenchyma was significant and the border of the VX-2 tumor was clear. The image (4) is the ADC map from VX-2 tumor DWI of the image (3).

DISCUSSION

Diffusion is caused by water molecular random motion, so-called "Brownian motion", and it is able to change the intensity of local magnetic field around hydrogen proton so that its phase position in the magnetic field is changed. When we added a powerful polar and quick switching gradient radiofrequent (RF) pulse besides routine RF pulse, we were able to amplify these phase changes so that we could detect water molecular diffusion motion, the so-called DWI. DWI was initially used to evaluate early ischemic stages of the brain and its value has been recognized in recent years. However, because of its poor image quality, DWI is rarely used in diagnosing and evaluating the lesions of the liver[24-28].

b value is the sensitivity of diffusion and it is the most important parameter of DWI scanning because changing it will directly lead to a change of the complemented gradient magnetic field and affect the ability of detecting water molecular diffusion. Ichikawa *et al*.[27,28], reported that high *b* value or *b* value deviation has an important influence on the quality of DWI and ADC value or DC value. When *b* value or its deviation is higher, ADC value would be stabler and could get closer to the DC value, which could better reflect water molecular diffusion motion, little affected by the microcirculation. When *b* value or its deviation is lower, ADC value will, to some degree, reflect the perfusion of the microcirculation while the ability of reflecting water molecular diffusion motion is worse than that of the former and the ADC value is also unstable. However, with increasing *b* value, gradient RF pulse will prolong, thus enlarging TE value, and the quality of images will be reduced[15,27,28]. Our results showed that ADC value, QI and SNR of the images would reduce with *b* value increase but, when *b* value was 100, QI of the images was basically the same as that when *b* value was 10 or 50 and SNR of the images was also better. Moreover, QI and SNR of the images were still high when *b* value was 300. Thus, we consider that at a *b* value of 100, QI and SNR of the images are good, together with a *b* value of 300, at which lesions are more sensitively detected as a good choice on DWI (Figures 1 and 3).

TR enlarging will raise the quality of the images because it prolongs the signal collecting time. But it leads to prolongation of the scanning time or reduction of the scanning coverage and it is not beneficial to control breathing. Our results indicated that the distinction of ADC between TR 4 000, 6 000 and 8 000 was significant ($P<0.01$) and that of QI or SNR was not significant. Because breathing has little influence on DWI after the rabbits are anesthetized generally and deeply, TR 6 000 is an appropriate choice and we may also choose a large NEX at the same time.

In our study, ADC value of hepatic parenchyma and SNR of images were significantly higher when the thickness was 5 mm than when it was 2 mm ($P<0.01$) and QI of the images were slightly higher when the thickness was 2 mm than when it was 5 mm ($P<0.01$). When the thickness is raised, SNR of images increases along with the increase of artifacts and decrease of the liver anatomy manifestations, which are not beneficial to the diagnosis of lesions. However, if we increase the collective information through enlarging NEX in order to compensate for the reduction due to the 2 mm thickness, we can obtain enough SNR and a good QI, especially for rabbit liver, which is small in volume andthe number of scans is limited and is not suitable for use in breath gating (Figures 2 and 3).

Both the knee joint coil and the cranium coil have applied reference in reported literature. Our results indicated that SNR of the knee joint coil group was higher than that of the cranium coil group ($P<0.01$), while QI of the knee joint coil group was lower than that of the cranium coil group ($P<0.01$). We found that the major reason for this was their clouding borders and artifacts because of small objective aperture of the knee joint coil, and effects of breathing movement. The cranium coil is a good choice for rabbit liver DWI because it is technically, the best.

As for FOV, it has a significant influence on the quality of DWI images. SNR of images increase with the increase in collective information as FOV enlarges, but QI do not increase continuously. This is because the liver anatomy manifestation decreases as the pixel enlarges and spatial resolution decreases due to the FOV increase. Small FOV (16 cm×12 cm) is not beneficial to diagnoses because of its small QI and SNR at the same time and we regard "20 cm×15 cm" as a more suitable FOV.

Due to the light weight, hair on body surface and quick breathing of rabbits, it was difficult to apply the technology of breath gating in rabbit liver DWI scanning. After rabbits were anesthetized by 3% soluble pentobarbitone injection into auricular vein, the breathing of rabbits was slow and stable; we acquired good images with SE-EPI series, the scan time was short, little affected by the respiratory movement. Our results indicated that the major reason for the artifact was the gas in the stomach and it was effective to use some precluding drug, fast the rabbits and use a stable and suitable posture to decrease the artifact.

In conclusion, the scanning techniques, including appropriate *b* value, thickness, coil, FOV, respiratory movement and control of stomach gas, are very important in DWI of rabbit liver and the overall quality of DWI with a *b* value (100 s/mm^2), thickness (2 mm), cranium coils and FOV (20 cm×15 cm) was considered the best in our study.

ACKNOWLEDGMENTS

We thank the staff of the Radiology Department and the Animal Department of the Second Xiangya Hospital for their help and support; particularly Miss. Ying-Si He.

REFERENCES

1 **Cai RL**, Meng W, Lu HY, Lin WY, Jiang F, Shen FM. Segregation analysis of hepatocellular carcinoma in a moderately high-incidence area of East China. *World J Gastroenterol* 2003; **9**: 2428-2432

2 **Braga L,** Guller U, Semelka RC. Modern hepatic imaging. *Surg Clin North Am* 2004; **84**: 375-400

3 **Choi BI.** The current status of imaging diagnosis of hepatocellular carcinoma. *Liver Transpl* 2004; **10**(2 Suppl 1): S20-S25

4 **Hussain SM,** Terkivatan T, Zondervan PE, Lanjouw E, de Rave S, Ijzermans JN, de Man RA. Focal nodular hyperplasia: findings at state-of-the-art MR imaging, US, CT, and pathologic analysis. *Radiographics* 2004; **24**: 3-17

5 **Koda M,** Matsunaga Y, Ueki M, Maeda Y, Mimura K, Okamoto K, Hosho K, Murawaki Y. Qualitative assessment of tumor vascularity in hepatocellular carcinoma by contrast-enhanced coded ultrasound: comparison with arterial phase of dynamic CT and conventional color/power Doppler ultrasound. *Eur Radiol* 2004; **14**: 1100-1108

6 **Vogl TJ,** Schwarz W, Blume S, Pietsch M, Shamsi K, Franz M, Lobeck H, Balzer T, del Tredici K, Neuhaus P, Felix R, Hammerstingl RM. Preoperative evaluation of malignant liver tumors: comparison of unenhanced and SPIO (Resovist)-enhanced MR imaging with biphasic CTAP and intraoperative US. *Eur Radiol* 2003; **13**: 262-272

7 **Vilana R,** Llovet JM, Bianchi L, Sanchez M, Pages M, Sala M, Gilabert R, Nicolau C, Garcia A, Ayuso C, Bruix J, Bru C. Contrast-enhanced power doppler sonography and helical computed tomography for assessment of vascularity of small hepatocellular carcinomas before and after percutaneous ablation. *J Clin Ultrasound* 2003; **31**: 119-128

8 **Minami Y,** Kudo M, Kawasaki T, Kitano M, Chung H, Maekawa K, Shiozaki H. Transcatheter arterial chemoembolization of hepatocellular carcinoma: usefulness of coded phase-inversion harmonic sonography. *Am J Roentgenol* 2003; **180**: 703-708

9 **Ward J,** Robinson PJ. How to detect hepatocellular carcinoma in cirrhosis. *Eur Radiol* 2002; **12**: 2258-2272

10 **Nijsen JF,** Seppenwoolde JH, Havenith T, Bos C, Bakker CJ, van het Schip AD. Liver tumors: MR imaging of radioactive holmium microspheres-phantom and rabbit study. *Radiology* 2004; **231**: 491-499

11 **Lee JW,** Moon WK, Weinmann HJ, Kim SJ, Kim JH, Park SH, Kim TJ, Yoon CJ, Kim YH, Cho EY, Ha SW, Kang WS, Chang KH. Contrast-enhanced MR imaging of postoperative scars and VX2 carcinoma in rabbits: comparison of macromolecular contrast agent and gadopentetate dimeglumine. *Radiology* 2003; **229**: 132-139

12 **Forsberg F,** Piccoli CW, Liu JB, Rawool NM, Merton DA, Mitchell DG, Goldberg BB. Hepatic tumor detection: MR imaging and conventional US versus pulse-inversion harmonic US of NC100100 during its reticuloendothelial system-specific phase. *Radiology* 2002; **222**: 824-829

13 **Sayegh Y,** Pochon S, Vallee JP, Becker M, Lazeyras F, Tournier H, Hyacinthe R, Fouillet X, Terrier F. Detection of experimental hepatic tumors using long circulating superparamagnetic particles. *Invest Radiol* 2001; **36**: 15-21

14 **Geschwind JF,** Artemov D, Abraham S, Omdal D, Huncharek MS, McGee C, Arepally A, Lambert D, Venbrux AC, Lund GB. Chemoembolization of liver tumor in a rabbit model: assessment of tumor cell death with diffusion-weighted MR imaging and histologic analysis. *J Vasc Interv Radiol* 2000; **11**: 1245-1255

15 **Kuszyk BS,** Boitnott JK, Choti MA, Bluemke DA, Sheth S, Magee CA, Horton KM, Eng J, Fishman EK. Local tumor recurrence following hepatic cryoablation: radiologic-histopathologic correlation in a rabbit model. *Radiology* 2000; **217**: 477-486

16 **Miao Y,** Ni Y, Mulier S, Yu J, De Wever I, Penninckx F, Baert AL, Marchal G. Treatment of VX2 liver tumor in rabbits with "wet" electrode mediated radio-frequency ablation. *Eur Radiol* 2000; **10**: 188-194

17 **Sun XJ,** Quan XY, Liang W, Wen ZB, Zeng S, Huang FH, Tang M. Quantitative study of diffusion weighted imaging on magnetic resonance imaging in focal hepatic lesions less than 3 cm. *Zhonghua Zhongliu Zazhi* 2004; **26**: 165-167

18 **Cheryauka AB,** Lee JN, Samsonov AA, Defrise M, Gullberg GT. MRI diffusion tensor reconstruction with PROPELLER data acquisition. *Magn Reson Imaging* 2004; **22**: 139-148

19 **Chow LC,** Bammer R, Moseley ME, Sommer FG. Single breath-hold diffusion-weighted imaging of the abdomen. *J Magn Reson Imaging* 2003; **18**: 377-382

20 **Kamel IR,** Bluemke DA, Ramsey D, Abusedera M, Torbenson M, Eng J, Szarf G, Geschwind JF. Role of diffusion-weighted imaging in estimating tumor necrosis after chemoembolization of hepatocellular carcinoma. *Am J Roentgenol* 2003; **181**: 708-710

21 **Boulanger Y,** Amara M, Lepanto L, Beaudoin G, Nguyen BN, Allaire G, Poliquin M, Nicolet V. Diffusion-weighted MR imaging of the liver of hepatitis C patients. *NMR Biomed* 2003; **16**: 132-136

22 **Taouli B,** Vilgrain V, Dumont E, Daire JL, Fan B, Menu Y. Evaluation of liver diffusion isotropy and characterization of focal hepatic lesions with two single-shot echo-planar MR imaging sequences: prospective study in 66 patients. *Radiology* 2003; **226**: 71-78

23 **Inoha S,** Inamura T, Nakamizo A, Ikezaki K, Amano T, Fukui M. Magnetic resonance imaging in cases with encephalopathy secondary to immunosuppressive agents. *J Clin Neurosci* 2002; **9**: 305-307

24 **Murtz P,** Flacke S, Traber F, van den Brink JS, Gieseke J, Schild HH. Abdomen: diffusion-weighted MR imaging with pulse-triggered single-shot sequences. *Radiology* 2002; **224**: 258-264

25 **Moteki T,** Horikoshi H, Oya N, Aoki J, Endo K. Evaluation of hepatic lesions and hepatic parenchyma using diffusion-weighted reordered turboFLASH magnetic resonance images. *J Magn Reson Imaging* 2002; **15**: 564-572

26 **Chan JH,** Tsui EY, Luk SH, Fung AS, Yuen MK, Szeto ML, Cheung YK, Wong KP. Diffusion-weighted MR imaging of the liver: distinguishing hepatic abscess from cystic or necrotic tumor. *Abdom Imaging* 2001; **26**: 161-165

27 **Ichikawa T,** Haradome H, Hachiya J, Nitatori T, Araki T. Diffusion-weighted MR imaging with a single-shot echoplanar sequence: detection and characterization of focal hepatic lesions. *AJR Am J Roentgenol* 1998; **170**: 397-402

28 **Ichikawa T,** Haradome H, Hachiya J, Nitatori T, Araki T. Diffusion-weighted MR imaging with single-shot echo-planar imaging in the upper abdomen: preliminary clinical experience in 61 patients. *Abdom Imaging* 1999; **24**: 456-461

Science Editor Zhu LH and Guo SY **Language Editor** Elsevier HK

PO Box 2345, Beijing 100023, China
www.wjgnet.com
wjg@wjgnet.com

ELSEVIER

World J Gastroenterol 2005;11(35):5512-5516
World Journal of Gastroenterology ISSN 1007-9327
© 2005 The WJG Press and Elsevier Inc. All rights reserved.

• *CLINICAL RESEARCH* •

Amelioration effects of traditional Chinese medicine on alcohol-induced fatty liver

Hyun-Jeong Kwon, Yun-Young Kim, Se-Young Choung

Hyun-Jeong Kwon, Yun-Young Kim, Se-Young Choung, Department of Hygienic Chemistry, College of Pharmacy, Kyung Hee University, Seoul 130-701, South Korea
Correspondence to: Se-Young Choung, PhD, Department of Hygienic Chemistry, College of Pharmacy, Kyung Hee University, Seoul 130-701, South Korea. sychoung@khu.ac.kr
Telephone: +82-2-961-0372 Fax: +82-2-961-0372
Received: 2004-11-08 Accepted: 2004-12-23

Abstract

AIM: To examine the effects of traditional Chinese medicine (TCM) on alcohol-induced fatty liver in rats. TCM consists of *Astragalus membranaceus*, *Morus alba*, *Crataegus pinnatifida*, *Alisma orientale*, *Salvia miltiorrhiza*, and *Pueraria lobata.*

METHODS: The rats were separated randomly into five groups. One (the CD group) was fed a control diet for 10 wk, another (the ED group) fed an ethanol-containing isocaloric liquid diet for 10 wk, and the last three (the TCM group) were fed an ethanol-containing isocaloric liquid diet for 10 wk and dosed orally with TCM (222 mg/kg·d, TCM222; 667 mg/kg·d, TCM667; and 2 000 mg/kg·d, TCM2000, respectively) weekly during the last 4 wk.

RESULTS: ED group developed fatty liver according to lipid profile and liver histological findings. Compared with the control group, liver/body weight, serum triglyceride (TG) and total cholesterol (TC), liver TG and TC, serum alanine aminotransferase (ALT) and aspartic aminotransferase (AST) significantly increased in the ED group. Whereas, in the rats administered with TCM, liver/body weight, serum TG and TC, liver TG and TC, serum ALT and AST were significantly decreased, and the degree of hepatic lipid droplets was markedly improved compared with those in the ED group.

CONCLUSION: TCM treatment causes significant reduction in alcohol-induced lipid hepatic accumulation, reversing fatty liver and liver damage, and can be used as a remedy for alcoholic fatty liver.

© 2005 The WJG Press and Elsevier Inc. All rights reserved.

Key words: Fatty liver; Alcohol; *Astragalus membranaceus*; *Morus alba*; *Crataegus pinnatifida*; *Alisma orientale*; *Salvia miltiorrhiza*; *Pueraria lobata*

Kwon HJ, Kim YY, Choung SY. Amelioration effects of traditional Chinese medicine on alcohol-induced fatty liver. *World J Gastroenterol* 2005; 11(35): 5512-5516
http://www.wjgnet.com/1007-9327/11/5512.asp

INTRODUCTION

Fatty liver is a common histological finding in human liver biopsies, it has been defined as both, more than 5% of cells containing fat droplets or total lipid exceeding 5% of liver weight[1,2]. In the majority of cases the accumulating lipid is predominantly TG. Fatty liver can occur in association in the majority of cases due to alcohol excess, and patients with it are susceptible to liver fibrosis and cirrhosis. Fatty liver is also associated with liver cancer[3-6]. Recovery from fatty liver seems to decrease susceptibility to liver fibrosis and cirrhosis, the more severe liver diseases in terms of liver function and treatment. However, there is as yet no clearly established therapy for reversing fatty liver. We screened a number of liver protective and anti-hepatic steatosis agents from natural products used for the treatment of liver diseases, and selected *Astragalus membranaceus*[7-9], *Morus alba* (Oh *et al*., 2002), *Crataegus pinnatifida*[10,11], *Alisma orientale*[12,13], *Salvia miltiorrhiza*[14,15] and *Pueraria lobata*[16-18]. All of these have been reported to effect liver protection; however, the question of whether a mixture of these continues to be effective is unknown. Thus, the current study investigates the effects of traditional Chinese medicine (TCM) on induced (by administration of alcohol) fatty liver in male Sprague-Dawley rats. Although the active ingredients of TCM is not completely known, any of their synergistic mixtures could play a role in resolving fatty liver, and the potential clinical therapeutic value for subjects with alcoholic fatty liver warrants further attention.

MATERIALS AND METHODS

Preparation of traditional Chinese medicine

TCM is a mixture of traditional medicine, consisting of *Astragalus membranaceus*, *Morus alba*, *Crataegus pinnatifida*, *Alisma orientale*, *Salvia miltiorrhiza*, and *Pueraria lobata* (2:2:2:2:1:1). The materials were obtained from Pharmaceutical Company in Korea, and cut into small pieces. After standing at room temperature for 30 min, the materials were extracted in 10 volumes of distilled water at 95-99 ℃, 0.5-0.6 kgf/cm^2, 3 h. The fluids were then filtered, and thickened under reduced pressure at 70-80 ℃. The extracts were spray dried to a dry powder, and maintained in humidity below 5%.

Animals and diets

Male Sprague-Dawley rats (Daehan Biolink, Chungbuk, Korea), weighing about 100 g, were purchased. All animals received humane care in compliance with the institution's guideline criteria for humane care, as outlined in the National Institute of Health Guidelines for the Care and

Use of Laboratory Animals[19]. The rats were acclimatized for at least 7 d after delivery and were given free access to standard rodent pellet food (Samtaco, Gyeonggi-do, Korea) and water during the adaptation period. The cages were placed in a room with controlled temperature (22±2 ℃), relative humidity (60±5%), and 12 h light/dark cycle (08:00 on-20:00 off). The body weight and general condition of the animals were monitored twice weekly and liquid diet intake was determined daily. The rats were randomly assigned to three groups: one (the CD group) fed a control diet for 10 wk and administered orally daily with saline on each of the last 4 wk, another (the ED group) fed an ethanol-containing isocaloric liquid diet for 10 wk and dosed orally with saline in each of the last 4 wk, and the last three (the TCM groups) were fed an ethanol-containing isocaloric liquid diet for 10 wk and dosed orally with TCM [0.222 g/(kg·d), TCM222; 0.667 g/(kg·d), TCM667; and 2.000 g/(kg·d), TCM2000, respectively] on each of the last 4 wk. Each group included 10 rats. The liquid diet (Table 1) was prepared according to the method described by Lieber-DeCarli[20] and provided 1 kcal/mL, containing 28% carbohydrate, 20% protein, 15% fat plus 37% ethanol (ED group) or isocaloric maltose dextrin as the control. Animals were started on the diet at a body weight of 125-140 g and ethanol was introduced progressively with 3% for the first 2 d (21% of total energy), 4% for the subsequent 2 d (28% of energy) followed by the final formula containing 5% (36% of energy) thereafter. Ethanol was incorporated into the diet just before the supply of the liquid diet to the rats. The diet was kept refrigerated in the dark and used within 1 wk of preparation.

Table 1 Composition of experimental diets (g/L)

Ingredients	Control	Ethanol
Casein	41.40	41.40
DL-Methionine	0.30	0.30
L-Cystine	0.50	0.50
Cellulose	10.00	10.00
Maltose dextrin	115.20	25.60
Corn oil	8.50	8.50
Olive oil	28.40	28.40
Safflower oil	2.70	2.70
Mineral mix[1]	8.75	8.75
Vitamin mix[2]	2.50	2.50
Choline bitartrate	0.53	0.53
Xanthan gum	3.00	3.00
Ethanol	–	45.5

[1]AIN-76 mineral mix provided the following g/kg mix: calcium phosphate, dibasic, 500; sodium chloride, 74; potassium citrate • H_2O, 220; potassium sulfate, 52; magnesium oxide, 24; manganous carbonate, 3.5; ferric citrate, 6; zinc carbonate, 1.6; cupric carbonate, 0.3; potassium iodate, 0.01; sodium selenite, 0.01; chromium K sulfate.12H_2O, 0.55; sucrose, finely powdered, 118.03; Dyets, Bethlehem, PA, USA. [2]AIN-76A vitamin mix provided the following g/kg mix: thiamine HCl, 0.6; riboflavin, 0.6; pyridoxine HCl, 0.7; niacin, 3; calcium pantothenate, 1.6; folic acid, 0.2; biotin, 0.02; vitamin B12 (0.1%), 1; vitamin A palmitate (500 000 IU/g), 0.8; vitamin D3 (400 000 IU/g), 0.25; vitamin E acetate (500 IU/g), 10; menadione sodium bisulfite, 0.08; sucrose, finely powdered, 981.15; Dyets, Bethlehem, PA, USA.

Sampling procedures

On 0, 6, 8, and 10 wk of treatment, animals were killed and blood and tissue removed for analysis. The rats were anesthetized with ether and killed after 12 h of fasting. Blood samples were collected from hepatic portal vein into vacutainer (Becton Dickinson & Co., Rutherford, NJ, USA) for the separation of serum and centrifuged (3 000 r/min for 15 min at 4 ℃). The serum was frozen at -70 ℃ for biochemical analysis. The liver was removed and then weighed after being cleaned with ice-cold saline, and stored at -70 ℃ for the lipid analysis.

Biochemical analysis

Biochemical analysis was carried out using commercial kits. The analysis of serum TG, TC, and high-density lipoprotein cholesterol (HDL-C) concentration were done by automatic analyzer techniques (Asan Pharm. Co., Ltd, Korea). The concentrations were measured spectrophotometrically at a wavelength of 550, 500, and 500 nm respectively (Jasco V-530 UV/VIS, Japan). The low-density lipoprotein cholesterol (LDL-C) and very low-density lipoprotein cholesterol (VLDL-C) were estimated using the Friedewald formula as follows: LDL-C = TC-(VLDL-C+HDL-C) and VLDL-C = TG/5[21]. The activities of the serum aspartic aminotransferase (AST) and alanine aminotransferase (ALT) were measured using kits (Asan Pharm. Co., Ltd, Korea). To analyze hepatic lipid content, the lipids were extracted by homogenizing the liver with 2:1 chloroform-methanol (v/v) by the method devised by Folch *et al*.[22]. Then, TG and TC were measured using commercial kits (Asan Pharm. Co., Ltd, Korea).

Liver histology

A portion of the liver was fixed in 40 g/L formaldehyde and embedded in paraffin wax. Frozen liver sections from fixed tissues were cut into 10-μm pieces and mounted on the slide. The samples were stained for lipid with Oil Red O in propylene glycol with Mayer's hematoxylin as the counter stain, and it calculated the area by densitometer.

Statistical analysis

Statistical evaluation of data was performed by Duncan's multiple range tests to make comparisons among the groups. Values were given as the mean±SD. Differences of $P<0.05$ were considered statistically significant.

RESULTS

Effects on body weight and liver weight

Table 2 shows the body weight and liver weight (g/100 g body weight) in all rats during the 10 wk. At 10th wk, the body weight gain was significantly lower in the rats fed alcohol than in the rats fed without alcohol. However, a trend toward increased weights was seen in rats administrated TCM than those in the ED group. The liver weights tended to be higher in alcohol-fed rats than in the CD group. However, after the administration of TCM for 4 wk, the TCM groups showed significantly decreased liver weights above all, and TCM667 group was the lowest of all the TCM groups. It is considered that there is an inhibition of hepatic lipids accumulation in rats treated with TCM.

Table 2 Effect of TCM on body weight and liver weight of rats fed experimental diets for 10 wk and treated with TCM for the last 4 wk

Wk	Group	Body weight (g)	Liver/body weight (g/BW 100 g)
0	–	134.8±5.6	4.03±0.33
6	CD	306.6±14.2	2.69±0.22
	ED	265.4±13.5[b]	3.14±0.11[b]
8	CD	309.4±16.3[a,c]	2.74±0.22[e]
	ED	293.2±17.2[c]	3.20±0.26[a]
	TCM2000	315.0±15.2[a]	2.97±0.14[c]
	TCM667	299.2±20.9[a,c]	2.90±0.25[c,e]
	TCM222	294.0±15.1[c]	2.93±0.18[c,e]
10	CD	350.8±19.7[a]	2.55±0.13[e]
	ED	308.0±12.7[c,e]	2.99±0.31[a]
	TCM2000	317.8±15.6[c]	2.80±0.08[a,c]
	TCM667	319.0±17.8[c]	2.74±0.21[c,e]
	TCM222	299.4±20.1[e]	2.84±0.17[a,c]

[a]P<0.05, [c]P<0.05, [e]P<0.05, *vs* others, [b]P<0.001 *vs* control.

Effects on serum lipid profiles

Serum concentrations of TG and TC in rats administrated with alcohol increased to 3.8- and 1.5-fold higher levels respectively than those seen in rats given the control diet (Figure 1). Consumption of alcohol for 6 wk caused significant increases in TG and TC. At 10th wk, TG and TC were significantly reduced by consumption of TCM. TG concentration was reduced by 70%, and the TC concentration was significantly decreased to the level of control rats. Especially, a "middle dose" of TCM667 is more effective in decreasing serum TG than a high dose of TCM2000. In the current study, LDL-C and VLDL-C concentration in rats given alcohol significantly increased 5.8- and 3.8-fold higher levels than those seen in control diet-treated rats (Table 3). However, a trend toward decreased LDL and VLDL was seen after TCM administration; especially, TCM667 is more effective in this, than a high dose of TCM2000. On the other hand, HDL-C concentration in rats given alcohol declined significantly. However, the administration of TCM partially returned to normal.

Table 3 Effect of TCM on serum LDL-C, VLDL-C and HDL-C concentration of rats fed experimental diets for 10 wk and treated with TCM for the last 4 wk

Wk	Group	LDL-C	VLDL-C mg/dL	HDL-C
0		16.66±9.58	7.41±1.87	31.20±9.73
6	CD	26.46±13.45	8.62±3.67	35.21±6.98
	ED	41.39±17.36[b]	22.33±1.33[d]	28.65±7.68[b]
8	CD	20.21±9.15[e]	8.72±4.21[e]	48.36±4.47[a]
	ED	49.53±17.02[a]	25.90±2.88[a]	24.94±7.93[e]
	TCM2000	30.15±4.21[c]	16.43±2.23[c]	31.70±3.74[c]
	TCM667	44.78±10.26[a]	8.47±1.71[e]	32.94±6.71[c]
	TCM222	45.55±9.66[a]	10.94±1.88[e]	30.67±5.65[c]
10	CD	12.02±8.78[g]	4.75±0.60[e]	55.36±10.48[a]
	ED	69.94±11.90[a]	18.05±3.30[a]	20.42±6.21[e]
	TCM2000	26.23±9.99[e]	7.78±1.54[c]	38.27±9.33[c]
	TCM667	35.59±8.91[c]	6.59±1.93[c]	37.71±6.74[c]
	TCM222	39.14±8.47[c]	6.95±1.57[c]	35.67±3.04[c]

[a]P<0.05, [c]P<0.05, [e]P<0.05, [g]P<0.05, *vs* others, [b]P<0.001, [d]P<0.001 *vs* control.

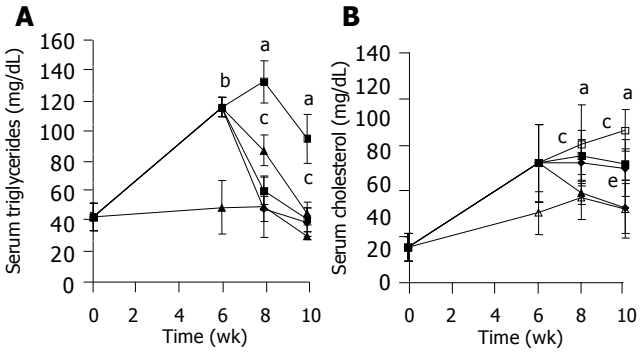


Figure 1 Effect of TCM on concentration of serum TGs (**A**) and TC (**B**) of rats fed experimental diet for 10 wk and treated with TCM for the last 4 wk. △, CD; □, ED; ▲, TCM2000; ●, TCM667; ■, TCM222. [a]P<0.05, [c]P<0.05, [e]P<0.05 *vs* others, [b]P<0.0001 *vs* control.

Effects on hepatic triglycerides and total cholesterol

In alcohol-fed rats, hepatic lipid content raised significantly compared to rats fed with an isocaloric diet without alcohol (Figure 2). Hepatic triglycerides (TGs) and total cholesterol (TC) concentration showed 2.3- and 2.7-fold increase, respectively, in rats fed an alcohol diet compared to those fed a control diet. Therefore, ingestion of alcohol containing diets for 6 wk causes the onset of fatty liver. At 10th wk, TG and TC were significantly reduced by consumption of TCM. Both the TG and TC concentration was significantly decreased to the level of control rats. Especially, TCM667 is more effective in decreasing serum TG than a high dose of TCM2000.

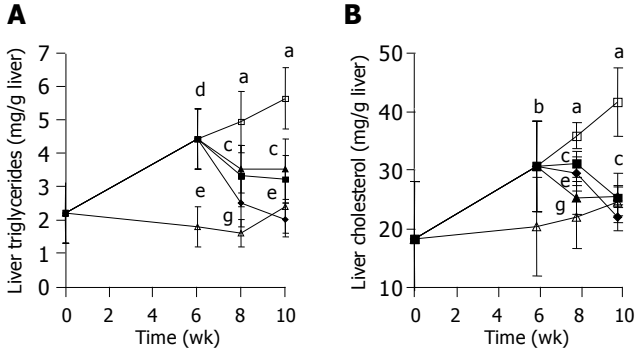


Figure 2 Effect of TCM on TGs and TC concentrations in liver of rats fed experimental diet for 10 wk and treated with TCM for the last 4 wk. △, CD; □, ED; ▲, TCM2000; ●, TCM667; ■, TCM222. [a]P<0.05, [c]P<0.05, [e]P<0.05, [g]P<0.05 *vs* others, [b]P<0.001, [d]P<0.0001 *vs* control.

Effects on hepatoprotective activities

The administration of alcohol to the rats significantly raised the activities of AST and ALT (Table 4). Supplementing with TCM reduced the activity of serum AST and ALT in rats with fatty liver. Moreover, TCM exhibited DPPH free radical scavenging effect (data not shown).

Hepatopathological manifestations

Histological examination of liver tissue (Figure 3) showed lipid accumulation greater in rats, which fed the ethanol-containing diets for 10 wk (Figure 3B), compared to control

Table 4 Effect of TCM on serum AST and ALT activities of rats fed experimental diets for 10 wk and treated with TCM for the last 4 wk

Wk	Group	AST (U/mL)	ALT (U/mL)
0		71.79±9.39	32.67±8.52
6	CD	89.72±6.17	28.00±6.63
	ED	133.30±12.78[b]	68.96±9.22[b]
8	CD	94.85±8.12[c,e]	38.45±8.97[c]
	ED	119.52±14.73[a]	62.60±9.48[a]
	TCM2000	86.20±9.89[e]	33.92±9.26[c,e]
	TCM667	99.21±6.41[c]	29.84±9.44[e]
	TCM222	103.61±6.92[c]	59.37±7.07[a]
10	CD	96.97±9.97[a,c]	23.50±3.02[e]
	ED	105.24±12.06[a]	56.74±9.76[a]
	TCM2000	86.13±9.71[e]	36.23±9.92[c]
	TCM667	86.54±9.66[e]	27.73±9.87[e]
	TCM222	88.34±6.72[c,e]	40.80±9.44[c]

[a]P<0.05, [c]P<0.05, [e]P<0.05, *vs* others, [b]P<0.001 *vs* control.

diet-fed rats (Figure 3A). In contrast, in rats administrated with TCM for 4 wk, accumulation of lipid droplets was remarkably decreased (Figures 3C-E). Quantification of liver lipids was concordant with the histological findings (Figure 3F). Ethanol feeding increased the liver lipids content by threefold, these results are consistent with the rate of elevation of plasma and hepatic TG in the ethanol-fed rats. In striking contrast, when TCM was administered for the last 4 wk of the ethanol feeding, the lipids content was significantly decreased to the level of control rats.

DISCUSSION

Fatty liver is the most common pathological change induced by alcohol and is also one of the earliest pathological revelations of alcoholic liver disease. Autopsy studies in previously healthy adults, killed accidentally, have revealed an incidence of 1/3[1]. Potential pathophysiological mechanisms include: (1) increased uptake of fatty acids, (2) inhibition of fatty acid oxidation, (3) increased endogenous synthesis of fatty acids, and (4) decreased capacity of the liver to export TG in very-low density lipoprotein particles[23]. Fatty liver can lead to liver fibrosis and cirrhosis; therefore, it is important to treat the condition before it progresses into a more serious form. However, there is no established therapy for the recovery of fatty liver. In this regard, the present study aimed to evaluate the effects of TCM, which depletes levels of serum and hepatic lipid profiles on alcohol-induced fatty liver in rats.

The liquid diet containing alcohol resulted in the accumulation of liver lipids and thus provided a model for alcohol-induced lesions[20]. Despite strict isocaloric pair feeding, alcohol-fed rats did not gain as much weight as those in their pair fed control groups even though they received diets with the same energy content. The slower weight gain of the animals in this study compared to those reported by some authors may be due to the reduction of intake and absorption of nutrients[24,25]. The supplement of alcohol for 6 wk to the rats caused a significant increase in liver weight, and this accounted for by TG accumulation. However, body weight and liver weight of TCM groups were close to those of the control groups. Moreover, both serum and liver, lipid concentrations were significantly (P<0.0001) increased by alcohol feeding. In the present study, however, TCM administration decreased serum and hepatic lipids concentrations to levels lower than those seen before

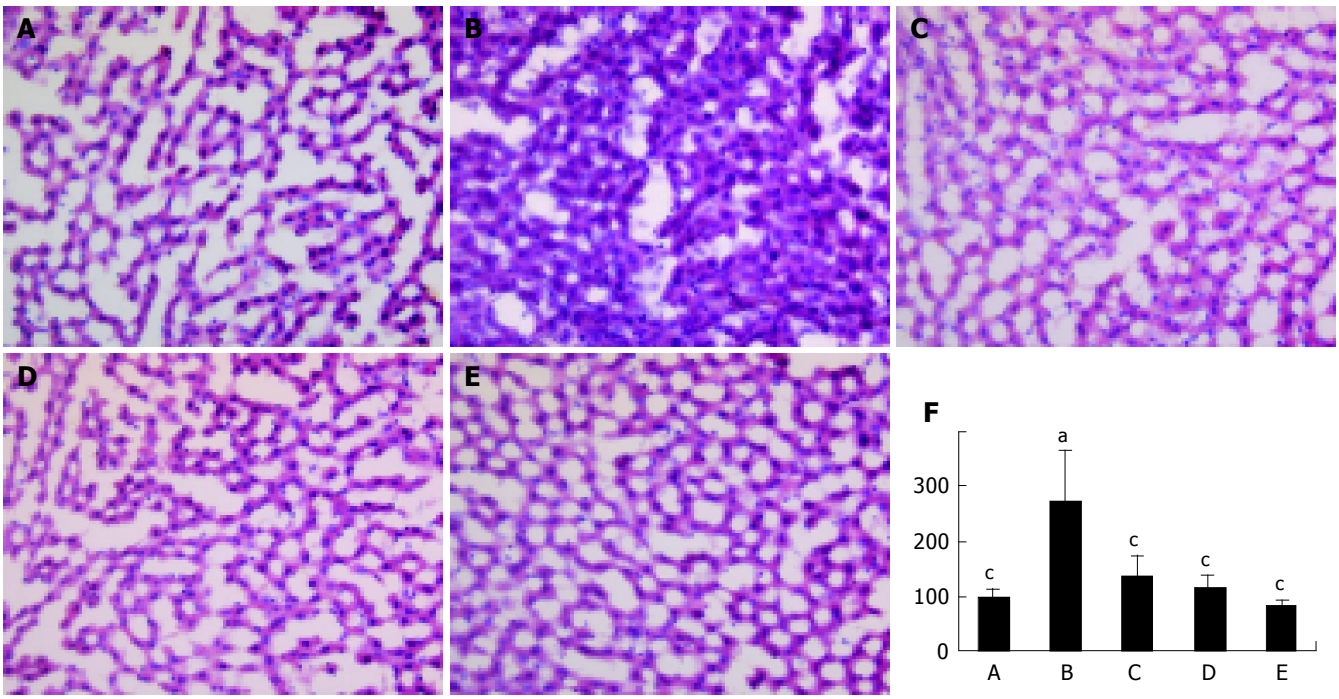


Figure 3 Liver histology in rats treated with alcohol or alcohol plus TCM. Frozen sections of liver (×40) taken from (**A**) CD+saline, (**B**) ED+saline, (**C**) ED+TCM2000, (**D**) ED+TCM667, (**E**) ED+TCM222-treated rats on 10 wk, (**F**) densitometer analysis: the representative experiment A–E were quantified and the integrated area were percentized in control rats (100%). In **A-E**, frozen sections were stained with Oil Red O and counterstained with Mayer's hematoxylin. Lipid droplets were stained red. [a]P<0.05, [c]P<0.05 *vs* others.

TCM administration or returned to normal range, even when rats consumed ethanol diets during the period of TCM administration.

Accordingly, we suggest that the treatment of rats with TCM for 4 wk reversed fatty liver to normal values, as appraised biochemically and histologically. In addition, VLDL was made up of TG-rich lipoproteins and transferred TG from the liver to peripheral tissues. Previous studies indicate that the impaired ability of hepatocytes to secrete lipid components as VLDL is likely to be one major mechanism linked to alcoholic fatty liver[4,26-28]. Accordingly, one important mechanism involved in TCM-induced recovery from an alcoholic fatty liver is decrease in serum LDL and VLDL concentrations. In the current study, the ED group showed increased VLDL and LDL, but the administration of TCM returned to normal. These findings suggest that TCM might enhance the secretion of VLDL from the liver and contribute to the improvement of alcoholic fatty liver. In addition, it seems remarkable that TCM administration increased serum HDL levels. HDL are cholesterol-rich lipoproteins and transferred cholesterol from peripheral tissues to the liver. Therefore, TCM might affect not only TG but also total lipid metabolism, including cholesterol metabolism. Additionally, the current study evaluated whether TCM could protect against liver damage, consequently, TCM takes effects to decrease AST and ALT.

In conclusion, administration of TCM diminishes the accumulation of lipids in the liver. These results suggested that intake of TCM (*Astragalus membranaceus*, *Morus alba*, *Crataegus pinnatifida*, *Alisma orientale*, *Salvia miltiorrhiza*, and *Pueraria lobata*) may be useful in preventing and improving fatty liver induced by alcohol. It is not certain by what mechanism this takes place from the current observation; therefore, follow-up investigations identifying the mechanism related to the reduction of lipids in liver are recommended.

REFERENCES

1 **Underwood Ground KE.** Pilot-induced factors in fatal light aircraft accidents in the United Kingdom: 1969-1981. *Aviat Space Environ Med* 1984; **55**: 52-58
2 **Hoyumpa AM,** Greene HL, Dunn GD, Schenker S. Fatty liver: biochemical and clinical considerations. *Am J Dig Dis* 1975; **20**: 1142-1170
3 **Lieber CS.** Metabolic effects of ethanol on the liver and other digestive organs. *Clin Gastroenterol* 1981; **10**: 315-342
4 **Day CP,** Yeaman SJ. The biochemistry of alcohol-induced fatty liver. *Biochim Biophys Acta* 1994; **1215**: 33-48
5 **Sorensen TI,** Orholm M, Bentsen KD, Hoybye G, Eghoje K, Christoffersen P. Prospective evaluation of alcohol abuse and alcoholic liver injury in men as predictors of development of cirrhosis. *Lancet* 1984; **2**: 241-244
6 **Teli MR,** Day CP, Burt AD, Bennett MK, James OF. Determinants of progression to cirrhosis or fibrosis in pure alcoholic fatty liver. *Lancet* 1995; **346**: 987-990
7 **Zee-Cheng RK.** Shi-quan-da-bu-tang (ten significant tonic decoction), SQT. A potent Chinese biological response modifier in cancer immunotherapy, potentiation and detoxification of anticancer drugs. *Methods Find Exp Clin Pharmacol* 1992; **14**: 725-736
8 **Lu DC,** Su ZJ, Rui T. Effect of jian yan ling on serum lipids, apoprotein and lipoprotein-a. *Zhongguo Zhongxiyi Jiehe Zazhi* 1994; **14**: 142-144
9 **Zhang ZL,** Wen QZ, Liu CX. Hepatoprotective effects of astragalus root. *J Ethnopharmacol* 1990; **30**: 145-149
10 **Shanthi S,** Parasakthy K, Deepalakshmi PD, Devaraj SN. Hypolipidemic activity of tincture of Crataegus in rats. *Indian J Biochem Biophys* 1994; **31**: 143-146
11 **Ciplea AG,** Richter KD. The protective effect of Allium sativum and Crataegus on isoprenaline-induced tissue necroses in rats. *Arzneimittelforschung* 1988; **38**: 1583-1592
12 **Lim SJ,** Park JE. Effects of butanol fraction of Alisma canaliculatum with vitamin E of plasma levels of glucose and lipid in streptozotocin-induced diabetic rats. *Korean J Food S Technol* 2003; **4**: 713-719
13 **Chang IM,** Kim YS, Yun HS, Kim SO. Liver-protective activities of Alisol compounds against CCl_4 intoxication. *Korean J Pharmacognosy* 1982; **13**: 112-115
14 **Wasser S,** Ho JM, Ang HK, Tan CE. Salvia miltiorrhiza reduced experimentally-induced hepatic fibrosis in rats. *J Hepatol* 1998; **29**: 760-771
15 **Nan JX,** Park EJ, Kang HC, Park PH, Kim JY, Sohn DH. Antifibrotic effects of a hot-water extract from Salvia miltiorrhiza roots on liver fibrosis induced by biliary obstruction in rats. *J Pharmacy Pharmacol* 2001; **53**: 197-204
16 **Keung WM,** Klyosov AA, Vallee BL. Daidzin inhibits mitochondrial aldehyde dehydrogenase and suppresses ethanol intake of Syrian golden hamsters. *Proc Natl Acad Sci USA* 1997; **94**: 1675-1679
17 **Lee JS,** Mamo J, Ho N, Pal S. The effect of *Puerariae radix* on lipoprotein metabolism in liver and intestinal cells. *BMC Complement Altern Med* 2002; **2**: 12-18
18 **Arao T,** Udayama M, Kinjo J, Nohara T, Funakoshi T, Kojima S. Preventive effects of saponins from puerariae radix (the root of Pueraria lobata Ohwi) on *in vitro* immunological injury of rat primary hepatocyte cultures. *Biol Pharm Bull* 1997; **20**: 988-991
19 National institutes of health: guide for the care and use of laboratory animals. 1985. Public health service, NIH publication no. 86-23, Bethesda, MD.
20 **Lieber CS,** DeCarli LM, Sorrel MF. Experimental methods of ethanol administration. *Hepatology* 1989; **10**: 501-510
21 **Friedewald WT,** Levy RI, Fredrickson DS. Estimation of low density lipoprotein cholesterol in plasma, without use of the preparative ultracentrifuge. *Clin Chem* 1972; **18**: 499-502
22 **Folch J,** Lees M, Sloane Stanley GH. A simple method for the isolation and purification of total lipids from animal tissue. *J Biol Chem* 1957; **226**: 497-509
23 **Abrams MA,** Cooper C. Quantitative analysis of metabolism of hepatic triglyceride in ethanol-treated rats. *Biochem J* 1976; **156**: 33-46
24 **Lieber CS.** Alcohol and the liver: 1994 update. *Gastroenterology* 1994; **106**: 1085-1105
25 **Pikaar NA,** Wedel M, van der Beek EJ, van Dokkum W, Kempen HJ, Kluft C, Ockhuizen T, Hermus RJ. Effects of moderate alcohol consumption on platelet aggregation fibrinolysis and blood lipids. *Metabolism* 1987; **36**: 538-543
26 **Schapiro RH,** Drummey GD, Shimizu Y, Isselbacher KJ. Studies on the pathogenesis of the ethanol-induced fatty liver. II. Effect of ethanol on palmitate-1-C-14 metabolism by the isolated perfuse rat liver. *J Clin Invest* 1964; **43**: 1338-1347
27 **Grunnet N,** Kondrup J, Dich J. Effect of ethanol on lipid metabolism in cultured hepatocytes. *Biochem J* 1985; **228**: 673-681
28 **Venkatesan S,** Ward RJ, Peters TJ. Effect of chronic ethanol feeding on the hepatic cretion of very-low-density lipoproteins. *Biochim Biophys Acta* 1988; **960**: 61-66

Science Editor Guo SY **Language Editor** Elsevier HK

PO Box 2345, Beijing 100023, China
www.wjgnet.com
wjg@wjgnet.com

ELSEVIER

World J Gastroenterol 2005;11(35):5517-5520
World Journal of Gastroenterology ISSN 1007-9327
© 2005 The WJG Press and Elsevier Inc. All rights reserved.

• *CLINICAL RESEARCH* •

Acupuncture therapy for experimental stomach ulcer and c-Fos expression in rats

Hong Wang, Chun-Yang Wang, Jin-Shan Zhang, Lan Sun, Jing-Ping Sun, Qing-Hua Tian, Xiang-Lan Jin, Ling Yin

Hong Wang, Jing-Ping Sun, Qing-Hua Tian, Xiang-Lan Jin, Ling Yin, Neuroinformatics Center, Chinese PLA General Hospital, Beijing 100853, China
Chun-Yang Wang, Department of Urology, Chinese PLA General Hospital, Beijing 100853, China
Jin-Shan Zhang, Lan Sun, Department of Embryology and Histology, the Fourth Military Medical University, Xi'an 710032, Shaanxi Province, China
Supported by National Natural Science Foundation of China, No. 30171135; National Key Program for Basic Research of China, No. 2001CCA00700
Correspondence to: Professor Ling Yin, 28 Fuxing Road, Institute of Neurology Neuroinformatics Center, Chinese PLA General Hospital, Beijing 100853, China. yinling1955@sina.com
Telephone: +86-10-66937546 Fax: +86-10-88271317
Received: 2004-03-03 Accepted: 2004-08-30

Abstract

AIM: To determine the role of acupuncture therapy in treating experimental gastric ulcer in rats.

METHODS: Twenty-eight adult male Sprague-Dawley rats were randomly divided into four groups (pre-acupuncture group; acupuncture group; paradistance-acupuncture group; and control group), and pre-acupuncture, paradistance-acupuncture, and control groups received 5 μL acetic acid (200 mL/L HAc) injection after a same course of electroacupuncture (EA) treatment (4 Hz, 0.6 mA, 0.45 ms, 45 min for 4 d). The rats in these three groups recovered within 4 d. The acupuncture group received EA therapy for 4 d, after HAc injection. The stomach was dissected to compare the pathological structures of ulcer. Also c-Fos activation in the nuclei of solitary tract (NTS) was observed under microscope after regular immunohistochemistry staining of brain stem sections.

RESULTS: The number of ulcers was different among the four groups, especially between control group and paradistance-acupuncture group or pre-acupuncture group. In the latter group, the number of ulcers was much less. The gastric ulcer area was consistent with the histopathological results, indicating that pre-acupuncture had an obvious therapeutic effect on gastric ulcers. Acupuncture had a very modest effect and paradistance-acupuncture had no effect on gastric ulcers. No therapeutic effect was found in the control group. Fos-Li neurons in NTS induced by noxious gastric ulcer showed a significant difference between pre-acupuncture and control groups.

CONCLUSION: Acupuncture before ulceration can obviously alleviate ulcer. The production of c-Fos proves that the vagus nerve mediates the induction of c-Fos in nuclei of solitary tract following experimental ulceration, suggesting that parasympathetic afferents promote the process of noxious visceral stimulation.

© 2005 The WJG Press and Elsevier Inc. All rights reserved.

Key words: Zusanli acupuncture; Ulceration; c-Fos; Nucleus of solitary tract

Wang H, Wang CY, Zhang JS, Sun L, Sun JP, Tian QH, Jin XL, Yin L. Acupuncture therapy for experimental stomach ulcer and c-Fos expression in rats. *World J Gastroenterol* 2005; 11(35): 5517-5520
http://www.wjgnet.com/1007-9327/11/5517.asp

INTRODUCTION

Acupuncture has been used for the treatment of a wide variety of conditions[1] including fever, inflammation and infection, especially stomach diseases. But the efficacy and mechanism of acupuncture in prevention of acid-induced ulcers are unknown. Here the previous animal ulceration model[2] by injection of acetic acid (HAc) was used to study the effectiveness of acupuncture. The zusanli (St36) acupuncture was chosen, because it may have therapeutic functions for stomach diseases and it may be related with the anti-inflammation effect of vagus nerve[3]. C-Fos has been used as a marker for activity in the central nervous system following noxious somatic and visceral stimulation. Experimental gastric ulcer could induce significant c-Fos activity in the nuclei of the solitary tract (NTS) and lumbosacral spinal cord, which receives more parasympathetic afferent inputs than sympathetic afferent inputs.

The study was carried out to examine the effect of electroacupuncture (EA) on attenuating the inflammation of animals subjected to acid-induced gastric ulcer. The acupuncture effect on gastric ulcer was compared among different groups and their relations with c-Fos-activated neurons in vagus-mediated nuclear NTS were analyzed.

MATERIALS AND METHODS

Animals

Twenty-eight adult male Sprague-Dawley rats weighing 150-250 g were included in this study. The rats were divided into four groups randomly and housed in a 12-h light and dark cycle with free access to food and water. They were deprived of food but not water 12 h prior to experiment. The experiment was approved by Chinese Animal Committee.

Animal models

Among several models[4,5], a previously established model to induce gastric ulcer in rats was used. The rats were anesthetized with 45-50 mg/kg pentobarbital intraperitoneally. A midline incision was made to expose the stomach, and 5 μL of 200 mL/L HAc in sterile saline was injected into the subserosal layer of the dorsal and ventral stomach wall and then the epigastric incision was closed. After a recovery period of 4 d, just before the repair time for ulcer[6,7], EA was performed for the acupuncture group. Then the animals were anesthetized, the stomach was opened along the greater curvature, and then pinned to a corkboard. Macroscopic mucosal damage and gastric ulcer were immediately evaluated and gastric ulcer tissues were stained with hematoxylin and eosin (HE). The rat body was perfused immediately after the stomach was removed.

Electroacupuncture

EA treatment (4 Hz, 0.6 mA, 0.45 ms) was carried out for 45 min/day for 4 consecutive d prior to acid injection. The rats were anesthetized, EA was applied with stainless steel needles inserted bilaterally into points corresponding to zusanli (St 36) in human beings. Since EA stimulation produced slight muscle twitch, and did not raise the blood pressure of the anaesthetized animals, it was mostly an innocuous stimulation.

Assessment of gastric mucosal damage

Gastric mucosal damage was quantitated by measuring the area and the number of mucosal lesions. The length and width of each gastric lesion were measured to assess the area of mucosal damage and then the total area of superficial ulceration was calculated. The area of aggregate lesions was expressed as square millimeters.

Histological processing for c-Fos protein

Under deep sodium pentobarbital anesthesia, the animals were perfused transcardially with 100 mL saline, followed by 500 mL fixative containing 40 g/L paraformaldehyde in 0.1 mol/L phosphate buffer (PB, pH 7.4). The brain tissue containing the medulla oblongata was removed and stored in 300 g/ L sucrose (4 ℃) until sedimentation of the blocks, and cut into serial 30 μm coronal sections on a cryostat. For anti-Fos immunostaining, the sections were treated with methanol, H_2O_2 and 3 g/L Triton X-100 for 30 min, then successively incubated with polyclonal primary rabbit anti-Fos antibody (1:10 000, Sigma) for 16 h, donkey anti-rabbit antibody (1:200, Vector) for 3 h, mixture complex liquid of avidin-biotin(1:100, Vector) for 1 h at room temperature. Then the sections were visualized by 0.5 g/L diaminobenzidine(DAB) and 0.3 g/L H_2O_2 (DAB kit, Dako) in distilled water, and rinsed in phosphate buffered saline (PBS) for 10 min thrice after each step. One set of sections were stained with Nissle to get the comparative nuclei in brain stem sections.

Statistical analysis

Results were expressed as mean±SD. The analysis of variance (ANOVA) was employed for statistical evaluations and comparisons of the data. The differences in mean values between two experimental g roups were evaluated by *t*-test. $P<0.05$ was considered statistically significant.

RESULTS

Significantly histological changes were observed after submucosal injection of HAc into the 4 groups. Microscopic examination showed that gastric ulcers induced by HAc-injection in acupuncture group had much more repairing area of submucosa than the untreated rats (Figure 1), and the whole area of gastric ulceration was found in the former group ($P<0.01$, Table 1). The ulceration area of paradistance acupuncture group increased obviously at the same time. The measured results were 5.6±0.5 mm^2 in early acupuncture prior to ulcer, 22.1±5.9 mm^2 in paradistance acupuncture group, and 16.9±0.8 mm^2 in acupuncture after ulceration. The submucosa of stomach in rats subjected to early stage acupuncture was well protected, but acupuncture therapy after HAc-injection failed to prevent mucosal ulcer injury ($P>0.1$, Figure 2). In comparison to the area of gastric ulceration, the acupuncture-dependent inhibition of ulceration could be observed (Figure 2).

Table 1 Area of gastric ulceration after acupuncture (mean±SD, mm^2, $n = 7$)

Group	Gastric ulcer area	*P*
Pre-acupuncture	5.6±0.5	$P<0.001^b$
Paradistance acupuncture	22.1±5.9	$P<0.05^a$
Acupuncture	16.9±0.8	$P>0.10^d$
Control(without acupuncture)	20.3±5.3	Control

$^aP<0.05$, $^bP<0.001$, $^dP>0.10$ *vs* control group.

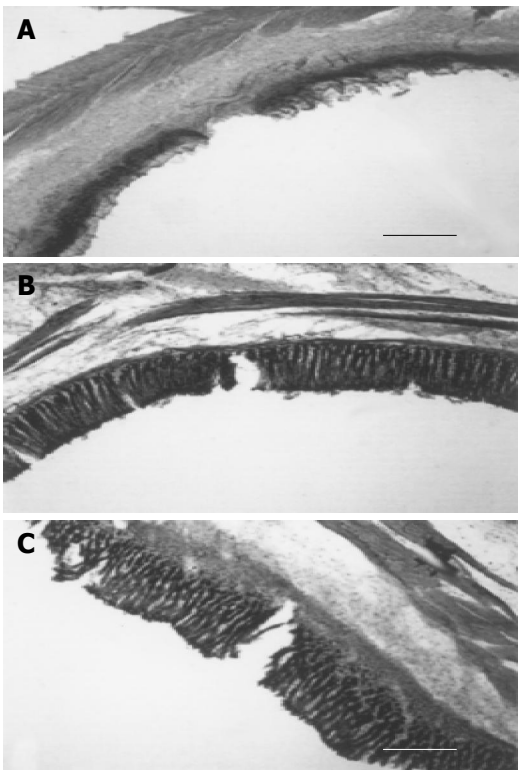


Figure 1 Histological change after submucosal injection of HAc. **A**: A repaired area of ulcer in submucosa of stomach; **B**: Ulcer-free areas after HAc-injection; **C**: Gastric ulcer in untreated rats.

Most Fos-Li neurons were distributed mainly around NTS (Figures 3: B, D, F). There were also some sparsely distributed Fos-Li neurons in surrounding area. At the lower (Figures 3: A, C) or higher magnification (Figures 3: B, D, E, F), the high density of Fos-Li neurons was obviously shown in non-acupuncture group (Figure 3D) and paradistance group (Figure 3F). The acupuncture therapy in early stage could prevent the production of c-Fos (Figure 3E). The number of c-Fos-stained nuclei was counted from NTS at three levels of brain stem in each group (seven rats) animals. For each section three fields were chosen to count the Fos-Li expressing neurons. In pre-acupuncture group the induced Fos-Li neurons were fewer (Figure 4, $P<0.05$). In both paradistance acupuncture group (Figure 4, $P<0.05$) and acupuncture group, the number of Fos-Li neurons significantly increased (Figure 4). In the control group the number of Fos-Li neurons was also higher (Figure 4).

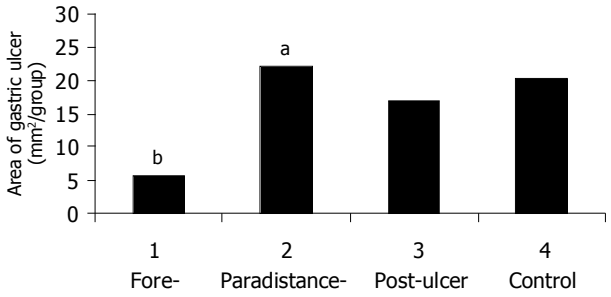


Figure 2 Effects of acupuncture on HAc-induced gastric ulcer in rats $^{a}P<0.05$, $^{b}P<0.01$ *vs* control group.

DISCUSSION

In our study, the acupuncture point was accurate and reasonable. When the rats were anesthetized, EA was applied with stainless steel needles inserted bilaterally into points corresponding to zusanli (St36) in human beings. EA stimulation produced slight muscle twitch, but did not raise the blood pressure in anaesthetized animals, indicating that it is an innocuous stimulation. Fos-Li cells induced by these factors should die after so long a repair time and also some of them might spread to other brain areas especially in the latter situation. It means that even if acupuncture and surgery could induce c-Fos protein expression, but it could be neglected over the long enough recovery time. The results are consistent with the hypotheses, otherwise sham group should have had fewer c-Fos-positive neurons than acupuncture group. But the opposite results we obtained indicate that the ulceration in control group can induce more noxious signals from ulcer inflammation than the acupuncture-treated animals.

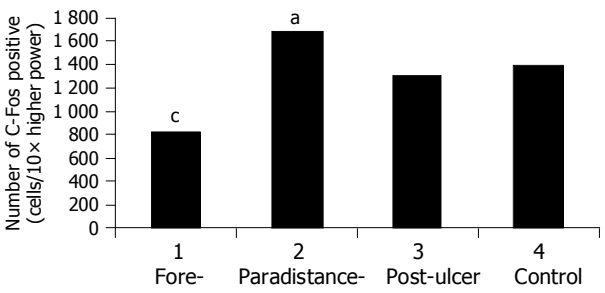


Figure 4 Total number of c-Fos positive cells in NTS $^{a}P<0.05$, $^{c}P<0.05$ *vs* control group.

HAc injected into the gastric wall induced significant inflammation and ulceration in rats. Four days were chosen for the ulceration time, because this is the most possible period for inducing ulceration[4,5]. Pathological examination showed that the acupuncture (St36) attenuated gastric ulcer in

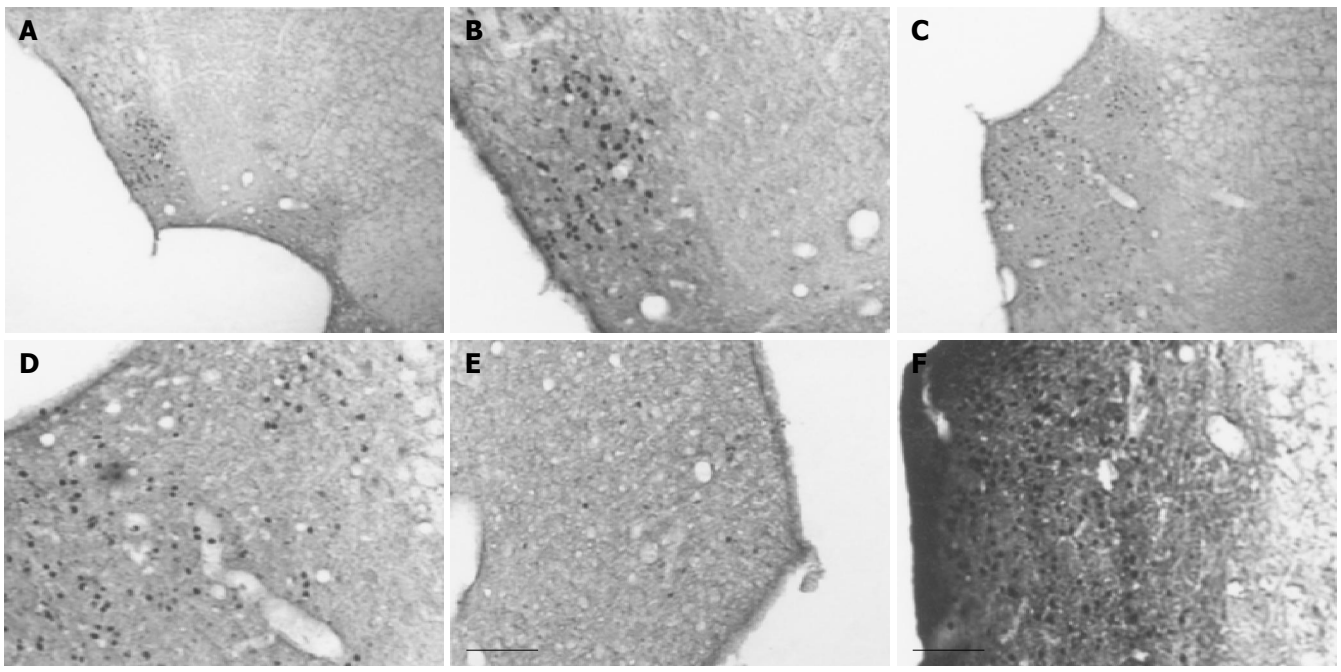


Figure 3 Fos-Li neurons within nuclei of solitary tract. **A**, **B**: Acupuncture after ulceration; **C**, **D**: No acupuncture after ulceration; **E**: Acupuncture prior to ulceration; **F**: Paradistance acupuncture prior to ulceration.

experimental rats. The repair in submucosa was more complete than that in non acupuncture group (Figures 1 and 3). The number and area of ulceration were different (Table 1).

Acupuncture has been used to treat gastrointestinal symptoms in China for more than 3 000 years. However, the mechanism of its beneficial effects remains unknown. It was reported that acupuncture at the right lower abdomen causes a transient relaxation of the stomach, and acupuncture-induced gastric relaxations can be abolished by guanethidine, propranolol, splanchnic ganglionectomy, spinal cord transection, and spinomedullary transection[8]. In contrast, N (G)-nitro-L-arginine, phentolamine, truncal vagotomy, and pontomedullary transection have no effect. Popova *et al*.[9], have proved the effect of acupuncture on activity of antioxidant system in rats with gastroduodenal ulcer. More recently the effect of acupuncture on young pigs with enteropathogenic *Escherichia coli* diarrhea has been evaluated by staining with hematoxylin and eosin[10]. All these results indicate that acupuncture treatment is effective in controlling some stomach diseases at their early stage.

Concerning both of these studies and our results, the number of c-Fos immunopositive cells at the NTS in medulla was changed because of prevailing acupuncture. NTS receives gastrointestinal mechno- and chemosensory information *via* the vagus nerve and vagal afferents may be involved in chemonoreception, which means that pain signals induced by gastric ulcer can be traced by the most related nucleus-NTS in medulla and this effect can be deduced by accurate acupuncture *via* vagus nerve, suggesting that acupuncture-induced gastric ulcer reduction is mediated *via* the somato-parasympathetic reflex system. But acupuncture afferent limb is composed of abdominal cutaneous and muscle afferent nerves. Though the direct or indirect efferent limb is questionable, our hypothesis is *via* the gastric parasympathetic nerve and the reflex center is within the medulla. NTS neurons may play an important role in mediating this reflex and are the 'brain of the gut' for autonomic control of digestion. Because 88-90% of axons in the vagus nerves are afferent nerve fibers that project to the nucleus tractus solitaries and area postrema[11,12], acupuncture prevents mainly brain structures from formation and increase of the products of Fos-Li neurons, suggesting that vagus nerve mediates induction of c-Fos in NTS following experimental ulceration, and that parasympathetic afferents promote noxious visceral stimulation. Results from this study are in agreement with some reports[13].

Although there is evidence that induction of Fos-Li neurons does not depend on the integrity of vagus nerves[8,14]. Tada *et al*.[8], suggested that acupuncture treatment of gastric ulcer can be mediated *via* the somatosympathetic reflex system. Its afferent limb is composed of abdominal cutaneous and muscle afferent nerves. Its efferent limb is the gastric sympathetic nerve and the reflex center is within the ventral lateral medulla. Our present study strongly supports that vagus nerve itself plays a very important role in peripheral gastric organ and central brain communication and cytokine-brain communication[15], because ulcer itself is a kind of cytokine-induced inflammation. The hypothesis that inflammation of gastric ulcer activates afferent vagal fibers that terminate in the nucleus tractus solitarius and may be adjusted by early stage acupuncture has been proved. Previous studies showed that vagal nerve may be a neural route and vagotomy blocks the afferent signaling to the central nerve system and the effects of peripheral cytokines. Peripheral cytokines induced by ulcer inflammation may influence the central nerve system by blood-borne routes of communication.

In conclusion, our study provides the possible neural mechanism of acupuncture underlying gastric ulcer formation. NTS neurons may play an important role in mediating gastric ulcer.

REFERENCES

1 **Pei WF,** Xu GS, Sun Y, Zhu SL, Zhang DQ. Protective effect of electroacupuncture and moxibustion on gastric mucosal damage and its relation with nitric oxide in rats. *World J Gastroenterol* 2000; **6**: 424-427

2 **Takahashi S,** Shigeta J, Inoue H, Tanabe T, Okabe S.Localization of cyclooxygenase-2 and regulation of its mRNA expression in gastric ulcers in rats. *Am J Physiol* 1998; **275**: G1137-G1145

3 **Borovikova LV,** Ivanova S, Zhang M, Yang H, Botchkina GI, Watkins LR, Wang H, Abumrad N, Eaton JW, Tracey KJ. Vagus nerve stimulation attenuates the systemic inflammatory response to endotoxin. *Nature* 2000; **405**: 458-462

4 **Sisco M,** Mustoe TA. Animal models of ischemic wound healing. Toward an approximation of human chronic cutaneous ulcers in rabbit and rat. *Methods Mol Med* 2003; **78**: 55-65

5 **Li Z,** Shi A, Karlsson FA. Transient increase of rat gastric amylin in the neonatal period and in experimental ulcers. *J Gastroenterol* 2002; **37**: 172-176

6 **Bielefeldt K,** Ozaki N, Gebhart GF. Experimental ulcers alter voltage-sensitive sodium currents in rat gastric sensory neurons. *Gastroenterology* 2002; **122**: 394-405

7 **Pawlik M,** Ptak A, Pajdo R, Konturek PC, Brzozowski T, Konturek SJ. Sensory nerves and calcitonin gene related peptide in the effect of ischemic preconditioning on acute and chronic gastric lesions induced by ischemia-reperfusion. *J Physiol Pharmacol* 2001; **52**: 569-581

8 **Tada H,** Fujita M, Harris M, Tatewaki M, Nakagawa K, Yamamura T, Pappas TN, Takahashi T. Neural mechanism of acupuncture-induced gastric relaxations in rats. *Dig Dis Sci* 2003; **48**: 59-68

9 **Popova SP.** Effect of acupuncture on dynamics of changes in lipid peroxidation and activity of antioxidant system in rats with gastroduodenal ulcer. *Fiziol Zh* 2002; **48**: 54-59

10 **Park ES,** Jo S, Seong JK, Nam TC, Yang IS, Choi MC, Yoon YS. Effect of acupuncture in the treatment of young pigs with induced *Escherichia coli* diarrhea. *J Vet Sci* 2003; **4**: 125-128

11 **Holzer P,** Michl T, Danzer M, Jocic M, Schicho R, Lippe IT. Surveillance of the gastrointestinal mucosa by sensory neurons. *J Physiol Pharmacol* 2001; **52**: 505-521

12 **Berthoud HR,** Neuhuber WL. Functional and chemical anatomy of the afferent vagal system. *Auton Neurosci* 2000; **85**: 1-17

13 **Furness JB,** Clerc N, Kunze WA. Memory in the enteric nervous system. *Gut* 2000; **47**(Suppl 4): iv60-iv62; discussion iv 76

14 **Hermann GE,** Emch GS, Tovar CA, Rogers RC. c-Fos generation in the dorsal vagal complex after systemic endotoxin is not dependent on the vagus nerve. *Am J Physiol Regul Integr Comp Physiol* 2001; **280**: R289-R299

15 **Ge X,** Yang Z, Duan L, Rao Z. Evidence for involvement of the neural pathway containing the peripheral vagus nerve, medullary visceral zone and central amygdaloid nucleus in neuroimmunomodulation. *Brain Res* 2001; **914**: 149-158

Science Editor Wang XL, Zhu LH and Guo SY **Language Editor** Elsevier HK

PO Box 2345, Beijing 100023, China
www.wjgnet.com
wjg@wjgnet.com

ELSEVIER

World J Gastroenterol 2005;11(35):5521-5524
World Journal of Gastroenterology ISSN 1007-9327
© 2005 The WJG Press and Elsevier Inc. All rights reserved.

• *BRIEF REPORTS* •

Improvement of quantitative testing of liver function in patients with chronic hepatitis C after installment of antiviral therapy

Matthias Ocker, Marion Ganslmayer, Steffen Zopf, Susanne Gahr, Christopher Janson, Eckhart G. Hahn, Christoph Herold

Matthias Ocker, Marion Ganslmayer, Steffen Zopf, Susanne Gahr, Christopher Janson, Eckhart G. Hahn, Christoph Herold, Department of Medicine I, University Erlangen-Nuernberg, Ulmenweg 18, Erlangen 91054, Germany
Correspondence to: Christoph Herold, MD, PhD, Department of Medicine I, Ulmenweg 18, Erlangen D-91054, Germany. christoph.herold@med1.imed.uni-erlangen.de
Telephone: +49-9131-8535145
Received: 2005-01-22 Accepted: 2005-02-18

Abstract

AIM: To investigate if and to what extent antiviral therapy influenced a broad panel of quantitative testing of liver function (QTLF).

METHODS: Fifty patients with chronic hepatitis C were either treated with interferon (n = 8), interferon/ribavirin (n = 19) or peg-interferon/ribavirin (n = 23). Quantitative testing of liver function, including aminopyrine breath test (ABT), galactose elimination capacity (GEC), sorbitol clearance (SCl) and indocyanine green clearance (ICG) was performed before and 3 mo after initiation of antiviral therapy.

RESULTS: After 3 mo of antiviral treatment, 36 patients showed normal transaminases and were negative for HCV-RNA, 14 patients did not respond to therapy. ABT and GEC as parameters of microsomal and cytosolic liver function were reduced in all patients before therapy initiation and returned to normal values in the 36 therapy responders after 3 mo. Parameters of liver perfusion (SCl and ICG) were not affected by antiviral therapy. In the 14 non-responders, no changes in QTLF values were observed during the treatment period.

CONCLUSION: ICG and SCl remained unaffected in patients with chronic hepatitis C, while ABT and GEC were significantly compromised. ABT and GEC normalized in responders to antiviral therapy. Early determination of ABT and GEC may differentiate responders from non-responders to antiviral treatment in hepatitis C.

© 2005 The WJG Press and Elsevier Inc. All rights reserved.

Key words: Aminopyrine breath test; Galactose elimination capacity; Indocyanine green clearance; Sorbitol clearance; Hepatitis C; Interferon; Ribavirin

Ocker M, Ganslmayer M, Zopf S, Gahr S, Janson C, Hahn EG, Herold C. Improvement of quantitative testing of liver function in patients with chronic hepatitis C after installment of antiviral therapy. *World J Gastroenterol* 2005; 11(35): 5521-5524
http://www.wjgnet.com/1007-9327/11/5521.asp

INTRODUCTION

Chronic infection with HCV is among the leading causes for impaired liver function and a major risk factor for developing liver cirrhosis and subsequently hepatocellular carcinoma[1,2]. Treatment of patients with chronic HCV infection has significantly improved, since the introduction of INF-based therapies[3-6]. Yet, more than 50% of patients infected with HCV genotype 1 and approximately 20% of patients with genotypes 2 and 3 do not achieve sustained virologic responses. Risk factors for non-response are HCV genotype, HCV RNA level and liver cirrhosis, which is usually accompanied by impaired liver function and blood flow[7]. Stage and prognosis of liver cirrhosis can be assessed by clinical examination, conventional blood tests and ultrasound or computed tomography. Yet, these conventional parameters (e.g., serum albumin, cholinesterase or coagulation factors) often lack sensitivity in early stages of liver diseases and are only changed in advanced stages. Therefore QTLF, which are based on the hepatic clearance or metabolism of test substances, have been successfully used to predict prognosis and outcome of a variety of different liver diseases[8-14].

So far, response to antiviral therapy is mainly based on HCV RNA levels and transaminases. Here, we investigated if and to what extent changes in either hepatic metabolic enzyme function and in liver perfusion can be achieved by different antiviral therapies, and if changes in QTLF may help to discriminate responders from non-responders to antiviral treatment strategies.

MATERIALS AND METHODS

Fifty consecutive patients (age 39±13 years) with chronic hepatitis C (HCV-RNA positive and raised transaminases, mild to moderate fibrosis, all with HCV genotype 1) were included in the study. Eight patients (16%) were treated with INF monotherapy, 19 patients (38%) with INF/RIB and 23 patients (46%) with peg-INF/RIB combination therapy. All patients underwent QTLF before and 3 mo after initiation of antiviral therapy. Drugs that could possibly interfere with QTLF were discontinued 120 h before testing. Twenty-five healthy adults with normal hepatic serum parameters served as controls[8].

HCV-RNA was assessed qualitatively and quantitatively using the HCV Monitor and the Cobas Amplicor systems,

respectively (both from Roche, Germany). Response to antiviral treatment was defined as being negative for qualitative HCV testing or less than two log steps drop in quantitative HCV-RNA levels.

The following tests were performed to quantitatively assess changes in liver function during antiviral therapy: aminopyrine breath test (ABT), galactose elimination capacity (GEC), sorbitol clearance (SCl) and indocyanine green clearance (ICG). ABT measures the metabolic capacity of hepatocytes by determining the activity of microsomal enzymes[15]. In detail, radioactively labeled ^{14}C-aminopyrine (1.5 μCr), applied intravenously, is demethylated by amino-N-demethylase, which reflects the activity of three different cytochrome P450-dependent microsomal enzymes, and further metabolized to $^{14}CO_2$ which is exhaled and measured with a β-counter.

GEC determines the cytosolic metabolic capacity of the liver[16]. The catabolic enzyme system is saturated by an intravenous bolus injection of galactose (45% galactose, 0.5 g/kg body weight). The cytoplasmic enzyme galactokinase phosphorylates galactose determines the elimination of this hexose, serving as a measure of functional liver cell mass. Serum concentrations of galactose are determined photometrically at 366 nm at 0 min and from 20 to 60 min p.i. in 5 min intervals.

SCl is regarded as a parameter of liver parenchymal perfusion (liver plasma flow). Sorbitol (500 g/L) is administered via a perfusor at 7.5 mL/h. The hepatic clearance corresponds to the measurement of the arteriovenous concentration difference[17]. Serum and urinary concentrations of sorbitol are determined photometrically at the beginning of the perfusion and after reaching steady-state conditions (150 min).

ICG is exclusively absorbed in the liver and quickly excreted in unmodified form (97%) in the bile and can therefore be used as a marker for liver perfusion and biliary secretion capacity after infusion of a bolus of 0.5 mg/kg body weight. Its serum concentration is measured photometrically at 800 nm in 3 min intervals until 21 min after ICG injection[18].

Transaminase levels (AST, ALT) were determined by routine methods in the Department of Medical Chemistry, University Erlangen.

Statistical analysis was performed using SPSS for Windows with $P<0.05$ regarded as significant. Spearman's correlation coefficient (r) was calculated with Microsoft Excel 2003 for Windows XP. The present study was performed in concordance with the ethical standards formulated in the version of 1964 Declaration of Helsinki. All patients gave their informed consent prior to inclusion in the study.

RESULTS

Of the 50 treated patients, 36 (72%) responded to the respective antiviral therapy, showing normal transaminases and negative HCV-RNA after 3 mo. Fourteen patients (28%) did not respond to the therapy regimens (Table 1). Transaminase levels correlated well with HCV-RNA copy numbers, with $r = 0.966$ and $r = 0.937$ for AST and ALT, respectively.

ABT (Figure 1A) and GEC (Figure 1B) were reduced in all patients before beginning the treatment (ABT: 0.65±0.24% dose-kg/mmol CO_2; GEC: 5.43±2.06 mg/min-kg; $P<0.05$ *vs* healthy controls). In patients responding to antiviral therapy, ABT and GEC returned to normal values after 3 mo (0.82±0.14% dose-kg/mmol CO_2 and 7.84±1.71 mg/min-kg.), showing a statistically significant change compared to the initial values ($P<0.05$). Non-responders still showed reduced parameters of microsomal and cytosolic liver function after the therapy interval (ABT: 0.68±0.19% dose-kg/mmol CO_2; GEC: 5.89±1.64 mg/min-kg). Paralleling transaminase levels, ABT and GEC showed a high correlation with HCV-RNA levels with $r = 0.974$ and $r = 0.99$, respectively.

In contrast to these metabolic liver function tests, no changes were observed in QTLF investigating parameters of liver perfusion. While SCl (Figure 1C) and ICG (Figure 1D) were lower in patients with hepatitis C compared to healthy controls (not significant, $P>0.05$), neither responders nor non-responders to antiviral therapies improved during the 3 mo treatment period. SCl was 12.86±2.58 mL/min-kg in healthy controls, 10.8±2.19 mL/min-kg in HCV patients before treatment and 11.3±2.13 and 10.72±2.37 mL/min-kg in responders and non-responders to antiviral therapy. ICG was determined as 0.21±0.11 L/min in controls, 0.17±0.07 L/min before treatment, 0.20±0.07 L/min in responders and 0.18±0.09 L/min in non-responding patients, respectively. Values for ICG and SCl did not correlate with HCV-RNA or transaminases. Although both parameters show slight differences in responders before and after antiviral therapy, these changes were statistically not significant.

Overall, antiviral therapy ameliorated QTLF of microsomal (ABT) and cytosolic (GEC) metabolic capacities, but did not influence parameters of liver perfusion (SCl) and secretion (ICG). Amelioration of ABT and GEC was independent of the applied antiviral regimen in the examined patient groups, but only dependent on overall response to treatment as evidenced by high correlation coefficients with serum transaminase levels.

DISCUSSION

We have shown previously that the application of a broad

Table 1 Transaminase levels and RNA copy numbers in HCV patients before and after 3 mo of antiviral therapy

	HCV patients ($n = 50$)	Responders ($n = 36$)	Non-responders ($n = 14$)	Controls ($n = 25$)
Age (yr)	39±13	41±12	37±11	39±10
Sex (m/f)	33/17	25/11	10/4	17/8
AST (U/L)	74±37	35±13	59±17	27±11
ALT (U/L)	97±45	30±11	63±21	23±13
RNA level (×1 000)	723±234	Neg/2 log drop	649±305	Negative

Transaminase levels and RNA copy numbers in HCV patients before and after 3 mo of antiviral therapy. Patients were divided in responders (negative or 2 log steps drop in HCV-RNA copy numbers) or non-responders according to RNA levels. HCV-RNA negative persons served as controls. Normal transaminase values: AST<31 U/L (male), <35 U/L (female); ALT <34 U/L (male), <45 U/L (female).

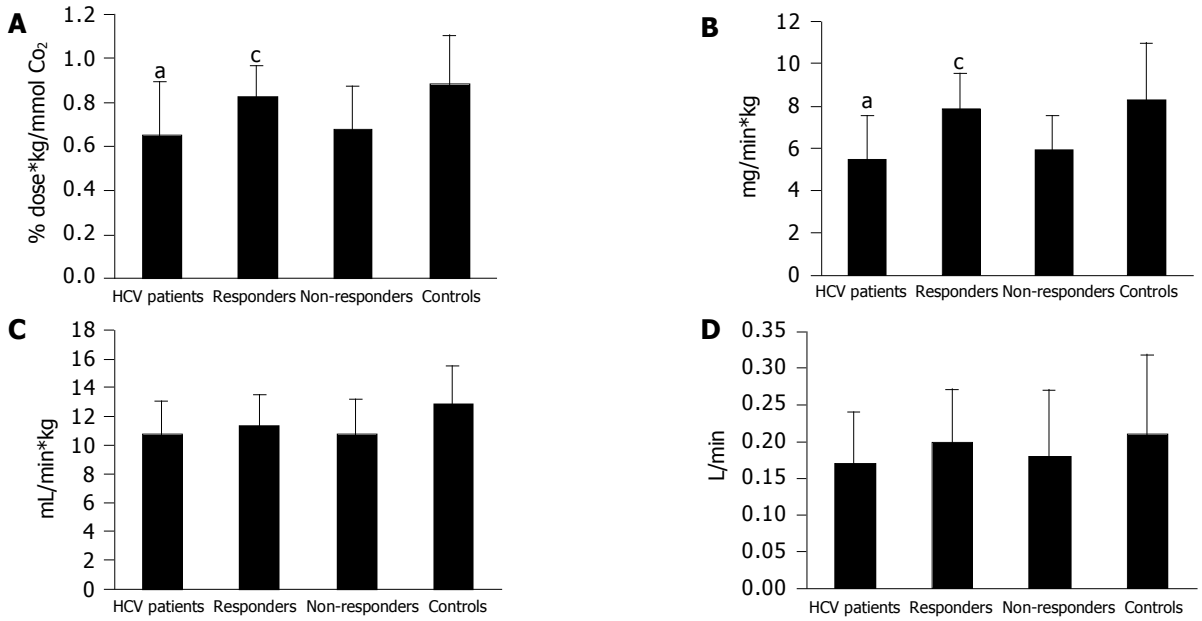


Figure 1 Quantitative testing of liver function in patients with hepatitis C. Shown are mean±SD of QTLF values in healthy controls (n = 25) and HCV patients (n = 50) before and 3 mo after antiviral therapy, divided into responders (n = 36) and non-responders (n = 14). [a]P<0.05 *vs* healthy controls; [c]P<0.05 *vs* pre-treatment values. **A:** Aminopyrine breath test. ABT (% dose-kg/mmol CO_2); **B:** Galactose elimination capacity. GEC (mg/min-kg); **C:** Sorbitol clearance. SCl (mL/min-kg); **D:** Indocyanine green clearance. ICG (L/min).

panel of QTLF is a useful diagnostic tool to assess prognosis and outcome in different liver diseases[8,13,14]. Although liver damage due to chronic viral hepatitis is considered more predictable than toxic injuries, so far only the application of a single QTLF has been described in small collectives[19,20] and we have shown recently that untreated viral hepatitis influences QTLF in a large cohort[12]. Additionally, we have shown previously that QTLF are inversely correlated with Child-Pugh grades in cirrhotic patients[8]. As there is no information available on the impact of antiviral therapies using INF, INF/RBV or PEG-INF/RBV, we applied a broad panel of QTLF to 50 consecutive patients with chronic HCV infection, 3 mo after beginning the antiviral therapy. At this time point, therapy response is usually re-evaluated to distinguish responders from non-responders to antiviral treatment. HCV has been shown to lead to parenchymal inflammation and to decrease microsomal as well as cytosolic hepatic enzyme capacities, which was independent of the etiology of hepatitis[12].

Compared to healthy controls, we found a significant reduction in metabolic liver function tests (ABT, GEC) in all HCV patients before the initiation of either antiviral therapy. ABT is mainly used to evaluate the prognosis of alcohol-induced hepatitis, paracetamol poisoning or cirrhosis[12,21-23]. ABT can be influenced by pharmacologic induction (e.g., barbiturates, phenytoine) or inhibition (e.g., contraceptives) of microsomal enzymes[14].

GEC was proposed as a prognostic parameter in chronic hepatitis as well as acute liver failure and has been demonstrated to be already reduced in patients with mild fibrosis or acute liver dysfunction[11,22,24].

In HCV patients, reduction of ABT and GEC can be explained by decreased enzymatic capacities caused by active viral replication and expression of viral proteins. Additionally, the total number of vital hepatocytes is decreased in chronic HCV due to ongoing parenchymal inflammation, tissue remodeling and scarring by advancing fibrosis/cirrhosis due to immunologic responses[25]. As responders to antiviral treatment, HCV-RNA was not detectable after 3 mo, independent of the therapy regimen and both metabolic parameters increased to the levels of healthy controls indicating that viral replication strongly influences both microsomal and cytosolic enzymes. HCV is a rapidly replicating virus whose genome is translated into a large polyprotein precursor which undergoes extensive post-translational modifications[26] by using different cellular enzyme systems which might explain lower metabolic QTLF values in HCV patients.

In contrast to the metabolic parameters, QTLF investigating hepatic perfusion (SCl and ICG) were not significantly reduced in the 50 patients with chronic HCV infection and remained unaffected by any response to antiviral therapies. This corroborates previous findings, where hepatic perfusion remained in the normal range even in patients with early fibrotic lesions and irrespective of inflammatory grade of size of the lesions[12]. ICG is considered to be insensitive to pharmacological influences, because its metabolism solely depends on hepatic transport and biliary secretion. Here, we found that 3 mo of different antiviral therapies did not influence ICG, as was shown previously for long-term treatment with beta-blockers, nitrates or antithyroid medications[9,27].

In summary, our results suggest that QTLF monitoring metabolic liver functions (ABT, GEC) may be a useful tool to discriminate responders from non-responders to antiviral therapy regimens in chronic HCV infection after a 3-mo treatment period. While liver perfusion is not altered by either HCV infection or antiviral treatment, ABT and GEC may help to optimize economic and medical treatment strategies in chronic viral hepatitis.

REFERENCES

1 **Okuda K.** Hepatocellular carcinoma. *J Hepatol* 2000; **32**: 225-237
2 **Everson GT.** Treatment of chronic hepatitis C in patients with decompensated cirrhosis. *Rev Gastroenterol Disord* 2004; **4** Suppl 1: S31-S38
3 **McHutchison JG,** Poynard T, Esteban-Mur R, Davis GL, Goodman ZD, Harvey J, Ling MH, Garaud JJ, Albrecht JK, Patel K, Dienstag JL, Morgan T. Hepatic HCV RNA before and after treatment with interferon alone or combined with ribavirin. *Hepatology* 2002; **35**: 688-693
4 **Zeuzem S,** Hultcrantz R, Bourliere M, Goeser T, Marcellin P, Sanchez-Tapias J, Sarrazin C, Harvey J, Brass C, Albrecht J. Peginterferon alfa-2b plus ribavirin for treatment of chronic hepatitis C in previously untreated patients infected with HCV genotypes 2 or 3. *J Hepatol* 2004; **40**: 993-999
5 **Manns MP,** McHutchison JG, Gordon SC, Rustgi VK, Shiffman M, Reindollar R, Goodman ZD, Koury K, Ling M, Albrecht JK. Peginterferon alfa-2b plus ribavirin compared with interferon alfa-2b plus ribavirin for initial treatment of chronic hepatitis C: a randomised trial. *Lancet* 2001; **358**: 958-965
6 **Fried MW,** Shiffman ML, Reddy KR, Smith C, Marinos G, Goncales FL, Haussinger D, Diago M, Carosi G, Dhumeaux D, Craxi A, Lin A, Hoffman J, Yu J. Peginterferon alfa-2a plus ribavirin for chronic hepatitis C virus infection. *N Engl J Med* 2002; **347**: 975-982
7 **Shiffman ML.** Management of patients with chronic hepatitis C virus infection and previous nonresponse. *Rev Gastroenterol Disord* 2004; **4** Suppl 1: S22-S30
8 **Herold C,** Heinz R, Radespiel-Troeger M, Schneider HT, Schuppan D, Hahn EG. Quantitative testing of liver function in patients with cirrhosis due to chronic hepatitis C to assess disease severity. *Liver* 2001; **21**: 26-30
9 **Merkel C,** Gatta A, Zoli M, Bolognesi M, Angeli P, Iervese T, Marchesini G, Ruol A. Prognostic value of galactose elimination capacity, aminopyrine breath test, and ICG clearance in patients with cirrhosis. Comparison with the Pugh score. *Dig Dis Sci* 1991; **36**: 1197-1203
10 **Merkel C,** Marchesini G, Fabbri A, Bianco S, Bianchi G, Enzo E, Sacerdoti D, Zoli M, Gatta A. The course of galactose elimination capacity in patients with alcoholic cirrhosis: possible use as a surrogate marker for death. *Hepatology* 1996; **24**: 820-823
11 **Reichen J,** Widmer T, Cotting J. Accurate prediction of death by serial determination of galactose elimination capacity in primary biliary cirrhosis: a comparison with the Mayo model. *Hepatology* 1991; **14**: 504-510
12 **Herold C,** Heinz R, Niedobitek G, Schneider T, Hahn EG, Schuppan D. Quantitative testing of liver function in relation to fibrosis in patients with chronic hepatitis B and C. *Liver* 2001; **21**: 260-265
13 **Herold C,** Regn S, Ganslmayer M, Ocker M, Hahn EG, Schuppan D. Can quantitative testing of liver function discriminate between different etiologies of liver cirrhosis? *Dig Dis Sci* 2002; **47**: 2669-2673
14 **Herold C,** Ganslmayer M, Ocker M, Zopf S, Gailer B, Hahn EG, Schuppan D. Inducibility of microsomal liver function may differentiate cirrhotic patients with maintained compared with severely compromised liver reserve. *J Gastroenterol Hepatol* 2003; **18**: 445-449
15 **Hepner GW,** Vesell ES. Quantitative assessment of hepatic function by breath analysis after oral administration of (14C) aminopyrine. *Ann Intern Med* 1975; **83**: 632-638
16 **Tygstrup N,** Andersen PK, Thomsen BL. Prognostic evaluation in alcoholic cirrhosis. *Acta Med Scand Suppl* 1985; **703**: 149-156
17 **Zeeh J,** Lange H, Bosch J, Pohl S, Loesgen H, Eggers R, Navasa M, Chesta J, Bircher J. Steady-state extrarenal sorbitol clearance as a measure of hepatic plasma flow. *Gastroenterology* 1988; **95**: 749-759
18 **Leevy CM,** Mendenhall CL, Lesko We, Howard MM. Estimation of hepatic blood flow with indocyanine green. *J Clin Invest* 1962; **41**: 1169-1179
19 **Horsmans Y,** Brenard R, Geubel AP. Short report: interferon-alpha decreases 14C-aminopyrine breath test values in patients with chronic hepatitis C. *Aliment Pharmacol Ther* 1994; **8**: 353-355
20 **Reichen J,** Bianchi L, Buhler H, Dolivo N, Gonvers JJ, Lavanchy D, Male PJ, Renner EL, Solioz M, Schmid M, Zimmermann A. Fixed versus titrated interferon-alpha 2B in chronic hepatitis C. A randomized controlled multicenter trial. The Swiss Association for the Study of the Liver. *J Hepatol* 1996; **25**: 275-282
21 **Saunders JB,** Lewis KO, Paton A. Early diagnosis of alcoholic cirrhosis by the aminopyrine breath test. *Gastroenterology* 1980; **79**: 112-114
22 **Saunders JB,** Wright N, Lewis KO. Predicting outcome of paracetamol poisoning by use 14C-aminopyrine breath test. *Br Med J* 1980; **280**: 279-280
23 **Giannini E,** Fasoli A, Chiarbonello B, Malfatti F, Romagnoli P, Botta F, Testa E, Polegato S, Fumagalli A, Testa R. 13C-aminopyrine breath test to evaluate severity of disease in patients with chronic hepatitis C virus infection. *Aliment Pharmacol Ther* 2002; **16**: 717-725
24 **Ranek L,** Andreasen PB, Tygstrup N. Galactose elimination capacity as a prognostic index in patients with fulminant liver failure. *Gut* 1976; **17**: 959-964
25 **Thimme R,** Oldach D, Chang KM, Steiger C, Ray SC, Chisari FV. Determinants of viral clearance and persistence during acute hepatitis C virus infection. *J Exp Med* 2001; **194**: 1395-1406
26 **Moradpour D,** Brass V, Gosert R, Wölk B, Blum HE. Hepatitis C: molecular virology and antiviral targets. *Trends Mol Med* 2002; **8**: 476-482
27 **Andersen V,** Sonne J, Court-Payen M, Sletting S, Prip A, Molholm-Hansen J. Liver volume, portal vein flow, and clearance of indocyanine green and antipyrine in hyperthyroidism before and after antithyroid treatment. *Scand J Gastroenterol* 1999; **34**: 618-622

Science Editor Guo SY **Language Editor** Elsevier HK

PO Box 2345, Beijing 100023, China
www.wjgnet.com
wjg@wjgnet.com

ELSEVIER

World J Gastroenterol 2005;11(35):5525-5529
World Journal of Gastroenterology ISSN 1007-9327
© 2005 The WJG Press and Elsevier Inc. All rights reserved.

• *BRIEF REPORTS* •

Locoregional IL-2 low dose applications for gastrointestinal tumors

Zachary Krastev, V Koltchakov, R Tomova, S Deredjian, A Alexiev, D Popov, B Tomov, Jan-Willem Koten, John Jacobs, Willem Den Otter

Zachary Krastev, V Koltchakov, R Tomova, S Deredjian, A Alexiev, D Popov, B Tomov, Clinic of Gastroenterology, Faculty of Medicine, University Hospital, Blvd. Iv. Geshov 15, Sofia 1431, Bulgaria
Jan-Willem Koten, John Jacobs, Willem Den Otter, Department of Pathobiology, PO Box 80.178, 3508 TD Utrecht, The Netherlands
Correspondence to: Professor Zachary Krastev, Clinic of Gastroenterology, University Hospital "St.I.Rilski", #15 Blvd. "Iv. Geshov", Sofia 1431, Bulgaria. zahkrastev@yahoo.com
Telephone: +359-2-58-12-827 Fax: +359-2-851-06-15
Received: 2005-01-07 Received: 2005-04-18

Abstract

AIM: To explore the feasibility of local interleukin 2 (IL-2) in patients with different forms of abdominal cancer. This required experimentation with the time interval between IL-2 applications and the methods of application.

METHODS: Sixteen patients with stages III and IV of gastrointestinal malignancies (primary or metastatic) who were admitted to our Department of Gastroenterology were treated with locoregionally applied IL-2 in low doses.

RESULTS: No major problems applying locoregional IL-2 were encountered. In 6 out of 16 patients, a modest but clinically worthwhile improvement was obtained. Adverse effects were minimal. The therapeutic scheme was well tolerated, even in patients in a poor condition.

CONCLUSION: This study demonstrates the feasibility of low dose locoregional IL-2 application in advanced abdominal cancer. Local IL-2 therapy gives only negligible adverse effects. The results suggest that it is important to apply intratumorally. Local IL-2 may be given adjunct to standard therapeutic regimes and does not imply complex surgical interventions. These initial results are encouraging.

© 2005 The WJG Press and Elsevier Inc. All rights reserved.

Key words: Interleukin-2; Local IL-2 therapy; Gastrointestinal cancer

Krastev Z, Koltchakov V, Tomova R, Deredjian S, Alexiev A, Popov D, Tomov B, Koten JW, Jacobs J, Den Otter W. Locoregional IL-2 low dose applications for gastrointestinal tumors. *World J Gastroenterol* 2005; 11(35): 5525-5529
http://www.wjgnet.com/1007-9327/11/5525.asp

INTRODUCTION

Treatment of cancer with intratumoral or peritumoral IL-2 application is very effective in mice with e.g. transplanted lymphoma[1] and colon carcinoma[2], and in guinea pigs with transplanted liver carcinoma[3]. In veterinary practice, it is also very effective in bovine ocular squamous cell carcinoma[4,5] and in equine sarcoids (fibro-epithelial tumors)[6]. Finally, it is effective in human patients with recurrent superficial bladder carcinoma following transurethral tumor resection[7,8], in patients with advanced nasopharyngeal carcinoma[9], and in patients with lung metastases of renal cell carcinoma[10]. Obviously, local IL-2 treatment does not cure all tumors. That is, in an experiment or a trial, usually only 50-70% of animals with large, metastasized tumors are cured or show complete tumor regression, whereas some tumors like EL4-lymphoma and MOT-carcinoma are not sensitive[11].

A well-known effect of IL-2 is vascular leakage. This side effect severely limits systemic application of IL-2. However, on a local level, this vascular leakage seems to be crucial for the therapeutic effect[2,12,13]. Locally applied IL-2 induces local vascular leakage and local edema, which results in massive tumor necrosis, a characteristic feature in most experimental animals after 5-20 d of local IL-2 treatment. Locally applied IL-2 also induces angiogenesis and attracts numerous macrophages and lymphocytes that invade the tumor debris and boost specific immunity against the tumor[2,14]. Animals that are cured from a transplanted tumor are immune to this tumor[1,3,15], suggesting that an immune response is essential for cure.

Recently we have successfully applied local IL-2 therapy to a patient with hepatocellular carcinoma[16] and to a patient with mesothelioma[17]. These results justified to proceed with local IL-2 therapy. In the present study, we have applied locoregional IL-2 therapy in 16 cancer patients with gastrointestinal malignancies (primary or metastatic) who were hospitalized in the University Gastroenterology Department in Sofia, Bulgaria. No alternative treatment was available for these patients. Our primary aim was to study the feasibility of locoregional IL-2 application in advanced abdominal cancer. Secondly, we wanted to establish, whether clinical improvement could be obtained with this treatment. We present the results of local IL-2 treatment of patients with a variety of advanced abdominal cancers.

MATERIALS AND METHODS

Patients

All the 16 patients were admitted to the Clinic of Gastroenterology for primary or metastatic gastrointestinal cancer. All patients who were admitted to this IL-2 trial were advanced cases with progressive disease (PD, stages III and IV), either inoperable or not fit for standard chemo- or

radiotherapy at the time of admission. Always a clinical oncologist was consulted to exclude that further radio- or chemotherapy was still a valid option. In all cases there was a histopathological diagnosis. Previous chemotherapy or radiotherapy was stopped at least 3 mo before IL-2 treatment. The patients were admitted to the trial, only if non-tumor-related serious conditions were absent such as heart, pulmonary, endocrine, or kidney disease. IL-2 was applied only following extensive information of the patients and with their full consent. All patients were treated in the period of 1999-2003. In Table 1 the characteristics of these patients are summarized.

Interleukin-2

Recombinant human IL-2 (rhIL-2; Proleukin; specific activity 18×10^6 IU/mg) from Chiron was used. RhIL-2 was dissolved according to the manufacturer's instructions and, if necessary, further diluted with 1% albumin and 0.9% NaCl.

Treatment

Our primary intention was to apply IL-2 as close as possible to the tumor (primary or metastatic) and at the site of the anti-tumor immune reaction. Direct intra-peritoneal IL-2 was applied in carcinosis of the peritoneum. In patients W5, W7, and W8, IL-2 could be instilled directly into the malignant ascites. In patients W1, W2, W3, and M3 'ascites' was artificially made by infusing between 500 and 2 000 mL 0.9% NaCl into the peritoneal cavity. Thereafter IL-2 was injected into this 'ascites', in order to ensure an intra-peritoneal spread of IL-2.

In hepatic tumors (primary or metastatic), IL-2 was injected directly into the tumor using a fine needle under ultrasound control or via the hepatic artery under X-ray control. In colon cancer patients with unresected primary tumor, IL-2 was endoscopically applied directly into the tumor. When it was possible, IL-2 was also directly injected into accessible peritoneal tumors.

We applied IL-2 weekly and monthly for 2 mo. In patients with weekly applications, IL-2 was injected every week in 7-d interval and in patients with monthly applications IL-2 was applied every month in 30-d intervals. This was followed by application of IL-2 at 3-mo intervals.

At the beginning of the treatment, when it was possible, we artificially induced necrosis in order to stimulate the immune reactivity[18,19]. For this purpose, 10 d before the start of IL-2 treatment, we applied single procedures of local ablation-percutaneous ethanol injection in five patients with liver tumors (primary or metastatic) and in one patient with unresected primary colorectal cancer-endoscopic ablation.

Ethical committee

The treatment protocol was accepted by the ethical committee of our hospital in Sofia.

Effect of treatment

(1) The effect of therapy was assessed as follows: complete response (CR: disappearance of all tumors and signs of disease); partial response (PR: reduction >50% in the sum of the products of perpendicular diameters of bidimensionally measurable disease or for unidimensionally measurable disease a reduction of ⩾50% in linear tumor measurement compared to those prior to treatment); stable disease (SD: <50% reduction, or an increase of <25% in the sum of the products of perpendicular diameters of bidimensionally measurable disease or in linear tumor measurement for

Table 1 Patients' characteristics

A. Once weekly local IL-2 application

No.	Sex	Primary tumor	Metastases	Neoplastic ascites	Route and dose of IL-2 application	Necrosis induction
W1	M	Pancreatic Ca	Liver, abdominal lymph nodes	-	1.5 MIU i.p.	-
W2	F	Stomach Ca	Liver, abdominal lymph nodes	-	4.5 MIU i.p.	-
W3	F	Colorectal Ca	Liver, lung	-	4.5 MIU i.p.+i.t.	Yes
W4	F	Colorectal Ca	Liver, abdominal lymph nodes	-	4.5 MIU i.t.	Yes
W5	M	Colorectal Ca	Peritoneum	+	1.5 MIU i.p.+i.t.	-
W6	F	Ovarian Ca	Lung, peritoneum, spleen	+	4.5 MIU i.t.	-
W7	F	Mammary Ca	Liver, lung, peritoneum	+	4.5 MIU i.p.	-
W8	M	Hemangiosarcoma	Liver, peritoneum, abdominal lymph nodes	+pleural effusion	4.5 MIU i.p.+i.t.	-

B. Once monthly local IL-2 application

No.	Sex	Primary tumor	Metastases	Neoplastic ascites	Route of IL-2 application	Necrosis induction
M1	M	HCC, liver cirrhosis		-	4.5/9 MIU i.t.	-
M2	M	HCC, liver cirrhosis		-	4.5 MIU i.t.	Yes
M3	M	Abdominal mesothelioma	Peritoneum	-	9 MIU i.t.+i.p.	-
M4	F	Colorectal Ca	Liver	-	9 MIU i.t.	Yes
M5	F	Mammary Ca	Liver, bone, skin	–	1.5 MIU i.t.	-
M6	F	Mammary Ca	Liver	-	4.5/9 MIU i.t.	-
M7	M	HCC, liver cirrhosis		-	4.5 MIU i.t.	Yes
M8	F	HCC, liver cirrhosis		-	1.5 MIU i.t.	-

Ca, carcinoma; HCC, hepatocellular carcinoma; i.p., intraperitoneal; i.t., intratumoral; W, weekly IL-2 application; M, monthly IL-2 application.

unidimensionally measurable disease compared to those prior to treatment with no new lesions for at least 4 wk); or PD (increase of ⩾25% in the sum of the products of perpendicular diameters of bidimensionally measurable disease or in linear tumor measurement for unidimensionally measurable disease compared to those prior to treatment/or the appearance of new lesions). Response to treatment was assessed with CT scan and ultrasound control; (2) IL-2 is thought to be effective in palliative therapy of neoplastic effusions[21]. For this reason in patients with malignant ascites we also assessed the effect of our treatment on fluid accumulation according to the following criteria: if there was a complete disappearance of ascites with no further reaccumulation of fluid for more than 30 d, it was defined as CR; if the ascites decreased but there was still minimal asymptomatic fluid, not requiring further drainage within 30 d, it was a PR; if there was further accumulation of fluid requiring paracenteses within 30 d, it was considered as a failure. The patients were assessed by ultrasound control and number of paracenteses. Our criteria for evaluation are similar to those reported by Lissoni *et al*.[20], but we did not drain the ascitic fluid before IL-2 applications in order to enable better spread of IL-2.

This assessment was performed 3 and 6 mo after the commencement of treatment. Separately we assessed the Karnofsky Index in patients in order to follow the changes in quality of life.

RESULTS

Feasibility

Application of IL-2 at the site of the tumor was feasible in all patients. No major obstacles were encountered. Locoregional IL-2 application in doses 1.5-9 MIU IL-2 did not cause undue discomfort, even in patients in poor general condition.

Therapeutic effect

The clinical effects of local IL-2 application are shown in Table 2. (1) After IL-2 treatment, most patients (12/16) had PD. One patient of the 'weekly' scheme (W4) and three patients of the "monthly" scheme (M2, M7, and M8) had SD. These four patients had PD at the start of therapy and stabilization of their disease is a success that was proved by their survival (Table 2). Patient W4 was cachectic at the first presentation. After IL-2 treatment, her condition improved (Karnofsky index of 50 became 80), she had SD for 7 mo. Thereafter liver metastases slowly progressed, liver function tests worsened, but the primary tumor in the colon did not progress. Her survival was 28 mo. Patient M2 showed SD for 8 mo. He was in a relatively good clinical condition and this remained so. Patient M7 had SD for more than 2 years (at the time of diagnosis of HCC he was decompensated, had cirrhosis Child C, and diabetes), and enjoyed an improved quality of life. This patient did not die from the tumor, but due to liver cirrhosis. Patient M8 had SD for 23 mo. At the time of writing this paper a progression of the tumor was registered, but she is still in good general condition. (2). Neoplastic ascites. All patients with malignant effusion were of the 'weekly' scheme. Two of them showed complete reduction of ascites (2/4) after IL-2 treatment, and the other two showed failure to IL-2 treatment. Responding patients were patients W5 and W8. In these two patients, IL-2 was initially applied directly into

Table 2 Therapeutic effect after 3rd mo and survival

A. Once weekly local IL-2 application

No.	Sex	Primary tumor	Clinical effect	Neoplastic effusion	Karnofsky before and after treatment (%)	*Survival mo
W1	M	Pancreatic Ca	PD	-	30-30	4
W2	F	Stomach Ca	PD	-	80-60	3
W3	F	Colorectal Ca	PD	-	80-60	L
W4	F	Colorectal Ca	SD	-	50-80	28
W5	M	Colorectal Ca	PD	Complete reduction	70-90	10
W6	F	Ovarian Ca	PD	Failure	60-50	2
W7	F	Mammary Ca	PD	Failure	60-40	1
W8	M	Hemangiosarcoma	PD	Complete reduction	50-80	12

B. Once monthly local IL-2 application

No.	Sex	Primary tumor	Clinical effect	Karnofsky before and after treatment (%)	*Survival mo
M1	M	HCC Liver cirrhosis	PD	70-70	4
M2	M	HCC Liver cirrhosis	SD	80-80	24A
M3	M	Abdominal mesothelioma	PD	80-50	6
M4	F	Colorectal Ca	PD	80-70	L
M5	F	Mammary Ca	PD	40-40	1
M6	F	Mammary Ca	PD	80-80	L
M7	M	HCC Liver cirrhosis	SD	90-90	27
M8	F	HCC Liver cirrhosis	SD	80-90	24A

I survival since the start of IL-2 therapy till death; W, weekly IL-2 application; M, monthly IL-2 application; A, alive; L, lost for follow-up; Ca, carcinoma; HCC, hepatocellular carcinoma; PD, progressive disease; SD, stable disease.

the neoplastic effusion, but with the reduction of the ascites, subsequent IL-2 applications were made into artificially made ascites. Patient W8 had complete reduction of ascites and significant reduction of the pleural effusion, though liver metastases progressed. The quality of life after IL-2 treatment had improved (Karnofsky index of 50% became 80%). Patient W5 had complete reduction of ascites and improved quality of life (Karnofsky of 70% became 90%) enabling him to resume his usual activities. (3) In conclusion, 6 out of 16 patients seemed to benefit more or less from IL-2 application at the site of the tumor. Three out of eight patients of the 'weekly' scheme improved -one had SD and two had reduction of ascites, and also 3/8 patients of the "monthly" scheme showed SD. Therapeutic results did not differ between the 'weekly' and the 'monthly' treatment schedule. Comparison with historical controls in our study was not possible due to the heterogeneity of our patients. In future larger prospective trial should be done.

Adverse effects

Adverse effects were minimal. The therapeutic scheme was well tolerated, even in patients in a poor condition. Often moderate fever was observed, though rarely above 38.2 ℃. A transient local skin rash was observed in one patient after intra-peritoneal IL-2 application.

DISCUSSION

This study shows that treatment of cancer, presented at a gastro-intestinal clinic, with locoregionally applied IL-2 in doses 1.5-9 MIU was feasible. No major problems arose. Locoregional IL-2 treatment induced a modest but worthwhile clinical gain: 6/16 patients benefited from this treatment. Four patients had SD for some time after IL-2 treatment and two had reduction of ascites. Four patients had an improved Karnofsky Index. Two patients lived considerably longer than was clinically expected (>24 and 27 mo).

Probably vascular leakage causing edema and subsequent tumor necrosis are indirect effects of local IL-2 application. IL-2 has pleiotropic immune effects *in vivo* and probably leads to macrophage reaction and homing of specific lymphocytes. Induction of tumor necrosis by irradiation[19] or Cisplatin[6,18] further enhances the therapeutic effect of following local IL-2 injections. Therefore, necrosis was induced in five of our patients. We applied only single procedure of local ablation, which cannot create significant necrosis, and therefore cannot lead to the therapeutic effect observed in our patients alone.

Whereas chemotherapy of cancer is usually connected with serious side effects such as extensive nausea and fatigue, leucopenia and related to this infections, such features were not observed in the patients treated with local IL-2 applications in these doses. Another advantage of this treatment is that IL-2 can usually be applied without complex surgical intervention. Further this treatment is cheap since only limited amounts of IL-2 are required.

Therapeutic gain might even be better if we can fine-tune our protocol. The results of this feasibility study thus warrant proceeding with a larger trial to further establish the effect of local IL-2 application in advanced gastro-intestinal cancer in combination with standard anti-cancer treatment.

In conclusion, this study demonstrates the feasibility of low dose locoregional IL-2 application in advanced abdominal cancer.

Local IL-2 application in patients with advanced GI malignancies led to modest but worthwhile clinical improvement in 6 out of 16 patients.

Important are the absence of adverse effects or serious discomfort, and the limited expenses.

REFERENCES

1 **Maas RA,** Dullens HF, De Jong WH, Den Otter W. Immunotherapy of mice with a large burden of disseminated lymphoma with low-dose interleukin-2. *Cancer Res* 1989; **49**: 7037 -7040

2 **Kusnierczyk H,** Pajtasz Piasecka E, Koten JW, Bijleveld C, Krawczyk K, Den Otter W. Further development of local IL-2 therapy of cancer: multiple versus single IL-2 treatment of transplanted murine colon carcinoma. *Cancer Immunol Immunother* 2004; **53**: 445-452

3 **Balemans LTM,** Mattijssen V, Steerenberg PA, Van Driel BE, De Mulder PHM, Den Otter W. Locoregional therapy with polyethyleneglycol-modified interleukin-2 of an intradermally growing hepatocellular carcinoma in the guinea pigs induces T-cell-mediated antitumour activity. *Cancer Immunol Immunother* 1993; **37**: 7

4 **Den Otter W,** Hill FW, Klein WR, Koten JW, Steerenberg PA, De Mulder PH, Rutten VP, Ruitenberg EJ. Low doses of interleukin-2 can cure large bovine ocular squamous cell carcinoma. *Anticancer Res* 1993; **13**: 2453-2455

5 **Den Otter W,** Hill FW, Klein WR, Koten JW, Steerenberg PA, De Mulder PH, Rhode C, Stewart R, Faber JA, Ruitenberg EJ. Therapy of bovine ocular squamous cell carcinoma with local doses of interleukin-2: 67% complete regressions after 20 mo of follow-up. *Cancer Immunol Immunother* 1995; **41**: 10-14

6 **Spoormakers TJ,** Klein WR, Jacobs JJ, Van Den Ingh TS, Koten JW, Den Otter W. Comparison of the efficacy of local treatment of equine sarcoids with IL-2 or cisplatin/IL-2. *Cancer Immunol Immunother* 2003; **52**: 179-184

7 **Den Otter W,** Dobrowolski Z, Bugajski A, Papla B, Van der Meijden APM, Koten JW, Boon TA, Siedlar M, Zembala M. Intravesical interleukin-2 in T1 papillary bladder carcinoma: regression of marker lesion in 8 out of 10 patients. *J Urol* 1998; **159**: 1183

8 **Pizza G,** Severini G, Menniti D, De Vinci C, Corrado F. Tumour regression after intralesional injection of interleukin 2 (IL-2) in bladder cancer. Preliminary report. *Int J Cancer* 1984; **34**: 359-367

9 **Jacobs JJ,** Hordijk GJ, Jurgenliemk-Schulz IM, Terhaard CH, Koten JW, Battermann JJ, Den Otter W. Treatment of stage III-IV nasopharyngeal carcinomas by external beam irradiation and local low dose of IL-2. *Cancer Immunol Immunother* 2005; **54**: 792-798

10 **Huland E,** Heinzer H, Huland H. Treatment of pulmonary metastatic renal-cell carcinoma in 116 patients using inhaled interleukin-2 (IL-2). *Anticancer Res* 1999; **19**: 2679-2683

11 **Den Otter W,** De Groot JW, Bernsen MR, Heintz AP, Maas R, Hordijk GJ, Hill FW, Klein WR, Ruitenberg EJ, Rutten VP. Optimal regimes for local IL-2 tumour therapy. *Int J Cancer* 1996; **66**: 400-403

12 **Baselmans AHC,** Koten JW, Battermann JJ, Van Dijk JE, Den Otter W. The mechanism of regression of solid SL2 lymphosarcoma after local IL-2 therapy. *Cancer Immunol Immunother* 2002; **51**: 492-498

13 **Jacobs JJ,** Sparendam D, Den Otter W. Local interleukin-2 therapy is therapeutically most effective against cancer

when injected intratumorally. *Cancer Immunol Immunother* 2005; **54**: 647-654

14 **Balemans LT,** Steerenberg PA, Koppenhagen FJ, Kremer BH, De Mulder PH, Claessen AM, Scheper RJ, Den Otter W. PEG-IL-2 therapy of advanced cancer in the guinea pig. Impact of the primary tumour and beneficial effect of cyclophosphamide. *Int J Cancer* 1994; **58**: 871-876

15 **Van Es RJ,** Baselmans AH, Koten JW, Van Dijk JE, Koole R, Den Otter W. Perilesional IL-2 treatment of a VX2 head and neck cancer model can induce a systemic anti-tumor activity. *Anticancer Res* 2000; **20**: 4163

16 **Krastev Z,** Koltchakov V, Popov D, Alexiev A, Koten JW, Den Otter W. A case of hepatocellular carcinoma (HCC): Treatment with local application of alcohol and interleukin-2 (IL-2). *Hepatogastroenterology* 2003; **50**: 1647

17 **Krastev Z,** Koltchakov V, Vladov N, Popov D, Milev A, Koten JW, Den Otter W. A mesothelioma that is sensitive to locally applied IL-2. *Cancer Immunol Immunother* 2001; **50**: 226

18 **Bernsen MR,** Van Der Velden AW, Everse LA, Dullens HF, Den Otter W, Heintz AP. Interleukin-2: hope in cases of cisplatin resistant tumours. *Cancer Immunol Immunother* 1998; **46**: 41-47

19 **Everse LA,** Renes IB, Jürgenliempk-Schultz IM, Rutgers DH, Bernsen MR, Dullens HF, Den Otter W, Battermann JJ. Local low dose interleukin-2 induces systemic immunity when combined with radiotherapy of cancer. A preclinical study. *Int J Cancer* 1997; **72**: 1003

20 **Lissoni P,** Mandala M, Curigliano G, Ferretti G, Moro C, Arddizoia A, Malugani F, Tancini G, Tisi E, Arrigoni C, Barni S. Progress report on the palliative therapy of 100 patients with neoplastic effusions by intracavitary low-dose interleukin 2. *Oncology* 2001; **60**: 308

Science Editor Guo SY **Language Editor** Elsevier HK

PO Box 2345, Beijing 100023, China
www.wjgnet.com
wjg@wjgnet.com

ELSEVIER

World J Gastroenterol 2005;11(35):5530-5534
World Journal of Gastroenterology ISSN 1007-9327
© 2005 The WJG Press and Elsevier Inc. All rights reserved.

• *BRIEF REPORTS* •

Association between thyroid function and gallstone disease

Henry Völzke, Daniel M Robinson, Ulrich John

Henry Völzke, Ulrich John, Ernst Moritz Arndt University Greifswald, Institute of Epidemiology and Social Medicine, Walther Rathenau Str. 48, D-17487 Greifswald, Germany
Daniel M Robinson, Ernst Moritz Arndt University Greifswald, Department of Medicine B, Friedrich Loeffler Str. 23a, D-17487 Greifswald, Germany
Supported by the German Federal Ministry for Education and Research, No. 01ZZ96030, from the Ministry for Education, Research and Cultural Affairs and the Ministry for Social Affairs of the State Mecklenburg-West Pomerania
Correspondence to: Henry Völzke, MD, Institute of Epidemiology and Social Medicine, Ernst Moritz Arndt University, Walther Rathenau Str. 48, D-17487 Greifswald, Germany. voelzke@uni-greifswald.de
Telephone: +49-3834-867707 Fax: +49-3834-866684
Received: 2005-01-28 Accepted: 2005-02-18

Abstract

AIM: To investigate those associations using data of the population-based Study of Health in Pomerania.

METHODS: A study population of 3 749 residents aged 20-79 years without previously diagnosed thyroid disease was available for analyses. Serum TSH was used to assess thyroid function. Cholelithiasis was defined by either a prior history of cholecystectomy or the presence of gallstones on ultrasound. Logistic regression was performed to analyze independent associations between thyroid function and cholelithiasis.

RESULTS: There were 385 persons (10.3%) with low (<0.3 mIU/L), 3 321 persons (88.6%) with normal and 43 persons (1.2%) with high serum TSH levels (>3 mIU/L). The proportion of cholelithiasis among males and females was 14.4% and 25.3%, respectively. Among males, there was an independent relation between high serum TSH and cholelithiasis (OR 3.77; 95%-CI 1.06-13.41; $P<0.05$). Also among males, there was a tendency towards an elevated risk of cholelithiasis in persons with low serum TSH (OR 1.40; 95%-CI 0.96-2.02; $P = 0.07$). In the female population, no such relation was identified.

CONCLUSION: There is an association between thyroid and gallstone disease with a gender-specific relation between hypothyroidism and cholelithiasis.

© 2005 The WJG Press and Elsevier Inc. All rights reserved.

Key words: Thyroid function; Gallstones; Cholelithiasis; SHIP

Völzke H, Robinson DM, John U. Association between thyroid function and gallstone disease. *World J Gastroenterol* 2005; 11(35): 5530-5534
http://www.wjgnet.com/1007-9327/11/5530.asp

INTRODUCTION

For decades, there has been a discussion, whether thyroid disorders could cause gallstone disease. Particularly, there are several explanations for a possible relation between hypothyroidism and gallstone disease. These explanations include the known link between thyroid failure and disturbances of lipid metabolism[1] that may consecutively lead to a change of the composition of the bile. Recent studies[2] also demonstrated low bile flow in hypothyroid subjects. Furthermore, the sphincter of Oddi expresses thyroid hormone receptors and thyroxine has a direct prorelaxing effect on the sphincter[3]. Both low bile flow and sphincter of Oddi dysfunction are regarded as important functional mechanisms that may promote gallstone formation[4].

In a series of 668 female patients who had undergone cholecystectomy for gallstone disease, the proportion of treated hypothyroidism was 2.4% compared to 0.8% in the 782 controls[5]. Other studies[6] found a proportion of previously diagnosed hypothyroidism of 8% and 6% in patients having common bile duct and gallbladder stones, respectively, compared to a proportion of only 1% in the controls. The usage of thyroxine was even suspected to dissolve gallstones[7]. However, a spontaneous passage of the stone to the duodenum could not be excluded in this case report[7]. In an animal model of rabbits in whom a fatty diet induced gallstone formation, administering thyroxine was associated with a low gallstone weight, but did not dissolve the gallstones[8].

Previous studies[5,6] that investigated the association between thyroid function and gallstone disease in human beings, were conducted in a series of patients with potential for selection bias that may have produced false positive results. Furthermore, the statistical analyses were only controlled for age, but not for further confounders in both studies[5,6]. To our knowledge, there is only one large case-control study[9] that was appropriately adjusted for other risk factors of gallstone disease. In this study[9], no independent relation between thyroid disorders and gallstone formation was found. Unfortunately, the exposure was only defined as previous history of thyroid disease, and assessments of the current thyroid function status were not included. Moreover, there are currently no investigations that also include ultrasound to evaluate asymptomatic gallstones in this context.

Therefore, the aim of our study is to analyze the association between thyroid function and the risk of cholelithiasis using the data on the population-based Study of Health in Pomerania (SHIP).

MATERIALS AND METHODS

The Study of Health in Pomerania (SHIP) is a cross-sectional

examination in West Pomerania, the north-eastern part of Germany[10]. The study region is a formerly iodine deficient area with a high prevalence of iodine deficiency-related disorders such as goiter, thyroid nodules and decreased serum TSH levels[11]. A stable and adequate iodine supply has been achieved in the study area for the past decade. A random sample from the population aged 20-79 years was drawn. The sample was selected using population registries. Only individuals with German citizenship and main residency in the study area were included. There were 7 008 subjects sampled, with 292 persons of each gender in each of the 12 five-year age strata. The net sample (without migrated or deceased persons) comprised 6 267 eligible subjects. Selected persons received a maximum of three written invitations. In case of no response, letters were followed by a phone call or by home visits, if contact by phone was not possible. The final SHIP sample comprised 4 310 participants (final response proportion 68.8%). All participants gave informed written consent. The study protocol is consistent with the principles of the Declaration of Helsinki and was approved by the Ethics Committee of the University of Greifswald.

All 423 persons with known thyroid disorders or current thyroid medication according to the anatomic, therapeutic and chemical (ATC) code H03 (iodine, thyroid hormone replacement, suppression therapy or thyrostatics), 44 more persons without data on serum TSH levels and 94 more persons with no liver ultrasound or uncertainty with regard to cholelithiasis were excluded. This resulted in a study population of 3 749 subjects who were available for the present analysis.

Sociodemographic characteristics and medical histories were assessed by computer-assisted personal interviews. Education was categorized into three levels [low (<10 years), medium (10 years), high (>10 years), categories based on the East German three-level school system]. Individuals who participated in physical training during summer or winter for at least 1 h a week were classified as being physically active. According to the smoking habits participants were categorized into current, former and non-smokers. Diabetes was defined as a self-reported physician's diagnosis of diabetes, or serum hemoglobin A1c >7%. Body height and weight were measured for the calculation of the body mass index (BMI = weight [kg]/ height^2 [m^2]). Blood samples were taken, and laboratory parameters were analyzed in a central laboratory. Serum low-density lipoprotein (LDL) and high-density lipoprotein (HDL) cholesterol were precipitated and measured photometrically (Boehringer GmbH, Mannheim, Germany). Serum thyrotropin (TSH) was analyzed by immunochemiluminescent procedures (LIA-mat, Byk Sangtec Diagnostica GmbH, Frankfurt, Germany). All TSH measurements were performed in one central laboratory. The functional sensitivity of the TSH assay was 0.03 mIU/L. The reference range was 0.3-3 mIU/L.

The liver was examined using a 5 MHz transducer and a high-resolution instrument (Vingmed VST Gateway, Santa Clara, USA). The sonographers were unaware of the participant's clinical and laboratory characteristics. Gallstones were present if the gallbladder contained echoes that moved with gravity except when the stones were large, a septum existed in the gallbladder or there was an enclosed infundibulum[12]. Cholelithiasis was defined as previous history of cholecystectomy or current, sonographically diagnosed gallstones.

Statistical analyses

Data on quantitative characteristics are expressed as mean±SD. Data on qualitative characteristics are expressed as percentage values or absolute numbers as indicated. The study population was divided according to the TSH reference values that were provided by the manufacturer. The three groups consisted of persons with low (<0.3 mIU/L), normal (0.3-3 mIU/L) and high (>3 mIU/L) serum TSH levels. Comparisons between groups were made using χ^2-test (nominal data) and analysis of variance (ANOVA, continuous data). Sex-stratified logistic regression was performed in order to evaluate independent relationships between thyroid function and cholelithiasis. All analyses were adjusted for age and further potential confounders. Since missing values were present in some variables, data of 30 males (1.54%) and 21 females (1.17%) were lost for multivariable analyses. Serum lipids as mediators were not considered. The odds ratio (OR) was calculated, values being given as lower and upper 95%-confidence interval (CI). A value of $P<0.05$ was considered statistically significant. All statistical analyses were performed with SPSS software, version 11.0.5 (SPSS GmbH Software, Munich, Germany).

RESULTS

There were 385 persons (10.3%) with low, 3 321 persons (88.6%) with normal and 43 persons (1.1%) with high serum TSH levels. The three groups were compared with respect to baseline demographic and clinical characteristics (Table 1). Persons with low serum TSH levels were older, less educated, less physically active and had lower serum HDL cholesterol levels than persons with serum TSH levels within the reference range (Table 1). Compared to the latter persons, individuals with high serum TSH levels were more often of female gender and had higher serum total cholesterol concentrations (Table 1).

The proportion of persons with cholelithiasis among the total sample was 19.7% (Table 2). Women were affected nearly twice as often as men (OR females *vs* males 2.01; 95%CI 1.71-2.37). While gallstones were only slightly more often detected by ultrasound in women than in men (OR 1.54; 95%CI 1.24-1.92), females reported particularly more often a previous history of cholecystectomy compared to males (OR 2.63; 95%CI 2.09-3.30; Table 2). Given these gender-related differences, all multivariable analyses were performed separately among males and females. These analyses revealed an advanced age, high BMI and low serum HDL cholesterol levels as independent risk factors for cholelithiasis in males as well as in females (Table 3).

The prevalence proportions of cholelithiasis among males with low, normal and high serum TSH levels were 22.5%, 13.3% and 30.8%, respectively. Bivariate analyses revealed an increased proportion of cholelithiasis in male persons with low serum TSH levels. This association bordered statistical significance after adjustment for potential

Table 1 Baseline clinical characteristics of study participants with low (< 0.3 mIU/L), normal (0.3–3 mIU/L) and high (> 3 mIU/L) serum TSH levels

	Low serum TSH n = 385	Normal serum TSH n = 3321	High serum TSH n = 43
Age (yr)	57.2±15.2[a]	48.4±16.3	51.1±12.7
Sex (male)	218 (56.6%)	1 723 (51.9%)	13 (30.2%)[a]
Education			
<10 yr	209 (54.6%)[a]	1 206 (36.6%)	14 (32.6%)
10 yr (Ref.)	132 (34.5%)	1 556 (47.2%)	19 (44.2%)
>10 yr	42 (11.0%)	535 (16.2%)	10 (23.3%)
Physical activity	130 (33.9%)[a]	1 445 (43.7%)	19 (44.2%)
Current cigarette smoking			
Never (Ref.)	125 (32.6%)	1 138 (34.4%)	15 (34.9%)
Former	151 (39.4%)	1 109 (33.5%)	17 (39.5%)
Current	107 (27.9%)	1 061 (32.1%)	11 (25.6%)
Diabetes mellitus	38 (10.0%)	269 (8.2%)	0
Body mass index; kg/m^2	27.4±4.5	27.1±4.7	27.9±4.6
Total cholesterol; mg/dL	221±44	223±49	240±53[a]
mmol/L	5.71±1.14	5.76±1.26	6.20±1.38[a]
LDL-Cholesterol; mg/dL	138±41	138±45	152±50
mmol/L	3.56±1.05	3.56±1.18	3.92±1.30
HDL-Cholesterol; mg/dL	54±17[a]	56±17	60±17
mmol/L	1.41±0.44[a]	1.45±0.44	1.56±0.43

χ^2-test (nominal data) or ANOVA (interval data) for inter-group comparisons; [a]P<0.05 *vs* reference group: normal serum TSH. LDL denotes low density lipoprotein, HDL; high density lipoprotein.

Table 2 Prevalence of previous history of cholecystectomy and sonographically detected gallstones among males and females

	History of cholecystectomy (%)	Ultrasound diagnosis of gallstones (%)	Total (%)
Males	122 (6.8)	160 (8.7)	282 (14.4)
Females	257 (16.1)	198 (12.9)	455 (25.3)
All	379 (11.2)	358 (10.6)	737 (19.7)

Table 3 Sex-specific independent risk factors for cholelithiasis

	Males OR (95%CI)	Females (95%CI)
Age; yr (Ref. <30)		
30–<40	4.15 (1.17–14.69)	1.97 (1.04–3.75)
40–<50	8.32 (2.47–28.03)	4.67 (2.55–8.52)
50–<60	16.68 (5.04–55.22)	7.16 (3.85–13.30)
60–<70	28.02 (8.44–93.05)	13.01 (6.81–24.88)
⩾70	40.09 (12.02–133.76)	19.60 (9.92–38.72)
Education; yr (Ref. 10)		
<10	0.88 (0.62–1.26)	0.93 (0.67–1.30)
>10	0.72 (0.44–1.16)	0.68 (0.44–1.05)
Physical activity	0.96 (0.71–1.29)	0.78 (0.60–1.02)
Smoking (Ref. non)		
Ex-smoker	1.15 (0.79–1.68)	0.73 (0.53–1.01)
Current smoker	1.03 (0.66–1.61)	0.78 (0.56–1.10)
Diabetes mellitus	1.37 (0.94–2.01)	1.10 (0.72–1.71)
Body mass index; per kg/m^2	1.04 (1.01–1.08)	1.08 (1.06–1.11)
LDL cholesterol; per 10 mg/dL	0.97 (0.94–1.02)	0.97 (0.94–1.01)
HDL cholesterol; per 10 mg/dL	0.87 (0.78–0.97)	0.87 (0.78–0.97)

Logistic regression analysis, OR denotes odds ratio; 95%CI, confidence interval; LDL, low density lipoprotein; HDL, high density lipoprotein.

confounding variables (Table 4). The full model in the male study population further revealed an independent association between high serum TSH levels and cholelithiasis (Table 4). The prevalence proportions of cholelithiasis among females with low, normal and high serum TSH levels were 31.7%, 24.7% and 26.7%, respectively. The relation between low serum TSH levels and cholelithiasis that was found in bivariate analyses was not stable after appropriate adjustment for relevant confounders. Likewise, there was no independent association between high serum TSH levels and cholelithiasis in women (Table 4).

Further analyses were performed using ultrasound diagnosis of gallstones as the dependent variable. In the male population, multivariable analyses did not attain statistical significance for the association between low serum TSH levels and the endpoint (OR 1.25, 95%CI 0.78-2.02; P = 0.36). High serum TSH levels, however, were again detected as an independent risk factor for sonographically detected gallstones (OR 4.85, 95%CI 1.19-19.74; P<0.05). In the female population, no such association was present. Additional multivariable analyses that were run with previous history of cholecystectomy as the dependent variable also did not find an association between serum TSH levels and this endpoint in women. However, in the male population, the relation between low serum TSH levels and previous history of cholecystectomy bordered statistical significance (OR 1.55, 95%CI 0.94-2.56; P = 0.07), whereas no association between high serum TSH levels and this endpoint was observed (OR 1.91, 95%CI 0.22-16.59; P = 0.56).

Moreover, persons with a previous history of thyroid disease were compared to the study population with respect to their risk of cholelithiasis. Among both the sexes, persons with thyroid disease had cholelithiasis more often than persons without known thyroid disease (23.0% *vs* 14.5% in males and 38.4% *vs* 25.6% in females; P<0.05). After adjustment for the full model, however, there was no independent relation between thyroid and gallstone disease in males as well as females.

DISCUSSION

The present study investigated possible associations between serum TSH levels and gallstone disease. There was an independent relation of high serum TSH levels with cholelithiasis among males, predominantly among those who had sonographically detected gallstones. In the female population, no such associations were identified.

At least in the male population, the finding of high serum TSH levels as an independent risk factor for cholelithiasis confirm previous research[5,6]. An absence of such an association among females might be explained by two points. Firstly, the study population only comprised persons with as yet undiagnosed thyroid disorders. Females were more often excluded due to a known thyroid disorder than males. Thus, there might be earlier diagnosis and treatment of hypothyroidism in women compared to men, reflected by a longer and more intense exposure in males. Likewise, the higher proportion of cholelithiasis in women compared to men was mainly due to the higher proportion of previous history of cholecystectomy in females. Thus, in women,

Table 4 The association between serum TSH levels and cholelithiasis according to sex

	Regression models	Low (<0.3 mIU/L) OR (95%CI)	Serum TSH normal (0.3–3.0 mIU/L) OR (95%CI)	High (> 0.3 mIU/L) OR (95%CI)
Males;	Crude	1.89 (1.34–2.67)[1]	1.0 (Reference)	2.90 (0.90–9.49)
OR	Adjusted for confounding variables[2]	1.40 (0.96–2.02)	1.0 (Reference)	3.77 (1.06–13.41)[1]
Females;	Crude	1.42 (1.01–2.01)[1]	1.0 (Reference)	1.11 (0.49–2.52)
OR	Adjusted for confounding variables[2]	0.89 (0.61–1.32)	1.0 (Reference)	0.91 (0.38–2.19)

[1]Logistic regression analysis, [2]Age (decades), education (three categories), physical activity (yr/*n*), smoking (three categories), diabetes (yr/*n*), body mass index (cont.). OR denotes odds ratio; 95%–CI, confidence interval.

gallstones may become symptomatic earlier than in men and the consecutive diagnostic procedures may further lead to an earlier detection and treatment of hypothyroidism. This assumption is supported by the fact that the association between high serum TSH levels and cholelithiasis was mainly found in males with sonographically detected gallstones. Secondly, there are also gender differences with respect to the type of gallstones. In one study[13], males had less often cholesterol stones than women. One may assume that, if hypothyroidism would indeed be a causal factor for gallstone disease, then this may lead to a specific type of stone other than cholesterol stones. In the same study[13], however, there was no association between thyroid function and the stone type.

In the male population, also an association between low serum TSH levels and cholelithiasis bordered statistical significance in the full model. This was not expected, because experimental evidence suggested a direct association between thyroid function and the bile flow to the duodenum. While the flow was reduced in hypothyroidism, it was enhanced in hyperthyroidism[14]. However, this study[14] was performed in rats without gall bladder. In hamsters, extremely high doses of thyroxine may induce the formation of gallbladder stones[15]. In the present study, particularly males with low serum TSH levels had a higher risk of previous cholecystectomy. Thus, a cholelithiasis may become symptomatic in an earlier state in hyperthyroid persons. In general, the role of hyperthyroidism with respect to gallstone formation in human beings is currently not well investigated and further research is needed.

The exclusion of patients with known thyroid disorders resulted in small numbers of individuals with hypothyroidism, limiting the power of the statistical analysis. We therefore repeated the analyses including these persons. The results confirmed an increased cholelithiasis prevalence in persons with previously diagnosed thyroid disease, however, there was no independent relation between these two parameters. In patients with known thyroid disease the thyroid function status may change dramatically over time mainly due to the effects of treatment. Further confounding variables in patients with known thyroid disease may include medical treatment, better health education and more frequent and intense contact with medical personnel.

Previous studies[16] that were conducted in a neighborhood region identified a high cholelithiasis prevalence proportion of greater than 30% and 55% in men and women who were ⩾65-years old, respectively. This high prevalence is in good agreement with the results of our study. Also in accordance with other studies[17], an advanced age, high BMI and serum lipids were identified as major independent risk factors for cholelithiasis. This argues for the good validity of the diagnostic method to define cholelithiasis used in the present study.

We conclude, that there is a gender-specific relation between hypothyroidism and cholelithiasis. Especially males with gallstones should be further examined for thyroid disorders. Further research is needed to explain the role of low serum TSH levels with respect to gallstone disease in men.

REFERENCES

1 **Canaris GJ,** Manowitz NR, Mayor G, Ridgway EC. The Colorado thyroid disease prevalence study. *Arch Intern Med* 2000; **160**: 526-534

2 **Laukkarinen J,** Sand J, Saaristo R, Salmi J, Turjanmaa V, Vehkalahti P, Nordback I. Is bile flow reduced in patients with hypothyroidism? *Surgery* 2003; **133**: 288-293

3 **Inkinen J,** Sand J, Arvola P, Porsti I, Nordback I. Direct effect of thyroxine on pig sphincter of Oddi contractility. *Dig Dis Sci* 2001; **46**: 182-186

4 **Cicala M,** Habib FI, Fiocca F, Pallotta N, Corazziari E. Increased sphincter of Oddi basal pressure in patients affected by gall stone disease: a role for biliary stasis and colicky pain? *Gut* 2001; **48**: 414-417

5 **Honore LH.** A significant association between symptomatic cholesterol cholelithiasis and treated hypothyroidism in women. *J Med* 1981; **12**: 199-203

6 **Inkinen J,** Sand J, Nordback I. Association between common bile duct stones and treated hypothyroidism. *Hepatogastroenterology* 2001; **47**: 919-921

7 **Vassilakis JS,** Nicolopoulos N. Dissolution of gallstones following thyroxinee administration. A case report. *Hepatogastroenterology* 1981; **28**: 60-61

8 **Borgman RF,** Haselden FH. Cholelithiasis in rabbits: effects of bile constituents and hormones on dissolution of gallstones. *Am J Vet Res* 1969; **30**: 107-112

9 **La Vecchia C,** Negri E, D'Avanzo B, Franceschi S, Boyle P. Risk factors for gallstone disease requiring surgery. *Int J Epidemiol* 1991; **20**: 209-215

10 **John U,** Greiner B, Hensel E, Lüdemann J, Piek M, Sauer S, Adam C, Born G, Alte D, Greiser E, Haertel U, Hense HW, Haerting J, Willich S, Kessler C. Study of Health In Pomerania (SHIP): a health examination survey in an east German region: objectives and design. *Soz Präventivmed* 2001; **46**: 186-194

11 **Völzke H,** Lüdemann J, Robinson DM, Spieker KW, Schwahn C, Kramer A, John U, Meng W. The prevalence of undiagnosed thyroid disorders in a previously iodine deficient area. *Thyroid* 2003; **13**: 803–810

12 **Loria P,** Dilengite MA, Bozzoli M, Carubbi F, Messora R, Sassatelli R, Bertolotti M, Tampieri A, Tartoni PL, Cassinadri

M, Della Ciana M, Contemori M, Save N, Sordi B, Alimenti G, Fabrizi F, Buciuni A, Carulli N. Prevalence rates of gallstone disease in Italy. The Chianciano population study. *Eur J Epidemiol* 1994; **10**: 143-150

13 **Trotman BW,** Soloway RD. Pigment vs cholesterol cholelithiasis: clinical and epidemiological aspects. *Am J Dig Dis* 1975; **20**: 735-740

14 **Laukkarinen J,** Koobi P, Kalliovalkama J, Sand J, Mattila J, Turjanmaa V, Porsti I, Nordback I. Bile flow to the duodenum is reduced in hypothyreosis and enhanced in hyperthyreosis. *Neurogastroenterol Motil* 2002; **14**: 183-188

15 **Bergman F,** van der Linden W. Further studies on the influence of thyroxine on gallstone formation in hamsters. *Acta Chir Scand* 1966; **131**: 319-328

16 **Berndt H,** Nürnberg D, Pannwitz H. Prävalenz der Cholelithiasis. Ergebnisse einer epidemiologischen Studie mittels Sonographie in der DDR. [Prevalence of cholelithiasis. Results of an epidemiologic study using sonography in East Germany]. *Z Gastroenterol* 1989; **27**: 662-666

17 **Martinez de Pancorbo C,** Carballo F, Horcajo P, Aldeguer M, de la Villa I, Nieto E, Gaspar MJ, de la Morena J. Prevalence and associated factors for gallstone disease: results of a population survey in Spain. *J Clin Epidemiol* 1997; **50**: 1347-1355

18 **Kratzer W,** Mason RA, Kachele V. Prevalence of gallstones in sonographic surveys worldwide. *J Clin Ultrasound* 1999; **27**: 1-7

Science Editor Guo SY **Language Editor** Elsevier HK

PO Box 2345, Beijing 100023, China
www.wjgnet.com
wjg@wjgnet.com

ELSEVIER

World J Gastroenterol 2005;11(35):5535-5539
World Journal of Gastroenterology ISSN 1007-9327
© 2005 The WJG Press and Elsevier Inc. All rights reserved.

• *BRIEF REPORTS* •

Mechanism of diarrhea in microscopic colitis

Marijana Protic, Njegica Jojic, Daniela Bojic, Svetlana Milutinovic, Dusanka Necic, Bozidar Bojic, Petar Svorcan, Miodrag Krstic, Obren Popovic

Marijana Protic, Center for Gastroenterology and Hepatology, Zvezdara University Clinical Center, Belgrade
Njegica Jojic, Daniela Bojic, Metabolic Department, Center for Gastroenterology and Hepatology, Zvezdara University Clinical Center, Belgrade
Svetlana Milutinovic, Institute for Pathology, Zvezdara University Clinical Center, Belgrade
Dusanka Necic, Metabolic Laboratory, Center for Gastroenterology and Hepatology, Zvezdara University Clinical Center, Belgrade
Bozidar Bojic, Endoscopic Unit, Center for Gastroenterology and Hepatology, Zvezdara University Clinical Center, Belgrade
Petar Svorcan, Center for Gastroenterology and Hepatology, Zvezdara University Clinical Center, Belgrade
Miodrag Krstic, Center for Gastroenterology and Hepatology, Clinical Center of Serbia, Belgrade
Obren Popovic, Center for Gastroenterology and Hepatology, Zvezdara University Clinical Center, Belgrade
Correspondence to: Marijana Protic, MD, Assistant Professor, Center for Gastroenterology and Hepatology, Zvezdara Clinical Center, 161 Dimitrija Tucovica, Belgrade 11 000, Serbia and Montenegro. marijanaprotic@beotel.yu
Telephone: +381-63-345985 Fax: +381-11-3806340
Received: 2005-01-19 Accepted: 2005-02-28

Abstract

AIM: To search the pathophysiological mechanism of diarrhea based on daily stool weights, fecal electrolytes, osmotic gap and pH.

METHODS: Seventy-six patients were included: 51 with microscopic colitis (MC) [40 with lymphocytic colitis (LC); 11 with collagenous colitis (CC)]; 7 with MC without diarrhea and 18 as a control group (CG). They collected stool for 3 d. Sodium and potassium concentration were determined by flame photometry and chloride concentration by titration method of Schales. Fecal osmotic gap was calculated from the difference of osmolarity of fecal fluid and double sum of sodium and potassium concentration.

RESULTS: Fecal fluid sodium concentration was significantly increased in LC 58.11±5.38 mmol/L (P<0.01) and CC 54.14±8.42 mmol/L (P<0.05) than in CG 34.28±2.98 mmol/L. Potassium concentration in LC 74.65±5.29 mmol/L (P<0.01) and CC 75.53±8.78 mmol/L (P<0.05) was significantly less compared to CG 92.67±2.99 mmol/L. Chloride concentration in CC 36.07±7.29 mmol/L was significantly higher than in CG 24.11±2.05 mmol/L (P<0.05). Forty-four (86.7%) patients had a secretory diarrhea compared to fecal osmotic gap. Seven (13.3%) patients had osmotic diarrhea.

CONCLUSION: Diarrhea in MC mostly belongs to the secretory type. The major pathophysiological mechanism in LC could be explained by a decrease of active sodium absorption. In CC, decreased Cl/HCO_3 exchange rate and increased chloride secretion are coexistent pathways.

© 2005 The WJG Press and Elsevier Inc. All rights reserved.

Key words: Lymphocytic colitis; Collagenous colitis; Secretory diarrhea

Protic M, Jojic N, Bojic D, Milutinovic S, Necic D, Bojic B, Svorcan P, Krstic M, Popovic O. Mechanism of diarrhea in microscopic colitis. *World J Gastroenterol* 2005; 11(35): 5535-5539
http://www.wjgnet.com/1007-9327/11/5535.asp

INTRODUCTION

Microscopic colitis is a new form of idiopathic inflammatory bowel disease. First studies dealing with microscopic colitis appeared in the late seventies[1-3]. Clinical manifestations are substantially milder than other forms of idiopathic inflammatory bowel diseases. The main characteristics include chronic watery diarrhea and abdominal cramps. Endoscopic[4-8] and radiological examination of gastrointestinal tract are normal. The major criteria for diagnosis are set on the basis of histological findings of colonic mucosal biopsies[9] and stool examinations. There are two basic types of microscopic colitis: collagenous and lymphocytic colitis. They could be differentiated on the basis of pathohistological findings. Collagenous colitis is defined by the appearance of diffuse thickening of subepithelial collagenous band (>10 μm)[10], desquamation and degeneration of surface epithelium, increased number of intraepithelial lymphocytes and mild or moderate mononuclear infiltration of lamina propria[10,11-13]. Collagenous colitis shows striking predominance in women (F:M 7:1) in their fifth and sixth decades[4,10,14]. They are often associated with other autoimmune diseases: rheumatoid arthritis[15-17], systemic and discoid lupus erythematosus[18,19], juvenile scleroderma[20], CREST syndrome[21], abnormal function of thyroid gland[14]. Lymphocytic colitis is defined by increased number of intraepithelial lymphocyte of colonic mucosa (>20 IEL per 100 epithelial cells)[10]. Other histological features include flattened surface epithelium with mucine depletion, mononuclear infiltration of lamina propria, and minimal crypt distortion or cryptitis[10,11]. Lymphocytic colitis typically occurs in the sixth decade with roughly equivalent female to male ratio[10,14,19-21]. According to data from the literature there is an association between lymphocytic colitis and other

autoimmune diseases: sicca syndrome[15], celiac disease[24-26] idiopathic pulmonary fibrosis, uveitis, and idiopathic thrombocytopenic purpura[12]. Ethiopathogenesis of microscopic colitis still remains unclear. The long-term use of NSAID[27], and other medication (cyclo3fort[28], ranitidine[29], ticlodipin) could be important. A good number of authors[19,20,30] claim that autoimmune process is the cause of prime importance in ethiopathogenetic mechanism.

Intraepithelial lymphocytes in lymphocytic and collagenous colitis belong to T suppressor cells, CD_8 group[19]. Stimulated by some luminal antigen they can cause cross reaction with endogen antigen present in the epithelial cells, damage them or reveal direct toxic action on the enterocytes[31]. The hypothesis of the infective etiology of microscopic colitis is based on the results of success of antibiotic therapy[4]. Bile acids also may play a role as shown by malabsorption of bile acids and proper therapeutic response to the cholestiramine[32], which is also suggested by combined manifestation with primary ileal villous atrophy[33]. Deregulation of a collagen synthesis[19,33] has also been mentioned as a possible etiological factor. The precise pathophysiological mechanism of secretory diarrhea typical for microscopic colitis has not been clarified. Most of the authors[31,34,35] believe that the following processes prevail in the development of secretory diarrhea:

- Reduced active sodium absorption
- Inhibited chloride and bicarbonate exchange
- Increased electrogenic chloride secretion followed by passive sodium and water transport.
- Decreased passive permeability of colonic mucosa.

Evidence for each of these hypotheses is contained in a Bo-Linn perfusion study[34]. Results of net and unidirectional electrolyte fluxes and electrical potential difference suggested that colonic fluid absorption was abnormal. The main reasons for these are: reduced active and passive sodium and chloride absorption and reduced Cl/HCO_3 exchange. Zeroogian and Chopra thought that mediators secreted by inflammatory cells in lamina propria may play an important role in disturbances of absorptive colonic capacity and reducing passive transport[21]. Other authors consider that watery diarrhea is a consequence of increased active chloride intraluminal secretion and accompanying passive sodium and water transport[31,35]. Increased concentration of prostaglandin E2 secreted by pericryptal fibroblasts may stimulate active chloride secretion. Pericryptal fibroblasts compose pericryptal sheets which can cause functional abnormalities. In some cases an increased concentration of prostaglandin E2 is found in jejunal aspirate and feces[31]. The same group considers that injured surface epithelium and collagen deposit band of colonic mucosa may prevent absorption of luminal water and electrolytes. The most important pathophysiological role could be played by inflammatory cells infiltrated in the lamina propria, common characteristic for both lymphocytic and collagenous colitis. Precise mechanism of diarrhea remains unclear due to unknown etiological factors yet to be discovered. It is possible that different mechanisms cause diarrhea in the course of the disease, depending on whether pericryptal absorption site are blocked by the collagen deposit or inflammatory cells infiltrate.

MATERIALS AND METHODS

The study was performed in the Center for Gastroenterology and Hepatology (Zvezdara, University Clinical Center, Belgrade) between 1993 and 2004. Seventy-six people were included in the study (58 with diagnoses of microscopic colitis and 18 healthy people composing a control group).

The following diagnostic procedures were performed in both groups: routine biochemical examinations with electrolyte status, lactose tolerance test, thyroid status, presence of antinuclear antibody (ANA), antimitochondrial antibody (AMA) and antibodies to tyreoglobulin; standard and specific (*Yersinia enterocolitica* and *Campylobacter jejuni*) stool examinations for bacteria and parasites; duodenal tube with quantitative and qualitative bacterial culture of aspirate; small bowel barium enema, enteroscopy with small bowel biopsies; colonoscopy with terminal ileoscopy and serial biopsies of colonic and terminal ileum mucosa. Biopsy specimens were fixed with 40 g/L formaldehyde and embedded in paraffin. Five micrometer sections were stained with hematoxylin and eosin. Thickness of the subepithelial collagen layer was measured with light microscopy using screw micrometer by an experienced pathologist. Number of intraepithelial lymphocytes was determined with regard to 100 epithelial cells of colonic mucosa.

Functional examinations of stool

Stool samples All patients collected stool for 3 d (72 h) in preweight plastic bucket that held 3-5 L. Buckets with stools were kept cold under refrigeration (+4 ℃) during the collection period. During that time patients were on a diet with 70-100 g fats per day.

Determination of sodium, potassium and chloride concentration in fecal fluid Concentration of sodium and potassium were determined by flame photometry (Corning 480 Flame Photometer)[36,37] and chloride concentration by the titration method of Schales[38]. Data of sodium, potassium and chloride were multiplicities with water dilution factor. Daily losses of electrolytes by stool were calculated from the concentration of electrolytes in fecal fluid. Fecal osmotic gap was calculated from the difference of measured osmolality of fecal fluid and double sum of the sodium and potassium concentration [290-(Na+K)×2].

Estimation of pH of fecal fluid For estimating fecal pH we used balanced Beckman Expandomatic pH meter[37].

Determination of daily fecal fat The amount of fat in daily stool was quantified by titration method of Van de Kamer[39]. Normal values of fecal fat in our laboratory are less than 6 g/d. Normal values by the data of Fine are 6.4 g/d[40,43].

Statistical analysis

For all tested parameters we calculated mean and standard error (SE). For the statistical significant difference ($P<0.05$) among different group of patients, unpaired Student's *t*-test was used.

RESULTS

There were 51 patients with complete conditions for diagnosis

of microscopic colitis [40 patients with lymphocytic colitis (LC) and 11 patients with collagenous colitis (CC)]. Seven patients had histological diagnoses of MC (5 patients with LC and 2 with CC) without diarrhea at that moment. Control group consisted of 18 healthy persons.

Based upon the status of the collagen plate and the number of IEL of biopsy specimen of right colon, patients are classified as a group with LC or CC or CG (Table 1). In the group of patients with LC the median number of IEL/100 epithelial cells was (32±12) and the mean thickness of collagen plate was (8±2) μm with moderate inflammation of lamina propria. Patients with CC had average thickness of collagen band (25±9) μm and (14±4) IEL/100 epithelial cells with severe inflammation of lamina propria. Control group of patients had (4±1) IEL/100 epithelial cells and mean thickness of collagen plate (8±3) μm.

Physical examination, all biochemical tests, radiological and endoscopic findings were normal in all patients. Diagnoses of microscopic colitis was established based on the data of verified diarrhea [daily stool weight (DSW)> 200 g/24 h] and histopathology analysis of biopsy specimens of colonic mucosa. Mean values of DSW (mean±SE) in the group of patients with LC and CC were statistically significantly higher than in the other two groups: CG and group of 7 patients with histological signs of microscopic colitis without diarrhea ($P<0.01$, Table 2). The average values of sodium concentration in the patients with LC ($P<0.01$) and CC ($P<0.05$) were statistically significantly different than in the CG. Daily fecal loss of this electrolyte patient with LC and CC was statistically significantly different than among the healthy people ($P<0.05$, Figure 1) The mean values of potassium concentration in patients with LC ($P<0.01$) and CC ($P<0.05$) were statistically significantly different than CG. Daily fecal loss of potassium in patients with LC and CC was statistically significantly different with regard to CG ($P<0.05$). The average value of chloride concentration in patients with CC was statistically significantly different with regard to CG ($P<0.05$). Daily fecal loss of this electrolyte in patients with LC and CC was statistically significantly different than among the healthy people ($P<0.05$). We tried to clarify the mechanism of diarrhea by calculation of the fecal osmotic gap (FOG). Secretory diarrhea (FOG <50 memo/kg) was found in 44 (86.7%) of patients with microscopic colitis. Osmotic diarrhea was present in 7 (13.3%) of patients. The reason in determining the concentration of fecal fat in patients with LC and CC was to establish possible impact of some other disease (small bowel or pancreatic) on pathophysiological mechanism of diarrhea. Six (11.7%) patients with LC had slightly increased daily fecal fat (9-11 g/24 h). DSW in the group of patients [9 (17.46%)] with LC and accompanying disease (mean: 315.10 g/24 h) was not statistically significantly different than in the group of patients with LC (mean: 372.64 g/24 h). The average values of fecal pH in the patients with LC (6.31±0.14) and CC (6.36±0.11) were not statistically significantly different compared to CG.

Table 1 Mean±SD of number of IEL/100 EC and thickness of collagen plate in patients with LC and CC

	n	No. of IEL/100 EC (mean±SD)	Thickness of collagen band (mean±SD)	Inflammation of propria
Lymphocytic colitis	46	32±12	8±2	Moderate
Collagenous colitis	13	14±4	25±9	Severe
Control group	18	4±1	8±3	Mild/none

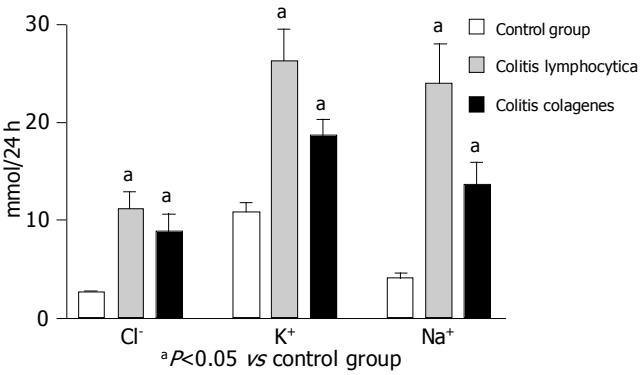


Figure 1 Average values of fecal daily loss of Na^+, K^+, Cl^- (mean±SE).

DISCUSSION

Precise mechanism of diarrhea in patients with microscopic colitis still remains unclear. Most of the authors[31,34,35] believe that dominant processes in the development of diarrhea are: 1. Reduced active sodium absorption 2. Inhibited chloride and bicarbonate exchange 3. Increased electrogenic chloride secretion followed by passive sodium and water transport. 4. Decreased passive permeability of colonic mucosa. First data about mechanism of secretory diarrhea were established by Bo-Linn perfusion study[34]. The average values of DSW in this and other similar studies[21,33,34] were higher than values from our study (LC: 200, 2-1 400 g/24 h; CC: 206-350 g/24 h). Using "steady-state" perfusion method, the authors have proved that electrolyte and fluid absorption in colon were seriously disturbed in patients with microscopic colitis. The reasons for reduced electrolyte and fluid absorption are microscopic changes of colonic mucosa. Degenerative injuries of surface epithelium, subepithelial

Table 2 mean±SE values of daily stool weight, electrolyte concentration in fecal fluid and fecal pH in examined group of patients

	DSW (g/24 h)	Conc Na^+(mmol/L)	Conc K^+(mmol/L)	Conc Cl^-(mmol/L)	pH
Lympocytic colitis	386.25±5.39[b]	58.11±5.38[b]	74.65±5.29[b]	28.85±2.55	6.31±0.14
Collagenous colitis	245.66±18.43[b]	54.14±8.42[a]	75.53±8.78[a]	36.07±7.29[a]	6.36±0.11
Control group	118.34±8.79	34.28±2.98	92.67±2.99	24.11±2.05	6.36±0.15
MC without diarrhea	139.19±15.92				

[a]$P<0.05$ *vs* Control group; [b]$P<0.01$ *vs* control group.

collagen deposit and persistence of inflammatory cells (prostaglandin E2)[31,34,35] infiltrate in lamina propria play the most important role in decreased absorption of luminal water and electrolyte. Pathohistological findings of colonic biopsy specimen in our patients are in accordance with the results of previous studies[8-10]. Decreased active sodium absorption is visible by a reduction of the flux lumen/plasma of sodium and chloride. Inhibited chloride and bicarbonate exchange is shown by the reduced bicarbonate secretion rate and lowered chloride absorption[34]. In our study, sodium concentration of the fecal fluid in patients with LC and CC was highly increased in relation to control group. These facts are in accordance with data of other authors. Potassium concentration in fecal fluid of patients with LC and CC was significantly less compared to CG. But the average values of potassium concentration were higher with regard to data from other studies. The mean values of chloride concentrations in patients with CC were statistically significantly higher with regard to CG. These results in our study were less than the data of other authors[34,35]. Daily fecal loss of electrolyte in patients with LC and CC were significantly higher compared to a group of healthy persons. These results were expected for sodium and chloride, due to great concentration of these electrolytes in fecal fluid. Despite smaller potassium fecal concentration, great potassium fecal loss appeared, due to daily stool weight. This fact could have clinical significance and could explain uncommon severe hypokalemia in some patients with microscopic colitis. Finally, our results of fecal electrolytes concentration and their daily fecal loss also confirm the hypothesis of disturbed active sodium absorption and absorption/secretion of chloride[31,34,35,41]. The dominant process in electrolyte malabsorption in patients with LC could be reduced by active sodium absorption. In the group of patients with CC prevailing mechanisms are decreasing the rate of Cl/HCO3 exchange and increased electrogenic Cl secretion, in addition to, reduced active sodium absorption. There were no significant differences between main values of fecal pH of examined patients with LC and CC with regard to healthy persons. Still it is interesting to note that all patients with proper therapeutic response to cholestyramine had slightly increased fecal pH (>6.8). This data could suggest possible co-factorial influence of bile acid malabsorption[17,33] on the mechanism of diarrhea in microscopic colitis. Only 6 (11.7%) patients had slightly increased daily fecal fat (9-11 g/24 h). All of them had lymphocytic colitis. In the group of patients with microscopic colitis and associated disease there were no differences in average values of daily stool weight compared to patients with microscopic colitis without accompanied disease. On the basis of our results it could be concluded that influence of accompanied disease on the mechanism of diarrhea is of secondary importance. Most of the authors[31,34,41-43,45] claim that secretory diarrhea is characteristic of microscopic colitis. By Erer's criteria, the border value of fecal osmotic gap (FOG) for distinction between secretory and osmotic diarrhea is 50 mOsmol/kg[43,44]. In our study 86.7% of patients had secretory diarrhea and 13.3% osmotic diarrhea. All patients with secretory diarrhea belong to the group of patients with lymphocytic colitis. There was a group of 7 patients with histological diagnosis of microscopic colitis and without approved diarrhea. All of them had intermittent diarrhea. We recommended them to collect stool during the period of diarrhea. The schedule for future examination of these patients remains imprecise.

In conclusion, on the basis of our results it could be stated that diarrhea in microscopic colitis (LC, CC) belongs to the secretory type. The major pathophysiological mechanism in patients with LC may be a decrease of active sodium absorption. In collagenous colitis decreased Cl/HCO_3 exchange rate and increased electrogenic chloride secretion is coexistent pathway in the genesis of diarrhea.

REFERENCES

1 **Lindstrom CG.** "Collagenous colitis" with watery diarrhoea - a new entity? *Pathol Eur* 1976; **11**: 87-89
2 **Read NW,** Krejs GJ, Read MG, Santa Ana CA, Morawski SG, Fordtran JS. Chronic diarrhea of unknown origin. *Gastroenterology* 1980; **78**: 264-271
3 **Kingham JG,** Levison DA, Ball JA, Dawson AM. Microscopic colitis-a cause of chronic watery diarrhoea. *Br Med J (Clin Res Ed)* 1982; **285**: 1601-1604
4 **Bohr J,** Tysk C, Eriksson S, Abrahamsson H, Jarnerot G. Collagenous colitis: a retrospective study of clinical presentation and treatment in 163 patients. *Gut* 1996; **39**: 846-851
5 **Olesen M,** Eriksson S, Bohr J, Jarnerot G, Tysk C. Lymphocytic colitis: a retrospective clinical study of 199 Swedish patients. *Gut* 2004; **53**: 536-541
6 **Barta Z,** Mekkel G, Csipo I, Toth L, Szakall S, Szabo GG, Bako G, Szegedi G, Zeher M. Microscopic colitis: a retrospective study of clinical presentation in 53 patients. *World J Gastroenterol* 2005; **11**: 1351-1355
7 **Baert F,** Wouters K, D'Haens G, Hoang P, Naegels S, D'Heygere F, Holvoet J, Louis E, Devos M, Geboes K. Lymphocytic colitis: a distinct clinical entity? A clinicopathological confrontation of lymphocytic and collagenous colitis. *Gut* 1999; **45**: 375–381
8 **Veress B,** Loffberg R, Bergman L. Microscopic colitis syndrome. *Gut* 1995; **36**: 880-886
9 **Lazenby AJ,** Yardley JH, Giardiello FM, Jessurun J, Bayless TM. Lymphocytic ("microscopic") colitis: a comparative histopathologic study with particular reference to collagenous colitis. *Hum Pathol* 1989; **20**: 18–28
10 **Bogomoletz WV,** Flejou JF. Newly recognized forms of colitis: collagenous colitis, microscopic (lymphocytic) colitis and lymphoid follicular proctitis. *Semin Diagn Pathol* 1991; **8**: 178-189
11 **Fernandez-Banares F,** Salas A, Esteve M, Espinos J, Forne M, Viver JM. Collagenous and lymphocytic colitis. Evaluation of clinical and histological features, response to treatment, and long-term follow-up. *Am J Gastroenterol* 2003; **98**: 340-347
12 **Robert ME.** Microscopic colitis: pathologic considerations, changing dogma. *J Clin Gastroenterol* 2004; **38**: S18-S26
13 **Olesen M,** Eriksson S, Bohr J, Järnerot G, Tysk C. Microscopic colitis: a common diarrhoeal disease. An epidemiological study in Örebro, Sweden 1993–1998. *Gut* 2004; **53**: 346-350
14 **Zins BJ,** Sandborn WJ, Tremaine WJ. Collagenous and lymphocytic colitis: Subject review and therapeutic alternatives. *Am J Gastroenterol* 1995; **90**: 1394-1400
15 **Castanet J,** Lacour JP, Ortonne JP. Arthritis, collagenous colitis, and discoid lupus. *Ann Intern Med* 1994; **120**: 89-90
16 **Sowa JM.** Arthritis and collagenous colitis. *Ann Intern Med* 1994; **121**: 237
17 **Bowling TE,** Price AB, Al-Adnani M. Interchange between collagenous and lymphocytic colitis in severs disease with autoimmune associations requiring colectomy: a case report. *Gut* 1996; **38**: 788-791
18 **Heckerling P,** Urtubey A, Te J. Collagenous colitis and systemic lupus erythematosus. *Ann Intern Med* 1995; **122**: 71-72

19 **Schiller LR.** Diagnosis and management of microscopic colitis syndrome. *J Clin Gastroenterol* 2004; **38**: S27-S30
20 **Bohr J,** Tysk C, Yang P, Danielsson D, Jarnerot G. Autoantibodies and immunoglobulins in collagenous colitis. *Gut* 1996; **39**: 73-76
21 **Zeroogian JM,** Chopra S. Collagenous colitis and Lymphocytic colitis. *Annu Rev Med* 1994; **45**: 105 -118
22 **Tagkalidis P,** Bhathal P, Gibson P. Microscopic colitis. *J Gastroenterol Hepatol* 2002; **17**: 236-248
23 **Pardi DS,** Ramnath VR, Loftus EV, Tremaine WJ, Sandborn WJ. Lymphocytic colitis: clinical features, treatment, and outcomes. *Am J Gastroenterol* 2002; **97**: 2829-2833
24 **Freeman HJ.** Collagenous colitis as the presenting feature of biopsy defined celiac disease. *J Clin Gastroenterol* 2004; **38**: 664-668
25 **Matteoni CA,** Goldblum JR, Wang N, Brzezinski A, Achkar E, Soffer EE. Celiac disease is highly prevalent in lymphocytic colitis. *J Clin Gastroenterol* 2001; **32**: 225-227
26 **Abdulkarim AS,** Burgart LJ, See J, Murray JA. Etiology of nonresponsive celiac disease: results of a systematic approach. *Am J Gastroenterol* 2002; **97**: 2016-2021
27 **Mulder CJ,** Harkema IM, Meijer JW, De Boer NK. Microscopic colitis. *Rom J Gastroenterol* 2004; **13**: 113-117
28 **Beaugerie L,** Luboinski J, Brousse N, Cosnes J, Chatelet FP, Gendre JP, Le Quintrec Y. Drug induced lymphocytic colitis. *Gut* 1994; **35**: 426-428
29 **Beaugerie L,** Patey N, Brousse N. Ranitidine, diarrhoea, and lymphocytic colitis. *Gut* 1995; **37**: 708-711
30 **Jarenot G,** Bohr J, Tysk C, Eriksson S. Faecal stream diversion in patients with collagenous colitis. *Gut* 1996; **38**: 154-155
31 **Stampfl DA,** Friedman LS. Collagenous colitis: pathophysiologic considerations. *Dig Dis Sci* 1991; **36**: 705-711
32 **Baert D,** Coppens M, Burvenich P, De Cock G, Lagae J, Rasquin K, Vanderstraeten E. Chronic diarrhoea in non collagenous microscopic colitis: therapeutic effect of cholestyramine. *Acta Clin Belg* 2004; **59**: 258-262
33 **Marteau P,** Lavergne-Slove A, Lemann M, Bouhnik Y, Bertheau P, Becheur H, Galian A, Rambaud JC. Primary ileal villous atrophy is often associated with microscopic colitis. *Gut* 1997; **41**: 561-564
34 **Bo-Linn GW,** Vendrell DD, Lee E, Fordtran JS. An evaluation of the significance of microscopic colitis in patients with chronic diarrhea. *J Clin Invest* 1985; **75**: 1559-1569
35 **Ernest DL,** Hixon LJ. Collagenous and lymphocytic colitis. In Sleisenger MN, Fordtran JS (Eds): Gastrointestinal disease. 5th ed. WB Saunders Co. *Philadelphia* 1993: 1563-1570
36 **Jesenovac N.** Determination of sodium in fecal fluid. Special methods of biochemical laboratory analysis. Yugoslav society of medical biochemistries. *Karlovac* 1988; **1**: 192-193
37 **Jesenovac N.** Determination of potassium in fecal fluid. Special methods of biochemical laboratory analysis. Yugoslav society of medical biochemistries. *Karlovac* 1988: **1**: 182-183
38 **Jesenovac N.** Determination of chloride in fecal fluid. Special methods of biochemical laboratory analysis. Yugoslav society of medical biochemistries. *Karlovac* 1988: **1**: 257-258
39 **Van de Kamer JH.** Quantitative determination of the saturated and unsaturated higher fatty acids in fecal fat. *Scand J Clin Lab Invest* 1953; **5**: 30-36
40 **Fine KD,** Fordtran JS. The effect of diarrhea on fecal fat excretion. *Gastroenterology* 1992; **102**: 1936-1939
41 **Delgado J,** Delgado B, Fich A, Odes S. Microscopic colitis. *Isr Med Assoc J* 2004; **6**: 482-484
42 **Koskela RM,** Niemela SE, Karttunen TJ, Lehtola JK. Clinical characteristics of collagenous and lymphocytic colitis. *Scand J Gastroenterol* 2004; **39**: 837-845
43 **Fine KD,** Krejs GJ, Fordtran JS. Diarrhea. In Sleisenger MH, Fordtran JS (eds.): Gastrointestinal disease. 5th ed. WB Saunders Co. *Philadelphia* 1993: 1043-1072
44 **Eherer AJ,** Fordtran JS. Fecal osmotic gap and pH in experimental diarrhea of various causes. *Gastroenterology* 1992; **103**: 545-551
45 **Menduina Guillen MJ,** Alaminos Garcia P, Valenzuela Barranco M. Microscopic colitis. A possible diagnosis in secretory diarrhea. *An Med Interna* 2004; **21**: 387-390

Science Editor Guo SY **Language Editor** Elsevier HK

PO Box 2345, Beijing 100023, China
www.wjgnet.com
wjg@wjgnet.com

ELSEVIER

World J Gastroenterol 2005;11(35):5540-5544
World Journal of Gastroenterology ISSN 1007-9327
© 2005 The WJG Press and Elsevier Inc. All rights reserved.

• *BRIEF REPORTS* •

On tolerability and safety of a maintenance treatment with 6-thioguanine in azathioprine or 6-mercaptopurine intolerant IBD patients

Nanne KH de Boer, Luc JJ Derijks, Lennard PL Gilissen, Daniel W Hommes, Leopold GJB Engels, Sybrand Y de Boer, Gijsbertus den Hartog, Piet M Hooymans, Anja BU Mäkelburg, Barend D Westerveld, Anton HJ Naber, Chris JJ Mulder, Dirk J de Jong

Nanne KH de Boer, Chris JJ Mulder, Department of Gastroenterology and Hepatology, VU University Medical Centre, Amsterdam, The Netherlands
Luc JJ Derijks, Department of Clinical Pharmacy, Maxima Medical Centre, Veldhoven, The Netherlands
Lennard PL Gilissen, Department of Gastroenterology and Hepatology, Academic Hospital, Maastricht, The Netherlands
Daniel W Hommes, Department of Gastroenterology and Hepatology, Academic Medical Centre, Amsterdam, The Netherlands
Leopold GJB Engels, Department of Gastroenterology and Hepatology, Maasland Hospital, Sittard, The Netherlands
Sybrand Y de Boer, Gijsbertus den Hartog, Department of Gastroenterology and Hepatology, Rijnstate Hospital, Arnhem, The Netherlands
Piet M Hooymans, Department of Clinical Pharmacy, Maasland Hospital, Sittard, The Netherlands
Anja BU Mäkelburg, Barend D Westerveld, Department of Gastroenterology and Hepatology, Isala Clinics Location Sophia, Zwolle, The Netherlands
Anton HJ Naber, Dirk J de Jong, Department of Gastroenterology and Hepatology, Radboud University Nijmegen Medical Centre, The Netherlands
Correspondence to: Professor Chris JJ Mulder, Department of Gastroenterology and Hepatology, VU University Medical Centre, PO Box 7057, 1007 MB Amsterdam, The Netherlands. cjmulder@vumc.nl
Telephone: +31-20-4440613 Fax: +31-20-4440554
Received: 2005-01-04 Accepted: 2005-02-18

Abstract

AIM: To determine the tolerability and safety profile of a low-dose maintenance therapy with 6-TG in azathioprine (AZA) or 6-mercaptopurine (6-MP) intolerant inflammatory bowel disease (IBD) patients over a treatment period of at least 1 year.

METHODS: Database analysis.

RESULTS: Twenty out of ninety-five (21%) patients discontinued 6-TG (mean dose 24.6 mg; mean 6-TGN level 540 pmol/8×10^8 RBC) within 1 year. Reasons for discontinuation were GI complaints (31%), malaise (15%) and hepatotoxicity (15%). Hematological events occurred in three patients, one discontinued treatment. In the 6-TG-tolerant group, 9% (7/75) could be classified as hepatotoxicity. An abdominal ultrasound was performed in 54% of patients, one patient had splenomegaly.

CONCLUSION: The majority of AZA or 6-MP-intolerant IBD patients (79%) is able to tolerate maintenance treatment with 6-TG (dosages between 0.3 and 0.4 mg/kg per d). 6-TG may still be considered as an escape maintenance immunosuppressant in this difficult to treat group of patients, taking into account potential toxicity and efficacy of other alternatives. The recently reported hepatotoxicity is worrisome and 6-TG should therefore be administered only in prospective trials.

© 2005 The WJG Press and Elsevier Inc. All rights reserved.

Key words: 6-Thioguanine; Azathioprine; 6-Mercaptopurine; Crohn's disease; Ulcerative colitis; Side effects; Tolerance; Safety

de Boer NKH, Derijks LJJ, Gilissen LPL, Hommes DW, Engels LGJB, de Boer SY, den Hartog G, Hooymans PM, Mäkelburg ABU, Westerveld BD, Naber AHJ, Mulder CJJ,de Jong DJ. On tolerability and safety of a maintenance treatment with 6-thioguanine in azathioprine or 6-mercaptopurine intolerant IBD patients. *World J Gastroenterol* 2005; 11 (35): 5540-5544
http://www.wjgnet.com/1007-9327/11/5540.asp

INTRODUCTION

Until now, no definite medical or surgical therapy is available for the treatment of inflammatory bowel disease (IBD) as the etiology remains essentially unknown. Therefore, the aims of medical therapy in IBD are relief of symptoms and to prevent long-term complications. Maintenance therapy should preferably be efficient, safe, and cost-effective. The immune modulating thiopurines 6-mercaptopurine (6-MP) and its pro-drug azathioprine (AZA) have proven efficacy in active IBD and in maintenance of an induced clinical remission[1]. These thiopurines are prescribed on a large scale in IBD and are considered as a mainstay treatment option. However, issues concerning delayed onset of activity, refractoriness, and toxicity have limited the general use of AZA and 6-MP. In previous reports, up to 20% of patients discontinued AZA or 6-MP prematurely due to adverse events[2]. The metabolism of thiopurines has been partly elucidated in recent years (Figure 1). The toxicity profile depends at least partly on the generated metabolites of AZA and 6-MP[3]. At first, AZA is converted to 6-MP by a non-enzymatic reaction, which is then

converted by a multi-step enzymatic pathway into a number of active, inactive, or toxic metabolites. The efficacy of AZA and 6-MP appears to be correlated with the formation of the 6-thioguanine nucleotides (6-TGNs). During this complex metabolization process, possible hepatotoxic metabolites are generated under the influence of the enzyme thiopurine methyltransferase (TPMT). The methylation products of 6-MP, 6-methylmercaptopurine (6-MMP) and their ribonucleotides, may be associated with hepatotoxicity[3]. Furthermore, flu-like symptoms, rashes, pancreatitis, and neutropenia induced by AZA or 6-MP have recently been related to mutations in the inosine triphosphate pyrophosphatase (ITPase) gene leading to accumulation of the proposed metabolite thio inosine triphosphate[4]. A possible strategy to avoid AZA or 6-MP-induced toxicity is the administration of a thiopurine, which is metabolically closer to the 6-TGNs. The thiopurine 6-thioguanine (6-TG) is an attractive candidate, which has the advantage of being directly converted to 6-TGNs[5]. Therefore, treatment and safety outcomes might be less sensitive for intra- and inter-individual metabolic variations. Furthermore, due to the relative simple metabolization, the number of possible toxic metabolites is strongly reduced. Several open label studies in patients with IBD have shown promising efficacy and acceptable short-term toxicity of 6-TG[6,7]. More recently, the use of 6-TG has been associated with the induction of nodular regenerative hyperplasia (NRH) of the liver. The aim of the present study was to determine the tolerability and safety profile of a low-dose maintenance therapy with 6-TG in AZA or 6-MP intolerant IBD patients over a treatment period of at least 1 year.

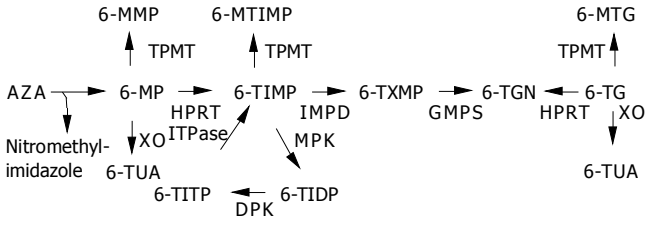


Figure 1 Metabolization process of thiopurines.

AZA is degraded to 6-MP and nitromethyl-imidazole, via a non-enzymatic step. Three competing enzymes metabolize 6-MP. Xanthine oxidase (XO) inactivates 6-MP to 6-thiouric acid (6-TUA). TPMT methylates 6-MP, the formed 6-MMP is associated with hepatotoxicity. By hypoxanthine guanine phosphoribosyl transferase (HPRT), 6-MP is catalyzed to 6-thioinosine monophosphate (6-TIMP), then via inosine monophosphate dehydrogenase to 6-thioxanthosine monophosphate, ultimately leading to the pharmacologically active 6-TGN via the enzyme guanosine monophosphate synthetase. 6-TIMP can also be methylated to 6-methyl-TIMP. In a normal useless cycle, 6-TIMP is phosphorylated by monophosphate kinase to 6-thioinosine diphosphate, subsequently by diphosphate kinase to 6-thioinosine triphosphate (6-TITP) and ultimately back to 6-TIMP due to the ITPase. When ITPase activity is impaired or lacking, 6-TITP accumulates. 6-TG is directly converted by HPRT to 6-TGN. XO and TPMT metabolize 6-TG to 6-methyl-TG and 6-TUA, respectively. ITPase has no known role in the metabolism of 6-TG.

MATERIALS AND METHODS

Patient selection

The study is a retrospective database analysis exploring the tolerability and safety of 6-TG over at least a 1-year treatment period in AZA or 6-MP-intolerant IBD patients, treated in participating university and district hospitals in the Netherlands. In each patient, the attending physician judged the indication for administration of 6-TG. Some patients have been described earlier in a short safety assessment of 6-TG[6]. Patients were eligible for the study, if they met the following in- and exclusion criteria. Inclusion criteria were: age between 18 and 75 years, presence of confirmed CD or UC with an indication for immunosuppressive therapy, but in whom standard AZA or 6-MP therapy failed, due to adverse events. Immunosuppression was indicated in case of chronic active disease, corticosteroid dependency or recurrent disease. Exclusion criteria were pregnancy, lactation, presence of active infection, history of tuberculosis, HIV, hepatitis B or C, history of severe pancreatitis (necrotizing pancreatitis or pancreatitis leading to multi-organ-failure), ongoing treatment with concomitant immunosuppressive drugs (e.g., cyclosporine, methotrexate (MTX), thalidomide or infliximab), impaired renal function (serum creatinine >2 times normal upper limit), impaired hepatic function (>2 times normal upper limit) and persistent bone marrow suppression.

Study design

In all patients, 6-TG (Lanvis®, tablet 40 mg, Glaxo Wellcome) was administered orally in a dose of 20-40 mg once daily based on the decision of the attending physician. The following data were collected: patient demographics, history of thiopurine exposure, type of thiopurine intolerance, the use of concomitant medication, blood cell counts, and liver enzymes were recorded. Dose of 6-TG, duration of 6-TG, occurrence of adverse events, blood cell counts, and liver enzymes were reviewed after a minimum of 12 mo after initiation of 6-TG treatment. During the described period, the genotyping of TPMT became available and in a subgroup of patients the TPMT status was determined. RBC 6-TGN levels were determined at least 4 wk after giving a stable dose in order to obtain steady-state levels of 6-TGN. Dose adjustments were left to the discretion of the attending physician, but when 6-TGN levels were above 1 000-1 500 pmol/8×10^8 RBC, dose reduction was contemplated. In case of a leukocyte count below 3.5×10^9/L, dose reduction was advocated and in case of severe leukopenia (below 1.0×10^9/L) 6-TG had to be discontinued. Additionally, in order to explore signs of hepatotoxicity, an abdominal ultrasonography was advised after at least 1-year 6-TG administration. Special attention was paid to splenomegaly, signs of portal hypertension, and hepatic changes.

Outcome measurements

Primary outcome measures were the ability to tolerate 6-TG and the occurrence of adverse events leading to discontinuation of 6-TG over the 1-year period. The relationship of any adverse event with the use of 6-TG was established by the following method: unrelated, no temporal relation and other etiology likely; possibly related, potential temporal relation and other etiologies possible; probably related, potential temporal relation and other etiologies unlikely; related, clear temporal relation not otherwise explained. Secondary outcome measures were the occurrence of hematological events (defined as leukocyte count $<4.0\times10^9$/L or platelet count $<100\times10^9$/L), the occurrence of hepatotoxicity (defined as a rise of at least two times the upper normal limit of a single liver enzyme level), pancreaticotoxicity (serum amylase >220 U/L) and signs of liver-related abnormalities on the abdominal ultrasound. The following data concerning disease activity were analyzed as well: ESR, C-reactive protein (CRP), serum albumin and a global physician assessment score (features were same, better or worse).

6-TG metabolite monitoring and genotyping of TPMT

Blood samples for 6-TGN measurements were obtained at least 4 wk after the onset of a stable 6-TG dose. The samples were centrifuged to isolate erythrocytes and after washing with PBS, erythrocyte counts were done. Samples were stored at -20 ℃ until required. RBC 6-TGN levels were measured in the laboratory of the Department of Clinical Pharmacy, Maasland Hospital Sittard, using a proprietary modified previously published assay[8]. The lower limit of quantification of the assay was 30 pmol/8×10^8 RBC for 6-TGN levels with a run-to-run coefficient of variation of 6.6%. Extra blood samples were drawn once during the 1-year period to assess TPMT (*G238C, G460A* and *A719G,* i.e., *TPMT*1, TPMT*2, TPMT*3A, TPMT*3B, TPMT*3C*) genotypes in a sub-group of patients, independent of the biochemical or clinical status. The genotyping was performed at the Department of Gastroenterology and Hepatology at the Academic Medical Centre in Amsterdam.

Statistical analysis

Data are expressed as mean±SD. Significance was evaluated by a *t* test for paired or independent data; *P* values of less than 0.05 were considered significant. Pearson's correlation was used to determine relationships between parameters. A χ^2 test was used to determine the significance between the TPMT genotype and 6-TG intolerance. SPSS for Windows version 11.0 was used for statistical analysis.

RESULTS

Patients

In 95 patients, treatment with 6-TG was initiated in the period from June 2001 to July 2003. Fifty-eight patients (61%) were female (mean age: 40 years, range: 20-74 years) and 37 (39%) were male (mean age: 47 years, range: 20-71 years). Forty-two (44%) patients were diagnosed with UC compared to 53 (56%) patients with CD. All patients were intolerant to AZA, 6-MP or both. The adverse events leading to discontinuation of AZA or 6-MP use were gastrointestinal complaints, general malaise, allergic reactions, hepatotoxicity or myelotoxicity. The patient's characteristics are given in detail in Table 1. The mean initial 6-TG dose was 24.6 mg (range 20-40 mg). The mean initial 6-TG dose adjusted to bodyweight was 0.37 mg/kg (SD 0.16 mg/kg).

Table 1 Patients' characteristics

	n = 95 patients
Female:male	58:37 patients
Age (yr)	43 years (range 20–74 yr)
UC:CD	42:53 patients
Duration of IBD at start 6-TG	10.4 yr (SD 9.4 yr)
AZA intolerance	78 patients (82%)
6-MP intolerance	4 patients (4%)
AZA and 6-MP intolerance	13 patients (14%)
AZA or 6-MP rechallenge	36 patients (38%)
Adverse events on AZA or 6MP:	30% gastrointestinal complaints
	20% general malaise
	14% allergic reactions
	10% pancreaticotoxicity
	6% hepatotoxicity
	5% myelotoxicity
	14% rest (e.g., myalgia or alopecia)
6-TG dosage at the start	24.6 mg (range 20-40 mg)

Primary outcome

Seventy-five (79%) of the ninety-five patients were able to tolerate 6-TG during 1-year use. In 20 (21%) patients, the administration was discontinued due to side effects. The 20 intolerant patients (9 females and 11 males) encountered 26 side effects. The data concerning the adverse events leading to withdrawal and the relationship with 6-TG use are summarized in Table 2. No mortality was reported. The mean 6-TG dosage was 0.30 mg/kg in the tolerant group compared to 0.34 mg/kg in the intolerant group (NS).

Table 2 Adverse events (*n* = 26) leading to discontinuation of 6-TG use in 20 patients (AE, adverse event; 6-TG, 6-thioguanine; GI complaints, gastrointestinal complaints)

AE on 6-TG	Frequency (%)	Mean time to AE (d)	Relationship with 6-TG
GI complaints	8/26 (31)	43	Probably 6/8 possibly 2/8
Hepatotoxicity	4/26 (15)	182	Probably 2/4 possibly ¼ unrelated 1/4
Myelodepression	1/26 (4)	50	Related
Pancreaticotoxicity	1/26 (4)	103	Possibly
General malaise	4/26 (15)	51	Probably 3/4 possibly ¼
Allergic reaction	1/26 (4)	1	Related
Other AE	7/26 (27)	39	Related 1/7 probably 2/7 possibly 4/7

Secondary outcomes

Hematological events Three patients had signs of myelosuppression. One patient had a leukocyte count of 3.2×10^9/L and a platelet count of 70×10^9/L after 50 d of 6-TG use (20 mg). Subsequently, 6-TG was discontinued.

The second patient had a leukopenia (leukocytes 3.5×10^9/L) and a third patient had a thrombocytopenia (platelets 87×10^9/L) at 1-year measurements, both did not discontinue 6-TG. All other patients, both tolerant and intolerant to 6-TG, had platelet and leukocyte counts above the set lower limits. However, the mean platelet count decreased significantly from baseline (309×10^9/L) to 1 year of 6-TG treatment (290×10^9/L, $P = 0.033$). The mean leukocyte count decreased as well (from 11.9 to 7.8×10^9/L) though not significantly. The 6-TGN level did not correlate with the decrease in both leukocytes or platelets counts. Hemoglobin levels remained unchanged in both patient groups.

Hepatotoxicity and pancreaticotoxicity In the 6-TG tolerant group the ASAT, ALAT, GGT, and AP levels were determined in 65%, 71%, 60%, and 68% of patients at 1-year 6-TG use, respectively. The mean levels of ASAT, ALAT, GGT, and AF were 24.7 U/L (range 6-118 U/L), 24.5 U/L (range 5-206 U/L), 48 U/L (range 6-535 U/L), and 84 U/L (range 42-322 U/L), respectively. A significant increase in liver enzymes during treatment in the tolerant group was not established. At 1-year use, in 9% of patients (7/75) hepatotoxicity occurrence on 6-TG treatment could be classified. Four patients (4/20) of the intolerant group discontinued 6-TG use due to hepatotoxicity. All had normal liver tests at entry and three of these patients encountered allergic reactions but no hepatotoxicity on the prior AZA therapy. Three patients had a serum amylase level above 220 U/L before the start of 6-TG that all became normal during treatment. One patient developed a transitory symptomatic pancreatitis with a serum amylase level of 430 U/L during 6-TG treatment and discontinued treatment.

Abdominal ultrasonography In 51 patients (54%), an abdominal ultrasonography was performed after at least 1 year 6-TG use. Five ultrasounds (10%) were considered as abnormal; three patients with steatosis, one patient had a choledocholithiasis and the last patient had a hydrops of the gallbladder and a splenomegaly (spleen size 13 cm). The latter two patients were classified as hepatotoxicity on 6-TG treatment.

Disease activity parameters No significant decrease in CRP (15-11 mg/L) or ESR level (15-14 mm) was established in the 6-TG tolerant group. The albumin level increased (37.6-40.1 g/L) significantly in the tolerant group ($P = 0.002$). A significant decrease of albumin level (38.5-36.6 g/L) was established in the intolerant group ($P = 0.03$). The global physician score was determined at 1-year 6-TG use in 85% (64/75) of the tolerant patients. Forty-seven patients (73%) were classified as better, 15 patients (23%) as the same and 4 patients (6%) as worse during 6-TG treatment.

6-TG metabolite monitoring and genotyping of TPMT The mean steady state 6-TGN level, determined in 63% (47/75) of the tolerant patients, was 540 pmol/8×10^8 RBC (SD 245, range 0-1 404). In the eight intolerant patients in whom metabolite levels were measured (40%), the 6-TGN level was 725 pmol/8×10^8 RBC (SD 422, range 229-1 563). The difference in 6-TGN levels between tolerant and intolerant patients was not significant. No statistical significant correlations were established between laboratory parameters (leukocytes, platelets, hemoglobin, AF, GGT, ASAT, and ALAT) and 6-TGN level. The TPMT genotyping was performed in 51 patients (54%). Two patients (3.9%) had one mutant non-functional allele (TPMT*3A and TPMT*3C) and both patients were intolerant for 6-TG (myelodepression and hepatotoxicity) (significant, $P = 0.003$). The 6-TGN level was not determined in both patients. Patients with two mutant non-functional alleles of TPMT (homozygous mutants) were not found in our population.

DISCUSSION

In this group of AZA or 6-MP-intolerant IBD patients, we demonstrated that 6-TG in dosages of 0.3-0.4 mg/kg daily was well tolerated over a period of 1 year as a maintenance immunosuppressant in 79% of the patients. This result suggests that during the metabolization process of AZA or 6-MP metabolites are generated that induce side effects, which at least in part are not generated during the 6-TG metabolism. No mortality was reported due to 6-TG use. When 6-TG was discontinued, the side effects leading to withdrawal resolved spontaneously. One patient developed a myelodepression that may be explained by the impaired TPMT activity, probably shunting 6-TG away from methylation by TPMT toward the formation of 6-TGNs, which have been associated with myelotoxicity. Unfortunately, no 6-TGN level was determined in this patient. The real incidence of 6-TG-related histological liver abnormalities like NRH or veno-occlusive disease (VOD) in the present study remains unknown, as liver biopsies were not performed. The incidence of 6-TG related increase in liver enzymes probably will be lower than 7 out of 75 patients, as 2 patients already had abnormal liver tests before the start of 6-TG and 1 patient had symptomatic choledocholithiasis.

In the present study, we found a mean 6-TGN level of 540 pmol/8×10^8 RBC in the tolerant group, which is above the proposed therapeutic threshold of 250 pmol/8×10^8 RBC and even higher than the proposed upper limit of efficacy (450 pmol/8×10^8 RBC) under AZA or 6-MP therapy[3,9]. This is consistent with previous observations[6,7]. It remains to be elucidated whether the same 6-TGN limits should be used when 6-TG is administered. In our study, 73% clinically benefited from 6-TG by using the global physician score and the mean albumin level increased significantly. However, due to the retrospective nature of the study, we must be reserved in drawing firm conclusions as no standard efficacy parameters as the Crohn's disease activity index or Truelove-Witts index were used. Despite the fact that we have not demonstrated a significant relationship between 6-TGN levels, laboratory results and adverse events, we believe that therapeutic drug monitoring may be a helpful tool in dosing 6-TG. Extremely high 6-TGN levels, which have been associated with an increased risk of developing myelotoxicity, can be prevented and compliance can be monitored.

The TPMT status has been associated with the ability to tolerate AZA or 6-MP. Patients with impaired TPMT activity are more prone to develop a myelodepression[10]. However, our study demonstrates that in AZA or 6-MP-intolerant patients only two patients (3.9%) had one mutant TPMT allele, which is even lower than the incidence in the normal Caucasian population[11]. Interestingly, both patients did not develop a myelodepression on AZA therapy. This

indicates that other metabolic pathways may lead to toxicity of AZA or 6-MP as was recently demonstrated for the ITPase routing (Zelinkova *et al*., submitted for publication). However, both patients with one mutant TPMT allele discontinued the use of 6-TG. Unfortunately, in these patients no 6-TGN concentrations were measured before discontinuation of 6-TG. Possibly, an impaired TPMT activity leads to more 6-TG being metabolized by the enzymes HGPRT or XO leading to higher 6-TGN and 6-TUA levels, respectively (Figure 1). The accumulation of these metabolites may lead to intolerance of 6-TG.

Recently, the use of 6-TG in IBD patients has been associated with the induction of NRH and VOD[12]. In the present study, we performed an abdominal ultrasonography after at least 1-year 6-TG use to screen for possible hepatotoxicity in 51 patients. Only one patient showed signs of portal hypertension indicated by an enlarged spleen. NRH has been associated with thrombocytopenia[16] and in our evaluation only two patients had platelets counts below 100 U/L. We are well aware of the fact that by using biochemistry and ultrasound outcomes, we probably underestimate the real incidence of 6-TG-induced NRH, as the golden standard is based on histology. Additionally, liver tests abnormalities were shown not to be indicative for NRH. Conversely, it should be taken into account that AZA and 6-MP can induce NRH or VOD as well, but performing liver biopsies during treatment with these compounds is not recommended in clinical practice.

Currently, the use of 6-TG in IBD patients is abandoned due to potential hepatotoxicity[12]. However, low-dose 6-TG may still be considered as an escape maintenance strategy in AZA- or 6-MP-intolerant IBD patients whom are refractory for alternative therapies. The number of proven effective medical maintenance options is scarce for these patients. MTX has a reasonable toxicity profile and seems effective in CD, comparable with AZA or 6-MP[13] but the potential use of MTX in UC patients has yet to be proven. In addition, long-term use of MTX may be limited[14]. Cyclosporine seems to have no role as a maintenance immunosuppressive alternative in IBD[15]. Infliximab can be administered as a maintenance option in CD with acceptable toxicity and may be effective in treating UC. However, concomitant immunosuppressive therapy with thiopurines or MTX next to infliximab therapy seems mandatory to reduce the immunogenic response[16].

Treatment with 6-TG is well tolerated in AZA and 6-MP-intolerant IBD patients and seems to be effective. We believe that low-dosed 6-TG (0.3-0.4 mg/kg per d) maintenance therapy may still be an escape option for this difficult to treat group of patients. The benefit of 6-TG use in this sub-group may balance its toxicity profile, especially taking into account the toxicity and efficacy of other therapeutic alternatives. Still, the reported hepatotoxicity is worrisome and 6-TG should therefore be administered only in prospective clinical trials.

REFERENCES

1 **Sandborn WJ.** A review of immune modifier therapy for inflammatory bowel disease: azathioprine, 6-mercaptopurine, cyclosporine, and methotrexate. *Am J Gastroenterol* 1996; **91**: 423-433

2 **Present DH,** Meltzer SJ, Krumholz MP, Wolke A, Korelitz BI. 6-Mercaptopurine in the management of inflammatory bowel disease: short- and long-term toxicity. *Ann Intern Med* 1989; **111**: 641-649

3 **Dubinsky MC,** Lamothe S, Yang HY, Targan SR, Sinnett D, Theoret Y, Seidman EG. Pharmacogenomics and metabolite measurement for 6-mercaptopurine therapy in inflammatory bowel disease. *Gastroenterology* 2000; **118**: 705-713

4 **Marinaki AM,** Ansari A, Duley JA, Arenas M, Sumi S, Lewis CM, Shobowale-Bakre E, Escuredo E, Fairbanks LD, Sanderson JD. Adverse drug reactions to azathioprine therapy are associated with polymorphism in the gene encoding inosine triphosphate pyrophosphatase (ITPase). *Pharmacogenetics* 2004; **14**: 181-187

5 **de Jong D,** Mulder CJ, van Sorge AA. Why measure thiopurine methyltransferase activity? Direct administration of 6-thioguanine might be the alternative for 6-mercaptopurine or azathioprine. *Gut* 2001; **49**: 874

6 **Derijks LJ,** de Jong DJ, Gilissen LP, Engels LG, Hooymans PM, Jansen JB, Mulder CJ. 6-Thioguanine seems promising in azathioprine- or 6-mercaptopurine-intolerant inflammatory bowel disease patients: a short-term safety assessment. *Eur J Gastroenterol Hepatol* 2003; **15**: 63-67

7 **Dubinsky MC,** Feldman EJ, Abreu MT, Targan SR, Vasiliauskas EA. Thioguanine: a potential alternate thiopurine for IBD patients allergic to 6-mercaptopurine or azathioprine. *Am J Gastroenterol* 2003; **98**: 1058-1063

8 **Derijks LJ,** Gilissen LP, Engels LG, Bos LP, Bus PJ, Lohman JJ, Curvers WL, Van Deventer SJ, Hommes DW, Hooymans PM. Pharmacokinetics of 6-mercaptopurine in patients with inflammatory bowel disease: implications for therapy. *Ther Drug Monit* 2004; **26**: 311-318

9 **Cuffari C,** Hunt S, Bayless T. Utilisation of erythrocyte 6-thioguanine metabolite levels to optimise azathioprine therapy in patients with inflammatory bowel disease. *Gut* 2001; **48**: 642-646

10 **Ansari A,** Hassan C, Duley J, Marinaki A, Shobowale-Bakre EM, Seed P, Meenan J, Yim A, Sanderson J. Thiopurine methyltransferase activity and the use of azathioprine in inflammatory bowel disease. *Aliment Pharmacol Ther* 2002; **16**: 1743-1750

11 **Weinshilboum R.** Thiopurine pharmacogenetics: clinical and molecular studies of thiopurine methyltransferase. *Drug Metab Dispos* 2001; **29**: 601-605

12 **Dubinsky MC,** Vasiliauskas EA, Singh H, Abreu MT, Papadakis KA, Tran T, Martin P, Vierling JM, Geller SA, Targan SR, Poordad FF. 6-thioguanine can cause serious liver injury in inflammatory bowel disease patients. *Gastroenterology* 2003; **125**: 298-303

13 **Ardizzone S,** Bollani S, Manzionna G, Imbesi V, Colombo E, Bianchi PG. Comparison between methotrexate and azathioprine in the treatment of chronic active Crohn's disease: a randomised, investigator-blind study. *Dig Liver Dis* 2003; **35**: 619-627

14 **Bell SJ,** Kamm MA. Review article: the clinical role of anti-TNFalpha antibody treatment in Crohn's disease. *Aliment Pharmacol Ther* 2000; **14**: 501-514

15 **Hanauer SB,** Present DH. The state of the art in the management of inflammatory bowel disease. *Rev Gastroenterol Disord* 2003; **3**: 81-92

16 **Rutgeerts P,** Van Assche G, Vermeire S. Optimizing anti-TNF treatment in inflammatory bowel disease. *Gastroenterology* 2004; **126**: 1593-1610

Science Editor Guo SY **Language Editor** Elsevier HK

PO Box 2345, Beijing 100023, China
www.wjgnet.com
wjg@wjgnet.com

ELSEVIER

World J Gastroenterol 2005;11(35):5545-5548
World Journal of Gastroenterology ISSN 1007-9327
© 2005 The WJG Press and Elsevier Inc. All rights reserved.

• *BRIEF REPORTS* •

Evaluation of urine ELISA test for detecting *Helicobacter pylori* infection in Taiwan: A prospective study

Fu-Chen Kuo, Sheng-Wen Wang, I-Chen Wu, Fang-Jung Yu, Yuan-Chieh Yang, Jeng-Yih Wu, Wen-Ming Wang, Deng-Chyang Wu

Fu-Chen Kuo, Department of Gynecology and Obstetrics, E-Da Hospital, I-Shou University, Kaohsiung, Taiwan, China
Sheng-Wen Wang, I-Chen Wu, Fang-Jung Yu, Jeng-Yih Wu, Wen-Ming Wang, Deng-Chyang Wu, Division of Gastroenterology, Department of Internal Medicine, Kaohsiung Medical University Hospital, Taiwan, China
Yuan-Chieh Yang, Department of Clinical Pathology, Kaohsiung Medical University Hospital, Taiwan, China
Supported by the grants from the National Science Council of the Taiwan, No. NSC91-2315-B-037-003
Correspondence to: Dr. Deng-Chyang Wu, Chief of Gastroenterology, Kaohsiung Medical University Hospital, 100 Zih-You 1st Road, Kaohsiung City, 807 Taiwan, China. dechwu@yahoo.com
Telephone: +886-7-3121101-7451 Fax: +886-7-3135612
Received: 2004-12-14 Accepted: 2005-01-05

Abstract

AIM: To evaluate the diagnostic accuracy and clinical utility of a new ELISA (URINELISA) test for detecting *Helicobacter pylori* (*H pylori*) antibody in the urine of Taiwanese population.

METHODS: In this prospective study, 317 consecutive dyspeptic patients (171 men, 146 women; mean age, 51.0 years) were included. They underwent gastroendoscopy for evaluation. Invasive tests, including culture, histology, and rapid urease test (RUT), and non-invasive ^{13}C-urea breath test were preformed. At the same time, urine specimens were collected for URINELISA. The status of *H pylori* infection was considered as positive when either culture was positive, or when two of the other, RUT, histology or 13C-UBT, were positive.

RESULTS: The sensitivity, specificity, positive predictive value, and negative predictive value of URINELISA are 91.7% (211/230), 90.8% (79/87), 96.3% (211/219), and 80.6% (79/98) respectively.

CONCLUSION: This URINELISA test is reliable, inexpensive and easy-to-use. The high diagnostic accuracy warrants the use of URINELISA as a first-line screening tool for diagnosis of *H pylori* infection in untreated patients.

© 2005 The WJG Press and Elsevier Inc. All rights reserved.

Key words: *H pylori*; URINELISA

Kuo FC, Wang SW, Wu IC, Yu FJ, Yang YC, Wu JY, Wang WM, Wu DC. Evaluation of urine ELISA test for detecting *Helicobacter pylori* infection in Taiwan: A prospective study. *World J Gastroenterol* 2005; 11(35): 5545-5548
http://www.wjgnet.com/1007-9327/11/5545.asp

INTRODUCTION

Since the discovery of *Helicobacter pylori* (*H pylori*) by Marshall and Warren in 1983[1], overwhelming evidence has confirmed that *H pylori* infection plays a significant role in the development of chronic active gastritis, peptic ulcer, and gastric adenocarcinoma[2]. *H pylori* infection is very common throughout the world, occurring in 40-50% of the population in developed countries, 80-90% of the population in developing regions[3], and about 54.4% of the population in Taiwan[4].

A large number of methods have been developed to diagnose *H pylori* infection, including invasive and non-invasive tests. The former requires endoscopy exam for gastric mucosal biopsy. Because of the patchy nature of the infection, biopsy-based tests may suffer sampling errors[5]. There is an increasing interest in non-invasive tests, as they are not influenced by sampling error and can profitably replace endoscopy making the diagnosis and determining the management of some types of patients[6]. The urea breath test (UBT) is based on the carbon dioxide labeled with carbon-13 or carbon-14 in expired air to detect *H pylori* urease activity[7]. Serological tests are based on the detection of a specific anti-*H pylori* immunological response, mostly by IgG antibodies in patient's serum. Same as serum antibody testing, an enzyme immunoassay method (URINELISA test, Otsuka Pharmaceutical Co., Ltd, Japan) for detecting *H pylori* antibody in the urine has been marketed in Japan, but at present, data on its clinical utility are limited[8,9]. It is possible that different genetic background of patients and *H pylori* strains could induce different antigen-antibody responses that would affect the results of URINELISA[10-14]. The aim of this study is to evaluate the usefulness of this new test in detecting *H pylori* antibody in the urine as a predictor of *H pylori* status in pretreatment settings in Taiwan.

MATERIALS AND METHODS

Patient selection and exclusion criteria

Three hundred and seventeen dyspeptic patients (171 men and 146 women; mean age, 51.0 years; range, 16-81 years) were recruited for this study. Exclusion criteria were as follows: antibiotic, bismuth salts, proton pump inhibitor therapy 2 mo before recruitment, previous anti-*H pylori*

treatment, chronic use of corticosteroids or immunosuppressant drugs, prior gastric surgery, presence of a bleeding peptic ulcer, severe concomitant disease, pregnancy, and lactation. Informed consent was obtained from each patient, and the study was performed in accordance with the Declaration of Helsinki.

Study design

All patients underwent gastroendoscopic examination, and gastric mucosal biopsies were performed. Non-invasive tests including URINELISA and ^{13}C-urea breath test (^{13}C-UBT) were also carried out. *H pylori* infection status was considered positive, when either culture was positive or when two of the following three tests, histology, rapid urease test (RUT), and ^{13}C-UBT, were positive. Urine samples were collected on the same day after endoscopic examination. The endoscopic biopsy protocol is shown in detail as follows: two specimens from the antrum and body for culture, five specimens from the angle and both greater and lesser curvatures of the antrum and body for histology and four specimens, excluding angle, for RUT.

Diagnostic tests for H pylori infection

Histology One set of specimens was fixed with formalin and embedded in paraffin. Sections were then stained with hematoxylin and eosin (H&E).

Rapid urease test CLO-test (Delta West, Bentley, Australia) was selected for determination of the presence of urease in the biopsied gastric mucosa. The results of the CLO-test were interpreted as positive if the color of the gel changed from yellow to pink or red within 6 h at room temperature.

Culture Culture of *H pylori* was made by rubbing the specimen on the surface of a Campy-BAP agar plate [Brucella agar (Difco)+IsoVitalex (Gibco)+10% whole sheep blood], and then incubating it at 35 ℃ under microaerobic conditions (5% O_2, 100 mL/L CO_2, and 85% N_2) for 4-5 d. The *H pylori* culture was considered positive if one or more colonies of gram-negative, oxidase (+), catalase (+), and urease (+) spiral or curved rods were present.

^{13}C-urea breath test (^{13}C-UBT) The ^{13}C-urea was 100 mg 99% ^{13}C-labeled urea produced by the Institute of Nuclear Energy Research (INER), Taiwan, and 100 mL of fresh milk was used as the test meal. This procedure has been modified since our previous study[15]. Patients were asked to fast at least 6 h beforehand, then a baseline sample was collected in duplicate by exhaling through a straw into a vacuum container tube 5 min after consuming the test meal. Five minutes later, the patients drank the urea solution prepared by dissolving 100 mg ^{13}C-urea in 50 mL of sterile water. Immediately after ^{13}C-urea consumption, subjects were asked to gargle rinsing the mouth to avoid detecting oral urease activity. The patient then rested on their sides for 15 min, changing sides every 5 min. Fifteen minutes after ^{13}C-urea was ingested, a breathing sample was collected in duplicate as the method of collecting baseline samples. All samples were sent to INER, where a continuous-flow isotope ratio mass spectrometer (CF-IRMS, Europa Scientific Ltd, Crewe, UK) was used for analysis. Based on findings from our previous study, the cut-off value was 4.2/mL at 15 min after ingesting ^{13}C -urea.

URINELISA *H pylori* antibody test All patients were asked to deliver a fresh urine specimen on the day of endoscopy. Urine samples were stored at 4 ℃ before analysis. Urinary antibodies to *H pylori* were determined by URINELISA *H pylori* antibody test (Otsuka Pharmaceutical Co., Ltd, Japan). This kit is an enzyme-linked immunosorbent assay (ELISA) kit using a 96-well microplate, and, as a solid phase of an antigen, a protein extracted from an *H pylori* strain isolated from a Japanese patient with gastritis is used. The assay procedure was performed according to the manufacturer's recommendations. To each well of the solid-phase microplate, 25 μL each of a buffer solution and 100 μL each of the urine specimen, the negative controls or positive controls were added in turn. After a reaction at 37 ℃ for 1 h, the plate was washed. One hundred microliters of an enzyme-labeled antibody solution was added to each of the wells subjected to the reaction at 37 ℃ for 1 h, and then washed. One hundred microliters of a substrate solution was then added. After the reaction was conducted for 15 min, 100 μL of a reaction stopping solution was added to each well. Absorbance was determined at a wavelength of 450 nm by an ELISA reader. Two positive controls and three negative controls were measured simultaneously. The cut-off value for urine-based ELISA was determined as the value calculated by the following formula: (mean absorbance of two positive controls)/8.5+ (mean absorbance of three negative controls). The equation employed was based on the results of numerous clinical studies[16]. Absorbance below the cut-off value was assessed as negative, and absorbance greater than the cut-off value was assessed as positive.

RESULTS

Of 317 patients, 230 (72.6%) were *H pylori*-infected and 87 (27.4%) were uninfected. Of the infected patients, 75 (23.7%) had non-ulcer dyspepsia, 224 (70.7%) had duodenal and gastric ulcers, and 18 (5.7%) had gastric adenocarcinoma. URINELISA was positive in 219 cases (8 of which were false positives) and negative in 98 (19 of which were false negatives). A summary of the diagnostic efficacy of individual tests is shown in Table 1. The urine test showed

Table 1 Summary of diagnostic efficacy of all tests used in this study

	URINELISA(%)	^{13}C-UBT (%)	RUT (%)	Culture (%)	Histology (%)
Sensitivity	91.7 (88.7–94.8)	96.7 (94.7–98.7)	94.4 (91.9–96.9)	55.6 (50.1–61.1)	86.7 (83–90.4)
Specificity	90.8 (87.6–94.0)	95.2 (92.8–97.6)	95.2 (92.8–97.6)	100 (100)	79.7 (75.3–84.1)
PPV	96.4 (94.3–98.5)	96.7 (94.7–98.7)	96.6 (94.6–98.6)	100 (100)	85.6 (81.7–89.5)
NPV	80.6 (76.2–85.0)	95.2 (92.8–97.6)	92.3 (89.4–95.2)	61.2 (55.8–66.6)	80.6 (76.2–85)

Results are expressed by percentages, with a 95%CI.

sensitivity of 91.7%, specificity of 80.8%, positive predictive value of 96.4% and negative predictive value of 80.6%. That is, the diagnostic efficacy of URINELISA was similar to ^{13}C-UBT and RUT.

DISCUSSION

Since the early 1980s, when *H pylori* was first discovered, significant progress has been made in identifying this infection, especially with respect to non-invasive techniques. The UBT, first described by Graham *et al*., in 1987[17], is presently considered as the most effective non-invasive test for *H pylori*[18]. Based on the direct identification of a bacterial enzyme activity (urease), the UBT detects an active, ongoing infection and is highly accurate even shortly after therapy[19]. However, the availability of ^{14}C-UBT is limited by the strict regulations governing the use, handling, and storage of radioactive isotopes, which in practice precludes use outside hospitals and the testing of children and women of childbearing age. ^{13}C on the other hand is a safe isotope that can be used for breath testing, but it is expensive ($ 250-350) when compared with other non-invasive tests ($ 20-100)[20], and does require the use of a CF-IRMS, thereby limiting widespread applicability. Furthermore, UBT for detection of *H pylori* is less effective in patients who have had a prior gastrectomy[21] and in those with severe atrophic gastritis[22]. In addition, equivocal or false-negative UBT results often occur in patients taking acid-suppression therapy[23-26]. Moreover, in most of the approved UBT protocols, demands are made on patients' time and cooperation (i.e., fasting before the test, the necessity of an office/laboratory visit, consumption of a test meal, and collection of a second breath sample after a time lag). Therefore, it is not easy to perform a UBT test on patients who cannot cooperate, such as children, psychological patients and unconscious patients.

Serology has clear advantages over breath tests, both in terms of cost and in being a non-invasive screening strategy, and it is the most important tool for epidemiological studies[27]. However, old-fashioned serological tests have suffered from cross-reactivity with *Campylobacter* species[28], resulting in a high rate of false positives. The reported sensitivity of serological tests is approximately 98-100%, but specificity varies from 26% to 96.4%[29]. Results of these assays may be due to the reference method used to confirm *H pylori* status, the source of the antigen on which the assay is based, and the reference population studies[29]. Furthermore, the specificity of most serologic tests decreases by approximately 10%, when sera from subjects more than 45 years are examined[30].

Recently, urine-based antibody tests have been developed for the screening of infectious diseases, including *H pylori*[31]. The benefits of using urine as the specimen are as follows: (1) Urine can be obtained easily, and its collection requires little skill. (2) Urine does not require centrifugation. (3) The cost of using urine as a sample is much lower than that of serum. (4) Urine tests can be simply formatted for use in doctors' offices or even for home testing. (5) Using urine provides a simpler alternative sample for epidemiological and screening studies. Laboratory-based urine testing using ELISA technology to detect IgG antibody is inexpensive (under $ 20), non-invasive, and well suited to primary care practice. Urine-based testing also combines the advantages of simplicity, cost-effectiveness and applicability under circumstances in which serological testing is largely impracticable. It has been reported that antibodies in urine are stable for 55 days at room temperature, and for one year at 2-8 ℃[32]. Katsuragi *et al*.[8], also confirmed that *H pylori* antibodies in urine were viable for at least 60 d at 4 ℃ and 25 ℃, and for at least 3 d at 37 ℃ and 45 ℃. In contrast, stool samples must be kept at 4 ℃ within 12 h after defecation, or diagnostic efficacy decreases.

Two studies have been performed in different populations with similar diagnostic efficacy with our results reported[33,34]. These studies show that URINELISA has a high degree of consistency in detecting *H pylori* infection in both Asian and European populations. Therefore, URINELISA is suitable for mass screening of *H pylori* infection. Such consistency has not been observed in stool antigen tests. In our own experience[35], and based on other reports made of an Asian population[34,36], the diagnostic efficacy of Premier Platinum HpSA® has been less consistent in an Asian population. However, there is a new stool antigen test, ImmunoCard HpSA STAT®, which seems to have higher diagnostic accuracy in Asian population[38]. In conclusion, URINELISA test is reliable, inexpensive and easy-to-use, and its high degree of diagnostic accuracy warrants its use as a first-line screening tool for the diagnosis of *H pylori* infection in untreated patients.

REFERENCES

1 Unidentified curved bacilli on gastric epithelium in active chronic gastritis. *Lancet* 1983; **1**: 1273-1275
2 International Agency for Research on Cancer WHO. Infection with *Helicobacter pylori*. In: Schistosomes, liver flukes and *Helicobacter pylori*. *Lyon: IARC* 1994: 177-202
3 **Vaira D,** Miglioli M, Mule P, Holton J, Menegatti M, Vergura M, Biasco G, Conte R, Logan RP, Barbara L. Prevalence of peptic ulcer in *Helicobacter pylori* positive blood donors. *Gut* 1994; **35**: 309-312
4 **Lin JT,** Wang JT, Wang TH, Wu MS, Lee TK, Chen CJ. *Helicobacter pylori* infection in a randomly selected population, healthy volunteers, and patients with gastric ulcer and gastric adenocarcinoma. A seroprevalence study in Taiwan. *Scand J Gastroenterol* 1993; **28**: 1067-1072
5 **van Zwet AA,** Thijs JC, Roosendaal R, Kuipers EJ, Pena S, de Graaff J. Practical diagnosis of *Helicobacter pylori* infection. *Eur J Gastroenterol Hepatol* 1996; **8**: 501-507
6 Current European concepts in the management of *Helicobacter pylori* infection. The Maastricht Consensus Report. European *Helicobacter pylori* Study Group. *Gut* 1997; **41**: 8-13
7 **Logan RPH.** The 13C urea breath test: In Lee A, Megraud F, and Eds. *Helicobacter pylori*: technique for clinical diagnosis and basic research. *WB Saunders* 1996: 74-81
8 **Katsuragi K,** Noda A, Tachikawa T, Azuma A, Mukai F, Murakami K, Fujioka T, Kato M, Asaka M. Highly sensitive urine-based enzyme-linked immunosorbent assay for detection of antibody to *Helicobacter pylori*. *Helicobacter* 1998; **3**: 289-295
9 **Miwa H,** Hirose M, Kikuchi S, Terai T, Iwazaki R, Kobayashi O, Takei Y, Ogihara T, Sato N. How useful is the detection kit for antibody to *Helicobacter pylori* in urine (URINELISA) in clinical practice? *Am J Gastroenterol* 1999; **94**: 3460-3463
10 **Yang JC,** Wang TH, Wang HJ, Kuo CH, Wang JT, Wang WC. Genetic analysis of the cytotoxin-associated gene and the

vacuolating toxin gene in *Helicobacter pylori* strains isolated from Taiwanese patients. *Am J Gastroenterol* 1997; **92**: 1316-1321

11 **Shyu RY,** Jiang SY, Lai CH, Hsu CT, Young TH, Yeh MY. High frequency of cytotoxin-associated gene A in *Helicobacter pylori* isolated from asymptomatic subjects and peptic ulcer patients in Taiwan. *J Clin Gastroenterol* 1998; **27**: 54-59

12 **Maeda S,** Ogura K, Yoshida H, Kanai F, Ikenoue T, Kato N, Shiratori Y, Omata M. Major virulence factors, VacA and CagA, are commonly positive in *Helicobacter pylori* isolates in Japan. *Gut* 1998; **42**: 338-343

13 **Miwa H,** Kikuchi S, Ohtaka K, Kobayashi O, Ogihara A, Hojo M, Nagahara A, Sato N. Insufficient diagnostic accuracy of imported serological kits for *Helicobacter pylori* infection in Japanese population. *Diagn Microbiol Infect Dis* 2000; **36**: 95-99

14 **Leung WK,** Ng EK, Chan FK, Chung SC, Sung JJ. Evaluation of three commercial enzyme-linked immunosorbent assay kits for diagnosis of *Helicobacter pylori* in Chinese patients. *Diagn Microbiol Infect Dis* 1999; **34**: 13-17

15 **Wang WM,** Lee SC, Ding HJ, Jan CM, Chen LT, Wu DC, Liu CS, Peng CF, Chen YW, Huang YF, Chen CY. Quantification of *Helicobacter pylori* infection: Simple and rapid 13C-urea breath test in Taiwan. *J Gastroenterol* 1998; **33**: 330-335

16 **Kato M,** Asaka M, Saito M, Sekine H, Ohara S, Toyota T, Akamatsu T, Kaneko T, Kiyosawa K, Nishizawa O, Kumagai T, Katsuyama T, Abe M, Kosaka M, Hariya S, Minami K, Sanai Y, Sawamura M, Tachikawa T. Clinical usefulness of urine-based enzyme-linked immunosorbent assay for detection of antibody to *Helicobacter pylori*: a collaborative study in nine medical institutions in Japan. *Helicobacter* 2000; **5**: 109-119

17 **Graham DY,** Klein PD, Evans DJ, Evans DG, Alpert LC, Opekun AR, Boutton TW. Campylobacter pylori detected noninvasively by the 13C-urea breath test. *Lancet* 1987; **1**: 1174-1177

18 **Atherton JC,** Spiller RC. The urea breath test for *Helicobacter pylori*. *Gut* 1994; **35**: 723-725

19 **Vaira D,** Malfertheiner P, Megraud F, Axon AT, Deltenre M, Gasbarrini G, O'Morain C, Pajares Garcia JM, Quina M, Tytgat GN. Noninvasive antigen-based assay for assessing *Helicobacter pylori* eradication: a European multicenter study. The European *Helicobacter pylori* HpSA Study Group. *Am J Gastroenterol* 2000; **95**: 925-929

20 **Smoot DT,** Cutler AF. *Helicobacter pylori*. Diagnostic tests. Gastroenterology and Endoscopy News. *McMahon Publishing Group, New York* 1997; **48**: 28

21 **Chen X,** Haruma K, Kamada T, Mihara M, Komoto K, Yoshihara M, Sumii K, Kajiyama G. Factors that affect results of the 13C urea breath test in Japanese patients. *Helicobacter* 2000; **5**: 98-103

22 **Logan RP,** Walker MM, Misiewicz JJ, Gummett PA, Karim QN, Baron JH. Changes in the intragastric distribution of *Helicobacter pylori* during treatment with omeprazole. *Gut* 1995; **36**: 12-16

23 **Graham DY,** Genta R, Evans DG, Reddy R, Clarridge JE, Olson CA, Edmonds AL, Siepman N. *Helicobacter pylori* does not migrate from the antrum to the corpus in response to omeprazole. *Am J Gastroenterol* 1996; **91**: 2120-2124

24 **Chey WD,** Spybrook M, Carpenter S, Nostrant TT, Elta GH, Scheiman JM. Prolonged effect of omeprazole on the 14C-urea breath test. *Am J Gastroenterol* 1996; **91**: 89-92

25 **Chey WD,** Woods M, Scheiman JM, Nostrant TT, DelValle J. Lansoprazole and ranitidine affect the accuracy of the 14C-urea breath test by a pH-dependent mechanism. *Am J Gastroenterol* 1997; **92**: 446-450

26 **Feldman RA,** Evans SJ. Accuracy of diagnostic methods used for epidemiological studies of *Helicobacter pylori*. *Aliment Pharmacol Ther* 1995; **9**(Suppl 2): 21-31

27 **Yamamoto I,** Fukuda Y, Mizuta T, Fukada M, Nishigami T, Shimoyama T. Serum anti-*Helicobacter pylori* antibodies and gastritis. *J Clin Gastroenterol* 1995; **21**(Suppl 1): S164-168

28 **Marchildon PA,** Ciota LM, Zamaniyan FZ, Peacock JS, Graham DY. Evaluation of three commercial enzyme immunoassays compared with the 13C urea breath test for detection of *Helicobacter pylori* infection. *J Clin Microbiol* 1996; **34**: 1147-1152

29 **Schembri MA,** Lin SK, Lambert JR. Comparison of commercial diagnostic tests for *Helicobacter pylori* antibodies. *J Clin Microbiol* 1993; **31**: 2621-2624

30 **Alemohammad MM,** Foley TJ, Cohen H. Detection of immunoglobulin G antibodies to *Helicobacter pylori* in urine by an enzyme immunoassay method. *J Clin Microbiol* 1993; **31**: 2174-2177

31 **Kostolansky F,** Li JJ, Friedman-Kien AE. Detection of false antibodies to HIV-1 in urine. *Aids* 1993; **7**: 1531-1532

32 **Bravo LE,** Realpe JL, Campo C, Mera R, Correa P. Effects of acid suppression and bismuth medications on the performance of diagnostic tests for *Helicobacter pylori* infection. *Am J Gastroenterol* 1999; **94**: 2380-2383

33 **Leodolter A,** Vaira D, Bazzoli F, Schutze K, Hirschl A, Megraud F, Malfertheiner P. European multicentre validation trial of two new non-invasive tests for the detection of *Helicobacter pylori* antibodies: urine-based ELISA and rapid urine test. *Aliment Pharmacol Ther* 2003; **18**: 927-931

34 **Adachi K,** Kawamura A, Ono M, Masuzaki K, Takashima T, Yuki M, Fujishiro H, Ishihara S, Kinoshita Y. Comparative evaluation of urine-based and other minimally invasive methods for the diagnosis of *Helicobacter pylori* infection. *J Gastroenterol* 2002; **37**: 703-708

35 **Yu FJ,** Wu DC, Kuo CH, Lu CY, Su YC, Lee YC, Lin SR, Liu CS, Jan CM, Wang WM. Diagnosis of *Helicobacter pylori* infection by stool antigen test in southern Taiwan. *Kaohsiung J Med Sci* 2001; **17**: 344-350

36 **Wong BC,** Xia HH, Cheung HK, Ng FH, Wong SY, Chow KC, Lin SK, Yin Y, Wong WM, Yuen MF, Lam SK. Evaluation of two stool antigen tests for the detection of *Helicobacter pylori* infection in the Chinese population. *J Gastroenterol Hepatol* 2003; **18**: 26-31

37 **Wu IC,** Ke HL, Lo YC, Yang YC, Chuang CH, Yu FJ, Lee YC, Jan CM, Wang WM, Wu DC. Evaluation of a newly developed office-based stool test for detecting *Helicobacter pylori*: an extensive pilot study. *Hepatogastroenterology* 2003; **50**: 1761-1765

38 **Li YH,** Guo H, Zhang PB, Zhao XY, Da SP. Clinical value of *Helicobacter pylori* stool antigen test, ImmunoCard STAT HpSA, for detecting *H pylori* infection. *World J Gastroenterol* 2004; **10**: 913-914

Science Editor Guo SY **Language Editor** Elsevier HK

PO Box 2345, Beijing 100023, China
www.wjgnet.com
wjg@wjgnet.com

ELSEVIER

World J Gastroenterol 2005;11(35):5549-5552
World Journal of Gastroenterology ISSN 1007-9327
© 2005 The WJG Press and Elsevier Inc. All rights reserved.

• *BRIEF REPORTS* •

Effects of soy components on blood and liver lipids in rats fed high-cholesterol diets

Ching-Yi Lin, Cheng-Yu Tsai, Shyh-Hsiang Lin

Ching-Yi Lin, Cheng-Yu Tsai, Shyh-Hsiang Lin, Graduate Institute of Nutrition and Health Sciences, Taipei Medical University, (110) 250 Wu-Hsing Street, Taipei, Taiwan, China
Correspondence to: Shyh-Hsiang Lin, Graduate Institute of Nutrition and Health Sciences, Taipei Medical University, (110) 250 Wu-Hsing Street, Taipei, Taiwan, China. lin5611@tmu.edu.tw
Telephone: +886-2-27361661-6551-126 Fax: +886-2-27373112
Received: 2004-12-10 Accepted: 2005-03-21

Abstract

AIM: To assess the effects of soy protein, isoflavone, and saponin on liver and blood lipid in rats that consumed high-cholesterol diets.

METHODS: High-cholesterol diets (1%) with or without soy material were fed to 6-wk-old male Sprague-Dawley rats for 8 wk. Blood lipids, liver lipids, glutamic oxaloacetic transaminase (GOT), and glutamic pyruvic transaminase (GPT) levels were measured. The *in vitro* bile acid-binding ability of soy materials was analyzed.

RESULTS: The results of *in vitro* studies showed that soy protein isolate had a significantly higher bile acid-binding ability (8.4±0.8%) than soy saponin (3.1±0.7%) and isoflavone (1.3±0.4%, $P<0.05$). On the other hand, at the end of the experimental period, rats that consumed soy protein diets had lower GOT and GPT levels than rats that consumed casein under high-cholesterol diets. Rats that consumed soy protein also had lower total cholesterol (TC) levels in the liver than those that consumed casein under high-cholesterol diets. Rats that consumed the soy protein diet containing both saponin and isoflavone had lower hepatic TC level than those that consumed the soy protein diet without isoflavone alone. The effect of different types of proteins on triglyceride was not significant.

CONCLUSION: Consumption of soy provided benefits to control lipid levels under high-cholesterol dieting conditions in this rat model of hypercholesterolemia. The major component that reduced hepatic TC was not saponin, but possibly isoflavone.

© 2005 The WJG Press and Elsevier Inc. All rights reserved.

Key words: Soy; Isoflavone; Saponin; Triglyceride; Cholesterol

Lin CY, Tsai CY, Lin SH. Effects of soy components on blood and liver lipids in rats fed high-cholesterol diets. *World J Gastroenterol* 2005; 11(35): 5549-5552
http://www.wjgnet.com/1007-9327/11/5549.asp

INTRODUCTION

Soybeans contain many ingredients that are considered to have health benefits. Among them, soy protein, soy saponin, and isoflavone are most commonly noted. All of them consist of aglycones and glycosides. Soy protein has been shown to have a cholesterol-lowering ability because some ingredients in soy protein bind with cholesterol so that the complex is absorbed[1]. Wang and Ng[2] also demonstrated that the alcohol-extractable materials in soy protein were effective in lowering cholesterol. Previous studies showed that soy protein loses its cholesterol-lowering effect if it is extracted with alcohol[3-5]. Saponin and isoflavone are alcohol-soluble components in soy beans. Unlike isoflavone, soy saponin is amphiphilic. Recent studies suggest that soy saponin is effective in lowering cholesterol[6] and inhibiting tumor because it binds with cholesterol[1,7]. Venter[8] indicated that soy protein decreases LDL cholesterol in people with elevated serum cholesterol[9]. The objective of this study was to identify the effect of individual components of the alcohol-soluble portion of soy protein on bile acid binding and lipid oxidation in order to delineate their potential role in the health benefits from soy consumption.

MATERIALS AND METHODS

Extraction of saponin

Soybeans were ground up in a blender for 2 min. The isoflavone/saponin mixture was then extracted from soy powder (1:20, soy powder:methanol) with 80% methanol at 40 ℃ for 2 h. After the methanol solution had been removed in a rotary evaporator, a certain amount of distilled water (e.g., 5 g of soy powder as starting material would need 10 mL of distilled water) was added to separate saponin from isoflavone. A quick test for saponin was performed by shaking the liquid sample for 1 min. Foaming for 10 min indicated a positive result of saponin. Saponin samples were analyzed for isoflavone residues with HPLC before further application. Commercial saponin was also purchased from Wako (Japan) for use as the HPLC standard.

In vitro bile acid binding of saponin

Ten grams of soy saponin was mixed with 5 mL of bile salt (10^{-4} mol)-containing buffer solution (0.1 mol/L of Tris-HCl and 0.1 mol/L NaN_3) at pH 4.0 and 37 ℃ for 2 h, followed

by dialysis (Spectra/POR, MW cut-off 6 000-8 000, Spectrum Medical, Los Angeles, CA, USA) for 4 d. The content of the bile salt was determined by enzymatic analysis as previously described[10].

Animals

Thirty-two 6-wk-old male Sprague-Dawley rats (Animal Center, National Scientific Council, Taipei, Taiwan) were randomly assigned to five groups according to the isoflavone and saponin contents in their diets: (1) soy protein (with isoflavone and saponin)+1% cholesterol (SP); (2) alcohol-washed soy protein (no isoflavone or saponin)+1% cholesterol (ASP); (3) alcohol-washed soy protein+soy saponin+1% cholesterol (SS); (4) casein+1% cholesterol (PC); and (5) casein (negative control, NC). The composition of each diet is shown in Table 1. Guidelines for the ethical care and treatment of animals from the Animal Care Committee at Taipei Medical University were strictly followed. Rats were individually housed and maintained in a temperature-controlled (23±2 ℃) room with a 12-h light/dark cycle. They were fed a chow diet for 1 wk before switching to the experimental diets. Five rats were randomly chosen and killed after completing the 1 wk of chow diet to acquire the baseline total cholesterol (TC) and triglyceride (TG) values of the liver. Water and food were available *ad libitum*. Two milliliters of blood samples were collected from the tail vein during wk 2, 4, and 6 after the start of the experimental diets. After wk 8, all rats were killed, and liver and blood samples were collected.

Table 1 Composition of the experimental diets

	NC[3]	CC	SP	ASP	SS
Corn starch	588	588	588	588	588
Dextrin	191.1	191.1	191.1	191.1	191.1
Casein	294	294	0	0	0
Soy protein[1]	0	0	294	0	0
Soy protein[2]	0	0	0	294	294
Sucrose	147	73.5	73.5	73.5	66.15
Saponin	0	0	0	0	7.35
Soybean oil	88.2	147	147	147	147
Mineral mix	58.8	58.8	58.8	58.8	58.8
Cellulose	73.5	73.5	73.5	73.5	73.5
Vitamins	14.7	14.7	14.7	14.7	14.7
Cholesterol	0	14.7	14.7	14.7	14.7
Methionine	14.7	14.7	14.7	14.7	14.7
Choline	0	0.735	0.735	0.735	0.735
Cholic acid	0	0.735	0.735	0.735	0.735

[1]Soy protein with isoflavone and saponin; [2]Alcohol-extracted soy protein; [3]NC, negative control (casein); PC, positive control (casein+1% cholesterol); SP, soy protein diet; ASP, alcohol-extracted soy protein diet; SS, soy saponin diet.

Blood lipid and liver function analyses

TC, TG, glutamic oxaloacetic transaminase (GOT), and glutamic pyruvic transaminase (GPT) were measured with commercial kits (Randox).

Statistical analysis

Data are presented as the mean±SD. One- and two-way ANOVA were performed using SAS® 8.1 software. Least significant difference test was performed to determine within-group differences.

RESULTS

Bile acid binding

The percentages of bile acid binding were as follows: soy saponin, 3.1±0.7%; soy isoflavone aglycones, 1.3±0.4%; and soy protein isolate, 8.4±0.8%. The differences in bile acid-binding percentages between each group were all significant ($P<0.05$).

In vivo studies

Table 2 shows the body weight changes of rats in each group during the feeding period. None of the mean body weights differed significantly among the groups. The effects of different diets on serum GOT, GPT, TG, and TC are shown in Table 3. In wk 0, the GOT and TC in five groups did not differ from each other. The GPT in the NC group was a bit, but significantly higher than that in the ASP group ($P<0.05$). The TG in the PC group was significantly higher (though the differences were not very big) than those in the ASP and SS groups ($P<0.05$). In wk 2, the GPT and TG levels did not differ among all groups, while the TC level in the SS group and the GOT level in the PC group were the highest ($P<0.05$). In wk 4, the PC group had higher GOT and GPT levels than the other groups ($P<0.05$), but the TC and TG levels still did not significantly differ among all groups. In wk 6, the PC group had higher GOT, GPT, and TG levels than the ASP, AS, and NC groups ($P<0.05$). The SS and NC groups also had higher TG levels than the SP and ASP groups ($P<0.05$). In wk 8, the PC group still had higher GPT levels than the other groups ($P<0.05$). The SS group had a lower TG level than the SP, NC, PC ($P<0.05$), and ASP ($P>0.05$) groups. The groups fed 1%-cholesterol diets had higher TC values than the NC group ($P<0.05$). Generally speaking, dietary consumption of soy protein either with or without alcohol extraction resulted in lower GOT and GPT levels than casein and showed a tendency to lower serum TG levels.

Table 2 Body weight (g) changes of rats during the experiment (all $n = 9$)

	Wk 1	Wk 2	Wk 4	Wk 6	Wk 8
NC[1]	349±23	376±37	421±51	455±59	482±59
PC	357±18	392±19	444±32	488±33	521±33
SP	352±26	376±36	426±35	471±39	494±41
ASP	358±23	396±27	449±40	491±44	522±49
SS	364±12	399±20	448±29	489±24	518±22

[1]NC, negative control (casein); PC, positive control (casein+1% cholesterol); SP, soy protein; ASP, alcohol-extracted soy protein; SS, alcohol-extracted soy protein plus saponin.

The changes in GOT, GPT, TG, and TC during the experiment are also presented in Table 3. In the NC group (regular AIN76), GOT, GPT, and TC levels did not significantly change throughout the experiment. By contrast, the TG level gradually increased from wk 2 to 6

Table 3 Effects of experimental diets on serum GOT, GPT, TG, and TC through the experiment (all *n*=9)

		Wk 0	Wk 2	Wk 4	Wk 6	Wk 8
ASP[1]	GOT[2]	67.8±20.8[a]	49.9 ±11.2[a]	73.8±13.2[a]	65.1±22.0[a]	70.7±22.8[a]
	GPT	13.8±5.5[a]	13.8±7.4	21.0±9.8[a]	21.1±9.8[a]	20.5±6.2[a]
	TC	57.9±15.1[a]	39.1±10.4[a]	54.2±9.3[a]	62.3±12.0[a]	64.0±7.8[a]
	TG	32.0±14.2[a]	52.1±14.7[a]	34.4±12.4[a]	30.4±6.6[a]	35.2±23.4[a]
SS	GOT	61.0±16.7	52.3±12.1[a]	61.6±27.7[a]	88.8±77.3[a]	103.7±90.8[a]
	GPT	16.9±3.7[a]	15.7±12.8[a]	18.2±7.6[a]	18.2±7.6[a]	26.8±11.6[a]
	TC	62.1±31.6[a]	53.2±11.4[a]	52.3±9.6[a]	58.6±14.7[a]	74.7±5.7[a]
	TG	33.5±14.1[a]	42.3±15.5	42.1±17.3	34.3±26.3[a]	22.3±14.5[a]
NC	GOT	68.7±13.5[a]	49.9±12.7[a]	60.4±15.1[a]	54.4±10.1[a]	55.0±20.8[a]
	GPT	19.8±4.2[a]	25.8±13.6	17.2±7.0[a]	17.2±7.0[a]	16.8±8.2[a]
	TC	46.5±12.9	46.4±12.4[a]	49.4±16.2	53.6±15.6	50.6±13.3[a]
	TG	43.2±12.5[a]	68.5±19.6[a]	40.7±21.2[a]	76.6±29.0[a]	52.2±25.1[a]
PC	GOT	71.0±11.9[a]	59.8±11.6[a]	109.5±41.8[a]	125.2±48.0[a]	114.6±38.4[a]
	GPT	16.3±5.3[a]	21.5±12.5[a]	65.1±37.9[a]	65.1±37.9[a]	49.5±29.0[a]
	TC	43.2±19.0[a]	43.7±10.6[a]	55.8±16.0[a]	68.7±18.6[a]	69.4±11.2[a]
	TG	53.2±12.1[a]	60.3±34.5	56.2±20.4	63.1±35.3[a]	42.5±14.0[a]
SP	GOT	79.7±10.4[a]	44.6±14.9[a]	64.5±10.5[a]	61.5±15.8[a]	93.3±35.1[a]
	GPT	17.5±5.4[a]	19.5±6.5[a]	25.8±11.3[a]	25.8±11.3[a]	35.6±15.7[a]
	TC	47.5±12.8[a]	46.9±11.5[a]	50.2±8.0[a]	64.0±9.1[a]	71.9±10.5[a]
	TG	43.4±10.2[a]	43.8±22.6[a]	45.0±12.2[a]	34.7±12.2[a]	52.3±8.9[a]

[1]ASP, alcohol-extracted soy protein; SS, alcohol-extracted soy protein plus saponin; NC, negative control (casein); PC, positive control (casein+1% cholesterol); SP, soy protein. [2]GOP and GPT, IU/dL; TG and TC, mg/dL. [a]$P<0.05$ within.

($P<0.05$). In the SP (intact soy protein) group, GOT, GPT, and TC levels had significantly increased ($P<0.05$) by the end of the experiment. Changes in the TG level did not show a clear trend. In the ASP (alcohol-washed soy protein) group, GOT and GPT levels did not change significantly during the experiment. The TC level significantly increased from wk 2 to 8 ($P<0.05$), while the TG level significantly decreased ($P<0.05$) during the experiment. In the SS group (ASP+saponin), the GOT level did not change throughout the experiment and the GPT level gradually increased toward the end of the experiment ($P<0.05$). By contrast, the TG level reached a maximum in wk 6 ($P<0.05$). In the PC group (high-cholesterol casein diet), the GOT, GPT, and the TC levels were elevated from wk 4 until the end of the feeding period ($P<0.05$).

Table 4 shows the hepatic TC and TG levels at baseline and at the end of the feeding period. The hepatic TG level in the SS group was the highest among the five groups in wk 8 ($P<0.05$), and was significantly higher than at baseline ($P<0.05$). TG levels in the other groups did not change significantly from baseline. Hepatic TC levels in all groups increased ($P<0.05$) compared to baseline. Rats that consumed soy protein (SP, SS, and ASP groups) had lower TC levels in the liver than those consumed casein (PC group) under high-cholesterol diets ($P\leqslant 0.05$). The SS and PC groups had higher hepatic TC levels than the other groups ($P<0.05$). Hepatic TC level in the SP and NC groups were significantly lower than those of the other groups ($P<0.05$). No significant differences were observed between the effects of casein and soy protein on hepatic TC and TG levels.

Table 4 TC and TG levels in the liver at the baseline and at the end of the feeding period

	TC (mg/g liver)	TG (mg/g liver)
Baseline	1.4±1.2	18.1±5.3
NC[1]	2.5±1.7[a]	15.8±5.9[a]
PC	5.3±1.1[a]	14.8±5.1[a]
SP	3.3±0.6[a]	17.1±3.5[a]
SS	4.8±1.1[a]	25.8±3.7[a]
ASP	3.6±0.9[a]	18.9±2.4[a]

[1]NC, negative control (casein); PC, positive control (casein+1% cholesterol); SP, soy protein; SS, alcohol-extracted soy protein plus saponin; ASP, alcohol-extracted soy protein. [a]$P<0.05$ *vs* others.

DISCUSSION

In this study, different types of dietary protein and the addition of saponin did not affect the growth of rats. We found that alcohol-extracted soy proteins (without isoflavone and saponin) with or without the addition of saponin had a protective effect on maintaining GOT and GPT under elevated cholesterol conditions. A diet high in cholesterol causes an increase in oxidative stress in the liver[11] and results in increases in GOT and GPT levels. In this study, the increasing levels of GOT and GPT in the rats fed casein with 1% cholesterol also produced elevated TC levels at the end of the feeding period compared to baseline.

The serum cholesterol content in the body is balanced by dietary cholesterol absorption, cholesterol synthesis in the body, and biliary cholesterol excretion. The cholesterol-lowering effect of saponin is due to the increase in bile acid excretion[12], which occurs through interference with the absorption of cholesterol[13]. Potter[14] also indicated that saponin might alter the absorption of cholesterol and bile acid. One of the possible mechanisms for this effect is that saponin forms micelles with bile acid[4]. Our *in vitro* data also suggested that soy protein and saponin bind a certain amount of bile acid, while the TC levels did not differ among

groups. Jimenez *et al*.[15], reported that soy saponin in the diet of rats did not have the same blood cholesterol-lowering effect of another amphiphilic compound, lecithin. This may have been due to soy saponin not being absorbed well in the small intestine through oral intake and reaching the colon directly[16]. Thus, the cholesterol-lowering effect of saponin appears to occur mainly through its bile acid- or cholesterol-binding ability in the digestive tract. In addition, the cholesterol-lowering effect may be changed if amino acids appear together[8]. Sautier *et al*.[17], also showed that the effect of soy saponin on lowering serum cholesterol might be greatly depressed if soy protein is added. In our experiments, soy saponin was added with soy protein and, therefore, no significant effect on TC was observed. Yamakoshi *et al*.[18], found that soy isoflavone had more significant cholesterol-lowering effects in plasma compared to saponin because saponin is not absorbed in the small intestine.

Soy isoflavone has been shown to have a cholesterol-lowering effect in the liver[19,20]. Soy protein also increases the activity of cholesterol receptors in the liver[21]. In our study, only the soy protein diet containing both isoflavone and saponin (SP group) lowered TC levels. Since we used healthy rats as the animal model, the liver cholesterol receptors should have been normal. This implies that the cholesterol-lowering effect in the liver in our study was from the effect of isoflavone rather than from saponin or soy protein. Sugano *et al*.[10], also suggested that the cholesterol-lowering effect of saponin might be reduced if it was ingested with soy protein.

In this study, we used SD rats as the animal model. It has been suggested that hypercholesterolemia is more easily induced in hamsters than in SD rats[22]. However, high cholesterol levels were observed in our SD rats fed high-cholesterol diets, which suggests that this animal model is also suitable for use in research. Since the hypercholesterolemic effect was not as apparent as that of hamsters; however, the results might have been affected. On the other hand, Gao *et al*.[22], suggested that SD rats might be a better animal model for investigating TG levels. In this study, the effect of different diets on blood TG levels of SD rats was highly significant.

In conclusion, this study found that soy protein was better than casein for liver protection in terms of GOT and GTP under high-cholesterol diet conditions. Soy protein and saponin showed some bile acid-binding abilities *in vitro*. However, the major component that reduced liver TC was isoflavone. The effects of various protein types on lowering TG still need further investigation. In addition, the SD rat is a useful animal model for studying hypercholesterolemia.

REFERENCES

1 **Potter JD,** Topping DL, Oakenfull D. Soya, saponins and plasma cholesterol. *Lancet* 1979; **1**: 223

2 **Wang HX,** Ng TB. Natural products with hypoglycemic, hypotensive, hypocholesterolemic, antiatherosclerotic and antithrombotic activities. *Life Sci* 1999; **65**: 2663-2677

3 **Lucas EA,** Khalil DA, Daggy BP, Arjmandi BH. Ethanol-extracted soy protein isolate does not modulate serum cholesterol in golden Syrian hamsters: a model of postmenopausal hypercholesterolemia. *J Nutr* 2001; **131**: 211-214

4 **Oakenfull D.** Soy protein, saponins and plasma cholesterol. *J Nutr* 2001; **131**: 2971-2972

5 **Arjmandi BH.** Reply to Dr. David Oakenfull. *J Nutr* 2001; **131**: 2972

6 **Anderson RL,** Wolf WJ. Compositional changes in trypsin inhibitors, phytic acid, saponins and isoflavones related to soybean processing. *J Nutr* 1995; **125**: 581S-588S

7 **Messina M,** Barnes S. The role of soy products in reducing risk of cancer. *J Natl Cancer Inst* 1991; **83**: 541-546

8 **Venter CS.** Health benefit of soybeans and soy products: a review. *J Family Ecol Consumer Sci* 1999; **127**: 24-33

9 **Carroll KK.** Review of clinical studies on cholesterol-lowering response to soy protein. *J Am Diet Assoc* 1991; **91**: 820-827

10 **Sugano M,** Goto S, Yamada Y, Yoshida K, Hashimoto Y, Matsuo T, Kimoto M. Cholesterol-lowering activity of various undigested fractions of soybean protein in rats. *J Nutr* 1990; **120**: 977-985

11 **AI Kanhal MA,** Ahmad F, AI Othman AA, Arif Z, AI Orf S, AI Murshed KS. Effect of pure and oxidized cholesterol-rich diets on some biochemical parameters in rats. *Int J Food Sci Nutr* 2002; **53**: 381-388

12 **Erdman JW.** AHA Science Advisory: Soy protein and cardiovascular disease: A statement for healthcare professionals from the Nutrition Committee of the AHA. *Circulation* 2000; **102**: 2555-2559

13 **Shin DH,** Heo HJ, Lee YJ, Kim HK. Amaranth squalene reduces serum and liver lipid levels in rats fed a cholesterol diet. *Br J Biomed Sci* 2004; **61**: 11-14

14 **Potter SM.** Overview of proposed mechanisms for the hypocholesterolemic effect of soy. *J Nutr* 1995; **125**: 606S-611S

15 **Jimenez MA,** Scarino ML, Vignolini F, Mengheri E. Evidence that polyunsaturated lecithin induces a reduction in plasma cholesterol level and favorable changes in lipoprotein composition in hypercholesterolemic rats. *J Nutr* 1990; **120**: 659-667

16 **Oh YJ,** Sung MK. Soybean saponins inhibit cell proliferation by suppressing PKC activation and induce differentiation of HT-29 human colon adenocarcinoma cells. *Nutr Cancer* 2001; **39**: 132-138

17 **Sautier C,** Doucet C, Flament C, Lemonnier D. Effects of soy protein and saponins on serum, tissue and feces steroids in rat. *Atherosclerosis* 1979; **34**: 233-241

18 **Yamakoshi J,** Piskula MK, Izumi T, Tobe K, Saito M, Kataoka S, Obata A, Kikuchi M. Isoflavone aglycone-rich extract without soy protein attenuates atherosclerosis development in cholesterol-fed rabbits. *J Nutr* 2000; **130**: 1887-1893

19 **Iqbal MJ,** Yaegashi S, Ahsan R, Lightfoot DA, Banz WJ. Differentially abundant mRNAs in rat liver in response to diets containing soy protein isolate. *Physiol Genomics* 2002; **11**: 219-226

20 **Xiao CW,** L'Abbe MR, Gilani GS, Cooke GM, Curran IH, Papademetriou SA. Dietary soy protein isolate and isoflavones modulate hepatic thyroid hormone receptors in rats. *J Nutr* 2004; **134**: 743-749

21 **Sirtori CR,** Bosisio R, Pazzucconi F, Bondioli A, Gatti E, Lovati MR, Murphy P. Soy milk with a high glycitein content does not reduce low-density lipoprotein cholesterolemia in type II hypercholesterolemic patients. *Ann Nutr Metab* 2002; **46**: 88-92

22 **Gao Y,** Li K, Tang S, Xiao Y. Study on animal models for hyperlipidemia. *Weisheng Yanjiu* 2002; **31**: 97-99

Science Editor Guo SY **Language Editor** Elsevier HK

PO Box 2345, Beijing 100023, China
www.wjgnet.com
wjg@wjgnet.com

ELSEVIER

World J Gastroenterol 2005;11(35):5553-5556
World Journal of Gastroenterology ISSN 1007-9327
© 2005 The WJG Press and Elsevier Inc. All rights reserved.

• *BRIEF REPORTS* •

Disproportional exaggerated aspartate transaminase is a useful prognostic parameter in late leptospirosis

Ming-Ling Chang, Chih-Wei Yang, Jeng-Chang Chen, Yu-Pin Ho, Ming-Jeng Pan, Cheng-Hui Lin, Deng-Yn Lin

Ming-Ling Chang, Yu-Pin Ho, Cheng-Hui Lin, Deng-Yn Lin, Department of Hepatogastroenterology, Chang Gung Memorial Hospital, 5 Fu-Shin Street, Kweishan, Taoyuan, Taiwan, China
Chih-Wei Yang, Department of Nephrology, Chang Gung Memorial Hospital, Taoyuan, Taiwan, China
Jeng-Chang Chen, Department of Surgery, Chang Gung Memorial Hospital, Taoyuan, Taiwan, China
Ming-Jeng Pan, National Taiwan University, Taipei, Taiwan, China
Supported by the Chang Gung Medical Research Project fund, No. CMRPG 33014
Correspondence to: Dr. Deng-Yn Lin, Department of Hepatogastroenterology, Chang Gung Memorial Hospital, 5 Fu-Shin Street, Kweishan, Taoyuan, Taiwan, China. kitty8210@yahoo.com
Telephone: +886-3-3281200-8227 Fax: +886-3-3288957
Received: 2005-01-05 Accepted: 2005-02-18

Abstract

AIM: To evaluate the hepatic dysfunction in leptospirosis is usually mild and resolved eventually. However, sequential follow-up of liver biochemical data remained lacking..

METHODS: The biochemistry data and clinical symptoms of 11 sporadic patients were collected and analyzed, focusing on the impacts of leptospirosis upon liver biochemistry tests.

RESULTS: The results disclosed that of the 11 cases, 5 or 45% died. The liver biochemistry data in the beginning of the disease course were only mildly elevated. Nevertheless, late exaggerated aspartate transaminase (AST) elevations were noted in three cases who finally died when compared with the typical course. Besides, significant higher AST/alanine transaminase (ALT) ratios (AARs) of the peak levels for transaminase were also noted in the cases who eventually succumbed. The mean±SD of AARs for the survival group and dead group were 5.65±2.27 (n = 5) and 1.86±0.64 (n = 6) respectively (P = 0.006). The ratios of the cases who finally died were all more than 3.0. Conversely, the survival group's ratios were less than 3.0.

CONCLUSION: Serial follow-up of transaminase might provide evidence to predict some rare evolutions in leptospirosis. If AST elevated progressively without a concomitant change of ALT, it might indicate an acute disease course with ensuing death. Additionally, AAR is another prognostic parameter for leptospirosis. Once the value was higher than 3.0, a grave prognosis is inevitable.

© 2005 The WJG Press and Elsevier Inc. All rights reserved.

Key words: Leptospirosis; Liver; Aspartate transaminase; Alanine transaminase; AST/ALT ratios

Chang ML, Yang CW, Chen JC, Ho YP, Pan MJ, Lin CH, Lin DY. Disproportional exaggerated aspartate transaminase is a useful prognostic parameter in late leptospirosis. *World J Gastroenterol* 2005; 11(35): 5553-5556
http://www.wjgnet.com/1007-9327/11/5553.asp

INTRODUCTION

Leptospirosis is caused by a variety of pathogenic spirochetes of the genus *Leptospira*[1], the human beings are generally the dead-end host after transmission from animal contact[2]. This disease is characterized by a broad spectrum of manifestations, which are usually subclinical[1,2]. Its diagnosis relies upon strong suspicions of this disease from some nonspecific clinical presentations[3]. Confirmation of this infection is usually established by serological studies[4] or PCR[5,6].

In terms of pathologic findings and biochemical manifestations, liver is not the main target of spirochete infection[2,3,7,8]. Hepatic dysfunction in leptospirosis was usually mild and resolved eventually. However, if jaundice occurs, serum bilirubin levels might be markedly elevated as compared with aspartate transaminase (AST) and alanine transaminase (ALT)[9]. Weil's disease, defined as severe icteric leptospirosis with renal failure, accounts for mortality associated with leptospirosis[1]. In some cases, aside from severe jaundice, the elevation of AST was so remarkable as acute viral hepatitis could be, which attracted our attention in the endemic area of the HBV. However, the data regarding sequential follow-up of liver biochemical data of leptospirosis remained lacking. Herein, our experiences of the sporadic leptospirosis are presented and the possible implication of exaggerated AST change in leptospirosis is discussed.

MATERIALS AND METHODS

During the period from May 1998 to January 2000, 11 patients with sporadic leptospirosis in intensive care unit, Chang Gung Memorial Hospital, Taiwan, were reviewed to evaluate the impact of severe leptospirosis on liver biochemistry tests. There were seven males and four females, and their age ranged from 30 to 78 years (mean: 57 years). None of the patients were alcoholics, nor suggestive of acute viral infection or chronic virus carrier by serological tests excluding the following: hepatitis A, B, and C, Epstein-Barr virus, cytomegalovirus and Hanta virus. Bacterial and fungal cultures were all sterile. There was no history of previous

liver disease in any of the patients. Leptospirosis was confirmed by either urine PCR tests or serum microscopic agglutinin test (single serum titer ≥100-fold or paired serum titers rise ≥4-fold).

The hepatic biochemistry parameters including AST (normal 0-34 U/L), ALT (normal 0-36 U/L), alkaline phosphatase (Alk-p, normal 28-94 U/L), γ-glutamyl transpeptidase (r-GT, normal <26 U/L), direct bilirubin (bili-D, normal 0-0.4 mg/dL), total bilirubin (bili-T, normal 0-1.3 mg/dL), creatine phosphokinase (CPK, normal 15-130 U/L) were chronologically collected and then analyzed. Student's *t*-test was used to compare the means. A probability value of less than 0.05 was considered statistically significant. Furthermore, the influence of leptospirosis on liver function tests was discussed.

RESULTS

The disease onset was severe and abrupt in all patients with fever and chills. The clinical manifestations included conjunctival suffusion in 9, jaundice in 9, abdominal pain in 7, myalgia in 7, consciousness disturbance in 4, hepatomegaly in 4, upper gastrointestinal bleeding 2, rhabdomyolysis in 2, and hemophagocytosis, hemolytic uremic syndrome each for one case. This disease progressed to acute renal failure in all and acute respiratory failure in six. All patients received parenteral penicillin and hemodialysis. Finally, five icteric cases died exclusively of multiple organ failure.

Table 1 illustrates the characteristics and liver biochemical data of the patients. Of the 11 patients, 5 (cases 1-5) or 45% contributes to the mortality rate. One of four (25%) younger than 50 years, and four out of seven (57%) older than 50 years expired. One hundred percent of the cases got abnormal liver biochemistry parameters in spite of various degrees. Alk-p and r-GT were only elevated mildly during the entire course and never exceeded 4-folds of the normal limit. Upon admission, eight had hyperbilirubinemia; however, in the 3rd wk of the disease, one of the patients who originally had normal bilirubin levels became icteric. Therefore, there were nine cases of Weil's disease by the definition mentioned before. The highest bilirubin level attained 35.1 mg%. CPK ranged from 178 to 2 889 U/L.

The most evident difference of liver biochemistry parameters between the dead and survival group was bilirubin levels (Table 1). The mean±SD of Bili (D) of the peak level for the former are significantly higher than the latter ($P = 0.03$). All those who died had jaundice; however, four cases with jaundice recovered.

Upon admission, both AST and ALT levels of all the patients elevated modestly with an average of 117.27 and 70.63 U/L respectively. However, three patients (cases 1, 3, and 5) with Weil's disease had unusually exaggerated AST elevation more than 2-3 wk after the onset of disease (Table 1, the peak AST level for case 1, 3, and 5 were 901, 1 216 and 580 U/L respectively). A representative case (case 1) showed disproportional progressive elevations of AST levels since the first admission day, which was the 12th d since the disease onset (Figure 1). Although ALT peaked at 144 U/L, it did not increase in proportion with AST, which peaked at 901 U/L. Meanwhile, CPK was 628 U/L. Due to pancytopenia, a bone marrow biopsy was performed for this patient and revealed hemophagocytosis. Case 3 displayed peak AST and ALT levels (1 216 and 308 U/L) (Table 1) after an episode of septic shock. However, they returned to normal 4 d later. Case 5 obtained peak levels of AST (580 U/L) and ALT (139 U/L) 18 d after the onset of disease. CPK was only 99 U/L then. A peripheral blood smear for pancytopenia demonstrated burr cells and toxic granules in WBCs. A disseminated intravascular coagulopathy (DIC) profile revealed positive finding, while both direct and indirect Coomb's tests yielded negative findings. All three patients eventually died of multiple organ failure.

In addition to exaggerated transaminase elevations of the late stage in the three cases mentioned above, significant higher AST/ALT ratios (AARs) of the peak levels for transaminase were also noted in the cases who eventually succumbed (Table 1 and Figure 2). The mean±SD of the AAR for the survival group and dead group were 5.65±2.27

Table 1 Biochemistry parameters of the patients with leptospirosis, presented with data upon entry (initial admission)/*peak levels*

Case No.	Age (yr)	Sex	Biochemical parameters (entry/*peak*) AST (U/L)	ALT (U/L)	AAR	Alk-P (U/L)	r-GT (U/L)	Bili (D) (mg%)	Bili (T) (mg%)	CPK (U/L)	DA	Remark
1	60	f	190/901	78/144	6.26	232/232	100/100	2.7/4.6	4.3/7.6	628	12	A B[1]
2	70	m	103/132	9/22	6.0	198/212	125/174	10.6/13.8	17.3/28.2	99	47	A
3	42	f	86/1216	50/308	3.94	40/446	6/285	14.6/16.4	28.4/35.1	N.A.	65	A B[3]
4	58	f	63/63	1/8	7.88	74/241	30/98	0.2/3	0.4/5.1	985	78	A
5	75	m	226/580	139/139	4.17	195/195	80/80	6/15.7	11.7/36.4	99	19	A B[5]
Mean	61		133.6/578	55.4/214.6	5.65	147.8/265.2	68.2/286.8	6.82/10.7	12.43/22.5	452.8	44.2	
(SD)	12.7		70.5/493.8	21/166	2.27	85.0/102.6	49.3/84.9	5.83/6.39	11.07/15.1	433.7	28.5	
6	78	m	74/127	23/45	2.82	104/114	32/24	2.5/2.7	4.4/4.6	178	35	
7	41	m	165/208	149/149	1.39	68/78	32/64	6/14.3	10.8/27.2	2889	33	
8	30	m	203/253	185/102	2.48	40/45	6/7	0.1/0.1	0.4/0.4	704	10	
9	65	m	29/34	25/25	1.36	198/198	50/70	0.3/0.3	0.7/0.7	N.A.	16	
10	65	m	21/29	16/17	1.7	104/104	20/20	1.4/1.4	2.2/2.3	61	38	
11	43	f	130/156	102/112	1.39	141/141	80/80	3.3/3.3	5.2/5.2	69	21	
Mean	53.661		103.6/134.5	83.3/175	1.85	109.2/136	36.7/144.2	2.26/13.68	3.95/6.73	780.2	25.5	
(SD)	0.35		74.3/90.8	72.9/53.6	0.64	55.6/52.8	25.8/30.7	2.2/5.35	3.87/10.22	1028.2	11.43	

N.A.: not assessed; D.A.: d of admission; AAR: AST/ALT ratio of peak levels; m: male; f: female. A: Complicated with multiple organ failure and fatal; B: exaggerated AST peak levels; B[1]: hemophagocytosis. B[2]: shock, hemorrhage. B[3]: DIC.

(n = 5) and 1.86±0.64 (n = 6) respectively (P = 0.006). The ratios of the cases who finally died were all higher than 3.0. Conversely, the survival group's ratios were lower than 3.0 (Figure 2).

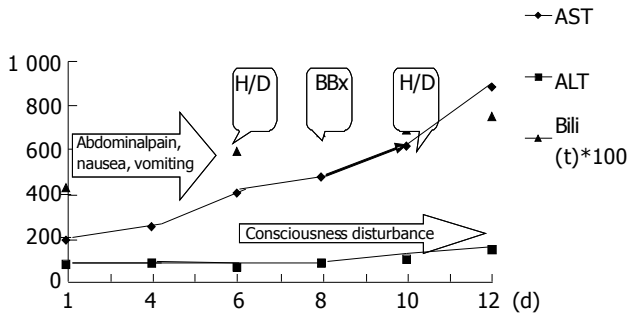


Figure 1 Clinical manifestations and biochemical changes in the whole course of case 1. Unit: AST (U/L), ALT (U/L), Bili(T) (mg/dL), H/D: hemodialysis, BBx: bone marrow biopsy.

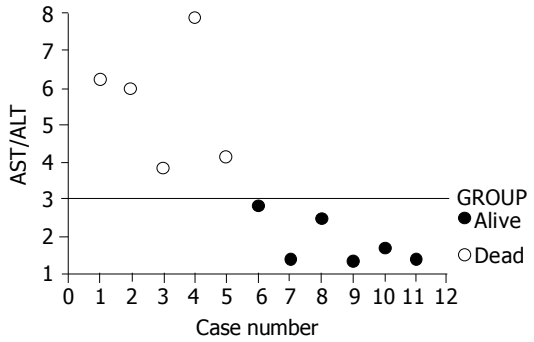


Figure 2 Scattered figure of AST/ALT (AAR) values. All the dead cases are shown as AAR >3.0. On the contrary, the ratios of all the survival cases were <3.0.

DISCUSSION

Age is reported as the most significant host factor related to mortality of leptospirosis. The mortality rate rose from 10% (in patients less than 50 years) to 56% (in those over 51 years)[1]. As the average age (57 years) of our cases was much higher than those of teenagers and young adults, who were considered as the major victims of leptospirosis, they were rarely admitted to hospital on account of their subclinical symptoms[1,3,6]. Furthermore, all the cases were enrolled from the intensive care unit, it is reasonable why the overall mortality (45%) of this hospitalized series was much higher than other published reports (5-16%)[1,2].

On hospitalization, the liver biochemistry tests disclosed only modest elevations in AST, ALT, Alk-p, and r-GT. However, total bilirubin ranged from normal limits to as high as 28.2 mg/dL. Such a pattern was compatible with the fact that the liver dysfunction in leptospirosis is typically mild, resolved finally and serum bilirubin can be markedly elevated as compared with other liver enzymes[1,2,3,9]. Hyperbilirubinemia is not only related to hepatocellular dysfunction but also magnified by impairing bilirubin excretion from renal failure, and bilirubin overproduction from tissue hemorrhage and intravascular hemolysis[8]. Five Weil's disease accounted for the mortality (Table 1, cases 1-5), it was also consistent with that leptospirosis is never fatal without jaundice[1,8]. It is because the pathogenesis in jaundice resulted from leptospirosis is as complex as mentioned above[8].

Nevertheless, among the five cases dying of Weil's disease, three (cases 1, 3, and 5) had exaggerated AST elevation 2-3 wk after the onset of disease. In contrast, among the four Weil's disease of the survival group (cases 6, 7, 9, and 10), none had been found with exaggerated AST elevation through the whole disease course. All the cases 1, 3, and 5 developed progressive AST elevation without concomitant ALT change. Therefore, the extrahepatic origin of AST should be considered. Myositis is a common presentation in leptospirosis and usually abated by the 2nd wk[10,11]. If the extrahepatic AST had come from muscle, AST would return to normal within 2 wk rather than being progressively elevated as seen in the two cases. Moreover, it has been reported that for severe myositis in leptospirosis, CPK elevation up to 8 880 U/L only correlated with AST elevation as high as 440 U/L[12]. Myositis alone could not contribute to AST elevation in the two cases, as their AST elevations (901 and 580 U/L) were not in proportion to CPK (628 and 99 U/L) elevations in terms of myositis. Therefore, the muscle origin of AST could not simply explain this phenomenon, and the exaggerated AST elevation must have had another source.

The pathogenesis of the systemic lesions in leptospirosis was ascribed to directly damaging the parenchymal cellular membranes. It may initially cause functional disorder of these membranes, and only later lead to necrosis[13]. Nevertheless, complete cell necrosis is not prominent in leptospirosis, which is in accordance with the low level of serum transaminase in this disease[7]. Notably, hemophagocytosis and DIC were proved in the two cases (cases 1 and 5) respectively. Both are rare presentations in human leptospirosis[13,14], and they indicated a severe form of infections and disease progression. Besides, clinical presentations (respiratory failure, renal failure, consciousness disturbance, *etc*.,), they indicated grave multiple organ failure. It was suggested that, in rare and deteriorated situations, the systemic parenchymal cellular dysfunction in leptospirosis could evolve into extensive cellular necrosis. Namely, severe and extensive destruction of cells in various organs -not only muscle and liver -might lead to the unusual AST elevations. It had been documented that, in acute and/or fatal leptospirosis, the pathogenesis of the pathologic features are related to the presence of the organisms in the tissues, and was usually multi-system involvement[15,16].

All the five fatal cases displayed multiple organ failure (Table 1). The major difference between those who with (cases 1, 3, and 5) and without (cases 2 and 4) exaggerated AST elevation was the natural course of disease. The duration from disease onset to death appeared much shorter in the former (12-19 d) as compared to the latter (47-78 d). The clinical course of leptospirosis can be divided into two stages, a 3-7-d septic stage followed by an immune stage lasting for 4-30 d[2]. All the exaggerated AST occurred in the immune stage of leptospirosis. The balance between

the host and parasite determines, whether the infection runs an acute or a protracted course[17]. In acute leptospirosis, the main pathogenesis was probably due to the direct toxic damage of spirochetes[13,18,19]. However, an immune complex-mediated mechanism was suggested when the course was protracted[18]. Because the infections ran acute courses in cases 1, 3, and 5, it might indicate that although the exaggerated AST elevations occurred in the immune stages (after 1 wk of disease onset), the hosts could not clear the spirochetes then from the blood by immune reactions efficiently. The spirochetes were consistently virulent to the systemic parenchymal cells. Finally unavoidable deaths with fulminant courses of the hosts ensued.

Aside from AST, AAR of peak levels for transaminase might predict the outcome of leptospirosis. AAR was significantly higher in the fatal cases. The ratios were higher than 3.0 (Table 1 and Figure 2) in all of the deaths. In contrast, all the cases who finally recovered had the ratios of less than 3.0. The ratios seemed to stop at 3. Both multiple major organ failure and systemic parenchymal cells necrosis might contribute to the higher ratios in the fatal cases.

In endemic areas of hepatitis B infection such as Taiwan, viral hepatitis was the first consideration for icteric patients with abrupt disease onset associated with transaminase elevation. Such impression might delay the appropriate management of the true culprit-leptospirosis. Typically acute viral hepatitis presented as exaggerated transaminase elevations initially and recovered thereafter regardless of the existence of jaundice. Besides, the ALT elevation usually sustains longer than that of AST. On the contrary, leptospirosis showed as initial modest transaminase elevations accompanied with extremely high CPK levels[1,2,8]. The initial amplitude of transaminase could be a clue to differentiate viral hepatitis and leptospirosis. However, in a chronic HBV carrier, the delayed transaminase elevation would confuse the physician, if the elevation is due to acute exacerbation of chronic HBV infection. We were convinced that delayed and disproportional AST elevation is in favor of nonhepatic origin. In leptospirosis, it might hint a fulminant disease course with high mortality.

Conclusively, in addition to clinical symptoms, serial follow-up of transaminase could provide some evidence to predict the rare evolution in leptospirosis. Late disproportional AST elevation indicates an ominous sign, mortality that typically ensues from a fulminant disease course. AAR is a parameter responsive to the prognosis of leptospirosis, the ratio >3.0 means a grave prognosis. Furthermore, in endemic areas of viral hepatitis, Weil's disease still should be considered in icteric cases of unknown origin regardless of AST level, since exaggerated AST might herald the unusual fulminant mortality.

REFERENCES

1 **Isselbacher KJ,** Braunwald E, Wilson JD. Harrison's principles of internal medicine. 14th ed. *St. Louis: McGraw-Hill* 1993: 1036-1038
2 **Taber LH,** Feigin RD. Spirochetal infections. *Pediatr Clin North Am* 1979; **26**: 377-413
3 **Farr RW.** Leptospirosis. *Clin Infect Dis* 1995; **21**: 1-8
4 **Lupidi R,** Cinco M, Balanzin D, Delprete E, Varaldo PE. Serological follow-up of patients involved in a localized outbreak of leptospirosis. *J Clin Microbiol* 1991; **29**: 805-809
5 **Merien F,** Baranton G, Perolat P. Comparison of polymerase chain reaction with microagglutionation test and culture for diagnosis of leptospirosis. *J Infect Dis* 1995; **172**: 281-285
6 **Ralph D,** McClelland M, Welsh J, Baranton G, Perolat P. Leptospira species categorized by arbitrarily primed Polymerase chain reaction (PCR) and by mapped restriction polymorphisms in PCR-amplified rRNA genes. *J Bacteriol* 1993; **175**: 973-981
7 **Brito de T,** Penna DO, Hoshino S, Pereira VG, Caldas AC, Rothstein W. Cholestasis in human leptospirosis: a clinical, histochemical, biochemical and electron microscopy study based on liver biopsies. *Beitr Pathol Anat* 1970; **140**: 345-361
8 **Sherlock S,** Dooley J. Disease of the liver and biliary system. 10th ed. *Malden: Blackwell Sci Pub* 1997: 507-510
9 **den Haan PJ,** van Vliet AC, Hazenberg BP. Weil's disease as a cause of jaundice. *Neth J Med* 1993; **42**: 171-174
10 **Johnson WD,** Silva IC, Rocha H. Serum creatine phosphokinase in leptospirosis. *JAMA* 1975; **233**: 981-982
11 **Heath CW**, Alexander AD, Galton MM. Leptospirosis in the United States. *N Engl J Med* 1965; **273**: 857-864
12 **Farkas PS,** Knapp AB, Lieberman H, Guttman I, Mayan S, Bloom AA. Markediy elevated creatinine phosphokinase, cotton wool spots, and pericarditis in a patient with leptospirosis. *Gastroenterology* 1981; **80**: 587-589
13 **Nicodemo AC,** Duarte MI, Alves VA, Takakura CF, Santos RT, Nicodemo EL. Lung lesions in human leptospirosis: microscopic, immunohistochemical, and ultrastructural features related to thrombocytopenia. *Am J Trop Med Hyg* 1997; **56**: 181-187
14 **Yang CW,** Pan MJ, Wu MS, Chen YM, Tsen YT, Lin CL, Wu CH, Huang CC. Leptospirosis: an ignored cause of acute renal failure in Taiwan. *Am J Kidney Dis* 1997; **30**: 840-845
15 **Nally JE,** Chantranuwat C, Wu XY, Fishbein MC, Pereira MM, Da Silva JJ, Blanco DR, Lovett MA. Alveolar septal deposition of immunoglobulin and complement parallels pulmonary hemorrhage in a guinea pig model of severe pulmonary leptospirosis. *Am J Pathol* 2004; **164**: 1115-11127
16 **Brown PD,** Carrington DG, Gravekamp C, van de Kemp H, Edwards CN, Jones SR, Prussia PR, Garriques S, Terpstra WJ, Levett PN. Direct detection of leptospiral material in human postmortem samples. *Res Microbiol* 2003; **154**: 581-586
17 **Yasuda PH,** Hoshino-Shimizu S, Yamashiro EH, De Brito T. Experimental leptospirosis (L. interrogans serovar icterohaemorrhagiae) of the guinea pig: leptospiral antigen, gamma globulin and complement C3 detection in the kidney. *Exp Pathol* 1986; **29**: 35-43
18 **Alves VA,** Vianna MR, Yasuda PH, De Brito T. Detection of leptospiral antigen in the human liver and kidney using an immunoperoxidase staining procedure. *J Pathol* 1987; **151**: 125-131
19 **Alves VA,** Gayotto LC, De Brito T, Santos RT, Wakamatsu A, Vianna MR, Sakata EE. Leptospiral antigens in the liver of experimentally infected guinea pig and their relation to the morphogenesis of liver damage. *Exp Toxicol Pathol* 1992; **44**: 425-434

Science Editor Guo SY **Language Editor** Elsevier HK

PO Box 2345, Beijing 100023, China
www.wjgnet.com
wjg@wjgnet.com

ELSEVIER

World J Gastroenterol 2005;11(35):5557-5560
World Journal of Gastroenterology ISSN 1007-9327
© 2005 The WJG Press and Elsevier Inc. All rights reserved.

• *BRIEF REPORTS* •

Analysis of clinical manifestations of symptomatic acquired jejunoileal diverticular disease

Chia-Yuan Liu, Wen-Hsiung Chang, Shee-Chan Lin, Cheng-Hsin Chu, Tsang-En Wang, Shou-Chuan Shih

Chia-Yuan Liu, Wen-Hsiung Chang, Shee-Chan Lin, Cheng-Hsin Chu, Tsang-En Wang, Shou-Chuan Shih, Division of Gastroenterology, Department of Internal Medicine, Mackay Memorial Hospital, Taipei, Taiwan, China
Chia-Yuan Liu, Department of Medical Research, Mackay Memorial Hospital, Taipei, Taiwan, China
Shou-Chuan Shih, Mackay Medicine, Nursing and Management College, Taipei, Taiwan, China
Correspondence to: Dr. Shou-Chuan Shih, Division of Gastroenterology, Department of Internal Medicine, Mackay Memorial Hospital, No. 92, Section 2, Chung-San North Road, Taipei, Taiwan, China. sschuan@ms2.mmh.org.tw
Telephone: +886-2-25433535 Fax: +886-2-27752142
Received: 2004-12-10 Accepted: 2005-02-28

Abstract

AIM: To analyze systematically our experience over 22 years with symptomatic acquired diverticular disease of the jejunum and ileum, exploring the clinical manifestations and diagnosis of this rare but life-threatening disease.

METHODS: The medical records of patients with surgically confirmed symptomatic jejunoileal diverticular disease were retrospectively reviewed. Data collected included demographic data, laboratory results, clinical course (acute or chronic), preoperative diagnosis, and operative findings. Inclusion criteria were as follows: (1) surgical confirmation of jejunoileal diverticular disease and (2) exclusion of congenital diverticula (e.g. Meckel's diverticulum).

RESULTS: From January 1982 to July 2004, 28 patients with a total of 29 operations met the study criteria. The male:female ratio was 14:14, and the mean age was 62.6±3.5 years. The most common manifestation was abdominal pain. In nearly half of the patients, the symptoms were chronic. Two patients died after surgery. Only four cases were correctly diagnosed prior to surgery, three by small bowel series.

CONCLUSION: Symptomatic acquired small bowel diverticular disease is difficult to diagnose. It should be considered in older patients with unexplained chronic abdominal symptoms. A small bowel series may be helpful in diagnosing this potentially life-threatening disease.

© 2005 The WJG Press and Elsevier Inc. All rights reserved.

Key words: Acquired; Symptomatic; Jejunoileal; Diverticular disease

Liu CY, Chang WH, Lin SC, Chu CH, Wang TE, Shih SC. Analysis of clinical manifestations of symptomatic acquired jejunoileal diverticular disease. *World J Gastroenterol* 2005; 11(35): 5557-5560
http://www.wjgnet.com/1007-9327/11/5557.asp

INTRODUCTION

According to the literature review by Longo and Vernava[1], the first report of jejunal diverticulosis was published by Sir Astley Cooper in 1807, and the first operation for small bowel diverticula was performed by Gordinier and Sampson in 1906. The small bowel is the least common site for diverticula in the entire GI tract. According to the literature, the duodenum is the most common location for a small bowel diverticulum[2,3]. After excluding Meckel's diverticulum, less than 30% of reported diverticula occurred in the jejunum and ileum. The reported incidence of jejunoileal diverticula on small bowel studies by enteroclysis is 2-2.3%[4,5], comparable to autopsy data demonstrating an incidence of 1.3-4.6% for acquired diverticula of the jejunum and ileum[6,7].

Most small bowel diverticula, whether duodenal or jejunoileal, are asymptomatic[1,8] and are simply incidental findings. Complicated acquired diverticular disease of the jejunum and ileum is, on the other hand, a diagnostic dilemma. The exact prevalence of complicated small bowel diverticula is difficult to ascertain, estimates in the literature range from less than 10% to nearly 40%[9,10]. In a series of 47 patients, operative intervention was required because of complications in 7 (15%) patients[11]. We conducted a retrospective review of our experience with this rare entity, with a view to expanding the cumulative information in the literature.

MATERIALS AND METHODS

General data

The chart and operative records of Mackay Memorial Hospital from January 1982 to July 2004 were reviewed for cases of surgically proven jejunoileal diverticula. During this period, 28 patients with symptomatic, acquired jejunoileal diverticular disease were managed. We retrospectively reviewed their age, sex, admission data, and outcome. We reviewed the major symptoms and recorded whether they were acute or chronic. The definition of chronic symptoms was vague complaints with no other identifiable cause persisting for at least 1 mo[7]. The preoperative laboratory data was also recorded and compared according to gender and whether the disease was acute or chronic. The preoperative diagnosis and surgical findings were recorded, including the location, number, and size of diverticula and the operative method.

Statistical analysis

Data were expressed as percentages or the mean±SD. Sigma Stat software (version 2.03, SPSS Inc., Chicago, IL) was used to perform a Student's *t*-test to compare the difference between groups of patients. Differences were considered significant at a *P* value of less than 0.05.

RESULTS

The records of 28 patients with surgically proven jejunoileal diverticula were retrieved for this study. The male:female ratio was 14:14. One woman with multiple jejunal diverticula had two episodes requiring surgery, once at age 66 and again at 77. Therefore, a total of 29 operations were reviewed. The mean age was 62.6±3.5 years (ranging from 22 to 93 years). Symptoms were acute in 15 episodes and chronic in 14. Two patients died, for a mortality of 7% (2 of 29). The length of hospital stay was 23.2±3.7 d, and the length of time between admission and surgery was 5.0±2.7 d. Six patients (21%) had colonic diverticular disease, with one tentatively diagnosed with colonic diverticulitis before surgery.

Some patients had multiple presenting symptoms. The most common was abdominal pain (25 of 29 episodes, 86%). Four patients had GI bleeding on arrival and six were febrile. One patient had a palpable left lower quadrant mass and was found to have diverticulitis of the terminal ileum with rupture. Other manifestations included nausea or vomiting in nine patients, abdominal fullness in seven, constipation in two, shock in two, and others in five.

Table 1 shows the surgical findings noted in the records. In the 29 episodes where the information was available, the diverticula were located in the jejunum in 16, the ileum in 11, and both jejunum and ileum in 2. In the 27 records where the number of diverticula was stated, 19 patients had multiple diverticula. The majority (12 of 21) of diverticula in cases where the size was recorded were greater than 3 cm. More than three quarters (22 of 29) of surgeries involved segmental resection of the intestine, and three patients had resection of the diverticula only. Additional procedures, such as enteroclysis and drainage, were done in four cases. Diverticulitis with or without perforation was the most common final surgical diagnosis (17 of 29).

Table 1 Surgical findings in 29 episodes of acquired symptomatic jejunoileal diverticular disease

Surgical findings	*n*	%
Location (*n* = 29)		
Jejunal:ileal:both	16:11:2	55:38:7
Number of diverticula (*n* = 27)		
Single:multiple	8:19	30:70
Size of diverticula (*n* = 21)		
Less than 1 cm:1–3 cm:over 3 cm	2:7:12	10:33:57
Operative method (*n* = 29)		
Segmental resection of intestine	22	76
Resection of diverticulum only	3	10
Others	4	14
Postoperation finding (*n* = 29)		
Diverticulitis with/without perforation	17	58
Hemorrhage	4	14
Intestinal obstruction	8	28

Table 2 shows the preoperative diagnoses, with acute appendicitis being the most common (6 of 29). Five patients were thought to have ileus, one of whom had an enterolith. Only four patients had a correct diagnosis before surgery, three of which were suggested by a small bowel series. The other patient had an upper GI series that disclosed a proximal jejunal diverticulum.

Table 2 Preoperative diagnoses in 29 episodes of acquired jejunoileal diverticular disease

Preoperative diagnosis	
Acute appendicitis	6
Ileus	5
Small bowel diverticula	4
GI tract bleeding	4
Perforated peptic ulcer	3
Intussusceptions	2
Colonic diverticulitis	1
Intra-abdominal tumor	1
Volvulus	1
Others	2

Table 3 lists the laboratory data. The mean blood sugar, leukocyte count and amylase were slightly elevated, while the mean albumin, calcium were mildly decreased. When we compared the data between patients with acute or chronic symptoms and between males and females, we found no significant statistical differences.

Table 3 Laboratory data in 29 episodes of acquired symptomatic jejunoileal diverticular disease

Laboratory data	mean±SD	Normal range
Hemoglobin	11.6±3.0	11.0-16.0 g/dL
Leukocyte count	11 540±4 656	4.0-10.0×10^3/μL
Platelet count	237 541±99 860	140-450×10^3/μL
Blood sugar	133.6±47.0	70-120 mg/dL
Blood urea nitrogen	16.9±12.6	7-24 mg/dL
Creatinine	1.1±0.4	0.5-1.2 mg/dL
Albumin	3.0±0.6	3.4-4.8 g/L
Calcium	7.8±0.7	8.4-10.0 g/L
Aspartate aminotransferase	26.9±18.7	5-35 IU/L
Bilirubin	0.80±0.5	0.2-1.3 mg/dL
Amylase	129.2±165.4	25-125 U/L

DISCUSSION

Our study confirms the rarity of symptomatic acquired jejunoileal diverticular disease, with only 28 patients seen with this disorder in our hospital in the past 22 years. It is more common in older patients, with a mean age in our series being 62.6±3.5 years. This is in general agreement with the findings of previous studies, with few young patients reported[1,7,12]. Although other investigators have reported a male predominance[1,2], this was not the case in our series. Because of the small number of patients in any one of the series, it is difficult to collect enough data to determine a clear pattern of gender distribution.

Most acquired jejunoileal diverticula are false diverticula,

occurring along the mesenteric border of the small bowel[1,10]. The incidence decreases distally progressively from the ligament of Treitz. The pathogenesis of jejunoileal diverticula has been ascribed to a pulsion phenomenon with local increases in intraluminal pressure. The mucosa and submucosa are forced through vascular channels in the muscle layer[13-15]. It is also possible that smooth muscle abnormalities create localized weakness in the wall. Diverticula are thought to occur more frequently in the proximal jejunum because of the larger size of the vasa recta at this area[7]. Another theory is that abnormalities of the myenteric plexus may result in uncoordinated smooth muscle activity, producing high pressure in localized area[1,2]. In our series, the distribution of diverticula was similar to the findings of others, with 55% in the jejunum, 38% in the ileum, and 7% in both.

Of patients with jejunoileal diverticula reported in the literature, more than 60% have been asymptomatic, another 30% minimally symptomatic, and only 10% have developed serious complications[13]. The rarity of symptomatic acquired jejunoileal diverticula often results in missed or delayed diagnosis. de Bree *et al*., advocated earlier diagnosis and timely treatment to reduce the morbidity and mortality[16]. Only four patients in our series (14%) were correctly diagnosed before surgery. Geroulakos reported an even worse record, with none of their patients being correctly diagnosed preoperatively. Three of the thirteen patients in their series were once labeled as psychoneurotic because diagnostic studies failed to demonstrate obvious pathology. The correct diagnosis was made only at emergency laparotomy[17]. This demonstrates the importance of remembering that there are such uncommon entities that are difficult to diagnose but which, if unrecognized, may result in serious complications.

Acute complications of diverticula include diverticulitis with or without perforation, hemorrhage, and intestinal obstruction[18-21]. In a patient with diverticular bleeding, endoscopy is unlikely to reveal the source, although it is of benefit in excluding other source of bleeding. Mesenteric angiography or Tc^{99m} RBC scan can be more helpful in such cases[22]. The differential diagnosis of intestinal obstruction includes volvulus, adhesions, intussusception, compression by a large diverticulum, or enterolith[1,7,23]. Small bowel dyskinesia, caused by bacterial overgrowth, visceral myopathy, or neuropathy may induce pseudo-obstruction[15]. Pseudo-obstruction is in fact a more common complication than mechanical obstruction and has been reported in 10-25% of cases[24]. Most of the patients in our study (58%) had diverticulitis with or without perforation. Hemorrhage and intestinal obstruction were only minor findings in our series, with only four patients presenting with GI bleeding. One of eight patients had an enterolith in his diverticulum that resulted in obstruction.

Chronic symptoms included intermittent abdominal fullness, vague abdominal discomfort or pain, passage of oily stool, weight loss, and weakness, which resolve after treatment. These might have been caused by pseudo-obstruction or bacterial overgrowth[1,7]. In one report, 14 of 27 patients had chronic refractory symptoms[15]. In our series the result was comparable (14/29). Small bowel diverticula should be considered in patients presenting with such unexplained chronic symptoms.

Nobles described a radiographic finding suggestive of jejunoileal diverticulum, namely a segmental dilatation of the small bowel in the epigastrium or left upper quadrant. He also suggested that the diagnosis be considered whenever the triad of obscure abdominal pain, anemia, and dilated small bowel loops on abdominal radiographs is encountered[7,25]. An upper GI series with small bowel follow through is a simple method for identifying a diverticulum. Three of the four correct preoperative diagnoses in our series were made by this method. However, diverticula may protrude into the leaves of mesentery and be hidden by the mesenteric fat. They also often communicate with bowel lumen through a wide opening. These factors may prevent the lesion being seen on routine barium follow through[26]. Enteroclysis (i.e., a double contrast of small bowel series) is more reliable for detecting these lesions, because the barium is able to flow out of a wide-mouthed diverticulum after air insufflation[4,5,16]. A meticulous search of the mesenteric portion of the small bowel as well as air insufflation with a small gauge needle into isolated segments of the bowel have been used to demonstrate obscure diverticula during operation[7,14,18].

Asymptomatic non-Meckelian diverticula as an incidental finding on radiographic studies or at laparotomy usually do not need resection[20]. However, if a dilated, hypertrophied segment of bowel with large diverticula is found, it may indicate a progressive form of the disease, in which case resection of the diverticular segment found incidentally at laparotomy is recommended[1,9]. Although some patients with chronic symptoms can be treated conservatively, when symptoms are persistent or refractory to treatment, resection may be beneficial[1].

In conclusion, symptomatic acquired diverticular disease of the jejunum and ileum is an uncommon disorder. Diagnosis is often difficult and delayed, resulting in unnecessary morbidity and mortality[16]. All published studies are limited by being retrospective analyses of small numbers of cases. There has thus been an inherent bias in patient selection. Preoperative diagnosis is difficult, and the paucity of studies makes it difficult to define the optimal diagnostic method. Certainly a high index of suspicion for this often obscure disease is necessary.

ACKNOWLEDGMENT

The authors wish to thank Dr. Mary Jeanne Buttrey for critical reading and correction of the manuscript.

REFERENCES

1 **Longo WE,** Vernava AM. Clinical implications of jejunoileal diverticular disease. *Dis Colon Rectum* 1992; **35**: 381-388
2 **Chiu EJ,** Shyr YM, Su CH, Wu CW, Lui WY. Diverticular disease of the small bowel. *Hepatogastroenterology* 2000; **47**: 181-184
3 **Zhan J,** Xia ZS, Zhong YQ, Zhang SN, Wang LY, Shu H, Zhu ZH. Clinical analysis of primary small intestinal disease: A report of 309 cases. *World J Gastroenterol* 2004; **10**: 2585-2587
4 **Maglinte DD,** Chernish SM, DeWeese R, Kelvin FM, Brunelle RL. Acquired jejunoileal diverticular disease: subject review. *Radiology* 1986; **158**: 577-580
5 **Salomonowitz E,** Wittich G, Hajek P, Jantsch H, Czembirek H. Detection of intestinal diverticula by double-contrast small bowel enema: differentiation from other intestinal diverticula.

Gastrointest Radiol 1983; **8**: 271-278
6 **Noer T.** Non-Meckelian diverticula of the small bowel: The incidence in an autopsy material. *Acta Chir Scand* 1960; **120**: 175-179
7 **Ross CB,** Richards WO, Sharp KW, Bertram PD, Schaper PW. Diverticular disease of the jejunum and its complications. *Am Surg* 1990; **56**: 319-324
8 **Afridi SA,** Fichtenbaum CJ, Taubin H. Review of duodenal diverticula. *Am J Gastroenterol* 1991; **86**: 935-938
9 **Altemeier WA,** Bryant LR, Wulsin JH. The surgical significance of jejunal diverticulosis. *Arch Surg* 1963; **86**: 732-745
10 **Akhrass R,** Yaffe MB, Fischer C, Ponsky J, Shuck JM. Small-bowel diverticulosis: perceptions and reality. *J Am Coll Surg* 1997; **184**: 383-388
11 **Palder SB,** Frey CB. Jejunal diverticulosis. *Arch Surg* 1988; **123**: 889-894
12 **Kraus M,** Sampson D, Wilson SD. Perforation of diverticulum of terminal ileum presenting as acute appendicitis. *Surgery* 1976; **79**: 724-725
13 **Baskin RH,** Mayo CW. Jejunal diverticulosis: a clinical study of 87 cases. *Surg Clin North Am* 1952; **95**: 1185-1196
14 **Cooke WT,** Cox EV, Fone DJ, Meynell MJ, Gaddie R. The clinical and metabolic significance of jejunal diverticula. *Gut* 1963; **4**: 115-131
15 **Krishnamurthy S,** Kelly MM, Rohrmann CA, Schuffler MD. Jejunal diverticulosis. A heterogenous disorder caused by a variety of abnormalities of smooth muscle or myenteric plexus. *Gastroenterology* 1983; **85**: 538-547
16 **de Bree E,** Grammatikakis J, Christodoulakis M, Tsiftsis D. The clinical significance of acquired jejunoileal diverticula. *Am J Gastroenterol* 1998; **93**: 2523-2528
17 **Geroulakos G.** Surgical problems of jejunal diverticulosis. *Ann R Coll Surg Engl* 1987; **69**: 266-268
18 **Roses DF,** Gouge TH, Scher KS, Ranson JH. Perforated diverticula of the jejunum and lleum. *Am J Surg* 1976; **132**: 649-652
19 **Gliustra PE,** Killoran PJ, Root JA, Ward WW. Jejunal diverticulitis. *Radiology* 1977; **125**: 609-611
20 **Wilcox RD,** Shatney CH. Surgical implications of jejunal diverticula. *South Med J* 1988; **81**: 1386-1391
21 **Wilcox RD,** Shatney CH. Massive rectal bleeding from jejunal diverticula. *Surg Gynecol Obstet* 1987; **165**: 425-428
22 **Spiegel RM,** Schultz RW, Casarella WJ, Wolff M. Massive hemorrhage from jejunal diverticula. *Radiology* 1982; **143**: 367-371
23 **Harris LM,** Volpe CM, Doerr RJ. Small bowel obstruction secondary to enterolith impaction complicating jejunal diverticulitis. *Am J Gastroenterol* 1997; **92**: 1538-1540
24 **Eckhauser FE,** Zelenock GB, Freier DT. Acute complications of jejuno-ileal pseudodiverticulosis: Surgical implications and management. *Am J Surg* 1979; **138**: 320-323
25 **Nobles ER Jr.** Jejunal diverticula. *Arch Surg* 1971; **102**: 172-174
26 **Freimanis MG,** Plaza-Ponte M. Radiologic diagnosis of jejunal diverticulitis. *Gastrointest Radiol* 1988; **13**: 312-314

Science Editor Guo SY **Language Editor** Elsevier HK

PO Box 2345, Beijing 100023, China
www.wjgnet.com
wjg@wjgnet.com

ELSEVIER

World J Gastroenterol 2005;11(35):5561-5564
World Journal of Gastroenterology ISSN 1007-9327
© 2005 The WJG Press and Elsevier Inc. All rights reserved.

• *BRIEF REPORTS* •

Heat shock protein 70 chaperoned alpha-fetoprotein in human hepatocellular carcinoma cell line BEL-7402

Xiao-Ping Wang, Qiao-Xia Wang, Hai-Yan Li, Rui-Fen Chen

Xiao-Ping Wang, Hai-Yan Li, Rui-Fen Chen, Department of Pathology, Capital University of Medical Sciences, Beijing 100054, China
Qiao-Xia Wang, Department of Gastroenterology, the Third Clinical Hospital, Lanzhou Medical College, Lanzhou 730000, Gansu Province, China
Supported by the Research Fund for Young Scholars of Beijing, No. 02120031 and Research Program of Beijing Education Committee, No. 0410025002
Correspondence to: Dr. Xiao-Ping Wang, Department of Pathology, Capital University of Medical Sciences, Beijing 100054, China. wxpphd@yahoo.com.cn
Telephone: +86-10-63051455-11
Received: 2005-01-19 Accepted: 2005-02-18

Abstract

AIM: To investigate the interaction between heat shock protein 70 (HSP70) and α-fetoprotein (AFP) in human hepatocellular carcinoma (HCC) cell line BEL-7402.

METHODS: The expression and localization of HSP70 and AFP in human HCC cell line BEL-7402 were determined by immunocytochemistry and indirect immunofluorescence cytochemical staining. The interaction between HSP70 and AFP in HCC cells was analyzed by immunoprecipitation and Western blot.

RESULTS: Immunocytochemical staining detection showed that HCC cell BEL-7402 expressed a high level of HSP70 and AFP synchronously. Both were stained in cell plasma. AFP existed in the immunoprecipitate of anti-HSP70 mAb, while there was HSP70 in the immunoprecipitate of anti-AFP mAb.

CONCLUSION: HSP70 chaperones AFP in human HCC cell BEL-7402. The interaction between HSP70 and AFP in human HCC cell can be a new route to study the pathogenesis and immunotherapy of HCC.

© 2005 The WJG Press and Elsevier Inc. All rights reserved.

Key words: Heat shock protein 70; Alpha-fetoprotein; Hepatocellular carcinoma

Wang XP, Wang QX, Li HY, Chen RF. Heat shock protein 70 chaperoned alpha-fetoprotein in human hepatocellular carcinoma cell line BEL-7402. *World J Gastroenterol* 2005; 11(35): 5561-5564
http://www.wjgnet.com/1007-9327/11/5561.asp

INTRODUCTION

Alpha-fetoprotein (AFP) is a major serum protein synthesized by fetal liver cells, yolk sac cells, and in trace amounts by the fetal gastrointestinal tract[1]. AFP appears to function as an osmotic and carrier protein in the fetus and to regulate the immune system by immunosuppressive functions, such as preventing immunological attacks to the embryo by the maternal immune system[1]. Reappearance of AFP in adult serum often signals pathological conditions, particularly the presence of hepatocellular carcinoma (HCC) and germ cell tumors containing yolk sac cell elements[2]. Now AFP has been successfully used as a diagnostic and prognostic tool for HCC. Although many investigations for the function of AFP had been carried out, the biological role of AFP is still a riddle so far.

Heat shock proteins (HSPs) are molecular chaperones which are emerging as biochemical regulators of cell growth, apoptosis, protein homeostasis and cellular targets of peptides[3-5]. Up regulated expression of HSPs during the growth of cancer cells has a close relationship with cell proliferation[6-8]. It is interesting to note that several studies have shown that AFP plays some roles during cell survival and proliferation of HCC cells[9-11]. Previous studies have confirmed overexpression of HSP70 in HCC[12]. So there may be a possible correlation between the expression of HSP70 and AFP during the growth and differentiation of HCC cells. In this study, by immunocytochemistry and immunoprecipitation, we observed that HSP70 chaperoned AFP in HCC cell cytoplasm. The interaction between HSP70 and AFP in human HCC cells will provide a new route for studying the pathogenesis and immunotherapy of HCC.

MATERIALS AND METHODS

Reagents

Rabbit anti-human HSP70 antibody, mouse anti-human AFP monoclonal antibody, TRITC labeled goat anti-rabbit antibody and FITC labeled goat anti-mouse antibody were purchased from Santa Cruz Company. EnVisionTM kits were purchased from Dako Biological Technology Company. ProteinA/G-agarose beads were purchased from Gene Company.

Cell line and cell culture

Human HCC cell line BEL-7402 was provided by the Institute of Oncology, Chinese Academy of Medical Sciences, Beijing, China. The derived cell lines were grown in RPMI 1 640 medium supplemented with 100 mL/L heat-inactivated fetal calf serum, 50 000 U/L penicillin and 0.05 g/L streptomycin. The cells were maintained at 37 ℃ in a humidified atmosphere

containing 50 mL/L CO_2. Viability of the cells used in these experiments was consistently more than 95% when evaluated by the trypan blue exclusion method. Cells at a density of 2.5×10^5/mL were seeded into six-well plates for 24 h, washed with PBS, fixed by adding 2 mL of cold 500 mL/L methanol-acetone and stored at 4 ℃ for 20 min, then washed with PBS, and dried at room temperature.

Immunocytochemistry

All cells in six-well plates were hydrated with graded alcohol. Endogenous peroxidase was then blocked with 3 mL/L H_2O_2 diluted in methanol for 30 min at room temperature. Antigen retrieval was performed by treating the slides in citrate buffer in a microwave for 10 min. The cells were incubated in a moist chamber with HSP70 rabbit antibody (1∶100) or AFP mouse monoclonal antibody (1∶100) at 4 ℃ overnight, respectively. After a complete wash in PBS, the cells were treated with HRP labeled goat anti-rabbit and goat anti-mouse antibody (1∶100) for 45 min at 37 ℃. After a complete wash in PBS, all cells were developed in 0.5 g/L freshly prepared diaminobenzidine solution (DAB, Sigma Co.) for 8 min, and then counterstained with hematoxylin, dehydrated, air dried, and mounted. Anti-HSA was used to substitute for the primary antibody as a negative control.

Indirect double-immunofluorescence cytochemistry

All cells in six-well plates were hydrated with graded alcohol. The cells were blocked in 10 mL/L bovine serum albumin (BSA) for 30 min at room temperature, and then incubated with HSP70 rabbit antibody (1∶100) or AFP mouse monoclonal antibody (1∶100) at 4 ℃ overnight, respectively. After a complete wash in PBS, the cells were treated with TRITC labeled goat anti-rabbit antibody or FITC labeled goat anti-mouse antibody (1∶20) for 40 min at room temperature. After extensive washing, the stained cells were observed under an immunofluorescence microscope. Anti-HSA was used to substitute for the primary antibody as a negative control.

Immunoprecipitation and Western blot

Cells at a density of 2.5×10^5/mL were seeded into six-well plates for 24 h. Then cells were treated with 0.5 g/L trypsin and 0.2 g/L EDTA. After washing with cold PBS, the cells were centrifuged and harvested. They were then lysed with 500 μL of lysis buffer (10 mmol/L Tris-HCl, pH 7.4, 150 mmol/L NaCl, 1 mL/L Triton X-100, 10 g/L sodium deoxycholate) containing 1 μg/mL pepstatin and 1 mmol/L phenyl-methylsulfonyl fluoride (PMSF). Also, five units of apyrase (Sigma, Co.) were added to the lysate to deplete endogenous ATP. The cell lysates were sonicated and clarified by centrifugation. The supernatants were preabsorbed with 20 μL protein A/G-agarose beads at 4 ℃ for 4 h. After centrifugation, the supernatants were incubated with 100 μL HSP70 rabbit antibody (1∶100) or 100 μL AFP mouse monoclonal antibody (1∶100), respectively at 4 ℃ for 60 min. Then 50 μL protein A/G-agarose beads were added and incubated for 60 min at 4 ℃. The immunoprecipitates were collected by centrifugation and washed five times with PBS. The precipitated protein complexes were released from the immunopellet with SDS-sample buffer (62.5 mmol/L Tris-HCl, pH 6.8, 25 g/L SDS, 50 mL/L β-mercaptoethanol, 100 mL/L glycerol) at 100 ℃ for 5 min. The immunoprecipitates were then analyzed by 90 g/L SDS-polyacrylamide gel electrophoresis (SDS-PAGE). Proteins were transferred to nitrocellulose (NC) membrane (BioRad) and detected by immunoblotting with anti-AFP monoclonal antibody or anti-HSP70 antibody (1∶100) at 4 ℃ overnight, respectively. After a complete wash in PBS, the membranes were treated with HRP labeled goat anti-rabbit and goat anti-mouse antibody (1∶100) for 45 min at 37 ℃. After a complete wash in PBS, the membranes were developed in 0.5 g/L freshly prepared diaminobenzidine solution (DAB, Sigma Co.) for 8 min. Anti-HSA was used to substitute for the primary antibody as a negative control.

Statistical analysis

HSP70, AFP expression differences between HCC cell BEL-7402 and control group were analyzed statistically using χ^2-test. $P<0.05$ was considered statistically significant.

RESULTS

Expression of HSP70 and AFP in HCC cell line BEL-7402

Positive expression of HSP70 and AFP showed brown staining in the nuclei or cytoplasm, more than 500 cells calculated in different microscopic fields of each well, and the percentage of positive cells were evaluated.

Immunocytochemical staining showed that the positive rate of HSP70 was 96.0% (480/500), and AFP was 100.0% (500/500), while control group was 5.0% (25/500). There was a significant difference between experimental group and control group ($P<0.01$). HSP70 and AFP were mainly stained in cell cytoplasm (Figure 1).

Interaction between HSP70 and AFP in HCC cell line BEL-7402

Immunoprecipitate and Western blot showed that there were

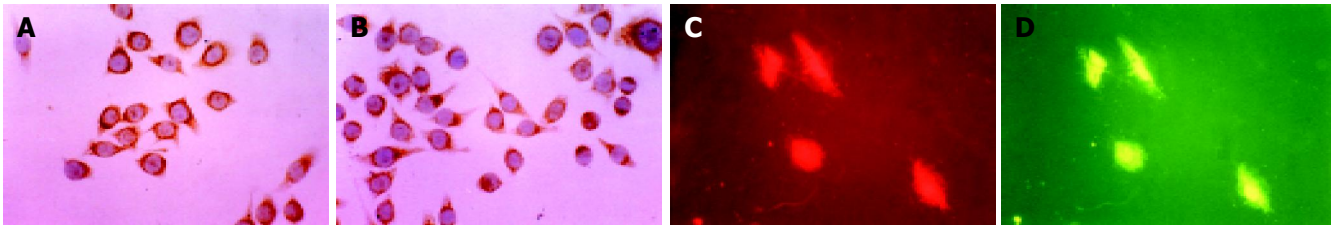


Figure 1 Expressions of HSP70 and AFP in HCC cell line BEL-7402 by immunocytochemistry and immunofluorescence cytochemistry, ×400. **A:** HSP70 positive expression in cytoplasm; **B:** AFP immunostaining in cytoplasm; **C:** HSP70 immunostaining in cytoplasm; **D:** AFP green immunofluorescence in cytoplasm.

two clear protein bands in the transferred NC membrane. Under-precipitated with anti-HSP70 antibody, there appeared a M_r 68 000 clear AFP band (lane 1) and under-precipitated with anti-AFP mAb, there existed a M_r 72 000 clear HSP70 band (lane 2), demonstrating that AFP existed in the immunoprecipitate of anti-HSP70 antibody and HSP70 existed in that of anti-AFP mAb. The results indicated that HSP70 interacted with AFP in HCC cell line BEL-7402 (Figure 2).

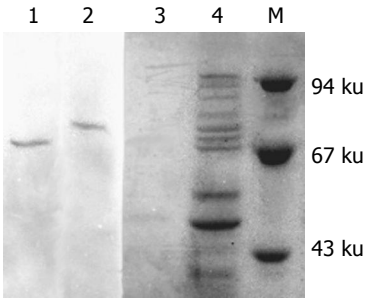


Figure 2 Analysis of immunoprecipitate of anti-HSP70 antibody and anti-AFP mAb by SDS-PAGE and Western blot (lane 1: precipitated with anti-HSP70 antibody; lane 2: precipitated with anti-AFP mAb; lane 3: precipitated with anti-HSA antibody; lane 4: cell lysates supernatants; M: molecular mass markers).

DISCUSSION

In this study we examined the expressions of HSP70 and AFP in HCC cell line BEL-7402 by immunocytochemistry, immunofluorescence cytochemistry and immunoprecipitate analysis. The results showed that almost all HCC cells detected expressed a high level of HSP70 and AFP, which had a significant difference compared with control group. HSP70 chaperoned AFP that mainly localized in cell cytoplasm.

AFP always accompanies the growth of liver cells, and it is possible that AFP may be related to the proliferation of tumor or fetal cells[8-10]. The mechanism for growth-promoting activity of AFP is still unclear. Escaping from the surveillance of immune system is the primary cause for malignant growth of HCC cells[12,13]. Several investigations have shown that AFP could be individually synergistic with other growth factors to promote the growth of many tumor cells[14,15]. AFP receptors have been found anchoring on the membrane of various tumor cells[16-17]. The receptor may mediate intercellular signal transduction which influences the expression of genes related to proliferation[16,17]. AFP can stimulate the expression of some oncogenes which controls cell cycle, and then enhance the proliferation of human HCC[19,20]. When BEL-7402 cell line were treated with AFP, oncogene protein, such as c-fos, c-jun, n-ras and mutative p53 and $p21^{ras}$ increased rapidly, which have an important function in modulating growth and differentiation of the cells.

Heat shock protein (HSP) is a group of highly conserved proteins synthesized after heat induction[3-5]. In normal cells, HSP70 is constitutively expressed at low levels but the expression was dramatically enhanced by stressful conditions[3]. HSPs are thought to act as molecular chaperone, helping in transporting, folding and processing of their target proteins. Although the cellular implication of the increased production of these proteins is unknown, it may be expected that each response would enhance the capacity of the pathway(s) in which these proteins function and perhaps protect the associated cellular compartments from damage via abnormal protein interactions. Enhanced expression of HSPs during the growth of cancer cells implies its close relationship with cell growth[6-8]. It is interesting to note that AFP plays some roles during tumor cell survival and proliferation[9-11]. These studies have suggested a possible correlation between the overexpression of HSP70 and AFP during the growth and differentiation of tumor cells. Continuous expression of HSP70 in tumor cells is required to serve as molecular chaperones in regulating and stabilizing tumor growth process. Some studies have suggested that high level expression of HSP70 could contribute to tumorigenecity of certain tumors[7,8], but its role in tumorigenecity is not clear. So, it is reasonable to propose that HSP70 and AFP up-expression in these tumor cells is closely related with the tumor cell survival and proliferation. Up-regulated expression of HSP70 in tumor cells may be required to serve as molecular chaperones in regulating and stabilizing oncofetal protein and mutant oncogene products during the tumor growth process[21,22]. Therefore, HSP70 could assist to stabilize AFP in cell cytoplasm, transport it to cell membrane and release its monomer to the serum, which indirectly prompts and protects AFP function. Conversely, AFP itself stimulates HCC cell proliferation through membrane receptor mediating cellular signal transduction pathways. This indicates that the proliferating HCC cells need much more HSP70 to maintain the formation of AFP activities. Our results showed that, in human HCC BEL-7402 cell line, there exists a high level of expression of HSP70 and AFP. It indicates that co-expression of HSP70 and AFP is likely to have some relationship with proliferation, development and poor prognosis of human HCC. The observed fact is that HSP70 chaperoned AFP may be useful to study the pathogenesis and immunity of human HCC.

Recent studies on the immunodominant epitopes of AFP have provided a solution to the obstacle of HCC immunotherapy. AFP is produced at low serum levels after birth throughout life[1]. The majority of human HCC overexpress the oncofetal antigen AFP, M_r 64 000-72 000 glycoprotein[2]. Despite being exposed to high plasma levels of this oncofetal protein during embryonic development, the body has a low immunity to it[3-5]. Butterfield *et al*.[23], recently found that four peptides of human AFP processed and presented in the context of HLA-A0201, could be recognized by the human T cell repertoire, and could be used to generate AFP-specific CTL in human T cell cultures. It was also found that murine immune system could generate T-cell responses to this oncofetal antigen[24]. Therefore, it may be a better target for immunotherapy. But AFP immunization alone still results in lower levels of specific response and poorly reproducible protective immunity[24,25].

How to enhance the host's active immunity to AFP may be an interesting strategy for HCC therapy. In our previous study, tumor rejection assay demonstrated that recombinant DNA vaccine AFP/HSP70 elicited strong specific antitumor

immunity against AFP-producing SP2/0 cells than AFP DNA vaccine. Results indicated that AFP immunogenicity can be improved greatly by HSP70 molecular and vaccination with DNA encoding HSP70 could increase both humoral and T-cell proliferation responses to AFP. We attributed the successful AFP specific T-cell responses in mice to the HSP70 molecule by mediating APCs for efficient uptake and process of AFP. Numerous investigations have been verified that HSP70 is a better molecular chaperone and adjuvant which can process and present weak tumor antigen to MHC-I of host APCs, eliciting specific T-cell response and CTL reaction[26,27]. HSP70-associated peptides can also anchor antigen on the cell membrane and directly present it to nature killer cells or γδ T cells as superantigen without being dependent on the stimulation of MHC-I molecules[28,29]. The observed fact is that HSP70 chaperoned AFP in HCC, may be useful to study tumor pathogenesis or design effective vaccine against liver cancers.

REFERENCES

1 **Deutsch HF.** Chemistry and biology of a-fetoprotein. *Adv Cancer Res* 1991; **56**: 253-312
2 **Goldenberg DM,** Kim EE, Deland F, Spremulli E, Nelson MO, Gockerman JP, Primus FJ, Corgan RL, Alpert E. Clinical studies on the radioimmunodetection of tumors containing alpha-fetoprotein. *Cancer* 1980; **45**: 2500-2505
3 **Schlesinger MJ.** Heat shock proteins. *J Biol Chem* 1990; **265**: 12111-12114
4 **Little E,** Ramakrishnan M, Roy B, Gazit G, Lee AS. The glucose-regulated proteins (GRP78 and GRP94): functions, gene regulation, and applications. *Crit Rev Eukaryot Gene Expr* 1994; **4**: 1-18
5 **Morimoto RI.** Cells in stress: transcriptional activation of heat shock genes. *Science* 1993; **259**: 1409-1410
6 **Lee AS.** The glucose-regulated proteins: stress induction and clinical applications. *Trends Biochem Sci* 2001; **26**: 504-510
7 **Isomoto H,** Oka M, Yano Y, Kanazawa Y, Soda H, Terada R, Yasutake T, Nakayama T, Shikuwa S, Takeshima F, Udono H, Murata I, Ohtsuka K, Kohno S. Expression of heat shock protein (Hsp) 70 and Hsp 40 in colonic cancer. *Cancer Lett* 2003; **198**: 219-228
8 **Thanner F,** Sutterlin MW, Kapp M, Rieger L, Kristen P, Dietl J, Gassel AM, Muller T. Heat-shock protein 70 as a prognostic marker in node-negative breast cancer. *Anticancer Res* 2003; **23**: 1057-1062
9 **Dudich E,** Semenkova L, Gorbatova E, Dudich I, Khromykh L, Tatulov E, Grechko G, Sukhikh G. Growth-regulative activity of human alpha-fetoprotein for different types of tumor and normal cells. *Tumour Biol* 1998; **19**: 30-40
10 **Wang XW,** Xie H. alpha-fetoprotein enhances the proliferation of human hepatoma cells *in vitro*. *Life Sci* 1999; **64**: 17-23
11 **Wang XW,** Xu B. Stimulation of tumor-cell growth by alpha-fetoprotein. *Int J Cancer* 1998; **75**: 596-599
12 **Semeniuk DJ,** Boismenu R, Tam J, Weissenhofer W, Murgita RA. Evidence that immunosuppression is an intrinsic property of the alpha-fetoprotein molecule. *Adv Exp Med Biol* 1995; **383**: 255-269
13 **Gotsman I,** Israeli D, Alper R, Rabbani E, Engelhardt D, Ilan Y. Induction of immune tolerance toward tumor-associated-antigens enables growth of human hepatoma in mice. *Int J Cancer* 2002; **97**: 52-57
14 **Keel BA,** Eddy KB, Cho S, May JV. Synergistic action of purified alpha-fetoprotein and growth factors on the proliferation of porcine granulosa cells in monolayer culture. *Endocrinology* 1991; **129**: 217-225
15 **Peng SY,** Chen WJ, Lai PL, Jeng YM, Sheu JC, Hsu HC. High alpha-fetoprotein level correlates with high stage, early recurrence and poor prognosis of hepatocellular carcinoma: significance of hepatitis virus infection, age, p53 and beta-catenin mutations. *Int J Cancer* 2004; **112**: 44-50
16 **Esteban C,** Geuskens M, Uriel J. Activation of an alpha-fetoprotein (AFP)/receptor autocrine loop in HT-29 human colon carcinoma cells. *Int J Cancer* 1991; **49**: 425-430
17 **Villacampa MJ,** Moro R, Naval J, Failly-Crepin C, Lampreave F, Uriel J. Alpha-fetoprotein receptors in a human breast cancer cell line. *Biochem Biophys Res Commun* 1984; **122**: 1322-1327
18 **Naval J,** Villacampa MJ, Goguel AF, Uriel J. Cell-type-specific receptor for alpha-fetoprotein in mouse T-lymphoma cell line. *Proc Natl Acad Sci USA* 1985; **82**: 3301-3305
19 **Caruso ML,** Valentini AM. Overexpression of p53 in a large series of patients with hepatocellular carcinoma: a clinicopathological correlation. *Anticancer Res* 1999; **19**: 3853-3856
20 **Zhang XW,** Xu B. Differential regulation of P53, c-Myc, Bcl-2, Bax and AFP protein expression, and caspase activity during 10-hydroxycamptothecin-induced apoptosis in Hep G2 cells. *Anticancer Drugs* 2000; **11**: 747-756
21 **Hwang TS,** Han HS, Choi HK, Lee YJ, Kim YJ, Han MY, Park YM. Differential, stage-dependent expression of Hsp70, Hsp110 and Bcl-2 in colorectal cancer. *J Gastroenterol Hepatol* 2003; **18**: 690-700
22 **Dorsey WC,** Tchounwou PB. CYP1a1, HSP70, P53, and c-fos expression in human liver carcinoma cells (HepG2) exposed to pentachlorophenol. *Biomed Sci Instrum* 2003; **39**: 389-396
23 **Butterfield LH,** Koh A, Meng W, Vollmer CM, Ribas A, Dissette V, Lee E, Glaspy JA, McBride WH, Economou JS. Generation of human T-cell responses to an HLA-A2.1-restricted peptide epitope derived from alpha-fetoprotein. *Cancer Res* 1999; **59**: 3134-3142
24 **Saeki A,** Nakao K, Nagayama Y, Yanagi K, Matsumoto K, Hayashi T, Ishikawa H, Hamasaki K, Ishii N, Eguchi K. Diverse efficacy of vaccination therapy using the alpha-fetoprotein gene against mouse hepatocellular carcinoma. *Int J Mol Med* 2004; **13**: 111-116
25 **Hanke P,** Serwe M, Dombrowski F, Sauerbruch T, Caselmann WH. DNA vaccination with AFP-encoding plasmid DNA prevents growth of subcutaneous AFP-expressing tumors and does not interfere with liver regeneration in mice. *Cancer Gene Ther* 2002; **9**: 346-355
26 **Milani V,** Noessner E, Ghose S, Kuppner M, Ahrens B, Scharner A, Gastpar R, Issels RD. Heat shock protein 70: role in antigen presentation and immune stimulation. *Int J Hyperthermia* 2002; **18**: 563-575
27 **Harmala LA,** Ingulli EG, Curtsinger JM, Lucido MM, Schmidt CS, Weigel BJ, Blazar BR, Mescher MF, Pennell CA. The adjuvant effects of Mycobacterium tuberculosis heat shock protein 70 result from the rapid and prolonged activation of antigen-specific CD8+ T cells *in vivo*. *J Immunol* 2002; **169**: 5622-5629
28 **Wei Y,** Zhao X, Kariya Y, Fukata H, Teshigawara K, Uchida A. Induction of autologous tumor killing by heat treatment of fresh human tumor cells: involvement of gamma delta T cells and heat shock protein 70. *Cancer Res* 1996; **56**: 1104~1110
29 **Gross C,** Hansch D, Gastpar R, Multhoff G. Interaction of heat shock protein 70 peptide with NK cells involves the NK receptor CD94. *Biol Chem* 2003; **384**: 267-279

Science Editor Guo SY **Language Editor** Elsevier HK

PO Box 2345, Beijing 100023, China
www.wjgnet.com
wjg@wjgnet.com

ELSEVIER

World J Gastroenterol 2005;11(35):5565-5567
World Journal of Gastroenterology ISSN 1007-9327
© 2005 The WJG Press and Elsevier Inc. All rights reserved.

• *BRIEF REPORTS* •

Detection of HBsAg, HBcAg, and HBV DNA in ovarian tissues from patients with HBV infection

Li-Zhang Chen, Xue-Gong Fan, Jian-Ming Gao

Li-Zhang Chen, Jian-Ming Gao, School of Public Health, Central South University, Changsha 410078, Hunan Province, China
Xue-Gong Fan, Department of Infectious Diseases, Xiangya Hospital, Central South University, Changsha 410078, Hunan Province, China
Correspondence to: Dr. Li-Zhang Chen, School of Public Health, Central South University, Changsha 410078, Hunan Province, China. chenliz@mail.csu.edu.cn
Telephone: +86-731-8836971 Fax: +86-731-8836266
Received: 2004-09-03 Accepted: 2005-01-26

Abstract

AIM: To investigate the presence of HBsAg, HBcAg, and HBV DNA in ovarian tissues from patients with HBV infection.

METHODS: HBsAg and HBcAg were examined in ovarian biopsy tissues from 26 patients with HBV infection by immunocytochemistry, and HBV DNA was detected in ovarian tissues by PCR.

RESULTS: HBsAg and HBcAg were present with the same positive rate of 34.6% (9/26). The total positive rate was 46.2% (12/26). HBsAg and HBcAg were positive in 6 (23.1%) of the 26 patients. Brown positive particles were diffusely distributed in ovarian cells. The positive rate of HBV DNA was 58.3% (7/12).

CONCLUSION: HBsAg, HBcAg, and HBV DNA can be detected in ovarian tissues from patients with HBV infection. The presence of HBsAg and HBcAg in ovarian tissues does not correlate with the HBV markers in serum.

© 2005 The WJG Press and Elsevier Inc. All rights reserved.

Key words: Ovarian tissue; HBsAg; HBcAg; HBV DNA

Chen LZ, Fan XG, Gao JM. Detection of HBsAg, HBcAg, and HBV DNA in ovarian tissues from patients with HBV infection. *World J Gastroenterol* 2005; 11(35): 5565-5567
http://www.wjgnet.com/1007-9327/11/5565.asp

INTRODUCTION

The prevalence of hepatitis B is high in China. The overall positive rate of serum HBsAg is about 10%. Hepatitis B virus (HBV) infection can cause acute hepatitis, chronic hepatitis, hepatocirrhosis and hepatocellular carcinoma[1,2]. HBV is not a kind of virus that locates strictly in the liver cells. HBV infection may cause either pathological hepatic lesion or extra-hepatic lesion. It has been well documented that the extra-hepatic lesion due to acute hepatitis is temporary, and that due to chronic hepatitis is associated with persistent HBV infection and draws more attention of researchers. Animal experiments have confirmed that HBV can exist and replicate in various organs and tissues[3,4]. With the development of molecular biology, HBV can be detected in patients with HBV infection outside the liver, such as in peripheral blood mononuclear cells, tissues or cells of pancreas, spleen, skin, kidney, etc.[5]. Moreover, it has been shown to be present in blood, saliva, semen, vagina secretion, sweat, breast milk, tear, and urine[6].

Although some studies on the infection and location of HBV in extra-hepatic tissues have been carried out and a few papers have been published at home or abroad[3-5], whether HBV replicates outside the liver after its infection is still controversial. The location and distribution of HBV in extra-hepatic tissues or cells are not consistent, and the pathologic lesions caused by the extra-hepatic infection of HBV and their pathogenesis are not fully understood. Whether HBV exists in ovarian tissues is unknown. If we can demonstrate this, then it is reasonable to assume that vertical transmission may be due to HBV transmitting from ovary to ovum and fetus. In this study, we investigated the presence of HBsAg, HBcAg, and HBV DNA in 26 ovarian biopsy specimens using immunocytochemistry and PCR in order to analyze and interpret the mechanism and significance of HBV infection in ovarian tissues.

MATERIALS AND METHODS

Subjects

We reviewed the medical history at the Department of Pathology, Xiangya Hospital, Central South University and found 170 patients who had ovarian biopsy from June 2002 to June 2003. Among them, 26 patients had positive serum HBV markers. Seven out of the twenty-six patients were positive for HBsAg, and the other 19 patients had two or more HBV markers in serum. Paraffin-embedded ovarian tissues from these 26 patients were enrolled for further analysis. The age of the 26 patients ranged from 2 mo to 71 years, with an average of 40 years. Five patients were diagnosed as ovarian cyst, and 21 patients as ovarian cancer.

Detection of HBsAg and HBcAg by immunocytochemistry

The presence of HBsAg and HBcAg was examined in ovarian biopsy tissues from the 26 patients by immunocytochemistry (streptavidin-peroxidase-biotin) according to the manufacturer's instructions. The main steps were as

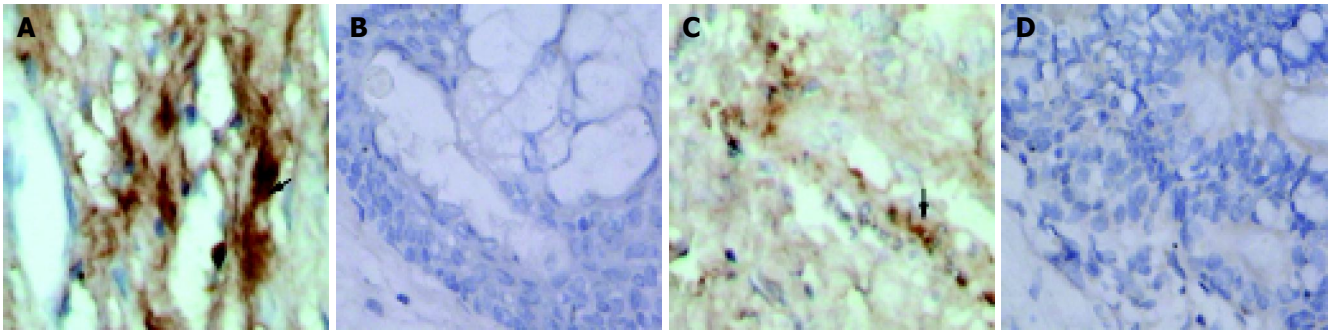


Figure 1 Positive HBsAg (**A**) expression and positive HBcAg (**B**) expression in ovarian tissue and negative control (**C** and **D**).

follows. Cover slips were dewaxed with xylene, and dehydrated in alcohol, washed thrice with PBS for 5 min each time. Endogenous peroxidase activity was quenched by incubating cover slips with 50 μL peroxide for 10 min, and washed with PBS. Samples were blocked by incubating cover slips with 50 μL goat serum for 30 min, washed with PBS and incubated with primary antibody for 60 min at room temperature, then washed with PBS and incubated with biotin-conjugated secondary antibody for 10 min at room temperature, washed again with PBS and incubated with streptavidin-peroxidase for 10 min at room temperature, washed with PBS and incubated with DAB for 5 min, counterstained with hematoxylin, dehydrated in alcohol and xylene. The coverslips were permanently mounted and observed under light microscope. Brown signals were considered as positive result.

When primary antibody was replaced by PBS, the result was negative.

Ovarian tissues from patients without HBV infection were used as negative control.

Liver tissues from patients with hepatitis B were used as positive control.

Mouse anti-HBsAg, mouse anti-HBcAg, and SP kit were purchased from Zhongshan Biological Technology Limited Company, Beijing.

Detection of HBV DNA by PCR

Paraffin-embedded ovarian tissues were digested with proteinase K, and HBV DNA was isolated using phenol and chloroform. Primer sequences were designed by us using Primer 3 software: forward primer, 5'-TCGGAAATACACCTCCTTTCCATGG-3' (HBV genome 1 353-1 377); reverse primer, 5'-GCCTCAA GGTCGGT-CGTTGACA-3' (HBV genome 1 702-1 681). The length of PCR product was 350 bp. Liver tissue DNA from patients with hepatitis B and ovarian tissue DNA from patients without HBV infection were used as positive control and negative control respectively. Thirty cycles of DNA amplification were performed in 50 μL PCR reaction mixture. The condition of each cycle was denaturation at 94 ℃ for 30 s, primer annealing at 55 ℃ for 30 s, and elongation at 72 ℃ for 30 s, followed by a final 10-min elongation at 72 ℃. DNA marker, proteinase K, Taq DNA polymerase and dNTP were purchased from TaKaRa Company, Dalian. Primer was synthesized by BioAsia Company, Shanghai.

RESULTS

The results of immunocytochemistry indicated that HBsAg and HBcAg were present in ovarian tissues (Figures 1). The positive rate of HBsAg and HBcAg in ovarian tissue was 34.6% (9/26), respectively. The total positive rate was 46.2% (12/26). HBsAg and HBcAg were positive in 6 (23.1%) of the 26 cases. Brown positive particles were predominantly within the ovarian cells, depositing linearly or in clusters. According to HBV markers in serum, the 26 patients were divided into two groups: patients with one indicator positive and patients with two or more positive indicators. The positive rate of HBsAg and HBcAg in ovarian tissues of these two groups showed no statistical difference ($P>0.05$) as listed in Table 1.

HBV DNA was examined in ovarian tissues from the 12 patients with positive immunocytochemical results. The positive rate of HBV DNA was 58.3% (7/12), as shown in Figure 2.

Table 1 HBsAg and HBcAg in ovarian tissues from 26 patients with HBV infection

	HBsAg in ovarian tissue[1]		HBcAg in ovarian tissue[2]	
	Positive	Negative	Positive	Negative
Patients with one HBV marker	2	5	1	6
Patients with two or more HBV markers	7	12	8	11

[1]P = 1.000 (Fisher's exact test), [2]P = 0.357 (Fisher's exact test).

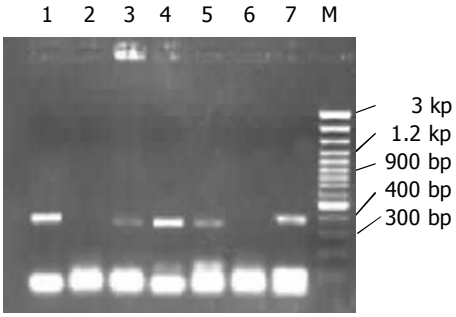


Figure 2 Detection of HBV DNA in ovarian tissue by PCR. M: DNA marker; lanes 1, 3, 4 and 5: positive samples; lane 6: negative control; lane 7: positive control.

DISCUSSION

Whether HBV can locate and replicate in ovarian tissue is not clear. This is the first report to detect HBsAg, HBcAg, and HBV DNA in ovarian tissues by immunocytochemistry and PCR. Our data indicate the positive rate of HBsAg and HBcAg was 34.6% (9/26) respectively, and the presence of HBsAg and HBcAg in ovarian tissues does not correlate with the HBV markers in serum.

PCR is a technique for quickly cloning a particular piece of DNA *in vitro*. The essential steps include thermal denaturation of the double-stranded molecules, the primers binding to their complementary template, and extension of the primers by enzymatic synthesis with DNA polymerase. The reaction is efficient, specific, and extremely sensitive[7-9]. Using PCR to assay clinical specimens has become a common method in the diagnosis of infectious diseases. HBV DNA is present in ovarian tissues with a positive rate of 58.3%. Our data provide evidence for extra-hepatic infection of HBV.

It is not clear what pathologic changes might be induced in ovary by HBV infection. An early study[10] reported that HBV can induce immune damage, even cell carcinogenesis through antigen expression in cells or integration to cell genome. In our research, all the samples were collected from patients with ovarian tumor. Whether HBV infection in ovary relates to ovarian tumor needs further study. HBV extra-hepatic infection plays a role in the preservation of the virus, but extra-hepatic tissues and cells with HBV infection often escape immune damage without obvious pathologic changes because of the small amount of viruses and the incomplete protein expression in extra-hepatic infection.

Extra-hepatic HBV infection should be targeted as liver pathologic changes in the treatment of hepatitis B. Since our study indicated the presence of HBV in ovary, and HBV might be possible to replicate in ovary, it is reasonable to assume that vertical transmission is due to HBV transmitting from ovary to ovum and fetus. There are three classical mechanisms underlying HBV transmission from mother to child[11,12]. (1) HBV transmit to the fetus through placenta, namely intrauterine infection, which has been confirmed by studies based on newborn, abortus and germ cells. (2) If there is a small cut in the skin of the fetus, and the cut is contaminated by the mother's blood or vaginal secretion in the process of childbearing, HBV infection may occur. This is the main type of vertical transmission. (3) Mother to child horizontal transmission is the main transmission route via breast milk feeding. Further studies should be focused on the transmission routes of HBV in order to control and prevent hepatitis B.

REFERENCES

1 **Lansang MA.** Epidemiology and control of hepatitis B infection: a perspective from the Philippines, Asia. *Gut* 1996; **38**(Suppl 2): S43-S47

2 **Maupas P,** Chiron JP, Barin F, Coursaget P, Goudeau A, Perrin J, Denis F, Mar ID. Efficacy of hepatitis B vaccine in prevention of early HBsAg carrier state in children. Controlled trial in an endemic area (Senegal). *Lancet* 1981; **1**: 289-292

3 **Hosoda K,** Omata M, Uchiumi K, Imazeki F, Yokosuka O, Ito Y, Okuda K, Ohto M. Extrahepatic replication of duck hepatitis B virus: more than expected. *Hepatology* 1990; **11**: 44-48

4 **Chen LB,** Chen PL, Wang GL, Song XT, Li YF, Liu CY, Jia KM. Ultrastructural study on extrahepatic infection of duck hepatitis B virus in ducks. *Chinese Med J* 1992; **105**: 212-216

5 **Lin CY.** Hepatitis B virus deoxyribonucleic acid in kidney cells probably leading to viral pathogenesis among hepatitis B virus associated membranous nephropathy patients. *Nephron* 1993; **63**: 58-64

6 **Boag F.** Hepatitis B: heterosexual transmission and vaccination strategies. *Int J STD AIDS* 1991; **2:** 318-324

7 **Gao H,** Kong J, Wang JY, Liu HY, Wen J. The study on hepatitis B maternal-infant longitudinal transmission by nested PCR technology. *Zhongguo Yike Daxue Xuebao* 1998; **27**: 59-62

8 **Ou ZS,** Song WG, Yin XM, Chen XL, Gao LY, Ding CF. Study of application of PCR technique to the diagnosis of vertical transmission of HBV. *Taishan Yixueyuan Xuebao* 1998; **19**: 10-13

9 **Feinman SV,** Berris B, Guha A, Sooknanan R, Bradley DW, Bond WW, Maynard JE. DNA: hybridization method for the diagnosis of hepatitis B infection. *J Virol Methods* 1984; **8**: 199-206

10 **Chu CM,** Liaw YF. Intrahepatic distribution of hepatitis B surface and core antigens in chronic hepatitis B virus infection. Hepatocyte with cytoplasmic/membranous hepatitis B core antigen as a possible target for immune hepatocytolysis. *Gastroenterology* 1987; **92**: 220-225

11 **Jiang JX.** Advance on the study of vertical transmission of HBV. *Zhongguo Xiandai Yixue Zazhi* 2001; **11**: 26-27

12 **Zhu DY,** Huang HY, Zheng JS. The transmission routes of mother to child transmission of HBV and its prevention. *Zhonghua Huli Zazhi* 2001; **36**: 209-210

Science Editor Wang XL and Guo SY **Language Editor** Elsevier HK

PO Box 2345, Beijing 100023, China
www.wjgnet.com
wjg@wjgnet.com

ELSEVIER

World J Gastroenterol 2005;11(35):5568-5570
World Journal of Gastroenterology ISSN 1007-9327
© 2005 The WJG Press and Elsevier Inc. All rights reserved.

• *CASE REPORT* •

Acute esophageal necrosis caused by alcohol abuse

Tetsu Endo, Juichi Sakamoto, Ken Sato, Miyako Takimoto, Koji Shimaya, Tatsuya Mikami, Akihiro Munakata, Tadashi Shimoyama, Shinsaku Fukuda

Tetsu Endo, Juichi Sakamoto, Ken Sato, Miyako Takimoto, Koji Shimaya, Tatsuya Mikami, Akihiro Munakata, Tadashi Shimoyama, Shinsaku Fukuda, First Department of Internal Medicine, Hirosaki University School of Medicine, 5 Zaifucho, Hirosaki, Aomori 036-8562, Japan
Correspondence to: Tadashi Shimoyama, First Department of Internal Medicine, Hirosaki University School of Medicine, 5 Zaifucho, Hirosaki, Aomori 036-8562, Japan. tsimo-hki@umin.ac.jp
Telephone: +81-172-39-5053 Fax: +81-172-37-5946
Received: 2005-03-03 Accepted: 2005-04-02

Abstract

Acute esophageal necrosis (AEN) is extremely rare and the pathogenesis of this is still unknown. We report a case of AEN caused by alcohol abuse. In our case, the main pathogenesis could be accounted for low systemic perfusion caused by severe alcoholic lactic acidosis. After the healing of AEN, balloon dilatation was effective to manage the stricture.

© 2005 The WJG Press and Elsevier Inc. All rights reserved.

Key words: Esophagus; Lactic acidosis; Alcohol drinking; Balloon dilatation

Endo T, Sakamoto J, Sato K, Takimoto M, Shimaya K, Mikami T, Munakata A, Shimoyama T, Fukuda S. Acute esophageal necrosis caused by alcohol abuse. *World J Gastroenterol* 2005; 11(35): 5568-5570
http://www.wjgnet.com/1007-9327/11/5568.asp

INTRODUCTION

Acute esophageal necrosis (AEN) in the absence of ingestion of a caustic or corrosive agent has been reported to be extremely rare. AEN is defined as a dark pigmentation of the esophagus associated with histologic mucosal necrosis. The exact pathogenesis is still unknown, but several etiologies have been suggested including ischemia[1,2], gastric outlet obstruction[3], hypersensitivity to antibiotics[4], gastric volvulus[5], and viral infection[6]. We reported a case of AEN caused by alcohol abuse.

CASE REPORT

A 41-year-old man visited the emergency room with a 12-h history of epigastric pain, violent vomiting, and coffee-ground emesis. His past medical history included alcoholic liver injury. He had felt nausea and appetite loss for a week. The previous day, he had consumed 1.8 L of shochu, distilled spirits containing 25% alcohol. He denied the ingestion of any caustic agents, antibiotics, and NSAIDs. He was afebrile with a regular pulse of 110 bpm, a blood pressure of 74/40 mmHg, a respiratory rate of 26 breaths/min and a core temperature of 37.0 ℃. Physical examination revealed a mild distended abdomen and epigastric tenderness. The liver edge was measured at 4 cm below the right costal margin. A Foley catheter was inserted into the bladder, but no urine was returned. Arterial blood gas measurements using with O_2 flow at 3 L/min was: pH 6.981, $PaCO_2$ 16.4 mmHg, PaO_2 156.4 mmHg, AG 55.7 mmol/L, HCO^{3-} 3.9 mmol/L, lactate 26.4 mmol/L. Laboratory data were: WBC 32 430/mm^3, hemoglobin 149 g/L, platelets 194 K/mm^3, TP 55 g/L (normal 67-83 g/L), SGOT 169 U/L (8-38 U/L), SGPT 47 U/L (4-44 U/L), T. chol 2 670 mg/L (1 270-2 380 mg/L), TG 20 370 mg/L (430-1 610 mg/L), BUN 320 mg/L (80-200 mg/L), creatinine 33 mg/L (6-10 mg/L), Na 129 mmol/L (138-149 mmol/L), K 5.4 mmol/L (3.5-5.0 mmol/L), Cl 71 mmol/L (99-110 mmol/L), Ca 65 mg/L (82-102 mg/L), amylase 484 U/L (43-116 U/L). Abdominal CT demonstrated a grossly dilated stomach, a few linear strands in peripancreatic fat suggesting inflammation, a small amount of fluid in the anterior pararenal space, a thickened distal esophagus with evidence of transmural inflammation, but no free air. A naso-gastric tube was placed and 800 mL of brown liquid was removed. The patient was admitted and received intravenous fluids with 80 mL of 7% sodium bicarbonate. He was rapidly rehydrated and urinalysis did not reveal ketones. Arterial blood gas, 5 h after his admission, showed pH 7.505, lactate 4.1 mmol/L.

Esophago-gastro-duodenoscopy (EGD), on the next day, demonstrated black and friable mucosa from 3 to 4 cm below the cricopharyngeus to the cardia (Figure 1A). Biopsies of the esophagus were not taken at this time due to concern over possible perforation. The stomach had a few linear ulcers and the mucosa was edematous. A barium swallow revealed thickened esophagus and decreased esophageal motility, but no evidence of perforation.

Platelets count was rapidly decreased (d 3: 74 K/mm^3) and we considered disseminated intravascular coagulation. Treatment was conservative management with oral intake restriction, intermittent naso-gastric tube suction, total parental nutrition, intravenous famotidine, antibiotics, and nafamostat mesilate. Laboratory data, including thrombocytopenia, were gradually recovered.

Ten days after admission, EGD revealed the presence of a thick, white exudate on the pink esophageal mucosa. Oral feeding was started on d 13. However, he sometimes complained about chest oppression after meal. Both an EGD

on d 24 (Figure 1B) and a barium swallow on d 27 (Figure 2A) demonstrated stricture of the middle esophagus. On d 39, we performed balloon dilatation to the stricture. With the assistance of esophagoscope and a guidewire, a 20-mm balloon dilator was inserted to the stricture. The balloon dilator was inflated to a pressure of 2 atm for 5 min. Balloon dilatation was accomplished without any complication. Two days after, the barium swallow demonstrated improvement of the stricture (Figure 2B). The patient was discharged without complaints on d 46 taking 20 mg of omeprazole once a day. His alcoholic hepatitis was reversible and laboratory data has been normal since discharge.

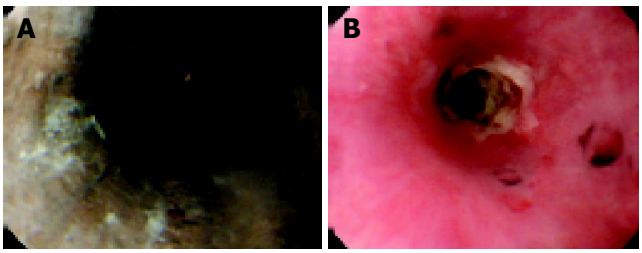


Figure 1 **A:** Endoscopy on d 2 shows that esophagus is circumferentially black and friable. **B:** Endoscopy on d 24 shows stricture formation at the middle esophagus. The mucosa is covered by white exudate.



Figure 2 Barium swallow study. **A:** Stricture formation at middle esophagus on d 27. The diameter of the lumen was 6 mm; **B:** On d 41, improvement of the stricture was seen after balloon dilatation.

DISCUSSION

AEN or Black esophagus was first described in 1990 by Goldenberg *et al*.[1], although two post-mortem cases had previously been reported[7,8]. The precise incidence and prevalence of this disease are unknown. Autopsy studies have estimated its prevalence at 0.1-0.2%[9,10]. Moreto *et al*.[11], have identified 10 cases of AEN in a review of more than 80 000 upper endoscopies, an incidence rate of only 0.0125%. Among variety of mechanisms for the development of this condition including direct toxic effect[12,13] or indirect acidic effect[14,15], low systemic perfusion seems to play the dominant role. The main complications are esophageal stenosis and stricture formation[3].

Lactic acidosis is the cause of sudden death in alcoholics[16]. It is caused by an elevation of the NADH/NAD+ ratio with increased formation of lactate from pyruvate, diminished gluconeogenesis and decreased lactate uptake into the liver[17,18]. Thiamine deficiency due to malnutrition and the direct action of alcohol are responsible for the occurrence of lactic acidosis[19,20]. Five typical symptoms of alcoholic lactic acidosis are vomiting, nausea, abdominal pain, tachycardia and the Kussmaul form of respiration. In this case, we suspect that his acidosis appeared at least a week before his admission because his nausea and appetite loss had started. Lactic acidosis might have been worsened by his malnutrition and alcohol abuse.

The fall in blood pH had profound effects on circulation systems. Intrinsic cardiac contractility may be depressed, but inotropic function can be normal because of catecholamine release. Both peripheral arterial vasodilatation and central venoconstruction can be present. Several reports described cases of stroke[21], intestinal necrosis[22], heart failure, and pancreatitis[23] in severe metabolic acidosis and those may be associated with physiologic response to hypovolemia and subsequent poor organ perfusion caused by severe acidosis. Low esophageal perfusion pressure, a presumed cause of our case, was suggested by his original hypotension. In addition, coagulation abnormality by acute pancreatitis can aggravate esophageal mucosal perfusion. Severe peripheral circulatory failure also makes massive gastric distension and renal insufficiency. Moreover, alcohol overindulgence induces irritation of the gastric mucosa and the accumulation of large volume of gastric secretions. This can overwhelm the normal defense of the esophagus, and could be another cause of our case.

In conclusion, we reported a case of AEN caused by alcohol abuse. The main pathogenesis can be accounted for low systemic perfusion caused by severe lactic acidosis. The stricture area of middle esophagus was managed with balloon dilatation.

REFERENCES

1 **Goldenberg SP,** Wain SL, Marignani P. Acute necrotizing esophagitis. *Gastroenterology* 1990; **98**: 493-496
2 **Cappell MS.** Esophageal necrosis and perforation associated with the anticardiolipin antibody syndrome. *Am J Gastroenterol* 1994; **89**: 1241-1245
3 **Lacy BE,** Toor A, Bensen SP, Rothstein RI, Maheshwari Y. Acute esophageal necrosis: report of two cases and a review of the literature. *Gastrointest Endosc* 1999; **49**: 527-532
4 **Mangan TF,** Colley AT, Wytock DH. Antibiotic-associated acute necrotizing esophagitis. *Gastroenterology* 1990; **99**: 900
5 **Kram M,** Gorenstein L, Eisen D, Cohen D. Acute esophageal necrosis associated with gastric volvulus. *Gastrointest Endosc* 2000; **51**: 610-612
6 **Cattan P,** Cuillerier E, Cellier C, Carnot F, Landi B, Dusoleil A, Barbier JP. Black esophagus associated with herpes esophagitis. *Gastrointest Endosc* 1999; **49**: 105-107
7 **Lee KR,** Stark E, Shaw FE. Esophageal infarction complicating spontaneous rupture of the thoracic aorta. *JAMA* 1977; **237**: 1233-1234
8 **Brennan JL.** Case of extensive necrosis of the oesophageal mucosa following hypothermia. *J Clin Pathol* 1967; **20**: 581-584
9 **Etienne JP,** Roge J, Delavierre P, Veyssier P. Esophageal necrosis of vascular origin. *Sem Hop* 1969; **45**: 1599-1606
10 **Postlethwait RW,** Musser AW. Changes in the esophagus in 1,000 autopsy specimens. *J Thorac Cardiovasc Surg* 1974; **68**:

953-956
11 **Moreto M,** Ojembarrena E, Zaballa M, Tanago JG, Ibanez S. Idiopathic acute esophageal necrosis: not necessarily a terminal event. *Endoscopy* 1993; **25**: 534-538
12 **Orlando RC,** Powell DW, Carney CN. Pathophysiology of acute acid injury in rabbit esophageal epithelium. *J Clin Invest* 1981; **68**: 286-293
13 **Tobey NA,** Orlando RC. Mechanisms of acid injury to rabbit esophageal epithelium. Role of basolateral cell membrane acidification. *Gastroenterology* 1991; **101**: 1220-1228
14 **Bass BL,** Schweitzer EJ, Harmon JW, Kraimer J. H+ back diffusion interferes with intrinsic reactive regulation of esophageal mucosal blood flow. *Surgery* 1984; **96**: 404-413
15 **Katsinelos P,** Pilpilidis I, Dimiropoulos S, Paroutoglou G, Kamperis E, Tsolkas P, Kapelidis P, Limenopoulos B, Papagiannis A, Pitarokilis M, Trakateli C. Black esophagus induced by severe vomiting in a healthy young man. *Surg Endosc* 2003; **17**: 521
16 **Doehn M,** Schwartau M. Alcohol-induced lactic acidosis in thiamine deficiency. *Z Rechtsmed* 1982; **89**: 125-130
17 **Duffens K,** Marx JA. Alcoholic ketoacidosis -a review. *J Emerg Med* 1987; **5**: 399-406
18 **Fulop M.** Alcoholism, ketoacidosis, and lactic acidosis. *Diabetes Metab Rev* 1989; **5**: 365-378
19 **Hoyumpa AM.** Mechanisms of thiamin deficiency in chronic alcoholism. *Am J Clin Nutr* 1980; **33**: 2750-2761
20 **Klein M,** Weksler N, Gurman GM. Fatal metabolic acidosis caused by thiamine deficiency. *J Emerg Med* 2004; **26**: 301-303
21 **Keane S,** Gallagher A, Ackroyd S, McShane MA, Edge JA. Cerebral venous thrombosis during diabetic ketoacidosis. *Arch Dis Child* 2002; **86**: 204-205
22 **DiMeglio LA,** Chaet MS, Quigley CA, Grosfeld JL. Massive ischemic intestinal necrosis at the onset of diabetes mellitus with ketoacidosis in a three-year-old girl. *J Pediatr Surg* 2003; **38**: 1537-1539
23 **Tanaka M,** Miyazaki Y, Ishikawa S, Matsuyama K. Alcoholic ketoacidosis associated with multiple complications: report of 3 cases. *Intern Med* 2004; **43**: 955-959

Science Editor Guo SY **Language Editor** Elsevier HK

PO Box 2345, Beijing 100023, China
www.wjgnet.com
wjg@wjgnet.com

ELSEVIER

World J Gastroenterol 2005;11(35):5571-5572
World Journal of Gastroenterology ISSN 1007-9327
© 2005 The WJG Press and Elsevier Inc. All rights reserved.

• *CASE REPORT* •

Complex pattern of colon cancer recurrence including a kidney metastasis: A case report

Helfried Waleczek, Moritz N Wente, Jürgen Kozianka

Helfried Waleczek, Department of Surgery, Evangelic Hospital, Bredenscheider Straße 54, D-45525 Hattingen, Germany
Moritz N Wente, Department of General Surgery, University of Heidelberg, Im Neuenheimer Feld 110, D-69120 Heidelberg, Germany
Correspondence to: Jürgen Kozianka, Department of Surgery, St-Anna-Hospital, Hospitalstraße 19, D-44649 Herne, Germany. waleczek@krankenhaus-hattingen.de
Telephone: +49-2324-502-216 Fax: +49-2324-502-385
Received: 2004-04-15 Accepted: 2004-07-15

Abstract

We report a case of a 77-year-old female with a local recurrence of cancer after right hemicolectomy which infiltrated the pancreatic head affording pancreatoduodenectomy, who developed 3 years later recurrent tumor masses localized in the mesentery of the jejunum and in the lower pole of the left kidney. Partial nephrectomy and a segment resection of the small bowel were performed. Histological examination of both specimens revealed a necrotic metastasis of the primary carcinoma of the colon. Although intraluminal implantation of colon cancer cells in the renal pelvic mucosa from ureteric metastasis has been described, metastasis of a colorectal cancer in the kidney parenchyma is extremely rare and can be treated in an organ preserving manner. A complex pattern of colon cancer recurrence with unusual and rare sites of metastasis is reported.

© 2005 The WJG Press and Elsevier Inc. All rights reserved.

Key words: Colonic neoplasm; Local recurrence; Kidney metastasis

Waleczek H, Wente MN, Kozianka J. Complex pattern of colon cancer recurrence including a kidney metastasis: A case report. *World J Gastroenterol* 2005; 11(35): 5571-5572
http://www.wjgnet.com/1007-9327/11/5571.asp

INTRODUCTION

Adequate resection of colon and mesentery including standardized lymphadenectomy remains the cornerstone of treatment for colorectal cancer[1-3]. Although most patients can be treated surgically with a chance of cure, colorectal neoplasms are still the second leading cause of cancer-related death because 25-50% of the patients suffer from local recurrences or metastasis after complete resection[1,4]. Without adjacent organ invasion and limited nodal disease, local recurrence should be rare depending on technical aspects and quality of the performed operation[5,6]. Among patients with recurrences, the most frequent sites are the liver and the lungs, local and/or regional retroperitoneal and peripheral lymph nodes[7]. Metastases of colorectal cancer in the kidney are considered to be extremely rare. Lee did not identify renal metastasis when analyzing colorectal tumor manifestations in the genitourinary tract[8].

CASE REPORT

In July 1998, 6 mo after laparoscopic cholecystectomy, a 77-year-old female presented herself having a palpable mass in the right upper abdomen with a heavy loss of weight. CT scan showed a tumor involving the right colonic flexure. Colonoscopy revealed an adenocarcinoma, which was intraoperatively found to be perforated locally. Right hemicolectomy and resection of the anterior wall of the duodenum were performed and a highly differentiated adenocarcinoma without lymph node involvement was found histologically. Due to the negative lymph node status, no adjuvant therapy was initiated.

Again 6 mo later a local recurrence at the anastomosis was diagnosed with infiltration of the head of the pancreas. This situation afforded re-resection including a pylorus-preserving pancreatoduodenectomy. No lymph node involvement was found and the TNM tumor stage was rpT3, G2, N0 and M0. CEA levels were normal postoperatively, adjuvant therapy was started with standard intravenous administration of 5-FU/FA for 6 mo.

In October 2001, two tumor sites were found in a MRI localized in the mesentery of the jejunum and in the lower pole of the left kidney. Partial nephrectomy and a segment of the small bowel were done. Histological examination of the kidney specimen as well as of the mesentery of the jejunum showed necrotic metastasis of the colon carcinoma in the kidney with a size of 2.5 cm in diameter. The patient refused any further adjuvant chemotherapy.

In January 2003, multiple jejunal tumors were found in a CT scan, one of them causing complete small bowel obstruction. Because of endoscopic inaccessibility, an open segment resection was needed and performed. Palliative chemotherapy with oral anti-tumor drug administration was started. It was consented not to perform any further surgery. No hepatic or pulmonary metastasis could be found during any hospital stay.

DISCUSSION

In the present case, colon cancer of the right flexure was

not diagnosed during laparoscopic surgery. The rate of missed colonic neoplasms during laparoscopic cholecystectomy is reported to be as low as 0.24-0.4%. Because of this low incidence, most surgeons do not screen patients prior to cholecystectomy for colorectal cancer routinely, although careful attention to preoperative physical findings and laboratory data as well as meticulous techniques during laparoscopic cholecystectomy is regarded to be essential to identify patients with concomitant malignant disease[9,10]. If cancer of the colon is overseen during an initial operation, 46% of the patients are readmitted during the first, and another 30% during the second year postoperatively[11]. In these advanced cases, extended surgical procedures such as hemicolectomy with duodenal or pancreatic resection have been shown to be adequate, since they can be performed safely with an increased survival time[12]. In the present case, local tumor growth could not be controlled by the surgical procedure, thus a local recurrence infiltrating the anastomosis was seen 6 mo after primary resection of the tumor.

Isolated anastomotic recurrence is rare after resection of colonic lesions, but more common for rectal cancer, whereas the average time for anastomotic recurrence is about 16 mo[13]. In the case of local or distant recurrent disease, 20% of the patients can be reoperated upon with curative intent, a solitary lesion being a favorable prognostic factor[14,15]. The purpose of postoperative follow-up after curative resection is to identify recurrences at an early and localized stage, because surgical excision remains the only effective treatment, although a substantial impact of any tumor follow-up has been questioned. Nevertheless, using computed tomography and frequent measurements of serum CEA or both, an absolute reduction in mortality of 9-13% can be achieved[16,17].

Localizations of distant colon cancer recurrences are most likely the liver and the lungs, but also metastasis to other organs, such as the thyroid gland or the spleen, has been described[18,19]. In combination with metastasis to the ureter, intraluminal implantation of colon cancer cells in the renal pelvic mucosa has been discovered[20]. Only one case of an intraluminal renal metastasis of a carcinoma of the rectum has been described before[21].

REFERENCES

1 **Jemal A,** Tiwari RC, Murray T, Ghafoor A, Samuels A, Ward E, Feuer EJ, Thun MJ. Cancer statistics, 2004. *CA Cancer J Clin* 2004; **54**: 8-29

2 **Daneker GW**, Ellis LM. Colon cancer nodal metastasis: biologic significance and therapeutic considerations. *Surg Oncol Clin N Am* 1996; **5**: 173-189

3 **Wu JS,** Fazio VW. Colon cancer. *Dis Colon Rectum* 2000; **43**: 1473-1486

4 **August DA,** Ottow RT, Sugarbaker PH. Clinical perspective of human colorectal cancer metastasis. *Cancer Metastasis Rev* 1984; **3**: 303-324

5 **Bokey EL,** Chapuis PH, Dent OF, Mander BJ, Bissett IP, Newland RC. Surgical technique and survival in patients having a curative resection for colon cancer. *Dis Colon Rectum* 2003; **46**: 860-866

6 **Read TE,** Mutch MG, Chang BW, McNevin MS, Fleshman JW, Birnbaum EH, Fry RD, Caushaj PF, Kodner IJ. Locoregional recurrence and survival after curative resection of adenocarcinoma of the colon. *J Am Coll Surg* 2002; **195**: 33-40

7 **Galandiuk S,** Wieand HS, Moertel CG, Cha SS, Fitzgibbons RJ Jr, Pemberton JH, Wolff BG. Patterns of recurrence after curative resection of carcinoma of the colon and rectum. *Surg Gynecol Obstet* 1992; **174**: 27-32

8 **Lee PH,** Khauli RB, Baker S, Menon M. Prognostic and therapeutic observations of manifestations in the genitourinary tract of adenocarcinoma of the colon and rectum. *Surg Gynecol Obstet* 1989; **169**: 511-518

9 **Ishida H,** Ohsawa T, Murata N, Fujioka M, Hashimoto D. Risk of missing colorectal cancer during laparoscopic cholecystectomy. *Surg Today* 2002; **32**: 392-396

10 **Mylonaki D,** Alexakis N, Archodovassilis F, Konstadoulakis MM, Leandros E, Androulakis G. Latent adenocarcinoma of the colon discovered during or after laparoscopic cholecystectomy. *Endoscopy* 2002; **34**: 315-317

11 **Denning DA,** Lipshy KA. Missed pathology following laparoscopic cholecystectomy: a cause for concern? *Am Surg* 1995; **61**: 117-120

12 **Koea JB,** Conlon K, Paty PB, Guillem JG, Cohen AM. Pancreatic or duodenal resection or both for advanced carcinoma of the right colon: is it justified? *Dis Colon Rectum* 2000; **43**: 460-465

13 **Obrand DI,** Gordon PH. Incidence and patterns of recurrence following curative resection for colorectal carcinoma. *Dis Colon Rectum* 1997; **40**: 15-24

14 **Goldberg RM,** Fleming TR, Tangen CM, Moertel CG, Macdonald JS, Haller DG, Laurie JA. Surgery for recurrent colon cancer: strategies for identifying resectable recurrence and success rates after resection. Eastern Cooperative Oncology Group, the North Central Cancer Treatment Group, and the Southwest Oncology Group. *Ann Intern Med* 1998; **129**: 27-35

15 **Sardi A,** Minton JP, Nieroda C, Sickle-Santanello B, Young D, Martin EW. Multiple reoperations in recurrent colorectal carcinoma. An analysis of morbidity, mortality, and survival. *Cancer* 1988; **61**: 1913-1919

16 **Staib L,** Link KH, Beger HG. Follow-up in colorectal cancer: cost-effectiveness analysis of established and novel concepts. *Langenbecks Arch Surg* 2000; **385**: 412-420

17 **Renehan AG,** Egger M, Saunders MP, O'Dwyer ST. Impact on survival of intensive follow up after curative resection for colorectal cancer: systematic review and meta-analysis of randomised trials. *BMJ* 2002; **324**: 813

18 **Akimaru K,** Onda M, Tajiri T, Shimanuki K, Iwama H, Furukawa K, Sugiyama Y. Colonic adenocarcinoma metastatic to the thyroid: report of a case. *Surg Today* 2002; **32**: 151-154

19 **Place RJ.** Isolated colon cancer metastasis to the spleen. *Am Surg* 2001; **67**: 454-457

20 **Shiraishi T,** Hasegawa Y, Itoh H, Nakakuki K. Implantation of colon cancer cells onto renal pelvic mucosa. A case report. *APMIS* 1989; **97**: 181-184

21 **Rioux-Leclercq N,** Le Gall F, Ziade J, Patard JJ, Guille F, Lobel B, Ramee MP. Intraluminal renal metastasis from a rectal adenocarcinoma: an unusual site. *Ann Pathol* 2000; **20**: 361-364

Science Editor Wang XL **Language Editor** Elsevier HK

PO Box 2345, Beijing 100023, China
www.wjgnet.com
wjg@wjgnet.com

ELSEVIER

World J Gastroenterol 2005;11(35):5573-5576
World Journal of Gastroenterology ISSN 1007-9327
© 2005 The WJG Press and Elsevier Inc. All rights reserved.

• *CASE REPORT* •

Solitary colonic neurofibroma in a patient with transient segmental colitis: Case report

Vasilios Panteris, Thivi Vassilakaki, Nikos Vaitsis, Ioannis Elemenoglou, Irini Mylonakou, Dimitrios Georgios Karamanolis

Vasilios Panteris, Irini Mylonakou, Dimitrios Georgios Karamanolis, Department of Gastroenterology, "Tzaneion" General Hospital, Zanni and Afentouli 1, Piraeus 18536, Greece
Thivi Vassilakaki, Nikos Vaitsis, Ioannis Elemenoglou, Department of Pathology, "Tzaneion" General Hospital, Zanni and Afentouli 1, Piraeus 18536, Greece
Correspondence to: Vasilios Panteris, MD, M. Botsari 38, 132 31 Petroupoli, Athens, Greece. kresson@panafonet.gr
Telephone: +30-21-05011944 Fax: +30-21-05011944
Received: 2005-03-04 Accepted: 2005-03-23

Abstract

Neurofibromas of the large bowel are very rare and usually are part of the colonic involvement in neurofibromatosis type 1 (Nf1, von Recklinghausen's disease). Solitary neurofibromas of the colon are extremely rare. We describe a case of an isolated neurofibroma that was found in the large bowel of a patient who suffered from segmental colitis and presented with bloody diarrhea. A review of the literature is also included, concerning the disclosure of isolated neurofibromas in the gut and other body parts and the type of gastrointestinal involvement in von Recklinghausen's disease.

© 2005 The WJG Press and Elsevier Inc. All rights reserved.

Key words: Solitary neurofibroma; Isolated neurofibroma; Neurofibromatosis; Intestinal neurofibromatosis; von Recklinghausen's disease

Panteris V, Vassilakaki T, Vaitsis N, Elemenoglou I, Mylonakou I, Karamanolis DG. Solitary colonic neurofibroma in a patient with transient segmental colitis: Case report. *World J Gastroenterol* 2005; 11(35): 5573-5576
http://www.wjgnet.com/1007-9327/11/5573.asp

INTRODUCTION

Neurofibromas exist rarely in the colon as isolated neoplasms outside the classical clinical picture of von Recklinghausen's disease (neurofibromatosis type 1, Nf1)[1]. Intestinal neurofibromatosis characterized by multiple neurofibromas usually in the small intestine and stomach may rarely present as a sporadic case in a patient without features of the generalized neurofibromatosis. Isolated colonic neurofibromatosis is even more unusually described in the literature[2]. Here we describe a rare case of a solitary colonic neurofibroma in a patient without features of Nf1 or isolated colonic neurofibromatosis.

CASE REPORT

A 65-year-old Caucasian female came to the emergency department of our hospital complaining of bloody diarrhea. Twelve hours before admission the patient experienced a dull abdominal pain of sudden onset, located at the hypogastrium, and her temperature rose to 37.8 ℃. She reported 10 bowel movements, which were diarrheal at first and became hemorrhagic later. Physical examination revealed moderate tenderness on palpation of the hypogastrium and increased bowel sounds on auscultation. Inspection of the skin revealed two firm, subcutaneous masses with ill-defined borders, each one located at the apex of the scapula with a diameter of 2 cm. Physical examination of the lungs, heart, skin, and other body systems revealed no abnormal features. It was the first episode of bloody diarrhea experienced by the patient. Her past medical history included essential hypertension, hyperlipidemia, and an acute coronary syndrome and she was receiving an angiotensin-converting enzyme inhibitor, enteric-coated aspirin and a statin. Furthermore, she had atopy to grass, tree pollens and fungal spores, manifested by bronchoconstriction. There was no family history of intestinal diseases.

Laboratory investigation including complete blood count, biochemical examination, tumor markers (CEA, CA 19-9, aFP, CA125, CA 15-3), coagulation tests, microbiological cultures for bacterial and parasites in feces and cultures of the urine were normal except for a slightly elevated blood glucose level (120 mg%) and CRP (12, normal <4). Chest x-ray and ECG had no abnormal features. An abdominal plain radiograph showed only an air-filled large bowel.

Colonoscopy was performed after cessation of the hemorrhage. The endoscope reached the hepatic flexure and revealed a segmental colitis. At the splenic flexure and proximal portion of the descending colon there were erythema and edema of the mucosa with hemorrhagic petechiae. A sessile polyp 1 cm in diameter was detected at the descending colon, near the site of inflammation and was endoscopically removed. The transverse colon and the rectum were macroscopically normal. At the sigmoid colon a few, small diverticulae were noticed, without inflammation. Ultrasonography of the abdomen revealed no pathological findings.

Pathology findings

Microscopically, the biopsy from the polyp showed fragments of mucosa of the large bowel lined by normal epithelium. In the lamina propria there was a nodule, with ill-defined borders, which was composed of longitudinal cells with elongated, pointed nucleus. These cells were

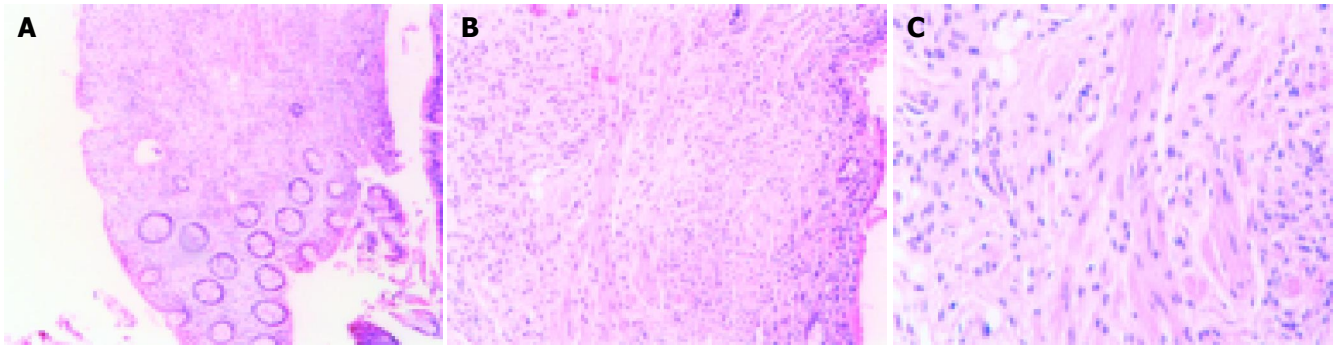


Figure 1 **A**: Neurofibroma, hematoxylin-eosin (H-E) ×100; **B**: Neurofibroma, H-E ×250; **C**: Neurofibroma, H-E ×400.

deposited in interlaced bundles and in near proximity with collagen fibers. There were no signs of atypia, nor significant mitotic activity. Immunohistochemical stains were positive for vimentin and S-100 protein but negative for desmin, smooth muscle actin, c-kit and CD34. The above morphological and immunohistochemical characteristics were consistent with the diagnosis of neurofibroma (Figures 1A-C). Biopsy samples from the site of colitis showed focal erosions of the surface mucosal epithelium and focal decrease in mucus production. The architecture of the glands was intact. There was edema and dense infiltrate of inflammatory cells (lymphocytes, polymorphonuclear and plasma cells) in the lamina propria. There was an increased number of eosinophils in the same area. Crypt abscesses were rarely encountered. Granulomas were not recognized microscopically. These findings could not support a definite diagnosis of idiopathic inflammatory bowel disease and were classified as nonspecific colitis (Figures 2A-C).

Clinically the patient had no café-au-lait spots on her skin, axillary freckling or peripheral neurofibromas. Also there were no pigmented hamartomas of the iris and no family history of neurofibromatosis. The patient received crystalloid solutions, antibiotics and mesalazine, had an uneventful recovery and was discharged 5 d later. Two months later in a follow-up examination, the patient had no symptoms from the intestine and her physical examination was unremarkable. Colonoscopy was again performed and the colon was examined to the hepatic flexure. The previous findings were absent and the mucosal surface was normal. The patient was advised to have a barium enema done for the visualization of the remaining large bowel which showed only diverticula of the right colon and sigmoid. Due to the polypoid neurofibroma the patient underwent spiral CT of the brain, thorax and abdomen for pathological features associated with neurofibromatosis. No abnormalities were found. Biopsy samples, taken from one of the subcutaneous masses located at the back of the patient showed a lipoma with fibrous components and S-100 negative immunoreactivity. New serum laboratory tests were normal except glucose, which was 142 mg%. Gastroscopy revealed erosive duodenitis and no other suspicious pathologic lesion.

DISCUSSION

Neurofibromas are usually manifestations of the von Recklinghausen's disease. They are benign neoplasms consisting of neural and connective tissue components like Schwann and perineural cells and myofibroblasts. They are usually multiple on presentation and are part of a hereditary disorder with two clinical forms: Nf1 (or von Recklinghausen's neurofibromatosis or peripheral neurofibromatosis, Nf1) and neurofibromatosis type 2 (or central neurofibromatosis or bilateral acoustic neurofibromatosis). These disease entities have variable clinical expressions with manifestations involving the skin, nervous system, eyes, bones, gastrointestinal tract, and other body parts. Cardiovascular disease manifested as hypertension, myocardial infarction, hemorrhage, or cerebral ischemia, are the most frequent causes of death in Nf1 patients[3]. Survival is lesser than expected in the normal population as much as 15 years. There is also a disease type called segmental neurofibromatosis, which involves a specific

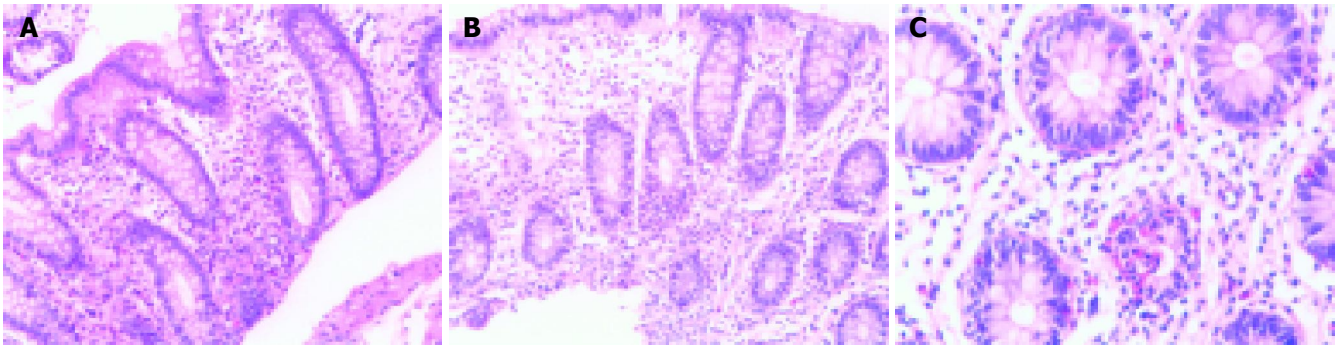


Figure 2 **A**: Nonspecific colitis, H–E ×250; **B**: Nonspecific colitis, H-E ×250; **C**: Nonspecific colitis, crypt abscess, H-E ×400.

body organ without the variety of multiple pathologic expressions of the generalized form.

Neurofibromas of the digestive system are usually found as part of the Nf1. This is a relative common inherited disorder based on genetic transmission of the autosomal dominant type. The incidence of the disease is 1:3 000 births and the population prevalence is 1:5 000[1,4]. The diagnostic criteria for Nf1 include the following: (1) the so-called "café-au-lait" spots (at least six spots, size $\geqslant$1.5 cm in postpubertal patients), (2) the characteristic neurofibromas (at least two or one plexiform), (3) axillary or groin freckling, (4) pigmented hamartomas of the iris, the so-called Lisch nodules (at least two), (5) an osseous lesion which may include thinning of the long bone cortex or sphenoid wing dysplasia, (6) first degree relative with Nf1, (7) optic glioma. The patient should have at least two of the previous criteria to be considered as Nf1. The penetrance of the disease is 100% until age 5[5]. The majority of patients have café-au-lait spots (95%), neurofibromas (95%), Lisch nodules (95%) and axillary freckling (70%). Optic gliomas affect 15% of the patients[1]. Café-au-lait spots most commonly present before 2 years of age[6].

Neurofibromas may be cutaneous, nodular derived from peripheral nerves or plexiform with aggressive, infiltrative growth that extends outside the nerve sheath to the surrounding tissue. Although benign, neurofibromas of the nodular and particular the plexiform type may demonstrate a malignant transformation in 2-16% of affected individuals[1,2,7]. About 50% of the cases of Nf1 are not familial but sporadic as a result of germ-cell mutations. Segmental Nf seems to involve a group of somatic cells that have exclusively acquired the specific neurofibromatosis mutations presenting a mosaicism[4]. The Nf1 gene has been located on chromosome 17q11.2 and produces a peptide of 2 818 aminoacids, called neurofibromin, which works as a tumor suppressor[1,3]. Neurofibromin seems to interact with the RAS/GTP membrane-signaling pathway in cells by activating the GTPase that converts GTP to inactive GDP and therefore shutting down the RAS effector system which is involved in cell growth and differentiation. Mutations of the Nf1 gene result in deficient neurofibromin, which in turn seems unable to control responses to proliferation signaling thus giving birth to neoplastic growth.

Participation of the gastrointestinal tract has been documented in 25% of patients with Nf1. Ganglioneuromatosis and neurofibromatosis are the pathologic forms of gastrointestinal involvement[8]. Ganglioneuromatosis refers to extended hyperplasia and hypertrophy of the nerve plexuses and ganglion cells in the mucosa or throughout the intestinal wall. Characteristic neurofibromas have been found in the digestive tract in 11% of patients with Nf1[5].

Intestinal neurofibromatosis exists, in the majority of cases, in association with Nf1 and only rarely presents outside this disease as a separate pathologic entity (familial or sporadic)[2]. Multiple neurofibromas are discovered in the gut, more often located in the jejunum, stomach, ileum, duodenum, and colon according to the frequency of their appearance[1,5]. Neurofibromas are usually originating from either the plexus of Meissner in the submucosa or the plexus of Auerbach's in the muscularis propria or even from the serosa[2,9]. The lesions are often sessile and wide based but also pedunculated polyps have been observed[2]. These lesions most often are discovered in the 4th-6th decade of life[8-10]. It is common to remain clinically silent and rarely cause symptoms before puberty. Nf1 is also associated with the occurrence of other neoplasms that involve the gastrointestinal tract. These include carcinoids and somatostatinomas that are located mainly in the duodenum and ampulla of Vater, stromal tumors mainly leiomyomas and sarcomas and pancreatic adenocarcinomas[5,8,10]. The clinical picture includes abdominal pain, palpable masses, hemorrhage due to necrosis or ulceration of the mucosa, obstruction due to intussusception or extraluminar pressure, perforation, megacolon, peptic ulcer disease, diarrhea, steatorrhea, obstructive jaundice and obstruction of the pancreatic tract. Iron deficiency anemia has also been reported and caused by occult blood loss[2,5,11].

Neurofibromatosis of the colon as part of the Nf1 is rare[7,9,12–14]. Isolated colonic neurofibromatosis without other features suggestive of Nf1 has been very rarely encountered in the clinical practice. Only 13 such cases of isolated colonic neurofibromatosis with no evidence of Nf1 have been documented in the literature[2,15]. Isolated neurofibromas of the colon are even rarer and only two such cases have been published[11]. In the first case an asymptomatic polyp was discovered to represent a neurofibroma while in the second case the neurofibroma presented as a large polypoid mass in the transverse colon. The mass had intussuscepted into the rectum causing massive bleeding of the gastrointestinal tract. There are also other parts of the digestive tract in which solitary neurofibromas have been detected. There have been 8 cases of solitary mesentery neurofibroma (7 ileal, 1 gastrocolic)[6], 1 case of ileal isolated neurofibroma[16], 3 cases of the anal canal[17], 1 case of the esophagus[18], 1 case of the soft palate[19], 7 cases of the gallbladder[20], and 1 case of the common bile duct[21].

Isolated neurofibromas in other body organs are also very rare. Very few cases have been reported so far, namely to the kidney[22], spermatic cord[23], nasal cavity[24], palatine tonsil[25], parapharyngeal space[26], larynx[27], humerus[28], submandibular salivary gland[29], conjuctiva[30], retroperitoneal space[31], cranial ventricles[32], and chest wall[33].

In our case a solitary neurofibroma was discovered in the descending colon in the form of a sessile polyp. The patient has no associated features of von Recklinghausen's disease. The patient presented with lower gastrointestinal bleeding. In colonoscopy a segmental colitis was revealed, involving the splenic flexure and associated proximal part of the descending colon. Although a definite diagnosis of ischemic colitis cannot be made, there are many clues that support this explanation. The medical history of atherosclerotic disease including hypertension, ischemic heart attack, diabetes and hyperlipidemia (syndrome X), which justify the presence of predisposing factors for the development of vascular blood flow defects as a pathogenetic mechanism for ischemic attacks. The age of the patient is compatible with ischemia. The symptoms and physical findings are among those found in ischemic, perfusion-compromised bowel: sudden onset of pain in the lower

abdomen, passage of red blood with stools within 24 h and abdominal tenderness. The endoscopic findings of transient, segmental colitis located around the splenic flexure are a characteristic pattern in 11% of colonic ischemia. The histologic evaluation of the biopsy specimens revealed a nonspecific inflammatory process, which is mostly encountered in mild cases of ischemic colitis. The clinical course with remission of symptoms within 72 h and the reversal of mucosal damage after 8 wk correlates with the usual prognosis of mild ischemic colitis. In less than 10% of patients with colonic ischemia, there is a potentially obstructing lesion located distally to the ischemic segment with normal intervening mucosa between them. In our case the polypoid neurofibroma and the diverticula of the sigmoid appear at a site distal to the colitis.

Aspirin, which is a drug implicated in the induction of inflammatory colitis, might have attributed to the patient's symptoms. In a recent review, 5 cases of inflammatory colitis have been attributed to hypersensitivity reactions caused by salicylates[34]. The clinical presentation in these cases has included, among others, abdominal pain, distention, and pyrexia. Endoscopy has revealed erythema, friability and ulcers and the histologic examination included an eosinophilic infiltration and crypt abscesses. Many of the above symptoms and signs also exist in our case and therefore aspirin colitis may also be an explanation for our findings.

REFERENCES

1 **Reynolds RM,** Browning GG, Nawroz I, Campbell IW. Von Recklinghausen's neurofibromatosis: neurofibromatosis type 1. *Lancet* 2003; **361**: 1552-1554
2 **Bononi M,** De Cesare A, Stella MC, Fiori E, Galati G, Atella F, Angelini M, Cimitan A, Lemos A, Cangemi V. Isolated intestinal neurofibromatosis of colon. Single case report and review of the literature. *Dig Liver Dis* 2000; **32**: 737-742
3 **Friedman JM,** Arbiser J, Epstein JA, Gutmann DH, Huot SJ, Lin AE, McManus B, Korf BR. Cardiovascular disease in neurofibromatosis 1: report of the NF1 Cardiovascular Task Force. *Genet Med* 2002; **4**: 105-111
4 **Hirsch NP,** Murphy A, Radcliffe JJ. Neurofibromatosis: clinical presentations and anaesthetic implications. *Br J Anaesth* 2001; **86**: 555-564
5 **Pinsk I,** Dukhno O, Ovnat A, Levy I. Gastrointestinal complications of von Recklinghausen's disease: two case reports and a review of the literature. *Scand J Gastroenterol* 2003; **38**: 1275-1278
6 **Magro G,** Piana M, Venti C, Lacagnina A, Ruggieri M. Solitary neurofibroma of the mesentery: report of a case and review of the literature. *Pathol Res Pract* 2000; **196**: 713-718
7 **Kim HR,** Kim YJ. Neurofibromatosis of the colon and rectum combined with other manifestations of von Recklinghausen's disease: report of a case. *Dis Colon Rectum* 1998; **41**: 1187-1192
8 **Gogus S,** Sarikayalar F, Akcoren Z, Yalnizoglu D, Hicsonmez A. Intestinal involvement and vasculopathy in von Recklinghausen's neurofibromatosis. *Turk J Pediatr* 1997; **39**: 117-122
9 **Jacob S,** Prabhakar BR, Singh SK, Mammen KJ. Neurofibromatosis of the colon: an unusual manifestation of von Recklinghausen's diseases-a case report. *Indian J Pathol Microbiol* 1998; **41**: 113-116
10 **Giuly JA,** Picand R, Giuly D, Monges B, Nguyen-Cat R. Von Recklinghausen disease and gastrointestinal stromal tumors. *Am J Surg* 2003; **185**: 86-87
11 **Abramson LP,** Orkin BA, Schwartz AM. Isolated colonic neurofibroma manifested by massive lower gastrointestinal bleeding and intussusception. *South Med J* 1997; **90**: 952-954
12 **Baril A,** Bayle JJ, Boucheron S, Dano P, Meley J. Colonic localization of pseudopolypoid type disclosing Recklinghausen's neurofibromatosis. *Sem Hop* 1982; **58**: 2665-2668
13 **Grouls V,** Vaih S, Bindewald H. Involvement of the large intestine in neurofibromatosis type 1. *Pathologe* 1996; **17**: 133-138
14 **Finkel M,** Finkel ER, Harris AI. Von Recklinghausen's disease with involvement of the colon: an endoscopic view. *Mt Sinai J Med* 1978; **45**: 387-389
15 **Becheur H,** Marteau P, Lavergne-Slove A, Bouhnik Y, Attar A, Rambaud JC. Isolated and spontaneously regressive colonic neurofibromatosis. *Gastroenterol Clin Biol* 1995; **19**: 718-120
16 **Watanuki F,** Ohwada S, Hosomura Y, Okamura S, Kawashima Y, Tanahashi Y, Nakamura S, Iino Y, Johshita T, Morishita Y. Small ileal neurofibroma causing intussusception in a non-neurofibromatosis patient. *J Gastroenterol* 1995; **30**: 113-116
17 **Frick EJ Jr,** Lapos L, Vargas HD. Solitary neurofibroma of the anal canal: report of two cases. *Dis Colon Rectum* 2000; **43**: 109-112
18 **Saitoh K,** Nasu M, Kamiyama R, Hatakeyama S, Maruyama M, Tsuruta K, Takeshita K. Solitary neurofibroma of the esophagus. *Acta Pathol Jpn* 1985; **35**: 527-531
19 **Sinha R,** Paul R, Sen I, Sikdar B. A solitary huge neurofibroma of the soft palate. *J Laryngol Otol* 2002; **116**: 637-638
20 **Acebo E,** Fernandez FA, Val-Bernal JF. Solitary neurofibroma of the gallbladder. A case report and review of the literature. *Gen Diagn Pathol* 1998; **143**: 337-340
21 **Carbia S,** Pagola J, Flaster N, Guida A, Jufe L, Gonzalez B, Caniparoli A. Isolated neurofibroma of the common bile duct. *Medicina* 1995; **55**: 689-692
22 **Kostakopoulos A,** Chorti M, Protogerou V, Kokkinou S. Solitary neurofibroma of kidney: clinical, histological and chromosomal appearance. *Int Urol Nephrol* 2003; **35**: 11-13
23 **Milathianakis KN,** Karamanolakis DK, Mpogdanos IM, Trihia-Spyrou EI. Solitary neurofibroma of the spermatic cord. *Urol Int* 2004; **72**: 271-274
24 **Hirao M,** Gushiken T, Imokawa H, Kawai S, Inaba H, Tsukuda M. Solitary neurofibroma of the nasal cavity: resection with endoscopic surgery. *J Laryngol Otol* 2001; **115**: 1012-1014
25 **Surwald CJ,** Salam MA, Rowe RC. A solitary neurofibroma of the palatine tonsil. *J Laryngol Otol* 2002; **116**: 1050-1052
26 **Wenke KA,** Jackel MC. Solitary neurofibroma of the parapharyngeal space. *HNO* 2004; **52**: 443-446
27 **Puri R,** Berry S, Srivastava G. Solitary neurofibroma of the larynx. *Otolaryngol Head Neck Surg* 1997; **117**: 713-714
28 **Paksoy Y,** Sahin M, Avunduk MC, Aksoy F, Odev K. Solitary juxtacortical neurofibroma of the humerus. *Skeletal Radiol* 2002; **31**: 112-115
29 **Tsutsumi T,** Oku T, Komatsuzaki A. Solitary plexiform neurofibroma of the submandibular salivary gland. *J Laryngol Otol* 1996; **110**: 1173-1175
30 **Kalina PH,** Bartley GB, Campbell RJ, Buettner H. Isolated neurofibromas of the conjunctiva. *Am J Ophthalmol* 1991; **111**: 694-698
31 **Ameur A,** Lezrek M, Jira H, el Alami M, Beddouch A, Abbar M. Solitary giant retroperitoneal neurofibroma. *Prog Urol* 2002; **12**: 465-468
32 **Kocak A,** Cayli SR, Sarac K, Aydin NE. Intraventricular solitary fibrous tumor: an unusual tumor with radiological, ultrastructural, and immunohistochemical evaluation: case report. *Neurosurgery* 2004; **54**: 213-216
33 **Kamiyoshihara M,** Hirai T, Kawashima O, Morishita Y. Primary solitary neurofibroma of the chest wall: report of a case resected with video-assisted thoracoscopic surgery. *Kyobu Geka* 1997; **50**: 421-423
34 **Cappell MS,** Colonic toxicity of administered drugs and chemicals. *Am J Gastroenterol* 2004; **99**: 1175-1190

Science Editor Guo SY **Language Editor** Elsevier HK

PO Box 2345, Beijing 100023, China
www.wjgnet.com
wjg@wjgnet.com

ELSEVIER

World J Gastroenterol 2005;11(35):5577-5581
World Journal of Gastroenterology ISSN 1007-9327
© 2005 The WJG Press and Elsevier Inc. All rights reserved.

• *CASE REPORT* •

Autoimmune pancreatitis with IgG4-positive plasma cell infiltration in salivary glands and biliary tract

Masashi Taguchi, Gentaro Aridome, Shintaro Abe, Keiichiro Kume, Mitsuo Tashiro, Mitsuyoshi Yamamoto, Yasuyuki Kihara, Hayato Nakamura, Makoto Otsuki

Masashi Taguchi, Gentaro Aridome, Shintaro Abe, Keiichiro Kume, Mitsuo Tashiro, Mitsuyoshi Yamamoto, Yasuyuki Kihara, Hayato Nakamura, Makoto Otsuki, Third Department of Internal Medicine, University of Occupational and Environmental Health, Japan School of Medicine, Kitakyushu, Japan
Correspondence to: Makoto Otsuki, MD, PhD, Professor, Third Department of Internal Medicine, University of Occupational and Environmental Health, Japan School of Medicine, 1-1 Iseigaoka, Yahatanishi-ku, Kitakyushu 807-8555, Japan. mac-otsk@med.uoeh-u.ac.jp
Telephone: +81-93-691-7251 Fax: +81-93-692-0107
Received: 2005-03-01 Accepted: 2005-03-23

Taguchi M, Aridome G, Abe S, Kume K, Tashiro M, Yamamoto M, Kihara Y, Nakamura H, Otsuki M. Autoimmune pancreatitis with IgG4-positive plasma cell infiltration in salivary glands and biliary tract. *World J Gastroenterol* 2005; 11(35): 5577-5581
http://www.wjgnet.com/1007-9327/11/5577.asp

Abstract

A 62-year-old male was referred to our hospital because of liver dysfunction, diffuse pancreatic swelling, and trachelophyma. At admission, the patient was free of pain. Physical examination showed enlarged and palpable bilateral submandibular masses, but no palpable mass or organomegaly in the abdomen. Laboratory findings were as follows: total protein 90 g/L with γ-globulin of 37.3% (33 g/L), total bilirubin 4 mg/L, aspartate aminotransferase 39 IU/L, alanine aminotransferase 67 IU/L, γ-glutamyl transpeptidase 1 647 IU/L, and amylase 135 IU/L. Autoantibodies were negative, and tumor markers were within the normal range. Serum IgG4 level was markedly elevated (18 900 mg/L). Computed tomography (CT) showed diffuse swelling of the pancreas and dilatation of both common and intra-hepatic bile ducts. Endoscopic retrograde pancreatography (ERP) revealed diffuse irregular and narrow main pancreatic duct and stenosis of the lower common bile duct. Biopsy specimens from the pancreas, salivary gland and liver showed marked periductal IgG4-positive plasma cell infiltration with fibrosis. We considered this patient to be autoimmune pancreatitis (AIP) with fibrosclerosis of the salivary gland and biliary tract, prescribed prednisolone at an initial dose of 40 mg/d. Three months later, the laboratory data improved almost to normal. Abdominal CT reflected prominent improvement in the pancreatic lesion. Swelling of the salivary gland also improved. At present, the patient is on 10 mg/d of prednisolone without recurrence of the pancreatitis. We present here a case of AIP with fibrosclerosis of salivary gland and biliary tract.

© 2005 The WJG Press and Elsevier Inc. All rights reserved.

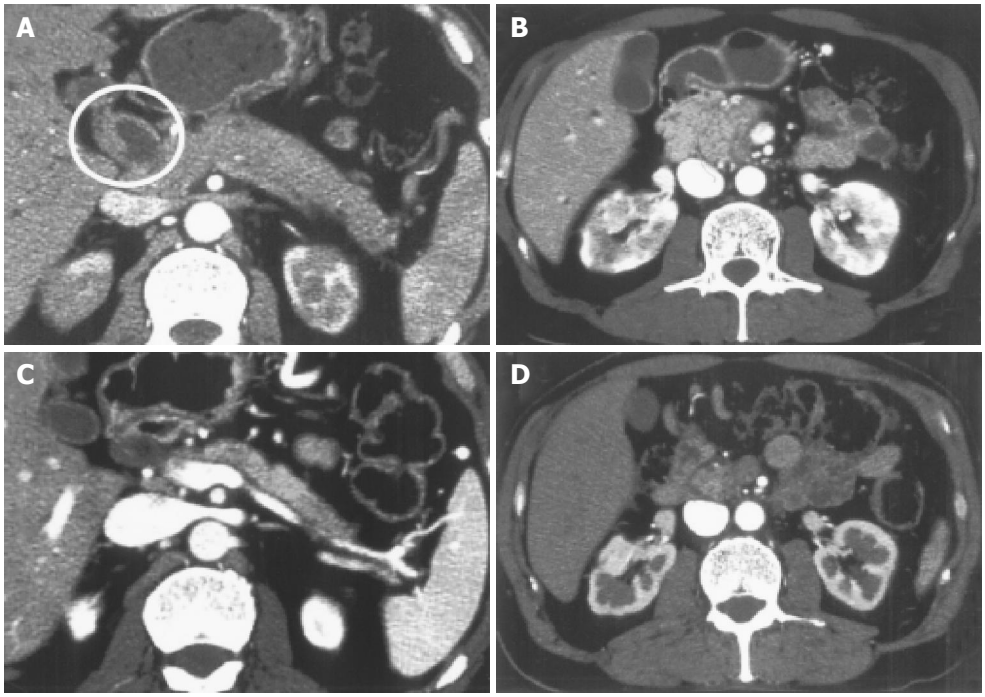
Key words: Autoimmune pancreatitis; Fibrosclerosis; IgG4-positive plasma cell; Salivary gland

CASE REPORT

A 62-year-old Japanese male was referred to our hospital because of liver dysfunction, common and intra-hepatic bile duct dilatation, diffuse pancreatic swelling, and trachelophyma. He had complained about fatigability and appetite loss without abdominal pain and noticed enlarged bilateral submandibular masses. There was no past history of pancreatitis, biliary tract disease or collagen disease. He was not a habitual drinker, and his family history was not contributory.

On admission, the patient was free of pain. Physical examination showed enlarged and palpable bilateral submandibular masses, but no palpable mass or organomegaly in the abdomen. Laboratory tests showed elevation of hepatobiliary enzyme levels without hyperbilirubinemia: total-bilirubin 7 mg/L, aspartate aminotransferase 39 IU/L, alanine aminotransferase 67 IU/L, alkaline phosphatase 1 293 IU/L, γ-glutamyl transpeptidase 1 647 IU/L. BUN and creatinine (Cre) levels were also elevated; BUN 230 mg/L, Cre 17 mg/L. Serum IgG level was elevated to 33 680 mg/L, serum IgG4, a subclass of IgG, was especially elevated to 1 890 mg/mL, although autoantibodies such as anti-nuclear antibodies (ANA), rheumatoid factor (RF), SS-A and SS-B antibody were negative. Pancreatic enzyme levels were elevated except for amylase (Amy); Amy 135 IU/L, lipase 95 IU/L, trypsin 584 ng/mL, elastase I 5 200 ng/L, and pancreatic exocrine function determined by the urinary para-aminobutyric acid excretion rate (BT-PABA test) was 27.5%. Tumor markers were also elevated: CA19-9 125 U/mL, DUPAN-2 330 U/mL, and SPAN-1 97 U/mL. The 75 g oral glucose tolerance test showed a diabetic pattern. The glucagon-loading test revealed impaired insulin secretory function.

Contrast-enhanced abdominal CT demonstrated diffuse enlargement of the pancreas, wall thickness of the dilated common bile duct, and heterogeneous enhancement of both kidneys (Figures 1A and B). Endoscopic retrograde pancreatography (ERP) revealed an irregular narrowing of the entire main pancreatic duct (Figure 2A). Drip infusion cholangiography-CT (DIC-CT) showed a smooth stenosis



Figures 1 Abdominal CT scans on admission. Note the diffuse enlargement of the pancreas and wall thickness of the enlarged common bile duct (CBD) (white circle) (**A**, **B**). Abdominal CT scans taken at 3 mo after treatment. Note the improvement in pancreatic swelling and CBD (**C**, **D**).

of the lower common bile duct with upstream dilatation (Figure 2B). Ultrasonography (US) of the neck showed diffuse swelling of bilateral salivary glands and Ga scintigraphy revealed abnormal uptake in the salivary glands (Figures 3A and B).

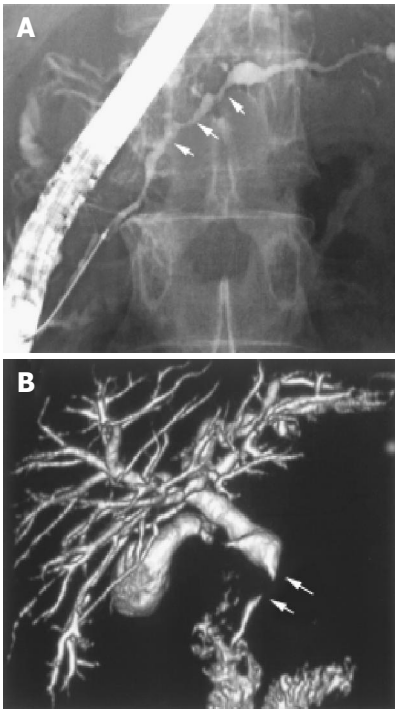


Figure 2 ERP (**A**) and DIC-CT (**B**) on admission. **A**: Note the diffuse irregular narrowing of the main pancreatic duct (arrow); **B**: Note the smooth stenosis of the common bile duct (arrow) and dilatation of the distal portion of the biliary tract.

Pancreatic tissue samples obtained by needle biopsy under US showed periductal lymphoplasmacytic infiltration and marked interstitial fibrosis with acinar atrophy (Figures 4A and B). Immunohistochemically, diffuse infiltrates in the pancreas consisted predominantly of CD4- or CD8-positive T lymphocytes, and IgG4-positive plasma cells rather than CD20-positive B lymphocytes (Figures 4C-F). Liver and salivary gland tissue samples by

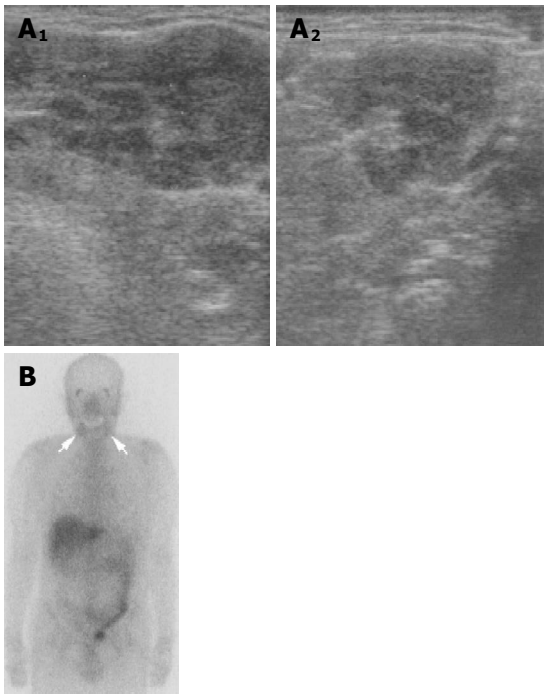


Figure 3 Neck US (**A**) and Ga scintigraphy (**B**) on admission. Note the diffuse swelling (**A**) and abnormal uptake (**B**: arrow) in the bilateral salivary glands.

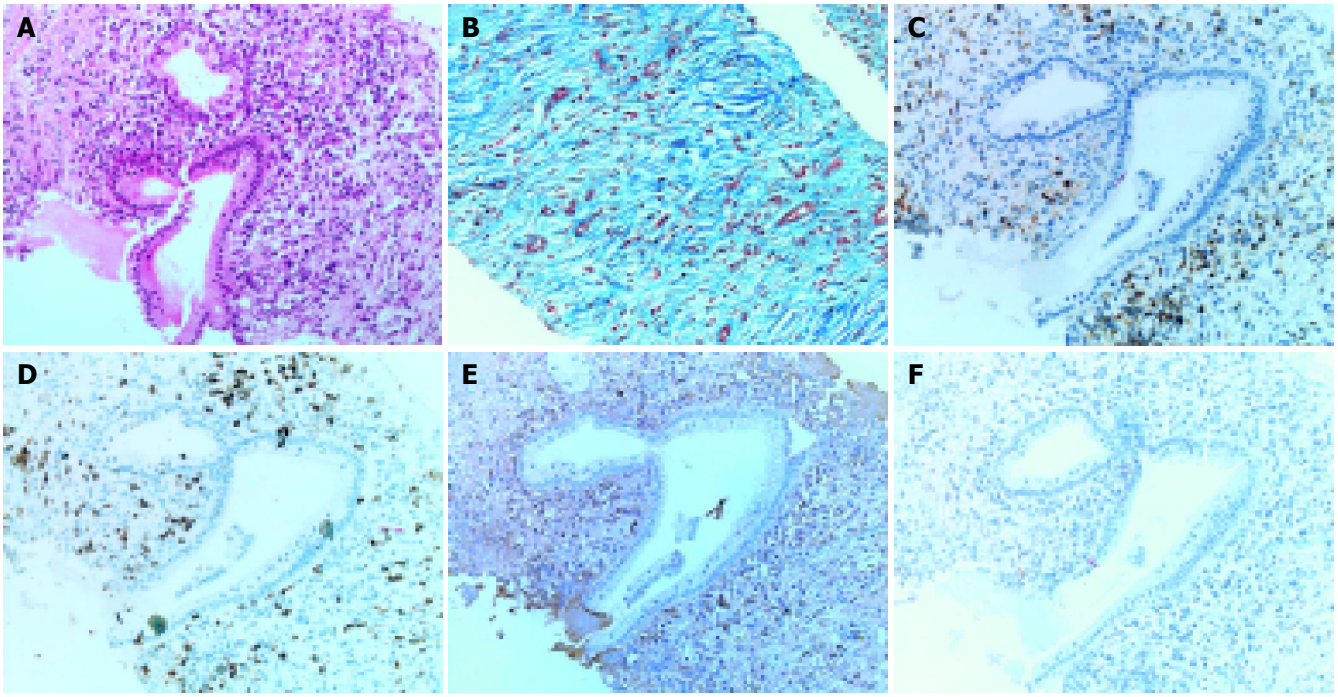


Figure 4 Histological examination of pancreatic specimen obtained by needle biopsy. Note the extensive fibrosis, acinar atrophy, infiltration of lymphocytes and plasma cells were seen. The infiltrates were observed predominantly around the pancreatic duct (**A**: hematoxylin and eosin staining; **B**: Masson staining). These infiltrates consisted mainly of CD4- or CD8-positive T lymphocytes, and CD20-negative and IgG4-positive plasma cells (**C**-**F**: immunostaining of CD4, 8, IgG4, and CD20 respectively).

needle biopsy also showed the periductal IgG4-positive plasma cell infiltration with interstitial fibrosis (Figures 5A-D).

Oral administration of prednisolone at an initial dose of 40 mg/d, following a diagnosis of autoimmune pancreatitis (AIP), led to an immediate improvement in all blood chemistries including tumor markers and serum γ-globulin concentration. In addition, the endocrine function improved from HbA1c 6.6% to 5.7%, the exocrine function determined by BT-PABA test also improved from 27.5% to 52.9% and renal function determined by serum Cre improved from 17 to 11 mg/L after steroid therapy. Subsequent follow-up CT showed improvement in pancreatic swelling, stenosis of lower common bile duct with upstream dilatation and wall thickness of the bile ducts and heterogeneous enhancement of both kidneys (Figures 1C and D). Moreover, the salivary glands swelling also improved. Prednisolone was gradually reduced to 10 mg/d over the course of 9 wk without any exacerbation.

DISCUSSION

AIP is a recently noted clinical entity and a rare group of pancreatitis in which autoimmunity is a suspected pathogenic mechanism. The diagnostic criteria for AIP according to the Japan Pancreas Society (2002) are as follows: (1) Diffuse or segmental narrowing of the main pancreatic duct with irregular wall (more than 1/3 length of the entire pancreas) and diffuse or localized enlargement of the pancreas by imaging studies, such as US, CT and magnetic resonance imaging. (2) High serum γ-globulin and/or IgG, or the presence of autoantibodies, such as ANA and RF. (3) Marked inter-lobular fibrosis and prominent infiltration of lymphocytes and plasma cells in the periductal area occasionally with lymphoid follicles in the pancreas. Diagnosis of AIP is established when criterion 1, together with criteria 2 and/or 3, are fulfilled[1-3]. We diagnosed our patient as AIP by these criteria.

Recent studies have revealed extrapancreatic involvements in AIP, such as sclerosing cholangitis, retroperitoneal fibrosis, and salivary gland swelling[4,5]. In AIP patients, the high serum levels of IgG4, subclass of IgG, and IgG4-positive lymphoplasmacytic infiltration are observed not only in the pancreas, but also in extra-pancreatic organs, such as the biliary duct, salivary gland and lymph nodes. These observations suggest a common pathogenesis related to the IgG4 subclass of immune complexes[6,7]. In our case, immunohistochemical examination of biopsied specimens showed infiltration of IgG4-positive plasma cells in the periductal area of the salivary gland (Figure 5D) and the portal area of the liver (Figure 5B), as well as in the pancreas (Figure 4E).

Nishimori *et al*.[8], found jaundice in 30% of AIP patients and stenosis of the lower common bile duct in 68% of 64 AIP patients. Two possible mechanisms of stenosis were hypothesized: one is the direct effect of the swollen pancreas on the bile duct, the other is wall inflammatory swelling of the bile duct wall, independent of the pancreas. In our case, smooth stenosis of the lower common bile duct was accompanied by wall thickening of bile duct (Figure 1A), which improved completely after steroid therapy (Figure 1C). These results support the latter hypothesis. It is reported that the histological features of bile duct lesions are similar to those typically seen in the pancreas[9]. Moreover, the liver biopsy specimen showed IgG4-positive cell infiltration

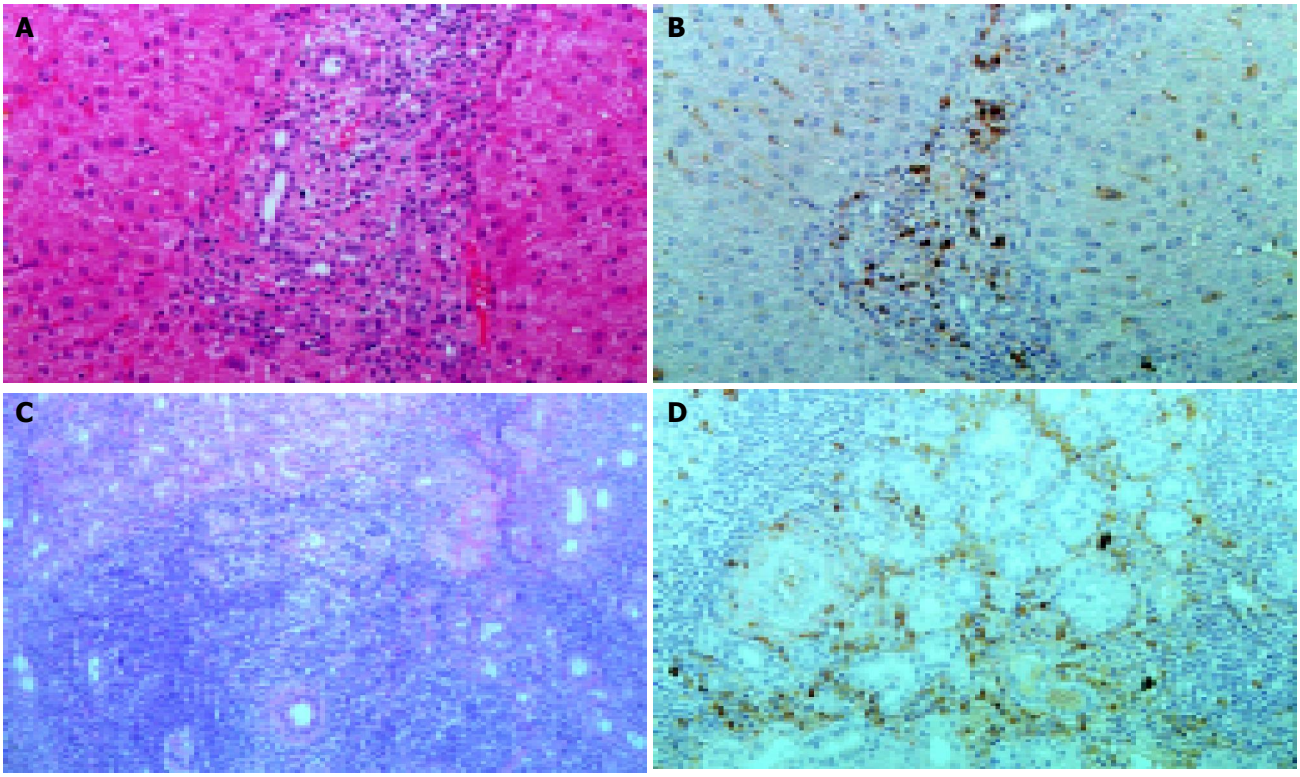


Figure 5 Histopathological examination of the liver (**A** and **B**) and salivary gland (**C** and **D**) specimens obtained by needle biopsy. Note the infiltrated lymphocytes and IgG4-positive plasma cells in the portal area, around the ducts of the salivary gland (**A** and **C**: hematoxylin and eosin staining, **B** and **D**: immunostaining of IgG4).

around the small bile duct in the portal area (Figure 5B). In fact, the focus of the bile duct, one of the extrapancreatic lesion of AIP, is diffuse from the common to intrahepatic bile ducts. Stenosis of the upper common bile was seen in 53% of AIP patients[8].

Pancreatic islets as well as acinar cells are involved in the same inflammatory process in AIP[10]. Kamisawa *et al*.[11], reported that 42% and 88% of AIP showed pancreatic endocrine and exocrine dysfunction, respectively. The endocrine and exocrine function improved in 60% and 50% of these patients after steroid therapy, respectively. Although we were unable to demonstrate extensive islet destruction in the pancreas due to lack of islets in the biopsy specimen, HbA1c, a marker of glycemic control, improved without anti-diabetic treatment and the exocrine function evaluated by BT-PABA test also improved after steroid therapy.

Salivary gland function, which is known to be frequently impaired in patient with AIP, even when clinical symptoms are not obvious as determined by β_2-microglobulin level in the saliva and parotid gland scintigraphy improves after steroid therapy in almost all AIP patients[11,12]. In our case, the patient noticed swelling of the salivary glands and abundant infiltration of IgG4-positive plasma cells, which has not been detected in Sjögren's syndrome[7]. In addition, specific marker of Sjögren's syndrome, anti SS-A and SS-B antibodies were negative. Swelling of the salivary glands disappeared after steroid therapy. These results suggest that the salivary swelling was due to extrapancreatic lesion of AIP rather than due to Sjögren's syndrome. Ductal system of salivary gland and pancreas are similar in histological structure, so common autoantigen might be involved in the pathogenesis of these organs.

On admission, mild renal dysfunction was seen and contrast-enhanced CT demonstrated heterogeneous enhancement of both kidneys (Figure 1B). Treatment with steroid improved CT findings (Figure 1D) and renal function. Renal dysfunction in AIP is reported to be due to retroperitoneal fibrosis[13] and/or IgG4-associated tubulointerstitial nephritis[14,15]. Although we could not prove histologically, renal dysfunction in the present case was probably due to tubulointerstitial nephritis, one of the extrapancreatic involvements in AIP.

Following steroid therapy, most of all clinical symptoms and laboratory data improved and the pancreas became small and atrophic (Figure 1C). Takayama *et al*.[16], reported pancreatic stones in 20% of AIP patients during observation for 4.5 years. This suggests that AIP is a progressive disease and a possibility of an early stage of idiopathic chronic pancreatitis. We continued maintenance steroid therapy at 10 mg/d, but prognosis with AIP is also unknown at this stage.

In conclusion, we presented here a case of AIP with IgG4-associated fibrosclerosis of the salivary gland and biliary tract. AIP may be one lesion of systemic multifocal fibrosclerosis in some cases.

REFERENCES

1 Members of the criteria committee for autoimmune pancreatitis of the Japan pancreatic society. Diagnostic criteria for autoimmune pancreatitis by the Japan pancreas society. *J Jpn Panc Soc* 2002; **17**: 585-587

2 **Otsuki M.** Chronic pancreatitis in Japan: Epidemiology,

prognosis, diagnostic criteria, and future problems. *J Gastroenterol* 2003; **38**: 315-326
3 **Otsuki M.** Chronic pancreatitis. The problems of diagnostic criteria. *Pancreatology* 2004; **4**: 28-41
4 **Okazaki K,** Chiba T. Autoimmune related pancreatitis. *Gut* 2002; **51**: 1-4
5 **Kawa S,** Hamano H. Autoimmune pancreatitis and bile duct lesions. *J Gastroenterol* 2003; **38**: 1201-1203
6 **Hamano H,** Kawa S, Horiuchi A, Unno H, Furuya N, Akamatsu T, Fukushima M, Nikaido T, Nakayama K, Usuda N, Kiyosawa K. High serum IgG4 concentrations in patients with sclerosing pancreatitis. *N Engl J Med* 2001; **344**: 732-738
7 **Kamisawa T,** Funata N, Hayashi Y, Tsuruta K, Okamoto A, Amemiya K, Egawa N, Nakajima H. Close relationship between autoimmune pancreatitis and multifocal fibrosclerosis. *Gut* 2003; **52**: 683-687
8 **Nishimori I,** Suda K, Oi I. Research on the clinical state of autoimmune pancreatitis. *J Jpn Panc Soc* 2002; **17**: 619-627
9 **Kuroiwa T,** Suda T, Takahashi T, Hirono H, Natsui M, Motoyama H, Nomoto M, Aoyagi Y. Bile duct involvement in a case of autoimmune pancreatitis successfully treated with an oral steroid. *Dig Dis Sci* 2002; **47**: 1810-1816
10 **Tanaka S,** Kobayashi T, Nakanishi K, Okubo M, Murase T, Hashimoto M, Takeuchi K. Corticosteroid-responsive diabetes mellitus associated with autoimmune pancreatitis. *Lancet* 2000; **356**: 910-911
11 **Kamisawa T,** Egawa N, Inokuma S, Tsuruta K, Okamoto A, Kamata N, Nakamura T, Matsukawa M. Pancreatic endocrine and exocrine function and salivary gland function in autoimmune pancreatitis before and after steroid therapy. *Pancreas* 2003; **27**: 235-238
12 **Kamisawa T,** Tu Y, Egawa N, Sakaki N, Inokuma S, Kamata N. Salivary gland involvement in chronic pancreatitis of various etiologies. *Am J Gastroenterol* 2003; **98**: 323-326
13 **Uchida K,** Okazaki K, Asada M, Yazumi S, Ohana M, Chiba T, Inoue T. Case of chronic pancreatitis involving an autoimmune mechanism that extended to retroperitoneal fibrosis. *Pancreas* 2003; **26**: 92-94
14 **Takeda S,** Haratake J, Kasai T, Takaeda C, Takazakura E. IgG4-associated idiopathic tubulointerstitial nephritis complicating autoimmune pancreatitis. *Nephrol Dial Transplant* 2004; **19**: 474-476
15 **Uchiyama-Tanaka Y,** Mori Y, Kimura T, Sonomura K, Umemura S, Kishimoto N, Nose A, Tokoro T, Kijima Y, Yamahara H, Nagata T, Masaki H, Umeda Y, Okazaki K, Iwasaka T. Acute tubulointerstitial nephritis associated with autoimmune-related pancreatitis. *Am J Kidney Dis* 2004; **43**: e18-25
16 **Takayama M,** Hamano H, Ochi Y, Saegusa H, Komatsu K, Muraki T, Arakura N, Imai Y, Hasebe O, Kawa S. Recurrent attacks of autoimmune pancreatitis result in pancreatic stone formation. *Am J Gastroenterol* 2004; **99**: 932-937

Science Editor Guo SY **Language Editor** Elsevier HK

PO Box 2345, Beijing 100023, China
www.wjgnet.com
wjg@wjgnet.com

ELSEVIER

World J Gastroenterol 2005;11(35):5582
World Journal of Gastroenterology ISSN 1007-9327
© 2005 The WJG Press and Elsevier Inc. All rights reserved.

Acknowledgments to Reviewers of *World Journal of Gastroenterology*

Many reviewers have contributed their expertise and time to the peer review, a critical process to ensure the quality of *World Journal of Gastroenterology*. The editors and authors of the articles submitted to the journal are grateful to the following reviewers for evaluating the articles (including those were published and those were rejected in this issue) during the last editing period of time.

Vito Annese, M.D.
Department of Internal Medicine, Unit of Gastroenterology, CSS-IRCCS Hospital, Viale Cappuccini, 1, San Giovanni Rotondo 71013, Italy

Masahiro Asaka, Professor
Department of Internal Medicine, Gastroentology Section, Hokkaido University Graduate School of Medicine, N-15, W-7, Kita-ku, Sapporo 060-8638, Japan

Anthony Thomas Roger Axon, Professor
Department of Gastroenterology, Infirmary At Leeds, Room 190a, Clarendon Wingthe General Infirmary At Leedsgreat George Stree, Leeds Ls1 3ex, United Kingdom

Giovanni Barbara, Professor
Internal Medicine and Gastroenterology, University of Bologna, St.Orsola Hospital - Building No. 5Via Massarenti, 9 - 40138, Bologna 40138, Italy

Tomasz Brzozowski, Professor
Department of Physiology, Jagiellonian University Medical College, 16 Grzegorzecka Str, Cracow 31-531, Poland

Antoni Castells, M.D.
Gastroenterology Department, Hospital Clínic, University of Barcelona, Villarroel 170, Barcelona 08036, Spain

Xian-Ming Chen, M.D.
Mayo Medical School, Clinic and Foundation, 200 First Street, SW, Rochester, MN 55905, United States

Chi-Hin Cho, Chair and Professor
Departmentof Pharmacology, The University of Hong Kong, 21 Sassoon Road, Hong Kong, China

Zong-Jie Cui, Professor
Institute of Cell Biology, Beijing Normal University, Beijing 100875, China

Amar Paul Dhillon, Professor
Department of Histopathology, Royal Free Hospital, Pond Street, London NW3 2QG, United Kingdom

Abraham Rami Eliakim, Professor
Gastroenterology, Rambam Medical Center, Technion School of Medicine, P.O.B.9602, Haifa 31096, Israel

Ulrich Robert Fölsch, Professor
1st Department of Medicine, Christian-Albrechts-University of Kiel, Schittenhelmstrasse 12, Kiel 24105, Germany

Xue-Gong Fan, Professor
Xiangya Hospital, Changsha 410008, China

Yoshihide Fujiyama, Professor
Internal Medicine, Division of Gastroenterol, Shiga University of Medical Science, Tsukinowa, Seta, Otsu 520-2192, Japan

Edoardo G Giannini, Assistant Professor
Department of Internal Medicine, Gastroenterology Unit, Viale Benedetto XV, no. 6, Genoa, 16132, Italy

Neil Kaplowitz, M.D.
USC Kec k School of Medicine, GI/Liver Division, 2011 Zonal Avenue, HMR 101, Los Angeles CA 90033 , United States

Leonid Lazebnik, Professor
Moscow Health Department, CRI of Gastroenterology, Shosse Entusiastov 86, Moscow 111123, Russian Federation

Yoshiharu Motoo, Associate Professor
Cancer Research Institute, Kanazawa University, 13-1 Takara-machi, Kanazawa 920-0934, Japan

Piero Portincasa, Professor
Internal Medicine - DIMIMP, University of Bari Medical School, Hospital Policlinico Piazza G. Cesare 11, Bari 70124, Italy

Lun-Xiu Qin, Professor
Liver Cancer Institute and Zhongshan Hospital, Fudan University, 180 Feng Lin Road, Shanghai 200032, China

Qin Su, Professor
Department of Pathology, Cancer Hospital and Cancer Institute, Chinese Academy of Medical Sciences and Peking Medical College, PO Box 2258, Beijing 100021, China

Harald Vogelsang, Professor
Gastroenterology, AKH- KIM IV, Wahringer G. 18-20, Vienna A-1090, Austria

Harry H-X Xia, M.D.
Department of Medicine, The University of Hong Kong, Pokfulam Road, Hong Kong, China

Yuan Yuan, Professor
Cancer Institute of China Medical University, 155 North Nanjing Street, Heping District, Shenyang 110001, Liaoning Province, China

PO Box 2345, Beijing 100023, China
www.wjgnet.com
wjg@wjgnet.com

ELSEVIER

World J Gastroenterol 2005;11(35):5583
World Journal of Gastroenterology ISSN 1007-9327
© 2005 The WJG Press and Elsevier Inc. All rights reserved.

Meetings

MAJOR MEETINGS COMING UP

APDW 2005 - Asia Pacific Digestive Week 2005
September 25-28, 2005
asiapdw@kornet.net
www.apdw2005.org

13th United European Gastroenterology Week
October 15-20, 2005
uegw@discongress.com
www.webasistent.cz/guarant/uegw2005/

American College of Gastroenterology Annual Scientific Meeting
October 28 -November 2, 2005
annualmeeting@acg.gi.org
www.acg.gi.org

EVENTS AND MEETINGS IN THE UPCOMING 6 MONTHS

United European Gastroenterology Week
October 15-20, 2005
uegw@discongress.com
www.webasistent.cz/guarant/uegw2005/

ISGCON2005
November 11-15, 2005
isgcon2005@yahoo.co.in
isgcon2005.com

II Latvian Gastroenterology Congress
November 29, 2005
gec@stradini.lv
www.gastroenterologs.lv

70th ACG Annual Scientific Meeting and Postgraduate Course
October 28-November 2, 2005

Advanced Capsule Endoscopy Users Course
November 18-19, 2005
www.asge.org/education

2005 CCFA National Research and Clinical Conference - 4th Annual Advances in the Inflammatory Bowel Diseases
December 1-3, 2005
c.chase@imedex.com
www.imedex.com/calendars/therapeutic.htm

EVENTS AND MEETINGS IN 2005

XIII Argentine Hepatology Congress
XIII Congreso Argentino de HepatologÃa
June 10-13, 2005
mci@mcimeetings.com
www.hepatologia.org

9th Annual Coolum Update in Gastroenterology & Hepatology
June 11-13, 2005
info@e-Kiddna.com.au

Canadian Digestive Disease Week Conference
February 26-March 6, 2005
www.cag-acg.org

2005 World Congress of Gastroenterology
September 12-14, 2005
wcog2005@congrex.nl

International Colorectal Disease Symposium 2005
February 3-5, 2005
info@icds-hk.org

15th World Congress of the International Association of Surgeons and Gastroenterologists
September 7-10, 2005
iasg2005@guarant.cz
www.iasg2005.cz

7th International Workshop on Therapeutic Endoscopy
September 10-12, 2005
alfa@alfamedical.com
www.alfamedical.com

EASL 2005 the 40th annual meeting
April 13-17, 2005
www.easl.ch/easl2005/

ISGCON2005
November 11-15, 2005
isgcon2005@yahoo.co.in
isgcon2005.com

Pediatric Gastroenterology, Hepatology and Nutrition
March 13, 2005

II Latvian Gastroenterology Congress
November 29, 2005
gec@stradini.lv
www.gastroenterologs.lv

21st annual international congress of Pakistan society of Gastroenterology & GI Endoscopy
March 25-27, 2005
psgc05@hotmail.com
www.psgc2005.com

8th Congress of the Asian Society of HepatoBiliary Pancreatic Surgery
February 10-13, 2005

1º Workshop de Gastrenterologia para Clí nica Geral
April 29, 2005
luis.m.lopes@sapo.pt

APDW 2005 - Asia Pacific Digestive Week 2005
September 25-28, 2005
asiapdw@kornet.net
www.apdw2005.org

World Congress on Gastrointestinal Cancer
June 15-18, 2005
meetings@imedex.com

British Society of Gastroenterology Conference
March 14-17, 2005
www.bsg.org.uk

Training Director's Workshop:Developing and Teaching Principles in the New Era of GI Training
February 4-6, 2005
www.asge.org/education

The Pharmacological, Surgical and Endoscopic Management of GERD
April 8-9, 2005
www.asge.org/education

Digestive Disease Week
DDW 106th Annual Meeting
May 15-18, 2005
ddwadmin@gastr.org
www.ddw.org

ASGE Advanced Endscopy Skills Hands-on Sessions
May 15, 2005
www.asge.org/education

ASGE GERD Hands-on Session
May 17, 2005
www.asge.org/education

Annual Postgraduate Course
May 18-19, 2005
www.asge.org/education

Advanced Capsule Endoscopy Users Course
June 4-5, 2005
www.asge.org/education

Advanced Capsule Endoscopy Users Course
August 12-13, 2005
www.asge.org/education

GI Practice Management Symposium: Solutions for a Successful Practice
August 18, 2005
www.asge.org/education

70th ACG Annual Scientific Meeting and Postgraduate Course
October 28-November 2, 2005

Advanced Capsule Endoscopy Users Course
November 18-19, 2005
www.asge.org/education

2005 CCFA National Research and Clinical Conference - 4th Annual Advances in the Inflammatory Bowel Diseases
December 1-3, 2005
c.chase@imedex.com
www.imedex.com/calendars/therapeutic.htm

EVENTS AND MEETINGS IN 2006

10th World Congress of the International Society for Diseases of the Esophagus
February 22-25, 2006
isde@sapmea.asn.au
www.isde.net

Easl 2006 - The 41st Annual Meeting
April 26-30, 2006

Canadian Digestive Disease Week Conference
March 4-12, 2006
www.cag-acg.org

XXX pan-american congress of digestive diseases
XXX congreso panamericano de anfermedades digestivas
November 25-December 1, 2006
amg@gastro.org.mx
www.gastro.org.mx

World Congress on Gastrointestinal Cancer
June 14-17, 2006
c.chase@imedex.com

7th World Congress of the International Hepato-Pancreato-Biliary Association
September 3-7, 2006
convention@edinburgh.org
www.edinburgh.org/conference

Annual Postgraduate Course
May 25-26, 2006
www.asge.org/education

71st ACG Annual Scientific Meeting and Postgraduate Course
October 20-25, 2006

PO Box 2345, Beijing 100023, China
www.wjgnet.com
wjg@wjgnet.com

ELSEVIER

World J Gastroenterol 2005;11(35):5584-5585
World Journal of Gastroenterology ISSN 1007-9327
© 2005 The WJG Press and Elsevier Inc. All rights reserved.

Instructions to authors

GENERAL INFORMATION

World Journal of Gastroenterology (*WJG,* ISSN 1007-9327 CN 14-1219/R) is a weekly journal of more than 48 000 circulation, published on the 7th, 14th, 21st and 28th of every month.

Original Research, Clinical Trials, Reviews, Comments, and Case Reports in esophageal cancer, gastric cancer, colon cancer, liver cancer, viral liver diseases, *etc*., from all over the world are welcome on the condition that they have not been published previously and have not been submitted simultaneously elsewhere.

Published jointly by
The WJG Press and Elsevier Inc.

SUBMISSION OF MANUSCRIPTS

Manuscripts should be typed double-spaced on A4 (297×210 mm) white paper with outer margins of 2.5 cm. Number all pages consecutively, and start each of the following sections on a new page: Title Page , Abstract, Introduction, Materials and Methods, Results, Discussion, Acknowledgements, References, Tables, Figures and Figure Legends. Neither the Editors nor the Publisher is responsible for the opinions expressed by contributors. Manuscripts formally accepted for publication become the permanent property of The WJG Press and Elsevier Inc., and may not be reproduced by any means, in whole or in part without the written permission of both the Authors and the Publisher. We reserve the right to put onto our website and copy-edit accepted manuscripts. Authors should also follow the guidelines for the care and use of laboratory animals of their institution or national animal welfare committee.

Authors should retain one copy of the text, tables, photographs and illustrations, as rejected manuscripts will not be returned to the author(s) and the editors will not be responsible for the loss or damage to photographs and illustrations.

Online submission
Online submission is strongly advised. Manuscripts should be submitted through the Online Submission System at: http://www.wjgnet.com/index.jsp. Authors are highly recommended to consult the ONLINE INSTRUCTIONS TO AUTHORS (http://www.wjgnet.com/wjg/help/instructions.jsp) before attempting to submit online. Authors encountering problems with the Online Submission System may send an email describing the problem to wjg@wjgnet.com for assistance. If you submit manuscript online, do not make a postal contribution. A repeated online submission for the same manuscript is strictly prohibited.

Postal submission
Send 3 duplicate hard copies of the full-text manuscript typed double-spaced on A4(297×210 mm) white paper together with any original photographs or illustrations and a 3.5 inch computer diskette or CD-ROM containing an electronic copy of the manuscript including all the figures, graphs and tables in native Microsoft Word format or *.rtf format to:

World Journal of Gastroenterology
Apartment 1066 Yishou Garden,
58 North Langxinzhuang Road,
PO Box 2345, Beijing 100023, China
E-mail: wjg@wjgnet.com
http: //www.wjgnet.com

MANUSCRIPT PREPARATION

All contributions should be written in English. All articles must be submitted using a word-processing software. All submissions must be typed in 1.5 line spacing and in word size 12 with ample margins. The letter font is Tahoma. For authors originating from China, one copy of the Chinese translation of the manuscript is also required (excluding references). Style should conform to our house format. Required information for each of the manuscript sections is as follows:

Title page
Full manuscript title, running title, all author(s) name(s), affiliations, institution(s) and/or department(s) where the work was accomplished, disclosure of any financial support for the research, and the name, full address, telephone and fax numbers and email address of the corresponding author should be involved. Titles should be concise and informative (removing all unnecessary words), emphasize what is NEW, and avoid abbreviations. A short running title of less than 40 letters should be provided. List the author(s)' name(s) as follows: initials and/or first name, middle name or initial(s) and full family name.

Abstract
An informative, structured abstract of no more than 250 words should accompany each manuscript. Abstracts for original contributions should be structured into the following sections: AIM: Only the purpose should be included. METHODS: The materials, techniques, instruments and equipments, and the experimental procedures should be included. RESULTS: The observatory and experimental results, including data, effects, outcome, *etc*. should be included. Authors should present *P* value where necessary, and the significant data should accompany. CONCLUSION: Accurate view and the value of the results should be included.

The format of structured abstracts is at: http://www.wjgnet.com/wjg/help/11.doc

Key words
Please list 3-10 key words that could reflect content of the study.

Text
For most article types, the main text should be structured into the following sections: INTRODUCTION, MATERIALS AND METHODS, RESULTS and DISCUSSION, and should include appropriate Figures and Tables. Data should be presented in the body text or Figures and Tables, not both.

Illustrations
Figures should be numbered as 1, 2, 3 and so on, and mentioned clearly in the main text. Provide a brief title for each figure on a separate page. No detailed legend should be involved under the figures. This part should add into the text where the figures are applicable. Digital images: black and white photographs should be scanned and saved in TIFF format at a resolution of 300 dpi; color images should be saved as CMYK (print files) and not RGB (screen-viewing files). Place each photograph in a separate file. Print images: supply images of size no smaller than 126×76 mm printed on smooth surface paper; label the image by writing the Figure number and orientation using an arrow. Photomicrographs: indicate the original magnification and stain in the legend. Digital Drawings: supply files in EPS if created by Freehand and Illustrator, or TIFF from Photoshop. EPS files must be accompanied by a version in native file format for editing purposes. Scans of existing line drawings should be scanned at a resolution of 1200 dpi and as close as possible to the size at which they will appear when printed, not smaller. Please use uniform legends for the same subjects. For example: Figure 1 Pathological changes of atrophic gastritis after treatment. A: ...; B: ...;C: ...; D: ...; E: ...; F: ...; G: ...

Tables
Three-line tables should be numbered as 1, 2, 3 and so on, and mentioned clearly in the main text. Provide a brief title for each table. No detailed legend should be involved under the tables. This part should add into the text where the tables are applicable. The information should complement but not duplicate that contained in the text. Use one horizontal line under the title, a second under the column heads, and a third below the Table, above any footnotes. Vertical and italic lines should be omitted.

Notes in tables and illustrations
Data which is not statistically significant should not be noted. $^{a}P<0.05$, $^{b}P<0.01$ ($P>0.05$ should not be noted). If there are other series of *P* values, $^{c}P<0.05$ and $^{d}P<0.01$ are used; Third series of *P* values can be expressed as $^{e}P<0.05$ and $^{f}P<0.01$. Other notes in tables or under

illustrations should be expressed as ^1F, ^2F, ^3F; or some other symbols with a superscript (Arabic numerals) in the upper left corner. In a multi-curve illustration, each curve should be labeled with ●, ○, ■, □, ▲, △, *etc*. in a certain sequence.

Acknowledgments

Brief acknowledgments of persons who have made genuine contributions to the manuscripts and who endorse the data and conclusions are included. Authors are responsible for obtaining written permission to use any copyrighted text and/or illustrations.

References

Cited references should mainly be drawn from journals covered in the Science Citation Index (http://www.isinet.com) and/or Index Medicus (http://www.ncbi.nlm.nih.gov/PubMed) databases. Mention all references in the text, tables and figure legends, and set off by consecutive, superscripted Arabic numerals. References should be numbered consecutively in the order in which they appear in the text. Abbreviate journal title names according to the Index Medicus style (http://www.ncbi.nlm.nih.gov/entrez/query.fcgi?db=journals). Unpublished observations and personal communications are not listed as references. The style and punctuation of the references conform to ISO standard and the Vancouver style (5th edition); see examples below. Reference lists not conforming to this style could lead to delayed or even rejected publication status. Examples:

Standard jounal article (list all authors and include the PubMed ID [PMID] where applicable)

1 **Das KM,** Farag SA. Current medical therapy of inflammatory bowel disease. *World J Gastroenterol* 2000; 6: 483-489 [PMID: 11819634]

2 **Pan BR**, Hodgson HJF, Kalsi J. Hyperglobulinemia in chronic liver disease: Relationships between *in vitro* immunoglobulin synthesis, short lived suppressor cell activity and serum immunoglobulin levels. *Clin Exp Immunol* 1984; 55: 546-551 [PMID: 6231144]

3 **Lin GZ,** Wang XZ, Wang P, Lin J, Yang FD. Immunologic effect of Jianpi Yishen decoction in treatment of Pixu-diarrhoea. *Shijie Huaren Xiaohua Zazhi* 1999; 7: 285-287 [CMFAID:1082371101835979]

Books and other monographs (list all authors)

4 **Sherlock S,** Dooley J. Diseases of the liver and billiary system. 9th ed. Oxford: Blackwell Sci Pub, 1993: 258-296

Chapter in a book (list all authors)

5 **Lam SK.** Academic investigator's perspectives of medical treatment for peptic ulcer. In: Swabb EA, Azabo S. Ulcer disease: investigation and basis for therapy. New York: Marcel Dekker, 1991: 431-450

Electronic journal (list all authors)

6 **Morse SS.** Factors in the emergence of infectious diseases. Emerg Infect Dis serial online, 1995-01-03, cited 1996-06-05; 1(1):24 screens. Available from: URL: http//www.cdc.gov/ncidod/EID/eid.htm

PMID requirement

From the full reference list, please submit a separate list of those references embodied in PubMed, keeping the same order as in the full reference list, with the following information only: (1) abbreviated journal name and citation (e.g. *World J Gastroenterol* 2003;9(11): 2400-2403; (2) article title (e.g. Epidemiology of gastroenterologic cancer in Henan Province, China; (3) full author list (e.g. Lu JB, Sun XB, Dai DX, Zhu SK, Chang QL, Liu SZ, Duan WJ; (4) PMID (e.g. 14606064). Provide the full abstracts of these references, as quoted from PubMed on a 3.5 inch disk or CD-ROM in Microsoft Word format and send by post to The *WJG* Press. For those references taken from journals not indexed by *Index Medicus*, a printed copy of the first page of the full reference should be submitted. Attach these references to the end of the manuscript in their order of appearance in the text.

Inappropriate references

Authors should always cite references that are relevant to their article, and avoid any inappropriate references. Inappropriate references include those that are linked with a hyphen and the difference between the two numbers at two sides of the hyphen is more than 5. For example, [1-6], [2-14] and [1, 3, 4-10, 22] are all considered as inappropriate references. Authors should not cite their own unrelated published articles.

Statistical data

Present as mean±SD and mean±SE.

Statistical expression

Express *t* test as *t*(in italics), *F* test as *F*(in italics), chi square test as χ^2 (in Greek), related coefficient as *r*(in italics), degree of freedom as γ(in Greek), sample number as *n*(in italics), and probability as *P*(in italics).

Units

Use SI units. For example: body mass, m(B) = 78 kg; blood pressure, p (B)=16.2/12.3 kPa; incubation time, t(incubation)=96 h, blood glucose concentration, c(glucose) 6.4±2.1 mmol/L; blood CEA mass concentration, p(CEA) = 8.6 24.5 μg/L; CO_2 volume fraction, 50 mL/L CO_2 not 5% CO_2; likewise for 40 g/L formaldehyde, not 10% formalin; and mass fraction, 8 ng/g, *etc*. Arabic numerals such as 23,243,641 should be read 23 243 641.

The format about how to accurately write common units and quantum is at: http://www.wjgnet.com/wjg/help/15.doc

Abbreviations

Standard abbreviations should be defined in the abstract and on first mention in the text. In general, terms should not be abbreviated unless they are used repeatedly and the abbreviation is helpful to the reader. Permissible abbreviations are listed in Units, Symbols and Abbreviations: A Guide for Biological and Medical Editors and Authors (Ed. Baron DN, 1988) published by The Royal Society of Medicine, London. Certain commonly used abbreviations, such as DNA, RNA, HIV, LD50, PCR, HBV, ECG, WBC, RBC, CT, ESR, CSF, IgG, ELISA, PBS, ATP, EDTA, mAb, can be used directly without further mention.

Italicization

Quantities: *t* time or temperature, *c* concentration, *A* area, *l* length, *m* mass, *V* volume.
Genotypes: *gyr*A, *arg* 1, *c myc*, *c fos*, *etc*.
Restriction enzymes: *Eco*RI, *Hin*dI, *Bam*HI, *Kbo* I, *Kpn* I, *etc*.
Biology: *Helicobacter pylori, H pylori, E coli, etc*.

SUBMISSION OF THE REVISED MANUSCRIPTS AFTER ACCEPTED

Please revise your article according to the revision policies of *WJG*. The revised version including manuscript and high-resolution image figures (if any) should be copied on a floppy or compact disk. Author should send the revised manuscript, along with printed high-resolution color or black and white photos, copyright transfer letter, the final check list for authors, and responses to reviewers by a courier (such as EMS) (submission of revised manuscript by e-mail or on the WJG Editorial Office Online System is NOT available at present).

Language evaluation

The language of a manuscript will be graded before sending for revision. (1) Grade A: priority publishing; (2) Grade B: minor language polishing; (3) Grade C: a great deal of language polishing; (4) Grade D: rejected. The revised articles should be in grade B or grade A.

Copyright assignment form

It is the policy of WJG to acquire copyright in all contributions. Papers accepted for publication become the copyright of WJG and authors will be asked to sign a transfer of copyright form. All authors must read and agree to the conditions outlined in the Copyright Assignment Form (which can be downloaded from http://www.wjgnet.com/wjg/help/9.doc).

Final check list for authors

The format is at: http://www.wjgnet.com/wjg/help/13.doc

Responses to reviewers

Please revise your article according to the comments/suggestions of reviewers. The format for responses to the reviewers' comments is at: http://www.wjgnet.com/wjg/help/10.doc

Proof of financial support

For paper supported by a foundation, authors should provide a copy of the document and serial number of the foundation.

Publication fee

Authors of accepted articles must pay publication fee.

PO Box 2345, Beijing 100023, China
www.wjgnet.com
wjg@wjgnet.com

ELSEVIER

World J Gastroenterol 2005;11(35):5586
World Journal of Gastroenterology ISSN 1007-9327
© 2005 The WJG Press and Elsevier Inc. All rights reserved.

World Journal of Gastroenterology standard of quantities and units

Number	Nonstandard	Standard	Notice
1	4 days	4 d	In figures, tables and numerical narration
2	4 days	four days	In text narration
3	day	d	After Arabic numerals
4	Four d	Four days	At the beginning of a sentence
5	2 hours	2 h	After Arabic numerals
6	2 hs	2 h	After Arabic numerals
7	hr, hrs,	h	After Arabic numerals
8	10 seconds	10 s	After Arabic numerals
9	10 year	10 years	In text narration
10	Ten yr	Ten years	At the beginning of a sentence
11	0,1,2 years	0,1,2 yr	In figures and tables
12	0,1,2 year	0,1,2 yr	In figures and tables
13	4 weeks	4 wk	
14	Four wk	Four weeks	At the beginning of a sentence
15	2 months	2 mo	In figures and tables
16	Two mo	Two months	At the beginning of a sentence
17	10 minutes	10 min	
18	Ten min	Ten minutes	At the beginning of a sentence
19	50% (*V/V*)	500 mL/L	
20	50% (m/*V*)	500 g/L	
21	1 M	1 mol/L	
22	10 μM	10 μmol/L	
23	1N HCl	1 mol/L HCl	
24	1N H_2SO_4	0.5 mol/L H_2SO_4	
25	4rd edition	4^{th} edition	
26	15 year experience	15- year experience	
27	18.5 kDa	18.5 ku,18 500u or M_r18 500	
28	25 $g.kg^{-1}/d^{-1}$	25 g/(kg·d) or 25 g/kg per day	
29	6900	6 900	
30	1000 rpm	1 000 r/min	
31	sec	s	After Arabic numerals
32	1 pg $\cdot L^{-1}$	1 pg/L	
33	10 kilograms	10 kg	
34	13 000 rpm	13 000 *g*	High speed; *g* should be in italic and suitable conversion.
35	1000 *g*	1 000 r/min	Low speed. *g* cannot be used.
36	Gene bank	GenBank	International classified genetic materials collection bank
37	Ten L	Ten liters	At the beginning of a sentence
38	Ten mL	Ten milliliters	At the beginning of a sentence
39	umol	μmol	
40	30 sec	30 s	
41	1 g/dl	10 g/L	10-fold conversion
42	OD_{260}	A_{260}	"OD" has been abandoned.
43	One g/L	One microgram per liter	At the beginning of a sentence
44	*A*260 nm	A_{260}nm	*A* should be in italic.
	^bP<0.05	^aP<0.05	In Table, no note is needed if there is no significance in statistics: ^aP<0.05, ^bP<0.01 (no note if P>0.05). If there is a second set of P value in the same table, ^cP<0.05 and ^dP<0.01 are used for a third set: ^eP<0.05, ^fP<0.01.
45	**F*=9.87, §*F*=25.9, #*F*=67.4	^1F=9.87,^2F=25.9, ^3F=67.4	Notices in or under a table
46	KM	km	kilometer
47	CM	cm	centimeter
48	MM	mm	millimeter
49	Kg, KG	kg	kilogram
50	Gm, gr	g	gram
51	nt	N	newton
52	l	L	liter
53	db	dB	decibel
54	rpm	r/min	rotation per minute
55	bq	Bq	becquerel, a unit symbol
56	amp	A	ampere
57	coul	C	coulomb
58	HZ	Hz	
59	w	W	watt
60	KPa	kPa	kilo-pascal
61	p	Pa	pascal
62	ev	EV	volt (electronic unit)
63	Jonle	J	joule
64	J/mmol	kJ/mol	kilojoule per mole
65	10×10×10cm^3	10 cm×10 cm×10 cm	
66	N·km	KN·m	moment
67	$\bar{x}\pm s$	mean±SD	In figures, tables or text narration
68	Mean±SEM	mean±SE	In figures, tables or text narration
69	*im*	im	intramuscular injection
70	*iv*	iv	intravenous injection
71	Wang et al	Wang *et al.*	
72	EcoRI	*Eco*RI	*Eco* in italic and RI in positive. Restriction endonuclease has its prescript form of writing.
73	Ecoli	*E.coli*	Bacteria and other biologic terms have their specific expression.
74	Hp	*H pylori*	
75	Iga	*Iga*	writing form of genes
76	*igA*	IgA	writing form of proteins
77	-70 kDa	~70 ku	

PO Box 2345, Beijing 100023, China
www.wjgnet.com
wjg@wjgnet.com

ELSEVIER

World J Gastroenterol 2005;11(36):5587-5591
World Journal of Gastroenterology ISSN 1007-9327
© 2005 The WJG Press and Elsevier Inc. All rights reserved.

• *REVIEW* •

Metastatic bone cancer as a recurrence of early gastric cancer - characteristics and possible mechanisms

Michiya Kobayashi, Takehiro Okabayashi, Takeshi Sano, Keijiro Araki

Michiya Kobayashi, Takehiro Okabayashi, Keijiro Araki, Department of Tumor Surgery, Kochi Medical School, Nankoku 783-8505, Japan
Takeshi Sano, Gastric Surgery Division, National Cancer Center Hospital, Chuo-ku, Tokyo 104-0045, Japan
Supported by the KOBAYASHI MAGOBE Memorial Medical Foundation
Correspondence to: Michiya Kobayashi MD, PhD, Department of Tumor Surgery, Kochi Medical School, Oko-cho, Nankoku, Kochi 783-8505, Japan. kobayasm@kochi-ms.ac.jp
Telephone: +81-888-80-2370 Fax: +81-888-80-2371
Received: 2005-03-25 Accepted: 2005-04-18

Abstract

The surgical outcome of most early gastric cancer (EGC) is usually satisfactory. Some cases show bone metastasis even though the depth of cancer invasion is confined to the mucosa. The most frequent site for recurrence of EGC is the liver. Cases of EGC with bone metastasis are reviewed to clarify the clinicopathological characteristics of EGC giving rise to bone metastasis. Possible mechanisms and risk factors underlying this rare condition are proposed. Forty-six cases of bone metastasis from EGC are reviewed from published reports and meeting proceedings in Japan. This investigation suggests that risk factors for bone metastasis from EGC include depressed-type signet-ring cell carcinoma, poorly differentiated carcinoma, and/or the likely involvement of lymph node metastasis, even though the cancer is confined to the gastric mucosa. The risk factors do not include recurrence of EGC in the liver. We speculate that the mechanism of bone metastasis from EGC is via lymphatic channels and systemic circulation. Post-operative follow-up of cases should consider the development of bone metastasis from EGC. We propose the use of elevated alkaline phosphatase levels for the detection of bone metastasis and recommend bone scintigraphy in positive cases.

© 2005 The WJG Press and Elsevier Inc. All rights reserved.

Key words: Gastric cancer; Early gastric cancer; Bone metastasis; Recurrence of early gastric cancer

Kobayashi M, Okabayashi T, Sano T, Araki K. Metastatic bone cancer as a recurrence of early gastric cancer - characteristics and possible mechanisms. *World J Gastroenterol* 2005; 11 (36): 5587-5591
http://www.wjgnet.com/1007-9327/11/5587.asp

INTRODUCTION

Early gastric cancer (EGC) is defined as a cancer confined to the mucosa or submucosa regardless of lymph node metastasis and/or distant metastasis. Although the 5-year survival rate for EGC is 90% or greater[1], EGC can recur. Most of the recurrences from EGC are hematogenous metastasis of the liver. Bone metastasis is a common event in advanced cancers of the breast, lung and prostate, but not in gastric cancer (GC). We have previously reported a rare case of mucosal EGC giving rise to multiple bone metastases[2].

In this article, we reviewed bone metastasis from EGC through a literature search of published reports and meeting proceedings in Japan. We have discussed the possible mechanisms and risk factors underlying this rare condition.

RECURRENCE OF EGC

Ichiyoshi *et al*., reviewed 503 consecutive cases of curative resection for EGC at a single institution from 1965 to 1988[3]. Seventeen patients (3.4%) died from a recurrence of GC. Of these 17 cases, 9 with submucosal invasion developed hematogenous metastasis in the liver, lung or bone. These cases showed that high-risk factors for hematogenous recurrence included submucosal cancers with a macroscopically elevated lesion, lymph node metastasis, and vessel invasion[4].

Sano *et al*., investigated the follow-up records of 1 475 EGC cases treated at the National Cancer Center Hospital Tokyo[4]. Twenty patients (1.4%) developed a recurrence of GC, including 14 (70%) with the lymph node metastases and 13 (65%) with blood-borne metastases. The incidence of recurrence of GC was shown to be significantly higher in submucosal, node-positive, and histologically differentiated carcinomas than in mucosal, node-negative, and undifferentiated groups. Hematogenous metastasis was thought to be the most common mode of recurrence and the investigation by Sano *et al*., showed that hematogenous recurrence of EGC accounted for 68% of 91 histologically differentiated tumors and 34% of 32 undifferentiated tumors[4]. This review also showed that lymph node metastasis at the time of surgery was not related to the mode of recurrence.

Lee *et al*., investigated 1 452 EGC patients with curative resection at Seoul National University Hospital in Korea from 1986 to 1995[5]. Twenty-one patients (1.4%) showing recurrence of GC included four cases with locoregional disease, two with peritoneal disease, nine with distant recurrence, and six with a mixed pattern of recurrence. Using multivariate analysis Lee *et al*., concluded that EGC with lymph node metastasis carries a high risk of recurrence.

Guadagni *et al*.[6], investigated 172 EGC patients who underwent gastrectomy at seven institutes in Italy. Twelve patients (7.0%) developed a recurrence of GC after surgery. Of these, three had liver metastasis, two had lymph node

recurrence, four had peritoneal disease and five had recurrence of GC in the gastric stump. The two cases with lymph node metastasis also had peritoneal dissemination. The most frequent site of recurrence was the gastric stump and Guadagni *et al*., concluded that recurrence in this location may be related to inadequate histological examination of resection margins. They suggested that submucosal and intestinal type cancers were a high risk factor for recurrence of GC.

Kodama *et al*., investigated 167 EGC cases and proposed growth patterns for EGC[7]. They classified a carcinoma growing expansively with complete destruction of the muscularis mucosae as Pen A-type. The characteristics of Pen A-type carcinoma were elevated lesions (87.5%), histological differentiation (81.3%), a high incidence of lymphatic metastasis and frequent hematogenous metastasis. The most common site of recurrence for this type of cancer was liver metastasis within 3 years[7].

According to the reports discussed above, the recurrence of EGC occurs in 1.4-3.4% of surgically resected cases. Macroscopically elevated, submucosal, lymph node positive, and histologically differentiated cancer types show a higher incidence of recurrence than their counterparts. The most common mode of recurrence is hematogenous metastasis of the liver. Bone metastasis is rare, even in cases with hematogenous recurrence of GC.

LYMPH NODE METASTASIS IN EGC

The most important prognostic factor for patients with EGC is the presence of lymph node metastasis. Lymph node metastasis of EGC is found in 5.4-24.0% of cases. Sano *et al*., investigated the clinicopathological features of 748 solitary EGC cases and found that only depth of invasion (submucosal invasion) and tumor size (more than 2 cm) significantly correlated with lymph node metastasis[8]. Maehara *et al*., analyzed 396 EGC cases and found that lymphatic involvement, in addition to depth of invasion and tumor size, were independent risk factors for the occurrence of lymph node metastasis[9]. Lehnert *et al*., reported that the rate of lymph node metastasis of mucosal and submucosal EGC is 4.2% (of a total of 1 447 cases) and 16.8% (of a total of 1 509 cases), respectively[10]. Gotoda *et al*., reported that the rate of lymph node metastasis from intramucosal cancer was 2.2%[11] and for differentiated and undifferentiated mucosal carcinoma was 0.4% and 4.2%, respectively. They showed that lymph node metastases from differentiated and undifferentiated submucosal cancer were 17.0% and 15.1%, respectively[11].

Although metastases occurs most commonly in peri-gastric nodes, Kawata *et al*., identified 16 EGC cases, until 1991 in Japan, with distant lymph node metastasis. Most of these cases showed submucosal invasion, only two had mucosal EGC, one case had bilateral inguinal lymph node metastasis, and one had paraaortic lymph node metastasis[12].

BONE METASTASIS IN GC

Bone metastasis is a rare condition in GC and is clinically underestimated. Mori *et al*., investigated 719 cases of malignant tumors among 2 240 consecutive autopsies[13] in Tokyo Medical and Dental University. These included 176 cases of GC of which 28 cases (15.9%) exhibited metastasis in bone, the third-most common site of GC metastases. The metastatic rate in the liver and lungs was 34.7% and 31.3%, respectively. Consistent with these findings, Yoshikawa and Kitaoka and Yamamura *et al*., showed that the metastatic rate in bone from curatively resected GC cases was high among autopsy cases, but was comparatively low in clinical practice at a rate of 1.2-1.4%[14,15]. Also in support of these findings, Maeyama *et al*., reported the rate of bone metastasis in clinical practice and autopsy as 0.7% and 17.6%, respectively.

Choi *et al*., evaluated bone metastasis from GC by bone scintigraphy[16]. They investigated 234 bone scans from a total of 17 176 GC patients. The 234 patients were classified according to their original clinical stage rather than by standard stage and were identified as having advanced stage disease. Of these cases, 106 (45.3%) had metastatic bone lesions.

The findings discussed above suggest that asymptomatic bone metastasis is underestimated as examination by bone scintigraphy is not a routine clinical practice. It is also possible that peritoneal dissemination or liver metastasis masks the clinical manifestation of bone metastasis. For these reasons, the rate of bone metastasis in clinical cases may be higher than expected.

OTHER DETECTION METHODS FOR BONE METASTASIS FROM GC

Maehara *et al*., investigated bone micrometastasis using a monoclonal anti-cytokeratin antibody[17]. They found that 9 (20%) of 45 EGC cases examined had cytokeratin-positive cells in the bone marrow at the time of primary surgery. Microvessel density in the primary tumor was significantly higher in cytokeratin-positive than in cytokeratin-negative patients. These findings suggested that the presence of micrometastatic cells in the bone marrow was closely related to angiogenesis in the primary tumor.

Immunocytochemistry was performed by Macadam *et al*., to investigate recurrence of GC[18]. In this study, the monoclonal antibody Ber-EP4 that recognizes 34 and 39 ku glycopeptides present in human epithelium, was used to detect cells derived from squamous and columnar epithelial tumors. Of 74 patients with esophago-gastric cancer, 27 (36.5%) had Ber-EP4 positive cells in their bone marrow at the time of operation. Fourteen patients with benign gastrointestinal disease were used as a control group. There were no patients with clinical evidence of overt bone metastases, pathological fractures or signs of bone marrow fracture. Multivariate analysis of risk factors revealed that bone marrow cytology was a significant factor for recurrence and death.

While investigations on bone marrow micrometastasis by immunocytochemistry may play a role in predicting disease recurrence, at present it cannot be clinically applied to detect bone metastasis.

REVIEW OF EGC CASES GIVING RISE TO BONE METASTASIS IN THE JAPANESE LITERATURE

Cases of EGC giving rise to bone metastasis in Japan were

reviewed from literature and meeting proceedings in English or Japanese. Kodama *et al*., reported 13 cases of GC recurrence out of 167 EGC cases of which 5 had liver metastasis and 1 had bone metastasis[7]. The case of bone metastasis was classified as 'small mucosal type', defined as a carcinoma lesser than 4.0 cm in diameter with mucosal invasion or slight submucosal invasion. This case was thought to be a premature type of carcinoma that had invaded the submucosa in a wide-penetrating fashion[7]. Most 'small mucosal type' carcinomas are depressed lesions (73.8%) unlike the Pen A-type, which possess the potential for liver metastasis[7].

In a previous report we, reviewed 46 bone metastasis cases arising from EGC in Japan to the end of 2003[2]. These cases were used to clarify the clinicopathological characteristics of EGC leading to bone metastasis. It is possible that in some cases, metastatic bone cancer is not recognized as a recurrence of EGC. Table 1 summarizes the clinicopa-thological data from this study. Although more than half of the patients were females, the male to female ratio for ECG is 2:1. The incidence of mucosal and submucosal cancer was almost identical. Macroscopically, 34 out of 36 lesions were depressed or flat type. Histological characteristics were described for 48 lesions in the 44 cases. Twenty-three lesions were classified as signet-ring cell carcinoma, 14 as poorly differentiated adenocarcinoma and 2 as undifferentiated carcinoma. These characteristics differed from the histological type of EGC overall[4,5]. The macroscopic features (poor histological differentiation and depressed shape) of lesions of EGC cases with bone metastasis were clearly different from those exhibiting liver metastasis[3,4,19]. A description of lymph node status was available for 29 cases. The rate of lymph node metastasis was 55.2% (16 cases) and represented a higher rate of lymph node involvement compared with EGC as a whole[8,9,11,20].

The time interval between diagnosis of EGC and bone metastasis was described for 40 cases out of 46 cases. Fourteen cases had bone metastasis at the time of diagnosis for EGC. In 26 cases, bone metastasis was diagnosed metachronously. The mean time interval to the development of metachronous bone metastasis after surgery was 46.9 mo, classified as a late recurrence of EGC. There were seven cases in which bone metastasis was diagnosed more than 5 years after surgery and two cases that presented with bone metastasis 96 mo after surgery (one from a meeting proceeding in Japan and the other a case report written in Japanese).

Concomitant metastasis, other than lymph node metastasis, was described in 16 out of the 46 cases and are summarized in Table 2. Lung metastasis was present in 11 cases (68.8%) and liver metastasis was observed only in 4 cases (25.0%). These findings are consistent with the finding by Seto *et al*., that 60% of cases with bone metastasis cases arising from GC did not have liver metastasis[21]. Similarly, a lack of liver metastasis is characteristic of cases of EGC with bone metastasis. It appears that liver metastasis has a different pathogenesis from bone metastasis arising from EGC.

Table 1 Clinicopathological features of early gastric cancer cases giving rise to bone metastasis in Japan

Age (range) (n = 37)		56.6 (33-78)
Sex	Male	18
(n = 43)	Female	25
Location	Upper third	4
(n = 28)	Middle third	13
	Lower third	7
	Whole stomach	4
Depth	Mucosa	18
(n = 35)	Submucosa	17
Timing	Synchronous	14
(n = 40)	Recurrence	26
Diagnosis	Plain bone X-ray	8
(n = 24)	Bone scintigraphy	13
	Autopsy	1
	Fracture	1
	Bone marrow aspiration	1
Macroscopic type[1]	IIa	2
(n = 36)	IIb	6
	IIc	21
	IIc+III	5
	IIa+IIc	1
	IIb+IIc	1
Histological type[2]	Tub	9
(n = 48)	Por	14
	Sig	23
	Ud	2
Lymph node metastasis[3]	n0	13
(n = 29)	n1	5
	n2	4
	n3	3
	n4	4

[1]IIa: elevated type, IIb: flat type, IIc: depressed type, III: excavated type, [2]tub: tubular adenocarcinoma, por: poorly differentiated adenocarcinoma, sig: signet-ring cell carcinoma, ud: undifferentiated carcinoma, and include cases with multiple lesions. [3]*The General Rules for the Gastric Cancer Study* (The 12th Edition), Japanese Research Society for Gastric Cancer.

Table 2 Distant metastatic sites other than lymph node of early gastric cancer with bone metastasis (n = 16, nine cases that had more than two distant metastasis are included)

Lung	11
Liver	4
Brain	2
Kidney	2
Pleura	2
Ovary	2
Meninx	2
Spleen	2
Thyroid	1
Peritoneum	1
Diaphragm	1

POSSIBLE MECHANISMS RESPONSIBLE FOR BONE METASTASIS

Lehnert *et al*., used light and transmission electron microscopy to investigate lymph and blood capillaries of human gastric mucosa and found that the upper and middle levels of the lamina propria of the gastric mucosa contained no lymph capillaries[10]. The mucosa has a rich supply of blood capillaries, many of which are adjacent to the basal lamina of gastric glands and surface epithelium[6]. Lehnert *et al*., suggests that the low incidence of lymph node metastases in the early mucosal GC might be explained by the rarity of lymph vessels in the mucosa, and that blood-borne metastases in

recurrent EGC might be related to the rich vascularity of the gastric mucosa[10].

As there are no lymphatic vessels in the bone marrow, bone metastasis is usually regarded as a hematogenous spread[22]. Rino *et al*., reported five EGC cases without vascular invasion (v_0) resulting in bone metastasis[23] and concluded that high risk factors for bone metastasis were accompanying ulceration, lymph node metastasis, and distant metastasis to other organs[23].

Our review of the literature found that EGC resulting in bone metastasis had different macroscopic and histological types, suggesting that the mechanisms responsible for bone metastasis might not be through regular hematogenous routes via the portal vein as in liver metastasis. This is supported by the fact that concomitant metastasis was much more frequent in the lung than in the liver. We speculated that GC might metastasize to the bones through the vertebral vein system as suggested by Batson[24]. Yamamura *et al*., reported that GC with bone metastasis resulted in the invasion of the lymphatic vessels more frequently than invasion of venules[15]. They also speculated that GC might metastasize to the bone through the thoracic duct.

For EGC, cancer cells may invade the capillary network or postcapillary venules in the gastric mucosa as mentioned in the investigation of Lehnert *et al*.[10]. Alternatively, they may metastasize to regional lymph nodes following cancer cell invasion into the venules of lymph nodes as reported by Rino *et al*.[23]. The latter is supported by the higher rate of lymph node metastasis in those cases with bone metastasis compared to that for EGC as a whole. For advanced cancer that has invaded adjacent organs, cancer cells may invade a fairly large vein, such as those found in the vertebral vein system outlined by Seto *et al*.[21].

The possible mechanisms of hematogenous metastasis of GC are: (1) through the portal vein, (2) through the venous system, other than the portal vein, and (3) through lymphatic channels into the systemic circulation. Most cases of bone metastasis do not show liver metastasis, most venous drainage from the stomach is via the portal vein, and many cases of bone metastasis are associated with lymph node metastasis, suggesting that the mechanisms underlying bone metastasis involves lymphatic channel into the systemic circulation.

CLINICAL FEATURES AND TREATMENTS OF BONE METASTASIS

Ell reviewed skeletal imaging of metastatic diseases and identified MRI as sensitive in detecting bone marrow involvement[25]. Despite this finding, bone scintigraphy continues to be the modality of choice in view of its simplicity, low cost, and ability to screen the entire body[25]. Choi *et al*., evaluated bone metastasis from GC by Tc-99m MDP imaging[16]. They investigated 234 bone scans of GC patients. One hundred and six patients (45.3%) had bone scan abnormalities that qualified as metastatic bone lesions. The most frequent metastatic sites were the spine (66%), the ribs (59%), pelvis (43%), femur (30%), and skull (22%)[16]. The least frequent metastatic sites were the shoulder girdle (17%), such as the scapula and clavicle, sacroiliac joint (7.2%), humerus (6.0%), sternum (4.2%), and tibia (3.0%)[16]. On the other hand, roentgenographic evaluation of bone metastases has limited value because symptoms caused by bone metastases frequently occur before abnormal imaging. Bone metastases were diagnosed by bone scintigraphy in 13 out of 24 cases described in our review.

Laboratory data may be helpful in the diagnosis of bone metastasis. Although tumor markers do not play an important role, many cases with bone metastasis show elevated serum alkaline phosphatase (ALP). In the study by Choi *et al*., ALP was elevated in 64% of 106 patients with bone metastasis[16]. Seto *et al*., also found that ALP was significantly elevated in GC cases with bone metastasis compared to those without[21].

Once cancer disseminates to the bone marrow, disseminated intravascular coagulation (DIC) may occur. Clinically, patients show a tendency to bleed that is confirmed on a combination of laboratory data for platelet count and fibrin degradation products. Several chemotherapy regimens for bone metastasis of GC have been reported as case reports. Kobayashi *et al*., and Hironaka *et al*., demonstrated that sequential methotrexate and 5-fluorouracil chemotherapy resulted in a high rate of alleviation (80% and 89%, respectively) of DIC caused by bone metastasis from GC[26,27].

CONCLUSION

The incidence of bone metastasis from GC may be underestimated, and may occur after surgical resection in EGC. The mechanisms underlying bone metastasis arising from EGC most likely involve the lymphatic channels. Some cases give rise to late bone metastasis after surgery. As only 46 cases of bone metastasis arising from EGC are reported in Japan up to 2003, the exact incident rate cannot be estimated accurately. It can be considered that bone metastasis arising from EGC is a rare condition and as a result adjuvant chemotherapy is not recommended. In the post-operative follow-up of EGC cases that are histologically less differentiated and display involvement of lymph nodes, recurrences as bone metastasis should be considered. Elevation of ALP can be used to detect bone metastasis and bone scintigraphy is recommended for its diagnosis.

ACKNOWLEDGMENTS

We would like to thank Dr. Alan GK Li, Aberdeen Royal Infirmary, for his valuable advice.

REFERENCES

1 **Nakajima T**. Gastric cancer treatment guidelines in Japan. *Gastric Cancer* 2002; **5**: 1-5
2 **Kobayashi M**, Araki K, Matsuura K, Kawai S, Moriki T. Early gastric cancer giving rise to bone and brain metastases -A review of the Japanese literature. *Hepatogastroenterology* 2002; **49**: 1751-1754
3 **Ichiyoshi Y**, Toda T, Minamisono Y, Nagasaki S, Yakeishi Y, Sugimachi K. Recurrence in early gastric cancer. *Surgery* 1990; **107**: 489-495
4 **Sano T**, Sasako M, Kinoshita T, Maruyama K. Recurrence of early gastric cancer. *Cancer* 1993; **72**: 3174-3178
5 **Lee HJ**, Kim YH, Kim WH, Lee KU, Choe KJ, Kim JP, Yang HK. Clinicopathological analysis for recurrence of early gastric cancer. *Jap J Clin Oncol* 2003; **33**: 209-214

6 **Guadagni S**, Catarci M, Kinoshita T, Valenti M, De Bernardinis G, Carboni M. Causes of death and recurrence after surgery for early gastric cancer. *World J Surg* 1997; **21**: 434-439

7 **Kodama Y**, Inokuchi K, Soejima K, Matsusaka T, Okamura T. Growth patterns and prognosis in early gastric carcinoma. Superficially spreading and penetrating growth types. *Cancer* 1983; **51**: 320-326

8 **Sano T**, Kobori O, Muto T. Lymph node metastasis from early gastric cancer: endoscopic resection of tumor. *Br J Surg* 1992; **79**: 241-244

9 **Maehara Y**, Orita H, Okuyama T, Moriguchi S, Tsujitani S, Korenaga D, Sugimachi K. Predictors of lymph node metastasis in early gastric cancer. *Br J Surg* 1992; **79**: 245-247

10 **Lehnert T**, Erlandson RA, Decosse JJ. Lymph and blood capillaries of the human gastric mucosa. A morphologic bases for metastasis in early gastric carcinoma. *Gastroenterology* 1985; **89**: 939-950

11 **Gotoda T**, Yanagisawa A, Sasako M, Ono H, Nakanishi Y, Shimoda T, Kato Y. Incidence of lymph node metastasis from early gastric cancer: estimation with a large number of cases at two large centers. *Gastric Cance*r 2000; **3**: 219-225

12 **Kawata N**, Suzuki Y, Saitoh S, Funatsu T, Kobayashi N. A case of early gastric cancer with bilateral inguinal lymph node and multiple bone metastases. *Jpn J Gastroenterol Surg* 1992; **85**: 2973-2977

13 **Mori W**, Adachi Y, Okabe H, Ohta K. An analysis of 755 autopsied cases of malignant tumors. -A statistical study of their metastasis. *Gan No Rinsho* 1963; **9**: 351-374

14 **Yoshikawa K**, Kitaoka H. Bone metastasis of gastric cancer. *Jpn J Surg* 1983; **13**: 173-176

15 **Yamamura Y**, Kito T, Yamada E. Clinical evaluation of bone and bone marrow metastasis of gastric carcinoma. *Jpn J Gastroenterol Surg* 1985; **18**: 2288-2293

16 **Choi CW**, Lee DS, Chung JK, Lee MC, Kim NK, Choi KW, Koh CS. Evaluation of bone metastases by Tc-99m MDP imaging in patients with stomach cancer. *Clin Nucl Med* 1995; **20**: 310-314

17 **Maehara Y**, Hasuda S, Abe T, Oki E, Kakeji Y, Ohno S, Sugimachi K. Tumor angiogenesis and micrometastasis in bone marrow of patients with early gastric cancer. *Clin Cancer Res* 1998; **4**: 2129-2134

18 **Macadam R**, Sarela A, Wilson J, MacLennan K, Guillou P. Bone marrow micrometastases predict early post-operative recurrence following surgical resection of oesophageal and gastric carcinoma. *Eur J Surg Oncol* 2003; **29**: 450-454

19 **Ohno S**, Fujii T, Ueda S, Nakamoto T, Kinugasa S, Yoshimura H, Tachibana M, Kubota H, Dhar DK, Nagasue N. Predictive factors and timing for liver recurrence after curative resection of gastric carcinoma. *Am J Surg* 2003; **185**: 258-263

20 **Deguchi H**, Kawamura K, Hashimura C, Murakuni H, Kaburagi S, Tsugu Y. Cases of early gastric cancer with lymph node metastasis. *J Medical Soc Toho Univ* 1990; **37**: 221-228

21 **Seto M**, Tonami N, Koizumi K, Sui O, Hisada K. Bone metastasis from gastric cancer. -Clinical evaluation on bone scintigram -*Jpn J Nucl Med* 1983; **20**: 795-801

22 **Abramson DI**. Blood vessels and lymphatics. New York: *Academic Press* 1962: 531-556

23 **Rino Y**, Okukawa T, Okada K, Kobayashi O, Sairenji M, Motohashi H, Kameda Y, Yamaguchi M, Iida M. A case report of bone metastasis from early gastric cancer preliminary to diagnosis of the primary lesion. *Shokakigeka* 1996; **19**: 1493-1497

24 **Batson OV**. The function of the vertebral veins and their role in the spread of metastases. *Clin Orthop Relat Res* 1995; **312**: 4-9

25 **Ell PJ**. Skeletal imaging in metastatic disease. *Curr Opin Radiol* 1991; **3**: 791-796

26 **Kobayashi T**, Sasaki T, Ibuka T, Imai K, Monma K, Sasaki N, Tabata I, Ishiwata J, Onozawa Y, Ohno T, Shimoyama T. Sequential MTX and 5-FU therapy for gastric cancer patients with systemic bone metastasis and DIC . *Jpn J Cancer Chemother* 1992; **19**: 69-74

27 **Hironaka S**, Boku N, Ohtsu A, Ngashima F, Sano Y, Muto M, Fujii T, Tajiri H, Yoshida S. Sequential methotrexate and 5-fluorouracil therapy for gastric cancer patients with bone metastasis. *Gastric Cancer* 2000; **3**: 19-23

Science Editor Guo SY **Language Editor** Elsevier HK

PO Box 2345, Beijing 100023, China
www.wjgnet.com
wjg@wjgnet.com

ELSEVIER

World J Gastroenterol 2005;11(36):5592-5600
World Journal of Gastroenterology ISSN 1007-9327
© 2005 The WJG Press and Elsevier Inc. All rights reserved.

• *GASTRIC CANCER* •

DNA ploidy analysis and expression of MMP-9, TIMP-2, and E-cadherin in gastric carcinoma

Jing-Fang Zhang, Yuan-Ping Zhang, Feng-Yun Hao, Cai-Xin Zhang, Yu-Jun Li, Xiang-Rui Ji

Jing-Fang Zhang, Department of Pathology, Taishan Medical University, Taian 271000, Shandong Province, China
Yuan-Ping Zhang, Department of Prosthodontics, Taian Hospital of Stomatology, Taian 271000, Shandong Province, China
Feng-Yun Hao, Department of Pathology, Weifang Municipal People's Hospital, Weifang 261031, Shandong Province, China
Cai-Xin Zhang, Department of Pathology, Qingdao Municipal Hospital, Qingdao 266003, Shandong Province, China
Yu-Jun Li, Xiang-Rui Ji, Department of Pathology, the Affiliated Hospital of Medical College, Qingdao University, Qingdao 266003, Shandong Province, China
Supported by the Bureau of Education of Shandong Province, No. 03K02
Co-first-authors: Jing-Fang Zhang and Yuan-Ping Zhang
Correspondence to: Professor Xiang-Rui Ji, the Affiliated Hospital of Medical College, Qingdao University, 16 Jiangsu Road, Qingdao 266003, Shandong Province, China. jixiangrui@yahoo.com.cn
Telephone: +86-532-2911533
Received: 2004-09-10 Accepted: 2004-11-04

Abstract

AIM: To investigate DNA ploidy and expression of MMP-9, TIMP-2, and E-cadherin in gastric carcinoma and to explore the mechanism of invasion and metastasis of gastric carcinoma.

METHODS: Immunohistochemical methods were used to detect the expressions of MMP-9, TIMP-2, and E-cadherin in 156 cases, including 99 cases of gastric carcinoma, 16 cases of adjacent noncancerous mucosa, 16 cases of distant metastases and 25 cases of metastatic lymph node (LN) from gastric carcinoma. Flow cytometry DNA ploidy and S-phase fraction (SPF) analysis were performed on 57 cases, including 47 cases of gastric cancer, 6 cases of adjacent noncancerous mucosa, and 4 cases of distant metastatic cancer.

RESULTS: The expression of MMP-9 was significantly correlated with Lauren's classification, Borrmann's classification, LN metastasis, tumor metastasis, and TNM stage, as well as depth of invasion (all $P<0.05$). The positive rate was lower in noncarcinoma than in carcinoma (31.3% *vs* 66.7%, $P<0.01$). The expression of TIMP-2 was significantly correlated with Borrmann's classification, LN metastasis, and the depth of invasion (all $P<0.05$). The expression of E-cadherin was significantly correlated with differentiation, Lauren's classification, Borrmann's classification, and LN metastasis, as well as the depth of invasion ($P<0.01$ or $P<0.05$). E-cadherin was less expressed in carcinoma than in noncarcinoma (42.4% *vs* 87.5%, $P<0.01$). There was a positive correlation between MMP-9 and TIMP-2 and a negative correlation between MMP-9 and E-cadherin, but no correlation between TIMP-2 and E-cadherin. Also there was a positive correlation between DNA aneuploid rate and differentiation and LN metastasis. SPF that was higher than 15% was positively correlated with tumor size, differentiation and LN metastasis. And there was a significant difference between carcinoma and noncarcinoma in DNA aneuploid rate and SPF.

CONCLUSION: With tumor progression and development of heterogeneity, the abnormal expressions of MMP-9, TIMP-2, and E-cadherin or DNA aneuploid rate or high SPF gradually increases, suggesting that they play a crucial role in gastric carcinoma progression.

© 2005 The WJG Press and Elsevier Inc. All rights reserved.

Key words: MMP-9; TIMP-2; E-cadherin; DNA ploidy; Gastric carcinoma

Zhang JF, Zhang YP, Hao FY, Zhang CX, Li YJ, Ji XR. DNA ploidy analysis and expression of MMP-9, TIMP-2, and E-cadherin in gastric carcinoma. *World J Gastroenterol* 2005; 11(36): 5592-5600
http://www.wjgnet.com/1007-9327/11/5592.asp

INTRODUCTION

Gastric cancer is the second most common malignancy worldwide. Although the achievement in early diagnosis and treatment of gastric cancer has improved the patients' outcome, it is still among the leading causes of mortality in countries such as China and Japan; even in the developed Western countries the 5-year survival rate for gastric cancer is only 10-19%[1]. The mechanisms of its development, progression, and metastasis are under investigation[2].

Breakdown of cell-cell adhesion and degradation of extracellular matrix (ECM) represent an essential step for tumor metastasis and invasion. The cadherin superfamily is a major class of adhesion molecules that play an important role in homotypic cell-cell interactions and hence cancer cell metastasis and invasion[3]. E-cadherin is a member of the cadherin family that is expressed in all epithelial cells. It is a calcium-dependent cell adhesion molecule and has been recognized as an important suppressor gene. A variety of human cancers exhibit altered expression of E-cadherin, which correlates with high grade and advanced stage of tumor.

Matrix metalloproteinases (MMPs) are a large family

of zinc-dependent proteolytic enzymes, which are believed to play a pivotal role in malignant behavior of cancer cells such as rapid growth, invasion, and metastasis by degrading ECM[4,5]. Increased expression of MMPs has been found in various carcinomas. The family of human MMPs comprises mainly four classes according to their structure and *in vitro* substrate specificity: collagenases, gelatinases, stromelysins, and membrane-type MMPs. MMP-9 belongs to gelatinases and most investigations supported that there was a positive correlation between MMP-9 and tumor progression[9]. Tissue inhibitors of matrix metalloproteinases (TIMPs) are the major natural inhibitors of MMPs. To date, four types of TIMPs have been recognized[6]. TIMPs are secreted proteins that are complex MMPs and are involved in the inhibition of individual MMPs and regulation of their activity. Indeed, it is thought that the balance between activated MMPs and TIMPs determines the overall MMP activity and proteolysis *in vivo*. However, recent experimental data suggest that TIMPs not only have MMP inhibitory functions, but also are multifunctional molecules, with apparent paradoxical effects on tumor progression. Recently some studies suggest a positive correlation between TIMP-2 level and poor outcome in certain types of tumors[7,8].

In this study, we detected the expression of MMP-9, TIMP-2, and E-cadherin proteins in gastric cancer, its adjacent noncancerous mucosa, metastatic lymph nodes (LNs), and metastatic cancer by using immunohistochemical staining. Moreover we detected DNA ploidy and S-phase fraction (SPF) in gastric cancer by flow cytometry to explore the molecular and cellular mechanisms of tumor progression so as to develop novel therapies and provide scientific basis for prognostic evaluation of gastric carcinoma.

MATERIALS AND METHODS

Patients and specimens

One hundred and fifty-six surgically removed specimens from the year 2000-2003 were collected from the Department of Pathology, Affiliated Hospital of Medical College, Qingdao University, including 99 cases of gastric carcinoma, 16 cases of adjacent noncancerous mucosa, 25 cases of metastatic LNs, and 16 cases of metastatic carcinoma from gastric cancer. Patients consisted of 87 male and 28 female with a mean age of 58.2 years (range 32-82 years) and were untreated before surgery. Sections from the surgical specimens were fixed in 4% formaldehyde solution for 24-48 h, and embedded in paraffin. A 4-μm section from each specimen block was stained with H&E for histological evaluation, and representative blocks were chosen for immunohistochemical study. In addition, normal gastric epithelium, colon adenocarcinoma, and breast carcinoma were used as positive controls for E-cadherin, TIMP-2, and MMP-9, respectively. For negative controls, sections were incubated with PBS (0.01 mol/L, pH 7.4) instead of the primary antibodies.

For flow cytometry, 57 specimens were selected from immunohistochemical study cases, including 47 cases of gastric carcinoma, 6 cases of adjacent noncancerous mucosa, and 4 cases of metastatic carcinoma from gastric cancer. For each case, we selected the most representative area of the specimen for flow cytometry analysis with H&E section. Five 50-μm sections from each specimen block and one 50-μm section from normal LN block, which was fixed and embedded with the same method and used for internal standard were cut for preparation of single cell suspensions.

Antibodies and other chemicals

The goat anti-human polyclonal antibody against TIMP-2, rabbit anti-human monoclonal antibodies against MMP-9 and E-cadherin were from Santa Cruz (CA, USA); Histostain^{TM}-Plus kit was from Zymed (CA, USA); Coulter DNA-Prep Reagent kit was from Beckman Coulter (Miami, USA).

Immunohistochemical staining

Immunohistochemical staining was performed with SP method, according to instruction of the kit and antibodies against MMP-9, TIMP-2, and E-cadherin were used at a concentration of 1:60, 1:30, and 1:120, respectively.

Sample preparation for flow cytometry analysis

Modified Hedley protocol was a workable method for making nuclear suspensions from paraffin blocks. Sections were deparaffinized and rehydrated through changes of xylene and graded alcohol, then immersed in water, and converted to a nuclear suspension by digestion in 0.5% pepsin (pH 1.5). The dispersive nuclear suspension was pelleted by centrifugation (1 500 r/min, 5 min) and filtered through a nylon filter, and then incubated with DNA-prep reagents kit for 30 min for DNA quantitation. The exciting spectrum was 488 nm and about 20 000 signals were collected per specimen with a coefficient of variation (CV) of 2% or less. Data collection was performed on a flow cytometer (FCM, Beckman Coulter EPICS XL).

Evaluation of immunostaining

Clear brown staining was restricted to cytoplasm, and was considered as positive for MMP-9 and TIMP-2. Slides were scored semi-quantitatively based on staining intensity and distribution. Two investigators without knowledge of the clinical data independently performed analysis of immunohistochemical staining. Staining was graded based on the method by Massi *et al*.[9], as follows: negative (-): no positive cells were found; focal (+): positive tumor cells accounted for <20% of the total; moderate (++): 21-50% of tumor cells were positive; diffuse (+++): >50% tumor cells were positive. The positive staining of E-cadherin appeared pale brown and was located in the cell membrane. Staining was scored according to the method described by Li *et al*.[10]: 0 score: no expression; 1 score: expression in cytoplasm; 2 scores: decreased expression; 3 scores: expression in cell membrane, namely normal expression. A score of 0-2 was considered as negative expression.

Evaluation of flow cytometry

FCM-derived parameters were DNA ploidy and SPF. According to DNA index (DI), aneuploid and diploid tumors were evaluated[11].

Statistical analysis

Statistical analysis was performed using the χ^2 test. A P value lesser than 0.05 was considered as statistically significant.

All statistical analyses were performed using the SPSS 11.0 statistical software.

RESULTS

Immunohistochemical staining of MMP-9

Immunoreactivity for MMP-9 was present in the cytoplasm of neoplastic and non-neoplastic mucosa cells. MMP-9 expression showed moderate or diffuse distribution in neoplastic cells (Figure 1A), but was single or focal in noncancerous mucosa cells (Figure 1B). In the invasion front, MP-9 showed strong positive staining (Figure 1C) and positive staining was also noted in vascular endothelial cells and inflammatory cells (Figure 1D). The expression of MMP-9 was significantly correlated with Lauren's classification (in intestinal and diffuse types, the positive rate was 58.2% and 90.9%, respectively, $\chi^2 = 8.025$, $P<0.05$), Borrmann's classification (in Borrmann's types I-II, III, and IV, the positive rate was 33.3%, 65.7%, and 85.0% respectively, $\chi^2 = 7.554$, $P<0.05$), LN metastasis (in negative and positive cases, the positive rate was 54.3% and 79.2% respectively, $\chi^2 = 6.986$, $P<0.05$), metastasis (in primary gastric carcinoma, metastatic LN, and metastatic carcinoma, the positive rate was 66.7%, 92.0%, and 81.7%, respectively, $\chi^2 = 7.121$, $P<0.05$) and TNM stage (in stages II, III, and IV, the positive rate was 37.5%, 50.0%, and 73.3%, respectively, $\chi^2 = 6.647$, $P<0.05$, Tables 1 and 2). A significant association between the depth of invasion and expression of MMP-9 (in submucosa, superficial muscular layer, and deep muscular layer or serosa, the positive rate was 28.6%, 59.3%, and 73.8% respectively, $\chi^2 = 6.743$, $P<0.05$) was detected. The positive rate was lower in noncarcinoma than in carcinoma (31.3% *vs* 66.7%, $\chi^2 = 7.314$, $P<0.01$).

Immunohistochemical staining of TIMP-2

Immunoreactivity for TIMP-2 was also present in the cytoplasm of neoplastic and non-neoplastic mucosa cells. TIMP-2 expression showed moderate or diffuse distribution in neoplastic cells (Figure 2A), but focal or moderate distribution in noncancerous mucosa cells (Figure 2B). The expression of TIMP-2 was significantly correlated with Borrmann's classification (in Borrmann's types I-II, III, and IV, the positive rate was 66.7%, 47.1%. and 20.0% respectively, $\chi^2 = 6.839$, $P<0.05$) and LN metastasis (in negative and positive cases, the positive rate was 56.5% and 32.1% respectively, $\chi^2 = 5.992$, $P<0.05$). A significant association between the depth of invasion and expression of TIMP-2 (in submucosa, superficial muscular layer, and deep muscular layer or serosa, the positive rate was 71.4%, 59.3%, and 33.8% respectively, $\chi^2 = 7.417$, $P<0.05$) was also revealed (Tables 1 and 2).

Immunohistochemical staining of E-cadherin

Immunoreactivity for E-cadherin was present in the membrane of neoplastic and non-neoplastic mucosa cells. In noncancerous mucosa epithelia, E-cadherin expression showed strong membranous staining, especially at the intercellular border (Figure 3A), but abnormal expression was observed in neoplastic tissues with reduction or loss of membranous expression and cytoplasmic or nuclear staining (Figures 3B-D). The expression of E-cadherin was significantly correlated with differentiation (in well-, moderately-, and poorly-differentiated, and signet ring cell carcinoma, the positive rate was 75.0%, 61.1%, 30.6%, and 27.6% respectively, $\chi^2 = 14.215$, $P<0.01$), Lauren's classification (in intestinal and diffuse type, positive rate was 53.7% and 13.6% respectively, $\chi^2 = 11.603$, $P<0.05$), Borrmann's classification (in Borrmann's

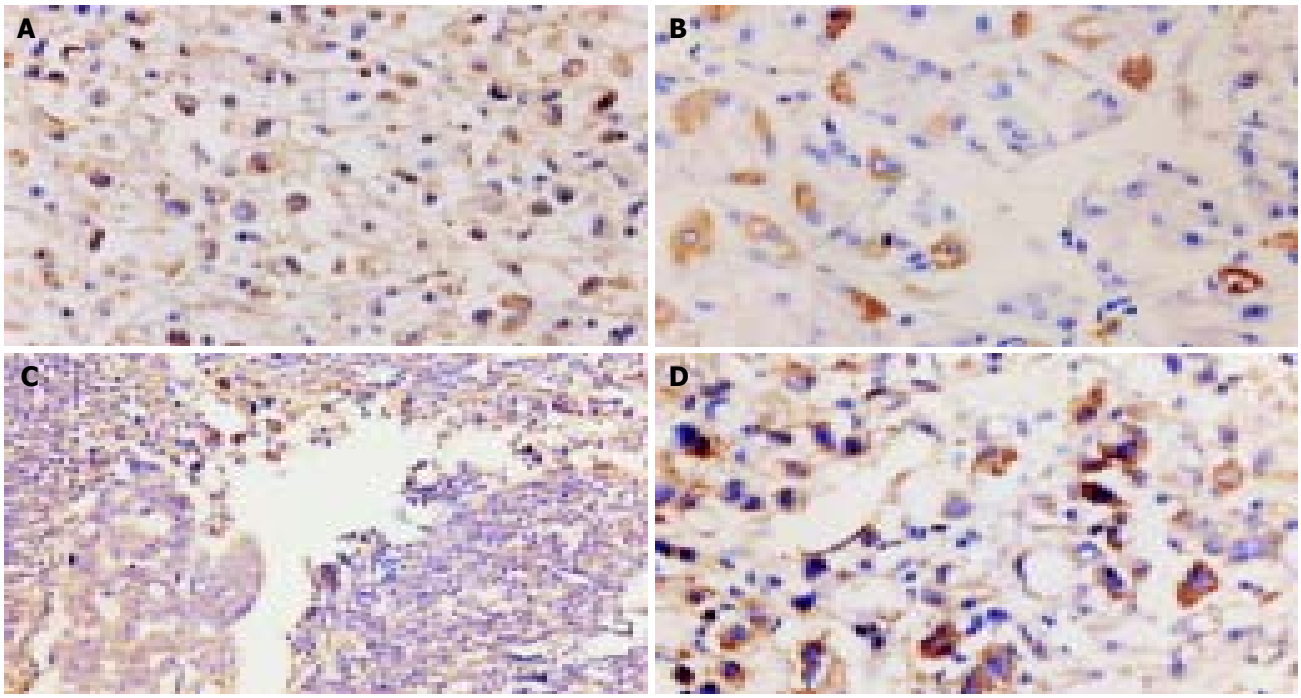


Figure 1 MMP-9 expression in gastric carcinoma. **A:** MMP-9 expression showed moderate or diffuse distribution of immunostaining in neoplastic cells (×200); **B:** single or focal distribution in noncancerous mucosa cells (×400); **C:** in the invasion front, MMP-9 showed strong positive staining (×200); **D:** positive staining was also noted in vascular endothelial cells and inflammatory cells (×400).

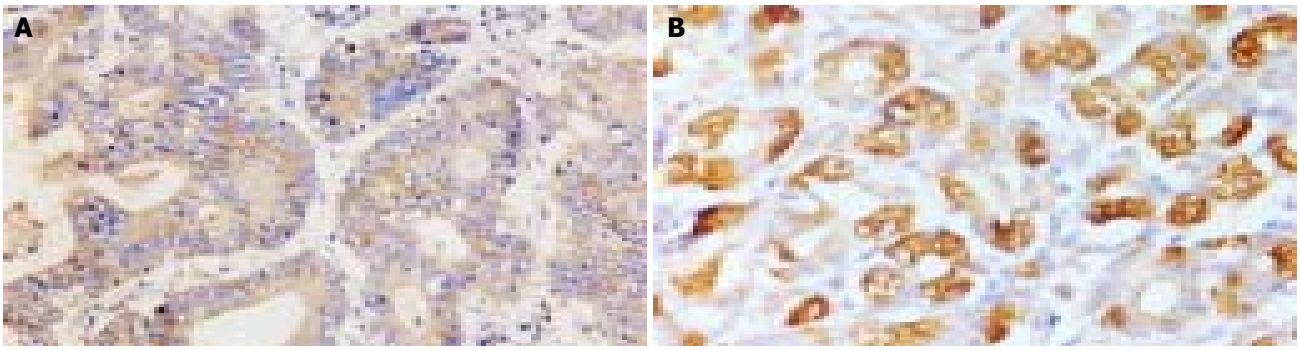


Figure 2 TIMP-2 expression in gastric carcinoma. **A:** TIMP-2 expression showed moderate or diffuse distribution in neoplastic cells (×200), **B:** focal or moderate distribution in noncancerous mucosa cells (×400).

Table 1 Relationship between expression of MMP-9, TIMP-2 or E-cadherin, and histopathological features in gastric carcinoma

		Positive			Rate (%)		
	n	MMP-9	*P*	TIMP-2	*P*	E-cadherin	*P*
Differentiation							
Well	16	50.0	>0.05	62.5	>0.05	75.0	<0.01
Moderate	18	66.7		55.6		61.1	
Poor	36	69.4		38.9		30.6	
Signet ring cell type	29	72.4		31.0		27.6	
Tumor recurrence							
Primary carcinoma	91	65.9	>0.05	44.0	>0.05	44.0	>0.05
Recurrent carcinoma	8	75.0		37.5		25.0	
Carcinoma and non-neoplastic							
Gastric carcinoma	99	66.7	<0.01	43.4	>0.05	42.4	<0.001
Non-neoplastic gastric mucosa	16	31.3		31.3		87.5	
Lauren's classification							
Intestinal type	67	58.2[a]	<0.05	46.3	>0.05	53.7[a]	<0.05
Diffuse type	22	90.9		36.4		13.6	
Mixed type	10	70.0		40.0		30.0	
Borrmann's classification							
Types I–II	9	33.3[c]	<0.05	66.7	<0.05	55.6[c]	<0.05
Type III	70	65.7		47.1		42.9	
Type IV	20	85.0		20.0		25.0	

[a]$P<0.05$ *vs* diffuse type; [c]$P<0.05$ *vs* type IV.

Table 2 Relationships between expression of MMP-9, TIMP-2 or E-cadherin, and clinical features in gastric carcinoma

		Positive			Rate (%)		
	n	MMP-9	*P*	TIMP-2	*P*	E-cadherin	*P*
Tumor size							
⩾5 cm	53	66.0	>0.05	41.5	>0.05	39.6	>0.05
<5 cm	46	67.4		45.7		45.7	
LN metastasis							
Negative	46	54.3	<0.01	56.5	<0.05	54.3	<0.05
Positive	53	79.2		32.1		32.1	
Metastasis							
Primary carcinoma	99	66.7	<0.05	43.4	>0.05	42.4	>0.05
Metastatic LN	25	92.0		36.0		20.0	
Metastatic carcinoma	16	81.7		43.8		37.5	
Depth of invasion							
Submucosa	7	28.6[c]	<0.05	71.4[c]	<0.05	85.7[c]	<0.05
Superficial muscular layer	27	59.3		59.3		48.1	
Deep muscular layer or serosa	65	73.8		33.8		35.4	
TNM stage							
Stage II	8	37.5[e]	<0.05	50.0	>0.05	62.5	>0.05
Stage III	16	50.0		43.8		50.0	
Stage IV	75	73.3		42.7		38.7	

[c]$P<0.05$ *vs* deep muscular layer or serosa; [e]$P<0.05$ *vs* stage IV.

types I-II , III, and IV, the positive rate was 66.7%, 44.3%, and 25.0% respectively, $\chi^2 = 7.097$, $P<0.05$) and LN metastasis (in negative and positive cases, the positive rate was 54.3% and 32.1% respectively, $\chi^2 = 5.012$, $P<0.05$). A significant association between the depth of invasion and expression of E-cadherin (in submucosa, superficial muscular layer, and deep muscular layer or serosa, the positive rate was 85.7%, 48.1%, and 35.4% respectively, $\chi^2 = 7.051$, $P<0.05$) was observed. E-cadherin was less expressed in carcinoma than in noncarcinoma (42.4% *vs* 87.5%, $\chi^2 = 11.223$, $P<0.001$, Tables 1 and 2).

Correlation between MMP-9 and TIMP-2

The expression of MMP-9 was significantly and positively correlated with expression of TIMP-2 (Table 3). Positive rate of TIMP-2 in cases with MMP-9 positive was higher than those with MMP-9 negative, and the coefficient of correlation was 0.22.

Table 3 Correlations between MMP-9 and TIMP-2 expression

	TIMP-2	
MMP-9	-	+
+	32	34
-	24	9

Correlation between E-cadherin and MMP-9

The expression of MMP-9 was significantly and negatively correlated with the expression of E-cadherin (Table 4). Negative rate of E-cadherin in MMP-9 positive cases was higher than in MMP-9 negative cases, and the coefficient of correlation was -0.33.

Correlation between E-cadherin and TIMP-2

The expression of E-cadherin was not correlated with the expression of TIMP-2 (Table 5). The coefficient of correlation was only 0.07 without significance by χ^2 test.

Table 4 Correlations between E-cadherin and MMP-9 expression

	E-cadherin	
MMP-9	-	+
+	46	20
-	11	22

Table 5 Correlations between TIMP-2 and E-cadherin expression

	TIMP-2	
E -cadherin	-	+
+	22	20
-	35	22

FCM results

Typical DNA histogram of non-neoplastic mucosa showed a large diploid peak and a smaller tetraploid peak, and SPF was less than 15% (Figure 4A), but the histogram from gastric carcinoma showed a definitely abnormal (aneuploid or hyperdiploid) peak (Figure 4B) or/and increased SPF (Figure 4C). Aneuploid rate was significantly correlated with differentiation (in well- or moderately- and poorly-differentiated or signet ring cell carcinomas, the aneuploid rates were 42.1% and 75.0%, respectively, $\chi^2 = 5.183$, $P<0.05$) and LN metastasis (in negative and positive cases, the aneuploid rates were 80.0% and 29.4% respectively, $\chi^2 = 11.752$,

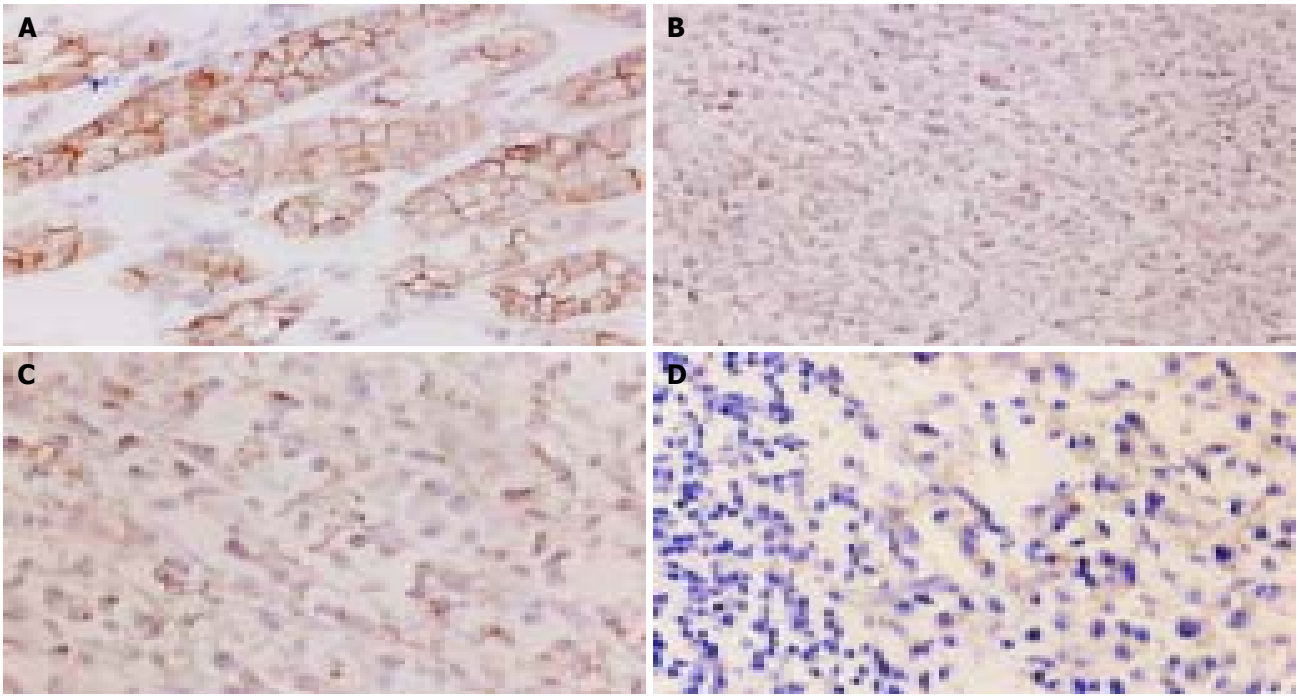


Figure 3 E-cadherin expression in gastric carcinoma. **A:** E-cadherin expression showed strong membranous staining in noncancerous mucosa cells, especially at the intercellular border (×400); **B-D:** abnormal expression was observed in neoplastic tissues which showed reduction or loss of membranous expression and showed cytoplasmic or nuclear staining (**B** and **D**, ×200; **C**, ×400).

$P<0.001$, Table 6). It was significantly different between carcinoma and noncarcinoma (aneuploid rate were 61.7% and 16.7%, respectively, $\chi^2 = 4.393$, $P<0.05$). SPF was significantly correlated with tumor size (the number of cases with SPF>15% and tumor size <5 cm was 9 and it was 23 in tumors with SPF>15% and tumor size >5 cm, $\chi^2 = 4.931$, $P<0.05$), differentiation (the number of cases with SPF>15% and well- or moderately-differentiated carcinoma was 8 and it was 21 in poorly-differentiated or signet ring carcinoma, $\chi^2 = 6.299$, $P<0.05$) and LN metastasis (the number of cases with SPF>15% and negative LN metastasis was 24 and it was 8 in cases with SPF>15% and positive LN metastasis, $\chi^2 = 5.419$, $P<0.05$). And the number of cases with SPF higher than 15% was significantly different between carcinoma and noncarcinoma (32 *vs* 1, $\chi^2 = 5.987$, $P<0.05$).

DISCUSSION

One of the typical characteristics of malignant tumor is invasion and metastasis, which is the main cause for their lethality. Tumor progression is considered to be a dynamic, complex, and a multi-step process, but the essential steps are the breakdown of cell-cell adhesion and degradation of basement membrane (BM) and ECM.

In the present study, immunohistochemical analysis revealed a progressive increase in expression of MMP-9 with increasing severity of lesions of carcinoma (Figure 1A). And in tumor invasion front or the surrounding of tumor nests, MMP-9 showed a strong staining (Figure 1C), while in non-neoplastic tissues it was weakly positive (Figure 1B). Although the antibodies do not distinguish between proenzyme and active forms of MMP-9, an increase in intensity of immunohistochemical reactions of MMPs may play a crucial role in the progression of carcinoma. MMP-9 upregulation will confer on tumor cells the ability to degrade BM and ECM and lead to tumor progression. MMP-9 immunoreactivity in vascular endothelial cells and inflammatory cells was also noted (Figure 1D), suggesting that those cells might secrete MMP-9 induced by malignant cells, the so-called host reaction[12]. As reported, MMP-9 promoted inflammatory reaction by upregulation of cytokines such as IL-1β[13], and this then stimulated host reaction, thus forming a pernicious cycle. Therefore, in view of MMP-9, it is not a good phenomenon that tumor cells can induce inflammatory reaction. MMP-9 participates in the whole process of carcinogenesis and development of gastric carcinoma and even in intramucosal gastric carcinomas MMP-9 showed strong staining and promoted LN metastasis[14,15], suggesting an early tumor progression. Our result demonstrated that MMP-9 activity increased as the depth of invasion extended,

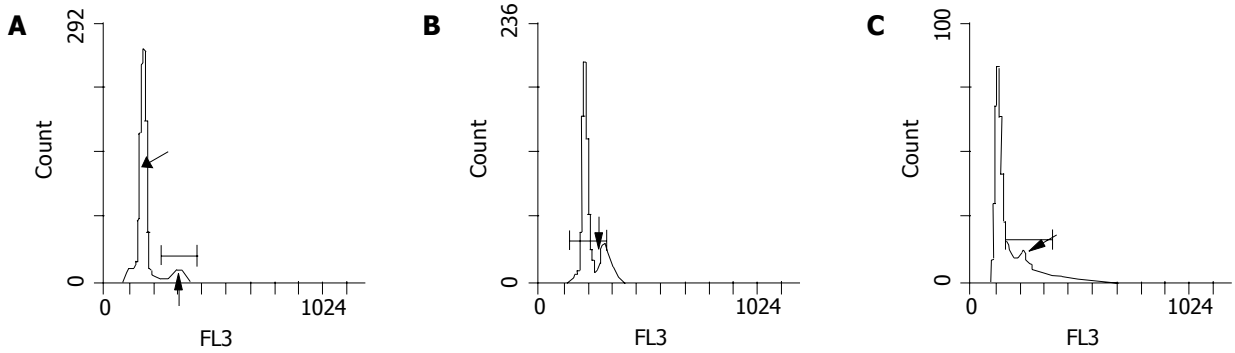


Figure 4 Histograms from FCM. **A:** A large diploid peak and a smaller tetraploid peak; **B:** an aneuploid peak (see arrow); **C:** higher SPF (see arrow).

Table 6 Correlation between DNA ploidy or SPF and histopathological or clinical features in gastric carcinoma

	n	Aneuploid rate (%)	*P*	*n* (SPF>15%)	*P*
Tumor size					
⩾5 cm	29	65.5	>0.05	23	>0.05
<5 cm	18	55.6		9	
Differentiation					
Well or moderate	19	42.1	<0.05	9	<0.05
Poor or signet ring cell type	28	75.0		23	
Depth of invasion					
Submucosa	7	28.6	>0.05	3	>0.05
Muscular layer or serosa	40	67.5		29	
LN metastasis					
Negative	30	80.0	<0.001	24	<0.05
Positive	17	29.4		8	
Metastasis					
Primary carcinoma	47	61.7	>0.05	32	>0.05
Metastatic carcinoma	4	100		3	
Carcinoma and noncarcinoma					
Gastric carcinoma	47	61.7	<0.05	32	<0.05
Noncarcinoma gastric mucosa	6	16.7		1	

indicating that MMP-9 participated in tumor invasion. It was also revealed that MMP-9 activity increased as LN metastasis progressed, indicating that MMP-9 participated in tumor metastasis. Expression rate of MMP-9 was significantly different between carcinoma and noncarcinoma (66.7% and 31.3% respectively), implying that MMP-9 may be related to carcinogenesis. Recent findings support the view that MMPs are not only responsible for the proteolytic degradation of BM as an important step in metastasis, but also essentially regulate the growth of tumor by maintaining its access to growth factors from ECM and regulation of angiogenesis[16]. Single MMP strong expression does not necessarily suggest invasion or metastasis, because its activity is influenced by its inhibitors such as RECK and TIMPs[17]. TIMPs are endogenous specific inhibitors of MMPs. They have such abilities to form tight binding, non-covalent inhibitory complexes with multiple members of the MMP family that they inhibit ECM degradation by MMPs and have anti-metastasis function[18]. TIMP-2 inhibits active and proenzyme forms of MMPs. It was reported that transfection of TIMP-2 gene into human gastric cancer cell line SGC-7901 by lipofection technology reduced their invasion potential *in vivo* and *in vitro*[19]. The expression of type IV collagenase in the untransfected group was higher than in the transfected group. The high expression of TIMP-2 may represent a mechanism by which tumor cells control the proteolysis and remodeling of ECM that occurs during invasion and progression of tumors. Another report suggested that transfection of TIMP-2 into the liver tissue could treat colorectal cancer liver metastasis[20]. However, some studies suggested that high expression level of TIMP-2 related to poor prognosis. It showed that high level of TIMP-2 mRNA correlated with the development of distant metastasis[21]. A study on gastric cancer showed that TIMP-1 and TIMP-2 were identified in 41% and 57% of tumors, respectively, whereas normal gastric mucosa was negative. No correlation was observed between the presence of TIMP-2 and tumor stage, histological type, LN status or survival[22]. However, our results demonstrated that there was correlation between the presence of TIMP-2 and depth of invasion and LN metastasis and different from MMP-9; there was no correlation between TIMP-2 and other clinical or histopathological features. Our results also suggested that as MMP-9 activity increased during tumor progression a corresponding increase in TIMP-2 level also occurred. Therefore, it appears that the expression of MMPs and TIMPs during tumor progression is coordinately regulated. Imbalance between MMP-9 and TIMP-2 could be an essential factor in tumor progression and may be more important than the concentrations of single components of MMPs and TIMPs[23,24]. The increased ratios could be interpreted as a sign of proteolytic inequilibrium in the early stage of carcinogenesis and in the advanced stage of tumor progression. We believed that the high expression of MMP-9 was the basis of tumor invasion and metastasis and that relatively high level of TIMP-2 was induced by MMP-9. Our results are contradictory to previous reports. It might be due to different study methods and antibodies used, and double effects of TIMP-2. TIMP-2 not only inhibits MMPs activities but also takes part in other activities such as cell growth and survival that cannot always be clearly reconciled with their abilities to abrogate MMP activity[25,26]. Therefore, further investigations are required to explore this controversy.

E-cadherin plays a critical role in the establishment and maintenance of intercellular adhesion, cell polarity, and tissue architecture. Abnormalities of E-cadherin adhesive system have been detected in a number of cancers. Loss of E-cadherin adhesive function has been found in premalignant conditions such as colorectal adenoma, Barrett's esophagus, and gastric dysplasia[27] and in tumors such as ductal carcinoma *in situ* of the breast, prostate carcinoma, and gastric carcinoma. In gastric carcinoma, the overall expression of E-cadherin ranges from 20% up to 90% due to different score systems and different antibodies used. The present study showed that the expression rates of E-cadherin in carcinoma and noncarcinoma were 42.4% and 87.5% respectively, suggesting that E-cadherin played a role in carcinogenesis and tumor progression. The downregulation of expression of E-cadherin may contribute to disruption of normal cell-cell adhesion in malignantly transformed cells, which may associate with tumor cells' enhanced migration and proliferation, leading to invasion and metastasis. It was also revealed that the expression of E-cadherin was significantly correlated with tumor differentiation and Lauren's classification. That is, abnormal expression rate was significantly higher in poorly differentiated (or diffuse-type) adenocarcinomas than in well-differentiated (or intestinal-type) ones, in another word, strong E-cadherin staining correlated with well-differentiated cancers and tumor cell cohesiveness, while loss of staining or changes in localization were associated with poorly differentiated, discohesive and highly invasive tumors. Multiple *in vitro* and *in vivo* studies demonstrated that a loss of E-cadherin expression correlated with the development of metastasis[28]. We proved that abnormal expression rate of E-cadherin was higher in LN metastasis positive cases than in negative ones. E-cadherin participates in the whole process from early stage to advanced stage of tumor development and in addition to its interaction with β-catenin, experimental work has also indicated that E-cadherin is involved in inducing cell-cycle arrest, at least partially, through upregulation of the cyclin-dependent kinase inhibitor, p27[29]. These interactions provide a direct link between the proliferative phenotype, presumed to be a precursor of neoplasia, and E-cadherin. It was reported[30] that the presence of paranuclear E-cadherin in cancer-associated benign epithelium suggested that alteration in E-cadherin molecule responsible for the paranuclear distribution might be an early change in gastric adenocarcinoma progression. Our result also showed the presence of paranuclear E-cadherin in cancer, especially in low-differentiated tumors (Figures 3B-D). E-cadherin has been associated with dedifferentiation, loss of adhesion and invasion in tumor cells, suggesting a role for loss of E-cadherin expression in the acquisition of potentially invasive and metastatic phenotype. Despite some contrary results, the bulk of evidence from clinical studies suggests that loss of E-cadherin is linked to prognosis and has been found to be an independent predictor in patients with various cancers[31]. Level of serum soluble E-cadherin is a potentially valid prognostic marker for gastric cancer and high concentration predicts advanced stage and indicates palliative/conservative treatment[32]. However, the reasons that E-cadherin showed strong expression in

inflammatory breast cancer are still under investigation[33].

Correlation between E-cadherin and MMP-9

It was reported that MMP-9 degraded membranous E-cadherin and caused an increase of serum soluble E-cadherin fragment which could upregulate the level of MMPs, forming a vicious cycle[34]. The present study showed that expression of E-cadherin and MMP-9 was reversely or negatively correlated, supporting previous findings. MMP-9 and E-cadherin interact and accelerate tumor progression. Llorens[35] investigated the correlation between MMP-9 and E-cadherin from another perspective, and detected that the activity of enhancer for MMP-9 was upregulated in rat skin carcinoma HaCa[Ecad(-)] cell line, accompanied with upregulation of the expression of MMP-9 mRNA and MMP-9 protein, but was downregulated in HaCa[Ecad(+)] cell line. The expression of MMP-9 protein and its activity were upregulated while signal transmission was blocked by cDNA for anti-E-cadherin monoclonal antibody. E-cadherin regulates MMP-9 at transcriptional level, which aggravates tumor invasion and metastasis. From this point of view, E-cadherin seems to be an initiating factor and more important than MMP-9. The reason may lie in Snail or SIP1, because during HCC progression, Snail/SIP1 directly represses E-cadherin gene transcription and activates cancer invasion via upregulation of MMP gene family[36].

In brief, E-cadherin and MMP-9 form a malignant cycle and detecting the levels of those two molecules simultaneously would have important significance for predicting prognosis[37]. However, some scholars reported that E-cadherin down-regulated MMPs in high-invasive bronchogenic carcinoma cell line[38], which is controversial to our report.

Correlation between E-cadherin and TIMP-2

According to our investigation, a positive correlation existed between MMP-9 and TIMP-2 and negative correlation between MMP-9 and E-cadherin, thus there is supposed to be a negative correlation between E-cadherin and TIMP-2. E-cadherin and TIMP-2 genes both belong to tumor suppressor gene (TSG)[39], however we did not find any association between them. It may be limited by our experimental method and further investigation is required.

DNA ploidy analysis

Normal human cells undergo a series of sequential changes culminating in mitotic division. These complex changes can be roughly identified using DNA measurements in which the cell population can be divided into three basic cell-cycle compartments: G_1, S, and G_2+M. Figure 4A shows typical DNA distribution of normal cells. The first peak on the left represents the G_0/G_1 population and the smaller peak to the right represents the G_2+M populations. The S phase cells are residing in between these two peaks. In contrast to normal tissues, neoplastic lesions often undergo chromosomal aberrations resulting in the appearance of nondiploid (aneuploid) clones within the tumor population and/or an increase in the proportion of S-phase cells. Numerous investigations suggested that slight changes of DNA content would lead to malignant tumors. Therefore, detecting DNA ploidy and content would be of great value for diagnosis of malignant tumors. Recent studies showed that DNA content of carcinoma cells is an independent prognostic factor[40-42]. According to our investigation result that since SPF was significantly correlated with tumor size, differentiation, LN metastasis, and depth of invasion, we conclude that percentage of cells synthesizing DNA (S phase cells) is an indirect reflection of tumor proliferation, hence aggressive behavior. However, some scholars reported that SPF was not correlated with tumor differentiation. Normal or near-normal DNA modes often correlate with a high degree of histological differentiation and abnormal DNA modes with low degree of histological differentiation. In carcinoma aneuploid rate was 61.7%, much higher than in noncarcinoma (16.7%). These results indicate that the DNA pattern is a valuable predictor of early stage of cancer and prognosis.

In summary, with tumor progression and development of heterogeneity, the abnormal expressions of MMP-9, TIMP-2 or E-cadherin or the rate of DNA aneuploidy or high SPF gradually increase correspondingly, suggesting that they play a crucial role in gastric carcinoma progression and can be objective markers for biological behaviors of gastric carcinoma. Furthermore, these factors correlate with one another, accelerating the process of tumor progression. In early stage of cancer or precancerous lesion, we may detect those factors to prevent tumor development and improve prognosis.

ACKNOWLEDGMENTS

The authors are grateful to the Affiliated Hospital of Medical College, Qingdao University and Qingdao Municipal Hospital, Qingdao 266003, China, for their help in accomplishing the study.

REFERENCES

1 **Hansson LE,** Sparen P, Nyren O. Survival in stomach cancer is improving: results of a nationwide population-based Swedish study. *Ann Surg* 1999; **230**: 162-169
2 **Chen XY,** van Der Hulst RW, Shi Y, Xiao SD, Tytgat GN, TenKate FJ. Comparision of precancerous conditions:atrophy and intestinal metaplasia in *Helicobacter pylori* gastritis among Chinese and Dutch patients. *J Clin Pathol* 2001; **54**: 367-370
3 **Steinberg M,** McNutt P. Cadherins and their connections: adhesions have broader functions. *Curr Opin Cell Biol* 1999; **17**: 554-560
4 **Stamenkovic I.** Extracellular matrix remodeling: the role of matrix metalloproteinases. *J Pathol* 2003; **200**: 448-464
5 **Curran S,** Murray GI. Matrix metalloproteinases: molecular aspects of their roles in tumor invasion and metastasis. *Eur J Cancer* 2000; **36**: 1621-1630
6 **Noel A,** Maillard C, Rocks N, Jost M, Chabottaux V, Sounni NE, Maquoi E, Cataldo D, Foidart JM. Membrane associated proteases and their inhibitors in tumor angiogenesis. *J Clin Pathol* 2004; **57**: 577-584
7 **Ravery V,** Angulo J, Shamsa F, Pontes JE, Crissman JC, Fridman R. High levels of tissue inhibitor of metalloproteinses-2 (TIMP-2) expression are associated with poor outcome in invasive bladder cancer. *Cancer Res* 1996; **56**: 1654-1659
8 **Brew K,** Dinakarpandian D, Nagase H. Tissue inhibitors of metalloproteinase: evolution, structure and function. *Biochim Biophys Acta* 2000; **1477**: 267-283
9 **Massi D,** Fetabchi A, Paglierani M, Pimpinelli N, Santucci M. Expression and pronostic significance of matrix metalloproteinases and their tissue inhibitors in primary neuroendocrine carcinoma of the skin. *Human Pathol* 2003; **34**: 80-88

10 **Li YJ,** Ji XR. Relationship between expression of E-cadherin-catenin complex and clinicpathologic characteristics of pancreatic cancer. *World J Gastroenterol* 2003; **9**: 368-372
11 **Liu M,** Lawson G, Delos M, Jamart J, Chatelain B, Remacle M, Marbaix E. Prognostic value of cell proliferation markers, tumour suppressor proteins and cell adhesion molecules in primary squamous cell carcinoma of the larynx and hypopharynx. *Eur Arch Otorhinolaryngol* 2003; **260**: 28-34
12 **Shen KH,** Chi CW, Lo SS. Serum matrix metalloproteinase-9 level associated with stromal reaction in patients with gastric cancer. *Anticancer Res* 2000; **20**: 1307-1310
13 **Opdenakker G,** Van den Steen PE, Dubois B, Nelissen L, Van Coillie E, Masure S, Proost P, Van Damme J. Gelatinase B functions as regulator and effector in leukocyte biology. *Leukoc Biol* 2001; **69**: 851-859
14 **Kabashima A,** Maehara Y, Kakeji Y, Baba H, Koga T, Sugimachi K. Clinicopathological features and overexpression of matrix metalloproteinases in intramucosal gastric carcinoma with lymph node metastasis. *Clin Cancer Res* 2000; **6**: 3581-3584
15 **Kleiner DE,** Stetler-Stevenson WG. Matrix metalloproteinases and metastasis. *Cancer Chemother Phamacol* 1999; **43**: 42-47
16 **Egeblad M,** Werb Z. New functions for the matrix metalloproteinases in cancer progression. *Nat Rev Cancer* 2002; **2**: 161-174
17 **Baker AH,** Edwards DR, Murphy G. Metalloproteinase inhibitors: biological actions and therapeutic opportunities. *J Cell Sci* 2002; **115**: 3719-3727
18 **Jiang Y,** Goldberg ID, Shi YE. Complex roles of tissue inhibitors of metalloproteinases in cancer. *Oncogene* 2002; **21**: 2245-2252
19 **Li N,** Xu C, Liu W. The effect of tissue inhibitor of metalloproteinase-2 gene (TIMP-2 gene) on gastric carcinoma cells *in vitro* and *in vivo*. *Zhonghua Binglixue Zazhi* 1998; **27**: 362-365
20 **Brand K,** Baker AH, Perez-Canto A, Possling A, Sacharjat M, Geheeb M, Arnoid W. Treatment of colorectal liver metastases by adenoviral transfer of tissue inhibitor of metalloproteinases-2 into the liver tissues. *Cancer Res* 2000; **60**: 5723-5730
21 **Ree AH,** Florenes VA, Breg JP, Maelandsmo GM, Nesland JM, Fodstad O. High levels of messenger RNA for tissue inhibitors metalloproteinases in primary breast carcinomas are associated with development of distant metastasis. *Clin Cancer Res* 1997; **3**: 1623-1628
22 **Murray GI,** Duncan ME, Arbuckle E, Melvin WT, Fothergill JE. Matrix metalloproteinases and their inhibitors in gastric cancer. *Gut* 1998; **43**: 791-797
23 **Kugler A.** Matrix metalloproteinases and their inhibitors. *Anticancer Res* 1999; **19**: 1589-1592
24 **Giannelli G,** Erriquez R, Fransvea E, Daniele A, Trerotoli P, Schittulli F, Grano M, Quaranta M, Antonaci S. Proteolytic imbalance is reversed after therapeutic surgery in breast cancer patients. *Int J Cancer* 2004; **109**: 782-785
25 **Ohuchi E,** Shinagawa A. Cell growth-promoting activity of tissue inhibitor of metalloproteinases-2 (TIMP-2). *J Cell Sci* 1994; **107**: 2373-2379
26 **Coussens LM,** Fingleton B, Matrisian LM. Matrix metalloproteinase inhibitors and cancer: trials and tribulations. *Science* 2002; **295**: 2387-2392
27 **Chan AO,** Wong BC, Lan HY, Loke SL, Chan WK, Hui WM, Yuen YH, Ng I, Hou L, Wong WM, Yuen MF, Luk JM, Lam SK. Deregulation of E-cadherin-catenin complex in precancerous lesions of gastric adenocarcinoma. *J Gastroenterol Hepatol* 2003; **18**: 534-539
28 **Wijnhoven BP,** Dinjens WN, Pignatelli M. E-cadherin-catenin cell adhesion complex and human cancer. *Br J Surg* 2000; **87**: 992-1005
29 **Rak JW,** Florenes VA, Slingerland JM, Kerbel RS. E-cadherin dependent growth inhibition is mediated by the cyclin dependent kinase inhibitor p27 (KIP1). *J Cell Biol* 1998; **142**: 557-571
30 **Carpenter PM,** Al-Kuran RA, Theuer CP. Paranuaclear E-cadherin in gastric adenocarcinoma. *Am J Clin Pathol* 2002; **118**: 887-894
31 **Ozawa M.** How do cell control the cadherin-mediated cell adhesion? *Tanpakushitsu Kakusan Koso* 2003; **48**: 1673-1682
32 **Chan AO,** Chu KM, Lam SK, Wong BC, Kwork KF, Law S, Ko S, Hui WM, Yueng YH, Wong J. Soluble E-cadherin is an independent pretherapentic factor for long-trem survival in gastric cancer. *J Clin Oncol* 2003; **21**: 2288-2293
33 **Colpaert CG,** Vermeulen PB, Benoy L, Soubry A, Van Roy F, Van Beest P, Goovaerts G, Dirix LY, Van Dam P, Fox SB, Harris AL, van Marck EA. Inflammatory breast cancer shows angigenesis with high endothelial proliferation rate and strong E-cadherin expression. *Breast Cancer Res* 2003; **18**: 58-64
34 **Nawrocki-Raby B,** Gilles C, Polette M, Bruyneel E, Laroze JY, Bonnet N, Poidart JM, Mareel M, Birembaut P. Upregulation of MMPs by soluble E-cadherin in human lung tumor cells. *Int J Cancer* 2003; **105**: 790-795
35 **Llorens A,** Rodrigo I, Lopez-Barcons L, Gonzalez-Garrigues M, Lozano E, Vinyals A, Quintanilla M, Cano A, Fahra A. Down-regulation of E-cadherin in mouse skin carcinoma cells enhance a migratory and invasive phenotype linked to matrix metalloproteinase-9 gelatinase expression. *Laboratory Investigation* 1998; **78**: 1131-1138
36 **Miyoshi A,** Kitajima Y, Sumi K, Sato K, Hagiwara A, Koga Y, Miyazaki K. Snail and SIP1 increase cancer invasion by upregulating MMP family in hepatocellular carcinoma cells. *Br J Cancer* 2004; **90**: 1265-1273
37 **Polette M,** Nawrocki-Raby B, Gilles C, Clavel C, Birembaut P. Tumour invasion and matrix metalloproteinases. *Crit Rev Oncol Hematol* 2004; **49**: 179-186
38 **Nawrochi-Raby B,** Gilles C, Polette M, Martinella-Catusse C, Bonnet N, Puchelle E, Foidart JM, Van Roy E, Birembaut P. E-Cadherin mediates MMP down-regulation in highly invasive bronchial tumor cells. *Am J Pathol* 2003; **163**: 653-661
39 **Lee HS,** Lee HK, Kim HS, Yang HK, Kim WH. Tumour suppressor gene expression correlates with gastric cancer prognosis. *J Pathol* 2003; **200**: 39-46
40 **Jiao YF,** Sugai T, Suzuki M, Uesugi N, Habano W, Nakamura S, Takagane A, Suto T, Yoshida T. Application of the crypt isolation technique to the flow cytometric analysis of DNA content in gastric carcinoma. *Hum Pathol* 2004; **35**: 587-593
41 **Danesi DT,** Spano M, Fabiano A, Altavista P, Pasqualetti P, Toscano MG, Antonini F, Catalano P, Mecozzi A, Picconi A, Daffina A, Cucchiara G. Flow cytometric DNA ploidy, p53, PCNA, and c-erbB-2 protein expressions as predictors of survival in surgically resected gastric cancer patients. *Cytometry* 2000; **42**: 27-34
42 **Molnar B,** Bocsi J, Karman J, Nemeth A, Pronai L, Zagoni T, Tulassay Z. Immediate DNA ploidy analysis of gastrointestinal biopsies taken by endoscopy using a mechanical dissociation device. *Anticancer Res* 2003; **23**: 655-660

Science Editor Zhu LH and Guo SY **Language Editor** Elsevier HK

PO Box 2345, Beijing 100023, China
www.wjgnet.com
wjg@wjgnet.com

ELSEVIER

World J Gastroenterol 2005;11(36):5601-5606
World Journal of Gastroenterology ISSN 1007-9327
© 2005 The WJG Press and Elsevier Inc. All rights reserved.

Local recurrence is an important prognostic factor of hepatocellular carcinoma

Eiichirou Arimura, Kazuhiro Kotoh, Makoto Nakamuta, Shusuke Morizono, Munechika Enjoji, Hajime Nawata

Eiichirou Arimura, Kazuhiro Kotoh, Makoto Nakamuta, Shusuke Morizono, Munechika Enjoji, Hajime Nawata, Department of Medicine and Bioregulatory Science, Graduate School of Medical Sciences, Kyushu University, Fukuoka 812-8582, Japan
Correspondence to: Makoto Nakamuta, Department of Medicine and Bioregulatory Science, Graduate School of Medical Sciences, Kyushu University, 3-1-1 Maidashi, Higashi-ku, Fukuoka 812-5282, Japan. nakamuta@intmed3.med.kyushu-u.ac.jp
Telephone: +81-92-642-5282 Fax: +81-92-642-5287
Received: 2004-11-15 Accepted: 2005-02-18

Abstract

AIM: To clarify the importance of complete treatment by PEIT.

METHODS: A total of 140 previously untreated cases of HCC were enrolled in this study from 1988 to 2002. The inclusion criteria were: a solitary tumor less than 4 cm in diameter or multiple tumors, fewer than four in number and less than 3 cm in diameter, without extrahepatic metastasis or vessel invasion. As general principles for the treatment of HCC, the patients underwent transcatheter arterial chemoembolization (TACE) prior to PEIT. After the initial treatment of the patients, ultrasonography and computed tomography were performed, and measurement of serum levels of α-fetoprotein (AFP) was determined. When tumor recurrences were detected, PEIT and/or TACE were repeated whenever the hepatic functional reserve of the patient permitted. We then analyzed the variables that could influence prognosis, including tumor size and number, the serum levels of AFP, the parameters of hepatic function (albumin, bilirubin, ALT, hepaplastin test, platelet number, and indocyanine green retention at 15 min [ICG-R15]), combined therapy with TACE, distant recurrence, and local recurrence.

RESULTS: Univariate analysis identified the ICG test, serum levels of AFP and albumin, tumor size and number, and local recurrence, but not distant recurrence, as significant prognostic variables. In multivariate analysis using those five parameters, the ICG test, tumor size, tumor number, and local recurrence were identified as significant prognostic factors. In both univariate and multivariate analyses, the relative risk for the ICG test was the highest, followed by local recurrence.

CONCLUSION: We found that local recurrence is an independent prognostic factor of HCC, indicating that achieving complete treatment for HCC on first treatment is important for improving the prognosis of patients with HCC.

© 2005 The WJG Press and Elsevier Inc. All rights reserved.

Key words: Hepatocellular carcinoma; Local recurrence; Percutaneous ethanol injection therapy; Transcatheter arterial chemoembolization

Arimura E, Kotoh K, Nakamuta M, Morizono S, Enjoji M, Nawata H. Local recurrence is an important prognostic factor of hepatocellular carcinoma. *World J Gastroenterol* 2005; 11(36): 5601-5606
http://www.wjgnet.com/1007-9327/11/5601.asp

INTRODUCTION

Hepatocellular carcinoma (HCC) is a highly malignant tumor with a high morbidity and mortality rate, carrying a poor prognosis[1]. Improvement of imaging techniques has enabled the diagnosis of HCC at an early stage, making it possible to treat tumors locally. The first local treatment for HCC consisted of percutaneous ethanol injection therapy (PEIT), which was reported by Livraghi *et al*., in 1986[2]. Although PEIT has been limited to small-sized HCC and liver resection remains a good treatment for HCC[3], the long-term prognosis due to recurrence or survival after treatment is close to that for hepatic resection[4-6]. Furthermore, PEIT can be used for HCC patients with reduced hepatic functional reserve attributable to pre-existing liver cirrhosis[7]. In 1996, however, Ishii *et al*., pointed out that a significant number of patients experienced local recurrence after PEIT[8]. This local recurrence is caused predominantly by intra-tumor septa, which may inhibit the infiltration of the injected ethanol into the entire tumor.

When the technique of percutaneous microwave coagulation therapy (PMCT) was established, it was expected that the rate of local recurrence would decrease because thermal coagulation should be achieved regardless of intra-tumor septa[9]. Contrary to that expectation, however, the effect of PMCT was limited to tumors of 15 mm or less in diameter. Radio frequency ablation (RFA) was later developed, which can achieve thermal necrosis throughout a mass of 35 mm in diameter[10,11]. Although the development of techniques for local treatment of HCC was aimed at decreasing the rate of local recurrence, it has remained unclear whether local recurrence does indeed worsen the prognosis

of patients with HCC[12], and whether an additional treatment for local recurrence can overcome the failure of initial treatment. Several studies have attempted to identify the significant prognostic factors for HCC[13-17]; however, to our knowledge, none of those studies considered local recurrence as a prognostic factor[18,19].

In this study, we aimed to clarify how local recurrence after initial treatment influences the prognosis of HCC patients. If the survival rate of patients with local recurrence is the same as that of those without local recurrence, the advantage of PMCT or RFA over PEIT would be diminished greatly, since PMCT and RFA were developed to reduce local recurrence.

MATERIALS AND METHODS

Patients

The inclusion criteria were as follows: (1) the patients not diagnosed with HCC previously; (2) a solitary HCC less than 4 cm in diameter, or fewer than four tumors with diameter less than 3 cm; and (3) patients without extrahepatic metastasis or vessel invasion. Of the 452 consecutive patients who were diagnosed with HCC in Kyushu University Hospital between January 1988 and December 2002, a series of 140 consecutive HCC patients meeting the inclusion criteria were enrolled. The enrolled patients included 95 males and 45 females, ranging in age from 35 to 83 years (mean 63.2 years, Table 1). Computed tomography (CT) and ultrasonography (US) were performed on all of the patients. To confirm the findings obtained by CT and US, angiography was also performed on patients, who gave consent for angiography examination. The diagnosis of HCC was finally confirmed histologically by aspiration tumor biopsy using a 21 G needle prior to the PEIT procedure.

Table 1 Characteristics of 140 patients at base line (means±SD)

		(Range)
Age (yr)	63.3±8.54	(35-83)
Male/female	95/45	
Child (A/B/C)	77/48/15	
Albumin (g/dL)	3.56±0.43	(2.5-4.5)
Bilirubin (mg/dL)	1.19±0.99	(0.4-10.3)
Platelet (10^4/L)	9.74±6.0	(0.8-69.9)
ALT (U/L)	84.58±47.04	(14-266)
HPT (%)	60.98±17.14	(25-116)
ICG-R15 (%)	28.13±15.29	(3.5-76.5)
AFP (ng/mL)	155.37±565.3	(2-5 653)
Tumor size (mm)	20.51±8.26	
Tumor number	1.51±0.79	

In accordance with general principles for the treatment of HCC, the patients underwent transcatheter arterial chemoembolization (TACE) prior to local treatment to enhance the effects of PEIT. In total, TACE was carried out on 81 patients 7 to 14 d before local treatment. With a therapeutic goal of complete necrosis of HCC, PEIT was carried out on all tumors for each patient. Ethanol (4-8 mL) was injected into each tumor during one session of PEIT. The total number of PEIT sessions was decided based on achieving a total amount of injected ethanol for each HCC that was more than two times the mass volume and all tumors consequently received more than two sessions of PEIT. CT was performed to evaluate treatment after finishing all sessions of PEIT. Successful treatment with PEIT was confirmed by CT and demonstrated that the tumor was completely covered by at least a 5 mm region (i.e., the ethanol-injected region) that was non-enhanced with contrast medium. When evidence of treatment success was not obtained, additional PEIT was performed until success was achieved, as assessed by CT. Major complications, such as intraperitoneal bleeding, hemobilia or liver abscesses were not observed in any case after PEIT.

After the initial treatment of the patients, US and measurement of serum α-fetoprotein (AFP) levels were carried out on an outpatient basis. The patients were also observed regularly by CT at 1, 3, 6, and 12 mo after the initial treatment, and every 6 mo after the first year of the treatment. Whenever changes were observed on US or CT imaging, or in the serum AFP levels, CT and/or angiography were carried out to confirm the recurrence, which was verified by enhanced uptake of contrast medium. Among the cases of recurrence, we defined "local recurrence" as those cases in which tumors occurred within or in contact with the treated lesion as determined by CT findings (Tables 2 and 3). The number and size (diameter) of locally and/or distantly recurrent tumors were also determined by CT examination (Table 3). Where recurrences were detected, PEIT and/or TACE were repeated whenever the hepatic functional reserve of the patient permitted. Among the local recurrence group, four patients suffered rapid and diffuse tumor growth involving the portal and hepatic veins. Two of them had been treated only with PEIT and the other two patients had undergone both PEIT and TACE at first treatment. In the local recurrence-free group, on the other hand, venous invasion was not seen. Although PEIT and/or TACE were available for all patients in the local recurrence-free group, four patients in the local recurrence group could not be given further treatment because of their decreased hepatic functional reserve.

Table 2 Comparison of clinical backgrounds between local recurrence group and local recurrence-free group

	Local recurrence	
	(+)	(-)
n	44	96
Albumin (g/dL)	3.47±0.49	3.60±0.40
Bilirubin (mg/dL)	1.15±0.53	1.20±1.15
Platelets (10^4/L)	10.01±9.89	9.62±4.37
ALT (U/L)	85.16±41.76	84.31±49.50
HPT (%)	62.28±18.64	60.35±16.44
ICG-R15 (%)	29.04±15.23	27.72±15.39
AFP (ng/mL)	153.83±539.31	63.24±118.58
Tumor size (mm)	24.00±9.48	18.92±7.15[d]
Tumor number	1.77±0.94	1.39±0.69[b]
TACE prior to PEIT	22 (50%)	59 (61%)

[b]$P<0.01$ *vs* local recurrence (+); [d]$P<0.001$ *vs* local recurrence (+).

The variables that could influence the prognosis were compared between the local recurrence group and the local

Table 3 Comparison of features of recurrence after initial treatment for HCC between local recurrence group and local recurrence-free group

	Local recurrence	
	(+)	(-)
Recurrent tumor number	3.6±0.6[1]	2.3±1.9[d]
Recurrent tumor size	33.0±22.0[2]	19.4±8.8[d]
Recurrence-free period	325.6±216.8	710.5±813.3[b]
Treatment for recurrence		
PEIT (+/-)	25/16	65/16
TACE (+/-)	21/20	24/57

[1]Including both local and distant recurred tumors; [2]calculated from the size of locally recurred tumors; [b]$P<0.01$ *vs* local recurrence (+), [d]$P<0.001$ *vs* local recurrence (+).

recurrence-free group; these included tumor size and number, serum AFP levels, the parameters of hepatic function (albumin, bilirubin, ALT, hepaplastin test, platelet number, and ICG-R15), and combination with TACE.

Statistical analysis

Baseline data were presented as mean±SD for quantitative variables. Differences in baseline characteristics between the local recurrence group and local recurrence-free group were analyzed using the Wilcoxon rank sum test and the Fisher's exact test for qualitative variables.

The prognostic values of baseline characteristics, local and distant recurrence after initial treatment were assessed using the univariate and multivariate Cox proportional hazards regression models. Variables that met the selected cut-off value ($P<0.05$) in the univariate comparison were entered into the multivariate analysis. Both univariate and multivariate results were presented as relative risks with corresponding 95%CIs and *P* values from the Wald test. All significant tests were two-sided and differences with a $P<0.05$ were considered statistically significant.

RESULTS

Among the 140 patients enrolled, 44 (31.4%) suffered from local recurrence. Of the remaining 96 patients, non-local recurrence was found in 80, and only 16 patients (11.4%) remained free of recurrence throughout the period of observation.

For comparison of baseline characteristics, we divided the patients with recurrence into two groups, the local recurrence group and local recurrence-free group. There was no significant difference between these two groups with respect to the hepatic functional reserve (Table 2). The proportion of patients in the local recurrence group who underwent TACE was higher than that in the local recurrence-free group (50% *vs* 39%), but the difference was not significant. On the other hand, the differences in tumor size and numbers were significant between these two groups (Table 2). The local recurrence group had significantly larger average tumor size and greater tumor numbers compared to the local recurrence-free group (tumor size: 24.00±9.48 mm *vs* 18.92±7.15 mm, $P<0.001$; tumor number 1.77±0.94 *vs* 1.3±0.69, $P<0.01$). Combination with TACE did not affect the rate of local recurrence.

We then compared the features of recurrence after initial treatment between these two groups. At the time of recurrence, the tumor number in the local recurrence group was 3.6±0.6 and the largest tumor size among them was 33.0±22.0 mm in diameter, whereas the tumor number in the local recurrence-free group was 2.3±1.9 and the largest size was 19.4±8.8 mm in diameter (both $P<0.001$, Table 3). All cases of the local recurrence group ($n = 44$) showed

Table 4 Univariate analysis of prognostic factors for HCC

Variables		*n*	*P*	Exp	95%CI
Albumin (g/dL)	>3.5	74	0.0455	1.694	1.011-2.841
	≤3.5	60			
Bilirubin (mg/dL)	<1.0	62	0.4059	1.246	0.742-2.091
	≥1.0	70			
Platelet (10^4/L)	>8.0	79	0.8301	1.057	0.637-1.753
	≤8.0	60			
ALT (U/L)	<75	65	0.2317	1.373	0.817-2.310
	≥75	74			
HPT (%)	>55	76	0.1665	0.688	0.406-1.168
	≤55	59			
ICG-R15 (%)	<30	67	0.0003	2.905	1.637-5.156
	≥30	45			
AFP (ng/mL)	<30	59	0.0269	1.879	1.075-3.287
	≥30	56			
Tumor size (mm)	<20	73	0.0174	1.882	1.117-3.170
	≥20	67			
Tumor number	1	91	0.0170	1.863	1.117-3.106
	≥2	49			
Local recurrence	(+)	45	0.0003	2.579	1.540-4.317
	(-)	95			
Distant recurrence	(+)	111	0.2250	1.630	0.740-3.951
	(-)	29			
TACE	(+)	81	0.5885	1.156	0.683-1.958
	(-)	59			

solitary local recurrence, but 31 cases also showed distant recurrence, in addition to local recurrence, when the recurrence was confirmed. In all cases of local recurrence combined with distant recurrence, the tumor size of local recurrence was larger than that of distant recurrence. Therefore, the recurrent tumor size (33.0±22.0 mm) in the local recurrence group was derived from the locally recurrent tumor (Table 3). The period from the initial treatment to the detection of recurrence (recurrence-free period) was 325.6±216.8 d in the local recurrence group, which was significantly shorter than that in the local recurrence-free group (710.5±813.3 d, $P<0.01$, Table 3). There was no significant difference between the two groups in the method of treatment after recurrence (Table 3).

Using univariate analysis, we identified the ICG test, serum levels of AFP and albumin, tumor size and number, and local recurrence, but not distant recurrence, as significant prognostic variables (Table 4). Additionally, in multivariate analysis using those five parameters, the ICG test, tumor size and number, and local recurrence were identified as significant prognostic factors (Table 5). In both univariate and multivariate analyses, the relative risk for the ICG test was the highest, followed by local recurrence.

Table 5 Multivariate analysis of prognostic factors for HCC

Variables	*P*	Exp	95%CI
Albumin	0.2424	1.490	0.764-2.906
ICG-R15 (%)	0.0074	2.498	1.278-4.882
AFP (ng/mL)	0.1816	1.557	0.813-2.983
Tumor size (mm)	0.0124	2.267	1.193-4.308
Tumor number	0.0469	1.845	1.008-3.375
Local recurrence	0.0081	2.362	1.250-4.462

DISCUSSION

Multivariate analysis showed that the ICG test, tumor size, tumor number, and local recurrence after initial treatment were significant prognostic factors. Those factors could be classified into three categories: the hepatic functional reserve, the progression of HCC, and local recurrence. In this study, "local recurrence" was defined as those cases in which tumor (s) occurred within or in contact with the treated lesion as detected by CT. It is impossible to determine whether local recurrence was attributable to residual HCC that had not been detected after initial evaluation or to newly developed HCC. We believe that local recurrence reflected failure (residual HCC) not recognized initially after treatment, since it seemed to be rare to newly develop within or in contact with the treated lesion, and because the recurrence-free period in the local recurrence group was significantly shorter compared to the local recurrence-free group. In earlier reports investigating the prognostic factors of HCC, tumor size and hepatic functional reserve were commonly identified as significant factors[15-19]. Those results, however, depended on the hypothesis that the treatment for HCC was performed completely. On the other hand, it has been reported repeatedly that a significant number of patients experience local recurrence after non-surgical treatment, which indicates that it cannot be expected that all treatments are performed completely. Therefore, multivariate analysis of HCC prognosis should be performed, and it should include factors relating to the completeness of the treatment, which is directly referable to local recurrence. Local treatments, including PEIT, require technical skill in both US and puncture, and it is well known that considerable variation in the PEIT technique occurs among different surgeons. In our univariate and multivariate analyses, the relative risk of local recurrence was the greatest, next to the ICG-R15 value, indicating that cautious PEIT technique is required when treating new cases of HCC.

In the treatment of HCC using PEIT, there are three difficulties that prevent the achievement of complete tumor necrosis. The first is the existence of septa in the tumor which partitions it into several closed spaces. The existence of septa is very common when the diameter of the tumor is larger than 20 mm. When a tumor has septa, injected ethanol is not able to spread across the tumor and it is necessary to repeat the puncture, aiming at each separate partition[20,21]. Such a tedious procedure would risk that viable HCC cells may remain. The second problem relates to the location of the tumor. Because PEIT is performed under the guidance of US, it is sometimes difficult to image tumors located close to the diaphragm. Poor imaging of the tumor leads inevitably to insufficient injection of ethanol. Tumors on the surface of the liver also are difficult to puncture because a direct puncture of the projecting area should be avoided to prevent bleeding from the needle track. Furthermore, the tumors located near the portal vein or gall bladder are not easy to be treated completely without the possibility of viable HCC cells remaining. In such situations, surgeons tend to hesitate to inject a sufficient volume of ethanol (more than twice the mass volume)[22,23], fearing the possibility of causing inflammation in the wall of the intrahepatic vessel or gall bladder. The third problem is that the injected ethanol does not always spread fully into the target space. When the tumor includes a relatively large vein, injected ethanol leaks out through the vessels before it can infiltrate the tumor. Taking into account the aforementioned difficulties, multiple sessions are required to decrease the local recurrence after PEIT.

When we compared the local recurrence group and the local recurrence-free group, the latter had smaller diameter and fewer numbers of tumors; whereas there were no significant differences in the variables indicating their hepatic functional reserve (Table 2). Considering the difficulties in the PEIT procedure mentioned above, our results are clinically acceptable. As the number of tumors increases, the probability of tumor occurrence in the areas difficult to puncture also increases. Similarly, larger HCCs contain more septa and are more likely to involve vessels as compared with smaller HCCs. Furthermore, as the number of tumors to be treated increases, it becomes more difficult for the surgeon to maintain concentration.

There are several possible explanations for the poor prognosis of patients with local recurrence. The first possible explanation is that the residual part of the tumor might change to a poor differentiation after treatment. It is well known that there are cases in which rapid sarcomatous change

developed from residual HCC after TACE[24]. Recently, similar results also have been reported after RFA[12,25]. These phenomena are considered to be the result of the hypoxemia caused by TACE. HCC cells basically require a rich blood supply. Therefore, artificial hypoxic pressure could result in undifferentiation of malignant cells. In our study, it should be emphasized that the recurrences in the local recurrence group were more likely to be multiple and emerged more rapidly than that in the local recurrence-free group, indicating that the character of the residual tumor cells had changed to a more malignant one. On the other hand, it is well known that locally recurrent HCC often occurs with an extrahepatic arterial supply. Such vessel reconstruction is observed after treatments that could damage the original feeding artery. In short, all TACE, PEIT, PMCT and RFA procedures could be a cause of revascularization. Once the residual tumor is supplied by blood flowing from the extrahepatic artery, it is very difficult to perform complete treatment following chemoembolization.

Combined TACE and PEI is a therapeutic option that has been proposed to overcome the weakness of each of the two procedures in the treatment of HCC[21,26-30]. The rationale for a combination of these two treatments relies on the fact that tumor consistency is markedly decreased and intratumoral septa are usually disrupted after TACE. Consequently, these changes make subsequent treatment with PEIT easier, as they provide enhanced ethanol diffusion within the tumor and higher doses of ethanol than those used in conventional PEIT. In our general principles for the treatment of HCC, the patients underwent TACE prior to local treatment to enhance the effects of PEIT, however, combining with TACE did not affect the rate of local recurrence or the prognosis in our study. Koda *et al*.[21], reported that in patients with HCC less than 2 cm in diameter, combination with TACE showed lesser rate of local and distant recurrence and better prognosis than PETI alone. Further study will be needed including more number of cases and/or longer observation.

In conclusion, we showed that, in addition to factors such as the hepatic functional reserve and tumor size, it is important to achieve complete necrosis upon initial treatment in order to improve the prognosis of HCC patients. This result warrants the surgeons to be more cautious when performing the first treatment. New RFA devices that cover a greater volume might contribute to this goal, and further study of local recurrence after RFA is critical for improving the local treatment of HCC.

REFERENCES

1 **Tang ZY**. Hepatocellular carcinoma-cause, treatment and metastasis. *World J Gastroenterol* 2001; **7**: 445-454
2 **Livraghi T**, Festi D, Monti F, Salmi A, Vettori C. US-guided percutaneous alcohol injection of small hepatic and abdominal tumors. *Radiology* 1986; **161**: 309-312
3 **Parks RW**, Garden OJ. Liver resection for cancer. *World J Gastroenterol* 2001; **7**: 766-771
4 **Kotoh K**, Sakai H, Sakamoto S, Nakayama S, Satoh M, Morotomi I, Nawata H. The effect of percutaneous ethanol injection therapy on small solitary hepatocellular carcinoma is comparable to that of hepatectomy. *Am J Gastroenterol* 1994; **89**: 194-198
5 **Daniele B**, De Sio I, Izzo F, Capuano G, Andreana A, Mazzanti R, Aiello A, Vallone P, Fiore F, Gaeta GB, Perrone F, Pignata S, Gallo C. CLIP investigators. Hepatic resection and percutaneous ethanol injection as treatments of small hepatocellular carcinoma: a Cancer of the Liver Italian Program (CLIP 08) retrospective case-control study. *J Clin Gastroenterol* 2003; **36**: 63-67
6 **Yamamoto J**, Okada S, Shimada K, Okusaka T, Yamasaki S, Ueno H, Kosuge T. Treatment strategy for small hepatocellular carcinoma: comparison of long-term results after percutaneous ethanol injection therapy and surgical resection. *Hepatology* 2001; **34**: 707-713
7 **Giorgio A**, Tarantino L, Francica G, Scala V, Mariniello N, Aloisio T. Percutaneous ethanol injection under sonographic guidance of hepatocellular carcinoma in compensated and decompensated cirrhotic patients. *J Ultrasound Med* 1992; **11**: 587-595
8 **Ishii H**, Okada S, Nose H, Okusaka T, Yoshimori M, Takayama T, Kosuge T, Yamasaki S, Sakamoto M, Hirohashi S. Local recurrence of hepatocellular carcinoma after percutaneous ethanol injection. *Cancer* 1996; **77**: 1792-1796
9 **Seki T**, Wakabayashi M, Nakagawa T, Itho T, Shiro T, Kunieda K, Sato M, Uchiyama S, Inoue K. Ultrasonically guided percutaneous microwave coagulation therapy for small hepatocellular carcinoma. *Cancer* 1994; **74**: 817-825
10 **Jiang HC**, Liu LX, Piao DX, Xu J, Zheng M, Shu AL, Qi SY, Zhang WH, Wu LF. Clinical short-term results of radiofrequency ablation in liver cancers. *World J Gastroenterol* 2002; **8**: 624-630
11 **Buscarini L**, Buscarini E. Therapy of HCC-radiofrequency ablation. *Hepatogastroenterology* 2001; **48**: 15-19
12 **Ruzzenente A**, Manzoni GD, Molfetta M, Pachera S, Genco B, Donataccio M, Guglielmi A. Rapid progression of hepatocellular carcinoma after Radiofrequency Ablation. *World J Gastroenterol* 2004; **10**: 1137-1140
13 **Ikeda K**, Saitoh S, Tsubota A, Arase Y, Chayama K, Kumada H, Watanabe G, Tsurumaru M. Risk factors for tumor recurrence and prognosis after curative resection of hepatocellular carcinoma. *Cancer* 1993; **71**: 19-25
14 **Qin LX**, Tang ZY. The prognostic significance of clinical and pathological features in hepatocellular carcinoma. *World J Gastroenterol* 2002; **8**: 193-199
15 **Rabe C**, Pilz T, Klostemann C, Berna M, Schild HH, Sauebruch T, Caselmann WH. Clinical characteristics and outcome of a cohort of 101 patients with hepatocellular carcinoma. *World J Gastroenterol* 2001; **7**: 208-215
16 **Ueno S**, Tanabe G, Nuruki K, Oketani M, Komorizono Y, Hokotate H, Fukukura Y, Baba Y, Imamura Y, Aikou T. Prognosis of hepatocellular carcinoma associated with Child class B and C cirrhosis in relation to treatment: a multivariate analysis of 411 patients at a single center. *J Hepatobiliary Pancreat Surg* 2002; **9**: 469-477
17 **Zhao WH**, Ma ZM, Zhou XR, Feng YZ, Fang BS. Prediction of recurrence and prognosis in patients with hepatocellular carcinoma after resection by use of CLIP score. *World J Gastroenterol* 2002; **8**: 237-242
18 **Liao CS**, Yang KC, Yen MF, Teng LL, Duffy SW, Chen TH. Prognosis of small hepatocellular carcinoma treated by percutaneous ethanol injection and transcatheter arterial chemoembolization. *J Clin Epidemiol* 2002; **55**: 1095-1104
19 **Kuriyama H**, Okada S, Okusaka T, Ueno H, Ikeda M. Prognostic factors in patients with small hepatocellular carcinoma treated by percutaneous ethanol injection. *J Gastroenterol Hepatol* 2002; **17**: 1205-1210
20 **Shiina S**, Tagawa K, Unuma T, Takanashi R, Yoshiura K, Komatsu Y, Hata Y, Niwa Y, Shiratori Y, Terano A. Percutaneous ethanol injection therapy for hepatocellular carcinoma. A histopathologic study. *Cancer* 1991; **68**: 1524-1530
21 **Koda M**, Murawaki Y, Mitsuda A, Oyama K, Okamoto K, Idobe Y, Suou T, Kawasaki H. Combination therapy with transcatheter arterial chemoembolization and percutaneous ethanol injection compared with percutaneous ethanol injection alone for patients with small hepatocellular carcinoma: a randomized control study. *Cancer* 2001; **92**: 1516-1524

22 **Ebara M**, Ohto M, Sugiura N, Kita K, Yoshikawa M, Okuda K, Kondo F, Kondo Y. Percutaneous ethanol injection for the treatment of small hepatocellular carcinoma. Study of 95 patients. *J Gastroenterol Hepatol* 1990; **5**: 616-626
23 **Livraghi T**, Bolondi L, Lazzaroni S, Marin G, Morabito A, Rapaccini GL, Salmi A, Torzilli G. Percutaneous ethanol injection in the treatment of hepatocellular carcinoma in cirrhosis. A study on 207 patients. *Cancer* 1992; **69**: 925-929
24 **Morishita Y**, Etori F, Sawada K, Kachi H, Yamada T, Kawamori T, Tanaka T. Sarcomatous hepatocellular carcinoma with malignant ascites. A report of two cases. *Acta Cytol* 1998; **42**: 759-764
25 **Koda M**, Maeda Y, Matsunaga Y, Mimura K, Murawaki Y, Horie Y. Hepatocellular carcinoma with sarcomatous change arising after radiofrequency ablation for well-differentiated hepatocellular carcinoma. *Hepatol Res* 2003; **27**: 27163-27167
26 **Qian J**, Feng GS, Vogi T. Combined interventional therapies of hepatocellular carcinoma. *World J Gastrolenterol* 2003; **9**: 1885-1891
27 **Lencioni R**, Paolicchi A, Moretti M, Pinto F, Armillotta N, Di Giulio M, Cicorelli A, Donati F, Cioni D, Bartolozzi C. Combined transcatheter arterial chemoembolization and percutaneous ethanol injection for the treatment of large hepatocellular carcinoma: local therapeutic effect and long-term survival rate. *Eur Radiol* 1998; **8**: 439-444
28 **Kirchhoff T**, Chavan A, Galanski M. Transarterial chemoembolization and percutaneous ethanol injection therapy in patients with hepatocellular carcinoma. *Eur J Gastroenterol Hepatol* 1998; **10**: 907-909
29 **Lencioni R**, Cioni D, Donati F, Bartoiozzi C. Combination of interventional therapies in hepatocellullar carcinoma. *Hepatogastroenterolgy* 2001; **48**: 8-14
30 **Kamada K**, Kitamoto M, Aikata H, Kawakami Y, Kono H, Imamura M, Nakanishi T, Chayama K. Combination of transcatheter arterial chemoembolization using cisplatin-lipiodol suspension and percutaneous ethanol injection for treatment of advanced small hepatocellular carcinoma. *Am J Surg* 2002; **184**: 284-290

Science Editor Kumar M and Guo SY **Language Editor** Elsevier HK

PO Box 2345, Beijing 100023, China
www.wjgnet.com
wjg@wjgnet.com

ELSEVIER

World J Gastroenterol 2005;11(36):5607-5613
World Journal of Gastroenterology ISSN 1007-9327
© 2005 The WJG Press and Elsevier Inc. All rights reserved.

• *LIVER CANCER* •

1.5 Harmonic Imaging Sonography with microbubble contrast agent improves characterization of hepatocellular carcinoma

Kouji Yamamoto, Katsuya Shiraki, Shigeo Nakanishi, Hiroyuki Fuke, Takeshi Nakano, Akira Hashimoto, Atsuya Shimizu, Toshinobu Hamataki

Kouji Yamamoto, Katsuya Shiraki, Shigeo Nakanishi, Hiroyuki Fuke, Takeshi Nakano, First Department of Internal Medicine, Mie University School of Medicine, Tsu, Mie 514-8507, Japan
Akira Hashimoto, Atsuya Shimizu, Department of Internal Medicine, Saiseikai Matsusaka General Hospital, Matsusaka, Mie 515-8557, Japan
Toshinobu Hamataki, Sales Engineering Department, Toshiba Medical Systems Corporation, Nagoya, Aichi 450-0003, Japan
Correspondence to: Katsuya Shiraki, MD, PhD, First Department of Internal Medicine, Mie University School of Medicine, 2-174 Edobashi, Tsu, Mie 514-8507, Japan. katsuyas@clin.medic.mie-u.ac.jp
Telephone: +81-59-231-5015 Fax: +81-59-231-5201
Received: 2005-01-07 Accepted: 2005-02-18

AIM: To investigate the usefulness of 1.5 Harmonic Imaging Sonography with the use of the contrast agent Levovist for the diagnosis of hepatocellular carcinoma (HCC) and for the evaluation of therapeutic response.

METHODS: Phantom experiments were performed to compare the contrast effects of 2nd harmonic imaging and 1.5 Harmonic Imaging Sonography. 1.5 Harmonic Imaging Sonography was employed to examine 36 patients with HCC (42 nodules) before and after the treatment and to compare against the findings obtained using other diagnostic imaging modalities.

RESULTS: In 1.5 Harmonic Imaging Sonography, the tumor vessels of HCCs were clearly identified during the early phase, and late-phase images clearly demonstrated the differences in contrast enhancement between the tumor and surrounding hepatic parenchyma. Blood flow within the tumor was detected in 36 nodules (85.7%) during the early phase and in all 42 nodules (100%) during the late phase using 1.5 Harmonic Imaging Sonography, in 38 nodules (90.5%) using contrast-enhanced CT, in 34 nodules (81.0%) using digital subtraction angiography (DSA), and in 42 nodules (100%) using US CO_2 angiography. Following transcatheter arterial embolization, 1.5 Harmonic Imaging Sonography detected blood flow and contrast enhancement within the tumors that were judged to contain viable tissue in 20 of 42 nodules (47.6%). However, 6 of these 20 cases were not judged in contrast-enhanced CT. 1.5 Harmonic Imaging Sonography was compared with the US CO_2 angiography findings as the gold standard, and the sensitivity and specificity of these images for discerning viable and nonviable HCC after transcatheter arterial embolization were 100% and 100%, respectively.

CONCLUSION: 1.5 Harmonic Imaging Sonography permits the vascular structures of HCCs to be identified and blood flow within the tumor to be clearly demonstrated. Furthermore, 1.5 Harmonic Imaging Sonography is potentially useful for evaluating the therapeutic effects of transcatheter arterial embolization on HCC.

© 2005 The WJG Press and Elsevier Inc. All rights reserved.

Key words: 1.5 Harmonic imaging sonography; Hepatocellular carcinoma; Microbubble

Yamamoto K, Shiraki K, Nakanishi S, Fuke H, Nakano T, Hashimoto A, Shimizu A, Hamataki T. 1.5 Harmonic Imaging Sonography with microbubble contrast agent improves characterization of hepatocellular carcinoma. *World J Gastroenterol* 2005; 11(36): 5607-5613
http://www.wjgnet.com/1007-9327/11/5607.asp

The usefulness of the peripheral ultrasound contrast agent Levovist was originally thought to be limited to signal enhancement in color/power Doppler ultrasonography[1,2]. Levovist is now employed for the diagnosis of hepatic tumors, in which it has been found to enhance blood flow signals and thus improve the visualization of hepatic tumor vessels[3-5]. However, recent advances in ultrasonographic technologies have led to the development of new imaging techniques collectively referred to as "harmonic imaging", in which images are obtained using the 2nd harmonic components of the ultrasound signal. Among these new techniques, flash echo imaging (FEI) employs intermittent transmission at high acoustic power to permit the microbubbles to enter the scanning plane and thus to obtain echoes with high sensitivity. In other words, FEI makes it possible to acquire detailed images with high spatial resolution in which only blood flow information is extracted, making it easier to visualize tumor vessels. In contrast ultrasonographic examination of hepatocellular carcinoma (HCC), the microbubbles in Levovist cause higher frequency signals to be generated by the tumor than by normal hepatic parenchyma. Consequently, the contrast resolution of the tumor and normal parenchyma is further improved and minute blood vessels within the tumor can be visualized[6-11]. One technique is digital subtraction imaging,

which permits the contrast effect to be clearly identified and is therefore employed for the diagnosis of hepatic tumors[12-15]. In 2nd harmonic imaging, however, the presence of tissue harmonic components may lead to poorer contrast enhancement in some cases. In another method, Doppler technology is used to eliminate tissue echoes and to visualize the nonlinear behavior of the microbubbles[16-18], but this method is susceptible to motion artifacts near the heart. A new technology known as 1.5 Harmonic Imaging Sonography has been developed to overcome these problems. In this method, images are obtained using a band that is intermediate between the fundamental and the 2nd harmonic components (Figure 1). In the 1.5 Harmonic Imaging technique, a frequency band whose center frequency is higher than the fundamental by a factor of 3/2 is extracted and visualized. This frequency band is intermediate between the fundamental and the second harmonic. It includes only bubble echoes and is free of tissue echoes. This imaging technique reduces tissue echoes without generating motion artifacts such as those that are seen in the pseudo-Doppler imaging technique. Contrast between tissues and bubbles is improved by 20 dB or more compared with the 2nd harmonic imaging technique. 1.5 Harmonic Imaging Sonography involves the use of a transmission waveform in which the bandwidth is limited and the leakage of fundamental components is therefore reduced. The fundamental components of tissue echoes are effectively separated from the 2nd harmonic components, permitting images to be obtained in an intermediate band that is almost completely free from tissue echoes. When images are obtained in this intermediate band, higher contrast can be achieved between contrast agent and tissue echoes than in conventional 2nd harmonic imaging. The echo from the tissue has only fundamental and 2nd harmonic component. In the intermediate band, there exists no tissue echo with the dedicated transmission where the fundamental band width and leakage are well controlled. On the other hand, bubble echo has broadband harmonics in high mechanical index (MI) contrast imaging. So high bubble/tissue signal ratio is achieved in image with the component of that intermediate band. Nevertheless, to our knowledge, there have been no studies on the clinical application of 1.5 Harmonic Imaging Sonography for the evaluation of hepatic tumors and the assessment of therapeutic effects. The present study was therefore conducted to investigate the clinical usefulness of the ultrasound contrast agent Levovist for the examination of HCCs and for the assessment of therapeutic effects.

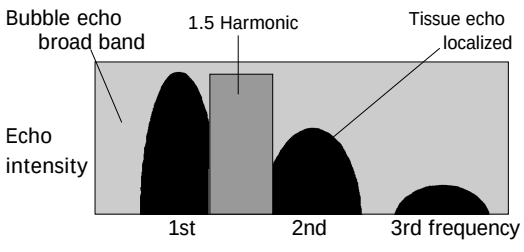


Figure 1 Basic concept of 1.5 Harmonic Imaging Sonography. A high microbubble/tissue ratio is obtained in the intermediate domain.

Patients

This study was performed with approval from the institutional review board, and informed consent was obtained from each patient before undergoing this procedure.

From September 2002 and November 2003, we enrolled in this study 36 patients with unresectable HCC, who had a total of 42 hypervascular HCC nodules. The subjects in the present study were 36 patients with 42 nodules that were diagnosed as HCC based on histopathological examination (n = 18) and diagnostic imaging findings (n = 24). The study group comprised 36 patients with type C cirrhosis: 24 men and 12 women ranging in age from 41 to 78 years and with a mean age of 62 years. The minimum tumor diameter was 10 mm, the maximum tumor diameter was 73 mm, and the mean tumor diameter was 25.8±15.1 mm (±SD). All those HCC nodules have been diagnosed by the sonography. Before therapy, serum α-fetoprotein levels (normal, <7 ng/mL) ranged from 4.7 to 928.6 ng/mL (mean, 186.1 ng/mL). 12/36(33.3%) case showed normal α-fetoprotein level.

Methods

Contrast-enhanced sonography examination

Ultrasound images were acquired using a diagnostic ultrasound system (SSA-770A, Aplio, Toshiba) with phased-array transducers operating at frequencies of approximately 2.5 and 3.0 MHz (PST-25AT and PST-30AT sector transducers, Toshiba). The MI was set to 1.6, and the transmission/reception frequencies were 1.4 MHz/3.0 MHz for 2nd harmonic imaging and 2.3 MHz/3.3 MHz in phantom experiments and 1.7 MHz/2.5 MHz in clinical study for 1.5 Harmonic Imaging Sonography. Contrast images were acquired using FEI.

Phantom experiments were conducted to compare images obtained by 2nd harmonic imaging and 1.5 Harmonic Imaging Sonography (i.e., to compare tissue and microbubble echo contrast between 2nd harmonic imaging and 1.5 Harmonic Imaging Sonography). The phantom consisted of agar mixed with powdered graphite to simulate attenuation in the living body (Nihonkai Medical; 0.6, 0.9 dB/cm/MHz). The tube in this phantom was filled with the ultrasound contrast agent Levovist, which contains particles composed of a mixture of galactose and palmitic acid (SHU 508A, Levovist, Schering, Berlin, Germany; concentration 300 mg/mL). Images of this phantom were acquired using FEI.

In the clinical study, a total of 7 mL of Levovist at a concentration of 300 mg/mL was injected as a single bolus via a peripheral vein at a rate of 1 mL/s. Images were acquired using FEI at intervals of 0.2 s. The early phase was specified as the period of up to 60 s after the injection of contrast agent, and the tumor vessels were observed with the focal point set at the bottom of the tumor. Then, after an interval of 4 min, the late phase was specified as the period beginning at the 5-min time point, and ultrasound transmission was performed once manually to observe vascular enhancement (staining) of the tumor tissues. Images

were recorded on S-VHS videotape immediately after the injection of contrast agent. The patient was instructed to hold his or her breath for 10-50 s after the injection of Levovist in order to maintain a constant respiratory phase, and early-phase images were obtained continuously. Subsequently, the system was temporarily set to freeze mode and the images stored in cine loop memory were recorded onto the system hard disk. Five minutes after the injection, late-phase images were observed for several seconds during breath-holding and recorded onto the system hard disk.

Contrast-enhanced CT Contrast-enhanced CT was performed in all patients before treatment. Contiguous 5-mm-thick axial CT scans were obtained with a HiSpeed Advantage RP scanner (Lemage Supreme, General Electric Yokogawa Medical Systems, Tokyo, Japan). A nonionic contrast material, 100 mL of iopamidol (Iopamiron, Nippon Schering, Osaka, Japan), was administered at a rate of 3 mL/s, and CT scans of the entire liver were obtained twice: first at 20-40 s (arterial phase) after IV injection of contrast material and then at 90 s (portal phase). Lesions were considered to be hypervascular if they appeared denser than the surrounding liver during the arterial phase.

Digital subtraction angiography Digital subtraction angiography (DSA) images were obtained using a DSA system (Infinix NB, Toshiba). The contrast agent was injected via a catheter placed in the hepatic artery. The presence or absence of tumor vessels was assessed. When tumor vessels were identified, the tumor was considered to be hypervascular. We performed transcatheter arterial chemoembolization in all patients by selectively introducing a coaxial microcatheter into a segmental branch or a subsegmental branch of the hepatic artery and injecting a mixture of iodized oil (Lipiodol, Guerbet, Aulnay-sous-Bois, France; 3.0-10.0 mL/body) or epirubicin hydrochloride (Farmorubicin, Pharmacia and Upjohn, Tokyo, Japan: 30-60 mg per body weight). We then preformed embolization using 0.5 mm×0.5 mm×0.5 mm gelatin sponge (Spongel, Yamamouchi Pharmaceuticals) in all patients. These embolic materials were injected until the feeding arteries were completely obliterated. If the blood supply was from two different subsegmental arteries, both were embolized. The effectiveness of transcatheter arterial chemoembolization was evaluated by 1.5 Harmonic Imaging Sonography and contrast-enhanced CT at 7 d after treatment.

US CO_2 angiography In ultrasound angiography, after the tumor was identified in a cross-sectional ultrasound image, CO_2 microbubbles were injected at a constant rate during breath-holding via a catheter placed in the hepatic artery. The CO_2 microbubbles were prepared by adding 5 mL of autologous blood to 10 mL of CO_2, connecting the container to a three-way stopcock, and transferring the mixture repeatedly approximately 30 times with a pump. Ultrasound images were acquired using a diagnostic ultrasound system (SSA-250A, Toshiba) with a 3.75-MHz convex transducer. Images were simultaneously recorded on videotape and magneto-optical disk from the time immediately before the injection of CO_2 microbubbles until the time when tumor enhancement was observed. When the tumor showed stronger enhancement than the surrounding hepatic parenchyma, it was considered to be hypervascular.

CT during arterial portography CT during arterial portography (CTAP) was performed using a CT scanner (Asteion, Toshiba, Tokyo Japan). For CTAP, 100 mL of Iopamidol contrast medium (Iopamiron 150; Nihon Schering, Osaka, Japan) was administered via a catheter in the superior mesenteric artery at an estimated rate of 2.0 mL/s during sequential helical scanning of the liver. For CT arteriography, 30-50 mL of contract medium (Iopamiron 150) was administered via a catheter in the proper hepatic, left, or right hepatic artery at an estimated rate of 1.5-2.5 mL/s during sequential helical scanning of the liver. Tumors that did not contain portal blood flow were identified as low-absorption areas in the hepatic parenchyma (portal perfusion defects).

Imaging analysis All the sonographic data were recorded on videotape from the beginning of B-mode scanning. The still images were stored on the hard disk of the unit by reviewing the cine loop memory. The images obtained using the above modalities were interpreted by three specialists in diagnostic imaging. When a discrepancy occurred among the interpreters, re-evaluation and discussion were done for agreement. On contrast-enhanced imaging with 1.5 Harmonic Imaging Sonography, the presence of the intratumoral blood flow signals on either the vessel image or on the tumor parenchymal stain image was considered as hypervascular or residual tumor due to inadequate treatment. In contrast, the absence of the intratumoral blood flow signals was evaluated as hypovascular or complete response to the treatment. The contrast enhancement on CT was reviewed by three radiologists without knowledge of the 1.5 Harmonic Imaging Sonography results.

The sensitivity and specificity of 1.5 Harmonic Imaging Sonography in detecting intratumoral blood flow signals on the vessel tumor were determined using US CO_2 angiography as a gold standard[21,22]. The detectability of residual tumor using contrast-enhanced 1.5 Harmonic Imaging Sonography was compared with that of the tumors using contrast-enhanced CT.

The data were analyzed with the χ^2 test. A P value less than 0.05 was considered significant.

In vitro study

In the phantom experiments, the area occupied by the contrast agent was shown as a gleaming white zone, with the surrounding area corresponding to a tissue-equivalent phantom composed of agar mixed with powdered graphite. In oblique images, the echoes from the microbubbles appeared as an oblique bright zone, and the surrounding dark area corresponded to echoes from the agar phantom. The images clearly demonstrated the improvement in tissue-microbubble contrast in 1.5 Harmonic Imaging Sonography as compared with 2nd harmonic imaging. In 1.5 Harmonic Imaging Sonography, the contrast between tissues and microbubbles was found to be clearly superior to that in 2nd harmonic imaging (Figure 2).

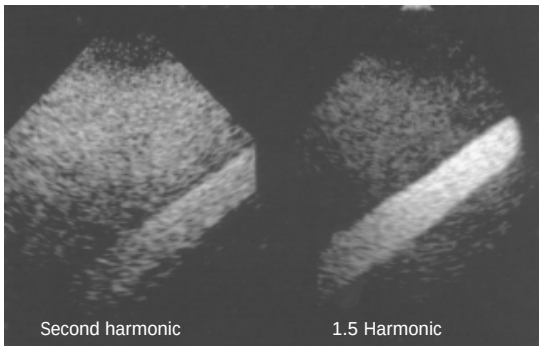


Figure 2 Comparison of contrast images obtained by 1.5 Harmonic Imaging Sonography and 2nd harmonic imaging.

Clinical study

Blood vessels in all HCCs were more clearly depicted by 1.5 Harmonic Imaging Sonography than by 2nd harmonic imaging (Figures 3A and C). Moreover, during the late phase, 1.5 Harmonic Imaging Sonography demonstrated the surrounding hepatic parenchyma with higher contrast enhancement than 2nd harmonic imaging, clearly depicting the area of the tumor (Figures 3B and D).

In hypervascular HCCs, the blood vessels within the tumor were clearly demonstrated during the early phase (Figures 4B-D and 5A). In addition, late-phase images revealed partial residual enhancement in all tumors, but with less enhancement than the surrounding hepatic parenchyma (Figures 3B and 5B).

With regard to the detection of blood flow signals within the tumor in the 42 nodules, early-phase 1.5 Harmonic Imaging Sonography revealed the tumor vessels in 36 nodules (85.7%). Late-phase images demonstrated significantly lower enhancement of the tumor than the surrounding hepatic parenchyma in all 42 nodules (100%). Early-phase 1.5 Harmonic Imaging Sonography did not show hypervascular enhancement in six nodules (14.3%), and late-phase images confirmed that these six nodules were not enhanced ($P>0.05$). As for the findings of other imaging modalities, blood flow signals were detected within the tumor in 39 nodules (92.9%) by contrast-enhanced CT, in 34 nodules (81.0%) by DSA, and in 42 nodules (100%) by US CO_2 angiography. CTAP showed a perfusion defect image in all 42 nodules (100%, Table 1).

Contrast-enhanced CT did not show hypervascular enhancement in three nodules (one small HCC nodule measuring 10 mm in diameter and two nodule near the heart), but 1.5 Harmonic Imaging Sonography was able to

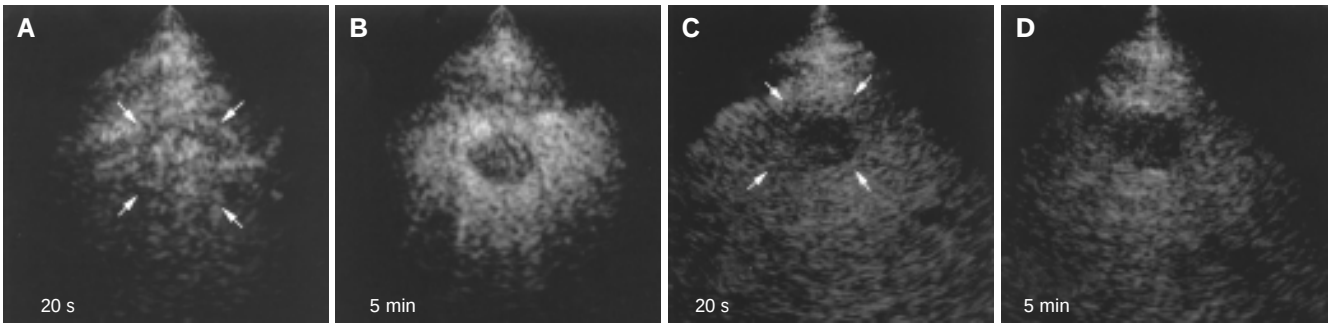


Figure 3 A 74-year-old man with C-type cirrhosis and HCC (15.4 mm in diameter) in the right liver. Comparison of contrast images obtained by 1.5 Harmonic Imaging Sonography and 2nd harmonic imaging. A: 1.5 Harmonic Imaging Sonography image obtained by real-time continuous sonography in the early phase (20 s after injection). Abundant tumor vessels (arrows) with peripheral branching are seen; B: 1.5 Harmonic Imaging Sonography image obtained by real-time continuous sonography in the late phase (5 min after injection). Residual enhancement of some tumor vessels is seen, but the boundary between the tumor and the hepatic parenchyma is clearly demonstrated; C: 2nd harmonic imaging obtained by real-time continuous sonography in the early phase (20 s after injection). The abundant and peripherally branching tumor vessels (arrows) cannot be clearly depicted; D: 2nd harmonic imaging obtained by real-time continuous sonography in the late phase (5 min after injection). The boundary between the tumor and the hepatic parenchyma is somewhat obscure.

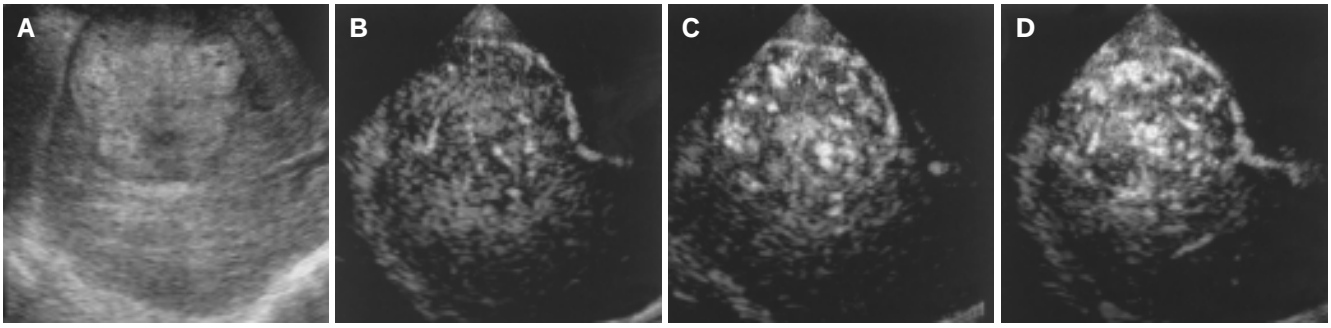


Figure 4 A 78-year-old man with C-type cirrhosis and HCC (73.3 mm in diameter) in the right liver. A: Right oblique conventional sonography image of the liver shows a mixed-pattern nodule 73.3 mm in diameter in segment 6 that exhibits the typical characteristics of HCC; B: 1.5 Harmonic Imaging Sonography image obtained by real-time continuous sonography in the early phase (20 s after injection) shows the tumor vessels; C and D: 1.5 Harmonic Imaging Sonography images obtained by real-time continuous sonography in the early phase, 28 s (C) and 32 s (D) after injection, show abundant tumor vessels with peripheral branching.

demonstrate the tumor vessels even in these three nodules. Furthermore, DSA failed to demonstrate tumor vessels in eight nodules, while these vessels were successfully visualized by 1.5 Harmonic Imaging Sonography. 1.5 Harmonic Imaging Sonography were compared with the US CO_2 angiography findings as the gold standard, and the sensitivity and specificity of these images for discerning viable and nonviable HCC after transcatheter arterial embolization were 100% and 100%, respectively.

With regard to treatment, 1.5 Harmonic Imaging Sonography revealed residual blood flow signals within the tumor in 20 (47.6%) of the 42 nodules that had been treated by transcatheter arterial embolization. MRI, US CO_2 angiography also revealed residual blood flow signals within the tumor, but contrast-enhanced CT demonstrated residual blood flow signals in only 14 nodules (33.3%). In the remaining 22 nodules (52.4%), no blood flow signal was observed within the tumor by 1.5 Harmonic Imaging Sonography or contrast-enhanced CT (Table 2, Figures 6 and 7).

In the present study, phantom experiments were conducted to investigate the usefulness of 1.5 Harmonic Imaging Sonography. In 1.5 Harmonic Imaging Sonography, unlike 2nd harmonic imaging, images are obtained using a frequency band that is lower than that of the 2nd harmonics, resulting in a significant improvement of the contrast enhancement non-uniformity that is frequently observed when a sector transducer is used. In 1.5 Harmonic Imaging Sonography,

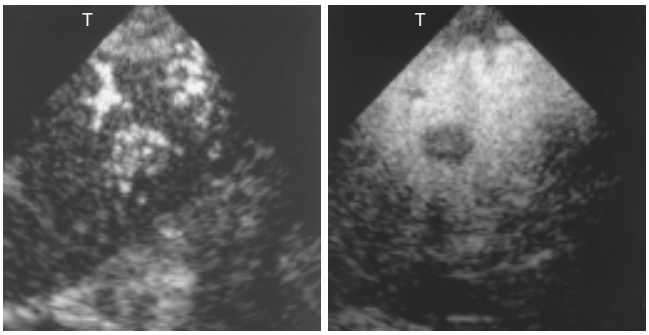


Figure 5 A 62-year-old man with C-type cirrhosis and HCC (18.9 mm in diameter) in segment 4 of the liver. A: 1.5 Harmonic Imaging Sonography image obtained by real-time continuous sonography in the early phase (28 s after injection) shows abundant tumor vessels with peripheral branching; B: 1.5 Harmonic Imaging Sonography image obtained by real-time continuous sonography in the late phase (5 min after injection) shows residual enhancement of some tumor vessels, but the boundary between the tumor and the hepatic parenchyma is clearly depicted.

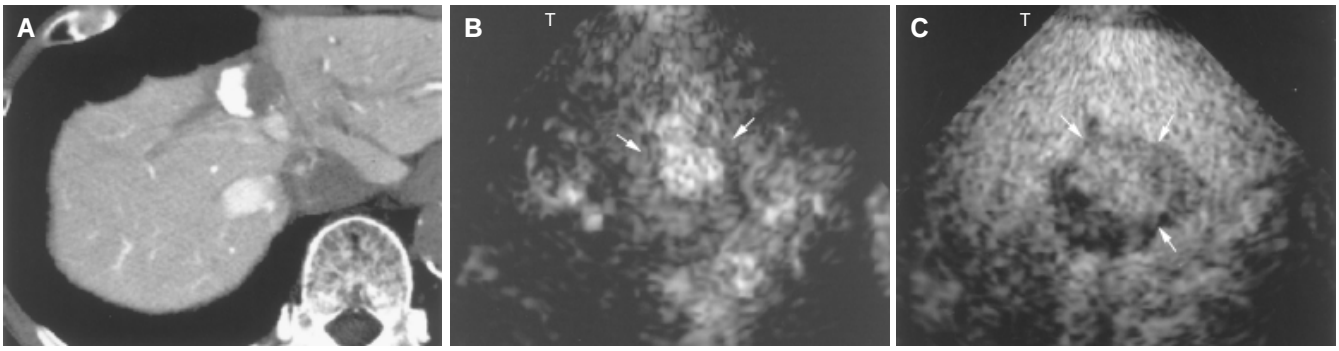


Figure 6 A 73-year-old man with C-type cirrhosis and HCC (16.5 mm in diameter) in the right liver who had undergone transcatheter arterial chemoembolization therapy with iodized oil and an anticancer drug. A: Transverse CT image with iodized oil obtained 7 d after treatment shows incomplete retention of iodized oil within the nodule; B and C: 1.5 Harmonic Imaging Sonography images obtained 35 s (B) and 5 min (C) after injection show partial enhancement. Right oblique 1.5 Harmonic Imaging Sonography image depicts residual tumor vessels within the tumor and subcapsular area (arrows), which is suggestive of possible future recurrence in this region.

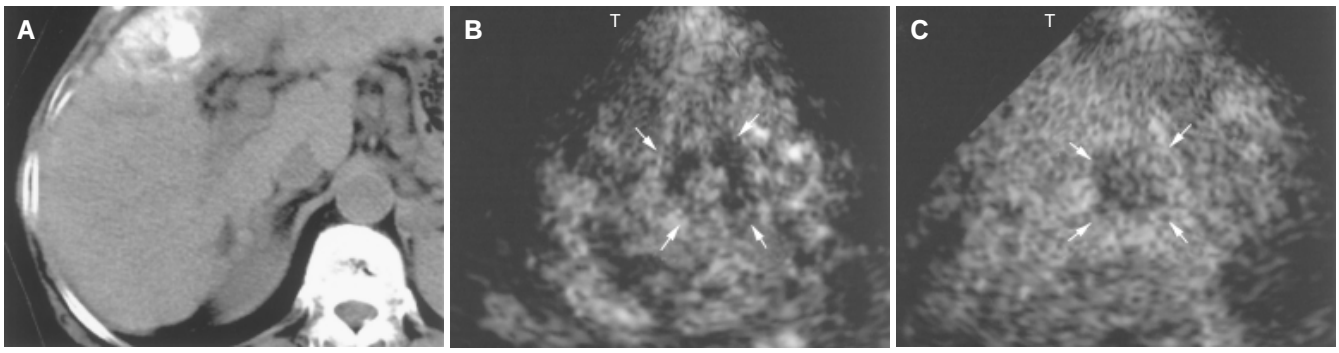


Figure 7 A 59-year-old woman with C-type cirrhosis and HCC (17.7 mm in diameter) in the right liver who had undergone transcatheter arterial chemoembolization therapy with iodized oil and an anticancer drug. A: Transverse CT scan with iodized oil obtained 7 d after treatment shows incomplete retention of iodized oil within the nodule; B and C: 1.5 Harmonic Imaging Sonography images obtained 34 s (B) and 5 min (C) after injection show partial enhancement. Right oblique 1.5 Harmonic Imaging Sonography image depicts residual tumor vessels within the tumor and subcapsular area (arrows), which is suggestive of possible recurrence in this region.

Table 1 Detection of HCC tumors with different imaging modalities (n = 42)

	1.5 Harmonic (early phase) enhancement	Imaging sonography (late phase) no enhancement	CTAP	US CO_2 angiography	DSA	CECT
Positive cases	36	42	42	42	34	39
(%)	(85.7)	(100)	(100)	(100)	(81.0)	(92.9)

Table 2 Evaluation of TAE response in HCCs by using 1.5 Harmonic Imaging Sonography compared with contrast-enhanced CT

Findings at contrast-enhanced CT	Vascular findings at 1.5 enhancement	Harmonic imaging sonography no enhancement
Incomplete (n = 14)	14	0
Complete (n = 28)	6	22

on the other hand, since there are almost no tissue echoes, the gain can be increased. As a result, enhancement is significantly improved in deep regions from which only weak echoes are received. In addition, images are generated using the B-mode processing system, resulting in good spatial resolution and minimal motion artifacts and blooming, which are often a problem in the pseudo-Doppler method. Furthermore, the combined use of flash echo mode and monitor mode ensures that slices can be maintained or adjusted in real time even though images are acquired at high acoustic power and the microbubbles are destroyed. Therefore, the enhanced slice can easily be adjusted during the continuous injection of contrast agent. When a frequency near the mean value is used, adequate contrast enhancement is obtained in all areas, from the near field to the far field, in 1.5 Harmonic Imaging Sonography. Furthermore, this method avoids the problems associated with the Doppler method and provides extremely clear contrast-enhanced images[19,20].

The results of the present clinical study have clearly demonstrated that the use of 1.5 Harmonic Imaging Sonography is effective for evaluating the vascularity of HCCs, including the assessment of tumor vessels during continuous early-phase arterial imaging as well as the assessment of late-phase enhancement (staining) due to blood flow signals in the tumor tissues. In early-phase real-time continuous imaging, the movement of microbubbles provides the signals used to obtain enhancement. In other words, the image can depict the flow of the microbubbles in the tumor vessels. The results of our study have also shown that 1.5 Harmonic Imaging Sonography can clearly depict the hypervascular tumor vessels of HCCs. The findings obtained by late-phase imaging show partial residual enhancement of the tumor tissues, but with less enhancement than the surrounding hepatic parenchyma. It is thought that the microbubbles flow from the tumor into the hepatic parenchyma over time, resulting in lower enhancement. Residual enhancement in the area of the tumor during the late phase is believed to reflect the enhancement (staining) due to the microbubbles that are trapped in the very small, tortuous blood vessels that are characteristically found in HCCs. In the present study, however, there were six nodules (14.3%) in which the tumor vessels were identified by US CO_2 angiography but not by 1.5 Harmonic Imaging Sonography. In principle, 1.5 Harmonic Imaging Sonography selectively eliminates the fundamental components in order to generate images, thus reducing the quality of B-mode images and the degree of visualization of the tumor area. In addition, the use of a sector transducer makes it difficult to assess deep regions. Generally, line density of sector scan is lower than that of convex in the deep region. Furthermore, lateral resolution of sector image is inferior to that of convex image. For these reasons, it was expected that the tumor vessels associated with small tumors in deep regions would not be detectable during the early phase. But, due to the reduction in motion artifacts, 1.5 Harmonic Imaging Sonography has significant advantages in the detection of nodules near the heart, which are difficult to detect by contrast-enhanced CT.

In the present study, the usefulness of 1.5 Harmonic Imaging Sonography and contrast-enhanced CT for evaluating treatment effects following transcatheter arterial chemoembolization of HCCs were compared, and the results showed that areas of insufficient treatment could be clearly identified by 1.5 Harmonic Imaging Sonography. Early-phase images clearly showed microbubbles flowing into the residual tumor vessels in insufficiently treated areas. Such areas were identified particularly well in late-phase images, and the information provided by such images was found to be useful for planning additional treatment. When percutaneous ethanol injection therapy and radiofrequency thermal ablation are performed under ultrasonographic guidance, 1.5 Harmonic Imaging Sonography permits viable areas within the tumor to be accurately identified during treatment and is therefore expected to improve treatment accuracy. Furthermore, 1.5 Harmonic Imaging Sonography has the advantage of being unaffected by lipiodol accumulation in the area of the tumor, which is associated with an increased risk of false-negative findings. In the present study, contrast-enhanced CT was found not to be useful for the evaluation of six nodules following transcatheter arterial chemoembolization with lipiodol.

With regard to the detection of early-stage tumor vessels, the results obtained by 1.5 Harmonic Imaging Sonography were comparable to those obtained by Sonography angiographic evaluation of blood flow signals within the tumor, except for six nodules measuring approximately 10 mm in diameter that were located 80 mm or more from the body surface. However, evaluation of all cases is difficult because of a sector probe, and an ultrasound image quality needs to be improved. The reasons for the difficulty in evaluating tumors in deep regions are thought to be (1) the use of 2.5- and 3.0-MHz sector transducers; (2) the attenuation of ultrasound signals in deep regions due to the elimination of the fundamental components, which is characteristic of 1.5 Harmonic Imaging Sonography; and (3) MI values insufficient to destroy the microbubbles.

These problems may be overcome in future when 1.5 Harmonic Imaging Sonography with the use of a convex transducer becomes available.

The next step will involve the use of a next-generation contrast agent with fluorocarbon-containing gas, which has already been employed clinically in Europe and USA. The main advantage of this contrast agent is that real-time contrast images can be obtained at low acoustic power without the need to destroy the microbubbles, and imaging techniques employing this contrast agent are therefore expected to be comparable or superior to US CO_2 angiography in terms of diagnostic capabilities.

In conclusion, 1.5 Harmonic Imaging Sonography is therefore considered to be an extremely useful diagnostic imaging modality for the assessment of patients with HCC.

1 **Choi BI,** Kim TK, Han JK, Kim AY, Seong CK, Park SJ. Vascularity of hepatoceller carcinoma :assessment with contrast-enhanced second-harmonic versus conventional power Doppler US. *Radiology* 2000; **214**: 381-386

2 **Hosten N,** Puls R, Lemke AJ, Steger W, Zendel W, Zwicker C, Felix R. Contrastenhanced power Doppler sonography: Improved detection of characteristic flow patterns in focal liver lesions. *J Clin Ultrasound* 1999; **27**: 107-115

3 **Ding H,** Kudo M, Onda H, Suetomi Y, Minami Y, Chung H, Kawasaki T, Maekawa K. Evaluation of Posttreatment Response of hepatocellular carcinoma with contrast-enhanced coded phase-inversion harmonic US: comparison with dynamic CT. *Radiology* 2001; **221**: 721-730

4 **Heckemann RA,** Cosgrove DO, Blomley MJ, Eckersley RJ, Harvey CJ, Mine Y. Liver lesions: intermittent second-harmonic gray-scale US can increase conspicuity with microbubble contrast material – early experience. *Radiology* 2000; **216**: 592-596

5 **Harvey CJ,** Blomley MJ, Eckersley RJ, Heckemann RA, Butler-Barnes J, Cosgrove DO. Pulse-inversion mode imaging of liver specific microbubbles:improved detection of subcentimetre metastases. *The Lancet* 2000; **355**: 807-808

6 **Blomley MJ,** Albrecht T, Cosgrove DO, Patel N, Jayaram V, Butler-Barnes J, Eckersley RJ, Bauer A, Schlief R. Improved imaging of liver metastases with stimulated acoustic emission in the late phase of enhancement with the US contrast agent SH U 508A: early experience. *Radiology* 1999; **210**: 409-416

7 **Burns PN,** Wilson SR, Muradali D, Microbubble destruction is the origin of Harmonic signals from FS 069. *Radiology* 1996; **201**: 158-159

8 **Calliada F,** Campani R, Bottinelli O, Bozzini A, Sommaruga MG. Ultrasound contrast agents basic principals. *Eur J Radiol* 1998; **27**: 157-160

9 **Wilson SR,** Burns PN, Muradali D, Wilson JA, Lai X. Harmonic hepatic US with microbubble contrast agents:initial experience showing improved characterization of hemangioma, hepatocellular carcinoma,and metastasis. *Radiology* 2000; **215**: 153-161

10 **Blomley MJ,** Albrecht T, Cosgrove DO, Eckersley RJ, Butler-Barnes J, Jayaram V, Patel N, Heckemann RA, Bauer A, Schlief R. Stimulated acoustic emission to image a late liver and spleen-specific phase of Levovist in normal volunteers and patients with and without liver disease. *Ultrasound Med Biol* 1999; **25**: 1341-1352

11 **Blomley MJ,** Sidhu PS, Cosgrove DO, Albrecht T, Harvey CJ, Heckemann RA, Butler-Barnes J, Eckersley RJ, Basilico R. Do different types of liver lesions differ in their uptake of the microbubble contrast agent SH U 508A in the late liver phase? early experience. *Radiology* 2001; **220**: 661-667

12 **Kim TK,** Choi BI, Han JK, Hong HS, Park SH, Moon SG. Hepatic tumors: contrast agent-enhancement patterns with pulse- inversion harmonic US. *Radiology* 2000; **216**: 411-417

13 **Harvey CJ,** Blomley MJ, Eckersley RJ, Cosgrove DO, Patel N, Heckemann RA, Butler-Barnes J. Hepatic malignancies: improved detectio with pulse-inversion US in late phase of enhancement with SH U 508A-Early Experience. *Radiology* 2000; **216**: 903-908

14 **Yamamoto K,** Shiraki K, Deguchi M, Sugimoto K, Sakai T, Ohmori S, Murata K, Hashimoto A, Shimizu A, Okuda Y, Nakano T. Diagnosis of hepatocellular carcinoma using digital subtraction imaging with the contrast agent, Levovist: Comparison with helical CT,Digital subtraction angiography, and US angiography. *Oncol Reports* 2002; **9**: 789-792

15 **Yamamoto K,** Shiraki K, Nakanishi S, Deguchi M, Sugimoto K, Sakai T, Ohmori S, Murata K, Fuke H, Hashimoto A, Shimizu A, Okuda Y, Nakano T. The usefulness of digital subtraction imaging with Levovist in the diagnosis of focal hepatic tumors. *Int J Oncol* 2003; **22**: 353-358

16 **Kim AY,** Choi BI, Kim TK, Han JK, Yun EJ, Lee KY, Han MC. Hepatocellular carcinoma:power Doppler US with a contrast agent-preliminary results. *Radiology* 1998; **209**: 135-140

17 **Kim TK,** Han JK, Kim AY, Choi BI. Limitations of characterization of hepatic hemangiomas using a sonographic contrast agent (Levovist) and power Doppler ultrasonography. *J Ultrasound Med* 1999; **18**: 737-743

18 **Choi D,** Lim HK, Kim SH, Lee WJ, Jang HJ, Lee JY, Paik SW, Koh KC, Lee JH. Hepatocellular carcinoma treated with percutaneous radio-frequency ablation: usefulness of power Doppler US with a microbubble contrast agent in evaluating therapeutic response-preliminary results. *Radiology* 2000; **217**: 558-563

19 **Tetsuya K.** Technical Description of 1.5-Harmonic Imaging, an Effective Technique for Contrast-Enhanced Ultrasound Diagnosis. *Medical Review* 2002; **87**: 22-25

20 **Tetsuya K,** Yoshitaka M, Naohisa. New Imaging Method for High MI Contrast Imaging:1.5 Harmonic Imaging. *J Ultrasound Med* 2002; **29**: 241

21 **Kudo M,** Tomita S, Tochio H, Kashida H, Hirasa M, Todo A. Hepatic focal nodular hyperplasia:specific findings at dynamic contrast-enhanced US with carbon dioxide microbubbles. *Radiology* 1991; **179**: 377-382

22 **Kudo M,** Tomita S, Tochio H, Mimura J, Okabe Y, Kashida H, Hirasa M, Ibuki Y, Todo A. Small hepatoceller carcinoma: diagnosis with US angiography with intraarterial CO_2 microbubbles. *Radiology* 1992; **182**: 155-160

Science Editor Guo SY **Language Editor** Elsevier HK

PO Box 2345, Beijing 100023, China
www.wjgnet.com
wjg@wjgnet.com

ELSEVIER

World J Gastroenterol 2005;11(36):5614-5620
World Journal of Gastroenterology ISSN 1007-9327
© 2005 The WJG Press and Elsevier Inc. All rights reserved.

Dendritic cells pulsed with hsp70-peptide complexes derived from human hepatocellular carcinoma induce specific anti-tumor immune responses

Xian-Hua Wang, Yan Qin, Mei-Hao Hu, Yong Xie

Xian-Hua Wang, Yan Qin, Mei-Hao Hu, College of Life Sciences, Peking University, Beijing 100871, China
Xian-Hua Wang, PhD candidate of Peking University
Xian-Hua Wang, Yan Qin, Yong Xie, Department of Biology, The Hong Kong University of Science and Technology, Hong Kong, China
Correspondence to: Professor Yong Xie, Department of Biology, The Hong Kong University of Science and Technology, Clear Water Bay, Kowloon, Hong Kong, China. boyxie@ust.hk
Telephone: +852-2358-7340 Fax: +852-2358-1559
Received: 2004-11-11 Accepted: 2004-12-23

Abstract

AIM: To investigate the anti-tumor effect of dendritic cells (DCs) pulsed with hsp70-peptide complexes derived from human hepatocellular carcinoma (HCC) cells on human T cells.

METHODS: Hsp70-peptide complexes were purified from human HCC cells with column chromatography using ADP-agarose and DEAE-Sepharose. DCs were derived from peripheral blood mononuclear cells of healthy donors in the presence of human GM-CSF and IL-4. The anti-tumor effect of DCs pulsed with hsp70-peptide complexes on human T-cell was assayed by CTL and enzyme-linked immunospot (ELISPOT) tests.

RESULTS: Hsp70-peptide complexes derived from human HCC cells activated phenotypic and functional maturation of DCs. The matured DCs stimulated a high level of autologous T-cell proliferation and type I cytokine secretion, and induced HCC-specific cytotoxic T lymphocytes (CTLs), which specifically killed HCC cells by a MHC class I restricted mechanism.

CONCLUSION: Hsp70-peptide complexes derived from human HCC cells can serve as a potent tumor antigen source for pulsing DCs, the pulsed DCs are very effective in activating specific T-cell responses against HCC cells.

© 2005 The WJG Press and Elsevier Inc. All rights reserved.

Key words: Hsp70-peptide complexes; Dendritic cells; Cytotoxic T lymphocytes; ELISPOT assay; Hepatocellular carcinoma

Wang XH, Qin Y, Hu MH, Xie Y. Dendritic cells pulsed with hsp70-peptide complexes derived from human hepatocellular carcinoma induce specific anti-tumor immune responses. *World J Gastroenterol* 2005; 11(36): 5614-5620
http://www.wjgnet.com/1007-9327/11/5614.asp

INTRODUCTION

Hepatocellular carcinoma (HCC) is one of the most common malignancies in the world, especially in sub-Saharan Africa and Southeast Asia, and it rarely responds to conventional treatment, such as surgery, radiation, or chemotherapy[1,2]. The ability of tumors to escape from immune surveillance contributes to their uncontrolled growth, recurrence, and metastasis[3]. Finding an efficient therapeutic method for HCC has become the focus of researchers around the world. An ideal cancer therapy should have the potency to eradicate systemic tumors in multiple sites in the body and the specificity to discriminate between neoplastic and non-neoplastic cells. In these respects, immunotherapy that stimulates tumor-specific immune responses has become an attractive approach.

Dendritic cells (DCs) are professional antigen presenting cells (APCs), which direct the cellular immune response through antigen presentation in the presence of appropriate costimulation. These cells reside in an immature state in non-lymphoid tissues, where they can efficiently capture invading pathogens. After antigen uptake, they rapidly migrate to the draining secondary lymphoid tissues and convert into mature DCs with decreased antigen processing ability, enhanced expression of MHC and costimulatory molecules, and increased capacity of priming naïve T cells and initiating an adaptive immune response[4]. The extraordinary functional profile of DCs suggests that they may represent an ideal vector in the immunotherapy of cancer and infectious diseases[4]. Studies have shown that DC-based vaccines can induce potent anti-tumor immunity. Various strategies have been developed to introduce tumor-specific antigens into DCs and thereby to generate cytotoxic T lymphocyte (CTL) responses against malignant cells.

Heat shock proteins (HSPs) are important molecular chaperones that play essential roles in the regulation of protein synthesis and folding, and vesicular trafficking[5-7]. They are ubiquitously expressed at a basal level but are specifically induced in response to various stress conditions such as heat, anoxia, and metabolic stress[3]. The observation that preparations of HSPs from various tumors can elicit specific anti-tumor immune responses suggests their immunotherapeutic activity[8]. The observed immunogenicity of HSP preparations is derived from the antigenic peptides

they chaperone[9]. Studies concerning the mechanisms of HSP preparations' immunogenicity have shown that HSPs transfer antigenic peptides to professional APCs, such as DCs, and channel them into the class I antigen presenting pathway through receptors[10-14]. HSPs can also elicit cytokine production by, and adhesion molecule expression of, a range of cell types, and they can deliver maturation signals to APCs through receptor-mediated interactions[5,11,15].

In the current study, we used DCs pulsed with hsp70-peptide complexes derived from human HCC cell line SMMC-7721 to activate autologous T cells. We found that the pulsed DCs stimulated a high level of T-cell proliferation and type I cytokine secretion, and induced HCC-specific CTLs which specifically killed HCC cells by a MHC class I restricted mechanism. Also the hsp70-peptide complexes induced the maturation of DCs by enhanced expression of HLA class II, CD86, and CD83. Our findings provide a new approach for pulsing DCs as tumor vaccines and a rationale for HSP-based vaccination against human HCC.

MATERIALS AND METHODS

Culture of cell lines

Human HCC cell line SMMC-7721, human NK cell sensitive cell line K562 and human cervix cell line Hela (American Type Culture Collection) were cultured in RPMI 1640 medium (GIBCO, Invitrogen Corporation, CA, USA) supplemented with 10% heat-inactivated fetal calf serum (FCS) (HyClone, UT, USA), 2 mol/L L-glutamine (GIBCO, Invitrogen Corporation), 100 U/mL penicillin G, 100 μg/mL streptomycin and 250 ng/mL amphotericin B (GIBCO^{TM}, Invitrogen Corporation). Cultures were incubated at 37 ℃ in humidified air with 50 mL/L CO_2.

Preparation of DCs and T cells

DCs were generated as described with some modifications[16]. Briefly, peripheral blood mononuclear cells (PBMCs) were isolated from healthy donors (Beijing Red Cross Blood Center, China) by Ficoll-Hypaque (1.077 g, Shang Hai Heng Xin Co., China) density gradient centrifugation and cultured in RPMI 1640 medium containing 10% FCS for 2 h. The non-adherent cells were removed for isolation of T cells and the adherent cells were cultured for 6 d in RPMI 1640 medium containing 10% FCS, 1 000 U/mL human GM-CSF (Biosea Biotechnology Co., Beijing, China) and 500 U/mL human IL-4 (Peprotech Inc., NJ, USA). Culture medium and cytokines were refreshed every other day. DCs were harvested from the non-adherent and loosely adherent cells.

T cells were purified by nylon wool column (Polysciences Inc., Warrington, USA) from non-adherent cells according to manufacturer's instructions. Briefly, non-adherent cells were resuspended in RPMI 1640 medium containing 10% FCS and added to the prepared nylon wool column. After incubating for 1 h at 37 ℃, the non-adherent cells, which contained mainly T cells, were collected by washing with RPMI 1640 medium containing 10% FCS.

Purification of hsp70-peptide complexes

The method for hsp70-peptide complex purification was as described with minor modifications[17]. In brief, SMMC-7721 tumor cells were harvested by culturing tumor cells in roller bottles and then 10 g tumor cells were suspended in 40 mL (4 volumes) of 30 mmol/L sodium bicarbonate (pH 7.0) and lysed by Dounce homogenization. The homogenate was centrifuged at 100 000 *g* for 90 min at 4 ℃ and the supernatant obtained. The sample was subjected to column chromatography using Sephadex G25 (Amersham Pharmacia Biotech, NJ, USA) for buffer exchange, affinity chromatography ADP-agarose (Sigma Chemical Co., St. Louis, Missouri, MO, USA), Sephadex G25 for buffer exchange, and ion-exchange chromatography with DEAE-Sepharose (Amersham Pharmacia Biotech, NJ, USA). The eluted proteins were identified by 12% reducing SDS-PAGE followed by silver staining and Western blot with an anti-hsp70 antibody (PharMingen, San Diego, CA, USA). Fractions containing more than 50% hsp70 were stored at -20 ℃ and used for additional experiments. Protein concentration was determined by Bio-Rad protein assay (Bio-Rad Laboratories, Inc., CA, USA). Endotoxin level in the preparations was determined by Limulus amebocyte lysate (LAL) assay (Ocean Biologicals Co., China).

T-cell proliferation assay

DCs were pulsed with hsp70-peptide complexes purified from SMMC-7721 cells at 37 ℃ for 4 h and then harvested followed by washing with PBS. Autologous T cells isolated by nylon wool column were cocultured with the pulsed DCs in a 96-well flat bottomed culture plate (NUNC, Roskilde, Denmark). Proliferation was determined after 5 d by uptake of tritiated thymidine (Amersham Pharmacia Biotech, Buckinghamshire, UK) measured at 18 h after a pulse of 1 μCi/well.

In vitro cytotoxicity test

DCs were pulsed with hsp70-peptide complexes purified from SMMC-7721 cells at 37 ℃ for 4 h. After washing with PBS, DCs were then cocultured with autologous T cells isolated by nylon wool column for 7-10 d in the presence of 20 U/mL human IL-2 (Kexing Co., China) in 24-well culture plate (NUNC, Roskilde, Denmark). The stimulated T cells were harvested with Ficoll-Hypaque density gradient centrifugation and used as effector cells in the CTL assay using LDH cytotoxicity detection kit (Roche, Indianapolis, USA). SMMC-7721, K562, Hela and autologous DCs pulsed with or without hsp70-peptide complexes were used as target cells in the assay. Briefly, target cells and effector cells were resuspended in assay medium (RPMI 1640 with 1% BSA), and then target cells (1×10^4 cells/well) were cocultured with effector cells at different ratios in a 96-well round bottomed culture plate (NUNC, Roskilde, Denmark) at 37 ℃. In the indicated experiment, target cells were preincubated with anti-MHC class I antibody (W6/32, PharMingen, San Diego, CA, USA) for 30 min at 37 ℃ before being cocultured with effector cells to test if the cytotoxicity was MHC class I restricted. After 5 h of incubation, the culture plate was centrifuged and the supernatant (100 μL/well) was transferred to another ELISA plate (NUNC, Roskilde, Denmark). LDH detection mixture (100 μL/well) was then added and incubated in the dark for 30 min at room temperature. After adding 50 μL stop

solution per well, the absorbance of the samples was measured by ELISA reader (Bio-Rad Laboratories, Inc., CA, USA) at 490 nm with 630 nm as reference wavelength. The spontaneous release of LDH by target cells or effector cells was assessed by incubation of target cells in the absence of effector cells and vice versa. The maximum release of LDH was determined by incubation of target cells in 1% Triton X-100 in assay medium. The percentage of specific cell-mediated cytotoxicity was determined by the following equation: cytotoxicity (%) = [(effector and target mixture-effector spontaneous-target spontaneous)/(maximum-target spontaneous)]×100.

Enzyme-linked immunospot (ELISPOT) assay

ELISPOT assay was performed to assess the IFN-γ production of T cells using IFN-γ ELISPOT kit (U-CyTech BV, Utrecht, Netherlands). DCs were pulsed with hsp70-peptide complexes purified from SMMC-7721 cells at 37 ℃ for 4 h. After washing with PBS, DCs were then cocultured with autologous T cells isolated with nylon wool column in the presence of 20 U/mL human IL-2 for 7-10 d. The stimulated T cells (1×10^4/well) as effector cells and irradiated SMMC-7721 cells (5×10^3/well) as target cells were transferred to ELISPOT plate and incubated for 18 h at 37 ℃. The IFN-γ secreting spots were developed as described in the IFN-γ ELISPOT kit manual and evaluated in a blind fashion by Dakewe Biotech Co., China, with an automated ELISPOT reader system (Biosys Co. Ltd, Germany).

Flow cytometry DCs were pulsed with hsp70-peptide complexes at 37 ℃ for 4 h and then cultured for another 48 h. The DCs unpulsed or pulsed with hsp70-peptide complex were washed with cold PBS and incubated with murine antibodies directed against human HLA-DR, CD86, CD83 (all from PharMingen, San Diego, USA), for 1 h in ice. After washing with cold PBS, the cells were incubated with FITC conjugated with goat anti-mouse IgG (Zymed Laboratories, Inc., South San Francisco, USA) for 30 min in ice. The cells were then washed with cold PBS and fixed with 2% paraformaldehyde (Sigma). The fluorescence intensity was analyzed by FACS Calibur and the CellQuest software (Becton Dickinson, NJ, USA).

RESULTS

Purification of hsp70-peptide complexes

As described in Materials and methods, the hsp70-peptide complexes were purified from HCC SMMC-7721 cells and identified by reduced SDS-PAGE stained with silver and Western blot using an hsp70-specific antibody. The result showed that the purified protein was approximately 72 ku (Figure 1A) and could hybridize with the hsp70-specific antibody (Figure 1B), demonstrating that the obtained protein was hsp70. The purity of the protein preparations was estimated to be >99% by silver-stained SDS-PAGE. The endotoxin level in the preparations was lower than 0.03 EU/μg of hsp70-peptide complexes, as determined by LAL assay.

Stimulation of autologous T cells by DCs pulsed with hsp70-peptide complexes derived from SMMC-7721 cells

To determine if DCs pulsed with hsp70-peptide complexes derived from SMMC-7721 cells are effective in stimulating autologous T cells, the pulsed DCs were cocultured with autologous T cells. As a control, the T cells were used alone or cocultured with unpulsed DCs. After a 5-d coculture, the T-cell proliferation was tested by uptake of tritiated thymidine. As shown in Figure 2A, DCs pulsed with hsp70-peptide complexes derived from SMMC-7721 cells stimulated autologous T cells to proliferate significantly stronger than did T cells cultured by themselves or cocultured with unpulsed DCs. By contrast, unpulsed DCs exhibited little capacity to stimulate autologous T cells. To further assess the selectivity of this stimulation response, we changed the ratio of DCs:T cells in coculture (Figure 2B). The result showed that the proliferation of T cells cocultured with DCs pulsed with hsp70-peptide complexes was enhanced rapidly by increasing the ratio of DCs:T cells. Contrarily, T-cells coculture with unpulsed DCs proliferated at almost the same level despite an increase in the ratio of DCs:T cells. These results demonstrate that DCs pulsed with hsp70-peptide complexes are capable of specifically stimulating T-cell responses.

Induction of specific CTLs and type I cytokine secretion against SMMC-7721 by DCs pulsed with hsp70-peptide complexes derived from SMMC-7721 cells

Cell-mediated immunity, which is particularly important in suppressing tumors, is characterized by induction of CTLs and production of type I cytokines. To explore whether DCs pulsed with hsp70-peptide complexes derived from SMMC-7721 cells are capable of generating SMMC-7721-specific CTLs and inducing type I cytokine secretion, we examined cytotoxic activities and IFN-γ production of autologous T cells cocultured with DCs. DCs pulsed with

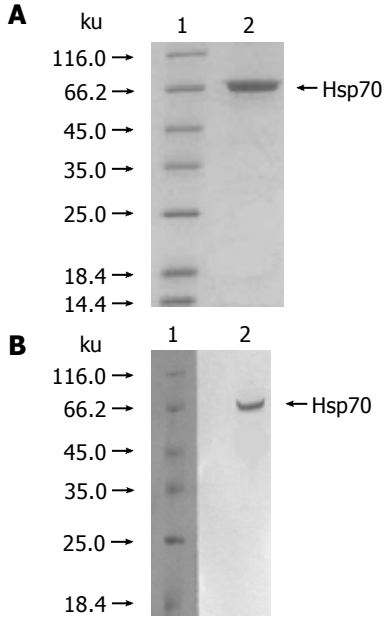


Figure 1 Purification of hsp70-peptide complexes from HCC cell line SMMC-7721. (**A**) 12% reducing SDS-PAGE analysis of purified hsp70-peptide complexes preparation with silver staining. (**B**) Western blotting analysis of purified hsp70-peptide complexes preparation. The preparation of hsp70-peptide complexes was immunoblotted with anti-hsp70 antibody. Lane 1 represents the protein molecular marker, and lane 2 represents hsp70-peptide complexes preparation.

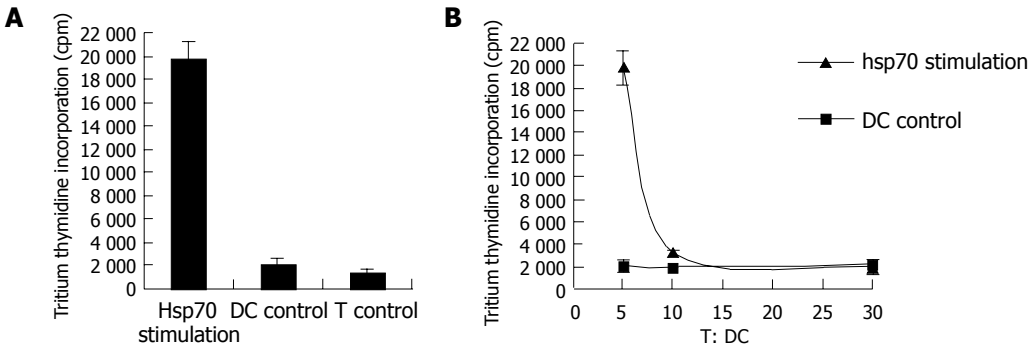


Figure 2 Stimulation of T cells by autologous DCs pulsed with hsp70-peptide complexes derived from SMMC-7721 cells. DCs were incubated with 20 μg/mL hsp70-peptide complexes derived from SMMC-7721 for 4 h at 37 ℃ and cocultured with autologous T cells at different ratios for 5 d, and then tritiated thymidine was added and its incorporation was measured 18 h later. (**A**) 1×10^5 T cells were cocultured with 2×10^4 autologous DCs, pulsed with hsp70-peptide complexes (indicated as hsp70 stimulation) or unpulsed (indicated as DC control), or by themselves (indicated as T control) per well; (**B**) 1×10^5 autologous T cells were cocultured with 2×10^4, 1×10^4, or 3.3×10^3 DCs pulsed with hsp70-peptide complexes (indicated as hsp70 stimulation) or unpulsed (indicated as DC control) per well separately. The results are expressed as mean±SD and each value represents the mean of three replicates.

hsp70-peptide complexes were cocultured with autologous T cells for 7-10 d in the presence of 20 U/mL human IL-2 and then the T cells were isolated by density gradient centrifugation for cytotoxicity testing and type I cytokine secretion assessing. As a control, the T cells were used alone or cocultured with unpulsed DCs.

The result of cytotoxicity testing showed that T cells cocultured with unpulsed DCs or by themselves failed to exhibit evident cytotoxicity against SMMC-7721 cells, but significantly, T cells cocultured with DCs pulsed with hsp70-peptide complexes were capable of killing SMMC-7721 cells at high levels (Figure 3A). To test if the lysis

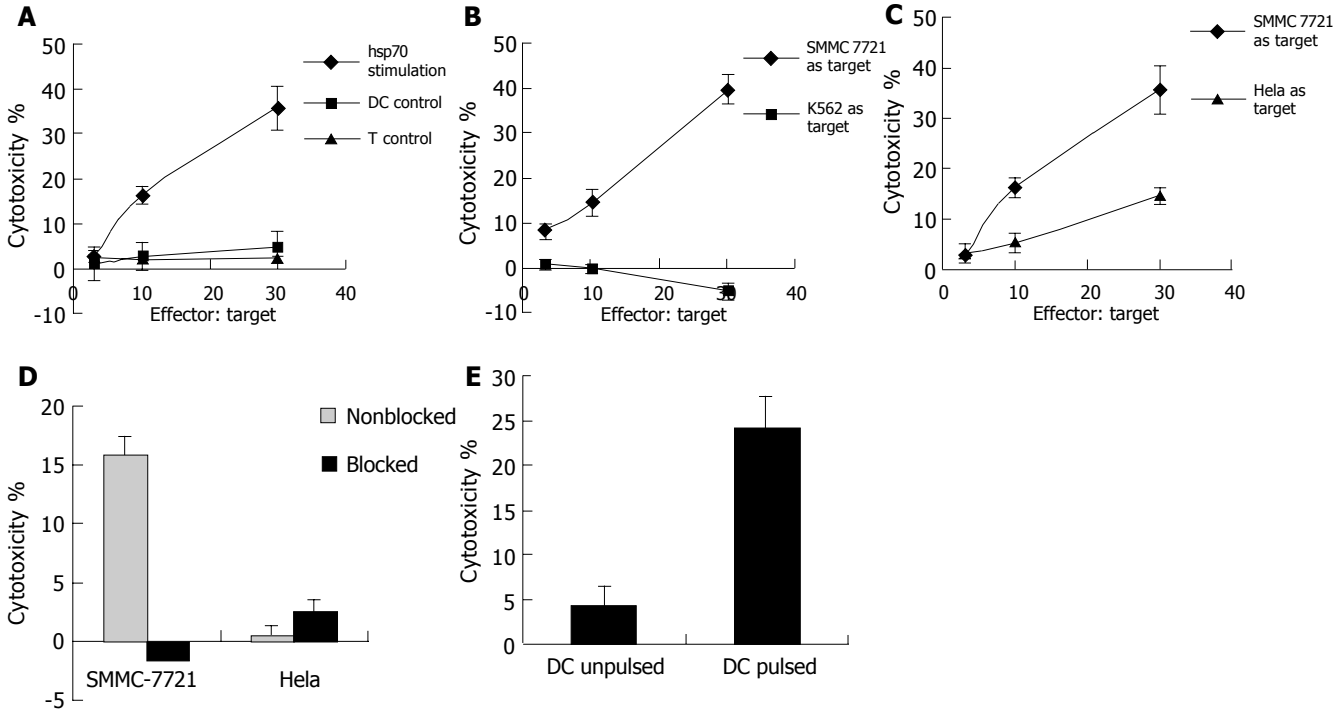


Figure 3 Generation of specific CTLs against SMMC-7721 by DCs pulsed with hsp70-peptide complexes derived from SMMC-7721 cells. 1×10^5 DCs were incubated with 20 μg/mL hsp70-peptide complexes derived from SMMC-7721 for 4 h at 37 ℃ and then cocultured with 1×10^6 autologous T cells in each well of 24-well culture plate for 7-10 d in the presence of 20 U/mL human IL-2. The stimulated T cells were harvested by density gradient centrifugation and the cytotoxicity was determined by testing LDH release. As a control, T cells cocultured with unpulsed DCs or by themselves were also used as effectors. (**A**) T cells were cocultured with autologous DCs pulsed with hsp70-peptide complexes (indicated as hsp70 stimulation) or unpulsed (indicated as DC control), or by themselves (indicated as T control), and SMMC-7721 cells were used as target cells; (**B**) T cells were cocultured with autologous DCs pulsed with hsp70-peptide complexes, and SMMC-7721 cells (indicated as SMMC-7721 as target) or NK-sensitive cell line K562 cells (indicated as K562 as target) were used as target cells; (**C**) T cells were cocultured with autologous DCs pulsed with hsp70-peptide complexes and SMMC-7721 cells (indicated as SMMC-7721 as target) or Hela cells (indicated as Hela as target) were used as target cells; (**D**) T cells cocultured with autologous DCs pulsed with hsp70-peptide complexes were used as effector cells and SMMC-7721 cells or Hela cells were used as target cells. The ratio of effector cells:target cells was 10:1. The target cells were preincubated with an anti-MHC class I antibody (W6/32; 1:50 dilution) or not, indicated as blocked and nonblocked separately. (**E**) T cells cocultured with autologous DCs pulsed with hsp70-peptide complexes were used as effector cells and autologous DCs pulsed with hsp70-peptide complexes or unpulsed were used as target cells (indicated as DC pulsed or DC unpulsed separately). The ratio of effector cells:target cells was 10:1. The results are expressed as mean±SD and each value represents the mean of three replicates.

against SMMC-7721 was due to the presence of NK cells, the NK cell-sensitive cell line K562 was used as target cell in the cytotoxicity assay (Figure 3B). The result showed that the cytotoxicity against K562 cells was very little, much lower than that against SMMC-7721 cells, indicating that it was not NK cells but rather CTLs that killed SMMC-7721 cells.

To further prove that CTLs killed the SMMC-7721 cells and to define the specificity of the CTLs generated by the coculture of T cells with autologous DCs pulsed with hsp70-peptide complexes, we compared the cytotoxicity of the T-cell against SMMC-7721 cells and another human cervix cell line Hela cells (Figure 3C), and assessed if the cytotoxicity was MHC class I restricted (Figure 3D). As shown in Figure 3C, T cells stimulated by DCs pulsed with hsp70-peptide complexes showed significant cytotoxicity against SMMC-7721 cells, whereas they exhibited little lysis against Hela cells. As shown in Figure 3D, preincubation of SMMC-7721 cells with anti-MHC class I antibody resulted in abrogation of tumor cell lysis; however, the anti-MHC class I antibody had little if any effect on lysis of Hela cells, demonstrating that the cytotoxicity against SMMC-7721 cells was MHC class I restricted and therefore due to $CD8^+$ T cells which directed against tumor-specific antigens. The quite weak lysis against Hela cells may result from non-specific killing activity. These results demonstrated that CTLs induced by autologous DCs pulsed with hsp70-peptide complexes were specific to SMMC-7721 cells from which hsp70-peptide complexes were derived.

To exclude the possibility that the SMMC-7721 specific cytotoxicity was due to allogeneic response, autologous DCs pulsed or unpulsed with hsp70-peptide complexes were used as target cells in CTL assay. As shown in Figure 3E, the CTLs induced by DCs pulsed with hsp70-peptide complexes exhibited significant cytotoxicity against DCs pulsed with hsp70-peptide complexes which expressed tumor antigens on their surface, whereas little cytotoxicity was exhibited against unpulsed DCs which did not express tumor antigens. The result confirmed that the cytotoxicity against SMMC-7721 was a tumor-specific response rather than an allogeneic response.

In addition to the cytotoxicity test, we also examined if DCs pulsed with hsp70-peptide complexes could induce autologous T cells to secret IFN-γ. As shown in Figure 4, T cells cocultured with DCs pulsed with hsp70-peptide complexes secreted a high level of IFN-γ against SMMC-7721; however, T cells cocultured with unpulsed DCs or by themselves secreted very little IFN-γ. Consistent with the CTL testing result, this finding suggested that DCs pulsed with hsp70-peptide complexes efficiently induce SMMC-7721 specific CTLs, which secrete type I cytokines at a high level.

These findings illuminate that DCs pulsed with hsp70-peptide complexes are very effective in inducing functional CTLs which direct to tumor cells from which hsp70-peptide complexes are isolated and secrete type I cytokine at high levels.

Maturation of human DCs pulsed with hsp70-peptide complexes derived from SMMC-7721 cells

To examine the effect of hsp70-peptide complexes derived from SMMC-7721 cells on DCs, immature DCs generated by culturing human PBMCs in the presence of human GM-CSF and IL-4 for 6 d, were incubated with hsp70-peptide complexes for 4 h at 37 ℃ and then cultured for 48 h. The expression level of HLA-DR, CD86, and CD83 was determined by flow cytometry. The result showed that hsp70-peptide complexes promoted upregulation of HLA-DR, co-stimulation molecule CD86 and maturation marker CD83 (Figure 5), indicating that hsp70-peptide complexes induced maturation of DCs. This maturation effect of hsp70-peptide complexes on DCs suggests that they can activate DCs effectively.

DISCUSSION

Cancer, which is difficult to cure completely using conventional treatment such as surgery, radiation or chemotherapy, has become one of the most common causes

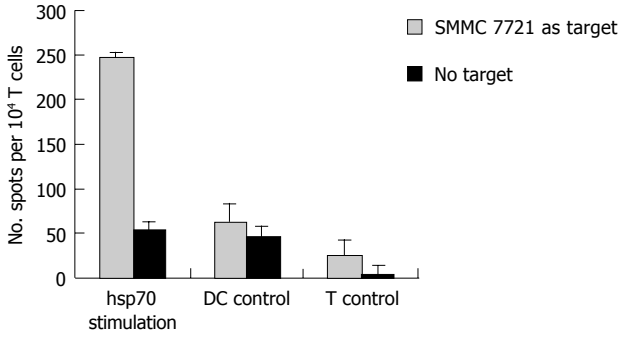


Figure 4 Secretion of IFN-γ by T cells induced with autologous DCs pulsed with hsp70-peptide complexes derived from SMMC-7721 cells. 1×10^5 DCs were incubated with 20 μg/mL hsp70-peptide complexes derived from SMMC-7721 for 4 h at 37 ℃ and then cocultured with 1×10^6 autologous T cells in each well of 24-well culture plate for 7–10 d in the presence of 20 U/mL human IL-2. The stimulated T cells were harvested by density gradient centrifugation and their IFN-γ production was determined by ELISPOT assay (indicated as hsp70 stimulation). As a control, T cells cocultured with unpulsed DCs (indicated as DC control) or by themselves (indicated as T control) were also used as effectors. The results are expressed as mean±SD and each value represents the mean of three replicates.

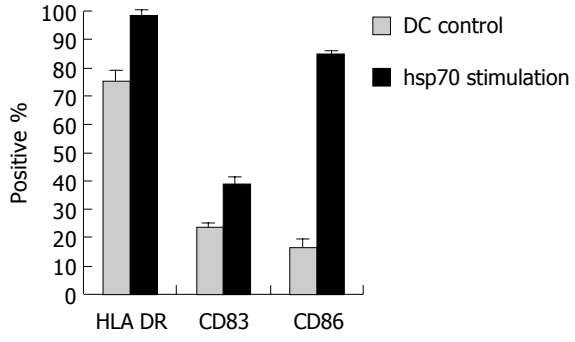


Figure 5 Maturation of human DCs by hsp70-peptide complexes derived from SMMC-7721 cells. DCs were incubated with 20 μg/mL hsp70-peptide complexes derived from SMMC-7721 cells for 4 h at 37 ℃, and cultured for 48 h. The DCs were then harvested and analyzed for expression of the indicated surface molecules using FACS analysis. The percentages shown were positive for the indicated surface markers. The results are expressed as mean±SD and each value represents the mean of three replicates.

of death in industrialized societies[3]. Immunotherapy, which utilizes the immune response in combating cancer, seems to be a potentially effective approach for treatment of cancer. Numerous vaccination approaches have been explored and developing more effective anti-tumor vaccines has become one of the major goals in tumor immunotherapy.

It is commonly accepted that tumor rejection is mediated by lymphocytes, and most notably by CTLs. Therefore, activating tumor-specific CTLs to kill tumor cells is considered to be one of the most important events in tumor immunotherapy[18]. T-cell activation requires two signals. Signal one is generated when TCR interacts with the MHC-peptide complex and signal two is provided by costimulatory molecules expressed by professional APCs. Most tumors do not express costimulatory molecules and thus fail to activate tumor-specific T lymphocytes[19]. The HCC cell line SMMC-7721 expresses MHC class I molecules, but does not express costimulatory molecules, such as CD80 or CD86 (data not shown). So to generate tumor-specific CTLs, it is essential to find a good tumor antigen source and then present them in the context of costimulatory molecules.

The features of HSPs suggest that they are very potent tumor antigen sources for pulsing DCs to stimulate anti-tumor response. Three features characterize HSPs as a tumor antigen source: first, they can induce multiple anti-tumor immune responses without prior identification of tumor antigens; second, they can chaperone tumor antigens associated with them and present them with high efficiency through specific receptors on DCs; third, they can induce phenotypical and functional maturation of DCs. In the present study, we used hsp70-peptide complexes derived from HCC cell line SMMC-7721 as the tumor antigen source to pulse DCs, which are known to be critical activators of T-cell responses. Various studies suggest that hsp70 has immunotherapeutic potential as hsp70 purified from malignant and virally infected cells can transfer and deliver antigenic peptides to APCs to elicit peptide-specific immunity[20]. We demonstrated that DCs pulsed with hsp70-peptide complexes derived from human HCC cell line SMMC-7721 stimulated significant autologous T-cell proliferation and that unpulsed DCs had little stimulatory effect (Figure 2). More importantly, we proved that DCs pulsed with hsp70-peptide complexes were able to induce tumor cell-specific CTLs with high efficiency and specificity (Figure 3) and the generated CTLs could secrete a high level of type I cytokine (Figure 4). Our results demonstrated that the cytotoxicity against SMMC-7721 cells was due to the presence of CTLs but not NK cells because NK cell-sensitive cell line K562 could not be killed (Figure 3B). In addition, we tested the phenotype of the cytotoxic cells using T-cell lineage marker CD3, NK cell lineage marker CD56 and NK-T-cell lineage marker CD56+CD3 by flow cytometry (data not shown). The result showed that most of the cytotoxic cells were T cells and there were very few NK cells or NK-T cells. Also we demonstrated that the generated CTLs exhibited specific cytotoxicity against SMMC-7721 cells (Figure 3C) and the cytotoxicity was MHC class I restricted (Figure 3D). Furthermore we excluded the possibility that the induced anti-tumor response was an allogeneic response (Figure 3E). The result indicated that the generated CTLs exhibited significant cytotoxicity against autologous DCs pulsed with hsp70-peptide complexes, but little lysis against unpulsed DCs, demonstrating that the CTLs were directed against tumor-specific antigens expressed on DCs rather than allo-antigens. This result also implied that DCs took up hsp70-peptide complexes, and then processed and presented tumor-specific antigens in the MHC class I pathway, making them available for CTL recognition. Our findings indicated that the SMMC-7721 specific antigens chaperoned by hsp70 had been functionally presented to T cells through the active interaction of hsp70 and DCs. The implication of the original studies was that immunization of HSPs was able to generate anti-tumor CTLs via cross-priming by transferring the antigenic peptides with which they were associated into the MHC class I antigen presenting pathway within APCs, a pathway usually restricted to antigens derived from the cytoplasm of the APCs[21]. The mechanism of receptor-mediated endocytosis contributes to the high efficiency of antigen transfer[10,22]. More recently, different receptors involved in the capacity of hsp70 to induce peptide-specific immunity have been identified[11,23]. Consistent with these observations, our results indicated that hsp70 was a potent adjuvant for presenting tumor-associated antigens and then inducing specific anti-tumor immune responses.

Activation of DCs is a key step in the stimulation of tumor-specific CTLs. As professional APCs, with a potent capacity to present antigens and activate naive T cells, DCs can both initiate and modulate immune responses[24]. In the present study, we showed that hsp70-peptide complexes derived from HCC cell line SMMC-7721 induced maturation of allogeneic DCs by enhancing the expression of HLA class II, costimulatory molecule CD86, and maturation maker CD83. The matured DCs were able to stimulate high levels of autologous T-cell proliferation and type I cytokine secretion, and to induce tumor-specific CTLs with high efficiency. The results indicate that hsp70-peptide complexes derived from HCC cell line SMMC-7721 have the capacity to induce human DCs maturation phenotypically and functionally. The phenotypical and functional maturation is critical for DCs to efficiently activate immune responses[25].

Consistent with previous reports[26], MHC matching between the SMMC-7721 cells used as source of hsp70-peptide complexes and the responding T cells was not required, suggesting that the peptides complexed by hsp70 were not restricted to the MHC haplotype of the donor cells and hsp70-peptide complexes were able to induce tumor-specific CTLs across MHC barriers by active interaction with DCs.

In conclusion, our present study demonstrated varied attributes of hsp70 which included chaperoning a broad array of antigenic peptides, delivering them into MHC class I antigen presentation pathway within DCs via cross-priming through receptor-mediated interaction, and activating DCs phenotypically and functionally. These properties of hsp70 suggest that hsp70-peptide complexes are appealing antigen sources for immunization against tumors and infectious diseases. In this study, we combined the characteristics of DCs and hsp70 for stimulating anti-tumor

immune responses and offered a new kind of anti-tumor immunotherapeutic strategy against human HCC. Our results suggest that DCs pulsed with hsp70-peptide complexes derived from human HCC cells can be used as potential vaccines in anti-tumor immunotherapy, as these pulsed DCs are capable of inducing multiple CTLs efficiently without the need for identifying tumor-specific antigens. In the present study, we used allogeneic rather than autologous HCC cells to isolate hsp70-peptide complexes for pulsing DCs derived from healthy donors. We hope to apply this approach to HCC patients in future clinical research.

ACKNOWLEDGMENTS

We thank the Beijing Red Cross Blood Center for supplying the blood samples. We also thank the FACS laboratory of the Medical School of Peking University for performing the FACS analysis.

REFERENCES

1 **Liu BB,** Ye SL, He P, Liu YK, Tang ZY. MAGE-1 and related MAGE gene expre ssion may be associated with hepatocellular carcinoma. *J Cancer Res Clin Oncol* 1999; **125**: 685-689
2 **Takayama T,** Sekine T, Makuuchi M, Yamasaki S, Kosuge T, Yamamoto J, Shimada K, Sakamoto M, Hirohashi S, Ohashi Y, Kakizoe T. Adoptive immunotherapy to lower postsurgical recurrence rates of hepatocellular carcinoma: a randomized trial. *Lancet* 2000; **356**: 802-807
3 **Pandey M,** Mathew A, Nair MK. Cancer vaccines: a step towards prevention and treatment of cancer. *Eur J Surg Oncol* 1999; **25**: 209-214
4 **Banchereau J,** Steinman RM. Dendritic cells and the control of immunity. *Nature* 1998; **392**: 245-252
5 **Pockley AG.** Heat shock proteins as regulators of the immune response. *Lancet* 2003; **362**: 469-476
6 **Fujihara SM.** Nadler SG. Intranuclear targeted delivery of functional NF-κB by 70 kDa heat shock protein. *EMBO J* 1999; **18**: 411-419
7 **Wallin RP,** Lundqvist A, More SH, von Bonin A, Kiessling R, Ljunggren HG. Heat-shock proteins as activators of the innate immune system. *Trends Immunol* 2002; **23**: 130-135
8 **Janetzki S,** Palla D, Rosenhauer V, Lochs H, Lewis JJ, Srivastava PK. Immunization of cancer patients with autologous cancer-derived heat shock protein gp96 preparations: a pilot study. *Int J Cancer* 2000; **88**: 232-238
9 **Tamura Y,** Peng P, Liu K, Daou M, Srivastava PK. Immunotherapy of tumors with autologous tumor-derived heat shock protein preparations. *Science* 1997; **278**: 117-120
10 **Arnold-Schild D,** Hanau D, Spehner D, Schmid D, Rammensee HG, de la Salle H, Schild H. Cutting edge: receptor-mediated endocytosis of heat shock proteins by professional antigen-presenting cells. *J Immunol* 1999; **162**: 3757-3760
11 **Basu S,** Binder RJ, Ramalingam T, Srivastava PK. CD91 is a common receptor for heat shock proteins gp96, hsp90, hsp70, and calreticulin. *Immunity* 2001; **14**: 303-313
12 **Singh-Jasuja H,** Scherer HU, Hilf N, Arnold-Schild D, Rammensee HG, Toes RE, Schild H. The heat shock protein gp96 induces maturation of dendritic cells and down-regulation of its receptor. *Eur J Immunol* 2000; **30**: 2211-2215
13 **Singh-Jasuja H,** Toes RE, Spee P, Munz C, Hilf N, Schoenberger SP, Ricciardi-Castagnoli P, Neefjes J, Rammensee HG, Arnold-Schild D, Schild H. Cross-presentation of glycoprotein 96-associated antigens on major histocompatibility complex class I molecules requires receptor-mediated endocytosis. *J Exp Med* 2000; **191**: 1965-1974
14 **Suto R,** Srivastava PK. A mechanism for the specific immunogenicity of heat shock protein-chaperoned peptides. *Science* 1995; **269**: 1585-1588
15 **Cho KB,** Palliser D, Guillen E, Wisniewski J, Young RA, Chen JZ, Eisen HN. A proposed mechanism for the induction of cytotoxic T lymphocyte production by heat shock fusion proteins. *Immunity* 2000; **12**: 263-272
16 **Thurner B,** Roder C, Dieckmann D, Heuer M, Kruse M, Glaser A, Keikavoussi P, Kampgen E, Bender A, Schuler G. Generation of large numbers of fully mature and stable dendritic cells from leukapheresis products for clinical application. *J Immunol Methods* 1999; **223**: 1-15
17 **Srivastava PK,** Jaikaria NS. Methods of purification of heat shock protein-peptide complexes for use as vaccines against cancers and infectious diseases. *Methods Mol Biol* 2001; **156**: 175-186
18 **Hanson HL,** Donermeyer DL, Ikeda H, White JM, Shankaran V, Old LJ, Shiku H, Schreiber RD, Allen PM. Eradication of established tumors by $CD8^+$ T cell adoptive immunotherapy. *Immunity* 2000; **13**: 265-276
19 **Cavallo F,** Martin-Fontecha A, Bellone M, Heltai S, Gatti E, Tornaghi P, Freschi M, Forni G, Dellabona P, Casorati G. Co-expression of B7-1 and ICAM-1 on tumors is required for rejection and the establishment of a memory response. *Eur J Immunol* 1995; **25**: 1154-1162
20 **Ciupitu AM,** Petersson M, Kono K, Charo J, Kiessling R. Immunization with heat shock protein 70 from methylcholanthrene-induced sarcomas induces tumor protection correlating with *in vitro* T cell responses. *Cancer Immunol Immunother* 2002; **51**: 163-170
21 **Srivastava PK,** Menoret A, Basu S, Binder RJ, McQuade KL. Heat shock proteins come of age: primitive functions acquire new roles in an adaptive world. *Immunity* 1998; **8**: 657-665
22 **Binder RJ,** Harris ML, Menoret A, Srivastava PK. Saturation, competition, and specificity in interaction of heat shock proteins (hsp) gp96, hsp90, and hsp70 with $CD11b^+$ cells. *J Immunol* 2000; **165**: 2582-2587
23 **Becker T,** Hartl FU, Wieland F. CD40, an extracellular receptor for binding and uptake of Hsp70–peptide complexes. *J Cell Biol* 2002; **158**: 1277-1285
24 **Liu YJ.** Dendritic cell subsets and lineages, and their functions in innate and adaptive immunity. *Cell* 2001; **106**: 259-262
25 **Wan T,** Zhou XY, Chen GY, An HZ, Chen TY, Zhang WP, Liu SX, Jiang YM, Yang F, Wu YF, Cao XT. Novel heat shock protein Hsp70L1 activates dendritic cells and acts as a Th1 polarizing adjuvant. *Blood* 2004; **103**: 1747-1754
26 **Castelli C,** Ciupitu AM, Rini F, Rivoltini L, Mazzocchi A, Kiessling R, Parmiani G. Human heat shock protein 70 peptide complexes specially activate antimelanoma T cells. *Cancer Res* 2001; **61**: 222-227

Science Editor Guo SY **Language Editor** Elsevier HK

PO Box 2345, Beijing 100023, China
www.wjgnet.com
wjg@wjgnet.com

ELSEVIER

World J Gastroenterol 2005;11(36):5621-5626
World Journal of Gastroenterology ISSN 1007-9327
© 2005 The WJG Press and Elsevier Inc. All rights reserved.

Synergistic effect of bromocriptine and tumor necrosis factor-α on reversing hepatocellular carcinoma multidrug resistance in nude mouse MDR1 model of liver neoplasm

Lei Ding, Xiao-Ping Chen, Zhi-Wei Zhang, Jian Guan, Wan-Guang Zhang, Hai-Ping Wang, Zhi-Hui Wang, Chun-Lei Li

Lei Ding, Xiao-Ping Chen, Zhi-Wei Zhang, Jian Guan, Wan-Guang Zhang, Hai-Ping Wang, Hepatic Surgery Center, Affiliated Tongji Hospital, Tongji Medical College, Huazhong University of Science and Technology, Wuhan 430030, Hubei Province, China
Zhi-Hui Wang, Chun-Lei Li, Department of Ultrasonography, Affiliated Tongji Hospital, Tongji Medical College, Huazhong University of Science and Technology, Wuhan 430030, Hubei Province, China
Supported by the Clinical Key Program Point Subject Foundation of Ministry of Public Health, No. 2001-2003
Correspondence to: Professor Xiao-Ping Chen, Department of General Surgery, Tongji Hospital, Tongji Medical College, Huazhong University of Science and Technology, Wuhan 430030, Hubei Province, China. chenxp@medmail.com
Telephone: +86-27-83662599 Fax: +86-27-83662851
Received: 2004-11-16 Accepted: 2005-01-26

Abstract

AIM: To investigate the effect of bromocriptine (BCT) and tumor necrosis factor-α (TNF-α) on hepatocellular carcinoma (HCC) multidrug resistance (MDR) in nude mouse MDR model of liver neoplasm.

METHODS: Human hepatocarcinoma cell line $HepG_2$, drug resistant hepatocarcinoma cell line $HepG_2$/adriamycin (ADM) and hepatocarcinoma cell line transfected with TNF-α gene $HepG_2$/ADM/TNF were injected into the liver of nude mice via orthotopic implantation and MDR model of liver neoplasm *in vivo* was established ($HepG_2$, ADM, TNF, BCT groups). Among these groups, BCT group and TNF group were treated with BCT through gastric canal. Each group was divided into control group and chemotherapy group. Size and weight of the tumor were measured. Furthermore, tumor histological character and growth of the nude mice were observed and their chemosensitivity was tested. MDR-associated genes and proteins (MRP, LRP) of implanted tumors were detected by immunohistochemistry, reverse transcriptase polymerase chain reaction, and apoptosis rate of hepatocarcinoma cells was detected by TUNEL assay.

RESULTS: The nude mouse model of each cell line was inoculated successfully. The tumor growth rate and weight were significantly different among groups. After chemotherapy, abdominal cavity tumor growth inhibition rate was higher in BCT group (67%) compared to ADM and TNF groups, and similar to $HepG_2$ group (54%). MDR1 and LRPmRNA could be detected in all groups, but TNF-α was detected only in TNF and BCT groups. Furthermore, MDR1 and LRP protein expression of tumors in TNF and BCT groups was low similar to $HepG_2$ group. The apoptosis rate of hepatocarcinoma cells was much higher in BCT group than in other groups with TUNEL assay.

CONCLUSION: BCT and TNF-α can reverse HCC MDR in nude mouse MDR1 model of liver neoplasm.

© 2005 The WJG Press and Elsevier Inc. All rights reserved.

Key words: Bromocriptine; Tumor necrosis factor-α; Hepatocellular carcinoma

Ding L, Chen XP, Zhang ZW, Guan J, Zhang WG, Wang HP, Wang ZH, Li CL. Synergistic effect of bromocriptine and tumor necrosis factor-α on reversing hepatocellular carcinoma multidrug resistance in nude mouse MDR1 model of liver neoplasm. *World J Gastroenterol* 2005; 11(36): 5621-5626
http://www.wjgnet.com/1007-9327/11/5621.asp

INTRODUCTION

The development of multidrug resistance (MDR) in human tumors may be a major obstacle to successful cancer chemotherapy[1]. MDR is often associated with increased expression of the MDR1 (also known as P-glycoprotein) gene, encoding P-glycoprotein (Pgp)[2]. Since the MDR1 gene appears to represent a major cause of MDR in tumor cells, MDR1 messenger RNA (mRNA) and Pgp may be important targets in MDR reversal strategies. But almost all MDR reverse studies are only performed *in vitro*[3-5], and few are performed *in vivo*. A study[6] indicates that overexpression of Pgp, a product of MDR1, is intimately associated with liver cancer development and therefore inhibitors of Pgp should inhibit the development of liver cancer. Accordingly, we determined the effect of bromocriptine (BCT), a potent inhibitor of Pgp[7,8], and tumor necrosis factor-a (TNF-α)[9-11] which could downregulate expression of the MDR-associated genes LRP and MRP in multidrug resistant model of nude mice via orthotopic implantation of multidrug resistant human hepatocellular carcinoma (HCC) cells $HepG_2$/adriamycin (ADM).

TNF is a cytokine playing an important role in immunoregulation and antitumor mechanisms, and has been extensively tested in *in vitro* and *in vivo* investigations as well as in clinical trials for immunotherapy of malignant diseases[12,13]. More recently, it has been demonstrated that TNF can modulate

MDR1 expression and enhance cytotoxicity of certain MDR-related drugs to various cell lines[10,14]. The ability of cytokines to influence MDR phenotype is strongly supported by a previous study[15].

BCT, as a D_2 dopaminergic receptor agonist, has been reported to inhibit activity of ATPase and function of Pgp[7]. Moreover, because of its slight side-effects and the MDR-reversing effect[8], we chose BCT and TNF-α to detect their synergistic antitumor effects.

MATERIALS AND METHODS

Reagents

1640 medium, fetal bovine serum (FBS), lipofectamine 2000, and G418 were purchased from Invitrogen Inc., USA. Upstream and downstream primers were produced by Shanghai Boya Biosynthesis Co., Shanghai, China. dNTPs, RNasin, AMV reverse transcriptase, Taq and DNA enzymes were purchased from Sigma Company, USA. TRIzol reagent was purchased from Gibco Company, USA. BCT mesilate was purchased from Novartis, Italy; 5-fluorouracil (5-FU), ADM, mitomycin (MMC) were from Pharmacia & Upjohn, Italy; and S-P immune test kit was from Beijing Zhongshan Company, Beijing, China. LRP mouse antibody, P170 mouse antibody and Pan actin antibody-5 were purchased from Neomarker Inc., Germany.

Cell lines and cell culture

Human HCC cell line, $HepG_2$ (GDC024), was purchased from the China Center for Type Culture Collection (Wuhan University, Hubei). $HepG_2$ was induced to form a multidrug resistant cell line ($HepG_2$/ADM) by exposure to gradually increased concentration of ADM. Firstly, eukaryotic expression vector pBK-TNF-α was constructed by recombinant DNA technique, and transfected into multidrug resistant cell line ($HepG_2$/ADM) to obtain cell line $HepG_2$/ADM/TNF and cultured in the presence of 800 mg/mL G418. All cells were maintained in 1640 medium containing 10% heat-inactivated FBS at 37 ℃ in a humid atmosphere of 50 mL/L CO_2.

Multidrug resistant model establishment and grouping

BALB/c, nu/nu, nude mice, male and female from Centers for Disease Control and Prevention of Hubei province, age ranging 4-5 wk, weighing 12.1-15.0 g, bred in specific pathogen-free condition, were used in this study. Firstly, a left subcostal incision was made under anesthesia with 20% urethane, then left lobe of the liver was exposed, and each kind of cells was injected into mice liver and an orthotopic MDR1 hepatoma was obtained successfully ($HepG_2$, ADM, TNF, BCT groups respectively). Each group contained 16 nude mice inoculated with each kind of cell lines, and was divided into control group and experiment group, 8 in each group. Chemotherapy was performed when tumor diameter was 1.5 cm. Among these groups, BCT group and TNF group were treated with BCT (6.25 mg/kg·d) through gastric canal. Association of 5-FU (0.15 g/kg·d)+MMC (1.5 mg/kg·d) +ADM (10 mg/kg·d) were administered through intraperitoneal injection in experiment groups, but 0.9% NS 15 μL/g was given to control groups for 3 d. Nude mice were weighed and the size of tumors was measured every week by B-ultrasound after orthotopic implantation, when the mice were killed 14 d after chemotherapy. Furthermore, some specimens were fixed in 40 g/L formaldehyde and embedded with paraffin for immunohistochemistry (IHC), and other markers were detected by molecular biological techniques.

Evaluation of growth and sensitivity of chemotherapy

The living condition, diet and reaction with stimuli from environment were observed everyday from the first day of chemotherapy. The size of tumors was measured every week by B-ultrasound after chemotherapy using the formula $V = a \times b^2/2$ (V: volume; a: long diameter; b: short diameter). Meanwhile xenograft tumors were observed and weighed until the mice were killed. Lastly, the inhibition rate of volume and weight was calculated by the formula (inhibition rate of volume or weight = [1-volume or weight of chemotherapy group/volume or weight of control group]×100%).

HE staining and immunohistochemistry (IHC) for detection of MDR1 expression

Firstly, each kind of orthotopic tumor tissues was stained with HE, and fixed in formalin and embedded in paraffin. The expression of Pgp protein was studied using mouse anti-human MDR1 C219 and sections of 5 μm from the tumor tissues were implanted in each kind of cell lines and MDR1 expression was assayed by immunoperoxidase staining with the SP method (SP kit, Zhongshan Biocompany). IHC process was strictly done as the indication of SP kit. In summary, endogenous peroxidase was blocked with H_2O_2 and non-specific antigens were blocked with normal serum. The primary antibodies were diluted to 1∶100 for Pgp, then incubated at 4 ℃ overnight, washed thrice with PBS. The secondary antibody (1∶500) was incubated for 15 min at 37 ℃, sections were stained with diaminobenzidine tetrahydrochloride (DAB) and restained with hematoxylin for visualization of nuclei. For negative controls, primary antibodies were substituted by PBS instead of Pgp antibodies. The Pgp protein expression intensity was observed through ocular lens and the positive cells per square millimeter were calculated and expressed as mean±SD.

Expressions of TNFmRNA, MDR1 mRNA and LRP mRNA

Total RNA was respectively extracted from tumors in nude mice with TRIzol according to the manufacturer's instructions. Reverse transcription (RT) was performed with random primers by a complementary DNA (cDNA) synthesis kit (Promega). RT-reaction reagents (25 μL) were added as follows: 0.1 μg OligdT (100 g/L), 25 U rRNasin, 1.25 μL dNTP (10 mmol/L), 5 μL M-MLV 5×buffer, 200 U M-MLVRT. After all the components were mixed, the mixture was incubated at 42 ℃ for 1 h in a DNA thermal cycler (PTC-100, MJ Research Inc., Watertown, MA, USA), and the reverse transcriptase was inactivated by heating the reaction mixture to 95 ℃ for 5 min. Then each tube was kept at -20 ℃ until PCR was performed. The primers of the target genes MDR1, LRP, and the endogenous reference β-actin were designed using the Primer Express Software (Applied Biosystems) (Table 1). The final volume of the reaction (25 μL) of PCR included: 25 μL transcription solution containing 15 pmol upstream and downstream respectively, 2.5 μL 10×buffer, 2 μL cDNA, 0.5 μL dNTP (10 mmol/L),

Table 1 MDR1, LRP primers

Gene	Quantification method	Sequence (5′-3′)	Size (bp)
MDR1	Forward primer	CATTGGTGTGGTGAGTCAGG	176
	Reverse primer	CTCTCTCTCCAACCAGGGTG	
LRP	Forward primer	TAAGGGCTTCCAGCACCAAC	237
	Reverse primer	GGAGTTCTCGCTTCTCGTCC	
TNF-α	Forward primer	GC*GGATT*CATGAGCACTGAAAGCATGATCC	725
	Reverse primer	CCC*AAGCTT*TCACAGGGCAATGATCCCAAAG	
β-actin	Forward primer	GTGCGTGACATTAAGGAG	530
	Reverse primer	CTAAGTCATAGTCCGCCT	

2 μL $MgCl_2$ (25 mmol/L), 1 μL Taq polymerase (10×10^6 U/L), ddH_2O to a final volume of 25 μL. Thirty-five PCR cycles were performed, for each cycle, the sample was denatured at 94 ℃ for 1 min, annealed at 55 ℃ for 1 min, extended at 72 ℃ for 1 min, and finally extended at 72 ℃ for 10 min.

TUNEL assay for apoptosis detection

The paraffin-embedded specimens were cut into 5-μm-thick sections, rehydrated and then incubated with protease K solution for 30 min at room temperature. After being washed twice with PBS, the sections were incubated with TUNEL reaction solution at 37 ℃ for 60 min. The transforming solution (POD) was added and incubated at 37 ℃ for 30 min. The sections were stained with DAB for 10 min. Then counterstained with hematoxylin for 10 min, dehydrated in graded alcohol and covered with resin. The criterion of positive staining was that the nuclei were stained pale brown.

Statistical analysis

Data were presented as mean±SD, significance of statistical difference was assessed by Student's *t*-test and analyzed with SPSS11.0. $P<0.05$ was considered statistically significant.

RESULTS

TNF-α mRNA expression in orthotopic tumor tissues

TNF-α mRNA could be amplificated only from the tumors of TNF and BCT groups in the orthotopic tumor tissues injected into three kinds of cell lines, and no positive band could be seen from the other two groups. Electrophoresis showed that there was a positive band at 725 bp in the tissues injected into multidrug resistant cells transfected with TNF-α gene (Figure 1) and no band was found, indicating TNF-α mRNA was integrated into the nude mice implanted with multidrug resistant cells transfected with TNF-α gene. Thus, the model of implanted orthotopic tumor was successfully established.

Evaluation of growth and sensitivity of chemotherapy

No death occurred. The successful rate of tumor implantation was 100%, and tumor could be seen via B ultrasound after 10 d. The rate of tumor growth in the group transfected with TNF-α was lower compared to other groups ($P<0.05$). Low appetite and emotion occurred in the mice receiving chemotherapy, especially in BCT group. The tumor volume and weight of BCT group decreased compared to the other group ($P<0.01$), and tumor growth inhibition rate in $HepG_2$ group was similar to TNF group ($P>0.05$), but lower than that in BCT group ($P<0.05$, Table 2, Figures 2 and 3).

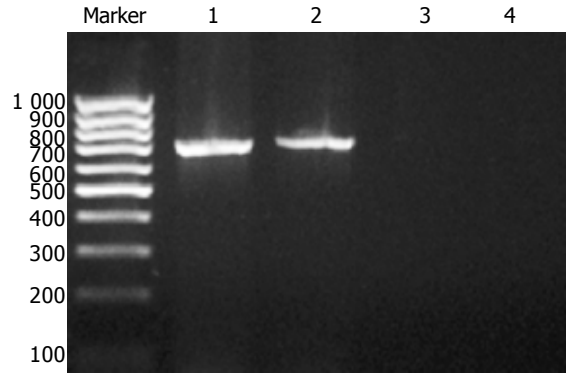


Figure 1 RT-PCR of TNFmRNA. M: Marker; lanes 1 and 2: TNF group, BCT group; lanes 3 and 4: $HepG_2$ group, ADM group.

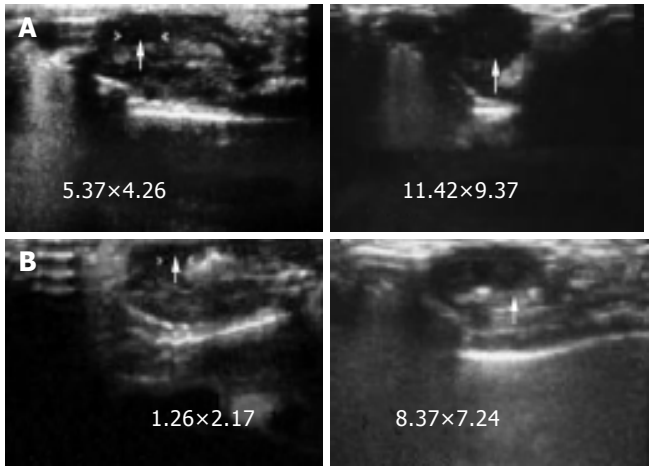


Figure 2 Size of tumor after chemotherapy in groups of $HepG_2$ (**A**) and BCT (**B**).

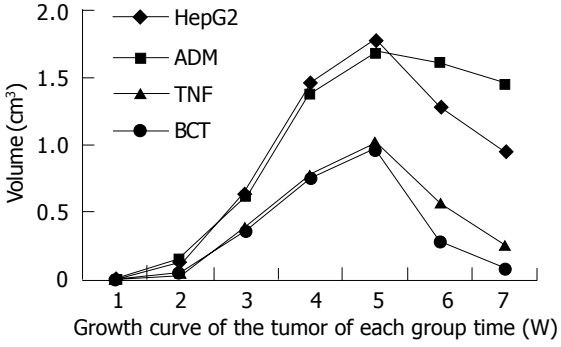


Figure 3 Growth curve of tumor in each group after chemotherapy.

Table 2 Volume and size of orthotopic tumor tissues (mean±SD)

Groups	Mice and incidence of tumor, *n* (%)	Volume (cm^3)	Rate of volume inhibition (%)	Weight (g)	Rate of weight inhibition (%)
$HepG_2$			57		54
Experiment	8 (100)	1.25±0.13		0.72±0.12	
Control	8 (100)	2.92±0.21		1.55±0.17	
ADM			14		18
Experiment	8 (100)	2.03±0.11		1.22±0.11	
Control	8 (100)	2.37±0.18		1.48±0.21	
TNF			58[a]		57
Experiment	8 (100)	0.67±0.22		0.45±0.16	
Control	8 (100)	1.37±0.18		0.93±0.18	
BCT			66[c]		67
Experiment	8 (100)	0.49±0.17[b]		0.29±0.21	
Control	8 (100)	1.45±0.26		0.88±0.17	

[a]$P>0.05$ *vs* $HepG_2$ group, $\chi^2=4.32$; [b]$P<0.01$ *vs* ADM group, $t=2.38$; [c]$P<0.05$ *vs* $HepG_2$ group, $\chi^2=2.49$.

Histologic characteristics and Pgp protein expression in orthotopic tumor tissues

Histological characteristics of the tumor model in different groups were similar (Figure 4). Pgp protein expression was low. Pgp protein expression was lower in $HepG_2$ group, but high in ADM group, and lower in groups TNF and BCT than in ADM group. There was a significant difference between the groups ($P<0.01$), but no difference among $HepG_2$, BCT and TNF groups ($P>0.05$, Figure 5)

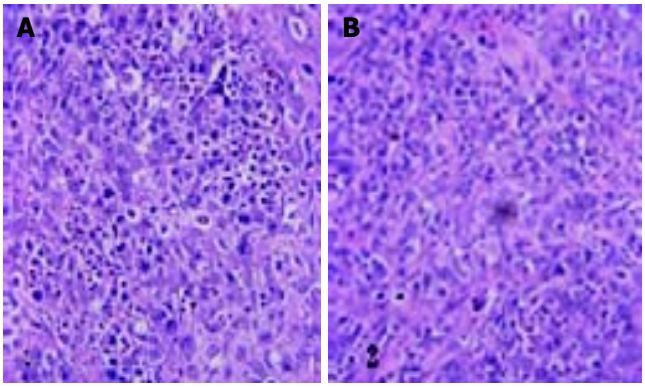


Figure 4 Histological characteristics of tumor in $HepG_2$ group (**A**) and BCT group (**B**).

Downregulation of MDR1mRNA expression in orthotopic tumor tissues transfected with TNF-α

Electrophoresis in each group showed 176, 237, and 530 bp bands, which were coincident with the amplification fragments of designed MDR1mRNA, LRPmRNA and β-actin genes. The relative quantity of MDR1mRNA in groups of BCT, TNF, $HepG_2$ was 0.21±0.02, 0.15±0.03, 0.13±0.02 respectively. The relative quantity of LRPmRNA in groups BCT, TNF, $HepG_2$ was 0.17±0.04, 0.15±0.01, 0.11±0.01. There was no difference among these groups ($P>0.05$), but the relative quantity of MDR1mRNA, LRPmRNA was significantly lower in groups of BCT, TNF, and $HepG_2$ than in ADM group ($P<0.05$, Figure 6, Table 3).

Apoptosis of tumor cells

After intra-abdominal chemotherapy with ADM, 5-FU, and mitomycin, the apoptotic rate of tumor cells expressing TNF-α was significantly higher compared to those not expressing TNF-α. The average of apoptotic cells in TNF-α and BCT group was (21.9±2.1) and (30.5±4.2) per field of high-power microscope respectively. There was a difference between the groups ($P<0.05$). TNF-α could reduce the tolerance of hepatoma cells to chemotherapy and increase apoptosis of tumor cells. BCT and TNF-α could induce apoptosis of HCC (Figure 7, Table 4).

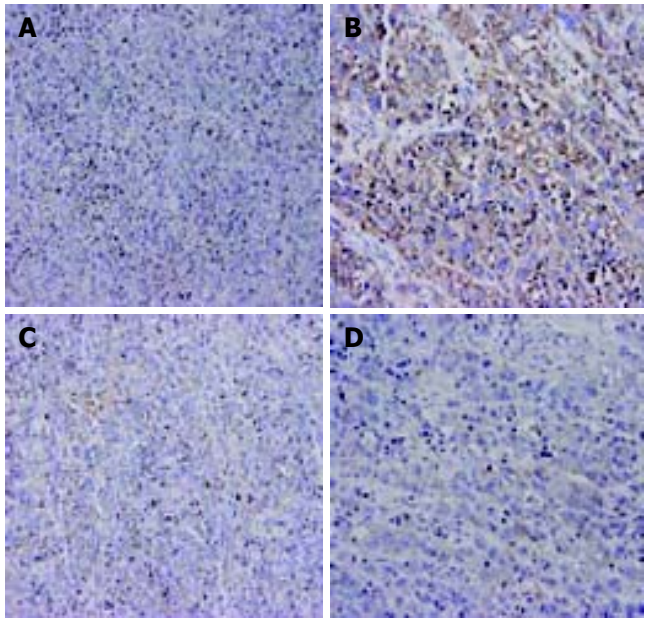


Figure 5 Pgp protein expression in groups of $HepG_2$ (**A**), ADM (**B**), BCT (**C**), and TNF (**D**).

DISCUSSION

Since MDR is the leading cause of failure of comprehensive therapy for HCC, investigations aimed at circumvention of intrinsic tumor-mediated drug resistance are warranted. But the efficacy of some drugs used to reverse MDR is limited due to their side-effects[16-18]. BCT has been used to treat hyperprolactinemia for more than two decades because of its slight side-effects[19,20]. It was reported that BCT can

Table 3 mRNA level of MDR-associated genes in response to TNF-α gene induction (mean±SD)

Groups	MDR1mRNA	LRPmRNA
BCT	0.21±0.02[a,c]	0.17±0.04
TNF	0.15±0.03[a,c]	0.15±0.01
ADM	0.89±0.15	0.83±0.12
$HepG_2$	0.13±0.02[c]	0.11±0.01

[a]P>0.05 *vs* $HepG_2$ group; [c]P<0.05 *vs* ADM group.

Table 4 Apoptosis index of each kind of tumors (mean±SD)

Group	Mice (no)	Experimental (index of apoptosis)
BCT	8	30.5±4.2[a,b,c]
TNF	8	21.9±2.1[b,c]
ADM	8	2.3±1.8
$HepG_2$	8	23.7±2.9

[a]P<0.05 *vs* TNF group; [b]P<0.01 *vs* ADM group; [c]P>0.05 *vs* $HepG_2$ group.

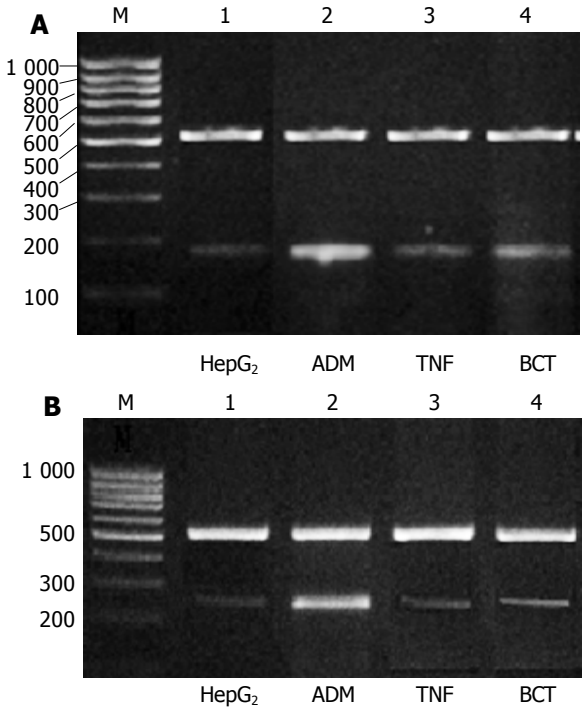


Figure 6 Expression of MDR1mRNA (**A,** 176 bp) and LRPmRNA (**B,** 237 bp).

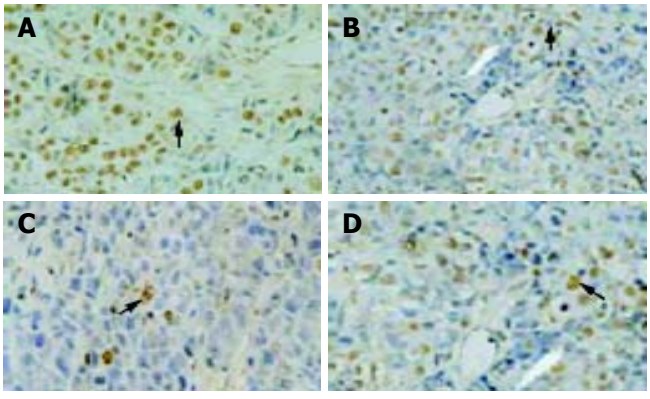


Figure 7 HHC cell apoptosis in groups of BCT (**A**), TNF (**B**), ADM (**C**), and $HepG_2$ (**D**).

be used as a chemosensitizer against MDR tumor cells[7,8] and a current study showed that TNF-α may play a role in MDR[21].

In this study, we first demonstrated that TNF-α was expressed in the orthotopic tumor tissues injected into $HepG_2$/ADM cells transfected with TNF-α. Moreover, tumor inhibition rate after treatment with 5-FU, ADM, MMC through intraperitoneal injection was higher in BCT group (67%, P<0.05) than in TNF group (57%) and ADM group (18%), and similar to $HepG_2$ group (54%). As the data shows, the drug-resistant hepatocarcinoma cell line $HepG_2$/ADM transfected with TNF-α could excrete cytokine TNF-α which could induce cancer cell apoptosis and inhibit the growth of tumor[22,23]. The result is in coincidence with Stein *et al*.[24]. Furthermore, TNF-α gene in combination with BCT could reverse HCC MDR. Moreover, IHC and reverse transcriptase polymerase chain reaction (RT-PCR) showed that transduction and expression of human TNF-α in drug-resistant HCC cell line $HepG_2$/ADM could reverse expression of MDR1mRNA, LRPmRNA, and Pgp, but had no synergistic effect compared to BCT, suggesting that TNF-α can downregulate the expression of MDR-associated genes and proteins[25], and BCT may act on for its potential interaction and transport by Pgp[26-31], but has no effect on MDR-associated genes. Additionally, an interesting discovery indicate that the rate of apoptosis after chemotherapy in BCT group is the highest in all experiment groups, and BCT and TNF-α can reverse HCC MDR in nude mice MDR1 model of liver neoplasm.

ACKNOWLEDGMENTS

We thank Professors Zhuo-Ya Li, Fei-Li Gong, Qing-Fen Li and teacher Xiao-Dan Jiang (Department of Immunity, Tongji Medical College, Huazhong University of Science and Technology, Wuhan 430030, Hubei Province, China) for their useful suggestions during the whole experiment.

REFERENCES

1 **Germann UA,** Pastan I, Gottesman MM. P-glycoproteins: mediators of multidrug resistance. *Semin Cell Biol* 1993; **4**: 63-76
2 **Marzolini C,** Paus E, Buclin T, Kim RB. Polymorphisms in human MDR1 (P-glycoprotein): recent advances and clinical relevance. *Clin Pharmacol Ther* 2004; **75**: 13-33
3 **Chan JY**, Chu AC, Fung KP. Inhibition of P-glycoprotein expression and reversal of drug resistance of human hepatoma HepG2 cells by multidrug resistance gene (mdr1) antisense RNA. *Life Sci* 2000; **67**: 2117-2124
4 **Huesker M**, Folmer Y, Schneider M, Fulda C, Blum HE, Hafkemeyer P. Reversal of drug resistance of hepatocellular carcinoma cells by adenoviral delivery of anti-MDR1 ribozymes. *Hepatology* 2002; **36** (4 Pt1): 874-884
5 **Wang H**, Chen XP, Qiu FZ. Overcoming multi-drug resistance by anti-MDR1 ribozyme. *World J Gastroenterol* 2003; **9**: 1444-1449
6 **Grude P**, Conti F, Mennecier D, Louvel A, Houssin D, Weill B, Calmus Y. MDR1 gene expression in hepatocellular carcinoma and the peritumoral liver of patients with and without cirrhosis. *Cancer Lett* 2002; **186**: 107-113
7 **Orlowski S,** Valente D, Garrigos M, Ezan E. Bromocriptine modulates P-glycoprotein function. *Biochem Biophys Res Commun* 1998; **244**: 481-488
8 **Shiraki N,** Okamura K, Tokunaga J, Ohmura T, Yasuda K, Kawaguchi K, Hamada A, Nakano M. Bromocriptine reverses

P-glycoprotein-mediated multidrug resistance in tumor cells. *Jpn J Cancer Res* 2002; **93**: 209-215

9 **Stein U,** Walther W, Laurencot CM, Scheffer GL, Scheper RJ, Shoemaker RH. Tumor necrosis factor-alpha and expression of the multidrug resistance-associated genes LRP and MRP. *J Natl Cancer Inst* 1997; **89**: 807-813

10 **Walther W,** Stein U, Pfeil D. Gene transfer of human TNF alpha into glioblastoma cells permits modulation of mdr1 expression and potentiation of chemosensitivity. *Int J Cancer* 1995; **61**: 832-839

11 **Hirsch-Ernst KI**, Ziemann C, Foth H, Kozian D, Schmitz-Salue C, Kahl GF. Induction of mdr1b mRNA and P-glycoprotein expression by tumor necrosis factor alpha in primary rat hepatocyte cultures. *J Cell Physiol* 1998; **176**: 506-515

12 **Gilboa E,** Lyerly HK, Vieweg J, Saito S. Immunotherapy of cancer using cytokine gene-modified tumor vaccines. *Semin Cancer Biol* 1994; **5**: 409-417

13 **Uckert W,** Walther W. Retrovirus-mediated gene transfer in cancer therapy. *Pharmacol Ther* 1994; **63**: 323-347

14 **Walther W,** Stein U. Influence of cytokines on mdr1 expression in human colon carcinoma cell lines: increased cytotoxicity of MDR relevant drugs. *J Cancer Res Clin Oncol* 1994; **120**: 471-478

15 **Mitchell MS.** Combining chemotherapy with biological response modifiers in treatment of cancer. *J Natl Cancer Inst* 1988; **80**: 1445-1450

16 **Madureira AM**, Spengler G, Molnar A, Varga A, Molnar J, Abreu PM, Ferreira MJ. Effect of cycloartanes on reversal of multidrug resistance and apoptosis induction on mouse lymphoma cells. *Anticancer Res* 2004; **24**: 859-864

17 **Woehlecke H,** Osada H, Herrmann A, Lage H. Reversal of breast cancer resistance protein-mediated drug resistance by tryprostatin A. *Int J Cancer* 2003; **107**: 721-728

18 **Schuetzer-Muehlbauer M,** Willinger B, Egner R, Ecker G, Kuchler K. Reversal of antifungal resistance mediated by ABC efflux pumps from Candida albicans functionally expressed in yeast. *Int J Antimicrob Agents* 2003; **22**: 291-300

19 **Schlesinger I**, Ravin PD. Dopamine agonists induce episodes of irresistible daytime sleepiness. *Eur Neurol* 2003; **49**: 30-33

20 **Deleu D**, Northway MG, Hanssens Y. An evidence-based review of Dopamine receptor agonists in the treatment of Parkinson's disease. *Saudi Med J* 2002; **23**: 1165-1175

21 **Lee JS**, Song CH, Lim JH, Kim HJ, Park JK, Paik TH, Kim CH, Kong SJ, Shon MH, Jung SS, Jo EK. The production of tumour necrosis factor-alpha is decreased in peripheral blood mononuclear cells from multidrug-resistant tuberculosis patients following stimulation with the 30-kDa antigen of Mycobacterium tuberculosis. *Clin Exp Immunol* 2003; **132**: 443-449

22 **Corti A**. Strategies for improving the anti-neoplastic activity of TNF by tumor targeting. *Methods Mol Med* 2004; **98**: 247-264

23 **Kim HR**, Park HJ, Park JH, Kim SJ, Kim K, Kim J. Characteristics of the killing mechanism of human natural killer cells against hepatocellular carcinoma cell lines HepG2 and Hep3B. *Cancer Immunol Immunother* 2004; **53**: 461-470

24 **Stein U**, Walther W, Shoemaker RH. Reversal of multidrug resistance by transduction of cytokine genes into human colon carcinoma cells. *J Natl Cancer Inst* 1996; **88**: 1383-1392

25 **Walther W,** Stein U, Fichtner I, Alexander M, Shoemaker RH, Schlag PM. Mdr1 promoter-driven tumor necrosis factor-alpha expression for a chemotherapy-controllable combined *in vivo* gene therapy and chemotherapy of tumors. *Cancer Gene Ther* 2000; **7**: 893-900

26 **Samini M,** Fakhrian R, Mohagheghi M, Dehpour AR. Comparison of the effect of levodopa and bromocriptine on naloxone-precipitated morphine withdrawal symptoms in mice. *Hum Psychopharmacol* 2000; **15**: 95-101

27 **Teodori E,** Dei S, Scapecchi S, Gualtieri F. The medicinal chemistry of multidrug resistance (MDR) reversing drugs. *Farmaco* 2002; **57**: 385-415

28 **Wu JY,** Fong WF, Zhang JX, Leung CH, Kwong HL, Yang MS, Li D, Cheung HY. Reversal of multidrug resistance in cancer cells by pyranocoumarins isolated from Radix Peucedani. *Eur J Pharmacol* 2003; **473**: 9-17

29 **Marian T,** Szabo G, Goda K, Nagy H, Szincsak N, Juhasz I, Galuska L, Balkay L, Mikecz P, Tron L, Krasznai Z. *In vivo* and *in vitro* multitracer analyses of P-glycoprotein expression-related multidrug resistance. *Eur J Nucl Med Mol Imaging* 2003; **30**: 1147-1154

30 **Psarros T,** Zouros A, Coimbra C. Bromocriptine-responsive akinetic mutism following endoscopy for ventricular neurocysticercosis. Case report and review of the literature. *J Neurosurg* 2003; **99**: 397-401

31 **Yavuz D,** Deyneli O, Akpinar I, Yildiz E, Gozu H, Sezgin O, Haklar G, Akalin S. Endothelial function, insulin sensitivity and inflammatory markers in hyperprolactinemic pre-menopausal women. *Eur J Endocrinol* 2003; **149**: 187-193

Science Editor Wang XL and Guo SY **Language Editor** Elsevier HK

PO Box 2345, Beijing 100023, China
www.wjgnet.com
wjg@wjgnet.com

ELSEVIER

World J Gastroenterol 2005;11(36):5627-5632
World Journal of Gastroenterology ISSN 1007-9327
© 2005 The WJG Press and Elsevier Inc. All rights reserved.

Upregulation of human telomerase reverse transcriptase mRNA expression by *in vitro* transfection of hepatitis B virus X gene into human hepatocarcinoma and cholangiocarcinoma cells

Zhen-Liang Qu, Sheng-Quan Zou, Nai-Qiang Cui, Xian-Zhong Wu, Ming-Fang Qin, Di Kong, Zhen-Li Zhou

Zhen-Liang Qu, Nai-Qiang Cui, Xian-Zhong Wu, Ming-Fang Qin, Di Kong, Zhen-Li Zhou, Department of Surgery, Tianjin Nankai Hospital, Tianjin 300100, China
Sheng-Quan Zou, Department of Surgery, Tongji Hospital, Wuhan 430030, Hubei Province, China
Correspondence to: Zhen-Liang Qu, MD, Department of Surgery, Tianjin Nankai Hospital, Tianjin 300100, China. zlqu2002@hotmail.com
Telephone: +86-22-27022268
Received: 2005-01-14 Accepted: 2005-02-18

Abstract

AIM: To study the changes of human telomerase reverse transcriptase (hTERT) mRNA expression in human hepatocarcinoma cell lines (HepG2) and cholangiocarcinoma cell lines (QBC939) after HBx gene transfection and to illustrate the significance of transcriptional regulation of hTERT gene by HBx gene in the carcinogenesis.

METHODS: HepG2 and QBC939 cell lines were cultured and co-transfected with eukaryotic expression vector containing the HBx coding region and cloning vector containing enhanced green fluorescent protein (EGFP) coding sequence using lipid-mediated gene transduction technique. Thirty-six hours after transfection, EGFP expression in cells was used as the indicator of successful transfection. Flow cytometry was performed to determine the transfection efficiency. Cells were harvested and total RNA was extracted using TRIzol® reagent. The expression of hTERT mRNA in HepG2 and QBC939 cell lines was assayed by reverse transcription-polymerase chain reaction. The expression of HBx protein in both cell lines was detected by immunocytochemical staining and Western blotting.

RESULTS: Flow cytometry showed that the transfection efficiency was 46.4% in HepG2 cells and 29.6% in QBC939 cells for both HBx gene expression vector and blank vector. The expression of hTERT mRNA was meaningfully increased in HepG2 and QBC939 cell lines when transfected with HBx gene expression vector compared to those transfected with OPTI-MEM medium and blank vector. Immunocytochemical staining and Western blotting revealed HBx protein expression in HepG2 and QBC939 cells only when transfected with HBx gene.

CONCLUSION: HBx gene transfection can upregulate the transcriptional expression of hTERT mRNA. The transactivation of hTERT gene by HBx gene is a newfound mechanism for pathogenesis of hepatocarcinomas and cholangiocarcinomas after HBV infection.

© 2005 The WJG Press and Elsevier Inc. All rights reserved.

Key words: Hepatocholangiocarcinoma; Human telomerase reverse transcriptase; Gene expression; Hepatitis B virus; X protein

Qu ZL, Zou SQ, Cui NQ, Wu XZ, Qin MF, Kong D, Zhou ZL. Upregulation of human telomerase reverse transcriptase mRNA expression by *in vitro* transfection of hepatitis B virus X gene into human hepatocarcinoma and cholangiocarcinoma cells. *World J Gastroenterol* 2005; 11(36): 5627-5632
http://www.wjgnet.com/1007-9327/11/5627.asp

INTRODUCTION

As an oncogenic DNA virus, HBV has been ascertained as the major causative factor for hepatocarcinogenesis[1]. Our recent study has also shown that HBV infection may be associated with biliary tract carcinogenesis[2]. The X gene of HBV (HBx gene) encodes a viral protein (HBx protein), which performs an essential function in the development of human hepatocarcinoma[3] and cholangiocarcinoma[4]. The finding that HBx gene can upregulate telomerase activation, when transferred into hepatocarcinoma cells reveals a new mechanism for HBx gene in carcinogenesis[5]. Human telomerase reverse transcriptase (hTERT) is the rate-limiting determinant for telomerase activity and its expression parallels frequently to telomerase activity[6,7]. Our previous findings that HBx gene can upregulate hTERT mRNA expression, when transferred into normal human cholangiocytes and cholangiocarcinoma cells[8], ascertain the regulation of hTERT gene by HBx gene. To learn more about the mechanism in carcinogenesis, we transferred the eukaryotic expression vector encompassing the entire HBx coding region into both hepatocarcinoma cell line (HepG2) and cholangiocarcinoma cell line (QBC939). By assaying the expression of hTERT mRNA, we attempted to elucidate the significance of transcriptional regulation of hTERT gene by HBx gene in the carcinogenesis.

MATERIALS AND METHODS

Cell and culture

HepG2 cell line was purchased from Foundation Institute, Chinese Academy of Medical Sciences. QBC939 cell lines

were obtained from Dr. Shuguang Wang (Southwest Hospital, the Third Military Medical University, Chongqing). Cells were maintained in Dulbecco's modified Eagle's medium containing 100 mL/L fetal bovine serum (FBS), 100 U/mL penicillin and 100 μg/mL streptomycin, and propagated at 37 ℃ in a humidified atmosphere of 50 mL/L CO_2 in air. Cells in monolayer culture passaged approximately thrice a week by incubation with 2.5 g/L trypsin/1 mmol/L versene at 37 ℃ for approximately 5 min until the cells were shrunken. Trypsin activity was quenched by the addition of fresh medium containing FBS and cells were seeded at 1/4 split ratio.

Plasmids and transfection

The empty vector pcDNA3 is eukaryotic expression vector used as a negative control. pCMV-X is constructed by inserting the entire HBx coding region (HBV nucleotides 1 372-1 833, 465 bp) into the *Eco*RI/*Eco*RV sites of the pcDNA3 vector. Cloning vector pEGFP carries an enhanced green fluorescent protein (EGFP) gene, which was cloned between the two MCS of the pPD16.43. EGFP encoded by pEGFP can emit bright green fluorescence in eukaryotic cells. All the plasmids contain ampicillin resistance genes for propagation and selection in *E. coli*.

Transient transfection of plasmids into both HepG2 and QBC939 was performed using LipofectAMINE PLUS™ reagent (Gibco BRL®) according to the manufacturer's instructions. The day before transfection, cells were trypsinized and seeded in six-well plates. At the day of transfection, cells reached over 80% confluence, and then 2.9 μg pcDNA3 or pCMV-X DNA and 0.1 μg pEGFP DNA were diluted into OPTI-MEM medium (Invitrogen) and mixed with Lipofect-AMINE PLUS™ reagent. After the cells were washed once by OPTI-MEM medium, a total of 1 mL transfection medium was added to the cells. The cells were incubated at 37 ℃ for 3 h in a humidified atmosphere containing 50 mL/L CO_2. After 3 h of incubation, the transfection medium was replaced with fresh complete medium containing serum and the cells were further incubated for 36 h. Then the cells were harvested, and the expression of hTERT mRNA was assayed. The cells transfected with OPTI-MEM medium were used as blank control (group A) and that transfected with pcDNA3 vector were used as negative control (group C), while that transfected with pCMV-X were defined as experimental group (group B). Co-transfection of pEGFP was used to evaluate the successful transfection.

Detection of transfection efficiency by flow cytometry

Cells were trypsinized, washed with PBS for twice, followed by dilution at 1×10^6 cells/mL. Transfection efficiency was detected using flow cytometry by following the manufacturer's instructions.

Extraction of total cellular RNA and RT-PCR analysis for hTERT mRNA

Total cellular RNAs were extracted from cells of different groups by TRIzol® reagent (Gibco BRL®) according to the manufacturer's instructions. Two micrograms of extracted RNA was reverse transcribed into cDNA first-strand using 200 U of Moloney Murine Leukemia Virus Reverse Transcriptase (Promega, Madison, USA) and 1 μg of oligo $(dT)_{15}$ primer (Promega) in a final volume of 25 μL of enzyme buffer (Promega) for 60 min at 42 ℃. hTERT cDNA analysis was performed by PCR amplification of a fragment of 145 bp using primer pairs: 5'-CGGAAGAGTGTCTGG-AGCAA-3' (sense) and 5'-GGATGAAGCGGAGTCTGGA-3' (antisense). A 320-bp fragment of GAPDH gene was amplified as an internal control. The primers for GAPDH are 5'-GGAAGCTTGTCATCAATGG-3' (sense) and 5'-CTGTGGTCATGAGTCCTTC-3' (antisense). PCR was performed with 5 μL of cDNA first-strand in a 50 μL reaction volume containing 2 mmol/L $MgCl_2$, 1 mmol/L dNTPs, 0.4 μmol/L of each primer, and 2.5 U of Taq DNA polymerase (Promega). The reaction mixture was heated at 94 ℃ for 5 min, followed by amplification through 33 cycles. Each cycle included denaturation at 94 ℃ for 40 s, annealing at 60 ℃ for 40 s and extension at 72 ℃ for 90 s. Then 10 μL of the PCR product was electrophoresed on a 15 g/L agarose gel containing ethidium bromide (0.5 μg/mL), and visualized under ultraviolet light. The quantitative difference of bands between groups was analyzed by NIH Image software. The reverse transcription-polymerase chain reaction (RT-PCR) was repeated in triplicate and quantitative data were expressed as mean±SD.

Detection of HBx protein by Western blotting

Total cellular protein was extracted by cell lysis (20 mmol/L Tris-HCl [pH 7.5], 1 mmol/L EDTA, 1 mmol/L EGTA, 150 mmol/L NaCl, 2.5 mmol/L sodium pyrophosphate, 1 mmol/L β-glycerolphosphate, 1 μg/mL leupeptin, 1 mol/L PMSF) and quantitated by BCA™ protein assay kit (Pierce Biotech). An equal amount of protein sample was separated on SDS-polyacrylamide gel electrophoresis and transferred onto nitrocellulose membrane. The membrane was incubated in a blocking buffer (1 g/L Tween-20, 50 g/L non-fat dry milk in TBS) for 3 h. Rabbit anti-human HBx polyclonal antibody was diluted by primary antibody dilution buffer (1 g/L Tween-20, 50 g/L BSA in TBS) at 1∶800. The membrane was then incubated with HBx antibody overnight at 4 ℃. The expression of HBx protein was detected using Phototope®-HRP Western Blot Detection Kit (Cell Signaling Technology).

Detection of HBx protein in transferred cells by immunocytochemistry

The cells in different groups were cultured on cover slips and fixed with fixative (acetone and methanol). Detection of HBx protein expression in the transfected cells was performed by UltraSensitive™ Immunochemistry kit according to the manufacturer's instructions. A rabbit anti-human HBx polyclonal antibody was used at dilution of 1∶800.

Statistical analysis

Comparison between means was tested by Student's *t*-test and *P* value lesser than 0.05 was considered statistically significant.

RESULTS

Transfection efficiency

Under fluorescence microscope, EGFP expression could only be observed in the cells of groups B and C (Figure 1). There

was no such green fluorescence could be seen in group A. Transfection efficiency was 46.4% for HepG2 and 29.6% for QBC939 when detected by flow cytometry (Figure 2).

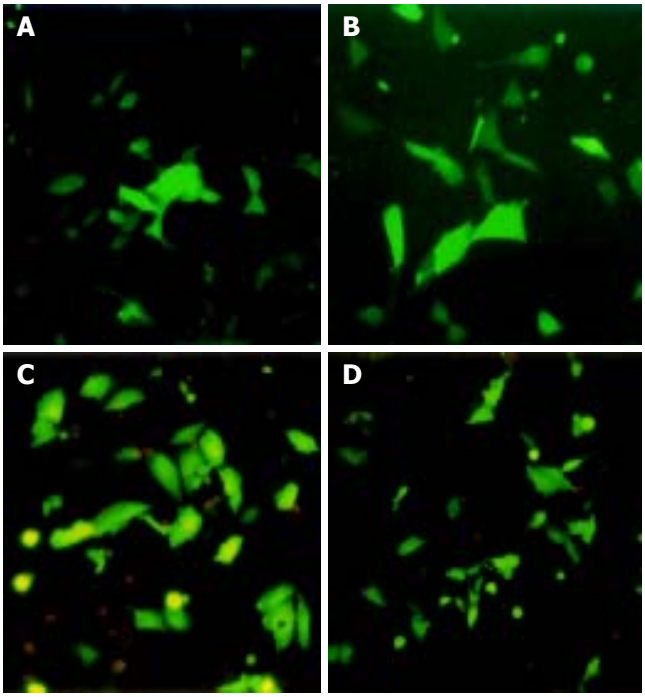


Figure 1 EGFP expressions in HepG2 (**A** and **B**) and QBC939 (**C** and **D**) cell lines under fluorescence microscope. After 36 h of transfection, EGFP-expressing cells were visible in group B (**A** and **C**) and group C (**B** and **D**), but not in group A.

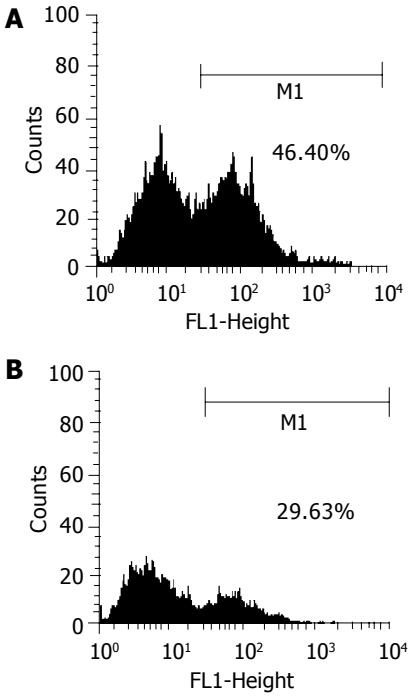


Figure 2 Transfection efficiency evaluated by flow cytometry. The transfection efficiencies were about 46.4% for HepG2 (**A**) and 29.6% for QBC939 (**B**).

hTERT mRNA expression

To examine the effects of HBx gene on hTERT transcription, pCMV-X expression vector was co-transfected with pEGFP into HepG2 and QBC939 cell lines. Thirty-six hours after transfection, the total cellular RNA was extracted and hTERT transcript was assayed using RT-PCR. The result showed that hTERT transcript was expressed in all groups (Figure 3). Expression of the human GAPDH gene was monitored for quantitation of the amount of RNA in all of the samples as an internal control. Relative expression of hTERT mRNA was determined by measuring band intensities of both hTERT transcript and GAPDH transcript and calculating the ratio of hTERT to GAPDH. After being analyzed by NIH Image software, hTERT mRNA expression was more distinct in group B than that in other two groups (Figure 4).

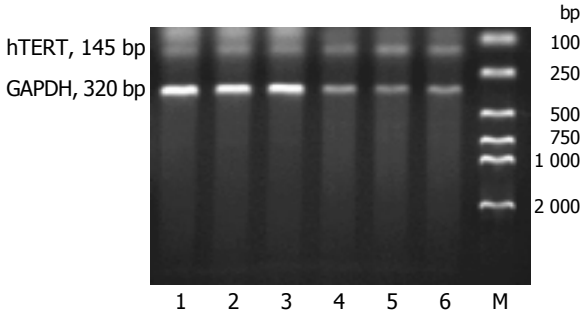


Figure 3 Analysis of hTERT mRNA expression by RT-PCR. RT-PCR was performed on total RNA extracted from both HepG2 (lanes 1-3) and QBC939 (lanes 4-6) cell lines transfected with OPTI-MEM medium (lanes 1 and 4), pCMV-X (lanes 2 and 5) and pcDNA3 (lanes 3 and 6) respectively. M: DL 2000 marker.

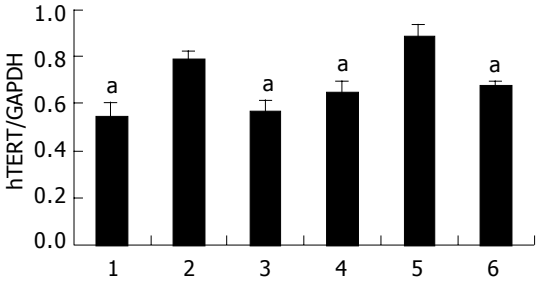


Figure 4 Relative quantitative changes of hTERT mRNA in HepG2 (lanes 1-3) and QBC939 (lanes 4-6) cell lines. A significant higher expression of hTERT mRNA was observed in both HepG2 and QBC939 cells after being transfected with pCMV-X vector (lanes 2 and 5) compared to those transfected with OPTI-MEM medium (lanes 1 and 4) and pcDNA3 (lanes 3 and 6). $^{a}P<0.05$ *vs* others.

Western blotting analysis

The result of Western blot analysis showed that the expression of HBx protein could only be detected in HepG2 and QBC939 cells when transfected with HBx gene, but undetected in those when transfected with OPTI-MEM medium and blank vector (Figure 5).

Immunocytochemical staining

A sensitive immunocytochemical staining was performed to identify whether there was HBx protein expression in transfected HepG2 and QBC939 cell lines. The results showed positive signals observed in cytoplasm of HepG2

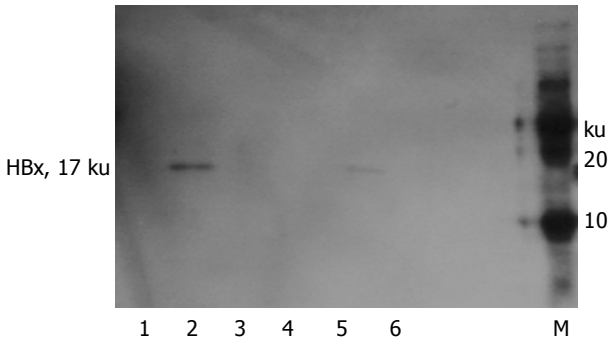


Figure 5 Western blot analysis of HBx protein expression in transfected HepG2 (lanes 1-3) and QBC939 (lanes 4-6) cell lines. A marked expression of HBx protein was observed in HepG2 and QBC939 cells when transfected with pCMV-X vector (lanes 2 and 5), but there were no such protein expression in those when transfected with OPTI-MEM medium (lanes 1 and 4) and blank vector (lanes 3 and 6). M: Protein marker.

(Figure 6) and QBC939 cells (Figure 7) in group B, while no such positive signals could be observed in HepG2 and QBC939 cells in groups A and C.

DISCUSSION

Telomerase/hTERT mechanisms have long been investigated for their potential role in cancer. Activation of telomerase is considered as the major episode for carcinogenesis[9] and over 85% of tumorigenic tissues and malignant cells express telomerase activity. hTERT is the rate-limiting determinant for regulating telomerase activity and also highly expressed in neoplastic tissues and tumor cells[10]. Most studies have shown that hTERT expression is usually correlated with telomerase activity and upregulation of hTERT expression is considered as the major step in carcinogenesis[11]. Multiple transcriptional factor binding sites are well identified in hTERT core promoter region and these regulatory factors make up a complex system of hTERT regulation[12]. The findings that HBV genome integration into upstream of hTERT core promoter region[13] and the *cis*-activation of hTERT gene transcription by HBV enhancer first elucidate a new mechanism for HBV in oncogenesis are the possible transcriptional regulation of hTERT gene[14].

HBV has been illustrated as the major causative factor for hepatocarcinogenesis[15]. Recent researches have also revealed that HBV infection might be associated with the development of cholangiocarcinoma. HBx protein, which is encoded by HBx gene, is considered as an essential oncogenic factor in oncogenesis of both human hepatocarcinomas and cholangiocarcinomas. HBx protein is a multifunctional viral oncoprotein and functions mainly as a transcriptional co-

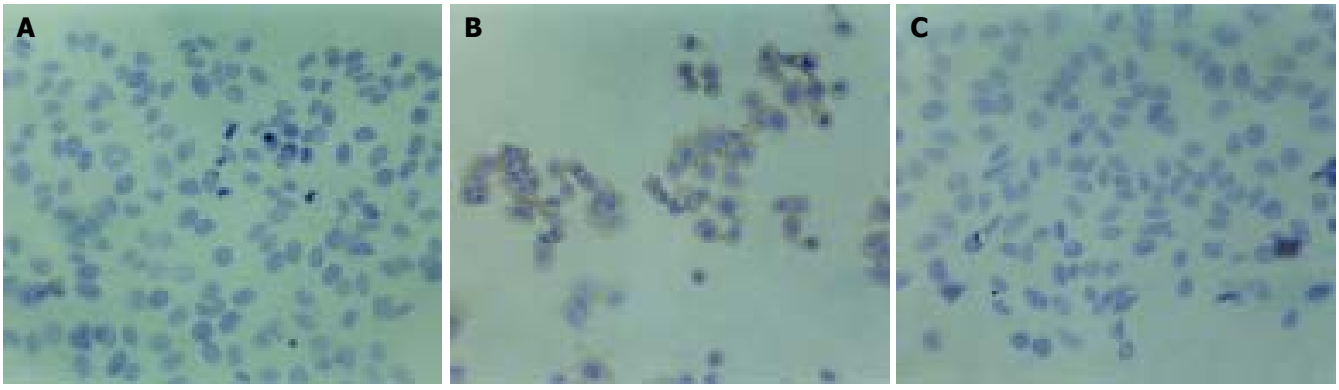


Figure 6 HBx protein expression in transfected HepG2 cells as assayed by UltraSensitive™ immunocytochemistry (SP×200). The cells transfected with OPTI-MEM medium (**A**) and blank vector (**C**) showed no expression of HBx protein, while some cells transfected with pCMV-X vector (**B**) showed visible brown positive signals.

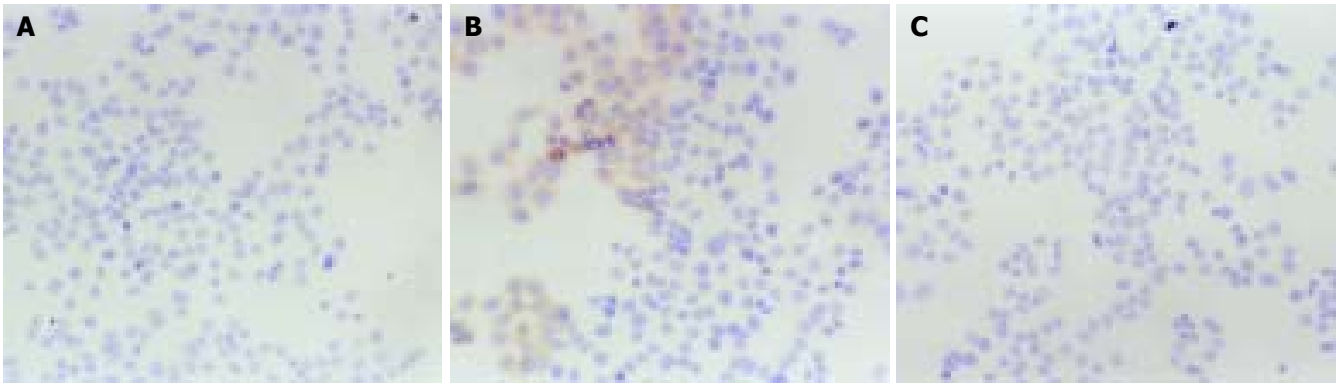


Figure 7 HBx protein expression in transfected QBC939 cells as detected by UltraSensitive™ immunocytochemistry (SP×200). The cells transfected with OPTI-MEM medium (**A**) and blank vector (**C**) showed no expression of HBx protein, but some cells transfected with pCMV-X vector (**B**) showed brown positive signals.

activator involving in multiple gene regulation and signaling pathways[16]. The integration of HBV genome into the hTERT promoter region[17] and upregulation of telomerase expression by HBx gene transfection[5] imply the possibility that HBx gene and protein may regulate hTERT gene transcription. In order to validate this surmise, we cultured HepG2 and QBC939 cells *in vitro* and transferred transiently the HBx gene into both the cell lines through lipid-mediated gene transduction technique. By observing the changes of hTERT mRNA expression, we attempted to elucidate the transcriptional regulation of hTERT gene by HBx gene. We observed that both HepG2 and QBC939 cell lines, when transfected with OPTI-MEM medium, could express hTERT mRNA quantitatively. Though there was no increase for hTERT mRNA expression in both cells when transfected with blank vector, a dramatic higher expression of hTERT mRNA was observed in both HepG2 and QBC939 cells when transfected with HBx gene. The results showed that HBx gene transfection could upregulate transcriptional expression of hTERT gene in both hepatocarcinomas and cholangiocarcinoma cells.

It is well known that some viruses contribute to carcinogenesis in two ways. One way is to transcriptionally activate proto-oncogenes of host cells by the integration of viral genome into the cellular genome and activation of the regulatory sequences (i.e., promoter or enhancer) of the viral genome[18]. This viral *cis*-activation mechanism can target the hTERT gene transcription[19]. Previous studies have found that HBV genome integrated in the hTERT promoter region and HBV enhancer could *cis*-activate the transcription of hTERT gene. Taken together with our present results, it is revealed that activation of telomerase by integration of HBV genome into telomerase gene is a new mechanism for oncogenic virus, HBV, in carcinogenesis. Another way is that some virus-encoded proteins contribute to cell transformation and carcinogenesis by modulating cellular signaling pathways that regulate cell-cycle progression, cell proliferation and differentiation, and cell apoptosis[20]. Recent evidence suggests that the activation of telomerase through transcriptional activation of the hTERT gene is another way in which human tumor-associated viruses can work[21]. Human papilloma viruses, especially its oncoproteins E6 and E7[22], which can abrogate the tumor suppressive function of p53 and Rb signaling pathways[23] and upregulate the hTERT promoter activity[24,25], play an important role in the development of cancers. The E-box elements within the hTERT promoter seem to be the target motifs responsible for the E6 activation of the hTERT transcription[26]. It is most likely that the aforementioned two ways are responsible for the upregulation of hTERT gene expression after HBx gene transfection into HepG2 and QBC939 cells. Although no direct evidence shows the existence of the integrated sites for HBx gene and the binding sites for HBx protein in hTERT promoter region, further investigations will identify these functional sites and validate the regulatory mechanisms eventually. HBx protein is a potential oncogenic factor and functions mainly as a transcriptional co-activator[16] involved in multiple gene regulation[27] and signaling pathway[28]. We suppose that upregulation of hTERT mRNA expression by HBx gene transfection is the result of the regulatory functions of binding motifs within the hTERT promoter for HBx protein or HBx-containing transcriptional complexes. But the exact mechanisms of these regulatory functions need to be elucidated through the study of transcription regulation for hTERT gene. Using immunocytochemical staining and Western blotting, we observed HBx protein expression only in HepG2 and QBC939 cells transfected with HBx gene. The expression of HBx protein in transfected cells indicates the achievement of transcription and duplication for HBx gene in some of these cells and meanwhile, demonstrates a key factor in regulating hTERT gene expression.

In conclusion, activation of telomerase and transcriptional regulation of hTERT gene involve in the development of carcinomas and act as the major targets for some tumor-associated viruses[19]. The transactivation of hTERT mRNA expression by HBx gene is a newfound mechanism for HBV in oncogenesis of hepatocarcinomas and cholangiocarcinomas. The elucidation of this mechanism may contribute to the deep understanding of the pathogenesis of HBV infection and subsequent formation of cancers.

ACKNOWLEDGMENTS

We thank Dr. Shu-Guang Wang for kindly providing us cholangiocarcinoma cell lines (QBC939) and Professor Xiao-Dong Zhang for providing us plasmids and technical assistance.

REFERENCES

1 **Arbuthnot P,** Kew M. Hepatitis B virus and hepatocellular carcinoma. *Int J Exp Pathol* 2001; **82**: 77-100
2 **Qu ZL,** Zou SQ, Wei GH, Sun ZC, Wu XZ. *In situ* nucleic acid detection of HBV X gene in extrahepatic biliary tract carcinomas and its clinicopathological significance. *Zhonghua Waike Zazhi* 2004; **42**: 88-91
3 **Block TM,** Mehta AS, Fimmel CJ, Jordan R. Molecular viral oncology of hepatocellular carcinoma. *Oncogene* 2003; **22**: 5093-5107
4 **Qu ZL,** Zou SQ, Zhen SL, Wu XZ, Cui NQ. The expression and significance of hepatitis B virus X protein in extrahepatic bile duct carcinomas and the surrounding non-cancerous tissues. *Zhonghua Shiyan Waike Zazhi* 2002; **19**: 401-402
5 **Zhou WP,** Shen QH, Gu BY, Ren H, Zhang DF. Effect of hepatitis B virus X gene on apoptosis and the activity of telomerase in HepG2 cells. *Zhonghua Ganzangbing Zazhi* 2000; **8**: 212-214
6 **Kyo S,** Kanaya T, Takakura M, Tanaka M, Inoue M. Human telomerase reverse transcriptase as a critical determinant of telomerase activity in normal and malignant endometrial tissues. *Int J Cancer* 1999; **80**: 60-63
7 **Nagao K,** Tomimatsu M, Endo H, Hisatomi H, Hikiji K. Telomerase reverse transcriptase mRNA expression and telomerase activity in hepatocellular carcinoma. *J Gastroenterol* 1999; **34**: 83-87
8 **Qu ZL,** Zou SQ, Wang X. The effect of hepatitis B virus X gene transfection on expression of human telomerase reverse transcriptase mRNA in human bile duct carcinoma cell lines. *Zhonghua Waike Zazhi* 2004; **42**: 1254-1257
9 **Guilleret I,** Yan P, Guillou L, Braunschweig R, Coindre JM, Benhattar J. The human telomerase RNA gene (hTERC) is regulated during carcinogenesis but is not dependent on DNA methylation. *Carcinogenesis* 2002; **23**: 2025-2030
10 **Dhaene K,** Van Marck V, Parwaresch R. Telomeres, telomerase and cancer: an up-date. *Virchows Arch* 2000; **437**: 1-16
11 **Yan P,** Saraga EP, Bouzourene H, Bosman FT, Benhattar J. Expression of telomerase genes correlates with telomerase

activity in human colorectal carcinogenesis. *J Pathol* 2001; **193**: 21-26

12 **Poole JC,** Andrews LG, Tollefsbol TO. Activity, function, and gene regulation of the catalytic subunit of telomerase (hTERT). *Gene* 2001; **269**: 1-12

13 **Ferber MJ,** Montoya DP, Yu C, Aderca I, McGee A, Thorland EC, Nagorney DM, Gostout BS, Burgart LJ, Boix L, Bruix J, McMahon BJ, Cheung TH, Chung TK, Wong YF, Smith DI, Roberts LR. Integrations of the hepatitis B virus (HBV) and human papillomavirus (HPV) into the human telomerase reverse transcriptase (hTERT) gene in liver and cervical cancers. *Oncogene* 2003; **22**: 3813-3820

14 **Horikawa I,** Barrett JC. Cis-activation of the human telomerase gene (hTERT) by the hepatitis B virus genome. *J Natl Cancer Inst* 2001; **93**: 1171-1173

15 **Anzola M.** Hepatocellular carcinoma: role of hepatitis B and hepatitis C viruses proteins in hepatocarcinogenesis. *J Viral Hepat* 2004; **11**: 383-393

16 **Murakami S.** Hepatitis B virus X protein: a multifunctional viral regulator. *J Gastroenterol* 2001; **36**: 651-660

17 **Horikawa I,** Cable PL, Afshari C, Barrett JC. Cloning and characterization of the promoter region of human telomerase reverse transcriptase gene. *Cancer Res* 1999; **59**: 826-830

18 **Van Tine BA,** Kappes JC, Banerjee NS, Knops J, Lai L, Steenbergen RD, Meijer CL, Snijders PJ, Chatis P, Broker TR, Moen PT Jr, Chow LT. Clonal selection for transcriptionally active viral oncogenes during progression to cancer. *J Virol* 2004; **78**: 11172-11186

19 **Horikawa I,** Barrett JC. Transcriptional regulation of the telomerase *hTERT* gene as a target for cellular and viral oncogenic mechanisms. *Carcinogenesis* 2003; **24**: 1167-1176

20 **Cheng W.** Human DNA oncogenic viruses and their transforming protein interactions with cell cycle control proteins. *Chin Med J* 1999; **112**: 291-296

21 **Veldman T,** Horikawa I, Barrett JC, Schlegel R. Transcriptional activation of the telomerase hTERT gene by human papillomavirus type 16 E6 oncoprotein. *J Virol* 2001; **75**: 4467–4472

22 **Al Moustafa AE,** Foulkes WD, Benlimame N, Wong A, Yen L, Bergeron J, Batist G, Alpert L, Alaoui-Jamali MA. E6/E7 proteins of HPV type 16 and ErbB-2 cooperate to induce neoplastic transformation of primary normal oral epithelial cells. *Oncogene* 2004; **23**: 350-358

23 **Psyrri A,** DeFilippis RA, Edwards AP, Yates KE, Manuelidis L, DiMaio D. Role of the retinoblastoma pathway in senescence triggered by repression of the human papillomavirus E7 protein in cervical carcinoma cells. *Cancer Res* 2004; **64**: 3079-3086

24 **Jeong Seo E,** Jung Kim H, Jae Lee C, Tae Kang H, Seong Hwang E. The role of HPV oncoproteins and cellular factors in maintenance of hTERT expression in cervical carcinoma cells. *Gynecol Oncol* 2004; **94**: 40-47

25 **Veldman T,** Horikawa I, Barrett JC, Schlegel R. Transcriptional activation of the telomerase hTERT gene by human papillomavirus type 16 E6 oncoprotein. *J Virol* 2001; **75**: 4467-4472

26 **Gewin L,** Galloway DA. E box-dependent activation of telomerase by human papillomavirus type 16 E6 does not require induction of c-myc. *J Virol* 2001; **75**: 7198–7201

27 **Kekule AS,** Lauer U, Weiss L, Luber B, Hofschneider PH. Hepatitis B virus transactivator HBx uses a tumour promoter signalling pathway. *Nature* 1993; **361**: 742-745

28 **Yun C,** Cho H, Kim SJ, Lee JH, Park SY, Chan GK, Cho H. Mitotic aberration coupled with centrosome amplification is induced by hepatitis B virus X oncoprotein via the Ras-mitogen-activated protein/extracellular signal-regulated kinase-mitogen-activated protein pathway. *Mol Cancer Res* 2004; **2**: 159-169

Science Editor Kumar M and Guo SY **Language Editor** Elsevier HK

PO Box 2345, Beijing 100023, China
www.wjgnet.com
wjg@wjgnet.com

ELSEVIER

World J Gastroenterol 2005;11(36):5633-5637
World Journal of Gastroenterology ISSN 1007-9327
© 2005 The WJG Press and Elsevier Inc. All rights reserved.

Synergistic effect of all-trans-retinoic acid and arsenic trioxide on growth inhibition and apoptosis in human hepatoma, breast cancer, and lung cancer cells *in vitro*

Le-Min Lin, Bao-Xin Li, Jian-Bing Xiao, Dan-Hua Lin, Bao-Feng Yang

Le-Min Lin, Department of General Surgery, The First Clinical College, Harbin Medical University, Harbin 150001, Heilongjiang Province, China
Bao-Xin Li, Jian-Bing Xiao, Dan-Hua Lin, Bao-Feng Yang, Department of Pharmacology, Harbin Medical University, Harbin 150086, Heilongjiang Province, China
Supported by the Key Scientific and Technological Projects of Heilongjiang Province during the 10th Five-Year Plan Period, No. GB05C401-10
Correspondence to: Dr. Bao-Feng Yang, Department of Pharmacology, Harbin Medical University, Harbin 150086, Heilongjiang Province, China. yangbf@cms.hrbmu.edu.cn
Telephone: +86-451-86671354 Fax: +86-451-86699644
Received: 2005-01-14 Accepted: 2005-04-02

AIM: To investigate the effect of all-trans-retinoic acid (ATRA) on arsenic trioxide (As_2O_3)-induced apoptosis of human hepatoma, breast cancer, and lung cancer cells in an attempt to find a better combination therapy for solid tumors.

METHODS: Human hepatoma cell lines HepG2, Hep3B, human breast cancer cell line MCF-7, and human lung adenocarcinoma cell line AGZY-83-a were treated with As_2O_3 together with ATRA. Cell survival fraction was determined by MTT assay, cell viability and apoptosis were measured by annexin V-fluorescein isothiocyanate (FITC) and PI staining, and intracellular glutathione (GSH) and glutathione-S-transferase (GST) activities were determined using commercial kits.

RESULTS: Cytotoxicity of ATRA was low. ATRA (0.1, 1, and 10 μmol/L) could synergistically potentiate As_2O_3 to exert a dose-dependent inhibition of growth and to induce apoptosis in each of the cell lines. HepG2 and Hep3B with low intracellular GSH or GST activities were remarkably sensitive to As_2O_3 or As_2O_3+ATRA, while AGZY-83-a with higher GSH or GST activities was less sensitive to As_2O_3 or As_2O_3+ATRA. Treatment with 2 μmol/L As_2O_3 for 72 h significantly decreased intracellular GSH and GST levels in each of the cell lines, and 1 μmol/L ATRA alone reduced minimal intracellular GSH and GST levels. ATRA potentiated the effect of As_2O_3 on intracellular GSH levels, but intracellular GST levels were not significantly affected by the combination of As_2O_3 and ATRA for 72 h as compared to As_2O_3 alone.

CONCLUSION: ATRA can strongly potentiate As_2O_3-induced growth-inhibition and apoptosis in each of the cell lines, and two drugs can produce a significant synergic effect. The sensitivity to As_2O_3 or As_2O_3+ATRA is inversely proportional to intracellular GSH or GST levels in each of the cell lines. The GSH redox system may be the possible mechanism by which ATRA synergistically potentiates As_2O_3 to exert a dose-dependent inhibition of growth and to induce apoptosis.

© 2005 The WJG Press and Elsevier Inc. All rights reserved.

Key words: Arsenic trioxide; All-trans-retinoic acid; Hepatocellular carcinoma; Cancer of breast and lung; Glutathione; Glutathione-S-transferase

Lin LM, Li BX, Xiao JB, Lin DH, Yang BF. Synergistic effect of all-trans-retinoic acid and arsenic trioxide on growth inhibition and apoptosis in human hepatoma, breast cancer, and lung cancer cells *in vitro*. *World J Gastroenterol* 2005; 11(36): 5633-5637
http://www.wjgnet.com/1007-9327/11/5633.asp

Liver, breast, and lung cancers are the most common malignant diseases in the human race. Surgical resection or radiation therapy is potentially curative for localized diseases. Advanced liver, breast, and lung cancers are associated with a poor prognosis, and conventional chemotherapies and radiation therapy are still of limited effectiveness. Innovative approaches for advanced disease are necessary.

During the last decade, investigators using As_2O_3 alone or the combination of all-trans-retinoic acid (ATRA) and As_2O_3 for patients with acute promyelocytic leukemia (APL), have achieved great success[1-3]. Because of the many pathways involved in mediating the effects of arsenic, the potential exists for synergism with other agents to provide enhanced therapeutic benefits. Retinoic acid and arsenic synergize to eradicate leukemic cells in a mouse model of APL[4,5].

Other studies have also shown that As_2O_3 or ATRA alone has antiproliferative and apoptotic activities in some solid tumors, including human hepatoma and breast cancer[6-8]. Because of the drug resistance of solid tumors to As_2O_3, it has not been widely used in the treatment of solid tumors. Therefore, this study was to investigate the effect of ATRA on As_2O_3-induced cell apoptosis in human

hepatoma, breast cancer, and lung cancer in an attempt to find a better combination therapy for solid tumors. To our knowledge, this is the first report on the effects of the combination of As_2O_3 and ATRA for solid tumors.

The glutathione (GSH) redox system is known to modulate the growth-inhibitory and apoptotic effect of As_2O_3. Different kinds of malignant cells have different GSH levels. It was reported that the GSH redox system is relative to sensitivity of malignant cells to As_2O_3[9]. Elevated GSH levels are associated with the chemoresistance of malignant cells. Optimal therapies for chemoresistant malignant cells should overcome or bypass the increased intracellular GSH levels. Glutathione-S-transferase (GST), an enzyme involved in metabolic detoxification of a variety of xenobiotics, is increased in an arsenic-resistant CHO cell line[10,11]. Therefore, we also measured intracellular GSH and GST levels in malignant cells, when they were treated in the absence or presence of As_2O_3, ATRA, or As_2O_3+ATRA.

Materials

Human hepatoma cell lines HepG2, Hep3B, human breast cancer cell line MCF-7 (American Type Culture Collection, Rockville, MD, USA) and human lung adenocarcinoma cell line AGZY-83-a (Harbin Medical University) were cultured in Dulbecco's modified Eagle's medium (DMEM) supplemented with 100 U/mL penicillin, 100 μg/mL streptomycin, 1 mmol/L L-glutamine, and 10% heat-inactivated fetal bovine serum in a humidified atmosphere of 50 mL/L CO_2 at 37 ¡æ Cells in logarithmic growth were seeded at 1×10^5 cells/mL for studies performed in duplicate and repeated at least thrice. As_2O_3 solution (0.1%) was purchased from Harbin Medical University (Harbin, China). ATRA, MTT, and dimethyl sulfoxide (DMSO) were purchased from Sigma Chemical Co. (St. Louis, MO, USA).

Cell proliferation and cell survival rate tested with MTT

Cell proliferation was measured by a MTT assay. For proliferation assays, cells were plated onto 96-well plates (2×10^3 cells/well, 200 μL cell suspension per well) and cultured overnight to allow for cell attachment. Cells were then treated with drugs of different concentrations in the absence (control) or presence of As_2O_3 (0.5, 1, 1.5, and 2 μmol/L), ATRA (0.1, 1, and 10 μmol/L), or As_2O_3+ATRA. All groups had concentrations of four compound wells. After incubation for 72 h, 20 μL of 0.5% MTT was added to each well and incubated for another 4 h. The supernatant was discarded and 150 μL of DMSO was added. When the stain was dissolved, the optical density ABS (absorbance) value of each well was read on Minireader II at 490 nm. Cell survival rate was calculated with the following equation: average *A* value of experimental group/ average *A* value of control group×100%. Each experiment was repeated at least thrice.

Quantitation of cell viability and apoptotic cells

Cell viability and apoptosis were measured by annexin V-fluorescein isothiocyanate (FITC) (Becton Dickinson) and PI staining. Cells were plated onto six-well dishes (1×10^5 cells/dish) and grown overnight to allow for cell attachment. They were then treated in the absence (control) or presence of As_2O_3 (2 μmol/L), ATRA (1 and 10 μmol/L), or As_2O_3+ATRA (1 and 10 μmol/L) for 72 h. After the indicated time, cells were harvested, washed once in PBS and stained with annexin V-FITC (Biovision) and PI (2 mg/mL) according to manufacturer's instructions. Samples were acquired on a FACScan flow cytometer (Becton Dickinson, San Jose, CA, USA) and analyzed with CellQuest software (Becton Dickinson).

Intracellular glutathione measurements

Intracellular GSH levels were determined in all cell lines. Cells were plated onto six-well dishes (1×10^5 cells/dish) and grown overnight to allow for cell attachment. They were then treated in the absence (control) or presence of As_2O_3 (2 μmol/L), ATRA (1 μmol/L), or As_2O_3+ATRA for 72 h. After the indicated time, cells were harvested, and intracellular GSH was measured using the GSH assay kit (Calbiochem, San Diego, CA, USA). Briefly, cells were pelleted, resuspended in 500 μL ice-cold 5% metaphosphoric acid, and homogenized with a Teflon pestle and an overhead stirrer. After centrifugation at 3 000 r/min for 10 min at 4 ¡æ, 60 μL supernatant, 60 μL solution R1, 2 μL solution R2, and 1 mL solution R3 were combined according to the manufacturer's instructions. Samples were incubated at room temperature for 5 min in the dark, and the final absorbance was measured at 412 nm and compared to a GSH standard curve. To quantitate the total protein, the pellet from the above centrifugation was resuspended in 1 mol/L NaOH, and the protein concentration was measured using the Bio-Rad DC protein assay (Bio-Rad, Hercules, CA, USA). Intracellular GSH was normalized to total protein content.

Measurement of intracellular GST

GST activity was determined using commercial kits (Calbiochem, San Diego, CA, USA). GST activity was measured using 1-chloro-2,4-dinitrobenzene (CDNB) and GSH as substrates. Cells were plated onto six-well dishes (1×10^5 cells/dish) and grown overnight to allow for cell attachment. They were then treated in the absence (control) or presence of As_2O_3 (2 μmol/L), ATRA (1 μmol/L), or As_2O_3+ATRA for 72 h. After the indicated time, cells were harvested. The cell pellets were resuspended in 300 μL of 100 mmol/L potassium phosphate buffer, pH 6.8, sonicated for 10 s at 4 ¡æ and centrifuged at 14 000 *g* for 30 min. Supernatant was used for GST measurement according to the manufacturer's instructions. The absorbance at 412 nm was continuously recorded for 2 min. The pellet was dissolved in 1 mol/L NaOH and analyzed for protein by Bio-Rad protein assay (Bio-Rad Laboratories, Hercules, CA, USA). The GST content was expressed as nanomoles per milligram protein per minute.

Statistical analysis

Data were presented graphically as mean±SD. Treatment groups were compared by independent *t*-test or paired *t* test as appropriate, with *P* reported in each figure legend. Statistical analyses were performed using SPSS 10.1 software.

Effects of ATRA and As_2O_3 on growth inhibition in each cell line

To examine the possible relationship between serum concentration and growth-inhibitory effects of the two drugs, cells were treated with drugs of different concentrations in the absence (control) or presence of As_2O_3 (0.5, 1, 1.5, and 2 μmol/L), ATRA (0.1, 1, and 10 μmol/L), or As_2O_3+ATRA for 72 h, and then cell growth was measured by MTT assays.

The ATRA alone at 0.1, 1, and 10 μmol/L could only moderately inhibit cell growth in each of the cell lines. As_2O_3 exerted a dose-dependent growth inhibition of the HepG2, Hep3B, MCF-7, AGZY-83-a cells (Figures 1A-D).

Interestingly, the combination of ATRA (0.1, 1, and 10 μmol/L) and As_2O_3 had at least an additive effect on growth inhibition in each of the cell lines. ATRA (0.1, 1, and 10 μmol/L) could synergistically potentiate As_2O_3 to exert a dose-dependent growth inhibition in each of the cell lines. High concentration of ATRA (10 μmol/L) exerted greater synergistic effects on growth inhibition than low concentration (0.1 μmol/L, Figures 1A-D).

Effects of two drugs on apoptosis in each cell line

Cytotoxicity of ATRA was low. The apoptotic rate of 1 or 10 μmol/L of ATRA approached to that of control in each of the cell lines, and the difference was not significant

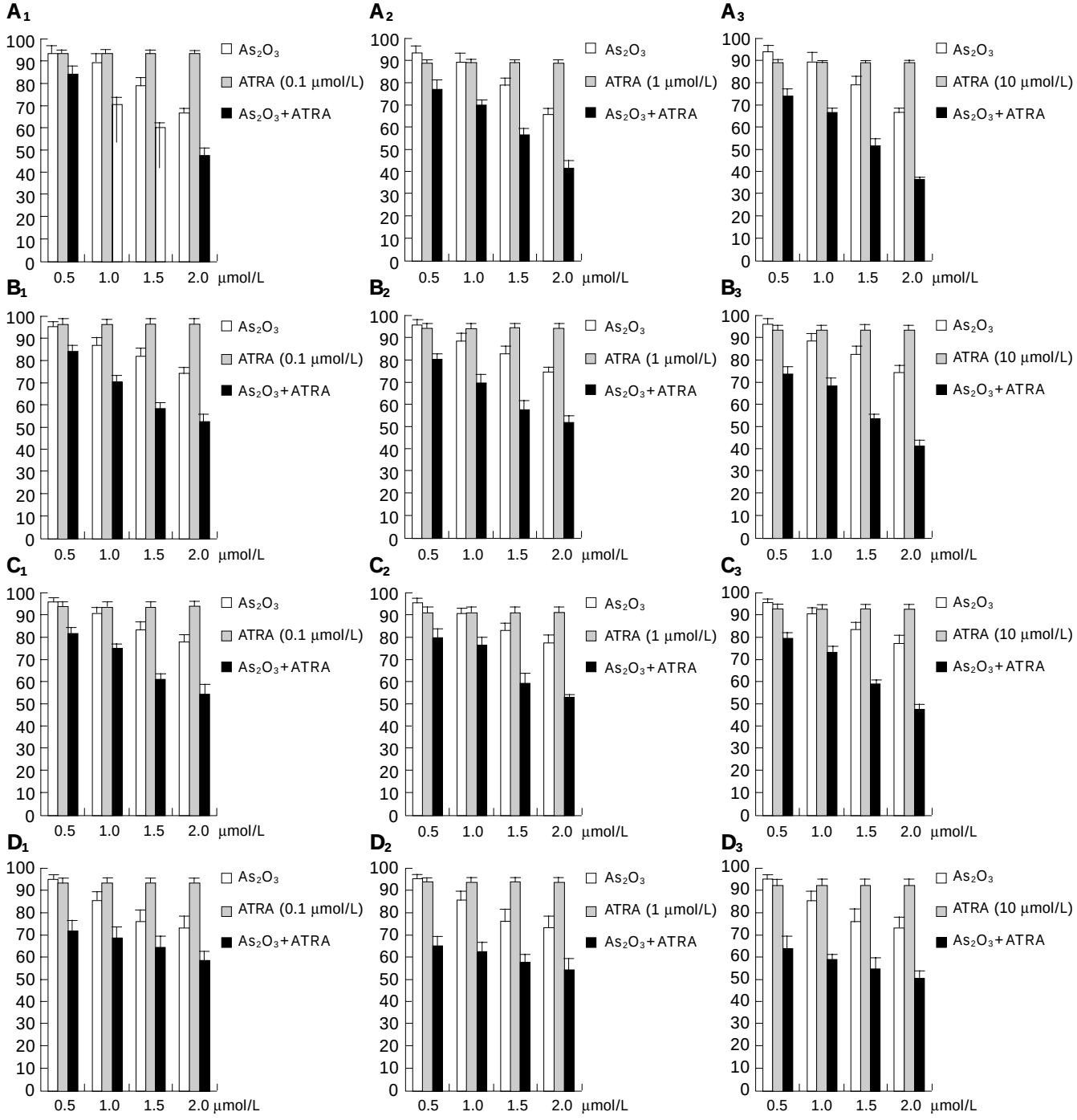


Figure 1 Effects of ATRA and As_2O_3 on growth inhibition in cancer cell lines HepG2 (A), Hep3B (B), MCF-7 (C), and AGZY-83-a (D).

Table 1 Basal activities of GSH or GST and As_2O_3+ ATRA or As_2O_3-induced apoptosis in different cell lines (mean±SD)

Cell lines	GSH	GST	As_2O_3	Apoptosis (%)	
				As_2O_3+ATRA (10 μmol/L)	As_2O_3+ ATRA (1 μmol/L)
HepG2	60.7±7.1	22.3±1.4	29.3±3.2	61.1±5.6	48.4±4. 1
Hep3B	62.4±5.4	21.4±2.8	27.3±6.5	57.1±4.9	49.3±4.2
MCF-7	76.0±5.1	31.0±2.6	22.6±3.3	45.5±3.0	40.2±3.3
AGZY-83-a	104.8±8.1	50.6±4.5	19.0±3.8	40.8±5.6	32.9±3.0

(P>0.05). ATRA greatly potentiated the apoptosis induced by As_2O_3. Exposure of the cells to the combination of As_2O_3 (2 μmol/L) and ATRA (10 μmol/L) for 72 h synergistically induced apoptosis in HepG2 (61.1±5.6%), Hep3B (57.1±4.9%), MCF-7 (45.5±3.0%), AGZY-83-a (40.8±5.6%) respectively, as measured by annexin V-FITC and PI staining as compared to exposure of the cells to either agent alone (Figure 2A). A similar, dramatic effect was observed, when they were treated in the absence (control) or presence of As_2O_3 (2 μmol/L), ATRA (1 μmol/L), or As_2O_3+ATRA for 72 h, with HepG2 being 48.4±4.1%, Hep3B being 49.3±4.2%, MCF-7 being 40.2±3.3%, AGZY-83-a being 32.9±3.0% respectively (Figure 2B). All these findings indicated that ATRA could synergistically potentiate As_2O_3 to induce apoptosis in each of the cell lines.

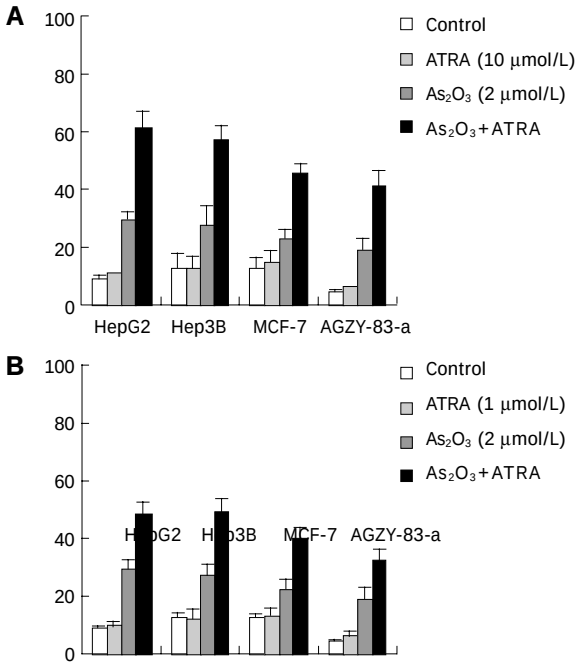


Figure 2 Effects of combined ATRA (10 mol/L: A, 1 mol/L: B) and As_2O_3, and either agent alone on apoptosis in cancer cell lines.

Changes of intracellular GSH and GST

HepG2 and Hep3B with low intracellular GSH or GST activities, were remarkably sensitive to 2 μmol/L As_2O_3 or As_2O_3 (2 μmol/L)+ATRA (10 μmol/L), the apoptotic rate was 29.3±3.2% and 61.1±5.6%, respectively. AGZY-83-a with higher GSH or GST activities was less sensitive to As_2O_3 or As_2O_3+ATRA, the apoptotic rate was 19.0±3.8% and 40.8±5.6%, respectively (Table 1). The sensitivity to As_2O_3 or As_2O_3+ATRA was inversely proportional to intracellular GSH or GST levels in each of the cell lines. A similar, dramatic effect was observed when they were treated in the presence of As_2O_3 (2 μmol/L), or As_2O_3 (2 μmol/L)+ATRA (1 μmol/L) for 72 h (Table 1).

Dramatic changes of intracellular GSH or GST activities were observed when the cell lines were treated in the absence (control) or presence of As_2O_3 (2 μmol/L), ATRA (1 μmol/L), or As_2O_3+ATRA for 72 h. Treatment with 2 μmol/L As_2O_3 for 72 h significantly decreased the intracelluar GSH and GST levels in each of the cell lines, and 1 μmol/L ATRA alone reduced minimal intracellular GSH and GST levels. ATRA potentiated the effect of As_2O_3 on intracellular GSH levels, but intracellular GST levels were not significantly affected by the combination of As_2O_3 (2 μmol/L) and ATRA (1 μmol/L) for 72 h as compared to As_2O_3 alone (Tables 2 and 3).

Table 2 Effect of As_2O_3 on intracellular GSH levels (mean±SD)

Cell lines	Control	ATRA[a]	As_2O_3[c]	As_2O_3+ATRA[e]
HepG2	60.7±7.1	54.4±4.9	46.7±9.0	26.8±4.4
Hep3B	62.4±5.4	55.6±0.5	35.3±3.0	25.9±3.6
MCF-7	76.0±5.1	69.9±1.7	52.5±2.4	44.1±3.8
AGZY-83-a	104.8±8.1	99.8±9.4	89.8±5.6	80.4±1.0

[a]P>0.05, [c]P<0.05 *vs* the control cells, [e]P<0.05 *vs* As_2O_3-treated cells.

Table 3 Changes in intracellular GST activities (mean±SD)

Cell lines	Control	ATRA[a]	As_2O_3[c]	As_2O_3+ATRA[e]
HepG2	22.3±1.4	21.2±1.7	5.5±1.8	8.6±2.3
Hep3B	21.4±2.8	20.4±4.4	8.6±1.8	10.3±3.4
MCF-7	31.0±2.6	29.7±3.0	16.4±1.6	19.3±1.4
AGZY-83-a	50.6±4.5	49.3±4.7	36.3±0.9	39.3±3.1

[a]P>0.05, [c]P<0.05 *vs* the control cells, [e]P>0.05 *vs* As_2O_3-treated cells.

Our *in vitro* studies showed that the combination of As_2O_3 and ATRA was statistically superior to either As_2O_3 or ATRA alone in the treatment of the three cell lines. Furthermore, ATRA (0.1, 1, and 10 μmol/L) could synergistically potentiate As_2O_3 to exert a dose-dependent growth inhibition in each of the cell lines. Cell survival rate could be reduced from 89.5±3.9% to 70.5±3.3% in HepG2 cells exposed to 1 μmol/L As_2O_3 or the combination of 1 μmol/L As_2O_3 and 0.1 μmol/L ATRA for 72 h.

Apoptosis is important for the development and

homeostasis of multicellular organisms. Specific therapies have been designed to enhance the susceptibility of human cancers to apoptosis. We showed that the combination of As_2O_3 and ATRA dramatically and significantly increased the number of apoptotic cells in each of the cell lines, especially the human hepatoma cell lines HepG2 and Hep3B.

Drug resistance of cancer cells and toxicity of cell apoptotic agents are the major factors contributing to the failure of chemotherapy. At least four distinct mechanisms contribute to the chemoresistance. Cellular response to steroids typically depends on the expression of the glucocorticoid receptor, and resistance to steroid therapies is classically associated with downregulation or loss of glucocorticoid receptor expression in some malignant cells[12,13]. The overexpression of drug efflux pumps, such as *mdr* gene product P-glycoprotein (PgP), is also a common trait of chemoresistant malignant cells[14,15]. In addition, it was reported that the expression of the antiapoptotic protein Bcl-xL is higher in some chemoresistant malignant cells[16]. Furthermore, increased expression or activity of GSH and GSH-related enzymes confers resistance to antineoplastic agents[17,18]. GSH is the major auto-oxidant of the cells, and functions to scavenge free radicals and to detoxify toxins and chemotherapeutic agents. GSH can bind to arsenic by the formation of a transient $As(GS)_3$ complex[19].

The GSH redox system is known to modulate the growth-inhibitory and apoptotic effect of As_2O_3. Different kinds of malignant cells have different GSH levels. It was reported that the GSH redox system is relative to sensitivity of malignant cells to As_2O_3[9]. Elevated GSH levels are associated with the chemoresistance of malignant cells. Optimal therapies for chemoresistant malignant cells should overcome or bypass the increased intracellular GSH levels. It is known that GST, an enzyme involved in metabolic detoxification of a variety of xenobiotics, is increased in an arsenic-resistant CHO cell line[10]. Our study showed that HepG2 and Hep3B with low intracellular GSH or GST activities were remarkably sensitive to As_2O_3 or As_2O_3+ATRA, while AGZY-83-a with higher GSH or GST activities was less sensitive to As_2O_3 or As_2O_3+ATRA. The sensitivity to As_2O_3 or As_2O_3+ATRA was inversely proportional to GSH or GST levels in each of the cell lines.

Arsenite can decrease GSH levels which can result in DNA damage as a result of increased intracellular reactive oxygen molecules. Our intracellular GSH and GST assays showed that treatment with 2 μmol/L As_2O_3 for 72 h significantly decreased intracellular GSH and GST levels in each of the cell lines, and 1 μmol/L ATRA alone reduced minimal intracellular GSH and GST levels (Tables 2 and 3). ATRA potentiated the effect of As_2O_3 on intracellular GSH levels, but intracellular GST levels were not significantly affected by the combination of As_2O_3 (2 μmol/L) and ATRA (1 μmol/L) for 72 h as compared to As_2O_3 alone. These findings indicate that GSH redox system may be the possible mechanism by which ATRA synergistically potentiates As_2O_3 to induce apoptosis or to exert a dose-dependent inhibition of growth. Either As_2O_3 alone or in combination with ATRA may become a useful adjuvant therapy for liver, breast, and lung cancers.

1 **Avvisati G,** Lo Coco F, Mandelli F. Acute promyelocytic leukemia: clinical and morphologic features and prognositic factors. *Semin Hematol* 2001; **38**: 4-12

2 **Fenaux P,** Chomienne C, Degos L. All-trans retinoic acid and chemotherapy in the treatment of acute promyelocytic leukemia. *Semin Hematol* 2001; **38**: 13-25

3 **Chen Z,** Chen GQ, Shen ZX, Chen SJ, Wang ZY. Treatment of acute promyelocytic leukemia with arsenic compounds: *in vitro* and *in vivo* studies. *Semin Hematol* 2001; **38**: 26-36

4 **Lallemand-Breitenbach V,** Guillemin MC, Janin A, Daniel MT, Degos L, Kogan SC, Bishop JM, de The H. Retinoic acid and arsenic synergize to eradicate leukemic cells in a mouse model of acute promyelocytic leukemia. *J Exp Med* 1999; **189**: 1043-1052

5 **Rego EM,** He LZ, Warrell RP Jr, Wang ZG, Pandolfi PP. Retinoic acid (RA) and As2O3 treatment in transgenic models of acute promyelocytic leukemia (APL) unravel the distinct nature of the leukemogenic process induced by the PML/RAR alpha and PLZF/RAR alpha oncoproteins. *Proc Natl Acad Sci USA* 2000; **97**: 10173-10178

6 **Zhang T,** Wang SS, Hong L, Wang XL, Qi QH. Arsenic trioxide induces apoptosis of rat hepatocellular carcinoma cells *in vivo*. *J Exp Clin Cancer Res* 2003; **22**: 61-68

7 **Vernhet L,** Allain N, Le Vee M, Morel F, Guillouzo A, Fardel O. Blockage of multidrug resistance-associated proteins potentiates the inhibitory effects of arsenic trioxide on CYP1A1 induction by polycyclic aromatic hydrocarbons. *J Pharmacol Exp Ther* 2003; **304**: 145-155

8 **Wang X,** Kong L, Zhao J, Yang P. Arsenic trioxide in the mechanism of drug resistance reversal in MCF-7/ADM cell line of human breast cancer. *Zhonghua Zhongliu Zazhi* 2002; **24**: 339-343

9 **Dai J,** Weinberg RS, Waxman S, Jing Y. Malignant cells can be sensitized to undergo growth inhibition and apoptosis by arsenic trioxide through modulation of the glutathione redox system. *Blood* 1999; **93**: 268-277

10 **Lee TC,** Wei ML, Chang WJ, Ho IC, Lo JF, Jan KY, Huang H. Elevation of glutathione levels and glutathione S-transferase activity in arsenic-resistant Chinese hamster ovary cells. *In Vitro Cell Dev Biol* 1989; **25**: 442-448

11 **Lo JF,** Wang HF, Tam MF, Lee TC. Glutathione S-transferase pi in an arsenic-resistant Chinese hamster ovary cell line. *Biochem J* 1992; **288**(Pt 3): 977-982

12 **Moalli PA,** Pillay S, Weiner D, Leikin R, Rosen ST. A mechanism of resistance to glucocorticoids in multiple myeloma: transient expression of a truncated glucocorticoid receptor mRNA. *Blood* 1992; **79**: 213-222

13 **Gomi M,** Moriwaki K, Katagiri S, Kurata Y, Thompson EB. Glucocorticoid effects on myeloma cells in culture: correlation of growth inhibition with induction of glucocorticoid receptor messenger RNA. *Cancer Res* 1990; **50**: 1873-1878

14 **Epstein J,** Xiao HQ, Oba BK. P-glycoprotein expression in plasma-cell myeloma is associated with resistance to VAD. *Blood* 1989; **74**: 913-917

15 **Dalton WS,** Durie BG, Alberts DS, Gerlach JH, Cress AE. Characterization of a new drug-resistant human myeloma cell line that expresses P-glycoprotein. *Cancer Res* 1986; **46**: 5125-5130

16 **Tu Y,** Renner S, Xu F, Fleishman A, Taylor J, Weisz J, Vescio R, Rettig M, Berenson J, Krajewski S, Reed JC, Lichtenstein A. BCL-X expression in multiple myeloma: possible indicator of chemoresistance. *Cancer Res* 1998; **58**: 256-262

17 **Gupta V,** Singh SV, Ahmad H, Medh RD, Awasthi YC. Glutathione and glutathione S-transferases in a human plasma cell line resistanct to melphalan. *Biochem Pharmacol* 1989; **38**: 1993-2000

18 **Bellamy WT,** Dalton WS, Gleason MC, Grogan TM, Trent JM. Development and characterization of a melphalan-resistant human multiple myeloma cell line. *Cancer Res* 1991; **51**: 995-1002

19 **Scott N,** Hatlelid KM, MacKenzie NE, Carter DE. Reactions of arsenic(III) and arsenic(V) species with glutathione. *Chem Res Toxicol* 1993; **6**: 102-106

Science Editor Wang XL and Guo SY **Language Editor** Elsevier HK

PO Box 2345, Beijing 100023, China
www.wjgnet.com
wjg@wjgnet.com

ELSEVIER

World J Gastroenterol 2005;11(36):5638-5643
World Journal of Gastroenterology ISSN 1007-9327
© 2005 The WJG Press and Elsevier Inc. All rights reserved.

Lysophosphatidic acid transactivates both c-Met and epidermal growth factor receptor, and induces cyclooxygenase-2 expression in human colon cancer LoVo cells

Dai Shida, Joji Kitayama, Hironori Yamaguchi, Hiroharu Yamashita, Ken Mori, Toshiaki Watanabe, Hirokazu Nagawa

Dai Shida, Joji Kitayama, Hironori Yamaguchi, Hiroharu Yamashita, Ken Mori, Toshiaki Watanabe, Hirokazu Nagawa, Department of Surgical Oncology, University of Tokyo Graduate School of Medicine, Tokyo 113-8655, Japan
Supported by a Grant-in-Aid for Scientific Research from the Ministry of Education, Culture, Sports, Science and Technology of Japan and a grant from the Ministry of Health, Labour and Welfare of Japan
Correspondence to: Dr. Dai Shida, Department of Surgical Oncology, University of Tokyo Graduate School of Medicine, 7-3-1 Hongo, Bunkyo-ku, Tokyo 113-8655, Japan. dshida-tky@umin.ac.jp
Telephone: +81-3-5800-8653 Fax: +81-3-3811-6822
Received: 2004-12-10 Accepted: 2005-03-09

Abstract

AIM: To examine whether lysophosphatidic acid (LPA) induces phosphorylation of c-Met and epidermal growth factor receptor (EGFR), both of which have been proposed as prognostic markers of colorectal cancer, and whether LPA induces cyclooxygenase-2 (COX-2) expression in human colon cancer cells.

METHODS: Using a human colon cancer cell line, LoVo cells, we performed immunoprecipitation analysis, followed by Western blot analysis. We also examined whether LPA induced COX-2 expression, by Western blot analysis.

RESULTS: Immunoprecipitation analysis revealed that 10 μmol/L LPA induced tyrosine phosphorylation of c-Met and EGFR in LoVo cells within a few minutes. We found that c-Met tyrosine phosphorylation induced by LPA was not attenuated by pertussis toxin or a matrix metalloproteinase inhibitor, in marked contrast to the results for EGFR. In addition, 0.2-40 μmol/L LPA induced COX-2 expression in a dose-dependent manner.

CONCLUSION: Our results suggest that LPA acts upstream of various receptor tyrosine kinases (RTKs) and COX-2, and thus may act as a potent stimulator of colorectal cancer.

© 2005 The WJG Press and Elsevier Inc. All rights reserved.

Key words: Lysophosphatidic acid; c-Met; EGFR; Transactivation; Cyclooxygenase-2; Colon cancer

Shida D, Kitayama J, Yamaguchi H, Yamashita H, Mori K, Watanabe T, Nagawa H. Lysophosphatidic acid transactivates both c-Met and epidermal growth factor receptor, and induces cyclooxygenase-2 expression in human colon cancer LoVo cells. *World J Gastroenterol* 2005; 11(36): 5638-5643
http://www.wjgnet.com/1007-9327/11/5638.asp

INTRODUCTION

Although the incidence of colorectal cancer was substantially lower in Asia than that in the USA in the mid-twentieth century, the incidence in Japan and China has been rapidly increasing[1,2]. Thus, colorectal cancer is now a major cause of cancer death worldwide. Surgery is the main modality of treatment for colorectal cancer, other modalities like chemotherapy being adjuvant in nature. Whereas fluorouracil has been reported to be the only effective systemic therapeutic agent for colorectal cancer until recently, considerable improvement has been achieved in the last decade with the development of newer chemotherapeutic agents, such as irinotecan and oxaliplatin. In addition to these conventional cytotoxic agents, growing interest and significant advances have been made in the use of targeted therapy for colorectal cancer during the last few years. Bevacizumab, a mAb against vascular endothelial growth factor (VEGF), and cetuximab, a chimeric mAb directed against epidermal growth factor receptor (EGFR), were shown to improve the survival of patients with metastatic colorectal cancer in large randomized clinical trials[3-5]. Now that molecular target therapy for colorectal cancer has started in clinical settings, new and more effective molecular targets are eagerly being investigated.

From this standpoint, we have focused on lysophosphatidic acid (LPA, 1- or 2-acyl-sn-glycero-3-phosphate). LPA, the simplest glycerophospholipid, has been shown to interact with at least three G protein-coupled receptors (GPCRs), such as LPA1/Edg-2, LPA2/Edg-4, and LPA3/Edg-7[6,7]. Through these receptors, LPA mediates a broad range of cellular responses, including smooth muscle cell contraction, platelet aggregation, neurite retraction/cell rounding, regulation of cell proliferation, protection from apoptosis, modulation of chemotaxis and transcellular migration[8-10]. Some of these cellular responses implicate LPA as a mediator of tumor progression[11]. We have previously reported several experimental studies using cell lines and surgically resected specimens. Using various human colon cancer cells, we revealed that LPA stimulated migration, adhesion, proliferation, and secretion of angiogenic factors *in vitro*, although the responses induced showed some differences among cells, which seemed to be based on their expression pattern of LPA receptors[12]. We also revealed aberrant

expression of LPA receptors in human colorectal cancer tissues; i.e., overexpression of LPA2 and underexpression of LPA1 in colorectal cancer compared with normal mucosa[13]. Thus, LPA and its receptors play crucial roles in the development and progression of colorectal cancer.

As for colorectal cancer, it is well known that the use of nonsteroidal anti-inflammatory drugs (NSAIDs) has been linked to a 40-50% reduction in relative risk for cancer development[14]. The molecular basis for this striking chemopreventive effect has been attributed to inhibition of cyclooxygenases (COX)[14]. Consistent with this, approximately 80% of colorectal cancers show increased levels of COX-2[14,15]. COX-2 is responsible for the synthesis of prostaglandin E_2 (PGE_2), a bioactive lipid molecule with diverse biological activities, including growth-promoting actions on the gastrointestinal mucosa. Although the precise mechanism of these trophic actions of PGs had remained unclear for a long time, it was recently demonstrated that PGE_2 could phosphorylate EGFR and trigger the extracellular signal-regulated kinase 2 (ERK2)-mitogenic signaling pathway, which reveals a previously unknown mechanism by which PGE_2 mediates a trophic action resulting in the growth of colonic polyps and cancers[16].

Thus, tyrosine phosphorylation of various receptor tyrosine kinases (RTKs) in response to activation of many GPCRs, which was designated as "transactivation", has been shown to have important physiological consequences and has received considerable attention in recent years. In addition to EGFR, PGE_2 was also shown to transactivate c-Met, the receptor for hepatocyte growth factor (HGF) resulting in increased invasiveness of colon cancer cells[16,17]. In colorectal cancer, c-Met expression level has been shown to be a predictor of tumor invasion and lymph node metastasis, suggesting that c-Met signals contribute to colorectal cancer progression[18,19].

LPA has been reported to transactivate EGFR in several cell types, and, in some epithelial cells, LPA has also been reported to induce COX-2 gene expression[13,20-24]. However, to the authors' knowledge, LPA signaling pathways in colon cancer cells have not been fully understood as yet. In the present study, using colon cancer LoVo cells which are known to express abundant c-Met at both mRNA and protein levels[25], we investigated whether LPA induces phosphorylation of c-Met as well as EGFR, and whether LPA induces COX-2 expression.

MATERIALS AND METHODS

Materials

A selective inhibitor of COX-2, NS-398, was purchased from Cayman Chemicals (Ann Arbor, MI, USA), and 1-oleoyl-LPA was purchased from Sigma Chemical Co. (St. Louis, MO). Recombinant human HGF was purchased from R&D Systems, Inc. (Minneapolis, MN, USA) and recombinant human EGF was purchased from PeproTechEC Ltd. (London, UK). Rabbit polyclonal anti-human c-Met antibody (C-28), rabbit polyclonal anti-human EGFR antibody, and mouse monoclonal anti-human phosphotyrosine antibody (PY20) were purchased from Santa Cruz Biotechnology, Inc. (Santa Cruz, CA, USA). Mouse monoclonal anti-human COX-2 antibody was purchased from Exalpha Biologicals, Inc. (Boston, MA, USA). Pertussis toxin (PTX) and the broad-spectrum matrix metalloproteinase (MMP) inhibitor GM6001 were purchased from Calbiochem (La Jolla, CA, USA).

Cell culture

The human colon cancer cell line, LoVo cells, were obtained from American Type Culture Collection (Manassas, VA, USA) and maintained in Dulbecco modified Eagle medium (DMEM) supplemented with 100 mL/L fetal calf serum (Sigma, St. Louis, MO, USA), 100 U/mL penicillin, and 100 μg/mL streptomycin (Gibco BRL Co., Grand Island, NY, USA).

Immunoprecipitation and Western blot analysis of RTK transactivation

Immunoprecipitation and Western blot analysis were performed as described previously[13,26,27]. In brief, LoVo cells were starved in serum-free medium for 24 h and then LPA was added to the culture. After incubation of starved LoVo cells with 10 μmol/L LPA for various times, cellular protein lysates were obtained and then proteins were incubated with antibodies against two RTKs, c-Met and EGFR. Immunoprecipitates were collected with protein A-agarose. Immunoprecipitated proteins were electrophoresed on sodium dodecyl sulfate (SDS)-75 g/L polyacrylamide gel for 35 min at 200 V. Then, the protein was transferred onto an Immobilon transfer membrane (Millipore Co., Bedford, MA, USA) for sequential incubation with 50 g/L reconstituted non-fat milk powder to block nonspecific sites, dilutions of rabbit polyclonal anti-phosphotyrosine antibody, and then horseradish peroxidase-labeled donkey anti-rabbit IgG, prior to the development with a standard ECL kit (Amersham, Inc., Buckinghamshire, UK). Some cells were pretreated with 100 ng/mL PTX for 24 h before stimulation, and other cells were pretreated with 5-50 μmol/L GM6001 for 30 min before stimulation. All membranes were stripped and immunoblotted with antibodies against RTKs as a control.

Western blot analysis of cyclooxygenase-2

LoVo cells were starved in serum-free medium overnight and then various concentrations of LPA were added to the culture. After incubation of starved LoVo cells with LPA for 24 h, cellular protein lysates were obtained. Then, cell proteins (15 μg per lane) were electrophoresed on SDS-150 g/L polyacrylamide gel for 45 min at 200 V. Then, the protein was transferred onto an Immobilon transfer membrane (Millipore Co.) for sequential incubation with 50 g/L reconstituted non-fat milk powder to block nonspecific sites, dilutions of mouse monoclonal anti-human COX-2 antibody, and then horseradish peroxidase-labeled donkey anti-rabbit IgG, prior to the development with a standard ECL kit (Amersham, Inc.). The same membrane was stripped and immunoblotted with antibodies against β-actin as a control.

Proliferation assay

LoVo cells (5×10^3 cells in 100 μL solution per well), which were pretreated with DMSO or 100 μmol/L NS-398, were seeded in a 96-well plate in DMEM containing 1 g/L fatty acid-free BSA with various concentrations of LPA, which

was added every 24 h. After incubation at 37 ℃ in 50 mL/L CO_2 for 120 h, the number of living cells was measured using an MTS assay (Promega Co., Madison, WI, USA) according to the manufacturer's instructions. Briefly, MTS solution was added to each well and the cells were further incubated for 3 h. The number of living cells was determined by measuring optical density at 490 nm.

RESULTS

LPA-induced tyrosine phosphorylation of c-Met in colon cancer cells

In order to investigate whether tyrosine phosphorylation of c-Met was induced by LPA, LoVo cells were incubated with 10 μmol/L LPA for 2-60 min. As shown in Figure 1, LPA induced a significant level of tyrosine phosphorylation of c-Met in LoVo cells. Time course experiments revealed that phosphorylation was maximal after 2 min of stimulation and declined thereafter, suggesting that LPA-induced rapid and transient tyrosine phosphorylation of c-Met. After stripping, c-Met in LoVo cells was detected by anti-human c-Met antibody at 190 ku. The amount of c-Met immunoprecipitation was not different with or without LPA (Figure 1). In reverse experiments, phosphotyrosine immunoprecipitation and anti-c-Met immunoblotting revealed the same results (Figure 1). Tyrosine phosphorylation of c-Met induced by 10 μmol/L LPA was as strong as that induced by 10 ng/mL HGF (Figure 2).

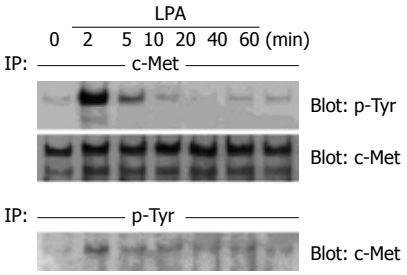


Figure 1 Rapid tyrosine phosphorylation of c-Met in response to LPA in human colon cancer cells. (**A**) Human colon cancer LoVo cells were serum-starved for 24 h and then incubated with 10 μmol/L LPA for 2-60 min. After cell lysis, c-Met was immunoprecipitated (IP) using polyclonal anti-c-Met antibody, and immunoprecipitates were immunoblotted with monoclonal anti-phosphotyrosine antibody. Then the membrane was stripped and immunoblotted with anti-c-Met as a control. (**B**) Human colon cancer LoVo cells were serum-starved for 24 h and then incubated with 10 μmol/L LPA for 2-60 min. These cell lysates were IP with anti-phosphotyrosine, and the immunoprecipitates were immunoblotted with anti-c-Met.

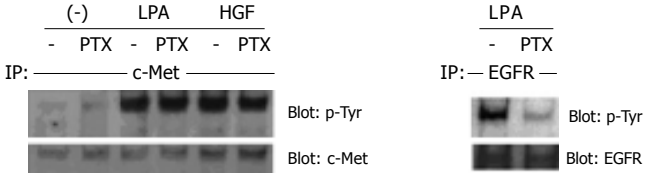


Figure 2 Effect of PTX, a Gi inhibitor, on LPA-stimulated c-Met transactivation in colon cancer cells. Human colon cancer LoVo cells were serum-starved for 24 h with or without 100 ng/mL PTX and then stimulated with 10 μmol/L LPA or 10 ng/mL HGF for 2 min. Cell lysates were IP with anti-c-Met. Immunoprecipitates were immunoblotted with anti-phosphotyrosine. Then the membrane was stripped and immunoblotted with anti-c-Met as a control. The same experiments were performed using anti-EGFR as a control for the inhibitory effect of PTX.

Tyrosine phosphorylation of c-Met induced by LPA was not inhibited by pertussis toxin

As shown in Figure 2, pretreatment with PTX partly decreased the LPA-induced phosphorylation of EGFR in LoVo cells. This is compatible with previous reports that LPA-induced EGFR transactivation in Cos-7 cells, and head and neck squamous cell carcinoma cells (HNSCC) was PTX sensitive, suggesting the involvement of Gi protein in this signaling pathway[28,29]. To address the question of whether a Gi-dependent mechanism is also involved in LPA-induced c-Met transactivation in colon cancer cells, we examined the effect of PTX in our system. In contrast to EGFR transactivation, PTX did not significantly inhibit tyrosine phosphorylation of c-Met in response to LPA in any experimental condition (24-48 h pretreatment with 100-200 ng/mL PTX) (Figure 2). Thus, LPA-induced c-Met transactivation in colon cancer cells seems to be Gi-independent.

Tyrosine phosphorylation of c-Met induced by LPA was not dependent on MMP activation

Previous reports have shown that GPCR-induced EGFR transactivation requires MMP activation and cleavage of the membrane-anchored growth factor precursor pro-HB-EGF in COS-7 cells, HEK-293 cells and HNSCC[20,30]. As shown in Figure 3, pretreatment with an MMP inhibitor, GM6001, decreased the phosphorylation of EGFR by LPA in LoVo cells in a dose-dependent manner, which is compatible with previous reports. In contrast to EGFR transactivation, GM6001 did not significantly inhibit LPA-induced tyrosine phosphorylation of c-Met at any concentration (Figure 3). Thus, LPA-induced c-Met transactivation in colon cancer cells does not require MMP activation.

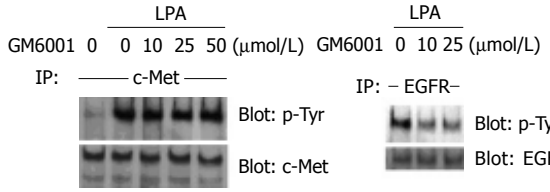


Figure 3 Effect of GM6001, an MMP inhibitor, on LPA-stimulated c-Met transactivation in colon cancer cells. Human colon cancer LoVo cells were serum-starved for 24 h and pre-incubated with the indicated concentrations of GM6001 for 30 min. After incubation with 10 μmol/L LPA for 2 min, cell lysates were obtained and IP with anti-c-Met. Immunoprecipitates were immunoblotted with anti-phosphotyrosine. Then the membrane was stripped and immunoblotted with anti-c-Met as a control. The same experiments were performed using anti-EGFR as a control for the inhibitory effect of GM6001.

LPA induced COX-2 expression in colon cancer cells

LPA has been shown to induce COX-2 expression in some epithelial cells[13,20,21]. However, as for cancer cells, to our knowledge, there is no report of LPA-induced COX-2 expression. Hence, we examined whether LPA induces COX-2 expression in LoVo cells. When LoVo cells were stimulated with various concentrations of LPA for 24 h, the 72-ku COX-2 protein was increased in a concentration-dependent manner (Figure 4). This effect was maximal at an LPA concentration of 40 μmol/L.

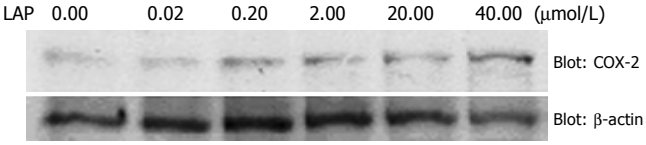


Figure 4 Effect of LPA on COX-2 expression in colon cancer cells. Human colon cancer LoVo cells were serum-starved for 24 h, and then treated with 0.02-40 μmol/L LPA for 24 h. After cell lysis, the expression level of COX-2 protein was examined by Western blotting using anti-COX-2 antibody. Then the membrane was stripped and immunoblotted with anti-β-actin as a control.

COX-2 inhibitor reduced LPA-induced proliferation in colon cancer cells

LPA has been shown to be a potent mitogen for various cell types. In order to investigate the role of LPA-induced COX-2 expression, we performed a proliferation assay using NS398, a selective COX-2 inhibitor, with the measurement by MTS assay. LPA itself induced a dose-dependent increase in proliferation, showing significant growth stimulation at 0.2 μmol/L and a stronger effect at 20 μmol/L (5.2±0.6 -fold increase compared with control) (Figure 5). NS398 alone did not show a significant effect in control conditions without LPA; however, NS398 markedly inhibited LPA-induced proliferation at 20 μmol/L LPA (51±6% inhibition) (Figure 5). Thus, NS398 significantly inhibited LPA-induced LoVo cell proliferation.

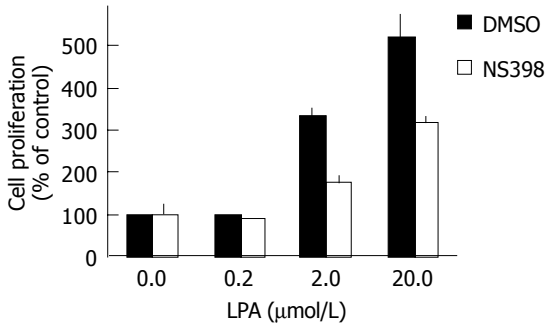


Figure 5 Inhibition of LPA-induced proliferation of LoVo cells by NS398, a COX-2 inhibitor. Human colon cancer LoVo cells, after being pretreated with DMSO or NS398, were seeded with the indicated concentrations of LPA. After incubation for 120 h, the cell proliferation was measured using MTS assay. Data are expressed as a percentage of control, where control indicates cell proliferation in the absence of LPA without NS398 pretreatment (100%).

DISCUSSION

In this study, using LoVo cells, we revealed LPA induced transactivation of c-Met as well as EGFR. Since both c-Met and EGFR serve as prognostic markers in human colorectal cancer, LPA may be a potent stimulator of colorectal cancer progression that acts upstream of these RTK signaling pathways (Figure 5)[18,31]. We also revealed that LPA induced COX-2 expression. Interestingly, PGE_2, which is synthesized by COX-2, is known to transactivate both c-Met and EGFR[16,17]. Taking these results together, LPA may act upstream of these RTK signaling pathways in a dual manner; one is a direct effect and the other an indirect effect accomplished via COX-2 upregulation (Figure 6).

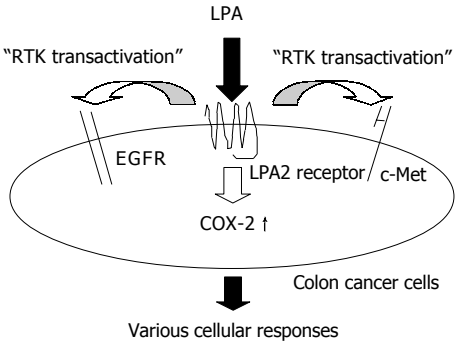


Figure 6 Mechanism of the effects of LPA on human colon cancer cells.

EGFR is well-known to not only transduce EGF signals, but also integrate diverse stimuli, such as LPA, bombesin, thrombin, and S1P[28,30,32-34]. This transactivation of EGFR represents a paradigm for cross-talk between GPCRs and RTK signaling pathways. From this knowledge, a novel picture of EGFR as a central cellular network element has been established in recent years, which broadens both its physiological as well as pathological significance[35-37]. In addition to EGFR transactivation, Pai *et al*.[17], recently reported c-Met transactivation which was induced by PGE_2 in colon cancer cells. They also showed that, whereas HGF induces autophosphorylation of tyrosine residues in c-Met and can enhance invasion into the extracellular matrix, ligand-independent activation of the c-Met signaling pathway could cause similar changes and increase colon cancer cell invasion[17]. Thus, c-Met signals, which were activated by various stimuli, also seem to play an important role in colorectal cancer progression. In this study, we revealed that tyrosine phosphorylation of c-Met induced by LPA was rapid and transient, which is exactly the same pattern as that of EGFR. Thus, LPA utilizes EGFR and c-Met as a downstream signaling partner in colon cancer cells.

Previous studies indicated that LPA-stimulated transactivation of EGFR in COS-7 cells and HNSCC was mediated partly via Gi protein and required MMP activation[28-30]. In our study of colon cancer cells, we also confirmed that LPA-induced transactivation of EGFR was mediated partly via Gi protein and required MMP activation. In contrast, LPA-induced transactivation of c-Met did not show significant inhibition by either PTX or GM6001. These data indicated that c-Met transactivation by LPA does not require Gi proteins and MMP activation, in marked contrast to EGFR transactivation induced by LPA. Since Gq is known to be coupled with LPA receptors and plays a role in EGFR transactivation, this Gq or other G proteins could be involved in the transactivation of c-Met. The contribution of MMP activation in EGFR transactivation has been shown to induce proteolytic cleavage of transmembrane precursors, such as pro-HB-EGF, which subsequently activates the EGFR family[20,30]. Our results, however, suggested that HGF or other c-Met ligands do not exist as a membrane-bound form, such as HB-EGF.

Accumulating evidence indicates that COX-2 plays key roles in intestinal tumorigenesis. In addition, COX-2 overexpression in colon cancer cells was shown to promote

cell motility and stimulate the production of angiogenic factors[38]. Thus, the expression level of COX-2 may determine, at least in part, the aggressiveness of cancer. In this study, we demonstrated LPA induced COX-2 expression in a dose-dependent manner. We also revealed that a COX-2 inhibitor significantly reduced LPA-induced proliferation of LoVo cells. These results suggest that LPA uses COX-2 as a downstream signaling partner, which results in making cancer cells aggressive.

We have previously demonstrated that LoVo cells exclusively expressed LPA2 among the three LPA receptors, by both Northern blot analysis and real-time RT-PCR method[12,13]. Therefore, LPA-induced transactivation of c-Met and EGFR in LoVo cells, as well as LPA-induced COX-2 expression, might be presumably mediated by the LPA2 receptor. We have previously demonstrated that, in colorectal cancer tissue, the LPA2 receptor is markedly overexpressed as compared with normal mucosa[12,13]. Moreover, overexpression of the LPA2 receptor was also shown in ovarian cancer, thyroid cancer, and breast cancer as compared to normal tissue[39-42]. Since, in general, the targets of newly developed drugs are mostly GPCRs, the LPA2 receptor, a member of GPCR, could be a novel molecular target for cancer therapy.

In summary, this study demonstrates that LPA, at a physiological concentration, induces transactivation of c-Met as well as EGFR, and induces COX-2 expression. Colorectal cancers are often associated with local bleeding and thus, at the tumor site, platelets are activated and secrete lysophospholipids such as lysophosphatidylcholine (LPC), lysophosphatidylethanolamine (LPE), and lysophosphatidylserine (LPS). These lysophospholipids are subsequently converted to LPA by lysophospholipase D[43]. Therefore, a significant amount of extracellular LPA is thought to be present in colorectal cancer tissue, and is able to induce various important biological responses in cancer tissues. Our findings indicate that the development of an antagonist for LPA or the appropriate spectrum of LPA receptors may be a new and effective therapy for colon cancer.

REFERENCES

1 **Lu JB,** Sun XB, Dai DX, Zhu SK, Chang QL, Liu SZ, Duan WJ. Epidemiology of gastroenterologic cancer in Henan Province, China. *World J Gastroenterol* 2003; **9**: 2400-2403
2 **Yiu HY,** Whittemore AS, Shibata A. Increasing colorectal cancer incidence rates in Japan. *Int J Cancer* 2004; **109**: 777-781
3 **Hurwitz H,** Fehrenbacher L, Novotny W, Cartwright T, Hainsworth J, Heim W, Berlin J, Baron A, Griffing S, Holmgren E, Ferrara N, Fyfe G, Rogers B, Ross R, Kabbinavar F. Bevacizumab plus irinotecan, fluorouracil, and leucovorin for metastatic colorectal cancer. *N Engl J Med* 2004; **350**: 2335-2342
4 **Saltz LB,** Meropol NJ, Loehrer PJ Sr, Needle MN, Kopit J, Mayer RJ. Phase II trial of cetuximab in patients with refractory colorectal cancer that expresses the epidermal growth factor receptor. *J Clin Oncol* 2004; **22**: 1201-1208
5 **Cunningham D,** Humblet Y, Siena S, Khayat D, Bleiberg H, Santoro A, Bets D, Mueser M, Harstrick A, Verslype C, Chau I, Van Cutsem E. Cetuximab monotherapy and cetuximab plus irinotecan in irinotecan-refractory metastatic colorectal cancer. *N Engl J Med* 2004; **351**: 337-345
6 **An S,** Bleu T, Hallmark OG, Goetzl EJ. Characterization of a novel subtype of human G protein-coupled receptor for lysophosphatidic acid. *J Biol Chem* 1998; **273**: 7906-7910
7 **Bandoh K,** Aoki J, Hosono H, Kobayashi S, Kobayashi T, Murakami-Murofushi K, Tsujimoto M, Arai H, Inoue K. Molecular cloning and characterization of a novel human G-protein-coupled receptor, EDG7, for lysophosphatidic acid. *J Biol Chem* 1999; **274**: 27776-27785
8 **Moolenaar WH.** Lysophosphatidic acid, a multifunctional phospholipid messenger. *J Biol Chem* 1995; **270**: 12949-12952
9 **Moolenaar WH.** Bioactive lysophospholipids and their G protein-coupled receptors. *Exp Cell Res* 1999; **253**: 230-238
10 **Goetzl EJ,** An S. Diversity of cellular receptors and functions for the lysophospholipid growth factors lysophosphatidic acid and sphingosine 1-phosphate. *FASEB J* 1998; **12**: 1589-1598
11 **Mills GB,** Moolenaar WH. The emerging role of lysophosphatidic acid in cancer. *Nat Rev Cancer* 2003; **3**: 582-591
12 **Shida D,** Kitayama J, Yamaguchi H, Okaji Y, Tsuno NH, Watanabe T, Takuwa Y, Nagawa H. Lysophosphatidic acid (LPA) enhances the metastatic potential of human colon carcinoma DLD1 cells through LPA1. *Cancer Res* 2003; **63**: 1706-1711
13 **Shida D,** Watanabe T, Aoki J, Hama K, Kitayama J, Sonoda H, Kishi Y, Yamaguchi H, Sasaki S, Sako A, Konishi T, Arai H, Nagawa H. Aberrant expression of lysophosphatidic acid (LPA) receptors in human colorectal cancer. *Lab Invest* 2004; **84**: 1352-1362
14 **DuBois RN,** Giardiello FM, Smalley WE. Nonsteroidal anti-inflammatory drugs, eicosanoids, and colorectal cancer prevention. *Gastroenterol Clin North Am* 1996; **25**: 773-791
15 **Eberhart CE,** Coffey RJ, Radhika A, Giardiello FM, Ferrenbach S, DuBois RN. Up-regulation of cyclooxygenase 2 gene expression in human colorectal adenomas and adenocarcinomas. *Gastroenterology* 1994; **107**: 1183-1188
16 **Pai R,** Soreghan B, Szabo IL, Pavelka M, Baatar D, Tarnawski AS. Prostaglandin E2 transactivates EGF receptor: a novel mechanism for promoting colon cancer growth and gastrointestinal hypertrophy. *Nat Med* 2002; **8**: 289-932
17 **Pai R,** Nakamura T, Moon WS, Tarnawski AS. Prostaglandins promote colon cancer cell invasion; signaling by cross-talk between two distinct growth factor receptors. *FASEB J* 2003; **17**: 1640-1647
18 **Takeuchi H,** Bilchik A, Saha S, Turner R, Wiese D, Tanaka M, Kuo C, Wang HJ, Hoon DS. c-MET expression level in primary colon cancer: a predictor of tumor invasion and lymph node metastases. *Clin Cancer Res* 2003; **9**: 1480-1488
19 **Di Renzo MF,** Olivero M, Giacomini A, Porte H, Chastre E, Mirossay L, Nordlinger B, Bretti S, Bottardi S, Giordano S. Overexpression and amplification of the met/HGF receptor gene during the progression of colorectal cancer. *Clin Cancer Res* 1995; **1**: 147-154
20 **Gschwind A,** Prenzel N, Ullrich A. Lysophosphatidic acid-induced squamous cell carcinoma cell proliferation and motility involves epidermal growth factor receptor signal transactivation. *Cancer Res* 2002; **62**: 6329-6336
21 **Kue PF,** Taub JS, Harrington LB, Polakiewicz RD, Ullrich A, Daaka Y. Lysophosphatidic acid-regulated mitogenic ERK signaling in androgen-insensitive prostate cancer PC-3 cells. *Int J Cancer* 2002; **102**: 572-579
22 **Ershov AV,** Bazan NG. Induction of cyclooxygenase-2 gene expression in retinal pigment epithelium cells by photoreceptor rod outer segment phagocytosis and growth factors. *J Neurosci Res* 1999; **58**: 254-261
23 **Goppelt-Struebe M,** Fickel S, Reiser CO. The platelet-derived-growth-factor receptor, not the epidermal-growth-factor receptor, is used by lysophosphatidic acid to activate p42/44 mitogen-activated protein kinase and to induce prostaglandin G/H synthase-2 in mesangial cells. *Biochem J* 2000; **345**: 217-224
24 **Hahn A,** Barth H, Kress M, Mertens PR, Goppelt-Struebe M. Role of Rac and Cdc42 in lysophosphatidic acid-mediated cyclo-oxygenase-2 gene expression. *Biochem J* 2002; **362**: 33-40
25 **Nabeshima K,** Shimao Y, Inoue T, Itoh H, Kataoka H, Koono M. Hepatocyte growth factor/scatter factor induces not only

scattering but also cohort migration of human colorectal-adenocarcinoma cells. *Int J Cancer* 1998; **78**: 750-759
26 **Shida D,** Kitayama J, Yamaguchi H, Hama K, Aoki J, Arai H, Yamashita H, Mori K, Sako A, Konishi T, Watanabe T, Sakai T, Suzuki R, Ohta H, Takuwa Y, Nagawa H. Dual mode regulation of migration by lysophosphatidic acid in human gastric cancer cells. *Exp Cell Res* 2004; **301**: 168-178
27 **Shida D,** Kitayama J, Yamaguchi H, Yamashita H, Mori K, Watanabe T, Yatomi Y, Nagawa H. Sphingosine 1-phosphate transactivates c-Met as well as epidermal growth factor receptor (EGFR) in human gastric cancer cells. *FEBS Lett* 2004; **577**: 333-338
28 **Daub H,** Wallasch C, Lankenau A, Herrlich A, Ullrich A. Signal characteristics of G protein-transactivated EGF receptor. *EMBO J* 1997; **16**: 7032-7044
29 **Gschwind A,** Hart S, Fischer OM, Ullrich A. TACE cleavage of proamphiregulin regulates GPCR-induced proliferation and motility of cancer cells. *EMBO J* 2003; **22**: 2411-2421
30 **Prenzel N,** Zwick E, Daub H, Leserer M, Abraham R, Wallasch C, Ullrich A. EGF receptor transactivation by G-protein-coupled receptors requires metalloproteinase cleavage of proHB-EGF. *Nature* 1999; **402**: 884-888
31 **Resnick MB,** Routhier J, Konkin T, Sabo E, Pricolo VE. Epidermal growth factor receptor, c-MET, beta-catenin, and p53 expression as prognostic indicators in stage II colon cancer: a tissue microarray study. *Clin Cancer Res* 2004; **10**: 3069-3075
32 **Daub H,** Weiss FU, Wallasch C, Ullrich A. Role of transactivation of the EGF receptor in signalling by G-protein-coupled receptors. *Nature* 1996; **379**: 557-560
33 **Endo A,** Nagashima K, Kurose H, Mochizuki S, Matsuda M, Mochizuki N. Sphingosine 1-phosphate induces membrane ruffling and increases motility of human umbilical vein endothelial cells via vascular endothelial growth factor receptor and CrkII. *J Biol Chem* 2002; **277**: 23747-23754
34 **Kim JH,** Song WK, Chun JS. Sphingosine 1-phosphate activates Erk-1/-2 by transactivating epidermal growth factor receptor in rat-2 cells. *IUBMB Life* 2000; **50**: 119-1124
35 **Zwick E,** Hackel PO, Prenzel N, Ullrich A. The EGF receptor as central transducer of heterologous signalling systems. *Trends Pharmacol Sci* 1999; **20**: 408-412
36 **Gschwind A,** Zwick E, Prenzel N, Leserer M, Ullrich A. Cell communication networks: epidermal growth factor receptor transactivation as the paradigm for interreceptor signal transmission. *Oncogene* 2001; **20**: 1594-1600
37 **Fischer OM,** Hart S, Gschwind A, Ullrich A. EGFR signal transactivation in cancer cells. *Biochem Soc Trans* 2003; **31**: 1203-1208
38 **Tsujii M,** Kawano S, Tsuji S, Sawaoka H, Hori M, DuBois RN. Cyclooxygenase regulates angiogenesis induced by colon cancer cells. *Cell* 1998; **93**: 705-716
39 **Fujita T,** Miyamoto S, Onoyama I, Sonoda K, Mekada E, Nakano H. Expression of lysophosphatidic acid receptors and vascular endothelial growth factor mediating lysophosphatidic acid in the development of human ovarian cancer. *Cancer Lett* 2003; **192**: 161-169
40 **Fang X,** Schummer M, Mao M, Yu S, Tabassam FH, Swaby R, Hasegawa Y, Tanyi JL, LaPushin R, Eder A, Jaffe R, Erickson J, Mills GB. Lysophosphatidic acid is a bioactive mediator in ovarian cancer. *Biochim Biophys Acta* 2002; **1582**: 257-264
41 **Schulte KM,** Beyer A, Kohrer K, Oberhauser S, Roher HD. Lysophosphatidic acid, a novel lipid growth factor for human thyroid cells: over-expression of the high-affinity receptor edg4 in differentiated thyroid cancer. *Int J Cancer* 2001; **92**: 249-256
42 **Kitayama J,** Shida D, Sako A, Ishikawa M, Hama K, Aoki J, Arai H, Nagawa H. Over-expression of lysophosphatidic acid receptor-2 in human invasive ductal carcinoma. *Breast Cancer Res* 2004; **6**: R640-R646
43 **Aoki J,** Taira A, Takanezawa Y, Kishi Y, Hama K, Kishimoto T, Mizuno K, Saku K, Taguchi R, Arai H. Serum lysophosphatidic acid is produced through diverse phospholipase pathways. *J Biol Chem* 2002; **277**: 48737-48744

Science Editor Guo SY and Kumar M **Language Editor** Elsevier HK

PO Box 2345, Beijing 100023, China
www.wjgnet.com
wjg@wjgnet.com

ELSEVIER

World J Gastroenterol 2005;11(36):5644-5650
World Journal of Gastroenterology ISSN 1007-9327
© 2005 The WJG Press and Elsevier Inc. All rights reserved.

Polo-like kinase 1 expression is a prognostic factor in human colon cancer

Wilko Weichert, Glen Kristiansen, Mathias Schmidt, Volker Gekeler, Aurelia Noske, Silvia Niesporek, Manfred Dietel, Carsten Denkert

Wilko Weichert, Glen Kristiansen, Aurelia Noske, Silvia Niesporek, Manfred Dietel, Carsten Denkert, Institute of Pathology, Charité University Hospital, Berlin 10117, Germany
Mathias Schmidt, Volker Gekeler, Altana Pharma AG, Konstanz 78467, Germany
Correspondence to: Dr. Wilko Weichert, Institute of Pathology, Charité University Hospital, Schumannstraße 20/21, Berlin 10117, Germany. wilko.weichert@charite.de
Telephone: +49-30450536006 Fax: +49-30450536922
Received: 2004-12-07 Accepted: 2005-01-05

Abstract

AIM: To clarify the expression patterns and prognostic implications of the mitotic regulator Polo-like kinase 1 (PLK1) in colon cancer.

METHODS: Expression of PLK1 was investigated by immunohistochemistry (158 cases) and immunoblotting in tissue of colon adenomas and adenocarcinomas. PLK1 expression patterns were correlated with clinicopathological parameters and patient prognosis. In addition, expression of PLK1 was evaluated by immunoblot and PCR in colon carcinoma cell lines, and coexpression of PLK1 with the proliferation marker Ki-67 was investigated.

RESULTS: Weak PLK1 expression was observed in normal colon mucosa and adenomas. In contrast, 66.7% of carcinomas showed strong expression of PLK1. Overexpression of PLK1 correlated positively with Dukes stage ($P<0.001$), tumor stage ($P = 0.001$) and nodal status ($P<0.05$). Additionally, PLK1 expression was a prognostic marker in univariate survival analysis ($P<0.01$) and had independent prognostic significance (RR = 3.3, $P = 0.02$) in patients with locoregional disease. Expression of PLK1 mRNA and protein was detected in all cell lines investigated. Coexpression of PLK1 and Ki-67 was observed in the majority of colon cancer cells, but a considerable proportion of cells showed PLK1 positivity without Ki-67 expression.

CONCLUSION: PLK1 is a new prognostic marker for colon carcinoma patients and may be involved in tumorigenesis and progression of colon cancer. Strategies focusing on PLK1 inhibition *in vivo* might therefore represent a promising new therapeutic approach for this tumor entity.

© 2005 The WJG Press and Elsevier Inc. All rights reserved.

Key words: Polo-like kinase; Colon carcinoma; Survival; Immunohistochemistry; Mitosis

Weichert W, Kristiansen G, Schmidt M, Gekeler V, Noske A, Niesporek S, Dietel M, Denkert C. Polo-like kinase 1 expression is a prognostic factor in human colon cancer. *World J Gastroenterol* 2005; 11(36): 5644-5650
http://www.wjgnet.com/1007-9327/11/5644.asp

INTRODUCTION

Colorectal cancer ranks third in cancer deaths for both sexes in the Western world, with 146 940 estimated new cases and 56 730 estimated deaths in USA in 2004[1]. Incidence and mortality of colon cancer have decreased only slightly over the last 20 years. Though surgery is potentially curative, the risk of recurrence is high. Apart from surgical resection, treatment strategies for high risk patients are still mainly based on adjuvant/neoadjuvant use of 5-fluorouracil and leukovorin as chemotherapeutic agents alone or in combination with radiotherapy. Unfortunately, use of the standard therapeutic protocols results only in a moderate decline in mortality and the risk to sustain a recurrence of disease remains high[2]. Furthermore, it is still uncertain which of the patients should be treated, as prediction of the prognosis for an individual patient remains problematic[3]. With increasing knowledge about molecular changes in the malignant phenotype, therapeutic strategies focusing on targeted modulation of signal transduction pathways, which are imperative to malignant cells, are becoming increasingly important. Genetic alterations, typically associated with a malignant cell phenotype, affect genes involved in DNA repair and apoptosis, cell adhesion and invasion, angiogenesis and finally cell proliferation and cell cycle control[4].

After its discovery in Drosophila 16 years ago by Sunkel and Glover[5] *polo* has become the founding member of a whole family of protein kinases centrally involved in the mitotic regulation of both normal and malignant transformed cells. Since then, polo homologs have been discovered in a broad variety of species, including certain bacteria, yeast, mice, and men[6,7]. Till date, there are four known polo homologs in human beings with Polo-like kinase 1 (PLK1) being the best characterized protein of this family[8].

There is convincing evidence that PLK1 plays a central role in the G_2/M transition by exerting an important control function in several steps of mitosis[7]. Additionally, PLK1 plays an important role in the regulation of microtubule dynamics and in the maturation of centrosomes[9].

Expression of PLK1 has been described in a variety of

human malignancies[10-21]. We and others have reported that PLK1 overexpression had a significant impact on patient prognosis in some of these tumor entities[0,13,15,17,20]. For colon cancer, the prognostic impact of PLK1 has not been investigated so far.

The central aim of this study was to evaluate the status of PLK1 expression in a cohort of 158 benign and malignant colon tumors and in colon cancer cell lines by immunohistochemistry and immunoblotting, and to investigate the association of PLK1 expression with clinicopathological parameters and patient survival.

MATERIALS AND METHODS

Patients

A total of 153 patients (age: 31-86 years, median 65.45 years) who were diagnosed for colon cancer at the Institute of Pathology, Charité University Hospital between 1996 and 1999, were included in this study. Only patients with primary colon adenocarcinomas and no other known malignancies were included. None of the patients received radiotherapy or chemotherapy prior to diagnosis. All patients were residents of the city of Berlin. The majority of patients represented consecutive cases of colon cancer in our institute. Based on tissue availability in our archive, a small number of cases (7.8%, 12 cases) had to be excluded from this study. Histologic diagnosis was established on standard H&E stained sections according to the guidelines of the World Health Organization. The details on the distribution of clinicopathological factors in the study cohort are listed in Table 1. Clinical follow-up data were available for all patients. The median follow-up time of survivors was 47 mo. Forty-one patients (27%) died after a median time of 60 mo of follow-up. As a control for non-malignant colon tumors, five adenomas of the colon were included in the study as well.

Cell lines

The human colon carcinoma cell lines RKO and HT29 were obtained from ATCC. CX2 and HRT18 were from the German Cancer Research Center (Heidelberg, Germany). Cells were cultured in either DMEM (RKO) or RPMI (CX2, HRT18, HT29) supplemented with 10% fetal bovine serum.

Polymerase chain reaction

Subconfluent colon carcinoma cells were harvested and total RNA was prepared with RNAeasy kit (Qiagen, Hilden, Germany) and reverse transcribed. PCR cycling conditions for PLK1 were 30 cycles of denaturation, annealing and extension at 95 ℃ for 60 s, at 54 ℃ for 60 s, and at 72 ℃ for 120 s. The primers used were human PLK1 sense 5'-AGTGCTGCAGTGACTGCA-3' and antisense 5'-GGAGGCCTTGAGACGGTT-3' (generating a 1 807-bp band). As control GAPDH sense 5'-ACCACAGTCC-ATGCCATCAC-3' and antisense 5'-TCCACCACCCTG-TTGCTGTA-3' (generating a 452-bp band) primers were used.

Immunoblotting

Tissues from colon carcinomas and normal colon mucosa were dissected by a senior pathologist in the operation theater from surgical specimens sent for frozen section analysis and were immediately frozen in liquid nitrogen and stored at -80 ℃ until analysis.

Subconfluent colon carcinoma cells were harvested and 100 μg protein/sample was loaded on a 10% polyacrylamide gel. Western blots were performed as previously described[22], using a mouse monoclonal anti-PLK1 antibody (BD Transduction, San Diego, CA, USA) diluted 1:500 and an anti-β-actin antibody (Chemicon, Temecula, CA, USA) diluted 1:3 000.

Immunohistochemistry on tissue slides

For immunohistochemical detection of PLK1 on tissue samples and cells, a monoclonal mouse antibody (BD Transduction) directed against human PLK1 protein was used on 5-μm paraffin sections. Antibody specificity has been ascertained by Western blot and immunohistochemistry in preceding expression studies[14,23]. For immunolabeling of Ki-67, a polyclonal rabbit antibody (Dako, Glostrup, Denmark) directed against human Ki-67 protein was used. As negative controls, slides were processed without primary antibody. For antigen retrieval, the deparaffinized slides were placed in 0.01 mol/L sodium citrate buffer, pH 6.0 and boiled for 5 min in a pressure cooker. Then slides were allowed to cool down for additional 5 min in the same buffer. After several rinses in TBS and pre-treatment with blocking reagent (Dako, Glostrup, Denmark) for 5 min, slides were incubated with primary antibody diluted 1:500 (PLK1) and 1:50 (Ki-67) in antibody diluent solution (Zymed, San Francisco, CA, USA) for 20 min at room temperature and then at 4 ℃ overnight. After the slides were washed in TBS, bound antibody was detected by applying a streptavidin-biotin system (BioGenex, San Ramon, CA, USA) following the standard protocol with standard antibody dilutions as supplied by the manufacturers. For color development, a fast red system (Sigma, Deisenhofen, Germany) was used. The slides were mounted using Aquatex (Merck, Gernsheim, Germany).

Double-immunostaining of cells

RKO cells were grown on Labtek chamber slides. Subconfluent cells were fixed in 100% methanol for 20 min at -20 ℃. For immunolabeling of PLK1, slides were processed as described above but without applying the pressure cooker. After the color developed, slides were washed in PBS and subsequently incubated with a 1:50 dilution of primary antibody directed against Ki-67 for 20 min at room temperature and subsequently at 4 ℃ overnight. After the slides were washed in TBS, bound antibody was detected by the peroxidase anti-peroxidase method following the standard protocol with standard antibody dilutions as supplied by the manufacturers (Dako). Color development was performed using a DAB+system (Dako). Finally, slides were mounted using Aquatex.

Evaluation of tissue staining

Staining intensity of tissue slides was evaluated independently by two pathologists who were blinded towards patients' characteristics and survival. Cases with disagreement were discussed using a multi-headed microscope until agreement

was achieved. To assess differences in staining intensity, an immunoreactivity scoring system (IRS) was applied. Intensity of staining was designated as negative (0), weak (1), moderate (2) or strong (3). Additionally, the percentage of positive cells was evaluated and scored as either no cells (0), less then 10% of cells (1), 10-50% of cells (2), 51-80% of cells (3) or over 80% of cells stained (4). By multiplication of these two parameters, the IRS for each case was calculated. Finally, cases were grouped as PLK negative (IRS 0-6) or PLK positive (IRS 7-12) for statistical analysis.

Statistical analysis

Statistical correlation between clinicopathological factors and expression of PLK1 was assessed by applying either Fisher's exact test, Spearman's rank order correlation or χ^2 test for trends. The probability of differences in overall survival as a function of time was determined by Kaplan-Meier analysis and log-rank test. Multivariate probing for significance was performed applying the Cox proportional hazard model. Generally $P<0.05$ was considered statistically significant. For all statistical procedures, SPSS v10.0 software was used.

RESULTS

PLK1 expression in colon tissue and cell lines

Normal colon mucosa from both the vicinity of benign and malignant tumors as well as from more distant sites showed a weak cytoplasmic staining of the epithelium at the basis of colon crypts (Figure 1). Staining was lost in the epithelium of apical parts of the crypts. A comparable staining in the epithelium was observed on serial sections for the proliferation marker Ki-67 (data not shown).

Occasionally, lymphocytes resident in normal colon mucosa showed moderate staining for PLK1 in the cytoplasm. Moderate PLK1 positivity was observed in autonomous neural plexus cells in the submucosa and muscularis propria of the colon. This staining served as an internal positive control.

None of the five adenomas of colon mucosa showed sufficient staining of PLK1 to be designated as PLK1 positive, although a weak patchy staining in the epithelium was observed in all cases (Figure 1).

Among the 153 colon cancers investigated, 102 (66.7%) were PLK1 positive in the neoplastic epithelium (Figure 1 and Table 1). Staining was inhomogeneous in a considerable number of cases with pronounced PLK1 positivity at the leading edge of tumor invasion. However, cases scored as PLK1 negative consistently showed a weak irregular staining for PLK1 in the cytoplasm as well (Figure 1). The tumor-associated inflammatory infiltrate occasionally expressed moderate amounts of PLK1, while all other stromal cells were PLK1 negative in all cases.

Overexpression of PLK1 in colon carcinoma compared to normal colon mucosa could be confirmed by immunoblotting in three of four matched samples of normal colon mucosa and colon carcinoma (Figure 2). In one case the tumor tissue showed a loss of expression in comparison to the normal colon mucosa.

In addition to the investigation of primary colon carcinoma tissue, we also tested four colon carcinoma cell lines for expression of PLK1 mRNA and protein. As shown in Figure 2, all cell lines expressed PLK1 mRNA measured by RT-PCR with a 1 807-bp band. On the protein level, PLK1 expression with an estimated size of 68 ku was

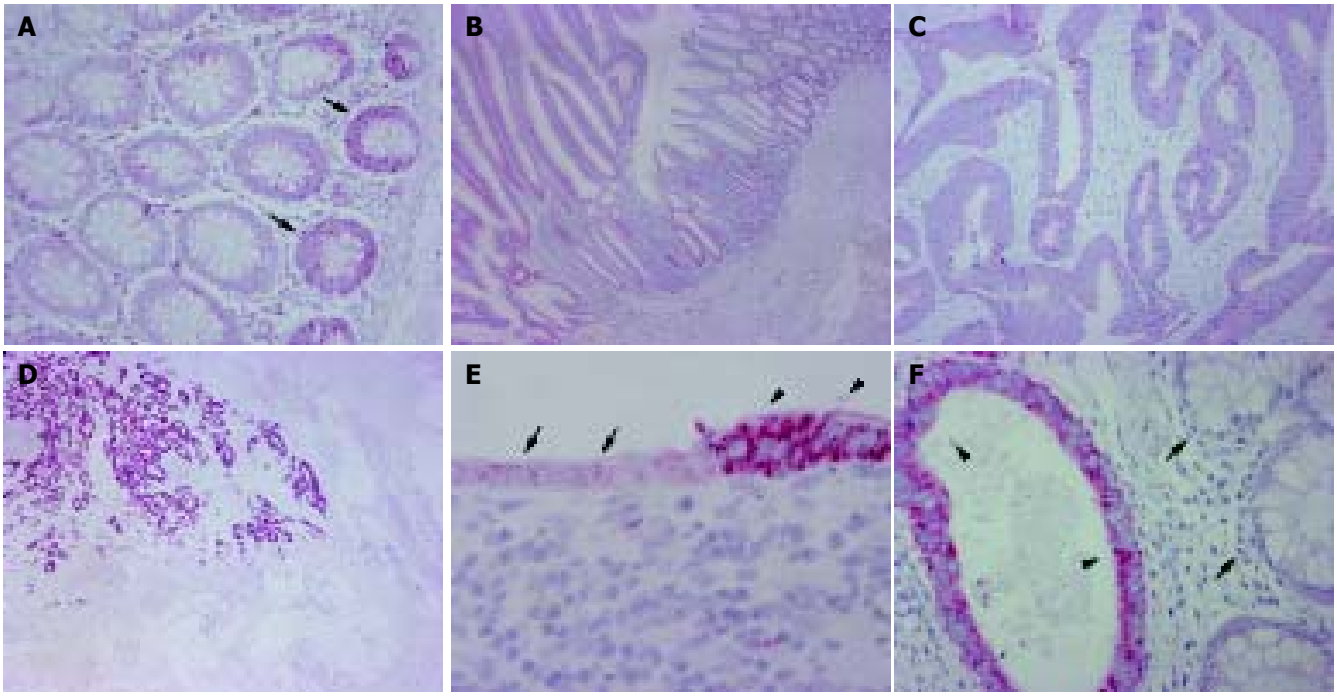


Figure 1 Expression of PLK1 in colon tissue. **A**: PLK1 expression in epithelium of the basis of normal colon crypts (arrows); **B**: Weak PLK1 positivity in colon adenoma; **C**: Weak expression of PLK1 in colon carcinoma; **D**: Strong positivity for PLK1 in colon carcinoma infiltrating pericolonic soft tissue; **E**: Transition of slightly dysplastic colon epithelium (small arrows) into colon carcinoma (arrowheads). Note the abrupt onset of PLK1 expression; **F**: Overexpression of PLK1 in colon carcinoma (arrowheads) infiltrating normal colon mucosa (small arrows). Original magnifications **A**: ×200, **B**: ×50, **C**: ×100, **D**: ×20, **E**/**F**: ×400.

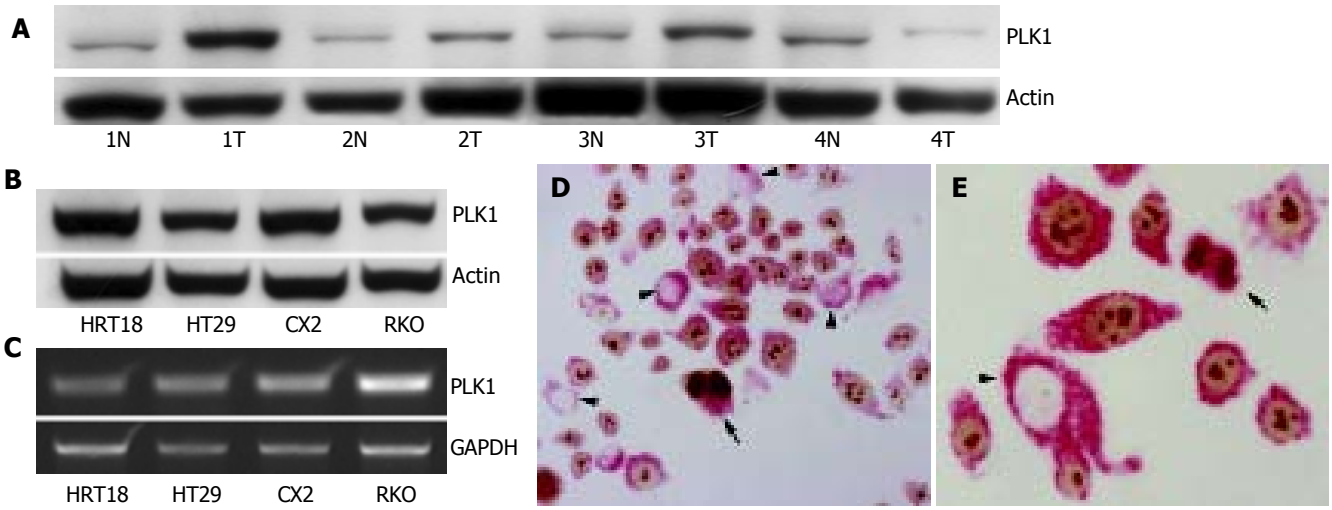


Figure 2 Expression of PLK1 in frozen colon tissue and colon carcinoma cell lines. **A**: Expression of PLK1 protein (68 ku) in colon carcinoma and normal colon mucosa; **B**/**C**: Strong expression of PLK1 protein (**B**, immunoblot, 68 ku) and mRNA (**C**: RT-PCR, 1 807 bp) in colon carcinoma cell lines; **D**/**E**: Coexpression of PLK1 (red staining of the cytoplasm) and Ki-67 (brown staining of the nucleus) in RKO colon carcinoma cell line. A considerable number of cells were PLK1 positive, but remained Ki-67 negative (arrowheads). Note cells in M-phase (small arrows) strongly expressing both proteins. Original magnifications **D**: ×200, **E**: ×500.

detected in all cell lines by immunoblot.

PLK1 and Ki-67 coexpression in primary colon carcinomas and RKO cell line

Since PLK1 plays a pivotal role in cell cycle control, we investigated the coexpression of Ki-67 and PLK1 in the colon cancer cell line RKO by immunolabeling both proteins consecutively on the same slide. As illustrated in Figure 2, simultaneous expression of PLK1 in cytoplasm and Ki-67 in nuclei was evident in the majority of cells. However, while almost all cells expressed PLK1, there was a considerable fraction of cells without simultaneous Ki-67 expression. Similar results were observed in serial sections of primary colon carcinoma tissue. Staining of serial sections of colon carcinomas with PLK1 and Ki-67 revealed no strict overlap between the expressions of both proteins though highly proliferating tumors (strong Ki-67 positivity) were more prone to overexpress PLK1.

Correlation of PLK1 expression with clinicopathological data

A highly significant positive correlation of PLK1 expression with either Dukes stage ($P<0.001$, χ^2 test for trends) and WHO tumor stage ($P = 0.001$, χ^2 test for trends) could be observed. More advanced tumors expressed significantly higher amounts of PLK1 than locally restricted carcinomas (Table 1). Additionally, a significant positive correlation of PLK1 expression with nodal status could be demonstrated ($P = 0.049$, χ^2 test for trends). This observation was further confirmed by a significant positive correlation ($P = 0.044$, $r = 0.163$, Spearman's rank order correlation) of the number of positive lymph nodes with ungrouped PLK1 score. We did not observe a correlation of PLK1 expression in colon cancer with patients' age, status of distant metastasis and tumor grade (Table 1)

Correlation of PLK1 expression with patient prognosis

Known prognostic parameters in colon cancer, as patients' age, Dukes stage, WHO tumor stage, lymph node status, status of distant metastasis and tumor grade were confirmed to have a significant impact on patient prognosis in this study (Table 2).

Additionally, PLK1 expression had a significant impact on patient prognosis both in the whole study cohort ($n = 153$, $P = 0.006$) and in the subgroup of patients without distant metastasis at the time of diagnosis ($n = 140$, $P = 0.012$). The mean survival time of patients in the PLK1 negative groups was 74.13 mo (whole group) and 76.36 mo (subgroup without distant metastasis), while the survival time was reduced to a mean of 63.75 mo (whole group) and 67.77 mo

Table 1 Overall expression of PLK1 in colon carcinoma as well as distribution of PLK1 expression in the study population, *n* (%)

Characteristics		All cases	PLK1 negative	PLK1 positive	*P*
All cases		153	51 (33.3)	102 (66.7)	
Age (yr)					
	≤65 yr	74 (48.4)	28 (37.8)	46 (62.2)	0.304[1]
	>65 yr	79 (51.6)	23 (29.1)	56 (70.9)	
Dukes stage					
	A	35 (22.9)	20 (57.1)	15 (42.9)	
	B	55 (35.9)	19 (34.5)	36 (65.5)	<0.001[2]
	C	50 (32.7)	10 (20)	40 (80)	
	D	13 (8.5)	2 (15.4)	11 (84.6)	
Tumor stage					
	T1	10 (6.5)	9 (90)	1 (10)	
	T2	36 (23.5)	14 (38.9)	22 (61.1)	0.001[2]
	T3	96 (62.7)	24 (25)	72 (75)	
	T4	11 (7.3)	4 (36.4)	7 (63.6)	
Nodal status					
	N0	91 (59.5)	38 (41.8)	53 (58.2)	
	N1	30 (19.6)	4 (13.3)	26 (86.7)	0.049[2]
	N2	32 (20.9)	9 (28.1)	23 (71.9)	
State of distant metastasis					
	Mx	140 (91.5)	49 (35)	91 (65)	0.221[1]
	M1	13 (8.5)	2 (15.4)	11 (84.6)	
Grade					
	G1	6 (3.9)	2 (33.3)	4 (66.7)	
	G2	123 (80.4)	43 (35)	80 (65)	0.423[2]
	G3	24 (15.7)	6 (25)	18 (75)	

[1]Fisher's exact test, [2]χ^2 test for trends.

(subgroup without distant metastasis) in the PLK1 positive groups, respectively (Figure 3). In the whole study cohort, patients with PLK1 positive tumors showed a rate of 65% survival after 5 years compared to 86% survival in the PLK1 negative group. In the subgroup without distant metastasis, the 5-year survival was reduced from 89% in the PLK1 negative group to 70% in the PLK1 positive group (Table 2).

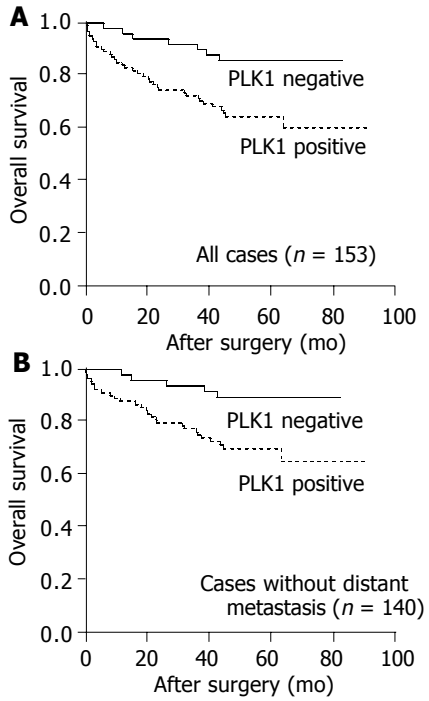


Figure 3 Correlation of PLK1 expression with patient survival in the whole study population (**A**) and in the subgroup of patients with locoregional disease (**B**).

Table 2 Correlation of PLK1 expression and selected tumor parameters with patient prognosis

		Cases	Events	Mean survival (mo)	Standard error	Log-rank test *P*
Age (yr)	≤65 yr	74	13	76.59	3.42	0.0142
	>65 yr	79	29	57.94	3.51	
Dukes stage	A	35	4	70.27	3.18	<0.0001
	B	55	5	83.89	2.67	
	C	50	23	48.26	4.28	
	D	13	10	22.96	6.60	
Tumor stage	T1	10	0	Not reached	–	0.0006
	T2	36	8	74.08	5.06	
	T3	96	27	63.84	3.06	
	T4	11	7	27.00	7.22	
Nodal status	N0	91	11	81.93	2.34	<0.0001
	N1	30	10	55.94	5.17	
	N2	32	21	28.74	3.97	
Metastasis	Mx	140	32	73.19	2.68	<0.0001
	M1	13	10	22.96	6.60	
Grade	G1	6	0	Not reached	–	0.0007
	G2	123	29	72.61	2.90	
	G3	24	13	33.37	4.68	
PLK1 (all cases)	Negative	51	7	74.13	2.90	0.0060
	Positive	102	35	63.75	3.66	
PLK1 (locoregional disease)	Negative	49	5	76.36	2.52	
	Positive	91	27	67.77	3.66	0.0119

In the whole study population, PLK1 expression failed to be a significant independent predictor of prognosis ($P = 0.091$, RR = 2.1). Independent prognostic predictors were patients' age, nodal status, state of distant metastasis and tumor grade (Table 3). In contrast, in the subgroup of patients without distant metastasis, PLK1 expression had a significant impact on patient prognosis in multivariate survival analysis. Patients with PLK1 positive tumors were approximately thrice (RR = 3.3, $P = 0.019$) more likely to die in the given time interval compared to their PLK1 negative counterparts. Again, patients' age, nodal status and tumor grade remained independent significant predictors of prognosis (Table 4).

Table 3 Multivariate survival analysis for all cases ($n = 153$)

	RR	95%CI	*P*
Age (yr)			
per yr	1.040	1.008–1.072	0.013
Tumor stage			
T1/T2	1.000		
T3/T4	1.061	0.466–2.413	0.888
Nodal status			
Per positive node	1.116	1.037–1.201	0.003
Metastasis			
Mx	1.000		
M1	3.223	1.202–8.643	0.020
Grade			
G1/G2	1.000		
G3	2.773	1.382–5.564	0.004
PLK1 expression			
Negative	1.000		
Positive	2.067	0.890–4.800	0.091

Table 4 Multivariate survival analysis for the subgroup of patients without distant metastasis ($n = 140$)

	RR	95%CI	*P*
Age (yr)			
per yr	1.044	1.009–1.079	0.013
Tumor stage			
T1/T2	1.000		
T3/T4	0.898	0.365–2.206	0.814
Nodal status			
Per positive node	1.231	1.125–1.348	<0.001
Grade			
G1/G2	1.000		
G3	2.614	1.172–5.829	0.019
PLK1 expression			
Negative	1.000		
Positive	3.306	1.214–9.002	0.019

DISCUSSION

To our knowledge, this is the first study showing an adverse effect of PLK1 overexpression on the prognosis of patients with colon cancer. This effect remains independently significant in the clinically important subgroup of patients without known distant metastasis.

In the present study, PLK1 was overexpressed in 66.7% of colon cancers and overexpression was positively linked to tumor stage and lymph node status, two parameters

that determine the extent of tumor burden. This is in line with the results of Takahashi *et al*.[21]. In another study by Macmillan *et al*.[24], increased PLK1 transcription levels were observed in colon carcinoma.

PLK1 overexpression in malignancies seems to be a common event, since it has been observed in a variety of different neoplasms, including cancer of stomach[10], esophagus[10], breast[11], endometrium[12], ovary[13], brain[14], head and neck[15], skin[16], lung[17], prostate[18], thyroid[19], liver[20], and colon[21]. Effects of PLK expression on patient prognosis have already been reported in a variety of other tumor entities, including esophageal carcinoma[10], ovarian carcinoma[13], carcinoma of head and neck[15], non-small cell lung carcinomas[17], and hepatoblastoma[20].

Among the possible functions of PLK1 overexpression in tumor biology, the most important factor might be the central role of PLK1 in mitotic regulation. PLK1 initiates mitosis by the activation of cdc25 and cyclin B1 via direct phosphorylation. Both events lead to an accumulation of cdc2/cyclin B1 complex in the nuclei, a precondition known to be crucial for the onset of mitosis[25,26]. Later in mitosis, PLK1 triggers the dissociation of cohesins from their chromosomal binding sites[27] and activates the anaphase-promoting complex[28]. The central involvement of PLK1 in mitosis of malignant cells is supported bys findings in several tumor entities including colon cancer[21], showing that PLK1 expression correlated positively with markers of cell proliferation.

Nevertheless, there are several arguments supporting the theory that additional functions of PLK1 must exist. First, only a part of the variety of PLK1 expression can be explained by mitotic activity. Second, we observed expression of PLK1 in irreversibly postmitotic cells such as neuronal ganglion cells. Third, PLK1 expression is unlikely to reflect cell proliferation exclusively, since we observed cases with strong PLK1 expression in almost 100% of tumor cells (Figure 1), a number that by far exceeds the rate of cells that can be expected to be in G_2/M phase. Finally, we could show that PLK1 expression is not strictly confined to cycling cells by double staining of colon cancer cells. Additional functions of PLK1 in tumor biology may have something to do with its ability to control microtubule dynamics[9], which is not only essential in mitosis but also important in golgi protein transport and cytoskeletal formation and rearrangement. These possible additional roles of PLK1 overexpression in tumor biology should be subjected to further functional studies.

Another explanation for the cause of PLK1 deregulation might be that either enhanced transcription by altered intracellular signal transduction or chromosomal over-representation of the respective gene locus leads to high cellular protein levels, which in turn enhance mitotic activity. In fact, chromosomal amplifications of 16p12, the gene locus of PLK1 has been described in human colorectal carcinomas[29].

Most recently, several groups found that inhibition of PLK1 expression in cancer cells of various tumor entities leads to a dramatic decline in cell proliferation[23,30] and to an induction of apoptosis[31]. These results suggest that PLK1 is an attractive target for novel chemotherapeutic approaches. Expression studies, like ours, may thus provide the translational basis for such new therapeutical approaches.

In summary, PLK1 is overexpressed in 66.7% of colon cancers, overexpression of PLK1 is linked to advanced tumor stages in this disease and can be considered as a new independent prognostic marker for colon cancer patients with locoregional disease.

ACKNOWLEDGMENTS

The authors thank Lisa Glanz for excellent technical assistance and Martina Eickmann for help in the preparation of the manuscript.

REFERENCES

1 **Jemal A,** Tiwari RC, Murray T, Ghafoor A, Samuels A, Ward E, Feuer EJ, Thun MJ. American Cancer Society. Cancer statistics, 2004. *CA Cancer J Clin* 2004; **54**: 8-29
2 **Chau I,** Chan S, Cunningham D. Overview of preoperative and postoperative therapy for colorectal cancer: the European and United States perspectives. *Clin Colorectal Cancer* 2003; **3**: 19-33
3 **Cascinu S,** Georgoulias V, Kerr D, Maughan T, Labianca R, Ychou M. Colorectal cancer in the adjuvant setting: perspectives on treatment and the role of prognostic factors. *Ann Oncol* 2003; **14**: 25-29
4 **Hanahan D,** Weinberg RA. The hallmarks of cancer. *Cell* 2000; **100**: 57-70
5 **Sunkel CE,** Glover DM. Polo, a mitotic mutant of Drosophila displaying abnormal spindle poles**.** *J Cell Sci* 1988; **89**: 25-38
6 **Nigg EA.** Polo-like kinases: positive regulators of cell division from start to finish. *Curr Opin Cell Biol* 1998; **10**: 776-783
7 **Barr FA,** Sillje HH, Nigg EA. Polo-like kinases and the orchestration of cell division. *Nat Rev Mol Cell Biol* 2004; **5**: 429-440
8 **Manning G,** Whyte DB, Martinez R, Hunter T, Sudarsanam S. The protein kinase complement of the human genome. *Science* 2002; **298**: 1912-1934
9 **Dai W,** Wang Q, Traganos F. Polo-like kinases and centrosome regulation. *Oncogene* 2002; **21**: 6195-6200
10 **Tokumitsu Y,** Mori M, Tanaka S, Akazawa K, Nakano S, Niho Y. Prognostic significance of polo-like kinase expression in esophageal carcinoma. *Int J Oncol* 1999; **15**: 687-692
11 **Wolf G,** Hildenbrand R, Schwar C, Grobholz R, Kaufmann M, Stutte HJ, Strebhardt K, Bleyl U. Polo-like kinase: a novel marker of proliferation: correlation with estrogen-receptor expression in human breast cancer. *Pathol Res Pract* 2000; **196**: 753-759
12 **Takai N,** Miyazaki T, Fujisawa K, Nasu K, Hamanaka R, Miyakawa I. Polo-like kinase (PLK) expression in endometrial carcinoma. *Cancer Lett* 2001; **169**: 41-49
13 **Weichert W,** Denkert C, Schmidt M, Gekeler V, Wolf G, Köbel M, Dietel M, Hauptmann S. Polo like kinase isoform expression is a prognostic factor in ovarian carcinoma. *Br J Cancer* 2004; **90**: 815-821
14 **Dietzmann K,** Kirches E, von Bossanyi, Jachau K, Mawrin C. Increased human polo-like kinase-1 expression in gliomas. *J Neurooncol* 2001; **53**: 1-11
15 **Knecht R,** Elez R, Oechler M, Solbach C, von Ilberg C, Strebhardt K. Prognostic significance of polo-like kinase (PLK) expression in squamous cell carcinomas of the head and neck. *Cancer Res* 1999; **59**: 2794-2797
16 **Kneisel L,** Strebhardt K, Bernd A, Wolter M, Binder A, Kaufmann R. Expression of polo-like kinase (PLK1) in thin melanomas: a novel marker of metastatic disease. *J Cutan Pathol* 2002; **29**: 354-358
17 **Wolf G,** Elez R, Doermer A, Holtrich U, Ackermann H, Stutte HJ, Altmannsberger HM, Rubsamen-Waigmann H, Strebhardt

K. Prognostic significance of polo-like kinase (PLK) expression in non-small cell lung cancer. *Oncogene* 1997; **14**: 543-549

18 **Weichert W,** Schmidt M, Gekeler V, Denkert C, Stephan C, Jung K, Loening S, Dietel M, Kristiansen G. Polo-like kinase 1 is overexpressed in prostate cancer and linked to higher tumor grades. *Prostate* 2004; **60**: 240-245

19 **Ito Y,** Miyoshi E, Sasaki N, Kakudo K, Yoshida H, Tomoda C, Uruno T, Takamura Y, Miya A, Kobayashi K, Matsuzuka F, Matsuura N, Kuma K, Miyauchi A. Polo-like kinase 1 overexpression is an early event in the progression of papillary carcinoma. *Br J Cancer* 2004; **90**: 414-418

20 **Yamada S,** Ohira M, Horie H, Ando K, Takayasu H, Suzuki Y, Sugano S, Hirata T, Goto T, Matsunaga T, Hiyama E, Hayashi Y, Ando H, Suita S, Kaneko M, Sasaki F, Hashizume K, Ohnuma N, Nakagawara A. Expression profiling and differential screening between hepatoblastomas and the corresponding normal livers: identification of high expression of the PLK1 oncogene as a poor-prognostic indicator of hepatoblastomas. *Oncogene* 2004; **23**: 5901-5911

21 **Takahashi T,** Sano B, Nagata T, Kato H, Sugiyama Y, Kunieda K, Kimura M, Okano Y, Saji S. Polo-like kinase 1 (PLK1) is overexpressed in primary colorectal cancers. *Cancer Sci* 2003; **94**: 148-152

22 **Denkert C,** Kobel M, Pest S, Koch I, Berger S, Schwabe M, Siegert A, Reles A, Klosterhalfen B, Hauptmann S. Expression of cyclooxygenase 2 is an independent prognostic factor in human ovarian carcinoma. *Am J Pathol* 2002; **160**: 893-903

23 **Elez R,** Piiper A, Kronenberger B, Kock M, Brendel M, Hermann E, Pliquett U, Neumann E, Zeuzem S. Tumor regression by combination antisense therapy against Plk1 and Bcl-2. *Oncogene* 2003; **22**: 69-80

24 **Macmillan JC,** Hudson JW, Bull S, Dennis JW, Swallow CJ. Comparative Expression of the Mitotic Regulators SAK and PLK in Colorectal Cancer. *Ann Surg Oncol* 2001; **8**: 729-740

25 **Toyoshima-Morimoto F,** Taniguchi E, Nishida E. Plk1 promotes nuclear translocation of human Cdc25C during prophase. *EMBO Rep* 2002; **3**: 341-348

26 **Yuan J,** Eckerdt F, Bereiter-Hahn J, Kurunci-Csacsko E, Kaufmann M, Strebhardt K. Cooperative phosphorylation including the activity of polo-like kinase 1 regulates the subcellular localization of cyclin B1. *Oncogene* 2002; **21**: 8282-8292

27 **Sumara I,** Vorlaufer E, Stukenberg PT, Kelm O, Redemann N, Nigg EA, Peters JM. The dissociation of cohesin from chromosomes in prophase is regulated by Polo-like kinase. *Mol Cell* 2002; **9**: 515-525

28 **Golan A,** Yudkovsky Y, Hershko A. The cyclin-ubiquitin ligase activity of cyclosome/APC is jointly activated by protein kinases Cdk1-cyclin B and Plk. *J Biol Chem* 2002; **277**: 15552-15557

29 **Knosel T,** Schluns K, Stein U, Schwabe H, Schlag PM, Dietel M, Petersen I. Chromosomal alterations during lymphatic and liver metastasis formation of colorectal cancer. *Neoplasia* 2004; **6**: 23-28

30 **Spankuch-Schmitt B,** Bereiter-Hahn J, Kaufmann M, Strebhardt K. Effect of RNA silencing of polo-like kinase-1 (PLK1) on apoptosis and spindle formation in human cancer cells. *J Natl Cancer Inst* 2002; **94**: 1863-1877

31 **Liu X,** Erikson RL. Polo-like kinase (Plk)1 depletion induces apoptosis in cancer cells. *Proc Natl Acad Sci USA* 2003; **100**: 5789-5794

Science Editor Wang XL and Guo SY **Language Editor** Elsevier HK

PO Box 2345, Beijing 100023, China
www.wjgnet.com
wjg@wjgnet.com

ELSEVIER

World J Gastroenterol 2005;11(36):5651-5654
World Journal of Gastroenterology ISSN 1007-9327
© 2005 The WJG Press and Elsevier Inc. All rights reserved.

Effect of *SNC19/ST14* gene overexpression on invasion of colorectal cancer cells

Ke-Feng Ding, Li-Feng Sun, Wei-Ting Ge, Han-Guang Hu, Su-Zhan Zhang, Shu Zheng

Ke-Feng Ding, Li-Feng Sun, Surgery of Oncology, The Second Affiliated Hospital, School of Medicine, Zhejinag University, Hangzhou 310009, Zhejiang Province, China
Wei-Ting Ge, Han-Guang Hu, Su-Zhan Zhang, Shu Zheng, Cancer Institute, School of Medicine, Zhejinag University, Hangzhou 310009, Zhejiang Province, China
Supported by the National Natural Science Foundation of China, No. 30200325
Co-first-authors: Ke-Feng Ding and Li-Feng Sun
Co-correspondent: Su-Zhan Zhang
Correspondence to: Professor Shu Zheng, Cancer Institute, School of Medicine, Zhejinag University, 88 Jiefang Road, Hangzhou 310009, Zhejiang Province, China. zhengshu@zju.edu.cn
Telephone: +86-571-87784501 Fax: +86-571-87214404
Received: 2005-01-07 Accepted: 2005-02-18

Abstract

AIM: To study the effect of *SNC19/ST14* gene overexpression on invasion *in vitro* of colorectal cancer cells.

METHODS: The adhesion of *SNC19/ST14* gene-transfected cells to ECM was measured by MTT assay. The cell movement was evaluated by wound healing assay. Cell invasion and migration were determined by invasion assay *in vitro*.

RESULTS: *SNC19/ST14* gene overexpression could enhance invasion of colorectal cancer cells *in vitro* significantly and influence early cell adherence to ECM, but could not change cell movement significantly.

CONCLUSION: *SNC19/ST14* gene overexpression increases the local invasion of colorectal cancer cells *in vitro*.

© 2005 The WJG Press and Elsevier Inc. All rights reserved.

Key words: Gene; *SNC19/ST14*; Colorectal cancer; Invasion

Ding KF, Sun LF, Ge WT, Hu HG, Zhang SZ, Zheng S. Effect of SNC19/ST14 gene overexpression on invasion of colorectal cancer cells. *World J Gastroenterol* 2005; 11(36): 5651-5654
http://www.wjgnet.com/1007-9327/11/5651.asp

INTRODUCTION

SNC19/ST14 is recently found to be a new member of the serine protease family[1]. *SNC19* gene has been isolated from a subtractive cDNA library of colorectal cancer by Cancer Institute of Zhejiang University, and is uploaded in the GenBank in 1995[2-4], and designated as *ST14* (suppression of tumorigenicity 14) by Gene Nomenclature Committee in 1998[5]. From then on, homologous products of *SNC19/ST14* have been found in many types of tissue cells, cell lines, and milk. SNC19/ST14 protein is designated as ST14/MT-SP1/matriptase/TADG-15, EC 3.4.21. SNC19/ST14 could convert hepatocyte growth factor (HGF)/scattering factor to its active form, and activate c-Met tyrosine phosphorylation[5]. Further, protease-activated receptor 2 (PAR2) and single-chain urokinase plasminogen activator (sc-uPA) have been identified as substrates of *SNC19/ST14/MT-SP1/matriptase/TADG-15*[6].

The uPA and HGF/SF are closely correlated with ECM degradation, growth, movement, and metastasis of cancer cells[7]. The SNC19/ST14 protein could also directly degrade ECM[8,9]. Studies suggest that *SNC19/ST14* is highly expressed in prostate, breast, and cervical cancer tissue[10-12]. The results suggest that *SNC19/ST14* and its human ortholog may play an important role in cell migration, cancer invasion, and metastasis. To know the detailed information on how the *SNC19/ST14* takes part in tumor invasion and metastasis, we compared the change of adhesion, movement, migration, and invasion of the stable *ST14*-transfected colorectal cancer cell clones to vector alone-transfected clones.

MATERIALS AND METHODS

Cell culture

RKO, a colorectal cancer cell line, *SNC19/ST14*-transfected (RKO-ST14-1) and vector alone-transfected colorectal cancer cell clones (RKO-pSecTag) were grown in Dulbecco's modified Eagle's medium (DMEM) supplemented with 10% fetal calf serum (Gibcol Inc.), penicillin (50 U/mL), streptomycin (50 g/mL), glucose (4 500 mg/L), L-glutamine (2 mmol/L) and Zeocin™ (600 mg/mL), then incubated at 37 ℃ in a humidified 95% air, 50 mL/L CO_2. Culture medium was changed on alternate days to avoid nutrient depletion.

Cell adhesion assay

Polystyrene 96-well plates (Costar) were coated with 50 μL/well of 8 μg/mL ECM (Sigma, USA), and left uncovered in a laminar flow hood overnight to allow evaporation. The plates were then rinsed with PBS and used for the attachment assays. Cells were washed thrice with PBS, trypsinized and seeded into 200 μL cells at a density of 2×10^5/mL on ECM. After 1, 2, 6, and 12 h of incubation at 37 ℃, the wells were gently rinsed thrice with PBS to remove unattached cells. The remaining cells in 96-well plates were reacted with

MTT for 4 h at 37 ℃, then solved with DMSO. The absorbance of each well was measured at 570 nm. Results were expressed as the percentage of total cells assuming that the adhesion of cells in control was 100%. The percentage of adhesion was determined using the formula: (A570 nm after being rinsed with PBS/A570 nm no rinse)×100%. The experiments were performed in triplicate.

Wound healing assays

Confluent monoplayers were serum starved for 24 h and washed with PBS, and wounds were made with a pipette tip. After cell debris were removed, the cultures were incubated in DMEM alone or containing fetal calf serum. After 24 and 48 h, healing was evaluated under a phase contrast microscope and photographed at 200×magnification under a Zeiss microscope (Germany). The movement distance of the wounded cells was measured by ImageJ software.

ECM invasion assay

Invasion assays were carried out, following the manufacturer's instructions of cell invasion assay kit (Chemicon International Inc., catalog: ECM550). For the invasion assay, we used a modified Boyden chamber. The chamber has two compartments divided by a polycarbonate filter (8 μm pore size) coated by a reconstituted basement membrane (ECMatrix™ solution). RKO, pSecTag vector controls (RKO-pSecTag), ST14-transfected cell clones (RKO-ST14-1) were grown in DMEM and harvested in PBS. After centrifugation the cell pellets were suspended in serum-free DMEM and 1.5×10^5 cells were placed into the upper chamber and 500 μL DMEM containing 10% fetal calf serum was added into the bottom chamber. Cells were incubated for 48 h at 37 ℃ in 50 mL/L CO_2. The non-invading cells and the ECMatrix gel were gently removed from the upper chamber with cotton-tipper swabs, and the filters were stained in the staining solution for 20 min and rinsed several times in water and air dried. Three filters were used for each cell type. The number of invading cells was counted in 10 random high-powered (HP) fields per filter under a Zeiss microscope.

Statistical analysis

The data were expressed as mean±SD and compared by ANOVA and Student's *t*-test. $P<0.05$ was considered statistically significant.

RESULTS

SNC19/ST14 transfectants adhesion to ECM in vitro

After 1 and 2 h, the percentage of ST14 transfectant (RKO-ST14-1) adhesion to ECM was about 5.1% and 32.3%, respectively, and significantly decreased compared to the wild type (RKO) and vector-transfected control (RKO-pSecTag) ($P<0.05$). But after 6 and 12 h, their difference in cell adhesion to ECM was not significant ($P>0.05$, Figure 1, and Table 1).

Table 1 Percentage of cell adhesion to ECM (mean±SD)

Cell type	1 h	2 h	6 h	12 h
RKO	12.0±1.8	52.7±6.5	59.7±2.9	98.5±0.6
RKO-pSecTag	7.6±1.8	42.8±1.6	56.5±3.4	93.4±0.6
RKO-ST14-1	5.1±1.9[a]	32.3±0.8[a]	55.6±5.7	88.5±2.0

[a]$P<0.05$ *vs* RKO and RKO-pSecTag.

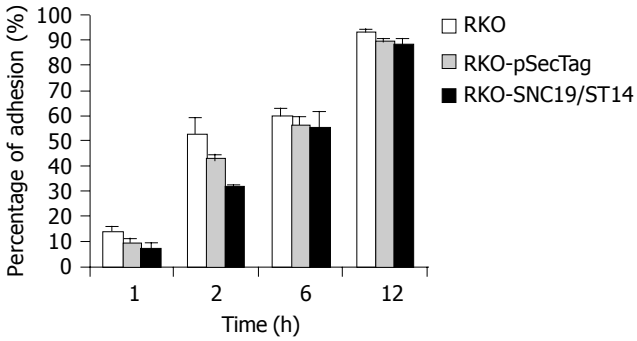


Figure 1 Percentage of cell adhesion to ECM.

SNC19/ST14 transfectants did not increase cell movement in vitro

There was no significant difference in movement distance between RKO-ST14-1 and vector-transfected cells (RKO-pSecTag) ($P>0.05$), but the movement distance of RKO-ST14-1 cells had a tendency to increase (Figure 2 and Table 2).

Table 2 *In vitro* cell movement assay (cm, mean±SD)

Cell	24 h	48 h	*P*
R-P-media	0.56±0.24	0.44±0.08	0.22
R-S-media	0.73±0.56	0.72±0.45	0.15
R-P-serum	0.97±0.07	1.01±0.27	0.37
R-S-serum	1.15±0.46	1.11±0.6	0.70

SNC19/ST14 transfectants increased cell invasion in vitro

The number of invasive cells per HP field of *SNC19/ST14* transfected clones (RKO-ST14-1), vector-transfected cells (RKO-pSecTag) and wild type cells (RKO) were 64.5±7.3, 44.9±7.0, and 32.6±4.1, respectively. RKO-ST14-1 cells show a significantly increased the cell invasion as compared to wild type cells (RKO) and vector-transfected control (RKO-pSecTag) (Figure 3 and Table 3), suggesting that the ST14 protein might promote invasion of colorectal cancer cells.

Table 3 *In vitro* cell invasion assay (n = 30, mean±SD)

Cell line	Cell number/HP	*P*
RKO	32.6±4.1	0.000018
RKO-pSecTag	44.9±7.0	0.00009
RKO-ST14-1	64.5±7.3	

DISCUSSION

Tumor progression and metastasis can be considered as a cascade of events and a continuous selection process, which includes ECM recognition, matrix degradation, migration,

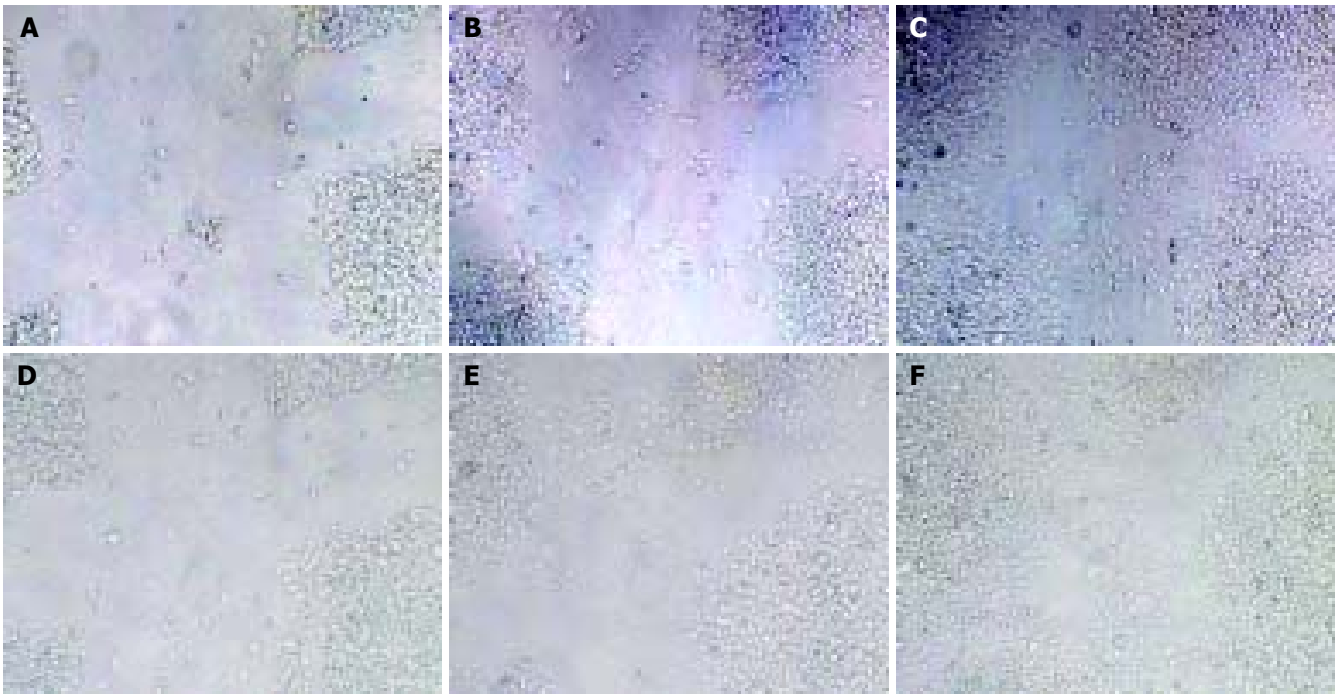


Figure 2 Wounding healing assay in wounds of RKO-ST14-1 (**A**), RKO-pSecTag (**D**), RKO-ST14-1 and RKO-pSecTag after 24 h (**B** and **E**) and 48 h (**C** and **F**).

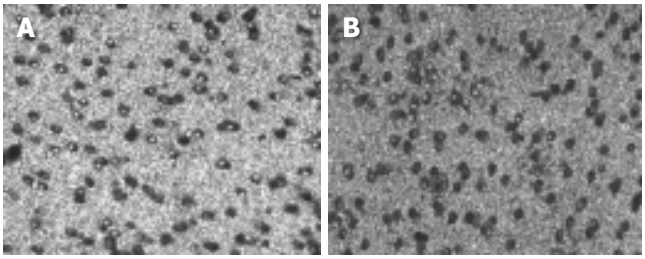


Figure 3 Cell invasion assay (200×). RKO-pSecTag (**A**) and RKO-ST14-1 (**B**).

hematogenous dissemination and organ selection metastasis[13]. It is accepted that malignant cell-ECM interaction must be considered as the key feature of malignancy. Malignant cells must recognize and degradate ECM before invasion and metastasis. Therefore, it is important to study matrix degrading enzymes for understanding and controlling the metastasis. The serine protease is a member of these ECM-degrading enzymes family. SNC19/ST14 protein has been recently found to be a new member of type II transmembrane serine protease (TTSPs)[1].

In our experiments, the SNC19/ST14 protein could enhance cell invasion *in vitro* when it was overexpressed in colorectal cancer cells. The final results of cell adhesion, degradation, and movement were evaluated by ECM invasion assay *in vitro*. In this study, although SNC19/ST14 overexpression could decrease cell adhesion to ECM in a short time, after 6 h this change was not observed. Besides, *SNC19/ST14* overexpression could not increase cell movement. Since *SNC19/ST14* overexpression could not induce cell cycle, apoptosis and proliferation, we believe that SNC19/ST14 enhancing cancer cell invasion results from increased ECM degradation.

There are several reasons to explain why *SNC19/ST14* overexpression could increase ECM degradation. Firstly, *SNC19/ST14* protein has extracellular matrix-degrading activity[8,9]. Secondly, SNC19/ST14 protein can activate HGF and uPA *in vitro*[6]. HGF and uPA have been implicated in cancer invasion and metastasis due to their cellular motility, extracellular matrix degradation, and tumor vascularization[14,15]. As a protease, uPA is best known to convert zymogen plasminogen into active plasmin. Plasmin promotes degradation of diverse ECM substrates such as fibrin, fibronectin, and laminin[16], activates certain matrix metalloproteases (MMPs) to allow further degradation of ECM, especially interstitial and type IV collagen. Therefore, uPA can promote metastasis by degrading ECM and permitting local invasion. Besides, HGF increases the expression of uPA and its receptor (uPAR)[18], and HGF precursor (pro-HGF) can be activated by uPA[19].

In conclusion, SNC19/ST14 can directly degrade ECM and activate uPA and HGF/SF to enhance ECM degradation, which might be one of the reasons why *SNC19/ST14* overexpression enhances local invasion and tumor metastasis.

REFERENCES

1 **Hooper JD**, Clements JA, Quigley JP, Antalis TM. Type II transmembrane serine proteases. Insights into an emerging class of cell surface proteolytic enzymes. *J Biol Chem* 2001; **276**: 857-860
2 **Cao J**, Cai X, Zheng L, Geng L, Shi Z, Pao CC, Zheng S. Characterization of colorectal-cancer-related cDNA clones obtained by subtractive hybridization screening. *J Cancer Res Clin Oncol* 1997; **123**: 447-451
3 **Zheng S**, Cai X, Cao J, Zheng L, Geng L, Zhang Y, Gu J, Shi Z. Screening and identification of down-regulated genes in colorectal carcinoma by subtractive hybridization: a method to identify putative tumor suppressor genes. *Chin Med J* 1997; **110**: 543-547
4 **Zhang Y**, Cai X, Schlegelberger B, Zheng S. Assignment1 of

human putative tumor suppressor genes ST13 (alias SNC6) and ST14 (alias SNC19) to human chromosome bands 22q13 and 11q24-->q25 by in situ hybridization. *Cytogenet Cell Genet* 1998; **83**: 56-57

5 **Lee SL**, Dickson RB, Lin CY. Activation of hepatocyte growth factor and urokinase/plasminogen activator by matriptase, an epithelial membrane serine protease. *J Biol Chem* 2000; **275**: 36720-36725

6 **Takeuchi T**, Harris JL, Huang W, Yan KW, Coughlin SR, Craik CS. Cellular localization of membrane-type serine protease 1 and identification of protease-activated receptor-2 and single-chain urokinase-type plasminogen activator as substrates. *J Biol Chem* 2000; **275**: 26333-26342

7 **Parr C**, Watkins G, Mansel RE, Jiang WG. The hepatocyte growth factor regulatory factors in human breast cancer. *Clin Cancer Res* 2004; **10** (1 Pt1): 202-211

8 **Shi YE**, Torri J, Yieh L, Wellstein A, Lippman ME, Dickson RB. Identification and characterization of a novel matrix-degrading protease from hormone-dependent human breast cancer cells. *Cancer Res* 1993; **53**: 1409-1415

9 **Lin CY**, Anders J, Johnson M, Sang QA, Dickson RB. Molecular cloning of cDNA for matriptase, a matrix-degrading serine protease with trypsin-like activity. *J Biol Chem* 1999; **274**: 18231-18236

10 **Oberst M,** Anders J, Xie B, Singh B, Ossandon M, Johnson M, Dickson RB, Lin CY. Matriptase and HAI-1 are expressed by normal and malignant epithelial cells *in vitro* and *in vivo*. *Am J Pathol* 2001; **158**: 1301-1311

11 **Bhatt AS**, Takeuchi T, Ylstra B, Ginzinger D, Albertson D, Shuman MA, Craik CS. Quantitation of membrane type serine protease 1 (MT-SP1) in transformed and normal cells. *Biol Chem* 2003; **384**: 257-266

12 **Santin AD**, Cane' S, Bellone S, Bignotti E, Palmieri M, De Las Casas LE, Anfossi S, Roman JJ, O'Brien T, Pecorelli S. The novel serine protease tumor-associated differentially expressed gene-15 (matriptase/MT-SP1) is highly overexpressed in cervical carcinoma. *Cancer* 2003; **98**: 1898-1904

13 **Timar J**, Csuka O, Orosz Z, Jeney A, Kopper L. Molecular pathology of tumor metastasis. *Pathol Oncol Res* 2002; **8**: 204-219

14 **Comoglio PM**, Boccaccio C. Scatter factors and invasive growth. *Semin Cancer Biol* 2001; **11**: 153-165

15 **Andreasen PA**, Egelund R, Petersen HH. The plasminogen activation system in tumor growth, invasion, and metastasis. *Cell Mol Life Sci* 2000; **57**: 25-40

16 **Andreasen PA**, Kjoller L, Christensen L, Duffy MJ. The urokinase-type plasminogen activator system in cancer metastasis: a review. *Int J Cancer* 1997; **72**: 1-22

17 **Carmeliet P,** Moons L, Lijnen R, Baes M, Lemaitre V, Tipping P, Drew A, Eeckhout Y, Shapiro S, Lupu F, Collen D. Urokinase-generated plasmin activates matrix metalloproteinases during aneurysm formation. *Nat Genet* 1997; **17**: 439-444

18 **Jeffers M**, Rong S, Vande Woude GF. Enhanced tumorigenicity and invasion-metastasis by hepatocyte growth factor/scatter factor-met signalling in human cells concomitant with induction of the urokinase proteolysis network. *Mol Cell Biol* 1996; **16**: 1115-1125

19 **Naldini L**, Tamagnone L, Vigna E, Sachs M, Hartmann G, Birchmeier W, Daikuhara Y, Tsubouchi H, Blasi F, Comoglio PM. Extracellular proteolytic cleavage by urokinase is required for activation of hepatocyte growth factor/scatter factor. *EMBO J* 1992; **11**: 4825-4833

Science Editor Wang XL and Guo SY **Language Editor** Elsevier HK

PO Box 2345, Beijing 100023, China
www.wjgnet.com
wjg@wjgnet.com

ELSEVIER

World J Gastroenterol 2005;11(36):5655-5658
World Journal of Gastroenterology ISSN 1007-9327
© 2005 The WJG Press and Elsevier Inc. All rights reserved.

B_7 molecule mRNA expression in colorectal carcinoma

Ju-Xiang Xiao, Pei-Song Bai, Bao-Chang Lai, Li Li, Juan Zhu, Yi-Li Wang

Ju-Xiang Xiao, Pei-Song Bai, Li Li, Juan Zhu, Department of Oncology, First Hospital of Xi'an Jiaotong University, Xi'an 710061, Shaanxi Province, China
Bao-Chang Lai, Yi-Li Wang, Institute for Cancer research, School of Life Science and Technology of Xi'an Jiaotong University, Xi'an 710061, Shaanxi Province, China
Supported by the National Natural Science Foundation of China, No. 30370549
Correspondence to: Dr. Ju-Xiang Xiao, Department of Oncology, First Hospital of Xi'an Jiaotong University, Xi'an 710061, Shaanxi Province, China. xiao_juxiang@yahoo.com
Telephone: +86-29-85324068 Fax: +86-29-85237369
Received: 2005-05-13 Accepted: 2005-06-06

Abstract

AIM: To observe the status of tumor-associated B_7 molecule mRNA expression in human colorectal cancer tissue by *in situ* hybridization.

METHODS: The mRNA expression patterns of cancer-associated $B_{7\text{-}1}$,B_7H_1,B_7H_2,ICOS in 22 specimens of human colorectal cancer tissue were monitored by *in situ* hybridization (ISH) with digoxin-labeled oligonucleotide probes.

RESULTS: $B_{7\text{-}1}$,B_7H_1,B_7H_2,ICOS mRNA were detected in both cancer cells and tumor infiltrating lymphocytes (TIL). The mRNA expression level of these molecules in tumor cells was higher than that in TIL (0.76±0.54-1.62±0.82 *vs* 0.38±0.19-0.65±0.33, $P<0.001$). There was no relationship between expression level of tested B_7 family molecules and patients' sex, age, differentiation status of cancer and regional lymph node metastasis.

CONCLUSION: Th2 cytokine predominant in tumor microenvironment might be related to the expression of B_7H_1,B_7H_2 co-signal molecules in tumor cells and TIL.

© 2005 The WJG Press and Elsevier Inc. All rights reserved.

Key words: Colorectal cancer; $B_{7\text{-}1}$, B_7H_1, B_7H_2 and ICOS; Tumor immunity; Immune evasion

Xiao JX, Bai PS, Lai BC, Li L, Zhu J, Wang YL. B_7 molecule mRNA expression in colorectal carcinoma. *World J Gastroenterol* 2005; 11(36): 5655-5658
http://www.wjgnet.com/1007-9327/11/5655.asp

INTRODUCTION

Although it has been well accepted that human tumor is immunogenic, most patients suffering from cancer are destined to die due to tumor progress. Establishment of the bisignal model for T-cell activation leads people to think that inactivation of infiltrating immune potential cells in tumor tissue might be immune anergic owing to the deficiency of co-stimulatory molecules. Tumor cells modified with B_7 co-stimulatory molecule gene could be rejected by tumor bearing host[1,2], but most human cancer tissues express co-stimulators[3,4], suggesting that co-stimulatory molecules might not be the only mechanism of immune evasion. The tumor-associated B_7H_1 and B_7H_2, new members of B_7 family can preferentially stimulate the production of IL-10, promote activated T cell apoptosis[5].

In the present study, the status of tumor-associated B_7 molecule mRNA expression in human colorectal cancer tissue was observed using B_7H_1, B_7H_2 and ICOS cDNA probe, *in situ* hybridization. The results showed that $B_{7\text{-}1}$, B_7H_1, B_7H_2, ICOS mRNA were expressed in both cancer cells and tumor infiltrating lymphocytes (TIL), indicating that Th2 cytokine predominant in tumor microenvironment might be related to the expression of B_7H_1, B_7H_2 co-signal molecules in tumor cells and TIL. Elucidation of tumor-associated B_7 molecules may contribute to the design of T cell-based cancer immunotherapy.

MATERIALS AND METHODS

Samples

Tissue samples were obtained from 22 patients with colorectal cancer. The specimen were fixed in 4 g/L formaldehyde in phosphate-buffered saline (PBS) immediately and embedded in paraffin. Serial sections (5 μm in thickness) were cut for *in situ* hybridization or histological evaluation, and mounted on slides covered with APES, dried overnight at 65 ℃, stored at -70 ℃ until use. The diagnosis of colorectal carcinoma was histopathologically verified in all cases. None of the patients had previously received radio-, chemo-, or immunotherapy.

Preparation of oligonuleotide probes

Primer 3 software was used to design oligonuleotide probes complementary to the mRNA of all kinds of target sequences including $B_{7\text{-}1}$, B_7H_1, B_7H_2, ICOS mRNA. The specificity of all oligonucleotide probes was analyzed by BLAST software (www.ncbi.nih.gov). The probes were labeled by tailing the oligonucleotides with digoxigenin-11-dUTP kit (Boehringer Mannheim, German). A labeling activity of 1.56 nmol/L was obtained (Primer3 http://www.genome.wi.mit.edu/cgi-bin/primer/Primer3;BLAST http://www.ncbi.nlm.gov/cgi-bin/BLAST). Sequence of oligonuleotide probes of co-stimulatory molecules was tested ($B_{7\text{-}1}$: 5'-CAT GAA GCT GTG GTT GGT TG -3'; B_7H_1:

5'-TGC TTG TCC AGA TGA CTT CG -3'; B_7H_2: 5'-CCA TCG CTC TGA CTT CCT TC -3'; ICOS: 5'-TTC AGC TGG CAA CAA AGT TG-3').

In situ hybridization (ISH)

Diethyl pyrocarbonate (DEPC) water was used for all solutions necessary for ISH. The sections were deparaffinized in xylene and rehydrated in descending ethanol, followed by digestion with 1 g/L proteinase K at 37 ℃ for 30 min and terminated with 20 g/L glycine in PBS for 5 min. Then, the sections were refixed in 40 g/L polyformaldehyde for 20 min, washed with PBS for 10 min, treated with 0.2 mol/L HCI for 10 min and washed with DEPC water for 3 min. The sections were dehydrated in ascending gradient ethanol, air-dried and followed by prehybridization at 42 ℃ for 2 h. Hybridization reaction was carried out at 42 ℃ for 22 h. Then the sections were washed with gradient SSC thoroughly and followed by treatment with digoxin antibody at 37 ℃ for 2 h. The color was developed in NBT-BCIP substrate, then counterstained with 10 g/L methyl green in distilled water, dehydrated and mounted with neutral gum.

For negative controls, probes and antibodies were replaced by PBS or the slides were treated with RNase A (20 mg/L) at 37 ℃ for 30 min. $B_{7\text{-}1}$ mRNA expression in mononuclear leucocytes was used as positive control.

Evaluation of results

Purple blue precipitation in cytoplasm under light microscope was considered as positive signal, and 5 high power fields were randomly chosen from each slide, The percentage of positive cells and the positive cell index (total positive granule number/positive cell number) were calculated. Intensity of the color reaction was classified into 4 grades: strongly positive (+++), positive (++), weakly positive (+) and negative (-) and scored as 3, 2, 1 and 0, respectively. The Accumulation index was determined as percentage of positive cells multiply intensity score.

Statistics analysis

All datas were expressed as mean±SD. Analysis was performed by using chi-square test and Spearman correlation analysis with SPSS 11.0 software. $P<0.05$ was considered statistically significant.

RESULTS

Expression of $B_{7\text{-}1}$, B_7H_1, B_7H_2, ICOS mRNA was detected in both cancer cells and tumor infiltrating lymphocytes (Figure 1). The mRNA expression level of these molecules in tumor cells was higher than that in TIL (0.76±0.54-1.62±0.82 *vs* 0.38±0.19-0.65±0.33, $P = 0.000$). However, when the expression of B_7 family mRNA was analyzed with respect to the tested members, there was a significant difference in B_7H_1 and ICOS expression between TIL and cancer cells ($P<0.05$). The expression of B_7H_1 and ICOS mRNA was higher in tumor cells and TIL. The expression of B_7 family molecules either in tumor cells or in TIL was not correlated with patients' sex, age, differentiation status of cancer and regional lymph node metastasis. B_7H_1 expression in TIL and tumor invasiveness was significantly associated with the intensity and the depth of tumor invasion ($P = 0.050$, Tables 1-3).

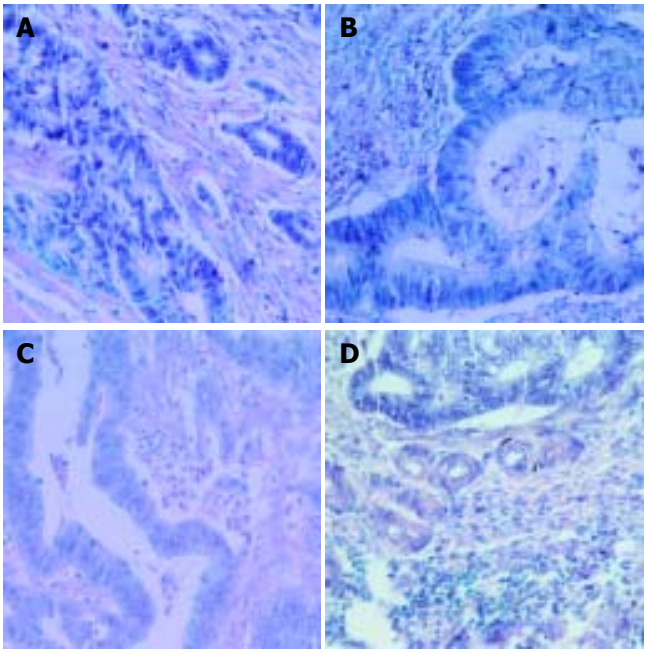


Figure 1 mRNA expression of $B_{7\text{-}1}$ (**A**), B_7H_1 (**B**), B_7H_2 (**C**) and ICOS (**D**) in human colorectal cancer tissues (ISH×400).

Table 1 B7 family molecule expression in colorectal cancer cells and TIL (mean±SD)

B7 molecule	Tumor cell	TIL
$B_{7\text{-}1}$:	1.29±0.63	0.45±0.28[a]
B_7H_1:	1.38±0.71	0.65±0.33[a]
B_7H_2:	0.76±0.54	0.38±0.19[a]
ICOS:	1.62±0.82	0.53±0.27[a]

[a]$P<0.05$ *vs* tumor cell.

Table 2 Relationship between depth of tumor invasion and B7 family molecule expression (mean±SD)

B7 molecule	Tumor cell			TIL		
	T2	T3	T4	T2	T3	T4
$B_{7\text{-}1}$:	1.22±0.82	1.28±0.70	1.35±0.42	0.36±0.43	0.50±0.25	0.43±0.24
B_7H_1:	1.43±0.63	1.55±0.76	1.01±0.63	0.66±0.25	0.76±0.36[a]	0.42±0.21
B_7H_2:	0.62±0.05	0.91±0.69	0.56±0.28	0.42±0.21	0.39±0.19	0.33±0.18
ICOS:	1.59±1.14	1.77±0.78	1.35±0.78	0.48±0.35	0.53±0.23	0.59±0.33

[a]$P<0.05$ *vs* T2, T4.

Table 3 Relation between tumor metastasis and B_7 family molecule expression (mean±SD)

B7 molecule	Tumor cell		TIL	
	Metastasis	Nometastasis	Metastasis	Nometastasis
$B_{7\text{-}1}$:	1.08±0.59	1.31±0.64	0.34±0.18	0.46±0.28
B_7H_1:	0.70±0.00	1.45±0.71[a]	0.29±0.04	0.68±0.35[a]
B_7H_2:	0.59±0.01	0.78±0.57	0.47±0.33	0.37±0.18
ICOS:	0.63±0.04	1.72±0.80[a]	0.24±0.06	0.56±0.27[a]

[a]P<0.05 *vs* metastasis.

DISCUSSION

It has been accepted that the efficacy of antitumor immunity is mainly affected by three factors, namely status of tumor immunogenecity, expression of co-stimulatory molecules and type of cytokines. Lack of co-stimulatory molecules in tumor cells might be a reasonable explanation of the tumor immune evasion, but the fact that most human cancer tissues express co-stimulators makes it contradictory. Si *et al.*[3], reported that $B_{7\text{-}1}$ molecule expresses at least in more than half of human solid tumors. MHC-I, II molecules are detectable in human cervical cancer and tumor-associated dendritic cell (DC)[4]. Analysis of tumor microenvironment has demonstrated that type II cytokines are predominant in non-small cell lung cancer and gastric carcinoma[5,6]. Interestingly there is a dynamic change with the progress of tumor, i.e. the expression of IFN-γ and IL-2 decreases, whereas the expression of Th2 cytokines such as IL-4, IL-10 and TNF-β increases significantly.

There is evidence that co-stimulators play a very important role in antigen-specific T cell activation. *In vitro* and *in vivo* experiments have shown that T cell interaction via T-cell receptor (TCR) with MHC/antigen complexes in the absence of co-stimulation may lead to induction of anergy rather than activation. $B_{7\text{-}1}$ gene-modified tumor cells can elicit tumor rejection response in xenograft tumor models. All these suggest that deficiency of co-stimulators is the key factor for immune evasion. However, Dong *et al.*[7], found that CD_{28} by its natural legend $B_{7\text{-}1}$ or $B_{7\text{-}2}$ triggers Th1 cytokine secretion including IFN-γ and IL-2, while IL-10 production is increased considerably after stimulation with immobilized B_7H_1Ig and antibody against CD_3. Dynamic observation has demonstrated that the production of IL-2 peaks 24 h after B_7H_1 co-stimulation, whereas IL-10 secretion starts to increase after 48 and 72 h. Additionally, monoclonal antibody against IL-2 could inhibit IL-10 secretion from T cells co-stimulated with B_7H_1Ig. ICOS, one of the B_7 legends, plays a critical and non-dispensable role in T cell activation and proliferation *in vitro*, especially in regulating Th2 differentiation. In addition, it is critical for efficient T-cell priming and production of Th2 cytokines *in vivo*, in particular IL-4 and IL-10. Results obtained from some experiments demonstrated that Ag stimulation of naive $CD4^+$ T cells in the absence of ICOS signal results in impaired Th2 development[8]. At the molecular level, ICOS is involved in upregulating the expression of CD40L as well as promoting the secretion of IL-4 and IL-13. ICOS is a co-stimulatory receptor essential for T-cell activation and function and also plays an important role in acquired immunity[9,10]. This could well elucidate our previous findings, i.e. although expression of $B_{7\text{-}1}$ by human tumor cells can activate T cells and enhance the secretion of Th1 cytokines such as IL-2 and IFN-γ, Th2 cytokine predominates ultimately since co-stimulators such as B_7H_1, B_7H_2 and ICOS act dominantly.

In the present study, we observed that $B_{7\text{-}1}$ co-stimulatory molecule mRNA was expressed in tumor cells and tumor infiltrating lymphocytes (TIL) of human colorectal carcinoma by *in situ* hybridization, which is consistent with many experiments of B_7-gene transfection vaccine[11,12]. However, the other members of B_7 family such as B_7H_1, and ICOS can also be detected. In our study, the expression of B_7 molecules in tumor cells was higher than that in TIL (P<0.005), and B_7H_1 and ICOS mRNA expression in tumor cells was even higher than that of $B_{7\text{-}1}$, suggesting that B_7 family plays a role in tumor immunity. In addition, the expression of B_7H_1 and ICOS mRNA is related with the invasion depth of tumor, the mRNA expression of B_7H_1 and ICOS in both tumor cells and TIL is associated with the metastasis of colorectal carcinoma. A recent study on B_7 family molecules in tumor biological behavior demonstrated that aberrant expression of B_7H_1 in renal cell carcinoma apparently impairs T cell function and survival[13]. Our results and these data provide the morphological and clinical support to elucidate the role of B_7 co-stimulatory molecules in tumor immune evasion.

The present findings indicate that new members of B7 family such as B_7H_1, B_7H_2 and ICOS are involved in promoting TH2-based responses preferentially. More interestingly, it has been reported that tumor-associated B_7H_1 can promote apoptosis of antigen-specific human T-cell clones *in vitro*[14,15], and mouse P815 tumor -expressed B_7H_1 increases apoptosis of activated tumor-reactive T- cells and promotes the growth of highly immunogenic $B_{7\text{-}1}^+$ tumor *in vivo*[10]. These results suggest that induction of apoptosis of tumor-infiltrating lymphocytes by B_7H_1 molecules overexpressed in human colorectal carcinoma may be a potentially active escape strategy of various tumors from immune attack as is shown by Wintterle *et al.*[16].

Tumor escape is attributed to a variety of immune evasion strategies, including downregulation of MHC-I class molecules, regulatory T cells, Th2 cytokines, secretion of immunosuppressive factors from tumor cells or TIL, and lack of T-cell co-stimulation. Tumor local microenvironment plays an essential role in determining the final destiny of antitumor immunity[17].

The discovery of new members of B_7 family presenting different co-stimulatory effects indicates that different co-signaling molecules lead to different results, such as enhancement of T-cell Receptor (TCR)-mediated immune responses or inhibition of TCR-mediated immune responses. Tumor-associated B_7H_1 might produce tumor immune escape by promoting apoptosis of tumor-reactive T-cells and type II cytokine secretion through PD-1 ligand[18,19]. Hirano *et al.*[20], reported that B_7H_1/PD-1 forms a molecular shield to prevent destruction by CTL, suggesting that to block B_7H_1 or PD-1 by specific monoclonal antibodies could reverse this resistance and profoundly enhance therapeutic efficacy. Strome *et al.*[21], have shown the

feasibility of the new immunotherapy. With the suggestion of the concept of co-inhibitors[22], investigation of the functional characteristics of tumor-associated signal molecules may contribute to exploitation of T cell-based tumor immunotherapy.

REFERENCES

1 **Chen LP,** McGowan P, Ashe S, Johnston J, Li Y, Hellström I, Hellström KE. Tumor immunogenicity determines the effect of B7 costimulation on T cell-mediated tumor immunity. *J Exp Med* 1994; **179**: 523-532

2 **Smyth MJ,** Godfrey DI, Trapani JA. A fresh look at tumor immunosurveillance and immunotherapy. *Nature Immunol* 2001; **2**: 293-299

3 **Si LS,** Chen YY, Wang YL, Guo JF, Sun Y. $B_{7\text{-}1}$ Molecule expression on tumor cells in human cancerous tissues. *Chin Med Sci J* 1998; **13**: 195-198

4 **Guo JF,** Si LS, Wang YL, Zhao YR, Liu Z, Xiu CF, Sun XL. An *in situ* study on immunostimulatory molecules in cancer cells within the cervical carcinoma tissues. *Zhonghua Yixue Zazhi* 2000; **80**: 342-345

5 **Liu P,** Xiao JX, Li R, Chen XL, Lai BC, Si LS, Wang YL. Analysis on local immune environment of human gastric carcinoma *in situ*. *J Tumor Marker Oncol* 2003; **18**: 80-85

6 **Li R,** Rüttinger D, Li R, Si LS, Wang YL. Analysis of the immunological microenvironment at the tumor site in patients with non-small cell lung cancer. *Langenbecks Arch Surg* 2003; **388**: 406-412

7 **Dong HD,** Zhu GF, Tamada K, Chen LP. B7H-1, a third member of the B7 family, co-stimulates T-cell proliferation and interleukin-10 secretion. *Nature Medicine* 1999; **5**: 1365-1369

8 **Watanabe M,** Watanabe S, Hara Y, Harada Y, Kubo M, Tanabe K, Toma H, Abe R. ICOS-mediated costimulation on Th2 differentiation is achieved by the enhancement of IL-4 receptor-mediated signaling. *J Immunol* 2005; **174**: 1989-1996

9 **Dong C,** Juedes AE, Temann UA, Shresta S, Allison JP, Ruddle NH, Flavell RA. ICOS co-stimulatory receptor is essential for T-cell activation and function. *Nature* 2001; **409**: 97-101

10 **Smith KM,** Brewer JM, Webb P, Coyle AJ, Gutierrez-Ramos C, Garside P. Inducible costimulatory molecule-B7-related protein 1 interactions are important for the clonal expansion and B cell helper functions of naive, Th1, and Th2 T cells. *J Immunol* 2003; **170**: 2310-2315

11 **Fujiwara K,** Higashi T, Nouso K, Nakatsukasa H, Kobayashi Y, Uemura M, Nakamura S, Sato S, Hanafusa T, Yumoto Y, Naito I, Shiratori Y. Decreased expression of B7 costimulatory molecules and major histocompatibility complex class-I in human hepatocellular carcinoma. *J Gastroenterol Hepatol* 2004; **19**: 1121-1127

12 **Ke XY,** Jia LP, Wang J, Wang DB. Transfection of B7-1 cDNA empowers antigen presentation of blood malignant cells for activation of anti-tumor T cells. *Chin Med J* 2003; **116**: 78-84

13 **Thompson RH,** Gillett MD, Cheville JC, Lohse CM, Dong HD, Webster WS, Krejci KG, Lobo JR, Sengupta S, Chen LP, Zincke H, Blute ML, Strome SE, Leibovich BC, Kwon ED. Costimulatory B7-H1 in renal cell carcinoma patients: Indicator of tumor aggressiveness and potential therapeutic target. *PNAS* 2004; **101**: 17174-17179

14 **Dong HD,** Strome SE, Salomao DR, Tamura H, Hirano F, Flies DB, Roche PC, Lu J, Zhu G, Tamada K, Lennon VA, Celis E, Chen LP. Tumor-associated B7-H1 Promotes T-cell apoptosis: A potential mechanism of immune evasion. *Nature Medicine* 2002; **8**: 793-800

15 **Dong HD,** Chen LP. B7-H1 pathway and its role in the evasion of tumor immunity. *J Mol Med* 2003; **81**: 281-287

16 **Wintterle S,** Schreiner B, Mitsdoerffer M, Schneider D, Chen LP, Meyermann R, Weller M, Wiendl H. Expression of the B7-related molecule B7-H1 by glioma cells: a potential mechanism of immune paralysis. *Cancer Res* 2003; **63**: 7462-7467

17 **Chu Y,** Hu HM, Winter H, Wood WJ, Doran T, Lashley D, Bashey J, Schuster J, Wood J, Lowe BA, Vetto JT, Weinberg AD, Puri R, Smith JW 2nd, Urba WJ, Fox BA. Examining the immune response in sentinel lymph nodes of mice and men. *Eur J Nucl Med* 1999; **26**(4 Suppl): S50-53

18 **Blank C,** Gajewski TF, Mackensen A. Interaction of PD-L1 on tumor cells with PD-1 on tumor-specific T cells as a mechanism of immune evasion: implications for tumor immunotherapy. *Cancer Immunol Immunother* 2005; **54**: 307-314

19 **Carter L,** Fouser LA, Jussif J, Fitz L, Deng B, Wood CR, Collins M, Honjo T, Freeman GJ, Carreno BM. PD-1:PD-L inhibitory pathway affects both CD4(+) and CD8(+) T cells and is overcome by IL-2. *Eur J Immunol* 2002; **32**: 634-643

20 **Hirano F,** Kaneko K, Tamura H, Dong H, Wang S, Ichikawa M, Rietz C, Flies DB, Lau JS, Zhu G, Tamada K, Chen L. Blockade of B7-H1 and PD-1 by monoclonal antibodies potentiates cancer therapeutic immunity. *Cancer Res* 2005; **65**: 1089-1096

21 **Strome SE,** Dong HD, Tamura H, Voss SG, Flies DB, Tamada K, Salomao D, Cheville J, Hirano F, Lin W, Kasperbauer JL, Ballman KV, Chen L. B7-H1 blockade augments adoptive T-cell immunotherapy for squamous cell carcinoma. *Cancer Res* 2003; **63**: 6501-6505

22 **Chen LP.** Co-inhibitory molecules of the B7-CD28 Family in the control of T-cell immunity. *Nature Review Immunol* 2004; **4**: 336-347

Science Editor Wang XL and Guo SY **Language Editor** Elsevier HK

PO Box 2345, Beijing 100023, China
www.wjgnet.com
wjg@wjgnet.com

ELSEVIER

World J Gastroenterol 2005;11(36):5659-5665
World Journal of Gastroenterology ISSN 1007-9327
© 2005 The WJG Press and Elsevier Inc. All rights reserved.

Screening of hepatocyte proteins binding to F protein of hepatitis C virus by yeast two-hybrid system

Yan-Ping Huang, Jun Cheng, Shu-Lin Zhang, Lin Wang, Jiang Guo, Yan Liu, Yuan Yang, Li-Ying Zhang, Gui-Qin Bai, Xue-Song Gao, Dong Ji, Shu-Mei Lin, Qing Shao

Yan-Ping Huang, Shu-Lin Zhang, Yuan Yang, Gui-Qin Bai, Shu-Mei Lin, The First Hospital of Xi'an Jiaotong University, Xi'an 710061, Shaanxi Province, China
Jun Cheng, Lin Wang, Jiang Guo, Yan Liu, Li-Ying Zhang, Xue-Song Gao, Dong Ji, Qing Shao, Institute of Infectious Diseases, Ditan Hospital, Anwai Street, Beijing 100011, China
Supported by the National Natural Science Foundation of China, Nos. C03011402 and C30070690; and the Research and Technique Foundation of PLA during the 9th-Five year plan period, No. 98D063; and the Launching Foundation for Student Studying Abroad of PLA, No. 98H038; and the Youth Research and Technique Foundation of PLA during the 10th-Five Year Plan Period, No. 01Q138; and the Research and Technique Foundation of PLA during the 10th-Five Year Plan Period, No. 01MB135
Correspondence to: Yan-Ping Huang, Department of Pediatrics, the First Hospital of Xi'an Jiaotong University, Xi'an 710061, Shaanxi Province, China. huangyp423@126.com
Telephone: +86-29-85324065
Received: 2004-07-17 Accepted: 2004-08-25

Key words: Hepatitis C virus; F protein; Yeast two-hybrid system

Huang YP, Cheng J, Zhang SL, Wang L, Guo J, Liu Y, Yang Y, Zhang LY, Bai GQ, Gao XS, Ji D, Lin SM, Shao Q. Screening of hepatocyte proteins binding to F protein of hepatitis C virus by yeast two-hybrid system. *World J Gastroenterol* 2005; 11(36): 5659-5665
http://www.wjgnet.com/1007-9327/11/5659.asp

AIM: To investigate the biological function of F protein by yeast two-hybrid system.

METHODS: We constructed F protein bait plasmid by cloning the gene of F protein into pGBKT7, then recombinant plasmid DNA was transformed into yeast AH109 (a type). The transformed yeast AH109 was mated with yeast Y187 (α type) containing liver cDNA library plasmid in 2×YPDA medium. Diploid yeast was plated on synthetic dropout nutrient medium (SD/-Trp-Leu-His-Ade) containing X-α-gal for selection and screening. After extracting and sequencing plasmids from positive (blue) colonies, we underwent sequence analysis by bioinformatics.

RESULTS: Thirty-six colonies were selected and sequenced. Among them, 11 colonies were zymogen granule protein, 5 colonies were zinc finger protein, 4 colonies were zinc-α-2-glycoprotein, 1 colony was sialyltransferase, 1 colony was complement control protein factor I, 1 colony was vitronectin, and 2 colonies were new genes with unknown function.

CONCLUSION: The yeast two-hybrid system is an effective method for identifying hepatocyte proteins interacting with F protein of hepatitis C virus. F protein may bind to different proteins.

© 2005 The WJG Press and Elsevier Inc. All rights reserved.

Hepatitis C virus (HCV) is the major etiologic agent of parenterally transmitted non-A, non-B hepatitis worldwide[1-3]. Most infected individuals are unable to eliminate the virus, resulting in a persistent infection in about 80% of cases. Chronically infected patients often develop progressive liver disease, cirrhosis, hepatic failure, and hepatocellular carcinoma (HCC)[4,5]. Because development of a robust cell culture system for HCV infection has remained elusive, little is known about HCV-host cell interactions and how they influence cell physiology or viral replication. There is no vaccine against HCV.

HCV, discovered by cDNA cloning in 1989, is a member of the Hepacivirus genus within the Flaviviridae family, and a 9.6-kb positive single-stranded RNA virus. The HCV genome carries a single open reading frame (ORF) flanked by nontranslated regions and encodes a single polyprotein of about 3 010-3 033 amino acids. HCV polyprotein is cleaved by both host cell and viral proteases into at least 10 distinct structural and nonstructural protein products. The major structural proteins are a core (C) protein and two envelope proteins called E1, E2 and a short hydrophobic peptide p7. Four major nonstructural proteins called NS2, NS3, NS4, and NS5 are also generated, two of which, NS4 and NS5 are further processed into smaller polypeptides called NS4A, NS4B, NS5A, and NS5B. Most nonstructural proteins have enzymatic activities critical for viral replication. An additional HCV protein, F (for "frameshift protein") or ARFP (for "alternate reading frame protein"), encoded by the ORF that overlaps the core gene in the +1 frame (core+1 ORF), is synthesized *in vitro* from the initiator codon of the polyprotein sequence followed by a +1 ribosomal frameshift operating in the region of core codons 8-14[6-9]. Antibodies to F protein have been detected in HCV patients, indicating the production of F protein during natural HCV infection[10,11]. The function of F protein in the life cycle of HCV remains unknown. To investigate the biological

importance of F protein, we screened and identified the proteins interacting with HCV F protein by yeast two-hybrid system. One of the positive interacting proteins, named HCV F-interacting protein (HCV FBP2), was without known function.

Bacterial yeast strains and plasmids

All yeast strains and plasmids for yeast two-hybrid experiments were obtained from Clontech Co. (Palo Alto, CA, USA) as components of the MATCHMAKER two-hybrid system 3. Yeast strain AH109 (MATa, *trp1-901*, *leu2-3*, *112*, *ura3-52*, *his3-200*, *gal4*△, *gal80*△, *LYS2*:*GAL1*$_{UAS}$-*GAL1*$_{TATA}$-*HIS3*, *GAL2*$_{UAS}$-*GAL2*$_{TATA}$-*ADE2*, *URA3*:*MEL1*$_{UAS}$-*MEL*$_{1TATA}$-*LacZ*) containing pGBKT7-53, coding for DNA-BD/mouse p53 fusing protein was used for cloning of bait plasmid. Yeast strain Y187 (MATa *ura3-52*, *his3-200*, *Ade2-101*, *trp1-901*, *leu2-3*, *112*, *gal4*△, *gal80*△, *met-*, *URA3*:*GAL1*$_{UAS}$-*GAL1*$_{TATA}$-*lacZ MEL1*) containing pTD1-1 in which pACT2 coding for AD/SV40 large T antigen fusing protein was used for cloning of library plasmids. Pretransformed human cDNA liver cell library Y187 and bacterial strain DH5a were used for cloning of each shuttle plasmid. Yeast-*Escherichia coli* shuttle plasmids pGBKT7 DNA-BD, pGADT7 AD, pGBKT7-53, pGADT7, pGBKT7-Lam, pCL1 were from Clontech Co. (K1612-1). pGEM T vector was from Promega Co., USA.

Chemical agents and culture media

Taq DNA polymerase was purchased from MBI Co. T4 DNA ligase, *Eco*RI, and *Bam*HI restriction endonuclease were from Takara Co. c-myc mAb secreted by 1-9E10.2 hybridoma (ATCC), goat anti-mouse IgG conjugated with horseradish peroxidase were from Zhongshan Co., China. Lithium acetate, semi-sulfate adenine, acrylamide and *N*, *N*'-bis-acrylamide were from Sigma Co., TEMED was from Boehringer Mannheim Co. Tryptone and yeast extracts were from OXOID Co. X-α-gal and cultural media YPDA, SD/-*Trp* SD/-*Leu*, SD/-*Trp*/-*Leu*, SD/-*Trp*/-*Leu*/-*His*, SD/-*Trp*/-*Leu*/-*His*/-*Ade* were from Clontech Co. Protein-G agarose was from Roche Co. pGEM-T vector was from Promega Co.

RT-PCR kit and TNT® coupled reticulocyte lysate systems were from Promega Co. [^{35}S]-methionine (1 000 Ci/mmoL, 10 mCi/mL) was from Isotope Company of China. Amplification fluorographic reagent (#NAMP100) was from Amersham Life Sciences Co. Others were from Sigma Co.

Construction of "bait" plasmid and expression of HCV F protein

HCV-F sequences were generated by PCR amplification of HCV plasmid (HCV strain 1b) containing coding sequences for all the structural and nonstructural proteins. The sequences of the primers, containing the *Eco*RI and *Bam*HI restriction enzyme sites, are sense primer: 5'-GAA TTC ATG GCA CGA ATC CTA AAC C-3', and antisense primer: 5'-GGA TCC CTA CGC CGT CTT CCA GAA C-3'. The PCR conditions were at 94 ℃ for 30 s, at 60 ℃ for 30 s, at 72 ℃ for 30 s. Ten nanograms of PCR product was cloned with pGEM-T vector. The primary structure of insert was confirmed by direct sequencing. The fragment of encoding F was released from pGEM-T-F by digestion with *Eco*RI and *Bam*HI, and ligated to pGBKT7. Vector pGBKT7 expressing proteins were fused with amino acids 1-147 of the GAL4 DNA binding domain (DNA-BD), pGADT7 expressing proteins were fused with amino acids 768-881 of the GAL4 activation domain (AD). Plasmid pGBKT7-F (Figure 1) containing full-length HCV F gene could directly express DNA binding domain, c-myc and F fusion protein. The plasmid was transformed into yeast strain AH109 by lithium acetate method[12]. Western blotting was performed to confirm the expression of the fusion protein using c-myc monoclonal antibody. Transformed AH109 (bait) was cultured on quadruple dropout media to exclude the auto-activation activity.

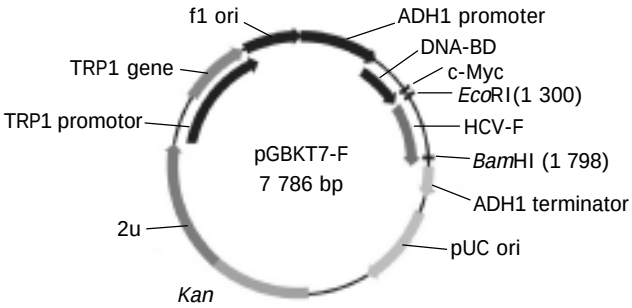


Figure 1 Map of "bait" plasmid pGBKT7-F.

Yeast two-hybrid library screening using yeast mating

One large (2-3 mm) fresh (<2 mo old) colony of AH109 [bait] was inoculated into 50 mL of SD/-*Trp* and incubated at 30 ℃ overnight (16-24 h) with shaking at 250-270 r/min. Then the cells were spun down by centrifuging the entire 50 mL culture at 1 000 r/min for 5 min. After the supernatant was decanted, the cell pellet was resuspended in the residual liquid by vortexing. A human liver cDNA library was cloned into pACT2 and yeast reporter strain Y187 (Clontech Co., USA). The entire AH109 [bait] culture and 1 mL human liver cDNA library (1×10^6 cfu/mL) were combined and cultured in a 2-L sterile flask and 45 mL of 2×YPDA/Kan was added and swirled gently. After 20 h of mating, the cells were spun down and resuspended, and then spread on 50 large (150-mm) plates containing 100 mL of SD/-*Ade*/-*His*/-*Leu*/-*Trp* (QDO). After growth for 6-15 d, the yeast colonies were transferred onto the plates containing X-α-gal to check for expression of the MEL1 reporter gene (blue colonies).

Plasmid isolation from yeast and transformation of E.coli with yeast plasmid

Approximately 1×10^6 colonies were screened and positive clones were identified. Yeast plasmid was isolated from positive yeast colonies by the lyticase method (Clontech Co.), and transformed into super-competence *E.coli* DH5α by chemical method. Transformants were plated on ampicillin SOB selection media and grown under selection. Subsequently, pACT2-cDNA constructs were re-isolated, and analyzed by

restriction digests and sequencing.

Bioinformatic analysis

After the positive colonies were sequenced, the sequences were blasted with GenBank to analyze the function of the genes (http://www.ncbi.nlm.nih.gov.blast).

Cell culture and new gene cloning

The hepatoblastoma cell line HepG2 was propagated in DMEM supplemented with 10% FBS, 200 μmol/L L-glutamine, penicillin, and streptomycin. HepG2 cells were plated at a density of 1×10^6/well in 35-mm dishes. Total cellular RNA was isolated using TRIzol (Invitrogen Co., USA) according to the manufacturer's instructions. cDNAs were reverse-transcribed from total RNA.

On the basis of liver cDNA library of genes of proteins interacting with HCV-F protein, the coding sequence of a new gene with unknown function, named HCV FBP2, was obtained by bioinformatics methods. The sequence of HCV FBP2 was deposited into GenBank, and the accession number was AY553876. The standard PCR cloning technique was used to amplify HCV FBP2 gene. Cytoplasmic RNA was isolated from HepG2 cells. RNA was used for RT-PCR. The primers were sense: 5'-GGA TTC ATG CCA TAT ATT CCT CTCA-3', and antisense: 5'-GGA TCC CTA ATA CAA ATG TAT GTG G-3' (HepG2 cDNA). The PCR conditions were at 94 ℃ for 60 s, at 58 ℃ for 60 s, at 72 ℃ for 60 s, for 30 cycles. The PCR product was cloned with pGEM-T vector (Promega Co.). The primary structure of insert was confirmed by direct sequencing. The gene was ligated into yeast plasmids pGBKT7 and pGADT7.

Confirmation of true interaction in yeast

To confirm the true protein-protein interaction and exclude false positives, the plasmids of positive colonies were transformed into yeast strain Y187, then mating experiments were carried out by mating with yeast strain AH109 containing pGBKT7-F or pGBKT7-Lam. After mating, the diploid yeast was plated on SD/-*Ade*-*His*-*Leu*-*Trp* (QDO) covered by X-α-gal to test the specificity of interactions.

In vitro translation

Twenty-five microliters of mixture of TNT® reticulocytes, 2 μL TNT® reaction buffer, 1 μL T7 TNT® RNA polymerase, 1 μL amino acid mixture (minus methionine, 1 mmol/L), 2 μL [^{35}S]-methionine, 1 μL RNasin RNase inhibitor (40 U/mL), 2 μL DNA template (pGBKT7-F or pGADT7-library gene) (0.5 μg/mL), 16 μL ddH_2O, were incubated at 30 ℃ for 90 min.

Co-immunoprecipitation

Following reactants were combined in a 1.5-mL microcentrifuge tube on ice: 5 μL *in vitro* translated bait protein, 5 μL *in vitro* translated library protein. Only 10 μL pGBKT7-F plasmid was added into the control. The mixtures were incubated at 30 ℃ for 1 h. Then, the following reagents were added into the reaction tubes: 470 μL co-immunoprecipitation buffer (20 mmol/L Tris-HCl [pH 7.5], 150 mmol/L NaCl, 1 mmol/L DTT, 5 μg/mL aprotinin, 0.5 mmol/L PMSF, 0.1% Tween 20), 10 μL protein-G agarose beads, 10 μL c-myc mAb, and incubated at 4 ℃ for 2 h with continuous shaking. The tubes were centrifuged at 14 000 *g* for 1-2 min. The supernatants were removed, 0.5 mL TBST was added to the tubes. Rinse was repeated thrice, 15 μL SDS-loading buffer was added. The samples were heated at 80 ℃ for 5 min. The tubes were placed on ice, and briefly centrifuged, and 10 μL was loaded onto an SDS-PAGE mini-gel for electrophoresis. After electrophoresis, the gel was transferred onto a tray containing gel fixation solution, and placed on a rotary shaker for 10 min at room temperature. The gel was rinsed with H_2O, then amplification fluorographic reagent was added and shook for 20 min at room temperature, then dried at 80 ℃ under constant vacuum. The gel was exposed to X-ray film overnight at room temperature. The film was developed by standard techniques.

Identification of recombinant plasmid

The full-length sequences of HCV F were generated by PCR amplification of HCV plasmid (HCV strain 1b), and a 840-bp fragment of HCV FBP2 was amplified by RT-PCR after total RNA was isolated from HepG2 cells, sequenced and analyzed by comparing to Vector NTI 6 and BLAST database homology search (http://www.ncbi.nlm.nih.gov/blast). After being cut by *Eco*RI/*Bam*HI, the fragments were in-frame ligated respectively into pGBKT7 and pGADT7 *Eco*RI/*Bam*HI sites. Restriction enzyme analysis of pGBKT7-F, pGBKT7-FBP2, and pGADT7-FBP2 plasmids with *Eco*RI/*Bam*HI yielded two bands respectively: 7 300 bp empty pGBKT7 and 486 bp HCV F, 7 300 bp empty pGBKT7 and 840 bp HCV FBP2, 7 900 bp empty pGADT7 and 840 bp HCV FBP2. The products of plasmid were amplified by PCR. Analysis of the PCR products by agarose gel electrophoresis showed the clear bands with the expected size (486 bp of F, 840 bp of FBP2). Sequences of the PCR products were correct (Figures 2A-D).

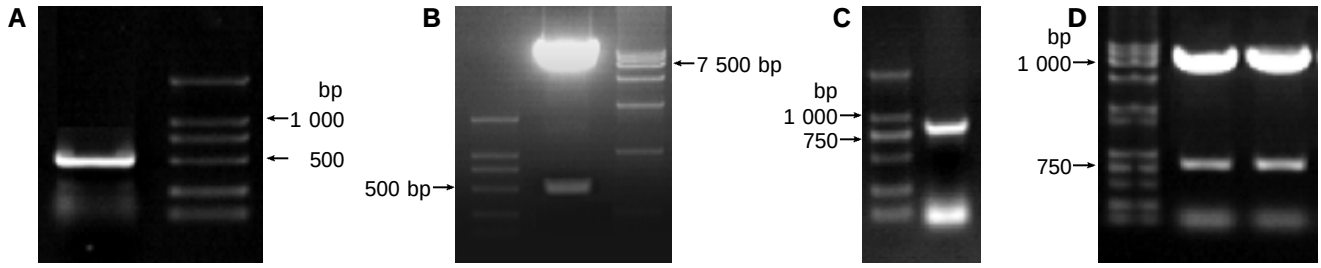


Figure 2 Sequences of PCR products A: a 486-bp fragment-F amplified by RT-PCR; B: pGBKT7-F cut by *Eco*RI/*Bam*HI; C: a 840-bp fragment-FBP2 amplified by RT-PCR; D1: pGBKT7-FBP2; D2: pGADT7-FBP2 cut by *Eco*RI/*Bam*HI.

Expression of "bait" fusion protein

Yeast strain AH109 transformed with pGBKT7-F and pGBKT7-FBP2 stably expressed the fusion protein at high level (Figure 3) and only grew on SD/-*Trp* medium but not on QDO medium. Thus, the transformed yeast could be used for yeast hybrid analysis.

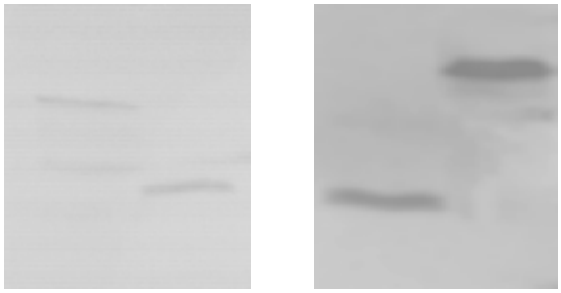


Figure 3 Expression of HCV F and HCV FBP2 proteins in yeast . Lane 1: HCV F protein; lane 2: positive control; lane 3: HCV FBP2 protein.

Screening of liver cell cDNA library

We isolated plasmids from the blue colonies containing only pGBKT7-F and one library plasmid other than other plasmids. Because plasmid pACT2- cDNA contains two restriction endonuclease sites of *Bgl*II, the gene fragments of the liver cell cDNA library (pACT2- cDNA) were released by *Bgl*II digestion (Figure 4). The gene fragments with different lengths proved that these screened clones were positive colonies but not false positive colonies growing on SD/-*Trp*/-*Leu*/-*His*/-*Ade* culture medium after mating .

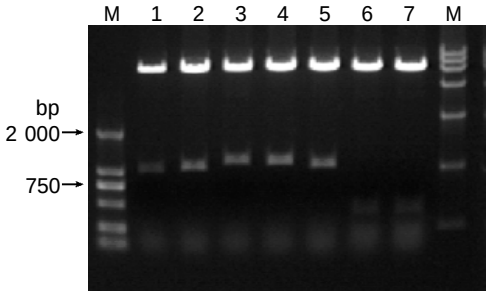


Figure 4 Identification of different colonies by *Bgl*II digestion.

Analysis of cDNA sequence and homology

A total of 36 positive colonies were grown on the selective SD/-*trp*-*leu*-*his*-*ade*/X-α-gal medium. These colonies were prescreened by *Bgl*II digesting to make sure that only colonies with different inserts were subjected to sequencing. Thirty-six colonies from cDNA library were sequenced. Using the BLAST program from the National Center for Biotechnology Information, two of the sequences were unknown genes and one of them was named as HCV FBP2. The full-length sequences accepted by GenBank were obtained by bioinformatics method. The other 34 sequences had a high similarity to known genes. The data are presented in Table 1.

Table 1 Comparison between positive clones and similar sequences in GenBank

High similarity to known genes	Similar number	Homolog (%)
Homo sapiens zymogen granule protein 16	11	99
Homo sapiens zinc-alpha-2-glycoprotein	4	99
Highly similar to *Homo sapiens* SL15 protein	5	100
Homo sapiens RAB14, member RAS oncogene family	1	98
Human mRNA for complement control protein factor I	1	98
Homo sapiens angiotensinogen (serine or cysteine) proteinase inhibitor, clade A (alpha-1 antiproteinase, antitrypsin), member 8)	1	97–99
Homo sapiens sialyltransferase 1	1	97
Similar to *Homo sapiens* zinc finger protein 83	5	100
Homo sapiens mRNA for peroxisomal ion protease	2	100
Homo sapiens cathepsin B mRNA	1	99
Homo sapiens vitronectin (serum spreading factor, somatomedin B, complement S-protein)	1	100
Homo sapiens serine (or cysteine) proteinase inhibitor, clade G (C1 inhibitor), member1	1	99
Homo sapiens genes of unknown functions	2	

Back-across testing

We confirmed the protein-protein interaction between HCV F and a new gene named as HCV FBP2 by back-across in yeast. Expressive vector pGADT7-HCV FBP2 was constructed and transformed into yeast Y187. This Y187 containing pGADT7-HCV FBP2 was mated with the yeast AH109 containing pGBKT7-F. The mated yeast was plated on the dropout medium. The positive colonies emerged and became blue.

In vitro co-immunoprecipitation

HCV F protein containing 161 aa, M_r = 17 710, being smaller than FBP2 containing 280 aa, M_r = 30 800 is shown in Figure 5.

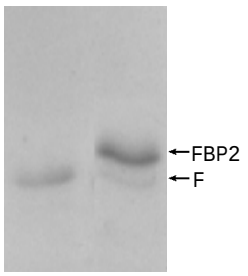


Figure 5 Interaction between HCV F protein and FBP2 protein identified by co-immunoprecipitation. Lane 1: HCV F protein; lane 2: interaction between HCV F and FBP_2 proteins.

The core protein of HCV is a multifunctional protein[13-15]. There is evidence that this protein can directly modulate intracellular signal transduction, gene transcription, cell proliferation, and cell death, interfere with lipid metabolism

and suppress host immune responses[16-19]. HCV F protein is a newly discovered HCV gene product encoded by the ORF that overlaps the core gene in the +1 frame[6-8]. F protein might have previously escaped attention because it possesses the immunodominant epitopes located in the N-terminus, in common with the core protein. A F protein analog synthesized *in vitro* reacts with the sera of HCV patients but not with the sera of hepatitis B patients, indicating that F protein is expressed during natural HCV infection. F protein is a very unstable protein with a half-life of <10 min in Huh7 hepatoma cells and *in vitro*, and is mediated by the proteasome pathway[20,21]. Immunofluorescence staining and subcellular fractionation experiments indicate that the subcellular localization of F protein is in the endoplasmic reticulum, and is similar to those of HCV core and NS5A proteins, suggesting that F protein may participate in HCV morphogenesis or replication. F protein shows more sequence diversity than the core protein[22-25]. Mutations of the core protein help virus to escape host immunologic reaction and may trigger cellular malignancy conversion. F protein might regulate cellular functions that are important for the viral life cycle or might play a role in viral morphogenesis or viral entry.

Because proteins often assemble into large complexes to perform different activities, characterization of the interaction pattern of a protein could contribute to the elucidation of the functions of protein[26]. Interaction between viral and hepatocellular proteins plays an important role in the pathogenesis of the virus and may mediate virus to enter hepatocytes. Their network interaction can change normal biological functions of proteins, influence self-replication of virus, prolong infection and develop diseases. Yeast two-hybrid 3 is an effective gene analysis method which can analyze interactions between protein and protein, protein and DNA, protein and RNA in eukaryotic cells, as well as a new genetics technique for studying interactions of proteins in physiologic condition *in vivo*.

Yeast two-hybrid system 3 based on the system originally designed by Fields and Song[27] takes the advantage of the properties of GAL4 protein of the yeast *Saccharomyces cerevisiae*. GAL4-yeast two-hybrid assay uses two expression vectors, one uses GAL4-DNA-binding domain (DBD) and the other uses GAL4-activation domain (AD). The GAL4-DBD is fused to protein 'X' and GAL4-AD is fused to protein 'Y' to form the bait and the target of the interaction trap, respectively. A selection of host cells with different reporter genes and different growth selection markers can detect and confirm protein-protein interactions and has fewer false positives[27-30].

In this study, the "bait" plasmid pGBKT7-F was transformed into yeast strain AH109. HCV F gene was expressed in yeast cells. After the "bait" plasmid pGBKT7-F yeast strain AH109 was mated with liver cDNA library yeast strain Y187, the diploid yeast cells were plated on QDO media containing X-α-gal, 36 true positives were obtained. By sequencing analysis of isolated library plasmids, we got the sequences of 34 genes with known functions and the sequences of two genes with unknown function, one of them was named as HCV FBP2. In order to further confirm the interaction between expressed protein and HCV F protein, we performed the experiment of co-immunoprecipitation of both proteins. A strong interaction between HCV F protein and HCV FBP2 protein *in vitro* was observed.

We screened *Homo sapiens* zymogen granule (ZG) protein 16 (ZG16p) interacting with F protein from liver cDNA library. ZG protein is highly expressed in the pancreas cells and regulates ATP-sensitive K(+) conductance of ZGs. ZG16p is one of the linker proteins with a submembranous protein matrix on the inner surface of ZG. The submembranous matrix composed of sulfated proteoglycans, glycoproteins and lectin ZG16p is essential for the binding and sorting of aggregated zymogens during granule formation. ZG16p is associated with lipid microdomains ('rafts') and affects the protein synthesis and intracellular transport of secretory proteins and maturation of zymogens in ZGs[31-34]. HCV infection and chronic hepatopathy caused by HCV are significantly associated with diabetes, and reduction of glucose tolerance is related to the severity of chronic hepatitis C[35,36]. The result of our experiment showed that interaction occurred between HCV F and ZG16p, thus providing a new clue for revealing the function of HCV F protein and relationship between pathogenesis of HCV and diabetes mellitus.

Another important protein interacting with F protein from liver cDNA library is the *Homo sapiens* zinc-alpha 2-glycoprotein (Zn-α2-GP). It is present at a high concentration in the seminal plasma and in other human body fluids. Hepatocytes are a source of protein in blood plasma and epithelia. Zn-α2-GP is present at carcinoma of prostate, breast cancer and hydroadenoma. Zn-α2-GP production is associated with tumor differentiation, decreased or absent Zn-α2-GP production is found in poorly differentiated (high Gleason grade) tumors. Zn-α2-GP production in tumors can elevate the systemic ZAG concentration and induce lipolysis leading to cachexia. Zn-α2-GP is a potential serum marker of prostate cancer that may elevate early in tumor development. Whether tumors can induce secretion of endogenous Zn-α2-GP by normal prostatic or other secretory ZAG expression can predict the risk of a progressive disease needs further study[37].

Vitronectin, also known as a serum spreading factor, is a glycoprotein present in both human plasma and serum. It is also present in different loose connective tissues, often in co-localization of elastic fibrils. Vitronectin binds to cells through interaction of the Arg-Gly-Asp (RGD) sequence in its cell-binding domain with vitronectin-specific cell surface receptors and may modulate blood coagulation and complement-induced cytolysis. Matrix-bound vitronectin plays a role in regulating pericellular proteolysis by binding to plasminogen activator inhibitor type I. Vitronectin may promote cell attachment, spreading, proliferation, and differentiation of normal and neoplastic cells[38,39].

C1 inhibitor (C1 INH) is a highly glucosylated protein. The content of glucose is up to 35-49%. It has 30% homology of amino acids of serine proteinase inhibitor superfamily members including α1 anti-trypsin, α1 anti-chymotrypsin and anti-thrombin III. C1 INH combines activated C1r or C1s to form a stable complex, leading to inactivation of serine proteinase C1. C1 INH may prevent auto-activation of C1. Because C1 INH still inhibits factors XIIa, XIa,

kallikrein and fibrinolysin, it plays an important role in regulation of blood coagulation, kinin, and fibrinolytic system[40,41].

Sialyltransferase is a member of glycosyltransferase family and presents at Golgi apparatus. Sialyltransferase possesses the functions of catalyzing cellular adhesive molecule-ganglioside polysialic acidification. Ganglioside, a kind of glycosphingolipid containing sialic acid, is an important factor for cellular adhesion and malignancy cell growth *in vitro* culture.

HCV F protein also interacts with complement control protein factor I, peroxisomal ion protease, cathepsin B, RAS oncogene. These interacting proteins are closely correlated with carbohydrate metabolism, immunoregulation, occurrence and development of tumor. How interactions between HCV F protein and interacting proteins affect the occurrence and development of chronic hepatitis C, hepatic fibrosis and hepatocarcinoma, needs to be further elucidated.

1 **Yokoyama Y,** Kuramitsu Y, Takashima M, Iizuka N, Toda T, Terai S, Sakaida I, Oka M, Nakamura K, Okita K. Proteomic profiling of proteins decreased in hepatocellular carcinoma from patients infected with hepatitis C virus. *Proteomics* 2004; **4**: 2111-2116

2 **Miller RH,** Purcell RH. Hepatitis C virus shares amino acid sequence similarity with pestiviruses and flaviviruses as well as members of two plant virus supergroups. *Proc Natl Acad Sci USA* 1990; **87**: 2057-2061

3 **Simmonds P,** Smith DB, McOmish F, Yap PL, Kolberg J, Urdea MS, Holmes EC. Identification of genotypes of hepatitis C virus by sequence comparisons in the core, E1 and NS-5 regions. *J Gen Virol* 1994; **75**(Pt 5): 1053-1061

4 **O'Brien TR,** Kirk G, Zhang M. Hepatocellular carcinoma: paradigm of preventive oncology. *Cancer J* 2004; **10**: 67-73

5 **Tanaka J,** Yoshizawa H. A national project for the management of viral hepatitis toward prevention of hepatocellular carcinoma in Japan. *Gan To Kagaku Ryoho* 2004; **31**: 864-870

6 **Varaklioti A,** Vassilaki N, Georgopoulou U, Mavromara P. Alternate translation occurs within the core coding region of the hepatitis C viral genome. *J Biol Chem* 2002; **277**: 17713-17721

7 **Walewski JL,** Keller TR, Stump DD, Branch AD. Evidence for a new hepatitis C virus antigen encoded in an overlapping reading frame. *RNA* 2001; **7**: 710-721

8 **Xu Z,** Choi J, Yen TS, Lu W, Strohecker A, Govindarajan S, Chien D, Selby MJ, Ou J. Synthesis of a novel hepatitis C virus protein by ribosomal frame shift. *EMBO J* 2001; **20**: 3840-3848

9 **Boulant S,** Becchi M, Penin F, Lavergne JP. Unusual multiple recoding events leading to alternative forms of hepatitis C virus core protein from genotype 1b. *J Biol Chem* 2003; **278**: 45785-45792

10 **Roussel J,** Pillez A, Montpellier C, Duverlie G, Cahour A, Dubuisson J, Wychowski C. Characterization of the expression of the hepatitis C virus F protein. *J Gen Virol* 2003; **84**(Pt 7): 1751-1759

11 **Choi J,** Xu Z, Ou JH. Triple decoding of hepatitis C virus RNA by programmed translational frameshifting. *Mol Cell Biol* 2003; **23**: 1489-1497

12 **Matsumoto M,** Hsieh TY, Zhu N, VanArsdale T, Hwang SB, Jeng KS, Gorbalenya AE, Lo SY, Ou JH, Ware CF, Lai MM. Hepatitis C virus core protein interacts with the cytoplasmic tail of lymphotoxin-beta receptor. *J Virol* 1997; **71**: 1301-1309

13 **Liu M,** Liu Y, Cheng J, Zhang SL, Wang L, Shao Q, Zhang J, Yang Q. Transactivating effect of hepatitis C virus core protein: A suppression subtractive hybridization study. *World J Gastroenterol* 2004; **10**: 1746-1749

14 **Okamoto K,** Moriishi K, Miyamura T, Matsuura Y. Intramembrane proteolysis and endoplasmic reticulum retention of hepatitis C virus core protein. *J Virol* 2004; **78**: 6370-6380

15 **Majeau N,** Gagne V, Boivin A, Bolduc M, Majeau JA, Ouellet D, Leclerc D. The N-terminal half of the core protein of hepatitis C virus is sufficient for nucleocapsid formation. *J Gen Virol* 2004; **85**(Pt 4): 971-981

16 **Carlos MP,** Yamamura Y, Vu Q, Conzen K, Anderson DE, Torres JV. Humoral immunity to immunodominant epitopes of Hepatitis C virus in individuals infected with genotypes 1a or 1b. *Clin Immunol* 2004; **111**: 22-27

17 **Kunkel M,** Watowich SJ. Biophysical characterization of hepatitis C virus core protein: implications for interactions within the virus and host. *FEBS Lett* 2004; **557**: 174-180

18 **Hahn CS,** Cho YG, Kang BS, Lester IM, Hahn YS. The HCV core protein acts as a positive regulator of fas-mediated apoptosis in a human lymphoblastoid T cell line. *Virology* 2000; **276**: 127-137

19 **Sabile A,** Perlemuter G, Bono F, Kohara K, Demaugre F, Kohara M, Matsuura Y, Miyamura T, Brechot C, Barba G. Hepatitis C virus core protein binds to apolipoprotein AII and its secretion is modulated by fibrates. *Hepatology* 1999; **30**: 1064-1076

20 **Ogata S,** Nagano-Fujii M, Ku Y, Yoon S, Hotta H. Comparative sequence analysis of the core protein and its frameshift product, the F protein, of hepatitis C virus subtype 1b strains obtained from patients with and without hepatocellular carcinoma. *J Clin Microbiol* 2002; **40**: 3625-3630

21 **Xu Z,** Choi J, Lu W, Ou JH. Hepatitis C virus f protein is a short-lived protein associated with the endoplasmic reticulum. *J Virol* 2003; **77**: 1578-1583

22 **Brass V,** Bieck E, Montserret R, Wolk B, Hellings JA, Blum HE, Penin F, Moradpour D. An amino-terminal amhipathic alphahelix mediates membrane association of the hepatitis C virus nonstructural protein 5A. *J Biol Chem* 2002; **277**: 8130-8139

23 **Lanford RE,** Notvall L, Chavez D, White R, Frenzel G, Simonsen C, Kim J. Analysis of hepatitis C virus capsid, E1, and E2/NS1 proteins expressed in insect cells. *Virology* 1993; **197**: 225-235

24 **Mclauchlan J,** Lemberg MK, Hope G, Martoglio B. Intramembrane proteolysis promotes trafficking of hepatitis C virus core protein to lipid droplets. *EMBO J* 2002; **21**: 3980-3988

25 **Shi ST,** Polyak SJ, Tu H, Taylor DR, Gretch DR, Lai MM. Hepatitis C virus NS5A colocalizes with the core protein on lipid droplets and interacts with apolipoproteins. *Virology* 2002; **292**: 198-210

26 **Emmert-Buck MR,** Gillespie JW, Pawletz CP, Ornstein DK, Basrur V, Appella E, Wang QH, Huang J, Hu N, Taylor P, Petricoin EE 3rd. An approach to proteomic analysis of human tumors. *Mol Carcinog* 2000; **27**: 158-165

27 **Fields S,** Song O. A novel genetic system to detect protein-protein interactions. *Nature* 1989; **340**: 245-246

28 **Osman A.** Yeast two-hybrid assay for studying protein-protein interactions. *Methods Mol Biol* 2004; **270**: 403-422

29 **Gietz RD,** Woods RA. Screening for protein-protein interactions in the yeast two-hybrid system. *Methods Mol Biol* 2002; **185**: 471-486

30 **Zhen Z.** Progress in proteomics. *Shengwu Gongcheng Xuebao* 2001; **17**: 491-493

31 **Kalus I,** Hodel A, Koch A, Kleene R, Edwardson JM, Schrader M. Interaction of syncollin with GP-2, the major membrane protein of pancreatic zymogen granules, and association with lipid microdomains. *Biochem J* 2002; **362**(Pt 2): 433-442

32 **Hodel A,** An SJ, Hansen NJ, Lawrence J, Wasle B, Schrader M, Edwardson JM. Cholesterol-dependent interaction of syncollin with the membrane of the pancreatic zymogen granule. *Biochem J* 2001; **356**(Pt 3): 843-850

33 **Schmidt K,** Schrader M, Kern HF, Kleene R. Regulated apical secretion of zymogens in rat pancreas: Involvement of the GPI-anchored glycoprotein GP-2, the lectin ZG16p and cho-

lesterol-glycosphingolipid enriched microdomains. *J Biol Chem* 2001; **276**: 14315-14323

34 **Kleene R,** Dartsch H, Kern HF. The secretory lectin ZG16p mediates sorting of enzyme proteins to the zymogen granule membrane in pancreatic acinar cells. *Eur J Cell Biol* 1999; **78**: 79-90

35 **Arao M,** Murase K, Kusakabe A, Yoshioka K, Fukuzawa Y, Ishikawa T, Tagaya T, Yamanouchi K, Ichimiya H, Sameshima Y, Kakumu S. Prevalence of diabetes mellitus in Japanese patients infected chronically with hepatitis C virus. *J Gastroenterol* 2003; **38**: 355-360

36 **Paraschiv C,** Graur M, Butnariu G, Mihai B, Constantinescu D. The pathological, mechanisms of glycoregulation disturbances in chronic B and C. *Rev Med Chir Soc Med Nat Iasi* 2002; **107**: 294-297

37 **Hale LP,** Price DT, Sanchez LM, Demark-Wahnefried W, Madden JF. Zinc alpha-2-glycoprotein is expressed by malignant prostatic epithelium and may serve as a potential serum marker for prostate cancer. *Clin Cancer Res* 2001; **7**: 846-853

38 **Stawowy P,** Kallisch H, Veinot JP, Kilimnik A, Prichett W, Goetze S, Seidah NG, Chretien M, Fleck E, Graf K. Endoproteolytic activation of alpha (v) integrin by proprotein convertase PC5 is required for vascular smooth muscle cell adhesion to vitronectin and integrin-dependent signaling. *Circulation* 2004; **109**: 770-776

39 **Faucheux N,** Schweiss R, Lutzow K, Werner C, Groth T. Self-assembled monolayers with different terminating groups as model substrates for cell adhesion studies. *Biomaterials* 2004; **25**: 2721-2730

40 **Sim RB,** Tsiftsoglou SA. Proteases of the complement system. *Biochem Soc Trans* 2004; **32**(Pt 1): 21-27

41 **Toomayan GA,** Chen LE, Jiang HX, Qi WN, Seaber AV, Frank MM, Urbaniak JR. C1-esterase inhibitor and a novel peptide inhibitor improve contractile function in reperfused skeletal muscle. *Microsurgery* 2003; **23**: 561-567

Science Editor Wang XL **Language Editor** Elsevier HK

PO Box 2345, Beijing 100023, China
www.wjgnet.com
wjg@wjgnet.com

ELSEVIER

World J Gastroenterol 2005;11(36):5666-5671
World Journal of Gastroenterology ISSN 1007-9327
© 2005 The WJG Press and Elsevier Inc. All rights reserved.

Cloning and characterization of a novel hepatitis B virus core binding protein C12

Yin-Ying Lu, Jun Cheng, Yong-Ping Yang, Yan Liu, Lin Wang, Ke Li, Ling-Xia Zhang

Yin-Ying Lu, Jun Cheng, Yong-Ping Yang, Yan Liu, Lin Wang, Ke Li, Ling-Xia Zhang, Gene Therapy Research Center, Institute of Infectious Diseases, The 302 Hospital of PLA, 100 Xisihuanzhong Road, Beijing 100039, China
Correspondence to: Dr. Jun Cheng, Gene Therapy Research Center, Institute of Infectious Diseases, The 302 Hospital of PLA, 100 Xisihuanzhong Road, Beijing 100039, China. cj@genetherapy.com.cn
Telephone: +86-10-66933391 Fax: +86-10-63801283
Received: 2004-11-16 Accepted: 2005-02-18

Abstract

AIM: To elucidate the biological function of HBV core antigen (HBcAg) on pathogenesis of hepatitis B, a novel gene C12 coding for protein with unknown function interacting with HBcAg in hepatocytes was identified and characterized.

METHODS: HBcAg bait plasmid pGBKT7-HBcAg was constructed and transformed into yeast AH109, then the transformed yeast was mated with yeast Y187 containing liver complementary DNA (cDNA) library plasmid in 2×YPDA medium. Diploid yeast was plated on synthetic dropout nutrient medium (SD/-Trp-Leu-His-Ade) and synthetic dropout nutrient medium (SD/-Trp-Leu-His-Ade) containing X-α-gal for screening twice. After extracting and sequencing of plasmid from blue colonies, we isolated a cDNA clone encoding a novel protein designated as C12 that directly interacted with HBcAg. The interaction between HBcAg and C12 was verified again by re-mating. pEGFP-N1-C12 fluorescent protein fusion gene was transfected in 293 and L02 cell, and observed by fluorescent microscope. MTT reduction assay was used to study the action of C12 protein effect on metabolism of mammal cell. Yeast two-hybrid and cDNA microarray were performed to search binding protein and differential expression genes regulated by C12 protein.

RESULTS: C12 gene was screened and identified by yeast two-hybrid system 3. The interaction between HBcAg and the novel protein coded by the new gene C12 was further confirmed by re-mating. After 48 h, fluorescence of fusion protein could be observed steadily in the 293 and L02 cell plasma. Under MTT assay, we found that the expression of C12 did not influence the growth of liver cells. Seventeen differential expression genes in HepG2 cells transfected with C12 protein expression plasmid by cDNA microarray, of which 16 genes were upregulated and 1 gene was downregulated by C12 protein. Twenty-one colonies containing 16 different genes coding for C12 protein binding proteins were isolated by yeast two-hybrid, there were 2 new genes with unknown function.

CONCLUSION: The novel protein C12 is located in cell plasma, and its overexpression has no significant effect on the metabolism of liver cell. It interacts with many proteins in hepatocytes and may be involved in many processes of gene expression.

© 2005 The WJG Press and Elsevier Inc. All rights reserved.

Key words: Hepatitis B virus core antigen; Yeast two-hybrid; cDNA microarray; MTT assay

Lu YY, Cheng J, Yang YP, Liu Y, Wang L, Li K, Zhang LX. Cloning and characterization of a novel hepatitis B virus core binding protein C12. *World J Gastroenterol* 2005; 11(36): 5666-5671
http://www.wjgnet.com/1007-9327/11/5666.asp

INTRODUCTION

There are more than 400 million carriers of HBV worldwide who are at high risk for the development of chronic liver diseases, but the precise mechanism of virus involvement remains elusive[1,2]. Identification of cellular HBV core antigen (HBcAg) interaction protein would provide insights into the mechanism of HBV cellular effects[3-5]. Based on the yeast two-hybrid screening and bio-information assay, we found a novel gene named C12 coding for protein binding with HBcAg, and located in cell plasma. After the finishing of human genome project, we obtained mass information of chromosome DNA including many sequences of coding gene with unknown functions. While DNA constitutes the information archive of the genome, it is the proteins that actually serve as the functional effectors of cellular processes. How to elucidate the structure, biological function and medical significance of protein coding by novel genes, are the most difficult and complex work in future. By means of MTT reduction assay, complementary DNA (cDNA) microarray and yeast two-hybrid technique, the potential biological function of C12 protein was initially investigated in the context of effect on cell metabolism and gene expression, the binding protein in hepatocytes. We expected the results would bring us some valuable information and pave the way for further study.

MATERIALS AND METHODS

Plasmid construction

The HBcAg gene from a known HBV DNA sequence

(subtype ayw) was amplified by PCR (P1 3'-GAA TTC ATG GAC ATC GAC CCT TAT AA-5', P2 3'-CTG CAG AAC ATT GAG ATT CCC GAG AT-5') and cloned into the DNA-binding domain vector pGBKT7 (Clontech, Palo Alto, CA, USA). This plasmid contains TRP1 gene, permitting it to grow in trp medium. A normal human adult liver cDNA stretch library was cloned into the activation domain vector pACT2 and transformed into yeast strain Y187 to build pretransformed cDNA liver cell library (Clontech Co., USA); pACT2 plasmid contain Leu2 gene (Clontech Co., USA), permitting it to grow in leu-medium[6-9].

Western blotting

The plasmid pGBKT7-HBcAg containing full length of HBcAg gene was constructed by insertion of HBcAg gene in-frame into *Eco*RI/*Bam*HI site, and could directly express DNA binding domain, *c-myc* and core fusion protein was transformed into yeast strain AH109 by using lithium acetate method. Yeast protein of AH109 was extracted and Western blotting was performed to confirm the expression of the fusion protein by using *c-myc* mAb. Transformed AH109 was cultured on quadrupole dropout media to exclude the auto-activity.

Two-hybrid library screen and cDNA isolation

One large (2-3 mm), fresh (<2 mo old) colony of AH109 containing bait plasmid was inoculated into 50 mL of SD/-Trp and incubated at 30 ℃ overnight (16-24 h) with shaking at 250-270 r/min. Then the cells were spun down by centrifuging the entire 50-mL culture at 1 000 r/min for 5 min and supernatant was decanted, the cell pellet was resuspended in the residual liquid by vortexing. The entire AH109 (bait) culture and the 1-mL library were combined and cultured in a 2-L sterile flask and 45 mL of 2× YPDA/Kan was added and swirled gently. After 20-h mating, the cells were spun down, resuspended and then spread on 50 large (150-mm) plates, containing 200 mL of SD/-Ade/-His/-Leu/-Trp. After 6-18 d of growth, the yeast colonies were transferred onto the plates containing X-α-gal to check for expression of the MEL1 reporter gene (blue colonies). Blue colonies were considered to be true positives and were discarded. Yeast plasmid DNA was isolated with lyticase method (Clontech), and transformed into *E. coli* by using electroporation; transformants were plated on ampicillin LB selection media and analyzed by DNA sequencing.

DNA sequencing and computation

cDNA inserts were sequenced with the Sequenase version 2.0 sequencing kit (Boya Biochemical Corp, China) based on the dideoxy method. Homology searches for the DNA sequences thus determined and their deduced amino acid sequences were performed at the National Center for Biotechnology Information with the BLAST network service.

RT-PCR and re-mating

Based on the information of GenBank, PCR primers of the novel gene C12 were designed (P3 5'-GAA TTC ATG ATA AGT GAA GGC GGA TG-3', P4 5'-GGA TCC CTA TTG TTA ACA GAG GAC T-3'), and the full-length gene of C12 was amplified by using reverse transcription polymerase chain reaction (RT-PCR) by using genomic DNA from HepG2 cell line as the template. C12 gene was inserted into yeast expression vector pGADT7 and transformed into yeast strain Y187, then re-mated with AH109 containing pGBKT7-HBcAg. After mating, the diploid yeasts were plated on QDO covered with X-α-gal for further verification[10].

Sub-cellular localization

Full-length C12 gene was amplified by PCR with primers (P5 5'-GAA TTC ATG ATA AGT GAA GGC GGA TG-3', P6 5'-GGA TCC TTG TTA ACA GAG GAC TTT T-3') and inserted into green fluorescent protein (GFP) expression vector pEGFP-N1 (Promega Co., USA). The human liver cell line L02 and African green monkey renal cell line 293 was incubated in DMEM medium with 10% fetal bovine serum (FBS), 200 μmol/L L-glutamine, penicillin, streptomycin, and plated at a density of 1×10^4/well in 35-mm dishes. Purified plasmid pEGFP-N1-C12 was transfected into 293 and L02 cell by using Lipofectamine PLUS (Gibco Co., USA) and observed under fluorescent microscope after 48-h incubation.

MTT reduction assay

L02 and Bel7402 cells were respectively divided into four groups; they were empty cell group, liposomes group, pEGFP-N1 group, and pEGFP-N1-C12 group. Each group included six wells and each well was incubated with 1×10^4 cells. Deionized water, liposomes, pEGFP-N1, and pEGFP-N1-C12 were transfected into corresponding groups and incubated for 18 h in DMEM medium with 10% FBS at 37 ℃ (Roche Co., USA). Cells were incubated for next 4 h with DMEM without FBS, and 750 μL DMSO was added in each well followed by discarding the medium and washing with 1× PBS. After mixing steadily, the absorbance of samples was measured (detection wavelength 550 nm, reference wavelength 650 nm) to quantify cell number.

Screening of binding protein

pGBKT7-C12 bait plasmid was constructed by inserting C12 full-length gene into yeast expression vector pGBKT7 and transfected into AH109 cell. Positive AH109 cell mated with pretransformed cDNA liver cell library Y187 cell for screening twice. Blue colonies were discarded and analyzed by DNA sequencing and bioinformatic assay.

cDNA microarray assay

HepG2 cell line transfected with pcDNA3.1(-)-C12 and pcDNA3.1(-) were incubated at DMEM medium for 48 h. mRNA from these cells were extracted by using Quick Prep micro mRNA Purification Kit (Amersham Pharmacia Co., USA). Cy3-dUTP was labeled into cDNA of pcDNA3.1(-) group and Cy5-dUTP was labeled into cDNA of pcDNA3.1(-)-C12 group during the RT-PCR procedure. These cDNA was hybridized with cDNA chip containing 1 152 cDNA and amplified by PCR with common primer. After dotting, hydrating, dehydrating, ultraviolet joining, and washing with SDS, water and sodium borocaptate solution, samples were degenerated in water at 95 ℃ for 5 min and hybridized

with mixed probe for 15-17 h. Followed by washing, drying at room temperature, specimens were analyzed by ScanArray 3000 (General Scanning, positive standard: Cy5/Cy3>2.0, negative standard: Cy5/Cy3<0.5).

RESULTS

Expression of the "bait" fusion protein

Yeast strain AH109 transformed with pGBKT7-HBcAg could stably express the fusion protein at high level (Figure 1). The transformed AH109 could only grow on SD/-Trp medium but not on QDO medium. Thus, the transformed yeast could be used for yeast hybrid analysis.

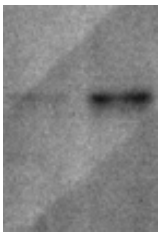


Figure 1 Western blotting showed the expression of HBV core protein in yeast. Lane 1: 5-μL sample; lane 2: 10-μL sample.

Two-hybrid library screen and re-mating

In order to unravel the molecular mechanisms of HBcAg, we adopted the yeast two-hybrid system to identify and characterize cellular targets of HBcAg. An adult human liver cDNA library containing cDNAs fused to the GAL4 activation domain in yeast vector pCAT2 was used to screen for clones interacting with HBcAg. Plasmid pACT2-cDNA was recovered from the true positive clone and was sequenced. The result of our screening led to the identification of a clone containing gene without homologs in GenBank. This cDNA was 591 bases long (Figure 3), which contained an open reading frame (ORF) able to encode a protein of 197 amino acids. The protein was named C12. Sequence homology searches in GenBank revealed that it was a novel gene. The entire ORF coding for C12 was obtained from HepG2 cells and subcloned into yeast plasmid pGADT7 to be expressed as a fusion protein with DNA activation domain of GAL4. pGADT7-C12 was transfected into Y187 and re-mated with AH109 transfected with pGBKT7-HBcAg to verify the reliability of the interaction between them.

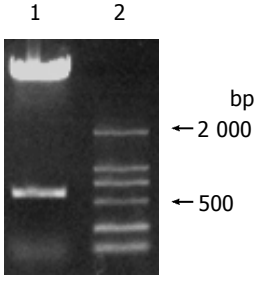


Figure 2 pEGFP-N1-C12 digested by *Eco*RI and *Bam*HI. Lane 1: pEGFP-N1-C12; lane 2: DNA marker.

```
      M  I  S  E  G  G  W  G  W  Q  G  W  G  R  S  Q  G
1     ATG ATA AGT GAA GGC GGA TGG GGA TGG CAG GGG TGG GGG CGA AGC CAA GGT
      L  R  P  A  P  C  S  W  V  S  R  M  V  S  P  P  A
52    CTG AGA CCT GCA CCC TGC AGC TGG GTC AGC AGG ATG GTA TCT CCA CCC GCG
      A  I  Q  E  T  Q  L  H  F  L  A  D  T  L  P  S  P
103   GCC ATC CAG GAA ACA CAG CTC CAT TTC CTT GCT GAC ACC CTC CCC TCC CCG
      L  S  I  L  L  P  P  H  K  Q  E  E  L  S  Q  S  Q
154   TTG TCC ATC CTG CTC CCT CCC CAC AAG CAA GAG GAG TTG TCC CAG AGT CAG
      L  L  I  A  D  L  L  P  A  S  D  L  G  N  F  Q  T
205   CTC CTC ATA GCT GAC CTC TTA CCA GCT TCG GAT CTA GGA AAC TTC CAG ACT
      S  R  E  T  Q  S  Y  Q  K  A  Q  P  T  P  I  S  F
256   TCT AGG GAG ACA CAG AGC TAC CAG AAA GCC CAA CCC ACC CCC ATC TCT TTC
      S  P  D  H  R  K  V  S  R  D  V  I  P  G  A  A  L
307   TCT CCA GAT CAT AGG AAA GTA TCA AGG GAT GTC ATT CCG GGA GCA GCC CTT
      G  T  A  S  S  R  C  W  Q  M  L  C  P  S  P  S  V
358   GGG ACA GCC AGC AGC AGG TGC TGG CAG ATG CTC TGT CCT TCA CCC TCT GTC
      P  G  T  R  W  G  R  P  Q  W  K  L  L  N  S  V  T
409   CCC GGC ACC AGA TGG GGA AGG CCA CAG TGG AAA CTT CTC AAT TCC GTC ACA
      G  Q  S  S  D  T  V  I  S  Q  F  S  L  A  M  S  F
460   GGG CAG AGC TCT GAC ACT GTT ATA AGT CAG TTC TCC CTG GCC ATG TCT TTT
      P  N  F  P  V  P  Q  L  R  F  L  N  T  C  S  T  D
511   CCT AAT TTT CCT GTC CCA CAA CTT AGG TTC CTT AAC ACT TGT TCT ACA GAT
      E  T  K  K  S  S  V  N  K  *
562   GAA ACA AAA AAG TCC TCT GTT AAC AAG TAG
```

Figure 3 Nucleic and amino acid sequences of C12 cDNA.

Sub-cellular localization

After the full-length gene of C12 was cloned into pEGFP-N1 (Figure 2), the fluorescent protein expression plasmid pEGFP-N1-C12 was transfected into 293 and L02 cells and incubated for 48 h. When we observed under the fluorescent microscope, the steady, powerful green fluorescent signal could be observed in most cells (Figures 4A and B). The result indicated that the C12 protein could be expressed in these cells and mainly localized in the cell plasma.

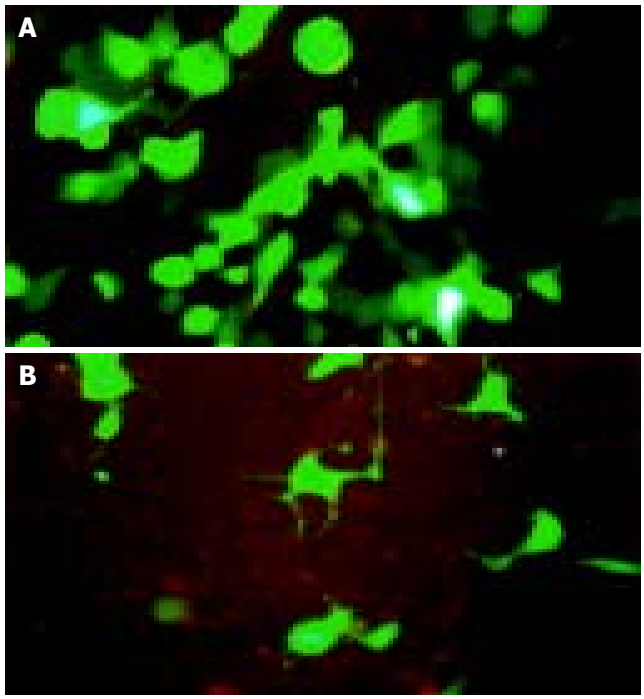


Figure 4 A pEGFP-N1-C12 expression in 293 cell line; **B**: pEGFP-N1-C12 expression in L02 cell line.

MTT reduction assay

MTT reduction assay was performed in Bel7402 and L02 cell line transfected with deionized water, liposomes, pEGFP-N1 and pEGFP-N1-C12 respectively. The results showed that the optical density in Bel7402 cell line

groups were 0.547±0.076, 0.575±0.122, 0.470±0.124, 0.503±0.093, while the optical density in L02 cell line groups were 0.216±0.028, 0.201±0.01, 0.197±0.011, 0.205±0.024. It revealed that the expression of C12 gene in both cells did not have inhibitory or promotional effect on the growth of these cells, compared with deionized water, liposomes and empty vector (P>0.01).

Screening of binding protein

Yeast strain AH109 transformed with pGBKT7-C12 could grow on SD/-Trp medium and could not grow on QDO medium, the result showed that C12 protein have no autoactivation in yeast cell and could be used for yeast two-hybrid screening. After being mated with pretransformed cDNA library strain Y187 and screened on QOD, 21 blue clones were obtained. Plasmid in these clones were cloned into *Escherichia coli* and analyzed by DNA sequencing. After comparing these sequences in GenBank, 16 different genes were screened. Fourteen genes were homolog of known genes, two genes did not find homolog in GenBank (Table 1)[11].

Table 1 Binding protein of C12 protein screened by yeast two-hybrid

Homeobox gene	Homogeneity %	Clones
Cathepsin B	99	1
Apolipoprotein M	98	1
Cytochrome C oxidase II	97–99	3
Receptor JAK (EPHB4) variation factor	99	1
KH splicing regulation protein (KSRP)	98	1
Phosphatidylinositol deacylase	97	1
poly-glucose Q transcriptional variation factor 1		
Ferritin light chain	99	2
Ornithine decarboxylase 1	99	1
Metallothionein 2A	98–100	3
Blood coagulation factor IX	100	1
Acetolactate synthase	99	1
Calpain	98	1
Exo-nucleus triphosphate diplo-phosphoinostide	99	1
hydrolase 5		
Plasma globulin inhibitive factor H4	99	1
Novel gene	100	2

cDNA microarray assay

Eight paddy genes from 1 152 cDNA on the chip that served as negative control showed very weak hybrid signal, which confirmed the reliability of the experiment. Total mRNA of HepG2 cells transfected with pcDNA3.1(-) and pcDNA3.1(-)-C12 were purified, respectively, then labeled with Cy3-dUTP and Cy5-dUTP during RT-PCR procedure. Cy5 fluorescein showed red fluorescence and Cy3 fluorescein showed green fluorescence. The difference of color showed the difference of gene expression level, such as yellow showed that there was no difference between the two groups. Based on the criteria, 16 differential expression genes upregulated by C12 and 1 gene downregulated by C12 were screened (Table 2). These genes were involved in cell signal conduction, cell proliferation, differentiation, and generation of carcinoma[12].

Table 2 Differential expression genes upregulated by C12 gene

GenBank number	Homeobox gene
000208	Insulin receptor (INSR),
005500	SUMO-1 activating enzyme subunit 1 (SAE1),
006292	Tumor susceptibility gene 101 (TSG101),
012248	Selenophosphate synthetase 2 (SPS2),
006217	Serine (or cysteine) proteinase inhibitor, clade I (neuroserpin), member 2 (SERPINI2),
016614	TRAF and TNF receptor-associated protein (TTRAP),
006437	ADP-ribosyltransferase-like 1 (ADPRTL1)
033306	Caspase 4, apoptosis-related cysteine protease (CASP4), transcript variant gamma,
L04731	Translocation T (4:11) of ALL-1 gene
002085	Glutathione peroxidase 4 (phospholipid hydroperoxidase) (GPX4),
004728	DEAD/H (Asp-Glu-Ala-Asp/His) box polypeptide 21 (DDX21),
002624	Prefoldin 5 (PFDN5), transcript variant 1,
006415	Serine palmitoyl transferase, long chain base subunit 1 (SPTLC1),
004127	G protein pathway suppressor 1 (GPS1),
014887	Hypothetical protein from BCRA2 region
000660	Transforming growth factor, beta 1 (TGF-β1),

DISCUSSION

The HBV infection is a public health problem worldwide, particularly in East Asia. The current therapy of HBV infection is mostly based on chemical agents and cytokines that have been shown to provide limited efficacy are also toxic to the human body[13-15]. Elucidating the interaction between hepatocytes and HBV was essential for finding new methods to inhibit the replication of HBV. The HBV nucleocapsid or core antigen (HBcAg) is extremely immunogenic during infection and after immunization. HBcAg has a unique three-dimensional folding that interacts with immunoglobulins outside the classical antibody-binding site, has the $CD4^+$ T cell epitopes and the encapsidated nucleic acids that can efficiently interact and activate antigen presenting cells, especially naive B cells. HBcAg also performs pivotal functions by mediating release of (sub) viral particles, regulation of supercoiled DNA amplification, and transcriptional transactivation[16-19]. To assess its multiple functions and host-protein assistance involved, we initiated a two-hybrid screen using the HBcAg domain as bait and had identified a novel gene named C12 with unknown function. To study the biological function of C12 gene and its role in the HBV infection, we performed the following researches and hoped to get some valuable clues for the further investigation.

First of all, the full-length gene of C12 was amplified from HepG2 cell and verified by DNA sequencing. Gene of C12 was cloned into GFP expression vector pEGFP-N1 and transfected into 293 and L02 cell line. After incubating for 48 h, cells were observed under the fluorescent microscope. We found that these cells were stained with steady, strong green fluorescence in the whole cell, the result indicated that C12 protein mainly expressed in cell plasma. Eighteen hours after incubation with medium, cell number, as measured by absorbance (A), was quantified by using colorimetric MTT assay. The result showed that the optical

density in Bel7402 and L02 cell line groups transfected with deionized water, liposomes, pEGFP-N1 and pEGFP-N1-C12 have no significant difference. This result could be explained as follows: C12 protein was a normal protein present in cells and may have the promotive or inhibitive effect on cell growth. It did not show significant effect because of the interference of network regulation of other proteins. The main expression of C12 protein does not intervene the growth and reproduction of normal cells.

Screening binding protein in hepatocytes, identification of interaction protein in the protein network, may provide valuable clues for the further research[20-23]. Based on the modified yeast two-hybrid technique, the "bait" plasmid pGBKT7-C12 was transformed into yeast strain AH109. After mating with liver cDNA library yeast strain Y187, the diploid yeast cells were plated on QDO media containing X-α-gal, 21 true positives were obtained. Sequencing analysis of isolated library plasmids, 16 different genes were found. Among them, cytochrome C oxidase, ornithine decarboxylase, and acetolactate synthase related to energy metabolism. C12 bind with these proteins indicating that C12 may participate in mitochondrion energy metabolism. KSRP was a factor that regulated the shearing process of enhancer exon[24,25]. Calpain, phosphatidylinositol deacylase poly-glucose Q transcriptional variation factor and receptor JAK (EPHB4) variation factor were important members involved in cellular signal transduction and cell cycle regulation. The interaction between C12 and these proteins suggest that C12 may serve in the above procedure. Ferritin related to hepatocellular damage and HCC[26]. Interaction between C12 and ferritin may play the bridge role in hepatocellular damage and HCC. C12 also take part in blood coagulation procedure for binding with coagulation factor IX. All of the above suggest that proteins found to binding C12 in the yeast two-hybrid system 3 appeared to reveal some probable functions of C12.

The cDNA microarray is a genomic technology, which is widely used in both basic and applied research. Recent advances in cDNA microarray technology have great impact on many areas of biomedical research and pharmacogenomics: discovering novel targets and genes, elucidating signatures of complex diseases, transcriptional profiling of models for diseases, and the development of individually optimized drugs based on differential gene expression patterns[17-29]. The commercial availability of several different precoated arrays and the ease of handling supported the broad distribution of this new technique. The basic protocol in this article involves the hybridization of complementary strands of fluorescent (Cy3 and Cy5) labeled cDNA from HepG2 cells transfected with expression plasmid pcDNA3.1(-)-C12 and empty vector pcDNA3.1(-) spotted onto a solid support and then detected by fluorescence scanning. Sixteen differential expression genes upregulated by C12 and 1 gene downregulated by C12 were screened (Table 2). These genes were involved in cell signal conduction, cell proliferation and differentiation, generation of carcinoma.

The preliminary data from the context studies suggest that the novel protein C12 is located in cell plasma, and its overexpression has no significant effect on the metabolism of liver cells; it interacted with many proteins in hepatocytes and may be involved in many processes of gene expression. These results stride the first step for the functional study of C12 gene and pave the way for the new gene biology research. We will further refine our understanding of currently known results as well as identify novel pathways and methods to elucidate the integral biological functions.

REFERENCES

1 **Li H,** Wang L, Wang SS, Gong J, Zeng XJ, Li RC, Nong Y, Huang YK, Chen XR, Huang ZN. Research on optimal immunization strategies for hepatitis B in different endemic areas in China. *World J Gastroenterol* 2000; **6**: 392-394

2 **Yu LC,** Gu CH. Mutation of hepatitis B virus and its association with liver diseases. *Shijie Huaren Xiaohua Zazhi* 1999; **7**: 978-979

3 **Milich DR.** Do T cells "see" the hepatitis B core and e antigens differently? *Gastroenterology* 1999; **116**: 765-768

4 **Riedl P,** Stober D, Oehninger C, Melber K, Reimann J, Schirmbeck R. Priming Th1 immunity to viral core particles is facilitated by trace amounts of RNA bound to its arginine-rich domain. *J Immunol* 2002; **168**: 4951-4959

5 **Dong J,** Cheng J, Wang Q, Huangfu J, Shi S, Zhang G, Hong Y, Li L, Si C. The study on heterogeneity of hepatitis B virus DNA. *Zhonghua Yixue Zazhi* 2002; **82**: 81-85

6 **Lu YY,** Li K, Cheng J, Wang L, Liu Y, Duan HJ, Zhang LX. Cloning and expression of hepatitis virus X gene in yeast. *Shijie Huaren Xiaohua Zazhi* 2002; **10**: 15-18

7 **Lu YY,** Wang L, Cheng J, Li K, Lu Y, Zhang LX. Screening of HBcAg interacting proteins in hepatocytes with yeast-two hybrid technique. *Shijie Huanren Xiaohua Zazhi* 2003; **11**: 426-429

8 **Lu YY,** Wang L, Li K, Liu Y, Cheng J, Zhang LX. Screening and cloning of HBeAg interacting proteins in hepatocytes. *Shijie Huaren Xiaohua Zazhi* 2003; **11**: 422-425

9 **Lu YY,** Shao Q, Chen J, Cheng TY, Wang L, Liang YD, Liu Y, Zhang J, Li K, Zhang LX. Screening and identification of a novel hepatitis B virus e antigen binding protein E-19 in hepatocyte by yeast two-hybrid technique. *Shijie Huaren Xiaohua Zazhi* 2003; **11**: 1118-1121

10 **Lu YY,** Chen TY, Cheng J, Shao Q, Liang YD, Wang L, Liu Y, Zhang J, Li K, Zhang LX. Screening and identification of a novel gene coding for Hepatitis B virus core antigen interacting protein C-12 in hepatocyte. *Shijie Huaren Xiaohua Zazhi* 2003; **11**: 1122-1125

11 **Liang YD,** Lu YY, Cheng J, Li Q, Wang L, Wu J, Cheng ML. Screening of a new gene C-12 coding for a hepatitis B virus core antigen interacting protein in hepatocytes by yeast-two hybrid technique. *Shijie Huaren Xiaohua Zazhi* 2003; **11**: 1862-1865

12 **Lu YY,** Liu Y, Cheng J, Ling YD, Chen TY, Shao Q, Wang L, Zhang LX. Gene expression profile of HepG2 cell transfected with a novel gene C-12 coding HBcAg binding protein. *Shijie Huaren Xiaohua Zazhi* 2004; **12**: 62-65

13 **Xu R,** Cai K, Zheng D, Ma H, Xu S, Fan ST. Molecular therapeutics of HBV. *Curr Gene Ther* 2003; **3**: 341-355

14 **Lagget M,** Rizzetto M. Current pharmacotherapy for the treatment of chronic hepatitis B. *Expert Opin Pharmacother* 2003; **4**: 1821-1827

15 **Lagget M,** Rizzetto M. Treatment of chronichepatitis B. *Curr Pharm Des* 2002; **8**: 953-958

16 **Pumpens P,** Grens E. HBV core particles as a carrier for B cell/T cell epitopes. *Intervirolog* 2001; **44**: 98-114

17 **Hacker HJ,** Deres K, Mildenberger M, Schroder CH. Antivirals interacting with hepatitis B virus core protein and core mutations may misdirect capsid assembly in a similar fashion. *Biochem Pharmacol* 2003; **66**: 2273-2279

18 **Murray K,** Shiau AL.The core antigen of hepatitis B virus as a carrier for immunogenic peptides. *Biol Chem* 1999; **380**: 277-283

19 **Vanlandschoot P,** Cao T, Leroux-Roels G. The nucleocapsid

of the hepatitis B virus: a remarkable immunogenic structure. *Antiviral Res* 2003; **60**: 67-74

20 **Gietz RD,** Woods RA. Screening for protein-protein interactions in the yeast two-hybrid system. *Methods Mol Biol* 2002; **185**: 471-486

21 **Nagpal S,** Ghosn CR, Chandraratna RA. Identification of nuclear receptor interacting proteins using yeast two-hybrid technology. *Methods Mol Biol* 2001; **176**: 359-376

22 **Serebriiskii IG,** Toby GG, Finley RL Jr, Golemis EA. Genomic analysis utilizing the yeast two-hybrid system. *Methods Mol Biol* 2001; **175**: 415-454

23 **Zhen Z.** Progress in proteomics. *Shengwu Gongcheng Xuebao* 2001; **17**: 491-493

24 **Min H,** Turck CW, Nikolic JM, Black DL. A new regulatory protein, KSRP, mediates exon inclusion through an intronic splicing enhancer. *Genes Dev* 1997; **11**: 1023-1036

25 **Ring HZ,** Vameghi-Meyers V, Nikolic JM, Min H, Black DL, Francke U. Mapping of the KHSRP gene to a region of conserved synteny on human chromosome19p13.3 and mouse chromosome 17. *Genomics* 1999; **56**: 350-352

26 **Cao Z,** Bai Y, Yang X, Liu J, Li B, Li F. Study of iron metabolism abnormality in the hepatocyte damage of hepatitis B. *Zhonghua Ganzangbing Zazhi* 2001; **9**: 37-39

27 **Hackl H,** Cabo FS, Sturn A, Wolkenhauer O, Trajanoski Z. Analysis of DNA microarray data. *Curr Top Med Chem* 2004; **4**: 1357-1370

28 **Chittur SV.** DNA microarrays: tools for the 21st Century. *Comb Chem High Throughput Screen* 2004; **7**: 531-537

29 **Duncan RC,** Salotra P, Goyal N, Akopyants NS, Beverley SM, Nakhasi HL. The application of gene expression microarray technology to kinetoplastid research. *Curr Mol Med* 2004; **4**: 611-621

Science Editor Wang XL and Guo SY **Language Editor** Elsevier HK

PO Box 2345, Beijing 100023, China
www.wjgnet.com
wjg@wjgnet.com

ELSEVIER

World J Gastroenterol 2005;11(36):5672-5676
World Journal of Gastroenterology ISSN 1007-9327
© 2005 The WJG Press and Elsevier Inc. All rights reserved.

The best method of detecting prior *Helicobacter pylori* infection

Chien-Yu Lu, Chao-Hung Kuo, Yi-Ching Lo, Hung-Yi Chuang, Yuan-Chieh Yang, I-Chen Wu, Fang-Jong Yu, Yi-Chen Lee, Chang-Ming Jan, Wen-Ming Wang, Deng-Chyang Wu

Chien-Yu Lu, Chao-Hung Kuo, Fang-Jong Yu, Yi-Chen Lee, Chang-Ming Jan, Wen-Ming Wang, Deng-Chyang Wu, Division of Gastroenterology, Department of Internal Medicine, Kaohsiung Medical University Hospital, Taiwan, China
Yi-Ching Lo, Department of Pharmacology, Kaohsiung Medical University, Taiwan, China
Hung-Yi Chuang, Department of Occupational Medicine and School of Public Health, Kaohsiung Medical University, Taiwan, China
Yuan-Chieh Yang, Department of Clinical Pathology, Kaohsiung Medical University Hospital, Taiwan, China
I-Chen Wu, Department of Internal Medicine, Kaohsiung Municipal United Hospital, Kaohsiung, Taiwan, China
Supported by Grants From the China American Petrochemical Co., Ltd. Foundation (CAPCO) and the National Science Council of the ROC (NSC-90-2314-B-037-044)
Correspondence to: Dr. Deng-Chyang Wu, Chief of Gastroenterology, Kaohsiung Medical University Hospital, 100 Zih-You 1st Road, Kaohsiung City, 807 Taiwan, China. dechwu@yahoo.com
Telephone: +886-7-3121101-7451 Fax: +886-7-3135612
Received: 2004-05-27 Accepted: 2004-06-18

Abstract

AIM: Prior *Helicobacter pylori* (*H pylori*) infection has often been underestimated. These underestimations have misled physicians attempting to determine the significance between *H pylori* and certain gastrointestinal lesions such as intestinal metaplasia, atrophic gastritis, and gastric cancer. Our study endeavored to detect past *H pylori* infections accurately, easily, and rapidly with the newly developed immunoblot kit, Helico Blot 2.1.

METHODS: Thirty-three patients, including 25 *H pylori* infected and 8 uninfected cases, were enrolled in our study. All patients received consecutive gastroendoscopic examinations and ^{13}C-urea breath test (UBT) tests at 6- or 12-mo intervals for up to 4 years. Serum samples were obtained from each patient at the same time. Intragastric *H pylori* infection was confirmed in accordance with the gold standard. Twenty-five *H pylori*-infected patients received triple therapies after initial bacterial confirmation, and were successful in eradicating their infections. Serially obtained sera were tested by means of Helico Blot 2.1.

RESULTS: Current infection marker detected by Helico Blot 2.1 was unreliable for representing ongoing *H pylori* infection. Only 35 and 37 ku antibodies of *H pylori* had significant seroconversion rates 1 year after having been cured. The seropositive rates of 116 ku (cytotoxin-associated antigen [CagA]) and Helico Blot 2.1 were nearly 100% during 4-year follow-up period. Both CagA antigen and Helico blot 2.1 could serve as indicators of long-term *H pylori* infection.

CONCLUSION: Helico Blot 2.1 can detect past *H pylori* infections for up to 4 years, and is the best method to date for detecting previous long-term *H pylori* infection.

© 2005 The WJG Press and Elsevier Inc. All rights reserved.

Key words: *Helicobacter pylori*; Long-term infection; Diagnosis; Serum

Lu CY, Kuo CH, Lo YC, Chuang HY, Yang YC, Wu IC, Yu FJ, Lee YC, Jan CM, Wang WM, Wu DC. The best method of detecting prior *Helicobacter pylori* infection. *World J Gastroenterol* 2005; 11(36): 5672-5676
http://www.wjgnet.com/1007-9327/11/5672.asp

INTRODUCTION

Since Warren and Marshall reported *Helicobacter pylori* (*H pylori*) in 1983[1], this gram negative, spiral-shaped bacterium has been designated as a causative agent in many benign and malignant gastrointestinal diseases, such as peptic ulcer[2,3] and gastric cancer[4-7]. However, low intragastric *H pylori* infection rates have been reported in connection with certain precancerous lesions, such as intestinal metaplasia[8] and atrophic gastritis[9,10]. This has been attributed to inappropriate use of medications or intragastric environmental changes. Recent meta-analysis reports[11-13] about serology studies have even argued that the association between *H pylori* and gastric cancer is relatively weak. Therefore, accurate detection of past *H pylori* infection is important in deciding the real prevalence rates of many gastrointestinal diseases.

Conventional ELISA serology study was previously known as the best method of determining past *H pylori* infection, because the IgG antibody decreases slowly and may remain detectable for months after bacterial cure[14-17]. The delay in fall in serum anti-*H pylori* IgG antibody following eradication therapy inspired the idea that serum antibodies to specific *H pylori* immunoreactive antigens could serve as tools in detecting past *H pylori* infections. The *H pylori* cytotoxin-associated antigen (CagA) is known to be more virulent[18-21], have a stronger immunoreactivity[22,23], and persist longer after *H pylori* eradication[24]. The other low molecular weight antigens of *H pylori* have also been helpful in detecting *H pylori* infection[25-27].

The primary goal of our study was to determine the feasibility and accuracy of a newly developed immunoblot

device in the detection of past *H pylori* infections.

MATERIALS AND METHODS

A total of 33 patients were enrolled in this study. Of these, 25 (19 men, 6 women, mean age 57.5±14.3 years) were the *H pylori* positive study group, and 8 (2 men, 6 women, mean age 63.8±15.8 years) made up the *H pylori* negative control group. The 25 *H pylori* positive patients included 23 cases of peptic ulcers and 2 cases of early gastric cancers. There were eight *H pylori* negative patients as a control group, including four cases with peptic ulcers, two cases with gastro-esophageal regurgitation diseases, one case with gastritis, and one case with early gastric cancer. The *H pylori* positive study group was followed up for 18-45 mo, on an average of 30.0±8.9 mo. The negative control group was followed up for 26-48 mo, on an average of 34.6±7.1 mo. During the follow-up periods, all of the patients received gastroendoscopic examinations and biopsy-based *H pylori* studies at 6-mo or 1-year intervals. ^{13}C-urea breath test (UBT) tests and sera collection for the diagnosis of *H pylori* infection were conducted at the same time. Exclusion criteria were the following: use of antibiotics or bismuth salts, or proton pump inhibitors therapy within the last 2 mo, previous anti-*H pylori* treatment, chronic use of corticosteroids or immunosuppressant drugs, prior gastric surgery, presence of a bleeding peptic ulcer, severe concomitant disease, and pregnancy or lactation.

The gold standard of identifying a *H pylori* infected patient is determined by positive culture results, or positive results in any two of the following: histology (hematoxylin and eosin, H&E stain), rapid urease test and ^{13}C-UBT test. The negative *H pylori*-infected patient was identified by a negative culture result and at least two negative results in the following: histology, rapid urease test, and ^{13}C-UBT test. All of the *H pylori* infected patients received *H pylori* eradication therapy with standard full-dose triple therapy regimen (omeprazole 20 mg, amoxicillin 500 mg, and clarithromycin 500 mg twice a day for 7 d).

The Helico Blot 2.1 kit (Genelabs Diagnostics, Singapore) was used to detect IgG antibodies to specific antigens of *H pylori* in accordance with manufacturer's instructions. Helico Blot 2.1 kit is a qualitative serologic test using a Western blot made from bacterial lysate, and including a recombinant antigen of *H pylori* with a predictive value for indicating current *H pylori* infection. The corresponding bands to these specific antigens of *H pylori* are 116 ku (CagA), 89 ku (vacuolating-associated antigen [VacA]), 37, 35, 30 ku (Urease A), and 19.5 ku (Figure 1). The determinations of *H pylori* seropositivity on Helico Blot 2.1 and corresponding specific antigens were in accordance with the manufacturer's criteria. The recommended criteria for determining a sample as *H pylori* seropositive on Helico Blot 2.1 kit is any one of the following conditions: (1) 116 ku (CagA) positive, where CagA has to be present with one or more of the following bands: 89 ku (VacA), 37, 35, 30 ku (Urease A), and 19.5 ku together, or with a current infection marker (CIM). (2) Presence of any one band at 89, 37 or 35 ku, with or without a CIM. (3) Presence of both 30 and 19.5 ku with or without a CIM. Each patient's serum samples were analyzed at the same time to avoid interassay variation. Furthermore, three specialists who did not know about the study's objectives were invited to examine and interpret the nitrocellulose strips to decrease the individual subjective bias (Figure 1).

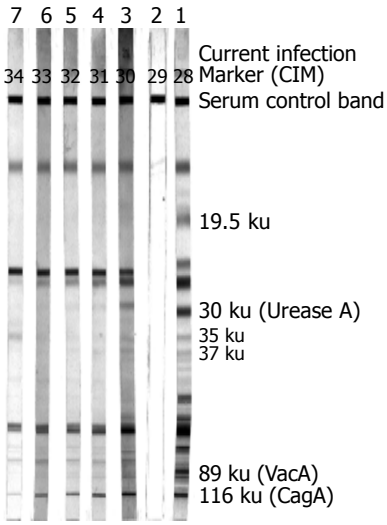


Figure 1 The nitrocellulose strips of Helico Blot 2.1 representative of immunoblot results: lane 1, positive control; lane 2, negative control; lanes 3-7, serial serum samples of a patient showing positive results.

Statistics

Due to the repeated measurements to determine antibody positive or negative status, the generalized estimating equation (GEE) was applied to statistically analyze intra- and inter-individual changes in specific antigens of *H pylori* during the follow-up periods (every 6 mo).

RESULTS

All 25 *H pylori* positive patients underwent successful bacterial eradication with triple therapy, as confirmed by gastroendoscopic biopsy-based studies and ^{13}C-UBT tests. A total of 112 sera samples obtained from the 25 patients in our study group were checked with Helico Blot 2.1. The test results are recorded in Tables 1 and 2, and depicted in Figure 2.

Except for 37 and 35 ku, other *H pylori* specific antibodies (19.5, 30, 89, 116 ku, and even CIM) showed as seropositive for over half of the serum samples tested with Helico Blot 2.1 test during a 4-year follow-up period (Figure 2). Both Helico Blot 2.1 and 116 ku (CagA) antibody seropositive rates were nearly 100% (98% and 99% respectively, as shown in Table 1). Also, at least 79% of *H pylori* 30 ku antibody can be detected positively before the end of a 3-year follow-up. The 89 ku (VacA) was also at least 67% positive during the 4-year follow-up (Table 2 and Figure 2).

The seropositive rate of 19.5 ku antibody decreased significantly, but wide fluctuation decreased its reliability (Figure 2). The seroconversion rates of 35 and 37 ku antibodies were significant (GEE testing significance, *P* values as 0.008 and 0.001 respectively) till 1 year after bacterial cure, in spite of initial lower seropositive rates (35 ku, 44% down to 29% and 37 ku, 68% down to 36%, Table 2 and Figure 2). The positive rate of CIM decreased significantly between

the 3rd and 4th years, but the small number of cases studied has influenced reliability (Figure 2).

The *H pylori* statuses in the negative control group were still negative as determined by the gold standard and Helico Blot 2.1 tests after a follow-up period similar to the study groups. Because of this, the data is not shown in tables or figures.

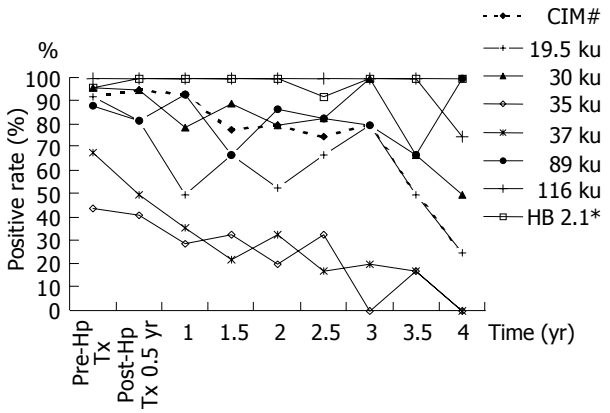


Figure 2 Fluctuating positive rates of various *H pylori*-specific antigens and Helico Blot 2.1 in 25 *H pylori*-infected patients were charted at half-year intervals during a 4-year follow-up period. The CIM was unreliable, because it maintained high positive rates for at least 3 years after *H pylori* eradication. Thirty-five and thirty-seven kilounits antibodies of *H pylori* showed significant seroconversion changes at 1 year after bacterial cure. The seropositive rates of 116 ku (CagA) and Helico Blot 2.1 were nearly 100% during the 4-year follow-up period.

DISCUSSION

Although *H pylori* was designated as a human class I carcinogen already in 1994[28], the exact nature and strength of the association with gastric cancer has remained debatable[11-13]. Because *H pylori* infection are primarily acquired in childhood[29,30], older subjects have had more time to develop mucosal atrophy and to loose their infection than younger subj-ects[9,10]. Also, decades may pass between initiation and detection of gastric cancers. *H pylori* may disappear spontaneously with progressing precancerous intragastric environmental change and invalidate various studies of its association with gastric cancer. The significance of detecting the past *H pylori* infection is to re-estimate the strength of the *H pylori*-gastric cancer relationship.

The CIM of Helico Blot 2.1 was developed and claimed to be able to detect ongoing *H pylori* infection. However, our study showed that the CIM band was oversensitive and unreliable, because it remained at a 75-80% positive rate for 3 years after *H pylori* eradication (Table 2). Our results differ from the conclusions of Oleastro's *et al*., study of pediatric patients[31]. There were two reasons for these discrepancies with our report. First were the different age groups of the studies. It is known that *H pylori* infection occurs beginning in childhood, and gradually accumulates as the patients get older[29,30]. Consequently, pediatric studies will have more true negative cases when compared with adult groups. Our adult patients may have had immunological memory due to past *H pylori* infection, and were mistaken for currently infected by the oversensitive CIM band. Second, these two studies had different designs. Oleastro's study[31] was a cross-sectional design, not a long term follow-up study like ours. Their study checked serum *H pylori* antibody at only one time point, and the serial seroconversion changes could not be detected in cross-sectional study designs.

The seropositive rate of 116 ku (CagA) was the highest (up to 100% before the end of a 3.5-year follow-up period) among various antibodies to *H pylori*-specific antigens and nearly parallel to Helico Blot 2.1 (Table 2 and Figure 2). This phenomenon explains why the CagA antibody was the

Table 1 The results of Helico Blot 2.1 and various *H pylori*-specific antigens in 25 *H pylori* infected patients with a total of 112 sera samples

	HB2.1[1]	116 ku (CagA)	89 ku (VacA)	37 ku	35 ku	30 ku (Urease A)	19.5 ku	CIM[2]
Positive sera (%)	110/112 (98)	111/112 (99)	94/112 (84)	44/112 (39)	35/112 (31)	97/112 (87)	78/112 (70)	93/112 (83)

[1]HB2.1: Helico Blot 2.1; [2]CIM: current infection marker.

Table 2 The positive numbers and rates of various *H pylori*-specific antigens and Helico Blot 2.1 in 25 *H pylori*-infected patients at half-year intervals during a 4-year follow-up period (*n*, %).

	Pre-Hp Tx	Post-Hp Tx							
		0.5 yr	1 yr	1.5 yr	2 yr	2.5 yr	3 yr	3.5 yr	4 yr
CIM[2]	23 (92)	21 (95)	13 (93)	7 (78)	12 (80)	9 (75)	4 (80)	3 (50)	1 (25)
19.5 ku	23 (92)	18 (82)	7 (50)	6 (67)	8 (53)	8 (67)	4 (80)	3 (50)	1 (25)
30 ku	24 (96)	21 (95)	11 (79)	8 (89)	12 (80)	10 (83)	5 (100)	4 (67)	2 (50)
35 ku	11 (44)	9 (41)	4 (29)	3 (33)	3 (20)	4 (33)	0 (0)	1 (17)	0 (0)
37 ku	17 (68)	11 (50)	5 (36)	2 (22)	5 (33)	2 (17)	1 (20)	1 (17)	0 (0)
89 ku	22 (88)	18 (82)	13 (93)	6 (67)	13 (87)	10 (83)	4 (80)	4 (67)	4 (100)
116 ku	25 (100)	22 (100)	14 (100)	9 (100)	15 (100)	12 (100)	5 (100)	6 (100)	3 (75)
HB2.1[1]	24 (96)	22 (100)	14 (100)	9 (100)	15 (100)	11 (92)	5 (100)	6 (100)	4 (100)
Total case nos.	25	22	14	9	15	12	5	6	4

[1]HB2.1: Helico Blot 2.1; [2]CIM: current infection marker; Pre-Hp Tx: before *H pylori* eradication therapy; Post-Hp Tx: after *H pylori* eradication therapy.

last antibody to disappear after *H pylori* eradication, and may serve as a single predictor in *H pylori* long-term infection. Our results showed that CagA antigen had the strongest immunoreactivity among various *H pylori* antigens, and was in agreement with numerous previous reports[22,24,32,33].

The roles of various low molecular weight antibodies of *H pylori* were ambiguous. The heat shock protein of *H pylori* was related to chronic gastric inflammation[34,35]. Mucosa-associated lymphoid lymphoma (MALToma) patients had higher prevalence rates of 19.5 and 30 ku antibodies of *H pylori*. After *H pylori* eradication, MALToma patients had significant negative seroconversion of 19.5, 30, and 35 ku antibodies[36]. The 35 ku antibody of *H pylori* also plays a role in peptic ulcers[37]. The immunoreaction with 30 ku (Urease A) of *H pylori* could provide a serological assessment of not only *H pylori* infection[25-27], but also of eradication[27]. In our study, the seroconversion of 35 and 37 ku was significant for up to 1 year after *H pylori* eradication.

According to our previous study[14], IgG seroconversion rates by conventional ELISA method were 42% and 94% at 6 and 12 mo after *H pylori* eradication, respectively. Although some papers[15,38] have proposed latent IgG seroconversion, many confounding factors, including small case numbers, different antigenic preparations, and variable cut-off values, made this conflict. Moreover, the follow-up periods of most studies were less than 2 years, which would mean that whether or not *H pylori* could be detected beyond 2 years after bacterial cure would be difficult to determine, and has rarely been addressed by the conventional ELISA method. Our study test kits can detect past intragastric *H pylori* infections for at least 3, or even 4 years after eradication.

The positive or negative results of Helico Blot 2.1 are given as the presence or absence of immunodetection of certain specific antigen bands, 116 ku (CagA), 89 ku (VacA), 37, 35, 30 ku (Urease A) and 19.5 ku, by the patient's serum (Figure 1). Even the decay or disappearance of serum CagA antibody, the positive result of Helico Blot 2.1 could still be achieved by other recommended criteria (criteria 2 or 3). There is one serum sample in our 4th-year study shows negative CagA antibody and positive Helico Blot 2.1 results (Table 2). Besides, Helico Blot 2.1 can differentiate various *H pylori* strains according to the presence of corresponding specific immunoreactive bands. So, Helico Blot 2.1 has more advantages over CagA only in detecting the past *H pylori* infection.

We expected that Helico Blot 2.1 will improve the detection of *H pylori* infection in many GI and non-GI diseases, such as ischemic heart disease and chronic urticaria. The present role of *H pylori* in these non-GI diseases is debatable[39,40], and improvements in detecting past *H pylori* infections would further clarify the correlations between these diseases and *H pylori*.

In summary, Helico Blot 2.1 is the best method thus far of detecting past intragastric *H pylori* infections for up to 4 years after treatment. This newly developed device with Western blot method improves the detection of *H pylori* and further clarifies its role in many *H pylori*-related diseases.

REFERENCES

1 Unidentified curved bacilli on gastric epithelium in active chronic gastritis. *Lancet* 1983; **1**: 1273-1275

2 **Marshall BJ**, Warren JR. Unidentified curved bacilli in the stomach of patients with gastritis and peptic ulceration. *Lancet* 1984; **1**: 1311-1315

3 **Olbe L**, Fandriks L, Hamlet A, Svennerholm AM, Thoreson AC. Mechanisms involved in *Helicobacter pylori* induced duodenal ulcer disease:an overview. *World J Gastroenterol* 2000; **6**: 619-623

4 **Forman D**, Newell DG, Fullerton F, Yarnell JW, Stacey AR, Wald N, Sitas F. Association between infection with *Helicobacter pylori* and risk of gastric cancer: evidence from a prospective investigation. *B M J* 1991; **302**: 1302-1305

5 **Nomura A**, Stemmermann GN, Chyou PH, Kato I, Perez-Perez GI, Blaser MJ. *Helicobacter pylori* infection and gastric carcinoma among Japanese Americans in Hawaii. *N Engl J Med* 1991; **325**: 1132-1136

6 **Parsonnet J**, Friedman GD, Vandersteen DP, Chang Y, Vogelman JH, Orentreich N, Sibley RK. *Helicobacter pylori* infection and the risk of gastric carcinoma. *N Engl J Med* 1991; **325**: 1127-1131

7 **Wang RT**, Wang T, Chen K, Wang JY, Zhang JP, Lin SR, Zhu YM, Zhang WM, Cao YX, Zhu CW, Yu H, Cong YJ, Zheng S, Wu BQ. *Helicobacter pylori* infection and gastric cancer: evidence from a retrospective cohort study and nested case-control study in China. *World J Gastroenterol* 2002; **8**: 1103-1107

8 **Testoni P**, Colombo E, Scelsi R, Cattani L, Bagnolo F, Lella F, Buizza M, Luinetti O. Tissue staining for *Helicobacter pylori* in intestinal metaplasia: correlation with its extension and histochemical subtypes. *Ital J Gastroenterol* 1995; **27**: 285-290

9 **Karnes WE** Jr, Samloff IM, Siurala M, Kekki M, Sipponen P, Kim SW, Walsh JH. Positive serum antibody and negative tissue staining for *Helicobacter pylori* in subjects with atrophic body gastritis. *Gastroenterology* 1991; **101**: 167-174

10 **Testoni PA**, Bonassi U, Bagnolo F, Colombo E, Scelsi R. In diffuse atrophic gastritis, routine histology underestimates *Helicobacter pylori* infection. *J Clin Gastroenterol* 2002; **35**: 234-239

11 **Huang JQ**, Sridhar S, Chen Y, Hunt RH. Meta-analysis of the relationship between *Helicobacter pylori* seropositivity and gastric cancer. *Gastroenterology* 1998; **114**: 1169-1179

12 **Eslick GD**, Lim LL, Byles JE, Xia HH, Talley NJ. Association of *Helicobacter pylori* infection with gastric carcinoma: a meta-analysis. *Am J Gastroenterol* 1999; **94**: 2373-2379

13 **Danesh J**. *Helicobacter pylori* infection and gastric cancer: systematic review of the epidemiological studies. *Aliment Pharmacol Ther* 1999; **13**: 851-856

14 **Wang WM**, Chen CY, Jan CM, Chen LT, Perng DS, Lin SR, Liu CS. Long-term follow-up and serological study after triple therapy of *Helicobacter pylori*-associated duodenal ulcer. *Am J Gastroenterol* 1994; **89**: 1793-1796

15 **Cutler AF**, Prasad VM. Long-term follow-up of *Helicobacter pylori* serology after successful eradication. *Am J Gastroenterol* 1996; **91**: 85-88

16 **Kato S**, Furuyama N, Ozawa K, Ohnuma K, Iinuma K. Long-term follow-up study of serum immunoglobulin G and immunoglobulin A antibodies after *Helicobacter pylori* eradication. *Pediatrics* 1999; **104**: e22

17 **Li S**, Lu AP, Zhang L, Li YD. Anti-*Helicobacter pylori* immunoglobulin G (IgG) and IgA antibody responses and the value of clinical presentations in diagnosis of *H pylori* infection in patients with precancerous lesions. *World J Gastroenterol* 2003; **9**: 755-758

18 **Blaser MJ**, Perez-Perez GI, Kleanthous H, Cover TL, Peek RM, Chyou PH, Stemmermann GN, Nomura A. Infection with *Helicobacter pylori* strains possessing cagA is associated with an increased risk of developing adenocarcinoma of the stomach. *Cancer Res* 1995; **55**: 2111-2115

19 **Maeda S**, Yoshida H, Ogura K, Yamaji Y, Ikenoue T, Mitsushima T, Tagawa H, Kawaguchi R, Mori K, Mafune K, Kawabe T, Shiratori Y, Omata M. Assessment of gastric carcinoma risk associated with *Helicobacter pylori* may vary depending on the antigen used: CagA specific enzyme-linked immunoadsorbent assay (ELISA) versus commercially avail-

able *H pylori* ELISAs. *Cancer* 2000; **88**: 1530-1535
20 **Parsonnet J**, Friedman GD, Orentreich N, Vogelman H. Risk for gastric cancer in people with CagA positive or CagA negative *Helicobacter pylori* infection. *Gut* 1997; **40**: 297-301
21 **Xia HHX**. Association between *Helicobacter pylori* and gastric cancer: current knowledge and future research. *World J Gastroenterol* 1998; **4**: 93-96
22 **Havlasova J**, Bures J, Rejchrt S, Voxova B, Krejsek J. *Helicobacter pylori* CagA antigen antibodies. *Cas Lek Cesk* 1998; **137**: 404-409
23 **Everhart JE**, Kruszon-Moran D, Perez-Perez G. Reliability of *Helicobacter pylori* and CagA serological assays. *Clin Diagn Lab Immunol* 2002; **9**: 412-416
24 **Ekstrom AM**, Held M, Hansson LE, Engstrand L, Nyren O. *Helicobacter pylori* in gastric cancer established by CagA immunoblot as a marker of past infection. *Gastroenterology* 2001; **121**: 784-791
25 **Andersen LP**, Espersen F, Souckova A, Sedlackova M, Soucek A. Isolation and preliminary evaluation of a low-molecular-mass antigen preparation for improved detection of *Helicobacter pylori* immunoglobulin G antibodies. *Clin Diagn Lab Immunol* 1995; **2**: 156-159
26 **Madico G,** Verastegui M. Serodiagnosis of *Helicobacter pylori* infection by enzyme-linked immunoelectrotransfer blot. Gastrointestinal Physiology Working Group of Cayetano Heredia University. *J Diarrhoeal Dis Res* 1995; **13**: 122-126
27 **Voland P**, Weeks DL, Vaira D, Prinz C, Sachs G. Specific identification of three low molecular weight membrane-associated antigens of *Helicobacter pylori*. *Aliment Pharmacol Ther* 2002; **16**: 533-544
28 Schistosomes, liver flukes and *Helicobacter pylori*. IARC Working Group on the Evaluation of Carcinogenic Risks to Humans. Lyon, 7-14 June 1994. *IARC Monogr Eval Carcinog Risks Hum* 1994; **61**: 1-241
29 **Xu CD**, Chen SN, Jiang SH, Xu JY. Seroepidemiology of *Helicobacter pylori* infection among asymptomatic Chinese children. *World J Gastroenterol* 2000; **6**: 759-761
30 **Sinha SK**, Martin B, Sargent M, McConnell JP, Bernstein CN. Age at acquisition of *Helicobacter pylori* in a pediatric Canadian First Nations population.PG - 76-85. *Helicobacter* 2002; **7**: 76-85
31 **Oleastro M**, Matos R, Cabral J, Barros R, Lopes AI, Ramalho P, Monteiro L. Evaluation of a Western blot test, Helico blot 2. 1, in the diagnosis of *Helicobacter pylori* infection in a pediatric population.PG - 210-5. *Helicobacter* 2002; **7**: 210-215
32 **Monteiro L**, Bergey B, Gras N, Megraud F. Evaluation of the performance of the Helico Blot 2.1 as a tool to investigate the virulence properties of *Helicobacter pylori*. *Clin Microbiol Infect* 2002; **8**: 676-679
33 **Fusconi M**, Vaira D, Menegatti M, Farinelli S, Figura N, Holton J, Ricci C, Corinaldesi R, Miglioli M. Anti-CagA reactivity in *Helicobacter pylori*-negative subjects: a comparison of three different methods. *Dig Dis Sci* 1999; **44**: 1691-1695
34 **Leri O**, Teichner A, Sinopoli MT, Abbolito MR, Pustorino R, Nicosia R, Paparo Barbaro S. Heat-shock-proteins-antibodies in patients with *Helicobacter pylori* associated chronic gastritis. *Riv Eur Sci Med Farmacol* 1996; **18**: 45-47
35 **Vorobjova T**, Ananieva O, Maaroos H, Sipponen P, Villako K, Utt M, Nilsson I, Wadstrom T, Uibo R. Seropositivity to *Helicobacter pylori* heat shock protein 60 is strongly associated with intensity of chronic inflammation, particularly in antrum mucosa: an extension of an 18-year follow-up study of chronic gastritis in Saaremaa, Estonia. *FEMS Immunol Med Microbiol* 2001; **30**: 143-149
36 **Sheu BS**, Shiesh SC, Wang JT, Yang HB, Lin ST, Wu JJ. Clinical Application of 20 MHz Endosonography and Anti-*Helicobacter pylori* Immunoblots to Predict Regression of Low-grade Gastric MALToma by *H pylori* Eradication. *Helicobacter* 2003; **8**: 36-45
37 **Delchier JC**, Lamarque D, Levy M, Tkoub EM, Copie-Bergman C, Deforges L, Chaumette MT, Haioun C. *Helicobacter pylori* and gastric lymphoma: high seroprevalence of CagA in diffuse large B-cell lymphoma but not in low-grade lymphoma of mucosa-associated lymphoid tissue type. *Am J Gastroenterol* 2001; **96**: 2324-2328
38 **Veenendaal RA**, Pena AS, Meijer JL, Endtz HP, van der Est MM, van Duijn W, Eulderink F, Kreuning J, Lamers CB. Long term serological surveillance after treatment of *Helicobacter pylori* infection. *Gut* 1991; **32**: 1291-1294
39 **Hook-Nikanne J**, Varjonen E, Harvima RJ, Kosunen TU. Is *Helicobacter pylori* infection associated with chronic urticaria? *Acta Derm Venereol* 2000; **80**: 425-426
40 **Zhu J**, Quyyumi AA, Muhlestein JB, Nieto FJ, Horne BD, Zalles-Ganley A, Anderson JL, Epstein SE. Lack of association of *Helicobacter pylori* infection with coronary artery disease and frequency of acute myocardial infarction or death. PG-155-8. *Am J Cardiol* 2002; **89**: 155-158

Science Editor Wang XL and Zhu LH **Language Editor** Elsevier HK

PO Box 2345, Beijing 100023, China
www.wjgnet.com
wjg@wjgnet.com

ELSEVIER

World J Gastroenterol 2005;11(36):5677-5684
World Journal of Gastroenterology ISSN 1007-9327
© 2005 The WJG Press and Elsevier Inc. All rights reserved.

• *BASIC RESEARCH* •

Role of nitric oxide in the impairment of circular muscle contractility of distended, uninflamed mid-colon in TNBS-induced acute distal colitis in rats

Luciano Onori, Annalisa Aggio, Simona D'Alo', Paola Muzi, Maria Grazia Cifone, Gabriella Mellillo, Rachele Ciccocioppo, Gennaro Taddei, Giuseppe Frieri, Giovanni Latella

Luciano Onori, Annalisa Aggio, Rachele Ciccocioppo, Gennaro Taddei, Giuseppe Frieri, Giovanni Latella, Department of Internal Medicine and Public Health, University of L' Aquila, 67100 L'Aquila, Italy
Simona D'Alo', Paola Muzi, Maria Grazia Cifone, Department of Experimental Medicine, University of L' Aquila , 67100 L'Aquila, Italy
Gabriella Mellillo, Department of Preclinical Pharmacology, Dompé SPA Research Center, 67100 L'Aquila, Italy
Correspondence to: Giovanni Latella, MD, Dipartimento di Medicina Interna e Sanità Pubblica, Cattedra di Gastroenterologia, Università degli Studi di L'Aquila, Via S. Sisto n. 22/E, 67100 L'Aquila, Italy. giolatel@tin.it
Telephone: +39-862-433358 Fax: +39-862-432858
Received: 2004-12-19 Accepted: 2005-02-18

Abstract

AIM: To evaluate the role of nitric oxide (NO) in the motor disorders of the dilated uninflamed mid-colon (DUMC) from trinitrobenzene sulfonic acid (TNBS)-induced acute distal colitis in rats.

METHODS: Colitis was induced in male Sprague-Dawley rats by a single intracolonic administration of TNBS. Control rats received an enema of 0.9% saline. The rats were killed 48 h after TNBS or saline administration. Macroscopic and histologic lesions of the colon were evaluated. Myeloperoxidase (MPO) and nitric oxide synthase (NOS) activity were measured on the colonic tissue. In TNBS rats, we evaluated spontaneous and evoked contractile activity in circular muscle strips derived from DUMC in comparison to the same colonic segment of control rats, both in the presence and in the absence of a non-selective NOS isoforms inhibitor *N*-nitro-L-arginine (L-NNA). Pharmacological characterization of electric field stimulation (EFS)-evoked contractile responses was also performed.

RESULTS: In TNBS rats, the distal colon showed severe histological lesions and a high MPO activity, while the DUMC exhibited normal histology and MPO activity. Constitutive NOS activity was similar in TNBS and control rats, whereas inducible NOS activity was significantly increased only in the injured distal colon of TNBS rats. Isometrically recorded mechanical activity of circular muscle strips from DUMC of TNBS rats showed a marked reduction of the force and frequency of spontaneous contractions compared to controls, as well as of the contractile responses to a contracting stimulus. In the presence of L-NNA, the contractile activity and responses displayed a significantly greater enhancement compared to controls. The pharmacological characterization of EFS contractile responses showed that a cooperative-like interaction between cholinergic muscarinic and tachykinergic neurokinin 1 and 2 receptors mediated transmission in DUMC of TNBS rats *vs* a simple additive interaction in controls.

CONCLUSION: The results of this study show that, during TNBS-induced acute distal colitis, circular muscle intrinsic contractile mechanisms and possible enteric neural excitatory activity are inhibited in the distended uninflamed mid-colon. Suppression of NO synthesis markedly improves spontaneous and evokes muscle contractions, in spite of any evident change in local NO activity.

© 2005 The WJG Press and Elsevier Inc. All rights reserved.

Key words: TNBS colitis; Colonic dilatation; Colonic motility; Nitric oxide synthase

Onori L, Aggio A, D'Alo' S, Muzi P, Cifone MG, Mellillo G, Ciccocioppo R, Taddei G, Frieri G, Latella G. Role of nitric oxide in the impairment of circular muscle contractility of distended, uninflamed mid-colon in TNBS-induced acute distal colitis in rats. *World J Gastroenterol* 2005; 11(36): 5677-5684
http://www.wjgnet.com/1007-9327/11/5677.asp

INTRODUCTION

Changes in motility patterns have been described in the gastrointestinal tract in association with inflammatory conditions, independent of the etiologic origin[1,2]. Indeed, ulcerative colitis (UC), an idiopathic inflammatory disease of the colon, is associated with impaired intestinal motility such as defective colonic contractility[3-5] sometimes leading to dramatic colonic dilatation (toxic megacolon, TMC)[1]. Data derived from human colitis and from animal models of colitis suggest a clear relationship between the impaired colonic motility and the abnormal local production or release of inflammatory mediators and neuropeptides[6,7].

However, changes in motility patterns are not related only to the inflamed site of the colon[8-10]. In fact, in UC, concomitant distension of the small bowel and, less frequently, of the stomach has been reported[11,12]. Small

bowel distension may even precede colonic dilation, and this has been termed as impending megacolon. This condition characterizes a subgroup of UC patients with a poor response to medical treatment and an increased risk for TMC, a need for surgery and mortality[11-14]. Furthermore, experimental colitis leads to changes in myenteric nerve function at inflamed and uninflamed gastrointestinal sites in the rat[15,16]. Several mechanisms have been hypothesized to explain motility disorders of an inflamed colonic segment[12,17,18].

In the last few years, growing evidence appears to suggest that nitric oxide (NO), synthesized by constitutive NO synthase (cNOS) expressed by certain descending interneurons in the myenteric plexus and by almost all enteric inhibitory non-adrenergic non-cholinergic motorneurons (iNANC), play a major role in the neuronal inhibitory control of intestinal mechanical activity in physiological conditions[19-21]. NO exerts its action both through direct inhibition of smooth muscle contractility and negative modulation in myenteric excitatory motorneurons activity, mainly releasing acetylcholine and tachykinins[22]. Furthermore, in human beings and experimental severe colitis, there is evidence that a burst of NO production by inducible NO synthase (iNOS) in inflammatory and smooth muscle cells is responsible for severe motility disorders of the inflamed colon[23,24]. In fact, several studies have suggested that NO may be involved in the pathogenesis of acute colonic distension in severe UC and in animal model of acute colitis[25,26]. Nevertheless, little is known about the role of NO on motility disorders in intestinal tracts far from the inflamed segment[16].

Aim of the present study was to establish whether, in trinitrobenzene sulfonic acid (TNBS)-induced acute distal colitis in rats, abnormal NO activity was also responsible for the colonic motor disorders of the dilated mid-colonic segment apparently devoid of inflammatory alterations. In TNBS distal colitis, we, therefore, evaluated spontaneous and evoked contractions in circular muscle strips derived from the dilated uninflamed mid-colon (DUMC) and compared findings with those in the same colonic segment of control rats, both in the presence and absence of *N*-nitro-L-arginine (L-NNA), a non-selective nitric oxide synthase (NOS) isoforms inhibitor. Furthermore, NOS activity was also evaluated on samples of tissues adjacent to those used for the evaluation of mechanical activity.

MATERIALS AND METHODS

Animals

Adult male Sprague-Dawley rats (250-300 g) were kept in a restricted access room at a constant temperature of 21-23 ℃ with light/dark cycles of 12 h. The animals were housed in rack-mounted wire cages and fed with standard chow pellets and water *ad libitum*.

Induction of colitis

Adhering to the Italian National Research Council criteria for the care and use of laboratory animals, colitis was induced as originally described by Morris[27]. Briefly, colitis was induced in 10 rats under light ether anesthesia by a single intracolonic administration of 0.25 mL of 50% ethanol containing 30 mg of TNBS. The solution was introduced via a catheter placed 8 cm from the anal verge. Ten rats in the control group were given an enema of the same volume of 0.9% saline instead of TNBS. The rats were anesthetized and then killed by decapitation 48 h after TNBS or saline administration.

Sample recovery and preparation

Laparotomy was performed under ether anesthesia, the colon was visualized, and the perimeter of the mid-colon was measured. Under anesthesia the entire colon was then rapidly excised and placed in a Petri capsule containing Tyrode solution (6.9 g/L NaCl, 0.35 g/L KCl, 0.16 g/L KH_2PO_4, 0.29 g/L $MgSO_4$, 1 g/L glucose, 0.28 g/L $CaCl_2$, 2.1 g/L $NaHCO_3$) continuously oxygenated with a mixture of 95% O_2 and 5% CO_2 and maintained at a temperature of 37 ℃. The colon was carefully opened along the mesenteric side and the luminal surface was flushed with pre-warmed Tyrode solution through a fine needle syringe to remove the feces. If perforation of the organ was observed, the rat was excluded from the study. Fragments from the mid-colon (corresponding to the dilated non-inflamed region of the colon in TNBS rats) and the distal colon in both treated and control rats were processed for structural and enzymatic activity (myeloperoxidase (MPO), NOS). The mid-colon, from TNBS and control rats, was used for motility studies.

Assessment of colonic damage and inflammation

All tissue fragments were immediately and rapidly examined under a stereomicroscope by a blinded expert observer, and any visible damage was scored according to the following scale: 0 = no damage, 1 = localized hyperemia without ulcers, 2 = linear ulcers without inflammation, 3 = linear ulcers plus inflammation, 4 = two or more sites of ulceration and/or inflammation, 5 = ulceration >1 cm extension.

Samples from the DUMC and from the inflamed distal colon of TNBS rats and from mid- and distal colon of control rats were taken for conventional histology and for MPO activity evaluation.

For histology, tissue specimens were fixed in formalin and embedded in paraffin. Coded sections were then stained with hematoxylin and eosin, and examined at light microscopy, by a blinded observer.

For the measurement of MPO activity, full-thickness tissue, obtained from the sites adjacent to the tissue retrieved for histological studies, was snap frozen in liquid nitrogen and stored at -80 ℃. The MPO activity was measured according to the protocol of Wallace[28]. One unit of MPO activity was defined as the quantity of enzyme needed to convert 1 mol of hydrogen peroxide to water in 1 min, at room temperature, and was expressed in units per milligram of tissue.

Assessment of NOS activity

Full thickness samples, obtained from DUMC and inflamed distal colon of TNBS rats and from mid- and distal colon of control rats, were used for the assessment of NOS activity.

NOS activity was determined by measuring the conversion of [3H]-L-arginine to [3H]-L-citrulline. Tissue samples were homogenized by sonication in homogenization ice-cold buffer (25 mmol/L Tris-HCl, pH 7.4, 1 mmol/L ethylenediaminetetraacetic acid (EDTA), 1 mmol/L ethylene glycol-bis (β-aminoethyl ether)-*N*,*N*,*N*',*N*'-tetraacetic acid containing protease inhibitors (0.2 mmol/L phenylmethanesulfonyl fluoride, 10 g/mL aprotinin, 10 g/mL pepstatin A, 10 g/mL leupeptin). The homogenates were centrifuged at 4 ℃ for 20 min at 15 000 *g*. The supernatants were passed through AG50WX-8 Dowex resin (Bio-Rad Laboratories, Melville, NY, USA) to remove endogenous arginine. The protein content was determined by the bicinchoninic acid procedure (Pierce) using BSA as standard. Enzymatic reactions were conducted at 37 ℃ for 30 min in 50 mmol/L Tris-HCl, pH 7.4, containing 1 mmol/L $CaCl_2$, 1 mmol/L $MgCl_2$, 6 mol/L tetrahydrobiopterin (BH4), 2 mol/L flavin adenine dinucleotide, 2 mol/L flavin adenine mononucleotide, 1 mmol/L L-citrulline (to inhibit the catabolism of [3H]-L-citrulline), 60 mmol/L L-valine, 60 mmol/L L-ornithine, 60 mmol/L L-lysine (to inhibit nonspecific arginase activity) and 10 Ci/mL of [3H]-L-arginine (specific activity 66 Ci/mmol/L (Amersham, Buckinghamshire, UK). When indicated, $CaCl_2$ (0.6 mmol/L) and calmodulin (CAM, 0.1 mol/L) were added to the assay system. This reaction was stopped by the addition of 0.4 mL of stop buffer (50 mmol/L Hepes, pH 5.5, 5 mmol/L EDTA). Citrulline was determined by introducing the samples into columns containing 0.1 mL of Dowex AG50WX-8, equilibrated resin to Na+ form, to bind all the unreacted radio-labeled L-arginine. The columns were vortexed and centrifuged (15 000 *g* for 30 s). Therefore, 100 μL of the eluate were counted by liquid scintillation to quantitate the formation of [3H]-L-citrulline. This assay measures both the calcium-dependent (constitutive) and the calcium-independent (inducible) isoenzymes. Any activity detected in the absence of Ca/CAM represented the iNOS activity. Quantitative results for citrulline-production are expressed as picomoles of citrulline per milligram proteins per minute (citrulline pmol/mg protein/min).

Evaluation of circular muscle contractile activity

Tissue preparation Full wall thickness strips containing the mucosa (1.5 mm×10 mm) were derived both from the DUMC of the TNBS rats and the corresponding mid-colon of the control rats. Strips were oriented in the axis of the circular muscle and were attached to an isometric force transducer (Model Gemini Basile, Varese, Italy) and placed in an organ bath containing 20 mL of Tyrode solution which was continuously oxygenated with a mixture of 95% O_2 and 5% CO_2 and maintained at a temperature of 37 ℃. Muscle strips were allowed to stabilize for 2 h before they were stretched by 2-mm increments to the optimal length for contraction (L_o). The force of muscle contraction was normalized for cross-sectional area obtained by the following equation: $XS = M/L_o \times d$[29,30], where XS (cm^2)=cross-sectional area of muscle, M (g) = mass of circular muscle layer (after removal of the mucosa and submucosa), L_o (cm)=optimal length for muscle contraction, d (g/mL) = density of colonic muscle in bath numerically equal to specific gravity of colonic muscle in Tyrode solution. The muscle strips from TNBS rats which were devoid of spontaneous activity were, nevertheless, used to study the effects of NOS inhibitor (L-NNA) when basal activity was absent. These muscle strips, after 2 h of equilibration, were stretched to 1.25× resting length. In this way, each muscle strip was stretched to a similar length.

Spontaneous contractile activity The parameters considered were the frequency and force of contraction. In a preliminary set of experiments, in order to evaluate the nature of the phasic contractions, i.e. myogenic or neurogenic, the preparations were treated with tetrodotoxin (TTX, 1 μmol/L), a sodium channel blocking agent, commonly used to block inhibitory and excitatory motorneurons activity.

Muscle stimulation High potassium (high $[K+]_o$, 80 mmol/L) was used as a mainly direct smooth muscle depolarizing and contracting agent without the need for receptor activation to assess whether the observed decrease in basal contractile efficacy of the circular muscle strips derived from the TNBS rats was due to a post-receptor event, i.e. intrinsic smooth muscle properties. In a set of experiments, TTX was added to the buffer in order to evaluate the potential neuro-mediated effects of high $[K+]_o$.

Electric field stimulation (EFS) was obtained through two platin electrodes placed in parallel with respect to the circular muscle strip. The electrodes were connected to a stimulator (Mod. 1193 Tuniati, Pavia Italy) and 4 Hz stimuli were applied (25; 60 V; 0.3 ms impulses) for a total duration of 5 s. This stimulus induced a submaximal contractile response evaluated in the context of a range of stimuli applied from 1 to 15 Hz. EFS were applied every 5 min. The EFS-induced responses were neuromediated in that no effect was observed when the stimulation was performed in the presence of TTX 1 μmol/L.

Effect of L-NNA To evaluate the role of NO on basal and evoked contractile activity, the experiments were performed both in the absence and in the presence of a non-selective NOS inhibitor, L-NNA (100 μmol/L)[31]. The full effect of the compound was obtained after 10 min of incubation.

Pharmacological characterization of EFS-evoked contractile response This study was performed only in the presence of L-NNA which made responses of circular muscle strips more stable[32] and excluded the inhibitory action of NO on neuromuscular function. The major putative excitatory neurotransmitters responsible for intestinal muscle contraction after EFS are considered to be acetylcholine and tachykinins (substance P and neurokinin A)[33]. The cholinergic component of EFS contractions was determined by adding atropine (1 mol/L) to the bath. The tachykinergic component of EFS evoked contractions was established by adding neurokinin 1 (NK_1) plus neurokinin 2 (NK_2) receptor antagonists (0.3 μmol/L) and SR48968 (0.3 mol/L), respectively, to the bath[34,35]. SR140333 and SR48968 are selective non-peptide tachykinin NK_1 and NK_2 receptor antagonists, respectively[34,35]. The concentrations of these antagonists used in our study have previously been demonstrated to be effective and receptor-selective in the mammalian intestinal preparations[34,35]. The antagonists were

left for at least 20 min before EFS. The antagonist concentration and time incubation were established following the demonstration of their ability to block the contractile effect of submaximal concentration of NK_1 and NK_2 receptor agonists, substance P methyl ester and [ALA]8-NKA[4-10] respectively, on circular muscle strips derived from controls. Atropine and NK_1 plus NK_2 receptor antagonists were, sequentially, added to the bath.

Drugs and solutions

The following drugs were obtained from Sigma Chemicals (Milan, Italy): atropine sulfate, TTX, L-NNA, substance P methylester and [ALA]8-NKA[4-10]. SR140333 and SR48968 were obtained by the courtesy of Dr. X. Edmond-Alt (Sanofi Research, Montpellier, France).

Substance P methylester, [ALA]8-NKA[4-10], SR140333 and SR48968 were dissolved in dimethyl sulfoxide (final solution 0.1%) and diluted in distilled water.

Statistical analysis

Statistical analysis was performed in a double-blind fashion using a suitable computer program (SAS/STAT software). Results were expressed as means±SD. Comparison of results between groups was made using the unpaired *t* test, Kruskal-Wallis test, Wilcoxon rank sum test, Mann-Whitney *U* test, Duncan's multiple range test, and ANOVA, when appropriate. All statistical tests were two sided. A value of $P<0.05$ was considered significant.

RESULTS

Course of colitis

All rats presented bloody diarrhea within 12 h of intracolonic administration of TNBS. All ($n = 10$) had lost 14±4 g body weight, while control rats ($n = 10$) gained 12±4 g, $P<0.01$. No animal died within 48 h of colitis induction.

Colonic lesions and inflammation

After laparotomy and upon visualization of the colon, TNBS rats presented a severely dilated mid-colon proximal to the grossly impaired distal colon. The *ex vivo* mean perimeter of the mid-colon in TNBS rats ($n = 10$) was 21±6 mm compared to 12±5 mm of the mid-colon in controls ($n = 10$) ($P<0.01$).

In TNBS rats, a dischromic, opaque, but not perforated, serosa was observed, nearly 8 cm from the anal verge, corresponding to the contact area of the instilled TNBS solution, the lumen of the colon was entirely filled with liquid feces, while in control rats the serosa appeared normal and well-formed fecal pellets, mainly at the distal colon, were observed.

In TNBS rats, the macroscopic damage score (0-5), at the macroscopically inflamed distal colon, was 4.1±0.2 while, at the DUMC the score was 0.3±0.1 ($P<0.01$).

In TNBS rats, the histological evaluation showed no lesions or inflammatory infiltrate at the mid-colon, which represents the area of interest for mechanical activity studies. The distal segment was grossly ulcerated and necrotic up to the smooth muscle layers appeared to be slightly damaged. The inflammatory infiltrate was composed mainly by neutrophils and, to a lesser extent, by monocytes. The entire colon of the control rats was devoid of any significant lesions.

MPO activity, in the TNBS inflamed distal colon (dilated and macroscopically and histologically inflamed segment), was significantly higher than that in the distal colon of control rats (Figure 1). Whereas, in the TNBS uninflamed mid-colon (dilated but macroscopically and histological normal), MPO activity was similar to that of the corresponding mid-colon of control rats.

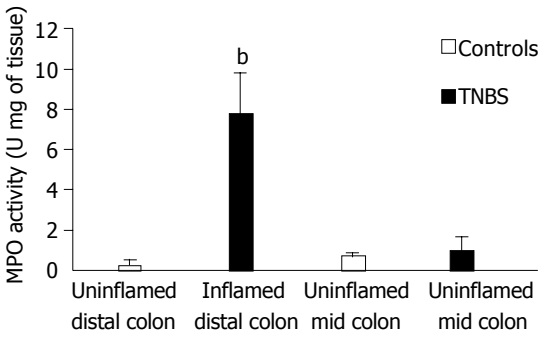


Figure 1 Colonic MPO activity in TNBS and control rats. $^bP<0.01$ *vs* controls distal colon.

NOS activity

In TNBS rats, NOS activity of the inflamed distal colon was significantly increased ($P<0.01$) compared to that of DUMC of TNBS and of controls (Figure 2). iNOS activity was observed only in the inflamed distal colon of TNBS rats where it was responsible for the marked increase of the overall NOS activity observed at this level. In the inflamed distal colon of TNBS rats, cNOS activity was not, in fact, significantly different from that in the controls and TNBS uninflamed mid-colon.

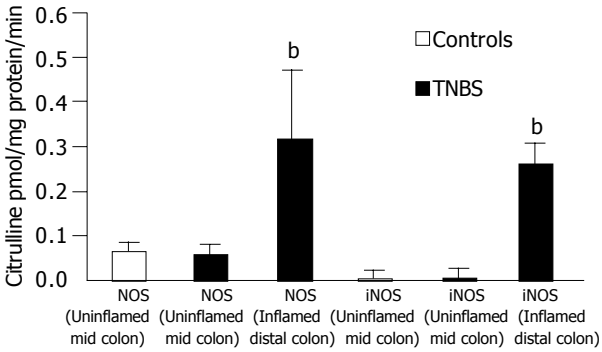


Figure 2 NOS activity in different colon segments in TNBS and control rats. $^bP<0.01$ *vs* uninflamed mid-colon.

Circular muscle contractile activity

Spontaneous contractile activity In controls, two types of spontaneous mechanical contractions were identified, i. e., low- and high-frequency spontaneous contractions. High-frequency contractions are intermittent and produce

summation contractions which are not constantly present and, therefore, these were not considered, in detail, in the present study.

Spontaneous activity was absent in 28% of the TNBS rat DUMC preparations or they showed a significant reduction of frequency and force compared to controls (Figures 3 and 4). In both groups, the spontaneous phasic activity was significantly increased both in frequency and force by TTX (1 μmol/L), the effects being significantly greater and long lasting in the strips from the DUMC of TNBS rats than in the controls. In the former, the increase in frequency and force was 40±9% and 22±7%, respectively, $P<0.01$; in the latter, the increase was 22±8% and 14±7%, respectively, $P<0.01$. Furthermore, TTX evoked spontaneous contractions in 80% of specimens which, in basal conditions, appeared to be inactive. Taken together, these data highlight the greater sensitivity to neuronal inhibitory input of DUMC of TNBS *vs* controls.

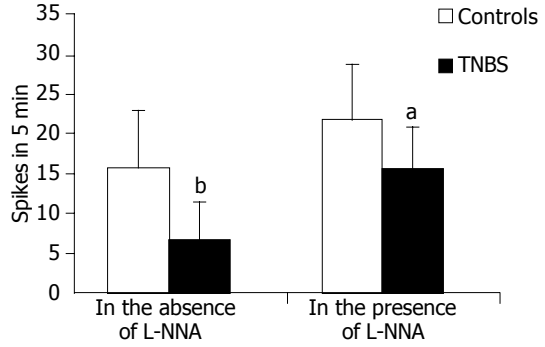


Figure 3 Frequency of phasic contractions of mid-colon circular muscle in controls compared to DUMC of TNBS rats. [a]$P<0.05$ *vs* controls, [b]$P<0.01$ *vs* controls.

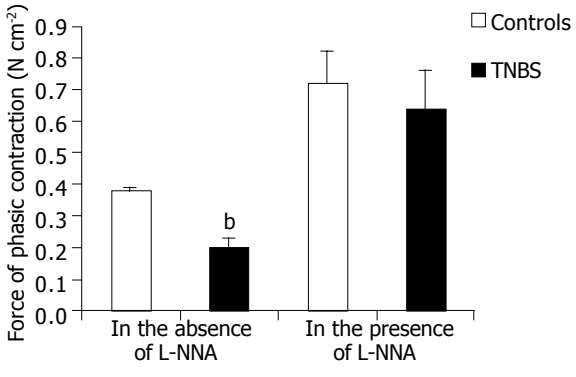


Figure 4 Force of phasic contractions of mid-colon circular muscle in controls compared to DUMC of TNBS rats. [b]$P<0.01$ *vs* controls.

L-NNA (100 μmol/L) induced a slow onset enhancing the effect of the frequency and force of spontaneous contractile activity which peaked after 5-7 min and remained unchanged for about 40 min in circular muscle strips from both animal groups, the effect being more pronounced in TNBS rats (Figures 3 and 4). In the presence of TTX, L-NNA induced, in both groups and to the same extent, a further slight increase (10%) in the force of muscle contraction suggesting a very small additional non-neuronal location of NO biosynthesis. L-NNA did not affect the frequency of contractions in the presence of TTX. Furthermore, L-NNA evoked phasic activity in almost all the strips (90%) from the DUMC of TNBS rats which had not originally shown any spontaneous contractions.

Overall, these findings suggest that endogenous NO negatively modulates the frequency and force of spontaneous phasic activity, and these effects were relatively more marked in tissues derived from TNBS rats than from controls.

Muscle stimulation High $[K+]_o$ (80 mmol/L)-induced contractile response was quantitatively and qualitatively different in circular muscle strips from DUMC of TNBS rats compared to those from controls. In the former, the force of contraction was markedly lower (Figure 5), and its time course to peak was longer. Furthermore, in control strips, high $[K+]_o$ induced a rapid onset inhibitory response followed by contraction. In the presence of TTX, the inhibitory response was abolished indicating its neuromediated nature. The inhibitory effect to high $[K+]_o$ was seldom observed in tissues from TNBS rats probably due to their lower basal tone. In both groups, in DUMC of TNBS and controls, the contractile responses to potassium were not significantly affected by TTX, indicating that this component of potassium responses was due to a mainly direct, non-neuromediated, circular muscle activation.

In the presence of L-NNA (100 μmol/L), high $[K+]_o$ contraction was enhanced by 112±22% in TNBS rats and by 28±2% in control animals ($P<0.001$) (Figure 5). However, the contractile response obtained in TNBS rats remained lower [by 23.5±1.8% ($P<0.01$)] than in controls without L-NNA.

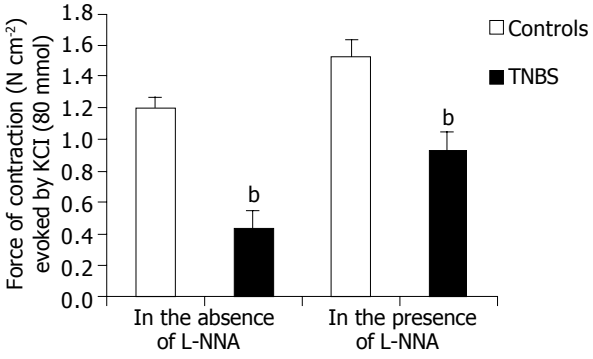


Figure 5 High $[K^+]_o$ induced contractile response of mid-colon circular muscle in controls compared to DUMC of TNBS rats. [b]$P<0.001$ *vs* controls.

EFS (1-15 Hz) evoked frequency-dependent contractile responses both in TNBS rat colonic muscle and in that of control rats (data not shown). In this study, a submaximal frequency of stimulus of 4 Hz was used. In controls, an initial inhibitory response precedes the contraction. The force of contractions was markedly smaller in TNBS rats (Figure 6) and tended to progressively fade after further stimulations until it became stable after the third stimulus. The value of the stabilized contraction has been assumed as EFS response. EFS induced contractions, in control rats, were stable and reproducible for at least 60 min. The EFS effects were abolished by TTX thus indicating the

neuromediated nature of the mechanical events (data not shown). In the presence of L-NNA, the force of contraction induced by EFS was enhanced by 121±19% in TNBS rats and by 27.4±1.9% in control rats ($P<0.001$) (Figure 6). However, the response obtained in TNBS rats remained lower [by 17.6±1.5% ($P<0.05$)] than in controls without L-NNA.

In the presence of L-NNA, the inhibitory response to potassium and EFS, observed in the controls, was not significantly lesser in amplitude than in the absence of NO synthesis inhibition, indicating the relative role of NO in inducing neuromediated relaxation in these colonic preparations.

Effects of cholinergic muscarinic and NK_1 plus NK_2 tachykinin receptor blockade on EFS evoked circular muscle contractile response In the presence of L-NNA, in control preparations, the sequential administration of atropine (1 μmol/L) and non-peptide tachykinin NK_1 and NK_2 receptor antagonists SR140333 (0.3 μmol/L) plus SR48968 (0.3 μmol/L) induced an apparent additional inhibitory effect of the EFS induced contraction leaving a non-cholinergic non-tachykinergic contractile component which was completely abolished by TTX. In TNBS rats, atropine alone induced a dramatic inhibition of contraction and the residual response was abolished by the sequential administration of SR140333 plus SR48968 (Figure 7). These results indicate the appearance of a cooperative-like interaction between the neuromuscular excitatory transmissions subserving EFS contraction in TNBS rats.

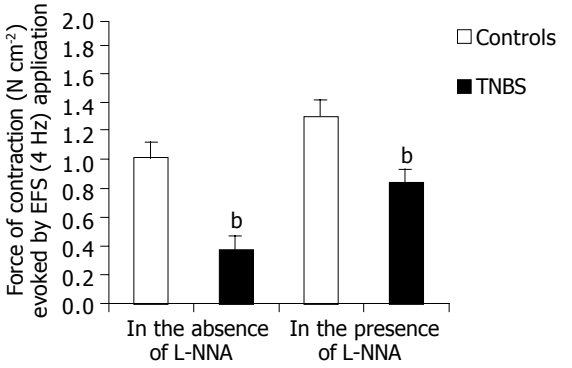


Figure 6 EFS evoked contraction of mid-colon circular muscle in controls compared to DUMC of TNBS rats. $^bP<0.001$ *vs* controls.

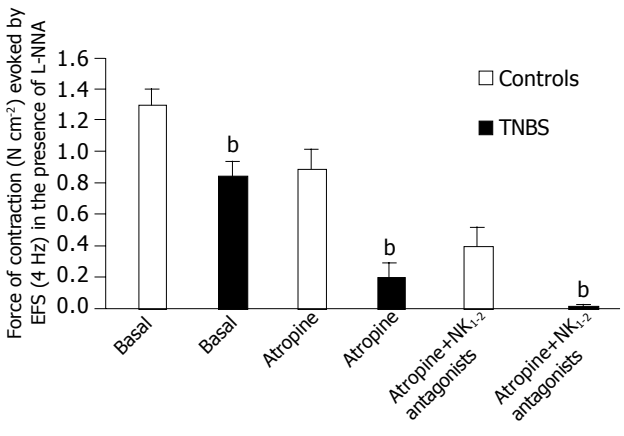


Figure 7 Pharmacological effects on EFS-evoked contractile responses recorded in the presence of L-NNA. $^bP<0.001$ *vs* controls.

DISCUSSION

The present study focused on changes in colonic motility of the uninflamed regions of the colon observed in the course of severe human and experimental focal colitis. In rats with TNBS-induced acute distal colitis, we evaluated the spontaneous and evoked contractile activity of circular muscle strips from a region of the mid-colon, which was dilated but showed a normal appearance at light microscopy and normal MPO activity.

Low-frequency spontaneous contractile activity was always present in controls, but conversely, was absent in 28.5% of specimens from the DUMC of TNBS rats, and, if present, showed a significant reduction both in frequency and force of contraction, with respect to that in controls. Removal of the overall neural control, on smooth muscle activity, by TTX, induced an increase in the frequency and force of contractions which were significantly greater in tissues from TNBS rats and this contractile activity became present in almost all specimens. These findings confirm previous evidence that the spontaneous contractions in rat circular muscle strips, as, in general, in the mammalian colon, are myogenic in nature and under tonic neuronal inhibition[4,21]. Thus, the impairment of spontaneous activity in tissues from TNBS rats may be due to a disorder of the intrinsic muscle contractile machinery and/or due to an inappropriate neural inhibitory control.

Evoked contractions were induced by a mainly direct smooth muscle plasma membrane depolarization by high $[K+]_o$ in the buffer, and by indirect neuronal- and receptor-mediated activation of circular muscle strips by EFS, the former being largely resistant to TTX and the latter abolished by it. In the controls, both stimulatory procedures, in addition to contraction, induced a rapid onset and transient relaxation due to the release of inhibitory neurotransmitters in that it was abolished by TTX and slightly reduced by L-NNA. In the DUMC of TNBS rats, the relaxing effects were not usually observed, probably because of the lower basal tone of the circular muscle and, moreover, the high $[K+]_o$ contractions appeared markedly impaired in amplitude and slower in the time course compared to controls. Likewise, the EFS contractile responses, in TNBS rats, were smaller in force than those in controls and tended to fade at subsequent stimulations until a stable response was reached after the third stimulation.

Impairment of evoked contractions in TNBS rats may still suggest a defect of contractile machinery (as suggested by the high $[K+]_o$ response). However, a simultaneous defect in the excitatory neurotransmission (neurotransmitter release and/or receptor–postreceptor functions) in the EFS response could not be ruled out.

On the base of increasing evidence that NO plays an important role in inhibiting colonic tone and motility of the inflamed region in human and experimental animal colitis[12,17,25,26], we evaluated the potential role of NO in the impairment of muscle contractility also in the dilated uninflamed region of the TNBS rat. NO is the most important inhibitory transmitter of enteric neurons in the mammalian gut[20-22] and, in human colitis, iNANC activity has been shown to be increased[36]. Furthermore, extraneuronal NO production, by iNOS, localized in

immune cells and enteric myocytes has recently been detected in inflamed colonic mucosa from patients with UC compared to controls, with significantly higher levels in TMC than in uncomplicated colitis[23-25]. Similarly, in TNBS-induced colitis, associated with colonic dilation, a striking increase in iNOS expression was found, whereas inhibition of NOS activity, by L-NNA, prevented colonic dilation[26]. The observation that interleukin 1 (IL-1), tumor necrosis factor-α (TNFα), and interferon-γ (INFγ), which are of prime importance in the inflammatory process of severe colitis, as well as free radicals and lipopolysaccharides, are able to induce iNOS expression in human colonic smooth muscle strips, further supports the role of iNOS in the genesis of TMC[25,26,37,38].

In this study, the role of NO on the contractility of circular muscle from DUMC of TNBS rats has been evaluated using L-NNA, a non selective NOS isoforms inhibitor. Previously, an analogous compound of L-NNA, the *N*-monomethyl-L-arginine, has been reported to increase spontaneous contractions of rat distal colon circular muscle strips, indicating that this colonic preparation is under tonic neural inhibition by NO biosynthesis[29]. L-NNA, added to the organ bath, induced both a relatively greater increase in the frequency and force of circular muscle phasic contractions in DUMC of TNBS than in controls and, indeed, their appearance, when absent, in the former. Furthermore, L-NNA induced a considerably greater increase of high $[K+]_o$ contractile responses in DUMC of TNBS compared to controls with a reduction in the time course. Likewise, in the presence of L-NNA, the contraction induced by EFS was enhanced in both groups, the effect being relatively more marked in strips from TNBS rats.

Studies on the pharmacological characterization of contractions induced by EFS were performed only in the presence of L-NNA in order to obtain more stable responses as already observed in rat duodenal preparations[32], and to better define potential dysfunctions in the excitatory neuromuscular transmissions and responses, i.e., independently of the NO-mediated inhibitory action, both on excitatory neurotransmitters release and muscular contractile response. The nature of the contractile responses induced by EFS were analyzed using atropine and SR140333 plus SR48968 as selective antagonists of cholinergic muscarinic and NK_1 and NK_2 tachykinin receptors, respectively. In controls, a simple additional interaction was observed between the cholinergic and tachykinergic transmission in inducing contractions and the sequential blockade of the respective receptors left a non-cholinergic-non-tachykinergic contractile component which was abolished by TTX. In TNBS rats, a cooperative-like interaction between cholinergic and tachykinergic excitatory transmissions appeared to be present. The existence of a non-simple additional interaction in the latter was suggested by the evidence that the blockade of only one of the neuronal transmissions (i.e., muscarinic transmission) induced a dramatic inhibitory effect on EFS responses, and the residual contraction was completely abolished after sequential tachykinergic transmission blockade, indicating that the contribution of both the excitatory transmissions was mandatory to induce contractile responses.

The biochemical studies performed to define the activity of NOS isoforms in the DUMC tissues of TNBS showed that only cNOS was present and its activity was not different from that in control rats. In the injured distal colonic segments of TNBS rats, cNOS activity was similar to that in controls, whereas iNOS activity was markedly present, confirming previous observations[26]. These findings indicate that enhancement of spontaneous and evoked muscle contractility, in the presence of blockade of NOS activity, is due to the inhibition of the cNOS in the two groups studied. The set-up used did not allow us to characterize the cellular source and isoform of cNOS (neural or endothelial/muscular) in the colonic preparations. However, the observation that L-NNA induced a slight but not a significant increase in the amplitude of spontaneous contractions in the presence of TTX may suggest a scanty role of non-neural cNOS in the overall enzyme activity in both groups of rats. The lack of appreciable quantitative differences, in the presence and activity of cNOS, between the two groups did not allow us to give a simple interpretation for the considerably greater enhancing effect, induced by L-NNA, on the spontaneous and evoked contractions of circular muscle strips from DUMC of TNBS compared to those from controls. However, it is tempting to hypothesize that a relatively greater inhibitory effect is exerted by NO on the functionally impaired myogenic and possibly excitatory neurogenic mechanisms subserving contractions in TNBS rats. The observation that also TTX induced a considerably greater enhancing effect on spontaneous and high potassium ($High[K+]_o$)-evoked contractions in DUMC of TNBS compared to controls may suggest that circular muscle strips from DUMC of TNBS present an abnormally high sensitivity to inhibitory neurotransmitters. On the other hand, it is unlikely that the increase in mechanical activity of the circular muscle induced by L-NNA in DUMC, is not due to the suppression of NO synthesis, but rather due to the inhibition of the production of peroxynitrite (ONOO-) in as much as the production of the latter requires the presence of the superoxide radical ($\cdot O_2$), (i.e. $NO+\cdot O_2 \rightarrow$ONOO-). The generation of $\cdot O_2$ requires the presence of local inflammation which was absent in the intestinal preparations in which mechanical activity was evaluated.

The importance of the neurogenic mechanisms in the distension and hypocontractility of uninflamed gastrointestinal segments in TNBS-induced intestinal inflammation in rats has recently been reported[18,39].

As far as concerning the potential mechanisms involved in the impairment of intrinsic muscle contractile machinery, in the rat model of acute TNBS colitis, a decrease in the activity of smooth muscle L-type Ca++ channels has been demonstrated. Ca++ mobilization, via the L-type Ca++ channel, is the primary mechanism for excitation-contraction coupling in gastrointestinal smooth muscle. The dysfunction of the L-type Ca++ channels appears to be mediated by the activation of the NF-kB-dependent pathway leading to a marked alteration in the assessment of cytokines, as observed in acute TNBS colitis. Theoretically, the hematogenic diffusion of cytokines from the inflammatory to the non-inflammatory region of the colon may also result in the inhibition of TNBS DUMC muscle contractility as observed in the present study.

In conclusion, results emerging from the present study show that impairment of spontaneous and evoked circular muscle contraction of the DUMC in TNBS-induced distal colitis, in rats, is mainly due to a disorder of the intrinsic muscle contractile machinery. Failure of enteric neural excitatory input to the smooth muscle cannot be ruled out. Local suppression of NO synthesis markedly improves both the spontaneous and evoked muscle contractions, in spite of any evident abnormal local NO activity. New therapeutic approaches aimed at inhibition of NO synthesis or effects may improve muscle contractility, not only in the inflamed, but also in the distended uninflamed intestinal regions in the course of acute severe inflammatory bowel disease.

REFERENCES

1 **Fazio VW.** Toxic megacolon in ulcerative colitis and Crohn's colitis. *Clin Gastroenterol* 1980; **9**: 389-407
2 **Sheth SG,** LaMont JT. Toxic megacolon. *Lancet* 1998; **351**: 509-513
3 **Snape WJ,** Williams R, Hyman PE. Defect in colonic muscle contraction in patients with ulcerative colitis. *Am J Physiol Gastrointest Liver Physiol* 1991; **261**: G987-G995
4 **Koch TR,** Carney JA, Go ULW, Szurszewski JH. Spontaneous contraction and some electrophysiological properties of circular muscle from normal sigmoid colon and ulcerative colitis. *Gastroenterology* 1988; **95**: 77-85
5 **Snape WJ,** Materazzo SA, Cohen S. Abnormal gastrocolonic response in patients with ulcerative colitis. *Gut* 1980; **21**: 392-396
6 **Snape WJ,** Kao HW. Role of inflammatory mediators in colonic smooth muscle function in ulcerative colitis. *Dig Dis Sci* 1988; **3**: 65S-70S
7 **Sharkey KA.** Substance P and Calcitonin Gene Related Peptide (GCRP) in gastrointestinal inflammation. *Ann NY Acad Sci* 1992; **664**: 425-442
8 **Lennard-Jones JE,** Cooper GW, Newell AC, Wilson CW, Jones FA. Observations on idiopathic proctitis. *Gut* 1962; **3**: 201-206
9 **Allison MC,** Vallance R. Prevalence of proximal faecal stasis in active ulcerative colitis. *Gut* 1991; **32**: 179-182
10 **Reddy SN,** Bazzochi G, Ghan S, Akashi K, Viuanueva Meyer J, Yanni G, Mena I, Dnape WJ Jr. Colonic motility and transit in health and ulcerative colitis. *Gastroenterology* 1991; **101**: 1289-1297
11 **Caprilli R,** Vernia P, Latella G, Torsoli A. Early recognition of toxic megacolon. *J Clin Gastroenterol* 1987; **9**: 160-164
12 **Latella G,** Vernia P, Viscido A, Frieri G, Cadau G, Cocco A, Tomei E, Capriui R. GI distension in severe ulcerative colitis. *Am J Gastroenterol* 2002; **97**: 1169-1175
13 **Chew CN,** Nolan GJ, Jewell DP. Small bowel gas in severe ulcerative colitis. *Gut* 1991; **32**: 1535-1537
14 **Caprilli R,** Latella G, Vernia P, Frieri G. Multiple organ dysfunction in ulcerative colitis. *Am J Gastroenterol* 2000; **95**: 1258-1262
15 **Jacobson K,** McHugh K, Collins SM. Experimental colitis alters myoenteric nerve function of inflamed and non-inflamed sites. *Gastroenterology* 1995; **109**: 718-722
16 **Aube AC,** Cherbut C, Barbier M, Xing JH, Roze C, Galmiche JP. Altered myoenterical activity in non-inflamed ileum of rats with colitis induced by trinitro benzene sulphonic acid. *Neurogastroenterol Motil* 1999; **11**: 55-62
17 **Caprilli R,** Onori L. Pathogenesis of GI distension in severe ulcerative colitis: a hypothesis. *Gastroenterol Int* 1992; **5**: 268-272
18 **Blandizzi C,** Fornai M, Colucci R, Baschiera F, Barbara G, De Giorgio R, De Ponti f, Breschi MC, Del Tacca M. Altered prejunctional modulation of intestinal cholinergic and noradrenergic pathways by α2receptors in the presence of experimental colitis. *Br J Pharmacol* 2003; **139**: 309-320
19 **Costa M,** Furness JB, Brookes SJH, Bornstein JC, Bredt DS. Projection and chemical coding of neurons with immunoreactivity for nitric oxide synthase in the guinea pig small intestine. *Neurosci Lett* 1992; **148**: 121-125
20 **Keef KD,** Du C, Ward SN, McGregor M, Sanders KM. Enteric inhibitor neural regulation of human colon circular muscle: role of nitric oxide. *Gastroenterology* 1993; **105**: 1009-1016
21 **Middleton SJ,** Cuthbert AW, Shorthouse M, Hunter JO. Nitric oxide affects mammalian distal colonic smooth muscle by tonic neural inhibition. *Br J Pharmacol* 1993; **108**: 974-979
22 **Wiklund CO,** Olgart C, Wiklund NP, Gustavsson LE. Modulation of cholinergic and substance P-like neurotransmission by nitric oxide in the guinea pig ileum. *Br J Pharmacol* 1993; **110**: 833-839
23 **Middleton SJ,** Shorthouse M, Hunter JO. Increased nitric oxide synthesis in ulcerative colitis. *Lancet* 1993; **341**: 465-466
24 **Boughton-Smith NK,** Evans SM, Hawkey CJ, Cole AT, Basitis M, Whittle BJR, Moncada S. Nitric oxide synthase activity in ulcerative colitis and Crohn's disease. *Lancet* 1993; **342**: 338-340
25 **Mourelle M,** Casella F, Guarner F, Salas A, Riveras-Moreno V, Moncada S, Malagelada JR. Induction of nitric oxide synthase in colonic smooth muscle from patients with toxic megacolon. *Gastroenterology* 1995; **109**: 1497-1502
26 **Mourelle M,** Villaseca J, Guarner F, Salas A, Malagelada JR. Toxic dilatation of colon in a rat model of colitis is linked to an inducible form of nitric oxide synthase. *Am J Physiol Gastrointest Liver Physiol* 1996; **270**: G425-G430
27 **Morris GP,** Beck PL, Herridge MS, Depew WT, Szewczuk MR, Wallace JL. Hapten-induced model of chronic inflammation and ulceration in the rat colon. *Gastroenterology* 1989; **96**: 795-803
28 **Wallace JL.** Glucocorticoid induced gastric mucosal damage in inhibition of leukotriene but not prostaglandin biosynthesis. *Prostaglandins* 1987; **43**: 311-323
29 **Middleton SJ,** Cuthbert AW, Shorthouse M, Hunter JO. Nitric oxide affects mammalian distal colon smooth muscle by tonical neural inhibition. *Br J Pharmacol* 1993; **108**: 974-979
30 **Cohen JD,** Kao HW, Tani ST, Lechago J, Snape WJ. Effect of acute experimental colitis on rabbit colonic smooth muscle. *Am J Physiol Gastrointest Liver Physiol* 1986; **251**: G538-G545
31 **Moncada S,** Palmer RMJ, Higgs EA. Nitric oxide: physiology, pathophysiology and pharmacology. *Pharmacol Rev* 1991; **43**: 109-142
32 **Giuliani S,** Tramontana M, Lecci A, Maggi CA. Tachykinin receptors mediate atropine-resistant rat duodenal reflex contractions *in vivo*. *Naunyn Schmiedeberg's Arch Pharmacol* 1996; **354**: 327-335
33 **Maggi CA,** Zagorodnyuk V, Giuliani S. Specialization of tachykinin NK1 and NK2 receptors in producing fast and slow atropine-resistant neurotransmission to the circular muscle of the giuinea-pig colon. *Neuroscience* 1994; **63**: 1137-1152
34 **Edmonds-Alt X,** Doutremepuich JD, Heaulme M, Neliat G, Santucci V, Steinberg R, Vilain P, Bichon D, Ducoux JP, Proietto V. *In vitro* and *in vivo* biological activity of SR140333, a novel potent non peptide tachykinin NK1 receptor antagonist. *Eur J Pharmacol* 1993; **250**: 403-413
35 **Edmonds-Alt X,** Vilain P, Goulaouic P, Proietto V, Van Broeck D, Advenier C, Naline E, Neliat G, Le Fur G, Breliere JC. A potent selective non-peptide antagonist of the neurokinin A (NK2) receptor. *Life Sci* 1992; **50**: 101-106
36 **Tomita R,** Munakata K, Tanjoh K. Role of non-adrenergic non-cholinergic inhibitory nerves in the colon of patients with ulcerative colitis. *J Gastroenterol* 1998; **33**: 48-52
37 **Cook HT,** Cattell V. Role of nitric oxide in immune-mediated disease. *Clin Sci* 1996; **91**: 375-384
38 **Lundberg JON,** Lundberg JM, Alving K, Weitzberg E. Nitric oxide and inflammation: the answer is blowing in the wind. *Nat Med* 1997; **3**: 30-31
39 **Moreels TG,** De Man JG, De Winter BY, Timmermans JP, Herman AG, Pelckmans PA. Effect of 2,4,6-trinitrobenzenesulphonic acid (TNBS)-induced ileitis on the motor function of non-inflamed rat gastric fundus. *Neurogastroenterol Mot* 2001; **13**: 339-352

Science Editor Wang XL and Guo SY **Language Editor** Elsevier HK

PO Box 2345, Beijing 100023, China
www.wjgnet.com
wjg@wjgnet.com

ELSEVIER

World J Gastroenterol 2005;11(36):5685-5687
World Journal of Gastroenterology ISSN 1007-9327
© 2005 The WJG Press and Elsevier Inc. All rights reserved.

• *BRIEF REPORTS* •

Re-evaluation of antitumor effects of combination chemotherapy with interferon-α and 5-fluorouracil for advanced hepatocellular carcinoma

Munechika Enjoji, Shusuke Morizono, Kazuhiro Kotoh, Motoyuki Kohjima, Yuzuru Miyagi, Tsuyoshi Yoshimoto, Makoto Nakamuta

Munechika Enjoji, Shusuke Morizono, Kazuhiro Kotoh, Motoyuki Kohjima, Yuzuru Miyagi, Tsuyoshi Yoshimoto, Makoto Nakamuta, Department of Medicine and Bioregulatory Science, Graduate School of Medical Sciences, Kyushu University, Fukuoka, Japan
Correspondence to: Munechika Enjoji, MD, Department of Medicine and Bioregulatory Science, Graduate School of Medical Sciences, Kyushu University, 3-1-1 Maidashi, Higashi-ku, Fukuoka 812-8582, Japan. enjoji@intmed3.med.kyushu-u.ac.jp
Telephone: +81-92-642-5282 Fax: +81-92-642-5287
Received: 2005-03-22 Accepted: 2005-04-02

Key words: Interferon-α; 5-Fluorouracil; Hepatocellular carcinoma; Chemotherapy

Enjoji M, Morizono S, Kotoh K, Kohjima M, Miyagi Y, Yoshimoto T, Nakamuta M. Re-evaluation of antitumor effects of combination chemotherapy with interferon-α and 5-fluorouracil for advanced hepatocellular carcinoma. *World J Gastroenterol* 2005; 11(36): 5685-5687
http://www.wjgnet.com/1007-9327/11/5685.asp

Abstract

AIM: To evaluate the efficacy of combination chemotherapy with interferon-α (IFNα) and 5-fluorouracil (5-FU) in patients with advanced hepatocellular carcinoma (HCC).

METHODS: Twenty-eight HCC patients in advanced stage were enrolled in the study. They were treated with IFNα/5-FU combination chemotherapy. One cycle of therapy lasted for 4 wk. IFNα (3×10^6 units) was subcutaneously injected thrice weekly on days 1, 3, and 5 for 3 wk, and 5-FU (500 mg/d) was administered via the proper hepatic artery for 5 consecutive days per week for 3 wk. No drugs were administered during the 4th wk. The effect of combination chemotherapy was evaluated in each patient after every cycle based on the reduction of tumor volume.

RESULTS: After the 1st cycle of therapy, 16 patients showed a partial response (PR, 57.1%) but none showed a complete response (CR, 0%). At the end of therapy, the number of patients who showed a CR, PR, or no response (NR) was 1, 10, and 17, respectively. The response rate for therapy (CR+PR) was 21.5%. Biochemical tests before therapy were compared between responsive (CR+PR) and non-responsive (NR) patients, but no significant differences were found for any of the parameters examined, indicating that no reasonable predictors could be identified in our analysis.

CONCLUSION: Attempts should be made to discriminate between responders and non-responders by evaluating tumor size after the first cycle of IFNα/5-FU combination chemotherapy. For non-responders, therapy should not proceed to the next cycle, and instead, different combination of anticancer drugs should be explored.

© 2005 The WJG Press and Elsevier Inc. All rights reserved.

INTRODUCTION

Hepatocellular carcinoma (HCC) is one of the most common tumors worldwide. Therapies for HCC have been developed, such as percutaneous ethanol injection therapy (PEIT), microwave coagulation therapy (MC), and radiofrequency ablation (RFA). For patients in whom these localized therapies cannot be used, transarterial chemoembolization (TACE) and liver transplantation may be selected. However, in cases with repeated recurrence, vascular invasion or distant metastasis were used; these methods often become ineffective or impossible, and the last treatment option is chemotherapy. Although it is thought that HCCs are generally resistant to anticancer drugs, combination chemotherapy has been used to increase the responsiveness of cancer cells.

Combination therapy with interferon-α (IFNα) and 5-fluorouracil (5-FU) was first reported for the treatment of patients with colorectal cancer[1]. Recent studies indicated that the combined chemotherapy involving arterial injection of 5-FU and subcutaneous injection of IFNα was also markedly effective in some patients with advanced HCC. In these studies, the response rates to therapy were 62.5%[2] and 53.1%[3]. In the present study, we describe the use of this combination therapy in HCC patients for whom there were no other treatment options.

MATERIALS AND METHODS

Between 2003 and 2004, 28 patients with unresectable HCC associated with multiple intrahepatic tumors and/or portal vein tumor thrombi received IFNα/5-FU combination therapy at the Third Department of Internal Medicine, Kyushu University Hospital. The treatment regimen is shown in Figure 1. IFNα (3×10^6 units) was subcutaneously injected thrice per week on d 1, 3, and 5 for 3 wk. 5-FU (500 mg/d) was given over 2 h through a catheter introduced

into the proper hepatic artery for 5 consecutive days per week for 3 wk. No drugs were administered during the 4th wk. One cycle of the therapy lasted for 4 wk and patients received 1-4 cycles. The effect of combination chemotherapy was evaluated in each patient after every cycle based on the reduction of tumor volume. The degree of the response was categorized as follows: (1) complete response (CR); depletion of all the tumors on computed tomography (CT); (2) partial response (PR); over 15% reduction of the total diameters of all detectable tumors on CT; and (3) no response (NR); those that did not show a CR or PR. Combination chemotherapy was stopped after the fourth cycle was completed, or when there was no reduction in the tumor volume after any cycle. At that time, final evaluations were performed.

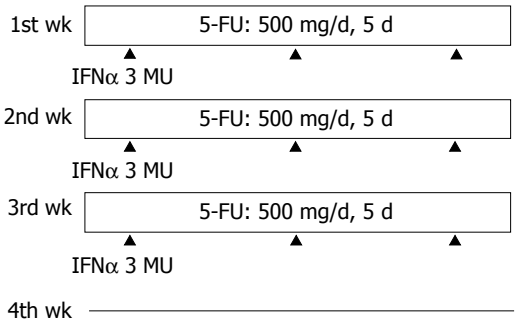


Figure 1 Regimen for IFNα plus 5-FU combination therapy (one cycle).

RESULTS

The baseline characteristics of the patients who received IFNα/5-FU combination chemotherapy are shown in Table 1. Because of the advanced stage of HCC in these patients, no other therapeutic options were available. Seven of the patients were being treated for HCC for the first time. Other therapies, such as surgical resection, PEIT, MC, RFA, and TACE, had been repeated at least twice in the other patients. Portal thrombi existed in Vp3-4 in seven patients. The combination chemotherapy was performed on these patients (see Patients and methods).

The response to chemotherapy is shown in Table 2. In these patients, chemotherapy was not stopped by adverse effects, such as thrombocytopenia and leukocytopenia. After the first cycle of therapy, 16 patients showed a PR (57.1%) but none showed a CR. In all the patients with PR, levels of the tumor marker α-fetoprotein (AFP) decreased (-2.6-91.2%, mean: -55.6%). When the therapy was completed, 1 of these 16 PR patients achieved a CR, and 10 of them showed a NR. The overall response rate for chemotherapy (CR+PR) was 21.5% (6/28). CT of a patient who achieved a CR is shown in Figure 2. After three cycles of therapy, the enhanced area of the HCC observed before chemotherapy disappeared and elevated levels of AFP decreased to the normal range (from 761.0 to 8.9 ng/mL). The backgrounds of the patients, including their laboratory test profiles before chemotherapy, were compared between responders (CR+PR) and non-responders; however, no significant differences were found for any of the parameters examined.

Table 1 Baseline characteristics of the patients

Patient (*n*)	28
Male/female	21/7
Portal thrombi (+/–)	7/21
TNM classification (II/III/IV)	5/11/12
Albumin	3.4±0.1 (g/dL)
Total bilirubin	1.3±0.2 (mg/dL)
ALT	48.2±6.4 (IU/L)
Platelet	11.3±1.7 (×10⁴/mL)
PT	70.9±2.8 (%)
AFP	7 105±2 756 (ng/mL)
PIVKA-II	11 922±4 274 (U/L)

ALT, alanine aminotransferase; PT, prothrombin time; AFP, alpha-fetoprotein.

Table 2 Evaluation of IFNα/5-FU combination therapy

	Evaluation after 1st cycle patient *n* (%)	Final results patient *n* (%)
CR		1 (3.6)
PR	16 (57.1)	5 (17.9)
NR	12 (42.9)	22 (78.6)

IFN, interferon; FU, fluorouracil; CR, complete response; PR, partial response; NR, no response.

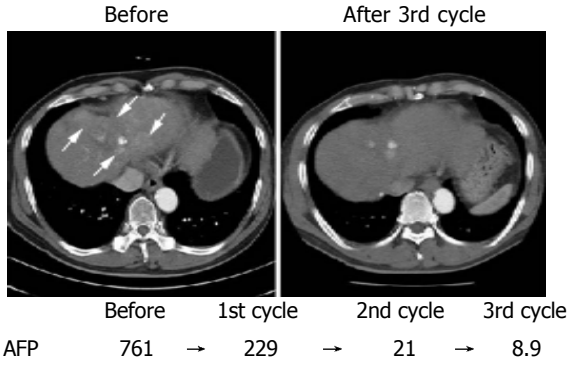


Figure 2 CT of a patient who showed a complete response. Enhanced lesions of HCC (arrows) disappeared after three cycles of combination therapy with IFNα and 5-FU. The serum levels of AFP are also presented.

DISCUSSION

The mechanism underlying the ability of IFNα to strengthen the anti-cancer effect of 5-FU has been studied previously. IFNα enhances the conversion of 5-FU to an active metabolite, fluorodeoxyuridine monophosphate (FdUMP), through an increase of thymidine phosphorylase and a suppression of dihydropyrimidine dehydrogenase[4,5]. FdUMP induces DNA damage and the expression of death receptors (tumor necrosis factor-related apoptosis-inducing ligand [TRAIL] receptors) on cancer cells, resulting in cell death[6]. IFNα reduces tumor cell proliferation through cell cycle elongation[7] and induces p53, which contributes to tumor suppression[8]. IFNα also exerts immunomodulatory effects by stimulating T cells, NK cells, and monocytes[9,10], and enhances production of TRAIL by immune cells[11-13].

Several studies have attempted to distinguish between responders and non-responders to 5-FU/IFNα combination chemotherapy. Low levels (<50 ng/mL) of serum AFP were reported as a predictor[14], but conflicting results have

also been reported[15]. A relationship between the expression levels of the IFN receptor on HCC cells and sensitivity to 5-FU/IFN therapy was reported previously[7], but another study group indicated that the expression levels of the type I IFN receptor were similar between responders and non-responders[3]. Yamamoto *et al*., reported that, among HCC patients who received 5-FU/IFNα combination chemotherapy, the expression of TRAIL mRNA in peripheral blood mononuclear cells (PBMC) was significantly higher in clinical responders than in non-responders[6]. It was suggested that upregulation of TRAIL mRNA in PBMC may be a predictor of the clinical response to combination therapy. In our patients, no predictors were found among the biochemical tests that were analyzed. We advocate that, in practice, responders and non-responders should be discriminated after the first cycle of the therapy by evaluating tumor size and the levels of tumor markers. For non-responders, therapy should not proceed to the next cycle and instead a different therapeutic option should be explored.

Some groups have reported much better results from combination chemotherapy than those observed in our study[2,3]. Apart from the dose of IFNα used, their regimens were nearly identical to ours. Those studies used 5×10^6 units of IFNα per treatment. We previously tested the effect of IFNα at doses of 3×10^6 and 6×10^6 units, and found no significant difference (data not shown). We therefore used the lower dose of 3×10^6 units to decrease the incidence of adverse effects. Since other types of therapies have been repeated in many of our patients, the HCCs in these patients may have existed in polyclonal nodules. In fact, in some patients, some HCC nodules were reduced in size, and others were enlarged during the chemotherapy. It is possible that the polyclonality weakened the clinical effects of therapy. In our patients, a relatively high response rate, 57.1%, was observed after the first cycle, but resulted in a rate of 21.5% at the end of the last cycle. Many of the patients who initially showed a PR after the first stage ended up having NR at the end of therapy. These findings suggest that the original clones with resistance against anticancer drugs and some cancer cells that acquire resistance during therapy can proliferate, and their rate of growth increases synergistically whenever a cycle is repeated.

What can be done to make combination chemotherapy more effective? A better regimen for IFNα/5-FU combination chemotherapy could be developed. Which is better, IFNα or IFNβ? IFN can be administered intravenously or intra-arterially. How many times should IFN be administered? What should be the dose of 5-FU at a time? What will be the best duration for 5-FU injection? It is also a problem whether the couple of 5-FU and IFNα is the best combination as chemotherapy for HCC. Many anticancer drugs can be selectable such as CDDP, MTX, LCV, and Gemcitabine. We should develop better regimen and combination for HCC.

REFERENCES

1 **Wadler S,** Schwartz EL, Goldman M, Lyver A, Rader M, Zimmerman M, Itri L, Weinberg V, Wiernik PH. Fluorouracil and recombinant alfa-2a-interferon: an active regimen against advanced colorectal carcinoma. *J Clin Oncol* 1989; **7**: 1764-1765

2 **Sakon M,** Nagano H, Dono K, Nakamori S, Umeshita K, Yamada A, Kawata S, Imai Y, Iijima S, Monden M. Combined intra-arterial 5-fluorouracil and subcutaneous IFN-alfa therapy for advanced hepatocellular carcinoma with tumor thrombi in the major portal branches. *Cancer* 2002; **94**: 435-442

3 **Moriyama M,** Hoshida Y, Kato N, Otsuka M, Yoshida H, Kawabe T, Omata M. Genes associated with human hepatocellular carcinoma cell chemosensitivity to 5-fluorouracil plus interferon-α combination chemotherapy. *Int J Oncol* 2004; **25**: 1279-1287

4 **Schwartz EL,** Baptiste N, Wadler S, Makower D. Thymidine phosphorylase mediates the sensitivity of human colon carcinoma cells to 5-fluorouracil. *J Biol Chem* 1995; **270**: 19073-19077

5 **Dou J,** Iwashita Y, Sasaki A, Kai S, Hirano S, Ohta M, Kitano S. Consensus interferon enhances the anti-proliferative effect of 5-fluorouracil on human hepatoma cells via downregulation of dihydropyrimidine dehydrogenase expression. *Liver Int* 2005; **25**: 148-152

6 **Yamamoto T,** Nagano H, Sakon M, Wada H, Eguchi H, Kondo M, Damdinsuren B, Ota H, Nakamura M, Wada H, Marubashi S, Miyamoto A, Dono K, Umeshita K, Nakamori S, Yagita H, Monden M. Partial contribution of tumor necrosis factor-related apoptosis-inducing ligand (TRAIL)/TRAIL receptor pathway to antitumor effects of interferon-α/5-fluorouracil against hepatocellular carcinoma. *Clin Cancer Res* 2004; **10**: 7884-7895

7 **Eguchi H,** Nagano H, Yamamoto H, Miyamoto A, Kondo M, Dono K, Nakamori S, Umeshita K, Sakon M, Monden M. Augmentation of anti-tumor activity of 5-fluorouracil by interferon alpha is associated with up-regulation of p27Kip1 in human hepatocellular carcinoma cells. *Clin Cancer Res* 2000; **6**: 2881-2890

8 **Takaoka A,** Hayakawa S, Yanai H, Stoiber D, Negishi H, Kikuchi H, Sasaki S, Imai K, Shibue T, Honda K, Taniguchi T. Integration of interferon alpha/beta signaling to p53 response in tumor suppression and antiviral defense. *Nature* 2003; **424**: 516-523

9 **Brassard DL,** Grace MJ, Bordens RW. Interferon-alpha as an immunotherapeutic protein. *J Leukoc Biol* 2002; **71**: 565-581

10 **Stark GR,** Kerr IM, Williams BR, Silverman RH, Schreiber RD. How cells respond to interferons. *Ann Rev Biochem* 1998; **67**: 227-264

11 **Grifith TS,** Wiley SR, Kubin MZ, Sedger LM, Maliszewski CR, Fanger NA. Monocyte-mediated tumoricidal activity via the tumor necrosis factor related cytokine, TRAIL. *J Exp Med* 1999; **189**: 1343-1354

12 **Kayagaki N,** Yamaguchi N, Nakayama M, Eto H, Okumura K, Yagita H. Type I interferons (IFNs) regulate tumor necrosis factor-related apoptosis-inducing ligand (TRAIL) expression on human T cells: a novel mechanism for the antitumor effects of type I IFNs. *J Exp Med* 1999; **189**: 1451-1460

13 **Sato K,** Hida S, Takayanagi H, Yokochi T, Kayagaki N, Takeda K, Yagita H, Okumura K, Tanaka N, Taniguchi T, Ogasawara K. Antiviral response by natural killer cells through TRAIL gene induction by IFN-alpha/beta. *Eur J Immunol* 2001; **31**: 3138-3146

14 **Patt YZ,** Yoffe B, Charnsangavej C, Pazdur R, Fischer H, Cleary K, Roh M, Smith R, Noonan CA, Levin B. Low serum alpha-fetoprotein level in patients with hepatocellular carcinoma as a predictor of response to 5-FU and interferon-alpha-2b. *Cancer* 1993; **72**: 2574-2582

15 **Kurokawa Y,** Matoba R, Nagano H, Sakon M, Takemasa I, Nakamori S, Dono K, Umeshita K, Ueno N, Ishii S, Kato K, Monden M. Molecular prediction of response to 5-fluorouracil and interferon-α combination chemotherapy in advanced hepatocellular carcinoma. *Clin Cancer Res* 2004; **10**: 6029-6038

Science Editor Guo SY **Language Editor** Elsevier HK

PO Box 2345, Beijing 100023, China
www.wjgnet.com
wjg@wjgnet.com

ELSEVIER

World J Gastroenterol 2005;11(36):5688-5690
World Journal of Gastroenterology ISSN 1007-9327
© 2005 The WJG Press and Elsevier Inc. All rights reserved.

• *BRIEF REPORTS* •

Malignancies associated with intraductal papillary mucinous neoplasm of the pancreas

Terumi Kamisawa, Yuyang Tu, Naoto Egawa, Hitoshi Nakajima, Kouji Tsuruta, Atsutake Okamoto

Terumi Kamisawa, Yuyang Tu, Naoto Egawa, Hitoshi Nakajima, Department of Internal Medicine, Tokyo Metropolitan Komagome Hospital, Tokyo, Japan
Kouji Tsuruta, Atsutake Okamoto, Department of Surgery, Tokyo Metropolitan Komagome Hospital, Tokyo, Japan
Correspondence to: Dr. Terumi Kamisawa, Department of Internal Medicine, Tokyo Metropolitan Komagome Hospital, 3-18-22 Honkomagome, Bunkyo-ku, Tokyo 113-8677, Japan. kamisawa@cick.jp
Telephone: +81-3-3823-2101 Fax: +81-3-3824-1552
Received: 2005-03-12 Accepted: 2005-04-02

Abstract

AIM: As intraductal papillary mucinous neoplasm (IPMN) has a favorable prognosis, associated malignancies have potential significance in these patients. We examined the incidence and characteristics of pre-existing, coexisting and subsequent malignancies in patients with IPMN.

METHODS: Seventy-nine cases of IPMN were diagnosed by detection of mucous in the pancreatic duct during endoscopic retrograde pancreatography. Histological diagnosis was confirmed in 30 cases (adenoma (n = 19) and adenocarcinoma (n = 11). Other primary malignancies associated with IPMN, occurring in the prediagnostic or postdiagnostic period, were investigated. Postdiagnostic follow-up period was 3.3±0.5 years (range, 0.2-20 years).

RESULTS: Other 40 malignancies occurred in 28 patients (35%). They were found before (n = 15), at (n = 19) and after (n = 6) the diagnosis of IPMT. Major associated malignancies were gastric cancer (n = 12), colonic cancer (n = 7), esophageal cancer (n = 4), pulmonary cancer (n = 4), and independent pancreatic cancer (n = 3). Pancreatic cancer was synchronous with IPMN in two patients and metachronous in one (3 years after diagnosis of IPMN). Thirty-one lesions were treated surgically or endoscopically. Fourteen patients died of associated cancers. Development of other malignancies was related to age (71.9±8.2 *vs* 66.8±9.3, P<0.05), but not to gender or site of the tumor.

CONCLUSION: IPMN is associated with a high incidence of other malignancies, particularly gastric and colonic cancers. Common genetic mechanisms between IPMN and other associated malignancies might be present. Clinicians should pay attention to the possibility of associated malignancies in preoperative screening and follow-up of patients with IPMN.

© 2005 The WJG Press and Elsevier Inc. All rights reserved.

Key words: Intraductal papillary mucinous neoplasms; Pancreas; Gastric cancer; Colonic cancer

Kamisawa T, Tu Y, Egawa N, Nakajima H, Tsuruta K, Okamoto A. Malignancies associated with intraductal papillary mucinous neoplasm of the pancreas. *World J Gastroenterol* 2005; 11 (36): 5688-5690
http://www.wjgnet.com/1007-9327/11/5688.asp

INTRODUCTION

Intraductal papillary mucinous neoplasm (IPMN) of the pancreas is a distinct entity characterized by intraductal papillary growth and thick mucous secretion. Copious mucous fills the main and branch pancreatic ducts and causes ductal dilatation. IPMN histologically shows a broad spectrum ranging from adenoma to invasive carcinoma. IPMN is classified into two subtypes of main duct type and branch duct type based on the site of tumor involvement. IPMN is a slow-growing tumor and many cases of branch duct type IPMN have been followed. IPMN, even when malignant, is often resectable, and has a favorable prognosis, compared with that of pancreatic ductal adenocarcinoma[1-3]. Prolonged postoperative survival can be anticipated in many IPMN cases. There are few papers reporting that IPMN is sometimes accompanied by malignant diseases of the other organs or pancreatic adenocarcinoma[4,5]. This report thus evaluates the incidence and features of associated malignancies in patients with IPMN.

MATERIALS AND METHODS

Between 1980 and 2004, 79 patients with IPMN were treated in Tokyo Metropolitan Komagome Hospital. They were diagnosed by detection of mucous in the pancreatic duct during endoscopic retrograde pancreatography. These patients comprised 54 males and 25 females, with an age of 68.5±9.2 (mean±SD) years. Twenty-three patients underwent surgical resection. Thirteen patients became unclear during follow up (1-5 years). Histological examination of the surgical (n = 23), biopsied (n = 2), and autopsied (n = 5) specimens revealed adenoma in 19 patients, non-invasive adenocarcinoma in 6, and invasive adenocarcinoma in 5. They were classified into main duct type (n = 30) and branch duct type (n = 49) based on the site of tumor involvement. Postdiagnostic follow-up period was 3.3±0.5 years (range, 0.2-20 years).

The inpatient records of these 79 patients were reviewed mainly for previous and coexisting nonpancreatic and

independent pancreatic neoplasms found at the time of diagnosis of IPMN. Furthermore, postdiagnostic follow-up data were obtained from outpatient charts.

Statistical analysis was performed using Student's *t*-test and Fisher's exact probability test. Differences were considered significant at $P<0.05$.

RESULTS

Other 40 malignancies were diagnosed in 28 (35%) of 79 patients with IPMN. They were found before ($n = 15$), at ($n = 19$) and after ($n = 6$) the diagnosis of IPMN. Major associated malignancies were gastric cancer ($n = 12$), colonic cancer ($n = 7$), esophageal cancer ($n = 4$), pulmonary cancer ($n = 4$), and independent pancreatic cancer ($n = 3$) (Table 1). Three other organs were involved in three patients, and two organs in four patients (Table 2). Double gastric cancers occurred in two patients. All of 15 other malignancies occurring 1-10 years (3.7±3.6 years) before the diagnosis of IPMN were resected surgically or endoscopically. Fifteen of nineteen other malignancies diagnosed simultaneously with IPMN were resected surgically or endoscopically. Only one other malignancy diagnosed after IPMN was surgically resected. Fourteen patients died of associated malignancies. Age at IPMN diagnosis in patients with other malignancies was significantly older than that in those without other malignancies ($P<0.05$). However, gender, follow-up period, site of IPMN, and resection of IPMN did not differ significantly between the two groups (Table 3).

Three patients had both IPMN and independent pancreatic cancer. Two patients had the two lesions synchronously, and pancreatic cancer occurred 3 years after the diagnosis of IPMN in one patient. All the three IPMNs were of branch type located in the pancreatic head and ranged from 1.5 to 3 cm. The lesion of IPMN was proximal to pancreatic cancer in two patients and distal in the other. Independence of IPMN and pancreatic cancer of two patients was proved histologically in the resected and autopsied pancreas, respectively. Two lesions were radiologically far from each other in the other patient (Figure 1). Although prognosis was poor in two patients in whom the presence of pancreatic cancer led to the diagnosis of IPMN, one patient with pancreatic cancer discovered during the follow-up of IPMN is doing well without any signs of recurrence, 36 mo after the operation (Table 4).

DISCUSSION

The incidence of occurrence of multiple primary malignant neoplasms occurring in different tissues has been reported

Table 1 Other malignacies in patients with IPMN

	Previous	At diagnosis	Post diagnosis	Total
Gastric cancer	4	7	1	12
Colonic cancer	4	3	0	7
Esophageal cancer	3	1	0	4
Pulmonary cancer	0	2	2	4
Pancreatic cancer	0	2	1	3
Breast cancer	2	0	0	2
Hepatocellular cancer	0	2	0	2
Uterine cancer	1	0	0	1
Pharyngeal cancer	1	0	0	1
Bile duct cancer	0	1	0	1
Prostatic cancer	0	1	0	1
Laryngeal cancer	0	0	1	1
Malignant lymphoma	0	0	1	1

Table 3 Clinicopathological findings of IPMN patients with and without other malignancies

	With other malignancies ($n = 28$)	Without other malignancies ($n = 51$)	*P*
Age (yr)	71.9±8.2	66.8±9.3	$P<0.05$
Male/Female	8/20	34/17	NS
Follow-up period[1]	3.2±0.5	3.4±0.5	NS
Site of IPMN			NS
Main duct	13	17	
Branch duct	15	34	
Resection/Nonresection of IPMN	7/20	16/35	NS
Cause of death			
Invasive IPMN	1	4	
Gastric cancer	4	0	
Pulmonary cancer	3	0	
Pancreatic cancer	2	0	
Colonic cancer	2	0	
Esophageal cancer	1	0	
Hepatocellular cancer	1	0	
Malignant lymphoma	1	0	
Pneumonia	1	1	
Renal failure	0	1	

Table 2 Other malignancies of more than two organs in patients with IPMN

Case	Age (yr)	Sex	Previous	At diagnosis	Postdiagnosis
1	76	M	Gastric cancer (EMR, 1 yr ago) Esophageal cancer (EMR, 1 yr ago)		Pulmonary cancer (4 yr after)
2	74	F	Uterine cancer (ope, 10 yr ago)	Hepatocellular cancer Colonic cancer	
3	70	M		Gastric cancer Colonic cancer Pulmonary cancer	
4	83	F		Esophageal cancer	Malignant lymphoma (1 yr after)
5	78	M		Hepatocellular cancer	Gastric cancer (6 yr after)
6	78	M	Esophageal cancer (EMR, 1 yr ago)		Laryngeal cancer (6 yr after)
7	68	M	Esophageal cancer (EMR, 2 yr ago)		Pancreatic cancer (3 yr after)

EMR: endoscopic mucosal resection.

Table 4 IPMN concomitant with independent pancreatic cancer

Case	Age (yr)	Sex	Syn/Met	Other malignancies	IPMN location	Site	Therapy	Pancreatic location	Cancer therapy	Stage	Prognosis
1	71	M	Syn	None	Head	Branch	None	Body	DP	III	Died 7 mo after operation
2	75	M	Syn	None	Head	Branch	None	Head	None	IV	Died 8 mo after diagnosis
3[1]	68	M	Met	Esophageal cancer	Head	Branch	PD	Head	PD	II	Alive now 3 yr after diagnosis of IPMN

Syn: synchronous, Met: metachronous, PD: pancreatoduodenectomy, DP: distal pancreatectomy. [1]: This case is the same as case 7 in Table 2.

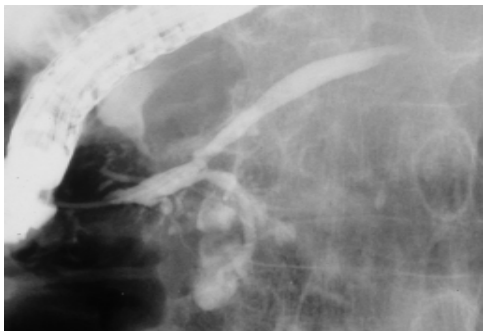


Figure 1 Endoscopic retrograde pancreatography showing branch-type intraductal papillary mucinous tumor of the pancreatic head and tapering obstruction of the main pancreatic duct involved with the concomitant pancreatic cancer of the body.

as 5.1%[6]. The incidence of other malignant neoplasms preceding, following or occurring simultaneously with the diagnosis of pancreatic cancer was reported to be 7%[4]. The present study revealed a high incidence of other malignancies (35%) in patients with IPMN. Other 40 malignancies were found before (n = 15), at (n = 19) and after (n = 6) the diagnosis of IPMN. Major associated malignancies were gastric cancer (n = 12) and colonic cancer (n = 7). Sugiyama and Atomi[4] reported that 15 (32%) of 42 patients with IPMN had nonpancreatic malignancies, including colonic cancer (n = 5) and gastric cancer (n = 4). Yamaguchi *et al*.[5], also reported that 13 (27%) of 48 patients with IPMN had malignant diseases, including gastric cancer (n = 5) and colonic cancer (n = 2). Incidence and associated other malignancies were similar to our results. In the present series, 14 patients died of associated malignancies. As IPMN is a slow-growing tumor with a relatively favorable prognosis, associated malignancies have potential prognostic significance. Systemic surveillance at the diagnosis of IPMN and careful follow-up is necessary for early detection of associated malignancies in patients with IPMN.

Interestingly, three patients with IPMN had also independent pancreatic cancer. All these IPMNs were of branch type located in the pancreatic head. The lesion of IPMN was proximal to pancreatic cancer in two patients and distal in the other. Pancreatic cancer occurred during the follow-up of IPMN could be diagnosed in relatively early stage. There is only one report describing the relationship between IPMN and pancreatic cancer[7]. In this report, independent pancreatic cancer was detected in 7 (10%) of 69 patients with IPMN, suggesting that the entire ductal epithelium of the pancreas with IPMN might already be in the premalignant condition.

The cause of frequent development of other malignancies in patients with IPMN is unknown. In the present study, age at IPMN diagnosis in patients with other malignancies was significantly older than the age in those without other malignancies. As elderly patients are more susceptible to neoplasms in most organs than younger patients and IPMN mainly affects elderly men, patients with IPMN have increased risk for other malignancies due to their age. Furthermore, oncogenetic changes of various organs of patients with IPMN might induce frequent development of other malignancies. Recent study has suggested that IPMN might form part of the spectrum of lesions encountered in attenuated familial adenomatous polyposis[8]. Common underlying genetic etiology might be present between IPMN and other associated malignancies. Further investigations focusing on this field are necessary in future.

In conclusion, IPMN is associated with a high incidence of other malignancies including pancreatic cancer. As IPMN has a relatively favorable prognosis, associated malignancies have potential prognostic significance. Clinicians should pay attention to the other associated malignancies in patients with IPMN.

REFERENCES

1 **Obara T,** Maguchi H, Saitoh Y, Itoh A, Arisato S, Ashida T, Nishino N, Ura H, Namiki M. Mucin-producing tumor of the pancreas: natural history and serial pancreatogram changes. *Am J Gastroenterol* 1993; **88**: 564-569

2 **Kimura W,** Sasahira N, Yoshikawa T, Muto T, Makuuchi M. Duct-ectatic type of mucin producing tumor of the pancreas-new concept of pancreatic neoplasia. *Hepatogastroenterology* 1996; **43**: 692-709

3 **Sugiyama M,** Atomi Y, Kuroda A. Two types of mucin-producing cystic tumors of the pancreas: diagnosis and treatment. *Surgery* 1997; **122**: 617-625

4 **Sugiyama M,** Atomi Y. Extrapancreatic neoplasms occur with unusual frequency in patients with intraductal papillary mucinous tumors of the pancreas. *Am J Gastroenterol* 1999; **94**: 470-473

5 **Yamaguchi K,** Yokohata K, Noshiro H, Chijiiwa K, Tanaka M. Mucinous cystic neoplasm of the pancreas or intraductal papillary-mucinous tumor of the pancreas. *Eur J Surg* 2000; **166**: 141-148

6 **Moertel CG,** Dockerty MB, Baggentoss AH. Multiple primary malignant neoplasms. I. Introduction and presentation of data. *Cancer* 1961; **14**: 221-230

7 **Yamaguchi K,** Ohuchida J, Ohtsuka T, Nakano K, Tanaka M. Intraductal papillary-mucinous tumor of the pancreas concomitant with ductal carcinoma of the pancreas. *Pancreatology* 2002; **211**: 484-490

8 **Chetty R,** Salahshor S, Bapat B, Berk T, Croitoru M, Gallinger S. Intraductal papillary mucinous neoplasm of the pancreas in a patient with attenuated familial adenomatous polyposis. *J Clin Pathol* 2005; **58**: 97-101

Science Editor Guo SY **Language Editor** Elsevier HK

PO Box 2345, Beijing 100023, China
www.wjgnet.com
wjg@wjgnet.com

ELSEVIER

World J Gastroenterol 2005;11(36):5691-5695
World Journal of Gastroenterology ISSN 1007-9327
© 2005 The WJG Press and Elsevier Inc. All rights reserved.

• *BRIEF REPORTS* •

Management of hepatocellular adenoma: Solitary-uncomplicated, multiple and ruptured tumors

Christian Toso, Pietro Majno, Axel Andres, Laura Rubbia-Brandt, Thierry Berney, Léo Buhler, Philippe Morel, Gilles Mentha

Christian Toso, Pietro Majno, Axel Andres, Thierry Berney, Léo Buhler, Philippe Morel, Gilles Mentha, Abdominal and Transplant Surgery, University Hospital, Geneva, Switzerland
Laura Rubbia-Brandt, Clinical Pathology, University Hospital, Geneva, Switzerland
Correspondence to: Christian Toso, Clinic of Digestive and Transplant Surgery, University Hospital, 24, rue Micheli-du-Crest, 1211 Geneva 14, Switzerland. christian.toso@hcuge.ch
Telephone: +41-22-3727702 Fax: +41-22-3727755
Received: 2004-12-10 Accepted: 2005-02-18

AIM: While hepatocellular adenomas (HAs) have often been studied as a unique entity, we aimed to better define current management of the various forms of HAs.

METHODS: Twenty-five consecutive patients operated for solitary-uncomplicated (9), multiple (6), and ruptured (10) HAs were reviewed according to management strategies and outcomes.

RESULTS: All solitary-uncomplicated HAs (ranged 2.2-14 cm in size) were removed. Out of 25 HAs, 2 (8%) included foci of carcinoma. In the multiple HA group, previously undiagnosed tumors were identified during surgery in 5/6 cases. In three cases with multiple spread HA, several lesions had to be left unresected. They remained unmodified after 4-, 6-, and 6-year radiological follow-up. Patients with ruptured HA (ranged 1.7-10 cm in size) were initially managed with hemodynamic support and angiography, allowing the embolization of actively bleeding tumors in two patients. All ruptured tumors were subsequently removed 5.5 d (range 4-70 d) after admission.

CONCLUSION: Tumors suspected of HA, regardless of the size, should be resected, because of high chances of rupture causing bleeding, and/or containing malignant foci. Although it is desirable to remove all lesions of multiple HA, this may not be possible in some patients, for whom long-term radiological follow-up is advised. Ruptured HA can be managed by hemodynamic support and angiography, allowing scheduled surgery.

© 2005 The WJG Press and Elsevier Inc. All rights reserved.

Key words: Liver; Adenoma; Management; Surgery

Toso C, Majno P, Andres A, Rubbia-Brandt L, Berney T, Buhler L, Morel P, Mentha G. Management of hepatocellular adenoma: Solitary-uncomplicated, multiple and ruptured tumors. *World J Gastroenterol* 2005; 11(36): 5691-5695
http://www.wjgnet.com/1007-9327/11/5691.asp

Hepatocellular adenomas (HAs) are generally considered as a single clinical entity, because they share a common histological appearance. However, HA can present as single or multiple tumors to be investigated in an elective setting (usually after the discovery of a silent hepatic lesion), or acutely as ruptured tumors causing right upper quadrant pain and/or intra-abdominal bleeding. Although the characteristics of HA have been described by several studies, still some controversy remains on its management. The aim of the present study is to offer a practical approach to the treatment of HA based on the various presentation forms of the disease, i.e., solitary-uncomplicated, multiple, or ruptured tumors.

From February 1980 to March 2003, 667 adults over 16-year underwent liver resection at our institution. Among them, 25 patients (3.7%) with HA represented the study population. All patients with a liver tumor compatible with a HA were operated in our hospital. No extra patient was found in the records of pathology, hepatology, and radiology.

For the purpose of the study, the patients were classified as cases with solitary-uncomplicated, multiple, and ruptured HA on the basis of clinical presentations and radiological evidences. The solitary-uncomplicated and multiple HA groups included patients with HA, but without a clinical bleeding episode. Patients with ruptured HA had clinical evidence of bleeding.

Data related to clinical picture, radiology, surgery and pathology were collected and compared between each group. Follow-up was performed in the outpatient clinic.

Over a 23-year period, 25 patients with HA were identified and included in the study. All patients were operated upon for a total of 58 HAs. Nine patients had solitary-uncomplicated (36%), 6 multiple (24%) and 10 ruptured HAs (40%). There were 23 females and 2 males, with a median age of 38 years (range, 19-55 years).

Clinical presentation

Signs and symptoms are summarized in Table 1. In the

Table 1 Clinical presentation of different forms of HA

	Solitary-uncomplicated HA	Multiple HA	Ruptured HA	Total
Cases (*n*)	9	6	10	25
No. of HA[1]	9	>39[2]	10	>58
Symptoms (no. of cases)				
None	3	3	0	6
Pain	6	3	10	19
Nausea / vomiting	3	0	5	8
Diarrhea	0	0	2	2
Asthenia	1	1	0	2
Median duration of symptoms (wk)[3]	8 (1-24)	5 (2-16)	1 (0.5-2)	2
Signs (no. of cases)				
None	6	5	0	11
Tenderness	3	1	10	14
Fever	2	0	4	6
Hepatomegaly	0	1	0	1

[1]Hepatocellular adenoma; [2]two patients presented more than 10 HA (adenomatosis); [3]median duration of symptoms up to diagnosis, excluding asymptomatic patients (three solitary-uncomplicated and three multiple HA).

solitary-uncomplicated and multiple HA groups, six patients (3/9 and 3/6, respectively) had no symptoms. Tumors were discovered because of increased liver function tests (LFT) in two, hepatomegaly in one, during laparotomy in one or at ultrasonography done for other reasons in two patients.

Twenty-two of the twenty-five patients (88%) were or had been taking exogenous sex hormones for a median duration of 9.25 years (range, 3 mo-22 years). They were equally distributed between all groups.

Laboratory findings

Seventy-two percent (18/25) of the patients had at least one increased LFT. Anemia and increased transaminases were more often associated to ruptured HA, while increased alkaline phosphatase and γ-glutamyl transpeptidase to solitary-uncomplicated and multiple HA (Table 2). Prothrombin time, albumin, and bilirubin were normal in all patients. α-Fetoprotein was normal in all nine patients in whom this marker was tested, including the two cases of HA with foci of hepatocellular carcinoma.

Table 2 Results of laboratory tests

Laboratory test (range)	Solitary-uncomplicated HA (9 cases)	Multiple HA (6 cases)	Ruptured HA (10 cases)
Anemia (Hb<12 g / dL)	4	2	7
Bilirubin (>25 μmol / L)	0	0	1
ALP (>125 μmol / L)	4	4	1
AST (>42 U / L)	0	0	4
ALT (>42 U / L)	0	0	4
γ-GT (>35 U / L)	5	3	4

ALP: alkaline phosphatase; AST: aspartate aminotransferase; AST: alanine aminotransferase; γ-GT: γ-glutamyl transpeptidase.

Radiological investigations

Ultrasonography was performed in 23 cases. Abnormal findings (a focal lesion or a hematoma) were detected in all cases, but a diagnosis of HA could never be established by ultrasonography alone. Computer tomography (CT), angiography, and magnetic resonance imaging (MRI) demonstrated possible images of HA in 3/25, 2/18, and 3/9 patients, respectively. Needle biopsy gave the correct diagnosis in five of eight cases who underwent this procedure.

Among the 10 patients with ruptured HA, no clear tumor could be identified by preoperative imaging in 7 cases, and the diagnosis of HA remained presumptive until gross examination of the resection specimen.

In patients with solitary-uncomplicated or multiple tumors (i.e., excluding patients with ruptured tumors), a correct pre-operative diagnosis could be made with radiology or liver biopsy in 9/15 cases.

Clinical management

The indication for surgery was either the presence of a possibly malignant tumor, or the preoperative diagnosis of HA. Liver resections were performed according to the principles of segmental surgery, with Kellyclasy or the ultrasonic dissector[1]. Intra-operative ultrasound was routinely performed to clarify the anatomical relationship of the known lesions and to guide the resection when the tumor could not be identified with certainty on preoperative imaging.

Patients with solitary-uncomplicated HA All the nine patients with solitary-uncomplicated HA required less extensive resections as compared to the patients of other groups (Table 3). Two HA patients (6.4 and 11.2 cm in tumor size) with tumor appearing heterogeneous on gross inspection demonstrated foci of hepatocellular carcinoma on frozen sections. In one of these patients, a local excision was extended for right hepatectomy after the results of the frozen sections. Both results on frozen section were further confirmed on paraffin-embedded sections.

Patients with multiple adenomas In these six patients, no clear diagnosis could be made before surgery, and intra-operative ultrasonography and frozen sections were performed in order to resect the largest lesions or the one most likely to be malignant. In five cases, previously unidentified tumors were discovered during the operation. In these patients, resections were extensive, involving three segments or more in four cases. A vascular exclusion maneuver was required more often in multiple HA group compared to the other groups (four hepatic inflow occlusion and one total vascular exclusion). In three cases with multiple

Table 3 Surgical management of different forms of HA

	Solitary-uncomplicated HA	Multiple HA	Ruptured HA	Total
Types of operation				
Enucleation	3	2[1,2,3]		5
Segmental resection	1	1[2]	2	4
Left hemihepatectomy	1		3	4
Hemihepatectomy (R)	4	4	4	12
Extended hemihepatectomy (R)			1	1
Median tumor size (cm, range)	6 (2.2-14)	3.05 (1.1-4)	7 (1.7-10)	5.25
Vascular exclusion (number of cases)	3	5	1	8
Median per-operative transfusions (*n*, range)	0 (0-2)	0 (0-4)	3 (1.7-10)	1.5
Median time between admission and operation (*d*, range)	3	3	5.5 (4-70)	
Median duration of post-operative hospital stay (*d*, range)	8 (6-15)	13 (7-20)	9 (8-28)	9
Complications				
Pleural effusion / atelectasis / pneumonia	1	2		3
Biliary leak		1	1	2
Pulmonary embolism			1	1
Coma	1			1

[1]Seven enucleations performed in the same patient; [2]performed in the same patient; [3]performed in an elective setting.

HA, several lesions were left unresected, and they were subsequently followed-up by yearly CT or MRI.

Patients with ruptured HA None of the 10 patients with ruptured HA was in hypovolemic shock on admission. The early management included hemodynamic monitoring and in two cases, transfusion of packed RBCs (two units in each patient). An angiography was performed in all cases of ruptured HA and in two, a vessel bleeding actively within liver parenchyma was identified and embolized. In all cases of ruptured HA, resection was delayed for a median of 5.5 d (range, 4-70 d) after presentation. In all cases, a hematoma was present in the tumor (two cases), in the liver parenchyma (six cases) or intraperitoneally (two cases). The risk of rupture was not associated with the size of the HA, and the ruptured HA ranged between 1.7 and 10 cm in size. The mean number of packed RBCs required during the operation was higher in the ruptured HA group compared to the others (Table 3).

Follow-up

The length of hospital stay was similar in all groups. There was no peri-operative death. The overall peri-operative complications rate was 28% (7/25), including three lung infections, two bile leakage (one in multiple HA and one in ruptured HA), one pulmonary embolism and one transitory coma of unknown origin, possibly due to a gas embolism on withdrawal of a central line. Both patients with foci of hepatocellular carcinoma were followed-up with a yearly CT during first 2 years and every second year thereafter, and were found to be disease-free for 2 and 11 years after surgery and without adjuvant treatment. In the three patients with multiple HA left unresected, no growth of lesion or new tumor appeared after 4, 6, and 6 years of follow-up, respectively. All other patients did not demonstrate any tumor recurrence.

The present study describes the management of the three modes of presentations of HA, such as solitary-uncomplicated, multiple, and ruptured tumors, in a series of 25 consecutive patients operated for 58 HAs.

HAs are rare tumors, representing 3.7% of all liver resections performed during the same period in our center and 10-25% of all operated benign tumors in other studies[2-4]. The various forms of presentation are often studied together according to the common pathological appearance rather than as separated clinical entities with specific presentations and deserving specific management. In addition to the solitary-uncomplicated cases, 12-42% of HA present acutely as ruptured tumors[3-5] and 8-36% are multiple tumors often requiring complex surgical decisions and procedures[3,6-10].

Management of solitary-uncomplicated HA

We defined solitary-uncomplicated HA as single adenomas without clinical or pathological evidence of bleeding on gross examination of the cut surface. In this group, the clinical challenge is the appropriate management of a solitary liver nodule and its differential diagnosis with other tumors, such as hemangioma and focal nodular hyperplasia, which, in contrary to HA, do not require surgical removal. Symptoms are non-specific, including pain that is rarely acute[2,7,10-12]. In one-third of the cases, the tumor is silent and discovered incidentally[2,11]. While LFTs are increased in many patients in the present study, they are most often normal, and do not help to identify the tumor[2,7,12,13].

Radiological investigations play a key role in detection of HA. Due to the wider use of ultrasonography to investigate a variety of abdominal conditions from uncomplicated pregnancy to non-specific abdominal pain, an increasing number of focal liver tumors are discovered accidentally. Diagnosis of HA remains difficult, with accurate tumor characterization in only 50-70% for CT, angiography, and scintigraphy[4,13,14]. These results can be explained by the highly variable radiological behaviors of HA according to the presence of steatosis, necrosis, bleeding, or malignant transformation, as well as by the similarities to some cases of focal nodular hyperplasia and fibrolamellar hepatocarcinoma. MRI appears to be more effective, and identifies HA in 75% of cases[8,12,13,15]. In the present study, the low preoperative diagnostic accuracy is explained by the long study period and the use of radiological examinations with low accuracy

for the initial patients.

In our institution, all patients suspected of having HA were operated and the outcome of conservative management could not be assessed. This is an important issue, as some studies advise resection of HA only, when they are larger than 5 cm, because of the tendency of regression of smaller HA[4,10,16,17]. However, only half of these tumors were found to regress on long-term follow-up[4], and we believe, together with others, that adenomas should be removed with an open[2,7,18,19] or laparoscopic approach[20,21], regardless of size. HA generally occur in young patients without hepatocellular dysfunction, and a resection, even major, has a mortality rate lower than 1%[2,4,6,9]. On the contrary, after rupture, resection is more complex, transfusion requirements increase and overall mortality figures up to 10% have been quoted[22-24]. Furthermore, foci of hepatocellular carcinoma have been identified within HA of any size with a prevalence of 4-16% of the cases[3,10,18,25], probably a conservative estimate, as later stages of malignant transformation can no longer be recognized as originating from HA and are diagnosed as *de novo* carcinomas. The follow-up of HA is also difficult because malignant transformation can appear without increase in size, and the tumor marker α-fetoprotein has low sensitivity[4,10,12,18,25]. Finally, the occurrence of rupture is not related to the size of HA, and can happen, as shown in our series, in HA as small as 1.7 cm.

Management of multiple HA

Multiple HAs pose a diagnostic and therapeutic challenge. A malignant lesion is difficult to be ruled out, excluding the possibility of conservative management, and in some cases, the totality of the lesions cannot be removed. Two options remain open: liver transplantation or surgical exploration with resection of the largest lesion. Transplantation is required in some symptomatic patients[9], in cases of massive or multifocal lesions, especially with an underlying metabolic disease[2,5,6,26-28]. In the other cases, such as the patients of this study, surgical exploration should be preferred, because of its lower morbidity[5,6,27]. The direct examination of liver and intra-operative ultrasonography often discover new tumors (5/6 cases in this study)[2-12]. Frozen section should be performed because of its superiority over fine needle biopsies in diagnosing the type of tumor, and its high consistency, as seen in our study, with the paraffin-embedded histological results. After identification of all tumors, if removal of all lesions is not possible, we advise surgical resection of the largest and most heterogeneous ones, and yearly radiological follow-up of the remaining lesions. In this study, three patients with unresected lesions were symptom-free without increase in tumor size after a follow-up of 4, 6, and 6 years, respectively. In cases of symptomatic patients or of tumor relapse, a further resection or transplantation should be considered.

Management of ruptured HA

Patients with ruptured HA do not represent a diagnostic challenge, because the association of acute abdominal pain (all patients in this group), increased LFTs and radiological evidence of intrahepatic or intraperitoneal bleeding often point to the diagnosis of a ruptured hepatic tumor. The differential diagnosis between a bleeding HA and hepatocellular carcinoma remains difficult in some cases, but hepatocellular carcinoma is rare in young women without underlying liver disease. The early management of all spontaneous hemorrhages, regardless of tumor origin, is the same with hemodynamic monitoring and support. Most patients are stable on admission and require only intravenous fluids and occasionally blood transfusions[22,24,29]. Rarely, patients in shock may require emergency laparotomy[29]. Angiography should be performed as soon as possible: it allows the control of a possible actively bleeding vessel (two patients in our series), and a better identification of the lesion and its blood supply, which can be helpful to establish the surgical strategy. Resection can be postponed to later in the hospital stay, when the patient has fully recovered from the bleeding episode, to minimize the surgical morbidity and to allow the contralateral part of the liver to increase size, if embolization has been performed[22,24,29,30].

In summary, the present study describes the specific presentations and managements of the different types of HA. Tumors diagnosed as or suspected of being HA should be resected, regardless of their size. Multiple tumors should be explored surgically by performing intra-operative ultrasonography and frozen sections, which are mandatory to solve the differential diagnosis of hepatocellular carcinoma and other malignant tumors. Ruptured HA are managed primarily with hemodynamic support and angiography, followed by scheduled resection.

1 **Bismuth H**. Surgical anatomy and anatomical surgery of the liver. *World J Surg* 1982; **6**: 3-9

2 **Weimann A**, Ringe B, Klempnauer J, Lamesch P, Gratz K, Prokop M, Mashek H, Tusch G, Pichlmayr R. Benign liver tumors: differential diagnosis and indications for surgery. *World J Surg* 1997; **21**: 983-991

3 **Reddy KR**, Kligerman S, Levi J, Livingstone A, Molina E, Franceschi D, Badalamenti S, Jeffers L, Tzakis A, Schiff ER. Benign and solid tumors of the liver: relationship to sex, age, size of tumors and outcome. *Am Surg* 2001; **67**: 173-178

4 **Terkivatan T**, de Wilt JH, de Man RA, van Rijn RR, Zondervan PE, Tilanus HW, Ijzermans JN. Indications and long-term outcome of treatment for benign hepatic tumors: a critical appraisal. *Arch Surg* 2001; **136**: 1033-1038

5 **Yoshidome H**, McMasters KM, Edwards MJ. Management issues regarding hepatic adenomatosis. *Am Surg* 1999; **65**: 1070-1076

6 **Leese T**, Farges O, Bismuth H. Liver cell adenomas. *Ann Surg* 1988; **208**: 558-564

7 **Belghiti J**, Pateron D, Panis Y, Vilgrain V, Fléjou JF, Benhamou JP, Fékété F. Resection of presumed benign liver tumours. *Br J Surg* 1993; **80**: 380-383

8 **Chung KY**, Mayo-Smith WW, Saini S, Rahmoui A, Golli M, Mathieu D. Hepatocellular adenoma: MR imaging features with pathologic correlation. *Am J Roentgenol* 1995; **165**: 303-308

9 **Nagorney DM**. Benign hepatic tumors: focal nodular hyperplasia and hepatocellular adenomas. *World J Surg* 1995; **19**: 13-18

10 **Ault GT**, Wren SM, Ralls PW, Reynolds TB, Stain SC. Selective management of hepatic adenomas. *Am Surg* 1996; **62**: 825-829

11 **Kerlin P**, Davis GL, McGill DB, Weiland LH, Adson MA, Sheedy PF. Hepatic adenoma and focal nodular hyperplasia: clinical, pathological, and radiologic features. *Gastroenterology* 1983; **84**: 994-1002

12 **Cherqui D**, Rahmouni A, Charlotte F, Boulahdour H, Métreau JM, Meignan M, Fagniez PL, Zafrani ES, Mathieu D,

Dhumeaux D. Management of focal nodular hyperplasia and hepatocellular adenoma in young women: a series of 41 patients with clinical, radiological, and pathological correlation. *Hepatology* 1995; **22**: 1674-1681

13 **Herman P**, Pugliese V, Machado M, Montagnini A, Salem M, Bacchella T, D'Abuquerque L, Saad W, Machado M, Pinotti H. Hepatic adenoma and focal nodular hyperplasia: differential daignosis and treatment. *World J Surg* 2000; **24**: 372-376

14 **Bartolozzi C**, Lencioni R, Paolicchi A, Moretti M, Armillotta N, Pinto F. Differentiation of hepatocellular adenoma and focal nodular hyperplasia of the liver: comparaison of power Doppler imaging and conventional color Doppler sonography. *Eur Radiol* 1997; **7**: 1410-1415

15 **Arrivé L**, Fléjou JF, Vilgrain V, Belghiti J, Najmark D, Zins M, Menu M, Tubiana JM, Nahum H. Hepatic adenoma: MR findings in 51 pathologically proved lesions. *Radiology*. 1994; **193**: 507-512

16 **Kawakatsu M**, Vilgrain V, Erlinger S, Nahum H. Disappearance of liver cell adenoma: CT and MR imaging. *Abdom Imaging* 1997; **22**: 274-276

17 **Aseni P**, Sansalone CV, Sammartino C, Di Benedetto F, Carrafiello G, Giacomoni A, Osio C, Vertemati M, Forti D. Rapid disappearance of hepatic adenoma after contraceptive withdrawal. *J Clin Garoenterol* 2001; **33**: 234-236

18 **Foster JH**, Berman MM. The malignant transformation of liver cell adenomas. *Arch Surg* 1994; **129**: 712-717

19 **Mentha G**, Rubbia-Brandt L, Howarth N, Majno P, Morel P, Terrier F. Management of focal nodular hyperplasia and hepatocellular adenoma. *Swiss Surg* 1999; **5**: 122-125

20 **Katkhouda N**, Hurwitz M, Gugenheim J, Mavor E, Mason R, Waldrep D. Laparoscopic management of benign solid and cystic lesions of the liver. *Ann Surg* 1999; **229**: 460-466

21 **Descottes B**, Glineur D, Lachachi F, Valleix D, Paineau D, Hamy A, Morino M, Bismuth H, Castaing D, Savier E, Honore P, Detry O, Legrand M, Azagra JS, Goergen M, Ceuterick M, Marescaux J, Mutter D, Hemptinne B, Troisi R, Weerts J, Dallemagne B, Jehaes C, Gelin M, Donckier V, Aerts R, Topal B, Bertrand C, Mansvelt B, Krunckelsven L, Herman D, Kint M, Totte E, Schockmel R, Gigot JF. Laparoscopic liver resection of benign liver tumors. *Surg Endosc* 2002; **17**: 668

22 **Flowers BF**, McBumey RP, Vera SR. Ruptured hepatic adenoma. A spectrum of presentation and treatment. *Am Surg* 1990; **56**: 380-383

23 **Shortell CK**, Schwartz SI. Hepatic adenoma and focal nodular hyperplasia. *Surg Gyneco Obstet* 1991; **173**: 426-431

24 **Marini P**, Vilgrain V, Belghiti J. Management of spontaneous rupture of liver tumors. *Dig Surg* 2002; **19**: 109-113

25 **Closset J**, Veys I, Peny MO, Braude P, Van Gansbeke D, Lambilliotte JP, Gelin M. Retrospective analysis of 29 patients surgically treated for hepatocellular adenoma of focal nodular hyperplasia. *Hepatogastroenterology* 2000; **47**: 1382-1384

26 **Tepetes K**, Selby R, Webb M, Madariaga JR, Iwatsuki S, Starzl TE. Orthotopic liver transplantation for benign hepatic neoplasm. *Arch Surg* 1995; **130**: 153-156

27 **Chiche L**, Doa T, Salamé E, Galais MP, Bouvard N, Schmutz G, Rousselot P, Bioulac-Sage P, Ségol P, Gignoux M. Liver adenomatosis: reappraisal, diagnosis, and management: eight new cases and review of the literature. *Ann Surg* 2000; **231**: 74-80

28 **Grazioli L**, Federla MP, Ichikawa T, Balzano E, Nalesnik M, Madariaga J. Liver adenomatosis: clinical, histopathologic, and imaging findings in 15 patients. *Radiology* 2000; **216**: 395-402

29 **Terkivatan T**, de Wilt JHW, de Man RA, van Rij RR, Tilanus HW, Ijzermans JNM. Treatment of ruptured hepatocellular adenoma. *Br J Surg* 2001; **88**: 207-209

30 **Toso C**, Rubbia-Brandt L, Negro F, Morel P, Mentha G. Hepatocellular adenoma and polycystic ovary syndrome. *Liver Int* 2003; **23**: 35-37

Science Editor Kumar M and Guo SY **Language Editor** Elsevier HK

PO Box 2345, Beijing 100023, China
www.wjgnet.com
wjg@wjgnet.com

ELSEVIER

World J Gastroenterol 2005;11(36):5696-5700
World Journal of Gastroenterology ISSN 1007-9327
© 2005 The WJG Press and Elsevier Inc. All rights reserved.

• *BRIEF REPORTS* •

*p*53 negativity, CDC25B positivity, and metallothionein negativity are predictors of a response of esophageal squamous cell carcinoma to chemoradiotherapy

Fumiko Sunada, Masayuki Itabashi, Hisanao Ohkura, Toshiyuki Okumura

Fumiko Sunada, Masayuki Itabashi, Hisanao Ohkura, Toshiyuki Okumura, Departments of Internal Medicine, Pathology, Radiology, Ibaraki Prefectural Central Hospital and Cancer Center, Koibuchi 6528, Tomobe-machi Nishiibaraki-gun, Ibaraki-ken, Japan
Correspondence to: Fumiko Sunada, MD, Department of Internal Medicine, Jichi Medical School Hospital, Yakushiji 3311, Minamikawachi-machi, Kawachi-gun, Tochigi 329-0498, Japan. f-sunada@jichi.ac.jp
Telephone: +81-285-587348 Fax: +81-285-448297
Received: 2004-12-15 Accepted: 2005-01-26

AIM: Esophageal squamous cell carcinoma is generally sensitive to chemoradiotherapy (CRT), but some cases are not. Using a retrospective analysis, we aimed to identify the predictors of the response by esophageal squamous cell carcinoma to definitive CRT.

METHODS: The intensities of expression of *p*53, Ki67, Bcl-2, Bax, cyclin D1, VEGF, CDC25B, and metallothionein (MT) were evaluated immunohistochemically in the biopsy specimens obtained before CRT, and the intensities of their expression were tested for correlations with the clinical effects of CRT.

RESULTS: The esophageal squamous cell carcinomas with negative *p*53, positive CDC25B, and negative MT expression were found to be significantly more sensitive to CRT. In addition, p53 positivity and CDC25B positivity respond well to CRT.

CONCLUSION: Esophageal squamous cell carcinomas with negative *p*53,positive CDC25B, and negative MT expressions respond well to CRT. Even with p53 positivity, if with CDC25B positivity, CRT can be expected.

© 2005 The WJG Press and Elsevier Inc. All rights reserved.

Key words: *p*53; CDC25B; Metallothionein; Chemoradiotherapy; Esophageal squamous cell carcinomas

Sunada F, Itabashi M, Ohkura H, Okumura T. *p*53 negativity, CDC25B positivity, and metallothionein negativity are predictors of a response of esophageal squamous cell carcinoma to chemoradiotherapy. *World J Gastroenterol* 2005; 11(36): 5696-5700

http://www.wjgnet.com/1007-9327/11/5696.asp

Chemoradiotherapy (CRT) is one of the most commonly used modalities of treatment for squamous cell carcinoma of the esophagus. Although the response rate to CRT with 5-fluorouracil and cisplatin is high (64%), there is no survival benefit for non-responders[1]. Hence, it would be useful to be able to predict the response to CRT so that the non-responders could avoid the side-effects of CRT. This has not been possible, however, on the basis of the clinicopathological factors that are routinely examined. Recent advances in tumor biology, especially in relation to apoptosis, offer a possible solution to this problem. Apoptosis induced by CRT involves various biological phenomena, such as DNA repair, altered drug metabolism, inflammation, molecular chaperoning and changes to the cell cycle, and a variety of biological markers, including *p*53, Ki67, Bcl-2, Bax, VEGF, cyclin D1, metallothionein (MT), and CDC25B have been investigated for an association with response to CRT[2-5]. *p*53 is a tumor suppressor gene that contributes to the preservation of genetic stability by facilitating both G_1 arrest and apoptosis in response to DNA damage[6,7]. The Bcl-2 family of proteins includes molecules with both the anti-apoptotic effects (e.g., Bcl-2 and Bcl-XL) and pro-apoptotic effects (e.g., Bax and Bak), and cell susceptibility to apoptosis has been found to be determined by competing dimerization of different members of the Bcl-2 family[8,9]. Previous studies have revealed that CDC25B, which activates CDC2 and the G_2-M progression, is significantly associated with radiation sensitivity among various molecules regulating the G_2-M checkpoint[10]. MT is an intracellular metal-binding protein involved in zinc homeostasis and the detoxification of heavy metals[11]. A study has shown that MT affects cisplatin-induced apoptosis[12]. Moreover, another recent study has reported that essential cytotoxic targets of both oxidants and heavy metals exist in the cytoplasm and establish the importance of nucleocytoplasmic partitioning for the function of MT[13], and a positive association has also been found between MT expression and resistance to CRT[14]. Thus, the purpose of our study was to identify the predictors of the response to definitive CRT with a retrospective analysis. Therefore, we have investigated a variety of biological markers, including *p*53, Ki67, Bcl-2, Bax, VEGF, cyclin D1, MT, and CDC25B.

Thirty-six patients with advanced squamous cell carcinoma of the esophagus, who refused surgery and gave informed consent to CRT at Ibaraki Prefectural Central between 1996 and 2001, were included in this study (Table 1). The diagnosis of squamous cell carcinoma was confirmed by histological examination of biopsy specimens obtained before starting CRT (the clinicopathological data are summarized in Table 1). Response to CRT was evaluated clinically after two courses and the evaluation included a barium esophagogram, esophagoscopy, and computed tomography (CT) of the chest and abdomen. A complete response was defined as no visible tumor by esophagoscopy, biopsy specimens free of tumor tissue, and normal CT findings; a partial response as >50% tumor regression as evaluated by CT, and >50% reduction of intraesophageal tumor extension assessed by barium swallow and esophagoscopy; no change as <50% regression of tumor extension, and no evidence of tumor progression; and progressive disease as increasing tumor growth indicated by barium swallow or esophagoscopy and increasing tumor diameter assessed by CT.

Table 1 Characteristics of patients (mean±SD, *n*)

Parameters	Values
Sex (male/female)	33/3
Age (range)	63.3±9.2 (42-78 yr)
Histopathology	
Well-differentiated	6
Moderately differentiated	23
Poorly differentiated	7
Stage (UICC)	
I	4
II	7
III	18
IVa	7

Chemoradiotherapy

Chemotherapy consisted of protracted infusion of 5-FU at a dose of 400 mg/m^2 per d on d 1-5 and 8-12, combined with a 2-h infusion of CDDP at 40 mg/m^2 per d on d 1 and 8, repeated twice every 5 wk. Concurrent radiotherapy was started on d 1 at 2 Gy/d for 5 d/wk. The total radiation dose was 60 Gy, with a 2-wk break after a dose of 30 Gy. The patients were followed up every 3 mo for the first 3 years after the end of treatment, and afterward every 6 mo thereafter. New chemotherapy agent (e.g., docetaxel) was applied for the patient with non-effective CRT.

Immunohistological staining and its evaluation

Immunostainings for *p*53, Ki67, Bcl-2, Bax, cyclin D1, VEGF, MT, and CDC25B were performed using streptavidin-peroxidase complex methods with an EnVision+™ peroxidase kit (Dako, Glostrup, Denmark) on a TeckMate Horizon automated staining system (Dako, Glostrup, Denmark). Primary antibodies were incubated overnight at 4 ℃ with E9 (dilution 1:50; Dako, Kyoto, Japan) for MT, and for 1 h at room temperature with DO-7 (dilution 1:50; Novocastra Laboratories, Newcastle upon Tyne, UK) for *p*53, with Ki-S5 (dilution 1:50; Dako, Kyoto, Japan) for Ki-67, with 124 (dilution 1:50; Dako, Kyoto, Japan) for Bcl-2, with A3533 (dilution 1:50; Dako, Kyoto, Japan) for Bax, with DSC-6 (dilution 1:200; Novocastra) for cyclin D1, with JH 121 (dilution 1:50; Upstate, Lake Placid, NY, USA) for VEGF, and with C45820 (5 μg/mL; Transduction Laboratories, Lexington, KY, USA) for CDC25B. The expressions of *p*53, Bcl-2, Bax, VEGF, cyclin D1, MT, and CDC25B were investigated in consecutive histological sections prepared from the biopsy specimens. After being pretreated thrice, each for 5 min, in a citrate buffer (pH 6.0) at 750 W, the slides were separately incubated overnight at 4 ℃ with the mAbs, and the expressions of *p*53, Ki-67, Bcl-2, Bax, VEGF, cyclin D1, MT, and CDC25B were assessed under light microscope by one observer (Itabashi), who was unknown about the clinical outcome. The percentages of positive tumor cells were determined semiquantitatively, and each sample was assigned to one of the following categories: negative (0-10%) and positive (11-100%). In addition, the intensities of immunostaining of antigens localized in the cytoplasm (Bcl-2, Bax, cyclin D1, VEGF, MT, and CDC25B) were classified as negative or positive. Staining intensity was not determined for *p*53 (nuclear immunostaining), because no significant differences in staining intensity were observed in the *p*53-positive cases.

Statistical analysis

Associations between two parameters were analyzed by the Spearman's rank correlation test. For continuous parameters, the difference between the two groups was analyzed by Student's *t*-test. Determination of the distribution of immunohistochemical staining between groups was analyzed using χ^2 analysis. Cumulative survival of the patients was calculated on July 31, 2002, by the Kaplan-Meier method and the statistical significance was analyzed by the log-rank test. $P<0.05$ was considered statistically significant in all analyses. All statistical analyses were performed using the StatView version 5.0 software package (Abacus Concepts, Berkeley, CA, USA).

The overall proportions of the cells positive for expression of *p*53, Bcl-2, Bax, Ki67, cyclin D1, VEGF, MT, and CDC25B were 58.3%, 27.8%, 30.6%, 86.1%, 41.7%, 58.3%, 27.8%, and 13.9%, respectively (Tables 2 and 3). Not MT negativity, but CDC25B positivity with p53 positivity is a predictor of a response to CRT (respectively p=0.39, 0.027).The median survival time of the *p*53-negative and *p*53-positive patients were 588 and 415 d, respectively ($P<0.001$, Student's *t*-test), but no significant difference was found between the survival curves of the *p*53-negative and *p*53-positive patients and esophageal cancer staging (Figures 1 and 2). However, there was a significant association between *p*53-negative and MT-negative patients and effect of CRT (Table 4). At the end of the follow-up period on July 31, 2002, 25% patients (9/36) were still alive. The follow-up time for all 36 patients ranged from 26.7 to 81 mo (median, 59.5±18.1 mo). In the group treated by CRT, there was a marked difference in mean survival time between the patients with *p*53-negative tumors (19.6±10.3 mo) and with *p*53-postive tumors (13.8±8. 6 mo). Esophageal squamous cell carcinomas relapsed in

Table 2 Relation between immunohistochemical expressions of biological markers and response of esophageal squamous cell carcinoma to CRT (*n*)

Markers	Responder (CR+PR)	Non-responder (NC+PD)	*P*
p53(-)	14	1	0.0095
p53(+)	11	10	
MT (-)	21	5	0.019
MT (+)	4	6	
CDC25B (-)	7	8	0.0129
CDC25B (+)	18	3	

Spearman's rank correlation test.
z

Table 3 Relation between expressions of biological markers and response of esophageal squamous cell carcinoma to CRT (*n*)

Markers	Responder (CR+PR)	Non-responder (NC+PD)	*P*
Bax (-)	17	8	0.799
Bax (+)	8	3	0.799
Bcl-2 (-)	18	8	0.836
Bcl-2 (+)	7	3	0.836
Cyclin D1 (-)	15	6	0.305
Cyclin D1 (+)	10	5	0.305
VEGF (-)	10	5	0.936
VEGF (+)	15	6	0.936
Ki67 (-)	4	1	0.586
Ki67 (+)	21	10	0.586

Spearman's rank correlation test.

Table 4 Relation between effects of CRT and immunohistochemical staining

	Immunoreactivity / response				*P*
*p*53	-	-	+	+	0.027
CDC25B	+	-	+	-	
Responder	9	5	9	2	
Non-responder	0	1	3	7	
MT	-	-	+	+	
0.0305					
CDC25B	+	-	+	-	
Responder	16	5	2	2	
Non-responder	2	3	1	5	

χ^2 test.

11 out of 25 (44%) responder cases after CRT.

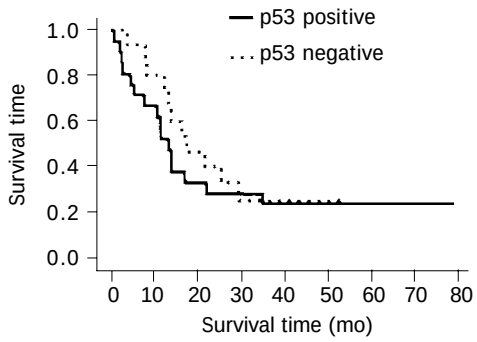


Figure 1 Cumulative survival curve of 36 patients. A significant difference that was not found was observed between the survival rates of the patients with *p*53-negative and *p*53-positive expression.

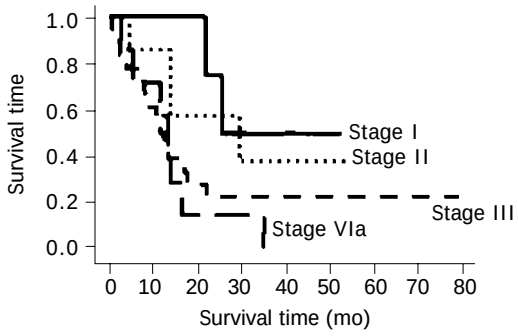


Figure 2 Relation between survival rates of 36 patients and staging of esophageal cancer. No significant difference was seen between survival curves of the *p*53-negative and *p*53-positive patients and esophageal cancer staging.

Esophageal cancer is a relatively uncommon but aggressive disease. Surgical resection has been widely accepted as the standard treatment for esophageal cancer, and techniques have improved during the past decades. However, long-term survival after resection of carcinoma of the thoracic esophagus is generally poor, with rates of only 20-42.4%[15-18]. Some reports on CRT have indicated that it offers various advantages in managing esophageal cancer[19]. Oncologists have advocated a non-surgical approach with definitive CRT as the standard treatment for this disease[20-23]. The value of CRT for the treatment of unresectable esophageal squamous cell carcinoma remains a matter of controversy. Only a few clinical studies have been published since the 1980s, and most patients in those studies had local-regional disease (UICC stage I or II). Several investigators have reported successful results with these modalities, either with or without surgery, against local-regional carcinoma[24-26]. The combination of 5-FU and CDDP has become the standard regimen, not only because of the clinical outcome but also because of the synergism between the two agents and their radiosensitizing effects[27,28]. Recently published results on CRT have indicated that it offers various advantages for the treatment of carcinoma of the esophagus[29,30]. A multicenter study on the indications for CRT as curative therapy for patients with locally advanced disease has suggested that concurrent CRT is potentially curative, even in cases of locally advanced carcinoma of the esophagus (i.e., T4 and/or M1 lymph node metastasis disease)[31]. Some studies have implicated various molecules, including *p*53, CDC25B, and MT, as candidates for biological markers for the response of human esophageal cancer to CRT[10,14]. We evaluated the role of cell-cycle-regulating molecules in the sensitivity of human squamous cell carcinoma of the esophagus to CRT by immunohistochemical methods and found *p*53, MT, and CDC25B to be significant independent markers for predicting sensitivity to CRT. Our results showed that negative

immunostaining for *p*53 in pre-CRT biopsy specimens predicted a good response. In addition to being the only established biological marker for response to CRT in clinical studies, *p*53 is the best characterized and most powerful marker[32,33], and it is commonly acknowledged to be a definite indicator of radiation sensitivity in various cancers[34,35]. The *p*53 immunoreactivity is generally thought to be attributable to the accumulation of abnormal *p*53 protein[36]. In our results, even the tumors with *p*53 positivity were sensitive to the CRT. In most of the esophageal squamous cell carcinoma, p53 are positive immunohistologically. Even with p53 positivity, CDC25B positivity respond well to CRT. So, we think that another pathway independent of *p*53 that regulate CRT sensitivity is sure to exist. G_2-M checkpoint, in which CDC25B is involved, is a candidate for this *p*53-independent pathway. Among the various molecules that regulate G_2-M arrest, overexpression of CDC25B has frequently been observed in human cancer[37,38], and also found to be related with response to CRT[10]. In our cases, no significant difference was observed between the survival curves of the *p*53-negative and *p*53-positive patients. It might be because a new chemotherapeutic agent (e.g., docetaxel) was applied for the patients with non-effective CRT. Docetaxel is an active drug for treating squamous cell carcinoma of head and neck. For the patients with recurrent or metastatic disease of squamous cell carcinoma, docetaxel could be used as a second line chemotherapy[39]. From a clinical standpoint, it is very important that a prospective study based on this result should be done. There are only retrospective studies that have been reported up to now. Standard therapy may be developed from the results of a prospective study based on the immunohistochemical characteristics of the tumor biopsy.

1 **Yano M**, Tsujinaka T, Shiozaki H, Inoue M, Doki Y, Yamamoto M, Tanaka E, Inoue T, Modern M. Concurrent chemotherapy (5-fluouracil and cisplatin) and radiation therapy followed by surgery for T4 squamous cell carcinoma of the esophagus. *J Surg Onclo* 1999; **13**: 455-460

2 **Sarbia M**, Stahl M, Fink U, Willers R, Seeber S, Gabbert HE. Expression of apoptosis-regulating proteins and outcome of esophageal cancer patients treated by combined therapy modalities. *Clin Cancer Res* 1998; **4**: 2991-2997

3 **Kitadai Y**, Amioka T, Haruma Y, Tanaka S, Yoshihara M, Sumi K, Matsutani N, Yasui W, Chayama K. Clinicopathological significance of vascular endothelial growth factor (VEGF)–C in human esophageal squamous cell carcinoma. *Int J Cancer* 2001; **93**: 662-666

4 **Rosa AR**, Schirmer CC, Gurski RR, Meurer L, Edelweiss MI, Kruel CD. Prognostic value of *p*53 protein expression and vascular endothelial growth factor expression in resected squamous cell carcinoma of the esophagus. *Dis Esophagus* 2003; **16**: 112-118

5 **Guner D**, Sturm I, Hemmati P, Hermann S, Haupmann S, Wurm R, Budach V, Dorken B, Lorenz M, Daniel PT. Multigene analysis of Rb pathway and apoptosis control in esophageal squamous cell carcinoma identifies patients with good prognosis. *Int J Cancer* 2002; **103**: 445-454

6 **el Deiry** WS, Tokino T, Velculescu VE, Levy DB, Parsons R, Trent JM, Lin D, Mercer WE, Kinzler KW, Vogelstein B. WAF1, a potential mediator of *p*53 tumor suppression. *Cell* 1993; **73**: 817-825

7 **Caelles C**, helmberg A, Karin M. *p*53-dependent apoptosis in the absence of transcriptional activation of *p*53-target genes. *Nature* 1994; **370**: 847-849

8 **Gross A**, McDonnell JM, Korsmeyer SJ. Bcl-2 family members and the mitochondria in apoptosis. *Genes Dev* 1999; **13**: 1899-1911

9 **Green DR**, Reed JC. Mitochondria and apoptosis. *Science* 1998; **281**: 5381

10 **Miyata H**, Doki Y, Shiozaki H, Inoue M, Yano M, Fujiwara Y, Yamamoto H, Nishioka K, Kishi K, Monden M. CDC25B and *p*53 are independently implicated in radiation sensivity for human esophageal cancers. *Clin Cancer Res* 2000; **6**: 4859-4865

11 **Hamer DH**. Metallothionein. *Annu Rev Biochem* 1986; **55**: 913-951

12 **Kondo Y**, Rusnak JM, Hoyt DG, Settineri CE, Pitt BR, Lazo JS. Enhanced apoptosis in metallothionein null cells. *Mol Pharmacol* 1997; **52**: 195-201

13 **Woo ES**, Lazo JS. Nucleocytoplasmic functionality of metallothionein. *Cancer Res* 1997; **57**: 4236-4241

14 **Yamamoto M**, Tsujinaka T, Shiozaki H, Doki Y, Tamura S, Inoue M, Hirao M, Monden M. Metallothionein expression correlates with the pathological response of patients with esophageal cancer undergoing preoperative chemoradiation therapy. *Oncology* 1999; **56**: 332-337

15 **Ando N**, Ozawa S, Kitagawa Y, Shinozawa Y, Kitajima M. Improvement in the results of surgical treatment of advanced squamous esophageal carcinoma during 15 consecutive years. *Ann Surg* 2000; **233**: 225-232

16 **Muller JM**, Erasmi H, Stelzner M, Zieren V, Pichlmaier H. Surgical therapy of oesophageal carcinoma. *Br J Surg* 1990; **77**: 845-857

17 **Akiyama H**, Tsurumaru M, Udagawa H, Kajiyama Y. Radical lymphnode dissection for cancer of the thoracic esophagus. *Ann Surg* 1994; **220**: 364-373

18 **Turnbull AD**, Ginsberg RJ. Options in the surgical treatment of esophageal carcinoma. *Chest Surg Clin North Am* 1994; **4**: 315-329

19 **Coia LR**. Chemoradiation as primary management of esophageal cancer. *Semin Oncol* 1994; **21**: 483-492

20 **Herskovic A**, Martz K, al-Sarraf M, Leichman L, Brindle J, Vaitkevicius V, Cooper J, Byhardt R, Davis L, Emami B. Combined chemotherapy and radiotherapy compared with radiotherapy alone in patients with cancer of the esophagus. *N Engl J Med* 1992; **326**: 1593-1598

21 **Cooper JS**, Guo MD, Herskovic A, Macdonald JS, Martenson JA Jr, Al-Sarraf M, Byhardt R, Russell AH, Beitler JJ, Spencer S, Asbell SO, Graham MV, Leichman LL. Chemoradiotherapy of locally advanced esophageal cancer: Long-term follow-up of a prospective randomized trial (RTOG 85-01). *JAMA* 1999; **281**: 1623-1627

22 **Araujo CM**, Souhami L, Gil RA, Carvalho R, Garcia JA, Froimtchuk MJ, Pinto LH, Canary PC. A randomized trial comparing radiation therapy versus concomitant radiation therapy and chemotherapy in carcinoma of the thoracic esophagus. *Cancer* 1991; **67**: 2258-2261

23 **Wilson KS**, Lim JT. Primary chemo-radiotherapy and selective oesophagectomy for oesophageal cancer: goal of cure with organ preservation. *Radiother Oncol* 2000; **54**: 129-134

24 **Leichman L**, Herskovic A, Leichman CG, Lattin PB, Steiger Z, Tapazoglou E, Rosenberg JC, Arbulu A, Asfaw I, Kinzie J. Nonoperative therapy for squamous-cell cancer of the esophagus. *J Clin Oncol* 1987; **5**: 365-370

25 **Leichman L**, Steiger Z, Seydel HG, Dindogru A, Kinzie J, Toben S, Mackenzie G, Shell J. Preoperative chemotherapy and radiation therapy for patients with cancer of the esophagus: a potentially curative approach. *J Clin Oncol* 1984; **2**: 75-79

26 **Poplin E**, Fleming T, Leichman L, Seydel HG, Steiger Z, Taylor S, Vance R, Stuckey WJ, Rivkin SE. Combined therapies for squamous-cell carcinoma of the esophagus, a Southweat Oncology Group Study (SWOG- 8037). *J Clin Oncol* 1987; **5**: 622-628

27 **Scanlon KJ**, Newman YL, Priest DG. Biochemical basis for cisplatin and 5-fluorouracil synergism in human ovarian car-

cinoma cells. *Proc Natl Acad Sci USA* 1986; **83**: 8923-8925
28 **Byfield JE**. Combined modality infusional chemotherapy with radiation. in: cancer chemotherapy by infusion, *Lokich JJ* (ed) 2nd edn. *Chicago, IL: Percepta Press* 1990: 521-551
29 **Forastiere AA**, Orringer MB, Perez-Tamayo C, Urba SG, Zahurak M. Preoperative chemoradiation followed by transhiatal esophagectomy for carcinoma of the esophagus: final report. *J Clin Oncol* 1993; **11**: 1118-1123
30 **Coia LR**. Chemoradiation as primary management of esophageal cancer. *Semin Oncol* 1994; **21**: 483-492
31 **Ohtsu A**, Boku N, Muto K, Yoshida S, Satake M, Ishikura S, Ogino T, Miyata Y, Seki S, Kaneko K, Nakamura A. Definitive chemoradiotherapy for T4 and / or M1 lymph node squamous cell carcinoma of the esophagus. *J Clin Oncol* 1999; **17**; 2915-2921
32 **Perdomo JA**, Naomoto Y, Haisa M, Fujiwara T, Yasuoka Y, Tanaka N. *In vivo* influence of *p*53 status on proliferation and chemoradiosensitivity in non-small-cell lung cancer. *J Cancer Res Clin Oncol* 1998; **124**: 10-18
33 **Shimoyama S**, Konishi T, Kawahara M, Aoki F, Harada N, Shimizu S, Murakami T, Kaminishi M. Expression and alteration of *p*53 and *p*21 (waf1/cip1) influence the sensitivity of chemoradiation therapy for esophageal cancer. *Hepatogastroenterology* 1998; **45**: 1497-1504
34 **Hamada M**, Fijiwara T, Hizuta A, Gochi A, Naomoto Y, Takakura N, Takahashi K, Roth JA, Tanaka N, Orita K. The *p*53 gene is a potent determinant of chemosensitivity and radiosensitivity in gastric and colorectal cancers. *J Cancer Res Clin Oncol* 1996; **122**: 360-365
35 **Bergh J**, Norberg T, Sjogren S, Lingren A, Holmerg L. Complete sequencing of the p53 gene provides prognostic information in breast cancer patients, particularly in relation to adjuvant systemic therapy and radiotherapy. *Nat Med* 1995; **1**: 1029-1034
36 **Begg AC**, Hofland I, Moonen L, Bartelink H, Schraub S, Bontemps P, Le Fur R, Van Den Bogaert W, Caspers R, Van Glabbeke M, Horiot JC. The predictive valve of cell kinetic measurements in a European trial of accelerated fractionation in advanced head and neck: an interim report. *Int J Radiat Oncol Bio Phys* 1990; **19**: 1449-1453
37 **Galaktinov K**, Lee AK, Eckstein J, Draette G, Meckler J, Loda M, Beach D. CDC25 phosphatases as potential human oncogenes. *Science* 1995; **269**: 1575-1577
38 **Gasparotto D**, Maestro R, Piccinin S, Vukosavljevic T, Barzan L, Sulfaro S, Boiocchi M. Overexpression of CDC25A and CDC25B in head and neck cancers. *Cancer Res* 1997; **57**: 2366-2368
39 **Calais G**. Docetaxel and squamous cell carcinoma of the head and neck. *Bull Cancer* 2004; **91**: 167-171

Science Editor Kumar M and Guo SY **Language Editor** Elsevier HK

PO Box 2345, Beijing 100023, China
www.wjgnet.com
wjg@wjgnet.com

ELSEVIER

World J Gastroenterol 2005;11(36):5701-5705
World Journal of Gastroenterology ISSN 1007-9327
© 2005 The WJG Press and Elsevier Inc. All rights reserved.

• *BRIEF REPORTS* •

Long-term results of pneumatic dilation for achalasia: A 15 years' experience

Panagiotis Katsinelos, Jannis Kountouras, George Paroutoglou, Athanasios Beltsis, Christos Zavos, Basilios Papaziogas, Kostas Mimidis

Panagiotis Katsinelos, George Paroutoglou, Athanasios Beltsis, Basilios Papaziogas, Kostas Mimidis, Department of Endoscopy and Motility Unit, Central Hospital, Thessaloniki, Greece
Jannis Kountouras, Christos Zavos, Department of Medicine, Second Medical Clinic, Aristotle University of Thessaloniki, Ippokration Hospital, Thessaloniki, Greece
Correspondence to: Jannis Kountouras, MD, PhD, Professor of Medicine, Gastroenterologist, 8 Fanariou Street, Byzantio 55133, Thessaloniki, Macedonia, Greece. jannis@med.auth.gr
Telephone: +30-2310-892238 Fax: +30-2310-992794
Received: 2005-03-18 Accepted: 2005-04-26

AIM: Although most patients with achalasia respond to pneumatic dilation, one-third experienced recurrence, and prolonged follow-up studies on parameters associated with various outcomes are scanty. In this retrospective study, we reported a 15-years' experience with pneumatic dilation treatment in patients with primary achalasia, and determined whether previously described predictors of outcome remain significant after endoscopic dilation.

METHODS: Between September 1989 and September 2004, 39 consecutive patients with primary symptomatic achalasia (diagnosed by clinical presentation, esophagoscopy, barium esophagogram, and manometry) who received balloon dilation were followed up at regular intervals in person or by phone interview. Remission was assessed by a structured interview and a previous symptoms score. The median dysphagia-free duration was calculated by Kaplan-Meier analysis.

RESULTS: Symptoms were dysphagia (n = 39, 100%), regurgitation (n = 23, 58.7%), chest pain (n = 4, 10.2%), and weight loss (n = 26, 66.6%). A total of 74 dilations were performed in 39 patients; 13 patients (28%) underwent a single dilation, 17 patients (48.7%) required a second procedure within a median of 26.7 mo (range 5-97 mo), and 9 patients (23.3%) underwent a third procedure within a median of 47.8 mo (range 37-120 mo). Post-dilation lower esophageal sphincter (LES) pressure, assessed in 35 patients, has decreased from a baseline of 35.8±10.4-10.0±7.1 mmHg after the procedure. The median follow-up period was 9.3 years (range 0.5-15 years). The dysphagia-free duration by Kaplan-Meier analysis was 78%, 61% and 58.3% after 5, 10 and 15 years respectively.

CONCLUSION: Balloon dilation is a safe and effective treatment for primary achalasia. Post-dilation LES pressure estimation may be useful in assessing response.

© 2005 The WJG Press and Elsevier Inc. All rights reserved.

Key words: Pneumatic dilation; Primary achalasia; Esophagoscopy; Barium esophagogram; Manometry

Katsinelos P, Kountouras J, Paroutoglou G, Beltsis A, Zavos C, Papaziogas B, Mimidis K. Long-term results of pneumatic dilation for achalasia: A 15 years' experience. *World J Gastroenterol* 2005; 11(36): 5701-5705
http://www.wjgnet.com/1007-9327/11/5701.asp

Achalasia is a disorder of the esophagus characterized by increased lower esophageal sphincter (LES) tone, lack of LES relaxation with swallowing and aperistalsis of the body of the esophagus. The etiology and pathogenesis of idiopathic achalasia are still unclear, although a viral cause, genetic influences (associations with HLA loci) and autoimmune processes have been postulated. Degeneration and significant loss of nerve fibers, associated with an inflammatory infiltration of the myenteric plexus in idiopathic achalasia, provide evidence of an immune-mediated destruction of the myenteric plexus, possibly through apoptotic process[1,2].

Current therapy is aimed at reducing the pressure gradient across the LES to allow passage of food. Therapeutic options for achalasia include pharmacologic therapy, surgical myotomy, mechanical rupture of LES smooth muscle by endoscopic balloon dilation, metal or plastic autoexpandable stent placement, and relaxation of the hypertonic muscles by injection of botulinum toxin, an inhibitor of acetylcholine release from nerve endings[3-6]. Drugs, including calcium-channel blockers, may be tried in mild cases, but their efficacy is modest and their side effects can be bothersome[3]. Besides, surgery has proved to be effective, although invasive[7]. In most cases therefore, gastroenterologists prefer pneumatic dilation as the first therapeutic step, due to its low cost[8] and high success rates, ranging from 70% to 90%. However, there is little information with regard to the patients' long-term course following a single pneumatic dilation or after repeated therapies[3].

In 1993, we reported our experience of 31 patients with achalasia, treated with pneumatic dilation[9]. Since then, the same patient cohort was regularly reassessed at 2-year intervals and eight patients were added until September 2004, thereby obtaining a median follow-up time of 9.3 years

(range 0.5-15 years).

The aim of the present study was to evaluate the long-term results of endoscopic balloon dilation treatment for achalasia, over a prolonged observation period.

Using records from a therapeutic endoscopy registry that has been kept in our department for a 15-year period, consecutive patients, who had undergone pneumatic dilation for achalasia from September 1989 to September 2004, were reviewed retrospectively. The diagnosis was based on clinical presentation, barium swallow contrast studies, endoscopic criteria and manometry studies. Exclusion criteria included pseudoachalasia, prior endoscopic or surgical therapy, and those with inadequate records. Patients under 14 years were also not included and they were referred to the pediatric gastrointestinal unit.

Evaluation of symptoms

Symptoms of dysphagia, retrosternal (chest) pain, regurgitation, and weight loss were evaluated at the first visit and during subsequent follow-up in the outpatient clinic of our department or by phone interview. The frequency of the symptoms was graded as following: grade 0, none; grade 1, less than once weekly; grade 2, two to three times weekly; grade 3, once daily; grade 4, more than once daily. Moreover, relative data on the effectiveness of treatment were classified as follows: (a) excellent, restoration to complete health (free of symptoms); (b) good, dysphagia or pain of short duration, defined as retrosternal hesitation of food lasting about 3 min and disappearing after drinking fluids, less than once weekly; (c) moderate, dysphagia lasting about 3 min without weight loss, more than once weekly; (d) poor, dysphagia lasting more than 3 min, accompanied by regurgitation or weight loss, more than once weekly. Clinical remission was considered as symptomatic scores of (a) and (b). Clinical recurrence in less than 3 mo following the second or subsequent dilations was considered as an indication for surgical myotomy.

Esophageal manometry

Esophageal manometry was performed in all patients after overnight fasting using a low compliance, pneumohydraulic, water infusion system (Arndofer, Medical Specialties, Milwaukee, WI, USA) and an eight lumen, manometric catheter. The catheter had four ports radially oriented (90°) near the tip and four more centrally positioned, 5 cm apart (5, 10, 15, and 20 cm from the tip). The recording sites were connected to an eight-channel polygraph (Synetics Medical AB, Stockholm, Sweden). The manometric catheter assembly was passed transnasally without any sedation into the stomach. The LES pressure was determined using the station pull through technique and recorded as the mean of four measurements at mid-respiration. Completeness of LES relaxation (normal >85%) was assessed as percent decrease from resting LES pressure to gastric baseline following wet swallows. Esophageal body motility was recorded at 3, 8, 13, and 18 cm above the LES in response to 5 mL swallows of water at 30-s intervals. LES pressures and peristalsis were determined at the time of diagnosis, and 1 mo after the dilation.

The diagnostic criteria for primary achalasia were incomplete LES relaxation and aperistalsis of the esophageal body. Once the diagnosis was confirmed, the patients were asked to choose between pneumatic dilation or Heller myotomy as treatment options and gave informed consent for the procedures; they were informed that pneumatic dilation carries a 5% perforation rate with an 80% success rate, whereas Heller myotomy generally requires 1 wk of hospitalization with 3-4 wk needed for recovery and has a 90% success rate and a 10% chance of postoperative gastroesophageal reflux. All patients chose balloon distension as an initial therapeutic procedure.

Pneumatic dilation

All dilations were performed with a Rigiflex (Microvasive, Boston Scientific Corporation, Boston, MA, USA) achalasia balloon dilator by two experienced gastroenterologists. After a liquid diet for 48 h and an overnight fast, sedation for upper gastrointestinal endoscopy was administered using intravenous pethidine (25-50 mg), diazepam (5-10 mg) and recently midazolam (2-5 mg), as required. Following complete upper gastrointestinal endoscopy to exclude malignancy or peptic strictures, a stiff guidewire was placed into the stomach through the endoscope. The balloon dilator was passed over the guidewire under endoscopic guidance and positioned at the esophagogastric junction under fluoroscopic control and partly inflated with dilute water-soluble contrast medium. The position of the catheter was adjusted so that the waist of the partly inflated balloon caused by the LES lay at the midpoint of the balloon. Maintaining the balloon catheter into position by fixation against the bite guard, the balloon was fully inflated with dilute water-soluble contrast. Full inflation was confirmed visually by the loss of the waist at the midpoint of the balloon and inflation was maintained for 1-3 min.

Because there is currently no consensus regarding the size of balloon that should be used for the dilation, the choice was solely based on the individual endoscopist's preference. A water-soluble contrast examination immediately after the dilation to look for perforation was ordered only if there was clinical suspicion of perforation.

Statistical analysis

All data were expressed as the mean±SD, and the paired *t*-test was used for statistical comparisons before and after dilation. The median dysphagia-free duration following balloon dilation was calculated by Kaplan-Meier analysis.

A total of 39 patients (17 men, 22 women) who underwent pneumatic balloon dilation for achalasia during the 15-year study period were included in the analysis. Age ranged from 27 to 87 years, with a mean age of 56±11 years. Symptoms at presentation were dysphagia (n = 39, 100%), regurgitation (n = 23, 58.7%), weight loss (n = 26, 66.6%), and chest pain (n = 4, 10.2%). The mean duration of symptoms prior to treatment was 32.1±56.2 mo (Table 1). Three patients with retrosternal pain were diagnosed as a vigorous achalasia by esophageal manometry. Thirteen patients underwent a single dilation, and 17 and 9 patients underwent 2 and 3 procedures respectively (Table 1).

Table 1 Demographic data, presenting symptoms, number of procedures and follow-up of the patients

Age (yr) [median (range)]	56 (27-87)
Gender (M/F)	17/22
Dysphagia	39 (100%)
Regurgitation	23 (58.7%)
Chest pain	4 (10.2%)
Weight loss	26 (66.6%)
Mean duration of symptoms (mo)	32.1±56.2
No of procedures	74
No of patients undergoing	
1 procedure	13
2 procedures	17
3 procedures	9
Median follow-up (yr) (range)	9.3 (0.5-15)

The choice of the balloon size was at the discretion of individual endoscopist; a 30-mm balloon-dilator was utilized in 26 of 74 procedures (35.1%), a 35-mm balloon in 39 procedures (52.8%), and a 40-mm balloon in 9 procedures (12.1%). The balloon was inflated once per procedure in 21 of 74 (28.3%) dilations and twice per procedure in 53 of 74 (72.7%). The duration of the inflation ranged from 30 s to 2 min (median 93 s) and in each procedure obliteration of the balloon "waist" was fluoroscopically noted. Upon withdrawal, traces of blood were noted on the balloon in 21 of 74 procedures (81.1%), by using 30- and 35-mm balloon dilators in 11 and 10 procedures, respectively. Four patients (5.4%) presented post-dilation esophageal perforation (Table 2), which occurred during the initial dilation with a 30-mm balloon dilator. The esophageal perforations were successfully managed with surgical intervention. In one (1.3%) patient tachycardia (120/min) and hypotension (70/40 mmHg) were developed 5 h after the procedure by using a 35-mm balloon dilator, followed by hematemesis and a drop of the Ht from 44% to 30%. After administration of crystalloids solutions and 4 units of blood, an emergency endoscopy disclosed a mucosal tear (Mallory-Weiss) 0.7 cm in length, with an overlying clot on the anterior wall of the esophagogastric junction. Bleeding stopped spontaneously and the patient's course was uneventful. The median hospital stay was 1.9 d (range 1-21 d); all four patients who underwent operation for post-dilation esophageal perforation required parenteral nutrition for 7-11 d and no mortality was recorded.

Table 2 Post-dilation complications

Perforation	4 (5.4%)
Bleeding	1 (1.3%)

A significant improvement in symptom score and LES pressure was noted 1 mo post-treatment (Table 3). The median follow-up period was 9.3 years (range 0.5-15 years) (Table 1).

The overall cumulative success rates at 5, 10, and 15 years after balloon dilation for achalasia were 78%, 61%, and 58.3% respectively (Figure 1). At their last attendance for follow-up, 20 of 29 patients (68%) complained for mild intermittent dysphagia, and 9 of 29 (32%) for moderate intermittent dysphagia.

Table 3 Symptom score and LES pressure at baseline and 1 mo after dilation

	Baseline	After 1 mo	*P*
Dysphagia	2.8±1.3	0.8±0.4	<0.01
Regurgitation	2.1±0.7	1.1±0.5	<0.01
Chest pain	1.8±1.2	1.4±0.9	<0.05
Weight loss	8.3±2.2	0.3±0.1	<0.01
LES pressure	35.8±10.4 (15-63)	10.0±7.1 (0-13)	<0.01

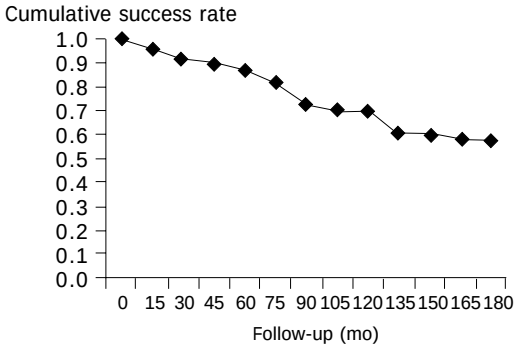


Figure 1 Cumulative success rate with pneumatic balloon dilation during the 15-yr study period.

Within the 15-year follow-up period, balloon dilation was considered to have failed in one patient, three patients died from unrelated causes and six young patients (2 men, 4 women) with a median age of 32 years (range 19-46 years) decided to undergo Heller myotomy after a median follow-up period of 34 mo (range 14-93), and could not be further contacted.

Physiologic studies have established the occurrence of denervation of the smooth muscle segment of the esophagus in patients with achalasia. A loss of ganglion cells (possibly through an apoptotic attack of T lymphocytes against nerve fibers and ganglia) in the region of the LES, particularly if the loss is predominantly of inhibitory neurons, would lead to an increased basal pressure and poor relaxation[2]. In particular, electron microscopic examination of the esophageal vagal branches reveals degeneration of myelin sheaths and disruption of axonal membranes, the valerian degenerative changes characteristic of experimental nerve transaction. Degenerative changes, including fragmentation and dissolution of nuclear material, have also been reported in ganglia of the vagal dorsal motor nucleus during the apoptotic process[10-12]. Ganglion cells degeneration in the esophageal body itself would ultimately result in permanent aperistalsis and allow for dilation of the esophagus. The damage in the LES might be the earliest event, and the aperistalsis of some early nondilated cases might be related to the obstruction of the esophagus at the level of the sphincter. After reduction in LES pressure by pneumatic dilation or myotomy in these patients, occasional peristalsis may be observed[13].

In this regard, pneumatic dilation has been the first-line therapeutic option for achalasia. The reported success rate varies widely, with figures ranging from 59% to 93% in a

review by Vaezi and Richter[14]; the differences may result from variations in the definition of success used, and in the techniques applied. The Rigiflex balloon dilator has been used in our department for the last 15 years, and data from the group of patients studied in this report compare favorably with data of previous studies, with an initial success rate of more than 80% in the 1st year and a overall cumulative success rates at 5, 10, and 15 years of 78%, 61%, and 58.3% respectively. A standardized protocol for the size of the Rigiflex dilator was not used.

The most extensive experience with objective evaluations of treatment responses after pneumatic dilation relates to determination of LES pressures[15-24]. In nine of these investigations, improvement in symptoms correlated significantly with decrease in LES pressure, and optimal response was found in patients exhibiting a post-dilation sphincter pressure of less than 10 mmHg, or of >50% reduction from baseline. With a post-dilation LES pressure of 10±7.1 mmHg achieved in our patients, the current study extends these observations by showing that post-dilation LES pressure appears to be helpful in assessing the long-term clinical response.

Apart from a significant fall in LES pressure, several authors have tried to determine other factors that predict clinical outcome following pneumatic dilation. In these studies, advanced age, a moderately dilated esophagus and a long history of symptoms prior to diagnosis were all found to predict a favorable treatment result[14,25-27], whereas male gender was found to predict a poor outcome[15]. However, the most significant factor predicting response to treatment appears to be the age at diagnosis. The results of our study with patients' advanced age (70% of cases), confirm and strengthen this observation. Although the reason for these differences in treatment remains unknown, it has been speculated that a general difference in muscle strength across the age groups may account for this observation[28].

The perforation rate with the Rigiflex balloon dilator ranges from 0% to 6.6%[29], and graded balloon dilation starting with a 30-mm balloon dilator and progressing to 35 and 40 mm if necessary appears to be the safest approach[30]. In the present series, 5.4% of dilations were complicated by perforation. Despite the common belief that dilation with a larger balloon (35 or 40 mm) increases the chance of perforation, all perforations observed in the present series occurred during the initial dilation with a 30-mm balloon dilator. In our study, gastrografin swallowing was performed following dilation only when there was clinical suspicion of perforation, despite the fact that the use of immediate contrast studies to exclude perforation had become routine in the late 1970s and that this approach is recommended in several studies and textbooks. It must be emphasized that an immediate contrast study may not always exclude a perforation that may become clinically evident several hours later[30].

Less common complications including intramural hematoma, diverticula of the gastric cardia, mucosal tears, reflux esophagitis, prolonged post-procedure chest pain, fever, hematemesis with or without changes in hematocrit, and angina may occur after pneumatic dilation[30]. In our series, a patient developed hematemesis due to a Mallory-Weiss lesion, which is an uncommon complication.

Eckardt *et al*.[16], reported that the size of the balloon dilator can predict a favorable outcome after a single dilation. In contrast, the present study suggests that the use of both 30- and 35-mm balloons exerts a similar good outcome.

Finally, there is no consensus as to whether repeated pneumatic dilations are associated with longer remission or not[31,32]. A number of studies have shown that the additional sessions of pneumatic dilations are followed by a longer duration of remission, while others believe that subsequent pneumatic dilations after the second or third dilation are less likely to result in a sustained remission, and surgical intervention should be considered for patients who have had two or three unsuccessful sessions of pneumatic dilations[15,16,24,33]. According to our clinical experience, better long-term results of pneumatic dilation can be achieved with repeated procedures, because additional procedures improve the initial success and are followed by progressively longer duration of remission.

In conclusion, this study shows that pneumatic dilation is a safe and effective treatment for achalasia, with a long duration of efficacy; once, twice and rarely thrice pneumatic dilation appears to provide good results in the majority of patients.

1 **Prakash C,** Clouse RE. Esophageal motor disorders. *Curr Opin Gastroenterol* 1999; **15:** 339-346

2 **Kountouras J,** Zavos C, Chatzopoulos D. Apoptosis and autoimmunity as proposed pathogenetic links between *Helicobacter pylori* infection and idiopathic achalasia. *Med Hypotheses* 2004; **63:** 624-629

3 **Dunaway PM,** Wong RK. Achalasia. *Curr Treat Options Gastroenterol* 2001; **4:** 89-100

4 **Cheng YS,** Li MH, Chen WX, Chen NW, Zhuang QX, Shang KZ. Selection and evaluation of three interventional procedures for achalasia based on long-term follow-up. *World J Gastroenterol* 2003; **9:** 2370-2373

5 **Zhao X,** Pasricha PJ. Botulinum toxin for spastic GI disorders: a systematic review. *Gastrointest Endosc* 2003; **57:** 219-235

6 **Wong RK.** Pneumatic dilation for achalasia. *Am J Gastroenterol* 2004; **99:** 578-580

7 **Patti MG,** Fisichella PM, Perretta S, Galvani C, Gorodner MV, Robinson T, Way LW. Impact of minimally invasive surgery on the treatment of esophageal achalasia: a decade of change. *J Am Coll Surg* 2003; **196:** 698-703

8 **O'Connor JB,** Singer ME, Imperiale TF, Vaezi MF, Richter JE. The cost-effectiveness of treatment strategies for achalasia. *Dig Dis Sci* 2002; **47:** 1516-1525

9 **Eugenidis N,** Katsinelos P, Paroutoglou G, Contizas G, Kajagidou E, Triantopoulos J. Pneumatic dilatation in the management of achalasia: experience in 31 cases. *Hellenic J Gastroenterol* 1993; **6:** 343-347

10 **Cassella RR,** Brown AL Jr, Sayre GP, Ellis FH Jr. Achalasia of the esophagus: pathologic and etiologic considerations. *Ann Surg* 1964; **160:** 474-487

11 **Kountouras J,** Kouklakis G, Zavos C, Chatzopoulos D, Moschos J, Molyvas E, Zavos N. Apoptosis, inflammatory bowel disease and carcinogenesis: overview of international and Greek experiences. *Can J Gastroenterol* 2003; **17:** 249-258

12 **Kountouras J,** Zavos C, Chatzopoulos D. Apoptosis in hepatitis C. *J Viral Hepat* 2003; **10:** 335-342

13 **Clouse RE,** Diamant NE. Esophageal motor and sensory function and motor disorders of the esophagus. In Feldman M, Friedman LS, Sleisenger MD, eds. Sleisenger and Fordtran's Gastrointestinal & Liver Disease. 7th edn, *W B Saunders Company* 2002: 561-598

14 **Vaezi MF,** Richter JE. Current therapies for achalasia: com-

parison and efficacy. *J Clin Gastroenterol* 1998; **27:** 21-35
15 **Ghoshal UC,** Kumar S, Saraswat VA, Aggarwal R, Misra A, Choudhuri G. Long-term follow-up after pneumatic dilation for achalasia cardia: factors associated with treatment failure and recurrence. *Am J Gastroenterol* 2004; **99:** 2304-2310
16 **Eckardt VF,** Aignherr C, Bernhard G. Predictors of outcome in patients with achalasia treated by pneumatic dilation. *Gastroenterology* 1992; **103:** 1732-1738
17 **Alonso P,** Gonzalez-Conde B, Macenlle R, Pita S, Vazquez-Iglesias JL. Achalasia: the usefulness of manometry for evaluation of treatment. *Dig Dis Sci* 1999; **44:** 536-541
18 **Shahi HM,** Aggarwal R, Misra A, Agarwal DK, Naik SR. Relationship of manometric findings to symptomatic response after pneumatic dilation in achalasia cardia. *Indian J Gastroenterol* 1998; **17:** 19-21
19 **Kim CH,** Cameron AJ, Hsu JJ, Talley NJ, Trastek VF, Pairolero PC, O'Connor MK, Colwell LJ, Zinsmeister AR. Achalasia: prospective evaluation of relationship between lower esophageal sphincter pressure, esophageal transit, and esophageal diameter and symptoms in response to pneumatic dilation. *Mayo Clin Proc* 1993; **68:** 1067-1073
20 **Ponce J,** Garrigues V, Pertejo V, Sala T, Berenguer J. Individual prediction of response to pneumatic dilation in patients with achalasia. *Dig Dis Sci* 1996; **41:** 2135-2141
21 **Gelfand MD,** Kozarek RA. An experience with polyethylene balloons for pneumatic dilation in achalasia. *Am J Gastroenterol* 1989; **84:** 924-927
22 **Kadakia SC,** Wong RK. Graded pneumatic dilation using Rigiflex achalasia dilators in patients with primary esophageal achalasia. *Am J Gastroenterol* 1993; **88:** 34-38
23 **Holloway RH,** Krosin G, Lange RC, Baue AE, McCallum RW. Radionuclide esophageal emptying of a solid meal to quantitate results of therapy in achalasia. *Gastroenterology* 1983; **84:** 771-776
24 **Eckardt VF,** Gockel I, Bernhard G. Pneumatic dilation for achalasia: late results of a prospective follow up investigation. *Gut* 2004; **53:** 629-633
25 **Barnett JL,** Eisenman R, Nostrant TT, Elta GH. Witzel pneumatic dilation for achalasia: safety and long-term efficacy. *Gastrointest Endosc* 1990; **36:** 482-485
26 **Katz PO,** Gilbert J, Castell DO. Pneumatic dilatation is effective long-term treatment for achalasia. *Dig Dis Sci* 1998; **43:** 1973-1977
27 **Fellows IW,** Ogilvie AL, Atkinson M. Pneumatic dilatation in achalasia. *Gut* 1983; **24:** 1020-1023
28 **Richter JE.** Comparison and cost analysis of different treatment strategies in achalasia. *Gastrointest Endosc Clin N Am* 2001; **11:** 359-370
29 **Seelig MH,** DeVault KR, Seelig SK, Klingler PJ, Branton SA, Floch NR, Bammer T, Hinder RA. Treatment of achalasia: recent advances in surgery. *J Clin Gastroenterol* 1999; **28:** 202-207
30 **Kadakia SC,** Wong RK. Pneumatic balloon dilation for esophageal achalasia. *Gastrointest Endosc Clin N Am* 2001; **11:** 325-346
31 **Sanderson DR**, Ellis FH Jr, Olsen AM. Achalasia of the esophagus: results of therapy by dilation, 1950-1967. *Chest* 1970; **58:** 116-121
32 **Parkman HP**, Reynolds JC, Ouyang A, Rosato EF, Eisenberg JM, Cohen S. Pneumatic dilatation or esophagomyotomy treatment for idiopathic achalasia: clinical outcomes and cost analysis. *Dig Dis Sci* 1993; **38:** 75-85
33 **Mikaeli J**, Bishehsari F, Montazeri G, Yaghoobi M, Malekzadeh R. Pneumatic balloon dilatation in achalasia: a prospective comparison of safety and efficacy with different balloon diameters. *Aliment Pharmacol Ther* 2004; **20:** 431-436

Science Editor Guo SY **Language Editor** Elsevier HK

PO Box 2345, Beijing 100023, China
www.wjgnet.com
wjg@wjgnet.com

ELSEVIER

World J Gastroenterol 2005;11(36):5706-5709
World Journal of Gastroenterology ISSN 1007-9327
© 2005 The WJG Press and Elsevier Inc. All rights reserved.

• *BRIEF REPORTS* •

High concentration of antimitochondrial antibodies predicts progressive primary biliary cirrhosis

Robert Flisiak, Maria Pelszynska, Danuta Prokopowicz, Magdalena Rogalska, Urszula Grygoruk

Robert Flisiak, Maria Pelszynska, Danuta Prokopowicz, Magdalena Rogalska, Urszula Grygoruk, Department of Infectious Diseases, Medical University of Bialystok, Poland
Correspondence to: Professor Robert Flisiak, Department of Infectious Diseases, Medical University of Bialystok, Bialystok 15-540, Zurawia str., 14, Poland. flisiakr@priv.onet.pl
Telephone: +48-85-7409481 Fax: +48-85-7434613
Received: 2005-01-04 Accepted: 2005-01-26

Abstract

AIM: To evaluate the serum concentration of antimitochondrial antibodies (AMAs) as a prognostic indicator of progressive primary biliary cirrhosis (pPBC).

METHODS: Serum concentrations of AMA subtypes (anti-M2, anti-M4, and anti-M9), biochemical indices of liver function and Mayo risk factor (MRF) were determined in 30 women with diagnosed primary biliary cirrhosis (PBC) selected among 348 females with elevated alkaline phosphatase but without signs of hepatic decompensation. They were followed up for 5 years for possible development of hepatic decompensation.

RESULTS: Anti-M2 concentration was significantly correlated with bilirubin and albumin levels as well as MRF, whereas anti-M4 was significantly correlated with albumin level, prothrombin time and MRF. During the 5-year follow-up, progressive PBC (pPBC) was diagnosed in 3 among 23 patients available for evaluation. These 3 patients were positive for both anti-M2 and anti-M4. Anti-M2 serum concentration exceeded 1 300 RU/mL in patients with pPBC and only in 1 among 20 non-progressive PBC persons (5%). Anti-M4 serum concentration exceeded 400 RU/mL in 2 of the progressive patients and none in the non-progressive group. In contrast, anti-M9 serum concentration was below 100 RU/mL in all patients with pPBC, and higher than 100 RU/mL in 11 women (55%) among the non-progressive group.

CONCLUSION: Females with elevated alkaline phosphatase and high anti-M2 and anti-M4 concentrations are at a high risk for developing pPBC. Quantitative AMA detection should be considered as a method for early diagnosis of pPBC.

© 2005 The WJG Press and Elsevier Inc. All rights reserved.

Key words: Primary biliary cirrhosis; Autoantibodies; Liver

Flisiak R, Pelszynska M, Prokopowicz D, Rogalska M, Grygoruk U. High concentration of antimitochondrial antibodies predicts progressive primary biliary cirrhosis. *World J Gastroenterol* 2005; 11(36): 5706-5709
http://www.wjgnet.com/1007-9327/11/5706.asp

INTRODUCTION

Primary biliary cirrhosis (PBC) is an autoimmune disease of unknown etiology leading to progressive destruction of small intrahepatic bile ducts and liver cirrhosis. It is characterized by female predominance (90%) with most cases observed between the ages of 40 and 60[1,2]. PBC incidence in different parts of the world is estimated to be 4-58 cases/million per year that can be affected by diagnostic efficacy[3-7]. Antimitochondrial antibodies (AMAs) are highly specific hallmarks for PBC diagnosis, but their prevalence in the general population and its relationship to the development of PBC are not well known[8]. Nine different types of AMAs have been described in non-hepatic and hepatic disorders. Among them only anti-M2, anti-M4, anti-M8, and anti-M9 are considered specific for PBC[9]. Retrospective studies have reported that subtypes of AMAs can discriminate between a benign and a progressive course of the disease[9,10]. However, it was recently reported that profiles can predict PBC prognosis[11]. All these studies focused on qualitative evaluation of AMA subtypes whereas quantitative measurement was not investigated for PBC management.

This study was to evaluate the serum concentration of different types of AMAs as a prognostic indicator of progressive PBC (pPBC).

MATERIALS AND METHODS

Patients

Thirty women aged between 30 and 65 years with diagnosed PBC were selected among 348 females with elevated alkaline phosphatase (ALP) activities at admission to the Liver Unit of the Department of Infectious Diseases, Medical University of Bialystok in 1999. PBC diagnosis was established according to American Association for the Study of Liver Disease (AASLD) Practice Guidelines and the presence of AMAs, elevated ALP and normal bile ducts on ultrasound[12]. All 30 patients demonstrated normal activities of serum alanine transaminase and no clinical signs of liver disease decompensation (jaundice, pruritus, ascites, encephalopathy, and shank edema). Further evaluations performed in PBC patients included quantitative measurement of serum concentration of AMA subtypes (anti-M2, anti-M4,

and anti-M9). Mayo risk factor (MRF) usually applied for estimation of PBC patient survival probability was also determined. Among these 30 patients, only 23 became available for evaluation during the 5-year follow-up. Patients who demonstrated clinical signs of hepatic decompensation were identified as having pPBC. In contrast, patients without any signs of decompensation during the follow-up were diagnosed as non-progressive PBC (nPBC). Baseline results were analyzed for the diagnosis of pPBC or nPBC within the follow-up period. Ethical approval for the study was obtained from the Bioethical Committee of the Medical University of Bialystok.

AMA measurement

Serum concentration of AMA subtypes was determined by ELISA (Euroimmun, Lubeck, Germany) for human autoantibodies of the IgG class against the mitochondrial antigens M2 (pyruvate dehydrogenase complex), M4 (sulfite oxidase) and M9 (glycogen phosphorylase). For qualitative evaluation, serum samples with extinction values exceeding the recommended cut-off level (20 RU/mL) for at least one subtype of AMAs were considered positive. Quantitative determination of AMA subtype serum concentration was performed using calibration sera provided by the manufacturer.

Liver function tests

Bilirubin and albumin concentrations were determined using a Cobas Mira instrument (Roche) and the prothrombin time (PT) was detected using Kselmed K-3002 (Poland). MRF was calculated according to the formula of Dickson *et al*.[13], based on the following variables: age, bilirubin and albumin concentration, PT, presence of peripheral edema and diuretic treatment.

Statistical analysis

Values were expressed as mean±SE. The significance of difference was calculated by two-tailed Student's *t*-test. For correlation analysis, the Pearson product moment correlation was performed. $P<0.05$ was considered to be statistically significant.

RESULTS

Among the screened 348 women, quantitative evaluation of AMA demonstrated positive results in 30 (8.6%). Anti-M2 was demonstrated in 13 (3.7%), including 5 (1.4%) with accompanying anti-M4. The remaining 8 women (2.3%) were positive only for anti-M2. In the other 5 (1.4%) women, the only anti-M9 was demonstrated. Anti-M4 without any other AMA was present in sera of 12 women (3.4%, Table 1). Quantitative evaluation demonstrated significantly higher concentrations of all three types of AMAs in persons with at least one type of AMAs present in qualitative evaluation (Table 2). As demonstrated in Table 3, anti-M2 concentration was significantly correlated with bilirubin and albumin levels as well as MRF, whereas anti-M4 was significantly correlated with albumin level, PT, and MRF. Anti-M9 was not correlated to any of these parameters.

During the 5-year follow-up, clinical signs of hepatic decompensation were demonstrated in 3 among 23 patients available for evaluation, and they were recognized as having pPBC. The remaining 20 patients were diagnosed as nPBC. All three women were positive for both anti-M2 and anti-M4. Anti-M2 serum concentration exceeded 1 300 RU/mL in all pPBC women and only in 1 among 20 nPBC patients (5%). Anti-M4 serum concentration exceeded 400 RU/mL in 2 pPBC patients and in none of the nPBC patients. Anti-M9 serum concentration was below 100 RU/mL in all pPBC patients, and was higher than 100 RU/ml in 11 nPBC patients (55%). As demonstrated in Table 4, the mean concentrations of anti-M2 and anti-M4 were about five times higher in pPBC patients than in nPBC patients, however statistical significance was shown only with respect to anti-M2. The mean concentration of anti-M9 was two-fold higher in nPBC patients (Table 4). As demonstrated in Table 5, the difference found in both groups in relation to biochemical indices of liver injury and MRF was not statistically significant.

Table 1 Profiles of AMAs in 348 screened women

	n	%
Anti-M2	8	2.3
Anti-M4	12	3.4
Anti-M9	5	1.4
Anti-M2+Anti-M4	5	1.4
Any AMA	30	8.6

Table 2 Serum concentrations of different types of AMAs in women with positive (at least one type of AMAs present) or negative AMAs (mean±SE)

	Qualitative AMAs		*P*
	Positive	Negative	
Anti-M2 (RU/mL)	378.1±96.8	6.1±1.3	3×10^{-15}
Anti-M4 (RU/mL)	140.5±27.7	18.1±1.9	2×10^{-17}
Anti-M9 (RU/mL)	112.5±25.9	35.8±3.8	2×10^{-7}

Table 3 Correlation between AMA concentration and biochemical indices of liver injury and Mayo risk score in asymptomatic AMA positive women

	Anti-M2	Anti-M4	Anti-M9
Bilirubin	0.410[a]	0.339	0.011
Albumin	–0.500[a]	–0.406[a]	0.119
PT	0.321	0.514[a]	0.002
Mayo risk score	0.415[a]	0.572[a]	–0.088

[a]$P<0.05$.

Table 4 Serum concentrations of different types of AMAs in patients with pPBC or nPBC during 5-year follow-up (mean±SE)

	pPBC	nPBC	*P*
Anti-M2 (RU/mL)	1 399±48	265±81	6×10^{-12}
Anti-M4 (RU/mL)	474±149	103±17	0.09
Anti-M9 (RU/mL)	49±15	120±28	0.03

Table 5 Serum concentrations of bilirubin and albumin, PT, and MRF value in patients with pPBC or nPBC during 5-year follow-up (mean±SE)

	pPBC	nPBC	*P*
Bilirubin (mg%)	2.2±1.1	0.76±0.1	0.241
Albumin (g%)	2.7±0.2	3.5±0.1	0.027
PT (s)	17.0±0.8	14.7±0.2	0.056
Mayo risk score	7.2±0.8	4.8±0.2	0.058

DISCUSSION

According to AASLD Practice Guidelines, the diagnosis of PBC can be made in AMA positive patients with biochemical evidence of cholestasis, and normal biliary system in ultrasound examination. In these patients, a liver biopsy is not essential to make the PBC diagnosis[12].

The prevalence of AMAs in the general population is usually estimated below 1%. According to recent studies AMAs are detected in 0.64% Japanese and 0.16% Chinese workers who have an annual health check[8]. Sakugawa *et al*.[14], demonstrated that 6 AMA among 122 women with elevated γ-glutamyl transpeptidase levels (4.9%) are positive for AMAs. The prevalence of AMAs in our study, that varied from 3.7% (anti-M2 positive) to 8.6% (any positive AMA subtype), was due to inclusion of Caucasian women aged 30-65 years with elevated ALP[3-6]. However, the purpose of this study was not to demonstrate AMA prevalence, but to capture as many asymptomatic AMA positive women as possible.

Progressive PBC can be predicted even at its early stages when antibodies against M2 and M4 are present in patient sera[9]. In our study the three patients with PBC progression during follow-up, were positive for both anti-M2 and anti-M4, suggesting that the presence of anti-M2 plus anti-M4 profile in asymptomatic persons can predict pPBC. Concentrations of these antibodies were significantly higher in pPBC than in nPBC. However, this profile demonstrated that in PBC patients, it is not possible to predict fatal prognosis, and the proportion of patients, who died of liver disease or transplantation does not differ among the AMA profiles[11].

Anti-M2 serum levels in PBC patients are closely associated with the degree of liver insufficiency[15]. There is a significant correlation between Child-Pugh and Mayo scores and both are useful for the estimation of survival probabilities[16]. Our study also confirmed this observation with respect to asymptomatic AMA positive women, because there was a significant correlation between serum concentrations of anti-M2 or anti-M4 and bilirubin, albumin or PT values. Moreover, in this association we also demonstrated regarding the MRF. Prince *et al*.[17], have shown that patient age, alkaline phosphatase, albumin, and bilirubin as well as Mayo prognostic score at diagnosis can independently predict survival. However, according to Krzeski *et al*.[18], the Mayo model overestimates death risk in PBC patients, and serum bilirubin concentration appears to be the only variable of prognostic importance. Corpechot *et al*.[19], demonstrated that elevated bilirubin and decreased albumin are predictive factors for cirrhosis development under ursodeoxycholic acid treatment. We demonstrated a significant difference only regarding albumin among possible biochemical and clinical predictive factors. However, the most important factor for pPBC development is the high level of anti-M2 and anti-M4 antibodies in sera of asymptomatic persons. Similar results but without quantitative AMA evaluation are demonstrated by Kisand *et al*.[20]. According to our results, serum concentration of anti-M2 exceeding 1 300 RU/mL and anti-M4 exceeding 400 RU/mL are critical for detection of pPBC. However, border-line levels need to be validated in a larger number of patients.

In conclusion, persons with elevated ALP and high concentrations of anti-M2 and anti-M4 are at a high risk of developing pPBC. Quantitative detection of these antibodies should be considered as a method for early diagnosis of pPBC.

REFERENCES

1 **Selmi C,** Invernizzi P, Keeffe EB, Coppel RL, Podda M, Rossaro L, Ansari AA, Gershwin ME, Keefe EB. Epidemiology and pathogenesis of primary biliary cirrhosis. *J Clin Gastroenterol* 2004; **38**: 264-271

2 **Sherlock S.** Primary biliary cirrhosis, primary sclerosing cholangitis, and autoimmune cholangitis. *Clin Liver Dis* 2000; **4**: 97-113

3 **Kim WR,** Lindor KD, Locke GR 3rd, Therneau TM, Homburger HA, Batts KP, Yawn BP, Petz JL, Melton LJ 3rd, Dickson ER. Epidemiology and natural history of primary biliary cirrhosis in a US community. *Gastroenterology* 2000; **119**: 1631-1636

4 **Parikh-Patel A,** Gold EB, Worman H, Krivy KE, Gershwin ME. Risk factors for primary biliary cirrhosis in a cohort of patients from the United States. *Hepatology* 2001; **33**: 16-21

5 **Prince MI,** James OF. The epidemiology of primary biliary cirrhosis. *Clin Liver Dis* 2003; **7**: 795-819

6 **James OF,** Bhopal R, Howel D, Gray J, Burt AD, Metcalf JV. Primary biliary cirrhosis once rare, now common in the United Kingdom? *Hepatology* 1999; **30**: 390-394

7 **Boberg KM,** Aadland E, Jahnsen J, Raknerud N, Stiris M, Bell H. Incidence and prevalence of primary biliary cirrhosis, primary sclerosing cholangitis, and autoimmune hepatitis in a Norwegian population. *Scand J Gastroenterol* 1998; **33**: 99-103

8 **Shibata M,** Onozuka Y, Morizane T, Koizumi H, Kawaguchi N, Miyakawa H, Kako M, Mitamura K. Prevalence of antimitochondrial antibody in Japanese corporate workers in Kanagawa prefecture. *J Gastroenterol* 2004; **39**: 255-259

9 **Berg PA,** Klein R. Antimitochondrial antibodies in primary biliary cirrhosis and other disorders: definition and clinical relevance. *Dig Dis* 1992; **10**: 85-101

10 **Bunn CC,** McMorrow M. Anti-M4 antibodies measured by a sulphite oxidase ELISA in patients with both anti-centromere and anti-M2 antibodies. *Clin Exp Immunol* 1995; **102**: 131-136

11 **Joshi S,** Cauch-Dudek K, Heathcote EJ, Lindor K, Jorgensen R, Klein R. Antimitochondrial antibody profiles: are they valid prognostic indicators in primary biliary cirrhosis? *Am J Gastroenterol* 2002; **97**: 999-1002

12 **Heathcote EJ.** Management of Primary Biliary Cirrhosis. *Hepatology* 2000; **31**: 1005-1013

13 **Dickson ER,** Grambsch PM, Fleming TR, Fisher LD, Langworthy A. Prognosis in primary biliary cirrhosis: model for decision making. *Hepatology* 1989; **10**: 1-7

14 **Sakugawa H,** Nakasone H, Nakayoshi T, Yamashiro T, Maeshiro T, Kobashigawa K, Kinjo F, Saito A, Zukeran H, Nakanuma Y, Ohba K. Epidemiology of primary biliary cirrhosis among women with elevated gamma-glutamyl transpeptidase levels in Okinawa, Japan. *Hepatol Res* 2003; **26**: 330-336

15 **Flisiak R,** Wierciñska-Drapa³o A, Prokopowicz D. Antibodies against M2 antigen in differential diagnosis of primary biliary cirrhosis. *Pol Merk Lek* 2000; **8**: 373-375
16 **Reisman Y,** van Dam GM, Gips CH, Lavelle SM, Euricterus PM. Survival probabilities of Pugh-Child-PBC classified patients in the euricterus primary biliary cirrhosis population, based on the Mayo clinic prognostic model. Euricterus Project Management Group. *Hepatogastroenterology* 1997; **44**: 982-989
17 **Prince M,** Chetwynd A, Newman W, Metcalf JV, James OF. Survival and symptom progression in a geographically based cohort of patients with primary biliary cirrhosis: follow-up for up to 28 years. *Gastroenterology* 2002; **123**: 1044-1051
18 **Krzeski P,** Zych W, Kraszewska E, Milewski B, Butruk E, Habior A. Is serum bilirubin concentration the only valid prognostic marker in primary biliary cirrhosis? *Hepatology* 1999; **30**: 865-869
19 **Corpechot C,** Carrat F, Poupon R, Poupon RE. Primary biliary cirrhosis: incidence and predictive factors of cirrhosis development in ursodiol-treated patients. *Gastroenterology* 2002; **122**: 652-658
20 **Kisand KE,** Metskula K, Kisand KV, Kivik T, Gershwin ME, Uibo R. The follow-up of asymptomatic persons with antibodies to pyruvate dehydrogenase in adult population samples. *J Gastroenterol* 2001; **36**: 248-254

Science Editor Wang XL and Guo SY **Language Editor** Elsevier HK

PO Box 2345, Beijing 100023, China
www.wjgnet.com
wjg@wjgnet.com

ELSEVIER

World J Gastroenterol 2005;11(36):5710-5713
World Journal of Gastroenterology ISSN 1007-9327
© 2005 The WJG Press and Elsevier Inc. All rights reserved.

• *BRIEF REPORTS* •

Effects of variant UDP-glucuronosyltransferase *1A1* gene, glucose-6-phosphate dehydrogenase deficiency and thalassemia on cholelithiasis

Yang-Yang Huang, Ching-Shui Huang, Sien-Sing Yang, Min-Shung Lin, May-Jen Huang, Ching-Shan Huang

Yang-Yang Huang, May-Jen Huang, Department of Laboratory Medicine, Cathay General Hospital, Taipei, Taiwan, China
Ching-Shui Huang, Department of General Surgery, Cathay General Hospital, Taipei, Taiwan, China
Sien-Sing Yang, Department of Liver Unit, Cathay General Hospital, Taipei, Taiwan, China
Min-Shung Lin, Department of Family Medicine, Cathay General Hospital, Taipei, Taiwan, China
Ching-Shan Huang, Department of Medical Technology, Fooyin University, Kaohsiung, Taiwan, China
Supported by a grant from the Cathay Medical Research Center, Taipei, Taiwan, China
Correspondence to: Professor Ching-Shan Huang, Department of Medical Technology, Fooyin University, Kaohsiung, Taiwan, China. chsh.huang@msa.hinet.net
Telephone: +886-22-6360450 Fax: +886-28-87725983
Received: 2005-01-09 Accepted: 2005-04-09

Abstract

AIM: To test the hypothesis that the variant UDP-glucuronosyltransferase *1A1* (*UGT1A1*) gene, glucose-6-phosphate dehydrogenase (G6PD) deficiency, and thalassemia influence bilirubin metabolism and play a role in the development of cholelithiasis.

METHODS: A total of 372 Taiwan Chinese with cholelithiasis who had undergone cholecystectomy and 293 healthy individuals were divided into case and control groups, respectively. PCR and restriction fragment length polymorphism were used to analyze the promoter area and nucleotides 211, 686, 1 091, and 1 456 of the *UGT1A1* gene for all subjects and the gene variants for thalassemia and G6PD deficiency.

RESULTS: Variation frequencies for the cholelithiasis patients were 16.1%, 25.8%, 5.4%, and 4.3% for $A(TA)_6$ TAA/$A(TA)_7$TAA (6/7), heterozygosity within the coding region, compound heterozygosity, and homozygosity of the *UGT1A1* gene, respectively. Comparing the case and control groups, a statistically significant difference in frequency was demonstrated for the homozygous variation of the *UGT1A1* gene ($P = 0.012$, χ^2 test), but not for the other variations. Further, no difference was demonstrated in a between-group comparison of the incidence of G6PD deficiency and thalassemia (2.7% *vs* 2.4% and 5.1% *vs* 5.1%, respectively). The bilirubin levels for the cholelithiasis patients with the homozygous variant-*UGT1A1* gene were significantly different from the control analog (18.0±6.5 and 12.7±2.9 μmol/L, respectively; $P<0.001$, Student's *t* test).

CONCLUSION: Our results show that the homozygous variation in the *UGT1A1* gene is a risk factor for the development of cholelithiasis in Taiwan Chinese.

© 2005 The WJG Press and Elsevier Inc. All rights reserved.

Key words: *UGT1A1* gene; G6PD deficiency; Thalassemia; Cholelithiasis

Huang YY, Huang CS, Yang SS, Lin MS, Huang MJ, Huang CS. Effects of variant UDP-glucuronosyltransferase *1A1* gene, glucose-6-phosphate dehydrogenase deficiency and thalassemia on cholelithiasis. *World J Gastroenterol* 2005; 11(36): 5710-5713
http://www.wjgnet.com/1007-9327/11/5710.asp

INTRODUCTION

The life span of erythrocytes in individuals with chronic hemolytic disease is short relative to normal subjects. The accelerated red-cell turnover produces more bilirubin and is probably a risk factor for the development of gallstones. Cholelithiasis has been detected in 38% of subjects with chronic hemolytic anemia due to glucose-6-phosphate dehydrogenase (G6PD) deficiency[1]. It has been demonstrated that G6PD-deficient subjects without chronic hemolytic anemia also have a higher frequency of cholelithiasis development than normal individuals[1]. Because the enzyme UDP-glucuronosyltransferase 1A1 (UGT1A1) catalyzes unconjugated bilirubin into the diglucuronidated and conjugated forms, UGT1A1 defects decrease the elimination of bilirubin[2]. Genetic variation in the *UGT1A1* gene promoter, $A(TA)_7$TAA, instead of $A(TA)_6$TAA influences bilirubin levels causing hyperbilirubinemia, which is associated with Gilbert's syndrome in Caucasians[2]. Further, it has been determined that *UGT1A1* gene expression is a major modifying factor for bilirubin levels in heterozygous β-thalassemia[3] and that cholelithiasis is one of the manifestations of thalassemia[4].

In a previous study of the *UGT1A1* gene in Taiwan Chinese[5], we found that occurrence of the $A(TA)_7$TAA allele in the promoter area was relatively rare (14.3% *vs* 40%) and that the variation rate within the coding region was much higher (29.3% *vs* 0.1%) relative to Caucasians[2], respectively. The aim of this study was to analyze variations in the promoter area and coding region in the *UGT1A1* gene in Taiwan Chinese patients with cholelithiasis. The incidence and genetic expression of G6PD deficiency in

these subjects was also investigated. Additionally, we studied the genetic alteration of thalassemia. Variations in the *UGT1A1*, *G6PD* and thalassemia genes were compared with those of normal subjects. To our knowledge, this is the first report elucidating the relationship between these three genes and cholelithiasis.

MATERIALS AND METHODS

Study subjects, healthy controls, and laboratory tests

The study subjects (157 males and 215 females) were selected from Taiwan Chinese adults who had undergone cholecystectomy for symptomatic gallstone. Healthy controls (135 males and 158 females) were selected from adults who had undergone physical examination at Cathay General Hospital as previously described[5]. The control subjects were investigated for cholelithiasis by abdominal ultrasonography (model SSD-1700, Aloka Co., Tokyo, Japan) and no change in abdomen was determined with respect to gallstones. Blood samples were collected from all subjects in the morning after 10-12 h of fasting. An automatic cell-counter (NE 9000, Sysmex Co., Kobe, Japan) was used for hematology testing, and erythrocyte G6PD activity was quantitatively measured using the enzyme-coupled method[6]. G6PD deficiency was confirmed by polymerase chain reaction-restriction fragment length polymorphism (PCR-RFLP)[7]. The 15 single-nucleotide mutations, restriction enzymes, and restriction-fragment results are listed in Table 1, with priority arranged in descending order of mutation frequency of our Taiwan Chinese sample population[7]. The promoter area and nucleotides 211, 686, 1 091, and 1 456 of the *UGT1A1* gene were amplified by PCR and analyzed using RFLP[8]. The restriction enzymes and restriction-fragment results are listed in Table 2. Mean corpuscular volume $\leqslant$80 fL, the gene variants for α- and β-thalassemia were identified using PCR-RFLP[9,10].

Comparison of bilirubin values

Serum bilirubin levels were measured using an autoanalyzer (model 747, Hitachi Co., Tokyo, Japan). The bilirubin values in cholelithiasis patients with statistically significant differences in gene frequency relative to controls were obtained from the records made 2-3 mo after cholecystectomy and compared with that in the control group.

Statistical analysis

The χ^2 test, with or without Yate's correction, and Student's *t* test were used to analyze the data as appropriate. A *P* value less than 0.05 was defined as statistically significant.

RESULTS

G6PD deficiency was confirmed for 4 of the 157 males (2.5%) and 6 of the 215 females (2.8%) cholelithiasis patients, with respective gender distribution as follows: hemizygous 493, 871, 1 024, and 1 388 (n = 1 each), and heterozygous 1 376 (n = 5) and heterozygous 1 388 (n = 1) (data not shown in Tables). There was no significant between-gender difference in incidence of G6PD deficiency. Analysis of pooled data showed an overall incidence of G6PD deficiency of 2.7% (10/372) for the cholelithiasis group. The frequencies of the *UGT1A1* genotypes are presented in Table 3. Less than half (48.4%) of the cholelithiasis patients carried the wild genotype. The variation frequencies for A(TA)$_6$TAA/A(TA)$_7$TAA (6/7), heterozygosity within the coding region, compound heterozygosity, and homozygosity were 16.1%, 25.8%, 5.4%, and 4.3%, respectively. The incidence of thalassemia in the cholelithiasis patients was 5.1% (19/372) [heterozygous α-thalassemia 2.7% (n = 10); heterozygous β-thalassemia 1.6% (n = 6); homozygous β-thalassemia 0.53% (n = 2); and heterozygous α-thalassemia plus heterozygous β-thalassemia 0.27% (n = 1)] (detailed data not shown in Tables). Analysis for the combination of G6PD deficiency, homozygous variation in the *UGT1A1* gene, and presence of thalassemia revealed that two cholelithiasis patients carried the 211 G→A/211 G→A *UGT1A1* and the heterozygous α-thalassemia genes (data not shown in Tables).

Clinical data for the cholelithiasis patients and healthy controls are compared in Table 3. There was no difference in gender distribution, neither in the mean of age, comparing the two groups. A significant difference was demonstrated comparing the frequency of homozygous variation (7/7, 211 G→A/211 G→A, and 686 C→A plus 7/7) of the *UGT1A1* gene for the case and control groups (P = 0.012, χ^2 test), while those for the other three variation types were not statistically meaningful. There was no significant between-group difference in the incidence of G6PD deficiency and thalassemia (2.7% *vs* 2.4% and 5.1% *vs* 5.1%, respectively). Nine (56.3%) of the 16 cholelithiasis patients

Table 1 Fifteen single nucleotide mutations of G6PD deficiency in Taiwan Chinese

Mutation site	Restriction enzyme	Restriction fragment (bp)	
		Normal	Mutant
1 376 G→T	*Afl*II	214	194, 20
1 388 G→A	*Nde*I	227	206, 21
493 A→G	*Ava*II	120, 11	87, 33, 11
1 024 C→T	*Mbo*II	187	150, 37
95 A→G	*Mlu*I	198	174, 24
392 G→T	*Bst*EII	188, 15	203
871 G→A	*Bg*III	118	94, 24
487 G→A	*Hin*dIII	104	82, 22
519 C→G	*Sty*I	300	189, 111
835 A→T	*Taq*I	185	164, 21
1 360 C→T	*Hha*I	142, 45, 27	187, 27
592 C→T	*Pst*I	157, 83	157, 63, 20
517 T→C	*Xho*I	134	114, 20
1 004 C→A	*Hha*I	49, 20	69
1 387 C→T	*Hha*I	105, 22	127

Table 2 Variations of the *UGT1A1* gene

Variation site	Restriction enzyme	Restriction fragment (bp)	
		Normal	Variant
211 G→A	*Ava*II	128, 18	146
686 C→A	*Bsr*I	374, 51	242, 132, 51
1 091 C→T	*Bcl*I	209	190, 19
1 456 T→G	*Ava*II	270	197, 73
Promoter		77	79

Table 3 Comparison of clinical data for cholelithiasis patients and healthy controls

	Cholelithiasis patients (n = 372)		Control group (n = 293)		P (χ^2 test) (for age by student's t test)
	n	%	n	%	
Gender (M/F)	157/215		135/158		NS
Age (yr, mean±SD)	53.0±14.9		51.5±10.6		NS
UGT1A1 genotype					
Wild type	180	48.4	143	48.8	NS
Heterozygous variation in promoter area (6/7)	60	16.1	60	20.5	NS
Heterozygous variation within coding region	96	25.8	64	21.8	NS
211 G→A/normal	89		57		
1 091 C→T/normal	6		7		
1 456 T→G/normal	1				
Compound heterozygous variation	20	5.4	23	7.9	NS
6/7, 211 G→A/normal	10		4		
6/7, 686 C→A/normal	8		14		
6/7, 1 091 C→T/normal			1		
6/7, 211 G→A/normal, 686 C→A/ normal			1		
6/7, 686 C→A/normal, 1 091 C→T/normal	1		1		
211 G→A/normal, 1 091 C→T/ normal	1		1		
Homozygous variation	16	4.3	3	1.0	0.012
7/7	5				
211 G→A /G→A	4		3		
7/7, 686 C→A /normal	7		0		
G6PD deficiency	10	2.7	7	2.4	NS
Thalassemia	19	5.1	15	5.1	NS

6/7: $A(TA)_6TAA/A(TA)_7TAA$, 7/7: $A(TA)_7TAA/A(TA)_7TAA$ in the promoter area of *UGT1A1* gene.

with the homozygous variant-*UGT1A1* gene had bilirubin levels ⩾17.1 μmol/L (upper limit of normal reference value) with significant difference between means in comparing the 16 patients with the controls [18.0±6.5 μmol/L (range 6.8-32.5 μmol/L) and 12.7±2.9 μmol/L (range 6.8-17.1 μmol/L), respectively; P<0.001, Student's t test] (data not shown in Tables).

DISCUSSION

No gender difference has been demonstrated in the incidence of variant *UGT1A1* gene and thalassemia, while G6PD deficiency is X-linkage transmitted[11]. In this study, as the male/female ratio was approximately equal for the case and control groups, the genders were pooled for analysis. More than 50% of the members of both groups had at least one heterozygous variation in the *UGT1A1* gene, while the frequency of homozygous variation differed between groups. The 686 C→A variation was associated with the 6/7 or 7/7 variation for both study subjects and the controls, as observed in our previous studies[5,7,8,12,13]. In the present investigation, however, the 7/7 and 686 C→A plus 7/7 variations were found only in the case group (Table 3). Since bilirubin may be affected by cholelithiasis status, bilirubin values were obtained for cholelithiasis patients with the homozygous variant-*UGT1A1* gene from the records which were made 2-3 mo post cholecystectomy. UGT1A1 enzyme activity was found to be 18-33% of normal in individuals with the 7/7 variation of the *UGT1A1* gene[2]. In another *in vitro* gene-expression study[14], subjects bearing the homozygous 211 G→A variant-*UGT1A1* gene were demonstrated to have 32.2% of the UGT1A1 enzyme activity of normal analogs. Moreover, coinheritance of heterozygous α-thalassemia gene was observed in two of our four cholelithiasis patients who carried the homozygous 211 G→A variation. These findings may account for the significant difference in serum bilirubin levels in cholelithiasis patients with the homozygous variant-*UGT1A1* gene (7/7, 211 G→A/211 G→A, and 686 C→A plus 7/7) related to controls.

Although it has been determined that G6PD deficiency and thalassemia are risk factors for cholelithiasis development in Caucasians[1,4], these associations were not observed in our sample, with no between-group difference in incidences of these two factors were noted. This discrepancy may be due to the ethnic differences between the sample populations. Co-inheritance of the homozygous variant-*UGT1A1* gene and G6PD deficiency may lead to pronounced hyperbilirubinemia in adults[13], and co-inheritance of Gilbert's syndrome and hereditary spherocytosis may increase the risk for developing gallstones[15]. However, these co-inheritances were not noted in this study. Structural analysis of gallstones from a sample of Taiwan Chinese patients revealed that a relatively small proportion of the gallstones were composed of bilirubin (pure cholesterol 35%, combination 12%, mixed 17%, black 25%, calcium bilirubinate 8%, and unclassified 3%)[16]. It is not surprising, therefore, that only 4.3% of our cholelithiasis patients carried the homozygous variant-*UGT1A1* gene, which leads to the bilirubin accumulation and is a risk factor for cholelithiasis. We suggest that investigation of cholelithiasis status and carriage of variant *UGT1A1* gene for specific subpopulations, such as G6PD-deficient or thalassemic Taiwan Chinese, is a superior alternative in genetic research for gallstones. A research program of this type is ongoing at the Cathay General Hospital.

REFERENCES

1 **Meloni T,** Forteleoni G, Noja G, Dettori G, Sale MA, Meloni GF. Increased prevalence of glucose-6-phosphate dehydrogenase deficiency in patients with cholelithiasis. *Acta Haematol* 1991; **85**: 76-78

2 **Bosma PJ,** Chowdhury JR, Bakker C, Gantla S, de Boer A, Oostra BA, Lindhout D, Tytgat GN, Jansen PL, Oude-Elferink RP. The genetic basis of the reduced expression of bilirubin UDP-glucuronosyl transferase 1 in Gilbert's syndrome. *N Engl J Med* 1995; **333**: 1171-1175

3 **Sampietro M,** Lupica L, Perrero L, Comino A, di Montemuros F, Cappellini MD, Fiorelli G. The expression of uridine diphosphate glucuronosyl transferase gene is a major determinant of bilirubin level in heterozygous beta-thalassemia and in glucose-6-phosphate dehydrogenase deficiency. *Brit J Haematol* 1997; **9**9: 437-439

4 **Tunaci M,** Tunaci A, Engin G, Ozkorkmaz B, Dincol G, Acunas G, Acunas B. Imaging features of thalassemia. *Eur Radiol* 1999; **9**: 1804-1809

5 **Huang CS,** Luo GA, Huang MJ, Yu SC, Yang SS. Variations of the bilirubin uridine-diphosphoglucuronosyl transferase 1A1 gene in healthy Taiwanese. *Pharmacogenetics* 2000; **10**: 539-544

6 **Huang CS,** Chan TH, Wei C, Chein TJ, Tang JF. The clinical application of glucose-6-phosphate dehydrogenase quantitative test. *Taiwan Yixuehui Zazhi* 1982; **81**: 938-944

7 **Huang CS,** Chang PF, Huang MJ, Chen ES, Chen WC. Glucose-6-phosphate dehydrogenase deficiency, the UDP-glucuronosyl transferase 1A1 gene and neonatal hyperbilirubinemia. *Gastroenterology* 2002; **123**: 127-133

8 **Huang MJ,** Kua KE, Teng HC, Tang KS, Weng HW, Huang CS. Risk factors for severe hyperbilirubinemia in neonates. *Pediatr Res* 2004; **56**: 682-689

9 **Ko TM,** Tseng LH, Hsieh FJ, Hsu PM, Lee TY. Carrier detection and prenatal diagnosis of alpha-thalassemia of Southeast Asian deletion by polymerase chain reaction. *Hum Genet* 1992; **88**: 245-248

10 **Chang JG,** Chen PH, Chiou SS, Lee LS, Perng LI, Liu TC. Rapid diagnosis of β-thalassemia mutations in Chinese by naturally and amplified created restriction sites. *Blood* 1992; **80**: 2092-2096

11 **Beutler E.** G6PD deficiency. *Blood* 1994; **84**: 3616-3636

12 **Huang CS,** Chang PF, Huang MJ, Chen ES, Hung KL, Tsou KI. Relationship between bilirubin UDP-glucuronosyl transferase 1A1 gene and neonatal hyperbilirubinemia. *Pediatr Res* 2002; **52**: 601-605

13 **Huang MJ,** Yang YC, Yang SS, Lin MS, Chen ES, Huang CS. Coinheritance of variant UDP-glucuronosyltransferase 1A1 gene and glucose-6-phosphate dehydrogenase deficiency in adults with hyperbilirubinemia. *Pharmacogenetics* 2002; **12**: 663-666

14 **Yamamoto K,** Sato H, Fujiyama Y, Doida Y, Bamba T. Contribution of two missense mutations (G71R and Y486D) of the bilirubin UDP glycosyltransferase (UGT1A1) gene to phenotypes of Gilbert's syndrome and Crigler-Najjar syndrome type II. *Biochem Biophys Acta* 1998; **1406**: 267-273

15 **del Giudice EM,** Perrotta S, Nobili B, Specchia C, d'Urzo G, Iolascon A. Coinheritance of Gilbert's syndrome increases the risk for developing gallstones in patients with hereditary spherocytosis. *Blood* 1999; **94**: 2259-2262

16 **Liu JS,** Huang CS, Lien HH. Structural analysis of gallstones with thin-section petrographic microscopy: a study of 100 gallstones from Taiwanese patients. *J Lab Clin Med* 2002; **140**: 387-390

Science Editor Guo SY **Language Editor** Elsevier HK

PO Box 2345, Beijing 100023, China
www.wjgnet.com
wjg@wjgnet.com

ELSEVIER

World J Gastroenterol 2005;11(36):5714-5717
World Journal of Gastroenterology ISSN 1007-9327
© 2005 The WJG Press and Elsevier Inc. All rights reserved.

• *BRIEF REPORTS* •

Intracerebral xenotransplantation of semipermeable membrane- encapsuled pancreatic islets

Zhao-Liang Xin, Song-Lin Ge, Xiao-Kang Wu, Yan-Jie Jia, Han-Tao Hu

Zhao-Liang Xin, Neurosurgery Department of Yiwu Central Hospital, 3rd Faculty of Medical College, Zhejiang University, Yiwu 322000, Zhejiang Province, China
Song-Lin Ge, 3rd Faculty of Medical College, Zhejiang University, Hangzhou, 310016, Zhejiang Province, China
Xiao-Kang Wu, Department of Neurosurgery, Affiliated Hospital of Railway University, Shanghai, China
Yan-Jie Jia, Han-Tao Hu, Department of Anatomy, Medical College, Xi'an Jiaotong University, Xi'an 710007, Shaanxi Province, China
Supported by the Natural Science Foundation of Shaanxi Province, No. 98SZ-064
Correspondence to: Zhao-Liang Xin, Yiwu Central Hospital, Yiwu 322000, Zhejiang Province, China. wxk555@sohu.com
Telephone: +86-579-5209626 Fax: +86-579-5209618
Received: 2004-08-26 Accepted: 2004-12-21

Abstract

AIM: To identify the decreasing effect of xenotransplantion in combination with privileged sites on rejection and death of biological semipermeable membrane-(BSM) encapsulated implanted islets.

METHODS: After the BSM experiment *in vitro*, BSM-encapsulated SD rat's islet-like cell clusters (ICCs) were xenotransplanted into normal dog's brain. Morphological changes were observed under light and transmission electron microscope. The islets and apoptosis of implanted B cells were identified by insulin-TUNEL double staining.

RESULTS: The BSM used in our study had a favorable permeability, some degree of rigidity, lighter foreign body reaction and toxicity. The grafts consisted of epithelioid cells and loose connective tissue. Severe infiltration of inflammatory cells was not observed. The implanted ICCs were identified 2 mo later and showed typical apoptosis.

CONCLUSION: BSM xenotransplantation in combination with the privileged site can inhibit the rejection of implanted heterogeneous ICCs, and death of implanted heterogeneous B cells is associated with apoptosis.

© 2005 The WJG Press and Elsevier Inc. All rights reserved.

Key words: Islets of Langerhans; Xenotransplantation; Brain; Semipermeable membrane

Xin ZL, Wu XK, Hu HT, Jia YJ. Intracerebral xenotransplantation of semipermeable membrane- encapsuled pancreatic islets. *World J Gastroenterol* 2005; 11(36): 5714-5717
http://www.wjgnet.com/1007-9327/11/5714.asp

INTRODUCTION

Studies have shown that porcine ICCs xenotransplanted into rat's brain could survive for only eighteen days[1,2], suggesting that the immuno-privileged function of brain cannot ensure the long-time survival of heterogeneous islets. Immunity-isolation is an effective way to lessen the immunological rejection damage[3,4]. Better effect can be achieved through the combination of different immunity-isolation techniques[5]. Rat's pancreatic islet is easy to be separated, transgenic rats are also developed, and the cell line secreting insulin has been established[6]. However, the exact effects of apoptosis on the death of xenotransplanted islets cannot be shown[7-9]. In this study, BSM-encapsuled SD rat's ICCs were xenotransplanted into a normal dog's brain to identify their decreasing effect on rejection and death of implanted islets.

MATERIALS AND METHODS

Separation, purification and culture of rat ICCs[6]

SD rats, weighing 50-200 g were used in this study. Pancreas and its amiculas and vessels were washed twice in Hank's solution and then minced. The fragments were digested with collagenase V (1 g/L, Sigma) at 37 ℃ for 15-20 min, ground and filtrated through an 80-mesh steal net to remove connective tissue, washed in cold Hank's solution to stop the activity of collagenase. Then the filtrates were filtrated with a 400-mesh steal net to remove the small exocrine cells, red and white blood cells with the bigger ICCs kept on the net. The cell clusters on the net were collected and put into the Ficoll fluid (Euro-Collin) at the concentrations of 25 g/L, 23 g/L, 20 g/L and 11 g/L. The mixed liquors were centrifuged at 3 500 r/min at 4 ℃ for 15 min. ICCs were washed three times. The purity of ICCs obtained in this way was (88.2±7.6) %. These ICCs were cultured in non-insulin DMEM supplemented with 10% fetal bovine serum, 2 mmol/L glutamine, 10 mmol/L nicotinamide, 5 mmol/L hydroxyethyl methylmethane sulfonic acid, 100 000 U/L penicillin and 1 g/L streptomycin, and maintained at 37 ℃ in a high-humidity incubator with 50 mL/L CO_2. A total of 400-1 000 purified ICCs were obtained from each rat. These ICCs were stained with trypan blue and the activity was 90%.

Lymphocytes diffusion

Five semipermeable membrane encysts were filled with 1 mL of fresh blood plasma, put into 200 mL of blood and maintained at 37 ℃ in a high-humidity incubator with 50 mL/L CO_2 and kept agitated with magnetic force. Fluid

in encysts was suctioned respectively 5 h later, then smeared and observed under a light microscope by Wright's staining.

Glucose diffusion

Eight semipermeable membrane encysts were filled with 1 mL of isotonic sodium chloride, put into 400 mL of isotonic sodium chloride containing 29.1 mmol/L glucose and kept agitated with magnetic force. The encysts were taken out at 1, 4, 8, 12, 16, 20, 24 and 28 min, respectively, and washed with isotonic sodium chloride. The fluid in the encysts was obtained and the concentration of glucose was detected.

In vitro culture of BSM-encapsulated ICCs

About twelve thousands separated ICCs were divided into ten parts, five were encapsulated by BSM, five were routinely cultured. The culture medium was changed every three days. The concentration of insulin in the medium was detected on d 3, 6, and 15 respectively when the medium was changed.

Transplantation of BSM-encapsulted SD rat ICCs into dog's brain

After ICCs were cultured for 72 h, they were encapsulated by aseptic BSM. The volume of encysts was 1.5 cm×1.5 cm×1.5 cm. Each of them contained 6 000 to 10 000 ICCs.

The recipients were normal male local hybrid dogs weighing 7-14 kg. The dogs were intravenously anesthetized and their hair was shaved. The straight nick was made at frontal-occipital middle line perpendicular to the zygomatic arch. The temporalis muscles were pulled back to expose the skull, a hole was burred to enlarge the skull window to 3 cm×3 cm, and the dura mater was cut open. The pallium was exposed to make a nick under the cerebral lateral fissure, and a fistula was made into ventricle between the rectal fissure and rectal lateral fissure to form a 2 cm×2 cm×1.5 cm tunnel. The brain tissue was wet compressed with 0.5 g/L orthophosphoric acid dexamethasone for 15 min[7], then encysts were transplanted into the tunnel. The dura mater was relocated and compressed with gelatin sponges from the outside. Scalp and muscles were then sutured. Dogs were allowed to take food when consciousness was regained after anesthesia. Penicillin and streptomycin were used 30 min before and 1-3 d after operation.

The dogs were divided into control group (n = 2) and experimental group(n = 4). In control group, a fistula was made, the stoma at the ventricle side was covered with gelatin sponges. Then the encysts were cut open to let the contents efflux into the brain tissue and the stoma at cortex side was covered with gelatin sponges. In experimental group, brain tissue was obtained 1 mo and 2 mo after encapsulated ICCs were transplanted.

Observation of morphological changes after surgery

According to the schedule, the brain was perfused with 4 g/L paraformaldehyde phosphate buffer through the ambi-common carotid artery. The grafts' shape, color, location and changes of surrounding brain tissue were observed. Then part of the grafts and surrounding brain tissue were paraffin embedded, sectioned and stained with HE. Morphological changes of grafts and brain tissue were observed under a light microscope. Some grafts were divided into 1 mm×1 mm×1 mm piecers. These pieces were fixed with 25 g/L glutaraldehyde, dehydrated, embedded and then cut into ultrathin sections. The ultramicro-changes of the grafts were observed under a transmission electron microscope (JEM2000).

Identification of islets and apoptosis of implant ICCs

The first antibody was replced by normal mouse serum in the negative control group. Paraffin-embedded sections were used. The first antibody was mouse anti-human insulin used at 1:100 dilution and stained according to the avidin-biotin compound method (ABC), and then counterstained with hematoxylin to identify B cells in the grafts. The DNA fragmentation of transplanted B cells was identified by insulin-TUNEL double staining .

RESULTS

In vitro experiments of BSM

The BSM was not damaged during the whole process of the experiment *in vitro*. In lymphocyte-diffusion experiment, lymphocytes and any other blood cells were not immersed into the semipermeable membrane capsule, but glucose could rapidly diffuse into the capsule. The concentration of glucose in the capsule was 14.3 mmol/L after 8 min, which was 50% of the concentration out of the capsule. After 28 min. The concentration of glucose in the capsule reached the same environmental level. The concentration of insulin on d 3, 6 and 15 was (139.0±3.4) mU/L, (78.7±3.9) mU/L and (66.2±2.9) mU/L, respectively in the experimental group , and (145.4±4.2) mU/L, (79.4±2.1) mU/L and (48.2±4.1) mU/L, respectively in the control group. There was no conspicuous variability (P>0.05) between the two groups at various time points. Insulin secreted from pancreatic islet cells could diffuse rapidly out of the capsule.

ICCs xenotransplanted into dog's brain

The dogs of both groups had no conspicuous behavior disorder. No dog in the experimental group was infected. The graft was deep gray and homogenous in the experimental group. It was connected with the ventricle at the inner side and adhered to the thickening dura mater at the lateral side as well as in contact with the cerebral parenchyma. The boundary was clear. Brain tissue around the graft had no obvious hemorrhage, necrosis and inflammatory abscess. Only residual semipermeable membrane was observed in the control dogs.

Under light microscope, the graft was consisted of epithelial cells and loose connective tissue, including epithelial cells, fibroblasts, collagen fiber, and small vessels. In the middle of them, there were lymphocytes and other kinds of white blood cells. Epithelial cells mostly adhered to the fibroblasts, collagen fiber or small vessels, and were arranged loosely in the connective tissue along the collagen fibers. The structure of small vessels was normal, while that of some parts of the semipermeable membrane was different, but there was no clump-like infiltration of lymphocytes.

Slight hyperplasia and hydropsia of glial cells were observed in the brain tissue around the graft, but severe infiltration of inflammatory cells was not observed.

Under electron microscope, secreting granulae were observed in the endochylema. The granulae were not only different in size but also diferent from those of pancreatic islet cells. Intact and contracted caryons, aggregated chromosome and typical apoptotic bodies were found in some cells (Figure1).

No xenotransplanted cell disappeared in the control group.

Cytoplasms of many epithelial cells in the grafts of EG were stained yellow, indicating that they were islet B cells (Figure2). The implanted B cells showed typical apoptosis by insulin-TUNEL double staining.

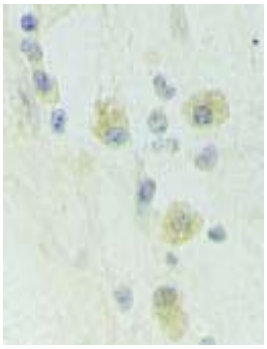


Figure 1 Typical morphology of apoptotic cells 1 mo after transplantation (×6 000). ↑ collagen fiber, ↑ WBC, ▲ apoptosis body.

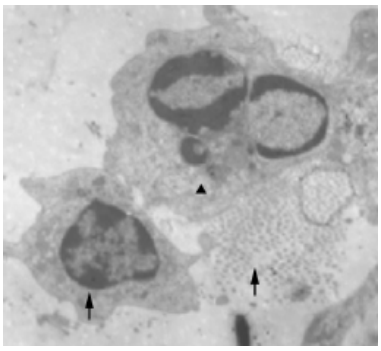


Figure 2 Yellow staining of cytoplasma of some graft cells 1 mo after transplantation (×6 000).

DISCUSSION

Studies have shown that porcine ICCs xenotransplanted into a rat's brain can survive for only 18 d[1,2], and fetal porcine ICCs transplanted into cynomolgus monkey's kidney encysts are completely rejected on d 6[5,8]. In the present study, no infiltration of clump-like polymorphic nuclear cells and lymphocytes was found, suggesting that rejection occurs in xenotransplanted ICCs. Immunohistochemical staining showed that pancreatic islet B cells still existed in the grafts after 2 mo. The dogs had no conspicuous behavior disorder after transplantation. Slight hyperplasia and hydropsia of glial cells were observed in the brain tissue around the graft. These facts suggest that ing Xenotransplantation of BSM in combination with the privileged site can inhibit the rejection of implanted heterogeneous ICCs.

In the present study, cells displayed different morphological features in different environments to adapt themselves to the microenvironment. The culture medium was gradually absorbed after graffing and replaced by loose connective tissue until solidification. The appearance of connective tissue was a kind of compensatory reaction, giving support and nutrition to islet cells and keeping them stable. Islet cells were arranged loosely in the connective tissue along the collagen fibers, while the in situ compact cell clumps were observed under the pressure of exocrine division.

It is easier to transplant pancreatic islets when they are capsuled and to dislodge them when the rejection is serious during the early period of transplantation. This is very important when a clinical trial is carried out. According to the *in vitro* experiments and transplant experiments, the semi permeable membrane used in our study had a favorable permeability, some degree of rigidity, lighter foreign body reaction and toxicity.

It was reported that cerebrospinal fluid (CSF) could ensure islet survival with sufficient oxygen and nutrients[10]. We made a tunnel into the ventricle, which could connect capsules with CSF immediately. Accordingly, islets were supplied with nutrients in the earlier period, which is beneficial for their survival. However, how many islet nutrients can be obtained in this way remians unclear. We also found that the implanted B cells showed classic apoptosis by insulin-TUNEL double staining and electron microscopy. The death of implanted heterogeneous B cells is associated with apoptosis. Why apoptosis occurs and how to delay or block this apoptosis are the subjects to be studied[11-14].

Surgical procedures injure brain tissue and integrality of the blood-brain barrier. Wet compressing with dexamethasone on the injured brain can decrease the blood-brain barrier permeability and non-specific exudation of inflammatory cells[15].

REFERENCES

1 **Triponez F,** Oberholzer J, Morel P, Toso C, Yu D, Cretin N, Buhler L, Majno P, Mentha G, Lou J. Xenogeneic islet re-transplantation in mice triggers an accelerated, species-specific rejection. *Immunology* 2000; **101**: 548-554

2 **Thomas FT,** Hutchings A, Contreras J, Wu J, Jiang XL, Eckhoff D, Thomas JM. Islet transplantation in the twenty-first century. *Immunol Res* 2002; **26**: 289-296

3 **Opara EC,** Kendall WF Jr. Immunoisolation techniques for islet cell transplantation. *Expert Opin Biol Ther* 2002; **2**: 503-511

4 **Bucher P,** Mathe Z, Bosco D, Andres A, Buhler LH, Morel P, Berney T. Islet of Langerhans transplantation for the treatment of type 1 diabetes. *Swiss Surg* 2003; **9**: 242-246

5 **Juang JH.** Islet transplantation: an update. *Chang Gung Med J* 2004; **27**: 1-15

6 **Xin ZL,** Jia YJ, Hu HT, Ren HM. The coculture of pancreatic islets with neurons and gliacytes. *Xi'an Yike Daxue Xuebao* 2001; **22**: 475-479

7 **Lehnert AM,** Yi S, Burgess JS, O'Connell PJ. Pancreatic islet xenograft tolerance after short-term co-stimulation blockade is associated with increased CD4+ T cell apoptosis but not immune deviation. *Transplantation* 2000; **69**: 1176-1185

8 **Vizzardelli C,** Molano RD, Pileggi A, Berney T, Cattan P, Fenjves ES, Peel A, Fraker C, Ricordi C, Inverardi L. Neonatal

porcine pancreatic cell clusters as a potential source for transplantation in humans: characterization of proliferation, apoptosis, xenoantigen expression and gene delivery with recombinant AAV. *Xenotransplantation* 2002; **9**: 14-24

9 **Xin ZL,** Jia YJ, Hu HT, Ren HM. Rat ICCs apoptosis of xenotransplantation into dogs brain. *Disi Junyi Daxue Xuebao* 2002; **23**: 2279-2281

10 **Atwater I,** Yanez A, Cea R, Navia A, Jeffs S, Arraya V, Szpak-Glasman M, Leighton X, Goping G, Bevilacqua JA, Moreno R, Brito J, Arriaza C, Ommaya A. Cerebral spinal fluid shunt is an immunologically privileged site for transplantation of xenogeneic islets. *Transplant Proc* 1997; **29**: 2111-2115

11 **Saudek F.** Gene therapy in the treatment of diabetes mellitus. *Cas Lek Cesk* 2003; **142**: 523-527

12 **Contreras JL,** Bilbao G, Smyth CA, Jiang XL, Eckhoff DE, Jenkins SM, Thomas FT, Curiel DT, Thomas JM. Cytoprotection of pancreatic islets before and soon after transplantation by gene transfer of the anti-apoptotic Bcl-2 gene. *Transplantation* 2001; **71**: 1015-1023

13 **Contreras JL,** Bilbao G, Smyth C, Eckhoff DE, Xiang XL, Jenkins S, Cartner S, Curiel DT, Thomas FT, Thomas JM. Gene transfer of the Bcl-2 gene confers cytoprotection to isolated adult porcine pancreatic islets exposed to xenoreactive antibodies and complement. *Surgery* 2001; **130**: 166-174

14 **Brandhorst D,** Hammes HP, Brandhorst H, Zwolinski A, Nahidi F, Alt A, Bretzel RG. Pretransplant induction of HSP-70 in isolated adult pig islets decreases early islet xenograft survival. *Cell Transplant* 2000; **9**: 423-430

15 **Xin ZL,** Duan GR, Lv J, Yang QY. Experimental study of local use of dexamethasone and its effects on brain edema and blood brain barrier permeability following brain injury. *Zhonghua Shiyan Waike Zazhi* 1997; **14**: 355-356

Science Editor Wang XL and Guo SY **Language Editor** Elsevier HK

PO Box 2345, Beijing 100023, China
www.wjgnet.com
wjg@wjgnet.com

ELSEVIER

World J Gastroenterol 2005;11(36):5718-5720
World Journal of Gastroenterology ISSN 1007-9327
© 2005 The WJG Press and Elsevier Inc. All rights reserved.

• *BRIEF REPORTS* •

Expression of HBsAg and HBcAg in the ovaries and ova of patients with chronic hepatitis B

Feng Ye, Ya-Fei Yue, Shu-Hong Li, Tian-Yan Chen, Shu-Ling Zhang, Gui-Qin Bai, Min Liu

Feng Ye, Tian-Yan Chen, Shu-Ling Zhang, Min Liu, Department of Infectious Disease, First Hospital of Xi'an Jiaotong University, Xi'an 710061, Shaanxi Province, China
Ya-Fei Yue, Shu-Hong Li, Gui-Qin Bai, Department of Obstetrics and Gynecology, First Hospital of Xi'an Jiaotong University, Xi'an 710061, Shaanxi Province, China
Supported by the National Natural Science Foundation of China, No. 30371277
Co-first-authors: Feng Ye and Ya-Fei Yue
Co-correspondents: Ya-Fei Yue
Correspondence to: Dr. Feng Ye, Department of Infectious Disease, First Hospital of Xi'an Jiaotong University, Jiankang Road 1#, Xi'an 710061, Shaanxi Province, China. yefeng.jiaotong@163.com
Telephone: +86-29-88042433 Fax: +86-29-5252812
Received: 2005-01-14 Accepted: 2005-02-18

Abstract

AIM: To investigate the expression and distribution of HBV in the ovaries and ova.

METHODS: The immunohistochemistry method was used to detect the HBsAg and HBcAg in the ovaries of patients with chronic hepatitis B.

RESULTS: Expression of HBsAg in the ova, granular and interstitial cells of the ovaries was located in the cytomembrane and cytoplasm. Expression of HBcAg in the ova, granular, interstitial and endothelial cells of interstitial blood vessels of the ovaries was found in the cytomembrane, cytoplasm, and nuclei.

CONCLUSION: HBV can infect the ova at different stages of development and replicate in it.

© 2005 The WJG Press and Elsevier Inc. All rights reserved.

Key words: HBV; Ovaries; Ova; Immunohistochemistry

Ye F, Yue YF, Li SH, Chen TY, Zhang SL, Bai GQ, Liu M. Expression of HBsAg and HBcAg in the ovaries and ova of patients with chronic hepatitis B. *World J Gastroenterol* 2005; 11(36): 5718-5720
http://www.wjgnet.com/1007-9327/11/5718.asp

INTRODUCTION

In Asian countries such as China, vertical infection plays a major role in transmitting HBV. The infected babies will eventually develop liver cirrhosis or hepatocellular carcinoma in their adulthood, and female babies will continue the cycle of vertical transmission to their offsprings[1-3]. Recent data indicate that intrauterine infection is one of the important routes of HBV vertical transmission, and the rate of intrauterine HBV infection is 10-44.4%[3,4]. Furthermore, studies have proved that most intrauterine infections can be prevented by inoculation with HBVac and HBIG in the perinatal stage, but 5-10% of the infections cannot be prevented by the combination of HBIG and HBVac[5,6]. The mechanism for this fact is controversial. Some researchers suspected that the infection of ova with HBV may be a factor in this mechanism[7]. But this was just a supposition, and little data exist to prove it.

To explore if HBV could infect the ovaries and ova, we detected the expression of HBsAg and HBcAg in the ovaries and ova of patients with chronic hepatitis B (CHB) by immunohistochemistry method.

MATERIALS AND METHODS

Ovary tissues were obtained from 18 patients with CHB who received surgery for ovary disease at the First Hospital of Xi'an Jiaotong University in China. The specimens were collected after surgery. Serum samples from these patients were tested for different HBV markers including HBsAg, HBeAg, anti-HBc, anti-HBe (HBVM) using a commercially available ELISA kit (Sino-America Biological Technology, Inc., Beijing, China) prior to surgery. HBsAg was positive while HCV, HIV, HAV, and HEV were negative in 18 patients. All reactions were performed at the Immunohistochemistry Laboratory in Xi'an Jiaotong University.

Ovary tissues were fixed in 40 g/L formaldehyde, embedded with paraffin and cut into 4 μm thick sections. Mouse (McAb) against HBsAg (Dako, Denmark) and rabbit polyclonal antibodies against HBcAg (Baoxin, China) were used for immunohistochemical test. DAB staining kits were purchased from Wuhan BoShiDe Biological Engineering Ltd. Company.

HBsAg and HBcAg were detected by immunhistochemical staining using the avidin-biotin complex (ABC) method on the sections of ovarian tissues. In brief, formalin-fixed, paraffin-embedded sections were deparaffinized in xylene and passed through ethanol series. After the endogenous peroxidase activity was blocked, the sections were rinsed in 0.01 mol/L PBS. Non-specific binding was blocked by treatment with 5% normal serum for 30 min. Primary antibody was applied to the sections and incubated in a moist chamber overnight at 4 ℃. After the sections were washed in 0.01 mol/L PBS, second antibody was applied and sections were incubated for 30 min at 37 ℃ in

a moist chamber. After being washed, the sections were incubated with avidin-biotin-peroxidase complex for 30 min at 37 ℃ in a moist chamber and washed again. The chromogen, 3-3-diaminobenzidine (DAB) was added to the sections for 10 min.

The sections of HBsAg and HBcAg positive livers from autopsy were used as positive control, and the sections of ovaries from HBVM negative women served as negative control. At the same time, PBS was used as blank control instead of the first antibody in immunohistochemical test. Dark brown yellow in cytoplasm, cytomembrane or nuclei was regarded as strongly positive, brown yellow as positive, and light brown yellow as weakly positive.

RESULTS

Expression of HBsAg in the ova and granular cells of the ovaries was located in the cytomembrane and cytoplasm. The positive rate was 11% (2/18). Negative control and blank control were negative. (Figures 1A and B)

Expression of HBcAg in the ova, granular, interstitial and endothelial cells of interstitial blood vessels of the ovaries was found in the cytomembrane, cytoplasm, and nuclei. HBsAg and HBcAg in the ovaries were strongly positive. The positive rate was 45% (8/18). Negative control and blank control were negative. (Figures 1C-H).

DISCUSSION

Much attention has been paid to the effective prevention of vertical HBV transmission[1-4]. It was reported that intrauterine HBV is transmitted through HBV-infected placenta and HBV could enter the blood of infant through placental leak[8]. But this cannot explain why HBV can infect the embryo (46 d). Chen *et al*.[7], showed that HBV cannot infect the embryo through placenta. They believe there is another mechanism by which HBV infects the embryo.

Yu *et al*.[9], proved that hemorrhagic fever virus exists in the ova of rodent. Bovine viral diarrhea virus can infect the ova of bovine[10]. Tagawa *et al*.[11], found that duck HBV

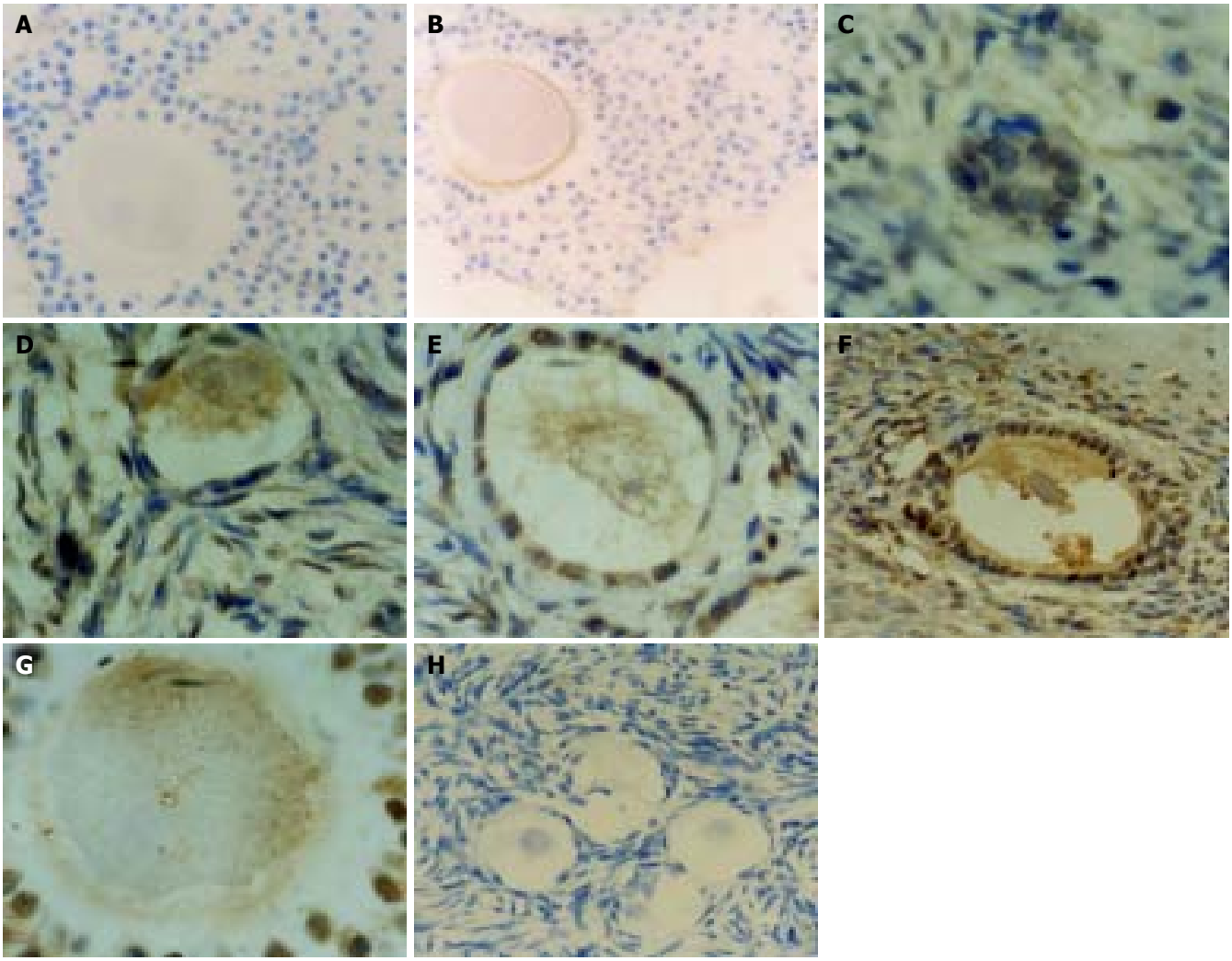


Figure 1 Expression of HBsAg and HBcAg in the ovaries and ova. **A**: HBsAg negative control (original magnification:10×40); **B**: expression of HBsAg in plasma and membrane of ova and granular cells (original magnification:10×40); **C**: expression of HBcAg in plasma, membrane and nuclei of sinus ova, granular and interstitial cells (original magnification: 10×100); **D** and **E**: expression of HBcAg in plasma, membrane and nuclei of primary ova, granular and interstitial cells (original magnification: 10×40); **F**: expression of HBcAg in plasma, membrane and nuclei of secondary ova, granular and interstitial cells (original magnification: 10×40); **G**: expression of HBcAg in plasma, membrane and nuclei of mature ova, granular and interstitial cells (original magnification: 10×100); **H**: HBcAg negative control (original magnification: 10×40).

(DHBV) is expressed in yolk of duck with hepatitis B, and that DHBVDNA is present in liver of embryo after 6 d of incubation, suggesting DHBV could infect the egg of duck and replicate in it. Zhao *et al*.[12], reported that DNA of TTV is found in the ovaries of CHB patients by hybridization *in situ*. Zhou *et al*.[13], reported that HBVDNA is present in plasma of ova and in interstitial cells of the ovaries of a patient who died of serious hepatitis B. Taylor *et al*.[14], have detected HBsAg in follicular fluid of CHB patients by immunohistochemistry method.

In this study, HBsAg and HBcAg were expressed in ova and granular cells of the ovaries. HBcAg was expressed in ova at different stages of development, suggesting that HBV can infect the ovaries and ova, and replicate in them. The fact suggests that HBV-infected ova may cause the vertical transmission of HBV, which cannot be prevented by inoculation of HBV vaccine and HBIG because the embryo is infected as zygote is formed.

In this study, the positive rate of HBsAg (11%) was lower than that of HBcAg (45%). We consider that the primary antibody against HBsAg is monoclonal antibody (McAb), but the primary antibody against HBcAg is polyclonal antibody. Since the binding epitope of McAb is less than that of polyclonal antibody, the positive rate of HBsAg is lower. On the other hand, in the ova, the synthetizing and expression of HBcAg by HBV may be higher than that of HBsAg in the ovaries. The amount of HBsAg is more than that of HBcAg in liver cells[15,16]. Of course, a little sample may be a reason.

In conclusion, HBV can infect the ovaries and ova and replicate in them. But how does HBV infect the ovaries and ova and whether HBV-infected ova results in HBV vertical transmission remain unknown.

ACKNOWLEDGMENTS

The authors thank Xiao-Ge Zhao for his excellent technical assistance, Zhao-Yang Liu and Zi-Yun Shi for their surgical assistance.

REFERENCES

1 **Li YX,** Gao QW, Zhang YH, Guo Y, Li BW, Wang HX, Wang YL, Wang YM. An investigation on the transmission routes and early diagnosis of intrauterine infection induced by hepatitis B virus. *Zhonghua Ganzangbing Zazhi* 2004; **12**: 18-20
2 **Yue YF,** Jiang H, Shi L, Li LF, Xi BS, Yu YL, Chen GF. Study on the mechanism of intrauterine infection of hepatitis B virus. *Zhonghua Fuchanke Zazhi* 2004; **39**: 224-226
3 **Xu DZ,** Yan YP, Choi BC, Xu JQ, Men K, Zhang JX, Liu ZH, Wang FS. Risk factor and mechanism of transplacental transmission of hepatitis B virus: a case control study. *J Med Virol* 2002; **67**: 20-26
4 **Wang Z,** Zhang J, Yang H, Li X, Wen S, Guo Y, Sun J, Hou J. Quantitative analysis of HBV DNA level and HBeAg title in hepatitis B surface antigen positive mothers and their babies: HBeAg passage through the placenta and the rate of decay in babies. *J Med Virol* 2003; **71**: 360-366
5 **Soderstrom A,** Norkrans G, Lindh M. Hepatitis B virus DNA during pregnancy and post partum: aspects on vertical transmission. *J Infect Dis* 2003; **35**: 814-819
6 **Xia GL,** Gong J, Wang JJ, Meng ZD, Jia ZY, Cao HL, Liu CB. Efficacy of recombinant hepatitis B vaccine and low-dose hepatitis B immune globulin in preventing mother-infant transmission of hepatitis B virus infection. *Zhonghua Liuxingbingxue Zazhi* 2003; **24**: 362-365
7 **Chen HY,** Shen DX, Wang SH, Wang XH. Detection on presence of hepatitis B virus in human infected by vertical transmission. *Zhongguo Gonggong Weisheng Zazhi* 2002; **18**: 417-419
8 **Wang XP,** Xu DZ, Li YG, Yan YP, Men K, Zhang JX. HBsAg uptake into human trophoblasts cultured *in vitro*. *Diyi Junyi Daxue Xuebao* 2003; **23**: 16-20
9 **Yu MM,** Zhang Y, Wu GH, Huang CA, She JJ, Zhang JJ, Jiang KJ. Experimental studies on transmission of EHF in rodent. *Zhonghua Yufang Yixue Zazhi* 1994; **28**: 132-134
10 **Givens MD,** Galik PK, Riddell KP, Brock KV, Stringfellow DA. Replication and persistence of different strains of bovine viral diarrhea virus in an *in vitro* embryo production system. *Theriogenology* 2000; **54**: 1093-1107
11 **Tagawa M,** Robinson WS, Marion PL. Duck hepatitis B virus replicates in the yolk sac of developing embryos. *J virol* 1987; **61**: 2273-2279
12 **Zhao YW,** Xu JZ,Yang ZG, Lang ZW,Yan HP,Huang ZH. Preparation of digoxignin labelled probe and detection of transfusion transmitted virus in extrahepatic tissue with *in situ* hybridization. *Jiangsu Yixue Zazhi* 2002; **26**: 428-430
13 **Zhou Sl,** Zhao LS, Li H, Liu L. Detection of HBVDNA in oocyte of a patient with chronic hepatitis B by *in situ* by hybridization. *J Heredity Disease* 1989; **6**: 46-48
14 **Taylor PJ,** Gill MJ, Mahadevan M, Pattinson HA. Hepatitis B virus in follicular fluid. *Fertil Steril* 1987; **48**: 54-56
15 **Yamada M,** Nakamura K, Nakajima Y, Yamamoto M, Komae H, Okuda K, Tsuji M, Arai M. Ground-glass hepatocytes in fibrinogen storage disease in Japanese Black calves. *J Comp Pathol* 2002; **126**: 95-99
16 **Alonso-Marti C,** Moreno A, Barat A, Solera JC, Oliva H. Coexistence of hepatocyte ground-glass inclusions from several causes. *Histopathology* 1990; **16**: 304-307

Science Editor Wang XL **Language Editor** Elsevier HK

PO Box 2345, Beijing 100023, China
www.wjgnet.com
wjg@wjgnet.com

ELSEVIER

World J Gastroenterol 2005;11(36):5721-5724
World Journal of Gastroenterology ISSN 1007-9327
© 2005 The WJG Press and Elsevier Inc. All rights reserved.

• *BRIEF REPORTS* •

Relationship of human leukocyte antigen class II genes with the susceptibility to hepatitis B virus infection and the response to interferon in HBV-infected patients

Yong-Nian Han, Jin-Long Yang, Shui-Gen Zheng, Qun Tang, Wei Zhu

Yong-Nian Han, Jin-Long Yang, Shui-Gen Zheng, Qun Tang, Wei Zhu, Research Unit of Liver Diseases, Shanghai 8th People's Hospital, Shanghai 200235, China
Supported by the Development Fund of Shanghai Science and Technology Committee, No. 014119052
Correspondence to: Yong-Nian Han, Research Unit of Liver Diseases, Shanghai 8th People's Hospital, Shanghai 200235, China. hanyn88@163.com
Telephone: +86-21-64363101-3031
Received: 2005-03-07 Accepted: 2005-04-02

Key words: Hepatitis B; Human leukocyte antigens; Genetic susceptibility; Interferon

Han YN, Yang JL, Zheng SG, Tang Q, Zhu W. Relationship of human leukocyte antigen class II genes with the susceptibility to hepatitis B virus infection and the response to interferon in HBV-infected patients. *World J Gastroenterol* 2005; 11(36): 5721-5724
http://www.wjgnet.com/1007-9327/11/5721.asp

Abstract

AIM: To study the relationship of human leukocyte antigen (HLA)-DRB1 and -DQB1 alleles with the genetic susceptibility to HBV infection and the response to interferon (IFN) in HBV-infected patients.

METHODS: Low-resolution DNA typing kit was used to determine HLA-DR-1 and -DQB1 genes in 72 patients with chronic hepatitis B (CHB) and HLA-DRB1 in 200 healthy people ready to donate their bone marrow in Shanghai. Among CHB patients, 35 were treated with IFNα-1b for 24 wk.

RESULTS: The frequencies of HLA-DRB1*06, DRB1*08 and DRB1*16 alleles in 72 patients were higher than in 200 healthy people (2.08% *vs* 0%, OR = 3.837, *P* = 0.018; 11.11% *vs* 5.50%, OR = 2.148, *P* = 0.034; and 6.94% *vs* 3.00%, OR = 0.625, *P* = 0.049, respectively); whereas that of DRB1*07 allele was lower (2.78% *vs* 7.75%, OR = 0.340, *P* = 0.046). The frequency of HLA-DRB1* 14 allele was higher in 11 responders to IFN compared with 24 non-responders (18.18% *vs* 2.08%, OR = 10.444, *P* = 0.031), whereas that of DQB1*07 allele was inverse (9.09% *vs* 37.50%, OR = 0.167, *P* = 0.021).

CONCLUSION: The polymorphism of HLA class II may influence the susceptibility to HBV infection and the response to IFN in studied CHB patients. Compared with other HLA-DRB1 alleles, HLA-DRB1*06, DRB1*08, and DRB1*16 may be associated with chronicity of HBV infection, HLA-DRB1*07 with protection against HBV infection, and HLA-DRB1*14 allele may be associated with a high rate of the response of CHB patients to IFN treatment. Compared with other HLA-DQB1 alleles, HLA-DQB1*07 may be associated with low response rate to IFN.

© 2005 The WJG Press and Elsevier Inc. All rights reserved.

INTRODUCTION

It is generally accepted that viral clearance or chronic viremia following HBV infection is determined by the host immune response against HBV, in which human leukocyte antigens (HLA) play a central role. The progressions of antigen-presenting cells presenting viral antigens to B and T cells, B and T cells recognizing antigens, and B and T cells being reactivated are all restricted by HLA. The genes of HLA are polymorphous and difficult types of HLA are combined with difficult motifs of the antigens. It is, therefore, presumed that the HLA polymorphism possibly determines the pathogenesis and outcome of HBV infection. It has been reported that the HLA polymorphism correlates with the outcome of HBV infection, but this relationship is not universal on the basis of the investigated population. In Caucasia[1,2] and Korea[3], for example, HLA-DRB1*1301-02 has been found to be associated with acute self-limited hepatitis B. In Taiwanese, HLA-DRB1*0406 is associated with recovery from HBV infection in Han Chinese, and so is HLA-B*4001 in Aborigines[4]. Han Chinese with HLA-DR12 (especially one of its alleles of DRB1*1201) or HLA-DRB1*1101/1104, respectively, have been shown to be able to resist HBV infection, and those with HLA-DR9, DQ9, HLA-DRB1*0301, HLA-DQB1*0301 (one of DQ7 isoforms)[5,6] and DRB1*10, respectively, have been revealed to have a relationship with susceptibility to chronic HBV infection[7]. DRB1*15 and its link-inequilibrium haploid-DRB1*15-DQB1*05 have been found to be associated with sustained response to interferon (IFN) treatment in Taiwanese patients with chronic hepatitis C[8]. It has not been known, however, whether HLA genes correlate with the responsiveness to IFN treatment in patients with chronic hepatitis B (CHB). The aim of this study was therefore to assess whether HLA class II alleles play a critical role in the susceptibility to HBV infection and the response rate to IFN treatment in CHB patients.

MATERIALS AND METHODS

Subjects

A total of 72 patients with chronic HBV infection in the present study were positive for HBV surface antigen (HBsAg), e antigen (HBeAg) or anti-HBe and anti-HBc paralleled with serum ALT elevation for at least 6 mo. None of the patients were positive for hepatitis C virus antibody, hepatitis D virus antibody and HIV antibody; 62 of them were males and 10 were females with mean age of 32±7 years; 200 healthy people ready to donate their bone marrow in Shanghai were selected as control group; 112 of them were males and 88 were females with mean age of 35±7 years. All participants had no relative relationship.

Thirty-five of seventy-two patients without immunosuppressive or antiviral therapy within 1 year before entry, and without alcoholism, intravenous drug abuse, fatty liver, cirrhosis, pregnancy, or other serious diseases that may interfere with IFN-α therapy or that were forbidden for IFN therapy were treated with IFN-α-1b (Sinogen, Kexing Company, Shenzhen) at a dose of 3 MU per 2 d for 24 wk. Thirty-one of thirty-five patients were males and four were females with mean age of 31±7 years. Response to IFN-α treatment was defined as normalization of serum elevated ALT, undetectable HBV DNA by PCR method, and HBeAg seroconversion to anti-HBe until 6 mo after the treatment had ended; and non-response as detectable HBV DNA by PCR, and/or presence of HBeAg regardless of serum ALT level.

Methods

HLA class II typing Genomic DNA was extracted from peripheral blood using guanidine sulfocyanate method and the reagents were supplied by Shanghai blood center. HLA class II alleles were determined by low resolution DNA typing method, one of polymerase chain reaction-sequence specific primers techniques (Pel-Freez, USA) according to the manufacturer's instruction. Gene typing was performed with the use of software supplied by the company.

Serological testing

HBsAg, HBeAg, and antibodies to HBsAg, HBeAg and HBcAg were tested by an ELISA (Roche, Switzerland).

Quantification of HBV DNA

Serum HBV DNA was quantitated by fluorescence PCR performed in LightCycle amplifier (Roche, Switzerland) using domestic commercial kit (Piji Company, Shenzhen).

Statistical analysis

The frequency of HLA class II alleles was calculated by direct counting. The statistical significance of the associations of HLA class II alleles with the clinical outcome or the response to IFN-α was determined by the two-tailed Fisher's exact test using the SPSS 10.0 data analysis software package (Chicago, USA); P values <0.05 were considered statistically significant.

RESULTS

Relationship between HLA-DRB1 and the susceptibility to HBV infection

Frequency distribution of HLA-DRB1 in CHB patients and wealthy controls is illustrated in Table 1. The frequency of DRB1*06 allele in CHB patients was higher than in wealthy controls (2.08% *vs* 0%, $P = 0.018$, odds ratio [OR] = 3.837, 95% confidence interval [95%CI] 3.329-4.422), so are those of DRB1*08 allele (11.11% *vs* 5.50%, $P = 0.034$, OR = 2.148, 95%CI 1.094-4.216) and DRB1*16 allele (6.94% *vs* 3.00%, $P = 0.049$, OR = 0.625, 95%CI 0.252-1.552); the frequency of DRB1*07 allele was lower in CHB patients than in wealthy controls (2.78% *vs* 7.75%, $P = 0.046$, OR = 0.340, 95%CI 0.118-0.981). No significant differences of other HLA-DRB1 alleles' distribution were found between the two groups.

Relationship of HLA-DRB1 and HLA-DQB1 with the response to IFN therapy in patients with CHB

Frequency distribution of HLA-DRB1 and -DQB1 in responders and non-responders to IFN treatment is shown in Table 2. The frequency of DRB1*14 allele in 11 responders was higher than in 24 non-responders (18.18% *vs* 2.08%, $P = 0.031$, OR = 10.444, 95%CI 1.092-99.855); that of DQB1*07 allele was inverse (9.09% *vs* 37.50%,

Table 1 Distribution of HLA-DRB1 alleles in CHB patients and wealthy people

HLA-DRB1	Patients with CHB		Wealthy people		OR (95%CI)	P
	N1	Allele frequency $n = 144$	*N2*	Allele frequency $n = 400$		
DRB1*01	2	1.39	3	0.75	1.864 (0.308–11.269)	0.612
DRB1*04	14	9.72	53	13.25	0.705 (0.378–1.314)	0.303
DRB1*06	3	2.08	0		3.837 (3.329–4.422)	0.018
DRB1*07	4	2.78	31	7.75	0.340 (0.118–0.981)	0.046
DRB1*08	16	11.11	22	5.50	2.148 (1.094–4.216)	0.034
DRB1*09	34	23.61	75	18.75	1.339 (0.846–2.120)	0.225
DRB1*10	4	2.78	4	1.00	2.829 (0.698–11.462)	0.217
DRB1*11	11	7.64	29	7.25	1.058 (0.514–2.178)	0.854
DRB1*12	20	13.89	66	16.50	0.816 (0.475–1.402)	0.507
DRB1*13	2	1.39	15	3.75	0.362 (0.082–1.601)	0.262
DRB1*14	9	6.25	25	6.25	1.000 (0.455–2.197)	1.000
DRB1*15	9	6.25	39	9.75	0.617 (0.291–1.308)	0.234
DRB1*16	10	6.94	12	3.00	2.413 (1.019–5.713)	0.049
DRB1*17	6	4.17	26	6.50	0.625 (0.252–1.552)	0.409

P = 0.021, OR = 0.167, 95%CI 0.035-0.796). No significant differences of other HLA-DRB1 and -DQB1 alleles' distribution were found between the responders and non-responders.

DISCUSSION

It has been well known that human HLA-II antigens are expressed in the member surface of antigen presentation cells and immune response cells, taking part in the regulation of host immune response against foreign antigens, which is determined by the HLA genes' polymorphism and their expression levels in the above-mentioned cell member surface. It is generally acknowledged that some HLA polymorphisms are associated with auto-immune diseases. A close attention has been recently paid to the relationship between HLA polymorphisms and viral hepatitis.

It has been reported that in western Caucasians the frequencies of HLA-DRB1*1301/1302 in German patients with acute self-limited hepatitis B and USA patients with spontaneous viral clearance after HBV infection are both higher than in respective patients with CHB[1,2], whereas in the USA, Afro-American persistent HBV infection is associated with HLA-II gene homozygotes, and DQA1*0501 and DQB1*0301, and their haploids DQA1*0501-DQB1*0301 and DQA1*0501-DQB1*0301-DRB1*1102[9]. It has also revealed that in Korea DR6 and DR13 (especially DR13) have a close relationship with spontaneous viral clearance and DR9 is associated with disease chronicity following HBV infection[2]. These findings suggest that there are different relationships between HLA gene polymorphisms and HBV infection in different racial population, implying that various HLA molecules could present different HBV epitopes to induce effective immune responses[4].

It has been found that in China, the frequencies of HLA-DR10, -DRB1*0301 and -DQB1*0301 all increase in patients with CHB compared with wealthy people, whereas that of HLA-DRB1*1101/1104 is inverse[6,7]; the frequency of HLA-DR12 (especially one of its alleles DRB1*1201) declines compared with those with spontaneous cure following HBV infection, whereas frequencies HLA-DR9, -DQ9 are inverse[5]. In the present study the frequencies of HLA-DRB1*06, -DRB1*08 and -DRB1*16 were all higher in CHB patients than in wealthy people, and that of HLA-DRB1*07 lower in CHB patients than in wealthy people, suggesting that individuals with HLA-DRB1*06, -DRB1*08 or -DRB1*16 alleles were susceptible to HBV infection, whereas those with HLA-DRB1*07 allele was resistant to HBV infection in Shanghai people. Four HLA genes mentioned above, however, are all infrequent among the Shanghai population, the proportion of which accounts for 16.25% of the whole population, suggesting that HLA polymorphism has a less of a role in pathogenesis of CHB.

A lot of domestic and foreign studies including this one demonstrate that some of HLA alleles were susceptible genes to HBV infection and some were resistant genes to HBV infection, but the different genes associated with the outcome of HBV infection were found in different studies. This divergence may be elucidated by gene background of different nations of subjects, research designs and the fact that disease chronicity following HBV infection is probably not influenced by HLA gene polymorphisms.

Whether hepatitis B onsets and disease chronicity occurs after HBV infection is dependent on immune response condition of host who is infected. If there are no primary and secondary immune defects, host's age can reflect his/her mature level of immune functions. Hyams *et al*., reviewed the literatures on chronic HBV infection and found that chronicity rate is about 80-90%, when infection occurs in infants and young persons less than 6 years; that there are usually no self-conscious symptoms accompanying HBV

Table 2 Distribution of HLA class II alleles in IFN responders and non-responders

HLA	Responder		Non-responder		OR (95%CI)	*P*
	N1	Allele frequency *n* = 22	*N2*	Allele frequency *n* = 48		
DRB1*01	0	0.00	1	2.08	1.468 (1.249–1.725)	1.000
DRB1*04	2	9.09	7	14.58	0.586 (0.111–3.080)	0.709
DRB1*06	0	0.00	1	2.08	1.468 (1.249–1.725)	1.000
DRB1*07	1	4.55	2	4.17	1.095 (0.094–12.760)	1.000
DRB1*08	2	9.09	3	6.25	1.500 (0.232–9.685)	0.646
DRB1*09	3	13.64	11	22.92	0.531 (0.132–2.135)	0.524
DRB1*10	1	4.55	2	4.17	1.095 (0.094–12.760)	1.000
DRB1*11	1	4.55	5	10.42	0.410 (0.045–3.731)	0.657
DRB1*12	2	9.09	9	18.75	0.433 (0.085–2.199)	0.483
DRB1*14	4	18.18	1	2.08	10.444 (1.092–99.855)	0.031
DRB1*15	2	9.09	1	2.08	4.700 (0.403–54.835)	0.231
DRB1*16	3	13.64	2	4.17	3.632 (0.561–23.500)	0.316
DRB1*17	1	4.55	3	6.25	0.714 (0.070–7.281)	1.000
DQB1*02	2	9.09	3	6.25	1.500 (0.232–9.685)	0.646
DQB1*04	1	4.55	1	2.08	2.238 (0.134–37.516)	0.533
DQB1*05	7	31.82	8	16.67	2.333 (0.720–7.557)	0.210
DQB1*06	4	18.18	2	4.17	5.111 (0.860–30.310)	0.073
DQB1*07	2	9.09	18	37.50	0.167 (0.035–0.796)	0.021
DQB1*08	1	4.55	5	10.42	0.410 (0.045–3.731)	0.657
DQB1*09	5	22.73	11	22.92	0.989 (0.297–3.295)	1.000

that clear on their own and immunity being acquired, and only a minority with HBV infection show clinical manifestations of acute hepatitis B, chronicity rate less than 5% when infection occurs in adults[10]. The result of a study has shown that only 0.3% of patients become chronic HBV carriers in which a total of about 300 000 patients with HBV infection due to inoculations of yellow fever vaccine populated by HBV were followed up for 40 years[11]. In China 30-50% of population are detected with one antibody or more antibodies to HBV in their whole life, suggesting that they have been infected with HBV and virus has been cleared spontaneously and immunity against HBV has been acquired, which demonstrates that acute transient infection is a principal pattern of HBV infection[12]. These phenomena are not obviously explained by individual discrepancy of human gene background, including HLA polymorphisms.

The effects of HLA genes on IFN treatment to CHB patients have not yet been reported, although domestic and foreign studies have shown that gene polymorphisms of HLA-I and -II antigens have an influence on host immune response to HBsAg vaccine[13-15]. Our study has revealed that HLA-DRB1*14 may be associated with a high rate of the response of CHB patients to IFN treatment, compared with other HLA-DRB1 alleles and HLA-DQB1*07 may be associated with low response rate to IFN, compared with other HLA-DQB1 alleles.

DRB1*14 is also an infrequent HLA gene in Shanghai, its frequencies in 200 wealthy people and 72 CHB patients being 6.25% and 7.14%, respectively. DRB1*14 was found in five patients treated with IFN, four of them were responders. Among these five patients, four of them were infected with type B HBV and one was infected with type C HBV, and serum HBV DNA level was low (data not shown). It has been generally accepted that low level of serum HBV DNA has benefit to IFN treatment and the response rate to IFN treatment is higher in patients with type B HBV infection than in those with type C HBV infection[16]. Therefore, it is not excluded that HLA-DRB1*14 had an occasional relationship with IFN therapy in our study.

Further studies are required for elucidating whether HLA-DQB1*07 allele can serve as one of the indices for selecting patients to be treated with IFN because of a small sample in our study, though it is a frequent HLA gene in the Chinese and has been found to be associated with low response rate to IFN treatment in the present study.

REFERENCES

1 **Hohler T,** Gerken G, Notghi A, Lubjuhn R, Taheri H, Protzer U, Lohr HF, Schneider PM, Meyer zum Buschenfelde KH, Rittner C. HLA-DRB1*1301 and *1302 protect against chronic hepatitis B. *J Hepatol* 1997; **26**: 503-507

2 **Thio CL,** Thomas DL, Karacki P, Gao X, Marti D, Kaslow RA, Goedert JJ, Hilgartner M, Strathdee SA, Duggal P, O'Brien SJ, Astemborski J, Carrington M. Comprehensive analysis of class I and class II HLA antigens and chronic hepatitis B virus infection. *J Virol* 2003; **77**: 12083-12087

3 **Ahn SH,** Han KH, Park JY, Lee CK, Kang SW, Chon CY, Kim YS, Park K, Kim DK, Moon YM. Association between hepatitis B virus infection and HLA-DR type in Korea. *Hepatology* 2000; **31**: 1371-1373

4 **Wu YF,** Wang LY, Lee TD, Lin HH, Hu CT, Cheng ML, Lo SY. HLA phenotypes and outcomes of hepatitis B virus infection in Taiwan. *J Med Virol* 2004; **72**: 17-25

5 **Meng XQ,** Chen HG, Ma YL, Liu KZ. Influence of HLA class II molecules on the outcome of hepatitis B virus infection in population of Zhejiang Province in China. *Hepatobiliary Pancreat Dis Int* 2003; **2**: 230-233

6 **Jiang YG,** Wang YM, Liu TH, Liu J. Association between HLA class II gene and susceptibility or resistance to chronic hepatitis B. *World J Gastroenterol* 2003; **9**: 2221-2225

7 **Shen JJ,** Ji Y, Guan XL, Huang RJ, Sun YP. The association of HLA-DRB1*10 with chronic hepatitis B in Chinese patients. *Linchuang Weishengwuxue Yu Mianyixue Zazhi* 1999; **19**: 58-59

8 **Yu ML,** Dai CY, Chen SC, Chiu CC, Lee LP, Lin ZY, Hsieh MY, Wang LY, Chuang WL, Chang WY. Human leukocyte antigen class I and II alleles and response to interferon-alpha treatment, in Taiwanese patients with chronic hepatitis C virus infection. *J Infect Dis* 2003; **188**: 62-65

9 **Thio CL,** Carrington M, Marti D, O'Brien SJ, Vlahov D, Nelson KE, Astemborski J, Thomas DL. Class II HLA alleles and hepatitis B virus persistence in African Americans. *J Infect Dis* 1999; **179**: 1004-1006

10 **Hyams KC.** Risks of chronicity following acute hepatitis B virus infection: a review. *Clin Infect Dis* 1995; **20**: 992-1000

11 **Seeff LB,** Beebe GW, Hoofnagle JH, Norman JE, Buskell-Bales Z, Waggoner JG, Kaplowitz N, Koff RS, Petrini JL Jr, Schiff ER. A serologic follow-up of the 1942epidemic of post-vaccination hepatitis in the United States Army. *N Engl J Med* 1987; **316**: 965-970

12 **Luo KX.** Hepatitis B: Basic Biology and Clinical Science. 2nd ed. Beijing: *People's Hygiene Press* 2001: 640-650

13 **Qian Y,** Zhang L, Liang XM, Hou JL, Luo KX. Association of immune response to hepatitis B vaccine with HLA-DRB1*02, 07, 09 genes in the population of Han nationality in Guangdong province. *J Mil Med Univ* 2002; **22**: 67-69

14 **Caillat-Zucman S,** Gimenez JJ, Wambergue F, Albouze G, Lebkiri B, Naret C, Moynot A, Jungers P, Bach JF. Distinct HLA class II alleles determine antibody response to vaccination with hepatitis B surface antigen. *Kidney Int* 1998; **53**: 1626-1630

15 **Martinetti M,** De Silvestri A, Belloni C, Pasi A, Tinelli C, Pistorio A, Salvaneschi L, Rondini G, Avanzini MA, Cuccia M. Humoral response to recombinant hepatitis B virus vaccine at birth: role of HLA and beyond. *Clin Immunol* 2000; **97**: 234-240

16 **Wai CT,** Chu CJ, Hussain M, Lok AS. HBV genotype B is associated with better response to interferon therapy in HBeAg (+) chronic hepatitis than genotype C. *Hepatology* 2002; **36**: 1425-1430

Science Editor Guo SY **Language Editor** Elsevier HK

PO Box 2345, Beijing 100023, China
www.wjgnet.com
wjg@wjgnet.com

ELSEVIER

World J Gastroenterol 2005;11(36):5725-5731
World Journal of Gastroenterology ISSN 1007-9327
© 2005 The WJG Press and Elsevier Inc. All rights reserved.

• *BRIEF REPORTS* •

Oral administration of geranylgeranylacetone plus local somatothermal stimulation: A simple, effective, safe and operable preconditioning combination for conferring tolerance against ischemia-reperfusion injury in rat livers

Ning Fan, Guang-Shun Yang, Jun-Hua Lu, Ning Yang, Hai-Bin Zhang

Ning Fan, Guang-Shun Yang, Jun-Hua Lu, Ning Yang, Hai-Bin Zhang, Department of Laparoscopy, Affiliated Eastern Hospital of Hepatobiliary Surgery, Second Military Medical University, Shanghai 200438, China
Co-first-authors: Ning Fan
Correspondence to: Professor Guang-Shun Yang, Department of Laparoscopy, Affiliated Eastern Hospital of Hepatobiliary Surgery, Second Military Medical University, Shanghai 200438, China. guangshun@smmu.edu.cn
Telephone: +86-21-25070803 Fax: +86-21-25070803
Received: 2005-03-11 Accepted: 2005-04-02

Abstract

AIM: To explore a simple, effective, safe and operable pretreatment for conferring tolerance against ischemia-reperfusion (I-R) injury in rat livers.

METHODS: Forty-five rats were divided into five groups (each group n = 9). Group C: control group; group G: geranylgeranylacetone (GGA) was administered without heat stress; group S: local heat stress alone; group WG: GGA plus whole-body heat stress; group SG: GGA administration plus local heat stress. After completion of the I-R procedure, the ischemic-reperfused liver lobes in five groups were resected and tested for heat shock protein (HSP70) by RT-PCR, Western blotting analysis and immunohistochemical staining. The blood samples were collected for ALT and AST measurement at the end of occlusion of blood supply, 30 min after reperfusion, 24, 48, 72 h after surgery from the inferior vena cava. Survival was monitored for 1 wk.

RESULTS: The production of HSP70 after I-R injury increased, the liver enzyme levels after reperfusion decreased rapidly, and the survival rates increased in groups C-SG.

CONCLUSION: The combination of GGA plus local somatothermal stimulation is a simple, effective, safe and operable pretreatment to induce HSP70 in patients with liver tumor and cirrhosis before hepatectomy and in donors before harvesting graft for liver transplantation.

© 2005 The WJG Press and Elsevier Inc. All rights reserved.

Key words: Ischemia-reperfusion injury; Heat shock protein; Geranylgeranylacetone; Local somatothermal stimulation

Fan N, Yang GS, Lu JH, Yang N, Zhang HB. Oral administration of geranylgeranylacetone plus local somatothermal stimulation: A simple, effective, safe and operable preconditioning combination for conferring tolerance against ischemia-reperfusion injury in rat livers. *World J Gastroenterol* 2005; 11(36): 5725-5731
http://www.wjgnet.com/1007-9327/11/5725.asp

INTRODUCTION

Ischemia-reperfusion (I-R) injury is the main cause of hepatic damage induced by temporary clamping of the hepatoduodenal ligament during liver resection (Pringle maneuver), and severe complications of liver transplantation such as primary graft nonfunction or malfunction are also the consequence of reperfusion injury[1,2]. Furthermore, even moderate reperfusion damage that does not severely affect the graft can impair long-term hepatic recovery and enhances the patient's susceptibility to infections and multiple organ failure[1]. Though improvements in liver preservation and surgical techniques have been achieved, hepatic ischemia/reperfusion remains an important clinical problem. Furthermore, because of the shortage of organs for transplantation, the use of steatotic livers, which have a lower tolerance to hypoxia and are more susceptible to reoxygenation damage, greatly increase the risks related to reperfusion injury[3,4]. Therefore, it is clinically significant to find a simple, effective, safe and operable preconditioning combination before liver surgery to protect liver against I-R injury.

Hepatic preconditioning can be induced by transient I-R[5-9], short-term hyperthermia[10,11], oxidative stress[12], or ANP infusion[13,14]. All these stimuli improve postischemic sinusoidal perfusion, leukocyte infiltration, bile production, and aminotransferase release 48 h after their application to liver. Among these stimuli, hyperthermic preconditioning has been proved to be a potential clinical application measurement. After heat shock preconditioning, organisms may produce endogenous cytoprotective substances which can ameliorate I-R injury in subsequent hepatectomy or liver transplantation.

The cytoprotective action of heat shock preconditioning is closely related to the endogenous cytoprotective protein, heat shock protein (HSP), which has been proved to play an important role in protection against I-R injury[16,17]. In

the HSP family, inducible form of HSP70 is the main cytoprotective protein[18,19]. Research on how to apply the cytoprotective action of HSP70 during liver surgery by certain heat shock preconditioning form is scarce. Therefore, how to find out a clinically feasible heat shock stress form remains to be elucidated.

Generally, heat shock stress includes two types: whole-body heat and local heat. By heating the whole body in warm water or on electronic pad, body temperature must be above 41 ℃-the critical temperature[11,20] to activate heat shock stress of viscera where the inducible form of HSP70 is induced to play the cytoprotective action[18,21]. Local somatothermal stimulation (LSTS), a kind of local heat stress on designated skin area, is speculated to be the consequence of a somatovisceral reflex through a heat-sensitive neural release of NO. It is well known that NO is a strong inducer of gene expression of HSP[22-24], and it is interesting that LSTS also has the same critical temperature 41 ℃. Chiu *et al*.[26], have applied LSTS on the right seventh intercostal nerve territory[25] and left median nerve territory[27] respectively (they are regarded in Chinese medicine as sites to cure hepatobiliary and cardiovascular diseases), and found that HSP70 gene expression increases in liver and heart, and I-R injury in liver and heart was also relieved. Thus, for the two types of heat stress, this study aimed to estimate which type is more simple, effective, safe and operable for clinical application.

Besides, in view of the induction of HSP70, the use of pharmacologic inducers might be different. Although most chemicals that are able to induce HSP expression are cellular toxins[28-30], geranylgeranylacetone (GGA, teprenone or Selbex; Eisai Co., Ltd, Tokyo, Japan) is a commercially available medication used to treat gastric ulcer, which has been used in clinic in Japan for decades. Hirakawa *et al*.[31], reported that GGA has the potential to activate HSP70 gene expression in gastric mucosal cells in response to ethanol stress or water-immersion stress. In addition, the cytoprotective effect of GGA has been reported in liver[32,33] and small intestine[34]. Mizushima *et al*.[35], reported that pretreatment with low concentrations of ethanol, as well as GGA-induced HSPs in cultured guinea pig gastric mucosal cells, can prevent DNA fragmentation[35], but further investigation is necessary to know whether ethanol is efficacious in liver pretreatment because the liver has a strong activity of alcohol dehydrogenase. Bimoclomol is a new nontoxic compound, introduced by Vígh *et al*.[36] in 1997, which facilitates the formation of chaperone molecules by inducing or amplifying expression of heat shock genes. It was reported that four- to fivefold HSP70 gene is transcribed by the simultaneous application of bimoclomol and heat. The potency of GGA to enhance HSP70 induction under heat shock stress is as high as that of bimoclomol[21]. In this sense, pharmacologic modulation of heat shock preconditioning by GGA may have a clinical priority because its nontoxicity to human subjects has been proven during the long-term clinical use.

Therefore, the other aim of this study was to explore whether there is any difference in the induction of HSP70 in liver between administration of GGA and heat shock stress, and whether there is an additive effect if GGA is used in combination with heat shock stress.

MATERIALS AND METHODS

Animals

Male Sprague-Dawley rats weighing 250-300 g were obtained from Animal Center of the Fudan University, Shanghai, China. They were housed in chip-bedded cages at room temperature (24±1 ℃) in a 12-h light/dark cycle. Rats were permitted free access to water and standard rat chow. The study was approved by the Committee on Experimental Animals of Second Military Medical University.

Grouping

Forty-five rats were divided into five groups (each group n = 9). Group C: experiment for I-R injury (as a control); group G: GGA was administered 2 h before experiments for I-R injury (administering GGA without heat stress); group S: LSTS was performed 12 h before experiment for I-R injury (local heat stress alone); group WG: GGA was administrated 2 h before whole-body heat shock exposure, and experiment for I-R injury was performed 48 h after whole-body heat shock exposure (GGA plus whole-body heat stress); group SG: GGA was administered 2 h before LSTS, and experiment for I-R injury was performed 12 h after LSTS (GGA administration plus local heat stress).

Extraction of mRNA and reverse transcriptase polymerase chain reaction

Total RNA was isolated from rat liver using a modified single-step guanidinium thiocyanate method (Tri Reagent, T-9424, Sigma Chemical Co., St. Louis, MO, USA)[37]. Reverse transcription (RT) was performed using a reverse transcription kit. One microgram of rat tissue RNA was used as a template and RT-generated cDNA encoding Hsp70 and β-microglobulin (β-MG internal control) were amplified using PCR. The primers used in this study were Hsp70 (354 bp), sense: 5'-AAC-GTG-CTG-CGG-ATC-ATC-AA-3', anti-sense: 5'-CGT-GAT-GGA-CGT-GTA-GAA-GT-3', and rat-β-MG (100 bp), sense: 5'-AAT-ATC-GAG-ATG-TCA-GAT-CTG-TC-3', anti-sense: 5'-GCT-TCA-ATG-AGT-GTT-TTG-ATC-AG-3'. The possible contamination of any PCR component was excluded by performing a PCR with these components in the absence of RT products in each set of experiments (negative control). Twenty microliters of RT-PCR products was checked by 2% agarose gel electrophoresis containing 0.2 mg/mL ethidium bromide, followed by photography under ultraviolet transillumination.

Antibody and Western blot analysis for hsp70 expression

Mouse monoclonal antibody against inducible HSP70 was purchased commercially (HSP 70 K-20: sc-1060, Santa Cruz Biotechnology, Inc.). Liver tissue was snap-frozen *in situ* using stainless steel tongs precooled in liquid nitrogen. Tissue homogenates from rat liver were obtained in the presence of protease inhibitors on ice, and the homogenate protein was assayed by the Bradford method[38]. After protein concentrations were measured, samples were applied to a 10% polyacrylamide gel with 0.1% sodium dodecylsulfate.

The gel-resolved proteins were transferred to polyvinylidene difluoride membranes (Marsh Biomedical Products Inc., Rochester, NY, USA). The blots were incubated with primary antibody (monoclonal K-20: sc-1060) and anti-mouse immunoglobulin horseradish peroxidase-linked secondary antibody (NA 931; Amersham International, Buckinghamshire, UK). They then reacted with enhanced chemiluminescence detection reagent (Amersham). The bands were recorded on X-ray film (Hyper film ECL, Amersham). Intensity of the blots was then measured densitometrically using a GS-700 imaging densitometer. To standardize the blotting as well as the visualization of each film, 0.005 μg of HSP70 (SPP-755, StressGen Biotechnologies Corp.) was simultaneously electrophoresed on each gel as an external standard. Anti-β-actin (monoclonal: clone AC-74, Sigma Inc.) was used as an internal control.

Immunohistochemical staining

Tissue samples fixed overnight in Bouin's solution[39] were immersed first in 50% ethanol for 24 h and then in 70% ethanol for 24 h for their dehydration and the removal of picric acid. Specimens were then embedded in paraffin and cut into 3.5-μm-thick sections. The slightly modified avidin-biotin complex method was used for immunohistochemical staining with a monoclonal antibody (1.0 μg/mL) against the inducible form of HSP70 (monoclonal K-20: sc-1 060.12) normal rabbit serum (diluted to 1:75) as an inhibitor of nonspecific binding of the secondary antibody. Biotin-labeled rabbit anti-mouse IgG serum (diluted to 1:300) as a secondary antibody and avidin-biotin-alkaline phosphatase complex (diluted to 1:100) were purchased from Dako (Kyoto, Japan). The substrate for alkaline phosphatase (black) was obtained from Vector Laboratories (Burlingame, CA, USA).

Administration of GGA

After overnight fasting, each rat in groups G, WG and SG was given 8 mL/kg of an emulsion composed of 200 mg/kg GGA in a 5% gum arabic solution (vehicle). The dose was administered intragastrically through a metal tube. In the groups not receiving GGA (groups C and S), only the vehicle was administered in a similar fashion. GGA used in this study was a generous gift from Eisai Co., Ltd (Tokyo, Japan). We chose a dose of 200 mg/kg, in which abundant HSP70 was produced with whole-body heat shock stress at 41-42 ℃ [21].

Whole-body heat shock exposure

Rats were anesthetized with intramuscular injections of atropine sulfate (0.05 mg/kg) and ketamine (50 mg/kg) 2 h after the GGA administration. They were then immersed in a warm water bath to elevate their rectal temperature to 41-42 ℃ for 15 min. Rectal temperature was measured by a digital thermometer. The timing of 2 h between GGA administration and heat shock treatment was decided according to the reports of *in vivo* metabolism of GGA in rats by Nishizawa *et al*.[40,41]. They showed that tissue level of GGA in the liver reaches plateau 2 h after oral administration in rats. Subsequent experiments for I-R injury were performed 48 h after whole-body heat shock exposure[19].

Local heat stress by local somatothermal stimulation

Local heat stress was confined to LSTS on a designated skin area but no direct contact with the skin surface. LSTS could induce relaxation of the sphincter of Oddi in cats and rabbits and as well as internal sphincter in rabbits[42,43]. In brief, LSTS was achieved by application of a heat generator 0.5 cm on and above the right seventh intercostal nerve territory, just at the junction of right midclavicular line and the seventh intercostal space (Figure 1, under light anesthesia with atropine sulfate, 0.05 mg/kg and ketamine 50 mg/kg, im). The skin temperature at the heating point fluctuating above and below the critical point 41 ℃ was obtained by intermittently turning the switch of the heat generator on and off, namely 4 min on and 5 min off for three courses. Usually, it took 27 min to compete one dose of LSTS. Subsequent experiment for I-R injury of the liver was performed 12 h after the preconditioned LSTS[25].

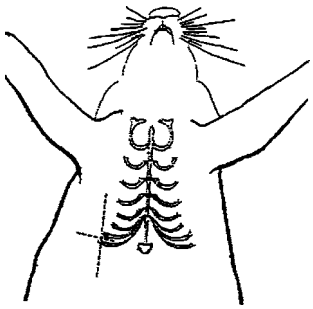


Figure 1 The heating site of LSTS.

Animal model and parameters for liver ischemia-reperfusion injury

The I-R injury rat model was established as described previously[44,45]. In brief, male Sprague-Dawley rats were anesthetized with diethyl ether (1.25 g/kg, ip), and the trachea was cannulated for artificial respiration with a ventilator. The liver was exposed through an upper midline incision, and one clamp for dog's ear was used to clamp the left branches of hepatic hilum and to allow occlusion of the blood supply to either the median or the left lobes (left branch). For I-R injury study, ischemia of left of the median lobes was maintained for 60 min, followed by reperfusion of the left/median lobes with occlusion of the right branches of hepatic hilum for another 30 min. After completion of the reperfusion procedure, the initial ischemia-reperfused left lobes were resected and tested for HSP70 by PT-PCR, Western blotting analysis and immunohistochemical staining. All rats were given 10 mL/kg of 5% glucose solution subcutaneously immediately after completion of the surgery, and all rats were allowed free access to 10% glucose solution after they recovered from the anesthesia. The blood samples were collected for ALT and AST measurement at 60 min after occlusion of the blood supply to the left branch; 30 min after reperfusion to the left branch: 24, 48, and 72 h after surgery from the vena caudalis. Signs of distress and survival were monitored for 1 wk.

Statistical analysis

The data were expressed as mean±SD. SPSS for Windows, version 11.0, was used with *t*-test, LSD, and Wilcoxon. $P<0.05$ was considered statistically significant.

RESULTS

Figure 2 shows the expression of HSP70 mDNA detected by RT-PCR and production of protein HSP70 detected by Western blotting in the five groups after I-R injury. Liver tissues in groups C and G exhibited the most pallid bands of HSP70 compared to that in the other three groups ($P<0.05$). Liver tissue in groups S and WG showed comparative bands of HSP 70 ($P>0.05$), while liver tissue in group SG showed the higher bands compared to that in groups C, G, and S ($P<0.05$). Generally, the production of HSP70 after I-R injury increased in groups C-SG.

Figure 3 shows immunohistochemical staining of HSP70 in liver tissue from groups C to SG. The accumulation of HSP70 in groups C, G, and S was significantly less than

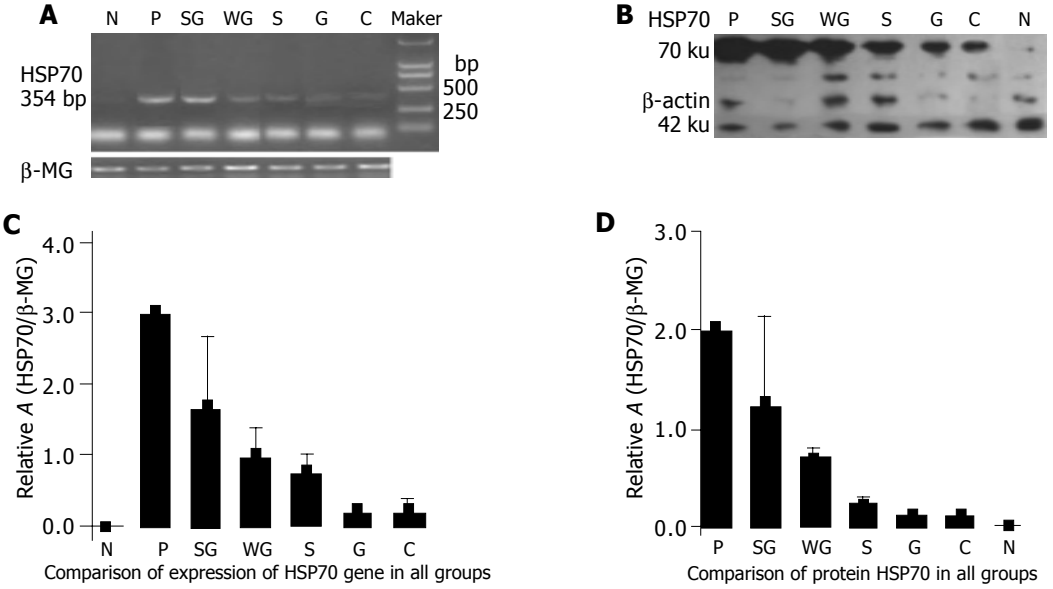


Figure 2 Detection of HSP70. **A**, **B**, The expression of HSP70 gene detected by RT-PCR is shown. **C**, **D**, The production of HSP70 protein detected by Westem blotting is shown. P, positive control. N, nagetive control. SG WG G S C N, group name. The mean difference is significant compared with group G and C at the 0.05 level. The mean difference is significant compared with group S at the 0.05 level.

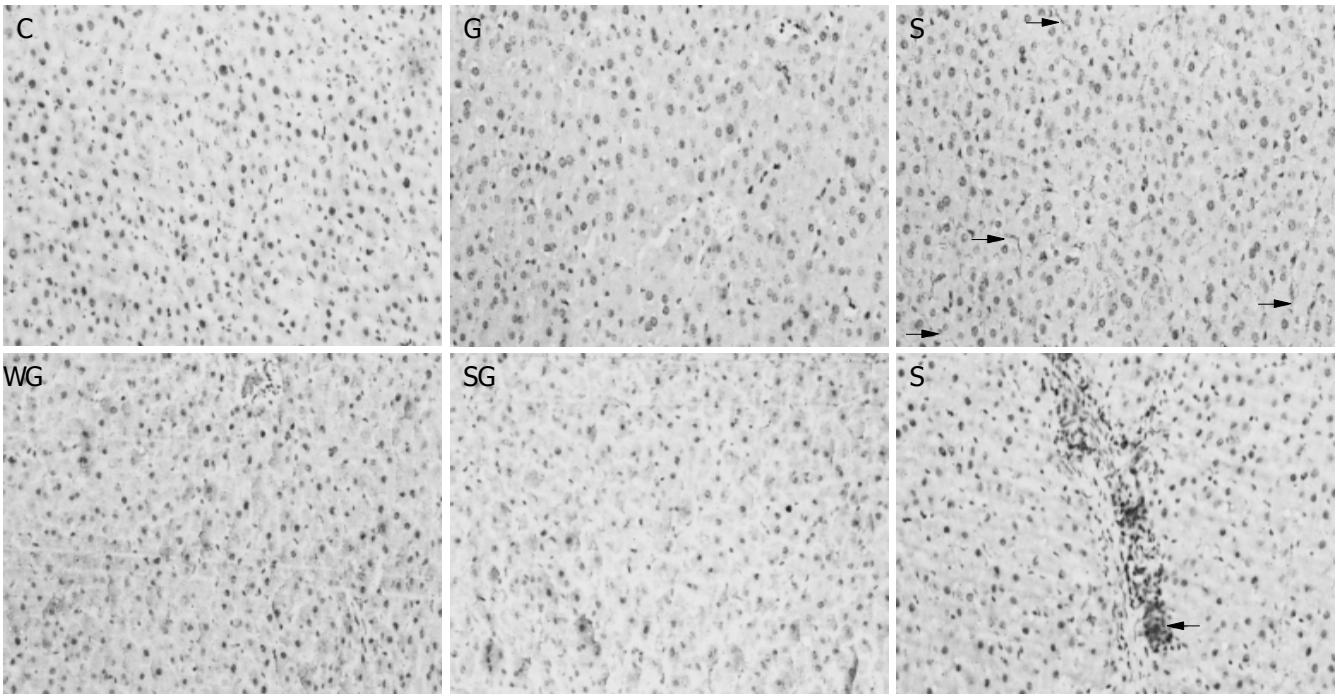


Figure 3 Immunohistochemical staining of HSP70 in liver tissue in group C,G, S,WG and SG HSP70-positive cells in group S were located in the hepatic sinusoid (→) and periportal areas (←).

Table 1 ALT values at different time points in all groups (mean±SD)

Group	60 min after clamping (n = 9)	30 min after reperfusion (n = 9)	24 h after surgery	48 h after surgery	72 h after surgery
C	365.67±13.34	2 601.00±99.21[a]	3 512.75±110.20 (n = 4)[a]	3 895.00±24.04 (n = 2)[a]	–
G	364.22±8.11	2 527.44±74.97[a]	3 521.33±59.53 (n = 3)[a]	3 820.50±72.64 (n=2)[a]	–
S	369.00±12.69	2 174.56±83.99[c]	3 227.50±104.94 (n = 6)[c]	3 589.20±72.64 (n = 5)[c]	3 193.50±101.12 (n = 2)[c]
WG	363.44±9.07	1 977.33±61.07	2 584.63±194.11 (n = 8)	3 040.83±154.93 (n = 6)	2 793.50±122.15 (n=4)
SG	359.11±10.87	1 723.56±94.33	2 013.78±198.22 (n = 9)	2 496.13±139.96 (n = 8)	1 987.25±95.44 (n=7)

[a]P<0.05 *vs* group S, WG, SG; [c]P<0.05 *vs* group WG and SG LSD.

Table 2 AST values at different time points in all groups (mean±SD)

Group	60 min after clamping (n = 9)	30 min after reperfusion (n = 9)	24 h after surgery	48 h after surgery	72 h after surgery
C	365.00±13.73	2 501.89±77.27[a]	3 509.00±125.68 (n = 4)[a]	3 881.00±55.15 (n = 2)[a]	–
G	363.56±12.86	2 525.67±66.83[a]	3 539.67±156.83 (n = 3)[a]	3 932.5±2.12 (n = 2)[a]	–
S	367.67±12.87	2 130.78±78.61[c]	3 221.5±96.67 (n = 6)[c]	3 595.80±60.44 (n = 5)[c]	3 188.00±63.64 (n = 2)[c]
WG	369.67±7.312	1 983.44±50.80	2 591.5±186.35 (n = 8)	3 060.50±145.10 (n = 6)	2 763.75±127.47 (n = 4)
SG	360.67±9.31	1 729.67±93.54	2 019.33±156.83 (n = 9)	2 482.38±113.96 (n = 8)	1 920.38±91.82 (n = 7)

[a]P<0.05 *vs* group S, WG, SG; [c]P<0.05 *vs* group WG and SG LSD.

that in groups WG and SG, whereas a great deal of parenchymal hepatocytes contained HSP70 preferentially in their nuclei and cytoplasm (Figure 3, WG and SG). These results were consistent with those of Western blot and RT-PCR analysis. HSP70-positive cells in group S were located in the hepatic sinusoid and periportal areas (Figure 3, S, arrow).

Tables 1 and 2 show the changes in serum levels of AST and ALT in the five groups. At the end of a 60-min period of clamping, all these parameters remained at low levels in the five groups, and there were no significant differences in these parameters among the groups. During reperfusion, however, these enzyme levels elevated rapidly. Thirty minutes after reperfusion, the levels of AST and ALT in five groups were significantly higher than before reperfusion. But the serum enzyme levels in groups S and G were significantly higher than those in any of the other three groups (P<0.05). The peak of serum enzyme level occurred at 48 h after surgery in groups S, WG, and SG.

Table 3 shows the survival rates at 24, 48, 72 h and 7 d after surgery in all groups. Within 72 h, all rats in groups C and G died, which may be due to the hepatic failure caused by I-R injury after surgery. While in groups SG and WG, the survival rates on d 7 after surgery were as high as 77.8% (7/9) and 44.4% (4/9) respectively, being significantly higher than that in group S (22.2%, P<0.05).

Table 3 Survived rats in all groups

Group (n = 9)	1 d after surgery	2 d after surgery	3 d after surgery	7 d after surgery
C	4	2	0	0
G	3	2	0	0
S	6	5	2	2
WG	8	6	4	4[a]
SG	9	8	7	7[a]

[a]P<0.05 *vs* group S Wilcoxon.

DISCUSSION

It is still controversial that whether certain stress is necessary to the induction of HSP70 after GGA administration, which is related to the application of GGA in clinic to ameliorate I-R injury. Yamagami *et al*.[21], reported that GGA itself does not directly induce HSP70, but it markedly augments the heat shock response in rat liver, leading to the suppression of I-R injury, suggesting that GGA has only a supplementary action in helping other stressors, such as heat stress, ethanol, or water-immersion stress, to activate the cascade of stress response. Oda *et al*.[46], also agree with this. On the other hand, Fudaba *et al*.[47,48], reported that HSP70 could be detected in liver before I-R, and much more after I-R, after administration of high dose of GGA (400 mg/kg per d, for 3 wk) without any form of stress. It was recently reported that administration of a high dose of GGA (200 mg/kg per day for 4 wk) enhances HSP70 induction in transplanted livers and prevented warm ischemic injury and primary graft nonfunction in recipient rats[49]. Our viewpoint is that may be high dose is effective, but it is not applicable because of the long administration schedule before liver transplantation or hepatectomy. But GGA is slowly absorbed from the gastric mucosa, and the uptake by the rat liver is only 5% of that by the gastric mucosa[40], indicating that administration of normal dose GGA without any stimuli cannot enhance HSP70 induction in rat liver and protect liver against I-R injury, which has been proved by our result in group G (200 mg/kg, once a day before surgery). Therefore, it is necessary to find an operable form of stress for clinical application of GGA. Our results showed that GGA plus whole-body heat (group WG) or LSTS (group SG) could significantly enhance HSP70 induction.

As mentioned above, the whole body must be heated in warm water or on electronic pad above 41 ℃ for a certain period of time, which makes this stress form cumbersome and impractical in some circumstances as in the case of

conscious animals or patients.

Compared to whole-body hyperthermia, LSTS has the following three merits. (1) LSTS has a simple and operable manipulation protocol (see Materials and methods) which can be accepted by patients and performed correctly by doctors or nurses before liver surgery. (2) LSTS is performed intermittently to keep the temperature above and below the critical point 41 ℃, so that the heat-sensitive neural transmission would not cause tolerance and patients would feel better. (3) LSTS is a specific stimulation site and can improve the expression of Hsp70 in designed visceral organs. For example, LSTS on left median nerve skin territories increases myocardial but not hepatic Hsp70 expression[25-27], which is the main difference from whole-body hyperthermia. These merits make LSTS be a potential stress form which can be used in clinic.

However, in order to heat the designated skin area above 41 ℃, LSTS needs certain stimulation intensity which is likely to make patients feel a bit of discomfort. This can be relieved by two methods: lowering the stimulating temperature and reducing the time or intensity of stimulation. The latter method is more likely to limit critical temperature. Yamagami *et al*.[21], reported that GGA can achieve a reduction in the duration of whole-body heat shock exposure, which makes us think about what could happen if GGA is administered before LSTS and whether GGA plus LSTS has an additive effect on the induction of HSP70. This hypothesis has been proved in this study by the facts that group SG exhibited a significant higher production of HSP70 than groups G and S (Figures 2 and 3). Liver-related enzymes in group SG presented better liver function recovery 24-72 h after surgery than those in groups G and S (Tables 1 and 2), which is coincident with the conclusion that HSP70 plays an important role lasting for up to 2-4 d in tolerance to reperfusion injury[19,50]. Survival rates 7 d after surgery in group SG was better than that in groups G and S (Table 3). These facts demonstrate that the combination of GGA plus LSTS pretreatment (group SG) has an addictive effect on the induction of HSP70 and the recovery of liver function compared to GGA (group G) or LSTS (group S) alone. Furthermore, GGA plus LSTS (group SG) is comparable to GGA plus whole-body hyperthermia (group WG), but is more simple, safe and operable as a pretreatment to induce HSP70.

In conclusion, the combination of GGA plus LSTS can be used in patients with liver tumor and cirrhosis before hepatectomy and in donor before harvesting graft for liver transplantation.

REFERENCES

1 **Serracino-Inglott F,** Habib NA, Mathie RT. Hepatic ischemia-reperfusion injury. *Am J Surg* 2001; **181**: 160–166
2 **Jaeschke H.** Preservation injury: mechanisms, prevention and consequences. *J Hepatol* 1996; **25**: 774–780
3 **Selzner M,** Clavien PA. Fatty liver in liver transplantation and surgery. *Semin Liver Dis* 2001; **21**: 105–113
4 **Koneru B,** Dikdan G. Hepatic steatosis and liver transplantation current clinical and experimental perspectives. *Transplantation* 2002; **73**: 325–330
5 **Schauer RJ,** Gerbes AL, Vonier D, Opden Winkel M, Fraunberger P, Bilzer M. Induction of cellular resistance against Kupffer cellderived oxidant stress: a novel concept of hepatoprotection by ischemic preconditioning. *Hepatology* 2003; **37**: 286–295
6 **Cutrin JC,** Perrelli MG, Cavalieri B, Peralta C, Rosell-Catafau J, Poli G. Microvascular dysfunction induced by reperfusion injury and protective effect of ischemic preconditioning. *Free Radic Biol Med* 2002; **33**: 1200–1208
7 **Peralta C,** Fernandez L, Panes J, Prats N, Sans M, Pique´ JM, Gelpi E, Rosello-Catafau J. Preconditioning protects against systemic disorders associated with hepatic ischemia-reperfusion through blockade of tumor necrosis factor-induced P selectin up-regulation in the rat. *Hepatology* 2001; **33**: 100–113
8 **Teoh N,** Leclercq I, Dela Pena A, Farrell G. Low-dose TNF-protects against hepatic ischemia-reperfusion injury in mice: implications for preconditioning. *Hepatology* 2003; **37**: 118–128
9 **Funaki H,** Shimizu K, Harada S, Tsuyama H, Fushida S, Tani T, Miwa K. Essential role for nuclear factor kappaB in ischemic preconditioning for ischemia-reperfusion injury of the mouse liver. *Transplantation* 2002; **74**: 551–556
10 **Yamagami K,** Yamamoto Y, Kume M, Kimoto S, Yamamoto H, Ozaki M, Yamamoto M. Heat shock preconditioning ameliorates liver injury following normothermic ischemia-reperfusion in steatotic rat livers. *J Surg Res* 1998; **79**: 47–53
11 **Terajima H,** Enders G, Thiaener A, Hammer C, Kondo T, Thiery J, Yamamoto Y, Yamaoka Y, Messmer K. Impact of hyperthermic preconditioning on postischemic hepatic microcirculatory disturbances in an isolated perfusion model of rat liver. *Hepatology* 2000; **31**: 407–415
12 **Ito K,** Ozasa H, Sanada K, Horikawa S. Doxorubicin preconditioning: a protection against rat hepatic ischemia-reperfusion injury. *Hepatology* 2000; **31**: 416–419
13 **Kiemer AK,** Vollmar AM, Bilzer M, Gerwing T, Gerbes AL. Atrial natriuretic peptide reduces expression of TNF-alpha mRNA during reperfusion of the rat liver upon decreased activation of NF-kappaB and AP-1. *J Hepatol* 2000; **33**: 236–246
14 **Yamagami K,** Yamamoto Y, Toyokuni S, Hata K, Yamaoka Y. Heat shock preconditioning reduces the formation of 8-hydroxy-2'-deoxyguanosine and 4-hydroxy-2-nonenal modified proteins in ischemia-reperfused liver of rats. *Free Radic Res* 2002; **36**: 169–176
15 **Cvoro A,** Matic G. Hyperthermic stress stimulates the association of both constitutive and inducible isoforms of 70 kDa heat shock protein with rat liver glucocorticoid receptor. *Int J Biochem Cell Biol* 2002; **34**: 279-285
16 **Beckmann RP,** Mizzen LA, Welch WJ. Interaction of Hsp 70 with newly synthesized proteins: implications for protein folding and assembly. *Science* 1990; **248**: 850-854
17 **Gething MJ**, Sanbrook J. Protein folding in the cell. *Nature* 1992; **355**: 33-45
18 **King YT,** Lin CS, Lin JH, Lee WC. Whole-body hyperthermia-induced thermotolerance is associated with the induction of heat shock protein 70 in mice. *J Exp Biol* 2002; **205**(Pt 2): 273–278
19 **Terajima H,** Enders G, Thiaener A, Hammer C, Kondo T, Thiery J, Yamamoto Y, Yamaoka Y, Messmer K. Impact of hyperthermic preconditioning on postischemic hepatic microcirculatory disturbances in an isolated perfusion model of the rat liver. *Hepatology* 2000; **31**: 407-415
20 **Lin MT.** Heatstroke-induced cerebral ischemia and neuronal damage. Involvement of cytokines and monoamines. *Ann N Y Acad Sci* 1997; **813**: 572-580
21 **Yamagami K,** Yamamoto Y, Ishikawa Y, Yonezawa K, Toyokuni S, Yamaoka Y. Effects of geranyl-geranyl-acetone administration before heat shock preconditioning for conferring tolerance against ischemia reperfusion injury in rat livers. *J Lab Clin Med* 2000; **135**: 465-475
22 **Fiorucci S,** Santucci L, Antonelli E, Distrutti A, Del Sero G, Morelli O, Romani L, Federici B, Del Soldato P, Morelli A. NO-aspirin protects from T cell-mediated liver injury by inhibiting caspase-dependent processing of Th1like cytokines. *Gastroenterology* 2000; **118**: 404–421
23 **Fiorucci S,** Mencarelli A, Palazzetti B, Del Soldato P, Morelli A, Ignarro LJ. An NO derivative of ursodeoxycholic acid pro-

tects against Fas-mediated liver injury by inhibiting caspase activity. *Proc Natl Acad Sci USA* 2001; **98**: 2652–2657
24 **Leesar MA,** Stoddard MF, Dawn B, Jasti VG, Masden R, Bolli R. Delayed preconditioning-mimetic action of nitroglycerin in patients undergoing coronary angioplasty. *Circulation* 2001; **103**: 2935–2941
25 **Lin YH,** Chiu JH, Tung HH, Tsou MT, Lui WY, Wu CW. Preconditioned somatothermal stimulation on right 7th intercostal nerve territory increases hepatic heat shock protein 70 and protects the liver from ischemia-reperfusion injury in rats. *J Surg Res* 2001; **99**: 328-334
26 **Chiu JH,** Tsou MT, Tung HH, Tai CH, Tsai SK, Chih CL, Lin JG, Wu CW. Preconditioned somatothermal stimulation on median nerve territory increases myocardial heat shock protein 70 and protects rat hearts against ischemia-reperfusion injury. *J Thorac Cardiovasc Surg* 2003; **125**: 678-685
27 **Tsou MT,** Ho JY, Lin CH, Chiu JH. Proteomic analysis finds different myocardial protective mechanisms for median nerve stimulation by electroacupuncture and by local somatothermal stimulation. *Int J Mol Med* 2004; **14**: 553-563
28 **Wiegant FA,** Spieker N, Van Wijk R. Stressor-specific enhancement of hsp induction by low doses of stressors in conditions of self- and cross-sensitization. *Toxicology* 1998; **127**: 107- 119
29 **Ribeiro SP,** Villar J, Downey GP, Edelson JD, Slutsky AS. Sodium arsenite induces heat shock protein-72 kilodalton expression in the lungs and protects rat against sepsis. *Crit Care Med* 1994; **22**: 922-929
30 **Mirkes PE,** Doggett B, Cornel L. Induction of a heat shock response (HSP 72) in rat embryos exposed to selected chemical teratogens. *Teratology* 1994; **49**: 135-142
31 **Hirakawa T,** Rokutan K, Nikawa T, Kishi K. Geranylgeranylacetone induces heat shock proteins in cultured guinea pig gastric mucosal cells and rat gastric mucosa. *Gastroenterology* 1996; **111**: 345-357
32 **Kurihara T,** Akimoto M, Kurokawa K, Ishiguro H, Niimi A, Maeda A, Shigemoto M, Yamashita K, Yokoyama I. Effects of a gastric mucosal protecting agent in rats with liver cirrhosis. *J Gastroenterol Hepatol* 1992; **7**: 405–410
33 **Kurihara T,** Kitamura Y, Adachi Y, Obuchi M, Abe K, Akimoto M, Hashimoto H, Ishiguro H, Niimi A, Maeda A, Shigemoto M, Yamashita K, Yokoyama I. Increase in hepatic tissue blood flow by teprenone. *J Gastroenterol Hepatol* 1996; **11**: 978–984
34 **Tsuruma T,** Yagihash A, Koide S, Araya J, Tarumi K, Watanabe N, Hirata K. Geranylgeranylacetone induces heat shock protein-73 in rat small intestine. *Transplant Proc* 1999; **31**: 572–573
35 **Mizushima T,** Tsutsumi S, Rokutan K, Tsuchiya T. Suppression of ethanol-induced apoptotic DNA fragmentation by geranylgeranylacetone in cultured guinea pig gastric mucosal cells. *Dig Dis Sci* 1999; **44**: 510-514
36 **Vígh L,** Literáti PN, Horváth I, Török Z, Balogh G, Glatz A, Kovacs E, Boros I, Ferdinandy P, Farkas B, Jaszlits L, Jednakovits A, Koranyi L, Maresca B. Biomclomol: a nontoxic, hydroxylamine derivative withstress protein-inducing activity and cytoprotective effects. *Nat Med* 1997; **3**: 1150-1154
37 **Chomczynski P,** Sacchi N. Single-step method of RNA isolation by acid guanidinium thiocyanate–phenol–chloroform extraction. *Anal Biochem* 1987; **162**: 156-159
38 **Bradford MM.** A rapid and sensitive method for quantitation of microgram quantities of protein utilizing the principle of protein–dye binding. *Anal Biochem* 1976; **72**: 248-254
39 **Luna LG.** Manual of histlogical staining methods of the Armed Forces Institute of Pathology. *New York: McGraw- Hill* 1968: 5
40 **Nishizawa Y,** Yamada K, Yamato C, Fujita T. Metabolic fate of geranylgeranylacetone. *Xenobiot Metab Dispos* 1986; **1**: 71-77
41 **Nishizawa Y,** Tanaka H, Kinoshita K. Absorption, distribution, metabolism, and secretion of tetraprenyacetone in rats and guinea pigs. *Prog Med* 1983; **3**: 1029–1035
42 **Chiu JH,** Lui WY, Chen YL, Hong CY. Local somatothermal stimulation inhibits sphincter of Oddi motility in cats, rabbits, and humans through the neural release of nitric oxide. *Life Sci* 1998; **63**: 413-428
43 **Jiang JK,** Chiu JH, Lin JK. Local thermal stimulation inhibits the motility of internal anal sphincter through nitrergic neural release of nitric oxide. *Dis Colon Rectum* 2000; **43**: 381-388
44 **Chiu JH,** Ho CT, Wei YH, Lui WY, Hong CY. *In vitro* and *in vivo* protective effect of honokiol on rat liver from peroxidative injury. *Life Sci* 1997; **61**: 1961-1971
45 **Canada AT,** Stein K, Martel D, Watkins WD. Biochemical appraisal of models for hepatic ischemia–reperfusion injury. *Circ Shock* 1992; **36**: 163-168
46 **Oda H,** Miyake H, Iwata T, Kusumoto K, Rokutan K, Tashiro S. Geranylgeranylacetone suppresses inflammatory responses and improves survival after massive hepatectomy in rats. *J Gastrointest Surg* 2002; **6**: 464-473
47 **Fudaba Y,** Tashiro H, Ohdan H, Miyata Y, Shibata S, Shintaku S, Nishihara M, Asahara T, Ito H, Fukuda Y, Dohi K. Prevention of warm ischemic injury in rat liver transplantation by geranylgeranylacetone. *Transplant Proc* 2000; **32**: 1615–1616
48 **Fudaba Y,** Ohdan H, Tashiro H, Mizunuma K, Ito H, Fukuda Y, Dohi K, Asahara T. High dose of geranylger-anylacetone accumulate HSP72 mRNA in rat liver. *Transplant Proc* 2001; **33**: 978
49 **Fudaba Y,** Ohdan H, Tadhiro H, Hirotaka T, Yasuhiro F, Ito H, Fukuda Y, Dohi K, Asahara T. Geranylgeranylacetone, a heat shock protein inducer, prevents primary graft nonfunction in rat liver transplantation. *Transplantation* 2001; **72**: 184–189
50 **Carini R,** Albano E. Recent Insights on the Mechanisms of Liver Preconditioning. *Gastroenterology* 2003; **125**: 1480-1491

Science Editor Wang XL and Guo SY **Language Editor** Elsevier HK

PO Box 2345, Beijing 100023, China
www.wjgnet.com
wjg@wjgnet.com

ELSEVIER

World J Gastroenterol 2005;11(36):5732-5734
World Journal of Gastroenterology ISSN 1007-9327
© 2005 The WJG Press and Elsevier Inc. All rights reserved.

• *BRIEF REPORTS* •

Role of perioperative parenteral nutrition in severely malnourished patients with Crohn's disease

Guo-Xiang Yao, Xiu-Rong Wang, Zhu-Ming Jiang, Si-Yuang Zhang, An-Ping Ni

Guo-Xiang Yao, Department of Surgery, Tongji Hospital, Tongji Medical College, Huazhong University of Science and Technology, Wuhan 430030, Hubei Province, China
Xiu-Rong Wang, Zhu-Ming Jiang, Si-Yuang Zhang, An-Ping Ni, Department of Surgery, Peking Union Medical College Hospital, CAMS and PUMC, Beijing 100730, China
Correspondence to: Guo-Xiang Yao, MD, Department of Surgery (New Surg Bld-14 F), Tongji Hospital, Tongji Medical College, Huazhong University of Science and Technology, 1095# Jiefang Grand Road, Hankou, Wuhan 430030, Hubei Province, China. gxyao@tjh.tjmu.edu.cn
Telephone: +86-27-61048672
Received: 2005-02-15 Accepted: 2005-04-11

Abstract

AIM: To evaluate the effect of perioperative parenteral nutrition on serum immunoglobulin, weight change, and post-operative outcome in severely malnourished patients with Crohn's disease.

METHODS: Thirty-two severely malnourished patients with Crohn's disease who had undergone surgery in our hospital were reviewed. Sixteen patients who received perioperative parenteral nutrition were enrolled in the study group, and the other 16 patients who did not receive parenteral nutrition were enrolled in the control group. Serum immunoglobulin, body mass index (BMI), liver function, weight change, and postoperative complications were evaluated.

RESULTS: Serum IgM levels elevated 1 wk before surgery in both groups, and decreased to normal value (from 139±41 to 105±29 mg/dL, $P = 0.04$) 4 wk after operation in the study group, while no significant changes was noted in the control group (from 133±16 to 129±13 mg/dL, $P = 0.34$). There were no significant changes in concentrations of IgG and IgA. The BMI of the study group increased from 13.9±0.6 to 15.3±0.7 kg/m^2 ($P = 0.02$) with no significant change in the control group (14.1±0.7 and 14.5±0.5, respectively, $P = 0.81$). The percentage of resuming work was higher in the study group than in the control group.

CONCLUSION: Perioperative parenteral nutrition possibly ameliorates the humoral immunity, reverses malnutrition, and facilitates rehabilitation.

© 2005 The WJG Press and Elsevier Inc. All rights reserved.

Key words: Parenteral nutrition; Malnourished patients; Crohn's disease

Yao GX, Wang XR, Jiang ZM, Zhang SY, Ni AP. Role of perioperative parenteral nutrition in severely malnourished patients with Crohn's disease. *World J Gastroenterol* 2005; 11(36): 5732-5734
http://www.wjgnet.com/1007-9327/11/5732.asp

INTRODUCTION

Most cases of Crohn's disease are complicated by malnutrition and require surgical intervention. Surgery is needed for complications such as perforation, complete bowel obstruction, etc.[1,2].

The effectiveness of parenteral nutrition used alone or in combination with other therapeutics in Crohn's disease patients has been recently reported by clinical trial[1]. However, little is known about the effect of perioperative parenteral nutrition on severely malnourished patients with Crohn's disease.

It was reported that Crohn's disease is caused by excessive immune reactivity in the gut wall[2]. Studies have shown that in active Crohn's disease peripheral B cells are activated as indicated by an increased expression of lymphocyte-activated antigens and by the enhanced *in vitro* spontaneous immunoglobulin production[3]. Immunoglobulin change in the severely malnourished patients receiving perioperative parenteral nutrition *in vivo* is still unclear.

In the present study, the serum immunoglobulin and outcome (weight changes, postoperative complications, and rate of work resumption after 6 mo) in severely malnourished patients with Crohn's disease were evaluated after they were given perioperative parenteral nutrition.

MATERIALS AND METHODS

Patients

Thirty-two patients with Crohn's disease who had undergone surgery were enrolled in the study. All of them were severely malnourished with their body mass indexes (BMI) being less than 15.0 kg/m^2. Sixteen patients entered the study group who received perioperative parenteral nutrition. The other 16 patients who did not receive perioperative parenteral nutrition entered the control group. All had different kinds of bowel surgery for intestinal obstruction and received perioperative parenteral nutrition after 3 wk. The clinical characteristics of the two groups are shown in Table 1. The study group received bowel resection procedures and began to receive perioperative parenteral

nutrition 1 wk before the operation and continued for 2 wk from the next day after surgery. The parenteral nutrition formula was as follows: Crystal amino acid (18 s) was used to provide nitrogen: 0.2 g/kg per d; energy: 30 kcal/kg per d; fat: 40%; glucose: 60%. Patients in the study group received parenteral nutrition through a central venous catheter with the dosages increased over 48 h to a daily goal. Patients in the control group received 5-d intravenous transfusions containing energy 20 kcal/kg per d, normal water, and diet containing the same amount of energy as used in the study group. Average intraoperative blood transfusion was 400 mL in the two groups, which also did not receive steroids 2 wk before and after surgery. All the patients were monitored for complications.

Table 1 Clinical characteristics of two groups before parenteral nutrition

Group	Non-malnutrition group	Malnutrition group	*P*
Patients	16	16	
Age (yr)	28 (20–73)	30 (18–71)	0.47
Sex (M/F)	9/7	10/6	0.60
Localization			
Small bowel	5	6	0.59
Colon	5	3	0.28
Ileocolic	6	7	0.61
Medication			
Corticosteroid	No	No	
Sulfasalazine	7/16	6/16	0.61
Former body weight (%)	92.6±5.3	77.9±6.1	0.03

Serum parameters

Blood samples were drawn before breakfast in the morning and at beginning and end of the study, centrifuged and stored at -20 ℃ before assay.

Serum IgM, IgG, and IgA values were quantitated by ELISA (Sigma, USA)[4].

Liver function and bilirubin levels were also assayed (BD, USA).

Weight change

Body height and weight were recorded; BMI was then calculated at the beginning and end of the study[5].

Follow-up

All the patients were followed up for 6 mo on work resumption after they were discharged from the hospital.

Statistical analysis

The results were expressed as mean±SD. Statistical analyses were performed with the analysis of variance or Student's *t*-test or χ^2 test. $P<0.05$ was considered statistically significant.

RESULTS

Crohn's disease was confirmed in all patients by pathological examination of the surgical samples.

IgM levels elevated before surgery in both groups (control group: 133±16 mg/dL; study group: 139±41 mg/dL; normal value: 110±35 mg/dL; $P = 0.04$), and decreased to normal value (105±29 mg/dL, $P = 0.02$) 3 wk after surgery in the study group with no significant changes in the control group (129±13 mg/dL, $P = 0.34$). There were no significant changes in concentrations of IgG and IgA ($P = 0.20$-0.57, Table 2).

The BMI increased from 13.9±0.6 to 15.3±0.7 kg/m^2 ($P = 0.02$) in the study group and had no significant change in the control group (14.1±0.7 and 14.5±0.5, respectively, $P = 0.81$).

The overall complication rates of both groups were similar (control group: 7 cases, 26.5%; study group: 6 cases, 27.3%; $P = 0.86$). Serum total bilirubin level (mainly indirect bilirubin) was slightly elevated in each group near the end of parenteral nutrition. These results are shown in Table 3.

Table 3 Complications observed during perioperative parenteral nutrition

Type of complications	Non-malnutrition group	Malnutrition group
Infectious		
Pneumonia	2 (*Pneumococcus*)	1 (*Pneumococcus*)
Bacteremia	1 (*Escherichia coli*)	0
Abdominal Abscess	1 (*Enterococcus*)	1 (*E.coli*)
Noninfectious		
Anastomotic leak	1	1
Wound dehiscence	1	2
Liver cholestasis	1 (Tbil = 1.6 mg/dL)	1 (Tbil = 1.4 mg/dL)
Catheter-related	0	0
Total	7	6

DISCUSSION

It was reported that significant B-cell activity is present in Crohn's disease patients and is accompanied with an increase or decrease in immunoglobulin production related to an augmented B-cell clone size, which subsequently induces the humoral immunological action toward the bowel wall[6,7]. However, there are different opinions as to which immunoglobulin is subjected to change[6]. Our study identified the change of IgM.

IgM is the only immunoglobulin that mainly exists in

Table 2 Levels of immunoglobulin before and after parenteral nutrition (mean±SD)

Immunoglobulins	Normal value (mg/dL)	Non-malnutrition group		Malnutrition group	
		Before PN	After PN	Before PN	After PN
IgA	203±50	195±42	218±53	201±38	215±41
IgM	110±35	133±16[1]	129±13	139±41[2]	105±29[3]
IgG	1 210±300	1 160±280	1 250±210	1 305±185	1 409±213

PN, parenteral nutrition. [1]$P = 0.04$ *vs* normal value. [2]$P = 0.04$ *vs* normal value. [3]$P = 0.02$ *vs* before PN.

the circulatory system and not in the tissue. IgG, however, exists in both blood and tissue. Therefore, the change in the concentration of serum IgM instead of IgG represents the total amount of its kind.

In the present study, serum IgM levels rose before surgery in both groups and decreased in the malnourished group after perioperative parenteral nutrition (we excluded the data of the patients complicated by infection to obviate its influence on the results) demonstrates that perioperative parenteral nutrition can ameliorate the humoral immunity of the severely malnourished patients. But the role of circulating B cells and cytokines such as IL-2, TNF-γ, and IL-4 needs to be clarified.

The main effects of parenteral nutrition on humoral immunity may be due to its ability to repair the bowel wall and promote recovery of the disease by avoiding the stimulation of food[8,9], reduce the energy supply for the bacterial proliferation can reduce the antigen load[10], and improve the nutritional status. Our study showed that perioperative parenteral nutrition was efficacious in ameliorating malnutrition without increasing the rate of catheter-related complications. This is beneficial for the repair of lesions, thus attenuating the immune reaction as the anabolism increases[11].

Parenteral nutrition can lead to liver cholestasis, has decreased with reduced energy supply and adequate use of fat emulsions[12,13]. In the present study, one patient had a mild elevation of serum bilirubin (predominantly indirect bilirubin) in each group, which decreased after the patients took a small amount of parenteral nutrition.

In the present study, the 6-mo follow-up showed that the rate of resuming work was higher in the perioperative parenteral nutrition group than in the control group, suggesting that perioperative parenteral nutrition support has a long-lasting effect on recovery, possibly due to the amelioration of immunity[14].

In conclusion, perioperative parenteral nutrition possibly ameliorates the humoral immunity, reverses malnutrition, and facilitates rehabilitation.

REFERENCES

1 **Hoffmann JC,** Zeitz M. Treatment of Crohn's disease. *Hepatogastroenterology* 2000; **47**: 90-100
2 **Bernell O,** Lapidus A, Hellers G. Risk factors for surgery and postoperative recurrence in Crohn's disease. *Ann Surg* 2000; **231**: 38-45
3 **Boirivant M,** Quintieri F, Pugliese O, Famularo G, Fais S, Pallone F. A limiting-dilution analysis of activated circulating B cells in Crohn's disease. *J Clin Immunol* 1990; **10**: 128-134
4 **Gouni-Berthold I,** Baumeister B, Berthold HK, Schmidt C. Immunoglobulins and IgG subclasses in patients with inflammatory bowel disease. *Hepatogastroenterology* 1999; **46**: 1720-1723
5 **Molina A,** Pita A, Farriol M, Virgili N, Soler J, Gomez JM. Serum leptin concentrations in patients with short-bowel syndrome. *Clin Nutr* 2000; **19**: 333-338
6 **Macdonald TT,** Monteleone G, Pender SL. Recent developments in the immunology of inflammatory bowel disease. *Scand J Immunol* 2000; **51**: 2-9
7 **Duerksen DR,** Nehra V, Bistrian BR, Blackburn GL. Appropriate nutritional support in acute and complicated Crohn's disease. *Nutrition* 1998; **14**: 462-465
8 **Wilmore DW.** Nutrition and metabolic support in the 21st century. *J Parenter Enteral Nutr* 2000; **24**: 1-4
9 **Nakamura K,** Moriyama Y, Kariyazono H, Hamada N, Toyohira H, Taira A, Yamada K. Influence of preoperative nutritional state on inflammatory response after surgery. *Nutrition* 1999; **15**: 824-841
10 **Bozzetti F,** Gavazzi C, Miceli R, Rossi N, Mariani L, Cozzaglio L, Bonfanti G, Piacenza S. Perioperative total parenteral nutrition in malnourished, gastrointestinal cancer patients: a randomized, clinical trial. *J Parenter Enteral Nutr* 2000; **24**: 7-14
11 Perioperative total parenteral nutrition in surgical patients. The veterans affairs total parenteral nutrition cooperative study group. *N Engl J Med* 1991; **325**: 525-532
12 **Leaseburge LA,** Winn NJ, Schloerb PR. Liver test alterations with total parenteral nutrition and nutritional status. *J Parenter Enteral Nutr* 1992; **16**: 348-352
13 **Han PD,** Burke A, Baldassano RN, Rombeau JL, Lichtenstein GR. Nutrition and inflammatory bowel disease. *Gastroenterol Clin North Am* 1999; **28**: 423-443
14 **Meryn S,** Lochs H, Pamperl H, Kletter K, Mulac K. Influence of parenteral nutrition on serum levels of proteins with Crohn's disease. *J Parenter Enteral Nutr* 1983; **7**: 553-556

Science Editor Wang XL and Guo SY **Language Editor** Elsevier HK

PO Box 2345, Beijing 100023, China
www.wjgnet.com
wjg@wjgnet.com

ELSEVIER

World J Gastroenterol 2005;11(36):5735-5738
World Journal of Gastroenterology ISSN 1007-9327
© 2005 The WJG Press and Elsevier Inc. All rights reserved.

• *BRIEF REPORTS* •

Clinicopathological significance of FHIT protein expression in gastric adenocarcinoma patients

Po Zhao, Wu Liu, Ya-Li Lu

Po Zhao, Wu Liu, Ya-Li Lu, Department of Pathology, Chinese People's Liberation Army General Hospital, Beijing 100853, China
Correspondence to: Dr. Po Zhao, Department of Pathology, Chinese People's Liberation Army General Hospital, Beijing 100853, China. zhaopo@plagh.com.cn
Telephone: +86-10-66937954 Fax: +86-10-68181689
Received: 2005-03-12 Accepted: 2005-04-11

Abstract

AIM: To investigate the expression of fragile histidine triad (FHIT) protein, and the possible relationship between FHIT expression and clinicopathological indices in gastric carcinoma.

METHODS: FHIT protein expression was examined in 76 cases of gastric carcinoma, 58 cases of intraepithelial neoplasia, and 76 cases of corresponding normal mucosae by immunohistochemical method to analyze its relationship to histological grade, clinical stage, metastatic status and prognosis.

RESULTS: The FHIT protein expression was positive in 28/76 (36.8%) cases of adenocarcinoma tissue, 22/58 (37.9%) cases of adjacent dysplastic tissue and 76/76 (100%) cases of distal normal gastric mucosa. There was a significant difference in the expression of FHIT protein between cancer or adjacent intraepithelial neoplasia and normal gastric mucosa ($P = 0.000$). FHIT protein expression was found in 64.3% (18/28) of grades I and II cancers, and 20.8% (10/48) of grade III cancers ($P = 0.000$), in 56.3% (18/32) of stages I and II cancers and 22.7% (10/44) of stages III and IV cancers ($P = 0.004$), and in 63.6% (14/22) of cancers without metastasis but only 25.9% (14/54) of those with metastasis ($P = 0.003$). The significant difference in the expression of FHIT was found between histological grade, clinical stage and metastatic status of cancer. Follow-up data showed that there was a significant difference in median survival time between cancer patients with expression of FHIT (71 mo) and those without (33 mo, log rank = 20.78, $P = 0.000$).

CONCLUSION: FHIT protein is an important tumor suppressor protein. Loss of FHIT protein expression may be associated with carcinogenesis, invasion, metastasis and prognosis of gastric adenocarcinoma.

© 2005 The WJG Press and Elsevier Inc. All rights reserved.

Key words: Gastric cancer; Gene expression; FHIT; Prognosis

Zhao P, Liu W, Lu YL. Clinicopathological significance of FHIT protein expression in gastric adenocarcinoma patients. *World J Gastroenterol* 2005; 11(36): 5735-5738
http://www.wjgnet.com/1007-9327/11/5735.asp

INTRODUCTION

Fragile histidine triad (FHIT) gene, localized on chromosome 3p14.2 is an important tumor suppressor gene identified after Rb, p53, and p16 genes[1,2]. It spans not only the *t* (3:8) (p14.2; q24) translocation breakpoint found in familial renal cell carcinoma but also the most common human fragile site, FRA3B[2,3]. Alterations in the FHIT gene and/or its expression have been found in primary tumors and cell lines of lung[4,5], breast[6-8], head and neck[9], esophagus[10-12], stomach[13-15], colon and rectum[16-18], pancreas[19], kidney[20,21], cervix[22-25], and hepatocellular carcinoma[26-30]. Abnormal protein expression and allelic deletion of FHIT in lung cancer are associated with the history of smoking and prognosis[31,32]. The finding of decreased expression of FHIT in 93% of precancerous lesions of the lung suggests that this gene might be used as an intermediate biomarker for early diagnosis and/or prevention of lung cancers[32]. Gastric cancer, like lung cancer, is thought to be induced by carcinogens such as *Helicobacter pylori*, alcohol, smoking, high salt and nitrosamine, and low antioxidant vitamins and is increasing in frequency among males in many countries. Therefore, it is imperative to determine whether FHIT plays a role in this second-ranked tumor in male cancer mortality, which has been increasing in China since the 1990s. Only a few reports have evaluated the FHIT gene in primary gastric carcinoma so far[13-15,34-36]. Photomicrographs of FHIT protein expression in gastric carcinoma have been reported[34-36]. However, there is no detailed investigation of FHIT protein expression during gastric carcinogenesis in Chinese patients. Based on the study carried out in 76 gastric adenocarcinomas with 58 abutting intraepithelial neoplasia tissues and 76 distal normal gastric mucosae, the FHIT protein expression in Chinese patients is altered in a high proportion of gastric carcinomas as well as adjacent intraepithelial neoplasia and the loss of FHIT expression is significantly correlated with more advanced clinical stage, poorer differentiation, metastasis and worse prognosis of gastric cancer.

MATERIALS AND METHODS

Biopsy specimens

Paraffin-embedded sections of 76 gastric carcinomas with corresponding 58 adjacent intraepithelial neoplasia mucosae

and 76 distal normal gastric tissues were obtained from the Department of Pathology, Chinese People's Liberation Army General Hospital (Beijing, China). The age of patients ranged from 35 to 84 years, averaged 59±11.58 years. Sixty-six were men and 10 women. Among them, 22 had grade I carcinoma, 6 had grade II carcinoma and 48 had grade III carcinoma, according to their histological grading; while 20 had stage I carcinoma, 12 had stage II carcinoma, 38 had stage III and 6 had stage IV carcinoma, according to the clinical staging of TNM, respectively. Lymphatic metastasis in regional nodes was confirmed during surgery in 54 cancers.

Immunohistochemistry

All samples were fixed in 10% buffered formalin and embedded in paraffin. Four-micrometer-thick sections were cut from wax blocks, mounted onto APES-coated glass slides. Slides were deparaffinized twice in xylene for 10 min, rehydrated through graded ethanol to distilled water before incubation for 30 min with 3% hydrogen peroxidase-methanol to inhibit endogenous peroxidase activity, and heated in 0.01 mol/L citrate buffer (pH 6.0) in a microwave oven for 5 min at 100 ℃ for antigen retrieval. Then the slides were taken out of the microwave oven to be cooled at room temperature for 30 min. After being incubated for 15 min in a blocking solution containing 10% normal goat serum in PBS, sections were incubated at 4 ℃ overnight in a humidified chamber with rabbit polyclonal antibody to human FHIT (Zymed Laboratories Inc., South San Francisco, CA, USA) diluted 1:200 in blocking solution. The sections were rinsed in PBS and incubated for 30 min with biotinylated secondary antibody (Histostain-SP, Zymed). After being washed in PBS, the sections were then incubated for 30 min in streptavidin–HRP (Histostain-SP, Zymed). 3,3'-Diaminobenzidine was used as the chromogen. Slides were counterstained for 3 min with hematoxylin solution. Normal liver tissue was used as a positive control for each lesion, whereas the primary antibody was replaced by normal rabbit serum IgG at a similar dilution or PBS as a negative control.

Evaluation of score

In scoring FHIT protein expression, both the extent and intensity of immunopositivity were considered, according to Hao *et al*.[18]. The intensity of positivity was scored as follows: 0, negative; 1, weak; 2, moderate; 3, strong as the normal stomach. The extent of positivity was scored as follows: 0, <5; 1, >5-25%; 2, >25-50%; 3, >50-75%; 4, >75% of the cells in the respective lesions. The final score was determined by multiplying the intensity of positivity and the extent of positivity scores, yielding a range from 0 to 12. Scores 9-12 were defined as preserved or strong staining pattern (++), 5-8 as weak staining pattern (+), and 0-4 were markedly reduced or negative expression (-).

Statistical analysis

Fisher's exact test (two-sided), Pearson's χ^2 test for trends in proportions and Kaplan-Meier method with log rank test for survival analysis were used to assess the associations between FHIT expression and pathological indices by SPSS 10.0 for Windows (Chicago, IL, USA). $P<0.05$ was considered statistically significant.

RESULTS

FHIT expression in normal, adjacent dysplastic mucosae and adenocarcinoma

FHIT protein was predominantly strongly expressed in the cytoplasm of epithelial cells in 76/76 distal normal stomach mucosae (Figure 1A) and 22/58 (37.9%) adjacent intraepithelial neoplasia. Some stromal cells, such as fibroblasts, endoepithelial cells, and macrophages, also expressed FHIT protein, both in nuclei and cytoplasm. FHIT protein was positively expressed in 28/76 (36.8%) of gastric adenocarcinomas. The carcinomas with markedly reduced or loss of FHIT protein were 48/76 (63.2%), in which the extent and intensity of FHIT expression were markedly reduced or absent in cancer cells (Figure 1B). A significant difference was found in the expression of FHIT protein between normal gastric mucosae and adenocarcinoma or adjacent intraepithelial neoplasia ($P = 0.000$). There was no difference in FHIT expression between carcinoma and adjacent intraepithelial neoplasia ($P = 1.000$).

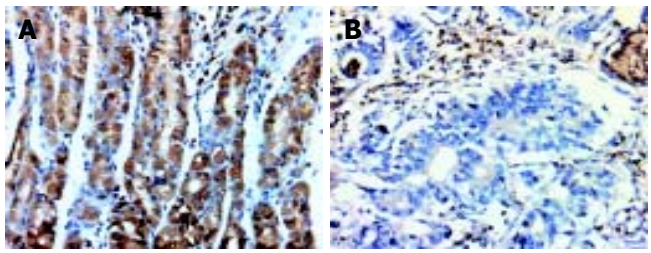


Figure 1 Positive FHIT expression in the normal gastric mucosa (**A**) and negative FHIT expression in cancer cells (**B**). (SP ×200).

Relationship between FHIT expression and histological grade, clinical stage and prognosis

The proportion of carcinomas with expression of FHIT protein showed a decreasing trend from 18 of 28 (64.3%) well- and moderately-differentiated cancers (grades I and II) to 10 of 48 (20.8%) poorly-differentiated carcinomas (grade III), and a significant inverse association was found between FHIT expression and histological grade ($P = 0.000$). A decreasing trend in FHIT expression was also observed in clinical stage, from 18 of 32 (56.3%) in stages I and II adenocarcinomas to 10 of 44 (22.7%) in stages III and IV adenocarcinomas and there was a significant difference in FHIT expression between clinical stages ($P = 0.004$) as well. FHIT expression was present in 14 of 54 (25.9%) cancers with metastasis or in 14 of 22 (63.6%) of tumors without metastasis, thus a significant difference in expression of FHIT was found between the adenocarcinomas with different biological behaviors ($P = 0.003$). Follow-up data showed that there was a significant difference in median survival time between the carcinoma patients with FHIT expression (71 mo) and those without FHIT expression (33 mo, log rank = 20.78, $P = 0.000$, Figure 2).

DISCUSSION

Although FHIT protein is expressed in most types of normal human tissues, it is frequently reduced or lost in a variety

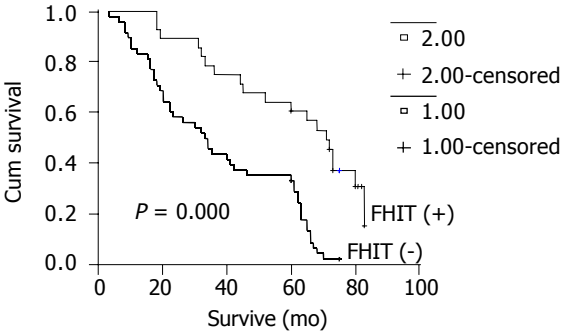


Figure 2 Difference in median survival time between carcinoma patients with and without FHIT expression (n = 76). The y-axis represents the percentage of patients, the x-axis represents their survival time. The red line represents FHIT-positive patients with a better survival, the green line represents FHIT-negative gastric carcinoma patients (log rank = 20.78; P = 0.000).

of human tumors due to alterations in its gene transcription or gene deletion[1-3]. It has thus been suggested that FHIT gene is a candidate tumor suppressor gene for multiple carcinomas. FHIT gene protein is a member of histidine triad family and the mechanism of its suppression on tumor cells remains obscure[1-3]. The following possible mechanisms have been considered as a tumor suppressor[33]. First, the tumor-suppressing function of FHIT might catabolize ApppA (Ap_3A) or related substrates. Ap_3A is an analog of ATP, which can provide phosphates as a substrate to raise the activity of protein kinase. Loss of FHIT protein may lead to the loss of Ap_3A hydrolase activity and the resulting elevated levels of Ap_3A or similar compounds may enhance the transductive signals of growth, thus contributing to carcinogenesis. Second, the activity of FHIT on mRNA cap analogs raises the possibility that failure of a decapping function might be tumorigenic, but the properties of FHIT are quite different from those of enzymes known to decap mRNA, making this an unlikely mechanism. Third, the tumor-suppressing function of FHIT might be the signaling of FHIT-substrate complexes or compounds as an active form of FHIT. Fourth, FHIT might have a nucleotide-independent role as a tumor suppressor[33]. The loss of FHIT protein corresponds to the carcinogenesis and evolution of gastric adenocarcinoma. Capuzzi *et al*.[34], found that 49% of tumors show complete loss plus 29% partial loss of expression in FHIT protein. The absence of FHIT protein is related to higher histological grade and higher tumor stage. Lee *et al*.[35], observed that FHIT expression correlates with the prognosis of gastric cancer. Rocco *et al*.[36], showed that loss of FHIT protein expression is associated with progression and poor differentiation of gastric cancer. Our results are consistent with those reported outside China[34-36], and our previous finding in Chinese colorectal cancer and hepatocellular carcinoma patients[17]. Besides adenocarcinoma, we have also investigated the adjacent intraepithelial neoplasia mucosa and found only 37.9% of which could express FHIT protein, slightly higher than that of carcinoma (36.8%). Therefore, it is also further suggested that like lung and esophageal cancers associated with environmental carcinogens, loss of FHIT protein plays an important role in gastric cancer transformation at its early stage and thus the treatment of FHIT in molecular approach can prevent the carcinogenesis of precancerous gastric lesions.

In conclusion, FHIT protein, like Rb, p53 and p16, may be a universal tumor-suppressor protein, and plays an important role in the carcinogenesis, progress and prognosis of Chinese gastric carcinoma patients. The FHIT expression status detected by immunohistochemistry may be used as a simple and useful molecular marker for the prognosis of gastric adenocarcinoma patients.

REFERENCES

1 **Croce CM,** Sozzi G, Huebner K. Role of FHIT in human cancer. *J Clin Oncol* 1999; **17**: 1618-1624
2 **Huebner K,** Druck T, Siprashvili Z, Croce CM, Kovatich A, McCue PA. The role of deletions at the FRA3B/FHIT locus in carcinogenesis. *Recent Results Cancer Res* 1998; **154**: 200-215
3 **Druck T,** Berk L, Huebner K. FHITness and cancer. *Oncol Res* 1998; **10**: 341-345
4 **Fong KM,** Biesterveld EJ, Virmani A, Wistuba I, Sekido Y, Bader SA, Ahmadian M, Ong ST, Rassool FV, Zimmerman PV, Giaccone G, Gazdar AF, Minna JD. FHIT and FRA3B 3p14.2 allele loss are common in lung cancer and preneoplastic bronchial lesions and are associated with cancer-related FHIT cDNA splicing aberrations. *Cancer Res* 1997; **57**: 2256-2267
5 **Sozzi G,** Tornielli S, Tagliabue E, Sard L, Pezzella F, Pastorino U, Minoletti F, Pilotti S, Ratcliffe C, Veronese ML, Goldstraw P, Huebner K, Croce CM, Pierotti MA. Absence of Fhit protein in primary lung tumors and cell lines with FHIT gene abnormalities. *Cancer Res* 1997; **57**: 5207-5212
6 **Negrini M,** Monaco C, Vorechovsky I, Ohta M, Druck T, Baffa R, Huebner K, Croce CM. The FHIT gene at 3p14.2 is abnormal in breast carcinomas. *Cancer Res* 1996; **56**: 3173-3179
7 **Bieche I,** Latil A, Becette V, Lidereau R. Study of FHIT transcripts in normal and malignant breast tissue. *Genes Chromosomes Cancer* 1998; **23**: 292-299
8 **Campiglio M,** Pekarsky Y, Menard S, Tagliabue E, Pilotti S, Croce CM. FHIT loss of function in human primary breast cancer correlates with advanced stage of the disease. *Cancer Res* 1999; **59**: 3866-3869
9 **Virgilio L,** Shuster M, Gollin SM, Veronese ML, Ohta M, Huebner K, Croce CM. FHIT gene alterations in head and neck squamous cell carcinomas. *Proc Natl Acad Sci USA* 1996; **93**: 9770-9775
10 **Zou TT,** Lei J, Shi YQ, Yin J, Wang S, Souza RF, Kong D, Shimada Y, Smolinski KN, Greenwald BD, Abraham JM, Harpaz N, Meltzer SJ. FHIT gene alterations in esophageal cancer and ulcerative colitis (UC). *Oncogene* 1997; **15**: 101-105
11 **Michael D,** Beer DG, Wilke CW, Miller DE, Glover TW. Frequent deletions of FHIT and FRA3B in Barrett's metaplasia and esophageal adenocarcinomas. *Oncogene* 1997; **15**: 1653-1659
12 **Menin C,** Santacatterina M, Zambon A, Montagna M, Parenti A, Ruol A, D'Andrea E. Anomalous transcripts and allelic deletions of the FHIT gene in human esophageal cancer. *Cancer Genet Cytogenet* 2000; **119**: 56-61
13 **Tamura G,** Sakata K, Nishizuka S, Maesawa C, Suzuki Y, Iwaya T, Terashima M, Saito K, Satodate R. Analysis of the fragile histidine triad gene in primary gastric carcinomas and gastric carcinoma cell lines. *Genes Chromosomes Cancer* 1997; **20**: 98-102
14 **Baffa R,** Veronese ML, Santoro R, Mandes B, Palazzo JP, Rugge M, Santoro E, Croce CM, Huebner K. Loss of FHIT expression in gastric carcinoma. *Cancer Res* 1998; **58**: 4708-4714
15 **Lee SH,** Kim WH, Kim HK, Woo KM, Nam HS, Kim HS, Kim JG, Cho MH. Altered expression of the fragile histidine triad gene in primary gastric adenocarcinomas. *Biochem Biophys Res Commun* 2001; **284**: 850-855
16 **Ohta M,** Inoue H, Cotticelli MG, Kastury K, Baffa R, Palazzo J, Siprashvili Z, Mori M, McCue P, Druck T, Croce CM, Huebner K. The FHIT gene, spanning the chromosome 3p14.2 fragile site and renal carcinoma-associated t (3; 8) breakpoint, is

abnormal in digestive tract cancers. *Cell* 1996; **84**: 587-597
17 **Zhao P,** Lu Y, Hu Y, Zhong M, Li Z, Li X. Loss of fragile histidine triad expression in colorectal carcinoma. *Zhonghua Binglixue Zazhi* 2002; **31**: 124-127
18 **Hao XP,** Willis JE, Pretlow TG, Rao JS, MacLennan GT, Talbot IC, Pretlow TP. Loss of fragile histidine triad epression in colorectal carcinomas and premalignant lesions. *Cancer Res* 2000; **60**: 18-21
19 **Sorio C,** Baron A, Orlandini S, Zamboni G, Pederzoli P, Huebner K, Scarpa A. The FHIT gene is expressed in pancreatic ductular cells and is altered in pancreatic cancers. *Cancer Res* 1999; **59**: 1308-1314
20 **Hadaczek P,** Siprashvili Z, Markiewski M, Domagala W, Druck T, McCue PA, Pekarsky Y, Ohta M, Huebner K, Lubinski J. Absence or reduction of Fhit expression in most clear cell renal carcinomas. *Cancer Res* 1998; **58**: 2946-2951
21 **Werner NS,** Siprashvili Z, Fong LY, Marquitan G, Schroder JK, Bardenheuer W, Seeber S, Huebner K, Schutte J, Opalka B. Differential susceptibility of renal carcinoma cell lines to tumor suppression by exogenous Fhit expression. *Cancer Res* 2000; **60**: 2780-2785
22 **Greenspan DL,** Connolly DC, Wu R, Lei RY, Vogelstein JT, Kim YT, Mok JE, Munoz N, Bosch FX, Shah K, Cho KR. Loss of FHIT expression in cervical carcinoma cell lines and primary tumors. *Cancer Res* 1997; **57**: 4692-4698
23 **Yoshino K,** Enomoto T, Nakamura T, Nakashima R, Wada H, Saitoh J, Noda K, Murata Y. Aberrant FHIT transcripts in squamous cell carcinoma of the uterine cervix. *Int J Cancer* 1998; **76**: 176-181
24 **Birrer MJ,** Hendricks D, Farley J, Sundborg MJ, Bonome T, Walts MJ, Geradts J. Abnormal Fhit expression in malignant and premalignant lesions of the cervix. *Cancer Res* 1999; **59**: 5270-5274
25 **Wu R,** Connolly DC, Dunn RL, Cho KR. Restored expression of fragile histidine triad protein and tumorigenicity of cervical carcinoma cells. *J Natl Cancer Inst* 2000; **92**: 338-344
26 **Chen YJ,** Chen PH, Chang JG. Aberrant FHIT transcripts in hepatocellular carcinomas. *Br J Cancer* 1998; **77**: 417-420
27 **Schlott T,** Ahrens K, Ruschenburg I, Reimer S, Hartmann H, Droese M. Different gene expression of MDM2, GAGE-1, -2 and FHIT in hepatocellular carcinoma and focal nodular hyperplasia. *Br J Cancer* 1999; **80**: 73-78
28 **Keck CL,** Zimonjic DB, Yuan BZ, Thorgeirsson SS, Popescu NC. Nonrandom breakpoints of unbalanced chromosome translocations in human hepatocellular carcinoma cell lines. *Cancer Genet Cytogenet* 1999; **111**: 37-44
29 **Gramantieri L,** Chieco P, Di Tomaso M, Masi L, Piscaglia F, Brillanti S, Gaiani S, Valgimigli M, Mazziotti A, Bolondi L. Aberrant fragile histidine triad gene transcripts in primary hepatocellular carcinoma and liver cirrhosis. *Clin Cancer Res* 1999; **5**: 3468-3475
30 **Yuan BZ,** Keck-Waggoner C, Zimonjic DB, Thorgeirsson SS, Popescu NC. Alterations of the FHIT gene in human hepatocellular carcinoma. *Cancer Res* 2000; **60**: 1049-1053
31 **Burke L,** Khan MA, Freedman AN, Gemma A, Rusin M, Guinee DG, Bennett WP, Caporaso NE, Fleming MV, Travis WD, Colby TV, Trastek V, Pairolero PC, Tazelaar HD, Midthun DE, Liotta LA, Harris CC. Allelic deletion analysis of the FHIT gene predicts poor survival in non-small cell lung cancer. *Cancer Res* 1998; **58**: 2533-2536
32 **Sozzi G,** Pastorino U, Moiraghi L, Tagliabue E, Pezzella F, Ghirelli C, Tornielli S, Sard L, Huebner K, Pierotti MA, Croce CM, Pilotti S. Loss of FHIT function in lung cancer and preinvasive bronchial lesions. *Cancer Res* 1998; **58**: 5032-5037
33 **Pace HC,** Garrison PN, Robinson AK, Barnes LD, Draganescu A, Rosler A, Blackburn GM, Siprashvili Z, Croce CM, Huebner K, Brenner C. Genetic, biochemical, and crystallographic characterization of Fhit-substrate complexes as the active signaling form of Fhit. *Proc Natl Acad Sci USA* 1998; **95**: 5484-5489
34 **Capuzzi D,** Santoro E, Hauck WW, Kovatich AJ, Rosato FE, Baffa R, Huebner K, McCue PA. Fhit expression in gastric adenocarcinoma: correlation with disease stage and survival. *Cancer* 2000; **88**: 24-34
35 **Lee HS,** Lee HK, Kim HS, Yang HK, Kim WH. Tumour suppressor gene expression correlates with gastric cancer prognosis. *J Pathol* 2003; **200**: 39-46
36 **Rocco A,** Schandl L, Chen J, Wang H, Tulassay Z, McNamara D, Malfertheiner P, Ebert MP. Loss of FHIT protein expression correlates with disease progression and poor differentiation in gastric cancer. *J Cancer Res Clin Oncol* 2003; **129**: 84-88

Science Editor Wang XL and Guo SY **Language Editor** Elsevier HK

PO Box 2345, Beijing 100023, China
www.wjgnet.com
wjg@wjgnet.com

ELSEVIER

World J Gastroenterol 2005;11(36):5739-5741
World Journal of Gastroenterology ISSN 1007-9327
© 2005 The WJG Press and Elsevier Inc. All rights reserved.

• *CASE REPORT* •

Post-metallic stent placement bleeding caused by stent-induced ulcers

Chun-Tao Wai, Christopher Khor, Siew-Eng Lim, Khek-Yu Ho

Chun-Tao Wai, Christopher Khor, Khek-Yu Ho, Department of Medicine, National University Hospital, 5 Lower Kent Ridge Road, Singapore 119074, Singapore
Siew-Eng Lim, Department of Hematology and Oncology, National University Hospital, 5 Lower Kent Ridge Road, Singapore 119074, Singapore
Correspondence to: Professor Khek-Yu Ho, Senior Consultant, Department of Medicine, National University Hospital, 5 Lower Kent Ridge Road, Singapore 119074, Singapore. mdchoky@nus.edu.sg
Telephone: +65-67724353 Fax: +65-67794112
Received: 2004-10-22 Accepted: 2004-11-19

Abstract

Placement of self-expandable metal stents (SEMS) is an effective mode of palliative treatment for patients with malignant gastrointestinal obstruction. Gastrointestinal mucosal bleeding complicates about 5% of placement of SEMS but is not well described. We report three cases of gastrointestinal bleeding post-SEMS placement and suggest that bleeding is caused by direct mucosal infringement by the sharp edges of the ends of the stents.

© 2005 The WJG Press and Elsevier Inc. All rights reserved.

Key words: Colorectal cancer; Gastric cancer; Stricture

Wai CT, Khor C, Lim SE, Ho KY. Post-metallic stent placement bleeding caused by stent-induced ulcers. *World J Gastroenterol* 2005; 11(36): 5739-5741
http://www.wjgnet.com/1007-9327/11/5739.asp

INTRODUCTION

Placement of self-expandable metal stents (SEMS) has emerged as an effective mode of palliative treatment for patients with malignant gastrointestinal obstruction[1,2]. This is particularly true in patients with locally advanced disease or patients with multiple co-morbidities, where open or laparoscopic surgical by-pass is associated with high post-operative mortality and morbidity[3,4]. Although placement of SEMS is successful in almost 100% of cases, complications of SEMS do occur and include re-obstruction (10%), stent migration (10%), pain (5%), perforation (4%), and rarely, death (1%)[5,6]. Bleeding has been reported to occur in 5% of patients following placement of SEMS. The mechanisms to explain such bleeding have not been well described. In this report, we describe three cases of bleeding post-SEMS placement and suggest that stent-induced ulcers were caused by infringement of the raw ends of the stents onto the mucosa that may be the cause of such bleeding.

CASE REPORT

The first patient was a 93-year-old female with a past history of diabetes mellitus, hypertension, cerebrovascular accident, who presented with subacute intestinal obstruction. Sigmoidoscopy showed a large tumor at the recto-sigmoid junction, causing almost complete obstruction of the intestinal lumen. The CF240 endoscope (Olympus Pte Ltd, Singapore) could not be passed to cross the structure (Figure 1). In view of her poor pre-morbid status, the family and the attending gastroenterologist opted for palliative stenting. Stenting was done with 85 mm×25 mm Ultraflex® stent (Boston Scientific Pte Ltd, Singapore), which was successful and uneventful. The patient was able to pass motion after the stenting and was discharged one day after the procedure. Unfortunately, she was readmitted 8 wk later for fresh per rectal bleeding. A repeat sigmoidoscopy showed a patent stent with a circumferential mucosal ulcer being impinged upon by the proximal sharp edges of the stent (Figure 2). The bleeding stopped spontaneously and no specific treatment was required. The patient was well till 4 wk post-discharge.

The second patient was a 51-year-old man who presented with gastric outlet obstruction one year after cholecystectomy with hepaticojejunostomy for gallbladder carcinoma. CT scan of the abdomen showed local recurrence at the head of pancreas with liver metastasis. Gastroscopy showed pyloric stenosis due to extrinsic compression, which was not passable by the XQ240 endoscope (Olympus Pte Ltd, Singapore). In view of the metastatic disease and previous laparotomy, the family and the attending gastroenterologist decided on placement of SEMS for palliation of the gastric outlet obstruction. A 60 mm×22 mm uncovered Enteral Wallstent® (Boston Scientific Pte Ltd, Singapore) was subsequently placed successfully. The patient was able to tolerate oral diet and remained well until 4 wk later, when he was noted to have a drop in hemoglobin to 3.9 g/dL from a baseline level of 9 g/dL. A repeat gastroscopy showed a patent stent with circumferential ulcers on the mucosa of the first part of duodenum being impinged upon by the distal end of the stent (Figure 3). Hemostasis was secured by application of argon plasma coagulation (Erbe, JDH Medical System, Singapore). He recovered well with stable hemoglobin and absence of rebleeding up to 4 wk post discharge.

The third patient was an 80-year-old man with adenocar-

cinoma at the gastroesophageal junction, presenting with dysphagia. Despite seven previous dilatations using savary dilators, his dysphagia persisted. A 16 cm×24 mm Flamingo stent (Boston Scientific Pte Ltd, Singapore) was subsequently inserted uneventfully with relief of his dysphagia. He was readmitted 16 wk later for melena and anemia, requiring blood transfusion. A repeat gastroscopy showed oozing from the esophageal mucosa at the proximal end of the stent (Figure 4). No endoscopic therapy was applied as no focal site of active bleeding was noted at that time. The patient was given oral sulcralfate and tranexamic acid. He succumbed to his metastatic disease 8 wk later although his rebleeding did not occur.



Figure 1 A large tumor at the recto-sigmoid junction was seen almost obstructing the entire lumen.



Figure 2 A circumferential ulcer in the rectum was seen being impinged upon by the sharp edges of the Wallstent.

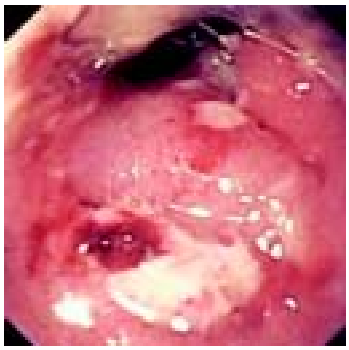


Figure 3 A circumferential ulcer with an adherent clot in the first part of duodenum was seen being impinged upon by the sharp edges of the Wallstent.

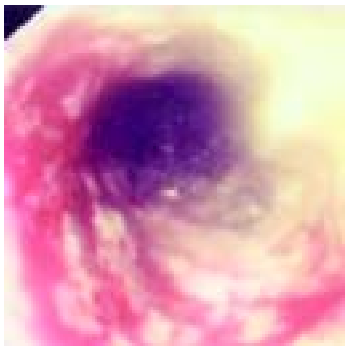


Figure 4 Circumferential ulcer with mild oozing was noted at the proximal end of the stent in the esophagus.

DISCUSSION

Gastrointestinal cancers are among the commonest cancers in most developed countries. Unfortunately, less than half of the patients are candidates for curative surgery, and maintaining patency of the gastrointestinal tract becomes one of the most important aspects of palliative management[7,8]. Among the different modes of palliation, SEMS placement offers the advantage of a high success rate and a low procedure-related complication rate[9]. However, 10-20% of complications, including stent migration, reobstruction by tumor ingrowth, and perforation, have been reported[10]. Bleeding post-stent placement is considered rare at <5%, and has not been studied well.

In this study, we encountered three cases of delayed bleeding post-stent placement, which occurred 4-16 wk after placement. The bleeding originated from ulcers that arose as a result of impingement by the sharp flaring edges of the stents. No active bleeding was noted from the tumor itself. Bleeding stopped spontaneously in one case, and was arrested by argon plasma coagulation application in one and sulcrafate plus tranexamic acid in another. The bleeding appeared to be self-limiting, as no rebleeding was seen after 4-8 wk of follow-up.

Mucosal response to stents is not well understood. Previous animal studies suggest that stents could cause inflammation and collagenous reaction at the underlying mucosa[11]. Another human autopsy study suggests that stents could cause pressure necrosis in the underlying tumor, followed by chronic inflammatory response in the tumor, and epithelialization of the stent lumen[12]. However, these studies did not evaluate the cause of bleeding post-tent insertion.

We believe that direct impingement of gastrointestinal mucosa by the sharp edges of the metallic stent may be an important cause of ulcer formation and bleeding post-stent placement. Manufacturers of SEMS should be aware of this potential technical complication and consider making stents with blunt and softer edges, which may help in avoiding such a complication.

REFERENCES

1 **Kim JH,** Yoo BM, Lee KJ, Hahm KB, Cho SW, Park JJ, Kim SS, Park HC, Kim JH. Self-expanding coil stent with a long delivery system for palliation of unresectable malignant gastric

outlet obstruction: a propective study. *Endoscopy* 2001; **33**: 838-842
2 **Baron TH,** Rey JF, Spinelli P. Expandable metal stent placement for malignant colorectal obstruction. *Endoscopy* 2002; **34**: 823-830
3 **Buechter KJ,** Boustany C, Caillouette R, Cohn I Jr. Surgical management of acutely obstructed colon: review of 127 cases. *Am J Surg* 1988; **156**: 163-168
4 **van Wagensveld BA,** Coene PP, van Gulik TM, Rauws EA, Obertop H, Gouma DJ. Outcome of palliative gastric bypass surgery for pancreatic head carcinoma in 126 patients. *Br J Surg* 1997; **84**: 1402-1406
5 **Khot UP,** Lang AW, Murali K, Parker MC. Systematic review of the efficacy and safety of colorectal stents. *Br J Surg* 2002; **89**: 1096-1102
6 **Gukovsky-Reicher S,** Lin RM, Sial S, Garrett B, Wu D, Lee T, Lee H, Arnell T, Stamos MJ, Eysselein VE. Self-expandable metal stents in palliation of malignant gastrointestinal obstruction: review of the current literature data and 5-year experience at Harbor-UCLA Medical Center. *Med Gen Med* 2003; **5**: 16
7 **Bond JH.** Colorectal cancer update. Prevention, screening, treatment and surveillance for high-risk groups. *Med J North Am* 2000; **84**: 1163-1182
8 **Morgan R,** Adam A. Use of metallic stents and balloons in the esophagus and gastrointestinal trace. *J Vasc Interv Radiol* 2001; **12**: 283-297
9 **Yim HB,** Jacobson BC, Saltzman JR, Johannes RS, Bounds BC, Lee JH, Shields SJ, Ruymann FW, Van Dam J, Carr-Locke DL. Clinical outcome of the use of enteral stents for palliation of patients with malignant upper GI obstruction. *Gastrointest Endosc* 2001; **53**: 329-332
10 **Baron TH,** Harewood GC. Enteral self-expandable stents. *Gastrointest Endosc* 2003; **58**: 421-433
11 **Cwikiel W,** Willen R, Stridbeck H, Lillo-Gil R, von Holstein CS. Self-expanding stents in the treatment of benign esophageal strictures: experimental study in pigs and presentations of clinical cases. *Radiology* 1993; **187**: 667-671
12 **Bethge N,** Sommer A, Gross U, von Kleist D, Vakil N. Human tissue responses to metal stents implanted *in vivo* for the palliation of malignant stenoses. *Gastrointest Endosc* 1996; **43**: 596-602

Science Editor Wang XL and Guo SY **Language Editor** Elsevier HK

PO Box 2345, Beijing 100023, China
www.wjgnet.com
wjg@wjgnet.com

ELSEVIER

World J Gastroenterol 2005;11(36):5742-5745
World Journal of Gastroenterology ISSN 1007-9327
© 2005 The WJG Press and Elsevier Inc. All rights reserved.

• *CASE REPORT* •

Megacolon in adulthood after surgical treatment of Hirschsprung's disease in early childhood

Christoph R. Werner, Gisela Stoltenburg-Didinger, Henning Weidemann, Christoph Benckert, Marco Schmidtmann, Ivo R. van der Voort, Viola Andresen, Burghard F. Klapp, Peter Neuhaus, Bertram Wiedenmann, Hubert Mönnikes

Christoph R. Werner, Bertram Wiedenmann, Hubert Mönnikes, Department of Medicine, Division of Hepatology and Gastroenterology, Charité, Campus Virchow-Klinikum, Universitätsmedizin Berlin, Augustenburger Platz 1, 13353 Berlin, Germany
Gisela Stoltenburg-Didinger, Department of Neuropathology, Charité, Campus Virchow-Klinikum, Universitätsmedizin Berlin, Augustenburger Platz 1, 13353 Berlin, Germany
Marco Schmidtmann, Ivo R. van der Voort, Viola Andresen, Burghard F. Klapp, Department of Medicine, Division of Psychosomatic Medicine and Psychotherapy, Charité, Campus Mitte , Luisenstraße 13 A, D-10117 Berlin, Germany
Christoph Benckert, Henning Weidemann, Peter Neuhaus, Department of General, Visceral and Transplantation Surgery, Charité, Campus Virchow-Klinikum, Universitätsmedizin Berlin, Augustenburger Platz 1, 13353 Berlin, Germany
Correspondence to: Hubert Mönnikes, MD MSc; Department of Medicine, Division of Hepatology and Gastroenterology; Charité, Campus Virchow-Klinikum; Universitätsmedizin Berlin, Augustenburger Platz 1, 13353 Berlin, Germany. moennikes@web.de
Telephone: +49-30-450653391 Fax: +49-30-450553991
Received: 2004-07-23 Accepted: 2005-01-05

Hirschsprung's disease (HD) is a disorder associated with congenital malformation of the enteric nervous system with segmental aganglionosis. Prevailing therapy includes a resection of the affected part of the bowel. However, patients often do not obtain complete functional improvement after surgical treatment. We present the case of a 25-year-old woman who had surgical treatment of HD in early childhood. After that procedure she had clinical features of constipation for years in the end, passing of stool once a week, requiring laxatives and enemas. We diagnosed an incomplete resection of the aganglionic bowel via rectal biopsy and resected the remaining aganglionic segment. Two months after surgery the patient's bowel function improved to a frequency of 1-4 stools per day. We conclude that regular follow-up is required to identify HD patients with persistent alterations of bowel function after surgery. In patients presenting with constipation, recognition of a remaining aganglionic segment or other alterations of the enteric nervous system should be aimed at in an early stage.

© 2005 The WJG Press and Elsevier Inc. All rights reserved.

Key words: Hirschsprung´s disease; Megacolon; Surgical treatment; Constipation
Werner CR, Stoltenburg-Didinger G, Weidemann H, Benekert C, Schmidtmann M, van der Voort IR, Andresen V, Klapp BF, Neuhaus P, Wiedenmann B, Mönnikes H. Megacolon in adulthood after surgical treatment of Hirschsprung's disease in early childhood. *World J Gastroenterol* 2005; 11(36): 5742-5745
http://www.wjgnet.com/1007-9327/11/5742.asp

Hirschsprung's disease (HD) is a birth defect affecting the bowel with segmental aganglionosis of the distal part of the gut due to disturbances in the development and migration of neural crest-derived cells which comprise the enteric nervous system. This dysfunction leads to constipation and, in the worst case, to *megacolon congenitum*. HD occurs in one of 5 000 live births and has a male predominance of about 4:1[1, 13]. Most patients are diagnosed in early childhood and treated by resection of the involved part of the colon. However, patients often do not obtain complete functional recovery after surgical treatment[2]. Studies on the therapeutic outcome in HD have so far mainly focused on the efficacy of different surgical techniques[3-6]. We present a case underscoring the necessity of appropriate diagnostic and therapeutic procedures in patients with HD where alterations of bowel function persist even after surgery.

A twenty-five year old woman, who suffered from constipation for years, was referred to our out patient clinic by her family physician. Symptoms worsened after an episode of diarrhea eight months ago. Currently she passed stool only once a week with the help of enemas.

A colon contrast-medium enema showed a dilated colon proximal to a stricture of the rectum, located at about 8 cm proximal of the anus forming a megacolon (Figure 1). The dilated section of the colon reached mid-transverse colon, proximally followed by colon of normal filling pattern.

Three months after birth the patient underwent abdominal surgery because of clinical features of acute constipation suggesting HD. A two-step procedure was performed with colostomy and sigmoideostomy three months after birth. Four months later a definitive surgical solution was intended by resection of the aganglionic bowel and reanastomosis of the proximal normal bowel to the normal anal canal after Rehbein[7]. Resection of 16 cm gut was performed, including a constricted distal part and a dilated proximal segment with a coprolith in it. The complete

excision of aganglionic bowel was confirmed by a pathologist.

At the age of nine years, a complete obstruction of the small intestine occurred, and therefore resection of 9 cm of jejunum and removal of adhesions were required. During surgery a dilated hypertrophic descending colon was observed. After this surgical procedure, colonoscopy was performed with removal of tissue samples from the site of anastomosis of colon and anal canal. The colonoscopist reported no dilatation of the bowel, differing from the surgeon's report. In contrast, the pathologist diagnosed aganglionosis in gut biopsies from aboral of the anastomosis. There was no enhanced activity of acetylcholinesterase in the segment proximal to the anastomosis. However, the patient was discharged with no definitive treatment for her constipation.

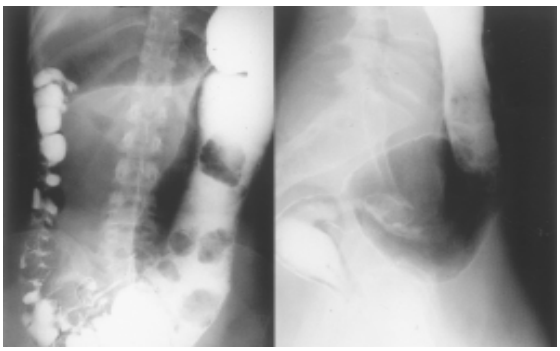


Figure 1 Contrast medium enema of the distal bowel shows a distal stenosis and a megacolon proximal to the stenosis.

At initial presentation in our out-patient clinic, physical examination of the 25-year old patient with moderate adipose revealed surgical scars at the left lower abdomen and a longish palpable mass in the left abdomen reaching from left lower up to the left upper quadrant. Initial laboratory tests were normal with exception of hypercholesterinaemia. Anorectal manometry displayed absence of the anorectal inhibitory reflex at inflation of the balloon in the distal rectum (Figure 2).

Rectal biopsies were taken and showed increased activity of acetylcholinesterase (Figure 3) in mucosal and submucosal layers and no ganglia of the plexus submucosus. Re-examination of slides of the specimen from the initial surgery 24 years ago revealed aganglionosis of both distal and proximal transection margins of the resected segment and extremely thickened nerve fibers replacing plexus myentericus.

We therefore concluded that at the abdominal surgery 24 years ago, removal of the entire aganglionic bowel was missed and an overseen aganglionic segment remained *in situ*. To remove the megacolon (Figure 4) and establish

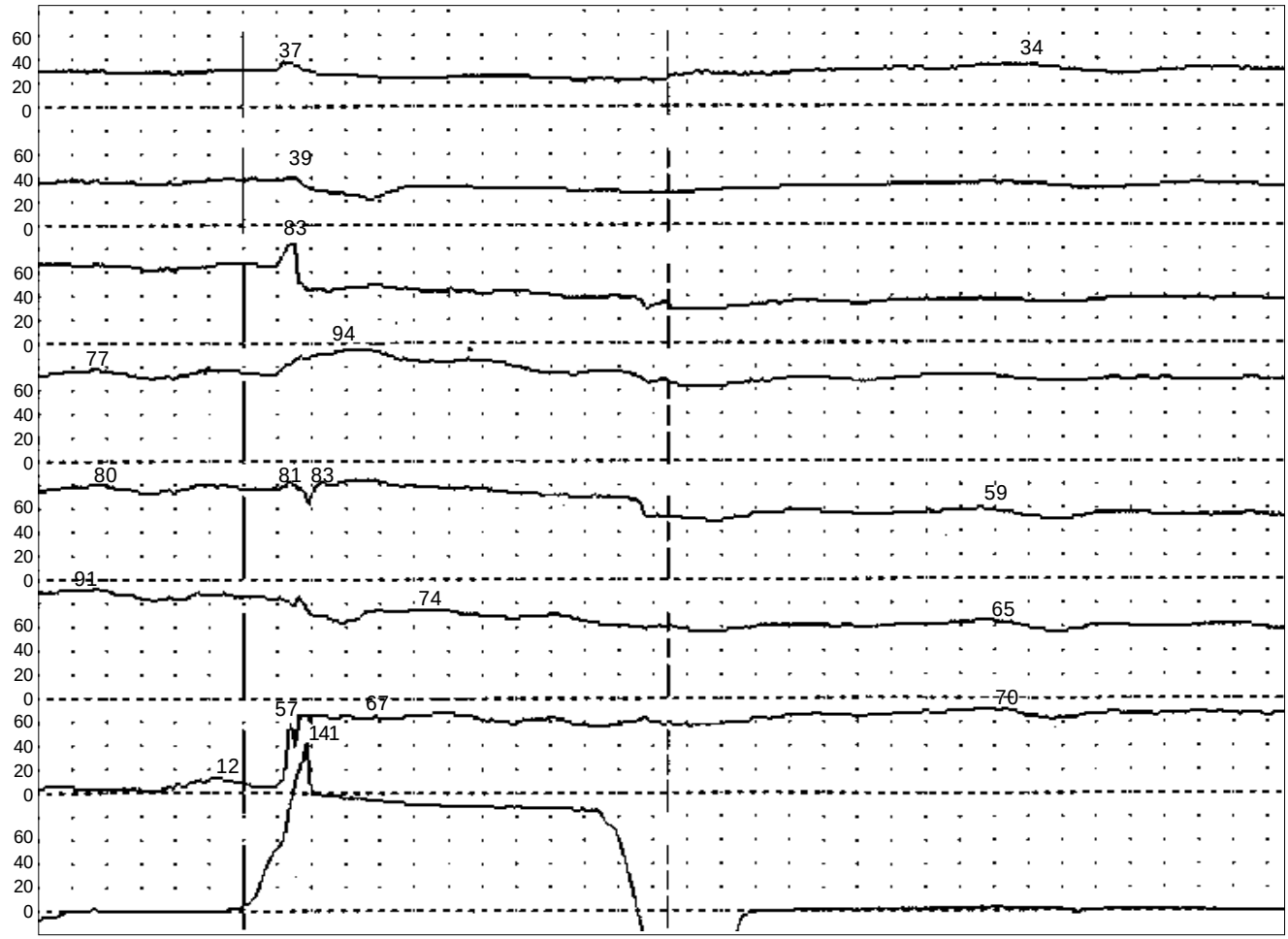


Figure 2 Anorectal manometry shows absence of the recto-anal inhibitory reflex after inflation of an intrarectally placed balloon with 40 mL of air.

normal transit of stool through the bowel, we referred the patient to the surgical department where resection of the aganglionic segment with end-to-end anastomosis was performed. Complete resection of the aganglionic segment was confirmed via instantaneous sections during surgery (Figure 5).

A 51 cm long segment of the distal colon was resected up to that point in the more proximal colon where the instantaneous sections showed a physiological account of ganglia.

After surgery, microscopic examination of the mucosal, submucosal and muscular layers showed presence of a hypoganglionic segment in the distal part of the resected segment (Figure 6A) and presumptive secondary aganglionosis in the mid-part of the specimen. At the proximal transection margin, a number of normal-sized ganglia were present (Figure 6B).

The patient had a rapid recovery from surgery and was discharged after a few days. Upon re-examination two months after the surgery, the patient reported an excellent functional improvement. She passed stool regularly 1-4 times a day without the use of laxatives.

Newborns who fail to pass meconium within the first 48 h should be suspected of having Hirschsprung's disease (HD) as one of the possible differential diagnoses[1]. However, if HD is not recognized at an early stage, it can present later in one or more of the following ways: delayed passage of meconium, complete intestinal obstruction (sometimes associated with a *megacolon congenitum*), and enterocolitis.

If diagnosis is confirmed by contrast enema, anorectal manometry and, as gold standard, a rectal biopsy with increased activity of acetylcholinesterase and absence of the plexus submucosus, sufficient resection has to be done, as the only successful treatment for HD is the resection of the aganglionic part of the bowel, including a dilated segment proximal to it. For definitive surgical treatment, several procedures have been developed[6-10].

In studies to elicit the long-term follow-up situation in patients who underwent surgical treatment of HD as infants[2-5], depending on the performed procedure, about 50% of patients report occasional complaints such as fecal soiling (43.5%), abdominal pain (34.8%), constipation (14.4%).

Constipation is a frequent finding among patients who underwent surgical treatment for HD (10.4%[3] to 14.4%[2]). Except for common reasons for constipation in adults, one has to consider additional differential diagnoses in patients who have had a surgical procedure because of HD in early childhood. Firstly, an incomplete resection of the aganglionic segment proximal to the anastomosis has to be ruled out. Secondly, a "transition zone", i.e. a congenital hypoganglionosis or hyperganglionosis adjacent to the aganglionic segment[11] that causes constipative symptoms due to malfunction of the enteric nervous systems of this segment of the bowel has also to be ruled out. Thirdly, an intestinal neuronal dysplasia type B (INDB) has to be considered. This disease

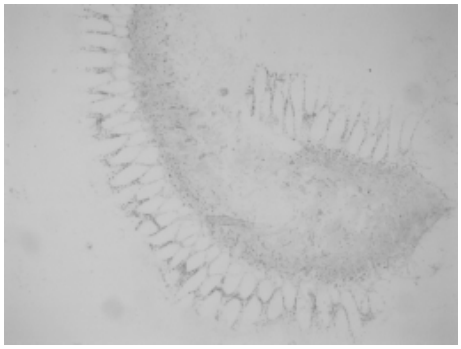


Figure 3 Rectal biopsy (AChE-staining) shows increased activity of acetylcholinesterase in the mucosal layer of the dilated segment.



Figure 4 Megacolon *in situ*.

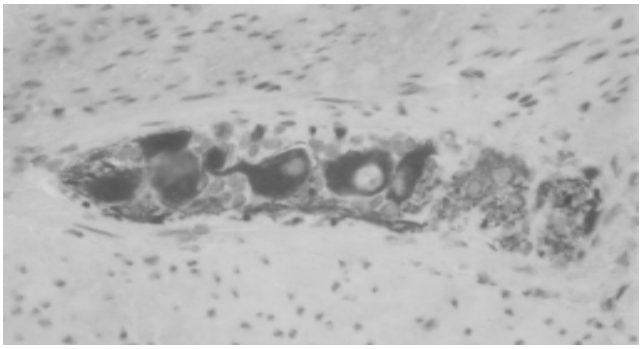


Figure 5 Instantaneous section (Peripherin-immmunohistochemistry) shows normal formation of plexus myentericus.

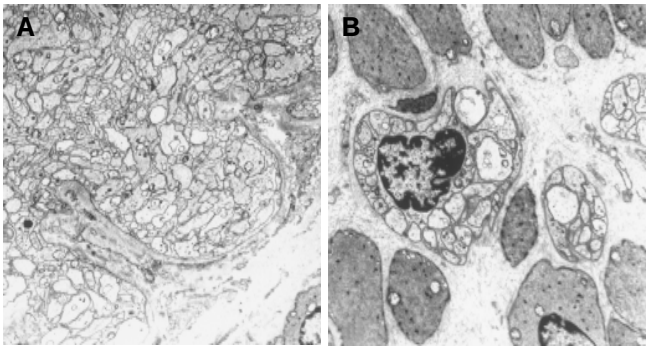


Figure 6 Electron microscopic sections show thickened parasympathetic nerve fibers in the distal part of the resected segment (A) and normal numbers of ganglia in the proximal part (B).

shows slowed intestinal transit time and an intractable constipation. Though aganglionosis is never present in INDB, there may be an increase of extrinsic nerve fibers in the affected gut as in HD[12,13] which could be mistaken for HD by rectal biopsy. Furthermore, HD often includes a region of INDB-like characteristic proximal to the aganglionic segment[11].

Another possibility is the secondary involution of the enteric nervous system and fibrosis of the bowel wall due to recurrent infections, causing features of constipation.

Depending on the diagnosis and if normal bowel function is not sustainable by conservative therapy, surgical treatment should be considered, as it was in our patient. Especially in young patients a long-lasting dependency on strong laxatives and enemas means a significant reduction in quality of life.

In Hirschsprung's disease, regular follow-up examinations are required to identify patients with persisting alterations of bowel function after surgery. In HD patients with consatipation or other symptoms of impaired bowel movement after surgery, remaining of an aganglionic segment should be considered in differential diagnosis. Identification of this and other alterations of the enteric nervous system mentioned above should already be aimed at in an early stage, in order to prevent secondary harms, such as development of a megacolon, as it happened in our patient.

1 **Milla PJ.** Hirschsprung disease and other neuropathies. In: Rudolph AM, Hoffman JIE., Rudolph CD, eds. Rudolph's pediatrics. *Stamford Appleton & Lange* 1996: 1115-1118
2 **Skaba R,** Simsova M. Long-term results and quality of life in patients after surgery in childhood for Hirschsprung's disease by the Kasai method of colo(ileo)rectoplasty. *Rozhl Chir* 2002; **81**: 622-627
3 **Bjornland K,** Diseth TH, Emblem R. Long-term functional, manometric, and endosonographic evaluation of patients operated upon with the Duhamel technique. *Pediatr Surg Int* 1998; **13**: 24-28
4 **Hsu WM,** Chen CC. Clinical and manometric evaluation of postoperative fecal soiling in patients with Hirschsprung's disease. *J Formos Med Assoc* 1999; **98**: 410-414
5 **Heikkinen M,** Rintala R, Luukkonen P. Long-term anal sphincter performance after surgery for Hirschsprung's disease. *J Pediatr Surg* 1997; **32**: 1443-1446
6 **Rehbein F.** Operative therapy of Hirschsprung's disease. *Langenbecks Arch Klin Chir Ver Dtsch Z Chir* 1953; **276**: 540-543
7 **Swenson O,** Bill AH. Resection of the rectum and rectosigmoid with preservation of the sphincter for benign spastic lesions producing megacolon. *Surgery* 1948; **24**: 212-220
8 **Duhamel B.** A new operation for the treatment of Hirschsprung's disease. *Arch Dis Child* 1960; **35**: 38-39
9 **Soave F.** A new surgical technique for treatment of Hirschsprung's disease. *Surgery* 1964; **56**: 1007-1014
10 **Boley SJ.** New modification of the surgical treatment of Hirschsprung's disease. *Surgery* 1964; **56**: 1015-1017
11 **Newgreen D,** Young HM. Enteric nervous system: development and developmental disturbances-part 1. *Pediatr Dev Pathol* 2002; **5**: 224-247
12 **Meier-Ruge WA,** Bronnimann PB, Gambazzi F, Schmid PC, Schmidt CP, Stoss F. Histopathological criteria for intestinal neuronal dysplasia of the submucosal plexus (type b). *Virchows Arch* 1995; **426**: 546-556
13 **Wiedenmann B,** Riedel C, John M, Ahnert-Hilger G, Stoltenburg G, Waldschmidt J, von Deimling K, Riecken EO, Schier F. Qualitative and quantitative analysis of synapses in Hirschsprung's disease. *Pediatr Surg Int* 1998; **13**: 468-473

Science Editor Wang XL and Guo SY **Language Editor** Elsevier HK

PO Box 2345, Beijing 100023, China
www.wjgnet.com
wjg@wjgnet.com

ELSEVIER

World J Gastroenterol 2005;11(36):5746
World Journal of Gastroenterology ISSN 1007-9327
© 2005 The WJG Press and Elsevier Inc. All rights reserved.

Acknowledgments to Reviewers of *World Journal of Gastroenterology*

Many reviewers have contributed their expertise and time to the peer review, a critical process to ensure the quality of *World Journal of Gastroenterology*. The editors and authors of the articles submitted to the journal are grateful to the following reviewers for evaluating the articles (including those were published and those were rejected in this issue) during the last editing period of time.

Taku Aoki, M.D.
Division of Hepato-Biliary-Pancreatic and Transplantation Surgery, Department of Surgery, Graduate School of Medicine, University of Tokyo,7-3-1 Hongo, Bunkyo-ku, Tokyo, Japan. Tokyo 113-8655, Japan

Chi-Hin Cho, Chair and Professor
Departmentof Pharmacology, The University of Hong Kong, 21 Sassoon Road, Hong Kong, China

Amar Paul Dhillon, Professor
Department of Histopathology, Royal Free Hospital, Pond Street, London NW3 2QG, United Kingdom

Jaime Guardia, Professor
Internal Medicine and Liver Unit, Hospital Universitari 'Vall d'Hebron'. Universitat Autonoma de Barcelona, Hospital Universitari Vall d'Hebron, Pg Vall d'Hebron, 119, Barcelona 08035, Spain

De-Wu Han, Professor
Shanxi Medical University, 86 Xinjian South Road, Taiyuan 030001, China

Naohiko Harada, PhD
Department of Gastroenterology, Fukuoka Higashi Medical Center, Chidori 1-1-1, Koga, Fukuoka 811-3195, Japan

Yik-Hong Ho, Professor
Department of Surgery, School of Medicine, James Cook University, Townsville 4811, Australia

Ernst Johan Kuipers, Professor
Department of Gastroenterology and Hepatology, Erasmus University Medical Center, PO Box 2400, Rotterdam 3000CA, Netherlands

Giacomo Laffi, Professor
University of Florence, Viale Morgagni 85, Firenze I-50134, Italy

Timothy H Moran, Professer
Department of Psychiatry, Johns Hopkins University School of Medicine, Ross 618, 720 Rutland Ave, Baltimore, Maryland 21205, United States

Yuji Naito, Professor
Kyoto Prefectural University of Medicine, Kamigyo-ku, Kyoto 602-8566, Japan

Chifumi Sato, Professor
Department of Analytical Health Science, Tokyo Medical and Dental University, Graduate School of Health Sciences, 1-5-45 Yushima, Bunkyo-ku, Tokyo 113-8519, Japan

Shuichi Seki, Associate professor
Department of Hepatology, Osaka City University, 1-4-3 Asahimachi, Abeno-ku, Osaka 545-8585, Japan

Francis Seow-Choen, Professor
Seow-Choen Colorectal Centre, Mt Elizabeth Medical Centre, Singapore, 3 Mt Elizabeth Medical Centre #09-10Singapore 228510, Singapore 228510, Singapore

Manfred Stolte, Professor
Institute of Pathology, Klinikum Bayreuth, Preuschwitzer Str. 101, Bayreuth 95445, Germany

Kyuichi Tanikawa, Professor
International Institute for Liver Research, 1-1 Hyakunen Kouen, Kurume 839-0864, Japan

Simon D Taylor-Robinson, M.D.
Department of Medicine A, Imperial College London, Hammersmith Hospital, Du Cane Road, London W12 0HS, United Kingdom

Roberto Testa, Professor
Department of Internal Medicine, University of Genoa, Viale Benedetto XV 6, Genoa 16132, Italy

Karel van Erpecum, M.D.
Department of Gastroenterology and Hepatology, University Hospital Utrecht, Utrecht 3508GA, Netherlands

Harald Vogelsang, Professor
Gastroenterology, AKH- KIM IV, Wahringer G. 18-20, Vienna A-1090, Austria

Yuan Wang, Professor
Institute of Biochemistry and Cell Biology, Shanghai Institutes for Biological Sciences, Chinese Academy of Sciences, Shanghai 200031, China

Harry H-X Xia, M.D.
Department of Medicine, The University of Hong Kong, Pokfulam Road, Hong Kong, China

Yuan Yuan, Professor
Cancer Institute of China Medical University, 155 North Nanjing Street, Heping District, Shenyang 110001, Liaoning Province, China

PO Box 2345, Beijing 100023, China
www.wjgnet.com
wjg@wjgnet.com

ELSEVIER

World J Gastroenterol 2005;11(36):5747
World Journal of Gastroenterology ISSN 1007-9327
© 2005 The WJG Press and Elsevier Inc. All rights reserved.

Meetings

MAJOR MEETINGS COMING UP

APDW 2005 - Asia Pacific Digestive Week 2005
September 25-28, 2005
asiapdw@kornet.net
www.apdw2005.org

13th United European Gastroenterology Week
October 15-20, 2005
uegw@discongress.com
www.webasistent.cz/guarant/uegw2005/

American College of Gastroenterology Annual Scientific Meeting
October 28 -November 2, 2005
annualmeeting@acg.gi.org
www.acg.gi.org

EVENTS AND MEETINGS IN THE UPCOMING 6 MONTHS

United European Gastroenterology Week
October 15-20, 2005
uegw@discongress.com
www.webasistent.cz/guarant/uegw2005/

ISGCON2005
November 11-15, 2005
isgcon2005@yahoo.co.in
isgcon2005.com

II Latvian Gastroenterology Congress
November 29, 2005
gec@stradini.lv
www.gastroenterologs.lv

70th ACG Annual Scientific Meeting and Postgraduate Course
October 28-November 2, 2005

Advanced Capsule Endoscopy Users Course
November 18-19, 2005
www.asge.org/education

2005 CCFA National Research and Clinical Conference - 4th Annual Advances in the Inflammatory Bowel Diseases
December 1-3, 2005
c.chase@imedex.com
www.imedex.com/calendars/therapeutic.htm

EVENTS AND MEETINGS IN 2005

XIII Argentine Hepatology Congress
XIII Congreso Argentino de HepatologÃa
June 10-13, 2005
mci@mcimeetings.com
www.hepatologia.org

9th Annual Coolum Update in Gastroenterology & Hepatology
June 11-13, 2005
info@e-Kiddna.com.au

Canadian Digestive Disease Week Conference
February 26-March 6, 2005
www.cag-acg.org

2005 World Congress of Gastroenterology
September 12-14, 2005
wcog2005@congrex.nl

International Colorectal Disease Symposium 2005
February 3-5, 2005
info@icds-hk.org

15th World Congress of the International Association of Surgeons and Gastroenterologists
September 7-10, 2005
iasg2005@guarant.cz
www.iasg2005.cz

7th International Workshop on Therapeutic Endoscopy
September 10-12, 2005
alfa@alfamedical.com
www.alfamedical.com

EASL 2005 the 40th annual meeting
April 13-17, 2005
www.easl.ch/easl2005/

ISGCON2005
November 11-15, 2005
isgcon2005@yahoo.co.in
isgcon2005.com

Pediatric Gastroenterology, Hepatology and Nutrition
March 13, 2005

II Latvian Gastroenterology Congress
November 29, 2005
gec@stradini.lv
www.gastroenterologs.lv

21st annual international congress of Pakistan society of Gastroenterology & GI Endoscopy
March 25-27, 2005
psgc05@hotmail.com
www.psgc2005.com

8th Congress of the Asian Society of HepatoBiliary Pancreatic Surgery
February 10-13, 2005

1º Workshop de Gastrenterologia para Clí nica Geral
April 29, 2005
luis.m.lopes@sapo.pt

APDW 2005 - Asia Pacific Digestive Week 2005
September 25-28, 2005
asiapdw@kornet.net
www.apdw2005.org

World Congress on Gastrointestinal Cancer
June 15-18, 2005
meetings@imedex.com

British Society of Gastroenterology Conference
March 14-17, 2005
www.bsg.org.uk

Training Director's Workshop:Developing and Teaching Principles in the New Era of GI Training
February 4-6, 2005
www.asge.org/education

The Pharmacological, Surgical and Endoscopic Management of GERD
April 8-9, 2005
www.asge.org/education

Digestive Disease Week
DDW 106th Annual Meeting
May 15-18, 2005
ddwadmin@gastr.org
www.ddw.org

ASGE Advanced Endscopy Skills Hands-on Sessions
May 15, 2005
www.asge.org/education

ASGE GERD Hands-on Session
May 17, 2005
www.asge.org/education

Annual Postgraduate Course
May 18-19, 2005
www.asge.org/education

Advanced Capsule Endoscopy Users Course
June 4-5, 2005
www.asge.org/education

Advanced Capsule Endoscopy Users Course
August 12-13, 2005
www.asge.org/education

GI Practice Management Symposium: Solutions for a Successful Practice
August 18, 2005
www.asge.org/education

70th ACG Annual Scientific Meeting and Postgraduate Course
October 28-November 2, 2005

Advanced Capsule Endoscopy Users Course
November 18-19, 2005
www.asge.org/education

2005 CCFA National Research and Clinical Conference - 4th Annual Advances in the Inflammatory Bowel Diseases
December 1-3, 2005
c.chase@imedex.com
www.imedex.com/calendars/therapeutic.htm

EVENTS AND MEETINGS IN 2006

10th World Congress of the International Society for Diseases of the Esophagus
February 22-25, 2006
isde@sapmea.asn.au
www.isde.net

Easl 2006 - The 41st Annual Meeting
April 26-30, 2006

Canadian Digestive Disease Week Conference
March 4-12, 2006
www.cag-acg.org

XXX pan-american congress of digestive diseases
XXX congreso panamericano de anfermedades digestivas
November 25-December 1, 2006
amg@gastro.org.mx
www.gastro.org.mx

World Congress on Gastrointestinal Cancer
June 14-17, 2006
c.chase@imedex.com

7th World Congress of the International Hepato-Pancreato-Biliary Association
September 3-7, 2006
convention@edinburgh.org
www.edinburgh.org/conference

Annual Postgraduate Course
May 25-26, 2006
www.asge.org/education

71st ACG Annual Scientific Meeting and Postgraduate Course
October 20-25, 2006

PO Box 2345, Beijing 100023, China
www.wjgnet.com
wjg@wjgnet.com

ELSEVIER

World J Gastroenterol 2005;11(36):5748-5749
World Journal of Gastroenterology ISSN 1007-9327
© 2005 The WJG Press and Elsevier Inc. All rights reserved.

Instructions to authors

GENERAL INFORMATION

World Journal of Gastroenterology (*WJG,* ISSN 1007-9327 CN 14-1219/R) is a weekly journal of more than 48 000 circulation, published on the 7th, 14th, 21st and 28th of every month.

Original Research, Clinical Trials, Reviews, Comments, and Case Reports in esophageal cancer, gastric cancer, colon cancer, liver cancer, viral liver diseases, *etc*., from all over the world are welcome on the condition that they have not been published previously and have not been submitted simultaneously elsewhere.

Published jointly by
The WJG Press and Elsevier Inc.

SUBMISSION OF MANUSCRIPTS

Manuscripts should be typed double-spaced on A4 (297×210 mm) white paper with outer margins of 2.5 cm. Number all pages consecutively, and start each of the following sections on a new page: Title Page , Abstract, Introduction, Materials and Methods, Results, Discussion, Acknowledgements, References, Tables, Figures and Figure Legends. Neither the Editors nor the Publisher is responsible for the opinions expressed by contributors. Manuscripts formally accepted for publication become the permanent property of The WJG Press and Elsevier Inc., and may not be reproduced by any means, in whole or in part without the written permission of both the Authors and the Publisher. We reserve the right to put onto our website and copy-edit accepted manuscripts. Authors should also follow the guidelines for the care and use of laboratory animals of their institution or national animal welfare committee.

Authors should retain one copy of the text, tables, photographs and illustrations, as rejected manuscripts will not be returned to the author(s) and the editors will not be responsible for the loss or damage to photographs and illustrations.

Online submission
Online submission is strongly advised. Manuscripts should be submitted through the Online Submission System at: http://www.wjgnet.com/index.jsp. Authors are highly recommended to consult the ONLINE INSTRUCTIONS TO AUTHORS (http://www.wjgnet.com/wjg/help/instructions.jsp) before attempting to submit online. Authors encountering problems with the Online Submission System may send an email describing the problem to wjg@wjgnet.com for assistance. If you submit manuscript online, do not make a postal contribution. A repeated online submission for the same manuscript is strictly prohibited.

Postal submission
Send 3 duplicate hard copies of the full-text manuscript typed double-spaced on A4(297×210 mm) white paper together with any original photographs or illustrations and a 3.5 inch computer diskette or CD-ROM containing an electronic copy of the manuscript including all the figures, graphs and tables in native Microsoft Word format or *.rtf format to:

World Journal of Gastroenterology
Apartment 1066 Yishou Garden,
58 North Langxinzhuang Road,
PO Box 2345, Beijing 100023, China
E-mail: wjg@wjgnet.com
http: //www.wjgnet.com

MANUSCRIPT PREPARATION

All contributions should be written in English. All articles must be submitted using a word-processing software. All submissions must be typed in 1.5 line spacing and in word size 12 with ample margins. The letter font is Tahoma. For authors originating from China, one copy of the Chinese translation of the manuscript is also required (excluding references). Style should conform to our house format. Required information for each of the manuscript sections is as follows:

Title page
Full manuscript title, running title, all author(s) name(s), affiliations, institution(s) and/or department(s) where the work was accomplished, disclosure of any financial support for the research, and the name, full address, telephone and fax numbers and email address of the corresponding author should be involved. Titles should be concise and informative (removing all unnecessary words), emphasize what is NEW, and avoid abbreviations. A short running title of less than 40 letters should be provided. List the author(s)' name(s) as follows: initials and/or first name, middle name or initial(s) and full family name.

Abstract
An informative, structured abstract of no more than 250 words should accompany each manuscript. Abstracts for original contributions should be structured into the following sections: AIM: Only the purpose should be included. METHODS: The materials, techniques, instruments and equipments, and the experimental procedures should be included. RESULTS: The observatory and experimental results, including data, effects, outcome, *etc*. should be included. Authors should present *P* value where necessary, and the significant data should accompany. CONCLUSION: Accurate view and the value of the results should be included.

The format of structured abstracts is at: http://www.wjgnet.com/wjg/help/11.doc

Key words
Please list 3-10 key words that could reflect content of the study.

Text
For most article types, the main text should be structured into the following sections: INTRODUCTION, MATERIALS AND METHODS, RESULTS and DISCUSSION, and should include appropriate Figures and Tables. Data should be presented in the body text or Figures and Tables, not both.

Illustrations
Figures should be numbered as 1, 2, 3 and so on, and mentioned clearly in the main text. Provide a brief title for each figure on a separate page. No detailed legend should be involved under the figures. This part should add into the text where the figures are applicable. Digital images: black and white photographs should be scanned and saved in TIFF format at a resolution of 300 dpi; color images should be saved as CMYK (print files) and not RGB (screen-viewing files). Place each photograph in a separate file. Print images: supply images of size no smaller than 126×76 mm printed on smooth surface paper; label the image by writing the Figure number and orientation using an arrow. Photomicrographs: indicate the original magnification and stain in the legend. Digital Drawings: supply files in EPS if created by Freehand and Illustrator, or TIFF from Photoshop. EPS files must be accompanied by a version in native file format for editing purposes. Scans of existing line drawings should be scanned at a resolution of 1200 dpi and as close as possible to the size at which they will appear when printed, not smaller. Please use uniform legends for the same subjects. For example: Figure 1 Pathological changes of atrophic gastritis after treatment. A: ...; B: ...;C: ...; D: ...; E: ...; F: ...; G: ...

Tables
Three-line tables should be numbered as 1, 2, 3 and so on, and mentioned clearly in the main text. Provide a brief title for each table. No detailed legend should be involved under the tables. This part should add into the text where the tables are applicable. The information should complement but not duplicate that contained in the text. Use one horizontal line under the title, a second under the column heads, and a third below the Table, above any footnotes. Vertical and italic lines should be omitted.

Notes in tables and illustrations
Data which is not statistically significant should not be noted. $^{a}P<0.05$, $^{b}P<0.01$ ($P>0.05$ should not be noted). If there are other series of *P* values, $^{c}P<0.05$ and $^{d}P<0.01$ are used; Third series of *P* values can be expressed as $^{e}P<0.05$ and $^{f}P<0.01$. Other notes in tables or under

illustrations should be expressed as ^1F, ^2F, ^3F; or some other symbols with a superscript (Arabic numerals) in the upper left corner. In a multi-curve illustration, each curve should be labeled with ●, ○, ■, □, ▲, △, *etc*. in a certain sequence.

Acknowledgments

Brief acknowledgments of persons who have made genuine contributions to the manuscripts and who endorse the data and conclusions are included. Authors are responsible for obtaining written permission to use any copyrighted text and/or illustrations.

References

Cited references should mainly be drawn from journals covered in the Science Citation Index (http://www.isinet.com) and/or Index Medicus (http://www.ncbi.nlm.nih.gov/PubMed) databases. Mention all references in the text, tables and figure legends, and set off by consecutive, superscripted Arabic numerals. References should be numbered consecutively in the order in which they appear in the text. Abbreviate journal title names according to the Index Medicus style (http://www.ncbi.nlm.nih.gov/entrez/query.fcgi?db=journals). Unpublished observations and personal communications are not listed as references. The style and punctuation of the references conform to ISO standard and the Vancouver style (5th edition); see examples below. Reference lists not conforming to this style could lead to delayed or even rejected publication status. Examples:

Standard jounal article (list all authors and include the PubMed ID [PMID] where applicable)

1 **Das KM,** Farag SA. Current medical therapy of inflammatory bowel disease. *World J Gastroenterol* 2000; 6: 483-489 [PMID: 11819634]

2 **Pan BR**, Hodgson HJF, Kalsi J. Hyperglobulinemia in chronic liver disease: Relationships between *in vitro* immunoglobulin synthesis, short lived suppressor cell activity and serum immunoglobulin levels. *Clin Exp Immunol* 1984; 55: 546-551 [PMID: 6231144]

3 **Lin GZ,** Wang XZ, Wang P, Lin J, Yang FD. Immunologic effect of Jianpi Yishen decoction in treatment of Pixu-diarrhoea. *Shijie Huaren Xiaohua Zazhi* 1999; 7: 285-287 [CMFAID:1082371101835979]

Books and other monographs (list all authors)

4 **Sherlock S,** Dooley J. Diseases of the liver and billiary system. 9th ed. Oxford: Blackwell Sci Pub, 1993: 258-296

Chapter in a book (list all authors)

5 **Lam SK.** Academic investigator's perspectives of medical treatment for peptic ulcer. In: Swabb EA, Azabo S. Ulcer disease: investigation and basis for therapy. New York: Marcel Dekker, 1991: 431-450

Electronic journal (list all authors)

6 **Morse SS.** Factors in the emergence of infectious diseases. Emerg Infect Dis serial online, 1995-01-03, cited 1996-06-05; 1(1):24 screens. Available from: URL: http//www.cdc.gov/ncidod/EID/eid.htm

PMID requirement

From the full reference list, please submit a separate list of those references embodied in PubMed, keeping the same order as in the full reference list, with the following information only: (1) abbreviated journal name and citation (e.g. *World J Gastroenterol* 2003;9(11): 2400-2403; (2) article title (e.g. Epidemiology of gastroenterologic cancer in Henan Province, China; (3) full author list (e.g. Lu JB, Sun XB, Dai DX, Zhu SK, Chang QL, Liu SZ, Duan WJ; (4) PMID (e.g. 14606064). Provide the full abstracts of these references, as quoted from PubMed on a 3.5 inch disk or CD-ROM in Microsoft Word format and send by post to The *WJG* Press. For those references taken from journals not indexed by *Index Medicus*, a printed copy of the first page of the full reference should be submitted. Attach these references to the end of the manuscript in their order of appearance in the text.

Inappropriate references

Authors should always cite references that are relevant to their article, and avoid any inappropriate references. Inappropriate references include those that are linked with a hyphen and the difference between the two numbers at two sides of the hyphen is more than 5. For example, [1-6], [2-14] and [1, 3, 4-10, 22] are all considered as inappropriate references. Authors should not cite their own unrelated published articles.

Statistical data

Present as mean±SD and mean±SE.

Statistical expression

Express *t* test as *t*(in italics), *F* test as *F*(in italics), chi square test as χ^2 (in Greek), related coefficient as *r*(in italics), degree of freedom as γ(in Greek), sample number as *n*(in italics), and probability as *P*(in italics).

Units

Use SI units. For example: body mass, m(B) = 78 kg; blood pressure, p (B)=16.2/12.3 kPa; incubation time, t(incubation)=96 h, blood glucose concentration, c(glucose) 6.4±2.1 mmol/L; blood CEA mass concentration, p(CEA) = 8.6 24.5 μg/L; CO_2 volume fraction, 50 mL/L CO_2 not 5% CO_2; likewise for 40 g/L formaldehyde, not 10% formalin; and mass fraction, 8 ng/g, *etc*. Arabic numerals such as 23,243,641 should be read 23 243 641.

The format about how to accurately write common units and quantum is at: http://www.wjgnet.com/wjg/help/15.doc

Abbreviations

Standard abbreviations should be defined in the abstract and on first mention in the text. In general, terms should not be abbreviated unless they are used repeatedly and the abbreviation is helpful to the reader. Permissible abbreviations are listed in Units, Symbols and Abbreviations: A Guide for Biological and Medical Editors and Authors (Ed. Baron DN, 1988) published by The Royal Society of Medicine, London. Certain commonly used abbreviations, such as DNA, RNA, HIV, LD50, PCR, HBV, ECG, WBC, RBC, CT, ESR, CSF, IgG, ELISA, PBS, ATP, EDTA, mAb, can be used directly without further mention.

Italicization

Quantities: *t* time or temperature, *c* concentration, *A* area, *l* length, *m* mass, *V* volume.
Genotypes: *gyr*A, *arg* 1, *c myc*, *c fos*, *etc*.
Restriction enzymes: *Eco*RI, *Hin*dI, *Bam*HI, *Kbo* I, *Kpn* I, *etc*.
Biology: *Helicobacter pylori, H pylori, E coli, etc*.

SUBMISSION OF THE REVISED MANUSCRIPTS AFTER ACCEPTED

Please revise your article according to the revision policies of *WJG*. The revised version including manuscript and high-resolution image figures (if any) should be copied on a floppy or compact disk. Author should send the revised manuscript, along with printed high-resolution color or black and white photos, copyright transfer letter, the final check list for authors, and responses to reviewers by a courier (such as EMS) (submission of revised manuscript by e-mail or on the WJG Editorial Office Online System is NOT available at present).

Language evaluation

The language of a manuscript will be graded before sending for revision. (1) Grade A: priority publishing; (2) Grade B: minor language polishing; (3) Grade C: a great deal of language polishing; (4) Grade D: rejected. The revised articles should be in grade B or grade A.

Copyright assignment form

It is the policy of WJG to acquire copyright in all contributions. Papers accepted for publication become the copyright of WJG and authors will be asked to sign a transfer of copyright form. All authors must read and agree to the conditions outlined in the Copyright Assignment Form (which can be downloaded from http://www.wjgnet.com/wjg/help/9.doc).

Final check list for authors

The format is at: http://www.wjgnet.com/wjg/help/13.doc

Responses to reviewers

Please revise your article according to the comments/suggestions of reviewers. The format for responses to the reviewers' comments is at: http://www.wjgnet.com/wjg/help/10.doc

Proof of financial support

For paper supported by a foundation, authors should provide a copy of the document and serial number of the foundation.

Publication fee

Authors of accepted articles must pay publication fee.

PO Box 2345, Beijing 100023, China
www.wjgnet.com
wjg@wjgnet.com

ELSEVIER

World J Gastroenterol 2005;11(36):5750
World Journal of Gastroenterology ISSN 1007-9327
© 2005 The WJG Press and Elsevier Inc. All rights reserved.

World Journal of Gastroenterology standard of quantities and units

Number	Nonstandard	Standard	Notice
1	4 days	4 d	In figures, tables and numerical narration
2	4 days	four days	In text narration
3	day	d	After Arabic numerals
4	Four d	Four days	At the beginning of a sentence
5	2 hours	2 h	After Arabic numerals
6	2 hs	2 h	After Arabic numerals
7	hr, hrs,	h	After Arabic numerals
8	10 seconds	10 s	After Arabic numerals
9	10 year	10 years	In text narration
10	Ten yr	Ten years	At the beginning of a sentence
11	0,1,2 years	0,1,2 yr	In figures and tables
12	0,1,2 year	0,1,2 yr	In figures and tables
13	4 weeks	4 wk	
14	Four wk	Four weeks	At the beginning of a sentence
15	2 months	2 mo	In figures and tables
16	Two mo	Two months	At the beginning of a sentence
17	10 minutes	10 min	
18	Ten min	Ten minutes	At the beginning of a sentence
19	50% (*V/V*)	500 mL/L	
20	50% (m/*V*)	500 g/L	
21	1 M	1 mol/L	
22	10 μM	10 μmol/L	
23	1N HCl	1 mol/L HCl	
24	1N H_2SO_4	0.5 mol/L H_2SO_4	
25	4rd edition	4^{th} edition	
26	15 year experience	15- year experience	
27	18.5 kDa	18.5 ku,18 500u or M_r18 500	
28	25 $g.kg^{-1}/d^{-1}$	25 g/(kg·d) or 25 g/kg per day	
29	6900	6 900	
30	1000 rpm	1 000 r/min	
31	sec	s	After Arabic numerals
32	1 $pg·L^{-1}$	1 pg/L	
33	10 kilograms	10 kg	
34	13 000 rpm	13 000 *g*	High speed; *g* should be in italic and suitable conversion.
35	1000 *g*	1 000 r/min	Low speed. *g* cannot be used.
36	Gene bank	GenBank	International classified genetic materials collection bank
37	Ten L	Ten liters	At the beginning of a sentence
38	Ten mL	Ten milliliters	At the beginning of a sentence
39	umol	μmol	
40	30 sec	30 s	
41	1 g/dl	10 g/L	10-fold conversion
42	OD_{260}	A_{260}	"OD" has been abandoned.
43	One g/L	One microgram per liter	At the beginning of a sentence
44	*A*260 nm	A_{260} nm	*A* should be in italic.
	^{b}P<0.05	^{a}P<0.05	In Table, no note is needed if there is no significance in statistics: ^{a}P<0.05, ^{b}P<0.01 (no note if P>0.05). If there is a second set of P value in the same table, ^{c}P<0.05 and ^{d}P<0.01 are used for a third set: ^{e}P<0.05, ^{f}P<0.01.
45	**F*=9.87, §*F*=25.9, #*F*=67.4	^{1}F=9.87,^{2}F=25.9, ^{3}F=67.4	Notices in or under a table
46	KM	km	kilometer
47	CM	cm	centimeter
48	MM	mm	millimeter
49	Kg, KG	kg	kilogram
50	Gm, gr	g	gram
51	nt	N	newton
52	l	L	liter
53	db	dB	decibel
54	rpm	r/min	rotation per minute
55	bq	Bq	becquerel, a unit symbol
56	amp	A	ampere
57	coul	C	coulomb
58	HZ	Hz	
59	w	W	watt
60	KPa	kPa	kilo-pascal
61	p	Pa	pascal
62	ev	EV	volt (electronic unit)
63	Jonle	J	joule
64	J/mmol	kJ/mol	kilojoule per mole
65	10×10×10cm^3	10 cm×10 cm×10 cm	
66	N·km	KN·m	moment
67	$\tilde{x}$±s	mean±SD	In figures, tables or text narration
68	Mean±SEM	mean±SE	In figures, tables or text narration
69	*im*	im	intramuscular injection
70	*iv*	iv	intravenous injection
71	Wang et al	Wang *et al.*	
72	EcoRI	*Eco*RI	*Eco* in italic and RI in positive. Restriction endonuclease has its prescript form of writing.
73	Ecoli	*E.coli*	Bacteria and other biologic terms have their specific expression.
74	Hp	*H pylori*	
75	Iga	*Iga*	writing form of genes
76	*igA*	IgA	writing form of proteins
77	-70 kDa	~70 ku	

PO Box 2345, Beijing 100023, China
www.wjgnet.com
wjg@wjgnet.com

ELSEVIER

World J Gastroenterol 2005;11(37):5751-5756
World Journal of Gastroenterology ISSN 1007-9327
© 2005 The WJG Press and Elsevier Inc. All rights reserved.

Significance and prognostic value of lysosomal enzyme activities measured in surgically operated adenocarcinomas of the gastroesophageal junction and squamous cell carcinomas of the lower third of esophagus

Aron Altorjay, Balazs Paal, Nicolette Sohar, Janos Kiss, Imre Szanto, Istvan Sohar

Aron Altorjay, Balazs Paal, Department of Surgery, Saint George University Teaching Hospital, Székesfehérvár, Seregélyesi u. 3., H-8000, Hungary
Nicolette Sohar, Istvan Sohar, Center for Advanced Biotechnology and Medicine, UMDNJ, Piscataway, NJ, USA
Janos Kiss, Imre Szanto, National Medical Center, Department of Surgery, Budapest, Szabolcs u. 33-35., H-1135, Hungary
Correspondence to: Aron Altorjay, MD, PhD, Professor of Surgery, Department of Surgery, Saint George University Teaching Hospital, Seregélyesi u. 3., Székesfehérvár, H-8000, Hungary. altorjay@mail.fmkorhaz.hu
Telephone: +36-22-504-100 Fax: +36-22-504-100
Received: 2004-12-23 Accepted: 2005-02-18

Abstract

AIM: To establish whether there are fundamental differences in the biochemistries of adenocarcinomas of the gastroesophageal junction (GEJ) and the squamous cell carcinomas of the lower third of the esophagus (LTE).

METHODS: Between February 1, 1997 and February 1, 2000, we obtained tissue samples at the moment of resection from 54 patients for biochemical analysis. The full set of data could be comprehensively analyzed in 47 of 54 patients' samples (81%). Of these, 29 were adenocarcinomas of the GEJ Siewert type I (n = 8), type II (n = 12), type III (n = 9), and 18 presented as squamous cell carcinomas of the LTE. We evaluated the mean values of 11-lysosomal enzyme and 1-cytosol protease activities of the tumorous and surrounding mucosae as well as their relative activities, measured as the ratio of activity in tumor and normal tissues from the same patient. These data were further analyzed to establish the correlation with tumor localization, TNM stage (lymph-node involvement), histological type (papillary, signet-ring cell, tubular), state of differentiation (good, moderate, poor), and survival ($\leqslant$24 or $\geqslant$24 mo).

RESULTS: In adenocarcinomas, the activity of α-mannosidase (AMAN), cathepsin B (CB) and dipeptidyl-peptidase I (DPP I) increased significantly as compared to the normal gastric mucosa. In squamous cell carcinomas of the esophagus, we also found a significant difference in the activity of cathepsin L and tripeptidyl-peptidase I in addition to these three. There was a statistical correlation of AMAN, CB, and DPP I activity between the level of differentiation of adenocarcinomas of the GEJ and lymph node involvement, because tumors with no lymph node metastases histologically confirmed as well-differentiated, showed a significantly lower activity. The differences in CB and DPP I activity correlated well with the differences in survival rates, since the CB and DPP I values of those who died within 24 mo following surgical intervention were significantly higher than of those who survived for 2 years or more.

CONCLUSION: Adenocarcinomas of the GEJ form a homogenous group from a tumor-biochemical aspect, and differ from the biochemical characteristics of squamous cell carcinomas of the LTE on many points. When adenocarcinomas of the GEJs are examined at the preoperative phase, the ratio of the performed AMAN, CB, and DPP I enzymatic activity of the tissue sample from the tumor and adjacent intact mucosa within 2 cm of the tumor may have a prognostic value even in the preoperative examination period, and may indicate that ranking of these patients into the neo-adjuvant treatment group should be considered.

© 2005 The WJG Press and Elsevier Inc. All rights reserved.

Key words: Prognostic value; Lysosomal enzymes; Cardiac adenocarcinomas; Siewert classification; Esophageal squamous cell carcinoma

Altorjay A, Paal B, Sohar N, Kiss J, Szanto I, Sohar I. Significance and prognostic value of lysosomal enzyme activities measured in surgically operated adenocarcinomas of the gastroesophageal junction and squamous cell carcinomas of the lower third of esophagus. *World J Gastroenterol* 2005; 11(37): 5751-5756
http://www.wjgnet.com/1007-9327/11/5751.asp

INTRODUCTION

While the majority of carcinomas located in the upper and middle third of the esophagus are squamous cell carcinomas, the incidence of adenocarcinomas in the lower third of the esophagus (LTE) is increasing in the Western world. Although their etiology is not clear, esophageal adenocarcinomas almost always arise in areas of Barrett's metaplasia, usually in the specialized intestinal-type mucosa in the lower esophagus, and predominantly affect elderly white men, often those with a history of heavy smoking. Barrett's metaplasia

is an accepted complication of gastroesophageal reflux disease, but gastric cancer is not linked to reflux disease. Thus, it is of interest to note that the incidence of proximal gastric adenocarcinomas is increasing. At Temple University Hospital, the percentage of cardiac carcinomas within gastric carcinomas has increased from 16% to 25% between 1976-80 and 1991-95[1]. Antonioli and Goldman[2] reported that the incidence of cardiac carcinomas has increased from 0% to 27% of all gastric carcinomas in Boston. They also showed that the number of signet-ring cell carcinomas is increased with a decrease in the male to female ratio, and an increase in the age of patients.

The classification system described by Siewert[3], which organizes adenocarcinomas of the gastroesophageal junction (GEJ) into tumors of the distal esophagus as type I (Si I), true carcinomas of the cardia as type II (Si II) and subcardial carcinomas as type III (Si III), has allowed for a comparative assessment of the data of the various sites and has facilitated the choice of surgical therapy. This classification brings light into the "Black Box" of GEJ carcinomas. The classification itself can easily be performed by summarizing all available information from contrast radiography, endoscopy, and intraoperative findings.

Following surgical resection, there is a clear survival advantage for patients with early-stage tumors over patients with late-stage tumors, regardless of tumor location. There is, therefore, no difference in the survival rates between any of the three locations[4]. Although much effort has been made to obtain a more accurate understanding and to apply more effective therapy for carcinomas in the lower esophagus and proximal stomach, patient survival rates are still not satisfactory.

A number of molecular markers have been analyzed as possible prognostic factors in patients with esophageal cancer including expression of proliferating cell nuclear antigen, epidermoid growth factor receptor, cyclin Dl, p53, and p21. However, none of these markers are of clinical value[5-7]. Merely aberrant expression of pRB and high serum immunosuppressive acidic protein concentration seems to be useful as a prognostic factor for esophageal squamous cell carcinoma[8,9].

As the etiology of tumors may well be different, it is important to establish whether there are fundamental differences in the biochemistries of adenocarcinomas of the GEJ and the squamous cell carcinomas of the LTE. In order to answer this question, it seems evident that proteolytic enzyme activities in the tumor tissue and the histologically intact mucosa bordering, it should be measured and compared, since peptidases are primarily responsible for intracellular catabolism and turnover. The increased level of lysosomal enzymes in tumors, together with their ability to degrade extracellular matrix proteins, has led to the hypothesis that they could be involved in the process of invasion and metastasis[10-12].

MATERIALS AND METHODS

Between February 1, 1997 and February 1, 2000, we obtained tissue samples at the moment of resection from 54 patients for biochemical analysis. The average age was 57.8 years and the M/F ratio was 35/19 (65%/35%). The full set of data could be comprehensively analyzed in 47 of 54 patients' samples (81%). Of these, 29 were adenocarcinomas of the GEJ Siewert type I (n = 8), type II (n = 12), type III (n = 9), and 18 presented as squamous cell carcinomas of the LTE. Tissue samples obtained during surgery were further separated into two groups: cancer tissue and normal tissue closely surrounding the cancer tissue, within 2 cm of the tumor border. The latter was checked histologically to confirm it to be tumor-free. For enzyme assays the mucosal layer was used. Reasons for exclusion included histologically confirmed synchronous multiple carcinoma (n = 3), death within early postoperative period (n = 2) and intolerance of study protocol (n = 2).

All patients in the study were so-called advanced cancer cases. Thus, the TNM stage and number of esophageal tumors were IIA:6, IIB:6, and III:6, while the tumors of the GEJ were II:10, IIIA:11, and IIIB:8.

The central-European reality is that almost 90% of malignant carcinomas in this area of the gastrointestinal tract are discovered at an advanced stage, and this fact is well reflected in this group of patients.

We evaluated the mean values of 11-lysosomal enzyme and 1-cytosol protease (as control) specific activities of the tumorous and surrounding mucosae as well as their relative activities, measured as the ratio of activity in tumor and normal tissues from the same patient. These data were further analyzed to establish the correlation with tumor localization, TNM stage (lymph-node involvement), histological type (papillary, signet-ring cell, tubular), state of differentiation (good, moderate, poor), and survival ($\leqslant$24 or $\geqslant$24 mo). The term of relative activity was used for the mean ratio of enzyme activity values for tumorous and intact mucosae in individual patients expressed as a decimal fraction.

Tissue samples from the tumor and intact surrounding area were frozen on dry ice immediately after dissection and stored at -70 ℃ prior to use.

Samples were thawed on ice, placed in 50 volumes (w/v) of 0.15 mol/L NaCl, 0.1% Triton X-100 and homogenized with a Brinkmann Polytron homogenizer. A soluble supernatant was prepared by centrifugation at 12 000 g for 25 min at 4 ℃.

Glycosidase activities were measured using 4-methylumbelliferyl (4-MU) substrates as previously described[13]. Protease assays using 7-amino-4-methylcoumarine (AMC) substrates were conducted as described by Sleat *et al*.[14], and Sohar *et al*.[15]. Reactions were initiated by adding 40 μL of substrate (various concentrations 20 μmol/L-1 mmol/L)-buffer (100 mmol/L) solution to 5 μL (cathepsin B) or 10 μL (other enzymes) of sample (supernatants diluted two-, four-, and eightfold in homogenization buffer in duplicate), incubated at 37 ℃, and terminated by the addition of 100 μL of 0.5 mol/L glycine, pH 10.5 (4-MU substrates) or 0.1 mol/L monochloroacetic acid in 0.1 mol/L acetate, pH 4.3 (AMC substrates). Buffers consisted of 0.1 mol/L citric acid or 0.1 mol/L sodium acetate adjusted to the indicated pH using sodium hydroxide, acetic acid, or HCl respectively, contained 0.1% Triton-X-100 with 0.15 mol/L NaCl. Substrates were purchased from Sigma and prepared as stocks in dimethyl sulfoxide (remaining substrates) that

were added to the reaction buffer immediately prior to assay. Samples added to substrate solutions after the addition of the termination buffer were used as blanks. Fluorescent reaction products were determined using a CytoFluor II fluorescence multiwell plate reader (PerSeptive Biosystems, Framingham, MA, USA) with excitation at 360 nm and emission at 460 nm.

Since our variables were normally distributed, Microsoft Excel *t*-test with two samples, correlated *t*-test and single factor analysis of variance were used for the statistical analysis. Permission for the investigations was sought and obtained from the appropriate local ethical committee.

RESULTS

The analysis of 11-lysosomal enzyme and 1-cytosol protease-thimet oligopeptidase (THP)-activity levels in adenocarcinomas of the GEJ and squamous cell carcinomas of the LTE showed that α-mannosidase (AMAN), cathepsin B (CB) and dipeptidyl-peptidase I (DPP I) had a significant increase in adenocarcinoma (Table 1). AMAN, CB, DPP I, cathepsin L (CL) and tripeptidyl-peptidase I (TPP I) showed a significant increase in squamous cell carcinoma as compared to the levels of activity measured in the bordering intact mucosa (Table 2).

When relative activity values were compared (Table 3) for α-glucosidase (AGLU), CB, CL, and DPP I enzymes, the activity level was twofold higher in squamous carcinomas than in adenocarcinomas.

The values of peptidase activity in cardiac tumors with Si I, II, and III localization did not differ significantly (Table 4). There was no significant correlation between lysosomal enzyme activities and adenocarcinomas of different histological types (papillary, signet-ring cell, tubular). There was no significant difference between carcinomas of stages II, IIIA, and IIIB. However, we found a significant and relatively strong relationship between the level of differentiation of adenocarcinomas of the GEJ and the level of activity of AMAN (H: 0.78), CB (H: 0.76), and DPP I (H: 0.67) lysosomal enzymes. The lysosomal enzyme activities in well-differentiated adenocarcinomas were significantly lower than those in poorly differentiated ones. The changes of the activity of certain enzymes correlated well with lymph node involvement. Tumors with no lymph-node metastases showed a significantly lower value of activity. A moderate relation was detected between the relative activities and the presence of lymph-node metastases (H: 0.61). The change in CB and DPP I activity sensitively reflected the differences in survival rates too.

Tables 2 and 3 show that the lysosomal enzyme activity increased significantly in the so-called advanced esophageal carcinomas compared to that in adenocarcinomas of the GEJ. However, we found no statistically measurable correlation between the rate of increased lysosomal enzyme activities and maturity of tumors, as well as the involvement of lymph nodes and TNM stage. Moreover, in contrast to adenocarcinomas of the GEJ, the significantly increased lysosomal enzyme activities in squamous cell carcinomas of the LTE did not correlate with survival time. Thus, these parameters in stages II and III had no prognostic value.

Table 1 Specific activities of lysosomal enzymes in 29 adenocarcinomas of the GEJ and surrounding normal mucosa (mean±SE)

Enzymes	Adenocarcinoma	Normal gastric mucosa	*P*
AGLU	27 315±3 139	31 210±2 490	NS
AMAN	89 594±8 518	66 653±4 066	<0.05
BGAL	318 224±43 694	245 442±15 421	NS
CB	324 095±39 402	167 582±14 842	<0.001
CL	392 438±44 328	296 166±29 044	NS
DPP I	2 140 499±287 604	1 291 759±126 796	<0.05
CH	491 813±51 110	404 285±40 939	NS
DPP II	80 982±9 916	110 728±15 265	NS
GCU	219 615±42 364	178 776±18 607	NS
HEX	213 292±28 785	186 396±18 779	NS
TPP I	921 939±328 332	443 130±134 508	NS
THP	36 271±14 639	23 382±10 817	NS

GEJ: gatroesophageal junction; NS: non significant; AGLU: α-glucosidase; AMAN: α-mannosidase; BGAL: β-galactosidase; CB: cathepsin B; CL: cathepsin L; DPP I: dipeptidyl-peptidase I; CH: cathepsin H; DPP II: dipeptidyl-peptidase II; GCU: β-glucuronidase; HEX: β-hexosaminidase B; TPP I: tripeptidyl-peptidase I; THP: thimet oligopeptidase (pmol /h·mg).

Table 2 Specific activities of lysosomal enzymes in 18 squamous cell carcinomas of the LTE and surrounding normal mucosa (mean±SE)

Enzymes	Squamous cell carcinoma	Normal esophageal mucosa	*P*
AGLU	54 216±16 793	21 596±4 106	NS
AMAN	86 987±14 625	36 905±2 287	<0.05
BGAL	225 913±43 791	135 696±24 644	NS
CB	535 860±134 809	114 697±13 037	<0.05
CL	292 996±56 644	60 964±14 115	<0.001
DPP I	2 328 558±634 873	401 436±172 042	<0.05
CH	578 119±50 491	453 922±54 228	NS
DPP II	41 816±7 226	34 539±6 833	NS
GCU	134 414±22 391	115 250±19 634	NS
HEX	149 704±30 362	86 965±15 449	NS
TPP I	191 061±20 874	112 048±11 472	<0.001
THP	45 828±7 921	31 459±7 164	NS

LTE: lower third of the esophagus; NS: non significant; AGLU: α-glucosidase; AMAN: α-mannosidase; BGAL: β-galactosidase; CB: cathepsin B; CL: cathepsin L; DPP I: dipeptidyl-peptidase I; CH: cathepsin H; DPP II: dipeptidyl-peptidase II; GCU: β-glucuronidase; HEX: β-hexosaminidase B; TPP I: tripeptidyl-peptidase I; THP: thimet oligopeptidase (pmol /h·mg).

Table 3 Relative activities of lysosomal enzymes in adenocarcinoma of the GEJ and in squamous cell carcinoma of the LTE (mean±SE)

Enzymes	GEJ Tumor/own normal mucosa	LTE Tumor/own normal mucosa	Ratio of LTE/GEJ
AGLU	0.91±0.09	2.55±0.78	2.8
AMAN	1.39±0.12	2.36±0.32	1.7
BGAL	1.33±0.16	2.01±0.42	1.5
CB	2.15±0.34	4.89±1.20	2.3
CL	1.48±0.17	6.21±2.00	4.2
DPP I	2.34±0.52	12.43±5.30	5.3
CH	1.30±0.12	1.44±0.31	1.1
DPP II	0.83±0.08	1.39±0.23	1.7
GCU	1.36±0.24	1.46±0.33	1.1
HEX	1.29±0.18	2.06±0.45	1.6
TPP I	1.66±0.33	1.77±0.21	1.1
THP	2.36±0.41	3.59±2.30	1.5

GEJ: gatroesophageal junction; LTE: lower third of the esophagus; SE: standard error; AGLU: α-glucosidase; AMAN: α-mannosidase; BGAL: β-galactosidase; CB: cathepsin B; CL: cathepsin L; DPP I: dipeptidyl-peptidase I; CH: cathepsin H; DPP II: dipeptidyl-peptidase II; GCU: β-glucuronidase; HEX: β-hexosaminidase B; TPP I: tripeptidyl-peptidase I; THP: thimet oligopeptidase.

Table 4 Prognostic value of lysosomal enzyme activities in adenocarcinomas of the GEJ (mean±SE)

Prognostic categories	Relative activity	AMAN	Specific activity	Relative activity	CB	Specific activity	Relative activity	DPP I	Specific activity
Siewert I	1.36±0.19	NS	110 136±20 902	1.68±0.37	NS	273 838±66 573	1.37±0.42	NS	1 896 366±446 446
Siewert II	1.49±0.23		88 413±17 021	2.42±0.48		417 978±65 610	2.58±0.64		2 673 743±638 594
Siewert III	1.34±0.19		79 101±9 469	2.20±0.68		278 994±63 462	2.68±1.1		1 861 382±384 367
Papillary	1.54±0.27	NS	92 754±22 466	2.79±1.19	NS	368 700±112 886	2.97±1.60	NS	2 156 354±763 729
Signet-ring cell	1.42±0.13		82 743±10 810	2.04±0.27		291 588±58 097	2.37±0.59		2 328 450±567 443
Tubular	1.30±0.26		90 069±8 722	1.80±0.45		325 476±68 549	2.10±1.12		1 916 498±504 487
Grade 1	0.91±0.11	$P<0.01$	61 931±8 716	0.95±0.08	$P<0.01$	210 697±54 630	0.72±0.06	$P<0.01$	981 478±111 507
Grade 2–3	1.63±0.13		103 425±10 283	2.75±0.42		380 793±46 390	3.14±0.69		2 720 009±332 437
N0	1.00±0.17	$P<0.05$	67 068±10 377	1.03±0.11	$P<0.01$	201 550±55 664	0.75±0.07	$P<0.01$	1 053 122±122 928
N1–N2	1.59±0.13		100 857±10 644	2.71±0.43		385 367±44 735	3.12±0.69		2 684 187±345 227
Survival $\leqslant$2 yr	1.55±0.14	NS	103 466±11 103	2.76±0.46	$P<0.01$	382 830±49 621	3.24±0.74	$P<0.01$	2 722 922±373 145
Survival $\geqslant$2 yr	1.13±0.17		67 052±9 135	1.16±0.14		228 650±51 792	0.87±0.07		1 194 060±160 577
Stage II	1.19±0.13	NS	80 194±8 553	1.90±0.50	NS	293 720±52 833	1.98±0.74	NS	1 860 244±358 265
Stage III	1.66±0.18		102 128±15 960	2.47±0.41		364 594±59 832	2.81±0.73		2 514 172±465 458

GEJ: gastroesophageal junction; NS: non significant; N0: lymph node negative; N1–N2: lymph node positive; AMAN: α-mannosidase; CB: cathepsin B; DPP I: dipeptidyl-peptidase I.

DISCUSSION

The incidence of adenocarcinomas of the esophagus (Si type I) is increasing[16,17]. These cancers are associated with Barrett's specialized epithelium and appear to be part of the continuum of gastroesophageal reflux disease. To date, no data suggest that the prevalence of gastroesophageal reflux disease has changed over the past 20 years and thus the cause of this current "epidemic" remains unclear[18].

The epidemiology of adenocarcinomas of the "classic" gastric cardia (Si type II-III) remains even less clear. Very few studies have examined this as a distinct entity. Overall, it seems that the incidence of cancer in this location, mainly Si type II, has not changed significantly in the past 50 years[1]. Some cases of gastric cardia cancer may be associated with chronic gastritis and *Helicobacter pylori* infection, whereas other cases may be related to Barrett's specialized epithelium in the proximal stomach[19-21].

A number of reports suggest that the synthesis, transport, and processing of lysosomal enzymes and their phosphorylated derivatives are altered in cancer, making these proteins interesting subjects for investigation[22]. The ability of tumor cells to invade tissues and metastasize is thought to involve an increased expression of proteinases and/or a decrease in the levels of proteinase inhibitors. Peptidases may facilitate metastasis in a number of different ways, including detachment of individual cells from the primary tumor, invasion of surrounding tissues to allow contact with vascular channels, degradation of the basement membrane during both intravasation and extravasation, and invasion of tissues during the formation of secondary tumor sites. Several classes of proteinases have been implicated in this process including matrix metalloproteinases, cysteine proteinases as CB or CL, aspartic proteinase cathepsin D, and serine proteinase plasminogen activators[23-28]. It is possible that human tumors may use combinations of these enzymes working synergistically to facilitate invasion or alternatively one specific proteinase may play a dominant role in tissue invasion for a given cancer, while some tumors exhibit an alteration in the synthesis or processing of many or all lysosomal enzymes. Defining the role of proteinases in the invasiveness of different tumors is important with regard to understanding the biology of this process and searching for potential prognostic markers and targets for therapeutic intervention.

The results of clinical investigations on cysteine cathepsins and their endogenous inhibitors in human breast, lung, brain, liver, and head and neck tumors, as well as in body fluids of ovarian, uterine, melanoma and colorectal carcinoma bearing patients, have shown that these molecules are highly predictive for the length of survival and may be used for risk assessment of relapse and death in cancer patients[29-32].

By examining the correlation of cysteine protease CB and laminin degradation, Khan *et al*.[33], demonstrated that increased CB expression and decreased tumor-associated laminin levels may suggest a mechanism underlying the progression of colorectal adenomas to carcinomas.

As for the relationship of gastric tumors and proteolytic enzymes, β hexosaminidase and its isoenzymes[34], and plasminogen activators are in the center of interest. Cathepsins B, L and tissue type plasminogen activator activities are higher in gastric cancer tissues than in normal gastric tissues. Chung and Kawai[35] also revealed that inhibitory activities of CL, CB, urinary and tissue type plasminogen activators are stronger in normal tissue closely surrounding the gastric cancer compared to normal tissue distant from the tumor border, as a result of a defense mechanism of the host against cancer invasion.

Yamamoto *et al*.[36], reported that the matrix metalloproteinase matrilysin may play a key role in the progression of esophageal carcinoma and that its detection may be useful in predicting recurrence and poor prognosis, and possibly in selecting patients for anti-matrix metalloproteinase therapy. Another study on esophageal adenocarcinoma demonstrated that amplicon at 8p22, the locus of the CB gene, is identified and associated with amplification and overexpression of the CB gene in esophageal adenocarcinoma[37].

Prior to this study, no lysosomal enzyme activity measurements have been performed in adenocarcinomas of the GEJ. During our examinations we measured the

activity of 11 different lysosomal enzymes and one cytosol protease THP in Si type I-III adenocarcinomas of the GEJ and in squamous cell carcinomas of the LTE. The activity of AMAN, CB, and DPP I in adenocarcinoma increased significantly as compared to that in normal gastric mucosa. In squamous cell carcinomas of the esophagus (Table 1) we also found a significant difference in the activity of CL and TPP I in addition to these three (Table 2). Moreover, when the relative activity values were compared for AGLU, CB, CL, and DPP I in adenocarcinoma of the GEJ and in squamous cell carcinoma of the LTE, marked differences in the relative activity levels by a factor of 2-5 respectively could be observed in squamous cell carcinomas as opposed to adenocarcinomas (Table 3).

From a tumor-biochemical aspect, adenocarcinomas within the Si I-III localization system did not show any differences, nor were there any significant differences in their lysosomal enzyme activities. Similarly to this there was no significant correlation between protease activities and adenocarcinomas of different histological types (papillary, signet-ring cell, tubular). However, we found a statistically measurable correlation to AMAN, CB and DPP I between the level of differentiation of adenocarcinomas of the GEJ and lymph node involvement, because histologically well-differentiated tumors with no lymph node metastases showed a significantly lower activity. The change of two proteases with cysteine catalytic site, namely CB and DPP I, activity correlated well with differences in survival rates, since the CB and DPP I values of those who died within 24 mo following surgical intervention were significantly higher than the same values for those who survived for 2 years or more (Table 4). At the same time, no statistically measurable correlation was found in relation to the proteases despite of displaying significantly higher activity levels as compared to the normal mucosa, the level of differentiation of tumors, their lymph node state or survival rates for squamous cell carcinomas of the LTE.

We conclude that adenocarcinomas of different locations in the GEJ form a homogenous group and differ in many aspects from malformations and neoformations within similar locations, though they possess a different histological structure. This conclusion is supported by data from Izutani *et al*.[38]. The difference in radiation sensitivity could be attributed to the tissue type difference. The increased MnSOD mRNA and MnSOD proteins in adenocarcinoma are believed to indicate the activity of strong defense mechanisms protecting the active form of cysteine catalytic center at CB and DPP I against reactive oxygen species, and this activity could be a cause of resistance against radiation therapy and quinone anticancer drugs.

Our results suggest that when adenocarcinomas of the GEJ are investigated at the preoperative phase, the ratio of the actual AMAN, CB, and DPP I enzyme activity in the samples taken from the tumor and its adjacent tissues may have some prognostic value. Relative activity values within the range of 1, signaling a comparatively more favorable prognosis pattern mean that a specific kind of "static warfare" prevails between the tumor tissue and the surrounding intact mucosa. This may be due not only to the diminished invasiveness of a given tumor, but also to the more effective defensive properties of the intact bordering mucosa, or it may be a consequence of a reduction in protease inhibitor synthetic activity. It seems, therefore, that the activity levels of AMAN, CB, and DPP I in adenocarcinoma may assist us in formulating our preoperative therapeutic strategy for adenocarcinomas of the GEJ.

ACKNOWLEDGMENTS

The authors are grateful for the opportunity to measure lysosomal enzyme activities in the laboratory of Dr. Peter Lobel at CABM, UMDNJ, Piscataway, NJ, USA. We also thank Professor Charles J. Filipi, Creighton Medical University, Omaha, Nicola Pen Jackson and Laszlo Novak for critical reading of the manuscript before its submission.

REFERENCES

1 **Locke GR,** Talley NJ, Carpenter HA, Harmsen WS, Zinsmeister AR, Melton LJ. Changes in the site- and histology-specific incidence of gastric cancer during a 50-year period. *Gastroenterology* 1995; **109**: 1750–1756
2 **Antonioli DA,** Goldman H. Changes in the location and type of gastric adenocarcinoma. *Cancer* 1982; **50**: 775–781
3 **Siewert JR,** Feith M, Werner M, Stein HJ. Adenocarcinoma of the esophagogastric junction. Results of surgical therapy based on anatomical/topographic classification in 1.002 consecutive patients. *Ann Surg* 2000; **232**: 353-361
4 **Clark GWB,** Smyrk TC, Burdiles P, Hoeft SF, Peters JH, Kiyabu M. Is Barrett's metaplasia the source of adenocarcinomas of the cardia? *Arch Surg* 1994; **129**: 609–614
5 **Hirai T,** Kuwahar M, Yoshida K, Osaki A, Toge T. The prognostic significance of p53, p21 (Wafl, Cipl), and cyclin D1 protein expression in esophageal cancer patients. *Anticancer Res* 1999; **19**: 4587–4591
6 **Wang LS,** Chow KC, Chi KH, Liu CC, Li WY, Chiu JH. Prognosis of esophageal squamous cell carcinoma: analysis of clinicopathological and biological factors. *Am J Gastroenterol* 1999; **94**: 1933–1940
7 **Zafirellis K,** Dolan K, Fountolakis A, Dexter SPL, Martin IG, Sue-Ling HM. Multivariate analysis of clinical, operative and pathologic features of esophagal cancer: who needs adjuvant therapy? *Dis Esoph* 2002; **15**: 155–159
8 **Shinohara M,** Aoki T, Sato S, Takagi Y, Osaka Y, Koyanagi Y. Cell cycle-regulated factors in esophageal cancer. *Dis Esoph* 2002; **15**: 149–154
9 **Shimada H,** Nabeya Y, Okazumi S, Matsubara H, Miyazawa Y, Shihratori T, Hayashi H, Aoki T, Sugaya M, Guniji Y, Kobayashi S, Ochiai T. Prognostic value of preoperative serum immunosuppressive acidic protein in patients with esophageal squamous cell carcinoma. *Dis Esoph* 2003; **16**: 102–106
10 **Mullins DE,** Rohrlich ST. The role of proteinases in cellular invasiveness. *Biochim Biophys Acta* 1983; **695**: 177–214
11 **Sloane BF,** Hohn KV. Cysteine proteinases and metastasis. *Cancer Metastasis Rev* 1984; **3**: 249–263
12 **Duffy MJ,** Ogrady P. Plasminogen activator and cancer. *Eur J Cancer Clin Oncol* 1984; **20**: 577–582
13 **Sleat DE,** Sohar I, Lackland H, Majercak J, Lobel P. Rat brain contains high levels of mannose-6-phosphorylated glycoproteins including lysosomal enzymes and palmitoyl-protein thioesterase, an enzyme implicated in infantile neuronal lipofuscinosis. *J Biol Chem* 1996; **271**: 19191–19198
14 **Sleat DE,** Sohar I, Pullarkat PS, Lobel P, Pullarkat RK. Specific alterations in levels of mannose 6-phosphorylated glycoproteins in different neuronal ceroid lipofuscinoses. *Biochem J* 1998; **334**: 547–551
15 **Sohar I,** Lin L, Lobel P. Enzyme-based diagnosis of late in-

fantile neuronal ceroid lipofuscinosis: comparison of tripeptidyl peptidase I and pepstatin-insensitive protease assays. *Clin Chem* 2000; **46**: 1005-1008

16 **Blot WJ,** Devesa SS, Kneller RW, Fraumeni JF Jr. Rising incidence of adenocarcinoma of the esophagus and gastric cardia. *JAMA* 1991; **265**: 1287–1289

17 **Siewert JR,** Feith M, Werner M, Stein HJ. Adenocarcinoma of the esophagogastric junction. Results of surgical therapy based on anatomical/topographic classification in 1.002 consecutive patients. *Ann Surg* 2000; **232**: 353–361

18 **Okabayashi T,** Gotoda T, Kondo H, Inui T, Ono H, Saito D. Early carcinoma of the gastric cardia in Japan. Is it different from that in the West? *Cancer* 2000; **89**: 2555–2559

19 **Appelman HD,** Kalish RJ, Clancy PE, Orringer MB. Distinguishing features of adenocarcinoma in Barrett's esophagus and in the gastric cardia. In: Speckler S J, Goyal RK, eds. Barrett's esophagus: pathophysiology, diagnosis and management. New York: *Elsevier Science Publishing Co Inc* 1985

20 **Parsonnet J,** Freidman GD, Vandersteen DP, Chang Y, Vogelman JH, Orentreich N. *Helicobacter pylori* infection and the risk of gastric carcinoma. *N Engl J Med* 1991; **325**: 1127–1131

21 **Forman D,** Newell DG, Fullerton F, Yarnell JWG, Stacey AR, Wald N. Association between infection with Helicobacter pylori and risk of gastric cancer. Evidence from a prospective investigation. *Br Med J* 1991; **302**: 1302–1305

22 **Boyer MJ,** Tannock IF. Lysosomes, lysosomal enzymes and cancer. *Adv Cancer Res* 1993; **60**: 269–291

23 **Liotta LA,** Stetler-Stevenson WG. Metalloproteinases and cancer invasion. *Semin Ancer Biol* 1990; **1**: 99-106

24 **Koblinski JE,** Ahram M, Sloane BF. Unraveling the role of proteases in cancer. *Clin Chim Acta* 2000; **291**: 113-135

25 **Premzl A,** Puizdar V, Zavasnik-Bergant V, Kopitar-Jerala N, Lah TT, Katunuma N. Invasion of ras-transformed breast epithelial cells depends on the proteolytic activity of cysteine and aspartic proteinases. *Biol Chem* 2001; **382**: 853-857

26 **Levicar N,** Nutall RK, Lah TT. Proteases in brain tumour progression. *Acta Neurochir* 2003; **145**: 825-838

27 **Yan S,** Sloane BF. Molecular regulation of human cathepsin B: Implication in pathologies. *Biol Chem* 2003; **384**: 845-854

28 **Turk V,** Turk B, Guncar G, Turk D, Kos J. Lysosomal cathepsins: structure, role in antigen processing and presentation, and cancer. *Adv Enzyme Reg* 2002; **42**: 285-303

29 **Lah TT,** Kos J. Cysteine proteinases in cancer progression and their clinical relevance for prognosis. *Biol Chem* 1998; **379**: 125–130

30 **Lah TT,** Cercek M, Blejec A, Kos J, Gorodetsky E, Somers R, Daskal I. Cathepsin B, a prognostic indicator in lymph node-negative breast carcinoma patients: comparison with cathpesin D, cathepsin L, and other clinical indicators. *Clin Cancer Res* 2000; **6**: 578–584

31 **Ledakis P,** Tester WT, Rosenberg N, Romero-Fischmann D, Daskal I, Lah TT. Cathepsin D, B, and L in malignant human lung tissue. *Clin Cancer Res* 1996; **2**: 561–568

32 **Gardett EA,** Reed MW, Brown NJ. Proteolysis in colorectal cancer. *Mol Pathol* 1999; **52**: 140–145

33 **Khan A,** Krishna M, Baker SP, Banner BF. Cathepsin B and tumor associated lamininexpression in the progression of colorectal adenoma to carcinoma. *Mol Pathol* 1998; **11**: 704–708

34 **Gil-Martin E,** Rodriguez-Berrocal FJ, Paez de la Cadena M, Fernandez-Briera A. N-acetyl-beta hexosaminidase activity and isoenzymes in human gastric adenocarcinoma. *Oncology* 1999; **56**: 142–154

35 **Chung SM,** Kawai K. Protease activities in gastric cancer tissues. *Clin Chim Acta* 1990; **189**: 205–210

36 **Yamamoto H,** Adachi Y, Itoh F, Iku S, Matsuno K, Kusano M, Arimura Y, Endo T, Hinoda Y, Hosokawa M, Imai K. Association of matrilysin expression with recurrence and poor prognosis in human esophageal squamous cell carcinoma. *Cancer Res* 1999; **59**: 3313–3316

37 **Hughes SJ,** Glover TW, Zhu XX, Kuick R, Thoraval D, Orringer MB. A novel amplicon at 8p22-23 results in overexpression of cathepsin B in esophagealadenocarcinoma. *Proc Natl Acad Sci USA* 1998; **95**: 12410-12415

38 **Izutani R,** Asano S, Imano M, Kato M, Ohyanagi H, Chihara J. Are adenocarcinomas of the cardia resistant as gastric cancers to quinone anti-cancer drugs and radiation therapy? In: Giuli R, eds. The esophagogastric junction. Paris: *John Libbey Eurotext* 1998: 1244–1249

Science Editor Wang XL and Guo SY **Language Editor** Elsevier HK

PO Box 2345, Beijing 100023, China
www.wjgnet.com
wjg@wjgnet.com

ELSEVIER

World J Gastroenterol 2005;11(37):5757-5762
World Journal of Gastroenterology ISSN 1007-9327
© 2005 The WJG Press and Elsevier Inc. All rights reserved.

• *GASTRIC CANCER* •

Polymorphism of CYPIA1 and GSTM1 genes associated with susceptibility of gastric cancer in Shandong Province of China

Hao Li, Xue-Liang Chen, Hui-Qing Li

Hao Li, Xue-Liang Chen, the Center of Tumour Treatment, Qilu Hospital of Shandong University, Jinan 250012, Shandong Province, China
Hui-Qing Li, the Institute of Basic Medicine, Shandong Academy of Medical Sciences, Jinan 250062, Shandong Province, China
Supported by the Association of Science and Technology of Shandong Province, No. Y97C21057
Correspondence to: Hao Li, the Center of Tumour Treatment, Qilu Hospital of Shandong University, Jinan 250012, Shandong Province, China. haoli611@yahoo.com
Telephone: +86-531-82169873
Received: 2005-01-14 Accepted: 2005-02-28

Abstract

AIM: To explore whether polymorphisms of the CYPIA1 and GSTM1 genes are associated with susceptibility of stomach cancer.

METHODS: A total of 102 stomach cancer cases and 62 healthy persons were diagnosed by pathology in 1998-2000 in the Qilu Hospital of Shandong University. Gene polymorphisms were detected by the PCR using sequence-specific primers. Data analysis of the case-control study was carried out using the unconditional logistic method.

RESULTS: After adjustment for age, sex, educational levels, and occupation, the risk factors for stomach cancer were shown to be smoking, *Helicobacter pylori* (*H pylori*), and presence of the CYPIM G/G and GSTM1 O/O genotypes. Interaction was observed between the combined genotypes of either CYPIA1 G/G and GSTM1 O/O or *H pylori* infection, or GSTM1 O/O and *H pylori* infection or smoking.

CONCLUSION: Polymorphisms of the CYPIA1 and GSTM1 genes, *H pylori* infection and smoking are related to susceptibility to stomach cancer.

© 2005 The WJG Press and Elsevier Inc. All rights reserved.

Key words: Stomach cancer; CYPIA1; GSTM1; Polymorphism

Li H, Chen XL, Li HQ. Polymorphism of CYPIA1 and GSTM1 genes associated with susceptibility of gastric cancer in Shandong Province of China. *World J Gastroenterol* 2005; 11(37): 5757-5762
http://www.wjgnet.com/1007-9327/11/5757.asp

INTRODUCTION

It has been found that the progression of precancerous lesions to gastric cancer is associated with cigarette smoking, alcohol drinking, and *Helicobacter pylori* (*H pylori*) infection in high-incidence areas of China[1-3].

Individual susceptibility to cancer may be partly due to exposure to environmental risk factors, which can be partly explained by genetic variability in metabolic activities related to phases I and II detoxification enzyme pathways. Polymorphisms in these metabolic susceptible genes have been linked to increased risk of cancer in several case-control studies[4].

Cytochrome p450 enzymes, which represent a large multigene family with different substrate specificities, are important in phase I detoxification reactions. The CYPIA1 gene product, aromatic hydrocarbon hydroxylase, catalyzes the first oxidative step in the metabolism of polycyclic aromatic hydrocarbons, such as those found in tobacco smoke, to carcinogens. This gene is induced by exposure to agents such as dioxin, benzo [α] pyrene and other aromatic hydrocarbons[5].

Various CYPIA1 gene polymorphisms have been found to be differentially associated with increased risk of several cancers (including cancer of the lung, breast, and colon) in different specific ethnic groups[6-9].

Phase II enzymes, glutathione *S*-transferase (GSTs), also have activated metabolites of carcinogens to be subjected to metabolic conjugation and other kinds of detoxifications. Homozygous deletions or null genotypes of GSTT1 (theta class) and GSTM1 (mu class) genes may be associated with an increased risk of cancer[5,7-9].

The polymorphisms of these metabolic enzymes result from a difference of the genotypes. Some of these forms cannot metabolize carcinogens into non-cytotoxic agents as is observed in the wild-type proteins[10]. Otherwise some of them metabolize cytotoxic agents into compounds that have the potential to damage DNA associated with high susceptibility to many kinds of diseases or drug resistance[11].

Few studies have evaluated the relationship between CYPIA1, GSTM1, and the risk of gastric cancer, as well as the potential interactions between these genetic markers and other risk factors for gastric cancer in the Chinese population. The present study was to investigate the interaction between CYPIA1- and GST-susceptible genotypes of gastric cancer and *H pylori* infection or smoking.

MATERIALS AND METHODS

Patients with stomach cancer were recruited between January 1998 and January 2000 in the Affiliated Hospital of Shandong University. A biopsy was taken under gastroscope from all patients for their pathologic diagnosis. Of these patients, 102 (86 males and 16 females) had stomach cancer as the

case group, and 62 (33 males and 29 females) had normal gastrointestinal mucous membrane and were used as the control group. All subjects were interviewed using a standardized questionnaire concerning their education, occupation, and cigarette smoking, etc. Blood samples (5 mL) were obtained from patients and controls, and 0.5 mL anti-clot solution of ACD was added. DNA was isolated from peripheral WBC by digestion with proteinase K, followed by phenol/chloroform extraction, and ethanol precipitation prior to resuspension in buffer containing 0.05 mol/L Tris, 5 mol/L EDTA, pH 7.6.

CYPIA1 genetic polymorphisms were determined as described previously[10]. Two pair primer sets were used to detect the polymorphism within exon 7 of the CYPIA1 gene by PCR. One pair primers were sense primer 1A1A: 5'-GAAGTGTATCGGTGAGACCA-3' and antisense primer c53: 5'-GTAGACAGAGTCTAGGCCTCA-3'; the other pair primers were sense primer 1A1G: 5'-GAAGTGTATCGGTGAGACCG-3' and antisense primer c53: 5'-GTAGACAGAGTCTAGGCCTCA-3' located about 190 bp downstream of the polymorphism site (Figure 1).

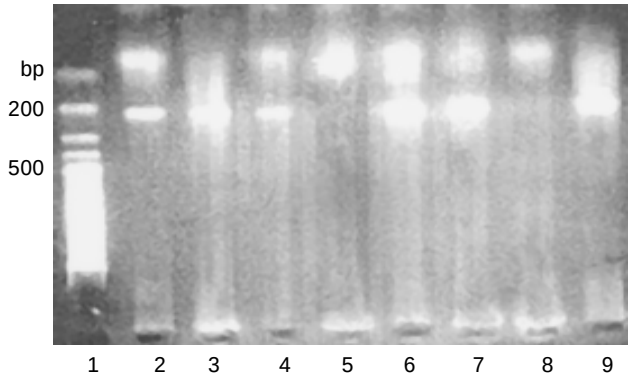


Figure 1 CYPP1A1 genotypes:lanes 2,3 and 6,7 recoded as A/G, lanes 4,5 recoded as A/A, lanes 8,h9 recoded as G/G, lane 1 indicates the molecular-weight marker.

PCR was carried out in two tubes with a total volume of 30 μL containing 0.4 μg of genomic DNA, 1 μL of each of 1A1A and C53 primers 1A1G and C53 were added into the other tube, 2.5 μL of 10×PCR buffer, 2.5 μL of 25 mmol/L Mg^{2+}, 1.5 μL of 10 mmol/L dNTP, 1 U Taq DNA polymerase. The program was initiated 8 min of denaturation at 95 ℃, followed by 35 cycles of amplification with denaturation for 90 s at 95 ℃, annealing for 60 s at 65 ℃ and an extension at 72 ℃ for 120 s, a final elongation at 72 ℃ for 6 min and 40 s on a water incubation PCR amplifier.

The PCR products were then subjected to electrophoresis on 1.8% agarose gels. If there was only a faint band of 190 bp in the 1A1A tube, the genotype was recorded as A/A. If there was only a faint band in the 1A1G tube, the genotype was determined to be G/G.

If both 1A1A and 1A1G tubes showed the faint bands, the genotype was recorded as A/G.

Two primers (G5: 5'-GAACTCCCTGAAAAGCTAAAGC-3' and G6: 5'-GTTGGGCTCAAATATACGGTGG-3') and the primer of β-protein (5'-CAACTTCATCCACGTTCACC-3' and 5'-GAAGAGCCAAGGACAGGTAC-3'), which is located about 215 and 286 bp, downstream of the polymorphic sites, were used to determine the GSTM1 genetic polymorphism as previously described[11] (Figure 2).

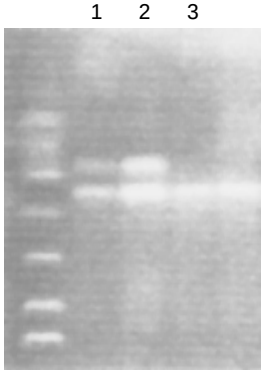


Figure 2 GSTM1 genotypes: lane 1: GSTM1+/o, lane 2: GSTM1 +/+, lane 3: GSTM1 0/0. (lane 1 and lane 2 indicating wild heterozygote; lane 3 indicating null homozygote), left arrow indicates biomarker 242 bp of PBR322 gene/MSPI internally tangent fragments.

PCR were carried out in two tubes of a total volume of 30 μL containing 0.4 μg of genomic DNA, 0.5 μL of each primer, 3.0 μL of 10×PCR buffer, 2.5 μL of 25 mmol/L Mg^{2+}, 3.0 μL of 10 mmol/L dNTP, 2 U of Taq DNA polymerase. The program was initiated for 4 min of denaturation at 94 ℃, followed by 30 cycles of amplification with denaturation for 30 s at 94 ℃, annealing for 30 s at 57 ℃ and an extension at 72 ℃ for 45 s, a final elongation at 72 ℃ for 5 min on a Perkin Elmer PCR amplifier.

The PCR products were then subjected to electrophoresis on 1.8% agarose gels. If there were light intensity bands at 215 and 268 bp, the genotype was recorded as +/+. If there was only a light band of 268 bp, the genotype was determined to be O/O. If there was a faint band of 215 bp and a more intense band of 268 bp, the genotype was recorded as +/O.

All subjects were tested with an antibody against *H pylori* for evidence of infection using an ELISA kit.

To examine the association between CYPIA1 and GSTM1 genotypes and stomach cancer, we calculated the odds ratio (OR) and 95% confidence interval (CI) by unconditional logistic regression. The ORs were adjusted for potential confounding factors, including age, sex, education, and occupation.

Possible modification of the association between genetic polymorphism and stomach cancer risk was also evaluated by stratifying cases and controls into tertiles based on *H pylori* infection and smoking.

RESULTS

We initially assessed the risk of stomach cancer using a variety of parameters. As reported previously, both smoking and *H pylori* infection led to a significant increase in risk (Table 1).

Table 1 Distribution of cases and controls by age, sex, education, and occupation

Variable	Value level	Gastric group		Control group		χ^2	*P*
		n	%	*n*	%		
Age (yr)	<35	4	3.9	18	29.0		
	35-	13	12.7	21	33.9		
	45-	85	83.3	23	37.1	38.945	<0.001
Sex	Male	86	84.3	33	53.2		
	Female	16	15.7	29	46.8	18.718	<0.001
Education years	<5	57	55.9	14	22.6		
	6-	29	28.4	28	45.2		
	13-	16	15.7	20	32.3	17.807	<0.001
Occupation	Farmer	63	61.8	24	38.7		
	Worker	21	20.6	18	29.0		
	Card	18	17.6	20	32.3	8.573	= 0.014

There was no evidence for an increased risk of gastric cancer associated with sauerkraut and mildew food consumption or imbibing white spirit in Chinese population. However, frequent consumption of raw garlic was associated with an apparently reduced risk. The most significant factor associated with increased risk of stomach cancer was a CYPIA1 G/G genotype where the OR was 4.84 compared to the A/A and A/G genotypes. The GSTM1 O/O genotype was also associated with an increased risk of gastric cancer (Table 2).

When the ORs were calculated for the combined CYPIA1 and GSTM1 genotypes, a combination of CYPIA1 A/A and GSTM1 +/+ or +/O gave a baseline of 1.0 as shown in Table 3. The OR for GSTM1 O/O genotype was 3.34 (95%CI: 1.13-9.87). The OR for CYPIA1 G/G was 4.16 (95%CI: 0.40-43.45). However, combined CYPIA1 G/G and GSTM1 O/O enhanced the risk of gastric cancer (OR = 16.48, 95%CI: 2.36-115.0). There was a significant interaction.

When the ORs were calculated for the combined CYPIA1 genotypes and *H pylori* infection, a combination

Table 2 Relative risk of stomach cancer in relation to observed factors

Factors	Controls	Cases	OR[1]	95%CI		OR[2]	95%CI	
Chinese sauerkraut								
None	53	95	1.00					
Sometime	6	4	0.37	0.08	1.58	0.24	0.04	0.95
Often (2+/wk)	3	3	0.56	0.09	3.62	0.39	0.41	3.30
Mildew food								
None	59	94	1.00					
Sometime	2	5	1.57	0.20	12.11	1.50	0.22	10.14
Often (2+/mo)	1	3	1.88	0.17	48.13	1.00	0.07	14.69
Eat raw garlic/yr								
<1 000	20	77	1.00					
>1 000	42	25	0.15	0.07	0.33	0.15	0.06	0.33
CYPIA1 genotype								
A/A	35	53	1.00					
A/G	24	27	0.74	0.35	1.58	0.59	0.26	1.34
G/G	3	22	4.84	1.24	22.07	5.91	1.28	27.24
H pylori infection								
-	26	13	1.00					
+	36	89	4.64	2.15	11.51	4.00	1.65	9.71
Drinking white alcohol[3]								
None	37	48	1.00					
1–100	8	9	0.87	0.27	2.77	1.03	0.26	4.02
100+	17	45	2.04	0.95	4.39	1.11	0.41	2.99
Smoking[4]								
None	42	46	1.00					
<270	14	15	0.98	0.39	2.46	0.66	0.22	1.94
⩾270	6	41	6.23	2.24	18.27	2.78	0.90	8.65
History of cancer family								
None	59	88	1.00					
Yes	3	14	3.13	0.79	14.38	2.98	0.69	12.82
GSTM1 genotype								
+/+ or +/O	36	33	1.00					
O/O	26	67	2.81	1.39	5.71	2.72	1.32	5.62

[1]Non-adjusted OR, [2]adjusted for age, sex, education, and occupation, [3]drinking index=white alcohol/month×number of drinking years, [4]smoking index = cigarette/day×number of smoking years.

of CYPIA1 A/A and no *H pylori* infection at a baseline of 1.0, the OR of *H pylori* infection alone was 7.19 (95%CI: 1.98-26.11), and the OR of CYPIA1 G/G genotype alone was 13.18 (95%CI: 0.42-414.9). The OR significantly enhanced for the combined CYPIA1 G/G genotype and *H pylori* infection compared to the baseline group (Table 4).

As shown in Table 4, when compared to the combined CYPIA1 A/A genotype and non-smoking at a baseline of 1.0, the OR of smoking alone was 1.53 (95%CI: 0.47-4.96), and the OR of CYPIA1 G/G genotype alone was 4.90 (95%CI: 0.90-26.73), both of them did not reach a significant level. However, the ORs were significantly higher for the combined CYPIA1 G/G genotype and smoking as compared to the baseline group (Table 5).

As shown in Table 5, when compared to the combined GSTM1 +/+ or +/O genotype with no *H pylori* infection at a baseline of 1.0, the OR of *H pylori* infection alone was 4.19 (95%CI: 1.16-15.13). In combined GSTM1 O/O genotype and *H pylori* infection group, the OR was 12-fold higher than that in the baseline group (Table 6).

As shown in Table 7, when compared to the combined GSTM1 +/+ or +/O genotype with no smoking at a baseline of 1.0, the OR of smoking alone was 1.22 (95%CI: 0.37-4.01), and the OR of GSTM1 O/O alone was 3.08 (95%CI: 1.11-8.54). An interaction between the GSTM1 O/O genotype and smoking was also observed with a fourfold increase compared to that in the baseline group.

DISCUSSION

In this study, since the biopsy from cases and controls was tested by gastroscopy, there was no bias caused by misclassification.

Table 3 Relative risk of stomach cancer for combined CYPIA1 and GSTM1 genotypes

CYPIA1	GSTM1	Controls	Cases	OR[1]	95%CI	
A/A	+/+or+/O	22	17	1.00		
	O/O	13	35	3.34	1.13	9.87
A/G	+/+or+/O	13	10	0.65	0.20	2.14
	O/O	11	16	1.67	0.52	5.36
G/G	+/+or+/O	1	6	4.16	0.40	43.45
	O/O	2	16	16.48	2.36	115.0

[1]Adjusted for age, sex, education, and occupation; CI: confidence interval.

Table 4 Relative risk of stomach cancer for combined CYPIA1 genotype and *H pylori* infection

CYPIA1	*H pylori*	Controls	Cases	OR[1]	95%CI	
A/A	-	18	5	1.00		
	+	17	22	7.19	1.98	26.11
A/G	-	7	5	1.59	0.29	8.91
	+	17	48	2.94	0.78	11.13
G/G	-	1	3	13.18	0.42	414.9
	+	2	19	28.11	3.95	199.8

[1]Adjusted for age, sex, education, and occupation; CI: confidence interval.

Table 5 Relative risk of stomach cancer for combined CYPIA1 genotype and smoking

CYPIA1	Smoking	Controls	Cases	OR[1]	95%CI	
A/A	None	21	21	1.00		
	Yes	14	32	1.53	0.47	4.96
A/G	None	18	12	0.62	0.20	1.89
	Yes	6	15	0.92	0.24	3.53
G/G	None	3	13	4.90	0.90	26.73
	Yes	0	9	19.0[2]	7.27	54.06

[1]Adjusted for age, sex, education, and occupation; CI: confidence interval; [2]weighed OR by adding to 0.5 for each cell number.

Table 6 Relative risk of stomach cancer for GSTM1 genotype and *H pylori* infection

GSTM1	H p	Controls	Cases[1]	OR[2]	95%CI	
+/+or+/O	-	16	5	1.00		
	+	20	28	4.19	1.16	15.13
O/O	-	10	7	3.53	0.70	17.81
	+	16	60	12.37	3.37	45.46

[1]Adjusted for age, sex, education, and occupation; CI: confidence interval; [2]two cases missing.

Table 7 Relative risk of stomach cancer for combined GSTM1 genotype and smoking

GSTM1	Smoking	Controls	Cases[1]	OR[2]	95%CI	
+/+ or +/O	-	23	16	1.00		
	+	13	17	1.22	0.37	4.01
O/O	-	19	30	3.08	1.11	8.54
	+	7	37	4.32	1.27	14.69

[1]Adjusted for age, sex, education, and occupation; CI: confidence interval; [2]two cases missing.

The results of this study showed that smoking and *H pylori* infection had an association with stomach cancer after being adjusted for age, sex, education, and occupation. Jarebinski *et al*.[12], in 1992 first reported that there is a weak association between smoking and stomach cancer. Liu and Wang[13] in 2002 made a meta-analysis of the relationship between smoking and stomach cancer, and found that cigarette smoking is a risk factor for gastric cancer, especially for male smokers. Finding from most case-control and cohort studies support the causal relation between smoking and gastric cancer[14-16]. Epidemiological evidence relating *H pylori* infection to the etiology of gastric cancer showed that at least 30% of gastric cancers in the developing world and 50% of gastric cancers in the developed world may be attributed to *H pylori* infection[17-20]. Studies indicate that *H pylori* infection is a frequent finding in patients with gastric adenocarcinoma and benign peptic ulcer[21-23]. With respect to carcinogenic mechanism, *H pylori* affects several aspects of gastric epithelial cell function[24-26]. The result from the present study is in agreement with these reports.

There are a number of studies on cytochrome p450 and GSTs associated with cancers, such as breast, lung, liver, esophagus, and stomach cancer[6-8,11].

It was reported that in the presence of p450, CYPIA, CYP2E1, and CYP3A in stomach cancer, the expression of CYPIA (51%) and CYP3A (28%) increases in stomach cancer[27-29]. Liakhovich *et al*.[30], reported that the frequency of CYPIA1-val allele in lung, stomach, and intestine cancer groups was three to five times higher than in the healthy control group. The carriers of homozygous GSTM1 gene deletion are also higher lung cancer risk.

Cai *et al*.[31], in 1999 reported that GSTM1 null genotype correlates with the susceptibility to gastric cancer (OR = 2.03, 95%CI of OR = 1.09-3.80). The risk for gastric cancer in those with GSTM1 null and GSTT1 non-null genotype is significantly higher than that in those with GSTM1 non-null and GSTT1 null genotype, with an OR of 2.91 (95%CI, 1.09-7.89). The risk for gastric cancer in smokers with GSTM1 null genotype increases significantly (OR = 8.06, 95%CI, 2.83-23.67)[31].

Setiawan *et al*.[32], reported that the prevalence of GSTM1 null genotype is 48% in gastric cancer cases, 60% in CG patients, and 51% in controls; after controlling for age, gender, education, pack-years of smoking, alcohol drinking, body mass index, *H pylori* infection, fruit and salt intake, the adjusted OR for GSTT1 and gastric cancer was 2.50 (95%CI, 1.01-6.22); when gastric cancer cases are compared to CG patients, the adjusted OR for GSTT1 is 2.33 (95%CI, 0.75-7.25).

In conclusion, CYPIA1 G/G and GSTM1 O/O genotypes are associated with the increase of stomach cancer in Chinese people. When the CYPIA1 G/G genotype for patients is combined with GSTM1 O/O genotype, then the risk factors involved are *H pylori* infection or smoking. A study needs to be carried out in future.

REFERENCES

1 **Agundez JA**. Cytochrome P450 gene polymorphism and cancer. *Curr Drug Metab* 2004; **5**: 211-224

2 **Wong BC,** Lam SK, Wong WM, Chen JS, Zheng TT, Feng RE, Lai KC, Hu WH, Yuen ST, Leung SY, Fong DY, Ho J, Ching CK, Chen JS. China Gastric Cancer Study Group. *Helicobacter pylori* eradication to prevent gastric cancer in a high-risk region of China: a randomized controlled trial. *JAMA* 2004; **291**: 187-194

3 **You WC**, Zhang L, Gail MH, Chang YS, Liu WD, Ma JL, Li JY, Jin ML, Hu YR, Yang CS, Blaser MJ, Correa P, Blot WJ, Fraumeni JF Jr, Xu GW. Gastric dysplasia and gastric cancer: *Helicobacter pylori*, serum vitamin C, and other risk factors. *J Natl Cancer Inst* 2000; **92**: 1607-1612

4 **Garte S**. The role of ethnicity in cancer susceptibility gene polymorphisms: the example of CYP1A1. *Carcinogenesis* 1998; **19**: 1329-1332

5 **Shi SF**, Xie QX, LI XB. The advance process in relation to the susceptibility of tumor. *Guowai Yixue Zhongliuxue Fence* 1997; **4**: 304-307

6 **Smith GB**, Harper PA, Wong JM, Lam MS, Reid KR, Petsikas D, Massey TE. Human lung microsomal cytochrome P4501A1 (CYP1A1) activities: impact of smoking status and CYP1A1, aryl hydrocarbon receptor, and glutathione S-transferase M1 genetic polymorphisms. *Cancer Epidemiol Biomarkers Prev* 2001; **10**: 839-853

7 **Taioli E**, Ford J, Trachman J, Li Y, Demopoulos R, Garte S. Lung cancer risk and CYP1A1 genotype in African Americans. *Carcinogenesis* 1998; **19**: 813-817

8 **Bell DA**, Taylor JA, Paulson DF, Robertson CN, Mohler JL, Lucier GW. Genetic risk and carcinogen exposure: a common inherited defect of the carconogen-metabolism gene glutathione S-transferase M1 (GSTM1) that increases susceptibility to bladder cancer. *J Natl Cancer Inst* 1993; **85**: 1159-1164

9 **Crofts F**, Taioli E, Trachman L, Cosma GN, Currie D, Toniolo P, garte SJ. Functional significance of different human CYPIA1 genotype. *Carcinogenesis* 1994; **15**: 2961-2963

10 **Hayashi SI**, Walanabe J, Nakachi K, Kawajiri K. PCR detection of an A/G polymorphism within exon 7 of the CYPIA1 gene. *Nucleic Acids Res* 1991; **19**: 4797

11 **Shields PG,** Ambrosone CB, Graham S, Bowman ED, Harrington AM, Gillenwater KA, Marshall JR, Vena JE, Laughlin R, Nemoto T, Freudenheim JL. A cytochrome P4502E1 genetic polymorphism and tobacco smoking in breast cancer. *Mol Car* 1996; **17**: 144-150

12 **Jarebinski M**, Adanja B, Vlajinac H, Pekmezovic T, Sipetic S. Evaluation of the association of cancer of the esophagus, stomach and colon with habits of patients. *Vojnosanit Pregl* 1992; **49**: 19-24

13 **Liu YX**, Wang JZ. Meta-analysis of the relationship between smoking and stomach cancer. *Zhongguo Yixue Kexueyuan Xuebao* 2002; **24**: 559-563

14 **Gonzalez CA**, Pera G, Agudo A, Palli D, Krogh V, Vineis P,

Tumino R, Panico S, Berglund G, Siman H, Nyren O, Agren A, Martinez C, Dorronsoro M, Barricarte A, Tormo MJ, Quiros JR, Allen N, Bingham S, Day N, Miller A, Nagel G, Boeing H, Overvad K, Tjonneland A, Bueno-De-Mesquita HB, Boshuizen HC, Peeters P, Numans M, Clavel-Chapelon F, Helen I, Agapitos E, Lund E, Fahey M, Saracci R, Kaaks R, Riboli E. Smoking and the risk of gastric cancer in the European prospective investigation into cancer and nutrition (EPIC). *Int J Cancer* 2003; **107**: 629-634

15 **Zaridze D**, Borisova E, Maximovitch D, Chkhikvadze V. Alcohol consumption, smoking and risk of gastric cancer: case-control study from Moscow,Russia. *Cancer Causes Control* 2000; **11**: 363-371

16 **Chow WH**, Swanson CA, Lissowska J, Groves FD, Sobin LH, Nasierowska-Guttmejer A, Radziszewski J, Regula J, Hsing AW, Jagannatha S, Zatonski W, Blot WJ. Risk of stomach cancer in relation to consumption of cigarettes, alcohol, tea and coffee in warsaw, poland. *Int J Cancer* 1999; **81**: 871-876

17 **Forman D**. *Helicobacter pylori* and gastric cancer. *Scand J Gastroenterol Suppl* 1996; **220**: 23-26

18 **Guisset M**, Coton T, Rey P, Debonne JM. *Helicobacter pylori* infection in developing countries. *Med Trop* 1997; **57**: 77-82

19 **Tokunaga Y**, Hahata K, Ryo J, Kitaoka A, Tokuka A, Ohsumi K. Density of *Helicobacter pylori* infection in patients with peptic ulcer perforation. *J Am Coll Surg* 1998; **186**: 659-663

20 **Lin CW**, Chang YS, Wu SC, Cheng KS. *Helicobacter pylori* in gastric biopsies of Taiwanese patients with gastroduodenal diseases. *Jpn J Med Sci Biol* 1998; **51**: 13-23

21 **Basso D**, Navaglia F, Brigato L, Piva MG, Toma A, Greco E, Di Mario F, Galeotti F, Roveroni G, Corsini A, Plebani M. Analysis of *Helicobacter pylori* vacA and cagA genotypes and serum antibody profile in benign and malignant gastroduodenal diseases. *Gut* 1998; **43**: 182-186

22 **Buckley MJ**, O'Shea J, Grace A, English L, Keane C, Hourihan D, O'Morain CA. A community-based study of the epidemiology of *Helicobacter pylori* infection and associated asymptomatic gastroduodenal pathology. *Eur J Gastroenterol Hepatol* 1998; **10**: 375-379

23 **Roher HD**, Verreet PR, Wormer O, Muller FP, Ohmann C, Fischbach W. *Helicobacter pylori* in the upper gastrointestinal tract: medical or surgical treatment of gastric lymphoma? *Langenbecks Arch Surg* 2000; **385**: 97-105

24 **Torgyekes E**, Molnar B. Effect of *Helicobacter pylori* infection on the apoptotic and cell proliferative processes of the gastric mucosa. *Orv Hetil* 1999; **140**: 755-760

25 **Calam J**. Host mechanisms: are they the key to the various clinical outcomes of *Helicobacter pylori* infection? *Ital J Gastroenterol Hepatol* 1997; **29**: 375-382

26 **De Gusmao VR**, Nogueira Mendes E, De Magalhaes Queiroz DM, Aguiar Rocha G, Camargos Rocha AM, Ramadan Ashour AA, Teles Carvalho AS. vacA genotypes in *Helicobacter pylori* strains isolated from children with and without duodenal ulcer in Brazil. *J Clin Microbiol* 2000; **38**: 2853-2857

27 **Suzuki S**, Muroishi Y, Nakanishi I, Oda Y. Relationship between genetic polymorphisms of drug-metabolizing enzymes (CYP1A1, CYP2E1, GSTM1, and NAT2), drinking habits, histological subtypes, and p53 gene point mutations in Japanese patients with gastric cancer. *J Gastroenterol* 2004; **39**: 220-230

28 **Hamajima N**. Genetic polymorphisms and cancer risk. *Gan To Kagaku Ryoho* 2004; **31**: 853-857

29 **Murray GI**, Taylor MC, Burke MD, Melvin WT. Enhanced expression of cytochrome P450 in stomach cancer. *Br J Cancer* 1998; **77**: 1040-1044

30 **Liakhovich VV**, Vavilin VA, Gutkina NI, Laktionova IP, Makarova SI, Mitrofanov DV, Ostashevskii VA, Chasovnikova OB. Genes and enzymes of the xenobiotic-metabolizing system in cancer pathology. *Vopr Med Khim* 1997; **43**: 330-338

31 **Cai L**, Yu S, Chen J. Relationship between glutathione S-transferase M1, T1 genotype and susceptibility to gastric cancer. *Zhonghua Yufang Yixue Zazhi* 1999; **33**: 331-333

32 **Setiawan VW**, Zhang ZF, Yu GP, Li YL, Lu ML, Tsai CJ, Cordova D, Wang MR, Guo CH, Yu SZ, Kurtz RC. GSTT1 and GSTM1 null genotypes and the risk of gastric cancer: a case-control study in a Chinese population. *Cancer Epidemiol Biomarkers Pre* 2000; **9**: 73-80

Science Editor Wang XL and Guo SY **Language Editor** Elsevier HK

PO Box 2345, Beijing 100023, China
www.wjgnet.com
wjg@wjgnet.com

ELSEVIER

World J Gastroenterol 2005;11(37):5763-5769
World Journal of Gastroenterology ISSN 1007-9327
© 2005 The WJG Press and Elsevier Inc. All rights reserved.

Inhibitory effects of *N*-(4-hydrophenyl) retinamide on liver cancer and malignant melanoma cells

Xing-Zhong Wu, Li Zhang, Bi-Zhi Shi, Ping Hu

Xing-Zhong Wu, Li Zhang, Bi-Zhi Shi, Ping Hu, Department of Biochemistry and Molecular Biology, Shanghai Medical College, Fudan University, Shanghai 200032, China
Supported by the National Natural Science Foundation of China, No. 30070183 and 30470398
Correspondence to: Professor Xing-Zhong Wu, MD, PhD, Department of Biochemistry and Molecular Biology, Shanghai Medical College, Fudan University, Shanghai 200032, China. xz_wu@shmu.edu.cn
Telephone: +86-21-54237697 Fax: +86-21-64278329
Received: 2004-11-16 Accepted: 2005-02-18

© 2005 The WJG Press and Elsevier Inc. All rights reserved.

Key words: *N*-(4-hydrophenyl) retinamide; Apoptosis; CST; p27^{kip1}

Wu XZ, Zhang L, Shi BZ, Hu P. Inhibitory effects of *N*-(4-hydrophenyl) retinamide on liver cancer and malignant melanoma cells. *World J Gastroenterol* 2005; 11(37): 5763-5769
http://www.wjgnet.com/1007-9327/11/5763.asp

Abstract

AIM: To investigate the effect of *N*-(4-hydrophenyl) retinamide (4-HPR), the derivative of retinoic acid, on inhibition of migration, invasion, cell growth, and induction of apoptosis in hepatocellular carcinoma cells (HCCs) and malignant melanoma cells.

METHODS: 4-HPR was chemically synthesized. Cellular migration and invasion were assayed by Borden chamber experiment. Cell growth was assayed by MTT chromometry. Apoptosis effect was measured using Hoechst 32258 staining and flow cytometry. Gene transfection was performed with lipofectamine.

RESULTS: We observed that the migration of HCC and melanoma cells was significantly suppressed by 4-HPR and the migration cells were reduced to 58±5.03 (control 201±27.2, $P<0.05$, $n = 4$) in SMMC 7721-k3 HCC, and to 254±25.04 (control 302±30.1, $P<0.05$, $n = 4$) in melanoma cells after 6-h incubation with 4-HPR. The invasion through reconstituted basement membrane was also significantly reduced by 4-HPR treatment to 11.2±3.3 in SMMC 7721-k3 HCC (control 27±13.1), and to 24.3±3.2 in melanoma cells (control 67.5±10.1, $P<0.05$, $n = 3$). Cell growth, especially in melanoma cells, was also significantly inhibited. Furthermore, 3 μmol/L of 4-HPR induced apoptosis in B16 melanoma cells (37.11±0.94%) more significantly than all-trans retinoic acid ($P<0.05$), but it failed to induce apoptosis in SMMC 7721-k3 HCC. The mechanism for 4-HPR-induced apoptosis was not clear, but we observed that 4-HPR could regulate p27^{kip1}, and overexpression of cerebroside sulfotransferase (CST) diminished the apoptosis induced by 4-HPR in melanoma cells.

CONCLUSION: 4-HPR is a potent inhibitor of HCC migration and inducer of melanoma cell apoptosis. CST and p27^{kip1} expression might be associated with 4-HPR-induced apoptosis.

INTRODUCTION

The incidence of malignancy is increasing, especially hepatocellular carcinoma and malignant melanoma. Patients with these tumors usually have poor prognosis and short survival because of early metastasis, and also have the highest morbidity rate among all tumors[1-3]. The tumor cells of these diseases have early metastasis potential, which makes the leading cause of cancer-related death[4,5]. However, there is some lack of knowledge regarding the mechanism of tumor cell migration and metastasis, although some metastasis modes or general process have been suggested by previous study[6]. The mechanism by which one or several neoplastic cells escape from the primitive tumor to start the metastatic process is still a matter of discussion[7,8]. The neoplastic cells escape, migration, invasion of blood vessel basement membrane, and growth at new locations are all involved in the process and potential of metastasis. It is completely unclear that what kind of circumstances and conditions will produce the escape and that what situation will favor tumor cells migration or invasion, although the invasion is correlated with matrix metalloproteinases activity[9,10]. The patients' situations get worse due to lack of effective therapy and prevention of tumor metastasis. Hence, it will be more important to find an alternative approach or therapeutic agent that can inhibit the growth or metastasis of HCC and malignant melanoma.

Synthetic derivative of retinoic acid holds a great promise in the treatment against tumors[11]. With an artificial modification of the structure, *N*-(4-hydrophenyl) retinamide (4-HPR) shows a different activity with retinoic acid and has apoptosis-inducing potential[12]. To investigate its anti-tumor effects on HCC and melanoma cells, we used the synthetic analog and compared 4-HPR with retinoic acid. This study is supposed to present the evidence of inhibition of HCC and melanoma cells by 4-HPR and provide the experimental base for further application of anti-tumor activities.

MATERIALS AND METHODS

Materials

Agarose, propidium iodide (PI), *p*-nitrophenyl phosphate (pNPP), all-trans retinoic acid, and 3-(*N*-morpholino) propane-sulfonic acid (MOPS) were from Sigma-Aldrich. Bovine serum albumin (BSA, V) was from Roche. Culture medium RPMI 1640 and fetal bovine serum (FBS) were the product of GIBCO. Transfection reagent lipofectamine was purchased from Life Technologies. Matrigel was from BD Bioscience. Transwell (Borden Chamber), 24- and 96-well cluster plates were from Costar Corning Company. Arsenic (III) oxide was from the Pharmaceutical factory, Harbin Medical University. 4-HPR was synthesized by us by achieving recrystal with the purity of 99.95%. Mouse mAbs against $p27^{kip1}$ and $p21^{waf1}$ were from NeoMarker Co. O4 mAb against lactosyl sulfatide and galactosyl sulfate was from Chemicon. Bicinchonic acid (BCA) protein assay reagent kit was from Pierce.

F1/B16 melanoma cell was purchased from ATCC. The 7721-k3 cell was a subline[13] selected from SMMC-7721 cells for the high migration capability.

Cell migration assay

Cell migration assay was performed as described in our previous report[13]. The assay was performed in Transwell with an insert in 6.5 mm diameter, which has a polycarbonate filter at the bottom. The filter is a microporous membrane and has 8.0 μm sized pores in the membrane. In the chamber under the insert, 600 μL DMEM containing 5 mL/L FBS was added as an attractant for cell migration. In control, 5 mL/L BSA, instead of 5 mL/L FBS, was added, which had no attraction to cells. The cells were digested with 2.5 mmol/L EDTA, washed twice with serum-free medium, resuspended in serum-free DMEM, and adjusted to a concentration of 2×10^5/mL. The cell suspension of 100 μL was added into the insert and incubated at 37 ℃ in 50 mL/L CO_2 for 6 h. After gentle scraping, the adherent cells on the top of the filter by cotton in 30 g/L acetic acid, the cells in the bottom of the filter were then fixed in methanol for 30 min and stained with 5 g/L crystal violet for 5 min. All the cells in the bottom of the filter were counted and the average cell number of four independent assays represented cell migration capacity. In the control group containing 5 mL/L BSA under the filter, few cells migrated through the polycarbonate filter with an average of 2.50±0.02, whereas in the test group containing 5 mL/L FBS under the filter, 334.70±24.57 (n = 3) cells migrated to the bottom of the filter. Therefore, in the following experiment, 5 mL/L FBS was used as chemoattractant in chemotaxis assay.

Invasion assay

Tumor cell invasion assay was also conducted in Transwell, but the polycarbonate filter was precoated by 20 μg matrigel per insert. After incubation at 37 ℃ for 1-2 h, the gel was dried and formed a thin layer to reconstitute base membrane. Like the migration assay, 600 μL of DMEM containing 5 mL/L FBS was added to the well under the filter as chemoattractant. Cell suspension (100 μL) containing 1×10^5 cells was added into the insert. To observe the inhibition of tumor cell invasion, 3 μmol/L 4-HPR was added into the cell suspension. In the control group, 3 μmol/L 4-HPR was replaced by same amount of ethanol. After incubation at 37 ℃ with 50 mL/L CO_2 for 36 h, the top surface of the filter was gently scrapped by a cotton stick and then the filter was fixed by methanol for 30 min and stained by 5 g/L crystal violet for 5 min. Cells on the bottom surface of the filter were all counted.

MTT assay

Cells are prepared in medium at a concentration of 3×10^4/mL and 0.1 mL of cell suspension was placed on the 96-well plate. After incubation, 10 μL of 3-(4,5-dimethyl-2-thiazolyl)-2,5-diphenyl-2H-tetrazolium bromide (MTT) solution (5 mg/mL) was added to each well and incubated at 37 ℃ for further 2 h. Then all the media in the well was discarded and the plate was washed with PBS. The plate was inverted onto an absorbent diaper to pull off the remaining solution in each well. Then 0.1 mL of DMSO was added to each well and the plate was gently shaken for 15 min. Data were read at 570 nm with a reference wavelength of 630 nm.

Acid phosphatase assay

Acid phosphatase assay was performed according to our previous report[14] and the activity correlated well with cell number and MTT assay. Briefly, 3×10^3 cells were placed on each well of a 96-well cluster plate. In the test group, 3 μmol/L 4-HPR was added, whereas the same amount of ethanol was added in the control group. After 12-48 h of incubation, the plate was washed twice with PBS (pH 7.4) and 100 μL reaction buffer (0.1 mol/L sodium acetate pH 5.0, 1 g/L Triton X-100, 5 mmol/L pNPP) was added into each well. After incubation at 37 ℃ for 2 h, the reaction was stopped by adding 10 μL of 1 mol/L NaOH. The data were read at 405 nm wavelength.

Flow cytometry analysis

Cells were cultured at an initial density of 2×10^5 cells/mL. The test group cells were incubated with 3 μmol/L 4-HPR (control with ethanol) at 37 ℃ for 6, 18, and 24 h, followed by washing twice with PBS. Cell pellets were then resuspended in 1 mL of hypotonic PI working solution (50 μg/mL PI, 1 g/L sodium citrate, 1 g/L Triton X-100) and incubated at 4 ℃ overnight. On the 2nd day, the cells were analyzed by a FACScalibur machine. Each sample containing at least 20 000 cells was acquired and measured by CellQuest software. The data of cell cycle were analyzed by ModFit LT version 2.0 software, fitting apoptosis mode.

Fluorescent staining

Cells attached onto a glass slide were treated with 3 μmol/L 4-HPR. After washing twice with PBS, the slide was stained by Hoechst 32 258 and examined under a fluorescent microscope to count the cells with condensed, shrunk, and crumpled apoptosis nucleus among 200 cells, which were examined.

Western blot

Cell cultures, maintained for the indicated time periods, were

washed twice with ice-cold PBS, lysed with lysate buffer (50 mmol/L Tris-HCl, pH 7.4; 2 g/L Triton X-100, 1 mmol/L EDTA, 1 mmol/L PMSF). After being sonicated in ice for 5 min, protein concentration was determined using the BCA assay. Equal amounts of protein extracts were loaded onto 100 g/L sodium dodecyl sulfate-polyacrylamide gel electrophoresis (SDS-PAGE), electroblotted onto PVDF membrane, probed with antibodies against $p27^{kip1}$ and $p21^{waf1}$, developed using the ECF Western blotting kit, and visualized in Kodak X-ray film.

Gene transfection

A full-length of cerebroside sulfotransferase (CST) gene expression frame[15] was inserted into an expressional vector pCXN2 and linearized by a restriction enzyme *Sxp*I. The vectors were then transfected into HCC and B16 melanoma cells. Transfection was performed with lipofectamine following the protocol provided by the manufacturer. After 48 h of transfection, all cells were screened with 400 μg/mL G418, and the colonies in clonal growth were selected, among which nine colonies with CST and six colonies with the vector pCXN2 transfection (Mock) were achieved. All the transfectants were further screened by Northern blot to determine mRNA expression level and by immunology assay with specific mAb O4 to confirm the products of CST enzyme.

Northern blot

A total of 20 μg RNA extracted from all transfectant cells was kept in a solution containing 500 mL/L formamide, 60 g/L formaldehyde, 20 mmol/L MOPS (pH 7.0), denatured at 65 ℃, and then loaded onto 10 g/L agarose. After electrophoresis, RNA was blotted onto a nylon membrane and hybridized with a digoxigenin-labeled probe, which was a RNA fragment synthesized from pSVK-hCST (*Xho*I) by T7 RNA polymerase *in vitro*. Digoxigenin-labeled nucleotide was incorporated into the probe during RNA synthesis. After hybridization at 68 ℃ overnight and washing, the membrane was then incubated with mAb Fab2 against digoxigenin. Bands on the membrane were detected by a DIG Detection kit according to the manufacturer's instructions.

Statistics

The data were expressed as mean±SD. Difference analysis was made by Student's *t*-test. $P<0.05$ was considered statistically significant.

RESULTS

Inhibition of cell migration

SMMC 7721-k3 HCC and B16 melanoma cells were both incubated at an initial concentration of 2×10^5/mL with 3 μmol/L 4-HPR, which was dissolved in ethanol. The control cells were not incubated with the same amount of 0.1 g/L ethanol instead of 4-HPR. After 6-, 18-, or 24-h treatment, the cells were assayed for migration. The inhibitory effects of 4-HPR are shown in Figure 1. After a short period (6 h) treatment with 4-HPR, the migration ability of both cells was significantly inhibited and the migration rate in B16 melanoma cells declined to 84.1% of the control (Figure 1). After 18-h treatment with 4-HPR, the inhibitory effect became stronger. The migration rate after 24-h treatment got further down to 30.5% of the control. In HCC, the inhibitory effect was most significant after 18-h treatment (Figure 1).

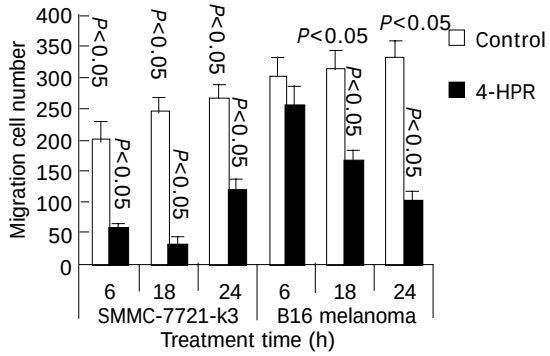


Figure 1 Inhibition migration of hepatocellular carcinoma and melanoma cells by 4-HPR treatment within a short period. SMMC 7721-k3 and B16 melanoma cells were treated with 4-HPR for 6, 18, and 24 h, respectively. After treatment, the cells were assayed for migration in the Transwell.

Effect on the invasion ability

The invasion behavior of tumor cells is important in the metastasis process of hepatocellular carcinoma or melanoma cells. Tumor cell invasion ability can be evaluated and measured *in vitro* by means of the migration and penetration through a reconstituted base membrane. After 4-HPR treatment, 7721-k3 HCC and B16 melanoma cells were assayed for invasion capacity through the reconstituted base membrane (matrigel-coated chemotaxis filter). We observed a significant reduction of cells invading and migrating through the reconstituted base membrane in both SMMC 7721-k3 HCC and melanoma cells even after a short time period of 6-h incubation with 4-HPR. Melanoma cell invasion ability was inhibited more significantly and the cells invading and migrating through the membrane were reduced to 36% of the control. Moreover, invasion of HCC decreased to 41.4% of the control (Figure 2).

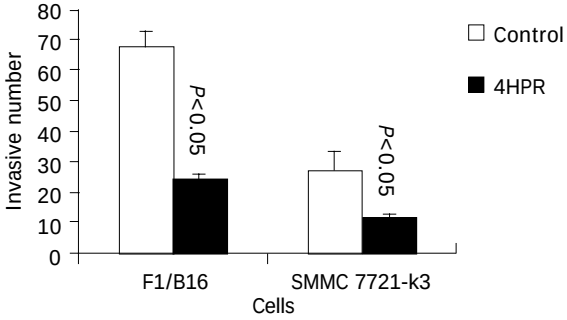


Figure 2 Effect of 3 μmol/L 4-HPR on cell invasion. SMMC 7721-k3 and B16 melanoma cells were treated with 4-HPR for 6 h. The cells penetrating matrigel membrane and migrating to the bottom of the filter were counted and data were expressed as an average from six independent assays.

Effect on the cell growth

Cell growth was evaluated *in vitro* in a time-dependent manner. The treated cells were measured by MTT assay as well as acid phosphatase assay to indicate cell number after the treatment. HCCs seemed to be slightly resistant to low concentration (3 μmol/L) of retinoic acid treatment (ATRA). High concentration of ATRA (10 μmol/L) was needed for the inhibitory effect on the growth of SMMC-7721-k3 HCC. However, 4-HPR was able to inhibit SMMC-7721-k3 HCC growth at 3 μmol/L (Figure 3). After 72-h treatment, the inhibitory effect became significant as shown by the MTT assay (Figure 3). B16 melanoma cells were quite sensitive to 4-HPR treatment and the growth rate was significantly inhibited by 3 μmol/L 4-HPR. After 48-72 h treatment with 3 μmol/L 4-HPR, B16 melanoma cell growth was completely inhibited because the cell number did not increase, but decreased. The growth of B16 melanoma cells also decreased after treatment with 10 μmol/L ATRA, but the cell could still grow. The inhibitory effects of ATRA on B16 melanoma cell growth was not as significant as the inhibitory effects of 4-HPR (Figure 4).

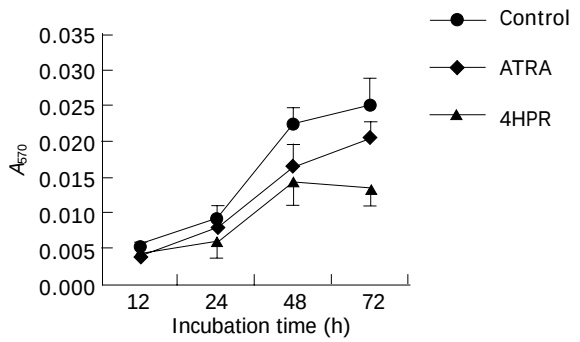


Figure 3 Growth inhibition of SMMC 7721-k3 cells by ATRA and 4-HPR. SMMC 7721-k3 cells were cultured in the 96-well cluster plate and incubated with 10 μmol/L ATRA, 3 μmol/L 4-HPR, or ethanol in the control.

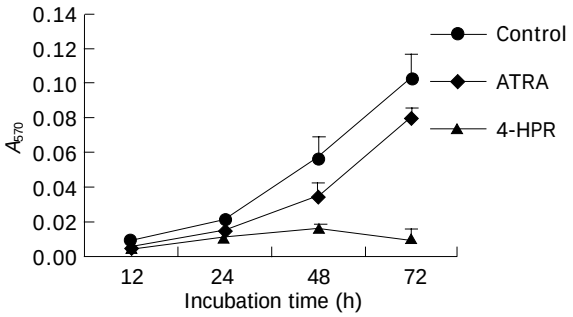


Figure 4 Growth inhibition of B16 melanoma cells by ATRA and 4-HPR. B16 melanoma cells were cultured in the 96-well cluster plate and incubated with 10 μmol/L ATRA, 3 μmol/L 4-HPR, or ethanol in the control. The data were achieved by an average from eight independent groups.

Regulation of cell cycles

SMMC 7721-k3 HCCs were proliferated and the cell cycle was analyzed by flow cytometry. After 18-h treatment with 4-HPR, SMMC 7721-k3 HCCs at G_0/G_1 stage were significantly fewer, but at G_2/M and S stage were significantly increased. After 24-h treatment with 4-HPR, cells at G_2/M stage increased significantly (Figure 5), indicating that the cells were accumulated at this stage. However, cells at G_0/G_1 stage were the majority of the cells in control group, which accounted for 73.3%. Cells at S stage accounted for 22.95% and cells at G_2/M stage were the minority (Figure 5). Total proteins extracted from the cells treated with ATRA or 4-HPR for 24 h was used to analyze $p27^{kip1}$ and $p21^{waf1}$ expression. We observed that 4-HPR treatment significantly induced $p27^{kip1}$ expression, while $p21^{waf1}$ retained the same expressional level after the treatment with either ATRA or 4-HPR (Figure 6). B16 melanoma cells were treated with 4-HPR for 18-24 h and the cycle did not change so much as SMMC 7721-k3 HCCs did. The percentage of different cell cycles remained at the similar level as control cells. However, 24 h after 4-HPR treatment, a peak of apoptosis appeared in B16 melanoma cells as detected by flow cytometry.

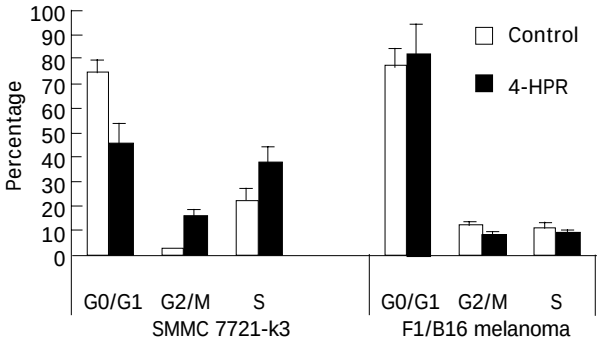


Figure 5 Regulation of cell cycles by 4-HPR. SMMC 7721-k3 cells and B16 melanoma cells were treated with 4-HPR for 24 h, respectively. Data were expressed as an average from three independent assays.

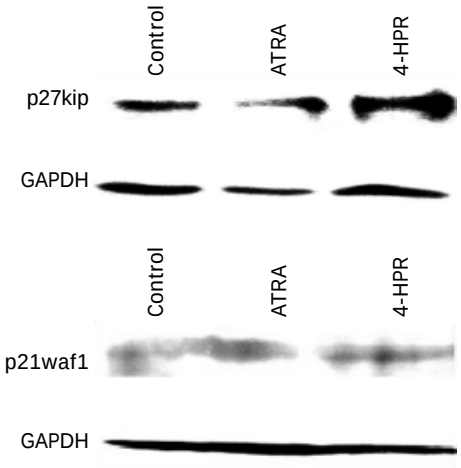


Figure 6 Western blot analysis of effects of 4-HPR on $p27^{kip1}$ and $p21^{waf1}$ expression. SMMC 7721-k3 cells were treated with 10 and 3 μmol/L 4-HPR for 24 h, respectively.

Induction of apoptosis by 4-HPR

Apoptosis was evaluated using both Hoechst fluorescent staining and flow cytometry analysis by PI staining. SMMC

7721-k3 cells were not sensitive to 3 μmol/L 4-HPR induction and only few cells were induced into apoptosis. After 6-48 h treatment with 3 μmol/L 4-HPR, apoptotic cell population was less than 8% of all SMMC 7721-k3 cells, which was not significantly different from that in negative control. In positive control, the cells were treated with 3 μmol/L arsenic (III) oxide, 24.3% of SMMC 7721-k3 cells was induced into apoptosis, which was significantly different from that of negative control. B16 melanoma cells were treated with 3 μmol/L 4-HPR for 24 h and apoptotic cell population reached to 12.52% of the total cells. After 48-h treatment with 3 μmol/L 4-HPR, apoptotic cells accounted for 37.11% (Table 1). This indicated that 4-HPR might be a potent inducer of apoptosis for melanoma cells, but not HCCs. As for comparison, we observed the effect of ATRA on both SMMC 7721-k3 cells and B16 melanoma cells at the same time. No significant apoptosis could be detected after treatment with 3 μmol/L ATRA for 24-48 h, whereas about 20% apoptosis was observed in both hepatocellular carcinoma and melanoma cells after treatment with 20 μmol/L ATRA for 72 h (Table 1).

Table 1 Apoptotic effects induced by 4-HPR (mean±SD, n = 3)

	Control	4-HPR	ATRA	As_2O_3
7721-k3 cells	4.27±0.06	8.53±0.12	5.05±0.03	24.27±0.39
P		>0.05	>0.05	<0.05
B16 melanoma cells	1.65±0.16	37.11±0.94	2.38±0.38	ND
P		<0.05	>0.05	

ND, not determined.

Influence of CST overexpression on 4-HPR induction

Our previous study demonstrated that retinoid compounds could inhibit cellular CST activity[16]; however, the inhibitory mechanism was unclear. Whether higher CST expression and activity would affect the action of retinoid compounds requires further investigation. In this study, we observed high CST expression influenced on 4-HPR induction in HCC and melanoma cells. After B16 melanoma and HCCs were transfected with whole expressional frame of CST cDNA in pCXN2 vector and CST mRNA expression was confirmed by Northern blot in the transfectants. All the cells were further screened using immune thin-layer chromatography with specific mAb against sulfolactosyl sulfatide and sulfogalactosyl sulfatide to select the clones with high expression of CST enzyme products. CST-transfected melanoma cell clones 1, 3 and CST-transfected HCC clone 6, 8 were chosen for the study. CST-transfected HCCs did not have any alteration in proliferation and cell growth, but the cell mobility, migration, and adhesion behaviors changed significantly, which led to promote metastasis of HCC in nude mice. The sensitivity to 4-HPR induction in CST-transfected HCCs remained the same as in vector-transfected cells (mock) or in parent HCC.

Table 2 4-HPR-induced apoptosis in CST overexpressed B16 melanoma cells (mean±SD, n = 3)

	Parent cells	Mock cells	CST1	CST3
Control	1.64±1.16	1.37±0.30	2.61±0.61	1.37±0.374
4-HPR	37.11±0.95	38.030±1.002	32.65±1.98[a]	33.59±0.91[a]

[a]P<0.05 *vs* mock cells.

CST-transfected B16 melanoma cells, however, proliferated and grew in a faster rate than mock and parent B16 melanoma cells. Interestingly, CST-transfected B16 melanoma cells became less sensitive to 4-HPR induction than mock and parent melanoma cells. After treatment with 3 μmol/L 4-HPR for 48 h, 38.03±1.002% apoptotic cells were detected in mock transfectants. Moreover, after treatment with 3 μmol/L 4-HPR, parent B16 melanoma cells showed 37.11±0.95% apoptosis (Table 2). However, no significant difference of apoptotic rate was observed between the mock cells and parent melanoma cells (n = 4). The CST transfectant CST1 and CST3 of B16 melanoma cells became less sensitive to 4-HPR induction. After treatment with 3 μmol/L 4-HPR, there were only 32.65±1.98% and 33.59±0.91% apoptosis in CST1 and CST3 transfectants, respectively, which were significantly lower than those in mock cells (P<0.05, n = 3). The results from flow cytometry analysis are similar to these. B16 melanoma cells were treated with 3 μmol/L 4-HPR and a peak of apoptosis appeared before peak G_1 (Figure 7). Mock cells had a similar peak of apoptosis as the parent cells. However, the size and height

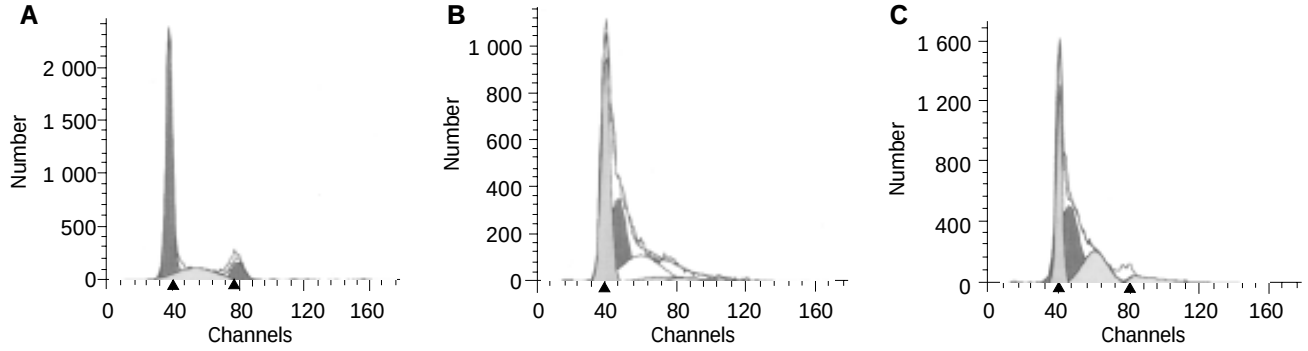


Figure 7 Comparison of apoptosis peak between CST- and vector-transfected cells. Control cells either of vector- or CST-transfected could not show any apoptosis (A). After being treated with 4-HPR, the vector-transfected cells produced a large apoptosis peak (B), while in CST-transfected cells only a small apoptosis peak could be seen (C).

of apoptosis peak in both CST transfectants, CST1 and CST3, were much smaller or shorter than those of mock cells, which indicated that CST transfectant B16 melanoma cells produced fewer apoptosis cells after 4-HPR treatment. But, to ATRA the sensitivity remained the same in CST transfectants as those in mock cells.

DISCUSSION

Hepatocellular carcinoma is one of the most common malignant tumors. Up to now, there is no effective approach for treatment of the patients with HCC except surgical therapy. We have previously used all-trans retinoic acid to induce differentiation of HCCs and in clinical trials in some cases[17]. Although ATRA could induce HCCs differentiation and resulted in shrinkage of tumor mass in some patients, a higher dose of ATRA was required to achieve the effectiveness. The *in vitro* concentration induction needed 10 μmol/L, which was 10 times higher than that for leukemia cells[18,19]. ATRA also was used for the induction of melanoma cells. Due to side effects, especially liver lesion, ATRA has a limited application for some patients. 4-HPR is a kind of synthetic retinoid derivative, which has been considered as the product with fewest side effects up to now. Several documents and clinical trials have suggested that 4-HPR is an effective agent for chemoprevention of breast cancer. Holven *et al*.[20], reported that 4-HPR could inhibit liver secretion of retinoic acid binding protein and enhance the induction effect of retinoic acid.

In this study, we used the synthetic 4-HPR to observe the effect on hepatocellular carcinoma and melanoma cells. Quite different actions and effects were noted between 4-HPR and ATRA. To inhibit cell growth or migration of hepatocellular carcinoma and melanoma cells required relatively lower 4-HPR concentration as compared with ATRA. Our data showed that 3 μmol/L 4-HPR could significantly inhibit the migration of HCC and melanoma cells. After 6-h incubation with 3 μmol/L 4-HPR, the migration of B16 melanoma cells was inhibited to 84.1%. After 18-h incubation with 3 μmol/L 4-HPR, B16 melanoma cell migration was decreased to 52.4%. Similarly, the invasion ability of B16 melanoma cells through reconstituted basement membrane was significantly inhibited by 4-HPR treatment. Tumor cell migration and invasion were closely related with the metastasis behavior[21,22]. Thus, we consider that 4-HPR potentially inhibits the biological behaviors related with metastasis of melanoma cells and HCC and may have a potential application as the alternative treatment and prevention of tumor metastasis. In this study, we also observed the difference in effects between 4-HPR and ATRA. When B16 melanoma cells were treated with 3 μmol/L 4-HPR only for 24 h, a significant apoptosis rate was observed, no significant apoptosis could be detected after treatment with 3 μmol/L ATRA for 24 h. Induction of apoptosis in B16 melanoma cells or HCC needed a much higher concentration of ATRA and much longer incubation time (72 h) compared to 4-HPR. However, the mechanism of 4-HPR-induced apoptosis is not fully understood, although some lines of evidence have suggested the involvement of super oxygen reaction[23].

In our previous investigation[24], we observed that CST expression was closely associated with metastasis of tumor cells. When HCCs were inhibited by 10 μmol/L ATRA, the activity and products of cellular CST were significantly reduced. Overexpression of CST in HCC altered cell behaviors of migration through chemotaxis filters and adhesion to extracellular matrix. Overexpression of CST in melanoma cells promoted cell growth. Therefore, we observed 4-HPR induction, sensitivity, and other biologic behavioral changes in CST-expressing B16 melanoma cells. Interestingly, the induction of 4-HPR in such cells seemed to be less effective than in mock or parent cells because there were fewer apoptosis cells in CST highly expressing B16 melanoma cells than the mock cells. Although the possible mechanism is unclear, this result suggests that CST expression might be involved in 4-HPR-induced apoptosis in melanoma cells. Several studies have suggested that CST is closely related with some growth factors, such as HGF[25] and EGF[26,27], which stimulate cell growth. A recent report has suggested that HER2/neu can reduce the sensitivity of breast cancer cells to 4-HPR by activation of Akt, which further induces cyclooxygenase-2 (COX-2) expression[28]. Furthermore, 4-HPR has been recently reported to increase cellular ceramide levels, which is considered to be a cytotoxic messenger that may regulate the proliferation, survival, and death of cells[29,30]. The increased ceramide biosynthesis is required for 4-HPR-induced endothelial apoptosis[29]. Therefore, the metabolism or catabolism of cellular ceramide could affect the induction and sensitivity of 4-HPR. CST catalyzes sulfation of lactosylceramide or galactosylceramide[31], and thus promotes the metabolism of cellular ceramide.

ACKNOWLEDGMENT

We appreciate the National Nature Science Foundation of China (No. 30070183 and 30470398) for their support to this work.

REFERENCES

1 **Li XT,** Mikkelsen IM, Mortensen B, Winberg JO, Huseby NE. Butyrate reduces liver metastasis of rat colon carcinoma cells *in vivo* and resistance to oxidative stress *in vitro*. *Clinical Experimental Metastasis* 2004; **21**: 331-338

2 **Timmers M,** Vekemans K, Vermijlen D, Asosingh K, Kuppen P, Bouwens L, Wisse E, Braet F. Interactions between rat colon carcinoma cells and Kupffer cells during the onset of hepatic metastasis. *Int J Cancer* 2004; **112**: 793-802

3 **Chuma M,** Sakamoto M, Yasuda J, Fujii G, Nakanishi K, Tsuchiya A, Ohta T, Asaka M, Hirohashi S. Overexpression of cortactin is involved in motility and metastasis of hepatocellular carcinoma. *J Hepatol* 2004; **41**: 629-636

4 **Mann CD,** Metcalfe MS, Leopardi LN, Maddern GJ. The clinical risk score - Emerging as a reliable preoperative prognostic index in hepatectomy for colorectal metastases. *Archives Surg* 2004; **139**: 1168-1172

5 **Murakami T,** Cardones AR, Hwang ST. Chemokine receptors and melanoma metastasis. *J Dermatol Sci* 2004; **36**: 71-78

6 **Takamura M,** Sakamoto M, Hirohashi S. Recent progress in study of mechanism of invasion and metastasis of hepatocellular carcinoma. *Nippon Rinsho* 2001; **59**: 169-175

7 **Fiol J,** Bolognese MG. Proto-metastatic core and comet effect: new theoretical model of the mechanism of metastasis generation. *Med Hypotheses* 2000; **54**: 353-357

8 **Xiong B,** Yuan HY, Hu MB, Zhang F, Wei ZZ, Gong LL, Yang GL. Transforming growth factor-beta1 in invasion and metastasis in colorectal cancer. *World J Gastroenterol* 2002; **8**: 674-678
9 **Hosotani R,** Kawaguchi M, Masui T, Koshiba T, Ida J, Fujimoto K, Wada M, Doi R, Imamura M. Expression of integrin alphaVbeta3 in pancreatic carcinoma: relation to MMP-2 activation and lymph node metastasis. *Pancreas* 2002; **25**: e30-e35
10 **Monig SP,** Baldus SE, Hennecken JK, Spiecker DB, Grass G, Schneider PM, Thiele J, Dienes HP, Holscher AH. Expression of MMP-2 is associated with progression and lymph node metastasis of gastric carcinoma. *Histopathology* 2001; **39**: 597-602
11 **Minton SE.** Chemoprevention of breast cancer in the older patient. *Hematol Oncol Clin North Am* 2000; **14**: 113-130
12 **Clifford JL,** Sabichi AL, Zou C, Yang X, Steele VE, Kelloff GJ, Lotan R, Lippman SM. Effects of novel phenylretinamides on cell growth and apoptosis in bladder cancer. *Cancer Epidemiol Biomarkers Prev* 2001; **10**: 391-395
13 **Wu XZ,** Chen YF. Fucosylated ogligosaccharides in the migration of hepatoma cells. *Progress Biochem Biophys* 2002; **29**: 932-937
14 **Lu H,** Wu XZ. Acid phosphatase assay for measuring of the proliferation of tumor cells. *Chin J Lab Med* 2001; **24**: 84-86
15 **Hirahara Y,** Tsuda M, Wada Y, Honke K. cDNA cloning, genomic cloning, and tissue-specific regulation of mouse cerebroside sulfotransferase. *Eur J Biochem* 2000; **267**: 1909-1917
16 **Wu XZ,** Li W, Ben J, Zha XL. Correlation between the expression level of sulfated lactosyl ceramide and metastasis potential of hepatocellular carcinoma. *Progress Biochem Biophys* 2003; **30**: 395-400
17 **Wu XZ,** Lu H, Zhou L, Huang Y, Chen H. Changes of phosphatidylcholine-specific phospholipase C in hepatocarcinogenesis and in the proliferation and differentiation of rat liver cancer cells. *Cell Biol Int* 1997; **21**: 375-381
18 **Wu XZ,** Wang X, Qien X, Liu H, Ying J, Yang Z, Yao H. Four years' experience with the treatment of all-trans retinoic acid in acute promyelocytic leukemia. *Am J Hematol* 1993; **43**: 183-189
19 **Wu XZ,** Qureshi IA, Liu HN, Yin JS, Qian XP, Xu RJ. Epidermal growth-factor in acute promyelocytic leukemia treated with retinoic acid. *Int J Hematol* 1995; **62**: 83-89
20 **Holven KB,** Natarajan V, Gundersen TE, Moskaug JO, Norum KR, Blomhoff R. Secretion of N-(4-hydroxyphenyl) retinamide-retinol-binding protein from liver parenchymal cells: evidence for reduced affinity of the complex for transthyretin. *Int J Cancer* 1997; **71**: 654-659
21 **Dellacasagrande J,** Schreurs OJ, Hofgaard PO, Omholt H, Steinsvoll S, Schenck K, Bogen B, Dembic Z. Liver metastasis of cancer facilitated by chemokine receptor CCR6. *Scand J Immunol* 2003; **57**: 534-544
22 **Yamaguchi H,** Kitayama J, Takuwa N, Arikawa K, Inoki I, Takehara K, Nagawa H, Takuwa Y. Sphingosine-1-phosphate receptor subtype-specific positive and negative regulation of Rac and haematogenous metastasis of melanoma cells. *Biochem J* 2003; **374**: 715-722
23 **Goto H,** Takahashi H, Fujii H, Ikuta K, Yokota S. N-(4-Hydroxyphenyl) retinamide (4-HPR) induces leukemia cell death via generation of reactive oxygen species. *Int J Hematol* 2003; **78**: 219-225
24 **Wu XZ,** Honke K, ZhangYL, Zha XL, Taniguchi N. Lactosylsulfatide expression in hepatocellular carcinoma cells enhances cell adhesion to vitronectin and intrahepatic metastasis in nude mice. *Int J Cancer* 2004; **110**: 504-510
25 **Kobayashi T,** Honke K, Miyazaki T, Matsumoto K, Nakamura T, Ishizuka I, Makita A. Hepatocyte growth factor specifically binds to sulfoglycolipids. *J Biol Chem* 1994; **269**: 9817-9821
26 **Kobayashi T,** Honke K, Gasa S, Kato N, Miyazaki T, Makita A. Epidermal growth factor elevates the activity levels of glycolipid sulfotransferases in renal-cell-carcinoma cells. *Int J Cancer* 1993; **55**: 448-452
27 **Tsuda M,** Egashira M, Niikawa N, Wada Y, Honke K. Cancer-associated alternative usage of multiple promoters of human GalCer sulfotransferase gene. *Eur J Biochem* 2000; **267**: 2672-2679
28 **Simeone AM,** Li YJ, Broemeling LD, Johnson MM, Tuna M, Tari AM. Cyclooxygenase-2 is essential for HER2/neu to suppress N- (4-hydroxyphenyl) retinamide apoptotic effects in breast cancer cells. *Cancer Res* 2004; **64**: 1224-1228
29 **Erdreich-Epstein A,** Tran LB, Bowman NN, Wang H, Cabot MC, Durden DL, Vlckova J, Reynolds CP, Stins MF, Groshen S, Millard M. Ceramide signaling in fenretinide-induced endothelial cell apoptosis. *J Biol Chem* 2002; **277**: 49531-49537
30 **Maurer BJ,** Metelitsa LS, Seeger RC, Cabot MC, Reynolds CP. Increase of ceramide and induction of mixed apoptosis/necrosis by N-(4-hydroxyphenyl)-retinamide in neuroblastoma cell lines. *J Natl Cancer Inst* 1999; **91**: 1138-1146
31 **Kabayama K,** Ito N, Honke K, Igarashi Y, Inokuchi J. Suppression of integrin expression and tumorigenicity by sulfation of lactosylceramide in 3LL Lewis lung carcinoma cells. *J Biol Chem* 2001; **276**: 26777-26783

Science Editor Guo SY and Kumar M **Language Editor** Elsevier HK

PO Box 2345, Beijing 100023, China
www.wjgnet.com
wjg@wjgnet.com

ELSEVIER

World J Gastroenterol 2005;11(37):5770-5776
World Journal of Gastroenterology ISSN 1007-9327
© 2005 The WJG Press and Elsevier Inc. All rights reserved.

Low prevalence of germline *hMSH6* mutations in colorectal cancer families from Spain

Ana Sánchez de Abajo, Miguel de la Hoya, Alicia Tosar, Javier Godino, Juan Manuel Fernández, Jose Lopez Asenjo, Beatriz Perez Villamil, Pedro Perez Segura, Eduardo Diaz-Rubio, Trinidad Caldes

Ana Sánchez de Abajo, Miguel de la Hoya, Alicia Tosar, Javier Godino, Juan Manuel Fernández, Beatriz Perez Villamil, Eduardo Diaz-Rubio, Trinidad Caldes, Laboratorio de Oncología Molecular, Hospital Clinico San Carlos, Madrid, Spain
Jose Lopez Asenjo, Servicio de Anatomía Patológica, Hospital Clinico San Carlos, Madrid, Spain
Pedro Perez Segura, Servicio de Oncología Médica, Hospital Clinico San Carlos, Madrid, Spain
Supported by the Instituto Nacional Carlos III (RTICC C03/10); Fondo de Investigación Sanitaria (FIS 04/0957) and Sanofi-Synthelabo
Correspondence to: Dr. Trinidad Caldes, Laboratorio de Oncología Molecular, Hospital Clinico San Carlos, Martín Lagos s/n, Madrid 28040, Spain. tcaldes@hcsc.es
Telephone: +34-91-3303348 Fax: +34-91-3303544
Received: 2005-04-12 Accepted: 2005-04-30

Abstract

AIM: To investigate the prevalence and penetrance of hMSH6 mutations in Spanish HNPCC families that was negative for mutation in hMLH1 or hMSH2.

METHODS: We used PCR-based DGGE assay and direct sequencing to screen for hMSH6 gene in 91 HNPCC families.

RESULTS: we have identified 10 families with germ-line mutations in the DNA sequence. These mutations included two intronic variation, three missense mutation, one nonsense mutation, and four silent mutations. Among the 10 germ-line mutations identified in the Spanish cohort, 8 were novel, perhaps, suggesting different mutational spectra in the Spanish population. Detailed pedigrees were constructed for the three families with a possible pathogenic hMSH6 mutation. The two silent mutations H388H and L758L, detected in a person affected of colorectal cancer at age 29, produce loss of the wild-type allele in the tumor sample. Immunohistochemical analysis showed that expression of MSH6 protein was lost only in the tumors from the carriers of V878A and Q263X mutations.

CONCLUSION: Altogether, our results indicate that disease-causing germ-line mutations of hMSH6 are very less frequent in Spanish HNPCC families.

© 2005 The WJG Press and Elsevier Inc. All rights reserved.

Key words: HNPCC; MMR; hMSH6; MSI; IHC; SPANISH

de Abajo AS, de la Hoya M, Tosar A, Godino J, Fernández JM, Asenjo JL, Villamil BP, Segura PP, Diaz-Rubio E, Caldes T. Low prevalence of germline *hMSH6* mutations in colorectal cancer families from Spain. *World J Gastroenterol* 2005; 11 (37): 5770-5776
http://www.wjgnet.com/1007-9327/11/5770.asp

INTRODUCTION

The link between defective DNA mismatch repair and the development of tumors has been firmly established. Inherited mutations in DNA mismatch repair genes are associated with the autosomal-dominant cancer susceptibility syndrome, hereditary non-polyposis colorectal cancer (HNPCC [MIM 114400; MIM 114500]). Patients with HNPCC are at high risk for colorectal and endometrial cancer and a variety of other malignancies. Tumors from HNPCC patients frequently show mutations in repetitive sequences, giving rise to a molecular phenotype referred to as microsatellite instability (MSI). Not surprisingly, a significant fraction of sporadic colorectal and endometrial cancers also show MSI.

The hMSH6 (MIM 600678) protein is a member of the MMR system; it interacts with hMSH2 to form the MutSα heterodimer[1-3]. Besides hMSH6, the hMSH2 protein also interacts with the hMSH3 protein to form the MutSβ heterodimer. The MutSα heterodimer is efficient in the repair of both base-base mismatches and insertion-deletion loops, whereas the MutSβ heterodimer is mainly active in the repair of insertion-deletion loops and not in the repair of base-base mismatches[4,5]. These data indicate that the hMSH6 and hMSH3 proteins are partially redundant in their DNA repair function.

Most families with clinically recognized HNPCC and MSI high, have mutations in either hMLH1 or hMSH2. Mutations in hMSH6 gene, appear to be associated with atypical HNPCC and in particular with the development of endometrial carcinoma[6-9]. The age of onset of cancers in HNPCC kindred's with hMSH6 mutations is higher than in hMSH2 or hMLH1 mutation carriers, and it has been reported that tumors from affected family members are less likely to have high MSI than tumors from hMSH2 or hMLH1 mutation carriers[10].

The estimate frequency of hMSH6 mutations in patients with colorectal cancer ranges between 0% based on a tumor immunohistochemistry study of a consecutive series and 1.5% based on mutation analysis of a combination of sporadic and familial cases[11,12]. Only a few of these germ-line mutations have been reported in families that fulfill the Amsterdam criteria[12,13]. To date, there have been no studies

to determine the frequency of germ-line hMSH6 mutations in Spanish HNPCC families. The aim of this study was to verify the contribution of hMSH6 defects to cancer susceptibility in 132 HNPCC Spanish families that have been previously tested for hMSH2 and hMLH1 mutations[14,15].

MATERIALS AND METHODS

Patients

Families were selected through the clinic for familial cancer at the San Carlos University Hospital in Madrid, and they were Spanish by descent. Informed consent was obtained from each participant. Personal and family cancer histories were obtained from the proband and participating relatives, and cancer diagnoses and deaths were confirmed by reviewing the medical records, pathology reports, or death certificates.

We classified each pedigree by whether they fulfilled the original Amsterdam I criteria (n = 56 families), Amsterdam II (n = 11 families), Bethesda guidelines (n = 37 families), or none of these criteria (n = 28 families)[16-18]. This last category we refer to as "HNPCC-like" where the tumor spectra are reminiscent of HNPCC but not fulfilling Amsterdam I, Amsterdam II, or young age at onset criteria.

All probands, had been previously tested for MSI status and hMLH1/hMSH2 mutations/deletions by either DGGE and direct genomic sequencing and multiplex ligation-dependent probe amplification (MLPA, MRC-Holland).

Control subjects

One hundred unrelated healthy individuals from the Blood Transfusion National Service in Madrid (Spain) were used as controls.

DNA isolation

Genomic DNA was isolated from peripheral blood lymphocytes according to the salting out procedure[19]. Paraffin-embedded tumor samples were used to confirm segregation of identified mutations and to study MSI and LOH. In these cases, DNA was extracted from paraffin blocks as described previously by de la Hoya *et al*.[20].

Tumor MSI analysis

One hundred and thirteen paired normal and tumor DNA were analyzed for MSI with the five markers of the Bethesda panel (BAT25, BAT26, D2S123, D5S346, and D17S250). Analysis of microsatellite sequences for instability was performed using an ABI Prism 310 Genetic Analyzer (Applied Biosystems, Foster City, CA, USA). PCR reactions were performed in a PTC-100 thermocycler (MJ Research, Waltman, MA, USA) and AB/ABI GeneScan software was used for data interpretation. Primer sequences were as described[21,22] and both fluorescent labeled and unlabeled primers were obtained from Applera Hispania SA. PCR reactions were carried out in a 10 μL reaction volume containing 50-100 ng of DNA, 1× PCR buffer (Ecogen SRL, Spain), 2.5 mol/L $MgCl_2$, 200 μmol/L of each deoxynucleotide triphosphate (Promega, Madison, WI, USA), 0.4 μmol/L of each primer, and 1 U Eco Taq DNA polymerase (Ecogen SRL, Spain). The thermocycling conditions were 1 cycle of 10 min 95 ℃, followed by 40 cycles consisting of 30 s 98 ℃; 1 min 55 ℃; 1 min 72 ℃, followed by 1 cycle of 7 min 72 ℃. Normal and tumor samples were prepared for analysis by pooling 0.5 μL of each reaction, 12 μL of formamide and 0.5 μL GeneScan 500 (Tamra; PE/ABI). The resulting suspension was heated at 95 ℃, for 3 min, and then loaded on an ABI 310 sequencer for automated detection. The GeneScan software analyzed the data. Microsatellite stable (MSS) was defined as no observed instability, MSI-H was defined as two unstable loci of the five reference loci.

DNA amplification

The entire *MSH6* coding region and the splice-junctions were amplified using the PCR from genomic DNA using 23 primer pairs. All amplicons were subjected to DGGE (below). The sequences of the primers are available upon request.

All DNA amplifications were performed in a 50-μL volume containing 100 ng DNA, 1× PCR buffer (Ecogen SRL, Spain), 0.4 μmol/L of each primer, 200 μmol/L of each deoxynucleotide (Promega, Madison, WI, USA), 1 U Eco Taq DNA polymerase (Ecogen SRL, Spain). Amplification was carried out in a PTC-100 thermocycler (MJ Research, Waltham, MA, USA). After denaturation at 95 ℃ for 5 min, 35 cycles at 95 ℃ for 30 s, 55 ℃, or 58 ℃ for 30 s and 72 ℃ for 60 s were performed, followed by a final extension step of 10 min at 72 ℃. Subsequently, PCR fragments were subjected to one round of complete denaturation and renaturation that is 98 ℃ for 10 min, 55 ℃ for 30 min, and 37 ℃ for 30 min to create heteroduplex molecules.

DGGE

DGGE analysis was performed in a denaturing gradient gel electrophoresis D-Code System (Bio-Rad Hercules, CA, USA). A 6-μL aliquot from the PCR reaction volume was mixed with 2 μL of standard dye-loading buffer and then loaded onto a 10% AA/bis-acrylamide (37.5:1) gel (0-60% or 20-80% urea-formamide chemical gradient according to melting profiles of each PCR fragment) in 1× TAE (40 mmol/L Tris-base, 20 mmol/L NaAC, 1 mmol/L EDTA pH 8) for 16 h at 80 V and 60 ℃. The DNA fragments were visualized and photo-documented under ultraviolet transillumination after staining with an ethidium bromide solution.

In addition to mutation analysis, we used DGGE to perform DGGE-LOH analysis where appropriate tissue was available, for tumors belonging to families with identified germ-line mutations in *hMSH6*. All available tumor tissue was sectioned and subjected to hematoxylin-eosin staining to determine the proportion of tumor cells. Only samples with >95% tumor cells were selected by macrodissection.

DNA sequencing

DNA fragments that displayed an abnormal DGGE pattern were analyzed by cycle sequencing. PCR products were purified with the QIAquick PCR purification Kit (Qiagen, Hilden, Germany) following the manufacturer's instructions. Cycle sequencing reactions were performed with the ABI Prism dRhodamine Terminator Sequencing Kit (Applied Biosystems, Forest City, CA, USA) and analyzed in the ABI

Prism 310 Genetic Analyzer (Applied Biosystems). All mutations were confirmed by two independent sequencing PCR reactions and sequenced in both directions.

hMSH6 immunohistochemistry

Immunohistochemical staining of *hMSH6* was performed for the 60 MSS cases and for the 12 MSI-H cases negative for mutation in hMLH1 and hMSH2. The tissue sections were cut at 6 μm and mounted on ChemMate Gap microscopy slides (DAKO A/S, Denmark) and dried at 37 ℃. After deparaffinization, slides were steam pretreated in EDTA buffer, pH 8-0, in a Magefesa Handy Steamer Plus (Magefesa, Spain) for 30 min, and then cooled and washed in PBS.

The antibody to *hMSH6* (clone 44; 1/100; catalog number G70220; Transduction Laboratories, Becton Dickinson, Lexington, UK) is a mouse mAb generated with an NH2-terminal fragment (codons 225-333) of the hMSH6 protein. For the immunohistochemical analysis, avidin-biotin complex immunoperoxidase technique was performed by using a commercial ChemMate detection kit (DAKO A/S) in a Techmate automate machine. Endogenous peroxidase was blocked by incubation in hydrogen peroxide with methanol. Incubation with no immune horse serum was followed by incubation with primary antibody. The sections were then incubated in biotinylated second antibody and peroxidase-labeled avidin-biotin complex. All dilutions were made in PBS (pH 7.2). The stainings were visualized with diaminobenzidine tetrahydrochloride solution. The sections were counterstained in Mayer's hematoxylin, rinsed with water, and mounted in an aqueous mounting media (Aquamount, BDH, Poole, UK). The percentage of positive nuclei was evaluated by two pathologists. Cases with more than 10% of nuclei staining were considered as positive protein expression. Normal colonic epithelium and lymphocytes exhibited strong nuclear staining for hMSH6 and, thus, served as positive internal controls for the staining of this protein.

RESULTS

MSI testing was carried out in 113 of the 132 families enrolled in our study. Of these 113 families, 60 had tumors that exhibited a non-MSI-high (MSS) phenotype and 53 had tumors that exhibited an MSI-high (MSI-H) phenotype. Nineteen families were not typed for MSI. All families were tested for mutations in hMLH1 and hMSH2, 24 families had a mutation in hMLH1 and 17 had a mutation in hMSH2 and were not studied further (Table 1). The remaining families were studied for mutations in hMSH6. In the 91 index cases tested for mutations in hMSH6, we identified 14 DNA variants. Of these, one was a novel definite deleterious mutation, nine were unclassified variants, six of them not described previously (Table 2) and four were polymorphisms described previously (Table 4). None of the unclassified variants were found in 100 control subjects.

The deleterious mutation Q236X, was found in an Amsterdam II family FC-100; change of cytosine for thymine at position c.706 leads to the formation of a termination codon at amino acid residue 236 that produces an 235 amino acid product instead of the normal 1 360 amino acid product. This mutation was found in a patient with two tumors, one colorectal and one endometrial (Figure 1). MSI testing was carried out in both tumors, colorectal and endometrial, and they exhibited a MSS phenotype; the immunohistochemical analysis of MSH6 showed an absence of staining (Table 3). In this family, we could test atleast two affected members, her father affected of colorectal cancer who was a carrier of the mutation and her sister also affected

Table 1 Classification of colorectal cancer families, frequencies of pathogenic mutations in hMLH1 and hMSH2 genes and MSI phenotype

Clinical criteria	Number of families	hMLH1 mutations	hMSH2 mutations	MSI-H	MSS	MSI untyped
Amsterdam I	56	17	15	42	13	1
Amsterdam II	11	2	2	2	7	2
Bethesda	37	5	0	6	20	11
HNPCC-like	28	0	0	3	20	5
Total	132	24	17	53	60	19

Table 2 hMSH6 mutations in Spanish HNPCC families

Family	Clinical criteria	Dx aged index patient (y)	No. of tumors in the family	Exon/intron	Nucleotide change	Amino acid change	Predicted consequence	Nfdht data base
3	Bethesda	42	1E, 1G, 1M, 1H, 1F, and 1A	Ex. 8	c.3725 G>T	R1242L	Inconclusive	No
11	HNPCC-like	58	1G, 2C, and 1B	Ex. 4	c.2319 C>T	L773L	Inconclusive	No
68	Bethesda	29	1L, and 1C	Ex. 4	c.1164 C>T	H388H	Inconclusive	No
				Ex. 4	c.2272 C>T	L758L		
81	HNPCC-like	50	4C	Int. 5	c.3439–16 C>T	NA	Inconclusive	No
94	Amsterdam II	45	3 P, 2E, 1G, and 3C	Ex. 4	c.2633 T>C	V878A	Pathogenic	Yes
100	Amsterdam II	54	4C, 1P, and 3G	Ex. 4	c.706 C>T	Q236X	Truncation	No
73	Amsterdam	29	2SM, 1G, 3C, and 1L	Ex. 4	c.2633 T>C	V878A	Pathogenic	Yes
121	HNPCC-like	58	3C, 1G, and 1B	Int. 5	c.3439–16 C>T	NA	Inconclusive	No
138	Bethesda	43	2C and 1 ureter in the same patient	Ex. 4	c.1677 C>T	C559C	Inconclusive	No

E, endometrial; G, glioma; M, meningioma; H, hemangioma; F, fibrosarcoma; A, adenoma; G, gastric; C, colon; B, breast; L, larynx; P, prostate; B, brain; SM, small intestine; y, years.

Table 3 Molecular alterations of tumors from persons carrying mutations of hMSH6 gene

Family/member	Tumor type	MSI status	Immunohistochemistry			hMSH6 mutation	Other MMR gene mutation
			MLH1	MSH2	MSH6		
3/270	CRC	MSI-H	P	P	P	R1242L	V716M (hMLH1)
11/310	CRC	MSI-H	P	P	P	L773L	NO
68/675	CRC	MSS	P	P	P	H388H and L758L	NO
73/526	3 CRCs	MSI-H	P	P	N	V878A	NO
81/757	CRC	MSS	P	P	P	c.3439–16 C>T	K618A (hMLH1)
94/854	UTERO	MSI-H	P	P	N	V878A	K618A (hMLH1)
100/940	CRC	MSS	P	P	N	Q236X	NO
121/1041	CRC	MSS	ND	ND	ND	c.3439–16 C>T	NO
138/1165	2 CRCs	MSI-H	P	P	P	C559C	P350P (hMLH1)

CRC, colorectal cancer; MSI-H, high microsatellite instability; MSS, negative microsatellite instability; P, positive for MMR protein; N, negative for MMR protein; ND, not done MMR expression.

Table 4 hMSH6 polymorphisms in Spanish HNPCC families

Location	Nucleotide change	Amino acid change	Previously reported	Frequency[1]
Exon 1	116 G→A	G 39 E	Yes	0.40
Exon 2	276 A→G	P 92 P	Yes	0.38
Exon 3	540 T→C	D 180 D	Yes	0.24
Exon 4	642 C→T	Y 214 Y	Yes	0.25

[1]Patients harboring/patients screened.

of colorectal cancer that resulted not to be a carrier. Both members had MSS tumors and MSH6 protein staining was absent in the carrier and was present in the non carrier.

The missense mutation V878A was detected in two Amsterdam families, FC-73 and FC-94, this mutation has been reported previously and had been considered as possibly pathogenic[6]. FC-94 (Figure 1) is also a carrier of the unclassified variant K618A in the MLH1 gene (Table 3). Both mutations (V878A in MSH6 and K618A in MLH1) were found in two affected members of the family, the proband (affected with colorectal and prostate cancer at ages 51 and 52) and his sister (affected with endometrial cancer at age 45). MSI study in tumors from carriers showed a MSI-H phenotype and the immunohistochemical analysis of hMSH6 showed absence of staining. Mutation V878A was also detected in FC-73 (Figure 1). This mutation was found in four affected members of the family, the proband was affected of three different cancers (two small intestine cancer and one colorectal cancer at ages 42, 47, and 49), his mother (affected of colorectal cancer at age 48), his brother (affected with gastric cancer at age 29) and his sister (affected with colorectal cancer at age 48). MSI study in tumors from carriers showed a MSI-H phenotype and the immunohistochemical analysis of hMSH6 showed absence of staining (Figure 2).

The missense mutation R1242L was detected in FC-3 (Table 2); it is located in a conserved amino acid in exon 8 of the gene and causes substitution of a polar amino acid arginine to a non-polar amino acid leucine. This family also carries the mutation V716M in hMLH1 gene. Both mutations (R1242L in hMSH6 and V716M in hMLH1) were found in two members of the family, in the proband (affected with glioma, colorectal adenoma, meningioma, fibrosarcoma, and colorectal cancer at ages 42, 43, 52, 52, and 53), and in his father who was healthy. The MSI status of the colorectal cancer showed a MSI-H phenotype and the MLH1 and MSH6 staining were present (Table 3).

The silent mutation L773L was detected in FC-11 (Table 2). This mutation was found in an HNPCC-like criteria family with two members affected with colorectal cancer (ages 58 and 64), one affected with gastric cancer (age 60) and one with breast cancer (age 60). The mutation was found only in the proband, the other affected members were of wild type. The MSI status of the colorectal cancer showed a MSI-H phenotype and the hMSH6 staining was present (Table 3).

The silent mutation C559C was detected in FC-138 (Table 2), the proband was affected of two colorectal and one ureter cancers and the first age at diagnostic was at 43 years. The MSI status of the colorectal cancer showed an MSI-H phenotype and the hMSH6 staining was present (Table 3). Mutations H388H and L758L were detected in FC-68 (Table 2). These mutations were found in a patient with early onset colorectal cancer (age 29), the MSI status of the tumor was MSS and the hMSH6 staining was present (Table 3). The intron five mutation IVS 5-16 C>T was detected in two families FC-81 and FC-121 (Table 2). FC-81 has four members affected by colorectal cancer in two generations. The mutation was found in two affected members of the family, the proband (affected with colorectal cancer at age 66), and his brother (affected with colorectal cancer at age 61); the two other members of the family, his father who was not tested and his other brother (affected with colorectal cancer at age 50) was wild type. The two members who carry the hMSH6 mutation, were also carriers of K618A in the MLH1 gene. The MSI status of the tumors from the three affected brothers was MSS. The hMSH6 staining was present in the member wild type and in the two carriers of hMSH6 mutation. The MLH1 staining was present in the tumors of the carriers and the non-carriers of K618A (Table 3). FC-121 has three members affected of colorectal cancer (ages 60, 75, and 55), one with gastric cancer (age 73) and one with brain cancer (age 70, Table 2). We could only test the proband (affected with colorectal cancer at age 60). The MSI status of the tumor was MSS and the MSH6 staining was not determined (Table 3).

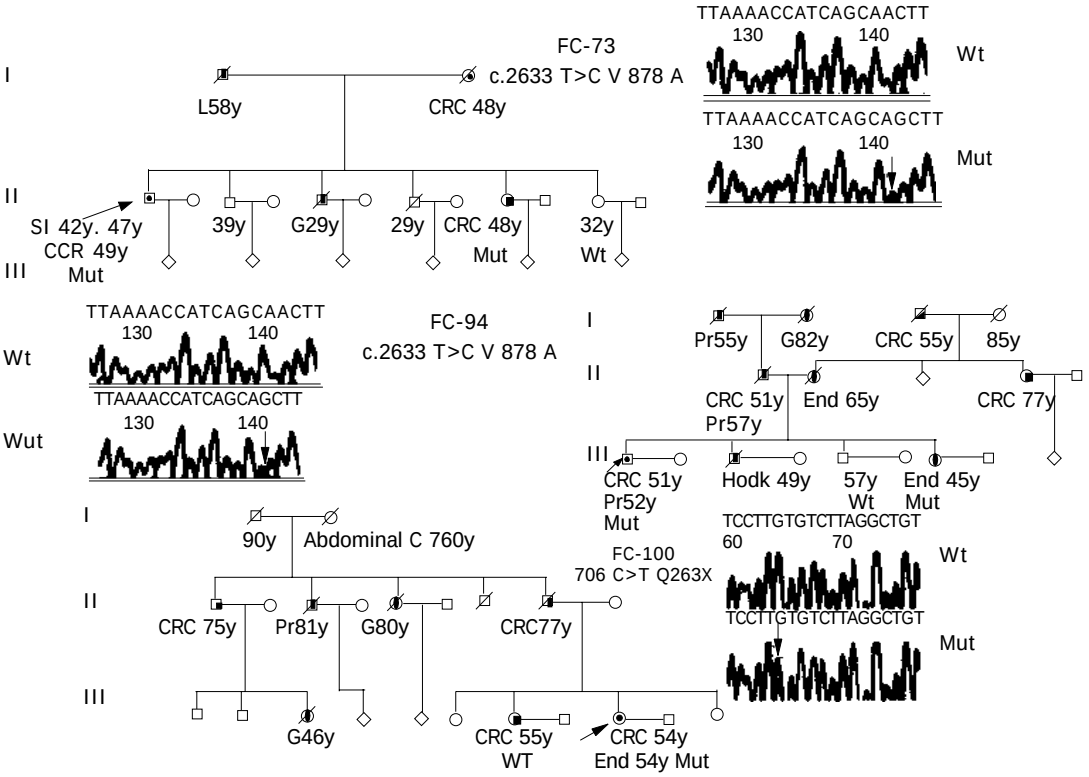


Figure 1 Pedigrees and DNA nucleotide sequence of the three families with disease-causing mutations of *hMSH6* gene. Squares, males; circles, females; diagonal bars, deceased; unblackened symbols, no tumor; semi-blackened symbols, patients with histological-verified carcinomas; arrows, probands; mut, carries the indicated mutation. Abbreviations indicating type of tumor: CRC, colorectal; SI, small intestine; G, gastric; H, Hodgkin; End, endometrium; Pr, prostate; L, liver. Number after abbreviation indicates age at which tumor was diagnosed. Electropherograms of the wild type and mutant nucleotide sequences for V878A and Q263X mutations located in exon 4 of the hMSH6 gene.

DGGE-LOH analysis was done to further characterize the role of these variants. Figure 3 shows a typical DGGE analysis of different hMSH6 exons amplified from tumor and peripheral blood DNA. Examples of missense mutations R1242L, V878A, and nonsense mutation K263X are shown. The silent mutations H388H and L758L were identified in the same individual. LOH analysis showed loss of the wild-type allele in both informative loci, indicating that these changes were located in the same chromosome. Taking into account our results, no evidence for LOH acting as a second-hit in the hMSH6 locus was found.

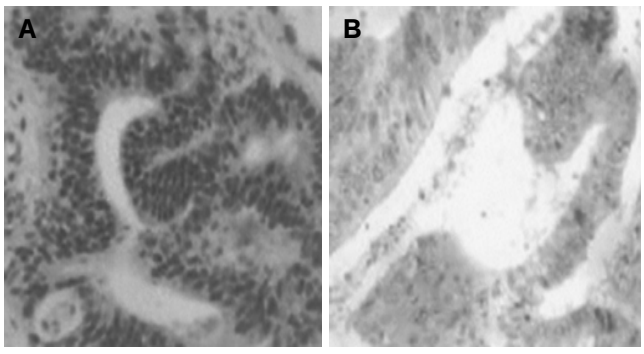


Figure 2 Representative examples of positive (A) and negative (B) immunohistochemical staining for hMSH6 protein (clone 44, Transduction laboratories/Becton Dickinson, Lexington, UK). A: Tumor from family 60, exhibited positive nuclear staining for hMSH6; B: tumor from family 73 carrier of V878A mutation, exhibited loss of hMSH6 expression.

DISCUSSION

Carrier frequencies of germ-line hMSH6 mutations in selected HNPCC families have been extensively described[6,10,12,23,24]. However, there is no evidence in the literature on this point regarding the Spanish population. We screened 91 HNPCC families (24 Amsterdam I, 7 Amsterdam II, 32 Bethesda guidelines, and 28 HNPCC-like) for the presence of germ-line mutations in the hMSH6 gene and identified 14 DNA changes. Seven of them were previously unreported DNA changes, including the intronic change at -16 base position of intron 5 (intronic mutation) found in two HNPCC-Like families, 1 amino acid substitution, 1 protein truncation mutation, and 4 silent mutations (Tables 2 and 3). The remaining seven DNA changes were reported previously, four of which were attested polymorphisms, one was the silent mutation H388L and the other 2 were V878A substitution that have been described as a possible disease causing mutation by other authors[6,9,25]. In our study, the Val878Ala substitution was detected in all affected members tested of both families, FC-73 (Amsterdam I) and FC-94 (Amsterdam II), suggesting that the hMSH6 germ-line mutation segregated with the disease. The MSI study of the tumors revealed an MSI-H phenotype. Moreover, immunohistochemical analysis revealed loss of hMSH6 protein in tumors from these patients. Our data suggest that this alteration may be a disease-causing mutation. However, we cannot discard that another mutation not detected could be linked to V878A in our population. Peterlongo *et al.*[24], has found the V878A in 4 out of 190

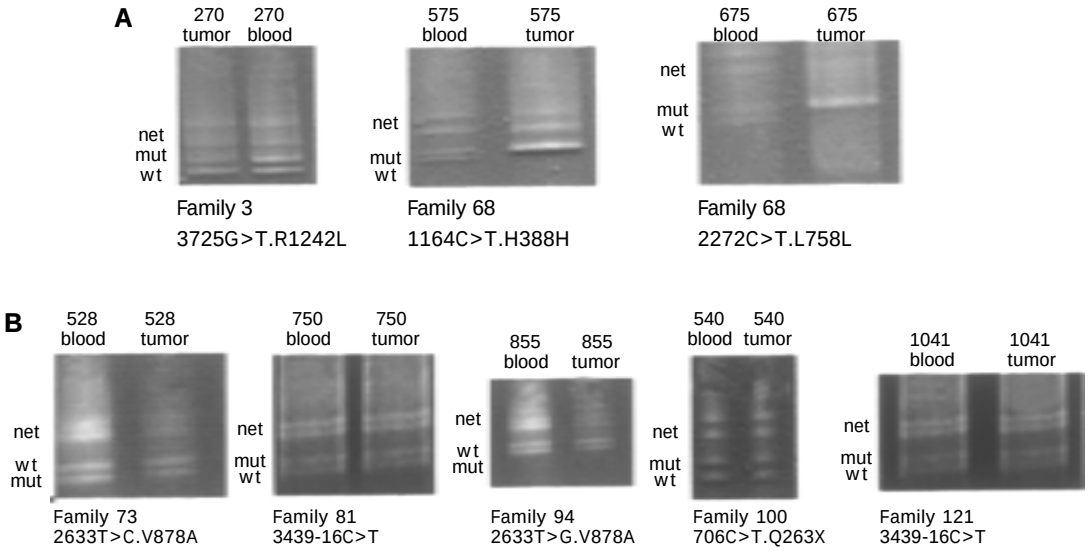


Figure 3 DGGE-LOH analysis of different *hMSH6* exons, amplified from both tumor and blood DNA. Analysis of 7 patients (270, 675, 526, 750, 855, 940, and 1 041) harboring the mutations R1242L, H388L, L758L, V878A, 3439-16 C>T, and Q263X. Bands corresponding to wild-type (Wt), mutant (Mut) alleles and the heteroduplex (Het) are indicated in all cases. Panel A shows LOH of the mutant allele in patient 270 and LOH of wild-type allele in patient 675. Panel B shows retention of both alleles (wt and mut) in all patients.

controls (from 18 000 volunteers of varying ethnic backgrounds who live in the New York metropolitan area), suggesting that this variant may not be linked to the disease in their population.

From the study presented here, we propose the following interpretations concerning the role of each previously unreported DNA change in the susceptibility to CRC. We interpret the $hMSH_6$ 3 435-16 C>T mutation found in two HNPCC-like families (FC-81 and FC-121) as a non disease-causing mutation for the following reasons: the 3 435-16 C>T did not segregate in the families, the tumors showed a MSS phenotype and the immunohistochemical analysis showed normal expression of the hMSH6; moreover, the wild type and mutant alleles were both retained in the tumor (LOH study, Figure 3). The $hMSH_6$ c.706 C>T mutation produces a stop codon, Q236X, and presumably causes the synthesis of a truncated hMSH6 protein of 235 amino acids (instead of 1 360), the immunohistochemical analysis showed lack of expression of hMSH6 and reduced expression of hMSH2 proteins from cancer cells. Reduced expression of hMSH2 was observed in CRC and endometrial cancer cases with a germ-line mutation in hMSH6[26,28]. We could study three affected members of the family, and we have seen that the mutation segregate with the disease because the father of the index case is also a carrier. Her sister, diagnosed of colorectal cancer at age 55, resulted not to be a carrier, this case could be a phenocopy. We can conclude that the mutation could be responsible for the susceptibility to cancer in this family. Mutation c.3725 G>T (R1242L) was found in a patient with multiple tumors and he is also a carrier of K618A in hMLH1 gene, his father is also a carrier of both mutations but he is still healthy. The immunohistochemical study showed expression of all MMR proteins and the study of LOH in the tumor cells showed loss of mutant allele. We could not study any other member of the family because the pedigree was very short (no more members, the index case was alone). Mutations c.1164 C>T and c.2272 C>T occur in the same chromosome in a patient from a short family (the index case diagnosed of colorectal cancer at 29, her brother was healthy, and her father was diagnosed of larynx cancer at 50 years). The hMSH6 protein was present in the tumor cells and the LOH study showed retention of mutant allele and perhaps, this fact could produce chromosomal instability, and therefore, mutational events that led to hyperproliferation. At the end, the silent mutation c.1677 C>T (C559C) was found in a patient with two CRCs at age 43 and one urothelial cancer at age 47. This patient was also a carrier of another silent mutation in hMLH1 gene (P350P) and both colorectal tumors showed a MSI-H phenotype and the immunohistochemical study showed expression of hMLH1 and hMSH6 proteins. With these results, we cannot conclude if the silent mutations are responsible for the tumors in our patient.

Our data indicate that the frequency of hMSH6 mutations is low in Spanish HNPCC, they can be found either in families with MSI-H or MSS tumors, which on average had an older age at diagnosis of cancer and are associated with other HNPCC tumors-overall gastric and endometrium. These data are consistent with the results of other published studies[24,27-29].

Thus, we can conclude from our study, that the two possible pathogenic mutations of hMSH6 were found in three families, in two of them the patients had tumors exhibiting a MSI-H phenotype and had been tested negative for mutations in hMLH1 and hMSH2. The remaining family was also negative for mutations in hMLH1 and hMSH2 but the tumors of the two carriers were MSS. The frequency of hMSH6 mutations in our series was low, as they were found only in 3 out of 91 families studied (1 of 19 Amsterdam I and 2 of 8 Amsterdam II). The mean age of dx cancer was higher than in hMLH1- and hMSH2-related families. On the other hand, we have not found these variants in site-specific CRC families but in families with a broad

spectrum of cancer types. Therefore, we suggest that hMSH6 testing should be pursued in Amsterdam families that have been negative for mutation in hMLH1 and hMSH2 genes or, as the literature suggests, in families with a history of endometrial, gastric, or other cancers in addition to a history of CRC.

ACKNOWLEDGMENTS

We thank the families for participating in the study. We thank C Corbacho, Dr. J Sanz Garcia and Dr. C Saez for their technical work.

REFERENCES

1 **Drummond JT,** Li GM, Longley MJ, Modrich P. Isolation of an hMSH2-p160 heterodimer that restores DNA mismatch repair to tumor cells. *Science* 1995; **268**: 1909-1912
2 **Palombo F,** Gallinari P, Iaccarino I, Lettieri T, Hughes M, D'Arrigo A, Truong O, Hsuan JJ, Jiricny J. GTBP, a 160-kilodalton protein essential for mismatch-binding activity in human cells. *Science* 1995; **268**: 1912-1914
3 **Papadopoulos N,** Nicolaides NC, Liu B, Parsons R, Lengauer C, Palombo F, D'Arrigo A, Markowitz S, Willson JK, Kinzler KW. Mutations of GTBP in genetically unstable cells. *Science* 1995; **268**: 1915-1917
4 **Das Gupta R,** Kolodner RD. Novel dominant mutations in Saccharomyces cerevisiae MSH6. *Nat Genet* 2000; **24**: 53-56
5 **Marsischky GT,** Filosi N, Kane MF, Kolodner R. Redundancy of Saccharomyces cerevisiae MSH3 and MSH6 in MSH2-dependent mismatch repair. *Genes Dev* 1996; **10**: 407-420
6 **Berends MJ,** Wu Y, Sijmons RH, Mensink RG, van der Sluis T, Hordijk-Hos JM, deVries EG, Hollema H, Karrenbeld A, Buys CH. Molecular and clinical characteristics of MSH6 variants: an analysis of 25 index carriers of a germline variant. *Am J Hum Genet* 2002; **70**: 26-37
7 **Miyaki M,** Konishi M, Tanaka K, Kikuchi-Yanoshita R, Muraoka M, Yasuno M, Igari T, Koike M, Chiba M, Mori T. Germline mutation of MSH6 as the cause of hereditary nonpolyposis colorectal cancer. *Nat Genet* 1997; **17**: 271-272
8 **Wagner A,** Hendriks Y, Meijers-Heijboer EJ, de Leeuw WJ, Morreau H, Hofstra R, Tops C, Bik E, Brocker-Vriends AH, van Der Meer C. Atypical HNPCC owing to MSH6 germline mutations: analysis of a large Dutch pedigree. *J Med Genet* 2001; **38**: 318-322
9 **Wijnen J,** de Leeuw W, Vasen H, van der Klift H, Moller P, Stormorken A, Meijers-Heijboer H, Lindhout D, Menko F, Vossen S. Familial endometrial cancer in female carriers of MSH6 germline mutations. *Nat Genet* 1999; **23**: 142-144
10 **Wu Y,** Berends MJ, Mensink RG, Kempinga C, Sijmons RH, van Der Zee AG, Hollema H, Kleibeuker JH, Buys CH, Hofstra RM. Association of hereditary nonpolyposis colorectal cancer-related tumors displaying low microsatellite instability with MSH6 germline mutations. *Am J Hum Genet* 1999; **65**: 1291-1298
11 **Cunningham JM,** Kim CY, Christensen ER, Tester DJ, Parc Y, Burgart LJ, Halling KC, McDonnell SK, Schaid DJ, Walsh Vockley C. The frequency of hereditary defective mismatch repair in a prospective series of unselected colorectal carcinomas. *Am J Hum Genet* 2001; **69**: 780-790
12 **Kolodner RD,** Tytell JD, Schmeits JL, Kane MF, Gupta RD, Weger J, Wahlberg S, Fox EA, Peel D, Ziogas A. Germ-line msh6 mutations in colorectal cancer families. *Cancer Res* 1999; **59**: 5068-5074
13 **Plaschke J,** Kruppa C, Tischler R, Bocker T, Pistorius S, Dralle H, Ruschoff J, Saeger HD, Fishel R, Schackert HK. Sequence analysis of the mismatch repair gene hMSH6 in the germline of patients with familial and sporadic colorectal cancer. *Int J Cancer* 2000; **85**: 606-613
14 **Caldes T,** Godino J, de la Hoya M, Garcia Carbonero I, Perez Segura P, Eng C, Benito M, Diaz-Rubio E. Prevalence of germline mutations of MLH1 and MSH2 in hereditary nonpolyposis colorectal cancer families from Spain. *Int J Cancer* 2002; **98**: 774-779
15 **Godino J,** de La Hoya M, Diaz-Rubio E, Benito M, Caldes T. Eight novel germline MLH1 and MSH2 mutations in hereditary non-polyposis colorectal cancer families from Spain. *Hum Mutat* 2001; **18**: 549
16 **Vasen HF,** Mecklin JP, Khan PM, Lynch HT. The International Collaborative Group on Hereditary Non-Polyposis Colorectal Cancer (ICG-HNPCC). *Dis Colon Rectum* 1991; **34**: 424-425
17 **Vasen HF,** Watson P, Mecklin JP, Lynch HT. New clinical criteria for hereditary nonpolyposis colorectal cancer (HNPCC, Lynch syndrome) proposed by the International Collaborative group on HNPCC. *Gastroenterology* 1999; **116**: 1453-1456
18 **Rodriguez-Bigas MA,** Boland CR, Hamilton SR, Henson DE, Jass JR, Khan PM, Lynch H, Perucho M, Smyrk T, Sobin L, Srivastava S. A National Cancer Institute Workshop on Hereditary Nonpolyposis Colorectal Cancer Syndrome: meeting highlights and Bethesda guidelines. *J Natl Cancer Inst* 1997; **89**: 1758-1762
19 **Miller SA,** Dykes DD, Polesky HF. A simple salting out procedure for extracting DNA from human nucleated cells. *Nucleic Acids Res* 1998; **16**: 1215
20 **de la Hoya M,** Diaz-Rubio E, Caldes T. Denaturing gradient gel electrophoresis-based analysis of loss of heterozygosity distinguishes nonobvious, deleterious BRCA1 variants from nonpathogenic polymorphisms. *Clin Chem* 1999; **45**: 2028-2030
21 **Boland CR,** Thibodeau SN, Hamilton SR, Sidransky D, Eshleman JR, Burt RW, Meltzer SJ, Rodriguez-Bigas MA, Fodde R, Ranzani GN. A National Cancer Institute Workshop on Microsatellite Instability for cancer detection and familial predisposition: development of international criteria for the determination of microsatellite instability in colorectal cancer. *Cancer Res* 1998; **58**: 5248-5257
22 **Hoang JM,** Cottu PH, Thuille B, Salmon RJ, Thomas G, Hamelin R. BAT-26, an indicator of the replication error phenotype in colorectal cancers and cell lines. *Cancer Res* 1997; **57**: 300-303
23 **Buttin BM,** Powell MA, Mutch DG, Babb SA, Huettner PC, Edmonston TB, Herzog TJ, Rader JS, Gibb RK, Whelan AJ, Goodfellow PJ. Penetrance and expressivity of MSH6 germline mutations in seven kindreds not ascertained by family history. *Am J Hum Genet* 2004; **74**: 1262-1269
24 **Peterlongo P,** Nafa K, Lerman GS, Glogowski E, Shia J, Ye TZ, Markowitz AJ, Guillem JG, Kolachana P, Boyd JA. MSH6 germline mutations are rare in colorectal cancer families. *Int J Cancer* 2003; **107**: 571-579
25 **Charames GS,** Millar AL, Pal T, Narod S, Bapat B. Do MSH6 mutations contribute to double primary cancers of the colorectum and endometrium? *Hum Genet* 2000; **107**: 623-629
26 **de Leeuw WJ,** Dierssen J, Vasen HF, Wijnen JT, Kenter GG, Meijers-Heijboer H, Brocker-Vriends A, Stormorken A, Moller P, Menko F. Prediction of a mismatch repair gene defect by microsatellite instability and immunohistochemical analysis in endometrial tumours from HNPCC patients. *J Pathol* 2000; **192**: 328-335
27 **Parc YR,** Halling KC, Wang L, Christensen ER, Cunningham JM, French AJ, Burgart LJ, Price-Troska TL, Roche PC, Thibodeau SN. HMSH6 alterations in patients with microsatellite instability-low colorectal cancer. *Cancer Res* 2000; **60**: 2225-2231
28 **Plaschke J,** Kruger S, Pistorius S, Theissig F, Saeger HD, Schackert HK. Involvement of hMSH6 in the development of hereditary and sporadic colorectal cancer revealed by immunostaining is based on germline mutations, but rarely on somatic inactivation. *Int J Cancer* 2002; **97**: 643-648
29 **Wang Q,** Lasset C, Desseigne F, Saurin JC, Maugard C, Navarro C, Ruano E, Descos L, Trillet-Lenoir V, Bosset JF. Prevalence of germline mutations of hMLH1, hMSH2, hPMS1, hPMS2, and hMSH6 genes in 75 French kindreds with nonpolyposis colorectal cancer. *Hum Genet* 1999; **105**: 79-85

Science Editor Guo SY **Language Editor** Elsevier HK

PO Box 2345, Beijing 100023, China
www.wjgnet.com
wjg@wjgnet.com

ELSEVIER

World J Gastroenterol 2005;11(37):5777-5781
World Journal of Gastroenterology ISSN 1007-9327
© 2005 The WJG Press and Elsevier Inc. All rights reserved.

• *BASIC RESEARCH* •

Consumption of purple sweet potato leaves modulates human immune response: T-lymphocyte functions, lytic activity of natural killer cell and antibody production

Chiao-Ming Chen, Sing-Chung Li, Ya-Ling Lin, Ching-Yun Hsu, Ming-Jer Shieh, Jen-Fang Liu

Chiao-Ming Chen, Graduate Institute of Pharmacy, Graduate Institute of Nutrition and Health Sciences, Taipei Medical University; Department of Dietetics, Taipei Medical University Hospital, Taipei, Taiwan, China
Sing-Chung Li, Ya-Ling Lin, Ming-Jer Shieh, Jen-Fang Liu, School of Nutrition and Health Sciences, Taipei Medical University, Taipei, Taiwan, China
Ching-Yun Hsu, Chang-Gung Institute of Technology, Taoyuan, Taiwan; Graduate Institute of Pharmacy, Taipei Medical University, Taipei, Taiwan, China
Supported by the Grant From the Taipei Medical University, No. TMU91-Y05-A110, TMU92-AE1-B33
Correspondence to: Dr. Jen-Fang Liu, School of Nutrition and Health Sciences, Taipei Medical University, 250 Wu-Shing Street, Taipei 110, Taiwan, China. liujenfa@tmu.edu.tw
Telephone: +886-2-27361661-6551 Fax: +886-2-27373112
Received: 2004-12-10 Accepted: 2005-01-05

Abstract

AIM: To study the immunological effects of physiological doses of purple sweet potato leaves (PSPL).

METHODS: The randomized crossover study (two periods, each lasting for 2 wk) involved 16 healthy non-smoking adults of normal weight. The 6-wk study consisted of a run-in (wk 1) PSPL diet (daily consumption of 200 g PSPL) or a control diet (low polyphenols, with the amount of carotenoids adjusted to the same level as that of PSPL) (wk 2-3), washout diet (wk 4), and switched diet (wk 5-6). Fasting blood was collected weekly in the morning. T-lymphocyte function was assessed via the proliferation and secretion of immunoreactive cytokines. Salivary IgA secretion and the specific cytotoxic activities of cytotoxic T lymphocytes and natural killer (NK) cells were determined.

RESULTS: The plasma β-carotene level increased with time in both groups, while the plasma polyphenol level decreased in the control group, and no significant difference was detected between the two groups. Although plasma polyphenol levels did not significantly increase in the PSPL group at the end of the study, they were significantly elevated in urine. PSPL consumption produced a significant increase in proliferation responsiveness of peripheral blood mononuclear cells (PBMC) and their secretion of immunoreactive IL-2 and IL-4. As well, lytic activity in NK cells was elevated in a time-dependent fashion. Salivary IgA secretion significantly decreased in control group after 2 wk, and returned to baseline following dietary switch to PSPL.

CONCLUSION: Consumption of PSPL modulates various immune functions including increased proliferation responsiveness of PBMC, secretion of cytokines IL-2 and IL-4, and the lytic activity of NK cells. The responsible determinants of PSPL remain to be elucidated, as does the biological significance of the present observations.

© 2005 The WJG Press and Elsevier Inc. All rights reserved.

Key words: Purple sweet potato leaves; Polyphenol; Immune function

Chen CM, Li SC, Lin YL, Hsu CY, Shieh MJ, Liu JF. Consumption of purple sweet potato leaves modulates human immune response: T-lymphocyte functions, lytic activity of natural killer cell and antibody production. *World J Gastroenterol* 2005; 11(37): 5777-5781
http://www.wjgnet.com/1007-9327/11/5777.asp

INTRODUCTION

The high consumption of vegetables and fruits has been linked epidemiologically to a decreased risk of cancer and cardiovascular disease[1]. Their beneficial effects have been attributed partly to the presence of numerous polyphenolic compounds, which display antioxidant and free radical scavenging properties[2]. Polyphenols are the major phytochemicals in fruits and vegetables. A variety of *in vitro* studies have shown that polyphenols such as flavonoids are antioxidants[3], immunomodulators[4], and exhibit antigenotoxic effects[5].

Purple sweet potato leaves (PSPL), which are easily grown in tropical areas such as Taiwan, have the highest polyphenolic content, in particular flavonoids, of all the commonly grown vegetables, and exhibit free radical scavenging ability[6]. Supplementation of diets with PSPL would seemingly be prudent. However, this recommendation is premature, since little is known from human experimental studies about the physiologic effects of dietary PSPL on the immune system.

As with many vegetables and fruits, PSPL are rich in carotenoids. The immunomodulatory activity of carotenoids in animals and human beings is well known[3-5]. Presently, we sought to evaluate whether physiological doses of polyphenol via consumption of PSPL affected the immune status of healthy subjects. In order to calibrate the

immunomodulatory effect of carotenoids, the amount of carotenoids consumed by the test and control groups was similarly adjusted. The results are consistent with a beneficial immune effect of PSPL.

MATERIALS AND METHODS

Subjects

Sixteen non-smoking healthy adults (seven men and nine women, aged 20-22 years), with normal weight (body mass index 20.9-21.6 kg/m^2) were recruited for the study. All subjects were in good medical health. Their screening histories did not reveal indications of any gastrointestinal disorder. Vitamin supplements or medications were not taken 1 mo preceding the study and during the study period. The study was approved by Medical Ethical Committee of the Taipei Medical University and all participants gave their written consent.

Sample collection and processing

Study design The leaves used were obtained from purple sweet potatoes planted and tended at the Taoyuan District Agriculture Improvement Station, Taipei Branch, Taiwan.

The randomized crossover study was conducted during September to November 2003. Subjects were randomly divided into control group and experimental group, all of them ran in a low polyphenol diet for 1 wk (wk 1). After that, control group consumed a control diet (low polyphenols, with the amount of carotenoids adjusted to the same level as that of PSPL) for 2 wk, experimental group consumed a PSPL diet (daily consumption of 200 g PSPL) for 2 wk (wk 2-3). The washout diet (a low polyphenol diet) was followed for 1 wk (wk 4), and then, the control and experimental groups were given switched diet for 2 wk (wk 5-6). Results were presented in a total study period of 6 wk.

Subjects were provided PSPL and control diet for lunch and dinner by the Department of Dietetics of Taipei Medical University Hospital. The meals were eaten in the hospital cafeteria. Each subject returned any uneaten food to allow food intake to be recorded. A list of the food products that the subjects were not allowed to eat was provided. Each subject kept a record of food consumption, which was checked to ensure compliance with the diet.

Collection and preparation of blood samples Blood from fasting subjects was collected once weekly in the morning between 07.00 a.m. and 09.00 a.m. Blood was drawn from an antecubital vein into the tubes containing 1.6 g/L of EDTA or Li-heparin, which were immediately placed on ice in the dark. Plasma collected by centrifugation at 1 500 r/min for 10 min at 4 ℃ was stored at -80 ℃ until analysis.

Collection and preparation of urine samples Before and at the end of the intervention period all volunteers were asked to provide a 24-h urine sample. During the collection period urine was stored at 4 ℃ and kept in dark bottles. Exact sampling time and urine volume were determined, and each sample was stored at -20 ℃ until analysis.

Analytical methods

Total polyphenols in urine and plasma Total polyphenols in urine and plasma were measured using the Folin-Ciocalteau method[10]. The absorption at 750 nm was measured spectrophotometrically. The total polyphenol content was expressed as gallic acid equivalents (GAE).

Plasma β-carotene Carotenoids were extracted from plasma with absolute ethanol (containing 1% pyrogallol) and hexane, separated by C18 reverse phase high-pressure liquid chromatography using spherical 3 micron packing. β-carotene was identified and quantified using an external standard[11].

Preparation of peripheral blood mononuclear cells (PBMC) PBMC were isolated by density gradient centrifugation using Ficoll-Paque (Amersham Biosciences, Buckinghamshire, UK) and resuspended in complete RPMI-1640 culture medium (Invitrogen, Carlsbad, CA, USA), containing 50 mL/L heat-inactivated fetal bovine serum (FBS, Invitrogen), 2 mmol/L L-glutamine, 100 000 U/L penicillin, and 100 mg/L streptomycin.

Lymphocyte proliferation PBMC (1×10^9 cells/L) in medium containing 5% of FBS were stimulated by T cell mitogen concanavalin A (Con A; 5 mg/L; Sigma Chemical Co., St. Louis, MO, USA) for 120 h at 37 ℃. Proliferation was measured using the BrdU proliferation enzyme immunoassay kit (Oncogene, Merck, Darmstadt, Germany).

Quantification of cytokine secretion PBMC were stimulated with Con A as described above for 48 h to measure IL-2 and IL-4 secretion. Cell-free supernatants were collected and stored at -80 ℃ until analysis. IL-2 and IL-4 were measured by ELISA kit (Biosource, Camarillo, CA, USA).

Cytotoxicity activity assay of NK cells The specific cytotoxic activities of natural killer (NK) cells were tested using a Promega CytoTox 96 kit (Promega, Madison, WI, USA). K562 cells were susceptible target cells to the cytotoxic effects of NK cells. K562 cells and PBMC including NK cells, resuspended in phenol red free RPMI-1640 culture medium containing 5% FBS were coincubated in 96-well round bottomed plates for 4 h at 37 ℃. The following PBMC/ K562 cell ratios 30:1, 20:1, 15:1, 10:1, and 7.5:1 were used to find a good effect between NK cells and K562 cells. During the incubation, the NK cells destroyed the target cells and lactate dehydrogenase (LDH) was released. Spontaneous release of PBMC or target cells was controlled by separate incubation of the respective population and detergent was added to lyse all target cells into a complete cytotoxicity. At the end of incubation, the cells were lysed and centrifuged. Fifty microliters of aliquot of each well was transferred into another 96 well flat-bottomed plate and 50 μL of fresh LDH substrate solution was added to each well. The plates were incubated at room temperature for 30 min, and the reaction was stopped by the addition of 1 mol/L acetic acid. The resulting light absorbance was measured in microplate reader at 490 nm. The percentage of cells exhibiting cytotoxic activity was calculated.

Salivary IgA secretion A small absorbent pad was used to collect saliva before brushing of the teeth in the morning. All samples were centrifuged at 13 000 *g* in a microliter tube. The supernatant was stored at -20 ℃ until analysis. Salivary immunoglobulin A (IgA)[12] was measured using an immunoassay kit (Salimetrics, State College, PA, USA).

Statistical analysis

All values were expressed as mean±SD. The data were analyzed using SPSS version. Statistical significance was determined using pairs *t* test. $P<0.05$ was considered statistically significant.

RESULTS

All participants tolerated the intervention well and completed the study. Physical characteristics of the subjects are summarized in Table 1. Body mass index and the percentage of body fat did not vary significantly during the study. PSPL-related daily dietary intake was 902 mg GAE of total polyphenol and 23.42 mg of β-carotene. Control subjects ingested the same amount of β-carotene from 40 to 45 g carrots (268.76 μg/g of β-carotene) each day.

The concentrations of plasma β-carotene and polyphenol measured throughout the study are summarized in Table 2. Plasma β-carotene level increased with time in the PSPL and control groups. However, plasma polyphenol levels decreased in the control group, although the decrease was not significantly different from the PSPL group. In the latter group, the urine levels of polyphenol were significantly elevated (8.20±0.95 to 10.27±1.39 mg GAE/dL).

Table 1 Physical characteristics of subjects (mean±SD)

Subjects	Before		After	
	Male	Female	Male	Female
n	7	9	7	9
Age (yr)	21±1.5	20±1.2	21±1.5	20±1.2
Height (cm)	175.4±5.7	161.9±7.2	175.4±5.7	161.9±7.2
Body weight (kg)	64.8±9.6	53.8±6.4	65.9±9.2	54.7±6.6
Body mass index (kg/m^2)	21.0±2.6	20.6±2.3	21.4±2.4	20.9±2.3
Body fat (%)	16.4±4.5	26.8±4.9	17.4±4.5	28.7±4.6

Table 2 Change of plasma and urine β-carotene and polyphenol levels in subjects (mean±SD)

	Baseline	Washout	1 wk	2 wk
β-carotene in plasma (μmol/L)				
Control	0.088±0.06	0.076±0.02	0.104±0.05	0.125±0.05[a]
PSPL	0.091±0.04	0.107±0.04	0.125±0.05[c]	0.139±0.04[c]
Polyphenol in plasma (mg GAE/dL)				
Control	61.61±1.39	61.04±1.94	58.86±1.38[c]	59.02±1.35[c]
PSPL	59.21±3.34	58.87±1.63	59.44±2.00	60.01±1.41
Polyphenol in urine (mg GAE/dL)				
Control	8.38±1.50	8.28±1.19	6.76±131[c]	6.95±1.36[c]
PSPL	8.20±0.95	8.25±1.58	10.30±0.89[c,e]	10.27±1.39[c,e]

[a]$P<0.05$ for 2 wk *vs* baseline, washout, 1 wk. [c]$P<0.05$ for baseline *vs* 1 and 2 wk. [e]$P<0.05$ for control *vs* PSPL.

Proliferation responsiveness of Con A-activated PBMC increased significantly after consumption of PSPL (Figure 1). Secretion of T-helper lymphocyte cytokine IL-2 increased after consumption of PSPL for 1 and 2 wk (Figure 2A). The ability of PBMC to secrete immunoreactive IL-4 also significantly increased during the same period (Figure 2B). Lytic activity of NK cells was also affected by PSPL consumption (Figure 3). The results showed that a PBMC/target cell ratio of 30:1 had the highest percentage of cytotoxicity, and the other ratios had the same trend but no

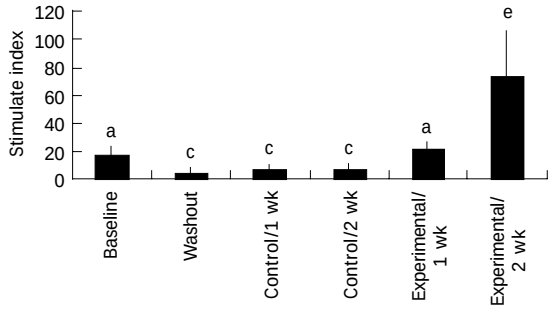


Figure 1 Proliferation responsiveness of PBMCs. [a]$P<0.05$ for baseline *vs* washout, control 1 and 2 wk. [c]$P<0.05$ for experimental 2 wk *vs* washout, control 1 and 2 wk. [e]$P<0.05$ for experimental 1 wk *vs* experimental 2 wk.

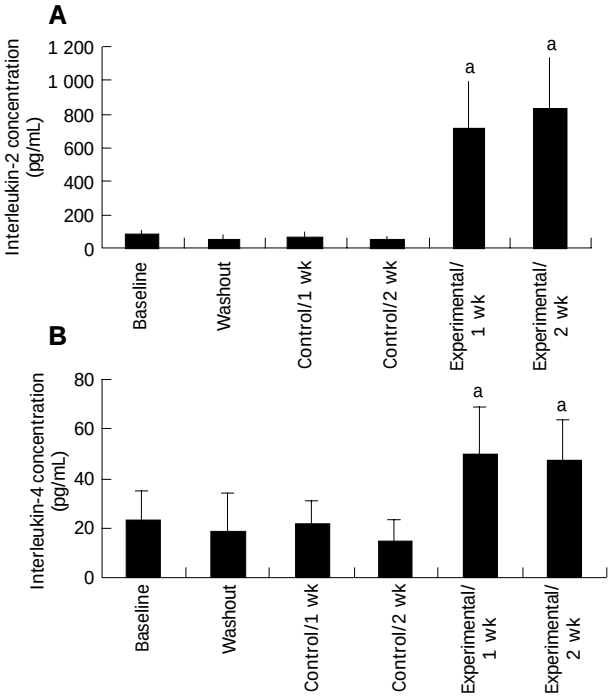


Figure 2 Concentration of interleukin-2 (A) and interleukin-4 (B) secreted by PBMCs. [a]$P<0.05$ for experimental 2 wk *vs* baseline, washout, control 1 and 2 wk.

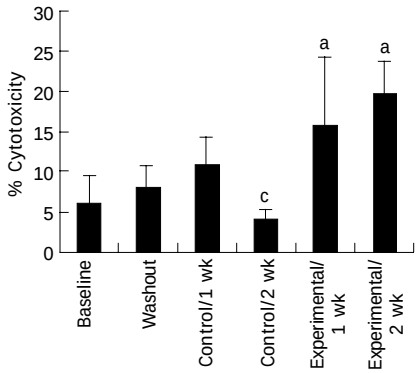


Figure 3 Lytic activity of NK cells. [a]$P<0.05$ for experimental 2 wk *vs* baseline, washout, control 1 and 2 wk. [c]$P<0.05$ for control 2 wk *vs* washout, control 1 wk, experimental 1 and 2 wk.

significance (data not shown). The percentage of lytic activity of NK cells in a PBMC/target cell ratio of 30:1 was elevated in the PSPL group after 1 wk, and then was further elevated. Salivary IgA secretion in the control group decreased significantly, but returned to the basal levels after 2 wk of PSPL consumption (Figure 4).

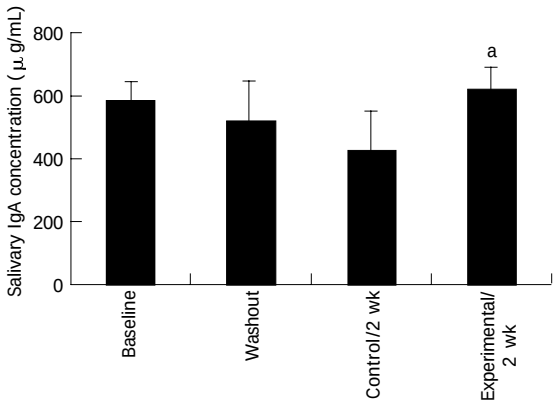


Figure 4 Concentration of salivary IgA detected by immunoassay kit. $^aP<0.05$ for experimental 1 wk *vs* experimental 2 wk.

DISCUSSION

The present study demonstrates that consumption of polyphenol-rich PSPL results in a marked total polyphenol increase in the urine. Most polyphenols peak in plasma 1-2 h after a single polyphenol intake, and are quickly eliminated from the circulation[13]. The prolonged ingestion of polyphenol-rich PSPL did not result in increased plasma polyphenol concentrations as expected. We also measured the total polyphenol in plasma 0, 2, 4, 8, 12, 24 h after consumption of PSPL in a previous study. The plasma polyphenol level raised 2 and 4 h after consumption of PSPL and further increased after 24 h, but there was no significance (data not shown). Although polyphenol was not different in plasma from fasting subjects throughout the whole study period, physiological functions were significantly modified.

β-Carotene-rich carrots were used to calibrate the effect of carotenoids from PSPL. As expected, β-carotene concentration in plasma was not significantly different. In another study, the dietary supplementation with β-carotene (8.2 mg) or lycopene (13.3 mg) for 12 wk does not enhance cell-mediated immunity in healthy free-living elderly humans beings[14]. A low-carotenoid diet reduces T-lymphocyte function, which cannot be restored by the daily supplementation with carrot juice containing 21.6 mg β-carotene, 15.7 mg α-carotene, and 0.5 mg lutein[9]. Presently, control subjects ingesting 23.42 mg of β-carotene each day do not display a significantly altered T-lymphocyte function.

The immune system provides markers for determining the biological health benefits of phytochemicals. Flavonoids suppress a variety of immune functions including lymphocyte proliferation, lytic activity of NK cells, and cytokine secretion *in vitro*[4]. The same study demonstrated that supplementing a low polyphenol diet with polyphenol-rich fruit juices results in significantly increased lymphocyte proliferative responsiveness, IL-2 secretion by activated lymphocytes, and the lytic activity of NK cells in healthy subjects[17]. These results are in agreement with the findings in our present study.

Many health benefits are associated with the consumption of tea, and are mainly attributed to the polyphenolic constituents. In animals, these constituents exert antioxidative activities and improve the antidotal capability of the liver. We found similar oxidative effects following the 2-wk regimen of PSPL consumption in humans beings (data not shown). Free radicals impair the integrity and functionality of membrane lipids and affect signal transduction and gene expression in immune cells[18]. One potential mechanism underlying the immunomodulatory effect of polyphenols is their ability to act as an antioxidant, resulting in a lower generation of free radicals.

IL-2 and IL-4 are both produced by activated T cells following *in vitro* stimulation by T-cell mitogens such as Con A. IL-2 is primarily produced by T-helper-1 cells, and IL-4 by T-helper-2 cells[19]. In our study, consumption of polyphenol-rich PSPL resulted in increased secretion of IL-2 and IL-4, which paralleled an enhanced proliferative response of these cells.

Pure flavonoids suppress a variety of immune mechanisms including lymphocyte proliferation, lytic activity of NK cells *in vitro*[4]. In animal models, quercetin also increases lytic activity of NK cells[20]. A study of healthy human subjects clearly showed that supplementing a low-polyphenol diet with polyphenol-rich fruit juices significantly increases lymphocyte responsiveness to mitogen activation and enhances lytic activity of NK cells[17]. The present findings are entirely consistent with the prior observations and support the suggestion that polyphenol possesses immunoactivity *in vivo* that differs from the activity observed *in vitro*. Possibly the polyphenol doses used *in vitro* are different from polyphenol in plasma concentrations and/or have the specific function of the metabolites of polyphenol.

IgA is the most important immunoglobulin in saliva, serving as a main immunological defense of mucosal surfaces[16]. Salivary IgA is a sensitive indicator of the humoral immune response to infection[17]. In our study, salivary IgA secretion significantly decreased when subjects consumed low polyphenol diet and returned to the basal level after PSPL consumption, indicating that PSPL consumption may protect mucosal surfaces.

In conclusion, dietary intervention in the form of PSPL consumption can modulate various immune functions. The active constituents in PSPL need to be determined in further investigations.

ACKNOWLEDGMENTS

We thank Drs. Yuan-Tsong Chen, Huey-Fang Shang, and Sung-Ling Yeh for their excellent technical assistance. We also thank the volunteers for taking part in this study and Dr. Tsan-Ju Chang, Agriculture Improvement Station, Taipei Branch, Taiwan, for generously providing the PSPL.

REFERENCES

1 **Block G,** Patterson B, Subar A. Fruit, vegetables, and cancer

prevention: a review of the epidemiological evidence. *Nutr Cancer* 1992; **18**: 1-29
2 **Surh Y.** Molecular mechanisms of chemopreventive effects of selected dietary and medicinal phenolic substances. *Mut Res* 1999; **428**: 305-327
3 **Rice-Evans CA,** Miller NJ, Paganga G. Structure-antioxidant activity relationships of flavonoids and phenolic acids. *Free Rad Biol Med* 1996; **20**: 933-956
4 **Middleton E Jr.** Effect of plant flavonoids on immune and inflammatory cell function. *Adv Exp Med Biol* 1998; **439**: 175-182
5 **Duthie SJ,** Johnson W, Dobson VL. The effect of dietary flavonoids on DNA damage (strand breaks and oxidised pyrimdines) and growth in human cells. *Mut Res* 1997; **390**: 141-151
6 **Chu YH,** Chang CL, Hsu HF. Flavonoid content of several vegetables and their antioxidant activity. *J Sci Food Agr* 2000; **80**: 561-566
7 **Bendich A.** Carotenoids and the immune response. *J Nutr* 1989; **119**: 112-115
8 **Kramer TR,** Burri BJ. Modulated mitogenic proliferative responsiveness of lymphocytes in whole-blood cultures after a low-carotene diet and mixed-carotenoid supplementation in women. *Am J Clin Nutr* 1997; **65**: 871-875
9 **Watzl B,** Bub A, Brandstetter BR, Rechkemmer G. Modulation of human T-lymphocyte functions by the consumption of carotenoid-rich vegetables. *Br J Nutr* 1999; **82**: 383-389
10 **Pearson DA,** Tan CH, German JB, Davis PA, Gershwin ME. Apple juice inhibits human low density lipoprotein oxidation. *Life Sci* 1999; **64**: 1913-1920
11 **Gatautis VJ,** Pearson KH. Separation of plasma carotenoids and quantitation of beta-carotene using HPLC. *Clin Chim Acta* 1987; **166**: 195-206
12 **Koh D,** Yang Y, Khoo L, Nyunt SZ, Ng V, Goh CL. Salivary immunoglobulin A and lysozyme in patients with psoriasis. *Ann Acad Med* 2004; **33**: 307-310
13 **Scalbert A,** Williamson G. Dietary intake and bioavailability of polyphenols. *J Nutr* 2000; **130**: 2073S-2085S
14 **Corridan BM,** O'Donoghue M, Hughes DA, Morrissey PA. Low-dose supplementation with lycopene or beta-carotene does not enhance cell-mediated immunity in healthy free-living elderly humans. *Eur J Clin Nutr* 2001; **55**: 627-635
15 **Mestecky J.** Saliva as a manifestation of the common mucosal immune system. *Ann N Y Acad Sci* 1993; **694**: 184-194
16 **Ludwig K,** Grabhorn E, Bitzan M, Bobrowski C, Kemper MJ, Sobottka I, Laufs R, Karch H, Muller-Wiefel DE. Saliva IgM and IgA are a sensitive indicator of the humoral immune response to Escherichia coli O157 lipopolysaccharide in children with enteropathic hemolytic uremic syndrome. *Pediatr Res* 2002; **52**: 307-313
17 **Bub A,** Watzl B, Blockhaus M, Briviba K, Liegibel U, Muller H, Pool-Zobel BL, Rechkemmer G. Fruit juice consumption modulates antioxidative status, immune status and DNA damage. *J Nutr Biochem* 2003; **14**: 90-98
18 **Meydani SN,** Wu D, Santos MS, Hayek MG. Antioxidants and immune response in aged persons: overview of present evidence. *Am J Clin Nutr* 1995; **62**(6 Suppl): 1462S-1476S
19 **Mosmann TR,** Sad S. The expanding universe of T-cell subsets: Th1, Th2 and more. *Immunol Today* 1996; **17**: 138-146
20 **Exon JH,** Magnuson BA, South EH, Hendrix K. Dietary quercetin, immune functions and colonic carcinogenesis in rats. *Immunopharmacol Immunotoxicol* 1998; **20**: 173-190
21 **Falchetti R,** Fuggetta MP, Lanzilli G, Tricarico M, Ravagnan G. Effects of resveratrol on human immune cell function. *Life Sci* 2001; **21**: 81-96

Science Editor Wang XL and Guo SY **Language Editor** Elsevier HK

PO Box 2345, Beijing 100023, China
www.wjgnet.com
wjg@wjgnet.com

ELSEVIER

World J Gastroenterol 2005;11(37):5782-5786
World Journal of Gastroenterology ISSN 1007-9327
© 2005 The WJG Press and Elsevier Inc. All rights reserved.

• *BASIC RESEARCH* •

Effect of *Astragalus complanatus* flavonoid on anti-liver fibrosis in rats

Chun-Yu Liu, Zhen-Lun Gu, Wen-Xuan Zhou, Ci-Yi Guo

Chun-Yu Liu, Department of Pharmacology, Medical College of Suzhou University, Suzhou 215007, Jiangsu Province, China
Zhen-Lun Gu, Suzhou Institute of Chinese Meteria Medica, Suzhou University, Suzhou 215007, Jiangsu Province, China
Wen-Xuan Zhou, Ci-Yi Guo, The Hong Kong Association for Health Care Ltd, Hong Kong, China
Correspondence to: Professor Zhen-Lun Gu, Suzhou Institute of Chinese Meteria Medica, Suzhou University, Suzhou 215007, Jiangsu Province, China. zhenlungu.2003@163.com
Telephone: +86-512-65190599 Fax: +86-512-65190599
Received: 2004-08-16 Accepted: 2004-10-07

Abstract

AIM: To observe the anti-liver fibrosis effect of *Astragalus complanatus* flavonoids (ACF) in rats.

METHODS: The liver fibrosis model in rats was established by injecting interperitoneally 0.2 mL/100 g 0.5% dimethylnitrosamine, thrice a week. Meanwhile, the rats were administered ACF (30, 60, 120 mg/kg) or colchicine (0.1 mg/kg) once a day for 1 mo. Serum *N*-propeptide of type I procollagen (PINP) and type III procollagen (PIIINP) was measured using ELISA. Malondialdehyde (MDA) and superoxide dismutase (SOD) in hepatic tissue were evaluated. Matrix metal protease-1 (MMP-1) mRNA expression was assayed by RT-PCR and the protein expression of tissue inhibitor of metal protease-1 (TIMP-1) was analyzed by immunohistochemistry.

RESULTS: In the ACF groups, SOD activity increased and MDA content decreased in comparison to the liver fibrosis model group. The serum PINP and PIIINP contents in ACF-2 and -3 group decreased compared to those in model group. In ACF-2 and -3 group, the expression of MMP-1 mRNA increased significantly and the protein expression of TIMP-1 decreased compared to that in model group.

CONCLUSION: The antifibrotic mechanisms of ACF are associated with its influence on lipid peroxidation and collagen synthesis and degradation.

© 2005 The WJG Press and Elsevier Inc. All rights reserved.

Key words: *Astragalus complanatus*; Liver fibrosis; *N*-propeptide of type I procollagen; *N*-propeptide of type III procollagen; Malondialdehyde; Superoxide dismutase; Matrix metal protease-1; Tissue inhibitor of metal protease-1

Liu CY, Gu ZL, Zhou WX, Guo CY. Effect of *Astragalus complanatus* flavonoid on anti-liver fibrosis in rats. *World J Gastroenterol* 2005; 11(37): 5782-5786
http://www.wjgnet.com/1007-9327/11/5782.asp

INTRODUCTON

Fibrosis is a common manifestation in most chronic liver diseases. The progression of hepatic fibrosis often leads to cirrhosis and is associated with liver cancer. Therefore, interrupting or reversing hepatic fibrosis is very important in preventing cirrhosis. Semen *Astragali* (SA) is a tonic traditional Chinese medicine for liver and kidney. We previously reported that SA has a protective effect on liver[1]. Our further investigation has revealed that the flavonoids extracted from SA are useful in preventing rat liver fibrosis induced by dimethylnitrosamine (DMN)[2]. However, how *Astragalus complanatus* flavonoids (ACF) interrupt the formation of liver fibrosis remains unknown. This study was designed to observe the anti-liver fibrosis effect and mechanisms of DMN in rats.

MATERIALS AND METHODS

Materials

Astragalus complanatus (AC) was obtained from Leiyunshang Pharmaceutical Corporation (Suzhou, China) and identified by a chief pharmacist (Suzhou Drug Administration Bureau). Colchicine was obtained from Kunming Pharmaceutical Corporation (Kunming, China). DMN was purchased from Shanghai Chemical Company (Shanghai, China). All other chemicals were of analytical grade.

Preparation of ACF

After being extracted with ligarine, the seed powder of AC was extracted with 80% ethyl acetate (EtOH). The 80% EtOH extract was further subjected to ZTC-5 adsorptive resin (Nankai University) column and eluented with water, 50% and 95% EtOH to afford three fractions. The 50% EtOH fraction was dried under vacuum, recrystallized with EtOH and ACF was obtained as a yellow powder containing complanatuside, neocomplanatuside, myricomplanoside, rhomnocitrin-3-O-β-D-glucoside and astragalin, etc. The complanatuside content in ACF was about 20% by RP-HPLC and determined on a Shim-pack VP-ODS analytical column (4.6 mm×150 mm, 5 μm) with the mobile phase consisting acetonitrile-1% acetic acid (18:82) as eluent at the flow rate of 1 mL/min. The UV detection was set at 266 nm. The total ACF was 80%, determined at 266 nm by UV spectroscopy with complanatuside as a standard substance.

Animals

Sixty male Wistar rats weighing 130-160 g were housed in conventional cages with free access to water and rodent chow at 20-22 ℃ with a 12-h light-dark cycle. All procedures involving the use of laboratory animals were in accordance with National Institutes of Health Guidelines. Rat liver fibrosis was produced according to the established protocol[3]. Except for the normal group, rats in other groups were injected interperitoneally 5 g/L DMN (0.2 mL/100 g, thrice a week). Meanwhile, the rats were administered 30 mg/kg ACF-1, 60 mg/kg ACF-2, 120 mg/kg ACF-3 or 0.1 mg/kg colchicine, respectively, once a day for 1 mo. The doses of ACF and its course of treatment were based on a pilot experiment. The rats in the normal control group and DMN model group received saline by gavage instead of ACF. After 4 wk of ACF treatment, all rats were anesthetized, sera were collected and liver tissues were removed rapidly. Liver tissue samples were immediately rinsed in sterile saline, snap-frozen in liquid nitrogen, and stored at -70 ℃ until analysis.

MDA and SOD determination

The livers were homogenized at 100 g/L in cold saline at 0-4 ℃ using a glass-potter-type homogenizer at 500-800 r/min in ice. The homogenates were centrifuged at 100 000 *g* for 20 min at 4 ℃ to obtain supernatants of tissue homogenates. The resultant supernatants were immediately pipetted for measuring the content of malondialdehyde (MDA) and the enzymatic activity of superoxide dismutase (SOD) by the test kits. Data were expressed as nanomolar MDA per gram wet liver tissue and units SOD per milligram wet liver tissue.

PINP and PIIINP determination

Serum *N*-propeptide of type I procollagen (PINP) and *N*-propeptide of type III procollagen (PIIINP) were measured by ELISA (LIFEKEY BioMeditech Corporation).

Immunohistochemistry

Five-micrometer-thick sections of formalin-fixed and paraffin-embedded livers were processed routinely. Tissue inhibitor of metal protease-1 (TIMP-1) was stained with polyclonal antibody (Santa Cruz Biotechnology, Inc.). Briefly, sections were deparaffinized in xylene and hydrated in a series of graded alcohol, and endogenous peroxidase was blocked with 5% hydrogen peroxide. The sections were then incubated with primary antibodies (1:50) against TIMP-1 at 37 ℃ for 1 h, followed by incubation with goat anti-rabbit IgG conjugated-horseradish peroxidase (1:200). The signals were visualized by ABC immunostaining system. The images were captured and digitized with an image analysis system (Jieda 501, version 3.10). The TIMP-1 positive cell ratios were automatically evaluated. For each specimen at least five fields were analyzed at 20× magnification.

RT-PCR reaction

Semiquantitative RT-PCR with β-actin as internal control was performed to examine the expression of matrix metal protease-1 (MMP-1) mRNA. Total RNA was extracted from liver by TRIzol method (GIBCO specification). The first-strand cDNA was synthesized from the total RNA using 40 μL reverse transcription mixture containing 2 μg total RNA, 1.0 μg M-MLV reverse transcriptase (Promega) and random primers (Sangon, Shanghai), 10 mmol/L dNTP. Reverse transcription reaction was preformed at 37 ℃ for 1 h. At the end of reverse transcription, the mixture was heated at 95 ℃ for 5 min and immediately cooled in ice for 5 min.

PCR amplification was carried out with 2 μL cDNA product in a 40 μL reaction volume containing 10 pmoL of each specific oligonucleotide primer (Table 1), 10 mmol/L dNTP, and 2.5 IU Taq DNA polymerase. Amplification was performed for 30 cycles of denaturation (at 94 ℃ for 30 s), annealing (at 58 ℃ for 30 s), and elongation (at 72 ℃ for 50 s). PCR products were electrophoresed on 20 g/L agarose gel and visualized by ethidium bromide staining under UV light. This semiquantitative measure was expressed as ratios compared to β-actin.

Table 1 Primers for PCR amplification of MMP-1 and β-actin mRNA

Primer name	Primer sequence	Product Size/bp	GenBank acc. no.
MMP-1	Sense: 5′-tactagccaccgcttcttcc-3′ (192–211)	311	U53605
	Anti-sense: 5′-ggccagaaatagctgaatgc-3′ (483–502)		
β-actin	Sense: 5′-ctgtgcccatctatgagggt-3′ (485–504)	199	NM-031144
	Anti-sense: 5′-gccatctcttgctcgaagtc-3′ (664–683)		

Statistical analysis

All numerical data were expressed as mean±SD. Statistical analyses were done using the SPSS for Window release 11.0 (SPSS Inc., USA). The parameters were evaluated with one-way ANOVA and Dunnett's *t* test. $P<0.05$ was considered statistically significant.

RESULTS

Effect of ACF on MDA and SOD in liver tissue of rats

As shown in Figure 1A, the SOD activity decreased and the MDA content increased significantly in model group in comparison to those in normal group ($P<0.01$, $P<0.01$). However, the SOD activity in ACF groups increased and MDA contents decreased in comparison to those in model group ($P<0.01$).

Effects of ACF on PINP and PIIINP contents in rat serum

The serum PINP and PIIINP contents in ACF-2 and -3 group decreased ($P<0.05$, $P<0.01$) compared to those in model group (Figure 1B).

Expression of MMP-1 mRNA in rat hepatic tissue

There was no significant difference in expression of MMP-1 mRNA between normal group and model group. But the expression of MMP-1 mRNA in ACF groups tended to increase. In ACF-2 and -3 group, the expression of MMP-1 mRNA increased significantly as compared to that in model group (Figure 2).

TIMP-1 protein expression in rat hepatic tissue

The positive expressions of TIMP-1 protein were observed in all groups. In normal group, the mild expression was

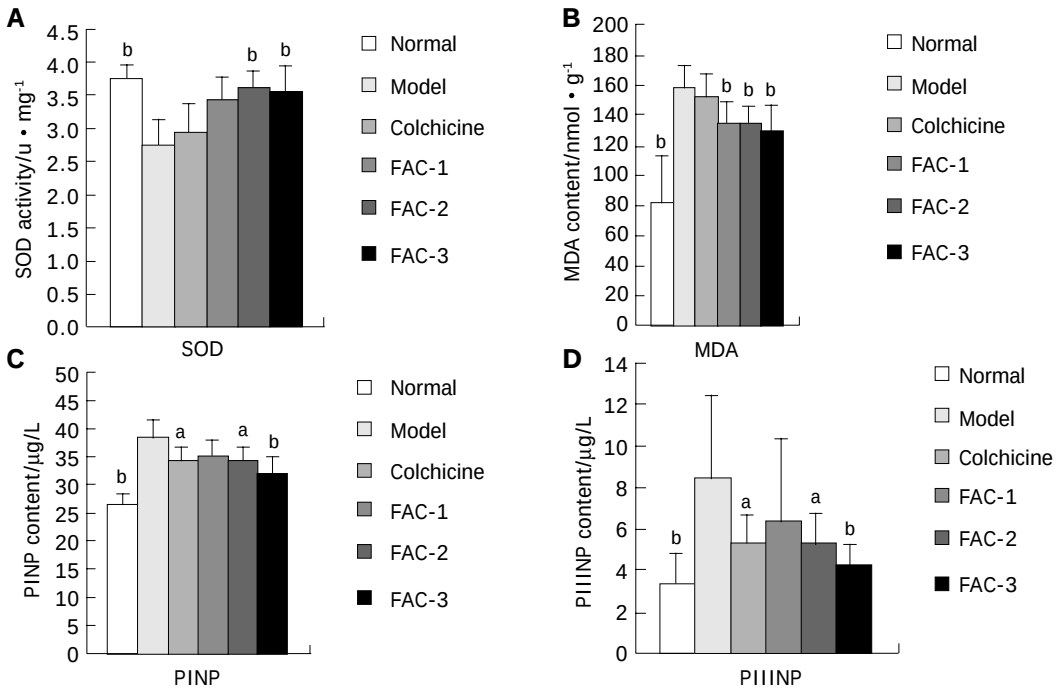


Figure 1 Effects of ACF on SOD activity and MDA content in rat liver tissue (A) and on PINP and PIIINP contents in rats serum (B). [a]$P<0.05$, [b]$P<0.01$ *vs* model group.

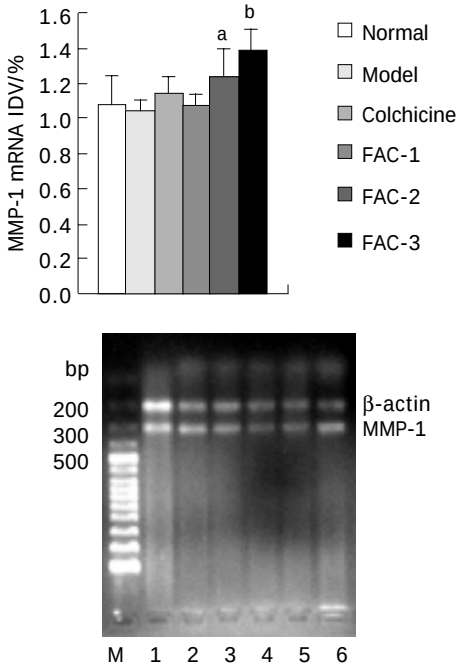


Figure 2 Analysis of MMP-1 mRNA expression in rat hepatic tissue. M: molecular weight markers (bp); lane 1: normal group; lane 2: model group; lane 3: colchicine group; lane 4: ACF-1 group; lane 5: ACF-2 group; lane 6: ACF-3 group; $n = 4$. [a]$P<0.05$, [b]$P<0.01$ *vs* model group.

presented in vascular endothelial cells and sinusoidal space. However, in model group the strong expression was noted around lobule median vein and in portal areas with a positive ratio of 8.84%. After the rats were treated with ACF, TIMP-1 protein expression decreased significantly ($P<0.01$, Figure 3).

DISCUSSION

Following chronic liver injury of any etiology, there is progressive fibrosis. The fibrotic process recognizes the involvement of various cells and different factors, leading to excessive fibrogenesis with disruption of intercellular contacts and interactions and of extracellular matrix composition[4-6]. However, hepatic stellate cells (HSCs), together with recruited mononuclear cells and Kupffer cells are by far the key players in liver fibrosis[7-10]. Their cross-talk is triggered and favored by a series of chemical mediators, with a prominent role played by the transforming growth factor beta. Both expression and synthesis of this inflammatory and pro-fibrogenic cytokine are mainly modulated through redox-sensitive reactions. Furthermore, involvement of reactive oxygen species and lipid peroxidation products can be clearly demonstrated in other fundamental events of hepatic fibrogenesis, like activation and effects of stellate cells, expression of metalloproteinases and their specific inhibitors[11-14]. Therefore, anti-oxidative stress can inhibit the process of fibrosis.

Liver fibrosis is characterized by the deposition of excess extracellular matrix (particularly collagen types I and III) in the liver. The aminoterminal procollagen type-I peptide and type-III peptide, which release during collagen types I and III deposition, have been suggested as serum markers of fibrogenesis[15-17]. Their concentrations in serum reflect the ongoing collagen formation in the liver. Extracellular degradation of matrix protein is regulated by MMPs produced by HSCs, which in turn are regulated by several mechanisms including regulation at level of the gene (transcription and proenzyme synthesis), cleavage of the proenzyme to an active form and specific inhibition of activated forms by TIMPs[18].

Extracellular degradation of matrix proteins is regulated by a family of enzymes known as MMPs[19-21]-types I, II,

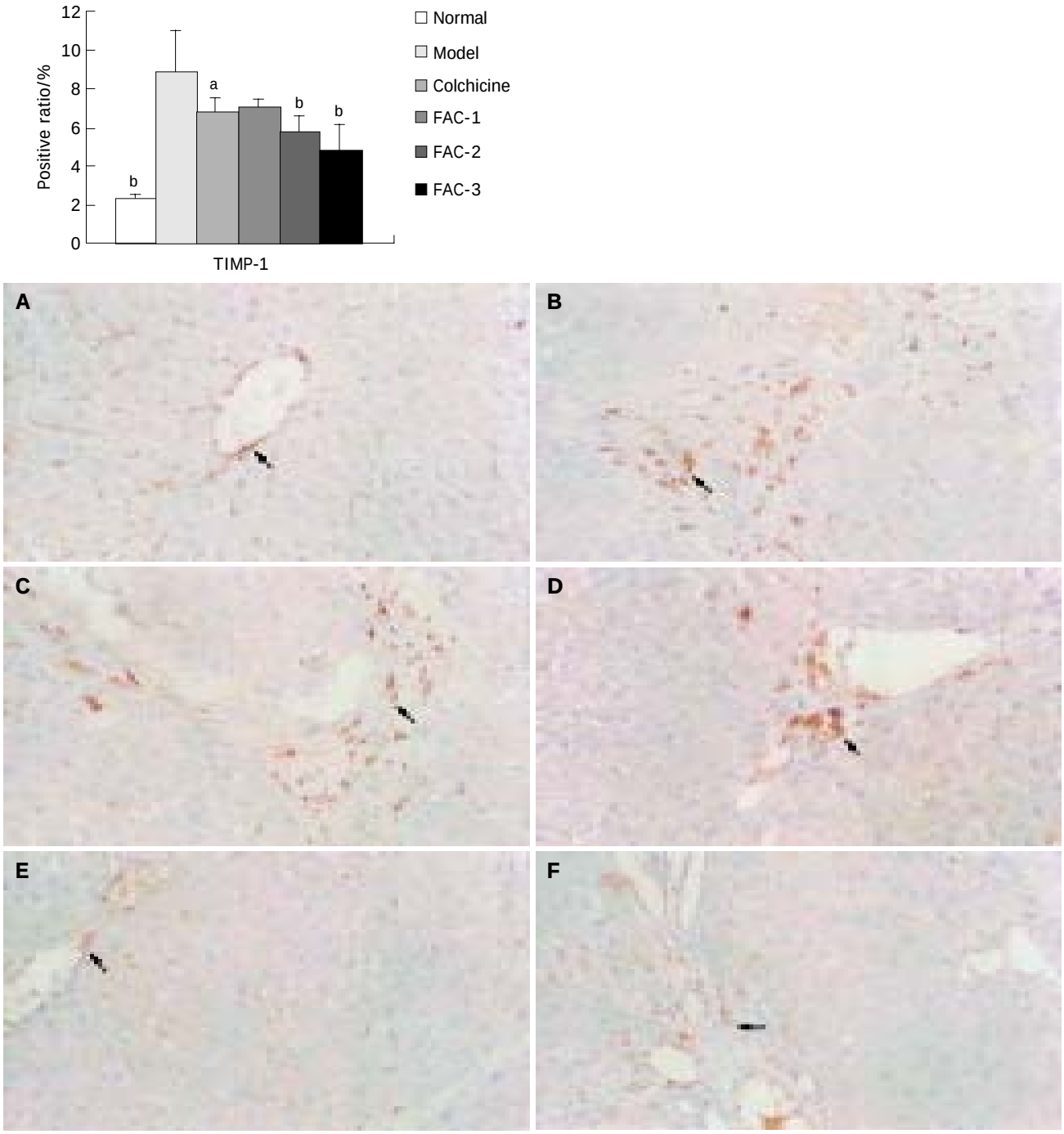


Figure 3 Immunohistochemical expression of TIMP-1 protein in rat hepatic tissue. (1) The positive ratio detected by Jieda 501 image-analysis system was used as the total protein expression. (2) TIMP-1 is shown as yellow grains in hepatic tissue (immunohistochemistry, ×200). A: normal group; B: model group; C: colchicine group; D: ACF-1 group; E: ACF-2 group; F: ACF-1 group; n = 5. $^{a}P<0.05$, $^{b}P<0.01$ *vs* model group.

and III collagenases degrade interstitial collagens. Type IV collagenases/gelatinases degrade basement membrane collagen and gelatins and stromelysins which degrade a broad range of substrates including proteoglycans, laminin, gelatins, and fibronectin. However, the activated forms of MMPs in turn are inhibited specifically by TIMPs, such as TIMP-1 and -2[22-26].

Based on this pathophysiological mechanism, therapeutic methods are developed to diminish collagen accumulation, stimulate the collagenolytic process, and/or inhibit stellate cell proliferation[27,28]. However, current therapies targeting at arresting or reversing liver fibrosis are largely ineffective and some have unacceptable side effects in long-term therapy. Recent clinical and experimental observations have demonstrated that Chinese medicines might be of some preventive and therapeutic values against fibrosis[29,30]. SA is a traditional Chinese medicine containing flavonoids, organic acids and triterpenoids, etc.[31]. It can protect animal livers against injury by CCl_4 and cirrhosis caused by DMN[1,2].

The present results indicate that ACF decreases the serum content of *N*-propeptide of types I and III procollagen,

elevates the activity of SOD and reduces the MDA content in DMN-treated rat hepatic tissue. In addition, the protein expression of TIMP-1 reduces and the MMP-1 mRNA expression increases in liver fibrosis rats with induced by DMN. The antifibrotic effect of ACF is associated with its influence on lipid peroxidation and collagen synthesis and degradation.

REFERENCES

1 **Liu CY,** Gu ZL, Han R, Zu LJ, Zhou WX, Guo CY. Protective effect of extract in seed of Astragalus complanatus on acute hepatic injury induced by carbon tetrachloride in mice. *Zhongcaoyao* 2002; **33**: 1104-1106
2 **Liu CY,** Gu ZL, Zhang KP, Zhou WX, Guo CY. Effect of flavonoids of astragali complanali on liver libroses induced by DMN in rats. *Zhonggu Yaolixue Tongbao* 2004; **20**: 110-114
3 **Li ZJ,** Jin SHG. Effect of Traditional Chinese Herb Panax Notogenseng (Burk) F.H. Chen on dimethylnitrosamine-induced liver injury in rats. *Chengdu Zhongyiyao Daxue Xuebao* 2000; **23**: 31-35
4 **Gerling B,** Becker M, Waldschmidt J, Rehmann M, Schuppan D. Elavated serum aminoerminal procollagen type-III-peptide parallels collagen accumulation in rats with secondary biliary fibrosis. *J Hepatol* 1996; **25**: 79-84
5 **Annoni G,** Colombo M, Cantaluppi MC, Khlat B, Lampertico P, Rojkind M. Serum type III procollagen peptide and laminin (Lam-P1) detect alcoholic hepatitis in chronic alcohol abusers. *Hepatology* 1989; **9**: 639-697
6 **Guechot J,** Laudat A, loria A, Serfaty L, Poupon R, Giboudeau J. Diagnostic accuracy of hyaluronan and type III procollagen amino-terminal peptide serum assays as markers of liver fibrosis in chronic viral viral hepatitis C evaluated by ROC curve analysis. *Clin Chem* 1996; **42**: 558-563
7 **Senoo H.** Structure and function of hepatic stellate cells. *Med Electron Microsc* 2004; **37**: 3-15
8 **Safadi R,** Friedman SL. Hepatic fibrosis-role of hepatic stellate cell activation. *MedGenMed* 2002; **4**: 27
9 **Marra F,** Pinzani M. Role of hepatic stellate cells in the pathogenesis of portal hypertension. *Nefrologia* 2002; **22**(Suppl 5): 34-40
10 **Reeves HL,** Friedman SL. Activation of hepatic stellate cells-a key issue in liver fibrosis. *Front Biosci* 2002; **7**: 808-826
11 **Zhang X,** Yu WP, Gaol, Wei KB, Ju JL, Xu JZ. Effects of lipopolysaecharides stimulated Kupffer cells on activation of rat hepatic stellate cells. *World J Gastroenterol* 2004; **15:** 610-613
12 **Poli G.** Pathogenesis of liver fibrosis role of oxidative stress. *Mol Aspects Med* 2000; **21**: 49-98
13 **Parola M,** Robino G. Oxidative stress-related molecules and liver fibrosis. *J Hepatol* 2001; **35**: 297-306
14 **Gebhardt R.** Oxidative stress, plant-derived antioxidants and liver fibrosis. *Planta Med* 2002; **68**: 289-296
15 **Refik Mas M,** Comert B, Oncu K, Vural SA, Akay C, Tasci I, Ozkomur E, Serdar M, Mas N, Alcigir G, Yener N. The effect of taurine treatment on oxidative stress in experimental liver fibrosis. *Hepatol Res* 2004; **28**: 207-215
16 **Xie SB,** Yao JL, Zheng RQ, Peng XM, Gao ZL. Serum hyaluronic acid, procollagen type III and IV in histological diagnosis of liver fibrosis. *Hepatobiliary Pancreat Dis Int* 2003; **2**: 69-72
17 **Stone PJ.** Potential use of collagen and elastin degradation markers for monitoring liver fibrosis in schistosomiasis. *Acta Trop* 2000; **77**: 97-99
18 **Oh S,** Afdhal NH. Hepatic fibrosis: are any of the serum markers useful? *Curr Gastroenterol Rep* 2001; **3**: 12-18
19 **McCrudden R,** Iredale JP. Liver fibrosis, the hepatic stellate cell and tissue inhibitors of metalloproteinases.*Histol Histopathol* 2000; **15**: 1159-1168
20 **Okazaki I,** Watanabe T, Hozawa S, Arai M, Maruyama K. Molecular mechanism of the reversibility of hepatic fibrosis: with special reference to the role of matrix metalloproteinases. *J Gastroenterol Hepatol* 2000; **15**(Suppl 1): D26-32
21 **Benyon RC,** Arthur MJ. Extracellular matrix degradation and the role of hepatic stellate cells. *Semin Liver Dis* 2001; **21**: 373-384
22 **Schuppan D,** Ruehl M, Somasundaram R, Hahn EG. Matrix as a modulator of hepatic fibrogenesis. *Semin Liver Dis* 2001; **21**: 351-372
23 **Okazaki I,** Arai M, Wada N, Maruyama K. Gene expression of MMPS and TIMPS in the process of hepatic fibrosis. *Nippon Rinsho* 1993; **51**: 428-434
24 **Murphy FR,** Issa R, Zhou X, Ratnarajah S, Nagase H, Arthur MJ, Benyon C, Iredale JP. Inhibition of apoptosis of activated hepatic stellate cells by tissue inhibitor of metalloproteinase-1 is mediated via effects on matrix metalloproteinase inhibition: implications for reversibility of liver fibrosis. *J Biol Chem* 2002; **277**: 11069-11076
25 **Arthur MJ.** Fibrogenesis II. Metalloproteinases and their inhibitors in liver fibrosis. *Am J Physiol Gastrointest Liver Physiol* 2000; **279**: 245-249
26 **Arthur MJ,** Iredale JP, Mann DA. Tissue inhibitors of metalloproteinase: role in liver fibrosis and alcoholic liver disease. *Alcohol Clin Exp Res* 1999; **23**: 940-943
27 **Iredale JP.** Tissue inhibitors of metalloproteinases in liver fibrosis. *Int J Biochem Cell Biol* 1997; **29**: 43-54
28 **Murphy F,** Arthur M, Iredale J. Developing strategies for liver fibrosis treatment. *Expert Opin Investig Drugs* 2002; **11**: 1575-1585
29 **Shimizu I.** Antifibrogenic therapies in chronic HCV infection. *Curr Drug Targets Infect Disord* 2001; **1**: 227-240
30 **Luo YJ,**Yu JP, Shi ZH, Wang L. Ginkgobiloba extra reverses CC_{14}-induced liver fibrosis in rats. *World J Gastroenterol* 2004; **10:** 1037-1042
31 **Stickel F,** Brinkhaus B, Krahmer N, Seitz HK, Hahn EG, Schuppan D. Antifibrotic properties of botanicals in chronic liver disease. *Hepatogastroenterology* 2002; **49**: 1102-1108
32 **Tang WX,** Dan ZL, Yan HM, Wu CH, Zhang G, Liu M, Li Q, Li SB. Experimental study of effect of Ganyanping on fibrosis in rat livers. *World J Gastroenterol* 2003; **9:** 1292-1295
33 **Du B,** You S. Present situation in preventing and treating liver fibrosis with TCM drugs. *J Tradit Chin Med* 2001; **21**: 147-152

Science Editor Wang XL and Guo SY **Language Editor** Elsevier HK

PO Box 2345, Beijing 100023, China
www.wjgnet.com
wjg@wjgnet.com

ELSEVIER

World J Gastroenterol 2005;11(37):5787-5794
World Journal of Gastroenterology ISSN 1007-9327
© 2005 The WJG Press and Elsevier Inc. All rights reserved.

• *BASIC RESEARCH* •

Amelioration of experimental colitis by *Astragalus membranaceus* through anti-oxidation and inhibition of adhesion molecule synthesis

Joshua Ka-Shun Ko, Flora Ying-Lee Lam, Andrew Pok-Lap Cheung

Joshua Ka-Shun Ko, Flora Ying-Lee Lam, Andrew Pok-Lap Cheung, School of Chinese Medicine, Hong Kong Baptist University, Hong Kong, China
Supported by the HKBU Faculty Research Grant FRG/02-03/II-64
Correspondence to: Dr. Joshua Ka-Shun Ko, School of Chinese Medicine, Hong Kong Baptist University, Kowloon Tong, Hong Kong, China. jksko@hkbu.edu.hk
Telephone: +852-3411-2907 Fax: +852-3411-2461
Received: 2004-12-22 Accepted: 2005-03-21

Abstract

AIM: To investigate the protective effects of *Astragalus membranaceus* (Am) against hapten-induced colitis in male Sprague-Dawley rats as well as its underlying mechanism.

METHODS: Experimental colitis was induced in rats by enema administration of 2,4-dinitrobenzene sulfonic acid (DNBS). Rats were either pretreated with Am extract (2 or 4 g/kg, p.o. once daily) starting from 10 d before DNBS enema, or received Am post-treatment (2 or 4 g/kg, p.o. twice daily) on the three consecutive days following DNBS administration. Colonic lesion area and histological damage were determined, while the activities of myeloperoxidase (MPO) and xanthine oxidase, as well as reduced glutathione (GSH) content were measured in the excised colonic tissues. Besides, protein expression of inducible nitrite oxide synthase (iNOS), intercellular adhesion molecule-1 (ICAM-1) and P-selectin was also detected by Western blot analysis.

RESULTS: Our findings had shown that both macroscopic lesion area and histological colonic damage induced by DNBS were significantly reduced by both Am pre- and post-treatments. These were accompanied by attenuation of the elevated colonic MPO activity and downregulation of the iNOS, P-selectin, and ICAM-1 protein expression. Besides, deprivation of colonic GSH level under colitis condition was also preserved.

CONCLUSION: These results demonstrate that Am possesses both preventive and therapeutic potential in experimental colitis. The anti-inflammatory actions involve anti-oxidation along with inhibition of adhesion molecule synthesis in the colonic tissues.

© 2005 The WJG Press and Elsevier Inc. All rights reserved.

Key words: IBD; *Astragalus membranaceus*; Reactive oxygen metabolites; Adhesion molecules

Ko JKS, Lam FYL, Cheung APL. Amelioration of experimental colitis by *Astragalus membranaceus* through anti-oxidation and inhibition of adhesion molecule synthesis. *World J Gastroenterol* 2005; 11(37): 5787-5794
http://www.wjgnet.com/1007-9327/11/5787.asp

INTRODUCTION

Inflammatory bowel disease (IBD) consists of a group of idiopathic diseases of the intestine characterized by chronic inflammation of the bowel with periods of exacerbation and remission[1]. Moreover, patients with IBD have a higher risk of developing colorectal cancer than the general population[2]. There are two major categories of IBD, ulcerative colitis (UC) and Crohn's disease (CD), which are both histologically and clinically dissimilar. Despite the fact that etiology of IBD still remains poorly understood, complex interactions among genetic, environmental and immunological have been implicated in the pathogenesis of IBD[3,4]. In fact, activation of the central immune cell populations will lead to the production of a wide variety of non-specific mediators of inflammation, including cytokines, chemokines, growth factors, arachidonic acid metabolites (e.g. prostaglandins and leukotrienes) and reactive oxygen metabolites (ROM)[3,5]. In the past few decades, new chemotherapeutic agents such as 5-aminosalicylic acid, corticosteroids, immunosuppressive and immunoregulatory agents, antibiotics and probiotics, anti-tumor necrosis factor (TNF)-α, anti-inflammatory cytokines, and anti-intercellular adhesion molecule (ICAM)-1 therapy, etc., had been developed to tackle with these problems. However, none of them appeared to have been successful in achieving complete remission or preventing relapse, while some may even cause serious side effects.

Neutrophil infiltration in the extravascular space involves a complex sequence of interaction between circulating neutrophils and the vascular endothelium, including rolling, adhesion and transendothelial migration. Myeloperoxidase (MPO) is an enzyme mainly found in azurophilic granules of neutrophils. It is a good marker of neutrophil infiltration in gastrointestinal tissues[6], as well as inflammation and tissue injury. Besides, significant amounts of superoxide can be generated by a variety of endogenous enzyme systems such as the peroxisomal enzyme xanthine oxidase (XO) following tissue ischemia. XO activity is often increased in intestinal inflammation through the induction by TNF-α and activated neutrophils[7]. It has been suggested that XO is a significant source of superoxide in the inflammation of IBD[8]. Nonetheless, the concentrations of endogenous antioxidants, such as reduced glutathione (GSH), alpha-tocopherol and

cysteine, are all significantly decreased in IBD patients. As a result, the balance between antioxidants and ROM becomes seriously impaired[9,10]. Most currently used therapeutic drugs for IBD, in particular sulfasalazine and its active moiety 5-aminosalicylic acid, control the disease partly by their property as potent ROM scavengers[11].

Nitric oxide (NO) will react with superoxide to form peroxynitrite, which is a highly cytotoxic oxidant[12]. Inducible nitrite oxide synthase (iNOS) is the inducible form of the enzyme responsible for the synthesis of pro-inflammatory NO, which is mainly induced in the infiltrated inflammatory cells, such as neutrophils, macrophages and mononuclear cells by stimulants such as cytokines[13]. Several studies had shown that NO production and iNOS activity were increased in colonic mucosa from UC and CD patients[14]. Immunohistochemical studies also indicated that iNOS was localized in neutrophils, macrophages and epithelial cells in the active area of the inflamed colon in UC patients[15]. Other than NO generated by the iNOS isozyme, leukocytes migration in IBD patients also requires the interaction between different cell adhesion molecules[16]. They are surface bound glycoprotein molecules on endothelial cells that are essential for the capture and migration of leukocytes. P-selectin and ICAM-1 are adhesion molecules which are essential for migration of leukocytes from the blood stream into the inflamed tissue. P-selectin captures circulating leukocytes in the early extravasation process, while ICAM-1 is involved further in the migration of leukocytes across the connective tissue in the lamina propria, and in the interaction between leukocytes and epithelial cells[17]. Furthermore, P-selectin is susceptible to be activated by endotoxin and cytokines[18]. Semiquantitative analyses have shown that P-selectin expression was significantly increased in both UC and CD patients, primarily expressed on venules and capillaries near the small lymphocyte aggregates[19,20]. Moreover, the elevated P-selectin and ICAM-1 levels could persist for more than 48 h in the colonic tissues after a single stimulus.

Astragalus membranaceus (Am, Fisch.) Bge. *var mongholicus* (Bge.) Hsiao or (Fisch., Am), also called Huang-qi in Chinese, is the dried root of a perennial herbaceous plant. It is an important "tonifying" herb being prescribed to strengthen body defense against pathogenesis and to promote the discharge of pus as well as tissue restitution. Traditional herbal formulations containing Am can be used to treat chronic ulceration and sores[21], mellitus diabetes and albuminuria in chronic nephritis, etc.[22]. Rats injected with the herb extract (0.5 g/kg, i.p.) for 1 mo had not been developing abnormalities[23]. Two groups of bioactive chemicals have been isolated from Am, which are polysaccharides (i.e. astragalan I-III) and saponins (i.e. astragalosides I-VIII, acetylastragaloside I, isoastragalosides I-II and soyasaponin I), respectively. Besides, about 0.18-2.0% of *Astragalus* root consists of coumarin and flavonoid derivatives[24]. These compounds are capable of minimizing free radical damage to membranes by inhibiting lipid peroxidation[25] and by protecting the intestinal endothelium[26]. There had been a number of clinical studies on the treatment of IBD using herbal formulations with Am as leading drug, with results ranging from the relief of symptoms to the prevention of UC recurrence with increased serum superoxide dismutase activity (anonymous Chinese case reports). However, there is no experimental or clinical study about the sole effect of Am on IBD.

The present investigation aimed to determine the preventive and therapeutic effects of Am extract on experimental colitis induced by 2,4-dinitrobenzene sulfonic acid (DNBS), and to delineate the underlying anti-oxidation mechanisms and modulation of colonic synthesis of inflammatory mediators and adhesion molecules.

MATERIALS AND METHODS

Animals and treatments

Male Sprague-Dawley rats, weighing 180-200 g, were acclimatized under constant temperature (22±1 ℃) and humidity (40-45%) with 12-h light-dark cycles for 10 d before experimentation. Groups of six animals each were housed in rack-mounted wire cages. They were reared on a standard laboratory diet (Purina, USA), and given tap water *ad libitum*. Both body weight and food intake of the rats were measured daily throughout the entire experimental period. In addition, the appearance of stools (normal, loose/watery, or bloody) was also observed as part of index to determine disease activity.

Animals were anesthetized with a mixture of 75 mg/kg ketamine and 10 mg/kg xylazine (Alfasan, the Netherlands) intraperitoneally before colitis induction. Following this, 250 μL of 500 mL/L ethanol containing 30 mg of DNBS dihydrate (Aldrich, USA) was slowly infused into the lumen of the colon through a siliconized catheter (12 cm long, 2-mm external diameter) inserting to an 8-cm position proximal to the anus. Animals of the normal untreated group (normal) received enema saline administration. The entire infusion process took approximately 10 s to complete, with the catheter remaining inside the colonic lumen for 5 min before the withdrawal in order to prevent possible leakage.

The concentrated powder of Am was obtained from Purapharm (Hong Kong) and was used throughout the entire experiment. The herbal compound was extracted from the dried roots of Am (Fisch.) Bge. var. *mongholicus* (Bge.) Hsiao, and was manufactured under Good Manufacturing Practice standard. A pilot study was undertaken to determine the dose-response relationship of the herbal extract prior to the actual investigation. It was found that 2 and 4 g/kg are being optimal pharmacological doses for the anti-inflammatory action against experimental colitis formation. Groups of rats received oral pre-treatment of the concentrated Am extract (2 or 4 g/kg in 10 mL/kg tap water) once daily for 10 d prior to DNBS induction. Alternatively, other groups of animals received oral Am treatment (2 or 4 g/kg in 10 mL/kg tap water) twice daily on the three consecutive days following DNBS induction. Control animals (control) received oral administration of normal drinking water instead. All animals were killed by intraperitoneal injection of 100 mg/kg of ketamine, followed by cervical dislocation, at 4 d after colitis induction. This time was chosen on the basis that development of acute inflammation arrives at peak level in DNBS-evoked colitis, whereas active tissue repair and regeneration begins afterwards[27].

Assessment of macroscopic colonic lesion area and inflammation

The entire segment of the colon from the rectum to the cecocolic junction was removed, opened and rinsed thoroughly with normal saline. The isolated colon was examined for the presence of gross macroscopic damage and inflammation. Lesion area was recorded by tracing onto a plastic transparency, and measured by using 1-mm^2 grids. Macroscopic lesion area was represented in square millimeter. Other disease activity index was also measured, including the ratio of colon weight to body weight, which was used as a parameter to assess the degree of tissue edema and reflects the severity of colonic inflammation. Moreover, a 6-8-mm sample block of the inflamed colonic tissue with the full thickness was excised from a region of grossly visible damage for histological analysis, while the remaining colonic segment was pulverized and stored at -80 ℃ for subsequent assays.

Histological study of the colonic tissue

After 48 h of 10% buffered formalin fixation, the excised tissue block was processed for histological analysis. After fixation, tissues were dehydrated by a 4-h successive immersion in ethanol and cleared with xylene for 45 min. The specimens were then immersed in melted paraffin at 80 ℃ for 3½ h for embedment into a cast. Six-micrometer sections were sliced with a microtome (Leica RM2135, Germany) and prepared on Vectabond-coated glass slides. The slides were then processed for subsequent staining. After hydration, the processed sections were immersed into periodic acid for 5 min. The sections were then dipped in Schiff's reagent for 5 s. After rinsing in running tap water and washed with distilled water, the tissue sections were dipped into Harris' hematoxylin for 3 s and rinsed in running tap water (for a few seconds) and washed with distilled water. Following hematoxylin counter-staining, tissues on slides were dehydrated and finally mounted in Permount (Sigma, USA). Colonic tissues were scored for histological damage using the criteria of Wallace and Keenan: 0=intact tissue with no apparent damage; 1 = damage limited to surface epithelium; 2 = focal ulceration limited to mucosa; 3=focal, transmural inflammation and ulceration; 4 = extensive transmural ulceration and inflammation bordered by normal mucosa; 5 = extensive transmural ulceration and inflammation involving entire section[28].

Measurement of MPO activity in the colonic tissue

MPO activity is used as a quantitative index of inflammation and a marker of neutrophil infiltration in the tissue[29]. MPO activity was measured by a modified method described by Suzuki and co-workers[30]. Pre-weighed colonic tissues were homogenized with a homogenizer (IKA Labortechnik T25 basic, Germany) in ice-cold 50 mmol/L PBS (pH 6) containing 0.5% hexadecyl-trimethylammonium bromide and 0.336% EDTA (9 μL/mg tissue) for 30 s. The homogenized samples were freeze-thawed and sonicated for 20 s thrice, and then centrifuged at 30 000 *g* (Beckman coulter, Avanti™ J-25I, USA) for 20 min at 4 ℃. Following this, 20 μL of resulting supernatant with dilution by 80 mmol/L PBS (pH 5.4) was mixed with 7.5 μL of 2 mmol/L 3, 3', 5, 5'-tetramethylbenzidine dissolved in 80 mL/L *N*,*N*-dimethylformamide and 2.5 μL of 0.3 mol/L hydrogen peroxide. The final mixture was incubated at 25 ℃ for 25 min. Finally, 125 μL of 0.5 mmol/L sulfonic acid was added to stop the reaction. The end-point absorbance of the mixture was measured at 450 nm in a spectrophotometer (Packard, Fusion™, Canada) using horseradish peroxidase (HRP, Sigma, UK) as standard. The final value of MPO activity was represented as unit per milligram protein.

Measurement of XO activity in the colonic tissue

One unit of XO activity is defined as that could convert 1 μmoL of xanthine to uric acid per min at pH 7.5 and 25 ℃. The XO activity assay was modified from the method of Parks and co-workers[31]. Colonic tissues were homogenized in the 50 mmol/L sodium phosphate buffer (pH 7; 3 μL/mg tissue) containing 0.1 mmol/L EDTA-2Na, 10 mmol/L dithioerythritol and 1 mmol/L phenylmethyl sulfonyl fluoride (PMSF) for 30 s. The mixture was centrifuged at 20 000 *g* (Beckman coulter, Avanti™ J-25I, USA) for 15 min. Then, 12 μL of the supernatant was mixed with 1 mmol/L xanthine (Sigma, UK), 2 mmol/L EDTA-2Na, 200 μg/mL of bovine saline albumin (BSA) and 50 mmol/L of $NaPO_4$ buffer. The mixture was incubated at 25 ℃ for 5 min. Finally, the reaction was terminated by the addition of 400 μL of 0.5 mol/L HCl. XO activity was assessed spectrophotometrically by measuring the absorbance at 295 nm (Packard, Fusion™, Canada). The final values of XO were expressed as milliunit per milligram protein.

Measurement of GSH level in the colonic tissue

The amount of GSH in colonic tissues was determined following the procedures of Cho's research team[32]. Colonic tissues were homogenized in ice-cold 125 mmol/L sodium phosphate buffer with 6.3 mmol/L EDTA (pH 7.5, 3 μL/mg tissue) for 30 s. The crude homogenate was centrifuged (Beckman coulter, Avanti™ J-25I, USA) at 30 000 *g* at 4 ℃ for 30 min. Then, 200 μL of 40 g/L sulfosalicylic acid was added to 100 μL of supernatant and allowed to stand on ice for 5 min to precipitate protein. The mixture was centrifuged again at 5 000 r/min (Eppendorf centrifuge, model 5417R, Germany) at 4 ℃ for 10 min. Subsequently, 100 μL of the de-proteinized supernatant was mixed well with 300 μL of 125 mmol/L sodium phosphate buffer (pH 8) and 2 μL of 10 mmol/L 5,5' dithiobis-(2-nitrobenzoic acid). The solution was allowed to stand at room temperature for 15 min to develop a yellow color. The absorbance was then read against the reagent blank at 412 nm in a spectrophotometer (Packard, Fusion™, Canada). A standard curve of reduced GSH (Sigma, UK) was used for the calculation of the concentration of GSH in the colonic tissues. The final values were expressed as nanomole per milligram protein.

Measurement of protein concentration in the colonic tissue

Total protein contents of the colonic samples were determined for a series of Western blot analyses. Colonic tissues were weighed and homogenized for 30 s at 4 ℃ in RIPA lysis buffer (50 mmol/L Tris, 150 mmol/L NaCl, 0.5% deoxycholate, 0.1% sodium dodecyl sulfate (SDS), 2 mmol/L EDTA, 1% Triton X-100 and 10% glycerol)

with 1 mmol/L PMSF, aprotinin (5 mg/mL), and pepstatin A (5 mg/mL) added freshly. The sample was then centrifuged at 13 000 *g* for 20 min and the resulting supernatant was collected. Five microliters of tissue sample supernatant was diluted with normal saline. Seventy-five microliters of a 1 000× diluted sample was mixed with 75 μL of Coomassie Plus Reagent (Pierce, UK). The mixture was then incubated at room temperature for 10 min. The samples' absorbance was measured at 595 nm by a spectrophotometer (Packard, Fusion™, Canada). The stock concentration of the standard protein BSA was made up to 100 μg/mL. A standard curve in the range of 0-25 μg protein was used for the calculation of the protein concentration present in the colonic tissue. The results are used to quantify the protein sample for electrophoresis in Western blotting and act as a unit of the biochemical assays.

Analysis of the protein expressions of iNOS, P-selectin, and ICAM-1 in the colonic tissue

The protein samples (ICAM-1: 50 μg of total protein; P-selectin and iNOS: 200 μg of total protein) were denatured and separated on 10% SDS-polyacrylamide gel electrophoresis, and then transferred to nitrocellulose membrane (Bio-Rad, USA). The membranes were blocked in blocking solution (5% skim milk powder in TBST containing 0.2 mol/L Tris, 1.37 mol/L NaCl, 1 mol/L HCl, and 0.1% Tween 20) for 30 min at room temperature. Subsequently, it was incubated in a 4 ℃ cold room overnight with the primary antibodies (anti-ICAM-1, anti-P-selectin, anti-iNOS; all in the dilution of 1:1 000) diluted in blocking solution. Membranes were washed six times and incubated with the secondary antibody (HRP-goat anti-rabbit IgG (H+L) conjugate; 1:5 000) in blocking solution for 45 min at room temperature. All antibodies were obtained from Santa Cruz, USA. Protein blots were developed by a chemiluminescence ECL Western blotting detection system (Amersham, USA). The protein bands were visualized by autoradiography using X-ray film (Fuji, Japan) and analyzed by the Bio-Rad Image Analysis System (USA).

Statistical analysis

Results were expressed as mean±SE. Differences between two groups were examined using the one-way analysis of variance (ANOVA) followed by the Dunnett's test. A *P*-value of less than 0.05 was considered significantly different.

RESULTS

Alleviation of DNBS-induced colitis by Am extract

Gross macroscopic observation had demonstrated that administration of DNBS resulted in mucosal lesion formation and inflammation in the distal colonic wall. There was also a drastic drop in body weight of the DNBS-induced rats. The animals also appeared to have diarrhea, soft stool, and rectal bleeding (in the first 2 d after colitis induction). Besides, ratio of the distal colon weight to animal body weight was also markedly increased due to tissue edema. Hyperemia of mesenteric arteries and fibrinous adhesion to other bowel tissues were frequently observed. Figure 1A shows that there was a significant reduction in macroscopic lesion area by both Am pre- and post-treatments in a dose-dependent manner. Microscopically, colonic tissues in all Am-treated groups had demonstrated significant reduction in histological damage scores (Figure 1B), as represented by well-organized mucosal architecture and less infiltrated leukocytes in the mucosal and submucosal layers of the inflamed colon. This was in contrast with the extensive morphological disorientation and generalized glandular disruption in the colonic tissues of the DNBS control group. These implicated that colonic protection produced by Am extract can be achieved at the histological level.

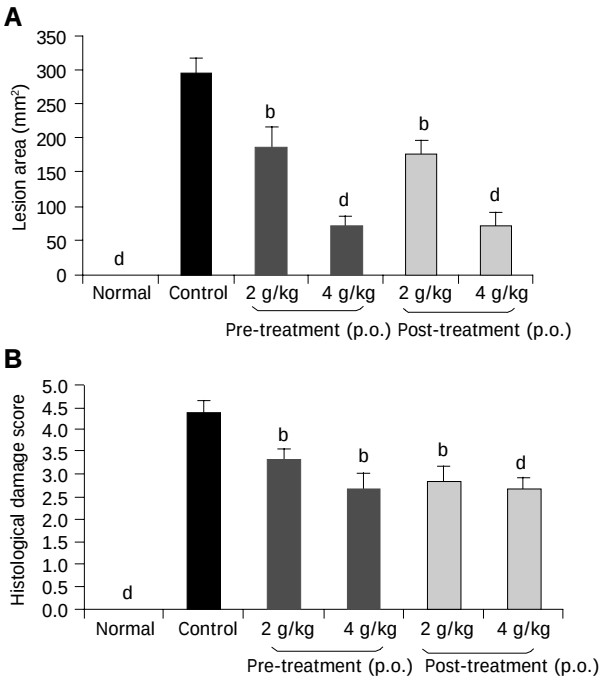


Figure 1 A: Effect of oral *Astragalus* extract (Am) treatment (2 or 4 g/kg) on DNBS-induced lesion formation in rat colon. Animals were either pre-treated with Am once daily for 10 d from 1 d after DNBS induction, or received Am post-treatment twice daily on the three consecutive days following DNBS induction. Control animals (control) received oral administration of normal drinking water only. Animals without colitis induction or drug treatment were regarded as normal animals (normal). All animals were killed 4 d after DNBS administration. Values are mean±SE (n = 6). ^{b}P<0.01, ^{d}P<0.001 *vs* control; B: Effect of oral *Astragalus* extract (Am) treatment (2 or 4 g/kg) on DNBS-induced histological damage score in rat colon. Animals were either pre-treated with Am once daily for 10 d from 1 d after DNBS induction, or received Am post-treatment twice daily on the three consecutive days following DNBS induction. Control animals (control) received oral administration of normal drinking water only. Animals without colitis induction or drug treatment were regarded as normal animals (normal). All animals were killed 4 d after DNBS administration. Values are mean±SE (n = 6). ^{b}P<0.01, ^{d}P<0.001 *vs* control.

Effects of Am extract on colonic activities of the oxidative enzymes MPO and XO and on content of the anti-oxidative enzyme GSH in inflamed colonic tissue

MPO activity was dramatically increased in the colonic tissue after DNBS administration (Figure 2A). Both Am pre- and post-treatments significantly reduced the elevated colonic MPO activity. The attenuating effect of Am on colonic MPO activity was consistent with its colonic protective actions both macroscopically and histologically (Figures 1A and B). Besides the MPO pathway, ROM can also be

generated through XO-catalyzed reactions. Nevertheless, there was no significant change in colonic XO activity after DNBS induction of colonic damages. Likewise, Am treatments also caused no alteration in XO activity. Therefore, it appeared that XO has no involvement in the pathogenesis of DNBS-induced colitis as well as in the mode of action of Am extract.

Figure 2B shows the effect of Am extract on the depletion of one of the key components of antioxidant defenses in the intestine, GSH. GSH concentration in the colonic tissue was dramatically decreased after DNBS enema. Pre- and post-treatment of Am (4 g/kg) significantly preserved the deprivation of the GSH level under colitis condition. The preservation of GSH in the colon by Am treatments could indeed strengthen the colonic defensive mechanism and thus reduce the susceptibility to tissue injury.

Effects of Am extract on protein expression of the pro-inflammatory enzyme iNOS, and adhesion molecules ICAM-1 and P-selectin in inflamed colon

There was a significant upregulation of colonic iNOS protein expression following DNBS administration. Such overexpression was attenuated by both Am pre- and post-treatments (Figure 3A). Similarly, the protein expression of both P-selectin and ICAM-1 was also dramatically upregulated under colitis condition (Figures 3B and C). Although there was a dose-dependent diminution of the P-selectin overexpression in all Am treatment groups (Figure 3B), only pre-treatment with 4 g/kg of Am was capable of inhibiting the elevated ICAM-1 protein expression in the colitic tissue, with no significant effect observed in other treatment groups (Figure 3C).

DISCUSSION

In the present study, DNBS was administrated intracolonically to stimulate cell-mediated immunity in rats[33]. This hapten molecule produces acute and chronic colonic inflammation as well as ulceration in rats[34]. Besides, the histopathologic

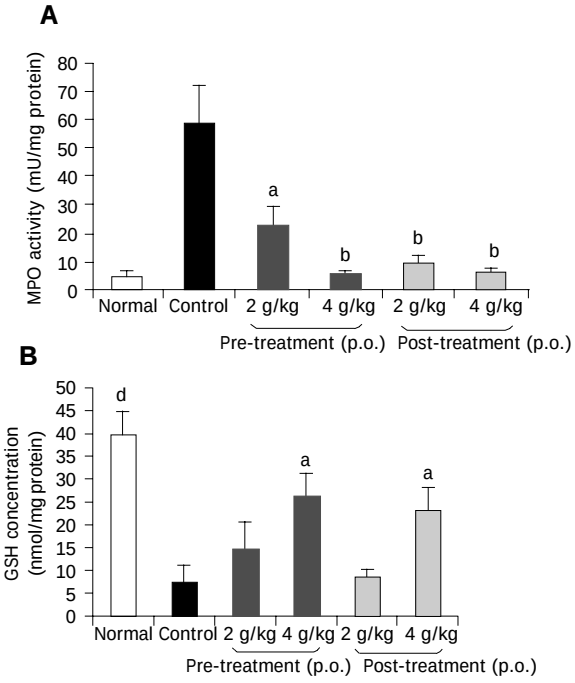


Figure 2 A: Effect of oral *Astragalus* extract (Am) treatment (2 or 4 g/kg) on MPO activity in rat colon. Animals were either pre-treated with Am once daily for 10 d from 1 d after DNBS induction, or received Am post-treatment twice daily on the three consecutive days following DNBS induction. Control animals (control) received oral administration of normal drinking water only. Animals without colitis induction or drug treatment were regarded as normal animals (normal). All animals were killed 4 d after DNBS administration. Values are mean±SE (n = 6). ^{a}P<0.05, ^{b}P<0.01 *vs* control; B: Effect of oral *Astragalus* extract (Am) treatment (2 or 4 g/kg) on GSH concentration in rat colon. Animals were either pre-treated with Am once daily for 10 d from 1 d after DNBS induction, or received Am post-treatment twice daily on the three consecutive days following DNBS induction. Control animals (control) received oral administration of normal drinking water only. Animals without colitis induction or drug treatment were regarded as normal animals (normal). All animals were killed 4 d after DNBS administration. Values are mean±SE (n = 6). ^{a}P<0.05, ^{d}P<0.001 *vs* control.

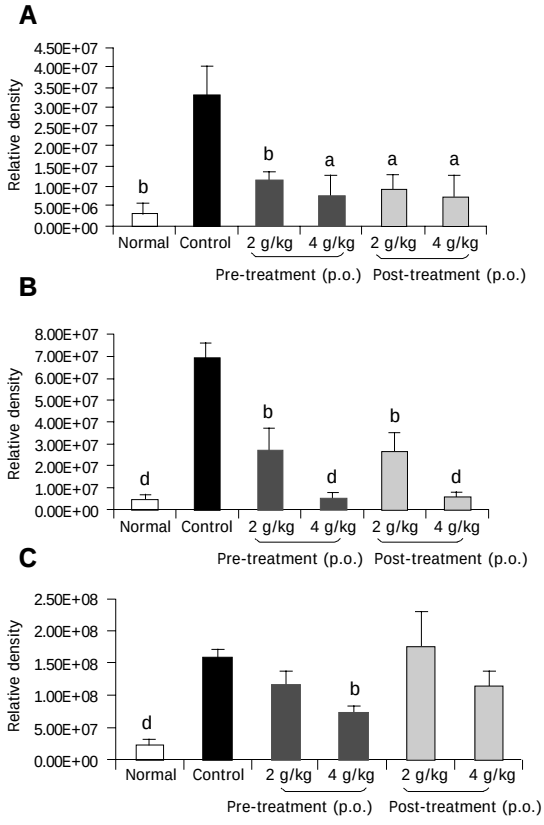


Figure 3 A: Effect of oral *Astragalus* extract (Am) treatment (2 or 4 g/kg) on iNOS protein expression in rat colon. Animals were either pre-treated with Am once daily for 10 d from 1 d after DNBS induction, or received Am post-treatment twice daily on the three consecutive days following DNBS induction. Control animals (control) received oral administration of normal drinking water only. Animals without colitis induction or drug treatment were regarded as normal animals (normal). All animals were killed 4 d after DNBS administration. Values are mean±SE (n = 6). ^{a}P<0.05, ^{b}P<0.01 *vs* control; B: Effect of oral *Astragalus* extract (Am) treatment (2 or 4 g/kg) on P-selectin protein expression in rat colon. Animals were either pre-treated with Am once daily for 10 d from 1 d after DNBS induction, or received Am post-treatment twice daily on the three consecutive days following DNBS induction. Control animals (control) received oral administration of normal drinking water only. Animals without colitis induction or drug treatment were regarded as normal animals (normal). All animals were killed 4 d after DNBS administration. Values are means±SE (n = 6). ^{b}P<0.01, ^{d}P<0.001 *vs* control; C: Effect of oral *Astragalus* extract (Am) treatment (2 or 4 g/kg) on ICAM-1 protein expression in rat colon. Animals were either pre-treated with Am once daily for 10 d from 1 d after DNBS induction, or received Am post-treatment twice daily on the three consecutive days following DNBS induction. Control animals (control) received oral administration of normal drinking water only. Animals without colitis induction or drug treatment were regarded as normal animals (normal). All animals were killed 4 d after DNBS administration. Values are mean±SE (n = 6). ^{b}P<0.01, ^{d}P<0.001 *vs* control.

conditions have more features in common with human UC than with CD. The use of natural immunomodulatory and anti-oxidative products provides an innovative and relatively non-toxic/less toxic alternative to modulate inflammatory disorders, including IBD. Am had exhibited marked antioxidant and immunomodulatory properties in both clinical and experimental studies. However, there is a lack of information regarding its effect on intestinal inflammatory disorders and the associated mechanism of action. The current study is the first one of its kind to demonstrate the effect of Am on experimental colitis. Our findings had indicated that DNBS could lead to a considerable degree of inflammation and tissue injury in the rat colon, with the concomitant infiltration of neutrophils into the colonic tissues. These were reflected by significant colonic lesion formation, high score in histological damage grading, as well as elevated MPO activity in the DNBS-induced animals. Such detrimental effects were alleviated by either pre- or post-treatment of oral Am.

The main pathological feature of IBD is an infiltration of polymorphonuclear neutrophils and mononuclear cells into the intestinal tissues. Neutrophils and monocytes migration is in turn triggered by chemotactic bacterial cell wall products and locally produced cytokines[35,36]. The neutrophil-generated ROM such as superoxide anions, hydrogen peroxide, *N*-chlorinated derivatives, as well as the release of granule enzymes[37] are responsible for the endothelial cell damage. Sedghi and co-workers reported the increase of chemiluminescence in inflamed colonic mucosa and suggested that neutrophils are the likely cellular sources of ROM in the inflamed colon in UC patients[38]. MPO activity was significantly increased and correlated with laboratory parameters and endoscopic grade of inflammation in stool from IBD patients[39]. Besides, MPO conversion of hydrogen peroxide to hypochlorus acid seems closely related to ROM-mediated tissue injury[38]. ROM can be generated through two pathways. The first one is via NADPH oxidase activation in the infiltrated neutrophils, which induces the release of large amount of ROM and oxidants derived from MPO[37]. Alternatively, the other pathway acts through XO induction after periods of hypoxia[40]. In this study, MPO-catalyzed reaction was found to be activated after DNBS administration and attenuated by Am treatments. However, induced production of ROM and reduction of oxidative damage caused by Am did not seem to act through the XO pathway. This result is consistent with a clinical study illustrating that colonic XO activity was not elevated in UC patients[41]. In fact, it had been suggested that XO may not be a major source of superoxide and ROM production in UC[42]. The data presented here actually implicates that the anti-oxidative effect of Am mainly involves the modulation of MPO in the inflamed colon.

The imbalance of ROM generation and antioxidant defense in the colon is an important contributor to the initiation and maintenance of inflammation in IBD[43]. Reduced colonic GSH level is crucial in inducing inflammatory changes. The decrease in colonic GSH concentration following colitis induction could be due to over-production of ROM that deplete GSH by inhibiting the synthetic enzymes for GSH production in the colonic tissue[44]. In the present study, depletion of GSH was significantly preserved by Am, with concurrent attenuation of the elevated MPO activity. This finding implicates that Am could maintain the free radical-scavenging ability of the colonic defense system. Consequently, this diminishes the burden of colonic ROM accumulation (e.g. superoxide), and could further improve the imbalance between ROM and endogenous antioxidants. It is implicit that Am exhibits anti-oxidative activities in several ways, including the inhibition of oxidative stress due to lipid peroxidation and protein oxidative modification, as well as direct removal of free radicals[45]. Among different Am constituents, the total flavonoids appear to possess the strongest free radical-scavenging potential, while total saponins and polysaccharides are somewhat weaker free radical-scavenging agents. In addition, *Astragalus* polysaccharides could modify the increase in malondialdehyde content and diminution of GSH level in the liver of *E-coli* endotoxin-induced rats, and is capable of antagonizing the reduction of GSH peroxidase and superoxide dismutase activities in spleen, thymus and intestinal lymph nodes of traumatic rats[46].

Our findings had demonstrated that iNOS protein expression was significantly upregulated in the colonic tissue after DNBS enema, which was attenuated by oral Am administration. iNOS synthesis can be induced by pro-inflammatory cytokines or bacterial toxins in a variety of cells such as neutrophils, macrophages, endothelial cells and enterocytes, etc.[47]. Therefore, the reduction of neutrophil infiltration, as indicated by the decrease of MPO activity during the anti-inflammatory action of Am, may contribute at least partly to the alleviating effect of Am on iNOS expression in the colonic tissue. Elevated iNOS expression will result in the production of a huge amount of colonic inflammatory NO radicals. Increased production of NO as a result of the overexpression of iNOS protein and mRNA had been demonstrated in affected areas of the intestine in patients suffering from UC or CD[14]. Overwhelming production of iNOS-produced NO causes mucosal vasodilation and modulation of intestinal water and electrolyte transport, which together increase vascular permeability[48]. One of the underlying mechanisms of NO in inducing colonic toxicity involves the interaction with superoxide to produce peroxynitrite, a potent oxidant that can initiate membrane lipid peroxidation, sulfhydryl oxidation of proteins and nitration of acromatic amino acids[29]. In turn, peroxynitrite was found to inhibit superoxide production in a dose-dependent manner[49]. Together with our findings concerning GSH level, Am treatment could reduce superoxide and NO production by preservation of GSH and attenuating iNOS protein expression. As a result, these actions could reduce peroxynitrite formation and in turn diminish the damaging effect of DNBS-induced colonic injury. In addition, it is possible that hydroxyl radicals could be formed by the interaction of NO and hydrogen peroxide[50], which was prevented by Am through inhibition of iNOS synthesis.

Gene expression of cell adhesion molecules is induced by pro-inflammatory cytokines and lipopolysaccharide, such as the cytokines TNF-α, interleukin (IL)-1 and interferon (IFN)-γ[51]. P-selectin was considerably increased in the

colonic endothelium early after colitis induction, which could last for at least 3 wk[52]. In this study, protein expression of P-selectin and ICAM-1 was significantly upregulated after DNBS induction, leading to continuous influx of leukocytes to maintain the local inflammation. Both Am pre-treatment and post-treatment significantly downregulated the protein expression of P-selectin, while ICAM-1 expression was only significantly inhibited in the 4 g/kg Am pre-treatment group. In general, these findings suggest that Am could reduce neutrophil infiltration into colonic tissues through the attenuation of P-selectin and ICAM-1 synthesis evoked by DNBS. Moreover, the subsequent attenuation of MPO activity could further lead to reduction of iNOS synthesis and ROM production. In the study of McCafferty's group, increased P-selectin expression was observed 3 d after induction of acetic acid induced colitis[53]. Moreover, Jones and co-workers reported that there was local upregulation of ICAM-1 in UC and CD patients[54]. ICAM-1 will be manifested during the early inflammatory status of the intestine, while P-selectin expression can only be detectable in a slightly later stage. It is imminent that ICAM-1 plays a pivotal role in determining the initial inflammatory events, while P-selectin will be manifested later in time and is responsible for the maintenance of such responses. Am pretreatment actually prepared the colonic mucosa for subsequent insult by suppressing ICAM-1 synthesis. Nevertheless, after colitis was induced, Am could no longer be capable of inhibiting ICAM-1 production as the inflammatory reactions had already been started.

In conclusion, the results of the present study have shown that Am have both preventive and therapeutic potential in experimental colitis by its modulation of inflammatory mediators and anti-oxidation. It could significantly inhibit P-selectin and ICAM-1 protein expression, attenuate neutrophil infiltration and iNOS synthesis, as well as preserve the deprivation of GSH in colonic tissue following DNBS challenge. Our findings indeed open up a new avenue in deriving new chemotherapeutic strategies against IBD.

ACKNOWLEDGMENTS

The authors want to express their sincere gratitude to Cecilia Chik and Jess Chung for their assistance throughout the present study.

REFERENCES

1 **Knigge KL.** Inflammatory bowel disease. *Clin Cornerstone* 2002; **4**: 49-60
2 **Farrell RJ,** Peppercorn MA. Ulcerative colitis. *Lancet* 2003; **359**: 331-340
3 **Fiocchi C.** Inflammatory bowel disease: etiology and pathogenesis. *Gastroenterology* 1998; **115**: 182-205
4 **Papadakis KA,** Targan SR. Current theories on the cause of inflammatory bowel disease. *Gastroenterol Clin N Am* 1999; **28**: 283-296
5 **Swidsinski A,** Ladhoff A, Pernthaler A, Swidsinski S, Loening–Baucke V, Ortner M, Weber J, Hoffmann U, Schreiber S, Dietel M, Lochs H. Mucosal flora in inflammatory bowel disease. *Gastroenterology* 2002; **122**: 44-54
6 **Morris GP,** Beck PL, Herridge MS, Depew WT, Szewezuk MR, Wallace JL. Hapten-induced model of chronic inflammation and ulceration in the rat colon. *Gastroenterology* 1989; **96**: 795-803
7 **Freidl HP,** Till GO, Ryan US, Ward PA. Mediator induced activation of xanthine oxidase in endothelial cells. *FASEB J* 1989; **3**: 2512-2518
8 **Simmonds NJ,** Rampton DS. Inflammatory bowel disease – a radical view. *Gut* 1993; **34**: 865-868
9 **Ramakrishna BS,** Varghese R, Jayakumar S, Mathan M, Balasubramanian KA. Circulating antioxidants in ulcerative colitis and their relationship to disease severity and activity. *J Gastroenterol Hepatol* 1997; **12**: 490-494
10 **Sturniolo GC,** Mestriner C, Lecis PE, D'Odorico A, Venturi C, Irato P, D'Inca R. Altered plasma and mucosal concentrations of trace elements and antioxidants in active ulcerative colitis. *Scand J Gastroenterol* 1998; **33**: 644-649
11 **Miles AM,** Grisham MB. Antioxidant properties of aminosalicylates. *Methods Enzymol* 1994; **234**: 555-572
12 **Beckman JS,** Koppenol WH. Nitric oxide, superoxide and peroxynitrite: the good, the bad and the ugly. *Am J Physiol* 1996; **271**: C1424-C1437
13 **Valentine JF,** Tannahill CL, Stevenot SA, Sallustio JE, Nick HS, Eaker EY. Colitis and interleukin 1â up-regulated inducible nitric oxide synthase and superoxide dismutase in rat myenteric neurons. *Gastroenterology* 1996; **111**: 56-64
14 **Rachmilewitz D,** Stamler JS, Bachwich D, Karmeli F, Ackerman Z, Podolsky DK. Enhanced colonic nitric oxide generation and nitric oxide synthase activity in ulcerative colitis and Crohn's disease. *Gut* 1995; **36**: 718-723
15 **Ikeda I,** Kasajima T, Ishiyama S, Shimojo T, Takeo Y, Nishikawa T, Kameoka S, Hiroe M, Mitsuuaga A. Distribution of inducible nitric oxide synthase in ulcerative colitis. *Am J Gastroenterol* 1997; **92**: 1339-1341
16 **Meenan J,** Mevissen M, Monajemi H, Radema SA, Soule HR, Moyle M, Tytgat GNJ, van Deventer SJH. Mechanisms underlying neutrophil adhesion to apical epithelial membranes. *Gut* 1996; **38**: 201-205
17 **Vainer B,** Nielsen OH. Changed colonic profile of P-selectin, platelet-endothelial cell adhesion molecules-1 (PECAM-1), intercellular adhesion molecule-1 (ICAM-1), ICAM-2, and ICAM-3 in inflammatory bowel disease. *Clin Exp Immunol* 2000; **121**: 242-247
18 **Ala A,** Dhillon AP, Hodgson HJ. Role of cell adhesion molecules in leukocyte recruitment in the liver and gut. *Int J Exp Pathol* 2002; **84**: 1-16
19 **Nakamura S,** Ohtani H, Watanabe Y, Fukushima K, Matsumoto T, Kitano A, Kobayashi K, Nagura G. *In situ* expression of the cell adhesion molecules in inflammatory bowel disease: evidence of immunologic activation of vascular endothelial cells. *Lab Invest* 1993; **69**: 77-85
20 **Schürmann GM,** Bishop AE, Facer P, Vecchio M, Lee JCW, Rampton DS, Polak JM. Increased expression of cell adhesion molecule P-selectin in active inflammatory bowel disease. *Gut* 1995; **36**: 411-418
21 **Bensky D,** Gamble A. Chinese herbal medicine: materia medica. Revised ed. Seattle: *Eastland Press* 1993
22 Pharmacopoeia Commission of the People's Republic of China. Pharmacopoeia of the People's Republic of China, vol. I. English ed. Beijing: *Chemical Industry Press* 2000
23 **Chang H,** But P. Pharmacology and applications of Chinese materia medica, vol. 2. Singapore: *World Scientific* 1987
24 **Huang KC.** The pharmacology of Chinese herbs. Boca Raton: *CRC Press* 1999
25 **Toda S,** Yase Y, Shirataki Y. Inhibitory effects of Astragali Radix, crude drug in oriental medicines on lipid peroxidation and protein oxidative modification of mouse brain homogenate by copper. *Phytother Res* 2000; **14**: 294-296
26 **Hei ZQ,** Zhang JJ, Lin SQ, Liu KX, Chen BX. Effects of Astragalus membranaceus injection on nitric oxide and endothelin concentration of intestinal mucosa after hemorrhage shock-reperfusion in rats. *Zhongguo Zhongyao Zazhi* 2004; **29**: 444-447
27 **Ko JKS,** Sham NF, Guo X, Cho CH. Beneficial intervention of

experimental colitis by passive cigarette smoking through the modulation of cytokines in rats. *J Invest Med* 2001; **49**: 21-29

28 **Wallace JL,** Keenan CM. An orally active inhibitor of leukotriene synthesis accelerates healing in a rat model of colitis. *Am J Physiol* 1990; **258**: G527-G534

29 **Rachmilewitz D,** Stamler JS, Karmeli F, Mullins ME, Singel DJ, Loscalzo J, Podolsky DK. Peroynitrite-induced rat colitis: a new model of colonic inflammation. *Gastroenterology* 1993; **105**: 1681-1688

30 **Suzuki K,** Ota H, Sasagawa S, Sakatani T, Fujikura T. Assay method for myeloperoxidase in human polymorphonuclear leukocytes. *Anal Biochem* 1983; **132**: 345-352

31 **Parks DA,** Williams TK, Beckman JS. Conversion of xanthine dehydrogenase to oxidase in ischemic rat intestine: a reevaluation. *Am J Physiol* 1988; **254**: G768-G774

32 **Cho CH,** Pfeiffer CJ, Misra HP. Ulcerative mechanism of ethanol and the action of sulphanilyl fluoride on the rat stomach *in-vivo*. *J Pharm Pharmacol* 1991; **43**: 495-498

33 **Kim HS,** Berstad A. Experimental colitis in animal models. *Scand J Gastroenterol* 1992; **27**: 529-537

34 **Hawkins JV,** Emmel EL, Feuer JJ, Nedelman MA, Harvey CJ, Kennedy AR, Lichtenstein GR, Billings PC. Protease activity in a hapten-induced model of ulcerative colitis in rats. *Dig Dis Sci* 1997; **42**: 1969-1980

35 **Grisham MB,** Granger DN. Neutrophil-mediated mucosal injury: role of reactive oxygen metabolites. *Dig Dis Sci* 1988; **33**: 6S-15S

36 **Riddel RH.** Pathology of idiopathic inflammatory bowel disease. In Kirsner JB, Shorter RG, eds. Inflammatory bowel disease. Philadelphia: *Lea and Febiger* 1988: 329-350

37 **Weiss SJ.** Tissue destruction by neutrophils. *N Engl J Med* 1989; **320**: 365-376

38 **Sedghi S,** Fields JZ, Klamut M, Urban G, Durkin M, Winship D, Fretland D, Olyaee M, Keshavarzian A. Increased production of luminal enhanced chemiluminescence by the inflamed colonic mucosa in patients with ulcerative colitis. *Gut* 1993; **34**: 1191-1197

39 **Saiki T.** Myeloperoxidase concentrations in the stool as a new parameter of inflammatory bowel disease. *Kurume Med J* 1998; **45**: 69-73

40 **Kooij A.** A re-evaluation of the tissue distribution and physiology of xanthine oxidoreductase. *Histochem J* 1994; **26**: 889-915

41 **Reynolds PD,** Rhenius ST, Hunter JO. Xanthine oxidase activity is not increased in the colonic mucosa of ulcerative colitis. *Aliment Pharmacol Ther* 1996; **10**: 737-741

42 **Kruidenier L,** Kuiper I, Lamers CB, Verspaget HW. Intestinal oxidative damage in inflammatory bowel disease: semi-quantification, localization, and association with mucosal antioxidants. *J Pathol* 2003; **201**: 28-36

43 **Buffinton GD,** Doe WF. Depleted mucosal antioxidant defences in inflammatory bowel disease. *Free Radic Biol Med* 1995; **19**: 911-918

44 **Sido B,** Hack V, Hochlehnert A, Lipps H, Herfarth C, Droge W. Impairment of intestinal glutathione synthesis in patients with inflammatory bowel disease. *Gut* 1998; **42**: 485-492

45 **Toda S,** Shirataki Y. Inhibitory effects of Astragali Radix, crude drug in oriental medicines on lipid peroxidation and protein oxidative modification by copper. *J Ethnopharmacol* 1999; **68**: 331-333

46 **Wang LX,** Han ZW. The effect of Astragalus polysaccharide on endotoxin-induced toxicity in mice. *Yaoxue Xuebao* 1992; **27**: 5-9

47 **Albina JE.** On the expression of nitric oxide synthase by human macrophages. Why no NO? *J Leuko Biol* 1995; **58**: 643-649

48 **Gaginella TS,** Kachur JF, Tamai H, Keshavarzian A. Reactive oxygen and nitrogen metabolites as mediators of secretory diarrhea. *Gastroenterology* 1995; **109**: 2019-2028

49 **Lee CI,** Liu XP, Zweier JL. Regulation of xanthine oxidase by nitric oxide and peroxynitrite. *J Biol Chem* 2000; **275**: 9369-9376

50 **Nappi AJ,** Vass E. Hydroxyl radical formation resulting from the interaction of nitric oxide and hydrogen peroxide. *Biochim Biophy Acta* 1998; **1380**: 55-63

51 **Lidington EA,** Moyes DL, McCormack AM, Rose ML. A comparison of primary endothelial cell lines for studies of immune interactions. *Trans Immunol* 1999; **7**: 239-246

52 **Sans M,** Salas A, Soriano A, Prats N, Gironella M, Pizcueta P, Elena M, Anderson D, Piqué P, Panés J. Differential role of selectins in experimental colitis. *Gastroenterology* 2001; **120**: 1162-1172

53 **McCafferty DM,** Smith CW, Granger DN, Kubes P. Intestinal inflammation in adhesion molecule-deficient mice: an assessment of P-selectin alone and in combination with ICAM-1 or E-selectin. *J Leuko Biol* 1999; **66**: 67-74

54 **Jones SC,** Banks RE, Haidar A, Gearing AJH, Hemingway IK, Ibbotson SH, Dixon MF, Axon ATR. Adhesion molecules in inflammatory bowel disease. *Gut* 1995; **36**: 724-730

Science Editor Guo SY **Language Editor** Elsevier HK

PO Box 2345, Beijing 100023, China
www.wjgnet.com
wjg@wjgnet.com

ELSEVIER

World J Gastroenterol 2005;11(37):5795-5800
World Journal of Gastroenterology ISSN 1007-9327
© 2005 The WJG Press and Elsevier Inc. All rights reserved.

• *BASIC RESEARCH* •

Protective effect of selenium-enriched lactobacillus on CCl_4-induced liver injury in mice and its possible mechanisms

Long Chen, Dao-Dong Pan, Juan Zhou, Ying-Zi Jiang

Long Chen, Juan Zhou, Ying-Zi Jiang, College of Life Sciences, Nanjing Normal University; Jiangsu Engineering Research Center for Bio-Medical Function Materials, Nanjing 210097, Jiangsu Province, China
Dao-Dong Pan, Department of Food Sciences, Nanjing Normal University, Nanjing 210097, Jiangsu Province, China
Supported by the Special Programs of State Science and Technology Ministry of China During the 10th 5-Year Plan Period, No. 2002BA518A12, and Open Foundation from Key Laboratory of Resource Biotechnology of Jiangsu Province, China, No. KJS00033
Correspondence to: Professor Long Chen, College of Life Sciences, Nanjing Normal University, Nanjing 210097, Jiangsu Province, China. lchen@njnu.edu.cn
Telephone: +86-25-83598216
Received: 2004-12-08 Accepted: 2005-04-02

Abstract

AIM: To study the protective effects and mechanisms of Se-enriched lactobacillus on liver injury caused by carbon tetrachloride (CCl_4) in mice.

METHODS: Seventy-two ICR mice were randomly divided into four groups: normal group, CCl_4-induced model group, low Se-enriched lactobacillus treatment group (L-Se group), and high Se-enriched lactobacillus treatment group (H-Se group). During a 3-wk experimental period, the common complete diet was orally provided daily for normal group and model group, and the mice in L-Se and H-Se groups were given a diet with 2 and 4 mg of organoselenium from Se-enriched lactobacillus per kg feed, respectively. From the 2nd wk of experiment, the model group, L-Se group, and H-Se group received abdominal cavity injection of olive oil solution containing 500 mL/L CCl_4 (0.07 mL/100 g body mass) to induce liver injury, and the normal group was given olive oil on every other day for over 2 wk. In the first 2 wk post injection with CCl_4, mice in each group were killed. The specimens of blood, liver tissue, and macrophages in abdominal cavity fluid were taken. Then the activities of the following liver tissue injury-associated enzymes including glutathione peroxidase (GSH-Px), superoxide dismutase (SOD), alanine aminotransferase (ALT) and aspartate aminotransferase (AST) as well as malondialdehyde (MDA) content were assayed. Changes of phagocytic rate and phagocytic index in macrophages were observed with Wright-Giemsa stain. Plasma TNF-α level was measured by radioimmunoassay. The level of intracellular free Ca^{2+} ($[Ca^{2+}]_i$) in hepatocytes was detected under a laser scanning confocal microscope.

RESULTS: During the entire experimental period, the AST and ALT activities in liver were greatly enhanced by CCl_4 and completely blunted by both low and high doses of Se-enriched lactobacillus. The Se-enriched lactobacillus-protected liver homogenate GSH-Px and SOD activities were higher or significantly higher than those in model group and were close to those in normal group. CCl_4 significantly increased MDA content in liver homogenates, while administration of Se-enriched lactobacillus prevented MDA elevation. Phagocytic rate and phagocytic index of macrophages decreased after CCl_4 treatment compared to those in normal control, but they were dramatically rescued by Se-enriched lactobacillus, showing a greatly higher phagocytic function compared to model group. CCl_4 could significantly elevate plasma TNF-α and hepatocyte $[Ca^{2+}]_i$ level, which were also obviously prevented by Se-enriched lactobacillus.

CONCLUSION: Se-enriched lactobacillus can intervene in CCl_4-induced liver injury in mice by enhancing macrophage function activity to keep normal and beneficial effects, elevating antioxidant-enzyme activities and reducing lipid peroxidation reaction, inhibiting excessive release of TNF-α, preventing the dramatic elevation of $[Ca^{2+}]_i$ in hepatocytes.

© 2005 The WJG Press and Elsevier Inc. All rights reserved.

Key words: Se-enriched lactobacillus; Liver injury; Carbon tetrachloride; Macrophage; Ca^{2+}

Chen L, Pan DD, Zhou J, Jiang YZ. Protective effect of selenium-enriched lactobacillus on CCl_4-induced liver injury in mice and its possible mechanisms. *World J Gastroenterol* 2005; 11(37): 5795-5800
http://www.wjgnet.com/1007-9327/11/5795.asp

INTRODUCTION

Hepatic fibrosis represents the response of the liver to diverse chronic insults such as parasitic disease, chronic viral infection (hepatitis B and C), immunologic attack (autoimmune hepatitis), hereditary metal overload, toxic damage, etc. Because of the worldwide prevalence of these insults, liver fibrosis is a common pathological process of hepatic disease, leading to the development of irreversible cirrhosis[1,2]. If treated properly at fibrosis stage, cirrhosis could be prevented[3]. However, there are no effective anti-fibrosis drugs till date. Selenium (Se), an essential nutrient element, can prevent the malignant transformation of normal cells and the activation of oncogenes with anticarcinogenic effects within a physiological dosage range[4,5]. It has been found in clinical investigations that the blood selenium of hepatocarcinoma patients is

low, and the progress of liver injury and carcinomatous change are related to the degree of selenium deficiency[6]. In addition, some studies indicate that selenium is closely related to the inhibition of hepatic fibrosis[7,8]. However, the supplement of selenium is relevant to selenium style and dosage[5]. Se-enriched lactobacillus is an organoselenium agent. We have demonstrated that concomitant Se-enriched lactobacillus administration to mice and rats subjected to CCl_4-induced liver injury results in a reliable hepatoprotection against hepatic damage, as well as an effective action on enhancing peripheral blood lymphocyte proliferation activity and RBC immune function[9,10]. Therefore, the aim of this study was to further evaluate the beneficial action of Se-enriched lactobacillus on reversing a well-established liver injury and the possible mechanisms by analyzing the activities of several liver tissue injury-associated enzymes, phagocytic function activities in macrophages, plasma TNF-α level and change of hepatocyte intracellular free Ca^{2+} $[Ca^{2+}]_i$ homeostasis.

MATERIALS AND METHODS

Preparation of a complete diet with Se-enriched lactobacillus

Lactobacillus was grown to a density of 5.88×10^7/mL in a medium containing sodium selenite to obtain Se-enriched lactobacillus. The Se-enriched lactobacillus was then processed into an organoselenium agent with 11.45 mg of selenium/g, then mixed into the common complete feed to produce the palletized complete diet with 2 and 4 mg of organoselenium/kg feed according to compound feed processing method in a feed processing plant.

Animals

Seventy-two ICR mice, equal number of males and females, weighing 27.74±0.37 g, were obtained from Experimental Animal Center of Nanjing Medical University, China. The mice were housed at room temperature (20-25 ℃) in a 12-h light and dark cycle. Free access to water and food was allowed during the experimental period. All mice were randomly divided into four groups: normal control group (n = 18), model control group (n = 18), low Se-enriched lactobacillus treatment group (L-Se group, n = 18), and high Se-enriched lactobacillus treatment group (H-Se group, n = 18). During a 3-wk experimental period, the common complete diet was orally provided daily for normal group and model group, and the mice in L-Se and H-Se groups were given a diet with 2 and 4 mg of organoselenium from Se-enriched lactobacillus/kg feed, respectively. In the 2nd wk of experiment, hepatic injury was induced in mice by carbon tetrachloride (CCl_4). The mice in model group, L-Se and H-Se groups were given abdominal cavity injection of olive oil solution containing 500 mL/L CCl_4 (0.07 mL/100 g body mass) every other day for over 2 wk. The mice in normal group received abdominal injection of olive oil at the same dose and frequency.

Phagocytic function detection of macrophage

The macrophage activities were observed in six mice of each group in the first 2 wk post injection with CCl_4. The mice received abdominal cavity injection of 1 mL saline suspension containing 5% chicken's erythrocytes, followed by 1 mL saline after 1 h. Abdominal cavity fluid was collected from the killed mice and incubated for 30 min at 37 ℃, then centrifuged at 1 000 r/min for 10 min to obtain the remaining deposit for smearing and staining with Wright-Giemsa stain. The phagocytic rate and phagocytic index of macrophages were counted under a light microscope.

Collection of specimens

In the first 2 wk post injection with CCl_4, six animals were chosen from each group and anesthetized with ether before they were killed to collect blood samples by enucleating eyeballs, which were put into test tubes containing anticoagulant heparin sodium (1:500). Plasma was obtained by centrifugation at 3 000 r/min for 20 min and stored for analysis. Then, the animals were killed and the liver was quickly washed *in situ* with ice-cold isotonic saline, followed by stripping the capsules. Parenchyma (0.5 g) was sheared into broken bits and put into test tubes with 4 mL physiological saline for tissue homogenates. Tubes were centrifuged at 4 000 r/min for 30 min at 4 ℃ to separate upper fluid, which was stored at -20 ℃ for analysis.

Laser scanning confocal microscopic analysis of intracellular free Ca^{2+} in hepatocytes

Hepatocyte isolation In the 1st wk post injection with CCl_4, six mice from each group were exsanguinated and liver was minced with dissecting scissors into approximately 1 mm^3 pieces. The pieces of liver were placed into 3 mL D-Hank's solution containing 0.25% trypsin (1:250, Amresco Co. USA) for 1 h digestion at 37 ℃, and then added into small 1640 medium (pH 7.2) containing 10% neonatal bovine serum (Sijiqing Co., Hangzhou, China). Streptomycin and penicillin (1×10^5 U/L for each) were used to terminate the digestion. The released cells were filtered through sterilized nylon membranes and washed in D-Hank's solution via two centrifugations at 1 000 r/min for 5 min after erythrocytes were dissolved with 0.85% amchlor solution, and then resuspended in 1640 medium containing 10% neonatal bovine serum.

Fluo-3/AM loading of hepatocytes Twenty microliters of suspension samples containing freshly isolated hepatocytes from each group was placed in 13 mm culture dishes. The glass bottom of the culture dishes were covered with a layer of 0.1 mg/mL ConA (Fluka Co., USA) and dried at 37 ℃ in order to allow cells to adhere. The cells were loaded with 15 μL of 0.1 μg/mL Fluo-3/AM (Calbiochem Co., USA) for 30 min at 37 ℃, and washed thrice with Hank's solution (pH 7.2) to remove the extracellular Fluo-3/AM.

The fluorescence intensity of $[Ca^{2+}]_i$ in hepatocytes was determined by ACAS Ultima-312 laser scanning confocal microscopy. Total images were scanned in each experiment and the data were stored in disks for analysis.

Parameters of plasma and liver homogenates in mice with hepatic injury

The activities of glutathione peroxidase (GSH-Px), superoxide dismutase (SOD), alanine aminotransferase (ALT) and aspartate aminotransferase (AST) as well as malondialdehyde (MDA) content in liver tissue homogenates were assayed by spectrophotometry using commercial kits (Nanjing Jiancheng Biotechnology Institute, China). Plasma TNF-α

level was measured by ^{125}I-based radioimmunoassay using commercial reagents (Radio-Immunity Institute of General Hospital of Chinese Liberation Army). In general, the procedures indicated by the kits were performed strictly according to the manufacturer's protocol.

Statistical analysis

Results were expressed as mean±SE. Statistical analysis was performed by Student's *t*-test (STATISTICA, Statsoft Inc., Tulsa, USA) on a conventional personal computer. $P<0.05$ was considered statistically significant.

RESULTS

Effect of Se-enriched lactobacillus on AST and ALT activities of liver homogenates in mice with CCl_4-induced hepatic injury

As shown in Table 1, during the entire experimental period, CCl_4 significantly increased AST activity in liver homogenates compared to normal control ($P<0.05$). This effect was completely prevented by both low and high doses of Se-enriched lactobacillus ($P<0.05$). Upon exposure to CCl_4, ALT activity in liver homogenates was not affected in the 1st wk of treatment, but significantly enhanced in the 2nd wk ($P<0.05$). This effect was also blunted by a high dose of Se-enriched lactobacillus ($P<0.05$).

Table 1 Changes of AST and ALT activities in mice with hepatic injury after Se-enriched lactobacillus treatment (mean±SE)

Index	Group	Post-injection with CCl_4	
		1 wk	2 wk
AST (U/mg tissue)	Normal	20.43±0.54[a]	17.68±1.21[a]
	Model	28.05±1.03[c]	26.81±0.46[c]
	L-Se	23.60±0.93[a]	17.86±1.75[a]
	H-Se	18.90±0.94[a]	18.90±2.26[a]
ALT (U/mg tissue)	Normal	31.64±0.23	42.93±0.42[a]
	Model	31.15±0.32	50.61±1.05[c]
	L-Se	30.71±0.39	49.47±0.26[c]
	H-Se	28.99±0.13[ac]	43.64±1.61[a]

[a]$P<0.05$ *vs* model group; [c]$P<0.05$ *vs* normal group.

Effect of Se-enriched lactobacillus on GSH-Px and SOD activities of liver homogenates in mice with CCl_4-induced hepatic injury

As demonstrated in Table 2, GSH-Px activity in the liver homogenates slightly decreased in the 1st wk, and significantly decreased in the 2nd wk after CCl_4 treatment. This effect was blunted by a high dose of Se-enriched lactobacillus ($P<0.05$). Similarly, during the entire period of treatment, SOD activity dramatically decreased after CCl_4 treatment ($P<0.05$), which was rescued by both low and high doses of Se-enriched lactobacillus.

Effect of Se-enriched lactobacillus on MDA content in liver homogenates of mice with CCl_4-induced hepatic injury

Figure 1 shows that CCl_4 significantly increased MDA content in liver homogenates compared to normal control during the entire experimental period ($P<0.05$). However, administration of Se-enriched lactobacillus prevented MDA elevation.

Table 2 Changes of GSH-Px and SOD activities in mice with hepatic injury after Se-enriched lactobacillus treatment (mean±SE)

Index	Group	Post-injection with CCl_4	
		1 wk	2 wk
GSH-Px (U/mg tissue)	Normal	6.43±0.67	6.40±0.38[a]
	Model	6.24±0.36	5.21±0.24[c]
	L-Se	7.68±0.33	5.67±0.25
	H-Se	8.10±0.21[a]	6.45±0.31[a]
SOD (U/mg tissue)	Normal	60.57±2.25[a]	61.34±0.83[a]
	Model	47.88±2.15[c]	48.95±1.19[c]
	L-Se	54.43±2.43	52.70±2.14[c]
	H-Se	52.61±3.46	51.50±2.20[c]

[a]$P<0.05$ *vs* model group; [c]$P<0.05$ *vs* normal group.

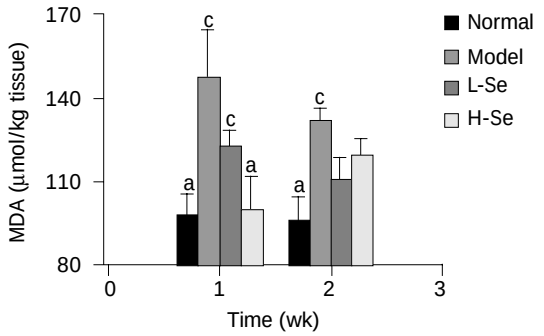


Figure 1 Change of MDA content in liver homogenates of mice with hepatic injury after Se-enriched lactobacillus treatment. [a]$P<0.05$ *vs* model group; [c]$P<0.05$ *vs* normal group.

Effect of Se-enriched lactobacillus on macrophage activities in mice with CCl_4-induced liver injury

During the entire experimental period, the phagocytic rate of macrophages significantly decreased after CCl_4 treatment compared to normal control ($P<0.05$), and was dramatically rescued by both low and high doses of Se-enriched lactobacillus, showing an obviously higher phagocytic rate than that in model group ($P<0.05$). The phagocytic index of macrophages slightly decreased in the 1st wk, and significantly decreased in the 2nd wk after CCl_4 treatment. This effect was protected by high dose of Se-enriched lactobacillus ($P<0.05$, Table 3).

Table 3 Changes of phagocytic function in mice with hepatic injury after Se-enriched lactobacillus treatment (mean±SE)

Index	Group	Post-injection with CCl_4	
		1 wk	2 wk
Phagocytic rate (%)	Normal	17.25±0.81[a]	15.25±1.18[a]
	Model	11.67±1.00[c]	10.64±0.56[c]
	L-Se	14.92±0.33[ac]	12.67±0.49[a]
	H-Se	20.42±0.86[ac]	15.17±0.60[a]
Phagocytic index	Normal	1.75±0.11	1.69±0.08[a]
(RBC/macrophage)	Model	1.46±0.08	1.17±0.06[c]
	L-Se	1.52±0.12	1.36±0.07
	H-Se	1.72±0.04[a]	1.55±0.09[a]

[a]$P<0.05$ *vs* model group; [c]$P<0.05$ *vs* normal group.

Effect of Se-enriched lactobacillus on plasma TNF-α in mice with CCl_4-induced liver injury

During the entire experimental period, CCl_4 significantly

elevated plasma TNF-α level compared to normal control ($P<0.05$). This effect was completely prevented by both low and high doses of Se-enriched lactobacillus, showing an obviously lower value than that in model group ($P<0.05$) and no significant difference as compared to normal group (Figure 2).

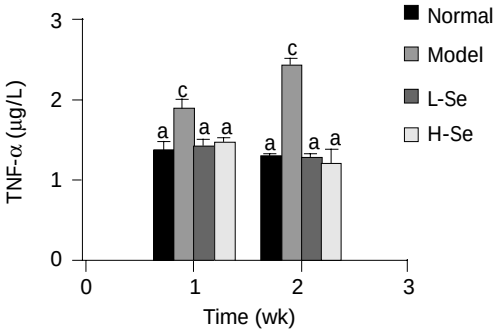


Figure 2 Change of plasma TNF-α level in mice with hepatic injury after Se-enriched lactobacillus treatment. [a]$P<0.05$ *vs* model group; [c]$P<0.05$ *vs* normal group.

Effect of Se-enriched lactobacillus on hepatocytes $[Ca^{2+}]_i$ in mice with CCl_4-induced liver injury

Figure 3A shows changes of hepatocyte $[Ca^{2+}]_i$ fluorescent visualizations in mice with hepatic injury after Se-enriched lactobacillus treatment. In model group, the hepatocyte $[Ca^{2+}]_i$ content significantly raised and was 5.5-fold higher than that in normal group ($P<0.05$), but hepatocytes $[Ca^{2+}]_i$ in mice with liver injury after Se-enriched lactobacillus treatment was significantly downregulated ($P<0.05$) and close to that in normal control (Figure 3B).

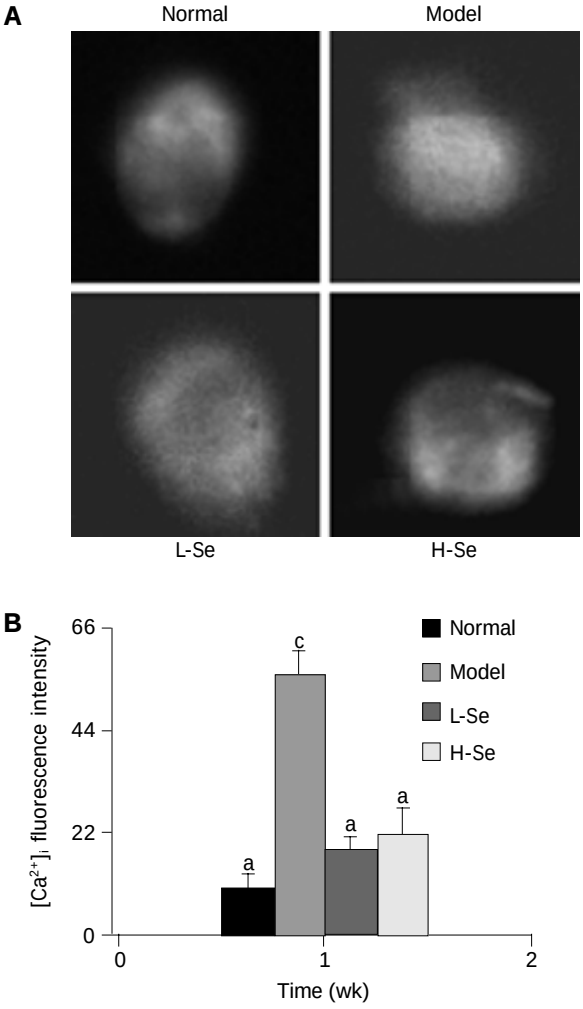


Figure 3 $[Ca^{2+}]_i$ fluorescence visualizations (A) and intensities (B) in mice with hepatic injury after Se-enriched lactobacillus treatment. [a]$P<0.05$ *vs* model group; [c]$P<0.05$ *vs* normal group.

DISCUSSION

Liver fibrosis is a common pathological process of hepatic disease, leading to the development of irreversible cirrhosis in patients. In recent years, the mechanism of hepatic fibrosis has been partly disclosed[11]. If treated properly at fibrosis stage, cirrhosis could be prevented[3]. Several drugs, including cytokines, antioxidants, chemical drugs, soluble type II receptor for TGF-β_1, and antibodies directed against TGF-β_1 have been used to block liver fibrosis, but their effects are not as good as expected[12]. The present study has demonstrated that Se-enriched lactobacillus is effective in treating mice hepatic injury and fibrosis based on both lipid peroxidation reaction and functional analysis. The underlying protective mechanism may involve enhanced immunity, and downregulation of TNF-α release and equilibration of hepatocyte $[Ca^{2+}]_i$ homeostasis.

There are various kinds of liver injuries all over the world, causing great affliction to patients. Searches for effective ways to inhibit fibrogenesis and to prevent the development of cirrhosis are of great significance. Selenium can prevent the malignant transformation of normal cells and the activation of oncogenes with anticarcinogenic effects within a physiological dosage range[4,5]. Selenium is closely related to the inhibition of hepatic fibrosis[7,8]. Se-enriched lactobacillus is an organoselenium agent. The present study showed that ALT, AST and MDA in mice after Se-enriched lactobacillus treatment dropped significantly when compared to those in model group, indicating that Se-enriched lactobacillus reduces the violent lipid peroxidation reaction induced by CCl_4 and prevents hepatic injury.

GSH-Px, a selenium-containing enzyme, is a primary selenium-dependent, glutathione-utilizing peroxidase in the liver[13-15]. The decreased GSH-Px activity has been implicated in animals fed with a selenium-deficient diet[16,17]. Conversely, selenium supplement can also impact GSH-Px activity directly[18,19]. In this study, CCl_4 caused an obvious decrease of GSH-Px activity in liver homogenates, but the enzyme activity was higher after Se-enriched lactobacillus treatment, suggesting that Se-enriched lactobacillus can ameliorate GSH-Px activity or enhance its activity by participating in GSH-Px biosynthesis in mice with CCl_4-induced liver injury. SOD is one of the potent antioxidant enzymes in cells and catalyzes the conversion of superoxide ions into oxygen and hydrogen peroxide. In our study, SOD activity was dramatically decreased by CCl_4, but the effect was rescued by both low and high doses of Se-enriched lactobacillus. GSH-Px and SOD are the important antioxidant enzymes of antioxidant

defense systems for stabilizing oxidative reactions. Decreased activity and content of these enzymes cause the descent of antioxidant ability in the body[20]. Therefore, Se-enriched lactobacillus may prevent experimental liver injury by modulating or enhancing GSH-Px and SOD activities.

Macrophages are important immune cells of the immune system and the first line of defense to infection and inflammation in the body, and play a very important role in regulating the body immune status. Many experiments have demonstrated that the macrophage phagocytosis in mice with CCl_4-induced liver injury can be reduced[16,21,22]. In our study, Se-enriched lactobacillus was found to be able to enhance the immunity of the body by increasing the phagocytic rate and phagocytic index in macrophages in L-Se group and H-Se group. This fact may be relevant to the protection of its biomembrane against oxidative destruction. Mayanski *et al*.[22], showed that structural and functional integrity of the cell membrane system including macrophages in mice with CCl_4-induced liver injury is damaged, thus depressing the activity of macrophages.

To understand the mechanism, we evaluated the effect of Se-enriched lactobacillus treatment on blood TNF-α concentration in mice with liver injury. There is evidence that TNF-α is a primary and key endogenous mediator inducing acute inflammatory conditions[23-25]. When an inflammatory reaction occurs, TNF-α is expressed by both infiltrating inflammatory cells such as macrophages in the blood and hepatocytes in liver injuries. Excessive TNF-α can indirectly induce liver damage by further enhancing the release of mass inflammatory mediators including free radicals, prostaglandin, leukotriene, thromboxane, interleukin-1, and TNF-α from macrophages, and also promote liver injury by increasing nitric oxide production from liver cells[26,27]. The present study showed that plasma TNF-α level due to CCl_4 increased obviously, but the effect was significantly blunted by Se-enriched lactobacillus, indicating that Se-enriched lactobacillus downregulates excessive release of TNF-α.

It was reported that changes of intracellular cation homeostasis are closely related to the mechanism of hepatic cell injury[28,29]. Elevation of $[Ca^{2+}]_i$ concentration is associated with the development of cell damage[30,31]. In the present study, CCl_4 caused the increase of hepatocyte $[Ca^{2+}]_i$, suggesting that the dramatic elevation of hepatocyte $[Ca^{2+}]_i$ due to CCl_4 is closely related to CCl_4-induced hepatocellular injury. However, the hepatocyte $[Ca^{2+}]_i$ level in mice with liver injury after Se-enriched lactobacillus treatment was significantly lower than that in model group, indicating that Se-enriched lactobacillus may prevent disturbance of $[Ca^{2+}]_i$ homeostasis. Other investigations showed that hepatocyte $[Ca^{2+}]_i$ elevation is caused by the decreased activities of Na^+/K^+- and Ca^{2+}-ATPases in hepatocyte membranes[32,33]. In addition, it is possible that CCl_4 may release Ca^{2+} by inhibiting the endoplasmic reticulum Ca^{2+} pump so that a passive leak of Ca^{2+} from the endoplasmic reticulum results in the increase of $[Ca^{2+}]_i$ and induces cell death[30,34,35]. Thus, Se-enriched lactobacillus may play an important role in preventing liver injury. The exact mechanisms remain to be explored.

In conclusion, Se-enriched lactobacillus can significantly reduce CCl_4-induced liver injury in mice by enhancing macrophage function activity to keep normal and beneficial effects, elevating antioxidant-enzyme activities and reducing lipid-peroxidation reaction, inhibiting excessive release of TNF-α and preventing dramatic elevation of hepatocyte $[Ca^{2+}]_i$ concentration.

ACKNOWLEDGMENT

We thank Dr. Chao-Ying Zhang at the College of Life Sciences, Nanjing Normal University for assistance with laser scanning confocal microscopic analysis of $[Ca^{2+}]_i$ in hepatocytes.

REFERENCES

1 **Shen L**, Fan JG, Shao Y, Zeng MD, Wang JR, Luo GH, Li JQ, Chen SY. Prevalence of nonalcoholic fatty liver among administrative officers in Shanghai: an epidemiological survey. *World J Gastroenterol* 2003; **9**: 1106-1110
2 **Wang FS**, Wu ZZ. Current situation in studies of gene therapy for liver cirrhosis and liver fibrosis. *Shijie Huaren Xiaohua Zazhi* 2000; **8**: 371-373
3 **Riley TR 3rd**, Bhatti AM. Preventive strategies in chronic liver disease: part II. Cirrhosis. *Am Fam Physician* 2001; **64**: 1735-1740
4 **Schrauzer GN**. Anticarcinogenic effects of selenium. *Cell Mol Life Sci* 2000; **57**: 1864-1873
5 **Schrauzer GN**. Nutritional selenium supplements: product types, quality, and safety. *J Am Coll Nutr* 2001; **20**: 1-4
6 **Shamberger RJ**, Frost DV. Possible protective effect of selenium against human cancer. *Can Med Assoc J* 1969; **100**: 682
7 **Zhang M**, Song G, Minuk GY. Effects of hepatic stimulator substance, herbal medicine, Selenium/Vitamin E, and ciproloxacin on cirrhosis in the rat. *Gastroenterology* 1996; **110**: 1150-1155
8 **Ianas O**, Olinescu R, Badescu I, Simionescu L, Popovici D. The influence of "selenium organicum" upon the hepatic function of carbon tetrachloride poisoned rats. *Rom J Intern Med* 1995; **33**: 113-120
9 **Sun YY**, Chen L, Jiang YZ, Cao M. Protection effect of lactobacillus of selenium enrichment in growth and lymphocyte transformation of rats with liver injuries. *Zhongguo Yingyong Shenglixue Zazhi* 2003; **19**: 366-367
10 **Zhou J**, Chen L, Chen LJ, Pan DD, Jiang YZ. Effects of lactobacillus rich in selenium on RBC lipid peroxidation and immune function in mice with CCl_4–injected liver injury. *Yingyang Xuebao* 2003; **25**: 405-408
11 **Zhu YH**, Hu DR, Nie QH, Liu GD, Tan ZX. Study on activation and c-fos, c-jun expression of *in vitro* cultured human hepatic stellate cells. *Shijie Huaren Xiaohua Zazhi* 2000; **8**: 299-302
12 **Bissell DM**, Roulot D, George J. Transforming growth factor â and the liver. *Hepatology* 2001; **34**: 859-867
13 **Ho YS**, Magnenat JL, Bronson RT, Cao J, Gargano M, Sugawara M, Funk CD. Mice deficient in cellular glutathione peroxidase develop normally and show no increased sensitivity to hyperoxia. *J Biol Chem* 1997; **272**: 16644-16651
14 **Esposito LA**, Kokoszka JE, Waymire KG, Cottrell B, MacGregor GR, Wallace DC. Mitochondrial oxidative stress in mice lacking the glutathione peroxidase-1 gene. *Free Radic Biol Med* 2000; **28**: 754-766
15 **Esposito LA**, Melov S, Panov A, Cottrell BA, Wallace DC. Mitochondrial disease in mouse results in increased oxidative stress. *Proc Natl Acad Sci USA* 1999; **96**: 4820-4825
16 **Hamazaki K**, Sato S, Yunoki M, Noda T, Moreira LF, Mimura H, Orita K. Kupffer cell function in chronic liver injury and after partial hepatectomy. *Res Exp Med* 1994; **194**: 237-246
17 **Noguchi T**, Cantor AH, Scott ML. Mode of action of selenium and vitamin E in prevention of exudative diathesis in chicks. *J Nut* 1973; **103**: 1502-1511
18 **Kvicala J**. Selenium and the organism. *Cas Lek Cesk* 1999; **138**: 99-106
19 **Tolando R**, Jovanovic A, Brigelius-Flohe R, Ursini F, Maiorino M. Reactive oxygen species and proinflammatory cytokine signaling in endothelial cells: effect of selenium supplementation. *Free Radic Biol Med* 2000; **28**: 979-986

20 **Menegola E**, Broccia ML, Prati M, Ricolfi R, Giavini E. Glutathione status in diabetes-induced embryopathies. *Biol Neonate* 1996; **69**: 293-297
21 **Noda T**, Mimura H, Orita K. Assessment of Kupffer cell function in rats with chronic liver injury caused by CCl_4. *Hepatogastroenterology* 1990; **37**: 319-323
22 **Mayanski DN**, Schwartz YS, Kutina SN, Zubakhin AA, Mayanskaya NN, Tsyrendorjiev DD. Mononuclear phagocyte system responsiveness in CCl_4-induced liver cirrhosis. *Int J Exp Pathol* 1993; **74**: 229-236
23 **Chen L,** Zhou J, Gao W, Jiang YZ. Action of NO and TNF-alpha release of rats with cadmium loading in malfunctiion of multiple system organ. *Shenli Xuebao* 2003; **55**: 535-540
24 **Kimura K,** Bowen C, Spiegel S, Gelmann EP. Tumor necrosis factor-alpha sensitizes prostate cancer cells to gamma-irradiation-induced apoptosis. *Cancer Res* 1999; **59**: 1606-1614
25 **Karck U**, Peters T, Decker K. The release of tumor necrosis factor from endotoxin-stimulated rat Kupffer cells is regulated by prostaglandin E_2 and dexamethasone. *J Hepatol* 1988; **7**: 352-361
26 **Al-Shabanah OA**, Alam K, Nagi MN, Al-Rikabi AC, Al-Bekairi AM. Protective effect of aminoguanidine, a nitric oxide synthase inhibitor, against carbon tetrachloride induced hepatotoxicity in mice. *Life Sci* 2000; **66**: 265-270
27 **Hoebe KH,** Witkamp RF, Fink-Gremmels J, Van Miert AS, Monshouwer M. Direct cell-to-cell contact between Kupffer cells and hepatocytes augments endotoxin-induced hepatic injury. *Am J Physiol Gastrointest Liver Physiol* 2001; **280**: G720-728
28 **Gasbarrini A**, Borle AB, Farghali H, Bender C, Francavilla A, Van Thiel D. Effect of anoxia on intracellular ATP, Na^+; Ca^{2+}; Mg^{2+}; and cytotoxicity in rat hepatocytes. *J Biol Chem* 1992; **267**: 6654-6663
29 **Carini R**, Bellomo G, Benedetti A, Fulceri R, Gamberucci A, Parola M, Dianzani MU, Albano E. Alteration of Na^+ homeostasis as a critical step in the development of irreversible hepatocyte injury after adenosine triphosphate depletion. *Hepatology* 1995; **21**: 1089-1098
30 **Ueda T**, Takeyama Y, Hori Y, Takase K, Goshima M, Kuroda Y. Pancreatitis-associated ascitic fluid increases intracellular Ca^{2+} concentration on hepatocytes. *J Sur Res* 2000; **93**: 171-176
31 **Orrenius S**, McCabe MJ Jr, Nicotera P. Ca^{2+}-dependent mechanisms of cytotoxicity and programmed cell death. *Toxicol Lett* 1992; **64**: 357-364
32 **Muriel P**, Favari L, Soto C. Erythrocyte alterations correlate with CCl_4 and biliary obstruction-induced liver damage in the rat. *Life Sci* 1993; **52**: 647-655
33 **Srivastava SP,** Chen NQ, Holtzman JL. The *in vitro* NADPH-dependent inhibition by CCl_4 of the ATP-dependent calcium uptake of hepatic microsomes from male rats. Studies on the mechanism of the inactivation of the hepatic microsomal calcium pump by the CCl3.radical. *J Biol Chem* 1990; **265**: 8392-8399
34 **Long RM**, Moore L. Cytosolic calcium after carbon tetrachloride, 1,1-dichloroethylene, and phenylephrine exposure. Studies in rat hepatocytes with phosphorylase a and quin2. *Biochem Pharmacol* 1987; **36**: 1215-1221
35 **Cheng JS**, Jan CR. Effect of nordihydroguaiaretic acid on intracellular Ca^{2+} concentrations in hepatocytes. *Toxicol In Vitro* 2002; **16**: 485-490

Science Editor Wang XL and Guo SY **Language Editor** Elsevier HK

PO Box 2345, Beijing 100023, China
www.wjgnet.com
wjg@wjgnet.com

ELSEVIER

World J Gastroenterol 2005;11(37):5801-5806
World Journal of Gastroenterology ISSN 1007-9327
© 2005 The WJG Press and Elsevier Inc. All rights reserved.

• *BASIC RESEARCH* •

Separation of growth-stimulating peptides for *Bifidobacterium* from soybean conglycinin

Wei-Yong Zuo, Wei-Hua Chen, Si-Xiang Zou

Wei-Yong Zuo, Wei-Hua Chen, Si-Xiang Zou, Key Laboratory of Animal Physiology and Biochemistry, Ministry of Agriculture, College of Veterinary Medicine, Nanjing Agricultural University, Nanjing 210095, Jiangsu Province, China
Supported by the National Key Basic Research Development Program of China, 973 Program, No. 2004CB117505
Correspondence to: Professor Si-Xiang Zou, Key Laboratory of Animal Physiology and Biochemistry, Ministry of Agriculture, College of Veterinary Medicine, Nanjing Agricultural University, Nanjing 210095, Jiangsu Province, China. sixiangzou@njau.edu.cn
Telephone: +86-25-84396763 Fax:+86-25-84398669
Received: 2004-12-07 Accepted: 2005-01-05

Abstract

AIM: To isolate and identify the soybean conglycinin peptides that selectively stimulates the growth of bifidobacteria *in vitro*, and to investigate the effect of soybean conglycinin peptides on intestinal ecosystem *in vivo*.

METHODS: Soybean conglycinin was purified from soybean seeds by gel filtration (Sepharose-CL-6B). These proteins were submitted to hydrolysis by pepsin. Several growth-stimulating peptides for bifidobacteria were isolated chromatographically from pepsin hydrolysis of soybean conglycinin and identified by means of matrix-assisted laser desorption ionization time of flight mass spectrometry (MALDI-TOF-MS). Parallel to *in vitro* study, *in vivo* experiments with soybean conglycinin peptides were performed in mice. Ninety male KM mice were randomly assigned into five groups of 16 mice each, and each group was administered for 21d intragastrically with physiological saline (control), conglycinin, pepsin-treated conglycinin (PTC), the most active fraction which isolated from pepsin-treated conglycinin (P2-PTC) and HCl-full hydrolysis of conglycinin (HCl-FHC), respectively. Intestinal microflora were evaluated by standard microbiologic methods and biochemical assays of cecal content samples after treatment.

RESULTS: The results showed that the peptides which were isolated from soybean conglycinin could stimulate the growth of bifidobacteria *in vitro*, and the molecular mass of purified peptides with MALDI-TOF-MS ranged from 693.32 to 1829.55. Compared with control group, *in vivo* experiments showed that P2-PTC group decreased cecal pH (7.08±0.08 *vs* 7.21±0.09, $P<0.05$) and *enterococci* counts (5.38±0.26 $\log_{10}$CFU/g *vs* 5.78±0.19 $\log_{10}$CFU/g, $P<0.05$), significantly increased sIgA level (172.08±35.40 ng/g *vs* 118.27±33.93 ng/g, $P<0.01$) and β-galactosidase activity (1.28±0.23 U/g *vs* 1.82±0.58 U/g, $P<0.05$).

CONCLUSION: The results have shown that conglycinin is good source for enzyme-mediated production of peptides which stimulate the growth of bifidobacteria. These peptides are inactive within the sequence of the parent protein but can be released during enzymatic hydrolysis, and *in vivo* experiments demonstrate that conglycinin peptides may be beneficial for improving gastrointestinal health.

© 2005 The WJG Press and Elsevier Inc. All rights reserved.

Key words: Conglycinin pepsin peptides bifidobacteria

Zuo WY, Chen WH, Zou SX. Separation of growth-stimulating peptides for *Bifidobacterium* from soybean conglycinin. *World J Gastroenterol* 2005; 11(37): 5801-5806
http://www.wjgnet.com/1007-9327/11/5801.asp

INTRODUCTION

In recent years, a large number of biologically active peptides have been isolated from bacterial, fungal, plant, and animal sources. The concept that peptides with potential biological activity might be present in food is not new. Soybean storage proteins are composed mainly of two major components, conglycinin and glycinin[1]. Many studies have demonstrated that the enzymatic hydrolysis of conglycinin improved its functional properties and had various physiological activities such as antihypertensive[2], immunostimulating[3] and antioxide activities[4].

It is now generally accepted that the human gastrointestinal tract is host to various species of microorganisms and these bacteria play a significant role in health and disease[5]. Bifidobacteria are gram-positive anaerobic bacteria, which normally inhabit the gut of human beings and animals, the presence of a great deal of bifidobacteria has been considered essential to promote intestinal health and to strengthen the local immune response[6]. The use of bifidobacteria as food supplements and therapeutical pharmaceuticals has been limited because of their slow growth. Several growth stimulating substances have been investigated, most of which derived from human and bovine milk[7,8], however, the effect of peptides isolated from soybean conglycinin has not been understood well.

In this paper, we report that peptides obtained from the digestion of conglycinin with pepsin are effective growth factors for bifidobacteria, based on experiments *in vitro*. We

also evaluated the *in vivo* effects of soybean conglycinin peptides on gut ecosystem in mice.

MATERIALS AND METHODS

Separation of conglycinin from soybean

The conglycinin was prepared from soybean seeds by the procedure of Iwabuchi[9] and Lovati[10] , as reported briefly below. Soybeans were finely ground and defatted with hexane at room temperature. Ground meals, extracted with 30 mmol/L Tris-HCl buffer (pH 8.0) containing 0.01 mol/L β-mercaptoethanol for 1 h at room temperature, were spun by centrifugation (20 min at 4 000 r/min, 20 ℃). The supernatant (adjusted to pH 6.4) was spun by centrifugation (15 000 r/min, 20 min, 4 ℃), the precipitates were discarded, and the supernatant was adjusted to pH4.8. The crude conglycinin was collected by the same centrifugation procedure as described above. The precipitated conglycinin was dissolved in 30 mmol/L Tris-HCl buffer (pH 8.0) containing 0.01 mol/L β-mercaptoethanol. The supernatant proteins were fractionated by ammonium sulphate precipitation. The 51-100% saturation fraction was dialyzed against water and applied to a Sepharose-CL-6B column (Pharmacia). Elution was performed with the phosphate buffer (2.6 mmol/L KH_2PO_4, 32.5 mmol/L K_2HPO_4, 0.4 mol/L NaCl, 10 mmol/L β-mercaptoethanol, pH 7.6). Finally the purified conglycinin was dialyzed against water. After readjusted to pH7.0 and analyzed for protein concentration by the method of micro-Kjeldahl, the protein solutions were freeze-dried and stored at 4 ℃. These materials were used as protein samples.

Sodium dodecyl sulfate gel electrophoresis(SDS-PAGE)

SDS-PAGE was performed according to Laemmli [11], using 10% polyacrylamide gels, The protein was stained with Coomassie brilliant blue(R-250), scanned, and the profiles of each lane were analyzed by densitometry in the Kodak Digital Science Software 1DTM.

Hydrolysis of conglycinin by pepsin

Conglycinin was hydrolyzed by pepsin (Amersico) using a 1:30 enzyme: substrate ratio. Enzymatic hydrolysis was performed after acidification to pH1.4 with 1 mol/L HCl, and mixture of pepsin and conglycinin was incubated for 2 h at 37 ℃. The reaction was terminated by heating at 70 ℃ for 30 min, and the solution was adjusted to pH 7 with 1 mol/L NaOH. After centrifugation (20 min, 3 000 r/min, 4 ℃), the supernatant was collected and lyophilized. The nitrogen concentrations of the conglycinin digestion were evaluated by the method of micro-Kjeldahl.

Full hydrolysis of conglycinin by hydrochloric acid

The conglycinin was fully hydrolyzed with 6 mol/L HCl at 110 ℃ for 24 h. The solution was composed of amino acid composition of conglycinin. The hydrolysates were neutralized and lyophilized.

Separation of peptides

Components of pepsin-treated conglycinin were separated using Sephadex-G15 (Pharmarcia) gel filtration chromatography, tracking the maximum growth stimulatory activity of the resulting fractions on *Bifidobacterium longum* (FCM1192) which was endorsed by Professor Ming-Sheng Dong (Nanjing Agricultural University). The elution was carried out with 0.05 mol/L acetate, and the absorbance of the column effluent was monitored at 280 nm. The molecular mass of the most active fraction was identified by means of MALDI-TOF-MS (BIFLEXTM III, BRUKER). In this study, α-cyano-4-hydroxy-cinnamic acid solution was used as matrix. Peptide concentrations in a sample throughout the purification were determined with the method of micro-Kjeldahl.

Bacterial growth assays in vitro

The basal medium used for a bioassay *in vitro* was a fully synthetic medium as described by Hassinen[12]. For growth assays, the assay medium (5 mL) was mixed with 0.15 mg/mL (nitrogen concentration) samples and inoculated with 100 μL of bacteria culture. The control contained ammonium acetate which has equal nitrogen concentration with samples. Culture was done under anaerobic conditions at 37 ℃. The extent of growth was measured by the absorbance at 460 nm after 48 h of cultivation. The growth experiments were done in triplicates.

Animals and diets

Ninety male KM mice (21 d old, body weight 10-13 g, Shanghai SLAC Experimental Animals Co.Ltd, China) were housed in a room with controlled lighting (12 h/d), and constant temperature. During the first week, all mice had a commercially available basal diet and then randomly assigned into five groups of 16 mice each. Each group was administered for 21 d intragastrically with physiological saline (control), conglycinin, pepsin-treated conglycinin (PTC), the most active fraction which was isolated from pepsin-treated conglycinin (P2-PTC), and HCl-full hydrolysis of conglycinin (HCl-FHC), respectively. The volume of every treatment for the latter four groups was 0.5 mL with equal amount of nitrogen (0.3 mg/mL).

Preparation of sample and enumeration of bacteria

At the end of the experimental period, mice were killed by decapitation. Blood samples were collected and spun by centrifugation at 3 000 r/min for 10 min to obtain sera. Serum level of IL-2 was assayed by radioimmunoassay (Beijing North Institute of Biotechnology) using RIA methods. Cecal samples were collected and immediately frozen and stored at -30 ℃ until analysis and subsequent testing for microbial composition. The following media were used: MacConkey agar for *E.coli*, bile esculine azide agar for *enterococci*. Cecal contents were cultured with triplicate plates for the microbial colony count. After incubation at 37 ℃ for 24 h, results were expressed as colony-forming units per gram of cecal contents. The pH of the cecal contents was measured using a pH meter. Contents of small intestine were also collected and diluted by water a ratio of 1:10. After centrifugation at 3 000 r/min for 10 min, sIgA level of supernatant was assayed by radioimmunoassay (Beijing North Institute of Biotechnology) using RIA methods.

Enzyme assays

A protocol for detecting fructose-6-phosphate phosphoketolase (F-6-PPK) activity in the extracts from cecum samples was employed based on the assay as previously described by Orban *et al*.[13]. A positive reaction was recorded if an immediate red-violet color change was visible, and color formation was recorded spectrophotometrically at 505 nm. Quantitative determinations of β-galactosidase enzyme activities were performed in cecal contents suspensions. The method was used for measuring β-galactosidase activity described by Brigidi *et al*.[14]. One unit of β-galactosidase activity was defined as the amount which released 1 μmoL of *p*-nitrophenol per minute and results were expressed as Units/g of wet sample.

Statistical analysis

Data were expressed as mean±SD. Statistical significance was determined by applying one-way analysis of variance (ANOVA). $P<0.05$ was considered statistically significant.

RESULTS

Soybean conglycinin separation

The procedure for fractionation of conglycinin was based on the isoelectric precipitation and size exclusion chromatography. The elution profile of crude conglycinin on sepharose-CL-6B is shown in Figure 1. The conglycinin was mainly detected in peak II. The gel electrophoretic pattern of purified conglycinin is illustrated in Figure 2. The major bands in the conglycinin were the α, α' and β subunits, the purification rate of conglycinin was 90.13%.

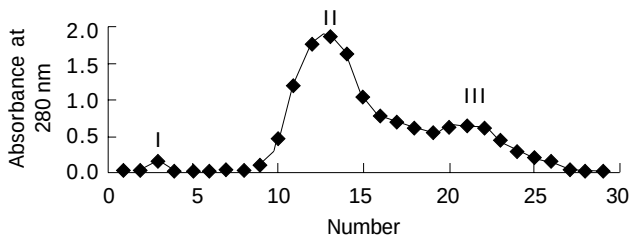


Figure1 Chromatography of soybean conglycinin on sepharose-CL-6B. Bed size,1 cmx100 cm, flow rate 30 mL/h, absorbance at 280 nm.

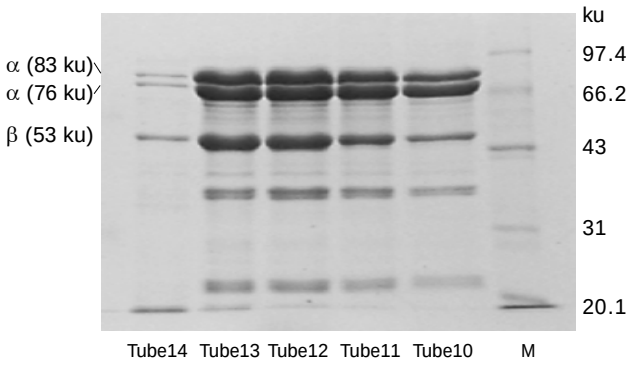


Figure 2 SDS-PAGE pattern of purified conglycinin. α, α' and β indicate subunits of conglycinin. M: standard molecular weight proteins.

Growth-stimulating activity of conglycinin hydrolysates in vitro

The results of the *in vitro* experiments of the effect of soybean conglycinin hydrolysates on the regulation of growth activity for *Bifidobacterium longum* is shown in Table 1. Compared with control, pepsin-treated conglycinin (PTC) could significantly promote the growth of *Bifidobacterium longum* ($P<0.01$), while HCl-full hydrolysis of conglycinin (HCl-FHC) had no significant effect on the growth of *Bifidobacterium longum* after 48 h .

Table 1 Effect of soybean conglycinin hydrolysates on the growth of *bifidobacterium longum* (n = 9)

Group	Control	Conglycinin	PTC	HCl-FHC
A_{460}	0.11±0.04	0.31±0.11	0.66±0.07[bd]	0.12±0.02

Values are expressed as the mean±SD. [b]*P<0.01 vs* control group, [d]*P<0.01 vs* HCl-FHC group.

Separation of peptides

Five fractions (P1-P5) were separated from pepsin-treated conglycinin using Sephadex-G15 gel filtration column chromatography based on absorbance at 280 nm (Figure 3). Results of bacterial growth assays showed that P2 had the maximum growth stimulatory activity (Table 2). MALDI-TOF-MS analysis of P2 is shown in Figure 4. The molecular mass ranged from 693.32 to 1829.55. It demonstrated that the fraction P2 was comprised of peptides with short lengths.

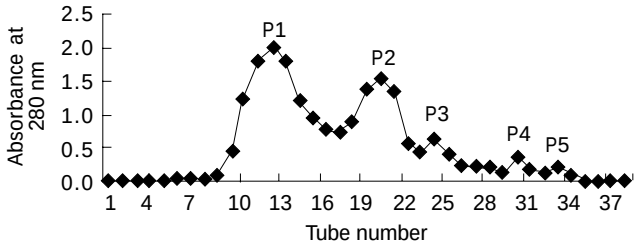


Figure 3 Chromatography of soybean conglycinin hydrolysates on sephadex-G15. Bed size, 1.0 cmx100 cm, flow rate 15 mL/h, absorbance at 280 nm.

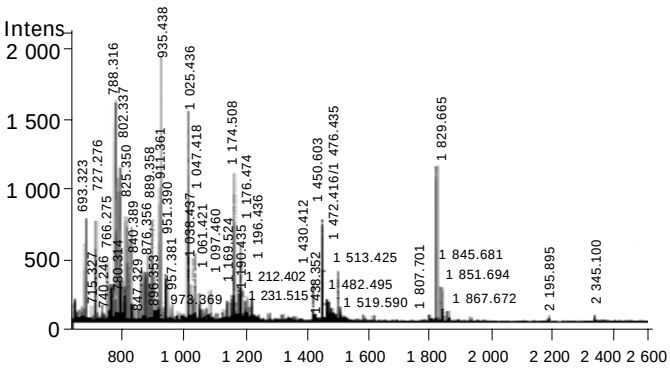


Figure 4 MALDI-TOF-MS analysis of fraction P2.

Table 2 Growth-stimulating activity of the isolated fractions from pepsin-treated conglycinin on bifidobacteria (n = 9)

	Control	P1	P2	P3	P4	P5	PTC	Conglycinin	HCl-FHC
$A_{460\,nm}$	0.35±0.05	0.38±0.05	0.50±0.10[a]	0.45±0.09[a]	0.33±0.08	0.36±0.07	0.42±0.06	0.37±0.05	0.36±0.08

Values are expressed as the mean±SD, [a]P<0.05 *vs* control group.

Effect of conglycinin peptides on serum IL-2 levels and sIgA concentrations of small intestine in mice

Serum IL-2 levels and small intestine sIgA concentrations are presented in Table 3. Level of sIgA in P2-PTC group was higher than that in control group (P<0.05) and HCl-FHC group (P<0.01). The level of serum IL-2 showed no significant difference among the five treated groups.

F-6-PPK activities in cecal contents

The detection of F-6-PPK was considered to be the most reliable indicator that the bacteria belong to the genus *Bifidobacterium*[15]. The results in Table 4 showed that the enzyme F-6-PPK was detected in all samples. Activities of F-6-PPK in the PTC and P2-PTC groups were significantly higher than that in the control group (P<0.01) and HCl-FHC group.

β-galactosidase activities in cecal contents

Compared with control group, β-galactosidase activities in cecal contents of P2-PTC group were significantly increased by 42.2% (1.82±0.58 U/g *vs* 1.28±0.23 U/g, P<0.05). The β-galactosidase activities of conglycinin group were significantly lower than that in P2-PTC group (1.27±0.34 U/g *vs* 1.82±0.58 U/g, P<0.05). But no significant difference was found between P2-PTC and PTC groups, and between P2-PTC and HCl-FHC group (1.82±0.58 U/g *vs* 1.43±0.38 U/g, 1.82±0.58 U/g *vs* 1.30±0.47 U/g, P>0.05) .The result is shown in Figure 5.

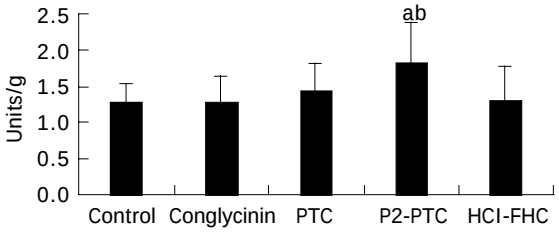


Figure 5 Effect of conglycinin peptides on β-galactosidase activities in cecal contents (n = 8). Values are expressed as the mean±SD, [a]P<0.05 *vs* control group, [b]P<0.01 *vs* conglycinin group.

Bacterial concentrations and cecal pH

As shown in Table 5, compared with control, cecal pH level and the population of *Enterococci* in P2-PTC group were significantly decreased (P<0.05).

DISCUSSION

In recent years, modification of the human intestinal microbiota has become an important objective of dietetics[16]. This goal can be achieved in two ways: (1) administration of beneficial bacteria with the expectation that they will be able to colonize the intestinal tract; (2) providing prebiotics, which have shown an ability to promote the growth of desirable bacteria[17-19]. Bifidobacteria are part of the beneficial microbiota of the human intestine[20], and they are considered to be important in maintaining intestinal microbiota balance [21]. Therefore, many attempts have been made to increase the number of bifidobacteria in the intestine.

Soybean proteins and their derived foods have been consumed for a long time in the diets of the people in China and other Asian countries. The health promoting properties of soybean proteins have been accepted worldwide. Peptides derived from soybean proteins with short lengths, produced during *in vitro* and *in vivo* digestion, are considered to have pharmacological and physiological activities[22]. However, the effect of conglycinin peptides on growth of bifidobacteria had not been reported yet. In this study, we used pepsin to hydrolyze the conglycinin *in vitro* and results demonstrated that conglycinin was a good raw material for enzyme-mediated production of growth-stimulating peptides for bifidobacteria. The peptides, which were obtained as a consequence of screening for highly active growth stimulators during the separation, were highly hydrophilic and comprised of 6-10 amino acid residues, and these peptides were inactive within the sequence of the parent protein, but could be released during enzymatic hydrolysis. Compared with the HCl-full hydrolysis of conglycinin, the results also indicated that the function of conglycinin peptides was not nutritional but it had physiological properties. Different enzymes in the gastrointestinal tract have different effects on various kinds

Table 3 Effect of conglycinin peptides on levels of serum IL-2 and small intestinal sIgA in mice (n = 8)

Group	Control	Conglycinin	PTC	P2-PTC	HCl-FHC
sIgA (ng/g)	118.27±33.93	133.17±36.15	139.01±32.65	172.08±35.40[ab]	104.43±30.75
IL-2 (ng/mL)	0.602±0.255	0.445±0.112	0.602±0.351	0.693±0.305	0.618±0.141

Values are expressed as the mean±SD, [a]P<0.05 *vs* control group, [b]P<0.01 *vs* HCl-FHC group.

Table 4 F-6-PPK activities in cecal contents (n = 8)

Group	Control	Conglycinin	PTC	P2-PTC	HCl-FHC
$A_{505\,nm}$	0.19±0.03	0.36±0.06[ac]	0.56±0.08[bd]	0.44±0.12[bd]	0.22±0.10

Values are expressed as mean±SD, [a]P<0.05, [b]P<0.01 *vs* control group, [c]P<0.05, [d]P<0.01 *vs* HCl-FHC group.

Table 5 Effect of conglycinin peptides on pH and total number of *enterococci* and *E.coli of cecum* in mice (n = 8)

Group	Control	Conglycinin	PTC	P2-PTC	HCL-FHC
pH	7.21±0.09	7.19±0.06	7.17±0.09	7.08±0.08[a]	7.18±0.09
E.coli $\log_{10}$CFU/g	6.32±0.34	6.21±0.5	6.19±0.16	6.14±0.22	6.27±0.30
Enterococci $\log_{10}$CFU/g	5.78±0.19	5.55±0.29	5.42±0.37	5.38±0.26[a]	5.66±0.14

Values are expressed as the mean±SD, [a]P<0.05 *vs* control group.

of foods, which contain numerous sorts of protein. The process above may release prolific bioactive peptides, which have physiological and metabolic programming function on the body.

In conjunction with *in vitro* studies, pepsin-treated conglycinin was administered to mice in an effort to determine the effects of these peptides on intestinal ecosystem. The results showed that administering these peptides could significantly increase β-galactosidase enzyme activity. It had been reported that the increase in galatosidase was presumably a consequence of elevated numbers of bifidobacteria, which have high levels of this enzyme[13]. This suggests that conglycinin peptides could induce the change of bifidobacteria in the intestine. From our results, conglycinin peptides could lower cecal pH markedly and decrease the population of *E.coli*. We also observed that conglycinin peptides decreased the population of *enterococci*, which not only appears to share the main characteristics of lactic acid bacteria (LAB), but also comprises pathogenic species. *Enterococci* show an extensive range of resistance to various antibiotics, and the evolution of its virulence has been documented[23]. In the present study, the result indicated that conglycinin peptides did not promote the growth of all species of LAB, especially pathogenic species. It had been reported that bifidobacteria could prevent colonization of pathogens in gastrointestinal tract by lowering gut pH, and have health-promoting effects such as enhancement of immune system[24,25]. Gibson *et al*.[26] suggested that the higher bifidobacteria population, detrimental to other anaerobic bacteria species, may lead to changes in the microbial ecology of the colon. The accepted mechanism that bifidobacteria are inhibitory is related to the higher production of acetic and lactic acids. Increased acid production resulted in a lower pH which prevented enteric colonization of potentially pathogenic microorganisms and growth of putrefactive bacteria[27]. Furthermore, bifidobacteria stimulate immune function. There is considerable evidence from animal studies that probiotic organisms could modulate the mucosal and systemic immune systems[28]. This stimulation of host immunity is thought to relate to the ability of microorganisms to adhere to intestinal cells and interact with the gut-associated lymphoid tissue (GALT)[29,30]. This ability can increase immunoglobulin output into the intestinal lumen [31-33]. sIgA is one of the principal factors preventing bacterial translocation, which can result in sepsis and death of the host. The classic view is that sIgA exerts its effect by aggregating bacteria, thereby mediating clearance of those bacteria from the gut and preventing invasion of bacteria to the body[34]. Some bifidobacteria strains have recently shown to stimulate sIgA production in intestine[35]. Therefore, bifidobacteria may stimulate active IgA production, thereby reducing infections. Our study also showed that local production of sIgA in the small intestine increased significantly, suggesting that the higher amount of bifidobacteria in the cecum of mice caused by ingestion of conglycinin peptides might produce beneficial effects within the gastrointestinal tract. Thus, the health-promoting effect of conglycinin peptides in human beings may have relationship with bifidobacteria of gastrointestinal tract.

In conclusion, our work placed emphasis on the activity (*in vitro* and *in vivo*), physiological and biochemical properties of the mixture peptides. The proteolysis of soybean conglycinin with the gastrointestinal protease pepsin results in the generation of growth-promoting peptides for bifidobacteria. Using the MALDI-TOF-MASS strategy, we were able to identify several low-molecular-mass peptides responsible for this activity. The digestion of conglycinin represents an important mechanism to obtain peptides which exhibit significant physiological roles in addition to their nutritional importance. Pepsin is an endopeptidase responsible for the hydrolysis of a wide range of proteins, we may infer that the mixture is a group of bioactive peptides that have identical C-terminus or N- terminus. Further characterization of the composition of the conglycinin hydrolysates, elucidation of the relationship between peptide structure and activity awaits future study.

ACKNOWLEDGMENTS

We thank Professor Wei-Yun Zhu of Nanjing Agricultural University and Professor Yu-Zhen Wang of University of Science and Technology of China for their help in this study.

REFERENCES

1 **Maruyama N,** Fukuda T, Saka S, Inui N, Kotoh J, Miyagawa M, Hayashi M, Sawadaa M, Moriyama T, Utsumi S. Molecular and structural analysis of electrophoretic variants of soybean seed storage proteins. *Phytochemistry* 2003; **64**: 701–708
2 **Kuba M,** Tanaka K, Tawata S, Takeda Y, Yasuda M. Angiotensin I-converting enzyme inhibitory peptides isolated from tofuyo fermented soybean food. *Biosci Biotechnol Biochem* 2003; **67**: 1278-1283
3 **Tsuruki T,** Kishi K, Takahashi M, Tanaka M, Matsukawa T, Yoshikawa M. Soymetide, an immunostimulating peptide derived from soybean beta-conglycinin, is an fMLP agonist. *FEBS Lett* 2003; **540**: 206-210
4 **Chen HM,** Muramoto K, Yamauchi F. Structural analysis of antioxidative peptides from Soybean β-conglycinin. *J Agric Food Chem* 1995; **43**: 574-578
5 **Kaur IP,** Chopra K, Saini A. Probiotics: potential pharmaceutical applications. *Eur J Pharm Sci* 2002; **15**: 1–9
6 **Arunachalam KD.** Role of Bifidobacteria in nutrition, medicine and technology. *Nutrition Research* 1999; **19**: 1559-1597
7 **Gomes AM,** Malcata FX, Klaver FA. Growth enhancement of Bifidobacterium lactis Bo and Lactobacillus acidophilus Ki by milk hydrolyzates. *J Dairy Sci* 1998; **81**: 2817-2825
8 **Liepke C,** Adermann K, Raida M, Magert HJ, Forssmann

WG, Zucht HD. Human milk provides peptides highly stimulating the growth of bifidobacteria. *Eur J Biochem* 2002; **269**: 712-718
9 **Iwabuchi S,** Yamauchi F. Determination of Glycinin and β-conglycinin in soybean proteins by Immunological methods. *J Agric Food Chem* 1987; **35**: 200-205
10 **Lovati MR,** Mnzoni C, Corsini A, Fumagalli R, Sirtori CR. 7S globulin from soybean is metabolized in human cell cultures by a specific uptake and degradation system. *J Nutr* 1996; **126**: 2871-2873
11 **Laemmli UK.** Cleavage of structural proteins during the assembly of the head of bacteriophage T4. *Nature* 1970; **227**: 680-685
12 **Hassinen JB,** Durbin GT, Tomarelli RM. The minimal nutritional requirements of *Lactobacillus Bifidus*. *J Bacteriol* 1951; **62**: 771-777
13 **Orban JI,** Patterson JA. Modification of the phosphoketolase assay for rapid identification of bifidobacteria. *J Microbiol Methods* 2000; **40**: 221–224
14 **Brigidi P,** Vitali B, Swennen E, Bazzocchi G, Matteuzzi D. Effects of probiotic administration upon the composition and enzymatic activity of human fecal microbiota in patients with irritable bowel syndrome or functional diarrhea. *Res Microbiol* 2001; **152**: 735-741
15 **Gavini F,** Van Esbroeck M, Touzel JP, Fourment A, Goossens H. Detection of Fructose-6-phosphate Phosphoketolase (F6PPK), a Key Enzyme of the Bifid-Shunt, in *Gardnerella vaginalis*. *Anaerobe* 1996; **2**: 191-193
16 **Ziemer CJ,** Gibson GR. An overview of probiotics, prebiotics and synbiotics in the functional food concept: perspectives and future strategies. *Int Dairy J* 1998; **8**: 473-479
17 **Saarela M,** Lahteenmaki L, Crittenden R, Salminen S, Mattila-Sandholm T. Gut bacteria and health foods--the European perspective. *Int J Food Microbiol* 2002; **78**: 99-117
18 **Sullivan A,** Nord CE. The place of probiotics in human intestinal infections. *Int J Antimicrob Agents* 2002; **20**: 313-319
19 **Zubillaga M,** Weill R, Postaire E, Goldman C, Caro R, Boccio J. Effect of probiotics and functional foods and their use in different diseases. *Nutrition Res* 2001; **21**: 569–579
20 **Favier CF,** Vaughan EE, De Vos WM, Akkermans ADL. Molecular monitoring of succession of bacterial communities in human neonates. *Appl Environ Microbiol* 2002; **68**: 219-226
21 **O'Sullivan D,** Kullen MJ. Tracking of probiotic bifidobacteria in the intestine. *Int Dairy J* 1998; **8**: 513-525
22 **Liu K.** Expanding soybean food utilization. *Food Technol* 2000; **54**: 46-58
23 **Aguirre M,** Collins MD. Lactic acid bacteria and human clinical infection. *J Appl Bacterial* 1993; **75**: 95-107
24 **Tuohy KM,** Probert HM, Smejkal CW, Gibson GR. Using probiotics and prebiotics to improve gut health. *DDT* 2003; **8**: 692-700
25 **McNaught CE,** MacFie J. Probiotics in clinical practice: a critical reviewof the evidence. *Nutrition Res* 2001; **21**: 343–353
26 **Gibson GR ,** Wang X. Regulatory effects of bifidobacteria on the growth of other colonic bacteria. *J Appl Bacteriol* 1994; **77**: 412-420
27 **Servin AL.** Antagonistic activities of Lactobacilli and bifidobacteria against microbial pathogens. *FEMS Microbiol Rev* 2004; **28**: 405-440
28 **Meydani SN,** Ha WK. Immunological effects of yoghurt. *Am J Clin Nutr* 2000; **71**: 861-872
29 **McGhee JR,** Mestecky J, Dertzbaugh MT, Eldridge JH, Hirasawa M, Kiyono H. The mucosal immune system: from fundamental concepts to vaccine development. *Vaccine* 1992; **10**: 75-88
30 **Herias MV,** Hessle C, Telemo E, Midtvedt T, Hanson LA, Wold AE. Immunomodulatory effects of Lactobacillus plantarum colonizing the intestine ofgnotobiotic rats. *Clin Exp Immunol* 1999; **116**: 283-290
31 **Fukushima Y,** Kawata Y, Mizumachi K, Kurisaki J, Mitsuoka T. Effect of bifidobacteria feeding on fecal flora and production of immunoglobulins in lactating mouse. *International J Food Microbiol* 1999; **46**: 193-197
32 **Gorbach SL.** Probiotics and gastrointestinal health. *Am J Gastroenterol* 2000; **95**: S2-S4
33 **Vitini E,** Alvarez S, Medina M, Medici M, de Budeguer MV, Perdigon G. Gut mucosal immunostimulation by lactic acid bacteria. *Biocell* 2000; **24**: 223-232
34 **Everetta ML,** Palestranta D, Millerb SE, Bollingera RR, Parkera W. Immune exclusion and immune inclusion: A new model of host-bacterial interactions in the gut. *Clin Applied Immunol Rev* 2004; **4**: 321-332
35 **Xiang MJ,** Ni YX, Li YZ, Yu SC. The effect of drinking living Bifidobacterial juice on intestinal bacteria floral and SIgA. *Shanghai Dier Yike Daxue Xuebao* 1996; **15**: 220-221

Science Editor Zhu LH and Guo SY **Language Editor** Elsevier HK

PO Box 2345, Beijing 100023, China
www.wjgnet.com
wjg@wjgnet.com

ELSEVIER

World J Gastroenterol 2005;11(37):5807-5810
World Journal of Gastroenterology ISSN 1007-9327
© 2005 The WJG Press and Elsevier Inc. All rights reserved.

•*Basic Research*•

Mesenchymal hamartoma of liver: Magnetic resonance imaging and histopathologic correlation

Bin-BinYe, Bing Hu, Li-Jun Wang, Hong-Sheng Liu, Yan Zou, Yu-Bin Zhou, Zhuang Kang

Bin-Bin Ye, Department of Radiology, No.1 Affiliated Hospital of Sun Yat-Sen University, Guangzhou 510080, Guangdong Province, China
Bing Hu , Li-Jun Wang ,Hong-Sheng Liu, Yan Zou, Yu-Bin Zhou, Zhuang Kang, Department of radiology, No.3 Affiliated Hospital of Sun Yat-Sen University, Guangzhou 510630 ,Guangdong Province, China
Correspondence to: Professor Bin-Bin Ye, Department of Radiology, No.1 Affiliated Hospital of Sun Yat-Sen University, Guangzhou 510080, Guangdong Province, China. zhj-ybb@163.com
Telephone: +86-20-87332200-8849 Fax: +86-20-87615805
Received:2005-01-14 Accepted:2005-04-02

Abstract

AIM: To describe the imaging features of hepatic mesenchymal hamartoma with emphasis on magnetic resonance imaging (MRI) compared to histopathologic results.

METHODS: Spin-echo sequence(SE),fast spin-echo sequence(FSE) were performed in 12 children (7 males,5 females) with mesenchymal hamartoma of the liver (MHL), aged 1.2 months to 12 years;(mean age, 6.3 years) axial, saggital, coronary plain imaging with an Elscint 2.0T MR equipment. Their main symptoms were abdominal mass (5 cases), enlarged liver (8 cases), abdominal pain (1 case) and anemia (2 cases), and negative alphafetoprotein. Dynamic enhancement examination was added in 2 cases.

RESULTS: Six cases had single mass type of MHL, in which 3 cases had solid masses showing slight low-signal-intensity in T1WI, and irregular high-signal-intensity in T2WI, 1 case had a cystic-solid mixed mass showing several border-clear cysts in a solid mass, 2 cases had cystic masses with multi-septa. Five cases had diffuse and multifocal lesions type of MHL with its signal intensity being similar to that of the solid mass. One case had a combined diffuse and single cystic mass. In the early dynamic enhancement examination, the lesions were slightly circum-enhanced , and the center was enhanced in the later scan images. Inner hepatic vessels were compressed in 5 cases, vena cava and abdominal aortae were compressed in 3 cases. Pathological findings included fiber hyperplasia, hyaline degeneration, biliary duct hyperplasia, lobule-like array.

CONCLUSION: MR imaging is a better way to differentiate and diagnose MHL. MHL may be recognized by its characteristic occurrence in infancy and MR imaging features.

© 2005 The WJG Press and Elsevier Inc. All rights reserved.

Key words: Hepatic mesenchymal hamartoma; Magnetic resonance imaging; Histopathologic correlation; Children

Ye BB, Hu B, Wang LJ, Liu HS, Zou Y, Zhou YB, Kang Z. Mesenchymal hamartoma of liver: Magnetic resonance imaging and histopathologic correlation.*World J Gastroenterol* 2005; 11(37): 5807-5810
http://www.wjgnet.com/1007-9327/11/5807.asp

INTRODUCTION

Mesenchymal hamartoma of the liver (MHL) is one of the rare hepatic benign tumors in children, which was first reported by Edmanson in 1956. It is usually present under 5 years of age, mostly under 2 years of age. One hundred and fifty cases of MHL are reported in English, 30 cases in Japanese, 21 cases in Chinese[1-3]. A few reports have discussed the X-ray, ultrasound and CT characteristics of MHL [5-9]. MHL is often misdiagnosed as other pathological lesions, because of its diversified image characteristics. MR has been widely used in the diagnosis of MHL . We have reviewed 12 MHL cases with MR scan in our hospital since 1996. The MR imaging features can help recognize and diagnose MHL.

MATERIALS AND METHODS

Twelve children with MHL (7 males and 5 females) were reviewed from January 1996 to 2002.They aged 1.2 months to 12 years with a mean age of 6.3 years.Their Clinical manifestations are list in Table 1.

MR imaging was performed with an Elscint 2.0T MR equipment. Patient was on his back, and chloral hydrate lysis was performed before scan. Spin-echo sequence (SE), fast spin-echo sequence (FSE) were performed with body coil. For T1-weighted MR imaging, the repetition time (TR) was 500 ms and the echo time (TE) was 15 ms. For T2-weighted imaging, the TR was 2500–3000 ms and the TE was 96 ms. Routine axial and coronary scan was performed 1-2 times. Dynamic enhancement examination was added in 2 cases, and CT scan was performed in 2 cases.

RESULTS

The pathologic types of MHL are showed in Table 2. The

Table 1 Clinical manifestations of 12 cases

Age	Cases	Gender		Clinical manifestations				
		Male	Female	Abdominal mass	Mega-liver	Abdominal pain	Anemia	Alphafetoprotein negative
1 mo¬12 mo	3	2	1	1	3			3
1 yr–2 yr	6	4	2	3	3		1	6
3 yr–4 yr	2	1	1	1	1	1		2
12 yr	1		1		1		1	1

Table 2 Pathologic types of MHL in 12 cases

	Cases	Hepatic lobes		Pathologic types		
		Right	Left	Solid	Cystic	Mixed cystic-solid
Single	6	5	2	3	2	1
Diffuse and multifocal	5	5	5	5		
Diffuse and single combined	1	1	1			1

envelopes of most masses were intact in general. Sections of the solid type mass were white and tough. The fluid in the cystic type was clear or turbid and pale yellow or coffee-like.

Fiber hyperplasia, hyaline degeneration, biliary duct hyperplasia and lobule-like array were seen. Lymphatic dilation was observed in a few cases. In crystic type, simple pavement epithelium or bile duct epithelium was seen at the inner layer of the cystic wall. The cyst contained fluid or gelatinoids. The separates consisted of mesenchyme and fibrostroma. In solid type, fibroadenoid structure consisting of remarkable hyperplastic biliary duct and fibrosis around it was seen. There were compacted hepatic tissues between the masses.

MRI finding in MHL

Single focal type of MHL was found in right hepatic lobe of 5 cases, in left hepatic lobe of 1 case with a big size and a clear border. The biggest one involved both lobes, with its diameter being 28 cm. Solid, cystic and mixed cystic-solid subtypes were classified based on the pathologic examination. In all lesions of solid subtype (n=3), MR images showed a slightly low signal intensity on T1-weighted images, an irregular high signal intensity on T2-

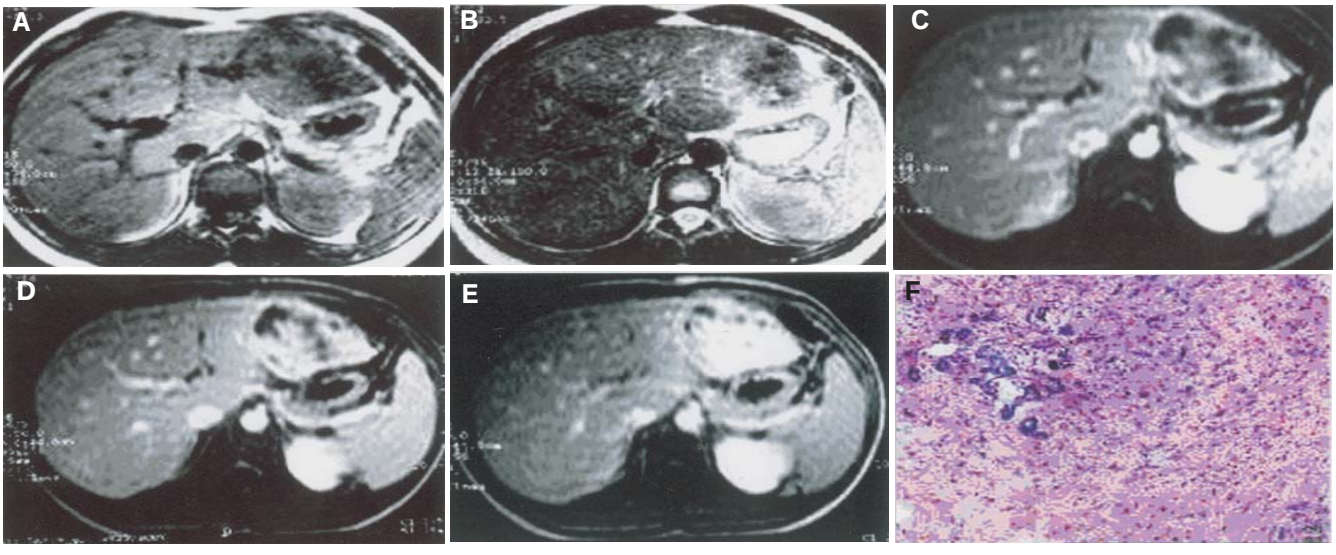


Figure 1 solid chief dingle mass type of MHL on T1WI(**A**), T2WI(**B**), and dynamic enhancement in artery phase(**C**), portal rein phase(**D**), and latency phase(**E**), and its pathologic lesions(**F**).

weighted images, and a higher signal intensity area inside. After intravenous administration of a gadolinium-based contrast agent, the lesions demonstrated mild annular enhancement in artery phase, moderate enhancement in portal phase, magnificent enhancement in delay phase (Figure 1). In the lesion of mixed cystic-solid subtype (n=1), MR images showed a slightly low signal intensity on T1-weighted images, a slightly high signal intensity on T2-weighted images. There were several cystic foci with varying sizes and clear borders. The gallbladder-like signal intensity was scattered or congregated, but not syncretized (Figure 2).

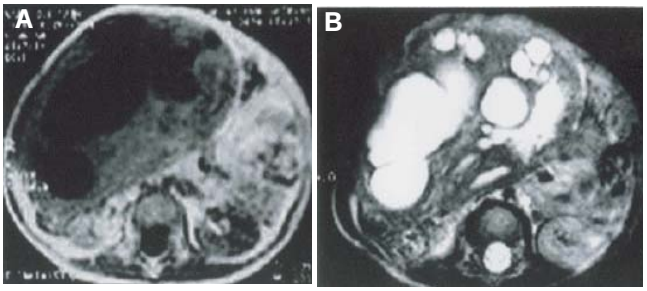


Figure 2 mixed cystic-solid single mass type of MHL on T1WI(**A**) and T2WI(**B**).

In the lesions of cystic subtype (n=2), MR images showed multi-cyst foci with varying sizes and thickness, low or normal signal intensity on T1-weighted images, high signal intensity on T2-weighted images, and varying signal intensity in different cysts, fluid-fluid plane in some cysts (Figure 3).

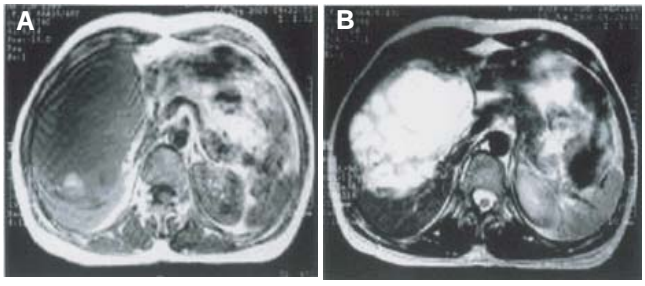


Figure 3 cystic single mass type of MHL on T1WI(**A**), T2WI(**B**).

Diffuse and multifocal type of MHL was found in 4 case. MR images showed enlarged liver with smooth border, multiple foci with slightly low signal intensity on T1-weighted images, slightly high signal intensity on T2-weighted images. After intravenous administration of a gadolinium-based contrast agent, the lesions demonstrated annular enhancement in artery phase, no enhancement in early stage, enhancement in delay phase. In 1 case, MR images showed multifocal masses in the liver, slightly low and normal signal intensity on T1-weighted images, very high signal intensity on T2-weighted images. The cotton-like masses with clear borders, did not syncretize each other (Figure 4).

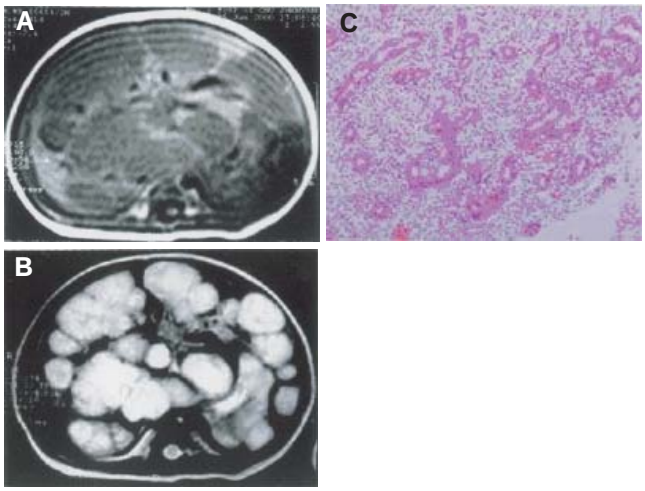


Figure 4 Diffuse and multifocal type of MHL on T1WI(**A**), T2WI(**B**) and Pathologic picture(**C**).

Combined diffuse and single type was found in 1 case. MR images showed big isolate multi-loculus cystic foci in the diffuse tubers, fluid-fluid plane in some cysts (Figure 5).

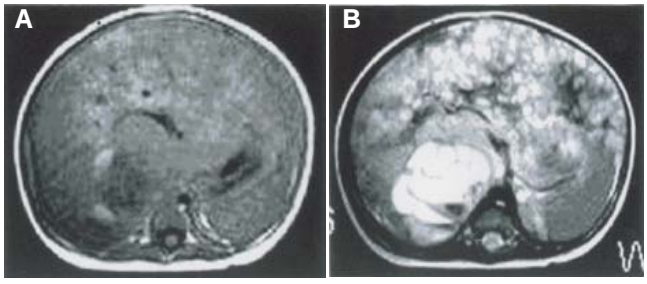


Figure 5 Diffuse and single combined type of MHL on T1WI(**A**) and T2WI(**B**).

The CT finding in MHL

In the multifocal type, CT images showed enlarged liver, multifocal low density foci of varying sizes from 1 cm × 1 cm to 2 cm×3 cm, lower density in the center. In the single focal type, CT images showed low density focus round in shape with a clear border.

Relationship between lesions and vessels

Inner hepatic vessels were compressed in 5 cases, vena cava and abdominal aortae were compressed in 3 cases. No portal vein was compressed in all the 12 cases.

DISCUSSION

MHL is a rare hepatic benign tumor, occurring most in children and rarely in adults [4]. MHL in fetus has also been reported [1].

Pathologensis

The exact pathologenesis is not clear. It has been reported that MHL is a kind of developmental deformity or the result of abnormal reaction procedure [8]. The abnormality appears in the late stage of embryo formation that grows along the portal vein system and surrounds the hepatic tissue island when the liver maintains lobular structure connecting to bile duct tree [7]. It was reported that MHL comes from the local area of bile duct atresia, inducing obstruction of distant bile ducts and necrosis of hepatic cells [5]. Some studies showed that MHL correlates with the developmental deformity of vessels and the rupture of 19q13.4 [12,13]. It was reported consider that most of MHL are diploid, but the set of chromosomes of MHL prompt that MHL is not the developmental deformity or the result of abnormal reaction procedure[7,12].

Clinical manifestations

MHL has no special clinical manifestations. The most common symptom is abdominal mass or enlarged liver. The mass increases rapidly in specific cases, leading to inappetence, obvious dyspnoea or obvious obstruction of inferior vena cava. Other symptoms are fever, vomit, constipation, diarrhea and weight loss [6]. Malnutrition, anemia and cachexia are occasionally found . AFP is normal. Some reports indicates that AFP increases in the infancy under 4 month [1]. Surgical operation is the best choice of treatment.

Radiologic finding

Solid type of MHL may have a single focus or multiple foci. In our study MHL was located at right lobe of liver in 5 of 6 cases of solid type, being consistant with other reports [6,8]. In the solid part of MHL, there were remarkably proliferated bile ducts and fibrosis around them to form fibroglandular structure. In 1 multifocal solid MHL, there was fluid retention in mesenchymal tissue (Figure 4). The higher the protein content in the fluid, the higher the signal intensity on T1-weighted images. Some studies showed that the solid part of MHL is formed during perinatal period. The mass enlarges rapidly, because of mesenchyme cystic degeneration with fluid retardation, obstruction and dilation of lymph duct or both [8]. With the growth of MHL, the cystic area in the mass enlarges significantly, taking up greater part of the lesion, because of mesenchyme atrophy, bile duct dilation, lympha retardation. Therefore, the lesion may be solid-cystic type or cystic type, which may be the pathological basis of it (Figure 3). There is no blood supply for MHL[6,8]. The masses shift the vessels in angiography. The septa are thick when there are more solid contents. There are areas surrounded by tumor vessels with no blood supply. Enhanced CT images can show cord-like enhancement [3]. We consider that the lesions with no blood supply may be cystic type, the lesions with less blood supply may be solid type. The part of annular enhancement may compress the hepatic tissue around the lesions. Intrahepatic vessels, inferior vena cava, abdominal aorta and other organs are compressed and shifted by huge MHL masses [1] with blood vessels or peripheral tissues invaded. Calcification is seldom found in MHL, but septum calcification is reported [9].

Treatment and prognosis

MHL seldom cancerates, but canceration can be found in specific cases [10]. In this research, no case was cancerated. Surgical operation is the best choice to treatment. MHL seldom relapses, and its prognosis is good. Surgery should be executed after diagnosis.

Differential diagnosis

Due to the different imagings of MHL, it should be differentiated from hepatic abscess, metastasis, caroli's disease, undifferentiated embryo sarcoma of the liver and hepatoblastoma. In conclusion, MR imaging is a better way to differentiate and diagnose MHL. MHL may be recognized by its characteristic occurrence in infancy and MR imaging features.

REFERENCES

1 **Kamata S,** Nose K, Sawai T, Hasegawa T, Kuroda S, Sasaki T, Okada A, Tawara M. Fetal mesenchymal hamartoma of the liver: report of a case. *J Pediatr Surg* 2003; **38:** 639-641

2 **Yen JB,** Kong MS, Lin JN. Hepatic mesenchymal hamartoma. *J Paediatr Child Health* 2003 ; **39:** 632-634

3 **Gornicka B,** Ziarkiewicz-Wroblewska B, Wroblewski T, Koperski L, Pawlak J, Nyckowski P, Krawczyk M, Zimmermann A, Wasiutynski A. Myoid hamartoma of the liver - a novel variant of hamartoma developing in the hilar region and imitating a malignant liver tumor. *Med Sci Monit* 2004; **10:** 23-26

4 **Cook JR,** Pfeifer JD, Dehner LP. Mesenchymal hamartoma of the liver in the adult: association with distinct clinical feature and histological changes. *Hum Pathol* 2002; **33:** 893-898

5 **Wholey MH,** Wojno KJ. Pediatric hepatic mesenchymal hamartoma demonstrated on plain film, ultrasound and MRI, and correlated with pathology. *Pediatr Radiol* 1994; **24:** 143-144

6 **Ros PR,** Goodman ZD, Ishak KG, Dachman AH, Olmsted WW, Hartman DS, Lichtenstein JE. Mesenchymal hamartoma of the liver: radiologic-pathologic correlation. *Radiology* 1986; **158:** 619-624

7 **DeMaioribus CA,** Lally KP, Sim K, Isaacs H, MahourGH Mesenchymal hamartoma of the liver. A 35-year review.*Arch Surg* 1990; **125:** 598-600

8 **Brunt EM.** Benign tumors of the liver. *Clin Liver Dis* 2001; **5:** 1-15,

9 **Konez O,** Goyal M, Vyas PK, Boinapally SB. Mesenchymal hamartoma of the liver. *Comput Med Imaging Graph* 2001; **25:** 61-65

10 **Ramanujam TM,** Ramesh JC, Goh DW, Wong KT, Ariffin WA, Kumar G, Taib NA. Malignant transformation of mesenchymal hamartoma of the liver: case report and review of the literature. *J Pediatr Surg* 1999; **34:** 1684-1686

11 **Otal TM,** Hendricks JB, Pharis P, Donnelly WH. Mesenchymal hamartoma of the liver. DNA flow cytometric analysis of eight cases. *Cancer* 1994; **74:** 1237-1242

12 **Bove KE,** Blough RI, Soukup S. Third report of t(19q)(13.4) in mesenchymal hamartoma of liver with comments on link to embryonal sarcoma. *Pediatr Dev Pathol* 1998; **1:** 438-442

13 **Mascarello JT,** Krous HF. second report of a translocatio involving 19q13,4 in a mesenchymal hamartoma of the liver. *Cancer Genetics and Cytogenetics* 1992; **58:** 141-142

Science Editor Guo SY **Language Editor** Elsevier HK

<ASCII-WIN>
<Version:4><FeatureSet:InDesign-Roman><ColorTable:=<Black:COLOR:CMYK:Process:0,0,0,1>>
<DefineParaStyle:<0x4E00><0x7EA7><0x6807><0x9898><0x6B63><0x6587>=<Nextstyle:<0x4E00><0x7EA7><0x6807><0x9898><0x6B63><0x6587>><cSize:10.500000><pHyphenationLadderLimit:0><pAutoLeadPercent:1.500000><cLeading:12.000000><pHyphenationZone:34.000000><cFont:Garamond><pMaxWordSpace:1.500000><pMinWordSpace:0.750000><pMaxLetterspace:0.250000><pMinLetterspace:-0.050000><pKeepFirstNLines:1><pKeepLastNLines:1><pRuleAboveColor:Black><pRuleAboveStroke:1.000000><pRuleAboveTint:100.000000><pRuleBelowColor:Black><pRuleBelowStroke:1.000000><pRuleBelowTint:100.000000><pRuleAboveOverprint:1><pRuleBelowOverprint:1><pKinsokuTable:Hard>>
<DefineParaStyle:<0x4E8C><0x7EA7><0x6807><0x9898>=<Nextstyle:<0x4E8C><0x7EA7><0x6807><0x9898>><cTypeface:Bold Italic><cSize:10.500000><pHyphenationLadderLimit:0><pAutoLeadPercent:1.500000><cLeading:12.500000><pHyphenationZone:34.000000><cFont:Arial Narrow><pMaxWordSpace:1.500000><pMinWordSpace:0.750000><pMaxLetterspace:0.250000><pMinLetterspace:-0.050000><pKeepFirstNLines:1><pKeepLastNLines:1><pRuleAboveColor:Black><pRuleAboveStroke:1.000000><pRuleAboveTint:100.000000><pRuleBelowColor:Black><pRuleBelowStroke:1.000000><pRuleBelowTint:100.000000><pRuleAboveOverprint:1><pRuleBelowOverprint:1><pKinsokuTable:Hard>>
<DefineParaStyle:<0x53C2><0x8003><0x6587><0x732E><0x6B63><0x6587>=<Nextstyle:<0x53C2><0x8003><0x6587><0x732E><0x6B63><0x6587>><cSize:8.000000><pHyphenationLadderLimit:0><pLeftIndent:18.000000><pFirstLineIndent:-18.000000><pAutoLeadPercent:1.500000><cLeading:10.000000><pHyphenationZone:34.000000><pTabRuler:18\,Left\,.\,0\,\;><cFont:Book Antiqua><pMaxWordSpace:1.500000><pMinWordSpace:0.750000><pMaxLetterspace:0.250000><pMinLetterspace:-0.050000><pKeepFirstNLines:1><pKeepLastNLines:1><pRuleAboveColor:Black><pRuleAboveStroke:1.000000><pRuleAboveTint:100.000000><pRuleBelowColor:Black><pRuleBelowStroke:1.000000><pRuleBelowTint:100.000000><pRuleAboveOverprint:1><pRuleBelowOverprint:1><pKinsokuTable:Hard>>
<ParaStyle:><cSize:14.000000><cTracking:50><cFont:FZCuYuan-M03S>INTRODUCTION<cSize:><cTracking:><cFont:><cSize:11.000000><cFont:AvantGarde Md BT>
<cSize:><cFont:><ParaStyle:<0x4E00><0x7EA7><0x6807><0x9898><0x6B63><0x6587>><cLeading:11.900000>Mesenchymal hamartoma of the liver (MHL) is one of the rare hepatic benign tumors in children, which was first reported by Edmanson in 1956. It is usually present under 5 years of age, mostly under 2 years of age. One hundred and fifty cases of MHL are reported in Britain, 30 cases in Japan, 21 cases in China<cLeading:><cLeading:11.900000><cPosition:Superscript>[1-3]<cLeading:><cPosition:><cLeading:11.900000>. A few reports have discussed the X-ray, ultrasound and CT characteristics of MHL <cLeading:><cLeading:11.900000><cPosition:Superscript>[5-9]<cLeading:><cPosition:><cLeading:11.900000>. MHL is often misdiagnosed as other pathological lesions, because of its diversified image characteristics. MR has been widely used in the diagnosis of MHL . We have reviewed 12 MHL cases with MR scan in our hospital since 1996. The MR imaging features can help recognize and diagnose MHL.
<cLeading:><ParaStyle:<0x4E00><0x7EA7><0x6807><0x9898><0x6B63><0x6587>><cLeading:11.900000>
<cLeading:><ParaStyle:<0x4E00><0x7EA7><0x6807><0x9898><0x6B63><0x6587>><cSize:14.000000><cTracking:25><cLeading:11.900000><cFont:FZCuYuan-M03S>MATERIALS AND METHODS<cSize:><cTracking:><cLeading:><cFont:><cSize:11.000000><cLeading:11.900000><cFont:AvantGarde Md BT>
<cSize:><cLeading:><cFont:><ParaStyle:<0x4E00><0x7EA7><0x6807><0x9898><0x6B63><0x6587>><cLeading:11.900000>Twelve children with MHL (7 males and 5 females) were reviewed from January 1996 to 2002.They aged 1.2 months to 12 years with a mean age of 6.3 years.Their clinical manifestations are listed in Table 1.
<cLeading:><ParaStyle:<0x4E00><0x7EA7><0x6807><0x9898><0x6B63><0x6587>><pFirstLineIndent:14.173228><cLeading:11.900000>MR imaging was performed with an Elscint 2.0T MR equipment. Patient was on his back, and chloral hydrate lysis was performed before scaning. Spin-echo sequence (SE) and fast spin-echo sequence (FSE) were performed with body coil. For T1-weighted MR imaging, the repetition time (TR) was 500 ms and the echo time (TE) was 15 ms. For T2-weighted imaging, the TR was 2500<0x2013>3000 ms and the TE was 96 ms. Routine axial and coronary scan was performed 1-2 times. Dynamic enhancement examination was added in 2 cases, and CT scan was performed in 2 cases.

<cLeading:><pFirstLineIndent:><ParaStyle:><cSize:10.500000><cLeading:11.900000><cFont:Garamond>
<cSize:><cLeading:><cFont:><ParaStyle:><cSize:14.000000><cTracking:25><cFont:FZCuYuan-M03S>RESULTS<cSize:><cTracking:><cFont:>
<ParaStyle:<0x4E00><0x7EA7><0x6807><0x9898><0x6B63><0x6587>>The pathologic types of MHL are shown in Table 2. The <cLeading:11.900000>envelopes of most masses were intact in general. Sections <cLeading:><ParaStyle:<0x4E00><0x7EA7><0x6807><0x9898><0x6B63><0x6587>><cLeading:11.900000>of the solid type mass were white and tough. The fluid in the cystic type was clear or turbid and pale yellow or coffee-like.
<cLeading:><ParaStyle:<0x4E00><0x7EA7><0x6807><0x9898><0x6B63><0x6587>><pFirstLineIndent:14.173228>
<cLeading:11.900000>Fiber hyperplasia, hyaline degeneration, biliary duct hyperplasia and lobule-like array were seen. Lymphatic <cLeading:><cLeading:11.900000>dilation was observed in a few cases. In crystic type, simple pavement epithelium or bile duct epithelium was seen at the inner layer of the cystic wall. The cyst contained fluid or gelatinoids. The separates consisted of mesenchyme <cLeading:><cTracking:40><cLeading:11.900000>and fibrostroma. In solid type, fibroadenoid structure<cTracking:><cLeading:><cLeading:11.900000> consisting of remarkable hyperplastic biliary duct and <cLeading:><cLeading:11.900000>fibrosis around it was seen. There were compacted hepatic tissues between the masses.
<cLeading:><pFirstLineIndent:><ParaStyle:<0x4E00><0x7EA7><0x6807><0x9898><0x6B63><0x6587>><cLeading:11.900000>
<cLeading:><ParaStyle:<0x4E8C><0x7EA7><0x6807><0x9898>><cLeading:11.900000>MRI finding in MHL
<cLeading:><ParaStyle:<0x4E00><0x7EA7><0x6807><0x9898><0x6B63><0x6587>><cLeading:11.900000>Single focal type of MHL was found in the right hepatic lobe of 5 cases, in the left hepatic lobe of 1 case with a big size and a clear border. The biggest one involved both lobes, with its diameter being 28 cm. Solid, cystic and mixed cystic-solid subtypes were classified based on the pathologic
<cLeading:><cTracking:30>examination.<cTracking:><cTracking:50> In all lesions <cTracking:><cTracking:30>of solid subtype (<cTracking:><cTypeface:Italic><cTracking:30>n<cTypeface:><cTracking:><cTracking:30>=3), MR <cTracking:><ParaStyle:<0x4E00><0x7EA7><0x6807><0x9898><0x6B63><0x6587>>images showed a slightly low signal intensity on T1-weighted images, an irregular high signal intensity on T2-weighted images, and a higher signal intensity area inside. After intravenous administration of a gadolinium-based contrast agent, the lesions demonstrated mild annular enhancement in artery phase, moderate enhancement in portal phase, magnificent enhancement in delay phase (Figure 1). In the lesion of mixed cystic-solid subtype (<cTypeface:Italic>n<cTypeface:>=1), MR images showed a slightly low signal intensity on T1-weighted images, a slightly high signal intensity on T2-weighted images. There were several cystic foci with varying sizes and clear borders. The gallbladder-like signal intensity was scattered or congregated, but not syncretized (Figure 2).
<ParaStyle:<0x4E00><0x7EA7><0x6807><0x9898><0x6B63><0x6587>><pFirstLineIndent:14.173228><cLeading:11.900000>
<cLeading:><pFirstLineIndent:><ParaStyle:<0x4E00><0x7EA7><0x6807><0x9898><0x6B63><0x6587>><pFirstLineIndent:14.173228>
<pFirstLineIndent:><ParaStyle:<0x4E00><0x7EA7><0x6807><0x9898><0x6B63><0x6587>><pFirstLineIndent:14.173228>
<pFirstLineIndent:><ParaStyle:<0x4E00><0x7EA7><0x6807><0x9898><0x6B63><0x6587>><pFirstLineIndent:14.173228>
<pFirstLineIndent:><ParaStyle:<0x4E00><0x7EA7><0x6807><0x9898><0x6B63><0x6587>><pFirstLineIndent:14.173228>
<pFirstLineIndent:><ParaStyle:<0x4E00><0x7EA7><0x6807><0x9898><0x6B63><0x6587>><pFirstLineIndent:14.173228>
<pFirstLineIndent:><ParaStyle:<0x4E00><0x7EA7><0x6807><0x9898><0x6B63><0x6587>><pFirstLineIndent:14.173228>
<pFirstLineIndent:><ParaStyle:<0x4E00><0x7EA7><0x6807><0x9898><0x6B63><0x6587>><pFirstLineIndent:14.173228>
<pFirstLineIndent:><ParaStyle:<0x4E00><0x7EA7><0x6807><0x9898><0x6B63><0x6587>><pFirstLineIndent:14.173228>
<pFirstLineIndent:><ParaStyle:<0x4E00><0x7EA7><0x6807><0x9898><0x6B63><0x6587>><pFirstLineIndent:14.173228>

<pFirstLineIndent:><ParaStyle:<0x4E00><0x7EA7><0x6807><0x9898><0x6B63><0x6587>><pFirstLineIndent:14.173228>
<pFirstLineIndent:><ParaStyle:<0x4E00><0x7EA7><0x6807><0x9898><0x6B63><0x6587>>
<ParaStyle:<0x4E00><0x7EA7><0x6807><0x9898><0x6B63><0x6587>><pFirstLineIndent:14.173228>
<pFirstLineIndent:><ParaStyle:<0x4E00><0x7EA7><0x6807><0x9898><0x6B63><0x6587>><pFirstLineIndent:14.173228>
<pFirstLineIndent:><ParaStyle:<0x4E00><0x7EA7><0x6807><0x9898><0x6B63><0x6587>><pFirstLineIndent:14.173228>
<pFirstLineIndent:><ParaStyle:<0x4E00><0x7EA7><0x6807><0x9898><0x6B63><0x6587>><pFirstLineIndent:14.173228>In the lesions of cystic subtype (<cTypeface:Italic>n<cTypeface:>=2), MR images showed multi-cyst foci with varying sizes and thickness, low or normal signal intensity on T1-weighted images, high signal intensity on T2-weighted images, and varying signal intensity in different cysts, fluid-fluid plane in some cysts (Figure 3).
<pFirstLineIndent:><ParaStyle:<0x4E00><0x7EA7><0x6807><0x9898><0x6B63><0x6587>><pFirstLineIndent:14.173228>
<pFirstLineIndent:><ParaStyle:<0x4E00><0x7EA7><0x6807><0x9898><0x6B63><0x6587>><pFirstLineIndent:14.173228>
<pFirstLineIndent:><ParaStyle:<0x4E00><0x7EA7><0x6807><0x9898><0x6B63><0x6587>><pFirstLineIndent:14.173228>
<pFirstLineIndent:><ParaStyle:<0x4E00><0x7EA7><0x6807><0x9898><0x6B63><0x6587>><pFirstLineIndent:14.173228>
<pFirstLineIndent:><ParaStyle:<0x4E00><0x7EA7><0x6807><0x9898><0x6B63><0x6587>><pFirstLineIndent:14.173228>
<pFirstLineIndent:><ParaStyle:<0x4E00><0x7EA7><0x6807><0x9898><0x6B63><0x6587>><pFirstLineIndent:14.173228>
<pFirstLineIndent:><ParaStyle:<0x4E00><0x7EA7><0x6807><0x9898><0x6B63><0x6587>><pFirstLineIndent:14.173228>
<pFirstLineIndent:><ParaStyle:<0x4E00><0x7EA7><0x6807><0x9898><0x6B63><0x6587>><pFirstLineIndent:14.173228>
<pFirstLineIndent:><ParaStyle:<0x4E00><0x7EA7><0x6807><0x9898><0x6B63><0x6587>><pFirstLineIndent:14.173228>
<pFirstLineIndent:><ParaStyle:<0x4E00><0x7EA7><0x6807><0x9898><0x6B63><0x6587>><pFirstLineIndent:14.173228>
<pFirstLineIndent:><ParaStyle:<0x4E00><0x7EA7><0x6807><0x9898><0x6B63><0x6587>>
<ParaStyle:<0x4E00><0x7EA7><0x6807><0x9898><0x6B63><0x6587>><cSize:8.000000><cFont:Arial>
<cSize:><cFont:><ParaStyle:<0x4E00><0x7EA7><0x6807><0x9898><0x6B63><0x6587>><pFirstLineIndent:14.173228>
<pFirstLineIndent:><ParaStyle:<0x4E00><0x7EA7><0x6807><0x9898><0x6B63><0x6587>><pFirstLineIndent:14.173228><cLeading:9.000000>
<cLeading:><pFirstLineIndent:><ParaStyle:<0x4E00><0x7EA7><0x6807><0x9898><0x6B63><0x6587>><pFirstLineIndent:14.173228><cLeading:12.100000>Diffuse and multifocal type of MHL was found in 4 case. MR images showed enlarged liver with smooth border, multiple foci with slightly low signal intensity on T1-weighted images, slightly high signal intensity on T2-weighted images. After intravenous administration of a gadolinium-based contrast agent, the lesions demonstrated annular enhancement in artery phase, no enhancement in early stage, enhancement in delay phase. In 1 case, MR images showed multifocal masses in the liver, slightly low and normal signal intensity on T1-weighted images, very <cLeading:><cLeading:11.900000>high signal intensity on T2-weighted images. The cotton-like masses with clear borders, did not syncretize each other (Figure 4).
<cLeading:><pFirstLineIndent:><ParaStyle:<0x4E00><0x7EA7><0x6807><0x9898><0x6B63><0x6587>><pFirstLineIndent:14.173228><cLeading:11.900000>
<cLeading:><pFirstLineIndent:><ParaStyle:<0x4E00><0x7EA7><0x6807><0x9898><0x6B63><0x6587>><pFirstLineIndent:14.173228><cLeading:11.900000>
<cLeading:><pFirstLineIndent:><ParaStyle:<0x4E00><0x7EA7><0x6807><0x9898><0x6B63><0x6587>><pFirstLineIndent:14.173228>

<pFirstLineIndent:><ParaStyle:<0x4E00><0x7EA7><0x6807><0x9898><0x6B63><0x6587>><pFirstLineIndent:14.173228>
<pFirstLineIndent:><ParaStyle:<0x4E00><0x7EA7><0x6807><0x9898><0x6B63><0x6587>><pFirstLineIndent:14.173228>
<pFirstLineIndent:><ParaStyle:<0x4E00><0x7EA7><0x6807><0x9898><0x6B63><0x6587>><pFirstLineIndent:14.173228>
<pFirstLineIndent:><ParaStyle:<0x4E00><0x7EA7><0x6807><0x9898><0x6B63><0x6587>><pFirstLineIndent:14.173228>
<pFirstLineIndent:><ParaStyle:<0x4E00><0x7EA7><0x6807><0x9898><0x6B63><0x6587>><pFirstLineIndent:14.173228>
<pFirstLineIndent:><ParaStyle:<0x4E00><0x7EA7><0x6807><0x9898><0x6B63><0x6587>><pFirstLineIndent:14.173228>
<pFirstLineIndent:><ParaStyle:<0x4E00><0x7EA7><0x6807><0x9898><0x6B63><0x6587>><pFirstLineIndent:14.173228>
<pFirstLineIndent:><ParaStyle:<0x4E00><0x7EA7><0x6807><0x9898><0x6B63><0x6587>><pFirstLineIndent:14.173228>
<pFirstLineIndent:><ParaStyle:<0x4E00><0x7EA7><0x6807><0x9898><0x6B63><0x6587>><pFirstLineIndent:14.173228>
<pFirstLineIndent:><ParaStyle:<0x4E00><0x7EA7><0x6807><0x9898><0x6B63><0x6587>><pFirstLineIndent:14.173228>
<pFirstLineIndent:><ParaStyle:<0x4E00><0x7EA7><0x6807><0x9898><0x6B63><0x6587>><pFirstLineIndent:14.173228>
<pFirstLineIndent:><ParaStyle:<0x4E00><0x7EA7><0x6807><0x9898><0x6B63><0x6587>><pFirstLineIndent:14.173228>
<pFirstLineIndent:><ParaStyle:<0x4E00><0x7EA7><0x6807><0x9898><0x6B63><0x6587>><pFirstLineIndent:14.173228>
<pFirstLineIndent:><ParaStyle:<0x4E00><0x7EA7><0x6807><0x9898><0x6B63><0x6587>><pFirstLineIndent:14.173228>
<pFirstLineIndent:><ParaStyle:<0x4E00><0x7EA7><0x6807><0x9898><0x6B63><0x6587>><pFirstLineIndent:14.173228>
<pFirstLineIndent:><ParaStyle:<0x4E00><0x7EA7><0x6807><0x9898><0x6B63><0x6587>><cLeading:8.000000>
<cLeading:><ParaStyle:<0x4E00><0x7EA7><0x6807><0x9898><0x6B63><0x6587>><cSize:8.000000><cFont:Arial>
<cSize:><cFont:><ParaStyle:<0x4E00><0x7EA7><0x6807><0x9898><0x6B63><0x6587>><pFirstLineIndent:14.173228>
<pFirstLineIndent:><ParaStyle:<0x4E00><0x7EA7><0x6807><0x9898><0x6B63><0x6587>><pFirstLineIndent:14.173228>
<pFirstLineIndent:><ParaStyle:<0x4E00><0x7EA7><0x6807><0x9898><0x6B63><0x6587>><pFirstLineIndent:14.173228><cLeading:9.000000>
<cLeading:><pFirstLineIndent:><ParaStyle:<0x4E00><0x7EA7><0x6807><0x9898><0x6B63><0x6587>><pFirstLineIndent:14.173228><cLeading:11.900000>Combined diffuse and single type was found in 1 case. MR images showed big isolate multi-loculus cystic foci in the diffuse tubers, fluid-fluid plane in some cysts (Figure 5).
<cLeading:><pFirstLineIndent:><ParaStyle:<0x4E8C><0x7EA7><0x6807><0x9898>><cLeading:11.900000>
<cLeading:><ParaStyle:<0x4E8C><0x7EA7><0x6807><0x9898>><cLeading:11.900000>
<cLeading:><ParaStyle:<0x4E8C><0x7EA7><0x6807><0x9898>>
<ParaStyle:<0x4E8C><0x7EA7><0x6807><0x9898>>
<ParaStyle:<0x4E8C><0x7EA7><0x6807><0x9898>>
<ParaStyle:<0x4E8C><0x7EA7><0x6807><0x9898>>
<ParaStyle:<0x4E8C><0x7EA7><0x6807><0x9898>>
<ParaStyle:<0x4E8C><0x7EA7><0x6807><0x9898>>
<ParaStyle:<0x4E8C><0x7EA7><0x6807><0x9898>>
<ParaStyle:<0x4E8C><0x7EA7><0x6807><0x9898>>
<ParaStyle:<0x4E8C><0x7EA7><0x6807><0x9898>><cLeading:8.000000>

<cLeading:><ParaStyle:<0x4E8C><0x7EA7><0x6807><0x9898>>
<ParaStyle:<0x4E8C><0x7EA7><0x6807><0x9898>>
<ParaStyle:<0x4E8C><0x7EA7><0x6807><0x9898>><cLeading:9.000000> CT finding in MHL<cLeading:><cLeading:11.800000>
<cLeading:><ParaStyle:<0x4E00><0x7EA7><0x6807><0x9898><0x6B63><0x6587>><cLeading:11.800000>In the multifocal type, CT images showed enlarged liver, multifocal low density foci of varying sizes from 1 cm <cLeading:><cSize:8.000000><cLeading:-1.000000><cFont:SimSun><0x00D7><cSize:><cLeading:><cFont:><cLeading:11.800000>1 cm to 2 cm<cLeading:><cSize:8.000000><cLeading:-1.000000><cFont:SimSun><0x00D7><cSize:><cLeading:><cFont:><cLeading:11.800000>3 cm, lower density in the center. In the single focal type, CT images showed low density focus round in shape with a clear border.
<cLeading:><ParaStyle:<0x4E8C><0x7EA7><0x6807><0x9898>><cLeading:11.800000>
<cLeading:><ParaStyle:<0x4E8C><0x7EA7><0x6807><0x9898>><cLeading:11.800000>Relationship between lesions and vessels
<cLeading:><ParaStyle:<0x4E00><0x7EA7><0x6807><0x9898><0x6B63><0x6587>><cLeading:11.800000>Inner hepatic vessels were compressed in 5 cases, vena cava and abdominal aortae were compressed in 3 cases. No portal vein was compressed in all the 12 cases.
<cLeading:><ParaStyle:<0x4E00><0x7EA7><0x6807><0x9898><0x6B63><0x6587>><cLeading:11.500000>
<cLeading:><ParaStyle:<0x4E00><0x7EA7><0x6807><0x9898><0x6B63><0x6587>><cSize:14.000000><cTracking:25><cLeading:11.800000><cFont:FZCuYuan-M03S>DISCUSSION<cSize:><cTracking:><cLeading:><cFont:><cSize:14.000000><cLeading:11.800000><cFont:AvantGarde Md BT>
<cSize:><cLeading:><cFont:><ParaStyle:<0x4E00><0x7EA7><0x6807><0x9898><0x6B63><0x6587>><cLeading:11.800000>MHL is a rare hepatic benign tumor, occurring most in children and rarely in adults <cLeading:><cLeading:11.800000><cPosition:Superscript>[4]<cLeading:><cPosition:><cLeading:11.800000>. MHL in fetus has also been reported <cLeading:><cLeading:11.800000><cPosition:Superscript>[1]<cLeading:><cPosition:><cLeading:11.800000>.
<cLeading:><ParaStyle:<0x4E8C><0x7EA7><0x6807><0x9898>><cLeading:11.900000>Pathologensis
<cLeading:><ParaStyle:<0x4E8C><0x7EA7><0x6807><0x9898>><cTypeface:Regular><cLeading:12.000000><cFont:Garamond>The exact pathologenesis of MHL is not clear. It has been reported that MHL is a kind of developmental deformity or the result of abnormal reaction procedure <cTypeface:><cLeading:><cFont:><cTypeface:Regular><cLeading:12.000000><cFont:Garamond><cPosition:Superscript>[8]<cTypeface:><cLeading:><cFont:><cPosition:><cTypeface:Regular><cLeading:12.000000><cFont:Garamond>. The abnormality appears in the late stage of embryo formation that grows along the portal vein system and surrounds the hepatic tissue island when the liver maintains lobular structure connecting to bile duct tree <cTypeface:><cLeading:><cFont:><cTypeface:Regular><cLeading:12.000000><cFont:Garamond><cPosition:Superscript>[7]<cTypeface:><cLeading:><cFont:><cPosition:><cTypeface:Regular><cLeading:12.000000><cFont:Garamond>. It was reported that MHL comes from the local area of bile duct atresia, inducing obstruction of distant bile ducts and necrosis of hepatic cells <cTypeface:><cLeading:><cFont:><cTypeface:Regular><cLeading:12.000000><cFont:Garamond><cPosition:Superscript>[5]<cTypeface:><cLeading:><cFont:><cPosition:><cTypeface:Regular><cLeading:12.000000><cFont:Garamond>. Some studies showed that MHL correlates with the developmental deformity of vessels and the rupture of 19q13.4 <cTypeface:><cLeading:><cFont:><cTypeface:Regular><cLeading:12.000000><cFont:Garamond><cPosition:Superscript>[12,13]<cTypeface:><cLeading:><cFont:><cPosition:><cTypeface:Regular><cLeading:12.000000><cFont:Garamond>. It was reported that most of MHLs are diploid, but the set of chromosomes of MHL prompt that MHL is not the developmental deformity or the result of abnormal reaction procedure<cTypeface:><cLeading:><cFont:><cTypeface:Regular><cLeading:12.000000><cFont:Garamond><cPosition:Superscript>[7,12]<cTypeface:><cLeading:><cFont:><cPosition:><cTypeface:Regular><cLeading:12.000000><cFont:Garamond>.
<cTypeface:><cLeading:><cFont:><ParaStyle:<0x4E8C><0x7EA7><0x6807><0x9898>><cLeading:12.000000>
<cLeading:><ParaStyle:<0x4E8C><0x7EA7><0x6807><0x9898>><cLeading:11.900000>Clinical manifestations
<cLeading:><ParaStyle:<0x4E8C><0x7EA7><0x6807><0x9898>><cTypeface:Regular><cLeading:12.000000><cFont:Garamond>MHL has no special clinical manifestations. The most common symptom is an abdominal mass or an enlarged liver. The mass increases rapidly in specific cases, leading to inappetence, obvious dyspnoea or obvious

obstruction of inferior vena cava. Other symptoms are fever, vomit, constipation, diarrhea and weight loss <cTypeface:><cLeading:><cFont:><cTypeface:Regular><cLeading:12.000000><cFont:Garamond><cPosition:Superscript>[6]<cTypeface:><cLeading:><cFont:><cPosition:><cTypeface:Regular><cLeading:12.000000><cFont:Garamond>. Malnutrition, anemia and cachexia are occasionally found . AFP is normal. Some reports indicates that AFP increases in the infancy under 4 months of age <cTypeface:><cLeading:><cFont:><cTypeface:Regular><cLeading:12.000000><cFont:Garamond><cPosition:Superscript>[1]<cTypeface:><cLeading:><cFont:><cPosition:><cTypeface:Regular><cLeading:12.000000><cFont:Garamond>. Surgical operation is the best choice of treatment.

<cTypeface:><cLeading:><cFont:><ParaStyle:<0x4E8C><0x7EA7><0x6807><0x9898>><cLeading:12.000000>
<cLeading:><ParaStyle:<0x4E8C><0x7EA7><0x6807><0x9898>><cLeading:12.000000>Radiologic finding
<cLeading:><ParaStyle:<0x4E8C><0x7EA7><0x6807><0x9898>><cTypeface:Regular><cLeading:12.100000><cFont:Garamond>Solid type of MHL may have a single focus or multiple foci. In our study MHL was located at the right lobe of liver in 5 of 6 cases of solid type, being consistant with other reports <cTypeface:><cLeading:><cFont:><cTypeface:Regular><cLeading:12.100000><cFont:Garamond><cPosition:Superscript>[6,8]<cTypeface:><cLeading:><cFont:><cPosition:><cTypeface:Regular><cLeading:12.100000><cFont:Garamond>. In the solid part of MHL, there were remarkably proliferated bile ducts and fibrosis around them to form fibroglandular structure. In 1 multifocal solid MHL, there was fluid retention in mesenchymal tissue (Figure 4). The higher the protein content in the fluid, the higher the signal intensity on T1-weighted images. Some studies showed that the solid part of MHL is formed during perinatal period. The mass enlarges rapidly, because of mesenchyme cystic degeneration with fluid retardation, obstruction and dilation of lymph duct or both<cTypeface:><cLeading:><cFont:><cTypeface:Regular><cLeading:12.100000><cFont:Garamond><cPosition:Superscript>
[8]<cTypeface:><cLeading:><cFont:><cPosition:><cTypeface:Regular><cLeading:12.100000><cFont:Garamond>. With the growth of MHL, the cystic area in the mass enlarges significantly, taking up greater part of the lesion, because of mesenchyme atrophy, bile duct dilation, lympha retardation. Therefore, the lesion may be solid-cystic type or cystic type, which may be its pathological basis (Figure 3). There is no blood supply for MHL<cTypeface:><cLeading:><cFont:><cTypeface:Regular><cLeading:12.100000><cFont:Garamond><cPosition:Superscript>[6,8]<cTypeface:><cLeading:><cFont:><cPosition:><cTypeface:Regular><cLeading:12.100000><cFont:Garamond>. The masses shift the vessels in angiography. The septa are thick when there are more solid contents. There are areas surrounded by tumor vessels with no blood supply. Enhanced CT images can show cord-like enhancement <cTypeface:><cLeading:><cFont:><cTypeface:Regular><cLeading:12.100000><cFont:Garamond><cPosition:Superscript>[3]<cTypeface:><cLeading:><cFont:><cPosition:><cTypeface:Regular><cLeading:12.100000><cFont:Garamond>. We consider that the lesions with no blood supply may be cystic type, the lesions with less blood supply may be solid type. The part of annular enhancement may compress the hepatic tissue around the lesions. Intrahepatic vessels, <cTypeface:><cLeading:><cFont:><cTypeface:Regular><cLeading:11.900000><cFont:Garamond>inferior vena cava, abdominal aorta and other organs are compressed and shifted by huge MHL masses <cTypeface:><cLeading:><cFont:><cTypeface:Regular><cLeading:11.900000><cFont:Garamond><cPosition:Superscript>[1]<cTypeface:><cLeading:><cFont:><cPosition:><cTypeface:Regular><cLeading:11.900000><cFont:Garamond> with blood vessels or peripheral tissues invaded. Calcification is <cTypeface:><cLeading:><cFont:><cTypeface:Regular><cHorizontalScale:0.900000><cLeading:11.900000><cFont:Garamond>seldom found in MHL, but septum calcification is reported <cTypeface:><cHorizontalScale:><cLeading:><cFont:><cTypeface:Regular><cHorizontalScale:0.900000><cLeading:11.900000><cFont:Garamond><cPosition:Superscript>[9]<cTypeface:><cHorizontalScale:><cLeading:><cFont:><cPosition:><cTypeface:Regular><cHorizontalScale:0.900000><cLeading:11.900000><cFont:Garamond>.<cTypeface:><cHorizontalScale:><cLeading:><cFont:><cTypeface:Regular><cLeading:11.900000><cFont:Garamond>

<cTypeface:><cLeading:><cFont:><ParaStyle:<0x4E00><0x7EA7><0x6807><0x9898><0x6B63><0x6587>><cLeading:11.900000>
<cLeading:><ParaStyle:<0x4E8C><0x7EA7><0x6807><0x9898>><cLeading:11.900000>Treatment and prognosis
<cLeading:><ParaStyle:<0x4E8C><0x7EA7><0x6807><0x9898>><cTypeface:Regular><cLeading:11.900000><cFont:Garamond>MHL seldom cancerates, but canceration can be found in specific cases<cTypeface:><cLeading:><cFont:><cTypeface:Regular><cLeading:11.900000><cFont:Garamond><cPosition:Superscript>
[10]<cTypeface:><cLeading:><cFont:><cPosition:><cTypeface:Regular><cLeading:11.900000><cFont:Garamond>. In this research, no case was cancerated. Surgical operation is the best choice of treatment. MHL seldom relapses, and

its prognosis is good. Surgery should be executed after diagnosis.
<cTypeface:><cLeading:><cFont:><ParaStyle:<0x4E8C><0x7EA7><0x6807><0x9898>><cLeading:11.900000>
<cLeading:><ParaStyle:<0x4E8C><0x7EA7><0x6807><0x9898>><cLeading:11.900000>Differential diagnosis
<cLeading:><ParaStyle:<0x4E8C><0x7EA7><0x6807><0x9898>><cTypeface:Regular><cLeading:11.900000><cFon
t:Garamond>Due to the different imagings of MHL, it should be differentiated from hepatic abscess, metastasis, caroli<0x2019>s disease, undifferentiated embryo sarcoma of the liver and hepatoblastoma.
<cTypeface:><cLeading:><cFont:><ParaStyle:<0x4E8C><0x7EA7><0x6807><0x9898>><cTypeface:Regular><cLea
ding:11.900000><cFont:Garamond> In conclusion, MR imaging is a better way to differentiate and diagnose MHL. MHL may be recognized by its characteristic occurrence in infancy and MR imaging features.
<cTypeface:><cLeading:><cFont:><ParaStyle:>
<ParaStyle:><cSize:14.000000><cTracking:25><cLeading:8.000000><cFont:FZCuYuan-
M03S>REFERENCES<cSize:><cTracking:><cLeading:><cFont:><cSize:14.000000><cLeading:8.000000>
<cSize:><cLeading:><ParaStyle:<0x53C2><0x8003><0x6587><0x732E><0x6B63><0x6587>><cLeading:8.000000>
<cLeading:><ParaStyle:<0x53C2><0x8003><0x6587><0x732E><0x6B63><0x6587>><cLeading:8.000000>1
<cLeading:> <cTypeface:Bold>Kamata S,<cTypeface:> Nose K, Sawai T, Hasegawa T, Kuroda S, Sasaki T, Okada A, Tawara M. Fetal mesenchymal hamartoma of the liver: report of a case. <cTypeface:Italic>J Pediatr Surg<cTypeface:> 2003;<cTypeface:Bold> 38:<cTypeface:> 639-641
<ParaStyle:<0x53C2><0x8003><0x6587><0x732E><0x6B63><0x6587>>2 <cTypeface:Bold>Yen JB,<cTypeface:> Kong MS, Lin JN. Hepatic mesenchymal hamartoma. <cTypeface:Italic>J Paediatr Child Health<cTypeface:> 2003 ; <cTypeface:Bold>39:<cTypeface:> 632-634
<ParaStyle:<0x53C2><0x8003><0x6587><0x732E><0x6B63><0x6587>>3 <cTypeface:Bold>Gornicka B,<cTypeface:> Ziarkiewicz-Wroblewska B, Wroblewski T, Koperski L, Pawlak J, Nyckowski P, Krawczyk M, Zimmermann A, Wasiutynski A. Myoid hamartoma of the liver - a novel variant of hamartoma developing in the hilar region and imitating a malignant liver tumor. <cTypeface:Italic>Med Sci Monit<cTypeface:> 2004;<cTypeface:Bold> 10:<cTypeface:> 23-26
<ParaStyle:<0x53C2><0x8003><0x6587><0x732E><0x6B63><0x6587>>4 <cTypeface:Bold>Cook JR, <cTypeface:>Pfeifer JD, Dehner LP. Mesenchymal hamartoma of the liver in the adult: association with distinct clinical feature
<ParaStyle:<0x53C2><0x8003><0x6587><0x732E><0x6B63><0x6587>> and histological changes. <cTypeface:Italic>Hum Pathol<cTypeface:> 2002; <cTypeface:Bold>33:<cTypeface:> 893-898
<ParaStyle:<0x53C2><0x8003><0x6587><0x732E><0x6B63><0x6587>>5 <cTypeface:Bold>Wholey MH,<cTypeface:> Wojno KJ. Pediatric hepatic mesenchymal hamartoma demonstrated on plain film, ultrasound and MRI, and correlated with pathology. <cTypeface:Italic>Pediatr Radiol<cTypeface:> 1994; <cTypeface:Bold>24:<cTypeface:> 143-144
<ParaStyle:<0x53C2><0x8003><0x6587><0x732E><0x6B63><0x6587>>6 <cTypeface:Bold> Ros PR,<cTypeface:> Goodman ZD, Ishak KG, Dachman AH, Olmsted WW, Hartman DS, Lichtenstein JE. Mesenchymal hamartoma of the liver: radiologic-pathologic correlation. <cTypeface:Italic>Radiology<cTypeface:> 1986; <cTypeface:Bold>158:<cTypeface:> 619-624
<ParaStyle:<0x53C2><0x8003><0x6587><0x732E><0x6B63><0x6587>>7 <cTypeface:Bold>DeMaioribus CA,<cTypeface:> Lally KP, Sim K, Isaacs H, MahourGH Mesenchymal hamartoma of the liver. A 35-year review.<cTypeface:Italic>Arch Surg<cTypeface:> 1990; <cTypeface:Bold>125:<cTypeface:> 598-600
<ParaStyle:<0x53C2><0x8003><0x6587><0x732E><0x6B63><0x6587>>8 <cTypeface:Bold>Brunt EM. <cTypeface:>Benign tumors of the liver. <cTypeface:Italic>Clin Liver Dis<cTypeface:> 2001;<cTypeface:Bold> 5:<cTypeface:> 1-15,
<ParaStyle:<0x53C2><0x8003><0x6587><0x732E><0x6B63><0x6587>>9 <cTypeface:Bold>Konez O,<cTypeface:> Goyal M, Vyas PK, Boinapally SB. Mesenchymal hamartoma of the liver. <cTypeface:Italic>Comput Med Imaging Graph<cTypeface:> 2001; <cTypeface:Bold>25:<cTypeface:> 61-65
<ParaStyle:<0x53C2><0x8003><0x6587><0x732E><0x6B63><0x6587>>10 <cTypeface:Bold>Ramanujam TM,<cTypeface:> Ramesh JC, Goh DW, Wong KT, Ariffin WA, Kumar G, Taib NA. Malignant transformation of mesenchymal hamartoma of the liver: case report and review of the literature. <cTypeface:Italic>J Pediatr Surg<cTypeface:> 1999;<cTypeface:Bold> 34:<cTypeface:> 1684-1686
<ParaStyle:<0x53C2><0x8003><0x6587><0x732E><0x6B63><0x6587>>11 <cTypeface:Bold>Otal TM,<cTypeface:> Hendricks JB, Pharis P, Donnelly WH. Mesenchymal hamartoma of the liver. DNA flow cytometric analysis of eight cases. <cTypeface:Italic>Cancer<cTypeface:> 1994;<cTypeface:Bold> 74:<cTypeface:> 1237-1242

<ParaStyle:<0x53C2><0x8003><0x6587><0x732E><0x6B63><0x6587>>12 <cTypeface:Bold>Bove KE,<cTypeface:> Blough RI, Soukup S. Third report of t(19q)(13.4) in mesenchymal hamartoma of liver with comments on link to embryonal sarcoma. <cTypeface:Italic>Pediatr Dev Pathol<cTypeface:> 1998; <cTypeface:Bold>1:<cTypeface:> 438-442
<ParaStyle:<0x53C2><0x8003><0x6587><0x732E><0x6B63><0x6587>>13 <cTypeface:Bold>Mascarello JT,<cTypeface:> Krous HF. second report of a translocatio involving 19q13,4 in a mesenchymal hamartoma of the liver. <cTypeface:Italic>Cancer Genetics and Cytogenetics <cTypeface:>1992; <cTypeface:Bold>58:<cTypeface:> 141-142
<ParaStyle:<0x53C2><0x8003><0x6587><0x732E><0x6B63><0x6587>>
<ParaStyle:<0x53C2><0x8003><0x6587><0x732E><0x6B63><0x6587>><cLeading:8.000000>
<cLeading:><cTypeface:Bold><cLeading:8.000000>Science Editor<cTypeface:><cLeading:><cLeading:8.000000> Guo SY <cLeading:><cTypeface:Bold><cLeading:8.000000>Language Editor<cTypeface:><cLeading:><cLeading:8.000000> Elsevier HK<cLeading:>
<ParaStyle:<0x53C2><0x8003><0x6587><0x732E><0x6B63><0x6587>>
<ParaStyle:<0x53C2><0x8003><0x6587><0x732E><0x6B63><0x6587>>

PO Box 2345, Beijing 100023, China
www.wjgnet.com
wjg@wjgnet.com

ELSEVIER

World J Gastroenterol 2005;11(37):5811-5815
World Journal of Gastroenterology ISSN 1007-9327
© 2005 The WJG Press and Elsevier Inc. All rights reserved.

• *BASIC RESEARCH* •

Microarray analysis of *Escherichia coli* O157:H7

Hui-Ying Jin, Kai-Hua Tao, Yue-Xi Li, Fa-Qing Li, Su-Qin Li

Hui-Ying Jin, Kai-Hua Tao, Yue-Xi Li, Fa-Qing Li, Su-Qin Li, Huadong Research Institute for Medicine and Biotechnics, Nanjing 210002, Jiangsu Province, China
Supported by the Key Military Medical Science and Technique Program during the 10th Five Year Plan Period, No. 01L006
Correspondence to: Hui-Ying Jin, Huadong Research Institute for Medicine and Biotechnics, Nanjing 210002, Jiangsu Province, China. laoyingj@hotmail.com
Telephone: +86-25-84542419 Fax: +86-25-84541183
Received: 2004-12-07 Accepted: 2005-02-18

Abstract

AIM: To establish the rapid, specific, and sensitive method for detecting O157:H7 with DNA microchips.

METHODS: Specific oligonucleotide probes (26-28 nt) of bacterial antigenic and virulent genes of *E. coli* O157:H7 and other related pathogen genes were pre-synthesized and immobilized on a solid support to make microchips. The four genes encoding O157 somatic antigen (*rfbE*), H7 flagellar antigen (*fliC*) and toxins (*SLT1*, *SLT2*) were monitored by multiplex PCR with four pairs of specific primers. Fluorescence-Cy3 labeled samples for hybridization were generated by PCR with Cy3-labeled single prime. Hybridization was performed for 60 min at 45 ℃. Microchip images were taken using a confocal fluorescent scanner.

RESULTS: Twelve different bacterial strains were detected with various combinations of four virulent genes. All the O157:H7 strains yielded positive results by multiplex PCR. The size of the PCR products generated with these primers varied from 210 to 678 bp. All the rfbE/fliC/SLT1/SLT2 probes specifically recognized Cy3-labeled fluorescent samples from O157:H7 strains, or strains containing O157 and H7 genes. No cross hybridization of O157:H7 fluorescent samples occurred in other probes. Non-O157:H7 pathogens failed to yield any signal under comparable conditions. If the Cy3-labeled fluorescent product of O157 single PCR was diluted 50-fold, no signal was found in agarose gel electrophoresis, but a positive signal was found in microarray hybridization.

CONCLUSION: Microarray analysis of O157:H7 is a rapid, specific, and efficient method for identification and detection of bacterial pathogens.

© 2005 The WJG Press and Elsevier Inc. All rights reserved.

Key words: Microarray; Multiplex PCR; *Escherichia coli* O157:H7; Shiga-like toxin

Jin HY, Tao KH, Li YX, Li FQ, Li SQ. Microarray analysis of *Escherichia coli* O157:H7. *World J Gastroenterol* 2005; 11 (37): 5811-5815
http://www.wjgnet.com/1007-9327/11/5811.asp

INTRODUCTION

In 1982, two outbreaks of hemorrhagic colitis occurred among patrons of a fast-food restaurant chain in Oregon and Michigan. The disease is characterized by watery diarrhea progressing rapidly to grossly bloody diarrhea and abdominal cramping with no fever. An investigation by state health departments and Centers for Disease Control (CDC) indicates that *E. coli* O157:H7, a rare strain not previously linked to human disease, is the cause of the disease[1]. In 1983, Karmali *et al*.[2], reported that *E. coli* O157:H7 is related with hemolytic uremic syndrome (HUS), a leading cause of kidney failure in children. Since then, *E. coli* O157:H7 has been recognized as the leading cause of HUS in the USA, Japan, and in our country. Infection with *E. coli* O157:H7 can be entirely asymptomatic or presents with watery diarrhea, bloody diarrhea, HUS, thrombotic thrombocytopenic purpura, leading to death[3]. Antimicrobial agents have no proven value in the treatment of *E. coli* O157:H7 infections. It was reported that patients receiving antimicrobial agents are more likely to develop HUS than patients not receiving such drugs[4]. It may be prudent to avoid the use of antimicrobial agents in patients with diagnosed or suspected *E. coli* O157:H7 infection. Traditionally, *E. coli* O157:H7 is identified by microbiological culture techniques and immunological methods that are used to detect the O157 and H7 antigens[5]. These methods are slow and complicated, and sometimes yield false-positive results when other variants of *E. coli* O157:H7 are occasionally isolated in the initial culture. Therefore, accurate and rapid identification is important for the diagnosis of O157:H7 infection.

DNA and oligonucleotide microchip (microarray) technology play an increasingly important role in gene expression, phylogenetic classification of bacteria, mapping of genes, analysis of single-nucleotide polymorphisms, drug discovery, multiple microbial diagnosis, and toxicological research[6-8]. Since microchips with short (8-30 nt) synthetic oligonucleotides are more sensitive to genetic differences, they are more appropriate for discriminating microorganisms.

In the present study, we used gene *rfbE* encoding an enzyme involved in the biosynthesis of O157 antigen (the somatic antigen), and gene *fliC* encoding the H7 flagellar antigen, and gene Shiga-like toxin (SLT) 1 and 2, encoding virulent factors, for the diagnosis of *E. coli* O157:H7 infection diagnosis by microarray analysis. It seems very useful for automatic identification and characterization of bacterial pathogens.

MATERIALS AND METHODS

Bacterial strains and other pathogens

O157:H7, *Vibrio cholerae, Shigella, Salmonella, DH5α,* and other *E. coli* strains were from National Institute for the Control of Pharmaceutical and Biological Products, CDC of Jiangsu and Shandong Provinces, and our laboratory. All strains were stored at -80 ℃ in Luria-Bertani broth containing 15% glycerol. *Schistosoma japonicum, hemorrhagic fever and renal syndrome virus (HFRSV), Leptospira interrogans, Rickettsia Tsutsugamushi,* and *Plasmodium* were also from CDC of Jiangsu, Guangdong, Fujian Provinces and our laboratory.

PCR primers and oligonucleotide probes

Primers used to amplify the fragments of antigenic genes and virulent genes are shown in Table 1. One primer was labeled with Cy3 (TaKaRa Co.). BLAST search was used to retrieve the homologous sequences of each of the four genes analyzed. For each gene, one conserved region containing approximately 26-28 nucleotides was chosen as the target sequence probe. The probes and their BLAST search results are also shown in Table 1.

Microchip design and fabrication

Microchips were printed on silylated (aldehyde-coated) glass slides (8 cm×2.5 cm, Sigma Co.) by the contact microspotting robotic system 7 500, the PixSys 5 500 workstation microspotting software (Cartesian Technologies, Inc.), and the ChipMaker Pin 40 microspotting device. Microchip design maps are shown in Table 2. The final spotting mixture contained 100 μmol/L specific oligonucleotide probe (TaKaRa Co.) in 0.25 mol/L acetic acid. A range of 70-75% humidity was maintained in an environmental chamber to prevent rapid evaporation of spotted drops and efficient coupling of amino-modified oligonucleotides with the aldehyde groups on the glass surface. Six identical probe area arrays were printed on each slide, allowing analysis of six samples on one glass slide simultaneously. The size of spots did not exceed 150 μm in diameter. Printed slides were incubated at 37 ℃ for 60 min, then overnight at room temperature. The next day, slides were washed twice with 0.2% sodium dodecyl sulfate (SDS) in water for 5 min, twice with distilled water for 5 min each, and then dried in air. Before hybridization, to make the bonds between oligonucleotides and glass surface irreversible, the slides were incubated for 30 min in a freshly prepared 0.6% aqueous solution of $NaBH_4$, then washed twice with 0.2% SDS for 1 min and twice with distilled water for 1 min. Microchips prepared according to this protocol could be stored for 2 mo at room temperature.

Multiplex PCR

E. coli cultures were grown overnight at 37 ℃ in Luria-Bertani broth. One milliliter of the culture sample was centrifuged, and the pellet was washed and resuspended in 100 μL of distilled water. The suspension was boiled for 10 min followed by centrifugation at 10 000 *g* for 10 min to remove denatured proteins and bacterial cell membranes. Five-microliter aliquot of the supernatant was used as the template for multiplex PCR amplification. Briefly, 50 μL of the reaction mixture containing 5 μL, 10×PCR buffer, 0.2 mmol/L dNTPs, 2.0 mmol/L $MgCl_2$, 0.5-1.0 pmol/L each primer and 1.5 U of Taq polymerase (TaKaRa Co.) was used. Temperature conditions consisted of an initial pre-denaturation step at 95 ℃ for 5 min, followed by 35 cycles at 94 ℃ for 30 s, at 57 ℃ for 45 s, and at 72 ℃ for 60 s, a final extension at 72 ℃ for 5 min. The PCR products were analyzed by electrophoresis on 1% agarose gel in TAE (40 mmol/L Tris-acetate, 2 mmol/L disodium EDTA). DNA bands in the gels were stained with 0.5 μg/mL of ethidium bromide. The interested DNAs were extracted using DNA fragment purification kit Ver. 2.0 (TaKaRa Co.) and dissolved in 50 μL of distilled water

Table 1 PCR primers and oligonucleotide probes for O157:H7 microarray

Target gene	Primer sequences for PCR amplification	Labeled primer	PCR product size (bp)	Oligonucleotides target adsorbed by array chip	GenBank No. of BLAST search
O157	L5′aacggttgctcttcatttag3′	R	678	ggtggaatggttgtcacgaatgacaaa	AE005429, AP002559, AB008676
(*rfbE*)	R5′gagaccatccaataagtgtg3′				AF061251 S83460
H7	L5′taccaccaaatctactgctg3′	R	560	gacgatgcaggcaacttgacgactaa	AE005415, AF228496, U47614
(*fliC*)	R5′taccacctttatcatccaca3′				AP002559, AB028474, L07388
SLT1	L5′tgtaactggaaaggtggagtatac3′	R	210	ggatgacgtaaccattaaaactaatgcc	AY123842, AF461172, AJ251754,
	R5′gctattctgagtcaacgaaaaataac3′				AB071624, AE005442, X07903
SLT2	L5′tttacgatagacttctcgac3′	L	228	agatggtcaaaacgcgcctgatagac	AF329817, AE005296, AJ272135
	R5′cacatataaattatttcgctc3′				AB052227, AP002554, Y10775

Table 2 Microchip design and spotting map

16 3×SSC	○	○	○	○	●	○	○	○	○	●	8 *Vibrio cholerae* ompW
15 3×SSC	○	○	○	○	●	○	○	○	○	●	7 *Schistosoma japonicum*
14 random probe	○	○	○	○	●	○	○	○	○	●	6 *Plasmodium* V
13 *SLT1* gene	○	○	○	○	●	○	○	○	○	●	5 *Plasmodium* F
12 *SLT2* gene	○	○	○	○	●	○	○	○	○	●	4 *Leptospira interrogans*
11 *fliC* gene (H7)	○	○	○	○	●	○	○	○	○	●	3*Rickettsia tsutsugamushi*
10 *rfbE* gene (O157)	○	○	○	○	●	○	○	○	○	●	2 *HFRSV* 1
9 *Vibrio cholerae* ctx	○	○	○	○	●	○	○	○	○	●	1 *HFRSV* 2

○: Detect probe, ●: Quality control probe.

for the next Cy3 labeling.

Synthesis of Cy3-labeled PCR samples

Fluorescence-labeled samples for hybridization were generated by PCR as described above, except that the annealing temperature was 42 ℃, and the template was the first multiplex PCR products (5 μL), the primer was only one Cy3-labeled (0.2 μmol/L) primer or four different Cy3-labeled (0.2-0.4 μmol/L) primers.

Microarray hybridization and scanning

Immediately before hybridization, 8 μL Cy3-labeled PCR samples was mixed with 3 μL hybridization buffer containing Cy3-labeled quality control (0.3 μmol/L) probe, and denatured for 5 min at 95 ℃, then chilled on ice for 1 min. This concentration could ensure rapid and efficient hybridization of a fluorescent sample with immobilized probes. Five-microliter aliquots from each sample was applied to the microarray area and covered with a glass coverslip to prevent evaporation of the sample during hybridization in the incubation chamber. Hybridization was performed for 60 min at 45 ℃. Slides were then washed twice with 2×SSC containing 0.1% SDS for 5 min at 60 ℃, twice with 0.1×SSC containing 0.1% SDS for 5 min at room temperature, and once with 0.1×SSC, once with distilled water and dried by an air stream to completely remove any remaining solution. Then microchip images were taken with the confocal fluorescent scanner ScanArray 3 000.

RESULTS

Multiplex PCR and microchip analysis of bacterial virulent genes

We detected 12 different bacterial strains with various combinations of four virulent genes. The results of multiplex PCR and microchip analysis generated by bacterial DNA and four primers or probes are shown in Table 3. All the O157:H7 strains yielded positive results. The size of the PCR products generated by these primers varied from 210 to 678 bp. The other non-O157:H7 strains were not positive. The pitfalls of agarose gel analysis of multiplex PCR are illustrated in Figure 1. The difference of SLT1 and SLT2 was too small (only 18 bp) to be distinguished in agarose gel electrophoresis.

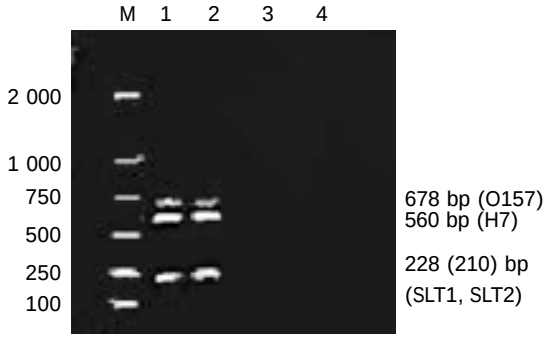


Figure 1 Result of multiplex PCR. Lane 1: O157:H7 882364 strain; lane 2: O157:H7 933 strain; lane 3: *Vibrio cholerae*; lane 4: DH5α.

Microarray hybridization specificity and sensitivity

All the rfbE/fliC/SLT1/SLT2 probes specifically recognized Cy3-labeled fluorescent samples from O157:H7 species, or strains containing O157 and H7 genes. Neither the cross hybridization of O157:H7 fluorescent samples to other probes (Figures 2A-C), nor cross hybridization of rfbE/fliC/SLT1/SLT2 probes to other pathogens (Figure 2D) was detected. If the Cy3-labeled fluorescent product of O157 single PCR was diluted 50-fold, no signal was visible in agarose gel electrophoresis, but a positive signal was found in microarray hybridization (Figure 2E).

DISCUSSION

E. coli is a normal inhabitant in the intestinal tract of human beings and warm-blooded animals. Although usually harmless, various strains such as *enterotoxigenic E. coli* (ETEC), *enteropathogenic E. coli* (EPEC) and *enterohemorrhagic E. coli* (EHEC), have virulent genes and render them pathogenic for both human beings and animals. *E. coli* O157:H7 is an important cause of hemorrhagic colitis and HUS. Conventional methods for detecting O157:H7 involve growth of non-sorbitol-fermenting *E. coli* colonies on sorbitol MacConkey agar culture (SMAC)[9]. These methods are time consuming, laborious, and expensive. More importantly, routine biochemical and serologic tests for pathogen identification can only type the species or serogroup level, but cannot directly characterize virulent genes. Thus, these assays cannot provide any information

Table 3 Results of multiplex PCR and microchip analysis by four primers and probes

Strain	PCR				Chipping			
	rfbE	fliC	SLT1	SLT2	rfbE	fliC	SLT1	SLT2
O157:H7 933	+	+	+		+	+	+	+
O157:H7 882364	+	+	+		+	+	+	+
O157:H19 44752	+	-	-	-	+	-	-	-
O1:H7 44766	-	+	-	-	-	+	-	-
O119:H6 44146	-	-	-	-	-	-	-	-
Vibrio cholerae 16017	-	-	-	-	-	-	-	-
Shigella dysenteriae 51252	-	-	-	-	-	-	-	-
Shigella flexneri 51302	-	-	-	-	-	-	-	-
Shigella boydii 51315	-	-	-	-	-	-	-	-
Shigella sonnei 51334	-	-	-	-	-	-	-	-
Salmonella 50087	-	-	-	-	-	-	-	-
DH5α	-	-	-	-	-	-	-	-

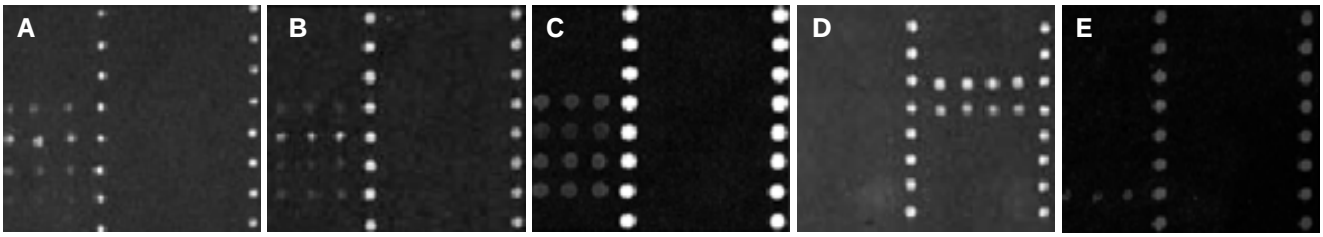


Figure 2 Results of microchip analysis. A: Microarray of O157:H7 933 strain, B: microarray of O157:H7 882364 strain, C: microarray of O157:H7 882364 strain, D: microarray of *Plasmodium*, E: microarray of O157.

about the potential pathogenicity or virulence of O157:H7[10]. Several genetic markers such as *rfbE*[11], *fliC*[12], and certain virulent genes as attachment and effacing gene (*eaeA*), hemolysin A (*hlyA*)[13,14], *SLT1*, *SLT2*[15] are useful targets for multiplex PCR amplification and differentiation of O157:H7. Although multiplex PCR amplification is a simple and sensitive method[16], it has some inherent shortcomings. When multiplex PCR is used for detection of several genetic markers, it tends to generate more nonspecific DNA products. If the size of PCR products is similar, it is difficult to discriminate these products. Therefore, it is necessary to establish high-throughput specific and sensitive methods for detecting O157:H7.

Hybridization of DNA samples to miniature arrays (microchips) of immobilized gene-specific DNA or oligonucleotide probes has recently become a powerful tool. A number of different ways can make oligonucleotide microchips, including *in situ* synthesis of oligonucleotides directly on the microchip surface[17] and immobilization of pre-synthesized oligonucleotides on a solid support[18]. We designed four genotype-specific oligonucleotide probes (*rfbE*, *fliC*, *SLT1*, and *SLT2*) for O157:H7, and immobilized them on a modified glass surface to create the microchip. *RfbE* and *fliC* are the specific marker genes encoding O157 somatic antigen and H7 flagellar antigen. *SLT1* and *SLT2* are the important virulent genes. Schmidt *et al*.[19], reported that the bacteriophage-encoded SLT plays a very important role in the pathogenesis of diseases caused by O157:H7, and in HUS through its cytotoxic effects on cells of the kidneys, intestines, central nervous system, and other organs. If infected with O157:H7 strain with SLT, many patients would develop HUS. Using these microchips, we can not only characterize the species of pathogens, but also identify their virulent factors SLT1 and SLT2. The major advantage of the microarray assay over agarose gel analysis of multiplex PCR products is that the microarray requires the internal sequences of DNA fragments to be complementary to the oligonucleotide probes on the microchip, but does not solely rely on the length of PCR products. In our study, only O157:H7 strains and SLT1, SLT 2 presented positive fluorescent signals. The successful demonstration of hybridization specificity led us to address the second critical parameter of microarray, assay sensitivity. When the Cy3-labeled product was diluted 50-fold, no positive signal was visible in agarose gel electrophoresis, but a positive hybridization signal was found in microchip, suggesting that microarray is more sensitive than agarose gel analysis.

In this study, to assess the synthesis of Cy3-labeled samples by multiplex and single PCR, we examined the same O157:H7 882364 strain in different ways. Multiplex and single PCR could display positive hybridization in microchip. Compared to multiplex PCR, the fluorescent signals of single PCR synthesis were more homogeneous and easier to control the PCR mixture concentration and microarray sample content. In conclusion, microarray analysis is a fast, sensitive, specific, and high throughput method for detecting O157:H7.

REFERENCES

1 **Besser RE,** Griffin PM, Slutsker L. Escherichia coli O157:H7 gastroenteritis and the hemolytic uremic ayndrome: an emerging infectious disease. *Annu Rev Med* 1999; **50**: 355-367
2 **Karmali MA,** Steele BT, Petric M, Lim C. Sporadic cases of haemolytic-uraemic syndrome associated with faecal cytotoxin and cytotoxin-producing Escherichia coli in stools. *Lancet* 1983; **1**: 619-620
3 **Ibekwe AM,** Watt PM, Grieve CM, Sharma VK, Lyons SR. Multiplex fluorogenic real-time PCR for detection and quantification of Escherichia coli O157:H7 in dairy wastewater wetlands. *Appl Enviro Microbio* 2002; **68**: 4853-4862
4 Guidance for the diagnosis and management of suspected or proven Escherichia coli O157 infection. Prepared by the Scottish Infection Standards and Strategy Group and supported by the Scottish Executive Health Department. *J R Coll Physician Edinb* 2004; **34**: 37-40
5 **Nei QH.** Infection of Escherichia coli O157:H7. *Shijie Huaren Xiaohua Zazhi* 2001; **9**: 944-945
6 **Hinchliffe SJ,** Isherwood KE, Stabler RA, Prentice MB, Rakin A, Nichols RA, Oyston PC, Hinds J, Titball RW, Wren BW. Application of DNA microarrays to study the evolutionary genomic of Yersinia pestis and Yersinia pseudotuberculosis. *Genome Res* 2003; **13**: 2018-2029
7 **McCaffrey RL,** Fawcett P, O'Riordan M, Lee KD, Havell EA, Brown PO, Portnoy DA. A specific gene expression program triggered by Gram-positive bacteria in the cytosol. *Proc Natl Acad Sci USA* 2004; **101**: 11386-11391
8 **Shioda T.** Application of DNA microarray to toxicological research. *J Environ Pathol Toxicol Oncol* 2004; **23**: 13-31
9 **Cody SH,** Glynn MK, Farrar JA, Cairns KL, Griffin PM, Kobayashi J, Fyfe M, Hoffman R, King AS, Lewis JH, Swaminathan B, Bryant RG, Vugia DJ. An outbreak of Escherichia coli O157:H7 infection from unpasteurized commercial apple juice. *Ann Intern Med* 1999; **130**: 202-209
10 **Holland JL,** Louie L, Simor AE, Louie M. PCR detection of Escherichia coli O157:H7 directly from stools: evaluation of commercial extraction methods for purifying fecal DNA. *J Clin Microbiol* 2000; **38**: 4108-4113
11 **Fortin NY,** Mulchandani A, Chen W. Use of real time polymerase chain reaction and molecular beacons for the detection of Escherichia coli O157:H7. *Anal Biochem* 2001; **289**: 281-288
12 **Wang L,** Rothemund D, Curd H, Reeves PR. Sequence diversity of the Escherichia coli H7 fliC genes: implication for a DNA-based typing scheme for *E. coli* O157:H7. *J Clin Microbiol* 2000; **38**: 1786-1790

13 **Blanco M,** Blanco JE, Mora A, Rey J, Alonso JM, Hermoso M, Hermoso J, Alonso MP, Dahbi G, Gonzalez EA, Bernardez MI, Blanco J. Serotypes, virulence genes, and intimin types of Shiga toxin (verotoxin)-producing Escherichia coli isolates from healthy sheep in Spain. *J Clin Microbiol* 2003; **41**: 1351-1356
14 **Fagan PK,** Hornitzky MA, Bettelheim KA, Djordjevic SP. Detection of shiga-like toxin (stx_1 and stx_2), intimin (eaeA), and enterohemorrhagic Escherichia coli (EHEC) hemolysin (EHEC hlyA) genes in animal feces by multiplex PCR. *Appl Environ Microbiol* 1999; **65**: 868-872
15 **Call DR,** Brockman FJ, Chandler DP. Detecting and genotyping Escherichia coli O157:H7 using multiplexed PCR and nucleic acid microarrays. *Int J Food Microbiol* 2001; 67: 71-80
16 **Syrmis MW,** Whiley DM, Thomas M, Mackay IM, Williamson J, Siebert DJ, Nissen MD, Sloots TP. A sensitive, specific, and cost-effective multiplex reverse transcriptase-PCR assay for the detection of seven common respiratory viruses in respiratory samples. *J Mol Diagn* 2004; **6**: 125-131
17 **Dolan PL,** Wu Y, Ista LK, Metzenberg RL, Nelson MA, Lopez GP. Robust and efficient synthetic method for forming DNA microarrays. *Nucleic Acids Res* 2001; **29**: E107
18 **Okamoto T,** Suzuki T, Yamamoto N. Microarray fabrication with covalent attachment of DNA using bubble jet technology. *Nat Biotechnol* 2000; **18**: 384-385
19 **Schmidt H,** Scheef J, Huppertz HI, Frosch M, Karch H. Escherichia coli O157:H7 and O157:H(-) strains that do not produce Shiga toxin: phenotypic and genetic characterization of isolates associated with diarrhea and hemolytic-uremic syndrome. *J Clin Microbiol* 1999; **37**: 3491-3496

Science Editor Wang XL and Li WZ **Language Editor** Elsevier HK

PO Box 2345, Beijing 100023, China
www.wjgnet.com
wjg@wjgnet.com

ELSEVIER

World J Gastroenterol 2005;11(37):5816-5820
World Journal of Gastroenterology ISSN 1007-9327
© 2005 The WJG Press and Elsevier Inc. All rights reserved.

• *BASIC RESEARCH* •

Enteroaggregative *Escherichia coli* isolated from Chinese diarrhea patients with high-pathogenicity island of *Yersinia* is involved in synthesis of siderophore yersiniabactin

Jing Hu, Biao Kan, Zhi-Hua Liu, Shou-Yi Yu

Jing Hu, Shou-Yi Yu, Department of Epidemiology, Southern Medical College, Guangzhou 510515, Guangdong Province, China
Biao Kan, Department of Genetics, Institute of Epidemiology and Microbiology, Chinese Center for Disease Control and Prevention, Beijing 102206, China
Zhi-Hua Liu, Department of Infectious Diseases, Nanfang Hospital, Southern Medical College, Guangzhou 510515, Guangdong Province, China
Supported by the National Basic Research Program of Ministry of Science and Technology of China, No. G1999054101
Co-first-author: Jing Hu
Co-correspondent: Shou-Yi Yu
Correspondence to: Professor Shou-Yi Yu, Department of Epidemiology, Southern Medical College, Guangzhou 510515, Guangdong Province, China. yushouyi@fimmu.com
Telephone: +86-20-61648313 Fax: +86-20-61648312
Received: 2005-01-08 Accepted: 2005-02-28

Abstract

AIM: To investigate the distribution of 12 high-pathogenicity island (HPI) genes and the relation between HPI genes and expression of yersiniabactin (Ybt) in enteroaggregative *E.coli* (EAggEC) isolated from Chinese diarrhea patients.

METHODS: The distribution of 12 HPI genes was investigated by PCR and DNA hybridization in two prototype strains of EAggEC, EAggEC 17-2, EAggEC O42, and 6 clinical EAggEC isolates from China. The production of siderophore Ybt in HPI-positive strains was detected by reporter gene bioassay to determine the relation between HPI genes and expression of Ybt. Flow cytometry was used to detect fluorescent signal of the reporter strain that could designate production of Ybt.

RESULTS: Seven strains were HPI-positive and one strain was HPI-negative. Six of the seven HPI-positive strains were inserted into *asnT-tRNA* site. Moreover, seven EAggEC HPI-positive strains revealed enhanced fluorescence signal but the EAggEC HPI-negative strain did not. However, there was a difference in Ybt expression condition and level among these seven EAggEC HPI-positive strains. Although UFT073 strain, the prototype strain of uropathogenic *E.coli* (UPEC), carried the complete HPI core part, we did not detect the expression of Ybt in it.

CONCLUSION: EAggEC HPI-positive strains can express the Ybt system, but the presence of HPI core part does not mean the functional expression of Ybt.

© 2005 The WJG Press and Elsevier Inc. All rights reserved.
Key words: High-pathogenicity island; Enteroaggregative *Escherichia coli*; Yersiniabactin

Hu J, Kan B, Liu ZH, Yu SY. Enteroaggregative *Escherichia coli* isolated from Chinese diarrhea patients with high-pathogenicity island of *Yersinia* is involved in synthesis of siderophore yersiniabactin. *World J Gastroenterol* 2005; 11(37): 5816-5820
http://www.wjgnet.com/1007-9327/11/5816.asp

INTRODUCTION

High-pathogenicity island (HPI) encoding synthesis and uptake of the siderophore yersiniabactin (Ybt) has been primarily identified in mouse lethal *Yersinia*: *Yersinia pestis*, *Yersinia pseudotuberculosis* serotypes O1-O3, and *Yersinia entercolitica* 1B biotype[1-5]. The *Yersinia* HPI consists of a 30.5 kb highly conserved functional core region termed Ybt locus and a 5- to 13-kb AT-rich variable part[1]. The core part comprises genes, *irp1-irp5* and *irp9* for the biosynthesis of the Ybt, *irp6-irp8* and *fyuA* for the uptake of Fe-Ybt, the AraC-like regulator *ybtA* and the integrase *intB* resides on the 5' end of the HPI right-end extremity next to the *asn-tRNA* bacterial attachment site[6-9]. Ybt-mediated iron acquisition is the main function of HPI[8,10]. Recently, HPI is subsequently identified in other bacterial genera such as *E.coli*, *Citrobacter diversus*, various species of *Klebsiella*[11-16]. Whether HPI in *E.coli* has the functional expression of Ybt is the premise to understand that HPI contributes to virulence or ecological fitness. Schubert *et al*.[14], reported that 93% EAggEC, 5% enteropathogenic *E.coli*, 27% enteroinvasive *E.coli* and 5% enterotoxigenic *E.coli* carry HPI by hybridization with an *irp2* probe, but none of enterohemorrhagic *E.coli* harbors it. It is still unclear why the distribution frequency of HPIs is different among various *E.coli* strains. Considering the high prevalence of HPI in EAggEC, in the present study, we detected all the12 genes of HPI by PCR and DNA hybridization in the EAggEC 17-2, EAggEC O42, and 6 EAggEC clinical isolates from Chinese diarrhea patients. By reporter bioassay, products of Ybt in these strains were determined under iron-rich or -poor conditions to demonstrate the function of *Yersiniae* HPI in EAggEC strains. The relation between HPI genes and their function was discussed.

MATERIALS AND METHODS

Bacterial strains and growth conditions

EAggEC O42 (O44:H18), 17-2 (O3:H2), CFT 073, JM109, and *Y. entercolitica* WA (O:8) were provided by Key Laboratory for Molecular Bacteriology in Chinese Center for Disease Control and Prevention. Six EAggEC strains isolated from Chinese diarrhea patients were confirmed by PCR and DNA hybridization with EAEC specific primer[17]. The codes of these strains were EAEC 47/37, EAEC 66, EAEC SS23, EAEC B86-2, EAEC E1073, and EAEC 52/46. The reporter strain *WA-CS irp1*:*KN* [14,18,19] was kindly provided by Professor A. Rakin. *Yersinia* strains were grown in Luria Bertani (LB) broth with shaking at 28 ℃ for 48 h and other *E.coli* strains at 37 ℃ for 24 h. The iron-deficient medium (LBD) was obtained by the addition of 0.2 mmol/L dipyridyl (Sigma) to LB broth. *Y. enterocolitica* WA (O:8) was used as positive control, while *E.coli* JM109 as negative control for PCR amplification and DNA blotting and Ybt assay.

Primers and PCR amplification

PCR was carried out in a 50 μL reaction volume containing template DNA (5 μL of boiled lysate), 1.5 mmol/L $MgCl_2$, 0.4 mmol/L of each of dNTPs, 0.5 μmol/L of each primer, and 25 U of Taq polymerase (TAKARA, Japan) with an automated thermal cycler (GeneAmp 9700, PE Biosystems, USA). The primers were designed according to the HPI sequence of *Yersinia* from GenBank and synthesized by Sangon (Shanghai, China).

Each set of primers and size of the amplified fragments are listed in Table 1. The pre-denaturation (94 ℃, 5 min) was followed by 30 cycles of denaturation (94 ℃, 1 min), annealing (53-58 ℃, 40 s-1 min), and extension (72 ℃, 30 s-2 min 30 s) with an additional extension step (72 ℃, 7 min). In this study, we amplified all the 12 genes within HPI functional core part. Among them, *asnT-tRNA-intB* fragment included 3' end partial sequence of *asnT-tRNA* gene and complete *intB* gene, while others contained the partial fragment within the internal of the corresponding gene. PCR products were electrophoresed in 1-1.5% agarose gels stained with ethidium bromide and visualized under UV light.

Dot blotting

Dot blotting for the *fyuA* and *irp2* genes was performed on DNA extracted from each strain and spotted on positively charged pyroxylin membranes. Hybridization was performed at 65 ℃ in 1% SDS/1 moL NaCl/Tris 50 mmol/L HCl, pH 7.5/1% blocking reagent. The membranes were washed in 2× SSC for 15 min at room temperature, then in 2× SSC/0.1% SDS for 30 min at 65 ℃, finally in 0.1× SSC for 5 min at room temperature. The probes were produced by PCR according to the manufacturer's instructions (PCR DIG Probe Synthesis kit, Roche), using the primers and amplification procedure described above. Digoxigenin labeling was probed and hybridized with a DNA labeling and detection kit (DIG Luminescent Detection kit for nucleic acids, Roche) according to the manufacturer's instructions.

Yersiniabactin assay

A reporter strain system, *Y. enterocolitica* strain *WA-CS irp1:KN* (pCJG3.3N), constructed by Schubert *et al.*[18], was used to monitor the expression of Ybt. This strain was deleted in the Ybt biosynthesis gene (*irp1*) and carried the *fyuA-gfp* reporter plasmid pCJG3.3N. As the expression of the *fyuA* gene was unregulated in the presence of the extracellular Ybt, supernatants of bacteria grown under normal (LB medium) or iron-deficient conditions (LBD medium) were applied to this reporter strain, which could lead to increased expression of the *fyuA-gfp*, if Ybt was present.

Table 1 Primers used in this study

Amplified fragment	Length (bp)	Primers	Reference
asnT-tRNA-int	1 505	5′-gctctcgacgtccgtatcgcctgacac-3′ 5′-gctctagatcaacctgtttcgggtcgg-3′	[1], GenBank no.: AJ132668
irp9	529	5′-gctgtcctgaaatacgga-3′ 5′-agtgcgctcgtttatgtt-3′	[1], GenBank no.: AJ132668
irp8	1 176	5′-tgtcatcagttctcttgccg-3′ 5′-ctggtatcggcgctgtctat-3′	[1], GenBank no.: AJ132668
irp7	1 572	5′-atggtggataaacggtgagc-3′ 5′-tatctccagcgccgttggcagtc-3′	[1], GenBank no.: AJ132668
irp6	1 588	5′-tcaccattgagagacgatgc-3′ 5′-tttcctctctggcaggtgat-3′	[1], GenBank no.: AJ132668
ybtA	555	5′-agtgcgctcgtttatgtt-3′ 5′-gcagcagtttctgacgtt-3′	[1], GenBank no.: AJ132668
irp2	267	5′-aaggattcgcctgttaccggac-3′ 5′-tcgtcgggcagcgtttcttct-3′	[19], GenBank no.: L18881
irp1	799	5′-ccggttattgtgaaggtt-3′ 5′-gtgaatgttacggcactaa-3′	[8], GenBank no.: Y12527
irp3	1 139	5′-ggaattcccatggaccggagaacacgttatg-3′ 5′-gctctagatcacagcgcctccttatcatc-3′	[8], GenBank no.: Y12527
irp4	827	5′-gctctagaatgtgcatcccgctgcgg-3′ 5′-aacgcagggtaccgtcacctttctgctgaagtgc-3′	[8], GenBank no.: Y12527
irp5	1 636	5′-cgcggatccggtaccaggtgacgcatgaattcttc-3′ 5′-aactgcagtcaacctgtttcgggtcgg-3′	[8], GenBank no.: Y12527
fyuA	948	5′-gctttatcctctggcctt-3′ 5′-ggcataacgattaacg-3′	[5], GenBank no.: Z35486
EAEC	623	5′-ctggcgaaagactgtatcat-3′ 5′-caatgtatagaaatccgctgtt-3′	[17]

We streaked the bacteria on Luria broth agar plates and inoculated about 5 mL LB medium for overnight culture as a start culture. From this preculture we inoculated the main culture on LB and LBD medium, respectively. The strains were incubated in the media for at least 7 d. Supernatants of the strains were added to the reporter strain, and flow cytometry for the reporter strain was done with an Epics flow cytometer (FACSCalibur, Becton Dickinson) and an argon 488-nm laser was used. The scale was logarithmic, and fluorescence data determined in arbitrary units were collected from 50 000 bacteria.

RESULTS

Integration analysis of HPI genes in EAggEC strains

We examined eight EAggEC strains for the presence of all the 12 HPI genes. *irp1-irp9*, *fyuA*, and *ybtA* genes were detected in seven strains of EAggEC by PCR and the amplification products were the same as *WA* positive control in lengths (Figure 1). One strain (EAEC 47/37) isolated from diarrhea patients did not yield any amplification products of these 12 gene primers.

In *Yersinia*, the site of HPI integration, bacterial chromosomes sharing homologies with the bacteriophage P4 attachment site are located within an *asn-tRNA* locus[4,20]. The *asnT-tRNA-int* fragment was also identified in six of seven HPI-positive strains, but not in EAEC B86-2, indicating that the strain might have a different insert site from others or the edge of HPI was damaged. We also confirmed the results by DNA-blot hybridization, using *irp2* and *fyuA* genes as probe (data not shown). All the 12 HPI genes were detected also in CFT073 strain, the prototype strain of UPEC, demonstrating that the core region of HPI was present in EAggEC strains with a high frequency. Moreover, HPIs in most of these strains were inserted in *asn-tRNA*, as in *Yersinia*.

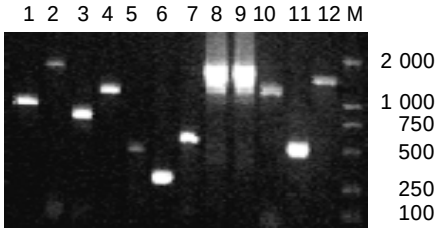


Figure 1 PCR amplification results of 12 genes within HPI core part. Lane 1: *fyuA*, lane 2: *irp5*, lane 3: *irp4*, lane 4: *irp3*, lane 5: *irp1*, lane 6: *irp2*, lane 7: *ybtA*, lane 8: *irp6*, lane 9: *irp7*, lane 10: *irp8*, lane 11: *irp9*, lane 12: *asnT-tRNA-int*, M: DL2000 marker.

Detection of yersiniabactin production in EAggEC strains carrying Yersinia HPI

We detected the expressions of Ybt in eight *EAggEC* strains and UFT073 strain under normal (LB medium) and iron-deficient conditions (LBD medium) using the reporter strain *WA-CS irp1:KN*. *WA* stain was used as positive control while *WA-CS irp1:KN* and *HB101* as negative control.

Figure 2 shows that the culture supernatants of these

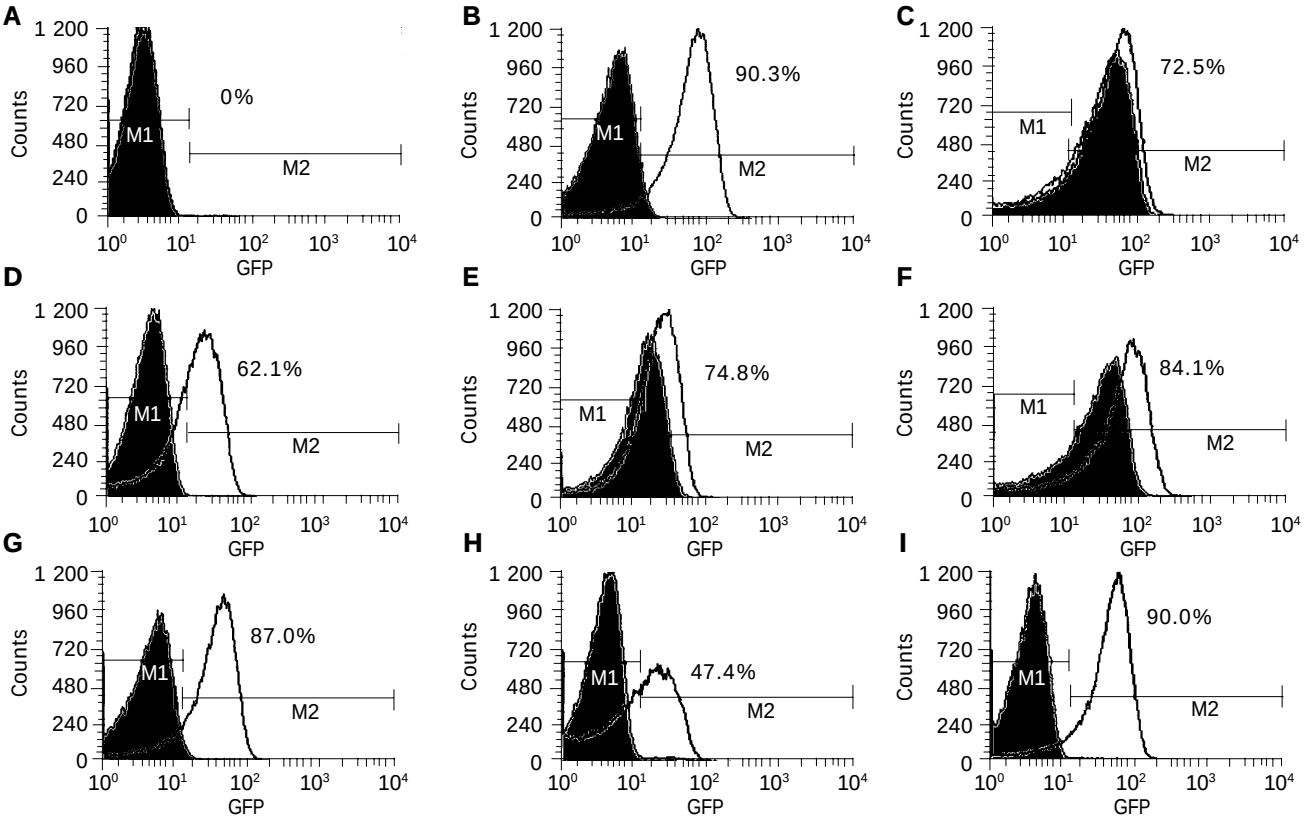


Figure 2 Fluorescence of *fyuA-gfp* in *E.coli* grown on LB media (green curve) and LBD media (black curve). A: *WA-CS irp1::KN(pCJG3.3N),* CFT073(HPI$^+$), HB101(HPI$^-$) and EAEC 47/37(HPI$^-$); B: WA(HPI$^+$); C: EAEC 66(HPI$^+$); D: EAEC SS23(HPI$^+$); E: EAEC B86-2(HPI$^+$); F: EAEC E1073(HPI$^+$); G: EAEC 52/46(HPI$^+$); H: EAEC 17-2 (HPI$^+$); I: EAEC O42 (HPI$^+$); M1: specified range of background of fluorescence signal; M2: specified range of enhanced florescence signal.

seven HPI-positive EAggEC strains grown on iron-deficient medium exhibited apparently enhanced fluorescent signals of the *fyuA-gfp* reporter strain. Among these seven strains, EAggEC O42 had the strongest expression of Ybt (90%), which was nearly equal to the positive control strain WA (90.3%), and EAggEC 17-2 had a comparatively weak signal (47.4%), indicating that the seven EAggEC strains could express Ybt under iron-deficient conditions. Interestingly, the supernatants of three isolates, EAEC66, EAEC B86-2 and EAEC E1073, grown on normal media could stimulate the reporter strain too, but the fluorescent signals were weaker than those grown on the iron-deficient medium. On the other hand, in WA strain, EAggEC 17-2, EAggEC O42, and two other HPI-positive isolates, EAEC SS23 and EAEC 52/46, the fluorescence signals were not enhanced when the bacteria were grown on LB medium. In addition, whether bacteria were grown under iron-rich conditions or iron-deficient conditions, the supernatants of two HPI-negative strains, HB101 and EAggEC 47/37, and one HPI-positive strain, CFT 073, did not affect the expression of the *fyuA-gfp* reporter gene.

The results suggested that EAggEC HPI-positive strains could express the Ybt system, but there was a difference in expression condition and level of Ybt among them.

DISCUSSION

In the genus *Yersinia*, *irp1-irp5* and *irp9* genes are essential for Ybt synthesis, and *irp6*, *irp7*, *fyuA* genes for Ybt transport. The pathway of Ybt uptake is blocked if any one of these genes mutates or misses. In this study, we investigated whether EAggEC strains carrying *Yersinia* HPI genes could express the corresponding products and whether the series of products could synthesize functional Ybt. In order to understand these events, we should know if these EAggEC strains carry the integrated functional core region of HPI.

The presence of HPI in enterobacteriaceae strains has been confirmed only by PCR amplification of *irp2*/*fyuA* and DNA hybridization, but the results of *irp2*/*fyuA* detection are not always identical[11,14]. Usually, the detection rate of *fyuA* is lower than that of *irp2*, which might be explained by the fact that *fyuA* gene is located in the boundary of HPI functional core region, and during the process of evolution it is liable to be damaged or changed due to the instability of HPI. As the exact mechanisms of transport, excision and synthesis of HPI are still unclear, the detection results of individual genes are not sufficient to confirm the presence of integrated functional core region. To avoid this problem, in this study, all the 12 genes in the functional core region of HPI were amplified by PCR. HPI was positive in seven of eight EAggEC strains, and six of seven HPI-positive EAggEC strains were positive *for asnT-tRNA-int* gene but not for EAEC B86-2 strain, indicating that the seven HPI-positive EAggEC strains carry the necessary genes for synthesis, transport and regulation of Ybt. HPIs in these EAggEC strains are often inserted into *asnT* locus on the chromosome, while HPI of EAEC B86-2 strain might be inserted into different loci of other strains or its border sequence is damaged.

To demonstrate the production of Ybt, we used a detection system based on Ybt-induced upregulation of a Ybt reporter gene *fyuA-gfp*. Schubert *et al.*[18], found that 49 of 60 HPI-positive enterobacteriaceae isolated from blood cultures and urine samples can produce Ybt using this system. Our study showed that Ybt could be synthesized in the seven HPI-positive EAggEC strains, including the strain of EAEC B86-2 with an incomplete *asn-tRNA-int* gene. However, not all HPI-positive strains could express Ybt. Based on the HPI transfer mechanism and bacterial evolution, we can make one intriguing hypothesis that under certain selective pressure, bacteria can obtain HPI, and then mutations occur during the process of evolution, thus resulting in the loss of function. However, bacteria could survive by changing themselves to adapt to the environment in the evolutionary process. Another hypothesis is that various bacteria can obtain HPI independently, a kind of random event rather than necessary for living, and the non-functional HPI remains in bacteria. The results suggest that the presence of *irp2*/*fyuA* does not necessarily mean that the integrated 'functional core region' of HPI is complete, and the presence of integrated functional core region of HPI does not necessarily mean that functional Ybt is synthesized.

Under iron-deficient condition (LBD medium), the seven HPI-positive EAggEC strains of Ybt were differently expressed, and some strains were different from WA strain in characteristics of Ybt expression. Only under iron-deficient condition, the Ybt system of WA strain could be activated. On the contrary, in our study expression of Ybt under normal condition could also be detected in three HPI-positive EAggEC strains. The reason why Ybt systems in these strains are easy to be activated remains to be clarified. A possible explanation might be that the difference in genetic structure of bacteria can result in the different need of iron. Though most enterobacteriaceae carry genes encoding high-affinity iron uptake systems, such as enterobactin system and aerobactin system, the fact that most *E.coli* HPI-positive strains have the ability to synthesize Ybt while others do not, may mean that the expression of Ybt possess more specific functions during different infection phases. It was reported that Yen-HPI core genes are insufficient to confer a positive chrome azurol S (CAS) phenotype and mouse virulence to the siderophore-deficient strain *Y. enterocolitica* NF-O (BG 1A), but sufficient to confer MRS40 (serotype O:9, BG 2; phenotype, CAS negative)[21]. Therefore, it is conceivable that the expression of Ybt may also be regulated by genes outside the HPI to adjust bacteria to make a living in iron-limited environment. More studies are needed to clarify the contribution of *Yersinia* HPI to the virulence of *E.coli*.

ACKNOWLEDGMENTS

The authors thank Rakin A (Max von Pettenkofer Institute, Germany) for kindly providing *WA-CS irp1:KN* (pCJG3.3N) reporter strain system and Schubert S (Max von Pettenkofer-Institute, Germany) for technical assistance and helpful discussion.

REFERENCES

1 **Rakin A,** Noelting C, Schubert S, Heesemann J. Common and specific characteristics of the high-pathogenicity island of Yersinia enterocolitica. *Infect Immun* 1999; **67**: 5265-5274
2 **Buchrieser C,** Rusniok C, Frangeul L, Couve E, Billault A, Kunst F, Carniel E, Glaser P. The 102-kb pgm locus of Yersinia pestis: sequence analysis and comparision of selected regions among different Yersina pestis and Yersinia pseudotuberculosis strains. *Infect Immun* 1999; **67**: 4851-4861
3 **Bach S,** Buchrieser C, Prentice M, Guiyoule A, Msadek T, Carniel E. The high-pathogenicity island of Yersinia enterocolitica Ye8081 undergoes low-frequency deletion but not precise excision, suggesting recent stabilization in the genome. *Infect Immun* 1999; **67**: 5091-5099
4 **Buchrieser C,** Brosch R, Bach S, Guiyoule A, Carniel E. The high-pathogenicity island of Yersinia pseudotuberculosis can be inserted into any of the three chromosomal asn tRNA genes. *Mol Microbiol* 1998; **30**: 965-978
5 **Rakin A,** Saken E, Harmsen D, Heesemann J. The pesticin receptor of Yersinia enterocolitica: a novel virulence factor with dual function. *Mol Microbiol* 1994; **13**: 253-263
6 **Bearden SW,** Fetherston JD, Perry RD. Genetic organization of the yersiniabactin biosynthetic region and construction of avirulent mutants in Yersinia pestis. *Infect Immun* 1997; **65**: 1659-1668
7 **Brem D,** Pelludat C, Rakin A, Jacobi CA, Heesemann J. Functional analysis of yersiniabactin transport genes of Yersinia enterocolitica. *Microbiology* 2001; **147**(Pt 5): 1115-1127
8 **Pelludat C,** Rakin A, Jacobi CA, Schubert S, Heesemann J. The yersiniabactin biosynthetic gene cluster of Yersinia enterocolitica: organization and siderophore-dependent regulation. *J Bacteriol* 1998; **180**: 538-546
9 **Perry RD,** Balbo PB, Jones HA, Fetherston JD, DeMoll E. Yersiniabactin from Yersinia pestis: biochemical characterization of the siderophore and its role in iron transport and regulation. *Microbiology* 1999; **145**(Pt 5): 1181-1190
10 **de Almeida AM,** Guiyoule A, Guilvout I, Iteman I, Baranton G, Carniel E. Chromosomal irp2 gene in Yersinia: distribution, expression, deletion and impact on virulence. *Microb Pathog* 1993; **14**: 9-21
11 **Bach S,** de Almeida A, Carniel E. The Yersinia high-pathogenicity island is present in different members of the family Enterobacteriaceae. *FEMS Microbiol Lett* 2000; **183**: 289-294
12 **Clermont O,** Bonacorsi S, Bingen E. The Yersinia high-pathogenicity island is highly predominant in virulence-associated phylogenetic groups of *Escherichia coli*. *FEMS Microbiol Lett* 2001; **196**: 153-157
13 **Karch H,** Schubert S, Zhang D, Zhang W, Schmidt H, Olschlager T, Hacker J. A genomic island, termed high-pathogenicity island, is present in certain non-O157 Shiga toxin-producing *Escherichia coli* clonal lineages. *Infect Immun* 1999; **67**: 5994-6001
14 **Schubert S,** Rakin A, Karch H, Carniel E, Heesemann J. Prevalence of the "high-pathogenicity island" of *Yersinia* species among *Escherichia coli* strains that are pathogenic to humans. *Infect Immun* 1998; **66**: 480-485
15 **Gophna U,** Oelschlaeger TA, Hacker J, Ron EZ. Yersinia HPI in septicemic *Escherichia coli* strains isolates from diverse hosts. *FEMS Microbiol Lett* 2001; **196**: 57-60
16 **Xu JG,** Cheng B, Wen X, Cui S, Ye C. High-pathogenicity island of Yersinia spp. in *Escherichia coli* strains isolated from diarrhea patients in China. *J Clin Microbiol* 2000; **38**: 4672-4675
17 **Nataro JP,** Kaper JB. Diarrheagenic *Escherichia coli*. *Clin Microbiol Rew* 1998; **11**: 142-201
18 **Schubert S,** Cuenca S, Fischer D, Heesemann J. High-pathogenicity island of *Yersinia pestis* in *Enterobacteriaceae* isolated from blood cultures and urine samples: prevalence and functional expression. *J Infect Dis* 2000; **182**: 1268-1271
19 **Guilvout I,** Mercereau-Puijalon O, Bonnefoy S, Pugsley AP, Carniel E. High-molecular-weight protein 2 of Yersinia enterocolitica is homologous to AngR of Vibrio anguillarum and belongs to a family of proteins involved in nonribosomal peptide synthesis. *J Bacteriol* 1993; **175**: 5488-5504
20 **Schubert S,** Rakin A, Fischer D, Sorsa J, Heesemann J. Characterization of the integration site of Yersinia high-pathogenicity island in *Escherichia coli*. *FEMS Microbiol Lett* 1999; **179**: 409-414
21 **Pelludat C,** Hogardt M, Heesemann J. Transfer of the core region genes of the Yersinia enterocolitica WA-C serotype O: 8 high-pathogenicity island to Y. enterocolitica MRS40, a strain with low levels of pathogenicity, confers a yersiniabactin biosynthesis phenotype and enhanced mouse virulence. *Infect Immun* 2002; **70**: 1832-1841

Science Editor Wang XL and Guo SY **Language Editor** Elsevier HK

PO Box 2345, Beijing 100023, China
www.wjgnet.com
wjg@wjgnet.com

ELSEVIER

World J Gastroenterol 2005;11(37):5821-5827
World Journal of Gastroenterology ISSN 1007-9327
© 2005 The WJG Press and Elsevier Inc. All rights reserved.

• *BASIC RESEARCH* •

Evaluation in vinyl chloride monomer (VCM)-exposed workers and the relationship between liver lesions and gene polymorphisms of metabolic enzymes

Shou-Min Zhu, Xue-Feng Ren, Jun-Xiang Wan, Zhao-Lin Xia

Shou-Min Zhu, Xue-Feng Ren, Jun-Xiang Wan, Zhao-Lin Xia, School of Public Health, Fudan University, Shanghai 200032, China
Supported by the National Natural Science Foundation of China, No. 30070650 and National Key Basic Research and Development Program of China, No. 2002CB512909
Co-first-authors: Shou-Min Zhu, Xue-Feng Ren
Correspondence to: Professor Zhao-Lin Xia, Department of Occupational and Environmental Health, School of Public Health, Fudan University, 138 Yixueyuan Road, Shanghai, 200032, China. zlxia@shmu.edu.cn
Telephone: +86-21-54237050
Received: 2004-10-09 Accepted: 2004-12-26

Abstract

AIM: The permissible exposure limit (PEL) of vinyl chloride monomer (VCM) in developed country was 1 p/m (2.79 mg/m^3); and threshold limit value-short term exposure limit (TLV-STEL) in China was 11 times higher [11 p/m (30 mg/m^3)] than it, till 2002. The mechanism of vinyl chloride monomer (VCM)-related carcinogenesis remains unclear. We aimed to analyze occupational health hazards exposure to doses lower than the Chinese occupational health standard in a selected VC polymerization plant in China, and also to elucidate the relationship between genetic polymorphisms and genetic susceptibility on liver lesions of workers exposed to VCM.

METHODS: In order to explore the mechanism of VCM-related health effects, we used a case-control design to investigate the association between the genetic polymorphisms of metabolic enzymes and liver lesions in workers occupationally exposed to VCM. Genotypes of *CYP2E1*, *GSTT1, GSTM1, ALDH2* and *ADH2* were identified using PCR and PCR-RFLP.

RESULTS: Even when the concentration of VCM was lower than the current Chinese occupational health standard, neurasthenia, pharyngeal irritation, liver ultrasonography abnormalities and hemoglobin disorders were significantly higher in exposure subjects compared to non-exposure subjects, and the relative risks (*RR* and 95% *CI*) were 1.74 (1.06-2.85), 1.97 (1.56-2.48), 10.69 (4.38-26.12), and 2.07 (1.20-3.57). *CYP2E1 c1c2/c2c2* genotype was significantly associated with liver damages (*OR* 3.29, 95% *CI* 1.51-7.20, *P*<0.01).

CONCLUSION: The incidences of neurasthenia and liver ultrasonography abnormalities significantly increase when the cumulative exposure dose increases. The genotypes of metabolic enzymes (*CYP2E1 c1c2/c2c2*, null *GSTT1* and *ADH2 1-1*) play important roles in VCM metabolism. Polymorphisms of *CYP 2E1*, *GSTT1* and *ADH2* may be a major reason of genetic susceptibility in VCM-induced hepatic damage.

© 2005 The WJG Press and Elsevier Inc. All rights reserved.

Key words: Vinyl chloride monomer; Hepatic lesions; Cytochrome p450 2E1; Glutathione S-transferase; Aldehyde dehydrogenase-2

Zhu SM, Ren XF, Wan JX, Xia ZL. Evaluation in vinyl chloride monomer (VCM)-exposed workers and the relationship between liver lesions and gene polymorphisms of metabolic enzymes. *World J Gastroenterol* 2005; 11(37): 5821-5827
http://www.wjgnet.com/1007-9327/11/5821.asp

INTRODUCTION

Vinyl chloride monomer (CH_2 = CHCl, VCM) is a colorless gas and a synthetic chemical that does not naturally occur. It is also known as monochloroethylene and chloroethene. At normal temperature it has a mild, sweet odor. Because VCM is easily polymerized to polyvinyl chloride, it is widely used in industry primarily. In fact, in the seventies of last century, 95% of the vinyl chloride produced was polymerized, and the rest is used in the formation of other chemicals. VCM was found to be easily absorbed through the respiratory tract, where it passed into the blood. Most studies concluded that the target organs for the VCM action are the liver, brain, lung, lymphohematopoietic system and skin, and hepatic lesion is its characteristic manifestation[1-3]. In 1974, the US National Institute of Occupational Safety and Health and US Centers for Disease Control and Prevention (CDC), reported that several deaths at one of their plants in a chemical company could be related to occupational exposures of vinyl chloride[4,5]. VCM has been classified by the International Agency for Research on Cancer (IARC) as a Group I carcinogen[6]. Since vinyl chloride is a known carcinogen, it has caused great concern to people who may be exposed to it.

PVC manufacture is a major industry in China, with total annual production of two or three million tons till now. In 1970's, China began to produce PVC, the output increased from 780 000 tons in 1990 to nearly 2 400 000 tons in 2000, and the figure will increase to 3 million tons

in the near future. Thousands of workers could be exposed to VCM. The permissible exposure limit (PEL) of VCM in developed country was 2.79 mg/m^3, and in China which was 11 times higher (30 mg/m^3) than it till 2002. Some studies of health hazards of workers exposure to VCM in China had been done. The results of these studies showed a high prevalence of abnormal liver function and neurasthenia as well as other symptoms due to exposure to VCM[7,8], and more tumors in VCM-exposed workers can be expected in future. However, the workers studied in the aforementioned studies were exposed to VCM at levels higher than the Chinese PEL. There is a general lack of information on estimates of health effects of workers exposed to lower levels of VCM exposure.

Earlier studies were more concerned with exposure levels and effects of vinyl chloride. More recently, there have been studies done on how vinyl chloride reacts in the body leading to cancer, both how it is bioactivated and how it interacts with DNA and forms DNA adducts. An earlier animal study has reported that VCM is primarily metabolized in the liver by CYP2E1 into active chloroethylene oxide (CEO), some of the CEO reacts to form adducts, 7-(2-oxoethyl) guanine. This adduct has been found in the most abundance, but it has not shown mispairing during DNA replication. Since CEO is unstable, it rearranges to chloroacetaldehyde (CAA)[9]. Once CAA is formed, it reacts with adenine, cytosine and guanine to form adducts. Reactions with guanine are less frequent than adenine and cytosine. There are four known etheno-adducts: 1, N^6-ethenoadenine (εA); 3, N^4-ethenocytosine (εC); N^2, 3-ethenoguanine (N^2, 3-εG); and 1, N^2 ethenoguanine (1, N^2 εG)[10]. These adducts contain an additional five-membered ring system. Although these adducts are known to be formed, it is still unclear which one induces errors during DNA and RNA synthesis, for both of which may be reactive with DNA to form DNA adducts[11], and are mutagenic in bacterial systems and mammalian cells[12].

Most of population-attributable cancer heritability is related not to the rare deleterious gene defects but to polymorphic variations in the DNA sequence. CYP2E1 has already been reported to be associated with lung cancer in smokers[13]. In a recent study performed in the Caucasian population, CYP2E1 can account for only a small proportion of the variability in mutagenic response to VCM exposure[14]. Furthermore, CEO may then be metabolized by GSTs, and simultaneously CAA may be metabolized by ALDH2 and ADH2. Thus, those with appropriate types of ALDH2, ADH2, and GSTs may also have elevated reactive intermediates, which can lead to increased liver damages. The metabolism of VCM is mostly concerned with the enzymes CYP2E1,GSTT1, GSTM1, ALDH2 and ADH2. Several studies have shown that all the enzymes exhibit their genetic polymorphisms[15-17], thereby causing different biological effects of metabolizing enzymes.

We aimed to analyze occupational health hazards exposure to doses lower than the Chinese occupational health standard in a selected VC polymerization plant in China, and provide information whether occupational health standard of VCM exposure needs to be revised in China, and also to elucidate the relationship between genetic polymorphisms and genetic susceptibility on liver lesions of workers exposed to VCM.

MATERIALS AND METHODS

Study subjects and epidemiological data

Information was collected from workers at the VC polymerization plant by using interviewer-administered questionnaires, subsequent to informed consent having been obtained during the medical surveillance process. The structured questionnaire contained questions that covered demographic characteristics, lifestyles, including cigarette-smoking habits and alcohol consumption, as well as compiling a detailed occupational history. Individuals who smoke once a day for over 6 mo were defined as smokers, and individuals who consumed once or more alcohol drinks a week for over 6 mo were considered drinkers.

Study subjects exposed to VCM for a period of >1 year in the plant were selected if the following criteria were met: detailed questionnaires had been completed; the hepatitis B, C viruses' status were known; and a blood sample could be provided. At final tally, a total of 163 male and 75 female workers in the industry, with an average age of 33 years (range, 19-54 years) and an average exposure time of 7 years, and who had been occupationally exposed to VCM were included for analysis. One hundred and twenty four male and 88 female employees, with an average age of 38 years (range, 23-60 years), were selected as the non-exposure group, who worked in the same industry as the exposure subjects but not occupationally or environmentally exposed to VCM previously. The workers infected with hepatitis B, C viruses were excluded from the study because hepatitis B, C also leads to liver lesions.

Based on the results of medical examination, we divided the workers in the VCM exposure group into two groups. Fifty eight workers were selected as "liver lesion group" for their liver ultrasonography abnormality and/or alanine aminotransferase (ALT) >40 for at least 2 years and did not get acute hepatitis, chronic hepatitis and cholelithiasis. The "control subjects" were employees who worked at the same worksites as the liver damage group and also had exposure to VCM. Each control was matched for gender, duration of work, worksite, and cumulative exposure dose.

Assessment of vinyl chloride exposure

Exposure levels of VCM in the plant were based on existing environmental monitoring data. The plant kept VCM air concentration data, and the data were generated at different worksites since the beginning of its establishment. The level of VCM was calculated at different worksites of the company, which ranged from 0.3 p/m (0.85 mg/m^3) to 17.8 p/m (48.41 mg/m^3) in air, with a geometric average concentration was 2.6 p/m (7.11 mg/m^3). And then the cumulative exposure dose of each worker was estimated relatively exact. The following equation was used to calculate cumulative exposure dose: Cumulative exposure dose (mg) = Σ (C * M * T) * A* 70%/10^6, where C (mg/m^3): Geometric mean of VCM exposure concentration each year in a special workplace, calculated for all different worksites; M: number of exposure months of each year for a VCM worker; T: 2 h exposure time at each working day, 20 d in each month (exposure time per month was 2 400 min); and A: alveolar ventilation (male average: 6 500 mL/min, female average: 4 300 mL/min, 30% dead space).

Cumulative exposure dose in VCM exposure group ranged from 1 047.41 mg to 33 357.11 mg. Then the VCM exposure subjects were divided into high-exposure and low-exposure groups. The individuals placed into the high-exposure group had been exposed to a cumulative dose of >15 000 mg and those in the low-exposure group with their cumulative dose of ⩽15 000 mg.

Genotyping of polymorphic metabolic enzymes

GSTT1 and *GSTM1* genotypes were determined by co-amplification of two genes as previously described[18,19]. Amplification of human *β-globin* (350 bp) was also performed as a positive control in each reaction to confirm the presence of amplifiable DNA in the samples. The primers used for *β-globin* were 5'-GCC CTC TGC TAA CAA GTC CTA C-3' and 5'-GCC CTA AAA AGA AAA TCG CCA ATC-3'. Individuals with one or more *GSTT1* alleles had a 459-bp fragment and individuals with one or more *GSTM1* alleles had a 350-bp fragment (Figure 1A).

Polymerase chain reaction-restriction fragment length polymorphism (PCR-RFLP) was applied to detect polymorphisms of the *CYP2E1*[20]. The primers used for *CYP2E1* were 5'-TTC ATT CTG TCT TCT AAC TG-3' and 5'-CAG TCG AGT CTA CAT TGT C -3'. The PCR products were digested with restricted endonuclease *P*st I. Homozygous *c1c1* individuals exhibited a product fragment of 410 bp, whereas homozygous *c2c2* individuals revealed a 290-bp and a 120-bp fragment, and heterozygous *c1c2* individuals demonstrated all the three fragments (Figure 1B).

The *ALDH2-Mbo*II polymorphism was determined by a modification of the methods developed by Harada and Zhang[21]. The sequences of *ALDH2* primers were 5'-CAA ATT ACA GGG TCA ACT GCT ATG-3' and 5'-CCA CAC TCA CAG TTT TCT CTT-3'. Homozygous *2-2* individuals demonstrated a single product fragment of 135 bp, whereas homozygous *1-1* individuals revealed both 125- and 10-bp fragments, and heterozygous *1-2* individuals exhibited all three of the fragments (Figure 1C).

According to Chen *et al*.[22], the sequences of *ADH2* primers were 5'- AAT CTT TTC TGA ATC TGA ACA G-3' and 5'- GAA GGG GGG TCA CCA GGT TGC-3', and the PCR products were digested with *Mae* III. Homozygous *1-1* individuals demonstrated a single product fragment of 95 bp, whereas homozygous *2-2* individuals revealed both 60- and 35-bp fragments, and heterozygous *1-2* individuals exhibited all three of the fragments (Figure 1D).

Statistical analysis

SPSS 10.0 version and Epi-info 6.0 software packages were used for statistical analysis. Maentel-Haenszel χ^2-test was used to compare the differences between basic characteristics of the non-exposure and exposure group. Stratified analyses were used to explore the correlation between liver damages and genotypes of *CYP2E1, GSTT1, GSTM1, ALDH2* and *ADH2* among the workers exposed to different levels of VCM. Logistic regression model was used to select the best model and to estimate the *OR* of related risk factors. A *P* value less than 0.05 was considered statistically significant.

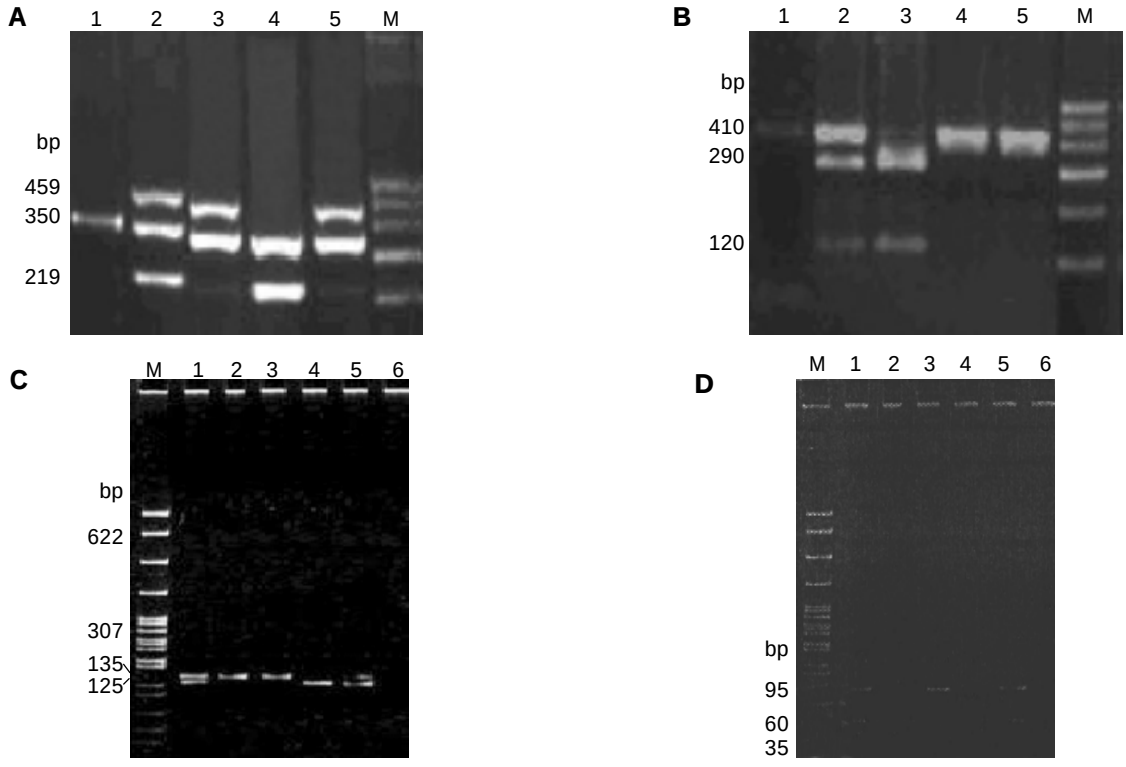


Figure 1 PCR products A: PCR products of GSTT1 and GSTM1. M: DNA marker; lanes 1-5 DNA products; lane 1: none; lane 2: GSTT1 and GSTM1; lane 4: GSTM1; lanes 3, 5: GSTT1. B: PCR-RLFP products of CYP2E1. M: DNA marker; lanes 1-5 DNA products. Homozygous c1c1 shows a single band with 410 bp; homozygous c2c2 shows two bands with 290 bp and 120 bp; and heterozygous c1c2 shows all three bands. C: PCR products of ALDH2. Lanes 1-6 DNA products; M: DNA marker. Homozygous 2-2 shows a single band with 135 bp; homozygous 1-1 shows two bands with 125 bp and 10 bp; and heterozygous 1-2 shows all the three bands. D: PCR products of ADH2. Lanes 1-6: DNA products; M: DNA marker. Homozygous 1-1 shows a single band with 95 bp; homozygous 2-2 shows two bands with 60 bp and 35 bp; and heterozygous 1-2 shows all the three bands.

RESULTS

Comparison of basic characteristics and clinical examinations between exposed and non-exposed groups

No significant difference was observed in age, duration of work, smoking, and drinking between the exposure and non-exposure subjects. All the standards of medical examination were selected as Chinese clinical diagnostic standards. There were significant differences in neurasthenia ($P<0.05$), pharyngeal irritation ($P<0.01$), liver ultrasonography abnormalities ($P<0.01$) and hemoglobin disorders ($P<0.05$) between the exposure and non-exposure groups, and relative risks were 1.74 (1.06-2.85), 1.97 (1.56-2.48), 10.69 (4.38-26.12), and 2.07 (1.20-3.57), respectively. Furthermore, abnormal ECG ($P<0.05$, *RR* 0.51, 95% *CI* 0.32-0.83) and fatty liver ($P<0.05$, *RR* 0.42, 95% *CI* 0.20-0.88) were found significantly higher in non-exposure subjects as compared to exposure subjects. Other symptoms and signs did not show any statistical difference (Table 1).

Stratified analysis of symptoms and signs caused by different cumulative exposure doses in exposure group

Trend chi-square test was used to compare symptoms and signs between the high-exposure and low-exposure groups. There were significant differences in neurasthenia, liver ultrasonography abnormality and pharyngitis between the high-exposure and low-exposure groups ($P<0.05$), with the chi-square values of 6.41, 5.33 and 4.56, respectively. Their incidences increased when the cumulative exposure dose increased (Table 2). However, the other symptoms and signs did not show any statistical difference.

Univariate analysis of genotypes of metabolic enzymes and variables for liver lesions in case-control design

Univariate analysis showed that *CYP2E1 c1c2/c2c2* genotype was significantly associated with liver damages (*OR* 3.29, 95% CI 1.51-7.20, $P<0.01$). Moreover, our results showed that the older or drinking subjects suffered from a higher frequency of liver damages but without statistical significance (OR 2.10, 95% *CI* 0.73-3.43, and *OR* 2.48, 95% *CI* 0.80-7.66). However, other factors did not show any association with liver damages (Table 3).

Correlation between cumulative exposure dose and genotypes of metabolic enzymes in the case-control design

ORs of liver lesions were calculated to investigate the joint effect of VCM exposure and genotypes. *CYP2E1* c1c2/c2c2 genotype was significantly associated with liver lesions (*OR* 4.6, 95% *CI* 1.4-15.1, $P<0.05$) in high-exposure group; and in low-exposure group, the distribution of non-null *GSTT1* was higher in the control group compared to liver lesion group (*OR* 0.3, 95% *CI* 0.1-0.9, $P<0.05$), and *ADH2 1-2/2-2* genotype was the same (*OR* 0.2, 95% *CI* 0.1 -1.0, $P<0.05$).

Table 1 Prevalence of symptoms and signs between exposure and control groups

Symptoms and signs	Exposure group	Control group	Relative risk (RR)
	n = 238(%)	n = 212(%)	
Neurasthenia[a]	40 (16.81)	21 (9.91)	1.74 (1.06-2.58)
Pharyngeal irritation[b]	138 (57.98)	63 (29.72)	1.97 (1.56-2.48)
Abnormal ECG[a]	24 (10.08)	40 (18.87)	0.51 (0.32-0.83)
Cholelithiasis	6 (2.52)	7 (3.30)	0.76 (0.26-2.24)
Renal cyst	2 (0.84)	3 (1.42)	0.59 (0.10-3.52)
Liver ultrasonography abnormality[b]	51 (21.41)	5 (2.36)	10.69 (4.38-26.12)
Fatty liver[a]	10 (4.20)	21 (9.91)	0.42 (0.20-0.88)
Hemoglobin disorders[a]	46 (19.33)	22 (10.38)	2.07 (1.20-3.57)
Hypertension	11 (4.62)	15 (7.07)	0.64 (0.29-1.42)
Hepatic hemangioma	3 (1.26)	3 (1.42)	0.89 (0.18-4.37)
Leucopenia	4 (1.68)	1 (0.47)	3.61 (0.40-32.53)

[a]$P<0.05$ *vs* control group; [b]$P<0.01$ *vs* control group.

Table 2 Prevalence of symptoms and signs among VCM-exposed workers stratified by VCM exposure

Symptoms and signs	VCM exposure					
	≤15 000 mg (n = 186)		>15 000 mg (n = 52)		Total (n = 238)	
Neurasthenia[a]	26	14.0%	14	26.92%	40	16.81%
Respiratory system	3	1.6%	1	1.92%	4	1.68%
Digestive system	4	2.15%	1	1.92%	5	2.10%
Pharyngitis[a]	104	55.9%	34	65.38%	138	57.98%
ECG	19	10.21%	5	9.61%	24	10.08%
Nephridium USG	1	0.53%	2	3.85%	3	1.26%
Gall bladder USG	4	2.15%	4	7.69%	8	3.36%
Liver USG[a]	34	18.3%	17	32.69%	51	21.43%
Fatty liver	7	3.76%	3	5.77%	10	4.20%
Hepatic hemangioma	1	0.53%	2	3.85%	3	1.26%
Splenomegaly	8	4.30%	2	3.85%	10	7.08%

[a]$P<0.05$ *vs* ≤ 15 000 mg group.

Table 3 Liver lesions status according to genotypes and variables of interest in VCM exposure group

	VCM exposure group		Adjusted *OR* (95%*CI*)
	Control (*n* = 58)	Liver lesions (*n* = 58)	
GSTT1			
Non-null	31 (53.4%)	37 (63.8%)	1.0 (reference)
Null	27 (46.6%)	21 (36.2%)	0.65 (0.31-1.37)
GSTM1			
Non-null	37 (63.8%)	36 (62.1%)	1.0 (reference)
Null	21 (36.2%)	22 (37.9%)	1.08 (0.51-2.29)
CYP2E1			
c1c1	43 (74.1%)	27 (46.6%)	1.0 (reference)
c1c2/ c2c2	13/2 (25.8%)	24/7 (53.4%)	3.29 (1.51-7.20) [b]
ALDH2			
1-1	37 (63.8%)	36 (62.1%)	1.0 (reference)
1-2/2-2	17/4 (36.2%)	17/5 (37.9%)	1.08 (0.51-2.29)
ADH2			
1-1	4 (6.9%)	9 (15.5%)	1.0 (reference)
1-2/2-2	24/30 (93.1%)	22/27 (84.5%)	0.40 (0.12-1.39)
Age (yr)			
<35	41 (70.7%)	35 (60.3%)	1.0 (reference)
⩾35	17 (29.3%)	23 (46.6)	2.10 (0.76-3.43)
Drinking			
No	53 (91.4%)	47 (81.0%)	1.0 (reference)
Yes	5 (9.6%)	11 (19.0%)	2.48 (0.80-7.66)
Smoking			
No	40 (69.0%)	41 (71.7%)	1.0 (reference)
Yes	18 (31.0%)	17 (29.3%)	0.92 (0.42-2.04)

[b]*P*<0.01 *vs* control.

The distribution of other genotypes did not have significant difference (Table 4).

Logistic regression analysis of liver lesions of workers exposed to VCM

Logistic regression analysis was employed to model the relationship between liver damages and genotypes of metabolic enzymes and related indicator among VCM workers. We observed a significant association between *CYP2E1 c1c2/ c2c2* and liver lesions (*P*<0.001, *OR* 3.173, 95%*CI* 1.329-7.572) and drinking (*P* = 0.10, *OR* 3.10, 95%*CI* 0.78-12.64), which might be associated with increased OR on liver lesions. But, we could not found any association between liver damages and age, duration of work, smoking and gender (Table 5).

Table 5 Logistic regression analysis of liver lesions

	Logistic regression analysis		
	Coefficient	*P*	*OR* (95% *CI*)
Age (yr)	0.47	0.33	1.60 (0.62-4.19)
Duration of work	0.24	0.60	1.27 (0.52-3.12)
Drinking	1.14	0.10	3.14 (0.78-12.64)
Smoking	-0.90	0.13	0.41 (0.13-1.29)
Gender	-0.06	0.91	0.94 (0.36-2.47)
GSTT1	-0.51	0.23	0.60 (0.26-1.39)
GSTM1	-0.15	0.75	0.86 (0.36-2.10)
CYP2E1	1.16	0.009[b]	3.17 (1.33-7.57)
ALDH2	0.09	0.84	1.09 (0.46-2.58)
ADH2	-0.72	0.31	0.49 (0.12-1.96)
Constant	0.24	0.84	

[b]*P*<0.01 *vs* control.

DISCUSSION

Several studies have proved VCM as a human carcinogen, and hence VCM exposure has strictly been regulated in many countries. In the USA, the Occupational Safety & Health Administration (OSHA) has adopted a permissible exposure limit (PEL) of 1 p/m for VCM as an 8 h time-weighed average (TWA). Taiwan has also adopted 1 p/m as the health standard. In many developing countries, for some reasons, they have not restricted the emissions of VCM to satisfy this standard. Therefore, their occupational health standard for VCM is still at a relatively higher level, for example, in China, the maximum allowable dose was 25 mg/m^3 which was 9-fold higher than that in the advanced countries (Since June 2002 the TWA has been revised to 10 mg/m^3 in China, and the

Table 4 ORs for analysis of correlation between exposure and genotypes

Genotypes	Cumulative VCM exposure					
	⩽15 000 mg			>15 000 mg		
	Control	Liver lesion	*OR* (95% *CI*)	Control	Liver lesion	*OR* (95%*CI*)
GSTT1						
Non-null	15	23	1.0	16	14	1.0
Null	17	9	0.3 (0.1-0.9)[a]	10	12	1.4 (0.5-4.1)
GSTM1						
Non-null	21	21	1.0	16	15	1.0
Null	11	11	1.0 (0.4-2.8)	10	11	1.2 (0.4-3.6)
CYP2E1						
c1c1	23	16	1.0	20	11	1.0
c1c2/ c2c2	9	16	2.6 (0.9-7.2)	6	15	4.6 (1.4-15.1)[a]
ALDH2						
1-1	20	22	1.0	17	14	1.0
1-2/2-2	12	10	0.8 (0.3-2.1)	9	12	1.6 (0.5-5.0)
ADH2						
1-1	2	8	1.0	2	1	1.0
1-2/2-2	30	24	0.2 (0.1-1.0)[a]	24	23	2.1 (0.2-24.5)

[a]*P*<0.05 *vs* ⩽ 15 000 mg group.

maximum allowable dose modified to 25 mg/m^3).

In this study, the level of VCM was lower than National Occupational Health Standard of China, but the incidences of neurasthenia, pharyngeal irritation and liver USG abnormality in the exposure group were still higher compared to non-exposure group, which indicated that even the concentration is around 9 p/m, we should also pay attention to the damage induced by VCM. By modeling the relationship between the symptoms and cumulative exposure dose, the results showed that when cumulative exposure dose increased, the incidence of the symptoms increased in accordance.

We found that, under the same working environment and exposure to the same level of VCM, not all but only some workers in VCM-exposure group had got liver damages, which indicated that there are genetic susceptible differences among the workers. Then we used case-control design to investigate the association between the gene polymorphisms of metabolic enzymes and liver lesions.

VCM is metabolized to CEO (chloroethylene oxide) and chloroacetaldehyde (CAA) by *CYP2E1*, which bind to macromolecular surface and form the electrophilic metabolites that can induce liver lesions, even worsen to hepatic angiosarcoma. A study showed the efficiency of conversion of c2 was higher than c1[23]. Studies by Huang *et al*.[24], and Li *et al*.[14], showed that the frequency of the *CYP2E1* c2c2 genotype was higher in the case group compared to the control group, but the degree of *CYP2E1* necessary to influence genetic susceptibility due to exposure to VCM was different between the Chinese and the Caucasian population. In our study, we found that the frequency of *CYP2E1 c1c2/c2c2* was higher in liver lesions group than that in controls. Stratified by cumulative exposure dose, in high dose group, the *CYP2E1 c1c2/ c2c2* genotype had higher frequency in liver lesions group than that in controls, indicating that *CYP2E1 c1c2/c2c2* genotype might be the main cause of genetic susceptibility of liver damage, which is consistent with previous reports.

All the metabolizing products are further metabolized and detoxified by GSTs; VCM metabolites can also directly bind to glutathione (GSH) after catalyzation by GSTs. This investigation showed that in liver lesions group, the frequency of the *GSTT1*-null genotype was 63.8%, which was higher than 47.4% as reported by Taiwan scholars[24]. And the frequency of the *GSTM1*-null genotype was 62.1%, which was consistent with 60.5% as reported by other scholars[23,24]. The study manifested that *GSTT1* non-null genotype protected the workers from exposure to low level VCM, but another study indicated that *GSTT1* non-null genotype could form reactive metabolites and produce adverse effects[25], which resulted in liver damages. However, we could not see any correlation between *GSTM1* and liver damage.

CEO may spontaneously transform into CAA, which may be subsequently metabolized by *ALDH2*. Although individuals with variant *ALDH2*2* allele have a lower enzyme activity, polymorphism of *ALDH2* has been reported to be associated with alcoholism[26]. Previous studies manifested that CEO produced DNA alkylating agent but CAA could not, suggesting that *ALDH2* had little effect on liver damage[27]. Our study also supports these results.

We found that *ADH2* genotypes *ADH2 1-2/2-2* and *1-1* were significantly different between liver lesions and controls in low-exposure group, which might be because the metabolized efficiency of *ADH2*2* was higher than *ADH2*1* [28]. Moreover, the incidence of liver damage in *ADH2 1-2/2-2* might be lower than *1-1*, if they were exposed to the same concentration of VCM.

The workers in our control group might have some potential VCM exposure based on environmental monitoring in the factory. However, our multivariate adjustment corroborates the possible mechanisms of VCM metabolism and carcinogenesis. In conclusion, VCM workers exposed to high concentration of VCM and with *CYP2E1 c1c2/c2c2* genotype may have a higher risk of liver lesions, and the incidence of liver damage in *ADH2 1-2/2-2* maybe lower than *1-1*, if they were exposed to the same concentration of VCM.

ACKNOWLEDGMENTS

We thank Dr. Shang-Jian Chai and Yu-Fang Li for their help in medical examination and VCM exposure data collection. We are very grateful to Dr. Li Jin (Department of Environmental Health, University of Cincinnati, 3223 Eden Ave, Cincinnati Ohio 45267-0056) for his critical review and scientific editing.

REFERENCES

1 **Uzych L**. Human male exposure to vinyl chloride and possible teratogenic and mutagenic risks: a review. *Hum Toxicol* 1988; **7**: 517-527
2 **Laplanche A**, Clavel-Chapelon F, Contassot JC, Lanouziere C. Exposure to vinyl chloride monomer: results of a cohort study after a seven year follow up. The French VCM Group. *Br J Ind Med* 1992; **49**: 134-137
3 **John Luo JC**, Cheng TJ, Du CL, Wang JD. Molecular epidemiology of plasma oncoproteins in vinyl chloride monomer workers in Taiwan. *Cancer Detect Prev* 2003; **27**: 94-101
4 An evaluation of chemicals and industrial processes associated with cancer in humans based on human and animal data: IARC Monographs Volumes 1 to 20. Report of an IARC Working Group. *Cancer Res* 1980; **40**: 1-12
5 **Cheng TJ**, Huang ML, You NC, Du CL, Chau TT. Abnormal liver function in workers exposed to low levels of ethylene dichloride and vinyl chloride monomer. *J Occup Environ Med* 1999; **41**: 1128-1133
6 **Dietz A**, Langbein G, Permanetter W. Vinyl chloride induced hepatocellular carcinoma. *Klin Wochenschr* 1985; **63**: 325-331
7 **Du CL**, Wang JD. Increased morbidity odds ratio of primary liver cancer and cirrhosis of the liver among vinyl chloride monomer workers. *Occup Environ Med* 1998; **55**: 528-532
8 **Mastrangelo G**, Fedeli U, Fadda E, Valentini F, Agnesi R, Magarotto G, Marchi T, Buda A, Pinzani M, Martines D. Increased risk of hepatocellular carcinoma and liver cirrhosis in vinyl chloride workers: synergistic effect of occupational exposure with alcohol intake. *Environ Health Perspect* 2004; **112**: 1188-1192
9 **Ghissassi F**, Barbin A, Bartsch H. Metabolic activation of vinyl chloride by rat liver microsomes: low-dose kinetics and involvement of cytochrome P450 2E1. *Biochem Pharmacol* 1998; **55**: 1445-1452
10 **Dosanjh MK**, Chenna A, Kim E, Fraenkel-Conrat H, Samson L, Singer B. All four known cyclic adducts formed in DNA by the vinyl chloride metabolite chloroacetaldehyde are released by a human DNA glycosylase. *Proc Natl Acad Sci USA* 1994; **91**: 1024-1028
11 **Guengerich FP**. Roles of the vinyl chloride oxidation prod-

ucts 1-chlorooxirane and 2-chloroacetaldehyde in the *in vitro* formation of etheno adducts of nucleic acid bases. *Chem Res Toxicol* 1992; **5**: 2-5

12 **Cheng KC**, Preston BD, Cahill DS, Dosanjh MK, Singer B, Loeb LA. The vinyl chloride DNA derivative N2,3-ethenoguanine produces G-A transitions in *Escherichia coli*. *Proc Natl Acad Sci USA* 1991; **88**: 9974-9978

13 **Wu X**, Shi H, Jiang H, Kemp B, Hong WK, Delclos GL, Spitz MR. Association between cytochrome P4502E1 genotype, mutagen sensitivity, cigarette smoking and susceptibility to lung cancer. *Carcinogenesis* 1997; **18**: 967-973

14 **Li Y**, Marion MJ, Ho R, Cheng TJ, Coulibaly D, Rosal R, Brandt-Rauf PW. Polymorphisms for vinyl chloride metabolism in French vinyl chloride workers. *Int J Occup Med Environ Health* 2003; **16**: 55-59

15 **Li Z**, Tan W, Shao K. Susceptibility to lung cancer in Chinese is associated with genetic polymorphism in cytochrome P4502E1. *Zhonghua Zhongliu Zazhi* 2000; **22**: 5-7

16 **Wall TL**, Peterson CM, Peterson KP, Johnson ML, Thomasson HR, Cole M, Ehlers CL. Alcohol metabolism in Asian-American men with genetic polymorphisms of aldehyde dehydrogenase. *Ann Intern Med* 1997; **127**: 376-379

17 **Wong NA**, Rae F, Simpson KJ, Murray GD, Harrison DJ. Genetic polymorphisms of cytochrome p4502E1 and susceptibility to alcoholic liver disease and hepatocellular carcinoma in a white population: a study and literature review, including meta-analysis. *Mol Pathol* 2000; **53**: 88-93

18 **Ambrosone CB**, Sweeney C, Coles BF, Thompson PA, McClure GY, Korourian S, Fares MY, Stone A, Kadlubar FF, Hutchins LF. Polymorphisms in glutathione S-transferases (GSTM1 and GSTT1) and survival after treatment for breast cancer. *Cancer Res* 2001; **61**: 7130-7135

19 **Guo JY**, Wan DS, Zeng RP, Zhang Q. The polymorphism of GSTM1, mutagen sensitivity in colon cancer and healthy control. *Mutat Res* 1996; **372**: 17-22

20 **Murata M**, Watanabe M, Yamanaka M, Kubota Y, Ito H, Nagao M, Katoh T, Kamataki T, Kawamura J, Yatani R, Shiraishi T. Genetic polymorphisms in cytochrome P450 (CYP) 1A1, CYP1A2, CYP2E1, glutathione S-transferase (GST) M1 and GSTT1 and susceptibility to prostate cancer in the Japanese population. *Cancer Lett* 2001; **165**: 171-177

21 **Harada S**, Zhang S. New strategy for detection of *ALDH2* mutant. *Alcohol Alcohol Suppl* 1993; **1**: 11-13

22 **Chen WJ**, Loh EW, Hsu YP, Cheng AT. Alcohol dehydrogenase and aldehyde dehydrogenase genotypes and alcoholism among Taiwanese aborigines. *Biol Psychiatry* 1997; **41**: 703-709

23 **Wan J**, Shi J, Hui L, Wu D, Jin X, Zhao N, Huang W, Xia Z, Hu G. Association of genetic polymorphisms in CYP2E1, MPO, NQO1, GSTM1, and GSTT1 genes with benzene poisoning. *Environ Health Perspect* 2002; **110**: 1213-1218

24 **Huang CY**, Huang KL, Cheng TJ, Wang JD, Hsieh LL. The GSTT1 and CYP2E1 genotypes are possible factors causing vinyl chloride induced abnormal liver function. *Arch Toxicol* 1997; **71**: 482-488

25 **Eaton DL**. Biotransformation enzyme polymorphism and pesticide susceptibility. *Neurotoxicology* 2000; **21**: 101-11

26 **Chen WJ**, Loh EW, Hsu YP, Chen CC, Yu JM, Cheng AT. Alcohol-metabolising genes and alcoholism among Taiwanese Han men: independent effect of ADH2, ADH3 and ALDH2. *Br J Psychiatry* 1996; **168**: 762-767

27 **Guengerich FP**, Mason PS, Stott WT, Fox TR, Watanabe PG. Roles of 2-haloethylene oxides and 2-haloacetaldehydes derived from vinyl bromide and vinyl chloride in irreversible binding to protein and DNA. *Cancer Res* 1981; **41**: 4391-4398

28 **Takeshita T**, Yang X, Inoue Y, Sato S, Morimoto K. Relationship between alcohol drinking, ADH2 and ALDH2 genotypes, and risk for hepatocellular carcinoma in Japanese. *Cancer Lett* 2000; **149**: 69-76

Science Editor Kumar M and Guo SY **Language Editor** Elsevier HK

PO Box 2345, Beijing 100023, China
www.wjgnet.com
wjg@wjgnet.com

ELSEVIER

World J Gastroenterol 2005;11(37):5828-5833
World Journal of Gastroenterology ISSN 1007-9327
© 2005 The WJG Press and Elsevier Inc. All rights reserved.

• *CLINICAL RESEARCH* •

Strictures, diaphragms, erosions or ulcerations of ischemic type in the colon should always prompt consideration of nonsteroidal anti-inflammatory drug-induced lesions

Manfred Stolte, Diana Karimi, Michael Vieth, Hildegard Volkholz, Klaus Dirschmid, Sigrid Rappel, Birgit Bethke

Manfred Stolte, Diana Karimi, Michael Vieth, Hildegard Volkholz, Klaus Dirschmid, Sigrid Rappel, Birgit Bethke, Institute of Pathology, Klinikum Bayreuth GmbH, Bayreuth 95445, Germany
Correspondence to: Professor Dr. Manfred Stolte, Institute of Pathology, Klinikum Bayreuth GmbH, Preuschwitzer Str. 101, Bayreuth 95445, Germany. pathologie.klinikum-bayreuth@t-online.de
Telephone: +49-921-4005600 Fax: +49-921-4005609
Received: 2004-11-12 Accepted: 2005-02-18

Abstract

AIM: To investigate whether NSAIDs/ASA lesions in the colon can histologically be diagnosed on the basis of ischemic necrosis similar to biopsy-based diagnosis of NSAIDs/ASA-induced erosions and ulcers of the stomach.

METHODS: In the period between 1997 and 2002, we investigated biopsy materials obtained from 611 patients (415 women, 196 men, average age 60.5 years) with endoscopic focal erosions, ulcerations, strictures or diaphragms in the colon. In the biopsies obtained from these lesions, we always established the suspected diagnosis of NSAID-induced lesions whenever necroses of the ischemic type were found. Together with the histological report, we enclosed a questionnaire to investigate the use of medication. The data provided by the questionnaire were then correlated with the endoscopic findings, the location, number and nature of the lesions, and the histological findings.

RESULTS: At the time of their colonoscopy, 86.1% of the patients had indeed been taking NSAID/ASA medication for years (43.9%) or months (29.5%). The most common indication for the use of these drugs was pain (64.3%), and the most common indication for colonoscopy was bleeding (55.5%). Endoscopic inspection revealed multiple erosions and/or ulcers in 60.6%, strictures in 15.8%, and diaphragms in 3.0% of the patients. The lesions were located mainly in the right colon including the transverse colon (79.9%). A separate analysis of age and sex distribution, endoscopic and histological findings for NSAIDs alone, ASA alone, combined NSAID/ASA, and for patients denying the use of such drugs, revealed no significant differences among the groups.

CONCLUSION: This uncontrolled retrospective study based on the histological finding of an ischemic necrosis shows that the histologically suspected diagnosis of NSAID-induced lesions in the colon is often correct. The true diagnostic validity of this finding and the differentiation from ischemic colitis should, however, be investigated in a prospective controlled study.

© 2005 The WJG Press and Elsevier Inc. All rights reserved.

Key words: Erosion; Ulceration; Stricture; Diaphragm; Ischemic necrose; NSAIDs; ASA

Stolte M, Karimi D, Vieth M, Volkholz H, Dirschmid K, Rappel S, Bethke B. Strictures, diaphragms, erosions or ulcerations of ischemic type in the colon should always prompt consideration of nonsteroidal anti-inflammatory drug-induced lesions. *World J Gastroenterol* 2005; 11(37): 5828-5833
http://www.wjgnet.com/1007-9327/11/5828.asp

INTRODUCTION

The first publications of NSAID-induced strictures in the small bowel[1,2] and colon[3,4] were followed by a number of reports that the intake of NSAIDs leads not only to such pathological changes as chemically-induced reactive gastritis, subepithelial bleeding, erosions and ulcerations complicated by bleeding or perforation in the stomach and duodenum[5,6], but also to erosions, ulcerations, perforations, bleeding[12,13,17], strictures and symptomatic diverticular disease[14-16] in the small and large bowel[7-11]. In animal experiments, it has been shown that as little as a single dose of NSAIDs can result in a high incidence of mortality after 3 d due to intestinal lesions and perforations[18-20].

With regard to the incidence of NSAID-induced lesions in the ileum and colon, the literature contains no reports on data obtained from controlled prospective endoscopic or endoscopy/biopsy studies. From the large Arthritis, Rheumatism, and Ageing Medical Information System databank of arthritic patients, however, it can be seen that 32% of gastrointestinal (GI) hospitalizations in osteoarthritis patients, and 13% of GI hospitalizations of patients with rheumatoid arthritis are due to lower GI diagnosis. In addition, studies of patients with spondyloarthropathy receiving conventional NSAID treatment over the long term have shown that 30-70% of these patients developed a macroscopic or microscopic ileitis, and, with varying frequency, inflammation of the cecum or colon[22-24].

In a post hoc analysis of 8 076 patients with rheumatoid arthritis who were treated with a non-selective NSAID (naproxen) or coxib (rofecoxib), serious lower intestinal events (bleeding, perforation, obstruction, ulceration, and

diverticulitis) were found. The rate of events per 100 patient years was 0.41 for rofecoxib and 0.89 for naproxen. Serious lower GI events accounted for 39.4% of all serious GI events among patients taking naproxen, and 42% among those taking rofecoxib[25].

NSAIDs preparations not only inhibit prostaglandin synthesis via COX inhibition[26], but also uncouple mitochondrial oxidative phosphorylation[27]. These substances also cause local topical toxicity[28], since they are lipid-soluble weak acids that can lead to interaction with surface membrane phospholipids and thus disruption of the gastric epithelial cell barrier and to back diffusion of acid into the mucosa[29,30].

Mucosal injuries in the gastrointestinal tract (GIT) are also a consequence of NSAID-induced liberation of vasoconstricting leukotrienes[31,32], free radicals, platelet thrombi and proteases[33,34,36]. Other publications have demonstrated a connection between NSAID-induced microcirculatory disorders and the adhesion of neutrophil granulocytes to vascular endothelium. In addition, liberation of TNF-α is triggered, which is responsible for the liberation of the intracellular adhesion molecule-1 at the vessel walls, and which can lead to local microcirculatory disorders due to vascular spasms[35,37]. All these synergistic interactions[38,39], particularly the microcirculatory disorders caused by spasms of the tiny blood vessels, can give rise to ischemic erosions and ulcerations in the GIT[40-44] and to diaphragm-like strictures[46,48-51]. Since these lesions may be the cause of blood in the stools or a positive hemoccult test, and the bleeding may lead to chronic hemorrhagic anemia[45,54], the indication for colonoscopy is now being established more frequently in this group of patients. Since colonoscopic biopsies are always taken from macroscopically identifiable lesions, the question arises as to whether the pathologist can establish a suspected diagnosis of NSAID-induced lesions in the biopsy material, and how reliable this suspected diagnosis is. Having already shown that NSAID-induced erosions[52] and ulcerations[56] of the gastric mucosa can often be identified on the basis of necrosis of the ischemic type, we have now examined the question whether this type of necrosis might not also be a suitable diagnostic criterion for NSAID-induced lesions in the colon.

MATERIALS AND METHODS

From 1997 to 2002, we investigated biopsy materials obtained from 611 patients (415 women, 196 men, average age 60.5 years) with focal erosions, ulcerations, strictures or diaphragms at endoscopy. In the biopsies obtained from these lesions, we always established the suspected diagnosis of NSAID-induced lesion whenever necroses of the ischemic type were found (homogeneous cell-poor eosinophilic necroses) to merge imperceptibly into the lamina propria (Figures 1 and 2), and when the clinical and endoscopic pictures and the location of the lesions militated against ischemic colitis. Together with the histological report, we enclosed a questionnaire with the aim of establishing the patient's use of medication (Table 1). The data provided by the questionnaire were subsequently correlated with the endoscopic findings, localization, number and nature of the lesions, and the histological findings.

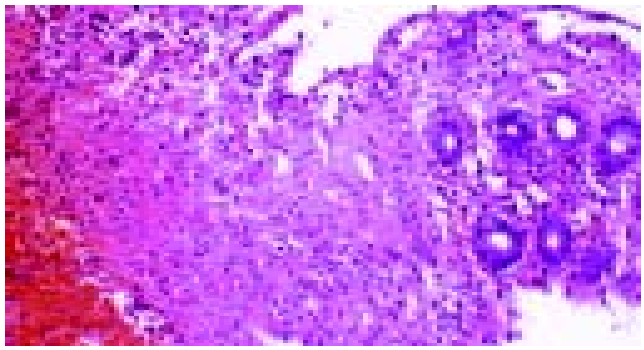


Figure 1 Biopsy from an erosion of mucosa of Bauhin's valve with ischemic necrosis (A).



Figure 2 Biopsy from the centre of an ulceration in cecum with ischemic necrosis and remains of a tablet (B).

Table 1 Questionnaire on NSAID/ASA use

Use of NSAID/ASA	Yes/no
If yes, which drug:.....	
- What dose……	
- How long……..	
Indication for NSAID/ASA…….....	
Indication for colonoscopy……..	

RESULTS

An analysis of the information provided on NSAID/ASA ingestion by the 501 patients with a histologically suspected diagnosis of NSAID/ASA-induced lesion in the colon is presented in Table 2 and shows that 86.1% of those patients actually were on NSAID/ASA medication at the time of their colonoscopy. In most cases, NSAIDs had been used for a period of years or months (Table 3). The most common indication for the use of these drugs was pain (Table 4). The symptoms that had led to an indication for colonoscopy are shown in Table 5. Lumping together the symptoms melena and anemia, and the positive occult blood test, it can be seen that bleeding complications occur in 55.5% of the cases, and are the most common indication for colonoscopy.

The most commonly cited medication (70.5%) was diclofenac (Table 6). In 60.6% of the cases, endoscopy revealed multiple lesions (erosions or ulcers), strictures (15.8%), while diaphragm-like formations (3.0%) were relatively rare. The distribution of the location of these

Table 2 Answers to the questionnaire in Table 1

	n	%
NSAID	326	58.3
ASA	122	20.0
NSAID/ASA	48	7.8

Table 3 Duration of ingestion of NSAID/ASA (%)

D	4.6
Wk	13.9
Mo	21.5
Yr	43.9
No information	16.1

Table 4 Indication for use of NSAID/ASA (%)

Pain	64.3
Polyarthritis	12.3
Coronary heart disease	10.2
Peripheral occlusive arterial disease	7.9
Others	5.7

Table 5 Indications for colonoscopy (%)

Melena	23.9
Positive occult blood test	11.0
Anemia	21.6
Diarrhea	19.4
Abdominal pain	17.7
Weight loss	1.9
Ileus or subileus	1.1
Others	1.1

Table 6 Frequency distribution of used NSAID preparations (%)

Diclofenac	70.5
Ibuprofen	7.3
Piroxicam	1.4
Ketoprofen	0.4
Phenylbutazone	0.2
Combinations	17.6

lesions identifies the right colon, in particular Bauhin's valve, as the most frequently affected site (Table 7).

An analysis of the frequency of the various lesions in terms of solitary or multiple lesions showed that multiple lesions were most commonly ulcers or ulcers in combination with erosions, while solitary lesions were mostly focal erosions. Strictures or diaphragms were also frequently associated with multiple lesions (Table 8).

Table 7 Localization of the lesions (%)

Ileum	4.5
Bauhin's valve	21.3
Cecum	14.8
Ascending colon	19.1
Right flexure	7.0
Transverse colon	15.7
Left flexure	2.8
Descending colon	6.7
Sigmoid colon	5.3
Rectum	2.8

Table 8 Frequency of lesion type (solitary and multiple lesions)

	Solitary (*n* = 207) (%)	Multiple (*n* = 319) (%)
Erosions	63.3	21.3
Ulcers	21.7	56.4
Erosions+ulcers	0	12.2
Regenerative mucosa	15.0	10.1
Strictures	11.1	18.8
Diaphragms	1.0	4.4

A separate analysis of patient's age and sex distribution and endoscopic findings, after dividing cases into those with NSAID use alone, ASA use alone, combined use of NSAID and ASA, and cases denying NSAID/ASA intake, are shown in Table 9. A similar analysis of the histological findings is shown in Table 10. These two analyses revealed no statistically significant differences among the four groups of patients.

DISCUSSION

Our analysis showed that the histologically established diagnosis of suspected NSAID/ASA-induced lesion of the colonic mucosa is probably correct in a high percentage of cases (86.1%), and focal lesions were found, mainly in the right colon, such as Bauhin's valve, cecum and ascending colon. However, since our study was an uncontrolled retrospective study based on histological findings, the results must be considered preliminary, and needs to be checked in prospective studies.

The topographic clustering of the lesions at Bauhin's valve, in the cecum and ascending colon prompts the hypothesis that the lesions are not very likely caused by a

Table 9 Age and sex distribution, location of lesions in right colon, and histological findings in the four groups of patients

	n	F:M	Age (yr)	Location right colon	Endoscopic solitary lesion	Endoscopic multiple lesions	Endoscopic stricture	Endoscopic diaphragm
	356	251:105	63±35	71.2%	36.8%	63.2%	15.4%	3.6%
NSAID	58.3%	2.4:1	28-98	*n* = 131	*n* = 225	*n* = 55	*n* = 13	
	122	75:47	56.5±33.5	76.8%	50%	50%	12.3%	0.8%
ASA	20%	1.6:1	23-90		*n* = 61	*n* = 61	*n* = 15	*n* = 1
	48	39:9	68±21	80.8%	31.2%	68.8%	25%	2.1%
NSAID+ASA	7.8%	4.3:1	47-89		*n* = 15	*n* = 33	*n* = 12	*n* = 1
	85	50:35	54.5±35.5	75.6%	68%	31.8%	8.2%	1.2%
NoNSAID/ASA	13.9%	1.4:1	19-90		*n* = 58	*n* = 27	*n* = 7	*n* = 1

Table 10 Frequency of histological findings in the four groups of patient

	Solitary erosion	Solitary ulcer	Solitary regenerative mucosa	Multiple erosions	Multiple ulcers	Multiple erosions+ ulcers	Multiple regenerative mucosa
NSAID (%)	23.7	76.3	13	36.5	46.6	10.8	6.1
	n = 27	*n* = 8	*n* = 17	*n* = 101	*n* = 129	*n* = 30	*n* = 17
ASA (%)	26.2	55.7	14.8	26.2	51	9.7	13.1
	n = 16	*n* = 34	*n* = 9	*n* = 16	*n* = 32	*n* = 6	*n* = 8
NSAID+ASA	26.6	66.6	6.8	21.2	57.6	15.2	6
(%)	*n* = 4	*n* = 10	*n* = 1	*n* = 7	*n* = 19	*n* = 5	*n* = 2
No	27.6	65.6	3.4	25.9	59.3	3.7	11.1
NSAID/ASA							
(%)	*n* = 16	*n* = 38	*n* = 2	*n* = 7	*n* = 16	*n* = 1	*n* = 3

generalized, but by a topical local injurious effect of the NSAID/ASA preparations. This hypothesis is supported by the fact that these lesions were, in many cases, associated with the use of retard preparations, and that in particular the "bottleneck" at Bauhin's valve was involved. In those patients using non-retard preparations, it might be interesting to establish whether diarrhea associated with rapid transit of the medication into the colon was present. This point would have to be clarified in a prospective study, since we did not request information about a temporal relationship to diarrhea and the use of the medication. In support of a topical mucosa-injuring effect of NSAID/ASA, there are also numerous case reports on the use of retard preparations and on the preferential sites of the lesions in the right colon[42,44,50,51,53].

An unclear finding of our analysis that appeared surprising at first sight was the relatively high percentage of patients taking ASA (20%). It has, however, been shown in earlier publications that ingestion of ASA can cause bleeding not only in the upper GIT, but also in the lower GIT[10,11]. In the present study, we did not specifically investigate the indication for ASA use. However, since chronic ingestion of ASA is usually found in patients with arteriosclerosis, in particular in patients with coronary heart disease[57], cerebral circulatory disorders[58] and peripheral arterial occlusive disease[59], the question must, of course, be considered whether these necroses of the ischemic type might not be due to the underlying disease rather than to the use of ASA. Militating against this possibility, however, is the fact that ischemic colitis in arteriosclerosis[60,61] has other predilection sites, particularly the left colon, in the "borderland area" of the arterial supply between the left colic artery and the inferior mesenteric artery, where the endoscopic picture is of an accumulation of erosions rather than focal erosions and ulcers, and that in these patients, acute perianal bleeding is often found.

Also surprising are the results of our comparative analysis of the four groups of patients (only NSAIDs, only ASA, NSAIDs in combination with ASA, and no known use of NSAID/ASA). Neither the endoscopic nor the histological findings differed among these four groups; this might indicate either that the patients in the no NSAID/ASA group often simply denied using such medication, or that the physicians had not questioned the patients specifically about over-the-counter painkillers.

Our retrospective study should prompt a prospective study. Ideal would be a prospective colonoscopic investigation of patients taking NSAIDs, with consideration being given to the nature and duration as also of the galenic formulation of the preparations employed. Of particular interest would be an investigation of the side effects of COX-1 inhibitors in comparison with COX-2 inhibitors, which also can cause lesions in the lower GIT[21,25]. Only in this way could we obtain data on the incidence, localization and type of lesions as a function of the medication. Such a study in patients with no colon-specific symptoms would, however, hardly be ethically justifiable. Worthy of discussion, however, is the question whether, in patients on NSAIDs, a hemoccult test could be performed and, in the event of positive results, an indication for colonoscopy established. Also, an investigation of the incidence of NSAID-induced lesions in the small intestine employing capsule endoscopy should receive consideration.

What the results of our retrospective study definitely show, however, is that the pathologist who finds focal erosions, ulcers and strictures, together with necroses of the ischemic type in biopsies from the (mainly right) colon, should, more than previously, suggest in his report the possibility of an NSAID-induced mucosal injury. This would then prompt the care-providing physician to look into the patient's use of NSAIDs, the type of preparation employed, its dosage and galenic formulation, and then possibly replace or discontinue the medication with the aim of clarifying the etiopathogenesis of the lesion and preventing such serious complications such as perforation, chronic bleeding, and strictures. In principle, however, the NSAID/ASA-induced lesions cannot be differentiated histologically from ischemic lesions. This, too, should be emphasized in the histological report. Although arteriosclerosis-induced ischemic colitis is usually located in the left colon, and often manifests as multiple lesions distributed over a large area, other rare causes of ischemic colitis (e.g., vasculitis, distension colitis, emboli) may also give rise to irregularly distributed focal lesions at atypical locations. In our experience as consultant pathologists investigating biopsy and surgical material, the most common endoscopic and histological wrong diagnosis in NSAID-induced colonopathy is Crohn's disease established on the basis of the discontinuous changes due to NSAID colonopathy. This diagnostic error can, however, be avoided by giving consideration to the age of the patient, since NSAID-induced colonopathy is seen mainly in the elderly people. However, also in the case of young patients with

no other clinical and laboratory findings suggestive of Crohn's disease, the physician should be prompted to enquire about the use of NSAIDs, and if such use is denied, to apply ASA serology to test for possible misuse of painkillers[54].

In conclusion, the present study shows that our retrospective suspected diagnosis of NSAID/ASA-induced lesions based on the histological finding of a focal ischemic necrosis of the colonic mucosa, located mainly in the right colon, is often correct, and may serve to prevent serious complications of NSAID-induced colonopathy. The actual utility of such histological findings and the differential diagnosis vis-α-vis ischemic colitis must, however, be checked in a prospective controlled study.

REFERENCES

1 **Lennert KA**, Kootz F. Nil nocere. Arzneimittelbedingte Dünndarmulcera. *Münch Med Wochenschr* 1967; **40**: 2058-2062
2 **Sturges HF,** Krone CL. Ulcerations and stricture of the jejunum in a patient of long-term indomethacin therapy. *Am J Gastroenterol* 1973; **59**: 162-169
3 **Huber T**, Ruchti C, Halter F. Non-steroidal anti-inflammatory drug-induced colonic structures: a case report. *Gastroenterology* 1991; **100**: 1119-1122
4 **Fellows IW**, Clarke JM, Roberts PF. Non-steroidal anti-inflammatory drug-induced jejunal and colonic diaphragm disease: a report of two cases. *Gut* 1992; **33**: 1424-1426
5 **Lanas A,** Bajador E, Serrano P, Fuentes J, Carreno S, Guardia J, Sanz M, Montoro M, Sainz R. Nitrovasodilators, low-dose aspirin, other nonsteroidal anti-inflammatory drugs, and the risk upper gastrointestinal bleeding. *N Engl J Med* 2000; **343**: 834-839
6 **Rockall TA,** Logan RF, Devlin HB. Incidence of and mortality from acute upper gastrointestinal haemorrhage in the united kingdom. Steering committee and members of the national audit of acute upper gastrointestinal haemorrhage. *BMJ* 1995; **311**: 222-226
7 **Bjarnason I**, Hayllar H, MacPherson AJ, Russell AS. Side effects of non steroidal anti-inflammatory drugs on the small and large intestine in humans. *Gastroenterology* 1993; **104**: 1832-1847
8 **Langman MJS**, Morgan L, Worrall A. Use of anti-inflammatory drugs by patients admitted with small or large bowel perforations and haemorrhage. *Br Med J* 1985; **290**: 347-349
9 **Allison MC**, Howatson AG, Torrance CJ, Lee FK, Russell RI. Gastrointestinal damage associated with the use of nonsteroidal antiinflammatory drugs. *N Engl J Med* 1992; **327**: 749-754
10 **Lanas A**, Sekar MC, Hirschowitz BI. Objective evidence of aspirin use in both ulcer and nonulcer upper and lower gastrointestinal bleeding. *Gastroenterology* 1992; **103**: 862-869
11 **Lanas A**, Serrano P, Bajador E, Esteva F, Benito R, Sainz R. Evidence of aspirin use in both upper and lower gastrointestinal perforation. *Gastroenterology* 1997; **112**: 683-689
12 **Wilcox CM**, Alexander LN, Cotsonis GA, Clark WS. Nonsteroidal antiinflammatory drugs are associated with both upper and lower gastrointestinal bleeding. *Dig Dis Sci* 1997; **42**: 990-997
13 **Holt S**, Rigoglioso V, Sidhu M, Irshad M, Howden CW, Mainero M. Nonsteroidal anti-inflammatory drugs and lower gastrointestinal bleeding. *Dig Dis Sci* 1993; **38**: 1619-1623
14 **Wilson RG**, Smith AN, Macintyre IMC. Complications of diverticular disease and non-steroidal anti-inflammatory drugs: a prospective study. *Br J Surg* 1990; **77**: 1103-1104
15 **Campbell K**, Steele RJC. Non-steroidal anti-inflammatory drugs and complicated diverticular disease: a case-control study. *Br J Surg* 1991; **78**: 190-191
16 **Aldoori WH**, Giovannucci EL, Rimm EB, Wing AL, Willett WC. Use of acetaminophen and nonsteroidal anti-inflammatory diverticular disease in men. *Arch Fam Med* 1998; **7**: 255-260
17 **Bombardier C**, Laine L, Reicin A, Shapiro D, Burgos-Vargas R, Davis B, Day R, Bosi Ferraz M, Hawkey CJ, Hochberg MC, Kvien TK, Schnitzer TJ. Comparison of upper gastrointestinal toxicity of rofecoxib and naproxen in patients with rheumatoid arthritis. *N Engl J Med* 2000; **343**: 1520-1528
18 **Robert A**. An intestinal disease produced experimentally by a prostaglandin deficiency. *Gastroenterology* 1975; **69**: 1045-1047
19 **Whittle BJR**. Temporal relationship between cyclo-oxygenase inhibition, as measured by prostacyclin biosynthesis, and the gastrointestinal damage induced by indomethacin in the rat. *Gastroenterology* 1981; **80**: 94-98
20 **Evans SM**, Whittle BJR. Interactive roles of superoxide and inducible nitric oxide synthase in rat intestinal injury provoked by non-steroidal anti-inflammatory drugs. *Eur J Pharmacol* 2001; **429**: 287-296
21 **Sigthorsson G**, Simpson RJ, Walley M, Anthony A, Foster R, Hotz-Behoftsitz C, Palizbau A, Pombo J, Watts J, Morham SG, Bjarnason J. COX-1 and 2, intestinal integrity, and pathogenesis of nonsteroidal anti-inflammatory drug enteropathy in mice. *Gastroenterology* 2002; **122**: 1913-1923
22 **De Vos M**, Cuvelier C. Mielanths H. Ileocolonoscopy in seronegative spondylarthopathy. *Gastroenterology* 1989; **96**: 339-344
23 **Leirisolo-Repo H**, Turunen U, Stenman S. High frequency of silent inflammatory bowel disease in spondylarthropathy. *Arthritis Rheum* 1994; **37**: 23-31
24 **Smale S**, Natt RS, Orchard TR, Russell AS, Bjarnason I. Inflammatory bowel disease and spondylarthropathy. *Arthritis Rheum* 2001; **44**: 2728-2736
25 **Laine L**, Connors LG, Reicin A, Howkey CJ, Burgos-Vargas R, Schnitzer TJ, Yu Q, Bombardier C. Serious lower gastrointestinal clinical events with nonselective NSAID or coxib use. *Gastroenterology* 2003; **124**: 288-292
26 **Vane JR**. Inhibition of prostaglandin synthesis as a mechanism of action of aspirin - like drugs. *Nature* 1971; **231**: 232-235
27 **Mahmud T**, Rafi SS, Scott DL, Wrigglesworth JM, Bjarnason I. Nonsteroidal antiinflammatory drugs and uncoupling of mitochondrial oxidative phosphorylation. *Arthritis Rheum* 1996; **39**: 1998-2003
28 **Brune K**, Schweitzer A, Eckert A. Parietal cells of the stomach trap salicylates during absorption. *Biochem Pharmacol* 1977; **26**: 1735-1740
29 **Lichtenberger LM**, Wang ZM, Romero JJ, Ulloa C, Perez JC, Giraud MN, Barreto JC. Non-steroidal anti-inflammatory drugs (NSAIDs) associate with zwitterionic phospholipids: Insight into the mechanism and reversal of NSAID-induced gastrointestinal injury. *Nat Med* 1995; **1**: 154-158
30 **Giraud MN**, Motta C, Romero JJ, Lichtenberger LM. Interaction of indomethacin and naproxen with gastric surface-active phospholipids: a possible mechanism from the gastric toxicity of nonsteroidal anti-inflammatory drugs (NSAIDs). *Biochem Pharmacol* 1999; **57**: 247-254
31 **Rampton DS**. Non-steroidal antiinflammatory drugs and the lower gastrointestinal tract. *Scand J Gastroenterol* 1987; **22**: 1-4
32 **Pihan GRC**, Szabo S. Vascular injury in acute gastric mucosa damage. Mediatory role of leucotrienes. *Dig Dis Sci* 1988; **33**: 625-632
33 **Davies NM**. Toxicity of nonsteroidal anti-inflammatory drugs in the large intestine. *Dis Colon Rectum* 1995; **38**: 1311-1321
34 **Wallace JL,** Arfors KE, McKnight GW. A monoclonal antibody against the CK 18 leucocyte adhesion molecule prevents indomethacin-induced gastric damage in the rabbit. *Gastroenterology* 1991; **100**: 878-883
35 **Davies NM**, Wallace JW. Nonsteroidal anti-inflammatory drug-induced gastrointestinal toxicity: New insights into an old problem. *J Gastroenterol* 1997; **32**: 127-133
36 **Appleyard CB**, McCafferty DM, Tigley AW, Swain MG, Wallace JL. Tumor necrosis factor mediation of NSAID-induced gastric damage: role of leukocyte adherence. *Am J Physiol* 1996; **270**: G42-48
37 **Rothlein R**, Czajkowski M, Kishimoto TK. Intercellular adhesion molecule-1 in inflammatory response. *Chem Immunol* 1991; **50**: 135-142

38 **Whittle BJR**. New dogmas or old? *Gut* 2003; **52**: 1379-1381
39 **Bjarnason I**, Takeuchi K, Simpson R. NSAIDs: the emperor's new dogma? *Gut* 2003; **52**: 1376-1378
40 **Aabakken L**, Osnes M. Non-steroidal anti-inflammatory drug-induced disease in the distal ileum and large bowel. *Scand J Gastroenterol* 1989; **163**: 48-55
41 **Gargot D**, Chaussade S, d'Alteroche L. Non-steroidal anti-inflammatory drug-induced colonic strictures: two cases and literature review. *Gastroenterology* 1995; **90**: 2035-2038
42 **Gut A**, Halter F, Ruchti C. Nonsteroidal antirheumatic drugs and acetylsalicylic acid: adverse affects distal to the duodenum. *Schweiz Med Wochenschr* 1996; **126**: 616-625
43 **Bjarnason I,** Hayllar J, MacPherson AJ, Russel AS. Side effects of nonsteroidal anti-inflammatory drugs on the small and large intestine in humans. *Gastroenterology* 1993; **104**: 1832-1847
44 **Gibson GR**, Whitacre EB, Ricotti CA. Colitis induced by non-steroidal anti-inflammatory drugs. Report of four cases and review of the literature. *Arch Intern Med* 1992; **152**: 625-632
45 **Sacanella E**, Munoz F, Cardellach F, Estruch R, Miro O, Urbano-Marquez A. Massive haemorrhage due to colitis secondary to nonsteroidal anti-inflammatory drugs. *Postgrad Med J* 1996; **72**: 57-58
46 **Sukumar L**. Recurrent small bowel obstruction with piroxicam. *Br J Surg* 1987; **74**: 186
47 **Bjarnason I**, Price AB, Zanelli G, Smethurst P, Burke M. Clinicopathological features of nonsteroidal anti-inflammatory drug induced small intestinal strictures. *Gastroenterology* 1988; **94**: 1070-1074
48 **Lang J**, Price AB, Levi AJ, Burke M, Gumpel JM, Bjarnason I. Diaphragm disease: pathology of disease of small intestine induced by non-steroidal anti-inflammatory drugs. *J Clin Pathol* 1988; **41**: 516-526
49 **Levi S**, de Lacey G, Price AB, Gumpel MJ, Levi AJ, Bjarnason I. "iaphragm-like" strictures of the small bowel in patients treated with non-steroidal anti-inflammatory drugs. *Br J Radiol* 1990; **63**: 186-189
50 **Withcomb DC**, Martin SP, Trellis AR, Evans BA, Becich MJ. "Diaphragmlike" stricture and ulcer of the colon during diclofenac treatment. *Arch Intern Med* 1992; **152**: 2341-2343
51 **Halter F**, Weber B, Huber T, Eigenmann F, Frey M, Ruchti C. Diaphragm disease of the ascending colon. Association with sustained-release diclofenac. *J Clin Gastroenterol* 1993; **61**: 74-80
52 **Anthony A**, Dhillon AP, Sim R, Nygard G. Pounder RE, Wakefield AJ. Ulceration, fibrosis and diaphragm-like lesions in the caecum of rats treated with indomethacin. *Aliment Pharmacol Ther* 1994; **8**: 417-424
53 **Robinson MWT**, Leach ICH. Nonsteroidal anti-inflammatory drug-induced colonic stricture. An unusual cause of large bowel obstruction and perforation. *Dig Dis Sci* 1995; **40**: 315-319
54 **Klee M**, Vogel CU, Diehl HG, Stolte M. Das Diaphragma-Kolon - Eine schwerwiegende Nebenwirkung nichtsteroidaler Antirheumatika (NSAR). *Leber Magen Darm* 1998; **28**: 137-141
55 **Stolte M**, Panayiotou S, Schmitz J. Can NSAID/ASA-induced erosions of the gastric mucosa be indentified at histology? *Pathol Res Pract* 1999; **195**: 137-142
56 **Vieth M**, Müller H, Stolte M. Can the diagnosis of NSAID-induced or Hp-associated gastric ulceration be predicted from histology? *J Gastroenterol* 2002; **40**: 783-788
57 The RISC Group. Risk of myocardial infarction and death during treatment with low dose aspirin and intravenous heparin in men with unstable cornary artery disease. *Lancet* 1990; **336**: 827-830
58 The SALT Collaborative Group. Swedish Aspirin Low-Dose Trial /SALT) of 75 mg aspirin as secondary prophylaxis after cerebrovascular ischaemic events. *Lancet* 1991; **338**: 1345-1349
59 **Patrono C**. Aspirin as an antiplatelet drug. *N Engl J Med* 1994; **330**: 1287-1294
60 **Newman JR**, Cooper MA. Lower gastroindestinal bleeding and ischemic colitis. *Can J Gastroenterol* 2002; **19**: 597-600
61 **MacDonald PH**. Ischaemic colitis. *Best Pract Res Clin Gastroenterol* 2002; **16**: 51-61
62 **Singh G**, Ramey DR. NSAID induced gastrointestinal complications: the ARAMIS perspective -1997. Arthritis, Rheumatism, and Aging Medical Information System. *J Rheumatol* 1998; **25**: 8-16

Science Editor Kumar M and Guo SY **Language Editor** Elsevier HK

PO Box 2345, Beijing 100023, China
www.wjgnet.com
wjg@wjgnet.com

ELSEVIER

World J Gastroenterol 2005;11(37):5834-5839
World Journal of Gastroenterology ISSN 1007-9327
© 2005 The WJG Press and Elsevier Inc. All rights reserved.

• *CLINICAL RESEARCH* •

Association between thrombotic risk factors and extent of fibrosis in patients with non-alcoholic fatty liver diseases

N Assy, I Bekirov, Y Mejritsky, L Solomon, S Szvalb, O Hussein

N Assy, O Hussein, Liver Unit and Internal Medicine A, Sieff Hospital, Safed, Israel
I Bekirov, Y Mejritsky, Liver Unit and Internal Medicine B, Sieff Hospital, Safed, Israel
L Solomon, Department of Hematology, Sieff Hospital, Safed, Israel
S Szvalb, Department of Pathology, Sieff Hospital, Safed, Israel
N Assy, O Hussein, Technion Faculty of Medicine, Haifa, Israel
Correspondence to: N Assy, MD, Liver Unit, Sieff Government Hospital, Safed 13100, Israel. assy.n@ziv.health.gov.il
Telephone: +972-4-6828581 Fax: +972-4-6828944
Received: 2004-11-15 Accepted: 2004-12-08

© 2005 The WJG Press and Elsevier Inc. All rights reserved.

Key words: NASH; NAFLD; Thrombotic risk factors; Fibrosis; Protein S; Protein C

Assy N, Bekirov I, Mejritsky Y, Solomon L, Szvalb S, Hussein O. Association between thrombotic risk factors and extent of fibrosis in patients with non-alcoholic fatty liver diseases. *World J Gastroenterol* 2005; 11(37): 5834-5839
http://www.wjgnet.com/1007-9327/11/5834.asp

Abstract

AIM: To evaluate the prevalence of genetic and acquired prothrombotic risk factors and their association with the extent of fibrosis and fatty infiltration in patients with non-alcoholic fatty liver disease (NAFLD).

METHODS: Forty-four patients with chronic hepatitis (28 men and 16 women, with mean age of 45±11 and 49±12 years, respectively) constituted the patient population of this study. The groups were divided as follows: 15 patients with fatty liver (FL); 15 with non-alcoholic steatohepatitis (NASH); 14 with chronic viral hepatitis (CH) diagnosed by histology and liver technetium scan or ultrasound; and 10 healthy individuals. Thrombophilic, coagulation factors and genetic mutations were diagnosed by standard hemostatic and molecular coagulation assays.

RESULTS: Activated protein C (APC) resistance and protein S were the most prevalent thrombotic risk factors (6% and 10% in NAFLD *vs* 21% and 14% in CH; $P<0.01$ and $P<0.05$, respectively). One thrombotic risk factor was identified in 41% of patients (23% mild fibrosis, 18% severe fibrosis) and two thrombotic risk factors in 6% of patients with NAFLD and severe fibrosis. While no differences in APC ratio, lupus anticoagulant, fibrinogen, factor V Leiden, prothrombin, and MTHFR mutation were found. Protein S levels were significantly lower in NASH patients than in patients with FL alone (92±19 *vs* 106±2, $P<0.01$). Protein C levels were markedly higher in patients with NAFLD and mild or severe fibrosis as compared to the patients with CH, respectively (128±40 *vs* 96±14, $P<0.001$ or 129±36 *vs* 88±13, $P<0.01$).

CONCLUSION: Up to 46% of patients with NAFLD may have thrombotic risk factors, and the presence of thrombotic risk factors is correlated with the extent of hepatic fibrosis, suggesting a crucial role of the coagulation system in the pathogenesis of hepatic fibrosis.

INTRODUCTION

The clinical implications of non-alcoholic fatty liver disease (NAFLD) are derived mostly from its common occurrence in the general population (10-24%) and the potential of the condition to progress to fibrosis (40%) and cirrhosis (30%)[1-3]. Non-alcoholic steatohepatitis (NASH) is the most common cause of cryptogenic cirrhosis and is an increasingly common indication for liver transplantation[3]. Obesity, diabetes mellitus, and hyperlipidemia are conditions frequently associated with NASH[4,5]. Although the pathogenesis of NASH is unknown, it has been suggested that hepatic fatty infiltration may stem from continuous delivery of free fatty acids to the liver after ingestion of fatty foods and from increased splanchnic lipolysis of visceral fat, both of which increase hepatic insulin resistance[6]. Recently, two additional mechanisms were reported: oxidative stress/lipid peroxidation; and TNF-α/endotoxin-mediated injuries[7]. To our knowledge, it is still unclear what causes progression from steatosis to steatohepatitis and from steatohepatitis to bridging fibrosis and cirrhosis. Alcohol consumption, hepatic iron deposition[8], drugs, endotoxin[9,10], and polymorphism in cytochrome p450 enzymes[11] have been proposed as putative mechanisms. However, the definitive mechanism is yet to be determined.

Thrombosis of the intrahepatic veins is frequently observed in cirrhosis and has been associated with its progression[12], while occlusion of small intrahepatic veins and sinusoids has been considered as a potential triggering factor of liver tissue remodeling[13]. More recently, Wanless and Shiota[14] proposed a four-step model in patients with NAFLD, including steatosis facilitated by insulin resistance (first step), necrosis induced by lipid peroxidation (second step), release of lipid from hepatocytes into the interstitium leading to direct and inflammatory injury to small hepatic veins (third step), and the venous obstruction with secondary collapse and ultimately fibrosis (fourth step). The involvement of various genetic and acquired thrombotic risk factors in the pathogenesis of vein thrombosis is well established but their role in

NAFLD progression, to our knowledge, has not yet been investigated. The present study was designed to determine whether genetic and acquired thrombotic risk factors might be observed at some stage of liver disease progression in patients with NAFLD as well as their possible association with the extent of fatty infiltration and the extent of hepatic fibrosis.

MATERIALS AND METHODS

Patient population

Forty-four patients (28 men and 16 women, mean age of 45±11 and 49±12 years, respectively) were divided into three groups for the purpose of this study: 15 patients with fatty liver (FL); 15 with steatohepatitis (NASH); 14 with chronic viral hepatitis (CH) diagnosed by histology and liver technetium scan or ultrasound. Ten healthy controls were also included in this study. Patients with antiviral therapy within the past 6 mo, hepatocellular carcinoma, other forms of chronic liver diseases, positive anti-human immunodeficiency antibodies, previous venous thrombosis, chronic immunosuppression therapy, contraceptives or any current anticoagulation therapy were excluded.

Laboratory studies

All laboratory studies including coagulation assays were done within 6 wk of liver biopsy. Full blood count, platelets count, prothrombin time (PT), or INR, partial thromboplastin time (PTT), fibrinogen, liver enzymes including aspartate aminotransferase (AST), alanine aminotransferase (ALT), alkaline phosphates, γ-glutamyl transferase (GGT), glucose, insulin, cholesterol, and triglycerides were measured using commercially available assays. The following parameters were considered as thrombotic risk factors: deficiency in anti-thrombin, protein S, protein C, presence of lupus anticoagulant, activated protein C (APC) resistance with factor V Leiden mutation, fibrinogen, G20210A mutation in the prothrombin gene and MTHFR mutations. Deficiency in anti-thrombin III, protein S, and protein C were diagnosed when the protein level was below 80%, 60%, and 70%, respectively. Blood samples were collected into the vacuum tubes containing trisodium citrate. Platelet poor plasma was prepared by double centrifugation at 2 000 r/min for 15 min at room temperature. The assay, performed on fresh plasma or aliquots stored at -70 ℃ until assay, included factor VIII coagulant activity using factor VIII deficient plasma (Dae Behring) and Platelin-LS (Organon Tecknica, Durham, NC, USA). Antithrombin activity using an amidolytic assay (Coamatic antithrombin, Chromogenix, Montpellier, France), protein C activity using a clotting assay (IL Pro Clot, Instrumentation Laboratory, Lexington, MA, USA) and protein C antigen using an immunoenzymatic assay (Asserachrom protein C, Diagnostica Stago, France), free protein S using an immunoenzymatic assay (Asserachrom free protein S, Diagnostica Stago), and the presence of lupus anticoagulant were determined as previously described[15]. Molecular diagnosis of the factor V Leiden mutation was performed as described by Ridker *et al*.[16]. The G20210A mutation in the prothrombin gene was detected as described by Poort *et al*.[17]. Body mass index (BMI) was calculated as weight in kilograms divided by the square of height in meters. Insulin resistance was estimated using the homeostasis model assessment index (HOMA index) derived from the following equation: HOMA index = (fasting plasma glucose level mg%×0.055)×(fasting plasma insulin level μIU/mL)/22.5.

Histological evaluation

Liver biopsy specimens were fixed in Bouin's and embedded in paraffin, and the sections were stained with hematoxylin-eosin and Masson's trichrome. The diagnosis of NASH was established, if abnormal liver enzymes were associated with steatosis more than 10% in the presence of lobular and/or portal inflammation, with or without Mallory bodies, ballooning degeneration or fibrosis and the exclusion of other viral, metabolic or immunologic liver diseases for more than 3 mo[18]. The histological classification of NASH was made according to Brunt classification[19]. Steatosis was graded as follows: mild (5-30% of hepatocytes affected); moderate: (30-60% of hepatocytes affected); and severe (>60% of hepatocytes affected). Fibrosis was scored on a scale from 0 to 4, with 0 denoting no fibrosis, 1 describing focal pericellular fibrosis in zone three, 2 describing perivenular and pericellular fibrosis confined to zones two and three with or without portal/periportal fibrosis, 3 describing bridging fibrosis with architectural distortion but no cirrhosis, and 4 determining cirrhosis. Inflammatory grade was scored on a scale from 0 to 4, with 0 denoting no inflammation, grade 1 = sparse zone three inflammation, grade 2 = mild focal zone three hepatocyte inflammation, grade 3 = moderate zone three hepatocyte inflammation, and grade 4 = severe zone three hepatocyte inflammation. The histological classification of chronic viral hepatitis was made according to the new classification of Desmet *et al*.[20].

Statistical analysis

Data were expressed as mean±SD or as median and range. Kruskall-Wallis test for two-way analysis of variance (ANOVA) was used to evaluate difference between three or four groups. The difference between two groups was assessed by the two-tailed Mann-Whitney *U*-test for continuous variables and by χ^2 test for categorical variables. Bonferroni method was employed to correct for multiple comparisons. Correlations coefficient was evaluated by the Spearman's test and by simple linear or multiple stepwise regression analysis. The Winstat computer program was used for all calculations. Two-tailed *P* values less than 0.05 were considered statistically significant.

RESULTS

Epidemiological, biochemical, and histological characteristics of all patient populations are presented in Table 1. The patients with NAFLD were older and had increased BMI and increased insulin resistive index as compared to the patients with chronic viral hepatitis and to healthy controls ($P<0.001$). Inflammation score and ALT levels were obviously less pronounced in patients with NASH as compared to the patients with chronic viral hepatitis (inflammation score, 8.7±2.4 *vs* 10.4±5.0, $P<0.01$; and ALT, 43±18 *vs* 79±25, $P<0.001$). There was no significant difference in the severity

Table 1 Clinical, biochemical, and demographic characteristics of study population (mean±SD, *n*)

Characteristics	FL *n* = 15	NASH *n* = 15	CH *n* = 14	Healthy controls *n* = 10	*P*
Age (yr)	50±11	53±9	40±13	39±7	0.01
Gender (M/F)	10M/5F	7M/8F	11M/3F	6M/4F	NS
BMI	32±5	33.0±6	24.0±3	25.0±4	0.001
IRI	4.0±3.3	4.7±2.4	1.7±0.9	1.8±0.4	0.001
Hb (g/dL)	14±1.0	14±2.0	14±1.0	13.9±1.0	NS
WBC ($\times 10^3$ cell/mm^3)	6.2±1.4	7.4±1.9	7.2±2.1	5.9±0.9	NS
Platelets (10^3 cell/mm^3)	245±49	247±57	226±44	279±72	NS
INR	0.9±0.08	0.9±0.08	0.9±0.09	0.9±0.05	NS
PTT (s)	32±5.0	32±4.0	31.0±4.0	33.0±6.0	NS
Fibrinogen (mg/dL)	336±69	326±57	296±49	291±69	NS
ALT (IU/mL)	45±21	43±18	79±25	20±1.0	0.001
AST (IU/mL)	36±16	35±8	83±8	20±1.0	0.001
ALKPH (IU/mL)	87±22	87±26	73±20	70±1.0	NS
GGT (IU/mL)	73±35	56±29	62±45	50±1.0	0.5
Activity grade	2.1±1.3	8.7±2.5 (3.9)[1]	10.4±5.1 (12)[1]	ND	0.01
Fibrosis stage	0.5±0.0	1.4±1.6 (0.5)[1]	1.5±1.6 (1.0)[1]	ND	NS

[1]Numbers in parenthesis represent the median value.

of fibrosis stage between patients with NASH and patients with chronic viral hepatitis (1.4±1.6 *vs* 1.5±1.6).

APC resistance and protein S were the two most prevalent thrombotic risk factors observed in patients with NAFLD and in patients with chronic viral hepatitis (6% and 10% in NAFLD *vs* 21% and 14% in CH, $P<0.01$ and $P<0.05$, respectively, Table 2). While the prevalence of antithrombin III was more frequent in NAFLD as compared to chronic hepatitis (6% *vs* 0%, $P<0.01$), there was no significant difference between the two groups in APC ratio, lupus anticoagulant, and fibrinogen levels. There were also no significant differences in the genetic risk factors including factor V Leiden, prothrombin 20210A mutation, and MTHFR mutation. Finally, one patient in the NAFLD group was heterozygous for MTHFR mutation.

Table 2 Prevalence of thrombotic risk factors in 44 patients of study population (*n*, %)

Thrombotic risk factors	NAFLD (%)	CH (%)	Total (%)
Protein C deficiency	1 (3)	1 (7)	2 (10)
Protein S deficiency	2 (6)	3 (21)	5 (27)
Anti-thrombin III deficiency	2 (6)	0 (0)	2 (6)
Lupus anticoagulant	2 (6)	1 (7)	3 (13)
APC resistance	3 (10)	2 (14)	5 (24)
PT20210A mutation	None	None	None
Factor V Leiden	None	None	None
MTHFR mutation	1 (3)[1]	None	1 (3)

[1]Heterozygous mutation.

One thrombotic risk factor was present in 23% of patients with NAFLD and mild fibrosis as compared to 36% of patients with chronic hepatitis and mild fibrosis. Two thrombotic risk factors were present in 6% of patients with NAFLD. Absence of thrombotic risk factors was seen in 47% of patients with NAFLD and mild fibrosis and 6% with severe fibrosis (Table 3). No healthy individuals showed evidence of thrombotic risk factors.

Table 3 Number of thrombotic risk factors per patient in patients with NAFLD with mild and severe fibrosis score (*n*)

Number of thrombotic risk factors per patient fibrosis (%)	Mild fibrosis(%)	Severe
No risk factors	8 (47)	1 (6)
One risk factor	4 (23)	3 (18)
Two risk factors	1 (6)	0 (0)

Levels of thrombophilic and coagulation factors as well as the prevalence of thrombotic risk factors for the study population are presented in Tables 2 and 4, respectively. The patients with NASH had significantly more decrease in protein S levels as compared to the patients with FL alone (92±19 *vs* 106±20, $P<0.01$). Anti-thrombin III tended to be lower in NASH patients but did not reach statistical significance.

The association of fibrosis staging with patient characteristics and with levels of thrombophilic and coagulation factors is presented in Table 5. The patients with NASH and severe fibrosis had markedly more decrease in protein S levels compared to the patients without fibrosis (84±16 *vs* 100±22, $P<0.01$). An important finding was that protein C levels were higher in NASH patients at mild or severe fibrosis stage as compared to patients with chronic viral hepatitis (for mild fibrosis, 128±40 *vs* 96±14, $P<0.001$; or for severe fibrosis, 129±36 *vs* 88±13, $P<001$, Table 5, Figure 1A) and that protein C levels were correlated strongly with the extent of fatty infiltration ($r = 0.6$, Figure 1B). Table 6 shows the capacity of combined thrombotic risk factors, including protein S, antithrombin III, and fibrinogen to predict correctly the diagnosis of simple FL *vs* NASH. They classified the outcome correctly in 70% of cases. Finally, we observed a significant correlation between fibrotic score and proteins S level in patients with NAFLD ($r = 0.4$, $P<0.05$, Figure 2).

DISCUSSION

Our study has evaluated the association between thrombotic risk factors and the extent of hepatic fibrosis and fatty

Table 4 Levels of thrombophilic and coagulation factors in all study population (mean±SD)

Factors	FL $n = 15$	NASH $n = 15$	CH $n = 14$	Healthy controls $n = 10$	P ANOVA
Protein C (%)[a] (normal 70-130)	150±34	130±37	101±24	121±12	0.001
Protein S (%)[b] (normal 60-140)	106±20	92±19	95±37	90±17	0.01
Anti-thrombin III (%) (normal 80-120)	115±11	108±17	110±10	116±10	NS
APC ratio (normal >2.0)	2.2±0.1	2.2±0.9	2.2±0.3	2.2±0.1	NS
Lupus anticoagulant (normal <1.2 U/mL)	1.0±0.1	1.05±0.1	1.0±0.1	1.0±0.1	NS
Fibrinogen (normal 200-400 mg/dL)	336±69	326±57	296±49	291±69	NS

[1]$P = 0.07$, FL *vs* NASH; [b]$P<0.01$, FL *vs* NASH.

Table 5 Clinical and biochemical characteristics in all study population in relation to their fibrosis staging (mean±SD)

Characteristics	NAFLD		CH	
	Normal-mild fibrosis	Moderate-severe fibrosis	Normal-mild fibrosis	Moderate-severe fibrosis
IRI	3.9±3.0	3.9±1.6	1.2±0.7	1.9±0.8
BMI	31±5.0	34±6.7	23.6±1.5	24±3.9
Protein C (%)	128±40	129±36	96±14[b]	88±13
Protein S (%)	100±22[d]	84±16	96±19	77±16
Antithrombin III	110±17	116±8.9	111±3.7	101±7.4
APC ratio	2.3±0.1	2.2±0.1	2.01±0.3	2.3±0.3
Lupus anticoagulant	1.0±0.09	1.0±0.09	0.99±0.4	0.99±0.8
PT (%)	105±13	107±13	103±22	97±10
PTT (s)	32±5	29.5±2.0	32±4.6	30±4.3
Fibrinogen, mg/dL	306±57	337±57	290±29	314±64
PT mutation 20210A	Normal	Normal	Normal	Normal
Factor V Leiden	Normal	Normal	Normal	Normal
MTHFR (*n*)	One mutation	Normal	Normal	Normal
Platelets	244±43	237±47	242±36	225±44
Activity score	5.5±4.2	7.5±2.3	8.0±5.0	12.8±4.3

[a]$P<0.01$, CH mild fibrosis *vs* CH severe fibrosis; [b]$P<0.01$, NAFLD mild fibrosis *vs* NAFLD severe fibrosis.

Table 6 Results of capacity of combined risk factors for thrombosis (protein S, anti-thrombin III, and fibrinogen) in predicting the presence of FL or NASH patients (outcome)[1]

Results/ LNB	Actual number of patients	Predicted group	
		NASH (%)	FL(%)
NASH	15	11 (73)	4 (27)
FL	15	5 (33)	10 (67)

[1]70% of the cases were classified correctly.

infiltration in patients with NAFLD. Thrombotic risk factors were detected in 46% of patients with NAFLD with APC resistance and protein S as the most common. While the patients with NASH and advanced fibrosis demonstrated a greater decrease in protein S levels compared to the patients with FL alone, the patients with NAFLD had a greater increase in protein C levels as compared to the patients with chronic viral hepatitis and healthy individuals.

The mechanism by which the patients with NAFLD display a decrease in some hemostatic parameters remains to be established. Since protein C, protein S, and antithrombin

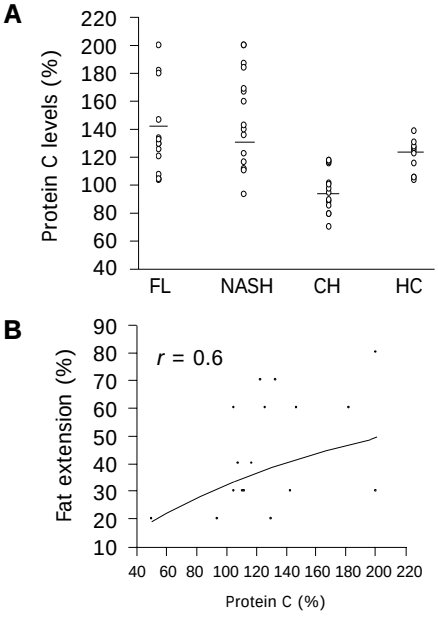


Figure 1 A: Protein C levels (normal 70-130%) in all study population (- median levels). B: Correlation between fat extension and protein C levels ($r = 0.6$, $P<0.001$).

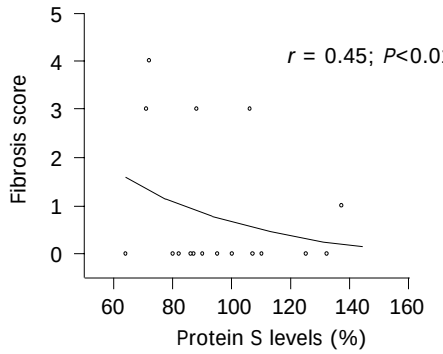


Figure 2 Correlation between fibrotic score and protein S levels in patients with NAFLD (r = 0.45, P<0.01).

III are produced by the liver, their levels may be decreased in patients with advanced chronic liver diseases[21]. This is considered to be the case in patients with established cirrhosis. However, patients with cirrhosis were excluded from our study and only four patients with NAFLD had severe bridging fibrosis. More important was the finding that protein C levels were obviously correlated with the extent of fatty infiltration and were higher in the patients with NAFLD when compared to the patients with chronic viral hepatitis and to healthy individuals (Figure 1A). This increase in protein C levels is related either to increased hepatic synthesis or impaired clearance of plasma protein C[22]. Bruckert *et al*.[23], has suggested that steatosis may be one of the factors leading to an increase in protein C levels resulting from accelerated turnover of triglycerides. Moreover, an increased level of protein C has been reported in patients with diabetes, hypertriglyceridemia, nephrotic syndrome, abuse of anabolic steroids, and alcoholism[22]. Diabetes and hypertriglyceridemia are predisposing conditions to fatty infiltration of the liver[4] and were present in 23% and 73% of our cases, respectively. The remaining conditions were excluded by clinical and biochemical findings.

Thrombotic risk factors have been found to be independently associated with the extent of fibrosis in patients with chronic viral hepatitis C and hepatitis B[21]. In particular, anti-thrombin III deficiency was associated with more extensive fibrosis. On contrary, in our study, anti-thrombin III deficiency was not associated with increased fibrosis, rather, protein S deficiency showed the greatest decrease in NASH with advanced fibrosis. The presence of combined thrombotic risk factors as the only independent variable associated with advanced fibrosis supports the hypothesis of vascular obstruction for the histological progression of NAFLD but does not indicate a cause and effect relationship.

Obliteration of small portal and hepatic veins due to thrombosis and phlebitis has been proposed as an important factor for the progression of chronic liver diseases[12-14]. Thus, changes in the composition of blood towards a hypercoagulability state in combination with changes in the endothelium of intrahepatic vessels and intrahepatic blood flow[24-26] certainly favor the development of thrombosis in intrahepatic veins. More recently, Wanless and Shiota[26] suggested a four-step model for the progression of FL towards NASH with fibrosis in which the fourth step is venous obstruction with secondary collapse and ultimately fibrous septation and cirrhosis. We have also demonstrated the beneficial effect of aspirin and enoxaparin on fibrosis progression in a rat model of cirrhosis, which supports the hypothesis of vascular thrombosis in hepatic fibrosis[27]. Again, a cause and effect relationship remains to be determined since more than half (54%) of the patients with NAFLD do not have thrombotic risk factors.

While APC, factor V Leiden, prothrombin mutation 20210A and MTHFR mutations had no association with advanced fibrosis, protein S deficiency was the only thrombotic risk factor associated with advanced staging (Table 5). Sixty percent of protein S plasma concentration is bound to a complement binding protein, which increases in inflammatory conditions (acute phase reactant), and only 40% of the concentration represent the active free form of protein S, which is a cofactor of APC but not a direct anticoagulant[28,29]. Thus, laboratory findings of protein S deficiency may not always reflect abnormal anticoagulation activity.

A link between thrombotic risk factors and hepatic fibrosis has been demonstrated. Liver inflammation resulting from NASH leads to activation of the coagulation system. In patients with protein S deficiency, the degree of activation is enhanced leading to increased thrombin activity and fibrin production. Thrombin is a stellate cell mitogen, and therefore activation of the coagulation cascade may stimulate stellate cell activation and fibrosis[30,31]. Recently, treatment with thrombin antagonist has been shown to reduce liver fibrogenesis in the rat via downregulation of TIMP-1 mRNA levels[32].

Increased levels of anticardiolipin or the presence of lupus anticoagulant were not associated with histological staging in our study. Anticardiolipin antibody has been reported to be present in up to 44% of patients with chronic hepatitis C, but the clinical significance remains controversial[33]. Positive anticardiolipin antibodies were detected in only 6% and 7% of our NAFLD and CH patients, respectively. None of our patients with positive anticardiolipin antibody had a history of thrombotic episodes or clinical signs of portal hypertension. Only one patient had advanced histological staging and one with low platelet count. Taken together, our data are in agreement with previous reports that anticardiolipin antibodies are epiphenomenona without any clinical relevance[34].

The deficiency in protein S is likely to result from an acquired defect, since in the healthy population, the prevalence of heterozygous deficiency has been estimated at 0.2%[35]. Decreased liver synthesis appears as the most plausible mechanism for the high prevalence of protein S deficiency in patients with NASH and advanced fibrosis. The 6% prevalence of protein S deficiency found in the group with NAFLD and the 21% in the group with CH strengthens this hypothesis. On the other hand, increase in protein C levels may explain the non-progression of fibrosis in some patients with NAFLD via its anti-coagulant and anti-inflammatory effects[36].

In conclusion, our data suggest that thrombotic risk factors are detected in approximately half of the patients with NAFLD and that the presence of one or more risk factors is associated with more fibrosis. This does not indicate a cause and effect relationship, but has a significant clinical implication. Whether it is a primary or secondary phenomenon needs further evaluation.

REFERENCES

1 **Willner IR**, Waters B, Patil SR, Reuben A, Morelli J, Riely CA. Ninety patients with nonalcoholic steatohepatitis: insulin resistance, familial tendency, and severity of disease. *Am J Gastroenterol* 2001; **96:** 2957-2961
2 **Bugianesi E**, Leone N, Vanni E. Expanding the natural history of nonalcoholic steatohepatitis: from cryptogenic cirrhosis to hepatocellular carcinoma. *Gastroenterology* 2002; **123:** 134-140
3 **Angulo P**. Nonalcoholic fatty liver disease. *N Engl J Med* 2002; **346:** 1221-1231
4 **Assy N**, Kaita K, Mymin D, Levy C, Rosser B, Minuk G. Fatty infiltration of liver in hyperlipidemic patients. *Dig Dis Sci* 2000; **45:** 1929-1934
5 **Bellentani S**, Saccoccio G, Masutti F. Prevalence and risk factors for hepatic steatosis in northern Italy. *Ann Intern Med* 2000; **132:** 112-117
6 **Marchesini G**, Brizi M, Morselli Labate AM. Association of non alcoholic fatty liver disease to insulin resistance. *Am J Med* 1999; **107:** 450-455
7 **Mehta K**, Van Thiel DH, Shah N, Mobarhan S. Nonalcoholic fatty liver disease: pathogenesis and the role of antioxidants. *Nutr Rev* 2002; **60:** 289-293
8 **George DK**, Goldwurn S, MacDonald GA, Cowley LL, Walker NI, Ward PJ, Jazwinska EC, Powell LW. Increased hepatic iron concentration in non-alcoholic steatohepatitis is associated with increased fibrosis. *Gastroenterology* 1998; **114:** 311-318
9 **Nolan JP**. Intestinal endotoxins as mediators of hepatic injury-an -idea whose time has come again. *Hepatology* 1989; **10:** 887-891
10 **Tiegs G**. Immunotoxicology of host response mediated experimental liver injury. *J Hepatol* 1994; **21:** 890-903
11 **Grove J**, Brown AS, Daly AK, Bassendine MF, James OF, Day CP. The RsaI polymorphism of CYP2E1 and susceptibility to alcoholic liver disease in Caucasians: Effect on age of presentation and dependence on alcohol dehydrogenase genotype. *Pharmacogenetics* 1998; **8:** 335-342
12 **Wanless IR**, Wong F, Blendis LM. Hepatic and portal vein thrombosis in cirrhosis: possible role in development of parenchymal extinction and portal hypertension. *Hepatology* 1995; **21:** 1238-1247
13 **Wanless IR**, Lio JJ, Butany J. Role of thrombosis in the pathogenesis of congestive hepatic thrombosis. *Hepatology* 1995; **21:** 1232-1237
14 **Wanless IR**, Shiota K. The pathogenesis of nonalcoholic steatohepatitis and other fatty liver diseases: a four-step model including the role of lipid release and hepatic venular obstruction in the progression to cirrhosis. *Semin Liver Dis* 2004; **24:** 99-106
15 **Robert A**. Two different incubation times for the activated partial thromboplastin time (APTT): a new criterion for diagnosis of lupus anticoagulant. *Thromb Haemost* 1994; **71:** 220-224
16 **Ridker PM**, Hennekens CH, Lindpaintner K, Stampfer MJ, Eisenberg PR, Miletich JP. Mutation in the gene coding for coagulation factor V and the risk of myocardial infarction, stroke, and venous thrombosis in apparently healthy men. *N Engl J Med* 1995; **332:** 912-917
17 **Poort SR**, Rosendaal FR, Reitsma PH, Bertina RM. A common genetic variation in the 3′-untranslated region of the prothrombin gene is associated with elevated plasma prothrombin levels and an increase in venous thrombosis. *Blood* 1996; **88:** 3698-3703
18 **Brunt EM**. Nonalcoholic steatohepatitis**.** *Semin Liver Dis* 2004; **24:** 3-20
19 **Brunt EM**, Janney CG, Di Bisceglie AM, Neuschwander-Tetri BA, Bacon BR. Nonalcoholic steatohepatitis: a proposal for grading and staging the histological lesions. *Am J Gastroenterol* 1999; **94:** 2467-2474
20 **Desmet VJ**, Gerber M, Hoofnagle JH, Manns M, Scheuer PJ. Classification of CH: diagnosis, grading, and staging. *Hepatology* 1994; **19:** 1513-1520
21 **Papatheodoridis GV**, Papakonstantinou E, Andrioti E, Cholongitas E, Petraki K, Kontopoulou I, Hadziyannis SJ. Thrombotic risk factors and extent of liver fibrosis in chronic viral hepatitis. *Gut* 2003; **52:** 404-409
22 **Cucuianu M**, Brudasca I, Trif I, Stancu A. Clinical studies on plasma protein C. Correlation with serum cholinesterase. *Nouv Rev Fr Hematol* 1993; **35:** 481-486
23 **Bruckert E**, Ankri A, Jung M, Turpin G, De Gennes JL. Mild liver abnormalities associated with elevated plasma factor VII and protein C in hypertriglyceridaemic patients. *Eur J Med* 1993; **2:** 461-465
24 **Friedman SL**. Liver fibrosis -from bench to bedside. *J Hepatol* 2003; **38:** S38-53
25 **Brenner DA**, Waterboer T, Choi SK, Lindquist JN, Stefanovic B, Burchardt E, Yamauchi M, Gillan A, Rippe RA. New aspects of hepatic fibrosis. *J Hepatol* 2000; **32:** 32-38
26 **Wanless IR**, Shiota K. The pathogenesis of nonalcoholic steatohepatitis and other fatty liver diseases: a four-step model including the role of lipid release and hepatic venular obstruction in the progression to cirrhosis. *Semin Liver Dis* 2004; **24:** 99-106
27 **Assy N**, Hussein O, Khalil A, Luder A, Szvalb S, Paizi M, Spira G. The beneficial effect of aspirin and enoxaparin on fibrosis progression and regenerative activity in a rat model of cirrhosis. *Dig Dis Sci* 2005 -in press
28 **Papatheodoridis GV**, Burroughs AK. Hemostasis in hepatic and biliary disorders. In: LH Blumgart, Fong Y, eds. Surgery of the liver and biliary tract. *London WB Saunders* 2000: 199-213
29 **Green AF**, Rantoff OD. Elevated antihaemophilic factor (AHF, factor VIII) procoagulant activity and AHF-like antigen in alcoholic cirrhosis of the liver. *J Lab Clin Med* 1974; **83:** 189-197
30 **Marra F**, DeFranco R, Grappone C. Expression of the thrombin receptor in human liver: up-regulation during acute and chronic injury. *Hepatology* 1998; **27:** 462-471
31 **Marra F**, Grandaliano G, Valente AJ. Thrombin stimulates proliferation of liver fat-storing cells and expression of monocyte chemotactic protein-1: potential role in liver injury. *Hepatology* 1995; **22:** 780-787
32 **Duplantier JG**, Dubuisson L, Senant N, Freyburger G, Laurendeau I, Herbert JM, Desmouliere A, Rosenbaum J. A role for thrombin in liver fibrosis. *Gut* 2004; **53**: 1682-1687
33 **Uthman IW**, Gharavi AE. Viral infections and antiphospholipid antibodies. *Semin Arthritis Rheum* 2002; **31:** 256-263
34 **Ordi-Ros J**, Villarreal J, Monegal F. Anticardiolipin antibodies in patients with chronic hepatitis C virus infection: characterization in relation to antiphospholipid syndrome. *Clin Diagn Lab Immunol* 2000; **7:** 241-244
35 **Beauchamp NJ**, Dykes AC, Parikh N, Campbell Tait R, Daly ME. The prevalence of, and molecular defects underlying, inherited protein S deficiency in the general population. *Br J Haematol* 2004; **125:** 647-654
36 **Yoshikawa A**, Kaido T, Seto SI, Katsuura Y, Imamura M. Activated protein C prevents multiple organ injury following extensive hepatectomy in cirrhotic rats. *J Hepatol* 2000; **33:** 953-960

Science Editor Kumar M and Guo SY **Language Editor** Elsevier HK

PO Box 2345, Beijing 100023, China
www.wjgnet.com
wjg@wjgnet.com

ELSEVIER

World J Gastroenterol 2005;11(37):5840-5844
World Journal of Gastroenterology ISSN 1007-9327
© 2005 The WJG Press and Elsevier Inc. All rights reserved.

• *CLINICAL RESEARCH* •

Surgical risk for patients with Chagasic achalasia and its correlation with the degree of esophageal dilation

José Garcia Neto, Roberto de Cleva, Bruno Zilberstein, Joaquim José Gama-Rodrigues

José Garcia Neto, Surgery Division, Hospital das Clínicas, Federal University of Goiás Medical School, Goiás, Brazil
Roberto de Cleva, Bruno Zilberstein, Joaquim José Gama-Rodrigues, Gastroenterology Department, Digestive Tract Surgery Division, Hospital das Clínicas, University of São Paulo Medical School, São Paulo, Brazil
Correspondence to: Professor. Dr. Roberto de Cleva, Gastroenterology Department, University of São Paulo Medical School, Rua Cel. Arthur Godoy, 125 Apto 152, São Paulo-SP CEP 04018-050, Brazil. roberto.cleva@hcnet.usp.br
Telephone: +55-11-30828000 Fax: +55-11-30828000
Received: 2004-10-23 Accepted: 2004-12-23

Abstract

AIM: To analyze the risk of cardiovascular complications in patients with indication for surgical treatment of Chagasic esophageal achalasia and to correlate the surgical risks with the degree of esophageal dilation, thereby proposing a risk scale index.

METHODS: One hundred and twenty-four patients with Chagasic esophageal achalasia, who received surgical treatment at the Hospital das Clinicas of the Federal University of Goiás, were included in this study. The patients were mostly related to the postoperative complications due to the cardiovascular system. All the patients were submitted to: (1) clinical history to define the cardiac functional class (New York Heart Association); (2) conventional 12-lead electrocardiogram at rest; and (3) contrast imaging of the esophagus to determine esophageal dilatation according to Rezende's classification of Chagasic megaesophagus.

RESULTS: An assessment of the functional classification (FC) of heart failure during the preoperative period determined that 67 patients (54.03%) were assigned functional class I (FC I), 46 patients (37.09%) were assigned functional class II (FC II), and 11 patients (8.87%) were assigned functional class III (FC III). None of the patients were assigned to functional class IV (FC IV). There was a positive correlation between the functional class and the postoperative complications (FC I×FC II: $P<0.001$; FC I×FC III: $P<0.001$). The ECG was normal in 44 patients (35.48%) and presented abnormalities in 80 patients (64.52%). There was a significant statistical correlation between abnormal ECG (arrhythmias and primary change in ventricular repolarization) and postoperative complications ($P<0.001$). With regard to the classification of the Chagasic esophageal achalasia, the following distribution was observed: group II, 53 patients (42.74%); group III, 37 patients (29.83%); and group IV, 34 patients (27.41%). There was a positive correlation between the degree of esophageal dilation and the increase in postoperative complications (grade II×grade III achalasia: $P<0.001$; grade II×grade IV achalasia: $P<0.001$; and grade III×grade IV achalasia: $P = 0.017$). Analyzing these results and using a multivariate regression analysis associated with the probability decision analysis, a risk scale was proposed as follows: up to 21 points (mild risk); from 22 to 34 points (moderate risk); and more than 34 points (high risk). The scale had 82.4% accuracy for mild risk patients and up to 94.6% for the high risk cases.

CONCLUSION: The preoperative evaluation of the cardiovascular system, through a careful anamnesis, an ECG and contrast imaging of the esophagus, makes possible to estimate the surgical risks for Chagas' disease patients who have to undergo surgical treatment for esophageal achalasia.

© 2005 The WJG Press and Elsevier Inc. All rights reserved.

Key words: Postoperative; Chagas' disease; Surgical risk; Chagasic achalasia; Cardiovascular risk

Neto JG, de Cleva R, Zilberstein B, Gama-Rodrigues JJ. Surgical risk for patients with Chagasic achalasia and its correlation with the degree of esophageal dilation. *World J Gastroenterol* 2005; 11(37): 5840-5844
http://www.wjgnet.com/1007-9327/11/5840.asp

INTRODUCTION

Preoperative clinical evaluation, a common practice in our midst, aims to estimate the risk of postoperative complications. The patient's clinical status is assessed and emphasis is given to cardiac function, as well as to the inherent risk of the surgical procedure performed, through the use of the several indexes available in the literature. According to Dias *et al*.[1], the clinical status during the preoperative period answers two questions: what is the surgical risk, and what can be done to reduce it? The adequate management of perioperative risk factors, such as normalizing blood pressure and diabetes mellitus, treating chronic pulmonary obstructive disease and the utilization of endovenous beta-blockers perioperatively in patients with coronary disease, can significantly decrease perioperative complications. Determining perioperative risk factors can be useful as it can provide elements to choose the best procedure or even if surgical treatment should be

performed[2]. The most commonly used risk indexes are those from the American Society of Anesthesia[3] and the Goldman index[4]. It is important to point out that Chagasic cardiopathy is not specifically evaluated in risk indexes, since Chagas' disease is not found in Western countries.

Cardiovascular complications in patients who have to undergo noncardiac surgery and changes in cardiac function caused by Chagas' disease have a direct influence over the morbidity and mortality rate of the surgical procedure[5]. Establishing guidelines, which identify Chagasic patients at high risk for complications arising from noncardiac surgery, as well as minimizing the onset of such complications during the perioperative period, are very important. The patients with Chagasic esophageal achalasia may have high cardiovascular system impairment.

In view of the scarce literature regarding the surgical risks for noncardiac procedures on the patients with Chagasic esophageal achalasia, and because of the frequent association between cardiopathy and digestive diseases, the purpose of the study was to analyze the risk of cardiovascular complications in patients with indication for surgical treatment of Chagasic esophageal achalasia and to correlate the surgical risks with the degree of esophageal dilation, and thereby proposing a risk scale index.

MATERIALS AND METHODS

A total of 124 patients with Chagasic esophageal achalasia submitted to surgical treatment at the Hospital das Clínicas, Federal University of Goiás from January 1995 and December 2000, were included in this study. Of them, 68 (54.83%) were males and 56 (45.16%) were females, with a mean age of 39 years. All the patients were subjected to: (1) clinical history to define the cardiac functional class [3] (New York Heart Association); (2) conventional 12-lead ECG at rest; and (3) contrast imaging of the esophagus to determine esophageal dilatation according to Rezende's classification of Chagasic megaesophagus[6,7] as follows: group I: esophagus with normal caliber but with slow contrast progression and small retention of barium contrast 1 min after ingestion; group II: esophagus with small to moderate dilatation and considerable radiological contrast retention; group III: hypotonic esophagus with important dilatation, poor motor activity and great retention of radiological contrast; and group IV: esophagus elongated that lies over the diaphragm with great retention of radiological contrast (dolico-megaesophagus, Figure 1).

All the patients were submitted, according to the radiological classification of the Chagasic megaesophagus, to surgical treatment of achalasia (Table 1), utilizing conservative techniques for the non-advanced esophageal achalasia (Grades II and III), employing Pinotti's operation (cardiomyectomy with fundoplication) and resective techniques using Serras Doria operation (Grondahl cardioplasty with hemigastrectomy and Roux en Y diversion) for advanced achalasia (Grade IV). Postoperative complications, directly related to the cardiovascular system, during the hospitalization period, were analyzed.

For statistical analysis, the variance analysis was used for comparisons between continuous numerical variables of distinct (independent) groups; the χ^2 and the Fisher's tests were used for comparisons between the quantities in which each patient was situated at a given level of classification; and multivariate regression and probabilistic decision analyses were used in the final phase of the study to create the surgical risk index.

Table 1 Patients according to the grade of esophageal dilatation and surgical treatment adopted

Esophageal dilatation	Surgical technique	Patients (%)
Group II		53
	Cardiomyectomy with fundoplication (Pinotti's technique)	53
Group III		37
	Cardiomyectomy with fundoplication	32
	Grondahl cardioplasty with hemigastrectomy and Roux-en-Y diversion (Serras Doria operation)	5
Group IV		34
	Grondahl cardioplasty with hemigastrectomy and Roux-en-Y diversion	26
	Mucosectomy	4
	Merendino's operation	2
	Gastrostomy	2

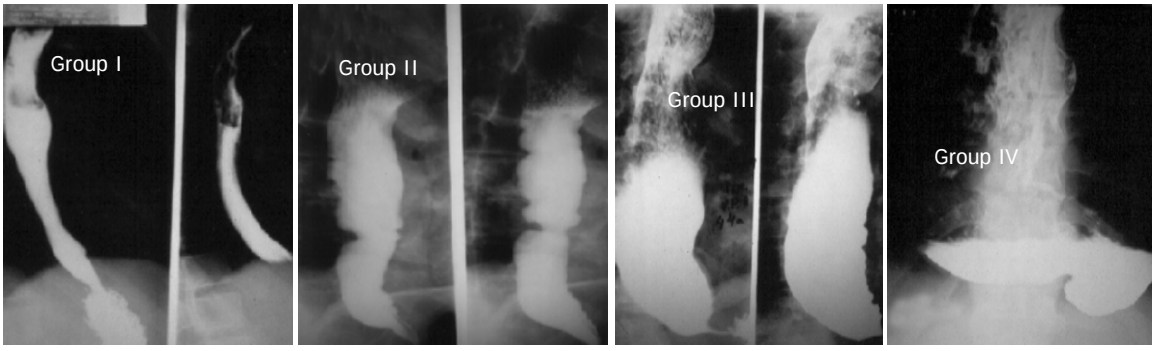


Figure 1 Contrast imaging of the esophagus according to Rezende's classification of Chagasic megaesophagus. Group I: esophagus with normal caliber but with slow contrast progression and small retention of barium contrast 1 min after ingestion; group II: esophagus with small to moderate dilatation and considerable radiological contrast retention; group III: hypotonic esophagus with important dilatation, poor motor activity and great retention of radiological contrast; and group IV: esophagus elongated over the diaphragm with great contrast retention.

RESULTS

An assessment of the functional classification (FC) of heart failure patients with Chagasic achalasia during the preoperative period determined that 67 patients (54.03%) were assigned functional class I (FC I), 46 patients (37.09%) were assigned functional class II (FC II), and 11 patients (8.87%) were assigned functional class III (FC III). None of the patients were assigned to functional class IV (FC IV). There was a positive correlation between the functional class and the postoperative complications (Table 2).

The ECG results are shown in Table 3. The ECG was normal in 44 patients (35.48%) and presented abnormalities in 80 patients (64.52%). We observed that a single patient could exhibit more than one change in the ECG and the most frequently observed abnormalities were complete right bundle branch block (CRBBB) and ventricular extrasystole in 28 patients (22.58%). We also observed a significant statistical correlation between abnormal ECG (arrhythmias and primary change in ventricular repolarization) and postoperative complications ($P<0.001$, Table 4).

With regard to the classification of the Chagasic esophageal achalasia, the following distributions were observed: 53 patients (42.74%) were classified into group II; 37 patients (29.83%) into group III; and 34 patients (27.41%) into group IV. The cardiovascular complications related to the esophageal dilation are shown in Table 5. A positive correlation between the degree of esophageal dilation and postoperative complications was observed, i.e., the higher the degree of esophageal dilation, the higher the risk of complications (grade II×grade III: $P<0.001$; grade II×grade IV: $P<0.001$; and grade III×grade IV: $P = 0.017$).

Cardiovascular complications, defined as any change detected in the cardiovascular system during the in-hospital postoperative recovery period, are described in Table 6. Four patients (3.22%) died. The cause of death was classified as: cardiogenic shock (one patient); pulmonary embolism (one patient); stroke (one patient); and non-defined causes (one patient) at the 5th postoperative day, although the presence of tachyarrhythmias was suspected.

Analyzing these results and using a multivariate regression analysis associated with the probability decision analysis, with direct and specific application to the Chagasic megaesophagus patient, we proposed a risk scale (Table 7). In terms of classifying preoperative risks, the point scale was as follows: up to 21 points (mild risk); from 22 to 34 points (moderate risk); and more than 34 points (high risk). The scale had 82.4% accuracy for mild risk patients and up to 94.6% for the high risk patients.

Table 2 Postoperative complications according to the functional class classification

Results	Functional class/number of patients					
	I (n = 67)[b,d]		II (n = 46)[1]		III (n = 11)	
	n	%	n	%	n	%
No complications	39	58.21	11	23.91	–	0.00
With complications	28	41.79	35	76.09	11	100.00
Heart failure/shock	0	0.00	4	11.43	7	63.64
Death	1	3.57	2	5.71	1	9.09
Others	27	96.43	29	82.86	3	27.27

[b]$P<0.001$ FCI *vs* FCII; [d]$P<0.001$ FCI *vs* FCIII; [1]$P=0.072$ FCII *vs* FCIII.

Table 3 Preoperative ECG results in patients with Chagasic esophageal achalasia

ECG results	Patients (n)	%
Normal ECG	44	35.48
Isolated ventricular extrasystoles	58	37.09
Complete right bundle branch block	35	28.22
Primary change in ventricular repolarization	12	9.67
First-degree atrioventricular block (1st degree AVB)	16	12.9
Second-degree atrioventricular block (2nd degree AVB) Mobitz I	02	1.61
Second-degree atrioventricular block (2nd degree AVB) Mobitz II	03	2.41
Complete atrioventricular block (CAVB)	08	6.4
Upper anterior divisional block (DB)	11	8.87
Complete left bundle branch block (CLBBB)	03	2.41
Paired ventricular extrasystoles	09	7.25
Supraventricular extrasystoles	06	4.83
Atrial fibrillation (AF)	04	3.22

Table 4 Correlation between postoperative complications and ECG changes

Results	ECG results			
	Normal (n = 44)		With abnormalities (n = 80)	
	n	%	n	%
No complications	27	61.4	23	28.8
With complications				
CHF/shock	2	11.8	8	14.0
Death	1	5.9	3	5.3
Others	14	82.4	46	80.7

$\chi^2 = 12.548$; $P<0.001$.

Table 5 Postoperative complications according to the degree of dilation of the Chagasic achalasia

Complications	Achalasia groups					
	II (n = 53)[b,d]		III (n = 37)[1]		IV (n = 34)	
	n	%	n	%	n	%
No complications	33	62.26	13	35.14	4	11.76
With complications	20	37.74	32	64.86	38	88.24
CHF/shock	–	0.00	6	18.75	7	18.42
Death	–	0.00	2	6.25	2	5.26
Others	20	100.00	24	75.00	29	76.32

[b]$P<0.001$ GII *vs* GIII; [d]$P<0.001$ GII *vs* GIV [1]$P=0.017$ GIII *vs* GIV.

Table 6 Postoperative cardiovascular complications after surgical treatment of Chagasic esophageal achalasia

Complications	Patients (%)
Decompensated congestive heart failure	12 (9.67)
Cardiogenic shock	03 (2.41)
Ventricular extrasystole	58 (46.77)
Sinus bradycardia	22 (17.74)
Non-sustained ventricular tachycardia	12 (9.67)
Sustained ventricular tachycardia	01 (0.80)
Acute atrial fibrillation	05 (4.03)
Supraventricular tachycardia	03 (2.41)
Temporary complete atrioventricular block	01 (0.80)
Acute arterial occlusion	04 (3.22)
Stroke	03 (2.41)
Pulmonary embolism	02 (1.67)
Acute renal failure	02 (1.67)

Table 7 Risk index for Chagasic achalasia

a) Points	
Achalasia	Points
Grade II	9
Grade III	13
Grade IV	17
Primary changes in ventricular repolarization	Points
Yes	15
No	0
Arrhythmias	Points
Yes	12
No	0
Functional class	Points
1	6
2	12
3	24
(b) Final index	
Points	Risk level
Up to 21	Mild
From 22 to 34	Moderate
Above 34	High
(c) Probability of accuracy of the risk level	
Risk levels	Probability (%)
Mild	82.4
High	94.6

DISCUSSION

The caseload of 124 patients is quite representative of the high incidence of megaesophagus with the indication for surgical treatment in a region where Chagas' disease is endemic. Although there may be an overlapping of clinical and morphological characteristics among dilated cardiomyopathies, it is very important to take into consideration the inherent characteristics of the Chagasic cardiomyopathy, such as autonomic denervation, fascicular and atrioventricular blocks, in addition to arrhythmogenic foci in the ventricles[8-11]. These peculiar characteristics are enough to elicit different responses to the surgical trauma relative to those observed in non-Chagasic patients[12-14].

Thus, it is our opinion that in order to estimate the surgical risk for these patients, it is imperative that the risk index developed should be simple and low-cost. These characteristics, however, should compromise neither its validity nor its feasibility.

In the score scale, the clinical history of the patients, used to determine precisely the functional class through the symptoms of myocardial dysfunction, associated to simple and inexpensive tests which are readily available, such as ECG, can estimate the risk for complications for the Chagasic achalasia patient. In view of the frequent association between a compromised digestive system and an equally compromised cardiovascular system[15], the positive predictive value of the scale is increased when the degree of dilation of the esophagus is included.

FC presents some problems because of the subjective interpretation of terms, such as "routine activity", and "excessive fatigue". They cause the consequent limitations in terms of precision and reproducibility[16]. However, our findings showed that the functional class of the patient was determined with a good degree of security.

Naturally, indexes, such as Goldman index, are not as precise for the analysis of specific groups, such as those with Chagasic cardiopathy[17-23]. These patients, according to the Goldman index, would have been classified as low risk.

Our findings equally suggested that the longer the degree of evolution of Chagasic esophageal achalasia, the higher the tendency for advanced cardiomyopathy. Our results showed a positive correlation between the degree of esophageal dilation and postoperative complications. The risk scale, which is being proposed[24] with a considerable degree of confidence, can provide an adequate and reliable predictor of cardiovascular complications in the patients with Chagasic esophageal achalasia during the postoperative period.

In conclusion, the evaluation of the cardiovascular system, through a careful anamnesis, an ECG and contrast imaging of the esophagus, makes it possible to estimate the surgical risks for the patients with Chagasic esophageal achalasia.

REFERENCES

1 **Dias LD**, Bittencourt LAK, Cavicchio JR, Figueiredo MJ, Simões NA. Importância e fundamentos da avaliação pré-operatória para pacientes submetidos a cirurgia não-cardíaca: quem deve ser avaliado e quem deve avaliar. *Rev Soc Cardiol Estado De São Paulo* 2000; **10**: 259-265

2 **Bittencuort LAK**, Simões AMR, Figueiredo MJO. O clínico e o período pré-operatório. In: Halbe HW, ed. Tratado de Ginecologia. São Paulo: Roca 2000: 2392-2401

3 **Eagle KA**, Brundage BH, Chaitman BR,, Ewy GA, Fleisher LA, Hertzer NR, Leppo JA, Ryan T, Schlant RC, Spencer WH 3rd, Spitell JA Jr, Twiss RD, Ritchie JL, Cheitlin MD, Gardner TJ, Garson A Jr, Lewis RP, Gibbons RJ, O´Rourke RA, Ryan TJ. Guidelines for Perioperative Cardiovascular Evaluation for noncardiac surgery. Report of the American College of Cardiology/ American Heart Association Task Force on Practice Guidelines. Committe on Perioperative Cardiovascular Evaluation for noncardiac Surgery. *Circulation* 1996; **93**: 1278-1317

4 **Goldman L,** Caldera DL, Nussbaum SR, Southwick FS, Krogstad D, Murray B, Burke DS, O'Malley TA, Caplan CH, Nolan J, Carabello B, Slater EE. Multifatorial index of cardiac risk in noncardiac surgical procedures. *N Engl J Med* 1977; **297**: 845-850

5 **Bestetti RB**, Dalbo CM, Freitas OC, Teno LA, Castilho OT, Oliveira JM. Noninvasive predictors of mortality for patients with Chagas heart disease: a multivariate stepwise logistic regression study. *Cardiology* 1994; **84**: 261-267

6 **de Rezende J**, Lauar KL, de Oliveira AR. Aspectos clínicos e radiológicos da aperistalsis do esôfago. *Rev Bras Gastroenterol* 1960; **12**: 247-262

7 **Rezende JM**. Classificação radiológica do megaesôfago. *Rev Goiana Med* 1982; **28**: 187-191

8 **Amorim DS**, Godoy RA, Manço JC, Tanaka A, Gallo L Jr. Effects of acute elevation in blood pressure and atropine on heart rate in Chagas´ disease. *Circulation* 1968; **38**: 289-294

9 **Bestetti RB,** Freitas OC, Muccillo G, Oliveira JM. Clinical and morphological characteristics associated with sudden cardiac death in patients with Chagas´ disease. *Eur Heart J* 1993; **14**: 1610-1614

10 **Blaustein AS**. Preoperative and perioperative management of cardiac patients undergoing noncardiac surgery. *Cardiol Clin* 1995; **13**: 149-461

11 **Braunwald E.** Heart Disease. A Textbook of Cardiovascular Disease. Saunders, 2th 1984: 1815-1825

12 **Detsky AS,** Abrams HB, Forbath N, Scott JG, Hilliard JR.

Cardiac assessment for patients undergoing noncardiac surgery. *Arch Inter Med* 1986; **146**: 2131-2134
13 **Forgosh LB,** Movahed A. Assessment of Cardiac risk in Noncardiac Surgery. *Clin Cardiol* 1995; **18**: 556-562
14 **Froehlic JB**. Clinical determinants in perioperative cardiac evaluation. *Prog Cardiovasc Dis* 1998; **40**: 373-381
15 **Rassi A,** Lorga AM, Rassi SG. Diagnóstico e tratamento das arritmias na cardiopatia crônica. In: Cançado JR, Chuster M. eds. Cardiopatia Chagásica. *Belo Horizonte*: *Fundação Carlos Chagas* 1985: 274-288
16 **Hlatky MA**, Boineau RE, Higinbotham MB, Lee KL, Mark DB, Califf RM. A brief self-administered questionnaire to determine functional capacity (The Duke Activity Status Index). *Am J Cardiol* 1989; **64**: 651-654
17 **Goldman L,** Caldera DL, Southwick FS, Nussbauam SR, Murray B, O'Malley TA, Goroll AH, Caplan CH, Nolan J, Burke DS, Krogstad D, Carabello B, Slater EE. Cardiac risk factors and complications in noncardiac surgery. *Medicine* 1978; **57**: 357-370
18 **Hollonberg SM**. Preoperative cardiac risk assessment. *Chest* 1999; **115**: 51S-57S
19 **Lee T**, Pujysum EM, Goldman L. Impact of inter-physician communication on the effectiveness of medical consultations. *Am J Med* 1983; **74**: 106-117
20 **Lee T**, Marcantonio ER, Mangione CM, Thomas EJ, Polanczyk CA, Cook EF. Derivation and prospective validation of a simple index for prediction of cardiac risk of major noncardiac surgery. *Circulation* 1999; **100**: 1043-1049
21 **Massie BM,** Mangano DT. Risk stratification for noncardiac surgery. *Circulation* 1993; **87**: 1752-1755
22 **Mehta RH**, Bossone E, Eagle KA. Perioperative cardiac risk assessment for noncardiac surgery. *Cardiologia* 1999; **44**: 409-418
23 **Prause G**, Ratzenhofer-Comenda B, Pierer G, Smolle-Junttner F. Can ASA grade or Goldman's cardiac risk index predict perioperative mortality? A study of 16227 patients. *Anaesthesia* 1997; **52**: 203-206
24 **Macpherson DS.** Preoperative laboratory testing: should any tests be "routine" before surgery? *Med Clin North Am* 1993; **77**: 289-308

Science Editor Kumar M and Guo SY **Language Editor** Elsevier HK

PO Box 2345, Beijing 100023, China
www.wjgnet.com
wjg@wjgnet.com

ELSEVIER

World J Gastroenterol 2005;11(37):5845-5852
World Journal of Gastroenterology ISSN 1007-9327
© 2005 The WJG Press and Elsevier Inc. All rights reserved.

• *CLINICAL RESEARCH* •

Focal adhesion kinase and Src phosphorylations in HGF-induced proliferation and invasion of human cholangiocarcinoma cell line, HuCCA-1

Urai Pongchairerk, Jun-Lin Guan, Vijittra Leardkamolkarn

Urai Pongchairerk, Vijittra Leardkamolkarn, Department of Anatomy, Faculty of Science, Mahidol University, Bangkok 10400, Thailand
Jun-Lin Guan, Department of Molecular Medicine, College of Veterinary Medicine, Cornell University, Ithaca, New York 14853, USA
Supported by the Royal Golden Jubilee PhD Program of the Thailand Research Fund (RGJ/PHD/0112/2542)
Correspondence to: Assoc. Professor. Vijittra Leardkamolkarn, Department of Anatomy, Faculty of Science, Mahidol University, Bangkok 10400, Thailand. scvlk@mahidol.ac.th
Telephone: +66-2-201-5936 Fax: +66-2-201-5923
Received: 2005-03-18 Accepted: 2005-04-09

Abstract

AIM: To study the role of focal adhesion kinase (FAK) and its association with Src in hepatocyte growth factor (HGF)-induced cell signaling in cholangiocarcinoma progression.

METHODS: Previously isolated HuCCA-1 cells were re-characterized by immunofluorescent staining and reverse transcriptase-polymerase chain reaction assay for the expression of cytokeratin 19, HGF and c-Met mRNA. Cultured HuCCA-1 cells were treated with HGF and determined for cell proliferation and invasion effects by MTT and invasion assays. Western blotting, immunoprecipitation, and co-immunoprecipitation were also performed to study the phosphorylation and interaction of FAK and Src. A novel Src inhibitor (AZM555130) was applied in cultures to investigate the effects on FAK phosphorylation inhibition and on cell proliferation and invasion.

RESULTS: HGF enhanced HuCCA-1 cell proliferation and invasion by mediating FAK and Src phosphorylations. FAK-Src interaction occurred in a time-dependent manner that Src was proved to be an upstream signaling molecule to FAK. The inhibitor to Src decreased FAK phosphorylation level in correlation with the reduction of cell proliferation and invasion.

CONCLUSION: FAK plays a significant role in signaling pathway of HGF-responsive cell line derived from cholangiocarcinoma. Autophosphorylated Src, induced by HGF, mediates Src kinase activation, which subsequently phosphorylates its substrate, FAK, and signals to cell proliferation and invasion.

© 2005 The WJG Press and Elsevier Inc. All rights reserved.

Key words: Human cholangiocarcinoma; Hepatocyte growth factor; C-Met; Focal adhesion kinase; Src

Pongchairerk U, Guan JL, Leardkamolkarn V. Focal adhesion kinase and Src phosphorylations in HGF-induced proliferation and invasion of human cholangiocarcinoma cell line, HuCCA-1. *World J Gastroenterol* 2005; 11(37): 5845-5852
http://www.wjgnet.com/1007-9327/11/5845.asp

INTRODUCTION

Hepatocyte growth factor (HGF) is a known multifunctional cytokine that affects a variety of cell types and plays roles in various cell behaviors. It has a potent mitogenic effect on hepatic cells during the process of regeneration after the liver injury[1]. It stimulates motility of some normal and tumor cells[2,3] and it contributes to the progression of cancers such as the invasiveness of hepatocellular carcinoma[4]. In addition, HGF has a protective effect on liver progenitor cells against apoptosis while enhancing angiogenesis and tumorigenesis[5-7]. Previous evidences have indicated that HGF is secreted from liver myofibroblasts and its functional role is initiated by the interaction with the receptor (c-Met) on the target cell surface[4]. The binding of HGF to c-Met induces receptor dimerization and autophosphorylation at the intracellular tyrosine kinase domain of the β-subunit of the receptors. This tyrosine kinase activation mediates the binding of signaling molecules such as Src, PI3K, PLC, and Grb2 to c-Met multifunctional docking site, which will further activate several signaling pathways leading to functional alterations of the cells[8,9] such as growth and motility[10].

Src is a 60-ku non-receptor protein tyrosine kinase, encoded by a proto-oncogene *c-Src*. It consists of a unique N-terminal segment, an SH3 domain, an SH2 domain, a catalytic domain, and a short C-terminal tail[11]. Src SH2 domain is available for binding with phosphotyrosine residues of the other molecules such as c-Met and focal adhesion kinase (FAK)[10,12]. It could be mutated and constitutively activated in transformed cells[13]. Increase in Src expression has been reported in several human cancers including colorectal cancer[14], pancreatic carcinoma[15] and breast cancer[16]. Studies on Src activation in cancer cell lines[17] and in animal model[18] have implicated it to the invasiveness of the cells.

FAK is a 125-ku cytoplasmic protein tyrosine kinase that is implicated in integrin-mediated signaling pathways involved in the process of cell cycle, cell spreading and migration and prevention of cell apoptosis[19-21]. FAK overexpression has been observed in a variety of invasive tumors[22-25] as well as in tumor cell lines[26,27]. The function of FAK in the promotion of cancer cells' proliferation has been previously demonstrated in an animal model[28].

Both Src and FAK seem to play a crucial role in the transformation and progression of tumor cells. The relationship between them has been extensively investigated, but the mechanism remains unclear. Evidences have indicated that in integrin-mediated signaling or adhesion-dependent pathway, the binding of integrin to its extracellular ligands recruits FAK to aggregate at the focal contact and initiates its autophosphorylation at tyrosine 397[29,30]. The activated FAK functions as a binding site for several downstream signaling molecules including Src[29,30], which interacts with autophosphorylated FAK by its SH2 domain[12,31]. Then, Src phosphorylates FAK at other tyrosine positions such as 576, 577, 861, and 925[32,33]. Phosphorylated FAK, especially at tyrosine 925, becomes a binding site for Grb2, one of the upstream molecules in Ras/MAPK pathway, which consequently activates this signaling pathway and eventually facilitates cell proliferation and migration[29-31]. The downstream pathway after Src and FAK interaction also involves the interaction of phosphorylated FAK with PI3K[34] or Grb7[35] that participated in actin cytoskeleton organization and cell migration. In the adhesion-independent pathway, however, evidence from the study in Phe397-FAK mutant cells has indicated that the SH3 domain of *v-Src* (a mutated and constitutive activated form of *c-Src*) could bind with the proline rich region of FAK and is able to mediate cell transformation without external stimuli[13]. The downstream pathway after Src and FAK interaction in these cells could be similarly involved with PI3K or Grb7 as in the adhesion-dependent pathway. Moreover, both FAK and Src have binding association with the exchange factors of the small GTPases in the Rho family, which are then activated by phosphorylation. These in turn regulate cytoskeleton organization and initiate cell migration[36,37].

In this study, we have attempted to clarify the associated function between Src and FAK in HGF-mediated cell proliferation and invasion, using human cholangiocarcinoma cell line, HuCCA-1, as a model. This cell line was isolated and established from a Thai patient who had cancer of the intrahepatic bile duct epithelium[38,39]. This is one of the most aggressive cancers that cause a high fatality rate in Thailand. It rapidly metastasizes to other parts of the body and there is no effective treatment available to date. The relative function of Src and FAK in the cancer cells was determined from their phosphotyrosine activities before and after Src inhibition by using a novel Src inhibitor (AZM555130).

MATERIALS AND METHODS

Materials

Mouse mAbs to cytokeratin 19, α-smooth muscle actin (SMA), FAK and phosphotyrosine (PY20) were purchased from DAKO, Sigma, Pharmingen, and Santa Cruz, respectively. Rabbit polyclonal antibody to FAK (α-KC) was produced in the laboratory at Cornell University, Ithaca, NY, USA. Rabbit polyclonal antibody to Src was purchased from Santa Cruz. Goat anti-mouse IgG-FITC, anti-mouse IgG-HRP, and anti-rabbit IgG-HRP were purchased from Zymed Laboratories Inc. Protein A-Sepharose 4B beads were purchased from Sigma. Recombinant human hepatocyte growth factor (rhHGF) was purchased from Biosource International. Src inhibitor (AZM555130) was a gift from AstraZeneca.

Cell culture

Human cholangiocarcinoma cell line, HuCCA-1, was cultured in HamF-12 medium (Hyclone) containing 10% fetal bovine serum (FBS) at 37 ℃ in 50 mL/L CO_2 incubator. To characterize the cells, immunofluorescent staining for cytokeratin 19 was performed to confirm the epithelial origin of these cells.

Immunofluorescent staining

HuCCA-1 cells were seeded on 12-mm coverslips and placed on a 24-well plate at the density of 5×10^4 cells/well. The cells were cultured until 80-90% confluence. The coverslips from each well were removed and placed on parafilms in cell-side up position. The cells were fixed by immersing in ice-cold methanol: acetone (1:1) and kept at -20 ℃ for 10 min, air dried at room temperature and rinsed thrice with PBS. Cells were covered with blocking buffer (1% BSA in PBS) at 37 ℃ for 30 min. After that, the blocking buffer was removed and the cells were incubated with mAbs against cytokeratin 19 (CK-19) or SMA, at room temperature for 1 h. The primary antibodies were removed and the cells were washed thrice with PBS. Then, cells on the coverslips were covered with FITC-conjugated goat anti-mouse IgG for 1 h at room temperature, and washed thrice with PBS. The stained cells were visualized under the Nikon fluorescent microscope at a wavelength of 450-490 nm.

Reverse transcriptase-polymerase chain reaction (RT-PCR)

Evaluation of mRNA expression for HGF and c-Met in HuCCA-1 cells were semiquantitated by RT-PCR. Total RNA was isolated from the cells using TRIzol reagent and RT-PCR was performed using OneStep RT-PCR kit (QIAGEN), following the manufacturer's instructions. Two micrograms of total RNA and 0.6 μmol/L of each primer were used in each reaction. The specific primer pairs included (1) for hHGF: "5'-GCCTGAAAGATATC-CCGACA-3' " and "5'-TTCCATGTTCTTGTCCCACA-3' "(523 bp), (2) for *c-Met*: "5'-TCTTGGGACATCAG-AGGGTC-3' "and "5'-TGACTGCAGGACTGGAAATG-3' "(222 bp), (3) for GAPDH (internal control): "5'-TGATGA-CATCAAGAAGGTGGTGAAG-3' "and "5'-TCCTTG-GAGGCCATGTG GCCAT-3' "(240 bp).

Immunoprecipitation and Western blotting assays of FAK and Src phosphorylation

Cultured HuCCA-1 cells were washed with ice-cold PBS and digested with radioimmunoprecipitation assay (RIPA) lysis buffer containing phosphatase and protease inhibitors

(50 mmol/L sodium fluoride, 1 mmol/L sodium orthovanadate, 1% aprotinin, 2 mmol/L phenylmethylsulfonyl fluoride and 10 μg/mL leupeptin). Whole cell lysates that contained ⩾500 μg of total protein were pre-cleared by incubation with protein A-Sepharose beads at 4 ℃ for 30 min. The beads containing lysates were centrifuged and supernatants were collected. Rabbit polyclonal anti-FAK or anti-Src antibody was added and incubated overnight at 4 ℃. Then, protein A-Sepharose beads were added and incubation was continued at 4 ℃ for an additional 1.30 h. Immunocomplexes were collected by centrifugation and the supernatants were discarded. The beads with immunocomplexes were washed with RIPA lysis buffer, mixed with SDS-PAGE sample buffer, boiled for 5 min and resolved by SDS-polyacrylamide gel electrophoresis. Western blotting was performed using mouse monoclonal anti-phosphotyrosine (PY20) antibody followed by HRP-conjugated goat anti-mouse IgG. The desired protein bands on the membrane were detected by using the enhanced chemiluminescence system (Lumiglo, KPL). To confirm the amount of total FAK or Src in each sample, the same membranes were stripped and reprobed with mouse monoclonal anti-FAK or rabbit polyclonal anti-Src antibody. The density of the bands was measured by densitometry.

Co-immunoprecipitation assay of Src and FAK

HuCCA-1 cells were washed with ice-cold PBS and lysed with NP-40 lysis buffer without salt (1% NP-40, 50 mmol/L Tris-HCl pH 7.4) containing phosphatase and protease inhibitors. Whole cell lysates were processed as above, but the immunoprecipitation was first complex with rabbit polyclonal anti-Src antibody. Then, the complex was resolved by SDS-PAGE and proteins were transferred to nitrocellulose membrane. The membrane was incubated with mouse monoclonal anti-FAK antibody followed by HRP-conjugated goat anti-mouse IgG. The desired protein bands were evaluated as above. The same membrane was stripped and reprobed with anti-Src antibody to confirm the amount of total Src used in each sample.

Cell proliferation assay

Cell proliferation assay was performed by using the *In Vitro* Toxicology Assay Kit MTT Based (Sigma) following the manufacturer's instruction. Briefly, HuCCA-1 cells were seeded in a 96-well plate at a density of 1×10^4 cells/well in 100 μL of HamF-12 media containing 10% FBS and cultured overnight in 37 ℃, 50 mL/L CO_2 incubator. Then, cells were starved in 100 μL of serum-free HamF-12 media for 24 h. Fresh medium (200 μL) with or without 10 or 20 ng/mL rhHGF were replaced and further incubated for 24-48 h. Then, the medium was changed to 100 μL of HamF-12, and 10 μL of reconstituted MTT was added into each well. The plate was incubated at 37 ℃ in 50 mL/L CO_2 incubator for 4 h. After incubation, 100 μL of MTT solubilizing solution (10% Triton X-100, 0.1 mol/L HCl in anhydrous isopropanol) was added into each well to dissolve the resulting formazan crystals. Absorbance at a wavelength of 570 nm was measured using a microplate reader. The negative control of the system was performed as the experimental one but without cells. Absorbance at 690 nm was measured to determine the background of the system, and was subtracted from each measurement. The data was statistically analyzed using Student's *t*-test and compared with the untreated group. A *P* value lesser than 0.05 was considered significant.

Cell invasion assay

HuCCA-1 cells, in the density of 1×10^5 cells/200 μL of HamF-12 and 0.1% BSA, were seeded on each upper chamber of 24-well transwell plate (8-μm pore-sized membrane, Costar) coated with 100 μL of 30 μg matrigel (Becton-Dickinson). In the lower chamber, 400 μL/well of HamF-12 with or without 20 ng/mL rhHGF was added. After incubation at 37 ℃ in 50 mL/L CO_2 incubator for 48 h, the media in both chambers were removed. The cells that remained on the upper surface of the membrane were wiped off with wet cotton buds. Invasive cells bounded on the lower surface of the membrane were fixed with 25% methanol and stained with 5% crystal violet in 25% methanol. The number of invading cells on each membrane was counted, under light microscope at 40× magnification, for six random microscopic fields per membrane and averaged. Each assay was performed in triplicate.

Inhibition assay of Src-FAK interaction

Cultured HuCCA-1 cells were treated with 0, 0.1, 0.5, and 1.0 μmol/L of Src inhibitor (AZM555130) for 1 h. Then, they were further incubated with 20 ng/mL rhHGF or without rhHGF for 48 h. The whole cell lysates were extracted for immunoprecipitation and Western blotting assay to determine the level of Src and FAK phosphorylation. Cell proliferation was performed by MTT assay as described above. The effect on cell invasion was performed by incubation of the cells with 0, 0.1, or 1.0 μmol/L of AZM555130 for 1 h and then seeded onto the upper chambers of 24-well transwell plates. HamF-12 medium with or without 20 ng/mL rhHGF was added in the lower chambers and the cells were cultured for 48 h. The number of cells invading through matrigel was analyzed as described above.

RESULTS

Characterization of HuCCA-1 cells

HuCCA-1 cells were intensely labeled with anti-cytokeratin-19 (CK19, Figure 1A) but not with SMA antibodies (Figure 1B), which indicated the epithelial origin of the cells. This confirms the previous characterization by the establishers[38,39]. The semi-quantitative determination of mRNA expression for HGF and its receptors (c-Met), by RT-PCR analysis, showed a high level of c-Met but a low level of HGF mRNA gene expression (Figures 2A-C). Liver myofibroblasts and hepatocellular carcinoma cell line, HepG2, were used as positive controls for HGF and c-Met gene expression, respectively.

Effect of HGF on HuCCA-1 cell proliferation and invasion

HuCCA-1 cell proliferation and invasion were enhanced by treatment with rhHGF, in a time-dependent fashion (Figures 3A and B). After 24-48 h treatment with 10 ng/mL

rhHGF, HuCCA-1 cell proliferation was significantly increased when compared to the control (P<0.05 and 0.01 at 24 and 48 h, respectively, Figure 3A). The number of invading cells was also increased significantly when 20 ng/mL rhHGF was added into the lower chamber without the serum (P<0.001 and 0.001 at 24 and 48 h, respectively, Figure 3B).

Effect of HGF on phosphorylation of FAK and Src

The immunoprecipitation and Western blotting assays demonstrated that HGF promoted FAK and Src phosphorylation in a time-dependent manner. The maximal level of tyrosine phosphorylation on FAK was reached after 60 min of HGF induction and then declined to the basal level after 120 min (Figures 4A and B). For Src phosphorylation, the level was peaked at 30 min after HGF induction (Figures 5A and B).

The interaction between Src and FAK after HGF induction

Co-immunoprecipitation of Src and FAK in HGF-induced cells revealed that HGF promoted Src and FAK interaction. The Src-FAK immunoprecipitation level reached a maximum at 30 min (Figures 6A-C). This was well correlated to the level of Src phosphorylation (Figure 5) indicating that the Src-FAK complex was formed before FAK became phosphorylated.

Effect of Src inhibitor (AZM555130) on Src and FAK phosphorylation

After 48 h treatment, Src inhibitor had no inhibition effect on Src phosphorylation (Figure 7A) both in HGF-induced and non-induced cells, but it had inhibition effect on FAK phosphorylation in a dose-dependent manner (Figure 7B). In HGF-induced FAK phosphorylation, a low dose at 0.1 μmol/L was not inhibited, but higher doses (0.5 and 1.0 μmol/L) were gradually inhibited. In non-HGF-induced cells, the inhibition effect was significant at a higher dose (1.0 μmol/L) than for HGF-induced cells.

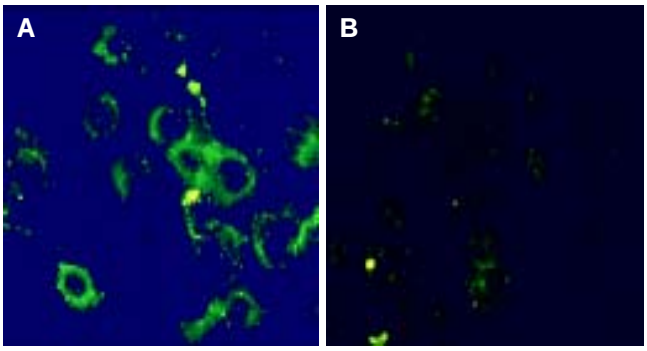


Figure 1 Immunofluorescent study in HuCCA-1 cells shows positive staining to human CK-19 mAb (A) and negative staining to SMA mAb (B) (40× magnification).

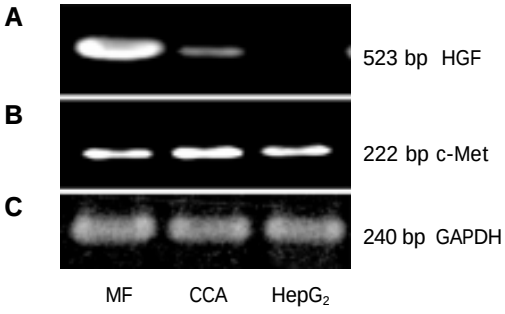


Figure 2 mRNA expression level of HGF (A) and c-Met (B) was observed by RT-PCR technique. HuCCA-1 (CCA) expressed low HGF but a high level of c-Met mRNA. Liver myofibroblasts (MF) and hepatocellular carcinoma cell line (HepG2) were used as positive controls for HGF and c-Met, respectively. Equal amount of total RNA from each cell was confirmed by GAPDH (C).

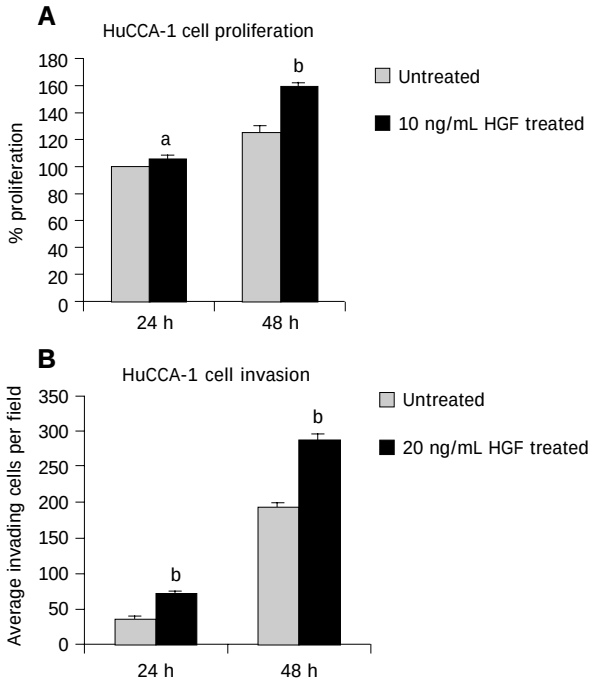


Figure 3 Cell proliferation assay showed significantly increased proliferating cell number after 10 ng/mL rhHGF treatment in HuCCA-1 cells for 24 and 48 h (A). Invasion assay also showed significantly increased invading cells after 24 and 48 h treatment of 20 ng/mL rhHGF (B). Data are expressed as mean±SE, ^aP<0.05 and ^bP<0.01, compared to the HGF-untreated cells at the corresponding time.

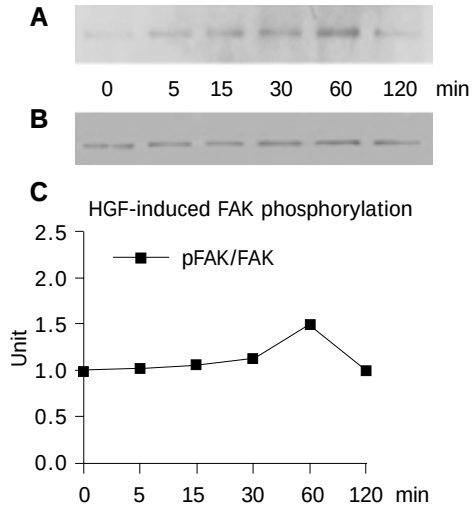


Figure 4 Treatment of HuCCA-1 cells with 20 ng/mL rhHGF for 0, 5, 15, 30, 60, and 120 min showed increased degree of FAK phosphorylation in a time-dependent manner. The maximal level of FAK phosphorylation was reached at 60 min and then sharply decreased at 120 min (A). Equal amount of FAK protein used in each time point was confirmed by reprobing the membrane with anti-FAK antibody (B). The density of bands was measured and pFAK/FAK value was plotted in a graph (C).

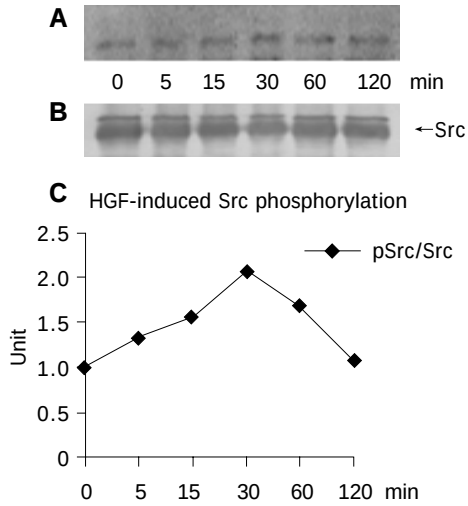


Figure 5 Treatment of HuCCA-1 cells with 20 ng/mL rhHGF for 0, 5, 15, 30, 60, and 120 min showed an increased degree of Src phosphorylation in a time-dependent manner. The maximal level of Src phosphorylation was reached at 30 min (A). Equal amount of Src protein (upper bands) used in each time point was confirmed by reprobing the membrane with anti-Src antibody (B). The density of bands was measured and pSrc/Src value was plotted in a graph (C).

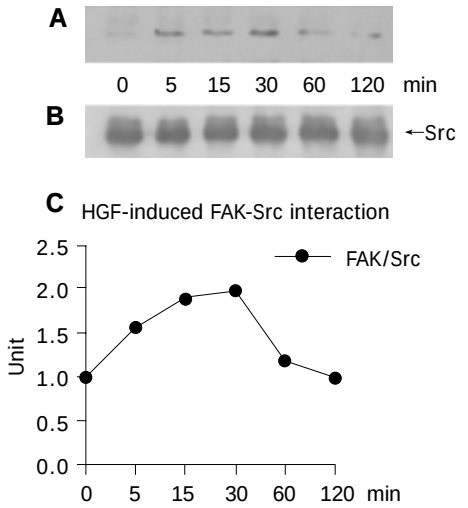


Figure 6 The interaction between Src and FAK was demonstrated in HGF-treated HuCCA-1 cells by co-immunoprecipitation at varied time points. The resulting bands showed a positive correlation of FAK with Src phosphorylation, which reached a maximum at 30 min and then declined (A). The amount of Src protein (upper bands) used in each time point was confirmed (B). The density of bands was measured and the ratio between FAK and Src was plotted in the graph (C).

Effect of Src inhibitor (AZM555130) on HuCCA-1 cell proliferation

HuCCA-1 cell proliferation in both HGF-induced and non-induced conditions was significantly inhibited by the treatment with AZM555130 (Figure 8). The non-induced cells were more affected than the induced cells. In HGF-induced cells, cell proliferation was reduced by 25% and 34% at the doses of 0.5 and 1.0 μmol/L, respectively (P<0.01, both). In the non-induced cells, the cell proliferation was reduced by 9% (P<0.05), 33% (P<0.01) and 41% (P<0.01) at the doses of 0.1, 0.5, and 1.0 μmol/L, respectively.

Effect of Src inhibitor (AZM555130) on HuCCA-1 cell invasion

Treatment of HuCCA-1 cells with AZM555130 reduced cell invasiveness in both HGF-induced and non-induced conditions, in a dose-dependent manner (Figure 9). The induced cells were more sensitive than the non-induced cells at the low dose, but the non-induced cells were more sensitive than the induced cells at the high dose. At the concentration of 0.1 and 1.0 μmol/L, AZM555130 significantly decreased the invasive ability of the HGF-induced cells by 32% and 85%, respectively and of the non-induced cells by 23% and 98%, respectively (P<0.01, all).

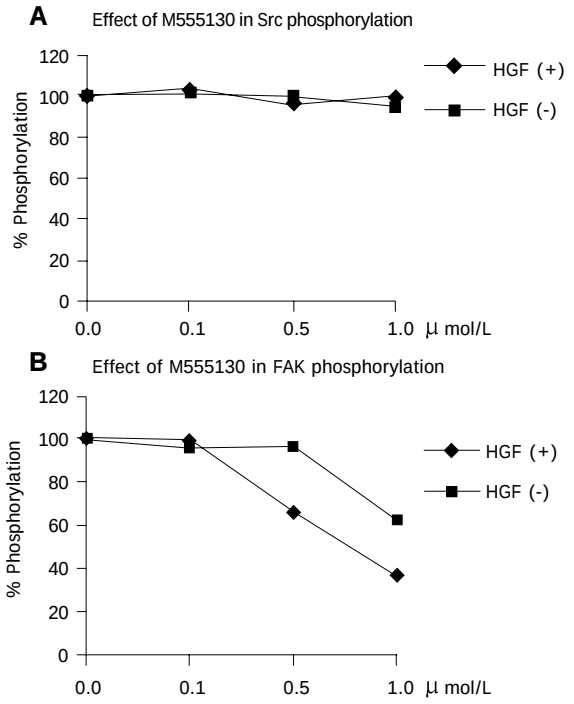


Figure 7 Treatment of cells with 0.1, 0.5, and 1.0 μmol/L of AZM555130 for 48 h showed no inhibition of Src phosphorylation both in HGF-treated and untreated cells (A). The HGF-induced FAK phosphorylation was not inhibited after 48 h treatment of 0.1 μmol/L AZM555130 but showed 34% and 63% inhibition by 0.5 and 1.0 μmol/L treatment, respectively. The 37% inhibition of FAK phosphorylation was observed by treatment of 1.0 μmol/L AZM555130 in non-induced cells (B). These values were compared with the levels of Src and FAK phosphorylation in AZM555130-untreated cells which is equal to 100%.

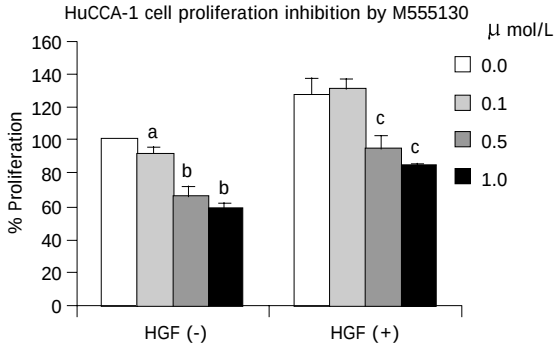


Figure 8 The HGF-mediated cell proliferation was not inhibited by 0.1 μmol/L AZM555130 but was significantly inhibited by 0.5 and 1.0 μmol/L of AZM555130 for 25% and 34%, respectively. Without HGF, cell proliferation was inhibited by 0.1, 0.5, and 1.0 μmol/L of AZM555130 for 9%, 33%, and 41%, respectively. All values are mean±SE, ^{a}P<0.05 and ^{b}P<0.01, compared to the control in HGF-untreated cells; ^{d}P<0.01, compared to the control in HGF-treated cells.

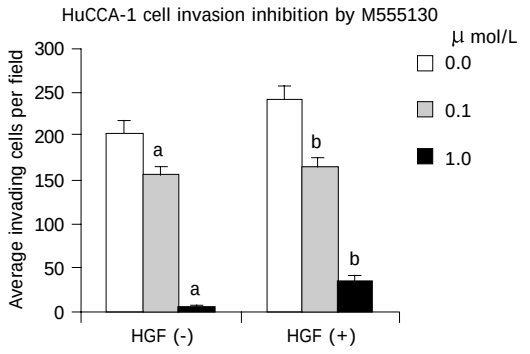


Figure 9 The HGF-mediated invasion of HuCCA-1 cells was significantly decreased by 0.1 and 1.0 μmol/L of AZM555130 for 32% and 85%, respectively. Without HGF, cell invasion was also significantly decreased by 0.1 and 1.0 μmol/L of AZM555130 for 23% and 98%, respectively. All values are mean±SE, $^{b}P<0.01$, compared to the control in HGF-untreated cells; $^{d}P<0.01$, compared to the control in HGF-treated cells.

DISCUSSION

Cholangiocarcinoma cells (HuCCA-1) showed high c-Met mRNA expression, thus they responded well to HGF induction. The profound effects of HGF in enhancing HuCCA-1 cell proliferation and invasion demonstrated here reflect the events in cholangiocarcinoma patients with high HGF (produced from the liver myofibroblasts) that exerted its action through c-Met to promote the rapid progression of cancer. Since various cancers respond differently to various growth factors and/or cytokines, their signaling mediators were believed to be very diverse[3,40]. The signaling molecules mediated by growth factors and/or cytokines to regulate normal-cell proliferation have been previously determined[41,42]. The implication of FAK activation via integrin-mediated signaling to promote cell migration in normal and embryonic cells has also been reported[29,43]. This study emphasized the signaling mechanism mediated by Src and FAK after the binding of HGF to c-Met. We found that in association with its promoting cell proliferation and invasiveness, HGF was also found to maximize the cytoplasmic tyrosine phosphorylation of Src and FAK in HuCCA-1 cells (Figures 4 and 5). FAK phosphorylation increased slightly at 30 min after the induction and reached the maximum level at 60 min. Src phosphorylation occurred prior to FAK phosphorylation and the level peaked at 30 min after the induction. Although the basal levels of both Src and FAK phosphorylation were high in the non-induced stage, the earlier and higher effect of HGF on Src phosphorylation was observed than on FAK phosphorylation in the induced stage. These results suggest that HGF-mediated signaling via Src. When Src was co-immunoprecipitated with FAK in the HGF-induced cells, Src phosphorylation pattern and time course level was similar to the pattern and level of the non-induced cell. It was suggested that Src phosphorylation and Src-FAK interaction occurred side by side and Src probably was the upstream effector molecule to FAK. Therefore, the sequences of signaling mechanism in HGF-induced HuCCA-1 cells could be (i) The binding of HGF to c-Met induced the conformational change and autophosphorylation of the receptors[44]. (ii) The binding of Src SH2 domain to the phosphorylated receptors at tyrosine 1349 and 1356 positions of the c-Met multifunctional docking site[45]. (iii) The phosphorylation of Src, and (iv) Src further activated FAK by Src kinase activity. However, previous investigation has indicated that FAK has no specific binding site on c-Met but Src was a substrate and a binding partner of FAK[29,46]. Apparently, the functional relationship between Src and FAK molecules was reversed in the induced HuCCA-1 cells. To act on its substrate FAK, Src might have to use its SH2 domain to bind c-Met and SH3 domain to bind the proline-rich region of FAK[12,21,47]. Subsequently, Src catalytic domain phosphorylates FAK at other tyrosine residues leading to the cascade of signaling pathways for cell proliferation such as activation of Ras/MAPK pathway. This pathway has been raised in the study of human embryonic kidney 293 cells under the induction of HGF, where FAK was suggested as an adaptor molecule in Src phosphorylation[48]. In addition, the activation through Src/p130Cas-signaling cascade was believed to use FAK as a mediator necessary for HGF-induced cell growth and invasiveness in MDCK cells[49].

To confirm that the signaling pathway mediated by HGF-c-Met interaction has Src as an upstream molecule to FAK, we inhibited Src by using a novel Src inhibitor (AZM555130). The results showed that AZM555130 could not inhibit Src phosphorylation (Figure 7A) but inhibit FAK phosphorylation (Figure 7B) since the inhibitor AZM555130 acted by specifically binding to its tyrosine kinase domain to block the enzyme activity[50], not to its tyrosine phosphorylation. Therefore, Src tyrosine phosphorylation remained stable (Figure 7A). However, when Src kinase activity was inhibited, the downstream signaling molecules, which were substrates for Src including FAK could not be further phosphorylated (Figure 7B). The effect of inhibitor to Src on FAK phosphorylation was concentration-dependent and more sensitive in HGF-induced cells than in the non-induced cells (Figure 7B). This further supported that Src was an intermediate linker between c-Met and FAK and Src enzyme activity was directly inhibited by AZM555130. Without HGF, the response of Src (as a kinase for FAK) to the inhibitor was low and required higher concentration of AZM555130 to reduce FAK phosphorylation.

The proliferation of HGF-induced cells was decreased after Src inhibitor treatment, at the concentration of 0.5-1.0 μmol/L, which was well correlated with FAK phosphorylation inhibition. In the non-induced cells, decreased cell proliferation by Src inhibitor was also detected but at the lower extent. Inhibition of HuCCA-1 cell invasion was found to be dependent on AZM555130 concentration both in cells with and without HGF induction indicating the high efficiency of the inhibitor.

The overall results implied that Src and FAK were the pivotal signaling molecules that mediated signaling pathway for HGF-induced cells. Src catalytic activity was enhanced in HGF-induced cells and functioned as a kinase for FAK. FAK was phosphorylated and further led to the downstream pathways to cell proliferation and invasion. In order to effectively stop the progression of cancers such as cholangiocarcinoma, in which FAK phosphorylation was specifically induced by the paracrine effect of HGF,

inhibition of FAK or blocking of Src-FAK interaction should be taken into consideration.

REFERENCES

1 **Kaido T,** Imamura M. Hepatocyte growth factor: clinical implications in hepatobiliarypancreatic surgery. *J Hepatobiliary Pancreat Surg* 2001; **8**: 65-75
2 **Li Y,** Bhargava MM, Joseph A, Jin L, Rosen EM, Goldberg ID. Effect of hepatocyte growth factor/scatter factor and other growth factors on motility and morphology of non-tumorigenic and tumor cells. *In Vitro Cell Dev Biol Anim* 1994; **30A**: 105-110
3 **Ueoka Y,** Kato K, Kuriaki Y, Horiuchi S, Terao Y, Nishida J, Ueno H, Wake N. Hepatocyte growth factor modulates motility and invasiveness of ovarian carcinomas via Ras-mediated pathway. *Br J Cancer* 2000; **82**: 891-899
4 **Neaud V,** Faouzi S, Guirouih J, Le Bail B, Balabaud C, Bioulac-Sage P, Rosenbaum J. Human hepatic myofibroblasts increase invasiveness of hepatocellular carcinoma cells: evidence for a role of hepatocyte growth factor. *Hepatology* 1997; **26**: 1458-1466
5 **Bardelli A,** Longati P, Albero D, Goruppi S, Schneider C, Ponzetto C, Comoglio PM. HGF receptor associates with the anti-apoptotic protein BAG-1 and prevents cell death. *EMBO J* 1996; **15**: 6205-6212
6 **Grant DS,** Kleinman HK, Goldberg ID, Bhargava MM, Nickoloff BJ, Kinsella JL, Polverini P, Rose EM. Scatter factor induces blood vessel formation *in vivo*. *Proc Natl Acad Sci USA* 1993; **90**: 1937-1941
7 **Rong S,** Bodescot M, Blair D, Dunn J, Nakamura T, Mizuno K, Park M, Chan A, Aaronson S, Vande Woude GF. Tumorigenicity of the met proto-oncogene and the gene for hepatocyte growth factor. *Mol Cell Biol* 1992; **12**: 5152-5158
8 **Pelicci G,** Giordano S, Zhen Z, Salcini AE, Lanfrancone L, Bardelli A, Panayotou G, Waterfield MD, Ponzetto C, Pelicci PG, Comoglio PM. The motogenic and mitogenic responses to HGF are amplified by the Shc adaptor protein. *Oncogene* 1995; **10**: 1631-1638
9 **Ponzetto C,** Bardelli A, Zhen Z, Maina F, Zonca PD, Giordano S, Graziani A, Panayotou G, Comoglio PM. A multifunctional docking site mediated signaling and transformation by the hepatocyte growth factor/scatter factor receptor family. *Cell* 1994; **77**: 261-271
10 **Rahimi N,** Hung W, Tremblay E, Saulnier R, Elliott B. c-Src kinase activity is required for hepatocyte growth factor-induced motility and anchorage-independent growth of mammary carcinoma cells. *J Biol Chem* 1998; **273**: 33714-33721
11 **Abram CL,** Courtneidge SA. Src family tyrosine kinases and Growth factor signaling. *Exp Cell Res* 2000; **254**: 1-13
12 **Xing Z,** Chen HC, Nowlen JK, Taylor SJ, Shalloway D, Guan JL. Direct interaction of v-Src with the focal adhesion kinase mediated by the Src SH2 domain. *Mol Biol Cell* 1994; **5**: 413-421
13 **Hauck CR,** Hunter T, Schlaepfer DD. The v-Src SH3 domain facilitates a cell adhesion-independent association with focal adhesion kinase. *J Biol Chem* 2001; **276**: 17653-17662
14 **Talamonti MS,** Roh MS, Curley SA, Gallick GE. Increase in activity and level of pp60 c-Src in progressive stages of human colorectal cancer. *Clin Invest* 1993; **91**: 53-60
15 **Lutz MP,** Esser IB, Flossman-Kast BB, Vogelmann R, Luhrs H, Friess H, Buchler MW, Adler G. Overexpression and activation of the tyrosine kinase Src in human pancreatic carcinoma. *Biochem Biophys Res Commun* 1998; **243**: 503-508
16 **Verbeek BS,** Vroom TM, Adriaansen-Slot SS, Ottenhoff-Kalff AE, Geertzema JG, Hennipman A, Rijksen G. c-Src protein expression is increased in human breast cancer. An immunohistochemical and biochemical analysis. *J Pathol* 1996; **180**: 383-388
17 **Ito H,** Gardner-Thorpe J, Zinner MJ, Ashley SW, Whang EE. Inhibiton of tyrosine kinase Src suppresses pancreatic cancer invasiveness. *Surgery* 2003; **134**: 221-226
18 **Myoui A,** Nishimura R, Williams PJ, Hiraga T, Tamura D, Michigami T, Mundy GR, Yoneda T. C-Src tyrosine kinase activity is associated with tumor colonization in bone and lung in an animal model of human breast cancer metastasis. *Cancer Res* 2003; **63**: 5028-5033
19 **Zhao JH,** Reiske H, Guan JL. Regulation of the cell cycle by focal adhesion kinase. *J Cell Biol* 1998; **143**: 1997-2008
20 **Panetti TS.** Tyrosine phosphorylation of paxillin, FAK, and p130CAS: effects on cell spreading and migration. *Front Biosci* 2002; **7**: D143-150
21 **Hanks SK,** Ryzhova L, Shin NY, Brabek J. Focal adhesion kinase signaling activities and their implications in the control of cell survival and motility. *Front Biosci* 2003; **8**: D982-996
22 **Owens LV,** Xu LH, Craven RJ, Dent GA, Weiner TM, Kornberg L, Liu ET, Cance WG. Overexpression of the focal adhesion kinase ($p125^{FAK}$) in invasive human tumors. *Cancer Res* 1995; **55**: 2752-2755
23 **Miyazaki T,** Kato H, Nakajima M, Sohda M, Fukai Y, Masuda N, Manda R, Fukuchi M, Tsukada K, Kuwano H. FAK overexpression is correlated with tumour invasiveness and lymph node metastasis in oesophageal squamous cell carcinoma. *Br J Cancer* 2003; **89**: 140-145
24 **Oktay MH,** Oktay K, Hamele-Bena D, Buyuk A, Koss LG. Focal adhesion kinase as a marker of malignant phenotype in breast and cervical carcinomas. *Hum Pathol* 2003; **34**: 240-245
25 **Schneider GB,** Kurago Z, Zaharias R, Gruman LM, Schaller MD, Hendrix MJ. Elevated focal adhesion kinase expression facilitates oral tumor cell invasion. *Cancer* 2002; **95**: 2508-2515
26 **Zetser A,** Bashenko Y, Miao HQ, Vlodavsky I, Ilan N. Heparanase affects adhesive and tumorigenic potential of human glioma cells. *Cancer Res* 2003; **63**: 7733-7741
27 **Moritake H,** Sugimoto T, Kuroda H, Hidaka F, Takahashi Y, Tsuneyoshi M, Yoshida MA, Cui Q, Akiyoshi K, Izumi T, Nunoi H. Newly established Askin tumor cell line and overexpression of focal adhesion kinase in Ewing sarcoma family of tumors cell lines. *Cancer Genet Cytogenet* 2003; **146**: 102-109
28 **Natarajan M,** Hecker TP, Gladson CL. FAK signaling in anaplastic astrocytoma and glioblastoma tumors. *Cancer J* 2003; **9**: 126-133
29 **Guan JL.** Role of focal adhesion kinase in integrin signaling. *Int J Biochem Cell Biol* 1997; **29**: 1085-1096
30 **Schaller MD.** Biochemical signals and biological responses elicited by the focal adhesion kinase. *Biochem Biophys Acta* 2001; **1540**: 1-21
31 **Schlaepfer DD,** Hanks SK, Hunter T, van der Geer P. Integrin-mediated signal transduction linked to Ras pathway by GRB2 binding to focal adhesion kinase. *Nature* 1994; **372**: 786-791
32 **Calalb MB,** Polte TR, Hanks SK. Tyrosine phosphorylation of focal adhesion kinase at sites in the catalytic domain regulates kinase activity: a role for Src family kinases. *Mol Cell Biol* 1995; **15**: 954-963
33 **Calalb MB,** Zhang X, Polte TR, Hanks SK. Focal adhesion kinase tyrosine-861 is a major site of phosphorylation by Src. *Biochem Biophys Res Commun* 1996; **228**: 662-668
34 **Reiske HR,** Kao SC, Cary LA, Guan JL, Lai JF, Chen HC. Requirement of phosphatidylinositol 3-kinase in focal adhesion kinase-promoted cell migration. *J Biol Chem* 1999; **274**: 12361-12366
35 **Han DC,** Guan JL. Association of focal adhesion kinase with Grb7 and its role in cell migration. *J Biol Chem* 1999; **274**: 24425-24430
36 **Parsons JT,** Martin KH, Slack JK, Taylor JM, Weed SA. Focal adhesion kinase: a regulator of focal adhesion dynamics and cell movement. *Oncogene* 2000; **19**: 5606-5613
37 **Zhai J,** Lin H, Nie Z, Wu J, Canete-Soler R, Schlaepfer WW, Schlaepfer DD. Direct interaction of focal adhesion kinase with p190RhoGEF. *J Biol Chem* 2003; **278**: 24865-24873
38 **Sirisinha S,** Tengchaisri T, Boonpucknavig S, Prempracha N, Ratanarapee S, Pausawasdi A. Establishment and characterization of a cholangiocarcinoma cell line from a Thai pa-

tient with intrahepatic bile duct cancer. *Asian Pac J Allergy Immunol* 1991; **9**: 153-157

39 **Sriurairatana S,** Tengchaisri T, Sirisinha S. Ultrastructural characteristics of liver fluke associated human cholangio-carcinoma cell lines. *Southeast Asian J Trop Med Public Health* 1996; **27**: 57-62

40 **Empereur S,** Djelloul S, Di Gioia Y, Bruyneel E, Mareel M, Van Hengel J, Van Roy F, Comoglio P, Courtneidge S, Paraskeva C, Chastre E, Gespach C. Progression of familial adenomatous polyposis (FAP) colonic cells after transfer of the src or polyoma middle T oncogenes: cooperation between src and HGF/Met in invasion. *Br J Cancer* 1997; **75**: 241-250

41 **Tangkijvanich P,** Melton AC, Chitapanarux T, Han J, Yee HF Jr. Platelet-derived growth factor-BB and lysophosphatidic acid distinctly regulate hepatic myofibroblasts migration through focal adhesion kinase. *Exp Cell Res* 2002; **281**: 140-147

42 **Hatai M,** Hashi H, Mogi A, Soga H, Yokota J, Yaoi Y. Stimulation of tyrosine- and serine-phosphorylation of focal adhesion kinase in mouse 3T3 cells by fibronectin and fibroblast growth factor. *FEBS Lett* 1994; **350**: 113-116

43 **Cary LA,** Han DC, Guan JL. Integrin-mediated signal transduction pathways. *Histol Histopathol* 1999; **14**: 1001-1009

44 **Stella MC,** Comoglio PM. HGF: a multifunctional growth factor controlling cell scattering. *Int J Biochem Cell Biol* 1999; **31**: 1357-1362

45 **Comoglio PM,** Boccaccio C. The HGF receptor family: unconventional signal transducers for invasive cell growth. *Genes Cells* 1996; **1**: 347-354

46 **Cary LA,** Guan JL. Focal adhesion kinase in integrin-mediated signaling. *Front Biosci* 1999; **4**: D102-113

47 **Thomas JW,** Ellis B, Boerner RJ, Knight WB, White II GC, Schaller MD. SH2- and SH3-mediated interactions between focal adhesion kinase and Src. *J Biol Chem* 1998; **273**: 577-583

48 **Chen HC,** Chan PC, Tang MJ, Cheng CH, Chang TJ. Tyrosine phosphorylation of focal adhesion kinase stimulated by Hepatocyte growth factor leads to mitogen-activated protein kinase activation. *J Biol Chem* 1998; **273**: 25777-25782

49 **Chan PC,** Liang CC, Yu KC, Chang MC, Ho WL, Chen BH, Chen HC. Synergistic effect of focal adhesion kinase overexpression and Hepatocyte growth factor stimulation on cell transformation. *J Biol Chem* 2002; **277**: 50373-50379

50 **Ple PA,** Green TP, Hennequin LF, Curwen J, Fennell M, Allen J, Lambert-Van Der Brempt C, Costello G. Discovery of a new class of anilinoquinazoline inhibitors with high affinity and specificity for the tyrosine kinase domain of c-Src. *J Med Chem* 2004; **47**: 871-887

Science Editor Guo SY **Language Editor** Elsevier HK

PO Box 2345, Beijing 100023, China
www.wjgnet.com
wjg@wjgnet.com

ELSEVIER

World J Gastroenterol 2005;11(37):5853-5858
World Journal of Gastroenterology ISSN 1007-9327
© 2005 The WJG Press and Elsevier Inc. All rights reserved.

• *CLINICAL RESEARCH* •

Effect of lysozyme chloride on betel quid chewing aggravated gastric oxidative stress and hemorrhagic ulcer in diabetic rats

Chen-Road Hung

Chen-Road Hung, Department of Pharmacology, College of Medicine, National Cheng Kung University, Tainan, Taiwan, China
Supported by a grant (NSC 91-2320-B006-103) from National Sciences Council of Taiwan, China
Correspondence to: Chen-Road Hung, PhD, Department of Pharmacology, College of Medicine, National Cheng Kung University, Tainan, Taiwan, China. crhung@mail.ncku.edu.tw
Telephone: +886-6-2353535-5483 Fax: +886-6-2749296
Received: 2005-03-28 Accepted: 2005-04-30

Abstract

AIM: To evaluate the protective effect of lysozyme chloride on betel quid chewing (BQC) aggravated gastric oxidative stress and hemorrhagic ulcer in rats with diabetes mellitus (DM).

METHODS: Male Wistar rats were challenged intravenously with streptozotocin (65 mg/kg) to induce DM. Rats were fed with regular pellet food or BQC-containing diets. After 90 d, rats were deprived of food for 24 h. Rat stomachs were irrigated for 3 h with normal saline or simulated gastric juice. Rats were killed and gastric specimens were harvested.

RESULTS: An enhancement of various gastric ulcerogenic parameters, including acid back-diffusion, mucosal lipid peroxide generation, as well as decreased glutathione levels and mucus content, were observed in DM rats. After feeding DM rats with BQC, an exacerbation of these ulcerogenic parameters was achieved. Gastric juice caused a further aggravation of these ulcerogenic parameters. Daily intragastric lysozyme chloride dose-dependently inhibited exacerbation of various ulcerogenic parameters in those BQC-fed DM rats.

CONCLUSION: (1) Gastric juice could aggravate both DM and BQC-fed DM rat hemorrhagic ulcer; (2) BQC exacerbated gastric hemorrhagic ulcer in DM rats via enhancing oxidative stress and reducing defensive factors; (3) lysozyme chloride effectively protected BQC aggravated gastric damage in DM rats.

© 2005 The WJG Press and Elsevier Inc. All rights reserved.

Key words: Glutathione; Lipid peroxide; Oxyradical; Prostaglandins; Gastric mucus; Mucosal damage; Acid back-diffusion

Hung CR. Effect of lysozyme chloride on betel quid chewing aggravated gastric oxidative stress and hemorrhagic ulcer in diabetic rats. *World J Gastroenterol* 2005; 11(37): 5853-5858
http://www.wjgnet.com/1007-9327/11/5853.asp

INTRODUCTION

Betel quid chewing (BQC) is a habit of human beings in most parts of the world. It has been estimated that more than 10% of the world's population chew betel quid for its mild psychoactive effects[39]. Ample documents demonstrate that BQC is a carcinogenic agent either in animal[4] or in human beings[7]. BQC can result in cancer of buccal cavity[26], esophagus[31], stomach[8], lung, and liver[4]. Since the stomach is the organ that directly contacts BQC, it is likely that gastric mucosa can also be damaged after its long-term consumption.

On the other hand, diabetes mellitus (DM) is an important fatal disease that is frequently found in the clinic. Gastrointestinal disturbance, such as gastric hemorrhagic ulcer, is one of the main manifestations observed in poor controlled DM patients. Previous document demonstrates the importance of acid back-diffusion in the formation of hemorrhagic ulcer in DM rats[22]. Whether BQC can aggravate DM-induced gastric hemorrhagic ulcer is unknown.

During gastric oxidative stress, the imbalance of aggressive and defensive factors in the stomach plays a pivotal role in gastric hemorrhage and ulcer formation. The aggressive factors include gastric acid back-diffusion and oxyradical generation, while defensive factors involve glutathione (GSH) and mucus biosynthesis[17]. Aggravation of aggressive factors and/or attenuation of defensive substances may result in high risk of gastric hemorrhage and ulcer formation.

When gastric mucosal barriers are inflamed or disrupted by acid, ethanol or aspirin, the intraluminal free acid may diffuse back into gastric mucosa through damaged mucosal barriers and consequently causes exacerbation of hemorrhage and ulceration. This acid back-diffusion is considered as a sensitive marker of gastric mucosal integrity[10,21]. In fact, gastric acid back-diffusion is greatly associated with hemorrhage and ulcer formation in various inflammatory diseases[12,17]. In the disease state, oxidative stress of the stomach may occur and result in an elevation of mucosal lipid peroxide (LPO) that are generated from the reaction of oxyradicals and cellular polyunsaturated fatty acid. Whereas reduced GSH is a sulfhydryl compound, which may act to prevent lipid peroxidation produced by noxious oxyradicals that can damage gastric mucosal cells[3]. Various studies have demonstrated a decrease in GSH level in inflammatory and ulcerated gastric mucosa[14,19]. The mucosal protective effect

of GSH on gastric damage induced by nonsteroidal anti-inflammatory drugs[35], ethanol[36] or lipopolysaccharide[17] has been well documented. Nevertheless, the role of mucosal GSH and oxyradicals in BQC-induced hemorrhagic ulcers are unknown. Gastric mucus, which plays an important role in the mucosal protection, can be eliminated by acid or noxious agents[1]. Nevertheless, the influence of BQC on gastric mucus secretion in DM rats also remains obscure.

Lysozyme (muramidase), which widely distributes in various human tissues[27] is a stable polypeptide containing 18 amino acids. High content of lysozyme is found in mammalian milk, chicken eggshell membrane, and matrix[13]. This compound may possess multiple pharmacological actions, including analgesic[5], anti-inflammatory[33], hemostatic, anti-allergy[2], anticancer[25], and antibiotic[24] effects. The aim was to study the influence of chronic consumption of BQC on gastric oxidative stress, mucus production, and mucosal hemorrhagic ulcer in DM rat gastric mucosa. The mucosal protective effects of lysozyme chloride on this ulcer model were also evaluated.

MATERIALS AND METHODS

Chemicals used

The following chemicals in reagent grade were used: acivicin, alcian blue, lysozyme chloride, 1-butanol, *o*-phthaldialdehyde, pyridine, rat hemoglobin (Hb), reduced GSH, sodium laurylsulfate, trichloroacetic acid, 1,1,3,3-tetramethoxypropane, and 2-thiobarbiturate were purchased from Sigma (St. Louis, MO, USA). The purity of all drugs was over 98%. All chemical solutions were freshly prepared before use.

Drug administration

Intragastric lysozyme chloride (0-500 mg/kg) was challenged once daily to normal and those rats fed with BQC for 90 d. The control group received normal saline instead of chemicals.

Animals

Male specific pathogen-free Wistar rats, weighing 150±20 g, were housed individually in a room with a 12-h dark-light cycle and with central air conditioning (25 ℃, 70% humidity). Animal care and experimental protocols were in accordance with the guidelines of the National Sciences Council of Taiwan (NSC 2002). Prior to the experiments, rats were injected intravenously with streptozotocin (65 mg/kgt) to induce DM. Non-DM rats received vehicle only. Blood glucose level over 2 500 mg/L was considered as DM. All rats were divided into groups. Control rats received laboratory rodent diet (the Richmond standard, PMI feeds, St. Louis, MO, USA). Test groups were fed with the BQC diet prepared by mixing the laboratory rodent diet with chopped and crushed BQC (30%, w/w), which contained areca nuts (40%, w/w), gambir lime (30%, w/w) and betel stems (30%, w/w). The calories of BQC-diet were compensated near the control pellet diet (4.25 kcal/g) by adding adequate amounts of sugar and eggs. The BQC-diet was then dried in cold air and stored in a refrigerator (4 ℃). The rats were given fresh diet every day at 8 a.m. While chewing the test food, rats mimicked human beings in chewing and spitting the fiber contained in the BQC diet. The consumption of the diet, water, and the body weight of the animal were recorded every day before feeding, respectively.

Surgical procedures

After 90 d, rats were deprived of food for 24 h and anesthetized with diethylether. Rat stomachs were surgically exposed for the ligation of pylorus and lower esophagus. To prevent the spontaneous gastric secretion, a bilateral diaphragmatic vagotomy was performed in all rats. A small incision was then made in the forestomach. A polypropylene tube (3.5 mm internal diameter×20 mm long) was inserted through the same incision and secured with a ligature. The stomach was subsequently rinsed meticulously with warm normal saline (37 ℃). Care was taken to avoid injury to blood vessels. The residues were gently removed.

Measurement of gastric acid back-diffusion

Gastric acid back-diffusion (the H^+ loss in the gastric lumen) was quantified by the method previously described[21]. Either normal saline or simulated gastric juice (7 mL) containing 100 mmol/L HCl, 17.4 mmol/L pepsin and 54 mmol/L NaCl was instilled into the cleansed stomach with a syringe. Luminal contents were mixed with the same syringe by three repeated aspirations and injections, and 3 mL of the fluid was taken as an initial sample. The forestomach was tightly closed. The abdominal wound was sutured. After 3 h, rats were killed with an overdose of diethylether. Gastric contents (final sample) were collected. Both initial and final samples were centrifuged at 3 000 r/min for 20 min. The volumes of the initial and final samples were measured. The acidity of samples was assessed by titrating 1.0 mL of gastric contents sample with 0.1 mol/L NaOH to pH 7.0 on an autoburette titrator (Radiometer, Copenhagen, Denmark). The net flux of ions through the gastric mucosa was calculated as follows:

$$\text{Ionic net flux} = F_v \times I_v - (7 - I_v) \times I_c$$

where F_v and I_v are the volume (mL) of the final sample and initial sample, respectively, and F_c and I_c are the ionic concentrations (in mmol/L) of the final sample and the initial sample, respectively. A negative value for net flux indicates luminal electrolyte loss and a positive value indicates luminal electrolyte gain.

Morphological and histological studies of gastric mucosa

As soon as the final sample was collected, the stomach was filled with 8 mL of 4 g/L formaldehyde for 10 min. The mucosa was exposed by opening the stomach along the greater curvature. The length (mm) and the width (mm) of ulcer on the mucosa were measured with a planimeter ($1\pi/4$).

The total ulcer area (mm^2) of each stomach was recorded. Histological studies of the stomach also were conducted by methods as previously described[21]. Sections were scored as 0-5, in which (0) indicated normal appearance, (1) mild injury in the epithelial cells, (2) mild injury in the upper part of mucosal cells, (3) hemorrhage or edema in the mid or lower part of mucosal cells, (4) degranulation or necrosis of the epithelial cells, and (5) serious cell disruption of lower part of the mucosa. The index score of each section was evaluated on a cumulative basis to give a maximal score of 15.

Determination of hemoglobin (Hb)

Cleansed rat stomachs were irrigated for 3 h with either normal saline or gastric juice. Initial and final samples were collected by methods described above.

The blood attached to the gastric mucosa was carefully scraped and added to the final sample. Subsequently, both initial and final samples were adjusted to pH 1.5 with 0.1 mol/L HCl. The Hb content of the samples was measured spectrophotometrically[22]. The absorption maximum of Hb was measured at 376 nm. Appropriate irrigating solutions, adjusted to pH 1.5, were used as blank. Absorbances of the samples were measured against a standard curve (r^2>0.98) constructed with freshly prepared rat Hb (0.05-1.00 mg/mL) treated in the same manner as gastric samples. The luminal Hb content was calculated as:

$$\text{Hb content} = F_v \times F_{Hb} (7\text{-}I_v) \times I_{Hb},$$

where F_v and I_v are the volume (mL) of final sample and initial sample, respectively, and F_{Hb} and I_{Hb} are the luminal Hb concentrations (mg/mL) in the final and initial samples, respectively. The results obtained from gastric samples were expressed in mg Hb per stomach.

Mucosal GSH assay

The quantitation of gastric mucosal GSH was performed by following the methods that were described previously[19]. As soon as the final sample was collected, the rat stomach was dissected. The corpus mucosa was scraped using two glass slides on ice, weighed and homogenized immediately in 2 mL phosphate buffer (0.1 mol/L NaH_2PO_4 plus 0.25 mol/L sucrose, pH 7.4). Acivicin (250 μmol/L), an irreversible inhibitor of γ-glutamyltransferase, was added to the homogenate to inhibit the catabolism of GSH. Samples were then centrifuged at 4 000 r/min for 15 min at 4 ℃.

To determine the recovery of reduced thiol, GSH (200 μmol reduced GSH contained in phosphate buffer solution, pH 7.0) was added to the supernatant. Subsequently, 0.5 mL, 0.25 mol/L trichloroacetic acid was added to 1.0 mL of the supernatant. The mixture was kept for 30 min at 4 ℃. After centrifugation for 15 min at 3 000 r/min, the supernatant was used to determine GSH using 2,2-dinitro-5,5-dithio-dibenzoic acid. The optical density was measured at 412 nm on a spectrophotometer (model U-3210, Hitachi, Tokyo, Japan). All samples were measured in duplicate. Recovery of added internal standard was greater than 90% in all experiments. Absorbances of the samples were measured against a standard curve constructed with freshly prepared GSH solutions (0.05-0.5 mmol/L) that were treated in the same manner as the tissue samples. The results obtained from tissue samples were expressed as μmol GSH/g wet tissue.

Determination of lipid peroxides (LPO)

The concentration of gastric mucosal LPO was determined by estimating malondialdehyde using the thiobarbituric acid test[30]. Briefly, the stomachs of rats were promptly excised and rinsed with cold normal saline. To minimize the possibility of interference of Hb with free radicals, any blood adhering to the mucosa was carefully removed. The corpus mucosa was scraped, weighed and homogenized in 10 mL 100 g/L KCl. The homogenate (0.5 mL) was added with a solution containing 0.2 mL 80 g/L sodium laurylsulfate, 1.5 mL 200 g/L acetic acid,1.5 mL 8 g/L 2-thiobarbiturate and 0.3 mL distilled water. The mixture was incubated at 98 ℃ for 1 h. Upon cooling, 5 mL of 1-butanol/pyridine (15:1) was added. The mixture was vortexed for 1 min and centrifuged for 10 min at 400 r/min. The supernatant was measured at 532 nm. The standard curve was obtained by using 1,1,3,3-tetramethoxypropane. The recovery was over 90%. All samples were measured in duplicate. The results were expressed as nmol malondialdehyde/g wet tissue.

Measurement of gastric mucus

Gastric mucus was assessed by the method as described by Corne *et al*.[9]. Briefly, the rat stomach was excised and washed with tap water. The sample was immersed in 10 mL of a solution containing alcian blue (1.0 mg/L), sucrose (0.16 mol/L) and sodium acetate (0.05 mol/L) for 2 h. To remove the unbound dye, the sample was washed for 15 min and then for 45 min in a 0.25 mol/L sucrose solution. The mucus-bound dye was eluted by immersing gastric mucosa in 10 mL of 0.5 mol/L $MgCl_2$ solution for 2 h. The obtained solution was mixed with 10 mL diethylether. The absorbance of the color aqua solution was measured on a spectrophotometer (U3210, Hitachi) at 605 nm. The amount of alcian blue was extracted from known graded concentrations (5-50 mg/L) of alcian blue solution. All samples were measured in duplicate. The results were expressed as μg alcian blue/g wet tissue.

Statistical analysis

The data were expressed as mean±SE. Significant differences in single measurement traits were analyzed statistically by using the Tukey truly significant difference test for pairwise comparison after ANOVA or by using the Student's *t*-test[28]. Statistical significance was set at P<0.05.

RESULTS

Changes in gastric parameters in normal, DM, and BQC-fed DM rat stomachs irrigated with either normal saline or gastric juice

Table 1 indicated that in normal diet rat stomachs irrigated with normal saline no gastric acid back-diffusion but only little gastric acid secretion was achieved. Mucosal GSH and LPO generation were at normal levels. No mucosal ulceration and hemorrhage was observed in these rats (photo not shown). In saline-irrigated stomachs of DM rats, an enhancement of LPO generation as well as an attenuation of GSH and mucus secretion was obtained. After receiving the BQC-diet, marked necrotic ulcers accompanied by a further decrease in mucosal GSH and mucus were achieved in DM rats. The generation of mucosal LPO also was further aggravated in those rats, despite that no acid back-diffusion occurred.

When gastric juice was present in the stomachs of normal diet rats, the mucosa looked normal. Except when a normal level of acid back-diffusion occurred, various gastric parameters were not significantly different from those in saline-irrigated stomachs of normal rats. When DM rat stomachs were irrigated with gastric juice, a significant (P<0.05) increased acid back-diffusion and LPO generation accompanied with an attenuation of mucosal GSH and mucus

Table 1 Gastric juice-aggravated various gastric biochemical parameters in stomachs of normal, DM and BQC fed DM rats

	Acid back-diffusion μmol /stomach	Glutathione μmol/g tissue	Lipid peroxide nmol MDA/g tissue	Mucus μg/g tissue	Hemoglobin mg/stomach	Ulcer area mm^2 /stomach
Normal saline						
Control	8.6±1.2	3.8±0.4	45.6±4.2	230.2±18.4	0.2±0.2	1.4±0.6
DM	5.0±0.8[a]	2.4±0.3[a]	95.4±5.2[a]	186.1±10.2[a]	2.2±0.5[a]	64.6±8.5[a]
BQC+DM	3.2±0.2[a]	1.6±0.2[a]	132±11.4[a]	155.0±14.8[a]	4.6±0.6[a]	154.8±18.4[a]
Gastric juice						
Control	-164.2±5.4	3.4±0.2	54.0±7.8	220.0±14.5	0.6±0.2b	2.2±1.2
DM	-235.4±10.6[ac]	2.8±0.1[ac]	120.0±10.2[ac]	140.0±12.6[ac]	5.3±0.7[ac]	264.8±27.1[ac]
BQC+DM	-384.2±18.6[ac]	0.8±0.1[ac]	184.0±16.3[ac]	75.0±6.8[ac]	9.0±1.2[ac]	378.6±45.6[ac]

Data are mean±SE (n = 8). [a]P<0.05 *vs* corresponding control group. [c]P<0.05 *vs* corresponding group in saline-treatment. MDA = malondialdehyde, BQC = betel quid chewing, DM = diabetes mellitus.

secretion was observed and an exacerbated hemorrhagic ulcer also was produced. Further aggravation of gastric acid back-diffusion and LPO generation as well as decreased GSH and mucus production was found in those BQC-fed DM rats. More severe gastric hemorrhage and ulcer also was observed in these rats.

Histological examination of gastric mucosa of DM and BQC-fed DM rats

Figure 1 shows the microscopic examination of normal, DM, and BQC-fed DM rat stomachs irrigated with gastric juice. Marked upper gastric mucosal damage was observed in DM rats. More severe mucosal damage in BQC-fed DM rat stomachs than those in DM rats was obtained. The comparisons of degrees of histological tissue damage in normal, DM and BQC-fed DM rat stomachs irrigated with saline or gastric juice are illustrated in Figure 2. When the stomachs of normal diet rats were irrigated with either saline or gastric juice, no appreciable damage of gastric mucosal cells was observed. In DM rats, normal saline-irrigation produced more mucosal cell damage than those were irrigated with normal saline or gastric juice in normal diet rats. A pronounced aggravation of mucosal cell damage was observed in gastric juice-irrigated stomach of DM rats. Further exacerbation of gastric damage was achieved in DM rats fed with BQC. In most cases, gastric edema also was observed in DM and BQC-fed DM rats.

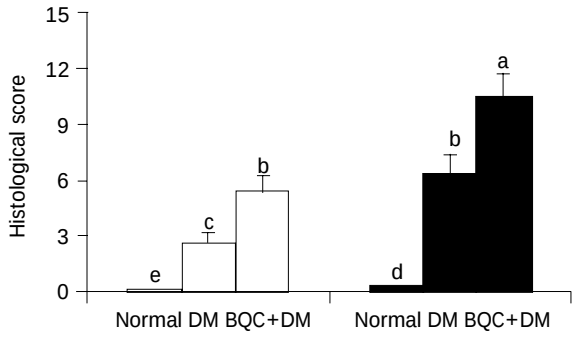


Figure 2 Histological scores of gastric mucosa in normal, DM, and BQC-fed DM rats. Rats were fed with normal diet or BQC diet for 90 d. Diabetes was induced by intravenous streptozotocin. Rat stomachs were irrigated for 3 h with normal saline (□) or gastric juice (■). Values are mean±SE, n = 6-8. Bars labeled with different letters are significantly different at P<0.05 based on Tukey statistic method.

Effects of lysozyme chloride on gastric parameters in gastric juice-irrigated stomachs of BQC-fed DM rats

As demonstrated in Table 2, low mucosal GSH levels and mucus secretion accompanied with high degree of acid back-diffusion and LPO generation were observed in 90-d BQC-fed DM rat stomachs irrigated with gastric juice. Severe gastric hemorrhage and mucosal ulceration also were achieved. Daily intragastric lysozyme chloride dose-dependently suppressed

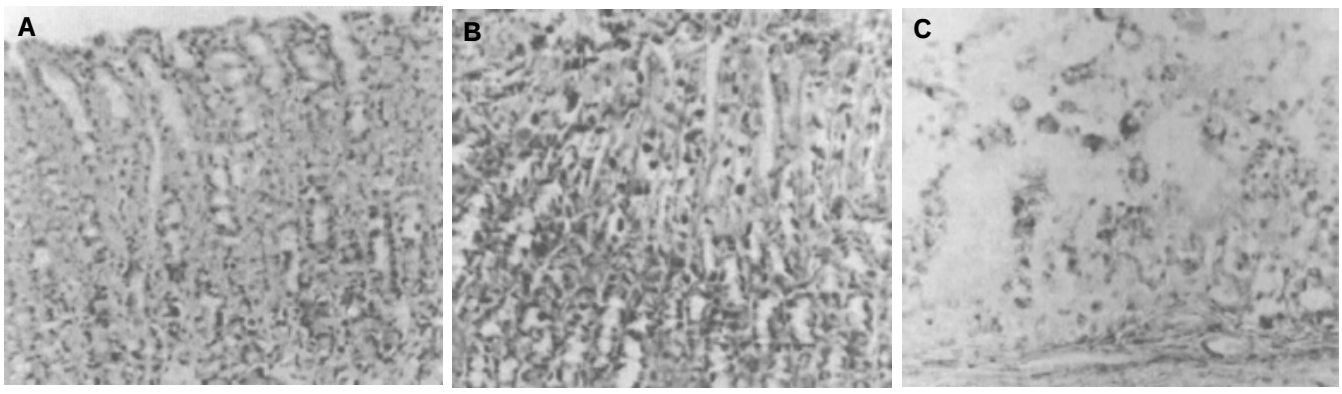


Figure 1 Histological studies of gastric mucosa exposed for 3 h gastric juice in normal, DM, and BQC-fed DM rats. Note that in normal rat stomachs irrigated with gastric juice (A), gastric mucosal cells look intact. However, gastric juice-irrigated DM rat mucosa (B), a disruption of gastric epithelial layer is observed. When stomachs of BQC-fed DM rats are irrigated with gastric juice (C), a complete disruption of the upper mucosal cells and lamina propria is obtained. The injured cells are characterized by karyorrhexis and dense homogenous acidophilic cytoplasm. In most cases, gastric edema also is observed (×150).

Table 2 Effects of lysozyme chloride on various biochemical parameters in gastric juice-irrigated stomachs of BQC-fed DM rats

	mg/kg	Acid back-diffusion μmol /stomach	Glutathione μmol/g tissue	Lipid peroxide nmol MD/g tissue	Mucus μg/g tissue	Hemoglobin mg /stomach	Ulcer area mm^2 /stomach
Control							
Saline		-132.0±3.4	3.6±0.3	62.6±7.0	206.4±14.6	0.4±0.2	3.2±0.5
Lysozyme chloride	500	-112.4±5.6[a]	4.6±0.5[a]	40.4±4.2[a]	245.4±16.5[a]	0.0±0.0[a]	0.0±0.0[a]
Indomethacin	5						
+ lysozyme chloride	500	-140.0±7.2	2.8±0.3[a]	74.5±6.8[a]	164.6±14.2	1.0±0.5	5.6±08
BQC+DM							
Saline		-365.2±20.4	0.8±0.2	160.4±11.6	83.2±10.2	8.0±0.8	396.8±34.2
Lysozyme chloride	50	-292.0±11.2[a]	1.7±0.3[a]	132.0±12.5[a]	126.6±7.4[a]	4.0±0.5[a]	306.0±25.2[a]
	100	-220.2±13.0[a]	2.4±0.3[a]	108.4±10.6[a]	182.8±9.2[a]	2.2±0.3[a]	168.6±12.4[a]
	500	-186.8±10.2[a]	3.4±0.3[a]	74.8±6.2[a]	216.3±16.4[a]	1.7±0.3[a]	44.5±6.4[a]
Indomethacin	5						
+ lysozyme chloride	500	-308.6±18.8[a]	1.5±0.2[a]	154.0±12.6[a]	140.8±11.5[a]	4.8±0.8[a]	320.4±30.4[a]

Data are mean±SE (n = 8). [a]P< 0.05 *vs* corresponding saline-group. MDA = malondialdehyde. MDA = malondialdehyde, DM = diabetes mellitus, BQC = betel quid chewing.

gastric hemorrhage and ulcer. This drug also inhibited the decreased mucosal GSH and mucus liberation as well as increased acid back-diffusion and mucosal LPO generations in BQC-fed DM rats in a dose-related manner. No visible side effects or toxicity of lysozyme chloride were observed in all experiments.

DISCUSSION

The pathological mechanisms underlying BQC-fed DM ulcer may be complex. Our previous paper demonstrates that chronic consumption of BQC can result in severe gastric hemorrhagic ulcer in rats[20]. In the present study, a remarkably increased acid back-diffusion was observed in those DM rat stomachs irrigated with gastric juice. Further aggravation of these ulcerogenic parameters was obtained in those DM rats fed with BQC. Obviously, chronic consumption of BQC diet could enhance various ulcerogenic parameters and result in greater gastric inflammation and breaking effects of gastric mucosal barriers in DM rats. Mechanisms of barrier-disruptive effect of BQC in DM rats are totally unknown. However, since BQC contained large amounts of gambir lime (which contains about 7-30% catechol, 20-50% catechu tannic acid and small amounts of quercetin waxes and oils; Merck Index, 1983) and calcium, the damage of mucosal barrier probably results from caustic injury from this component of BQC and DM-induced gastric cell degeneration. In clinical studies, it is reported that calcium polysulfite ingestion produces hemorrhagic necrosis of gastric mucosa[16]. BQC also contained arecoline, the main ingredient of areca fruit. Arecoline is a cholinergic agent that can cause gastric contraction and induce gastric secretion. Our previous paper demonstrates that arecoline causes seizure and results in gastric mucosal damage[17]. Therefore, after chronic consumption of BQC, gastric mucosal barriers might be severely disrupted and thus allowed copious free acid to diffuse back into the gastric mucosa during ulcer development.

Aggravation in LPO generation also was observed in gastric mucosa of BQC-fed DM rats. Apparently, the disruption of the mucosal barrier accompanied by gastric oxidative stress occurred in DM rats receiving BQC. In practice, oxyradicals can directly cause cell injury[3]. This cell damaging effect may associate with the occurrence of many diseases, including tissue inflammation and sepsis[17], hemorrhagic shock[11], and DM[29]. The initiation of gastric mucosal oxidative stress and inflammation might result from direct BQC-induced damage and degeneration of gastric mucosal cells induced by DM.

The lower mucosal GSH levels found in stomachs of DM or BQC-fed DM rats might be due to an increase in their consumption for scavenging oxyradicals and a decrease in cellular biosynthesis in damaged mucosal cells. In fact, depletion of neuronal GSH can cause an increase of neuronal nitric oxide synthase activity and cell death[6]. Moreover, GSH is used as a substrate or as a co-factor by several cytosolic and membrane-bound enzymes. A previous study demonstrated that exogenous GSH can produce a significant increase in mucosal GSH levels and a reduction in concentrations of mucosal LPO that associate with severe gastric hemorrhagic ulcers in acid-irrigated stomachs of septic rats[17]. Taken together, the imbalance between mucosal GSH biosynthesis and oxyradicals generation (gastric oxidative stress) was important in modulating BQC-induced ulcer in DM rats. A decreased gastric mucus also was found in DM or BQC-fed DM rats. Since BQC is an ulcerogenic substance, it might also damage gastric mucus cells and lead to attenuation of mucus biosynthesis. In fact, ulcerogens, such as aspirin and other non-steroidal anti-inflammatory drugs, have been reported to attenuate gastric mucus secretion[32]. Increase in mucus secretion can retard acid back-diffusion and is beneficial to the healing of mucosal damage[37].

In the present study, lysozyme chloride dose-dependently inhibited various aggressive parameters and elevated defensive factors in BQC-fed DM rats. It also ameliorated BQC-induced hemorrhagic ulcer in DM rats. This compound remarkably enhanced biosynthesis and secretion of gastric mucus, which is a potent gastroprotective substance. Lysozyme chloride also can enhance antral ulcer healing via stimulating mucus biosynthesis[18]. Indomethacin, a specific antagonist of prostaglandins, effectively reversed lysozyme chloride-induced cytoprotection of gastric mucosa. This implied that gastric mucosal protective effect of lysozyme chloride was partly mediated by stimulating biosynthesis and release of prostaglandins. Additionally, this drug has been reported to have analgesic and anti-inflammatory effects on pulpectomy and root canal filling[15]. It has also been shown to contribute

to the advantageous effects in the treatment of patients and experimental animals with cancer[34,38]. The attenuation of LPO generation produced by lysozyme chloride in BQC-fed DM rats explained that this compound might possess potent antioxidant effect, thus reduced consumption of GSH. Moreover, lysozyme chloride may stimulate GSH biosynthesis in mucosal cells. Considering the above-mentioned, this drug can increase the total levels of BQC-fed DM rat mucosal GSH and contribute to the ulcer healing.

In conclusion, long-term consumption of BQC produces aggravation of DM-induced hemorrhage and ulcer in rats via enhancing oxidative stress that can be ameliorated by lysozyme chloride.

REFERENCES

1 **Allen A**, McQueen S, Garner A. Gastroduodenal mucus: The effect of prostaglandins and role in mucosal protection. *Scand J Gastroenterol Suppl* 1984; **101**: 79-86
2 **Asakura K**, Kojima T, Shirasaki H, Kataura A. Evaluation of the effects of antigen specific immunotherapy on chronic sinusitis in children with allergy. *Auris Nasus Larynx* 1990; **17**: 33-38
3 **Bhatnagar A**. Biochemical mechanism of irreversible cell injury caused by free radical initiated reactions. *Mol Cell Biochem* 1994; **137**: 9-16
4 **Bhide SV**, Gothoskar SV, Shivapurkar NM. Arecoline tumorigenicity in Swiss strain mice on normal and vitamin B deficient diet. *J Cancer Res Clin Oncol* 1984; **107**: 169-171
5 **Biziulevichius GA**, Arestov IG. *In vivo* studies on lysosubtilin. Efficacy for prophylaxis and treatment of gastrointestinal disorders in newborn calves. *Vet Res* 1997; **28**: 19-35
6 **Bolanos JP**, Heales SJ, Peuchen S, Barker JE, Land JM, Clark JB. Nitric oxide-mediated mitochondrial damage, a potential neuroprotective role for glutathione. *Free Radic Biol Med* 1996; **21**: 995-1001
7 **Burton-Bradley BG**. Is 'betel chewing' carcinogenic? *Lancet* 1979; **2**: 903
8 **Chang CK**. Betel nut chewing and mouth cancer in Taiwan. *J Form Med Ass* 1964; **63**: 437-444
9 **Corne SJ**, Morrissey SM, Woods RJ. A method for the quantitative estimation of gastric barrier mucus. *J Physiol* 1974; **242**: 166-167
10 **Davenport HW**. Destruction of the gastric mucosal barrier by detergents and urea. *Gastroenterology* 1968; **54**: 175-181
11 **Itoh M**, Guth P. Role of oxygen-derived radicals in hemorrhagic shock-induced gastric lesions in the rat. *Gastroenterology* 1985; **88**: 1162-1167
12 **Gislason H**, Sorbye H, Abdi-Dezfuli F, Waldum HL, Svanes K. Role of prostaglandins and histamine in hyperemic response to superficial and deep gastric mucosal injury and H+ back-diffusion in cats. *Dig Dis Sci* 1995; **40**: 1669-1678
13 **Hincke MT**, Gautron J, Panheleux M, Garcia-Ruiz J, McKee MD, Nys Y. Identification and localization of lysozyme as a component of eggshell membranes and eggshell matrix. *Matrix Biol* 2000; **19**: 443-453
14 **Hirokawa K**, Kawasaki H. Changes in GSH in gastric mucosa of gastric ulcer patients. *Res Commun Mol Pathol Pharmacol* 1995; **88**: 163-176
15 **Horiuchi H**, Abe S, Maeda K, Watanabe M. Anti-inflammatory, analgesic effect of lysozyme chloride following direct pulpectomy and root canal filling. *Dent Outlook* 1981; **58**: 1007-1012
16 **Horowitz BZ**, Marquardt K, Swenson E. Calcium polysulfide overdose: a report of two cases. *J Toxicol Clin Toxicol* 1997; **35**: 299-303
17 **Hung CR**. Importance of histamine, glutathione and oxyradicals in modulating gastric hemorrhagic ulcer in septic rats. *Clin Exp Pharmacol Physiol* 2000; **27**: 306-312
18 **Hung CR**, Wang PS. Role of acid back-diffusion, glutathione, oxyradical and histamine in antral hemorrhagic ulcer in rats: the protective effect of lysozyme and antioxidants. *J Lab Clin Med* 2002; **140**: 142-151
19 **Hung CR**, Wang PS. Gastric oxidative stress and hemorrhagic ulcer in Salmonella typhimurium-infected rats. *Eur J Pharamcol* 2004; **491**: 61-68
20 **Hung CR**, Cheng JT. Betel quid chewing damaged gastric mucosa: protective effects of cimetidine and sodium bicarbonate. *Chin J Physiol* 1994; **37**: 213-218
21 **Hung CR**, Neu SL. Acid-induced gastric damage in rats is aggravated by starvation and prevented by several nutrients. *J Nutrition* 1997; **127**: 630-636
22 **Hung CR**, Huang EY. Role of acid back-diffusion in the formation of mucosal ulceration and its treatment with drugs in diabetic rats. *J Pharm Pharmacol* 1995; **47**: 493-498
23 **Hung CR**, Cheng JT, Shih CS. Gastric mucosal damage induced by arecoline seizure in rats. *Life Sci* 2000; **66**: 2337-2349
24 **Iacono VJ**, Zove SM, Grossbard BL, Pollock JJ, Fine DH, Greene LS. Lysozyme-mediated aggregation and lysis of the periodontal microorganism Capnocytophaga gingivalis 2010. *Infect Immu* 1985; **47**: 457-464
25 **Inouye K**. The effects of lysozyme chloride on the immune response of patients with head and neck cancer. *Jpn J Cancer Clin* 1987; **33**: 627-632
26 **Lee KW**, Chin CT. The effects of betel-nut chewing on the buccal mucosa: a histological study. *Br J Cancer* 1970; **24**: 433-441
27 **Mason DY,** Taylor CR. The distribution of muramidase (lysozyme) in human tissues. *J Clin Pathol* 1983; **28**: 124-132
28 **Montgomery DC**. Experiments to compare several treatments: the analysis of variance, In: Hinkelmann, K. and Kempthorne, O. (Eds), Design and Analysis of Experiments, Wiley, New York, NY 1984: 43-80
29 **Oberley LW**. Free radicals and diabetes. *Free Radic Biol Med* 1988; **5**: 113-124
30 **Ohkawa H**, Ohishi N, Yagi K. Assay for LPO in animal tissues by thiobarbituric acid reaction. *Anal Biochem* 1979; **95**: 351-358
31 **Ohshima H**, Friesen M, Bartsch H. Identification in rats of N-nitrosonipecotic acid as a major urinary metabolite of the areca-nut alkaloid-derived nitrosamines, N-nitrosoguvacoline and N-nitrosoguvacine. *Cancer Lett* 1989; **44**: 211-216
32 **Rainsford KD**. The effects of aspirin and other nonsteroid anti-inflammatory analgesic drugs on gastrointestinal mucus glycoprotein biosynthesis *in vivo*: relationship to ulcerogenic actions. *Biochem Pharmacol* 1978; **27**: 877-885
33 **Sato M**, Oe H, Nakano M, Kawasaki H, Hirayama C. A random controlled study of the prophylactic effect of lysozyme chloride on post-transfusion hepatitis. *Hepatogastroenterology* 1981; **28**: 135-138
34 **Sava G**, Ceschia V, Pacor S, Zabucchi G. Observations on the antimetastatic action of lysozyme in mice bearing Lewis lung carcinoma. *Anticancer Res* 1993; **11**: 1109-1013
35 **Strubelt O**, Hoppenkamps R. Relations between gastric GSH and the ulcerogenic action of nonsteroidal anti-inflammatory drugs. *Arch Int Pharmacodyn* 1983; **262**: 268-278
36 **Mizui T**, Sato H, Hirose F. Effects of antioxidative drugs on gastric damage induced by ethanol in rats. *Life Sci* 1987; **41**: 755-763
37 **Williams SE**, Turnberg LA. Retardation of acid diffusion by pig gastric mucus: a potential role in mucosal protection. *Gastroenterology* 1980; **79**: 299-304
38 **Yamaoka K**, Yoshioka T. Effects of lysozyme chloride on immune responses of patients with uterine cervical cancer. *Jpn J Cancer Chemother* 1983; **10**: 1803-1809
39 **Yoganathan P**. Betel chewing creeps into the New World. *New Zeal Dent J* 2002; **98**: 40-45

Science Editor Guo SY **Language Editor** Elsevier HK

PO Box 2345, Beijing 100023, China
www.wjgnet.com
wjg@wjgnet.com

ELSEVIER

World J Gastroenterol 2005;11(37):5859-5862
World Journal of Gastroenterology ISSN 1007-9327
© 2005 The WJG Press and Elsevier Inc. All rights reserved.

• *BRIEF REPORTS* •

Ulcerative colitis in a multiracial Asian country: Racial differences and clinical presentation among Malaysian patients

Yan-Mei Tan, Khean-Lee Goh

Yan-Mei Tan, Khean-Lee Goh, Division of Gastroenterology, Department of Medicine, University of Malaya, Kuala Lumpur 50603, Malaysia
Correspondence to: Professor Khean-Lee Goh, Head, Division of Gastroenterology, Department of Medicine, University of Malaya, Kuala Lumpur 50603, Malaysia. gohkl@um.edu.my
Telephone: +60-3-79502429 Fax: +60-3-79556936
Received: 2004-05-25 Accepted: 2004-07-05

Abstract

AIM: To determine the prevalence of ulcerative colitis (UC) in Malaysian patients and to establish the spectrum of the disease seen in Malaysian patients.

METHODS: Data were obtained retrospectively from a review of the medical records of in- and out-patients with a diagnosis of UC at the University Hospital, Kuala Lumpur between 1985 and 1998.

RESULTS: There were 45 confirmed cases of UC, of which 3 were foreigners, who were excluded from analysis. Thirty new cases of UC were diagnosed during the study period. Their mean age at presentation was 33.0±10.0 years. The highest prevalence of UC was 17.9/100 000 hospital admissions in the Indians, followed by 11.2/100 000 hospital admissions in the Chinese. The lowest prevalence was 3.7/100 000 hospital admissions in the Malays. The prevalence of UC was significantly higher in the Indians and the Chinese when compared with the Malays with an OR of 4.89 (CI = 2.02-12.24; χ^2 = 15.45, P<0.001) and 3.06 (CI = 1.24-7.78; χ^2 = 6.30; P = 0.012) respectively. The extent of colonic disease was similar in the Malay and Indian patients. In contrast, distal or left-sided colitis predominated in the Chinese with an OR of 8.17 (95%CI = 1.31-64.87; χ^2 = 5.53, P = 0.02). Extraintestinal manifestations were uncommon (11.9%).

CONCLUSION: UC is an uncommon disease in Malaysia, but racial differences exist. The Indians had the highest prevalence of UC with the Chinese demonstrating the least extensive disease.

© 2005 The WJG Press and Elsevier Inc. All rights reserved.

Key words: Ulcerative colitis; Asian races; Racial differences

Tan YM, Goh KL. Ulcerative colitis in a multiracial Asian country: Racial differences and clinical presentation among Malaysian patients. *World J Gastroenterol* 2005; 11(37): 5859-5862
http://www.wjgnet.com/1007-9327/11/5859.asp

INTRODUCTION

Ulcerative colitis (UC) is a common disease in the Western population. It is well recognized that the incidence of inflammatory bowel disease is among the highest in individuals of Anglo-Saxon descent and from the Scandinavian countries[1-3] and there is a suggestion that the incidence of UC may be on a rising trend[4-6]. The disease is also prevalent in Ashkenazi Jews[7,8]. There is a relative paucity of epidemiological studies from this region as compared to the West. Studies from Hong Kong and Singapore[9-14] suggest that this disease is uncommon in Asian countries. There have been only two published papers on the prevalence of UC in Malaysian patients[15,16]. Both are old papers reporting on a relatively small number of patients.

Malaysia epitomizes the multiraciality of an Asian country, where three major Asian races Malay, Chinese, and Indian -co-exist. Of the three major races in Malaysia, there appears to be a predisposition towards the Indian race. A more recent study by Lee *et al*.[14], in neighboring Singapore reported similar findings with an estimated prevalence among the Indians of 16.2/100 000 as compared to 6/100 000 among the Chinese and 7/100 000 among the Malays. The overall prevalence was 6/100 000. These figures are low in comparison to that of the West, where more than 10-fold excess in prevalence rates is reached. Observations of racial differences in the prevalence of upper gastrointestinal as well as liver diseases have been a major interest in Malaysia where three major Asian races co-exist[17-21].

The aim of this study was firstly to determine the prevalence of UC and the existence of ethnic differences in the prevalence of UC and secondly, to establish the spectrum of disease seen in Malaysian patients.

MATERIALS AND METHODS

Retrospective data were obtained from the careful review of the medical records of all patients who attended the outpatient clinics or were admitted to University Hospital, Kuala Lumpur between 1985 and 1998, and had the International Classification coding for UC (ICD-556). The diagnosis of UC was established based on a combination of clinical, radiographic, endoscopic, and histopathological evidence. As infective colitis is common in the tropics and can mimic the features of UC, this was routinely sought for and excluded. Stools were sent for microscopy and culture. Blood tests included serology for *Entamoeba histolytica* and the Widal-Weil-Felix test.

The following information was obtained: demographic characteristics, age at presentation, clinical presentation,

distribution of disease, requirement for surgical intervention and the presence of extraintestinal manifestations. The anatomical extent of the disease as determined by colonoscopy was classified as follows: distal colitis (i.e., limited to the rectum and sigmoid colon), left-sided colitis (i.e., disease distal to the mid-transverse colon) or "extensive"colitis (i.e., extending proximal to the mid-transverse colon).

Statistical analysis

The prevalence of UC for the three major ethnic groups was calculated per 100 000 hospital admissions of the respective racial group. The statistical significance of the difference in UC prevalence between the ethnic groups was assessed using the Yate's-corrected χ^2 test, the measure of association quoted as odd ratios (OR) with a 95% confidence interval (CI).

RESULTS

There were 45 confirmed cases of UC, of which 30 patients were diagnosed during the study period. All but three (6.7%) patients (an Albanian and two Pakistanis) were born in Malaysia. The non-Malaysians were excluded from analysis. There were 19 males and 23 females giving a male:female ratio of 0.8:1. The age distribution at presentation is shown in Figure 1. The mean age at presentation was 33.0 ± 10.0 years. They comprised 8 (19.0%) Malays, 16 (38.1%) Chinese, and 18 (42.9%) Indians. The prevalence of UC by ethnic origin is shown in Table 1. The highest prevalence of UC was 17.9/100 000 hospital admissions in the Indians, followed by 11.2/100 000 hospital admissions in the Chinese. The lowest prevalence was 3.7/100 000 hospital admissions in the Malays. The prevalence of UC was significantly higher in the Indians and the Chinese when compared with the Malays with an OR of 4.89 (CI = 2.02-12.24; χ^2 = 15.45, P < 0.00 1) and 3.06 (CI = 1.24-7.78; χ^2 = 6.30; P = 0.012) respectively.

Clinical presentation

Thirty-four (81.0%) patients presented with bloody diarrhea, 5 (11.9%) presented with rectal bleeding only and 3 (7.1%) had diarrhea without rectal bleeding. Other associated complaints were the passage of mucus (66.7%) and abdominal pain (54.8%).

Extent of UC, requirement for surgery and extraintestinal manifestations Eighteen (42.9%) patients had the disease confined to the distal colon, 8 (19.0%) had left-sided colitis and 16 (38.1%) had the disease extending beyond the mid-transverse colon. The extent of colonic involvement in the different ethnic groups is shown in Table 2. The extent of the disease was similar in the Malay and Indian patients. In contrast, distal or left-sided colitis predominated in the Chinese with an OR of 8.17 (95%CI = 1.31-64.87; χ^2 = 5.53, P = 0.02). No case of toxic megacolon was reported, but five (11.9%) patients required surgical intervention. These included two (4.8%) patients with intestinal perforation and one (2.4%) with massive rectal bleeding. Total colectomy was also required in two (4.8%) patients who developed colorectal cancer.

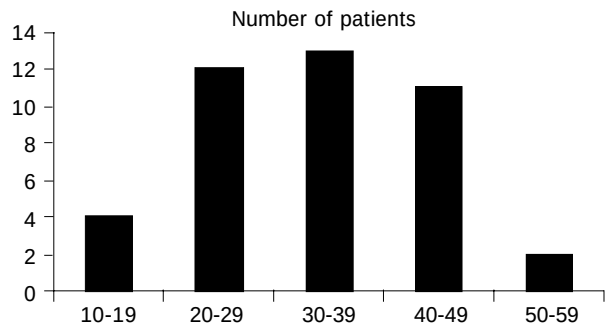


Figure 1 Age at presentation (by age-groups).

Table 2 Extent of colonic disease in the different ethnic groups

Ethnic origin	Distal colitis *n* (%)	Left-sided colitis *n* (%)	Pan-colitis *n* (%)
Malay	3 (37.5)	1 (12.5)	4 (50.0)
Chinese	11 (68.8)	3 (18.8)	2 (12.5)
Indian	4 (22.2)	4 (22.2)	10 (55.5)
Overall	18 (42.9)	8 (19.0)	16 (38.1)

(**%** of the ethnic group)y.

Extraintestinal manifestations occurred in only five (11.9%) patients. Three (7.1%) patients had arthropathy including one (2.4%) patient with sacroiliitis. Erythema nodosum occurred in two (4.8%) and pyoderma gangrenosum in one (2.4%).

DISCUSSION

This study is in agreement with previous studies around this region that UC is an uncommon entity in populations of Asian origin. Only 30 new cases were diagnosed in a 13 year span in a large public hospital. The majority of patients presented during young adulthood. Among the three major ethnic groups in Malaysia, UC was most prevalent in the Indians with an OR of 4.89 (CI = 2.02–12.24), followed by the Chinese with an OR of 3.06 (CI = 1.24-7.78) in comparison with the Malays who had the lowest prevalence for UC. The predominance of Indians with UC has been

Table 1 Prevalence of UC by ethnic origin at the University Hospital, Kuala Lumpur

Ethnic origin	Total number of hospital admissions by race	Number with UC	Prevalence per 100 000	Odds ratio (95%CI) (Malay as reference group)	*P*
Malay	218 019	8	3.7	1.00	-
Chinese	142 575	16	11.2	3.06 (1.24-7.78)	0.012
Indian	100 250	18	17.9	4.89 (2.02-12.24)	<0.001

observed previously[11,14].

It has been thought that the reason for the disparity of UC prevalence among Malaysians is largely due to genetic factors and seems to reflect the prevalence of the disease of their original native countries. There are very limited data of UC in the indigenous population (Malay), suggesting that the disease must be very rare in this race. Among the people of Mongoloid stock, UC is also uncommon. Morita *et al*.[22], reported an incidence and prevalence per 100 000 population per annum of 1.95 and 18.12, respectively in Japan. Studies from the Indian subcontinent have confirmed that UC is not uncommon in Indians, who are ethnically related to Caucasian stock[23-26]. However, there is growing evidence that environmental factors play an important role in the pathogenesis of the disease. An epidemiological study of Indian migrants to Leicestershire showed a significantly higher incidence of UC in the immigrant population than the local Europeans[27]. Montgomery *et al*.[28], reported that young Asians (ethnic origins in India and Pakistan) who were born in Britain were at a significantly higher risk of developing inflammatory bowel disease than the indigenous European population and suggested the role of environmental factors in uncovering the genetic predisposition to disease.

The extent of UC was similar in the Indian and Malay populations and not considerably different from those in Western countries. The Chinese on the other hand showed a significantly marked predominance of distal UC with an OR of 8.17 (CI = 1.31-64.87). The predominance of distal UC in the Chinese race has also been reported from China[29].

In our experience, treatment of UC was mainly medical (88.1%) with surgical intervention required because of complications of UC or the development of colorectal cancer. The remarkable features of the disease in our population are the relatively mild severity, indolent course of the disease and the paucity of extraintestinal manifestations. These observations are similar to those previously reported from the Asian region[11,12,29].

Time trend studies would be important to determine whether there would be an increase in the incidence of UC in our part of the world as has been observed in other gastrointestinal diseases such as gastroesophageal reflux disease[21,30]. If environmental factors predominate in the etiology of the disease, with the rapid Westernization and socio-economic development sweeping through the whole continent, an increase in the incidence of the disease would be inevitable.

In summary, UC remains uncommon despite greater awareness of the disease and better diagnostic facilities that distinguish UC from other diseases such as infective colitis, which is prevalent in developing countries. Among the three major ethnic groups in Malaysia, the Indians have the highest prevalence of UC and the Chinese demonstrate a less extensive disease. As Malaysia undergoes a transition to become a developed society in time, it remains to be seen if a shift in emphasis from racial factors to specific environmental factors in the etiology of UC is uncovered.

REFERENCES

1 **Morris T**, Rhodes J. Incidence of ulcerative colitis in the Cardiff region 1968-1977. *Gut* 1984; **25**: 846-848

2 **Haug K**, Schrumpf E, Barstad S, Fluge G, Halvorsen JF. Epidemiology of ulcerative colitis in western Norway. *Scand J Gastroenterol* 1988; **23**: 517-522

3 **Binder V**, Both H, Hansen PK, Hendriksen C, Kreiner S, Torp-Pedersen K. Incidence and prevalence of ulcerative colitis and Crohns disease in the County of Copenhagen, 1962 to 1978. *Gastroenterology* 1982; **83**: 563-568

4 **Bjornsson S**, Johannsson JH. Inflammatory bowel disease in Iceland, 1990-1994: a prospective, nationwide, epidemiological study. *Eur J Gastroenterol Hepatol* 2000; **12**: 31-38

5 **Stewenius J**, Adnerhill I, Ekelund G. Ulcerative colitis and indeterminate colitis in the city of Malmo, Sweden. A 25-year incidence study. *Scand J Gastroenterol* 1995; **30**: 38-43

6 **Trallori G**, Palli D, Saieva C. A population-based study of inflammatory bowel disease in Florence over 15 years (1978-92). *Scand J Gastroenterol* 1996; **3**: 892-899

7 **Odes HS**, Fraser D, Krawiiec J. Ulcerative colitis in the Jewish population of Southern Israel, 1961-1985 epidemiological and clinical study. *Gut* 1987; **28**: 1630-1636

8 **Jacobsohn WZ**, Levine Y. Incidence and prevalence of ulcerative colitis in the Jewish population of Jerusalem. *Isr J Med Sci* 1986; **22**: 559-563

9 **Lai CL**, Wu PC, Wong KL, Lok ASF. Clinical features of ulcerative proctocolitis in Hong Kong Chinese: a review of three decades. *Am J Proctol Gastroenterol Colon Rectal Surg* 1985; **1**: 14-19

10 **Fung WP**, Monteiro EH, Murugasu JJ, Ng KC, Kho KM, Lee SK. Non-specific ulcerative colitis in Chinese and Indians in Singapore. *Med J Aust* 1971; **2**: 361-365

11 **Teh LB**, Koh D, Ng HS. Ulcerative colitis in Singapore: a clinical study of sixty-one patients. *Ann Acad Med Singapore* 1987; **16**: 474-479

12 **Ng HS**. Chronic inflammatory bowel diseases in Singapore. *Sing Med J* 1989; **30**: 32-33

13 **Tan CC**, Kang JY, Guan R, Yap I, Tay HH. Inflammatory bowel disease: an uncommon problem in Singapore. *J Gastroenterol Hepatol* 1992; **7**: 360-362

14 **Lee YM**, Fock KM, See SJ, Ng TM, Khor C, Teo EK. Racial differences in the prevalence of ulcerative colitis and Crohn's disease in Singapore. *J Gastroenterol Hepatol* 2000; **15**: 622-625

15 **Ti TK**. Inflammatory diseases of the bowel: a Malaysian experience. *Aust NZ J Surg* 1979; **4**: 428-431

16 **Thein-Htut**, Kudva MV. Ulcerative colitis in Malaysians: a review of 23 patients. *Sing Med J* 1989; **30**: 385-387

17 **Ranjeev P**, Goh KL. Racial differences in the incidence of carcinoma of the esophagus in Malaysia. *Med J Mal* 1999; **54** (Suppl B): 10

18 **Ranjeev P**, Rosmawati M, Tan YM, Goh KL. Racial differences in the prevalence of hepatoma in a multiracial South East Asian population. *J Gastroenterol Hepatol* 1999; **14**: S93

19 **Rosaida MS**, Goh KL. Racial differences in the prevalence of gastric and duodenal ulcers in a multi-racial Malaysian population undergoing endoscopy. *Med J Malaysia* 2000; **55** (Suppl B): 17

20 **Goh KL**, Cheah PL, Noorfaridah M, Parasakthi N. Ethnic differences in gastric cancer in a multiracial Asian popoulation: a case-control study. *Gastroenterology* 2003; **124**: A168

21 **Rosaida MS**, Goh KL. Gastro-oesophageal reflux disease, reflux oesophagitis and non-erosive reflux disease in a multiracial Asian population: a prospective, endoscopy based study. *Eur J Gastroenterol Hepatol* 2004; **16**: 495-501

22 **Morita N**, Toki S, Hirohashi T. Incidence and prevalence of inflammatory bowel disease in Japan: nationwide epidemiological survey during the year 1991. *J Gastroenterol* 1995; **30**: 1-4

23 **Tandon BN**, Mathur AK, Mohapatra LN, Tandon HD, Wig KL. A study of the prevalence and clinical pattern of non-specific ulcerative colitis in northern India. *Gut* 1965; **6**: 448-453

24 **Chuttani HY**, Nigam SP, Sama S, Dhanda PC, Gupta PS. Ulcerative colitis in the tropics. *Br Med J* 1967; **4**: 204-207
25 **Maroo MK**, Nag NK, Soryur SV, Patil RS. Ulcerative colitis in Southern Maharashtra. *J Indian Med Assoc* 1974; **63**: 350-354
26 **Sharma MP**, Sarin SK. Ulcerative colitis in a North Indian hospital: current trends. *J R Coll Phys Lond* 1985; **19**: 99-102
27 **Probert CSJ**, Jayanthi V, Pinder D, Wicks AC, Mayberry JF. Epidemio logical study of ulcerative proctocolitis in Indian migrants and the indigenous population of Leicestershire. *Gut* 1992; **33**: 687-693
28 **Montgomery SM**, Moris DL, Pounder RE, Wakefield AJ. Asian ethnic origin and the risk of inflammatory bowel disease. *Eur J Gastroenterol Hepatol* 1999; **11**: 543-546
29 **Ouyang Q**. Inflammatory bowel disease in China (abstract). *Chinese J Gastroenterol* 2000; **5**: A50-S1
30 **Goh KL**, Chang SC, Fock KM, Ke MY, Park HJ, Lam SK. Gastro-oesophageal reflux disease in Asia. *J Gastroenterol Hepatol* 2000; **15**: 230-238

Science Editor Wang XL **Language Editor** Elsevier HK

PO Box 2345, Beijing 100023, China
www.wjgnet.com
wjg@wjgnet.com

ELSEVIER

World J Gastroenterol 2005;11(37):5863-5866
World Journal of Gastroenterology ISSN 1007-9327
© 2005 The WJG Press and Elsevier Inc. All rights reserved.

• *BRIEF REPORTS* •

Capsule endoscopy: Improving transit time and image view

Zvi Fireman, D Paz, Y Kopelman

Zvi Fireman, D Paz, Y Kopelman, Department of Gastroenterology, Hillel Yaffe, Hadera and Bruce Rappaport Faculty of Medicine Technion, Haifa, Israel
Correspondence to: Zvi Fireman, MD, Associate Professor of Medicine Head of Gastroenterology Department, Hillel Yaffe Medical Center, PO Box 16, Hadera 38100, Israel. fireman@hillel-yaffe.health.gov.il
Telephone: +972-4-6304480 Fax: +972-4-6304408
Received: 2004-11-27 Accepted: 2005-02-18

Abstract

AIM: To evaluate the effect of various methods of small bowel preparation on the transit time and the quality of visualization of the entire small bowel mucosa.

METHODS: Ninety-five patients underwent capsule endoscopy (CE) by easily swallowing the capsule. They were divided into three study groups according to the preparation used: group A (n = 26) by polyethylene glycol (PEG) liter or with sodium phosphate (SP) 12 h prior to the CE study; group B (n = 29) by erythromycin 1 h prior to the CE study; and group C (n = 40) without any preparation. Visualization ranged from good to satisfactory to poor.

RESULTS: The gastric emptying time in the group prepared with erythromycin was shorter but without statistical significance and the small bowel transit time was unaffected. In elderly subjects prepared by PEG or SP, the gastric emptying time was significantly longer (163.7 min, P = 0.05). The transit times of the three sub-groups were not affected by gender or pathology. The grade of cleaning of the entire study group was 3.27±1.1. The erythromycin group presented significantly the worst quality of images (P = 0.05) compared to the other sub-groups. Age, gender, and pathology had no effect on the quality of the cleaning of the small bowel in the sub-groups. One (1.05%) case had no natural excretion.

CONCLUSION: Erythromycin markedly reduces gastric emptying time, but has a negative effect on the quality of the image in the small bowel. The preparation of elderly subjects with PEG or SP has a negative effect on the small bowel transit time.

© 2005 The WJG Press and Elsevier Inc. All rights reserved.

Key words: Capsule endoscopy; Gastric emptying time; Small bowel transit time; View; Erythromycin; Polyethylene glycol

Fireman Z, Paz D, Kopelman Y. Capsule endoscopy: Improving transit time and image view. *World J Gastroenterol* 2005; 11(37): 5863-5866
http://www.wjgnet.com/1007-9327/11/5863.asp

INTRODUCTION

The capsule endoscopy (CE) is well accepted as a tool for evaluating small bowel pathology[1-5]. However, this new technology has several limitations, i.e., the time required to study the video, it takes an hour to watch the video of the small bowel and the residual material, especially in the ileum adversely affects the image[5-7]. Stomach emptying and small bowel motility depend upon a number of factors, such as the composition of the food and fluid in the gastrointestinal (GI) tract, diseases, etc. In addition, transit time differs according to whether the individual has eaten or is in a fasting state. The initial capsule experiences showed that the cecum could not be viewed in approximately 20% of the study population because of the short battery life, because the capsule had remained in the stomach for more than 60 min[5,6], and for a variety of other reasons. A shorter transit time would be directly beneficial in obviating the first two problems.

The CE is completely different from the standard endoscopy that allows the endoscopist to remove all the residual material to improve the image. In most CE studies, the image quality in the proximal small bowel is much superior to that in the distal ileum, due to residual material.

The reasons that some physicians refuse to adopt the CE study are the time consuming viewing procedures and the frustration of being unable to view the entire small bowel because of the residual material. So far there is still no definite answer to the question of which is the best way to prepare patients for the CE study. The Given Imaging Ltd recommendation is a 12-h fast prior to the CE study with no other preparation. Most of the published studies followed this recommendation and although other methods of preparations were mentioned, no comparative study was made.

In this study, we designed to determine the best preparation to provide the most complete visualization of the entire small bowel, as well the best preparation for rapid gastric emptying times.

MATERIALS AND METHODS

Study population

A retrospective study was performed on 97 patients who underwent the CE study (Given® M2A video capsule system, Given Imaging Ltd, Yokneam, Israel) between August 1st,

2001 and March 30, 2003. The study group participants were patients suffering from obscure GI bleeding, suspected small bowel illness of an unclear nature or unexplained abdominal pain for over 6 mo with negative GI evaluation. All patients underwent small bowel X-ray, and there were no signs of intestinal obstruction, major abdominal surgery, and diabetes mellitus. Pregnant women were excluded from the study. Two cases were excluded because in one case the CE "stuck" in the stomach for 6 h (without any pathological evidence) and the other had a mechanical software problem, i.e., image quality. All the patients signed the informed consent agreement.

Capsule endoscopy

After an overnight fast of 12 h, all patients ingested the CE (Given® M2A video capsule system). An array of eight sensors was attached to the abdominal wall, and a belt holding a recorder with a battery was fastened around their waists. Patients were allowed to drink 2 h after ingesting the capsule and to eat a light meal 3 h later. After ingesting the capsule with a small amount of water, patients were free to go about their own activities. Seven to eight hours after ingestion, the recorder was disconnected and the sensors removed. The recorded digital information was downloaded into the computer, and images from the stomach and all along the small bowel were analyzed using the proprietary RAPID® software.

Patients were asked to look for the capsule in the feces. All capsules were retrieved 24 h to 5 d after ingestion, except for one patient who had a non-natural excretion (the patient underwent surgery and was found to have Meckel's diverticulum). All patients signed an informed consent agreement approved by the Local and Governmental Helsinki and Ethical Committees.

Preparation of the sub-groups

They were divided into three study groups according to the preparation used. Group A (n = 26) was prepared with 3 L polyethylene glycol (PEG 400, Taro, Israel), given in two divided 2 doses, i.e., 1.5 L, 12 h before swallowing the capsule and 1.5 L, 1 h after swallowing the capsule, or with 90 mL of sodium phosphate (SP, Dexxon, Israel), given in two divided 2 doses, i.e., 45 mL, 12 h before swallowing the capsule and 45 mL, 1 h after swallowing the capsule. When we analyzed each preparation separately, we realized that there was no statistical significance and so made them into one group. Group B (n = 29) was prepared by 200 mg erythromycin (Teva, Israel) in liquid from 1 h prior to the CE study and group C (n = 40) without any preparation. All patients ingested the CE after an overnight fast of 12 h. We arbitrarily divided them into three age groups: 17-40, 41-60, and above 60 years of age.

There were several reasons for colonic preparation. The subjects who needed GI evaluation (e.g., unexplained iron deficiency anemia, etc.) underwent colonoscopy on the same day. Another reason was that part of the clinical study was to compare standard colonoscopy with wireless colonoscopy (unpublished data). In our initial experience with the capsule, we found that the distal part of the ileum was not clean enough for visualization and we, therefore, decided that one group of patients had to undergo colonic preparation. Another problem is the short battery life of the capsule (approximately 7 h), which may not be sufficient to image the entire small bowel. We hypothesized that some colonic preparation or erythromycin might accelerate the movement of the capsule and also provide a better view of the entire small bowel.

Reading of the capsule endoscopy

The transit time, from the first view of the gastric mucosa up to the pyloric region and the small bowel transit, was calculated from the first view of the duodenum up to the ileocecal region. The video results produced from the data recorded by each capsule were reviewed independently by one of the experts (FZ) who was unknown to the clinical data. Capsule transit times were evaluated by analysis of the videos generated during the CE passage.

The quality of the image, on a scale of 1-5, ranged from good (1) with more than 10% of the view with residual material, to poor (5) with more than 90% with residual material.

Statistical analysis

The gastric emptying time and the small bowel transit time was analyzed by computerized software SPSS. The differences in transit time and sub-groups preparation (correlated to age, gender, and normal or abnormal findings) were analyzed by ANOVA multi-changes test. The differences in transit time and preparation were analyzed separately, by ANOVA test, in each of the three sub-groups.

RESULTS

Ninety-five patients (55 men and 40 women, aged 18-91 years, mean age 50.1±17.5 years) were enrolled in the study (Table 1). The reasons for the CE studies: iron deficiency anemia (49 patients); abdominal pain/irritable bowel syndrome (27 patients); suspected Crohn's disease (9 patients); and miscellaneous disease (10 patients) (celiac disease, familial adenomatous polyposis, intestinal lymphoma, ulcerative colitis, Table 1).

There were pathological findings in 54 (56.8%) patients, such as angiodysplasia, ulcer, suspected Crohn's disease, erosions, polyps, edematous mucosa, etc. In 17 cases (17.9%), the capsule failed to reach the cecum before the end of the -420 min recording time.

Table 1 Characteristics of study groups (n)

No. of patients	95
Gender male/female	55/40
Mean age (yr)	50.1
Indications of the CE study	
Iron deficiency anemia	49
Abdominal pain/irritable bowel syndrome	27
Suspected Crohn's disease	9
Miscellaneous disease	10

Miscellaneous disease includes celiac disease, familial adenomatous polyposis, intestinal lymphoma, and ulcerative colitis.

The mean gastric emptying time was 41.7±51.5 min and the transit time of the small bowel was 225±80.6 min of the entire study group. The gastric emptying time in the group prepared with erythromycin was shorter but not statistically significant (Table 2). In elderly subjects prepared by PEG or SP, the gastric emptying time was significantly longer (163.7 min) compared to the other preparations ($P = 0.05$, Table 3). The small bowel transit times were similar in the three age sub-groups; however, a non-significant shorter transit time was seen in the mid-age group (41-60 years) prepared with PEG or SP (Table 3). The gender and pathology neither affected the transit time of the whole study group nor that of the three age sub-groups.

The grade of the cleaning of the entire study group was 3.27±1.1, on a scale of 1 (best image) to 5 (worst, Table 4). In comparison with the other sub-groups, the erythromycin group significantly presented the worst quality of image ($P = 0.05$). Age, gender, and pathology had neither effect on the quality of the cleaning of the entire small bowel study group nor on the arbitrarily selected three age sub-groups (Table 4).

The capsule passed through without difficulty in all cases except for one (1.05%) patient who had no natural excretion, and was found to have Meckel's diverticulum (the Meckel scan that was done prior to the CE study was interpreted as normal).

The average amount of time needed for an expert to review one video was about 50 min.

Table 2 Effect of preparation on transit time

Groups	Emptying gastric time (min)	Small bowel transit time (min)	*P*
Group A ($n = 26$)	53.1	216	NS
Group B ($n = 29$)	26.4	240	NS
Group C ($n = 40$)	45.5	218	NS

Group A: prepared by PEG or with SP, group B: prepared by erythromycin, group C: without any preparation, NS: non-significant.

Table 4 Effect of preparation on cleaning of small bowel

Groups	Grade of cleaning
Group A ($n = 26$)	3.1±1.18
Group B ($n = 29$)	3.7±1.09
Group C ($n = 40$)	3.0±1.06

Group A: prepared by PEG or with SP; group B: prepared by erythromycin; and group C: without any preparation; $P<0.05$, group B *vs* groups A and C.

DISCUSSION

The Given® Diagnostic Imaging System M2A™ Capsule is a new system designed to aid the gastroenterologist in diagnosing small bowel diseases[5,7-9].

The ingestible capsule records video images during natural propulsion through the digestive system. Averages of 50 000 images are obtained during the 8-h passage of the capsule. The CE is propelled by peristalsis through the intestinal tract and permits direct viewing of the entire small intestine[2-5]. From the initial capsule experience, we learned that in approximately 20% of the study population, the capsule did not reach the cecum (the view not the capsule) for several reasons: short battery life (7±1 h); the capsule remaining in the stomach for more than 60 min; and as well the quality of the image, especially in the distal part of the ileum. Practical experience has shown that visualization of the entire small bowel mucosa may sometimes be hindered by the presence of residual material. For these reasons, in some of the CE studies, it was impossible to visualize the entire small bowel[5-7].

More than 180 000 patients worldwide have swallowed the CE. It is estimated that 19 million people in the USA alone may suffer from diseases related to the small intestine, including obscure bleeding, irritable bowel syndrome, Crohn's disease, chronic diarrhea, and cancer. Hence, these will expand the need for CE, and endoscopy services are under increasing strain and to read one CE study takes approximately 1 h of the very expensive time of an expert endoscopist. This could well be the reason that some physicians refuse to adopt the CE study[5-9]. CE is a diagnostic tool with enormous potential and our expectations are that it will yield answers that other procedures are not capable of providing, and with time demand for CE, studies will grow.

There is a lack of data of the effect of colonic preparation on the stomach and the small bowel. Recently, Basit *et al*.[10], have demonstrated that PEG 400 has a marked accelerating effect on small intestinal liquid transit, which, in turn, has implications with PEG 400. In addition, SP effectively shortens small bowel transit time[11]. On the other hand, Sood *et al*.[12], found no significant difference in the mean transit time in the stomach, duodenum, and small bowel between PEG 400 and plain water. The macrolide antibiotic erythromycin has been known to be associated with increased GI motility because of its introduction more than 35 years ago and evidence for its therapeutic efficacy in gastroparesis[13,14]. However, regarding the effect of erythromycin on the transit time of small bowel and its cleaning effect, we have no data. At present, the two major requisites are image quality improvement and reduction of

Table 3 Effect of age on transit time

Groups	Emptying gastric time (min) Age (yr)			Small bowel transit time (min) Age (yr)		
	17–40	41–60	>60	17–40	41–60	>60
Group A ($n = 26$)	16.8	46.5	163.7[1]	234.0	178.1	315.5
Group B ($n = 29$)	31.6	27.7	22.5	235.3	220.1	214.8
Group C ($n = 40$)	54.2	46.9	34.5	218.0	239.4	250

Group A: prepared by PEG or with SP, group B: prepared by erythromycin, and group C: without any preparation, [1]$P = 0.05$.

the time spent in viewing the CE videos.

As shown by our study, the gender and the presence of pathology lesions had no impact on the cleaning and transit time. Preparation with erythromycin reduced the transit time in the stomach (especially in 40-60-year-old age group), but had a negative effect on the quality of the image in the small bowel. In elderly patients, small bowel transit time and gastric emptying time were significantly longer in those prepared with PEG or SP when compared to the other preparations ($P = 0.05$), but with no effect on the quality of the image.

To the best of our knowledge, this is the first time a study tried to deal with the problems of image quality improvement and reduction of CE viewing time through evaluation of various preparation techniques. After testing the various preparations, we had to concede that they neither offered any improvement in the time needed to read the study nor in image quality over the 12-h fasting period as recommended by the Given Company. Even though erythromycin has the best effect on gastric emptying time, the quality of the view in the small bowel is the worst, for which we have no explanation and preparation with PEG or SP has a negative effect on the transit time of the small bowel. We need other pharmaceutical tools and/or technical aid to improve the time and the quality of the CE study.

ACKNOWLEDGMENTS

The authors thank Carmela Reisler and Esther Eshkol for editorial assistance.

REFERENCES

1 **Iddan G,** Meron G, Glukhovsky A, Swain P. Wireless capsule endoscopy. *Nature* 2000; **405**: 417
2 **Scapa E,** Jacob H, Lewkowic S, Migdal M, Gat D, Gluckhovski A, Fireman Z. Results of the first clinical studies performed in Israel with wireless capsule endoscopy. *Am J Gastroenterol* 2002; **97**: 2776-2779
3 **Costamagna G,** Shah SK, Riccioni ME, Foschia F, Mutignani M, Perri V, Vecchioli A, Brizi MG, Picciocchi A, Marano P. A prospective trial comparing small bowel radiographs and video capsule endoscopy for suspected small bowel disease. *Gastroenterology* 2002; **123**: 1385-1388
4 **Ell C,** Remke S, May A, Helou L, Henrich R, Mayer G. The first prospective controlled trial comparing wireless capsule endoscopy with push enteroscopy in chronic gastrointestinal bleeding. *Endoscopy* 2002; **34**: 685–689
5 **Fireman Z,** Mahajna E, Broide E, Shapiro M, Fish L, Sternberg A, Kopelman Y, Scapa E. Diagnosing small bowel Crohn's disease with wireless capsule endoscopy. *Gut* 2003; **52**: 390–392
6 **Mylonaki M,** Fritscher-Ravens A, Swain P. Wireless capsule endoscopy: a comparison with push enteroscopy in patients with gastroscopy and colonoscopy negative gastrointestinal bleeding. *Gut* 2003; **502**: 1122-1126
7 **Swain P.** Wireless capsule endoscopy. *Gut* 2003; **52**: 48-50
8 **Hartmann D,** Schilling D, Bolz G, Hahne M, Jakobs R, Siegel E, Weickert U, Adamek HE, Riemann JF. Capsule endoscopy versus push enteroscopy in patients with occult gastrointestinal bleeding. *Z Gastroenerol* 2003; **41**: 377-382
9 **Eliakim R,** Fischer D, Suissa A, Yassin K, Katz D, Guttman N, Migdal M. Wireless capsule video endoscopy is a superior diagnostic tool in comparison to barium follow-through and computerized tomography in-patients with suspected Crohn's disease. *Eur J Gastroenterol Hepatol* 2003; **15**: 363-367
10 **Basit AW,** Newton JM, Short MD, Waddington WA, Ell PJ, Lacey LF. The effect of polyethylene glycol 400 on gastrointestinal transit: implications for the formulation of poorly-water soluble drugs. *Pharm Res* 2001; **18**: 1146-1150
11 **Linden TB,** Waye JDC. Sodium phosphate preparation for colonoscopy: onset and duration of bowel activity. *Gastrointest Endosc* 1999; **50**: 811-813
12 **Sood RR,** Joubert I, Franklin H, Doyle T, Lomas DJ. Small bowel MRI: Comparison of a polyethylene glycol preparation and water as oral contrast media. *J Magn Reson Imaging* 2002; **15**: 401-408
13 **Bungard TJ,** Kale-Pradhan PP. Prokinetic agents for the treatment of postoperative ileus in adults: A review of the literature. *Pharmacotherapy* 1999; **19**: 416-423
14 **Camilleri M.** The current role of erythromycin in the clinical management of gastric emptying disorders. *Am J Gastroenterol* 1993; **88**: 169-171

Science Editor Kumar M and Guo SY **Language Editor** Elsevier HK

PO Box 2345, Beijing 100023, China
www.wjgnet.com
wjg@wjgnet.com

ELSEVIER

World J Gastroenterol 2005;11(37):5867-5873
World Journal of Gastroenterology ISSN 1007-9327
© 2005 The WJG Press and Elsevier Inc. All rights reserved.

• *BRIEF REPORTS* •

Possible contribution of advanced statistical methods (artificial neural networks and linear discriminant analysis) in recognition of patients with suspected atrophic body gastritis

Edith Lahner, Enzo Grossi, Marco Intraligi, Massimo Buscema, Vito D Corleto, Gianfranco Delle Fave, Bruno Annibale

Edith Lahner, Vito D Corleto, Gianfranco Delle Fave, Bruno Annibale, Digestive and Liver Disease Unit, II Medical School, Sant'Andrea Hospital, University "La Sapienza", Rome, Italy
Enzo Grossi, Bracco Imaging Spa, Milan, Italy
Marco Intraligi, Massimo Buscema, Semeion Research Center, Rome, Italy
Supported by a grant from Bracco Imaging Spa, Milan, Italy, and a grant from the Italian Ministry of University and Research (No. 2002-2003)
Correspondence to: Professor Bruno Annibale, Ospedale Sant'Andrea, Via di Grottarossa 1035, Rome 00191, Italy. bruno.annibale@uniroma1.it
Telephone: +39-6-80345289 Fax: +39-6-80345001
Received: 2004-09-13 Accepted: 2004-12-01

Abstract

AIM: Diagnosis of atrophic body gastritis (ABG) is based upon histological examinations of body mucosa biopsies obtained during gastroscopy. However, gastroscopy is invasive and expensive, and biopsy sampling of body mucosa prolongs the procedure increasing discomfort to the patient. Artificial neural networks (ANNs) and linear discriminant analysis (LDA) may be used as computer-based decision-support systems. Thus, this pilot study aimed at investigating whether ANNs and LDA could recognize patients with ABG in a database, containing only clinical and biochemical variables, of a pool of patients with and without ABG, by selecting the most predictive variables and by reducing input data to the minimum.

METHODS: Data was collected from 350 consecutive outpatients (263 with ABG, 87 with non-atrophic gastritis and/or celiac disease [controls]). Structured questionnaires with 22 items (anagraphic, anamnestic, clinical, and biochemical data) were filled out for each patient. All patients underwent gastroscopy with biopsies. ANNs and LDA were applied to recognize patients with ABG. Experiment 1: random selection on 37 variables, experiment 2: optimization process on 30 variables, experiment 3: input data reduction on 8 variables, experiment 4: use of only clinical input data on 5 variables, and experiment 5: use of only serological variables.

RESULTS: In experiment 1, overall accuracies of ANNs and LDA were 96.6% and 94.6%, respectively, for predicting patients with ABG. In experiment 2, ANNs and LDA reached an overall accuracy of 98.8% and 96.8%, respectively. In experiment 3, overall accuracy of ANNs was 98.4%. In experiment 4, overall accuracies of ANNs and LDA were, respectively, 91.3% and 88.6%. In experiment 5, overall accuracies of ANNs and LDA were, respectively, 97.7% and 94.5%.

CONCLUSION: This preliminary study suggests that advanced statistical methods, not only ANNs, but also LDA, may contribute to better address bioptic sampling during gastroscopy in a subset of patients in whom ABG may be suspected on the basis of aspecific gastrointestinal symptoms or non-digestive disorders.

© 2005 The WJG Press and Elsevier Inc. All rights reserved.

Key words: Atrophic body gastritis; Computer-based decision support; Gastroscopy; Artificial neural networks

Lahner E, Grossi E, Intraligi M, Buscema M, Corleto VD, Fave GD, Annibale B. Possible contribution of advanced statistical methods (artificial neural networks and linear discriminant analysis) in recognition of patients with suspected atrophic body gastritis. *World J Gastroenterol* 2005; 11(37): 5867-5873
http://www.wjgnet.com/1007-9327/11/5867.asp

INTRODUCTION

Atrophic body gastritis (ABG), a condition characterized by atrophy of the gastric oxyntic mucosa, hypo/achlorhydria, and, in turn, hypergastrinemia, is a disorder considered as increased risk for gastric neoplasms[1,2].

In general, ABG does not give rise to symptoms of the upper gastrointestinal tract, such as epigastric pain or burning. Some patients may complain of dyspeptic symptoms, such as epigastric discomfort or postprandial bloating, complaints which are frequently found in the general population[1]. More frequently, the only relevant clinical finding is the presence of anemia[3-5], and, indeed, ABG is often considered synonymous with the presence of pernicious anemia[6,7]. Moreover, ABG may also present with iron-deficiency anemia, a consequence of the impaired iron absorption due to hypo/achlorhydria[8]. Finally, ABG may be associated with autoimmune disorders, such as autoimmune thyroid disease, vitiligo, and alopecia[7], and, in the presence of vitamin B_{12} deficiency, also with neurological symptoms[9].

However, the gold standard for the diagnosis of ABG is based, despite its limits, such as sampling error and inter-observer variability, on the histological examination of biopsy specimens of body mucosa obtained during gastroscopy[10,11]. Gastroscopy, however, is an invasive and expensive procedure, which is often accepted with reluctance

by patients without gastric symptoms. Moreover, the biopsy sampling of body and antral mucosa prolongs the endoscopic procedure increasing discomfort to the patient. Furthermore, the processing of multiple gastric biopsy specimens for histological examination is time- and cost-consuming.

Non-invasive screening methods, such as serum levels of gastrin and pepsinogen I and II, have been tested for gastric antral and body atrophy, respectively. Unfortunately, however, because of the high specificity but low sensitivity[12-14], these methods need to be further improved before their use in serological screening for atrophic gastritis can be considered feasible[15].

Thus, reliable tools to select patients with suspected ABG requiring gastroscopy with collection of body mucosa specimens for histological diagnosis of ABG are still lacking. Decision-support systems, based on conventional statistical methods, made their entry into medicine several years ago[16,17]. Recently, efforts to improve predictive and prognostic performance of these systems have led to the application of artificial neural networks (ANNs) as tools for clinical decision-making[17-19]. ANNs are highly flexible computerized mathematical models for understanding and predicting complex and chaotic dynamics in complex biological systems, and have been effectively used to solve non-linear problems related to diagnostic or prognostic queries even for single patients, and not necessarily for the groups of patients as in the case with conventional statistics[17,20]. Thus, ANNs would appear to be a promising tool for clinical decision-making and have been applied in various areas of medical research[21-24]. Recently, the role of ANNs has been investigated in two important aspects of clinical decision-making in gastroenterology: Das *et al*.[25], have proposed a prediction model of outcome in acute lower gastrointestinal hemorrhage based on ANNs; and Selaru *et al*.[26], have reported that ANNs are able to distinguish among subtypes of neoplastic colorectal lesions. To our knowledge, studies applying advanced statistical methods in patients with suspected ABG have not yet been performed. This pilot study, therefore, aimed to investigate the role of ANNs and LDA in recognizing patients with ABG in the database of a pool of patients with ABG comprising only clinical and biochemical variables, by selecting the most predictive variables and by reducing input data to the minimum.

MATERIALS AND METHODS

Patients

This study was carried out using a database prepared ad hoc, comprising data from 350 consecutive outpatients (86 male, 264 female, median age 53 years, range 20-81 years), with a diagnosis of ABG (n = 263), chronic non-atrophic gastritis (n = 42), and celiac disease with or without chronic non-atrophic gastritis (n = 45). The 87 patients without ABG were considered as controls. These patients were evaluated, from 1994 to 1998, for long-standing dyspepsia, microcytic or macrocytic anemia, presence of autoimmune diseases or neurological disorders in our gastroenterology unit, which is part of an academic, urban, tertiary-care medical institution.

For each of these patients, a structured questionnaire was filled out, composed of 22 items concerning anagraphic, anamnestic, clinical, and biochemical data. The items with their respective variables of the structured questionnaire are shown in Table 1. Replies of the patients to questionnaire items regarding symptoms were considered positive, when present for at least three consecutive months during the previous year.

All patients underwent gastroscopy with standardized biopsy sampling from the antrum (n = 3), body (n = 3), and duodenum (n = 2) for conventional histopathological examination, as previously described[3,4,27,28]. The degree of gastritis was assessed according to the Updated Sydney System[10]. Atrophy of the body and antral mucosa was defined as focal or complete replacement of oxyntic or pyloric glands by metaplastic pyloric or intestinal glands, respectively, as previously described[3,4]. Celiac disease was diagnosed and classified according to the classification of Marsh[29].

Furthermore, all patients also underwent serological studies: fasting gastrin levels were evaluated by means of a specific radioimmunoassay (RIA) using polyclonal antibody (No. 4562, kindly provided by Prof. J. Rehfeld, Copenhagen), which is able to detect the entire pool of molecular forms of gastrin, as described earlier (normal values $\leqslant$40 ng/L)[3]. Pepsinogen I levels were measured using a commercial RIA kit (Pepsik, Sorin, Saluggia, Italy), as previously reported (normal values 20-80 ng/mL)[3]. Antibodies against anti-parietal cells were assayed using a commercial kit (Autostat, Cogent Diagnostic Ltd, Edinburgh, UK), as previously described[3,4].

All patients gave written informed consent to the study, which was approved by the Local Ethics Committee.

Statistical methods

Artificial neural networks (ANNs) ANNs were applied to the data set from a structured questionnaire containing 22 clinical and biochemical items for each of the 350 patients (263 with ABG, 87 without ABG [controls], Table 1). The items with three or more levels were recoded in binary variables. The final data set was thus composed of 37 variables for each of the 350 patients, these being considered as independent variables (input). As dependent variable (output), we considered the presence or absence of diagnosis of ABG based on the histological examination of gastric biopsies obtained during gastroscopy. Endoscopic and histological data were not included in the data set.

Since the aim of our investigation was to study ANNs as a tool to recognize the presence of ABG on the basis of clinical and biochemical data, which in mathematical language is referred to as "classification problem", we applied the hetero-associated ANNs[19,20]. Thus, the samples of 350 patients were randomly subdivided several times into two equal and balanced sub-samples of patients with ABG and controls (random selection) as follows: one for the training phase (training) and one for the prediction phase (testing). During training phase, ANNs learn, on the basis of linear and non-linear relations existing between the variables of the data set, including the outcome variable, to perform the required classification, i.e., to correctly recognize the patients with ABG with respect to controls. ANNs were used with the following learning methods: (i) feed forward back propagation (BP)[30] e sine learning law (SP)[31]; (ii)

auto-recurrent (ARCR) and cluster recurrent (TASM)[32,33]. After several training cycles, the dependent variables (presence/absence of ABG) were excluded from the data set, and the ANNs showing the best performance during the training phase were applied to the second sub-sample of patients, not previously exposed to the network, whereby ensuring an unbiased testing phase during which the capability of trained ANNs to recognize patients with ABG with respect to controls was evaluated.

In order to reduce the number of input variables, selecting those most informative to predict the output, we used the "Training and Testing" (T&T) model, associated with the input selection (IS) system[34]. The T&T algorithm is a population of ANNs managed by an evolutionary system, in which a separate ANN represents a model of distribution of the complete data set in a training and a testing set. The score that each ANN reaches in the testing phase represents its goodness-of-fit and, consequently, its probability of evolution. The evolutionary algorithm called "Genetic Doping Algorithm" (GenD)[35], at each generation, combines the different hypotheses of distribution of each ANN according to the goodness-of-fit criterion. In this way, the best distribution of the entire data set, in a training set and in a testing set, is reached after a finite number of generations. The IS system becomes operative on a population of ANNs, each of them with the ability to select independent variables for the validation set. Each ANN learns from the training set, and is evaluated on the testing set[34]. Through the GenD evolutionary algorithm, different hypotheses of each ANN change over time, and generation after generation. When the evolutionary algorithm no longer improves, the process stops, and the best hypothesis of the input variables is selected and employed on the validation subset. The goodness-of-fit rule of GenD promotes, at each generation, the best testing performance with the minimal number of inputs[34].

All software used for the ANNs analysis, including the T&T model associated with the IS system, and the GenD have been developed and were applied by the Semeion Research Center, Rome, Italy[36].

Linear discriminant analysis (LDA) LDA was also used to analyze the predictive performance of conventional statistics. In order to optimize the predictive ability, different models were assessed and, as for the ANNs procedure, the samples were randomly divided into two sub-samples for the training and testing phases. For the analysis of LDA, the SAS version 6.04 (SAS Institute, Cary, NC, USA) using forward stepwise procedure was employed. This was performed by the Semeion Research Center, Rome, Italy. The application protocols of ANNs and LDA are schematically illustrated in Figure 1.

Study design

The first experiment was performed by random selection on the original database using all independent input variables. In the second experiment, the T&T algorithm, associated with the IS system, was applied using the independent input variables, which were reduced to the most informative ones.

The application of statistically-based decision supports, in clinical practice, should be simple and require little time for data entry. Thus, the number of inputs should be reduced to the bare minimum. Therefore, in order to verify the prediction capability of ANNs by using a reduced amount of input data, ANNs, in the third experiment, were performed using only the eight independent variables identified by LDA in the second experiment as having the most predictive power for the diagnosis of ABG. In the fourth experiment, the serological variables were removed from the eight independent variables used in the third experiment, thus verifying the prediction capability of ANNs and LDA for the presence of ABG by using only five clinical input variables. Finally, in the fifth experiment, only the serological variables were used. The study design is outlined in Figure 2.

RESULTS

Experiment 1

After random selection of patients, the ANNs training sets were used on a sub-sample of 175 patients (132 with ABG

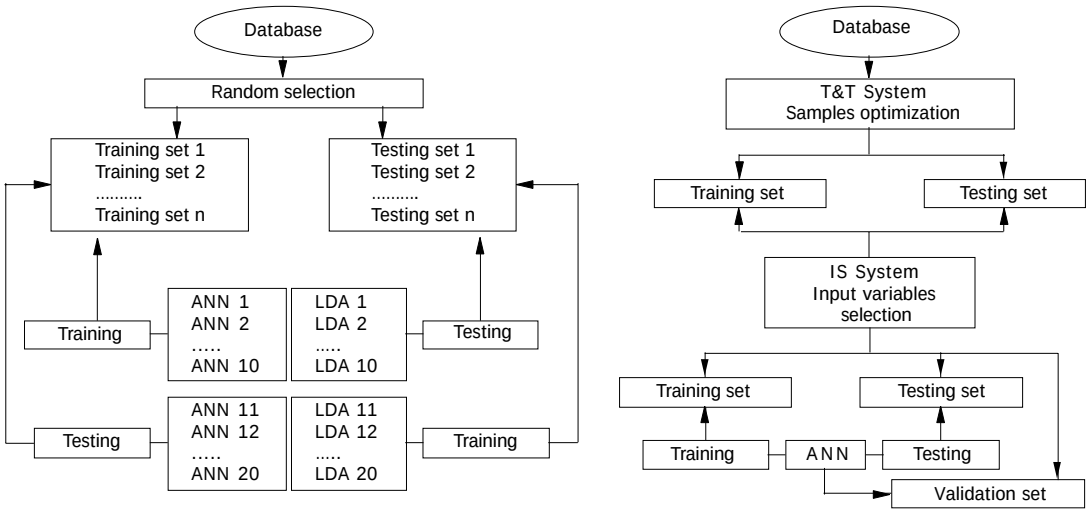


Figure 1 Application protocol of ANNs, LDA, T&T, and IS.

and 43 controls), and the ANNs tests were employed on the second sub-sample of 175 patients (131 with ABG and 44 controls) by using the original data set (37 independent variables). The best ANNs identified 128 of the 131 patients with ABG (sensitivity 97.7%), and correctly matched 42 of the 44 controls (specificity 95.5%), yielding an overall accuracy of 96.6%. The yield of LDA was slightly lower with a sensitivity of 95.4% (identifying 125 of the 131 patients with ABG), a specificity of 93.2% (recognizing 41 of the 44 controls), and the overall accuracy being 94.6% (Table 2).

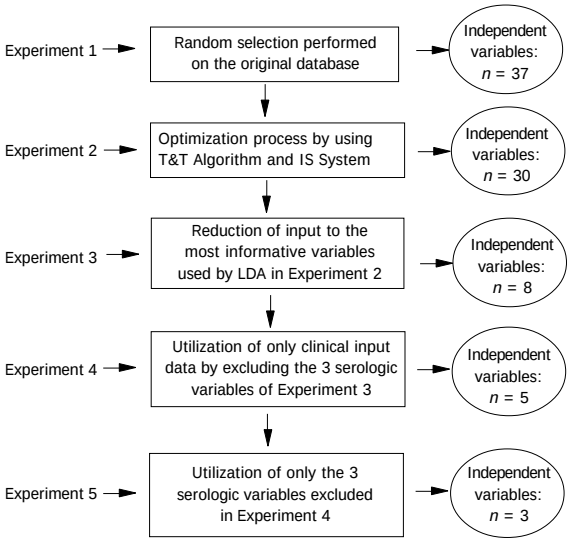


Figure 2 Study design: progressive reduction of independent input variables.

Experiment 2

The T&T algorithm, associated with the IS system, selected as the most informative 30 out of the 37 initial independent variables, removing the 7 variables such as mean corpuscular volume, absence of gastrointestinal symptoms, association with thyroid disease, family history for gastric ulcer, referred from the Department of Hematology, motility-like dyspepsia and hemoglobin was carried out.

The sub-samples of ANNs training, testing, and validation sets comprised 78, 60, and 125 patients with ABG, and 30, 17, and 40 controls, respectively. Following the optimization process, the performance of both the ANNs and the LDA increased with respect to the first experiment. In fact, on the validation set, ANNs' sensitivity rose to 98.4% (identifying 123 of the 125 patients with ABG) and specificity to 100% (correctly matching all 40 controls), thus yielding an overall accuracy of 98.8%. LDA recognized 119 of the 125 patients with ABG and failed to recognize only one out of the 40 controls, thus achieving a sensitivity, a specificity, and an overall accuracy of 96%, 97.5%, and 96.75%, respectively (Table 2).

Experiment 3

The eight independent variables used in this experiment are shown in Table 3. The performance of ANNs was good (overall accuracy 98.4%): only 4 out of the 125 patients with ABG (sensitivity 96.8%) were misclassified, but all 40 controls (specificity 100%) were correctly matched. The performance of LDA, which was the same as in the previous experiment, was slightly lower than that of ANNs (Table 2).

Table 1 Structured questionnaire containing anagraphic, anamnestic, clinical, and biochemical variables considered as independent variables (input)

Variables	Independent variables (input) levels
1. Sex (2)	Male; female
2. Age[1] yr	
3. Referred from the Department of… (5)	Hematology, gastroenterology, dermatology, endocrinology, other
4. Presentation symptom (5)	Anemia, GI symptoms/disorders, dermatological symptoms/disorders, endocrinological symptoms/disorders, other
5. Onset of presentation symptom (mo)	
6. GI symptoms (4)	Dyspepsia motility-like, dyspepsia ulcer-like, other GI symptoms, absence
7. Neurological symptoms (2)	Yes/no
8. Other symptoms (2)	Yes/no
9. Family history (1st degree relatives) autoimmune diseases (2)	Yes/no
10. Family history (1st degree relatives) for gastric neoplasms (2)	Yes/no
11. Family history (1st degree relatives) for duodenal ulcer or gastric ulcer (3)	No family history, family history for duodenal ulcer, family history for gastric ulcer
12. Association with thyroid disease (2)	Yes/no
13. Association with dermatological disease (2)	Yes/no
14. Association with neoplasms (2)	Yes/no
15. Association with duodenal ulcer or gastric ulcer (2)	Yes/no
16. Association with other diseases not mentioned previously (2)	Yes/no
17. Anemia (3)	No anemia, macrocytic (pernicious) anemia, microcytic (iron-deficiency) anemia
18. Hemoglobin[1]	
19. Mean corpuscular volume (MCV[1])	
20. Fasting gastrin[1]	
21. Pepsinogen I[1]	
22. Parietal cell antibodies (2)	Presence/absence

GI, gastrointestinal; ABG, atrophic body gastritis; [1]continuous variables. The number of levels of each variable is indicated in the brackets.

Table 2 Performance of ANNs and LDA for diagnosis of ABG

Experiments	ANNs			LDA		
	Accuracy (%)	Sensitivity (%)	Specificity (%)	Accuracy (%)	Sensitivity (%)	Specificity (%)
Experiment 1	96.6	97.7	95.5	94.6	95.4	93.2
Experiment 2	98.8	98.4	100	96.8	96.0	97.5
Experiment 3	98.4	96.8	100	96.8	96.0	97.5
Experiment 4	91.3	91.7	90.9	88.6	93.2	84.1
Experiment 5	97.7	95.4	100	94.5	94.9	94.2

Experiment 4

In this experiment, of the eight variables used in the previous experiment, the three serological variables, namely gastrin, pepsinogen I, and anti-parietal cell antibodies, were excluded. Using only the five clinical variables (Table 3), ANNs showed a sensitivity of 91.7% (121 of the 132 ABG patients identified), a specificity of 90.9% (40 of the 44 controls recognized), and an overall accuracy of 91.3%. On the other hand, LDA showed a sensitivity of 93.2% (123 of the 132 ABG patients identified), a specificity of 84.1% (37 of the 44 controls correctly matched), and an overall accuracy of 88.6% (Table 2).

Table 3 Independent variables identified by LDA as most predictive for the diagnosis of ABG with respective correlation coefficients

Independent variables	Correlation coefficients
Pepsinogen I[1]	0. 42
Gastrin[1]	–0.40
Age, yr	–0.37
Association with other diseases not previously mentioned[2]	0.35
Other (not gastrointestinal) symptoms[3]	0.34
Onset of presentation symptoms (mo)	0.25
Other gastrointestinal symptoms[4]	0.25
Antibodies against parietal cells[1]	0.23

[1]Serological variables; [2]represented in data set by cardiovascular diseases, diabetes type II and other causes of iron-deficiency anemia; [3]represented in data set by asthenia, fatigue, and headache; [4]represented in data set by diarrhea, abdominal pain, and bloating.

Experiment 5

In the final experiment, using only the three serological variables (gastrin, pepsinogen I, and anti-parietal cell antibodies), ANNs showed a sensitivity of 95.4%, a specificity of 100%, and an overall accuracy of 97.7%. LDA showed a sensitivity of 94.9%, a specificity of 94.2% and an overall accuracy of 94.5% (Table 2).

DISCUSSION

The results emerging from this pilot study suggest that advanced statistical methods, not only ANNs, but also LDA, are able to predict, with great accuracy, the presence of ABG using only clinical and serological variables. These methods may thus, after appropriate validation, be taken into consideration as potential clinical decision-support tools for identifying those patients with suspected ABG requiring gastroscopy with body mucosa biopsy sampling for the assessment of atrophy of the oxyntic mucosa. However, gastroscopy is an invasive and expensive procedure, which is often accepted with reluctance by patients without specific gastrointestinal symptoms or presenting with non-digestive disorders, such as thyroiditis, anemia or neurological symptoms. Furthermore, in this particular clinical setting, the cost-effectiveness of bioptic sampling during gastroscopy still needs to be determined[37]. Thus, a computer-based decision-support system, which is able to select with a high predictive accuracy, those patients with a high probability of having ABG, would enable the endoscopic/histologic investigation to be better addressed. Indeed, in the third experiment, the advanced statistical systems correctly identified all patients without ABG.

For the clinical applicability of computer-based decision support systems and their acceptance by physicians, it is necessary to offer a system, which is simple, with entry of data that requires little time, thus using a limited number of variables, which are readily available to the clinician. In the present study, we, therefore, progressively decreased the input variables in order to use less input data with a high predictive power for ABG. It is of interest that, despite the reduction in the number of input variables from the initial 37 to only 8, the accuracies of ANNs and LDA were still 98.4% and 96.8%, respectively. Surprisingly, the performance of ANN and LDA was still acceptable (91.3% and 88.6%, respectively) despite the reduction in the input variables to only five variables, readily available in the clinician's office by clinical history. However, four of these five clinical variables are non-specific, such as other gastrointestinal symptoms, namely diarrhea, abdominal pain and bloating, and other non-gastrointestinal symptoms, such as headache and asthenia. Thus, these findings need to be confirmed by a prospective study using these systems.

It was not surprising that of the most informative variables for the prediction of ABG, we find gastrin and pepsinogen I, which are parameters previously tested as serological screening tools for ABG[12-14]. In fact, in these studies, an overall accuracy of about 80% for the diagnosis of atrophic gastritis had already been obtained. The results of the present study support these findings: indeed, by using only the serological variables, gastrin and pepsinogen I together with parietal cell antibodies, the overall accuracy of ANNs was almost 98%. However, our study also shows that the accuracy of these serological markers for the identification of patients with suspected ABG may potentially be improved by almost 100%, associating them with a few clinical data and applying advanced statistical systems.

Albeit the clinical variables identified as those having the highest predictive power for the diagnosis of ABG were quite unexpected: age, onset of presentation symptoms, other gastrointestinal symptoms (diarrhea and bloating),

other non-gastrointestinal symptoms (headache, asthenia), and the association with other,not previously mentioned diseases(cardiovascular diseases and diabetes) . In general, the presence of a statistical relationship between a predictor variable and the outcome alone does not imply causality[38]. This is even more the case for ANN-based models, which process data in a non-linear way, and the network logic of prediction cannot be broken down into simple elements of clinical reasoning[17,18]. Thus, the variables with the most predictive power selected by the advanced statistical systems should not be viewed as independent predictive variables as perceived by a clinician[17,38].

However, these findings also show the crucial importance of coding variables during the setting up of a database to be used for advanced statistical analysis, which obviously affects the results of analyses. In fact, in our data set, three out of the five most informative variables were coded as cumulative variables (other gastrointestinal symptoms, other non-gastrointestinal symptoms, and association with other diseases not previously mentioned) and thus considered of little importance at the time of data collection. On the contrary, these five variables alone were able to distinguish between patients with and without ABG with an overall accuracy of approximately 90%. Thus, data sets for the use of advanced statistical methods need to be developed without considering a single data a priori as less important, but all available data should be entered in detail, since advanced statistical methods recognize complex linear and non-linear relationships, not valuable a priori[39].

It is of interest that, although a comparison of the two statistical approaches was not performed, ANNs somewhat outperformed LDA, but both technologies showed good predictive results. In fact, in 24 out of the 37 independent variables (64.9%), a non-linear relationship with the output (diagnosis of ABG) was observed, as shown by the values of the correlation coefficients, which were less than 0.06 (data not shown). However, the values of correlation coefficients of the remaining 13 independent variables ranged between 0.063 and 0.302, showing that these variables were, to some extent, related in a linear way to the output. This finding is in agreement with that of previous studies in which conventional statistical methods were compared to neural networks and no differences in overall predictive performance were observed[38,40,41]. However, it has been argued that performance improves merely by structuring information, making it difficult to assess how much improvement could be related to any specific statistical analysis[42].

However, the aim of the present study has been not to emphasize that advanced statistical decision support systems should replace or substitute experienced clinicians, but to stress that, in our opinion, these systems should be viewed as a potential decision aid, particularly in times of shortages of financial resources, in order to better address invasive investigations to save costs and to use resources when effectively necessary, as described in other fields of medical settings[43].

We are aware that the current study had some pitfalls, including the fact that external validation has not yet been carried out; in fact, our results need to be considered as preliminary and be validated in a prospective and large-population study. Secondly, these findings may not be generalized "tout-court" to the general population, since, in this pilot study, the frequency of ABG was higher than that of controls.

In conclusion, this preliminary study suggests that advanced statistical methods, not only ANNs, but also LDA, may contribute to better address bioptic sampling during gastroscopy in a subset of patients in whom ABG may be suspected on the basis of aspecific gastrointestinal symptoms or non-digestive disorders.

ACKNOWLEDGMENTS

We are grateful to Mrs. Marian Shield for editorial and linguistic revision.

REFERENCES

1 **Lee EL,** Feldman M. Gastritis and other gastropathies. In: *Sleisenger & Fordtran's Gastrointestinal and Liver Disease: pathophysiology, diagnosis, management*. Eds. Feldman M, Friedman LS, Sleisenger MH. 7th edition, Saunders, Philadelphia; 2002: 810-827

2 **Peterson WL,** Graham DY. Helicobacter pylori. In: *Sleisenger & Fordtran's Gastrointestinal and Liver Disease*: *pathophysiology, diagnosis, management*. Eds. Feldman M, Friedman LS, Sleisenger MH. 7th edition, Saunders, Philadelphia; 2002: 732-746

3 **Marignani M,** Delle Fave G, Mecarocci S, Bordi C, Angeletti S, D'Ambra G, Aprile MR, Corleto VD, Monarca B, Annibale B. High prevalence of atrophic body gastritis in patients with unexplained microcytic and macrocytic anemia: a prospective screening study. *Am J Gastroenterol* 1999; **94**: 766-772

4 **Annibale B,** Marignani M, Azzoni C, D'Ambra G, Caruana P, D'Adda T, Delle Fave G, Bordi C. Atrophic body gastritis: distinct features associated with *Helicobacter pylori* infection. *Helicobacter* 1997; **2**: 57-64

5 **Kekki M,** Samlof IM, Varis K, Ihamaki T. Serum pepsinogen I and serum gastrin in the screening of severe atrophic corpus gastritis. *Scand J Gastroenterol* 1991; **26**: 109-116

6 **Babio BM,** Bunn HF. Megaloblastic anemias. In: Fauci AS, Braunwald E, Isselbacher KJ. Eds. *Harrison's principles of internal medicine* (14th edition). *McGraw Hill* 1998: 653-659

7 **Whittingham S,** Mackay IR. Pernicious anemia and gastric atrophy. In: Rose NR, Mackay IR, Eds. *The Autoimmune Diseases*. Orlando, FL: Academic 1985: 243-266

8 **Schade SG,** Cohen RJ, Conrad ME. The effect of hydrochloric acid on iron absorption. *N Engl J Med* 1968; **279**: 672-674

9 **Toh BH,** van Driel IR, Gleeson PA. Pernicious anemia. *N Engl J Med* 1991; **337**: 1441-1448

10 **Dixon MF,** Genta RM, Yardley JH, Correa P. Classification and grading of gastritis. The Updated Sydney System. *Am J Surg Pathol* 1996; **20**: 1161-1181

11 **Rugge M,** Correa P, Dixon MF, Fiocca R, Hattori T, Lechago J, Leandro G, Price AB, Sipponen P, Solcia E, Watanabe H, Genta RM. Gastric mucosal atrophy: interobserver consistency using new criteria for classification and grading. *Aliment Pharmacol Ther* 2002; **16**: 1249-1259

12 **Westerveld BD,** Pals G, Lamers CB, Defize J, Pronk JC, Frants RR, Ooms EC, Kreuning J, Kostense PJ, Eriksson AW. Clinical significance of pepsinogen A isozymogens, serum pepsinogen A and C levels, and serum gastrin levels. *Cancer* 1987; **59**: 952-958

13 **Ley C,** Mohar A, Guarner J, Herrera-Goepfert R, Figueroa LS, Halperin D, Parsonnet J. Screening markers for chronic atrophic gastritis in Chiapas, Mexico. *Cancer Epidemiol Biomark Prev* 2001; **10**: 107-112

14 **Väänänen H,** Vauhkone M, Helske T, Kaariainen I, Rasmussen M, Tunturi-Hihnala H, Koskenpato J, Sotka M, Turunen M,

Sandstrom R, Ristikankare M, Jussila A, Sipponen P. Non-endoscopic diagnosis of atrophic gastritis with a blood test. Correlation between gastric histology and serum levels of gastrin-17 and pepsinogen I: a multicentre study. *Eur J Gastroenterol Hepatol* 2003; **15**: 885-891

15 **Kuipers EJ.** In through the out door: serology for atrophic gastritis. *Eur J Gastroenterol Hepatol* 2003; **15**: 877-879

16 **Wasson JH,** Sox HC, Neff RK, Goldman L. Clinical prediction rules: Applications and methodological standards. *N Engl J Med* 195; **313**: 793-799

17 **Dayhoff JE,** DeLeo JM. Artificial Neural Networks. Opening the black box. *Cancer* 2001; **91**: 1615-1635

18 **Cross SS,** Harrison RF, Kennedy RI. Introduction to neural networks. *Lancet* 1995; **346**: 1075-1079

19 **Wyatt JC.** Decision support systems. *J R Soc Med* 2000; **93**: 629-633

20 **Buscema M.** Special issue on artificial neural networks and complex social systems, I. Theory. *Substance Use Misuse* 1998; **33**: 1-220

21 **Detrano R,** Janosi A, Steinbrunn W, Pfisterer M, Schmid JJ, Sandhu S, Guppy KH, Lee S, Froelicher V. International application of a new probability algorithm for the diagnosis of coronary artery disease. *Am Cardiol* 1989; **64**: 304-310

22 **Han M,** Snow PB, Brandt JM, Partin AW. Evaluation of artificial neural networks for the rediction of pathologic state in prostate carcinoma. *Cancer* 2001; **91**: 1661-1666

23 **West D,** West V. Model selection for a medical diagnostic decision support system: a breast cancer detection case. *Artific Intell Med* 2000; **20**: 183-204

24 **Blekas K,** Stafylopatis A, KontoravdisD, Likas A, Karakitsos P. Cytological diagnosis based on fuzzy neural networks. *J Intellt Systems* 1998; **8**: 55-79

25 **Das A,** Ben-Menachem T, Cooper GS, Chak A, Sivak MV Jr, Gonet JA, Wong RC. Prediction of outcome in acute lower-gastrointestinal haemorrhage based on an artificial neural network: internal and external validation of a predictive model. *Lancet* 2003; **362**: 1261-1266

26 **Selaru FM,** Xu Y, Yin J, Zou T, Liu TC, Mori Y, Abraham JM, Sato F, Wang S, Twigg C, Olaru A, Shustova V, Leytin A, Hytiroglou P, Shibata D, Harpaz N, Meltzer SJ. Artificial neural networks distinguish among subtypes of neoplastic colorectal lesions. *Gastroenterology* 2002; **122**: 606-613

27 **Bordi C,** Annibale B, Azzoni C, Marignani M, Ferraro G, Antonelli G, D'Adda T, D'Ambra G, Delle Fave G. Endocrine cell growths in atrophic body gastritis. Critical evaluation of a histological classification. *J Pathol* 1997; **182**: 339-346

28 **Annibale B,** Severi C, Chistolini A, Antonelli G, Lahner E, Marcheggiano A, Iannoni C, Monarca B, Delle Fave G. Efficacy of a gluten-free diet alone on recovery from iron deficiency anemia in adult celiac patients. *Am J Gastroenterol* 2001; **96**: 132-137

29 **Marsh MN.** Gluten, major histocompatibility complex and the small intestine. A molecular and immunobiologic approach to the spectrum of gluten sensitivitiy ('celiac sprue'). *Gastroenterology* 1992; **102**: 330-354

30 **Buscema M.** Back propagation neural networks. *Substance Use Misuse* 1998; **33**: 233–270

31 **Buscema M.** Sine Net: a new learning rule for adaptive systems, Technical paper 21. Rome: Semeion 2000

32 **Buscema M.** Self-Recurrent neural network. *Substance Use Misuse* 1998; **33**: 495–501

33 **Breda M,** Buscema M. Reti neurali ricorrenti. In M. Buscema Semeion Group, *Reti Neurali Artificiali e Sistemi Sociali Complessi*, Vol. I: Teoria e Modelli, Milan: *Franco Angeli* 1999: 440–464

34 **Buscema M,** Grossi E, Intraligi M, Garbagna N, Andriulli A, Breda M. An optimized experimental protocol based on neuro-evolutionary algorithms. Application to the classification of dyspeptic patients and to the prediction of the effectiveness of their treatment. *Artif Intell Med* 2005; 34: 279-305

35 **Buscema M.** Genetic doping algorithm (GenD): theory and application. *Exp Systems* 2004; **2**: 63-79

36 **Buscema M.** SuperVised Feed Forward and Recurrent ANNs, Research Software package for Supervised ANNs. Semeion Software 12, ver 3.0. Roma 2000

37 **Annibale B,** Capurso G, Chistolini A, D'Ambra G, DiGiulio E, Monarca B, DelleFave G. Gastrointestinal causes of refractory iron deficiency anemia in patients without gastrointestinal symptoms. *Am J Med* 2001; **111**: 439-445

38 **Tu VJ.** Advantages and disadvantages of using artificial neural networks versus logistic regression for prediction medical outcomes. *J Clin Epidemiol* 1996; **49**: 1225-1231

39 **Levine RF.** Clinical problems, computational solutions. A vision for a collaborative future. *Cancer* 2001; **91**: 1595-1602

40 **Buchman TG,** Kubos KL, Seidler AJ, Siegforth MJ. A comparison of statistical and connectionist models for the prediction of chronicity in a surgical intensive care unit. *Crit Care Med* 1994; **22**: 750-762

41 **Sargent JD.** Comparison of artificial neural networks with other statistical approaches. *Cancer* 2001; **91**: 1636-1642

42 **Cross SS,** Harrison RF, Sanders DS. Supporting decisions in clinical medicine: neural network in lower gastrointestinal haemorrhage. *Lancet* 2003; **362**: 1250-1251

43 **Lisboa PJ.** A review of evidence of health benefit from artificial neural networks in medical intervention. *Neural Network* 2002; **15**: 11-39

Science Editor Kumar M **Language Editor** Elsevier HK

PO Box 2345, Beijing 100023, China
www.wjgnet.com
wjg@wjgnet.com

ELSEVIER

World J Gastroenterol 2005;11(37):5874-5877
World Journal of Gastroenterology ISSN 1007-9327
© 2005 The WJG Press and Elsevier Inc. All rights reserved.

• *BRIEF REPORTS* •

Is adiponectin level a predictor of nonalcoholic fatty liver disease in nondiabetic male patients?

Haluk Sargin, Mehmet Sargin, Hülya Gozu, Asuman Orcun, Gülcan Baloglu, Murat Ozisik, Mesut Seker, Oya Uygur-Bayramicli

Haluk Sargin, Mehmet Sargin, Hülya Gozu, Asuman Orcun, Gülcan Baloglu, Murat Ozisik, Mesut Seker, Oya Uygur-Bayramicli, Departments of Endocrinology and Diabetes, Biochemistry, Internal Medicine and Gastroenterology, Kartal Education and Research Hospital, Istanbul, Turkey
Correspondence to: Mehmet Sargin, Çakmak Mah. Soyak Yenisehir Palmiye Sitesi A-3 Blok Da: 20 Ümraniye, Istanbul, Turkey. sarginm@yahoo.com
Telephone: +90-216-3687811 Fax: +90-216-3684895
Received: 2004-11-15 Accepted: 2005-02-18

Abstract

AIM: To study the levels of adiponectin in nondiabetic patients with nonalcoholic fatty liver disease (NAFLD) in comparison with control group.

METHODS: Thirty-five patients who had elevated serum aminotransferase levels with bright liver and 34 healthy volunteers without liver disease were evaluated. Age, gender and body mass index (BMI) were recorded. Fasting plasma glucose, insulin, adiponectin, proinsulin and lipid profile were measured. A standard oral glucose tolerance test (OGTT) with insulin response was performed and the index of insulin resistance was calculated according to the homeostasis model assessment (HOMA) method.

RESULTS: According to the OGTT results, none of the participants had diabetes. Serum adiponectin levels were statistically significantly lower in patients with NAFLD than in control group (8.14±3.4 μg/mL *vs* 12.4±9.4 μg/mL, respectively, $P<0.01$). A statistically significant correlation was found between adiponectin and BMI (r: -0.33, $P<0.01$), HOMA (r: -0.26, $P<0.05$), proinsulin (r: -0.32, $P<0.01$), AST (r: -0.25, $P<0.05$), ALT (r: -0.26, $P<0.05$) or GGT (r: -0.22, $P<0.05$). In multiple regression analysis models, adiponectin levels were the only predictor of NAFLD in males, whereas in female group it was the BMI.

CONCLUSION: Low adiponectin level might be a predictor of NAFLD especially in male nondiabetics.

© 2005 The WJG Press and Elsevier Inc. All rights reserved.

Key words: Nonalcoholic fatty liver disease; Adiponectin; Gender

Sargin H, Sargin M, Gozu H, Orcun A, Baloglu G, Ozisik M, Seker M, Uygur-Bayramicli O. Is adiponectin level a predictor of nonalcoholic fatty liver disease in nondiabetic male patients? *World J Gastroenterol* 2005; 11(37): 5874-5877
http://www.wjgnet.com/1007-9327/11/5874.asp

INTRODUCTION

The growing epidemic of obesity has led to many studies on the role of adipose tissue as an endocrine organ that secretes many factors termed as adipokines, which mediate many of the vascular and metabolic complications of adiposity. These products, namely free fatty acids, TNF-α, interleukins, resistin, and leptin reduce insulin sensitivity[1-3].

Adiponectin is a plasma protein, which is secreted from adipose tissue, and serum levels are markedly reduced in obesity. Adiponectin levels are negatively correlated with body fat percent, central fat distribution, fasting plasma insulin, oral glucose tolerance and positively with glucose disposal during euglycemic insulin clamp[3-7]. It has two receptors; adipoR1 is abundantly expressed in skeletal muscle and at moderate levels in other tissues, whereas adipoR2 is predominantly expressed in the liver[8-10].

Adiponectin is a hepatic insulin sensitizer and also an inhibitor of tumor necrosis factor and therefore we studied its levels in nondiabetic patients with nonalcoholic fatty liver disease (NAFLD) and compared the results with healthy volunteers and looked for the effect of gender on adiponectin levels.

MATERIALS AND METHODS

Thirty-five patients admitted to the Department of Gastroenterology at Kartal Education and Research Hospital with elevated serum aminotransferase levels for longer than 6 mo and bright liver on ultrasound scan were included in this study. Thirty-four healthy volunteers without liver disease, who were gender and age matched with study group, were enrolled as the control group. Patients were excluded from this cohort if one of the following criteria was present: hepatitis B (hepatitis B surface antigen, antibody to hepatitis surface antigen, antibody to hepatitis B core antigen), hepatitis C (antibody to hepatitis C virus) and Epstein-Barr virus infection, non-organ specific autoantibodies (antimitochondrial antibody, antinuclear antibody, antismooth muscle antibody, and anti-liver/kidney microsomal antibody), hereditary defects (fasting serum iron, transferrin saturation, ferritin, ceruloplasmin, alpha-1-antitripsin levels), alcohol consumption (ethanol ingestion >20 g/d), use of amiodarone, corticosteroids, tamoxifen, methotrexate, or oral contraceptives, jejunoileal bypass or extensive small bowel resection, total parenteral nutrition, malignancy, hypo-hyperthyroid disease, pregnancy, other known liver diseases like cirrhosis and diabetes. The diagnosis of cirrhosis was based on the clinical and laboratory findings (hypoalbuminemia, prolongation of prothrombin time, hyperbilirubinemia, presence of ascites or other findings of portal hypertension). The absence of

diabetes was confirmed with oral glucose tolerance test (OGTT) in both groups.

The absence of liver disease in the control group was established based on clinical, laboratory and imaging criteria. All controls had normal liver biochemistries and lack of any evidence from physical examination of chronical liver disease. However, an abdominal ultrasound was performed to exclude bright liver in all of the controls. All subjects gave informed consent to take part in the study.

Age, gender, height, weight, and body mass index (BMI) were recorded. Fasting plasma glucose, insulin, proinsulin, lipid profile, uric acid, and serum proteins were measured. Adiponectin levels were measured by Adiponectin Human ELISA Kit. A standard 75 g OGTT with insulin response according to WHO criteria was performed on all patients.

The index of insulin resistance (IR) was calculated on the basis of fasting values of plasma glucose and insulin, according to the homeostasis model assessment (HOMA) method.

Ultrasound liver studies were carried out by the same experienced radiologist who was blinded to laboratory values. The diagnosis of bright liver was based on abnormally intense, high-level echoes arising from the hepatic parenchyma, with amplitude similar to that of echoes arising from the diaphragm.

Statistical analysis

Statistical analysis was performed with SPSS 11.5 program. Any *P* value less than 0.05 was considered statistically significant. Results are expressed as mean±SD. Comparison between the two groups was made with Student's *t*-test and Mann-Whitney *U* test. Pearson's and Spearman's rank correlations were used to detect the associations between serum adiponectin and various demographic, anthropometric, and metabolic variables. When necessary, multiple regression analysis was performed.

RESULTS

Demographic, anthropometric, metabolic, and laboratory characteristics of patients with NAFLD and their matched controls are shown in Table 1.

According to the OGTT results, none of the participants had diabetes. However, six patients in NAFLD group and three patients in control group had impaired glucose tolerance ($P>0.05$). The remaining had normal glucose tolerance.

Insulin (fasting, 60 and 120 min), HOMA, proinsulin and c-peptide levels were statistically significantly higher in NAFLD group than in control group (Table 2).

Serum adiponectin levels were statistically significantly lower in patients with NAFLD than in the control group (8.14±3.4 μg/mL *vs* 12.41±9.4 μg/mL, respectively, $P<0.01$; Table 2). A statistically significant correlation was found between adiponectin and BMI (r: -0.33, $P<0.01$), HOMA (r: -0.26, $P<0.05$), proinsulin (r: -0.32, $P<0.01$), AST (r: -0.25, $P<0.05$), ALT (r: -0.26, $P<0.05$) or GGT (r: -0.22, $P<0.05$). In multiple regressions analysis, gender was found to be a predictor of adiponectin but not the age and BMI (Table 3).

When we subclassified the patient and the control group according to gender, the adiponectin levels were found to be low in males compared to females ($P<0.05$). But there was no statistically significant difference in age, BMI, HOMA, and proinsulin between the subgroups of gender ($P>0.05$, Table 4). In multiple regression analysis, adiponectin levels were the only predictor of NAFLD in males (Table 5), whereas in female group it was the BMI (Table 6).

Table 1 Demographic, anthropometric, and biochemical measurements in NAFLD and control groups

	NAFLD (*n*: 35)	Controls (*n*: 34)	*P*
Age (yr)	39.1±7.8	36.1±6.0	NS
Gender (female/male)	20/15	20/14	NS
BMI (kg/m^2)	30.5±4.1	23.7±3.8	<0.001
Fasting glucose (mg/dL)	93±9	84±11	<0.01
Total cholesterol (mg/dL)	209±35	186±36	<0.01
HDL cholesterol (mg/dL)	50±12	51±12	NS
LDL cholesterol (mg/dL)	125±28	118±37	NS
Triglycerides (mg/dL)	177±100	103±57	<0.01
AST (IU/L)	36±10	18±5	<0.001
ALT (IU/L)	49±17	18±9	<0.001
GGT (IU/L)	43±16	16±8	<0.001

NS, nonsignificant.

Table 2 Comparison of IR parameters in NAFLD and control groups

	NAFLD (*n*: 35)	Controls (*n*: 34)	*P*
Fasting insulin (IU/L)	14.6±6.7	9.9±4.5	<0.01
Insulin 60 min (IU/L)	99.6±63.1	62.4±43.2	<0.01
Insulin 120 min (IU/L)	65.3±49	40.2±31.9	<0.01
HOMA index	3.3±1.5	2.1±1.1	<0.001
Proinsulin (pmol/L)	10.6±6.4	6.2±4.5	<0.001
C-peptide (ng/mL)	2.7±0.7	2.0±0.6	<0.001
Adiponectin (μg/mL)	8.14±3.4	12.41±9.4	<0.01

Table 3 Regression model of adiponectin as a dependent variable

Independent variables	*T*	Significance
Gender (male)	–2.791	0.009
Age (yr)	0.774	NS
BMI (kg/m^2)	–0.523	NS

NS, nonsignificant.

Table 4 Comparison of male and female patients in both NAFLD and control groups

	Female (*n:* 40)	Male (*n*: 29)	*P*
Age (yr)	37.0±7.1	38.6±7.1	NS
BMI (kg/m^2)	27.5±5.8	26.9±4.5	NS
HOMA	2.6±1.4	2.8±1.4	NS
Adiponectin (μg/mL)	11.7±8.9	8.2±3.3	0.025

NS, nonsignificant.

Table 5 Regression model of NAFLD as a dependent variable in

males

Independent variables	*B*	Exp (*B*)	Significance
Adiponectin (μg/mL)	0.466	1.593	0.045
Age (yr)	–0.086	0.918	NS
BMI (kg/m^2)	–0.237	0.789	NS
HOMA	–0.068	0.934	NS

NS, nonsignificant.

Table 6 Regression model of NAFLD as a dependent variable in females

Independent variables	*B*	Exp (*B*)	Significance
BMI (kg/m^2)	–0.505	0.972	0.007
Age (yr)	–0.028	0.604	NS
HOMA	–0.097	0.908	NS
Adiponectin (μg/mL)	0.003	1.003	NS

NS, nonsignificant.

DISCUSSION

Cytokines are mediators of cellular communication produced by multiple liver cell types such as Kupffer cells, stellate cells, hepatocytes and endothelial cells. Cytokines can directly induce necrosis or apoptosis. Increased levels of hepatotoxic cytokines such as tumor necrosis factor-α are documented in alcoholic liver disease and nonalcoholic steatohepatitis and have been shown to play a mechanistic role in both of these processes. There are also beneficial cytokines, such as interleukin (IL-10 and IL-6). Adiponectin, one of the beneficial cytokines, is made outside the liver and appear to protect against liver damage[11-13]. Adiponectin is an important adipokine specifically secreted by adipocytes that circulates at relatively high levels in the bloodstream[1]. Plasma levels of adiponectin are reduced in obese rodents and humans, as well as in humans with type 2 diabetes. It has been suggested that adiponectin might function as an adipostat in regulating energy balance and that its deficiency might contribute to the development of obesity and type 2 diabetes[14,15].

It has been shown that increased hepatic fat content is associated with hepatic IR in type 2 diabetic patients and IR was found in 85% of these patients by Willner *et al*.[16]. Insulin resistance and systemic hypertension features of the metabolic syndrome are also independently associated with advanced forms of NAFLD[17,18]. In our study, hyperinsulinemia was present in all the patients and a high value of HOMA index in NAFLD patients is present in comparison to control group which is an index of IR.

The euglycemic-hyperinsulinemic clamp is accepted as the gold standard in defining the IR, but it is difficult to perform and time consuming and can be used only in studies with limited number of patients. Therefore, we preferred to use HOMA, which is easy to perform and it has been shown that it is in correlation with the euglycemic-hyperinsulinemic clamp (*R*: 0.88, *P*<0.0001; *R*: 0.85, *P*<0.0001 and *R*: 0.73, *P*<0.0001). A literature search using Medline found that the use of the HOMA model has been reported in 572 published works. In >50% of reports, the model is used in nondiabetic populations[19-21].

For the diagnosis of NAFLD, we used the exclusion of known etiological factors, which are responsible for the liver disease and ultrasound examination. Liver biopsy was not done because the stage and grade of the NAFLD was not of importance in this study and according to Saverymuttu *et al*., ultrasound examinations can accurately identify steatosis with a sensitivity of 94% and a specificity of 84%[22]. Ricci *et al*., also demonstrated that standard ultrasonography may be used for the diagnosis of NAFLD[23].

In NAFLD, most of the liver damage in insulin-resistant and dyslipidemic patients is thought to be caused by accumulation of hepatic triglycerides, and adiponectin might be able to preserve liver function by preventing lipid accumulation in hepatocytes. Adiponectin is also a potent insulin sensitizer and modulates the inflammatory response[2,17,24-26]. In our study, low adiponectin levels in NAFLD patients are compatible with previous studies.

Adiponectin was found to circulate in inverse proportion to IR syndrome such as BMI, fasting glucose and triglycerides[15,25,27,28]. In our study, we also found an inverse correlation between adiponectin levels with BMI, insulin, HOMA, proinsulin and triglycerides.

A recent study showed that adiponectin levels are correlated in healthy humans with various liver function tests such as ALT and GGT[2]. We also found a statistically significant correlation between adiponectin and liver function tests like AST, ALT, and GGT.

This is the first study looking for adiponectin levels in nondiabetic NAFLD patients. Bajaj *et al*., demonstrated a relationship between plasma adiponectin levels with hepatic insulin sensitivity and hepatic fat content in patients with type 2 diabetes, for the first time[14]. Yamamoto *et al*., have reported that adiponectin predicts future IR in a Japanese population in a 2-year follow-up study[4].

In our study, it is remarkable that in males, NAFLD is definitely correlated with low adiponectin levels but the female gender did not show such a correlation. This gender predilection might be due to the correlation of low adiponectin with visceral adiposity in females.

As a summary, adiponectin level is lower in nondiabetic patients with NAFLD in comparison to healthy volunteers. Low adiponectin level might be a predictor of NAFLD especially in male nondiabetics.

REFERENCES

1 **Goldstein BJ,** Scalia R. Adiponectin: A Novel Adipokine Linking Adipocytes and Vascular Function. *JCEM* 2004; **89**: 2563-2568

2 **Bermejo AL,** Botas P, Funahashi T, Delgado E, Kihara S, Ricart W, Fernandez-Real JM. Adiponectin, hepatocellular dysfunction and insulin sensitivity. *Clinical Endocrinol* 2004; **60**: 256-263

3 **Ouchi N,** Kihara S, Arita Y, Maeda K, Kuriyama H, Okamoto Y, Hotta K, Nishida M, Takahashi M, Nakamura T, Yamashita S, Funahashi T, Matsuzawa Y. Novel modulator for endothelial adhesion molecules: adipocyte-derived plasma protein adiponectin. *Circulation* 1999; **100**: 2473-2476

4 **Yamamoto Y,** Hirose H, Saito I, Nishikai K, Saruta T. Adiponectin, an adipocyte-derived protein, predicts future insulin resistance: Two-year follow-up study in Japanase population. *JCEM* 2004; **89**: 87-90

5 **Hotta K,** Funahashi T, Arita Y, Takahashi M, Matsuda M,

Okamoto Y, Iwahashi H, Kuriyama H, Ouchi N, Maeda K, Nishida M, Kihara S, Sakai N, Nakajima T, Hasegawa K, Muraguchi M, Ohmoto Y, Nakamura T, Yamashita S, Hanafusa T, Matsuzawa Y. Plasma concentrations of a novel, adipose-specific protein, adiponectin, in type 2 diabetic patients. *Arterioscler Thromb Vasc Biol* 2000; **20**: 1595-1599

6 **Matsuzawa Y,** Funahashi T, Kihara S, Shimomura I. Adiponectin and metabolic syndrome. *Arteriscler Thromb Vasc Biol* 2004; **24**: 29-33

7 **Pittas AG,** Joseph NA, Greenberg AS. Adipocytokines and insulin resistance. *J Clin Endocrinol Metab* 2004; **89**: 447-452

8 **Yamauchi T,** Kamon J, Ito Y, Tsuchida A, Yokomizo T, Kita S, Sugiyama T, Miyagishi M, Hara K, Tsunoda M, Murakami K, Ohteki T, Uchida S, Takekawa S, Waki H, Tsuno NH, Shibata Y, Terauchi Y, Froguel P, Tobe K, Koyasu S, Taira K, Kitamura T, Shimizu T, Nagai R, Kadowaki T. Cloning of adiponectin receptors that mediate antidiabetic metabolic effects. *Nature* 2003; **423**: 762-769

9 **Yamauchi T,** Kamon J, Minokoshi Y, Ito Y, Waki H, Uchida S, Yamashita S, Noda M, Kita S, Ueki K, Eto K, Akanuma Y, Froguel P, Foufelle F, Ferre P, Carling D, Kimura S, Nagai R, Kahn BB, Kadowaki T. Adiponectin stimulates glucose utilization and fatty-acid oxidation by activating AMP-activated protein kinase. *Nat Med* 2002; **8**: 1288-1295

10 **Tomas E,** Tsao TS, Saha AK, Murrey HE, Zhang Cc C, Itani SI, Lodish HF, Ruderman NB. Enhanced muscle fat oxidation and glucose transport by ACRP30 globular domain: acetyl-CoA carboxylase inhibition and AMP-activated protein kinase activation. *Proc Natl Acad Sci USA* 2002; **99**: 16309-16313

11 **Song Z,** Joshi-Barve S, Barve S, Mc Clain CJ. Advances in alcoholic liver disease. *Curr Gastroenterol Rep* 2004; **6**: 71-76

12 **Xu A,** Wang Y, Keshaw H, Xu LY, Lam KS, Cooper GJ. The fat-derived hormone adiponectin alleviates alcoholic and nonalcoholic fatty liver diseases in mice. *J Clin Invest* 2003; **112**: 91-100

13 **Tilg H,** Diehl AM. Cytokines in alcoholic and nonalcoholic steatohepatitis. *New Engl J Med* 2000; **343**: 1467-1476

14 **Bajaj M,** Suraamornkul S, Piper P, Hardies LJ, Glass L, Cersosimo E, Pratipanawatr T, Miyazaki Y, Defronzo RA. Decreased plasma adiponectin concentrations are closely Related to hepatic Fat content and hepatic Insulin resistance in pioglitazone-treated type 2 diabetic patients. *JCEM* 2004; **89**: 200-206

15 **Weyer C,** Funanashi T, Tanaka S, Hotta K, Matsuzawa Y, Pratley RE, Tatarani PA. Hypoadiponectinemia in obesity and type 2 diabetes: close association with insulin resistance and hyperinsulinemia. *J Clin Endocrinol Metab* 2001; **86**: 1930-1935

16 **Willner IR,** Waters B, Patil SR, Reuben A, Morelli J, Riely CA. Ninety patients with nonalcoholic steatohepatatitis: insulin resistance, familial tendency and severity of disease. *Am J Gastroenterol* 2001; **96**: 2813-2814

17 **Angulo P.** Nonalcoholic fatty liver disease. *N Engl J Med* 2002; **346**: 1221- 1231

18 **Dixon JB,** Bhathal PS, O'Brien PE. Nonalcoholic fatty liver disease: predictors of nonalcoholic steatohepatitis and liver fibrosis in the severely obese. *Gastroenterology* 2001; **121**: 91-100

19 **Matthews DR,** Hosker JP, Rudenski AS, Naylor BA, Treacher DF, Turner RC. Homeostasis model assessment: insulin resistance and beta-cell function from fasting plasma glucose and insulin concentrations in man. *Diabetologia* 1985; **28**: 412-419

20 **Bonora E,** Targher G, Alberiche M, Bonadonna RC, Saggiani F, Zenere MB, Monauni T, Muggeo M. Homeostasis model assessment closely mirrors the glucose clamp technique in the assessment of insulin sensitivity. *Diabetes Care* 2000; **23**: 57-63

21 **Wallace TM,** Levy JC, Mathews DR. Use and Abuse of HOMA modelling. *Diabetes Care* 2004; **27**: 1487-1495

22 **Saverymuttu SH,** Joseph AE, Maxwell JD. Ultrasound scanning in the detection of hepatic fibrosis and steatosis. *BMJ* 1986; **292**: 13-15

23 **Ricci C,** Longo R, Gioulis E, Bosco M, Polesello P, Masutti F, Croce LS, Paoletti S, de Bernard B, Tiribelli C, Dalla Palma L. Noninvasive *in vivo* quantitative assessment of fat content in human liver. *J Hepatol* 1997; **27**: 108-113

24 **Lindsay RS,** Funahashi T, Hanson RL, Matsuzawa Y, Tanaka S, Tataranni PA, Knowler WC, Krakoff J. Adiponectin and development of type 2 diabetes in the Pima Indian population. *Lancet* 2002; **360**: 57-58

25 **Stefan N,** Vozarova B, Funahashi T, Matsuzawa Y, Weyer C, Lindsay RS, Youngren JF, Havel PJ, Pratley RE, Bogardus C, Tataranni PA. Plasma adiponectin concentrations associated with skeletal muscle insulin receptor tyrosine phosphorylation, and low plasma concentration precedes a decrease in whole-body insulin sensitivity in humans. *Diabetes* 2002; **51**: 1884-1888

26 **Spranger J,** Kroke A, Möhlig M, Bergmann MM, Ristow M, Boeing H, Pfeiffer AF. Adiponectin and protection against type 2 diabetes mellitus. *Lancet* 2003; **361**: 226-228

27 **Tshritter O,** Fritsche A, Thamer C, Haap M, Shirkavand F, Rahe S, Staiger H, Maerker E, Haring H, Stumvoll M. Plasma adiponectin concentrations predict insulin sensitivity of both glucose and lipid metabolism. *Diabetes* 2003; **52**: 239-243

28 **Hotta K,** Funahashi T, Bodkin NL, Ortmeyer HK, Arita Y, Hansen BC, Matsuzawa Y. Circulating concentrations of the adipocyte protein adiponectin are decreased in parallel with reduced insulin sensitivity during the progression to the type 2 diabetes in rhesus monkeys. *Diabetes* 2001; **50**: 1126-1133

Science Editor Wang XL and Guo SY **Language Editor** Elsevier HK

PO Box 2345, Beijing 100023, China
www.wjgnet.com
wjg@wjgnet.com

ELSEVIER

World J Gastroenterol 2005;11(37):5878-5881
World Journal of Gastroenterology ISSN 1007-9327
© 2005 The WJG Press and Elsevier Inc. All rights reserved.

• *BRIEF REPORTS* •

Comparison of a monoclonal antigen stool test (Hp StAR) with the ^{13}C-urea breath test (UBT) in monitoring *Helicobacter pylori* eradication therapy

Francesco Perri, Michele Quitadamo, Rosalba Ricciardi, Ada Piepoli, Rosa Cotugno, Annamaria Gentile, Alberto Pilotto, Angelo Andriulli

Francesco Perri, Michele Quitadamo, Rosalba Ricciardi, Ada Piepoli, Rosa Cotugno, Annamaria Gentile, Angelo Andriulli, Department of Internal Medicine, Gastroenterology Unit, "Casa Sollievo della Sofferenza" Hospital, IRCCS, San Giovanni Rotondo, Italy
Alberto Pilotto, Department of Internal Medicine, Geriatrics Unit, "Casa Sollievo della Sofferenza" Hospital, IRCCS, San Giovanni Rotondo, Italy
Co-first-author: Michele Quitadamo
Correspondence to: Professor Francesco Perri, "Casa Sollievo della Sofferenza" Hospital, IRCCS, San Giovanni Rotondo, Italy. f.perri@operapadrepio.it
Telephone: +39-882-410568 Fax: +39-882-411879
Received: 2004-11-21 Accepted: 2004-12-20

Abstract

AIM: To evaluate the agreement between a mAb-based stool test (HP StAR) and the urea breath test (UBT) in monitoring (*H pylori*) infection after eradication therapy.

METHODS: Patients with discordant results on UBT and Hp StAR underwent endoscopy with biopsies for rapid urease test, culture, and histology to confirm *H pylori* status.

RESULTS: Among 250 patients (50±14 years), 240 (96.0%) had concordant UBT and Hp StAR tests with a significant correlation between DOB and *A* values ($R = 0.87$; $P<0.0001$). The remaining 10 (4.0%) patients had discordant tests (positive Hp StAR and negative UBT) with the Hp StAR inaccurate in five cases (false positive) and UBT inaccurate in the other five cases (false negative). The "maximal expected" sensitivity, specificity, +PV, -PV, +LR, and -LR were 91%, 100%, 100%, 97.4%, ∞, and 8.2 respectively, for the UBT, and 100%, 97.4%, 91%, 100%, 38.8, and 0, respectively, for the Hp StAR. Overall accuracy for both tests was 98%.

CONCLUSION: Both the UBT and the Hp StAR are equally accurate in monitoring *H pylori* infection. Nowadays, the choice of the "best" non-invasive *H pylori* test in the post-treatment setting should be done not only in terms of diagnostic accuracy but also in view of cost and local facilities.

© 2005 The WJG Press and Elsevier Inc. All rights reserved.

Key words: Diagnosis; *Helicobacter pylori*; Stool antigen test; Urea breath test

Perri F, Quitadamo M, Ricciardi R, Piepoli A, Cotugno R, Gentile A, Pilotto A, Andriulli A. Comparison of a monoclonal antigen stool test (Hp StAR) with the ^{13}C-urea breath test (UBT) in monitoring *Helicobacter pylori* eradication therapy. *World J Gastroenterol* 2005; 11(37): 5878-5881
http://www.wjgnet.com/1007-9327/11/5878.asp

INTRODUCTION

Several non-invasive methods of testing for *Helicobacter pylori* (*H pylori*) have been developed and routinely used in clinical practice. They are based on: (1) the detection of ^{13}C- or ^{14}C-labeled CO_2 in expired air as a result of *H pylori* urease activity (^{13}C- or ^{14}C-UBT)[1,2], (2) the detection of antibodies in serum (serology)[3], saliva[4], and urine[5], and (3) the detection of *H pylori* antigens in stool[6]. Until now, the UBT has been considered to be the most reliable non-invasive test for the diagnosis of *H pylori* infection with an overall accuracy approaching 95% in both untreated and treated patients[7]. However, concerns regarding the cost of ^{13}C-urea, the radiological hazards of ^{14}C-urea, and the local availability of either mass spectrometers or β-counters induced clinicians to search for new alternative tests. Serological tests have been extensively used in the past but the diagnostic accuracy is no longer adequate to justify their clinical use. Stool antigen tests have proven to be reliable in the diagnosis of *H pylori* infection. In the previous years, mAb-based stool tests have been developed and introduced in clinical practice[8,9]. Sensitivity values ranged from 88% to 99% in pre-treatment setting and from 89% to 100% in post-treatment setting[10]. Concerning the specificity, values ranged from 92% to 99% in pre-treatment setting and from 95% to 100% in post-treatment setting[10]. The encouraging results obtained with mAb-based stool tests in post-treatment setting raise an important question: should the UBT be still considered on either clinical or economical ground as the most suitable non-invasive test for monitoring *H pylori* infection after treatment? Aim of this prospective, controlled, single-center study was to evaluate the agreement between the UBT and a commercially available mAb-based stool test in patients after *H pylori* eradication treatment in order to determine which of the two tests should be recommended in clinical practice.

MATERIALS AND METHODS

Consecutive outpatients, who were referred to our Center for non-invasively monitoring *H pylori* infection after a first-line or a second-line eradication treatment, were considered for recruitment into this study. Patients were prospectively interviewed on past medical history, smoking habits, and alcohol intake. Exclusion criteria were treatment with antibiotics, H_2-receptor antagonists, bismuth, or PPI in the 4 wk preceding the study, previous gastric surgery, severe renal or liver diseases, and malabsorption syndromes. All patients gave their informed consent to participate and the study was approved by the Ethical Committee of our institution.

Study design

At 4-6 wk after completion of eradication therapy, patients underwent both ^{13}C-UBT and antigen stool test. The UBT was performed with 75 mg ^{13}C-urea. Breath samples were taken before and 30 min after ingestion of the urea. The ^{13}C-enrichment in breath was determined by IRMS. The UBT was considered positive if the d-value over baseline (DOB) at 30 min was >5‰. On the same day of UBT, patients collected stool from the toilet paper or bowl into an airtight container. Stool specimens were analyzed for *H pylori* antigen using a sandwich-type enzyme immunoassay (Hp StAR, DakoCytomation, Milan, Italy), as described by the manufacturer. The results were analyzed by spectrophotometry. The absorbance was read at 450 nm and expressed as optical density (*A*). Specimens with absorbance values >0.19 were considered positive. Patients with concordant tests did not undergo further investigation. Patients with discordant tests were endoscoped with multiple biopsies (three from antrum and three from corpus) for rapid urease test (Cp-test, Yamanouchi, Milan, Italy), culture (Biomerieux Pylori, BioMerieux, Marseille, France), and histology (H&E and Giemsa).

Patient sample size

In the post-treatment setting, a sensitivity and specificity of 94% and 95% for the UBT and 95% and 98% for mAb-based stool tests have been reported[7]. Consequently, 4% and 1.2% of patients are expected to show a false positive or negative result on UBT, respectively, as compared to 1.6% and 1.0% of patients on stool test. In our study, the percentage of patients with discordant UBT and stool test was expected to range from 2.6% (5.2-2.6%) to 7.8% (5.2+2.6%) with a mean value of 5.2%. We assumed that at least 10 patients with discordant results would have been sufficient to evaluate the agreement between the UBT and the Hp StAR results. By taking into account a drop out rate of 20% (patients unwilling to undergo endoscopy), we decided that at least 13 patients with discordant results would have been evaluated. Therefore, the minimal sample size of patient population was 250 (13/5.2%).

Statistical analysis

Patients were considered as still infected if at least one of the biopsy-based tests was positive. Conversely, they were regarded as successfully eradicated if all the three tests were negative. Patients were sorted into two groups according to UBT and Hp StAR results: one group with concordant and the other with discordant results. Univariate analysis (*t*-test or χ^2-test) was carried out between the two groups for age, sex, smoking, alcohol consumption, and type of treatment. A *P*-value less than 0.05 was considered statistically significant. Linear regression analysis was carried out in the group of patients with concordant results to search for a significant correlation between UBT and Hp StAR results. Logistic analysis was performed to identify the factors determining discordance of test results. Finally, the "maximal expected" values of sensitivity, specificity, positive and negative predictive values, positive and negative likelihood ratios, and diagnostic accuracy were calculated for UBT and Hp StAR.

Funding

Stool kits were kindly provided by the manufacturer (DakoCytomation, Milan, Italy) who had no role in the collection, analysis and interpretation of the data. There was no other funding source.

RESULTS

Study population

Overall, 266 patients were asked to participate in this study but 16 (6%) refused to collect stool and were not included; 250 patients (50±14 years; range: 17-92 years; 113 males) were enrolled and none of them were excluded from the final analysis because of insufficient stool or breath collection. There were 75 (30%) smokers and 48 (19.3%) subjects reported alcohol consumption of more than 40 g daily. First-line eradication treatments were the "Maastricht therapy" (i.e., PPI with clarithromycin and either amoxicillin or metronidazole for 7 d) in 149 (59.6%) patients[11], and the 10-d sequential therapy proposed by Zullo *et al*., (i.e., PPI and amoxicillin for the first 5 d followed by PPI, clarithromycin, and tinidazole for the remaining 5 d) in 45 (18%) patients[12]. The quadruple therapy (i.e., PPI, bismuth citrate, tetracycline, and metronidazole for 7 d) was the second-line treatment used by the remaining 56 (22.4%) patients who were still *H pylori* positive after one course of the standard "Maastricht therapy".

UBT and stool test results

UBT and Hp StAR were concordant in 240 (96%) patients (189 negative and 51 positive) and discordant in the remaining 10 (4%, Table 1). All 10 patients tested positive on Hp StAR and negative on UBT. All patients with discordant results agreed to undergo endoscopic examination. After endoscopy was done, 5 out of 10 (50%) patients were classified as *H pylori* positive, and 5 (50%) *H pylori* negative. Compared with the gold standard biopsy-based tests, the Hp StAR was inaccurate in five cases (five false positive) and the UBT in the other five cases (five false negative). No coccoid forms were detected in the five patients with negative UBT and positive Hp StAR.

The absolute values of sensitivity and specificity for UBT and Hp StAR were not calculated since all patients, including those with concordant UBT and Hp StAR tests, would have undergone endoscopy with multiple biopsies.

Table 1 UBT and Hp StAR results in study population. Biopsy-based tests were performed only in patients with discordant UBT and Hp StAR results

Pts	DOB (POS>5)	*A* (POS>0.19)	Histology	Culture	RUT	Hp status
189 pts	0.01–2.53	0.03–0.17	np	np	np	NEG
Pt162	1.11	0.25	NEG	NEG	NEG	NEG
Pt177	0.74	0.26	NEG	NEG	NEG	NEG
Pt97	0.28	0.30	NEG	NEG	NEG	NEG
Pt98	1.52	0.33	NEG	NEG	NEG	NEG
Pt96	0.73	0.34	NEG	NEG	NEG	NEG
Pt179	0.11	0.29	POS	POS	NEG	POS
Pt223	0.31	0.30	POS	NEG	POS	POS
Pt201	1.07	0.34	POS	POS	NEG	POS
Pt72	3.56	0.61	NEG	POS	POS	POS
Pt47	4.24	0.23	POS	NEG	POS	POS
51 pts	6.81–86.15	0.23–2.93	np	np	np	POS

However, we extrapolated the "maximal expected" sensitivity, specificity, positive and negative predictive values, and positive and negative likelihood ratios (Table 2). The diagnostic accuracy for both tests was 98% (95%CI and 95.8-98.0%).

Both univariate and logistic analyses showed that patients with discordant results were not significantly different from those with concordant results as far as age, sex, smoking, alcohol consumption, and type of treatment were considered.

In patients with concordant results, a significant correlation (DOB = -0.42+14.9×A; R = 0.87, P<0.0001) was found between DOB and A values (Figure 1).

Table 2 Diagnostic accuracy of UBT and Hp StAR

	UBT	Hp StAR
Sensitivity		
Sens = TP/(TP+FN)	91.8 (87.4–91.8)	100 (95.2–100)
Specificity		
Spec = TN/(TN+FP)	100 (98.6–100)	97.4 (96–97.4)
Positive predictive value		
+PV = TP/(TP+FP)	100 (95.2–100)	91.8 (87.4–91.8)
Negative predictive value		
–PV = TN/(TN+FN)	97.4 (96–97.4)	100 (98.6–100)
Positive likelihood ratio		
+LR = Sens/(100–Spec)	∞ (60.9–∞)	38.8 (23.2–38.8)
Negative likelihood ratio		
–LR = (100–Sens)/Spec	8.2 (8.2–12.8)	0 (0–0.05)

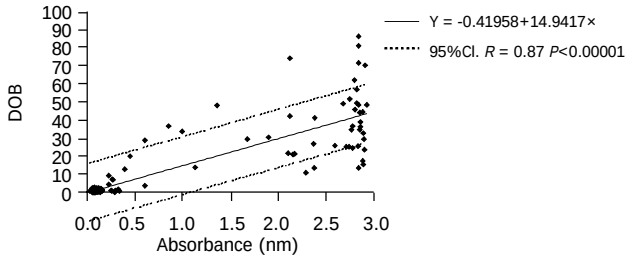


Figure 1 Correlation between UBT and Hp StAR results.

DISCUSSION

The UBT and the Hp StAR test are currently considered to be the only reliable non-invasive tests for monitoring *H pylori* infection[13]. The diagnostic accuracy is reportedly high, although some doubt still exists in the post-treatment setting since non-uniform results on the diagnostic accuracy of the stool test have been reported[14,15]. In a previous work, we found that the UBT and the antigen stool test were discordant or indeterminate in nearly 8% of patients after treatment[16]. This finding was mainly due to a lower diagnostic accuracy of stool test *vs* the UBT with the ratio between false UBT and stool test results of 1:6. The polyclonal antibody of the stool test (Premier Platinum HpSA test, Meridian Diagnostics, Cincinnati, OH, USA) used in that study could have been responsible for this disappointing result.

The present study was designed to evaluate the discordance rate between UBT and stool test results in the post-treatment setting by using a mAb-based stool test. Our results show that the UBT and Hp StAR results are discordant in 4% of patients. Nevertheless, the overall diagnostic accuracy of UBT and Hp StAR is identical (i.e., 98%) with the ratio between false UBT and stool test results of 1:1. Interestingly, we found that the Hp StAR is more sensitive than the UBT in monitoring *H pylori* infection with a higher negative predictive value. This finding is extremely important to assess the true eradication of the bacterium after antibiotic treatment and to definitely reassure patients on treatment effectiveness. Since mAb-based techniques generally have a high specificity, it is unclear why false positive results on Hp StAR test occurred in the post-treatment setting. The principle on which non-invasive *H pylori* diagnostic tests rely are different: the UBT measures a metabolic function of the bacterium (i.e., its urease activity) in the stomach; the Hp StAR detects antigens shed from the microorganism in stool; biopsy-based tests detect the bacterium in gastric mucosal specimens. It would be tempting to speculate that - after eradication treatment - *H pylori* survive in very low concentration in extra-gastric "sanctuary sites" such as dental plaque[17], Merkel's diverticulum[18] or rectum[19] persist in stool even when the other tests become negative. Another reason for the false positivity of the stool test might be due to the fact that it may take a few days for *H pylori* antigens to move from the stomach to the rectum and stay in the rectum for a few more days. Consequently while the UBT becomes negative, their stool could be still positive.

mAb stool tests are available as either laboratory-based or in-office-based[20] diagnostic tests. Both tests have

shown - at least in the post-treatment setting - a diagnostic accuracy comparable with the UBT. Moreover, in-office stool tests have also the advantage of being suitable for the use at the doctor's office affording physicians to prescribe eradication therapy even during the same visit[20]. Consequently, we believe that the UBT should not be regarded as the most suitable non-invasive test for monitoring *H pylori* infection when compared with stool test. The choice of the best non-invasive *H pylori* test after treatment should be done not only in terms of diagnostic accuracy but also after careful evaluation of costs and local facilities. In this regard, monoclonal-based stool tests seem to be more cost-effective than the UBT. In fact, spectrophotometers are generally more available locally and cheaper than IRMS which also require appropriate technical setting to guarantee optimal ^{13}C-measurements and accurate UBT results[21]. Moreover, for some patient subgroups, such as infants[22], elderly[23] or handicapped people, and in some specific clinical conditions, such as gastrointestinal bleeding[24] or severe obstructive respiratory diseases, the stool test seems to be more suitable than the UBT.

Another interesting finding of our work is the high significant correlation between UBT and stool test results. Since several investigators have shown a correlation between UBT results and intragastric bacterial load, it could be hypothesized that mAb-based stool test results give also a semiquantitative measure of bacterial load in the stomach[25]. Further studies comparing stool tests results with histological data are warranted to confirm this finding.

In conclusion, both breath and mAb-based stool antigen tests are reliable non-invasive tests for monitoring *H pylori* infection. In comparison with the UBT, the Hp StAR seems to be more sensitive and cost-effective in the post-treatment setting and more appropriate in non-cooperating patients and in some clinical conditions such as gastrointestinal bleeding or difficult breath collection.

REFERENCES

1 **Graham DY,** Klein PD, Evans DJ Jr, Evans DG, Alpert LC, Opekun AR, Boutton TW. Campylobacter pylori detected noninvasively by the ^{13}C-urea breath test. *Lancet* 1987; **8543**: 1174-1177

2 **Marshall BJ,** Surveyor I. Carbon-14 urea breath test for the diagnosis of Campylobacter pylori associated gastritis. *J Nucl Med* 1988; **29**: 11-16

3 **Loy CT,** Irwig LM, Katelaris PH, Talley NJ. Do commercial serological kits for *Helicobacter pylori* infection differ in accuracy? A meta-analysis. *Am J Gastroenterol* 1996; **91**: 1138-1144

4 **Luzza F,** Imeneo M, Marasco A, Crotta S, Ierardi E, Usai P, Virgilio C, Nardone G, Marchi S, Sanna G, Perri F, Zagari MR, Bazzoli F. Evaluation of a commercial serological kit for detection of salivary immunoglobulin G to *Helicobacter pylori*: a multicentre study. *Eur J Gastroenterol Hepatol* 2000; **12**: 1117-1120

5 **Miwa H,** Hirose M, Kikuchi S, Terai T, Iwazaki R, Kobayashi O, Takei Y, Ogihara T, Sato N. How useful is the detection kit for antibody to *Helicobacter pylori* in urine (URINELISA) in clinical practice? *Am J Gastroenterol* 1999; **94**: 3460-3463

6 **Vaira D,** Malfertheiner P, Megraud F, Axon AT, Deltenre M, Hirschl AM, Gasbarrini G, O'Morain C, Garcia JM, Quina M, Tytgat GN. Diagnosis of *Helicobacter pylori* infection with a new non-invasive antigen-based assay. *Lancet* 1999; **354**: 30-33

7 **Vaira D,** Gatta L, Ricci C, Miglioli M. Review article. Diagnosis of *Helicobacter pylori* infection. *Alim Pharmacol Ther* 2002; **16**(Suppl 1): 16-23

8 **Leodolter A,** Peitz U, Ebert MP, Agha-Amiri K, Malfertheiner P. Comparison of two enzyme immunoassay or the assessment of *Helicobacter pylori* status in stool specimens after eradication therapy. *Am J Gastroenterol* 2002; **97**: 1682-1686

9 **Makristathis A,** Pasching E, Schutze K, Wimmer M, Rotter ML, Hirschl AM. Detection of *Helicobacter pylori* in stool specimens by PCR and antigen enzyme immunoassay. *J Clin Microbiol* 1998; **36**: 2772-2774

10 **Gisbert JP,** Pajares JM. Stool antigen test for the diagnosis of *Helicobacter pylori* infection: a systematic review. *Helicobacter* 2004; **9**: 347-368

11 **Malfertheiner P,** Megraud F, O'Morain C, Hungin AP, Jones R, Axon A, Graham DY, Tytgat G. European *Helicobacter pylori* Study Group (EHPSG). Current concepts in the management of *Helicobacter pylori* infection - the Maastricht 2-2000 Consensus Report. *Aliment Pharmacol Ther* 2002; **16**: 167-180

12 **Zullo A,** Vaira D, Vakil N, Hassan C, Gatta L, Ricci C, De Francesco V, Menegatti M, Tampieri A, Perna F, Rinaldi V, Perri F, Papadia C, Fornari F, Pilati S, Mete LS, Merla A, Poti R, Marinone G, Savioli A, Campo SM, Faleo D, Ierardi E, Miglioli M, Morini S. High eradication rates of *Helicobacter pylori* with a new sequential treatment. *Aliment Pharmacol Ther* 2003; **17**: 719-726

13 **Vaira D,** Holton J, Menegatti M, Ricci C, Gatta L, Geminiani A, Miglioli M. Review article: invasive and non-invasive tests for *Helicobacter pylori* diagnosis. *Alim Pharmacol Ther* 2000; **14** (Suppl 3): 13-22

14 **Trevisani L,** Sartori S, Galvani F, Rossi MR, Ruina M, Chiamenti C, Caselli M. Evaluation of a new enzyme immunoassay for detecting *Helicobacter pylori* in feces: a prospective pilot study. *Am J Gastroenterol* 1999; **94**: 1830-1833

15 **Masoero G,** Lombardo L, Della Monica P, Vicari S, Crocilla C, Duglio A, Pera A. Discrepancy between *Helicobacter pylori* stool antigen assay and urea breath test in the detection of *Helicobacter pylori* infection. *Dig Liver Dis* 2000; **32**: 285-290

16 **Perri F,** Manes G, Neri M, Vaira D, Nardone G. *Helicobacter pylori* antigen stool test and ^{13}C-urea breath test in patients after eradication treatments. *Am J Gastroenterol* 2002; **97**: 2756-2762

17 **Nguyen AM,** Engstrand L, Genta RM, Graham DY, el-Zaatari FA. Detection of *Helicobacter pylori* in dental plaque by reverse transcription-polymerase chain reaction. *J Clin Microbiol* 1993; **31**: 783-787

18 **Hill P,** Rode J. *Helicobacter pylori* in ectopic gastric mucosa in Meckel's diverticulum. *Pathology* 1998; **30**: 7-9

19 **Dye KR,** Marshall BJ, Frierson HF Jr, Pambianco DJ, McCallum RW. Campylobacter pylori colonizing heterotopic gastric tissue in the rectum. *Am J Clin Pathol* 1990; **93**: 144-147

20 **Gatta L,** Perna F, Ricci C, Osborn JF, Tampieri A, Bernabucci V, Miglioli M, Vaira D. A rapid immunochromatographic assay for *Helicobacter pylori* in stool before and after treatment. *Aliment Pharmacol Ther* 2004; **20**: 469-474

21 **Perri F,** Zagari RM, Uebersax JS, Quitadamo M, Bazzoli F. *Helicobacter pylori* sige study group on $^{13}CO_2$ measurement standardization. An inter- and intra-laboratory comparison of breath $^{13}CO_2$ analysis. *Aliment Pharmacol Ther* 2003; **17**: 1291-1297

22 **Oderda G,** Rapa A, Ronchi B, Lerro P, Pastore M, Staiano A. de Angelis GL, Strisciuglio P. Detection of *Helicobacter pylori* in stool specimens by non-invasive antigen enzyme immunoassay in children: a multicentre Italian study. *Br Med J* 2000; **320**: 347-348

23 **Pilotto A,** Salles N. *Helicobacter pylori* infection in geriatrics. *Helicobacter* 2002; **7**(Suppl 1): 56-62

24 **Gisbert JP,** Trapero M, Calvet X, Mendoza J, Quesada M, Guell M, Pajares JM. Evaluation of three different tests for the detection of stool antigens to diagnose *Helicobacter pylori* infection in patients with upper gastrointestinal bleeding. *Aliment Pharmacol Ther* 2004; **19**: 923-929

25 **Ellenrieder V,** Glasbrenner B, Stoffels C, Weiler S, Bode G, Moller P, Adler G. Qualitative and semi-quantitative value of a modified ^{13}C-urea breath test for identification of *Helicobacter pylori* infection. *Eur J Gastroenterol Hepatol* 1997; **9**: 1085-1089

Science Editor Guo SY **Language Editor** Elsevier HK

PO Box 2345, Beijing 100023, China
www.wjgnet.com
wjg@wjgnet.com

ELSEVIER

World J Gastroenterol 2005;11(37):5882-5887
World Journal of Gastroenterology ISSN 1007-9327
© 2005 The WJG Press and Elsevier Inc. All rights reserved.

• *BRIEF REPORTS* •

Interferon-α plus lamivudine *vs* lamivudine reduces breakthroughs, but does not affect sustained response in HBeAg negative chronic hepatitis B

Michalis Economou, Spilios Manolakopoulos, Thomas A Trikalinos, Spyros Filis, Sotiris Bethanis, Dimitrios Tzourmakliotis, Alec Avgerinos, Sotiris Raptis, Epameinondas V Tsianos

Michalis Economou, Spilios Manolakopoulos, Sotiris Bethanis, Dimitrios Tzourmakliotis, Department of Gastroenterology, Polyclinic General Hospital, Athens, Greece
Michalis Economou, Spyros Filis, Epameinondas V Tsianos, Hepato-Gastroenterology Unit, Department of Internal Medicine, University of Ioannina School of Medicine, Ioannina, Greece
Thomas A Trikalinos, Department of Hygiene and Epidemiology, University of Ioannina School of Medicine, Ioannina, Greece
Alec Avgerinos, 2nd Department of Gastroenterology, "Evangelismos" General Hospital, Athens, Greece
Alec Avgerinos, Sotiris Raptis, 2nd Department of Internal Medicine, Propaedeutic, Athens University, Athens, Greece
Correspondence to: Michalis Economou, MD, Department of Internal Medicine, University of Ioannina School of Medicine, University Campus, Ioannina 45110, Greece. meconom@cc.uoi.gr
Telephone: +30-26510-79501 Fax: +30-26510-99736
Received: 2004-12-04 Accepted: 2005-01-05

Abstract

AIM: The HBeAg negative form of chronic hepatitis B (CHB) predominates in the Mediterranean area and has a rising frequency in Europe and North America. At present there are three approved therapies for patients with CHB: interferon-α (IFN-α), lamivudine and adefovir dipivoxil. Unfortunately, none of these drugs are effective in achieving a sustained response in patients with HBeAg negative CHB. Therefore, new therapeutic approaches have been examined. Our aim was to investigate the efficacy of combination treatment of IFN-α and lamivudine compared to lamivudine monotherapy, after 24 mo of administration in HBeAg-negative hepatitis B patients.

METHODS: Fifty consecutive patients were randomly assigned to receive IFN-α-2b (5 MU thrice per week, $n = 24$) plus lamivudine (100 mg daily) or lamivudine only ($n = 26$) for 24 mo. Patients were followed up for further 6 mo. The primary outcome was the proportion with sustained virological response (undetectable serum HBV DNA concentrations) and or sustained biochemical response (transaminase levels within normal range) at 30 mo (6 mo after the end of therapy). Secondary end-points were timed from initial virological (biochemical) response to VBR (BBR, respectively) and the emergence of YMDD mutants across the two arms.

RESULTS: Five of twenty-four (21%) patients in the combination arm *vs* 3/26 (12%) in the lamivudine arm had sustained response (i.e., normal serum transaminase levels and undetectable HBV DNA by PCR assay) 6 mo after treatment discontinuation. A reduction in the emergence of YMDD mutants and in the development of virological breakthroughs was observed in patients receiving combination treatment (10% *vs* 46%, $P = 0.01$ and 14% *vs* 46%, $P = 0.03$, respectively). Time from initial virologic response to virologic breakthrough (VBR) was greater among initial responders receiving combination treatment compared to those receiving lamivudine (22.9 mo *vs* 15.9 mo, respectively; $P = 0.005$).

CONCLUSION: Our results demonstrate that IFN-α plus lamivudine combination therapy did not increase the sustained response, compared to lamivudine. However, combination therapy reduces the likelihood of VBR due to YMDD mutants and prolongs the time period until the breakthrough development.

© 2005 The WJG Press and Elsevier Inc. All rights reserved.

Key words: Interferon; Lamivudine; Hepatitis B; Combination therapy

Economou M, Manolakopoulos S, Trikalinos TA, Filis S, Bethanis S, Tzourmakliotis D, Avgerinos A, Raptis S, Tsianos EV. Interferon-α plus lamivudine *vs* lamivudine reduces breakthroughs, but does not affect sustained response in HBeAg negative chronic hepatitis B. *World J Gastroenterol* 2005; 11(37): 5882-5887
http://www.wjgnet.com/1007-9327/11/5882.asp

INTRODUCTION

The HBeAg negative form of chronic hepatitis B (CHB) predominates in the Mediterranean area and has a rising frequency in Europe and North America. The HBeAg negative CHB is characterized by frequent exacerbation of hepatitis, which probably increases the risk of cirrhosis, hepatocellular failure, and hepatocellular carcinoma[1].

At present there are three approved therapies for patients with CHB: interferon-α (IFN-α), lamivudine, and adefovir dipivoxil. Unfortunately, none of these drugs are effective in achieving a sustained response in patients with HBeAg negative CHB[2-6]. Therefore, new therapeutic approaches have been examined. Combination of antiviral drugs with different mechanisms of action or prolongation of treatment periods[7-10] have been reported with controversial results[11,12]. The aim of this study was to investigate the efficacy of combination treatment of IFN-α and lamivudine compared

to lamivudine monotherapy, after 24 mo of administration in HBeAg-negative hepatitis B patients.

MATERIALS AND METHODS

Study design and patient selection

This was a multi-center open-labeled randomized controlled clinical trial, comparing IFN-α-2b 5 MU (Shering-Plough, Athens, Greece) t.i.w. plus oral lamivudine (GSK, Athens, Greece) 100 mg/d *vs* oral lamivudine 100 mg/d, for 24 mo. Randomization was performed centrally, using lottery cards.

Between January 2000 and May 2001, 50 consecutive adult patients with HBeAg-negative CHB fulfilling all the inclusion criteria were enrolled in the study. Adult patients were eligible if they met all the inclusion criteria: (1) HBsAg positive, anti-HBe positive and HBeAg negative serology for at least 6 mo before enrollment, (2) serum HBV DNA concentrations $>10^5$ copies/mL, (3) elevated alanine transaminase (ALT) activity (at least 1.5 times the upper normal limit) in three separate monthly occasions within the last 6 mo before randomization and (4) liver biopsy with evidence of chronic hepatitis within 12 mo before entering the study. The last patients enrolled ended their follow-up in December 2003.

Patients were excluded if they had antibodies against HIV or hepatitis C or D viruses, had decompensated liver disease (Child-Pugh score >8) or had previously received liver transplantation. We also excluded patients who had been treated with any antiviral drug other than IFN and those who had received immunosuppressive therapy within 6 mo before participation. Patients with active alcohol consumption (>50 g/d) or suspected hepatocellular carcinoma (by real-time ultrasonography and elevated α-fetoprotein) were also excluded. The study protocol conformed to the ethical guidelines of the Declaration of Helsinki and all patients gave informed consent.

Follow up and definitions

Clinical examination and routine laboratory tests were performed every 2 wk during the first 3 mo of treatment and every month thereafter. Compliance was monitored at each visit by assessing the number of used drugs. Laboratory tests included complete blood count, ALT, aspartate transaminase (AST), amylase, alkaline phosphatase, γ-glutamyl transpeptidase, creatinine, and prothrombin time. Serum HBV DNA and α-fetoprotein were evaluated every 6 mo, until the end of the follow-up period (30 mo). Potential side effects were recorded at each visit. All treated patients were followed up for additional 6 mo after they stopped their treatment.

We regarded as initial virologic response the clearance of serum HBV DNA by PCR, and as initial biochemical response the decline of transaminase levels to normal in two consecutive determinations. We considered as virologic breakthrough (VBR) the reappearance of detectable serum HBV DNA by PCR after an initial virologic response, and as biochemical breakthrough (BBR) the increase of ALT or AST levels to greater than 1.5 times the upper normal limit after an initial biochemical response[13]. The primary outcome was the proportion with sustained virological response (undetectable serum HBV DNA concentrations) and/or sustained biochemical response (transaminase levels within normal range) at 30 mo (6 mo after the end of therapy). Secondary end-points were timed from initial virological (biochemical) response to VBR (BBR, respectively) and the emergence of YMDD mutants across the two arms.

Laboratory assays

Serum ALT, AST, albumin, bilirubin, prothrombin time, and α-fetoprotein levels were measured by standard laboratory procedures. HBsAg, HBeAg, anti-HBe, anti-HBc, anti-HCV, anti-HDV, and anti-HIV titers were measured using commercially available microparticle enzyme immunoassays. Serum HBV DNA viral load levels were determined using AMPLICOR HBV MONITOR (Roche Diagnostics Systems, NJ, USA). The test incorporates a known amount of synthetic internal standard (IS), which is co-amplified. After amplification, a colorimetric reaction determines the amplified products. The HBV/IS ratio for each test specimen is compared against a standard curve and the HBV DNA viral load of the tested samples is calculated from the standard curve in copies per milliliter. The detection limit of this assay according to the manufacturer is 400 copies/mL[14].

YMDD mutants were evaluated at baseline and on any occasion of VBR. The YMDD motif of tested serum samples was determined by a line probe assay (INNO-LIPA HBV DR, Innogenetics NV, Belgium). DNA extraction, subsequent HBV polymerase region amplification, detection, and readout were performed according to the manufacturer's instructions[15].

Statistical analysis

The analyses were performed according to the intention-to-treat (ITT) principle, considering dropouts as failures for the primary endpoint. We used the last observation carried forward (LOCF) approach, where the last available measurement is imputed for missing values. We also performed secondary analyses excluding dropouts ("per protocol" analyses). We compared baseline characteristics between the two arms using Mann-Whitney or χ^2 tests, as appropriate. Dropouts across the two arms were compared with Fisher's exact test. HBV DNA values below detection (<400 copies/mL) were imputed to 399 copies/mL for the analyses. HBV DNA concentrations were log-transformed for normality. Univariate and multivariate logistic regressions were used to address possible relationships between baseline characteristics and the primary outcome. Time from initial virologic (or biochemical) response to VBR (or BBR, respectively) as well as time to YMDD emergence were explored with Kaplan-Meier analyses and multivariate Cox proportional hazards models. In all multivariate analyses (logistic regressions and Cox models), we considered as covariates the treatment allocation arm, age, gender, baseline transaminase level, baseline logarithm of HBV DNA, prior IFN therapy, histology activity index (appropriately coded with dummy variables), and presence of cirrhosis at baseline. Selection of covariates for the final models was performed with backward elimination based on likelihood ratio criteria. Serial measurements of ALT, AST, and log HBV DNA concentrations were compared employing repeated measures analysis of variance, using the Huynh-Feldt adjustment whenever sphericity assumptions

were violated. *P* values <0.05 were considered as statistically significant. All *P*-values were two-tailed. Analyses were performed in SPSS 10.0 (SPSS Inc., Chicago, IL, USA) and STATA 8.2 (STATA Corp., College Station, TX, USA).

RESULTS

Study population and baseline characteristics

During study period, 50 consecutive adult patients with HBeAg-negative CHB fulfilling all the inclusion criteria were randomly assigned to lamivudine plus IFN (n = 24) and to lamivudine monotherapy (n = 26, Figure 1). The baseline characteristics of the two arms were similar with respect to demographic and clinical features (Table 1). Twenty-eight patients had previously been treated with IFN-α: 6 had not responded and 22 had relapsed after discontinuing treatment. Three patients in the lamivudine plus IFN-α arm *vs* none in the lamivudine arm dropped out by the 10th wk (exact $P = 0.10$). None of the patients were dropped due to protocol violations.

Table 1 Baseline characteristics

	IFN-α+lamivudine (n = 24)	Lamivudine (n = 26)	*P*
Age (median, IQR)	53 (47, 60)	58 (41, 66)	0.36
Male (%)	15/24 (63)	18/26 (69)	0.62
ALT, median (IQR)	79 (57, 100)	59 (52, 94)	0.24
AST, median (IQR)	59 (51, 89)	60 (40, 94)	0.43
$\log_{10}$(HBV), median (IQR)	6.1 (5.2, 7.2)	5.9 (5.2, 6.6)	0.72
Previous IFN-α therapy (%)	13/24 (54)	15/26 (58)	0.80
Cirrhosis[1] (%)	11/24 (45.8)	13/26 (50)	0.7

IFN: interferon; IQR: interquartile range. *P*-values were derived from Mann-Whitney and χ^2 tests as appropriate. [1]Ishak classification, fibrosis 5 or 6.

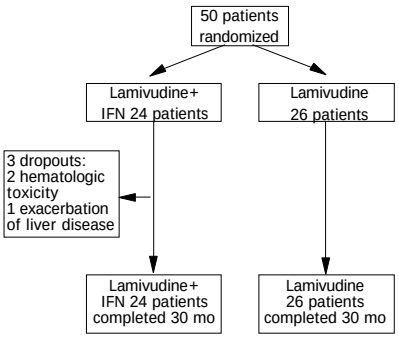


Figure 1 Outline of the trial.

Virologic response -virological breakthrough

In ITT analyses, 5/24 (21%) patients in the IFN-α plus lamivudine arm *vs* 3/26 (12%) patients in the lamivudine monotherapy arm had sustained response to therapy at 30 mo. Hence, the combination therapy was not more likely to lead to sustained response at the end of the follow-up period (rate ratio, RR = 1.81 [95%CI: 0.48-6.76]). The results were essentially the same for per protocol analyses (RR = 2.06 [95%CI: 0.56-7.65]). None of the patients cleared HBsAg at 30-mo study period. Univariate and multivariate logistic regression analyses did not identify a statistically significant relationship between any of the baseline characteristics and sustained response at 30 mo.

The mean log HBV DNA was not different across the two arms over time (P = 0.26; Figure 2A). The proportion of patients with serum HBV DNA below detection by ITT-LOCF for every assessment is shown in Figure 2B. In per protocol analyses, the proportion of patients who lowered their viral concentrations below detection was 21/21 = 100% *vs* 19/26 = 73% at 6 mo; 21/21 = 100% *vs* 20/26 = 77% at 12 mo; 20/21 = 95% *vs* 17/26 = 65% at 18 mo; and 18/21 = 86% *vs* 13/26 = 50% at 24 mo of treatment, between combination and monotherapy, respectively. In the combination arm, all patients except for the three dropouts had an initial virologic response during the first 6 mo of therapy. In the lamivudine arm, an initial virologic response was observed in 24/26 (92%) within the first 12 mo (19 patients by 6 mo, and 5 patients by 12 mo). The remaining two patients in the lamivudine group did not clear HBV DNA; however, their viral load concentrations dropped by at least 2 log during the first 12 mo of treatment.

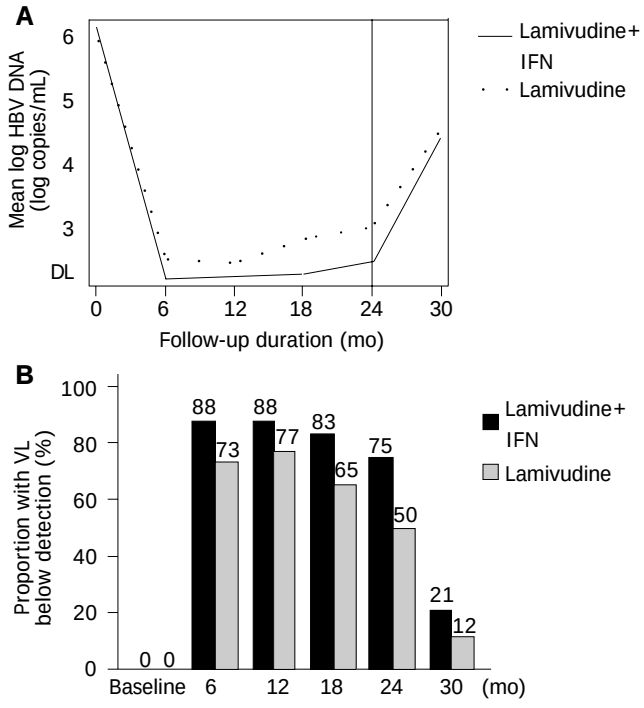


Figure 2 Virological course. A: Treatment was administered up to 24 mo (vertical line). The trajectories of the mean log HBV DNA viral load are similar between the two groups. The following 6 mo were the follow-up period. B: Proportion of patients with viral load below detection (by ITT). DL: Detection limit; IFN: interferon-α; mo: months; VL: HBV DNA viral load concentrations.

During 24 mo therapy, VBR were observed in 3 (14%) of the 21 patients with an initial virological response in the combination arm and in 11 (46%) of the 24 patients in the lamivudine arm respectively (P = 0.03). Time from initial virologic response to VBR was significantly greater among the 21 initial responders in the IFN-α plus lamivudine arm compared to the 24 initial responders in the lamivudine arm (Figure 3; log-rank P = 0.005). The mean time to

VBR was 22.9 mo (95%CI: 21.5-24.2) *vs* 15.9 mo (95%CI: 12.7-19.2), respectively. At the onset of VBR, median serum HBV DNA concentrations were similar between the two groups ($P = 0.10$). Furthermore at the onset of VBR, serum HBV DNA concentrations exceeded 100 000 copies/mL in only two patients, but became greater than 100 000 copies/mL in five more patients with at least 6 mo treatment after VBR.

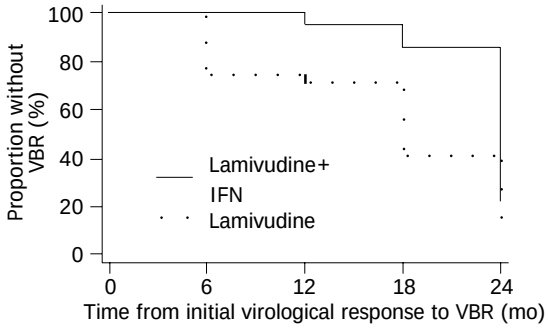


Figure 3 Combination treatment delayed the VBR compared to lamivudine monotherapy among patients who had lowered their HBV DNA concentrations below detection. IFN: interferon-α.

Biochemical response -biochemical breakthrough

Median ALT and AST values were statistically significantly lower in the IFN-α plus lamivudine arm compared to lamivudine monotherapy during the treatment period ($P = 0.04$; Figure 4). The proportion of patients with transaminase levels within normal range (per protocol analyses) was 14/21 = 67% *vs* 12/26 = 46% at 6 mo, 18/21 = 86% *vs* 21/26 = 81% at 12 mo, 19/21 = 90% *vs* 19/26 = 73% at 18 mo, 19/21 = 90% *vs* 16/26 = 62% at 24 mo and 6/21 = 28% *vs* 5/26 = 19% at 30 mo of follow-up for the two arms, respectively. All patients who cleared the serum HBV DNA at 30 mo had normal transaminase levels (complete response).

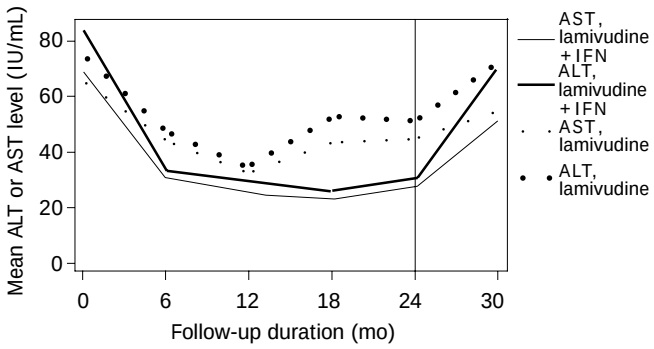


Figure 4 Biochemical course. Mean transaminase levels per assessment time. Layout as per Figure 2. IFN: interferon-α.

BBR was developed in seven patients with an initial biochemical response, two in the combination arm and five in the lamivudine arm respectively. None of the patients with BBR in both groups developed clinical signs of decompensation. At the onset of BBR, transaminase level exceeded 400 IU/L (>10 times the upper normal limit) in two patients receiving lamivudine monotherapy. Elevation of bilirubin to abnormal levels was observed in one of these patients. During BBR period, transaminase levels remained abnormal in all patients. Lamivudine therapy was continued in all patients with BBR in both groups. None of the patients with BBR received other anti-viral treatment. Combination therapy tended to delay BBR for a longer time period after the initial biochemical response, compared to those on lamivudine only. However, this was not formally statistically significant (Figure 5; log-rank $P = 0.18$). Similarly, time from initial biochemical response to BBR was not significantly dependent on any of the covariates in the multivariate Cox models.

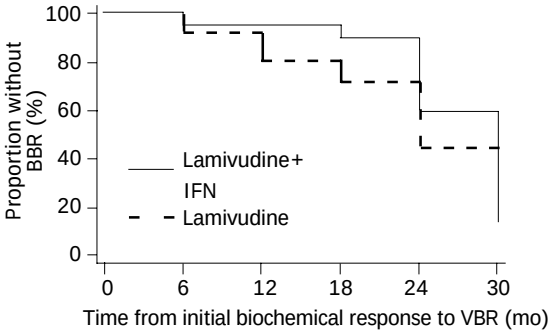


Figure 5 Combination therapy tended to delay BBR. IFN: interferon-α.

Genotypic analyses

None of the patients had YMDD mutants at baseline. YMDD mutations were detected in two of the three patients with VBR in the combination arm (one had the M552I mutant and the other the L528M+M552I mutant strains). In the lamivudine arm, YMDD mutants were detected in all 11 patients with VBR (three patients with VBR had the L528M+M552V mutant; three the L528M+M552I; two the M552I; and three the M552V mutant strains) and in one of the two patients who had detectable serum HBV DNA at all measurements (L528M+M552I mutant strains). Overall, the frequency of emergence of treatment of YMDD mutations in this study was 2/21 (10%) in the IFN-α plus lamivudine arm and 12/26 (46%) in the lamivudine arm (exact $P = 0.01$). The mean time to YMDD emergence was significantly longer in the combination arm compared to the monotherapy arm (23.7 mo [95%CI: 22.9-24.5] *vs* 21.5 mo [95%CI: 19.7-23.3], respectively, Figure 6; log-rank $P = 0.013$).

Adverse events

Three patients in the IFN-α plus lamivudine arm discontinued IFN-α because of hematologic toxicity in two cases and severe exacerbation of liver disease in one case. All 21 remaining patients in this arm reported minor side-effects. All patients tolerated lamivudine monotherapy very well throughout the study period.

DISCUSSION

Our results confirmed our initial hypothesis. The data presented

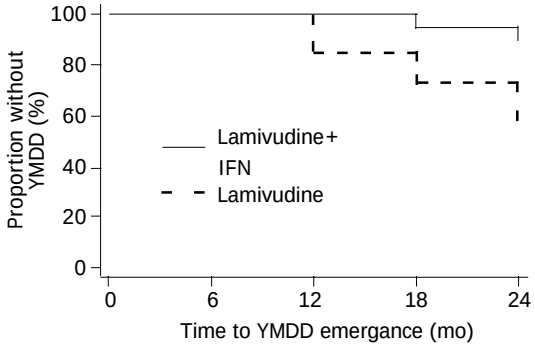


Figure 6 Time to YMDD emergence. IFN: interferon-α.

clearly suggest that 2 years treatment with the combination of IFN-α plus lamivudine induces higher rates of biochemical and virological response, reduces the possibility of YMDD mutations and delays the development of VBR in patients with HBeAg negative form of CHB.

This is the first study to suggest that the combination of IFN-α plus lamivudine may reduce and delay the VBR phenomenon during the treatment period. The only available evidence that this might happen comes from studies showing that the combination treatment is associated with a reduction in YMDD emergence[8-10] independently of HBeAg status. In accordance with these studies, we have also found a similar reduction in escape YMDD mutants. However, none of these studies have shown that this might be followed with a difference in VBR. The explanation might be attributed to the longer duration of treatment in our group of patients. As shown, the difference between the two groups of our patients became evident after 12 mo of continuous treatment. In favor of the above hypothesis is also the fact that in none of the studies conducted so far patients have been treated with the combination of IFN-α with lamivudine for a period longer than 12 mo.

It has been shown that the VBR phenomenon is usually associated with treatment failure[16,17]. It has therefore been anticipated that the reduction in the VBR may be associated with an increase in the number of patients with sustained response to treatment. However, we did not observe a difference in sustained response between the two groups of patients studied. According to our results, any kind of prolongation of remission does not appear to secure sustained remission of the disease. The reason of this phenomenon is difficult to understand. Perhaps in HBeAg negative form of CHB, the longer duration of infection is associated with a higher number of infected hepatocytes which may need longer duration of treatment in order to eradicate the virus[18]. Another possible explanation might be that interferon is not enough to restore the immune responsiveness.

We have identified a tendency in favor of the combination arm regarding sustained response rates at 6 months of follow-up, which did not reach formal statistical significance. If one synthesized findings from the other two relevant controlled trials[19,20] with the results from our trial in a formal meta-analysis, the summary sustained response rate ratio would be 30% greater for the combination arm (rate ratio = 1.28 [95%CI: 0.75-2.19], both by fixed and random effects meta-analysis[21] with no statistical dissimilarity -heterogeneity-across synthesized trials). The summary effect size cannot exclude a twofold difference in the sustained response rate between the two arms. This merely reflects the fact that all relevant trials are underpowered to detect the a posteriori observed differences across the two arms: a trial would have to randomize 440 people in order to be able to detect with 80% power, a difference of 20% *vs* 10% at the 0.05 significance level. For example, an adequately powered trial by Marcellin *et al*.[22], which examined the efficacy of the Pegylated-IFN-α2α in 537 patients with HBeAg negative CHB, was able to identify that the Pegylated IFN-α-2α/lamivudine combination was significantly superior to lamivudine and not different than Pegylated-IFN-α-2α monotherapy.

In our study, we used a sensitive PCR assay for HBV DNA determinations in contrast to less sensitive hybridization assays which were used by previous investigators. At the onset of VBR, only two patients had serum HBV DNA concentrations above 100 000 copies/mL. However, serum HBV DNA increased to levels greater than 100 000 copies/mL in five more patients during the treatment period. Our data are in accordance with those reported by Papatheodoridis *et al*.[16], who observed that only 2/32 patients had HBV DNA concentrations greater than 100 000 copies/mL at the onset of the breakthrough. Therefore, a close serum HBV DNA monitoring by a sensitive PCR assay is necessary in order to recognize the VBR early.

In conclusion, our study clearly shows that the combination of IFN-α plus lamivudine reduces the YMDD mutants and delays VBR, but does not affect significantly the sustained response in HBeAg negative CHB as compared to lamivudine monotherapy. Further well-designed studies are also urgently required in order to explore the mechanism involved in achieving a sustained response in this difficult-to-treat group of patients.

ACKNOWLEDGMENTS

We thank Mrs. P. Georgitsi and Mr. G. Filis for their technical assistance in the genotypic analyses.

REFERENCES

1 **Hadziyannis SJ**, Vassilopoulos D. Hepatitis B e antigen-negative chronic hepatitis B. *Hepatology* 2001; **34**: 617-624
2 **Manesis EK**, Hadziyannis SJ. Interferon alpha treatment and retreatment of hepatitis B e antigen-negative chronic hepatitis B. *Gastroenterology* 2001; **121**: 101-109
3 **Tassopoulos NC**, Volpes R, Pastore G, Heathcote J, Buti M, Goldin RD, Hawley S, Barber J, Condreay L, Gray DF. Efficacy of lamivudine in patients with hepatitis B e antigen-negative/hepatitis B virus DNA-positive (precore mutant) chronic hepatitis B. Lamivudine Precore Mutant Study Group. *Hepatology* 1999; **29**: 889-896
4 **Santantonio T**, Mazzola M, Iacovazzi T, Miglietta A, Guastadisegni A, Pastore G. Long-term follow-up of patients with anti-HBe/HBV DNA-positive chronic hepatitis B treated for 12 mo with lamivudine. *J Hepatol* 2000; **32**: 300-306
5 **Hadziyannis SJ**, Papatheodoridis GV. Treatment of HBeAg negative chronic hepatitis B with new drugs (adefovir and others). *J Hepatol* 2003; **39**(Suppl 1): S172-176
6 **Wong DK**, Cheung AM, O'Rourke K, Naylor CD, Detsky AS, Heathcote J. Effect of alpha-interferon treatment in patients with hepatitis B e antigen-positive chronic hepatitis B. A meta-analysis. *Ann Intern Med* 1993; **119**: 312-323

7 **Mutimer D**, Dowling D, Cane P, Ratcliffe D, Tang H, O'Donnell K, Shaw J, Elias E, Pillay D. Additive antiviral effects of lamivudine and alpha-interferon in chronic hepatitis B infection. *Antivir Ther* 2000; **5**: 273-277

8 **Schalm SW**, Heathcote J, Cianciara J, Farrell G, Sherman M, Willems B, Dhillon A, Moorat A, Barber J, Gray DF. Lamivudine and alpha interferon combination treatment of patients with chronic hepatitis B infection: a randomised trial. *Gut* 2000; **46**: 562-568

9 **Barbaro G**, Zechini F, Pellicelli AM, Francavilla R, Scotto G, Bacca D, Bruno M, Babudieri S, Annese M, Matarazzo F, Di Stefano G, Barbarini G. Lamivudine Italian Study Group Investigators. Long-term efficacy of interferon alpha-2b and lamivudine in combination compared to lamivudine monotherapy in patients with chronic hepatitis B. An Italian multicenter, randomized trial. *J Hepatol* 2001; **35**: 406-411

10 **Schiff ER**, Dienstag JL, Karayalcin S, Grimm IS, Perrillo RP, Husa P, de Man RA, Goodman Z, Condreay LD, Crowther LM, Woessner MA, McPhillips PJ, Brown NA. International Lamivudine Investigator Group. Lamivudine and 24 wk of lamivudine/interferon combination therapy for hepatitis B e antigen-positive chronic hepatitis B in interferon nonresponders. *J Hepatol* 2003; **38**: 818-826

11 **Lampertico P**, Del Ninno E, Manzin A, Donato MF, Rumi MG, Lunghi G, Morabito A, Clementi M, Colombo M. A randomized, controlled trial of a 24-mo course of interferon alfa 2b in patients with chronic hepatitis B who had hepatitis B virus DNA without hepatitis B e antigen in serum. *Hepatology* 1997; **26**: 1621-1625

12 **Janssen HL**, Gerken G, Carreno V, Marcellin P, Naoumov NV, Craxi A, Ring-Larsen H, Kitis G, van Hattum J, de Vries RA, Michielsen PP, ten Kate FJ, Hop WC, Heijtink RA, Honkoop P, Schalm SW. Interferon alfa for chronic hepatitis B infection: increased efficacy of prolonged treatment. The European Concerted Action on Viral Hepatitis (EUROHEP). *Hepatology* 1999; **30**: 238-243

13 **Hadziyannis SJ**, Papatheodoridis GV, Dimou E, Laras A, Papaioannou C. Efficacy of long-term lamivudine monotherapy in patients with hepatitis B e antigen-negative chronic hepatitis B. *Hepatology* 2000; **32**: 847-851

14 **Kessler HH**, Pierer K, Dragon E, Lackner H, Santner B, Stunzner D, Stelzl E, Waitzl B, Marth E. Evaluation of a new assay for HBV DNA quantitation in patients with chronic hepatitis B. *Clin Diagn Virol* 1998; **9**: 37-43

15 **Stuyver L**, Van Geyt C, De Gendt S, Van Reybroeck G, Zoulim F, Leroux-Roels G, Rossau R. Line probe assay for monitoring drug resistance in hepatitis B virus-infected patients during antiviral therapy. *J Clin Microbiol* 2000; **38**: 702-707

16 **Papatheodoridis GV**, Dimou E, Laras A, Papadimitropoulos V, Hadziyannis SJ. Course of virologic breakthroughs under long-term lamivudine in HBeAg-negative precore mutant HBV liver disease. *Hepatology* 2002; **36**: 219-226

17 **Manolakopoulos S**, Karatapanis S, Elefsiniotis J, Mathou N, Vlachogiannakos J, Iliadou E, Kougioumtzan A, Economou M, Triantos C, Tzourmakliotis D, Avgerinos A. Clinical course of lamivudine monotherapy in patients with decompensated cirrhosis due to HBeAg negative chronic HBV infection. *Am J Gastroenterol* 2004; **99**: 57-63

18 **Hadziyannis SJ**. Hepatitis B e antigen negative chronic hepatitis B: from clinical recognition to pathogenesis and treatment. *Viral Hepat Rev* 1995; **1**: 7-36

19 **Jaboli MF**, Fabbri C, Liva S, Azzaroli F, Nigro G, Giovanelli S, Ferrara F, Miracolo A, Marchetto S, Montagnani M, Colecchia A, Festi D, Reggiani LB, Roda E, Mazzella G. Long-term alpha interferon and lamivudine combination therapy in non-responder patients with anti-HBe-positive chronic hepatitis B: Results of an open, controlled trial. *World J Gastroenterol* 2003; **9**: 1491-1495

20 **Santantonio T**, Niro GA, Sinisi E, Leandro G, Insalata M, Guastadisegni A, Facciorusso D, Gravinese E, Andriulli A, Pastore G. Lamivudine/interferon combination therapy in anti-HBe positive chronic hepatitis B patients: a controlled pilot study. *J Hepatol* 2002; **36**: 799-804

21 **Lau J**, Ioannidis JP, Schmid CH. Quantitative synthesis in systematic reviews. *Ann Intern Med* 1997; **127**: 820-826

22 **Marcellin P**, Lau GK, Bonino F, Farci P, Hadziyannis S, Jin R, Lu ZM, Piratvisuth T, Germanidis G, Yurdaydin C, Diago M, Gurel S, Lai MY, Button P, Pluck N. Peginterferon Alfa-2a HBeAg-Negative Chronic Hepatitis B Study Group. Peginterferon alfa-2a alone, lamivudine alone, and the two in combination in patients with HBeAg-negative chronic hepatitis B. *N Engl J Med* 2004; **351**: 1206-1217

Science Editor Wang XL and Guo SY **Language Editor** Elsevier HK

PO Box 2345, Beijing 100023, China
www.wjgnet.com
wjg@wjgnet.com

ELSEVIER

World J Gastroenterol 2005;11(37):5888-5892
World Journal of Gastroenterology ISSN 1007-9327
© 2005 The WJG Press and Elsevier Inc. All rights reserved.

• *BRIEF REPORTS* •

Low preoperative platelet counts predict a high mortality after partial hepatectomy in patients with hepatocellular carcinoma

Kazuhiro Kaneko, Yoshio Shirai, Toshifumi Wakai, Naoyuki Yokoyama, Kohei Akazawa, Katsuyoshi Hatakeyama

Kazuhiro Kaneko, Yoshio Shirai, Toshifumi Wakai, Naoyuki Yokoyama, Katsuyoshi Hatakeyama, Division of Digestive and General Surgery, Niigata University Graduate School of Medical and Dental Sciences, Niigata, Japan
Kohei Akazawa, Department of Medical Informatics, Niigata University Medical and Dental Hospital, Niigata, Japan
Correspondence to: Yoshio Shirai, MD, PhD, Division of Digestive and General Surgery, Niigata University Graduate School of Medical and Dental Sciences, 1-757 Asahimachi-dori, Niigata City 951-8510, Japan. shiray@med.niigata-u.ac.jp
Telephone: +81-25-227-2228 Fax: +81-25-227-0779
Received: 2005-03-29 Accepted: 2005-04-30

© 2005 The WJG Press and Elsevier Inc. All rights reserved.

Key words: Hepatocellular carcinoma; Hepatectomy; Morbidity; Mortality; Indocyanine green clearance test; Blood platelet count

Kaneko K, Shirai Y, Wakai T, Yokoyama N, Akazawa K, Hatakeyama K. Low preoperative platelet counts predict a high mortality after partial hepatectomy in patients with hepatocellular carcinoma. *World J Gastroenterol* 2005; 11 (37): 5888-5892
http://www.wjgnet.com/1007-9327/11/5888.asp

Abstract

AIM: To assess the validity of our selection criteria for hepatectomy procedures based on indocyanine green disappearance rate (K_{ICG}), and to unveil the factors affecting posthepatectomy mortality in patients with hepatocellular carcinoma (HCC).

METHODS: A retrospective analysis of 198 consecutive patients with HCC who underwent partial hepatectomies in the past 14 years was conducted. The selection criteria for hepatectomy procedures during the study period were $K_{ICG} \geqslant 0.12$ for hemihepatectomy, $K_{ICG} \geqslant 0.10$ for bisegmentectomy, $K_{ICG} \geqslant 0.08$ for monosegmentectomy, and $K_{ICG} \geqslant 0.06$ for nonanatomic hepatectomy. The hepatectomies were categorized into three types: major hepatectomy (hemihepatectomy or a more extensive procedure), bisegmentectomy, and limited hepatectomy. Univariate (Fisher's exact test) and multivariate (the logistic regression model) analyses were used.

RESULTS: Postoperative mortality was 5% after major hepatectomy, 3% after bisegmentectomy, and 3% after limited hepatectomy. The three percentages were comparable ($P = 0.876$). The platelet count of $\leqslant 10\times10^4/\mu L$ was the strongest independent factor for postoperative mortality on univariate ($P = 0.001$) and multivariate (risk ratio, 12.5; $P = 0.029$) analyses. No patient with a platelet count of $>7.3\times10^4/\mu L$ died of postoperative morbidity, whereas 25% (6/24 patients) of patients with a platelet count of $\leqslant 7.3\times10^4/\mu L$ died ($P<0.001$).

CONCLUSION: The selection criteria for hepatectomy procedures based on K_{ICG} are generally considered valid, because of the acceptable morbidity and mortality with these criteria. The preoperative platelet count independently affects morbidity and mortality after hepatectomy, suggesting that a combination of K_{ICG} and platelet count would further reduce postoperative mortality.

INTRODUCTION

Postoperative morbidity and mortality remain a challenge following hepatectomy for hepatocellular carcinoma (HCC) of the injured liver[1-5]. Factors affecting morbidity and mortality after hepatectomy include hyperbilirubinemia[2,6], poor indocyanine green clearance[2-5,7], active hepatitis[1,2,5], low preoperative platelet count[6,8], hypoalbuminemia[8], high serum creatinine level[8], major hepatectomy[6,8], excessive blood loss during hepatectomy[4,6,9-11], and perioperative blood transfusion[8,12]. In our department, a hepatectomy procedure has been selected for each patient with HCC mainly based on indocyanine green disappearance rate. Despite this selection method, however, some patients have died of postoperative morbidity.

The aims of this study were to assess the validity of our selection criteria for hepatectomy procedures based on indocyanine green disappearance rate, and to unveil the risk factors for postoperative morbidity and mortality, in order to supplement the selection criteria for hepatectomy procedures for HCC.

MATERIALS AND METHODS

Patient population

From January 1990 to March 2004, 210 consecutive patients underwent partial hepatectomies for HCC in the study department. Eleven patients with concomitant primary malignant tumors in other organs and one with combined hepatocellular and cholangiocarcinoma were excluded. The remaining 198 patients formed the basis of this retrospective study, which included 145 men and 53 women with a median age of 65 years (range: 16-81 years). All patients were Japanese.

Hepatectomy procedures

In the study department, hepatectomy is the standard

treatment for HCC whenever the tumors are considered to be resectable and the patient's condition permits the resection. The hepatectomy procedures examined in this study included nonanatomic hepatectomy (removal of the tumor with a rim of non-neoplastic liver parenchyma) in 66 patients, anatomic monosegmentectomy (removal of 1 Couinaud's segment[13]) in 34, anatomic bisegmentectomy (removal of two Couinaud's segments) in 38, right hepatectomy (removal of Couinaud's segments V-VIII) in 31, left hepatectomy (removal of Couinaud's segments II–IV) in 6, extended right hepatectomy in 15, extended left hepatectomy in 6, and right trisectionectomy (removal of Couinaud's segments IV-VIII) in 2. In the case of combined nonanatomic and anatomic hepatectomies in the same patient, the anatomic hepatectomy represented the hepatectomy procedure for that patient.

The hepatectomies were categorized into three types: major hepatectomy (hemihepatectomy or a more extensive procedure), bisegmentectomy, and limited hepatectomy (monosegmentectomy or nonanatomic hepatectomy). Intra-operative ultrasonography was employed for all patients. Lymph-node dissection of the hepatic hilum was not performed routinely, and only 7 patients underwent this type of dissection. The median operative time was 306 min (range: 100-730 min). The median estimated blood loss was 887 mL (range: 10-14 263 mL).

The selection criteria for hepatectomy procedures based on indocyanine green disappearance rate

In our department, the indocyanine green clearance test[14,15] has been routinely performed preoperatively, in order to assess hepatic functional reserve in patients for whom hepatectomies are planned. After the intravenous injection of indocyanine green (0.5 mg/kg, Diagnogreen; Daiichi Pharmaceutical Co., Inc., Tokyo, Japan), indocyanine green disappearance rate (K_{ICG}) was calculated by linear regression from the plasma indocyanine green concentrations at 5, 10, and 15 min. For the current series, the median indocyanine green retention rate at 15 min was 14% (range: 1-47%; reference range: 10% or less), whereas the median K_{ICG} was 0.136 (range: 0.04-0.243).

The indocyanine green clearance test is useful for estimating hepatic functional reserve in patients with injured livers[2-5,7]. In our department, the selection of a hepatectomy procedure for each patient has depended mainly on K_{ICG}. The selection criteria for this series were $K_{ICG} \geqslant 0.12$ for hemihepatectomy, $K_{ICG} \geqslant 0.10$ for bisegmentectomy, $K_{ICG} \geqslant 0.08$ for monosegmentectomy, and $K_{ICG} \geqslant 0.06$ for nonanatomic hepatectomy (including the enucleation of hepatic tumors).

Laboratory tests before hepatectomy

All patients underwent the following laboratory tests about 1 wk before hepatectomy: blood platelet count (reference range: 16.4-35.4×10^4/μL), serum aspartate aminotransferase (reference range: 8-25 IU/L), serum alanine aminotransferase (reference range: 3-23 IU/L), serum total bilirubin (reference range: 3-9 mg/L), serum albumin (reference range: 41-50 g/L), blood urea nitrogen (reference range: 80-200 mg/L), serum creatinine (reference range: 5-8 mg/L), and prothrombin time (reference range: 81-131%).

Hepatitis B surface antigen and hepatitis C antibody in the serum were detected by radioimmunoassay (Lumipulse II HBsAg; Fujirebio Co., Inc., Tokyo, Japan) and a second-generation ELISA (Lumipulse II Ortho HCV; Ortho-Clinical Diagnostics Co., Inc., Tokyo, Japan), respectively. In the current series, 49 patients tested positive for hepatitis B surface antigen, 100 tested positive for hepatitis C antibody, and 2 tested positive for both. The remaining 47 patients tested negative for both.

Pathologic examination

The resected specimens were submitted to the Department of Surgical Pathology in our hospital for histologic evaluation. Each specimen was examined grossly and microscopically. The cancer stage was determined according to the pathologic tumor-node-metastasis (pTNM) staging system[16]. Cirrhosis in the resected liver was diagnosed microscopically based on the presence of fibrous septa and regenerative nodules. One hundred and six patients were found to be cirrhotic.

Definitions of postoperative morbidity and mortality

Postoperative morbidity was defined as any postoperative complication that lengthened the hospital stay, and included intra-abdominal bleeding (either interventional radiologic technique or reoperation required), hyperbilirubinemia (serum total bilirubin >50 mg/L, persisting for more than 7 d), hepatic encephalopathy, intractable ascites (abdominocentesis required), intractable pleural effusion (either insertion of a thoracic tube or two or more thoracocenteses required), biliary fistula, gastrointestinal hemorrhage, portal vein thrombosis, bowel obstruction (reoperation required), acute renal insufficiency (hemodialysis required), adult respiratory distress syndrome, sepsis, intra-abdominal infection, methicillin-resistant *Staphylococcus aureus* or pseudomembranous enterocolitis, pneumonia, and wound infection. Intra-abdominal infection was diagnosed when either an abscess was detected on imaging or positive bacterial culture of a drainage fluid was identified together with a fever (>38 ℃) without extra-abdominal septic complications. Tumor progression during the hospital stay (one patient) was not treated as a postoperative complication.

Postoperative mortality was defined as any death occurring during the hospital stay for resection of HCC.

Risk factors for postoperative morbidity and mortality

All 198 patients were tested for a total of 20 factors which might influence postoperative morbidity and mortality[17]: age (≤65 years *vs* >65 years), gender, the Child-Pugh classification[18] (A *vs* B+C), cirrhosis (absent *vs* present), hepatitis B viral status (positive *vs* negative for hepatitis B surface antigen), hepatitis C viral status (positive *vs* negative for hepatitis C antibody), blood platelet count (≤10×10^4/μL *vs* >10×10^4/μL), serum aspartate aminotransferase (≤50 IU/L *vs* >50 IU/L), serum alanine aminotransferase (≤46 IU/L *vs* >46 IU/L), serum total bilirubin (≤1.0 IU/L *vs* >1.0 IU/L), serum albumin (≤35 g/L *vs* >35 g/L), blood urea nitrogen (≤200 mg/L *vs* >200 mg/L), serum creatinine (≤10 mg/L *vs* >10 mg/L), prothrombin time (≤70% *vs* >70%), K_{ICG} (≤0.12 *vs* >0.12), the type of hepatectomy (major hepatectomy *vs* bisegmentectomy *vs* limited hepatectomy), operative time (≤300 min *vs* > 300 min), estimated blood loss (≤800 mL *vs* >800 mL),

blood transfusion (transfusion of packed red cells during the operation) (no *vs* yes), and pTNM stage[16] (I *vs* II+III+IV).

Statistical analysis

Medical records were obtained for all patients. Univariate analyses of risk factors for postoperative morbidity and mortality were performed using Fisher's exact test. Multivariate analyses of the risk factors for postoperative morbidity and mortality were performed using the logistic regression model. In this model, a stepwise selection was used for the variable selection, with entry and removal limits of $P<0.1$ and $P>0.15$, respectively. The stability of this model was confirmed using a step-backward and step-forward fitting procedure; the variables identified as having an independent influence on morbidity and mortality were identical with both procedures. The Mann-Whitney test was used to compare the blood platelet counts between patients with postoperative mortality and patients without postoperative mortality. All statistical evaluations were performed using the SPSS 11.5J software package (SPSS Japan Inc., Tokyo, Japan). All tests were two-sided, and the differences with P values lesser than 0.05 were considered statistically significant.

RESULTS

Postoperative complications occurred in 50 patients out of a total of 198 patients, resulting in a postoperative morbidity of 25%. Intra-abdominal infection was the most common complication ($n = 30$), followed by intractable pleural effusion ($n = 18$), wound infection ($n = 9$), gastrointestinal hemorrhage ($n = 9$), methicillin-resistant *Staphylococcus aureus* or pseudomembranous enterocolitis ($n = 8$), pneumonia ($n = 7$), biliary fistula ($n = 7$), hepatic encephalopathy ($n = 5$), intractable ascites ($n = 5$), hyperbilirubinemia ($n = 3$), portal vein thrombosis ($n = 3$), acute renal insufficiency ($n = 2$), bowel obstruction ($n = 2$), sepsis ($n = 1$), intra-abdominal bleeding ($n = 1$), and adult respiratory distress syndrome ($n = 1$).

Seven patients died during their hospital stay, which resulted in a postoperative mortality of 3.5%. Among the seven patients with postoperative mortality, six died of postoperative morbidity and the other died of tumor progression.

Postoperative morbidity and mortality according to the type of hepatectomy procedure

The incidence of postoperative morbidity was 28% (17/60 patients) after major hepatectomy, 32% (12/38 patients) after bisegmentectomy, and 21% (21/100 patients) after limited hepatectomy. The postoperative morbidity incidences for the three types of hepatectomy were comparable ($P = 0.365$).

The incidence of postoperative mortality was 5% (3/60 patients) after major hepatectomy, 3% (1/38 patients) after bisegmentectomy, and 3% (3/100 patients) after limited hepatectomy. The postoperative mortality incidences for the three types of hepatectomy were comparable ($P = 0.876$).

Risk factors for postoperative morbidity

Univariate analysis revealed that the estimated blood loss ($P<0.001$), blood transfusion ($P<0.001$), operative time ($P<0.001$), and blood platelet count ($P = 0.022$) were significantly associated with postoperative morbidity. These four variables entered into multivariate analysis, and the estimated blood loss (risk ratio: 3.935; $P = 0.003$), blood transfusion (risk ratio: 3.704; $P = 0.004$), and blood platelet count (risk ratio: 3.069; $P = 0.010$) remained as significantly independent factors for postoperative morbidity (Table 1).

Risk factors for postoperative mortality

Univariate analysis revealed that the blood platelet count ($P = 0.001$), prothrombin time ($P = 0.005$), and Child-Pugh classification ($P = 0.044$) were significantly associated with postoperative mortality. These three variables entered into multivariate analysis, and the blood platelet count (risk ratio: 12.50; $P = 0.029$) remained as the only significantly independent factor for postoperative mortality (Table 2).

Blood platelet count and postoperative mortality

The blood platelet counts were significantly lower in patients with postoperative mortality than in those without (the Mann-Whitney test, $P = 0.003$, Figure 1). Among the seven patients with postoperative mortality, the patient who died of tumor progression during the hospital stay showed a platelet count of $25.7\times10^4/\mu L$, whereas the other patients who died of postoperative morbidity showed platelet counts of $7.3\times10^4/\mu L$,

Table 1 Risk factors for morbidity after hepatectomy

Variable	Number of patients	Univariate analysis	Multivariate analysis			
		P	β	Risk ratio	95%CI	*P*
Estimated blood loss (mL)		<0.001	1.370	3.935	1.578-9.814	0.003
≤800 (*n* = 91)	8					
>800 (*n* = 107)	42					
Blood transfusion		<0.001	1.309	3.704	1.520-9.009	0.004
No (*n* = 94)	9					
Yes (*n* = 104)	41					
Operative time (min)		<0.001	-	-	-	-
≤300 (*n* = 96)	13					
>300 (*n* = 102)	37					
Blood platelet count ($\times10^4/\mu L$)		0.022	1.043	3.069	1.287-6.250	0.010
≤10 (*n* = 49)	19					
>10 (*n* = 149)	31					

CI: confidence interval.

Table 2 Risk factors for mortality after hepatectomy

Variable	Number of patients	Univariate analysis	Multivariate analysis			
		P	β	Risk ratio	95%CI	*P*
Blood platelet count (×10⁴/μL)		0.001	2.520	12.50	1.302-125.0	0.029
≤10 (*n* = 49)	6					
>10 (*n* = 149)	1					
Prothrombin time (%)		0.005	1.476	4.367	0.812-23.81	0.086
≤70 (*n* = 24)	4					
>70 (*n* = 174)	3					
Child–Pugh classification		0.044	-	-	-	-
A (*n* = 173)	4					
B+C (*n* = 25)	3					

CI: confidence interval.

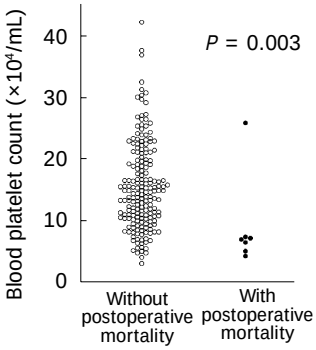


Figure 1 Patients with postoperative mortality had lower platelet counts than those without (the Mann-Whitney test, $P = 0.003$). The platelet counts were 8.9±7.5×10⁴/μL (mean±SD) in patients with postoperative mortality, whereas they were 15.4±7.0×10⁴/μL (mean±SD) in those without postoperative mortality. [1]This patient showed a platelet count of 25.7×10⁴/μL and died of tumor progression, and not of postoperative morbidity, during the hospital stay.

7.1×10⁴/μL, 6.9×10⁴/μL, 6.4×10⁴/μL, 5.0×10⁴/μL, and 4.2×10⁴/μL. Thus, no patient with a platelet count of > 7.3×10⁴/μL died of postoperative morbidity, whereas the postoperative mortality was 25% (6/24 patients) among patients with platelet counts of ≤ 7.3×10⁴/μL ($P<0.001$).

DISCUSSION

The indocyanine green clearance test has been reported to provide a reliable selection criterion for hepatectomy procedures for patients with resectable HCCs[2-4]. In the current series, a hepatectomy procedure was selected for each patient mainly based on K_{ICG}. As a result, both the postoperative morbidities and mortalities became comparable among the three types of hepatectomy. Although major hepatectomy is considered to be a high-risk treatment option for HCC patients with poor hepatic functional reserves[7,10,19], in our patients it resulted in an acceptable morbidity (28%) and mortality (5%). The above suggests that our selection criteria for hepatectomy procedures using K_{ICG} are generally valid. We regret, however, that some patients died of postoperative complications in spite of these selection criteria for hepatectomy procedures. This has prompted us to conduct the current study.

A low preoperative platelet count is related to portal hypertension and its resulting hypersplenism, hepatic fibrosis, and unfavorable indocyanine green clearance test results[20-22]. Jarnagin *et al.*[6], and Poon *et al.*[8], have documented the fact that a low preoperative platelet count is associated with a higher incidence of postoperative mortality. Bennett and Blumgart have stated, "We are cautious when planning resections in patients with counts less than 100 000/μL"[23]. Poon and Fan have also affirmed that cirrhotic patients with platelet counts of less than 10×10⁴/μL should not be considered for major hepatectomy[24]. Among various factors affecting perioperative mortality, the preoperative platelet count is clinically relevant, because it is readily available before surgery.

In this series, a hepatectomy procedure was selected for each patient based on K_{ICG} values, and a low preoperative platelet count (≤ 10×10⁴/μL) was the strongest independent factor for postoperative mortality; no patient with a count of >7.3×10⁴/μL died of postoperative complications, whereas the mortality was high (25%) among those with counts of ≤ 7.3×10⁴/μL. This suggests that the combined use of K_{ICG} and the preoperative platelet count would further reduce postoperative mortality in patients with HCC.

The estimated blood loss and blood transfusion also independently affected the postoperative morbidity in the current series. Recent evidence suggests that blood loss is associated with increased postoperative morbidity and mortality[4,6,9-11]. Blood transfusion is also related to the recurrence of HCC[25-27]. In order to reduce blood loss, adequate and wide exposure of the operative field is essential[25]. During parenchymal transection, intermittent use of the Pringle maneuver[28,29], the use of developed modalities[30-33], and a lowering of the central venous pressure[34-37] are important. Meticulous surgical techniques are required to minimize blood loss. Only experienced surgeons should perform hepatectomies for HCC of cirrhotic liver.

The current study has limitations, such as the retrospective nature of the study and the small number of patients. However, we feel that these limitations did not significantly influence the outcome of the study, because the differences between the groups were too marked to have resulted from these biases.

In conclusion, we believe that the selection criteria for hepatectomy procedures based on K_{ICG} are generally valid

because of the acceptable morbidity and mortality with these criteria. The preoperative platelet count independently affects morbidity and mortality after hepatectomy, suggesting that a combination of K_{ICG} and the platelet count would further reduce postoperative mortality in patients with HCC.

REFERENCES

1 **Noun R,** Jagot P, Farges O, Sauvanet A, Belghiti J. High preoperative serum alanine transferase levels: effect on the risk of liver resection in Child grade A cirrhotic patients. *World J Surg* 1997; **21**: 390-394
2 **Lau H,** Man K, Fan ST, Yu WC, Lo CM, Wong J. Evaluation of preoperative hepatic function in patients with hepatocellular carcinoma undergoing hepatectomy. *Br J Surg* 1997; **84**: 1255-1259
3 **Hemming AW,** Scudamore CH, Shackleton CR, Pudek M, Erb SR. Indocyanine green clearance as a predictor of successful hepatic resection in cirrhotic patients. *Am J Surg* 1992; **163**: 515-518
4 **Nonami T,** Nakao A, Kurokawa T, Inagaki H, Matsushita Y, Sakamoto J, Takagi H. Blood loss and ICG clearance as best prognostic markers of post-hepatectomy liver failure. *Hepatogastroenterology* 1999; **46**: 1669-1672
5 **Eguchi H,** Umeshita K, Sakon M, Nagano H, Ito Y, Kishimoto SI, Dono K, Nakamori S, Takeda T, Gotoh M, Wakasa K, Matsuura N, Monden M. Presence of active hepatitis associated with liver cirrhosis is a risk factor for mortality caused by posthepatectomy liver failure. *Dig Dis Sci* 2000; **45**: 1383-1388
6 **Jarnagin WR,** Gonen M, Fong Y, DeMatteo RP, Ben-Porat L, Little S, Corvera C, Weber S, Blumgart LH. Improvement in perioperative outcome after hepatic resection: analysis of 1,803 consecutive cases over the past decade. *Ann Surg* 2002; **236**: 397-406
7 **Fan ST,** Lai EC, Lo CM, Ng IO, Wong J. Hospital mortality of major hepatectomy for hepatocellular carcinoma associated with cirrhosis. *Arch Surg* 1995; **130**: 198-203
8 **Poon RT,** Fan ST, Lo CM, Liu CL, Lam CM, Yuen WK, Yeung C, Wong J. Improving perioperative outcome expands the role of hepatectomy in management of benign and malignant hepatobiliary diseases: analysis of 1 222 consecutive patients from a prospective database. *Ann Surg* 2004; **240**: 698-708
9 **Nagao T,** Inoue S, Mizuta T, Saito H, Kawano N, Morioka Y. One hundred hepatic resections. Indications and operative results. *Ann Surg* 1985; **202**: 42-49
10 **Nagao T,** Inoue S, Goto S, Mizuta T, Omori Y, Kawano N, Morioka Y. Hepatic resection for hepatocellular carcinoma. Clinical features and long-term prognosis. *Ann Surg* 1987; **205**: 33-40
11 **Shimada M,** Matsumata T, Akazawa K, Kamakura T, Itasaka H, Sugimachi K, Nose Y. Estimation of risk of major complications after hepatic resection. *Am J Surg* 1994; **167**: 399-403
12 **Gozzetti G,** Mazziotti A, Grazi GL, Jovine E, Gallucci A, Gruttadauria S, Frena A, Morganti M, Ercolani G, Masetti M, Pierangeli F. Liver resection without blood transfusion. *Br J Surg* 1995; **82**: 1105-1110
13 **Couinaud C.** Le foie. Etudes anatomiques et chirurgicales. Paris: Masson 1957
14 **Kawasaki S,** Sugiyama Y, Iga T, Hanano M, Sanjo K, Beppu T, Idezuki Y. Pharmacokinetic study on the hepatic uptake of indocyanine green in cirrhotic patients. *Am J Gastroenterol* 1985; **80**: 801-806
15 **Moody FG,** Rikkers LF, Aldrete JS. Estimation of the functional reserve of human liver. *Ann Surg* 1974; **180**: 592-598
16 **Greene FL,** Page DL, Fleming ID, Fritz AG, Balch CM, Haller DG, Morrow M. American Joint Committee on cancer staging manual. 6th ed. *Springer Verlag* 2002: 131-138
17 **Wei AC,** Tung-Ping Poon R, Fan ST, Wong J. Risk factors for perioperative morbidity and mortality after extended hepatectomy for hepatocellular carcinoma. *Br J Surg* 2003; **90**: 33-41
18 **Pugh RN,** Murray-Lyon IM, Dawson JL, Pietroni MC, Williams R. Transection of the oesophagus for bleeding varices. *Br J Surg* 1973; **60**: 646-649
19 **Matsumata T,** Kanematsu T, Shirabe K, Sonoda T, Furuta T, Sugimachi K. Decreased morbidity and mortality rates in surgical patients with hepatocellular carcinoma. *Br J Surg* 1990; **77**: 677-680
20 **Shimada M,** Matsumata T, Adachi E, Itasaka H, Watiyama S, Sugimachi K. Estimation of degree of liver cirrhosis using a fibrosis score; a multivariate analysis of clinical parameters and resected specimens. *Hepatogastroenterology* 1994; **41**: 177-180
21 **Kajiwara E,** Akagi K, Azuma K, Onoyama K, Fujishima M. Evidence for an immunological pathogenesis of thrombocytopenia in chronic liver disease. *Am J Gastroenterol* 1995; **90**: 962-966
22 **Kusaka K,** Harihara Y, Torzilli G, Kubota K, Takayama T, Makuuchi M, Mori M, Omata S. Objective evaluation of liver consistency to estimate hepatic fibrosis and functional reserve for hepatectomy. *J Am Coll Surg* 2000; **191**: 47-53
23 **J Bennett J,** Blumgart LH. Assessment of hepatic reserve prior to hepatic resection. *J Hepatobiliary Pancreat Surg* 2005; **12**: 10-15
24 **Poon RT,** Fan ST. Assessment of hepatic reserve for indication of hepatic resection: how I do it. *J Hepatobiliary Pancreat Surg* 2005; **12**: 31-37
25 **Fan ST,** Ng IO, Poon RT, Lo CM, Liu CL, Wong J. Hepatectomy for hepatocellular carcinoma: the surgeon's role in long-term survival. *Arch Surg* 1999; **134**: 1124-1130
26 **Matsumata T,** Ikeda Y, Hayashi H, Kamakura T, Taketomi A, Sugimachi K. The association between transfusion and cancer-free survival after curative resection for hepatocellular carcinoma. *Cancer* 1993; **72**: 1866-1871
27 **Yamamoto J,** Kosuge T, Takayama T, Shimada K, Yamasaki S, Ozaki H, Yamaguchi N, Mizuno S, Makuuchi M. Perioperative blood transfusion promotes recurrence of hepatocellular carcinoma after hepatectomy. *Surgery* 1994; **115**: 303-309
28 **Man K,** Fan ST, Ng IO, Lo CM, Liu CL, Wong J. Prospective evaluation of Pringle maneuver in hepatectomy for liver tumors by a randomized study. *Ann Surg* 1997; **226**: 704-711
29 **Li SQ,** Liang LJ, Huang JF, Li Z. Ischemic preconditioning protects liver from hepatectomy under hepatic inflow occlusion for hepatocellular carcinoma patients with cirrhosis. *World J Gastroenterol* 2004; **10**: 2580-2584
30 **Yamamoto Y,** Ikai I, Kume M, Sakai Y, Yamauchi A, Shinohara H, Morimoto T, Shimahara Y, Yamamoto M, Yamaoka Y. New simple technique for hepatic parenchymal resection using a Cavitron Ultrasonic Surgical Aspirator and bipolar cautery equipped with a channel for water dripping. *World J Surg* 1999; **23**: 1032-1037
31 **Sugo H,** Mikami Y, Matsumoto F, Tsumura H, Watanabe Y, Kojima K, Futagawa S. Hepatic resection using the harmonic scalpel. *Surg Today* 2000; **30**: 959-962
32 **Yamada T,** Sasaki Y, Yokoyama S, Miyashiro I, Murata K, Doki Y, Kameyama M, Ohigashi H, Hiratsuka M, Ishikawa O, Imaoka S. Practical usefulness of bipolar scissors in hepatectomy. *Hepatogastroenterology* 2002; **49**: 597-600
33 **Jones RM,** Moulton CE, Hardy KJ. Central venous pressure and its effect on blood loss during liver resection. *Br J Surg* 1998; **85**: 1058-1060
34 **Melendez JA,** Arslan V, Fischer ME, Wuest D, Jarnagin WR, Fong Y, Blumgart LH. Perioperative outcomes of major hepatic resections under low central venous pressure anesthesia: blood loss, blood transfusion, and the risk of postoperative renal dysfunction. *Am Coll Surg* 1998; **187**: 620-625
35 **Itamoto T,** Katayama K, Nakahara H, Tashiro H, Asahara T. Autologous blood storage before hepatectomy for hepatocellular carcinoma with underlying liver disease. *Br J Surg* 2003; **90**: 23-28
36 **Smyrniotis V,** Kostopanagiotou G, Theodoraki K, Tsantoulas D, Contis JC. The role of central venous pressure and type of vascular control in blood loss during major liver resections. *Am J Surg* 2004; **187**: 398-402

Science Editor Guo SY **Language Editor** Elsevier HK

PO Box 2345, Beijing 100023, China
www.wjgnet.com
wjg@wjgnet.com

ELSEVIER

World J Gastroenterol 2005;11(37):5893-5898
World Journal of Gastroenterology ISSN 1007-9327
© 2005 The WJG Press and Elsevier Inc. All rights reserved.

• *BRIEF REPORTS* •

Multidimensional assessment of neuro-psychiatric symptoms in patients with low-grade hepatic encephalopathy: A clinical rating scale

Sergei Mechtcheriakov, Ivo W Graziadei, André Kugener, Julia Wiedemann, Chantal Galbavy, Hartmann Hinterhuber, Josef Marksteiner, Wolfgang Vogel

Sergei Mechtcheriakov, André Kugener, Julia Wiedemann, Chantal Galbavy, Hartmann Hinterhuber, Josef Marksteiner, Department of General Psychiatry, Medical University Innsbruck, Austria
Ivo W Graziadei, Wolfgang Vogel, Department of Gastroenterology and Hepatology, Medical University Innsbruck, Anichstrasse 35, AT-6020, Innsbruck, Austria
Correspondence to: Dr. Sergei Mechtcheriakov, Department of General Psychiatry, Medical University Innsbruck, Anichstrasse 35, AT-6020, Innsbruck, Austria. s.mechtcheriakov@uibk.ac.at
Telephone: +43-512-50423636
Received: 2004-11-23 Accepted: 2005-01-26

Abstract

AIM: To evaluate the feasibility of a new clinical rating scale for a standardized assessment of cirrhosis-associated neuro-psychiatric symptoms.

METHODS: Forty patients with liver cirrhosis (LC, with or without low-grade hepatic encephalopathy) were investigated using a clinical neuro-psychiatric rating scale based on a comprehensive list of neurological, psychomotor, cognitive, affective, behavioral symptoms, and symptoms of disturbed bioregulation.

RESULTS: The analysis revealed that the majority of cirrhotic patients showed, besides characteristic neurological symptoms of hepatic encephalopathy, various psychomotor, affective and bioregulatory symptoms (disturbed sleep and sexual dysfunction). Patients were impaired in the following subscales: sleep and biorhythm disorder (75.0% of patients), Parkinsonoid symptoms (25.0%), affective symptoms (17.5%), and psychomotor retardation (12.5%). The increase of total neuro-psychiatric clinical score was significantly associated with the degree of hepatic encephalopathy.

CONCLUSION: This study suggests that a substantial number of patients with LC and low-grade hepatic encephalopathy manifest various clinical neuro-psychiatric symptoms. The use of a rating scale, which explores clinical dimensions of hepatic encephalopathy, would improve the management of patients with LC.

© 2005 The WJG Press and Elsevier Inc. All rights reserved.

Key words: Liver cirrhosis; Hepatic encephalopathy; Neuro-psychiatric symptoms; Clinical neuro-psychiatric rating; Bradykinesia

Mechtcheriakov S, Graziadei IW, Kugener A, Wiedemann J, Galbavy C, Hinterhuber H, Marksteiner J, Vogel W. Multidimensional assessment of neuro-psychiatric symptoms in patients with low-grade hepatic encephalopathy: A clinical rating scale. *World J Gastroenterol* 2005; 11(37): 5893-5898
http://www.wjgnet.com/1007-9327/11/5893.asp

INTRODUCTION

Patients with liver cirrhosis (LC) and hepatic encephalopathy frequently demonstrate various neuro-psychiatric symptoms and deficits[1-3]. The pathophysiology, natural history, and prognosis of cirrhosis-associated neuro-psychiatric deficits are not completely established and the data on this issue are controversial[4-7]. Recent studies have shown that these deficits are associated with changes in metabolic brain patterns[8-11] and can fluctuate correspondingly to the current ammonia level. On the other hand, long-term persistence of these symptoms after liver transplantation has been reported[12-14] and the neurodegenerative nature of this disorder has been suggested[15].

Mild forms of cirrhosis-associated encephalopathy include minimal hepatic encephalopathy (MHE) and grade I hepatic encephalopathy (grade I HE). Patients with grade I HE manifest minor symptoms of motor dysfunction and with attention and concentration deficits[16-18]. MHE is diagnosed in patients who demonstrate deficits in attention and visuomotor coordination[1,4,7,17], but otherwise show no evident or only transient neuro-psychiatric symptoms. Besides, cirrhosis-associated neurological symptoms, such as asterixis, tremor, Parkinsonoid symptoms and bradykinesia, patients with low-grade hepatic encephalopathy frequently demonstrate bioregulative (disturbed sleep and sexual dysfunction), behavioral and affective symptoms[2,18,19]. The adequate clinical neuro-psychiatric evaluation of patients with LC remains difficult, because, in part, neuro-psychiatric symptoms associated with LC are multiform and sometimes subtle and also because, in part, there are no available clinical diagnostic tools adjusted to investigate this group of patients. The previously used Brief Psychiatric Rating Scale[18], which was initially designed for the monitoring of chronic psychiatric patients does not allow sufficient assessment of slight and moderate symptoms and does not include specific cirrhosis-

associated neurological, psychomotor, and cognitive symptoms. Combination of several available clinical rating scales adjusted for other clinical disorders would inevitably lead to unreasonable extension of the investigation procedure, which is not always possible in patients with LC.

The purpose of this study was to explore the feasibility of a comprehensive clinical rating scale for the evaluation of frequency and severity of neuro-psychiatric symptoms in patients with low-grade hepatic encephalopathy. A multidimensional clinical neuro-psychiatric rating scale was developed based on previous findings and clinical experience. The scale includes neurological, psychomotor, affective, behavioral, and bioregulatory symptoms and allows a global evaluation of the neuro-psychiatric state of the patients with emphasis on symptoms characteristic of LC.

MATERIALS AND METHODS

Patients

Forty patients with LC at the out-patient clinic of the Department of Gastroenterology of Innsbruck Medical University, who were listed for liver transplantation, were considered to be eligible for this study. Prior to inclusion, patients underwent a comprehensive hepatologic work-up and gave informed consent. The following exclusion criteria were applied in this study: (1) clinical or laboratory signs of inflammation, gastrointestinal bleeding, anemia, electrolyte abnormalities, or renal insufficiency; (2) overt hepatic encephalopathy (persistent or episodic, clinical grades II-IV); (3) abuse of psychotropic substances; (4) known major psychiatric disorders, as defined by DSM-IV classification; and (5) less than 6 mo of complete alcohol abstinence. The severity of cirrhosis was assessed as follows: Child A (n = 6); Child B (n = 30); and Child C (n = 4). Table 1 shows clinical and demographic data of the patients.

Table 1 Clinical and demographic characteristics of patients with LC

	No. of patients	Percent
Age (mean±SD)	54.77±10.06	
Men/women	28/12	70.0/30.0
Etiology		
Hepatitis C	14	35.0
Alcohol-associated	16	40.0
Autoimmune	4	7.5
Cryptogenic	2	5.0
Hepatitis B	2	5.0
Hepatitis C and hepatocellular carcinoma	1	2.5
Polycystic liver disease	1	2.5

Clinical neuro-psychiatric rating ACIND and psychometric tests

The clinical neuro-psychiatric examination focuses on the symptoms frequently found in patients with LC[2,21] and contains the following clusters of symptoms: neurological symptoms, symptoms of psychomotor retardation, cognitive symptoms, affective symptoms, behavioral alterations, symptoms of sleep, and bioregulatory disorder.

Neurological symptoms, such as asterixis, postural tremor, adiadochokinesia (pronation-supination of both forearms), upper limb dysmetria, dysarthria, oculomotor deficits (nystagmus and altered smooth gaze pursuit) and gait ataxia, are assessed using a standard neurological investigation. The evaluation of psychomotor retardation is based on the assessment of psychomotor change (non-interactiveness and retardation parts)[21]. Cognitive deficits and affective symptoms as well as behavioral changes and bioregulatory deficits (disturbed sleep and sexual dysfunction) are assessed using a semi-structured clinical interview based on the AMDP system[22]. Depending on the nature of symptoms, the evaluation is based either on patient's reporting or rater's clinical assessment (Table 2, Appendix 1). The intensity of symptoms, defined as a combination of frequency and severity, is uniformly assessed as follows: absent (0); slight (1 score point); moderate (2 score points); and severe (3 score points). This rating scale was arbitrarily named as assessment of cirrhosis-associated neuro-psychiatric deficits (ACIND).

The ACIND rating scale was designed in order to evaluate several possible syndromes by combining the symptoms into subscales as follows: Parkinsonoid syndrome (rigidity [obligatory symptom]; facial and head hypomobility, bradykinesia and adiadochokinesia); ataxia (dysmetria, dysartria, adiadochokinesia, gait ataxia, oculomotor deficits [without muscular rigidity]); cognitive impairment (memory decline, attention deficits, concentration deficits, as well as apperception and acalculia); psychomotor retardation (bradykinesia, facial and head hypomobility, delayed verbal responses, reduced speech velocity [without muscular rigidity]); affective symptoms (depressive mood [obligatory symptoms], loss of interest, anhedonia, feeling of loss of feeling, energy deficit, affective lability); as well as sleep and biorhythm disorder (recurrent drowsiness, impaired sleep initiation, increased daily sleep, interrupted sleep). The diagnosis of the impairment on a subscale is based on a cut-off average score point (ASP, Appendix 1). The calculation of the ASP is performed as follows: $ASP = \Sigma / n$ (Σ, sum of all score points; n, the number of symptoms within a subscale). Patients with the ASP 1.0 and higher are arbitrarily assessed as being impaired in the corresponding subscale. The total clinical neuro-psychiatric score is calculated as a sum of score points in all symptoms with a possible maximum of 96 score points. The clinical investigation based on the ACIND rating scale (duration 10-20 min) was performed by a trained neuropsychiatrist and was applied prior to the administration of psychometric tests.

The psychometric test battery included trail-making tests A and B (TMT A and TMT B[23,24]) as well as the digit symbol test (DST). The age-adjusted percentile scores based on a large population data were used in order to calculate a cumulative visuomotor index defined as the sum of percentile scores for TMT A, TMT B, and DST. Visuomotor impairment was assessed using 1.5 z-score cut-off (visuomotor index <10.57), based on age-adjusted control group of 34 healthy subjects (mean visuomotor index 19.95, SD = 6.25). Patients without obvious symptoms of grade I hepatic encephalopathy and regular psychometric performance (visuomotor index >10.57) were assigned with absent HE (grade 0 HE; n = 14). Patients without clinical symptoms but with reduced psychometric performance (cumulative index below 10.57) were diagnosed with MHE (n = 11). Patients with apparent

Table 2 Frequency of neuro-psychiatric symptoms in patients with LC

	Neuro-psychiatric symptoms	Mode of assessment	Cumulative percent of patients showing slight, moderate, or severe symptoms		Percent of slight symptoms
			%	95%CI	
	Adiadochokinesia	r	72.5	56.11-85.40	45.0
Neurological and	Bradykinesia	r	75.0	58.8-87.31	50.0
psychomotor symptoms	Dysmetria of upper extremities	r	47.5	31.53-63-87	22.5
	Asterixis	r	30.0	16.56-46.53	20.0
	Facial and head hypomobility	r	60.0	43.33-75.14	50.0
	Postural tremor	r	32.5	18.57-49.13	30.0
	Increased tendon reflexes	r	45.0	29.26-61.51	35.0
	Dysarthria	r	20.0	9.05-35.65	10.0
	Rigidity	r	25.0	12.69-41.20	22.5
	Gait ataxia	r	37.5	22.73-54.50	27.5
	Oculomotor deficits	r	22.5	10.84-38.45	17.5
	Delay in responding verbally	r	35.0	20.63-51.68	32.5
	Reduced speech velocity	r	22.5	10.84-38.45	20.0
	Reduced modulation of voice	r	40.0	24.86-56.67	37.5
Cognitive symptoms	Memory decline	s/r	57.5	40.89-72.96	35.0
	Attention deficits	s/r	47.5	31.51-63.87	32.5
	Concentration deficits	s/r	45.0	29.26-61.51	30.0
	Impaired apperception	s/r	25.0	12.69-41.20	20.0
	Impaired calculation	r	22.5	10.84-38.45	10.0
Affective symptoms	Energy deficit (lack of drive)	s	65.0	48.32-79.37	30.0
	Affective lability	s/r	52.5	36.13-68.49	25.0
	Depressive mood	s/r	40.0	24.86-56.67	27.5
	Interest deficits	s	32.5	18.57-49.13	12.5
	Anhedonia	s	20.0	9.05-35.65	12.5
	Feeling of loss of feeling	s	25.0	12.69-41.20	25.0
Behavioral symptoms	Reduction of working ability	s	87.5	73.20-95.81	25.0
	Social withdrawal	s	50.0	33.80-66.20	15.0
Bioregulatory symptoms	Recurrent drowsiness	s	82.5	67.22-92.66	15.0
	Impaired sleep initiation	s	62.5	45.80-77.27	25.0
	Increased daily sleep	s	72.5	56.11-85.40	27.5
	Interrupted sleep	s	60.0	43.33-75.14	17.5
	Sexual dysfunction (total)	s	72.5	56.11-85.40	5.0
	Women (n = 12)		66.6	34.89-90.08	16.7
	Men (n = 28)		75.0	55.13-89.21	0.0

CI: confidence interval; r: evaluation by rater; s: assessment based on patient's self-report.

clinical symptoms of cerebral dysfunction but without somnolence and disorientation were diagnosed with grade I hepatic encephalopathy (grade I HE; n = 15).

Statistical analysis

The comparison between the subgroups of patients (grade 0 HE, MHE and grade I HE) with regard to the total ACIND score was performed using non-parametric statistics (Mann-Whitney U test and Wilcoxon matched-pairs test) and one-way ANOVA. The confidence intervals of the frequency of neuro-psychiatric symptoms were analyzed using the statistical assumption of standard binomial distribution. For data processing and statistical analysis, the SPSS 11.5 software package was applied.

RESULTS

The analysis of neuro-psychiatric findings showed a high rate of different neuro-psychiatric symptoms in patients with LC. Table 2 presents the frequency of neuro-psychiatric symptoms expressed as the percentage of patients showing a corresponding symptom, as well as the 95% confidence intervals (CI). Adiadochokinesia, bradykinesia, memory and attention deficits as well as recurrent drowsiness, energy deficit (lack of drive), reduction of working ability, sexual dysfunction and impaired sleep were the most frequent symptoms in this study, although these symptoms were only slightly pronounced in a majority of patients. Recurrent drowsiness, reduction of working ability and sexual dysfunction were in some patients reported as moderate or severe (Table 2).

Patients with LC showed various intensities of neuro-psychiatric symptoms and ranged in total ACIND scores from 0 to 56. For the whole group of patients, the mean ACIND score was 22.95 score points (SD = 12.43). Figure 1A presents the percentage of LC patients in respect with different ranges of the total ACIND score and shows that LC patients most frequently ranged between 21 and 30 total ACIND score points and that 77.5% of patients in this study ranged between 10 and 40 score points.

The frequency of symptoms in different ACIND subscales is presented in Table 3. The percentages of the LC patients demonstrating in average one or more score points per symptom in a particular subscale are listed. Symptoms of biorhythm and sleep disorder were the most

Table 3 Percentage of patients impaired on different ACIND subscales

Subscales	Symptoms	Percentage of impaired patients (95% CIs)
Sleep and biorhythm	Recurrent drowsiness, impaired sleep initiation, interrupted sleep, increased daily sleep	75.0 (58.80-87.31)
Parkinsonoid	Rigidity[1], bradykinesia, adiadochokinesia, facial and head hypomobility	25.0[3] (12.69-41.20)
Cognitive	Memory decline, impaired apperception, concentration deficits, impaired calculation, attention deficits	25.0 (12.69-41.20)
Affective	Depressive mood[1], loss of interest, anhedonia, feeling of loss of feeling, energy deficits, affective lability	17.5 (7.34-32.78)
Psychomotor[2]	Bradykinesia, facial and head hypomobility, reduced speech velocity, delayed verbal responses	12.5 (4.19-26.80)
Ataxia[2]	Dysmetria of upper extremities, oculomotor deficits, adiadochokinesia, dysarthria, gait ataxia	12.5 (4.19-26.80)

[1]Obligatory symptom; [2]patients showing muscular rigidity are excluded; [3]patients with average 0.75 or more score points per symptom are included.

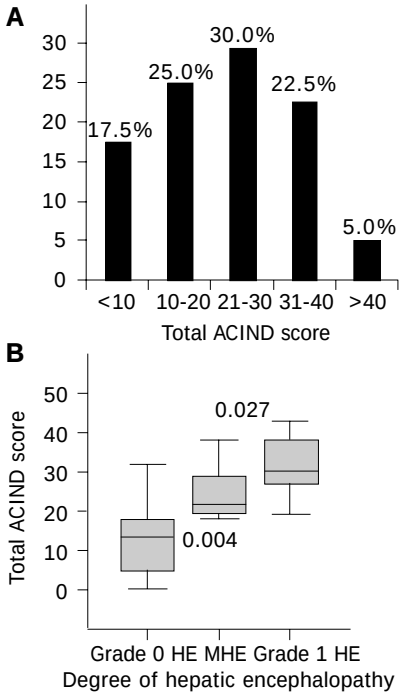


Figure 1 A: Clinical neuro-psychiatric symptoms in patients with LC; B: Box plot and Mann-Whitney *U* test with *P*-values showing the association between total ACIND score and the degree of hepatic encephalopathy (grade 0 hepatic encephalopathy, MHE, and grade I hepatic encephalopathy).

frequent (75.0%). Parkinsonoid syndrome, with rigidity as an obligatory symptom, was diagnosed in 10 patients out of 40 (25%). Cognitive impairment was found in 25% of patients. The average score on this subscale correlated significantly with the cumulative visuomotor index (Spearman's correlation: $r = 0.400$, $P = 0.021$). Depressive symptoms were found in 17.5% of patients. Both ataxia and psychomotor retardation scores were increased in 12.5% of patients.

The increase of the total ACIND score was significantly correlated with the degree of hepatic encephalopathy (Figure 1B). We observed a mean total ACIND score of 12.5 (SD = 9.1) in patients with grade 0 HE, 23.3 (SD = 9.0) in patients with MHE and 32.4 (the highest score, SD = 9.4) in patients with grade 1 HE. One-way ANOVA test demonstrated a highly significant ($P<0.001$) difference among the three subgroups of patients according to the degree of HE (grade 0 HE, MHE, and grade I). Also, the differences between the subgroups were found to be statistically significant, as proven by Mann-Whitney *U* test: grade 0 *vs* MHE ($P = 0.004$) and MHE *vs* grade I ($P = 0.027$).

DISCUSSION

This study provides a systematic description of the neuropsychiatric profile of patients with LC, including affective, behavioral, and bioregulatory symptoms and continues the investigation line of previous studies reporting various neurological, cognitive and psychomotor symptoms associated with LC[4,25-28]. A new clinical rating scale, i.e. ACIND, is proposed for the systematic assessment of the neuropsychiatric state of patients with LC. ACIND uniformly assesses a wide range of neuro-psychiatric symptoms and, due to retrospective evaluation of symptoms, is particularly sensitive for transient and subtle symptoms associated with LC. Since ACIND directly explores clinical dimensions of hepatic encephalopathy, there is a particular advantage in comparison to psychometric tests, which merely measure psychomotor performance.

Our data have shown that patients with LC frequently manifest mild neurological and psychomotor symptoms, such as adiadochokinesia, bradykinesia, and dysmetria of upper limb movements, which are consistent with previous reports on movement disorder in patients with LC[13,29,30]. Although, patients with hepatic encephalopathy grade II were not included in this study, a high rate of minor clinical symptoms of movement disorder was detected. Dysfunctions of basal ganglia, cerebellar pathways as well as in different cortical regions have been recently found to underlie neurological and psychomotor abnormalities in patients with LC and low-grade hepatic encephalopathy[9,30-35]. In our study, a bradykinetic syndrome was associated with Parkinsonoid symptoms in 25% patients (10/40). These findings support previous suggestions on the importance of Parkinsonoid syndrome in cirrhotic patients[13,30,36]. Some patients in our sample (12.5%) showed psychomotor slowing, which was associated with ataxia symptoms and not with crucial Parkinsonoid symptoms. This finding supports the suggestion of multifactorial genesis of bradykinesia in patients with low-grade hepatic encephalopathy[29].

A substantial number of our patients demonstrated a variety of affective symptoms. Depressive mood, energy deficits, loss of interest, feeling of loss of feeling, anhedonia, and social withdrawal were frequent, although in most cases slightly pronounced. These findings are in agreement with those recent reports that found affective symptoms in patients with LC[2,18,38]. Several factors may cause the occurrence of affective symptoms in patients with LC. First, a chronic disease, such as LC, is possibly associated with a high degree of impairment and might be *per se* a factor leading to the

development of a depressive syndrome. On the other hand, all patients in this study suffered from advanced LC and were challenged by indispensability of liver transplantation during several weeks or months prior to the neuro-psychiatric investigation. The inclusion in the liver transplantation waiting list requires substantial adjustment of everyday life and includes the possibility of being called for transplantation at any time. These conditions may also lead to the development of chronic adjustment disorder associated with the up-coming liver transplantation. Recent data supporting this assumption have shown manifest symptoms of post-traumatic stress disorder in a substantial number of LC patients after liver transplantation[39]. Furthermore, specific cirrhosis-associated biological mechanisms might also be responsible for the development of affective symptoms in patients with LC. Recent animal studies as well as investigations in humans have shown that acute and chronic hyperammoniemia can alter brain monoamine metabolism and cause disturbances of dopamine and serotonin neurotransmission[40-42]. Although current data on this issue are not sufficient and, to some degree, controversial, it can be assumed that metabolic brain dysfunction could lead to increased vulnerability for the development of affective symptoms in patients with LC. The high prevalence of depressive symptoms in our sample underlines the substantial demand on systematic screening of patients with LC with respect to affective symptoms.

Various cognitive symptoms, such as attention and memory deficits, have been previously reported in LC patients[37]. Our data were consistent with these findings and showed that 25% of LC patients reported increasing impairment of cognitive functions during the course of their illness.

Sleep and biorhythm dysfunction is an important clinical finding in our sample and has been reported earlier[19,43]. Disturbances of vigilance regulation have been supposed to be associated with a direct toxic effect of increased ammonia concentration, as well as with alterations in glutamine, dopamine, and serotonin neurotransmission occurring in low-grade hepatic encephalopathy[44].

Seventy-five percent of our patients reported sexual dysfunction. Previous reports suggest that an altered metabolism of steroid hormones in patients with LC could be responsible for sexual dysfunction in both men and women suffering from LC[45,46].

Our data demonstrate that clinical rating scale ACIND shows considerable sensitivity with respect to the degree of hepatic encephalopathy, which points toward its validity of clinical assessment of neuro-psychiatric deficits in patients with LC. Follow-up investigations of patients with LC after liver transplantation as well as further investigations including neuroimaging methods are needed to clarify the mechanisms underlying clinical neuro-psychiatric symptoms in LC.

Taking into account that the application of ACIND was not intended to substitute the established methods of investigation of cerebral dysfunction in LC, we suggest that the systematic use of a multidimensional clinical rating would profoundly improve the management of patients with LC.

ACKNOWLEDGMENTS

We are thankful to Mrs. Simone Auffinger and Mr. M. Mattedi for their technical assistance and to Dr. G. Kemmler for his support with statistical analyses. This study was partially supported by Dr. Kolasssa and Merz (Vienna).

REFERENCES

1 **Li YY**, Nie YQ, Sha WH, Zeng Z, Yang FY, Ping L, Jia L. Prevalence of subclinical hepatic encephalopathy in cirrhotic patients in China. *World J Gastroenterol* 2004; **10**: 2397-2340
2 **Wiltfang J**, Nolte W, Weissenborn K, Kornhuber J, Ruther E. Psychiatric aspects of portal-systemic encephalopathy. *Metab Brain Dis* 1998; **13**: 379-389
3 **Ferenci P**, Lockwood A, Mullen K, Tarter R, Weissenborn K, Blei AT. Hepatic encephalopathy-definition, nomenclature, diagnosis, and quantification: final report of the working party at the 11th World Congresses of Gastroenterology, Vienna, 1998. *Hepatology* 2002; **35**: 716-271
4 **Das A**, Dhiman RK, Saraswat VA, Verma M, Naik SR. Prevalence and natural history of subclinical hepatic encephalopathy in cirrhosis. *J Gastroenterol Hepatol* 2001; **16**: 531-535
5 **Hartmann IJ**, Groeneweg M, Quero JC, Beijeman SJ, de Man RA, Hop WC, Schalm SW. The prognostic significance of subclinical hepatic encephalopathy. *Am J Gastroenterol* 2000; **95**: 2029-2034
6 **Weissenborn K**. Minimal hepatic encephalopathy: a permanent source of discussion. *Hepatology* 2002; **35**: 494-496
7 **Duseja A**, Dhiman RK, Saraswat VA, Chawla Y. Minimal hepatic encephalopathy: natural history, impact on daily functioning, and role of treatment. *Indian J Gastroenterol* 2003; **22**: S42-44
8 **Thomas MA**, Huda A, Guze B, Curran J, Bugbee M, Fairbanks L, Ke Y, Oshiro T, Martin P, Fawzy F. Cerebral 1H MR spectroscopy and neuropsychologic status of patients with hepatic encephalopathy. *Am J Roentgenol* 1998; **171**: 1123-1130
9 **Huda A**, Guze BH, Thomas A, Bugbee M, Fairbanks L, Strouse T, Fawzy FI. Clinical correlation of neuropsychological tests with 1H magnetic resonance spectroscopy in hepatic encephalopathy. *Psychosom Med* 1998; **60**: 550-556
10 **Naegele T**, Grodd W, Viebahn R, Seeger U, Klose U, Seitz D, Kaiser S, Mader I, Mayer J, Lauchart W, Gregor M, Voigt K. MR imaging and (1) H spectroscopy of brain metabolites in hepatic encephalopathy: time-course of renormalization after liver transplantation. *Radiology* 2000; **216**: 683-689
11 **Mechtcheriakov S**, Schocke M, Kugener A, Graziadei I, Mattedi M, Hinterhuber H, Vogel W, Marksteiner J. Chemical shift magnetic resonance spectroscopy of cingulate gray matter in patients with minimal hepatic encephalopathy. *Neuroradiology* 2005; **47**: 27-34
12 **Tarter RE**, Switala JA, Arria A, Plail J, Van Thiel DH. Subclinical hepatic encephalopathy. Comparison before and after orthotopic liver transplantation. *Transplantation* 1990; **50**: 632-637
13 **Lazeyras F**, Spahr L, DuPasquier R, Delavelle J, Burkhard P, Hadengue A, Hochstrasser D, Mentha G, Giostra E, Terrier F, Vingerhoets F. Persistence of mild parkinsonism 4 mo after liver transplantation in patients with preoperative minimal hepatic encephalopathy: a study on neuroradiological and blood manganese changes. *Transpl Int* 2002; **15**: 188-195
14 **Mechtcheriakov S**, Graziadei IW, Mattedi M, Bodner T, Kugener A, Hinterhuber HH, Marksteiner J, Vogel W. Incomplete improvement of visuo-motor deficits in patients with minimal hepatic encephalopathy after liver transplantation. *Liver Transpl* 2004; **10**: 77-83
15 **Rose C**, Jalan R. Is minimal hepatic encephalopathy completely reversible following liver transplantation? *Liver Transpl* 2004; **10**: 84-87
16 **Weissenborn K**, Heidenreich S, Ennen J, Ruckert N, Hecker H. Attention deficits in minimal hepatic encephalopathy. *Metab Brain Dis* 2001; **16**: 13-19
17 **Kharbanda PS**, Saraswat VA, Dhiman RK. Minimal hepatic encephalopathy: diagnosis by neuropsychological and neurophysiologic methods. Indian. *J Gastroenterol* 2003; **22**: S37-41
18 **Krieger S**, Jauss M, Jansen O, Theilmann L, Geissler M, Krieger D. Neuropsychiatric profile and hyperintense globus pallidus

on T1- weighted magnetic resonance images in liver cirrhosis. *Gastroenterology* 1996; **111**: 147-155
19 **Wiltfang J**, Nolte W, von Heppe J, Bahn E, Pilz J, Hajak G, Ruther E, Ramadori G. Sleep disorders and portal-systemic encephalopathy following transjugular intrahepatic portosystemic stent shunt in patients with liver cirrhosis. Relation to plasma tryptophan. *Adv Exp Med Biol* 1999; **467**: 169-176
20 **Collis I**, Lloyd G. Psychiatric aspects of liver disease. *Br J Psychiatry* 1992; **161**: 12-22
21 **Parker G**, Hadzi-Pavlovic D. Melancholia: A Disorder of Movement and Mood. *New York: Cambridge University Press* 1996
22 **Fändrich E**, Stiegltz RD. Das AMDP-System. Manual zur Dokumentation psychiatrischer Befunde. Göttingen: Hogrefe-Verlag GmbH, 2000
23 Hamburg-Wechsler Intelligenztest für Erwachsene Rev. Bern, Stuttgart, Toronto: Verlag Hans Huber, 1991
24 **Lezak DL**. Neuropsychological Assessment, Second Edition ed. New York: Oxford University Press, 1983
25 **Gerber T**, Schomerus H. Hepatic encephalopathy in liver cirrhosis: pathogenesis, diagnosis and management. *Drugs* 2000; **60**: 1353-1370
26 **Groeneweg M**, Moerland W, Quero JC, Hop WC, Krabbe PF, Schalm SW. Screening of subclinical hepatic encephalopathy. *J Hepatol* 2000; **32**: 748-753
27 **Lockwood AH**. Early detection and treatment of hepatic encephalopathy. *Curr Opin Neurol* 1998; **11**: 663-666
28 **Weissenborn K**, Ennen JC, Schomerus H, Ruckert N, Hecker H. Neuropsychological characterization of hepatic encephalopathy. *J Hepatol* 2001; **34**: 768-773
29 **Joebges EM**, Heidemann M, Schimke N, Hecker H, Ennen JC, Weissenborn K. Bradykinesia in minimal hepatic encephalopathy is due to disturbances in movement initiation. *J Hepatol* 2003; **38**: 273-280
30 **Spahr L**, Vingerhoets F, Lazeyras F, Delavelle J, DuPasquier R, Giostra E, Mentha G, Terrier F, Hadengue A. Magnetic resonance imaging and proton spectroscopic alterations correlate with parkinsonian signs in patients with cirrhosis. *Gastroenterology* 2000; **119**: 774-781
31 **Trzepacz PT**, Tarter RE, Shah A, Tringali R, Faett DG, Van Thiel DH. SPECT scan and cognitive findings in subclinical hepatic encephalopathy. *J Neuropsychiatry Clin Neurosci* 1994; **6**: 170-175
32 **Lockwood AH**. Positron emission tomography in the study of hepatic encephalopathy. *Metab Brain Dis* 1998; **13**: 303-309
33 **Montes S**, Alcaraz-Zubeldia M, Muriel P, Rios C. Striatal manganese accumulation induces changes in dopamine metabolism in the cirrhotic rat. *Brain Res* 2001; **891**: 123-129
34 **Timmermann L**, Gross J, Kircheis G, Haussinger D, Schnitzler A. Cortical origin of mini-asterixis in hepatic encephalopathy. *Neurology* 2002; **58**: 295-298
35 **Lockwood AH**, Weissenborn K, Bokemeyer M, Tietge U, Burchert W. Correlations between cerebral glucose metabolism and neuropsychological test performance in nonalcoholic cirrhotics. *Metab Brain Dis* 2002; **17**: 29-40
36 **Burkhard PR**, Delavelle J, Du Pasquier R, Spahr L. Chronic Parkinsonism associated with cirrhosis- A distinct subset of acquired hepatocerebral degeneration. *Archives Neurol* 2003; **60**: 521-528
37 **Weissenborn K**, Heidenreich S, Giewekemeyer K, Ruckert N, Hecker H. Memory function in early hepatic encephalopathy. *J Hepatol* 2003; **39**: 320-325
38 **Groeneweg M**, Quero JC, De Bruijn, I, Hartmann IJ, Essink-Bot ML, Hop WC, Schalm SW. Subclinical hepatic encephalopathy impairs daily functioning. *Hepatology* 1998; **28**: 45-49
39 **Rothenhausler HB**, Ehrentraut S, Kapfhammer HP, Lang C, Zachoval R, Bilzer M, Schelling G, Gerbes AL. Psychiatric and psychosocial outcome of orthotopic liver transplantation. *Psychother Psychosom* 2002; **71**: 285-297
40 **Borkowska HD**, Albrecht J, Saransaari P, Oja SS. Ionotropic glutamate receptors and dopamine release in the frontal cortex in experimental hepatic encephalopathy. *Proc West Pharmacol Soc* 1998; **41**: 107-109
41 **Weissenborn K**, Berding G, Kostler H. Altered striatal dopamine D2 receptor density and dopamine transport in a patient with hepatic encephalopathy. *Metab Brain Dis* 2000; **15**: 173-178
42 **Jones EA**. Altered central serotoninergic neurotransmission: a potential mechanism for profound fatigue complicating chronic hepatitis C. *Med Hypotheses* 2001; **57**: 133-134
43 **Cordoba J**, Cabrera J, Lataif L, Penev P, Zee P, Blei AT. High prevalence of sleep disturbance in cirrhosis. *Hepatology* 1998; **27**: 339-345
44 **Jalan R**, Seery JP, Taylor-Robinson SD. Review article: pathogenesis and treatment of chronic hepatic encephalopathy. *Aliment Pharmacol Ther* 1996; **10**: 681-697
45 **Wang YJ**, Wu JC, Lee SD, Tsai YT, Lo KJ. Gonadal dysfunction and changes in sex hormones in postnecrotic cirrhotic men: a matched study with alcoholic cirrhotic men. *Hepatogastroenterology* 1991; **38**: 531-534
46 **Nolte W**, Schindler CG, Figulla HR, Wuttke W, Hufner M, Hartmann H, Ramadori G. Increase of serum estradiol in cirrhotic men treated by transjugular intrahepatic portosystemic stent shunt. *J Hepatol* 2001; **34**: 818-824

Science Editor Kumar M and Guo SY **Language Editor** Elsevier HK

PO Box 2345, Beijing 100023, China
www.wjgnet.com
wjg@wjgnet.com

ELSEVIER

World J Gastroenterol 2005;11(37):5899-5901
World Journal of Gastroenterology ISSN 1007-9327
© 2005 The WJG Press and Elsevier Inc. All rights reserved.

• *BRIEF REPORTS* •

Effect of *Helicobacter pylori* infection on Bax protein expression in patients with gastric precancerous lesions

Hai-Feng Liu, Wei-Wen Liu, Guo-An Wang, Xiao-Chun Teng

Hai-Feng Liu, Department of Gastroenterology, General Hospital of Chinese People's Armed Police Forces, Beijing 100039, China
Wei-Wen Liu, Guo-An Wang, Xiao-Chun Teng, Department of Gastroenterology, Southwest Hospital, Third Military Medical University, Chongqing 400038, China
Supported by the fund for Key Projects in the Army Medical and Health 9th 5-year Plan (No. 96Z047), and the Fund for Chongqing Applied Base Research
Correspondence to: Dr. Hai-Feng Liu, Department of Gastroenterology, General Hospital of Chinese People's Armed Police Forces, 69 Yongding Road, Beijing 100039,
China. haifengliu333@hotmail.com
Received: 2004-11-16 Accepted: 2005-02-18

Liu HF, Liu WW, Wang GA, Teng XC. Effect of *Helicobacter pylori* infection on Bax protein expression in patients with gastric precancerous lesions. *World J Gastroenterol* 2005; 11(37): 5899-5901
http://www.wjgnet.com/1007-9327/11/5899.asp

Abstract

AIM: To investigate the effect of *Helicobacter pylori* (*H pylori*) infection on Bax protein expression, and explore the role of *H pylori* in gastric carcinogenesis.

METHODS: *H pylori* was assessed by rapid urease test and Warthin-Starry method, and expression of Bax protein was examined immunohistochemically in 72 patients with pre-malignant lesions.

RESULTS: Bax protein was differently expressed in intestinal metaplasia and gastric dysplasia, and showed 63.99% positivity. The positivity of Bax protein expression in *H pylori*-positive gastric precancerous lesions (72.3%) was significantly higher than that in *H pylori*-negative gastric precancerous lesions (48.0%, $\chi^2 = 4.191$, $P<0.05$). *H pylori* infection was well correlated with the expression of Bax protein in gastric precancerous lesions ($r = 0.978$, $P<0.01$). After eradication of *H pylori*, the positivity of Bax protein expression significantly decreased in *H pylori*-positive gastric precancerous lesions ($\chi^2 = 5.506$, $P<0.05$). In the persisting *H pylori*-infected patients, the positivity of Bax protein expression was not changed.

CONCLUSION: *H pylori* infection may be involved in the upregulation of Bax gene, which might be one of the mechanisms of *H pylori* infection-induced gastric epithelial cell apoptosis. *H pylori* might act as a tumor promoter in the genesis of gastric carcinoma and eradication of *H pylori* could inhibit gastric carcinogenesis.

© 2005 The WJG Press and Elsevier Inc. All rights reserved.

Key words: *Helicobacter pylori*; Bax protein; Gastric precancerous lesions

INTRODUCTION

Helicobacter pylori (*H pylori*) is a Gram-negative bacterium that infects the human stomach and plays an important role in the pathogenesis of chronic gastritis and peptic ulcer diseases. In addition, epidemiological and clinical studies have consistently identified an association between infection with *H pylori* and subsequent development of gastric cancer[1]. Chronic and persistent infection with *H pylori* is considered to be one of the earliest steps in gastric carcinogenesis. *H pylori* has recently been classified as a group I carcinogen by an International Agency for Research on Cancer Working Group. In the Correa model of human gastric carcinogenesis, *H pylori* has been found to be involved in the evolution of the gastric tissue from normal to superficial gastritis, multifocal atrophic gastritis, intestinal metaplasia, and gastric dysplasia, and finally to adenocarcinoma[2-5]. However, the mechanisms underlying the carcinogenic potential of *H pylori* have not been completely understood as yet.

Our previous studies indicated that cell proliferation and apoptosis were essential events in the cellular turnover of gastric tissue. *H pylori* infection was associated with increased apoptosis. Abnormal regulation of apoptosis may play an important role in the pathogenesis of gastric carcinoma. Bax gene is an important apoptosis-regulatory gene. To the author's knowledge, the relationship between *H pylori* infection and Bax protein expression is still unclear. Hence, we conducted this study to investigate the effect of *H pylori* infection on Bax protein expression, and explore the role of *H pylori* in gastric carcinogenesis.

MATERIALS AND METHODS

Subjects

Seventy-two gastric antral biopsy specimens were taken from 51 patients with intestinal metaplasia and 21 patients with dysplasia referred for upper gastrointestinal endoscopy in Southwest Hospital from 1994 to 1996. Informed written consent was obtained from each patient for the upper gastrointestinal endoscopy and biopsy procedures. The patients who had undergone previous gastric surgery or were known to be taking nonsteroidal anti-inflammatory drugs, corticosteroids or prostaglandin analogs, which may damage the gastric

epithelium or impair the normal gastric cytoprotective response to injury, were excluded from this study. Moreover, the patients who had taken antibiotics or other anti-*H pylori* medications, such as a bismuth compound or a proton-pump inhibitor within the previous one month, were also excluded. This study was approved by the Research Ethics Committee of South-west Hospital. *H pylori* infection was assessed by rapid urease test and immunohistochemical method (Warthin-Starry stain). *H pylori* infection was defined when both rapid urease test and immunohistochemical staining were positive. The patients with *H pylori* infection were treated for 14 d with a triple therapy consisting of colloidal bismuth subcitrate, amoxycillin and metronidazole. One month after the end of triple therapy, the patients underwent the same investigations performed at entry. Eradication of infection by the triple therapy was considered successful when both the rapid urease test and immunohistochemical staining were negative.

Histology

Biopsy specimens were fixed in formalin and embedded in paraffin. The sections (4-μm thick) were stained with hematoxylin and eosin for histological evaluation and identification of *H pylori*. Histological evaluation and identification of *H pylori* were assessed at different times to ensure that the different grades were not influenced by each other.

All biopsy specimens were independently and blindly examined by two expert pathologists who were unaware of clinical, endoscopic, serological, and functional data of the patients. When discordance was found, the samples were re-examined by the two pathologists together using a double-headed microscope, and the grading obtained on this occasion was used for the analysis.

Immunohistochemistry

For each case, 4-μm-thick serial sections were cut from paraffin-fixed specimens, mounted on acid-cleaned glass slides, and heated at 55-60 ℃ for 60 min. Slides were dewaxed and rehydrated, then the endogenous peroxidase activity was inhibited by incubation with 30 mL/L H_2O_2 in methanol for 5 min at room temperature. To reduce non-specific background staining, slides were incubated with 50 mL/L normal goat serum for 10 min at room temperature. To enhance immunostaining, sections were treated with an antigen-retrieval solution (10 mmol/L citric acid monohydrate, pH 6.0, adjusted with 2 mol/L NaOH) and heated thrice in a microwave oven at high power for 5 min. Slides were incubated with primary rabbit antihuman Bax polyclonal antibody (1:50 dilution, Santa Cruz, USA) for 30 min at 37 ℃. A biotin–streptavidin detection system was employed with diaminobenzidine as the chromogen. Slides were washed twice with PBS and incubated with the linking reagent (biotinylated anti-immunoglobulin) for 10 min at 37 ℃. After rinsing in PBS, the slides were incubated with the peroxidase-conjugated streptavidin label for 10 min at 37 ℃, followed by incubation with diaminobenzidine and H_2O_2 for 10 min in darkness. The sections were then weakly counterstained with hematoxylin. With each batch of test samples, a positive control consisting of a tissue section from tonsil was evaluated. In addition, negative controls were prepared for each sample using an irrelevant antibody of the same isotype as the primary antibody.

The degree of Bax protein immunopositivity was evaluated semiquantitatively. Four hundred tumor cells were counted in random fields from representative areas of the lesions, and the immunoreactive cells were roughly assessed and expressed as percentages. The scoring system tested was: <10% (negative, -); 10-25% (low positivity, +); 26-50% (moderate positivity, ++); >50% (high positivity, +++).

Statistical analysis

Data were analyzed with the STATA package for Windows. The categorical variables were analyzed using χ^2 test or Fisher's exact test. Correlation between *H pylori* infection and Bax protein expression was assessed using the logistic regression. $P<0.05$ was considered statistically significant.

RESULTS

H pylori infection was identified by rapid urease test and an immunohistochemical staining. *H pylori* infection was detected in 68.62% (35/51) patients with intestinal metaplasia and 57.14% (12/21) patients with gastric dysplasia. There was no significant difference in *H pylori*-infection rate between intestinal metaplasia and gastric dysplasia.

The Bax protein immunoreactivity appeared brown or dark brown, which was mainly located in the cytoplasm, and a few specimens simultaneously expressed Bax protein in the cell nucleus of gastric epithelium (Figure 1). Bax protein was differently expressed in intestinal metaplasia and gastric dysplasia, and its positivity was 63.9%. The positivity of Bax protein expression in *H pylori*-positive gastric precancerous lesions (72.3%) was significantly higher than that in *H pylori*-negative gastric precancerous lesions (48.0%, $P<0.05$). *H pylori* infection was well correlated with the expression of Bax protein in gastric precancerous lesions ($r = 0.978$, $P<0.01$, Table 1). One month after the end of triple therapy, 37 patients became *H pylori* negative, while 10 patients were still infected. After eradication of *H pylori*, the positivity of Bax protein expression significantly decreased in *H pylori*-positive gastric precancerous lesions (42.3% *vs* 70.3%, $P<0.05$). In the persisting *H pylori*-infected patients, the positivity of Bax protein expression was not changed.

Table 1 Relationship between *H pylori* infection and Bax protein expression in gastric precancerous lesions

H pylori	*n*	Bax protein expression				Positive rate (%)
		-	+	++	+++	
Positive	47	13	15	10	9	72.3[a]
Negative	25	13	6	4	2	48.0

[a]$P<0.05$ *vs* negative.

DISCUSSION

The development of gastric carcinoma involves a multistep process from chronic gastritis to atrophy gastritis, intestinal metaplasia, and gastric dysplasia. It has been shown that atrophic gastritis with intestinal metaplasia and dysplasia significantly increased the risk of gastric carcinoma, and *H pylori*-induced gastritis is significantly more pronounced in gastric carcinoma

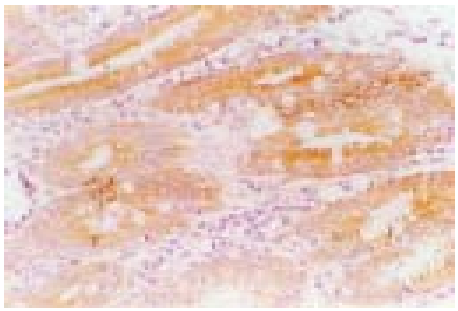


Figure 1 Staining of Bax protein located in the cytoplasm of gastric epithelium of intestinal metaplasia (SP ×200).

patients. Cell proliferation and apoptosis are essential events in the cellular turnover of gastric tissues. Not only excessive cell proliferation, but also abnormal apoptosis occur in the process of gastric carcinogenesis. The excessive cell proliferation and/or decreased cell apoptosis seem to be the biological basis of gastric carcinogenesis[5-8]. *H pylori* infection is an established risk factor for gastric cancer, and has been classified as a group I carcinogen[1,2]. Our previous studies demonstrated that *H pylori* infection not only increased gastric epithelial cell proliferation, but also induced apoptosis of gastric epithelial cells. *H pylori* infection brings about disorders between gastric epithelial cell proliferation and apoptosis, thereby increasing the risk of gastric carcinogenesis[4,7]. Although it is fairly well accepted that *H pylori* infection plays a significant role in gastric carcinogenesis, the exact mechanisms through which *H pylori* increases gastric epithelial cell proliferation and apoptosis are not completely understood to date.

Genetic control of apoptosis and cell survival play a crucial role in tumor growth. Among the molecules related to the apoptotic process, Bcl-2 family proteins are important and critical regulators in a variety of physiological and pathological contexts. Bcl-2 and Bax are members of the Bcl-2 family. Bcl-2 prevents cells from death through a variety of mechanisms, whereas overexpression of Bax protein increases the susceptibility of cells to apoptosis. Although Bax and Bcl-2 have different functions, they share similar structures. Bax is a homolog protein of Bcl-2 and possesses two conserved regions, BH1 and BH2 that appear to be important for Bax/Bcl-2 binding. Bax and Bcl-2 may form homodimers (Bax/Bax, or Bcl-2/Bcl-2) or heterodimers (Bax/Bcl-2). The ratio of Bcl-2 to Bax proteins appeared to control the relative sensitivity or resistance of many types of cells to apoptotic stimuli[9,10]. The Bcl-2 protein has been shown to prevent apoptosis and may play an important role in the regulation of gastric cancer growth. In this study, we have examined the relationship between *H pylori* infection and Bax protein expression in the precursor lesions of gastric cancer. Bax protein was differently expressed in intestinal metaplasia and gastric dysplasia. The positivity of Bax protein expression in *H pylori*-positive gastric precancerous lesions was significantly higher compared to the *H pylori*-negative gastric precancerous lesions. *H pylori* infection was well correlated with expression of Bax protein in gastric precancerous lesions. After eradication of *H pylori*, the positivity of Bax protein expression significantly decreased in *H pylori*-positive gastric precancerous lesions. However, in the persisting *H pylori* infected patients, the positivity of Bax protein expression was not changed. Thus, our results demonstrated that *H pylori* infection might increase Bax protein expression in intestinal metaplasia and gastric dysplasia, suggesting one of the mechanisms of *H pylori*-induced gastric epithelial cell apoptosis. However, the mechanism for the stimulation of Bax protein accumulation is still unknown and is not resolved by this study. Several studies have suggested that *H pylori* produces various toxins, and gastric mucosa can increase some cytokines, nitrous oxide synthase and oxygen radicals released after *H pylori* infection. At the same time, *H pylori* infection can lower the gastric antioxidant ability. All those factors damage DNA or enhance the susceptibility of DNA damage and gene mutation[11-12].

In conclusion, *H pylori* infection seems to be responsible for genomic instability in a subset of cases of *H pylori*-positive chronic atrophic gastritis and precancerous lesions like metaplasia and dysplasia. Our study suggests that patients with precancerous lesions should receive treatment for eradication of *H pylori*, which may correct the abnormal expression of Bax protein, reduce gastric epithelial-cell proliferation and apoptosis, thereby decreasing the subsequent risk of gastric carcinogenesis. Additional epidemiological studies need to elucidate whether prevention of gastric cancer is possible with the eradication of *H pylori*.

REFERENCES

1 **Vandenplas Y**. *Helicobacter pylori* infection. *World J Gastroenterol* 2000; **6**: 20-31
2 **Matsukura N**. *Helicobacter pylori* infection and gastric diseases-pathogenesis and effects of eradication. *Gan To Kagaku Ryoho* 2002; **29**: 1341-1349
3 **Miwa H**, Go MF, Sato N. *H pylori* and gastric cancer: the Asian enigma. *Am J Gastroenterol* 2002; **97**: 1106-1112
4 **Wang GT**. Progress in studies of mechanism of gastric precancerous lesions, carcinogenesis And their reversion. *Shijie Huaren Xiaohua Zazhi* 2000; **8**: 1-4
5 **Zhuang XQ**, Lin SR. Progress in research on the relationship between *Hp* and stomach cancer. *Shijie Huaren Xiaohua Zazhi* 2000; **8:** 206-207
6 **Chan AO**, Wong BC, Lam SK. Gastric cancer: past, present and future. *Can J Gastroenterol* 2001; **15**: 469-474
7 **Maeda S**, Yoshida H, Mitsuno Y, Hirata Y, Ogura K, Shiratori Y, Omata M. Analysis of apoptotic and antiapoptotic signalling pathways induced by *Helicobacter pylori*. *Gut* 2002; **50**: 771-778
8 **Hamajima N**, Matuo K, watanabe Y, Suzuki T, Nakamura T, Matsuura A, Yamao K, Ohashi K,Tominaga S. A pilot study to evaluate stomach cancer risk reduction by *Helicobacter pylori* eradication. *Am J Gastroenterol* 2002; **97**: 764-765
9 **Maeda S**, Amarsanaa J, Mitsuno Y, Hirata Y, Akanuma M, Ikenoue T, Ogura K, Yoshida H, Shiratori Y, Omata M. Relationship between nuclear factor-kappa B activation and virulence factors of *Helicobacter pylori* in Japanese clinical isolates. *J Gastroenterol Hepatol* 2002; **17**: 556-562
10 **El-Rifai W**, Powell SM. Molecular biology of gastric cancer. *Semin Radiat Oncol* 2002; **12**: 128-140
11 **Peek RM Jr**, Blaser MJ. *Helicobacter pylori* and gastrointestinal tract adenocarcinomas. *Nat Rev Cancer* 2002; **2**: 28-37
12 **Wang J**, Chi DS, Kalin GB, Sosinski C, Miller LE, Burja I, Thomas E. *Helicobacter pylori* infection and oncogene expressions in gastric carcinoma and its precursor lesions. *Dig Dis Sci* 2002; **47**: 107-113

Science Editor Kumar M and Guo SY **Language Editor** Elsevier HK

PO Box 2345, Beijing 100023, China
www.wjgnet.com
wjg@wjgnet.com

ELSEVIER

World J Gastroenterol 2005;11(37):5902-5904
World Journal of Gastroenterology ISSN 1007-9327
© 2005 The WJG Press and Elsevier Inc. All rights reserved.

• *BRIEF REPORTS* •

Effects of social isolation stress on immune response and survival time of mouse with liver cancer

Hui Liu, Zhun Wang

Hui Liu, Zhun Wang, Department of Clinical Immunology, Dalian Medical University, Dalian 116027, Liaoning Province, China
Supported by the National Natural Science Foundation of China, No. 30370484
Correspondence to: Professor Hui Liu, Department of Clinical Immunology, Dalian Medical University, Dalian 116027, Liaoning Province, China. liuhui60@mail.dlptt.ln.cn
Telephone: +86-411-84720083
Received: 2005-02-13 Accepted: 2005-03-24

Abstract

AIM: To investigate the effects of isolation stress on mouse with liver cancer and possible associated mechanisms.

METHODS: Transplantable murine hepatoma22 (H22) model was used to evaluate the effects of social isolation stress on murine liver cancer. Mice were immunized with sheep red blood cell (SRBC) and intraperitoneally inoculated with H22 cell, then divided into two groups, one reared individually as group (I) and the other reared in groups as group (G). Titer of antibody to SRBC and interleukin 2 (IL-2) in serum was monitored. The survival time of mouse with liver cancer was observed.

RESULTS: The titer of antibody to SRBC in group (G) was 1:24.5 and that in group (I) was 1:11.2. There was a significant difference between these two groups (t = 2.60, P = 0.02). A significant difference in IL-2 concentration was observed between group (G) (39.6 ng/L) and group (I) (47.1 ng/L, t = 2.14, P = 0.046). The survival time in group (G) (16.5 d) was markedly longer than that in group (I) (13.2 d, t = 3.46, P = 0.002).

CONCLUSION: Our study suggests that survival time of the mouse bearing H22 tumor is affected by the social isolation stress and the associated mechanism may be the immunological changes under the social isolation stress.

© 2005 The WJG Press and Elsevier Inc. All rights reserved.

Key words: Liver cancer; Psychoimmunology; IL-2

Liu H, Wang Z. Effects of social isolation stress on immune response and survival time of mouse with liver cancer. *World J Gastroenterol* 2005; 11(37): 5902-5904
http://www.wjgnet.com/1007-9327/11/5902.asp

INTRODUCTION

In humans, stressful life events have been shown to play a role in increased cancer risk and metastasis[1-3]. However, a number of studies have reported little or no support for the association among stressful life events, coping, biological changes, and cancer progression. The complex relationships between psychosocial stressors and the progression of cancer are difficult to investigate in humans because a number of issues, such as the stage of treatment in which the patients are examined as well as tumor and host factors, may affect interpretation of the data. Animal models allow investigation of the relationship among stressors, coping mechanisms, and tumor growth under more controlled conditions. In animals, psychosocial stressors such as housing condition and psychological stressors such as forced restraint and rotation have been shown to affect tumor growth rates or metastasis of both transplantable and chemically induced tumors[4,5].

There are now some evidences in animals and humans that psychological stress may affect many aspects of the integrative network among the central nervous system, endocrine system and immune system. The complex effects of psychological stress on the interactions among these three systems have been subject to study in the developing field of psychoneuroendocrinoimmunology. There is a large body of literature on the effects of psychological stress on immune function in humans[6-8]. Supposing that immunological changes play an important role in the survival time of mouse with liver cancer under the social isolation stress, we designed this experiment to understand the association among isolation stress, immunological response, and survival time of mouse with liver cancer.

MATERIALS AND METHODS

Animal management

Mice (KM strain, 18-22 g) were used for this study. All mice were offered the same commercial diet and tap water *ad libitum* in a temperature-controlled (22 ℃) holding room.

Immunization with SRBC

Each male mouse was injected intraperitoneally with 0.2 mL of 200 mL/L sheep red blood cell (SRBC). On the 10^{th} d, blood samples were obtained by decapitation and sera were prepared by routine methods.

Inoculation with tumor cell

After 2 d, male mice were inoculated intraperitoneally with liver cancer cells (5×10^4 cells/mouse) obtained from murine hepatoma22 (H22).

Grouping

One male mouse with two females, avoiding aggression, was reared in the same cage (21 cm×32 cm×14 cm) with wood shavings for group (G) or society group. One male

mouse reared individually in each cage to induce stress by isolation condition for group (I) or isolation group. Half of them were used to detect immunological parameter on the 10th d and the other half were used to observe survival time.

Detection of anti-SRBC antibody[9]

Normal saline (25 μL) was added in each cup of microtiter plate, and then was the sera (25 μL) in the first cup, followed by doubling dilution. After incubation with 10 mL/L SRBC (25 μL) for 1 h at 37 ℃, titers of the antibody were determined by the maximum dilution when the cells form a continuous carpet on the base of the cup.

Detection of interleukin-2 (IL-2)

Concentrations of IL-2 in sera were measured with ELISA kit (Jingmei Biotech Co., Ltd). All the procedures and conditions were consistent with the instructions of the kit.

Statistical analysis

Using Student's *t*-test with statistics package SPSS10.0, the differences in the survival time and titers of anti-SRBC antibody as well as concentration of IL-2 from isolation and society mice were evaluated. Differences were considered statistically significant at *P* values <0.05.

RESULTS

Survival time of mouse with liver cancer is shown in Table 1. There was a significant difference in survival time between the two groups ($P<0.01$).

Table 1 Survival time of mice of two groups (mean±SD)

Groups	*n*	mean±SD (d)	*t*	*P*
Society	12	16.5±2.7	3.46	0.002
Isolation	12	13.2±1.9		

Quantities of anti-SRBC antibody are shown in Table 2. The titers were converted to logarithms for analysis. We observed a significant difference in anti-SRBC antibody titers between the society and the isolation groups ($P<0.05$).

Table 2 Titers of anti-SRBC antibody

Groups	*n*	Titers	Ig, mean±SD	*t*	*P*
Society	10	1:24.5	1.39±0.38	2.60	0.02
Isolation	10	1:11.2	1.05±0.16		

Quantities of IL-2 in sera are shown in Table 3. Serum IL-2 of the mice in the society group was significantly lower compared to the isolation group ($P<0.05$).

Table 3 Concentrations of serum IL-2

Groups	*n*	mean±SD (ng/L)	*t*	*P*
Society	10	39.6±6.3	2.14	0.046
Isolation	10	47.1±9.1		

DISCUSSION

The effects of psychic factors on somatic diseases and rehabilitation have been more and more appreciated. Several clinical reports have demonstrated that psychic influences work on human bodies mainly through immune system[10-12]. However, many interfering factors in experiments on humans, especially on psychic activities, impair the rigor of the results, and retard further studies. Therefore, we used mice for this experimentation.

Ever since the introduction of the concept of the "animal model" into psychiatric medicine, various experimental models have been applied to clinic oncology trying to reveal the different effects of various psychic states on patient with cancer[4,5,13,14]. Mice are social or gregarious animals; so living alone will leave stressful effects on mice, while living in a society with appropriate sex ratio will not[15]. Our results showed that survival time of mouse with liver cancer in the society group was significantly longer than that in the isolation group ($P<0.01$, Table 1), suggesting that survival time of the mouse bearing H22 tumor was affected by the isolation stress.

Stressor-induced changes in hormones and cytokines have been demonstrated in various studies[6-8]. Our results revealed that the immune response to SRBC of mice in the isolation group was significantly lower than that of the mice in society group ($P<0.05$, Table 2), while IL-2 showed the opposite change ($P<0.05$, Table 3). Thus, differential immune activity in mice in the different experimental housing conditions could alter survival time of mouse with liver cancer.

IL-2 is an important immunoregulatory factor[16,17]. In our experiment, the average serum level of IL-2 in the isolation group mice was obviously higher than that in society group mice, which might be due to the compensative increase of IL-2 to maintain the necessary immune response under stress of social isolation. Even in animal models, data are complex, factors such as the type of tumor, strain or the species have been shown to influence results, and the mechanisms underlying the differential biological change under the stress may also be mediated in survival time of liver cancer. However, further studies are needed for the detailed psychoimmunological pathway and regulation.

REFERENCES

1 **Tian J,** Chen ZC, Wu B, Meng X. Comparison of quality of life between urban and rural gastric cancer patients and analysis of influencing factors. *World J Gastroenterol* 2004; **10:** 2940-2943

2 **Wu W,** Yamaura T, Murakami K, Murata J. Social isolation stress enhanced liver metastasis of murine colon 26-L5 carcinoma cells by suppressing immune responses in mice. *Life Sci* 2000; **66:** 1827-1838

3 **Arndt V,** Merx H, Stegmaier C, Ziegler H, Brenner H. Quality of life in patients with colorectal cancer 1 year after diagnosis compared with the general population: a population-based study. *J Clin Oncol* 2004; **22:** 4777-4784

4 **Stefanski V.** Social stress in laboratory rats: behavior, immune function, and tumor metastasis. *Physiol Behav* 2001; **73:** 385-391

5 **Ben-Eliyahu S**, Yirmiya R, Liebeskind JC, Taylor AN, Gale RP. Stress increases metastatic spread of mamary tumor in rats: evidence for mediation by the immune system. *Brain Behav Immun* 1991; **5:** 193-205

6 **Cohen S,** Miller GE, Rabin BS. Psychological stress and anti-

body response to immunization: a critical review of the human literature. *Psychosom Med* 2001; **63:** 7-18

7 **Bartolomucci A,** Sacerdote P, Panerai AE, Pederzani T, Palanza P, Parmigiani S. Chronic psychosocial stress-induced down-regulation of immunity depends upon individual factors. *J Neuroimmunol* 2003; **141:** 58-64

8 **Reiche EM,** Nunes SO, Morimoto HK. Stress, depression, the immune system, and cancer. *Lancet Oncol* 2004; **5:** 617-625

9 **Shimizu S,** Shiina T, Hosomichi K, Takahashi S, Koyama T, Onodera T, Kulski JK, Inoko H. MHC class IIB gene sequences and expression in quails (Coturnix japonica) selected for high and low antibody responses. *Immunogenetics* 2004; **56:** 280-291

10 **Diwanay S,** Gautam M, Patwardhan B. Cytoprotection and immunomodulation in cancer therapy. *Curr Med Chem Anti-Canc Agents* 2004; **4:** 479-490

11 **Gabrilovich D.** Mechanisms and functional significance of tumour-induced dendritic-cell defects. *Nat Rev Immunol* 2004; **4:** 941-952

12 **McKechnie A,** Robins RA, Eremin O. Immunological aspects of head and neck cancer: biology, pathophysiology and therapeutic mechanisms. *Surgeon* 2004; **2:** 187-207

13 **Vegas O,** Beitia G, Sanchez-Martin JR, Arregi A, Azpiroz A. Behavioral and neurochemical responses in mice bearing tumors submitted to social stress. *Behav Brain Res* 2004; **155:** 125-134

14 **Villano Bonamin L,** Barbuto JA, Malucelli BE. Effects of social isolation on ehrlich tumor growth and tumor leukocyte infiltration in mice: evidence of participation of the submaxillary salivary gland. *Neuroimmunomodulation* 2001; **9:** 313-318

15 **Kerr LR,** Hundal R, Siblva WA, Emerman JT, Weinberg J. Effects of social housing condition on chemotherapeutic efficacy in a Shionogi carcinoma (SC115) mouse tumor model: influences of temporal factors, tumor size, and tumor growth rate. *Psychosom Med* 2001; **63:** 973-984

16 **Malek TR.** The main function of IL-2 is to promote the development of T regulatory cells. *J Leukoc Biol* 2003; **74:** 961-965

17 **Nelson BH.** IL-2, regulatory T cells, and tolerance. *J Immunol* 2004; **172:** 3983-3988

Science Editor Kumar M and Guo SY **Language Editor** Elsevier HK

PO Box 2345, Beijing 100023, China
www.wjgnet.com
wjg@wjgnet.com

ELSEVIER

World J Gastroenterol 2005;11(37):5905-5909
World Journal of Gastroenterology ISSN 1007-9327
© 2005 The WJG Press and Elsevier Inc. All rights reserved.

• *BRIEF REPORTS* •

Primary early-stage intestinal and colonic non-Hodgkin's lymphoma: Clinical features, management, and outcome of 37 patients

Shu-Lian Wang, Zhong-Xing Liao, Xin-Fan Liu, Zi-Hao Yu, Da-Zhong Gu, Tu-Nan Qian, Yong-Wen Song, Jing Jin, Wei-Hu Wang, Ye-Xiong Li

Shu-Lian Wang, Xin-Fan Liu, Zi-Hao Yu, Da-Zhong Gu, Tu-Nan Qian, Yong-Wen Song, Jing Jin, Wei-Hu Wang, Ye-Xiong Li, Department of Radiation Oncology, Cancer Hospital, Peking Union Medical College and Chinese Academy of Medical Sciences, Beijing 10021, China
Zhong-Xing Liao, Department of Radiation Oncology, The University of Texas MD Anderson Cancer Center, Houston 77030, TX, USA
Correspondence to: Shu-Lian Wang, MD, Department of Radiation Oncology, Cancer Hospital, Peking Union Medical College and Chinese Academy of Medical Sciences, 17 Panjiayuan nanli, Chaoyang District, Beijing, 100021, China. slwang@mdanderson.org
Telephone: +86-10-87788122 Fax: +86-10-67706153
Received: 2005-01-03 Accepted: 2005-02-18

Abstract

AIM: To analyze the clinical features, management, and outcome of treatment of patients with primary intestinal and colonic non-Hodgkin's lymphoma (PICL).

METHODS: A retrospective study was performed in 37 patients with early-stage PICL who were treated in our hospital from 1958 to 1998. Their clinical features, management, and outcome were assessed. Prognostic factors for survival were analyzed by univariate analysis using the Kaplan-Meier product-limit method and log-rank test.

RESULTS: Twenty-five patients presented with Ann Arbor stage I PICL and 12 with Ann Arbor stage II PICL. Thirty-five patients underwent surgery (including 31 with complete resection), 22 received postoperative chemotherapy or radiotherapy or both. Two patients with rectal tumors underwent biopsy and chemotherapy with or without radiotherapy. The 5- and 10-year overall survival (OS) rates were 51.9% and 44.5%. The corresponding disease-free survival (DFS) rates were 42.4% and 37.7%. In univariate analysis, multiple-modality treatment was associated with a better DFS rate compared to single treatment (P = 0.001). While age, tumor size, tumor site, stage, histology, or extent of surgery were not associated with OS and DFS, use of adjuvant chemotherapy significantly improved DFS (P = 0.031) for the 31 patients who underwent complete resection. Additional radiotherapy combined with chemotherapy led to a longer survival than chemotherapy alone in six patients with gross residual disease after surgery or biopsy.

CONCLUSION: Combined surgery and chemotherapy is recommended for treatment of patients with PICL. Additional radiotherapy is needed to improve the outcome of patients who have gross residual disease after surgery.

© 2005 The WJG Press and Elsevier Inc. All rights reserved.

Key words: Intestinal neoplasm; Colonic neoplasm; Non-Hodgkin's lymphoma; Surgery; Chemotherapy; Radiotherapy

Wang SL, Liao ZX, Liu XF, Yu ZH, Gu DZ, Qian TN, Song YW, Jin J, Wang WH, Li YX. Primary early-stage intestinal and colonic non-Hodgkin's lymphoma: Clinical features, management, and outcome of 37 patients. *World J Gastroenterol* 2005; 11 (37): 5905-5909
http://www.wjgnet.com/1007-9327/11/5905.asp

INTRODUCTION

Primary intestinal and colonic non-Hodgkin's lymphoma (PICL) is an extra-nodal gastrointestinal (GI) lymphoma, which is less common than gastric lymphoma. In fact, the clinical features and treatment of patients with the disease in these two locations are different. Patients with PICL generally have a lower survival rate than those with gastric lymphoma and the best management is yet to be developed [1]. The role of surgery, chemotherapy, and radiotherapy in patients with PICL has not been defined. This study was to evaluate the clinical features, management and outcome of patients with PICL.

MATERIALS AND METHODS

During the period between 1958 and 1998, 37 patients with early-stage PICL were treated in our institution. Staging was based on physical examination, blood cell count, blood chemistry, chest X-ray or chest computed tomography (CT), ultrasonograms or CT of the abdomen. Some patients whose tumor was located in the colon or rectum underwent colonoscopy and biopsy or received an air-contrast barium enema. Bone marrow biopsy was performed for 22 patients. All diagnoses were confirmed by histology showing non-Hodgkin's lymphomas (NHLs). Immunophenotyping was performed in 34 patients, all showing B-cell origin. PICL was staged using the Ann Arbor classification system and graded according to the National Cancer Institute's Working

Formulation.

Surgery included tumor plus partial intestine or colon resection and tumor resection only. The chemotherapy regimens consisted of cyclophosphamide, doxorubicin, vincristine, and prednisolone (CHOP); bleomycin, epirubicin, cyclophosphamide, vincristine, and prednisone (BACOP); or cyclophosphamide, vincristine, and prednisone (COP). Treatment ranged from 1 to 9 courses (median, 5 courses). Radiotherapy was administered to the whole abdomen and the whole pelvis in 11 patients, to the whole pelvis or lower abdomen in 3 patients (1 patient had rectal, 1 had ascending colonic, and 1 had ileocecal lymphoma). No details were available for one patient. The median abdominal dose was 40 Gy (range, 26-45 Gy), and the median pelvic or lower abdominal dose was 40 Gy (range, 26-50.5 Gy). ^{60}Co γ, 6 MV X, or 8 MV X-rays were used to deliver irradiation. The dose per fraction varied from 1.5 to 2.0 Gy.

Follow-up evaluation included patient history, physical examination, blood cell count, blood chemistry analysis, reviews of chest X-ray films, and abdominal ultrasonograms, air-contrast barium enema, and/or endoscopic evaluation, CT of the abdomen. We obtained follow-up data from the hospital charts, reports from the local hospitals mailed to our hospital, forms filled in by patients and their local physicians, or telephone calls. OS was calculated from the date of treatment to death or to the date of last contact. DFS was calculated from the date of treatment to the date of disease relapse. Kaplan-Meier method was used to calculate the duration of survival, the difference in survival between groups was compared by log-rank test.

RESULTS

Clinical features

Patients including 27 males and 10 females ranged in age from 5 to 68 years (median, 42 years). The primary sites of tumor involvement were the ileocecal region in 20 patients, the ascending colon in 9, the ileum in 4, the rectum in 3, and the jejunum in 1. The median tumor size was 6 cm, ranging 1.8-22 cm. The most frequent symptom was abdominal pain (n = 26, 73%), for which five patients required emergency surgery, followed by abdominal mass (n = 17, 46%), intestinal bleeding (n = 8, 22%), and bowel obstruction (n = 2, 5%). According to the National Cancer Institute Working Formulation, PICL was classified in 24 patients as high-grade, low-grade in 7, and unknown in 6. Twenty-five patients had stage I PICL and 12 had stage II PICL based on the Ann Arbor staging system.

Treatment

Thirty-five patients underwent surgery (Table 1). Thirteen patients who underwent a complete tumor resection had surgery alone, 22 patients received postoperative chemotherapy and/or radiotherapy (Table 1). Two patients with rectal tumors had biopsy during colonoscopy: one received chemotherapy alone and the other received chemotherapy plus radiotherapy.

Table 1 Surgical and post-surgical treatment of 35 patients with PICL

Characteristics	*n*
Surgery result	
Complete resection	31
Gross residual disease	4
Post-surgical treatment	
Complete resection plus radiotherapy	8
Complete resection plus chemotherapy	6
Complete resection plus chemotherapy and radiotherapy	4
Incomplete resection plus chemotherapy	2
Incomplete resection plus chemotherapy and radiotherapy	2

Outcome

The median follow-up time was 17 mo for all patients and 45 mo for the surviving patients (range, 2-164 mo). The 5-year OS rate was 51.9%, the 10-year OS rate was 44.5%. The 5-year DFS rate was 42.4% and the 10-year DFS rate was 37.7% (Figure 1). Among the 21 patients who had relapse, 13 had loco-regional relapse, 4 had relapse at distant sites, and 4 had relapse at both loco-regional and distant sites. Among the 16 patients who received salvage therapy, 6 survived for 2, 3, 11, 71, 74, and 91 mo respectively, after disease relapse. Among the 14 patients who died, 12 died of lymphoma, 1 of cerebral arterial rupture, and 1 of hepatic failure due to hepatitis.

Univariate analysis showed that multiple modality treatment (surgery plus chemotherapy, surgery plus radiotherapy, surgery plus chemotherapy and radiotherapy, chemotherapy and radiotherapy) achieved a higher DFS rate than single

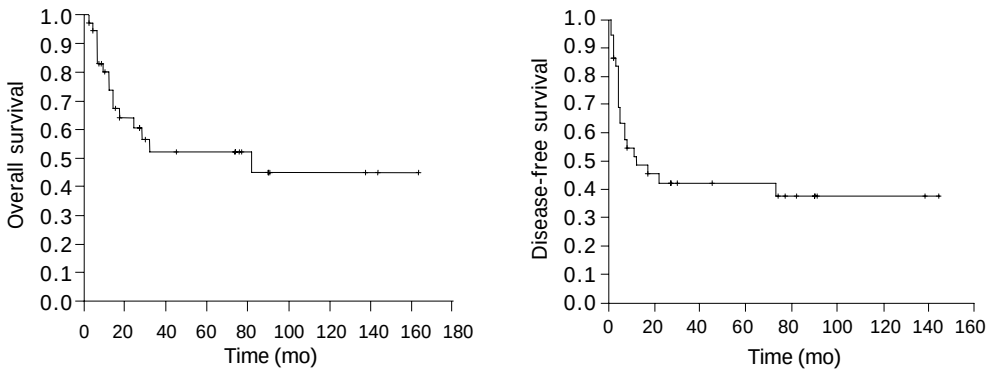


Figure 1 OS and DFS curves for 37 patients with early stage primary intestinal and colonic lymphomas.

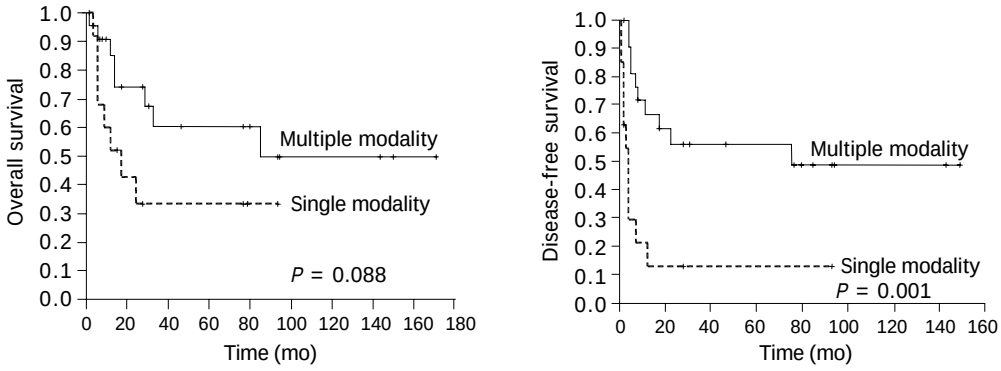


Figure 2 OS and DFS curves for 37 patients stratified by treatment.

modality therapy (surgery and chemotherapy alone, $P = 0.001$, Figure 2), and a higher OS rate than single modality therapy but the difference was not significant ($P = 0.088$). Other factors including age, tumor size, histology, tumor site, stage, and extent of surgery had no significant correlation with survival probability (Table 2).

In respect to the 31 patients who underwent complete tumor resection, there was a significant difference in DFS rates between patients who received chemotherapy and those who did not. The 5-year DFS rates were 68.6% and 27.2% respectively, being in favor of the chemotherapy group ($P = 0.031$). The 5-year OS rate was 70.0% for patients treated with chemotherapy and was 45.3% for patients without chemotherapy ($P = 0.062$, Figure 3). Postoperative radiotherapy tended to improve DFS but not OS. The 5-year DFS rates were 54.6% and 34.0% ($P = 0.087$), while the 5-year OS rates were 54.1% and 51.4% for patients with and without radiotherapy, respectively ($P = 0.831$).

Among the four patients with gross residual tumors after surgery and the two patients who underwent biopsy only, three patients received combined chemotherapy and radiotherapy and three patients received chemotherapy alone. The three patients who received chemotherapy alone had relapse 5, 12, and 22 mo after treatment and died of lymphoma 12, 17, and 28 mo after treatment. However, the three patients who received additional radiotherapy besides chemotherapy had no evidence of relapse 45, 91, and 144 mo after treatment.

DISCUSSION

This retrospective analysis of 37 patients with PICL showed the clinical features of PICL. It was reported that primary intestinal lymphoma accounts for 18.9-62.2% of all primary GI NHLs, and the most frequent sites of origin are the small bowel or ileocecal region, followed by the colon, rectum, and duodenum[2,3]. Most are classified as high-grade NHL. The main symptoms are pain, occult loss of blood or macroscopic bleeding, palpable abdominal mass, bowel

Table 2 Prognostic factors for DFS and OS of 37 patients with PICL by univariate analysis

Variable	Patients (*n*)	5-year DFS % (relapses)	*P*	5-year OS % (deaths)	*P*
Age (yr)					
≤45 yr	19	44.9 (11)	0.719	65.9 (6)	0. 270
>45 yr	18	39.5 (10)		36.8 (10)	
Tumor size					
≤6 cm	17	52.3 (8)	0.466	61.5 (6)	0.092
>6 cm	13	47.0 (7)		55.9 (5)	
Histology					
High grade	24	42.2 (13)	0.804	47.7 (11)	0.888
Low grade	7	42.9 (4)		66.7 (3)	
Unknown	6	40.0 (4)		62.5 (2)	
Tumor site					
Ileocecal region	20	40.0 (12)	0.742	57.6 (8)	0.479
Colon and rectum	12	40.7 (7)		37.1 (7)	
Intestine	5	60.0 (2)		66.7 (1)	
Stage					
I	25	37.9 (16)	0.200	48.0 (12)	0.350
II	12	49.9 (5)		59.3 (4)	
Surgery					
Complete resection	31	41.4 (18)	0.382	53.4 (13)	0.948
Gross residual or biopsy	6	50.0 (3)		50.0 (3)	
Treatment					
Single modality	14	16.8 (11)	0.001	35.9 (8)	0.088
Multiple modality	23	57.8 (10)		61.9 (8)	

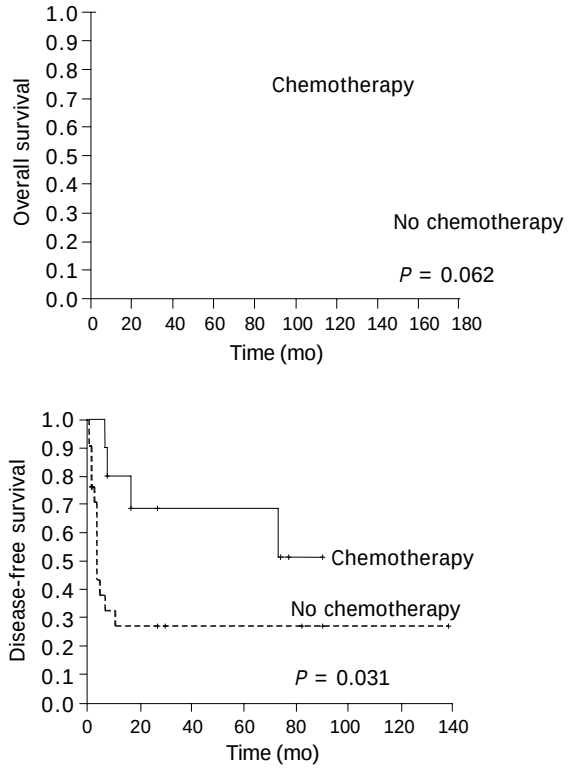


Figure 3 OS and DFS curves for 31 patients after complete surgery stratified by chemotherapy.

obstruction, and perforation. These symptoms occur more frequently in patients with intestinal NHL than in those with gastric NHL, and emergency surgery is necessary for some cases[4,5]. Prognostic factors include advanced disease stage[6], intestinal perforation[7,8], high grade histology[9], and T-cell lymphoma[10,11], which are associated with a lower survival rate. In our study, no patients had T-cell lymphoma. Due to the small number of patients, we did not detect any influence of stage, histological subtype, or sites of origin on the survival time.

Surgery plays an important role in the treatment of PICL. Emergency surgery is required in some cases to reduce the risk of complications and to improve the symptoms such as obstruction or bleeding. Most importantly, surgery can improve the survival of patients with PICL. It was reported that surgical resection is the only statistically significant prognostic variable for patients with intestinal lymphoma[12]. The favorable effects of debulking surgery (partial or complete resection) on OS and DFS were also emphasized[13]. It was reported that the 5-year survival rates were 46% and 0% for patients after radical resection and non-radical resection, respectively[14]. Jinnai *et al*.[15], found that the 5-year survival rate was 44.2% for patients with malignant lymphoma after curative resection, while none survived 5 years after non-curative resection. In our study, surgery was the primary treatment for almost all patients except for two patients with rectal tumor, and the 5-year OS rate was 51.9%. The extent of surgery did not affect survival, because all patients after incomplete surgery received chemotherapy or radiotherapy, or both, suggesting that multiple-modality treatment confer a superior survival advantage over surgery alone or chemotherapy alone.

Chemotherapy significantly improved the DFS rate of patients after complete surgical resection in our study, which is consistent with the reported findings[16]. The efficacy of surgery-chemotherapy combination has been confirmed by other studies[17-19].

In conclusion, surgery is the primary diagnostic and treatment modality for PICL, chemotherapy is necessary for improving the survival of PICL patients, and radiotherapy affords additional benefits to patients with gross residual disease after surgery.

ACKNOWLEDGMENTS

The authors thank Pamela Allen, PhD (The University of Texas MD Anderson Cancer Center, Houston, TX, USA) for helping us to analyze the data, and James D Cox, MD (The University of Texas MD Anderson Cancer Center, Houston, TX, USA) for revising the manuscript.

REFERENCES

1 **Bierman PJ**. Gastrointestinal lymphoma. *Curr Treat Options Oncol* 2003; **4**: 421-430
2 **Gurney KA**, Cartwringht RA, Gilman EA. Descriptive epidemiology of gastrointestinal non-Hodgkin's lymphoma in a population-based registry. *Br J Cancer* 1999; **79**: 1929-1934
3 **Koch BP**, del Valle F, Berdel WE, Willich NA, Reers B, Hiddemann W, Grothaus-Pinke B, Reinartz G, Brockmann J, Temmesfeld A, Schmitz R, Rübe C, Probst A, Jaenke G, Bodenstein H, Junker A, Pott C, Schultze J, Heinecke A, Parwaresch R. Markus tiemann for the german multicenter study group. Primary gastrointestinal non-Hodgkin's lymphoma: I. Anatomic and histologic distribution, clinical features, and survival data of 371 patients registered in the German multicenter study GIT NHL 01/92. *J Clin Oncol* 2001; **19**: 3861-3873
4 **Azab MB**, Henry-Amar M, Rougier P, Bognel C, Theodore C, Carde P, Lasser P, Cosset JM, Caillou B, Droz JP, Hayat M. Prognostic factors in primary gastrointestinal non-Hodgkin's lymphoma: a multivariate analysis, report of 106 cases, and review of the literature. *Cancer* 1989; **64**: 1208-1217
5 **Liang R**, Todd D, Chan TK, Chiu E, Lie A, Kwong YL, Choy D, Ho FCS. Prognostic factors for primary gastrointestinal lymphoma. *Hematol Oncol* 1995; **13**: 153-163
6 **Morton JE**, Leyland MJ, Vaughan Hudson G, Vaughan Hudson B, Anderson L, Bennett MH, MacLennan KA. Primary gastrointestinal non-Hodgkin's lymphoma: a review of 175 British national lymphoma investigation cases. *Br J Cancer* 1993; **67**: 776-782
7 **Amer MH**, El-Akkad S. Gastrointestinal lymphoma in adults: clinical features and management of 300 cases. *Gastroenterology* 1994; **106**: 846-858
8 **Domizio P**, Owen RA, Shepherd NA, Talbot IC, Norton AJ. Primary lymphoma of the small intestine: A clinicopathological study of 119 cases. *Am J Surg Pathol* 1993; **17**: 429-442
9 **Nakamura S**, Matsumoto T, Takeshita M, Kurahara K, Yao T, Tsuneyoshi M, Iida M, Fujishima M. A clinicopathologic study of primary small intestine lymphoma: prognostic significance of mucosa-associated lymphoid tissue-derived lymphoma. *Cancer* 2000; **88**: 286-294
10 **Daum S**, Ullrich R, Heise W, Dederke B, Foss HD, Stein H, Thiel E, Zeitz M, Riecken EO. Intestinal non-Hodgkin's lymphoma: a multicenter prospective clinical study from the german study group on intestinal non-Hodgkin's lymphoma. *J Clin Oncol* 2003; **21**: 2740-2746
11 **Kohno S**, Ohshima K, Yoneda S, Kodama T, Shirakusa T, Kikuchi M. Clinicopathological analysis of 143 primary malignant lymphomas in the small and large intestines based on

the new WHO classification. *Histopathology* 2003; **43**: 135-143
12 **Gobbi PG**, Ghirardelli ML, Cavalli C, Baldini L, Broglia C, Clo V, Berte R, Ilariucci F, Carotenuto M, Piccinini L, Stelitano C, Attardo-Parrinello G, Ascari E. The role of surgery in the treatment of gastrointestinal lymphomas other than low-grade MALT lymphomas. *Haematologica* 2000; **85**: 372-380
13 **Ibrahim EM**, Ezzat AA, El-Weshi AN, Martin JM, Khafaga YM, Al Rabih W, Ajarim DS, Al-Foudeh MO, Zucca E. Primary intestinal diffuse large B-cell non-Hodgkin's lymphoma: clinical features, management, and prognosis of 66 patients. *Ann Oncol* 2001; **12**: 53-58
14 **Radaszkiewicz T**, Dragosics B, Bauer P. Gastrointestinal malignant lymphomas of the mucosa-associated lymphoid tissue: factors relevant to prognosis. *Gastroenterology* 1992; **102**: 1628-1638
15 **Jinnai D**, Iwasa Z, Watanuki T. Malignant lymphoma of the large intestine: operative results in Japan. *Japan J Surg* 1983; **13**: 331-336
16 **d'Amore F**, Brincker H, Gronbaek K, Thorling K, Pedersen M, Jensen MK, Andersen E, Pedersen NT, Mortensen LS. Non-Hodgkin's lymphoma of the gastrointestinal tract: a population-based analysis of incidence, geographic distribution, clinicopathologic presentation features, and prognosis. *J Clin Oncol* 1994; **12**: 1673-1684
17 **Zinzani PL**, Magagnoli M, Pagliani G, Bendandi M, Gherlinzoni F, Merla E, Salvucci M, Tura S. Primary intestinal lymphoma: clinical and therapeutic features of 32 patients. *Haematologica* 1997; **82**: 305-308
18 **Pandey M**, Kothari KC, Wadhwa MK, Patel HP, Patel SM, Patel DD. Primary malignant large bowel lymphoma. *Am Surg* 2002; **68**: 121-126
19 **Doolabh N**, Anthony T, Simmang C, Bieligk S, Lee E, Huber P, Hughes R, Turnage R. Primary colonic lymphoma. *J Surg Oncol* 2000; **74**: 257-262

Science Editor Wang XL and Guo SY **Language Editor** Elsevier HK

PO Box 2345, Beijing 100023, China
www.wjgnet.com
wjg@wjgnet.com

ELSEVIER

World J Gastroenterol 2005;11(37):5910
World Journal of Gastroenterology ISSN 1007-9327
© 2005 The WJG Press and Elsevier Inc. All rights reserved.

Acknowledgments to Reviewers of *World Journal of Gastroenterology*

Many reviewers have contributed their expertise and time to the peer review, a critical process to ensure the quality of *World Journal of Gastroenterology*. The editors and authors of the articles submitted to the journal are grateful to the following reviewers for evaluating the articles (including those were published and those were rejected in this issue) during the last editing period of time.

Trond Berg, Professor
Department of Molecular Biosciences, University of Oslo, PO Box 1041 Blindern, Oslo 0316, Norway

Bruno Clement, Professor
INSERM U-620, University of Rennes I, Faculty of Medicine, 2 ave. L. Bernard, Rennes 35043, France

Xue-Gong Fan, Professor
Xiangya Hospital, Changsha 410008, China

Edoardo G Giannini, Assistant Professor
Department of Internal Medicine, Gastroenterology Unit, Viale Benedetto XV, no. 6, Genoa, 16132, Italy

Hans Gregersen, Professor
The Research Administration, Aalborg Hospital, Hobrovej 42 A, Aalborg 9000, Denmark

Anna S Gukovskaya, Professor
Department of Medicine, UCLA, 11301 Wilshire Blvd, Los Angeles 91301, United States

Werner Hohenberger, Professor
Chirurgische Klinik und Poliklinik, Krankenhausstrasse 12, Erlangen D-91054, Germany

Masayoshi Ito, M.D.
Department of Endoscopy, Yotsuya Medical Cube, 5-5-27-701 Kitashinagawa, Shinagawa-ku, Tokyo 1410001, Japan

Hiroaki Itoh, M.D.
First Department of Internal Medicine, Akita University Scool of Medicine, 1-1-1, Hondou, Akita City 010-8543, Japan

Tsuneo Kitamura, Associate Professor
Department of Gastroenterology, Juntendo University Urayasu Hospital, Juntendo University School of Medicine, 2-1-1 Tomioka, Urayasu-shi, Chiba 279-0021, Japan

Zahariy Krastev, Professor
Department of Gastroneterology, Universiti Hospital "St. Ivan Rilski", #15, blvd "Acad. Ivan Geshov", Sofia 1431, Bulgaria

Shoji Kubo, M.D.
Hepato-Billiary-Pancreatic Surgery, Osaka City University Graduate School of Medicine, 1-4-3 Asahimachi, Abeno-ku, Osaka 545-8585, Japan

Fin Stolze Larsen, Associate Professor
Hepatology A-2121, Rigshospitalet Univ. Hospital of Copenhagen, Blegdamsvej 9, Copenhagen 2100, Denmark

James Neuberger, Professor
Liver Unit, Queen Elizabeth Hospital, Birmingham B15 2TH, United Kingdom

Mikio Nishioka, M.D.
Ehime Rosai Hospital, 13-27 Minami Komatsubara, Niihama 792-8550, Japan

Gustav Paumgartner, Professor
University of Munich, Klinikum Grosshadern, Marchioninistr. 15, Munich D-81377, Germany

Zhiheng Pei, Assistant Professor
Department of Pathology and Medicine, New York University School of Medicine, Department of Veterans Affairs, New York Harbor Healthcare System, 6001W, 423 East 23rd street, New York NY 10010, United States

Lun-Xiu Qin, Professor
Liver Cancer Institute and Zhongshan Hospital, Fudan University, 180 Feng Lin Road, Shanghai 200032, China

Manfred Stolte, Professor
Institute of Pathology, Klinikum Bayreuth, Preuschwitzer Str. 101, Bayreuth 95445, Germany

Michael Trauner, Professor
Medical University Graz, Auenbruggerplatz 15, Graz A-8036, Austria

Takato Ueno, Professor
Research Center for Innovative Cancer Therapy, Kurume University, 67 Asahi-machi, Kurume 830-0011, Japan

Toshio Watanabe, Associate Professor
Department of Gastroenterology, Osaka City University, Graduate School of Medicine, 1-4-3 Asahimachi, Abenoku-ku, Osaka 545-8585, Japan

Harry H-X Xia, M.D.
Department of Medicine, The University of Hong Kong, Pokfulam Road, Hong Kong, China

PO Box 2345, Beijing 100023, China
www.wjgnet.com
wjg@wjgnet.com

ELSEVIER

World J Gastroenterol 2005;11(38):5915-5919
World Journal of Gastroenterology ISSN 1007-9327
© 2005 The WJG Press and Elsevier Inc. All rights reserved.

inhibitory effects of extracellular adenosine triphosphate on growth of esophageal carcinoma cells

Ming-Xia Wang, Lei-Ming Ren, Bao-En Shan

Ming-Xia Wang, Bao-En Shan, the Fourth Affiliated Hospital of Hebei Medical University, Shijiazhuang 050011, Hebei Province, China
Lei-Ming Ren, School of Pharmacy, Hebei Medical University, Shijiazhuang 050017, Hebei Province, China
Supported by the Science and Technology Development Project of Hebei Province, No. 032761192
Correspondence to: Lei-Ming Ren, MD, PhD, School of Pharmacy, Hebei Medical University, Shijiazhuang 050017, Hebei Province, China. ren-leiming@263.net
Telephone: +86-311-6034579 Fax: +86-311-6077634
Received: 2004-12-28 Accepted: 2005-03-24

© 2005 The WJG Press and Elsevier Inc. All rights reserved.

Key words: Extracellular adenosine triphosphate; Esophageal carcinoma cells; Apoptosis; Growth inhibition

Wang MX, Ren LM, Shan BE. inhibitory effects of extracellular adenosine triphosphate on growth of esophageal carcinoma cells. *World J Gastroenterol* 2005; 11(38): 5915-5919
http://www.wjgnet.com/1007-9327/11/5915.asp

Abstract

AIM: To study the growth inhibitory effects of ATP on TE-13 human squamous esophageal carcinoma cells *in vitro.*

METHODS: MTT assay was used to determine the inhibition of proliferation of ATP or adenosine (ADO) on TE-13 cell line. The morphological changes of TE-13 cells induced by ATP or ADO were observed under fluorescence light microscope by acridine orange (AO)/ethidium bromide (EB) double stained cells. The internucleosomal fragmentation of genomic DNA was detected by agarose gel electrophoresis. The apoptotic rate and cell cycle after treatment with ATP or ADO were determined by flow cytometry.

RESULTS: ATP and ADO produced inhibitory effects on TE-13 cells at the concentration between 0.01 and 1.0 mmol/L. The IC_{50} of TE-13 cells exposed to ATP or ADO for 48 and 72 h was 0.71 or 1.05, and 0.21 or 0.19 mmol/L, respectively. The distribution of cell cycle phase and proliferation index (PI) value of TE-13 cells changed, when being exposed to ATP or ADO at the concentrations of 0.01, 0.1, and 1 mmol/L for 48 h. ATP and ADO inhibited the cell proliferation by changing the distribution of cell cycle phase via either G_0/G_1 phase (ATP or ADO, 1 mmol/L) or S phase (ATP, 0.1 mmol/L) arrest. Under light microscope, the tumor cells exposed to 0.3 mmol/L ATP or ADO displayed morphological changes of apoptosis. A ladder-like pattern of DNA fragmentation was obtained from TE-13 cells treated with 0.1-1 mmol/L ATP or ADO in agarose gel electrophoresis. ATP and ADO induced apoptosis of TE-13 cells in a dose-dependent manner at the concentration between 0.03 and 1 mmol/L. The maximum apoptotic rate of TE-13 cells exposed to ATP or ADO for 48 h was 16.63% or 16.9%, respectively.

CONCLUSION: ATP and ADO inhibit cell proliferation, arrest cell cycle, and induce apoptosis of TE-13 cell line.

INTRODUCTION

Extracellular ATP and adenosine (ADO) are important signaling molecules in both intracellular and extracellular microenvironments of cells. Though the regulatory control is exerted by ectonucleotidases, which maintain its low physiologic concentrations, extracellular ATP may reach high concentrations when released exocytotically from various cell types such as neurons, platelets, basophils, and mast, or when released nonexocytotically from damaged cells[1]. Since the pioneering work of Rapaport and Fontaine[2,3] showing the anticancer activities of extracellular adenine nucleotides on tumor, inhibitory effects of extracellular ATP have been described in the majority of cells and tissues studied so far, including human histiocytic leukemia cell line U-937[4], macrophages[5], mouse neuroblastoma cell line N1E-115[6], pancreatic cancer cells[7], endothelial cells[8], pulmonary artery endothelial cells[9], colorectal carcinoma cells[10], prostate carcinoma cells[11], murine dendritic cells, etc.[12-16]. But in other cell lines, such as human ovarian tumor cells and breast tumor cells, ATP shows opposite effects[17,18]. Recently, Maaser *et al*.[19], reported that extracellular nucleotides inhibit growth of moderately differentiated human esophageal cancer cells. However, the effects of ATP on poorly differentiated esophageal cancer cells have not been reported. In this study, we observed the growth inhibitory and apoptotic effects of ATP and its final metabolite, ADO, on poorly-differentiated human TE-13 esophageal cancer cells.

MATERIALS AND METHODS

Drugs and reagents

ATP, ADO, acridine orange (AO), ethidium bromide (EB), 3-(4,5-dimethyiazol-2-yl)-2, 5-diphenyl tetrazolium bromide (MTT) were purchased from Sigma. RNase, SDS, proteinase K, trypsin and agarose were from Sino-American Biotec Co., RPMI 1640 medium was from GIBCO, and fetal bovine serum (FBS) was from Hangzhou Sijiqing Biotec Co. ATP and ADO were dissolved in sterile PBS, and stored at -20 ℃.

Cell culture

Human esophageal carcinoma TE-13 cells, obtained from Japanese Cancer Cell Database, were cultured in RPMI 1640 medium supplemented with 100 mL/L FBS, 100 U/mL penicillin, and 100 μg/mL streptomycin at 37 ℃ in a humidified CO_2-controlled (50mL/L) incubator.

MTT assays

The cell viability was determined by MTT assay[20]. TE-13 cells in exponential phase of growth were harvested and seeded in 96-well plates (Costar, USA) at a density of 10 000 cells/well, and cultured for 24 h. ATP or ADO (0.01, 0.03, 0.1, 0.3, and 1 mmol/L), and control (PBS) were added into the wells and incubated continuously for 48 or 72 h at 37 ℃ with 50 mL/L CO_2. The drugs were added daily and replaced with fresh medium every 2 d. A 20-μL sample of MTT solution (5 g/L dissolved in PBS) was added to each well and the plates were incubated at 37 ℃ for 4 h. The supernatant was discarded and 150 μL dimethylsulfoxide was added to dissolve the blue insoluble MTT formazan produced by mitochondrial succinate dehydrogenase. The absorbance was measured at 492 nm in a spectrophotometer (Zhengzhou Bosai Biotech Co., ht2010), and the negative control well contained only the medium. The percentage of viable cells was calculated as the relative ratio of their absorbances to the control. All determinations were performed in quadruplicate and each experiment was repeated at least thrice.

Morphological assessment of apoptotic cells induced by ATP or ADO

Morphological assessment of apoptotic cells was performed using the AO/EB double staining method[21]. TE-13 cells in exponential phase of growth were harvested and seeded in a 25-mL cultured flask. The cells were incubated for 24 h at 37 ℃ with 50 mL/L CO_2, and then treated with 0.3 mmol/L ATP or ADO for 48 h. Freshly isolated TE-13 cells (1×10^6) were harvested in an Ependorf centrifuge tube, centrifuged for 5 min at 1 000 r/min and suspended in PBS containing fluorescence dye AO/EB (both AO and EB were at the concentration of 100 mg/L in PBS). The cells were prepared, and dropped on slides. The morphology of the cells was observed under fluorescence light microscope (UFX-II; Nikon, Japan) and photographed.

Agarose gel electrophoresis of DNA[22]

After treatment with ATP or ADO (0.1, 0.3, and 1 mmol/L) for 72 h, TE-13 cells (1×10^6) were harvested in an Ependorf centrifuge tube and washed twice with PBS. The cells were resuspended in a cell lysis buffer (50 mmol/L Tris-HCl buffer, 20 mmol/L EDTA, pH 8.0, 1% SDS) and then mixed by vortexing briefly. After the cells stood for 30 min on ice, proteinase K was added at a final concentration of 0.25 g/L. The cell lysates were incubated at 37 ℃ overnight in a water bath, and RNase was added at a final concentration of 0.5 g/L and incubated at 37 ℃ for 1 h. The lysates were mixed with an equal volume of Tris-saturated phenol–chloroform (1:1, v/v) and mildly shaken for 30 min, and the mixture was centrifuged at 3 000 r/min for 10 min at room temperature to separate the aqueous phase from the organic phase. Extraction of each aqueous phase was repeated using the Tris-saturated phenol-chloroform-isopropanol (25:24:1, v/v/v) mixture, and the aqueous phase was further extracted with an equal volume of chloroform. Mixing with 2 volumes of ice-cold ethanol and 0.1 volume of 3 mol/L NaAc precipitated DNA in the final aqueous phase. At this point, the mixture could be stored overnight. DNA was recovered by centrifugation at 13 000 *g* for 20 min in an Ependorf centrifuge tube. The supernatant was discarded, the DNA pellet was washed once with 70% ethanol, air-dried, and then redissolved in an appropriate volume of deionized distilled water and electrophoresed for 3 h at a constant voltage of 60 mV on an 1.8% agarose gel containing 0.5 mg/L EB, using an electrophoresis buffer (40 mmol/L Tris/acetate buffer, 1 mmol/L EDTA, pH 8.0). Each DNA sample contained bromophenol blue as a front-running dye. Ladder formation of oligonucleosomal DNA was made visible by an ultraviolet transillumination and photographed using a gel imaging system (PE Co., USA).

Determination of apoptosis by flow cytometric analysis

After the cells were incubated with different concentrations of ATP or ADO for 48 h, they were harvested by centrifugation, washed with ice-cold PBS once and fixed in 70% ethanol at 4 ℃ overnight. The cells were then washed once with ice-cold PBS and resuspended in PBS (pH 7.4) containing 0.5% pepsin, 5 mg/L EB and RNase at room temperature for 30 min. Finally, cells were analyzed by flow cytometry on a FACS420 (Becton Dickinson Corporation, USA), equipped with an argon ion laser (488 nm), using the HP-300 Consort 30 software to determine percentage of the apoptotic cells and the proportion of cells in G_0/G_1, S, G_2/M phases of cell cycle. The proliferation index (PI) of cells was calculated by the following formula:

$$PI\ (\%) = ([S+G_2/M]/[G_0/G_1+S+G_2/M])\times100\%.$$

Statistical analysis

The data shown were mean values of at least three independent experiments and expressed as mean±SD. Statistical comparisons were made by ANOVA. $P<0.05$ was considered statistically significant.

RESULTS

Inhibitory effects of ATP or ADO on TE-13 cell proliferation

The proliferation of TE-13 cells was significantly inhibited in a dose- and time-dependent manner, by 0.01-1.0 mmol/L of ATP or 0.3-1.0 mmol/L of ADO for 48 h of incubation, as well as 0.01-1.0 mmol/L of ADO for 72 h of incubation. The inhibitory fraction of TE-13 cells exposed to ATP and ADO for 48 and 72 h was 59.6% and 46.5%, and 80.5% and 74%, respectively (Figures 1A and B). The IC_{50} of TE-13 cells exposed to ATP or ADO for 48 and 72 h was 0.71 or 1.05 mmol/L, and 0.21 or 0.19 mmol/L, respectively.

Effects of ATP or ADO on cell cycle and proliferation index (PI) of TE-13 cells

The cell cycle phase and PI value of TE-13 cells changed when exposed to ATP or ADO at the concentrations of 0.01, 0.1, 1 mmol/L for 48 h. The proportion of cells in

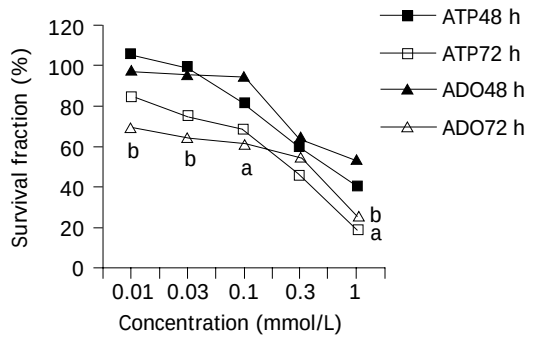


Figure 1 Effects of various concentrations of ATP or ADO on survival fraction of TE-13 cells. [a]*P*<0.05, [b]*P*<0.01 *vs* 48 h groups.

the S phase of cell cycle significantly increased, and that of the G_0/G_1, G_2/M phases and PI value did not alter after sustained incubation of TE-13 cells with ATP (0.1 mmol/L). In contrast, when exposed to ATP or ADO at the concentration of 1 mmol/L, the proportion of cells in the G_0/G_1 phase of cell cycle significantly increased, while that in the S phase of cell cycle and PI value significantly decreased. In accordance with cell proliferation results, neither the cell cycle phase nor PI value changed when exposed to ATP or ADO at the concentration of 0.01 mmol/L. The proportion of cells in G_2/M phase when exposed to ATP at various concentrations did not alter, but that significantly decreased when exposed to ADO at the concentration of 1 mmol/L. These results showed that ATP and ADO inhibited the cell proliferation by changing the distribution of cell cycle phase via either S phase delay (ATP, 0.1 mmol/L) or G_0/G_1 phase delay (ATP and ADO, 1 mmol/L, Table 1 and Figures 2A and B).

Table 1 Effects of ATP or ADO on PI value of TE-13 cells (*n* = 3, mean±SD)

Concentration (mmol/L)		PI (%)
ATP	0	37.57±2.02
	0.01	39.17±3.65
	0.1	31.24±1.04[a]
	1.0	28.69±1.33[a]
ADO	0	36.85±1.15
	0.01	29.91±1.78
	0.1	32.34±3.39
	1.0	21.76±5.20[b]

[a]*P*<0.05, [b]*P*<0.01 *vs* control group.

Morphological changes of TE-13 cells induced by ATP or ADO

Under fluorescence light microscope, the tumor cells exposed to 0.3 mmol/L ATP or ADO displayed morphological changes of apoptosis by AO/EB double staining, such as cell shrinkage, chromatin condensation, cell nuclear fragmentation, cell nucleolus disappearance, increased nuclei fluorescence or labeled orange or red-orange color (Figures 3A-C).

Agarose gel electrophoresis results of TE-13 cells induced by ATP or ADO

By agarose gel electrophoresis, a ladder-like pattern of DNA fragmentation was obtained from TE-13 cells treated with 0.1-1 mmol/L ATP or ADO, indicating that ATP or ADO induced apoptosis of TE-13 tumor cells (Figures 4A and B).

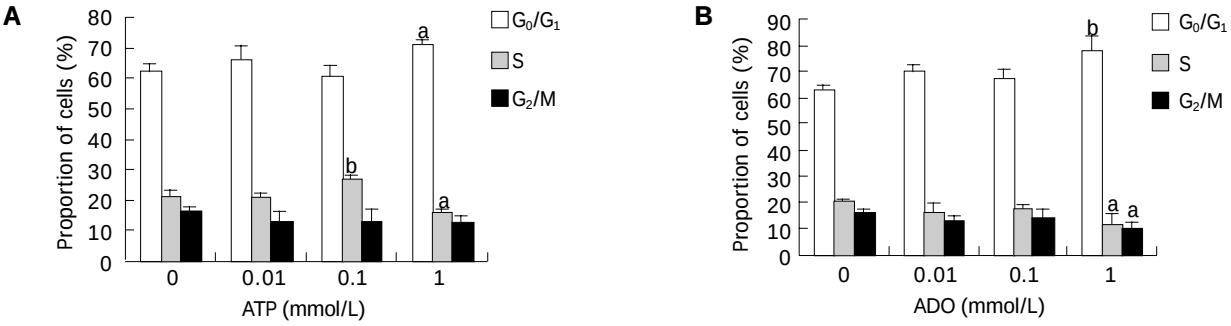


Figure 2 Effects of ATP (A) and ADO (B) on cell cycle of TE-13 cells (*n* = 3). [a]*P*<0.05, [b]*P*<0.01 *vs* 0 mmol/L.

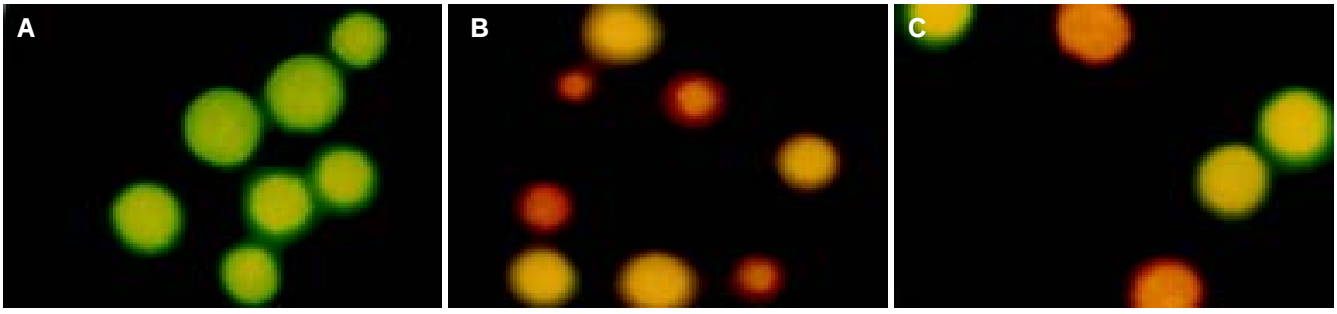


Figure 3 Fluorescence micrographs of TE-13 cells incubated for 48 h without treatment (A) and treated with ATP (B) or ADO (C) (×400).

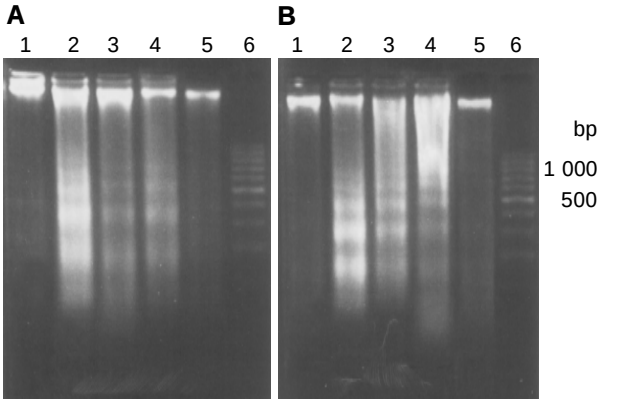


Figure 4 Agarose gel electrophoresis of DNA extracted from apoptotic TE-13 cells treated with ATP (A) or ADO (B) for 72 h. Lane 1: control; lanes 2-5: 1, 0.3, 0.1, and 0.03 mmol/L, respectively; lane 6: marker.

Apoptotic rate of TE-13 cells induced by ATP or ADO

ATP or ADO induced apoptosis of TE-13 cells in a dose-dependent manner at the concentration between 0.03 and 1 mmol/L for 48 h. The apoptotic rate of TE-13 cells treated with ATP or ADO was markedly higher than that of the control. The maximum apoptotic rate of TE-13 cells exposed to ATP or ADO (1 mmol/L) for 48 h was (16.6±1.1)% or (16.9±1.2)%, respectively (Table 2 and Figures 5A-C).

Table 2 Apoptosis of TE-13 cells induced by extracellular ATP or ADO (n = 3, mean±SD)

Concentration (mmol/L)		Apoptotic rate (%)
ATP	0	1.35±0.07
	0.03	3.89±0.29
	0.1	7.73±0.57[a]
	0.3	12.40±0.61[b]
	1.0	16.60±1.10[a]
ADO	0	2.43±0.85
	0.03	6.75±0.49[a]
	0.1	9.73±1.70[d]
	0.3	13.10±0.53[d]
	1.0	16.90±1.20[d]

[a]P<0.05, [b]P<0.01, and [d]P<0.001 *vs* control (0 mmol/L).

DISCUSSION

ATP and related compounds are widespread transmitters for extracellular communication in many cell types. By coupling to specific purinergic receptors, ATP is involved in a large variety of cellular functions. Receptors for purines and pyrimidines (P receptor) are divided into two major classes termed as ADO or P1 receptors at which ADO is the principal natural ligand, and P2 receptors at which ATP, ADP, UTP, and UDP are the principal natural ligands. To date four P1 receptor subtypes have been identified (A1, A2a, A2b, and A3), all of them are coupled to G proteins with distinct tissue distribution and pharmacological properties. The P2 receptors are divided into two families: the ligand-gated ion channels (P2X) and the G protein-coupled receptors (P2Y)[23-25]. ATP can inhibit cancer growth, induce apoptosis in various tumor models[26-30]. Both growth inhibition and programmed cell death are mediated by ionotropic P2-receptors and metabotropic P2-receptors[10,19]. Here we provide evidence that extracellular ATP induces apoptosis and causes cell cycle arrest in poorly differentiated human squamous cancer cells of the esophagus, and ADO plays an important role in them.

Recently, Maaser *et al*.[19], studied the effects of ATP and ADO on moderately differentiated esophageal cancer Kyse-140 cells, and found that ATP (100-500 μmol/L) inhibits cell growth, causes a delay in the S phase of cell cycle, and induces apoptosis. However, ADO has no contribution to the antiproliferative and apoptotic action of Kyse-140 cells. In our study, both ATP (0.1-1 mmol/L) and ADO (0.03-1 mmol/L) inhibited growth of TE-13 cells, caused cell cycle arrest in S phase (ATP, 0.1 mmol/L) or in G_0/G_1 phase (ATP or ADO, 1 mmol/L). The reasons why our results did not accord with those of Maaser *et al*.[19], may be due to the different kinds of esophageal cancer cell line and different concentrations of ATP used in our study. Additionally, a positive correlation between S-phase fraction and the response to anticancer agents has recently been documented[31]. Hence, in addition to the antiproliferative action of ATP on its own, possible synergistic effects of ATP and anticancer drugs should be investigated.

Besides its cell cycle interfering effects, ATP or ADO was shown to induce apoptosis in esophageal cancer TE-13 cells as assessed simultaneously by morphological study, agarose gel electrophoresis, and flow cytometry analysis. After being exposed to various concentrations of ATP or ADO for 48 or 72 h, TE-13 cells displayed a series of apoptotic vents, such as chromatin condensation, fragment nuclei, apoptotic body, apoptotic peak in the flow cytometry imaging

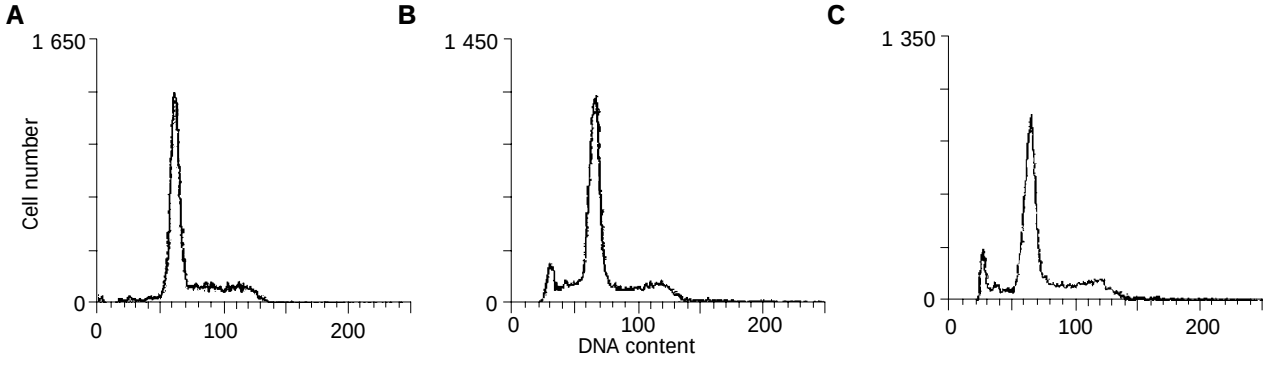


Figure 5 ATP- or ADO-induced apoptosis of TE-13 cells detected by flow cytometry in control (A) and treated with ADO (B) and ATP (C) for 48 h, respectively.

as well as DNA ladder. ADO is the final metabolite of ATP, and the result of ADO contributing to the growth inhibition and apoptosis suggests that the above effects of ATP might be partially related to its metabolite, ADO.

In conclusion, extracellular ATP inhibits cell growth, causes cell cycle arrest, and induces apoptosis. These actions might be partially related to its metabolite, ADO. Although the average concentration of nucleosides in plasma and other extracellular fluids is generally in the range of 0.4-6 μmol/L, these values can increase at sites of vascular inflammation and platelet degranulation[32]. Taken together, to further investigate the effects of ATP on tumor cells may provide an innovative treatment strategy for esophageal cancer.

REFERENCES

1 **Nihei OK**, de Carvalho AC, Savino W, Alves LA. Pharmacologic properties of P(2Z)/P2X(7) receptor characterized in murine dendritic cells: role on the induction of apoptosis. *Blood* 2000; **96**: 996-1005

2 **Rapaport E**, Fontaine J. Anticancer activities of adenine nucleotides in mice are mediated through expansion of erythrocyte ATP pools. *Proc Natl Acad Sci USA* 1989; **86**: 1662-1666

3 **Rapaport E**, Fontaine J. Generation of extracellular ATP in blood and its mediated inhibition of host weight loss in tumor-bearing mice. *Biochem Pharmacol* 1989; **38**: 4261-4266

4 **Schneider C**, Wiendl H, Ogilvie A. Biphasic cytotoxic mechanism of extracellular ATP on U-937 human histiocytic leukemia cells: involvement of adenosine generation. *Biochim Biophys Acta* 2001; **1538**: 190-205

5 **Coutinho-Silva R**, Perfettini JL, Persechini PM, Dautry-Varsat A, Ojcius DM. Modulation of P2Z/P2X$_7$ receptor activity in macrophages infected with Chlamydia psittaci. *Am J Physiol Cell Physiol* 2001; **280**: C81-C89

6 **Schrier SM**, Florea BI, Mulder GJ, Nagelkerke JF, Ijzerman AP. Apoptosis induced by extracellular ATP in the mouse neuroblastoma cell line N1E-115: studies on involvement of P2 receptors and adenosine. *Biochem Pharmacol* 2002; **63**: 1119-1126

7 **Yamada T**, Okajima F, Akbar M, Tomura H, Narita T, Yamada T, Ohwada S, Morishita Y, Kondo Y. Cell cycle arrest and the induction of apoptosis in pancreatic cancer cells exposed to adenosine triphosphate *in vitro*. *Oncol Rep* 2002; **9**: 113-117

8 **von-Albertini M**, Palmetshofer A, Kaczmarek E, Koziak K, Stroka D, Grey ST, Stuhlmeier KM, Robson SC. Extracellular ATP and ADP activate transcription factor NF-kappa B and induce endothelial cell apoptosis. *Biochem Biophys Res Commol* 1998; **248**: 822-829

9 **Rounds S**, Yee WL, Dawicki DD, Harrington E, Parks N, Cutaia MV. Mechanism of extracellular ATP- and adenosine-induced apoptosis of cultured pulmonary artery endothelial cells. *Am J Physiol* 1998; **275**(2 Pt1): L379-L388

10 **Hopfner M**, Maaser K, Barthel B, von Lampe B, Hanski C, Riecken EO, Zeitz M, Scherübl H. Growth inhibition and apoptosis induced by P2Y$_2$ receptors in human colorectal carcinoma cells: involvement of intracellular calcium and cyclic adenosine monophosphate. *Int J Colorectal Dis* 2001; **16**: 154-166

11 **Janssens R**, Boeynaems JM. Effects of extracellular nucleotides and nucleosides on prostate carcinoma cells. *Br J Pharmacol* 2001; **132**: 536-546

12 **Macino B**, Zambon A, Milan G, Cabrelle A, Ruzzene M, Rosato A, Mandruzzato S, Quintieri L, Zanovello P, Collavo D. CD45 regulates apoptosis induced by extracellular adenosine triphosphate and cytotoxic T lymphocytes. *Biochem Biophys Res Commol* 1996; **226**: 769-776

13 **Bronte V**, Macino B, Zambon A, Rosato A, Mandruzzato S, Zanovello P, Collavo D. Protein tyrosine kinases and phosphatases control apoptosis induced by extracellular adenosine 5′-triphosphate. *Biochem Biophys Res Commol* 1996; **218**: 344-351

14 **Sun AY**, Chen YM. Extracellular ATP-induced apoptosis in PC12 cells. *Adv Exp Med Biol* 1998; **446**: 73-83

15 **Schulze-Lohoff E**, Hugo C, Rost S, Arnold S, Gruber A, Brune B, Sterzel RB. Extracellular ATP causes apoptosis and necrosis of cultured mesangial cells via P2Z/P2X$_7$ receptors. *Am J Physiol* 1998; **275**(6 Pt2): F962-F971

16 **Nakamura N,** Wada Y. Properties of DNA fragmentation activity generated by ATP depletion. *Cell Death Differ* 2000; **7**: 477-484

17 **Dixon CJ**, Bowler WB, Fleetwood P, Ginty AF, Gallaghe JA, Carron JA. Extracellular nucleotides stimulate proliferation in MCF-7 breast cancer cells via P2-purinoceptors. *Br J Cancer* 1997; **75**: 34-39

18 **Popper LD** , Batra S. Calcium mobilization and cell proliferation activated by extracellular ATP in human ovarian tumor cells. *Cell Calcium* 1993; **14**: 209-218

19 **Maaser K**, Hopfner M, Kap H, Sutter AP, Barthel B, von Lampe B, Zeitz M, Scherübl H. Extracellular nucleotides inhibit growth of human oesophageal cancer cells via P2Y$_2$-receptors. *Br J Cancer* 2002; **86**: 636-644

20 **Situ ZQ**, Wu JZ. *Cell Culture*. Xi'an: *World Book's Publishing Company* 1996: 186-188

21 **Wang CY**, Sheng RL, Wang F, Ding XJ, Qiu NL. Fluorescence method of apoptotic morphology studying by acridine orange and ethidium bromide double stained cells. *Zhongguo Bingli Shengli Zazhi* 1998; **14**: 104-106

22 **Kim KT**, Yeo EJ, Choi H, Park SC. The effect of pyrimidine nucleosides on adenosine-induced apoptosis in HL-60 cells. *J Cancer Res Clin Oncol* 1998; **124**: 471-477

23 **Fredholm BB**, Abbracchio MP, Burnstock G, Daly JW, Harden TK, Jacobson KA, Leff P, Williams M. Nomenclature and classification of purinoceptors. *Pharmacol Rev* 1994; **46**: 143-156

24 **Burnstock G**. Purinergic signaling and vascular cell proliferation and death. *Arterioscler Thromb Vasc Biol* 2002; **22** 364-373

25 **Vandewalle B**, Hornez L, Revillion F, Lefebvre J. Effect of extracellular ATP on breast tumor cell growth, implication of intracellular calcium. *Cancer Lett* 1994; **85**: 47-54

26 **Ferraria D**, Los M, Bauer MK, Vandenabeele P, Wesselborg S, Schulze-Osthoff K. P2Z purinoreceptor ligation induces activation of caspases with distinct roles in apoptotic and necrotic alterations of cell death. *FEBS Lett* 1999; **447**: 71-75

27 **Peng L**, Bradley CJ, Wiley JS. P2Z purinoceptor, a special receptor for apoptosis induced by ATP in human leukemic lymphocytes. *Chin Med J* 1199; **112**: 356-362

28 **Fujita N**, Kakimi M, Ikeda Y, Hiramoto T, Suzuki K. Extracellular ATP inhibits starvation-induced apoptosis via P2X$_2$ receptors in differentiated rat pheochromocytoma PC12 cells. *Life Sci* 2000; **66**: 1849-1859

29 **Katzur AC**, Koshimizu T, Tomic M, Schultze-Mosgau A, Ortmann O, Stojilkovic SS. Expression and responsiveness of P2Y$_2$ receptors in human endometrial cancer cell lines. *J Clin Endocrinol Metab* 1999; **84**: 4085-4091

30 **Dawicki DD**, Chatterjee D, Wyche J, Rounds S. Extracellular ATP and adenosine cause apoptosis of pulmonary artery endothelial cells. *Am J Physiol* 1997; **273**(2 Pt1): L485-L494

31 **Kolfschoten GM**, Hulscher TM, Pinedo HM, Boven E. Drug resistance features and S-phase fraction as possible determinants for drug response in a panel of human ovarian cancer xenografts. *Br J Cancer* 2000; **83**: 921-927

32 **Traut TW**. Physiological concentrations of purines and pyrimidines. *Mol Cell Biochem* 1994; **140**: 1-22

Science Editor Wang XL and Guo SY **Language Editor** Elsevier HK

PO Box 2345, Beijing 100023, China
www.wjgnet.com
wjg@wjgnet.com

ELSEVIER

World J Gastroenterol 2005;11(38):5920-5925
World Journal of Gastroenterology ISSN 1007-9327
© 2005 The WJG Press and Elsevier Inc. All rights reserved.

• *GASTRIC CANCER* •

Prognostic implication of isolated tumor cells and micrometastases in regional lymph nodes of gastric cancer

Hye Seung Lee, Min A Kim, Han-Kwang Yang, Byung Lan Lee, Woo Ho Kim

Hye Seung Lee, Department of Pathology, Seoul National University Bundang Hospital, Gyeonggi 463-707, Korea
Min A Kim, Woo Ho Kim, Department of Pathology and Cancer Research Institute, Seoul National University College of Medicine, Seoul 110-799, Korea
Han-Kwang Yang, Department of Surgery and Cancer Research Institute, Seoul National University College of Medicine, Seoul, Korea
Byung Lan Lee, Department of Anatomy, Seoul National University College of Medicine, Seoul, Korea
Supported by a grant (FG03-11-02) from the 21C Frontier Functional Human Genome Project from the Ministry of Science and Technology of Korea
Correspondence to: Dr. Woo Ho Kim, Department of Pathology, Seoul National University College of Medicine, 28 Yongon-dong, Chongno-gu, Seoul 110-799, Korea. woohokim@snu.ac.kr
Telephone: +82-2-7408269 Fax: +82-2-7655600
Received: 2005-02-24 Accepted: 2005-05-12

ABSTRACT

AIM: To determine the prognostic significance of isolated tumor cells (ITCs) and lymph node micrometastases in gastric cancer.

METHODS: Hematoxylin and eosin-stained slides of lymph node dissections of 632 consecutive gastric cancers were reviewed. Cytokeratin immunostaining was performed in 280 node-negative cases and 5 cases indefinite for lymph node metastases. Lymph node metastases were divided into ITCs, micrometastases, or macrometastases, according to the sizes of tumor deposits in largest dimension. ITCs were further classified into four groups according to metastasis pattern.

RESULTS: Lymph node metastases were identified by immunostaining in 58 of 280 node-negative cases (20.7%) and were not significantly associated with patient survival (P = 0.3460). After cytokeratin immunostaining, 196 cases were classified as pN1, which consisted of 20 cases with micrometastases detected by immunostaining (pN1mi(i+)), 34 cases with only micrometastases (pN1mi), and 142 cases with pN1 with one or more macrometastases (pN1). Cases with pN1mi and pN1mi(i+) had a significantly better prognosis than the cases with pN1 (P = 0.0037). ITCs were found in 38 of these 58 cases, and could be divided into four groups: 12 cases with only a single cell pattern, 7 cases with multiple individual cells, 5 cases with single small cluster, and 14 cases with multiple small clusters. Among these four groups, cases with ITCs of multiple individual cell pattern showed the worst survival (median survival: 28 mo, P<0.0001).

CONCLUSION: Both size and pattern of lymph node metastases can give prognostic information on the survival of gastric cancer patients.

© 2005 The WJG Press and Elsevier Inc. All rights reserved.

Key words: Immunohistochemistry; Cytokeratin; Patient survival; Lymph node metastasis

Lee HS, Kim MA, Yang HK, Lee BL, Kim WH. Prognostic implication of isolated tumor cells and micrometastases in regional lymph nodes of gastric cancer. *World J Gastroenterol* 2005; 11(38): 5920-5925
http://www.wjgnet.com/1007-9327/11/5920.asp

INTRODUCTION

The most important prognostic factor in patients with gastric cancer is the presence of a regional lymph node metastasis[1]. Some patients with histologically node-negative gastric cancer will die as a result of local or distant tumor recurrence, even though their primary tumor is curatively resected. Adjuvant chemotherapy benefits some patients with node-negative gastric cancer, but the treatment of all node-negative patients is unnecessary, as most node-negative patients will never have recurrence after surgery. Therefore, additional markers would be helpful for predicting patients at risk of a poor prognosis.

For the above purpose, histological evaluations of multiple serial sections of lymph nodes at many levels have been undertaken by several investigators[2,3]. Although serial sectioning can increase the detection of occult lymph node metastases, it is also labor-intensive and expensive for routine diagnostic practice. Furthermore, a single cell or minute cluster cannot be detected even by an expert pathologist. Recent advances in immunohistochemistry and molecular biology allow the identification of discrete and occult tumor cells, which are undetectable by standard hematoxylin and eosin (HE) staining, in the lymph nodes of patients with breast[4,5], esophageal[6,7], and colorectal cancers[8,9]. Many investigators have correlated patient prognosis with the presence of metastases detected by immunostaining, but controversy remains over the importance of single cell or cluster of cancer cells in regional lymph nodes.

Recently, regional lymph node metastasis was further classified into isolated tumor cells (ITCs), micrometastases, or macrometastases according to the size of tumor deposits in largest dimension in patients with breast cancers[10]. ITCs are defined as single cells or small clusters not greater than 0.2 mm in largest dimension, usually with no histologic

evidence of malignant activity. Cases with only ITCs are designated as pN0(i+) and categorized into pN0 by AJCC[10]. Single cells and small ill-defined clusters in lymph node metastasis, classified as ITCs, are not uncommon in gastric cancer, since cancer cells in diffuse type cancer frequently loose intercellular adhesion molecules, which represents a critical event of the metastatic cascade[11-13]. However, the clinical importance of size or pattern of metastatic tumor deposits in lymph node metastases is not defined in gastric cancer patients. To clarify the prognostic impact of ITCs and micrometastases on regional lymph nodes, we investigated 632 consecutive gastric cancers resected during one year in the aspect of number, size, and patterns of lymph node metastases and examined their clinical significance.

MATERIALS AND METHODS

Specimens

The files of 659 surgically resected primary gastric cancer cases examined at the Department of Pathology, Seoul National University College of Medicine over a period of 1 year (January 1, 1995-December 31, 1995) were examined in order to evaluate their lymph node metastasis status. Of these 659 cases, 632 cases (95.9%) were available for slide review and immunohistochemical staining of lymph nodes. The series consisted of 280 cases of pN0 stage, 183 cases of pN1 stage, 113 cases of pN2 stage and 56 cases of pN3 stage. Mean age of the patients was 54.5 years, and 92.9% of the patients had undergone curative resection (R0 according to the AJCC guideline). The study included 409 advanced gastric carcinomas and 223 early gastric carcinomas. No patient had received preoperative chemo- or radiotherapy. Glass slides were reviewed to determine histologic types according to WHO classification[11]. The clinical outcomes of the patients were followed from the date of surgery to either the date of death or December 1, 2000, resulting in a follow-up period ranging from 1 to 72 mo (mean: 55 mo). Those cases who lost their follow-up and those who ended in death due to a cause other than gastric cancer were regarded as censored data during survival rate analysis.

Review of HE-stained slides of lymph node dissection

HE-stained slides of lymph node dissection of 632 consecutive gastric cancers (31 421 lymph nodes) were reviewed. In contrast to original report, metastatic nodules in the fat adjacent to a gastric carcinoma without evidence of residual lymph node tissue were regarded as regional lymph node metastases by the AJCC guideline. Lymph node metastases were subdivided into three groups according to the AJCC guidelines using the maximum size of tumor deposit, i.e., ITCs are not greater than 0.2 mm in diameter, micrometastases are greater than 0.2 mm but not greater than 2 mm in diameter, and macrometastases are greater than 2 mm in diameter[10]. Lymph nodes with ITCs were not regarded as lymph node metastases, and cases with only micrometastases (not greater than 2 mm in diameter) were classified as pN1mi.

Immunohistochemistry

Immunohistochemical staining was performed on 280 gastric cancer cases (9 604 lymph nodes) without regional lymph node metastasis (pN0) by conventional HE staining, and on an additional 5 cases, who were originally reported as pN1 but were indefinite for metastasis by reviewing HE-stained slides. A single serial section (4 μm) was cut from each paraffin block, deparaffinized and dehydrated. Immunostaining with antibodies against cytokeratin (mAb anti-human cytokeratin clone MNF116, DAKO, Glostrup, Denmark) at 1:100 dilution was performed using a streptavidin peroxidase procedure after an antigen retrieval process using microwaves. Cells were considered to be occult lymph node metastases, if they were immunoreactive mainly in their cytoplasmic membranes, were found within the substance of the lymph nodes and were morphologically consistent with cancer cells. Immunohistochemically detected lymph node metastases were also subdivided into three groups: ITCs, micrometastases, or macrometastases, according to the size of tumor deposits in the largest dimension. Tumor deposits in lymph nodes with histologic evidence of malignant activity, such as gland formation or stromal reaction, were defined as micrometastases even if they were smaller than 0.2 mm in maximum dimension. ITCs were subdivided into four groups according to metastasis pattern (single cell, multiple individual cells, single cluster and multiple clusters, Figure 1). The number of lymph nodes containing tumors and the total number of tumor cells or clusters in a lymph node were recorded.

Statistical analysis

Either the χ^2 test or Fisher's exact test (two-sided) was performed to determine the correlation between lymph node metastasis and clinicopathologic parameters. Survival curves were estimated using the Kaplan-Meier product-limit method, and the significance of differences between survival curves was determined using the log-rank test. Results were considered to be statistically significant when *P* values were less than 0.05. All statistical analyses were conducted using the SPSS 11.0 statistical software program (SPSS, Chicago, IL, USA).

RESULTS

Reclassified pN stage after immunohistochemistry and reviewing HE-stained slides

Occult lymph node metastases were identified by cytokeratin immunostaining in 58 (20.7%) of 280 cases or in 157 of 9 604 lymph nodes (1.63%), which were originally reported as pN0. Of the 58 cases with positive occult lymph node metastasis, macrometastasis was found in one case, micrometastases in 19 cases (pN1mi(i+)), and ITCs in 38 cases (pN0(i+)). Four cases, who were originally reported as pN1, were reclassified as pN0, and one case was reclassified as pN1mi(i+) after cytokeratin immunostaining.

The pN stage, after immunostaining for cytokeratin and reviewing HE-stained slides, was reclassified as pN0 in 264 cases, pN1 in 196 cases, pN2 in 113 cases, and pN3 in 59 cases. The reclassified pN stage was found to be significantly associated with patient survival (Figure 2A).

Subgroups of pN1

One hundred and ninety-six cases with pN1 were subdivided

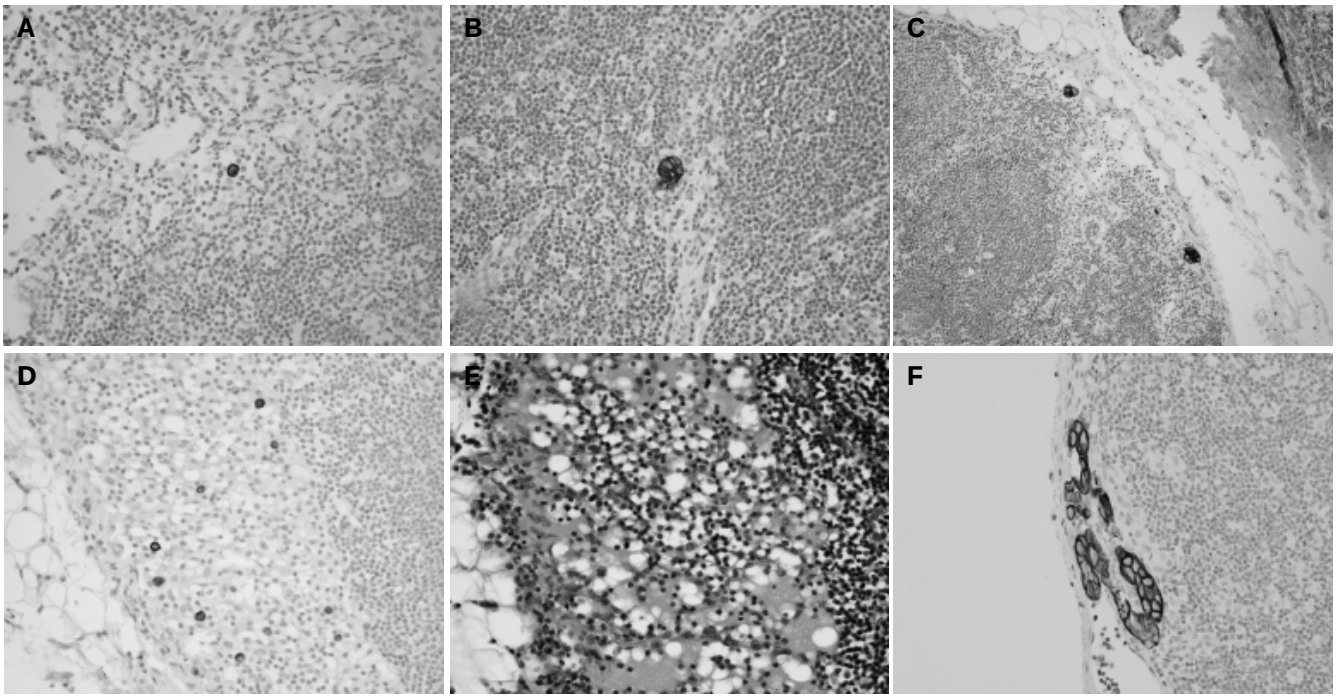


Figure 1 Immunohistochemical staining against cytokeratin. A: Single cell only (×400); B: single small cluster (×400); C: multiple small clusters (×200); D: multiple individual cells (×400); E: HE-stained slides of multiple individual tumor cells in lymph nodes (the same area of D, ×400); F: micrometastasis (×400).

into three groups: 20 cases with pN1mi(i+), 34 cases with pN1mi, and 142 cases with pN1 with one or more macrometastases. Cases with pN1mi, including pN1mi(i+), showed a significantly better prognosis than the 142 cases with macrometastases ($P = 0.0037$, Figure 2B). Furthermore, pN1mi detected by HE staining only was significantly associated with better survival than macrometastases ($P = 0.0218$, Figure 2C). No significant difference was observed between the survival of cases with pN1mi(i+) and pN1mi ($P = 0.3305$, Figure 2B). When compared to pN0(i-) cases, pN1mi cases showed significantly poorer survival ($P = 0.0104$, Figure 2C), but pN1mi (i+) and pN0(i-) cases did not show a survival difference ($P = 0.6738$).

Isolated tumor cells (ITCs)

Cases with lymph node metastases detected by immunohistochemistry (pN0(i+) and pN1(i+)) did not show a different survival when compared to cases without lymph node metastases ($P = 0.3460$, Figure 2D). Patients with immunohistochemically detected metastases had poorly differentiated adenocarcinomas more frequently than those without metastases ($P = 0.019$, Table 1).

Four groups of ITCs included 12 cases with a single cell pattern, 7 cases with multiple individual cells, 5 cases with a single cluster and 14 cases with multiple clusters. Among them, cases with multiple individual cells showed the poorest survival (median survival: 28 mo, $P<0.0001$, Figure 2E),

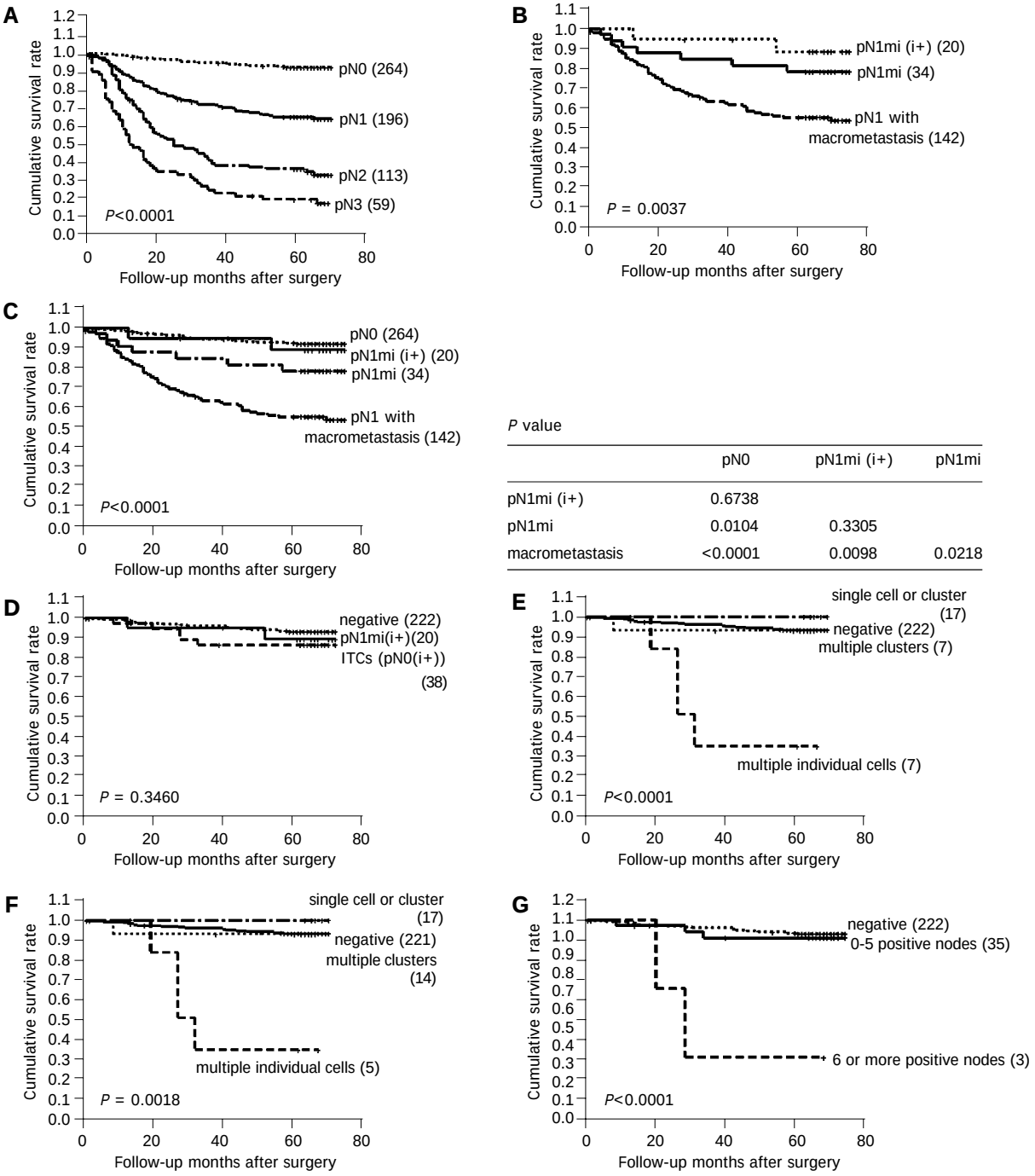
Table 1 Pathologic findings according to the size and pattern of lymph node metastasis after cytokeratin staining in pN0 cases on initial examination

	Negative	ITCs				Micro meta-stases	Macro meta-stases	*P*
		Single cell	Multiple cells	Single cluster	Multiple clusters			
WHO (%)								0.019
[1]W/D, M/D	112 (50.5)	6 (50.0)	0 (0)	1 (20)	6 (42.9)	8 (42.1)	0 (0)	
[2]P/D	54 (24.3)	4 (33.3)	7 (100)	2 (40)	5 (35.7)	8 (42.1)	1 (100)	
Mucinous	9 (4.0)	0 (0)	0 (0)	1 (20)	0 (0)	2 (10.5)	0 (0)	
[3]SRC	47 (21.2)	2 (16.7)	0 (0)	1 (20)	3 (21.4)	1 (5.3)	0 (0)	
Depth (%)								<0.001
Mucosa	97 (43.7)	4 (33.3)	0 (0)	2 (40)	1 (7.1)	3 (15.8)	0 (0)	
[4]SM	72 (32.4)	2 (16.7)	1 (14.4)	1 (20)	4 (28.7)	5 (26.3)	1 (100)	
[5]PM	21 (9.5)	1 (8.3)	0 (0)	0 (0)	1 (7.1)	2 (10.5)	0 (0)	
Subserosa	28 (12.6)	5 (41.7)	3 (42.8)	2 (40)	7 (50)	4 (21.1)	0 (0)	
Serosa	4 (1.8)	0 (0)	3 (42.8)	0 (0)	1 (7.1)	5 (26.3)	0 (0)	
Total (%)	222 (100)	12 (100)	7 (100)	5 (100)	14 (100)	19 (100)	1 (100)	

[1]Well and moderately differentiated tubular adenocarcinoma, [2]poorly differentiated tubular adenocarcinoma, [3]signet-ring cell carcinoma, [4]submucosa, [5]proper muscle.

and had poorly differentiated non-solid type adenocarcinomas with infiltrative border. Lymphatic invasion was not found in these cases. Histologically, cytokeratin-positive individual cells were found in the sinus of lymph nodes, and these could not be recognized by routine HE staining (Figure 1). In four of seven cases with multiple individual cells, the maximum number of tumor cells in a single lymph node exceeded 20 (Table 2), and prognosis was grave especially in these four cases. By Cox regression analysis, the pattern of metastasis was found to be a significant prognostic factor independent of pT stage and histologic type (P = 0.018, Table 3). Two of the seven patients with multiple individual cells had stage IV disease, and the pattern of multiple individual cells was associated with poor survival even after the patients with stage IV disease were deleted (P = 0.0018, Figure 2F).

Thirty-five of thirty-eight cases with ITCs had one to five positive metastatic nodes. The remaining cases had six or more positive metastatic nodes (9, 11, and 19 metastatic lymph nodes, respectively). Cases with ITCs in six or more lymph nodes showed a significantly poorer prognosis than those with ITCs in 1-5 lymph nodes (P<0.0001, Figure 2G).



P value

	pN0	pN1mi (i+)	pN1mi
pN1mi (i+)	0.6738		
pN1mi	0.0104	0.3305	
macrometastasis	<0.0001	0.0098	0.0218

Figure 2 Survival curves using the Kaplan-Meier method. A: Patient survival according to reclassified pN stage; B: survival curve of cases with pN1 with one or more macrometastases, pN1mi, and pN1mi(i+); C: survival curve of the cases with pN0 stage, pN1mi(i+), pN1mi, and pN1; D: prognostic impact of lymph node metastases as detected by immunostaining; E: survival curves according to the pattern of ITCs; F: survival curves according to the pattern of ITCs deleting patients with stage IV disease; G: survival curves according to the number of positive nodes.

Table 2 Clinicopathologic findings in seven cases with ITC with multiple scattered single cell pattern

Case	[1]F/U	[1]F/U months	Sex	Age (yr)	Tumor size (cm)	WHO	Depth	Stage	Number of positive nodes	Number of tumor cells in a lymph node
202	Alive	14	[2]M	67	2.0	[4]P/D	[5]SM	Ia	4	2
409	Alive	69	M	40	4.5	P/D	[6]SS	Ib	1	4
437	Died	20	[3]F	35	6.0	P/D	SS	Ib	19	>50
726	Died	33	F	40	14.0	P/D	[7]SE	II	3	>30
737	Died	28	F	30	3.0	P/D	SE	IV	9	>20
829	Died	28	M	46	6.0	P/D	SE	IV	2	45
850	Alive	63	M	49	5.0	P/D	SS	Ib	1	8

[1]Follow-up, [2]male, [3]female, [4]poorly differentiated tubular adenocarcinoma, [5]submucosa, [6]subserosa, [7]serosa.

Table 3 Multivariate analysis of predictive factors for survival in pN0 using Cox regression model

Prognostic factor	Hazard ratio (95%CI)	*P*
Pattern of ITCs		0.018
Multiple individual cells *vs* others	4.09 (1.28–13.10)	
PT stage		<0.001
II–IV *vs* I	8.77 (2.89–26.32)	
Lauren's classification		0.276
Diffuse *vs* intestinal	1.73 (0.65–4.61)	

DISCUSSION

When examining gastric cancer and related material, the pathologist aims to achieve as simply and reliably as possible, a comprehensive diagnosis and prognosis of therapeutic relevance. The routine histologic examination of lymph nodes has long been the gold standard for identifying metastases to regional lymph nodes resected as part of the staging procedure for tumors in diverse locations, including the stomach. However, this method has an inherent limitation, the potential for sampling error. Serial sectioning has been employed to scrutinize metastases[14], but it is impractical for routine surgical pathology practice. In this study, we performed immunohistochemical staining against cytokeratin on routine sections in the cases with original diagnosis of pN0. We found that micrometastases or macrometastases were overlooked in 20 of 280 node-negative cases (7.14%), and ITCs were found in 38 cases (13.6%).

The prognostic impact of lymph node metastases detected by immunohistochemistry remains controversial in gastric cancer. Some authors have reported an insignificant correlation between lymph node metastasis detected by immunostaining and patient survival[15-17], but others have reported a significant impact on patient survival[18-21]. In contrast to previous reports, we subdivided lymph node metastases according to the size of tumor deposits, and then subdivided cases with ITCs into four groups according to the pattern of tumor deposits. In this large scale study, lymph node metastases as detected by immunostaining were not significantly associated with patient survival.

Ishida *et al*.[21], have classified lymph node metastases into five groups according to the pattern of metastasis (single cell *vs* cluster), but did not analyze the implications on patient survival. Fukagawa *et al*.[17], demonstrated that the pattern of micrometastases (single cell *vs* cluster) does not affect the survival curve. In the present study, ITCs were classified into four groups: single cell, multiple individual cells, single cluster, and multiple clusters. Among ITCs, only cases with multiple individual cells comprised the poor prognosis group. Tumors with a pattern of multiple individual cells showed non-solid poorly differentiated type adenocarcinoma and had infiltrative border. Although the pattern of multiple individual cells was very uncommon (7 of 280 pN0, 2.5%), this pattern had a significant impact on patient survival and showed a distinct histologic feature. Therefore, cytokeratin immunostaining is recommended in node-negative gastric cancers especially in non-solid poorly differentiated type adenocarcinoma with infiltrative border, to identify occult metastasis with multiple individual cell pattern.

According to the cancer staging of AJCC, micrometastases are defined when the size of tumor deposits in largest dimension is greater than 0.2 mm and not greater than 2 mm in diameter, and cases in which only micrometastases are detected are defined as pN1mi in breast cancer. However, in previous reports on gastric cancer[17-21], micrometastases are defined as lymph node metastases detected by immunohistochemistry, not according to the size of tumor deposits. In the present study, micrometastases were defined according to cancer staging method recommended by AJCC. Cases with pN1mi including pN1mi(i+) showed a significantly better prognosis than cases with pN1 with macrometastases ($P = 0.0037$), and pN1mi by only HE staining was also significantly associated with better survival than macrometastases ($P = 0.0218$). Therefore, we recommend that pN1mi should be defined in gastric cancer as is currently done in breast cancer. Furthermore, the survival of patients with pN1mi(i+) was not significantly different from that of patients with pN0. Therefore, we also recommend classifying pN1mi(i+) separately from pN1mi.

Several lines of evidence support the interpretation that keratin-positive cells in lymph nodes represent metastatic carcinoma, though occasional normal constituents of lymph nodes may be stained positively for cytokeratin. Other than cancer cells, undesirable cytokeratin has been reported both in plasma cells[22,23] and in interstitial reticulum cells[22,24]. Cytokeratin-positive metastatic cells have an epithelial morphology, in contrast to the dendritic process appearance of keratin-positive reticulum cells. Plasma cells show weak and cytoplasmic expression of cytokeratin and have their characteristic features. Cells are considered as occult node metastases only when they show strong and membranous expression of cytokeratin, reside within the substance of the lymph nodes, and exhibit epithelial morphology.

In conclusion, immunohistochemical staining against cytokeratin can detect occult metastases in regional lymph nodes of patients with gastric cancer, and the presence of immunohistochemically detected ITCs does not affect patient survival, except for a subset of cases with metastasis of multiple individual cells. pN1mi or pN1mi(i+) is distinct from pN0 or pN1 in the aspect of patient survival. Therefore, the size and pattern of lymph node metastases can provide prognostic information in gastric cancer.

References

1 **Adachi Y,** Kamakura T, Mori M, Baba H, Maehara Y, Sugimachi K. Prognostic significance of the number of positive lymph nodes in gastric carcinoma. *Br J Surg* 1994; **81**: 414-416

2 **Isozaki H,** Okajima K, Fujii K. Histological evaluation of lymph node metastasis on serial sectioning in gastric cancer with radical lymphadenectomy. *Hepatogastroenterology* 1997; **44**: 1133-1136

3 Prognostic importance of occult axillary lymph node micrometastases from breast cancers. International (Ludwig) Breast Cancer Study Group. *Lancet* 1990; **335**: 1565-1568

4 **Cote RJ,** Peterson HF, Chaiwun B, Gelber RD, Goldhirsch A, Castiglione-Gertsch M, Gusterson B, Neville AM. Role of immunohistochemical detection of lymph-node metastases in management of breast cancer. International Breast Cancer Study Group. *Lancet* 1999; **354**: 896-900

5 **Dowlatshahi K,** Fan M, Snider HC, Habib FA. Lymph node micrometastases from breast carcinoma: reviewing the dilemma. *Cancer* 1997; **80**: 1188-1197

6 **Glickman JN,** Torres C, Wang HH, Turner JR, Shahsafaei A, Richards WG, Sugarbaker DJ, Odze RD. The prognostic significance of lymph node micrometastasis in patients with esophageal carcinoma. *Cancer* 1999; **85**: 769-778

7 **Doki Y,** Ishikawa O, Mano M, Hiratsuka M, Sasaki Y, Kameyama M, Ohigashi H, Murata K, Yamada T, Miyashiro I, Yokoyama S, Ishiguro S, Imaoka S. Cytokeratin deposits in lymph nodes show distinct clinical significance from lymph node micrometastasis in human esophageal cancers. *J Surg Res* 2002; **107**: 75-81

8 **Liefers GJ,** Cleton-Jansen AM, van de Velde CJ, Hermans J, van Krieken JH, Cornelisse CJ, Tollenaar RA. Micrometastases and survival in stage II colorectal cancer. *N Engl J Med* 1998; **339**: 223-228

9 **Nicholson AG,** Marks CG, Cook MG. Effect on lymph node status of triple levelling and immunohistochemistry with CAM 5.2 on node negative colorectal carcinomas. *Gut* 1994; **35**: 1447-1448

10 American Joint Committee on Cancer. AJCC cancer staging manual 6th ed. New York: Springer-Verlag, 2002

11 International Agency for Research on Cancer (IARC). World Health Organization Classification of Tumors; pathology and genetics of tumors of the digestive system. Lyon: IARC Press, 2000

12 **Woo DK,** Kim HS, Lee HS, Kang YH, Yang HK, Kim WH. Altered expression and mutation of beta-catenin gene in gastric carcinomas and cell lines. *Int J Cancer* 2001; **95**: 108-113

13 **Kumar V,** Abbas AK, Fausto N. Robbins and Cotran pathologic basis of disease 7th ed. Philadelphia: Elsevier, 2004

14 **Pickren JW.** Significance of occult metastases. A study of breast cancer. *Cancer* 1961; **14**: 1266-1271

15 **Morgagni P,** Saragoni L, Scarpi E, Zattini PS, Zaccaroni A, Morgagni D, Bazzocchi F. Lymph node micrometastases in early gastric cancer and their impact on prognosis. *World J Surg* 2003; **27**: 558-561

16 **Choi HJ,** Kim YK, Kim YH, Kim SS, Hong SH. Occurrence and prognostic implications of micrometastases in lymph nodes from patients with submucosal gastric carcinoma. *Ann Surg Oncol* 2002; **9**: 13-19

17 **Fukagawa T,** Sasako M, Mann GB, Sano T, Katai H, Maruyama K, Nakanishi Y, Shimoda T. Immunohistochemically detected micrometastases of the lymph nodes in patients with gastric carcinoma. *Cancer* 2001; **92**: 753-760

18 **Yasuda K,** Adachi Y, Shiraishi N, Inomata M, Takenchi H, Kitano S. Prognostic effect of lymph node micrometastasis in patients with histologically node-negative gastric cancer. *Ann Surg Oncol* 2002; **9**: 771-774

19 **Lee E,** Chae Y, Kim I, Choi J, Yeom B, Leong AS. Prognostic relevance of immunohistochemically detected lymph node micrometastasis in patients with gastric carcinoma. *Cancer* 2002; **94**: 2867-2873

20 **Nakajo A,** Natsugoe S, Ishigami S, Matsumoto M, Nakashima S, Hokita S, Baba M, Takao S, Aikou T. Detection and prediction of micrometastasis in the lymph nodes of patients with pN0 gastric cancer. *Ann Surg Oncol* 2001; **8**: 158-162

21 **Ishida K,** Katsuyama T, Sugiyama A, Kawasaki S. Immunohistochemical evaluation of lymph node micrometastases from gastric carcinomas. *Cancer* 1997; **79**: 1069-1076

22 **Xu X,** Roberts SA, Pasha TL, Zhang PJ. Undesirable cytokeratin immunoreactivity of native nonepithelial cells in sentinel lymph nodes from patients with breast carcinoma. *Arch Pathol Lab Med* 2000; **124**: 1310-1313

23 **Greenson JK,** Isenhart CE, Rice R, Mojzisik C, Houchens D, Martin EW Jr. Identification of occult micrometastases in pericolic lymph nodes of Duke's B colorectal cancer patients using monoclonal antibodies against cytokeratin and CC49. Correlation with long-term survival. *Cancer* 1994; **73**: 563-569

24 **Gould VE,** Bloom KJ, Franke WW, Warren WH, Moll R. Increased numbers of cytokeratin-positive interstitial reticulum cells (CIRC) in reactive, inflammatory and neoplastic lymphadenopathies: hyperplasia or induced expression? *Virchows Arch* 1995; **425**: 617-629

Science Editor Wang XL and Guo SY **Language Editor** Elsevier HK

PO Box 2345, Beijing 100023, China
www.wjgnet.com
wjg@wjgnet.com

ELSEVIER

World J Gastroenterol 2005;11(38):5926-5930
World Journal of Gastroenterology ISSN 1007-9327
© 2005 The WJG Press and Elsevier Inc. All rights reserved.

Overexpression of decoy receptor 3 in hepatocellular carcinoma and its association with resistance to Fas ligand-mediated apoptosis

Hong-Wei Shen, Shun-Liang Gao, Yu-Lian Wu, Shu-You Peng

Hong-Wei Shen, Shun-Liang Gao, Yu-Lian Wu, Shu-You Peng, Department of Surgery, 2nd Affiliated Hospital of Medical College, Zhejiang University, Hangzhou 310009, Zhejiang Province, China
Correspondence to: Hong-Wei Shen, Department of Surgery, 2nd Affiliated Hospital of Medical College, Zhejiang University, Hangzhou 310009, Zhejiang Province, China. shenhongwei2002@yahoo.com
Telephone: +86-571-87783585 Fax: +86-571-87022776
Received: 2004-03-26 Accepted: 2004-04-13

ABSTRACT

AIM: To characterize the expression and genomic amplification of decoy receptor 3 (DcR3) in hepatocellular carcinoma (HCC) and to evaluate the role of DcR3 in apoptosis.

METHODS: We examined 48 cases of HCC for DcR3 expression by RT-PCR and DcR3 gene amplification by quantitative genomic PCR. DcR3 protein was detected by immunohistochemistry. Terminal deoxynucleotidyl transferase-mediated dUTP digoxigenin nick and labeling (TUNEL) was used to identify the apoptosis cells in tissues. Primary hepatoma cell culture and MTT test were used to evaluate the protection against FasL- and chemical-induced apoptosis by DcR3 expression.

RESULTS: DcR3 mRNA overexpression was detected in 60% HCC (29/48) patients. The occurrence of HCC was not associated with amplification of the gene. One sample base substitution was found in three sites as a sequence in Genbank. The expression of DcR3 in HCC was associated with the apoptotic index (0.067±0.04 *vs* 0.209±0.12, $P<0.01$), size of mass, stage, and infiltration or metastasis (41.2% *vs* 71.0%, 40% *vs* 75%, 51.8% *vs* 84.6%, $P<0.05$). DcR3 expression could protect hepatoma cells against apoptosis induced by FasL, but not by chemicals.

CONCLUSION: These data suggest that in addition to gene amplification there may be another mechanism underlying DcR3 overexpression. The effect of overexpression of DcR3 on the apoptosis of cancer cells may have direct therapeutic implications for the management of HCC.

© 2005 The WJG Press and Elsevier Inc. All rights reserved.

Key words: DcR3; Hepatocellular carcinoma; Apoptosis

Shen HW, Gao SL, Wu YL, Peng SY. Overexpression of decoy receptor 3 in hepatocellular carcinoma and its association with resistance to Fas ligand-mediated apoptosis. *World J Gastroenterol* 2005; 11(38): 5926-5930
http://www.wjgnet.com/1007-9327/11/5926.asp

INTRODUCTION

DcR3, a member of the tumor necrosis factor receptor superfamily, is amplified and overexpressed in various human cancers as a negative regulator of Fas-mediated apoptosis[1-3]. It was reported that DcR3 can bind to LIGHT and FasL[4-8]. Therefore, DcR3 may act as an inhibitor of LIGHT-induced tumor cell death by blocking LIGHT interaction with its receptors. DcR3 is characterized by a soluble cognate receptor for both LIGHT and FasL/CD95L[9,10]. LIGHT and FasL mediate apoptosis, which is the most common physiological form of cell death and occurs during embryonic development, tissue remodeling, immune regulation, and tumor regression. Abnormalities in FasL and LIGHT system can result in a number of human pathological conditions such as tumor. The cause of DcR3 overexpression in human cancers remains unclear, but its value in tumor escaping from apoptosis and immune surveillance of organism is worthy of special remark.

In contrast, no data are available regarding the expression and amplification of DcR3 gene in HCC. We found that there was a high DcR3 protein level in serum of patients with HCC. In the present study, we examined 48 cases of HCC for DcR3 gene expression by RT-PCR and DcR3 gene amplification by quantitative genomic PCR. The expression of DcR3 protein was detected by immunohistochemistry. *In situ* TUNEL was used to identify the apoptosis cells in tissues of HCC. Primary hepatoma cell culture and MTT test were used to evaluate the role of DcR3 expression in protection against FasL and chemical-induced cell death. The findings in our study suggest that in addition to gene amplification there may be another mechanism underlying DcR3 gene expression. The effect of overexpression of DcR3 on the apoptosis of cancer cells may have direct therapeutic implications for the management of HCC, which remains a major unsolved health problem throughout the world.

MATERIALS AND METHODS

Quantitative genomic PCR

Quantitative genomic PCR was performed as previously described[2,11]. Genomic DNA was isolated from fresh tissues of HCC. Quantitative PCR was carried out by a lightcycler. Primers for DcR3 were designed using an intron sequence to avoid amplification from DcR3 mRNA. The DcR3-specific primers were 5'-CTTCTTCGCGCACGCTG-3' (sense) and 5'-ATCACGCCGGCACCAG-3' (antisense), and the fluorogenic probe was 5'-FAM-ACACGATGCGTGC-TCCAAGCAGAA-TAMARA-3'. The beta-globin primers were 5'-ACCCTTAGGCTGCTGGTGG-3' (sense) and 5'-GGAGTGGACAGATCCCCAAA-3' (antisense), and the

fluorogenic probe was 5'-FAM-CTACCCTTGGACCCA-GAGGTTCTTTGAGTC-TAMARA-3'. For each run, DNA isolated from normal matched tissues was used for comparison.

RT-PCR analysis

For RT-PCR analysis, total RNA was isolated using Trizol (Life Technologies, Inc.) from the tumor and its adjacent normal tissues of 48 HCC cases. RNA was converted to cDNA by reverse transcription and amplified for 35 cycles by PCR. Primers used for amplification of the DcR3 fragment were according to the RNA sequence of DcR3. Beta-actin was used as an internal control for RNA integrity. The DcR3-specific primers were 5'-TCCACCGCGCCACTACAC-3' (sense) and 5'-ACGGCACGCTCACACTCC-3' (antisense). The beta-actin specific primers were 5'-TTCCAGCCT-TCCTTCCTGG-3' (sense) and 5'-TTGCGCTCAGG-AGGAGCA AT-3'(antisense). PCR products were run on 2% agarose gel, stained with ethidium bromide, and visualized by UV illumination. RT-PCR product of one sample was sequenced to show reliability of the reaction.

Immunohistochemistry

HCC tissues were obtained from the Surgical Department of the Second Affiliated Hospital of Zhejiang University. Four micrometer-thick formalin-fixed and paraffin-embedded sections were deparaffinized and treated in microwave with citrate buffer, pH 6.0 (three times each for 5 min) for antigen retrieval and incubated for 15 min in 30 mL/L H_2O_2 Tris-buffered saline (TBS), pH 7.4 to block endogenous peroxidase activities. The sections were then incubated for 10 min at room temperature with blocking solution. Each section was incubated with anti-DcR3 antibody diluted 1:5000 for 30-60 min at room temperature. Bound antibodies were detected with the peroxidase-labelled streptavidin-biotin method, and stained with diaminobenzidine. Counterstaining was performed with Mayer's heamatoxylin, and the sections were mounted.

As a negative control for DcR3 protein expression, the primary antibody was replaced by normal non-immune rabbit serum. There were no known normal tissues expressing DcR3 protein, and no positive control was set up in the DcR3 immunostaining.

In situ TUNEL

HCC tissues were obtained from the Surgical Department of the Second Affiliated Hospital of Zhejiang University. Four micrometer-thick formalin-fixed and paraffin-embedded sections were deparaffinized and treated in microwave with citrate buffer, pH 6.0 (three times each for 5 min) for antigen retrieval and incubated for 15 min in 30 mL/L H_2O_2 TBS, pH 7.4 to block endogenous peroxidase activities. Each section was incubated with TUNEL reaction solution (Roche) for 60 min at 37 ℃, and washed three times with PBS. The signal translation solution was added to the slides for 30 min at 37 ℃. After being washed three times with PBS, each section was stained with freshly prepared diaminobenzidine. Counterstaining was performed with Mayer's heamatoxylin, and the sections were mounted.

As a negative control for *in situ* TUNEL, the TUNEL reaction solution was replaced by TBS. As a positive control, a slide (Roche) in the kit was used together with the samples.

FasL-induced apoptosis and drug-induced cell death of hepatoma cells

Hepatoma cells were obtained from patients with HCC who underwent surgery for tumor resection. After tumor removal, the tissues were placed immediately in petri dishes, minced mechanically, and digested by collagenase (3 h, 37 ℃). Subsequently, the dissociated cells were filtered through 100 μm of cell strainers to remove tissue debris. After centrifugation and lysis of erythrocytes by treatment with hypotonic water, the hepatoma cells were washed and resuspended in full medium (CAM).

The hepatoma cells were cultured with serum-free CAM in 96-well plates. A total 5×10^4 cells were seeded per well. Then 3 ng/mL FasL and ADM, MMC, and GEMZAR of 4-, 1- and 0.25-fold drug concentrations respectively were used to detect the cytotoxic effect on primary hepatoma cells. Each concentration and blank control were put in three parallel wells. The hepatoma cells were co-cultured with FasL or drugs in serum-free CAM for 5 d. The survival rate of the cells was detected with MTT method.

Statistical analysis

Results were expressed as mean±SE. Differences between groups were examined for statistical significance using analysis of variance (ANOVA) and *t*-test. $P<0.05$ was considered statistically significant.

[redacted]

We report that DcR3 mRNA is overexpressed in a substantial percentage of HCC, and that this overexpression can occur in the absence of detectable DcR3 gene amplification. In a case of sequence analysis, three base differences in the DcR3 gene of HCC were identified. The expression of DcR3 in HCC shows a relationship with the apoptosis index of the tissues of cancer. We also demonstrate that the hepatoma cells expressed DcR3 are protected from FasL-induced apoptotic cell death, but not the cell death induced by chemicals.

Relationship between clinical data and DcR3 mRNA expression

The mean age of cancer patients was 58.3±14 years. The clinical and pathological features of the total 48 cases were collected and summarized. The relationship between the DcR3 mRNA expression and the clinical and pathological features was analyzed. DcR3 mRNA expression in HCC showed a relationship with size of the mass, TNM stage and infiltration or metastasis of the tumor ($P<0.05$), but no relationship with membrane of the tumor, cancer embolus, and number of the tumor nodes (Table 1).

Overexpression of DcR3 mRNA and protein in HCC

Twenty-nine of 48 HCC cases were positive for DcR3 mRNA expression (Figure 1A). The ratio of positive expression was 60.4% (29/48). No positive expression was detected in adjacent normal tissues. As the level of DcR3 mRNA appeared to be elevated in HCC, we investigated

Table 1 Relationship between DcR3 mRNA expression and clinical and pathological features of HCC (n = 48)

Features	n	DcR3 mRNA expression (%)	P
Size of mass			
≤5 cm	17	41.2 (7/17)	<0.05
>5 cm	31	71.0 (22/31)	
Number of node			
Single	32	53.1 (17/32)	>0.05
Multiple	16	75 (12/16)	
Membrane of the mass			
Intact	14	50 (7/14)	>0.05
Not intact	34	64.7 (22/34)	
Cancer embolus			
Negative	38	60.5 (23/38)	>0.05
Positive	10	60 (6/10)	
TNM stage			
Stage I, II	20	40 (8/20)	<0.05
Stage III, IV	28	75 (21/28)	
Infiltration or metastasis			
Negative	35	51.4 (18/35)	<0.05
Positive	13	84.6 (11/13)	

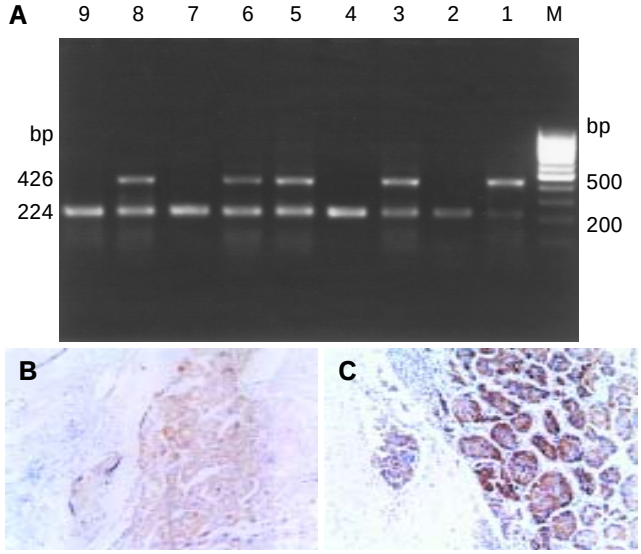


Figure 1 DcR3 gene expression in nine representative HCC samples. A: DcR3 gene mRNA expression detected by RT-PCR. Lanes 1,3,5,6, and 8: positive mRNA expression; lanes 2,4,7 and 9: negative expression. B, C: DcR3 protein expression detected by immunohistochemistry. (Magnification 100×).

whether it was true for DcR3 at the protein level. The expression of DcR3 protein was detected in five cases of HCC by immunohistochemistry. An obvious positive staining signal of DcR3 protein was detected in three out of five HCC cases (Figures 1B, and C). RT-PCR showed positive signals only in cancer cells. Furthermore, we found a high DcR3 protein level in serum of HCC patients by ELISA with anti-DcR3 antibody.

DcR3 overexpression without DcR3 gene amplification

DcR3 gene amplification was proposed to be the mechanism for DcR3 overexpression to promote tumor survival in lung and colon cancer. To determine whether DcR3 overexpression was due to gene amplification, quantitative PCR was carried out on genomic DNA from all the patients, with the relative number DcR3 gene copies determined by normalization of the beta-globin gene. Unexpectedly, the amplification was 2-fold higher only in 7 of 48 tumors patients than that in 29 of 48 tumors patients with positive DcR3 mRNA expression. Among the 29 HCC cases with postive DcR3 mRNA expression, the amplification was 2-fold higher only in six cases. From the result of sequence analysis, we found accidentally that there were three bases different from the DcR3 mRNA sequence in GenBank (Figure 2).

Table 2 Survival rate of hepatoma cells cultured in chemicals with different concentration (mean±SE)

	ADM	P	MMC	P	GENZAR	P
4×	51±0.2		44.6±0.19		52.2±0.17	
1×	72.7±0.18	<0.01	64.8±0.16	<0.01	66.7±0.17	<0.01
0.25×	82.6±0.17		81.8±0.16		77.9±0.18	

Apoptosis index and DcR3 mRNA expression in HCC

In situ TUNEL was used to identify the apoptosis cells in 29 tissue specimens of HCC. The apoptosis index was calculated by counting the positive cells in five visual fields under light microscope at 400-fold magnification. DcR3 mRNA positive expression was detected in 19 out of 29 HCC cases. The apoptosis index of the 29 HCC cases ranged from 0.021 to 0.362. The apoptosis index of the 19 patients with positive DcR3 mRNA expression was significantly lower than that (0.067±0.04) of the 10 patients with negative DcR3 mRNA expression (0.209±0.12) (P<0.01).

Expression of DcR3 protected hepatoma cells from FasL-induced apoptosis

Hepatoma cells of 19 HCC cases were studied. After treatment with FasL, the cell survival rate (CSR) of 10 HCC cases with DcR3 mRNA expression (83.7%±0.18) was significantly higher than that of another eight HCC cases without DcR3 expression (62.2%±0.16) (P<0.01).

From 0.25- to 4-fold drug concentrations, the hepatoma cell death induced by ADM, MMC, and GEMZAR had a positive relationship with the drug concentration (Table 2, P<0.01). But the effect of three drugs between hepatoma cells with positive and negative DcR3 mRNA expression had no significant difference (Table 3, P>0.05).

[illegible]

DcR3 gene is mapped on chromosome 20q13.3, a region known to be associated with gene amplification and rearrangement in human cancer[12,13]. Numerous reports have shown genomic amplifications of 20q13 in breast[14], gastric[15], colon, and lung[12] tumors and neuroblastomas[16]. Pitti *et al*.[1], found that the DcR3 gene is amplified in approximately half of human lung tumors and human colon adenocarcinomas and that DcR3 receptor overexpression might also occur, conferring growth advantage on tumor cells by blocking FasL-induced cell death. In this paper, we demonstrated DcR3 mRNA and protein overexpression in HCC. From the result our data, we found that there were only 20.7% (6/29) genomic amplifications in HCC with positive DcR3 mRNA

Table 3 Comparision of hepatoma cell death induced by chemicals between groups with negative and positive DcR3 expression (mean±SE)

	Survival rate of hepatoma cells					
	4-fold	*P*	1-fold	*P*	0.25-fold	*P*
ADM						
DcR3 negative	41.8±0.18	>0.05	65.9±0.17	>0.05	74.5±0.19	>0.05
DcR3 positive	58.4±0.19		78.1±0.17		89.1±0.12	
MMC						
DcR3 negative	36.2±0.07	>0.05	58.6±0.12	>0.05	77.9±0.18	>0.05
DcR3 positive	51.3±0.23		69.7±0.18		85±0.15	
GENZAR						
DcR3 negative	45.7±0.16	0.146	62.8±0.17	0.396	73.1±0.18	0.332
DcR3 positive	57.4±0.16		69.8±0.17		81.8±0.19	

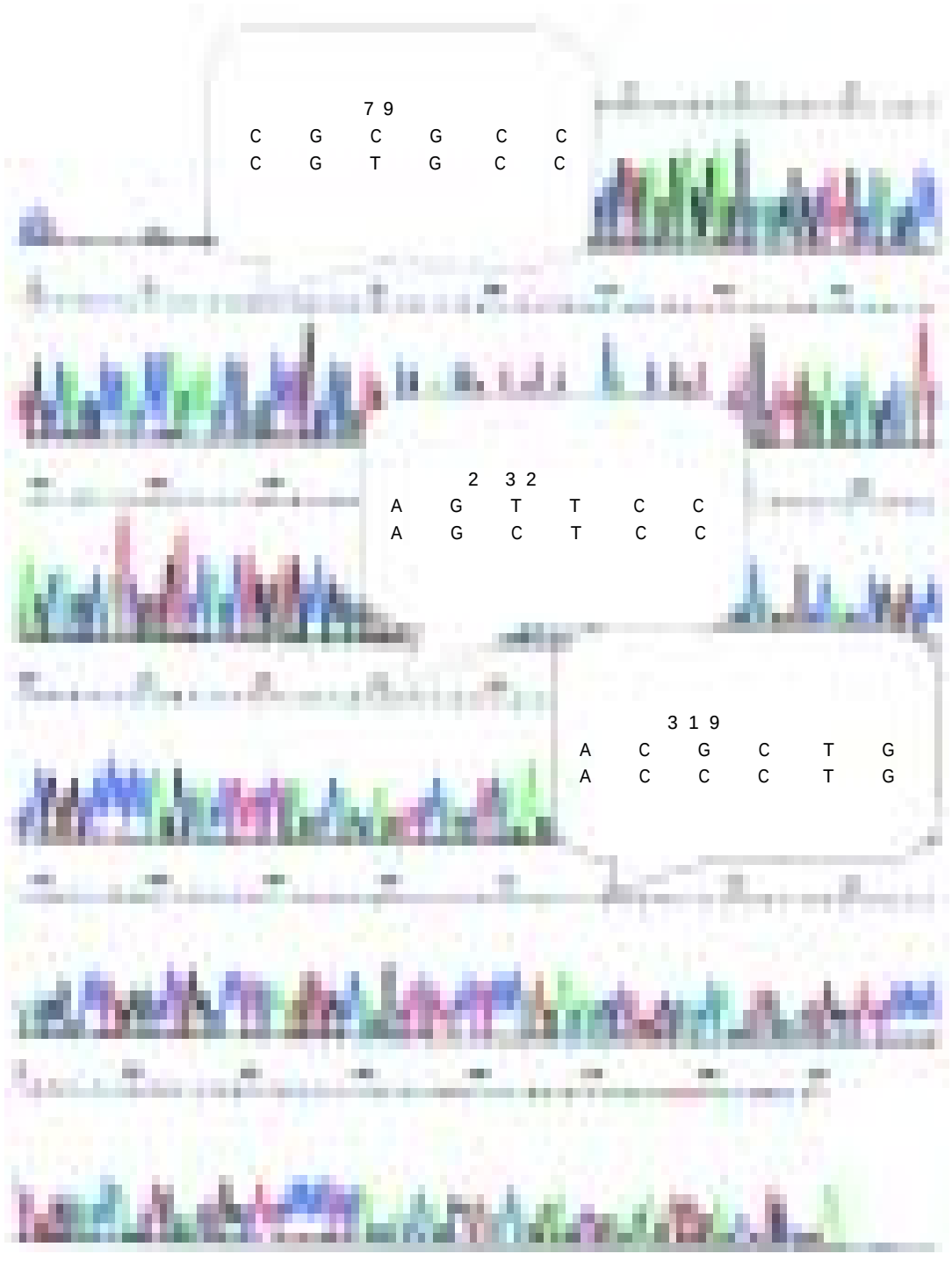


Figure 2 Sequence of DcR3 gene mRNA in HCC detected by sequencing RT- PCR product.

expression, suggesting that overexpression of DcR3 gene occurs without genomic amplification. Bai *et al*.[2], examined DcR3 genomic DNA, mRNA, and protein levels in a series of human gastrointestinal tract tumors and found that DcR3 gene is overexpressed in a substantial number of tumors in which gene amplification could not be detected by fluorescence *in situ* hybridization or quantitative genomic PCR. The identification of tumors with high-level DcR3 overexpression but no significant gene amplification raises the possibility that DcR3 protein overexpression might be an early event in oncogenesis, possibly driving selection of gene amplification. The cause of nongenomic DcR3 overexpression remains unclear. From the result of sequence analysis, we found accidentally that there were three bases different from the DcR3 mRNA sequence in GenBank. The base difference might represent a point mutation or a gene polymorphism in HCC. The meaning and mechanism of the base differences in HCC remain unclear and still need further work.

Since DcR3 is a soluble protein, it can be easily detected in serum with DcR3 antibody. The protein overexpression is likely to be the eventual choice of diagnostic method for DcR3. We found a high DcR3 protein level in serum of the HCC patients by ELISA with anti-DcR3 antibody. Although the diagnostic value of DcR3 protein still needs an overall evaluation, at least it can be used as an auxiliary diagnostic method in combination with other methods for HCC.

Fas-induced apoptosis plays a role in the hepatic pathology of Wilson's disease, in which Fas and FasL are induced in hepatocytes overloaded with copper[17,18]. Bai *et al*.[2,19-21], used an model of copper-induced hepatocellular injury to test whether expression of DcR3 could protect cells from apoptosis and found that DcR3 might indeed plays a physiologically important role in the regulation of apoptosis. In this study, we found that DcR3 mRNA expression in HCC showed a significant relationship with the apoptosis index. Patients with a positive DcR3 mRNA expression had a low apoptosis index compared to those with a negative expression. The difference in apoptosis index between positive and negative DcR3 mRNA expression groups showed a statistic significance. suggesting that DcR3 protein on apoptosis shows its therapeutic value of down-regulating DcR3 overexpression by genetic or immunotherapeutic means.

□□□□□□□□□□

1 **Pitti RM**, Marsters SA, Lawrence DA, Roy M, Kischkel FC, Dowd P, Huang A, Donahue CJ, Sherwood SW, Baldwin DT, Godowski PJ, Wood WI. Genomic amplification of a decoy receptor for Fas ligand in lung and colon cancer. *Nature* 1998; **396**: 699-703

2 **Bai C**, Connolly B, Metzker ML, Hilliard CA, Liu X, Sandig V, Soderman A, Galloway SM, Liu Q, Austin CP, Caskey CT. Overexpression of M68/DcR3 in human gastrointestinal tract tumors independent of gene amplification and its location in a four-gene cluster. *Proc Natl Acad Sci USA* 2000; **97**: 1230-1235

3 **Roth W**, Isenmann S, Nakamura M, Platten M, Wick W, Kleihues P, Bahr M, Ohgaki H, Ashkenazi A, Weller M. Soluble decoy receptor 3 is expressed by malignant gliomas and suppresses CD95 ligand-induced apoptosis and chemotaxis. *Cancer Res* 2001; **61**: 2759-2765

4 **Yu KY**, Kwon B, Ni J, Zhai Y, Ebner R, Know BS. A newly identified member of tumor necrosis factor receptor superfamily (TR6) suppresses LIGHT-mediated apoptosis. *J Biol Chem* 1999; **274**: 13733-13736

5 **Ohshima K**, Haraoka S, Sugihara M, Suzumiya J, Kawasaki C, Kanda M, Kikuchi M. Amplification and expression of a decoy receptor for fas ligand (DcR3) in virus (EBV or HTLV-I) associated lymphomas. *Cancer Lett* 2000; **160**: 89-97

6 **Otsuki T**, Tomokuni A, Sakaguchi H, Aikoh J, Matsuki T, Isozaki Y, Hyodoh F, Ueki H, Kusaka M, Kita S, Ueki A. Over-expression of the decoy receptor 3 (DcR3) gene in peripheral blood mononuclear cells (PBMC) derived from silicosis patients. *Clin Exp Immunol* 2000; **119**: 323-327

7 **Ibrahim SM**, Ringel J, Schmidt C, Ringel B, Muller P, Koczan D, Thiesen HJ, Lohr M. Pancreatic adenocarcinoma cell lines show variable susceptibility to TRAIL-mediated cell death. *Pancreas* 2001; **23**: 72-79

8 **Shen HW**, Wu YL, Peng SY. Overexpression and genomic amplification of decoy receptor 3 in hepatocellular carcinoma and significance. *Zhonghua Yixue Zazhi* 2003; **83**: 744-747

9 **Wu Y**, Han B, Shen H. Clinical significance of detecting elevated serum DcR3/TR6/M68 in malignant tumor patients. *Int J Cancer* 2003; **105**: 724-732

10 **Tsuji S**, Hosotani R, Yonehara S. Endogenous decoy receptor 3 blocks the growth inhibition signals mediated by Fas ligand in human pancreatic adenocarcinoma. *Int J Cancer* 2003; **106**: 17-25

11 **Chen J**, Zhang L, Kim S. Quantification and detection of DcR3, a decoy receptor in TNFR family. *J Immunol Methods* 2004; **285**: 63-70

12 **Muleris M**, Almeida A, Gerbault-Seureau M, Malfoy B, Dutrillaux B. Identification of amplified DNA sequences in breast cancer and their organization within homogeneously staining regions. *Genes Chromosomes Cancer* 1995; **14**: 155-163

13 **Shinomiya T**, Mori T, Ariyama Y, Sakabe T, Fukuda Y, Murakami Y, Nakamura Y, Inazawa J. Comparative genomic hybridization of squamous cell carcinoma of the esophagus: the possible involvement of the DPI gene in the 13q34 amplicon. *Genes Chromosomes Cancer* 1999; **24**: 337-344

14 **Schwendel A**, Richard F, Langreck H, Kaufmann O, Lage H, Winzer KJ, Petersen I, Dietel M. Chromosome alterations in breast cancer carcinomas: frequent involvement of DNA losses including chromosomes 4q and 21q. *Br J Cancer* 1998; **78**: 806-811

15 **Sakakura C**, Mori T, Sakabe T, Ariyama Y, Shinomiya T, Date K, Hagiwara A, Yamaguchi T, Takahashi T, Nakamura Y, Abe T, Inazawa J. Gains, losses, and amplifications of genomic materials in primary gastric cancers analyzed by comparative genomic hybridization. *Genes Chromosomes Cancer* 1999; **24**: 299-305

16 **Altura RA**, Maris JM, Li H, Boyett JM, Brodeur GM, Look AT. Novel regions of chromosomal loss in familial neuroblastoma by comparative genomic hybridization. *Genes Chromosomes Cancer* 1997; **19**: 176-184

17 **Kondo T**, Suda T, Fukuyama H, Adachi M, Nagata S. Essential roles of the Fas ligand in the development of hepatitis. *Nat Med* 1997; **3**: 409-413

18 **Strand S**, Hofmann WJ, Grambihler A, Hug H, Volkmann M, Otto G, Wesch H, Mariani SM, Hack V, Stremmel W, Krammer PH, Galle PR. Hepatic failure and liver cell damage in acute Wilson's disease involve CD95 (APO-1/Fas) mediated apoptosis. *Nat Med* 1998; **4**: 588-593

19 **Wu Y**, Han B, Luo H. DcR3/TR6 effectively prevents islet primary nonfunction after transplantation. *Diabetes* 2003; **52**: 2279-2286

20 **Shi G**, Wu Y, Zhang J. Death decoy receptor TR6/DcR3 inhibits T cell chemotaxis *in vitro* and *in vivo*. *J Immunol* 2003; **171**: 3407-3414

21 **Yang CR**, Hsieh SL, Teng CM. Soluble decoy receptor 3 induces angiogenesis by neutralization of TL1A, a cytokine belonging to tumor necrosis factor superfamily and exhibiting angiostatic action. *Cancer Res* 2004; **64**: 1122-1129

Science Editor Wang XL **Language Editor** Elsevier HK

PO Box 2345, Beijing 100023, China
www.wjgnet.com
wjg@wjgnet.com

ELSEVIER

World J Gastroenterol 2005;11(38):5931-5937
World Journal of Gastroenterology ISSN 1007-9327
© 2005 The WJG Press and Elsevier Inc. All rights reserved.

Expressions of inducible nitric oxide synthase and matrix metalloproteinase-9 and their effects on angiogenesis and progression of hepatocellular carcinoma

Min-Hua Sun, Xi-Chun Han, Ming-Ku Jia, Wei-Dong Jiang, Min Wang, Hong Zhang, Gang Han, Yi Jiang

Min-Hua Sun, Xi-Chun Han, Ming-Ku Jia, Wei-Dong Jiang, Min Wang, Hong Zhang, Gang Han, Yi Jiang, Department of General Surgery, Second Hospital, Jilin University, Changchun 130041, Jilin Province, China
Correspondence to: Professor Xi-Chun Han, Department of General Surgery, Second Hospital, Jilin University, Changchun 130041, Jilin Province, China. hanxichun@medmail.com.cn
Telephone: +86-431-8796988 Fax: +86-431-8934741
Received: 2005-03-12 Accepted: 2005-04-02

Abstract

AIM: To determine the expressions of inducible nitric oxide synthase (iNOS) and matrix metalloproteinase-9 (MMP-9) in hepatocellular carcinoma (HCC) and to investigate the relationship between iNOS and MMP-9 expression and their effects on angiogenesis and progression of HCC.

METHODS: In this study, we examined iNOS, MMP-9, and CD34 expression in specimens surgically removed from 32 HCC patients and 7 normal liver tissues by immunohistochemical staining. Meanwhile, microvessel density (MVD) was determined as a marker of angiogenesis by counting CD34-positive cells.

RESULTS: The positive rates of iNOS and MMP-9 expression were 71.88% (23/32) and 78.13% (25/32) in HCC. MMP-9 expression was significantly correlated with tumor size, capsule status, TNM stage, and risk of HCC recurrence ($P = 0.032$, $P = 0.033$, $P = 0.007$, and $P = 0.001$, respectively). There was also a significant relationship between iNOS expression and capsule status and risk of HCC recurrence ($P = 0.049$ and $P = 0.004$, respectively), but no correlation between iNOS expression and tumor size and TNM stage. There was a positive association between MVD and TNM stage and risk of HCC recurrence ($P = 0.037$ and $P = 0.000$, respectively). The count of MVD was significantly different in different iNOS and MMP-9 immunoreactivity groups ($F = 17.713$ and 17.097, $P = 0.000$ and $P = 0.000$, respectively). The examination of Spearman's rank correlation coefficient showed that there was a significant positive correlation between MVD and iNOS, MMP-9 immunoreactivity ($r = 0.754$ and 0.751, $P = 0.000$ and $P=0.000$, respectively). There was also a significant association between MMP-9 and iNOS expression in HCC ($P = 0.010$).

CONCLUSION: Nitric oxide (NO) produced by iNOS could modulate MMP-9 production and therefore contribute to tumor cell angiogenesis and invasion and metastasis in HCC. The strong expression of iNOS and MMP-9 in HCC may be helpful in evaluating the recurrence of HCC, predicting poor prognosis. For patients with strong expression of MMP-9 and iNOS, the optimal treatment scheme needs to be selected.

© 2005 The WJG Press and Elsevier Inc. All rights reserved.

Key words: Inducible nitric oxide synthase; Matrix metalloproteinase-9; Angiogenesis; Hepatocellular carcinoma

Sun MH, Han XC, Jia MK, Jiang WD, Wang M, Zhang H, Han G, Jiang Y. Expressions of inducible nitric oxide synthase and matrix metalloproteinase-9 and their effects on angiogenesis and progression of hepatocellular carcinoma. *World J Gastroenterol* 2005; 11(38): 5931-5937
http://www.wjgnet.com/1007-9327/11/5931.asp

INTRODUCTION

Hepatocellular carcinoma (HCC) is a highly vascular tumor characterized by a propensity for vascular invasion and distant metastasis. Angiogenesis is a prerequisite for tumor growth and metastasis[1]. In the process of invasion and metastasis of tumor cells, destruction of the extracellular matrix (ECM) is an essential initial step. Among the enzymes responsible for ECM degradation, several studies have shown a critical role played by matrix metalloproteinases (MMPs)[2]. MMP-9 (gelatinase B, 92-ku type IV collagenase) is capable of degrading the main components of the ECM, types IV and V collagen and gelatin[3-6]. Thus, its activities are closely related to the angiogenesis and invasiveness and metastasis of tumor cells[7,8]. However, it is secreted by cells as an inactive form, proMMP-9, which is then activated through an enzymatic cascade involving the generation of plasmin by urokinase-type plasminogen activator (u-PA)[9-12].

Nitric oxide (NO) is an important bioactive agent and a signaling molecule and may contribute to the pathogenesis of cancer[13]. Three distinct isoforms of NOS catalyze the formation of NO. Endothelial nitric oxide synthase (eNOS) and neuronal nitric oxide synthase (nNOS) are constitutively expressed in different tissues, whereas inducible nitric oxide synthase (iNOS) is related to a high-output pathway and is responsible for various pathological processes[14]. Although overexpression of iNOS has been demonstrated in various human neoplasms, such as colorectal cancer[15], pancreatic

cancer[16], and breast cancer[17], its exact function in tumor biology is complex and remains to be fully defined. During the initiation of tumor growth, natural killer cells and macrophages kill tumor cells by a NO-mediated mechanism[18]. However, NO may also suppress the antitumor defense, promote tumor angiogenesis and blood flow in the tumor neovasculature, and enhance tumor growth, invasion and metastasis[18]. Recently, investigators have tended to attribute NO-mediated stimulation of invasiveness to an alteration in the balance between the productions of MMPs and TIMPs[19-21]. Since NO has been assessed for the ability to upregulate u-PA in endothelial cells of post capillary venules during the process of NO-mediated stimulation of angiogenesis[22], the u-PA can convert plasminogen to plasmin, which can activate numerous MMPs.

There is evidence that NO produced by iNOS enhances the activity of MMP-9[19-21]. Both iNOS and MMP-9 expression have been reported to be increased in bone and joint disease and cardiovascular disease[23-25]. However, the relationship between them in tumors has been very seldom studied. To determine the role of iNOS and MMP-9 in HCC, we compared their expressions by the immunohistochemical method.

□□□□□□□□□ □□□ □□□□□□□

Materials

Thirty-two patients (24 males and 8 females, ranging in age from 16 years to 69 years, mean 53 years) who had undergone curative hepatectomy for HCC at the Second Hospital, Jilin University, and Tumor Hospital, Jilin Province, between May 2001 and October 2002 were involved in this study. As controls, seven normal adult liver specimens were wedge biopsies obtained during surgeries from patients with rupture of liver and cavernous hemangioma of liver. Of the 32 patients, 21 were positive for hepatitis B surface antigen (HBsAg), while 11 were infected with neither hepatitis C virus nor HBV. Five patients showed tumor thrombi in the portal vein, 3 patients showed lymph node metastasis in the porta hepatis, 14 patients showed microsatellite nodules. The patients were regarded as a high-risk group for HCC recurrence, if any one of the following factors existed: lymph node metastasis of the porta hepatis; tumor thrombi in the portal vein; surrounding the primary tumor two or more microsatellite tumor nodules were present in the same lobe of liver, or the microsatellite tumor nodules scattered over the two or more liver lobes. Eighteen cases were in high recurrence-risk group and 14 cases in low recurrence-risk group. The histological grade of malignancy was classified according to the criteria of World Health Organization. There were 17 cases of G1, 9 cases of G2, and 6 cases of G3. The degree of TNM classification was decided according to the general rules for the clinical and pathological study of primary liver tumor. One patient was staged I, 15 patients were staged II, and 16 patients were staged III. None of our patients received preoperative treatments, such as chemotherapy or embolization therapy. The resected surgical specimens were fixed in 10% buffered formalin and embedded in paraffin. Four-micrometer-thick sections were prepared for H&E and immunohistochemical staining.

Methods

Immunohistochemistry Immunostaining was performed according to the avidin-biotin-peroxidase complex method. Sections were dewaxed in xylene, and dehydrated in ethanol, and then heated at 98 ℃ in EDTA-retrieved solution for the antigens. Endogenous peroxidase was blocked by 3% hydrogen peroxide for 60 min at room temperature. The samples were incubated for 20 min at room temperature with a protein-blocking solution containing 5% normal horse serum and 1% normal goat serum. Subsequently, slides were incubated with primary anti-iNOS rabbit polyclonal antibody (Boster Bio, Wuhan) at 1:200 dilution for 60 min at room temperature, mouse anti-human MMP-9 mAb (Maixin Bio, Fuzhou) at 1:200 dilution overnight at 4 ℃, rat anti-mouse CD34 mAb (Maixin Bio, Fuzhou) at 1:100 dilution for 2 h at room temperature. Slides were then treated with a biotin-conjugated secondary antibody for 30 min followed by incubation with peroxidase-conjugated streptavidin for 60 min at room temperature. All steps were followed by washing in PBS. Finally, the sections were stained with a freshly prepared diaminobenzidine solution for 5 min and then counterstained with Mayer's hematoxylin. For CD34 staining, counterstaining was not done. As a negative control, PBS was used instead of the primary antibody. Known immunostaining-positive slides were used as positive controls.

Evaluation of iNOS and MMP-9 expression

Two independent observers screened all sections as semiqu-antitative evaluation of iNOS and MMP-9 immunostaining. The immunoreactive score was determined by the sum of intensity and extension of staining[26]. The intensity of staining was scored on a scale of 0-3, in which 0, negative staining; 1, weakly positive staining; 2, moderately positive staining; and 3, strongly positive staining. The extent of distribution of positive cells was estimated on a scale of 0-3, in which 0, negative or positive staining in 1-5% of cells; 1, positive staining in 6-25% of cells; 2, positive staining in 26-50% of cells; 3, positive staining in 51-100% of cells. The combined staining score (intensity+extension) $\geqslant$2 was considered as positive staining. The diagnosed grades accorded to the sum of two scores, -: 0-1; +: 2; ++: 3-4; and +++: >5.

Quantification of MVD

Microvessel density (MVD) was evaluated by two independent observers who were blinded to the patients' clinicopathologic data after sections were immunostained with anti-CD34 antibodies according to the procedure described by Weidner *et al*.[27]. In all tumors collected, the density of microvessels was higher in the peripheral tumor tissue close to the margin than in the central areas. Therefore, the peripheral tissue sections were used for counting of microvessels. Any brown-stained endothelial cells or endothelial cell clusters that was clearly separated from adjacent microvessels, tumor cells, or other stromal cells were counted as one microvessel. For MVD estimation, at low power magnification (×40 and ×100), the tissue sections were screened and five areas with the highest vessel density (hot spots) were selected. Microvessel counts of these areas were performed at a high power field (×200, the surface area of every vision

field being 0.708 mm^2) and the maximum microvessel count of the five richest vascular areas was taken as the MVD.

Statistical analysis

Qualitative data were expressed as the number of cases and quantitative data as mean±SD. These data were analyzed with the SPSS (version11.5) software. The qualitative data were compared using χ^2 test and Fisher's exact test, and the quantitative data were compared using one-way analysis of variance and independent sample *t*-test. Correlation between factors was evaluated using the Spearman's rank correlation coefficient. $P<0.05$ was considered statistically significant.

RESULTS

Correlation between MMP-9 and clinicopathologic parameters in HCC

The incidence of positive MMP-9 expression in cases with their tumor being more than 5 cm, their tumor capsules being not integral or their tumor without capsules was significantly higher than that in those with their tumor measured either less than or equal to 5 cm in diameter and their tumor capsules being integral ($\chi^2 = 5.283$ and $\chi^2 = 5.258$, $P = 0.032$ and $P = 0.033$, respectively). The incidence of MMP-9 expression was also significantly higher in high-risk group for HCC recurrence and TNM III stage group than in low-risk group for HCC recurrence and TNM I-II stage group ($\chi^2 = 11.160$ and $\chi^2 = 8.680$, $P = 0.001$ and $P = 0.007$, respectively). At the same time no significant correlation was demonstrated between the expression of MMP-9 and other parameters, such as sex, age, ascites, hepatitis B, cirrhosis of liver, value of AFP, and grade of histology (Table 1).

Correlation between iNOS and clinicopathologic parameters in HCC

The positive immunohistochemical staining for iNOS in cases with their tumor capsules being not integral or their tumors without capsules was significantly higher than that in those with their tumor capsules being integral ($\chi^2 = 4.652$, $P = 0.049$). The iNOS immunoreactivity was significantly higher in high-risk group for HCC recurrence than in low-risk group ($\chi^2 = 10.043$, $P = 0.004$). But there was no significant difference between iNOS expression and each of the parameters such as sex, age, value of AFP, TNM stage, tumor size, grade of histology, hepatitis B, cirrhosis

Table 1 Correlation between clinicopathologic parameters and MMP-9, iNOS expression and MVD in HCC

Variables	*n* (*n*=32)	MMP-9		*P*	iNOS		*P*	MVD	*P*
		+[1] (*n* = 25)	– (*n* = 7)		+ (*n* = 23)	– (*n* = 9)		(mean±SD)	
Sex									
Male	24	20	4		17	7		68.50±17.38	
Female	8	5	3	NS[2]	6	2	NS	80.64±29.51	NS
Age (yr)									
>50	19	17	2		16	3		76.11±18.86	
≤50	13	8	5	NS	7	6	NS	64.86±23.35	NS
Size of HCC (cm)									
>5.0	21	19	2		17	4		74.48±18.16	
≤5.0	11	6	5	0.032	6	5	NS	62.91±20.63	NS
Tumor capsule									
Present integrally	15	9	6		8	7		67.73±25.72	
Absent or not integral	17	16	1	0.033	15	2	0.049	74.88±16.31	NS
HbsAg[3]									
+	21	18	3		16	5		75.48±19.02	
–	11	7	4	NS	7	4	NS	64.00±23.96	NS
Cirrhosis									
+	19	16	3		15	4		72.79±16.30	
–	13	9	4	NS	8	5	NS	64.46±15.95	NS
Ascites									
+	6	4	2		3	3		64.83±22.73	
–	26	21	5	NS	20	6	NS	73.08±20.99	NS
Serum AFP[4] (μg/L)									
≤400	13	10	3		11	2		68.84±21.77	
>400	19	15	4	NS	12	7	NS	75.46±20.53	NS
Histological grade									
G1	17	12	5		11	6		65.94±19.14	
G2	9	7	2		6	3		73.56±20.97	
G3	6	6	0	NS	6	0	NS	84.33±24.48	NS
TNM stage									
I–II	16	9	7		9	7		63.81±21.78	
III	16	16	0	0.007	14	2	NS	79.25±18.08	0.037
Risk of recurrence									
High-risk group	18	18	0		17	1		82.56±17.29	
Low-risk group	14	7	7	0.001	6	8	0.004	57.36±17.19	0.000

[1]Score≥2: positive staining (+); [2]NS: not significant; [3]HBsAg: hepatitis B surface antigen; [4]AFP: serum α-fetoprotein.

of liver, and ascites in HCC (Table 1).

CD34 expression and its relationship to clinicopathologic parameters in HCC

No CD34 staining was found in the sinusoids of seven healthy liver tissues. In HCC tissues from 32 cases, sinusoid-like tumor vessels reacted intensively with anti-CD34 (mean±SD, 71.53±21.19; range, 31-126), and the positive staining of CD34 distributed with a diffuse pattern or an intensive cluster pattern and was defined as the buffy zonale staining on the cell membrane (Figure 1). In nonmalignant tissue, anti-CD34 stainings were confined to vessels of the portal triad with weak staining in few of the sinusoids at the periportal area in case of cirrhosis or chronic hepatitis. There was a significant difference in MVD between TNM III stage group (79.25±18.08) and TNM I-II stage group (63.81±21.78, t = 2.182, P = 0.037). There was also a significant difference in MVD between high-risk group for HCC recurrence (82.56±17.29) and low-risk group (57.36±17.19, t = 4.100, P = 0.000). But no significant association was noted between MVD and other clinicopathologic features (Table 1).

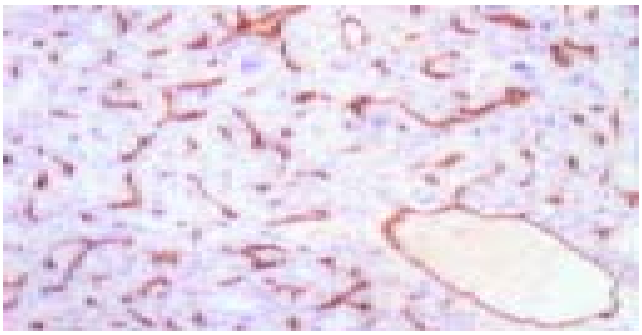


Figure 1 Immunohistochemical staining for CD34 in HCC (×100).

Relationship between iNOS, MMP-9 and MVD in HCC

As shown in Table 2, tumors were divided into three groups based on the degree of immunoreactivity. Along with the increase of immunoreactivity grades, the incidence of iNOS and MMP-9 expression enhanced gradually. The count of MVD was significantly different in different iNOS and MMP-9 immunoreactivity groups (F = 17.713 and 17.097, P = 0.000 and P = 0.000, respectively). The examination of Spearman's rank correlation coefficient showed that there was a significant positive correlation between iNOS, MMP-9 immunoreactivity and MVD (r = 0.754 and 0.751, P = 0.000 and P = 0.000, respectively).

Table 2 Relationship between MVD and MMP-9, iNOS staining intensity in HCC (mean±SD)

Degree of staining	n	iNOS	n	MMP-9
–	9	49.33±11.24	7	48.57±14.62
++	11	71.82±15.06[b]	8	62.50±11.98
+++	12	87.92±16.49[b]	17	85.24±16.02[b,d]

[b]P<0.01 *vs* degree of staining (–), [d]P<0.01 *vs* degree of staining (++).

Correlation between MMP-9 and iNOS expression in 32 HCC tissues

There was no MMP-9 staining in the normal liver tissue. MMP-9 immunoreactivity was detected in 25 (78.13%) of 32 HCCs. MMP-9 was mainly localized in cytoplasm and cytoplasmic membranes and its staining was detected in vascular endothelial cells, bile ducts, HCC cells, and stromal fibroblasts (Figures 2A and B). iNOS was expressed weakly in healthy liver tissue and mainly localized in tumor

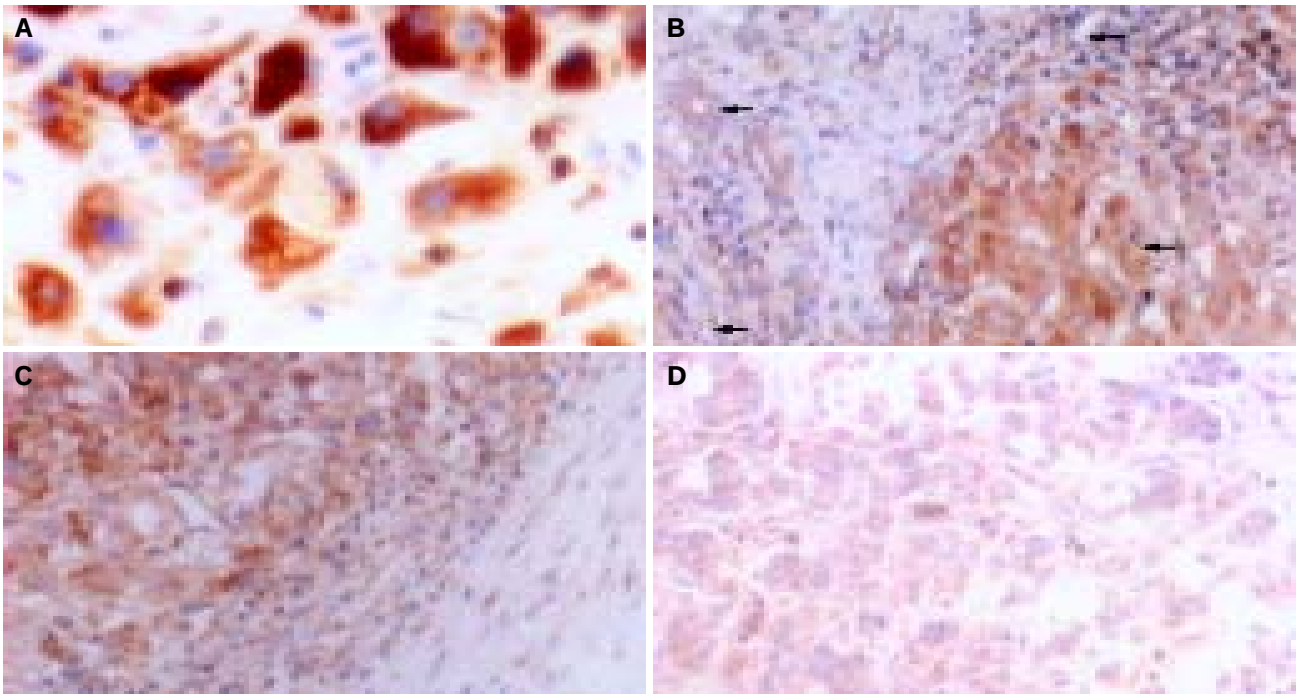


Figure 2 Immunohistochemical staining for MMP-9. A: MMP-9 in cytoplasm and cytoplasmic membranes in HCC (×400); B: MMP-9 in vascular endothelial cells, bile ducts, HCC cells, and stromal fibroblasts (arrow heads from top to bottom) within HCC (×200); C: MMP-9 expression in neighboring capsule of HCC (×200); and D: weak expression of MMP-9 in central areas of HCC tissues (×200).

cytoplasm with a diffuse distribution pattern and a granular pattern. It was also found in cell membranes occasionally. There was no expression of iNOS in tumor nuclei or interstitial cells (Figure 3A). The common characteristics of MMP-9 and iNOS expression were that their stainings were more frequent in tumor cells localized in the anterior borders of invasion or neighboring capsules of tumor tissues (Figures 2C and 3B) than in those cells in central areas (Figures 2D and 3C) and that they displayed various degrees of intensities and inter-tumor heterogeneity. There was a significant correlation between MMP-9 and iNOS expression ($\chi^2 = 8.052$, $P = 0.010$, Table 3).

Table 3 Correlation between MMP-9 and iNOS expression in 32 HCC tissues

iNOS	MMP-9		Total	*P*
	+	–		
+	21	2	23	
–	4	5	9	0.010
Total	25	7	32	

DISCUSSION

HCC is the fifth most common malignant disease in the world, causing almost one million deaths annually[28]. Surgical resection is the only proven cure for HCC, yet over 80%[29] of patients with HCC undergoing hepatectomy develop new tumors in the residual livers within 2 years. Further investigation of the pathological and biological factors of HCC in relation to recurrence and metastasis using molecular biology techniques will provide promising strategies for treatment and prevention of cancer invasion.

MMP-9 plays a key role in cancer invasion and metastasis by digesting native type IV collagen, which is a major structural component of basement membranes, since increased MMP-9 levels have been observed in various tumors such as HCC[30], bladder carcinoma[33], head, and neck cancer[19]. There is a trend toward a higher proportion of active MMP-9 with an increasing invasiveness of tumor cells. Our immunohistochemical study showed that the expression of MMP-9 was negative in the 7 normal liver tissues, and positive in 25 (78.13%) of 32 HCC tissues, suggesting that MMP-9 is produced by tumor cells. The strong staining in the marginal areas of tumor tissues suggests the close involvement of MMP-9 in the digestion of ECM. Moreover, positive staining of some fibroblasts and endothelial cells with anti-MMP-9 antibody suggests a participation of these cells in degradation of the ECM. The incidence of MMP-9 expression was significantly higher in high-risk group for HCC recurrence and TNM III stage group than in low-risk group and TNM I-II stage group, suggesting that overexpression of MMP-9 plays an important role in the progress of HCC, and that MMP-9 protein may serve as a marker for invasiveness and metastasis of HCC. These results are similar to the results reported by Arii *et al*.[30], and Hayasaka *et al*.[31]. In contrast to their study, there was also a significant correlation between MMP-9 expression and tumor size and capsule status of HCC. Both MMP-9 mRNA and activation of latent type of MMP-9 are significantly correlated with capsular infiltration of tumor[32]. Durkan *et al*.[33], reported that MMP-9 staining is associated with tumor size. Therefore, the above data further indicate that MMP-9 plays an important role in the dispersion of HCC cells and may accelerate the growth of tumors by enhancing angiogenesis of tumors.

MVD is an important indicator to reflect the level of tumor angiogenesis[34]. The result of our study revealed that there was a positive association between the extent of neovascularization and the clinicopathologic characteristics related to aggressiveness, such as TNM stage and risk of recurrence, indicating that the MVD reflects the potentiality for HCC recurrence and metastasis. We also found that the MVD was statistically different in different MMP-9 immunoreactivity groups. There was a significant positive relationship between MMP-9 and MVD, the higher the MMP-9 expression, the higher the MVD. MMP-9 plays a vital role in the turnover of basement membrane collagen types IV and I, which exert a crucial effect on the formation of new capillary sprouts and neoangiogenesis. Based on the above facts, we speculate that MMP-9 expression may initiate angiogenesis and promote vascularization.

A large body of clinical and experimental data suggest that NO plays a promoting role in tumor progression and metastasis[35-37], though a few reports indicate that the presence of NO in tumor cells or their microenvironment may exert deleterious effects on the tumor cell survival and consequently their metastatic ability[13]. In the current study, we found that iNOS was expressed weakly in healthy

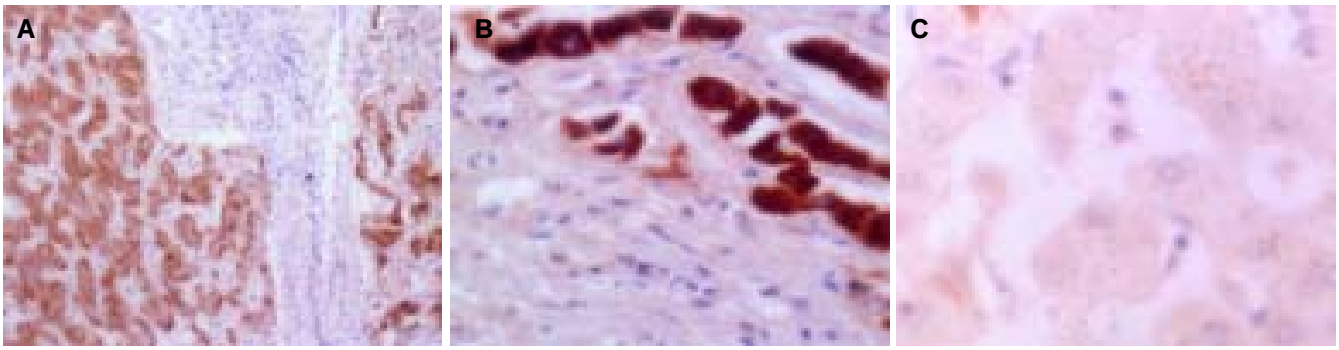


Figure 3 Immunohistochemical staining for iNOS. A: iNOS expression in tumor cytoplasm (×100); B: strong expression of iNOS in neighboring capsule of HCC tissues (×400); and C: weak expression of iNOS in central areas of HCC tissues (×400).

liver tissues, suggesting that iNOS is associated with the physiological function of normal liver tissues. The expression of iNOS showed strong cytoplasmic staining in cancerous cells but not in tumor nuclei and interstitial cells, suggesting that NO is produced by HCC cells and directly or indirectly influences the fate of HCC cells. Here, we also demonstrated that the rate of iNOS expression in cases with their tumor capsules being not integral or their tumors without capsules was significantly higher than that in those with their tumor capsules being integral. The expression of iNOS in high recurrence-risk group was significantly higher than that in low recurrence-risk group, indicating that iNOS positivity is upregulated along with the biological aggressiveness of HCC lesions. It seems more likely that iNOS may increase the viability and infiltrative potential of HCC.

In this study, the count of MVD was statistically different in different iNOS immunoreactivity groups, the higher the iNOS expression the higher the MVD. NO has been implicated in all processes of angiogenesis in a manner consistent with a pre-angiogenic phenotype[38]. iNOS-transfected human colon adenocarcinoma DLD-1 cells have a higher vessel density and a higher growth rate *in vivo* than parental cells in mammary tumor model, suggesting that NO is a key mediator of C3L5 tumor-induced angiogenesis in NOS inhibitor-treated mice[39]. Therefore, the above data further indicate that local NO production by iNOS in HCC cells is able to enhance angiogenesis. It was reported that MMP-9 can also facilitate angiogenesis[40]. In this study, we found that there was a significant association between MMP-9 and iNOS. Both MMP-9 and iNOS positive expressions were more frequent in tumor cells localized in the anterior borders of invasion or neighboring capsules of tumor tissues and were associated with the capsule status and the risk of HCC recurrence, demonstrating that the effect of iNOS on angiogenesis can promote metastatic potential as well as tumor invasiveness by inducing HCC cells to produce MMP-9. To evaluate the mechanism, further investigations are needed.

In conclusion, there is a significant positive correlation between MMP-9 and iNOS expression, suggesting that NO produced by iNOS modulates MMP-9 production and therefore contributes to tumor cell angiogenesis, invasion, and metastasis in HCC. The strong expression of iNOS and MMP-9 in HCC may be helpful in evaluating the recurrence of HCC, predicting poor prognosis. For patients with strong expression of MMP-9 and iNOS, the optimal treatment scheme needs to be selected.

REFERENCES

1 **Folkman J.** What is the evidence that tumors are angiogenesis dependent? *J Natl Cancer Inst* 1990; **82**: 4-6
2 **Stetler-Stevenson WG,** Liotta LA, Kleiner DE Jr. Extracellular matrix 6: role of matrix metalloproteinases in tumor invasion and metastasis. *FASEB J* 1993; **7**: 1434-1441
3 **Westermarck J,** Kahari VM. Regulation of matrix metalloproteinase expression in tumor invasion. *FASEB J* 1999; **13**: 781-792
4 **Curran S,** Murray GI. Matrix metalloproteinases: molecular aspects of their roles in tumor invasion and metastasis. *Eur J Cancer* 2000; **36**: 1621-1630
5 **Yoshizaki T,** Sato H, Furukawa M. Recent advances in the regulation of matrix metalloproteinase 2 activation: from basic research to clinical implication. *Oncol Rep* 2002; **9**: 607-611
6 **Mott JD,** Werb Z. Regulation of matrix biology by matrix metalloproteinases. *Curr Opin Cell Biol* 2004; **16**: 558-564
7 **Ramos-DeSimone N,** Hahn-Dantona E, Sipley J, Nagase H, French DL, Quigley JP. Activation of matrix metalloproteinase-9 (MMP-9) via a converging plasmin/stromelysin-1 cascade enhances tumor cell invasion. *J Biol Chem* 1999; **274**: 13066-13076
8 **Kallakury BV,** Karikehalli S, Haholu A, Sheehan CE, Azumi N, Ross JS. Increased expression of matrix metalloproteinases 2 and 9 and tissue inhibitors of metalloproteinases 1 and 2 correlate with poor prognostic variables in renal cell carcinoma. *Clin Cancer Res* 2001; **7**: 3113-3119
9 **Lee KH,** Hyun MS, Kim JR. Growth factor-dependent activation of the MAPK pathway in human pancreatic cancer: MEK/ERK and p38 MAP kinase interaction in uPA synthesis. *Clin Exp Metastasis* 2003; **20**: 499-505
10 **Legrand C,** Polette M, Tournier JM, de Bentzmann S, Huet E, Monteau M, Birembaut P. uPA/plasmin system-mediated MMP-9 activation is implicated in bronchial epithelial cell migration. *Exp Cell Res* 2001; **264**: 326-336
11 **Mazzieri R,** Masiero L, Zanetta L, Monea S, Onisto M, Garbisa S, Mignatti P. Control of type IV collagenase activity by components of the urokinase-plasmin system: a regulatory mechanism with cell-bound reactants. *EMBO J* 1997; **16**: 2319-2332
12 **Koolwijk P,** Miltenburg AM, van Erck MG, Oudshoorn M, Niedbala MJ, Breedveld FC, van Hinsbergh VW. Activated gelatinase-B (MMP-9) and urokinase-type plasminogen activator in synovial fluids of patients with arthritis. Correlation with clinical and experimental variables of inflammation. *J Rheumatol* 1995; **22**: 385-393
13 **Holian O,** Wahid S, Atten MJ, Attar BM. Inhibition of gastric cancer cell proliferation by resveratrol: role of nitric oxide. *Am J Physiol Gastrointest Liver Physiol* 2002; **282**: 809-816
14 **Michel T,** Feron O. Nitric oxide synthases: which, where, how, and why? *J Clin Invest* 1997; **100**: 2146-2152
15 **Cianchi F,** Cortesini C, Fantappie O, Messerini L, Sardi I, Lasagna N, Perna F, Fabbroni V, Di Felice A, Perigli G, Mazzanti R, Masini E. Cyclooxygenase-2 activation mediates the proangiogenic effect of nitric oxide in colorectal cancer. *Clin Cancer Res* 2004; **10**: 2694-2704
16 **Franco L,** Doria D, Bertazzoni E, Benini A, Bassi C. Increased expression of inducible nitric oxide synthase and cyclooxygenase-2 in pancreatic cancer. *Prostaglandins Other Lipid Mediat* 2004; **73**: 51-58
17 **Oktem G,** Karabulut B, Selvi N, Sezgin C, Sanli UA, Uslu R, Yurtseven ME, Omay SB. Differential effects of doxorubicin and docetaxel on nitric oxide production and inducible nitric oxide synthase expression in MCF-7 human breast cancer cells. *Oncol Res* 2004; **14**: 381-386
18 **Lala PK,** Orucevic A. Role of nitric oxide in tumor progression: lessons from experimental tumors. *Cancer Metastasis Rev* 1998; **17**: 91-106
19 **Franchi A,** Santucci M, Masini E, Sardi I, Paglierani M, Gallo O. Expression of matrix metalloproteinase 1, matrix metalloproteinase 2, and matrix metalloproteinase 9 in carcinoma of the head and neck. *Cancer* 2002; **95**: 1902-1910
20 **Eberhardt W,** Beeg T, Beck KF, Walpen S, Gauer S, Bohles H, Pfeilschifter J. Nitric oxide modulates expression of matrix metalloproteinase-9 in rat mesangial cells. *Kidney Int* 2000; **57**: 59-69
21 **Egi K,** Conrad NE, Kwan J, Schulze C, Schulz R, Wildhirt SM. Inhibition of inducible nitric oxide synthase and superoxide production reduces matrix metalloproteinase-9 activity and restores coronary vasomotor function in rat cardiac allografts. *Eur J Cardiothorac Surg* 2004; **26**: 262-269
22 **Vincent VA,** Lowik CW, Verheijen JH, de Bart AC, Tilders FJ, Van Dam AM. Role of astrocyte-derived tissue-type plasminogen activator in the regulation of endotoxin-stimulated nitric oxide production by microglial cells. *Glia* 1998; **22**: 130-137

23 **Marcet-Palacios M,** Graham K, Cass C, Befus AD, Mayers I, Radomski MW. Nitric oxide and cyclic GMP increase the expression of matrix metalloproteinase-9 in vascular smooth muscle. *J Pharmacol Exp Ther* 2003; **307**: 429-436

24 **Johanning JM,** Armstrong PJ, Franklin DP, Han DC, Carey DJ, Elmore JR. Nitric oxide in experimental aneurysm formation: early events and consequences of nitric oxide inhibition. *Ann Vasc Surg* 2002; **16**: 65-72

25 **Sasaki K,** Hattori T, Fujisawa T, Takahashi K, Inoue H, Takigawa M. Nitric oxide mediates interleukin-1-induced gene expression of matrix metalloproteinases and basic fibroblast growth factor in cultured rabbit articular chondrocytes. *J Biochem* 1998; **123**: 431-439

26 **Koomagi R,** Volm M. Expression of Fas (CD95/APO-1) and Fas ligand in lung cancer, its prognostic and predictive relevance. *Int J Cancer* 1999; **84**: 239-243

27 **Weidner N,** Semple JP, Welch WR, Folkman J. Tumor angiogenesis and metastasis correlation in invasive breast carcinoma. *N Engl J Med* 1991; **324**: 1-8

28 **Yu AS,** Keeffe EB. Management of hepatocellular carcinoma. *Rev Gastroenterol Disord* 2003; **3**: 8-24

29 Primary liver cancer in Japan. Clinicopathologic features and results of surgical treatment. Liver cancer study group of Japan. *Ann Surg* 1990; **211**: 277-287

30 **Arii S,** Mise M, Harada T, Furutani M, Ishigami S, Niwano M, Mizumoto M, Fukumoto M, Imamura M. Overexpression of matrix metalloproteinase 9 gene in hepatocellular carcinoma with invasive potential. *Hepatology* 1996; **24**: 316-322

31 **Hayasaka A,** Suzuki N, Fujimoto N, Iwama S, Fukuyama E, Kanda Y, Saisho H. Elevated plasma levels of matrix metalloproteinase-9 (92-kd type IV collagenase/gelatinase B) in hepatocellular carcinoma. *Hepatology* 1996; **24**: 1058-1062

32 **Hollingsworth HC,** Kohn EC, Steinberg SM, Rothenberg ML, Merino MJ. Tumor angiogenesis in advanced stage ovarian carcinoma. *Am J Pathol* 1995; **147**: 33-41

33 **Durkan GC,** Nutt JE, Marsh C, Rajjayabun PH, Robinson MC, Neal DE, Lunec J, Mellon JK. Alteration in urinary matrix metalloproteinase-9 to tissue inhibitor of metalloproteinase-1 ratio predicts recurrence in nonmuscle-invasive bladder cancer. *Clin Cancer Res* 2003; **9**: 2576-2582

34 **Zolota V,** Gerokosta A, Melachrinou M, Kominea A, Aletra C, Scopa CD. Microvessel density, proliferating activity, p53 and bcl-2 expression in *in situ* ductal carcinoma of the breast. *Anticancer Res* 1999; **19**: 3269-3274

35 **Feng CW,** Wang LD, Jiao LH, Liu B, Zheng S, Xie XJ. Expression of p53, inducible nitric oxide synthase and vascular endothelial growth factor in gastric precancerous and cancerous lesions: correlation with clinical features. *BMC Cancer* 2002; **2**: 8

36 **Yagihashi N,** Kasajima H, Sugai S, Matsumoto K, Ebina Y, Morita T, Murakami T. Increased in situ expression of nitric oxide synthase in human colorectal cancer. *Virchows Arch* 2000; **436**: 109-114

37 **Thomsen LL,** Miles DW. Role of nitric oxide in tumour progression: lessons from human tumours. *Cancer Metastasis Rev* 1998; **17**: 107-118

38 **Nicolson GL.** Tumor and host molecules important in the organ preference of metastasis. *Semin Cancer Biol* 1991; **2**: 143-154

39 **Jenkins DC,** Charles IG, Thomsen LL, Moss DW, Holmes LS, Baylis SA, Rhodes P, Westmore K, Emson PC, Moncada S. Roles of nitric oxide in tumor growth. *Proc Natl Acad Sci USA* 1995; **92**: 4392-4396

40 **Zhang Y,** Wu XH, Cao GH, Li S. Relationship between expression of matrix metalloproteinase-9 (MMP-9) and angiogenesis in renal cell carcinoma. *Aizheng* 2004; **23**: 326-329

Science Editor Wang XL and Guo SY **Language Editor** Elsevier HK

PO Box 2345, Beijing 100023, China
www.wjgnet.com
wjg@wjgnet.com

ELSEVIER

World J Gastroenterol 2005;11(38):5938-5943
World Journal of Gastroenterology ISSN 1007-9327
© 2005 The WJG Press and Elsevier Inc. All rights reserved.

Anti-hepatoma effect of arsenic trioxide on experimental liver cancer induced by 2-acetamidofluorene in rats

Bing Tan, Jie-Fei Huang, Qun Wei, Hong Zhang, Run-Zhou Ni

Bing Tan, Jie-Fei Huang, Qun Wei, Hong Zhang, Run-Zhou Ni, Department of Digestive Medicine, Affiliated Hospital of Nantong Medical College, Nantong 226001, Jiangsu Province, China
Co-first-authors: Bing Tan
Correspondence to: Dr. Jie-Fei Huang, Department of Digestive Medicine, Affiliated Hospital of Nantong Medical College, Nantong 226001, Jiangsu Province, China
Telephone: +86-513-5806629
Received: 2004-06-08 Accepted: 2004-08-05

Abstract

AIM: To study the anti-hepatoma efficiency of arsenic trioxide (As_2O_3) in the treatment of experimental rat hepatocellular carcinoma (HCC) induced by 2-acetamidofluorene (2-FAA) and to elucidate the possible mechanisms.

METHODS: SD rats (2 mo old) had been fed with 2-FAA for 8 wk to induce HCC, and then they were treated with As_2O_3 or matrine. On d 29, the rats were killed and the liver was weighed and liver tumors were counted. The histological changes of liver tissue were observed under microscope, and the cellular dynamic parameters were studied by flow cytometry. Immunohistochemistry (two-step method) was used to observe the expression of vascular endothelial growth factor (VEGF) and micro-vessel density (MVD) on consecutive sections. The pathological parameters were also analyzed, the levels of serum aspartate aminotransferase (AST), alanine aminotransferase (ALT), total bilirubin (TBi), and direct bilirubin (DBi).

RESULTS: The number of liver tumors decreased significantly in groups treated with As_2O_3, especially in medium-dose (1 mg/kg) group (t = 2.80, P<0.01). As_2O_3 caused HCC cell death via apoptosis; necrosis was seen and apoptosis was common when the dose was 1 mg/kg. Proliferation index decreased sharply in medium-dose (1 mg/kg) group (7.87±4.11 *vs* 24.46±6.49, t = 2087, P<0.01), but not in 0.2 mg/kg group. However, S-phase fraction decreased dramatically in both groups, it reached the bottom level only when the dose was 1 mg/kg compared with control (0.40±0.13 *vs* 3.01±0.51, t = 2.97, P<0.01), and it was obviously accompanied with accumulation of cells in G_0/G_1 (G_0/G_1 restriction). The expressions of VEGF and MVD in medium-dose (1 mg/kg) group were significantly lower than normal saline group (0.63±0.74 *vs* 2.44±0.88, P<0.05; 15.75±3.99 *vs* 47.44±13.41, t = 2.80, P<0.01). Compared with normal saline group, medium- and low-dose groups As_2O_3 and matrine lowered the levels of ALT in serum (61.46±9.46, 63.75±20.40, 61.18±13.00 *vs* 108.98±29.86, t = 2.14, P<0.05), but had no effect on the level of serum AST, TBi, and DBi.

CONCLUSION: As_2O_3 had inhibitory effect on growth of experimental HCC in rats induced by 2-FAA, but had no obvious effect on normal hepatic cells. The mechanisms may involve decrease of cell division, accumulation of cells in G_0/G_1 phase, apoptosis of tumor cells, and inhibitory effect on angiogenesis through blocking VEGF.

© 2005 The WJG Press and Elsevier Inc. All rights reserved.

Key words: Arsenic trioxide; Liver cancer; Cell proliferation

Tan B, Huang JF, Wei Q, Zhang H, Ni RZ. Anti-hepatoma effect of arsenic trioxide on experimental liver cancer induced by 2-acetamidofluorene in rats. *World J Gastroenterol* 2005; 11(38): 5938-5943
http://www.wjgnet.com/1007-9327/11/5938.asp

INTRODUCTION

Hepatocellular carcinoma (HCC), with the highest malignancy and worst prognosis, is a common digestive tumor[1]. In recent years, there have been many clinical drugs for the therapy of HCC patients who cannot tolerate operation, such as tamoxifen[2], flutamide[3], lipiodol for embolism[4], but the results were so far unsatisfactory. Arsenic trioxide (As_2O_3) has been extensively used for many malignant leukemia tumors and was proved to be effective[5]. Zhang found As_2O_3 inhibited growth of experimental HCC by inducing apoptosis of tumor cells[6]. Si applied matrine for late HCCs and noticed growth inhibition and apoptosis of malignant cells[7]. To elucidate the antineoplastic mechanisms of As_2O_3, we treated experimental HCC in rats induced by 2-acetamidofluorene (2-FAA) with As_2O_3, counted liver tumors, examined liver histological changes under microscope, examined expression of vascular endothelial growth factor (VEGF) and micro-vessel density (MVD) of tumor with immunohistochemistry, studied cellular dynamic parameters by flow cytometry, and also investigated the levels of serum aspartate aminotransferase (AST), alanine aminotransferase (ALT), total bilirubin (TBi), and direct bilirubin (DBi).

MATERIALS AND METHODS

Establishment of HCC rat models

Seventy SD rats from blocked population, about 2-mo old, weighing 140-180 g (supplied by the Experimental Animal

Center of Nantong Medical College), were fed with granules mixed by 0.05% (w/w) carcinogen 2-FAA (from Sigma Company, USA), and kept in constant environment (20 ℃, moisture content 50%). During the 3rd-5th wk, some rats died; 4 wk later some visible gray nodes appeared on the liver surface of the dead by autopsy. Moreover, the number and size of these nodes had an increasing tendency. At the end of the 8th wk, 34 rats were still alive, and they were then fed with normal granules.

Grouping of animals Thirty-four HCC rats were divided randomly into four groups: two groups were injected intraperitoneally with As_2O_3 (produced by Haerbing Yida Pharma AG), diluted with four volumes of normal saline before injection, including medium-dose (1 mg/kg per d) and small-dose (0.2 mg/kg per d) groups; the third group was injected with matrine (4.2 g/kg per d) in the same way; the last was injected with normal saline (1.5 mL/kg per d) similarly. Treatment effects in all groups were observed: group A (with medium-dose As_2O_3 for 4 wk, n = 8); group B (with small-dose for 4 wk, n = 9); group C (with matrine for 8 wk, n = 8); group D (with saline for 4 wk, n = 9). During the experiment, we weighed the rats and then adjusted the dosage each week.

Sampling of liver and serum specimens At the end of the treatment, 34 rats were killed under diethyl ether anesthesia. Blood (4-5 mL) was drawn from heart and serum sample was collected after blood clotting and stored at 20 ℃ until assay. Whole liver was taken out and weighed immediately after rats were killed. After recording the distribution, size, and number of neoplastic nodes on the liver surface, we fixed part of liver tissue in 10% neutral formaldehyde for pathological examination.

Histopathologic and immunohistochemical examination Formaldehyde-fixed liver tissue was embedded in paraffin, cut into 4-μm-thick sections, some were stained with routine hematoxylin and eosin (HE) to observe liver neoplasia and morphological apoptosis under microscope; the others were examined with the immunohistochemical method. Polyclonal antibodies of VEGF and FVIIIRAg were obtained from the Beijing Zhongshan Biotechnology Company Limited. The two-step staining method consisted of the following main procedures: paraffin section was dewaxed and hydrated; tissue antigens were retrieved with microwave; the first antigen was dropped on tissue section, subsequently, which was incubated in a wet box at 37 ℃ for 1 h. After addition of envision reagent, these sections were put into a wet box again at room temperature for 30 min. Between the above-mentioned steps, tissue sheets were washed thrice in Tris-buffered saline (TBS, 0.01 mol/L, pH 7.4). After that, these tissue samples were colored with dolichos bifows agglutinin, cellular nuclei were redyed with hematoxylin and then sealed. In the negative control group, TBS was used as the first antibody, while the positive controls were from confirmed positive tissue specimens.

Buffy granules in cytoplasm were indicative of positive VEGF expression. According to Wang's standards[8], the median percentage of VEGF-positive-stained cells in 10 high power fields (200×) was counted. These medians were divided into five classes: less than 10% was negative (-); equivalent to or more than 10% was positive: 10-25% was +, 26-50% was ++, 51-75% was +++, and 76% or above were ++++. The five classes were respectively graded as 0-4.

MVD count was in accordance with Weidner's method (ref no.). First under low power microscope, the most intensive micro-vessel area in tumor tissues was identified, and then counted under high power (400×). Any buffy-stained endothelial cell or cell tuft, as well as any structure-unconnected micro-vessel branch, which was distinct from the surrounding tumor cells and connective tissues, was regarded as one "micro-vessel", excluding those vessels with muscular layers or a cavity with more than eight RBCs. The average of three counts was MVD of a liver tissue sample, which was checked by two pathological doctors with double-blind method.

Flow cytometric study Single-cell suspension, about 0.2 g, was prepared from fresh liver neoplasm tissue, first washed twice in PBS, cut into fragments with a clipper, and then filtered twice through a 35-μm-pore nylon filter. Cell count ranged from 3×10^5 to 10×10^5 cells/mL per sample. The suspension was spun by centrifugation at the rate of 1 000 r/min for 5 min, and washed in PBS twice. The obtained pellet was fixed by 70% cold ethanol, and then stored at -20 ℃ for 12-18 h. After being spun and washed again as previously described, the fixed single-cell suspension was pipetted into 0.01% RNase solution (Becton Dickinson Corporation) 200 μL, vortex-mixed and incubated continuously at 4 ℃ for 30 min, stained with 50 μg/mL propidium iodide 200 μL (Becton Dickinson Corporation), and then placed in the dark at 4 ℃ for 10 min. The sample was analyzed from 30 min to 3 h after addition of propidium iodide. Flow cytometric analysis was performed with an FACS Caliber flow cytometer (Becton Dickinson Corporation), which was equipped with a 5 W argon-ion laser. The fluorescence intensity of propidium iodide-stained nuclei, excited by blue laser light (488 nm) with 200 mW of light-regulated power, was quantified after filtering through a 457-502 nm nylon blocking filter. Percent coefficient of variation (%CV) was adjusted to less than 4% with glutaral-fixed chicken erythrocyte nuclei (CEN). Two-micron beads function to verify instrument alignment. The modifier for color compensation was corrected with a fluorescence microsphere. A minimum of 1×10^4 stained nuclei was examined through the flow cytometer, and the data were saved in a computer. DNA data were acquired using CELLQuest, and analyzed with ModFit LT™. Normal peripheral blood lymphocytes and normal SD rat liver cells were used as the control samples to identify the staining efficiency of propidium iodide and the channel of diploid cells (G_0/G_1 phase cells). With the G_0/G_1 peak of CEN as an internal standard, both G_0/G_1 and G_2/M peaks of analyzed samples were determined, and then the DNA quantity was calculated. Cell cycle percentages were derived from DNA histograms. The peak of hypodiploid, anterior to the G_0/G_1 peak, was the apoptosis peak. Proliferative index (PI) was equal to the sum percentage of S-phase and G_2/M-phase nuclei to all; the S-phase fraction (SPF) was determined and calculated with the area under the curve between G_0/G_1 and G_2/M peaks.

Serum enzyme determination Serum AST, ALT, TBi,

and DBi total activity were measured by the direct method of nitrobenzenamine.

Statistical analysis

Experimental data were shown as mean±SD. Student's *t*-test, and rank sum test were performed to assess potentially significant differences between individual groups, with STATA 7.0 statistical analysis software. A P value of <5% was regarded as significant when comparing various groups.

RESULTS

General observation during treatment

During the 1st wk, several As_2O_3-administrated SD rats had a short-term sinus tachycardia, which self-recovered after 1 or 2 d. Skin induration could be avoided if injection sites were changed daily. Whether by As_2O_3 or matrine treatment, there was no significant difference between the treatment group and the control, in terms of body weight gain and the weight ratio of liver to body (Table 1).

Table 1 Changes of body and liver weights in SD rats (mean±SD)

Groups	Body weight	Weight gain	Liver weight	Liver weight /body weight
A	272.25±35.51	74.25±20.71	12.475±1.9	3.49±0.40
B	247.56±63.94	58.44±16.99	13.11±3.15	4.42±0.60
C	253.00±28.63	58.25±24.01	12.54±1.132	4.08±0.50
D	258.22±49.99	40.44±40.15	11.89±1.59	4.24±1.00

Morphological changes In contrast to the normal, HCC rat liver was gray, and hard, both volume and weight increased; slight hemorrhage and necrosis could be found on liver cross section; multiple nodes were distributed unevenly on liver surface, mostly 1-6 mm in diameters, one 9 mm-diameter node was found in the control group; the nodes were widespread on part of liver lobes, more evidently in the saline group; bulky tumor nodes appeared more frequently in the control groups. On the contrary, less node-widespread liver lobes and smaller tumor nodes were found in As_2O_3-treated rats (Table 2).

At the end of 4-wk treatment, five rats in group A and three rats in group B had no visible liver tumor nodes; while in the control group, all rats had widespread nodes on liver lobes and only one had sparsely distributed nodes on liver lobes (Figures 1A and B). Visible neoplastic nodes and node-widespread liver lobes in group A were less than those in groups B (P<0.05) and C (P<0.01), there was no significant difference between groups B and C.

Table 2 The number and distribution of tumor nodes on rat liver

Groups	*n*	2–4 mm diameter nodes	>4 mm diameter nodes	Liver lobes with diffuse nodes
A	8	0 (0)	1 (0.125)	0 (0)
B	9	50 (5.56)	9 (1)	17.5 (1.94)
C	8	137 (15.22)	13 (1.44)	29 (3.22)
D	9	223 (24.778)	49 (5.444)	39 (4.333)

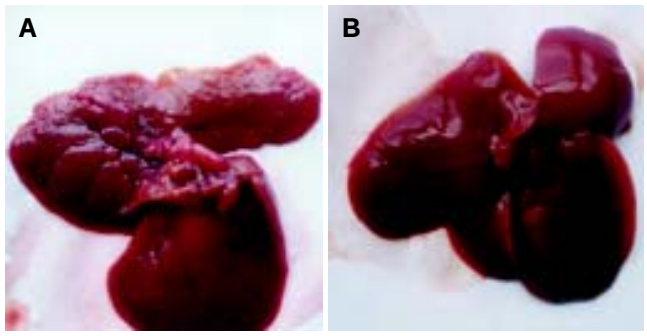


Figure 1 Gross changes of rat's liver after treatment. A: The control group (4 wk after NS injection); B: The treatment group (4 wk after medium-dose As_2O_3 injection).

Pathological examination Under microscope, all 2-FAA-induced HCC rat liver tissues had hepatic cell degeneration, oval cell proliferation, and inflammatory cell infiltration. There were more extensive infiltrations of inflammatory cells in control groups. Whereas in group A, these pathological changes were comparatively slight: there were fewer infiltrating inflammatory cells, more regenerated nodes, partly abnormal differentiated cells, and fewer carcinoma nodes (Figure 2A). There were more apoptotic cells in As_2O_3-treated tumor tissues, which were shrunk and separated from other surrounding cells, round or oval in shape, and had complete cellular membrane; chromatin of apoptotic cells was condensed, edge-gathered or broken, and formed into intra-cellular nucleosomes of different sizes; acidophilia of shrunk cytoplasm was raised; no infiltrating inflammatory cells were seen near apoptotic cells (Figure 2B).

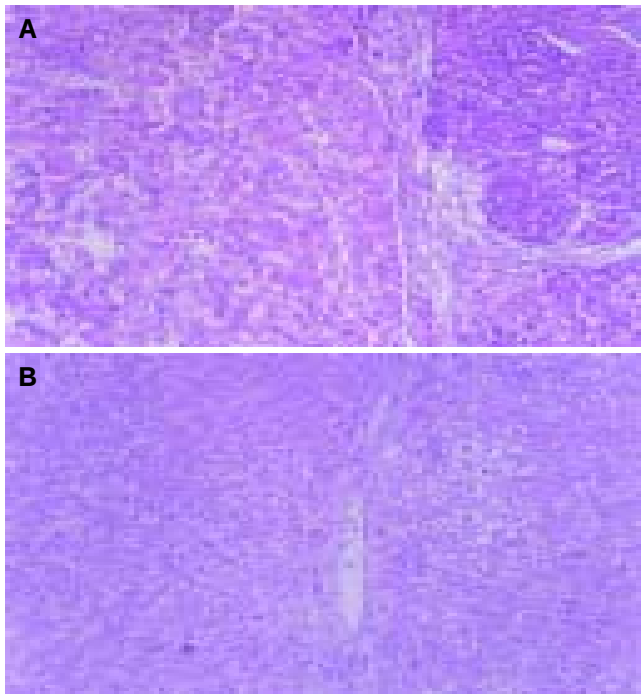


Figure 2 Pathological changes after treatment. A: The control group (4 wk after NS injection, HE×20); B: The treatment group (4 wk after medium-dose As_2O_3 injection, apoptotic cell observed).

Distribution of cell cycle phases The mean percentages of SPF, G_2/M phase, and PI of the 4-wk As_2O_3 group were less than those of the control ($P<0.05$), while G_0/G_1 phase mean ratio increased insignificantly ($P>0.05$, Table 3, Figures 3A and B).

The apoptotic rate in liver tumor tissues By means of DNA content assay, an obvious hypodiploid peak, before the G_0/G_1 peak, was called the apoptotic peak (Figures 3A and B). There was a significant increase in the apoptotic rate of the 4-wk As_2O_3-treated group compared with that of the control ($P<0.01$).

Levels of serum enzymes Compared with the control, serum ALT level of the 4-wk-treated groups was decreased ($P<0.05$), while AST, TBi, and DBi activity differed insignificantly ($P>0.05$, Table 4).

Immunohistochemical staining results Widespread brown cytoplasmic granules were VEGF positive, chiefly distributed inside tumor tissues and near the vessel endothelial cells (Figure 4A). In group A, more rats showed + to ++ degree VEGF signals, while four of eight rats were VEGF negative; in the control groups, more signals were from ++ to +++, with no negative expression (Figure 4B). There was a weakened intensity of VEGF in group A rats in comparison with the control and C groups ($P<0.05$, Table 5), but the difference was insignificant in all treatment groups ($P>0.05$), except for group A.

Vessel endothelial cells of tumor tissues, exhibited by FVIIIAg staining, formed into irregular micro-vessels, in the shapes of cluster and germination, which distributed unevenly, more intensively at the edge of tumor tissues (Figure 5A). As_2O_3 administration obviously inhibited neovascularization of liver tumor (Table 5, Figure 5B).

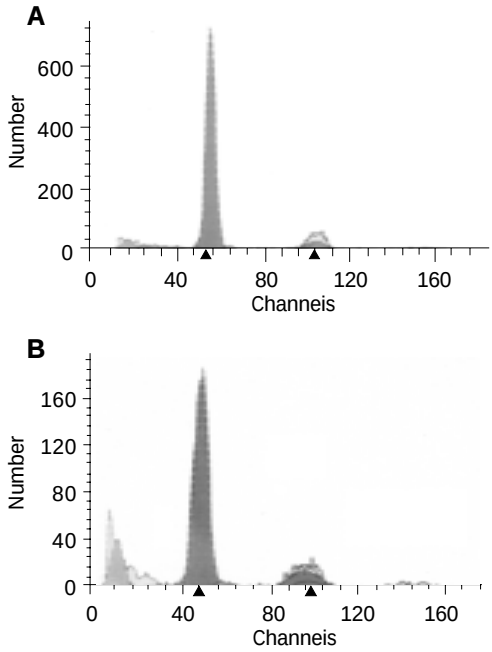


Figure 3 Changes of cell cycle phases after treatment. A: the control group (4 wk after NS injection); B: The treatment group (4 wk after medium-dose As_2O_3 injection, obvious hypodiploid peak).

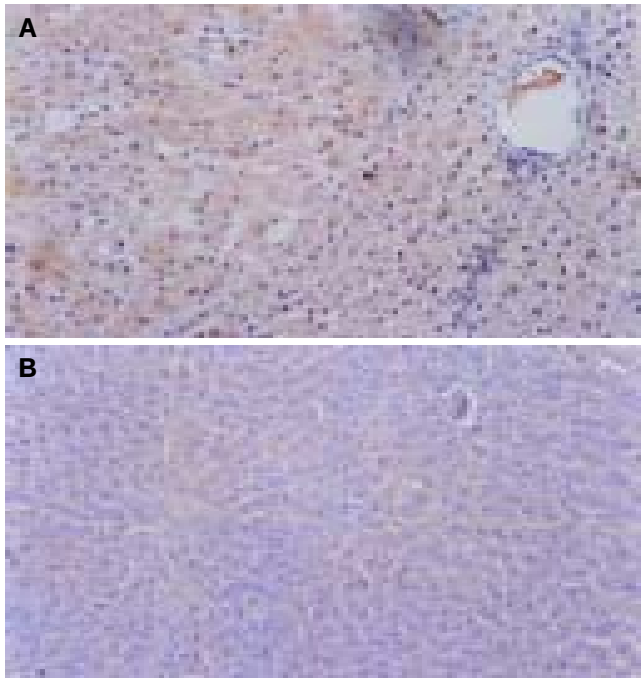


Figure 4 VEGF-positive signals after treatment. A: the control group (4 wk after NS injection, ×20); B: The treatment group (4 wk after medium-dose As_2O_3 injection, ×20).

Table 3 The percentages of cell cycle phases and PI

Groups	G_0/G_1 (%)	S (%)	G_2/M (%)	PI (%)
A	93.31±3.01[b]	0.40±0.13[b,d,f]	6.28±3.26[a]	7.87±4.11[b,d]
B	88.99±2.63	1.58±0.60[b]	9.43±2.29	17.14±6.08
C	87.34±4.75	2.05±0.62	10.61±4.33	20.77±5.28
D	84.26±2.53	3.01±0.51	12.73±2.40	24.46±6.49

[a]$P<0.05$, [b]$P<0.01$ *vs* group D; [d]$P<0.01$ *vs* group C; [f]$P<0.01$ *vs* group B.

Table 4 The levels of serum enzymes

Groups	AST (μ/L)	ALT (μ/L)	TBi (μmol/L)	DBi (μmol/L)
A	61.46±9.46[a]	31.65±9.25	0.52±0.11	0.35±0.15
B	63.75±20.40[a]	34±12.58	0.62±0.27	0.40±0.24
C	61.18±13.00[a]	33.45±16.44	0.51±0.14	0.30±0.12
D	108.98±29.86	40±16.12	0.47±0.13	0.60±0.28

[a]$P<0.05$ *vs* group D. AST: aspartate aminotransferase, ALT: alanine aminotransferase, TBi: total bilirubin, DBi: direct bilirubin.

Table 5 Expression intensity of VEGF and count of MVD in rat liver tumor tissues

Groups	*n*	VEGF					MVD	Marks
		–	+	++	+++	++++		
A	8	4	3	1	0	0	0.63±0.74[a]	15.75±3.99[b,d]
B	9	1	5	2	1	0	1.33±0.87	28.22±9.28[b]
C	8	1	1	3	3	0	2.00±1.07	41.13±7.70
D	9	0	1	4	3	1	2.44±0.88	47.44±13.41

[a]$P<0.05$, [b]$P<0.01$ *vs* group D; [d]$P<0.01$ *vs* group C.

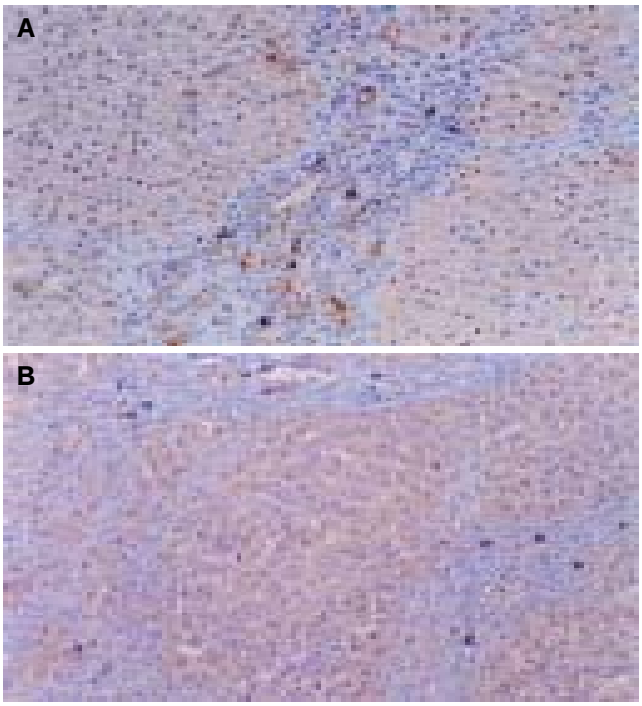


Figure 5 Micro-vessels by FVIIIAg staining after treatment, ×20. A: The control group (4 wk after NS injection); B: The treatment group (4 wk after medium-dose As_2O_3 injection).

DISCUSSION

The antineoplastic mechanisms of As_2O_3 are not yet clear. There are probably five major pathways: (1) inducing apoptosis of tumor cells[6,9-11]; (2) restraining the metastasis of HCC[12]; (3) effecting immunity of liver tumor cells[13]; (4) inhibiting angiogenesis through blocking VEGF; (5) having synergistic anti-hepatoma effect combined with chemical drugs.

PI and SPF often indicate the proliferation of tumor cells. In our study, the distribution of cell cycle phases showed cell proliferation tended to be inhibited after 4-wk of As_2O_3 administration. SPF, G_2/M phase, and PI all decreased ($P<0.05$), whereas G_0/G_1 phase increased insignificantly. More cells were blocked in G_0/G_1 phase. It is implied that As_2O_3 is able to prevent cells transisting from G_0/G_1 phase to S-phase, inhibiting the growth of tumor cells. In addition, apoptosis of tumor cells promoted by As_2O_3 occurred mainly at 1 mg/kg dose. PI decreased sharply in medium-dose (1 mg/kg) group ($P<0.01$), but not in the other (0.2 mg/kg) group ($P>0.05$). However, SPF decreased dramatically in both groups, suggesting 0.2 mg/kg dose also apparently inhibited synthesizing of DNA of tumor cells, but it was weaker. Therefore, antineoplastic mechanisms of As_2O_3 for HCC may involve the following two ways: inhibition of proliferation and induction of apoptosis of tumor cells.

In recent years, much importance has been attached to the relationship between angiogenesis and neoplasm. It has been confirmed that, solid carcinoma, once its diameter is over 2 mm, has to depend on neovascularization for its growth. It is through the blood vessel network that sufficient oxygen and nutrition are transported to meet the needs of high metabolism and fast proliferation of tumor cells. To some extent, the ability of inducing angiogenesis reflects tumor biological behaviors[14].

Various vessel growth factors act as the media to neovascularization, and VEGF is one of the most important one. Flt-1 and KDR/Flk-1, two receptors of VEGF, only exist in vessel endothelial cells, so VEGF promotes the proliferation of endothelial cells with a high specificity. VEGF can obviously improve the vessel permeability, which play an important role in tumor infiltration and metastasis[14,15]. It is necessary to find an objective and accurate indicator for the neovascularization. Thus, MVD count, which is for this purpose, has become a hot spot. In our study, VEGF and MVD were chosen to reflect the activity of tumor neovascularization. Our experiment showed that inhibitive effect of As_2O_3 on the angiogenesis was through inhibition of VEGF.

Morphological improvement by As_2O_3 in HCC rats could also be explained with its effects on cytokinetics. The number and distribution of liver tumor nodes decreased significantly in the As_2O_3-treated than in the controls, especially in medium-dose (1 mg/kg) group ($P<0.01$). As_2O_3 also lowered VEGF expression and MVD count in rat liver tumor tissues.

Compared with normal saline group, administration of As_2O_3 or matrine lowered the levels of AST in serum ($P<0.05$), but had no effect on the amount of serum AST, TBi, and DBi ($P>0.05$), indicating As_2O_3 has no obvious effect on normal hepatic cells.

In summary, through effective inhibition of proliferation, inducement of apoptosis, and restrain of neovascularization of tumor, As_2O_3 can serve as a new alternative for HCC treatment without serious adverse effects.

REFERENCES

1 **Lee JH,** Ku JL, Park YJ, Lee KU, Kim WH, Park JG. Establishment and characterization of four human hepatocellular carcinoma cell lines containing hepatitis B virus DNA. *World J Gastroenterol* 1999; **5**: 289-295
2 **Manesis EK,** Giannoulis G, Zoumpoulis P, Vafiadou I, Hadziyannis SJ. Treatment of hepatocellular carcinoma with combined suppression and inhibition of sex hormones: a randomized controlled trial. *Hepatology* 1995; **21**: 1535-1542
3 **Chao Y,** Chan WK, Huang YS, Teng HC, Wang SS, Lui WY, Whang-Peng J, Lee SD. Phase II study of flutamide in the treatment of hepatocellular carcinoma. *Cancer* 1996; **77**: 635-639
4 **Ram AM,** Bhattacharya S, Novell JR, Dick R, Winslet MC, Hobbs KEF. Intra-arterial radiotherapy with 131 iodinelipiodol for irresectable hepatocellular carcinoma. *Gut* 1996; **38** (Suppl 1): A17
5 **Dia J,** Weinberg RS, Waxman S, Jing Y. Malignant cells can be sensitized to undergo growth inhibition and apoptosis by arsenic trioxide through modulation of the glutathione redox system. *Blood* 1999; **93**: 268-277
6 **Zhang C,** Wang SS, Qi QH. The morphplogical and cellular dynamic changes in Arsenic Trioxide-treated rat liver cancer. *Zhongliu* 2001; **21**: 101-105
7 **Si WK,** Zhang GY, Ma WK, Kang GF. Effect of Matrine on the prolideration of $HepG_2$ cell line. *Disan Junyi Daxue Xueba* 2000; **22**: 451
8 **Wang Y,** Yang SQ, Wang ZG, Tang S, Sun WG, Liu GZ. Expressive meaning of ras p21, C-erbB-2 and P16 protein in Hepatocellular carcinoma. *Shijie Huaren Xiaohua Zazhi* 1999; **7**: 808-809

9 **Shen ZY,** Shen J, Cai WJ. The alteration of mitochondria is an early event of arsenic trioxide induced apoptosis in esophageal carcinoma cells. *Int J Mol Med* 2000; **5**: 155
10 **Liu LX,** Jiang HC, Zhuan AL, Zhou J, Wang XQ, Wu W. Arsenic trioxide induces apoptosis in hepatocellular carcinoma cells and to elucidate the possible mechanism. *Zhonghua Yixue Zazhi* 2001; **18**: 1526-1527
11 **Chen GQ,** Zhu J, Shi XG, Ni GH, Zhong HJ, Si GY, Jin XL, Tang W, Li XS, Xong SM, Shen ZC, Sun GL, Ma J, Zhang P, Zhang TD, Gazin C, Naoe T, Chen SJ, Wang ZY, Chen Z. *In vitro* studies on cellular and molecular mechanisms of arsenic trioxide (As2O3)in the treatment of acute promyelocytic leukemia: As2O3 induces NB4 cell apoptosis with downregulation of Bcl-2 expression and modulation of PML-RAR alpha/PML proteins. *Blood* 1996; **88**: 1052-1061
12 **Liu TF,** Cheng BL, Guan YG, Liang T. Study on relationship between expressions of CD44 and inhibition effect of arsenic trioxide on carcinoma. *Haerbing Yikedaxue Xuebao* 2001; **35**: 111-112
13 **Tang YH,** Liu TF. Effect of arsenic trioxide on the Immuni of H_{22} hepatocarcinoma rats. *Zhonghua Weishengwuxue He Mianyixue Zazhi* 2001; **21**: 63
14 **Kong HL,** Crystal RG. Gene therapy strategies for tumor antiangiogenesis. *J Natl Cancer Inst* 1998; **90**: 273-286
15 **Ng IO,** Poon RT, Lee JM, Fan ST, Ng M, Tso WK. Microvessel density, vascular endothelial growth factor and its receptors Flt-1 and Flk-1/KDR in hepatocellular carcinoma. *Am J Clin Pathol* 2001; **116**: 838-845

Science Editor Zhu LH and Guo SY **Language Editor** Elsevier HK

PO Box 2345, Beijing 100023, China
www.wjgnet.com
wjg@wjgnet.com

ELSEVIER

World J Gastroenterol 2005;11(38):5944-5950
World Journal of Gastroenterology ISSN 1007-9327
© 2005 The WJG Press and Elsevier Inc. All rights reserved.

Excess body weight, liver steatosis, and early fibrosis progression due to hepatitis C recurrence after liver transplantation

Pierluigi Toniutto, Carlo Fabris, Claudio Avellini, Rosalba Minisini, Davide Bitetto, Elisabetta Rossi, Carlo Smirne, Mario Pirisi

Pierluigi Toniutto, Carlo Fabris, Davide Bitetto, Elisabetta Rossi, Liver Transplantation Unit, Department of Pathology and Medicine Experimental and Clinical (DPMSC), University of Udine, Udine, Italy
Claudio Avellini, Pathology, University of Udine, Udine, Italy
Rosalba Minisini, Carlo Smirne, Mario Pirisi, Department of Medical Sciences, University of Eastern Piedmont "A. Avogadro", Novara, Italy
Correspondence to: Dr. Pierluigi Toniutto, Clinica di Medicina Interna, Università degli Studi, Piazzale Santa Maria della Misericordia, 1, Udine 33100, Italy. pierluigi.toniutto@uniud.it
Telephone: +39-432-559824 Fax: +39-432-42097
Received: 2004-12-22 Accepted: 2005-04-18

Abstract

AIM: To investigate how weight gain after OLT affects the speed of fibrosis progression (SFP) during recurrent hepatitis C virus (HCV) infection of the graft.

METHODS: Ninety consecutive patients (63 males, median age 53 years; 55 with HCV-related liver disease), transplanted at a single institution, were studied. All were followed for at least 2 years after OLT and had at least one follow-up graft biopsy, performed not earlier than 1 year after the transplant operation. For each biopsy, a single, experienced pathologist gave an estimate of both the staging according to Ishak and the degree of hepatic steatosis. The SFP was quantified in fibrosis units/month (FU/mo). The lipid metabolism status of patients was summarized by the plasma triglycerides/cholesterol (T/C) ratio. Body mass index (BMI) was measured before OLT, and 1 and 2 years after it.

RESULTS: In the HCV positive group, the highest SFP was observed in the first post-OLT year. At that time point, a SFP $\leqslant$0.100 FU/mo was observed more frequently among recipients who had received their graft from a young donor and had a pre-transplant BMI value >26.0 kg/m^2. At completion of the first post-transplant year, a BMI value >26.5 kg/m^2 was associated with a T/C ratio $\leqslant$1. The proportion of patients with SFP >0.100 FU/mo descended in the following order: female recipients with a high T/C ratio, male recipients with high T/C ratio, and recipients of either gender with low T/C ratio. Hepatic steatosis was observed more frequently in recipients who, in the first post-transplant year, had increased their BMI $\geqslant$1.5 kg/m^2 in comparison to the pre-transplant value. Hepatic steatosis was inversely associated with the staging score.

CONCLUSION: Among HCV positive recipients, excess weight gain post-OLT does not represent a factor favoring early liver fibrosis development and might even be protective against it.

© 2005 The WJG Press and Elsevier Inc. All rights reserved.

Key words: Liver transplantation; Hepatitis C infection; Liver fibrosis; Liver steatosis; Body mass index

Toniutto P, Fabris C, Avellini C, Minisini R, Bitetto D, Rossi E, Smirne C, Pirisi M. Excess body weight, liver steatosis, and early fibrosis progression due to hepatitis C recurrence after liver transplantation. *World J Gastroenterol* 2005; 11(38): 5944-5950

http://www.wjgnet.com/1007-9327/11/5944.asp

INTRODUCTION

Re-infection by hepatitis C virus (HCV) after liver transplantation (OLT) for HCV-related liver disease is almost universal, but the degree of necro-inflammatory damage and fibrosis deposition in the liver graft varies[1]. In the majority of cases, recurrent hepatitis C is mild. In up to one-third of OLT recipients with recurrent hepatitis C, however, a more severe course is observed, with progression to frank cirrhosis in less than 5 years[2]. The mechanisms associated with early fibrosis progression in this setting are actively investigated but remain poorly understood.

After liver transplantation, most patients gain weight[3], partly because of better health and freedom from pre-transplant dietary restrictions. As a result, within 2 years after the transplant operation, 60% of liver transplantation recipients are either overweight or obese. The role of excess weight post-transplant as a cardiovascular and metabolic risk factor has been widely addressed[4]: whether it may also contribute to graft damage, however, is unclear. Specifically, it is unknown if, in recipients with recurrent hepatitis C, fibrosis occurs earlier and is more severe when the patient is overweight or obese. This is conceivable, though, since data in immune-competent patients with chronic hepatitis C demonstrate that excess body weight leads to steatosis[5-7], acts as a cofactor for fibrosis progression[5,8,9] and represents an independent risk factor for non-response to antiviral treatment[10]. Independently of HCV infection, obesity may cause non-alcoholic steatohepatitis, a disease potentially capable of evolving toward cirrhosis and end-stage liver disease[11-13].

The present retrospective, longitudinal study aimed to investigate the possibility of a relationship between pre- and post-transplant body mass and fibrosis progression during recurrent hepatitis C. The study population included both

HCV positive and negative OLT recipients, in whom the value of body mass index (BMI) evaluated pre transplant and in the first 2 years post-transplant was related to the staging score measured in follow-up liver biopsies, taking into account other factors (pertaining to donor and host) which might have influenced the progression of recurrent hepatitis C.

MATERIALS AND METHODS

Patients

A total of 194 patients received a liver graft from a cadaveric donor between March 1996 and December 2002, at our institution. Insufficient data were available for 53 patients, who died either in the early post-transplant period or were lost to follow-up. Of the remaining 141 patients, 90 consecutive OLT recipients had a minimum follow-up of 2 years after OLT and had been subjected to at least one liver biopsy obtained not earlier than 1 year after OLT, and were included in the present study. Table 1 shows the demographic and clinical characteristics of the studied population. All were maintained in an immunosuppressive regimen that was either cyclosporine- or tacrolimus-based, associated, in the first few months, to corticosteroids. Cyclosporine dosage was calculated to obtain serum levels (measured 2 h after the drug administration) ranging from 800 to 1 200 μg/L in the first 6 wk after transplant and from 600 to 800 μg/L thereafter. Tacrolimus dosage was calculated to obtain pre-dose serum levels ranging from 10 to 15 μg/L in the first 6 wk after transplant and from 5 to 10 μg/L thereafter. Corticosteroid tapering was completed in 8 mo after the transplant in all except six patients (four HCV positive and two HCV negative). Thirty-two out of fifty-five HCV positive patients received antiviral treatment with interferon plus ribavirin due to recurrence of HCV hepatitis, defined as detectable serum HCV-RNA, serum alanine-aminotransferase (ALT) levels above the upper normal limit, Ishak grading score $\geqslant$2 and no evidence of rejection. Therapy was intended to be maintained for 12 mo. Antiviral treatment was started at a median time of 11.4 mo (range 0.7-75.9) after OLT and was completed in 17 patients. In the remaining 15 patients antiviral therapy had to be stopped prematurely due to adverse effects. Body weight was measured to the nearest 0.1 kg and height to the nearest 1 cm, with study participants wearing only underwear and no shoes. BMI was calculated as weight in kilograms divided by the square of the height in meters; it was measured pre transplant and one and 2 years after transplantation. In patients with ascites, pre-OLT BMI was calculated subtracting from the body weight the amount of ascitic fluid calculated on the basis of an ultrasound evaluation.

Liver histology In follow-up liver biopsies, grading and staging were scored according to the method of Ishak[14]. Fibrosis progression was evaluated annually in the first 4 years after OLT. It was based on the staging score at the corresponding "per protocol" liver biopsy, or, when unavailable, on the closest "on demand" liver biopsy. The speed of fibrosis progression (SFP), expressed in fibrosis units per month (FU/mo), was calculated for each 1-year time interval after OLT. It was obtained dividing the change observed in the fibrosis score at the end of the pertinent interval of time, with respect to either the transplant operation (for the first post-transplant year) or the previous liver biopsy (for the following years), by the number of months elapsed. The sum of micro- and macro-vesicular liver steatosis was calculated in each liver biopsy and graded as absent, $\leqslant$10% or >10%. All histological studies were performed by a single experienced histopathologist (CA).

Table 1 Clinical and demographic characteristics of the studied population

Recipient male gender, *n* (%)	63 (70.0)
Donor male gender, *n* (%)	53 (58.9)
Recipient age at transplantation (yr), median (range)	53 (23-66)
Donor age (yr), median (range)	41 (17-77)
Etiology of liver disease, *n* (%)	
HCV infection	55 (61.1)
HBV infection	12 (13.3)
Alcohol abuse	13 (14.5)
Other, unknown	10 (11.1)
Child–Pugh score pre-transplantation, median (range)	8 (5-14)
Immunosuppressive regimen, *n* (%)	
Tacrolimus-based	69 (76.7)
Cyclosporine-based	21 (23.3)
Antiviral therapy in HCV positive, *n* (%)	32 (58.2)

Categorical variables are expressed as frequencies (%); continuous variables as median (range). HCV: hepatitis C virus.

Statistical analysis

Statistical analysis of data was performed by means of the biomedical statistical software package BMDP Dynamic, Rel. 7.0 (Statistical Solutions, Cork, Ireland). Comparisons of continuous variables from two groups were explored by means of the Mann-Whitney's test. Correlations between continuous variables were performed either using the Spearman rank correlation coefficient or the Pearson product moment after logarithmic transformation of the values. Analysis of variance for repeated measures was employed to ascertain the significance of BMI increase post-OLT with respect to pre-OLT values. Wilcoxon matched pairs signed rank sum test was employed to evaluate modifications of fibrosis progression 2 and 3 years post-OLT in comparison to 1 year post-OLT. The associations between categorical variables were explored by means of the Pearson χ^2 test (in selected cases, with comparison of cross product ratios); if appropriate, the χ^2 test for linear trend was applied. Time-to-event analysis was performed to test whether the function to reach a staging score >2, in HCV positive patients, differed according to gender and BMI recorded pre- and 1 year post-OLT. Stepwise logistic regression analysis with a forward approach was used to evaluate the variables independently associated with a high one year post-OLT SFP. A level of 0.05 (two tailed) was chosen to indicate statistical significance.

RESULTS

BMI pre and post-OLT

BMI values, recorded before OLT, as well as 1 and 2 years post-OLT, are expressed in kg/m^2 and presented as medians (25-75th percentiles). For the entire study population, values were 25.0 (23.0-27.1), 25.4 (23.5-27.5) and 26.0 (23.7-28.4),

respectively (ANOVA for repeated measures, $P<0.05$). Among HCV positive recipients, the corresponding values were 24.7 (23.0-26.6), 25.1 (23.3-27.1) and 25.4 (23.4-28.1), respectively. Among HCV negative recipients, the corresponding values were 25.9 (23.0-28.4), 26.0 (24.0-28.0) and 26.6 (24.2-28.9), respectively. A BMI value $\geqslant$35 kg/m^2 (the limit indicating grade two obesity) was recognized before transplant operation in one HCV positive male recipient, who had a value of 38.4 kg/m^2. While 1 year after OLT, none of the recipients reached a BMI value $\geqslant$35 kg/m^2, 2 years after transplant, one HCV positive recipient had a BMI value of 36.5 kg/m^2 and one HCV negative patient a BMI value of 37.8 kg/m^2. The BMI values recorded pre-OLT and 1 and 2 years post-OLT were not statistically different between HCV positive and negative recipients. Among recipients belonging to both groups, no association was found between the pre-OLT BMI values and the severity of liver disease, calculated as the Child-Pugh score. Similarly, 1 and 2 years post-OLT BMI values did not differ considering the kind of immunosuppressive regimen in use (cyclosporine- or tacrolimus-based) or the rate of corticosteroid tapering (withdrawal completed before or after 90 d from OLT).

Liver histology

The histological follow-up lasted a median of 48 mo (range, 12-102 mo) in the HCV positive group and 30 mo (range, 12-78 mo) in the HCV negative group. A total of 465 follow-up liver biopsies were performed. In the group of HCV positive patients, the liver biopsies performed in a total of 315 patients, with a median number of five biopsies (range, 1-13) for each patient; protocol biopsies were 106/315 (median: two for each patient). In the group of HCV negative recipients, the liver biopsies performed were in a total of 150 patients, with a median number of four biopsies (range, 1-9) for each patient; protocol biopsies were 51 (median: one for each patient). In a median of 27 mo of follow up after OLT (range, 12-66mo), eight patients (8.8%; 6/8 were HCV positive) developed histological cirrhosis. The causes of cirrhosis in the two HCV negative patients were severe *de novo* autoimmune hepatitis and *de novo* HBV infection, respectively. At completion of the first post-transplant year, the median SFP was significantly faster in HCV positive in comparison to HCV-negative recipients: 0.083 (range, 0-0.455) *vs* 0.059 (range, 0-0.250) FU/mo ($P<0.02$). Table 2 shows the associations observed between 1 year post-OLT SFP >0.100 FU/mo and clinical and demographic characteristics of patients. Older donor age and lower BMI value pre-OLT were both significantly associated with faster fibrosis progression in HCV positive but not in HCV-negative recipients.

Figure 1 shows the fibrosis progression rates calculated at 1-4 years after OLT in the HCV-positive recipients. The fastest rate of fibrosis progression was observed during the 1st year after OLT. Later biopsies demonstrated a decrease in SFP with a non linear logarithmic trend ($r = 0.436$, $F = 37.1$, $P<0.0001$). Starting with the 3rd year after OLT, the SFP stabilized. Among the variables reported in Table 2, only a BMI value 1 year post-OLT >27.5 kg/m^2 was significantly associated with fibrosis progression <0.050 FU/mo (8/8 *vs* 18/35; $P<0.02$) in the 2nd year post-OLT. There was no difference in the SFP at 1 and 2 years post-OLT between patients that completed antiviral therapy as scheduled in comparison to those that either were untreated or terminated early interferon plus ribavirin treatment.

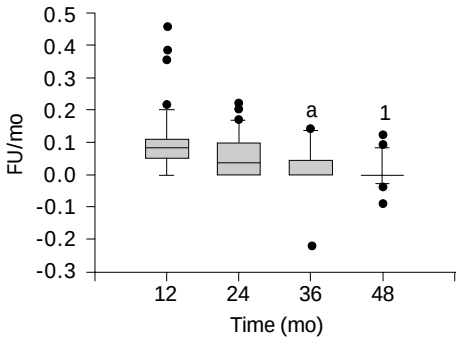


Figure 1 Vertical box plots of fibrosis progression rates in HCV-positive recipients, expressed as FU/mo, at different time points after the transplant operation. Median values, 10th, 25th, 75th, and 90th percentile are reported. Dots indicate outliers. [a]$P<0.005$ in comparison to FU/mo at 12 mo (Wilcoxon matched pairs signed rank sum test), [1]$P = 0.0001$ in comparison to FU/mo at 12 mo (Wilcoxon matched pairs signed rank sum test).

To further explore the relationship between gender and BMI, on the one hand, and fibrosis progression, on the other,

Table 2 Frequencies of patients with a SFP$\leqslant$0.100 FU/mo in the 1st year post-OLT, in relationship with a selection of demographic and clinical variables

	All patients ($n = 90$) FU/mo$\leqslant$0.100 $n = 70$	HCV-positive patients ($n = 55$) FU/mo$\leqslant$0.100 $n = 39$	HCV-negative patients ($n = 35$) FU/mo$\leqslant$0.100 $n = 31$
Recipient male gender ($n = 63$)	53[a]	29	24
Donor male gender ($n = 53$)	40	19	21
Recipient age $\leqslant$55 yr ($n = 54$)	42	19	23
Donor age $\leqslant$45 yr ($n = 54$)	47[d]	29[f]	18
Pre-OLT BMI >26.0 kg/m^2 ($n = 35$)	32[b]	16[c]	16
Tacrolimus therapy ($n = 69$)	56	31	25
Corticosteroid tapering >90 d ($n = 47$)	39	25	14
Diabetes mellitus ($n = 24$)	17	10	7

FU/mo: fibrosis units per month, HCV: hepatitis C virus, BMI: body mass index, [a]$P<0.05$ *vs* recipient female gender, [b]$P<0.02$ *vs* pre-OLT BMI $\leqslant$26 kg/m^2, [d]$P<0.01$ *vs* donor age >45 yr; [c]$P<0.05$ *vs* pre-OLT BMI $\leqslant$26 kg/m^2, [f]$P<0.001$ *vs* donor age >45 yr. P value refers to χ^2.

Table 3 Degree of hepatic steatosis in 105 biopsies performed between 12 and 36 mo after the transplant operation (HCV-positive recipients only), in relationship with a selection of variables

	Steatosis			
	Absent (n = 34)	≤10% (n = 60)	>10% (n = 11)	P
Ishak staging score≤2 (n = 79)	19	49	11	<0.005
Recipient male gender (n = 72)	20	42	10	<0.05
Recipient age≤55 yr (n = 50)	15	28	7	NS
Donor age≤45 yr (n = 65)	19	39	7	NS
BMI increase <1.5 kg/m^2 (n = 76)	29	41	6	<0.05
Recurrent hepatitis C≤1 yr post-OLT (n = 79)	31	41	7	<0.02
Diabetes mellitus (n = 31)	10	18	3	NS

BMI: body mass index, OLT: orthotopic liver transplantation, BMI increase: difference between BMI value 1 yr post-OLT and BMI value pre-OLT. P value refers to χ^2 for linear trend.

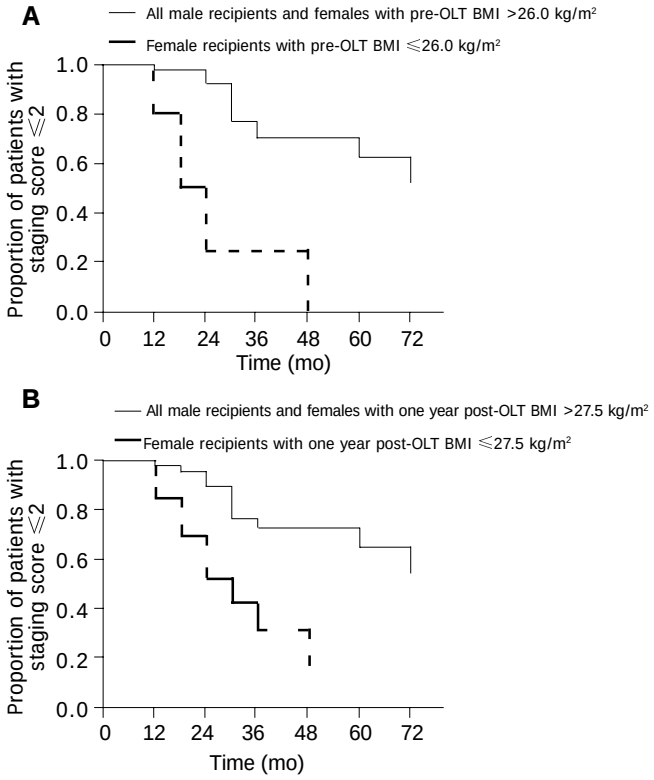


Figure 2 A: Time-to-event analysis to reach a staging score >2. HCV-positive recipients were divided as follows: all the male recipients and those females with pre-OLT BMI value >26.0 kg/m^2 (n = 45, continuous line); females with pre-OLT BMI value ≤26.0 kg/m^2 (n = 10, dotted line). B: Time-to-event analysis to reach a staging score >2. HCV-positive recipients were divided as follows: all the male recipients and those females with 1 year post-OLT BMI value >27.5 kg/m^2 (n = 42, continuous line); females with 1 year post-OLT BMI value ≤27.5 kg/m^2 (n = 13, dotted line).

we categorized OLT recipients as follows: females with BMI pre-OLT ≤26.0 kg/m^2 (group A^{pre}) or ≤27.5 kg/m^2 1 year post-OLT (group A^{post}); males with pre-OLT BMI value ≤26.0 kg/m^2 (group B^{pre}) or ≤27.5 kg/m^2 1 year post-OLT (group B^{post}); recipients of either gender and pre-OLT BMI >26.0 kg/m^2 (group C^{pre}) or >27.5 kg/m^2 1 year post-OLT (group C^{post}). Group A^{pre} showed the fastest SFP 1 year post-OLT, in comparison to group B^{pre} and group C^{pre} (7/10 *vs* 7/27 *vs* 16/18; P<0.002 for linear trend); a similar trend also was found considering 1 year post-OLT BMI and 2 years post-OLT fibrosis progression (A^{post} 6/10 *vs* B^{post} 11/25 *vs* C^{post} 8/8; P<0.02 for linear trend). Time-to-event analysis showed that, in females with lower BMI, the probability to reach a staging score >2 was the highest in comparison to all other recipients; this observation held true either considering BMI values pre-OLT (Figure 2A, Mantel-Cox, P<0.0001) or BMI values 1 year after OLT (Figure 2B, Mantel-Cox, P = 0.0005). Stepwise logistic regression analysis was performed among the predictive variables that, at univariate analysis, were associated, with a P value <0.10, to faster SFP (donor age, recipient gender, type of immunosuppressive therapy, and pre-OLT BMI). A SFP in the 1st year post-OLT >0.100 FU/mo was independently associated with older donor age (improvement of χ^2 11.63, P = 0.001), female recipient gender (improvement of χ^2 5.09, P<0.05) and lower pre-OLT BMI value (improvement of χ^2 4.26, P<0.05).

Post-OLT BMI, blood lipids, and liver steatosis One year post-OLT, having a BMI >26.5 kg/m^2, was found to be associated with a triglycerides/cholesterol (T/C) ratio ≤1 (14/15 *vs* 26/40, P<0.05). In relationship to the recipient gender, a low T/C ratio, i.e., higher serum levels of cholesterol than of triglycerides, was associated both to a delayed (>1 year) hepatitis C recurrence and to a slower post-OLT SFP. Female recipients with a high T/C ratio had the highest proportion of early hepatitis C recurrence and 1 year SFP >0.100 FU/mo, followed by male recipients with high T/C ratio and patients of either gender with low T/C ratio: 4/4 *vs* 11/11 *vs* 28/40 (P<0.05 for linear trend), and 4/4 *vs* 3/11 *vs* 9/40 (P<0.01 for linear trend), respectively.

One-hundred and five liver biopsies were performed in HCV-positive patients along the period of time elapsed between 12 and 36 mo post-OLT. Table 3 shows the relationship between hepatic steatosis and a selection of variables, including the Ishak fibrosis score. Male gender, delayed hepatitis C recurrence, and body weight gain post-OLT were positively associated with steatosis; on the contrary, progression to significant fibrosis was less frequent in the presence of hepatic steatosis.

[redacted]

Post-OLT fibrosis progression in patients transplanted for HCV-related liver cirrhosis has been recently reported to behave not linearly[15], reaching, a sharp increase in the first

2 years, a plateau at the 3rd year after OLT. In the present paper, we confirmed this observation, showing that fibrosis progression during the 1st year after OLT is faster than that observed in the longer follow-up, when the process tends to slow down. Furthermore, early fibrosis progression in the grafts of HCV recipients is confirmed to be related to factors pertaining both to the donor and to the host. First and most importantly, fibrosis progression is affected by the age of donors, in agreement with previous work by several authors who considered an aged donor as the strongest predictor of fibrosis progression in patients with post-OLT HCV recurrence[16]. Second, a novel finding and the focus of the present investigation, early fibrosis progression after OLT appears to be related to the BMI value measured either pre-OLT or post-OLT. The association is not direct, as one might expect, but inverse: the higher the BMI value, the lower is the degree of early fibrosis development. This association is peculiar to HCV-positive patients and was not observed in HCV-negative recipients. Third, the presence of steatosis in the graft, which occurs in association with the increase in BMI, does not predict, as reported in immune-competent patient, a higher fibrosis score. To reconcile these findings with the existing literature, the elements that need to be considered in detail concern the differences that exist between the natural history of HCV infection in immune-competent *vs* OLT patients, and the putative molecular mechanisms of HCV re-infection.

Obesity[5,8,9] and liver steatosis[6,17,18] are recognized factors of liver fibrosis progression in HCV-positive immune-competent patients. Some authors have hypothesized a direct steatogenic effect of HCV, supported by several lines of evidence: the development of progressive hepatic steatosis in transgenic mice expressing the HCV core gene[19], the inhibition of very low density lipoprotein (VLDL) secretion in a transgenic murine model expressing HCV core protein[20], the close relationship between intra-hepatic HCV RNA and development of steatosis[21], and the correlation between hepatic steatosis and hepatic HCV replication in patients infected with HCV genotype 3[22]. Others have investigated the mechanisms involved in the progression of liver fibrosis due to the concomitant presence of steatosis and HCV infection, suggesting that steatosis might contribute to fibrosis through a steatohepatitis-like pathway involving stellate cell activation and peri-sinusoidal fibrosis production[23]. In OLT patients, however, the situation is different. A recent report[24], while confirming that body weight is the best predictor of liver steatosis 12 mo post-OLT, demonstrated that allograft steatosis does not predict the severity of HCV recurrence in HCV-infected patients within the first 12 mo after OLT. The present results converge in the same direction, and suggest, for the first time, that overweight, while facilitates liver steatosis, on the other hand may protect the liver graft, during an initial phase, from the damage due to HCV recurrence. Further data outline the need to be cautious when transposing the information concerning the natural history of HCV in immune-competent patients to the natural history of HCV recurrence post-OLT. For example, female gender, known to be protective against fibrosis in immune-competent patients[25], is on the contrary a negative prognostic factor in the post-OLT setting[26]. The present data showed that, among the patients with the lowest BMI values, female recipients had a SFP faster than the corresponding males. Therefore, one might hypothesize that the stronger susceptibility of female recipients to HCV recurrence could be related, at least in part, to factors affected by the interrelationship between gender and BMI variations, for example the lipid profile.

According to recent studies, several aspects of HCV infection are connected with lipid metabolism and lipid profile modifications. Binding of HCV to cell membrane of hepatocytes is thought to occur via two putative HCV receptors: CD81, a cellular surface protein belonging to the tetraspanin protein super-family, and the low density lipoprotein receptor (LDL-r)[27-29]. The HCV envelope glycoprotein E2 may interact with the CD81 molecule, while HCV or HCV-LDL complexes interact preferentially with the LDL-r[30]. HCV circulates in blood in association with different lipoproteins: early in the course of the infection, the preferential association is with LDL, while later on the association is with high-density lipoproteins (HDL). In accordance, patients with immune-deficiencies present higher HCV RNA titers in the LDL and HDL fractions than the immune-competent counterparts[31]. During the early viremic phase of experimental HCV infection, several genes associated with lipid metabolism are upregulated; interestingly, the fatty acid synthesizing gene is expressed at higher levels among chimpanzees that attain sustained clearance of the virus[32]. Binding and internalization of HCV RNA containing particles seem strictly regulated by lipoproteins: an increase of LDL and other lipoproteins decreases the LDL-r HCV particles interaction[28,33,34] while an upregulation of the LDL-r increases the internalization of HCV[35]. According to a recently proposed model, virions are released by liver cells and may infect other liver cells via LDL-r; free β-lipoproteins may regulate the rate of the infection of liver cells by competing with the virus[29]. Considering altogether these observations, it is tempting to speculate that a particular lipid profile could be associated with a slower kinetic of HCV infection of the hepatocytes and as a consequence a lesser fibrosis progression of the graft. We calculated the ratio between serum triglycerides and serum cholesterol as a proxy index of the balance between VLDL and LDL in the circulation. An association was found between a low T/C ratio and a higher BMI 1 year post-OLT. As previously observed considering the association between BMI and fibrosis progression, the relationships between the value of T/C ratio and both the timing of hepatitis C recurrence and the 1 year fibrosis progression rate were gender-related: females with higher T/C ratio were found to present the fastest SFP. Following this line, one might hypothesize that a low BMI, especially for female patients, could be associated with a lipid profile characterized by reduced serum LDL/VLDL levels. In fact, the relationship between increasing body weight and blood lipid profile is stricter in men than in women[36-38]. Furthermore, we have previously found that recipient's carriage of at least one ε4 allele of the apo-lipoprotein E (an allelic variant associated with higher cholesterol levels) was associated with better histological outcome of recurrent hepatitis C in male, but not in female recipients[39]. An unfavorable lipoprotein profile could possibly enhance HCV infectivity through an

upregulation of LDL-r[40], or decreased interference of LDL at the level of the interaction between HCV and LDL-r[29].

In conclusion, post-OLT overweight in HCV-positive recipients does not represent a factor favoring early liver fibrosis development and could even be protective against it. The explanation of this unexpected finding might reside on the peculiar lipid profile of patients with excess body weight post-OLT, capable to modulate the severity of HCV recurrence and hence the speed at which liver fibrosis develops.

REFERENCES

1 **McCaughan GW**, Zekry A. Pathogenesis of hepatitis C virus recurrence in the liver allograft. *Liver Transpl* 2002; **8**: S7-13
2 **Berenguer M**. Natural history of recurrent hepatitis C. *Liver Transpl* 2002; **8**: S14-18
3 **Mazuelos F**, Abril J, Zaragoza C, Rubio E, Moreno JM, Turrion VS, Cuervas-Mons V. Cardiovascular morbidity and obesity in adult liver transplant recipients. *Transplant Proc* 2003; **35**: 1909-1910
4 **Nair S**, Verma S, Thuluvath PJ. Obesity and its effect on survival in patients undergoing orthotopic liver transplantation in the United States. *Hepatology* 2002; **35**: 105-109
5 **Hourigan LF**, Macdonald GA, Purdie D, Whitehall VH, Shorthouse C, Clouston A, Powell EE. Fibrosis in chronic hepatitis C correlates significantly with body mass index and steatosis. *Hepatology* 1999; **29**: 1215-1219
6 **Adinolfi LE**, Gambardella M, Andreana A, Tripodi MF, Utili R, Ruggiero G. Steatosis accelerates the progression of liver damage of chronic hepatitis C patients and correlates with specific HCV genotype and visceral obesity. *Hepatology* 2001; **33**: 1358-1364
7 **Monto A**, Alonzo J, Watson JJ, Grunfeld C, Wright TL. Steatosis in chronic hepatitis C: relative contributions of obesity, diabetes mellitus, and alcohol. *Hepatology* 2002; **36**: 729-736
8 **Ortiz V**, Berenguer M, Rayon JM, Carrasco D, Berenguer J. Contribution of obesity to hepatitis C-related fibrosis progression. *Am J Gastroenterol* 2002; **97**: 2408-2414
9 **Friedenberg F**, Pungpapong S, Zaeri N, Braitman LE. The impact of diabetes and obesity on liver histology in patients with hepatitis C. *Diabetes Obes Metab* 2003; **5**: 150-155
10 **Bressler BL**, Guindi M, Tomlinson G, Heathcote J. High body mass index is an independent risk factor for nonresponse to antiviral treatment in chronic hepatitis C. *Hepatology* 2003; **38**: 639-644
11 **Poonawala A**, Nair SP, Thuluvath PJ. Prevalence of obesity and diabetes in patients with cryptogenic cirrhosis: a case-control study. *Hepatology* 2000; **32**: 689-692
12 **Clark JM**, Diehl AM. Nonalcoholic fatty liver disease: an underrecognized cause of cryptogenic cirrhosis. *Jama* 2003; **289**: 3000-3004
13 **Ioannou GN**, Weiss NS, Kowdley KV, Dominitz JA. Is obesity a risk factor for cirrhosis-related death or hospitalization? A population-based cohort study. *Gastroenterology* 2003; **125**: 1053-1059
14 **Ishak K**, Baptista A, Bianchi L, Callea F, De Groote J, Gudat F, Denk H, Desmet V, Korb G, MacSween RN. Histological grading and staging of chronic hepatitis. *J Hepatol* 1995; **22**: 696-699
15 **Neumann UP**, Berg T, Bahra M, Seehofer D, Langrehr JM, Neuhaus R, Radke C, Neuhaus P. Fibrosis progression after liver transplantation in patients with recurrent hepatitis C. *J Hepatol* 2004; **41**: 830-836
16 **Machicao VI**, Bonatti H, Krishna M, Aqel BA, Lukens FJ, Nguyen JH, Rosser BG, Satyanarayana R, Grewal HP, Hewitt WR, Harnois DM, Crook JE, Steers JL, Dickson RC. Donor age affects fibrosis progression and graft survival after liver transplantation for hepatitis C. *Transplantation* 2004; **77**: 84-92
17 **Serfaty L**, Poujol-Robert A, Carbonell N, Chazouilleres O, Poupon RE, Poupon R. Effect of the interaction between steatosis and alcohol intake on liver fibrosis progression in chronic hepatitis C. *Am J Gastroenterol* 2002; **97**: 1807-1812
18 **Castera L**, Hezode C, Roudot-Thoraval F, Bastie A, Zafrani ES, Pawlotsky JM, Dhumeaux D. Worsening of steatosis is an independent factor of fibrosis progression in untreated patients with chronic hepatitis C and paired liver biopsies. *Gut* 2003; **52**: 288-292
19 **Moriya K**, Yotsuyanagi H, Shintani Y, Fujie H, Ishibashi K, Matsuura Y, Miyamura T, Koike K. Hepatitis C virus core protein induces hepatic steatosis in transgenic mice. *J Gen Virol* 1997; **78**(Pt 7): 1527-1531
20 **Perlemuter G**, Sabile A, Letteron P, Vona G, Topilco A, Chretien Y, Koike K, Pessayre D, Chapman J, Barba G, Brechot C. Hepatitis C virus core protein inhibits microsomal triglyceride transfer protein activity and very low density lipoprotein secretion: a model of viral-related steatosis. *Faseb J* 2002; **16**: 185-194
21 **Fujie H**, Yotsuyanagi H, Moriya K, Shintani Y, Tsutsumi T, Takayama T, Makuuchi M, Matsuura Y, Miyamura T, Kimura S, Koike K. Steatosis and intrahepatic hepatitis C virus in chronic hepatitis. *J Med Virol* 1999; **59**: 141-145
22 **Rubbia-Brandt L**, Quadri R, Abid K, Giostra E, Male PJ, Mentha G, Spahr L, Zarski JP, Borisch B, Hadengue A, Negro F. Hepatocyte steatosis is a cytopathic effect of hepatitis C virus genotype 3. *J Hepatol* 2000; **33**: 106-115
23 **Clouston AD**, Jonsson JR, Purdie DM, Macdonald GA, Pandeya N, Shorthouse C, Powell EE. Steatosis and chronic hepatitis C: analysis of fibrosis and stellate cell activation. *J Hepatol* 2001; **34**: 314-320
24 **Machicao VI**, Krishna M, Bonatti H, Aqel BA, Nguyen JH, Weigand SD, Rosser BG, Hughes C, Dickson RC. Hepatitis C recurrence is not associated with allograft steatosis within the first year after liver transplantation. *Liver Transpl* 2004; **10**: 599-606
25 **Poynard T**, Ratziu V, Benmanov Y, Di Martino V, Bedossa P, Opolon P. Fibrosis in patients with chronic hepatitis C: detection and significance. *Semin Liver Dis* 2000; **20**: 47-55
26 **Forman LM**, Lewis JD, Berlin JA, Feldman HI, Lucey MR. The association between hepatitis C infection and survival after orthotopic liver transplantation. *Gastroenterology* 2002; **122**: 889-896
27 **Agnello V**, Abel G, Elfahal M, Knight GB, Zhang QX. Hepatitis C virus and other flaviviridae viruses enter cells via low density lipoprotein receptor. *Proc Natl Acad Sci USA* 1999; **96**: 12766-12771
28 **Germi R**, Crance JM, Garin D, Guimet J, Lortat-Jacob H, Ruigrok RW, Zarski JP, Drouet E. Cellular glycosaminoglycans and low density lipoprotein receptor are involved in hepatitis C virus adsorption. *J Med Virol* 2002; **68**: 206-215
29 **Monazahian M**, Bohme I, Bonk S, Koch A, Scholz C, Grethe S, Thomssen R. Low density lipoprotein receptor as a candidate receptor for hepatitis C virus. *J Med Virol* 1999; **57**: 223-229
30 **Wunschmann S**, Medh JD, Klinzmann D, Schmidt WN, Stapleton JT. Characterization of hepatitis C virus (HCV) and HCV E2 interactions with CD81 and the low-density lipoprotein receptor. *J Virol* 2000; **74**: 10055-10062
31 **Pumeechockchai W**, Bevitt D, Agarwal K, Petropoulou T, Langer BC, Belohradsky B, Bassendine MF, Toms GL. Hepatitis C virus particles of different density in the blood of chronically infected immunocompetent and immunodeficient patients: Implications for virus clearance by antibody. *J Med Virol* 2002; **68**: 335-342
32 **Su AI**, Pezacki JP, Wodicka L, Brideau AD, Supekova L, Thimme R, Wieland S, Bukh J, Purcell RH, Schultz PG, Chisari FV. Genomic analysis of the host response to hepatitis C virus infection. *Proc Natl Acad Sci USA* 2002; **99**: 15669-15674
33 **Triyatni M**, Saunier B, Maruvada P, Davis AR, Ulianich L, Heller T, Patel A, Kohn LD, Liang TJ. Interaction of hepatitis C virus-like particles and cells: a model system for studying

viral binding and entry. *J Virol* 2002; **76**: 9335-9344

34 **Enjoji M**, Nakamuta M, Kinukawa N, Sugimoto R, Noguchi K, Tsuruta S, Iwao M, Kotoh K, Iwamoto H, Nawata H. Beta-lipoproteins influence the serum level of hepatitis C virus. *Med Sci Monit* 2000; **6**: 841-844

35 **Andre P**, Komurian-Pradel F, Deforges S, Perret M, Berland JL, Sodoyer M, Pol S, Brechot C, Paranhos-Baccala G, Lotteau V. Characterization of low- and very-low-density hepatitis C virus RNA-containing particles. *J Virol* 2002; **76**: 6919-6928

36 **Brown CD**, Higgins M, Donato KA, Rohde FC, Garrison R, Obarzanek E, Ernst ND, Horan M. Body mass index and the prevalence of hypertension and dyslipidemia. *Obes Res* 2000; **8**: 605-619

37 **Heitmann BL**. The effects of gender and age on associations between blood lipid levels and obesity in Danish men and women aged 35-65 years. *J Clin Epidemiol* 1992; **45**: 693-702

38 **Wilsgaard T**, Arnesen E. Change in serum lipids and body mass index by age, sex, and smoking status: the Tromso study 1986-1995. *Ann Epidemiol* 2004; **14**: 265-273

39 **Toniutto P**, Fabris C, Fumo E, Apollonio L, Caldato M, Mariuzzi L, Avellini C, Minisini R, Pirisi M. Carriage of the apolipoprotein E-epsilon4 allele and histologic outcome of recurrent hepatitis C after antiviral treatment. *Am J Clin Pathol* 2004; **122**: 428-433

40 **Olson RE**. Discovery of the lipoproteins, their role in fat transport and their significance as risk factors. *J Nutr* 1998; **128**: S439-443

Science Editor Guo SY **Language Editor** Elsevier HK

PO Box 2345, Beijing 100023, China
www.wjgnet.com
wjg@wjgnet.com

ELSEVIER

World J Gastroenterol 2005;11(38):5951-5957
World Journal of Gastroenterology ISSN 1007-9327
© 2005 The WJG Press and Elsevier Inc. All rights reserved.

• *BASIC RESEARCH* •

Upregulation of cathepsin W-expressing T cells is specific for autoimmune atrophic gastritis compared to other types of chronic gastritis

Doerthe Kuester, Michael Vieth, Ulrich Peitz, Stefan Kahl, Manfred Stolte, Albert Roessner, Ekkehard Weber, Peter Malfertheiner, Thomas Wex

Doerthe Kuester, Michael Vieth, Albert Roessner, Institute of Pathology, Otto-von-Guericke University Magdeburg, Leipziger Str. 44, Magdeburg D-39120, Germany
Ulrich Peitz, Stefan Kahl, Peter Malfertheiner, Thomas Wex, Department of Gastroenterology, Hepatology and Infectious Diseases, Otto-von-Guericke University Magdeburg, Leipziger Str. 44, Magdeburg D-39120, Germany
Manfred Stolte, Institute of Pathology, Klinikum Bayreuth GmbH, Preuschwitzerstr 101, Bayreuth D-95445, Germany
Ekkehard Weber, Institute of Physiological Chemistry, Medical Faculty, Martin-Luther University Halle-Wittenberg, Holly Str. 1, Halle D-06097, Germany
Supported by the "Deutsche Forschungsgemeinschaft", Germany (We2170/3-1) and the NBL-3 program of the "Bundesministerium für Forschung und Technik" (NBL3/01ZZ0407/PFG1)
Correspondence to: Dr. Thomas Wex, Department of Gastroenterology, Hepatology and Infectious Diseases, Otto-von-Guericke University, Magdeburg, Leipziger Str. 44, Magdeburg D-39120, Germany. thomas.wex@medizin.uni-magdeburg.de
Telephone: +49-391-6713106 Fax: +49-391-6713105
Received: 2005-03-04 Accepted: 2005-04-30

Abstract

AIM: To investigate a pathophysiological role of cathepsin W (CatW), a putative thiol-dependent cysteine protease, which is specifically expressed in cytotoxic lymphocytes, in different types of chronic inflammation of the gastric mucosa.

METHODS: Gastric and duodenal biopsies of patients with *Helicobacter pylori* (*H pylori*)-associated active gastritis (*Hp*, $n = 19$), chemically induced reactive gastritis (CG, $n = 17$), autoimmune atrophic gastritis (AIG, $n = 20$), lymphocytic corpus gastritis (LG, $n = 29$), celiac disease (CD, $n = 10$), and corresponding controls ($n = 24$) were analyzed by immunohistochemistry for the expression of CatW and CD45. Furthermore, immunohistochemical double staining with anti-CD3 and anti-cathepsin was performed for the samples of AIG.

RESULTS: Median values of CatW-expressing cells among CD45-positive immune cells were between 2% and 6% for normal gastric mucosa, CG, and LG, whereas the corresponding value was significantly increased for AIG (24.7%, $P<0.001$) and significantly decreased for HP (0.7%, $P<0.05$). Double staining with anti-CD3 and anti-CatW antibodies revealed that >90% of CatW-expressing cells in gastric mucosa of AIG were T cells. Duodenal mucosa had significantly more CatW/CD45-positive cells than normal gastric mucosa (median: 17.8% *vs* 2%, $P<0.01$). The corresponding proportion of CatW/CD45-positive cells was decreased in CD compared to duodenal mucosa (median: 2.1% *vs* 17.8%, $P<0.05$).

CONCLUSION: The opposite findings regarding the presence of CatW-positive cells in AIG (increase) and CD (decrease) reflects the different cellular composition of immune cells involved in the pathogenesis of these diseases.

© 2005 The WJG Press and Elsevier Inc. All rights reserved.

Key words: Cathepsin W; Inflammation; Gastritis; Immunohistochemistry; NK cells

Kuester D, Vieth M, Peitz U, Kahl S, Stolte M, Roessner A, Weber E, Malfertheiner P, Wex T. Upregulation of cathepsin W-expressing T cells is specific for autoimmune atrophic gastritis compared to other types of chronic gastritis. *World J Gastroenterol* 2005; 11(38): 5951-5957
http://www.wjgnet.com/1007-9327/11/5951.asp

INTRODUCTION

Gastritis, by definition, is a histopathological entity characterized by the chronic and active inflammation of the gastric mucosa. The classification of gastritis, according to the updated Sydney system[1], is organized along traditional lines with active and chronic gastritis and includes specific forms of chronic gastritis defined by topography, morphology, and etiology and is graded with the help of a semiquantitative visual scale. The discovery of *Helicobacter pylori* (*H pylori*) has dramatically altered the etiological concepts of several gastric diseases. *H pylori* is the major cause of gastritis, gastric ulcer and has been classified as a definite human carcinogen playing a key role in the pathogenesis of gastric cancer and MALT lymphoma[2,3]. The host response to *H pylori* and its bacterial products is composed of T-, B-lymphocytes and plasma cells defined as chronicity of the gastritis. The infiltration of the lamina propria and gastric epithelium by polymorph nuclear leukocytes (mostly neutrophil granulocytes) reflects the activity of the inflammation.

NSAID-associated or bile-induced chemical reactive gastritis, causing 20-30% of gastritis, as well as autoimmune and lymphocytic gastritis (LG) are distinct entities. The presence

of atrophy in the gastric corpus with diffuse atrophy of parietal and chief cells are the main characteristics of autoimmune atrophic gastritis (AIG) together with a hyperplasia of ECL cells. This disease is associated with serum anti-parietal and anti-intrinsic factor (IF) antibodies that cause IF deficiency, which can lead eventually to pernicious anemia in some patients. It has been shown that AIG is associated with infiltration of $CD4^+$ T lymphocytes into the gastric mucosa, where they contribute to tissue destruction and gastric atrophy[4].

Chemically induced reactive gastritis (CG), caused by the use of nonsteroidal anti-inflammatory agents (NSAIDs) or bile reflux, is characterized by regenerative processes that lead to foveolar hyperplasia, mucosal edema, hemorrhage, capillary ectasia, proliferation of ascending smooth muscle fibers, and apical fibrosis. Usually, these lesions exhibit a slight superficial infiltration of lymphocytes and plasma cells. NSAIDs might additionally cause epithelial damage such as erosions and ulcers[1].

LG is a rare form of gastritis. The essential diagnostic feature is the presence of increased intraepithelial lymphocytes (mostly T cells), at least 25 lymphocytes per 100 epithelial cells. In the lamina propria, there are often additional neutrophil granulocytes among lymphocytes and plasma cells at the surface epithelium and within foveolar epithelium[5-7]. LG is believed to represent a special form of Helicobacter-mediated gastritis, mostly found in the corpus and fundus, although *H pylori* is only rarely found morphologically[6,7]. Three different types of LG can be distinguished depending on the endoscopic appearance: LG without typical endoscopic findings, the varioliform gastritis with thickened rugal folds, and Ménétriers disease with prominent rugal folds.

In human beings, the group of thiol-dependent cathepsins comprises 11 different cysteine proteases that are mostly localized in the lysosomal compartment[8]. During the last decade, it has become evident that most of these enzymes in addition to their role in lysosomal protein degradation[9] can mediate or regulate specific processes in various tissues and cell types. These functions include 'limited proteolysis' leading to the activation of granzymes[10], the maturation of hormones[11,12] and the regulation of antigen presentation[13]. As today, there is limited knowledge concerning the role of thiol-dependent cathepsins in gastric physiology and related disorders. Notably, cathepsins B and L were found to be associated with the carcinogenesis and metastasis of gastric and esophageal cancer[14-16]. Furthermore, cathepsins X and K were found to be specifically expressed in gastric epithelium[17], whereas cathepsin W (CatW) was found to be specifically expressed in lymphocyte-like cells within the gastric and intestinal tissue[18]. This finding was in line with the restricted expression pattern of CatW, which is expressed in NK cells and in cytotoxic T cells[19-21]. Although, its enzymatic activity and major function has not been characterized, there are some data supporting a regulatory role of this putative protease in the cytotoxic process for the NK-92 cell model[22]. However, cells from CatW-deficient mice were not affected in their cell-mediated cytotoxicity *in vitro*[23]. The specific association between CatW and cytotoxic cells and the potential involvement of these cells in chronic inflammation, prompted us to investigate the expression of CatW in different types of gastritis.

MATERIALS AND METHODS

Materials

A total of 119 formalin-fixed, paraffin-embedded biopsy specimens from patients suffering from different gastrointestinal disorders were retrieved from the archives of the institutes of Pathology Bayreuth and Magdeburg. The selection was based on clinical and histological evidence of the corresponding diagnosis including *H pylori*-associated chronic active gastritis (n = 19), CG (n = 17), AIG (n = 20), lymphocytic corpus gastritis without endoscopic findings (n = 29) as well as samples of duodenal mucosa of 10 patients with celiac disease (CD). Furthermore, healthy controls of both gastric (n = 14) and duodenal (n = 10) mucosa were examined immunohistochemically. Histological diagnosis was made by hematoxylin-eosin and Warthin-Starry stainings.

Methods

Detection of cathepsin W and CD45 by immunohistochemistry After the removal of paraffin by xylol, two sets of serial sections of all tissue specimens were subsequently dehydrated using increasing concentrations of ethanol. In order to demask the antigens, the samples were boiled thrice in 0.01 mol/L sodium citrate buffer (pH 6.0) for 10 min in a microwave (600 W), and incubated for 30 min at room temperature in 1×staining buffer containing 5% RPMI, 5% FCS, and 0.05% sodium azide in aqua dest (pH 7.4-7.6). The subsequent staining procedure on each one serial slide was performed using the monoclonal anti-CatW antibody CW-401B1 (1:1 000 in 1×staining buffer, 1 h at room temperature) and the Vectastain ABC-AP Kit (Vector, Burlingame) following the manufacturer's instructions. In addition, a matching set of serial sections was stained with anti-CD45 (LCA, DakoCytomation, Glostrup, Denmark). The used antibody is a mixture of two mAbs (2B11 and PD7/26) representing all isoforms (2B11) and the isoform CD45R0 (PD7/26). Immunostaining was performed as described elsewhere[24]. All samples were counterstained with hematoxylin, dehydrated and mounted using DEPEX™ (Serva, Heidelberg, Germany).

Detection of cathepsin W and CD3 by double immunohistochemistry in autoimmune atrophic gastritis To distinguish between CatW-positive-stained natural killer cells and cytotoxic T lymphocytes, a third series of sections of the above used tissue specimens with AIG was pretreated and stained with the anti-CatW antibody and detected with Vectastain ABC-AP Kit as described above. After washing the slides thoroughly in PBS, subsequent staining with the anti-CD3-antibody (1:100; anti-human CD3, A 0452; DakoCytomation, Hamburg, Germany) was performed; marking the CD3-complex of T cells.

For revealing positive immunohistochemical reaction, the iVIEW™ DAB Detection Kit (Ventana, Germany) was used as chromogen substrate, and then specimens were counterstained with hematoxylin and mounted with DEPEX™.

For all immunohistochemical analyses, two persons counted the numbers of stained cells in three independent high-power fields. Mann-Whitney U test was used for group comparison. For all statistical analyses, $P<0.05$ was considered to indicate statistical significance.

Generally, a consistent staining pattern exhibiting CatW-positive cells with a lymphocytic phenotype was obtained in all samples. The tissue specimens of the different chronic gastrointestinal disorders contained various amounts of CatW-expressing cells. In normal gastric mucosa, CatW-expressing cells were rarely detected (0.5±1 cells/field), whereas the different forms of gastritis revealed higher absolute numbers of 4.1-41 cells per observation field (Figure 2). Other immune cells including polymorph nuclear neutrophils, macrophages, and plasma cells as well as epithelial and stroma cells did not express CatW. AIG showed extensive mucosal atrophy, replacement of the oxyntic glands by intestinal metaplastic epithelium and mononuclear infiltrate within the lamina propria with approximately 25% of $CD45^+$ cells expressing CatW (Figure 1C). CD with subtotal villous atrophy and dense inflammatory infiltrate revealed a fraction of about 5% $CatW^+/CD45^+$ cells (Figure 1D). In chronic *H pylori* gastritis, the gastric mucosa contained high absolute numbers of $CatW^+$ cells among the dense infiltrate consisting of $CD45^+$ lymphocytes, macrophages, plasma cells as well as neutrophils (Figure 1E).

Notably, the relative proportion of CatW-expressing cells among the infiltrating leukocytes, determined by CD45, differed remarkably for the investigated types of chronic inflammation (Figure 2). The highest proportion of CatW-expressing $CD45^+$ cells was found in AIG reaching 24.7% (ranging from 8% to 70%). Normal gastric mucosa, which comprised samples without gastritis, revealed a fraction of 2% (ranging from 1% to 5%). The difference between both groups was found to be significant ($P<0.001$). Surprisingly, for CD as another autoimmune-triggered intestinal disease investigated in this study, a significant reduction of the relative number of CatW-expressing cells was observed compared to healthy duodenal mucosa (2.1% *vs* 17.8%, $P<0.05$, Figure 2). Normal duodenal mucosa contained significantly more CatW-positive cells than normal gastric mucosa ($P<0.01$). Furthermore, the proportion of $CatW^+/CD45^+$ cells was analyzed in the specimens with *H pylori*-associated chronic active gastritis. Here, a significant decreased proportion of 0.7% (ranging from 0.5% to 2%, $P<0.05$) compared to normal gastric mucosa was detected (Figure 2).

For the other two chronic gastric disorders (CG and LG) analyzed in this study, the proportions of $CatW^+/CD45^+$ cells were not changed and similar to normal gastric mucosa (Figure 2). CatW was identified in about 6% and 2.2% of the $CD45^+$ cells in CG and LG, respectively.

As exemplarily shown in Figure 3, the double staining permitted a clear classification of the lymphocyte-like infiltrate of the lamina propria in AIG. The great majority (>90%) of CatW-expressing cells represented $CD3^+$ T lymphocytes, whereas $CatW^+$ NK cells ($CD3^-$) were rarely detected. Whereas $CatW^-/CD3^+$ positive T cells were abundantly seen in the samples of AIG, a high proportion of CatW-expressing cytotoxic T cells (CTL) was detected, too. $CatW^+$ NK cells (NK) were only rarely spotted in the lamina propria.

This study revealed two new and important findings. First, it provides evidence that the elevated number of CatW-expressing cells in AIG is a rather specific event for this disease and does not just represent a general phenomenon of mucosal inflammation. Second, data provide evidence that the cellular distribution of CatW is different in peripheral blood and mucosal compartment[25,26].

The elevated number of CatW-positive cells in AIG supports a pathophysiological role of these cells in this type of gastritis as discussed previously[18]. The specific expression pattern of CatW[19-21] and its potential involvement in cytotoxic processes[22] imply an involvement of CatW in Th1-mediated inflammation like AIG. According to the current model of AIG, first, self-antigen-reactive Th1 cells, which express IFN-γ, IL-2 and are capable for transendothelial migration, are activated by self-antigens of gastric mucosa and participate in tissue destruction and resulting inflammation. Second, Th2 cells, being sessile in the draining lymph nodes and activated by the self-antigens released from tissue destruction, support autoantibody production and might develop into memory cells[27]. Although, IFN-γ, which is mainly released by NK cells is one of the predominant cytokines increased in AIG[28-30], there are data implying that NK cells are dispensable for the onset of AIG. In mice models with neonatal thymectomy and subsequent depletion of NK cells, the disease incidence was not changed suggesting that other cells such as $CD8^+$ T cells are the primary source of IFN-γ[31]. Furthermore, it has been shown by several groups that in the experimental mouse model, CD4-positive T cells are mainly responsible for the development of gastric lesions[32-34]. Interestingly, the predominant role of CD4-positive T cells has not been fully confirmed. D'Elios and co-workers showed an association between AIG and Th1-differentiated T cells that possessed cytotoxic activity[35]. Other studies investigating patient-derived samples identified an upregulation of $CD16^+$ and $CD8^+$ cells suggesting a potential role of these cytotoxic cells in human AIG[36,37]. Based on these reports, an interaction of the $CD4^+$ cells with autoreactive $CD8^+$ effector cells might lead to the development of autoimmune gastritis that involves also regulatory T cells[38,39]. Taking into consideration the data from the human disease that showed a predominant involvement of T cells in AIG[35,36], the higher proportion of $CD8^+$ T cell in mucosal compartments[26] and the specific expression pattern of CatW in cytotoxic T and NK cells[21], we assume that in AIG mostly $CD8^+$ T cells contribute to the high proportion of $CatW^+/CD45^+$ cells. By performing double staining immunohistochemistry, we were able to confirm this hypothesis by showing a very low proportion of $CatW^+$ NK cells, whereas the number of CatW-expressing cytotoxic T lymphocytes was increased significantly. This observation supports a specific role of CTLs in the pathophysiological processes of AIG. For comparison, tissue samples of CD, another prototype of T-cell mediated autoimmune disease, were also investigated. Surprisingly, a decrease of the $CatW^+/CD45^+$ cells was determined in CD. This phenomenon is presumably caused by the massive increase of CatW-negative $CD4^+$ T cells, which make up the majority of infiltrating immune cells in this disease[39,40]. The observation, that the absolute number of CatW-expressing cells is significantly higher in normal intestinal samples compared to gastric samples, is in line with the distribution

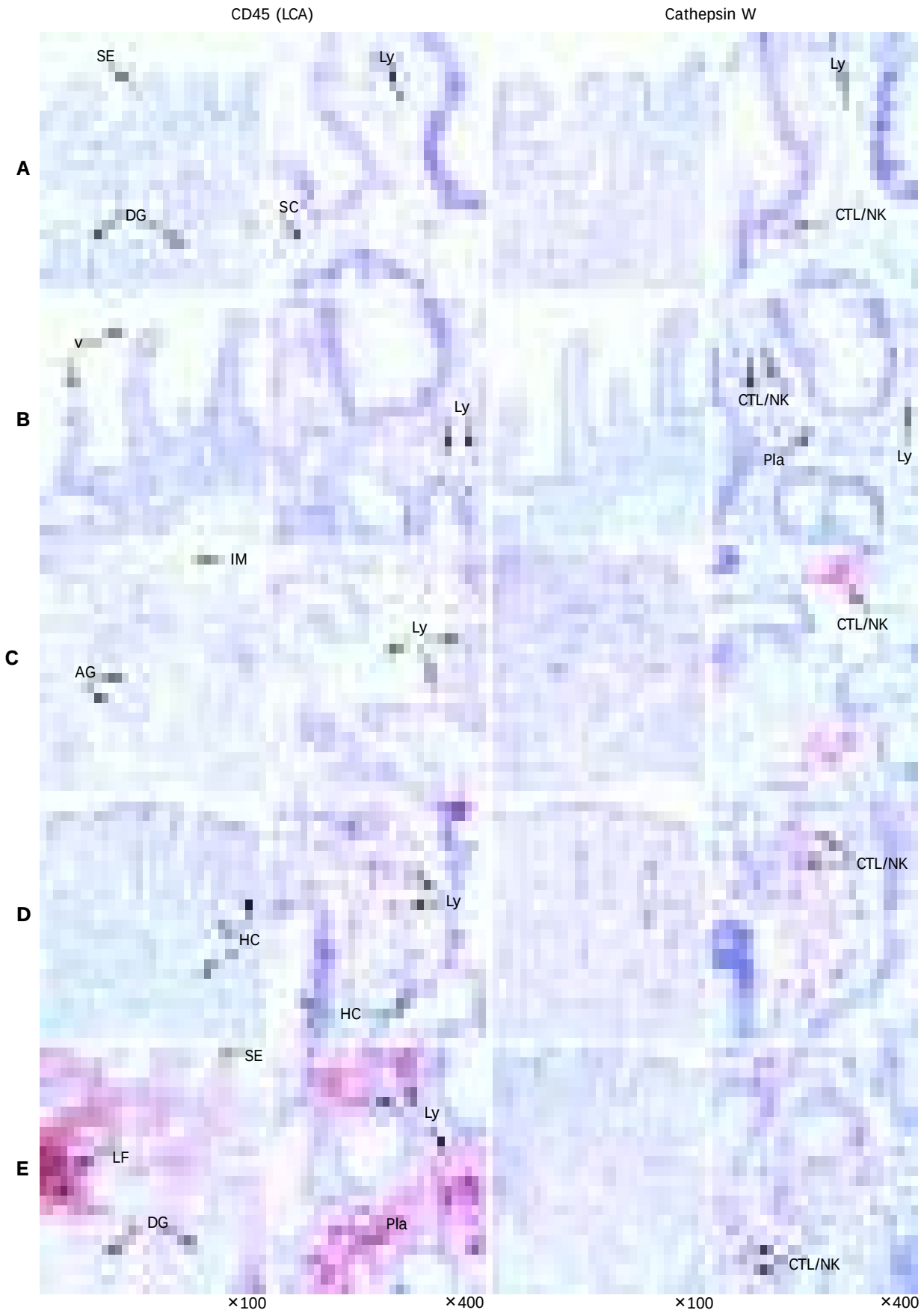


Figure 1 Immunohistochemical detection of CatW in gastrointestinal tissue specimens. The cellular distribution of CatW expression is presented by red staining, whereas the nuclei are counterstained with hematoxylin (blue). The distribution of CD45 (LCA) is shown as brownish staining. The negative controls (using isotype controls) did not reveal any signals (not shown). The tissue samples were as follows: normal gastric mucosa (A), duodenum (B), AIG (C), CD (D) and *H pylori* gastritis (E). AG: Atrophic glands, CTL: cytotoxic T-lymphocyte, DG: deep gastric glands, HC: hyperplastic crypts, IM: intestinal metaplasia, LF: lymph follicle, Ly: lymphocyte, Pla: plasma cell, NK: natural killer cell, SC: stroma cells, SE: surface epithelium, T-Ly: T lymphocyte, and V: duodenal villi.

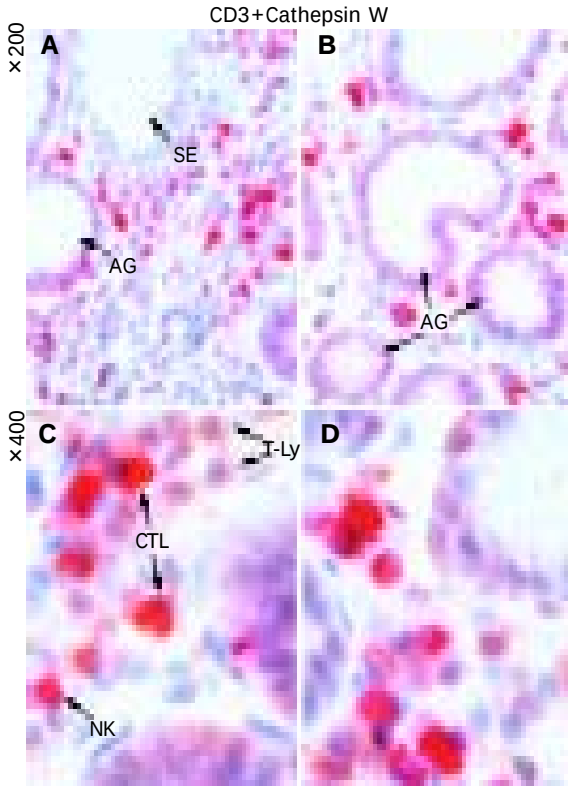


Figure 2 Detection of CatW and CD3$^+$ T cells in tissue specimens of AIG. The immunohistochemical double staining allowed a differentiation of both CatW-expressing cell types as well as a separation of CTLs from the other T cells (T-Ly) among the infiltrating cells of the lamina propria: Whereas CatW$^-$/CD3$^+$ positive T cells could be clearly distinguished by the brownish staining and were abundantly seen in the samples of AIG, an additional cytoplasmic red staining detected the CatW-expressing CTL. The exclusively red staining marked the CatW$^+$ NK cells, which were only rarely spotted in the lamina propria.

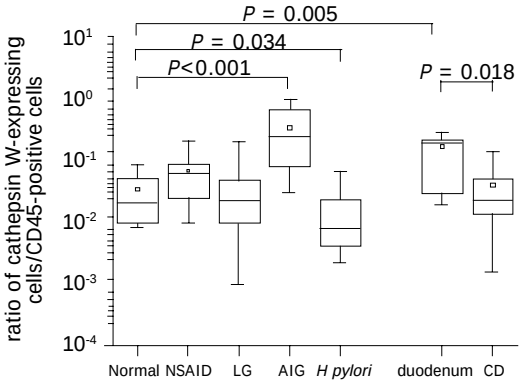


Figure 3 Presence of CatW-expressing cells among infiltrating immune cells in samples of patients with gastritis. The distribution of CatW- and LCA (leukocyte common antigen, CD45)-expressing cells was separately analyzed by immunohistochemistry in serial sections of tissue specimens. The number of CD45-positive cells was considered as 100% presented as a ratio of 1 at the Y-axis. The ratio of CatW$^+$/LCA$^+$ cells illustrates the proportion of CatW-expressing cells among leukocytes present in the gastric/duodenal mucosa. Data are shown as box plot for each group (antral mucosa: normal; chemically induced gastritis: NSAID; lymphocytic gastritis: LG; autoimmune gastritis: AIG; *H pylori*-induced gastritis: *H pylori*; normal duodenum: duodenum; celiac disease: CD). Boxes represent the 25th, 50th, and 75th percentile values (horizontal lines of the box) and means (squares). Mean values of absolute numbers of CatW-expressing cells per observation field were 0.5, 4.1, 4.2, 10.7, and 41 for normal antral mucosa, *H pylori* gastritis, NSAID-associated gastritis, LG and AIG, respectively. Tissue specimens from normal duodenum revealed 16 CatW-expressing cells per field, while samples from patient with CD had 6.3 CatW-positive cells in average per field.

of immune cells in these compartments.

It is well known that *H pylori* leads to an infiltration of neutrophils and a predominant Th1-dominated immune response[41]. The analysis of lymphocytic subsets in chronic gastritis revealed that most of the infiltrating lymphocytes were found to be CD4$^+$ T cells[42], whereas neutrophils and cytotoxic T cells seem to play an important role with respect to the activity of *H pylori* gastritis[43,44]. Furthermore, a significant increase of IL-2 receptor positive cells, including NK cells, was reported in chronic gastritis[44]. Taking into consideration the involvement of different subsets of immune cells in *H pylori*-mediated gastritis, the relative decrease of CatW-expressing cells can be attributed to the massive infiltration of CD45$^+$ leukocytes (CD4$^+$ T cells, B cells, and granulocytes). Although, there is no doubt that these cells in general participate in the immunological response by the secretion of cytokines and mediating cytotoxic effects, the lower numbers of CatW-expressing cells compared to AIG implies that they do not play a predominant role in the pathogenesis of *H pylori* gastritis[17].

No differences in the CatW$^+$/CD45$^+$ proportions for the CG and LG were detected compared to healthy controls. These findings are in line with the pathogenesis of both types of gastritis. NSAIDs, as the most common cause of CG, lead primarily to an inhibition of cyclooxygenases that subsequently leads to lower levels of prostaglandins and thromboxane and less lymphocytic infiltration compared to *H pylori* gastritis and AIG[45,46]. Therefore, CG showed normal numbers or only a minor increase of inflammatory cells, mostly being lymphocytes and plasma cells, in the mucosa[1]. Since the typical histological picture includes only a slight amount of inflammatory cells, the minimal presence of CatW-expressing cells, comparable to healthy gastric mucosa, is in concordance with these studies.

As the name implies, LG is characterized by the presence of large numbers of mature lymphocytes infiltrating the surface and foveolar epithelium[7]. Based on the guidelines, 25-40 intraepithelial lymphocytes per 100 epithelial cells are necessary for this diagnosis. Intraepithelial lymphocytes comprise mostly suppressor T cells showing cytotoxic ability through production of TIA1 and granzyme B[7,47]. The unchanged CatW$^+$/CD45$^+$ proportion in LG obviously corresponds to the normal fraction of CatW-expressing cells among the physiological infiltrate of inflammatory cells in gastric mucosa. It is notable that LG is thought to be related to *H pylori* infection, as shown by their improvement after eradication[6], indicating that LG may represent an atypical host immune response to this infection, even if *Helicobacter* is only rarely found morphologically[5,6].

The numeric differences of CatW-expressing cells and the differences of the relative portion of CatW-expressing cells among infiltrating CD45$^+$ leukocytes in the investigated types of chronic gastroduodenal inflammation imply a distinct involvement of cytotoxic cells expressing CatW in the pathogenesis among these diseases. Whereas CatW-expressing CTLs seem to contribute to the pathogenesis of AIG and to a lesser extent in *H pylori*-associated gastritis, the low

absolute and relative numbers of CatW-positive cells in the inflammatory infiltrate in CG and LG suggest that CatW-expressing cells do not play a major role in these diseases.

The identification of CTL as the predominant CatW-expressing cell type in gastric mucosa, as shown for AIG, supports the idea that the CatW-expression pattern might differ between certain subpopulations of cytotoxic cells. This hypothesis is further supported by the recent finding that cytotoxic cells of gastric mucosa can express an alternatively spliced isoform that has not been detected in peripheral NK cells so far[48].

ACKNOWLEDGMENTS

The authors thank Ursula Stolz, Claudia Miethke, and Carola Kügler for their skilful technical assistance while performing immunohistochemical procedures.

REFERENCES

1 **Dixon MF**, Genta RM, Yardley JH, Correa P. Classification and grading of gastritis. The updated Sydney System. International Workshop on the Histopathology of Gastritis, Houston 1994. *Am J Surg Pathol* 1996; **20**: 1161-1181
2 **Parsonnet J**, Friedman GD, Vandersteen DP, Chang Y, Vogelman JH, Orentreich N, Sibley RK. *Helicobacter pylori* infection and the risk of gastric carcinoma. *N Engl J Med* 1991; **325**: 1127-1131
3 **Asaka M**, Takeda H, Sugiyama T, Kato M. What role does *Helicobacter pylori* play in gastric cancer? *Gastroenterology* 1997; **113**: S56-60
4 **Toh BH**, van Driel IR, Gleeson PA. Pernicious anemia. *N Engl J Med* 1997; **337**: 1441-1448
5 **Dixon MF**, Wyatt JI, Burke DA, Rathbone BJ. Lymphocytic gastritis: relationship to Campylobacter pylori infection. *J Pathol* 1998; **154**: 125-132
6 **Müller H**, Volkholz H, Stolte M. Healing of Lymphocytic Gastritis by Eradication of *Helicobacter pylori*. *Digestion* 2001; **63**: 14-19
7 **Haot J**, Hamichi L, Wallez L, Mainguet P. Lymphocytic gastritis: a newly described entity: a retrospective endoscopic and histological study. *Gut* 1998; **29**: 1258-1264
8 **Turk V**, Turk B, Turk D. Lysosomal cysteine proteases: facts and opportunities. *EMBO J* 2001; **20**: 4629-4633
9 **Kirschke H**, Barrett AJ, Rawlings ND. Proteinases 1: lysosomal cysteine proteinases. *Protein Profile* 1995; **2**: 1581-1643
10 **Pham CT**, Ley TJ. Dipeptidyl peptidase I is required for the processing and activation of granzymes A and B *in vivo*. *Proc Natl Acad Sci USA* 1999 **96**: 8627-8632
11 **Yasothornsrikul S**, Greenbaum D, Medzihradszky KF, Toneff T, Bundey R, Miller R, Schilling B, Petermann I, Dehnert J, Logvinova A, Goldsmith P, Neveu JM, Lane WS, Gibson B, Reinheckel T, Peters C, Bogyo M, Hook V. Cathepsin L in secretory vesicles functions as a prohormone-processing enzyme for production of the enkephalin peptide neurotransmitter. *Proc Natl Acad Sci USA* 2003; **100**: 9590-9595
12 **Friedrichs B**, Tepel C, Reinheckel T, Deussing J, von Figura K, Herzog V, Peters C, Saftig P, Brix K. Thyroid functions of mouse cathepsins B, K, and L. *J Clin Invest* 2003; **111**: 1733-1745
13 **Honey K**, Rudensky AY. Lysosomal cysteine proteases regulate antigen presentation. *Nat Rev Immunol* 2003; **3**: 472-482
14 **Hughes SJ**, Glover TW, Zhu XX, Kuick R, Thoraval D, Orringer MB, Beer DG, Hanash S. A novel amplicon at 8p22-23 results in overexpression of cathepsin B in esophageal adenocarcinoma. *Proc Natl Acad Sci USA* 1998; **95**: 12410-12415
15 **Lauritzen C**, Pedersen J, Madsen MT, Justesen J, Martensen PM, Dahl SW. Active recombinant rat dipeptidyl aminopeptidase I (cathepsin C) produced using the baculovirus expression system. *Protein Expr Purif* 1998; **14**: 434-442
16 **Dohchin A**, Suzuki JI, Seki H, Masutani M, Shiroto H, Kawakami Y. Immunostained cathepsins B and L correlate with depth of invasion and different metastatic pathways in early stage gastric carcinoma. *Cancer* 2000; **89**: 482-487
17 **Buhling F**, Peitz U, Kruger S, Kuster D, Vieth M, Gebert I, Roessner A, Weber E, Malfertheiner P, Wex T. Cathepsins K, L, B, X and W are differentially expressed in normal and chronically inflamed gastric mucosa. *Biol Chem* 2004; **385**: 439-445
18 **Buhling F**, Kellner U, Guenther D, Kahl S, Bromme D, Weber E, Malfertheiner P, Wex T. Characterization of novel anti-cathepsin W antibodies and cellular distribution of cathepsin W in the gastrointestinal tract. *Biol Chem* 2002; **383**: 1285-1289
19 **Linnevers C**, Smeekens SP, Bromme D. Human cathepsin W, a putative cysteine protease predominantly expressed in CD8+ T-lymphocytes. *FEBS Lett* 1997; **405**: 253-259
20 **Brown J**, Matutes E, Singleton A, Price C, Molgaard H, Buttle D, Enver T. Lymphopain, a cytotoxic T and natural killer cell-associated cysteine proteinase. *Leukemia* 1998; **12**: 1771-1781
21 **Wex T**, Buhling F, Wex H, Gunther D, Malfertheiner P, Weber E, Bromme D. Human cathepsin W, a cysteine protease predominantly expressed in NK cells, is mainly localized in the endoplasmic reticulum. *J Immunol* 1998; **167**: 2172-2178
22 **Wex T**, Wex H, Hartig R, Wilhelmsen S, Malfertheiner P. Functional involvement of cathepsin W in the cytotoxic activity of NK-92 cells. *FEBS Lett* 2003; **552**: 115-119
23 **Ondr JK**, Pham CT. Characterization of murine cathepsin W and its role in cell-mediated cytotoxicity. *J Biol Chem* 2004; **279**: 27525-27533
24 **Borscheri N**, Roessner A, Rocken C. Canalicular immunostaining of neprilysin (CD10) as a diagnostic marker for hepatocellular carcinomas. *Am J Surg Pathol* 2001; **25**: 1297-1303
25 **Hayday A**, Theodoridis E, Ramsburg E, Shires J. Intraepithelial lymphocytes: exploring the Third way in immunology. *Nat Immunol* 2001; **2**: 997-1003
26 **Neutra MR**, Mantis NJ, Kraehenbuhl JP. Collaboration of epithelial cells with organized mucosal lymphoid tissues. *Nat Immunol* 2001; **2**: 1004-1009
27 **Katakai T**, Mori KJ, Masuda T, Shimizu A. Differential localization of Th1 and Th2 cells in autoimmune gastritis. *Int Immunol* 1998; **10**: 1325-1334
28 **Barrett SP**, Gleeson PA, de Silva H, Toh BH, van Driel IR. Interferon-gamma is required during the initiation of an organ-specific autoimmune disease. *Eur J Immunol* 1996; **26**: 1652-1655
29 **Chen H**, Paul WE. Cultured NK1.1+ CD4+ T cells produce large amounts of IL-4 and IFN-gamma upon activation by anti-CD3 or CD1. *J Immunol* 1997; **159**: 2240-2249
30 **Romagnani S**. Induction of TH1 and TH2 responses: a key role for the 'natural' immune response? *Immunol Today* 1992; **13**: 379-381
31 **La Gruta NL**, van Driel IR, Toh BH, Gleeson PA. The role of natural killer cells in the induction of autoimmune gastritis. *Autoimmunity* 2001; **34**: 147-154
32 **De Silva HD**, Van Driel IR, La Gruta N, Toh BH, Gleeson PA. CD4+ T cells, but not CD8+ T cells, are required for the development of experimental autoimmune gastritis. *Immunology* 1998; **93**: 405-408
33 **Martinelli TM**, van Driel IR, Alderuccio F, Gleeson PA, Toh BH. Analysis of mononuclear cell infiltrate and cytokine production in murine autoimmune gastritis. *Gastroenterology* 1996; **110**: 1791-1802
34 **Alderuccio F**, Toh BH, Gleeson PA, van Driel IR. A novel method for isolating mononuclear cells from the stomachs of mice with experimental autoimmune gastritis. *Autoimmunity* 1995; **21**: 215-221
35 **D'Elios MM**, Bergman MP, Azzurri A, Amedei A, Benagiano M, De Pont JJ, Cianchi F, Vandenbroucke-Grauls CM, Romagnani S, Appelmelk BJ, Del Prete G. H(+),K(+)-atpase (proton pump) is the target autoantigen of Th1-type cytotoxic T cells in autoimmune gastritis. *Gastroenterology* 2001; **120**: 377-386

36 **Vargas JA**, Alvarez-Mon M, Manzano L, Albillos A, Fernandez-Corugedo A, Albarran F, Durantez A. Functional defect of T cells in autoimmune gastritis. *Gut* 1995; **36**: 171-175
37 **Mitomi H**, Tanabe S, Igarashi M, Katsumata T, Arai N, Kikuchi S, Kiyohashi A, Okayasu I. Autoimmune enteropathy with severe atrophic gastritis and colitis in an adult: proposal of a generalized autoimmune disorder of the alimentary tract. *Scand J Gastroenterol* 1998; **33**: 716-720
38 **Shevach EM**, McHugh RS, Piccirillo CA, Thornton AM. Control of T-cell activation by CD4+ CD25+ suppressor T cells. *Immunol Rev* 2001; **182**: 58-67
39 **Shan L**, Molberg O, Parrot I, Hausch F, Filiz F, Gray GM, Sollid LM, Khosla C. Structural basis for gluten intolerance in celiac sprue. *Science* 2002; **297**: 2275-2279
40 **Maiuri L**, Ciacci C, Ricciardelli I, Vacca L, Raia V, Auricchio S, Picard J, Osman M, Quaratino S, Londei M. Association between innate response to gliadin and activation of pathogenic T cells in coeliac disease. *Lancet* 2003; **362**: 30-37
41 **Mohammadi M**, Czinn S, Redline R, Nedrud J. *Helicobacter* specific cell-mediated immune responses display a predominant Th1 phenotype and promote a delayed-type hypersensitivity response in the stomachs of mice. *J Immunol* 1996; **156**: 4729-4738
42 **Raptopoulou-Gigi M**, Polyzonis M, Orphanou-Koumerkeridou H, Agorastos J, Vacolas J, Gigis P. Immunohistological phenotyping of the stomach infiltrating lymphocytes in chronic gastritis. *Allergol Immunopathol* 1990; **18**: 87-89
43 **Fiocca R**, Villani L, Luinetti O, Gianatti A, Perego M, Alvisi C, Turpini F, Solcia E. *Helicobacter* colonization and histopathological profile of chronic gastritis in patients with or without dyspepsia, mucosal erosion and peptic ulcer: a morphological approach to the study of ulcerogenesis in man. *Virchows Arch A Pathol Anat Histopathol* 1992; **420**: 489-498
44 **Ohtani N**, Ohtani H, Nakayama T, Naganuma H, Sato E, Imai T, Nagura H, Yoshie O. Infiltration of CD8+ T cells containing RANTES/CCL5+ cytoplasmic granules in actively inflammatory lesions of human chronic gastritis. *Lab Invest* 2004; **84**: 368-375
45 **Wallace JL**, Zamuner SR, McKnight W, Dicay M, Mencarelli A, del Soldato P, Fiorucci S. Aspirin, but not NO-releasing aspirin (NCX-4016), interacts with selective COX-2 inhibitors to aggravate gastric damage and inflammation. *Am J Physiol Gastrointest Liver Physiol* 2004; **286**: G76-81
46 **Tomisato W**, Tsutsumi S, Hoshino T, Hwang HJ, Mio M, Tsuchiya T, Mizushima T. Role of direct cytotoxic effects of NSAIDs in the induction of gastric lesions. *Biochem Pharmacol* 2004; **67**: 575-585
47 **Oberhuber G**, Bodingbauer M, Mosberger I, Stolte M, Vogelsang H. High proportion of granzyme B-positive (activated) intraepithelial and lamina propria lymphocytes in lymphocytic gastritis. *Am J Surg Pathol* 1998; **22**: 450-458
48 **Meinhardt C**, Peitz U, Treiber G, Wilhelmsen S, Malfertheiner P, Wex T. Identification of a novel isoform predominately expressed in gastric tissue and a triple-base pair polymorphism of the cathepsin W gene. *Biochem Biophys Res Commun* 2004; **321**: 975-980

Science Editor Guo SY **Language Editor** Elsevier HK

PO Box 2345, Beijing 100023, China
www.wjgnet.com
wjg@wjgnet.com

ELSEVIER

World J Gastroenterol 2005;11(38):5958-5965
World Journal of Gastroenterology ISSN 1007-9327
© 2005 The WJG Press and Elsevier Inc. All rights reserved.

• *BASIC RESEARCH* •

Ischemic preconditioning inhibits development of edematous cerulein-induced pancreatitis: Involvement of cyclooxygenases and heat shock protein 70

Zygmunt Warzecha, Artur Dembinski, Piotr Ceranowicz, Stanislaw J Konturek, Marcin Dembinski, Wieslaw W Pawlik, Romana Tomaszewska, Jerzy Stachura, Beata Kuşnierz-Cabala, Jerzy W Naskalski, Peter C Konturek

Zygmunt Warzecha, Artur Dembiński, Piotr Ceranowicz, Stanisław J Konturek, Marcin Dembiński, Wiesław W Pawlik, Department of Physiology, Jagiellonian University Medical College, Kraków, Poland
Romana Tomaszewska, Jerzy Stachura, Department of Pathology, Jagiellonian University Medical College, Kraków, Poland
Beata Kuśnierz-Cabała, Jerzy W Naskalski, Department of Clinical Biochemistry, Jagiellonian University Medical College, Kraków, Poland
Peter C Konturek, Department of Internal Medicine I, University of Erlangen-Nuremberg, Erlangen, Germany
Correspondence to: Professor Artur Dembiński, MD, PhD, Department of Physiology, Jagiellonian University Medical College, ul. Grzegórzecka 16, Kraków 31-531, Poland. mpdembin@cyf-kr.edu.pl
Telephone: +48-12-4211006 Fax: +48-12-4225478
Received: 2004-12-17 Accepted: 2005-03-21

Abstract

AIM: To determine whether ischemic preconditioning (IP) affects the development of edematous cerulein-induced pancreatitis and to assess the role of cyclooxygenase-1 (COX-1), COX-2, and heat shock protein 70 (HSP 70) in this process.

METHODS: In male Wistar rats, IP was performed by clamping of celiac artery (twice for 5 min at 5-min intervals). Thirty minutes after IP or sham operation, acute pancreatitis was induced by cerulein. Activity of COX-1 or COX-2 was inhibited by resveratrol or rofecoxib, respectively (10 mg/kg).

RESULTS: IP significantly reduced pancreatic damage in cerulein-induced pancreatitis as demonstrated by the improvement of pancreas histology, reduction in serum lipase and poly-C ribonuclease activity, and serum concentration of pro-inflammatory interleukin (IL)-1β. Also, IP attenuated the pancreatitis-evoked fall in pancreatic blood flow and pancreatic DNA synthesis. Serum level of anti-inflammatory IL-10 was not affected by IP. Cerulein-induced pancreatitis and IP increased the content of HSP 70 in the pancreas. Maximal increase in HSP 70 was observed when IP was combined with cerulein-induced pancreatitis. Inhibition of COXs, especially COX-2, reduced the protective effect of IP in edematous pancreatitis.

CONCLUSION: Our results indicate that IP reduces pancreatic damage in cerulein-induced pancreatitis and this effect, at least in part, depends on the activity of COXs and pancreatic production of HSP 70.

© 2005 The WJG Press and Elsevier Inc. All rights reserved.

Key words: Acute pancreatitis; Ischemic preconditioning; Cyclooxygenase-2; Interleukin-1β; Heat shock protein-70

Warzecha Z, Dembinski A, Ceranowicz P, Konturek SJ, Dembinski M, Pawlik WW, Tomaszewska R, Stachura J, Kuśnierz-Cabala B, Naskalski JW, Konturek PC. Ischemic preconditioning inhibits development of edematous cerulein-induced pancreatitis: Involvement of cyclooxygenases and heat shock protein 70. *World J Gastroenterol* 2005; 11 (38): 5958-5965
http://www.wjgnet.com/1007-9327/11/5958.asp

INTRODUCTION

Various organs including the heart[1], brain[2], kidney[3], liver[4], skeletal muscle[5], and stomach[6] respond to brief exposure to ischemia with an increase in resistance to severe ischemia, and this phenomenon is called ischemic preconditioning (IP). Also, the protective effect of IP has been found in the pancreas against ischemia/reperfusion-induced pancreatitis[7]. However, no study so far has been undertaken to determine whether IP is also able to prevent the acute pancreatic damage induced by other primary non-vascular factors.

Cyclooxygenase (COX), the key enzyme for prostaglandin synthesis, exists in two isoforms as COX-1 and COX-2[8]. COX-1 is constitutively expressed in most tissues and has been suggested to mediate the synthesis of prostaglandins required for physiological functions and maintenance of organ integrity. COX-2 is undetectable in most tissues in normal condition, but is highly inducible by cytokines, mitogens, and endotoxins, and is responsible for an increased production of prostaglandins during inflammation[8]. However, it was reported that both COXs contribute to gastric mucosal defense[9]. Inhibition of COXs activity by nonselective nonsteroidal anti-inflammatory drugs leads to induction of gastric ulcers and delays the healing of gastric mucosa[10,11], while the selective inhibition of COX-2 delays gastric ulcer healing[12]. The role of COX-2 in pancreatic pathology is unclear. Studies performed by Song *et al*.[13], and Ethridge *et al*.[14], with mice have shown that pharmacological inhibition of COX-2 or

COX-2 gene disruption reduces the severity of pancreatitis and pancreatitis-associated lung injury. On the other hand, our own study has shown that inhibition of COX-2 abolishes the protective effect of hepatocyte growth factor (HGF) against cerulein-induced pancreatitis[15].

Heat shock proteins (HSPs) are cytoprotective molecules that help to maintain the metabolic and structural integrity of cells. HSPs are induced by a variety of stresses, including heat, free radicals, and toxins[16]. In the pancreas, HSPs have been shown to provide the protection against cerulein-[17,18] and arginine-induced[19] acute pancreatitis. However, it is not investigated whether IP interacts with HSPs and what is the biological consequence of this potential interaction in the development of cerulein-induced pancreatitis.

The present study was to determine the effect of IP on the development of acute cerulein-induced pancreatitis, to evaluate the role of COX-1 and COX-2 in pancreatic IP, and to assess the effect of IP on the pancreatic synthesis of HSP 70.

[illegible]

Animals and treatment

Studies were performed on male Wistar rats weighing 180-220 g and following the experimental protocol approved by the Committee for Research and Animal Ethics of Jagiellonian University. Rats were fasted for 18 h before final experiment, but they had free access to drinking water. Animals were housed in cages with wire mesh bottoms at normal room temperature in 12-h light–dark cycle.

Experiments were carried out in the following experimental groups (10 animals in each group); (1) sham-operated control group; (2) IP group; (3) sham-operated group treated with resveratrol (Cayman Chemicals, Ann Arbor, MI, USA, 10 mg/kg, intragastrically (i.g.) 1 h before sham operation); (4) sham-operated group treated with rofecoxib (Vioxx, Merck Sharp & Dohme Idea Inc., Glattbrugg, Switzerland, 10 mg/kg, i.g. 1 h before sham operation); (5) sham-operated group with cerulein-induced pancreatitis; (6) IP group with cerulein-induced pancreatitis; (7) sham-operated group with cerulein-induced pancreatitis and treated with resveratrol (10 mg/kg, i.g. 1 h before sham operation); (8) cerulein-induced pancreatitis group treated with rofecoxib (10 mg/kg, i.g. 1 h before sham operation); (9) IP group with cerulein-induced pancreatitis and treated with resveratrol (10 mg/kg, i.g. 1 h before IP); (10) IP group with cerulein-induced pancreatitis and treated with rofecoxib (10 mg/kg, i.g. 1 h before IP).

IP of the pancreas was performed under ketamine anesthesia (50 mg/kg i.p., Bioketan, Biowet, Gorzów Wlkp., Poland). After longitudinal laparotomy, the celiac artery was clamped twice for 5 min at 5-min intervals. In sham-operated rats, longitudinal laparotomy and mobilization of the pancreas without the clamping of any artery was performed.

Thirty minutes after IP or sham operation, acute pancreatitis was induced by cerulein (Takus, Pharmacia & Upjohn GmbH, Erlangen, Germany) i.p. five times at 1-h intervals at a dose 10 μg/kg per injection. Animals without induction of acute pancreatitis were treated with 0.9% NaCl i.p. at the same time as cerulein.

Determination of pancreatic blood flow

After the last injection of cerulein or saline, animals were anesthetized with ketamine and the abdomen was opened. The pancreas was exposed for the measurement of pancreatic blood flow by a laser Doppler flowmeter using PeriFlux 4001 Master monitor (Perimed AB, Järfälla, Sweden), as described previously[20]. Pancreatic blood flow was measured in five different portions of the pancreas. The area of laser emission of the probe was about 1 mm^2, while the depth of measurement reached about 3 mm. Data were presented as percent change from control value obtained in sham-operated rats injected with saline.

Determination of serum lipase activity and serum interleukin-1β and interleukin-10 concentration

Immediately after measurement of pancreatic blood flow, the abdominal aorta was exposed and blood was taken for determination of serum lipase activity and serum interleukin-1β (IL-1β) and IL-10 concentration. Serum lipase activity was determined with a Kodak Ectachem DT II System analyzer (Eastman Kodak Company, Rochester, NY, USA) using Lipa DT slides (Vitros DT Chemistry System, Johnson & Johnson Clinical Diagnostic, Inc., Rochester, NY, USA). Serum lipase activity was expressed as units per liter. Serum IL-1β and IL-10 concentrations were measured in duplicate, using appropriate BioSource Cytoscreen rat kits based on a solid phase sandwich ELISA (BioSource International, Camarillo, CA, USA). Concentration of IL was determined from standard curves for recombinant IL-1β or IL-10, respectively. Serum IL-1β or IL-10 concentration was expressed as picogram per milliliter.

Determination of serum poly-C specific ribonuclease activity

Poly-C specific ribonuclease activity was determined using Warsaw and Lee's procedure[21], employing polycytydylic acid (poly-C) as a ribonuclease substrate, as described previously in detail[22]. Poly-C specific ribonuclease activity was expressed in units per liter.

Protein extraction and analysis of pancreatic HSP 70 expression by Western blot analysis

Shock-frozen tissue from rat pancreas was homogenized in a lysis buffer (100 mmol/L Tris-HCl, pH 7.4, 15% glycerol, 2 mmol/L EDTA, 2% sodium dodecyl sulfate (SDS), 100 mmol/L D,L-dithiothreitol) by the addition of 1:20 dilution of aprotinin and 1:50 dilution of 100 mmol/L phenylmethylsulfonyl fluoride. Insoluble materials were removed by centrifugation at 12 000 *g* for 15 min. Approximately 50 μg of the total protein extract was loaded on SDS-polyacrylamide gels and run 40 mA, followed by transfer on nitrocellulose membrane (Protran, Schleicher & Schuell, Germany) by electroblotting. Bovine serum albumin (30 g/L, Sigma-Aldrich, Germany) in Tris buffered saline (TBS)-Tween-20 buffer (137 mmol NaCl, 20 mmol Tris-HCl, pH 7.4, 0.1% Tween-20) was used to block filters for at least 1 h at room temperature. Specific primary antibody against HSP 70 (mouse monoclonal, 1:200 dilution; Stressgen Biotechnologies Corp., Canada) or β-actin (mouse monoclonal, dilution 1:5 000; Sigma-Aldrich, Germany) was added to the membrane, followed by an anti-mouse-IgG or anti-mouse IgG horseradish

peroxidase-conjugated secondary antibody (dilution 1:20 000; Promega, WI, USA) dissolved in 1% non-fat milk in TBS-Tween-20 buffer. Incubation of primary antibody was followed by washing thrice with TBS-Tween-20 buffer for 10 min. Incubation of the secondary antibody was followed by five washes for 10 min. Immunocomplexes were detected by the SuperSignal West Pico chemiluminescent kit (Pierce, USA). Thereafter, the developed membrane was exposed to an X-ray film (Kodak, Wiesbaden, Germany). Comparison between different treatment groups was made by determining the HSP 70/β-actin ratio of the immunoreactive area by densitometry.

Determination of pancreatic DNA synthesis

The rate of DNA synthesis in samples of pancreatic tissue was determined as described previously[23]. Briefly, the minced pancreatic tissue was incubated at 37 ℃ for 45 min in 2 mL of medium containing 8 μCi/mL of [^{3}H]thymidine ([6-^{3}H] thymidine, 20-30 Ci/mmol; Institute for Research, Production and Application of Radioisotopes, Prague, Czech Republic). The incorporation of [^{3}H]thymidine into DNA was measured by counting DNA containing solution in a liquid scintillation system. DNA synthesis was expressed as [^{3}H]thymidine disintegrations per minute per microgram DNA (dpm/μg DNA).

Histological examination

Samples of pancreatic tissue for histological examination were fixed in 40 g/L formaldehyde, embedded in paraffin and sections were sliced and stained with hematoxylin and eosin. Slides were examined by two experienced pathologists without the knowledge of the treatment given (four slides per animal). The histological grading of edema was made using our scale ranging from 0 to 3: 0 = no edema, 1 = interlobular edema, 2 = interlobular and moderate intralobular edema, and 3 = severe interlobular and intralobular edema. Hemorrhage was graded: 0 = absent, 1 = 1-2 foci per slide, 2 = 3 to 5 foci per slide, 3 = more than 5 foci per slide. Leukocyte infiltration was graded: 0 = absent, 1 = scare perivascular infiltration, 2 = moderate perivascular and scare diffuse infiltration, 3 = abundant diffuse infiltration. Acinar necrosis was graded: 0 = absent, 1 = less than 15% of cells involved, 2 = 15–35% of cells involved, 3 = more than 35% of cells involved. Grading of vacuolization was based on the percentage of cells involved: 0 = absent, 1 = less than 25%, 2 = 25-50% and 3 = more than 50%.

Statistical analysis

Results were expressed as mean±SE. Statistical analysis was carried out by one-way analysis of variance followed by Tukey's multiple comparison test using GraphPadPrism (GraphPad Software, San Diego, CA, USA). $P<0.05$ was considered statistically significant.

[illegible]

Morphological features of pancreatic tissue

The pancreas of saline-treated sham-operated rats showed no tissue alteration macroscopically and at light microscopic level (Table 1). Exposure to IP combined with treatment with saline caused the mild interlobular edema and minimal vacuolization of acinar cells in cases 4 and 5, respectively. Rest of the animals exposed to IP and treated with saline did not show any histological alterations. Administration of the COX-1 inhibitor - resveratrol - in saline-treated animals did not affect pancreatic tissue morphology. Treatment with combination of the COX-2 inhibitor - rofecoxib - plus saline had no effect on pancreatic histology or caused mild interlobular edema. Administration of cerulein caused acute edematous pancreatitis in all rats that were tested (Table 1). The pancreas was grossly swollen and enlarged with a visible collection of edematous fluid. At light microscopic level, moderate or severe interlobular and intralobular edema was accompanied with moderate perivascular and scare diffuse inflammatory leukocyte infiltration. Vacuolization was observed in 25-50% of acinar cells. Additionally, in few cases, one or two foci of hemorrhages per slide were found. IP applied prior to cerulein-induced pancreatitis reduced histological signs of pancreatic damage such as pancreatic edema, inflammatory infiltration, and vacuolization of acinar cells. Also, administration of resveratrol or rofecoxib in combination with cerulein slightly reduced the cerulein-evoked pancreatic damage. In animals with IP applied prior to cerulein, inhibition of COXs abolished the beneficial effect of IP. This effect was especially pronounced after administration of rofecoxib and pancreatic damage was similar to that in animals treated with cerulein alone (Table 1).

Effect of ischemic preconditioning, resveratrol, and rofecoxib on serum lipase activity in rats without or with cerulein-induced pancreatitis

In sham-operated saline-treated rats, serum lipase activity reached 61.5±3.5 U/L (Figure 1A). IP, applied without

Table 1 Morphological features of pancreatic tissue of animals exposed to IP or sham-operated and treated with saline, resveratrol, rofecoxib or cerulein alone or in combination

	Edema	Inflammatory infiltration	Vacuolization	Hemorrhages	Necrosis
Sham-operation+saline (control)	0	0	0	0	0
IP+saline	0/1	0	0/1	0	0
Resveratrol+sham operation+saline	0	0	0	0	0
Rofecoxib+sham operation+saline	0/1	0	0	0	0
Sham-operation+cerulein	2/3	2	2	0/1	0
IP+cerulein	2	1	1	0	0
Resveratrol+sham operation+cerulein	2	1	2	0	0
Rofecoxib+sham operation+cerulein	2	1	2	0/1	0
Resveratrol+IP+cerulein	2	1/2	2	0	0
Rofecoxib+IP+cerulein	2/3	2	2	0/1	0

Numbers represent the predominant histological grading in each group.

induction of acute pancreatitis, did not affect serum lipase activity. Also, administration of the COX-1 inhibitor - resveratrol - or the COX-2 inhibitor - rofecoxib - had no effect on serum lipase activity in rats treated with saline. Administration of cerulein caused more than sevenfold increase in serum lipase activity, when compared to that of saline-treated control rats. IP markedly reduced the cerulein-evoked increase in serum lipase activity by 37% ($P<0.001$). Also, administration of resveratrol or rofecoxib reduced serum lipase activity in animals with cerulein-induced pancreatitis ($P<0.01$ or $P<0.05$, respectively). The effect of these blockers of COX on serum lipase activity was weaker than the effect of IP, but was still statistically significant. In contrast, administration of resveratrol or rofecoxib in combination with IP significantly abolished the IP-evoked reduction in serum lipase activity in animals with cerulein-induced pancreatitis ($P<0.001$). However, serum lipase activity in these animals was still lower than that in animals with cerulein-induced pancreatitis and treated with resveratrol or rofecoxib alone (Figure 1A).

Effect of ischemic preconditioning, resveratrol, and rofecoxib on serum concentration of IL-1β and IL-10 in rats without or with cerulein-induced pancreatitis

In control sham-operated rats treated with saline, the serum IL-1β concentration was 69.9±3.1 pg/mL (Figure 1B). IP or treatment with resveratrol or rofecoxib alone had no effect on serum IL-1β in rats without induction of acute pancreatitis. In sham-operated rats, cerulein caused more than threefold increase in serum IL-1β concentration and this increase was significantly diminished by IP ($P<0.001$). Lower but still significant reduction of serum IL-1β was also observed when administration of cerulein was combined with pretreatment with resveratrol ($P<0.05$). Administration of rofecoxib alone tended to reduce the cerulein-evoked increase in serum IL-1β concentration, but this effect was not statistically significant. Pretreatment with resveratrol or rofecoxib in animals with IP significantly reversed the

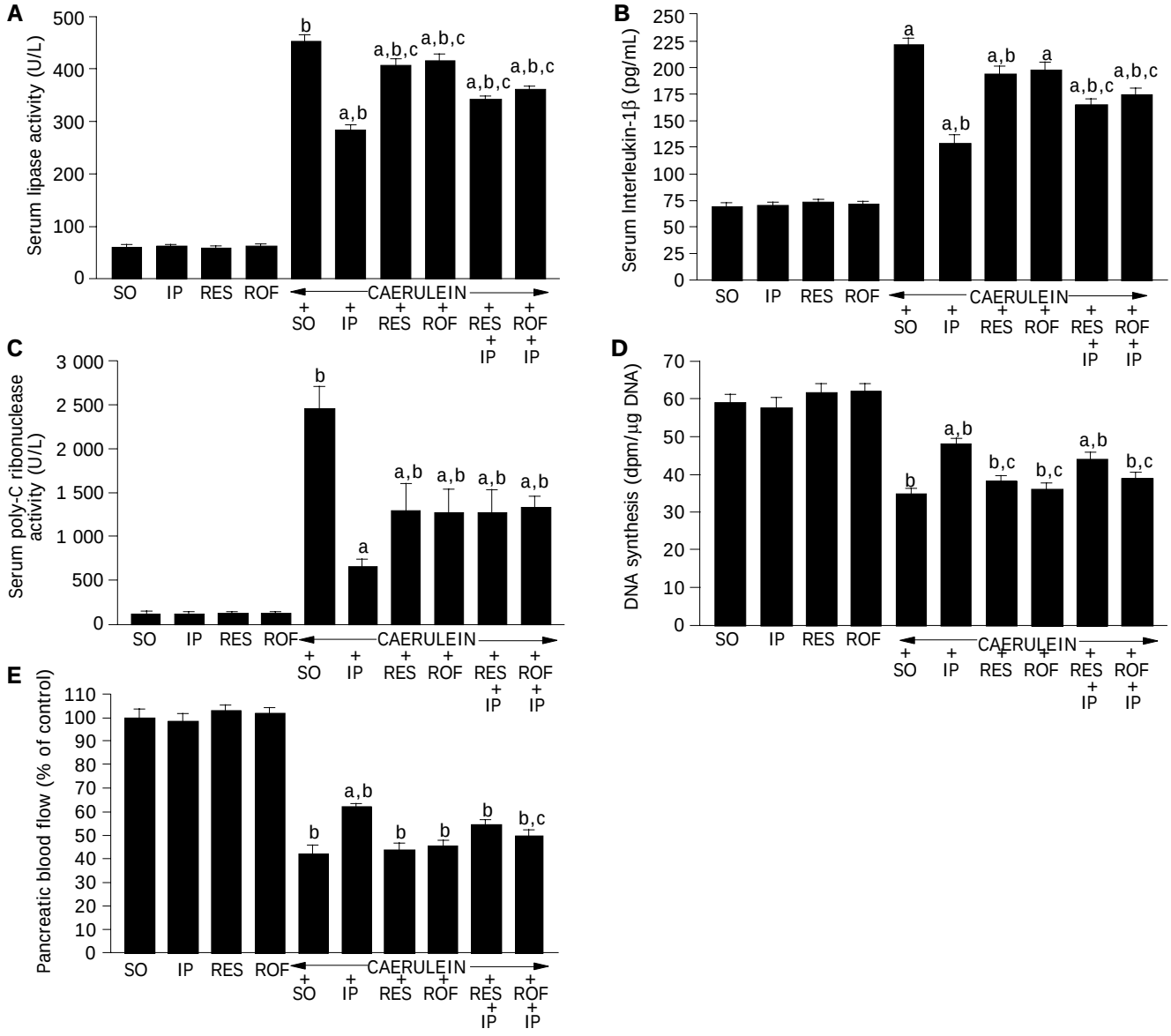


Figure 1 Effect of sham operation (SO), IP, resveratrol (RES) or rofecoxib (ROF) applied alone or in combination on serum lipase activity (A), IL-1β (B), poly-C ribonuclease (C), pancreatic DNA synthesis (D), and pancreatic blood flow (E) in rats with or without cerulein-induced pancreatitis. [a]$P<0.05$ *vs* sham-operated rats treated with cerulein alone, [b]$P<0.001$ *vs* sham-operated saline-treated control (SO), [c]$P<0.05$ *vs* rats exposed to IP and treated with cerulein.

IP-evoked decrease in serum IL-1β concentration in animals with cerulein-induced pancreatitis (P<0.001, Figure 1B).

In control sham-operated rats treated with saline, the serum IL-10 level reached 73.0±5.0 pg/mL (data not shown). Neither IP nor resveratrol or rofecoxib or cerulein applied alone or in their combination significantly affected the serum IL-10 concentration.

Effect of ischemic preconditioning, resveratrol, and rofecoxib on serum activity of poly-C ribonuclease in rats without or with cerulein-induced pancreatitis

In saline-treated sham-operated control rats, serum poly-C ribonuclease activity reached 125±25 U/L (Figure 1C). IP or administration of resveratrol or rofecoxib did not affect serum poly-C ribonuclease activity in animals without induction of acute pancreatitis. Cerulein-induced pancreatitis caused nearly 20-fold increase in serum poly-C ribonuclease activity and this effect was strongly and significantly inhibited by IP (P<0.001). Also administration of resveratrol or rofecoxib reduced the cerulein-induced increase in serum activity of poly-C ribonuclease, but the effect of these blockers of COX was weaker than that of IP (P<0.001). Combination of resveratrol or rofecoxib plus IP decreased the serum poly-C ribonuclease activity in cerulein-treated rats to the similar values as administration of resveratrol or rofecoxib in sham-operated rats with cerulein-induced pancreatitis (Figure 1C).

Effect of ischemic preconditioning, resveratrol, and rofecoxib on pancreatic DNA synthesis in rats without or with cerulein-induced pancreatitis

In saline-treated sham-operated control rats, pancreatic DNA synthesis reached 59.0±2.3 dpm/μg DNA (Figure 1D). IP as well as administration of resveratrol or rofecoxib did not affect pancreatic DNA synthesis in animals without induction of acute pancreatitis. In animals with cerulein-induced pancreatitis, pancreatic DNA synthesis was significantly reduced, reaching 34.7±1.6 dpm/μg DNA (P<0.001). IP significantly attenuated the pancreatitis-related reduction in pancreatic DNA synthesis (P<0.001). Resveratrol or rofecoxib given alone did not affect pancreatic DNA synthesis in animals treated with cerulein. Pretreatment with resveratrol tended to reduce the pancreatic DNA synthesis in animals treated with a combination of IP plus cerulein, but this effect was not statistically significant. In contrast, pretreatment with rofecoxib significantly reduced the pancreatic DNA synthesis in animals treated with IP plus cerulein (P<0.05).

Effect of ischemic preconditioning, resveratrol, and rofecoxib on pancreatic blood flow in rats without or with cerulein-induced pancreatitis

IP or treatment with resveratrol or rofecoxib did not affect pancreatic blood flow in rats without administration of cerulein (Figure 1E). Administration of cerulein for 5 h significantly reduced pancreatic blood flow by 58% when compared to that of saline-treated sham-operated control rats (P<0.001). Exposure to IP significantly reversed the cerulein-induced fall in pancreatic blood flow (P<0.001), whereas resveratrol or rofecoxib given alone had no effect on pancreatic blood flow in animals with cerulein-induced pancreatitis. Pretreatment with rofecoxib significantly abolished the IP-induced improvement of pancreatic blood flow in animals with pancreatitis (P<0.05).

Effect of ischemic preconditioning and cerulein-induced pancreatitis on synthesis of HSP 70 detected by Western blot

Figure 2 shows the effect of IP and cerulein-induced pancreatitis on the production of HSP 70 in the pancreatic tissue. In sham-operated control animals with an intact pancreas, the synthesis of HSP 70 was weak and the ratio of HSP 70 over β-actin reached a value of 0.11±0.01. IP or induction of acute pancreatitis by cerulein significantly increased the ratio of HSP 70 over β-actin in pancreatic tissue reaching 0.31±0.01 and 0.74±0.02, respectively (P<0.05 and P<0.001, respectively). The highest ratio of HSP 70 to β-actin in pancreatic tissue was observed in animals treated with combination of IP plus cerulein.

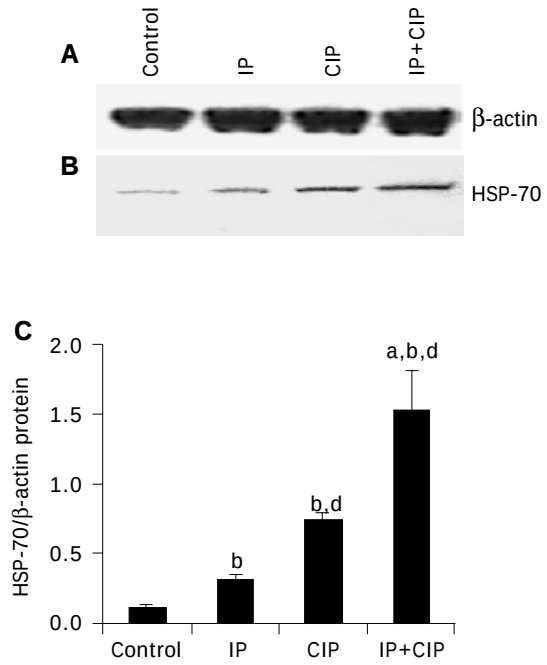


Figure 2 Representative Western blot analysis of β-actin protein (A) and HSP 70 (B), and the ratio of HSP 70 over β-actin protein (C) in pancreatic tissue of sham-operated control rats (lane 1), rats exposed to IP (lane 2), sham-operated rats with cerulein-induced pancreatitis (CIP, lane 3), and rats with IP applied prior to cerulein-induced pancreatitis (IP+CIP, lane 4). [b]P<0.001 *vs* sham-operated rats treated with cerulein alone (CIP), [a]P<0.05 *vs* sham-operated saline-treated control, [d]P<0.001 *vs* rats exposed to IP without induction of acute pancreatitis (CIP).

DISCUSSION

Our present study showed for the first time that: (1) IP could reduce the pancreatic damage in cerulein-induced acute pancreatitis; (2) IP and cerulein-induced pancreatitis could increase synthesis of HSP 70 in the pancreas and combination of these two factors could stimulate the production of HSP 70 to the highest extent; (3) inhibition of COXs, especially COX-2, could reduce the pancreatoprotective effect of IP against cerulein-induced pancreatitis.

Protective effect of IP against pancreatic damage evoked by cerulein was manifested by improvement of the biochemical and histological parameters. Exposure to IP prior to induction of acute pancreatitis significantly reduced the cerulein-evoked increase in serum lipase and poly-C ribonuclease activity, and serum concentration of pro-inflammatory IL-1β. A close relationship was found between the IP-evoked decrease in biochemical signs of pancreatitis and the improvement of pancreatic DNA synthesis, and pancreatic blood flow, as well as the reduction in histological score of pancreatic damage. Morphological features showed a decrease in pancreatic edema, vacuolization of acinar cells, and leukocyte infiltration of pancreatic tissue.

The increase in serum lipase activity is a well known manifestation of acute pancreatitis with high sensitivity and specificity[24]. Pancreatic-type poly-C specific ribonuclease is one of the few direct markers of severe pancreatic injury and pancreatic necrosis[21,25]. In our present study, acute pancreatitis was evoked by stimulation of pancreatitis by overdose of cerulein. This procedure leads to the development of mild edematous acute pancreatitis without pancreatic necrosis[26,27]. However, also in this case, we observed increase in serum activity of poly-C specific ribonuclease, suggesting that serum activity of pancreatic-type poly-C ribonuclease is not specific for severe pancreatic injury and pancreatic necrosis, and that serum activity of this enzyme increases in all types of acute pancreatitis, whereas severity of acute pancreatitis affects only the degree of poly-C ribonuclease activity in the serum. This discrepancy between our data and reports of Warshaw and Lee[21] or Naskalski *et al.*[25], may also be a result of species differences. On the other hand, our finding that IP applied before induction of acute pancreatitis reduced serum poly-C ribonuclease activity provides an additional support for the protective effect of IP on the pancreas in cerulein-induced pancreatitis.

In our present study, IP applied alone did not significantly affect pancreatic DNA synthesis. Induction of acute pancreatitis by cerulein caused a reduction in the pancreatic DNA synthesis, which is in agreement with previous observations[28,29] and may be considered as an index of pancreatic damage. In rats with induction of pancreatitis, IP attenuated the pancreatitis-evoked fall in pancreatic DNA synthesis. This observation brings the additional support for the concept that IP enhances resistance of the pancreas against tissue damage.

Our present observation that IP reduced pancreatic damage in cerulein-induced pancreatitis confirms and extends our previous finding that exposure to IP could protect the pancreas against damage evoked by severe ischemia followed by reperfusion[7]. These data suggest that IP, causing a mild damage, enhances resistance against pancreatic damage independently to the etiology of acute pancreatitis. This hypothesis is also supported by the observation that exposure to other mild damaging factors such as bacterial lipopolysaccharides[30], grapefruit-seed extract[22], or low doses of capsaicin[31] exhibits protective effect against acute pancreatitis.

The role of COX-2 in acute pancreatitis is unclear. Previous experimental studies on mice[13,14] have shown that pharmacological inhibition of COX-2 or COX-2 gene disruption ameliorates the severity of pancreatitis and the pancreatitis-associated lung injury. In contrast, in the rat model of pancreatitis, Foitzik *et al.*[32], have found some beneficial systemic effects of COX-2 inhibition on acute pancreatitis, such as an improvement of renal and respiratory function, but they have not observed any significant effect of COX-2 inhibition on histological score of pancreatic damage or plasma level of trypsinogen activation peptides. In our present study, blockade of COX-1 or COX-2 significantly reduced serum lipase and serum poly-C ribonuclease activity, as well as decreased pancreatic edema and inflammatory infiltration in morphological features in animals with cerulein-induced pancreatitis. The new and important finding of the present study is that inhibition of COXs, especially COX-2, reduces the protective effect of IP against pancreatic damage evoked by cerulein. This observation indicates that activity of COX-2 is necessary for the beneficial effect of IP. The involvement of COX-2 in IP effects on the pancreas is similar to that observed after treatment with HGF. Serum concentration of HGF is increased in patients with acute pancreatitis, and the HGF level reflects the clinical severity of pancreatitis and organ dysfunction[33,34]. Also experimental studies have shown the increase in plasma HGF level and tissue HGF overexpression in acute pancreatitis[35,36]. On the other hand, administration of antibodies that neutralize HGF aggravates the organ dysfunction and increases apoptosis in the course of acute pancreatitis[35], whereas treatment with HGF reduces pancreatic damage in cerulein-induced pancreatitis[37]. These data indicate that HGF is not a pro-inflammatory factor, but a result of pancreatic damage in acute pancreatitis and the elevation of HGF level plays a role of self-defense mechanism, limiting the intensity of inflammatory process. It was reported that inhibition of COX-2 abolishes the protective effect of HGF against acute pancreatitis[15]. Our present study showed that inhibition of COXs, especially COX-2, reduced the protective effect of IP against damage evoked by cerulein. These findings taken together suggest that pancreatoprotective effects evoked by IP and HGF involve similar but not strictly the same mechanisms. In contrast to the administration of HGF[37], exposure to IP did not increase the serum level of anti-inflammatory IL-10.

Another finding of our present study is the observation that cerulein-induced pancreatitis and IP increased pancreatic synthesis of HSP 70 and these two factors applied together caused maximal induction of HSP 70 synthesis in the pancreas. HSPs are highly conserved cytoprotective proteins that are induced by a variety of stresses including hyper- and hypothermia, toxin, heavy metals, and free radicals[16]. Previous studies demonstrated that both thermal and non-thermal stresses protect against cerulein-induced pancreatitis and prevent trypsinogen activation in the pancreas and this effect is mediated by HSP 70[38]. HSPs have also been shown to provide the protection against arginine-[19] and taurocholate-induced[39] pancreatitis. The potential protective mechanisms of HSPs on pancreas include stabilization and refolding of damaged proteins, resistance of cells to apoptosis or necrosis, decrease in the level of pro-inflammatory cytokines, antioxidant effects and interference with intra-acinar zymogen activation[16,38,40]. Our present results are consistent with the

previous studies showing an increase of HSP 70 at the mRNA and protein level after induction of cerulein-induced pancreatitis[41]. The major finding is, however, the observation of the further increase in HSP 70 synthesis in rats with IP, which indicates that the protective effects of IP could be mediated via this HSP.

In conclusion, exposure to IP reduces pancreatic damage in cerulein-induced acute pancreatitis and this protective effect of IP, at least in part, depends on COXs activity and production of HSP 70.

REFERENCES

1 **Murry CE**, Jennings RB, Reimer KA. Preconditioning with ischemia: a delay of lethal cell injury in ischemic myocardium. *Circulation* 1986; **74**; 1124-1136
2 **Kato H**, Liu Y, Kogure K, Kato K. Induction of 27-kDa heat shock protein following cerebral ischemia in a rat model of ischemic tolerance. *Brain Res* 1994; **634**: 235-244
3 **Turman MA**, Bates CM. Susceptibility of human proximal tubular cells to hypoxia: effect of hypoxic preconditioning and comparison to glomerular cells. *Ren Fail* 1997; **19**: 47-60
4 **Kume M**, Yamamoto Y, Saad S, Gomi T, Kimoto S, Shimabukuro T, Yagi T, Nakagami M, Takada Y, Morimoto T, Yamaoka Y. Ischemic preconditioning of the liver in rats: implications of heat shock protein induction to increase tolerance of ischemia-reperfusion injury. *J Lab Clin Med* 1996; **128**: 251-258
5 **Mounsey RA**, Pang CY, Boyd JB, Forrest C. Augmentation of skeletal muscle survival in the latissimus dorsi porcine model using acute ischemic preconditioning. *J Otolaryngol* 1992; **21**: 315-320
6 **Pajdo R**, Brzozowski T, Konturek PC, Kwiecien S, Konturek SJ, Sliwowski Z, Pawlik M, Ptak A, Drozdowicz D, Hahn EG. Ischemic preconditioning, the most effective gastroprotective intervention: involvement of prostaglandins, nitric oxide, adenosine and sensory nerves. *Eur J Pharmacol* 2001; **427**: 263-276
7 **Dembiñski A**, Warzecha Z, Ceranowicz P, Tomaszewska R, Dembinski M, Pabiañczyk M, Stachura J, Konturek SJ. Ischemic preconditioning reduces the severity of ischemia/reperfusion-induced pancreatitis. *Eur J Pharmacol* 2003; **473**: 207-216
8 **Smith WL**, Garavito RM, DeWitt DL. Prostaglandin endoperoxide H synthases (cyclooxygenases)-1 and 2. *J Biol Chem* 1996; **271**: 33157-33160
9 **Peskar BM**. Role of cyclooxygenase isoforms in gastric mucosal defence. *J Physiol Paris* 2001; **95**: 3-9
10 **Konturek SJ**, Piastucki I, Brzozowski T, Radecki T, Dembinska-Kiec A, Zmuda A, Gryglewski R. Role of prostaglandins in the formation of aspirin-induced gastric ulcers. *Gastroenterology* 1981; **80**: 4-9
11 **Wang JY**, Yamasaki S, Takeuchi K, Okabe S. Delayed healing of acetic acid-induced gastric ulcers in rats by indomethacin. *Gastroenterology* 1989; **96**: 393-402
12 **Mizuno H**, Sakamoto C, Matsuda K, Wada K, Uchida T, Noguchi H, Akamatsu T, Kasuga M. Induction of cyclooxygenase 2 in gastric mucosal lesions and its inhibition by the specific antagonist delays healing in mice. *Gastroenterology* 1997; **112**: 387-397
13 **Song AM**, Bhagat L, Singh VP, van Acker GGD, Steer ML, Saluja AK. Inhibition of cyclooxygenase-2 ameliorates the severity of pancreatitis and associated lung injury. *Am J Physiol Gastrointest Liver Physiol* 2002; **283**: G1166-1174
14 **Ethridge RT**, Chung DH, Slogoff M, Ehlers RA, Hellmich MR, Rajaraman S, Saito H, Uchida T, Evers BM. Cyclooxygenase-2 gene disruption attenuates the severity of acute pancreatitis and pancreatitis-associated lung injury. *Gastroenterology* 2002; **123**: 1311-1322
15 **Warzecha Z**, Dembinski A, Ceranowicz P, Konturek SJ, Tomaszewska R, Stachura J, Nakamura T, Konturek PC. Inhibition of cyclooxygenase-2 reduces the protective effect of hepatocyte growth factor in experimental pancreatitis. *Eur J Pharmacol* 2004; **486**: 107-119
16 **Rakonczay Z Jr**, Takacs T, Boros I, Lonovics J. Heat shock proteins and the pancreas. *J Cell Physiol* 2003; **195**: 383-391
17 **Wagner AC**, Weber H, Jonas L, Nizze H, Strowski M, Fiedler F, Printz H, Steffen H, Goke B. Hyperthermia induces heat shock protein expression and protection against cerulein-induced pancreatitis in rats. *Gastroenterology* 1996; **111**: 1333-1342
18 **Kubisch C**, Dimagno MJ, Tietz AB, Welsh MJ, Ernst SA, Brandt-Nedelev B, Diebold J, Wagner AC, Goke B, Williams JA, Schafer C. Overexpression of heat shock protein Hsp27 protects against cerulein-induced pancreatitis. *Gastroenterology* 2004; **127**: 275-286
19 **Tashiro M**, Ernst SA, Edwards J, Williams JA. Hyperthermia induces multiple pancreatic heat shock proteins and protects against subsequent arginine-induced acute pancreatitis in rats. *Digestion* 2002; **65**: 118-126
20 **Konturek SJ**, Szlachcic A, Dembinski A, Warzecha Z, Jaworek J, Stachura J. Nitric oxide in pancreatic secretion and hormone-induced pancreatitis in rats. *Int J Pancreatol* 1994; **15**: 19-28
21 **Warshaw AL**, Lee KH. Serum ribonuclease elevations and pancreatic necrosis in acute pancreatitis. *Surgery* 1979: **86**: 227-234
22 **Dembiñski A**, Warzecha Z, Konturek SJ, Ceranowicz P, Dembinski M, Pawlik WW, Kucœnierz-Cabała B, Naskalski JW. Extract of grapefruit-seed reduces acute pancreatitis induced by ischemia/reperfusion in rats; Possible implication of tissue antioxidants. *J Physiol Pharmacol* 2004; **55**: 799-809
23 **Warzecha Z**, Dembinski A, Ceranowicz P, Jaworek J, Konturek PC, Dembiñski M, Bilski J, Konturek SJ. Influence of leptin administration on the course of acute ischemic pancreatitis. *J Physiol Pharmacol* 2002; **53**: 775-790
24 **Dervenis C**, Johnson CD, Bassi C, Bradley E, Imrie CW, McMahon MJ, Modlin I. Diagnosis, objective assessment of severity, and management of acute pancreatitis. Santorini consensus conference. *Int J Pancreatol* 1999; **25**: 195-210
25 **Naskalski JW**, Kucœnierz-Cabała B, Panek J, Kędra B. Poly-C specific ribonuclease activity correlates with increased concentrations of IL-6, IL-8 and sTNFR55/sTNFR75 in plasma of patients with acute pancreatitis. *J Physiol Pharmacol* 2003; **54**: 439-448
26 **Watanabe O**, Baccino FM, Steer ML, Meldolesi J. Supramaximal caerulein stimulation and ultrastructure of rat pancreatic acinar cell: early morphological changes during development of experimental pancreatitis. *Am J Physiol* 1984; **246**: G457-G467
27 **Konturek SJ**, Dembinski A, Konturek PJ, Warzecha Z, Jaworek J, Gustaw P, Tomaszewska R, Stachura J. Role of platelet activating factor in pathogenesis of acute pancreatitis in rats. *Gut* 1992; **33**: 1268-1274
28 **Dembiñski A**, Warzecha Z, Konturek PC, Ceranowicz P, Konturek SJ, Tomaszewska R, Stachura J. Adaptation of pancreas to repeated caerulein-induced pancreatitis in rats. *J Physiol Pharmacol* 1996; **47**: 455-467
29 **Warzecha Z**, Dembinski A, Ceranowicz P, Konturek SJ, Tomaszewska R, Stachura J, Konturek PC. IGF-1 stimulates production of interleukin-10 and inhibits development of caerulein-induced pancreatitis. *J Physiol Pharmacol* 2003; **54**: 575-590
30 **Jaworek J**, Jachimczak B, Tomaszewska R, Konturek PC, Pawlik WW, Sendur R, Hahn EG, Stachura J, Konturek SJ. Protective action of lipopolysaccharides in rat caerulein-induced pancreatitis: role of nitric oxide. *Digestion* 2000; **62**: 1-13
31 **Warzecha Z**, Dembinski A, Ceranowicz P, Stachura J, Tomaszewska R, Konturek SJ. Effect of sensory nerves and CGRP on the development of caerulein-induced pancreatitis and pancreatic recovery. *J Physiol Pharmacol* 2001; **52**: 679-704
32 **Foitzik T**, Hotz HG, Hotz B, Witting F, Buhr HJ. Selective inhibition of cyclooxygenase-2 (COX-2) reduces prostaglandin E_2 production and attenuates systemic disease sequelae in experimental pancreatitis. *Hepatogastroenterology* 2003; **50**:

1159-1162
33 **Ueda T**, Takeyama Y, Toyokawa A, Kishida S, Yamamoto M, Saitoh Y. Significant elevation of serum human hepatocyte growth factor levels in patients with acute pancreatitis. *Pancreas* 1996; **12**: 76-83
34 **Ueda T**, Takeyama Y, Hori Y, Nishikawa J, Yamamoto M, Saitoh Y. Hepatocyte growth factor in assessment of acute pancreatitis: Comparison with C-reactive protein and interleukin-6. *J Gastroenterol* 1997; **32**: 63-70
35 **Ueda T**, Takeyama Y, Hori Y, Shinkai M, Takase K, Goshima M, Yamamoto M, Kuroda Y. Hepatocyte growth factor increases in injured organs and functions as an organotrophic factor in rats with experimental acute pancreatitis. *Pancreas* 2000; **20**: 84-93
36 **Menke A**, Yamaguchi H, Giehl K, Adler G. Hepatocyte growth factor and fibroblast growth factor 2 are overexpressed after cerulein-induced acute pancreatitis. *Pancreas* 1999; **18**: 28-33
37 **Warzecha Z**, Dembinski A, Konturek PC, Ceranowicz P, Konturek SJ, Tomaszewska R, Schuppan D, Stachura J, Nakamura T. Hepatocyte growth factor attenuates pancreatic damage in caerulein-induced pancreatitis in rats. *Eur J Pharmacol* 2001; **430**: 113-121
38 **Frossard JL**, Bhagat L, Lee HS, Hietaranta AJ, Singh VS, Song AM, Steer ML, Saluja AK. Both thermal and non-thermal stress protect against caerulein induced pancreatitis and prevent trypsinogen activation in the pancreas. *Gut* 2002; **50**: 78-83
39 **Rakonczay Z Jr**, Takacs T, Ivanyi B, Mandi Y, Papai G, Boros I, Varga IS, Jost K, Lonovics J. The effects of hypo- and hyperthermic pretreatment on sodium taurocholate-induced acute pancreatitis in rats. *Pancreas* 2002; **24**: 83-89
40 **Takayama S**, Reed JC, Homma S. Heat-shock proteins as regulators of apoptosis. *Oncogene* 2003; **22**: 9041-9047
41 **Weber CK**, Gress T, Muller-Pillasch F, Lerch MM, Weidenbach H, Adler G. Supramaximal secretagogue stimulation enhances heat shock protein expression in the rat pancreas. *Pancreas* 1995; **10**: 360-367

Science Editor Wang XL and Guo SY **Language Editor** Elsevier HK

PO Box 2345, Beijing 100023, China
www.wjgnet.com
wjg@wjgnet.com

ELSEVIER

World J Gastroenterol 2005;11(38):5966-5972
World Journal of Gastroenterology ISSN 1007-9327
© 2005 The WJG Press and Elsevier Inc. All rights reserved.

• *BASIC RESEARCH* •

Role of nuclear receptor CAR in carbon tetrachloride-induced hepatotoxicity

Yuichi Yamazaki, Satoru Kakizaki, Norio Horiguchi, Hitoshi Takagi, Masatomo Mori, Masahiko Negishi

Yuichi Yamazaki, Satoru Kakizaki, Norio Horiguchi, Hitoshi Takagi, Masatomo Mori, Department of Medicine and Molecular Science, Gunma University Graduate School of Medicine, Maebashi, Gunma 371-8511, Japan
Masahiko Negishi, Pharmacogenetics Section, Laboratory of Reproductive and Developmental Toxicology, National Institute of Environmental Health Sciences, National Institutes of Health, Research Triangle Park, NC 27709, USA
Supported by a Grant-in Aid for Scientific Research, No. 15790337 from the Ministry of Education, Science, Sports and Culture of the Japanese Government
Correspondence to: Satoru Kakizaki, MD, PhD, Department of Medicine and Molecular Science, Gunma University Graduate School of Medicine, 3-39-15 Showa-machi, Maebashi 371-8511, Japan. kakizaki@showa.gunma-u.ac.jp
Telephone: +81-27-220-8127 Fax: +81-27-220-8136
Received: 2005-03-25 Accepted: 2005-04-30

Abstract

AIM: To investigate the precise roles of CAR in CCl_4-induced acute hepatotoxicity.

METHODS: To prepare an acute liver injury model, CCl_4 was intraperitoneally injected in $CAR^{+/+}$ and $CAR^{-/-}$ mice.
RESULTS: Elevation of serum alanine aminotransferase and extension of centrilobular necrosis were slightly inhibited in $CAR^{-/-}$ mice compared to $CAR^{+/+}$ mice without PB. Administration of a CAR inducer, PB, revealed that CCl_4-induced liver toxicity was partially inhibited in $CAR^{-/-}$ mice compared with $CAR^{+/+}$ mice. On the other hand, androstanol, an inverse agonist ligand, inhibited hepatotoxicity in $CAR^{+/+}$ but not in $CAR^{-/-}$ mice. Thus, CAR activation caused CCl_4 hepatotoxicity while CAR inhibition resulted in partial protection against CCl_4-induced hepatotoxicity.There were no differences in the expression of CYP2E1, the main metabolizing enzyme for CCl_4, between $CAR^{+/+}$ and $CAR^{-/-}$ mice. However, the expression of other CCl_4-metabolizing enzymes, such as CYP2B10 and 3A11, was induced by PB in $CAR^{+/+}$ but not in $CAR^{-/-}$ mice. Although the main pathway of CCl_4-induced acute liver injury is mediated by CYP2E1, CAR modulates its pathway via induction of CYP2B10 and 3A11 in the presence of activator or inhibitor.

CONCLUSION: The nuclear receptor CAR modulates CCl_4-induced liver injury via induction of CCl_4-metabolizing enzymes in the presence of an activator. Our results suggest that drugs interacting with nuclear receptors such as PB might play critical roles in drug-induced liver injury or drug-drug interaction even though such drugs themselves are not hepatotoxic.
© 2005 The WJG Press and Elsevier Inc. All rights reserved.

Key words: CAR; Phenobarbital; Cytochrome P450; CCl_4; Drug-induced liver injury

Yamazaki Y, Kakizaki S, Horiguchi N, Takagi H, Mori M, Negishi M. Role of nuclear receptor CAR in carbon tetrachloride-induced hepatotoxicity. *World J Gastroenterol* 2005; 11 (38): 5966-5972
http://www.wjgnet.com/1007-9327/11/5966.asp

INTRODUCTION

Drug-induced liver injury is a clinical-relevant problem[1-3], and investigation of mechanisms of drug-induced liver injury is therefore of pharmacological and clinical importance. Animals induce drug-metabolizing enzymes to detoxify xenochemicals, including therapeutic drugs[4-6]. However, paradoxically, this can often result in bioactivation of toxic drugs and cause liver injury[4-6]. Thus, drug-metabolizing enzymes are a two-edge blade and have very crucial roles in drug-induced liver injury.

Recent studies indicate that the nuclear receptor constitutive androstane receptor (CAR) is a key regulator of drug-metabolizing enzymes such as cytochrome P450 (CYP)[7-9], UDP-glucuronosyltransferase (UGT)[10,11] and multidrug resistance-associated protein (MRP)[12,13]. CAR has also been reported as a key regulator for bile acid[14] and bilirubin liver injury[11,15,16]. As a cellular defense mechanism against toxicity and carcinogenicity, induction of and metabolism by CYPs usually leads to increased detoxification and elimination of xenobiotics[4-6]. The nuclear receptor CAR is implicated as an essential factor that mediates this inducible activation of drug-metabolizing enzymes[7-9]. CAR, acting as a heterodimer with the retinoid X receptor, binds to a nuclear receptor-binding site NR1 within the 51-bp phenobarbital-responsive enhancer module and activates genes such as CYP2B in response to phenobarbital (PB)-type inducers[7-9]. Expression analysis of hepatic genes in $CAR^{-/-}$ mice has also revealed that CAR is a key regulator of a group of xenochemical-metabolizing enzymes that include the CYP2B and CYP3A subfamilies[17]. Thus, CAR is closely associated with the regulation of drug-metabolizing enzymes. Because of its regulating roles for drug-metabolizing enzymes, CAR is thought to play an important role in the development of drug-induced liver injury.

Carbon tetrachloride (CCl_4) was once used widely as a solvent cleaner, anesthetic agent, and degreaser both for industrial and home use[18-20]. However, the high incidence of liver and renal problems following administration led to

discontinuation of its use. CCl_4 is used as a model drug for the study of hepatotoxicity in acute and chronic liver failure[18-20]. CCl_4 is metabolized by CYP2E1, CYP2B, and possibly CYP3A, to form the trichloromethyl radical, CCl_3*[18-20]. CCl_3* can bind to cellular molecules (nucleic acid, protein, and lipid), impairing crucial cellular processes. This radical can also react with oxygen to form the trichloromethylperoxy radical CCl_3OO*, a highly reactive species. Thus, the metabolites of CCl_4 cause the hepatic injury in the CCl_4 acute liver injury model. Inducers of drug-metabolizing enzymes, such as PB or dichlorodiphenyltrichloroethane, are also known to cause severe liver toxicity with CCl_4[18-20].

The nuclear receptor CAR has recently been shown to mediate the effects of PB and other PB-like inducers[21] and to act as a key regulator of drug-metabolizing enzymes[21-23]. However, the precise relationship between CAR and CCl_4-induced liver injury is not fully understood. We investigated the mechanism of CCl_4-induced acute liver injury and the roles of CAR in drug-induced liver injury using $CAR^{-/-}$ mice *in vivo*.

MATERIALS AND METHODS

Materials

PB was purchased from Sigma Chemicals Co. (St. Louis, MO, USA). 5α-Androstan-3δ-ol (androstanol) was purchased from Steraloids (Newport, RI, USA). CCl_4 was purchased from Kanto Chemistry (Tokyo, Japan). The total glutathione quantification kit was purchased from Dojindo Molecular Technologies Inc. (Gaithersburg, MD, USA).

Animals and treatment

$CAR^{-/-}$ and $CAR^{+/+}$ mice used in this study were generated as described previously[24]. The background strain contained 98% of the C3H/HeNCrlBR markers by microsatellite analysis[24]. All mouse work was performed in accordance with the guidelines for animal care and use established by Gunma University Graduate School of Medicine. Germline transmission of the disrupted allele was detected by PCR[17]. Mice were injected intraperitoneally with the indicated concentration of CCl_4 dissolved in olive oil at 8-10 wk of age and were killed, and their sera and livers were collected at specified time points. PB was administered in H_2O at a dose of 100 mg/kg body weight for 12 and 36 h before CCl_4 administration. Androstanol was administered in olive oil at a dose of 100 mg/kg body weight for 1 h before CCl_4 administration. For control mice, 100 μL of H_2O or olive oil per 25 g of body weight was injected. Serum alanine aminotransferase (ALT), total bilirubin, and blood urea nitrogen (BUN) levels were measured with an auto-analyzer at each point. Liver tissues were fixed in 40 g/L formaldehyde, embedded in paraffin and stained with hematoxylin-eosin. At a magnification of ×40, 10 areas of centrilobular necrosis were measured in a blinded fashion for each group using NIH Image 1.62 software (National Institute of Health, MD, USA). The index of centrilobular necrosis was scored as follows: area of centrilobular necrosis divided by whole area.

Reverse transcription-polymerase chain reaction

Total RNA extraction from liver and subsequent synthesis of first-strand cDNA were performed using TRIzol reagent (Invitrogen, Carlsbad, CA, USA) and SuperScript™ preamplification system (Invitrogen, Carlsbad, CA, USA), respectively. cDNAs were amplified using the following sets of primers: CYP2B10 mRNA, 5'-AAAGTCCCGTGGCAACTTCC-3' and 5'-CATCCCAAAGTCTCTCATGG-3'; CYP3A11 mRNA, 5'-CTCAATGGTGTGTATATCCCC-3' and 5'-CCGATGTTCTTAGACACTGCC-3'; GSTpi, 5'-CTTGCTCAAGCCCACTTGTC-3' and 5'-ATGGGACGGTTCACATGTTC-3'; CYP2E1, 5'-GGATGAATATGCCCTACATG-3' and 5'-TGATGGGCAGCAGGTCTCAT-3'. β-actin mRNA level was also measured as an internal control. One-twentieth of each cDNA synthesized from 5 μg of RNA was subjected to PCR. PCR was performed using Taq DNA polymerase (Promega, Madison, WI, USA) with TaqStart antibody (Clontech, Palo Alto, CA, USA) at 95 ℃ for 60 s, 55 ℃ for 60 s, and 72 ℃ for 60 s. The amplified DNA was separated on a 1.5% agarose gel and visualized with staining by ethidium bromide. The expected sizes of the amplified cDNA were 340, 423, 468, and 486 bp for CYP2B10, CYP3A11, CYP2E1, and GSTPi, respectively.

Hepatic glutathione concentration

Total hepatic reduced glutathione concentration was determined by the total glutathione quantification kit (Dojindo Molecular Technologies Inc.). Each liver was excised and homogenized with 5% trichloroacetic acid, and centrifuged at 4 ℃, 2 000 r/min for 15 min. The supernatant was used for total glutathione assay using the total glutathione quantification kit according to the manual provided by the manufacturer.

Statistical analysis

All experimental data are shown as mean±SD. Differences in serum ALT levels and the index of centrilobular necrosis were determined by one-way factorial analysis of variance for each group. The level of significance for all statistical analyses was set at $P<0.05$.

RESULTS

Phenobarbital pretreatment induces CCl_4 toxicity in $CAR^{+/+}$ mice

$CAR^{+/+}$ and $CAR^{-/-}$ mice were administered a 25-mg/kg dose of CCl_4 by intraperitoneal injection ($n = 6$ per treatment group) and the ALT level was measured at 24 h (Figure 1A). The serum levels of ALT increased following CCl_4 administration in both groups ($P<0.001$). The level of ALT was slightly higher in $CAR^{+/+}$ mice than in $CAR^{-/-}$ mice ($P<0.001$). There were no significant changes in the serum levels of total bilirubin and BUN in both groups (data not shown). $CAR^{+/+}$ and $CAR^{-/-}$ animals pretreated with PB (12 and 36 h before CCl_4 administration) were then administered the same dose of CCl_4. PB pretreatment caused marked elevation of ALT in $CAR^{+/+}$ mice. The $CAR^{-/-}$ mice showed some elevation of ALT with PB pretreatment, but the level was less than that in wild-type mice. The difference of ALT levels became clear between $CAR^{+/+}$ and $CAR^{-/-}$ mice with pre-treatment by PB ($P<0.001$). PB alone and control mice did not show such an elevation of ALT.

Histological changes associated with CCl_4 toxicity

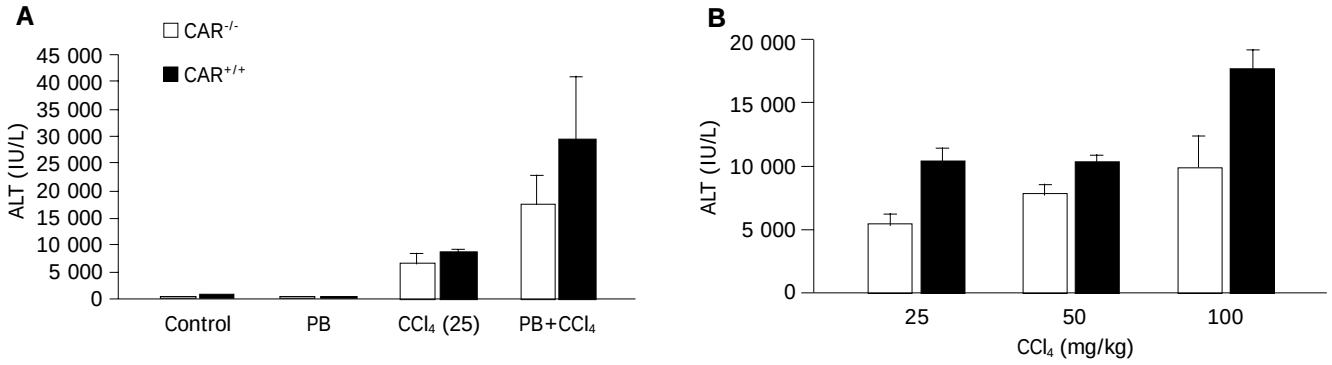


Figure 1 A: PB pretreatment induced CCl_4 toxicity. $CAR^{+/+}$ or $CAR^{-/-}$ mice were administered a 25-mg/kg dose of CCl_4 by intraperitoneal injection with or without PB pretreatment (n = 6 per treatment group). Serum was collected and ALT levels were measured after 24 h. The ALT level was slightly higher in $CAR^{+/+}$ mice than in $CAR^{-/-}$ mice with CCl_4 treatment (P<0.001). The difference in ALT levels became clearer between $CAR^{+/+}$ and $CAR^{-/-}$ mice with pre-treatment by PB (P<0.001). B: Dose dependency of CCl_4 toxicity. $CAR^{+/+}$ and $CAR^{-/-}$ mice were given 25-, 50-, or 100-mg/kg doses of CCl_4. Blood samples were collected 24 h later, and serum ALT levels were measured (n = 4). $CAR^{-/-}$ animals were significantly less sensitive than $CAR^{+/+}$ mice to CCl_4 toxicity (P<0.001). Data are mean±SD.

$CAR^{+/+}$ or $CAR^{-/-}$ mice were administered a 25-mg/kg dose of CCl_4 by intraperitoneal injection with or without pretreatment with PB (n = 6 per treatment group). Liver sections from each treatment were examined by hematoxylin and eosin staining. Liver samples from all treated animals were analyzed but representative histology is presented in Figure 2A showing marked centrilobular necrosis. The extent of the necrotic area with CCl_4 in the $CAR^{+/+}$ liver was slightly larger than that in $CAR^{-/-}$ mice. PB pretreatment caused extensive centrilobular necrosis in $CAR^{+/+}$ mice compared with $CAR^{-/-}$ mice. The indices of centrilobular necrosis (Figure 2B) in $CAR^{+/+}$ mice and $CAR^{-/-}$ mice treated with CCl_4 alone were 17.44±1.02 and 13.11±1.41, respectively (P<0.001). The indices of centrilobular necrosis in $CAR^{+/+}$ mice and $CAR^{-/-}$ mice treated with PB plus CCl_4 were 39.08±2.10 and 26.33±2.33, respectively (P<0.001).

Dose dependency and time course of CCl_4 toxicity

$CAR^{+/+}$ or $CAR^{-/-}$ mice were treated with 25-, 50-, or 100-mg/kg CCl_4 by intraperitoneal injection (n = 4 per treatment group). Five and twenty-four hours later, the mice were killed and blood samples were collected (Figure 1B).

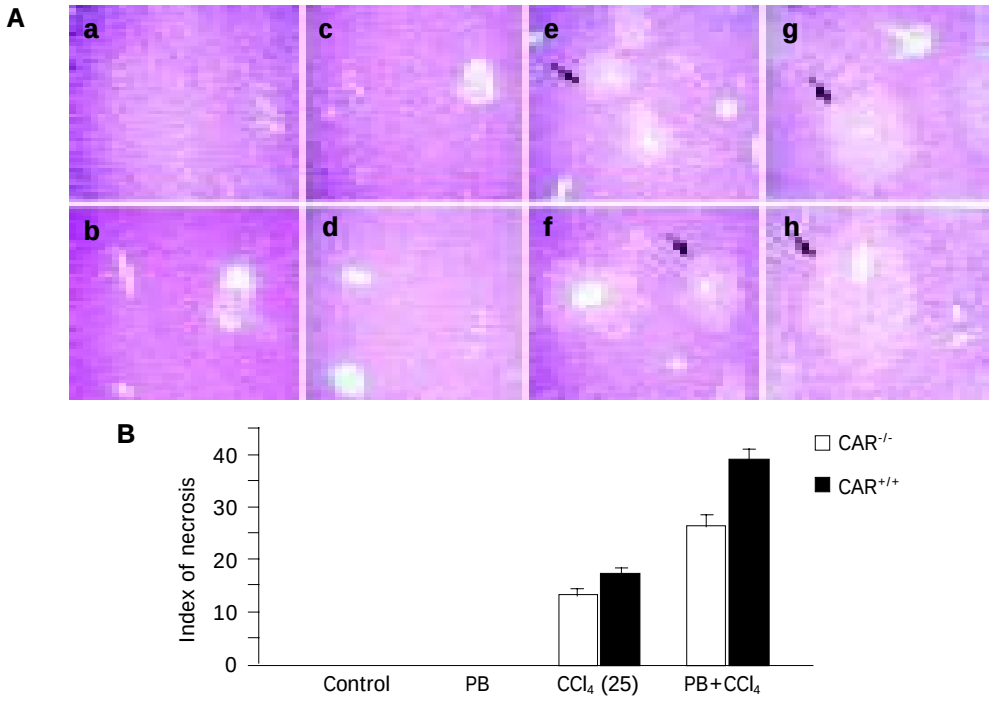


Figure 2 Histological changes associated with CCl_4 toxicity. A: Histological findings in the liver; (a) $CAR^{-/-}$ mice, control; (b) $CAR^{+/+}$ mice, control; (c) $CAR^{-/-}$ mice, PB; (d) $CAR^{+/+}$ mice, PB; (e) $CAR^{-/-}$ mice, CCl_4; (f) $CAR^{+/+}$ mice, CCl_4; (g) $CAR^{-/-}$ mice, PB plus CCl_4; and (h) $CAR^{+/+}$ mice, PB plus CCl_4. Liver sections from each treatment were examined by hematoxylin and eosin staining. Liver samples from all treated animals were analyzed, but only representative histology is presented. The extent of the necrotic area in the $CAR^{+/+}$ liver was larger than that in $CAR^{-/-}$ mice. PB pretreatment caused extensive centrilobular necrosis in $CAR^{+/+}$ mice. The arrows indicate centrilobular necrosis. Magnification, ×100. B: The indices of centrilobular necrosis in $CAR^{+/+}$ mice and $CAR^{-/-}$ mice. The indices of centrilobular necrosis were higher in $CAR^{+/+}$ mice than that in $CAR^{-/-}$ mice with PB pretreatment. The index in $CAR^{+/+}$ mice treated with CCl_4 plus PB was significantly increased. The index of centrilobular necrosis was scored as follows: area of centrilobular necrosis divided by whole area. Data are mean±SD.

No elevation of ALT was observed at 5 h (data not shown). At 24 h, ALT was significantly elevated and dose dependency was observed in CCl_4 toxicity in both groups of mice. The serum ALT concentrations of $CAR^{-/-}$ mice were lower than those of the $CAR^{+/+}$ mice ($P<0.001$). Thus, $CAR^{+/+}$ mice were apparently more sensitive to CCl_4 liver toxicity compared with $CAR^{-/-}$ mice.

Hepatic mRNA levels of CCl_4-metabolizing enzymes

CCl_4 is reported to be metabolized and activated by CYP2E1, CYP2B, and possibly CYP3A, to form the trichloromethyl radical, CCl_3*[18-20]. To evaluate the relationship between CAR and CCl_4-metabolizing enzymes, $CAR^{+/+}$ or $CAR^{-/-}$ animals were treated with a 100-mg/kg PB intraperitoneally ($n = 6$ per treatment group, Figure 3). There were no differences in the basal expression of CYP2E1, the main metabolizing enzyme of CCl_4, between $CAR^{+/+}$ and $CAR^{-/-}$ mice. Among the genes associated with CCl_4 metabolism, PB treatment did not influence CYP2E1 mRNA levels but induced CYP2B10, CYP3A11 mRNAs in $CAR^{+/+}$ mice. On the other hand, no induction of the enzymes CYP2E1, CYP2B10, and CYP3A11 was observed in $CAR^{-/-}$ mice. Thus, PB activated CCl_4-metabolizing enzymes, CYP2B10 and CYP3A11, via CAR. Because CAR is reported to regulate GSTPi, the enzyme that enhances glutathione depletion in acetaminophen toxicity[18-21], GSTPi mRNA, was also measured. GSTPi mRNA was induced by PB in $CAR^{+/+}$ mice stronger than in $CAR^{-/-}$ mice.

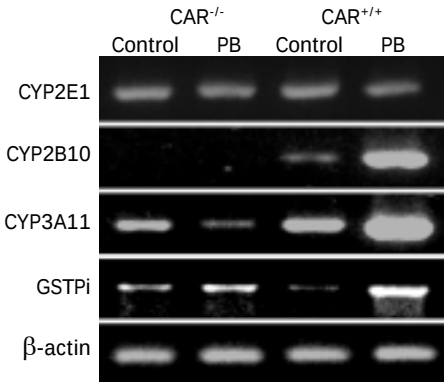


Figure 3 Hepatic mRNA level of drug-metabolizing enzymes with PB treatment. Total liver RNA was prepared from $CAR^{+/+}$ or $CAR^{-/-}$ animals treated with a 100-mg/kg dose of PB by intraperitoneal injection ($n = 6$ per treatment group). Total liver RNA was prepared 12 h after PB treatment and subjected to PCR analysis with the indicated primers in Materials and methods. β-Actin mRNA level was also measured as an internal control. The amplified DNA was separated on a 1.5% agarose gel and visualized with staining by ethidium bromide. The expected sizes of the amplified cDNA are described in Materials and methods.

Hepatic glutathione level

For detoxification, metabolites of CCl_4 such as CCl_3* decreased the amount of reduced glutathione. A decrease of glutathione in the liver reflects increased production of CCl_4 metabolites. Liver samples treated with CCl_4 and/or PB were collected 24 h after each treatment and glutathione levels were measured ($n = 6$ per treatment group, Figure 4). Hepatic glutathione levels in the PB plus CCl_4-treated $CAR^{+/+}$ mice were significantly different from those of the $CAR^{-/-}$ mice ($P<0.001$). $CAR^{+/+}$ mice treated with PB plus CCl_4 showed about a 50% decrease in hepatic glutathione level compared with $CAR^{-/-}$ mice.

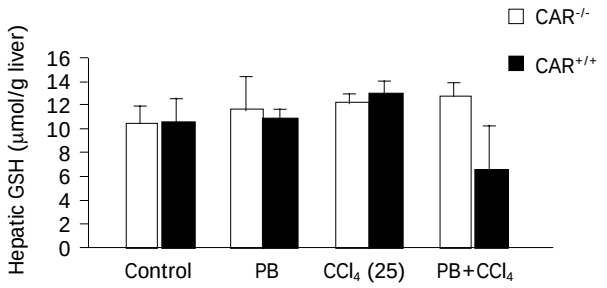


Figure 4 Hepatic glutathione (GSH) level. Liver samples treated with the indicated chemicals were collected 24 h after each treatment and glutathione levels were measured ($n = 6$ per treatment group) using the total glutathione quantification kit. Hepatic glutathione levels in the PB plus CCl_4 treated $CAR^{+/+}$ mice significantly decreased, compared with those of the $CAR^{-/-}$ mice ($P<0.001$). Data are mean±SD.

Androstanol reduced CCl_4-induced hepatotoxicity in $CAR^{+/+}$ mice to the level of $CAR^{-/-}$ mice

$CAR^{+/+}$ or $CAR^{-/-}$ mice were treated with 100-mg/kg CCl_4 intraperitoneally, with or without pretreatment with androstanol (100 mg/kg). Serum ALT levels were measured 24 h later ($n = 6$ per treatment group, Figure 5). Without androstanol, $CAR^{+/+}$ mice treated with CCl_4 showed significantly higher ALT concentrations than did $CAR^{-/-}$ mice ($P<0.0001$). Surprisingly, androstanol reduced the ALT concentration of $CAR^{+/+}$ mice to the level of $CAR^{-/-}$ mice. Liver sections from the same animals, as indicated, were stained with hematoxylin and eosin (Figure 5B). Androstanol pretreatment reduced the hepatic centrilobular necrosis (Figure 5C) of $CAR^{+/+}$ mice to the level of $CAR^{-/-}$ mice. The indices of centrilobular necrosis of $CAR^{+/+}$ mice and $CAR^{-/-}$ mice treated with CCl_4 alone were 33.39±5.04 and 26.49±2.87, respectively ($P<0.001$). With androstanol treatment, the indices of centrilobular necrosis in $CAR^{+/+}$ mice and $CAR^{-/-}$ mice decreased to 23.64±1.89 and 25.15±2.36, respectively ($P = 0.15$). Thus, androstanol, the inverse agonist of CAR, reduced the CCl_4-induced hepatotoxicity of $CAR^{+/+}$ mice to the level of $CAR^{-/-}$ mice.

To evaluate the effect of androstanol on CCl_4-metabolizing enzymes, hepatic mRNA levels were determined with RT-PCR. Androstanol treatment did not influence CYP2E1 mRNA levels but slightly repressed CYP3A11 mRNA in $CAR^{+/+}$ mice as previously reported[25]. Because of low basal expression of CYP2B10 mRNA, the repression of CYP2B10 mRNA by androstanol could not be demonstrated with RT-PCR in $CAR^{+/+}$ mice. However, androstanol was reported to repress the basal promoter activity of CYP2B10 by luciferase reporter assay[26]. On the other hand, no induction or repression of the enzymes CYP2E1, CYP2B10, and CYP3A11 was observed in $CAR^{-/-}$ mice. Thus, androstanol repressed basal expression of CCl_4-metabolizing enzymes, CYP3A11 and may be CYP2B10, via CAR. Androstanol

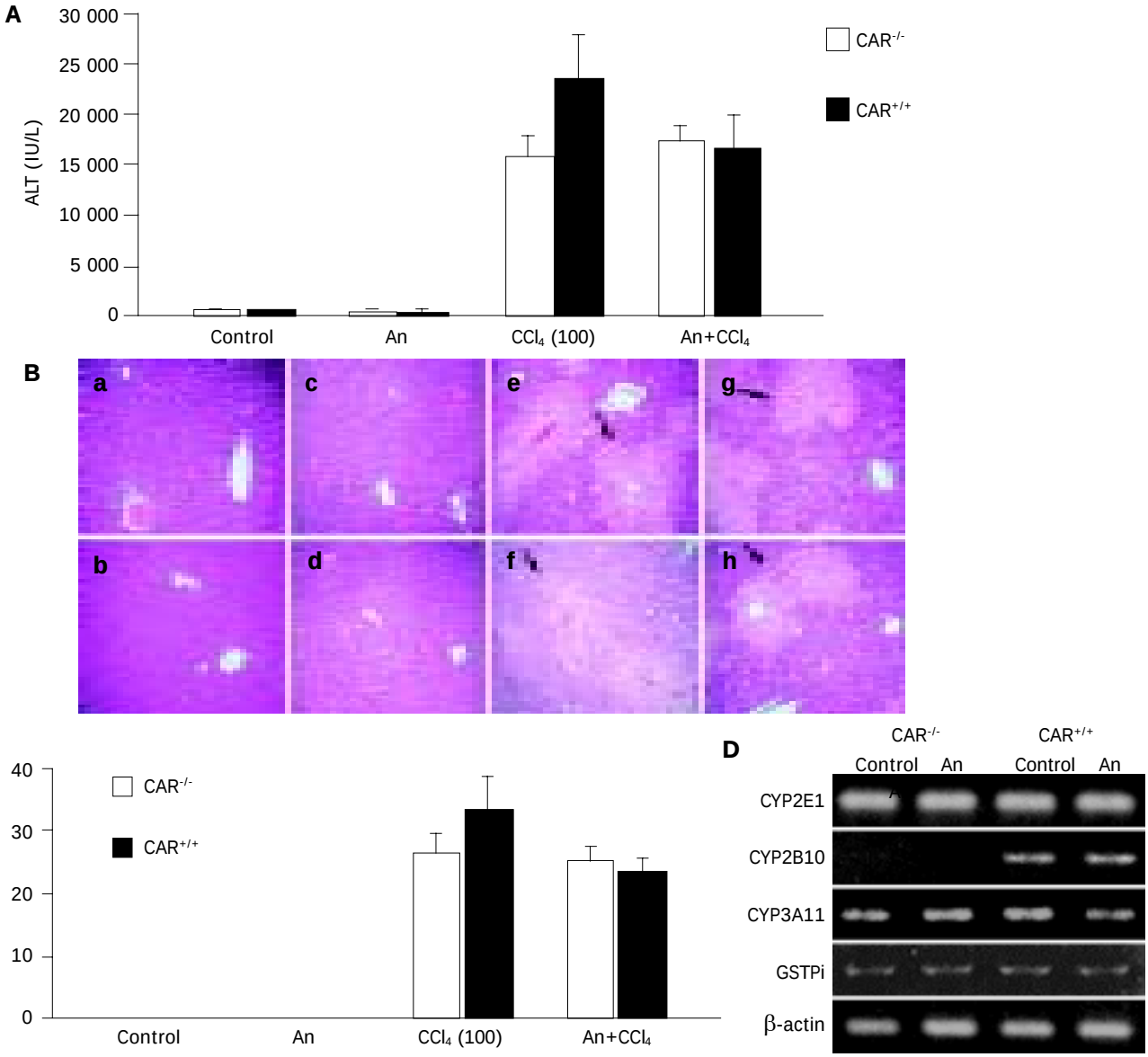


Figure 5 Androstanol prevented CCl_4-induced hepatotoxicity. A: $CAR^{+/+}$ or $CAR^{-/-}$ mice were given a 100-mg/kg dose of CCl_4 by intraperitoneal injection, with or without pretreatment with androstanol (100 mg/kg). Serum ALT levels were measured 24 h later (n = 6 per treatment group). Androstanol-pretreatment reduced the ALT level of $CAR^{+/+}$ mice to the level of $CAR^{-/-}$ mice. An: androstanol. B: Liver sections from the same animals 24 h after different treatments, as indicated, were stained with hematoxylin and eosin. (a) $CAR^{-/-}$ mice, control; (b) $CAR^{+/+}$ mice, control; (c) $CAR^{-/-}$ mice, androstanol; (d) $CAR^{+/+}$ mice, androstanol; (e) $CAR^{-/-}$ mice, CCl_4; (f) $CAR^{+/+}$ mice, CCl_4; (g) $CAR^{-/-}$ mice, androstanol plus CCl_4; and (h) $CAR^{+/+}$ mice, androstanol plus CCl_4. Androstanol pretreatment reduced the hepatic centrilobular necrosis in $CAR^{+/+}$ mice. Arrows indicate areas of hepatic necrosis. C: The indices of centrilobular necrosis in $CAR^{+/+}$ mice and $CAR^{-/-}$ mice. Androstanol-pretreatment reduced hepatic centrilobular necrosis of $CAR^{+/+}$ mice to the level of $CAR^{-/-}$ mice. Data in (A) and (C) are mean±SD. (D) Hepatic mRNA level of drug-metabolizing enzymes with androstanol treatment. Total liver RNA was prepared from $CAR^{+/+}$ or $CAR^{-/-}$ animals treated with a 100-mg/kg dose of androstanol by intraperitoneal injection (n = 6 per treatment group) and subjected to PCR analysis with the indicated primers in Materials and methods. β-actin mRNA level was also measured as an internal control. The amplified DNA was separated on a 1.5% agarose gel and visualized with staining by ethidium bromide. The expected sizes of the amplified cDNA are described in Materials and methods.

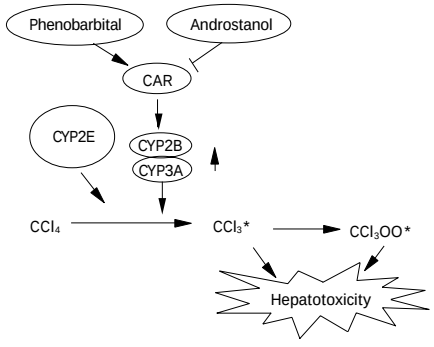


Figure 6 Schematic representation of CAR-mediated CCl_4 hepatotoxicity.

treatment did not influence GSTPi mRNA levels in $CAR^{+/+}$ and $CAR^{-/-}$ mice by RT-PCR.

DISCUSSION

In this study, we showed that CAR partially modulates the CCl_4 toxicity that is associated with induction of some CCl_4-metabolizing enzymes in the presence of agonist. The loss of CAR function results in partial resistance to CCl_4 toxicity. However, the CCl_4 liver toxicity is not fully inhibited in $CAR^{-/-}$ mice and differences between $CAR^{+/+}$ and $CAR^{-/-}$ mice were small in the absence of an inducer, PB. Metabolites of CCl_4 such as CCl_3* and CCl_3OO* are known to cause the

hepatic injury associated with CCl_4[18-20]. CCl_4 is metabolized by CYP2E1, CYP2B, and possibly CYP3A, to form the trichloromethyl radical, CCl_3*[18-20]. The main CCl_4-metabolizing enzyme is CYP2E1 and it is expressed in $CAR^{+/+}$ and $CAR^{-/-}$ mice in the same way. Therefore, CCl_4 liver toxicity occurs despite an absence of CAR. Thus, CYP2B or CYP3A may only have supplementary roles in CCl_4 metabolism in the absence of PB. On the other hand, in the presence of CAR inducers, it results in the induction of CYP2B and CYP3A, and CCl_4 liver toxicity is severe, as seen in $CAR^{+/+}$ mice. Inducers of drug-metabolizing enzymes including PB have long been known to cause severe liver toxicity with CCl_4[18-20]. In this study, we showed that PB activated CYP2B10 and 3A11 via receptor CAR and that it caused the severe CCl_4 liver toxicity (Figure 6). Thus, the xenobiotic receptor CAR will have a mean with the presence of its agonist/antagonist. PB treatment resulted in enhanced CCl_4 liver toxicity in $CAR^{-/-}$ mice although to a lesser degree than that in $CAR^{+/+}$ mice. PB may impact on pathways distinct from CAR to cause CCl_4 liver toxicity. Indeed, cDNA microarray analysis of $CAR^{-/-}$ mice showed CAR-independent genes in response to PB treatment[17]. A total of 138 genes were detected to be either induced or repressed in response to PB treatment, of which about half were not under CAR regulation[17]. Enzymes such as amino levulinate synthase 1 and squalene epoxidase displayed CAR-independent induction by PB[17]. CYP4A10 and CYP4A14 represented the group of genes induced by PB only in $CAR^{-/-}$ mice, indicating that CAR may be a transcription blocker that prevents these genes from being induced by PB[17]. The enzymes having CCl_4-metabolizing activity may be included in these CAR-independent PB response genes.

CAR was also identified as a key regulator of acetaminophen metabolism and hepatotoxicity[27]. CAR regulates GSTPi, the enzyme that enhances glutathione depletion and so promotes acetaminophen toxicity[27-29]. In this study, CAR also induced GSTPi with PB treatment. The metabolites of CCl_4 such as CCl_3* and CCl_3OO* induce hepatotoxicity and expend glutathione and cause a decrease of hepatic glutathione level. In addition, induction of GSTPi expression may cause further depletion of glutathione and severe toxicity in CCl_4-treated mice.

Although CAR acted as a hepatotoxic regulator in this study, CAR could act as a protective manner in other situations[30,31]. PB is a well-established therapy for hyperbilirubinemia in Crigler-Najjar type II patients[30]. CAR has the ability to activate expression of known components of the bilirubin pathway including UGT1A1, OATP2, MRP2, and GSTA1[15]. It was also reported that paralysis by the muscle relaxant zoxazolamine was avoided by pretreatment with CAR activators but was prolonged in $CAR^{-/-}$ mice[21]. Thus, CAR coordinates the induction of metabolic activity and increases elimination of the drugs in a protective manner in some cases.

Transactivation of target genes by CAR can be blocked by the inverse agonist androstanol[32]. Androstanol is reported to not only prevent induction but also to decrease basal expression of CAR target genes including CYP3A11[25]. Androstanol reduced the liver toxicity of $CAR^{+/+}$ mice to the level of $CAR^{-/-}$ mice in this study. This effect of androstanol may result in decrease of the basal expression of CAR target genes including CYP3A11. Androstanol treatment was also reported to decrease the toxicity of acetaminophen[24].

The nuclear receptor CAR has only a small role in CCl_4 toxicity without its agonist/antagonist. However, because of its nature as a xenobiotic sensor, CAR exhibits its ability to the full in the presence of agonist/antagonist. Since some kinds of CAR inducers such as PB and phenytoin are used clinically, CAR may have an important clinical role in drug-induced liver injury or drug-drug interaction. Nuclear receptors regulating drug-metabolizing enzymes such as CAR are a two-edge blade in animals. In some cases, activation of CAR increases production of drug-metabolizing enzymes and increases toxicity. Thus, CAR inverse agonists such as androstanol may have potential for treatment of these kinds of drug-induced liver injury. On the other hand, activation of CAR by appropriate inducers acts in a hepato-protective manner in some cases such as bilirubin toxicity. Conversely, induction of CAR activity reduced the liver injury in these cases.

Thus, a nuclear receptor that regulates drug-metabolizing enzymes is a key factor in drug-induced liver injury. Regulation of CAR activity may be an important clinical strategy for treatment of drug-induced liver injury. Both CAR and nuclear receptor regulating drug-metabolizing enzymes such as pregnane X receptor and peroxisome proliferator activated receptors are thought to be associated with drug-induced liver injury. Activating or inverse agonists for nuclear receptors may provide a clinically useful means to treat drug-induced liver injury.

REFERENCES

1 **Sgro C**, Clinard F, Ouazir K, Chanay H, Allard C, Guilleminet C, Lenoir C, Lemoine A, Hillon P. Incidence of drug-induced hepatic injuries: a French population-based study. *Hepatology* 2002; **36**: 451-455

2 **Chitturi S**, Farrell GC. Drug-induced cholestasis. *Semin Gastrointest Dis* 2001; **12**: 113-124

3 **Ibanez L**, Perez E, Vidal X, Laporte JR. Grup d'Estudi Multicenteric d'Hepatotoxicitat Aguda de Barcelona (GEMHAB). Prospective surveillance of acute serious liver disease unrelated to infectious, obstructive, or metabolic diseases: epidemiological and clinical features, and exposure to drugs. *J Hepatol* 2002; **37**: 592-600

4 **Guengerich FP**, Liebler DC. Enzymatic activation of chemicals to toxic metabolites. *Crit Rev Toxicol* 1985; **14**: 259-307

5 **Guengerich FP**, Shimada T. Oxidation of toxic and carcinogenic chemicals by human cytochrome P-450 enzymes. *Chem Res Toxicol* 1991; **4**: 391-407

6 **Zhou S**, Gao Y, Jiang W, Huang M, Xu A, Paxton JW. Interactions of herbs with cytochrome P450. *Drug Metab Rev* 2003; **35**: 35-98

7 **Honkakoski P**, Moore R, Washburn K, Negishi M. Activation by diverse xenochemicals of the 51-base pair phenobarbital-responsive enhancer module in the CYP2B10 gene. *Mol Pharmacol* 1998; **53**: 597-601

8 **Honkakoski P**, Zelko I, Sueyoshi T, Negishi M. The nuclear orphan receptor CAR-retinoid X receptor heterodimer activates the phenobarbital-responsive enhancer module of the CYP2B gene. *Mol Cell Biol* 1998; **18**: 5652-5658

9 **Sueyoshi T**, Kawamoto T, Zelko I, Honkakoski P, Negishi M. The repressed nuclear receptor CAR responds to phenobarbital in activating the human CYP2B6 gene. *J Biol Chem* 1999; **274**: 6043-6046

10 **Sugatani J**, Kojima H, Ueda A, Kakizaki S, Yoshinari K, Gong QH, Owens IS, Negishi M, Sueyoshi T. The phenobarbital response enhancer module in the human bilirubin UDP-

glucuronosyltransferase UGT1A1 gene and regulation by the nuclear receptor CAR. *Hepatology* 2001; **33**: 1232-1238

11 **Xie W**, Yeuh MF, Radominska-Pandya A, Saini SP, Negishi Y, Bottroff BS, Cabrera GY, Tukey RH, Evans RM. Control of steroid, heme, and carcinogen metabolism by nuclear pregnane X receptor and constitutive androstane receptor. *Proc Natl Acad Sci USA* 2003; **100**: 4150-4155

12 **Kast HR**, Goodwin B, Tarr PT, Jones SA, Anisfeld AM, Stoltz CM, Tontonoz P, Kliewer S, Willson TM, Edwards PA. Regulation of multidrug resistance-associated protein 2 (ABCC2) by the nuclear receptors pregnane X receptor, farnesoid X-activated receptor, and constitutive androstane receptor. *J Biol Chem* 2002; **277**: 2908-2915

13 **Cherrington NJ**, Hartley DP, Li N, Johnson DR, Klaassen CD. Organ distribution of multidrug resistance proteins 1, 2, and 3 (Mrp1, 2, and 3) mRNA and hepatic induction of Mrp3 by constitutive androstane receptor activators in rats. *J Pharmacol Exp Ther* 2002; **300**: 97-104

14 **Saini SP**, Sonoda J, Xu L, Toma D, Uppal H, Mu Y, Ren S, Moore DD, Evans RM, Xie W. A novel constitutive androstane receptor-mediated and CYP3A-independent pathway of bile acid detoxification. *Mol Pharmacol* 2004; **65**: 292-300

15 **Huang W**, Zhang J, Chua SS, Qatanani M, Han Y, Granata R, Moore DD. Induction of bilirubin clearance by the constitutive androstane receptor (CAR). *Proc Natl Acad Sci USA* 2003; **100**: 4156-4161

16 **Huang W**, Zhang J, Moore DD. A traditional herbal medicine enhances bilirubin clearance by activating the nuclear receptor CAR. *J Clin Invest* 2004; **113**: 137-143

17 **Ueda A**, Hamadeh HK, Webb HK, Yamamoto Y, Sueyoshi T, Afshari CA, Lehmann JM, Negishi M. Diverse roles of the nuclear orphan receptor CAR in regulating hepatic genes in response to phenobarbital. *Mol Pharmacol* 2002; **61**: 1-6

18 **Weber LW**, Boll M, Stampfl A. Hepatotoxicity and mechanism of action of haloalkanes: carbon tetrachloride as a toxicological model. *Crit Rev Toxicol* 2003; **33**: 105-136

19 **Jones IW**. Chloroform anaesthesia in Liverpool. *Anaesthesia* 1983; **38**: 578-580

20 **Clawson GA**. Mechanisms of carbon tetrachloride hepatotoxicity. *Pathol Immunopathol Res* 1989; **8**: 104-112

21 **Wei P**, Zhang J, Egan-Hafley M, Liang S, Moore DD. The nuclear receptor CAR mediates specific xenobiotic induction of drug metabolism. *Nature* 2000; **407**: 920-923

22 **Wang H**, LeCluyse EL. Role of orphan nuclear receptors in the regulation of drug-metabolising enzymes. *Clin Pharmacokinet* 2003; **42**: 1331-1357

23 **Moore LB**, Parks DJ, Jones SA, Bledsoe RK, Consler TG, Stimmel JB, Goodwin B, Liddle C, Blanchard SG, Willson TM, Collins JL, Kliewer SA. Orphan nuclear receptors constitutive androstane receptor and pregnane X receptor share xenobiotic and steroid ligands. *J Biol Chem* 2000; **275**: 15122-15127

24 **Yamamoto Y**, Moore R, Goldsworthy TL, Negishi M, Maronpot RR. The orphan nuclear receptor CAR is essential for liver tumor promotion by phenobarbital in mice. *Cancer Res* 2004; **64**: 7197-7200

25 **Wei P**, Zhang J, Dowhan DH, Han Y, Moore DD. Specific and overlapping functions of the nuclear hormone receptors CAR and PXR in xenobiotic response. *Pharmacogenomics J* 2002; **2**: 117-126

26 **Tzameli I**, Chua SS, Cheskis B, Moore DD. Complex effects of rexinoids on ligand dependent activation or inhibition of the xenobiotic receptor, CAR. *Nucl Recept* 2003; **1**: 2

27 **Zhang J**, Huang W, Chua SS, Wei P, Moore DD. Modulation of acetaminophen-induced hepatotoxicity by the xenobiotic receptor CAR. *Science* 2002; **298**: 422-424

28 **Morel F**, Fardel O, Meyer DJ, Langouet S, Gilmore KS, Meunier B, Tu CP, Kensler TW, Ketterer B, Guillouzo A. Preferential increase of glutathione S-transferase class alpha transcripts in cultured human hepatocytes by phenobarbital, 3-methylcholanthrene, and dithiolethiones. *Cancer Res* 1993; **53**: 231-234

29 **Hayes JD**, Pulford DJ. The glutathione S-transferase supergene family: regulation of GST and the contribution of the isoenzymes to cancer chemoprotection and drug resistance. *Crit Rev Biochem Mol Biol* 1995; **30**: 445-600

30 **Berk PD**, Martin JF, Blaschke TF, Scharschmidt BF, Plotz PH. Unconjugated hyperbilirubinemia. Physiologic evaluation and experimental approaches to therapy. *Ann Intern Med* 1975; **82**: 552-570

31 **Guo GL**, Lambert G, Negishi M, Ward JM, Brewer HB Jr, Kliewer SA, Gonzalez FJ, Sinal CJ. Complementary roles of farnesoid X receptor, pregnane X receptor, and constitutive androstane receptor in protection against bile acid toxicity. *J Biol Chem* 2003; **278**: 45062-45071

32 **Forman BM**, Tzameli I, Choi HS, Chen J, Simha D, Seol W, Evans RM, Moore DD. Androstane metabolites bind to and deactivate the nuclear receptor CAR-beta. *Nature* 1998; **395**: 612-615

Science Editor Guo SY **Language Editor** Elsevier HK

PO Box 2345, Beijing 100023, China
www.wjgnet.com
wjg@wjgnet.com

ELSEVIER

World J Gastroenterol 2005;11(38):5973-5977
World Journal of Gastroenterology ISSN 1007-9327
© 2005 The WJG Press and Elsevier Inc. All rights reserved.

• *BASIC RESEARCH* •

Damaging effects of gliadin on three-dimensional cell culture model

Ersilia Dolfini, Luca Elli, Leda Roncoroni, Barbara Costa, Maria Pia Colleoni, Vito Lorusso, Simona Ramponi, Paola Braidotti, Stefano Ferrero, Maria Letizia Falini, Maria Teresa Bardella

Ersilia Dolfini, Leda Roncoroni, Department of Biology and Genetics for Health Sciences, University of Milan, Milan, Italy
Luca Elli, Maria Teresa Bardella, Department of Gastroenterology, University of Milan, Ospedale Maggiore Policlinico, Mangiagalli e Regina Elena IRCCS, Milan, Italy
Barbara Costa, Department of Biotechnology and Bioscience, University of Milan-Bicocca, Milan, Italy
Maria Pia Colleoni, Department of Pharmacology, Chemotherapy and Toxicology, University of Milan, Milan, Italy
Vito Lorusso, Simona Ramponi, Bracco Imaging SpA, Milan Research Centre, Milan, Italy
Paola Braidotti, Stefano Ferrero, Department of Medicine, Surgery and Dentistry, S. Paolo Hospital and Ospedale Maggiore Policlinico, Mangiagalli e Regina Elena IRCCS, Milan, Italy
Maria Letizia Falini, Department of Agrifood Molecular Science, University of Milan, Milan, Italy
Supported by the San Paolo Foundation grant to "Centro per lo Studio della Celiachia"
Correspondence to: Maria Teresa Bardella, MD, Department of Gastroenterology, Ospedale Maggiore Policlinico, Mangiagalli e Regina Elena IRCCS, Via F. Sforza 35, Milan 20122, Italy. mariateresa.bardella@unimi.it
Telephone: +39-2-55033384 Fax: +39-2-50320403
Received: 2004-11-18 Accepted: 2005-01-26

Abstract

AIM: To evaluate the effects of gliadin on the oxidative environment in the "*in vivo*-like" model of a three-dimensional cell culture system.

METHODS: LoVo cell line (intestinal adenocarcinoma) multicellular spheroids were treated with digested gliadin (with albumin used as a control). Spheroid volumes, cell viability and morphology, lactate dehydrogenase (LDH) release, content of reduced glutathione (GSH) and activity of GSH-related enzymes were examined. The data were statistically analyzed using the Student's *t*-test ($P<0.05$). was considered statistically significant.

RESULTS: Gliadin reduced cell viability (from 20% to 60%) and led to morphological alterations characterized by apoptotic findings and cytoskeletal injuries. LDH activity increased. The content of GSH reduced (-20% *vs* controls), and activity of GSH-related enzymes was significantly inhibited.

CONCLUSION: Gliadin treatment induces an imbalance in the antioxidative mechanism of cells cultured by the three-dimensional technique. This alteration may explain the cell damage directly caused by gliadin and the subsequent morphological abnormalities.

© 2005 The WJG Press and Elsevier Inc. All rights reserved.

Key words: Gliadin; Celiac disease; Cytotoxicity; Multicellular spheroids

Dolfini E, Elli L, Roncoroni L, Costa B, Colleoni MP, Lorusso V, Ramponi S, Braidotti P, Ferrero S, Falini ML, Bardella MT. Damaging effects of gliadin on three-dimensional cell culture model. *World J Gastroenterol* 2005; 11(38): 5973-5977
http://www.wjgnet.com/1007-9327/11/5973.asp

INTRODUCTION

Since Hudson *et al*.[1], first observed the inhibited growth and morphological modifications in different human cell lines induced by gliadin exposure, a number of *in vitro* studies have confirmed the cytotoxicity of the peptide. Gliadin has agglutinating activity on K562 cells (human chronic myeloid leukemia), reduces F-actin content in intestine 407 cells, inhibits cell growth, induces apoptosis and alters redox equilibrium in Caco-2 cells (human intestinal adenocarcinoma), and causes a rearrangement of the cytoskeleton through the zonulin pathway and the loss of tight junction permeability in IEC-6 cells[2].

Three-dimensional cell cultures (multicellular tumor spheroids, MCTSs) were first introduced by Sutherland *et al*.[3], in the early 1970s, and are now considered as an interesting model in biomedical research[4]. Unlike conventional monolayer cell culture systems, MCTSs maintain the specific morphological and biochemical properties of the corresponding *in vivo* tissue, and remain in a differentiated and functionally active state for many weeks, thus making it possible to study the long-term effects of various xenobiotics[5]. We have recently used MCTSs from the LoVo cell line to test gliadin, and have shown that it has a direct cytotoxic effect on cell growth and morphology[6].

Redox equilibrium plays a pivotal role in cell homeostasis, and can affect biological functions[7,8]. Glutathione (GSH), which consists of L-glutamine, L-cysteine and glycine, is the most important low-molecular-weight peptide involved in redox equilibrium. It has a reductive action on the cell environment and neutralizes the reactive oxygen compounds and free radicals formed during metabolism. GSH depletion induces low thiol protein stores, a determinant of cell homeostasis, and triggers cytotoxicity[9,10]. GSH depletion has also been shown in a number of human diseases

(alcoholic liver disease, HIV infection, acute respiratory distress syndrome, and inflammatory bowel disease), and it has been shown that depressed intracellular GSH levels in liver and mammary tissues promote carcinogenesis[11].

The aim of this study was to evaluate the content of reduced GSH and the activity of GSH-related enzymes in LoVo MCTSs treated with gliadin.

[illegible]

Protein digestion

Gliadin was purified from *Triticum aestivum* flour (Hereward cultivar) according to Capelli *et al*.[12]. Bovine serum albumin (BSA) used as a control was purchased from Sigma (Milan, Italy). Pepsin was supplied by Sigma (Milan, Italy) and pancreatin by Merck (Milan, Italy). All the chemicals were of analytical grade. Digestion was performed as previously described[6]: briefly, gliadin was first incubated with pepsin at 37 ℃ for 24 h, and then with pancreatin at 37 ℃ for 3 h, adjusting to pH 8.0.

The digested proteins were analytically controlled by reverse-phase HPLC, size-exclusion HPLC and SDS-PAGE before being freeze-dried and stored.

Cell culture, treatment, volumetric analysis and viability test

LoVo human colon adenocarcinoma cell line (ATCC, Rockville, USA) was maintained in exponential monolayer growth and routinely checked for mycoplasma contamination as previously described[6].

MCTSs were initiated according to Dolfini *et al*.[6], by seeding 2×10^5 cells/mL in 25 mL of complete medium in polycarbonate Erlenmeyer flasks (Corning, Milan, Italy), and incubated in a gyratory rotation incubator. MCTS volumes were evaluated according to Chignola *et al*.[13].

On the 7th d, MCTSs (mean±SD: 220±70 μm) were exposed to digested gliadin (PT-gliadin, 500 μg/mL) or BSA (PT-BSA, 500 μg/mL) in completely renewed medium for further 5 d, and subsequently taken for the evaluation of lactate dehydrogenase (LDH) release, GSH content and GSH-related enzyme activity, and morphological analysis.

MCTS viability was tested (colony-forming assay) by plating a cell suspension obtained after trypsin disaggregation of MCTSs (on the 5th d of treatment at PT-gliadin concentrations of 125, 500, 750, and 1 000 μg/mL, and a PT-BSA concentration of 1 000 μg/mL) in triplicate in six-well plates (500 cells/well). The surviving cell fraction was calculated after 10 d and compared with the plating efficiency of the controls.

Lactate dehydrogenase activity

LDH released from damaged cells was measured in free aliquots of medium from the cell cultures, and cell-free complete medium was included as a negative control.

Briefly, 50 μL of the aliquots of cell supernatants was mixed with 25 μL of LDH reagent (Sigma, Milan, Italy) and incubated at room temperature for 30 min. LDH activity was calculated by measuring the increase in absorbance at 490 nm according to Legrand *et al*.[14], and related to the protein content of MTCSs[15]. LDH activity was reported as percentages of control values.

GSH content and GSH-related enzyme activity

MTCSs were washed with PBS (Sigma, Milan, Italy), and then sonicated and centrifuged. The cytosolic supernatant was used to measure GSH content and activity of the GSH-related enzymes, namely reductase (GSR), peroxidase (GPOX) and GSH-*S*-transferase (GST).

GSH content and enzyme activity were analyzed according to previously described methods[16], and expressed as percentages of control values.

Light and electron microscopy

LoVo cell line MCTS samples were prepared as previously described[6], fixed in 2.5% glutaraldehyde in a phosphate buffer, and then washed in the same buffer. In order to avoid injury or loss of spheroids, they were encapsulated in a solidifying agar solution and small spheroid-containing cubes were routinely processed for transmission electron microscopy (TEM)[17]. The semi-thin (0.5 μm) sections used for light microscopy analysis were stained with toluidine blue, the ultra-thin sections (50-70 nm) used for the ultrastructural study were counterstained with uranyl acetate and lead citrate. The MCTSs were studied for the presence of microvilli and intercellular junctions, and the appearance of nuclei, cytoplasm and intracytoplasmic organelles.

Scanning electron microscopy (SEM) was performed using a Philips mod. XL20 scanning electron microscope. MCTSs were washed twice with PBS, and then fixed in 2.5% glutaraldehyde in a phosphate buffer at 4 ℃ for a minimum of 24 h. At the time of analysis, a representative spheroid sample was recovered, immediately placed on a filter paper, and observed in low vacuum modality at a high voltage of 10 kV.

Statistical analysis

Each experiment was repeated four times. All the data were expressed as mean±SD and analyzed using the two-tailed Student's *t*-test. $P<0.05$ was considered statistically significant.

[illegible]

Volume, viability, and LDH activity in medium

The untreated and control MCTSs (treated with PT-BSA) did not show any statistical difference in terms of diameter ($27\pm7\times10^{-3}$ mm^3 *vs* $26\pm10\times10^{-3}$ mm^3), viability (98% of the colonies formed by untreated MCTSs), LDH release (102% of the activity of untreated MCTSs), or microscopic appearance (data not shown). The volumes of MCTSs treated with PT-gliadin were similar to those of the untreated or control MCTSs (Figure 1), but their viability was 20-50% less than that of the controls and inversely related to PT-gliadin concentrations (Figure 2A). LDH activity in the medium of treated MCTSs was significantly increased by about 30% (Figure 2B).

GSH content and GSH-related enzyme activity

As shown in Figure 3A, the GSH content of treated MCTSs was about 20% less than that observed in the controls ($P<0.05$). The activity of GSH-related enzymes (GSR, GST, and GPOX) was also significantly decreased (by respectively 56%, 34%, and 27%, Figure 3B).

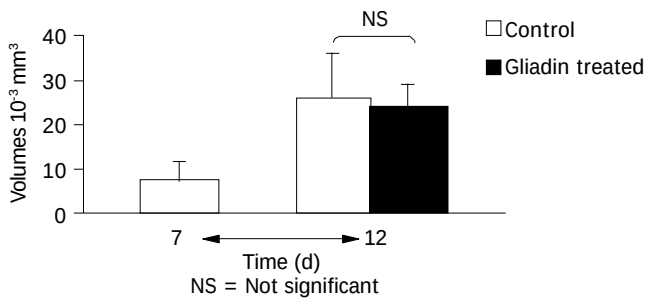


Figure 1 Volumes of MCTSs treated with PT-gliadin.

Morphological analysis

At light microscopy, both the treated and control MCTSs were spherical or oval in shape, but the control cells grew in a solid manner (with pseudoglandular differentiation, and without necrosis or apoptosis), whereas those in PT-gliadin-treated MCTSs showed nucleic displacement, a foamy cytoplasm and loss of cell adhesion: 20-50% had pycnotic nuclei and condensed chromatin (Figures 4A and B).

TEM showed that the control MCTSs had microvilli on their external surface and normal nuclei, cytoplasmatic organelles (rough endoplasmic reticulum, mitochondria,

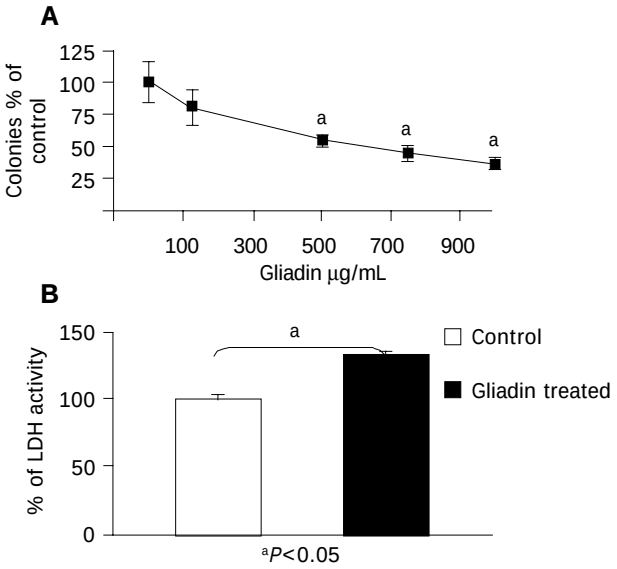


Figure 2 Viability test of MCTSs after treatment with different doses of digested gliadin (A) and lactate dehydrogenase (LDH) activity after gliadin treatment (B).

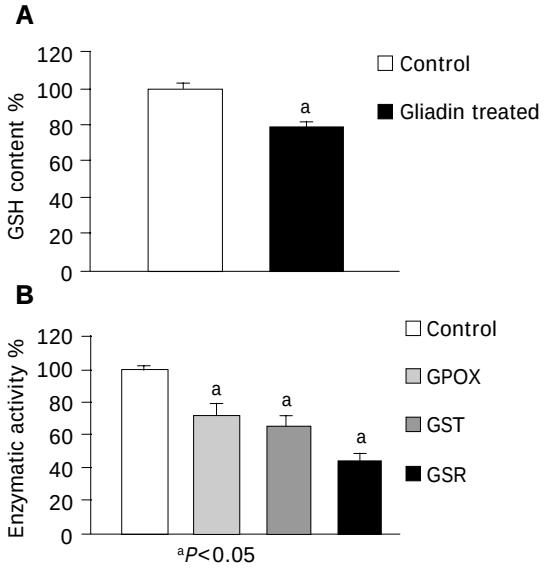


Figure 3 Content of reduced GSH (A) and GSH-related enzyme activity (B) in MCTSs treated with PT-gliadin.

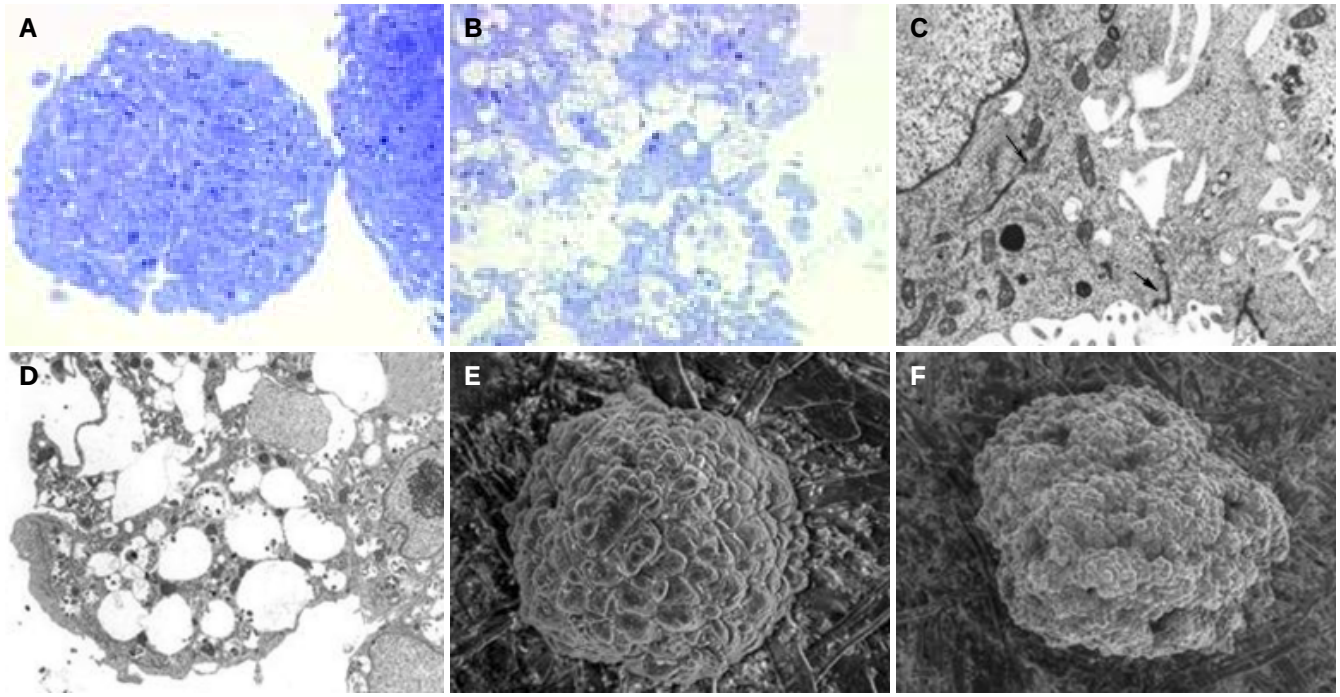


Figure 4 Microscopic analysis of MCTSs treated with digested gliadin or untreated. (A and B) Untreated and gliadin-treated MCTSs with cytoplasmatic vacuoles, (C and D) images of untreated and treated MCTSs, and (E) no holes and blebs on untreated controls, (F) holes and blebs on the surface of treated MCTSs.

Golgi complex, and lysosomes), and cytokeratin tonofilaments. The cells were joined by complexes of tight, intermediate and desmosome junctions. In the treated MCTSs, microvilli disappeared from the cell surface and there were cytoskeletal and tight junction injuries. The cytoplasm contained electron-dense material in numerous phagosomes and frequent vacuoles of various sizes. Some cells showed cytoplasmatic lipid-like droplets and cannibalism (Figures 4C and D).

SEM of the control MCTSs revealed an ovoid or spherical shape with compact cells, which were densely organized and tightly packed together, but clearly distinguishable from each other. The treated MCTSs were irregular in shape with loosely packed cells, and the external surface was focally interrupted by irregularly distributed holes and blebs (Figures 4E, F, and 5).

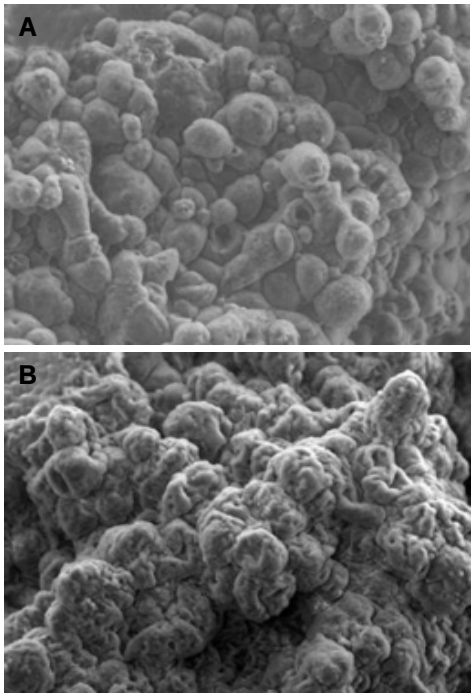


Figure 5 Smooth surface of untreated MCTS (A) and bleb on surface of MCTS treated with digested gliadin (B).

DISCUSSION

Our findings show that gliadin had significant functional and morphological cytotoxic effects on intestinal adenocarcinoma cell line (LoVo) cultured in a three-dimensional model.

Gliadin is a protein characterized by a particularly high proline and glutamine content (respectively 15% and 35% of the residues) that forms a kink in the polypeptide structure that prevents peptidase attack[18].

Over the last few years, a number of studies based on the *in vitro* two-dimensional cell culture system have investigated the cellular effects of gliadin in order to clarify its role in the pathogenetic "puzzle" of celiac disease (CD)[19]. Gliadin alters the cytoskeleton through the network of actin filaments, and damages tight junctions (TJ) by creating leaks in intercellular spaces, and these effects may be responsible for the loss of epithelial permeability and the changes in cell-cell signaling associated with CD[20]. Furthermore, gliadin also has a pro-apoptotic and agglutinating effect, inhibits cell growth and viability[2], and modifies the redox status of Caco-2 cells, thus causing a loss in reductive potential and an increase in the levels of reactive oxygen species[21].

Oxidative balance plays a pivotal role in cell homeostasis, and it has been suggested that its imbalance may be involved in various human diseases (liver diseases, HIV infection, pulmonary diseases, tumors, Parkinson's disease, myocardial ischemia, and inflammatory bowel disease)[9,11]. GSH and its enzymatic machinery represent one of the most important cellular defenses against oxidative agents and harmful xenobiotics. Three enzymes are mainly involved in the GSH cycle: GPOX, which converts peroxides into less dangerous fatty acids, water, and GSH disulfide (GSSG); GSR, which reduces GSSG to GSH in NADPH-dependent reaction; and GST, which is involved in detoxification from xenobiotic compounds[22]. GSH has also been implicated in other cell functions: apoptosis, cell differentiation, prostaglandin synthesis, DNA repair, amino acid transport, enhanced immune response, and enzymatic activation[23].

The reduced GSH content and GSH-related enzyme activity observed in our gliadin-treated MCTSs confirm the dangerous effect of this peptide in an experimental model that maintains some of the biochemical and morphological features of the corresponding *in vivo* tissue[5], and support the hypothesis that relates a deficiency in an oxidable substrate[24]. The disturbed redox equilibrium is associated with the reduced cell viability in treated MCTSs and the alteration in the integrity of plasma membrane, as demonstrated by the leakage of large molecules such as LDH into the medium[25].

These functional alterations affect the morphology of MCTSs and their cells, whose clearly foamy cytoplasm and peripherally displaced nuclei, together with the fact that many are pycnotic with marginally condensed chromatin, support the presence of apoptotic processes[26]. TEM confirmed cell injury by revealing the presence of numerous phagosomes and frequent vacuoles of different sizes in the cytoplasm, as well as intra-cytoplasmic lipid-like droplets. The external ring normally consisting of columnar cells with serrated intercellular TJs and surface microvilli resembling normal enterocyte epithelia was altered in our treated MCTSs, which showed disrupted TJs and microvilli (Figure 4). SEM also showed that the treatment causes a loss of organization in cells contained in the external layer of spheroid, with the formation of hole-like structures and an abundant presence of apoptotic blebs[27].

Although our data cannot explain whether the redox imbalance is due to a resource-consuming mechanism, decreased nuclear expression or protein synthesis (an effect previously associated with gliadin exposure[28]), they clearly demonstrate that gliadin has a direct damaging effect on human intestinal cells. Furthermore, we have confirmed that the three-dimensional cell culture system is a good experimental model for investigating the effects of different peptides, and can therefore be added to the techniques used to study CD.

ACKNOWLEDGMENTS

The authors would like to thank the "Centro per lo Studio

della Celiachia", University of Milan, for its logistic support and Kevin Smart (LINK Srl, Milan) for his help in preparing the manuscript.

References

1 **Hudson DA,** Purdham DR, Cornell HJ, Rolles CJ. Non specific cytotoxicity of wheat gliadin components towards cultured human cells. *Lancet* 1976; **1**: 339-341

2 **Elli L,** Dolfini E, Bardella MT. Gliadin cytotoxicity and *in vitro* cell cultures. *Toxicol Lett* 2003; **146**: 1-8

3 **Sutherland RM,** Inch WR, McCreide JA, Kruuv J. A multicomponent radiation survival curve using an *in vitro* tumor model. *Int J Radiat Biol Relat Stud Phys Chem Med* 1970; **18**: 491-495

4 **Kunz-Schughart LA,** Kreutz M, Knuechel R. Multicellular spheroids: a three-dimensional *in vitro* culture system to study tumor biology. *Int J Exp Pathol* 1998; **79**: 1-23

5 **Kunz-Schughart LA.** Multicellular tumor spheroids: intermediates between monolayer culture and *in vivo* tumor. *Cell Biol Int* 1999; **23**: 157-161

6 **Dolfini E,** Elli L, Ferrero S, Braidotti P, Roncoroni L, Dasdia T, Falini ML, Forlani F, Bardella MT. Bread wheat gliadin cytotoxicity: a new three-dimensional cell model. *Scand J Clin Lab Inv* 2003; **63**: 135-142

7 **Burdon RH.** Superoxide and hydrogen peroxide in relation to mammalian cell proliferation. *Free Rad Biol Med* 1995; **18**: 775-794

8 **Halliwell B.** Free radicals, antioxidants, and human disease: curiosity, cause or consequence? *Lancet* 1994; **344**: 721-724

9 **Burg D,** Mulder G. Glutathione conjugates and their synthetic derivatives as inhibitors of glutathione dependent enzymes involved in cancer and drug resistance. *Drug Met Rev* 2002; **34**: 821-863

10 **Ketterer B.** Protective role of glutathione and glutathione transferases in mutagenesis and carcinogenesis. *Mutation Res* 1988; **202**: 343-361

11 **Lomaestro BM,** Malone M. Glutathione in health and disease: pharmacotherapeutic issue. *Ann Pharmacol* 1995; **29**: 1263-1272

12 **Capelli L,** Forlani F, Perini F, Guerrieri N, Cerletti P, Righetti PG. Wheat cultivar discrimination by capillary electrophoresis of gliadins in isoelectric buffer. *Electrophoresis* 1998; **19**: 1-8

13 **Chignola R,** Schenetti A, Chiesa E, Forini R, Sartoris S, Brendolan A, Tridente G, Andrighetto G, Liberati D. Oscillating growth patterns of multicellular tumor spheroids. *Cell Prolif* 1999; **32**: 39-48

14 **Legrand C,** Bour JM, Jacob C, Capiaumont J, Martial A, Marc A, Wudtke M, Kretzmer G, Demangel C, Duval D. Lactate dehydrogenase (LDH) activity of the cultured eukaryotic cells as marker of the number of dead cells in the medium. *J Biotechnol* 1992; **25**: 231-243

15 **Lowry OH,** Rosebrough NJ, Farr AL, Randall RJ. Protein measurement with the folin phenol reagent. *J Biol Chem* 1951; **193**: 265-275

16 **Dolfini E,** Elli L, Dasdia T, Bufardeci B, Colleoni MP, Costa B, Floriani I, Falini ML, Guerrieri N, Forlani F, Bardella MT. *In vitro* cytotoxic effect of bread wheat gliadin on Lovo human adenocarcinoma cell line. *Toxicol In vitro* 2002; **16**: 331-337

17 **Ryter A,** Kellemberg E. Encapsulating methods for isolated cells. In: Glauter AM, ed. Fixation, dehydration and embedding of biological specimens, 3rd ed. *Oxford: North Holland Publishing Company* 1998: 95

18 **Dewar D,** Pereira SP, Ciclitira P. The pathogenesis of coeliac disease. *Int J Biochem Cell Biol* 2004; **36**: 17-24

19 **Elli L,** Dolfini E, Bardella MT. Direct gliadin cytotoxicity as a cofactor in the pathogenesis of celiac disease. *Int Arch All Immunol* 2004; **134**: 88

20 **Clemente MG,** De Virgiliis S, Kang JS, Macatagney R, Musu MP, Di Pierro MR, Drago S, Congia M, Fasano A. Early effects of gliadin on enterocyte intracellular signalling involved in intestinal barrier function. *Gut* 2003; **52**: 218-223

21 **Rivabene R,** Mancini E, De Vincenzi M. *In vitro* cytotoxic effect of wheat gliadin-derived peptides on Caco 2 intestinal cell line is associated with intracellular oxidative imbalance: implications for coeliac disease. *Biochim Biophys Acta* 1999; **1453**: 152-160

22 **Sies H.** Strategies of antioxidative defence. *Eur J Biochem* 1993; **215**: 213-219

23 **Peterson JD,** Herzenberg LA, Vasquez K, Waltenbaugh C. Glutathione levels in antigen-presenting cells modulate Th1 versus Th2 response patterns. *Proc Natl Acad Sci USA* 1998; **95**: 3071-3076

24 **Toborek M,** Hennig B. Fatty acid-mediated effects on the glutathione redox cycle in cultured endothelial cells. *Am J Clin Nutr* 1994; **59**: 60-65

25 **Gissel H,** Clausen T. Excitation-induced Ca^{2+} influx and skeletal muscle cell damage. *Acta Physiol Scand* 2001; **171**: 327-334

26 **Ashkenazi A,** Dixit VM. Death receptors: signaling and modulation. *Science* 1998; **281**: 1305-1308

27 **Hentze H,** Latta M, Kunstle G, Dhakshinamoorthy S, Yomg P, Porter AG, Wendel A. Topoisomerase inhibitor camptothecin sensitizes mouse hepatocytes *in vitro* and *in vivo* to TNF-mediated apoptosis. *Hepatology* 2004; **39**: 1311-1320

28 **Giovannini C,** Mancini E, De Vincenzi M. Inhibition of the cellular metabolism of Caco-2 cells by prolamin peptides from cereals toxic for coeliacs. *Toxicol In vitro* 1996; **10**: 533-538

Science Editor Wang XL and Guo SY **Language Editor** Elsevier HK

PO Box 2345, Beijing 100023, China
www.wjgnet.com
wjg@wjgnet.com

ELSEVIER

World J Gastroenterol 2005;11(38):5978-5983
World Journal of Gastroenterology ISSN 1007-9327
© 2005 The WJG Press and Elsevier Inc. All rights reserved.

• *BASIC RESEARCH* •

Insulin promotes sinusoidal endothelial cell proliferation mediated by upregulation of vascular endothelial growth factor in regenerating rat liver after partial hepatectomy

Jian-Guo Qiao, Long Wu, Dao-Xiong Lei, Lu Wang

Jian-Guo Qiao, Long Wu, Dao-Xiong Lei, Lu Wang, Department of General Surgery, Zhongnan Hospital Affiliated to Wuhan University, Wuhan 430071, Hubei Province, China
Co-first-authors: Jian-Guo Qiao and Long Wu
Correspondence to: Jian-Guo Qiao, Department of General Surgery, Zhongnan Hospital Affiliated to Wuhan University, Wuhan 430071, Hubei Province, China. jian_guoqiao@yahoo.com
Telephone: +86-27-67812959 Fax: +86-27-87307622
Received: 2004-12-28 Accepted: 2005-03-24

Abstract

AIM: To determine whether insulin could promote sinusoidal endothelial cell (SEC) proliferation mediated by upregulation of vascular endothelial growth factor (VEGF) in regenerating rat liver after partial hepatectomy (PHx).

METHODS: Adult male Sprague-Dawley rats undergoing 70% PHx were injected with insulin (300 MU/kg) or saline via the tail veins every 8 h after surgery for 7 d and killed at 0, 24, 48, 72, 96, 120, 144, and 168 h after surgery. Proliferation of both hepatocytes and SECs was monitored by evaluating the proliferating cell nuclear antigen (PCNA) labeling index (LI). The expression of VEGF protein was evaluated by immunohistochemistry. The mRNA expressions of VEGF and its receptors Flt-1 and Flk-1 were evaluated by semi-quantitative reverse transcription-PCR.

RESULTS: Insulin markedly increased the expression of VEGF mRNA between 24 and 120 h after hepatectomy compared to controls. Similarly, insulin significantly increased the expression of Flt-1 between 24 and 96 h. However, insulin had no significant effect on Flk-1. Furthermore, the immunohistochemical staining revealed that expression of VEGF protein increased in the insulin groups. Insulin significantly increased the PCNA LI of hepatocytes and SECs compared to controls.

CONCLUSION: Exogenous insulin may promote SEC proliferation with an enhanced expression of VEGF and its receptor Flt-1 in regenerating rat liver after PHx.

© 2005 The WJG Press and Elsevier Inc. All rights reserved.

Key words: Insulin; Sinusoidal endothelial cell; VEGF

Qiao JG, Wu L, Lei DX, Wang L. Insulin promotes sinusoidal endothelial cell proliferation mediated by upregulation of vascular endothelial growth factor in regenerating rat liver after partial hepatectomy. *World J Gastroenterol* 2005; 11 (38): 5978-5983
http://www.wjgnet.com/1007-9327/11/5978.asp

INTRODUCTION

Hepatic regeneration is a key step in the recovery process that occurs after various forms of liver injury, including partial hepatectomy (PHx)[1]. The exact mechanism of liver regeneration remains unclear. Several important cytokines and growth factors are involved in the regulation of hepatocyte proliferation[2-6]. Angiogenesis is a fundamental course required for wound healing and regeneration[5]. The liver microvasculature consists of large vessels such as portal and central venules and hepatic arterioles lined with continuous endothelial cells, and sinusoids lined with sinusoidal endothelial cells (SECs) expressing undiaphragmed fenestrations[6]. SECs are the second largest number of resident liver cells, and are vital in supplying nutrients and growth factors to proliferating hepatocytes by the formation of new blood vessels during liver regeneration[5]. Vascular endothelial growth factor (VEGF) is a potent angiogenic factor stimulating the proliferation and migration of endothelial cells, and is also known as a vascular permeability factor[7-9]. The effects of VEGF are mediated through at least two specific receptors, Flt-1 and Flk-1, expressed on the endothelial cell surface[7]. Recent studies have revealed that VEGF stimulates endothelial cell proliferation and plays an important role in the supply of blood to the newly replicating hepatocytes during regeneration[5,7]. Moreover, it is reported that exogenous VEGF can stimulate liver cell proliferation following PHx[5,7,10].

Insulin is a hepatocyte growth modulator, which is essential in liver regeneration, and is transported into the liver during the process of liver regeneration[11]. There is evidence that treatment with insulin contributes to the normal regeneration of liver by decreasing hepatocellular injury and by increasing hepatocyte proliferative capacity[11-13]. In addition, insulin therapy has also been shown epidemiologically as an independent risk factor for the progression of intraocular neovascularization in diabetic retinopathy[13,14]. Yamagishi *et al*.[13], have demonstrated that insulin stimulates the growth and tube formation of human microvascular endothelial cells through autocrine VEGF *in vitro*. Nevertheless the effect of insulin on blood vessels during regeneration after PHx in rats is still unknown.

Based on these studies, we believe that insulin promotes SECs and subsequently liver regeneration by accelerating the expression of VEGF. In the present study, we investigated the expression of VEGF and its receptors, Flt-1 and Flk-1, as well as the expression of proliferating cell nuclear antigen (PCNA) during rat liver regeneration after 70% PHx.

[illegible]

Animals

Adult male Sprague-Dawley rats aged 7-8 wk (180-200 g; from the Center of Animal Laboratory, Wuhan University) were used for all experiments. The rats were maintained in temperature-controlled rooms in a 12-h light/dark cycle with free access to food (standard laboratory chow) and water. Seventy percent PHx was performed by the standard two-thirds PHx under light anesthesia with ether. The animals were randomly divided into two groups: PHx group was injected with insulin (300 MU/kg) in saline via the tail vein of rats every 8 h after PHx for a week, while control group was given saline alone. Five rats in each group were used at each of the eight time points (0, 24, 48, 72, 96, 120, 144, and 168 h after surgery, with a total of 80 animals). All surgeries were performed between 08:30 and 11:30 a.m..

Immunohistochemical examination of VEGF

Anti-VEGF antibody (Santa Cruz Biotechnology Inc., Delaware, CA, USA) was used for the immunohistochemical staining of VEGF on formalin-fixed and paraffin-embedded liver tissue. Briefly, liver tissues excised at designated times after surgery were fixed in 40 g/L formaldehyde solution and embedded in paraffin wax. Sections were cut at 4 μm, mounted on poly-L-lysine-coated glass slides, air dried overnight at room temperature, dehydrated in graded alcohols, and cleared in xylene. The three-step immunoperoxidase method using a LSAB kit (Dako, Copenhagen, Denmark) was performed according to the manufacturer's instructions. Anti-VEGF antibody used was diluted at 1:100 and incubated overnight at 4 ℃.

PCNA labeling index

Immunohistochemical staining of the PCNA was performed using an indirect two-step labeling technique with peroxidase-conjugated IgG (Amersham NA 931, Amersham Life Science, NY, USA). The monoclonal anti-PCNA antibodies were purchased from Amersham Life Science (PC-10). The sections were deparaffinized in xylene and dehydrated by passage through graded alcohol. Endogenous peroxidase was blocked by incubation of the slides with 3% H_2O_2 in methanol for 30 min. After being washed in PBS, 10% normal goat serum (Amersham Life Science) in PBS was applied for 20 min at room temperature. Slides were incubated overnight with monoclonal anti-PCNA antibodies and subsequently exposed to prediluted peroxidase-conjugated IgG for 40 min at room temperature. The peroxidase reaction was developed by incubation in 0.005% H_2O_2 and 0.02% 3,3'-diaminobenzidine tetrachloride. The proliferative activity in the remnant liver was expressed as the labeling index (LI). The LI was the ratio of the number of PCNA positive nuclei of either hepatocytes or SECs to the total number of cells counted. In each liver, the hepatocytes and SECs in 200 consecutive high power fields were counted. In this study, the spindle-shaped sinusoid-lining cells in the open sinusoids were regarded as SECs.

RNA extraction, cDNA synthesis and PCR amplification of different angiogenic factors

About 20 mg liver tissues was immediately flash frozen in liquid nitrogen and stored at -70 ℃ after excision for RNA isolation. Total RNA was extracted with the RNeasy® Mini kit (Qiagen Cat. No. 74104) according to the manufacturer's protocol and eluted in 25 μL RNase-free water. Single-stranded cDNA was synthesized from 8 μL of RNA by the RevertAid™ first strand cDNA synthesis kit (MBI Cat. No. K1621) with random hexamer primers and 3 μL of the product was used for PCR.

The PCR primer pairs are listed in Table 1. Thirty cycles of DNA amplification using a Taq DNA polymerase (recombinant, MBI Cat. No. EP0404) was performed under the following conditions: denaturation at 94 ℃ for 1 min, annealing (β-actin, 52 ℃; VEGF, 60 ℃; Flt-1, 53 ℃; Flk-1, 52 ℃) for 1 min, extension at 72 ℃ for 1 min. Negative controls (cDNA-free solutions) were included in each reaction. β-actin, a house-keeping gene equally expressed in most eukaryotic cells, was used as an external standard and amplified in parallel with different angiogenic factors in all PCR samples.

Table 1 Oligonucleotides used as primers in RT-PCR procedure

Primer	Nucleotide sequence	PCR product lengths (bp)
Rat VEGF	Sense: 5′-ACTGGACCCTGGCTTTACTG-3′	256
Antisense:	5′-ACGCACTCCAGGGCTTCATC-3′ GenBank NM031836	
Rat Flt-1	Sense: 5′-AGGAGAGGACCTGAAACTGTCTT-3′ Antisense: 5′-ATTCCTGGGCTCTGCAGGCATAG-3′[10]	214
Rat Flk-1	Sense: 5′-GTGATTGCCATGTTCTTCTGGC-3′ Antisense: 5′-TCAGACATGAGAGCTCGATGCT-3′ GenBank U93306	337
Rat β-actin	Sense: 5′-TTCCACACACACCAGCTTCG-3′ Antisense: 5′-GGGGTGGTGTGGAGATTTAG-3′ GenBank NM031144	366

Semi-quantification of PCR products

After PCR amplification from 50 μL reaction volume, 10 μL was electrophoresed on 1.5% agarose gel in 1× TBE buffer. The amplified bands were detected by ethidium bromide staining. The intensity of ethidium bromide fluorescence was measured by the Photo Documentation and Imaging System (Bio-1D, VL, France). For quantification of the PCR products from all samples, the samples were evaluated by comparing the PCR product to β-actin.

Statistical analysis

The results were expressed as mean±SD. Statistical analysis was performed for the unpaired data using SPSS11.0 for Windows (SPSS Inc., Chicago, IL, USA). $P<0.05$ was considered statistically significant.

Hepatic VEGF, Flt-1 and Flk-1 mRNA expression

The changes in hepatic VEGF, Flt-1 and Flk-1 mRNA following surgery are shown in Figures 1 and 2. The expression of VEGF mRNA increased after 24 h of 70% PHx, with a peak from 48 to 72 h. Insulin significantly increased VEGF mRNA from 24 to 120 h after hepatectomy compared to controls ($P<0.01$; Figures 1C, D and 2A). Similarly, hepatic Flt-1 mRNA expression increased after hepatectomy. Insulin significantly increased Flt-1 mRNA from 24 to 96 h after hepatectomy compared to controls ($P<0.01$; Figures 1E, F and 2B). Insulin had no significant effect on Flk-1 when compared to controls (Figures 1G, H and 2C).

PCNA labeling index

The PCNA LI was lower than 5% in both hepatocytes and SECs before hepatectomy. However, liver cell proliferation was evident as early as 24 h postoperation. Insulin significantly promoted hepatocyte proliferation from 24 to 120 h compared to controls ($P<0.01$, Figure 3).

Immunohistochemical staining of VEGF protein in remnant liver

Before hepatectomy, there were very few VEGF-positive

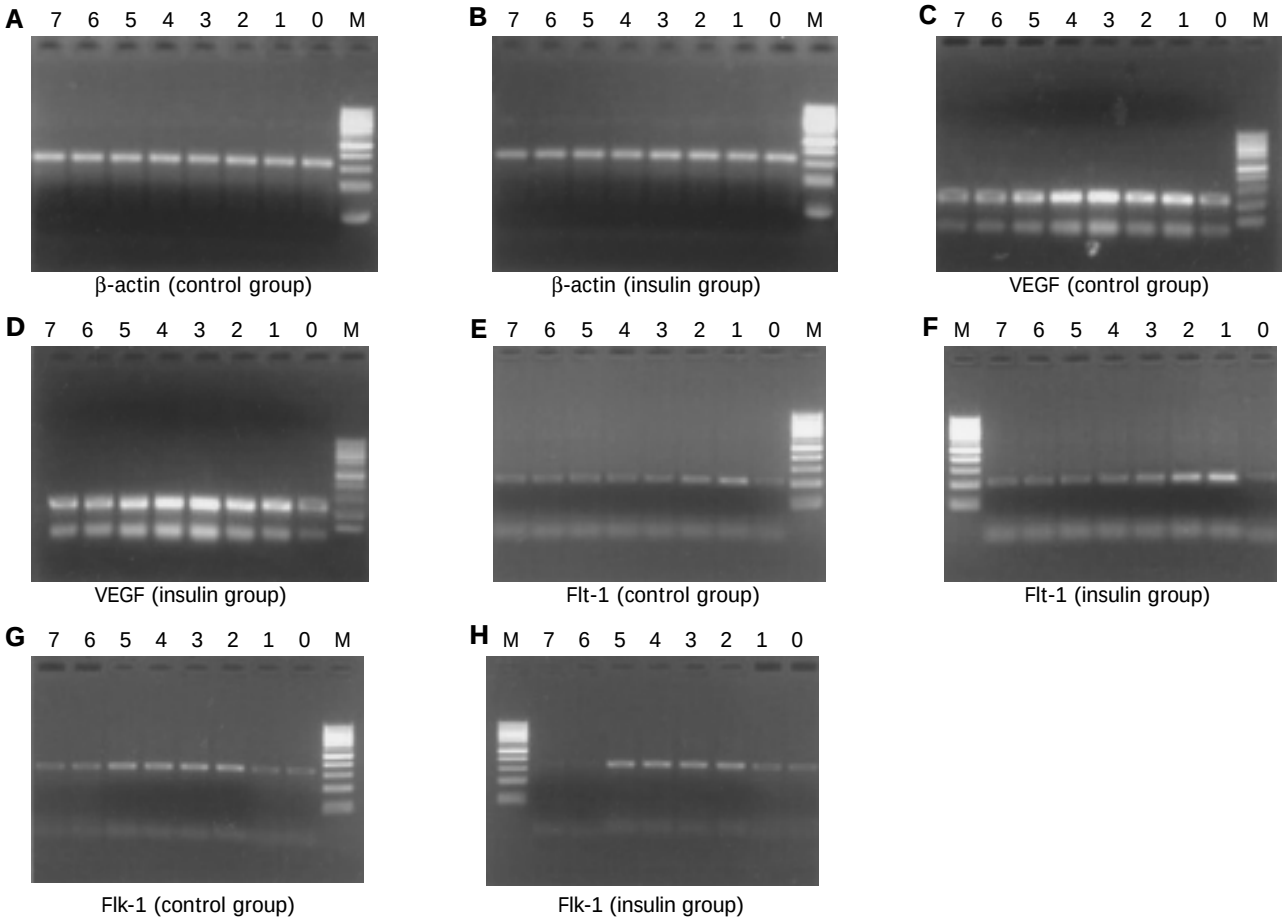


Figure 1 RT-PCR results of VEGF, Flt-1, and Flk-1 mRNA expressions in liver of different groups. M: 100-bp DNA ladder (upper to lower: 1 000, 900, 800, 700, 600, 500, 400, 300, 200, and 100 bp); lane 0: 0 h; lane 1: 24 h; lane 2: 48 h; lane 3: 72 h; lane 4: 96 h; lane 5: 120 h; lane 6: 144 h; lane 7: 168 h.

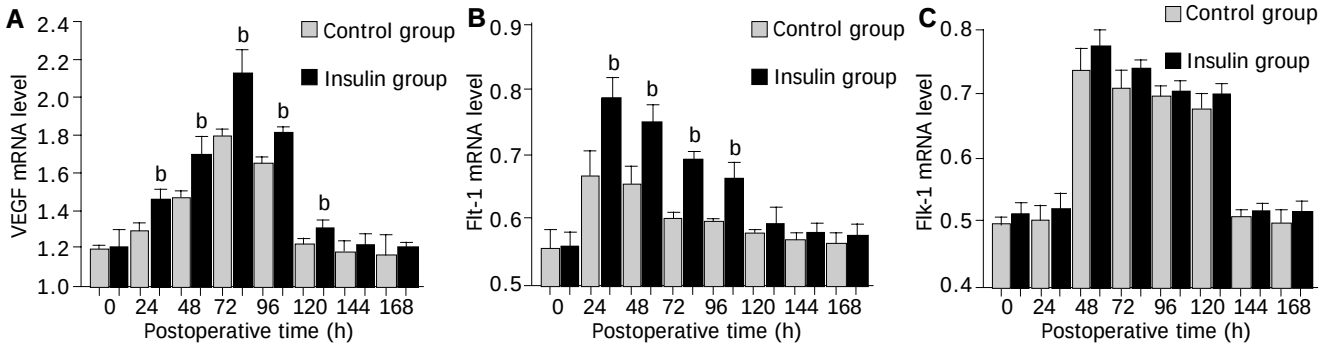


Figure 2 VEGF (A), Flt-1 (B), and Flk-1 (C) mRNA expressions after 70% hepatectomy in rats by RT-PCR.

cells, but increased expression of VEGF was observed 24 h after surgery (P<0.01, Figure 4A). Insulin increased the expression of VEGF, with a peak at 72 h (P<0.01, Figure 4D).

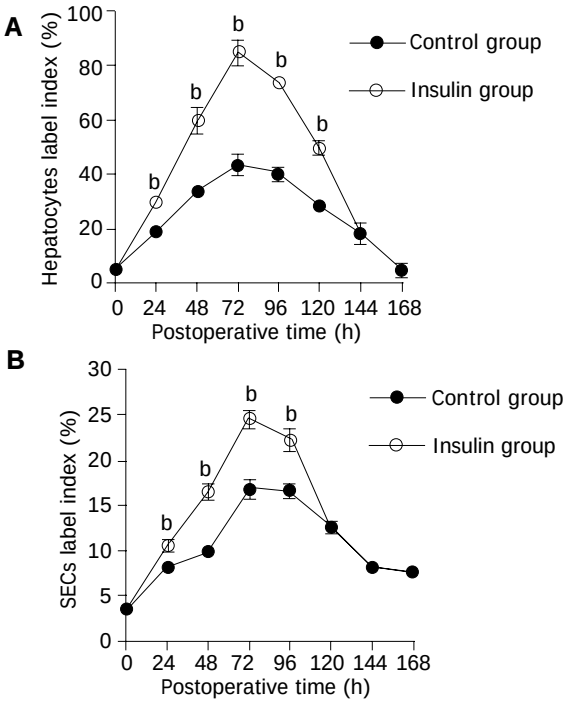


Figure 3 PCNA LI of hepatocytes (A) and SECs (B) after 70% hepatectomy in rats.

DISCUSSION

Liver remodeling following PHx comprises a complex set of events including activation and secretion of numerous factors, cell proliferation, thus finally re-establishing liver architecture[15-19]. Angiogenesis is the integrated process of endothelial cell division, vascular sprouting, and migration from pre-existing cells[20], indicating that SEC proliferation is strongly associated with hepatocyte proliferation during liver regeneration. Liver regeneration involves two processes: liver architecture remodeling and liver cell proliferation. In our study, SECs influenced the regenerative capacity of liver following PHx. Rebuilding the network of blood supply is necessary in liver regeneration. SECs play an important role in the formation of a complex network of blood vessels for remodeling liver architecture following liver resection. Additionally, SECs surround avascular clusters of hepatocytes, subsequently re-establish normal vascular architecture and directly supply nutrition and growth factors to liver cells[6].

The role of VEGF in liver regeneration has been reported[20-25]. SECs have a unique response to growth factors[6-8,18]. Information on the association of angiogenic factors with liver regeneration is available[5,6,18]. VEGF isoform signal has several receptors, including Flt-1 and Flk-1[26-30]. These receptors can operate in a paracrine and cooperative manner with VEGF produced by hepatocytes in regulating SEC growth and subsequent vascularization of the liver[13]. The receptors are structurally similar to members of the platelet-derived growth factor receptor family and consist of an extracellular domain composed of seven immunoglobulin-like motifs, a transmembrane domain, a juxtamembrane domain, a tyrosine kinase that is split by a kinase insert region, and a C-terminal tail. It is uncertain what role each VEGF receptor actually plays in cell signaling during liver revascularization. In some studies, Flk-1/KDR and Flt-1 have been shown to act in unique capacities[6]. These studies have determined that Flk-1/KDR can activate both mitogenicity and motility pathways, whereas

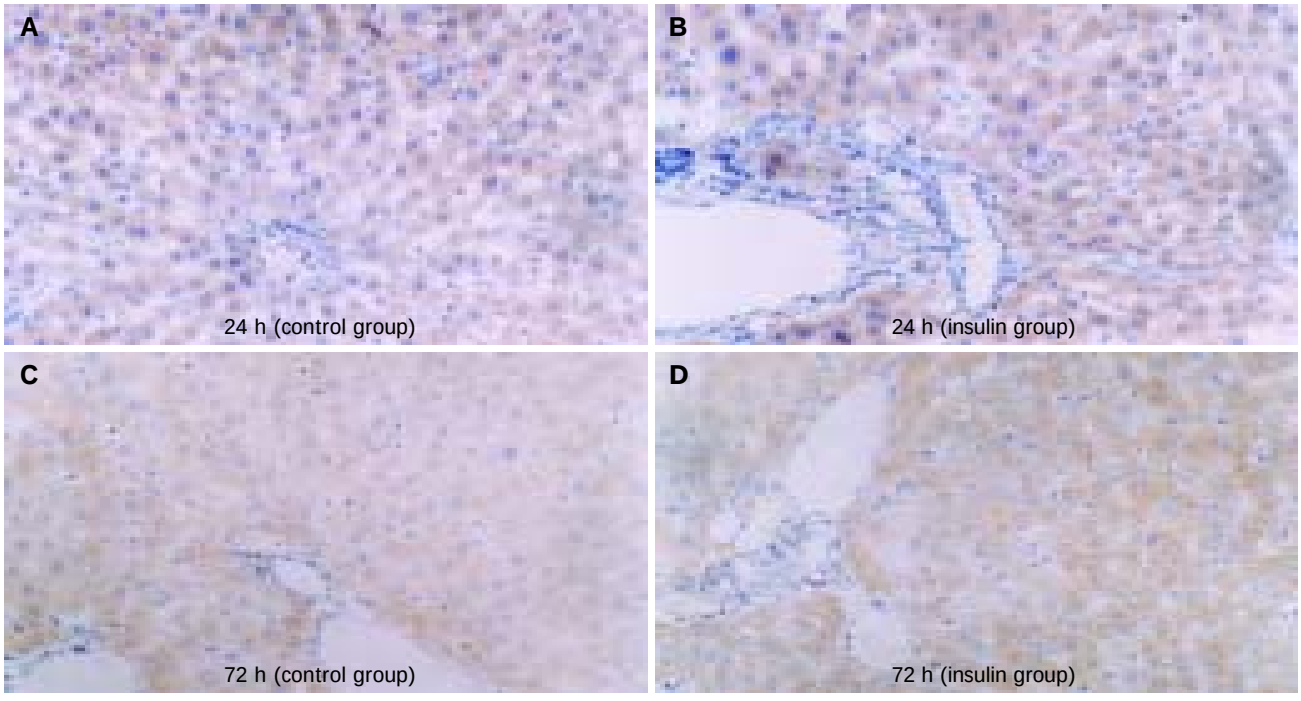


Figure 4 Expression of VEGF protein at 24 h in control group (A) and insulin group (B), at 72 h in control group (C), and insulin group (D).

Flt-1 appears to mediate actin reorganization[6]. Moreover, Flt-1 is induced by hypoxia, which emerges during regeneration, whereas Flk-1/KDR is not[6]. Exogenous $VEGF_{165}$ can stimulate liver cell proliferation following PHx and antibodies to VEGF significantly inhibit hepatocyte proliferation following PHx[5,29]. However, $VEGF_{165}$ does not induce either a motogenic or a mitogenic response in isolated hepatocytes, though Flt-1 is phosphorylated[6,29], indicating that VEGF may stimulate liver cell proliferation by acting on surrounding SECs, which influence hepatocytes by improving nutrient availability or through vascular permeability.

The present study demonstrated that exogenous insulin could stimulate SECs following PHx in rats. Insulin can induce a host of effects on glucose transport and utilization, protein synthesis, and cell proliferation, *etc*.[12].

However, the effect of insulin on blood vessels during regeneration after PHx in rats is still unknown. It has been reported that vascular abnormalities and pathologies are commonly associated with diabetes[31,32]. Jiang *et al*.[25], demonstrated that insulin can stimulate several signaling cascades in endothelial cells and vascular smooth muscle cells by phosphorylating both insulin receptor substrate-1 and -2. The vascular-specific action of insulin may be attributed to the growth factors, especially VEGF, and cytokines of which the expression is regulated by insulin. The exact mechanism underlying insulin-induced VEGF mRNA upregulation in microvascular EC is currently unknown. It was reported that insulin-induced VEGF expression is mediated through the activation of phosphatidylinositol (PI) 3-kinase/Akt being downstream to the insulin receptors[33,34]. It was reported that the activation of PI 3-kinase/Akt pathway can upregulate the expression of hypoxia-inducible factor-1α, a principal factor that causes angiogenesis[34]. Insulin may upregulate the VEGF mRNA through a nuclear factor-κB-mediated pathway, and mAb against VEGF can completely neutralize the proliferation and tube formation of endothelial cells induced by insulin[11,33].

In conclusion, insulin induces expression of VEGF and its receptor after PHx, and promotes liver regeneration besides the traditional metabolic action on hepatocytes.

ACKNOWLEDGMENTS

The authors thank Ms. Ou, Mr. Zhang, Mr. Gao, and Mr. Yu for their technical assistance.

REFERENCES

1 **Michalopoulos GK,** DeFrances MC. Liver regeneration. *Science* 1997; **276**: 60-66
2 **Kim I,** Kim HG, Kim H, Kim HH, Park SK, Uhm CS, Lee ZH, Koh GY. Hepapatic expression, synthesis and secretion of a novel fibrinogen/angiopoietin-related protein that prevents endothelial-cell apoptosis. *Biochem J* 2000; **346**(Pt 3): 603-610
3 **Mirpuri E,** Garcia-Trevijano ER, Castilla-Cortazar I, Berasain C, Quiroga J, Rodriguez-Ortigosa C, Mato JM, Prieto J, Avila MA. Altered liver gene expression in CCL_4-cirrhotic rats is partially normalized by insulin-like growth factor-I. *Int J Biochem Cell Biol* 2002; **34**: 242-252
4 **Rastegar M,** Lemaigre FP, Rousseau GG. Control of gene expression by growth hormone in liver: key role of a network transcription. *Mol Cell Endocrinol* 2000; **164**: 1-4
5 **Kraizer Y,** Mawasi N, Seagal J, Paizi M, Assy N, Spira G. Vascular endothelial growth factor and angiopoietin in liver regeneration. *Biochem Biophs Res Commun* 2001; **287**: 209-215
6 **Ross MA,** Sander CM, Kleeb TB, Watkins SC, Stolz DB. Spatiotemporal expression of angiogenesis growth factor receptors during the revascularization of regenerating rat liver. *Hepatology* 2001; **34**: 1135-1148
7 **Mustonen T,** Alitalo K. Endothelial receptor tyrosine kinases involved in angiogenesis. *J Cell Biol* 1995; **129**: 895-898
8 **Neufeld G,** Cohen T, Gengrinovitch S, Poltorak Z. Vascular endothelial growth factor (VEGF) and its receptors. *FASEB J* 1999; **13**: 9-22
9 **Stouffer RL,** Martinez-Chequer JC, Molskness TA, Xu F, Hazzard TM. Regulation and action of angiogensic factors in the primate ovary. *Arch Med Res* 2001; **32**: 567-575
10 **Sato T,** El-Assal ON, Ono T, Yamanoi A, Dhar DK, Nagasue N. Sinusoidal endothelial cell proliferation and expression of angiopoietin/Tie family in regenerating rat liver. *J Hepatol* 2001; **34**: 690-698
11 **Jiang ZY,** He Z, King BL, Kuroki T, Opland DM, Suzuma K, Suzuma I, Ueki K, Kulkarni RN, Kahn CR, King GL. Characterization of multiple signaling pathways of insulin in the regulation of vascular endothelial growth factor expression in vascular cells and angiogenesis. *J Biol Chem* 2003; **278**: 31964-31971
12 **Klein D,** Schubert T, Horch RE, Jauch KW, Jeschke MG. Insulin treatment improves hepatic morphology and function through modulation of hepatic signals after severe trauma. *Ann Surg* 2004; **240**: 340-349
13 **Yamagishi S,** Kawakami T, Fujimori H, Yonekura H, Tanaka N, Yamamoto Y, Urayama H, Watanabe Y, Yamamoto H. Insulin stimulates the growth and tube formation of human microvascular endothelial cells through autocrine vascular endothelial growth factor. *Microvasc Res* 1999; **57**: 329-339
14 **Sasso FC,** Carbonara O, Persico E, D'Ambrosio R, Coppola L, Nasti R, Campana B, Moschella S, Torella R, Cozzolino D. Increased vascular endothrlial growth factor mRNA expression in the heart of streptozotocin-induced diabetic rats. *Metabolism* 2003; **52**: 675-678
15 **Mitchell C,** Nivison M, Jackson LF, Fox R, Lee DC, Campbell JS, Fausto N. HB-EGF links hepatocyte priming with cell cycle progression during liver regeneration. *J Biol Chem* 2005; **280**: 2562-2568
16 **White P,** Brestelli JE, Kaestner KH, Greenbaum LE. Identification of transcriptional networks during liver regeneration. *J Biol Chem* 2005; **280**: 3715-3722
17 **Tracy TF Jr,** Fox ES. Molecular and cellular control points in pediatric liver injury and repair. *Semin Pediatr Surg* 1996; **5**: 175-181
18 **LeCouter J,** Moritz DR, Li B, Phillips GL, Liang XH, Gerber HP, Hillan KJ, Ferrara N. Angiogenesis-independent endothelial protection of liver: role of VEGFR-1. *Science* 2003; **299**: 890-893
19 **Leu JI,** Crissey MA, Craig LE, Taub R. Impaired hepatocyte DNA synthetic response posthepatectomy in insulin-like growth factor binding protein 1-deficient mice with defects in C/EBP beta and mitogen-activated protein kinase/extracellular signal-regulated kinase regulation. *Mol Cell Biol* 2003; **23**: 1251-1259
20 **Grosskreutz CL,** Anand-Apte B, Duplaa C, Quinn TP, Terman BI, Zetter B, D'Amore PA. Vascular endothelial growth factor-induced migration of vascular smooth muscle cells *in vitro*. *Microvasc Res* 1999; **58**: 128-136
21 **Unsoeld AS,** Junker B, Mazitschek R, Martin G, Hansen LL, Giannis A, Agostini HT. Local injection of receptor tyrosine kinase inhibitor MAE 87 reduces retinal neovascularization in mice. *Mol Vis* 2004; **10**: 468-475
22 **Manley PW,** Bold G, Bruggen J, Fendrich G, Furet P, Mestan J, Schnell C, Stolz B, Meyer T, Meyhack B, Stark W, Strauss A, Wood J. Advances in the structural biology, design and clinical development of VEGF-R kinase inhibitors for the treatment of angiogenesis. *Biochim Biophys Acta* 2004; **1697**: 17-27
23 **Sigrist S,** Mechine-Neuville A, Mandes K, Calenda V, Legeay

G, Bellocq JP, Pinget M, Kessler L. Induction of angiogenesis in omentum with vascular endothelial growth factor: influence on the viability of encapsulated rat pancreatic islets during transplantation. *J Vasc Res* 2003; **40**: 359-367

24 **Carmeliet P,** Storkebaum E. Vascular and neuronal effects of VEGF in the nervous system: implications for neurological disorders. *Semin Cell Dev Biol* 2002; **13**: 39-53

25 **Jiang ZY,** Lin YW, Clemont A, Feener EP, Hein KD, Igarashi M, Yamauchi T, White MF, King GL. Characterization of selective resistance to insulin signaling in the vasculature of obese zucker (fa/fa) rats. *J Clin Invest* 1999; **104**: 447-457

26 **Nakagawa M,** Kaneda T, Arakawa T, Morita S, Sato T, Yomada T, Hanada K, Kumegawa M, Hakeda Y. Vascular endothelial growth factor (VEGF) directly enhances osteoclastic bone resorption and survival of mature osteoclasts. *FEBS Lett* 2000; **473**: 161-164

27 **Tarnawski AS,** Chai J, Pai R, Chiou SK. Rebamipide activates genes encoding angiogenic growth factors and Cox2 and stimulates angiogensis: a key to its ulcer healing action? *Dig Dis Sci* 2004; **49**: 202-209

28 **Kraneburg O,** Gebbink MF, Voest EE. Stimulation of angiogensis by Ras proteins. *Biochim Biophys Acta* 2004; **1654**: 23-37

29 **Assy N,** Spira G, Paizi M, Shenkar L, Kraizer Y, Cohen T, Neufeld G, Dabbah B, Enat R, Baruc Y. Effect of vascular endothelial growth factor on hepatic regenerative activity following partial hepatectomy in rats. *J Hepatol* 1999; **30**: 911-915

30 **Shimizu H,** Miyazaki M, Wakabayashi Y, Mitsuhashi N, Kato A, Ito H, Nakagawa K, Yoshidome H, Kataoka M, Nakajima N. Vascular endothelial growth factor secreted by replicating hepatocytes induces sinusoidal endothelial cell proliferation during regeneration after partial hepatectomy in rats. *J Hepatol* 2001; **34**: 683-689

31 **Carrillo MC,** Favre C, Monti JA, Alvarez ML, Carnovale CE. Insulin hyperresponsiveness in partially hepatectomized diabetic rats. *Life Sci* 2001; **68**: 1417-1426

32 **Chiarelli F,** Santilli F, Mohn A. Role of growth factors in the development of diabetic complications. *Horm Res* 2000; **53**: 53-67

33 **Stiehl DP,** Jelkmann W, Wenger RH, Hellwig-Burgel T. Normoxic induction of the hypoxia-inducible factor 1alpha by insulin and interleukin-1beta involves the phosphatidylinositol 3-kinase pathway. *FEBS Lett* 2002; **512**: 157-162

34 **Poulaki V,** Qin W, Joussen AM, Hurlbut P, Wiegand SJ, Rudge J, Yancopoulos GD, Adamis AP. Acute intensive insulin therapy exacerbates diabetic blood-retinal barrier breakdown via hypoxia-inducible factor-1alpha and VEGF. *J Clin Invest* 2002; **109**: 805-815

Science Editor Wang XL and Guo SY **Language Editor** Elsevier HK

PO Box 2345, Beijing 100023, China
www.wjgnet.com
wjg@wjgnet.com

ELSEVIER

World J Gastroenterol 2005;11(38):5984-5987
World Journal of Gastroenterology ISSN 1007-9327
© 2005 The WJG Press and Elsevier Inc. All rights reserved.

• *CLINICAL RESEARCH* •

Sealing of the hepatic resection area using fibrin glue reduces significant amount of postoperative drain fluid

Frank Eder, Frank Meyer, Gerd Nestler, Zuhir Halloul, Hans Lippert

Frank Eder, Frank Meyer, Gerd Nestler, Zuhir Halloul, Hans Lippert, Department of Surgery, University Hospital, Magdeburg D-39120, Germany
Correspondence to: Frank Eder, MD, Department of Surgery, University Hospital, Leipziger Strasse 44, Magdeburg D-39120, Germany. frank.eder@medizin.uni-magdeburg.de
Telephone: +49-391-6715500 Fax: +49-391-6715570
Received: 2005-03-22 Accepted: 2005-04-18

ABSTRACT

AIM: To investigate whether the routine use of fibrin glue applied onto the hepatic resection area can diminish postoperative volume of bloody or biliary fluids drained via intraoperatively placed perihepatic tubes and can thus lower the complication rate.

METHODS: Two groups of consecutive patients with a comparable spectrum of recent hepatic resections were compared: (1) 13 patients who underwent application of fibrin glue immediately after resection of liver parenchyma; (2) 12 patients who did not. Volumes of postoperative drainage fluid were determined in 4-h intervals through 24 h indicating the intervention caused bloody and biliary segregation.

RESULTS: Through the first 8 h postoperatively, there was a tendency of higher amounts of fluids in patients with no additional application of fibrin glue while through the following intervals, a significant increase of drainage volumes was documented in comparison with the first two 4-h intervals, e.g., after 12 h, 149.6 mL +/-110 mL *vs* 63.2 mL +/-78 mL. Using fibrin glue, postoperative fluid amounts were significantly lower through the postoperative observation period of 24 h (851 mL +/-715 mL *vs* 315 mL +/-305 mL).

CONCLUSION: For hepatic resections, the use of fibrin glue appears to be advantageous in terms of a significant decrease of surgically associated segregation of blood or bile out of the resection area. This might result in a better outcome.

© 2005 The WJG Press and Elsevier Inc. All rights reserved.

Key words: Fibrin glue; Hepatic resection

Eder F, Meyer F, Nestler G, Halloul Z, Lippert H. Sealing of the hepatic resection area using fibrin glue reduces significant amount of postoperative drain fluid. *World J Gastroenterol* 2005; 11(38): 5984-5987
http://www.wjgnet.com/1007-9327/11/5984.asp

INTRODUCTION

Hepatic resections are considered as a standard intervention in abdominal surgery. Despite this, there is still a remarkable complication rate. In addition to patient-dependent factors, aspects of the surgical technique play a major role, in particular, with regard to the occurrence of postoperative bleeding and bile leakages. A precise dissection is as important as supplements such as hemostatics and tissue glue for the daily surgical practice to avoid complications, e.g., bleeding and biliary segregation from the resection area of the liver.

The aim of the study was to investigate, whether the sealing of the hepatic resection area using biocompatible glue leads to a significant decrease of postoperative release of blood and/or biliary fluid volume, which was measured in the local drainage(s).

MATERIALS AND METHODS

In a pilot study, a comparative non-randomized study of two case series, all consecutive patients with hepatic resections were enrolled with prospective data documentation over a defined observational period until the planned number of individuals was reached (n = 12 per group). Patients were retrospectively (to avoid a study bias) subdivided into two groups with or without sealing of the hepatic resection area using fibrin glue. Patient characteristics are listed in Table 1A.

Hepatic resections were carried out according to standardized technique following anatomically adequate resection margins (segmental resection, bi-/tri-segmental resection or hemihepatectomy) or as atypical hepatic resection with a tumor-free resection margin of minimally 5 mm ("wedge" resection).

Perioperative prophylaxis with antibiotics was performed (2 g of Cefotiam iv., Spizef®, Grünthal GmbH, Aachen, Germany). After explorative laparotomy, definitely exclusion of extrahepatic tumor manifestation and exploration of the hepatic tumor lesion needs to be approached (if necessary including intraoperative ultrasound of liver parenchyma). The liver was mobilized in a typical manner at the "Ligg. triangularia" and "falciforme", a tourniquet loop was placed around the hepatoduodenal ligament. After marking the resection margins, dissection of liver parenchyma was carried out using cavitron ultrasonic surgical aspirator (CUSA) technology. The intraparenchymatic vessels and ducts of the biliary tree were clipped and cut. Bleeding control at the hepatic resection area was achieved by bi- and/or mono-polar electrocoagulation. During the dissection,

Pringle's maneuver (temporary cessation of the blood flow in hepatic artery and portal vein) of maximally 20-min periods was executed to minimize the intraoperative blood loss. Bigger vessels and biliary ducts were ligated. After completion of the hepatic resection, the resection area was repeatedly coagulated (bi- or mono-polar electrocoagulation or infrared coagulation). Depending on the size of the resection area, one (or two) drain (s) was (were) placed into the subhepatic (and subphrenic) space.

According to the aim of the study, the hepatic resection area of the patients was sealed with fibrin glue (Tissucol or Tachocomb seal) or not.

For thrombosis prophylaxis heparin (low dose, low molecular heparin-derivative) was not given for 24 h postoperatively whereas antithrombosis socks were obligatory.

Patients were monitored at the surgical ICU for 24 h postoperatively.

Table 1 Comparison of patient groups with hepatic resection

(A) Patient characteristics.

		Fibrin glue	
		Without	With
Sex ratio			
Patients (*n*)	Male	8	7
	Female	4	6
Mean age (range) (yr)			
	Male	65 (37–77)	68 (41–75)
	Female	55 (44–70)	62 (46–75)

(B) Diagnosis

Diagnosis	Number of patients (sealing with fibrin glue)	
	Without	With
Hepatocellular carcinoma	5	2
Cholangiocellular carcinoma		
Liver metastases	5	9
Adenoma/FNH	2	2

(C) Types of resections

Type of resections	No. of patients (sealing with fibrin glue)	
	Without	With
Hemihepatectomy	4	1
Segmental resection (more than one segment)	4 (3 bisegmental resections)	10 (2 trisegmental and 5 bisegmental resections)
Atypical resection	4	2

(D) Values of significance

Postoperative time interval (h)	Value of significance (one side)
4	0.0094
8	0.0129
12	0.0059
16	0.0054
20	0.0026
24	0.0028

[a]*P*<0.05 *vs* no sealing, [b]*P*<0.01 *vs* no sealing, [c]*P*<0.005 *vs* no sealing, [d]*P*<0.001 *vs* no sealing.

Sealing with fibrin glue

Tissucol® (Baxter Deutschland GmbH, Heidelberg, Germany) was applied by spraying it on the hepatic resection area. Tachocomb seal (Tachocomb®, fibrin glue on a collagen fleece, Nycomed, Ismaning, Germany) was applied on the hepatic resection area after moistening it.

In the group of the patients with fibrin glue sealing, 13 patients (6 females and 7 males; mean age 62 years) with hepatic resections enrolled (Table 1A), were compared with a group of 12 subjects (4 females and 8 males; mean age, 60 years) with no fibrin glue application who were enrolled in the same study period.

The diagnoses and types of resections of both groups are listed in Tables 1B and C.

The fluid volumes drained via the intra-abdominally placed drains were documented in 4-h periods in a separate (Table 1D) and additive manner (Figure 1), in total through a time period of 24 h.

Informed consent for hepatic resection was obtained from each patient.

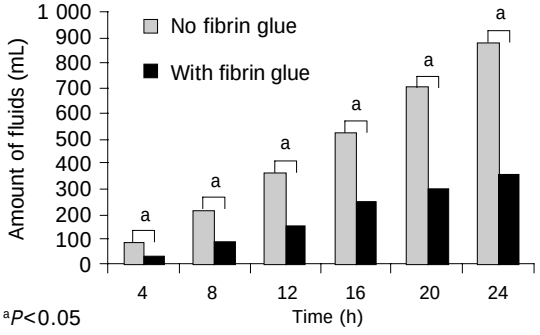


Figure 1 Time course of the mean of the added drain volumes depending on the application of fibrin glue. There was a significant reduction of the segregated amount of fluids in the group of patients in whom sealing with fibrin glue was used. [a]*P*<0.05 *vs* no sealing.

Statistical analysis

In addition to the descriptively statistical presentation of the results (SPSS 10.0 for Windows), fluid volumes of the drains in both patient groups with and without sealing with fibrin glue after hepatic resection were compared by a non-parametric test according to Mann-Whitney (*U* test) as appropriate. A value of $P<0.05$ was considered statistically significant.

RESULTS

The mean age and sex ratio of both patient groups appeared to be comparable. The spectrum and surgical extension of hepatic resections in both groups were similar.

The listed diagnoses demonstrate the patient profile, which is treated in our center of hepatobiliary surgery and varies from primary liver tumors, cholangio- and hepatocellular carcinomas ($n = 2$ and $n = 5$ in the group with and without fibrin glue, respectively), FNH ($n = 2$; no fibrin glue) or hepatocellular adenoma ($n = 2$; no fibrin glue), to metastases of colorectal ($n = 8$ in the group with

fibrin glue *vs* $n = 5$ without) or gastric carcinomas ($n = 1$; with fibrin glue, Table 1B). All patients showed an acceptable preoperative liver function, and no patient showed a postoperative decompensation of liver function.

In the spectrum of resections, there were one right hemihepatectomy, 10 segmental resections (trisegmental resections, $n = 2$; bisegmental resections, $n = 5$; one segment, $n = 3$) and two atypical resections in the patient group with no fibrin glue application *vs* four hemihepatectomies, four segmental resections (bisegmental resections, $n = 3$; one segment, $n = 1$) and four atypical resections in the comparison group with fibrin glue (Table 1C, Figure 2).

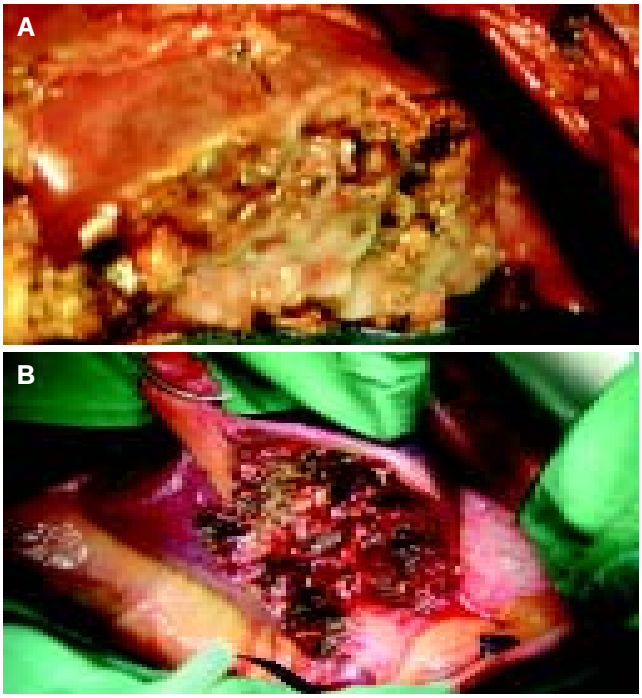


Figure 2 Hepatic resection area after segmental resection. A: With fibrin glue (sealing with Tissucol®). B: Without fibrin glue.

For sealing the hepatic resection area with fibrin glue, Tissucol® was used in 11 patients whereas in two further cases, Tachocomb® was chosen (data not shown).

In none of the patients included in the study, a severe postoperative complication occurred neither as acute nor intermediate problem. The drain fluid was either of serous or bloody-serous nature or serous quality with slight bile impurity. The comparison of the single drain volumes of both groups including the *P* values is shown in Table 1D.

Through the first 8 h postoperatively, there was a tendency of a higher drain fluid volume in the patient group with no fibrin glue, which was indicated by the single (of each 4-h time period) as well as the added amounts of fluids (total volume at specific time points during the postoperative course). Through the following time periods, the segregation increased significantly in this group compared with the first two time periods of 4 h each, resulting in the fact that a significant reduction of the segregated volumes via the drains in the patient group with fibrin glue was observed after 12 h ($P = 0.0059$). This difference became even more distinct through the following time periods up to 24 h ($P = 0.0028$). Figure 1 shows the comparison of the added postoperative amount of fluids drained postoperatively from the hepatic resection area. While the summation of the single drain volumes of the patients with fibrin glue through the 24-h time period shows a linear curve, the curve in the comparison group (no fibrin glue) shows an exponential increase.

Using fibrin glue, a significant reduction of the postoperative drain volume of segregated fluids out of the hepatic resection area was found during the study period of 24 postinterventional hours.

[redacted]

By means of a pilot study, two patient groups with similar demographic and treatment characteristics were compared to investigate whether the application of fibrin glue on the hepatic resection area has a significant impact on the postoperative segregation of fluids via the drains. Using a precise surgical technique with accurate dissection of liver parenchyma, in particular, according to the anatomic margins of the liver segments, with CUSA and a subtle control of bleeding, the complication rate in hepatic resections can be kept low.

The hypothesis was that, by the mean of an additive sealing the hepatic resection area with fibrin glue, the rate of local complications such as postoperative bleeding and biliary fistulas can be reduced. As a first step to prove this hypothesis, the amounts of segregated fluid via the drain(s) was compared between the groups of patients with or without application of fibrin glue on the hepatic resection area despite complete control of bleeding and biliary excretion occurred immediately after accomplishing the resection. It showed a significant difference with lower volumes of segregated fluids after 24 h, indicating a further possible reduction of the surgical risk and complication rate, which can be achieved by the use of fibrin glue. However, the main result of this pilot study needs to be confirmed in a currently ongoing study, in which more patients are being included.

The possible impact of a heparin medication was excluded by the department-specific standard since the continuation of the preoperatively initiated heparin administration for antithrombotic prophylaxis was postponed by 24 h postoperatively according to the duration of the study period[1]. In addition, acetylsalicylic acid-based medication was stopped a couple of days prior to the admission. The pathophysiological background to use postinterventional sealing with fibrin glue is as follows: hepatic resection can lead to an activation of fibrinolysis. Even in the case of a perfect hepatic resection from a technical point of view, postoperative bleeding and segregations of fluids can occur though the resection that was accomplished by leaving a dry hepatic resection area[2]. By the mean of fibrin application, the hepatic resection area can be sealed and, thus, smallest microlesions can be closed. In addition, the fibrin excess can avoid early fibrinolysis.

One limitation of the study might be the possibly varying size of the hepatic resection area but which is, because of the similar spectrum of different types of hepatic resections, almost comparable. In addition, the underlying liver disease

might affect the drain volume, which cannot be satisfyingly clarified in this study, which included only a limited number of patients. Furthermore, following studies need to focus on the composition of the segregated fluid with regard to the content of hemoglobin and bilirubin and the discrimination between the various types of sealing (Tissucol *vs* Tachocomb), which has not been the main focus and can be considered as an acceptable approximation in this pilot study.

From a technical point of view, the fast availability of the fibrin-coated collagen fleece seems to be advantageous as compared with the fibrin glue, which needs to be thawed[3].

There is a varying opinion on the additive use of fibrin glue in several surgical departments. In a Japanese study, 231 hospitals were asked about their routine use in hepatic resections. While in 203 hospitals, CUSA was used for resection (87%), only 135 (60%) applied fibrin glue on the hepatic resection area after the resection[4]. Comparison studies on the use of fibrin glue in hepatic resections were undertaken using animal experiments. The difficulty in the judgment of the fibrin effect was the usage of various additional agents, the different experimental designs, and varying animal strains and species. Davidson showed the advantage of a sealing with fibrin glue and cellulose gauze application after hepatic resections with regard to a tendency of a lower rate of postoperative bleeding using a pig model[5].

Turner has described the advantage of a composition consisting of thrombin and autologous plasma for control of bleeding after hepatic resections in sheep[6]. In addition, Martis has reported the benefit of Tachocomb in hepatic resections of dogs[7].

In conclusion, the presented pilot study in a clinical setting supports the thesis that an additional application of fibrin glue can contribute to the safe postoperative outcome as shown by the impressive statistically significant reduction of the postoperative volumes of segregated fluids via the perihepatic drain (s). Following studies using a prospective randomized study design, in a greater number of patients, and on various aspects such as the postoperative complication rate in patients with and without fibrin glue on the hepatic resection area may result in further facts and arguments for the impact and the beneficial effect of this additional tool.

ACKNOWLEDGEMENTS

We are grateful to Dr. Kropf, Institute for Biometry and Medical Informatics, University Hospital, Magdeburg, for appropriate statistical advice. For critical prereview of the manuscript, we thank M Reymond.

REFERENCES

1 **Lippert H,** Scheele J. Lebertumoren. In: Lippert H (ed.) Praxis der Chirurgie, Allgemein- und Viszeralchirurgie. 1st ed. *Stuttgart, New York: Thieme* 1998: 549-562
2 **Köckerling F,** Schneider C, Scheidbach H, Hohenberger W. Stellenwert der Fibrinklebung in der Leberchirurgie. In: Köckerling F (ed.) Leberchirurgie. 1st ed. Heidelberg, Leipzig: *Johann Ambrosius Barth* 1999: 103-108
3 **Ringe B.** Gewebeklebung in der hepatobiliären und Transplantationschirurgie. In: Ringe B (ed.) Gewebeklebung in der Chirurgie: Grundlagen und Anwendung. 1st ed. *Stuttgart, New York: Thieme* 2001: 63-75
4 **Nakajima Y,** Shimamura T, Kamiyama T, Matsushita M, Sato N, Todo S. Control of intraoperative bleeding during liver resection: analysis of a questionnaire sent to 231 Japanese hospitals. *Surg Today* 2002; **32**: 48-52
5 **Davidson BR,** Burnett S, Javed MS, Seifalian A, Moore D, Doctor N. Experimental study of a novel fibrin sealant for achieving haemostasis following partial hepatectomy. *Br J Surg* 2000; **87**: 790-795
6 **Turner AS,** Parker D, Egbert B, Maroney M, Armstrong R, Powers N. Evaluation of a novel hemostatic device in an ovine parenchymal organ bleeding model of normal and impaired hemostasis. *J Biomed Mater Res* 2002; **63**: 37-47
7 **Martis G,** Miko I, Szendroi T, Kathy S, Kovacs J, Hajdu Z. Results with collagen fleece coated with fibrin glue (TachoComb). A macroscopical and histological experimental study. *Acta Chir Hung* 1997; **36**: 221-222

Science Editor Guo SY **Language Editor** Elsevier HK

PO Box 2345, Beijing 100023, China
www.wjgnet.com
wjg@wjgnet.com

ELSEVIER

World J Gastroenterol 2005;11(38):5988-5992
World Journal of Gastroenterology ISSN 1007-9327
© 2005 The WJG Press and Elsevier Inc. All rights reserved.

• *CLINICAL RESEARCH* •

Low circulating levels of gastrin-17 in patients with Barrett's esophagus

Pentti Sipponen, Matti Vauhkonen, Timo Helske, Ilpo Kääriäinen, Matti Härkönen

Pentti Sipponen, Division of Pathology, Department of Pathology, HUSLAB, Helsinki University Central Hospital (HUCH), Jorvi Hospital, Espoo 02740, Finland
Matti Vauhkonen, Timo Helske, Ilpo Kääriäinen, Department Internal Medicine, Helsinki University Central Hospital (HUCH), Jorvi Hospital, Espoo 02740, Finland
Matti Härkönen, Department of Clinical Chemistry, Helsinki University Central Hospital (HUCH), Meilahti Hospital, Helsinki 00290, Finland
Correspondence to: Dr. Pentti Sipponen, Department of Pathology, HUSLAB, Jorvi Hospital, Espoo 02740, Finland. pentti.sipponen@hus.fi
Telephone: +358-9-8612671 Fax: +358-9-8615912
Received: 2004-11-30 Accepted: 2005-01-26

Abstract

AIM: To examine whether the fasting levels of serum gastrin-17 (G-17) are lower in Barrett's esophagus (BE) patients than in non-Barrett controls.

METHODS: Nineteen patients with BE (presenting with a tubular segment ⩾2 cm long in lower esophagus and intestinal metaplasia of incomplete type ("specialized columnar epithelium") in endoscopic biopsies from the tubular segment below the squamocolumnar junction were collected prospectively from outpatients referred to diagnostic gastroscopy. The controls comprised 199 prospectively collected dyspeptic outpatients without BE or any endoscopically visible lesions in the upper GI tract. Fasting levels of serum G-17 (G-17fast) were assayed with an EIA test using a Mab highly specific to amidated G-17. None of the patients and controls received therapy with PPIs or other antisecretory agents.

RESULTS: The mean and median levels of G-17fast in serum were significantly lower (P = 0.001) in BE patients than in controls. The positive likelihood ratios (LR+) of low G-17fast to predict BE in the whole study population at G-17fast levels <0.5, <1, or <1.5 pmol/L were 3.5, 3.0, and 2.8, respectively. Among patients and controls with healthy stomach mucosa, the LR+ were 5.6, 3.8, and 2.6, respectively. In the whole study population, serum G-17 was below 2 pmol/L in 15 of 19 BE patients (79%). The corresponding prevalence was 66 of 199 (33%) in controls (P<0.001). The G-17fast was 5 pmol/L or more in only one of the 19 BE patients (5%). In controls, 76 of the 199 patients (38%) had such high serum G-17fast levels (P<0.01).

CONCLUSION: Serum levels of G-17fast tend to be lower in native patients with BE than in healthy controls.

© 2005 The WJG Press and Elsevier Inc. All rights reserved.

Key words: Gastrin-17; Barrett's esophagus; Chronic gastritis; Atrophic gastritis; Diagnostics

Sipponen P, Vauhkonen M, Helske T, Kääriäinen I, Härkönen M. Low circulating levels of gastrin-17 in patients with Barrett's esophagus. *World J Gastroenterol* 2005; 11(38): 5988-5992
http://www.wjgnet.com/1007-9327/11/5988.asp

INTRODUCTION

High intragastric acidity inhibits the release of gastrin into circulation from antral G cells, and conversely, low acidity and high intragastric pH enhance this release[1,2]. Amidated gastrin-17 (G-17) is the biologically active main gastrin fragment, and G-17 is a gastrin compound secreted nearly entirely from the antral G cells[3-5]. It is conceivable that fasting levels of G-17 (G-17fast) in serum or plasma reflect indirectly the intragastric acidity. Correspondingly, it is conceivable that low serum levels of G-17 occur particularly in patients with acid-related diseases.

Gastroesophageal reflux disease is one of the most important acid-related diseases[6]. Patients with Barrett's esophagus (BE) are a subgroup of reflux patients in whom the refluxed acid gastric juice is a factor causing mucosal damages in the lower esophagus, and at the esophagogastric junction[7-9]. Some studies indicate that the prevalence of BE ranges from 0.5% to 5.0% in patients undergoing upper-GI endoscopy for dyspepsia, and from 12% to 15% in patients with gastroesophageal reflux disease and reflux symptoms[10-13].

In the present study, we investigated whether the serum levels of G-17 are lower in patients with BE than in non-BE controls.

MATERIALS AND METHODS

Patient and control series were collected prospectively in 2002 in Helsinki University Central Hospital (HUCH), Jorvi Hospital, Espoo, Finland, from patients who were referred to diagnostic gastroscopy for dyspeptic or reflux-type symptoms.

Patient series

The patient series consisted of 19 subjects with a BE diagnosed by endoscopy and histology. All had a Barrett's segment 2 cm or more in length in the lower columnar, tubular esophagus.

Of the available 19 patients, 14 were males and 5 females. The mean age was 60±12 years. Three of the nineteen BE patients (16%) had *Helicobacter pylori* (*H pylori*)-related gastritis. In one of these three patients, gastritis was strongly antrum dominant, and this patient showed moderate atrophy and intestinal metaplasia in the antrum. The histopathology was evaluated by biopsies from antrum and corpus (at least two biopsies from each site), and by the principles of the updated Sydney System. The biopsy specimens were stained with HE and Alcian blue (pH 2.5)-PAS methods and modified Giemsa for *H pylori*.

Control series

The control series consisted of 199 patients without any visible endoscopic lesions in the upper GI tract. Of the 199 patients, 71 were males and 128 females. The mean age was 54±15 years. Altogether, 94 patients (47%) had chronic *H pylori*-related or autoimmune chronic gastritis, or atrophic gastritis. The rest had normal and healthy gastric mucosa in gastric biopsies (no chronic gastritis, no *H pylori*, no intestinal metaplasia or atrophy). Of the total number of patients with chronic gastritis, 48 had atrophic gastritis of some grade and type. Advanced (moderate or severe) atrophic gastritis in corpus was found in 23 patients.

Inclusions and exclusions

A patient in the Barrett series was included if he/she had a segment of Barrett's mucosa 2 cm or more in length that was verified by endoscopy and histology of the biopsies taken below the squamocolumnar junction (*z*-line). The biopsies had to show the presence of intestinal metaplasia of incomplete type ("specialized columnar epithelium"), i.e. intestinal metaplasia of type II or III in the Alcian blue (pH 2.5)-PAS-stained sections[14]. In incomplete type of intestinal metaplasia, both goblet cells and columnar epithelium between the goblet cells showed secretory mucins that were stained blue with Alcian blue (pH 2.5)-PAS.

The following patients were excluded: patients with a short segment Barrett (the presence of "specialized columnar epithelium" in biopsies from a segment that is less than 2 cm long); patients with erosive esophagitis, ulcers, or polyps, or those with any endoscopically visible local lesions in stomach or esophagus.

Use of PPIs

Patients and controls with a long-term use of PPIs were excluded from the study, and none of the patients or controls was recorded having used PPI at the time of the diagnosis (information obtained from the patient at endoscopy). Thus, the present BE patients represented the native cases of dyspeptic subjects in whom BE was accidentally diagnosed in a diagnostic endoscopy, and in the subjects who did not receive any effective treatment.

Endoscopy

Diagnostic upper-GI endoscopy was done in all patients and controls. In both patient and control series, two groups were formed: the whole study population that included all patients and controls, and a subgroup of patients and controls in which the histology showed normal and healthy gastric mucosa (updated Sydney criteria) in both antrum and corpus biopsies (no gastritis, no atrophy, no intestinal metaplasia, nor *H pylori*). In the Barrett series, 16 of 19 patients (84%) were classified into the subgroup 2 (subjects with healthy and normal gastric mucosa). In controls, 105 of 199 (53%) subjects were classified into the subgroup 2.

Assay of amidated gastrin-17

G-17 was determined using specific EIA tests (G-17 EIA test kit Cat. No. 601 030, Biohit Plc, Helsinki, Finland) performed in batches of 40 samples on a microwell plate according to the instructions of the manufacturer. The EIA technique was based on measuring the absorbance after a peroxidation reaction at 450 nm. Between the reaction steps the plates were washed in a BW50 microplate strip washer (Biohit Plc, Helsinki, Finland). The absorbances were measured using a microplate reader (BP800 Microplate Reader, Biohit Plc, Helsinki, Finland). For determination of G-17 values, a 2nd order fit on standard concentrations was used to interpolate/extrapolate unknown sample concentrations automatically with the help of the BP800 in-built software (Biohit Plc, Helsinki, Finland).

The monoclonal antibody (Mab) of G-17 in the EIA tests was highly specific. The G-17 antibody used detected only amidated G-17, but no other gastrin molecules or fragments (e.g., glycine extended G-17, a kind gift from Prof. Jens F Rehfeld, Copenhagen, Denmark; human synthetic gastrin-34, G-5024, Sigma; human synthetic gastrin-13, G-0267, Sigma; or cholecystokinin fragment 26-33 amide, C-2901, Sigma) were detected. In immunohistochemistry (formalin-fixed, paraffin-embedded specimens: dilutions up to 10 000), the G-17 antibody stained only antral G cells and glands, not other cells or tissues in stomach, duodenum, small or large bowel, or pancreas. The G-17 EIA results correlated well with those of the G-17 RIA (by the courtesy of Prof. Jens F Rehfeld and Dr. Jens-Peter Gotze, Copenhagen, Denmark).

The G-17 assays from serum samples were done first after an overnight fast (G-17fast) and 20 min after a drink of a glass of a protein-rich juice (Biohit Plc, Helsinki, Finland) in which the protein content corresponded to that in an ordinary beef.

Specificity of G-17 antibody

The specificity of the antibody to G-17 secreted from antral G cells alone has been recently verified[15]. The G-17 assay measured only amidated G-17, and not other gastrin fragments.

Invasive and non-invasive tests for gastritis and atrophic gastritis

In addition to endoscopy and histology, the patient and control series were also classified into those with normal and healthy stomach or into those with non-atrophic or atrophic gastritis by serological tests which applied assays of *H pylori* antibodies, pepsinogens I (PGI) and II (PGII) and postprandial G-17 in serum (GastroPanel, Biohit Plc, Helsinki, Finland). The patients without *H pylori* antibodies and with PGI 50 microg/L, or more or above, were considered to have normal and healthy stomach mucosae.

Ethics

The study was approved by the Ethical Committee of the

Helsinki District University Hospital (HUCH), Helsinki, Finland. The purpose of the study was explained to all patients before taking blood samples, and all patients signed a written consent before enrolment into the study.

Statistical analysis

Non-parametric tests (Wilcoxon-Mann-Whitney test; χ^2 test; SPSS 10.1 Software) were used in the calculations of the significance between the groups. In order to examine the clinical value of low serum G-17 in the diagnosis of BE, the likelihood ratio (LR+) of the positive test result (low G-17fast or G-17prand) between the cases and controls was calculated at arbitrary cut-off levels of G-17. The LR+ indicates a factor by which the pre-test odds of BE has to be multiplied to obtain the post-test odds and, further, the post-test probability of the disease.

[illegible]

The mean and median values of serum G-17fast were significantly lower in patients with long-segment BE than in controls. This was the case both in males and females, or when the analysis was done in the whole study population (all patients and controls), or if the analysis was limited to subgroups of patients and controls with histologically normal and healthy gastric mucosa. The results in the whole study population and among those with healthy stomach mucosa are shown in Figures 1 and 2 in a box-plot form.

In contrast to G-17fast, the serum levels of postprandial G-17 (G-17prand) were significantly lower in BE patients than in controls in the whole study population only but not in the subjects with normal and healthy stomach mucosae (Figure 2).

The positive LR+ of low serum G-17 to predict odds of BE in the whole study population below the arbitrary cut-off levels of G-17fast are presented in Table 1. The corresponding results in the subgroups of cases and controls with histologically normal, healthy gastric mucosa are shown in Table 2. It appears that the LR+ gradually increased with a decreasing concentration of G-17fast. The sensitivity and specificity of low serum G-17fast (<1 pmol/L) to indicate BE in the whole study population were 47% and 89%, respectively.

The study population was also classified into those with normal and healthy stomach mucosae (16 BE patients and 108 controls) and those with gastritis or atrophic gastritis (3 BE patients and 91 controls) by applying the serological tests (GastroPanel, Biohit Plc, Helsinki, Finland). By these tests, the stomach mucosa was healthy when *H pylori* antibodies were not present and the serum pepsinogen I was 50 μg/L, or more. Among the patients diagnosed to have a healthy stomach mucosa by these tests, the LR+s of BE are presented in Table 3. The sensitivity and specificity of low serum G-17fast (<1 pmol/L) to indicate BE were 50% and 82%,

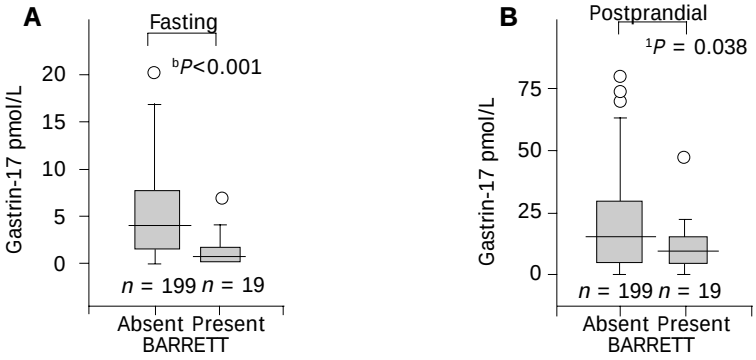


Figure 1 Fasting (A) and postprandial (B) serum G-17 levels in patients with or without long-segment BE in the whole study population. A box plot presentation. The boxes show the central 50% of the cases. The length of the box shows the range within which the center 50% of the values fell. The whiskers show the range of values that fall within 1.5×difference of the values of median from the two hinges of the box. Differences: ^bP<0.001; ^1P = 0.038; non-parametric test (Mann-Whitney *U*). To make the figure clear, the very most extreme outliers are not shown in the pictures.

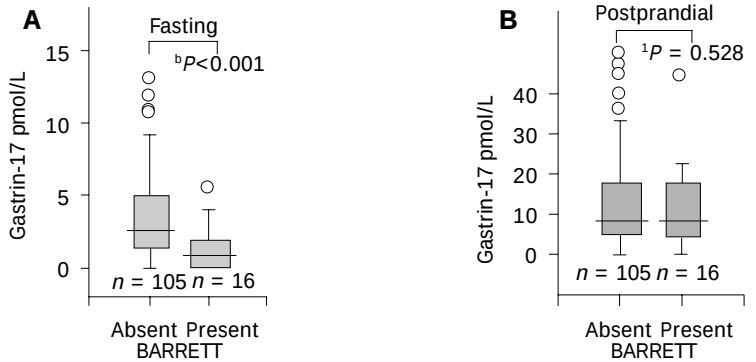


Figure 2 Fasting (A) and postprandial (B) serum G-17 levels in patients with or without long-segment BE among patients and controls with normal and healthy stomach mucosae (no gastritis, no *H pylori*, and no atrophy). A box plot presentation (see Figure 1). Differences: ^bP<0.001; ^1P = 0.528; non-parametric test (Mann-Whitney *U*). To make the figure clear, the very most extreme outliers are not shown in the pictures.

Table 1 LR+ of low serum level of fasting G-17 in whole study population

G-17fast pmol/L	Barrett *n*	Controls *n*	LR+(95%CI)
<0.5	7	21	3.5 (1.3-9.3)
<1	9	31	3.0 (1.3-7.3)
<1.5	13	48	2.8 (1.3-6.1)
<2	15	66	2.4 (1.1-4.9)
<3	17	89	2.0 (1.0-4.0)
<5	18	123	1.5 (0.8-3.0)
All	19	199	1

Table 2 LR+ of low serum level of fasting G-17 in patients and controls (males and females) with normal and healthy gastric mucosae (histology)

G-17fast pmol/L	Barrett *n*	Controls *n*	LR+(95%CI)
<0.5	6	7	5.6 (1.7-19)
<1	7	12	3.8 (1.3-11)
<1.5	10	25	2.6 (1.1-6.5)
<2	12	42	1.9 (0.8-4.3)
<3	14	61	1.5 (0.7-3.3)
<5	15	79	1.2 (0.6-2.7)
All	16	105	1

Table 3 LR+ of low serum level of fasting G-17 in patients and controls with healthy gastric mucosa, no *H pylori* antibodies and serum pepsinogen I ⩾50 μg/L

G-17fast pmol/L	Barrett *n*	Controls *n*	LR+(95%CI)
<0.5	6	13	3.1 (1.0-9.4)
<1	8	19	2.8 (1.1-7.6)
<1.5	11	34	2.2 (0.9-5.1)
<2	13	49	1.8 (0.8-4.0)
<3	15	65	1.6 (0.7-3.4)
<5	15	81	1.3 (0.6-2.7)
All	16	108	1

respectively, and at the cut-off level <2 pmol/L 81% and 55%, respectively. The corresponding overall accuracies were 77% and 55%, respectively.

In the whole study population, the G-17fast was very low (<0.5 pmol/L) in 7 of the 19 BE (37%) and 15 of the 199 controls (8%). Correspondingly, the G-17fast was lower than 2 pmol/L in 15 of 19 BE patients (79%) and in 66 of 199 controls (33%, $P<0.001$; χ^2). The G-17fast was 5 pmol/L or more in 1 of 19 BE patients (5%) but in 76 of 199 controls (38%, $P<0.01$; χ^2). In this BE patient, the G-17fast was 5.4 pmol/L.

Three BE patients had *H pylori*-positive chronic gastritis in the biopsy specimens from antrum and corpus. In one of these patients, gastritis was strongly antrum dominant and showed intestinal metaplasia of moderate grade in the antral biopsy specimens. In spite of the presence of gastritis, all three of these BE patients had a low serum level of G-17fast (0.02, 0.6, and 1.4 pmol/L).

Among controls with normal and healthy stomach mucosae (antrum and corpus mucosae were histologically healthy), age and serum G-17fast did not correlate (Pearson correlation 0.05; $P = 0.587$); neither was there any difference in the serum G-17fast between males and females (mean±SD: 4.7±5.7 and 4.1±5.4 pmol/L, respectively).

[redacted]

The present data indicate that the mean and median levels of serum G-17fast tend to be lower in patients with "native" (without previous or ongoing medication, nor previous knowledge of the disease) BE than in controls among outpatients referred to diagnostic endoscopy for dyspeptic symptoms. The BE is associated inversely with the serum level of G-17fast.

An inverse association between the likelihood of BE and serum level of G-17 was seen among the subjects with healthy stomach mucosa (normal gastric histology) and in the whole study population including subjects with gastritis and *H pylori* infection. Several earlier studies have shown that gastric inflammation (gastritis) tends to raise the serum levels of gastrin and other gastric peptides[4,16-18]. In accordance with this, the serum G-17fast levels were higher in the non-BE patients with gastritis than in those without. However, a surprise was that gastritis did not clearly raise the G-17fast concentrations in the present BE patients. Three of the nineteen BE patients had chronic *H pylori* gastritis and all had low serum G-17fast levels that did not differ from those in BE patients without gastritis.

The observations suggest that the inverse relationship between G-17fast and BE is a genuine characteristic of the Barrett's disease itself, and is not a result from gastric inflammation or atrophy, or *H pylori*. The low mean and median levels of G-17fast in BE patients are best explained by assuming that the basal intragastric acidity (basal acid output, BAO) tends to be higher in BE patients than in ordinary dyspeptic patients referred to diagnostic endoscopy. High intragastric acidity may, on the other hand, inhibit the release of G-17 from stomach mucosa, resulting thereby in low serum levels of fasting G-17. In other words, the BE patients may frequently have BAO levels that inhibit the release of G-17 from antral G cells. In two earlier studies, an elevated BAO has been shown to be a characteristic of patients with BE when compared to healthy controls[19,20].

Gastrins themselves have been linked to the pathogenesis of BE in some studies. Gastrins may have direct influences on growth and replication of the metaplastic Barrett epithelium[21], and may impair the esophageal motility and the function of the lower esophageal sphincter[22]. The present study indicates, however, that a low G-17fast in the circulation is a characteristic of BE, and that serum levels of G-17fast above 5 pmol/L are quite rare in BE patients.

Postprandial serum G-17 did not differ between BE and non-BE groups when investigated among subjects with healthy gastric mucosa. This may indicate that the post-stimulation level of serum G-17 does not reflect the intragastric acidity similarly as the fasting level of G-17 (G-17fast). Instead, the G-17prand may merely indicate the number of G cells in the antral mucosa, similarly as the peak acid output and maximal acid output (MAO) are measures of the number and mass of parietal cells in the oxyntic mucosa. Supporting this conclusion, atrophic antral gastritis results in a loss of antral G cells and, consequently, the serum G-17prand levels are low in these patients[23,24].

It was reported that the serum levels of total gastrin are similar in BE patients and controls even though the BAO and MAO are significantly increased[20]. Total serum gastrin was not assayed in the present study. Total immunoreactive gastrin consists of several gastrin fragments of which one-third are G-17 molecules under fasting conditions[25]. The fasting levels of G-17 tend to be very low in normal, healthy subjects in general, and these low G-17 concentrations may be easily eclipsed by other gastrin compounds.

In summary, the present investigation suggests that the serum level of G-17fast tends to be low in native BE patients who are not under PPI medication.

□□□□□□□□□□

1 **Hirschowitz BI**, Molina E. Relation of gastric acid and pepsin secretion to gastrin levels in dogs given bombesin and gastrin-17. *Am J Physiol* 1983; **244**: G546-551
2 **Muller J**, Kirchner T, Muller-Hermelink HK. Gastric endocrine cell hyperplasia and carcinoid tumors in atrophic gastritis type A. *Am J Surg Pathol* 1987; **11**: 909-917
3 **Malmström J**, Stadil F. Gastrin content and gastrin release. Studies on the antral content of gastrin and its release to serum during stimulation by food. *Scand J Gastroenterol* 1976; **37**: 71-76
4 **Petersen B**, Andersen BN. Increased concentrations of the NH2-terminal fragment of gastrin-17 in acute duodenal ulcer and acute gastritis. *Scand J Gastroenterol* 1983; **18**: 635-641
5 **Stepan V**, Sugano K, Yamada T, Paerk J, Dickson CJ. Gastrin biosynthesis in canine G cells. *Am J Physiol Gastrointest Liver Physiol* 2002; **282**: 766-775
6 **Spechler SJ**. Barrett´s esophagus and esophageal adenocarcinoma: pathogenesis, diagnosis, and therapy. *Med Clin North Am* 2002; **86**: 1423-1445
7 **Fitzgerald RC**. Significance of acid exposure in Barrett´s esophagus. *Am J Gastroenterol* 2003; **98**: 699-700
8 **Falk GW**. Barrett´s esophagus. *Gastroenterology* 2002; **122**: 1569-1591
9 **Zaninotto G**, Portale G, Parenti A, Lanza C, Costantini M, Molena D, Ruol A, Battaglia G, Costantino M, Epifani M, Nicoletti L. Role of acid and bile reflux in development of specialized metaplasia in distal oesophagus. *Dig Liver Dis* 2002; **34**: 251-257
10 **Cameron AJ**. Epidemiology of columnar-lined esophagus and adenocarcinoma. *Gastroenterol Clin North Am* 1997; **26**: 487-494
11 **Romero Y**, Cameron AJ, Schaid DJ, McDonnell SK, Burgart LJ, Hardtke CL, Murray JA, Locke GR 3rd. Barrett's esophagus: prevalence in symptomatic relatives. *Am J Gastroenterol* 2002; **97**: 1127-1132
12 **Gerson LB**, Shetler K, Triadafilopoulos G. Prevalence of Barrett's esophagus in asymptomatic individuals. *Gastroenterology* 2002; **123**: 636-639
13 **Bersentes K**, Fass R, Padda S, Johnson C, Sampliner RE. Prevalence of Barrett's esophagus in Hispanics is similar to Caucasians. *Dig Dis Sci* 1998; **43**: 1038-1041
14 **Spechler SJ**. Columnar-lined epithelium. Definitions. *Chest Surg Clin N Am* 2002; **12**: 1-13
15 **Goetze JP**, Paloheimo LI, Linnala A, Sipponen P, Hanssen CP, Rehfeld JF. Gastrin-17 specific antibodies are too specific for gastrinoma but stain G-cells. *Scand J Gastroenterol* 2005; 40: 596-598
16 **Mulholland G**, Ardill JE, Fillmore D, Chittajallu RS, Fullarton GM, McColl KE. *Helicobacter pylori* related hypergastrinaemia is the result of a selective increase in gastrin 17. *Gut* 1993; **34**: 757-761
17 **Beardshall K**, Moss S, Gill J, Levi S, Ghosh P, Playford RJ, Calam J. Suppression of *Helicobacter pylori* reduces gastrin releasing peptide stimulated gastrin release in duodenal ulcer patients. *Gut* 1992; **33**: 601-603
18 **Laheij RJ**, Van Rossum LG, De Boer WA, Jansen JB. Corpus gastritis in patients with endoscopic diagnosis of reflux oesophagitis and Barrett's oesophagus. A*liment Pharmacol Ther* 2002; **16**: 887-891
19 **Collen MJ**, Johnson DA. Correlation between basal acid output and daily ranitidine dose required for therapy in Barrett's esophagus. *Dig Dis Sci* 1992; **37**: 570-576
20 **Mulholland MW**, Reid BJ, Levine DS, Rubin CE. Elevated gastric acid secretion in patients with Barrett's metaplastic epithelium. *Dig Dis Sci* 1989; **34**: 1329-1334
21 **Haigh CR**, Attwood SE, Thompson DG, Jankowski JA, Kirton CM, Pritchard DM, Varro A, Dimaline R. Gastrin induces proliferation in Barrett's metaplasia through activation of the CCK2 receptor. *Gastroenterology* 2003; **124**: 615-625
22 **Straathof JW**, Lamers CB, Masclee AA. Effect of gastrin-17 on lower esophageal sphincter chracteristics in man. *Dig Dis Sci* 1997; **42**: 2547-2551
23 **Sipponen P**, Ranta P, Helske T. Kääriäinen I, Mäki T, Linnala A, Suovaniemi O, Alanko A, Härkönen M. Serum level of amidated gastrin-17 and pepsinogen I in atrophic gastritis; an observational case-control study. *Scand J Gastroenterol* 2002; **37**: 785-791
24 **Väänänen H**, Vauhkonen M, Helske T, Kääriäinen I, Rasmussen M, Tunturi-Hihnala H, Koskenpato J, Sotka M, Turunen M, Sandström R, Ristikankare M, Jussila A, Sipponen P. Non-endoscopic diagnosis of atrophic gastritis with a blood test. Correlation between gastric histology and blood levels of gastrin-17 and pepsinogen I: a multicentre study. *Eur J Gastroenterol Hepatol* 2003; **15**: 885-891
25 **Rehfeld JF**, Christiansen LA, Malmström J, Schwartz T, Stadil F. The heterogeneity of gastrin, with reference to conversion of gastrin-17. *Clin Endocrinol* 1976: **5**(Suppl): 185S-193S

Science Editor Wang XL and Guo SY **Language Editor** Elsevier HK

PO Box 2345, Beijing 100023, China
www.wjgnet.com
wjg@wjgnet.com

ELSEVIER

World J Gastroenterol 2005;11(38):5993-5996
World Journal of Gastroenterology ISSN 1007-9327
© 2005 The WJG Press and Elsevier Inc. All rights reserved.

• *BRIEF REPORTS* •

Expression profiling of gastric cancer samples by oligonucleotide microarray analysis reveals low degree of intra-tumor variability

Karolin Trautmann, Christine Steudel, Dana Grossmann, Daniela Aust, Gerhard Ehninger, Stephan Miehlke, Christian Thiede

Karolin Trautmann, Christine Steudel, Dana Grossmann, Gerhard Ehninger, Stephan Miehlke, Christian Thiede, Medical Department I, University of Dresden, Dresden, Germany
Daniela Aust, Department of Pathology, University of Dresden, Dresden, Germany
Supported by a MeDDrive grant From the University of Dresden 2003 and by a grant from the Dr. Mildred Scheel Stiftung No. 70-2923
Correspondence to: Dr. Christian Thiede, Medical Department I, Fetscherstr. 74, 01307 Dresden,
Germany. thiede@mk1.med.tu-dresden.de
Telephone: +49-351458-4680 Fax: +49-351458-5362
Received: 2004-10-04 Accepted: 2004-12-23

Abstract

AIM: Gene expression profiling provides an unique opportunity to gain insight into the development of different types of gastric cancer. Tumor sample heterogeneity is thought to decrease the sensitivity and tumor specificity of microarray analysis. Thus, microdissection and preamplification of RNA is frequently performed. However, this technique may also induce considerable changes to the expression profile. To assess the effect of gastric tumor heterogeneity on expression profiling results, we measured the variation in gene expression within the same gastric cancer sample by performing a gene chip analysis with two RNA preparations extracted from the same tumor specimen.

METHODS: Tumor samples from six intestinal T2 gastric tumors were dissected under liquid nitrogen and RNA was prepared from two separate tumor fragments. Each extraction was individually processed and hybridized to an Affymetrix U133A gene chip covering approximately 18 000 human gene transcripts. Expression profiles were analyzed using Microarray Suite 5.0 (Affymetrix) and GeneSpring 6.0 (Silicon Genetics).

RESULTS: All gastric cancers showed little variance in expression profiles between different regions of the same tumor sample. In this case, gene chips displayed mean pair wise correlation coefficients of 0.94±0.02 (mean±SD), compared to values of 0.61±0.1 for different tumor samples. Expression of the variance between the two expression profiles as a percentage of "total change" (Affymetrix) revealed a remarkably low average value of 1.18±0.78 for comparing fragments of the same tumor sample. In contrast, comparison of fragments from different tumors revealed a percentage of 24.4±4.5.

CONCLUSION: Our study indicates a low degree of expression profile variability within gastric tumor samples isolated from one patient. These data suggest that tumor tissue heterogeneity is not a dominant source of error for microarray analysis of larger tumor samples, making total RNA extraction an appropriate strategy for performing gene chip expression profiling of gastric cancer.

© 2005 The WJG Press and Elsevier Inc. All rights reserved.

Key words: Gastric cancer; Microarray analysis; Tissue heterogeneity

Trautmann K, Steudel C, Grossmann D, Aust D, Ehninger G, Miehlke S, Thiede C. Expression profiling of gastric cancer samples by oligonucleotide microarray analysis reveals low degree of intra-tumor variability. *World J Gastroenterol* 2005; 11(38): 5993-5996
http://www.wjgnet.com/1007-9327/11/5993.asp

INTRODUCTION

Gastric cancer is one of the most common malignancies, accounting for almost 10% of new cancer cases diagnosed worldwide[1,2]. However, knowledge about the molecular mechanisms underlying tumor development and progression is limited and molecular features of gastric cancer are not commonly used for diagnosis and treatment.

cDNA and oligonucleotide microarrays are capable of profiling gene expression patterns of tens of thousands of genes in a single experiment. They are an ideal tool to study cancer progression and development and to identify new molecular markers for tumor classification and prognosis. Microarrays have been successfully applied to study various tumors, including gastric cancers[3-13].

Like most solid tumors, gastric cancer consists of many different cell types including endothelium, different types of stromal cells and inflammatory cells. Such tissue heterogeneity is thought to decrease the sensitivity and tumor specificity of the microarray analysis[14-16]. One strategy to overcome the problem of tissue heterogeneity is the use of laser capture microdissection (LCM) for isolation of a defined cell population[17,18], followed by amplification of the RNA for subsequent microarray analysis[19,20]. However, amplification-associated bias may induce considerable changes to the expression profile[15,21]. Depending on both the degree of tissue heterogeneity and the robustness of the microarray analysis protocol, it may therefore sometimes be advantageous to avoid RNA amplification and instead extract total RNA directly from a larger tumor sample.

To assess the influence of gastric tumor heterogeneity on the outcome of the microarray analysis, we measured the variation between gene expression profiles derived from

two RNA preparations extracted from the same gastric tumor specimen.

[illegible]

Gastric tumor samples

Tumor samples from six patients who underwent surgery for gastric cancer at the University Hospital of Dresden were used for microarray analysis. Immediately after gastrectomy, a certified pathologist obtained representative samples of 1 cm^3 from the tumor centers. Special care was taken to avoid tumor necrosis. Tumors were snap-frozen in liquid nitrogen and stored at -80 ℃. To ensure consistency of the study population, only tumors classified as intestinal and T2 by pathology were included in the study[22]. Clinical and histopathological tumor characteristics are summarized in Table 1.

Table 1 Clinical data and histopathological features of gastric cancers included in the study

Tumor number	Age/Sex	Site	Lauren	TNM
1	72/Female	Antrum	Intestinal	T2 N2 G3
2	78/Male	Body	Intestinal	T2 N1 G2
3	81/Male	Antrum	Intestinal	T2 N1 G2
4	75/Female	Antrum	Intestinal	T2 N0 G3
5	76/Male	Cardia	Intestinal	T2 N2 G3
6	76/Male	Cardia	Intestinal	T2 N0 G3

RNA preparation

For RNA isolation, tumor samples were fragmented into smaller pieces under liquid nitrogen using a mortar and pestle. Subsequently, total RNA was extracted from two independent, randomly selected tumor fragments using RNAzol reagent according to the manufacturer's instructions (TelTest Inc., Friendswood, TX). Both extractions (extractions A and B) were processed individually until hybridization on two separate microarrays. To determine the influence of experimental variability, RNA was extracted only once from tumor no. 3 and aliquots of the same RNA preparation were used for further processing.

High-density oligonucleotide microarray analysis

Microarray analysis was performed according to the Affymetrix instructions for eukaryotic sample preparation[23]. In summary, double-stranded cDNA was synthesized from 5 μg of total RNA with oligo$(dT)_{24}$ T7 primer (Affymetrix), followed by *in vitro* transcription of cRNA synthesis using Enzo BioArray High Yield RNA Transcript Labeling Kit (Affymetrix) and the biotinylated cRNA was hybridized to Affymetrix U133A gene chip arrays containing 22 253 probe sets (approximately 18 000 human gene transcripts). The hybridized probe array was stained with streptavidin–phycoerythrin conjugate and scanned by the Affymetrix gene chip scanner.

Statistical analysis

Expression profiles were analyzed using Microarray Suite 5.0 (Affymetrix) and GeneSpring 6.0 (Silicon Genetics). We used the Affymetrix software to identify changes in expression levels between fragments of the same tumor specimen using standard protocols recommended by Affymetrix[24]. For normalization, data from each expression array were scaled, so that the overall fluorescence intensity across each chip was equivalent (average target intensity set at 500). Only relative changes equal or greater than twofold level of expression were considered. For a given gene transcript in any chip-to-chip comparison, Microarray Suite Software generates a "change call" parameter ("Increase" or "Decrease") based on a consideration of signal specificity as well as intensity. In other words, the "change call" is based on an evaluation of the intensities of the signals generated from each gene transcript on one chip relative to the corresponding signal intensities on the other chip. Instances where the signal on the higher intensity chip is falsely elevated are called "Increased" in a comparison between two chips derived from the same target preparation. "Decrease" calls represent instances where the signal on the lower intensity array has been falsely elevated. Consequently we define all "Increase" or "Decrease" calls in a comparison between arrays derived from the same target preparation as false positive. According to the Affymetrix specification, a percentage of "total change" up to 2% between two chips derived from the same hybridization cocktail is acceptable. To confirm results derived by Microarray Suite, GeneSpring was used to perform multiple comparisons between arrays and to generate pairwise correlation coefficients (Spearman correlation) for all arrays.

[illegible]

RNA and hybridization quality control parameters

Extracted total RNA was evaluated on a 2% agarose gel for the presence of 28S and 18S rRNA bands, which were clearly visible in all RNA samples. RNA purity was assessed by UV spectrophotometry. An $A_{260/280}$ ratio >1.9 was achieved in all samples. Total RNA was also used for RT-PCR of a housekeeping mRNA species to assess RNA quality. Human GAPDH (Applied Biosystems Inc., Foster City, CA, USA) was robustly amplified in all cases.

We followed the Affymetrix guidelines for efficient hybridization: Among the 22 253 probe sets, there was a consistent percentage of "present" calls for each of the 12 cRNA samples tested with a median of 50.68 (range 42.9-54.7). No array image showed grossly visible artifacts. The ratio of the 3' probe set to the 5' probe set of the GAPDH internal control gene, which acts as an indicator for overall RNA quality was below three in all cases. RNA and gene chip hybridization quality control parameters are summarized in Table 2.

Intra-tumor variability

Expression profiles from five gastric tumors were used to determine the degree of intra-tumor variability. As shown in Table 3, all gastric cancers demonstrated very little variance in expression profiles between different regions of the same tumor sample. In this case, expression arrays displayed mean pairwise correlation coefficients of 0.95±0.02, in contrast to values of 0.61±0.1 when different tumor samples were compared to each other. In accordance, the variance between two expression profiles calculated with the Affymetrix software

Table 2 RNA and hybridization quality control parameters

Extraction /Tumor number	$A_{260/280}$ ratio	GAPDH CT	Present calls (%)	GAPDH 3′5′ ratio
A/1	2.18	15.86	52.5	1.08
B/1	2.18	15.7	52.3	1.26
A/2	2.09	15.8	49.2	0.89
B/2	2.07	15.6	54.4	1.19
A/3	2.1	15.2	53.5	1.09
B/3	2.1	15.2	52.5	1.08
A/4	2.07	15.5	48.8	0.99
B/4	2.08	15.2	49.8	0.96
A/5	2.15	16.07	51.7	1.95
B/5	2.24	16.15	54.7	1.46
A/6	2.19	16.08	42.9	1.58
B/6	2.13	16.2	45.9	1.34

(percentage of "total change") revealed a remarkably low average value of 1.18±0.78 for comparing fragments of the same tumor sample. This result is even more striking in light of the Affymetrix guidelines, which suggest that a percentage of "total change" up to 2% is tolerable for comparing chips derived from the same hybridization cocktail. In contrast, when we compared tumor fragments from different tumors the percentage of "total change" was 24.4±4.5. As an example, Figure 1 illustrates different analyses results for two regions of the same gastric cancer sample (Figure 1A) and for two different gastric cancer samples (Figure 1B). In conclusion, there is a surprisingly low degree of expression profile variability within all gastric tumor samples studied.

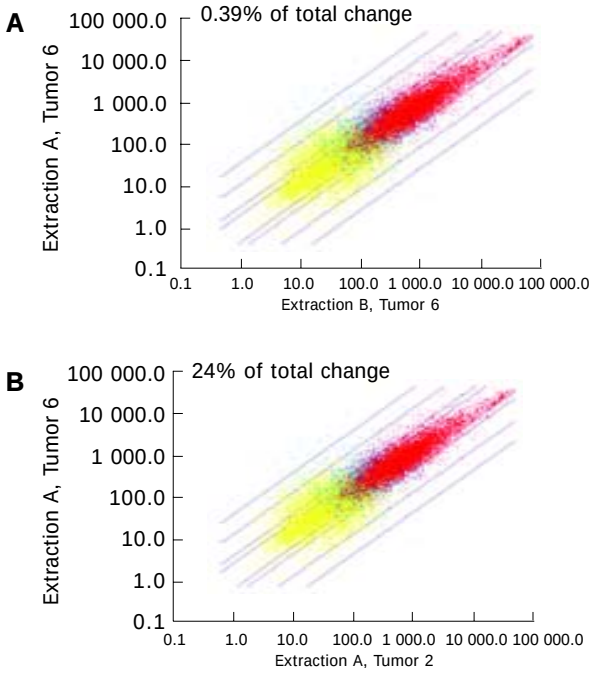


Figure 1 Scatter plots of the expression profiles derived from two different regions of the same gastric cancer sample (extraction A *vs* extraction B from tumor no. 6) (B) and from two different gastric cancer samples (extraction A from tumor no. 6 *vs* extraction A from tumor no. 2). The solid lines indicate 2-, 3-, 10-, and 30-fold expression level differences. Red dots represent gene transcripts detected in both arrays, yellow dots represent gene transcripts undetectable in both arrays, and blue dots represent transcripts detectable in one but undetectable in the other array. Gene transcripts detectable in both arrays (red dots) show a high correlation and thus a low percentage of "total change" for two different regions of the same tumor sample (B), whereas they show a poor correlation and thus a high percentage of "total change" for fragments of different tumors (A).

Experimental variability

During the whole procedure of the microarray experiment, so called experimental variability is generated by multiple factors including chip manufacture, preparation of cRNA, hybridization, washing steps, *etc*. To measure the degree of experimental variability, RNA was extracted only once from tumor no. 3. Subsequently, two aliquots from the same RNA preparation were used for further processing and hybridization on two separate Affymetrix U133A arrays. In this case, gene chip expression profiles differed in only 0.18% of all genes analyzed. Likewise the correlation coefficient was 0.99, respectively. Table 3 summarizes comparison of results from all samples.

Table 3 Comparison results for all tumor samples analyzed

Comparison	Pairwise correlation coefficient	Percentage of "total change"
Tumor 1, extraction A *vs* B	0.96	1.07
Tumor 2, extraction A *vs* B	0.91	2.65
Tumor 3, extraction A *vs* B	0.99	0.08
Tumor 4, extraction A *vs* B	0.96	0.55
Tumor 5, extraction A *vs* B	0.94	1.28
Tumor 6, extraction A *vs* B	0.95	0.39

Tumor no. 3 was used to evaluate experimental variability.

DISCUSSION

Microarray studies on gastric cancer are currently based on two main methods of RNA preparation: the recently developed technique of LCM allows for the isolation of cancer cells and other subpopulations of interest from a heterogeneous piece of tumor tissue. The advantage of microdissection is that it directly focuses on the gastric cancer cells[5,10]. The disadvantage of LCM is at the level of resources and expertise. A certified pathologist is required to select the cells to be microdissected under the microscope, and microdissection itself requires an expensive technology and special training. Furthermore the amount of RNA obtained after LCM is not sufficient for microarray analysis and generally requires amplification. However, the amplification of small amounts of RNA from laser-captured samples is difficult and has been proved to be less reproducible than measurement of unamplified mRNA[15,21]. Even a minor degree of amplification bias might result in a substantial variation to the expression profile.

The approach we used here is based on total RNA extraction with RNA isolated directly from the gastric tumor tissue without the need for subsequent amplification. Hence, the microarray profile reflects all different tissue components present in the tumor. Most gastric cancer microarray studies are based on this method of RNA extraction[3,4,6-9,11-13]. This strategy is less laborious, because it does not require isolation of specific cell types. Moreover, there is usually a sufficient amount of high quality RNA obtained for microarray analysis. However, since the actual proportion of tumor cells in the gastric cancer tissue studied remains unknown, expression profiling based on this strategy may not reliably represent "true" tumor changes. In other words, the level of intra-tumor variability is crucial for the sensitivity and tumor specificity of the microarray experiment. If there is a significant amount of intra-tumor variability, LCM becomes the strategy of choice.

In this study we found an unexpectedly low degree of

expression profile variability within all gastric tumor samples studied. Randomly selected fragments from the same tumor sample displayed a striking similarity in expression profiles, while expression profiles derived from distinct tumor samples differed significantly. These data suggest that tissue heterogeneity is not a dominant source of error for microarray analysis of larger gastric tumor samples, making total RNA extraction an appropriate strategy for performing gene chip expression profiling of gastric cancer.

Our findings are in contrast to a recently published microarray study on human muscle biopsies[25], where tissue heterogeneity was a major source of expression profile variability. This indicates that our results may be exclusive for larger tumor samples and should not be generalized. It might also reflect the influence of study design and appropriate material selection on the outcome of any microarray experiment. We believe that an experienced pathologist who is able to carefully select an appropriate piece of gastric tumor for microarray experiments directly from a large tumor avoiding necrosis and infiltration by normal gastric mucosa is crucial for the quality of our results.

In our study, the degree of experimental variability was only minimal. In the early times of gene chip technology, Mills and Gordon[26] found a substantial level of experimental variability, with an average of 12% increase/decrease calls between the same RNA processed in parallel and hybridized on two Mu11k-A Affymetrix arrays. However, studies using newer, more robust Affymetrix array generations have achieved results consistent with our studies[25,27]. The low degree of experimental variability reflects the inherent advantage of the Affymetrix Gene Chip technology. Due to commercial mass production, they contain a robust series of controls designed to minimize chip-to-chip variation. The availability of standardized protocols together with the use of stringent laboratory quality control parameters also helps to reduce experimental variability.

In conclusion, we assume that gastric tumor expression profiling based on total RNA extraction reliably represents "true" tumor changes. Therefore, total RNA extraction may be the strategy of choice for microarray studies including large gastric cancer samples.

REFERENCES

1 **Neugut AI**, Hayek M, Howe G. Epidemiology of gastric cancer. *Semin Oncol* 1996; **23**: 281-291
2 **Pisani P**, Parkin DM, Bray F, Ferlay J. Estimates of the worldwide mortality from 25 cancers in 1990. *Int J Cancer* 1999; **83**: 18-29
3 **Boussioutas A**, Li H, Liu J, Waring P, Lade S, Holloway AJ, Taupin D, Gorringe K, Haviv I, Desmond PV, Bowtell DD. Distinctive patterns of gene expression in premalignant gastric mucosa and gastric cancer. *Cancer Res* 2003; **63**: 2569-2577
4 **El-Rifai W**, Frierson HF Jr, Harper JC, Powell SM, Knuutila S. Expression profiling of gastric adenocarcinoma using cDNA array. *Int J Cancer* 2001; **92**: 832-838
5 **Hasegawa S**, Furukawa Y, Li M, Satoh S, Kato T, Watanabe T, Katagiri T, Tsunoda T, Yamaoka Y, Nakamura Y. Genome-wide analysis of gene expression in intestinal-type gastric cancers using a complementary DNA microarray representing 23,040 genes. *Cancer Res* 2002; **62**: 7012-7017
6 **Hippo Y**, Yashiro M, Ishii M, Taniguchi H, Tsutsumi S, Hirakawa K, Kodama T, Aburatani H. Differential gene expression profiles of scirrhous gastric cancer cells with high metastatic potential to peritoneum or lymph nodes. *Cancer Res* 2001; **61**: 889-895
7 **Hippo Y**, Taniguchi H, Tsutsumi S, Machida N, Chong JM, Fukayama M, Kodama T, Aburatani H. Global gene expression analysis of gastric cancer by oligonucleotide microarrays. *Cancer Res* 2002; **62**: 233-240
8 **Inoue H**, Matsuyama A, Mimori K, Ueo H, Mori M. Prognostic score of gastric cancer determined by cDNA microarray. *Clin Cancer Res* 2002; **8**: 3475-3479
9 **Kim B**, Bang S, Lee S, Kim S, Jung Y, Lee C, Choi K, Lee SG, Lee K, Lee Y, Kim SS, Yeom YI, Kim YS, Yoo HS, Song K, Lee I. Expression profiling and subtype-specific expression of stomach cancer. *Cancer Res* 2003; **63**: 8248-8255
10 **Mori M**, Mimori K, Yoshikawa Y, Shibuta K, Utsunomiya T, Sadanaga N, Tanaka F, Matsuyama A, Inoue H, Sugimachi K. Analysis of the gene-expression profile regarding the progression of human gastric carcinoma. *Surgery* 2002; **131**: S39-47
11 **Suganuma K**, Kubota T, Saikawa Y, Abe S, Otani Y, Furukawa T, Kumai K, Hasegawa H, Watanabe M, Kitajima M, Nakayama H, Okabe H. Possible chemoresistance-related genes for gastric cancer detected by cDNA microarray. *Cancer Sci* 2003; **94**: 355-359
12 **Tay ST**, Leong SH, Yu K, Aggarwal A, Tan SY, Lee CH, Wong K, Visvanathan J, Lim D, Wong WK, Soo KC, Kon OL, Tan P. A combined comparative genomic hybridization and expression microarray analysis of gastric cancer reveals novel molecular subtypes. *Cancer Res* 2003; **63**: 3309-3316
13 **Liu LX**, Liu ZH, Jiang HC, Qu X, Zhang WH, Wu LF, Zhu AL, Wang XQ, Wu M. Profiling of differentially expressed genes in human gastric carcinoma by cDNA expression array. *World J Gastroenterol* 2002; **8**: 580-585
14 **Liotta L,** Petricoin E. Molecular profiling of human cancer. *Nat Rev Genet* 2000; **1**: 48-56
15 **Alizadeh AA**, Ross DT, Perou CM, van de Rijn M. Towards a novel classification of human malignancies based on gene expression patterns. *J Pathol* 2001; **195**: 41-52
16 **Lakhani SR**, Ashworth A. Microarray and histopathological analysis of tumours: the future and the past? *Nat Rev Cancer* 2001; **1**: 151-157
17 **Simone NL**, Bonner RF, Gillespie JW, Emmert-Buck MR, Liotta LA. Laser-capture microdissection: opening the microscopic frontier to molecular analysis. *Trends Genet* 1998; **14**: 272-276
18 **Emmert-Buck MR**, Bonner RF, Smith PD, Chuaqui RF, Zhuang Z, Goldstein SR, Weiss RA, Liotta LA. Laser capture microdissection. *Science* 1996; **274**: 998-1001
19 **Van Gelder RN**, von Zastrow ME, Yool A, Dement WC, Barchas JD, Eberwine JH. Amplified RNA synthesized from limited quantities of heterogeneous cDNA. *Proc Natl Acad Sci USA* 1990; **87**: 1663-1667
20 **Wang E**, Miller LD, Ohnmacht GA, Liu ET, Marincola FM. High-fidelity mRNA amplification for gene profiling. *Nat Biotechnol* 2000; **18**: 457-459
21 **Nygaard V**, Loland A, Holden M, Langaas M, Rue H, Liu F, Myklebost O, Fodstad O, Hovig E, Smith-Sorensen B. Effects of mRNA amplification on gene expression ratios in cDNA experiments estimated by analysis of variance. *BMC Genomics* 2003; **4**: 11
22 **Sarbia M**, Becker KF, Hofler H. Pathology of upper gastrointestinal malignancies. *Semin Oncol* 2004; **31**: 465-475
23 Gene chip expression analysis technical manual Affymetrix Inc.; 2003
24 GeneChip Expression Analysis Data Analysis Fundamentals Affymetrix Inc.; 2002
25 **Bakay M**, Chen YW, Borup R, Zhao P, Nagaraju K, Hoffman EP. Sources of variability and effect of experimental approach on expression profiling data interpretation. *BMC Bioinformatics* 2002; **3**: 4
26 **Mills JC**, Gordon JI. A new approach for filtering noise from high-density oligonucleotide microarray datasets. *Nucleic Acids Res* 2001; **29**: E72
27 **Unger MA**, Rishi M, Clemmer VB, Hartman JL, Keiper EA, Greshock JD, Chodosh LA, Liebman MN, Weber BL. Characterization of adjacent breast tumors using oligonucleotide microarrays. *Breast Cancer Res* 2001; **3**: 336-341

Science Editor Guo SY **Language Editor** Elsevier HK

PO Box 2345, Beijing 100023, China
www.wjgnet.com
wjg@wjgnet.com

ELSEVIER

World J Gastroenterol 2005;11(38):5997-6002
World Journal of Gastroenterology ISSN 1007-9327
© 2005 The WJG Press and Elsevier Inc. All rights reserved.

• *BRIEF REPORTS* •

Effect of herpesvirus infection on pancreatic duct cell secretion

Péter Hegyi, Balázs Ördög, Zoltán Rakonczai Jr, Tamás Takács, János Lonovics, Annamária Szabolcs, Réka Sári, András Tóth, Julius G Papp, András Varró, Mária K Kovács, Mike A Gray, Barry E Argent, Zsolt Boldogköi

Péter Hegyi, Zoltán Rakonczai Jr, Tamás Takács, János Lonovics, Annamária Szabolcs, Réka Sári, First Department of Medicine, Faculty of Medicine, University of Szeged, Szeged, Hungary
Péter Hegyi, Zoltán Rakonczai Jr, Mike A Gray, Barry E Argent, School of Cell and Molecular Biosciences, University Medical School, Newcastle upon Tyne NE2 4HH, UK
Balázs Ördög, Mária K Kovács, Zsolt Boldogköi, Department of Biology, Faculty of Medicine, University of Szeged, Szeged, Hungary
András Tóth, Julius G Papp, András Varró, Mária K Kovács, Division of Cardiovascular Pharmacology, Department of Pharmacology and Pharmacotherapy, Faculty of Medicine, Hungarian Academy of Sciences, University of Szeged, Szeged, Hungary
Co-first-authors: Péter Hegyi and Balázs Ördög
Supported by a Wellcome Trust IRDA Grant to P.H. (No. 022618), Hungarian Scientific Research Funds to P.H. and J.L. (No. D42188, T43066), a Wellcome Trust Travelling Fellowship to Z.R. (No. 069470), a Bolyai Postdoctoral Fellowship to P.H. (No. 00276/04) and a National Fund for Scientific Research (OTKA) to Z.B. (No. T049171)
Correspondence to: Zsolt Boldogköi, Department of Biology, Faculty of Medicine, University of Szeged, Somogyi Bela str. 4, H-6720 Szeged, Hungary. boldog@sb4.szote.u-szeged.hu
Telephone: +36-62-545595 Fax: +36-62-545131
Received: 2004-12-09 Accepted: 2005-02-18

AIM: To examine the effect of acute infection caused by herpesvirus (pseudorabies virus, PRV) on pancreatic ductal secretion.

METHODS: The virulent Ba-DupGreen (BDG) and non-virulent Ka-RREp0lacgfp (KEG) genetically modified strains of PRV were used in this study and both of them contain the gene for green fluorescent protein (GFP). Small intra/interlobular ducts were infected with BDG virus (10^7 PFU/mL for 6 h) or with KEG virus (10^{10} PFU/mL for 6 h), while non-infected ducts were incubated only with the culture media. The ducts were then cultured for a further 18 h. The rate of HCO_3^- secretion [base efflux -$J(B^-)$] was determined from the buffering capacity of the cells and the initial rate of intracellular acidification (1) after sudden blockage of basolateral base loaders with dihydro-4,4,-diisothiocyanatostilbene-2,2,-disulfonic acid (500 μmol/L) and amiloride (200 μmol/L), and (2) after alkali loading the ducts by exposure to NH_4Cl. All the experiments were performed in HCO_3^--buffered Ringer solution at 37 ℃ (n = 5 ducts for each experimental condition). Viral structural proteins were visualized by immunohistochemistry. Virally-encoded GFP and immunofluorescence signals were recorded by a confocal laser scanning microscope.

RESULTS: The BDG virus infected the majority of accessible cells of the duct as judged by the appearance of GFP and viral antigens in the ductal cells. KEG virus caused a similarly high efficiency of infection. After blockage of basolateral base loaders, BDG infection significantly elevated -$J(B^-)$ 24 h after the infection, compared to the non-infected group. However, KEG infection did not modify -$J(B^-)$. After alkali loading the ducts, -$J(B^-)$ was significantly elevated in the BDG group compared to the control group 24 h after the infection. As we found with the inhibitor stop method, no change was observed in the group KEG compared to the non-infected group.

CONCLUSION: Incubation with the BDG or KEG strains of PRV results in an effective infection of ductal epithelial cells. The BDG strain of PRV, which is able to initiate a lytic viral cycle, stimulates HCO_3^- secretion in guinea pig pancreatic duct by about four- to fivefold, 24 h after the infection. However, the KEG strain of PRV, which can infect, but fails to replicate, has no effect on HCO_3^- secretion. We suggest that this response of pancreatic ducts to virulent PRV infection may represent a defense mechanism against invasive pathogens to avoid pancreatic injury.

© 2005 The WJG Press and Elsevier Inc. All rights reserved.

Key words: Pancreas; Hypersecretion; Ductal cells; Infection; Pseudorabies virus

Hegyi P, Ördög B, Rakonczai Z Jr, Takács T, Lonovics J, Szabolcs A, Sári R, Tóth A, Papp JG, Varró A, Kovács MK, Gray MA, Argent BE, Boldogköi Z. Effect of herpesvirus infection on pancreatic duct cell secretion. *World J Gastroenterol* 2005; 11(38): 5997-6002
http://www.wjgnet.com/1007-9327/11/5997.asp

INTRODUCTION

Pseudorabies virus (PRV) is an α-herpesvirus closely related to the herpes simplex virus (HSV), a well-known human pathogen[1,2]. The natural host of PRV is the pig, but it has a very wide host range including several mammalian families, such as carnivores, ungulates and rodents, but humans are resistant to PRV infection[1]. PRV infection is a multistep process initiated by the receptor-mediated attachment of the virus to the cell surface. Upon entering the cells, the PRV nucleocapsid approaches the nuclear membrane and the viral DNA is released into the nuclei by a poorly understood mechanism. The lytic cycle of the virus is controlled by a transcriptional cascade mechanism[2].

Acute pancreatitis is most commonly associated with

biliary stone and alcoholism. Other causes, including infections, drugs, lipid abnormalities, congenital anomalies, trauma, tumors, and idiopathic form, account for at least 10-20% of the total number of cases[3]. The incidence of pancreatitis may even be higher since the diagnosis of acute pancreatitis may go undetected in many patients. Several viruses have been reported to cause acute pancreatitis, including coxsackievirus B3[4] and B4[5], mumpsvirus[6], varicella[7], hepatitis A[8] and B[9], cytomegalovirus[10], varicella-zoster virus[11] and HSV[12].

We have previously shown that hypersecretion can be observed during the early phase of experimental edematous and necrotizing pancreatitis[13]. However, the source and the role of this hypersecretion are unknown. Either acinar cells and/or the ductal epithelium could be responsible for hypersecretion.

Our aim in this study was to examine the effect of acute infection caused by PRV on pancreatic ductal secretion.

□□□□□□□□□ □□□ □□□□□□□

Virus strain

Ba-Dup Green (BDG), a genetically modified replicating strain of PRV, was used in this study. The Bartha virus[14], which is an attenuated live vaccine strain of PRV, was used as the parental virus for the generation of BDG. Two copies of a genetically modified green fluorescent protein (GFP) gene-containing expression cassettes were inserted into the PRV antisense promoter region located in the inverted repeat segment of the virus[15,16]. Ka-EP0lacgfp (KEG) strain of PRV was used as a non-replicating control virus for these experiments. KEG was constructed by deleting the small subunit of ribonucleotide reductase[17] and the early protein 0 (EP0)[18] genes. An expression cassette containing a GFP and a lacZ gene was inserted in place of the EP0 gene[19]. These mutations render the virus incapable of replication in non-dividing cells[19].

Isolation and infection of pancreatic ducts

Small intra/interlobular ducts were isolated from the pancreas of guinea pigs weighing 150-250 g. The guinea pig was humanely killed by cervical dislocation, the pancreas was removed and intra/interlobular ducts were isolated by enzymatic dissociation, microdissection and then cultured at 37 ℃ in 50 mL/L CO_2[20]. Ducts were incubated in McCoy's-based culture medium containing BDG viruses at a dose of 10^7 PFU/mL for 6 h or KEG virus (10^{10} PFU/mL for 6 h), while the non-infected ducts were exposed to culture media only. The ducts were then cultured for a further 18 h as described earlier[20], during which time the ducts seal to form a closed sac that swells due to accumulation of ions and water secretions within the duct lumen[20].

Immunohistochemistry

The immunofluorescent detection of structural viral proteins was performed as follows. Isolated pancreatic ducts were fixed in 40 g/L paraformaldehyde in PBS, pH 7.4 for 1 h at room temperature. Following three rinses in PBS, the ducts were blocked with 10 g/L bovine serum albumin and 1 mL/L Triton X-100 in PBS for 1 h at room temperature. Thereafter, a rabbit polyclonal antiviral antibody (Affinity Bioreagents, Golden, USA) diluted at 1:500 (v/v) in blocking solution was applied for 24 h at 4 ℃. After being washed with PBS, the ducts were incubated with an anti-rabbit antibody conjugated with a red light-emitting dye (Alexa Fluor® 633; Molecular probes, USA) diluted at 1:1 000 (v/v) in a blocking solution for 24 h at 4 ℃. After further washing in PBS, the ducts were mounted on slides using Aqua-Poly/ Mount (Polysciences Inc., Niles, USA). The specificity of immunohistochemical procedure was assessed by simultaneous staining of non-infected ducts. No immunohistochemical labeling was observed in control experiments.

Microscopy

For monitoring virally expressed GFP and immunofluorescence signals, fluorescent images and optical sections of the infected ducts were recorded by a confocal laser scanning microscope (Zeiss, LSM 400).

Measurement of intracellular pH

Cultured ducts were attached, using Cell-Tak, to a coverslip (24 mmol/L) forming the base of a perfusion chamber mounted on a Nikon Diaphot microscope (Nikon UK Ltd, Budapest, Hungary). The ducts were bathed in the standard Hepes solution at 37 ℃ and loaded with the pH-sensitive fluorescent dye 2',7'-bis-(2-carboxyethyl)-5-(and-6)-carboxyfluorescein (BCECF) by exposure to 2 μmol/L BCECF-AM for 20-30 min. After loading, the ducts were continuously perfused with solutions at a rate of 4-5 mL/min. Intracellular pH (pH_i) was measured using a microspectrofluorimeter system (Cairn, Kent, UK). A small area of 5-10 cells was excited with light at wavelengths of 490 and 440 nm, and the 490/440 fluorescence emission ratio was measured at 535 nm. Four pH_i measurements were obtained per second. *In situ* calibration of the fluorescence signal was performed using the high K^+-nigericin technique[21,22]. During calibration, the ducts were bathed in high K^+ HEPES solution and extracellular pH stepped between 5.95 and 8.46.

Determination of base efflux

The intrinsic buffering capacity (β_i) of duct cells was estimated according to the NH_4^+ pre-pulse technique[23,24]. β_i refers to the ability of intrinsic cellular components (excluding HCO_3^-/CO_2) to buffer changes of pH_i. Briefly, pancreatic duct cells were exposed to various concentrations of NH_4Cl, while Na^+ and HCO_3^- were omitted from the solution in order to block the Na^+-dependent pH regulatory mechanisms. β_i was estimated by the Henderson-Hasselbach equation. The total buffering capacity (β_{total}) was calculated from: $\beta_{total} = \beta_i+\beta_{HCO3^-} = \beta_i+2.3\times[HCO_3^-]_i$, where β_{HCO3}- is the buffering capacity of the HCO_3^-/CO_2 system and $[HCO_3^-]_i$ is the intracellular HCO_3^- concentration[24].

Measurement of HCO_3^- efflux

Inhibitor stop method Exposing the ducts to dihydro-4, 4,-diisothiocyanatostilbene-2,2,-disulfonic acid (H_2DIDS, 0.5 mmol/L) and amiloride (0.2 mmol/L) for 5 min caused a marked acidification of pH_i (Figure 2A). This acidification occurred due to inhibition of the basolateral Na^+/HCO_3^- co-transporters and Na^+/H^+ exchangers, which normally

act to transport HCO_3^- into the duct cell from the blood[25,26]. The rate of pH_i acidification after the exposure to H_2DIDS and amiloride could reflect the intracellular buffering capacity and the rate at which HCO_3^- effluxes (i.e., secreted) across the apical membrane via Cl^-/HCO_3^- exchangers and CFTR channels[24,25].

The initial rate of intracellular acidification (dpH/dt), over the first 60 s of exposure to amiloride and H_2DIDS, was calculated by linear regression analysis using 240 data points (four pH_i measurements per second)[24].

Alkali load method Exposing the ducts to 20 mol/L NH_4Cl caused an alkalization of pH_i due to the rapid influx of NH_3 into cells (Figure 3A). Recently, we demonstrated that the recovery of pH_i under these conditions was dependent on the presence of HCO_3^- in the bathing solution, suggesting that it results from HCO_3^- efflux (i.e., secretion) out of the duct cells[24]. In the present study, the initial rate of recovery from alkalosis (dpH/dt) over the first 30 s (120 pH_i measurements) in the continued presence of NH_4Cl was calculated as described previously[24].

The rates of pH_i change measured in these inhibitors stopped and alkali load experiments were converted to transmembrane base flux $J(B^-)$ using the equation: $J(B^-)= dpH/dt \times \beta_{total}$. We denoted base influx as $J(B^-)$ and base efflux (secretion) as $-J(B^-)$.

Solutions and chemicals

The standard Hepes-buffered solution contained (mmol/L) 130 NaCl, 5 KCl, 1 $CaCl_2$, 1 $MgCl_2$, 10 D-glucose, and 10 Na-Hepes. The high K^+ Hepes-buffered solution contained (mmol/L) 130 KCl, 5 NaCl, 1 $CaCl_2$, 1 $MgCl_2$, 10 D-glucose, and 10 Na-Hepes. Hepes-buffered solutions were gassed with 100% O_2 and their pH was set to 7.4 at 37 ℃ with HCl. The standard HCO_3^--buffered solution contained (mmol/L) 115 NaCl, 25 $NaHCO_3$, 5 KCl, 1 $CaCl_2$, 1 $MgCl_2$, and 10 D-glucose. The ammonia pulse solution contained (mmol/L) 95 NaCl, 20 NH_4Cl, 25 $NaHCO_3$, 5 KCl, 1 $CaCl_2$, 1 $MgCl_2$, and 10 D-glucose. HCO_3^--buffered solutions were gassed with 95% O_2/50 mL/L CO_2 to set pH to 7.4 at 37 ℃.

Chromatographically pure collagenase was obtained from Worthington (Lakewood, NJ, USA), culture media from Sigma (Budapest, Hungary). Nigericin (Sigma, Budapest, Hungary) was dissolved in absolute ethanol, H_2DIDS (from Molecular Probes,Eugene, OR, USA) and amiloride in dimethyl sulfoxide (DMSO). CellTak was obtained from Becton Dickinson Labware (Bedford, MA, USA). BCECF-AM was obtained from Molecular Probes (Eugene, OR, USA) and was made up as a 2 mmol/L stock solution using DMSO. The 10-fold concentrated PBS stock solution contained (g/L) 80 NaCl, 2 KCl, 2.4 NaH_2PO_4, 14.4 Na_2HPO_4 (pH 7.2). Chemicals were obtained from Merck (Darmstadt, Germany). Blocking solution contained 10 g/L bovine serum albumin from Sigma (Budapest, Hungary) and 1 mL/L scintillation grade Triton X-100 (BDH Chemicals, Poole, UK).

Statistical analysis

Results were expressed as mean±SE (n = 5 ducts). Statistical analyses were performed using ANOVA. $P<0.05$ was accepted as statistically significant.

Efficacy of viral infection

Two GFP-expressing cassettes were inserted into the PRV genome[15] enabling virus infection to be visualized in both living and fixed cells. Monitoring of GFP expression of BDG was utilized to assess the extent of viral infection of ductal epithelial cells. We observed that BDG virus practically infected all accessible cells of the duct when used at a titer of 10^7 PFU/mL after 24 h (Figure 1A). We used a higher concentration (10^{10} PFU/mL) of KEG virus and found a similarly high efficiency of infection (Figure 1C).

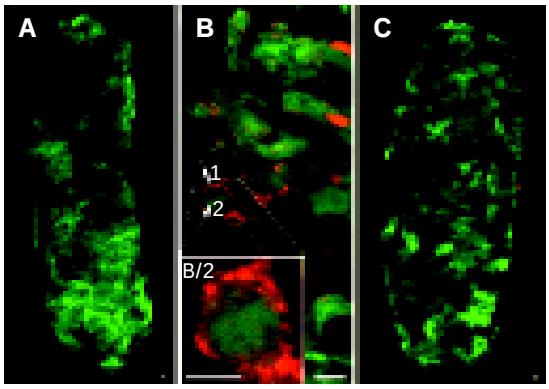


Figure 1 Infection of guinea pig pancreatic ducts with BDG and Ka-EP0lacgfp (KEG). A: Infection of the pancreatic ductal epithelial cells with BDG; B: appearance of viral antigens indicating the productive BDG infection and GFP fluorescence; C: non-virulent KEG strain-produced high efficiency of infection. Scale bars represent 10 μm.

Cytotoxic effect of PRV infection

BDG is a virulent strain; therefore, virus uptake by cells results in the immediate initiation of the lytic viral cycle and the unavoidable death of the infected cells. Productive virus infection was detected in the BDG group by labeling the structural viral proteins by means of immunohistochemistry. The GFP gene was placed under the control of the constitutive human cytomegalovirus immediate early promoter, which conferred a very early expression of the reporter gene. In contrast, viral structural proteins, which are recognized by the anti-PRV antibodies, appeared at a later stage of viral infection[15]; therefore, a shift between the appearance of GFP and immunofluorescence could be observed (Figure 1B). In contrast, in the KEG group, we did not observe any cytopathic effects and could not detect viral antigens. However, GFP expression indicated the presence of the virus within the infected cells (Figure 1C).

Pancreatic ductal bicarbonate secretion

Exposing the ducts to 0.5 mmol/L H_2DIDS and 0.2 mmol/L amiloride caused an acidification of pH_i (Figure 2A), due to inhibition of the basolateral Na^+/HCO_3^- co-transporters and Na^+/H^+ exchangers. The effect of H_2DIDS and amiloride was reversible, removal of the inhibitors caused pH_i to return to the control value. In these series of experiments, we tested whether virus infection affected the net HCO_3^- secretion of pancreatic duct cells. Base efflux was significantly elevated

in the BDG group compared to the non-infected ducts, 24 h after the infection (7.84±1.24 mmol/L B^-/min *vs* 2.2±0.18 mmol/L B^-/min, respectively; $n = 5$). However, no change was observed in the KEG group (2.4±0.32 mmol/L B^-/min; $n = 5$) compared to the non-infected ducts. These data are summarized in Figure 2B.

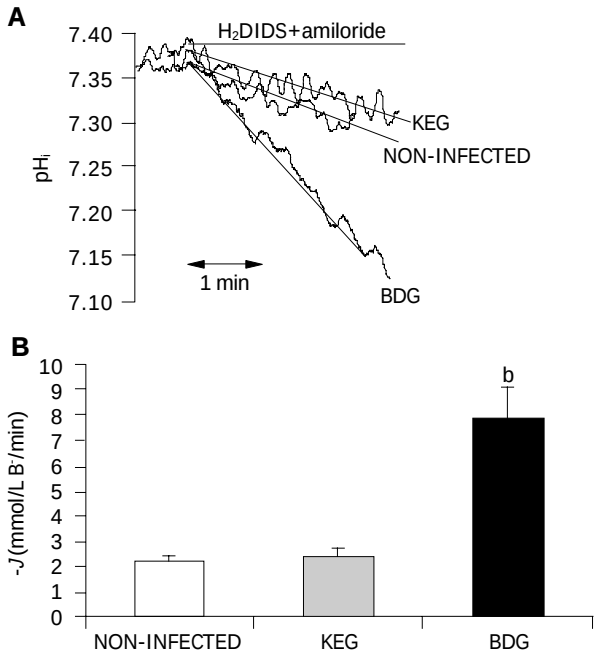


Figure 2 Inhibitor stop method for determining bicarbonate secretion. A: Representative pH_i traces; B: summary of the results obtained using the inhibitory stop method. $^bP<0.001$ *vs* the control (ANOVA).

Exposure of duct cells to 20 mmol/L NH_4Cl induced an immediate rise in pH_i due to the rapid entry of NH_3 into the duct cells (Figure 3A). In this series of experiments, base efflux was significantly elevated in the BDG group compared to the control group 24 h after the infection (160.04±19.16 mmol/L B^-/min *vs* 36.37±1.08 mmol/L B^-/min, respectively; $n = 5$). However, as we found with the inhibitor stop method, no change was observed in the KEG group (39.34±3.49 mmol/L B^-/min, $n = 5$) compared to the non-infected ducts (Figure 3B).

Using the ammonium pulse technique, we also tested whether PRV affected the ability of duct cells to recover from an acid load following removal of NH_4Cl from the superfusate. The transporters most likely to be involved in this process are the Na^+/HCO_3^- co-transporter, the Na^+/H^+ exchanger and the H^+ pump located on the basolateral membrane of the duct cells. No significant change was observed between the PRV infected and non-infected groups (Figure 3A, $n = 5$).

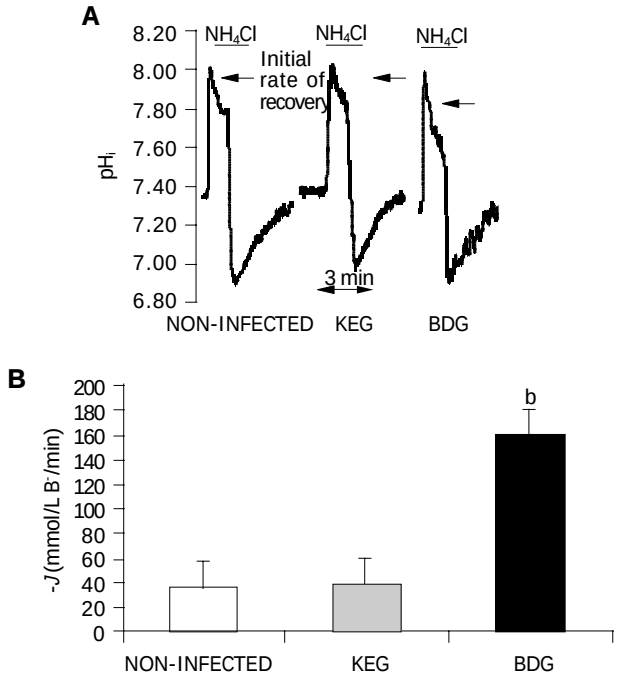


Figure 3 Alkali load method for determining bicarbonate secretion. A: Representative pH_i traces; B: summary of the results obtained using the alkali load method. $^bP<0.001$ *vs* the control (ANOVA).

[redacted]

Though the broad spectrum of etiological factors is involved in acute pancreatitis, the pathophysiology of the disease is less understood. Most investigators believe that acute pancreatitis results from an early intra-acinar cell activation of zymogens[26]. Following this early activation, a trypsin cascade occurs in the gland leading to the auto-digestion of acinar cells[26]. However, a possible pathophysiological role of the ductal epithelium has not been investigated. The permeability of the pancreatic ductal epithelium to HCO_3^- and Cl^- is increased by exposure to various bile salts at concentrations within the range normally found in the duodenum[27]. Moreover, *E. coli*-infected bile causes further increases of the permeability of the ductal epithelium to HCO_3^- and Cl^-[27]. Ethanol could induce fluid hypersecretion from guinea pig pancreatic duct cells. Low concentrations of ethanol directly augment pancreatic ductal fluid secretion stimulated by physiological and pharmacological concentrations of secretin (cAMP pathway) and via Ca^{2+} mobilization[28]. The effects of other etiologic factors for acute pancreatitis on pancreatic ductal HCO_3^- secretion have not been characterized as yet.

Viruses can alter ion transport by epithelial cells. Kunzelmann *et al*.[29], reported that parainfluenza virus I (Sendai virus) produces rapid changes in ion transport across tracheal epithelium. The Sendai virus, at concentrations observed during respiratory infections, activates Cl^- secretion and inhibits Na^+ absorption[29] by triggering the release of ATP, which then acts on apical P2Y receptors to produce changes in ion transport[29]. Bacterial infection (e.g., *Pseudomonas aeruginosa* or *Staphylococcus aureus*) triggers mucus and interleukin production[30,31]. Mucus clearance is a primary innate defense mechanism for mammalian airways[32].

In this study, we developed a model to investigate the effect of acute infection with a herpes virus (PRV) on the pancreatic ductal epithelium. Incubating BDG at a dose of 10^7 PFU/mL for 6 h resulted in the infection of the majority

of accessible epithelial cells within the duct. As expected, the virulent PRV strain resulted in a productive infection of epithelial cells, indicated by the appearance of viral antigens. We used two different measures of HCO_3^- secretion (inhibitor stop and alkali load methods) to study the effect of acute PRV infection on pancreatic ducts. Both methods showed that BDG infection stimulated HCO_3^- secretion in guinea pig pancreatic duct by about four or fivefold. However, BDG had no effect on the pH_i recovery after an acid load, suggesting that neither the basolateral Na^+/HCO_3^- co-transporter nor the basolateral Na^+/H^+ exchanger is involved in the hypersecretory effect. We have previously reported that pancreatic hypersecretion is observed during the early phase of acute necrotizing pancreatitis[33]. Furthermore, the early phase hypersecretion is accompanied with a simultaneous decrease in protein output[34], suggesting that the pancreatic ducts are at least in part involved in the change of secretory pattern. In our study, the genetically engineered control virus (KEG) did not evoke hypersecretion in the ductal cells, indicating that the presence of the virus in the cell is not enough to trigger hypersecretion. Hypersecretion was only induced by the BDG virus, which is able to initiate a lytic viral cycle.

Our finding that BDG stimulates HCO_3^- secretion from pancreatic ducts may represent a defense mechanism against invasive pathogens in order to avoid pancreatic injury. We speculate that the stimulated secretion can wash out activated enzymes, viruses and other toxic factors from the pancreas. Moreover, the high efficiency of PRV infection in the pancreatic ductal epithelium may open the possibility for gene transfer and gene therapy of the duct cells using non-replicating or conditionally replicating PRV variants (KEG)[2,19].

ACKNOWLEDGEMENTS

We would like to thank Dr. János Szabad for his helpful discussions.

REFERENCES

1 **Boldogkoi Z**, Bratincsak A, Fodor I. Evaluation of pseudorabies virus as a gene transfer vector and an oncolytic agent for human tumor cells. *Anticancer Res* 2002**;** **22**: 2153-2159
2 **Boldogkoi Z**, Nogradi A. Gene and Cancer Therapy - Pseudorabies Virus: A Novel Research and Therapeutic Tool? *Curr Gene Ther* 2003; **3**: 155-182
3 **Steer ML**. Etiology and pathophysiology of acute pancreatitis. In: The Exocrine *Pancreas: Biology, Pathobiology and Diseases*. Edited by Go VLW, Dimagno EP, Gardner JD, Lebenthal E, Reber HA, Scheele GA. *Raven Press New York* 1993: 581-593
4 **Vuorinen T**, Kallajoki M, Hyypia T, Vainionpaa R. Coxsackievirus B3-induced acute pancreatitis: analysis of histopathological and viral parameters in a mouse model. *Br J Exp Pathol* 1989; **70**: 395-403
5 **Vella C**, Brown CL, McCarthy DA. Coxsackievirus B4 infection of the mouse pancreas: acute and persistent infection. *J Gen Virol* 1992; **73**: 1387-1394
6 **Imrie CW**, Ferguson JC, Sommerville RG. Coxsackie and mumpsvirus infection in a prospective study of acute pancreatitis. *Gut* 1977; **18**: 53-56
7 **Kirschner S**, Raufman JP. Varicella pancreatitis complicated by pancreatic pseudocyst and duodenal obstruction. *Dig Dis Sci* 1988; **33**: 1192-1195
8 **Khanna S**, Vij JC. Severe acute pancreatitis due to hepatitis A virus infection in a patient of acute viral hepatitis. *Trop Gastroenterol* 2003; **24**: 25-26
9 **de Oliveira LC**, Rezende PB, Ferreira AL, de Freitas AA, de Carvalho AM, Guedes CA, Costa WO. Concurrent acute hepatitis and pancreatitis associated with hepatitis B virus: case report. *Pancreas* 1988; **16**: 559-561
10 **Wilcox CM**, Forsmark CE, Grendell JH, Darragh TM, Cello JP. Cytomegalovirus-associated acute pancreatic disease in patients with acquired immunodeficiency syndrome. Report of two patients. *Gastroenterology* 1990; **99**: 263-267
11 **Pulik M**, Teillet F, Teillet-Thiebaud F, Lionnet F, Genet P, Petitdidier C. Varicella-zoster virus pancreatitis in hematologic diseases (in French). *Ann Med Interne* 1995; **146**: 292-294
12 **Shintaku M**, Umehara Y, Iwaisako K, Tahara M, Adachi Y. Herpes simplex pancreatitis. *Arch Pathol Lab Med* 2003; **127**: 231-234
13 **Hegyi P**, Czako L, Takacs T, Szilvassy Z, Lonovics J. Pancreatic secretory responses in L-arginine-induced pancreatitis: comparison of diabetic and nondiabetic rats. *Pancreas* 1999; **19**: 167-174
14 **Bartha A**. Experimental reduction of virulence of Aujeszky's disease (in Hungarian). *Magy Allatorv Lapja* 1961; **16**: 42-45
15 **Boldogkoi Z**, Reichart A, Toth IE, Sik A, Erdelyi F, Medveczky I, Llorens-Cortes C, Palkovits M, Lenkei Z. Construction of recombinant pseudorabies viruses optimized for labeling and neurochemical characterization of neural circuitry. *Brain Res Mol Brain Res* 2002; **109**: 105-118
16 **Boldogkoi Z**, Sik A, Denes A, Reichart A, Toldi J, Gerendai I, Kovacs KJ, Palkovits M. Novel tracing paradigms-genetically engineered herpesviruses as tools for mapping functional circuits within the CNS: present status and future prospects. *Prog Neurobiol* 2004; **72**: 417-445
17 **Boldogkoi Z**, Medveczky I, Glavits R, Braun A, Fodor I. *In vivo* studies on Aujeszky's disease virus mutants. *Acta Microbiol Immunol Hung* 1996; **43**: 307-318
18 **Boldogkoi Z**, Braun A, Fodor I. Replication and virulence of early protein 0 and long latency transcript deficient mutants of the Aujeszky's disease (pseudorabies) virus. *Microbes Infect* 2000; **2**: 1321-1328
19 **Boldogkoi Z**, Szabo A, Vrbova G, Nogradi A. Pseudorabies virus-based gene delivery to rat embryonic spinal cord grafts. *Hum Gene Ther* 2002; **13**: 719-729
20 **Argent BE**, Arkle S, Cullen MJ, Green R. Morphological, biochemical and secretory studies on rat pancreatic ducts maintained in tissue culture. *Q J Exp Physiol* 1986; **71**: 633-648
21 **Thomas JA**, Buchsbaum RN, Zimniak A, Racker E. Intracellular pH-measurements in Ehrlich ascites tumor cells utilizing spectroscopic probes generated *in situ*. *Biochemistry* 1979; **18**: 2210-2218
22 **Hegyi P**, Rakonczay Z Jr, Gray MA, Argent BE. Measurement of intracellular pH in pancreatic duct cells: A new method for calibrating the fluorescence data. *Pancreas* 2004; **28**: 427-434
23 **Weintraub WH**, Machen TE. pH regulation in hepatoma cells: roles for Na-H exchange, Cl-HCO_3 exchange, and Na-HCO_3 cotransport. *Am J Physiol* 1989; **257**: G317-G327
24 **Hegyi P**, Gray MA, Argent BE. Substance P inhibits bicarbonate secretion from guinea-pig pancreatic ducts by modulating an anion exchanger. *Am J Physiol* 2003; **285**: C268-C276
25 **Szalmay G**, Varga G, Kajiyama F, Yang XS, Lang TF, Case RM, Steward MC. Bicarbonate and fluid secretion by cholecystokinin, bombesin and acetylcholine in isolated guinea-pig pancreatic ducts. *J Physiol* 2001; **535**: 795-807
26 **Lerch MM**, Albrecht E, Ruthenburger M, Mayerle J, Halangk W, Kruger B. Pathophysiology of alcohol-induced pancreatitis. *Pancreas* 2003; **27**: 291-296
27 **Reber HA**, Mosley JG. The effect of bile salts on the pancreatic

duct mucosal barrier. *Br J Surg* 1980; **67**: 59-62

28 **Yamamoto A**, Ishiguro H, Ko SB, Suzuki A, Wang Y, Hamada H, Mizuno N, Kitagawa M, Hayakawa T, Naruse S. Ethanol induces fluid hypersecretion from guinea-pig pancreatic duct cells. *J Physiol* 2003; **551**: 917-926

29 **Kunzelmann K**, Konig J, Sun J, Markovich D, King NJ, Karupiah G, Young JA, Cook DI. Acute effects of parainfluenza virus on epithelial electrolyte transport. *J Biol Chem* 2004; **279**: 48760-48766

30 **McNamara N**, Khong A, McKemy D, Caterina M, Boyer J, Julius D, Basbaum C. ATP transduces signals from ASGM1, a glycolipid that functions as a bacterial receptor. *Proc Natl Acad Sci USA* 2001; **98**: 9086-9091

31 **Ratner AJ**, Bryan R, Weber A, Nguyen S, Barnes D, Pitt A, Gelber S, Cheung A, Prince A. Cystic fibrosis pathogens activate Ca2+-dependent mitogen-activated protein kinase signaling pathways in airway epithelial cells. *J Biol Chem* 2001; **276**: 19267-19275

32 **Knowles MR**, Boucher RC. Mucus clearance as a primary innate defense mechanism for mammalian airways. *J Clin Invest* 2002; **109**: 571-577

33 **Hegyi P**, Rakonczay Z Jr, Sari R, Gog C, Lonovics J, Takacs T, Czako L. L-arginine induced experimental pancreatitis. *World J Gastroenterol* 2004; **10**: 2003-2009

34 **Czako L**, Yamamoto M, Otsuki M. Exocrine pancreatic function in rats after acute pancreatitis. *Pancreas* 1997; **15**: 83-90

Science Editor Wang XL and Guo SY **Language Editor** Elsevier HK

PO Box 2345, Beijing 100023, China
www.wjgnet.com
wjg@wjgnet.com

ELSEVIER

World J Gastroenterol 2005;11(38):6003-6008
World Journal of Gastroenterology ISSN 1007-9327
© 2005 The WJG Press and Elsevier Inc. All rights reserved.

• *BRIEF REPORTS* •

Haplotype of prostaglandin synthase 2/cyclooxygenase 2 is involved in the susceptibility to inflammatory bowel disease

David G Cox, J Bart A Crusius, Petra HM Peeters, H Bas Bueno-de-Mesquita, A Salvador Peña, Federico Canzian

David G Cox, International Agency for Research on Cancer, Lyon, France (Current address: Molecular Epidemiology, Harvard School of Public Health, Boston, MA, USA)
J Bart A Crusius, Laboratory of Immunogenetics, VU University Medical Center, Amsterdam, The Netherlands
Petra HM Peeters, Julius Center for Health Sciences and Primary Care, University Medical Center, Utrecht, The Netherlands
H Bas Bueno-de-Mesquita, Department of Epidemiology, National Institute of Public Health and Environmental Protection, Bilthoven, The Netherlands
A Salvador Peña, Laboratory of Immunogenetics and Department of Gastroenterology, VU University Medical Center, Amsterdam, The Netherlands
Federico Canzian, International Agency for Research on Cancer, Lyon, France (Current address: German Cancer Research Center, Heidelberg, Germany)
Supported by The Grants from the International Agency for Research on Cancer (Special Training Award to DGC), the French Association for Research on Cancer (grant #7478), and the Crohn's and Colitis Foundation of America (to ASP)
Correspondence to: Federico Canzian, PhD, German Cancer Research Centre (DKFZ), Im Neuenheimer Feld 280, D-69120 Heidelberg, Germany. f. canzian@dkfz.de
Telephone: +49-6221-421791 Fax: +49-6221-421810
Received: 2005-01-21 Accepted: 2005-02-18

Abstract

AIM: Prostaglandin G/H synthase 2 (PTGS2 or COX2) is one of the key factors in the cellular response to inflammation. PTGS2 is expressed in the affected intestinal segments of patients with inflammatory bowel diseases (IBD). In IBD patients, non-steroidal anti-inflammatory drugs, which have been shown to reduce both the production and activity of PTGS2, may activate IBD and aggravate the symptoms. We aimed at examining genetic variants of *PTGS2* that may be risk factors for IBD.

METHODS: We genotyped 291 individuals diagnosed with IBD and 367 controls from the Dutch population for the five most frequent polymorphisms of the *PTGS2* gene. Clinical data were collected on all patients. DNA was extracted via normal laboratory methods. Genotyping was carried out using multiplex PCR followed by the Invader Assay and the 5' exonuclease assay (TaqMan). New polymorphism screening was performed by pre-screening with denaturing high-performance liquid chromatography, followed by fluorescent sequencing.

RESULTS: Allele 5209G was weakly associated with Crohn's disease (odds ratio [OR] 1.63, 95% confidence interval [CI] 1.03-2.57), and allele 8473T with ulcerative colitis (OR 1.50, 95%CI 1.00-2.27). The haplotype including both alleles showed a strong association with IBD (OR 13.15, 95%CI 3.17-116.15). This haplotype, while rare (-0.3%) in the general population, is found more frequently in patients (3.5%).

CONCLUSION: Our data suggest that this haplotype of *PTGS2* contributes to the susceptibility of IBD.

© 2005 The WJG Press and Elsevier Inc. All rights reserved.

Key words: Inflammatory bowel disease; Prostaglandin G/H synthase; Cyclooxygenase; SNP; Haplotype

Cox DG, Crusius JBA, Peeters PHM, Bueno-de-Mesquita HB, Peña AS, Canzian F. Haplotype of prostaglandin synthase 2/cyclooxygenase 2 is involved in the susceptibility to inflammatory bowel disease. *World J Gastroenterol* 2005; 11(38): 6003-6008
http://www.wjgnet.com/1007-9327/11/6003.asp

INTRODUCTION

Risk factors for inflammatory bowel diseases (IBD) include several environmental and genetic exposures. Diet, tobacco smoking, and childhood diseases or poor hygiene have been identified as risk factors for IBD, with some important differences between ulcerative colitis (UC) and Crohn's disease (CD)[1-3]. Caucasians have been shown to be at higher risk than non-Caucasians, with North-South gradients seen in Europe[4,5].

Familial aggregation of IBD suggests a genetic component in the susceptibility to IBD. One major locus of susceptibility to IBD has been mapped by linkage analysis to chromosome 16, at the *CARD15/NOD2* gene[6-8], which has a role in inflammatory responses, through activation of nuclear factor NF-κB. Two more susceptibility genes have recently been identified[9,10]. Population-based association studies focused on polymorphisms of inflammatory genes, such as genes of the interleukin-1β pathway. Few showed significant associations with some degree of contradiction between studies[11-15].

Key genes involved in the regulation of the inflammatory processes, such as prostaglandin G/H synthase/cyclooxygenase (PTGS/COX), are obvious candidates to look for variants predisposing to IBD. One of the two PTGS isoforms, PTGS2/COX2, is expressed in epithelial cells and mononuclear cells in IBD[4], and it is induced in response to pro-inflammatory cytokines, including interleukin-1β[16-18]. PTGS2 is the rate-

limiting enzyme in the production of prostaglandins. Prostaglandins are thought to be essential in the process of wound healing in the gastrointestinal tract[19]. The use of non-steroidal anti-inflammatory drugs (NSAIDs), which inhibit both the transcription and activity of PTGS2, exacerbates the symptoms in UC[20] and may even activate quiescent IBD[21]. Thus, the expression of PTGS2 in the inflamed intestine might be a protective response within the wound-healing process[22]. Consequently, polymorphisms that change the amount of prostaglandins produced in inflamed cells could cause susceptibility to IBD.

To address this hypothesis, we have studied 145 UC patients, 146 CD patients, and 367 controls from the Dutch Caucasian population, which has a high incidence of IBD[23]. The present study was to search for associations between IBD and common single nucleotide polymorphisms (SNPs) in the *PTGS2* gene.

[illegible]

Samples

The recruitment of cases took place at the Department of Gastroenterology of the VU University Medical Center (VUmc), a referral center for IBD, between April 1992 and September 2000. Patients with indeterminate colitis were excluded from this study. Seventy-five UC patients were females and seventy males, with a median age of 46 years (range 19-89 years). The gender repartition of CD patients was 101 females and 45 males, with a median age of 40 years (range 15-80 years). The control population consisted of 175 healthy individuals who were students or staff at the VUmc, with a median age of 51 years (range 24-88 years). All subjects were unrelated Dutch Caucasians. Genomic DNA was extracted using the DNAzol procedure (Invitrogen).

In order to ensure that the control group was representative of the general population, a second control group was also used, consisting of 192 Dutch subjects (96 males and 96 females). These samples were selected from the European Prospective Investigation on Cancer (EPIC) cohort[24] to provide information on the genetic background in the overall Dutch population. These samples were selected to provide a similar age distribution and sex ratio as the original control group. DNA was extracted from buffy coat using Puregene chemistry (Gentra Systems, Minneapolis, MN, USA). This population-based sample was indistinguishable from the VUmc controls from the point of view of frequencies of *PTGS2* alleles and genotypes (data not shown). We take this as confirmation that both groups were drawn from the general Dutch population, at least from the genetic point of view.

Patient classification

Diagnosis and assessment of maximal extent of IBD were based on endoscopic, histopathological, and radiological criteria[25]. Patients with indeterminate colitis were not included in this study, as they can be categorized as UC or CD only at a later stage. UC patients were subdivided into three groups: proctitis, limited to the rectum (12 cases), left-sided colitis with disease activity up to the splenic flexure (72 cases), and pancolitis (61 cases), extending beyond the splenic flexure. In addition, the patients with UC were subdivided into one group with their colon *in situ* (116 cases), and a second group in which (procto)colectomy had to be performed during the course of disease (29 cases), indicative of severe or intractable disease (i.e., unresponsive to medical therapy). No patient was operated on prophylactic indication. In CD, patients were subdivided according to the Vienna classification[26]. This classification subdivides patients with CD according to age at onset (<40 years [125 cases] or ⩾40 years [21 cases]), disease behavior (non-stricturing, non-penetrating [51 cases], stricturing [63 cases], penetrating [32 cases]) and location of disease (terminal ileum [50 cases], colon [32 cases], ileocolonic [62 cases], or upper gastrointestinal tract [2 cases]). Anatomical classification is defined as the maximal extent of the disease prior to the first surgical procedure, while behavior is assessed at any time during the course of the disease.

SNP selection and genotyping

SNPs were selected from our previously collected data[27] to include those SNPs with a prevalence of greater than 5% in Caucasians. Among the SNPs we studied, the only one with a proven functional role is a SNP located in the promoter of *PTGS2*, at position 926 of GenBank entry D28235 (dbSNP rs20417), which has been shown to affect the expression of *PTGS2* mRNA[28].

The order of samples of patients and controls was randomized in the PCR plates, so that a uniform number of patients and controls could be analyzed simultaneously in each run. EPIC samples were genotyped separately.

Three SNPs were genotyped with the Invader Assay[29]. PCR for the Invader assay (Third Wave Technologies, Madison, WI, USA) was carried out in 25 μL reactions, using the following concentrations: 20 ng DNA, 20 μmol/L dNTPs, 1×Taq Platinum buffer, 1.5 mmol/L $MgCl_2$, 1.25 U Taq Platinum polymerase (Life Technologies, Inc., Gaithersburg, MD, USA), 0.5 μmol/L of each primer. The primers used were as follows (nomenclature of SNPs refers to base numbers in GenBank entry D28235):

PTGS2.401 (rs689465)
401F: AAG GAC TTA GGA CAT AAC TGA ATT TTC
401R: ATG GGT AGT GCT CAG GGA GGA G
PTGS2.3050 (rs5277)
3050F: CGT TGT GAA TAA CAT TCC CTT
3050R: ATT TTT CTT TGA GAA GGC TAA AA
PTGS2.5209 (rs20432)
5209F: ATG ATG TAT GCC ACA ATC TGG CTG
5209R: TTG TCT GGA ACA ACT GCT CAT CAC.

This multiplex reaction was then carried out in a Tetrad DNA Engine PCR machine (MJ Research, Waltham, MA, USA), with the following cycling conditions: 96 ℃ for 5 min, then 30 cycles of 96 ℃ for 30 s, 50 ℃ for 60 s, and 72 ℃ for 10 s, with a final extension of 72 ℃ for 5 min. PCR volumes were then brought up to 150 μL, and Invader reactions were carried out as per manufacturer's instructions. Plates were read in a fluorometer with excitation and emission spectra as recommended by Third Wave.

The SNPs *PTGS2*.926 and *PTGS2*.8473 were tested using the TaqMan assay with MGB chemistry (Applied Biosystems,

Foster City, CA, USA). The assay was carried out in a 10 μL reaction, with 20 ng DNA, 1×TaqMan master mix (Applied Biosystems), 0.1 μmol/L of each primer, and 0.2 μmol/L of each probe. Primer and probe sequences are as follows:
PTGS2.926 (rs20417)
926F: TTA ACT ATT TAC AGG GTA ACT GCT TAG G
926R: CTT CAC CCC CTC CTT GTT TC
926VIC: CCT TTC CCG CCT CT
926FAM: CTT TCC CCC CTC TC
PTGS2.8473 (rs5275)
8473F: ATG CAC TGA TAC CTG TTT TTG TTT G
8473R: GTT TCC AAT GCA TCT TCC ATG A
8473VIC: TGA CAG AAA AAT AAC CAA AA
8473FAM: TGA CAG AAA AAT GAC CAA A

The cycling conditions for these PCR reactions were as follows: 95 ℃ for 10 min, then 35 cycles of 95 ℃ for 15 s, and 60 ℃ (58 ℃ for *PTGS2*.926) for 60 s. Plates were then read in the ABI 7900HT sequence detection system.

Data analysis

For genotype data from the Invader assay, raw intensity counts were corrected with a negative control, and the ratio between the two signals (one color for each allele) was used to call each genotype. For the TaqMan assay, groups of genotypes (homozygote common, heterozygote, and homozygote rare) were determined manually within the SDS software (Applied Biosystems). Each SNP was tested in the control group to ensure that it does not deviate from Hardy-Weinberg equilibrium. Linkage disequilibrium tests were performed using macros developed by the authors in conjunction with the PHASE program[30] to reconstruct haplotype frequencies. Odds ratios (OR) and 95% confidence interval (CI) were calculated in Stata 7.0, using logistic regressions correcting for sex and age in analyzing genotypes at single SNPs. Simple OR were calculated when data consisted of frequencies of alleles or haplotypes in the population. All *P* values reported are two sided. SNPs were tested for effects on splicing using the Delila Server (http://www.lecb.ncifcrf.gov/-toms/delilaserver.html) at the Laboratory of Experimental and Computational Biology of the National Cancer Institute[31].

New polymorphism screening

Individuals termed "at risk" based on association testing (i.e., the 19 cases carrying the haplotype, which includes the two alleles showing increase in risk at SNPs 5 209 and 8 473) were screened for novel polymorphisms using denaturing high-performance liquid chromatography (DHPLC) via the WAVE system (Transgenomic, Omaha, NE, USA). The areas studied were the promoter region, exons 6 and 10, and the 3' UTR. The protocols followed were as published previously[27].

Figure 1 shows a graphical representation of the structure of the *PTGS2* gene. The five major SNPs as well as the polymorphisms discovered as part of this study are depicted. The allele frequencies of the five major SNPs in the control group were 11.4% (*PTGS2*.401), 13.4% (*PTGS2*.926), 14.6% (*PTGS2*.3050), 13.5% (*PTGS2*.5209), and 33.9% (*PTGS2*.8473). All SNPs, except *PTGS2*.3050, were in Hardy-Weinberg equilibrium in the control group. Table 1 shows the genotype counts of the SNPs studied, among cases and controls. The SNP at position 5 209 shows an increase in the carriers of the G allele in cases as compared to controls, with a weak but significant association was found only in CD (OR = 1.63, 95%CI 1.03-2.57, $P = 0.04$). The SNP at position 8 473 shows an increase in the frequency of the T/T homozygote genotype in cases as compared to controls, with an association of borderline significance found only in UC (OR = 1.50, 95%CI 1.00-2.27, $P = 0.05$). No association was seen with the SNPs at position 401, 926, or 3 050, although it should be noted that there is a lack of homozygous rare genotypes at bp 3 050 in the control group, which is the reason for its departure from Hardy-Weinberg equilibrium.

We analyzed differences in genotype counts among the different clinical variables for CD and UC. No statistically significant differences between classification levels were observed (data not shown).

Significant levels of linkage disequilibrium were seen among the most common SNPs in the *PTGS2* gene (data not shown). Table 2 shows the frequencies of haplotypes of the *PTGS2* gene in both IBD patients and controls. The SNP at bp 3 050 was not included in haplotype analysis, as it was not in Hardy-Weinberg equilibrium in the control population, and this has been shown to affect the accuracy of haplotype reconstruction methods[32]. All individuals were genotyped for the SNP at bp 3 050, eliminating the risk that its lack of Hardy-Weinberg equilibrium is caused by bias due to the genotyping technique missing preferentially one genotype. Haplotype frequencies were calculated using all four valid SNPs, and all data are shown. There were no differences in haplotype frequency between the two groups of IBD patients and the controls, except for haplotype AGGT, which shows an OR of 11.9 (95%CI 2.83-105.76, $P<0.00005$, for UC and CD combined). Interestingly, this haplotype includes the two alleles showing an increase in risk at SNPs 5 209 and 8 473. If we consider the haplotype including the 5209.G and 8473.T alleles (by lumping haplotypes

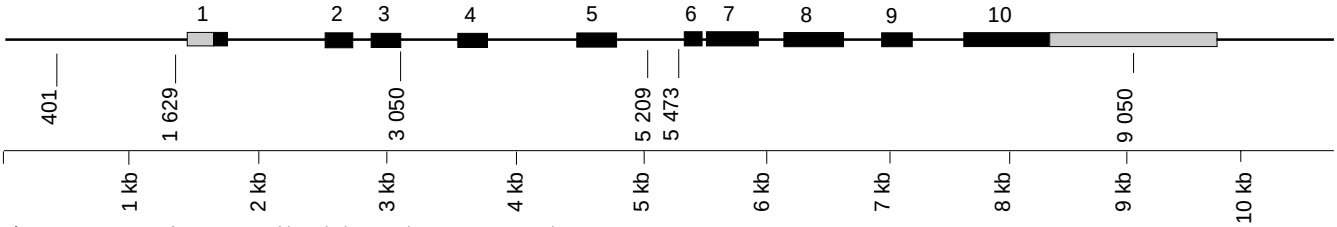


Figure 1 Structure of *PTGS2*. Positions in base pairs as per GenBank sequence D28235. Exons are shown as dark boxes, untranslated regions as light boxes. Vertical lines represent SNPs, with their positions in the sequence indicated.

Table 1 Genotype frequencies and OR for UC and CD of *PTGS2* SNPs

Genotype	Controls		UC			CD		
	n[1]	%	*n*[1]	%	OR (95%CI)[2]	*n*[1]	%	OR (95%CI)[2]
PTGS2.401								
A/A	277	79	115	82	1.00	107	77	1.00
A/G	66	19	24	17	0.82 (0.48-1.39)[3]	30	22	1.17 (0.70-1.94)[3]
G/G	7	2	1	1		1	1	
Total	350	100	140	100		138	100	
PTGS2.926								
G/G	256	75	112	81	1.00	106	76	1.00
G/C	75	22	23	17	0.77 (0.47-1.28)[3]	31	22	1.06 (0.65-1.73)[3]
C/C	8	2	4	3		3	2	
Total	339	100	139	100		140	100	
PTGS2.3050								
G/G	250	71	109	75	1.00	102	71	1.00
G/C	99	28	32	22	0.83 (0.52-1.32)[3]	38	26	0.97 (0.62-1.53)[3]
C/C	1	1	4	3		4	3	
Total	350	100	145	100		144	100	
PTGS2.5209								
T/T	265	75	110	76	1.00	95	66	1.00
T/G	81	23	30	21	1.00 (0.62-1.61)[3]	46	33	1.63 (1.03-2.57)[3]
G/G	7	2	5	3		2	1	
Total	353	100	145	100		143	100	
PTGS2.8473								
C/C	44	13	18	14	1.00[3]	21	15	1.00[3]
T/C	147	42	49	34		54	38	
T/T	155	45	78	54	1.50 (1.00-2.27)	68	47	1.10 (0.72-1.68)
Total	346	100	145	100		143	100	

[1]Numbers may not sum up to the totals of controls or cases due to genotyping failure. All samples that did not give a reliable result in the first round of genotyping were resubmitted to up to three additional rounds of genotyping. Data points that were still not filled up after this procedure were left blank. [2]All ORs are adjusted for sex and age. [3]Heterozygotes and homozygotes for the rare allele have been grouped in order to improve statistical power.

Table 2 *PTGS2* haplotype frequencies and OR for IBD

Haplotype[1]	Controls	UC cases		CD cases		UC+CD cases[2]	
	n (%)	*n* (%)	OR (95%CI)	*n* (%)	OR (95%CI)	*n* (%)	OR (95%CI)[3]
AGTT	471 (64.7)	193 (65.6)	1.00 (ref.)	183 (62.7)	1.00 (ref.)	376 (64.2)	1.00 (ref.)
AGTC	147 (20.2)	55 (18.7)	0.91 (0.64-1.30)	54 (18.5)	0.95 (0.66-1.35)	109 (18.6)	0.93 (0.69-1.24)
GCGC	64 (8.8)	22 (7.5)	0.84 (0.50-1.39)	27 (9.2)	1.09 (0.67-1.75)	49 (8.4)	0.96 (0.63-1.45)
ACGC	25 (3.4)	8 (2.7)	0.78 (0.35-1.73)	7 (2.4)	0.72 (0.31-1.66)	15 (2.6)	0.75 (0.36-1.51)
AGGT	2 (0.3)	10 (3.4)	12.2 (2.97-inf.)	9 (3.1)	11.58 (2.79-inf.)	19 (3.2)	11.9 (2.83-105.76)
Rare[4]	19 (2.6)	6 (2.0)	0.77 (0.31-1.90)	12 (4.1)	1.63 (0.78-3.37)	18 (3.1)	1.19 (0.61-2.29)

[1]The order of SNPs in the haplotypes is *PTGS2*.401, *PTGS2*.926, *PTGS2*.5209, and *PTGS2*.8473. [2]UC and CD combined. [3]ORs are not corrected as they are based on population level haplotype frequencies and are relative to the most common haplotype (AGTT). [4]Rare haplotypes (frequency ≤1% in both cases and controls).

AGGT and GCGT), we observe an increase in its frequency in patients with IBD (0.035, UC and CD combined) as compared to controls (0.003). This increase in frequency yields an OR of 13.15 (95%CI 3.17-116.15, $P<0.00005$, for UC and CD combined).

In order to test the possibility that these positive associations are in reality indicative of linkage disequilibrium with yet undiscovered nearby polymorphisms, we studied by DHPLC the 19 cases who could carry the risk haplotype. Regions of *PTGS2* surrounding the three SNPs, and in addition the promoter region, exon 1 and the UTRs were analyzed. No novel polymorphisms were discovered in the coding sequence of the gene. One SNP was discovered at bp 9 850 (A-G), with a minor allele frequency of lower than 2%. Therefore, we considered it unlikely that polymorphisms other than 5 209 or 8 473 could explain the observed associations.

[redacted]

PTGS2 is a critical enzyme involved in the production of prostaglandins, which are essential in the process of healing bowel wounds. The use of NSAIDs, which inhibit both the translation and activity of PTGS2, can induce a flare-up[21] and actually exacerbate the symptoms of IBD[20]. We hypothesized that polymorphisms in *PTGS2* might influence prostaglandin production in inflamed cells, thus affecting susceptibility to IBD. In this study, we have found a slightly increased risk of IBD associated to *PTGS2*.5209 and *PTGS2*.8473, and a strong association with a haplotype including alleles of these two SNPs.

PTGS2.5209 is in intron 5 of *PTGS2*. *In silico* analysis

of this SNP for splice site mutations[31] reveals that the T-G substitution creates a new splicing acceptor sequence with nearly the same strength as that found in normal splice sites. While this is most probably not enough of a change to exclude completely the normal splicing of exons 5-6, it could cause some "leaking", reducing the amount of normal *PTGS2* mRNA. *PTGS2*.8473, being in the 3' untranslated region (UTR), could affect the stability of *PTGS2* mRNA[33]. In fact, the unusually long 3' UTR plays an important role in determining the half-life of the mRNA. Various proteins bind to it and cause either acceleration or protection of the degradation of the mRNA[34,35].

The associations we have found between CD and *PTGS2*.5209 G/G, and UC and *PTGS2*.8473 T/T are statistically significant, but of moderate importance. We propose that it is the combination of the G allele at *PTGS2*.5209 with the T allele at *PTGS2*.8473, on the same chromosome (GT haplotype), that would have the most influence on disease status.

The association between IBD and the GT haplotype could be due to linkage disequilibrium with another polymorphism that lies nearby. To test this hypothesis, we have analyzed subjects who carry the GT haplotype for the presence of novel functional polymorphisms of *PTGS2*, but this search has not yielded any additional candidates. Linkage disequilibrium with polymorphisms in neighboring genes is not a likely explanation either, as there is no gene mapping of at less than 100 kbp on either side of *PTGS2*.

We are inclined to think that this association is not a finding by chance. First of all, we have found a higher level of linkage disequilibrium between alleles at bp 5 209 and 8 473 in controls than in cases. This could mean that natural selection has exerted pressure toward the disappearance of the GT haplotype, i.e. this haplotype might negatively affect the fitness of individuals carrying it. Additionally, we have observed that this haplotype is virtually absent not only in the Dutch population, but in other Northern European populations as well (Cox *et al*., unpublished data).

These results are the first linking of *PTGS2* to IBD. While the GT haplotype of *PTGS2* is rare, the two alleles that compose it are much more frequent, they both show a modest association with the disease, and could therefore be important for a large proportion of the population. Future steps are to replicate these findings by independent studies, to determine experimentally the extent to which *PTGS2* polymorphisms alter the expression or function of the gene, and to discover genetic or environmental factors that may alter the risk of IBD interacting with *PTGS2* alleles.

ACKNOWLEDGEMENTS

The authors thank Pietro Ferrari (Nutrition and Cancer Group, IARC) for discussion on statistical issues, Stéphanie Monnier (Genome Analysis Team, IARC) for bioinformatic support and AA van Bodegraven MD, PhD for facilitating the clinical database of the IBD patients at the VUmc.

REFERENCES

1 **Van Kruiningen HJ**, Freda BJ. A clustering of Crohn's disease in Mankato, Minnesota. *Inflamm Bowel Dis* 2001; **7**: 27-33
2 **Mahmud N**, Weir DG. The urban diet and Crohn's disease: is there a relationship? *Eur J Gastroenterol Hepatol* 2001; **13**: 93-95
3 **Koutroubakis I**, Manousos ON, Meuwissen SG, Pena AS. Environmental risk factors in inflammatory bowel disease. *Hepatogastroenterology* 1996; **43**: 381-393
4 **Farrokhyar F**, Swarbrick ET, Irvine EJ. A critical review of epidemiological studies in inflammatory bowel disease. *Scand J Gastroenterol* 2001; **36**: 2-15
5 **Karlinger K**, Gyorke T, Mako E, Mester A, Tarjan Z. The epidemiology and the pathogenesis of inflammatory bowel disease. *Eur J Radiol* 2000; **35**: 154-167
6 **Ogura Y**, Bonen DK, Inohara N, Nicolae DL, Chen FF, Ramos R, Britton H, Moran T, Karaliuskas R, Duerr RH, Achkar JP, Brant SR, Bayless TM, Kirschner BS, Hanauer SB, Nunez G, Cho JH. A frameshift mutation in NOD2 associated with susceptibility to Crohn's disease. *Nature* 2001; **411**: 603-606
7 **Hugot JP**, Chamaillard M, Zouali H, Lesage S, Cezard JP, Belaiche J, Almer S, Tysk C, O'Morain CA, Gassull M, Binder V, Finkel Y, Cortot A, Modigliani R, Laurent-Puig P, Gower-Rousseau C, Macry J, Colombel JF, Sahbatou M, Thomas G. Association of NOD2 leucine-rich repeat variants with susceptibility to Crohn's disease. *Nature* 2001; **411**: 599-603
8 **Hampe J**, Cuthbert A, Croucher PJ, Mirza MM, Mascheretti S, Fisher S, Frenzel H, King K, Hasselmeyer A, MacPherson AJ, Bridger S, van Deventer S, Forbes A, Nikolaus S, Lennard-Jones JE, Foelsch UR, Krawczak M, Lewis C, Schreiber S, Mathew CG. Association between insertion mutation in NOD2 gene and Crohn's disease in German and British populations. *Lancet* 2001; **357**: 1925-1928
9 **Peltekova VD**, Wintle RF, Rubin LA, Amos CI, Huang Q, Gu X, Newman B, Van Oene M, Cescon D, Greenberg G, Griffiths AM, St George-Hyslop PH, Siminovitch KA. Functional variants of OCTN cation transporter genes are associated with Crohn disease. *Nat Genet* 2004; **36**: 471-475
10 **Stoll M**, Corneliussen B, Costello CM, Waetzig GH, Mellgard B, Koch WA, Rosenstiel P, Albrecht M, Croucher PJ, Seegert D, Nikolaus S, Hampe J, Lengauer T, Pierrou S, Foelsch UR, Mathew CG, Lagerstrom-Fermer M, Schreiber S. Genetic variation in DLG5 is associated with inflammatory bowel disease. *Nat Genet* 2004; **36**: 476-480
11 **Watts DA**, Satsangi J. The genetic jigsaw of inflammatory bowel disease. *Gut* 2002; **50**(Suppl 3): III31-III36
12 **Nemetz A**, Nosti-Escanilla MP, Molnar T, Kope A, Kovacs A, Feher J, Tulassay Z, Nagy F, Garcia-Gonzalez MA, Pena AS. IL1B gene polymorphisms influence the course and severity of inflammatory bowel disease. *Immunogenetics* 1999; **49**: 527-531
13 **Tagore A**, Gonsalkorale WM, Pravica V, Hajeer AH, McMahon R, Whorwell PJ, Sinnott PJ, Hutchinson IV. Interleukin-10 (IL-10) genotypes in inflammatory bowel disease. *Tissue Antigens* 1999; **54**: 386-390
14 **Heresbach D**, Alizadeh M, Dabadie A, Le Berre N, Colombel JF, Yaouanq J, Bretagne JF, Semana G. Significance of interleukin-1beta and interleukin-1 receptor antagonist genetic polymorphism in inflammatory bowel diseases. *Am J Gastroenterol* 1997; **92**: 1164-1169
15 **Klein W**, Tromm A, Griga T, Fricke H, Folwaczny C, Hocke M, Eitner K, Marx M, Runte M, Epplen JT. The IL-10 gene is not involved in the predisposition to inflammatory bowel disease. *Electrophoresis* 2000; **21**: 3578-3582
16 **Kujubu DA**, Fletcher BS, Varnum BC, Lim RW, Herschman HR. TIS10, a phorbol ester tumor promoter-inducible mRNA from Swiss 3T3 cells, encodes a novel prostaglandin synthase/cyclooxygenase homologue. *J Biol Chem* 1991; **266**: 12866-12872
17 **Maier JA**, Hla T, Maciag T. Cyclooxygenase is an immediate-early gene induced by interleukin-1 in human endothelial cells. *J Biol Chem* 1990; **265**: 10805-10808
18 **Masferrer JL**, Seibert K, Zweifel B, Needleman P. Endogenous glucocorticoids regulate an inducible cyclooxygenase enzyme. *Proc Natl Acad Sci USA* 1992; **89**: 3917-3921

19 **Wallace JL**. Prostaglandin biology in inflammatory bowel disease. *Gastroenterol Clin North Am* 2001; **30**: 971-980
20 **Eberhart CE**, Dubois RN. Eicosanoids and the gastrointestinal tract. *Gastroenterology* 1995; **109**: 285-301
21 **Kaufmann HJ**, Taubin HL. Nonsteroidal anti-inflammatory drugs activate quiescent inflammatory bowel disease. *Ann Intern Med* 1987; **107**: 513-516
22 **Singer II**, Kawka DW, Schloemann S, Tessner T, Riehl T, Stenson WF. Cyclooxygenase 2 is induced in colonic epithelial cells in inflammatory bowel disease. *Gastroenterology* 1998; **115**: 297-306
23 **Russel MG**, Dorant E, Volovics A, Brummer RJ, Pop P, Muris JW, Bos LP, Limonard CB, Stockbrugger RW. High incidence of inflammatory bowel disease in The Netherlands: results of a prospective study. The South Limburg IBD Study Group. *Dis Colon Rectum* 1998; **41**: 33-40
24 **Bingham S**, Riboli E. Diet and cancer-the European Prospective Investigation into Cancer and Nutrition. *Nat Rev Cancer* 2004; **4**: 206-215
25 **Lennard-Jones JE**. Classification of inflammatory bowel disease. *Scand J Gastroenterol Suppl* 1989; **170**: 2-6
26 **Gasche C**, Scholmerich J, Brynskov J, D'Haens G, Hanauer SB, Irvine EJ, Jewell DP, Rachmilewitz D, Sachar DB, Sandborn WJ, Sutherland LR. A simple classification of Crohn's disease: report of the Working Party for the World Congresses of Gastroenterology, Vienna 1998. *Inflamm Bowel Dis* 2000; **6**: 8-15
27 **Cox D**, Boillot C, Canzian F. Data mining: Efficiency of using sequence databases for polymorphism discovery. *Hum Mutat* 2001; **17**: 141-150
28 **Papafili A**, Hill MR, Brull DJ, McAnulty RJ, Marshall RP, Humphries SE, Laurent GJ. Common promoter variant in cyclooxygenase-2 represses gene expression: evidence of role in acute-phase inflammatory response. *Arterioscler Thromb Vasc Biol* 2002; **22**: 1631-1636
29 **Mein CA**, Barratt BJ, Dunn MG, Siegmund T, Smith AN, Esposito L, Nutland S, Stevens HE, Wilson AJ, Phillips MS, Jarvis N, Law S, de Arruda M, Todd JA. Evaluation of single nucleotide polymorphism typing with invader on PCR amplicons and its automation. *Genome Res* 2000; **10**: 330-343
30 **Stephens M**, Smith NJ, Donnelly P. A new statistical method for haplotype reconstruction from population data. *Am J Hum Genet* 2001; **68**: 978-989
31 **Rogan PK**, Faux BM, Schneider TD. Information analysis of human splice site mutations. *Hum Mutat* 1998; **12**: 153-171
32 **Single RM**, Meyer D, Hollenbach JA, Nelson MP, Noble JA, Erlich HA, Thomson G. Haplotype frequency estimation in patient populations: the effect of departures from Hardy-Weinberg proportions and collapsing over a locus in the HLA region. *Genet Epidemiol* 2002; **22**: 186-195
33 **Rodriguez-Pascual F**, Hausding M, Ihrig-Biedert I, Furneaux H, Levy AP, Forstermann U, Kleinert H. Complex contribution of the 3'-untranslated region to the expressional regulation of the human inducible nitric-oxide synthase gene. Involvement of the RNA-binding protein HuR. *J Biol Chem* 2000; **275**: 26040-26049
34 **Nabors LB**, Gillespie GY, Harkins L, King PH. HuR, a RNA stability factor, is expressed in malignant brain tumors and binds to adenine- and uridine-rich elements within the 3' untranslated regions of cytokine and angiogenic factor mRNAs. *Cancer Res* 2001; **61**: 2154-2161
35 **Sheng H**, Shao J, Dixon DA, Williams CS, Prescott SM, Dubois RN, Beauchamp RD. Transforming growth factor-beta1 enhances Ha-ras-induced expression of cyclooxygenase-2 in intestinal epithelial cells via stabilization of mRNA. *J Biol Chem* 2000; **275**: 6628-6635

Science Editor Guo SY **Language Editor** Elsevier HK

PO Box 2345, Beijing 100023, China
www.wjgnet.com
wjg@wjgnet.com

ELSEVIER

World J Gastroenterol 2005;11(38):6009-6013
World Journal of Gastroenterology ISSN 1007-9327
© 2005 The WJG Press and Elsevier Inc. All rights reserved.

• *BRIEF REPORTS* •

Helicobacter pylori antibiotic resistance in Iran

Marjan Mohammadi, Delaram Doroud, Nazanin Mohajerani, Sadegh Massarrat

Marjan Mohammadi, Delaram Doroud, Nazanin Mohajerani, Biotechnology Research Center, Pasteur Institute of Iran, Tehran, Iran
Sadegh Massarrat, Gastroenterology Department, Shariati Hospital, Tehran University of Medical Sciences, Tehran, Iran
Supported by a Research Grant From the Pasteur Institute of Iran, No. 198
Co-first-authors: Marjan Mohammadi and Delaram Doroud
Correspondence to: Marjan Mohammadi, Biotechnology Research Center, Pasteur Institute of Iran, Tehran, Iran. marjan@institute.pasteur.ac.ir
Telephone: +98-21-6480780 Fax: +98-21-6480780
Received: 2004-11-16 Accepted: 2005-01-26

ABSTRACT

AIM: To examine the frequency of antibiotic resistance in Iranian *Helicobacter pylori* (*H pylori*) strains isolated from two major hospitals in Tehran.

METHODS: Examination of antibiotic resistance was performed on 120 strains by modified disc diffusion test and PCR-RFLP methods. In addition, in order to identify the possible causes of the therapeutic failure in Iran, we also determined the resistance of these strains to the most commonly used antibiotics (metronidazole, amoxicillin, and tetracycline) by modified disc diffusion test.

RESULTS: According to modified disc diffusion test, 1.6% of the studied strains were resistant to amoxicillin, 16.7% to clarithromycin, 57.5% to metronidazole, and there was no resistance to tetracycline. Of the clarithromycin resistant strains, 73.68% had the A2143G mutation in the *23S rRNA* gene, 21.05% A2142C, and 5.26% A2142G. None of the sensitive strains were positive for any of the three point mutations. Of the metronidazole resistant strains, deletion in *rdxA* gene was studied and detected in only 6 (5%) of the antibiogram-based resistant strains. None of the metronidazole sensitive strains possessed *rdxA* gene deletion.

CONCLUSION: These data show that despite the fact that clarithromycin has not yet been introduced to the Iranian drug market as a generic drug, nearly 20% rate of resistance alerts toward the frequency of macrolide resistance strains, which may be due to the widespread prescription of erythromycin in Iran. *rdxA* gene inactivation, if present in Iranian *H pylori* strains, may be due to other genetic defects rather than gene deletion.

© 2005 The WJG Press and Elsevier Inc. All rights reserved.

Key words: *H pylori*; Clarithromycin; Metronidazole; Resistance; Iran

Mohammadi M, Doroud D, Mohajerani N, Massarrat S. *Helicobacter pylori* antibiotic resistance in Iran. *World J Gastroenterol* 2005; 11(38): 6009-6013
http://www.wjgnet.com/1007-9327/11/6009.asp

INTRODUCTION

Helicobacter pylori (*H pylori*) infects the majority of the adult population in developing countries including Iran. The rate of infection in Iranian adults according to serology data is up to 80%[1]. The outcomes include gastritis, peptic ulcers and gastric adenocarcinomas, which are highly prevalent in Iran[2]. Patient compliance with the prescribed medications, presence of pre-existing resistance to the key anti-*H pylori* antibiotics (clarithromycin and metronidazole), final duration of therapy and prescribed dose of antibiotics are all the factors which influence the effectiveness of therapy[3]. Host genetic polymorphisms, i.e. IL-1-511 and CYP450 and CYP2C19, may affect the efficiency of the therapy as well [4]. Antibiotic resistance varies geographically and there is a great need for local studies.

Clarithromycin is recommended as a key component in anti-*H pylori* eradication[5]. In different geographic locations, resistance to clarithromycin differs. In countries with a higher use of macrolides, the rate of resistance to clarithromycin is reported to be proportionally higher[6]. The basis of the resistance is the presence of defined mutations in the *23S rRNA* gene, which results in a decrease in the antibiotic binding to the bacterial ribosome[7-9]. Mutations in the form of A-G transition at nucleotide positions 2143, 2144, and A-C at nucleotide position 2142 have been found to confer clarithromycin resistance in *H pylori* strains[10]. Recently in *H pylori* isolates from northeast China, three new mutation points (G2224A, C2245T, and T2289C) were found to be related to the clarithromycin resistance[11]. Several different PCR-based methods have been developed for the detection of the above-mentioned mutations in order to amplify part of the V domain of *23Sr RNA* gene[12]. The amplified fragments are digested by restriction enzymes, indicating mutations in the positions 2143 and 2144 which yield a high level clarithromycin resistance[10,13]. A2142C is reported to be less frequent and is detectable by PCR using 3'-mismatched specific primers[14,15].

Though most countries include clarithromycin in the prescribed anti-*H pylori* treatment regimens, this drug is infrequently prescribed in Iran due to its high cost.

As regards to metronidazole, the basis of resistance in *H pylori* has been partly associated with inactivation of *rdxA*, the gene encoding an oxygen-insensitive NADPH nitroreductase may be enhanced by mutations in *frxA* gene

encoding a NAD(P)H-flavin oxidoreductase[16].

This study presents the first documented report from Iran on the *rdxA* gene deletion. Frameshift mutations in *frxA* gene were not studied as their frequent occurrence has questioned its reliability as a resistance marker[17].

We have used modified disc diffusion test for primary analysis followed by the described molecular assays to examine resistance among Iranian *H pylori* strains with particular emphasis on clarithromycin and metronidazole.

MATERIALS AND METHODS

Bacterial strains and growth conditions

Gastric antral biopsies were taken from 120 non-*H pylori* pretreated patients (52 males and 68 females, aged 42±20 years) with epigastralgia referring to gastric endoscopy (during 2001-2002) followed by rapid urease test. These patients did not undergo any prior treatment. Urease positive samples were cultured on brucella agar (Merck) supplemented with 5% sheep blood, (6 mg/L) vancomycin (Fluka BioChemika), (5 mg/L) trimethoprim (Fluka BioChemika) and (2 mg/L) amphotericin-B (Gibco) under microaerophilic conditions (85% N_2, 100 mL/L CO_2, 5% O_2) at 37 ℃ for 3-5 d. Single colonies of *H pylori* were then isolated and confirmed for identity according to colony morphology, wet mount, microscopic observation after Gram staining and biochemical analysis (urease and catalase tests).

Disc diffusion susceptibility test

Bacterial resistance to clarithromycin[18], metronidazole[19], amoxicillin, and tetracycline[20] was determined using modified Kirby-Bauer procedure as previously described[21,22]. Suspensions of 4-d-old cultures were prepared in sterile saline to opacity of No. 4 (108 CFU/mL) McFarland standard. Muller-Hinton agar plates supplemented with 5% sheep blood were then inoculated with a swab from the prepared suspension. House-made discs containing 2 μg clarithromycin, 5 μg metronidazole, 10 μg amoxicillin, and 30 μg tetracycline were placed separately on the culture plates for each strain. Plates were then incubated at 37 ℃ for 72 h under microaerophilic conditions generated by Gas Pak jars. The disc diffusion tests were made thrice for each strain. The inhibition zone diameters were measured in millimeters with a ruler. If similar results were observed in two experiments out of three, the isolates were considered susceptible or resistant but as mixed populations. A *H pylori* control strain susceptible to metronidazole (Sydney strain, ss1) was used. The breakpoints with the Mueller-Hinton agar for the inhibition diameters are described in Table 3, briefly: 20 mm for tetracycline, 11 mm for amoxicillin, for metronidazole zones areas; <16 mm resistant, 16-21 mm intermediate and >21 mm susceptible (but in this study isolates in the intermediate and resistant zone were both considered as resistant), for clarithromycin development of any size zone is considered resistant[23].

DNA extraction and PCR assays

Genomic DNA was extracted as previously described[10]. PCR primers used for this study were chosen from published reports with the implementation of the same PCR cycles[10] (Table 1). Primer sets 1 and 2 were designed to detect point mutations in the *23S rRNA* gene responsible for clarithromycin resistance. Set 1 was used to amplify a 1 400-bp PCR fragment following digestion with *Bsa*I produced three fragments of 700, 400, and 300 bp, if the A2143G mutation was present. *Mbo*II digestion of the 1 400-bp fragment produced two 700-bp fragments, if A2142G mutation was present. A 750 and a 850 bp were produced, if A2144G mutations existed[10]. Set 2 was used in 3'-mismatched PCR to obtain a 700-bp-amplified fragment, an indication of the A2141C mutation[15].

For detection of *rdxA* gene deletion, set 3 was used. In this case, the native gene yielded a 850-bp PCR product and its deletion resulted in a 650-bp fragment[24].

Table 1 Primer sets used in this study

Gene	Primers	Expected fragment (bp)	References
23S rRNA	CLA 18: 5″-AGTCGGGAC CTAAGGCGAG-3″	1 400	10
(set 1)	CLA 21: 5″-TTCCCGCTTA GATGCTTTCAG-3″		
23S rRNA	CLA 18: 5″-AGTCGGGACC TAAGGCGAG-3″	700	15
(set 2)	CLA 3: 5″-AGGTCCACGGG GTCTTG-3″		
RdxA	RdxA1: 5″-AATTTGAGCATG GGGCAGA-3″	850	24
(set 3)	RdxA2: 5″-GAAACGCTTGAA AACACCCCT-3″		

Statistical analysis

Data were analyzed by SPSS version 11.0. The Pearson χ^2 test and Fisher's exact test were used to assess the relationships between the results of disc diffusion and PCR/RFLP methods. Standard error of mean for each frequency was determined accordingly.

RESULTS

Primary antibiotic resistance by disc diffusion

According to the disc diffusion test, all 120 strains were sensitive to tetracycline. Of these, 2 strains (1.6%) were resistant to amoxicillin, 20 (16.7%) to clarithromycin and 69 (57.5%) to metronidazole. Five of the one hundred and twenty (4.2% of the strains) showed dual resistance to metronidazole and clarithromycin. Table 2 presents the frequency of single and multiple resistances to the tested antibiotics.

Detection of 23S rRNA mutations via PCR-RFLP

All the DNA samples were positive by the PCR assay for the amplification of the 1 400 bp of *23S rRNA* gene. RFLP analysis pattern showed that 19 out of 120 (15.8%) strains were mutated (Table 2). In this group, 73.68% had the A2143G mutation and 5.26% the A2142G mutations. Moreover, none of the clarithromycin resistant samples showed the A2144G mutation, 21.05% of the samples were positive for the 3'-mismatched PCR, revealing the presence

of the A2142C mutation. Among the 20 clarithromycin resistant strains, only one did not show any of these mutations. None of the sensitive strains were positive for any of the mentioned mutations.

PCR detection of rdxA gene deletion

Among the 69 metronidazole resistant strains (based on antibiograms), only 6 (5% of total) demonstrated 200 bp deletion in the *rdxA* gene (Table 2).

According to the data analysis by the SPSS program, there were no relations between the *23S rRNA* mutations, *rdxA* deletion and antibiotic resistance with age, gender, and cagA status.

Table 2 Frequency of single and multi-drug resistance based on listed methods of detection

Antibiotics	Method of detection					
	Disc diffusion		*23S rRNA* PCR-RFLP		*rdxA* gene deletion	
	n	%	*n*	%	*n*	%
Amoxicillin only	1/120	0.8				
Amoxicillin and metronidazole	1/120	0.8				
Clarithromycin only	15/120	12.5	19/120	15.8		
Clarithromycin and metronidazole	5/120	4.2				
Metronidazole only	63/120	52.5			6/120	5
Metronidazole and amoxicillin	1/120	0.8				
Metronidazole and clarithromycin	5/120	4.2				
Tetracycline	0/120	0				

Table 3 Susceptibility rates of 120 isolates to selected antibiotics by modified disk diffusion method

Antibiotics	Disc content (μg)	Zone size breakpoint (resistance) (mm)	Resistant isolates (%)
Metronidazole	5	16	34.2 resistant 23.3 intermediate
Clarithromycin	2	Any zone	16.7
Amoxicillin	10	11	1.6
Tetracycline	30	20	0

DISCUSSION

Several studies comparing the different susceptibility techniques for *H pylori* have been published, but the results are controversial, as *H pylori* is a very slow growing bacterium with particular growth needs[23,25-28]. The oxygen-dependent metabolism of metronidazole in *H pylori* via several nitroreductases possibly results in great difference in MIC when isolates are tested repeatedly. Nevertheless, strains continue to be classified as resistant or susceptible[25].

As regards to culture-based antimicrobial susceptibility testing (especially to metronidazole), routine methods of agar dilution, disc diffusion, and *E*-test seem to be poorly standardized[29]. Though time consuming agar dilution is accepted as the gold standard and is reported to be highly reproducible in several studies[23,30,31], nowadays, *E*-test is used most frequently as a substitute as it is easier to perform and relatively reproducible[32]. Finally, a cheap and easy way to perform susceptibility testing is via disc diffusion, but no MIC value can be obtained. Recently in UK, susceptibility testing to metronidazole, tetracycline, macrolide, and amoxicillin is performed by the modified disc diffusion method and the results are adequate to determine the resistance rates in a large cohort of patients from a single clinical center whom resistance patterns have been evaluated over time[33]. Then again in a study in France, reproducibility study on randomly selected strains declared that disc diffusion is more reproducible than *E*-test for both clarithromycin and erythromycin[34]. Due to these observations and high cost of *E*-test, modified disc diffusion test was chosen for this study.

Worldwide antibiotic resistance has been carefully reviewed by Megraud[35], and our resistance rate to clarithromycin and metronidazole is comparable to the resistance rate of 50% to metronidazole and 8% to clarithromycin in China[36].

Current regimens for the eradication of *H pylori* in Iran consist of a proton pump inhibitor (omeprazole) or an H_2 receptor blocker (ranitidine), a bismuth salt plus two antibacterial agents, such as amoxicillin, furazolidone/metronidazole or recently clarithromycin[37]. Treatment regimens of 4 or 7 d are unacceptable for *H pylori* infection in Iran, even in the presence of a favorable sensitivity profile[38]. Although the presented data do not support the association with the failure of eradication in our country, according to our results, such rates of resistance to metronidazole and clarithromycin could be the major cause of eradication failure in Iran. For developing countries, the standard triple therapy remains as the best option for the eradication regimen because of its low cost. However, in Iran bismuth triple therapy in the presence of high prevalence of metronidazole resistance has a poor efficacy unless higher doses of metronidazole are prescribed to increase the cure rate of therapy[39].

Our results indicate that making clarithromycin available may not be an effective strategy to improve the eradication rates in Iran, as the level of resistance is already significant. There is a worldwide need for simple and cost effective anti-*H pylori* therapies. Since the effectiveness relates to the level of antibiotic resistance, knowledge of the resistance patterns is essential for choosing empiric therapy. Metronidazole is widely used in Iran because of the prescription in most periodontal and parasitic diseases. Resistance to metronidazole among Iranian patients, as most of the developing countries, is relatively high and this is the major cause of eradication failure in these countries. Thus, the need for a suitable alternative for this drug is highly perceptible and crucial to plan a more effective therapeutic strategy. (OABC) Omeprazole, Amoxicillin, Bismuth, Clarithromycin and (OABF)Omeprazole, Amoxicillin, Bismuth, Furazolidone are both effective in eradicating *H pylori* in countries where metronidazole resistance is a problem. OABF is a good alternative in the face of growing resistance to clarithromycin in developed countries, and is attractive for developing countries where clarithromycin is not readily available and is particularly recommended for Iran[37].

In recent years, *rdxA* gene analysis of the fresh samples showed that the metronidazole resistance is mainly attributed to the mutations in this gene including gene deletion[24]. Antibiogram analysis of our strains demonstrated 57% metronidazole resistance; however, the majority of the metronidazole resistant strains did not show the 200 bp deletion in the *rdxA* gene. One obvious explanation is that the deletion in this gene is not the only defect causing gene inactivation and is not an informative indication of metronidazole resistance in Iranian *H pylori* strains (with ~60% metronidazole resistance). The data are supported by data from Germany[40] and France[16] (with 40-50% metronidazole resistance) and contradicted by data from China[41] and Taiwan[42] (with 50-60% resistance). Due to the reported disparity, it seems that *rdxA* gene mutation is not a suitable marker for molecular prediction of metronidazole resistance. Although *rdxA* gene deletion is not a good resistance indicator, it is only detected in resistant strains and all of the strains with *rdxA* deletion clusterized in specific rapedemes (analyzed by RAPD-PCR), suggesting that they are genetically similar (data not shown). Unlike clarithromycin, metronidazole resistance *in vitro* does not reflect *in vivo* resistance. Other existing genetic defects causing metronidazole resistant phenotypes and the high incurring cost of molecular diagnostic assays lead us to the conclusion that standard culture-based techniques (simple and inexpensive disc diffusion method) remain the recommended method of choice in Iran.

In conclusion, the discovery of such a high rate of resistance to clarithromycin, which is most likely due to the vast consumption of erythromycin in cases of upper respiratory infections, calls for an effective eradication program and disqualifies clarithromycin as an alternative to metronidazole. These results further confirm the essence of continuous monitoring of antibiotic resistance patterns in order to reduce the rate of eradication failure in Iran or any other target population.

ACKNOWLEDGMENTS

The authors would like to thank Dr. David Graham, Digestive Diseases Section, Veterans Affairs Medical Center, Houston, TX, USA, for his kind review of this manuscript.

REFERENCES

1 **Massarrat S,** Saberi-Firoozi M, Soleimani A, Himmelmann GW, Hitzges M, Keshavarz H. Peptic ulcer disease, irritable bowel syndrome and constipation in two populations in Iran. *Eur J Gastroenterol Hepatol* 1995; **7**: 427-433
2 **Sadjadi A,** Malekzadeh R, Derakhshan MH, Sepehr A, Nouraie M, Sotoudeh M, Yazdanbod A, Shokoohi B, Mashayekhi A, Arshi S, Majidpour A, Babaei M, Mosavi A, Mohagheghi MA. Cancer occurrence in Ardabil: results of a population-based cancer registry from Iran. *Int J Cancer* 2003; **107**: 113-118
3 **Perri F,** Villani MR, Festa V, Quitadamo M, Andriulli A. Predictors of failure of *Helicobacter pylori* eradication with the standard 'Maastricht triple therapy. *Aliment Pharmacol Ther* 2001; **15**: 1023-1029
4 **Furuta T,** Shirai N, Xiao F, El-Omar EM, Rabkin CS, Sugimura H, Ishizaki T, Ohashi K. Polymorphism of interleukin-1beta affect the eradication rates of *Helicobacter pylori* by triple therapy. *Clin Gastroenterol Hepatol* 2004; **2**: 22-30
5 **Gisbert JP,** Pajares JM. *Helicobacter pylori* therapy: first-line options and rescue regimen. *Dig Dis* 2001; **19**: 134-143
6 **Grove DI,** Koutsouridis G. Increasing resistance of *Helicobacter pylori* to clarithromycin: is the horse bolting? *Pathology* 2002; **34**: 71-73
7 **Piana A,** Are BM, Maida I, Dore MP, Sotgiu G, Realdi G, Mura I. Genotypic characterization of clarithromycin-resistant *Helicobacter pylori* strains. *New Microbiol* 2002; **25**: 123-130
8 **Perri F,** Qasim A, Marras L, O'Morain C. Treatment of *Helicobacter pylori* infection. *Helicobacter* 2003; **8**: 53-60
9 **Taylor D**E, Ge Z, Purych D, Lo T, Hiratsuka K. Cloning and sequence analysis of two copies of a 23S rRNA gene from *Helicobacter pylori* and association of clarithromycin resistance with 23S rRNA mutations. *Antimicrob Agents Chemother* 1997; **41**: 2621-2628
10 **Versalovic JSD,** Kibler K, Griffy MV, Beyer J, Flamm RK, Tanaka SK, Graham DY, Go MF. Mutations in 23S rRNA are associated with clarithromycin resistance in *Helicobacter pylori*. *Antimicrob Agents Chemother* 1996; **40**: 477-480
11 **Hao Q,** Li Y, Zhang ZJ, Liu Y, Gao H. New mutation points in 23S rRNA gene associated with *Helicobacter pylori* resistance to clarithromycin in northeast China. *World J Gastroenterol* 2004; **1**: 1075-1077
12 **Chisholm SA,** Owen RJ, Teare EL, Savarymuttu S. PCR-based diagnosis of *Helicobacter pylori* infection and real-time determination of clarithromycin resistance directly from human gastric biopsy samples. *J Clin Microbiol* 2001; **39**: 1217-1220
13 **Occhialini AM,** Urdaci M, Doucet-Populaire F, Bebear CM, Lamouliatte H, Megraud F. Macrolide resistance in *Helicobacter pylori*: rapid detection of point mutations and assays of macrolide binding to ribosomes. *Antimicrob Agents Chemother* 1997; **41**: 2724-2728
14 **Menard A,** Santos A, Megraud F, Oleastero M. PCR-restriction fragment length polymorphism can also detect point mutation A2142C in the 23S rRNA gene, associated with *Helicobacter pylori* resistance to clarithromycin. *Antimicrob Agents Chemother* 2002; **46**: 1156-1157
15 **Alarcon T,** Domingo D, Prieto N, Lopez-Brea M. PCR using 3′-mismatched primers to detect A2142C mutation in 23S rRNA conferring resistance to clarithromycin in *Helicobacter pylori* clinical isolates. *J Clin Microbiol* 2000; **38**: 923-925
16 **Marais A,** Bilardi C, Cantet F, Mendz GL, Megraud F. Characterization of the genes *rdxA* and *frxA* involved in metronidazole resistance in *Helicobacter pylori*. *Res Microbiol* 2003; **154**: 137-144
17 **Chisholm SA,** Owen RJ. Frameshift mutations in *frxA* occur frequently and do not provide a reliable marker for metronidazole resistance in UK isolates of *Helicobacter pylori*. *J Med Microbiol* 2004; **53**: 135-140
18 **Grignon B,** Tankovic J, Megraud F, Glupczynski Y, Husson MO, Conroy MC, Emond JP, Loulergue J, Raymond J, Fauchere JL. Validation of diffusion methods for macrolide susceptibility testing of *Helicobacter pylori*. *Microb Drug Resist* 2002; **8**: 61-66
19 **Midolo PD,** Turnidge J, Lambert JR. Validation of a modified Kirby-Bauer disk diffusion method for metronidazole susceptibility testing of *Helicobacter pylori*. *Diagn Micr Infec Dis* 1995; **21**: 135-140
20 **Eltahawy AT.** Prevalence of primary *Helicobacter pylori* resistance to several antimicrobials in a Saudi Teaching Hospital. *Med Princ Pract* 2002; **11**: 65-68
21 **McNulty C,** Owen R, Tompkins D, Hawtin P, McColl K, Price A, Smith G, Teare L. *Helicobacter pylori* susceptibility testing by disc diffusion. *J Antimicrob Chemother* 2002; **49**: 601-609
22 **Debets-Ossenkopp YJ,** Herscheid AJ, Pot RG, Kuipers EJ, Kusters JG, Vandenbroucke-Grauls CM. Prevalence of *Helicobacter pylori* resistance to metronidazole, clarithromycin, amoxycillin, tetracycline and trovafloxacin in The Netherlands. *J Antimicrob Chemother* 1999; **43**: 511-515
23 **Chaves S,** Gadanho M, Tenreiro R, Cabrita J. Assessment of metronidazole susceptibility in *Helicobacter pylori*: statistical validation and error rate analysis of breakpoints determined by the disk diffusion test. *J Clin Microbiol* 1999; **37**: 1628-1631

24 **Debets-Ossenkopp YJ,** Pot RG, van Westerloo DJ, Goodwin A, Vandenbroucke-Grauls CM, Berg DE, Hoffman PS, Kusters JG. Insertion of mini-IS *605* and deletion of adjacent sequences in the nitroreductase (*rdxA*) gene cause metronidazole resistance in *Helicobacter pylori* NCTC11637. *Antimicrob Agents Chemother* 1999; **43**: 2657-2662

25 **Van der Wouden EJ,** de Jong A, Thijs JC, Kleibeuker JH, van Zwet AA. Subpopulations of *Helicobacter pylori* are responsible for discrepancies in the outcome of nitroimidazole susceptibility testing. *Antimicrob Agents Chemother* 1999; **43**: 1448-1456

26 **Piccolomini R,** Di Bonaventura G, Catamo G. Comparative evaluation of the E-test, agar dilution, and broth microdilution for testing susceptibilities of *Helicobacter pylori* strains to 20 antimicrobial agents. *J Clin Microbiol* 1997; **35**: 1842-1846

27 **DeCross AJ,** Marshall BJ, McCallum RW, Hoffman SR, Barrett LJ, Guerrant RL. Metronidazole susceptibility testing for *Helicobacter pylori*: comparison of disk, broth, and agar dilution methods and their clinical relevance. *J Clin Microbiol* 1993; **31**: 1971-1974

28 **Weiss K,** Laverdiere M, Restieri C. Comparison of activity to 10 antibiotics against clinical strains of *H pylori* by three different techniques. *Can J Gastroenterol* 1998; **12**: 181-185

29 **Edwards DI.** Nitroimidazole drugs-action and resistance mechanisms. II. Mechanisms of resistance. *J Antimicrob Chemother* 1993; **31**: 9-20

30 **Knapp CC,** Ludwig MD, W JA. *In vitro* activity of metronidazole against *Helicobacter pylori* as determined by agar dilution and agar diffusion. *Antimicrob Agents Chemother* 1991; **35**: 1230-1231

31 **Hachem CY,** Clarridge JE, Reddy R, Flamm R, Evans DG, Tanaka SK, Graham DY. Antimicrobial susceptibility testing of *Helicobacter pylori*. Comparison of E-test, broth microdilution, and disk diffusion for ampicillin, clarithromycin, and metronidazole. *Diagn Microbiol Infect Dis* 1996; **24**: 37-41

32 **Glupczynski Y,** Broutet N, Cantagrel A, Andersen LP, Alarcon T, Lopez-Brea M, Megraud F. Comparison of the E test and agar dilution method for antimicrobial suceptibility testing of *Helicobacter pylori*. *Eur J Clin Microbiol Infect Dis* 2002; **21**: 549-552

33 **Parsons HK,** Carter MJ, Sanders DS, Winstanley T, Lobo AJ. *Helicobacter pylori* antimicrobial resistance in the United Kingdom: the effect of age, sex and socio-economic status. *Aliment Pharmacol Ther* 2001; **15**: 1473-1478

34 **Grignon B,** Tankovic J, Megraud F, Glupczynski Y, Husson MO, Conroy MC, Emond JP, Loulergue J, Raymond J, Fauchere JL. Validation of diffusion methods for macrolide susceptibility testing of *Helicobacter pylori*. *Microb Drug Resist* 2002; **8**: 61-66

35 **Megraud F.** *H pylori* antibiotic resistance: prevalence, importance, and advances in testing. *Gut* 2004; **53**: 1374-1384

36 **Yakoob J,** Fan X, Hu G, Liu L, Zhang Z. Antibiotic susceptibility of *Helicobacter pylori* in the Chinese population. *J Gastroenterol Hepatol* 2001; **16**: 981-985

37 **Fakheri H,** Malekzadeh RKM, Merat S, Fazel A, Alizadeh BZ, Massarrat S. Clarithromycin *vs* furazolidone in quadruple therapy regimens for the treatment of *Helicobacter pylori* in a population with a high metronidazole resistance rate. *Aliment Pharmacol Ther* 2001; **15**: 411-416

38 **Malekzadeh R,** Merat S, Derakhshan MH, Siavoshi F, Yazdanbod A, Mikaeli J, Sotudemanesh R, Sotude M, Farahvash MJ, Nasseri-Moghaddam S, Pourshams A, Dolatshahi S, Abedi B, Babaei M, Arashi S, Majidpour A. Low *Helicobacter pylori* eradication rate with 4-7 d regimen in an Iranian population. *J Gastroenterol Hepatol* 2003; **18**: 13-17

39 **Roghani HS,** Massarrat S, Pahlewanzadeh MR, Dashti M. Effect of two different doses of metronidazole and tetracycline in bismuth triple therapy on eradication of *Helicobacter pylori* and its resistant strains. *Eur J Gastroenterol Hepatol* 1999; **11**: 709-712

40 **Bereswill S,** Krainick C, Stahler F, Herrmann L, Kist M. Analysis of the *rdxA* gene in high-level metronidazole-resistant clinical isolates confirms a limited use of *rdxA* mutations as a marker for prediction of metronidazole resistance in *Helicobacter pylori*. *FEMS Immunol Med Microbiol* 2003; **36**: 193-198

41 **Dai N,** Zhou G, Yan J. Correlation of *rdxA* gene mutation and metronidazole resistance of *Helicobacter pylori*. *Zhejiang Daxue Xuebao Yixueban* 2003; **32**: 37-40

42 **Yang YJ,** Wu JJ, Sheu BS, Kao AW, Huang AH. The *rdxA* gene plays a more major role than *frxA* gene mutation in high-level metronidazole resistance of *Helicobacter pylori* in Taiwan. *Helicobacter* 2004; **9**: 400-407

Science Editor Wang XL and Guo SY **Language Editor** Elsevier HK

PO Box 2345, Beijing 100023, China
www.wjgnet.com
wjg@wjgnet.com

ELSEVIER

World J Gastroenterol 2005;11(38):6014-6017
World Journal of Gastroenterology ISSN 1007-9327
© 2005 The WJG Press and Elsevier Inc. All rights reserved.

• *BRIEF REPORTS* •

Receptor-binding cancer antigen expressed on SiSo cells can be detected in metastatic lymph nodes from gastrointestinal cancers

Kawin Leelawat, Surang Engprasert, Supathip Tujinda, Cheepsumon Suthippintawong, Munechika Enjoji, Manabu Nakashima, Takeshi Watanabe, Vijittra Leardkamolkarn

Kawin Leelawat, Department of Surgery, Rajavithi Hospital, Bangkok 10400, Thailand
Kawin Leelawat, Vijittra Leardkamolkarn, Department of Anatomy, Mahidol University, Bangkok 10400, Thailand
Surang Engprasert, Department of Pharmacognosy, Kyushu University, Fukuoka 8128582, Japan
Supathip Tujinda, Cheepsumon Suthippintawong, Department of Pathology, Rajavithi Hospital, Bangkok 10400, Thailand
Munechika Enjoji, Manabu Nakashima, Takeshi Watanabe, Department of Medical Bioregulation, Kyushu University, Fukuoka 8128582, Japan
Supported by the Thailand Research Fund in the Royal Golden Jubilee Program
Correspondence to: Kawin Leelawat, MD, PhD, Department of Surgery, Rajavithi Hospital, Rajavithi Road, Rajathevi, Bangkok 10400, Thailand. kawin@tubtim.cri.or.th
Telephone: +66-2-245-6078 Fax: +66-2-245-6075
Received: 2004-02-02 Accepted: 2004-03-02

Abstract

AIM: To investigate the expression of receptor-binding cancer antigen expressed on SiSo cells (RCAS1) in metastatic lymph nodes from gastrointestinal cancer.

METHODS: Metastatic lymph nodes from gastrointestinal cancer were detected for RCAS1 by immunohistochemical staining and mRNA *in situ* hybridization.

RESULTS: A total of 102 metastatic lymph nodes from bile duct, gastric, colon, and pancreatic cancer were investigated for RCAS1 expression. The immunoreactivity of RCAS1 was identified in 100% of metastatic lymph nodes. Both local and distant metastatic lymph nodes showed RCAS1 expression. On the contrary, specimens of non-cancerous lymph nodes were negative for RCAS1. The result of mRNA *in situ* hybridization was also confirmed by the finding of immunohistochemical staining. RCAS1 mRNA was detected in all tumor cells that metastasized to lymph nodes.

CONCLUSION: All metastatic lymph nodes express RCAS1 in tumor cells at both protein and mRNA levels, and RCAS1 should be used as a complementary factor for identification of metastatic lymph nodes from gastrointestinal cancers.

© 2005 The WJG Press and Elsevier Inc. All rights reserved.

Key words: RCAS1; Gastrointestinal cancer; Lymph node metastasis

Leelawat K, Engprasert S, Tujinda S, Suthippintawong C, Enjoji M, Nakashima M, Watanabe T, Leardkamolkarn V. Receptor-binding cancer antigen expressed on SiSo cells can be detected in metastatic lymph nodes from gastrointestinal cancers. *World J Gastroenterol* 2005; 11(38): 6014-6017
http://www.wjgnet.com/1007-9327/11/6014.asp

INTRODUCTION

One of the major factors for the poor prognosis of gastrointestinal cancer patients is lymph node metastasis[1-3]. To indicate the lymph node metastasis, pathologists must carefully identify tumor cells spreading to lymph nodes in each serial section of pathological specimens. The suitable method for the identification of tumor cells in lymph nodes is to stain the specimen with antibody, which highly recognizes the tumor antigen. At this time, the antibody to cytokeratin is widely used for detection of lymph node metastasis from breast cancer[4,5]. However,a current study showed that the sensitivity of cytokeratin to lymph node metastasis from gastrointestinal cancer is low[6].

Recently, receptor-binding cancer antigen expressed on SiSo cells (RCAS1) is recognized as type II membrane protein and secreted as a soluble protein[7,8]. This tumor-associated antigen has been demonstrated in several kinds of gastrointestinal cancer by immunohistochemical study using the specific mouse mAb, 22-1-1. The result of RCAS1 expression was evaluated for the percent incidence in various cancers including gall bladder cancer (70%)[9], cholangiocarcinoma (85.9-96.4%)[10,11], gastric cancer (54.3%)[12], pancreatic cancer (100%)[13], and colorectal cancer (100%)[14]. However, until now, there has been no intensive study about the expression of RCAS1 in lymph node metastasis from gastrointestinal cancer. Therefore, the purpose of the present study was to investigate the expression of RCAS1 at both protein and mRNA levels in lymph node metastasis from gastrointestinal cancer.

MATERIALS AND METHODS

Tissue specimens

Fifteen specimens of non-cancerous lymph nodes and 102 specimens of metastatic lymph nodes from different gastrointestinal cancers (surgically resected in Rajavithi Hospital, Bangkok, Thailand) were collected for RNA investigation and immunohistochemical staining. The study was carried out with the approval of the Ethical Committee of Rajavithi Hospital. Pathological diagnosis and evaluation

were routinely performed.

Immunohistochemical staining

The sections (4 μm) were deparaffinized and immunostained for RCAS1 as described previously[14]. Briefly, the sections were incubated overnight at 4 ℃ with 1:1 000 dilution of 22-1-1 mouse mAb (Medical & Biological Laboratories Co., Ltd.). Biotinylated rabbit anti-mouse IgM (DAKO) was applied to the sections followed by avidin-biotin-peroxidase conjugate (ABC Elite, Vector Labs). The immunohistochemical reactions were developed with freshly prepared 3,3'-diaminobenzidine tetrahydrochloride solution (Histofine SAB-PO kit) and counterstained with hematoxylin. As a negative control, primary antibody was replaced with mouse IgM. The positive cell staining in each slide was identified under a high power field (×400) of Olympus BH2 microscope (field width = 0.5 mm).

RCAS1 mRNA in situ hybridization

Fluorescent probe preparation RCAS1 cDNA fragments from metastatic lymph nodes were synthesized by RT-PCR as described previously[14], using forward primer 5'-ACCTTACTGCCCTCCGTCTA-3' and reverse primer 5'-CTTCTTCATTAGCCGTTGTG-3'. The nucleotide sequence was confirmed with a Model 310 genetic analyzer (PE Biosystems) using a BigDye terminator cycle sequencing kit and used for generating fluorescent probes using Gene Images™ random prime labeling kit (Amersham, Biosciences). Twenty nanograms per microliter of denatured RCAS1 cDNA was mixed with 10 μL of nucleotide mix, 5 μL of primer, and 1 μL of 5 U/μL Klenow enzyme solution. The reaction was incubated at 37 ℃ for 1 h and stored at -20 ℃ until used.

***In situ* hybridization** The specimens were deparaffinized in xylene. The sections were treated with proteinase K for 20 min at 37 ℃ then diluted fluorescent-RNA probe (1 ng/mL with hybridization buffer) was applied onto each specimen. The slides were incubated at 55 ℃ for 2 h. The sections were rinsed with TBS and incubated for 15 min with blocking mixture (10% fetal calf serum). For detection of mRNA, the sections were incubated at room temperature for 30 min with anti-FITC/alkaline phosphatase. The immunoreactions were visualized by incubating the sections at room temperature with substrates and immersed in tap water for 5 min. The slides were counterstained with hematoxylin before observation under a light microscope.

Statistical analysis

Statistical analysis for comparing the expression of RCAS1 in the specimens was performed using SPSS 10.0 for Windows. $P<0.05$ was considered statistically significant.

结果

A total of 102 metastatic lymph nodes from various kinds of cancer were investigated for RCAS1 expression as shown in Table 1. The metastatic lymph nodes were divided into two groups (local and distant metastatic nodes) according to the TNM staging systems. The immunostaining pattern for RCAS1 was observed in the cytoplasm of tumor cells but not in lymphocytes (Figure 1). Most metastatic tumor cells showed a high intensity of RCAS1 immunostaining. The staining level was not related with tumor stage or differentiation status. All sections in negative control (non-cancerous lymph nodes) showed no immunoreactivity. RCAS1 was identified in 100% of metastatic lymph nodes. Interestingly, several primary cancers, which identified RCAS1 expression in some parts of tumor tissues, were found to express RCAS1 in most of the metastatic tumor cells in lymph nodes.

The RCAS1 cDNA of metastatic lymph nodes from various gastrointestinal cancers was determined by reverse-transcription-PCR. The 802 bp product was sequenced and its homology was compared with the RCAS1 cDNA sequence databases present at NCBI GenBank (gi: 13528905). This cDNA fragment started from nucleotide 41 to 842 of RCAS1 cDNA. As demonstrated in Figure 2, the cDNA fragment from metastatic lymph nodes revealed a high similarity throughout the 802 bp in the coding region.

To confirm further the expression of RCAS1 in metastatic lymph nodes, RCAS1 mRNA *in situ* hybridization was performed using the cDNA probes showing a high similarity with RCAS1 cDNA. The expression of RCAS1 mRNA was clearly identified in cytoplasm of tumor cells but not in lymphocytes. Figure 3 represents the typical RCAS1 mRNA expression, which could be detected in cytoplasm of tumor cells and represented the negative signal for RCAS1 mRNA in lymphocytes.

Table 1 RCAS1 expression in metastatic lymph nodes from gastrointestinal cancers

Type of cancer	Total no. of lymph nodes		No. of lymph nodes express RCAS1 (%)
	Local metastasis	Distance metastasis	
Bile duct cancer	10	4	14 (100)
Colon cancer	56	6	62 (100)
Pancreatic cancer	12	2	14 (100)
Stomach cancer	10	2	12 (100)

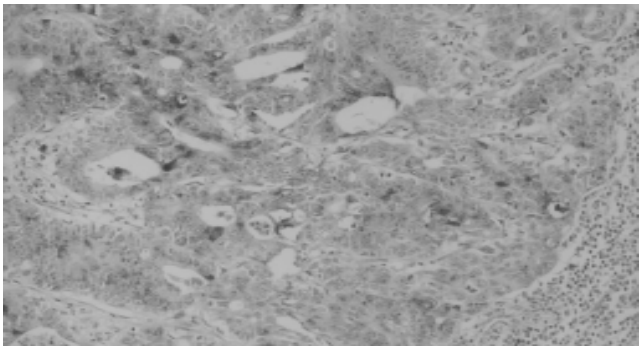


Figure 1 Typical result of immunohistochemical staining of RCAS1 (×200) in metastatic lymph nodes. Expression of RCAS1 was demonstrated both in cytoplasm and on cell membrane of tumor cells.

讨论

RCAS1 expression in lymph node metastasis from various

```
RCAS1     1   cgcagcctcc aaagccgcct tcctcaggga aatttgcgtg  accttactgc  cctccgtcta  60
RT- PCR   1   ---------- ---------- ---------- ----------  accttactgc  cctccgtcta  20
RCAS1     61  caggccttgt acctctccag gccgattttt ccacaattta  aatcccagtt  cacctggtat  120
RT- PCR   21  caggccttgt acctctccag gccgattttt ccacaattta  aatcccagtt  cacctggtat  80
RCAS1     121 ccagctccag caacttagag cgtttcacgt cacgccgggc  gccaggcgtc  ggcttgtata  180
RT- PCR   81  ccagctccag caacttagag cgtttcacgt cacgccgggc  gccaggcgtc  ggcttgtata  140
RCAS1     181 acctgaaaac gctcctgttt ttctcatctg tgcagtgggt  tttgattccc  accatggcca  240
RT- PCR   141 acctgaaaac gctcctgttt ttctcatctg tgcagtgggt  tttgattccc  accatggcca  200
RCAS1     241 tcacccagtt tcggttattt aaattttgta cctgcctagc  aacagtattc  tcattcctaa  300
RT- PCR   201 tcacccagtt tcggttattt aaattttgta cctgcctagc  aacagtattc  tcattcctaa  260
RCAS1     301 agagattaat atgcagatct ggcagaggac ggaaattaag  tggagaccaa  ataactttgc  360
RT- PCR   261 agagattaat atgcagatct ggcagaggac ggaaattaag  tggagaccaa  ataactttgc  320
RCAS1     361 caactacagt tgattattca tcagttccta agcagacaga  tgttgaagag  tggacttcct  420
RT- PCR   321 caactacagt tgattattca tcagttccta agcagacaga  tgttgaagag  tggacttcct  380
RCAS1     421 gggatgaaga tgcacccacc agtgtaaaga tcgaaggagg  gaatgggaat  gtggcaacac  480
RT- PCR   381 gggatgaaga tgcacccacc agtgtaaaga tcgaaggagg  gaatgggaat  gtggcaacac  440
RCAS1     481 aacaaaattc tttggaacaa ctggaacctg actattttaa  ggacatgaca  ccaactatta  540
RT- PCR   441 aacaaaattc tttggaacaa ctggaacctg actattttaa  ggacatgaca  ccaactatta  500
RCAS1     541 ggaaaactca gaaaattgtt attaagaaga gagaaccatt  gaattttggc  atcccagatg  600
RT- PCR   501 ggaaaactca gaaaattgtt attaagaaga gagaaccatt  gaattttggc  atcccagatg  560
RCAS1     601 ggagcacagg tttctctagt agattagcag ctacacaaga  tctgcctttt  attcatcagt  660
RT- PCR   561 ---------- ---------- ---------- ----------  ----------  ----------  620
RCAS1     661 cttctgaatt aggtgactta gatacctggc aggaaaatac  caatgcatgg  gaagaagaag  720
RT- PCR   621 ---------- ---------- ---------- ----------  ----------  ----------  680
RCAS1     721 aagatgcagc ctggcaagca gaagaagttc tgagacagca  gaaactagca  gacagagaaa  780
RT- PCR   681 ---------- ---------- ---------- ----------  ----------  ----------  740
RCAS1     781 agagagcagc cgaacaacaa aggaagaaaa tggaaaagga  agcacaacgg  ctaatgaaga  840
RT- PCR   741 ---------- ---------- ---------- ----------  ----------  ----------  800
RCAS1     841 ag
RT- PCR   801 --
```

Figure 2 Nucleotide sequence alignment of RCAS1 cDNA from databases present at NCBI GenBank (gi: 13528905) and RT-PCR products from metastatic lymph nodes. The residues boxed in black indicate positional identity for both sequences. Numbers of nucleotide sequences are indicated on the left and right margins.

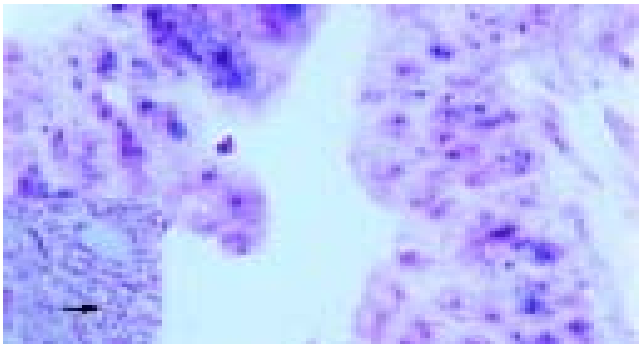


Figure 3 RCAS1 mRNA *in situ* hybridization in metastatic lymph nodes from colon cancer. The positive signal was identified in the cytoplasm of tumor cells. All leukocytes showed negative signal for RCAS1 (as presented in the Figure).

gastrointestinal cancers was first explored at protein level by immunohistochemical staining. The RCAS1 cDNA obtained from metastatic lymph nodes from various gastrointestinal tumors showed high homology with the RCAS1 cDNA sequence databases present at NCBI GenBank (gi: 13528905). This finding increases the reliability of *in situ* hybridization for identification RCAS1 of mRNA expression in metastatic tumor cells.

As suspected, it was expressed in all cases of metastatic lymph nodes. RCAS1 was shown to be a ligand for a putative receptor on immune cells such as T cells and natural killer cells[7-14]. Scientists suggest that RCAS1 may play a protective role in tumor cells against immune surveillance by inhibition of clonal expression and inducing receptor-expressing cell death. It has been previously reported that activated lymphocytes process receptors for RCAS1[7]. Thus, binding interaction between them induces apoptosis of lymphocytes. The mechanism by which tumor cell expressed RCAS1 mediates lymphocyte apoptosis is a main biologic pathway to escape the immune surveillance in both local and distant metastatic lymph nodes.

Although previous results[13,14] have demonstrated the correlation between the staining level and tumor stage or differentiation status, this study did not find any significant correlation between them. Most metastatic tumor cells showed a high intensity of RCAS1 immunostaining. This result may explain why tumor cells expressing RCAS1 metastasize the lymph nodes. The role of RCAS1 in lymph node metastasis needs further study.

Since the expression of RCAS1 is found in gastrointestinal cancers and their metastatic lymph nodes, it can be used as an additional step for identification of the status of lymph nodes.

REFERENCES

1 **Ding YB,** Chen GY, Xia JG, Zang XW, Yang HY, Yang L, Liu YX. Correlation of tumor-positive ratio and number of perigastric lymph nodes with prognosis of patients with surgically-removed gastric carcinoma. *World J Gastroenterol* 2004; **10**: 182-185

2 **Cuschieri A,** Weeden S, Fielding J, Bancewicz J, Craven J, Joypaul V, Sydes M, Fayers P. Patient survival after D1 and D2 resections for gastric cancer: long-term results of the MRC randomized surgical trial. Surgical Co-operative Group. *Br J Cancer* 1999; **79**: 1522-1530

3 **Ichikura T,** Ogawa T, Chochi K, Kawabata T, Sugasawa H, Mochizuki H. Minimum number of lymph nodes that should be examined for the International Union Against Cancer/ American joint committee on cancer TNM classification of gastric carcinoma. *World J Surg* 2003; **27**: 330-333

4 **Lara JF,** Young SM, Velilla RE, Santoro EJ, Templeton SF. The relevance of occult axillary micrometastasis in ductal carcinoma in situ: a clinicopathologic study with long-term follow-up. *Cancer* 2003; **98**: 2105-2113
5 **Euhus DM.** Cytokeratin staining and other sentinel node controversies. *Clin Breast Cancer* 2003; **4**(Suppl 1): S49-54
6 **Mukai M,** Sato S, Nakasaki H, Tajima T, Saito Y, Nishiumi N, Iwasaki M, Tokuda Y, Ogoshi K, Inoue H, Makuuchi H. Occult neoplastic cells in the lymph node sinuses and recurrence of primary breast, lung, esophageal, and gastric cancer. *Oncol Rep* 2004; **11**: 81-84
7 **Nakashima M,** Sonoda K, Watanabe T. Inhibition of cell growth and induction of apoptotic cell death by the human tumor-associated antigen RCAS1. *Nat Med* 1999; **5**: 938-942
8 **Sonoda K,** Nakashima M, Kaku T, Kamura T, Nakano H, Watanabe T. A novel tumor-associated antigen expressed in human uterine and ovarian carcinomas. *Cancer* 1996; **77**: 1501-1509
9 **Oshikiri T,** Hida Y, Miyamoto M, Hashida H, Katoh K, Suzuoki M, Nakakubo Y, Hiraoka K, Shinohara T, Itoh T, Kondo S, Katoh H. RCAS1 as a tumor progression marker: an independent negative prognostic factor in gallbladder cancer. *Br J Cancer* 2001; **85**: 1922-1927
10 **Enjoji M,** Nakashima M, Nishi H, Choi I, Oimomi H, Sugimoto R, Kotoh K, Taguchi K, Nakamuta M, Nawata H, Watanabe T. The tumor-associated antigen, RCAS1, can be expressed in immune-mediated diseases as well as in carcinomas of biliary tract. *J Hepatol* 2002; **36**: 786-792
11 **Suzuoki M,** Hida Y, Miyamoto M, Oshikiri T, Hiraoka K, Nakakubo Y, Shinohara T, Itoh T, Okushiba S, Kondo S, Katoh H. RCAS1 expression as a prognostic factor after curative surgery for extrahepatic bile duct carcinoma. *Ann Surg Oncol* 2002; **9**: 388-393
12 **Fukuda K,** Tsujitani S, Maeta Y, Yamaguchi K, Ikeguchi M, Kaibara N. The expression of RCAS1 and tumor infiltrating lymphocytes in patients with T3 gastric carcinoma. *Gastric Cancer* 2002; **5**: 220-227
13 **Akashi T,** Oimomi H, Nishiyama K, Nakashima M, Arita Y, Sumii T, Kimura T, Ito T, Nawata H, Watanabe T. Expression and diagnostic evaluation of the human tumor-associated antigen RCAS1 in pancreatic cancer. *Pancreas* 2003; **26**: 49-55
14 **Leelawat K,** Watanabe T, Nakajima M, Tujinda S, Suthipintawong C, Leardkamolkarn V. Upregulation of tumor-associated antigen RCAS1 is implicated in high stages of colorectal cancer. *J Clin Pathol* 2003; **56**: 764-768

Science Editor Wang XL and Guo SY **Language Editor** Elsevier HK

PO Box 2345, Beijing 100023, China
www.wjgnet.com
wjg@wjgnet.com

ELSEVIER

World J Gastroenterol 2005;11(38):6018-6021
World Journal of Gastroenterology ISSN 1007-9327
© 2005 The WJG Press and Elsevier Inc. All rights reserved.

• *BRIEF REPORTS* •

Normal serum alanine aminotransferase activity in uncomplicated obesity

Gianluca Iacobellis, Antonio Moschetta, Maria Cristina Ribaudo, Alessandra Zappaterreno, Concetta Valeria Iannucci, Frida Leonetti

Gianluca Iacobellis, Maria Cristina Ribaudo, Alessandra Zappaterreno, Concetta Valeria Iannucci, Frida Leonetti, Endocrinology, Department of Clinical Sciences, La Sapienza University, Rome, Italy
Gianluca Iacobellis, Center for Human Nutrition, the University of Texas Southwestern Medical Center, Dallas, TX, USA
Antonio Moschetta, Clinica Medica "*Augusto Murri*", Department of Internal and Public Medicine, University of Bari, Italy
Correspondence to: Dr. Gianluca Iacobellis, MD, PhD, Dipartimento Scienze Cliniche,Università La Sapienza,Policlinico I, Viale del Policlinico 155,00161,Roma, Italy, gianluca.iaco@tin.it
Telephone: +39-6-44240932 Fax: +39-6-44240932
Received: 2005-01-12 Accepted: 2005-03-23

AIM: To evaluate serum alanine aminotransferase (ALT) activity in a well-characterized group of uncomplicated obese subjects and its correlation with insulin resistance, plasma adiponectin, and leptin concentrations.

METHODS: One hundred and five uncomplicated obese subjects (87 women, 18 men, age 34.3±9.6 years, BMI 39.9±8.3 kg/m^2) were studied. Serum ALT activity was evaluated. Insulin sensitivity was assessed by euglycemic hyperinsulinemic clamp (M index) and fasting insulin. Plasma leptin and adiponectin levels were also measured.

RESULTS: Serum ALT concentration in the whole group of uncomplicated obese subjects was 17.73±6.33 U/L with none of the subjects presenting ALT levels greater than 43 U/L and only 9 (11%) women and 3 (19%) men showed ALT levels >19 and >30 U/L for women and men, respectively. No significant difference was detected in serum ALT levels between severe obese subjects (BMI >40 kg/m^2) and those with BMI <40 kg/m^2 (18.63±6.25 *vs* 17.26±6.02 U/L). ALT was significantly correlated with fasting insulin (r = 0.485, P = 0.02) and triglycerides (r = 0.358, P = 0.03).

CONCLUSION: Serum ALT activity is practically normal in uncomplicated obese subjects, independently of their obesity degree. These findings suggest the role of obesity-related comorbidities and not of BMI as main risk factors for elevated ALT levels in obese subjects.
© 2005 The WJG Press and Elsevier Inc. All rights reserved.

Key words: Serum alanine aminotransferase activity; Obesity; Insulin resistance

Iacobellis G, Moschetta A, Ribaudo MC, Zappaterreno A, Iannucci CV, Leonetti F. Normal serum alanine aminotransferase activity in uncomplicated obesity. *World J Gastroenterol* 2005; 11(38): 6018-6021
http://www.wjgnet.com/1007-9327/11/6018.asp

Overweight and obesity have been reported to be major risk factors for elevated serum alanine aminotransferase (ALT) activity[1,2] and non-alcoholic fatty liver disease (NAFLD)[3-6]. High serum ALT levels have also been proposed as a marker of risk for type 2 diabetes[7,8]. A recent atherosclerosis study showed a significant relationship between ALT activity and insulin resistance[7]. In addition, unexplained ALT elevation has been found to be associated with increased visceral adiposity and other features of the metabolic syndrome[9]. Nevertheless, no studies evaluating serum ALT activity in metabolically healthy obese subjects have been performed. Uncomplicated obesity, as previously shown by our group[10], could be a good model to clarify the influence of obesity *per se* on ALT levels, without the confounding effect of the obesity-related comorbidities.

In this study, we sought to evaluate the serum ALT activity in a well-characterized uncomplicated obese subjects and its possible correlation with insulin resistance, plasma adiponectin, and leptin concentrations.

Patients

We selected 105 consecutive Caucasian uncomplicated obese subjects (body mass index [BMI] >30 kg/m^2) from 600 obese subjects who were referred to our Day Hospital from Rome and surrounding areas between January 2001 and June 2004. The selected subjects had the following features: 87 women, 18 men; age, 34.3±9.6 years (range, 20-55 years); BMI, 39.9±8.3 kg/m^2 (range, 30-80.1 kg/m^2); duration of obesity, 15±5 years (range, 10-30 years). Uncomplicated obesity was defined according to the following parameters: no signs, symptoms and history of liver diseases (alcoholic hepatitis, viral hepatitis, positive serum hepatitis B surface antigen, positive serum hepatitis C surface antibody, auto-immune hepatitis, drug-induced hepatitis, familial metabolic disorders, history of fatty liver during pregnancy, portal hypertension, liver cancer, elevated serum transferrin

PO Box 2345, Beijing 100023, China
www.wjgnet.com
wjg@wjgnet.com

ELSEVIER

World J Gastroenterol 2005;11(38):6022-6026
World Journal of Gastroenterology ISSN 1007-9327
© 2005 The WJG Press and Elsevier Inc. All rights reserved.

• *BRIEF REPORTS* •

Endoscopic treatment and follow-up of gastrointestinal Dieulafoy's lesions

Panagiotis Katsinelos, George Paroutoglou, Kostas Mimidis, Athanasios Beltsis, Basilios Papaziogas, George Gelas, Yiannis Kountouras

Panagiotis Katsinelos, George Paroutoglou, Kostas Mimidis, Athanasios Beltsis, George Gelas, Department of Endoscopy and Motility Unit, "G. Gennimatas" Hospital, Ethnikis Aminis 41, Thessaloniki 54635, Greece
Basilios Papaziogas, 2nd Surgical Clinic, "G.Gennimatas" Hospital, Aristotle University of Thessaloniki, Ethnikis Aminis 41, Thessaloniki 54635, Greece
Yiannis Kountouras, 2nd Department of Internal Medicine, Ippokration Hospital, Aristotle University of Thessaloniki, Greece
Correspondence to: Dr. Panagiotis Katsinelos, Department of Endoscopy and Motility Unit, "G. Gennimatas" Hospital, Ethnikis Aminis 41, Thessaloniki 54635, Greece. pantso@the.forthnet.gr
Telephone: +30-2310-211221 Fax: +30-2310-210401
Received: 2004-11-30 Accepted: 2005-01-26

Abstract

AIM: To investigate retrospectively the clinical and endoscopic features of bleeding Dieulafoy's lesions and to assess the short- and long-term effectiveness of endoscopic treatment.

METHODS: Twenty-three patients who had gastrointestinal bleeding from Dieulafoy's lesions underwent endoscopic therapy. Demographic data, mode of presentation, risk factors for gastrointestinal bleeding, blood transfusion requirements, endoscopic findings, details of endoscopic therapy, recurrence of bleeding, and mortality rates were collected and analyzed retrospectively.

RESULTS: Hemostasis was attempted by dextrose 50% plus epinephrine in 10 patients, hemoclipping in 8 patients, heater probe in 2 patients and ethanolamine oleate in 2 patients. Comorbid conditions were present in 17 patients (74%). Overall permanent hemostasis was achieved in 18 patients (78%). Initial hemostasis was successful with no recurrent bleeding in patients treated with hemoclipping, heater probe or ethanolamine injection. In the group of patients who received dextrose 50% plus epinephrine injection treatment, four (40%) had recurrent bleeding and one (10%) had unsuccessful initial hemostasis. Of the four patients who had rebleeding, three had unsuccessful hemostasis with similar treatment. Surgical treatment was required in five patients (22%) owing to uncontrolled bleeding, recurrent bleeding with unsuccessful retreatment and inability to approach the lesion. One patient (4.3%) died of sepsis after operation during hospitalization. There were no side-effects related to endoscopic therapy. None of the patients in whom permanent hemostasis was achieved presented with rebleeding from Dieulafoy's lesion over a mean long-term follow-up of 29.8 mo.

CONCLUSION: Bleeding from Dieulafoy's lesions can be managed successfully by endoscopic methods, which should be regarded as the first choice. Endoscopic hemoclipping therapy is recommended for bleeding Dieulafoy's lesions.

© 2005 The WJG Press and Elsevier Inc. All rights reserved.

Key words: Endoscopic treatment; Dieulafoy lesion; Gastrointestinal tract

Katsinelos P, Paroutoglou G, Mimidis K, Beltsis A, Papaziogas B, Gelas G, Kountouras Y. Endoscopic treatment and follow-up of gastrointestinal Dieulafoy's lesions. *World J Gastroenterol* 2005; 11(38): 6022-6026
http://www.wjgnet.com/1007-9327/11/6022.asp

INTRODUCTION

Dieulafoy's lesion was first described by Gallard in 1884 and later fully characterized by French surgeon George Dieulafoy in 1896, as an arterial lesion associated with massive gastric hemorrhage. It is described as a minute defect of the gastrointestinal mucosa with rupture of a large submucosal artery into the lumen. Although usually described in the stomach, Dieulafoy's lesions are also described in the rest of the gastrointestinal tract including esophagus[1-3], duodenum[4], small bowel[5], colon[6], rectum[7], and anus[8].

Until a few years ago, surgical treatment was advocated for such lesions because of the inability to recognize the lesion via endoscopy, or because of massive and recurrent bleeding. However, endoscopic therapy has recently become the treatment of choice by many endoscopists, being effective in the majority of cases[9]. The aim of our study was to assess the short- and long-term effectiveness of endoscopic treatment of Dieulafoy's lesions.

MATERIALS AND METHODS

Between January 1994 and December 2003, 936 patients with acute GI bleeding of non-variceal origin were admitted to our endoscopy unit. After resuscitation with intravenous fluids and blood transfusions, emergency endoscopy without preparation was performed within 24 h of the onset of bleeding, using standard video-endoscopes. If there was fresh blood or clots obscuring bleeding lesion, a lavage with a large bore tube (34F) for upper GI bleeding or rigorous

cleansing of the colon with polyethylene glycol solution was performed. ECG, blood pressure, and oxygen saturation were monitored. Twenty-three patients were diagnosed as having Dieulafoy's lesions.

The endoscopic diagnosis of Dieulafoy's lesions was based on the following established criteria: active arterial spurting or micropulsatile streaming from a minute (<3 mm) mucosal defect, visualization of a protruding vessel with or without active bleeding within a minute mucosal defect or normal surrounding mucosa or densely adherent clot with a narrow point of attachment to a minute mucosal defect or normal-appearing mucosa. To avoid possible inclusion of variceal bleeding at either the index episode of bleeding or an episode of recurrent bleeding, all patients with esophagogastric varices were excluded from the study. If Dieulafoy's lesion was diagnosed at emergency endoscopy according to the criteria outlined above, the choice of the endoscopic method of treatment was left to the endoscopist's discretion.

The therapeutic methods used in the first six years of our study were injection of a solution of dextrose 50% plus epinephrine (1:10 000) and ethanolamine oleate, while heater probe treatment and hemoclipping were used in the last 4 years. In the injection group, 1 mL aliquot was injected via a plastic cannula (23-gauge, 5-mm tip) into and around the Dieulafoy's lesion. A limit of 10 mL of mixture per endoscopic session was set. A 3.2 mm diameter heater probe set at 30 J/pulse was used to coat the bleeding vessel. Hemoclip therapy (HX-3L, 5LR-1; Olympus Optical Co., Ltd, Tokyo, Japan) was performed by mechanical clipping of spurting, oozing or visible vessels.

Therapeutic endoscopy was defined as successful if there was no further bleeding from the Dieulafoy's lesion until the withdrawal of the endoscope. After endoscopic treatment, the patients with Dieulafoy's lesion in the upper GI tract were treated with intravenous administration of a standard dose of PPIs. Follow-up endoscopy was performed within 24 h after the initial procedure and at least once within 5 d. Criteria for recurrent bleeding included fresh hematemesis or hematochezia, fresh blood aspirated through the nasogastric tube, instability of vital signs or a reduction of hemoglobin in excess of 30 g/L within 24 h after endoscopic hemostasis. When recurrent bleeding was suspected, immediate endoscopic retreatment was performed. If bleeding persisted after the second intervention, an operation was performed. In order to determine whether new bleeding episodes occurred after discharge, long-term follow-up was carried out by retrieving the medical records from the files, and when necessary by telephone calls to the patients. The patients who underwent surgery were not subjected to long-term follow-up.

Data including age, gender, comorbidities, mode of presentation, hemodynamic parameters, blood transfusion requirements before and after endoscopic therapy, risk factors for gastrointestinal bleeding (such as coagulopathy, use of aspirin or other non-steroidal anti-inflammatory drugs), endoscopic findings, details of endoscopic therapy, complications, recurrence of bleeding, and 30-d mortality were collected (Table 1).

Informed consent was obtained from the patients and/or their relatives. Because this study was a retrospective review, institutional review board approval was not necessary.

Student's *t*-test was utilized to compare the mean values of continuous variables and Fisher exact test was utilized for the comparison of discrete variables.

[illegible]

The study group consisted of 17 male (74%) and 6 female (26%) patients. The mean age was 70.26 years (range 42-84 years). There was a history of hypertension in nine patients, ischemic heart disease in four, heart failure in six, diabetes in two, gout in two, chronic renal failure in one, BII gastrectomy in two, duodenal ulcer in one, and aorto-iliac bypass in one (Table 1).

Melena was present in 11 patients (47.8%), hematemesis and melena in 9 (39%), and rectal bleeding in the remaining 3 patients (13.2%). Mean hemoglobin concentration was 101 g/L (normal 130-160 g/L). Blood transfusion requirements ranged from 1 to 8 U of packed RBC (mean 2.9 U per patient) during hospitalization. There was no significant difference with respect to coagulation parameters in patients who had recurrent bleeding and those who did not.

The Dieulafoy's lesions were located in the stomach in 18 patients (78%, fundus in 6, body in 9, and antrum in 3), in the colon in 3 (Figure 1), in the jejunum in 1 and in the descending duodenum in 1 (Table 1). Eleven patients (47.8%) had active bleeding (oozing in 7 and spurting in 4) at the initial endoscopy. In the remaining 12 patients (52.2%), a non-bleeding vessel was found (Table 1). In a 84-year-old patient with a medical history of heart failure and aorto-iliac bypass, endoscopy revealed two simultaneous Dieulafoy's lesions in the fundus, 2 cm apart. The initial endoscopy was diagnostic in 69% of patients. The mean number of endoscopies required for diagnosis was 1.7 (range 1-3). Failure to diagnose when the appropriate site was evaluated at endoscopy was due to excessive blood on 11 occasions (47.8%) and a missed lesion on 8 occasions (34.7%).

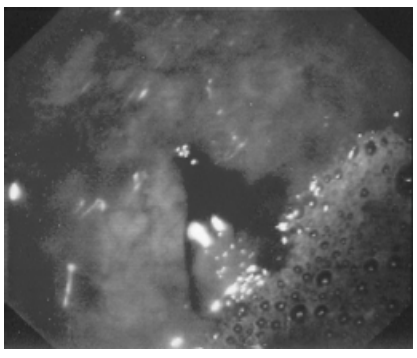


Figure 1 Endoscopic view of Dieulafoy's lesion with oozing in sigmoid.

Ten patients were treated with dextrose 50% plus epinephrine 1:10 000 injection. Mean injection volume was 7.6 mL (range 6-9 mL). Initial hemostasis was achieved in nine patients (90%), but four patients (44%) had rebleeding, which was successfully controlled at repeat endoscopy in one patient, but not in the other three using similar therapy,

Table 1 Clinical characteristics, endoscopic data, and after endoscopic therapy of patients with acute bleeding from Dieulafoy's lesion in GI tract

N	Sex	Age (yr)	Location	Bleeding symptom	Hb g/L	Transfusion (RBC)	Medical history	Endoscopic picture of bleeding	Type of therapy	Hemostasis	Rebleeding	Outcome
1	F	84	Fundus	Melena	98	3	Heart failure, hypertension	Oozing	Dextrose 50%+EPI (7 cm^3)	Successful	No	Discharge
2	F	54	Upper gastric body	Hematemesis /melena	117	1	–	Spurting	Dextrose 50%+EPI (6 cm^3)	Failure	–	Operation
3	F	42	Rectum	Rectal bleeding	121	–	–	Oozing	Dextrose 50%+EPI (7 cm^3)	Successful	No	Discharge
4	M	72	Jejunum	Hematemesis /melena	96	3	Hypertension, angina	Visible vessel	Dextrose 50%+EPI (7 cm^3)	Successful	Yes	Operation /death
5	M	48	Descending duodenum	Melena	117	–	–	Visible vessel	Dextrose 50%+EPI (8 cm^3)	Successful	No	Discharge
6	M	69	Gastric body	Hematemesis /melena	78	8	Angina, BII gastrectomy	Spurting	Dextrose 50%+EPI (9 cm^3)	Successful	Yes	Operation /discharge
7	M	86	Upper gastric body	Melena	104	2	Hypertension, angina	Visible vessel	Dextrose 50%+EPI (7 cm^3)	Successful	No	Discharge
8	F	81	Fundus	Melena	87	4	Hypertension, heart failure	Oozing	Dextrose 50%+EPI (8 cm^3)	Successful	No	Discharge
9	M	82	Fundus	Hematemesis /melena	78	8	Heart failure	Visible vessel	Dextrose 50%+EPI (8 cm^3)	Successful	Yes	Operation /discharge
10	M	83	Gastric body	Hematemesis /melena	96	3	Heart failure	Visible vessel	Dextrose 50%+EPI (8 cm^3)	Successful	Yes	Discharge
11	F	72	Fundus	Melena	77	6	Hypertension	Visible vessel	Ethanolamine oleate (9 cm^3)	Successful	No	Discharge
12	M	66	Upper gastric body	Melena	106	2	Gout, hypertension	Visible vessel	Ethanolamine oleate (6 cm^3)	Successful	No	Discharge
13	M	79	Upper gastric body	Melena	92	4	Hypertension, angina	Visible vessel	EPI+HP (8×30 J)	Successful	No	Discharge
14	M	74	Fundus	Hematemesis /melena	98	3	Renal failure, gout, diabetes	Visible vessel	EPI+HP (6×30 J)	Successful	No	Discharge
15	M	48	Antrum	Melena	110	1	–	Oozing	EPI+3 hemoclips	Successful	No	Discharge
16	M	60	Antrum	Hematemesis /melena	104	3	Duodenal ulcer	Oozing	EPI+4 hemoclips	Successful	No	Discharge
17	M	65	Antrum	Melena	103	2	Diabetes, hypertension	Spurting	EPI+3 hemoclips	Successful	No	Discharge
18	M	67	Sigmoid colon	Rectal bleeding	115	2	Colonic polyps	Oozing	EPI+4 hemoclips	Successful	No	Discharge
19	M	74	Sigmoid	Rectal bleeding	113	2	Angina	Oozing	EPI+3 hemoclips	Successful	No	Discharge
20	M	84	Fundus	Hematemesis /melena	88	4	Heart failure, aorto-iliac bypass	Two visible vessels	4 hemoclips	Successful	No	Discharge
21	F	79	Gastric body	Melena	118	1	Hypertension	Visible vessel	2 hemoclips	Successful	No	Discharge
22	M	75	Gastric body	Melena	103	2	Heart failure	Visible vessel	2 hemoclips	Successful	No	Discharge
23	M	72	Gastric body	Hematemesis /melena	100	3	BII gastrectomy angina	Visible vessel	Inability to approach the visible vessel	–	–	Operation /discharge

EPI, epinephrine solution 1:10 000.

and surgical intervention was required (Table 1). Four patients were treated with injection of ethanolamine oleate and the heater probe respectively, and permanent hemostasis was achieved on a single session (Table 1). The power settings for the heater probe were clearly stated in two patients (30 J in both) and the number of applications ranged from 6 to 8. Among the patients in the hemoclip group, the mean number of hemoclips used was 3.1 (range 2-4). Hemostasis was achieved at the initial endoscopic procedure by hemoclip (Figure 2) in all eight patients. Epinephrine plus normal saline (1:10 000) was used as an useful adjunct when the lesion was oozing or spurting, to slow or stop bleeding prior to hemoclip application or heater probe treatment. Five patients (22%) underwent surgery, four after unsuccessful endoscopic therapy and one because it was impossible to approach the lesion on the posterior wall of the patient's gastrectomized stomach. One patient (4.3%) died of sepsis and multiple organ failure in the postoperative period.

Endoscopic hemoclipping therapy was shown to be generally more effective than injection therapy in terms of the rates of permanent hemostasis (100% *vs* 66.6%, $P<0.01$), recurrent bleeding (0% *vs* 33.3%, $P<0.01$) and surgery (0% *vs* 33.3%, $P<0.01$, Table 2).

In the five patients, who underwent surgery, gastrotomy showed a muscular artery protruding from the mucosa but not ulceration, findings being consistent with Dieulafoy's lesion. Wedge resection was performed and histopathologic examination confirmed the presence of an abnormally large submucosal artery.

None of the patients presented with recurrent gastrointestinal bleeding from Dieulafoy's lesions during a mean long-term follow-up of 29.8 mo (range 2-120 mo). Seven patients died during the follow-up from causes unrelated to the Dieulafoy's lesions or endoscopic procedures.

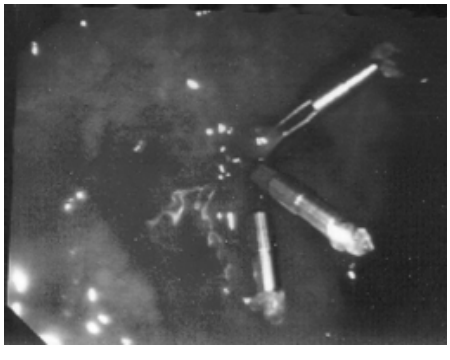


Figure 2 Endoscopic view showing complete closure of a minute mucosal defect with a protruding vessel with three hemoclips.

Table 2 Outcome of endoscopic therapy in injection and mechanical groups, *n* (%)

Parameters	Injection group	Mechanical group	*P*
Initial hemostasis	11 (92.5)	8 (100)	NS
Recurrent bleeding	4 (33.3)	0 (0)	<0.01
Permanent hemostasis	8 (66.6)	8 (100)	<0.01
Operation	4 (33.3)	0 (0)	<0.01

NS, non significant.

DISCUSSION

Dieulafoy's lesion is an uncommon cause of gastrointestinal bleeding, although some authors consider it as an under-recognized entity[1,9]. It is a disease of mainly aged and elderly males[10,11]. Our results with a mean age of 70.3 years and a more pronounced male predominance of 1:3 are consistent with former findings. Though the fact that they have been described in other parts of the gastrointestinal tract, Dieulafoy's lesions are located in the proximal stomach in more than three-fourths of patients[1,2]. Accordingly, in 78% of our patients the lesion was found in the stomach and in 39% in the classic site within 6 cm of the gastroesophageal junction. As in other reports, we identified Dieulafoy's lesions in the colon, jejunum and duodenum. Interestingly, one patient presented two simultaneous Dieulafoy's lesions in the gastric fundus.

The diagnostic yield of the first endoscopy varies from 63% to 92%[9]. Norton *et al*.[12], and Kasapidis *et al*.[13], found that a mean of 1.9 or 1.3 endoscopic sessions is required for diagnosis. In the present study, the diagnosis of Dieulafoy's lesion was established in 69% of patients during the first endoscopy, with a mean of 1.7 endoscopic sessions. A protruding vessel is found in 50% of patients and about two-thirds of patients manifest active bleeding, either as oozing or as spurting[10,11,14,15]. By contrast, in the present study the frequency of active bleeding was low (39%), with the majority of our patients having a non-bleeding visible vessel (61%), though the fact that the comorbid conditions and the mean age of our patients were consistent with former studies.

Some investigators have documented significant diseases in patients with Dieulafoy's lesion[5,10,16,17]. Comorbidity of cardiovascular diseases, diabetes, chronic renal failure and hypertension is present in almost 90% of patients with Dieulafoy's lesion[12]. In more than 40% of patients with Dieulafoy's lesion, the use of medication that influences blood coagulation has also been noted[12,16]. However, other studies have found no association of Dieulafoy's lesion with concomitant disease or the use of medications[14,18]. The results of the present investigation are consistent with the former studies. The significant comorbidity in 17 patients (74%) is likely a reflection of the elderly population studied, since any pathogenic significance remains speculative. Pathologic studies have failed to demonstrate atherosclerosis or aneurismal dilatation of the involved vessel[16,18].

Surgical wedge resection has been the standard treatment of Dieulafoy's lesions in the past[1]. However, its mortality rate is as high as 23%[1]. Since the late 1980s, a variety of endoscopic techniques have been used in the management of Dieulafoy's lesions. Endoscopic hemostatic methods could be divided into three groups: thermal, regional injection and mechanical[9,12,17,19,20]. Each method has both advantages and disadvantages related to the hemostatic mechanism and the technical procedure itself and varying results have been reported. The results of endoscopic hemostatic therapies depend on many and variable factors. The major factors include the level of expertise in performing the endoscopic procedure, coincident clinical risk factors, the use of advanced equipment and the inherent differences in various procedures.

All these factors influence the success of endoscopic outcome, but endoscopic modalities can achieve permanent hemostasis in approximately 95% of patients[9]. The overall lower rate of permanent hemostasis (78%) in our study was due to the low hemostatic effect (60%) of dextrose 50% plus epinephrine injection. It must be emphasized that the osmotic dehydrating and sclerosant effect of hypertonic glucose water (50%) has been reported[21] to be superior than a classic sclerosant agent, like sodium tetradecyl sulfate (15%), in controlling bleeding and rebleeding in patients with advanced liver cirrhosis and gastric variceal bleeding. Therefore, the low rate of hemostasis achieved in our study by dextrose 50% plus epinephrine cannot be explained. A careful search of the MEDLINE database from 1970 to 2003 did not retrieve any report of dextrose 50% plus epinephrine used in the treatment of Dieulafoy's lesions. Thus, the present study seems to be the first report on the use of dextrose 50% plus epinephrine as a therapeutic modality for Dieulafoy's lesions.

In the present investigation, none of the patients treated with heater probe coagulation or ethanolamine oleate injection developed recurrent bleeding. The mechanical method of hemoclips used in our study achieved complete hemostasis in 100% of patients. None of our patients treated with hemoclips had recurrent bleeding, while four patients (33.3%) in the injection group had recurrent bleeding ($P<0.01$, Table 2).

Although the number of patients in our study was small, we believe that the successful management especially by hemostatic clips (Table 2) favors a primary endoscopic approach to Dieulafoy's disease. It must be underscored, however, that an experienced endoscopist is necessary as a Dieulafoy's lesion can easily be overlooked or may be difficult to be approached, as was the case for one of our patients.

Hemoclips are mechanical devices, it must be argued that they cannot eradicate a Dieulafoy's lesion with a large caliber artery as effectively as sclerosant injections or thermal coagulation and that bleeding may recur after this type of treatment. However, in our study no patient had recurrent bleeding after hemoclip treatment during the follow-up period.

In conclusion, endoscopic therapy has become the treatment of choice for Dieulafoy's lesions and the endoscopic hemoclip treatment is effective and appears to be more successful in achieving hemostasis than injection treatment. More definite conclusions require further large controlled studies.

□□□□□□□□□□

1 **Fockens P,** Tytgat GN. Dieulafoy's disease. *Gastroenterol Clin North Am* 1996; **6**: 739-752
2 **Reilly HF,** Al-Kawas FH. Dieulafoy's lesion, diagnosis and management. *Dig Dis Sci* 1991; **36**: 1702-1707
3 **Ertekin C,** Barbaros U, Tavigoglu K, Guloglu R, Kasoglu A. Dieulafoy's lesion of the esophagus. *Surg Endosc* 2002; **16**: 219-221
4 **Goldenberg SP,** DeLuca VJ, Marignani P. Endoscopic treatment of Dieulafoy's lesion of the duodenum. *Am J Gastroenterol* 1990; **85**: 452-454
5 **Gadenstatter M,** Wetscher G, Cookes PF, Mason RJ, Schwab G, Pointner R. Dieulafoy's disease of the large and small bowel. *J Clin Gastroenterol* 1998; **27**: 169-172
6 **Nozoe T,** Kitamura M, Matsumata T, Sugimachi K. Dieulafoy – like lesions of colon and rectum in patients with chronic renal failure on long–term hemodialysis. *Hepatogastroenterology* 1999; **46**: 3121-3133
7 **Kayali Z,** Sangchantz W, Matsumoto B. Lower gastrointestinal bleeding secondary to Dieulafoy–like lesion of the rectum. *J Clin Gastroenterol* 2000; **30**: 328-330
8 **Azimuddin K,** Stasik JJ, Rosen L, Riether RD, Khubchandani IT. Dieulafoy's lesion of the anal canal: a new clinical entity. Report of two cases. *Dis Colon Rectum* 2000; **43**: 423-426
9 **Savides TJ,** Jensen DM. Therapeutic endoscopy for non – variceal gastrointestinal bleeding. *Gastroenterol Clin North Am* 2000; **29**: 465-487
10 **Stark ME,** Gostout CJ, Balm RK. Clinical features and endoscopic management of Dieulafoy's disease. *Gastrointest Endosc* 1992; **38**: 545-550
11 **Schmulewitz N,** Baillie J. Dieulafoy lesion: A review of 6 years of experience at a tertiary referral center. *Am J Gastroenterol* 2001; **96**: 1688-1694
12 **Norton ID,** Petersen BT, Sorbi D, Balm RK, Alexander GL, Gostout CJ. Management and long–term prognosis of Dieulafoy lesion. *Gastrointest Endosc* 1999; **50**: 762-767
13 **Kasapidis P,** Georgopoulos P, Delis V, Balatsos V, Kostantinidis A, Skandalis N. Endoscopic management and long–term follow–up of Dieulafoy's lesions in the upper GI tract. *Gastrointest Endosc* 2002; **55**: 527-531
14 **Veldhuyzen van Zanten SJ,** Bartelsman JF, Schipper ME, Tytgat GN. Recurrent massive hematemesis from Dieulafoy vascular malformations- a review of 101 cases. *Gut* 1986; **27**: 213-222
15 **Mumtaz R,** Shaukat M, Ramirez F. Outcomes of endoscopic treatment of gastrointestinal Dieulafoy's lesion with rubber band ligation and thermal/injection therapy. *J Clin Gastroenterol* 2003; **36**: 310-314
16 **Juler GI,** Labitzke HG, Lamb R, Allen R. The pathogenesis of Dieulafoy's gastric erosion. *Am J Gastroenterol* 1984; **79**: 195-200
17 **Parra-Blanco A,** Takahashi H, Mendez Jerez PV, Kojima T, Aksoz K, Kirihara K, Palmerin J, Takekuma E, Fuijta R. Endoscopic management of Dieulafoy lesions of the stomach: a case study of 26 patients. *Endoscopy* 1997; **29**: 834-839
18 **Katz PO,** Salas L. Less frequent causes of upper gastrointestinal bleeding. *Gastroenterol Clin North Am* 1993; **22**: 875-889
19 **Baettig B,** Haecki W, Lammer F, Jost R. Dieulafoy's disease: endoscopic treatment and follow–up. *Gut* 1993; **34**: 1418-1421
20 **Chung ILK,** Kim EJ, Lee MS, Kim HS, Park SH, Lee MH, Kim SJ, Cho MS. Bleeding Dieulafoy's lesion and the choice of endoscopic method: comparing the hemostatic efficacy of mechanical and injection method. *Gastrointest Endosc* 2000; **52**: 721-724
21 **Chang KY,** Wu CS, Chen PC. Prospective randomized trial of hypertonic glucose water and sodium tetradecyl sulfate for gastric variceal bleeding in patients with advanced liver cirrhosis. *Endoscopy* 1996; **2**: 481-486

Science Editor Wang XL and Guo SY **Language Editor** Elsevier HK

PO Box 2345, Beijing 100023, China
www.wjgnet.com
wjg@wjgnet.com

ELSEVIER

World J Gastroenterol 2005;11(38):6027-6030
World Journal of Gastroenterology ISSN 1007-9327
© 2005 The WJG Press and Elsevier Inc. All rights reserved.

• *BRIEF REPORTS* •

Manometric assessment of idiopathic megarectum in constipated children

Giuseppe Chiarioni, Giuseppe de Roberto, Alessandro Mazzocchi, Antonio Morelli, Gabrio Bassotti

Giuseppe Chiarioni, Gastroenterological Rehabilitation Division of the University of Verona, Valeggio sul Mincio Hospital, Azienda Ospedaliera of Verona, Valeggio sul Mincio, Verona 37067, Italy
Giuseppe de Roberto, Alessandro Mazzocchi, Antonio Morelli, Gabrio Bassotti, Gastroenterology and Hepatology Section, Department of Clinical and Experimental Medicine, University of Perugia, Perugia 06100, Italy
Correspondence to: Dr. Gabrio Bassotti, Clinica di Gastroenterologia ed Epatologia Via Enrico Dal Pozzo, Padiglione W, Perugia 06100, Italy. gabassot@tin.it
Telephone: +39-75-584-7570
Received: 2005-01-26 Accepted: 2005-04-18

Abstract

AIM: Chronic constipation is a frequent finding in children. In this age range, the concomitant occurrence of megarectum is not uncommon. However, the definition of megarectum is variable, and a few data exist for Italy. We studied anorectal manometric variables and sensation in a group of constipated children with megarectum defined by radiologic criteria. Data from this group were compared with those obtained in a similar group of children with recurrent abdominal pain.

METHODS: Anorectal testing was carried out in both groups by standard manometric technique and rectal balloon expulsion test.

RESULTS: Megarectum patients displayed discrete abnormalities of anorectal variables and sensation with respect to controls. In particular, the pelvic floor function appeared to be impaired in most patients.

CONCLUSION: Constipated children with megarectum have abnormal anorectal function and sensation. These findings may be helpful for a better understanding of the pathophysiological basis of this condition.

© 2005 The WJG Press and Elsevier Inc. All rights reserved.

Key words: Constipation; Manometry; Megarectum

Chiarioni G, de Roberto G, Mazzocchi A, Morelli A, Bassotti G. Manometric assessment of idiopathic megarectum in constipated children. *World J Gastroenterol* 2005; 11(38): 6027-6030
http://www.wjgnet.com/1007-9327/11/6027.asp

INTRODUCTION

Chronic constipation is a frequently encountered symptom in children[1]. Due to a general belief that childhood constipation gradually disappears before or during puberty, this symptom is often underestimated and scarcely taken into consideration. However, recent evidence suggests that up to one-third of the constipated children followed beyond puberty continue to have severe complaints of constipation[2].

The definition of constipation in childhood is also less standardized than in adults; for the latter, in fact, the Rome II criteria[3,4] seem quite accepted and widespread whereas the criteria for children[5] are believed to be too restrictive, in that they might exclude several children with constipation[6].

For practical purposes, childhood constipation may be grossly divided into two groups, represented by functional fecal retention (FFR, most frequent) and slow transit constipation (STC), which also reflect the main pathophysiological abnormalities[7]. In fact, constipation in children is very rarely caused by a colonic motility disorder, as frequently found in adults[8]. Childhood constipation is mostly due to a maladaptive behavior triggered by an unpleasant defecation that in some subjects led to delay further defecation by withholding the stools. These patients, who were different than those with STC, have normal colonic motility[9].

In chronically constipated children with FFR, the abnormal motor activity is often found in the rectum, which may become so dilated that it is unable to generate enough pressure to propel the stools into the anal canal[9]. This megarectum is found in 30-100% of constipated children, depending on the definition used[10-14]. Thus, no uniform definition of megarectum for constipated children is available, it is unknown whether a large rectum is the result or the cause of constipation, and which underlying mechanism is responsible for fecal impaction[15].

Therefore, purpose of the present study was the assessment of chronically constipated pediatric patients with megarectum defined by radiologic criteria.

MATERIALS AND METHODS

Patients

Fifteen constipated children (11 males and 4 females, age 9±0.6 years) entered the study. Average duration of symptoms was 4 years (range 2-8 years). Patients were recruited when they met at least two of the following criteria[16,17]: (1) less than three defecations per week; (2) soiling and/or encopresis episodes more than twice per week; (3) passage of large amounts of feces once per 7-30 d; and (4) presence of a palpable rectal mass. Moreover, barium enema showed the presence of an enlarged rectum

(diameter more than 6.5 cm in the lateral view, as measured on a line extending perpendicular to S_2[18]) in all patients.

On physical examination, all patients had a large amount of soft stool that filled the rectum. Soiling, defined as the loss of a small amount of loose stool in the underwear[17], was present in 3 (13%) patients and encopresis, defined as the loss of a normal amount of stool in the underwear after the age of 4 years (without an underlying organic disorder)[17], was present in 13 (87%) patients. Before performing manometric and rectal compliance determination, a rectal disimpaction schedule was performed in all patients. This schedule consisted of oral osmotic laxatives (lactitol, 5 g/10 kg body weight in two divided daily doses) and tap water enemas given by the parents for a maximum of 7 d. The last enema was given at least 5 h before physiological assessment was done. Rectal digital examination was performed in all patients, to ascertain that an adequate rectal disimpaction was achieved.

Controls

The control group was represented by 12 children (nine males and three females, age 10±0.7 years) with recurrent abdominal pain (RAP) and without rectal fecal impaction. These patients were recruited on the basis of Rome II criteria for RAP[5]: at least 12 wk of: (1) continuous or nearly continuous abdominal pain in a school-aged child or adolescent; and (2) no or only occasional relation of pain with physiological events (e.g., eating, menses, or defecation); and (3) some loss of daily functions; and (4) the pain is not feigned (e.g., malingering); and (5) the patient had insufficient criteria for other functional gastrointestinal disorders that would explain the abdominal pain. All controls had at least one bowel movement per day, and they did not meet the criteria for constipation as defined above.

Methods

Anorectal manometry and tests of rectal compliance were carried out according to a standard technique. Briefly, a commercially available four-lumen pediatric anorectal catheter with terminal balloon (Menfis bioMedica, Bologna, Italy, type 5R-9-100CB), connected via physiological pressure transducers to a low-compliance infusion pump and to a computerized recording system (Dyno Compact System, Menfis) was used.

After recording the rectoanal pressure profile with stepwise withdrawal (1 cm/30 s), the anal resting tone was recorded for 2-5 min with the catheter fixed at the highest pressure point obtained during two pull-throughs. Then, the rectosphincteric reflex was evaluated by inflating and rapidly deflating the catheter balloon with 10, 20, 30, 50, and 100 mL of air. Finally, the sphincteric response to straining was assessed by asking the patients to strain as if to defecate thrice at 1-min intervals.

To test rectal compliance and sensation, a single-lumen PVC catheter (outer diameter 4 mm) with a 7-cm-long cut terminal unstretched condom was used, connected to the above-mentioned pressure transducer and recorder, as previously described[19]. The balloon was placed with its distal portion about 5 cm from the anal margin and, through a syringe equipped with a three-channel stopcock, inflated with 50 mL of air increments every 60 s until the maximum rectal tolerable volume (MRTV) was reached. Rectal expulsion ability was assessed, with the patient lying on the left side, by inserting a well-lubricated Foley catheter in the rectum, then filling it with 50 mL of water and asking the patient to defecate it[20].

Ethical considerations

After careful explanations about the aims of the study, the parents of the children gave written informed consent, and the studies were carried out in accordance with local ethical guidelines, following the recommendations of the Declaration of Helsinki.

Data analysis

All tracings were analyzed in blind by one of the investigators. For anorectal manometry and test of rectal compliance and sensation, the following variables were taken into account[19,21]: (1) maximum basal pressure of the internal anal sphincter, defined as the mean of the highest resting pressures recorded from each of the four ports during the two pull-throughs[19,21,22]; (2) minimum relaxation volume (MRV), defined as the lower quantity of air inflated in the rectal balloon necessary to elicit the rectoanal inhibitory reflex, a drop in pressure >5 mmHg, which represents relaxation of the internal sphincter[23,24]; (3) defecatory sensation threshold (DST), defined as the smallest volume at which the first desire to defecate was reported by the patient[25,26]; (4) response to straining, evaluated by observing whether straining to defecate caused a decrease in intra-anal pressure (normal response) or a paradoxical increase in intra-anal pressure[27]; (5) MRTV, defined as the maximum volume of air that could be infused into the rectal balloon and responsible either for an intolerable urge to defecate, painful distension, or expulsion of the balloon itself[11]; (6) rectal compliance, defined as the intraballoon pressure at 100 mL when inflated intrarectally minus the intraballoon pressure at 100 mL when inflated in open air[28,29]; and (7) rectal expulsion. Without any time limitation, the test was considered abnormal when the patient was not able to expel the balloon (Foley catheter filled with 50 mL of water) and refused further straining attempts.

Statistical analysis

The Kolmogorov-Smirnov test for normality was applied, and showed that the data were not normally distributed. Therefore, comparisons of data between controls and patients were done by means of nonparametric tests. The Wilcoxon rank sum test (two-tailed) and the χ^2 test were applied, where necessary. Values of P less than 0.05 were chosen for rejection of the null hypothesis. Data are expressed as mean±SE.

RESULTS

No differences between groups were found concerning age (9.6±0.7 years in controls *vs* 9.5±0.6 years in patients, $P = 0.10$). Soiling and/or encopresis was found in none of the controls and in 13/15 (87%) patients ($P<0.0001$). Analysis of anorectal physiological variables showed that

the maximum basal pressure of the anal sphincter was significantly higher in controls with respect to the patients (58±3.4 *vs* 31±3 mmHg, $P<0.001$), whereas the MRV was lower in controls (13.3±1.4 *vs* 39±5.3 mmHg, $P<0.001$). Concerning the DST, this was found to be significantly lower in controls compared to that found in megarectum patients (54±4 mmHg *vs* 130±27 mmHg, $P<0.01$). As expected, controls displayed lower values of MRTV compared to the megarectum patients (171±11 mL *vs* 523±68 mL, $P<0.001$) and higher compliance values (18±1.3 mmHg *vs* 10.5±2 mmHg, $P<0.02$).

The response to straining was abnormal in 1/12 (8.3%) controls and in 9/15 (60%) patients ($P = 0.017$); the rectal expulsion test was abnormal in 1/12 (8.3%) controls and in 15/15 (100%) patients ($P<0.0001$).

DISCUSSION

The term megarectum is frequently employed in children with constipation or fecal impaction without any quantification measure, and there are only a few data obtained in groups with more objective definitions[17]. In the present study, we adopted a validated radiological definition, at least for adults and adolescents: the limit of this definition is due to the fact that lesser degrees of megarectum in the pediatric population may have been excluded. However, we had a well-defined group of patients with objective criteria, and we feel that this is important since to the best of our knowledge there are no such reports from Italy.

The comparison of anorectal parameters between patients and controls showed significant abnormalities in the former that displayed lower basal pressures of the anal sphincter and compliance values, whereas higher values were found for MRV, DST, and MRTV. In addition, most megarectum patients had clinical and instrumental evidence of abnormal pelvic floor function.

These results are in agreement with some previous studies[11,30-33], where others were not able to find such differences[16,17,34]. We are at present unable to explain such discrepancies, although patients' selection, severity of symptoms, and assessment methods may be responsible for these differences between studies.

We feel of interest that this group of children with megarectum shares anorectal abnormalities similar to those we found in adult patients with megarectum[19]. In this rather homogeneous group of pediatric patients, the findings seem consistent with similar mechanisms proposed for adults, i.e. that megarectum may be a mechanism for constipation by outlet obstruction[35], as shown by the impairment of anorectal dynamics in such patients. The rectal function, in fact, seems to be severely deranged, as shown by the MRTV recorded in these children, due to an atonic rectum that sometimes adapted to masses of over 800 mL, too large to be defecated. The MRV and rectal sensation were also impaired, with some of the patients needing higher volumes to relax the sphincter and feeling the defecatory stimulus only at high volumes of distension, thereby enforcing the mechanisms leading to further dilatation of the rectal ampulla.

The clinical significance of a dyssynergic phenomenon in these patients is unclear. Previous studies have proposed this phenomenon as one of the main causes of impaired rectal expulsion in megarectum and megacolon patients[36], but other studies have challenged this hypothesis, since rectal emptying may happen against a contracting pelvic floor[37,38]. However, since fecal consistency is likely to influence the efficiency of rectal emptying[39,40], it is possible that the presence of large, hard stools in a megarectum may elicit a dyssynergic pattern.

In conclusion, we described a group of constipated children with well-defined megarectum, and showed that these patients display important abnormalities of anorectal variables and sensation. We feel these findings may be of some interest for a better understanding of the pathophysiological mechanisms of this condition and, possibly, for a more targeted therapeutic approach.

REFERENCES

1 **Loening-Baucke V.** Chronic constipation in children. *Gastroenterology* 1993; **38**: 1568-1580
2 **van Ginkel R,** Reitsma JB, Buller HA, van Wijk MP, Taminiau JA, Benninga MA. Childhood constipation: longitudinal follow-up beyond puberty. *Gastroenterology* 2003; **125**: 357-363
3 **Thompson WG,** Longstreth GF, Drossman DA, Heaton KW, Irvine EJ, Muller-Lissner SA. Functional bowel disorders and functional abdominal pain. *Gut* 1999; **45**(Suppl 2): II43-II47
4 **Whitehead WE,** Wald A, Diamant NE, Enck P, Pemberton JH, Rao SSC. Functional disorders of the anus and rectum. *Gut* 1999; **45**(Suppl 2): II55-II59
5 **Rasquin-Weber A,** Hyman PE, Cucchiara S, Fleisher DR, Hyams JS, Milla PJ, Staiano A. Childhood functional gastrointestinal disorders. *Gut* 1999; **45**(Suppl 2): II60-II68
6 **Voskuijl WP,** Heijmans J, Heijmans TS, Taminiau JA, Benninga MA. Use of Rome II criteria in childhood defecation disorders: applicability in clinical and research practice. *J Pediatr* 2004; **145**: 213-217
7 **Sutcliffe JR,** King SK, Southwell BR, Hutson JM. Paediatric constipation for adult surgeons–Article 1: targeting the cause. *ANZ J Surg* 2004; **74**: 777-780
8 **Bassotti G,** Iantorno G, Fiorella S, Bustos-Fernandez L, Bilder CR. Colonic motility in man: features in normal subjects and in patients with chronic idiopathic constipation. *Am J Gastroenterol* 1999; **94**: 1760-1770
9 **Di Lorenzo C,** Ciamarra P. Pediatric gastrointestinal motility. In Schuster MM, Crowell MD, Koch KL, eds. *Schuster atlas of gastrointestinal motility*, 2nd edition. *Hamilton, BC Decker Inc.* 2002: 411-428
10 **Liebman WM.** Disorders of defecation in children: evaluation and management. *Postgrad Med* 1979; **66**: 105-108
11 **Meunier P,** Louis D, Jaubert de Beaujeau M. Physiologic investigation of primary chronic constipation in children : comparison with the barium enema study. *Gastroenterology* 1984; **87**: 1351-1357
12 **Loening-Baucke VA,** Cruikshank BM. Abnormal defecation dynamics in chronically constipated children with encopresis. *J Pediatr* 1986; **108**: 562-566
13 **Benninga MA,** Buller HA, Heymans HS, Tytgat GN, Taminiau JA. Is encopresis always the result of constipation? *Arch Dis Child* 1994; **71**: 186-193
14 **Staiano A,** Andreotti MR, Greco L, Basile P, Auricchio S. Long-term follow-up of children with chronic idiopathic constipation. *Dig Dis Sci* 1994; **39**: 561-564
15 **Partin JC,** Hamill SK, Fischel JE, Partin JS. Painful defecation and fecal soiling in children. *Pediatrics* 1992; **89**: 1007-1009
16 **van der Plas RN,** Benninga MA, Buller HA, Bossuyt PM, Akkermans LM, Redekop WK, Taminiau JA. Biofeedback training in treatment of childhood constipation: a randomised controlled study. *Lancet* 1996; **348**: 776-780
17 **van der Plas RN,** Benninga MA, Staalman CR, Akkermans

LMA, Redekop WK, Taminiau JA, Buller HA. Megarectum in constipation. *Arch Dis Child* 2000; **83**: 52-58
18 **Gattuso JM,** Kamm MA. Clinical features of idiopathic megarectum and idiopathic megacolon. *Gut* 1997; **41**: 93-99
19 **Chiarioni G,** Bassotti G, Germani U, Brunori P, Brentegani MT, Minniti G, Calcara C, Morelli A, Vantini I. Idiopathic megarectum in adults. An assessment of manometric and radiologic variables. *Dig Dis Sci* 1995; **40**: 2286-2292
20 **Barnes PR,** Lennard-Jones JE. Balloon expulsion from the rectum in constipation of different types. *Gut* 1985; **26**: 1049-1052
21 **Chiarioni G,** Chistolini F, Menegotti M, Salandini L, Vantini I, Morelli A, Bassotti G. One-year follow-up study on the effects of electrogalvanic stimulation in chronic idiopathic constipation with pelvic floor dyssynergia. *Dis Colon Rectum* 2004; **47**: 346-353
22 **Read NW,** Harford WV, Schmulen AC, Read MG, Santa Ana C, Fortran JS. A clinical study of patients with fecal incontinence and diarrhea. *Gastroenterology* 1979; **76**: 747-756
23 **Dickinson VA.** Maintenance of anal continence. A review of pelvic floor physiology. *Gut* 1978; **19**: 1163-1174
24 **Bassotti G,** Maggio D, Battaglia E, Giulietti O, Spinozzi F, Reboldi G, Serra AM, Emanuelli G, Chiarioni G. Manometric investigation of anorectal function in early and late stage Parkinson's disease. *J Neurol Neurosurg Psych* 2000; **68**: 768-770
25 **Pescatori M,** Parks AG. The sphincteric and sensory components of preserved continence after ileoanal reservoir. *Surg Gynecol Obstet* 1984; **158**: 517-521
26 **Chiarioni G,** Bassotti G, Monsignori A, Menegotti M, Salandini L, Di Matteo G, Vantini I, Whitehead WE. Anorectal dysfunction in constipated women with anorexia nervosa. *Mayo Clin Proceed* 2000; **75**: 1015-1019
27 **Whitehead WE,** Heymen S, Schuster MM. Motility as a therapeutic modality: biofeedback treatment of gastrointestinal disorders. In Schuster MM, Crowell MD, Koch KL, eds. Schuster Atlas of Gastrointestinal Motility, Second edition. *Hamilton, BC Decker Inc* 2002: 381-397
28 **Whitehead WE,** Chaussade S, Corazzieri E, Kumar D. Report of an international workshop on management of constipation. *Gastroenterol Int* 1991; **4**: 99-113
29 **Chiarioni G,** Scattolini C, Bonfante F, Vantini I. Liquid stool incontinence with severe urgency: anorectal function and effective biofeedback therapy. *Gut* 1993; **34**: 1576-1580
30 **Callaghan RP,** Nixon HH. Megarectum: physiological observations. *Arch Dis Child* 1964; **39**: 153-157
31 **Molnar D,** Taitz LS, Urwin OM, Wales JK. Anorectal manometry results in defecation disorders. *Arch Dis Child* 1983; **58**: 257-261
32 **Clayden GS.** Management of chronic constipation. *Arch Dis Child* 1992; **67**: 340-344
33 **Loening-Baucke V,** Yamada T. Is the afferent pathway from the rectum impaired in children with chronic constipation and encopresis? *Gastroenterology* 1995; **109**: 397-403
34 **Benninga MA,** Buller HA, Taminiau JA. Biofeedback training in chronic constipation. *Arch Dis Child* 1993; **68**: 126-129
35 **Verduron A,** Devroede G, Bouchoucha M, Arhan P, Schang JC, Poisson J, Hémond M, Hébert M. Megarectum. *Dig Dis Sci* 1988; **33**: 1164-1174
36 **Barnes PR,** Lennard-Jones JE. Function of the striated anal sphincter during straining in controls subjects and constipated patients with a radiologically normal rectum and idiopathic megacolon. *Int J Colorect Dis* 1988; **3**: 207-209
37 **Jones PN,** Lubowski DZ, Swash M, Path MRC, Henry MM. Is paradoxical contraction of the puborectalis muscle of functional importance? *Dis Colon Rectum* 1987; **30**: 667-670
38 **Miller R,** Duthie GS, Bartolo DCC, Roe AM, Locke-Edmunds J, Mortensen NJ. Anismus in patients with normal and slow transit constipation. *Br J Surg* 1991; **78**: 690-692
39 **Bannister JJ,** Davison P, Timms JM, Gibbons CG, Read NW. Effect of the stool size and consistency on defaecation. *Gut* 1987; **28**: 1246-1249
40 **Ambroze WL,** Pemberton JH, Bell AM, Brown ML, Zinsmeister AR. The effect of stool consistency on rectal and neorectal emptying. *Dis Colon Rectum* 1990; **34**: 1-7

Science Editor Guo SY **Language Editor** Elsevier HK

PO Box 2345, Beijing 100023, China
www.wjgnet.com
wjg@wjgnet.com

ELSEVIER

World J Gastroenterol 2005;11(38):6031-6037
World Journal of Gastroenterology ISSN 1007-9327
© 2005 The WJG Press and Elsevier Inc. All rights reserved.

• *BRIEF REPORTS* •

Different effects of a CD14 gene polymorphism on disease outcome in patients with alcoholic liver disease and chronic hepatitis C infection

C Meiler, M Mühlbauer, M Johann, A Hartmann, B Schnabl, N Wodarz, G Schmitz, J Schölmerich, C Hellerbrand

C Meiler, M Mühlbauer, B Schnabl, J Schölmerich, C Hellerbrand, Department of Internal Medicine I, University of Regensburg, Regensburg 93042, Germany
M Johann, N Wodarz, Department of Psychiatry, University of Regensburg, Regensburg 93042, Germany
A Hartmann, Department of Pathology, University of Regensburg, Regensburg 93042, Germany
G Schmitz, Institute for Clinical Chemistry and Laboratory Medicine, University of Regensburg, Regensburg 93042, Germany
Supported by grants from the Else Kröner Fresenius-Stiftung to Hellerbrand C and the Deutsche Forschungsgemeinschaft (Schn 620/3-1) to Schnabl B
Co-first-authors: C Meiler and M Mühlbauer
Correspondence to: C Hellerbrand, MD, Department of Internal Medicine I, University of Regensburg, Regensburg D-93042, Germany. claus.hellerbrand@klinik.uni-regensburg.de
Telephone: +49-941-944-7155 Fax: +49-941-944-7154
Received: 2005-03-10 Accepted: 2005-04-09

Abstract

AIM: Clinical and experimental data suggest that gut-derived endotoxins are an important pathogenic factors for progression of chronic liver disease. Recently, a C-T (-159) polymorphism in the promoter region of the CD14 gene was detected and found to confer increased CD14 expression and to be associated with advanced alcoholic liver damage. Here, we investigated this polymorphism in patients with less advanced alcoholic liver disease (ALD) and chronic hepatitis C virus (HCV) infection.

METHODS: CD14 genotyping was performed by PCR-RFLP analysis in (a) 121 HCV patients, (b) 62 patients with alcohol-associated cirrhosis (Alc-Ci), (c) 118 individuals with heavy alcohol abuse without evidence of advanced liver damage (Alc-w/o Ci), and (d) 247 healthy controls. Furthermore, serum levels of soluble CD14 (sCD14) and transaminases were determined.

RESULTS: The TT genotype was significantly more frequent in Alc-Ci compared to Alc-w/o Ci or controls (40.3% *vs* 23.7% or 24.0%, respectively). In Alc-w/o Ci, serum levels of transaminases did not differ significantly between patients with different CD14 genotypes. In HCV patients, TT-homozygotes had significantly higher sCD14 levels and sCD14 serum levels were significantly higher in patients with advanced fibrosis or cirrhosis. However, no association was found between CD14 genotypes and histological staging or grading.

CONCLUSION: Considering serum transaminases as surrogate markers for alcoholic liver damage, the CD14 polymorphism seems to exhibit different effects during the course of ALD. Differences in genotype distribution between cirrhotic HCV patients and alcoholics and the known functional impact of this polymorphism on CD14 expression levels further indicate differences in the pathophysiological role of CD14 and CD14-mediated lipopolysaccharides signal transduction with regard to the stage as well as the type of the underlying liver disease.

© 2005 The WJG Press and Elsevier Inc. All rights reserved.

Key words: CD14 gene; Alcoholic liver disease; Chronic hepatitis C infection

Meiler C, Mühlbauer M, Johann M, Hartmann A, Schnabl B, Wodarz N, Schmitz G, Schölmerich J, Hellerbrand C. Different effects of a CD14 gene polymorphism on disease outcome in patients with alcoholic liver disease and chronic hepatitis C infection. *World J Gastroenterol* 2005; 11(38): 6031-6037
http://www.wjgnet.com/1007-9327/11/6031.asp

INTRODUCTION

Individuals affected by chronic liver disease show a broad spectrum of responses to the same etiologic agent. As one cause for this finding and increasing evidence indicates that genetic factors influence the natural history of chronic liver disease[1].

In case of alcoholic liver disease (ALD), early studies have focused on polymorphic forms of enzymes involved in alcohol metabolism[2-4]. Recent studies have shown that genetically determined variations in the inflammatory response contribute to different susceptibility for the development of various liver diseases, notably viral hepatitis[5,6] and ALD[7-10]. These findings together with accumulating clinical and experimental data indicate that the extent of the inflammatory response to the etiological agent is crucial in the pathogenesis of chronic hepatitis C virus (HCV) as well as alcoholic and other liver disease.

Several lines of evidence indicate that bacterial products, primarily endotoxins (lipopolysaccharides; LPS) induce and perpetuate hepatic inflammation. Endotoxin levels are correlated with the severity of ALD in experimental models[11] as well as in patients with chronic liver disease[12], and reducing gut endotoxin alleviates hepatic injury[13]. Endogenous LPS are constitutively produced within the gut by the death of Gram-negative bacteria and are absorbed into intestinal capillaries. In low concentrations, LPS can also be demonstrated in the portal venous blood in healthy

humans[14].

Increased LPS levels have been shown in patients with ALD as well as patients with chronic hepatitis C infection[12,15-17]. Several factors promote endotoxemia in this setting, including increased translocation of endotoxins and reduced hepatic clearance[11,18].

Circulating endotoxin is bound mainly to the LPS binding protein. This complex has a high affinity for the CD14 receptor[19]. CD14 is expressed on mature monocytes and macrophages, such as Kupffer cells[20,21]. Furthermore, hepatocytes as well as activated hepatic stellate cells (HSC) get stimulated by LPS via membrane-bound CD14[20,23].

A soluble CD14 (sCD14) is constitutively present in the circulation, and is apparently derived both from secretion of CD14 and from enzymatically cleaved glycosylphosphatidylinositol-anchored tissue CD14[24,25]. sCD14 is believed to play a key role as an intermediate in the neutralization of LPS under physiological conditions. sCD14 accelerates the transfer between LPS micelles and lipoproteins by acting as a carrier. sCD14 also enhances the release of monocyte-bound LPS, transferring LPS into plasma and into lipoproteins[26]. This results in a decreased cellular response to LPS, such as induction of TNF and interleukin-6 synthesis[27].

Recently, a polymorphism of the CD14 gene (C-T transition at bp -159 from the major transcription start site) was described. This polymorphism is located within the Sp1 transcription factor binding site, known to affect CD14 expression. The T allele promotes CD14 gene transcription as shown in *in vitro* on monocytes[28,29].

Functional relevance of the polymorphism has been suggested in several studies finding an association with myocardial infarction[29,30], ulcerative colitis[31], asthma[32], and chronic spondyloarthropathy[33]. Notably, all these diseases have an inflammatory component.

Recently, Järveläinen *et al*., investigated the frequency of this CD14 polymorphism in autopsy series of Finnish patients with ALD[34]. Interestingly, the T allele was associated with advanced ALD, especially with cirrhosis, but not with steatosis or less advanced stages of fibrosis. A subsequent analysis of a relatively small cohort of 30 patients with primary biliary cirrhosis revealed no significant association of the CD14 polymorphism with the severity of the disease and found no differences in the genotype distribution as compared to healthy controls[35]. Poullis *et al*., analyzed the effect of the CD14 polymorphism on liver function tests and found some evidence indicating that the TT genotype, associated with higher serum levels of sCD14, may offer protection from the development of fatty liver disease[36]. This hypothesis is supported by recent studies indicating an association between sCD14 levels and insulin sensitivity[37,38].

As in ALD in HCV patients, elevated serum levels of endotoxin as well as sCD14 have been reported[12,16,39] but the C-T (-159) promotor polymorphism of the CD14 gene had not been investigated in this group of patients so far.

Here we analyzed the association of this CD14 polymorphism with the histological stage of fibrosis and the grade of inflammation in hepatic tissue of HCV patients, and their corresponding sCD14 serum levels, respectively.

Furthermore, the aim of this study was to verify the association of the CD14 polymorphism with the degree of alcoholic liver damage, previously found in the Finnish study[35], in our cohort of patients with ALD from southern Germany.

[illegible]

Patients and controls

The following groups of patients were studied retrospectively: (a) 121 patients (80 males and 41 females; mean age: 37.2±11.5 years) with chronic hepatitis C (positive for HCV-RNA and anti-HCV) consecutively admitted to the medical department of the University of Regensburg. All patients were negative for hepatitis B surface antigen or antibodies to HIV and none of them had evidence of other types of liver disease. Risk factors for acquisition of hepatitis C infection were previous intravenous drug abuse in 25.6%, receipt of blood or blood products before the introduction of donor screening in 15.7%, and other factors or unknown in 58.7%. Liver biopsies were obtained from all patients before initiation of antiviral therapy (naive patients) by percutaneous Menghini-needle biopsy. In these patients fibrosis and inflammation were graded and staged numerically according to a score proposed by Desmet *et al*.[40], by a single pathologist.

The majority of patients received treatment with interferon-α+ribavirin. For 91 patients, data of qualitative HCV-PCR analysis 3 mo after initiation of antiviral therapy were available.

(b) sixty-two patients with alcoholic cirrhosis consecutively admitted to the medical department of the University of Regensburg (49 males and 13 females; mean age: 53.1±8.9 years). Patients were considered to have alcohol-related cirrhosis, if alcohol intake had been in excess of 100 g/d for more than 10 years and if testing for viral, metabolic, and immune etiologies was negative. Liver cirrhosis was diagnosed based on typical clinical, laboratory, ultrasound, and gastroscopical findings.

(c) one hundred and eighteen heavy drinkers without evidence of liver damage (90 males and 28 females; mean age: 42.5±9.1 years). These unrelated individuals of German descent were recruited from an in-patient abstention program at the Department of Psychiatry of the University of Regensburg. Each subject met the criteria of alcohol dependence according to ICD-10[41]. At the day of admission, several serum parameters were analyzed including transaminases (alanine aminotransferase [ALT], AST, and γ-glutamyl transferase [γ-GT]), and anti-HCV- and HBV-antibodies. Previous and current drinking habits, as well as family history of non-ALDs, and potential previous complications of advanced liver damages as ascites or esophageal varices were examined. Furthermore, within 14 d after admission, a clinical and ultrasound examination of the abdomen was performed.

Only alcohol-dependent subjects with an alcohol consumption of at least 80 g/d for more than 5 years were included. Furthermore, clinical or sonomorphological indications for advanced liver damage and serological evidence of HBV or HCV infection were exclusion criteria.

(d)two hundred and forty seven healthy subjects (119

females and 128 males), genotyped already in a previous study[42], served as controls.

Patients and controls were Caucasians and their geographical origin was southern Germany. Informed consent was obtained from all patients and the study was approved by the local ethics committee.

DNA isolation and CD14 genotyping

Genomic DNA specimens were prepared from 200 μL blood using the QIAamp blood kit following the manufacturer's instructions (Qiagen, Hilden, Germany). The C-T polymorphisms at position -159 of the CD14 gene was analyzed by performing PCR and subsequent restriction fragment length polymorphism analysis. PCR was performed under standard conditions (35 cycles, annealing temperature: 55 ℃) in a total reaction volume of 50 μL containing 2 μL of diluted genomic DNA, using the following pair of primers: forward: 5'-CCG AGA TGT TCC CAG CAC AG-3' and reverse: 5'-CTG CTT TGC TTG TGC CTC TT-3'. PCR products were digested by *Hae*III, and the resulting fragments were separated by electrophoresis in a 2% agarose gel and visualized by ethidium bromide staining. With the -159 T polymorphic base, the recognition sequence 5'-GG/CC-3' is modified to 5'-GG/TC-3', which is not cut by *Hae*III.

Serum sCD14 levels

sCD14 concentrations were analyzed in the serum of 97 patients with chronic hepatitis C infection using a sandwich ELISA following the instructor's manual (Biosource Europe, Nivelles, Belgium).

Statistical analysis

Results are expressed as mean±SD (range), median, or percent. Genotype frequencies are reported with their group percentages. Comparisons between clinical subgroups were made using the Student's unpaired *t*-test. A two-sided χ^2 test was used for comparison of qualitative variables. A P value <0.05 was considered statistically significant.

All computations were performed by using the SPSS-10 for Windows statistical computer package (SSPS, Inc., Chicago, IL, USA).

RESULTS

CD14 genotype frequency in patients with chronic alcohol abuse and controls

Initially, we wanted to confirm the finding of the previous Finnish study by Järveläinen *et al*., indicating higher prevalence of the C-159T promotor polymorphism of the CD14 endotoxin receptor in patients with advanced ALD[34].

CD14 genotyping was performed in patients with chronic alcohol abuse and liver cirrhosis (n = 62), or without clinical or sonomorphological signs of liver cirrhosis (n = 118), respectively. Furthermore, 247 healthy controls were genotyped. Results are summarized in Table 1.

Distribution of the individual genotypes in the control group (CC: 64/247 [25.6%], CT 128/247 [51.8%], and TT: 55/247 [22.3%]) was similar as in cohorts of other healthy individuals in previous reports[36,43,44].

Frequency of the C-159T polymorphism did not differ significantly between alcoholics without cirrhosis and controls. However, in accordance to the study by Järveläinen *et al*.[34], the TT genotype was significantly more frequent in alcoholics with cirrhosis (40.3%), compared to alcoholics without cirrhosis (23.7%; P = 0.020) and controls (22.3%; P = 0.006), respectively.

Comparison of ALT and AST levels between TT-homozygotes and alcoholics with genotype CC or CT revealed no significant differences (42.0±61.0 U/L *vs* 33.6±33.8 U/L, and 34.9±27.9 U/L *vs* 28.2±28 U/L, respectively).

Table 1 Frequency of (-159) CD14 genotypes (%) in patients with chronic alcohol abuse and cirrhosis, compared to alcoholics without clinical or sonomorphological signs of cirrhosis and controls

	CD14 genotype frequency		
	CC	CT	TT
Alcoholics with cirrhosis (n = 62)	5 (8.1%)	32 (51.6%)	25 (40.3%)
Alcoholics w/o cirrhosis (n = 118)	32 (27.1%)	58 (49.2%)	28 (23.7%)
Controls (n = 247)	64 (25.6%)	128 (51.8%)	55 (22.3%)

CD14 genotype frequency in patients with chronic hepatitis C infection

Next we wanted to analyze the frequency of the C-159T CD14 polymorphism in patients with a different etiology of chronic liver disease. Genotyping of 121 patients with chronic hepatitis C infection revealed no significant differences compared to healthy controls (CC: 26/121 [21.5%], CT: 66/121 [54.5%], and TT: 29/121 [24.0%]).

Comparing TT-homozygote HCV patients and HCV patients with genotype CC or CT we found no differences in demographic features such as age (38.0±12.3 years *vs* 37.1±11.4 years) and distribution of sexes (58.6% *vs* 68.5% males), and in the frequencies of potential routes of HCV infection (24.1% *vs* 26.1% i.v. drug users; 17.2% *vs* 15.2% recipients of blood transfusions), serum HCV-RNA levels (2.0×10^6 copies/mL *vs* 1.6×10^6 copies/mL) or frequencies of different HCV-genotypes (58.7% *vs* 66.3% type 1; 34.5% *vs* 25.0% type 2, Table 2). The number of initial virological responders to interferon therapy (no HCV-RNA detectable in the serum, 3 mo after initiation of therapy) did not differ between the genotypes (14/21 [66.7%] *vs* 46/70 [65.7%]).

Moreover and in contrast to patients with chronic alcohol abuse, frequency of TT-homozygotes did not differ between HCV patients with different severity of liver damage (Figure 1). TT-homozygotes were similarly frequent in patients with no or only mild, periportal fibrosis (staging 1 or 2) and HCV patients with more advanced septal fibrosis or cirrhosis (staging 3 or 4), respectively (20/85 [23.5%] *vs* 9/36 [25.5%], respectively).

The frequency of the CD14 genotypes was similar in HCV patients with mild or only minimal hepatic inflammation (grading 1 or 2) and patients with more severe hepatic inflammation or necrosis (grading >2): 14/63 [22.2%] *vs* 15/58 [25.9%], respectively. As in patients with chronic alcohol abuse, the comparison of ALT and AST levels between TT-homozygotes and hepatitis C patients with

genotype CC or CT revealed no significant differences (80.4±65.3 U/L *vs* 80.2±78.1 U/L, and 33.9±20.7 U/L *vs* 36.1±28.7 U/L, respectively).

Table 2 Clinical and biological characteristics of 121 patients with chronic hepatitis C infection according to CD14 –159 genotypes (TT *vs* CC and CT)

Clinical and biological characteristics	All patients	CD14 -159 genotype	
		TT	CC or CT
Age (yr; mean±SD)	37.2±11.5	38.0±12.3	37.1±11.4
Male gender (%)	66.1	58.6	68.5
HCV transmission route (%)			
- i.v. drug use	25.6	24.1	26.1
- Post-transfusion	15.7	17.2	15.2
- Other factors or unknown	58.7	58.6	58.7
HCV genotypes (%)			
- Type 1	64.5	58.7	66.3
- Type 3	27.3	34.5	25.0
- Others than type 1 or 3	8.3	6.9	8.7
Viral load			
(10^6 copies/mL; median)	1.7	2.0	1.6
Initial virological response to anti-HCV treatment[1] (%)	65.9	66.7	65.7

[1]HCV-RNA negative, 3 mo after the start of antiviral therapy; data available from 91/121 patients.

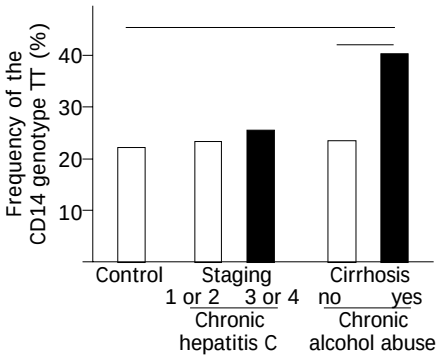


Figure 1 Frequency of the TT genotype at position -159 of the CD14 gene in patients with chronic hepatitis C infection, chronic alcohol abuse, and controls. The TT genotype was significantly more frequent in alcoholics with cirrhosis (25/62; [40.3%]), compared to alcoholics without clinical or sonomorphological signs of cirrhosis (28/118; [23.7%]; $P = 0.020$) and controls (55/247 [22.3%]; $P = 0.006$). In contrast, in HCV patients with no or only mild fibrosis (stage 1 or 2) and patients with prominent fibrosis or cirrhosis (stage 3 or 4) the frequency of the TT genotype was not significantly different (20/85 [23.5%] *vs* 9/36 [25.5%]).

Soluble CD14 serum levels in patients with chronic hepatitis C infection

It has been reported that sCD14 levels were elevated in patients with chronic liver disease[39]. Furthermore, studies investigating sCD14 levels in children recruited from a general population sample or in patients with ulcerative colitis found an association between sCD14 serum levels and CD14 -159 genotypes[28,31].

Therefore, we investigated sCD14 levels in the serum of 87 patients with chronic hepatitis C infection. Mean serum CD14 levels (3.8±0.4 μg/mL) were comparable to previous studies analyzing serum of patients with chronic liver disease[39].

HCV patients with no or only mild, periportal fibrosis, had significantly lower sCD14 serum levels than HCV patients with more advanced septal fibrosis or cirrhosis, respectively (3.5±0.4 μg/mL *vs* 3.8±0.9 μg/mL; $P = 0.004$).

Moreover, TT-homozygote HCV patients ($n = 20$) had significantly higher sCD14 serum levels than HCV patients with -159 CD14 genotype CT or TT ($n = 77$), respectively (3.5±0.4 μg/mL *vs* 3.7±0.7 μg/mL; $P = 0.012$, Figure 2).

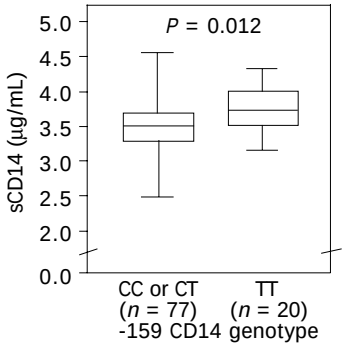


Figure 2 Serum levels of sCD14 comparing TT-homozygote HCV patients and patients with genotypes CC or CT, respectively. Box plots illustrate median values and interquartile distance.

[illegible]

There is a remarkable variation in the course of chronic liver disease in different patients. Recent studies suggest that the natural history of chronic liver disease is influenced by a number of gene polymorphism[1]. These genetic factors could explain the broad spectrum of response of the same etiologic agent seen in these individuals.

Recently, the C-T (-159) polymorphism in the promotor region of the CD14 gene was identified as a risk factor for the development of alcoholic liver cirrhosis in the Finnish population based on autopsy series[34]. The Finnish population has a limited number of founders and is characterized by national and regional isolation[45,46].

The first aim of our study was to re-evaluate the results of this previous study in a cohort of patients with chronic alcohol abuse from southern Germany.

In line with the previous Finnish study[35], the -159 CD14 genotype TT was significantly more frequent in patients with alcoholic liver cirrhosis compared to healthy controls or alcohol-dependent subjects without evidence of advanced liver damage.

Interestingly, serum aminotransferase levels did not vary significantly between patients with different genotypes in the group of alcoholics without evidence of advanced liver damage. Considering serum levels of aminotransferases as surrogate markers for hepatocellular damage, our data are in line with those of Järveläinen *et al*., who also could not find an association between the -159 genotypes and histological steatosis or less advanced stages of fibrosis, respectively[34]. Taken together, these findings indicate that the functional CD14 polymorphism and the associated CD14 expression, respectively, may exhibit different effects during the course of ALD.

On one hand, the CD14 polymorphism has been shown

to affect expression levels of membrane-bound CD14[28,44]. Higher expression levels of membrane-bound CD14 predispose hepatic cells for higher cytokine expression in response to endotoxins and cause increased inflammatory activity[23,47].

On the other hand, the CD14 polymorphism plays a significant role in regulating serum levels of sCD14 as TT-homozygotes have raised levels of sCD14[28,31]. Increased sCD14 can decrease the inflammatory response of monocytes to endotoxin by enhanced clearance[26]. Furthermore, a strong correlation between sCD14 and the endotoxin neutralizing capacity of plasma has been shown[48].

Increased expression of sCD14 in TT-homozygotes may lead to enhanced clearance of portal endotoxin and subsequently low-grade hepatic stimulation. In line with this hypothesis, Poullis *et al*., found the TT polymorphism to be associated with significantly reduced serum levels of ALT and γ-GT[36]. Similarly, Fernandez-Real *et al*., reported an inverse correlation between serum levels of sCD14 and ALT in individuals without known liver disease during routine-checkup visits[38].

These data indicate that the CD14 polymorphism seems to affect two mechanisms with opposite effects on hepatic inflammation by regulating the expression of membrane bound as well as sCD14. During the course of ALD the relative pathophysiological impact of each of these two mechanisms may vary.

Interestingly, there is an association between CD14 expression and the degree of fibrosis[49], and CD14 is *de novo* expressed on HSC during their activation process[23]. These cells are present in acute as well as chronically diseased livers, and there is a positive correlation between the degree of fibrosis and the accumulation of activated HSC[50,51]. Activated HSC synthesize and secrete excessive ECM molecules. In addition, it is recognized that they also play an important role in hepatic inflammation[52], and LPS-mediated NF-κB activation in HSC increases their resistance to apoptosis[23]. Therefore, with progressing liver damage and fibrosis, the number as well as type of CD14-expressing cells varies leading to differences in the LPS effects and CD14-mediated signal transduction.

In summary, the balance between potentially anti-inflammatory effects of sCD14 and proinflammatory effects of mCD14 may shift toward mCD14 during progression of ALD.

This imbalance may be further enhanced by higher endotoxin levels in patients with severe liver damage[11,16,17]. High LPS levels in more advanced liver damage may saturate the scavenger effects of sCD14. Furthermore, higher LPS levels promote hepatic inflammation leading to increased SP1-binding activity[53]. Since the -159 CD14 promotor polymorphism potentially affects binding of the transcription factor SP-1, high LPS levels in more advanced liver disease might promote CD14 expression particularly in carriers of the T-allele.

In summary, this hypothesis could explain that TT genotype promotes fibrosis in late stages of ALD, while in earlier stages pro- and anti-inflammatory mechanisms may be in balance regardless of the genotype.

The second aim of this study was to investigate the role of the -159 CD14 promotor polymorphism in HCV patients.

TT-homozygote HCV patients had significantly higher sCD14 serum levels than HCV patients with -159 CD14 genotype CT or TT, respectively. Moreover, HCV patients with advanced liver fibrosis or cirrhosis had significantly higher sCD14 levels than patients with less advanced stages of liver fibrosis. Similarly, a correlation between sCD14 levels and hepatic fibrosis has been shown previously in patients with ALD[39]. However, in contrast to patients with ALD, liver cirrhosis was not associated with the TT-homozygous state in patients with chronic hepatitis C infection. These findings indicate that the functional CD14 polymorphism and the expression of CD14 may exhibit different effects during the course of ALD and chronic HCV infection.

One explanation for this finding could be different expression patterns of membrane bound and sCD14, respectively, depending on the underlying cause of chronic liver disease. Furthermore, pathophysiological mechanism of viral and ALD may be differently affected by endotoxins, binding of sCD14 or CD14-mediated signal transduction.

It is known that sCD14 reveals inhibitory action on lymphocyte function[54,55]. Hepatic inflammation in HCV patients is characterized by lymphocyte infiltration while in alcoholic hepatitis there is a predominant infiltration with neutrophils. Furthermore, endotoxemia has been shown to exaggerate hepatic inflammation in murine viral infections[56,57] and to be associated with the response to antiviral therapy in HCV patients[58].

The origin of endotoxemia in HCV patients seems to be multifactorial, likely depending on impaired phagocytic functions and reduced T-cell-mediated antibacterial activity[57]. Furthermore, one cannot exclude the passage of LPS from the gut flora to the blood stream, condition owing to altered intestinal permeability, similar as shown in models of ALD[11,18]. In patients with alcoholic cirrhosis, the mean endotoxin concentration was significantly higher than in patients with non-alcoholic cirrhosis and higher endotoxin concentrations were more frequently observed in patients with alcoholic cirrhosis[12]. Therefore, it may be speculated that different LPS levels in patients with ALD and patients with chronic HCV infection may indirectly account for varying pathophysiological effects of CD14-mediated signal transduction.

There are several studies indicating that alcohol potentiates the proinflammatory effects of endotoxins in hepatic diseases. Peripheral blood mononuclear cells or purified monocytes from patients with alcoholic liver cirrhosis, stimulated *in vitro* with LPS, displayed a marked increase of proinflammatory cytokines compared with healthy controls[59]. Furthermore, alcohol was shown to increase the expression of CD14 on Kupffer cells and subsequently increased their responsiveness to endotoxins[60,61]. Interestingly, elegant studies by Järveläinen *et al*., in an animal model indicate that the synergistic effect of endotoxins and alcohol may vary depending on the time of exposure[62].

Finally, as for most genetic association studies, it has to be considered that the single nucleotide polymorphism investigated is in linkage disequilibrium to a different disease-associated genetic variation. Theoretically, this

potential genetic variation may affect particularly the pathophysiology of alcoholics but not viral liver disease. However, the functional relevance of the CD14/-159 polymorphism demonstrated in several studies and the important role of LPS and CD14 signaling in the pathophysiology of chronic liver disease clearly argue against this hypothesis.

In summary, comparison of the frequency of the -159 CD14 genotypes revealed significant differences between the two etiologies of liver diseases investigated in this study. In ALD, the impact of the -159 CD14 polymorphism may vary during the course of the disease, potentially via varying effects of soluble and membrane-bound forms of CD14. It will be interesting to elucidate the importance of this CD14 polymorphism in patients with other underlying liver diseases as non alcoholic fatty or autoimmune liver disease. These studies could potentially lead to therapeutic or prevention strategies selectively for those subgroups of patients that are particularly prone for the pathophysiological effects of gut-derived endotoxins.

[redacted]

1 **Bataller R,** North KE, Brenner DA. Genetic polymorphisms and the progression of liver fibrosis. a critical appraisal. *Hepatology* 2003; **37**: 493-503
2 **Yamauchi M,** Maezawa Y, Mizuhara Y, Ohata M, Hirakawa J, Nakajima H, Toda G. Polymorphisms in alcohol metabolizing enzyme genes and alcoholic cirrhosis in Japanese patients. a multivariate analysis. *Hepatology* 1995; **22**: 1136-1142
3 **Day CP,** Bashir R, James OF, Bassendine MF, Crabb DW, Thomasson HR, Li TK, Edenberg HJ. Investigation of the role of polymorphisms at the alcohol and aldehyde dehydrogenase loci in genetic predisposition to alcohol-related end-organ damage. *Hepatology* 1991; **14**: 798-801
4 **Carr LG,** Hartleroad JY, Liang Y, Mendenhall C, Moritz T, Thomasson H. Polymorphism at the P450IIE1 locus is not associated with alcoholic liver disease in Caucasian men. *Alcohol Clin Exp Res* 1995; **19**: 182-184
5 **Muhlbauer M,** Bosserhoff AK, Hartmann A, Thasler WE, Weiss TS, Herfarth H, Lock G, Scholmerich J, Hellerbrand C. A novel MCP-1 gene polymorphism is associated with hepatic MCP-1 expression and severity of HCV-related liver disease. *Gastroenterology* 2003; **125**: 1085-1093
6 **Yee LJ,** Tang J, Herrera J, Kaslow RA, van Leeuwen DJ. Tumor necrosis factor gene polymorphisms in patients with cirrhosis from chronic hepatitis C virus infection. *Genes Immun* 2000; **1**: 386-390
7 **Takamatsu M,** Yamauchi M, Maezawa Y, Ohata M, Saitoh S, Toda G. Correlation of a polymorphism in the interleukin-1 receptor antagonist gene with hepatic fibrosis in Japanese alcoholics. *Alcohol Clin Exp Res* 1998; **22**: 141-144
8 **Grove J,** Daly AK, Bassendine MF, Gilvarry E, Day CP. Interleukin 10 promoter region polymorphisms and susceptibility to advanced alcoholic liver disease. *Gut* 2000; **46**: 540-545
9 **Grove J,** Daly AK, Bassendine MF, Day CP. Association of a tumor necrosis factor promoter polymorphism with susceptibility to alcoholic steatohepatitis. *Hepatology* 1997; **26**: 143-146
10 **Takamatsu M,** Yamauchi M, Maezawa Y, Saito S, Maeyama S, Uchikoshi T. Genetic polymorphisms of interleukin-1beta in association with the development of alcoholic liver disease in Japanese patients. *Am J Gastroenterol* 2000; **95**: 1305-1311
11 **Nanji AA,** Khettry U, Sadrzadeh SM, Yamanaka T. Severity of liver injury in experimental alcoholic liver disease. Correlation with plasma endotoxin, prostaglandin E2, leukotriene B4, and thromboxane B2. *Am J Pathol* 1993; **142**: 367-373
12 **Fukui H,** Brauner B, Bode JC, Bode C. Plasma endotoxin concentrations in patients with alcoholic and non-alcoholic liver disease: reevaluation with an improved chromogenic assay. *J Hepatol* 1991; **12**: 162-169
13 **Nanji AA,** Khettry U, Sadrzadeh SM. Lactobacillus feeding reduces endotoxemia and severity of experimental alcoholic liver (disease). *Proc Soc Exp Biol Med* 1994; **205**: 243-247
14 **Jacob AI,** Goldberg PK, Bloom N, Degenshein GA, Kozinn PJ. Endotoxin and bacteria in portal blood. *Gastroenterology* 1977; **72**: 1268-1270
15 **Caradonna L,** Mastronardi ML, Magrone T, Cozzolongo R, Cuppone R, Manghisi OG, Caccavo D, Pellegrino NM, Amoroso A, Jirillo E, Amati L. Biological and clinical significance of endotoxemia in the course of hepatitis C virus infection. *Curr Pharm Des* 2002; **8**: 995-1005
16 **Lin RS,** Lee FY, Lee SD, Tsai YT, Lin HC, Lu RH, Hsu WC, Huang CC, Wang SS, Lo KJ. Endotoxemia in patients with chronic liver diseases: relationship to severity of liver diseases, presence of esophageal varices, and hyperdynamic circulation. *J Hepatol* 1995; **22**: 165-172
17 **Chan CC,** Hwang SJ, Lee FY, Wang SS, Chang FY, Li CP, Chu CJ, Lu RH, Lee SD. Prognostic value of plasma endotoxin levels in patients with cirrhosis. *Scand J Gastroenterol* 1997; **32**: 942-946
18 **Rivera CA,** Bradford BU, Seabra V, Thurman RG. Role of endotoxin in the hypermetabolic state after acute ethanol exposure. *Am J Physiol* 1998; **275**: 1252-1258
19 **Wright SD,** Ramos RA, Tobias PS, Ulevitch RJ, Mathison JC. CD14, a receptor for complexes of lipopolysaccharide (LPS) and LPS binding protein. *Science* 1990; **249**: 1431-1433
20 **Matsuura K,** Ishida T, Setoguchi M, Higuchi Y, Akizuki S, Yamamoto S. Upregulation of mouse CD14 expression in Kupffer cells by lipopolysaccharide. *J Exp Med* 1994; **179**: 1671-1676
21 **Tracy TF** Jr, Fox ES. CD14-lipopolysaccharide receptor activity in hepatic macrophages after cholestatic liver injury. *Surgery* 1995; **118**: 371-377
22 **Nanbo A,** Nishimura H, Muta T, Nagasawa S. Lipopolysaccharide stimulates HepG2 human hepatoma cells in the presence of lipopolysaccharide-binding protein via CD14. *Eur J Biochem* 1999; **260**: 183-191
23 **Paik YH,** Schwabe RF, Bataller R, Russo MP, Jobin C, Brenner DA. Toll-Like receptor 4 mediates inflammatory signaling by bacterial lipopolysaccharide in human hepatic stellate cells. *Hepatology* 2003; **37**: 1043-1055
24 **Pugin J,** Heumann ID, Tomasz A, Kravchenko VV, Akamatsu Y, Nishijima M, Glauser MP, Tobias PS, Ulevitch RJ. CD14 is a pattern recognition receptor. *Immunity* 1994; **1**: 509-516
25 **Ulevitch RJ,** Tobias PS. Receptor-dependent mechanisms of cell stimulation by bacterial endotoxin. *Annu Rev Immunol* 1995; **13**: 437-457
26 **Kitchens RL,** Wolfbauer G, Albers JJ, Munford RS. Plasma lipoproteins promote the release of bacterial lipopolysaccharide from the monocyte cell surface. *J Biol Chem* 1999; **274**: 34116-34122
27 **Wurfel MM,** Hailman E, Wright SD. Soluble CD14 acts as a shuttle in the neutralization of lipopolysaccharide (LPS) by LPS-binding protein and reconstituted high density lipoprotein. *J Exp Med* 1995; **181**: 1743-1754
28 **Baldini M,** Lohman IC, Halonen M, Erickson RP, Holt PG, Martinez FD. A Polymorphism* in the 5′ flanking region of the CD14 gene is associated with circulating soluble CD14 levels and with total serum immunoglobulin E. *Am J Respir Cell Mol Biol* 1999; **20**: 976-983
29 **Hubacek JA,** Rothe G, Pit'ha J, Skodova Z, Stanek V, Poledne R, Schmitz G. C(-260)->T polymorphism in the promoter of the CD14 monocyte receptor gene as a risk factor for myocardial infarction. *Circulation* 1999; **99**: 3218-3220
30 **Unkelbach K,** Gardemann A, Kostrzewa M, Philipp M, Tillmanns H, Haberbosch W. A new promoter polymorphism in the gene of lipopolysaccharide receptor CD14 is associated with expired myocardial infarction in patients with low

atherosclerotic risk profile. *Arterioscler Thromb Vasc Biol* 1999; **19**: 932-938
31 **Obana N,** Takahashi S, Kinouchi Y, Negoro K, Takagi S, Hiwatashi N, Shimosegawa T. Ulcerative colitis is associated with a promoter polymorphism of lipopolysaccharide receptor gene, CD14. *Scand J Gastroenterol* 2002; **37**: 699-704
32 **Woo JG,** Assa'ad A, Heizer AB, Bernstein JA, Hershey GK. The -159 C->T polymorphism of CD14 is associated with nonatopic asthma and food allergy. *J Allergy Clin Immunol* 2003; **112**: 438-444
33 **Repo H,** Anttonen K, Kilpinen SK, Palotie A, Salven P, Orpana A, Leirisalo-Repo M. CD14 and TNfa promoter polymorphisms in patients with acute arthritis. Special reference to development of chronic spondyloarthropathy. *Scand J Rheumatol* 2002; **31**: 355-361
34 **Järveläinen HA,** Orpana A, Perola M, Savolainen VT, Karhunen PJ, Lindros KO. Promoter polymorphism of the CD14 endotoxin receptor gene as a risk factor for alcoholic liver disease. *Hepatology* 2001; **33**: 1148-1153
35 **Corpechot C,** Poupon R. Promoter polymorphism of the CD14 endotoxin receptor gene and primary biliary cirrhosis. *Hepatology* 2002; **35**: 242-243
36 **Poullis AP,** Shetty AK, Risley PD, Collinson PO, Mendall MA. Effect of the CD14 promoter polymorphism on liver function tests and its association with alcohol and obesity. *Eur J Gastroenterol Hepatol* 2003; **15**: 1317-1322
37 **Fernandez-Real JM,** Broch M, Richart C, Vendrell J, Lopez-Bermejo A, Ricart W. CD14 monocyte receptor, involved in the inflammatory cascade, and insulin sensitivity. *J Clin Endocrinol Metab* 2003; **88**: 1780-1784
38 **Fernandez-Real JM,** Lopez-Bermejo A, Broch M, Vendrell J, Richart C, Ricart W. Circulating soluble CD14 monocyte receptor is associated with increased alanine aminotransferase. *Clin Chem* 2004; **50**: 1456-1458
39 **Oesterreicher C,** Pfeffel F, Petermann D, Muller C. Increased in vitro production and serum levels of the soluble lipopolysaccharide receptor sCD14 in liver disease. *J Hepatol* 1995; **23**: 396-402
40 **Desmet VJ,** Gerber M, Hoofnagle JH, Manns M, Scheuer PJ. Classification of chronic hepatitis. diagnosis, grading and staging. *Hepatology* 1994; **19**: 1513-1520
41 **Janca A,** Ustun TB, Early TS, Sartorius N. The ICD-10 symptom checklist: a companion to the ICD-10 classification of mental and behavioural disorders. *Soc Psychiatry Psychiatr Epidemiol* 1993; **28**: 239-242
42 **Hubacek JA,** Stuber F, Frohlich D, Book M, Wetegrove S, Rothe G, Schmitz G. The common functional C(-159)T polymorphism within the promoter region of the lipopolysaccharide receptor CD14 is not associated with sepsis development or mortality. *Genes Immun* 2000; **1**: 405-407
43 **Lichy C,** Meiser H, Grond-Ginsbach C, Buggle F, Dorfer C, Grau A. Lipopolysaccharide receptor CD14 polymorphism and risk of stroke in a South-German population. *J Neurol* 2002; **249**: 821-823
44 **Hubacek J,** Pitha J, Skodova Z, Poledne R. Is the CD14 receptor gene a marker for smoking dependence? *Med Sci Monit* 2002; **8**: 172-174
45 **Nevanlinna HR.** The Finnish population structure. A genetic and genealogical study. *Hereditas* 1972; **71**: 195-236
46 **De la Chapelle A.** Disease gene mapping in isolated human populations. the example of Finland. *J Med Genet* 1993; **30**: 857-865
47 **Yin M,** Bradford BU, Wheeler MD, Uesugi T, Froh M, Goyert SM, Thurman RG. Reduced early alcohol-induced liver injury in CD14-deficient mice. *J Immunol* 2001; **166**: 4737-4742
48 **Hiki N,** Berger D, Mimura Y, Frick J, Dentener MA, Buurman WA, Seidelmann M, Kaminishi M, Beger HG. Release of endotoxin-binding proteins during major elective surgery: role of soluble CD14 in phagocytic activation. *World J Surg* 2000; **24**: 499-506
49 **Su GL,** Rahemtulla A, Thomas P, Klein RD, Wang SC, Nanji AA. CD14 and lipopolysaccharide binding protein expression in a rat model of alcoholic liver disease. *Am J Pathol* 1998; **152**: 841-849
50 **Ballardini G,** Degli ES, Bianchi FB, de Giorgi LB, Faccani A, Biolchini L, Busachi CA, Pisi E. Correlation between Ito cells and fibrogenesis in an experimental model of hepatic fibrosis. A sequential stereological study. *Liver* 1983; **3**: 58-63
51 **Knittel T,** Kobold D, Piscaglia F, Saile B, Neubauer K, Mehde M, Timpl R, Ramadori G. Localization of liver myofibroblasts and hepatic stellate cells in normal and diseased rat livers. distinct roles of (myo-) fibroblast subpopulations in hepatic tissue repair. *Histochem Cell Biol* 1999; **112**: 387-401
52 **Marra F.** Hepatic stellate cells and the regulation of liver inflammation. *J Hepatol 1999*; **31**: 1120-1130
53 **Sakuta T,** Matsushita K, Yamaguchi N, Oyama T, Motani R, Koga T, Nagaoka S, Abeyama K, Maruyama I, Takada H, Torii M. Enhanced production of vascular endothelial growth factor by human monocytic cells stimulated with endotoxin through transcription factor SP-1. *J Med Microbiol* 2001; **50**: 233-237
54 **Rey Nores JE,** Bensussan A, Vita N, Stelter F, Arias MA, Jones M, Lefort S, Borysiewicz LK, Ferrara P, Labeta MO. Soluble CD14 acts as a negative regulator of human T cell activation and function. *Eur J Immunol* 1999; **29**: 265-276
55 **Arias MA,** Rey Nores JE, Vita N, Stelter F, Borysiewicz LK, Ferrara P, Labeta MO. Cutting edge: human B cell function is regulated by interaction with soluble CD14: opposite effects on IgG1 and IgE production. *J Immunol* 2000; **164**: 3480-3486
56 **Gut JP,** Schmitt S, Bingen A, Anton M, Kirn A. Probable role of endogenous endotoxins in hepatocytolysis during murine hepatitis caused by frog virus 3. *J Infect Dis* 1984; **149**: 621-629
57 **Jirillo E,** Caccavo D, Magrone T, Piccigallo E, Amati L, Lembo A, Kalis C, Gumenscheimer M. The role of the liver in the response to LPS: experimental and clinical findings. *J Endotoxin Res* 2002; **8**: 319-327
58 **Amati L,** Cozzolongo R, Manghisi OG, Cuppone R, Pellegrino NM, Caccavo D, Jirillo E. The immune responsiveness in hepatitis C virus infected patients: effects of interferon-alfa/ribavirin combined treatment on the lymphocyte response with special reference to B cells. *Curr Pharm Des* 2004; **10**: 2093-2100
59 **Deviere J,** Content J, Denys C, Vandenbussche P, Schandene L, Wybran J, Dupont E. Excessive *in vitro* bacterial lipopolysaccharide-induced production of monokines in cirrhosis. *Hepatology* 1990; **11**: 628-634
60 **Jarvelainen HA,** Oinonen T, Lindros KO. Alcohol-induced expression of the CD14 endotoxin receptor protein in rat Kupffer cells. *Alcohol Clin Exp Res* 1997; **21**: 1547-1551
61 **Kono H,** Wheeler MD, Rusyn I, Lin M, Seabra V, Rivera CA, Bradford BU, Forman DT, Thurman RG. Gender differences in early alcohol-induced liver injury: role of CD14, NF-kappaB, and TNF-alpha. *Am J Physiol Gastrointest Liver Physiol* 2000; **278**: 652-661
62 **Jarvelainen HA,** Fang C, Ingelman-Sundberg M, Lindros KO. Effect of chronic coadministration of endotoxin and ethanol on rat liver pathology and proinflammatory and anti-inflammatory cytokines. *Hepatology* 1999; **29**: 1503-1510

Science Editor Guo SY **Language Editor** Elsevier HK

PO Box 2345, Beijing 100023, China
www.wjgnet.com
wjg@wjgnet.com

ELSEVIER

World J Gastroenterol 2005;11(38):6038-6042
World Journal of Gastroenterology ISSN 1007-9327
© 2005 The WJG Press and Elsevier Inc. All rights reserved.

• *BRIEF REPORTS* •

Hyperhomocysteinemia in ulcerative colitis is related to folate levels

Petros Zezos, Georgia Papaioannou, Nikolaos Nikolaidis, Themistoclis Vasiliadis, Olga Giouleme, Nikolaos Evgenidis

Petros Zezos, Nikolaos Nikolaidis, Themistoclis Vasiliadis, Olga Giouleme, Nikolaos Evgenidis, Division of Gastroenterology, 2nd Propaedeutic Department of Internal Medicine, Hippokration General Hospital, Aristotle University of Thessaloniki, 49 Konstantinoupoleos Str., Thessaloniki 54642, Greece
Georgia Papaioannou, Department of Haematology, Papageorgiou General Hospital of Thessaloniki, Ring Road Nea Efkarpia, Thessaloniki 56403, Greece
Correspondence to: Associate Professor Nikolaos Evgenidis, Division of Gastroenterology, 2nd Propaedeutic Department of Internal Medicine, Aristotle University of Thessaloniki, Hippokration General Hospital, 49 Konstantinoupoleos Str., Thessaloniki 54642, Greece. zezosp@hol.gr
Telephone: +30-2310-892073 Fax: +30-2310-848354
Received: 2004-12-17 Accepted: 2005-03-21

ABSTRACT

AIM: To study the prevalence and clinical significance of hyperhomocysteinemia (hHcys), an independent factor for arterial and venous thrombosis, in a group of patients with ulcerative colitis (UC).

METHODS: Fasting homocysteine (Hcys), folate, and vitamin B_{12} serum levels were measured in 40 UC patients and 50 healthy controls. Clinical data regarding UC were gathered.

RESULTS: Median serum Hcys levels in UC patients were similar to those in controls (12.26 μmol/L *vs* 12.32 μmol/L), but the prevalence of hHcys was higher in UC patients than in controls (30% *vs* 10%, $P = 0.028$). UC significantly increased the risk of hHcys (adjusted odds ratio: 4.125; 95%CI: 1.26-13.44). Multivariate regression analysis showed that male sex, folate and vitamin B_{12} deficiency or lower serum values were significant independent predictors of higher Hcys levels in UC patients ($r^2 = 0.4$; $P<0.001$).

CONCLUSION: hHcys is common in UC patients and it is related to folate and vitamin B_{12} deficiency or lower serum values. It would be reasonable for patients with UC to receive folate and vitamin B complex supplements as a prophylactic measure.

© 2005 The WJG Press and Elsevier Inc. All rights reserved.

Key words: Folate; Homocysteine; Hyperhomocysteinemia; Thrombosis; Ulcerative colitis; Vitamin B_{12}

Zezos P, Papaioannou G, Nikolaidis N, Vasiliadis T, Giouleme O, Evgenidis N. Hyperhomocysteinemia in ulcerative colitis is related to folate levels. *World J Gastroenterol* 2005; 11 (38): 6038-6042
http://www.wjgnet.com/1007-9327/11/6038.asp

INTRODUCTION

The risk for thromboembolic complications is increased in patients with inflammatory bowel disease (IBD). The incidence of arterial and venous thromboembolic disease in patients with ulcerative colitis (UC) and Crohn's disease (CD) has been reported between 1% and 8%[1,2], rising to an incidence of 39% in some autopsy studies[3]. Several studies have shown that a hypercoagulable state involving all components of clotting system exists in IBD[4-6]. This hypercoagulable state may be related to an increased tendency for thromboembolic events and may be linked to the disease pathogenesis through promoting microthrombi formation in intestinal microcirculation[7,8]. The etiology and pathogenesis of the hypercoagulable state in IBD have not been fully elucidated but may be induced through a procoagulant effect of proinflammatory cytokines[9-13] in combination with acquired or genetic defects of clotting factors (protein S, protein C, antithrombin, factor V Leiden, prothrombin mutation 20210A, and antiphospholipid antibodies)[14-16]. Recently, the factor V Leiden has been implicated in the increased risk of venous thrombosis in IBD patients[17-19].

Homocysteine (Hcys) is a non-essential, sulfur-containing amino acid formed during the metabolism of methionine. Mild hyperhomocysteinemia (hHcys), which occurs in approximately 5-7% of the general population, has been proved to be thrombogenic and an independent risk factor for coronary artery disease[20], arterial and venous thrombosis[21-26]. Elevated levels of Hcys may result from abnormalities in metabolism pathways due to inherited abnormalities of the enzymes involved or nutrient deficiencies such as insufficiency of folate and vitamins B_2, B_6, and B_{12}[27,28].

The mechanism by which hHcys promotes thrombosis is uncertain, but it may be related to a hypercoagulatory state due to endothelial dysfunction[28-30].

Vitamin B_{12} and folate deficiency are relatively common conditions in IBD (especially in active disease) through malnutrition, malabsorption or antifolate drugs such as methotrexate and sulfasalazine (SASP). Deficiencies of key nutrients/cofactors in Hcys metabolism pathways (B_2, B_6, B_{12}, and folate) might lead to raised Hcys levels in IBD. The association between IBD and hHcys has been shown

in some recent studies, reporting an increased prevalence of hHcys in IBD (both UC and CD)[31-36].

The aim of this study was to evaluate whether Hcys levels were elevated compared to a group of healthy controls and whether Hcys levels were related to vitamin B_{12} and folate serum concentrations, disease activity, disease extent or history of thrombotic complications.

[illegible]

Patients and control population

Forty patients with UC (20 females and 20 males, mean age 41.65±15.21 years, range 17-71 years) were consecutively recruited from our outpatient clinic between February 1999 and February 2000. Diagnosis of UC was based on standard clinical, endoscopic and histological criteria. A detailed clinical history was taken from each patient regarding current symptoms, activity and duration of disease, extraintestinal manifestations, present medication, smoking status, and thrombotic complications. Patients with significant liver or kidney diseases were excluded. Endoscopy was performed in all patients in order to evaluate endoscopic activity, disease extension and histological confirmation and grading. Blood samples from fasting UC patients were collected. Serum Hcys, folate and vitamin B_{12} levels were determined.

Serum Hcys levels were also measured in blood samples from 50 healthy control subjects (HC) with similar age and gender (25 females and 25 males, age 39.96±14.33 years, range 17-72 years), under similar conditions and in the same laboratory. Healthy control subjects were visitors in the outpatient clinic of Hematology Department and had no known diseases, or any clinical or laboratory evidence of metabolic, neoplastic or inflammatory disease. They also had no history of thromboembolic disease. Patients and healthy controls were from the same geographical area (Northern Greece) and had Greek ancestry. Patients and controls reported that they had no daily alcohol intake above 35 g, and no use of drugs affecting Hcys status (phenytoin, theophylline, and vitamin supplements).

Measurements

Total serum Hcys concentrations were measured by the IMx homocysteine assay, which is a fluorescence polarization immunoassay (FPIA, Abbott Laboratories). Reference serum Hcys concentrations for both men and women were <15 μmol/L. Vitamin B_{12} and folate serum levels were measured by enzymatic immunoassays (ELISA). Reference ranges for vitamin B_{12} and serum folate were >223 pg/mL and >2.8 ng/mL respectively.

Statistical analysis

Descriptive statistics for continuous variables (including means and medians) were calculated. Categorical variables were described using proportions. Odds ratios and the 95%CI for the risk of hHcys in UC patients, as compared to healthy controls, were calculated. Multivariate logistic regression was used to adjust these crude odds for confounding differences in sex. Comparisons of continuous variables between the two groups were made by Student's *t*-test for normally distributed data or by Mann-Whitney *U*-test when data were not normally distributed. Fisher's exact test was used for the comparison of proportions. Pearson's correlation coefficient was calculated to describe the relationship between variables. Multiple linear regression analysis was performed in order to study the influence of individual factors on Hcys levels (treated as continuous variable). Since the concentrations of Hcys, folate and B_{12} were not normally distributed, correlation and regression analysis were performed with log-transformed data. Statistical analysis was performed using the SPSS for Windows package (version 11.0, SPSS, Chicago, IL, USA).

[illegible]

Demographics

The baseline characteristics of the patients and controls are shown in Table 1. There were no significant differences in age between healthy controls and patients, or between sexes or between study groups. There were also no significant differences in duration of disease, disease activity, endoscopic score, disease extent, smoking, and use of medication between sexes in UC group.

Table 1 Epidemiological and clinical data of study subjects

	UC patients (95%CI)	Healthy controls (95%CI)
Subjects (*n*)	40	50
Gender (female/male)	20/20	25/25
Mean age (yr±SD)(range)	41.65±15.21	39.96±14.33
	[36.78–46.52]	[35.89–44.03]
	(17–71)	(17–72)
Mean disease duration (mo±SD)	56.65±63.18	
(range)	[36.44–76.86]	
	(3–216)	
Current smoking (%)	9 (22.5)	
Extent of UC (%)		
Rectum/sigmoid	9 (22.5)	
Left colitis	22 (55.5)	
Pancolitis	9 (22.5)	
Activity of UC (%)		
Active	28 (70)	
Inactive	12 (30)	
Extraintestinal complications (%)	6 (15)	
Thrombotic complications (%)	2 (5)	
Medical treatment		
None	1 (2.5)	
5-ASA	35 (87.5)	
SASP	1 (2.5)	
Steroids	17 (42.5)	
Immunosuppressors (AZA/6-MP)	11 (27.5)	

Homocysteine determination and associations

The median serum levels of Hcys in UC patients were similar to those in controls (12.26 μmol/L [range 7.15-35.8 μmol/L] *vs* 12.32 μmol/L [range 5.97-22.06 μmol/L], $P = 0.518$), but hHcys was more prevalent in UC patients (30% [12/40] *vs* 10% [5/50], $P = 0.028$) than in controls. Male sex had higher median serum levels of Hcys both in HC and in UC groups (Table 2). Logistic regression analysis showed an odds ratio of 3.857 [95%CI: 1.22-12.12] for hHcys in the UC group as compared to healthy controls. Advanced age and

male sex were associated with higher Hcys levels, and there was not any difference in age and sex, but males had significant higher Hcys values in both study groups and we believe that sex might be a significant confounder. The adjusted odds ratio for the sex difference was 4.125 (95%CI: 1.26-13.44).

Table 2 Serum Hcys levels in male and female subjects in study groups

	Hcys (μmol/L)		*P*
	Male	Female	
Controls	13.7 (8.17–22.06)	11.94 (5.97–16.99)	0.005
UC	14 (9.13–35.8)	11.07 (7.15–26.6)	0.011
Total	13.72 (8.17–35.8)	11.87 (5.97–26.6)	0.0003

Values are expressed as medians (range). Comparisons were performed using Mann–Whitney's test.

Serum homocysteine, folate and vitamin B_{12} levels in ulcerative colitis patients

In UC patients, the median serum levels of folate and vitamin B_{12} were 7.2 ng/mL (range 2.4-13.4 ng/mL) and 431 pg/mL (range 195-1 430 pg/mL) respectively. One patient had serum folate below the lower limit (2.4 ng/mL) and two others had normal folate near the lower limit (2.9 and 3.4 ng/mL respectively). All three had high levels of Hcys (the three highest values). One patient had vitamin B_{12} below the lower limit (195 pg/mL) and two others had normal B_{12} near the lower limit (226 and 237 pg/mL, respectively). The patient with low B_{12} and one of the two others had high levels of Hcys. These patients had no overlapping low values for both folate and B_{12} levels. The disease duration, activity, extent, endoscopic severity, medical treatment, and smoking status did not significantly influence Hcys, folate, and vitamin B_{12} levels. There were no significant differences in levels of folate and vitamin B_{12} between sexes.

Predictors of hyperhomocysteinemia in ulcerative colitis

Because the concentrations of Hcys, folate and B_{12} were not normally distributed, correlation and regression analysis were performed with log-transformed data. To directly assess the effect of age, folic acid and B_{12} on Hcys levels, the Pearson correlation coefficients between these variables were determined, as shown in Table 3. A relatively strong inverse correlation was observed between log-transformed serum levels of Hcys and log-transformed serum concentrations of folate (r = -0.466, P = 0.002). To further define the role of folic acid and B_{12} in determining Hcys levels, a multiple regression analysis was performed where log-Hcys was the dependent variable whereas age, gender, log-B_{12}, log-folic acid, smoking and history of thrombosis were the independent variables. Multiple linear regressions revealed the following variables to be significant independent predictors of Hcys levels in UC patients: male sex, folate, and B_{12} deficiency or lower serum values (r^2 = 0.4; P<0.001).

Table 3 Pearson coefficient analysis of variables within UC group

	log-Hcys	Age (yr)	log-folic acid	log-B_{12}
log-Hcys				
Coefficient	1.000	–0.016	–0.466	–0.163
P	0.000	0.920	0.002	0.314
Age (yr)				
Coefficient	–0.016	1.000	0.189	–0.039
P	0.920	0.000	0.244	0.811
log-folic acid				
Coefficient	–0.466	0.189	1.000	–0.193
P	0.002	0.244	0.000	0.234
log-B_{12}				
Coefficient	–0.163	–0.039	–0.193	1.000
P	0.314	0.811	0.234	0.000

Homocysteine metabolism in ulcerative colitis patients with previous thrombotic events

Two patients had a history of previous thrombotic events. hHcys was found in one of them. This patient had folate deficiency and the highest value of Hcys. The other one had vitamin B_{12} close to lower normal limit without hHcys.

[redacted]

This study showed that although Hcys levels were similar in UC patients and healthy control subjects, hHcys (serum Hcys ⩾15 μmol/L) was more common in UC patients than in healthy controls (adjusted odds ratio, 4.125; prevalence 30% *vs* 10%). Increased Hcys levels and high prevalence of hHcys in IBD patients have been reported in previous studies[31-36]. In our study, similar findings were observed in this cohort of UC patients with a slightly higher prevalence of hHcys (30%) than in other studies (10-26%)[31,32,35,36].

Our analysis showed that male sex and low serum levels of folic acid and vitamin B_{12} were correlated with high Hcys levels. Multiple regression analysis and Pearson's correlation coefficient showed that serum folic acid was the most significant predictor of Hcys levels. We did not find significant correlation between age, disease activity, medication, smoking status, and Hcys levels in this UC cohort. Chowers *et al*.[33], have observed similar findings in a group of patients with CD.

We did not study the frequency of MTHFR C677T variant in our study groups. In a previous study, Mahmud *et al*.[31], reported that the frequency of the homozygous C677T mutation, which results in slower synthesis of 5-methyltetrahydrofolate, is increased from 7.3% in controls to 17.5% in patients with UC and is related with high Hcys levels especially in folate deficiency status. However, in that study, Hcys levels were also elevated in patients with IBD with no mutation to MTHFR enzyme. The levels of Hcys decreased after folate supplementation, regardless of the fact that the genotype of the mutation was detected or not. It has been suggested that folate status should be addressed in all IBD patients and prophylactic folate supplementation has been recommended to all patients with IBD. In our study, the prevalence of hHcys in UC patients was much higher than the frequency of homozygous mutation of MTHFR as detected by Mahmud *et al*.[31]. The differences between prevalences of hHcys and MTHFR mutant can be explained by the existence of additional factors affecting Hcys levels. Vitamin deficiencies can be a significant

contributing factor as it has been supported by our study and previous reports. The suboptimal vitamin status in IBD patients can be due to a combination of several factors. Folate levels may be low due to either inadequate dietary intake, or increased utilization, or drug effects, mainly SASP[33]. In our study, one patient was receiving SASP and had low folate levels and hHcys. Other studies have conflicting conclusions about the significance of SASP antifolate effects[31,32]. Disease activity may contribute to increased demand for folate due to inflammation, but like Chowers *et al*.[33], we did not find any correlation between disease activity and folate or Hcys levels. Furthermore, Chowers *et al*.[33], found no change in Hcys levels, despite a significant improvement in the disease activity in a group of CD patients. These data point out that an inadequate intake of folate may be the most significant factor affecting folate levels in IBD patients.

The prevalence of thromboembolic complications in IBD patients is higher than that in the normal population, in large retrospective studies 1.3-8% of the patients develop these complications[1,2]. The pathogenesis of thromboembolism in IBD is unknown, but it seems to be multifactorial[37]. In our study we found a high prevalence (2/40; 5%) of thromboembolic events in this group of UC patients. hHcys was found in one of them. There are case reports that hHcys was noted in the test results in IBD patients with thrombosis[38,39]. In our study a correlation between hHcys and history of thrombosis was noted, but the number of patients is too small to supply safe conclusions. Nevertheless high Hcys levels may predispose IBD patients to thrombotic complications in combination with other existing circumstantial or permanent risk factors[37].

In conclusion, UC patients have a higher prevalence of hHcys than healthy controls. hHcys in these patients is related to low folate and B_{12} status but not to disease activity. All UC patients, irrespective of disease activity, are at risk for vitamin deficiencies. It is recommended that all patients should have an assessment of the nutritional status in order for the vitamin deficiencies to be detected and that they should also receive folate and vitamin B complex supplements for protection from complications of HHcys.

ACKNOWLEDGMENTS

The authors thank Associate Professor Rigas AG, Department of Electrical and Computer Engineering, School of Engineering of Democritus University of Thrace, and his associates Ms. Kotti VK and Mr. Vassiliadis VG, for their support in the detailed statistical analysis of data.

REFERENCES

1 **Talbot RW,** Heppell J, Dozois RR, Beart RW Jr. Vascular complications of inflammatory bowel disease. *Mayo Clin Proc* 1986; **61**: 140-145
2 **Vecchi M,** Cattaneo M, de Francis R, Mannucci PM. Risk of thromboembolic complications in patients with inflammatory bowel disease. Study of hemostasis measurements. *Int J Clin Lab Res* 1991; **21**: 165-170
3 **Graef V,** Baggenstoss AH, Sauer WG. Venous thrombosis occurring in non-specific ulcerative colitis. *Arch Intern Med* 1965; **117**: 377-382
4 **Hudson M,** Hutton RA, Wakefield AJ, Sawyerr AM, Pouder RE. Evidence for activation of coagulation in Crohn's disease. *Blood Coagul Fibrinolysis* 1992; **3**: 773-778
5 **Souto JC,** Martinez E, Roca M, Mateo J, Pujol J, Gonzalez D, Fontcuberta J. Prothrombotic state and signs of endothelial lesion in plasma of patients with inflammatory bowel disease. *Dig Dis Sci* 1995; **40**: 1883-1889
6 **Collins CE,** Cahill MR, Newland AC, Rampton DS. Platelets circulate in an activated state in inflammatory bowel disease. *Gastroenterology* 1994; **106**: 840-845
7 **Dhillon AP,** Anthony A, Sim R, Wakefield AJ, Sankey EA, Hudson M, Allison MC, Pounder RE. Mucosal capillary thrombi in rectal biopsies. *Histopathology* 1992; **21**: 127-133
8 **Wakefield AJ,** Sawyerr AM, Dhillon AP, Pittilo RM, Rowles PM, Lewis AA, Pounder RE. Pathogenesis of Crohn's disease: multifocal gastrointestinal infarction. *Lancet* 1989; **2**: 1057-1062
9 **Van Deventer SJ.** Tumor necrosis factor and Crohn's disease. *Gut* 1997; **40**: 443-448
10 **Nassif A,** Longo WE, Mazuski JE, Vernava AM, Kaminski DL. Role of cytokines and platelet-activating factor in inflammatory bowel disease. Implications for therapy. *Dis Colon Rectum* 1996; **39**: 217–223
11 **Bevilacqua MP,** Pober JS, Majeau GR, Fiers W, Cotran RS, Gimbrone MA Jr. Recombinant tumor necrosis factor induces procoagulant activity in cultured human vascular endothelium: characterization and comparison with the actions of interleukin 1. *Proc Natl Acad Sci USA* 1986; **83**: 4533–4537
12 **Nawroth PP,** Stern DM. Modulation of endothelial cell hemostatic properties by tumor necrosis factor. *J Exp Med* 1986; **163**: 740–745
13 **Dosquet C,** Weill D, Wautier JL. Cytokines and thrombosis. *J Cardiovasc Pharmacol* 1995; **25**(Suppl 2): S13-19
14 **Aadland E,** Odegaard OR, Roseth A, Try K. Free protein S deficiency in patients with chronic inflammatory bowel disease. *Scand J Gastroenterol* 1992; **27**: 957-960
15 **Aadland E,** Odegaard OR, Roseth A, Try K. Free protein S deficiency in patients with Crohn's disease. *Scand J Gastroenterol* 1994; **29**: 333-335
16 **Heneghan MA,** Cleary B, Murray M, O'Gorman TA, McCatrhy CF. Activated protein C resistance, thrombophilia, and inflammatory bowel disease. *Dig Dis Sci* 1998; **43**: 1356-1361
17 **Liebman HA,** Kashani N, Sutherland D, McGehee W, Kam AL. The factor V Leiden mutation increases the risk of venous thrombosis in patients with inflammatory bowel disease. *Gastroenterology* 1998; **115**: 830-834
18 **Koutroubakis IE,** Sfiridaki A, Mouzas IA, Maladaki A, Kapsoritakis A, Roussomoustakaki M, Kouroumalis EA, Manousos ON. Resistance to activated protein C and low levels of free protein S in Greek patients with inflammatory bowel disease. *Am J Gastroenterol* 2000; **95**: 190-194
19 **Novacek G,** Miehsler W, Kapiotis S, Katzenschlager R, Speiser W, Wogelsang H. Thromboembolism and resistance to activated protein C in patients with inflammatory bowel disease. *Am J Gastroenterol* 1999; **94**: 685-690
20 **Gallagher PM,** Meleady R, Shields DC, Tan KS, McMaster D, Rozen R, Evans A, Graham IM, Whitehead AS. Homocysteine and risk of premature coronary disease: Evidence for a common gene mutation. *Circulation* 1996; **94**: 2154-2158
21 **Ridker PM,** Hennekens CH, Selhub J, Miletich JP, Malinow MR, Stampfer MJ. Interrelation of hyperhomocyst(e)inemia, factor V Leiden, and risk of future venous thromboembolism. *Circulation* 1997; **95**: 1777-1782
22 **Cantu C,** Alonso E, Jara A, Martinez L, Rios C, Fernandez Mde L, Garcia I, Barinagarrementeria F. Hyperhomocysteinemia, low folate and vitamin B12 concentrations, and methylene tetrahydrofolate reductase mutation in cerebral venous thrombosis. *Stroke* 2004; **35**: 1790-1794
23 **den Heijer M,** Koster T, Blom HJ, Bos GM, Briet E, Reitsma PH, Vandenbroucke JP, Rosendaal FR. Hyperhomocysteinemia as a risk factor for deep-vein thrombosis. *N Engl J Med* 1996; **334**: 759-762
24 **Ray JG.** Meta-analysis of hyperhomocysteinemia as a risk

factor for venous thromboembolic disease. *Arch Intern Med* 1998; **158**: 2101-2106
25 **Langman LJ,** Ray JG, Evrovski J, Yeo E, Cole DE. Hyperhomocyst(e)inemia and the increased risk of venous thromboembolism: more evidence from a case-control study. *Arch Intern Med* 2000; **160**: 961-964
26 **McCully KS.** Homocysteine and vascular disease. *Nat Med* 1996; **2**: 386-389
27 **Seshadri N,** Robinson K. Homocysteine, B vitamins and coronary artery disease. *Med Clin North Am* 2000; **84**: 215-237
28 **Welch GN,** Loscalzo J. Homocysteine and atherothrombosis. *N Engl J Med* 1998; **338**: 1042-1050
29 **McCully KS.** Homocysteine, folate, vitamin B6, and cardiovascular disease. *JAMA* 1998; **279**: 392-393
30 **Loscalzo J.** The oxidant stress of hyperhomocyst(e)inemia. *J Clin Invest* 1996; **98**: 5-7
31 **Mahmud N,** Molloy A, McPartlin J, Corbally R, Whitehead AS, Scott JM, Weir DG. Increased prevalence of methylenetetrahydrofolate reductase C677T variant in patients with inflammatory bowel disease, and its clinical implications. *Gut* 1999; **45**: 389-394
32 **Oldenburg B,** Fijnheer R, van der Griend R, vanBerge-Henegouwen GP, Koningsberger JC. Homocysteine in inflammatory bowel disease: a risk factor for thromboembolic complications? *Am J Gastroenterol* 2000; **95**: 2825-2830
33 **Chowers Y,** Sela BA, Holland R, Fidder H, Simoni FB, Bar-Mier S. Increased levels of homocysteine in patients with Crohn's disease are related to folate levels. *Am J Gastroenterol* 2000; **95**: 3498-3502
34 **Koutroubakis IE,** Dilaveraki E, Vlachonikolis IG, Vardas E, Vrentzos G, Ganotakis E, Mouzas IA, Gravanis A, Emmanouel D, Kouroumalis EA. Hyperhomocysteinemia in Greek patients with inflammatory bowel disease. *Dig Dis Sci* 2000; **45**: 2347-2351
35 **Romagnuolo J,** Fedorak RN, Dias VC, Bamforth F, Teltscher M. Hyperhomocysteinemia and inflammatory bowel disease: prevalence and predictors in a cross-sectional study. *Am J Gastroenterol* 2001; **96**: 2143-2149
36 **Papa A,** De Stefano V, Danese S, Chiusolo P, Persichilli S, Casorelli I, Zappacosta B, Giardina B, Gasbarrini A, Leone G, Gasbarrini G. Hyperhomocysteinemia and prevalence of polymorphisms of homocysteine metabolism-related enzymes in patients with inflammatory bowel disease. *Am J Gastroenterol* 2001; **96**: 2677-26782
37 **Koutroubakis IE.** Unraveling the mechanisms of thrombosis in inflammatory bowel disease. *Am J Gastroenterol* 2001; **96**: 1325-1327
38 **Slot WB,** van Kasteel V, Coerkamp EG, Seelen PJ, van der Werf SD. Severe thrombotic complications in a postpartum patient with active Crohn's disease resulting in ischemic spinal cord injury. *Dig Dis Sci* 1996; **40**: 1395-1399
39 **Gonera RK,** Timmerhuis TP, Leyten AC, van der Heul C. Two thrombotic complications in a patient with active ulcerative colitis. *Neth J Med* 1997; **50**: 88-91

Science Editor Wang XL and Guo SY **Language Editor** Elsevier HK

PO Box 2345, Beijing 100023, China
www.wjgnet.com
wjg@wjgnet.com

ELSEVIER

World J Gastroenterol 2005;11(38):6043-6048
World Journal of Gastroenterology ISSN 1007-9327
© 2005 The WJG Press and Elsevier Inc. All rights reserved.

• *BRIEF REPORTS* •

CD14 promoter polymorphism in Chinese alcoholic patients with cirrhosis of liver and acute pancreatitis

You-Chen Chao, Heng-Cheng Chu, Wei-Kuo Chang, Hsin-Hung Huang, Tsai-Yuan Hsieh

You-Chen Chao, Heng-Cheng Chu, Wei-Kuo Chang, Hsin-Hung Huang, Tsai-Yuan Hsieh, Division of Gastroenterology, Department of Internal Medicine, Tri-Service General Hospital, National Defense Medical Center, Taipei, Taiwan, China
Supported by grants from the Taiwan National Science Council (NSC- 91-2314-B-016-109) and from the ShuYuan Education and Academic Promotion Foundation
Co-first-authors: You-Chen Chao
Co-correspondents: You-Chen Chao
Correspondence to: You-Chen Chao, MD, No. 325, Section 2, Cheng-Kung Road, Neihu 114, Taipei, Taiwan, China. chaoycmd@ndmctsgh.edu.tw
Telephone: +886-2-87927008 Fax: +886-2-87927009
Received: 2004-12-28 Accepted: 2005-02-28

AIM: To investigate the relationship between genetic polymorphism of the CD14 promoter and the occurrence of alcoholic cirrhosis and alcoholic pancreatitis, and to challenge the conclusion made earlier that the patients with acute alcoholic pancreatitis and patients with alcoholic cirrhosis of liver are two different subpopulations.

METHODS: Using the polymerase chain reaction-restriction fragment length polymorphism (PCR-RFLP) method, we determined the polymorphism of CD14 gene and aldehyde dehydrogenase gene 2 (ALDH 2) in 335 alcoholic patients with different organ complications i.e., cirrhosis of liver (n = 100), acute pancreatitis (n = 100), esophageal cancer (n = 82) and avascular necrosis of hip joint (AVN) (n = 53) and 194 non-alcoholic controls in a Chinese group.

RESULTS: The results showed that the carriage of T allele was not different among alcoholic patients with cirrhosis of liver, alcoholic patients with other complication and non-alcoholic controls. On the other hand, the carriage of the C allele was significantly more prevalent for alcoholic pancreatitis than for esophageal cancer (0.79 *vs* 0.60, P<0.001), alcoholic AVN (0.79 *vs* 0.65, P<0.025) and non-alcoholic controls (0.79 *vs* 0.68, P<0.025). Furthermore, when only subjects with ALDH2 1-1 genotype were examined, the C allele frequency was significantly more prevalent for alcoholic pancreatitis than for alcoholic liver cirrhosis (0.82 *vs* 0.69, P<0.025), esophageal cancer (0.82 *vs* 0.61, P<0.01), alcoholic AVN (0.82 *vs* 0.64, P<0.01) and non-alcoholic controls (0.82 *vs* 0.69, P<0.05).

CONCLUSION: The C allele may be associated with some mechanism, which is important in the pathogenesis of alcoholic pancreatitis, and that alcoholic patients with acute pancreatitis and cirrhosis of liver are probably two different subpopulations.

© 2005 The WJG Press and Elsevier Inc. All rights reserved.

Key words: CD14 promoter; Polymorphism; Alcoholic patients

Chao YC, Chu HC, Chang WK, Huang HH, Hsieh TY. CD14 promoter polymorphism in Chinese alcoholic patients with cirrhosis of liver and acute pancreatitis. *World J Gastroenterol* 2005; 11(38): 6043-6048
http://www.wjgnet.com/1007-9327/11/6043.asp

INTRODUCTION

It is well known that alcoholism causes numerous physical complications[1]. However, it is still a mystery why certain organ-specific complications occur only in some alcoholics. Twin concordance studies suggest a contribution by genetic factors. In a large study, consisting of 16 000 male twin pairs, the concordance rate of alcoholic cirrhosis was significantly greater among monozygous (14.6%) than dizygous (5.4%) twins[2]. Later, Reed *et al*., also confirmed the findings in 1996[3]. Based on the above findings, many studies were designed to search for candidate genes that contribute to the susceptibility to alcoholic liver disease (ALD)[4-8]. As we know, the alcohol metabolizing enzymes alcohol dehydrogenase (ADH), aldehyde dehydrogenase (ALDH) and cytochrome P4502E1 are polymorphic at the ADH2, ADH3, ALDH2 loci and the 5'-fling region of the P4502E1[9,10]. Many studies have investigated the differences in these alcohol-metabolizing enzymes to explain susceptibility to alcoholism and to alcohol-induced liver disease[9-12]. The studies have been inconclusive in the linkage of the susceptibility to ALD and polymorphism of alcohol-metabolizing enzymes[13-16].

More recently, accumulating clinical and experimental data indicate that inflammatory responses are involved in the pathogenesis of ALD. Elevated serum endotoxin levels are found in alcoholic patients and in alcohol-treated experimental animals[17,18], as a consequence of intestinal wall leakage, bacterial overgrowth, or reduced phagocytic clearance[19]. Circulating endotoxin is bound mainly to the lipopolysacchride binding protein. This complex has a high affinity for the CD14 receptor, which is expressed on monocytes and macrophages[20]. Binding of the lipopolysaccharide–lipopolysaccharide binding protein complex to CD14 initiates transcription and release of several proinflammatory cytokines, such as tumor necrosis factor-α and interleukin-1β[21].

A polymorphic C/T form at position-159 in the promoter region of the human CD14 gene was recently detected. The polymorphism is within the Spl transcription factor binding site, known to affect CD14 expression. The T variants of the -159 polymorphism promote CD14 gene transcription and cause higher expression of CD14 on monocytes, which seems to lead to an enhanced inflammatory response[22,23]. The T allele has a suggested association with myocardial infarction, which also is known to have an inflammatory component[23,24]. Later, Jarvelainen *et al*., investigated the allele frequency of the CD14 promoter genotype in a Finnish group and found that the T allele was associated with advanced ALD. The T allele confers increased risk of alcoholic liver damage. The TT homozygotes are at a high risk to develop cirrhosis[25]. On the other hand, Koppelman *et al*., reported the importance of the C allele influencing the expression and severity of the atopic phenotype in a Dutch group[26]. The CD14 genotype does not appear to represent a susceptibility gene for the development of atopy, yet it appears to produce a more severe atopic phenotype. Considering the ethnic variations, we conducted a study in a Chinese group to investigate the relationship between genetic polymorphism of the CD14 promoter and the occurrence of alcoholic cirrhosis and alcoholic pancreatitis, two common necro-inflammatory complications in alcoholic patients. Because the preliminary data revealed that the C allele was higher in alcoholic pancreatitis patients, we also included patients with non-alcoholic pancreatitis for comparison. By investigating the polymorphism of CD 14 gene, we also want to challenge the conclusion we made before that the Chinese alcoholic patients with cirrhosis of liver and acute pancreatitis are two different subpopulation[27].

[illegible]

Blood samples were obtained from 335 alcoholic and 194 non-alcoholic patients at the Tri-Service General Hospital in Taipei, from September 2002 to March 2004. Of the 335 alcoholic patients, 100 were diagnosed with cirrhosis of liver, 100 with acute pancreatitis, 82 with esophageal cancer, and 53 with avascular necrosis of the hip joint (AVN), with all instances of the respective diseases deemed to be alcohol-induced. Of the 194 non-alcoholic controls, 77 were diagnosed with gallstone pancreatitis and 117 were non-alcoholic controls that had been admitted to hospital during the same observation period (clinical diagnoses for the controls included peptic ulcer, inguinal hernia, acute appendicitis, bone fracture and acute gastroenteritis). All of the alcoholic patients had consumed in excess of 60 g alcohol per day, on average, for at least 6 years. None of the patients in the non-alcoholic subgroup had a history of alcoholism and consumption of alcoholic beverages was infrequent for these individuals. The 100 patients in the alcoholic cirrhosis subgroup were all negative for serum antinuclear and anti-mitochondrial antibodies, and negative for antibodies to the hepatitis C virus and its RNA (determined using a second-generation test kit, Abbott Laboratories, Chicago, IL, USA) and PCR, respectively. The hepatitis B surface antigen and HBV DNA were negative for all 100 of these patients. All the cirrhotic patients presented with typical sonographic signs suggestive of cirrhosis, and all had endoscopically proven esophageal varices. The distributions of these cirrhotic patients according to Child-Pugh score (A/B/C) were 4/70/26. Liver biopsy was not performed for most cases because of decompensated hepatic function or massive ascites. None of the patients in the alcoholic cirrhosis subgroup had a history of acute pancreatitis. The acute pancreatitis patients presented with typical symptoms and signs, with elevations of serum amylase and lipase at least three-fold normal levels. Abdominal sonography, computerized tomography (CT), and endoscopic retrograde cholangiopancreatography were used for patient evaluation. For the alcoholic pancreatitis subgroup (n = 100), risk factors for the pancreatitis, other than alcoholism, were carefully assessed before being ruled out. Of these 100 patients, 40 had experienced two or more episodes, with mild but persistent elevation for serum transaminases noted among 12 during a 6-mo follow-up period after discharge, indicating the possibility of a coexisting alcohol-induced liver disease. The serum albumin, total bilirubin, prothrombin time and peripheral platelet count for these 12 acute alcoholic pancreatitis patients were within normal limits. No evidence of esophageal varices or congestive gastropathy was noted for any of the 100 patients in this subgroup. All the patients in the alcoholic AVN subgroup had undergone total hip replacement, with diagnosis proven from pathology; for 11 of these, hip-joint involvement was bilateral. None of the 53 patients in alcoholic AVN subgroup had a history of acute pancreatitis. Eleven patients were diagnosed with alcoholic liver disease because of persistently abnormal transaminase levels; however, there was no clinical evidence of cirrhosis. The pathology diagnosis of the patients in esophageal cancer subgroup revealed that 72 of the 82 were squamous cell carcinoma and the other 10 were adenocarcinoma. The 82 patients showed no clinical evidence of liver cirrhosis on abdominal sonography, gastroscopy, and biochemical studies. However, seven of them had mildly elevated serum transaminase levels. None of them had any history of acute pancreatitis. Alcohol consumption histories were obtained using a standard questionnaire. The physician on duty ensured that the informed consent was obtained and the questionnaire was reliably completed by interviewing both the patient and a member of the family, usually the spouse or mother.

DNA isolation and CD14 genotyping

DNA was extracted from WBC pellets, obtained after lysis of the red cells with ammonium bicarbonate. The genotyping of a polymorphism in the promoter region of the CD14 receptor characterized by a C to T transition at -159 was accomplished by restriction fragment length polymorphism analyses. The genomic DNA was amplified using the following primer pair: forward, 5' GTGCCAACAGATGA-GGTTCAC 3'. And reverse, 5' GCCTCTGACAGTTTAT-GTAATC 3'. The PCR was carried out in a final volume of 50 μL, containing 1 mmol/L $MgCl_2$, 0.2 mmol/L of each deoxynucleotide triphosphate, 0.2 μmol/L of each primer, and 1 U Taq DNA polymerase. After an initial denaturation of 5 min at 94 ℃, the samples were subjected to 35 cycles at 94 ℃ for 30 s, 60 ℃ for 30 s, and 72 ℃ for

30 s, with a final extension of 7 min at 72 ℃. The 497-bp product was restricted with Eca 471 (Ava II; Fermentas, Amherst, NY) overnight at 37 ℃. The unrestricted 497-bp product represents the C allele, where a T allele was cut into 144- and 353-bp fragments. The three genotypes were scored after running on a 2.5 % agarose gel. A T/T homozygote was included in PCR as a positive control of digestion.

ALDH2 genotyping

ALDH2 genotyping was determined by our previously published method, using PCR-directed mutagenesis[14].

Statistical analysis

χ^2 analysis was performed to compare the allele frequencies between groups.

□□□□□□□

The patient's age, sex, and alcoholism history are listed in Table 1. The CD14 genotype and allele frequencies for alcoholic and non-alcoholic patients are presented in Table 2. Carriage of C allele was significantly more prevalent in alcoholic pancreatitis than in esophageal carcinoma ($P<0.001$), alcoholic AVN ($P<0.025$), non-alcoholic pancreatitis ($P<0.001$) and non-alcoholic controls ($P<0.025$). When the subjects with genotype CC compared with genotype TT, the CC genotype was more prevalent in alcoholic pancreatitis than in esophageal cancer ($P<0.005$), non-alcoholic pancreatitis ($P<0.005$), and non-alcoholic controls ($P<0.025$).

We also compared subjects with genotype CC *vs* CT and TT (T- *vs* T+). The CC genotype was more prevalent in alcoholic pancreatitis than in alcoholic esophageal cancer ($P<0.001$), alcoholic AVN ($P = 0.005$), non-alcoholic pancreatitis ($P<0.001$) and non-alcoholic controls ($P<0.002$). The CC genotype was more prevalent in alcoholic liver cirrhosis than in alcoholic esophageal cancer ($P<0.05$) (Table 2).

For further clarification of the role of C allele in the development of different alcohol-related complications, we checked the allele frequency of CD14 only in subjects with the ALDH2 1-1 genotype (Table 3). The C allele frequency was significantly more prevalent in alcoholic pancreatitis than in alcoholic liver cirrhosis ($P<0.025$), esophageal cancer ($P<0.01$), alcoholic AVN ($P<0.01$), non-alcoholic pancreatitis ($P<0.001$) and non-alcoholic controls ($P<0.05$). In a subgroup of subjects with genotype ALDH2 1-1, the genotype CC *vs*

Table 1 Age, sex, and alcohol consumption in the different groups

Groups (*n*)	Alcohol consumption			
	Age (yr)	Sex (M/F)	Daily (g)	Duration (yr)
Alcoholic cirrhosis (100)	50.5±12.9	97/3	189±119	25.8±11.6
Alcoholic pancreatitis (100)	40.2±11.7	95/5	143±93	15.8±8.8
Alcoholic esophageal Ca (82)	64.4±12.7	82/0	200±175	35.8±13.8
Alcoholic AVN (53)	44.7±9.7	53/0	197±139	19.6±8.2
Non-alcoholic pancreatitis (77)	53.2±17.5	38/39	-	-
Non-alcoholic controls (117)	60.6±18.3	75/32	-	-

Table 2 CD14 polymorphism

Groups (*n*)	CC	CT	TT	*C	*T
Alcoholic pancreatitis (100)	59[c,d,f,h,2,3]	39	2	0.79[a,b]	0.21
Alcoholic cirrhosis (100)	46[e]	49	5	0.71[1]	0.29
Alcoholic esophageal Ca. (82)	25	49	8	0.60	0.40
Alcoholic AVN (53)	18	33	2	0.65	0.35
Non-alcoholic pancreatitis (77)	25	43	9	0.60	0.40
Non-alcoholic controls (117)	49	62	6	0.68	0.32

C allele frequency, [a]$P<0.025$ *vs* alcoholic AVN and non-alcoholic controls; [b]$P<0.001$ *vs* esophageal carcinoma and non-alcoholic pancreatitis; [1]$P = 0.055$ *vs* esophageal carcinoma. Genotype CC *vs* TT, [c]$P<0.005$ *vs* esophageal cancer and non-alcoholic pancreatitis; [d]$P<0.001$ *vs* alcoholic AVN. Genotype CC *vs* CT and TT (T- *vs* T+), [f]$P<0.001$ *vs* alcoholic esophageal cancer; [h]$P<0.001$ *vs* non-alcoholic pancreatitis; [2]$P = 0.005$ *vs* alcoholic AVN; [3]$P = 0.017$ *vs* non-alcoholic controls. Genotype CC *vs* CT and TT (T- *vs* T+), [e]$P<0.05$ *vs* alcoholic esophageal cancer.

Table 3 CD14 polymorphism in ALDH2 1-1 homozygotes

Group (*n*)	CC	CT	TT	*C	*T
Alcoholic pancreatitis (65)	41[e,g,i,k]	24	0	0.82[a,b,c,d]	0.18
Alcoholic cirrhosis (77)	33	40	4	0.69	0.31
Alcoholic esophageal Ca (23)	8	12	3	0.61	0.39
Alcoholic AVN (42)	14	26	2	0.64	0.36
Non-alcoholic pancreatitis (40)	13	21	6	0.59	0.41
Non-alcoholic controls (54)	22	30	2	0.69	0.31

C allele frequency, [a]$P<0.025$ *vs* alcoholic cirrhosis; [b]$P<0.001$ *vs* non-alcoholic pancreatitis; [c]$P<0.05$ *vs* non-alcoholic controls; [d]$P<0.01$ *vs* esophageal cancer and alcoholic AVN. Genotype CC *vs* CT and TT, [e]$P<0.05$ *vs* alcoholic cirrhosis and alcoholic esophageal cancer; [g]$P<0.025$ *vs* alcoholic AVN; [i]$P<0.005$ *vs* non-alcoholic pancreatitis; [k]$P<0.05$ *vs* non-alcoholic controls.

Table 4 CD14 polymorphism in alcoholic patients with and without pancreatitis

Group (*n*)	CC	CT	TT	*C	*T
Alcoholics without pancreatitis (235)	89[b,c]	131	15	0.66[a]	0.34
Alcoholics with pancreatitis (100)	59	39	2	0.79	0.21
Alcoholics with genotype ALDH2 1-1					
Alcoholics without pancreatitis (142)	59[g,i]	78	9	0.66[e]	0.34
Alcoholics with pancreatitis (65)	41	24	0	0.82	0.18

C allele frequency, [a]$P<0.005$ *vs* alcoholics with pancreatitis. Genotype CC *vs* TT, [b]$P<0.001$ *vs* alcoholics with pancreatitis. [c]$P<0.05$ *vs* alcoholics with pancreatitis. Genotype CC *vs* CT and TT (T- *vs* T+), C allele frequency, [e]$P<0.005$ *vs* alcoholics with pancreatitis. Genotype CC *vs* TT, [g]$P<0.05$ *vs* alcoholics with pancreatitis. Genotype CC *vs* CT and TT (T- *vs* T+), [i]$P<0.005$ *vs* alcoholics with pancreatitis.

CT and TT (T- *vs* T+) was also more prevalent for the alcoholic pancreatitis than for the alcoholic liver cirrhosis ($P<0.05$), alcoholic esophageal cancer ($P<0.05$), alcoholic AVN ($P<0.01$), non-alcoholic pancreatitis ($P<0.005$) and non-alcoholic controls ($P<0.05$). We did not check CC *vs* TT, and TT *vs* CC and CT in subjects with ALDH2 1-1 genotype because there were no TT homozygous patients in alcoholic pancreatitis group. We also compared alcoholic patients with and without pancreatitis in Table 4. The frequency of C allele was more prevalent for the alcoholic patients with pancreatitis than for the alcoholic patients without pancreatitis ($P<0.005$). Genotype CC was more prevalent for alcoholic patients with pancreatitis than for patients without pancreatitis ($P<0.05$). The genotype CC *vs* CT and TT (T- *vs* T+) was also more prevalent in alcoholic patients with pancreatitis than patients without pancreatitis ($P<0.001$). In subjects with genotype ALDH2 1-1, the C allele frequency was significantly higher in alcoholic patients with pancreatitis than without pancreatitis ($P<0.005$). The CC genotype was more prevalent for alcoholic patients with pancreatitis than patients without pancreatitis ($P<0.05$). And, the genotype CC *vs* CT and TT (T- *vs* T+) was more prevalent in alcoholic patients with pancreatitis than patients without pancreatitis ($P<0.005$).

[illegible]

The genotype distribution of the CD14 promoter polymorphism was unique in that the TT genotype was less prevalent in the Chinese than in the Finnish group (4.8% in Chinese alcoholics *vs* 19.7% in Finnish alcoholics and 7.7% in Chinese non-alcoholics *vs* 16.4% in Finnish non-alcoholics)[25]. In this study, we investigated the genotype distribution of CD14 in alcoholic patients with necro-inflammatory complications, pancreatitis and liver cirrhosis and other complications i.e., esophageal cancer and avascular necrosis of hip joint. We did not confirm the results in Chinese alcoholic patients that the T allele confers increased risk of alcoholic liver damage, reported by Jarvelainen *et al*., in the Finnish group[25]. This indicates that this polymorphism is probably not, at least in the Chinese population, an important factor determining the severity of liver disease in alcoholic patients. But we found that the C allele frequency was significantly higher in alcoholic patients with pancreatitis than alcoholic patients with other complications.

The significant role of the T allele in CD14 promoter region was suggested by two findings: (1) it has been found to confer increased CD14 expression on monocytes[22,23] and (2) an increased risk for myocardial infarction has been observed among individuals who are CD14-promoter TT homozygotes[23,24]. The T allele seems to favor the inflammatory process. On the other hand, Ito *et al*., reported that no association between CD14 genotypes and serum CD14 levels was observed in the Japanese population[28]. Risley *et al*., suggested no significant differences in serum CD14 concentration between Caucasian healthy carriers and noncarriers of the T allele[29]. Furthermore, Fernandez-Real *et al*., also found that there was no difference in CD14 levels among healthy Spanish people with different CD14 genotypes[30]. However, the T/T homozygotes have higher levels of circulating CD14 in a subset of diabetic patients[27]. The CD14 genotype was associated with insulin sensitivity in both Caucasian healthy subjects and type 2 diabetic patients[29]. Taking these together, whether CD14 polymorphism was associated with circulating CD14 levels remains controversial. More functional studies are needed to study the effect of CD14/-159 on promoter activity.

Previous publications discuss the relationship between diseases and the CD14 genotypes and have revealed conflicting results. Hubacek *et al*., found the T allele and TT genotype elevated in Czech patients with myocardial infarction ($n = 178$) if compared with the control subjects, suggesting the -159 C/T nucleotide polymorphism to be a genetic risk factor[23]. In a large study which included 1 793 patients, conducted in Germany by Koch *et al*., data indicated that the -159 C/T polymorphism is not related to coronary artery disease or myocardial infarction[31]. In a Dutch population, Koppelman *et al*., found homozygotes for the C allele had a higher number of positive skin tests and higher total serum IgE levels and subsequently, more allergic symptoms including rhinitis and hay fever, compared with subjects with CT and TT alleles[26]. In our study, we found that the C allele frequency was significantly higher in alcoholic patients with pancreatitis than alcoholic patients with other complications. This difference persisted between alcoholic patients with pancreatitis and alcoholic patients with other complications when compared with CC to TT or T- to T+. This suggested that the C allele may be associated with some mechanism which is important and specific in the pathogenesis of alcoholic pancreatitis.

Previously, we reported that most Chinese alcoholic patients with liver cirrhosis never had an episode of acute alcohol-induced pancreatitis despite the fact that they are older and their daily alcohol consumption is larger than that of pancreatitis patients. Further analysis revealed that the ADH2*1 allele frequency is significantly different between Chinese alcoholic patients with cirrhosis and pancreatitis.

We also suggest that alcoholic patients with these two different complications are two different subpopulations[27]. In this study, we also want to investigate whether the CD14 allele frequency is different between alcoholic patients with liver cirrhosis and alcoholic pancreatitis. Initially when comparing the C allele frequency of CD14 in alcoholic patients with pancreatitis and liver cirrhosis, no significant difference was found in these two groups. As the alcohol-specific complications are considered to be influenced by multiple genes and also because the ALDH2 gene is one of the most important alcohol-metabolizing genes, we evaluated the relationship between CD14 genotypes and different complications only in alcoholic patients with genotype ALDH 2 1-1, the most common genotype in the Chinese alcoholic patients. The result showed that the C allele frequency is significantly different between alcoholic patients with cirrhosis of the liver and alcohol-induced pancreatitis. This further indicated that the C allele is associated with the development of alcoholic pancreatitis and alcoholic patients with cirrhosis and pancreatitis are of two different subpopulations.

Unlike alcoholic pancreatitis patients, those with gallstone pancreatitis share the similar frequency of C allele with general population. This indicates that the increased C allele frequency is specific for alcoholic, but not all types of pancreatitis.

The pathogenesis of alcoholic pancreatitis is not clear. There are several plausible explanations for a possible role of CD14 in alcoholic pancreatitis. CD14 is a multifunctional receptor and may play a role in different biological and pathophysiological processes such as: apoptosis, sepsis and inflammatory disease[32-35]. CD14 on monocytes and polymorphonuclear cells functions as a receptor for lipopolysaccharides, thereby inducing mediator and cytokine release. Thus, CD14 may be involved in a proinflammatory pathway through the release of cytokines.

The reason why alcoholic patients develop different organ complications is still unknown. It seems highly probable that the development of specific complications in alcoholic patients is determined by multiple genes, with most of these still not well understood.

REFERENCES

1 **Schuckit MA.** Alcohol and alcoholism. In Braunwald E, Isselbacher KJ, Eds. Harrison's principles of internal medicine, 13th Ed. *New York: McGraw-Hill* 1995: 2420-2425
2 **Hrubec Z,** Omenn GS. Evidence of genetic predisposition to alcoholic cirrhosis and psychosis: twin concordances for alcoholism and its biological end points by zygosity among male veterans. *Alcohol Clin Exp Res* 1981; **5**: 207-215
3 **Reed T,** Page WF, Viken RJ, Christian JC. Genetic predisposition to organ-specific endpoints of alcoholism. *Alcohol Clin Exp Res* 1996; **20**: 1528-1533
4 **Lieber CS.** Alcohol and the liver:1994 update. *Gastroenterology* 1994; **106**: 1085-1105
5 **Bosron WF,** Li TK. Genetic polymorphism of human liver alcohol and aldehyde dehydrogenase, and their relationship to alcohol metabolism and alcoholism. *Hepatology* 1986; **6**: 502-510
6 **Bosron WF,** Ehrig T, Li TK. Genetic factors in alcohol metabolism and alcoholism. *Semin Liver Dis* 1993; **13**: 126-135
7 **Goedde HW,** Agarwal DP. Acetaldehyde metabolism: genetic variation and physiological implications. In: Goedde HW, Agarwal DP, eds. Alcoholism: Biomedical and genetic aspects. *Elmsford: Pergamon Press* 1989: 21-56
8 **Smith M.** Genetics of human alcohol and aldehyde dehydrogenases. *Adv Hum Genet* 1986; **15**: 249-290
9 **Maezawa Y,** Yamauchi M, Toda G. Association between restriction fragment length polymorphism of the human cytochrome P450IIE1 gene and susceptibility to alcoholic liver cirrhosis. *Am J Gastroenterol* 1994; **89**: 561-565
10 **Tsutsumi M,** Takada A, Wang JS. Genetic polymorphisms of cytochrome P4502E1 related to the development of alcoholic liver disease. *Gastroenterology* 1994; **107**: 1430-1435
11 **Day CP,** James OF, Bassendine MF, Crabb DW, Li TK. Alcohol dehydrogenase polymorphisms and predisposition to alcoholic cirrhosis. *Hepatology* 1993; **18**: 230-232
12 **Crabb DW.** Ethanol oxidizing enzymes: roles in alcohol metabolism and alcoholic liver disease. *Prog Liver Dis* 1995; **13**: 151-172
13 **Enomoto N,** Takase S, Takada N. Alcoholic liver disease in heterozygotes of mutant and normal aldehyde dehydrogenase-2 genes. *Hepatology* 1991; **13**: 1071-1075
14 **Chao YC,** Liou SR, Chung YY, Tang HS, Hsu CT, Li TK, Yin SJ. Polymorphism of alcohol and aldehyde dehydrogenase genes and alcoholic cirrhosis in Chinese patients. *Hepatology* 1994; **19**: 360-366
15 **Chao YC,** Young TH, Chang WK, Tang HS, Hsu CT. An investigation of whether polymorphisms of cytochrome P4502E1 are genetic markers of susceptibility to alcoholic end-stage organ damage in a Chinese population. *Hepatology* 1995; **22**: 1409-1414
16 **Yamauchi M,** Maezawa Y, Mizuhara Y, Ohata M, Hirakawa J, Nakajima H, Toda G. Polymorphisms in alcohol metabolizing enzyme genes and alcoholic cirrhosis in Japanese patients: a multivariate analysis. *Hepatology* 1995; **22**: 1136-1142
17 **Bode C,** Kugler V, Bode JC. Endotoxemia in patients with alcoholic and non-alcoholic cirrhosis and in subjects with no evidence of chronic liver disease following acute alcohol excess. *J Hepatol* 1987; **4**: 8-14
18 **Nanji AA,** Khettry U, Sadrzadeh SM, Yamanaka T. Severity of liver injury in experimental alcoholic liver disease. Correlation with plasma endotoxin, prostaglandin E2, leukotriene B4, and thromboxane B2. *Am J Pathol* 1993; **142**: 367-373
19 **Schenker S,** Bay MK. Alcohol and endotoxin: another path to alcoholic liver injury? *Alcohol Clin Exp Res* 1995; **19**: 1364-1366
20 **Matsuura K,** Ishida T, Setoguchi M, Higuchi Y, Akizuki S, Yamamoto S. Upregulation of mouth CD14 expression in Kupffer cells by lipopolysaccharide. *J Exp Med* 1994; **179**: 1671-1676
21 **Kielian TL,** Blecha F. CD 14 and other recognition molecules for lipopolysaccharide: a review. *Immunopharmacology* 1995; **29**: 187-205
22 **Baldini M,** Lohman IC, Halonen M, Erickson RP, Holt PG, Martinez FD. Polymorphism in the 5′ flanking region of the CD 14 gene is associated with circulating soluble CD14 levels and with total serum immunoglobulin E. *Am J Respir Cell Mol Biol* 1999; **20**: 976-983
23 **Hubacek JA,** Rothe G, Pit'ha J, Skodova Z, Stanek V, Poledne R, Schmitz G. C(-260)T polymorphism in the promoter of the CD14 monocyte receptor gene as a risk factor for myocardial infarction. *Circulation* 1999; **99**: 3218-3220
24 **Unkelbach K,** Gardemann A, Kostrzewa M, Philipp M, Tillmanns H, Haberbosch W. A new promoter polymorphism in the gene of lipopolysaccharide receptor CD14 is associated with expired myocardial infarction in patients with low atherosclerotic risk profile. *Arterioscler Thromb Vasc Biol* 1999; **19**: 932-938
25 **Jarvelainen HA,** Orpana A, Perola M, Savolainen VT, Karhunen PJ, Lindros KO. Promoter polymorphism of the CD14 endotoxin receptor gene as a risk factor for alcoholic liver disease. *Hepatology* 2001; **33**: 1148-1153
26 **Koppelman GH,** Reijmerink NE, Colin Stine O, Howard TD, Whittaker PA, Meyers DA, Postma DS, Bleecker ER. Association of a promoter polymorphism of the CD14 gene and atopy. *Am J Respir Crit Care Med* 2001; **163**: 965-969
27 **Chao YC,** Young TH, Tang HS, Hsu CT. Alcoholism and alcoholic organ damage and genetic polymorphisms of alco-

hol metabolizing enzymes in Chinese patients. *Hepatology* 1997; **25**: 112-117

28 **Ito D,** Murata M, Tanahashi N, Sato H, Sonoda A, Saito I, Watanabe K, Fukuuchi Y. Polymorphism in the promoter of lipopolysaccharide receptor CD14 and ischemic cerebrovascular disease. *Stroke* 2000; **31**: 2661-2664

29 **Risley P,** Jerrard-Dunne P, Sitzer M, Buehler A, von Kegler S, Markus HS. Carotid Atherosclerosis Progression Study. Promoter polymorphism in the endotoxin receptor (CD14) is associated with increased carotid atherosclerosis only in smokers. The carotid atherosclerosis progression study (CAPS). *Stroke* 2003; **34**: 604-606

30 **Fernandez-Real JM,** Broch M, Richart C, Vendrell J, Lopez-Bermejo A, Ricart W. CD14 monocyte receptor, involved in the inflammatory cascade, and insulin sensitivity. *J Clin Endocrinol Metab* 2003; **88**: 1780-1784

31 **Koch W,** Kastrati A, Mehilli J, von Beckerath N, Schomig A. CD14 gene -159 C/T polymorphism is not associated with coronary artery disease and myocardial infarction. *Am Heart J* 2002; **143**: 971-976

32 **Schlegel RA,** Krahling S, Callahan MK, Williamson P. CD14 is a component of multiple recognition systems used by macrophages to phagocytose apoptotic lymphocytes. *Cell Death Differ* 1999; **6**: 583-592

33 **Gibot S,** Cariou A, Drouet L, Rossignol M, Ripoll L. Association between a genomic polymorphism within the CD14 locus and septic shock susceptibility and mortality rate. *Crit Care Med* 2002; **30**: 969-973

34 **Obana N,** Takahashi S, Kinouchi Y, Negoro K, Takagi S, Hiwatashi N, Shimosegawa T. Ulcerative colitis is associated with a promoter polymorphism of lipopolysaccharide receptor gene, CD14. *Scand J Gastroenterol* 2002; **37**: 699-704

35 **Klein W,** Tromm A, Griga T, Fricke H, Folwaczny C, Hocke M, Eitner K, Marx M, Duerig N, Epplen JT. A polymorphism in the CD14 gene is associated with Crohn disease. *Scand J Gastroenterol* 2002; **37**: 189-191

Science Editor Guo SY **Language Editor** Elsevier HK

PO Box 2345, Beijing 100023, China
www.wjgnet.com
wjg@wjgnet.com

ELSEVIER

World J Gastroenterol 2005;11(38):6049-6052
World Journal of Gastroenterology ISSN 1007-9327
© 2005 The WJG Press and Elsevier Inc. All rights reserved.

• *BRIEF REPORTS* •

Balthazar computed tomography severity index is superior to Ranson criteria and APACHE II scoring system in predicting acute pancreatitis outcome

Ting-Kai Leung, Chi-Ming Lee, Shyr-Yi Lin, Hsin-Chi Chen, Hung-Jung Wang, Li-Kuo Shen, Ya-Yen Chen

Ting-Kai Leung, Chi-Ming Lee, Hsin-Chi Chen, Hung-Jung Wang, Li-Kuo Shen, Ya-Yen Chen, Department of Diagnostic Radiology, Taipei Medical University Hospital, Taipei, Taiwan, China
Shyr-Yi Lin, Department of Internal Medicine, Taipei Medical University Hospital, Taipei, Taiwan, China
Correspondence to: Chi-Ming Lee, MD, Department of Diagnostic Radiology, Taipei Medical University Hospital, 252, Wu Hsing Street, Taipei 110, Taiwan, China. yayen0220@yahoo.com.tw
Telephone: +886-2-27372181-1131 Fax: +886-2-23780943
Received: 2005-01-31 Accepted: 2005-04-18

Abstract

AIM: Acute pancreatitis (AP) is a process with variable involvement of regional tissues or organ systems. Multifactorial scales included the Ranson, Acute Physiology and Chronic Health Evaluation (APACHE II) systems and Balthazar computed tomography severity index (CTSI). The purpose of this review study was to assess the accuracy of CTSI, Ranson score, and APACHE II score in course and outcome prediction of AP.

METHODS: We reviewed 121 patients who underwent helical CT within 48 h after onset of symptoms of a first episode of AP between 1999 and 2003. Fourteen inappropriate subjects were excluded; we reviewed the 107 contrast-enhanced CT images to calculate the CTSI. We also reviewed their Ranson and APACHE II score. In addition, complications, duration of hospitalization, mortality rate, and other pathology history also were our comparison parameters.

RESULTS: We classified 85 patients (79%) as having mild AP (CTSI <5) and 22 patients (21%) as having severe AP (CTSI $\geqslant$5). In mild group, the mean APACHE II score and Ranson score was 8.6±1.9 and 2.4±1.2, and those of severe group was 10.2±2.1 and 3.1±0.8, respectively. The most common complication was pseudocyst and abscess and it presented in 21 (20%) patients and their CTSI was 5.9±1.4. A CTSI $\geqslant$5 significantly correlated with death, complication present, and prolonged length of stay. Patients with a CTSI $\geqslant$5 were 15 times to die than those CTSI <5, and the prolonged length of stay and complications present were 17 times and 8 times than that in CTSI <5, respectively.

CONCLUSION: CTSI is a useful tool in assessing the severity and outcome of AP and the CTSI $\geqslant$5 is an index in our study. Although Ranson score and APACHE II score also are choices to be the predictors for complications, mortality and the length of stay of AP, the sensitivity of them are lower than CTSI.

© 2005 The WJG Press and Elsevier Inc. All rights reserved.

Key words: Acute pancreatitis; Ranson score; APACHE II score; Balthazar computed tomography severity index

Leung TK, Lee CM, Lin SY, Chen HC, Wang HJ, Shen LK, Chen YY. Balthazar computed tomography severity index is superior to Ranson criteria and APACHE II scoring system in predicting acute pancreatitis outcome. *World J Gastroenterol* 2005; 11(38): 6049-6052
http://www.wjgnet.com/1007-9327/11/6049.asp

INTRODUCTION

Acute pancreatitis (AP) is a process of acute inflammation of the pancreas, with variable involvement of regional tissues or organ systems. The clinical expression of AP varies from edematous mild AP to severe AP, and is frequently associated with necrosis of the pancreas, a protracted clinical course, organ failure, a high incidence of local complications, and a high mortality rate[1]. Multifactorial scales including the Ranson[2] and Acute Physiology and Chronic Health Evaluation (APACHE II) systems[3] have been used for AP since the 1970s. Balthazar computed tomography severity index (CTSI) was developed since 1990[4]. Computed tomography (CT) with intravenous contrast medium injection is accepted as the imaging procedure of choice: first to document the extent of pancreatic and extrapancreatic acute fluid collections and, second, to detect pancreatic necrosis. These two parameters have been identified as prognostic indicators of the severity of AP. CTSI, based on combined assessment of peripancreatic fluid collections, and the degree of pancreatic necrosis were developed to improve prognostic accuracy. The purpose of this review study was to assess the early predictability of a variety of parameters in AP, such as Ranson, APACHE II, and CTSI. We compared the accuracy of CTSI, Ranson score, and APACHE II score in course and outcome of AP prediction and the prognostic value of CT in the assessment of AP.

MATERIALS AND METHODS

We performed a retrospective review of all 121 patients who underwent helical CT within 48 h after onset of symptoms of a first episode of AP between 1999 and 2003.

Fourteen inappropriate subjects who did not meet criteria of clinical blood data for diagnosis of pancreatitis were excluded, CT was performed without contrast because of renal dysfunction and missing chart in medical records, and we reviewed the 107 contrast-enhanced CT images. Of these, there were 57 males, 50 females, with ages ranging from 21 to 87 years, mean age 56 years. The abdominopelvic CT scans were (HiSpeed CT/I; GE Medical Systems, Milwaukee, WI, USA) acquired from patients after oral administration of 4% iothalamate meglumine (Mallinckrodt, USA) 1 000 mL and intravenous administration of iohexol (Nycoveien, Norway) 100 mL (350 mg/mL); flow rate, 2 mL/s, with a section thickness of 10 mm and a pitch of 1.5. We reviewed the CTSI of their CT images. CTSI is a 10-point scoring system derived by assessing the degree of pancreatic and peripancreatic inflammation (0-4 points), and the presence and degree of pancreatic parenchymal nonenhancement or necrosis (0-6 points)[4]. In addition, we also collected the clinical chart records (temperature, heart rate, mean blood pressure, respiratory rate, etc.) to calculate the APACHE II and Ranson score. Complications, duration of hospitalization (according to Simchuk's study[5], we defined the prolonged length of stay as ≥20 d; short length of stay as <20 d), mortality rate, and other pathology history also were our comparison parameters.

RESULTS

According to Casas's study[6], we classified 85 patients (79%) as having mild AP (CTSI <5) and 22 patients (21%) as having severe AP (CTSI ≥5). We found that the CTSI in all patients was 0-8 points and mean score was 3.7. The mean CTSI in mild group was 1.9±0.4 and that in severe group was 6.1±0.5. In APACHE II score aspect, the mean score among all patients was 9.4±2.4. In CTSI mild AP group, the mean APACHE II score was 8.6±1.9 and that of CTSI severe AP was 10.2±2.1. In Ranson score aspect, the mean score in all patients was 2.7±1.4. In CTSI mild group, the mean Ranson score was 2.4±1.2 and that of CTSI severe group was 3.1±0.8. Complications included pseudocyst formation in 21 (20%) including abdominal abscess in two cases. The CTSI in these patients was 5-8, and the mean score was 5.9. Mean APACHE II score and Ranson score of them were 9.4 and 2.7 respectively. Four patients (3.7%) died because of multiorgan failure and sepsis. They died at 21st, 23rd, 19th, and 12th d after admission. The CTSI of them was 3, 5, 6, and 7 respectively. The APACHE II in these four patients was 6, 7, 7, and 9 and the Ranson score was 2, 2, 2, and 3. The APACHE II and Ranson score in the patient who died but with a CTSI of 3 were not significantly higher than other patients. In the length of stay aspect, 19 patients stayed for over 20 d and the mean CTSI was 5.6. Others stayed for 3-15 d and the mean CTSI was 2.7. By comparison, there is no significant difference of APACHE II and Ranson score in the short length of stay (<20 d) group and prolonged length of stay (≥20 d) group. Mean APACHE II score in short and prolonged length of stay was 8.9 and 9.8 and the mean Ranson score was 2.9 and 2.6, respectively. Comparison of CTSI, APACHE II score and Ranson score in our patients are listed in Table 1.

Table 2 shows the relationship between CTSI and outcomes. These data showed that the CTSI significantly correlated with all outcomes measured. Patients with a CTSI ≥5 was 15 times to die than those CTSI <5, and the prolonged length of stay and complications present were 17 times and 8 times than that in CTSI <5, respectively. AP was due to gallstone in 36 patients (34%), to alcohol consumption in 36 patients (34%), to both causes in 16 patients (15%) and to unknown reasons in 19 patients (18%). In other pathology history aspect, the most popular disease in our patients is diabetes mellitus (DM). Thirty-six patients (34%) were with DM and two of them underwent neuropathy. The mean CTSI in these DM patients was 5.3. Three of the DM patients died and their CTSI were 5, 6, and 7. In addition, AP relapse occurred in 17 patients (16%) and they all belonged to alcoholic type. The mean CTSI of them was 4.2.

Table 1 The comparison of severity, complication, mortality, and the length of stay in CTSI, Ranson score, and APACHE II score

		CTSI[1]	Ranson score	APACHE II score
Severity	Mild	1.9±0.4	2.4±1.2	8.6±1.9
	Severe	6.1±0.5	3.1±0.8	10.2±2.1
Complications	Present	5.9±1.4	2.7±0.9	9.4±2.4
	Absent	2.1±0.6[1]	2.5±1.1	8.7±1.6
Mortality	Present	5.3±1.7	2.3±0.5	7.3±1.3
	Absent	1.8±0.6[1]	2.5±0.7	8.5±0.9
Length of stay	≥20 d	5.6±1.6	2.6±1.1	9.8±0.9
	<20 d	2.7±1.1[1]	2.9±0.9	8.9±1.2

[1]Significant differences between two lines in the same parameter.

Table 2 CTSI and outcome prediction

		No. of patients	*P*	Odd's ratio
Death	CTSI ≥5	3	<0.05	15
	CTSI <5	103		
Prolonged length of stay (≥20 d)	CTSI ≥5	19	<0.05	17
	CTSI <5	88		
Complications	CTSI ≥5	21	<0.05	8
	CTSI <5	86		

DISCUSSION

Predicting the severity and outcome of AP still represents a challenge for the physician. Since the work of Ranson[2] establishing a scoring system of severity for patients with AP, there has been several other scoring systems: Imrie[7], APACHE II[3], and Balthazar CTSI[4] systems were used to assess the severity of disease that had a high sensitivity and positive predictive value (PPV). A milestone achievement in assessing the severity of AP occurred in 1974, when Ranson developed his prognostic signs. He examined the relationship of 43 different measurements made during the first 48 h of treatment, finding 11 variables that significantly correlated with overall morbidity and mortality. Imrie *et al*., later modified Ranson's criteria by removing serum transaminase and adding serum methemalbumin, albumin, and cyclic AMP to Ranson's prognostic variables. However, the Ranson and Imrie criteria cannot be calculated until data from admission and 48 h after admission are compared. Larvin and McMahon[3]

applied the APACHE II score in the setting of AP and found that those with scores >7 were likely to have a severe course. They defined a severe course as the development of major organ system failure and a pancreatic collection. An advantage of the APACHE II score was flexibility, as it could be recalculated at any time during a hospital stay. However, Larvin and McMahon also showed that the APACHE II score had just a 67% PPV at 24 h after admission. They also showed that the APACHE II score was even less accurate for identifying patients with specific complications including peripancreatic fluid collections or major organ failure. Thus, better prognostic tools are needed. The Balthazar CTSI was reported to be of value in identifying patients with severe and fatal outcome, only a few studies have investigated whether CTSI performance is superior to that of the APACHE II or Ranson score in predicting AP outcome. This is the major challenge of this study.

Robert *et al.*[8], demonstrated that the Ranson score in mild AP (defined as the course of the disease was uncomplicated) and in severe AP (defined as organ failure) were 1.9±0.9 and 2.2±0.5. The APACHE II score was 6.9±0.7 and 7.4±0.4 in mild and severe group. In Chatzicostas's study[9], the Ranson score in mild (defined as normal amylase and lipase level) and severe (defined as organ failure and complications) groups were 2.0±1.4 and 2.1±1.6. The APACHE II score was 10.1±0.2 and 9.8±0.6 in mild and severe group. There were no significant differences between these data. According to these data, Robert and Chatzicostas demonstrated that the Ranson score and APACHE II score are not absolute predictors for severity of AP. In our study, we also did not find significant differences of Ranson and APACHE II score in mild and severe groups. So we suppose that our results are similar to Robert's and Chatzicostas's. In addition, in Wilson's study[10], they demonstrated that the patients with Ranson score ⩾3 was always in a severe situation. On evaluation of mean Ranson score in our study, we found that in severe AP it was 3.1±0.8. However, only one-thirds of the patients with severe pancreatitis had Ranson score ⩾3. Compared to Wilson's results, there were still a lot of variability in Ranson score prediction.

Complications are often the major reasons that resulted in the death of AP patients. The management of complications is important to reduce the mortality rate. In our study, we found that the higher CTSI associated with higher complication rate and the CTSI ⩾5 is an index. However, we did not find the same situation in Ranson and APACHE II score. There were no significant differences between mild and severe groups of Ranson and APACHE II score. According to Nicolas[11], they found that complications occurred rarely in Ranson score <3 and APACHE II score <8. In our study, the mean Ranson score and APACHE II score in complications-occurred patients were 2.7 and 9.4. Our APACHE II score result was similar to Nicolas' but in Ranson score aspect, the results showed that the relationship between complications present and Ranson score appeared to involve multiple variables. In the length of stay aspect, we demonstrated that CTSI is a more sensitive predictor than APACHE II and Ranson score. The mean CTSI in short and in prolonged length of stay showed significant difference (2.7 *vs* 5.6). However, there is no significant difference of APACHE II and Ranson score in the short length of stay group and prolonged length of stay group. In Simchuk's study[5], they mentioned that the PPV of APACHE II and Ranson score for the length of stay were 31% and 38%, and the PPV of CTSI was 71%. However, in Fleszler's study[12], they mentioned that APACHE II score is the most appropriate index to predict the length of stay, but they also mentioned that this score requires an arterial blood gas level, which was not available on some patients, thus the practicality of APACHE II is lower than Ranson score and CTSI.

The reported mortality rates for patients with AP vary greatly from 15% to 56%[12]. In Casas's study[6], they demonstrated that CTSI ⩾5 is the index, if the patients are under the danger of death. In Bradley's study[13], their results showed that CTSI >8 is the index for death. In our study, three of the four died patients had a CTSI ⩾5. So we supposed that our results were more similar to Casas's. According to Simchuk *et al.*[5], they mentioned that the CTSI <3 had a 3% mortality rate, whereas patients with a CTSI >7 had a mortality rate of 17%, it is likely 5-6 times mortality rate in CTSI >7 group. From the CTSI definitional value described above, there was still a lot of variability in death prediction of CTSI. According to our results, we demonstrated that the reason resulted in the variability may be the different characteristics of patients. Age, chronic diseases such as DM present or not, alcohol consumption and organ dysfunction all may affect the mortality rate of AP. We found that three of our four died patients had DM and their CTSI were 5, 6, and 7, all of them were alcoholics, and the average age of the four died patients was 55 years. Mortality rate associated with higher CTSI and worse pathological rate, the different characteristics of individual should not be ignored.

In conclusion, the CTSI is a useful tool in assessing the severity and outcome of AP and the CTSI ⩾5 are likely to have a severe course in our study. Although Ranson and APACHE II scores also are choices to be the predictors for complications, mortality and the length of stay of AP, the sensitivity of them are lower than CTSI. In addition, we found that if we are using CTSI to be an indicator for mortality rate, the different characteristics of an individual should not be ignored.

REFERENCES

1 **Yousaf M**, McCallion K, Diamond T. Management of severe acute pancreatitis. *Br J Surg* 2003; **90**: 407-420

2 **Ranson JH**, Rifkind KM, Roses DF, Fink SD, Eng K, Spencer FC. Prognostic signs and the role of operative management in acute pancreatitis. *Surg Gynecol Obstet* 1974; **139**: 69-81

3 **Larvin M**, McMahon MJ. APACHE II score for assessment and monitoring of acute pancreatitis. *Lancet* 1989; **2**: 201-205

4 **Balthazar EJ**, Robinson DL, Megibow. Acute pancreatitis: value of CT in establishing prognosis. *Radiology* 1990; **174**: 331-336

5 **Simchuk EJ**, Traverso LW, Nukui Y, Kozarek RA. Computed tomography severity index is a predictor of outcomes for severe pancreatitis. *Am J Surg* 2000; **179**: 352-355

6 **Casas JD**, Diaz R, Valderas G, Mariscal A, Cuadras P. Prognostic value of CT in the early assessment of patients with acute pancreatitis. *Am J Roentgenol* 2004; **182**: 569-574

7 **Imrie CW**, Benjamin IS, Ferguson JC, McKay AJ, Mackenzie I, O'Neill J. A single-centre double-blind trial of Trasylol therapy in primary acute pancreatitis. *Br J Surg* 1978; **65**:

337-341
8 **Robert JH**, Frossard JL, Mermillod B. Early prediction of acute pancreatitis: prospective study comparing computed Tomography scans, Ranson, Glasgow, APACHE II scores, and various serum markers. *World J Surg* 2002; **26**: 612-619
9 **Chatzicostas C**, Roussomoustakaki M, Vardas E, Romanos J, Kouroumalis EA. Balthazar computed tomography severity index is superior to Ranson criteria and APACHE II scoring systems in predicting acute pancreatitis outcome. *J Clin Gastroenterol* 2003; **36**: 253-260
10 **Wilson C**, Heath DI, Imrie CW. Prediction of outcome in acute pancreatitis: a comparative study of APACHE II, clinical assessment and multiple factor scoring systems. *Br J Surg* 1990; **77**: 1260-1264
11 **Nicolas MB**, Panis Y, Soyer P, Riche F, Laisne MJ, Boudiaf M, Valleur P. Serial computed tomography is rarely necessary in patients with acute pancreatitis: a prospective study in 102 patients. *J Am Coll Surg* 2001; **193**: 146-152
12 **Fleszler F**, Friedenberg F, Krevsky B, Friedel D, Braitman LE. Abdominal computed tomography prolongs length of stay and is frequently unnecessary in the evaluation of acute pancreatitis. *Am J Med Sci* 2003; **325**: 251-255
13 **Bradley E 3rd**. A clinically based classification system for on acute pancreatitis. Summary of the international symposium on acute pancreatitis. *Arch Surg* 1993; **128**: 586-590

Science Editor Guo SY **Language Editor** Elsevier HK

PO Box 2345, Beijing 100023, China
www.wjgnet.com
wjg@wjgnet.com

ELSEVIER

World J Gastroenterol 2005;11(38):6053-6055
World Journal of Gastroenterology ISSN 1007-9327
© 2005 The WJG Press and Elsevier Inc. All rights reserved.

• *BRIEF REPORTS* •

Downregulation of alpha-fetoprotein siRNA inhibits proliferation of SMMC-7721 cells

Yun-Shan Wang, Xiao-Li Ma, Tong-Gang Qi, Xiang-Dong Liu, Yue-Sheng Meng, Guang-Ju Guan

Yun-Shan Wang, Xiao-Li Ma, Central Laboratory, Jinan Central Hospital, Clinical Medical College of Shandong University, Jinan 250013, Shandong Province, China
Tong-Gang Qi, Yue-Sheng Meng, Guang-Ju Guan, Laboratory of Clinical Molecular Biology, The Second Hospital of Shandong University, Jinan 250015, Shandong Province, China
Xiang-Dong Liu, Shandong Provincial Hospital, Jinan 250020, Shandong Province, China
Supported by the Natural Science Foundation of Shandong Province, No. Z2003C01
Correspondence to: Professor Yun-Shan Wang, Jinan Central Hospital, 105# Jinan Jiefang Road, Jinan 250013, Shandong Province, China. sdjnwys@163.com
Telephone: +86-531-86557322 Fax: +86-531-86557322
Received: 2005-02-27 Accepted: 2005-04-11

AIM: To study the function of α-fetoprotein (AFP) in SMMC-7721 hepatoma cells.

METHODS: A hairpin siRNA expressing plasmid pSilencer3.0-H1-*afp* was constructed and transfected into SMMC-7721 cells with Lipofectamine 2000. The expression of AFP was monitored by real-time RT-PCR and immunoassays, its effect on SMMC-7721 cell proliferation and cell death was detected by MTT and fluorescence-activated cell sorter (FACS).

RESULTS: The AFP-siRNA expressing plasmid downregulated the expression of AFP obviously (about 34%), and inhibited SMMC-7721 cell proliferation, but did not induce apoptosis.

CONCLUSION: Downregulation of AFP siRNA inhibits proliferation of SMMC-7721 cells, but cannot cause apoptosis.

© 2005 The WJG Press and Elsevier Inc. All rights reserved.

Key words: siRNAs; AFP; SMMC-7721 cell; Proliferation; Apoptosis

Wang YS, Ma XL, Qi TG, Liu XD, Meng YS, Guan GJ. Downregulation of alpha-fetoprotein siRNA inhibits proliferation of SMMC-7721 cells. *World J Gastroenterol* 2005; 11(38): 6053-6055
http://www.wjgnet.com/1007-9327/11/6053.asp

INTRODUCTION

Primary hepatocellular carcinoma (PHCC) is one of the most common malignancies in the world, with a high fatality rate and a short survival time[1].

α-fetoprotein (AFP) is a major serum protein produced by the liver or yolk sac in mammals and other vertebrates, and is not detectable in normal adults[2]. However, AFP is often elevated to a significant level in association with development of PHCC, and has been defined as an oncofetal antigen[3,4]. The biological role of AFP has been widely investigated. However, the relationship between AFP and PHCC is still unclear. Some recent investigations indicate that human AFP can enhance the proliferation of mouse hepatoma H-22 and human hepatoma SMMC-7721, BEL-7404, or QGY-7703 cells *in vitro*[5]. Similar growth stimulatory effect of AFP at low concentrations has also been found in human hepatoma Hep G_2 cells. These results have an important implication that AFP may function as a hepatoma growth stimulator, thus suppression of AFP gene expression and its biological activities may become a new strategy for the treatment of AFP-associated tumors such as PHCC.

RNA-mediated interference is the inhibition of expression of specific genes by double-stranded RNAs (dsRNAs)[6]. Since short dsRNAs can silence the expression of its homologous gene in mammalian cells, and do not induce nonspecific interferon response, it is widely used in genome and therapy study. Here we have designed a plasmid pSilencer3.0-H1-*afp*, which can express siRNAs in mammalian cells to study the function of AFP and its therapeutic effect on hepatoma cells *in vitro*.

MATERIALS AND METHODS

Plasmid construction

The plasmid pSilencer3.0-H1-*afp* was constructed as previously described[7]. The targeted sequence of AFP gene (GenBank accession no. NM_005030) is 5'-AACTCAGTG-AGGACAAACTAT-3'. Positive and negative technical controls were supplied by Ambion Incorporation, and the positive control plasmid was aimed at GAPDH gene.

Hepatoma cell culture and plasmid transfection

Human hepatoma SMMC-7721 cells were cultured in RPMI-1640 (Invitrogen) supplemented with 10% FCS. Transfection was done with Lipofectamine 2000 (Invitrogen). One day before transfection, SMMC-7721 cells were seeded in the wells of 24-well culture plates, about 7×10^4 cells/well. Before transfection, 1 μg plasmid and 2 μL Lipofectamine 2000 were diluted with 50 μL serum-free Opti-MEM I (Invitrogen) and incubated for 5 min. They were mixed and incubated for 20 min at room temperature,

added to the medium, mixed gently, and then incubated at 37 ℃ for 4 h. The medium was replaced with a new medium and incubated for 12, 24, and 48 h.

Quantitative real-time PCR

For validation of the silencing effect by quantitative PCR, cDNA was prepared from the SMMC-7721 cell line. RT-PCR was carried out using RT and SYBR Green PCR Master Mix (ABI) according to the manufacturer's instructions. RT reaction was performed at 48 ℃ for 30 min. The cDNA was analyzed by real-time quantitative PCR immediately and stored at -20 ℃ until use. Each PCR was carried out in triplicate in a 25 μL volume for 15 min at 95 ℃ for initial denaturing, followed by 40 cycles at 95 ℃ for 30 s and at 60 ℃ for 1 min in the ABI 7000 sequence detection system. Each primer set was first tested to determine optimal concentrations, and products were run out on a 3% agarose gel to confirm the appropriate size. Subsequently, the ABI dissociation curves software was used following a brief thermal protocol (95 ℃ for 15 s and 60 ℃ for 20 s, followed by a slow ramp to 95 ℃) to control their multiple species in each PCR amplification. cDNA from hepatoma cells was used to construct a standard curve for each gene. Values for each gene were normalized to expression levels of actin-β, and then a ratio comparing the expression in negative and positive control, and pSilencer3.0-H1-*afp*-transfected hepatoma cells was calculated. The sequences of the primers used for RT-PCR were as follows: actin-β forward: 5'-CGT ACC ACT GGC ATC GTG AT-3'; reverse: 5'-GTG TTG GCG TAC AGG TCT TTG-3'; GAPDH forward: 5'-CTT CAC CAC CAT GGA GAA GGC-3'; reverse primer: 5'-GGC ATG GAC TGT GGT CAT GAG-3'; AFP forward: 5'-AAA TAC ATC CAG GAG AGC CA-3'; reverse: 5'-CTG AGC TTG GCA CAG ATC CT-3'.

Immunoassay of AFP concentration in supernatant

AFP concentration in the supernatant in each well was determined by chemiluminescence immunoassay according to the manufacturer's instructions.

MTT assays

Eight hours after plasmid transfection, the cells were harvested and replated in 96-well microtiter plates in triplicate at 1×10^4 cells in 0.1 mL medium/well. Twenty microliters of MTT dye (5 mg/mL) was added and incubated for 0, 24, 48, and 72 h respectively. Following 4 h of incubation at 37 ℃, formazan crystals were dissolved in dimethyl sulfoxide (0.1 mL/well). The plates were mechanically agitated for 5 min and the optical density at 540 nm was determined on the microtiter plate reader. Each experiment was done thrice.

Fluorescence-activated cell sorter (FACS) analysis

Forty-eight hours after transfection, cells were harvested by trypsin digestion, washed twice with cold PBS, and resuspended in 1× binding buffer, regulated to the concentration 1×10^6/mL. Then 100 μL was extracted to a new tube, 5 μL PI and 5 μL annexin V-FITC were added, mixed gently, incubated at 25 ℃ for 15 min. Four hundred microliters of binding buffer was added and analyzed within 1 h with FACS.

RESULTS

SiRNAs expressing vector pSilencer3.0-H1-afp could silence the expression of AFP in hepatoma cells efficiently

To specifically deplete AFP in hepatoma cells, we took advantage of the recently developed vector-based siRNA technology. The targeting sequence of human AFP (GenBank accession no. NM_005030) is 5'-AACTCAGTG-AGGACAAACTAT-3'. The vector pSilencer3.0-H1-*afp*, pSilencer3.0-H1-*gapdh* (positive control) and negative control vector were transfected into SMMC-7721 cells, which were cultured for 48 h, then RT-PCR and AFP in supernatant fluid were assayed. Positive control vector pSilencer3.0-H1-*gapdh* could silence the GAPDH efficiently. The inhibition rate of the positive control plasmid and pSilencer3.0-H1-*afp* was 60% and 34% respectively. In order to confirm the inhibitory effect, we assayed the AFP concentration in the supernatant. The AFP level in the supernatant reduced about 40%, 48 h after transfection. These results showed that the expression of AFP in hepatoma cells was downregulated.

MTT assays and FACS

Figure 1A shows that vector pSilencer3.0-H1-*afp* inhibited the proliferation of SMMC-7721 cells obviously compared to the negative control plasmid, and that the suppression effect was most obvious at 32 h. The results of FACS showed no difference between the negative control and pSilencer3.0-H1-*afp*-treated cells (Figure 1B).

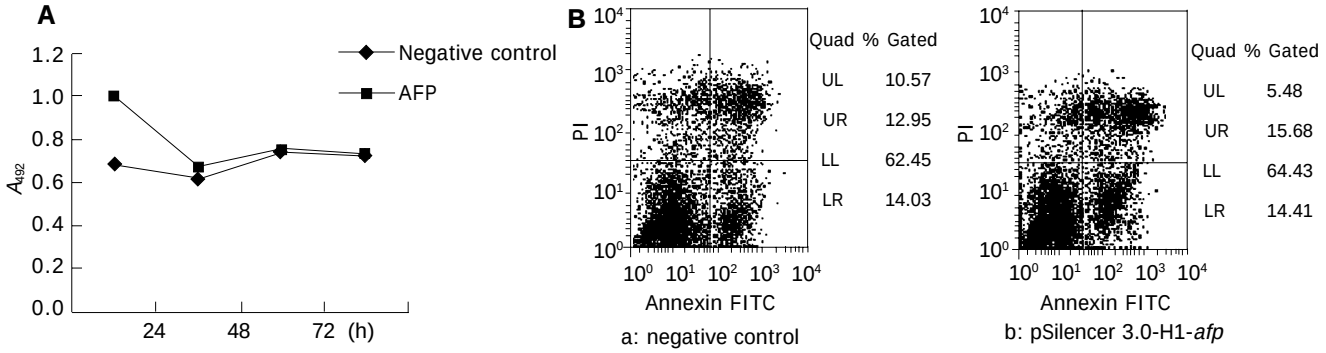


Figure 1 Proliferation (A) and apoptosis (B) of transfected cells. LR indicates the value of cell apoptosis.

DISCUSSION

Since AFP was found in the mid-1950s, this oncofetal protein has been used as a PHCC marker in clinical diagnosis[10]. But its biological activities in mammals still remain unclear. To date, only two functional roles of AFP have been ascertained[10]. In the last decade, the growth regulatory properties of AFP have aroused interests as a result of studies involving ontogenetic and oncogenic growth in both cell cultures and animal models. Particularly, the effect of AFP on the development of experimental tumors in mammals has been investigated *in vivo* with the use of carcinogens[11]. When AFP-treated mice develop larger tumors, they require a longer period for regression and have a significantly higher mortality[10]. Chicken AFP-treated quails develop tumors with shorter latent periods than the untreated quails[8]. The *in vivo* tumor growth stimulation by AFP can be explained by its immunosuppression. Cell-mediated immunity is an important mechanism of host resistance to malignant neoplasms. Recently, anonymous studies found that antihepatoma effects of AFP antisense S-ODNs are more significant in normal mice than in nude mice[10], suggesting that there exists a relationship between AFP and the susceptibility of hepatoma cells to immunity-mediated cytotoxicity. Recent studies indicate that AFP directly stimulates the proliferation of hepatoma cells *in vitro*, independent of its immunosuppression[11].

However, the precise relationship between AFP and PHCC is not clear. AFP is highly expressed in hepatic oval cells during the early stages of carcinogenesis, and high levels of AFP in the fully developed PHCC, or in the serum of the host, are associated with more aggressive behaviors, and increased anaplasia[9]. The present study also demonstrated that silencing the expression of AFP could effectively inhibit the growth of hepatoma cells *in vitro*, suggesting that AFP may play a role in the pathogenesis of PHCC.

The present results indicate that AFP siRNAs expressing plasmid exhibit significant antihepatoma activities *in vitro* by the sequence-specific silencing of AFP gene expression. But the results of FACS have no obvious difference between the negative control and the pSilencer3.0-H1-*afp* treated wells. Therefore, the mechanisms of antihepatoma action of AFP siRNAs expressing plasmid are not through the induction of hepatoma cell apoptosis.

ACKNOWLEDGMENTS

The authors express appreciation to Professor Bing-Yu Mao, Kunming Institute of Zoology, Chinese Academy of Sciences and Senior Lecturer Bin Yu, Sydney University, Australia for their critical revision of the manuscript.

REFERENCES

1 **Colleoni M,** Gaion F, Liessi G, Mastropasqua G, Nelli P, Manente P. Medical treatment of hepatocellular carcinoma: any progress? *Tumori* 1994; **80**: 315-326
2 **Wang W,** Alpert E. Downregulation of phorbol 12-myristate 13-acetate-induced tumor necrosis factor-alpha and interleukin-1beta production and gene expression in human monocytic cells by human alpha-fetoprotein. *Hepatology* 1995; **22**: 921-928
3 **Ogata A,** Yamashita T, Koyama Y, Sakai M, Nishi S. Suppression of experimental antigen-induced arthritis in transgenic mice producing human alpha-fetoprotein. *Biochem Biophys Res Commun* 1995; **213**: 362-366
4 **Jacobson HI,** Bennett JA, Mizejewski GJ. Inhibition of estrogen-dependent breast cancer growth by a reaction product of alpha-fetoprotein and estradiol. *Cancer Res* 1990; **50**: 415-420
5 **Wang XW,** Xie H. Effect of alpha-fetoprotein on the growth of human hepatoma cells *in vitro*. *Shiyan Shengwu Xuebao* 1999; **32**: 15-22
6 **Fire A,** Xu S, Montgomery MK, Kostas SA, Driver SE, Mello CC. Potent and specific genetic interference by double-stranded RNA in Caenorha-bditis elegans. *Nature* 1998; **391**: 806–810
7 **Qi TG,** Wang YS. Construction and identification of a plasmid expressing SiRNAs in mammalian cells aimed at AFP gene. *Shandong Daxue Xuebao* 2004; **42**: 107-109
8 **Yamada A,** Hayami M. Suppression of natural killer cell activity by chicken alpha-fetoprotein in Japanese quails. *J Natl Cancer Inst* 1983; **70**: 735-738
9 **Matsumoto Y,** Suzuki T, Asada I, Ozawa K, Tobe T, Honjo I. Clinical classification of hepatoma in Japan according to serial changes in serum alpha-fetoprotein levels. *Cancer* 1982; **49**: 354-360
10 Wang XW, Yuan JH, Zhang RG, Guo LX, Xie Y, Xie H. Antihepatoma effect of alpha-fetoprotein antisense phosphorothioate oligodeoxyribonucleotides *in vitro* and in mice. *World J Gastroenterol* 2001; **7**: 345-351
11 **Li MS,** Li PF, Chen Q, Du GG, Li G. Alpha-fetoprotein stimulated the expression of some oncogenes in human hepatocellular carcinoma Bel 7402 cells. *World J Gastroenterol* 2004; **15**: 819-824

Science Editor Wang XL and Guo SY **Language Editor** Elsevier HK

PO Box 2345, Beijing 100023, China
www.wjgnet.com
wjg@wjgnet.com

ELSEVIER

World J Gastroenterol 2005;11(38):6056-6060
World Journal of Gastroenterology ISSN 1007-9327
© 2005 The WJG Press and Elsevier Inc. All rights reserved.

• *BRIEF REPORTS* •

Interaction models of *CYP1A1*, *GSTM1* polymorphisms and tobacco smoking in intestinal gastric cancer

Jing Shen, Run-Tian Wang, Yao-Chu Xu, Li-Wei Wang, Xin-Ru Wang

Jing Shen, Yao-Chu Xu, Xin-Ru Wang, Department of Epidemiology and Biostatistics, School of Public Health, Nanjing Medical University, Nanjing 210029, Jiangsu Province, China
Jing Shen, Department of Environmental Health Sciences, Mailman School of Public Health, Columbia University, New York, NY 10032, USA
Run-Tian Wang, Department of Epidemiology and Biostatistics, School of Public Health, Peking University, Beijing 100083, China
Li-Wei Wang, Yang Zhong Cancer Research Institute, Yang Zhong City Municipal Hospital, Yang Zhong 212200, China
Supported by the National Natural Science Foundation of China, No. 30170827 and 30070671
Correspondence to: Dr. Jing Shen, Department of Environmental Health Sciences, Mailman School of Public Health, Columbia University, 701 West 168th Street (Room 505), New York, NY 10032, USA. js2182@columbia.edu
Telephone: +1-212-3058158 Fax: +1-212-3055328
Received: 2005-01-07 Accepted: 2005-04-02

AIM: To explore the interaction models of the cytochrome P-450 (CYP) *1A1 Val* variant and glutathione S-transferase (GST) *M1* null polymorphisms with tobacco smoking in the occurrence of intestinal gastric cancer.

METHODS: A community-based case-control study was conducted in Yangzhong. Subjects included 114 intestinal types of gastric cancer with endoscopic and pathological diagnosis during January 1997 and December 1998, and 693 controls selected from their spouse, siblings or siblings-in-law who had no history of digestive system cancer. Logistic regression was used to estimate the interaction models.

RESULTS: The frequency of the *CYP1A1 Val* variant allele in cases did not differ from that in controls. The OR of *GSTM1* null genotype was 2.0 (95% confidence interval [95%CI]: 1.2-3.1, $P<0.01$). It showed a significant type 2 form of interaction model when both *CYP1A1 Val* variant allele and former tobacco smoking existed (i.e., among the multiplicative effects, the disease risk is increased by the tobacco exposure alone but not by the *CYP1A1* variant alone). The interaction index γ was 2.8, and OR_{eg} (95%CI) was 5.0 (1.9-13.4). *GSTM1* null genotype and former tobacco smoking were significant in a type 4 interaction model (i.e., the disease risk is increased by *GSTM1* null genotype or tobacco exposure alone among the multiplicative effects). The interaction index γ and OR_{eg} (95%CI) were 3.4 and 8.4 (3.4-20.9), respectively.

CONCLUSION: Different interaction models of *CYP1A1 Val* variant allele and *GSTM1* null genotype with tobacco smoking will contribute to understanding carcinogenic mechanism, but there is a need to further investigate in larger scale studies.

© 2005 The WJG Press and Elsevier Inc. All rights reserved.

Key words: Interaction models; *CYP1A1*; *GSTM1*; Tobacco smoking; Intestinal gastric cancer

Shen J, Wang RT, Xu YC, Wang LW, Wang XR. Interaction models of *CYP1A1*, *GSTM1* polymorphisms and tobacco smoking in intestinal gastric cancer. *World J Gastroenterol* 2005; 11(38): 6056-6060
http://www.wjgnet.com/1007-9327/11/6056.asp

INTRODUCTION

Worldwide, gastric cancer is the second in rank overall (798 000 new cases per year), and ranks second in males, fourth in females. It remains the most common malignancy in many countries of the world[1,2], though the frequency of incidence and mortality is declining in almost all populations. Thirty-eight percent of gastric cancer cases occurred in China, where it remains to be most common and is the leading cause of cancer death in both sexes[1]. Yangzhong is among the areas with the highest gastric cancer mortality and incidence rate in south-east of China[3]. The crude mortality rate of gastric cancer changed from 96.9 to 110.9/100 000 during 1991 and 1997, and the average adjusted incidence rate in the same period was over 115/100 000 (unadjusted rate is 155.5/100 000). Previous studies have shown that high incidence rate of gastric cancer is associated with exposure to environmental factors (tobacco, alcohol consumption, and *H pylori* infection), and individual susceptibility[2,4].

Genetic polymorphisms in cytochrome P-450 (CYP) *1A1* and glutathione S-transferase (GST) *M1* genes that metabolize known and potentially carcinogenic environmental exposures may affect enzymatic activities and alter an individual's ability to metabolize pro-carcinogenic and related compounds, which may change the biologic effect of exposures[5]. A large number of studies have examined the role of polymorphisms in *CYP1A1*, *GSTM1*, and cancer risk, including gastric cancer[6-10], but the results are equivocal[11–14]. The interaction between *GSTM1* null genotype and tobacco smoking for the risk of gastric cancer has only been explored in three studies, with inconsistent evidence of departure from a

multiplicative model, possibly because of the small size (70, 91, and 136 gastric cancer cases, respectively), and the gene-environmental interaction (GEI) models best describing the risk of gastric cancer is not clear[6,11,14]. For this reason, we conducted a community-based case-control study in a Chinese population. Genetic polymorphisms in *CYP1A1* and *GSTM1* were analyzed to test the hypothesis that these genotypes have different interaction models with tobacco smoking in the development of intestinal gastric cancer.

[illegible]

Subjects

All gastric cancer patients and controls in this study are Han ethnic Chinese selected from Yangzhong County. Gastric cancer was prevalent in cases diagnosed according to International Classification of Diseases for Oncology IX, code = 151, and classified by the criteria of Laurén[15]. One hundred and fourteen intestinal gastric cancer patients (76 men and 38 women; mean age and SD 59.4±9.9 years) were identified by endoscopic and pathological diagnosis in Yangzhong City Municipal Hospital from January 1997 to December 1998. To reduce misclassification of the histological types, two pathologists reviewed and confirmed all diagnosed cases. Controls were selected from case's siblings (150 male and 140 female) and non-blood relatives (403 spouses and the siblings-in-law, 160 male and 243 female) without digestive tract cancers. Both kinds of controls differed slightly in demographic features, and their results were combined to increase the sample size and decrease type I error. The study was approved by the regional ethics committees of Yangzhong. All participants were given an explanation of the study and informed consent was obtained. Study subjects completed a questionnaire administered by specially trained interviewers through a face-to-face interview. The questionnaire was designed to elicit detailed information on tobacco smoking habit, alcohol drinking habit, family history of cancer, and occupational exposures. Cigarette smokers were defined as subjects who reported smoking of at least one cigarette per day for 1 year or more, or whose accumulated tobacco cigarette consumption was over 18 packs per year. Former smokers were those who had stopped smoking for one or more years before the interview. Cumulative smoking exposure (pack years) was defined as one pack per day for 1 year equals 1 pack years.

CYP1A1 and GSTM1 genotypes

DNA extraction was performed using Puregene DNA isolation kits (Gentra Systems, Minneapolis, MN, USA). PCR-RFLP approach was used to detect the 7th *CYP1A1 Ile/Val* variant at position 4 889. PCR was used to amplify the transcription regulatory region of *CYP1A1* that includes the restriction enzyme recognition site for *Hin*cII. The two allele-specific primers are respectively F5'-TCCT ACCTG-AACGGTTTCTCACCC-3' (T_m = 63.0) and R5'-TTTTTT-TTTTTGAAAGACCTCCCAGG GGTCA-3' (T_m = 65.1) modified from those previously reported[16]. The homozygous null polymorphism of *GSTM1* was determined using a PCR approach as previously reported[16].

Statistical analysis

The relative associations between cases and controls were assessed by crude odds ratio (OR), interaction OR_{eg} and the corresponding 95%CI. Unconditional logistic regression analysis was performed to assess the association between the *CYP1A1 Ile/Val* and *GSTM1* null polymorphism and intestinal gastric cancer after adjusting for confounding factors. All models included as co-variables: gender, age (entered as a continuous variable), living areas (relative lower or higher incidence areas in Yangzhong), education level (years), former tobacco smoking, former alcohol drinking, BMI (weight [kg]/height [m^2]) and family history of cancer. Test of trend was calculated through logistic models based on semi-continuous and dummy variables. A common way to describe the interaction between the effect of an environmental agent and a genetic risk factor is to use a term called interaction index (γ), which is determined by coefficient (β) in a multiple logistic regression model. The coefficient of this interactive term was calculated according to the method of Taioli *et al*.[17]. If the types of interaction belong to multiplicative effects suggested by Khoury and Ottman[18-20], it included several types of interactions. Such as type 1 interaction which means that the disease risk is increased only in the presence of the genotype and the environmental exposure. Type 2 interaction: the disease risk is increased by the environmental exposure alone but not by the genotype alone. Type 3 interaction: the disease risk is increased by the genotype in the absence of the environmental exposure but not by the environment alone. Type 4 interaction means that the disease risk is increased by genotype or environmental exposure alone[18-20]. False positive report probability (FPRP) was used as an index for judging the noteworthy or not noteworthy results at the 0.5 FPRP level among significant GEI results[21]. All data analysis was performed with the SAS package Genmod (SAS Institute, Cary, NC, USA) for the personal computer.

[illegible]

CYP1A1, GSTM1 polymorphisms and risk of intestinal gastric cancer

Compared with controls, patients were significantly older (median age 59 years for cases and 53 years for controls) and with a BMI less than 20. Former tobacco smoking is significantly associated with the risk of intestinal gastric cancer (OR = 2.4, 95%CI: 1.0-5.8). A significant dose-response was observed in relation to increasing gastric cancer risk, especially in 20 pack-years or more smokers (Table 1). The frequencies of *CYP1A1 Ile/Val* and *Val/Val* genotypes in controls were 33.4% and 5.6%, respectively, which showed no significant difference from that in cases (32.1% and 5.4%, respectively). The homozygote null *GSTM1* genotype was observed in 63.4% of cases, which was significantly higher than that in controls (53.5%). The adjusted OR was 2.0 (95%CI: 1.2-3.1).

Interaction models of CYP1A1 and GSTM1 polymorphisms with former tobacco smoking

Among former tobacco smokers with *CYP1A1 Ile* or *GSTM1* present genotypes, the OR_{eg} of intestinal gastric

Table 1 Characteristics of the interviewed subjects

	Characteristics	Gastric cancer cases (114)	Control subjects (693)	OR (95%CI)
Median age	yr±SD	59±10	53±10	1.1 (1.0-1.1) [1]
	Min (yr)	35	30	
	Max (yr)	82	78	
Gender	Female (%)	38 (33)	383 (55)	1.0 (Ref.)
	Male (%)	76 (67)	310 (45)	1.2 (0.7-2.1)
	F/M ratio	1:2	1:0.8	
Educational level	>5 yr	44 (38.6)	246 (35.5)	1.0 (Ref.)
	≤5 yr	70 (61.4)	447 (64.5)	1.0 (0.6-1.7)
Occupation				
	Manual	51 (44.7)	375 (54.1)	1.0 (Ref.)
	Office	9 (7.9)	87 (12.6)	0.6 (0.2-1.3)
	Retired	54 (47.4)	231 (33.3)	1.2 (0.7-1.9)
Marriage status				
	Married	100 (87.7)	649 (94.7)	1.0 (Ref.)
	Divorce or bereft spouse	14 (12.3)	36 (5.3)	1.4 (0.6-3.0)
Family history of cancer				
	No	84 (76.4)	613 (90.3)	1.0 (Ref.)
	Yes	26 (23.6)	66 (9.7)	3.9 (2.1-7.3) [1]
BMI (kg/m^2)				
	<20	56 (49.1)	95 (13.7)	1.0 (Ref.)
	20-	44 (38.6)	254 (36.7)	0.3 (0.2-0.5)[1]
	23-	14 (12.3)	344 (49.6)	0.1 (0.03-0.12)[1]
Tobacco smoking habits				
	Never	51 (44.7)	437 (63.0)	1.0 (Ref.)
	Current	36 (31.6)	225 (32.5)	0.6 (0.3-1.3)
	Former	27 (23.7)	31 (4.5)	2.4 (1.0-5.8)[1]
Amount of former smoking (pack years)				
	No	87 (76.4)	662 (95.6)	1.0 (Ref.)
	1-19	7 (6.1)	10 (1.4)	2.6 (0.8-8.6)
	20-29	8 (7.0)	11 (1.6)	3.1 (1.1-9.0)[1]
	≥30	12 (10.5)	10 (1.4)	4.4 (1.7-11.9)[1]
Alcohol drinking habits				
	Never	78 (68.5)	505 (72.9)	1.0 (Ref.)
	Current	11 (9.6)	156 (22.5)	0.2 (0.1-0.5)[1]
	Former	25 (21.9)	32 (4.6)	2.3 (1.2-4.7)[1]
Plasma *H pylori* CagA antibody				
	Negative	136 (82.4)	107 (49.3)	1.0 (Ref.)
	Positive	29 (17.6)	110 (50.7)	0.2 (0.1-0.3)[1]
CYP1A1 genotype				
	Ile/Ile	70 (62.5)	412 (61.0)	1.0 (Ref.)
	Ile/Val	36 (32.1)	226 (33.4)	0.9 (0.5-1.4)
	Val/Val	6 (5.4)	38 (5.6)	0.7 (0.2-1.8)
GSTM1 genotype				
	Present	41 (36.6)	314 (46.5)	1.0 (Ref.)
	Null	71 (63.4)	361 (53.5)	2.0 (1.2-3.1) [1]

[1]Showed significant difference after adjusting co-variables.

cancer were 1.8 and 3.5, respectively. With both exposure to tobacco smoking and the *CYP1A1 Val* allele or *GSTM1* null genotype, the OR_{eg} of suffering intestinal gastric cancer increased sharply, 5.0 (95%CI: 1.9-13.4) and 8.4 (95%CI: 3.4-20.9), respectively. The γ were 2.8 and 3.4, respectively, which showed multiplicative effects of type 2 GEI model for *CYP1A1* and type 4 model for *GSTM1* (Table 2).

Assessment of the probability of a potential positive result

A high FPRP (e.g., >0.5) could be a consequence of any combination of a low prior probability, low statistical power, or a relatively high *P* value[21]. We calculated FPRP to assess the probability that a positive result might be false using the observed *P* value or CI for the observed ORs, and to determine whether to consider a significant finding to be noteworthy with the specific prior probability (Table 3). The results showed that the FPRP was less than 0.5 for *GSTM1* null and former smokers, which indicated the most noteworthy finding in the present study even with a prior probability between 0.0001 and 0.00001.

□□□□□□□□□□

A large number of molecular epidemiological studies completed in the past decade have identified the relative etiologic roles of the *CYP1A1 Val* variant allele and *GSTM1* null genotype for cancer risk (including gastric cancer), although some results indicate no overall associations, only specific relationships were found in subgroups, such as in smokers, *H pylori*-infected patients or low consumption of

Table 2 Interaction models of *CYP1A1* and *GSTM1* polymorphism with former smoker in intestinal gastric cancer

Genotype	Former smoker	Cases	Controls	OR_{og}	95%CI
Ile[1]	No	57	391	1.0	Ref.
Val[2]	No	29	254	0.7	0.4-1.1
Ile	Yes	13	21	1.8	0.7-4.3
Val	Yes	13	10	5.0[5]	1.9-13.4
Present[3]	No	31	302	1.0	Ref.
Null[4]	No	54	345	1.9	1.1-3.1
Present	Yes	10	12	3.5	1.2-10.1
Null	Yes	17	16	8.4[6]	3.4-20.9

[1][*Ile*]: *CYP1A1* homozygous (*Ile*/*Ile*) genotype; [2][*Val*]: *CYP1A1* heterozygous (*Ile*/*Val*)+homozygous (*Val*/*Val*) genotypes; [3][present]: present genotype for *GSTM1*; [4][null]: null genotype for *GSTM1*; [5]adjusted by age, gender, living areas, family history of cancer, and former alcohol drinking; $\chi^2_{trend} = 24.0$, df = 1, $P = 0.00$; $\gamma = 1.61/0.57 = 2.8$; [6]adjusted by age, gender, living areas, family history of cancer, and former alcohol drinking; $\chi^2_{trend} = 45.7$, df = 1, $P = 0.00$; $\gamma = 2.13/0.63 = 3.4$.

Table 3 FPRP values for interactions between GSTM1 and former tobacco smoking in intestinal gastric cancer

GSTM1	Former	Observed	Assuming	Prior probability					
genotype	Smoking	OR	OR	0.25	0.1	0.01	0.001	0.0001	0.00001
GSTM1 null	No	1.9	1.2	0.481[1]	0.736[2]	0.968	0.997	1.000	1.000
			1.5	0.151	0.348	0.854	0.983	0.998	1.000
			2.0	0.050	0.136	0.634	0.946	0.994	0.999
GSTM1 present	Yes	3.5	2.4	0.202	0.432	0.893	0.988	0.999	1.000
			3.0	0.137	0.322	0.840	0.981	0.998	1.000
			4.0	0.093	0.236	0.773	0.972	0.997	1.000
GSTM1 null	Yes	8.4	4.8	0.000	0.000	0.004	0.040	0.293	0.805
			6.0	0.000	0.000	0.002	0.020	0.168	0.669
			8.4	0.000	0.000	0.001	0.009	0.087	0.487

[1]Bold with gray fill color indicate "noteworthy at the 0.5 FPRP level"; [2]with no fill color indicate "not noteworthy at the 0.5 FPRP level".

fruit[6-10]. Other studies have reported contrary findings[11-14]. These inconsistent results might be contributed to ethnically diverse populations involved in studies, different histological subtypes of cases used, and different co-variables categorized the sub-population. Until now, only a few studies discussed interactions between tobacco smoking and the polymorphisms in the occurrence of gastric cancer[6,11,14]. In the present study, we observed some evidence of a relationship between *GSTM1* null genotype and a risk of gastric cancer. Both the *CYP1A1 Val* variant allele and *GSTM1* null polymorphism have statistically significant interactions with former tobacco smoking. The GEI model of *CYP1A1* with smoking belongs to type 2, and *GSTM1* with smoking belongs to type 4 as Khoury and Ottman described. Present study as most molecular epidemiology studies based on multiple comparison corrective procedures is relied on the standard *P* value criterion of 0.05 to define statistical significance without consideration of power or prior probability, which may create a lot of false positives[21]. We further calculated FPRP as one of indices to decide about whether a positive finding in association study can be called "a noteworthy finding" or "deserve of more attention". We confirmed that the interaction between *GSTM1* null and former smokers was the most noteworthy positive finding in the present study even with a prior probability less than 0.0001. The interaction between *CYP1A1 Val* variant allele and former smokers was also a possible noteworthy positive finding with a prior probability less than 0.01 (data not shown). These results suggest that the risk of intestinal gastric cancer was greatly dependent upon both tobacco smoking exposures and susceptibility genes. Only complete smoking cessation may decrease susceptibility to gastric cancer in persons carrying the *CYP1A1 Val* variant allele or *GSTM1* null genotype. The different types of GEI models indicated that the interactions between genes and environmental factors are neither simply gene specific, nor exposure specific, and must be related to the mechanism of action of the gene product and features of exposure leading to gastric cancer.

Although the mechanism for tobacco-related gastric cancer risk is not well understood, tobacco-specific nitrosamines and other nitroso-compounds, plus other carcinogens contained in tobacco and tobacco smoke, are swallowed and may thus be involved in the process of gastric carcinogenesis[22,23]. Among gastric cancer cases, smoking-related DNA-adduct levels were higher in smokers than in non-smokers[24], and a study in China found smoking to be a risk factor for intestinal metaplasia and gastric dysplasia arising from chronic atrophic gastritis[25]. The biological mechanisms responsible for different interaction models observed in our study were not known, but it was possible to speculate that these interaction effects might be a reflection for individuals with and without environmental susceptible genotypes. This analytical approach may be used to determine higher risk individuals and take further preventive measures to decrease cancer risks in these susceptible individuals.

One limit of the study is the small number of subjects in some cells when GEI models were analyzed. The models resulting from the present study might be affected by chance, and need to be identified by more large-scale molecular epidemiological studies. Another potential limit was the

selection of controls, which include case's siblings. This kind of selection might create over-matching because siblings were more likely to have the same genotypes as cases than non-related controls, therefore leading to some loss of statistical efficiency, i.e. larger sample sizes required to attain the same statistical precision[26]. But others consider that the use of sibling controls generally improves efficiency for GEI evaluations[27,28].

In conclusion, our studies identified two kinds of GEI models between the *CYP1A1 Val* variant allele, *GSTM1* null genotype and tobacco smoking. Although the proposed carcinogen metabolism pathway seems a plausible explanation of our findings, further large studies are required to replicate these observations.

ACKNOWLEDGMENTS

We thank Zhaoxi Wang for his excellent technical assistance; thank Professor Regina M Santella for editing the manuscript. We also thank all the doctors for their kind help in collecting the biological samples and epidemiological data. We thank all participants in our study for their cooperation.

REFERENCES

1 **Parkin DM**. The global burden of cancer. *Seminars Cancer Biol* 1998; **8**: 219-235
2 **Stadtlander CT**, Waterbor JW. Molecular epidemiology, pathology and prevention of gastric cancer. *Carcinogenesis* 1999; **20**: 2195-2207
3 **Setiawan VW**, Zhang ZF, Yu GP, Lu QY, Li YL, Lu ML, Wang MR, Guo CH, Yu SZ, Kurtz RC, Hsieh CC. GSTP1 polymorphisms and gastric cancer in a high-risk Chinese population. *Cancer Causes Control* 2001; **12**: 673-681
4 **Zhang ZF**, Kurtz RC, Klimstra DS, Yu GP, Sun M, Harlap S, Marshall JR. *Helicobacter pylori* infection on the risk of stomach cancer and chronic atrophic gastritis. *Cancer Detect Prev* 1999; **23**: 357-367
5 **Nebert DW**, Ingelman-Sundberg M, Daly AK. Genetic epidemiology of environmental toxicity and cancer susceptibility: human allelic polymorphisms in drug-metabolizing enzyme genes, their functional importance, and nomenclature issues. *Drug Metab Rev* 1999; **31**: 467-487
6 **Tamer L**, Ates NA, Ates C, Ercan B, Elipek T, Yildirim H, Camdeviren H, Atik U, Aydin S. Glutathione S-transferase M1, T1 and P1 genetic polymorphisms, cigarette smoking and gastric cancer risk. *Cell Biochem Funct* 2005; 23: 267-272
7 **Gonzalez CA**, Sala N, Capella G. Genetic susceptibility and gastric cancer risk. *Int J Cancer* 2002; **100**: 249-260
8 **Parl FF**. Glutathione S-transferase genotypes and cancer risk. *Cancer Lett* 2005; **221**: 123-129
9 **Agundez JA**. Cytochrome P450 gene polymorphism and cancer. *Curr Drug Metab* 2004; **5**: 211-224
10 **Ng EK**, Sung JJ, Ling TK, Ip SM, Lau JY, Chan AC, Liew CT, Chung SC. *Helicobacter pylori* and the null genotype of glutathione-S-transferase-mu in patients with gastric adenocarcinoma. *Cancer* 1998; **82**: 268-273
11 **Deakin M**, Elder J, Hendrickse C. Glutathione S-transferase GSTT1 genotypes and susceptibility to cancer: studies of interactions with GSTM1 in lung, oral, gastric and colorectal cancers. *Carcinogenesis* 1996; **17**: 881-884
12 **Suzuki S**, Muroishi Y, Nakanishi I, Oda Y. Relationship between genetic polymorphisms of drug-metabolizing enzymes (CYP1A1, CYP2E1, GSTM1, and NAT2), drinking habits, histological subtypes, and p53 gene point mutations in Japanese patients with gastric cancer. *J Gastroenterol* 2004; **39**: 220-230
13 **Wu MS**, Chen CJ, Lin MT, Wang HP, Shun CT, Sheu JC, Lin JT. Genetic polymorphisms of cytochrome p450 2E1, glutathione S-transferase M1 and T1, and susceptibility to gastric carcinoma in Taiwan. *Int J Colorectal Dis* 2002; **17**: 338-343
14 **Setiawan VW**, Zhang ZF, Yu GP, Li YL, Lu ML, Tsai CJ, Cordova D, Wang MR, Guo CH, Yu SZ, Kurtz RC. GSTT1 and GSTM1 null genotypes and the risk of gastric cancer: a case-control study in a Chinese population. *Cancer Epidemiol Biomarkers Prev* 2000; **9**: 73-80
15 **Lauren P**. The two histological main types of gastric carcinoma: diffuse and so-called intestinal-type carcinoma. An attempt at a histoclinical classification. *Acta Pathol Microbiol Scand* 1965; **64**: 31-49
16 **Morita S**, Yano M, Shiozaki H, Tsujinaka T, Ebisui C, Morimoto T, Kishibuti M, Fujita J, Ogawa A, Taniguchi M, Inoue M, Tamura S, Yamazaki S, Kikkawa N, Mizunoya S, Monden M. CYP1A1, CYP2E1 and GSTM1 polymorphisms are not associated with susceptibility to squamous-cell carcinoma of the esophagus. *Int J Cancer* 1997; **71**: 192-195
17 **Taioli E**, Zocchetti C, Garte S. Models of interaction between metabolic genes and environmental exposure in cancer susceptibility. *Environ Health Perspect* 1998; **106**: 67-70
18 **Khoury MJ**, James LM. Population and familial relative risks of disease associated with environmental factors in the presence of gene-environment interaction. *Am J Epidemiol* 1993; **137**: 1241-1250
19 **Khoury MJ**, Wagener DK. Epidemiological evalution of the use of genetics to improve the predictive value of disease risk factors. *Am J Hum Genet* 1995; **56**: 835-844
20 **Ottman R**. An epidemiologic approach to gene-environment interaction. *Genet Epidemiol* 1990; **7**: 177-185
21 **Wacholder S**, Chanock S, Garcia-Closas M, El Ghormli L, Rothman N. Assessing the probability that a positive report is false: an approach for molecular epidemiology studies. *J Natl Cancer Inst* 2004; **96**: 434-442
22 **Hecht SS**, Hoffmann D. The relevance of tobacco-specific nitrosamines to human cancer. *Cancer Surv* 1989; **8**: 273-294
23 **Hecht SS**. Tobacco smoke carcinogens and lung cancer. *J Natl Cancer Inst* 1999; **91**: 1194-1210
24 **Dyke GW**, Craven JL, Hall R, Garner RC. Smoking-related DNA adducts in human gastric cancers. *Int J Cancer* 1992; **52**: 847-850
25 **Kneller RW**, You WC, Chang YS, Liu WD, Zhang L, Xu GW, Fraumeni JF, Blot WJ. Cigarette smoking and other risk factors for progression of precancerous stomach lesion. *J Natl Cancer Inst* 1992; **84**: 1261-1266
26 **Thomas DC**, Witte JS. Point: population stratification: a problem for case-control studies of candidate-gene associations? *Cancer Epidemiol Biomarkers Prev* 2002; **11**: 505-512
27 **Gauderman W**, Witte J, Thomas D. Family-based association studies. *Monogr Natl Cancer Inst* 1999; **26**: 31-37
28 **Witte JS**, Gauderman WJ, Thomas DC. Asymptotic bias and efficiency in case-control studies of candidate genes and gene-environment interactions: basic family designs. *Am J Epidemiol* 1999; **148**: 693-705

Science Editor Guo SY **Language Editor** Elsevier HK

PO Box 2345, Beijing 100023, China
www.wjgnet.com
wjg@wjgnet.com

ELSEVIER

World J Gastroenterol 2005;11(38):6061-6065
World Journal of Gastroenterology ISSN 1007-9327
© 2005 The WJG Press and Elsevier Inc. All rights reserved.

• *BRIEF REPORTS* •

Effect of peroxisome proliferator-activated receptor-gamma ligand on inflammation of human gallbladder epithelial cells

Guang-Dong Pan, Hong Wu, Jiang-Wen Liu, Nan-Sheng Cheng, Xian-Ze Xiong, Sheng-Fu Li, Guo-Fu Zhang, Lu-Nan Yan

Guang-Dong Pan, Hong Wu, Jiang-Wen Liu, Nan-Sheng Cheng, Xian-Ze Xiong, Lu-Nan Yan, Department of General Surgery, West China Hospital, Sichuan University, Chengdu 610041, Sichuan Province, China
Sheng-Fu Li, Laboratory of Transplant and Immunology, West China Hospital, Sichuan University, Chengdu 610041, Sichuan Province, China
Guo-Fu Zhang, Laboratory of Isotope, West China Hospital, Sichuan University, Chengdu 610041, Sichuan Province, China
Supported by the Grants From the Scientific Research Foundation for Returned Overseas Chinese Scholars, Education Ministry of China, No. 2001-345
Co-first-authors: Guang-Dong Pan and Hong Wu
Correspondence to: Dr. Guang-Dong Pan, PO Box 119, West China Medical University, Chengdu 610041, Sichuan Province, China. pgdhx@126.com
Telephone: +86-28-88054973
Received: 2004-08-30 Accepted: 2005-01-14

ABSTRACT

AIM: To investigate the effect of peroxisome proliferator-activated receptor gamma (PPAR-γ) and its ligand, ciglitazone, on inflammatory regulation of human gallbladder epithelial cells (HGBECs) and to assess the effect of human epithelial growth factor (hEGF) on growth of HGBECs.

METHODS: HGBECs were cultured in media containing hEGF or in hEGF-free media. HGBECs were divided into normal control group, inflammatory control group and ciglitazone group (test group). Inflammatory control group and ciglitazone group were treated with 5 μg/L of human interleukin-1β (hIL-1β) to make inflammatory model of HGBECs. The ciglitazone group was treated with various concentrations of ciglitazone, a potent ligand of PPAR-γ. Subsequently, interleukin-8 (IL-8), IL-6, and tumor necrosis factor-α (TNF-α) concentrations in all groups were measured. The data were analyzed statistically.

RESULTS: HGBECs were cultured in medium successfully. The longevity of HGBECs in groups containing hEGF was longer than that in hEGF-free groups. So was the number of HGBECs. The longest survival time of HGBEC was 25 d. The inflammatory model of HGBECs was obtained by treating with hIL-1β. The concentrations of IL-6 and IL-8 in ciglitazone group were lower than those in inflammatory control group ($P<0.05$). The secretion of IL-6 in inflammatory control group was higher (350.31±37.05 μg/L) than that in normal control group (50.0±0.00 μg/L, $P<0.001$). Compared to normal control group, IL-8 concentration in inflammatory control was higher ($P<0.05$).

CONCLUSION: hEGF improves the growth of HGBECs *in vitro*. Ciglitazone inhibits the inflammation of HGBECs *in vitro* and has potential therapeutic effect on cholecystitis *in vivo*.

© 2005 The WJG Press and Elsevier Inc. All rights reserved.

Key words: PPAR-γ; Human gallbladder epithelial cells; Inflammation; Effect

Pan GD, Wu H, Liu JW, Cheng NS, Xiong XZ, Li SF, Zhang GF, Yan LN. Effect of peroxisome proliferator-activated receptor-gamma ligand on inflammation of human gallbladder epithelial cells. *World J Gastroenterol* 2005; 11(38): 6061-6065
http://www.wjgnet.com/1007-9327/11/6061.asp

INTRODUCTION

The peroxisome proliferator-activated receptor-γ (PPAR-γ) is a member of the nuclear receptor superfamily of ligand-dependent transcription factors[1]. With ligand binding, PPAR-γ forms a heterodimer with the retinoid X receptor-α (RXR-α) and joins to the PPAR response element in promoters of target genes, thus directly regulating their expressions[2]. PPAR-γ plays an important role in cell growth, differentiation, inflammation, and apoptosis. Binding to its ligand, PPAR-γ is associated with the regulation of cardiovascular disease, diabetes, and carcinogenesis[3]. Expression in many kinds of cells such as colon epithelial cells, monocytes, hepatic stellate cells, aortic smooth-muscle cells, thyrocytes, and airway epithelial cells, PPAR-γ gene can regulate their inflammation[4-8].

The commonly used method to elucidate the physiological role of PPAR-γ is to investigate the effects of its well-characterized ligands. The most specific PPAR-γ agonists are thiazolidinediones (TZDs)-insulin-sensitizing drugs including pioglitazone, rosiglitazone, troglitazone, and ciglitazone[9]. Previously, cyclopentenone prostanoids were thought to be the most potent one among the naturally occurring PPAR-γ activators[10]. However, 15d-PGJ2 is proved to be a potent inducer of interleukin-6 (IL-6) and IL-8 production and can be a mediator of inflammatory response recently, but this effect is independent of PPAR-γ activation[11].

In activated macrophages and vascular smooth muscle cells, the agonists of PPAR-γ inhibit the expression of many proinflammatory genes, like inducible nitric oxide synthase (iNOS), tumor necrosis factor-α (TNF-α), IL-6 or metalloproteinase-9. Endothelium lines, the inner surface of blood vessels, and is a primary target for inflammatory

agents. Exposure of endothelial cells to cytokines or bacterial lipopolysaccharide (LPS) induces the secretion of proinflammatory mediators, among them both IL-6 and IL-8 are crucial to acute inflammation[12,13]. IL-6 and IL-8 are produced either by endothelial cells directly or by endothelial cells activated by human interleukin-1β (hIL-1β) and TNF-α[14].

The present study was to investigate whether and how the PPAR-γ agonist, ciglitazone, one of the TZDs, affected the inflammatory regulation of human gallbladder epithelial cells (HGBECs). The effect was assessed by changes of IL-6, IL-8, and TNF-α in media after being treated with ciglitazone and IL-1β in order to determine the potential therapeutic function of PPAR-γ agonists for cholecystitis.

[illegible]

Materials

Dulbecco's modified Eagle's medium (DMEM), antibiotic-antimycotic solution, trypsin-ethylenediaminetetraacetic acid (EDTA) were purchased from Gibco BRL Life Technologies. Epidermal growth factor (EGF), type IV collagenase were purchased from Sigma Chemical Co. hIL-1β was purchased from Roche Biology Co. Ciglitazone was purchased from Cayman Chemical Co. IL-8, IL-6 RIA kit and TNF-α RIA kit were purchased from East Asia Radio-immunology Institution, Beijing, China. The lower detection limit of the assay was 0.3 μg/L for TNF-α, 50 μg/L for IL-6, and 0.2 μg/L for IL-8.

Cell isolation and primary culture

The isolation of HGBECs was processed immediately after its surgical removal. Bile was aspirated through a cannula placed in the cystic duct and the mucosal cavity was washed repeatedly with cold PBS containing 10^5 U/L penicillin and 100 mg/L streptomycin. Subsequently, 15 mL of 2.5 g/L trypsin-EDTA was introduced into the gallbladder and then placed in a sterile glass container immersed in a water bath at 37 ℃ for 20 min. Trypsin treatment led to a clear separation of the lining columnar epithelial cells from the underlying fibrous connective tissue. The cells were further dissociated by agitating in a turbulent stream of culture medium containing the pepsin for 5-10 min. The cell suspension was then centrifuged at 4 000 r/min for 5 min and the pellet was washed twice with DMEM containing 100 mL/L FCS. Subsequently, the cells were counted and tested for viability using concentrated trypan blue solution. In a typical study, >95% of cells would exclude trypan blue. Cells were placed on the Vitrogen-100 coated 24-well culture plate with DMEM containing 100 mL/L FCS, 10 μg/L human epithelial growth factor (hEGF) as test groups. Another 24-well cells were cultured in media without hEGF as control groups. Cell concentration was $(5\text{-}10)\times10^5$/mL. After being incubated for 2 h, media were changed to exclude non-epithelial cells. Media were changed after 48 h and subsequently, the cells were fed every 3 d.

Cells in three wells were digested by 2.5 g/L trypsin/0.1 g/L EDTA and counted every 24 h for 3 d to protract cell growth curve. Cells were studied serially by inverted phase microscopy and immunohistochemical reaction with epithelial keratins.

Cell group and treatment

HGBECs obtained through the above procedure were incubated in DMEM supplemented with 100 mL/L FCS, 10 μg/L hEGF, 10^5 U/L of penicillin, 10 mg/L of streptomycin at 37 ℃ in 50 mL/L CO_2. They were placed into 48-well culture plates in 5×10^5/mL of cell density. Then, they were randomly divided into normal control group, inflammatory control group, test group 1, test group 2, test group 3, and test group 4, among which each group had 8 wells containing 2 mL of media in a well. On the 5th d of culture, media were changed to DMEM without hEGF. Various final concentrations including 10, 20, 30, 50 mmol/L of ciglitazone were added into test groups 1-4, respectively. Cells were incubated in DMEM at 37 ℃ in 50 mL/L CO_2. The cells were treated with ciglitazone and incubated for 24 h, then inflammatory control group and all test groups were treated with the final concentration 5 μg/L of hIL-1β. Media were collected after 2-h incubation for measuring concentration of IL-6, TNF-α, and IL-8 by radioimmunoassay. Cell morphology was studied serially by inverted phase contrast microscopy.

Statistical analysis

The data were analyzed by Student's *t*-test for paired sample, by ANOVA for multiple comparison between groups. The statistical significance of the difference between mean values was determined by the *P* value less than 0.05.

[illegible]

Growth and conformation of cultured cells

HGBECs were cultured successfully in DMEM containing hEGF or without hEGF. In groups containing hEGF, the number of HGBECs reached the peak on the 5th d of culture and maintained for 10-12 d. After 20 d, apoptosis of HGBECs was noted. The longest longevity of HGBECs was 25 d. Compared to hEGF-free group, the growth and number of HGBECs were increased by hEGF (Figure 1).

After 6 h of culture, HGBECs attached to the monolayer were flat and multiangular in morphology. Some of the HGBECs were columnar with vigorous growth (Figure 2A). After 20 d of culture, vacuoles and drawbenches were found in cytoplast.

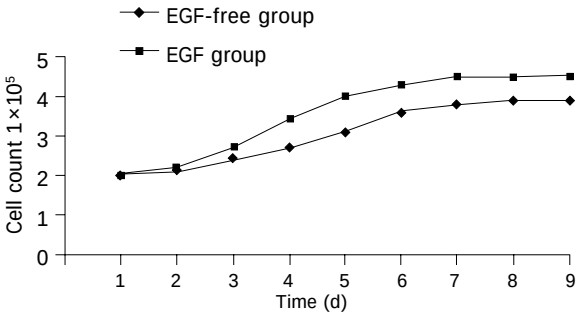


Figure 1 Growth curve of HGBECs.

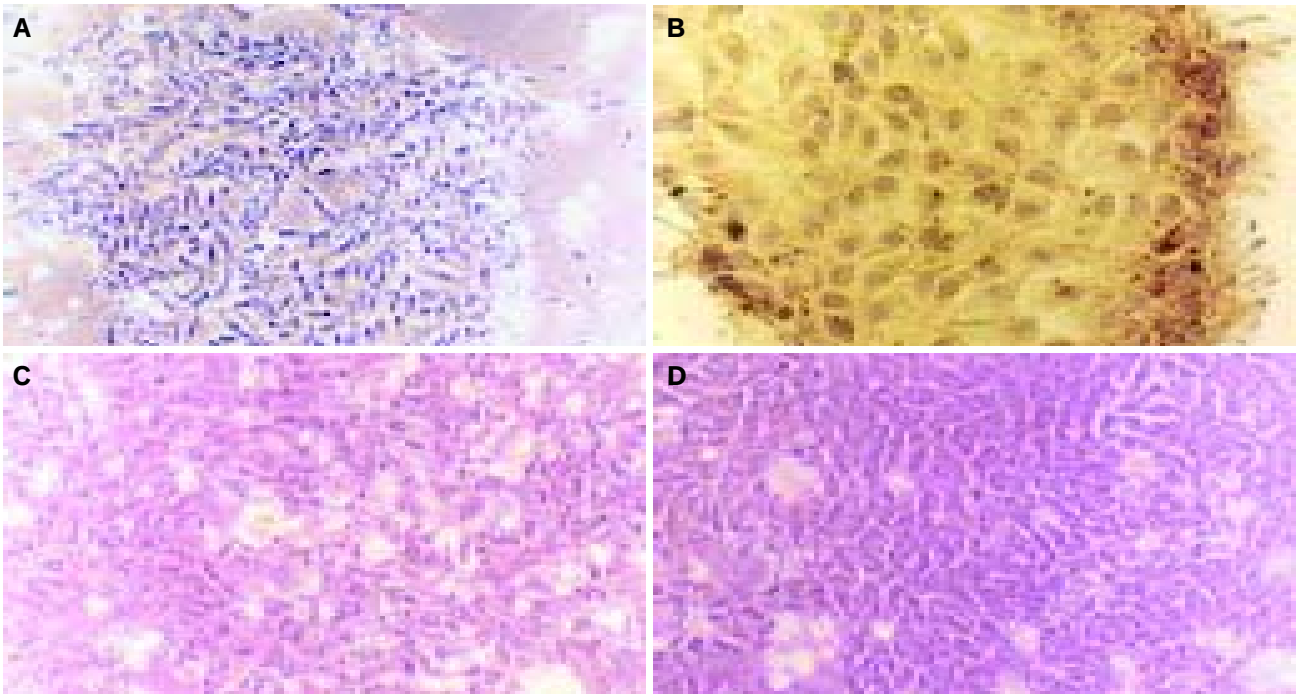


Figure 2 Attachment to monolayer (A), positive response (B), normal shape and structure (C) and edema (D) of HGBEC.

Identification of HGBECs

The cultured cells were identified by immunohistochemistry as keratin CK19. Specific positive reaction that could identify HGBECs was found in the cultured cells (Figure 2B).

Morphology of inflammatory HGBECs and inflammatory model of HGBECs

After HGBECs were treated with hIL-1β for 2 h, inflammatory changes of HGBECs such as swelling, unclear edge and irregular shape were found in test groups and inflammatory control group compared to normal control groups (Figures 2C and D).

Concentration of IL-6, IL-8 and TNF-α

Concentration of IL-6, IL-8 and TNF-α was measured by radioimmunoassay (Table 1). The data of TNF-α concentration were not shown because of its error and dispersion.

Table 1 IL-6 and IL-8 concentration in all groups (mean±SE)

Group	IL-6 (μg/L)	IL-8 (μg/L)
Normal control	50.0±0.00	0.20±0.00
Inflammatory control	350.31±37.05[b]	13.97±0.63[b]
Ciglitazone 10 mmol/L	231.46±39.41[a]	10.94±1.59[a]
20 mmol/L	207.22±26.72[a]	11.74±2.01[a]
30 mmol/L	188.89±29.33[a,d]	9.62±1.71[a]
50 mmol/L	170.46±20.24[a,e]	9.34±2.91[a,e]

[a]P<0.05 *vs* inflammatory control group; [b]P<0.001 *vs* normal control group; [d]P<0.001, [e]P<0.025 *vs* 10 mmol/L group.

[redacted]

The isolation and culture of HGBECs play a crucial role in studying biliary tract and liver disease. HGBECs have been cultured successfully since 1993[15], but its short duration limits the related research about the pathophysiology of biliary tract and liver. hEGF is a potent proliferation-activated factor of epithelial cells[16]. The first part of this study was performed to determine the hypothesis that hEGF could improve the growth of HGBECs. The proliferative activity of HGBECs promoted by hEGF was assessed by calculating the number and the life span of HGBECs, and compared to those in hEGF-free group. Results are in agreement with the hypothesis because hEGF increased the number of HGBECs and prolonged the longevity of HGBECs in which the longest was 25 d (8.2 d in EGF-free group). Also, the effect of hEGF on the growth of HGBECs is in agreement with the light microscopic findings. Thus, HGBECs cultured in medium containing hEGF are beneficial to the biological study of HGBECs.

The discovery that the insulin-sensitizing TZDs-specific PPAR-γ agonists have antiproliferative, anti-inflammatory and immunomodulatory effects has led to the evaluation of their potential use in the treatment of diabetic complications and inflammatory, proliferative diseases in non-insulin-resistant, euglycemic individuals. Apart from improving insulin resistance, plasma lipids and systemic inflammatory markers, ameliorating atherosclerosis and preventing coronary artery restenosis in diabetic subjects, currently approved TZDs that have been shown to improve psoriasis and ulcerative colitis in euglycemic human subjects[17]. In endothelial cells, troglitazone reduces expression of vascular cell adhesion molecule-1 and intercellular adhesion molecule-1, which are adhesion molecules that facilitate monocyte attachment and migration[18].

In addition to their impact on TNF-α and IL-6, IL -8, PPAR-γ agonists have also been reported by Pasceri *et al*.[18], to inhibit other macrophage proinflammatory mediators, including iNOS, gelatinase B, and the macrophage scavenger

receptor-A. PPAR-γ activation suppresses gastric mucosal inflammatory responses to *Helicobacter pylori* (*H pylori*) LPSs, suggesting that pharmacological manipulation of PPAR-γ activation may provide therapeutic benefits in the resolution of inflammation associated with *H pylori* infection[19]. In airway, PPAR-α and -γ (co) agonists might be of therapeutic interest for the regulation of allergic or inflammatory reactions by targeting both regulatory and effector cells involved in the immune response[20,21]. An important step in the monthly turnover of the endometrial lining during the menstrual cycle is the cyclical recruitment and activation of inflammatory cells. The use of PPAR-γ ligands to reduce chemokine production and inflammation may be a productive strategy for future therapy of endometrial disorders, such as endometriosis[22,23].

The mechanism of PPAR-γ and its ligand to regulate cellular inflammation may involve multiple pathways in different kinds of cells and the state of differentiation/ activation of the same source of cells. In macrophages and epithelial cells, the effect of 15 d-PGJ2 is targeted to the NF-κB/I-κB pathway and to the mitogen-activated protein kinase ERK1/2. The role of PPAR-γ activation in tissue factor inhibition by 15 d-PGJ2 is excluded[24]. 15 d-PGJ2 and rosiglitazone rapidly induce the transcription of suppressor of cytokine signalings 1 and 3, which in turn inhibit Janus kinase (JAK) activity in activated glial cells. In addition, Src homology 2 domain-containing protein phosphatase 2, another negative regulator of JAK activity, is also involved in their anti-inflammatory action[25]. Although it is not a direct causal effect, the insufficient PPAR-γ activity contributes to ongoing dysregulated inflammation in pulmonary sarcoidosis by failing to suppress NF-κB[26]. Dendritic cells (DCs), the most potent antigen-presenting cells, involve the anti-inflammatory activation of PPAR-γ. Recent reports showed that activation of PPAR-γ alters the maturation process of DCs, prevents induction of Th2-dependent eosinophilic airway inflammation and contributes to immune homeostasis in the lung[27]. However, conflicting findings on the consequences of PPAR-γ activation on inflammatory responses have led to a confusion regarding the role of the transcription factor in inflammation. Cyclopentenone prostaglandins, synthetic ligand of PPAR-γ, induce apoptosis of human DCs in a PPAR-γ-independent manner. Since these compounds are released during an inflammatory event and show anti-inflammatory properties, they may contribute to the downregulation of DC function through apoptotic cell death[28]. In a murine model of asthma, IL-8 release and activation of NF-κB-responsive reporter gene are inhibited only at micromolar concentrations, suggesting that these effects are not mediated by PPAR[29].

Based on the hypothesis that PPAR-γ expresses in HGBECs and inhibits inflammation of HGBECs, the following part of this study was designed to investigate whether the activation of PPAR-γ inhibited inflammation of HGBECs. IL-1β is a potent proinflammation factor that can induce multiple inflammatory mediators. After being treated with IL-1β for 2 h, HGBECs secreted a higher concentration of IL-6 and IL-8 in media ($P<0.001$). An inflammatory model of HGBECs was achieved successfully and showed a higher concentration of IL-6 and IL-8 in media, and inflammatory morphological changes such as edema and unclear edge in cellular formation. TNF-α, a potent inflammatory mediator, is often produced by white blood cells and smooth muscle cells in the early stage of inflammation. TNF-α could not be detected in the present study because HGBECs did not secrete it.

In vivo, IL-1β, TNF-α, and LPS initiate the secretion of cytokines including IL-6, IL-8, and IL-2. IL-1 can induce inflammation of gallbladder epithelial cells and biliary epithelial cells. Gallbladder inflammation is an early feature of gallstone formation[30]. These findings have been proved by molecular biology at mRNA level[31,32]. Also, these cytokines interact to form a network, which is named as cytokine storm[33]. The storm activates inflammatory cells and mediates inflammatory cell chemotaxis, then causes systemic inflammation. This process is defined as systemic inflammation response syndrome by the Association of American Physician and Critical Care in 1992[34].

PPAR-γ is a nuclear hormone receptor, with a well-established role in adipogenesis and glucose metabolism. Over the past 3 years several laboratories have reported that this protein can influence macrophage responses to a variety of inflammatory stimuli[32]. Immunolocalization of PPAR-γ primarily to colonocytes, especially in the presence of inflammation, strongly suggests that these epithelial cells are the target of PPAR-γ ligands[35-37]. In order to verify that HGBECs could express PPAR-γ and that PPAR-γ could affect the inflammation of HGBECs after binding to the ligand, we investigated the characteristics of PPAR-γ receptor using traditional endocrinological technique to study unknown receptor by binding to known ligand. We noted that ciglitazone with a final concentration of 10-50 mmol/L could suppress the IL-6 and IL-8 gene expression induced by IL-1β in a dose-dependent manner. This is consistent with our experimental hypothesis. Our results suggest that activation of PPAR-γ downregulates inflammation of HGBECs *in vitro*.

PPARs are nuclear receptor isoforms with key roles in the regulation of lipid and glucose metabolism. Synthetic ligands for PPAR-γ promote insulin sensitization in the context of obesity. In this study, ciglitazone showed potential therapeutic effects on inflammation of HGBECs *in vivo*.

REFERENCES

1 **Lemberger T,** Desvergne B, Wahli W. Peroxisome proliferator-activated receptors: a nuclear receptor signaling pathway in lipid physiology. *Annu Rev Cell Dev Biol* 1996; **12**: 335-363

2 **Michalik L,** Wahli W. Peroxisome proliferator-activated receptors: three isotypes for a multitude of functions. *Current Opin Biotechnol* 1999; **10**: 564-570

3 **Dalei S,** Rangwala SM, Bailey ST, Krakow SL, Reginato MJ. Interdomain comunication regulating ligand binding by PPAR-gamma. *Nature* 1998; **396**: 377-380

4 **Marra F,** Efsen E, Romanelli RG, Caligiuri A, Pastacaldi S, Batignani G, Bonacchi A, Caporale R, Laffi G, Pinzani M, Gentilini P. Ligands of peroxisome proliferator-activated receptors-gamma modulate profibrogenic and proinflammatory actions in hepatic stellate cells. *Gastroenterology* 2000; **119**: 466-478

5 **Staels B**, Koenig W, Habib A, Merval R, Lebret M, Torra IP, Delerive P, Fadel A, Chinetti G, Fruchart JC, Najib J, Maclouf J, Tedgui A. Activation of human aortic smooth-muscle cells is inhibited by PPAR-αbut not by PPAR-gamma activators.

Nature 1998; **393**: 790-793
6 **Hsueh WA,** Jackson S, Law RE. Control of vascular cell proliferation and migration by PPAR-gamma: a new approach to the macrovascular complications of diabetes. *Diabetescare* 2001; **24**: 392-397
7 **Wang AC,** Dai X, Liu B, Conrad DJ. Peroxisome proliferator-activated receptor-gamma regulates airway epithelial cell activation. *Am J Res Cell Mol Bilo* 2001; **24**; 688-693
8 **Kasai K,** Banba N, Hishinuma A, Matsumura M. Kakishita H, Matsumura M, Motohashi S, Sato N, Hattori Y. 15-Deoxy-Delta(12,14)-Prostaglandin J(2) facilitates thyroglobulin prodution by cultured human thyroicytes. *Am J Physiol Cell Physiol* 2000; **279**: 1859-1869
9 **Lehmann JM,** Moore LB, Smith-Olivier TA, Wilkison WO, Willson TM, Kliewer SA. An antidiabetic thiazolidinedione is a high affinity ligand for peroxisome proliferator-activated receptor-γ(PPAR-γ). *J Biol Chem* 1995; **270**: 12953-12956
10 **Kliewer SA,** Lenhard JM, Willson TM, Patei I, Morris DC, Lehmann JM. A prostaglandin-J_2 metabolite binds peroxisome proliferator-activated receptor γ and promotes adipocyte differentiation. *Cell* 1995; **83**: 813-817
11 **Jozkowicz A,** Dulak J, Proger M, Nanobashvili J, Nigisch A, Winter B, Weigel G, Huk I. Prostaglandin-J2 induces synthesis of interleukin-8 by endothelial cells in a PPAR-gamma independent manner. *Prostagl Other Lipid Med* 2001; **165**: 165-177
12 **Jiang C,** Ting AT, Seed B. PPAR-γ agonists inhibits production of monocyte inflammatory cytokines. *Nature* 1998; **391**: 82-86
13 **Kawahito Y,** Kondo M, Tsubouchi Y, Hashiramoto A, Bishop-Bailey D, Inoue KI, Kohno M, Yamada R, Hla T, Sano H. 15-deoxy-Ä^{12,14}–PGJ_2 induces synviocyte apoptosis and suppreses adjuvant-induced arthritis in rats. *J Clin Invest* 2000; **106**: 189
14 **Fitzegerald DJ,** Cecere G. Hemofiltration and inflammatory mediators. *Perfusion* 2002; **17**(Suppl): 23-28
15 **Purdum PP**, Ulissi A, Hylemon PB, Shiffman ML, Moore EW. Cultured human gallbladder epithelia. *Lab Invest* 1993; **68**: 345-353
16 **Liu HB,** Wang BS. Culture *in vitro* and biological feature of human bile duct epithelial cells. *Gandanyi Waike Zazhi* 1998; **10**: 165-166
17 **Pershadsingh HA.** Peroxisome proliferator-activated receptor-gamma: therapeutic target for diseases beyond diabetes: quo vadis?. *Expert Opinion on Investigational Drugs* 2004; **13**: 215-228
18 **Pasceri V,** Wu HD, Willerson JT, Yeh ETH. Modulation of vascular inflammation *in vitro* and *in vivo* by peroxisome proliferator-activated receptor-gamma activators. *Circulation* 2000; **101**: 235-238
19 **Slomiany BL,** Slomiany A. Suppression of gastric mucosal inflammatory responses to *Helicobacter pylori* lipopolysaccharide by peroxisome proliferator-activated receptor gamma activation. *IUBMB Life* 2002; **53**: 303-308
20 **Su CG,** Wen X, Bailey ST, Jiang W, Rangwala SM, Keilbaugh SA, Flanigan A, Murthy S, Lazar MA, Wu GD. A novel therapy for colitis utilizing PPAR-gamma ligands to inhibit the epithelial inflammatory response. *J Clin Invest* 1999; **104**: 383-389
21 **Mueller C,** Weaver V, Vanden Heuvel JP, August A, Cantorna MT. Peroxisome proliferator-activated receptor gamma ligands attenuate immunological symptoms of experimental allergic asthma. *Arch Biochem Biophys* 2003; **418**: 186-196
22 **Woerly G,** Honda K, Loyens M, Papin JP, Auwerx J, Staels B, Capron M, Dombrowicz D. Peroxisome proliferator-activated receptors alpha and gamma down-regulate allergic inflammation and eosinophil activation. *J Exp Med* 2003; **198**: 411-421
23 **Pritts EA,** Zhao D, Ricke E, Waite L, Taylor RN. PPAR-gamma decreases endometrial stromal cell transcription and translation of RANTES *in vitro*. *J Clin Endocrinol Metab* 2002; **87**: 1841-1844
24 **Hornung D,** Waite LL, Ricke EA, Bentzien F, Wallwiener D, Taylor RN. Nuclear peroxisome proliferator-activated receptors alpha and gamma have opposing effects on monocyte chemotaxis in endometriosis. *J Clin Endocrinol Metab* 2001; **86**: 3108-3114
25 **Eligini S,** Banfi C, Brambilla M, Camera M, Barbieri SS, Poma F, Tremoli E, Colli S. 15-deoxy-delta12,14-Prostaglandin J2 inhibits tissue factor expression in human macrophages and endothelial cells: evidence for ERK1/2 signaling pathway blockade. *Thromb Haemost* 2002; **88**: 524-532
26 **Park EJ,** Park SY, Joe EH, Jou I. 15d-PGJ2 and rosiglitazone suppress Janus kinase-STAT inflammatory signaling through induction of suppressor of cytokine signaling 1 (SOCS1) and SOCS3 in glia. *J Biol Chem* 2003; **278**: 14747-14752
27 **Trifilieff A,** Bench A, Hanley M, Bayley D, Campbell E, Whittaker P. PPAR-alpha and -gamma but not -delta agonists inhibit airway inflammation in a murine model of asthma: *in vitro* evidence for an NF-kappaB-independent effect. *Br J Pharmacol* 2003; **139**: 163-171
28 **Hammad H,** de Heer HJ, Soullie T, Angeli V, Trottein F, Hoogsteden HC, Lambrecht BN. Activation of peroxisome proliferator-activated receptor-gamma in dendritic cells inhibits the development of eosinophilic airway inflammation in a mouse model of asthma. *Am J Pathol* 2004; **164**: 263-271
29 **Nencioni A,** Lauber K, Grunebach F, Brugger W, Denzlinger C, Wesselborg S, Brossart P. Cyclopentenone prostaglandins induce caspase activation and apoptosis in dendritic cells by a PPAR-gamma-independent mechanism: regulation by inflammatory and T cell-derived stimuli. *Exp Hematol* 2002; **30**: 1020-1028
30 **Rege RV.** Inflammatory cytokines alter human gallbladder epithelial cell absorption/secretion. *J Gastrointest Surg* 2000; **4**: 185-192
31 **Morland CM,** Fear J, Joplin R, Adams DH. Inflammatory cytokines stimulate human biliary epithelial cells to express interleukin-8 and monocyte chemotactic protein-1. *Biochem Soc Trans* 1997; **25**: 232S
32 **Savard CE,** Blinman TA, Choi HS, Lee SK, Pandol SJ, Lee SP. Expression of cytokine and chemokine mRNA and secretion of tumor necrosis factor-alpha by gallbladder epithelial cells: response to bacterial lipopolysaccharides. *BMC Gastroenterol* 2002; **2**: 23
33 **Yoon JH,** Kim KS, Kim HU, Linton JA, Lee JG. Effects of TNF-alpha and IL-1 beta on mucin, lysozyme, IL-6 and IL-8 in passage-2 normal human nasal epithelial cells. *Acta Oto-Laryngol* 1999; **119**: 905-910
34 **Bone RC,** Balk RA, Cerra FB, Dellinger RP, Fein AM, Knaus WA, Schein RM, Sibbald WJ. Definitions for sepsis and organ failure and guidelines for the use of innovative therapies in sepsis. *Chest* 1992; **101**: 1644-1655
35 **Moore KJ,** Fitzgerald ML, Freeman MW. Peroxisome proliferator-activated receptors in macrophage biology: friend or foe? *Curr Opin Lipidol* 2001; **12**: 519-527
36 **Hinz B,** Brune K, Pahl A. 15-Deoxy-Delta(12,14)-prostaglandin J2 inhibits the expression of proinflammatory genes in human blood monocytes via a PPAR-gamma-independent mechanism. *Biochem Biophys Res Commun* 2003; **302**: 415-420
37 **Takagi T,** Naito Y, Tomatsuri N, Handa O, Ichikawa H, Yoshida N, Yoshikawa T. Pioglitazone, a PPAR-gamma ligand, provides protection from dextran sulfate sodium-induced colitis in mice in association with inhibition of the NF-kappaB-cytokine cascade. *Redox Report* 2002; **7**: 283-289

Science Editor Wang XL and Guo SY **Language Editor** Elsevier HK

PO Box 2345, Beijing 100023, China
www.wjgnet.com
wjg@wjgnet.com

ELSEVIER

World J Gastroenterol 2005;11(38):6066-6068
World Journal of Gastroenterology ISSN 1007-9327
© 2005 The WJG Press and Elsevier Inc. All rights reserved.

• *CASE REPORT* •

Multiseptate gallbladder with anomalous pancreaticobiliary ductal union: A case report

Takafumi Yamamoto, Jun Matsumoto, Shinya Hashiguchi, Atsumasa Yamaguchi, Koro Sakoda, Chiaki Taki

Takafumi Yamamoto, Jun Matsumoto, Shinya Hashiguchi, Atsumasa Yamaguchi, Koro Sakoda, Chiaki Taki, Department of Endoscopy, Kagoshima University Hospital, Kagoshima 890-8520, Japan; Departments of Internal Medicine, Surgery, and Pathology, Kagoshima Medical Association Hospital, Kagoshima 890-0081, Japan
Correspondence to: Dr. Takafumi Yamamoto, Department of Endoscopy, Kagoshima University Hospital, 8-35-1 Sakuragaoka Kagoshima City, Kagoshima 890-8520, Japan. tyama@m2.kufm.kagoshima-u.ac.jp
Telephone: +81-99-275-5325 Fax: +81-99-275-3504
Received: 2005-02-15 Accepted: 2005-04-09

Abstract

Multiseptate gallbladder, characterized by the presence of multiple septa dividing the gallbladder lumen, is a very extremely rare congenital anomaly of the gallbladder. On the other hand, anomalous pancreaticobiliary ductal union is also one of the congenital anomalous biliary diseases and thought to be related with choledochal cyst or biliary tract malignancies. In this paper, we describe a unique and first patient of multiseptate gallbladder with anomalous pancreaticobiliary ductal union and a review of the literature. To clarify more characters of the multiseptate gallbladder, examination of a larger patient population will be needed and further studies will be required.

© 2005 The WJG Press and Elsevier Inc. All rights reserved.

Key words: Multiseptate gallbladder; Anomalous pancreaticobiliary ductal union; Congenital anomaly

Yamamoto T, Matsumoto J, Hashiguchi S, Yamaguchi A, Sakoda K, Taki C. Multiseptate gallbladder with anomalous pancreaticobiliary ductal union: A case report. *World J Gastroenterol* 2005; 11(38): 6066-6068
http://www.wjgnet.com/1007-9327/11/6066.asp

INTRODUCTION

Multiseptate gallbladder is a very extremely rare congenital anomaly of the gallbladder. In the published cases, concomitant biliary diseases of the multiseptate gallbladder were reported as cholecystolithiasis, choledochal cyst, and hypoplasia. On the other hand, anomalous pancreaticobiliary ductal union is also one of the congenital anomalous biliary diseases and thought to be related with choledochal cyst or biliary tract malignancies. Along with the review of literature, reported here is a first patient of multiseptate gallbladder with anomalous pancreaticobiliary ductal union.

CASE REPORT

A 46-year-old Japanese female with gastric carcinoma underwent preoperative examinations at our institution. She had no complaints and her past history and family history were noncontributory. She reported no history of smoking and alcohol. Neither anemia nor jaundice was present. The abdomen was flat and soft. Liver, spleen, and mass could not be palpable. No lymph node swelling was palpated. Plain abdominal X-ray was normal. Laboratory data including tumor makers showed within normal range. Abdominal US and CT suspected septa in the gallbladder and showed neither cholecystolithiasis nor tumor lesion in the gallbladder. EUS demonstrated clearly multiple thin septa of the gallbladder (Figure 1A). ERCP revealed multiple faint septation in the neck portion of the gallbladder and combined with anomalous pancreaticobiliary ductal union. The common bile duct was not significantly dilated (Figures 1B and C).

Total gastrectomy and cholecystectomy were performed. In the macroscopic findings, the resected gallbladder was of normal size with smooth surface. Multiple thin septa were present only at the neck of the gallbladder. Neither tumor nor cholelithiasis was observed (Figure 1D). Microscopically, the septa were lined by typical columnar epithelium containing normal muscular layer of the gallbladder. There were mild chronic inflammation changes with the gallbladder. Pathological findings were consistent with multiseptate gallbladder (Figure 1E).

DISCUSSION

In recent years, congenital malformations of the gallbladder are increasingly diagnosed according to the rapid improvement of the imaging. The congenital malformations of the gallbladder are classified as anomalous forms, abnormal position, and absence. Multiseptate gallbladder is a very rare congenital anomaly form, which was first described by Simon and Tandon[1]. To our knowledge, only 30 cases including our case have been reported in the literature. A review of the cases described a female predominance; 21 of the patients were females. A mean age showed 29.4 years (range 3-70 years), and pediatric patients in four cases[2-5].

Most patients usually present with right upper abdominal pain, epigastralgia, and back pain, only six cases including our case were asymptomatic. Though the symptoms of multiseptate gallbladder patients were relieved after cholecystectomy, histological findings of the resected gallbladder in patients were usually of normal size with smooth surface and not

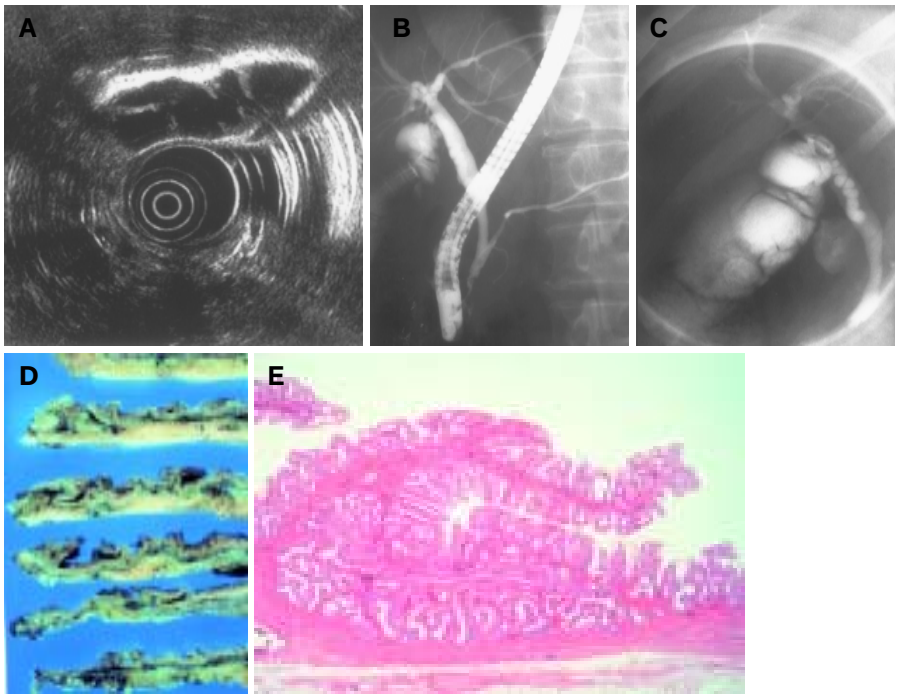


Figure 1 A: Endoscopic ultrasonography of the gallbladder showing multiple thin septa in the neck portion. B: Endoscopic retrograde cholangiopancreatography showing anomalous pancreaticobiliary ductal union. The common bile duct was not dilated. C: Endoscopic retrograde cholangiopancreatography showing multiple faint septation in the neck of the gallbladder. D: Longitudinal resected gallbladder shows multiple thin septa appearance at the neck portion. E: Microscopic findings of the resected gallbladder demonstrate the septa lined by normal typical columnar epithelium containing normal muscular layer (H&E stain, original magnification ×40).

always recognized as acute cholecystitis or cholecystolithiasis, and the exact mechanism of the biliary symptoms of multiseptate gallbladder is unknown. Saimura and co-workers investigated the mechanism of the symptoms of the patients with multiseptate gallbladder using biliary manometry and scintigraphy[6]. According to their study, both biliary manometry and scintigraphy indicated the impairment of the bile flow between the common bile duct and the gallbladder. One of the mechanism of the symptoms of multiseptate gallbladder is considered to be the impairment of the bile flow.

In nearly all literatures, pathological findings of multiseptate gallbladder reveal numerous septa, which consisted of a normal muscularis layer of the gallbladder wall, like a honeycomb appearance. Though the septa usually existed in the whole of the gallbladder, in some cases, the septations were confined to the neck, the body and the fundus alone[2,7,8]. This case presented the multiple septa in the neck portion of the gallbladder.

To make a diagnosis of multiseptate gallbladder exactly, it is important to detect clearly the septa in the gallbladder. Diagnostic imaging modalities for this disease were reported as abdominal US, abdominal CT[9], ERCP[7,10], oral cholecystography, and 99mTc hepatobiliary imaging[11]. In some asymptomatic cases, the diagnosis were made incidentally by abdominal US[3,4,8,12]. This case presented more clearly multiple thin septa in the neck portion of the gallbladder on EUS rather than other imagings. EUS is considered to be a very useful modality for the diagnosis of the cases with partial multiseptation.

Concomitant biliary disease of the patients with multiseptate gallbladder besides our case was reported in six patients; cholelithiasis in two patients[3,13], choledochal cyst in two[5,14], and hypoplasia of the gallbladder in two[15,16]. No cases that coexisted with malignancies were reported in the literature. On the other hand, anomalous pancreaticobiliary ductal union is also known as the congenital malformation of the pancreaticobiliary duct system and is thought to be related to choledochal cyst and biliary tract carcinoma. Though anomalous pancreaticobiliary ductal union is frequently observed in patients with congenital choledochal cyst, the cases without choledochal cyst are recognized to have great malignant potential of the gallbladder[17,18]. In this case, ERCP demonstrated anomalous pancreaticobiliary ductal union without choledochal cyst.

Our case is asymptomatic and has the septations at the only neck of the gallbladder. Besides these unique findings, this present case is the first report of multiseptate gallbladder associated with anomalous pancreaticobiliary ductal union in the world literature. To clarify more characters of the multiseptate gallbladder, examination of a larger patient population will be needed and further studies will be required.

REFERENCES

1 **Simon M**, Tandon BN. Multiseptate gallbladder: A case report. *Radiology* 1963; **80**: 84-86
2 **Strauss S**, Starinsky R, Alon Z. Partial multiseptate gallbladder: sonographic appearance. *J Ultrasound Med* 1993; **12**: 201-203
3 **Miwa W**, Toyama K, Kitamura Y, Murakami K, Kamata K, Takada T, Tanabe H, Kanayama M. Multiseptate gallbladder with cholelithiasis diagnosed incidentally in an elderly patient. *Intern Med* 2000; **39**: 1054-1059
4 **Saddik D**. Multiseptate gall-bladder: incidental diagnosis on ultrasound. *Australas Radiol* 1998; **42**: 374-376
5 **Pery M**, Kaftori JK, Marvan H, Sweed Y, Kerner H. Ultrasonographic appearance of multiseptate gallbladder:

report a case with coexisting choledochal cyst. *J Clin Ultrasound* 1985; **13**: 570-573
6 **Saimura M**, Ichimiya H, Naritomi G, Ogawa Y, Chijiiwa K, Yamaguchi K. Multiseptate gallbladder: biliary manometry and scintigraphy. *J Gastroenterol* 1996; **31**: 133-136
7 **Naritomi G**, Kimura H, Konomi H, Takeda T, Ogawa Y, Chijiiwa K. Multiseptate gallbladder as a cause of biliary pain. *Am J Gastroenterol* 1994; **89**: 1891-1892
8 **Adear H**, Barki Y. Mutiseptate gallbladder in a child: incidental diagnosis on sonography. *Pediatr Radiol* 1990; **20**: 192
9 **Isomoto I**, Matsunaga N, Ochi M, Hayashi K, Amamoto Y, Tachibana K, Furukawa M. Multiseptate gallbladder: computed tomographic appearance. *Radiat Med* 1990; **8**: 55-57
10 **Hahm KB**, Yim DS, Kang JK, Park IS. Cholangiographic appearance of multiseptate gallbladder: case report and a review of the literature. *J Gastroenterol* 1994; **29**: 665-668
11 **Vasinrapee P**, Linden K, Cook RE. Multiseptate gallbladder demonstrated on Tc-99m hepatobiliary imaging. *Clin Nucl Med* 1990; **15**: 272
12 **Lev-Toaff AS**, Friedman AC, Rindsberg SN, Caroline DF, Maurer AH, Radecki PD. Multiseptate gallbladder: incidental diagnosis on sonography. *Am J Roentgenol* 1987; **148**: 1119-1120
13 **Croce EJ**. The multiseptate gallbladder. *Arch Surg* 1973; **107**: 104-105
14 **Tan CE**, Howard ER, Driver M, Murray-Lyon IM. Non-communicating Multiseptate gallbladder and choledochal cyst: a case report and review of publications. *Gut* 1993; **34**: 853-856
15 **Bhagavan BS**, Amin PB, Land AS, Weinberg T. Multiseptate gallbladder. Embryogenetic hypotheses. *Arch Pathol* 1970; **89**: 382-385
16 **Jena PK**, Hardie RA, Hobsley M. Multiseptate hypoplastic gallbladder. *Br J Surg* 1977; **64**: 192-193
17 **Yamauchi S**, Koga A, Matsumoto S, Tanaka M, Nakayama F. Anomalous junction of pancreaticobiliary duct without congenital choledochal cyst: a possible risk factor for gallbladder cancer. *Am J gastroenterol* 1987; **82**: 20-24
18 **Chijiiwa K**, Kimura H, Tanaka M. Malignant potential of the gallbladder in patients with anomalous pancreaticobiliary ductal junction. The difference in risk between patients with and without choledochal cyst. *Int Surg* 1995; **80**: 61-64

Science Editor Guo SY **Language Editor** Elsevier HK

PO Box 2345, Beijing 100023, China
www.wjgnet.com
wjg@wjgnet.com

ELSEVIER

World J Gastroenterol 2005;11(38):6069-6071
World Journal of Gastroenterology ISSN 1007-9327
© 2005 The WJG Press and Elsevier Inc. All rights reserved.

• *CASE REPORT* •

Autoimmune hepatitis triggered by acute hepatitis A

Hiroto Tanaka, Hiroto Tujioka, Hiroki Ueda, Hiroko Hamagami, Youhei Kida, Masakazu Ichinose

Hiroto Tanaka, Hiroto Tujioka, Hiroki Ueda, Hiroko Hamagami, Youhei Kida, Masakazu Ichinose, 3rd Department of Internal Medicine, Wakayama Medical University, Japan
Correspondence to: Masakazu Ichinose, MD, PhD, 3rd Department of Internal Medicine, Wakayama Medical University, 811-1 Kimiidera, Wakayama 641-0015, Japan. h-tana@yf6.so-net.ne.jp
Telephone: +81-73-441-0619 Fax: +81-73-446-2877
Received: 2005-02-17 Accepted: 2005-05-12

Abstract

The patient was a 57-year-old woman presenting with jaundice as the chief complaint. She began vomiting on July 10, 2003. Jaundice was noted and admitted to our hospital for thorough testing. Tests on admission indicated severe hepatitis, based on: aspartate aminotransferase (AST), 1 076 IU/L; alanine aminotransferase (ALT), 1 400 IU/L; total bilirubin (TB), 20.9 mg/dL; and prothrombin time rate (PT%), 46.9%. Acute hepatitis A (HA) was diagnosed based on negative hepatitis B surface antigen and hepatitis C virus RNA and positive immunoglobulin (Ig) M HA antibody, but elevation of anti-nuclear antigen (×320) and IgG (3 112 mg/dL) led to suspicion of autoimmune hepatitis (AIH). Plasma exchange was performed for 3 d from July 17, and steroid pulse therapy was performed for 3 d starting on July 18, followed by oral steroid therapy. Liver biopsy was performed on August 5, and the results confirmed acute hepatitis and mild chronic inflammation. Levels of AST and ALT normalized, so dose of oral steroid was markedly reduced. Steroid therapy was terminated after 4 mo, as the patient had glaucoma. Starting 3 mo after cessation of steroid therapy, levels of AST and ALT began to increase again. Another liver biopsy was performed and AIH was diagnosed based on serum data and biopsy specimen. Oral steroid therapy was reinitiated. Levels of AST and ALT again normalized. The present case was thus considered to represent AIH triggered by acute HA.

© 2005 The WJG Press and Elsevier Inc. All rights reserved.

Key words: Acute hepatitis A; Autoimmune hepatitis; International criteria for AIH; HLA

Tanaka H, Tujioka H, Ueda H, Hamagami H, Kida Y, Ichinose M. Autoimmune hepatitis triggered by acute hepatitis A. *World J Gastroenterol* 2005; 11(38): 6069-6071
http://www.wjgnet.com/1007-9327/11/6069.asp

INTRODUCTION

Autoimmune hepatitis (AIH) is a chronic progressive hepatitis characterized clinically by positive anti-nuclear antibody (ANA) and hypergammaglobulinemia, and histologically by portal inflammatory cell infiltration (plasmacyte dominant) and piecemeal necrosis. However, the exact mechanisms of onset are unknown. Based on past reports, AIH appears to be induced by antibody-dependent cell-mediated cytotoxicity, which involves both antibody-mediated and cellular immunity against specific liver antigens on hepatocyte membranes[1]. Several studies have documented the involvement of genetic factors, including human lymphocyte antigen (HLA) types such as DR3 and DR4[2]. Furthermore, cases of AIH have been reported in which viruses causing acute hepatitis such as hepatitis A (HA) virus[3-7], HBV[8] and Epstein-Barr virus[9] have acted as a trigger. We report herein the case of a patient with AIH that appears to have been triggered by acute HA.

CASE REPORT

The patient was a 57-year-old woman with jaundice as the chief complaint.

History of present illness

The patient had been seeing a local doctor for hypertension, with no sign of hepatic pathology. On July 2, 2003, she developed hives and was given fexofenadine hydrochloride. Around this time, she began to feel sick. While she had eaten raw foods within the previous month, she had not eaten raw oysters. Starting on July 10, she began vomiting and visited the local doctor on July 14. Jaundice was noted, and the patient was referred and admitted to our hospital for thorough testing.

Physical findings on admission

The patient was 163 cm tall and weighed 100 kg. She was thus very obese, and although yellowing of the bulbar conjunctiva was noted, no other abnormalities were identified.

Test findings on admission (Table 1)

Aspartate aminotransferase (AST), 1 076 IU/L; alanine aminotransferase (ALT), 1 400 IU/L; total bilirubin (TB), 20.9 mg/dL; prothrombin time rate (PT%), 46.9%; hepatitis B surface antigen (HBsAg) negative; hepatitis C virus (HCV) RNA negative; and immunoglobulin (Ig) M HA antibody positive (titer, 1.9 cut of index). Acute HA was therefore diagnosed. Furthermore, as levels of ANA (×320) and IgG (3 112 mg/dL) were elevated, AIH was suspected. Drug lymphocyte stimulation test (DLST) yielded negative results for fexofenadine hydrochloride. The patient scored 1 point according to the diagnostic criteria for acute drug-induced

hepatic injury established by the International Consensus Meeting (ICM)[10], excluding the possibility of drug-induced hepatic injury. Computed tomography showed no hepatic atrophy, but thickening of the gallbladder wall was apparent, suggesting acute hepatitis (Figure 1). HLA assessment conducted after admission revealed: A24(9); B52(5); B61 (40); DR15(2); and DR9.

Table 1 Labo data on admission

WBC	6900/uL	BS	129 mg/dL
Neutro	60.9%	HbA1c	6.4%
Eosin	3.6%	CRP	1.59 mg/dL
Baso	0.5%	Na	137 mEq/L
Mono	9.1%	K	3.6 mEq/L
Lympho	25.9%	Cl	99 mEq/L
RBC	502×10⁴/uL		
Hb	15.2 g/dL		
Ht	44.7%		
Plt	16.5×10⁴/uL	ANA	320 times
		AMA	-
TP	8.5 g/dL	IgG	3 112 mg/dL
Alb	3.4 g/dL	IgM	234 mg/dL
BUN	11 mg/dL	IgA	631 mg/dL
Cr	0.9 mg/dL		
T-Bil	20.9 mg/dL	IgM HA	+
D-Bil	16.9 mg/dL	HBsAg	-
AST	1 076 IU/L	HCV Ab	-
ALT	1 400 IU/L	CMV IgM	-
PT%	46.9%	EBV IgM	-
LDH	498 U/L		
Γ-GTP	129 IU/L		
ChE	242 U/L	DLST	-

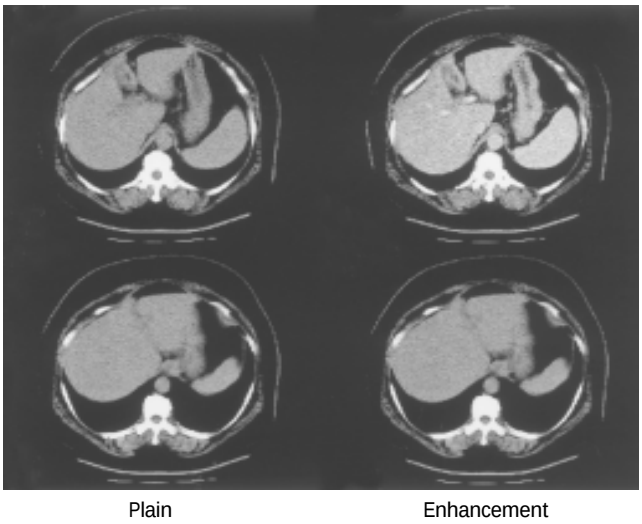


Figure 1 Liver parenchyma is not atrophic. Thickening of the gall bladder wall is also seen. This finding is compatible with acute hepatitis.

Clinical course following admission

Although AST and ALT levels started to improve, TB and PT% deteriorated to 27.5 mg/dL and 40.8%, respectively. To avoid onset of fulminant hepatitis, plasma exchange was performed for 3 d starting on July 17. From July 18, steroid pulse therapy was performed for 3 d, followed by oral steroid therapy. Levels of AST, ALT, TB, and PT% improved. Results of liver biopsy on August 5 confirmed acute hepatitis and mild chronic inflammation (mild fibrous enlargement of portal area was shown in two of eight portal areas and marked inflammatory cell infiltration of liver parenchyma was identified). The patient scored seven points according to international diagnostic criteria for AIH[11], which was thus excluded at this time. Acute HA was therefore diagnosed. At first, 50 mg/d of oral steroid (prednisolone) was administered, with dose reduced by 10 mg/d every week. Levels of AST, ALT, and TB gradually improved, and the patient was discharged while receiving 20 mg/d of steroid. After discharge, dose of oral steroid was reduced by 5 mg/d every week. As the patient also had glaucoma, oral steroid therapy was terminated after 4 mo. Levels of AST and ALT remained low, but began to increase around 3 mo after cessation of therapy. Since IgM HA antibody was negative at this time, AIH was suspected to be based on serum data such as ANA and IgG levels, and liver biopsy was performed on April 13 (Figure 2). AIH was diagnosed, and 600 mg/d of ursodeoxycholic acid was administered. This therapy proved ineffective, and oral steroid therapy (40 mg/d) was reinstated. AST and ALT levels normalized, and dose of oral steroid was gradually reduced. The patient is currently undergoing treatment in an outpatient basis with oral steroid therapy 1 mg/d, and no further elevation of AST or ALT levels has been seen.

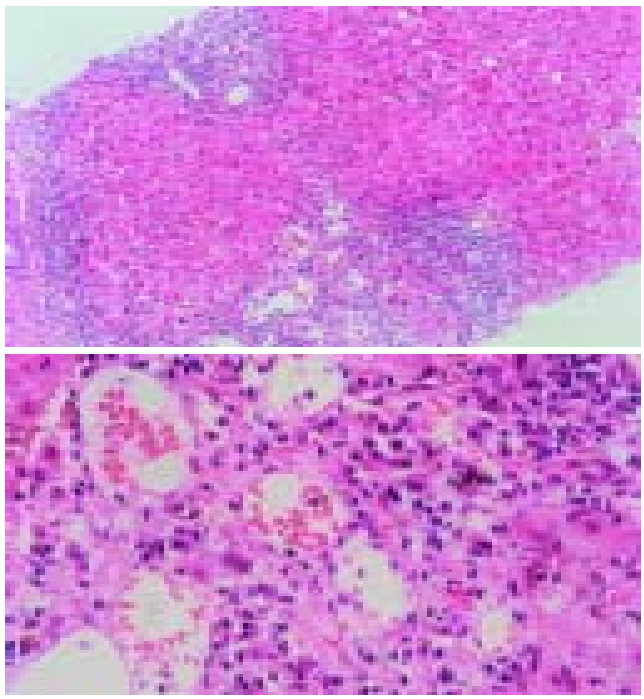


Figure 2 This liver biopsy specimen show the histopathologic appearance of chronic hepatitis. Interface hepatitis is present with bridging fibrosis, which fibrosis connects portal and cetral arreas. However, dominant plasmacyte infiltrates and rossete formation are not present.

[illegible]

On admission, although drug-induced hepatic injury was suspected in the present patient, acute HA was diagnosed due to positive IgM HA antibody. However, since ANA

was ×320 and IgG was 3 110 mg/dL, AIH could not be excluded as a possibility, and we could not be certain that the acute hepatic injury was caused by HA alone. DLST for the prescribed drug was negative, and the patient scored one point according to the diagnostic criteria for acute drug-induced hepatic injury established by the ICM [9]. Drug-induced hepatic injury thus seemed unlikely.

In the present patient, AIH was suspected at the onset of acute hepatitis, and assessment was performed in accordance with the international diagnostic criteria for AIH[11]. However, as the patient scored seven points, AIH was not initially diagnosed. Oral steroid therapy was terminated after 4 mo because transaminase levels remained normal and the patient also had glaucoma. However, transaminase levels again increased 3 mo after terminating oral steroid therapy. Since AIH had been suspected based on serum data such as ANA and IgG, liver biopsy was performed again. At this time, the patient scored 21 points according to international diagnostic criteria for AIH[11], and AIH was thus diagnosed.

While viral infection has been known to trigger AIH, few cases of AIH following acute HA have been described[3-7]. In most of these cases, AIH did not occur at the same time as acute hepatitis, with AIH often occurring several months after the onset of acute HA. According to international diagnostic criteria, the present patient did not display AIH at the time of acute hepatitis. However, since levels of ANA and IgG were high, excessive immune reactions were present. We suspect that these excessive immune reactions may lead to onset of AIH. No studies have investigated AIH during the early stages of acute hepatitis, and excessive immune reactions during acute HA have not been documented. One report documented a case of AIH that occurred after several months of abnormal liver function following acute HA[5]. While immune reactions are not often assessed in acute HA, as was the case with the present patient, excessive immune reactions may occur during acute HA.

Vento and colleagues[3] reported a patient with a deficiency of specific suppressor T cells for asialoglycoprotein receptor who developed type I AIH following subclinical HA, suggesting the possibility that immunological abnormalities including antigen presentations were involved in the onset of AIH following acute HA. HLA typings of patients with AIH triggered by acute HA were compared, but no specific tendencies were identified (Table 2). Since the sample of patients was small, larger subject populations need to be studied in future.

Herein, we presented the case of a patient with AIH that appears to have been triggered by acute HA. Given the existence of such patients and the need for careful follow-up of patients with acute HA, the clinical features of AIH patients after acute hepatitis need to be investigated for early diagnosis of AIH.

Table 2 Sample of patients

Author	Age (yr)	Sex Male/Female	Term (wk)	HLA
Vento S *et al.*	18	M	16	A2, B15, B40, DR7, DR4
Vento S *et al.*	13	F	15	A1, A19, B8, B44, DR7, DR3
Rahaman SM *et al.*	55	F	10	NT
Huppertz HI *et al.*	7	M	10	A1, A2, Bw52, Bw62, Cw3, Cw6, DR7, DRw8, DQw2
Hilzenrat N *et al.*	55	F	7	A26, B38, DRB1*0401, DRB44*01, DQB1*02
Bertran EM *et al.*	27	M	10	NT
Our case	57	F	28	A24, B52, B61, DR15, DR9

1 **Eggink HF,** Houthoff HJ, Huitema S, Gips CH, Poppema S. Cellular and humoral immune reactions in chronic liver disease. I. Lymphocyte subsets in liver biopsies of patients with untreated idiopathic autoimmune hepatitis, chronic active hepatitis B and primary biliary cirrhosis. *Clin Exp Immunol* 1982; **50**: 17-24

2 **Czaja AJ,** Carpenter HA, Santrach PJ, Moore SB. DR human leukocyte antigens and disease severity in chronic hepatitis C. *J Hepatol* 1996; **24**: 666-673

3 **Vento S,** Garofano T, Di Perri G, Dolci L, Concia E, Bassetti D. Identification of hepatitis A virus as a trigger for autoimmune chronic hepatitis type I in susceptible individuals. *Lancet* 1991; **337**: 1183-1187

4 **Huppertz HI,** Treichel U, Gassel AM, Jeschke R, Meyer KH. Autoimmune hepatitis following hepatitis A virus infection. *J Hepatol* 1995; **23**: 240-248

5 **Rahaman SM,** Chira P, Koff RS. Idiopathic autoimmune chronic hepatitis triggered by hepatitis A. *Am J Gastroenterl* 1994; **89**: 106-108

6 **Hilzenrat N,** Zilberman D, Klein T, Zur B, Sikuler E. Autoimmune hepatitis in a genetically susceptible patient. Is it triggered by acute viral hepatitis A? *Dig Dis Sci* 1999; **44**: 1950-1952

7 **Munoz Bertran E,** Rosa Salazar V, Hostalet Robles F, Correa Estan JA, Belda Abad G, Munoz Ramirez E. autoimmune hepatitis caused by acute hepatitis due to hepatitis A virus. *Gastroenterol Hepatol* 2002; **25**: 501-504

8 **Laskus T,** Slusarczyk J. Autoimmune chronic active hepatitis developing after acute type B hepatitis. *Dig Dis Sci* 1989; **34**: 1294-1297

9 **Vento S,** Guella L, Mirandola F, Cainelli F, Di Perri G, Solbiati M, Ferraro T, Concia E. Epstein-Barr virus as a trigger for autoimmune hepatitis in susceptible individuals. *Lancet* 1995; **346**: 608-609

10 **Danan G,** Benichou C. Causality assessment of adverse reactions to drugs. I. A novel method based on the conclusions of international consensus meeting: application to drug-induced liver injuries. *J Clin Epidemiol* 1993; **46**: 1323-1330

11 **Alvarez F,** Berg PA, Bianchi FB, Bianchi L, Burroughs AK, Cancado EL, Chapman RW, Cooksley WG, Czaja AJ, Desmet VJ, Donaldson PT, Eddleston AL, Fainboim L, Heathcote J, Homberg JC, Hoofnagle JH, Kakumu S, Krawitt EL, Mackay IR, MacSween RN, Maddrey WC, Manns MP, McFarlane IG, Meyer zum Buschenfelde KH, Zeniya M. International Autoimmune Hepatitis Group Report: review of criteria for diagnosis of autoimmune hepatitis. *J Hepatol* 1999; **31**: 929-938

Science Editor Guo SY **Language Editor** Elsevier HK

PO Box 2345, Beijing 100023, China
www.wjgnet.com
wjg@wjgnet.com

ELSEVIER

World J Gastroenterol 2005;11(38):6072-6073
World Journal of Gastroenterology ISSN 1007-9327
© 2005 The WJG Press and Elsevier Inc. All rights reserved.

• *LETTERS TO THE EDITOR* •

Role of von Willebrand factor levels in the prognosis of stage IV colorectal cancer: Do we have enough evidence?

I. Gil-Bazo, J.A Díaz González, J. Rodríguez, J. Cortés, E. Calvo, J.A. Páramo, J. García-Foncillas

I. Gil-Bazo, J.A Díaz González, J. García-Foncillas, Department of Medical Oncology, University Clinic, University of Navarra, Pío XII, 36. 31008 Pamplona, Spain
J.A. Páramo, Service of Haematology, University Clinic, University of Navarra, Pío XII, 36. 31008 Pamplona, Spain
J. Cortés, Department of Medical Oncology, Vall d'Hebron, University Hospital, Pg Vall d'Hebron, 119-129, E-08035 Barcelona, Spain
E. Calvo, Institute for Drug Development, Cancer Therapy and Research Center. University of Texas Health Science Center at San Antonio, 7979 Wurzbach Road, Zeller Building, San Antonio, TX 78229, United States
Correspondence to: I. Gil-Bazo, MD, PhD, Cancer Biology and Genetics Program, Memorial Sloan-Kettering Cancer Center, 1275 York Avenue, Box 241, New York, NY 10021, United States. gilbazoi@mskcc.org
Telephone: +1-21-26392390 Fax: +1-646-4222063
Received: 2005-04-30 Accepted: 2005-06-09

© 2005 The WJG Press and Elsevier Inc. All rights reserved.

Key words: Von Willebrand factor; Colorectal cancer; Prognosis

Gil-Bazo I, Diaz-Gonzalez JA, Rodríguez J, Cortés J, Calvo E, Páramo JA, García-Foncillas J. Role of von Willebrand factor levels in the prognosis of stage IV colorectal cancer: Do we have enough evidence? *World J Gastroenterol* 2005; 11 (38): 6072-6073
http://www.wjgnet.com/1007-9327/11/6072.asp

[illegible]

Cancer patients usually present a prothrombotic condition. Several clotting-related proteins, such as von Willebrand factor (vWF), presenting higher plasma concentrations in these patients, may play a key role in this process. Moreover, some of those proteins are currently being characterized as response rate and overall survival markers in metastatic colorectal cancer (MCRC). In this comment article, we discuss the last piece of evidence that supports the use of vWF as a prognostic indicator in MCRC patients, provided by a paper recently published by Wang *et al*., in the *World Journal of Gastroenterology*. Summarizing, although vWF should be seriously considered as potential future prognostic and predictive indicator in colorectal cancer, more dynamic and better designed studies in longer series of patients should be conducted before standardizing its universal use among these patients.

Wang *et al*.[1], have recently published an encouraging paper in the World Journal of Gastroenterology regarding the possible and novel use, as a prognostic factor, of vWF plasma levels in MCRC.

As the authors expose, cancer patients often show an imbalance between coagulation and fibrinolysis systems, which results in their prothrombotic condition[2-6]. Several clotting-related proteins, such as vWF, presenting higher plasma concentrations in these patients[7-11], may play a key role in this process. Moreover, some of those proteins are currently being characterized as response rate and overall survival markers in MCRC[12-16].

Accordingly, the data shown by Wang *et al*.[1], seem to indicate that plasma vWF concentrations are increased among colorectal cancer patients and correlate with tumor stage. In addition, those vWF higher levels may be related to significantly poor prognosis of subjects presenting metastasis.

However, although authors are aware of the important variability of vWF levels in humans due to the presence of a variety of diseases like diabetes mellitus, connective tissue disease, cardiovascular dysfunctions, thrombo-embolic events, acute infections, and other conditions like age or gender[17-20], patients suffering any of those illnesses were not apparently excluded from the study nor controlled by those factors in the multivariate analysis.

More strikingly, even though platelets are partially responsible for vascular endothelial growth factor (VEGF) levels[21-25], and VEGF is considered the most potent activator of the endothelium (main vWF producer), neither platelet count nor VEGF levels were measured and included in the statistical analysis.

Other issue that remains unclear in this article is whether the chemotherapy (CMT) regime used (5-fluorouracil alone or in combination with irinotecan, oxaliplatin or capecitabine) in each group of patients could have accounted for the differences observed between the survival curves for individuals presenting vWF$\geqslant$160% and those with levels below that threshold. Thus, in order to avoid the possible bias, the CMT regime administered to each patient should have also been taken into account in the multivariate statistical analysis.

Finally, given the fact that the CMT could catalyze the original risk for progression and death in these patients due to its alleged antiangiogenic effect, measuring vWF concentrations during treatment may modify the prognostic value of this protein.

According to this, in the University Clinic of the University of Navarra, 64 colorectal cancer patients were enrolled from 2002 and 2004. Blood samples were taken dynamically before and after fluoropirimidine-based CMT in 32 patients presenting metastasis, and stored until further

processing. vWF, VEGF, plasminogen activator inhibitor (PAI) 1, D-dimer, fibrinogen levels and platelet count were measured before and after CMT using standardized techniques. Gender, age, ECOG performance status, tumor burden, CMT course, and regime and CEA/CA 19.9 levels were also considered for the statistical analysis. Patients received a median of 3 cycles of CMT (range: 2-10) between both blood samples. After a median follow-up of 10 mo, baseline levels of vWF >202% showed an associated hazard ratio (HR), for death higher than patients with vWF ≤202%, with tendency to the statistical significance ($P = 0.08$). Meanwhile, post-CMT vWF levels above 189% were related to a fourfold HR for progression with respect to those subjects showing concentrations ≤189% after CMT treatment. These results were adjusted for the rest of the different protein levels measured, age, gender, ECOG performance status, tumor burden, and CMT course and regime.

In conclusion, although vWF and other coagulation/fibrinolysis factors should be seriously considered as potential future prognostic and predictive indicators in colorectal cancer, more dynamic and better designed studies in longer series of patients should be conducted before standardizing their universal use among these patients.

REFERENCES

1 **Wang WS**, Lin JK, Lin TC, Chiou TJ, Liu JH, Yen CC, Chen PM. Plasma von Willebrand factor level as a prognostic indicator of patients with metastatic colorectal carcinoma. *World J Gastroenterol* 2005; **11**: 2166-2170

2 **Bick RL.** Alterations of hemostasis associated with malignancy: etiology, pathophysiology, diagnosis and management. *Semin Thromb Hemost* 1978; **5**: 1-26

3 **Ho CH,** Yuan CC, Liu SM. Diagnostic and prognostic values of plasma levels of fibrinolytic markers in ovarian cancer. *Gynecol Oncol* 1999; **75**: 397-400

4 **Lip GY,** Chin BS, Blann AD. Cancer and the prothrombotic state. *Lancet Oncol* 2002; **3**: 27-34

5 **Lykke J,** Nielsen HJ. Haemostatic alterations in colorectal cancer: perspectives for future treatment. *J Surg Oncol* 2004; **88**: 269-275

6 **Paramo JA,** Cuesta B, Hernandez M, Fernandez J, Paloma MJ, Rifon J, Rocha E. Coagulation inhibitors in patients with neoplasms. *Med Clin* 1989; **92**: 164-166

7 **Gadducci A,** Baicchi U, Marrai R, Del Bravo B, Fosella PV, Facchini V. Pretreatment plasma levels of fibrinopeptide-A (FPA), D-dimer (DD), and von Willebrand factor (vWF) in patients with ovarian carcinoma. *Gynecol Oncol* 1994; **53**: 352-356

8 **Gil-Bazo I,** Páramo Fernández JA, García-Foncillas J. Hemostasis, angiogenesis and cancer: role of the von Willebrand factor. *Rev Clin Esp* 2003; **203**: 199-201

9 **Rohsig LM,** Damin DC, Stefani SD, Castro CG Jr, Roisenberg I, Schwartsmann G. von Willebrand factor antigen levels in plasma of patients with malignant breast disease. *Br J Med Biol Res* 2001; **34**: 1125-1129

10 **Schwartsmann G,** Damin DC, Roisemberg I. Malignant disease and von Willebrand factor. *Lancet Oncol* 2001; **2**: 716-717

11 **Zietek Z,** Iwan-Zietek I, Paczulski R, Kotschy M, Wolski Z. von Willebrand factor antigen in blood plasma of patients with urinary bladder carcinoma. *Thromb Res* 1996; **83**: 399-402

12 **Blackwell K,** Hurwitz H, Lieberman G, Novotny W, Snyder S, Dewhirst M, Greenberg C. Circulating D-dimer levels are better predictors of overall survival and disease progression than carcinoembryonic antigen levels in patients with metastatic colorectal carcinoma. *Cancer* 2004; **101**: 77-82

13 **Hogdall CK,** Christensen IJ, Stephens RW, Sorensen S, Norgaard-Pedersen B, Nielsen HJ. Serum tetranectin is an independent prognostic marker in colorectal cancer and weakly correlated with plasma suPAR, plasma PAI-1 and serum CEA. *APMIS* 2002; **110**: 630-638

14 **Loktionov A,** Watson MA, Stebbings WS, Speakman CT, Bingham SA. Plasminogen activator inhibitor-1 gene polymorphism and colorectal cancer risk and prognosis. *Cancer Lett* 2003; **189**: 189-196

15 **Seetoo DQ,** Crowe PJ, Russell PJ, Yang JL. Quantitative expression of protein markers of plasminogen activation system in prognosis of colorectal cancer. *J Surg Oncol* 2003; **82**: 184-193

16 **Gil Bazo I,** Catalan Gonzalez V, Alonso Gutierrez A, Rodriguez Rodriguez J, Paramo Fernandez JA, de la Camara Gomez J, Hernandez-Lizoain JL, Garcia-Foncillas Lopez J. Impact of surgery and chemotherapy on von Willebrand factor and vascular endothelial growth factor levels in colorectal cancer. *Clin Transl Oncol* 2005; **7**: 150-155

17 **Gordon JL,** Pottinger BE, Woo P, Rosenbaum J, Black CM. Plasma von Willebrand factor in connective tissue disease. *Ann Rheum Dis* 1987; **46**: 491-492

18 **Kadir RA,** Economides DL, Sabin CA, Owens D, Lee CA. Variations in coagulation factors in women: effects of age, ethnicity, menstrual cycle and combined oral contraceptive. *Thromb Haemost* 1999; **82**: 1456-1461

19 **Lufkin EG,** Fass DN, O'Fallon WM, Bowie EJ. Increased von Willebrand factor in diabetes mellitus. *Metabolism* 1979; **28**: 63-66

20 **Pottinger BE,** Read RC, Paleolog EM, Higgins PG, Pearson JD. von Willebrand factor is an acute phase reactant in man. *Thromb Res* 1989; **53**: 387-394

21 **George ML,** Eccles SA, Tutton MG, Abulafi AM, Swift RI. Correlation of plasma and serum vascular endothelial growth factor levels with platelet count in colorectal cancer: clinical evidence of platelet scavenging? *Clin Cancer Res* 2000; **6**: 3147-3152

22 **Verheul HM,** Hoekman K, Luykx-de Bakker S, Eekman CA, Folman CC, Broxterman HJ, Pinedo HM. Platelet: transporter of vascular endothelial growth factor. *Clin Cancer Res* 1997; **3**: 2187-2190

23 **Verheul HM,** Pinedo HM. Tumor growth: A putative role for platelets? *Oncologist* 1998; **3**: 2

24 **Verheul HM,** Pinedo HM. The importance of platelet counts and their contents in cancer. *Clin Cancer Res* 2003; **9**: 3219-3221

25 **Werther K,** Christensen IJ, Nielsen HJ. Determination of vascular endothelial growth factor (VEGF) in circulating blood: significance of VEGF in various leucocytes and platelets. *Scand J Clin Lab Invest* 2002; **62**: 343-350

Science Editor Guo SY **Language Editor** Elsevier HK

PO Box 2345, Beijing 100023, China
www.wjgnet.com
wjg@wjgnet.com

ELSEVIER

World J Gastroenterol 2005;11(38):6074
World Journal of Gastroenterology ISSN 1007-9327
© 2005 The WJG Press and Elsevier Inc. All rights reserved.

Acknowledgments to Reviewers of *World Journal of Gastroenterology*

Many reviewers have contributed their expertise and time to the peer review, a critical process to ensure the quality of *World Journal of Gastroenterology*. The editors and authors of the articles submitted to the journal are grateful to the following reviewers for evaluating the articles (including those were published and those were rejected in this issue) during the last editing period of time.

Trond Berg, Professor
Department of Molecular Biosciences, University of Oslo, PO Box 1041 Blindern, Oslo 0316, Norway

Bruno Clement, Professor
INSERM U-620, University of Rennes I, Faculty of Medicine, 2 ave. L. Bernard, Rennes 35043, France

Xue-Gong Fan, Professor
Xiangya Hospital, Changsha 410008, China

Edoardo G Giannini, Assistant Professor
Department of Internal Medicine, Gastroenterology Unit, Viale Benedetto XV, no. 6, Genoa, 16132, Italy

Hans Gregersen, Professor
The Research Administration, Aalborg Hospital, Hobrovej 42 A, Aalborg 9000, Denmark

Anna S Gukovskaya, Professor
Department of Medicine, UCLA, 11301 Wilshire Blvd, Los Angeles 91301, United States

Werner Hohenberger, Professor
Chirurgische Klinik und Poliklinik, Krankenhausstrasse 12, Erlangen D-91054, Germany

Masayoshi Ito, M.D.
Department of Endoscopy, Yotsuya Medical Cube, 5-5-27-701 Kitashinagawa, Shinagawa-ku, Tokyo 1410001, Japan

Hiroaki Itoh, M.D.
First Department of Internal Medicine, Akita University Scool of Medicine, 1-1-1, Hondou, Akita City 010-8543, Japan

Tsuneo Kitamura, Associate Professor
Department of Gastroenterology, Juntendo University Urayasu Hospital, Juntendo University School of Medicine, 2-1-1 Tomioka, Urayasu-shi, Chiba 279-0021, Japan

Zahariy Krastev, Professor
Department of Gastroneterology, Universiti Hospital "St. Ivan Rilski", #15, blvd "Acad. Ivan Geshov", Sofia 1431, Bulgaria

Shoji Kubo, M.D.
Hepato-Billiary-Pancreatic Surgery, Osaka City University Graduate School of Medicine, 1-4-3 Asahimachi, Abeno-ku, Osaka 545-8585, Japan

Fin Stolze Larsen, Associate Professor
Hepatology A-2121, Rigshospitalet Univ. Hospital of Copenhagen, Blegdamsvej 9, Copenhagen 2100, Denmark

James Neuberger, Professor
Liver Unit, Queen Elizabeth Hospital, Birmingham B15 2TH, United Kingdom

Mikio Nishioka, M.D.
Ehime Rosai Hospital, 13-27 Minami Komatsubara, Niihama 792-8550, Japan

Gustav Paumgartner, Professor
University of Munich, Klinikum Grosshadern, Marchioninistr. 15, Munich D-81377, Germany

Zhiheng Pei, Assistant Professor
Department of Pathology and Medicine, New York University School of Medicine, Department of Veterans Affairs, New York Harbor Healthcare System, 6001W, 423 East 23rd street, New York NY 10010, United States

Lun-Xiu Qin, Professor
Liver Cancer Institute and Zhongshan Hospital, Fudan University, 180 Feng Lin Road, Shanghai 200032, China

Manfred Stolte, Professor
Institute of Pathology, Klinikum Bayreuth, Preuschwitzer Str. 101, Bayreuth 95445, Germany

Michael Trauner, Professor
Medical University Graz, Auenbruggerplatz 15, Graz A-8036, Austria

Takato Ueno, Professor
Research Center for Innovative Cancer Therapy, Kurume University, 67 Asahi-machi, Kurume 830-0011, Japan

Toshio Watanabe, Associate Professor
Department of Gastroenterology, Osaka City University, Graduate School of Medicine, 1-4-3 Asahimachi, Abenoku-ku, Osaka 545-8585, Japan

Harry H-X Xia, M.D.
Department of Medicine, The University of Hong Kong, Pokfulam Road, Hong Kong, China

PO Box 2345, Beijing 100023, China
www.wjgnet.com
wjg@wjgnet.com

ELSEVIER

World J Gastroenterol 2005;11(39):6079-6084
World Journal of Gastroenterology ISSN 1007-9327
© 2005 The WJG Press and Elsevier Inc. All rights reserved.

• *REVIEW* •

Research progress of vasculopathy in portal hypertension

Tao Li, Zhen Yang

Tao Li, Zhen Yang, Department of General Surgery, Tongji Medical College, Huazhong University of Science and Technology, Wuhan 430030, Hubei Province, China
Supported by the National Natural Science Foundation of China, No. A30170920
Correspondence to: Professor Zhen Yang, Department of General Surgery, Tongji Medical College, Huazhong University of Science and Technology, Wuhan 430030, Hubei Province, China. litaoforgood@tom.com
Telephone: +86-27-83663502 Fax: +86-27-83622624
Received: 2004-09-06 Accepted: 2004-12-26

Abstract

Portal hypertension, one of the vascular diseases, not only has lesions in liver, but also changes in vascular structures and functions of extrahepatic portal system, systemic system and pulmonary circulation. The pathological changes of vasculopathy in portal hypertension include remodeling of arterialized visceral veins, intimal injury of visceral veins and destruction of contractile structure in visceral arterial wall. The mechanisms of vasculopathy in portal hypertension may be attributed to the changes of hemodynamics in portal system, immune response, gene modulation, vasoactive substances, and intrahepatic blood flow resistance. Portal hypertension can cause visceral hyperdynamic circulation, and the development and progression of visceral vasculopathy, while visceral vasculopathy can promote the development and progression of portal hypertension and visceral hyperdynamic circulation in turn. The aforementioned three factors interact in the pathogenesis of hepatic cirrhosis-induced portal hypertension and are involved in hemorrhage due to varicose vein rupture.

© 2005 The WJG Press and Elsevier Inc. All rights reserved.

Key words: Portal hypertension; Visceral vasculopathy; Visceral hyperdynamic circulation

Li T, Yang Z. Research progress of vasculopathy in portal hypertension. *World J Gastroenterol* 2005; 11(39): 6079-6084
http://www.wjgnet.com/1007-9327/11/6079.asp

INTRODUCTION

Portal hypertension is characterized not only by lesions in liver, but also by the changes in vascular structures and functions of extrahepatic portal system, systemic system and pulmonary circulation. During a long-term animal experiment as well as in clinical practice, Yang *et al*.[1], discovered that obvious pathological changes occurred in visceral vessels with the increment of the portal pressure, such as formation of extensive portal-systemic communicating branches, the changes in modeling of visceral veins and arteries, etc., which were named vasculopathy in portal hypertension. Generally, vascular lesions also include microvascular lesions in viscera, especially in stomach and intestine, named as portal hypertensive gastropathy and portal hypertensive intestinal vasculopathy, respectively, which can cause hematochezia, occult blood in stool or hemorrhage of digestive tract. Portal hypertension can also be complicated with pulmonary vascular lesions, leading to pulmonary hypertension and elevation of pulmonary venous pressure, the former might contribute to the inevitable injury of pulmonary arterioles and arteries due to the passage of vasoactive substances into lung through collateral circulation, as well as the synthesis of vasoactive substances produced by lung itself, while the latter can result in varicose vein in lung, trachea and bronchi, and hemorrhage following the disruption of the varicose veins[2,3]. Perforating vein is the special vascular structure of gastric wall in portal hypertension[4], and is considered as a vascular lesion. The connection of varicose vessels outside gastric tunica serosa with the perforating vein leads to the abnormal flow into the submucous layer of the gastric wall to form the varicose vein. In this paper, we have briefly reviewed the research progress in the pathology and pathogenesis of vasculopathy in portal hypertension.

Pathology of vascular lesions in portal hypertension-induced remodeling of arterialized visceral veins

The changes in visceral venous structures, such as collagen, elastic fibers, and smooth muscles, are involved in the vein lesions. Under light microscope, the smooth muscle cells in portal wall display hypertrophy and hyperplasia. Under electron microscope, the traverse areas of the smooth muscle cells have onefold increase as compared with the normal one and that of vascular media is increased subsequently. The rat model of partial portal ligation revealed the changes in vascular structure, contractility, contractile components and structural proteins, and the proportion of desmin and actin was found to be increased. The thickened vascular intima contained hyperplastic collagenous fibers and large numbers of disordered smooth muscles. The interstitial was also obviously thickened with thickened and condensed muscle fibers. In the adventitial layers, there was infiltration of inflammatory cells and onefold increase in the active contractility[5].

The arterialized remodeling exists in both splenic veins and coronary vein of stomach in the patients with portal hypertension[6], which includes: (1) Obviously thickened intima, showing diffuse thickening and locally thickened areas, forming neointima containing hyperplastic collagenous fibers and large numbers of disordered smooth muscle cells.

The hillock-shaped hyperplastic spots extrude towards the vascular cavity, also containing large numbers of collagenous fibers and disordered smooth muscle cells. Platelet aggregation and blood cell attachment to the surface of injured endothelial cells gradually lead to the formation of microthrombi, similar to the plaque of atherosclerosis. The vascular intima is widely injured with infiltration of inflammatory cells; (2) The interstitial layer is significantly thickened, internal circular muscles are arranged lengthwise and breadthwise, and longitudinal muscles undergo up-growth with thickened and condensed muscle fibers; (3) There is infiltration of inflammatory cells in the adventitial layer and few lymphatic nodes are complicated with inflammation. The feeding vessels are squeezed with the formation of thrombi; (4) The phenotypes of part muscle cells convert from contractile type to synthetic type, that is, many rough reticulum and ribosomes and decreased myofilaments exist in the cytoplasm, and migrate from interstitia to intima.

Intimal injury of visceral veins

Vascular endothelial cell, attaching to the surface of vascular intima, is a semi-transparent barrier membrane and possesses complicated metabolic and endocrine functions simultaneously. Researchers are paying attention to the importance of endothelial cells in cardiovascular diseases increasingly, but the correlation between endothelial cells and portal hypertension has not been elucidated clearly. It has been confirmed that the vascular intima in the patients with non-hepatic cirrhosis is intact, there is a thin layer of smooth muscle in subintima, and the feeding vessels are intact and open. While in the patients with hepatic cirrhosis, the vascular intima is severely injured, endothelial cells are detached, the subintima is nude and edematous, and there are large numbers of inflammatory cells and fibroblasts in the vascular cavity, many blood cells adhere to the nude subintima, and mural thrombi form in the vascular cavity. In the vascular adventitia, the feeding vessels become flat by extrusion and thrombi formation also takes place. McCarthy *et al*.[7], found that when the vascular endothelial cells and basement membrane were injured, the sensitivity of vessels to angiotensin-II (AngII) was increased, suggesting that the damage to the intima could influence the contractile function of the vessels.

Destruction of contractile structure in visceral arterial wall

The patients with portal hypertension are in a state of high flow and low resistance in systemic circulation (i.e., the cardiac output and arterial pressure are decreased). Moreover, they are commonly associated with splenomegaly and hypersplenism. The splenic artery has obvious histopathological changes, i.e., destruction of contractile structure in arterial wall[8] as follows: (1) Damage of arterial endothelial cells. Partial endothelial cells detach, platelets attach to intima, which is thickened and the smooth muscles in interstitia migrate to it; (2) Weigert staining certifies that the folded ripples from elastic membrane in arterial wall become flat or completely disappear. The elastic membrane is split into multiple layers. Some parts are ruptured completely. The elastic fibers in arterial wall are also diffusely ruptured and degenerated. Under an electron microscope, split, even partly ruptured elastic membrane, is clearly seen; (3) Under light microscope, the smooth muscles in interstitia can be seen to be migrated to intima. Some medial smooth muscle cells are atrophic and anatrophic, others are hypertrophic and hyperplastic. The smooth muscle cells are separated by collagenous fibers, and arranged disorderly. Under electron microscope, the size and morphology of the smooth muscle cells are uneven, i.e., some are atrophic and anatrophic, vacuoles form in the necrotized local cytoplasm, and even whole muscle cell is lysed, while others are compensatively hypertrophic and hyperplastic. In some muscle cells, cytoplasmic cellular organs are obviously increased, mitochondria are increased and swollen, and their cristae disappear with the formation of vacuoles. In others, there exist many rough reticulum, ribosomes and Golgi bodies in cytoplasm, while the filaments are decreased, indicating that the phenotypes of muscle cells convert from contractile type to synthetic type. The cytoplasm and nuclei in some muscle cells display the characteristics of cell apoptosis; (4) Under light microscope, collagenous fibers and extracellular matrix in whole vascular wall are increased, leading to collagenization of vascular wall, and its thickening and rigidness, and decreased elasticity. Under electron microscope, the extracellular matrix in arterial wall is obviously increased, but the elastic fibers are degenerated and ruptured.

Mechanism of vasculopathy in portal hypertension

The mechanism of vasculopathy in portal hypertension is not clear. The changes in hemodynamics of portal system, immune responses, gene regulation, and vasoactive substances might contribute to the process of vasculopathy in portal hypertension.

Changes in portal hemodynamics

Vascular wall, composed of different biomaterials, possesses multiple layers of compound structure. Within a certain pressure range, vascular tension, transmural blood pressure, and the geometrical parameters follow the Laplace's law of biomechanics: $T = P(R/W)$. The vascular tension (T) has its regulatory limitation. Within an elastic range, when the transmural blood pressure (P) is increased, compensation can be achieved by increasing the vascular width (W) and decreasing vascular radius (R). So, the high pressure of portal vein can thicken the vascular wall.

The increase of vascular resistance in portal system at any part can result in portal hypertension. Neurohumoral factors and vasoactive substances can actively regulate the contractility of vascular smooth muscles. The active changes in vascular resistance can happen in hepatic microcirculation, also in prehepatic portal-systemic communicating vessels, portal vein and their branches. Effect on vascular resistance can be expressed by Poiseuille law: $r = 8\,\mu L/\pi r^4$, in which μ represents the viscosity coefficient of blood, L the length of vessel and r the radius. It can be seen that the changes in vascular radius of extrahepatic portal system are the main factors influencing the resistance of portal resistance. Intimal hyperplasia, spot formation, internal wall roughness, decreased elasticity and contractility in visceral veins can limit the vascular diastolization, promote the mural thrombosis, occlude vessels and narrow vascular cavity, leading to hypostasis, even obstruction, and finally increasing the blood

flow resistance. When visceral veins and portal-systemic communicating vessels are contracted, the portal resistance is obviously increased. The collateral vessels are flexural and tortuous, so their increases in length can also significantly increase the blood flow resistance. The changes of hemoglobin and plasma protein concentration in portal blood, especially the increased blood viscosity following gastrointestinal hemorrhage, can also increase the blood flow resistance in portal veins.

Hypertrophy and hyperplasia of vascular smooth muscle cells are the important features of vasculopathy in portal hypertension. Krieger and Dzau[9] found that the increase in mechanical load of vessels could directly induce the expression of myosin gene, increase the expression of RNA and protein, and finally induce the growth of muscle cells. It is suggested that the hyperplasia and hypertrophy of vascular smooth muscle cells may be one of the adaptive compensatory responses of vessels to increased pressure.

Persistent stimulation of high pressure and blood flow of portal veins may be the main factors responsible for the vascular intimal injury of the patients with portal hypertension. Compression of feeding vessels can decrease the supply of blood to vascular wall and partial pressure of oxygen, causing ischemic damage and nutrient disturbance of vascular intima. In hepatic cirrhosis, dysfunction of liver and kidney, decreased clearance of oxygen-free radical, and increased injurants and oxygen-free radicals in portal blood can directly injure the vascular intima.

Immune response

Researchers pay increasingly more attention to the roles that vascular endothelial cells play in the pathogenesis of cardiovascular diseases. The damages to endothelial cells in portal hypertension can destroy the structure of vascular wall, cause dysfunction, influence substance exchange and result in inflammation and immune response. In the patients with hepatic cirrhosis, the cells are markedly increased in the peripheral tissue around vessels, mainly lymphocytes and inflammatory cells, associated with the proliferation of lymph follicles. Immunohistochemistry reveals that there exists strong expressions of platelet-derived growth factor, basic fibroblastic growth factor, epidermal growth factor, transforming growth factor-α (TGF-α), etc., on the vascular wall of gastric coronary vein in the patients with portal hypertension[10], indicating that the elevated pressure in gastric coronary vein can activate the smooth muscle cells of vascular wall to release many kinds of vasoactive substances. These growth factors can stimulate the proliferation, differentiation, and migration of vascular smooth muscle cells in turn, resulting in abnormal metabolism of collagenous fibers and elastic fibers. The phenotypic shift of smooth muscle cells is a chronic response to mechanical stimulation, which can induce not only cell migration, but also the synthesis of collagen and elastin, leading to the thickening of venous wall, decreased elasticity and compliance, and finally causing the increase in blood flow resistance.

Studies have also confirmed that the levels of inflammatory factors (e.g., C3, C4, IgG, IgE, IgA) in visceral venous wall in portal hypertension are significantly higher than that in the normal controls[11], suggesting that there are obvious immune inflammations in the vessels of portal system in the patients with portal hypertension, and the immune complex deposit and immune response may participate in the process of vasculopathy in portal hypertension.

In some studies, immunohistochemistry and double labeling immunofluorescence combined with laser scanning confocal microscopy are applied to detect the expressions of eNOS, ET-1, PKC, NF-κB in splenic vein of the patients with portal hypertension and portal endothelial cells of mouse portal hypertension model in order to investigate the relationship between the changes in the expression of eNOS and ET-1 in vascular endothelial cells in portal hypertension and signaling molecules PKC and NF-κB. The results showed that in the splenic vein of patients with portal hypertension and portal endothelial cells of mouse portal hypertension model, the expression of PKC was positive or strong positive, while in the controls, the expression of PKC was negative or weak positive[12]. Double labeling immunofluorescence combined with laser scanning confocal microscopy revealed that eNOS, ET-1, and NF-κB were mainly expressed in vascular endothelia and the fluorescent signaling intensity of them in the splenic vein of patients with portal hypertension and portal endothelial cells of mouse portal hypertension model was stronger than controls, suggesting that the increases of ET-1 and NO in venous blood was attributed to the increased synthesis from endothelial cells in portal system. The increased NO production in endothelial cells is related to the upregulation of eNOS expression. In portal hypertension, the mechanical stress signaling pathway in vascular endothelial cells is activated, which is responsible for the upregulation of ET-1 and eNOS expression in endothelial cells.

Recent studies showed that during the development of vasculopathy, endothelial cells and vascular smooth muscle cells are major effector cells. Various traumatic factors, such as shear stress, hydrostatic pressure, endotoxin, cytokines, growth factors, and inflammatory mediators, can result in injury and detachment of endothelial cells, leading to the bareness of collagenous fibers and aggregation of platelets. Endothelial cells express adhesion molecules (e.g., ICAM-1), release chemotactic factors (e.g., MCP-1)[13] and complement fragment C5a after complement activation[14]. As chemotactic factors, they can promote the mononuclear cells to bind to endothelial cells, translocating through endothelial cells to subintima, also enhance the migration of vascular smooth muscle cells to subintima and the phenotypic shift. The migration to subintima and proliferation of vascular smooth muscle cells and synthesized large quantities of extracellular matrix depositing in vascular wall to form neointima can induce remodeling of vessels before vasculopathy occurs. During this process, the interactive regulation between endothelial cells and vascular smooth muscle cells runs through the development of vasculopathy. Endothelial cells are the permissive cells to various stimulators, while vascular smooth muscle cells are the effector cells. This is a repair response of vessels to varied injures, at the same time, a pathological process of vasculopathy.

Gene regulation

c-fos is a message transferring factor. Dzau *et al*.[15], have

found that after vascular smooth muscle cells receive message, nuclear c-fos is expressed, the synthesis of DNA and mRNA is increased and cells proliferate. In the patients with hepatic cirrhosis, the expression of c-fos in splenic vein is increased, indicating that the proliferation, migration, and phenotypic shift of smooth muscle cells are related to the activation of oncogenes. The signaling pathway of c-fos that connects the mechanical signaling with the expression of proliferating gene is the biological basis of vascular remodelization.

Some suppressive oncogenes, such as p53, the effective regulatory factor for apoptosis, can promote the apoptosis of vascular smooth muscle cells, while prokaryotic genes, such as *c-myc* and *bcl-2*, can inhibit the apoptosis of these cells[16,17]. In patients with portal hypertension, the bax gene is strongly expressed and takes part in the regulation of apoptosis of smooth muscle cells in portal hypertension, indicating that the process of vasculopathy in portal hypertension involves gene modulation.

MAPK pathway is one of the important signaling conductive pathways modulating cellular proliferation, differentiation, and apoptosis[18,19]. Many extracellular stimulators, such as ultraviolet radiation[20], oxygen stress[21,22], cytokines[23,24], inflammatory mediators[25-27], can stimulate the cells to upregulate the expression and activation of MAPK. In an experiment using the specific antibody directed against Tyr-phosphorylated site at $ERK_{1/2}$204, the results revealed that in portal hypertension, the expressions of phosphorylated $ERK_{1/2}$ and its downstream factor c-fos were increased in vascular wall of splenic vein, indicating that the activation of $ERK_{1/2}$/c-fos signaling transduction pathway might contribute to the development of vasculopathy in portal hypertension.

Collagen, an important vascular extracellular matrix protein, can retain the flexibility and intensity of vascular wall. In normal human vascular wall, the predominant collagen subtypes are types I, III, and V[28]. When vascular endothelia are damaged, collagenous fibers, as a strong promoter factor, can promote the aggregation of platelets. During the process of intervention-induced vascular injury and atherogenesis[29,30], the synthesis of vascular wall types I and III collagen and procollagen is increased. Types I and III collagen and procollagen are all the components of extracellular matrix, synthesized and secreted mainly by vascular smooth muscle cells in vasculopathy. A study has shown that a slight change in the constitutional ratio of types I and III collagen can trigger atherogenesis[12]. In the study on vasculopathy in portal hypertension, it was found that in the gastric coronary venous wall, the synthesis of connectin and laminin was increased, suggesting that extracellular matrix might play an important role in the pathogenesis of vasculopathy in portal hypertension. In several studies, RT-PCR was used to detect the expression of types I and III procollagen in portal hypertensive vasculopathy to investigate the mechanism of vasculopathy. The results showed that in portal hypertension, the expression of type III procollagen mRNA in splenic venous wall was 5-6 times higher than that in the patients with non-portal hypertension ($P<0.01$), while there was no significant difference in the expression of type I procollagen mRNA between them. It demonstrated that in the development of vasculopathy in portal hypertension, type III procollagen, depositing in vascular wall when extracellular matrical components are greatly expressed, is one of the important factors promoting the remodelization of splenic veins.

Vasoactive substances

Vasoactive substances act on vascular smooth muscle cells through paracrine and autocrine system. Immunohistochemistry confirmed that in portal hypertension, the activities of iNOS, P substance, and VIP in visceral arterial wall were increased[8]. Among them, the expression of iNOS in vascular smooth muscle cells of splenic vein was increased, indicating that the production of NO was increased correspondingly. NO, a stronger vascular diastolic factor, can attenuate the response of vessels to endogenous systolic active substances, which is contributed to the activation of soluble guanylate cyclase in vascular smooth muscle cells by NO, leading to the increased production of cGMP, and intracellular Ca^{2+}, diastolization of smooth muscles, dilation of vessels, and decreased resistance. However, in hepatic cirrhosis-induced portal hypertension, the expression and activity of eNOS is reduced[31]. Transfection of eNOS[32] or heterogenic nNOS[33] genes by genetic techniques[3] could significantly reduce the animal portal pressure. By using PCR assay, Morales-Ruiz *et al*.[34], confirmed the expression of iNOS mRNA in thoracic aorta, abdominal aorta, and mesenteric arteries. The studies by Suga *et al*.[35], proved that the diastolic effect of mesenteric arteries to vasodilators in response was stronger than that of portal system. It is suggested that the over-release of NO may play an important role in the pathogenesis of visceral vascular low systolization and diastolization in portal hypertension[36].

Endothelin (ET) is the strongest vasoconstrictive polypeptide, crucially regulating the hepatic microcirculation and portal pressure. By using RT-PCR and RIA assays, Tieche *et al*., reported that in the mouse model of hepatic cirrhosis caused by bile duct ligation, the expression of ET gene was increased 6 times at 3 d after ligation and 30 times at 28 d after ligation. Moreover, it was directly correlated with the activation of hepatic stellate cells (HSCs) and the increased portal pressure. The increased expression and activity of ET gene were more obvious in portal vein and hepatic microcirculation than that in visceral arteries, and its systolic effect on veins was significantly stronger than that on arteries[37], suggesting that ET and NO are two important antagonists against portal hypertension.

AngII is an endogenous eight peptide and induces the increase in the targeting cellular Ca^{2+} concentration by binding to the specific receptor on the membrane of targeting cells to form a receptor-ligand compound. The increased Ca^{2+}, as a second messenger, can produce the intensive effects of vasoconstriction and promote smooth muscle cell proliferation by different cascade reactions. In hepatic cirrhosis-induced portal hypertension, the vasodilator substances, such as NO and PGT2, can directly or indirectly reduce the expression of AngII receptors (AT1 and AT2) in vascular endothelial cells and decrease their affinity to AngII on the surface of smooth muscle cells. Both receptors in combination with the phenotypic changes of obviously

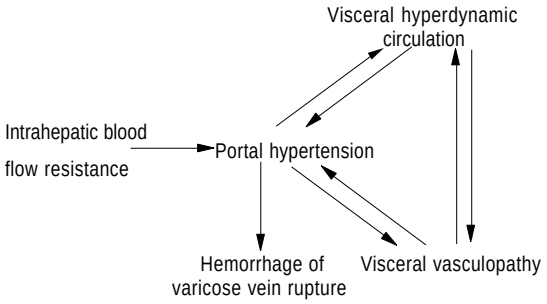
hypertrophic or hyperplastic vascular smooth muscle cells can influence the responses of vessels to AngII[38].

TGF-β plays a crucial role in regulating the deposition of external vascular matrix[39], promotes the transcription of types I and III procollagen, and contributes to fibrosis in liver and other organs noticeably. In animal models of hepatic cirrhosis and patients with chronic hepatitis, the increased TGF-β concentration was associated with the deposition of internal vascular matrix in the targeting organs. In HSCs, TGF-β could promote the synthesis of collagen[40]. Administration of TGF-β antibody or antagonists of TGF-β receptors can inhibit the synthesis of collagen. In contrast, the addition of exogenous TGF-β can increase the synthesis of collagen in smooth muscle cells[41,42]. TGF-β has many functions and exerts its biological effects via TGF-β receptors. TGF-β binds with its receptors before phosphorylation of the Smad protein and then enters into nuclei to regulate the transcription of proteins[43]. Also, TGF-β can increase the synthesis of extracellular matrix by activating Ras, Raf-1, and MEK in sequence[44,45].

NF-κB, as an important transcriptional regulatory factor, plays a key role in vasculopathy in portal hypertension[46]. After activation, the inhibition subunit I-κB of NF-κB is released into the nuclei to promote the transcription of fibrosis-associated genes via the JNK, AP-1 pathway. NK-κB is also the transcription of intercellular adhesion molecule-1 and vascular cell adhesion molecule-1[47]. It is known that besides the increased deposition of external vascular collagen for the vascular remodeling, the main factors for angiosclerosis are extracellular matrix and the binding sites of smooth muscle cells. During this process, adhesion molecules take part in regulating the binding of smooth muscles with extracellular matrix, promoting the development of vasculopathy.

Activator protein-1 (AP-1) binds with the AP-1 binding sites at the VEGF gene promoter that can promote transcription of VEGF[48]. VEGF acts through various pathways. Firstly, VEGF, the known strongest factor enhancing the vascular permeability, can increase the permeability of vascular wall[49]. VEGF functions through its receptors FLt-1 and FLk-1. In hepatic fibrosis, visceral vessels mainly express FLt-1, by which VEGF can promote the cell proliferation and collagen synthesis[50]. Secondly, VEGF possesses the chemotaxis to mononuclear macrophages and increases the adhesion of macrophages. The increased vascular permeability and the entry of mononuclear cells and macrophages into vascular intima result in the release of inflammatory factors, which can promote the smooth muscle cells proliferation and increase the synthesis of collagen[51]. VEGF can interact with basic cellular growth factor, TGF-β and hyaluronic acid to coordinately promote the proliferation of smooth muscle cells and collagen synthesis.

To sum up, the pathological changes of vasculopathy in portal hypertension include arterialized remodeling of visceral veins, the intimal injury of visceral veins and the destruction of contractile structure in visceral arterial wall. The mechanism of vasculopathy in portal hypertension may be attributed to the changes of hemodynamics in portal system, immune response, gene modulation, vasoactive substances, and intrahepatic blood flow resistance. On the one hand, portal hypertension can cause visceral hyperdynamic circulation and the development and progression of visceral vasculopathy. The visceral vasculopathy includes the destruction of contractile structure in visceral arterial wall and the remodelization of visceral veins. Vasculopathy results from the increased portal pressure and blood flow. On the other hand, visceral vasculopathy can promote the development and progression of portal hypertension and visceral hyperdynamic circulation in turn. The aforementioned three factors interact in the pathogenesis of hepatic cirrhosis-induced portal hypertension and are involved in hemorrhage of varicose vein rupture. The interaction between them is demonstrated as follows[6]:



REFERENCES

1 **Yang Z**, Liu R, Yang R. Pathology of endothelium, extracellular matrix and smooth muscle in gastric coronary vein of cirrhotic patients. *Zhonghua Waike Zazhi* 1996; **34**: 138-140
2 **Lebrec D**. Pharmacological treatment of portal hypertension: hemodynamic effects and prevention of bleeding. *Pharmacol Ther* 1994; **61**: 65-107
3 **Youssef AI**, Escalante-Glorsky S, Bonnet RB, Chen YK. Hemoptysis secondary to bronchial varices associated with alcoholic liver cirrhosis and portal hypertension. *Am J Gastroenterol* 1994; **89**: 1562-1563
4 **Burtin P**, Cales P, Oberti F, Joundy N, Person B, Carpentier S, Boyer J. Endoscopic ultrasonographic signs of portal hypertension in cirrhosis. *Gastrointesit Endosc* 1996; **44**: 257-261
5 **Malmqvist U**. Effect of long-term portal hypertension on structure, active force and content of contractile and structural proteins in smooth muscle of the rat portal vein. *Acta Physiol Scand* 1994; **150**: 171-179
6 **Yang Z**, Zhang L, Li D, Qiu F. Pathological morphology alteration of the splanchic vascular wall in portal hypertensive patients. *Chin Med J* 2002; **115**: 559-562
7 **McCarthy AL**, Woolfson RG, Raju SK, Posten L. Abnormal endothelial cell fuction of resistance arteries from women with preclampsia. *Am J Obstet Gynecol* 1993; **168**: 1323-1330
8 **Yang Z**, Ren D, Li D, Qiu F. Portal hypertensive vasculopathy of splenic artery. *Zhonghua Waike Zazhi* 1999; **37**: 412-414
9 **Krieger JE**, Dzau VJ. Molecular biology of hypertension. *Hypertension* 1991; **18**(3 Suppl): 13-17
10 **Yang Z**, Lei T, Lin P, Qiu F. Immunohistochemical analysis of growth factor expression and localization in gastric coronary vein of cirrhotic patients. *J Tongji Med Univ* 1996; **16**: 229-233
11 **Mba Mba C**, Yang Z. Role of injury of gastric parietal vessels by im-munocomplexes in the mechanism of gastric mucosal lesion in portal hypertension with cirrhosis. *J Tongji Med Univ* 1997; **17**: 44-48
12 **Li T**, Li HY, Zhang T, Ni JY, Yang Z. Splenic angiopathy in portal hypertension. *Shjie Huaren Xiaohua Zazhi* 2004; **12**: 1616-1622
13 **Watanabe T**, Pakala R, Katagiri T, Benedict CR. Monocyte chemotactic protein 1 amplifies serotonin-induced vascular smooth muscle cell proliferation. *J Vasc Res* 2001; **38**: 341-349
14 **Niculescu F**, Rus H. Complement activation and atherosclerosis.

Mol Immunol 1999; **36**: 949-955
15 **Dzau VJ**, Gibbons GH, Morishita R, Pratt RE. New perspectives in hypertension research. Potentials of vascular biology. *Hypertension* 1994; **23**: 1132-1140
16 **Bennett MR**, Evan GI, Schwartz SM. Apoptosis of rat vascular smooth muscle cells is regulated by p53-dependent and -independent pathways. *Cir Res* 1995; **77**: 266-273
17 **Chen HW**, Huang HC. Effect of curcumin on cell cycle progression and apoptosis in vascular smooth muscle cells. *Br J Pharmacol* 1998; **124**: 1029-1040
18 **Johnson GL**, Lapadat R. Mitogen-activated protein kinase pathways mediated by ERK, JNK and p38 protein kinases. *Science* 2002; **298**: 1911-1912
19 **Agell N**, Bachs O, Rocamora N, Villalonga P. Modulation of the Ras/Raf/MEK/ERK passway by Ca^{2+}, and calmodulin. *Cell Signal* 2002; **14**: 649-654
20 **Sasu S**, LaVerda D, Qureshi N, Golenbock DT, Beasley D. Chlamydia pneumoniae and chlamydial heat shock protein 60 stimulate proliferation of human vascular smooth muscle cells via toll-like receptor 4 and p44/p42 mitogen-activated protein kinase activation. *Circ Res* 2001; **89**: 244-250
21 **Blaschke F,** Stawowy P, Goetze S, Hintz O, Grafe M, Kintscher U, Fleck E, Graf K. Hypoxia activates beta(1)-intergrin via ERK1/2 and p38 MAP kinase in human vascular smooth muscle cells. *Biochem Biophys Res Commun* 2002; **296**: 890-896
22 **Komai N**, Morishita R, Yamada S, Oishi M, Iguchi S, Aoki M, Sasaki M, Sakurabayashi I, Higaki J, Ogihara T. Mitogenic activity of oxidized lipoprotein (a) on human vascular smooth muscle cells. *Hypertension* 2002; **40**: 310-314
23 **Goetze S**, Xi XP, Kawano Y, Kawano H, Fleck E, Hsueh WA, Law RE. TNF-alpha-induced migration of vascular smooth muscle cells is MAPK dependent. *Hypertension* 1999; **33** (1Pt 2): 183-189
24 **Jiang B**, Xu S, Brecher P, Cohen RA. Growth factors enhance interleukin-1 beta-induced persistent activation of nuclear factor-kappa B in rat vascular smooth muscle cells. *Arterioscler Thromb Vasc Biol* 2002; **22**: 1811-1816
25 **Christopher J**, Velarde V, Jaffa AA. Induction of B (1)-kinin receptors in vascular smooth muscle cells: cellular mechanisms of map kinase activation. *Hypertension* 2001; **38**(3Pt 2): 602-605
26 **Douillet CD**, Velarde V, Christopher JT, Mayfield RK, Trojanowska ME, Jaffa AA. Mechanisms by which bradykinin promotes fibrosis in vascular smooth muscle cells: role of TGF-beta and MAPK. *Am J Physiol Heart Circ Physiol* 2000; **279**: H2829-2837
27 **Agata J**, Miao RQ, Yayama K, Chao L, Chao J. Bradykinin B (1) recepter mediates inhibition of neointima formation in rat artery after balloon angioplasty. *Hypertension* 2000; **36**: 364-370
28 **Karim MA**, Miller DD, Farrar MA, Eleftheriades E, Reddy BH, Breland CM, Samarel AM. Histomorphometric and biochemical correlates of arterial procollagen gene expression during vascular repair after experimental angioplasty. *Circulation* 1995; **91**: 2049-2057
29 **Shi Y**, O'Brien JE Jr, Ala-Kokko L, Chung W, Mannion JD, Zalewski A. Origin of extracellular matrix synthsis during coronary repair. *Circulation* 1997; **95**: 997-1006
30 **Bahadori L**, Milder J, Gold L, Botney M. Active macrophage-associated TGF-beta β co-localizes with type I procollagen gene expression in atherosclerotic human pulmonary arteries. *Am J Pathol* 1995; **146**: 1140-1149
31 **Rockey DC**, Chung JJ. Reduced nitric oxide production by endothelial cells in cirrhotic rat liver: endothelial dysfunction in portal hypertension. *Gastroenterology* 1998; **114**: 344–351
32 **Van de Casteele M**, Omasta A, Janssens S, Roskams T, Desmet V, Nevens F, Fevery J. *In vivo* gene transfer of endothelial nitric oxide synthase decreases portal pressure in anaesthetised carbon tetrachloride cirrhotic rats. *Gut* 2002; **51**: 440-445
33 **Yu Q**, Shao R, Qian HS, George SE, Rockey DC. Gene transfer of the neuronal NO synthase isoform to cirrhotic rat liver ameliorates portal hypertension. *J Clin Invest* 2000; **105**: 741-748
34 **Morales-Ruiz M**, Jimenez W, Perez-Sala D, Ros J, Leivas A, Lamas S, Rivera F, Arroyo V. Increased nitric oxide synthase expression in arterial vessels of cirrhotic rats with ascites. *Hepatology* 1996; **24**: 1481-1486
35 **Suga T**, Itoh H, Shimomura A, Kusagawa M, Zto M, Takase K, Konishi T, Nakano T. Comparison of the effects of various vasodilators on the rat portal vein and mesenteric artery. *Eur J Pharmacol* 1993; **242**: 129-136
36 **Hartleb M**, Michielsen PP, Dziurkowska-Marek A. The role of nitric oxide in portal hypertensive systemic and portal vascular pathology. *Acta Gastroenterol Belg* 1997; **60**: 222-232
37 **Luscher TF**, Yang Z, Tschudi M, von Segesser L, Stulz P, Boulanger C, Siebenmann R, Turina M, Buhler FR. Interaction between endothelin-1 and endothelium-derived relaxing factor in human arteries and veins. *Circ Res* 1990; **66**: 1088-1094
38 **Cahill PA**, Redmond EM, Sitzmann JV. Endothelial dysfunction in cirrhosis and portal hypertension. *Pharmacol Ther* 2001; **89**: 273-293
39 **George J**, Roulot D, Koteliansky VE, Bissell DM. *In vivo* inhibition of rat stellate cell activation by soluble transforming growth factor beta type? receptor: a potential new therapy for hepatic fibrosis. *Proc Natl Acad Sci USA* 1999; **96**: 12719-12724
40 **Schlumberger W**, Thiem M, Rauterberg J, Robenek H. Collagen synthesis in cultured aortic smooth muscle cells. Modulation by collagen lattice culture transforming growth factor-beta 1 and epidermal growth factor. *Arterioscler Thromb* 1991; **11**: 1660-1666
41 **O'Callaghan CJ**, Williams B. Mechanical strain-induced extracellular matrix production by human vascular smooth muscle cells: role of TGF-beta(1). *Hypertension* 2000; **36**: 319-324
42 **Simonson MS**. Endothelins: multifunctional renal peptides. *Physiol Rev* 1993; **73**: 375-411
43 **Reimann T**, Hempel U, Krautwald S, Axmann A, Scheibe R, Seidel D, Wenzel KW. Transforming growth factor-beta1 induces activation of Ras, Raf-1, MEK and MAPK in rat hepatic stellate cells. *FEBS Lett* 1997; **403**: 57-60
44 **Davis BH,** Chen AP, Beno DW. Raf and mitogen-activated protein kinase regulate stellate cell collagen gene expression. *J Biol Chem* 1996; **271**: 11039-11042
45 **Gomez-Garre D**, Largo R, Tejera N, Fortes J, Manzarbeitia F, Egido J. Activation of NF-KappaB in tubular epithelial cells of rats with intense proteinuria: role of angiotensin II and endothelin-1. *Hypertension* 2001; **37**: 1171-1178
46 **Liu H**, Lo CR, Czaja MJ. NF-KappaB inhibition sensitizes hepatocytes to TNF-induced apoptosis through a sustained activation of JNK and c-Jun. *Hepatology* 2002; **33**: 772-778
47 **Tomita N**, Morishita R, Tomita S, Kaneda Y, Higaki J, Ogihara T, Horiuchi M. Inhibition of TNF-alphainduced cytokine and adhesion molecule. Expression in glomerular cells *in vitro* and *in vivo* by transcription factor decoy for NFkappaB. *Exp Nephrol* 2001; **9**: 181-190
48 **Tischer E**, Mitchell R, Hartman T, Silva M, Gospodarowicz D, Fiddes JC, Abraham JA. The human gene for vascular endothelial growth factor. Multiple protein forms are encoded through alternative exon splicing. *J Biol Chem* 1991; **266**: 11947-11954
49 **Keck PJ**, Hauseris D, Krivi G, Sanzo K, Warren T, Feder J, Connolly DT. Vascular permeability factor an endothelial cell mitogen related to PDGF. *Science* 1989; **246**: 1309-1312
50 **Corpechot C**, Barbu V, Wendum D, Kinnman N, Rey C, Poupon R, Housset C, Rosmorduc O. Hypoxia-induced VEGF and collagen I expressions are associated with angiogenesis and fibrogenesis in experimental cirrhosis. *Hepatology* 2002; **35**: 1010-1021
51 **Barleon B**, Sozzani S, Zhou D, Weich HA, Mantovani A, Marme D. Migration of human monocytes in response to vascular endothelial growth factor (VEGF) is mediated via the receptor flt-1. *Blood* 1996; **87**: 3336-3343

Science Editor Zhu LH and Kumar M, Guo SY **Language Editor** Elsevier HK

PO Box 2345, Beijing 100023, China
www.wjgnet.com
wjg@wjgnet.com

ELSEVIER

World J Gastroenterol 2005;11(39):6085-6089
World Journal of Gastroenterology ISSN 1007-9327
© 2005 The WJG Press and Elsevier Inc. All rights reserved.

• *REVIEW* •

Chronic hepatitis C virus infection and post-liver transplantation diabetes mellitus

Yun Ma, Wen-Wei Yan

Yun Ma, Basement 3 The Marco Polo Hotel, 6 Xuanwumen Nei Avenue, Xicheng District, Beijing 10003, China
Wen-Wei Yan, Department of Organ Transplantation, Tianjin First Central Hospital, Tianjin 300192, China
Correspondence to: Wen-Wei Yan, MD, Department of Organ Transplantation, Tianjin First Central Hospital, Tianjin 300192, China. wenweiyanboy@yahoo.com
Telephone: +86-22-23626549 Fax: +86-22-23682662
Received: 2005-03-01 Accepted: 2005-04-11

Abstract

Patients with chronic hepatitis C virus (HCV) infection have a significantly increased prevalence of type 2 diabetes mellitus compared to controls or HBV-infected patients. Moreover, the incidence rate of post-liver transplantation diabetes mellitus (PTDM) also appears to be higher among patients with HCV infection. PTDM is often associated with direct viral infection, autoimmune disorders, and immunosuppressive regimen. Activation of tumor necrosis factor-α may be the link between HCV infection and diabetes. In this article, we reviewed the epidemiologic association between HCV infection and PTDM, highlighting the most recent pathophysiologic insights into the mechanisms underlying this association.

© 2005 The WJG Press and Elsevier Inc. All rights reserved.

Key words: Hepatitis C virus; Post-liver transplantation diabetes mellitus; Tumor necrosis factor; Immunosuppressive therapy

Ma Y, Yan WW. Chronic hepatitis C virus infection and post-liver transplantation diabetes mellitus. *World J Gastroenterol* 2005; 11(39): 6085-6089
http://www.wjgnet.com/1007-9327/11/6085.asp

INTRODUCTION

The last two decades have seen an increase in various types of organ transplantation for the treatment of end stage organ diseases. Prevention of organ rejection requires long-term immunosuppressive therapy, which places recipients at the increasing risk of infection and metabolic disorders, such as recurrent hepatitis C virus (HCV) infection and post-liver transplantation diabetes mellitus (PTDM). Recipients with HCV infection have a higher incidence of PTDM, which depends on the degree and duration of immunosuppressant[1]. On the other hand, the occurrence of PTDM is associated with direct viral infection, autoimmune disorders[3], and immunosuppressive regimen, notably tacrolimus[4]. PTDM characteristically shows insidious onset and aggressive behavior thereafter. PTDM in HCV-infected patients might be partially or completely recovered after reduction or switching of immunosuppressive therapy[5].

PTDM AND HCV ASSOCIATION: RISK FACTORS

The high prevalence of diabetes mellitus, especially type 2 diabetes mellitus (type 2 DM) in HCV-infected patients comes from epidemiologic studies (Table 1), most of which are case control studies,[6,7,9,10-12,14] in addition to two multicenters and cohort[8,13]. Risk factors resulting in the increasing prevalence of type 2 DM in HCV-infected patients include positive family history of diabetes and black ethnicity[15]. Thus, it is conceivable that HCV leads to type 2 DM in susceptible hosts. Immunogenetic studies suggest that an infectious process coexists in patients with type 2 DM and chronic liver disease and HLA-DR2, -DR51, -DQB6 haplotypes provide a two- and three-fold relative risk for the development of diabetes[16].

It is reported that liver transplantation recipients with HCV infection have a four- to eight-fold prevalence of diabetes compared with recipients with other viral or cholestatic liver diseases 1 year after liver transplantation. A recent study of 260 HCV-infected patients has confirmed that insulin resistance is an independent predictor of the degree of fibrosis, and that insulin sensitivity has a significant correlation with serum aspartate aminotransferase, histological activity index and degree of fibrosis[18] in non-diabetic HCV-infected patients. Gray *et al*.[17], observed that abnormal liver function tests are found in 72.3% of HCV-positive diabetic patients and in only 24.7% of HCV-negative diabetic patients ($P<0.001$). In summary, the occurrence of PTDM seems to be associated with HCV infection.

PATHOPHYSIOLOGY

The pathophysiologic mechanism underlying the development of PTDM in patients with HCV infection has not been clearly illustrated. Possible mechanisms are shown in Figure 1.

Tumor necrosis factor-alpha (TNF-α)

A study of liver biopsy specimens from non-diabetic HCV-infected patients has revealed significant impairments in the insulin-signaling pathway[19], which is strikingly similar to the known effect of tumor necrosis factor-α (TNF-α) on insulin resistance[20]. The role of TNF-α in the pathogenesis of this HCV-associated insulin resistance state is strongly

Table 1 Studies of PTDM in patients with chronic HCV infection

PTDM (%)		RR (95%CI)	Study description	Reference
HCV+	HCV-			
33	12	3 (0.98-9.6)[b]	Case control	Zein *et al.*, 2000
34	9.8	0.95 (0.2-3.9)[a]	Case control	Bigam *et al.*, 2000
20.9	-	1.9 (0.4-14.2)	Multicenter	Khalili *et al.*, 2004
43	13	1.9 (1-2.6)[b]	Case control	AlDosary *et al.*, 2002
64	28	2 (0.9-4.6)[b]	Case control	Baid *et al.*, 2002
29	10	2 (0.96-4.3)[b]	Case control	Bigam *et al.*, 2000
72	37	4.8 (0.8-30)[d]	Case control	Yildiz *et al.*, 2002
62	8	11.6 (1.7-79)[b]	Cohort	Delgado-Borrego *et al.*, 2004
18.29	-	-	Case control	Parolin *et al.*, 2004

[a]$P<0.05$, [b]$P<0.01$, [d]$P<0.001$ *vs* control.

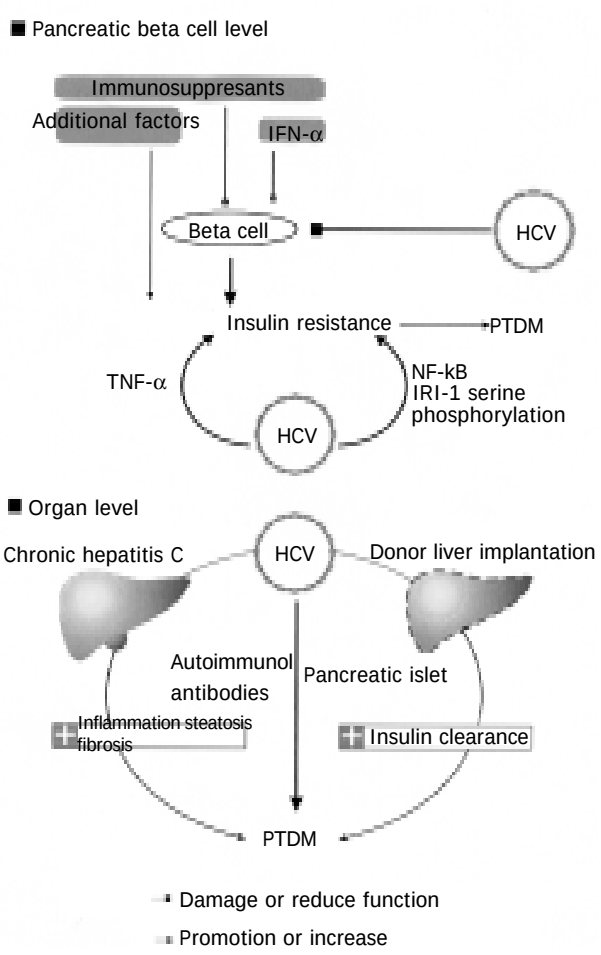


Figure 1 Possible mechanism underlying the development of PTDM in HCV infection (at least four mechanisms contribute to exacerbation of insulin resistance). (1) Chronic activation of TNF-α, which plays a key role not only in the production of and response to HCV itself, but also in the development of insulin resistance. Additional factors for developing PTDM in HCV-infected patients, including obesity, black ethnicity, and aging, are known to be associated with increased TNF-α independent mechanisms; (2) the increased clearance of insulin that occurs in post-transplant recipients thus creates a reactive hyperinsulinemic medium, and that in turn might enhance insulin resistance; (3) a bi-directional relationship between liver disease and diabetes is possible, as both insulin resistance and PTDM can adversely affect HCV liver disease; (4) directly diabetogenic effect of immunosuppressive therapy on pancreatic β cell.

supported by findings of elevated intra-hepatic TNF-α and amelioration of the metabolic abnormalities after TNF-α antibodies are administered[2]. The interrelationship between HCV and other predisposing conditions of PTDM could partly be mediated by TNF-α and most of the established risk factors for PTDM, such as obesity, aging[21], black ethnicity[22], and a family history of type 2 DM[23].

HCV per se

HCV replicates in hepatocytes, but its genome has been identified in a number of other tissues, including pancreatic acinar cells and epithelial cells of the pancreatic duct[24]. The destruction of pancreatic β cells could be mediated either directly by HCV or by HCV-induced immune responses, but evidence is scanty[3]. More recently, a transgenic mouse model that specifically expresses the HCV core protein in hepatocytes has been studied[2]. These animals had insulin resistance at an early age, and when challenged by a high fat diet, they developed glucose intolerance. Further characterization of the metabolic defects in these animals revealed that insulin resistance was caused mainly by failure of insulin to suppress hepatic glucose production. Piquer *et al.*[25], assessed the prevalence of islet cell autoantibodies in 303 non-selected HCV-infected patients (277 non-diabetic and 26 type 2 DM patients) and 273 sex- and age-matched control subjects, and found that patients with HCV have no significantly higher pancreatic autoantibodies compared with controls. However, it was reported that type 1 DM occurs more frequently in HCV patients treated with interferon (IFN) as a result of amplification of previously existing autoimmunity against pancreatic β cells, and that treatment of healthy volunteers with IFN can stimulate counter-regulatory hormone secretion, impair glucose tolerance and insulin sensitivity and induce insulin clearance, suggesting that HCV-induced immune response might be involved in the development of insulin resistance[26].

Immunosuppressive therapy

The overall effects of immunosuppression may potentiate the diabetogenic effects of HCV infection by enhancing the level of viral replication. A study on the effects of corticosteroids on post-transplant levels of viremia and PTDM showed that pulsed intravenous methylprednisolone therapy is associated with transient 4- to 100-fold rise in HCV RNA levels and the reduced translocation of glucose transporter 4 from cytosol into membrane, and that higher HCV RNA level is correlated with increased severity of graft and islet injury[30,45,46]. Immunosuppressive agents, especially steroids and calcineurin

inhibitors, are diabetogenic. The direct and indirect effects of corticosteroids, CyA on pancreatic β cells are well documented. With regard to FK506, the available data are not as extensive as for CyA, and its role in low blood insulin levels *vs* insulin resistance has not been fully evaluated. Human pancreatic allograft biopsies demonstrating both FK506 and CyA can induce structural damage of the graft islets, for example, cytoplasmic swelling, vacuolization, apoptosis, and abnormal immunostaining for insulin and the absent or reduced dense core secretory granules in the β cells. These changes are related to the doses of FK506 and/or CyA used. Although CyA and FK506 bind to different target molecules, both drugs inhibit or perturb the intermediate molecular events of insulin signal transduction (serine phosphorylations/dephosphorylations) in the same fashion. As a result, insulin signal fails to dephosphorylate the cytoplasmic component of the nuclear factor of activated signal transduction and transcription of insulin-sensitive gene, thus incorporating insulin resistance[27,28].

Organ level

Nonalcoholic fatty liver disease is associated with type 2 DM and the metabolic syndrome in patients with HCV[29]. However, the role of HCV as a risk factor for fatty liver has been questioned. It was reported that obesity and hyperlipidemia have a confounding effect on the association between HCV and steatosis[30]. In one study, serum ferritin levels were determined in 123 HCV-infected patients (55 diabetic and 68 non-diabetic patients)[32]. Increased iron store, which occurs in up to 40% of patients with chronic HCV infection[31], has been linked to the pathogenesis of diabetes development in those patients. The hepatic parasympathetic nerves are mediated by the activation of the Ach/NO/cGMP pathway involved in the secretion of a hepatic insulin sensitizing substance to mediate peripheral insulin sensitivity[41,42]. Schneiter *et al.*[33], found that liver transplantation recipients have severe insulinopenia as a result of the increased insulin clearance[33].

CLINICAL FEATURES

PTDM shares many similarities with type 2 DM in that the onset can be insidious, and individuals may experience glucose intolerance and may be asymptomatic for years[5]. The development of PTDM involves two distinct phases: (a) patients are initially at the greatest risk during the first 6 mo post-transplantation, and (b) the number of patients developing diabetes increases progressively thereafter. This has been illustrated by a study of 618 liver allograft recipients in which 7.2% of patients developed diabetes in the first 6 mo after transplantation, but then the percentage of cases increased linearly, leading to cumulative percentages of 7.1%, 10.4%, 13.2%, 20.5%, and 29.8%, respectively after 1, 3, 5, 10, and 15 years[34]. In a recent study, unadjusted cumulative incidences of diabetes 3, 12, and 36 mo after kidney transplantation were 15.6%, 25.6%, and 35.4% compared to 8.8%, 15.4%, and 23.4% in patients who were HCV negative at transplantation ($P<0.0001$)[35]. The potentially asymptomatic and/or transient nature of diabetes after transplantation makes the condition difficult to diagnose, thus underlining the importance of establishing a precise definition. It is recommended that the definition and diagnosis of PTDM should be based on the currently accepted definition of diabetes mellitus by the American Diabetes Association[5]. Diabetes mellitus is diagnosed by three fasting glucose measurements in the plasma above 7.0 mmol/L and/or antidiabetic medication (oral antidiabetic drugs or insulin), excluding periods requiring total parenteral nutrition or high steroid dosages for treatment of acute rejection, which may transiently impair glucose tolerance. After liver transplantation, patients with diabetes mellitus are classified either as non-insulin-requiring PTDM when taking only oral antidiabetic drugs or diet or as insulin-requiring PTDM when they require insulin injections. This classification of the patients should be done more than 1 year after liver transplantation[36]. Some preliminary reports suggest that pre-emptive therapy with IFN or a combination of IFN plus ribavirin may lead to less severe HCV infection recurrence after liver transplantation[43,44]. However, there are no controlled studies evaluating the prophylaxis of IFN in PTDM with HCV infection.

IMPLICATIONS

The HCV-diabetes association represents a major public health problem. Hundreds and thousands of patients in the USA alone are probably affected, and many more may have impaired glucose tolerance. Diabetes-related micro- and macrovascular complications are likely to occur, and the ongoing hepatic inflammatory response may contribute to atherogenesis. Furthermore, a putative bi-directional relationship between HCV-induced liver disease and diabetes may occur. Both insulin resistance and diabetes can adversely affect the course of chronic hepatitis C, and lead to enhanced steatosis, steatohepatitis, and liver fibrosis[37,38]. Moreover, recent evidence strongly suggests that steatosis and diabetes may also significantly enhance the risk of hepatocellular cancer[39,40].

FUTURE DIRECTIONS

There is evidence that HCV infection is related with the presence of PTDM. However, several questions remain to be answered. Firstly, randomized trials aimed to evaluate interactions of immunosuppressive regimens for the prophylaxis and treatment of PTDM are scarce. Secondly, the antiviral therapy for intervention remains to be determined. Finally, information is needed to clarify and diminish the effect of PTDM on quality of life and long-term outcomes. Further studies are necessary to evaluate the prognostic meaning of PTDM and the predictive factors for PTDM and to elucidate the pathophysiologic mechanisms.

REFERENCES

1 **Mathew JT**, Rao M, Job V, Ratnaswamy S, Jacob CK. Post-transplant hyper- glycaemia: a study of risk factors. *Nephrol Dial Transplant* 2003; **18**: 164-171
2 **Shintani Y**, Fujie H, Miyoshi H, Tsutsumi T, Tsukamoto K, Kimura S, Moriya K, Koike K. Hepatitis C virus infection and diabetes: direct involvement of the virus in the development of insulin resistance. *Gastroenterology* 2004; **26**: 840-848
3 **Hadziyannis SJ**. The spectrum of extrahepatic manifestations in hepatitis C virus infection. *J Viral Hepat* 1997; **4**: 9-28
4 **Kreis H**, Oberbauer R, Campistol JM, Mathew T, Daloze P,

Schena FP, Burke JT, Brault Y, Gioud-Paquet M, Scarola JA, Neylan JF. Rapamune Maintenance Regimen trial. Long-term benefits with sirolimus-based therapy after early cyclosporine withdrawal. *J Am Soc Nephrol* 2004; **15**: 809-817

5 **Davidson J**, Wilkinson A, Dantal J, Dotta F, Haller H, Hernandez D, Kasiske BL, Kiberd B, Krentz A, Legendre C, Marchetti P, Markell M, van der Woude FJ, Wheeler DC. International Expert Panel. New-onset diabetes after transplantation: 2003 International consensus guidelines. Proceedings of an international expert panel meeting. Barcelona, Spain, 19 February 2003. *Transplantation* 2003; **75**(10 Suppl): SS3-24

6 **Zein NN**, Abdulkarim AS, Wiesner RH, Egan KS, Persing DH. Prevalence of diabetes mellitus in patients with end-stage liver cirrhosis due to hepatitis C, alcohol, or cholestatic disease. *J Hepatol* 2000; **32**: 209-217

7 **Bigam DL**, Pennington JJ, Carpentier A, Wanless IR, Hemming AW, Croxford R, Greig PD, Lilly LB, Heathcote JE, Levy GA, Cattral MS. Hepatitis C-related cirrhosis: a predictor of diabetes after liver transplantation. *Hepatology* 2000; **32**: 87-90

8 **Khalili M**, Lim JW, Bass N, Ascher NL, Roberts JP, Terrault NA. New onset diabetes mellitus after liver transplantation: the critical role of hepatitis C infection. *Liver Transpl* 2004; **10**: 349-355

9 **AlDosary AA**, Ramji AS, Elliott TG, Sirrs SM, Thompson DM, Erb SR, Steinbrecher UP, Yoshida EM. Post-liver transplantation diabetes mellitus: an association with hepatitis C. *Liver Transpl* 2002; **8**: 356-361

10 **Baid S**, Tolkoff-Rubin N, Farrell ML, Delmonico F, Williams WW, Hayden D, Ko D, Cosimi AB, Pascual M. Tacrolimus-associated posttransplant diabetes mellitus in renal transplant recipients: role of hepatitis C infection. *Transplant Proc* 2002; **34**: 1771-1773

11 **Bigam DL**, Pennington JJ, Carpentier A, Wanless IR, Hemming AW, Croxford R, Greig PD, Lilly LB, Heathcote JE, Levy GA, Cattral MS. Hepatitis C-related cirrhosis: a predictor of diabetes after liver transplantation. *Hepatology* 2000; **32**: 87-90

12 **Yildiz A**, Tutuncu Y, Yazici H, Akkaya V, Kayacan SM, Sever MS, Carin M, Karsidag K. Association between hepatitis C virus infection and development of post-transplantation diabetes mellitus in renal transplant recipients. *Transplantation* 2002; **74**: 1109-1113

13 **Delgado-Borrego A**, Casson D, Schoenfeld D, Somsouk M, Terella A, Jordan SH, Bhan A, Baid S, Cosimi AB, Pascual M, Chung RT. Hepatitis C virus is independently associated with increased insulin resistance after liver transplantation. *Transplantation* 2004; **77**: 703-710

14 **Parolin MB**, Zaina FE, Araujo MV, Kupka E, Coelho JC. Prevalence of new-onset diabetes mellitus in Brazilian liver transplant recipients: association with HCV infection. *Transplant Proc* 2004; **36**: 2776-2777

15 **Mehta SH**, Brancati FL, Strathdee SA, Pankow JS, Netski D, Coresh J, Szklo M, Thomas DL. Hepatitis C virus infection and incident type 2 diabetes. *Hepatology* 2003; **38**: 50-56

16 **Bosi E**, Minelli R, Bazzigaluppi E, Salvi M. Fulminant autoimmune Type 1 diabetes during interferon-alpha therapy: a case of Th1-mediated disease? *Diabet Med* 2001; **18**: 329-332

17 **Gray H**, Wreghitt T, Stratton IM, Alexander GJ, Turner RC, O'Rahilly S. High prevalence of hepatitis C infection in Afro-Caribbean patients with type 2 diabetes and abnormal liver function tests. *Diabet Med* 1995; **12**: 244-249

18 **Hui JM**, Kench JG, Chitturi S, Sud A, Farrell GC, Byth K, Hall P, Khan M, George J. Long-term outcomes of cirrhosis in nonalcoholic steatohepatitis compared with hepatitis C. *Hepatology* 2003; **38**: 420-427

19 **Aytug S**, Reich D, Sapiro LE, Bernstein D, Begum N. Impaired IRS-1/PI3-kinase signaling in patients with HCV: a mechanism for increased prevalence of type 2 diabetes. *Hepatology* 2003; **38**: 1384-1392

20 **Ruan H**, Lodish HF. Insulin resistance in adipose tissue: direct and indirect effects of tumor necrosis factor-alpha. *Cytokine Growth Factor Rev* 2003; **14**: 447-455

21 **Ersoy C**, Imamoglu S, Budak F, Tuncel E, Erturk E, Oral B. Effect of amlodipine on insulin resistance & tumor necrosis factor-alpha levels in hypertensive obese type 2 diabetic patients. *Indian J Med Res* 2004; **120**: 481-488

22 **Kimball P**, Elswick RK, Shiffman M. Ethnicity and cytokine production gauge response of patients with hepatitis C to interferon-alpha therapy. *J Med Virol* 2001; **65**: 510-516

23 **Kobayashi S**, Suzuki M, Tsuneki H, Nagai R, Horiuchi S, Hagino N. Overproduction of N(epsilon)-(carboxymethyl) lysine-induced neovascularization in cultured choroidal explant of streptozotocin diabetic rat. *Biol Pharm Bull* 2004; **27**: 1565-1571

24 **Gowans EJ**, Jones KL, Bharadwaj M, Jackson DC. Prospects for dendritic cell vaccination in persistent infection with hepatitis C virus. *J Clin Virol* 2004; **30**: 283-290

25 **Piquer S**, Hernandez C, Enriquez J, Ross A, Esteban JI, Genesca J, Bonifacio E, Puig-Domingo M, Simo R. Islet cell and thyroid antibody prevalence in patients with hepatitis C virus infection: effect of treatment with interferon. *J Lab Clin Med* 2001; **137**: 38-42

26 **Weir MR**, Fink JC. Risk for posttransplant Diabetes mellitus with current immuno- suppressive medications. *Am J Kidney Dis* 1999; **34**: 1-13

27 **Drachenberg CB**, Klassen DK, Weir MR, Wiland A, Fink JC, Bartlett ST, Cangro CB, Blahut S, Papadimitriou JC. Islet cell damage associated with tacrolimus and cyclosporine: morphologicalfeatures in pancreas allograft biopsies and clinical correlation. *Transplantation* 1999; **68**: 396-402

28 **Aytug S**, Reich D, Sapiro LE, Bernstein D, Begum N. Impaired IRS-1/PI3-kinase signaling in patients with HCV: a mechanism for increased prevalence of type 2 diabetes. *Hepatology* 2003; **38**: 1384-1392

29 **Sanyal AJ**, Contos MJ, Sterling RK, Luketic VA, Shiffman ML, Stravitz RT, Mills AS. Nonalcoholic fatty liver disease in patients with hepatitis C is associated with features of the metabolic syndrome. *Am J Gastroenterol* 2003; **98**: 2064-2071

30 **Monto A**, Alonzo J, Watson JJ, Grunfeld C, Wright TL. Steatosis in chronic hepatitis C: relative contributions of obesity, diabetes mellitus, and alcohol. *Hepatology* 2002; **36**: 729-736

31 **Riggio O**, Montagnese F, Fiore P, Folino S, Giambartolomei S, Gandin C, Merli M, Quinti I, Violante N, Caroli S, Senofonte O, Capoccaccia L. Iron overload in patients with chronic viral hepatitis: how common is it? *Am J Gastroenterol* 1997; **92**: 1298-1301

32 **Furutani M**, Nakashima T, Sumida Y, Hirohama A, Yoh T, Kakisaka Y, Mitsuyoshi H, Senmaru H, Okanoue T. Insulin resistance/beta-cell function and serum ferritin level in non-diabetic patients with hepatitis C virus infection. *Liver Int* 2003; **23**: 294-299

33 **Schneiter P**, Gillet M, Chiolero R, Jequier E, Mosimann F, Temler E, Teta D, Matter M, Wauters JP, Tappy L. Mechanisms of postprandial hyperglycemia in liver transplant recipients:comparison of liver transplant patients with kidney transplant patients and healthy controls. *Diabetes Metab* 2000; **26**: 51-56

34 **Huo TI**, Yang WC, Wu JC, King KL, Lin CY, Loong CC, Lui WY, Chang FY, Lee SD. Long-term outcome of kidney transplantation in patients with hepatitis C virus infection. *Hepatogastroenterology* 2001; **48**: 169-173

35 **Duijnhoven EM**, Boots JM, Christiaans MH, Wolffenbuttel BH, Van Hooff JP. Influence of tacrolimus on glucose metabolism before and after renal transplant- tation: a prospective study. *J Am Soc Nephrol* 2001; **12**: 583-588

36 **Stockmann M**, Steinmuller T, Nolting S, Neuhaus P. Posttransplant diabetes mellitus after orthotopic liver transplantation. *Transplant Proc* 2002; **34**: 1571-1572

37 **Adinolfi LE**, Gambardella M, Andreana A, Tripodi MF, Utili R, Ruggiero G. Steatosis accelerates the progression of liver damage of chronic hepatitis C patients and correlates with specific HCV genotype and visceral obesity. *Hepatology* 2001; **33**: 1358-1364

38 **Castera L**, Hezode C, Roudot-Thoraval F, Bastie A, Zafrani

ES, Pawlotsky JM, Dhumeaux D. Worsening of steatosis is an independent factor of fibrosis progression in untreated patients with chronic hepatitis C and paired liver biopsies. *Gut* 2003; **52**: 288-292

39 **Tazawa J**, Maeda M, Nakagawa M, Ohbayashi H, Kusano F, Yamane M, Sakai Y, Suzuki K. Diabetes mellitus may be associated with hepatocarcinogenesis in patients with chronic hepatitis C. *Dig Dis Sci* 2002; **47**: 710-715

40 **Ohata K**, Hamasaki K, Toriyama K, Matsumoto K, Saeki A, Yanagi K, Abiru S, Nakagawa Y, Shigeno M, Miyazoe S, Ichikawa T, Ishikawa H, Nakao K, Eguchi K. Hepatic steatosis is a risk factor for hepatocellular carcinoma in patients with chronic hepatitis C virus infection. *Cancer* 2003; **97**: 3036-3043

41 **Lautt WW**, Macedo MP, Sadri P, Takayama S, Duarte Ramos F, Legare DJ. Hepatic parasympathetic (HISS) control of insulin sensitivity determined by feeding and fasting. *Am J Physiol Gastrointest Liver Physiol* 2001; **281**: 29-36

42 **Guarino MP**, Afonso RA, Raimundo N, Raposo JF, Macedo MP. Hepatic glutathione and nitric oxide are critical for hepatic insulin-sensitizing substance action. *Am J Physiol Gastrointest Liver Physiol* 2003; **284**: G588-G594

43 **Sheiner PA**, Boros P, Klion FM, Thung SN, Schluger LK, Lau JY, Mor E, Bodian C, Guy SR, Schwartz ME, Emre S, Bodenheimer HC Jr, Miller CM. The efficacy of prophylactic interferon alfa-2b in preventing recurrent hepatitis C after liver transplantation. *Hepatology* 1998; **28**: 831-838

44 **Singh N**, Gayowski T, Wannstedt CF, Shakil AO, Wagener MM, Fung JJ, Marino IR. Interferon- alpha for prophylaxis of recurrent viral hepatitis C in liver transplant recipients: a prospective, randomized, controlled trial. *Transplantation* 1998; **65**: 82-86

45 **Charlton M**. Liver biopsy, viral kinetics, and the impact of viremia on severity of hepatitis C virus recurrence. *Liver Transpl* 2003; **9**: S58-S62

46 **Konrad T**, Zeuzem S, Toffolo G, Vicini P, Teuber G, Briem D, Lormann J, Lenz T, Herrmann G, Berger A, Cobelli C, Usadel K. Severity of HCV-induced liver damage alters glucose homeostasis in noncirrhotic patients with chronic HCV infection. *Digestion* 2000; **62**: 52-59

Science Editor Wang XL and Guo SY **Language Editor** Elsevier HK

PO Box 2345, Beijing 100023, China
www.wjgnet.com
wjg@wjgnet.com

ELSEVIER

World J Gastroenterol 2005;11(39):6090-6095
World Journal of Gastroenterology ISSN 1007-9327
© 2005 The WJG Press and Elsevier Inc. All rights reserved.

Value of endoscopic methylene blue and Lugol's iodine double staining and detection of GST-π and telomerase in the early diagnosis of esophageal carcinoma

Xuan Zhu, Shuang-Hong Zhang, Kun-He Zhang, Bi-Ming Li, Jiang Chen

Xuan Zhu, Shuang-Hong Zhang, Bi-Ming Li, Department of Gastroenterology, the First Affiliated Hospital, Jiangxi Medical College, Nanchang 330006, Jiangxi Province, China
Kun-He Zhang, Jiang Chen, Department of Digestive Institution, the First Affiliated Hospital, Jiangxi Medical College, Nanchang 330006, Jiangxi Province, China
Supported by the Scientific and Technological Foundation of the Education Department of Jiangxi Province
Co-first-authors: Xuan Zhu and Shuang-Hong Zhang
Co-correspondents: Xuan Zhu
Correspondence to: Dr. Xuan Zhu, Department of Gastroenterology, the First Affiliated Hospital, Jiangxi Medical College, Nanchang 330006, Jiangxi Province, China. jyyfyzx@163.com
Telephone: +86-791-8692505
Received: 2004-12-30 Accepted: 2005-02-28

Abstract

AIM: To explore the expressions of GST-π and telomerase activity in esophageal carcinoma and premalignant lesions and to investigate the value of endoscopic methylene blue (MB) and Lugol's iodine double staining.

METHODS: Seventy-two patients with esophagopathy were sprayed endoscopically with MB and Lugol's iodine in proper order and the areas stained blue and brown, and the area between the blue and brown stains were obtained. Depending on the pattern of mucosal staining, biopsy specimen was obtained. GST-π and telomerase activity in specimens were examined by immunohistochemistry and PCR-based silver staining telomeric repeat amplification protocol, respectively.

RESULTS: After MB and Lugol's iodine staining, the area between both the colors was obtained in 64 of the 72 patients and the areas were stained blue and brown in all of the 72 patients. Association test of two simultaneous ordinal categorical data showed a correlation between the esophageal mucosal staining and the esophageal histology (P<0.005). The expression of GST-π and telomerase activity in esophageal carcinoma and premalignant lesions increased. The expression of GST-π and telomerase activity in dysplasia and carcinoma was significantly higher than that in normal epithelium (P<0.005). The expression in hyperplasia was slightly higher than that in normal epithelium. With the lesions progressing from low- to moderate- to high-grade dysplasia, the positive rate increased (P<0.025). Expression of GST-π was correlated with that of telomerase activity in dysplasia and carcinoma (φ = 0.4831, P<0.005; φ = 0.3031, P<0.025, respectively); but there was no correlation between them in normal epithelium and hyperplasia.

CONCLUSION: The expression of GST-π and telomerase may be an early event in the carcinogenesis of esophagus. They may play an induced and synergistic role with each other in the carcinogenesis of esophagus. Endoscopic MB and Lugol's iodine double staining and detection of GST-π and telomerase activity may contribute to the early diagnosis of esophageal carcinoma.

© 2005 The WJG Press and Elsevier Inc. All rights reserved.

Key words: Esophageal carcinoma; Endoscopy; Glutathione *S*-transferases; Telomerase

Zhu X, Zhang SH, Zhang KH, Li BM, Chen J. Value of endoscopic methylene blue and Lugol's iodine double staining and detection of GST-π and telomerase in the early diagnosis of esophageal carcinoma. *World J Gastroenterol* 2005; 11 (39): 6090-6095
http://www.wjgnet.com/1007-9327/11/6090.asp

INTRODUCTION

The early diagnosis of esophageal carcinoma correlates closely to improvement in prognosis. Much dependent on endoscopy, esophageal carcinoma is clinically diagnosed till now, but the choice of biopsy site, partly, has a limitation. The esophageal mucosal staining technique not only obtains the characteristic of the morphology of the lesions, but also helps to direct its biopsy in esophageal carcinoma. Carcinogen is one of the induced etiological factors. The glutathione *S*-transferases (GSTs) are a family of enzymes, which participate in metabolic detoxication and play important roles in the prevention of carcinogenesis by detoxifying numerous potentially carcinogenic compounds[1]. The present studies showed that telomerase activity had a close correlation with cell immortalization and carcinogenesis. The length of telomerase extends to maintain a proportional balance because telomerase is activated[2,3], therefore, the cells may unlimitedly proliferate to induce carcinogenesis. The aim of this study was to examine the expressions of GST-π and telomerase in esophageal carcinoma and premalignant lesions using immunohistochemistry and telomeric repeat amplification protocol (TRAP)-silver staining assay, respectively, and to investigate the value of endoscopic methylene blue (MB) and Lugol's iodine double

staining and detection of GST-π and telomerase in the early diagnosis of esophageal carcinoma.

MATERIALS AND METHODS

Specimen collection and processing

Tissue specimens were obtained endoscopically from in- and outpatients with abnormal findings, such as mucosal congestion, erosions, swelling or masses in the esophagus in the Affiliated Hospital of Jiangxi Medical College from 2002 to 2003. A total of 72 patients were included in this study, aged between 27 and 78 years, composed of 49 men and 23 women. All 72 patients underwent upper endoscopy and MB and Lugol's iodine staining with biopsy. After the endoscopic examination, the esophageal lumen was washed with 50 mL of distilled water. At first, 5 g/L MB solution was sprayed on the esophageal lesion. After 1 min, approximately 120-200 mL of distilled water was sprayed on the esophageal mucosa to wash off excess dye. Then 30 mL/L Lugol's iodine solution was sprayed on the esophageal lesion. After MB and Lugol's iodine staining, the pattern of mucosal staining was classified as blue, brown and the areas between both the colors. Depending on the color, two to four biopsy specimens of positive staining were obtained using the large cup biopsy forceps. Endoscopic specimens were immediately placed in the Eppendorf tube and a 10% buffered formalin solution, but immediately these specimens in the Eppendorf tube were kept in liquid nitrogen, and after 24 h, were stored at -80 ℃ until extraction for telomerase.

GST-π determination

Expression of GST-π was examined using indirect immunohistochemical staining accompanied by positive and negative controls. The key steps in the staining procedure were as follows: 4-μm-thick sections cut from each formalin-fixed and paraffin-embedded tissue specimen; deparaffinized in xylene, dehydrated through graded alcohol and washed thrice with distilled water; incubated for 5 min with 30 mL/L hydrogen peroxide to block endogenous peroxidase activity; again incubated with citrate buffer (pH 6.0) for 3 min using a household microwave oven at 800 W, followed by incubation for 1 h at 37 ℃ with the primary GST-π antibody at a dilution of 1∶100, and then washed thrice with PBS. After a second incubation with the GST-π anti-rabbit antibody HRP, 3, 3'-diaminobenzidine tetrachloride was used for color development and finally counterstained with hematoxylin. The immunohistochemical expression of GST-π was examined by means of light microscopy. The staining results were assigned to one of the following groups: (-), less than 25% of cells stained or the cells staining intensity being consistent with that of the background; (+), 25-50% of cells stained with light yellow fine granule showing in cells; (++), 50-70% of cells stained with dark brown granule showing in cells; (+++), more than 70% of cells stained with a great amount of dark brown granule showing in cells. Positive staining provided an internal positive control for GST-π staining. The primary antibody was replaced by PBS for the negative control.

Telomerase activity assay

Expression of telomerase activity was measured using TRAP-silver staining assay. Frozen specimens were homogenized and incubated with 20 μL of ice-cold lyses buffer (10 mmol/L Tris-HCl, pH 7.5, 1 mmol/L EGTA, 0.1 mmol/L benzamidine, 5 mmol/L β-mercaptoethanol, 5 g/L CHAPS, 100 mL/L glycerol). After 30 min of incubation on ice, the lysate was centrifuged at 14 500 *g* for 30 min at 2-8 ℃, and the supernatant was frozen and stored at -80 ℃. A total volume of PCR reactions was 25 μL. TRAP reaction was performed using 2 μL extracts, 2.5 μL 10× TRAP buffer (200 mmol/L Tris-HCl, pH 8.3, 15 mmol/L $MgCl_2$, 630 mmol/L KCl, 5 g/L Tween 20, 10 mmol/L EGTA, 1 g/L BSA), 1 μL of 4 mmol/L dNTP, 0.5 μL TS primer, and 18 μL double-distilled water. After 10 min incubation at 23 ℃ for telomerase-mediated extension of the TS primer, the reaction mixture was heated for 5 min at 94 ℃ to inactivate the telomerase, then added 2 U of Taq, 0.5 μL CX primer and finally 30 μL wax barrier. All the above steps were performed on ice. PCR reactions were performed for 27 amplification cycles, each cycle consisting of denaturation at 94 ℃ for 30 s, primers annealing at 50 ℃ for 30 s and extension at 72 ℃ for 90 s, followed by an extra incubation at 72 ℃ for 10 min to ensure full extension of the products. The PCR products were electrophoresed on a 120 g/L gel polyacrylamide for 2-3 h and then gel was stained using $AgNO_3$ and was photographed. The extract, which showed a ladder of products with 6-bp increments after being stained on the gel, was considered telomerase positive. For the negative controls of telomerase, the extract was heat-treated by incubation at 65 ℃ for 10 min prior to TRAP assay to inactivate the telomerase, and no PCR product was observed in the negative controls of telomerase.

Criteria of pathological histology

This was performed by evaluating the H&E-stained tissue sections under a microscope according to the criteria described previously by Qiu and Yang[4]. We classified the tissue sections into eight groups: normal epithelium; pure hyperplasia; low-grade dysplasia; moderate-grade dysplasia; high-grade dysplasia; carcinoma *in situ*; squamous cell carcinoma; and adenocarcinoma.

Statistical analysis

Proportion (relative number, %) was used for result analysis, and statistical significance was tested using χ^2 test, exact method analysis, rank sum test or association test of categorical data. A P value less than 0.05 was considered statistically significant.

RESULTS

Endoscopic methylene blue and Lugol's iodine double staining

After staining with MB and Lugol's iodine, the area between both the colors was obtained in 64 of the 72 patients. We observed areas stained blue and brown in all the 72 patients. Association test of two simultaneous ordinal categorical data showed a significant correlation between the esophageal mucosal staining and the esophageal histology (P<0.005, Table 1, Figure 1).

Table 1 Endoscopic MB and Lugol's iodine double staining (*n*, %)

Histology	*n*	Areas stained blue (%)	Areas between both the colors (%)	Areas stained brown (%)
Normal epithelium	53	49 (92.5)	4 (7.5)	0
Hyperplasia	21	13 (61.9)	6 (28.6)	2 (9.5)
Dysplasia	79	10 (12.6)	45 (57.0)	24 (30.4)
Low-grade	17	7 (41.2)	7 (41.2)	3 (17.6)
Moderate-grade	21	3 (14.3)	13 (61.9)	5 (29.4)
High-grade	41	0	25 (61.0)	16 (39.0)
Carcinoma	55	0	9 (16.4)	46 (83.6)
Carcinoma *in situ*	1	0	1 (100)	0
Squamous cell carcinoma	51	0	8 (15.7)	43 (84.3)
Adenocarcinoma	3	0	0	3 (100)
Total	208	72	64	72

$\chi^2 = 170.58$, $P<0.005$.

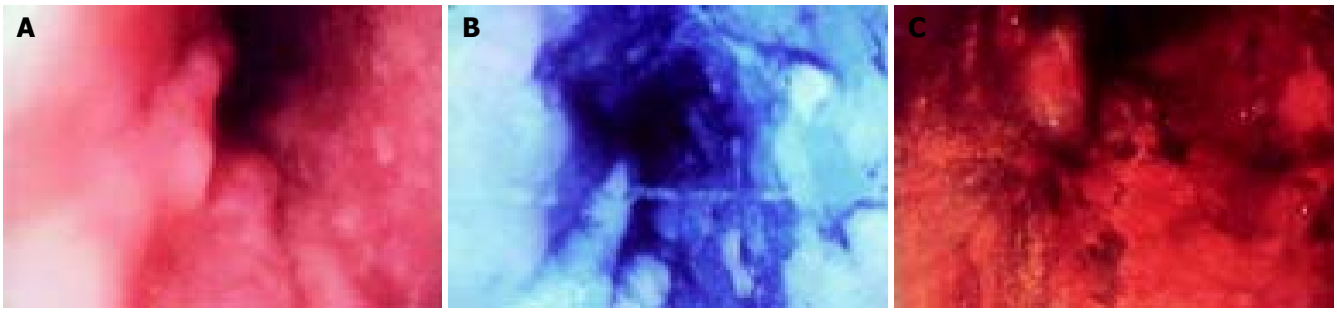


Figure 1 Endoscopic view of esophageal wall after MB and Lugol's iodine double staining. A: Before staining, a large broad-based erosion was observed on esophageal wall and the outlines of erosion were unclearly discernible; B: after MB staining, the same lesion stained more deeper blue than surrounding mucosa; C: after Lugol's iodine double staining, the normal mucosa appeared brown, the same lesion stained more deeper blue than surrounding mucosa and the areas between both the colors were not stained.

Expression of GST-π in esophageal carcinoma and premalignant lesions

GST-π was expressed in 5.7% normal epithelium (3/53), 62.0% dysplasia (49/79) and 83.6% carcinoma (46/55, $P<0.005$); the positive rate of hyperplasia was slightly higher than that of normal epithelium. With the lesions progressing from low- to moderate- to high-grade dysplasia, the positive rate increased ($P<0.025$, Tables 2 and 3, Figure 2).

Table 2 GST-π protein expression in esophageal carcinogenesis (*n*, %)

Histology	*n*	GST-π expression				Positive rate (%)
		–	+	++	++	
Normal epithelium	53	50	3	0	0	5.7
Hyperplasia	21	19	2	0	0	9.5[1]
Dysplasia	79	30	34	12	3	62.0[b]
Carcinoma	55	9	30	13	3	83.6[b]

[1]$P>0.9$, [b]$P<0.001$ *vs* normal epithelium.

Table 3 GST-π protein expression in various histology mucosa of esophagus (*n*, %)

Histology	*n*	GST-π expression				Positive rate (%)
		–	+	++	++	
Low-grade dysplasia	17	11	5	1	0	35.3
Moderate-grade dysplasia	21	9	8	3	1	57.1
High-grade dysplasia	41	10	21	8	2	75.6

$P<0.025$.

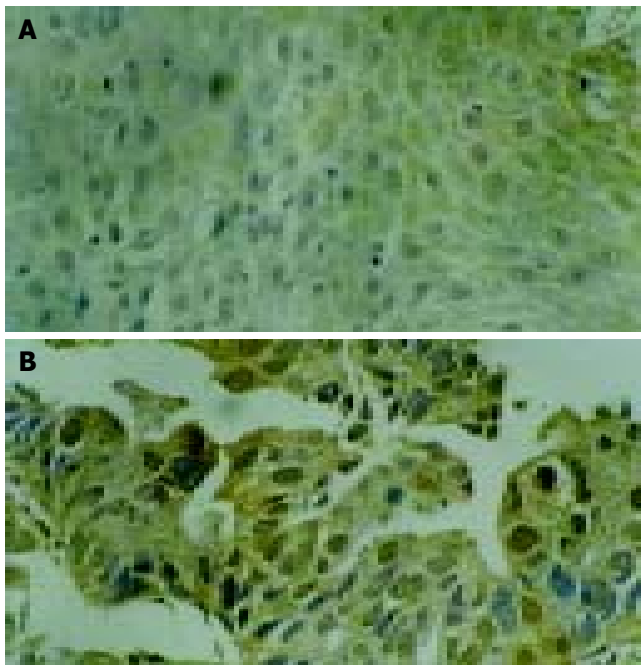


Figure 2 Expression of GST-π in histological esophageal tissues (×400). A: Esophageal dysplasia showing yellow or brown granule in cell substance and nucleus; B: esophageal carcinoma showing yellow or brown granules in cell substance and nucleus.

Expression of telomerase in esophageal carcinoma and premalignant lesions

Telomerase activity was expressed in 3.8% normal epithelium

(2/53), 51.9% dysplasia (41/79), and 89.1% carcinoma (49/55, $P<0.005$); the positive rate of hyperplasia was slightly higher than that of normal epithelium. With the lesions progressing from low-to moderate-to high-grade dysplasia, the positive rate increased ($P<0.005$, Tables 3 and 4, Figure 3).

Table 4 Telomerase activity expression in esophageal carcinogenesis (*n*, %)

Histology	*n*	Telomerase activity expression		Positive number of telomerase (%)
		+	–	
Normal epithelium	53	25	1	2 (3.8)
Hyperplasia	21	1	20	1 (4.8)[1]
Dysplasia	79	41	28	41 (51.9)[a]
Carcinoma	55	49	6	49 (89.1)[c]

[1]$P = 0.998$, hyperplasia *vs* normal epithelium; [a]$P<0.005$, $\chi^2 = 33.45$, dysplasia *vs* normal epithelium; [c]$P<0.005$, $\chi^2 = 78.83$, carcinoma *vs* normal epithelium.

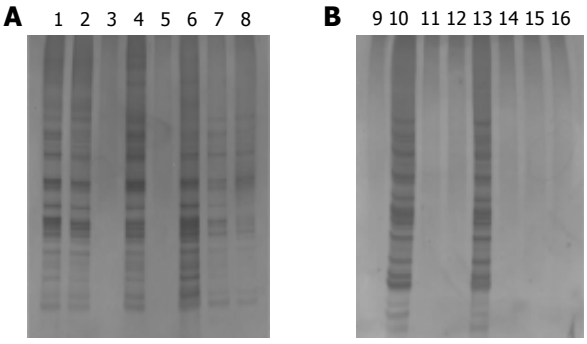


Figure 3 Analysis of telomerase activity of esophageal wall tissues using TRAP-silver staining assay. A: Esophageal carcinoma showing telomerase positivity (lanes 1, 2, 4, 6-8) and telomerase negativity (lanes 3 and 5); B: esophageal dysplasia showing telomerase positivity (lanes 10 and 13), and telomerase negativity (lanes 9, 11, 12, 14, and 15), and negative control (lane 16).

There was a positive correlation between the expression of GST-π and telomerase activity in esophageal carcinoma and premalignant lesions ($r = 0.9687$, $P<0.001$, Table 5). Expression of GST-π correlated to that of telomerase activity in dysplasia and carcinoma ($\varphi = 0.4831$, $P<0.005$; $\varphi = 0.3031$, $P<0.025$, respectively); but there was no correlation between the expression of GST-π and telomerase activity in normal epithelium and hyperplasia. Expression of GST-π was higher than that of telomerase activity in low- and moderate-grade dysplasia (Table 6).

DISCUSSION

In recent years, most scholars have advocated that the esophageal mucosal staining technique can be used for diagnosis of esophageal carcinoma to increase the sensitivity of the detection. Endoscopic MB and Lugol's iodine staining is one of the mucosal staining technique. The basis of the mucosal double staining technique is that MB stains lesion blue and Lugol's iodine reversibly stains glycogen brown. Normal squamous epithelium appears unstained because it does not absorb MB, but in abnormal mucosa, including intestinal metaplasia cells, columnar cells, erosions, ulcers and squamous carcinoma, the superficial epithelium is often stained blue because it absorbs MB. In normal squamous esophageal mucosa, the superficial epithelium contains large glycogen, so the mucosa stains dark brown, but in abnormal mucosa, the superficial epithelium often loses much of its glycogen, and remains partially or totally unstained. Therefore, the area stained blue indicates the existence of carcinoma; the area stained brown belongs to normal squamous esophageal mucosa and the area between both the colors clarifies the invasive lesion of carcinoma. Canto[5] reported that the diagnostic yield in 43 patients with Barrett's esophagus using MB-directed biopsies were compared with surveillance using a random biopsy technique in a controlled trial and the result indicated MB-directed biopsy was a more accurate technique than random biopsy for diagnosing specialized columnar epithelium and dysplasia and cancer. By means of the analysis of comparing the routine endoscopy to the endoscopy with 12 mL/L Lugol's iodine solution, Dawsey *et al*.[6], found that mucosal iodine solution improved endoscopic detection and this simple technique was highly sensitive in identifying these precursors and invasive squamous carcinoma. Our findings showed a correlation between the esophageal mucosal staining and esophageal histology ($P<0.005$), i.e. the areas between both the colors was a majority of dysplasia, especially moderate- and high-grade dysplasia, and the area stained blue was mostly carcinoma, and the area stained brown was mainly normal epithelium and hyperplasia. Overall,

Table 5 Telomerase activity expression in various histological mucosa of esophagus (*n*, %)

Histology	*n*	Telomerase activity expression		Positive number of telomerase (%)
		+	–	
Low-grade dysplasia	17	2	15	2 (11.8)
Moderate-grade dysplasia	21	7	14	7 (33.3)
High-grade dysplasia	41	32	9	32 (78.0)

Comparing among dysplasias $\chi^2 = 25.10$, $P<0.005$; there was significant difference between high- and low- or moderate-grade dysplasia ($\chi^2 = 21.77$, $P<0.005$; $\chi^2 = 11.90$, $P<0.005$, respectively), but no obvious difference between low- and moderate-grade dysplasia ($\chi^2 = 1.37$, $P>0.1$).

Table 6 Expressions of GST-π and telomerase activity in esophageal carcinoma and premalignant lesions

	Normal epithelium		Hyperplasia		Dysplasia		Carcinoma	
	GST-π (+)	GST-π (–)	GST-π (+)	GST- π(–)	GST- π(+)	GST-π (–)	GST-π (+)	GST-π (–)
TA (+)	0	2	0	1	36	5	43	6
TA (–)	3	48	2	18	13	25	3	3

TA: telomerase activity. Expression of GST-π correlated to that of telomerase activity in dysplasia and carcinoma ($\varphi = 0.4831$, $P<0.00$; $\varphi = 0.3031$, $P<0.025$ respectively); but there was no correlation between the expression of GST-π and telomerase activity in normal epithelium and hyperplasia ($P>0.05$).

endoscopic MB and Lugol's iodine double staining improves our ability to see the true size and borders of these esophageal lesions and to take biopsy accurately, which contributes to the early diagnosis of the high risk population and patients with esophageal carcinoma and premalignant lesion, thereby preventing the carcinogenesis of esophagus and reducing the mortality of the esophageal carcinoma.

In 1984, Sato *et al*.[7] firstly reported high level expression of GST-π protein in preneoplastic foci of rat liver, and subsequently the evidence suggested GST-π as an important marker of rat hepatocarcinogenesis. With a close crossing-immunity between GST-π in human tissues and GST-π in rat tissues, GST-π was regarded as a major research focus on the study of human carcinogenesis. A recent study has suggested that GST-π closely correlates with human alimentary carcinoma and is overexpressed in carcinoma and premalignant lesions. Ishioka *et al*.[8], showed that the RNA transcript levels of GST-π in tumor tissues were obviously higher than those in normal tissues in 80% cases (20/25), but no correlation between GST-π mRNA level and clinical stage or histologic characteristics was apparent. Li *et al*.[9], reported that the expression of GST-π increased in esophageal carcinoma and premalignant lesions and was associated with tumor differentiation, but no correlation between GST-π expression and clinical stage or lymphatic metastasis, while found that the mean serum GST-π levels in esophageal squamous cell carcinoma patients were significantly higher than those in normal subjects ($P<0.05$). Our data showed increased expression of GST-π in esophageal carcinoma and premalignant lesions, and with the lesions progressing from low- to moderate- to high-grade dysplasia, the positive rate obviously increased ($P<0.005$). In conclusion, when the cells are in the course of premalignancy, it is possible that some preneoplastic changes in metabolic enzyme have taken place, which are undetectable by using routinely stained sections and it is consistent with the fact of their increased GST-π expression level. Therefore, increased GST-π levels may be recognized as a useful marker of esophageal carcinogenesis.

Telomerase is a ribonuclear protein complex, which contains human telomerase RNA component and binding protein. Telomerase binding protein controls cell senescence, immortalization, and carcinogenesis by means of regulating telomerase activity and changing telomere length[10,11]. Normal somatic cells express undetectable levels of telomerase activity, whereas malignant cells express high levels[12]. Telomerase activity is strongly expressed in most human carcinomas, such as thyroid, breast, esophageal, gastric, lung, pancreatic, hepatocellular, and colorectal carcinoma[13-20]. Lord *et al*.[21], demonstrated that telomerase activation was an important early event in the development of Barrett's esophagus and esophageal adenocarcinoma, suggesting that very high telomerase levels might be a clinically useful biomarker for the detection of occult adenocarcinoma. Using microdissection-TRAP-silver staining assay, Li *et al*.[22], reported telomerase activity was high in both esophageal squamous cell carcinoma and preneoplastic lesions and was related to lymphatic metastasis, but not to cancer differentiation. The data from our studies showed that the positive rates of telomerase activity in low-, moderate-, high-grade dysplasia and carcinoma were 11.8%, 33.3%, 78.0% and 89.1%, respectively, but the positive rates of that in normal epithelium and hyperplasia were 3.8% and 4.8%. These observations reveal a crucial role for telomerase in the esophageal carcinogenesis. High expression levels in dysplasia show that telomerase may be activated in the early stage of esophageal carcinogenesis, indicating that telomerase activation is an early event in the carcinogenesis of the esophagus. It is, therefore, concluded that esophageal premalignant lesion may be effectively prevented from the progression to invasive malignancy in the light of irregularly surveying the variations of expression levels of telomerase activity in esophageal dysplasia patients and the prognosis of early esophageal carcinoma and premalignant lesion will improve significantly.

Our study provided evidence that expression of GST-π was higher than that of telomerase in low-moderate dysplasia. We infer that GST-π may be an early event in the carcinogenesis of esophagus in comparison with telomerase, but the relationship between GST-π and telomerase activity was not statistically significant. With the lesion progressing from dysplasia to carcinoma, expression level of GST-π showed an increased trend in degrees, whereas telomerase activity remained unchanged. We found that expression of GST-π was correlated to that of telomerase activity in dysplasia and carcinoma; but there was no correlation between the expression of GST-π and telomerase activity in normal epithelium and hyperplasia. Consequently, the results suggest that GST-π and telomerase may play an induced and synergistic role with each other in the carcinogenesis of esophageal carcinoma, but we do not know at present the mechanism to correlate GST-π with telomerase.

At present, many methods are widely used for the early diagnosis of esophageal carcinoma, but the sensitivity and specificity of a single method make it difficult to clinically diagnose an esophageal carcinoma. So, several authors have been exploring whether the combined method may improve the early diagnosis of esophageal carcinoma. Koyanagi *et al*.[23], reported that 10 of 18 iodine-nonreactive samples obtained from surgically resected specimens showed telomerase activity and in all 10 telomerase-positive samples, carcinoma *in situ* were observed in iodine-nonreactive mucosa by light microscopy and in 8 telomerase-negative samples, no tumor tissue were observed in iodine-nonreactive lesions. Inai *et al*.[24], also reported similar findings. Our study demonstrated that the expression levels of GST-π and telomerase were high in areas stained blue which was mostly carcinoma and the area between both the colors which was a majority of moderate- and high-grade dysplasia, and with the lesions progressing from low- to moderate- to high-grade dysplasia, the positive rate increased. In summary, the combined method of endoscopic MB and Lugol's iodine double staining and the detection of GST-π and telomerase activity are helpful to the early diagnosis of esophageal carcinoma and provide the chosen method for the physician.

REFERENCES

1 **Coles B,** Ketterer B. The role of glutathione and glutathione transferases in chemical carcinogenesis. *Crit Rev Biochem Mol*

Biol 1990; **25**: 47-70
2 **Colgin LM,** Reddel RR. Telomerase maintenance mechanisms and cellular immortalization. *Curr Opin Genet Dev* 1999; **9**: 97-103
3 **Meyerson M.** Role of telomerase in normal and cancer cells. *J Clin Oncol* 2000; **18**: 2626-2634
4 **Qiu SL,** Yang GR. Precursor lesions of esophageal cancer in high-risk populations in Henan Province, China. *Cancer* 1988; **62**: 551-557
5 **Canto MI.** Methylene blue-directed biopsies improve detection of intestinal metaplasis and dysplasia in Barrett's esophagus. *Gastrointest Endosc* 2000; **51**: 560-568
6 **Dawsey SM,** Fleischer DE, Wang GQ, Zhou B, Kidwell JA, Lu N, Lewin KJ, Roth MJ, Tio TL, Taylor PR. Mucosal lodine staining improves endoscopic visualization of squamous dysplasia and squamous cell carcinoma of the esophagus in Linxian, China. *Cancer* 1998; **83**: 220-230
7 **Sato K,** Kitahara A, Sathoh Kl. The placental form of glutathione S-transferase as a new marker protein for preneoplasia in rat chemical hepatocarcinogenesis. *Jpn J Cancer Res* 1984; **75**: 199-202
8 **Ishioka C,** Kanamaru R, Shibata H, Konishi Y, Ishikawa A, Wakui A, Sato T, Nishihira T. Expression of glutathione S-transferase-π messenger RNA in human esophageal cancers. *Cancer* 1991; **67**: 2560-2564
9 **Li Z,** Zhang R, Luo X. Expression of glutatgione S-transferase-π in human esophageal squamous cell carcinoma. *Chin J Oncol* 2001; **23**: 39-42
10 **Van SB,** Lang TD. Control of telomere length by the human telomeric protein TRF1. *Nature* 1997; **385**: 740-743
11 **Grieder CW.** Telomerase activation: one step on the road to cancer? *Trends Genetics* 1999; **15**: 109-112
12 **Chiu CP,** Harley CB. Replicative senescence and cell immortality: the role of telomeres and telomerase. *Proc Soc Exp Biol Med* 1997; **214**: 99-106
13 **Suzuki S,** Fukushima T, Ami H, Onogi H, Nakamura I, Takenoshita S. New attempt of preoperative differential diagnosis of thyroid neoplasms by telomerase activity measurement. *Oncol Rep* 2002; **9**: 539-544
14 **Shah NG,** Choksi TJ, Patel DD, Vora HH, Ghosh N, Trivedi TI, Trivedi KA. Telomerase activity in breast cancer in Western India (Gujarat). *Int J Biol Markers* 2002; **17**: 49-55
15 **Tominaga T,** Kashimura H, Suzuki K, Nakahara A, Tanaka N, Noguchi M, Itabashi M, Ohkawa J. Telomerase activity and expression of human telomerase catalytic subunit gene in esophageal tissues. *J Gastroenterol* 2002; **37**: 418-427
16 **Suzuki K,** Kashimura H, Ohkawa J, Itabashi M, Watanabe T, Sawahata T, Nakahara A, Muto H, Tanaka N. Expression of human telomerase catalytic subunit gene in cancerous and precancerous gastric conditions. *J Gastroenterol Hepatol* 2000; **15**: 744-751
17 **Fujita Y,** Fujikane T, Fujiuchi S, Nishigaki Y, Yamazaki Y, Nagase A, Shimizu T, Ohsaki Y, Kikuchi K. The diagnostic and prognostic relevance of human telomerase reverse transcriptase mRNA expression detected *in situ* in patients with nonsmall cell lung carcinoma. *Cancer* 2003; **98**: 1008-1013
18 **Zhou JH,** Zhang HM, Chen Q, Han DD, Pei F, Zhang LS, Yang DT. Relationship between telomerase activity and its subunit expression and inhibitory effect of antisense hTR on pancreatic carcinoma. *World J Gastroenterol* 2003; **9**: 1808-1814
19 **Miura N,** Shiota G, Nakagawa T, Maeda Y, Sano A, Marumoto A, Kishimoto Y, Murawaki Y, Hasegawa J. Sensitive detection of human telomerase reverse transcriptase mRNA in the serum of patients with hepatocellular carcinoma. *Oncology* 2003; **64**: 430-434
20 **Abe N,** Watanabe T, Nakashima M, Masaki T, Mori T, Sugiyama M, Atomi Y. Quantitative analysis of telomerase activity: a potential diagnostic tool for colorectal carcinoma. *Hepatogastroenterology* 2001; **48**: 692-695
21 **Lord RV,** Salonga D, Danenberg KD, Peters JH, DeMeester TR, Park JM, Johansson J, Skinner KA, Chandrasoma P, DeMeester SR, Bremner CG, Tsai PI, Danenberg PV. Telomerase reverse transcriptase expression is increased early in the Barrett's metaplasia, dysplasia, adenocarcinoma sequence. *J Gastrointest Surg* 2000; **4**: 135-142
22 **Li C,** Liang Y, Wu M, Xu L, Cai W. Telomerase activity analysis of esophageal carcinoma using microdissection-TRAP assay. *Chin Med J* 2002; **115**: 1405-1408
23 **Koyanagi K,** Ozawa S, Ando N, Mukai M, Kitagawa Y, Ueda M, Kitajima M. Telomerase activity as an indicator of malignant potential in iodine-nonreactive Lesions of the esophagus. *Cancer* 2000; **88**: 1524-1529
24 **Inai M,** Kano M, Shimada Y, Sakurai T, Chiba T, Imamura M. Telomerase activity of the Lugol-stained and -unstained squamous epithelia in the process of oesophageal carcinogenesis. *Br J Cancer* 2001; **85**: 1006-1013

Science Editor Kumar M and Guo SY **Language Editor** Elsevier HK

PO Box 2345, Beijing 100023, China
www.wjgnet.com
wjg@wjgnet.com

ELSEVIER

World J Gastroenterol 2005;11(39):6096-6103
World Journal of Gastroenterology ISSN 1007-9327
© 2005 The WJG Press and Elsevier Inc. All rights reserved.

• *GASTRIC CANCER* •

Epstein-Barr virus-associated gastric carcinoma: Evidence of age-dependence among a Mexican population

Roberto Herrera-Goepfert, Suminori Akiba, Chihaya Koriyama, Shan Ding, Edgardo Reyes, Tetsuhiko Itoh, Yoshie Minakami, Yoshito Eizuru

Roberto Herrera-Goepfert, Department of Pathology, Instituto Nacional de Cancerologia, Mexico City, Mexico
Suminori Akiba, Chihaya Koriyama, Shan Ding, Department of Epidemiology and Preventive Medicine, Kagoshima University Graduate School of Medical and Dental Sciences, Kagoshima, Japan
Edgardo Reyes, Department of Pathology, Instituto Nacional de Ciencias Médicas y de la Nutrición "Salvador Zubirán", Mexico City, Mexico
Tetsuhiko Itoh, Department of Pathology, Kagoshima Institute of Preventive Medicine, Kagoshima, Japan
Yoshie Minakami, Yoshito Eizuru, Division of Oncogenic and Persistent Viruses, Center for Chronic Viral Diseases, Kagoshima University Graduate School of Medical and Dental Sciences, Kagoshima, Japan
Supported by a Grant No. 12218231 from Grants-in-Aid for Scientific Research of the Ministry of Education, Science, Sports, and Culture of Japan
Correspondence to: Roberto Herrera-Goepfert, MD, Departamento de Patología Instituto Nacional de Cancerología, Av. San Fernando #22, Colonia Sección XVI, Tlalpan, México DF 14080, Mexico. rhgoepfert@yahoo.com.mx
Telephone: +52-55-5628-0466 Fax: +52-55-5573-4662
Received: 2005-04-13 Accepted: 2005-05-24

Abstract

AIM: To investigate features of Epstein-Barr virus (EBV)-associated gastric carcinoma (EBVaGC) among a Mexican population.

METHODS: Cases of primary gastric adenocarcinoma were retrieved from the files of the Departments of Pathology at the Instituto Nacional de Cancerología and the Instituto Nacional de la Nutrición in Mexico City. The anatomic site of the gastric neoplasia was identified, and carcinomas were histologically classified as intestinal and diffuse types and subclassified as proposed by the Japanese Research Society for Gastric Cancer. EBV-encoded small non-polyadenylated RNA-1 (EBER-1) *in situ* hybridization was conducted to determine the presence of EBV in neoplastic cells.

RESULTS: We studied 330 consecutive, non-selected, primary gastric carcinomas. Among these, there were 173 male and 157 female patients (male/female ratio 1.1/1). EBER-1 was detected in 24 (7.3%) cases (male/female ratio: 1.2/1). The mean age for the entire group was 58.1 years (range: 20-88 years), whereas the mean age for patients harboring EBER-1-positive gastric carcinomas was 65.3 years (range: 50-84 years). Age and histological type showed statistically significant differences, when EBER-1-positive and -negative gastric carcinomas were compared. EBER-1 was detected in hyperplastic- and dysplastic-gastric mucosa surrounding two EBER-1-negative carcinomas, respectively.

CONCLUSION: Among Latin-American countries, Mexico has the lowest frequency of EBVaGC. Indeed, the Mexican population >50 years of age was selectively affected. Ethnic variations are responsible for the epidemiologic behavior of EBVaGC among the worldwide population.

© 2005 The WJG Press and Elsevier Inc. All rights reserved.

Key words: Epstein-Barr virus; Stomach; Lymphoepithelioma-like carcinoma; Gastric carcinoma; EBV-A; EBER-1; LMP-1

Herrera-Goepfert R, Akiba S, Koriyama C, Ding S, Reyes E, Itoh T, Minakami Y, Eizuru Y. Epstein-Barr virus-associated gastric carcinoma: Evidence of age-dependence among a Mexican population. *World J Gastroenterol* 2005; 11(39): 6096-6103
http://www.wjgnet.com/1007-9327/11/6096.asp

INTRODUCTION

Gastric cancer (GC) is the second leading cause among cancer deaths in the world[1] and is one of the most frequent malignant neoplasms in Mexico[2]. Although the etiology of gastric carcinoma is now accepted as multifactorial, infectious agents play a central role in the mechanism of neoplastic transformation. The bacterium *Helicobacter pylori* (*H pylori*) has been implicated in a high percentage of gastric adenocarcinomas[3], in intestinal- as well as diffuse-type adenocarcinomas, according to the Lauren histoepidemiologic classification[4]. Another infectious agent, Epstein-Barr virus (EBV) or gamma type 4 herpes virus, has also been proved to be associated with gastric carcinoma in approximately 10% of cases[5]. This association has been reported in intestinal- and diffuse-type adenocarcinomas, as well as in nearly 100% of cases labeled lymphoid stroma-rich, lymphoepithelioma-like (LEL) carcinomas. The etiological role of EBV in GC development has been suspected on the basis of the uniform expression of Epstein-Barr nuclear antigen (EBNA)-1 protein, and EBV-encoded small non-polyadenylated RNA (EBER)-1 in all GC cells, the episomal monoclonality of the EBV genome, the elevated serum antibodies against EBV-related antigens among EBV-GC patients, and the unique 'lace pattern' morphology in some

early-stage EBV-GCs.

EBV-associated gastric carcinoma (EBVaGC) accounts for 1.7-16% of gastric carcinomas throughout the world, excluding LEL carcinomas[6]. The lowest frequency has been recorded in the UK, whereas the highest was in the USA. The definitive explanation for this figure remains unclear, but is probably related with genetic variations among different populations, as well as cultural and environmental influences among different geographic regions. Among Latin Americans, Mexican individuals are less likely to develop GC in association with EBV infection; in a previous study, we reported a prevalence of 8.15%[7]. In these series, diffuse-type EBV-GCs were seen exclusively, and EBER-1 was demonstrated in 100% of LEL carcinomas. In the present study, we expanded the number of cases under scrutiny and provided evidence that the risk for EBVaGC was significantly increased among patients >50 years of age in Mexico.

MATERIALS AND METHODS

Patient population

We retrieved cases of gastric adenocarcinoma from the files of the Departments of Pathology at the Instituto Nacional de Cancerología (1983-2000) and the Instituto Nacional de la Nutrición (1980-1995) in Mexico City. The results of a partial analysis of 135 cases were published previously elsewhere[7]. Eligible cases were included whenever they possessed complete demographic and pathologic information, as well as paraffin blocks with appropriate and well-preserved neoplastic tissue for molecular analysis. The age and gender of patients, and anatomic site, histological type, and depth of invasion of gastric carcinomas were obtained from records at the corresponding Department of Pathology.

Pathologic features

The anatomic site of gastric neoplasia was identified as upper (proximal) third, middle third, or lower (distal) third[8]. On the basis of predominant histological pattern, carcinomas were classified as intestinal- or diffuse-type according to the Lauren criteria[4] and subclassified as proposed by the Japanese Research Society for Gastric Cancer as follows[9]: intestinal types tub1 (well-differentiated adenocarcinoma with distinct glandular pattern and columnar epithelium throughout, moderate or small amount of stroma); tub2 (moderately differentiated adenocarcinoma with small or incomplete tubular structures with cubical or flat epithelium, amount of stroma variable from case to case), and muc (mucinous carcinoma); diffuse types, including por1 (poorly differentiated adenocarcinoma with solid, sheet-like proliferation with an alveolar pattern and indistinct tubular differentiation), por2 (poorly differentiated adenocarcinoma with acinar and trabecular pattern, usually showing diffuse infiltration with abundant fibrous stroma), and sig (signet-ring cell carcinoma). A special category, LEL carcinoma, similar to por1 adenocarcinoma but with dense lymphoid infiltrate exceeding total mass of carcinoma cells, was included. The depth of invasion was specified as mucosa; submucosa; or muscularis propria, subserosa, or serosa.

In situ hybridization

Molecular analysis was conducted as previously described[10]. Briefly, we retrieved one representative formalin-fixed, paraffin-embedded tissue sample from each carcinoma containing the neighboring non-neoplastic gastric mucosa. Two slides with 5 μm sections were prepared from each paraffin block. A set of slides were conventionally stained with hematoxylin and eosin, whereas the remainder were enhanced for EBER-1 *in situ* hybridization. The remaining paraffin-block sections were deparaffinized, rehydrated, predigested with pronase, prehybridized, and hybridized overnight at 37 ℃ with a concentration of 0.5 ng of digoxigenin-labeled probe. After sections were washed with 0.5×saline sodium citrate, hybridization was detected by anti-digoxigenin, antibody-alkaline phosphatase conjugate. Sections from a patient with known EBV-positive gastric carcinoma were used for a positive control, and sense probe to EBER-1 was used for a negative control for each procedure.

EBV genotyping

Preparation of DNA Each formalin-fixed and paraffin-embedded specimen was cut into 10-μm-thick slices, and a DNA sample was prepared following the method reported previously[11]. Each deparaffinized sample was treated with proteinase K (200 μg/mL) at 37 ℃ overnight followed by phenol/chloroform extraction and ethanol precipitation. Finally, the extracted DNA sample was dissolved in 50 μL of TE buffer.

Genotype-specific primer sets and probes Four different regions, the EBNA-3C, *Bam*HI-F, *Bam*HI-I, and *Xho*I sites in LMP-1, were used to determine viral genotypes. Types A and B can be determined by using the EBNA-2, -3A, -3B, or -3C gene[12-14]. In the present study, we chose EBNA-3C for genotyping because we experienced a higher detection rate of the primer set than those of the EBNA-2 region found in previous studies[15,16]. Types A and B, identified by PCR amplification of EBNA-3C region, corresponded to a 153- and a 246-bp band, respectively, and were confirmed by Southern blot hybridization with type-specific internal probes [14]. Wild-type F and f variant were identified by the presence of a 186-bp fragment in amplification of the *Bam*HI F region; after *Bam*HI cleavage, a 186-bp fragment could be identified in the case of wild-type F, and a 127-bp fragment could be identified in the case of the f variant. Wild-type F and f variants were confirmed by Southern blot hybridization with the internal probe as described previously[15].

For the *Bam*HI-I region, a 205-bp fragment was amplified by using primer sets as described previously[17], and types C and D were distinguished after cleavage by *Bam*HI-restriction enzyme. Type C had a 205-bp fragment, and type D had cleaved fragments with 130 and 75 bp. Types C and D were also confirmed by Southern blot hybridization with a cloned *Bam*HI-I DNA fragment probe.

To detect the *Xho*I polymorphism in exon 1 of the LMP-1 gene, we amplified a 497-bp DNA fragment with a primer set as previously described[18]. When two fragments, 340- and 157-bp long, were observed after *Xho*I digestion of the PCR product, the case was considered to contain the *Xho*I cleavage site. The 497-bp fragment of the PCR product of the B95-8 cell line was used as a probe to confirm the *Xho*I

cleavage site of LMP-1 by Southern blot hybridization[19].

PCR and Southern blot hybridization The PCR template contained the appropriate primer pair (1 μmol/L each), deoxyribonucleotide triphosphates (200 μmol/L each), and *Taq* polymerase (Takara Shuzo, Kyoto, Japan) in a total of 100 μL of PCR buffer. PCR products or PCR products digested with *Bam*HI and *Xho*I were confirmed by electrophoresis in 2% agarose gel and by staining with 0.5 μg/mL of ethidium bromide. Then, electrophoretic pattern was photographed under ultraviolet light. Electrophoretic DNA was transferred onto a Hybond N^+ nylon membrane (Amersham Pharmacia Biotech, UK) by capillary blotting using 0.4 N NaOH solution. Membranes were prehybridized with hybridization buffer for 0.5-1 h at 42 ℃. After the probe was added, hybridization was carried out overnight at 42 ℃. Probes of types A and B, and *Bam*HI-F were labeled with Dig oligonucleotide 3'-end labeling kit and detected using a Dig luminescent detection kit (Boehringer Mannheim, Germany). For detecting the *Bam*HI-I fragment and *Xho*I polymorphism in LMP-1, hybridization was carried out using the ECL direct labeling and detection kit (Amersham Pharmacia Biotech, UK) according to the manufacturer's instructions.

Statistical analysis

Odds ratios (ORs) and 95% confidence intervals (95%CIs) were obtained from logistic regression analysis, making comparisons between EBER-1-positive and EBER-1-negative gastric carcinomas with regard to age, gender, decade, anatomic site, histologic type, and depth of invasion.

RESULTS

Patient characteristics

We studied 330 consecutive, non-selected cases of gastrectomies due to primary gastric carcinoma. Among the 330 cases, there were 173 male and 157 female patients. The mean age was 58.1 years (range: 20-88 years) for all the patients, 59.9 years (range: 22-88 years) for male patients, and 56.1 years (range 20-88 years) for female patients. EBER-1 was detected in 24 (7.3%) of the 330 cases, 13 in men (7.5%) and 11 in women (7.0%). The mean age for patients harboring EBER-1-positive gastric carcinomas was 65.3 years: male patients 66.2 years (range: 51-74 years) and female patients 64.4 years (range: 50-84 years). The male/female ratio was 1.1/1 for the entire group and 1.2/1 for those with EBER-1-positive carcinomas.

Pathologic findings

With regard to the anatomic site of the primary neoplasia, 44 (13.3%) carcinomas were localized in the upper-third, 128 (38.8%) were in the middle portion, and 156 (47.3%) were in the lower-third of the stomach. In two cases (one male and one female), the anatomic location could not be determined; the entire stomach showed neoplastic infiltration in the male patient, and information on the original location of primary neoplasia was not available in the female patient. Both cases were EBER-1-negative. The distribution of carcinomas according to anatomic site and histological type, and the anatomic site and histological type of EBER-1-positive carcinomas are shown in Tables 1 and 2, respectively. Fourteen cases corresponded to early carcinomas, and only 4 were confined to mucosa; 10 cases invaded the submucosal layer. The remaining 316 cases were advanced carcinomas affecting muscular, subserosal, and serosal layers, as well as adjacent organs. EBER-1 was positive in all LEL carcinomas, in 4 out of 141 intestinal-type adenocarcinomas and in 11 out of 180 diffuse-type adenocarcinomas. The EBER-1 *in situ* hybridization signal was uniformly distributed in the nuclei of all 24 positive cases (Figures 1-6). A characteristic

Table 1 Distribution of EBER-1-positive gastric carcinomas by anatomic site[1] and gender

	Total (EBER-1+/total) %		Males (EBER-1+/total) %		Females (EBER-1+/total) %	
Total	24/330	7.3	13/173	7.5	11/157	7.0
Upper	3/44	6.8	3/31	9.7	0/13	0
Middle	13/128	10.2	7/67	10.4	6/61	9.8
Lower	8/156	5.1	3/74	4.1	5/82	6.1

[1]In two cases, anatomic location could not be determined. All (one male and one female) were EBER-1-negative.

Table 2 Distribution of EBER-1-positive gastric carcinomas by histologic type and gender

	Total (EBER-1+/total) %		Males (EBER-1+/total) %		Females (EBER-1+/total) %	
I-type	4/141	2.8	3/87	3.5	1/54	1.9
Tub1	0/42	0	0/28	0	0/14	0
Tub2	4/80	5.0	3/47	6.4	1/33	3.0
Muc	0/19	0	0/12	0	0/7	0
D-type	20/189	10.6	10/86	11.6	10/103	9.7
Por1	8/64	12.5	3/31	9.7	5/33	15.2
Por2	2/45	4.4	2/19	10.5	0/26	0
Sig	1/71	1.4	1/32	3.1	0/39	0
LEL	9/9	100	4/4	100	5/5	100

I-type: Intestinal-type adenocarcinoma; *D-type*: Diffuse-type adenocarcinoma.

lace pattern was evident in the intramucosal component of three EBER-1-positive carcinomas, two por1 plus tub2 and one tub2 plus por1 adenocarcinomas. Twenty-two of twenty-four EBER-1-positive cases extended beyond the submucosa, whereas two carcinomas, one from a female and one from a male patient, did not exceed the submucosal layer.

There were two EBER-1-negative carcinomas accompanied by EBER-1-positive gastric lesions. The first case, a 52-year-old male patient (Figures 7 and 8), had EBER-1 expression in regenerative epithelium of gastric mucosa adjacent to an EBER-1-negative primary adenocarcinoma (por1). The second case was a 46-year-old female patient whose EBER-1-negative adenocarcinoma (por1) was in the immediate vicinity of dysplastic gastric glands with EBER-1 expression (Figures 9 and 10).

Among the demographic and pathologic variables analyzed, age and histologic type had statistically significant differences, when EBER-1-positive and EBER-1 negative gastric carcinomas were compared (Table 3). In addition, comparison among patients more or less than 60 years of age showed significant differences ($P = 0.008$).

EBV genotype

We examined the genotype of seven EBV strains detected from

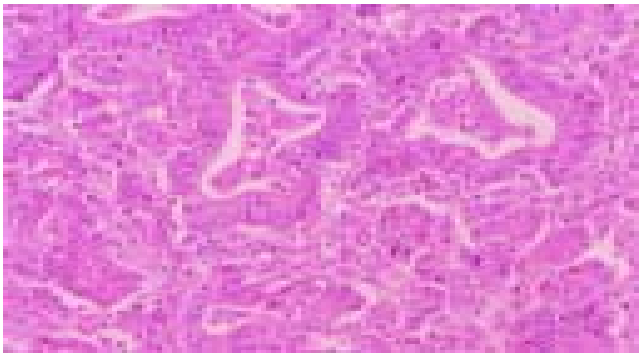


Figure 1 Moderately differentiated, intestinal-type (tub2) adenocarcinoma. Irregular neoplastic tubular structures are seen throughout the field (hematoxylin and eosin stain).



Figure 4 Same case as in Figure 3. A uniform nuclear signal of EBER-1 is seen in neoplastic cells (*in situ* hybridization).

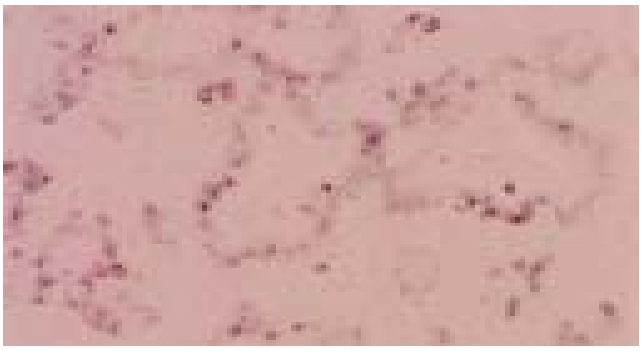


Figure 2 Same case as in Figure 1. EBER-1 nuclear positivity is limited to neoplastic cells lining the tubular structures (*in situ* hybridization).

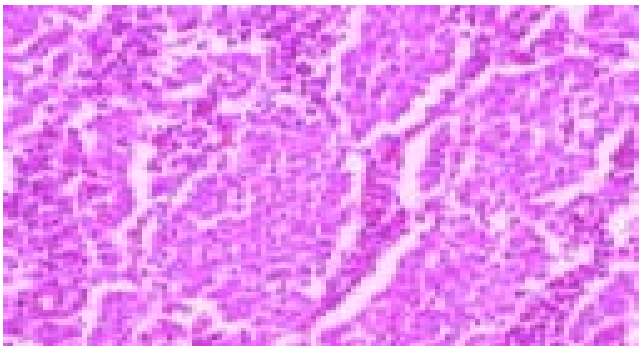


Figure 5 Poorly differentiated, LEL carcinoma. Clusters of neoplastic cells are separated by lymphoplasmacytic infiltrate.



Figure 3 Diffuse-type (por1) adenocarcinoma. Sheets of neoplastic cells are distributed in an indistinct pattern (hematoxylin and eosin stain).

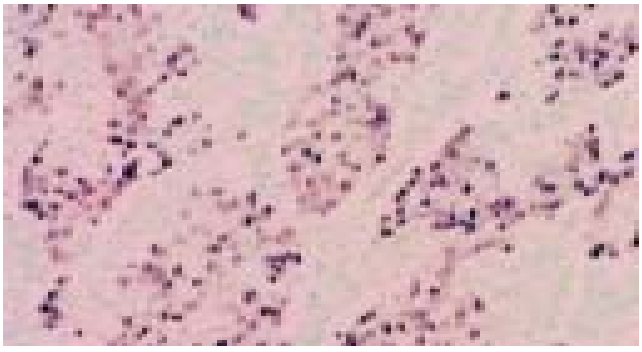


Figure 6 Same case as in Figure 5. An EBER-1-positive signal is detected in the nuclei of neoplastic cells (*in situ* hybridization).

EBER-1-positive cases; genotype could be determined in five of them. All were type A, wild-type F, and type D. In analysis of the *Xba*I cleavage site in LMP-1, we found that the cleavage site was lost in four cases and was maintained in one case.

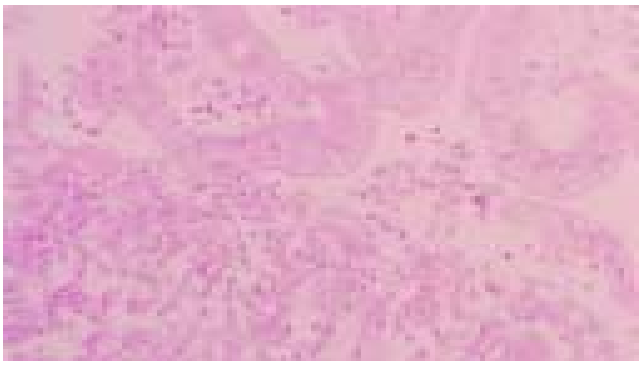


Figure 7 Lining gastric epithelium shows regenerative changes characterized by nuclear growth without atypia. There are few neoplastic cells in the underlying lamina propria (hematoxylin and eosin stain).



Figure 8 Same case as in Figure 7. The EBER-1-positive nuclear signal is restricted to regenerative epithelium. Note the EBER-1 nuclear negativity of neoplastic cells infiltrating the lamina propria (*in situ* hybridization).

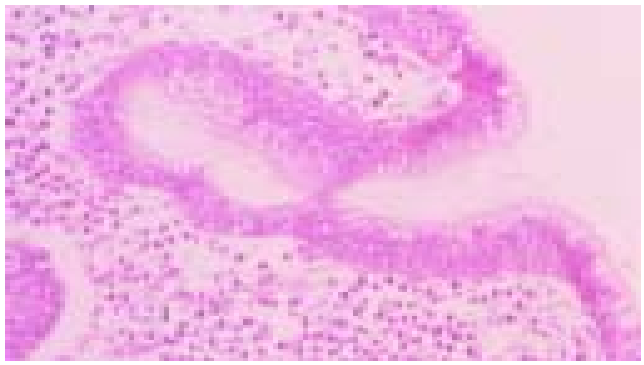


Figure 9 Lining gastric epithelium shows high-grade dysplasia, characterized by cell stratification and crowding, increased nuclear/cytoplasm ratio, nuclear atypia, and prominent eosinophilic nucleoli (hematoxylin and eosin stain).



Figure 10 Same case as in Figure 9. Dysplastic epithelium is intensely positive for the EBER-1 nuclear signal (*in situ* hybridization).

Table 3 Comparison of demographic and pathologic variables between EBER-1-positive and EBER-1-negative gastric carcinomas[1]

	EBER-1+/total	OR	95%CI	*P*
Gender				0.859
Female	11/157	1	Reference	
Male	13/173	0.9	0.4-2.2	
Age (yr)				0.013
20-49	0/87	<0.1		
50-69	14/170	0.6	0.2-1.3	
70-88	10/73	1	Reference	
Decade				0.787
1980-1989	11/130	1	Reference	
1990-2000	13/200	0.9	0.4-2.1	
Tumor site				0.229
Cardia	3/35	1.9	0.5-7.5	
Middle	13/137	2.2	0.9-5.5	
Antrum	8/156	1	Reference	
Lauren classification				0.005
Intestinal	4/141	1	Reference	
Diffuse	20/189	4.9	1.6-14.8	
Depth				0.273
Early	2/14	2.4	0.5-11.8	
Advanced	22/316	1	Reference	

[1]Odds ratios and 95% confidence intervals were obtained from logistic analysis. Age was adjusted in the analysis of variables other than age.

DISCUSSION

In this study, we found a 7.3% prevalence of EBVaGC in Mexico. In Latin America, this frequency is in contrast with that reported by Koriyama *et al*., (11.2%)[20] and Lopes *et al*., (11.3%)[21] in Brazil, Carrascal *et al*., in Colombia (13%)[22], and Corvalan *et al*., in Chile (16.8%)[23]. Excluding LEL carcinomas, the prevalence of EBVaGC in Mexico was 4.7%, whereas in Chile it was 15.8%. In a Brazilian study by Koriyama *et al*.[20], and a Colombian study by Carrascal *et al*.[22], there were no LEL carcinomas. Nonetheless, in the study by Lopes *et al*.[21], a high prevalence of LEL carcinomas (66.7%) among EBVaGC patients was found in a Brazilian population; thus, the prevalence of EBVaGC excluding LEL carcinomas is the lowest (3.8%). Conversely, the prevalence of LEL carcinoma was 7.6% in Brazil, 2.7% in Mexico, and 1.1% in Chile. The male/female ratio (1.2/1) was, as previously noted[7], the lowest among the series reported worldwide. Moreover, after excluding LEL carcinomas, Mexico remains among countries with the low prevalence of EBVaGC worldwide[6].

The frequency of EBVaGC among GC patients of Mexican ancestry in the USA ranged from 10.2%[24] to 12%[25], which is higher than the frequency (7.3%) reported by us. This peculiar migratory phenomenon has also been seen in other countries such as Japan and China. In Japan, the mean frequency of EBVaGC is 6.2%, but among patients of Japanese descent, those who are living in Hawaii, the frequency is 10.2%. In Taiwan, the frequency of EBVaGC among patients of Chinese descent is 11.2%, in comparison to 6.8% in China[26]. This figure probably indicates that besides ethnic and genetic backgrounds, environmental factors are involved in the development of EBVaGC.

A high frequency of EBVaGC at older ages is evident in our Mexican study. Not a single case of EBVaGC was observed among patients aged <50 years. This feature was previously highlighted by Gulley *et al*.[25], who examined American patients of Mexican descent in the USA and found EBVaGC cases only among those aged 56 years or older. Age dependence of EBVaGC frequency was statistically significant in their study ($P = 0.04$). The absence of EBVaGC in a set of patients of Mexican ancestry aged <56 years was also reported by Vo *et al*.[24], although the age difference they reported was not statistically significant. A similar age dependence was reported in China[26], where EBVaGC frequency was higher among those aged 60 years or older than those aged <60 years ($P = 0.03$); interestingly, the frequency of EBVaGC (7.8%) in their study is quite similar to that reported by us (7.3%).

In Brazil, Lopes *et al*.[21], also did not find any patient less than 52 years of age, although other Latin-American studies such as those of Koriyama *et al*.[20], and Corvalan *et al*.[23], did not show any age dependence, reporting EBVaGC cases in patients <50 years. Contrary to the age dependence observed in the present study, a large-scale Japanese study reported a high prevalence of EBVaGC in young men[27]. Furthermore, the same authors showed a significant decreasing trend in EBV prevalence with increasing age for males ($P = 0.04$). Carrascal *et al*.[22], also reported an age-dependent decrease of EBVaGC frequency among Colombian individuals with GC (P for trend = 0.022).

The fact that EBV-associated cancer cannot be detected in other digestive tract organs including the colon and esophagus indicates the importance of epithelial change(s) specific to the stomach[28]. EBV-latent infection products were reported to be expressed in predisposing conditions for gastric carcinoma[29,30]. Our observation showing that EBVaGC could not be found among patients <50 years of age supports the involvement of gastric-mucosal changes occurring late in human life in Mexico, as well as in Brazil and China, and relatively early in Japan and Colombia.

EBVaGC has been related to atrophic gastritis, and EBV DNA has been isolated from epithelial cells in gastric mucosa carrying chronic atrophic gastritis[29-31]. Indeed, intestinal metaplasia may enhance EBV entrance into epithelial cells via adherence of the virus to the secretory component of polymeric immunoglobulin A[32]. Our finding of two cases of EBV non-associated gastric carcinoma, one positive for EBER-1 in adjacent hyperplastic mucosa -a finding not previously described -and the other with an EBER-1-positive signal in dysplastic mucosa -a finding originally reported by Shibata and Weiss[33] -also suggests that the most plausible mechanisms for EBV entry into gastric epithelial cells are those related to previous mucosal damage and cooperation with some unknown promoter factors. In the present study, we did not observe any EBER-1 expression in normal gastric mucosa, even surrounding LEL-EBVaGC or infiltrating lymphocytes. Furthermore, we analyzed endoscopic gastric biopsies from 116 Mexican individuals >40 years of age carrying gastritis with mild atypia, and we did not find any EBER-1-positive case (unpublished data).

In addition to the age dependence of EBVaGC, the present study shows other characteristics of EBVaGC such as distal presentation among female patients and no male preponderance, altogether supporting that ethnicity and genetic backgrounds may address this particular outcome of EBV infection in the Mexican population. Among genetic backgrounds, an immunogenetic constitution may influence the outcome of EBV infection. Human leukocyte antigens (HLA) of the major histocompatibility complex have been implicated in susceptibility to develop EBV-related malignancies[34]. Very recently, we reported an association between the *HLA-DQB1**0501 allele and GC, predominantly in those labeled as diffuse-type carcinomas[35]; unfortunately, EBV status could not be assessed.

In Mexico, EBV antibody prevalence at 4-6 years of age is about 75%[36]. All EBV strains detected in EBVaGC and subjected to EBV genotyping were type A. Previous molecular studies on nasal T-lymphocyte/natural killer-cell lymphomas (nT/NKL) in Mexico[37] documented that EBV type A (EBV-1) is more frequent than EBV type B (EBV-2), as in nT/NKL and sino-nasal-B-cell lymphomas, and as in reactive tonsils from healthy individuals, thus suggesting that viral infection with EBV-1 strain is highly predominant among the Mexican population. In addition, the same authors[37] found a similar incidence of EBV LMP-1 deletions in Mexican individuals harboring nT/NKL as compared with normal subjects. Mori *et al*.[38], found no significant differences in DNA sequences of the LMP-1 region of EBV strains isolated from EBVaGC patients and throat washing samples of healthy individuals. So far no studies

have revealed differences in the genotype of EBV detected in EBVaGC *vs* that found in healthy individuals.

In conclusion, EBVaGC occurs less in Mexico than among other Latin-American populations, but it is as frequent in male as it is in female patients >50 years. In Mexican women, EBVaGC affects the middle and distal portions of the stomach but not the proximal portion. Finally, the participation of sequential steps in the mechanism of neoplastic transformation in EBVaGC, in a similar manner to the cascade of events described by Correa[39] in gastric carcinogenesis, cannot be ruled out.

REFERENCES

1 **Fuchs CS**, Mayer RJ. Gastric carcinoma. *N Engl J Med* 1995; **333**: 32–41
2 **Oñate-Ocaña LF**. Gastric Cancer in Mexico. *Gastric Cancer* 2001; **4**: 162–164
3 **Uemura N**, Okamoto S, Yamamoto S, Matsumura N, Yamaguchi S, Yamakido M, Taniyama K, Sasaki N, Schlemper RJ. *Helicobacter pylori* infection and the development of gastric cancer. *N Engl J Med* 2001; **345**: 784–789
4 **Laurén P**. The two histological main types of gastric carcinoma: diffuse and so-called intestinal type carcinoma. An attempt at a histo-clinical classification. *Acta Pathol Microbiol Scand* 1965; **64**: 31-49
5 **Takada K**. Epstein-Barr virus and gastric carcinoma. *J Clin Pathol* 2000; **53**: 255-261
6 **Burgess DE**, Woodman CB, Flavell KJ, Rowlands DC, Crocker J, Scott K, Biddulph JP, Young LS, Murray PG. Low prevalence of Epstein-Barr virus in incident gastric adenocarcinomas from the United Kingdom. *Br J Cancer* 2002; **86**: 702-704
7 **Herrera-Goepfert R**, Reyes E, Hernández-Avila M, Mohar A, Shinkura R, Fujiyama C, Akiba S, Eizuru Y, Harada Y, Tokunaga M. Epstein-Barr virus-associated gastric carcinoma in Mexico: analysis of 135 consecutive gastrectomies in two hospitals. *Mod Pathol* 1999; **12**: 873-878
8 Japanese Research Society for Gastric Cancer. Japanese Classification of Gastric Carcinoma. 1st english ed. *Tokyo Kanehara & Co Ltd* 1995: 3
9 Japanese Research Society for Gastric Cancer. Japanese Classification of Gastric Carcinoma. 1st english ed. *Tokyo Kanehara & Co Ltd* 1995: 39–43
10 **Chang KL**, Chen YY, Shibata D, Weiss LM. Description of an *in situ* hybridization methodology for detection of Epstein-Barr virus RNA in paraffin-embedded tissues, with a survey of normal and neoplastic tissues. *Diagn Mol Pathol* 1992; **1**: 246-255
11 **Greer CE**, Wheeler CM, Manos MM. PCR amplification from paraffin-embedded tissues: sample preparation and the effects of fixation In: Carl WD, and Gabriela SD, eds. PCR primer: a laboratory manual. *New York Cold Spring Harbor Laboratory Press* 1995: 99-112
12 **Adldinger HK**, Delius H, Freese UK, Clarke J, Bornkamm GW. A putative transforming gene Jijoye virus differs from that of Epstein-Barr virus prototypes. *J Virol* 1985; **14**: 221-234
13 **Rowe M**, Young L, Cadwallader K, Petti L, Kieff E, Rickinson A. Distinction between Epstein- Barr virus type-A (EBNA-2A) and type-B (EBNA-2B) isolates extends to the EBNA-3 family of nuclear proteins. *J Virol* 1989; **63**: 1031–1039
14 **Sample J**, Young L, Martin B, Chatman T, Kieff E, Rickinson A, Kieff E l. Epstein-Barr virus types 1 and 2 differ in their EBNA 3A, EBNA 3B, and ENBA 3C genes. *J Virol* 1990; **64**: 4084-4092
15 **Sidagis J**, Ueno K, Tokunaga M, Ohyama M, Eizuru Y. Molecular epidemiology of Epstein-Barr virus (EBV) in EBV-related malignancies. *Int J Cancer* 1997; **72**: 72–76
16 **Kunimoto M**, Tamura S, Tabata T, Yoshie O. One step typing of Epstein- Barr virus by polymerase chain reaction: Predominance of type 1 virus in Japan. *J Gen Virol* 1992; **73**: 455-461
17 **Lung ML**, Chang GC, Miller TR, Wara WM, Phillips TL. Genotypic analysis of Epstein-Barr virus isolates associated with nasopharyngeal carcinoma in Chinese immigrants to the United States. *Int J Cancer* 1994; **59**: 743-746
18 **Chen ML**, Tsai CN, Liang CL, Shu CH, Huang CR, Sulitzeanu D, Liu ST, Chang YS. Cloning and characterization of the latent membrane protein (LMP) of a specific Epstein-Barr virus variant derived from the nasopharyngeal carcinoma in the Taiwanese population. *Oncogene* 1992; **7**: 2131-2140
19 **Wu SJ**, Lay JD, Chen CL, Chen JY, Liu MY, Su IJ. Genomic analysis of Epstein-Barr virus in Nasal and Peripheral T-cell Lymphoma: a comparison with nasopharyngeal carcinoma in an endemic area. *J Med Virol* 1996; **50**: 314–321
20 **Koriyama C**, Akiba S, Iriya K, Yamaguti T, Hamada GS, Itoh T, Eizuru Y, Aikou T, Watanabe S, Tsugane S, Tokunaga M. Epstein-Barr virus-associated gastric carcinoma in Japanese Brazilians and non-Japanese Brazilians in Sao Paulo. *Jpn J Cancer Res* 2001; **92**: 911–917
21 **Lopes LF**, Bacchi MM, Elgui-de-Oliveira D, Zanati SG, Alvarenga M, Bacchi CE. Epstein-Barr virus infection and gastric carcinoma in Sao Paolo State, Brazil. *Braz J Med Biol Res* 2004; **37**: 1707-1712
22 **Carrascal E**, Koriyama C, Akiba S, Tamayo O, Itoh T, Eizuru Y, Garcia F, Sera M, Carrasquilla G, Piazuelo MB, Florez L, Bravo JC. Epstein-Barr virus-associated gastric carcinoma in Cali, Colombia. *Oncol Rep* 2003; **10**: 1059-1062
23 **Corvalan A**, Koriyama C, Akiba S, Eizuru Y, Backhouse C, Palma M, Argandoña J, Tokunaga M. Epstein-Barr virus in gastric carcinoma is associated with location in the cardia with a diffuse histology. A study in one area of Chile. *Int J Cancer* 2001; **94**: 527-530
24 **Vo QN**, Geradts J, Gulley ML, Boudreau DA, Bravo JC, Schneider BG. Epstein-Barr virus in gastric adenocarcinomas: association with ethnicity and CDKN2A promoter methylation. *J Clin Pathol* 2002; **55**: 669-675
25 **Gulley ML**, Pulitzer DR. Eagan PA, Schneider BG. Epstein-Barr virus infection is an early event in gastric carcinogenesis and is independent of *bcl*-2 expression and *p*53 accumulation. *Hum Pathol* 1996; **27**: 20-27
26 **Qiu K**, Tomita Y, Hashimoto M, Ohsawa M, Kawano K, Wu DM, Aozasa K. Epstein-Barr virus in gastric carcinoma in Suzhuo, China and Osaka, Japan: association with clinicopathologic factors and HLA-subtype. *Int J Cancer* 1997; **71**: 155-158
27 **Tokunaga M**, Uemura Y, Tokudome T, Ishidate T, Masuda H, Okazaki E, Kaneko K, Naoe S, Ito M, Okamura A, Shimada A, Sato E, Land CE. Epstein-Barr virus related gastric cancer in Japan: a molecular patho-epidemiological study. *Acta Pathol Japonica* 1993; **43**: 574-581
28 **Kijima Y**, Hokita S, Takao S, Baba M, Natsugoe S, Yoshinaka H, Aridome K, Otsuji T, Itoh T, Tokunaga M, Eizuru Y, Aikou T. Epstein-Barr virus involvement is mainly restricted to lymphoepithelial type of gastric carcinoma among various epithelial neoplasms. *J Med Virol* 2001; **64**: 513-518
29 **Kaizaki Y**, Sakurai S, Chong JM, Fukayama M. Atrophic gastritis, Epstein-Barr virus infection, and Epstein-Barr virus-associated gastric carcinoma. *Gastric Cancer* 1999; **2**: 101-108
30 **Yanai H**, Takada K, Shimizu N, Mizugaki Y, Tada M, Okita K. Epstein-Barr virus infection in non-carcinomatous gastric epithelium. *J Pathol* 1997; **183**: 293-298
31 **Hirano A**, Yanai H, Shimizu N, Okamoto T, Matsubara Y, Yamamoto K, Okita K. Evaluation of Epstein-Barr virus DNA load in gastric mucosa with chronic atrophic gastritis using a real-time quantitative PCR assay. *Int J Gastrointest Cancer* 2003; **34**: 87-94
32 **Sixbey JW**, Yao QY. Immunoglobulin A-induced shift of Epstein-Barr virus tissue tropism. *Science* 1992; **255**: 1578-1580

33 **Shibata D**, Weiss LM. Epstein-Barr Virus-associated Gastric Adenocarcinoma. *Am J Pathol* 1992; **140**: 769–774
34 **Koriyama C**, Shinkura R, Hamasaki Y, Fujiyoshi T, Eizuru Y, Tokunaga M. Human leukocyte antigens related to Epstein-Barr virus-associated gastric carcinoma in Japanese patients. *Eur J Cancer Prev* 2001; **10**: 69-75
35 **Herrera-Goepfert R**, Zúñiga J, Hernández-Guerrero A, Rodriguez-Reyna T, Osnaya N, Ruiz-Morales J, Vargas-Alarcón G, Yamamoto-Furusho JK, Mohar-Betancourt A, Granados J. Asociación del alelo HLA-DQB1*0501 del complejo principal de histocompatibilidad con cáncer gástrico en México. *Gac Med Mex* 2004; **140**: 299-303
36 **Niederman JC**, Evans AS. Epstein-Barr virus In: Evans AS, Kaslow RA eds. Viral Infections of Humans: Epidemiology and Control. 4th edition. *New York Plenum Medical Book Company* 1997: 253-283
37 **Elenitoba-Johnson KS**, Zarate-Osorno A, Meneses A, Krenacs L, Kingma DW, Raffeld M, Jaffe ES. Cytotoxic granular protein expression, EBV strain type and latent membrane protein-1 oncogene deletions in nasal T-lymphocyte/natural killer cell lymphomas from Mexico. *Mod Pathol* 1998; **11**: 754-761
38 **Mori S**, Itoh T, Tokunaga M, Eizuru Y. Deletions and single-base mutations within the carboxy-terminal region of the latent membrane protein 1 oncogene in Epstein-Barr virus-related gastric cancers of southern Japan. *J Med Virol* 1999; **57**: 152-158
39 **Correa P**. Human gastric carcinogenesis: A multistep and multifactorial process. First American Cancer Society Award Lecture on Cancer Epidemiology and Prevention. *Cancer Res* 1992; **52**: 6735-6740

Science Editor Guo SY **Language Editor** Elsevier HK

PO Box 2345, Beijing 100023, China
www.wjgnet.com
wjg@wjgnet.com

ELSEVIER

World J Gastroenterol 2005;11(39):6104-6109
World Journal of Gastroenterology ISSN 1007-9327
© 2005 The WJG Press and Elsevier Inc. All rights reserved.

Combined TACE and PEI for palliative treatment of unresectable hepatocellular carcinoma

Gerhild Becker, Tarik Soezgen, Manfred Olschewski, Joerg Laubenberger, Hubert Erich Blum, Hans-Peter Allgaier

Gerhild Becker, Tarik Soezgen, Manfred Olschewski, Joerg Laubenberger, Hubert Erich Blum, Hans-Peter Allgaier, for the Hcc Study Group, Department of Medicine II, Department of Medical Biometry and Statistics and Department of Radiology, University Hospital Freiburg, Germany
Correspondence to: Professor. Dr. Drs. h.c. Hubert Erich Blum, Abteilung Innere Medizin II, Medizinische Universitätsklinik, Hugstetter Str. 55, D-79106 Freiburg, Germany. hubert.blum@uniklinik-freiburg.de
Telephone: +49-761-270-3403 Fax: +49-761-270-3610
Received: 2005-01-19 Accepted: 2005-05-20

Abstract

AIM: To assess whether the effectiveness of a combination of transarterial chemoembolization (TACE) and percutaneous ethanol injection (PEI) in the treatment of unresectable hepatocellular carcinoma (HCC) is superior to TACE alone a randomized controlled trial was performed.

METHODS: The effect of combination therapy on long-term survival rates and duration of hospitalization was evaluated in 52 previously untreated HCCs, randomly allocated to TACE-PEI (27 pts) or TACE alone (25 pts).

RESULTS: The cumulative survival rate of the TACE group was 75.8% at 6 mo, 62.9% at 12 mo, and 18.0% at 24 mo and of the TACE-PEI group 76.9%, 61.5%, and 38.7%, respectively. Comparison of overall survival in both groups showed no statistically significant difference. Regarding the patients with HCCs Okuda stage I (n = 26), the median survival of the TACE-PEI group was significantly longer (>24 mo, median not yet reached in the study period) compared to the TACE group (18.4 mo [range 11.6-21.7 mo]; P = 0.04). TACE-PEI reduced the relative risk for mortality to 0.4 (95%CI 0.15-0.96) compared to patients who received TACE alone. Median survival in patients with HCCs Okuda stage II or III was 5.0 mo in the TACE group (1.7 mo-not defined) compared to 10.4 mo in the TACE-PEI group.

CONCLUSION: The combination TACE-PEI improved survival time compared to TACE alone. Our study revealed a statistically significant improved survival in HCCs Okuda stage I. Side effects were minor and the combination therapy did not prolong duration of hospitalization considerably.

© 2005 The WJG Press and Elsevier Inc. All rights reserved.

Key words: Hepatocellular carcinoma; Chemoembolization; Ethanol injection; Combination therapy

Becker G, Soezgen T, Olschewski M, Laubenberger J, Blum HE, Allgaier HP. Combined TACE and PEI for palliative treatment of unresectable hepatocellular carcinoma. *World J Gastroenterol* 2005; 11(39): 6104-6109
http://www.wjgnet.com/1007-9327/11/6104.asp

INTRODUCTION

Hepatocellular carcinoma (HCC) is one of the major malignancies worldwide with the highest incidence in Asia and sub-Saharan Africa[1]. Potentially curative therapeutic strategies such as orthotopic liver transplantation and hepatic resection are possible only in a minority of patients[2-7]. Due to tumor size and multicentricity, comorbidity and advanced or decompensated liver cirrhosis 70-80% of HCCs are inoperable at the time of diagnosis[8]. Because HCCs are chemo- and radio-resistant, systemic chemotherapy and radiation therapy are not options for the treatment[9]. Therefore, in most HCC patients, percutaneous ethanol injection (PEI) or thermal ablation, e.g., radiofrequency thermal ablation, and transarterial chemoembolization (TACE) are palliative treatment options[5,10-14].

Ultrasound guided PEI has been shown to be highly effective in the treatment of small HCCs[15-17]. However, PEI treatment was shown to be of limited efficacy in patients with large HCC (>5 cm) because ethanol diffusion within the tumor mass is incomplete and residual viable neoplastic tissue often persists in the periphery of the tumor lesion.

Advanced HCCs have been widely treated with TACE, using various combinations of chemotherapeutic drugs and embolic agents. The standard protocol adopted in many institutions includes repeated intra-arterial injections of a chemotherapeutic agent such as cisplatin, doxorubicin, or mitomycin C mixed with lipiodol. Lipiodol is added because of its relative selective uptake in HCCs and its antitumor effect[18]. The injection of chemotherapeutic oil emulsion is followed by embolization of feeding arteries with small gelatin-sponge particles.

A potential benefit of combining TACE with PEI in the treatment of HCC was first suggested by Tanaka *et al*.[19]. Adding PEI after TACE has been expected to achieve complete necrosis of the main tumors and to alter the texture of the tumor parenchyma, so that a large volume of ethanol can be administered to penetrate entire tumor lesions resulting in a complete necrosis[20]. In a previous study, we prospectively analyzed the clinical factors determining the prognosis of 132 inoperable HCC patients treated at our institution. Multivariate analysis revealed that patients treated with TACE-PEI had a significantly longer survival than patients treated with PEI or TACE alone[15]. These observations

prompted us to do a multicenter randomized controlled trial evaluating the effect of combination therapy with TACE-PEI *vs* TACE on long-term survival rates, duration of hospitalization and quality of life.

MATERIALS AND METHODS

Patient characteristics and study design

The study was performed as a multicenter randomized controlled trial comparing treatment with TACE and TACE-PEI. The mean 3-year-survival rate in patients treated with TACE is about 30%[18,21-24]. To demonstrate an improvement of the 3-year-survival from 30% to 40% with a statistical power of 80%, it was calculated that 308 patients in each group were needed (group 1 = TACE treatment, group 2 = treatment with TACE in combination with PEI). As a period of recruitment, 36 mo were calculated, and 24 mo were planned as follow-up period.

Participants for the trial were recruited from five centers listed in the Appendix. Patients included in the study fulfilled the following criteria: Untreated patients with HCC, confirmed histologically or diagnosed by significantly elevated α-fetoprotein (AFP) levels (>250 ng/mL) and imaging by CT, MRI, ultrasound, or angiography. No indication for surgery or any local treatment, no evidence for extrahepatic metastases, assessed by clinical and chest X-ray examinations. In patients with clinically suspected bone metastases, a bone scan was performed. There was no age limit. Exclusion criteria were: Second malignancy, any local, or systemic pretreatment, extrahepatic metastases, Child-Pugh C score, complete portal vein thrombosis (main trunk or both branches), serum creatinine >1.5 mg/dL, severe- and therapy-resistant hepatic encephalopathy, contraindications for peripheral artery catheterization. The study protocol conformed to the ethical guidelines of the 1975 Declaration of Helsinki and was approved by the ethics committee of the University Hospital Freiburg. All participants provided written informed consent. By external blockwise randomization centrally performed by fax, patients were assigned to treatment with TACE only or treatment with TACE-PEI.

Therapeutic procedures

TACE A diagnostic angiography was performed in all patients. For TACE, the tip of the catheter was placed in the left or right hepatic artery. Under fluoroscopic guidance, 5-10 mL of a solution containing 10 mg mitomycin C (Medac, Hamburg, Germany) in 10 mL iodized oil was injected into the artery feeding the lesion(s). The mitomycin/oil mixture was prepared immediately before injection by vigorous mixing for a few minutes. Embolization was performed with gelatin-sponge particles (Gelfoam; Upjohn, Kalamazoo, MI, USA). In case of unilateral portal vein thrombosis and contralateral localization of the HCC(s), chemoperfusion without embolization (TAC) of the corresponding lobe was performed. At the end of the procedure, the extent of vascular occlusion was demonstrated angiographically. The patients stayed in general, 1 d in the hospital for observation. Two weeks after TACE, a CT scan was performed. The results were interpreted as follows: (1) tumor necrosis: hypo-attenuated and contrast medium-non-enhanced lesion(s) in the early arterial phase; (2) residual tumor: contrast medium-enhanced lesion(s).

The procedure was repeated every 6-10 wk until one of the following end points was reached: (1) no viable tumor cells detectable by CT or biopsy; (2) contraindications for the procedure developed; (3) patient's death. In patients who developed thrombosis of the main portal trunk, TACE was performed only in cases of compensated cirrhosis Child-Pugh A score and adequate collateral circulation around the thrombosis (cavernous transformation with prograde intrahepatic portal perfusion on ultrasound Doppler flow examination). Patients not qualifying for TACE received best supportive care, including treatment of complications of liver cirrhosis and pain relief.

Combination of TACE-PEI Patients assigned to TACE-PEI additionally received PEI treatment for all visible lesions, 10 d after TACE. PEI was performed under real-time ultrasound guidance. A 3-MHz convex probe (Ultramark 4; ATL, Solingen, Germany) with a lateral guide attachment or a 3.5-MHz convex probe (EUB 525; Hitachi, Wiesbaden, Germany) with an incorporated guide was used. Two needle types were used: a 15-cm, 20-gauge spinal needle (Becton Dickinson, Franklin Lakes, NJ, USA) or a 20-cm, 20-gauge needle with a closed conical tip and side holes at the tip over a length of 1 or 2 cm (Pflugbeil, Ottobrunn, Germany). Ethanol (96%, 1-10 mL) was slowly injected. The PEI result was photodocumented. In general, PEI treatment involved 6-12 injections per lesion 1-6 d apart. After PEI treatment, patients regularly stayed in general 1 day in the hospital for observation. The procedure was repeated after every TACE, until one of the end points described above was reached.

Follow up

As primary end point of the study, death of any cause was chosen. Secondary end points were tumor response, quality of life, side effects, and duration of hospitalization because of treatment or side effects.

Follow-up period was 24 mo. Patients were seen on an outpatient basis 1 mo after initiation of the therapy, later on for every 3 mo. Routine follow-up included clinical examination, determination of AFP, and abdominal ultrasound. Abdominal CT or MRI was performed after 1, 3, and 6 mo, and then for every 6 mo. If HCC recurrence was suspected based on ultrasonography or AFP elevation, CT or MRI was performed earlier. Chest X-rays were done after 6, 12, and 24 mo. Quality of life evaluation (EORTC QLQ 30) was performed at inclusion in the study and then after 6, 12, and 24 mo. The therapeutic effect was assessed by CT or MRI every 3 mo according to WHO criteria[25]. A complete response was defined as disappearance of all HCC lesions documented by imaging analyses (ultrasound, CT, or MRI), and confirmation 4 or more weeks later. A partial response was defined as more than 50% reduction of the tumor size based on the measurement of the two longest perpendicular diameters of the tumor.

Statistical analyses

Study design was a multicenter randomized controlled trial to compare therapeutic effect of TACE and TACE-PEI.

Between January 1997 and August 2001, 58 patients

were recruited for the study. Recruitment was stopped after 56 mo. Follow-up period of 24 mo was planned.

Comparison between groups was made on an intention-to-treat basis. Survival time for the TACE- and TACE-PEI group was assessed by the Kaplan-Maier method and log-rank test for univariate analysis. Therapeutic effect was estimated by Cox's proportional hazards regression model for multivariate analysis. All significance tests were two-sided and $P<0.05$ was considered statistically significant. Data processing and analysis were performed using the statistical analysis system (SAS Institute, Cary, NC, USA).

RESULTS

From January 1997 to August 2001, 58 patients were enrolled in the study and were randomly assigned to TACE (n = 29) or to TACE-PEI (n = 29). Five patients were excluded because of complete portal vein thrombosis (1 patient), operability (1 patient), death (1 patient) or retraction of consent (2 patients). The remaining 53 patients (26 TACE and 27 TACE-PEI) received allocated intervention. One patient in the TACE group was lost to follow-up after moving. Thus, the data of 52 patients could be analyzed (Figure 1).

Patient characteristics showed no statistically significant differences between the two treatment groups (Table 1).

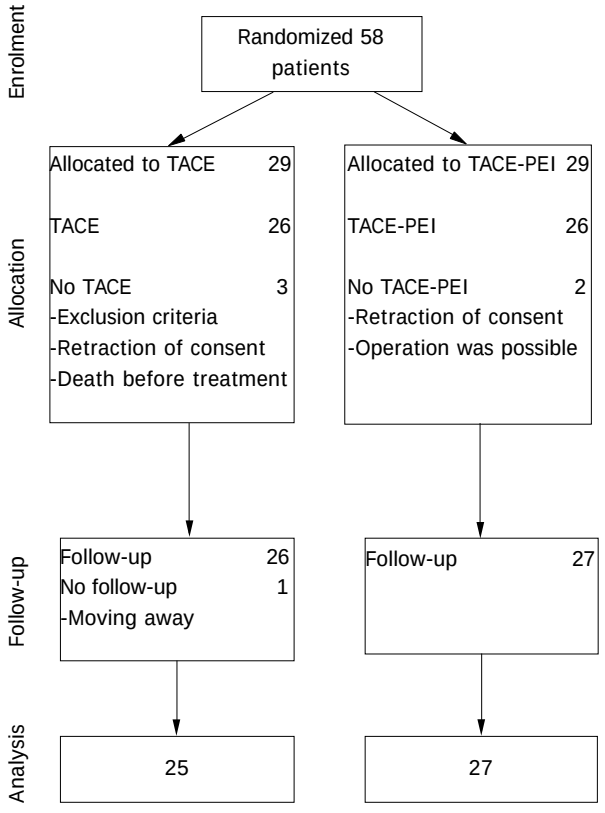


Figure 1 Flowchart of study patients.

Survival

At the time of final analysis (median follow-up time 32 mo [range 5-57 mo]), 18 patients of the TACE group and 17 patients of the TACE-PEI group had died. Median survival time was 18.4 mo (range 5.8-22.0 mo) of the TACE group as compared to 15.3 mo (range 9.2-49.0 mo) of the TACE-PEI group.

The cumulative survival rate of the TACE group was 75.8% at 6 mo, 62.9% at 12 mo and 18.0% at 24 mo and of the TACE-PEI group 76.9%, 61.5%, and 38.7%, respectively (Figure 2A). Comparison of overall survival in both groups showed no statistically significant difference.

Subgroup analysis of patients with HCC Okuda stage I (n = 26) showed a significant longer survival of the TACE-PEI group (>24 mo, median not yet reached in the study period) as compared to the TACE group (18.4 mo [range 11.6-21.7 mo]; P = 0.04; Figure 2B). TACE-PEI treatment reduced the relative risk for mortality to 0.4 (95%CI 0.15-0.96) compared to patients receiving TACE only.

Median survival of patients with HCCs Okuda stage II or III was 5.0 mo in the TACE group (1.7 mo-not defined) compared to 10.4 mo in the TACE-PEI group (Figure 2C). This difference was not statistically significant (P = 0.39).

Table 1 Patients' characteristics according to treatment

	TACE	TACE-PEI
Patients (n)	25	27
ean age yr (range)	63.6 (48-79)	64 (47-76)
M:F (%)	84:16	74.1:25.9
Cirrhosis/no cirrhosis	22/3	23/4
Etiology of cirrhosis (n/%)		
Alcohol	12 (55)	13 (57)
Hepatitis B or C	7 (32)	7 (30)
Hemochromatosis	2 (9)	1 (4)
Unknown	1 (4)	2 (9)
Liver function (n/%)		
Child Pugh A	22 (88)	17 (63)
Child Pugh B	3 (12)	10 (37)
Child Pugh C	0	0
Tumor stage (n)		
Okuda I	19	17
Okuda II	6	9
Okuda III	0	1
AFP		
<100 ng/mL	14	15
⩾100 ng/mL	11	12
Portal vein thrombosis (partial or complete)	8	6
Number of tumor lesions		
1	9	13
2	6	5
3	5	2
>3	4	5
Diffuse	0	2
Not documented	1	0
Largest diameter >5 cm (US)	17	17

Tumor response and side effects

Four patients in the TACE and five patients in the TACE-PEI group showed stable disease, respectively. The remaining 18 patients in the TACE and 20 patients in the combination group had a progressive disease, respectively (Table 2). In both groups, no major treatment-related complication occurred. The most common side effects of TACE were fever, abdominal pain, and elevation of total bilirubin levels. These side effects were transient and disappeared within a week. Side effects of PEI were spontaneously remitting mild local pain in all patients and mild transient fever in most patients.

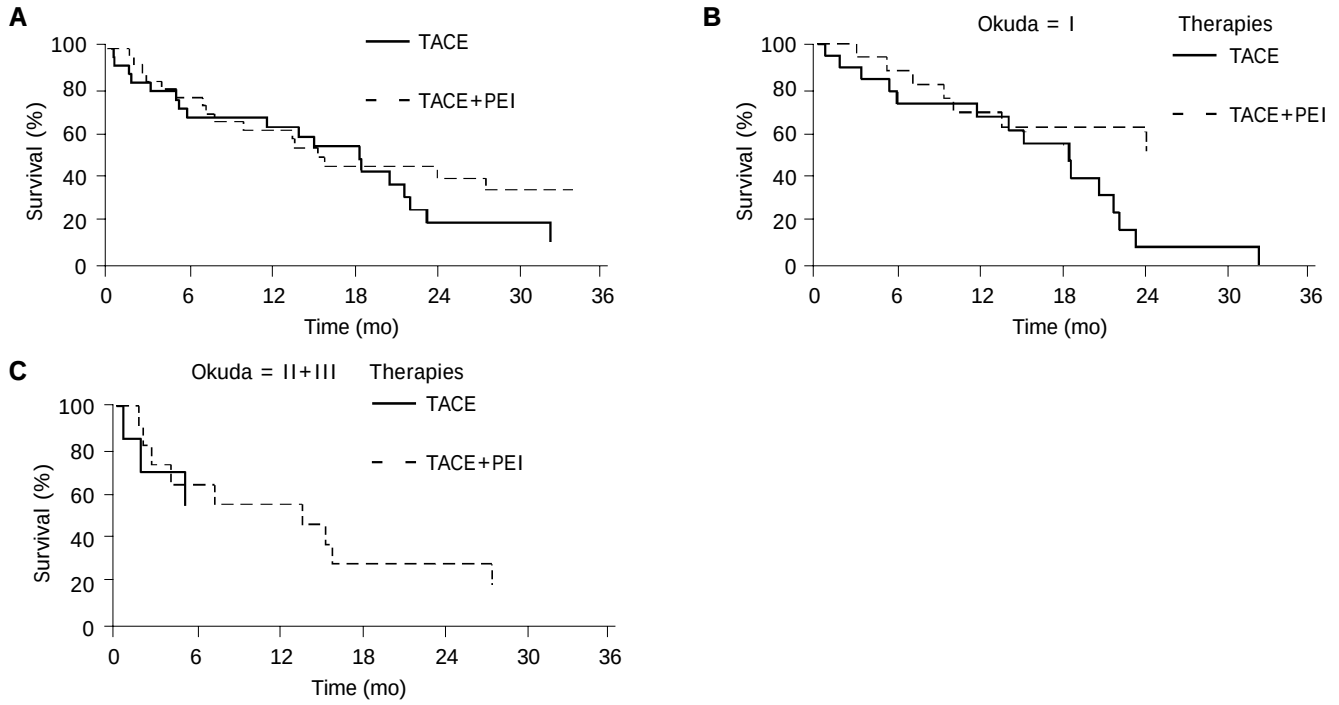


Figure 2 A: Overall survival according to treatment; B: Survival of patients with HCCs Okuda stage I according to treatment; C: Survival of patients with HCCs Okuda stage II or III according to treatment.

Table 2 Tumor response according to treatment

	TACE	TACE+PEI	*P* (χ^2-test)
Patients (*n*)	22	25	
Complete response	-	-	-
Partial response	-	-	-
Stable disease	4	5	NS
Progressive disease	18	20	NS

Duration of hospitalization

For all the 52 study patients, we recorded in-patient stays and out-patient visits during follow-up and discriminated between (1) treatment-related hospital stays/visits including adverse effects or complications and (2) hospital stays/visits because of other reasons (Table 3). As expected, patients treated with TACE-PEI had on average slightly longer hospital stays. Overall, however, there was no statistically significant difference between both treatment groups with respect to in-patient days and out-patient visits, respectively.

Table 3 Hospitalization or out-patient visits according to treatment

	TACE	TACE-PEI	*P* (Wilcoxon rank test)
IST (d)	33	44.67	0.46
OST (d)	2.72	3.07	0.75
ISO (d)	9.16	5.74	0.91

IST = average inpatient hospitalization because of treatment or complications; OST = average outpatient visits because of treatment or complications; ISO = average inpatient hospitalization for other reasons.

Quality of life

To evaluate quality of life, we used a validated self-rating questionnaire (EORTC QLQ 30). According to the design of the study, patients were expected to complete the questionnaire at enrolment into the study and at mo 6, 12, and 24. Unfortunately, only 17 completely filled out questionnaires were obtained. Most patients suffered from poor and worsening physical condition, including hepatic encephalopathy, so that only a minority of patients was able to complete the self-rating questionnaire. Therefore, we could not statistically analyze quality of life.

DISCUSSION

In a previous study, we prospectively analyzed the clinical factors determining the prognosis of 132 patients with inoperable HCCs who were treated with TACE, PEI, the combination of both, or best supportive care[15]. Multivariate analysis revealed that patients treated with a combination of TACE and PEI had a significantly better survival than patients receiving either PEI or TACE only. These observations prompted us to undertake a multicenter randomized controlled trial evaluating the effect of combination therapy with TACE-PEI on long-term survival.

The purpose of the combination is to overcome the shortcomings of both therapies and to get improved therapeutic results by combined effects. TACE is one of the most common therapies in patients with unresectable HCC. This regional therapy combines targeted chemotherapy and arterial embolization in order to induce both selective ischemic and chemotherapeutic effects on HCC. Although survival benefit has been reported after TACE[5], it is difficult to achieve complete necrosis of the target tumor by TACE alone, because HCC often has intercapsular or extracapsular invasion and viable tumor cells remain after TACE[26]. PEI is also widely used and is an effective means of treating

Table 4 Patients' characteristics and survival according to treatment

	Becker *et al.*,	Kamada [26]	Bartolozzi [27]	Tanaka [28]	Koda [29]	Yamamoto [20]
Number of patients						
	52	69	53	43	36	100
Cause of cirrhosis						
Hepatitis:alcohol	14:25	65	5:48	No data	No data	100
1-yr survival in % of patients						
TACE+PEI	62	90	100	100	100[1]	95
TACE	63	86	92.6	68	75[1]	92.5
2-yr survival in % of patients						
TACE+PEI	39	3-yr:65	86.7	85	82[2]	72.5
TACE	18	3-yr:44	69.7	37	50[2]	57.5
P	NS (0.371)	NS	NS	<0.001	<0.05	<0.05

[1]Observation period only 10 mo. [2]Observation period only 20 mo.

unresectable HCC. The method is effective in cases of capsular invasion. The injection of absolute alcohol causes cellular dehydration, coagulation necrosis, and vascular thrombosis within the treated tumor[27]. But several factors limit the therapeutic effect of PEI, such as tumor consistency, intratumoral septa, tumoral capsule, and tumor vascularization[28]. The rationale for combination of TACE and PEI relies on the fact that after TACE tumor consistency is markedly decreased and intratumoral septa are usually disrupted providing enhanced ethanol diffusion within the tumor. Therefore, combined therapy with TACE-PEI has been expected to improve survival rates of patients with advanced HCC.

In our randomized controlled multicenter trial comparing TACE and TACE-PEI, we observed no difference in overall survival. However, subgroup analysis based on HCC Okuda stage revealed that TACE-PEI results in statistically significant improved survival in patients with HCC Okuda stage I.

Similar to our findings, a recently published retrospective analysis based on medical records showed that patients receiving TACE alone had a median survival rate of 16 mo, whereas the median survival rate in patients receiving TACE followed by PEI was 24 mo[29].

The prospective randomized trials by Kamada *et al.*[30], and by Bartolozzi *et al.*[31], also showed improved survival for patients treated with TACE-PEI compared to TACE alone. Because of the small number of patients included in these studies, the difference did not reach statistical significance. Further, Tanaka *et al.*[32], Koda *et al.*[33], and Yamamoto *et al.*[20], showed a significant improved survival for patients treated with TACE-PEI as compared to TACE alone (Table 4).

Even though these studies included patients with Child-Pugh C score liver cirrhosis[20,32,33], mean survival time in our study, which excluded Child-Pugh C score patients, was shorter. This may be due to the following facts: (1) We only excluded patients with complete portal vein thrombosis (main trunk or both branches) whereas others excluded patients with any evidence of (partial) thrombosis[30-33]; that is predicting poor survival[15,20]. (2) Liver disease in our study was caused in about 50% by alcohol, whereas in all other studies most patients had chronic hepatitis B or C (Table 4). Our findings, therefore, may suggest that combination therapy with TACE-PEI may be less effective in patients with alcohol-induced than in patients with HBV- or HCV-induced cirrhosis. (3) Tanaka *et al.*[32], Koda *et al.*[33], and Yamamoto *et al.*[20], used doxorubicin, whereas in our study mitomycin C was used. Advantages for anthracyclin-based regimes were advocated in one randomized controlled trial[34], but a recently published meta-analysis showed no good evidence for best chemotherapeutic agent[5].

The primary end point of our study was survival time. Secondary end point was the duration of hospitalization and/or the number of out-patient visits. As expected, patients treated with TACE-PEI had on average slightly longer hospital stays than patients with TACE only. There was no statistically significant difference between both treatment groups, however. This aspect is important not only with respect to financial costs, but also with respect to patient's quality of life.

In conclusion, the combination of TACE-PEI compared with TACE alone prolongs survival in patients at Okuda stage I. Side effects were mild and combined therapy with TACE-PEI did not prolong duration of hospitalization or the number of out-patient visits considerably.

REFERENCES

1 **Wanebo HJ**, Falkson G, Order SE. Cancer of the hepatobiliary system. In: Devita VT Jr, Hellman S and Rosenberg SA (Eds.): Cancer Principles and Practice of Oncology *(*3rd ed.), *Philadelphia Lippincott* 1989: 836-874

2 **Andriulli A**, de Sio I, Solmi L, de Carlis L, Troisi R, Grasso A, Festa V, Caturelli E, Giacomoni A, de Veccio Blanco C, de Hemptinne B, Burroughs A, Perri F. Survival of Cirrhotic Patients With Early Hepatocellular Carcinoma Treated by Percutaneous Ethanol Injection or Liver Transplantation. *Liver Transplantation* 2004; **10**: 1355-1363

3 **Bruix J**. Treatment of hepatocellular carcinoma. *Hepatology* 1997; **25**: 259-262

4 **Kulik** L, Abecassis M. Living Donor Liver Transplantation for Hepatocellular Carcinoma. *Gastroenterology* 2004; **127**: S277-S282

5 **Llovet JM**, Burroughs A, Bruix J. Hepatocellular carcinoma. *Lancet* 2003; **362**: 1907-1917

6 **Schafer DF**, Sorrell MF. Hepatocellular carcinoma. *Lancet* 1999; **353**: 1253-1257

7 **Wiesner RH**, Freeman RB, Mulligan DC. Liver Transplantation for hepatocellular carcinoma: the impact of the meld allocation policy. *Gastroenterology* 2004; **127**: S261-S267

8 **Llovet JM**, Real MI, Montana X, Planas R, Coll S, Aponte J, Ayuso C, Sala M, Muchart J, Sola R, Rodes J, Bruix J. Arterial embolisation or chemoembolisation versus symptomatic treatment in patients with unresectable hepatocellular

carcinoma: a randomised controlled trial. *Lancet* 2002; **359**: 1734-1739
9 **Trevisani F**, De Notariis S, Rossi C, Bernardi M. Randomized control Trials on Chemoembolization for Hepatocellular Carcinoma. *J Clin Gastroenterol* 2001; **32**: 383-389
10 **Bruix J**, Sala M, Llovet JM. Chemoembolization for Hepatocellular Carcinoma. *Gastroenterology* 2004; **127**: S179-S188
11 **Llovet JM**, Bustamante J, Castells A, Villana R, Ayuso Mdel C, Sala M, Bru C, Rodes J, Bruix J. Natural history of untreated nonsurgical hepatocellular carcinoma: rationale for the design and evaluation of therapeutic trials. *Hepatology* 1999; **29**: 62-67
12 **Omata M**, Tateishi R, Haruhiko Y, Shiina S. Treatment of hepatocellular carcinoma by percutaneous tumor ablation methods: ethanol injection therapy and radiofrequency ablation. *Gastroenterology* 2004; **127**: S159-S166s•
13 **Lencioni R**, Allgaier HP, Cioni D, Olschewski M, Deibert P, Crocetti L, Frings H, Laubenberger J, Zuber I, Blum HE, Bartolozzi C. Small hepatocellular carcinoma in cirrhosis: randomized comparison of radio-frequency thermal ablation versus percutaneous ethanol injection. *Radiology* 2003; **228**: 235-240
14 **Tanaka K**, Nakamura S, Numata K, Kondo M, Morita K, Kitamura T, Saito S, Kiba T, Okazaki H, Sekihara H. The long term efficacy of combined transcatheter arterial embolization and percutaneous ethanol injection in the treatment of patients with large hepatocellular carcinoma and cirrhosis. *Cancer* 1998; **82**: 78-85
15 **Allgaier HP**, Deibert P, Olschewski M, Spamer C, Blum U, Gerok W, Blum HE. Survival benefit of patients with inoperable hepatocellular carcinoma treated by a combination of transarterial chemoembolization and percutaneous ethanol injection - a single center analysis including 132 patients. *Int J Cancer* 1998; **79**: 601-605
16 **Seki T**, Nonaka T, Kubota Y, Mizuno T, Sameshima Y. Ultrasonically guided percutaneous ethanol injection therapy for hoepatocellular carcinoma. *Am J Gastroenterol* 1989; **84**: 1400-1407
17 **Shiina S**, Tagawa K, Unuma T, Fujino H, Uta Y, Niwa Y, Hata Y, Komatsu Y, Shiratori Y, Terano A. Percutaneous ethanol injection therapy of hepatocellular carcinoma: analysis of 77 patients. *Am J Roentgenol* 1990; **155**: 1221-1226
18 **Mondazzi L**, Bottelli R, Brambilla G, Rampoldi A, Rezakovic I, Zavaglia C, Alberti A, Ideo G. Transarterial oily chemoembolization for the treatment of hepatocellular carcinoma: a multivariate analysis of prognostic factors. *Hepatology* 1994; **19**: 1115-1123
19 **Tanaka K**, Okazaki H, Nakamura S, Endo O, Inoue S, Takamura Y, Sugiyama M, Ohaki Y. Hepatocellular carcinoma: treatment with a combination therapy of transcatheter arterial embolization and percutaneous ethanol injection. *Radiology* 1991; **179**: 713-717
20 **Yamamoto K**, Masuzawa M, Kato M, Kurosawa K, Kaneko A, Ishida H, Imamura E, Park NJ, Shirai Y, Fujimoto K, Michida T, Hayashi N, Ikeda M. Evaluation of combined therapy with chemoembolization and ethanol injection for advanced hepatocellular carcinmoa. *Sem Oncol* 1997; **24**: 6 (Suppl): 50-55
21 **Bronowicki JP**, Vetter D, Dumas F, Boudjema K, Bader R, Weiss AM, Wenger JJ, Boissel P, Bigard MA, Doffoel M. Transcatheter oily chemoembolization for hepatocellular carcinoma. *Cancer* 1994; **74**: 16-24
22 **Chang JM**, Tzeng WS, Pan HB, Yang CF, Lai KH. Transcatheter arterial embolization with or without cisplatin treatment of hepatocellular carcinoma. *Cancer* 1994; **74**: 2449-2453
23 **Lencioni R**, Paolicchi A, Moretti M, Pinto F, Armillotta N, Di Giulio M, Cicorelli A, Donati F, Cioni D, Bartolozzi C. Combined transcatheter arterial chemoembolization and percutaneous ethanol injection for the treatment of large hepatocellular carcinoma: local therapeutic effect and long-term survival rate. *Eur Radiol* 1998; **8**: 439-444
24 **Stefanini GF**, Amorati P, Biselli M, Mucci F, Celi A, Arienti V, Roversi R, Rossi C, Re G, Gasbarrini G. Efficacy of transarterial targeted treatments on survival of patients with hepatocelllular carcinoma. *Cancer* 1995; **75**: 2427-2434
25 **Miller AB**, Hoogstraten B, Staquet M, Winkler A. Reporting results of cancer treatment. *Cancer* 1981; **47**: 207-214
26 **Jansen MC**, van Hillegersberg R, Chamuleau RA, van Delden OM, Gouma DJ, van Gulik TM. Outcome of regional and local ablative therapies for hepatocellular carcinoma: a collective review. *EJSO* 2005; **31**: 331-347
27 **Guan YS**, Sun L, Zhou XP, Li X, Zheng XH. Hepatocellular carcinoma treated with interventional procedures: CT and MRI follow-up. *World J Gastroenterol* 2004; **15**: 3543-3548
28 **Koda M**, Murawaki Y, Oyama K, Okamoto K, Idobe Y, Suou T, Kawasaki H. Combination therapy with transcatheter arterial chemoembolization and percutaneous ethanol injection compared with percutaneous ethanol injection alone for patients with small hepatocellular carcinoma. *Cancer* 2001; **92**: 1516-1524
29 **Greten TF**, Papendorf F, Bleck JS, Kirchhoff T, Wohlberedt T, Kubicka S, Klempnauer J, Galanski M, Manns MP. Survival rate in patients with hepatocellular carcinoma: a retrospective analysis of 389 patients. *Br J Cancer* 2005; **92**: 1862-1868
30 **Kamada K**, Kitamoto M, Aikata H, Kawakami Y, Kono H, Imamura M, Nakanishi T, Chayama K. Combination of transcatheter arterial chemoembolization using cisplatin-lipiodol suspension and percutaneous ethanol injection for treatment of advanced small hepatocellular carcinoma. *Am J Surg* 2002; **184**: 284-290
31 **Bartolozzi C**, Lencioni R, Caramella D, Vignali C, Cioni R, Mazzeo S, Carrai M, Maltinti G, Capria A, Conte PF. Treatment of large HCC: transcatheter arterial chemoembolization combined with percutaneous ethanol injection versus repeated transcatheter arterial chemoembolization. *Radiology* 1995; **197**: 812-818
32 **Tanaka K**, Nakamura S, Numata K, Okazaki H, Endo O, Inoue S, Takamura Y, Sugiyama M, Ohaki Y. Hepatocellular carcinoma: treatment with percutaneous ethanol injection and transcatheter arterial embolization. *Radiology* 1992; **185**: 457-460
33 **Koda M**, Okamoto K, Miyoshi Y, Kato S, Murawaki Y, Horie Y, Suou T, Kawasaki H. Combination therapy with transcatheter arterial embolization and percutaneous ethanol injection for advanced hepatocellular carcinoma. *Hepatogastroenterology* 1994; **41**: 25-29
34 **Kawai S**, Tani M, Okamura J, Ogawa M, Ohashi Y, Monden M, Hayashi S, Inoue J, Kawarada Y, Kusano M. Prospective and randomized clinical trial for the treatment of hepatocellular carcinoma -a comparison of L-TAE with farmorubicin and L-TAE with adriamycin (second cooperative study). *Cancer Chemother Pharmacol* 1994; **33**: S97-102

Science Editor Guo SY **Language Editor** Elsevier HK

PO Box 2345, Beijing 100023, China
www.wjgnet.com
wjg@wjgnet.com

ELSEVIER

World J Gastroenterol 2005;11(39):6110-6114
World Journal of Gastroenterology ISSN 1007-9327
© 2005 The WJG Press and Elsevier Inc. All rights reserved.

Effects of adenovirus-mediated human cyclooxygenase-2 antisense RNA on the growth of hepatocellular carcinoma

Xiao-Hu Wang, Sheng-Bao Li, Qiang Tong, Guo-Jian Xie, Qing-Ming Wu

Xiao-Hu Wang, Sheng-Bao Li, Qiang Tong, Guo-Jian Xie, Qing-Ming Wu, Department of Gastroenterology, Taihe Hospital, Yunyang Medical College, Shiyan 442000, Hubei Province, China
Supported by the Bureau of Science and Technology of Shiyan City
Correspondence to: Sheng-Bao Li, Department of Gastroenterology, Taihe Hospital, Yunyang Medical College, Shiyan 442000, Hubei Province, China. libao@sycatv.net
Telephone: +86-719-8801431
Received: 2004-07-30 Accepted: 2004-12-29

Abstract

AIM: To investigate the relation between the expression of cyclooxygenase-2 (COX-2) and liver cancer, to construct the recombinant adenovirus encoding human COX-2 antisense RNA, and to explore its effects on liver cancer cell proliferation.

METHODS: We studied the expression of COX-2 in 34 cases of hepatocellular carcinoma (HCC) and SMMC7402 and SMMC7721 by immunohistochemical technique. Recombinant adenovirus Ad-AShcox-2 was constructed and transfected into human HCC cell lines SMMC7402 and SMMC7721, and its effects on COX-2 expression, cell apoptosis and cell cycle were analyzed by flow cytometry. Cell proliferation was determined by colony-forming efficiency.

RESULTS: We observed COX-2 expression in 82.4% of HCC and SMMC7402 cells, but no COX-2 expression in SMMC7721 cells. In addition, recombinant adenovirus encoding antisense COX-2 fragment Ad-AShcox-2 was obtained with the titer of 1.06×10^{12} PFU/mL. Ad-AShcox-2 could reduce the expression of COX-2 and enhance the percentage of cells in G_1/G_0 phase in SMMC7402 cell line. The difference of apoptotic index between the Ad-AShcox-2 group and control group was statistically significant ($t_{control\ group}$ = 32.62 and $t_{Ad\text{-}LacZ}$ = 10.93, $P<0.001$) in SMMC7402 but not in SMMC7721. Similarly, colony-forming rates of SMMC7402 and SMMC7721 cell lines, after the transfer of Ad-AShcox-2, were (2.7±0.94)% and (33.6±4.24)%, respectively.

CONCLUSION: Reduction in the expression of COX-2 can inhibit COX-2 expressing HCC cells.

© 2005 The WJG Press and Elsevier Inc. All rights reserved.

Key words: Adenovirus; Cyclooxygenase-2; Antisense RNA; Hepatocellular carcinoma

Wang XH, Li SB, Tong Q, Xie GJ, Wu QM. Effects of adenovirus-mediated human cyclooxygenase-2 antisense RNA on the growth of hepatocellular carcinoma. *World J Gastroenterol* 2005; 11(39): 6110-6114
http://www.wjgnet.com/1007-9327/11/6110.asp

INTRODUCTION

Liver cancer is a kind of malignant tumor with a high mortality at present. Its morbidity is rather high in our country. Although a great number of researches on liver cancer as well as many achievements have been made, the exact molecular pathogenesis of liver cancer is not clear. Cyclooxygenase-2 (COX-2) has a high expression in quite a few tumors such as colorectal cancer[1,2], esophageal cancer[3], and other cancers[4]. It is likely to be related to the genesis and development of tumor, but the causing-carcinoma effect can be resisted by COX-2 selective inhibitors[5-7]. Our prophase researches showed that COX-2 antisense RNA obviously inhibits the growth of carcinoma of esophagus with a high expression of COX-2[8,9]. COX-2 is likely to become a new target of treating tumor. The present study aimed to investigate the relationship between the expression of COX-2 and liver cancer, to the construction of the recombinant adenovirus encoding human COX-2 anti-sense RNA, and to treat hepatocellular carcinoma (HCC) with or without the expression of COX-2 and to explore its mechanism.

MATERIALS AND METHODS

Intraremovelase

*Bam*HI, *Xba*I, and T_4 DNA ligase were purchased from Huamei Biological Engineering Company. RPMI 1640 and Lipofectamine were provided by GIBCO/BRL. CsCl was from Sigma Company. COX-2 cDNA and primer of adenovirus PCR were designed and synthesized by Saibaisheng Biology Company.

Plasmid, adenovirus, and cell line

Ad-LacZ was a gift from Dr. Jia-Ning Wang in our Molecular Biological Laboratory. COX-2 plasmid PCR™II vector was supplied by Dr. You-Fei Guan in Vanderbilt University, USA. pHCMVSP1A and pJM17 were donated by academician Wu Zuze in the Second Institute of Academy of Military Medical Sciences. DH_{5a} was donated by Dr. Peng Xu in Cardiology Internal Medicine Department of No. 1 Hospital Peking University. 293 cells and HCC cell lines SMMC7721 and SMMC7402 were purchased from Shanghai Cell Bank

of Chinese Academy of Medical Sciences.

Equipments

High-speed refrigerated centrifuge (Jouan, Italy), carbon dioxide incubator (Sany D, Japan), ultrahigh refrigerated centrifuge (Hitachi, Japan), inversion difference microscope (Olympus IX-To, Japan), PCR amplifier (Amplitron II, USA), flow cytometer (EPICS XL, Beckman Coulter Company, USA), ultraviolet spectrophotometer (752, Shanghai), air bath, and water bath cradle were used in our study.

Expression of COX-2 in HCC tissue

Immunohistochemical transfection was conducted by streptomy-glair-in-biotin-horseradish peroxidase (SP) compound method. The tissue was fixed with paraffin and cut into 5-μm-thick sections. HCC tissue slides were fixed in 4% PFA in PBS for 10 min, washed twice with PBS, and incubated in 3% H_2O_2 to eliminate the endogenous peroxidase activities. The tissues were then incubated either at room temperature for 1 h or at 4 ℃ overnight with 1% goat serum in PBS to block the nonspecific binding of antibodies. The slides were further incubated sequentially with rabbit anti-man COX-2 polyclonal antibody. PBS was used as a control. Color development was performed by incubation with 3,3-diaminobenzidine tetrahydrochloride in 0.03% H_2O_2 and 50 mmol/L Tris-HCl, pH 7.4. The percentage of positive tumor cells was determined semiquantitatively by assessing the whole tumor section, and each sample was assigned to one of the following categories: 0 (0-4%), 1 (5-24%), 2 (25-49%), 3 (50-74%), 4 (75-100%). Transfection strength was indicated with 0 (negative), 1 (weak positive), and 2 (positive). The expression levels were indicated with positive rate of tumor cells of one tumor tissue showing the different transfection strength. Its expression level was the transfection strength fraction by positive rate fraction. For example, if 50 tumor cells of one tumor tissue showed positive staining, we could mark 3 by 2 equaling 6; if 25 showed weak positive staining, we could mark 2 by 1 equaling 2; if 25% showed negative staining, we could mark 2 by 0 equaling 0. Thus the total was 6 plus 2 plus 0 equaling 8. The specific result statistics were carried out as previously described[10].

Construction, identification, amplification, purification, and titer assay

First, we obtained a COX-2 cDNA fragment using *Xba*I and *Bam*HI to bi-mold-cut the plasmid PCR™IICOX-2, and cloned the COX-2 cDNA fragment in the reverse direction onto two spots of *Xba*I and *Bam*HI of the pHCMUSP1A, the connection product was pAd-Ashcox-2. Then the latter was plasmid-amplified by transformed bacillus coli DH_{5a} and identified as positive plasmid by mold-cutting. The shuttle plasmid pAd-Ashcox-2 mediated Lipofectamine and pJM17 were co-transferred into 293 cells. When 293 cells had pathologic lesions and exfoliative cells made up 20%, we collected the upper clear liquid. Then we extracted viral DNA from the upper clear liquid and identified it by PCR. COX-2 primer's upstream sequences are 5'-TTG GCT TCA AGA CTG AGA TA-3' and 5'-AGC CCA AAT TAT TGG TTC-3'. Adenovirus primer's upstream sequence is 5'-TCG TTT CTC AGC AGC TGT TG-3', downstream sequence is 5'-CAT CTG AAC TCA AAG CGT GG-3'. PCR reaction system contained 10 μL viral DNA, 10 μL 20 μmol/L primer respectively (5 μL adenovirus), 5 μL 10× PCR buffer, 2 μL $MgCl_2$, 5 μL 2 mmol/L dNTP and 1 μL Taq enzyme. Water was added until the final volume of PCR reaction was 50 μL. Thirty cycles of PCR were carried out, each consisting of 30 s at 94 ℃, 30 s at 56 ℃, 1 min at 72 ℃, then a final extension at 72 ℃ for 10 min. Electrophoresis in 1.0% agarose gel was performed to amplify cDNA and adenovirus fragments as positive reconstructive cloning. Without adding mould, PCR amplification was used as a negative control. After positive reconstructive adenovirus was identified, we transferred 293 cells again. 293 cells were collected, refrigerated, melted, fragmented and ultracentrifuged twice with CsCl, viruses were collected and purified. At last the virus titer was assayed.

Efficiency of virus transfection

The recombinant adenovirus Ad-LacZ with genes encoding LacZ was used to infect liver cancer cell lines SMMC7721 and SMMC7402 according to multiplicity of infection-MOI 25, 50, 100, and 200. After 48 h, the cells were fixed and stained with X-gal. The number of cells stained blue was recorded under microscope. Then the percentage of cells with blue staining was calculated.

Transfection of recombinant adenovirus and expression of COX-2

Human liver cancer cell lines SMMC7721 and SMMC7402 were incubated in a 50 mL/L CO_2 at 37 ℃. When the density reached 40-50%, the medium was replaced by serum-free RPMI 1640 and incubated for 24 h. The experimental group infected the two cell lines with 100MOI, and was incubated for 2 h with serum. During the process, the culture fluid was shaken every 15 min. Two hours later, the medium was replaced by 10% FCS RPMI 1640. The control groups were Ad-LacZ group and non-virus group. Carcinoma cells were incubated for 24, 48, 72, 96 h respectively, fixed for 10 min in 4 ℃ cold acetone, and dried for 10 min at room temperature. Then the cells were stored at -85 ℃. The experiment was carried out with SP immunohistochemical method.

Flow cytometry

When the density of the two cell lines reached 40-50%, the medium was replaced by RPMI 1640 containing serum and incubated for 24 h. Forty-eight hours after the experimental group and control group finished virus transfection, the cells were collected (using trypsin digestion method) and centrifuged (1 000 r/min, 5 min). The upper clear fluid was discarded, PBS was added to adjust cell density to 10^6/mL. One hundred microliters of cell suspension was put into the tube, 200 μL DNA-PREP™I-PR was added to it and mixed. Two microliters DNA-PREP™ stain reagent (PI stain) was added and mixed after 30 s. After 30 min, the cell cycle and apoptosis was detected with flow cytometry (FCM).

Colony-forming experiment

The two cell lines was digested into single-cell suspension

respectively, and inoculated into a six-well board. Each well was inoculated with 500 cells. Each group had three pang-punches. After being treated with culture fluid Ad-AShcox-2, they were incubated for 10 d and fixed with 1:3 acetic acid:methanol, stained with Rui stain fluid. Then the number of colonies with more than 50 cells was recorded.

Statistical analysis

Expression level of COX-2 in liver cancer tissue was expressed as mean±SD. *t*-Test was used to show the cell apoptosis rate and cell cycle distribution rate.

RESULTS

Expression of COX-2 in liver cancer tissue

COX-2 was positive in 28 of 34 cases of liver cancers and was negative in 6 of 34 cases of liver cancer. Positive rate was 82.4%. The positive staining of COX-2 was mainly in cytoplasm. High expression of COX-2 was correlated with clinical pathological features of liver cancer (Figure 1). COX-2 expression level was high, if the cancer cells were well differentiated. COX-2 expression was not related to AFP levels, source cells and transference in liver (Table 1).

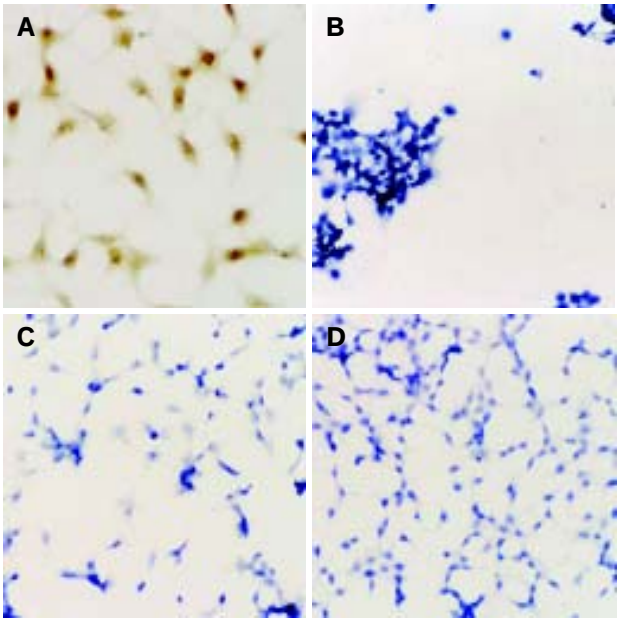


Figure 1 Expression of COX-2 in SMMC7402 and SMMC7721 before (A and B) and after (C and D) the transfer of Ad-AShcox-2.

Identification of recombinant adenovirus by PCR co-amplification method

DNA was extracted and precipitated, then PCR amplification was performed on this DNA model. The product of PCR amplification was evaluated with 0.8% agarose electrophoresis, and 277-bp COX-2 cDNA fragments and 860-bp virus gene frame fragments were obtained. After pAd-AShcox-2 and pJM17 were co-transferred to 293 cells, we produced anti-sense RNA recombinant adenovirus which could express COX-2.

Table 1 Relationship between high expression of COX-2 and clinical pathological features of liver cancer (mean±SD)

Clinical pathological features	*n*	Stain fraction	*t*	*P*
AFP (ng/mL)				
<20	4	6.48±1.46	0.74	>0.05
⩾20	24	6.36±1.15		
Cell category				
Liver cell category	27	6.79±1.60		
Bile duct cell category	1	6.26±1.25		
Transference in liver				
Yes	3	6.43±1.42	1.08	<0.05
No	25	7.15±1.80		
Pathological differentiation				
High	22	8.25±0.86	5.23	<0.05
Middle and low	6	6.11±1.02		

Titer and transfection rate of Ad-AShcox-2

After Ad-AShcox-2 was amplified, extracted, purified, and assayed with ultraviolet spectrophotometer, the virus titer was 1.06×10^{12} PFU/mL. When the MOI was 50 or greater, the transfection rate of SMMC7721 and SMMC7402 reached 100%.

Expression of COX-2 in HCC cell lines

Immunohistochemistry showed that SMMC7402 had a high expression of COX-2. But after Ad-AShcox-2 was transferred, the expression of COX-2 decreased obviously. Before and after Ad-AShcox-2 was transferred, SMMC7721 did not express COX-2 (Figures 1A-D).

Apoptosis of liver cancer cells

Forty-eight hours after SMMC7402 cells were treated with Ad-AShcox-2, FCM showed that apoptotic cells reached apoptosis peak prior to G_0/G_1 peak. The apoptosis rates of Ad-AShcox-2, Ad-LacZ, and the control group were (33.3±3.02)%, (0.42±0.14)%, and (0.25±0.08)%, respectively. The apoptosis rate of the experimental group increased obviously in comparison to the control group. However, after SMMC7721 was treated with Ad-AShcox-2, we could not detect the apoptosis peak with FCM. The apoptosis rates were (0.61±0.25)%, (0.48±0.09)%, and (0.56±0.11)%, respectively. The apoptosis rates of these two liver cancer cell lines, induced by Ad-AShcox-2, differed sharply when compared to each other (t = 32.05, P<0.001).

Effect of Ad-AShcox-2 on cell cycle

Cell cycle from FCM is listed in Table 2. After SMMC7402 cells were treated with Ad-LacZ and non-virus culture fluid, the cell proliferation rate decreased in G_0/G_1 phase, but it was high in S phase indicating that the proliferation of cells was active. After they were treated with Ad-AShcox-2, the number of cells in G_0/G_1 phase increased obviously, while in S phase, the number of cells decreased, suggesting that there was a significant difference compared to control group (P<0.05). The cells were blocked in G_1 phase. But after SMMC7721 was treated with Ad-AShcox-2, the cell proliferation rates in G_1/G_0 phase were low both in experimental group and in control group (Table 3); yet they were high in

Table 2 Cell apoptosis rate and cell cycle after SMMC7402 was treated in experimental group and control group (n = 9, mean±SD)

Groups	Apoptosis rate	Cell cycle (%)		
	(%)	G_0/G_1	S	G_2/M
Control group	0.25	40.39±3.86	49.61±4.27	13.10±1.03
Ad-LacZ	0.42	40.17±4.03	50.18±3.66	12.57±2.85
Ad-ASHcox-2	33.3	66.52±5.48	22.15±3.26	10.33±1.12

Table 3 Cell apoptosis rate and cell cycle after SMMC7721 was treated in experimental group and control group (mean±SD)

Groups	Apoptosis rate	Cell cycle (%)		
	(%)	G_0/G_1	S	G_2/M
Control group	0.56	40.39±3.86	49.61±4.27	13.10±1.03
Ad-LacZ	0.48	42.17±2.63	50.26±2.85	12.27±2.72
Ad-ASHcox-2	0.91	39.92±4.11	49.28±4.13	12.64±1.25

S phase. There was no difference (P>0.05) when compared to each other.

Effect of Ad-AShcox-2 on colony-forming ability of liver cancer cells

After Ad-AShcox-2 infected SMMC7721 and SMMC7402, the colony-forming rates were (2.7±0.94)% and (33.6±4.24)%. There were significant differences between the two groups (P<0.05, n = 6).

DISCUSSION

Cyclooxygenase is a kind of a rate-limiting enzyme, which catalyzes and synthesizes prostaglandin. It has two isomers -COX-1 and COX-2. COX-1 is constitutively expressed in most mammalian tissues and is thought to carry out "housekeeping" functions such as cytoprotection of the gastric mucosa, regulation of renal blood flow, and control of platelet aggregation. In contrast, COX-2 mRNA and protein are normally undetectable in most tissues, but can be rapidly induced by proinflammatory or mitogenic stimuli including cytokines, endotoxins, interleukins, and phorbolester. It has high expression levels in many cancer tissues. Researches showed that COX-2 can promote the formation and opening of tumor vessels[11,12], inhibit tumor immunity[13,14], stimulate transference of tumors and inhibit apoptosis[15-18].

Studies indicate that COX-2 selective inhibitor can inhibit proliferation of colon cancer cells[19,20], and induce their apoptosis[21,22]. In our prophase researches, by using the carrier of COX-2 antisense RNA adenovirus-transferred esophageal carcinoma cells, we successfully inhibited the expression of COX-2 in esophageal carcinoma cells[8,9]. The growth and proliferation of esophageal carcinoma cells were obviously inhibited, showing that reducing the expression of COX-2 or inhibiting the activity of COX-2 is likely to become a new way to treat tumors.

COX-2 is strongly positive in 28 of 34 cases of HCC. The positive rate reached 82.4%, suggesting that the high expression of COX-2 is related to the carcinogenesis and development of HCC. We also found that most HCCs with positive expression of COX-2 were well differentiated, but poorly differentiated HCC had a low expression of COX-2, indicating that COX-2 can promote the proliferation and differentiation of liver cancer cells, which is in line with the report of Koga *et al*.[23]. We can infer that HCC is related to COX-2 inhibiting cell apoptosis and increasing cytoplasmic matrix protein.

We successfully constructed the recombinant adenovirus expressing COX-2 anti-sense RNA. When the two liver cancer cells were treated with it, the expression of COX-2 decreased obviously. Meanwhile, the growth of cells was inhibited and the colony-forming rates of cells decreased apparently as well. But the colony-forming rates of SMMC7721 did not decrease, indicating that inhibiting the expression of COX-2 could inhibit the growth of liver cancer cells with positive expression of COX-2. However, cells with negative expression of COX-2 could not be inhibited. We further confirmed that the feasibility of COX-2 independent way in which NSAIDs could inhibit the colon cancer cells without the expression of COX-2[24].

After SMMC7402 was transferred in Ad-AShcox-2, the rate of cell apoptosis increased notably. There was a significant difference when control group, Ad-LacZ treatment group, and blank group were compared to each other (P<0.001), but the apoptosis rate of SMMC7721 did not increase, showing that by reducing the expression of COX-2, we can increase the apoptosis of cancer cells. This is in line with the result of a previous study[17].

Cell cycle test showed that Ad-AShcox-2 could reduce the expression of COX-2 in SMMC7402, the cell number increased evidently in G_0/G_1 phase. It could prevent cells passing from G_1 to S phase. It is likely to be linked with the expression of raised P_{27} and the inhibition of cyclin/CDK activity[25,26].

In conclusion, the adenovirus carrier with the expression of COX-2 anti-sense RNA is able to inhibit SMMC7402 and induce apoptosis.

REFERENCES

1 **Giardiello FM**, Spannhake EW, DuBois RN, Hylind LM, Robinson CR, Hubbard WC, Hamilton SR, Yang VW. Prostaglandin levels in human colorectal mucosa: effects of sulindac in patients with familial adenomatous polyposis. *Dig Dis Sci* 1998; **43**: 311-316

2 **Zhan J**, Liu JP, Zhu ZH, Yao HR, Chen CY. Relationship between COX-2 expression and clinicopathological features of colorectal cancers. *Chin Med J* 2004; **117**: 1151-1154

3 **Wu QM**, Li SB, Wang Q, Wang DH, Li XB, Liu CZ. The expression of cox-2 in esophageal carcinoma and its realation to clinicopathologic characteristic. *Shijie Huaren Xiahua Zazhi* 2001; **1**: 11-14

4 **Takahashi T**, Kozaki K, Yatabe Y, Achiwa H, Hida T. Increased expression of COX-2 in the development of human lung cancers. *J Environ Pathol Toxicol Oncol* 2002; **21**: 177-181

5 **Dang CT**, Shapiro CL, Hudis CA. Potential role of selective COX-2 inhibitors in cancer management. *Oncology* 2002; **16** (5 Suppl 4): 30-36

6 **Howe LR**, Dannenberg AJ. A role for cyclooxygenase-2 inhibitors in the prevention and treatment of cancer. *Semin Oncol* 2002; **29**(3 Suppl 11): 111-119

7 **Minter HA**, Eveson JW, Huntley S, Elder DJ, Hague A. The cyclooxygenase 2-selective inhibitor NS398 inhibits proliferation of oral carcinoma cell lines by mechanisms dependent and independent of reduces prostaglandin E2 synthesis. *Clin Cancer*

Res 2003; **9**: 1885-1897
8 **Wu QM**, Li SB, Liu CZ, Wang XH, Xie GJ, Yu JP. The effects of adenovirus-mediated human COX-2 antisense RNA on growth of esophageal carcinoma cells. *Zhongguo Zhongliu Shengwu Zhiliao Zazhi* 2001; **8**: 285-289
9 **Li SB**, Wu QM, Wang Q, Wang XH, Xie GJ. Effects of adenovirus-mediated human cox-2 antisense RNA on synthesis of DNA and proteins in esophageal carcinoma cell line. *Shijie Huaren Xiahua Zazhi* 2003; **5**: 517-521
10 **Krajewska M**, Krijewski S, Epstein JL, Shabaik A, Sauvageot J, Song K, Kitada S, Reed JC. Immunohistochemical analysis of bcl-2, bax, bcl-x and mcl-1expression in prostate cancers. *Am J Pathol* 1996; **148**: 1567-1576
11 **Leung WK**, To KF, Go MY, Chan FK, Ng EK, Chung SC, Sung JJ. Cyclooxygenase-2 upregulates vascular endothelial growth factor expression and angiogenesis in human gastric carcinoma. *Int J Oncol* 2003; **23**: 1317-1322
12 **Tsujii M**, Kawano S, Tsuji S, Sawaoka H, Hori M, DuBois RN. Cyclooxygenase regulates angiogenesis induced by colon cancer cells. *Cell* 1998; **93**: 705-716
13 **Kusumoto H**, Machara Y, Anai H, Kusumoto T, Sugimachi K. Potentiation of adriamycin cytotoxicity by dipyridamole against HeLa cells *in vitro* and sarcoma 180 cells *in vivo*. *Cancer Res* 1988; **48**: 1208-1212
14 **Kakiuchi Y**, Tsuji S, Tsujii M, Murata H, Kawai N, Yasumaru M, Kimura A, Komori M, Irie T, Miyoshi E, Sasaki Y, Hayashi N, Kawano S, Hori M. Cyclooxygenase-2 activity altered the cell surface carbohydrate antigens on colon cancer cells and enhanced liver metastasis. *Cancer Res* 2002; **62**: 1567-1572
15 **Hamasaki Y**, Kitzler J, Hardman R, Nettesheim P, Eling TE. Phorbol ester and epidermal growth factor enhance the expression of two inducible prostaglandin H synthase genes in rat tracheal epithelial cells. *Arch Biochem Bioghys* 1993; **304**: 226-234
16 **Jones DA**, Carlton DP, McIntyre TM, Zimmerman GA, Prescott SM. Molecular cloning of human prostaglandin endoperoxide synthase type II and demonstration of expression in response to cytokines. *J Biol Chem* 1993; **268**: 9049-9055
17 **Tsujii M**, DuBois RN. Alterations in cellular adhesion and apoptosis in epithelial cells overexpressing prostahlandin endoperoxide synthase 2. *Cell* 1995; **83**: 493-450
18 **Aoki T**, Tsukinoki K, Karakida K, Ota Y, Otsuru M, Kaneko A. Expression of cyclooxygenase-2, Bcl-2 and Ki-67 in pleomorphic adenoma with special reference to tumor proliferation and apoptosis. *Oral Onco* 2004; **40**: 954-959
19 **Kawamori T**, Rao CV, Seibert K, Reddy BS. Chemopreventive activity of celecoxib, a specific cyclooxygenase-2 inhibitor, against colon carcinogenesis. *Cancer Res* 1998; **58**: 409-412
20 **Minter HA**, Eveson JW, Huntley S, Elder DJ, Hague A. The cyclooxygenase 2-selective inhibitor NS398 inhibits proliferation of oral carcinoma cell lines by mechanisms dependent and independent of reduced prostaglandin E2 synthesis. *Clin Cancer Res* 2003; **9**: 1885-1897
21 **Grosch S**, Tegeder I, Niederberger E, Brautigam L, Geisslinger G. COX-2 independent induction of cell cycle arrest and apoptosis in colon cancer cells by the selective COX-2 inhibitor celecoxib. *FASEB J* 2001; **15**: 2742-2744
22 **Richter M**, Weiss M, Weinberger I, Furstenberger G, Marian B. Growth inhibition and induction of apoptosis in colorectal tumor cells by cyclooxygenase inhibitors. *Carcinogenesis* 2001; **22**: 17-25
23 **Koga H**, Sakisaka S, Ohishi M, Kawaguchi T, Taniguchi E, Sasatomi K, Harada M, Kusaba T, Tanaka M, Kimura R, Nakashima Y, Nakashima O, Kojiro M, Kurohiji T, Sata M. Expression of cyclocygenase-2 in human hepatocellular carcinoma: relevance to tumor differentiation. *Hepatology* 1999; **29**: 688-696
24 **Tsujii M**, Kawano S, DuBois RN. Cyclooxygenase-2 expression in human colon cancer cells increases metastatic potential. *Proc Natl Acad Sci USA* 1997; **94**: 3336-3340
25 **DuBois RN**, Shao J, Tsujii M, Sheng H, Beauchamp RD. G1 delay in cells overexpressing prostaglandin endoperoxide synthase-2. *Cancer Res* 1996; **56**: 733-737
26 **Hung WC**, Chang HC, Pan MR, Lee TH, Chuang LY. Induction of p27(KIP1) as a mechanism underlying NS398-induced growth inhibition in human lung cancer cells. *Mol Pharmacol* 2000; **58**: 1398-1403

Science Editor Wang XL and Zhu LH **Language Editor** Elsevier HK

PO Box 2345, Beijing 100023, China
www.wjgnet.com
wjg@wjgnet.com

ELSEVIER

World J Gastroenterol 2005;11(39):6115-6119
World Journal of Gastroenterology ISSN 1007-9327
© 2005 The WJG Press and Elsevier Inc. All rights reserved.

• *LIVER CANCER* •

Usefulness of serum des-γ-carboxy prothrombin in detection of hepatocellular carcinoma

Chaur-Shine Wang, Chih-Lin Lin, Hsi-Chang Lee, Kuan-Yang Chen, Ming-Feng Chiang, Hung-Sheng Chen, Tsung-Jung Lin, Li-Ying Liao

Chaur-Shine Wang, Chih-Lin Lin, Hsi-Chang Lee, Kuan-Yang Chen, Ming-Feng Chiang, Hung-Sheng Chen, Tsung-Jung Lin, Li-Ying Liao, Department of Gastroenterology, Ren-Ai Branch, Taipei City Hospital, Taipei, Taiwan, China
Supported by the Taipei Institute of Pathology, Taipei, Taiwan and Eisai Co., Tokyo, Japan
Correspondence to: Dr. Chaur-Shine Wang, Department of Gastroenterology, Ren-Ai Branch, Taipei City Hospital, No. 10, Sec. 4, Ren-ai Road, Da-an District Taipei City 106, Taiwan, China. lcl@tpech.gov.tw
Telephone: +886-2-27093600-1157 Fax: +886-2-27047859
Received: 2005-01-24 Accepted: 2005-04-09

Abstract

AIM: To evaluate whether DCP is better than AFP for differentiating HCC from nonmalignant liver disease and further evaluate the usefulness of DCP in early diagnosis of small HCC.

METHODS: Serum DCP and AFP levels were determined in 127 patients. Among these patients, 32 were with non-cirrhotic chronic hepatitis, 34 were with compensated cirrhosis, and 61 were with HCC. The cut-off value for the DCP and AFP were set as 40 mAU/mL and 20 ng/mL, respectively. To compare the diagnostic value of DCP and AFP in distinguishing HCC from nonmalignant chronic liver disease, receiver operating characteristic (ROC) curves were constructed for each assay.

RESULTS: The accuracy, sensitivity, and specificity of DCP were higher than AFP in detecting HCC (81.9%, 77%, and 86.4% *vs* 68.5%, 59%, and 77.3%, respectively). The area under the ROC (AUROC) curves revealed that DCP had a better accuracy than AFP in diagnosis of HCC (0.85 [95%CI, 0.78-0.91] *vs* 0.73 [95%CI, 0.65-0.81], $P = 0.013$). In 39 patients with solitary HCC, the positive rates of DCP were 100% in patients with tumor size larger than 3 cm, 66.7% in patients with tumor size 2-3 cm and 50% in patients with tumor size less than 2 cm. The positive rates of AFP in patients with tumor size larger than 3 cm, 2-3 cm and less than 2 cm were 55.6%, 50%, and 33.3%, respectively. The median level of DCP in HCC patients with tumor size larger than 3 cm was significantly higher than those with tumor size 2-3 cm and those with the size of less than 2 cm.

CONCLUSION: Our study indicates that DCP has a better diagnostic value than AFP in differentiating HCC from nonmalignant chronic liver disease. DCP has not only a stronger correlation with HCC than AFP in tumor size but also more effectiveness than AFP in detecting small size of HCC.

© 2005 The WJG Press and Elsevier Inc. All rights reserved.

Key words: Des-γ-carboxy prothrombin; α-Fetoprotein; Hepatocellular carcinoma

Wang CS, Lin CL, Lee HC, Chen KY, Chiang MF, Chen HS, Lin TJ, Liao LY. Usefulness of serum des-γ-carboxy prothrombin in detection of hepatocellular carcinoma. *World J Gastroenterol* 2005; 11(39): 6115-6119
http://www.wjgnet.com/1007-9327/11/6115.asp

INTRODUCTION

Hepatocellular carcinoma (HCC) is one of the most common cancers in the world[1]. The major causes of HCC are through chronic infection with HBV or hepatitis C virus (HCV)[2], cirrhosis and finally culminating into HCC[3,4]. HCC tends to occur in a definable population, so-called high risk population. Periodic screening among the high risk population would benefit in detecting HCC in an early curable stage and yield a long-term survival[5,6]. However, the worldwide 5-year survival rate of HCC only slightly increased from 2% to 5% over the past two decades[7]. This is partially due to the poor performance of currently available tumor markers, including α-fetoprotein (AFP), which cause the delay in diagnosis[8]. There is a need to develop an additional sensitive serum marker to improve the early detection of small HCC.

In 1984, Liebman *et al*., firstly reported the increasing levels of DCP in patients with HCC[9]. Since then, numerous studies indicated that DCP would be a useful marker in detecting HCC[10-14]. The conventional enzyme immunoassay (EIA) for DCP can detect advanced HCC with a high specificity. But the conventional EIA was limited in detecting small HCC[14-17]. A new method, revised EIA (Eitest PIVKA-II, Eisai, Tokyo, Japan), had been developed in recent years. The new sensitive DCP kit can measure the low concentration of serum DCP in normal persons. Thereafter, the diagnostic sensitivity of DCP for HCC had been much improved. It had been reported to be more sensitive and specific than AFP for the diagnosis of HCC[18,19]. However, the efficacy of DCP in diagnosis of small HCC still remains unclear.

Thus, we conducted a cross-sectional case control study to evaluate whether DCP is better than AFP for differentiating HCC from nonmalignant liver disease and further evaluate the usefulness of DCP in early diagnosis of small HCC.

MATERIALS AND METHODS

Patients

A total of 127 patients who were regularly followed up at Ren-Ai Branch, Taipei City Hospital were consecutively enrolled. Among the 127 patients, 32 had chronic hepatitis with higher serum alanine aminotransferase (ALT) levels than normal (upper limit of normal: 40 U/L) for at least 6 mo before enrollment, 34 had compensated cirrhosis (Child-Pugh score < 7) (20) and 61 had HCC. Cirrhosis was defined by clinical development of esophageal varices, thrombocytopenia (platelet count less than 100 000/mm^3), splenomegaly or small liver size with irregular liver surface to be noted by imaging studies at enrollment. Among all patients with chronic hepatitis and cirrhosis, HCC must be ruled out on the basis of imaging examinations including sonography and/or computed tomography (CT) performed on a regular examination. Also, cirrhotic patients who developed HCC within 6 mo after getting serum were excluded. The diagnosis of HCC was made on 47 (77%) histologically confirmed patients. The remaining 14 (23%) patients, who had advanced HCC with tumor size larger than 3 cm or patients with portal vein invasion, were confirmed by various combination of imaging studies, such as ultrasonography, enhanced CT, magnetic resonance imaging and/or angiography. Tumor size was estimated by using ultrasonography. Blood samples from HCC patients were drawn before initial treatment. The rest of the data obtained at enrollment included hepatitis B surface antigen (HBsAg), antibody to HCV (anti-HCV), ALT, albumin, total bilirubin, platelet count, prothrombin time, and serum level of tumor markers, AFP and DCP. Patients who had a history of alcohol consumption in excess of 80 g/ethanol per day for more than 5 years, serum total bilirubin level of more than 20 mg/L or under vitamin K medication were excluded. All subjects had given informed consent for the participation in the study. Serum samples were collected and stored at -70 ℃ until examined.

Biochemical and serological testing

The biochemical tests were measured by using routine automated methods. The HBsAg, anti-HCV were assayed by commercial kits (General Biological HBsAg RIA, General Biological Cooperation, Taiwan; HCV EIA II, Abbott Laboratories, North Chicago, IL, USA).

AFP assay

AFP was tested by using commercially available immunometric assay (Architect AFP assay, Abbott Laboratories, North Chicago, IL, USA). The cut-off value of AFP for HCC was set at 20 ng/mL, the most commonly set value[21-24].

DCP assay

DCP level was measured by using an ELISA (Eitest PIVKA-II, Eisai Co., Tokyo, Japan), according to the manufacturer's instructions. The detection limit is 10 mAU/mL. The cut-off value is determined as 40 mAU/mL for differentiation of HCC and nonmalignant liver disease based on previous studies[19].

Histological grading of HCC

Based on the criteria proposed by the Liver Cancer Study Group of Japan[25], each HCC was histologically graded into well differentiated, moderately differentiated, or poorly differentiated. Patients with multiple tumors consisted of more than two grades of histological differentiation; therefore, the most dedifferentiated grade was used.

Statistical analysis

Values were presented as mean ± SD and median:range. Data were analyzed by χ^2 test, Fisher's exact test, Student's *t*-test, Kruskal-Wallis ANOVA median test, and Pearson correlation where appropriate. All of the tests of significance were two-tailed and a *P* value of less than 0.05 was considered statistically significant. To compare the accuracy of DCP and AFP in the diagnosis of HCC, receiver operating characteristic (ROC) curves were constructed by using all possible cut-offs for each assay. The area under the ROC (AUROC) curves were calculated and compared by using a computer program of the MedCalc software version 7.5 (Mariakerke, Belgium).

RESULTS

Patient characteristics

Serum DCP and AFP levels were determined in 32 patients with chronic hepatitis, 34 patients with cirrhosis and 61 patients with HCC (their clinical characteristics were summarized in Table 1). The three groups were comparable in terms of gender, prevalence of HBsAg and anti-HCV. The mean age of HCC patients was significantly higher than those of chronic hepatitis patients and cirrhotic patients (63 ± 13 years *vs* 52 ± 10 years and 57 ± 12 years respectively, $P < 0.001$).

DCP and AFP in patients with chronic hepatitis, cirrhosis, and HCC

Both DCP and AFP levels increased progressively from nonmalignant chronic liver disease to HCC (Table 1). The mean values of DCP in patients with HCC was significantly higher than patients with chronic hepatitis and cirrhosis (2 808 ± 6 216 *vs* 21 ± 9 and 33 ± 14 mAU/mL, respectively, $P < 0.001$). In all, 2 of 32 (6.3%) patients with chronic hepatitis, 7 of 34 (20.6%) patients with cirrhosis, and 47 of 61 (77%) with HCC had DCP levels above the cut-off value of 40 mAU/mL.

The mean values of AFP were comparable among the three groups of patients (54 174 ± 296 329 *vs* 15 ± 24 and 13 ± 14 ng/mL, respectively $P > 0.05$). The AFP level above 20 ng/mL was found in 36 of 61 (59%) HCC, in 9 of 34 (26.5%) cirrhosis and in 6 of 32 (18.8%) chronic hepatitis patients. The overall accuracy, sensitivity, specificity, and positive and negative predictive values for the usefulness in the diagnosis of patients with HCC are shown in Table 2. ROC curves were plotted to compare the accuracy of DCP and AFP in the diagnosis of HCC, AUROC curves indicated

a better accuracy for DCP than AFP in diagnosis of HCC (0.85 [95%CI, 0.78-0.91] *vs* 0.73 [95%CI, 0.65-0.81], $P = 0.013$, Figure 1).

Relation between serum levels of AFP and DCP

Both DCP and AFP levels above cut-off value were found in 32 (52.5%) of 61 patients with HCC. Fifteen (60%) of twenty-five patients with AFP level less than 20 ng/mL had elevated concentrations of DCP. We failed to find any correlation between serum levels of AFP and DCP in 61 HCC patients (Figure 2, $r = 0.12$, $P = 0.36$).

Positive rates of DCP and AFP in patients with HCC

The positive rates of DCP and AFP in patients with HCC were detailed as follows: (1) When the largest size of HCC was more than 3 cm ($n = 22$), between 2 and 3 cm ($n = 16$) and less than 2 cm ($n = 23$), the rates were 100%, 75%, and 56.5% for DCP, 77.3%, 56.3%, and 43.5% for AFP; (2) When HCC was moderately to poorly differentiated ($n = 39$) and well differentiated ($n = 8$), the rates were 76.9% and 37.5% for DCP, 53.8% and 12.5% for AFP; (3) When the number of HCC were more than 2 ($n = 22$) and single ($n = 39$), the rates were 95.5% and 66.7% for DCP, 86.4% and 43.6% for AFP (Table 3).

The relation between the tumor size of HCC and levels of DCP and AFP were further analyzed. In the 39 patients with solitary HCC, 9 more than 3 cm, 12 between 2 and 3 cm, and 18 less than 2 cm, the positive rates were 100%, 66.7%, and 50% for DCP, 55.6%, 50%, and 33.3% for AFP respectively. DCP also had a better correlation with tumor size in comparison with AFP. The median (range) levels of DCP in patients with a size of HCC more than 3 cm was significantly higher than those with 2-3 cm and less than 2 cm [6 729 (40.4-20 000) *vs* 159 (12-655) and 89 (7-348) mAU/mL, respectively, $P = 0.01$] (Figure 3).

Table 1 Clinical characteristics of 127 patients with different stages of liver disease

	Chronic hepatitis ($n = 32$)	Cirrhosis ($n = 34$)	HCC ($n = 61$)	*P*
Age (yr/o)	52±10	57±12	63±13	<0.001[a]
Male/female	2.2	2.8	3.4	NS
Positive for HBsAg	17	18	28	NS
Positive for anti-HCV	15	13	24	NS
Positive for both HBsAg and anti-HCV	0	1	4	
Negative for both HBsAg and anti-HCV	0	2	4	
DCP level (mAu/mL), mean±SD	21±9	33±14	2 808±6 216	<0.001[a]
AFP level (ng/mL), mean±SD	15±24	13±14	54 174±296 329	NS

[a]$P<0.05$, HCC *vs* chronic hepatitis and cirrhosis. HBsAg: hepatitis B surface antigen; anti-HCV: antibody to hepatitis C virus; DCP: des-γ-carboxy prothrombin; AFP: α-fetoprotein.

Table 2 Diagnostic values of DCP and AFP for the detection of HCC

Groups	Case number	DCP		AFP		DCP/AFP	
		40 mAU/mL		20 ng/mL		DCP 40 mAU/mL or AFP 20 ng/mL	
		Positive	Negative	Positive	Negative	Positive	Negative
Nonmalignant liver disease							
Chronic hepatitis	32	2	30	6	26	8	24
Cirrhosis	34	7	27	9	25	13	21
HCC	61	47	14	36	25	51	10
Overall accuracy (%)		81.9		68.5		75.6	
Sensitivity		77.0		59.0		83.6	
Specificity		86.4		77.3		68.2	
Positive prediction rate		83.9		70.6		70.8	
Negative prediction rate		80.3		67.1		81.8	

DCP: des-γ-carboxy prothrombin; AFP: α-fetoprotein; HCC: hepatocellular carcinoma.

Table 3 Positive rates for serum concentrations of DCP and AFP in relation to largest size, histologic differentiation, and number of HCC

	Total HCC	Largest size of HCC			Histologic differentiation of HCCz		Number of HCC	
		2 cm	Between 2 and 3 cm	⩾3 cm	Well	Moderately and poorly	1	⩾2
2Case number	61	23	16	22	8	39	39	22
DCP (%)	77.0	56.5	75.0	100	37.5	76.9	66.7	95.5
AFP (%)	59.0	43.5	56.3	77.3	12.5	53.8	43.6	86.4

DCP: des-γ-carboxy prothrombin; AFP: α-fetoprotein; HCC: hepatocellular carcinoma.

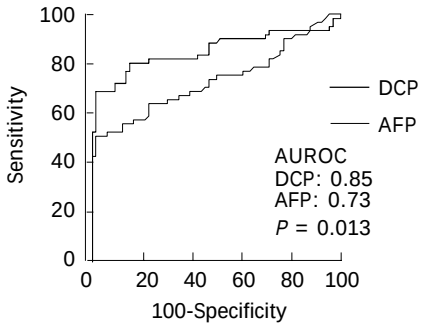


Figure 1 AUROC curves comparing DCP and AFP in patients with HCC and those with nonmalignant liver disease.

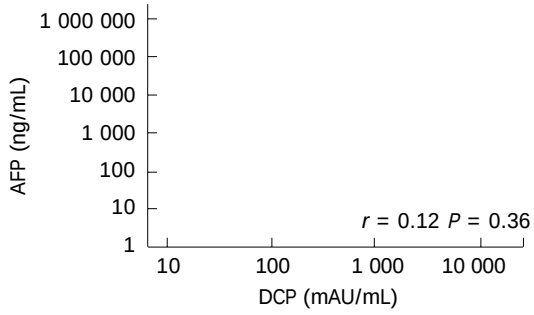


Figure 2 Relationship between DCP and AFP levels in 61 patients with HCC.

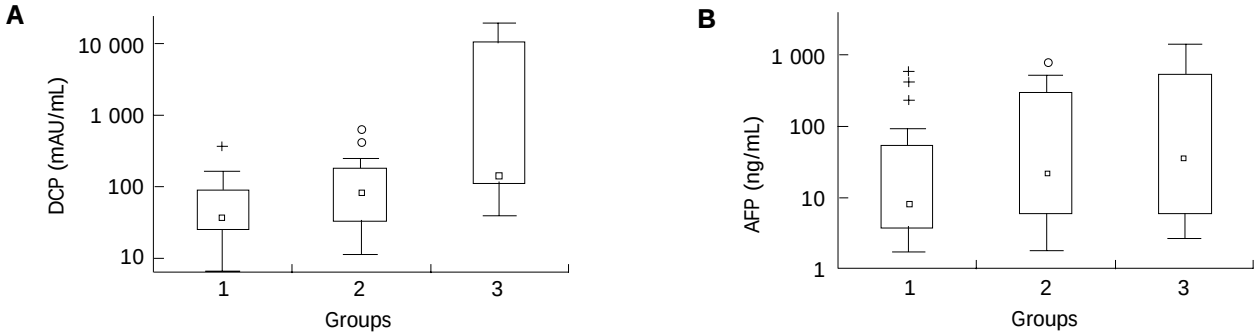


Figure 3 Box plot for DCP and AFP values in relation to size of tumor in 39 patients with solitary HCC (group 1, tumor less than 2 cm; group 2, tumor between 2 and 3 cm; and group 3, tumor more than 3 cm). The data were presented as the median and the range from the 25th-75th percentile(A and B).

DISCUSSION

Almost no symptoms would be noticed in patients with small HCC. The symptomatic HCC was usually incurable and lethal, and most previous studies reported that the median survival was only 3-6 mo after the onset of symptoms[26-28]. Early diagnosis is the most important issue in improving the long-term survival rate of HCC. Up to now, periodic screening among high risk population of HCC is the only way to detect the small HCC[5,6]. AFP is the most commonly used marker in diagnosing HCC. However, in 35-45% of HCC patients, the AFP level may be normal[21-24]; particularly in patients with small HCC[29]. On the other hand, patients with cirrhosis or chronic hepatitis, the elevated AFP level may be observed as well[30]. The dilemma is the reason why some cases of HCC could not be correctly diagnosed by AFP alone.

Based on our results, AUROC curves indicated a better accuracy for DCP than AFP in diagnosis of HCC (0.85 [95%CI, 0.78-0.91] *vs* 0.73 [95%CI, 0.65-0.81], $P = 0.013$). The cut-off value of DCP and AFP for HCC was set at 40 mAU/mL and 20 ng/mL, respectively. These values yielded a sensitivity and specificity for DCP of 77% and 86.4%, and for AFP of 59% and 77.3%, respectively. The sensitivity, specificity, and accuracy of DCP were significantly higher than APP in diagnosis of HCC (Table 2). Meanwhile, 25 of 61 (41%) patients with HCC had AFP level lower than 20 ng/mL. On the other hand, 15 of 66 (22.7%) patients with nonmalignant chronic liver disease had serum AFP level higher than 20 ng/mL. Taken together, DCP would be a better marker than AFP for HCC. Our results are also in accordance with recent studies that showed the unsatisfactory performance of AFP in diagnosis of HCC[8].

We did not find any correlation between the DCP and AFP in HCC patients (Figure 2). AFP secretion in HCC resulted from re-expression in the tumor of fetal origin[31]. DCP was produced by the malignant hepatocyte that resulted from an acquired post-translational defect in the vitamin K-dependent carboxylase system[32]. Because no correlation was observed between DCP and AFP, the simultaneous determination of both markers might be more effective in the diagnosis of HCC[33]. In our data, the increase in sensitivity from 77% to 83.6% (Table 2) in detecting HCC was found by the complementary use of the two markers.

We further analyzed 39 patients with solitary HCC in our study. We found that DCP levels had a better correlation with tumor size when compared with AFP levels (Figure 3). DCP also had a higher diagnostic sensitivity than AFP in patients with tumor size less than 2 cm in diameter. Particularly, for five patients with well-differentiated HCC less than 2 cm, the positive detection rate of DCP was 40%, which was much higher than 0% of AFP. It seems that DCP might be a better marker than AFP in detecting early-stage HCC. Because of the limited number of early-stage HCC in our report, further study is necessary to determine whether DCP plays an important role in early diagnosis of HCC.

In conclusion, our study indicates that DCP has a better diagnostic value than AFP in differentiating HCC from

nonmalignant chronic liver disease. DCP has not only a stronger correlation with HCC than AFP in tumor size but also more effectiveness than AFP in detecting small size of HCC.

REFERENCES

1 **Bosch FX,** Ribes J, Diaz M, Cleries R. Primary liver cancer: worldwide incidence and trends. *Gastroenterology* 2004; **127**: S5-16
2 **Bosch FX,** Ribes J, Borras J. Epidemiology of primary liver cancer. *Semin Liver Dis* 1999; **19**: 271-285
3 **Zaman SN,** Melia WM, Johnson RD, Portmann BC, Johnson PJ, Williams R. Risk factors in development of hepatocellular carcinoma in cirrhosis: prospective study of 613 patients. *Lancet* 1985; **1**: 1357-1360
4 **Benvegnu L,** Gios M, Boccato S, Alberti A. Natural history of compensated viral cirrhosis: a prospective study on the incidence and hierarchy of major complications. *Gut* 2004; **53**: 744-749
5 **Liaw YF,** Tai DI, Chu CM, Lin DY, Sheen IS, Chen TJ, Pao CC. Early detection of hepatocellular carcinoma in patients with chronic type B hepatitis. A prospective study. *Gastroenterology* 1986; **90**: 263-267
6 **Zhang BH,** Yang BH, Tang ZY. Randomized controlled trial of screening for hepatocellular carcinoma. *J Cancer Res Clin Oncol* 2004; **130**: 417-421
7 **El-Serag HB,** Mason AC, Key C. Trends in survival of patients with hepatocellular carcinoma between 1977 and 1996 in the United States. *Hepatology* 2001; **33**: 62-65
8 **Bruix J,** Sherman M, Llovet JM, Beaugrand M, Lencioni R, Burroughs AK, Christensen E, Pagliaro L, Colombo M, Rodes J. EASL panel of rxperts on HCC. Clinical management of hepatocellular carcinoma. Conclusions of the barcelona-2000 EASL conference. European sssociation for the dtudy of the liver. *J Hepatol* 2001; **35**: 421-430
9 **Liebman HA,** Furie BC, Tong MJ, Blanchard RA, Lo KJ, Lee SD, Coleman MS, Furie B. Des-gamma-carboxy (abnormal) prothrombin as a serum marker of primary hepatocellular carcinoma. *N Engl J Med* 1984; **310**: 1427-1431
10 **Soulier JP,** Gozin D, Lefrere JJ. A new method to assay des-gamma-carboxyprothrombin. Results obtained in 75 cases of hepatocellular carcinoma. *Gastroenterology* 1986; **91**: 1258-1262
11 **Okuda H,** Obata H, Nakanishi T, Furukawa R, Hashimoto E. Production of abnormal prothrombin (des-gamma-carboxy prothrombin) by hepatocellular carcinoma. A clinical and experimental study. *J Hepatol* 1987; **4**: 357-363
12 **Nakao A,** Suzuki Y, Isshiki K, Kimura Y, Takeda S, Kishimoto W, Nonami T, Harada A, Takagi H. Clinical evaluation of plasma abnormal prothrombin (des-gamma-carboxy prothrombin) in hepatobiliary malignancies and other diseases. *Am J Gastroenterol* 1991; **86**: 62-66
13 **Marrero JA,** Su GL, Wei W, Emick D, Conjeevaram HS, Fontana RJ, Lok AS. Des-gamma carboxyprothrombin can differentiate hepatocellular carcinoma from nonmalignant chronic liver disease in american patients. *Hepatology* 2003; **37**: 1114-1121
14 **Tsai SL,** Huang GT, Yang PM, Sheu JC, Sung JL, Chen DS. Plasma des-gamma-carboxyprothrombin in the early stage of hepatocellular carcinoma. *Hepatology* 1990; **11**: 481-488
15 **Chan CY,** Lee SD, Wu JC, Lin HC, Huang YS, Lo GH, Lee FY, Tsai YT, Lo KJ. The diagnostic value of the assay of des-gamma-carboxy prothrombin in the detection of small hepatocellular carcinoma. *J Hepatol* 1991; **13**: 21-24
16 **Kuromatsu R,** Tanaka M, Shimauchi Y, Shimada M, Tanikawa K, Watanabe K, Yokoo T. Usefulness of ED036 kit for measuring serum PIVKA-II levels in small hepatocellular carcinoma. *J Gastroenterol* 1997; **32**: 507-512
17 **Nomura F,** Ishijima M, Kuwa K, Tanaka N, Nakai T, Ohnishi K. Serum des-gamma-carboxy prothrombin levels determined by a new generation of sensitive immunoassays in patients with small-sized hepatocellular carcinoma. *Am J Gastroenterol* 1999; **94**: 650-654
18 **Mita Y,** Aoyagi Y, Yanagi M, Suda T, Suzuki Y, Asakura H. The usefulness of determining des-gamma-carboxy prothrombin by sensitive enzyme immunoassay in the early diagnosis of patients with hepatocellular carcinoma. *Cancer* 1998; **82**: 1643-1648
19 **Okuda H,** Nakanishi T, Takatsu K, Saito A, Hayashi N, Watanabe K. Measurement of serum levels of des-gcarboxy prothrombin in patients with hepatocellular carcinoma by a revised enzyme immunoassay kit with increased sensitivity. *Cancer* 1999; **85**: 812-818
20 **Pugh RNH,** Muray-Lyon IM, Dawson JL. Transection of the esophagus in the bleeding esophageal varices. *Br J Surg* 1973; **60**: 648-652
21 **Cedrone A,** Covino M, Caturelli E, Pompili M, Lorenzelli G, Villani MR. Utility of alpha-fetoprotein (AFP) in the screening of patients with virus-related chronic liver disease: does different viral etiology influence AFP levels in HCC? A study in 350 western patients. *Hepatogastroenterology* 2000; **47**: 1654-1658
22 **Nguyen MH,** Garcia RT, Simpson PW, Wright TL, Keeffe EB. Racial differences in effectiveness of alpha-fetoprotein for diagnosis of hepatocellular carcinoma in hepatitis C virus cirrhosis. *Hepatology* 2002; **36**: 410-417
23 **Peng YC,** Chan CS, Chen GH. The effectiveness of serum alpha-fetoprotein level in anti-HCV positive patients for screening hepatocellular carcinoma. *Hepatogastroenterology* 1999; **46**: 3208-3211
24 **Trevisani F,** D'Intino PE, Morselli-Labate AM, Mazzella G, Accogli E, Caraceni P. Serum alpha-fetoprotein for diagnosis of hepatocellular carcinoma in patients with chronic liver disease: influence of HBsAg and anti-HCV status. *J Hepatol* 2001; **34**: 570-575
25 Liver Cancer Study Group of Japan. Primary liver cancer in Japan: clinicopathologic features and results of surgical treatment. *Ann Surg* 1990; **211**: 277-287
26 **Naofumi N,** Hirofumi Y, Tadao H. The natural history of hepatocellular carcinoma: a study of 100 untreated cases. *Cancer* 1984; **54**: 1461-1465
27 **Wood WJ,** Rawlings M, Evans H, Lim CNH. Hepatocellular carcinoma: importance of histological classification as a prognostic factor. *Am J Surg* 1988; **155**: 663-666
28 **Douglas GF,** Michael HR, Abraham S, Ronald WB. Current treatment modalities for hepatocellular carcinoma. *Ann Surg* 1994; **219**: 236-247
29 **Chen DS,** Sung JL, Sheu JC, Lai MY, How SW, Hsu HC, Lee CS, Wei TC. Serum alpha-fetoprotein in the early stage of human hepatocellular carcinoma. *Gastroenterology* 1984; **86**: 1404-1409
30 **Di Bisceglie AM,** Hoofnagle JH. Elevations in serum alpha-fetoprotein levels in patients with chronic hepatitis B. *Cancer* 1989; **64**: 2117-2120
31 **Abelev GI.** Production of embryonal serum alpha-globulin by hepatomas: review of experimental and clinical data. *Cancer Res* 1968; **28**: 1344-1350
32 **Weitz IC,** Liebman HA. Des-gamma-carboxy (abnormal) prothrombin and hepatocellular carcinoma: a critical review. *Hepatology* 1993; **18**: 990-997
33 **Ishii M,** Gama H, Chida N, Ueno Y, Shinzawa H, Takagi T, Toyota T, Takahashi T, Kasukawa R. Simultaneous measurements of serum alpha-fetoprotein and protein induced by vitamin K absence for detecting hepatocellular carcinoma. South Tohoku District Study Group. *Am J Gastroenterol* 2000; **95**: 1036-1040

Science Editor Guo SY **Language Editor** Elsevier HK

PO Box 2345, Beijing 100023, China
www.wjgnet.com
wjg@wjgnet.com

ELSEVIER

World J Gastroenterol 2005;11(39):6120-6124
World Journal of Gastroenterology ISSN 1007-9327
© 2005 The WJG Press and Elsevier Inc. All rights reserved.

• *COLORECTAL CANCER* •

Genetic alterations and expression of inhibitor of growth 1 in human sporadic colorectal cancer

Li-Sheng Chen, Jian-Bao Wei, Yong-Chun Zhou, Sen Zhang, Jun-Lin Liang, Yun-Fei Cao, Zong-Jiang Tang, Xiao-Long Zhang, Feng Gao

Li-Sheng Chen, Jian-Bao Wei, Yong-Chun Zhou, Sen Zhang, Jun-Lin Liang, Yun-Fei Cao, Zong-Jiang Tang, Xiao-Long Zhang, Feng Gao, Department of Coloproctological Surgery, the First Affiliated Hospital, Guangxi Medical University, Nanning 530021, Guangxi Province, China
Supported by the Guangxi Provincial Scientific Fund for the Returned Overseas Chinese Scholars, No. 0342018 and Key Research Fund from Public Health Bureau of Guangxi, No. 200206
Correspondence to: Dr. Li-Sheng Chen, Department of Coloproctological Surgery, the First Affiliated Hospital, Guangxi Medical University, Nanning 530021, Guangxi Province, China. clisheng@vip.sina.com
Telephone: +86-771-5356529 Fax: +86-771-5358968
Received: 2005-03-31 Accepted: 2005-04-18

Abstract

AIM: To explore the effect and significance of inhibitor of growth 1 (ING1) gene in carcinogenesis and progression of human sporadic colorectal cancer.

METHODS: mRNA expression, mutation, and loss of heterozygosity (LOH) of ING1 gene in 35 specimens of sporadic colorectal cancer tissues and the matched normal mucous membrane tissues were detected by semi-quantitative reverse transcriptase-polymerase chain reaction (RT-PCR), PCR-single strain conformation polymorphism (PCR-SSCP) and PCR-simple sequence length polymorphism (PCR-SSLP) using microsatellite markers, respectively.

RESULTS: The average ratios of light intensities of $p33^{ING1b}$ and $p47^{ING1a}$ mRNA expression in the cancerous tissues were significantly lower than those in normal tissues. The difference between the two mRNA splices was not significant in the matched tissues. In addition, the ratios of light intensities of $p33^{ING1b}$ and $p47^{ING1a}$ mRNA expression in the cancerous tissues of Dukes' stages C and D were significantly lower than those in cancerous tissues of Dukes' stages A and B. However, no mutation of ING1 gene was detected in all 35 cases; only 4 cases of LOH (11.4%) were found.

CONCLUSION: $p33^{ING1b}$ and $p47^{ING1a}$ mRNA expressions are closely related with the carcinogenesis and progression of human sporadic colorectal cancer. No mutation of ING1 gene is found, and there are only few LOH in sporadic colorectal cancers. These might not be the main reasons for the down regulation of ING1 expression. Its low expression may happen in transcription or post-transcription.

© 2005 The WJG Press and Elsevier Inc. All rights reserved.

Key words: Colorectal cancer; Inhibitor of growth 1 (ING1); Expression; Mutation; Loss of heterozygosity

Chen LS, Wei JB, Zhou YC, Zhang S, Liang JL, Cao YF, Tang ZJ, Zhang XL, Gao F. Genetic alterations and expression of inhibitor of growth 1 in human sporadic colorectal cancer. *World J Gastroenterol* 2005; 11(39): 6120-6124
http://www.wjgnet.com/1007-9327/11/6120.asp

INTRODUCTION

A candidate tumor suppressor gene, inhibitor of growth 1 (ING1), has recently been cloned and mapped on human chromosome $13q^{33-34}$[1-3]. It has at least three exons and two introns. Its three alternative spliced transcripts encode $p47^{ING1a}$, $p33^{ING1b}$, and $p24^{ING1c}$ protein, respectively[4]. $p33^{ING1b}$ is a nuclear protein, which physically interacts with p53, and cooperates with it in many ways[2,5]. Overexpression of $p33^{ING1b}$ could efficiently block the growth of cells and induce apoptosis[6-8]. Conversely, inhibition of its expression by antisense constructs could promote cells growth and protect cells from apoptosis[7]. Downregulation of $p33^{ING1b}$ has been reported to be closely related with occurrence of various cancers, such as head and neck[4], esophageal[9], lung[10], gastric[11,12], bladder[13], ovary[14], breast[14,15], liver cell cancer[16,17], and so on. Genetic alterations, such as mutation or allelic imbalance, have been found in some cancers listed above. To the author's knowledge, only a few studies of ING1 gene on colorectal cancer have been reported as yet, and the results are different from each other[18]. Moreover, there is some lack of knowledge about $p47^{ING1a}$ expression in colorectal cancer till now. Accordingly, in order to evaluate the effect and significance of ING1 gene in carcinogenesis and progression of human sporadic colorectal cancer, we examined mRNA expression, mutation, and LOH of ING1 gene by using RT-PCR, PCR-SSCP, and PCR-RFLP.

MATERIALS AND METHODS

Patients and tissues

The tumor and matched normal mucosal tissues (at least 10 cm away from tumor margin) were obtained from 35 patients with sporadic colorectal cancer, who underwent surgical resection in our hospital, from December 2002 to March 2003. The patients consisted of 20 males and 15 females with the mean age of 59 years (range, 25-79 years). All the diagnoses were verified by pathological diagnosis.

Sixteen were colon and 19 were rectal carcinomas with Dukes' stages as follows: stage A (2 cases); stage B (15 cases); stage C (13 cases); and stage D (5 cases). All the specimens were frozen in liquid nitrogen after removal, followed by storage at -80 ℃.

RNA and DNA extraction

Total RNA and genomic DNA were isolated from the specimens using TRIzol reagent (Invitrogen, USA) and spin column genomic DNA isolation kit (BBI, Canada) according to the manufacturer's instructions. The integrity of total RNA and genomic DNA were checked on 10 g/L agarose gel.

RT-PCR

ING1 mRNA expression in tumor and matched normal tissues was examined using RT-PCR. RNase-free DNase I was used to remove DNA contamination at first. Then, cDNA was synthesized using first strand cDNA synthesis kit, following the manufacturer's instructions. At last, PCR was performed in 20 μL reaction mixtures comprising 2 μL of cDNA, 2.5 μL of 10×buffer, 1.5 μL of 2.5 mol/L deoxynucleotide triphosphate mixture (dNTP mixture), 2 U of Taq DNA polymerase (TaKaRa, Dalian, China), 0.5 μL of 10 mol/L each primer of ING1, 0.5 μL of 10 mol/L primer of GAPDH, and 12 μL of sterilized ddH_2O. Intron-spanning primers were: for $p47^{ING1a}$, 5'-CCGCATCTTT-GCTGACCCGA-3' and 5'-GCCTTCTTCTCCTTG-GGTGT-3' (444 bp); and for $p33^{ING1b}$, 5'-CTCCATCGAG-TCCCTGCCTT-3' and 5'-GCCTTCTTCTCCTTGG-GTGT-3' (480 bp). Primers for GAPDH were 5'-CGG-AGTCAACGGATTTGGTGCGTAT-3' and 5'-AGCCTT-CTCCATGGTGGYGAAGAC-3' (306 bp). The samples were amplified through 32 cycles, each amplification consisting of denaturation at 94 ℃ for 1 min, primer annealing at 62 ℃ for 1 min and extension at 72 ℃ for 1 min. Cycles were preceded by incubation at 94 ℃ for 5 min to ensure full denaturation of the target gene, followed by an extra incubation at 72 ℃ for 10 min to ensure full extension of the products. Primers for GAPDH were added to PCR tubes at the end of the 10^{th} cycle. Products of RT-PCR were electrophoresed on 20 g/L agarose gel. The light intensities of DNA bands were scanned by electrophoretic image analysis system (Bio-Rad Gel DOC 2000, USA). Reproducibility was confirmed by processing all samples at least twice.

PCR-SSCP

PCR reactions were carried out in a volume of 20 μL containing 100 ng of genomic DNA, 2.5 μL of 10× buffer, 1.5 μL of 2.5 mol/L dNTP mixture, 2 U of Taq DNA polymerase (TaKaRa, Dalian, China), 0.5 μL of 10 mol/L each primer, and 14 μL of sterilized ddH_2O. The samples were amplified through 32 cycles, each amplification consisting of denaturation at 94 ¡æ for 30 s, primer annealing at 62 ¡æ or 64 ¡æ for 30 s and extension at 72 ¡æ for 1 min. Finally, the samples underwent an extra incubation at 72 ¡æ for 10 min. The sequences of ING1 primers used for PCR-SSCP: exon 1, 5'-TGCAGTGCTATTTTT-TGAGGGG-3' and 5'-CGCCCCCGCCCATCCATCA-3' (248 bp); exon 2a, 5'-ACGCCTGTCCTTCTTGCCCC-3' and 5'-CTTGCCGCTGTTGCCCGCTG-3' (272 bp); exon 2b, 5'-TTCGAGGCGCAGCAGGAGCT-3' and 5'-CTTGGCCTTCTTCTCCTTGGG-3' (210 bp); exon 2c, 5'-TGAGCCCCACGCACGAGAAG-3' and 5'-CAGCA-ACCACGACCACGACG-3' (242 bp); exon 2d, 5'-CCTCC-CCATCGACCCCAACG-3' and 5'-ACATTTTACACT-CCTTGCACCTCA-3' (327 bp). Ten microliters of PCR products was mixed with 10 μL of loading dye (950 mL/L formamide, 20 mol/L EDTA, 0.5 g/L bromophenol blue, and 0.5 g/L xylene cyanol), heat denatured at 98 ¡æ for 10 min, chilled on ice, put onto 120 g/L polyacrylamide gel, and run at a constant rate of 12 V/cm for 10-14 h at variable temperatures. The DNA bands were detected by silver staining as previously described[19]. Reproducibility was confirmed by processing all samples at least twice.

LOH analysis

We examined genomic DNA for LOH by PCR-SSCP using five microsatellite markers (D13S158, D13S278, D13S285, D13S779, and D13S796), which are located in the ING1 locus. The primer pairs were available through the internet genome database (http://www.gdb.org). PCR was performed in 20 μL of reaction mixture comprising 100 ng of genomic DNA, 2.5 μL of 10× buffer, 1.5 μL of 2.5 mol/L dNTP mixture, 2 U of Taq DNA polymerase (TaKaRa, Dalian, China), 0.5 μL of 10 mol/L each primer, and 14 μL of sterilized ddH_2O. The samples were amplified through 32 cycles, each amplification consisting of denaturation at 62 ℃ for 30 s, primer annealing at 52 ℃ or 54 ℃ for 30 s and extension at 72 ℃ for 1 min. Finally, the samples underwent an extra incubation at 72 ℃ for 5 min. Ten microliters of PCR products was mixed with 10 μL of loading dye as described above, heat denatured for 10 min at 98 ℃, chilled on ice, put onto 120 g/L polyacrylamide gel containing 8 mol/L urea, and run at a constant rate of 25 V/cm for 3-4 h at room temperature. The DNA bands were visualized by silver staining. Reproducibility was confirmed by processing all samples at least twice. LOH was scored, if the heterozygous alleles showed at least 50% reduced intensity in tumor DNA bands as compared with the corresponding normal ones.

Statistical analysis

The SPSS 10.0 software package was used for all statistical analyses. Differences in expression of ING1 mRNA between the different groups were compared by using independent *t*-test. A *P* value less than 0.05 was considered statistically significant.

RESULTS

ING1 mRNA expression detected by RT-PCR

All the samples of tumor tissues and normal tissues showed ING1 mRNA expression. Moreover, the average ratios of light intensities of $p33^{ING1b}$ mRNA and $p47^{ING1a}$ mRNA expression in the cancerous tissues were significantly lower than those in normal tissues (0.52 *vs* 1.28, $P<0.01$; 0.51 *vs* 1.21, $P<0.01$, respectively; Figure 1); difference between the two mRNA splices was not significant in the matched tissues.

The average ratios of light intensities of $p33^{ING1b}$ mRNA and $p47^{ING1a}$ mRNA expression in the cancerous tissues of Dukes' stages C and D were significantly lower than those in cancerous tissues of Dukes' stages A and B (0.38 *vs* 0.65, $P<0.01$; 0.40 *vs* 0.63, $P<0.01$, respectively).

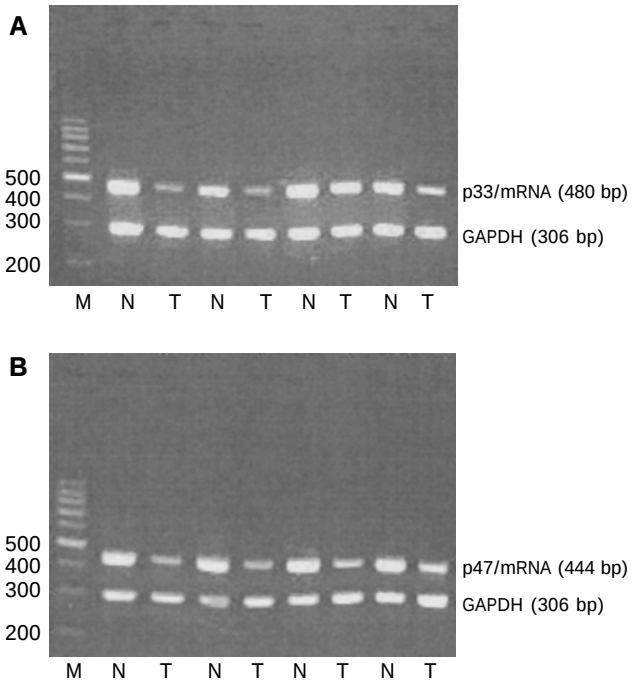


Figure 1 RT-PCR analysis of p33/ING1 and p47/ING1 mRNA expressions. N: normal tissue; T: tumor tissue (A and B).

Detection of ING1 gene mutation

To investigate whether the ING1 gene is the target of functional loss in tumors, we searched for mutation in the encoding regions of the gene in all 35 samples of colorectal cancer by using PCR-SSCP. However, no mutation was found (Figure 2).

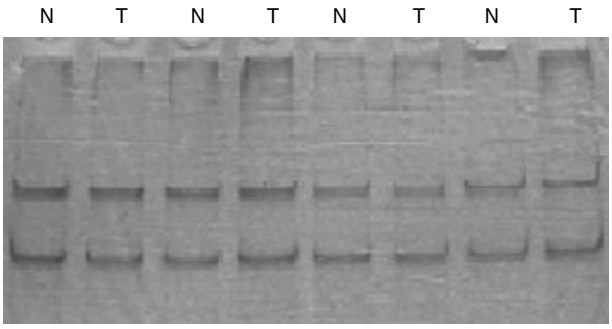


Figure 2 No mutation of ING1 gene was detected by PCR-SSCP (fragment exon 2a).

LOH analysis

To investigate whether allelic imbalance of terminal regions of chromosome 13q is reserved, we examined DNA from 35 pairs of matched tumor tissues and normal tissues for losses at five microsatellite markers (D13S158, D13S278, D13S285, D13S779, and D13S796). But only four cases of LOH (11.4%) were observed, two in D13S158, one in D13S278 and one in D13S285 (Figure 3).

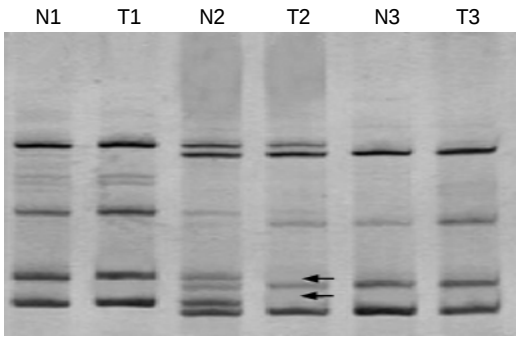


Figure 3 Electrophoretic picture of LOH analysis (LOH is seen in T2).

DISCUSSION

In this study, we found downregulation of $p33^{ING1}$ mRNA, and $p47^{ING1}$ mRNA expressions in the cancerous tissues of sporadic colorectal cancer, and the later Dukes' stage they were in, the less mRNA expression they presented. Our results are consistent with the previous data on head and neck[4], esophageal[9], lung[10], gastric[11,12], breast[14,15], and liver cell[16,17] cancers, neuroblastomas[20], and astrocytoma[21], but not with the other studies on colorectal cancer[18]. The precise mechanisms of tumor suppression by $p33^{ING1}$ and $p47^{ING1}$ remain unclear. Previous several reports thought that $p33^{ING1}$ might inhibit cells growth and promote apoptosis through both p53-dependent[5,8,17,21] and -independent pathways[21-24]. One is: $p33^{ING1}$ could stabilize p53 via disrupting the regulation of p53 by MDM2[23], and promote acetylation of p53 through inhibition of hSIR2[21,24]. Another one is: $p33^{ING1}$ and $p47^{ING1}$ could directly repress transcription promoters, and upregulate $p21^{WAF1}$ promoter activity[21]. Moreover, $p33^{ING1}$ could cooperate with p53. We, therefore, think that reduced expressions of $p33^{ING1}$ and $p47^{ING1}$ may lead to decreased inhibition of cell cycle and apoptosis, and strongly associated with the carcinogenesis and progression of human sporadic colorectal cancer.

Some previous studies have reported about several mis-sense mutations and silent changes in esophageal[9], head and neck[4], esophagogastric junction[25], gastric[11], skin[26], pancreatic[27], and breast[14] cancers. These mutations were all located in PDH finger and/or nuclear localization signal in the COOH-terminal half of ING1, and might lead to loss of the functions of ING1. But the rate of mutations was rare or no mis-sense mutation was found in oral squamous cell carcinoma[28], lymphoid malignancies[29], colorectal carcinoma[18], and hematological malignancies[30]. In our study, we could not detect mis-sense mutation of ING1 gene. Although PCR-SSCP analysis was reported to be less than 100% sensitive for mutation detection, this result suggests that mutation of ING1 occur with a very

low frequency in sporadic colorectal cancer. We, hereby, propose that gene mutation is not the main reason for the downregulation of ING1 expression.

Loss of heterozygosity (LOH), i.e., loss of one allele at a constitutional heterozygous locus, indicates the probability of loss of a tumor suppressor gene, which might promote neoplastic progression and metastasis. LOH is a critical event in the development of human cancers. It is thought to have resulted from either a large deletion or recombination between homologous alleles during repair of DNA double-strand breaks. These types of genetic alterations may produce mutations in some gene mutation assay. Previous studies demonstrated that high rates of LOH were found in human chromosome $13q^{33\text{-}34}$ region[4,9,31], such as the rates in esophageal/head and neck squamous cell cancers were 58.9% (20/34) and 68% (23/34), respectively[4,9]. Because the gene encoding ING1 is located in $13q^{33\text{-}34}$ region, we detected for LOH in this region using five microsatellite markers (D13S158, D13S278, D13S285, D13S779, and D13S796), which are at different locations on chromosome $13q^{33\text{-}34}$. In our study, the rate of LOH was only 11.4% (4/35), which is obviously lower than those in the previous reports. LOH at ING1 locus and the vicinity may affect the function of ING1, but these might not be the main reason for the downregulation of ING1 expression as well.

In conclusion, downregulation of $p33^{ING1}$ and $p47^{ING1}$ mRNA expressions in human sporadic colorectal cancer is substantial, relating with the carcinogenesis and progression, but mutation and LOH of gene might not be the main reason for the downregulation of ING1 expression. The reason for loss of function of ING1 gene is very complex. We speculate that the alterations at transcriptional or post-transcriptional levels, such as acetylation, methylation, ubiquitination, or phosphorylation, might be involved in the downregulation of ING1 gene. Further studies are needed to elucidate the possibility.

REFERENCES

1 **Garkavtsev I**, Kazarov A, Gudkov A, Riabowol K. Suppression of the novel growth inhibitor p33ING1 promotes neoplastic transformation. *Nat Genet* 1996; **14**: 415-420
2 **Garkavtsev I**, Demetrick D, Riabowol K. Cellular localization and chromosome mapping of a novel candidate tumor suppressor gene (ING1). *Cytogenet Cell Genet* 1997; **76**: 176-178
3 **Zeremski M**, Horrigan SK, Grigorian IA, Westbrook CA, Gudkov AV. Localization of the candidate tumor suppressor gene ING1 to human chromosome 13q34. *Somat Cell Mol Genet* 1997; **23**: 233-236
4 **Gunduz M**, Ouchida M, Fukushima K, Hanafusa H, Etani T, Nishioka S, Nishizaki K, Shimizu K. Genomic structure of the human ING1 gene and tumor-specific mutations detected in head and neck squamous cell carcinomas. *Cancer Res* 2000; **60**: 3143-3146
5 **Garkavtsev I**, Grigorian LA, Ossovskaya VS, Chernov MV, Chumakov PM, Gudkov AV. The candidate tumor suppression p33/ING1 cooperates with p53 in cell growth control. *Nature* 1998; **391**: 295-298
6 **Garkavtsev I**, Riabowol K. Extension of the replicative life span of human diploid fibroblasts by inhibition of the p33ING1 candidate tumor suppressor. *Mol Cell Biol* 1997; **17**: 2014-2019
7 **Helbing CC**, Veillette C, Riabowol K, Johnston RN, Garkavtsev I. A novel candidate tumor suppression. ING1, is involved in the regulation of apoptosis. *Gancer Res* 1997; **57**: 1255-1258
8 **Shinoura N**, Muramatsu Y, Nishimura M, Yoshida Y, Saito A, Yokoyama T, Furukawa T, Horii A, Hashimoto M, Asai A, Kirino T, Hamada H. Adenovirus-mediated transfer of p33ING1 with p53 drastically augments apoptosis in glionas. *Cancer Res* 1999; **59**: 5521-5528
9 **Chen LS**, Matsubara N, Yoshino T, Nagasaka T, Hoshizima N, Shirakawa Y, Naomoto Y, Isozaki H, Riabowol K, Tanaka N. Genetic alterations of candidate tumor suppressor ING1 in human esophageal squamous cell cancer. *Cancer Res* 2001; **61**: 4345-4349
10 **Kameyama K**, Huang CL, Liu D, Masuya D, Masuya D, Nakashima T, Sumitomo S, Takami Y, Kinoshita M, Yokomise H. Reduced ING1b gene expression plays an important role in carcinogenesis of non-small cell lung cancer patients. *Clin Cancer Res* 2003; **9**: 4926-4934
11 **Oki E**, Maehara Y, Tokunaga E, Kakeji Y, Sugimachi K. Reduced expression of p33(ING1) and the relationship with p53 expression in human gastric cancer. *Cancer Res* 1999; **147**: 157-162
12 **Ding HZ**, Yang D, Wu FR, Li H, Feng K, Zheng SJ, Ni CR, Yu GZ. p33(ING1) gene expression and mutation in stomach cancer tissues and precarcinomatous tissues. *Zhonghua Yixue Zazhi* 2003; **83**: 320-323
13 **Sanchez-Carbayo M**, Socci ND, Lozano JJ, Li W, Charytonowicz E, Belbin TJ, Prystowsky MB, Ortiz AR, Childs G, Cordon-Cardo C. Gene discovery in bladder cancer progression using cDNA microarrays. *Am J Pathol* 2003; **163**: 505-516
14 **Toyama T**, Iwase H, Wastson P, Muzik H, Saettler E, Magliocco A, DiFrancesco L, Forsyth P, Garkavtsev I, Kobayashi S, Riabowol K. Suppression of ING1 expression in sporadic breast cancer. *Oncogene* 1999; **18**: 5187-5193
15 **Nouman GS**, Anderson JJ, Crosier S, Shrimankar J, Lunec J, Angus B. Downregulation of nuclear expression of the p33 (ING1b) inhibitor of growth protein in invasive carcinoma of the breast. *J Clin Pathol* 2003; **56**: 507-511
16 **Ohgi T**, Masaki T, Nakai S, Morishita A, Yukimasa S, Nagai M, Miyauchi Y, Funaki T, Kurokohchi K, Watanabe S, Kuriyama S. Expression of p33(ING1) in hepatocellular carcinoma: relationships to tumour differentiation and cyclin E kinase activity. *Scand J Gastroenterol* 2002; **37**: 1440-1448
17 **Zhu Z**, Zhu M, Ni C. Significance of p33(ING1b) and p53 gene expression in hepatocellular carcinoma. *Zhonghua Yizxue Zazhi* 2002; **82**: 1332-1336
18 **Sarela AI**, Farmery SM, Markham AF, Guillou PJ. The candidate tumour suppressor gene, ING1, is retained in colorectal carcinomas. *Eur J Cancer* 1999; **35**: 1264-1267
19 **Bassam BJ**, Caetano-Anolles G, Gresshoff PM. Fast and sensitive silver straining of DNA in polyacrylamide gels. *Anal Biochem* 1991; **196**: 80-83
20 **Takahashi M**, Ozaki T, Todo S, Nakagawara A. Decreased expression of the candidate tumor suppressor gene ING1 is associated with poor prognosis in advanced neuroblastomas. *Oncol Rep* 2004; **12**: 811-816
21 **Tallwn G**, Riabowol K, Wolff JE. Expression of p33ING1 mRNA and chemosensitivity in brain tumor cells. *Anticancer Res* 2003; **23**: 1631-1635
22 **Kataoka H**, Bonnefin P, Vieyra D, Feng X, Hara Y, Miura Y, Joh T, Nakabayashi H, Vaziri H, Harris CC, Riabowol K. ING1 represses transcription by direct DNA binding and through effects on p53. *Cancer Res* 2003; **63**: 5785-5792
23 **Leung KM**, Po LS, Tsang FC, Siu WY, Lau A, Ho HT, Poon RY. The candidate tumor suppressor ING1b can stabilize p53 by disrupting the regulation of p53 by MDM2. *Cancer Res* 2002; **62**: 4890-4893
24 **Vieyra D**, Loewith R, Scott M, Bonnefin P, Boisvert FM, Cheema P, Pastyryeva S, Meijer M, Johnston RN, Bazett-Jones DP, McMahon S, Cole MD, Young D, Riabowol K. Human ING1 proteins differentially regulate histone acetylation. *J Biol Chem* 2002; **277**: 29832-29839
25 **Hara Y**, Zheng Z, Evans SC, Malatjalian D, Riddell DC, Guernsey DL, Wang LD, Riabowol K, Casson AG. ING1 and p53

tumor suppressor gene alterations in adenocarcinomas of the esophagogastric junction. *Cancer Lett* 2003; **192**: 109-116

26 **Chen B**, Campos EI, Crawford R, Martinka M, Li G. Analyses of the tumour suppressor ING1 expression and gene mutation in human basal cell carcinoma. *Int J Oncol* 2003; **22**: 927-931

27 **Yu GZ**, Zhu MH, Zhu Z, Ni CR, Zheng JM, Li FM. Genetic alterations and reduced expression of tumor suppressor p33 (ING1b) in human exocrine pancreatic carcinoma. *World J Gastroenterol* 2004; **10**: 3597-3601

28 **Krishnamurthy J**, Kannan K, Feng J, Mohanprasad BK, Tsuchida N, Shanmugam G. Mutational analysis of the candidate tumor suppressor gene ING1 in Indian oral squamous cell carcinoma. *Oral Oncol* 2001; **37**: 222-224

29 **Ohmori M**, Nagai M, Tasaka T, Koeffler HP, Toyama T, Riabowol K, Takahara J. Decreased expression of p33ING1 mRNA in lymphoid malignancies. *Am J Hematol* 1999; **62**: 118-119

30 **Bromidge T**, Lynas C. Relative levels of alternative transcripts of the ING1 gene and lack of mutations of p33/ING1 in haematological malignancies. *Leuk Res* 2002; **26**: 631-635

31 **Sanchez-Cespedes M**, Okami K, Cairns P, Sidransky D. Molecular analysis of the candidate tumor suppressor gene ING1 in human head and neck tumors with 13q deletions. *Genes Chromosomes Cancer* 2000; **27**: 319-322

Science Editor Kumar M and Guo SY **Language Editor** Elsevier HK

PO Box 2345, Beijing 100023, China
www.wjgnet.com
wjg@wjgnet.com

ELSEVIER

World J Gastroenterol 2005;11(39):6125-6129
World Journal of Gastroenterology ISSN 1007-9327
© 2005 The WJG Press and Elsevier Inc. All rights reserved.

Mechanism of counterattack of colorectal cancer cell by Fas/Fas ligand system

Qiang Zhu, Ji-Yong Liu, Hong-Wei Xu, Chong-Mei Yang, An-Zhong Zhang, Yi Cui, Hong-Bo Wang

Qiang Zhu, Ji-Yong Liu, Hong-Wei Xu, Chong-Mei Yang, An-Zhong Zhang, Yi Cui, Hong-Bo Wang, Department of Gastroenterology, Shandong Provincial Hospital, Jing 5 Wei 7 Road, 324#, Jinan 250021, Shandong Province, China
Correspondence to: Qiang Zhu, Department of Gastroenterology, Shandong Provincial Hospital, Jing 5 Wei 7 Road, 324#, Jinan 250021, Shandong Province, China. zhuqiang@medmail.com.cn
Telephone: +86-531-5186355 Fax: +86-531-7904002
Received: 2004-12-24 Accepted: 2005-01-26

Abstract

AIM: To determine the role of Fas/Fas ligand (FasL) in the immune escape of colon cancer cells.

METHODS: Immunohistochemistry was used to observe the expression of Fas and FasL in the tissues of colon cancer patients. *In situ* hybridization was used to detect the localization of FasL mRNA expression in cancer tissues. Terminal deoxynucleotide transferase-mediated dUTP nick end labeling (TUNEL) assay and CD45 staining were performed to detect the apoptosis of tumor-infiltrating lymphocytes (TILs). Co-culture assays of colon cancer cells (SW480) and Jurkat cells (Fas-sensitive cells) were performed to observe the counterattack of colon cancer cells to lymphocytes.

RESULTS: Of 53 cases of colon carcinomas, 23 cases (43.4%) expressed Fas which was significantly lower as compared to the normal colonic mucosa (73.3%, $P<0.01$), and 45 cases (84.9%) of colon carcinomas expressed FasL, whereas only two cases (3.75%) in normal mucosa expressed FasL. FasL expression in the colon cancer cells was found to be associated with increased cell death of TILs. The apoptotic rate of TIL in the FasL-positive staining regions of tumor cells was significantly higher than that in the FasL-negative staining region (54.84±2.79% *vs* 25.73±1.98%, $P<0.01$). The co-culture of SW480 cells and Jurkat cells confirmed the function of FasL on the SW480 cells. The apoptotic rates of Jurkat cells were found to be related with the amount of SW480 cells.

CONCLUSION: Colon cancer cells can escape the immune surveillance and killing via decreasing Fas expression, and can counterattack the immune system via increasing FasL expression. Fas/FasL can serve as potential targets for effective antitumor therapy.

© 2005 The WJG Press and Elsevier Inc. All rights reserved.

Key words: Colon neoplasm; Fas system; Immune counterattack

Zhu Q, Liu JY, Xu HW, Yang CM, Zhang AZ, Cui Y, Wang HB. Mechanism of counterattack of colorectal cancer cell by Fas/Fas ligand system. *World J Gastroenterol* 2005; 11(39): 6125-6129
http://www.wjgnet.com/1007-9327/11/6125.asp

INTRODUCTION

Fas (Apo-1/CD95) is a 45-ku type I membrane protein, and Fas ligand (FasL) is a 37-40-ku type II membrane protein, which belong to the tumor necrosis factor receptor and ligand families. Activation of Fas by certain anti-Fas antibodies or by FasL results in apoptotic cell death in susceptible cells. Fas/FasL interaction constitutes one of the main systems mediating the cytotoxicity of T cells and regulating immune responses, tissue development, and homeostasis[1,2].

Fas system is one of the killing pathways by cytotoxic T lymphocytes (CTL) to tumor cells in human body; however, in recent reports, the most enticing interpretation of FasL expression by tumor cells is that it offers a further novel mechanism of immune evasion. Tumor cells could counterattack the immune system of human body by inducing apoptosis of immune effector cells through Fas/FasL system[3]. We used *in vivo* and *in vitro* methods to determine the role of Fas/FasL in the immune escape of colon cancer cells.

MATERIALS AND METHODS

Immunohistochemical detection of Fas/FasL protein

Fifty-three colon carcinomas were collected after surgical resection performed at Shandong Provincial Hospital. None of the patients had received chemo-, radio- or immuno-therapy before resection. Paraffin wax-embedded surgically resected tumor sections were deparaffinized in xylene and rehydrated before analysis. The primary antibodies were purified rabbit polyclonal anti-human Fas and FasL-specific IgG (Santa Cruz Biotechnology, Santa Cruz, CA, USA) at 0.1 μg/mL in a wash buffer. Antibody binding was localized using a biotinylated secondary antibody, avidin conjugated horseradish peroxidase, and diamiobenzidine substrate, contained within the ABC detection kit. The immunizing peptide (Santa Cruz Biotechnology), to which the antibody was raised, was included at 1 μg/mL during primary antibody incubation as a direct internal competitive control for antibody specificity.

Localization of FasL mRNA expression by in situ hybridization

In situ hybridization was performed on paraffin-embedded human colonic tumor sections (4 μm thick), mounted on aminopropylethoxysilane-treated slides. A digoxigenin-labeled RNA hybridization probe (344 bp) was used, corresponding to codons 96-210 of the human FasL cDNA sequence. The nucleotide sequence of the FasL probe showed insignificant homology to any other sequence in the EMBL DNA sequence database. Prehybridization and hybridization were performed as previously described[3]. In order to confirm the specificity of hybridization, a 10-fold excess of unlabeled riboprobe was added to the digoxigenin-labeled probe prior to hybridization.

In situ apoptosis assessment of tumor-infiltrating lymphocyte

To identify tumor-infiltrating lymphocytes (TILs), CD45 staining was performed on consecutive sections with a mouse anti-human CD45 monoclonal IgG (clone 2B11+PD7/26, Dako Corp., Carpinteria, CA, USA, dilution 1/70) according to the standard immunohistochemical methods as described above. Alkaline phosphatase conjugated anti-alkaline phosphatase complex (DO651, Dako Corp.) was used to display the color of CD45 staining. The membrane of the CD45-positive cells was red. Apoptosis of TILs was detected *in situ* in frozen sections of resected tissues using Terminal deoxynucleotide transferase-mediated dUTP nick end labeling (TUNEL) assay (Boehringer Mannheim GmbH, Mannheim, Germany) applied to the histological sections. Visualization of the final reaction product was achieved by diaminobenzidine. TUNEL-positive TILs (with red membrane and brown nucleus) were counted at high power (×400) from fields of view chosen according to a systematic random sampling method. Approximately 1 000 TILs were counted and a TUNEL index (TI) was expressed as the percentage of TUNEL lymphocytes.

Cell culture and growth assay

Colon cancer SW480 cells were grown in RPMI medium supplemented with penicillin G (100 U/mL), streptomycin (100 μg/mL) and 100 mL/L fetal bovine serum at 37 ℃ in humidified atmosphere containing 50 mL/L CO_2 in air. Cell growth was determined by the 3-(4,5-methylthiazol-2yl)-2, 5-diaphenyl-tertrazolium bromide (MTT) colorimetric assay. The assay was initiated by adding MTT solution to each well at a final concentration of 0.625 μg MTT/mL medium. After 4 h, the optical density was determined with an ELISA plate reader after removal of the medium and dissolving of the dye crystals in acidified isopropylalcohol.

Co-culture assays of colon cancer and Jurkat cells

Different concentrations of SW480 cells (0, 1×10^5/mL, 2×10^5/mL, 4×10^5/mL) were plated in triplicate on 24-multiwell tissue culture dishes. After 24 h, 2×10^4/mL Jurkat cells were seeded onto the plates. The wells with colon cancer cells alone (without overlying Jurkat cells) were maintained as additional controls. After 48 h, the non-adherent phase of the mixed culture was aspirated and assayed for viability using MTT assay. In experiments using recombinant FasFc (ZB4) as a competitor, similar experimental conditions were used with the following exception. MTT assay was used to evaluate the amount of Jurkat cells at the co-culture time of 24, 48, 72, and 96 h.

Detection of apoptosis of Jurkat cells

After being co-cultured with SW480 for 48 h, the Jurkat cells were collected and added with Hoechst 33258 (Sigma) on a slide glass. The specimens were examined under a Nikon fluorescence microscope with B2-type filter (magnification ×200). When apoptotic bodies or chromatin condensations were observed, the observation was defined as apoptosis. Apoptotic cells were assessed morphologically by staining with Hoechst 33258 using cells fixed with Clarke fixative (ethanol:acetic acid = 3:1). Apoptotic index (AI) was defined as follows: AI = 100×apoptotic cells/200 cells.

Statistical analysis

All experiments for cell cultures were performed at least in triplicate. Data were expressed as mean±SD. Statistical analysis was performed by one-way variance (ANOVA), and the comparisons between groups were performed by independent sample *t*-test. The regressive relation between two variables was performed by linear regression. A two-tailed *P* value less than 0.05 was considered statistically significant.

RESULTS

Decrease of Fas expression and increase of FasL expression in colon cancer tissues

Of 53 cases of colon carcinomas, 23 cases (43.4%) expressed Fas which was significantly lower as compared to that in normal colonic mucosa (73.3%) ($P<0.01$), and 45 cases (84.9%) of colon carcinomas expressed FasL, whereas only 2 cases (3.75%) in normal mucosa expressed FasL. Intensity and extent of positive staining varied within individual tumors. Neoplastic areas with positive and negative staining for FasL frequently co-existed within the same tumor. The extent of FasL expression varied significantly between different cancer stages and differentiations (data not shown, Figures 1A and B). FasL expression also existed on TILs in all cases. TILs were smaller in volume than cancer cells, which could distinguish the two kinds of FasL-expressing cells.

In situ hybridization was performed on paraffin-embedded human colonic tumor sections in order to detect the localization of FasL mRNA expression. FasL mRNA was detected in the colon cancer cells and in TILs (Figure 2). The location of FasL mRNA and expression of FasL protein coincided.

To further study the role of FasL expressed in cancer cells in tissues, 23 cases of lymph node metastases from colorectal carcinomas were obtained to detect the expression of FasL immunohistochemically. All cases of lymph node metastases showed FasL immunoreactivity in greater than 60% of the metastatic cells (Figure 1C).

Apoptosis of tumor-infiltrating lymphocytes induced by FasL on colon cancer

To evaluate apoptosis of TILs, we detected the presence of apoptotic cells in tissue sections using CD45 staining

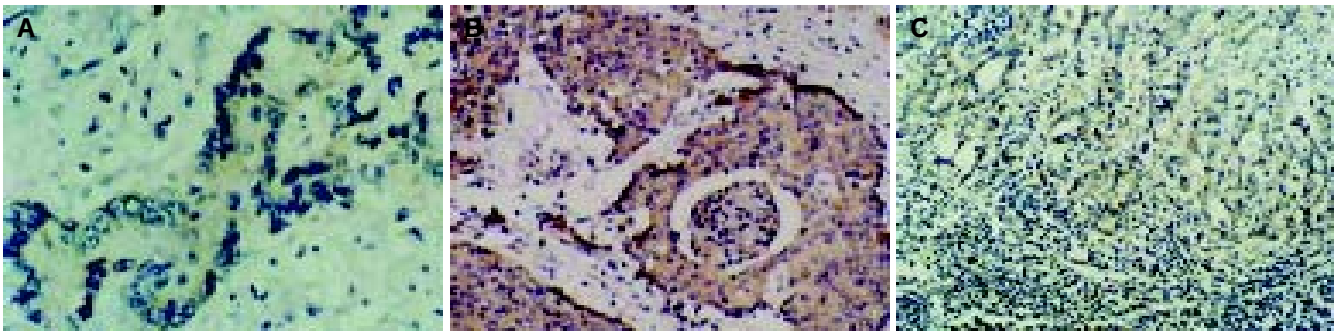


Figure 1 Immunohistochemical staining of Fas and FasL expression in colon cancer cells. A: Low expression of Fas in colon cancer cells; B: high expression of FasL in colon cancer cells; and C: high expression of FasL in lymph node metastases from colon cancer cells.

(WBC common antigen) and TUNEL techniques. Tonsil sections were included as positive controls, stained strongly, and omission of the primary antibody abolished staining. To quantify the extent of apoptosis of TILs, the percentage of TUNEL-positive and CD45-positive cells was calculated. The apoptotic rate of TILs in FasL-positive staining regions of tumor cells was significantly higher than that in FasL-negative region of tumor cells (54.84±2.79% *vs* 25.73±1.98%, $P<0.01$, Figure 3). *In vivo* FasL expression in colon cancer cells was found to be associated with increased cell death of TILs.

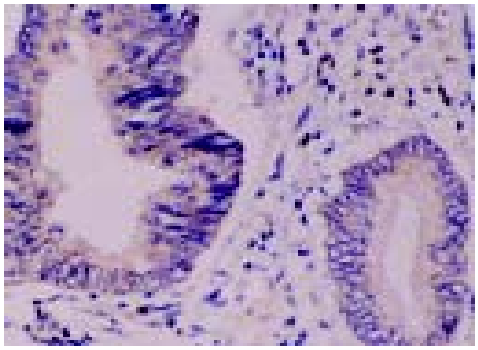


Figure 2 Localization of FasL mRNA by *in situ* hybridization.

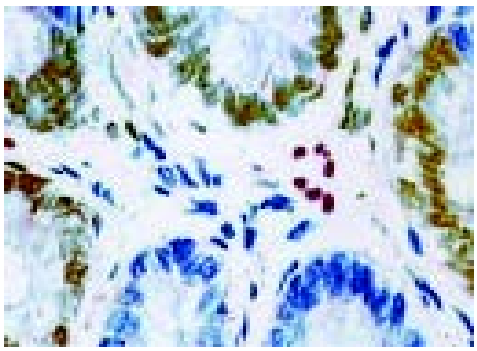


Figure 3 Detection of TILs. They were displayed by double staining (CD45 staining and TUNEL).

Colon cancer cell-mediated killing of Jurkat cells

Jurkat cells grown in the absence of human colon cancer cells showed a marked proliferation after 48 h. However, when co-cultured over a mono-layer of the FasL-expressing colon cancer cell line SW480, we observed a marked decrease in Jurkat cells while using MTT assay (Figure 4). The Jurkat cell killing was largely inhibited by pre-incubating the colon cancer mono-layer with a low concentration of recombinant Fas neutral antibody ZB4, which is capable of binding to FasL and blocking Fas/FasL interaction.

We used fluorescence microscopy to observe the shape of apoptotic Jurkat cells by the untreated SW480 cells. Condensation of chromatin, nuclear fragmentation and typical apoptotic bodies were observed in the tested group (Figure 5). The fluorescence microscopy results revealed that the apoptotic rates of Jurkat cells induced by SW480 cells after being co-cultured had a significant difference with the natural apoptotic rate of Jurkat cells (Table 1).

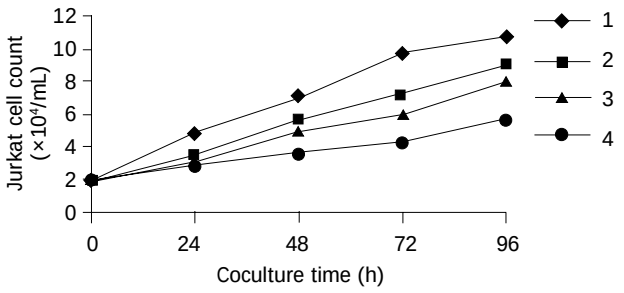


Figure 4 Jurkat cells growth curve after being co-cultured with SW480. 1: Control group; 2: 0.5×10^5/mL SW480 planting group; 3: 1×10^5/mL SW480 planting group; and 4: 2×10^5/mL SW480 planting group.

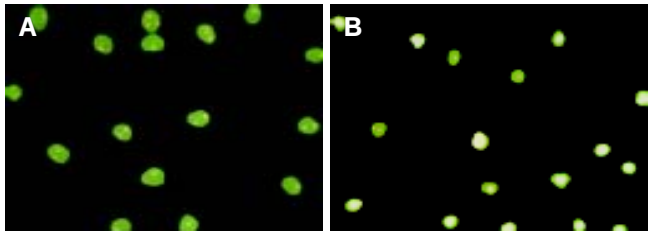


Figure 5 Detection of apoptotic Jurkat cells by fluorescence microscopy. A: Negative control of Jurkat cells; B: apoptotic Jurkat cells after being co-cultured with SW480 cells.

Table 1 Apoptotic rates of Jurkat cells detected by fluorescence microscopy

Planting concentration of SW480	Apoptotic rate of Jurkat cell (%)
0 (controls)	1.58±0.12
0.5×10^5/mL	5.22±0.13[b]
1×10^5/mL	9.74±0.21[b]
2×10^5/mL	19.33±0.18[b]

[b]$P<0.01$ *vs* controls.

DISCUSSION

Fas molecule was identified for the first time in 1989 by two research groups of Germany and Japanese separately[4,5]. In the beginning days of the twentieth century, researchers worldwide paid attention to the role of Fas system in the process of CTL killing cancer cells. It has been concluded that CTL-induced apoptosis of cancer cells via Fas system is one of the two main ways of CTL killing cancer cells, namely, Fas-based cytotoxicity is one of the two molecular mechanisms of T cell-mediated cytotoxicity, the other is perforin-based[1].

In recent years, some reports found that caner cells could decrease Fas expression which could escape the immune surveillance and killing, but could express FasL which could induce apoptosis of CTL, especially TILs[3,6,7]. In these cases, Fas and FasL may contribute to tumor immune privilege by inducing FasL-mediated apoptosis of host CTL and NK cells. We found that Fas expression on the colon cancer cells decreased significantly compared to the normal colonic epithelial cells ($P<0.05$), which was in agreement with the previous reports by Houston *et al.*[8], and Okada *et al.*[9]. Colon cancer could escape the immune surveillance and killing by decreasing Fas expression.

In addition to decrease in Fas expression, functional FasL expression by certain cancer cell types has been implicated in tumor escape via destruction of infiltrating Fas-bearing lymphocytes. In this study, we also found that FasL expression was absent in normal colonic epithelial cells, whereas markedly increased in colon carcinomas ($P<0.05$), and it was obviously correlated with apoptosis of TILs in colon cancer tissues. To evaluate the functional significance of FasL expression in colon cancer cells, we performed co-culture experiments using the Fas-sensitive Jurkat cell line (of human T-cell origin) as a target cell. These cells have been demonstrated to be capable of apoptosis following exposure to FasL. *In vitro*, colon cancer cells without any treatment could mediate apoptosis of Jurkat cells by Fas and FasL. Expression of FasL potentially enables colon cancer cells to counterattack Fas-sensitive anti-tumor immune effector cells by delivering a Fas-mediated apoptotic death signal. Ohta *et al.*[10], reported that 37 (82%) of the primary pancreatic cancers and both of the hepatic metastases expressed FasL, and the patients with FasL-positive tumor had significantly shorter survival times as compared with the FasL-negative, suggesting FasL as a significant prognostic factor of pancreatic cancer.

FasL expression may have effects on the immune system beyond the tumor site, and soluble FasL has been identified in certain types of FasL-positive leukemias and lymphomas[11]. Circulating forms of FasL (soluble FasL) were also found in blood from cancer patients, this could contribute to the generalized depression of cellular immunity. Thus, FasL expression might facilitate tumor invasion by inducing apoptosis in surrounding Fas-positive tissue, allowing the tumor to grow into the resulting space.

We found that large areas of most colonic tumors co-expressed FasL and Fas, indicating that these cells must have disabled the intracellular Fas apoptotic pathway due to intracellular defects in Fas signal transduction. Strand *et al.*[12], reported that MMP-7 cleavage of Fas resulted in reduced Fas surface expression and decreased Fas-mediated apoptosis sensitivity of tumor cells. Moreover, overexpression of inhibitors of apoptosis or intracellular apoptotic signal transduction may further contribute to the observed resistance to Fas-dependent apoptosis in colon cancer[13]. Several additional mechanisms of the Fas resistance have been described. Expression of soluble Fas by liver cancer cells may be involved in the Fas resistance of liver cancer *in vivo*[14].

A "Fas counterattack" model of colon cancer immune escape can be proposed, in which colon cancer cells, by expressing FasL, may remove Fas-sensitive immune effector cells by apoptosis. Increased expression of FasL is associated with decreased Fas levels in colon cancer cells that can escape immune surveillance and facilitate tumor progression and metastasis. Fas/FasL can serve as potential targets for effective antitumor therapy[15].

REFERENCES

1 **Nagata S,** Golstein P. The Fas death factor. *Science* 1995; **267**: 1449-1456

2 **Maher S,** Toomey D, Condron C, Bouchier-Hayes D. Activation-induced cell death: the controversial role of Fas and Fas ligand in immune privilege and tumour counterattack. *Immunol Cell Biol* 2002; **80**: 131-137

3 **Perabo FG,** Kamp S, Schmidt D, Lindner H, Steiner G, Mattes RH, Wirger A, Pegelow K, Albers P, Kohn EC, von Ruecker A, Mueller SC. Bladder cancer cells acquire competent mechanisms to escape Fas-mediated apoptosis and immune surveillance in the course of malignant transformation. *Br J Cancer* 2001; **84**: 1330-1338

4 **Trauth BC,** Klas C, Peters AM, Matzku S, Moller P, Falk W, Debatin KM, Krammer PH. Monoclonal antibody-mediated tumor regression by induction of apoptosis. *Science* 1989; **245**: 301-305

5 **Yonehara S,** Ishii A, Yonehara M. A cell-killing monoclonal antibody (anti-Fas) to a cell surface antigen co-downregulated with the receptor of tumor necrosis factor. *J Exp Med* 1989; **169**: 1747-1756

6 **Krishnakumar S,** Kandalam M, Mohan A, Iyer A, Venkatesan N, Biswas J, Shanmugam MP. Expression of Fas ligand in retinoblastoma. *Cancer* 2004; **101**: 1672-1676

7 **Abrams SI.** Positive and negative consequences of Fas/Fas ligand interactions in the antitumor response. *Front Biosci* 2005; **10**: 809-821

8 **Houston A,** Bennett MW, O'Sullivan GC, Shanahan F, O'Connell J. Fas ligand mediates immune privilege and not inflammation in human colon cancer, irrespective of TGF-beta expression. *Br J Cancer* 2003; **89**: 1345-1351

9 **Okada K,** Komuta K, Hashimoto S, Matsuzaki S, Kanematsu T, Koji T. Frequency of apoptosis of tumor-infiltrating lymphocytes induced by fas counterattack in human colorectal carcinoma and its correlation with prognosis. *Clin Cancer Res* 2000; **6**: 3560-3564

10 **Ohta T,** Elnemr A, Kitagawa H, Kayahara M, Takamura H, Fujimura T, Nishimura G, Shimizu K, Yi SQ, Miwa K. Fas ligand expression in human pancreatic cancer. *Oncol Rep* 2004; **12**: 749-754
11 **Hallermalm K,** De Geer A, Kiessling R, Levitsky V, Levitskaya J. Autocrine secretion of Fas ligand shields tumor cells from Fas-mediated killing by cytotoxic lymphocytes. *Cancer Res* 2004; **64**: 6775-6782
12 **Strand S,** Vollmer P, van den Abeelen L, Gottfried D, Alla V, Heid H, Kuball J, Theobald M, Galle PR, Strand D. Cleavage of CD95 by matrix metalloproteinase-7 induces apoptosis resistance in tumour cells. *Oncogene* 2004; **23**: 3732-3736
13 **Kase S,** Osaki M, Adachi H, Kaibara N, Ito H. Expression of Fas and Fas ligand in esophageal tissue mucosa and carcinomas. *Int J Oncol* 2002; **20**: 291-297
14 **Lee SH,** Shin MS, Lee HS, Bae JH, Lee HK, Kim HS, Kim SY, Jang JJ, Joo M, Kang YK, Park WS, Park JY, Oh RR, Han SY, Lee JH, Kim SH, Lee JY, Yoo NJ. Expression of Fas and Fas-related molecules in human hepatocellular carcinoma. *Hum Pathol* 2001; **32**: 250-256
15 **Kim R,** Emi M, Tanabe K, Uchida Y, Toge T. The role of Fas ligand and transforming growth factor beta in tumor progression: molecular mechanisms of immune privilege via Fas-mediated apoptosis and potential targets for cancer therapy. *Cancer* 2004; **100**: 2281-22891

Science Editor Kumar M and Guo SY **Language Editor** Elsevier HK

PO Box 2345, Beijing 100023, China
www.wjgnet.com
wjg@wjgnet.com

ELSEVIER

World J Gastroenterol 2005;11(39):6130-6133
World Journal of Gastroenterology ISSN 1007-9327
© 2005 The WJG Press and Elsevier Inc. All rights reserved.

Specific ssDNA concentration in liver tissue as an index of apoptosis in hepatitis C virus-infected patients

Tadeusz Wojciech Lapiński, Anatol Panasiuk, Jerzy Jaroszewicz, Oksana Kowalczuk, Robert Flisiak, Magdalena Rogalska

Tadeusz Wojciech Lapiński, Anatol Panasiuk, Jerzy Jaroszewicz, Robert Flisiak, Magdalena Rogalska, Department of Infectious Diseases, Medical University of Bialystok, Poland
Oksana Kowalczuk, Institute of Molecular Biology, Medical University of Bialystok, Poland
Correspondence to: Tadeusz Wojciech Lapiński, MD, Department of Infectious Diseases, Medical University of Bialystok, Bialystok 15-540, Żurawia str, 14, Poland. twlapinski@wp.pl
Telephone: +48-85-741-69-21
Received: 2005-01-19 Accepted: 2005-02-18

Abstract

AIM: To evaluate the activity of apoptosis in liver tissue and explore its possible association with hepatic necroinflammation and fibrosis as well as serum hepatitis C virus (HCV) load.

METHODS: The studied population included 50 chronic hepatitis C patients (20 women and 30 men, aged 18-66 years). HCV-RNA quantification was performed by two-step real-time quantitative RT-PCR method using the TaqMan technology (reagents of Applera Corporation firm, USA). The morphology of liver tissue was assessed descriptively and scored (necroinflammatory activity and fibrosis). The early apoptosis activity in liver tissue was examined by ssDNA apoptosis ELISA kit, (Chemicon, Germany).

RESULTS: The correlation between apoptosis and fibrosis in liver tissue was observed. High intensification of apoptosis was proportional to the increase of fibrosis (ssDNA: 16.65×10^{-5} μg/g; 12.71×10^{-5} μg/g), however, this difference was not statistically significant ($P>0.05$). Activity of apoptosis in the liver tissue, expressed by ssDNA concentration did not depend on hepatic necroinflammatory changes, HCV-RNA viral load, ALT, and AST activity as well as prothrombin time and INR index.

CONCLUSION: Fibrosis in the tissue is closely associated with early apoptosis in HCV-infected patients.

© 2005 The WJG Press and Elsevier Inc. All rights reserved.

Key words: Apoptosis; Hepatitis C virus; ssDNA; Fibrosis

Lapiński TW, Panasiuk A, Jaroszewicz J, Kowalczuk O, Flisiak R, Rogalska M. Specific ssDNA concentration in liver tissue as an index of apoptosis in hepatitis C virus-infected patients. *World J Gastroenterol* 2005; 11(39): 6130-6133
http://www.wjgnet.com/1007-9327/11/6130.asp

INTRODUCTION

Activity of apoptosis during hepatitis C virus (HCV) infection is a result of inhibitory and stimulatory effects of viral proteins. Apoptosis of HCV-infected hepatocytes influences the elimination of viruses. Insufficient activity of this process can lead to persistent liver inflammation[1]. On the contrary, excessive activity of apoptosis causes uncontrolled damage to liver cells. Moreover, there is evidence that apoptosis influences fibrosis progression.

This study was to evaluate the activity of apoptosis in liver tissue and explore its possible association with hepatic necroinflammation and fibrosis activity as well as serum HCV viral load.

MATERIALS AND METHODS

Patients

The study included 50 chronic hepatitis C patients (20 women and 30 men, aged 18-66 years). Their HCV infection did not exceed 5 years. Inclusion criteria were the following: no focal changes in ultrasonography investigation of liver, absence of drugs or alcohol abuse, autoimmune disease, HIV and hepatitis B co-infection as well as neoplasmatic and other serious diseases, which might alter apoptosis activity. Informed consent was obtained from each patient and the Bioethics Committee at the Medical University of Bialystok approved the study protocol.

The presence of anti-HCV antibodies in serum was detected by MEIA (Abbott, USA). Test was based on recombinant core proteins for HCr43, structural proteins for c200 (NS3 and NS4) and unstructured proteins for c100-3 (NS4) and NS5.

HCV-RNA quantification methods

Blood samples were obtained from 47 patients with known chronic hepatitis C. All blood samples were collected to Vacutainer tubes with no additives and centrifuged within 2 h of collection. The serum was aliquoted and kept at -80 ℃ until further use.

RNA was extracted from 280 μL of each serum sample using Qiagen (Hilden, Germany) QIAamp viral RNA mini kit according to the manufacturer's protocol and dissolved in 50 μL of RNase-free water. This resulted in nearly sixfold concentration of the original output material. RNA was stored at -80 ℃ until further testing. Each isolation was carried out in duplicate.

HCV-RNA quantification was performed by two-step real-time quantitative RT-PCR method using the TaqMan technology[2]. First, 3.5 μL of total RNA was subjected to reverse transcription in 10 μL of reaction mixture using the Applied Biosystems (Applera Corporation, USA) TaqMan

reverse transcription reagents and random hexamers $(dN)_6$. RNA was previously denatured at 70 ℃ for 10 min. The reaction mixture was prepared as follows: 1×reverse transcription buffer, 5.5 mmol/L $MgCl_2$, 0.5 mmol/L of each dNTPs, 2.5 mmol/L of primer $(dN)_6$, 0.4 U of RNase inhibitor per μL and 1.25 U of MultiScribe transcriptase per μL. The reaction was carried out at 48 ℃ for 30 min preceded by the incubation at 25 ℃ for 10 min. Incubation at 95 ℃ for 5 min terminated the reaction. The resulting cDNA was used as a template for PCR amplification.

cDNA amplification was performed by the Applied Biosystem (Applera Corporation, USA) ABI Prism 7 900HT sequence detection system in TaqMan universal PCR master mix, which is optimized for TaqMan reactions and contains Applied Biosystems (Applera Corporation, USA) AmpliTaq gold DNA polymerase, AmpErase UNG, dNTPs with UTP, passive reference ROX and optimized buffer components. For each PCR reaction, 4 μL of cDNA was added to 16 μL of PCR mix containing 450 nmoL each of HCV-specific forward and reverse primers and 300 nmoL of HCV-specific FAM-MGB probe. The primers and probe were designed and manufactured by Applied Biosystems (Applera Corporation, USA) and optimized for HCV genotype RNA detection. Thermal cycling conditions were designed as follows: inactivation of possible contaminating amplicons by AmpErase UNG at 50 ℃ for 2 min, initial cDNA denaturation at 95 ℃ for 10 min, followed by 40 cycles at 95 ℃ for 15 s and at 60 ℃ for 60 s. All amplification reactions were carried out in triplicate.

Fluorescent measurements were recorded during the annealing step of each cycle. At the end of each PCR run, data were automatically analyzed by the system to generate the amplification plots and the threshold cycle (Ct) for each sample was calculated. Sample RNA concentrations were then automatically calculated by interpolation of the experimentally determined standard curve.

An external standard curve was generated with each run by amplification of 10-fold serial dilutions of RNA isolated from the viral quality control serum (PeliSpy, Sanguin), containing 38 000 geq/mL HCV. RNA isolation and cDNA synthesis were carried out as described for unknown samples. All amplification reactions were carried out in duplicate. The standard curve was created automatically by the ABI Prism 7 900HT detection system by plotting the Ct values against each standard dilution of known concentration.

Precautions were undertaken to minimize the risk of PCR contamination during analysis.

Liver morphology

Liver tissue was obtained from the right lobe of the liver (with 1.6-1.8 mm needles from Hypafix packs by Braun, Germany). A part of the liver tissue was subjected to morphologic examination. The morphology of liver tissue was assessed descriptively and scored (necroinflammatory activity and fibrosis) according to Scheuer[3].

Another part of the liver tissue was transferred to 0.9% NaCl buffer and then subjected to apoptosis activity measurement.

Apoptosis in liver tissue

The early apoptosis activity in liver tissue was measured by ssDNA apoptosis ELISA kit, (Chemicon, Germany) based on the mAb to single-stranded DNA (ssDNA). The intensity of the reaction between ssDNA and mAb was evaluated. The amount of ssDNA was calculated with reference to absorbance line of positive and negative control.

The liver tissue was homogenized in 0.9% NaCl buffer. The concentrations of ssDNA and total proteins in the homogenized liver tissue were analyzed in duplicate. The homogenates of liver tissue were transferred to wells 24 h prior to the succeeding steps of the procedure to allow cell attachment. Then formamide was added to denature DNA in apoptotic cells, but not in necrotic cells or in cells with DNA damage in the absence of apoptosis. This process enabled specific receptors of apoptotic ssDNA binding to mAb. Following this reaction, 3-ethylbenziazoline-6-sulfonic acid was added to color the products of this reaction[4].

Absorbance was defined at 405 nm. The concentration of ssDNA was calculated from a prepared standard curve of absorbance (basis of different increasing positive and negative control). The results of ssDNA were referred to 1.0 g of proteins in the liver tissue sample.

Statistical analysis

Statistical analysis was performed by non-parametric Mann-Whitney *U*, Wilcoxon rank, and Pearson tests. $P<0.05$ was considered statistically significant.

RESULTS

Diagnostic biopsy was obtained from 47 patients. In three of the remaining cases, the liver biopsy sample did not contain five portobiliary areas, therefore it was impossible to obtain reliable histology results.

The activity of apoptosis in liver tissue of the studied group was independent of sex and age. ssDNA concentration in liver tissue did not correlate with ALT, AST activity, prothrombin time, and INR index. Moreover, apoptosis was independent of necroinflammatory changes in liver tissue (Table 1).

Table 1 Correlation between ALT, AST activity, prothrombin time, and INR index in chronic hepatitis C patients

	ALT	AST	Prothrombin time	INR index
Pearson test	0.08	0.14	-0.01	0.03

The correlation between fibrosis and apoptosis was observed. Concentration of ssDNA was higher (16.65×10^{-5} μg/g) in patients with more intensified fibrosis of liver tissue than in those with fibrosis (12.71×10^{-5} μg/g). However, this difference was not statistically significant ($P>0.05$). (Figures 1 and 2)

The serum HCV-RNA concentration did not correlate with ALT, AST activity, prothrombin time, and INR index. Moreover, no correlation between serum HCV-RNA and ssDNA concentrations in liver tissue was observed (Table 2).

DISCUSSION

Table 2 Concentration of apoptosis ssDNA in respect to serum HCV-RNA concentration, necroinflammatory changes (G) and fibrosis (S) in liver tissue

n	G1+G2	Concentration of ssDNA (μg/g)	Concentration of HCV-RNA (geq/mL)	Pearson test	*n*	*S*	Concentration of ssDNA (μg/g)	Concentration of HCV-RNA (geq/mL)	Pearson test
16	0-3	13.16×10^{-5} 3.95×10^{-5} SD±	$4.96\text{-}54.2\times10^{3}$	-0.11	39	0-1	12.71×10^{-5} $4.85\text{-}10^{-5}$ SD±	$4.96\text{-}227\times10^{3}$	0.01
13	4	13.41×10^{-5} 6.0×10^{-5} SD±	$2.48\times10^{2}\text{-}227\times10^{3}$	-0.14	8	2-3	16.65×10^{-5} 5.98×10^{-5} SD±	$14.7\text{-}266\times10^{3}$	0.01
18	5-7	13.56×10^{-5} 5.85×10^{-5} SD±	$14.7\text{-}266\times10^{3}$	-0.13					

Necroinflammatory activity: G1 = 0-4; G2 = 0-4; G1/2 = 0-8; *S* = 0-4.

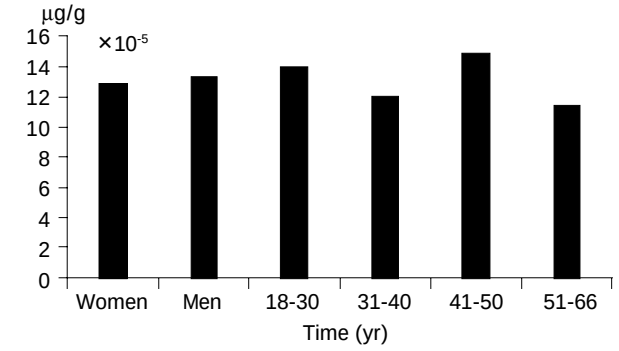


Figure 1 Concentration of ssDNA in HCV-infected patients with respect to age and sex.

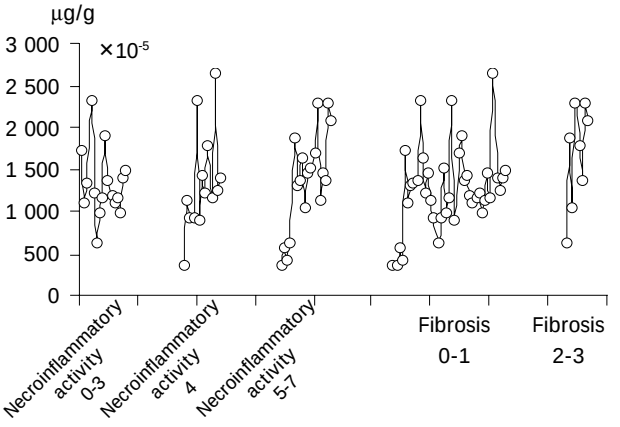


Figure 2 Concentration of ssDNA in liver tissue stratified according to liver morphology changes. Necroinflammatory activity: G1 = 0-4; G2 = 0-4; G1/2 = 0-8; *S* = 0-4.

Apoptosis is one of the factors regulating the course of chronic viral hepatitis. Since this process runs gradually, modification of its course is possible. Different HCV proteins can accelerate or suppress apoptosis.

HCV core proteins overactivate Fas particles expressed on hepatocytes, leading to degradation of cell DNA[5,6]. The Fas particles are "death domains" and indicators of apoptosis. Higher Fas concentration in patients with HCV infection can increase the activity of apoptosis.

HCV non-structural proteins (NS5A) are able to suppress apoptosis by diminishing synthesis of caspase 3, protein kinase A and suppressing TNF-α stimulating polymerase[7,8]. Insufficient activity of apoptosis can influence the persistence of chronic inflammation related to HCV infection[1].

Di Martino *et al*.[9], showed that activity of apoptosis in chronic hepatitis C patients is proportional to HCV-RNA levels. Caronia *et al*.[10], have shown that HCV strongly inhibits apoptosis. In previous investigations, the concentration of ssDNA, as an early indicator of apoptosis was not correlated with HCV viral load, functional state of the liver and necroinflammatory changes in liver tissue samples.

Tsamandas *et al*.[11], evaluated the location and concentration of Bcl-2 and Bax protein, markers of apoptosis activity, in patents with HBV and HCV infection, and found that Bcl-2 and Bax concentrations are enhanced in the regions of intense fibrosis. Takehara *et al*.[12], have shown the linear dependence between the concentration of Bcl-2 family members and activity of fibrosis in the liver. Our results are in accordance with their observations.

Bcl-2 and Bax proteins can mark the late period of apoptosis. Correlation between apoptosis and fibrosis in liver tissue seems unquestionable. However, whether cells with high activity of apoptosis are molecular inductors of fibrosis in HCV-infected patients remains to be solved.

In conclusion, fibrosis of liver tissue is associated with HCV-infection, but apoptosis is not associated with necroinflammatory changes in chronic hepatitis C patients.

REFERENCES

1 **Zuckerman E**, Zuckerman T, Sahar D, Streichman S, Attias D, Sabo E, Yeshurun D, Rowe J. bcl-2 and immunoglobulin gene rearrangement in patients with hepatitis C virus infection. *Br J Haematol* 2001; **112**: 364-369

2 **Castelain S**, Descamps V, Thibault V, Francois C, Bonte D, Morel V, Izopet J, Capron D, Zawadzki P, Duverlie G. TaqMan amplification system with an internal positive control for HCV RNA quantitation. *J Clin Virol* 2004; **31**: 227-234

3 **Scheuer PJ**. Classification of chronic viral hepatitis: A need for reassessment. *J Hepatol* 1991; **13**: 372-374

4 **Frankfurt OS**, Krishan A. Apoptosis enzyme-linked immunosorbent assay distinguishes anticancer drugs from toxic chemicals and predicts drug synergism. *Chem Biol Interact* 2003; **145**: 89-99

5 **Hahn CS**, Cho YG, Kang BS, Lester IM, Hahn YS. The HCV core protein acts as a positive regulator of fas-mediated apoptosis in a human lymphoblastoid T cell line. *Virology* 2000; **276**: 127-137

6 **Zhu N**, Ware CF, Lai MM. Hepatitis C virus core protein enhances FADD-mediated apoptosis and suppresses TRADD signaling of tumor necrosis factor receptor. *Virology* 2001; **283**: 178-187

7 **Ghosh AK**, Majumder M, Steele R, Meyer K, Ray R, Ray RB. Hepatitis C virus NS5A protein protects against TNF-alpha

mediated apoptotic cell death. *Virus Res* 2000; **67**: 173-178
8 **Ezelle HJ**, Balachandran S, Sicheri F, Polyak SJ, Barber GN. Analyzing the mechanisms of interferon-induced apoptosis using CrmA and hepatitis C virus NS5A. *Virology* 2001; **281**: 124-137
9 **Di Martino V**, Brenot C, Samuel D, Saurini F, Paradis V, Reynes M, Bismuth H, Feray C. Influence of liver hepatitis C virus RNA and hepatitis C virus genotype on Fas-mediated apoptosis after liver transplantation for hepatitis C. *Transplantation* 2000; **15**: 1390-1396
10 **Caronia S**, McGarvey MJ, Goldin RD, Foster GR. Negative correlation between intrahepatic expression of hepatitis C antigens and apoptosis despite high-level expression of Fas and HLA antigens. *J Viral Hepatol* 2004; **11**: 511-518
11 **Tsamandas AC**, Thomopoulos K, Zolota V, Kourelis T, Karatzas T, Ravazoula P, Tepetes K, Petsas T, Karavias D, Karatza C, Bonikos DS, Gogos C. Potential role of bcl-2 and bax mRNA and protein expression in chronic hepatitis type B and C: a clinicopathologic study. *Mod Pathol* 2003; **16**: 1273-1288
12 **Takehara T**, Tatsumi T, Suzuki T, Rucker EB 3rd, Hennighausen L, Jinushi M, Miyagi T, Kanazawa Y, Hayashi N. Hepatocyte-specific disruption of Bcl-xL leads to continuous hepatocyte apoptosis and liver fibrotic responses. *Gastroenterology* 2004; **127**: 1189-1197

Science Editor Wang XL and Guo SY **Language Editor** Elsevier HK

PO Box 2345, Beijing 100023, China
www.wjgnet.com
wjg@wjgnet.com

ELSEVIER

World J Gastroenterol 2005;11(39):6134-6143
World Journal of Gastroenterology ISSN 1007-9327
© 2005 The WJG Press and Elsevier Inc. All rights reserved.

NF-κB and ERK-signaling pathways contribute to the gene expression induced by *cag* PAI-positive-*Helicobacter pylori* infection

Wataru Shibata, Yoshihiro Hirata, Haruhiko Yoshida, Motoyuki Otsuka, Yujin Hoshida, Keiji Ogura, Shin Maeda, Tomoya Ohmae, Ayako Yanai, Yuzo Mitsuno, Naohiko Seki, Takao Kawabe, Masao Omata

Wataru Shibata, Yoshihiro Hirata, Haruhiko Yoshida, Motoyuki Otsuka, Yujin Hoshida, Keiji Ogura, Shin Maeda, Tomoya Ohmae, Ayako Yanai, Yuzo Mitsuno, Takao Kawabe, Masao Omata, Department of Gastroenterology, Graduate School of Medicine, University of Tokyo, Japan
Naohiko Seki, Department of Functional Genomics, Graduate School of Medicine, University of Chiba, Japan
Supported by a Grant-in-Aid for Scientific Research from the Ministry of Education, Science, Sport, and Culture of Japan
Correspondence to: Wataru Shibata, MD, PhD, Department of Gastroenterology, Graduate School of Medicine, University of Tokyo, 7-3-1 Hongo, Bunkyo-ku, Tokyo 113-8655, Japan. wshibata-tky@umin.ac.jp
Telephone: +81-3-3815-5411-33070 Fax: +81-3-3814-0021
Received: 2005-03-24 Accepted: 2005-04-26

Abstract

AIM: To elucidate the sequential gene expression profile in AGS cells co-cultured with wild-type *Helicobacter pylori* (*H pylori*) as a model of *H pylori*-infected gastric epithelium, and to further examine the contribution of *cag*-pathogenicity islands (*cag*PAI)-coding type IV secretion system and the two pathways, nuclear factor kappa B (NF-κB) and extracellular signal-regulated kinases (ERK) on wild-type *H pylori*-induced gene expression.

METHODS: Gene expression profiles induced by *H pylori* were evaluated in AGS gastric epithelial cells using cDNA microarray, which were present in the 4 600 independent clones picked up from the human gastric tissue. We also analyzed the contribution of NF-κB and ERK signaling on *H pylori*-induced gene expression by using inhibitors of specific signal pathways. The isogenic mutant with disrupted *cag*E (△*cag*E) was used to elucidate the role of *cag*PAI-encoding type IV secretion system in the gene expression profile.

RESULTS: According to the expression profile, the genes were classified into four clusters. Among them, the clusters characterized by continuous upregulation were most conspicuous, and it contained many signal transducer activity-associated genes. The role of *cag*PAI on cultured cells was also investigated using isogenic mutant *cag*E, which carries non-functional *cag*PAI. Then the upregulation of more than 80% of the induced genes (476/566) was found to depend on *cag*PAI. Signal transducer pathway through NF-κB or ERK are the major pathways which are known to be activated by *cag*PAI-positive *H pylori*. The role of these pathways in the whole signal activation by *cag*PAI-positive *H pylori* was analyzed. The specific inhibitors against NF-κB or ERK pathway blocked the activation of gene expression in 65% (367/566) or 76% (429/566) of the genes whose activation appealed to depend on *cag*PAI.

CONCLUSION: These results suggest that more than half of the genes induced by *cag*PAI-positive *H pylori* depend on NF-κB and ERK signaling activation, and these pathways may play a role in the gene expression induced by host-bacterial interaction which may associate with *H pylori*-related gastro-duodenal diseases.

© 2005 The WJG Press and Elsevier Inc. All rights reserved.

Key words: *Helicobacter pylori*; *Cag*-pathogenicity islands; cDNA microarray, Cluster analysis; Signal transduction

Shibata W, Hirata Y, Yoshida H, Otsuka M, Hoshida Y, Ogura K, Maeda S, Ohmae T, Yanai A, Mitsuno Y, Seki N, Kawabe T, Omata M. NF-κB and ERK-signaling pathways contribute to the gene expression induced by *cag* PAI-positive-*Helicobacter pylori* infection. *World J Gastroenterol* 2005; 11(39): 6134-6143
http://www.wjgnet.com/1007-9327/11/6134.asp

INTRODUCTION

Helicobacter pylori (*H pylori*) is the causative agent for various gastro-duodenal diseases[1] and has been classified as a definite carcinogen by the International Agency for Research on Cancer[2]. Previous studies have shown that the eradication of *H pylori* virtually eliminates the recurrence of peptic ulcer diseases, suppresses the recurrence of gastric cancer after mucosal resection, and cures mucosa-associated lymphoid tissue lymphoma[3-10]. The molecular mechanisms underlying these *H pylori*-related diseases have been extensively studied.

The *cag*-pathogenicity island (*cag*PAI), a cluster of about 28 genes, is one of the best known virulence factors; it encodes a type IV secretion system that transports CagA protein, peptidoglycan and possibly other molecules into host epithelial cells[11-16]. Transported CagA binds to molecules such as SH2 domain-containing protein-tyrosine phosphatase-2 (SHP-2), growth factor receptor bound 2 (Grb2), and cortactin[17-19]. Then it induces epithelial disruption as well as cytoskeletal changes[20], which might result in inducing ulcer diseases and gastric cancer[21,22].

The *cag*PAI is also associated with activation of the transcription factors nuclear factor kappa B (NF-κB) and

activator protein-1 (AP-1)[23-26], two key regulators of the expression of various inflammatory genes. NF-κB acts as a transcriptional modulator in the host response to bacterial invasion[27-33]. Its activation may in turn increase inflammation by inducing cytokines similar to the stimulation of interleukin-1 (IL-1) and tumor necrotizing factor-alpha (TNF-α)[34], and induce cell proliferation via activating anti-apoptotic effect[35]. The attachment of *H pylori* to gastric epithelial cells also induces the rapid activation of p38, c-Jun NH2-terminal kinase, and mitogen-activated protein kinase (MAPK)[36]; the downstream effectors of these signals include oncogene c-*fos* and its promoter element serum response element (SRE)[37,38]. These are possibly involved in cellular proliferation and survival[39-41], which might be associated with gastric carcinogenesis.

Some of the host cell responses to infection with *H pylori* induce many gene expressions and appear to function in contradictory directions, such as inflammation and cell proliferation, or apoptosis and anti-apoptosis[35]; the relative importance of each response is thus not immediately obvious. Recently, cDNA microarray analysis has been used to comprehensively characterize the individual responses in host cells[42,43]. The authors and coworkers have previously profiled *H pylori*-induced gene expression *in vitro*[44-51] and *in vivo*[52-54]. However, the contribution of the *cag*PAI-encoding type IV secretion system and the importance of intracellular signaling activation have not been fully elucidated.

In this study, we analyzed sequential gene expression profile in AGS cells co-cultured with wild-type *H pylori* as a model of *H pylori*-infected gastric epithelium. Furthermore, we examined the contribution of *cag*PAI-coding type IV secretion system and the two pathways, NF-κB and extracellular signal-regulated kinases (ERK) on wild-type *H pylori*-induced gene expression.

MATERIALS AND METHODS

Bacterial strains and cell culture

The *H pylori* TN2 strain, which is positive for entire *cag*PAI, and *vacA*, was generously denoted by Dr. M. Nakao (Takeda Chemical Industries, Ltd, Osaka, Japan). The isogenic *cagE* mutant TN2-△*cagE* was prepared by insertion of a kanamycin-resistant gene into the *cagE* gene locus of TN2, as described previously[55]. These strains were cultured on Columbia agar with 50 mL/L horse blood and Dent's selective antibiotic supplement (Oxoid, Basingstoke, UK) at 37 ℃ for 3 d under microaerobic conditions (Campy-Pak Systems; BBL, Cockeysville, MD, USA). The bacterial stocks were stored at -80 ℃ in Brucella broth with 50 mL/L fetal bovine serum (FBS) containing 160 mL/L glycerol. For co-culture experiments, *H pylori* was cultured in Brucella broth containing 7.5% FBS for 24 h, pelleted, resuspended in cell culture medium without FBS, and used to inoculate the host cells at a multiplicity of infection of 50 to 100:1 according to the previous reports[56,57]. At each time point, the AGS cells were collected by scraping, isolated by centrifugation, and stored at -80 ℃ for subsequent isolation of total RNA. Human gastric cancer cells (AGS; ATCC CRL 1739), established from poorly differentiated gastric adenocarcinoma, were maintained in Ham's F12 supplemented with 10% FBS. The medium was replaced with serum-free Ham's F12 at 24 h before the inoculation of the AGS cells with *H pylori*.

Treatment of AGS cells with specific NF-κB and ERK inhibitors

AGS cells were treated with ammonium pyrolidinedithiocarbamate (APDC; 400 μmol/L), which inhibits NF-κB activation, or with the ERK inhibitor PD98059 (25 μmol/L; Calbiochem, San Diego, CA, USA)[58] for 60 min before infection with *H pylori*, as described above. Total RNA was extracted from the AGS cells at 1.5, 3, 6, and 12 h of the co-culture period, as described above.

RNA extraction

Total cellular RNA was extracted using an acid guanidium thiocyanate-phenol-chloroform method, according to the manufacturer's instructions (ISOGEN Reagents; Nippon Gene, Tokyo, Japan), and column chromatography (RNeasy; Qiagen, Tokyo, Japan). The poly(A) mRNA was isolated from the total RNA using the Oligotex-dT30 mRNA purification kit (Takara Shuzo Co., Tokyo, Japan). The integrity of the purified mRNA was confirmed by agarose gel electrophoresis with ethidium bromide staining.

cDNA microarray

A cDNA microarray containing 4 600 cDNAs was made as previously described[44,59-61]. Briefly, human cDNAs were purchased from Research Genetics (Invitrogen Japan K. K., Tokyo, Japan). PCR-amplified cDNA products were mixed with nitrocellulose in dimethyl sulfoxide just before printing and were then spotted onto carbodiimide-coated glass slides using a robotics system (SPBIO-2000, Hitachi Software Engineering, Yokohama, Japan). In this study, we spotted 4 600 sequence-validated cDNAs on the array, including glyceraldehyde-3-phosphate dehydrogenase (GAPDH) and beta-actin to serve as an internal standard and the luciferase gene of *Photinus pyralis* as a negative control.

Sequential changes in gene expression in vitro

For the analysis of the time course of infection-induced gene expression in AGS cells, Cy5-labeled fluorescent cDNAs were prepared from 2 μg mRNA isolated from the infected AGS cells after 1.5, 3, 6, and 12 h of co-culture. The Cy5-labeled sample probes were then applied to the microarray slides for analysis. The Cy3-labeled control probes were similarly prepared from mRNA isolated from uninfected AGS cells. Two independent experiments were performed, and the array data were subject to a simple algorithm (see Data analysis) to set a lower bound threshold and to normalize for unequal incorporation label. Then average ratio was calculated and they were used for the following analysis.

Data analysis

The fluorescence signals from the microarrays were quantified with IMAGENE ver. 4.01 (Biodiscovery, Los Angeles, CA, USA) and analyzed with GENESIGHT LIGHT (Biodiscovery). Briefly, a cDNA spot was included in the analysis only if the raw fluorescence signal intensity was at least 1.5 times that of the local background. The signals were normalized between the arrays using a correction factor calculated from the sum

intensity of all spots. To control the uneven incorporation of the fluorescent dyes, the Cy5 and Cy3 fluorescence intensities for each spot were adjusted so that the mean Cy3:Cy5 ratio was equal to 1.0. We adjusted the raw fluorescence ratios by log transformation, median centering, and normalization to a mean of zero and a variance of one. Changes in expression (Cy3:Cy5 fluorescence ratio) with a factor of 3 or greater in either direction were considered significant, and if the maximum minus minimum values of the log-transformed fluorescence ratios were greater than 1. 0. (Full microarray data are deposited in the Gene Expression Omnibus at NCBI. The platform ID numbers are GPL 1303, and the sample ID numbers are GSM 25915-20). We performed cluster analysis using the average linkage method with uncentered correlation as the distance function by using the Cluster program (ver. 2.11) with TreeView (ver. 1.50) (http://rana.stanford.edu/software)[62]. The Onto-Express program (http://vortex.cs.wayne.edu/Projects.html) was used to perform functional characterization accompanied by the computation of significance values for each functional category, allowing significant biological processes to be distinguished from random events[63-65].

Reverse transcriptase-polymerase chain reaction (RT-PCR)

To validate the results obtained in the microarray experiments, first-strand cDNA was synthesized using 1 μg of total RNA, 1 mmol/L of oligo-dT primer, and reverse transcriptase (Superscript II; Invitrogen, Carlsbad, CA, USA). Each cDNA sample was amplified by PCR using specific primers, as the following, for 10 min at 95 ℃ for initial denaturing, followed by 35-40 cycles of 95 ℃ for 30 s, 52-54 ℃ for 30 s and 72 ℃ for 30 s, yielding products of approximately 300-500 bp. The PCR products were examined, with appropriate molecular size markers, by agarose gel electrophoresis and ethidium bromide staining. The primer pairs used for PCR analysis are listed in Table 1.

RESULTS

Sequential changes in gene expression in AGS cells co-cultured with cagPAI-positive H pylori

We used microarray technology to characterize the time course of changes in gene expression induced by wild-type *H pylori* in AGS cells infected *in vitro* and obtained 3 228 genes that were valid for the analysis. Changes in expression with a factor of 3 or greater in either direction were considered significant. Of the 3 228 genes, about 20% (641 genes) were altered significantly (Figure 1A). The percentage of the significantly altered genes at each time point is shown in Figure 1B. The number of upregulated genes reached their peak at 3 h after infection, while the downregulated genes peaked at 6 h after infection. It implicates that *H pylori*-associated phenomena like inflammatory changes following the induction of IL-8 or *c fos* might occur as the early event *in vitro*. Hierarchical clustering was used to classify the genes into upregulated and downregulated groups (Figure 1C). Each group was further divided into two minor clusters, resulting in a total of four clusters, designated as C-1 to C-4, based on the time course of expression induced by *H pylori*. Genes in both C-1 and C-2 were upregulated during the early phase (1.5-3 h); however, the genes in C-1 were downregulated in the late phase (6-12 h), while those in C-2 remained upregulated. The C-1 cluster contained 764 genes which include *c fos*, DSS1 (DELETED IN SPLIT-HAND/SPLIT-FOOT 1 REGION), NF-κB p65 subunit, Rac1 (Rho family small GTP-binding protein), and MAP2K1 (mitogen-activated protein kinase kinase 1). The C-2 cluster contained 943 genes which include Interleukin-8, NFKBIA (factor of kappa light polypeptide gene enhancer in B-cells inhibitor, alpha), VCL (vincullin), DUSP1 (dual specificity phosphatase 1), and NDRG1 (N-myc downstream regulated gene 1). The sequential changes in the expression of 2 of C-1 genes and 4 of C-2 genes were confirmed by RT-PCR (Figure 1D). In contrast, the expression of the genes in clusters C-3 (950 genes) showed downregulation at early-phase of infection, and C-4 (651 genes) were downregulated at late phase of infection. At late phase of infection, other functional events were modulated by response to these early events. We next performed to characterize the clusters to identify their function.

Gene expression profile and annotated function

The functional profiles of the *H pylori*-induced changes in gene expression *in vitro* are shown in Table 2. The Onto-Express program was used for functional profiling as described in Materials and Methods, using hypergeometric distribution to determine the significance of differences ($n \geqslant 5$, $P<0.05$). This result indicated that the transiently upregulated C-1 cluster included genes that participate in transcription regulator activity, such as Smad4, *c fos*, and RelA, and others involved in chaperon activity, such as DNAJB1 (DnaJ (Hsp40) homolog, subfamily B, member 1) and CD74 antigen (invariant polypeptide of major histocompatibility complex, class II antigen-associated), more frequently than did the other clusters. The C-2 cluster, the members of which were upregulated during both the early and late phases,

Table 1 Primer sequences for RT-PCR

Genes	Forward	Reverse
IL-8	5′-GCT TTC TGA TGG AAG AGA GC-3′	5′-GGC ACA GTG GAA CAA GGA CT-3′
c-fos	5′-GTC AAG AGC ATC AGC AGCA T-3′	5′-TCG GGG TAG GTG AAG ACG AA-3′
HNRPDL	5′-GTT TCA GAG GAC CTG GAA TA-3′	5′-TCA CTA CCC TAG ACA CCG CA3′
Vinculin	5′-CAA GTG TGA CCG AGT GGA CC-3′	5′-TTG GTA TCA ATG GCT TCG TC-3′
DSS1	5′-CAA GTC TCT ATG GTA GCG TCA GC-3′	5′-ACC ATG TTT CTC TAG TTC AG-3′
NDRG1	5′-GGC GCG ACC TGG AGA TGAG-3′	5′-CTA GCA GGA GAC CTC CAT GG-3′
EMK-1	5′-GAG ATG GAG GTG TGC AAA CT-3′	5′-TGG TTT AGG CGA AAT ACT CT-3′
GAPDH	5′-ACC ACA GTC CAT GCC ATC AC-3′	5′-TCC ACC ACC CTG TTG CTG TA-3′

contained genes related to signal transduction activity, such as TNF receptor-associated factor 4, and those related to structural molecular activity, such as VCL and ARPS2. The genes in the C-3 and C-4 clusters were downregulated by *H pylori*. The C-3 cluster contained genes related to antioxidant activity, such as TXNRD1 (thioredoxin reductase 1) and GPX (glutathione peroxidase) 1/2, and the C-4 cluster contained genes encoding lyase activity, such as GLO1 and

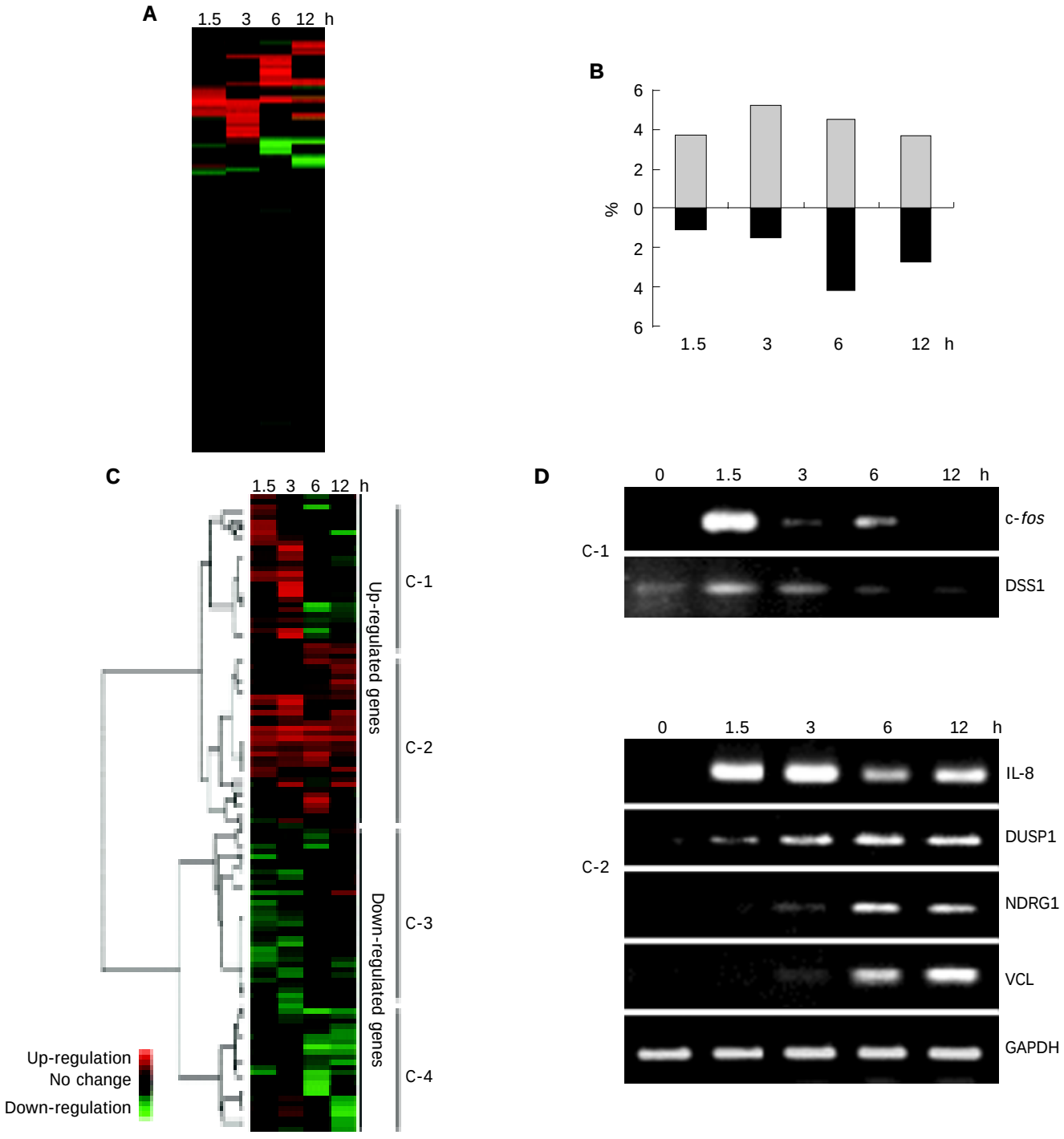


Figure 1 A: Schematic representation of the genes affected by wild-type *H pylori*-infection during 12 h in AGS cells. Red or green indicates up- or downregulation, respectively. About 20% of all the analyzed genes were significantly altered during infection experiments *in vitro*. Changes in expression with a factor of 3 or greater in either direction were considered significant; B: The percentage of the altered genes at each time point. The upregulated genes reached maximum number at 3 h after wild-type *H pylori*-infection, but the downregulated genes peaked at 6 h after infection; C: Cluster diagram of gene expression in AGS cells. The rows correspond to 3 228 genes for which the level of expression in AGS was changed by infection with wild-type *H pylori*, and the columns represent the various time points (1.5, 3, 6, and 12 h after wild-type *H pylori*-infection from left to right, respectively). Red or green indicates up- or downregulation, respectively, compared with the expression level in uninfected AGS cells. The dendrogram on the left and the horizontal distances between the nodes represent the statistical similarities between the neighboring genes and clusters. The genes were divided into two large clusters, comprising upregulated or downregulated genes. Each of the large clusters contained two smaller clusters, resulting in four clusters (C-1 to C-4; see Results for description); D: Validation of the microarray results by RT-PCR. Total RNAs from wild-type *H pylori*-infected AGS cells were isolated at the indicated times and subjected to reverse transcription and PCR with specific primers. The bands of the size corresponding to the expected length of the amplified fragment for each specific transcript were analyzed by agarose gel electrophoresis, along with GAPDH as a loading control.

Table 2 The functional profiles of the *H pylori*-induced changes in gene expression *in vitro*. Cluster represents the assigned cluster numbers in Figure 1C. Functions were defined by using the Onto-Express program, using hypergeometric distribution to determine the significance of differences ($n \geqslant 5$, $P<0.05$, see Materials and methods)

Cluster	Function	No. of the genes (total)	*P*
C-1	Chaperon activity	12 (31)	0.019
	Transcription regulator activity	29 (92)	0.033
C-2	Apoptosis regulator activity	7 (9)	<0.01
	Cell adhesion molecule activity	18 (39)	<0.01
	Signal transducer activity	47 (132)	0.034
	Transcription regulator activity	9 (20)	0.037
	Structural molecular activity	40 (113)	0.049
C-3	Antioxidant activity	6 (8)	<0.01
C-4	Lyase activity	8 (10)	0.011
	Chaperon activity	10 (31)	0.037

ENO1, and chaperone proteins. The genes undergoing most striking upregulation during *H pylori* infection *in vitro* are listed in Table 3.

Contribution of cagPAI-coding type IV secretion system in host gene expression

The contribution of *cag*PAI-coding type IV secretion system in host gene expression was examined by comparing the pattern of expression induced by the wild-type *H pylori vs* the isogenic *cag*E mutant strain. We tried to compare the gene expression profile 3 h post-infection when the number of the upregulated genes were most frequent, and when interleukin-8 (IL-8) which is the gene induced by the functional type IV secretion system was upregulated. Five hundred and sixty-six genes on the microarray were upregulated at least threefold by the wild-type *H pylori* infection 3 h post-infection. Four hundred and seventy-six out of five hundred and sixty-six genes (86%) required *cag*PAI-coding type IV secretion system for their upregulation, whereas only 90 out of 566 genes (14%) were upregulated without functional type IV secretion system (Figure 2A). For example, IL-8, RelA, VCL, and Rac1 were upregulated 3- to 15-fold by infection with the wild-type *H pylori*, while the *cagE* mutant induced only one to threefold increases from the control level. On the other hand, some signal transduction-associated genes were significantly upregulated by the *cag*E mutant infection such as STC2, HKR3, and LZTR1. These genes might be induced by the *cag*-independent virulence factor.

Contribution of NF-κB and ERK pathways in H pylori-induced gene expression

It has been reported that wild-type *H pylori* activates NF-κB and ERK pathways; however, the contribution of these signaling pathways on gene expression profiles has not been investigated. Our analysis of the sequential changes in the gene expression profile revealed that signal transducer activity-associated genes show the continuous expression infected with wild-type *H pylori*. We thus analyzed the contribution of NF-κB and ERK signaling on *H pylori*-induced gene expression by using specific inhibitors as previously described[23,36]. As a control sample, we used AGS cells without adding inhibitor reagents because it could avoid the downregulation of the gene expression of nontreated AGS cells by the inhibitors. Among the 566 genes upregulated by wild-type *H pylori*, the expression of 367 genes (65%) was suppressed by pre-incubation with APDC, an inhibitor of NF-κB (Figure 2B).

Table 3 Genes undergoing most striking upregulation during *H pylori*-infection *in vitro*. Values show the mean change in gene expression from two separate microarray experiments *in vitro* (shown at "1.5, 3, 6, and 12 h"). Significantly upregulated values are shown in bold (above threefold)

Acc. Number	Gene Symbol	Name	Function	1.5 h	3 h	6 h	12 h
U79243	LZTR1	Leucine-zipper-like transcriptional regulator 1	Transcription	5.08	3.08	0.95	2.30
X61118	LMO2	LIM domain only 2 (rhombotin-like 1)	Tumor associated	2.53	16.24	0.28	1.04
BC004247	RAC1	Ras-related C3 botulinum toxin substrate 1 (rho family small GTP binding protein Rac1)	Adhesion/cytoskeleton	1.13	4.78	0.89	1.29
AF005043	PARG	Poly (ADP-ribose) glycohydrolase	Metabolism	0.58	0.62	14.72	0.53
U86782	POH1	26S proteasome-associated pad1 homolog	RNA/Protein processing	2.55	3.59	7.24	3.56
M62839	APOH	Apolipoprotein H (beta-2-glycoprotein I)	Immunity	0.49	3.49	0.65	1.47
BC004980	SLC25A1	Solute carrier family 25 (mitochondrial carrier; citrate transporter) member 1	Metabolism	4.07	0.81	0.95	1.54
Z26649	PLCB3	Phospholipase C beta 3 (phosphatidylinositol-specific)	Tumor associated	2.49	3.32	0.75	2.52
M62399	RELA	V-rel reticuloendotheliosis viral oncogene homolog A nuclear factor of kappa light polypeptide gene enhancer in B-cells 3 p65 (avian)	Apoptosis	2.84	3.24	1.43	1.13
BC000665	TCP1	T-complex 1	RNA/Protein processing	1.73	3.21	1.05	1.41
V01512	c-fos	V01512|HSCFOS Human cellular oncogene c-fos (complete sequence).	Tumor associated	37.81	2.48	0.57	0.91
BC000117	GMDS	GDP-mannose 46-dehydratase	Metabolism	2.63	4.37	2.28	3.75
L29218	CLK2	CDC-like kinase 2	Growth/maintenance	1.46	4.03	1.96	0.60
BC000771	NTRK1	Neurotrophic tyrosine kinase receptor type 1	Tumor associated	3.33	3.47	1.42	3.59
X68836	MAT2A	Methionine adenosyltransferase II alpha	Metabolism	3.14	2.95	0.85	1.28
X94232	MAPRE2	Microtubule-associated protein RP/EB family member 2	Growth/maintenance	0.58	3.23	0.69	0.29
X80200	TRAF4	TNF receptor-associated factor 4	Signal transduction	3.20	3.02	3.67	1.08
D76444	ZFP103	Zinc finger protein 103 homolog (mouse)	Growth/maintenance	1.38	2.63	3.99	1.78

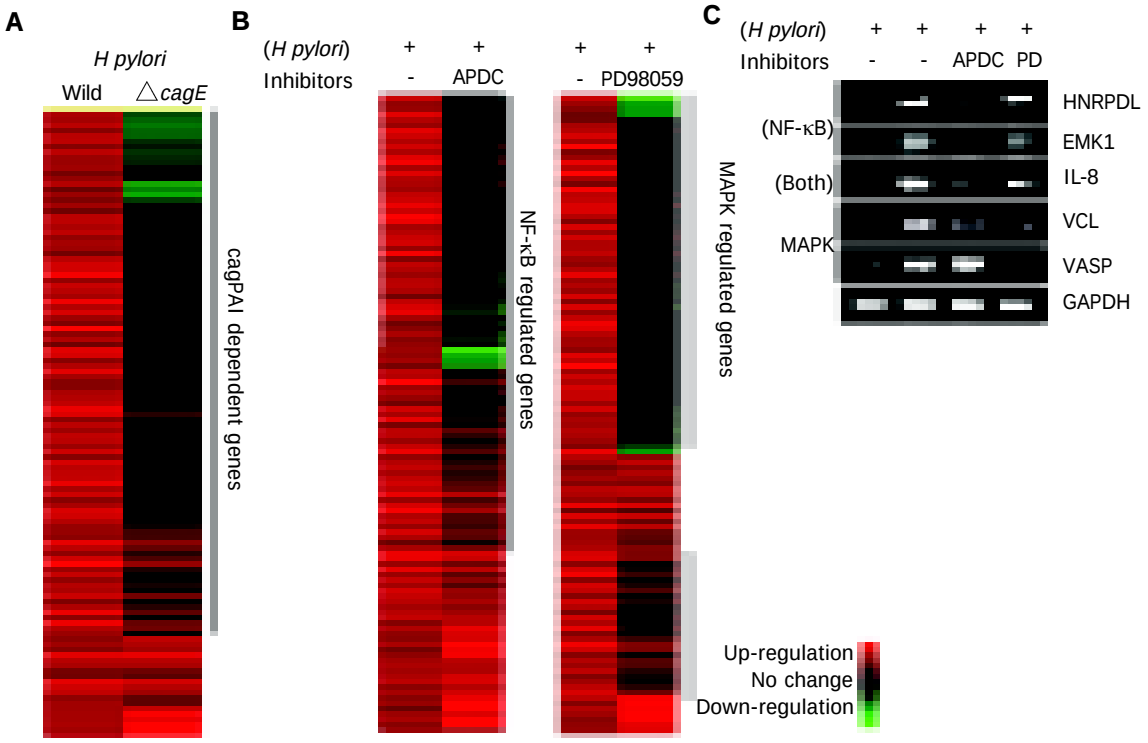


Figure 2 A: The contribution of the *cag*PAI-coded type IV secretion system to the gene expression profile in AGS cells. Hierarchical clustering of genes induced by *H pylori* with or without a functional type IV secretion system (wild type or *cag*E mutant, respectively). Left lane; gene expression profile of AGS cells co-cultured with wild-type *H pylori* relative to control. Right lane; gene expression profile of AGS cells co-cultured with the isogenic mutant *cag*E. Only the 566 significantly upregulated genes at 3 h are shown. About 84% of the genes were induced only by the wild-type *H pylori* infection. These genes were supposed to be induced by the presence of *cag*PAI-coded type IV secretion system. B: The contribution of NF-κB or ERK pathways to the gene expression profile. Inhibitors specific for NF-κB or ERK were added to AGS cells co-cultured with *H pylori*. The gene expression profiles in the presence or absence of the inhibitors were compared. C: The changes in the expression of some representative genes were confirmed by RT-PCR. All genes were induced by wild-type *H pylori* infection, and suppressed by the incubation with inhibitors of specific signal pathways.

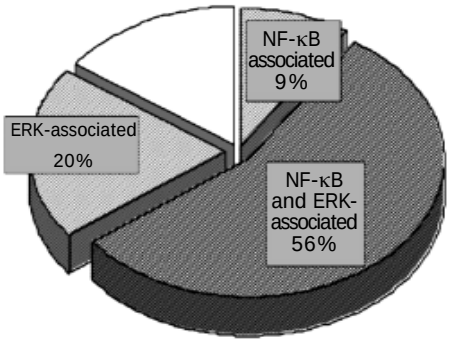


Figure 3 Schematic representation of the distribution of genes affected by wild-type *H pylori* infection. The complete upregulated genes at 3 h after infection is represented by the circle as a whole. The expression of 367 genes (65%) of the 566 genes upregulated by wild type *H pylori* was suppressed by pre-incubation with APDC, an inhibitor of NF-κB. On the other hand, pre-incubation with PD98059, an inhibitor of ERK, suppressed the expression of 429 genes (76%) of the 566 genes upregulated by wild type *H pylori*. Expression of 475 of the 566 genes (84%) was induced under NF-κB and/or ERK signaling activation, whereas changes in the remaining 16% are NF-κB or ERK signaling independent.

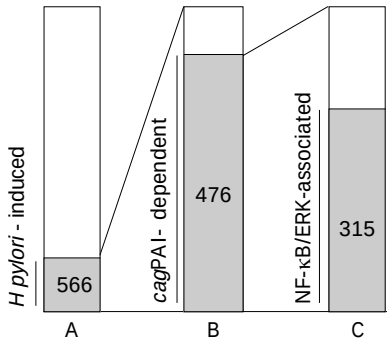


Figure 4 Characterization of the upregulated genes co-cultured with *H pylori* for 3 h (n = 566). A: The bar represents the number of 566 upregulated genes among 3 228 analyzed genes (566 genes). B: The genes induced by *cag*PAI-positive *H pylori* infection among the 566-*H pylori*-induced genes (476 genes). C: The contribution of NF-κB or ERK signaling pathway among the *cag*PAI-dependent gene expression. Among the 476-*cag*PAI-dependent genes, 66% (315 genes) were also involved in the NF-κB- and/or ERK-signaling activation, whereas 34% (161 genes) of 476 genes were dependent on *cag*PAI but not involved in either NF-κB or ERK signaling activation.

The suppressed genes included IL-8, NFKB1A, HNRPDL (heterogeneous nuclear ribonucleoprotein D-like protein) and EMK1 (ELKL motif kinase). On the other hand, pre-incubation with PD98059, an inhibitor of ERK, suppressed the expression of 429 genes (76%). The effects of the inhibitors on several genes were confirmed by RT-PCR (Figure 2C). Among the 566 upregulated genes, 315 genes (56%) were upregulated under NF-κB and ERK signaling activation, and 481 genes (85%) were upregulated under NF-κB and/or ERK signaling activation (Figure 3). HNRPDL was induced at 3.5-fold by wild-type *H pylori* infection, 1.2-fold with APDC, and 2.2-fold with PD98059, and the same

suppression was confirmed by RT-PCR.

It was reported that the activation of NF-κB and ERK by *H pylori* is dependent on the presence of *cag*PAI. Thus, we compared the gene expression profiles under the presence or absence of *cag*PAI-coding type IV secretion system, and we analyzed the contribution of NF-κB or ERK on their gene expression (Figure 4). About 66% (315 genes) of the 476 upregulated genes were induced under NF-κB and/or ERK activation, while 34% (161 genes) of the 476 upregulated genes were dependent on *cag*PAI but not on either NF-κB or ERK.

DISCUSSION

H pylori is now recognized as a definite exogenous carcinogen; hence intensive research effort is currently devoted to investigations of the molecular mechanism of *H pylori*-related gastric pathogenesis. In particular, recent reports have shown the importance of *cag*PAI as a potent bacterial virulence factor and the activation of NF-κB and MAPK signaling as the corresponding host responses[23,36]. However, the relative importance of these factors in gastric pathogenesis among all the events that are raised under *H pylori* infection has not been well established. In the present study, we showed that the genes upregulated by wild-type *H pylori* infection were mostly induced under the presence of *cag*PAI-coding type IV secretion system and that the expression of these genes mostly occurred via NF-κB and/or ERK activation *in vitro*.

Firstly, we analyzed the sequential gene expression changes in cultured cells. The experiments *in vitro* are supposed to simulate the environment in the acute phase of infection and cannot necessarily represent the conditions *in vivo* of chronic infection in which atrophic gastritis and/or gastric cancer actually develops. Therefore we analyzed the sequential changes of gene expression *in vitro* to seek the time-dependent characters of gene function. The genes in the C-1 cluster, which were upregulated during the early phase of infection, included interesting genes which might affect the pathogenesis of *H pylori* infection. *c fos* and DSS1 were included in this cluster. The expression of *c fos* is regulated by ERK (MAPK) signaling and *H pylori* activates the proto-oncogene *c fos* through SRE transactivation[38,66]. DSS1 has not previously been reported to be associated with *H pylori* infection. It has been shown to directly interact with BRCA2 and may play a role in the completion of the cell cycle[67]. The genes in C-2, which were persistently upregulated *in vitro*, contained the genes associated with intracellular signal transduction or cytoskeletal change, including Rho-family GTPases *rac1* and *cdc42*. The activation of them are known to be dependent on *cag*PAI[68]; Rac1 in turn regulates the vacuolation caused by the *vacA* virulence factor of *H pylori*[69]. NDRG1 was upregulated during the late phase of infection as shown in Figure 1D; the protein encoded by this gene is a cytoplasmic protein involved in stress responses, hormone responses, cell growth, and differentiation[70].

We show here that the upregulation of a large part of the genes depends on the presence of functional type IV secretion system. *Cag*PAI codes a type IV secretion system which transports CagA inside the host cells[11-15]; the transported CagA activates SRE[37]. Guilemin *et al*., reported that *cag*A gene, which encodes an effector molecule secreted by the type IV secretion system, induced the expression of many of the cytoskeletal genes. Recently, it has been reported that one of the effectors for NF-κB activation is peptidoglycan[16], and CagA is probably not involved[37,71,72]. In addition, *cag*E, which codes a structural component of the type IV secretion system, is required for the expression of many immune responsive genes. These results suggest that several distinct molecules are involved in *cag*PAI-dependent upregulation. Moreover, the interaction of some molecules of the secretion system with the molecules of the host cell might directly activate some intracellular signaling cascades.

The microarray analysis is useful to identify the downstream genes in the specific intracellular signaling pathway because it could detect a large number of the gene expression at a time. Then we analyzed the alteration of the gene expression by the inhibitor reagents against the signaling molecules to identify the genes which are induced through NF-κB or ERK signaling pathway. In this study, we have shown that the majority of the *H pylori*-induced gene were upregulated under NF-κB and/or ERK activation[23,36] NF-κB activation *in vivo* is associated with gastric inflammation via the production of cytokines, IL-8[24] and is associated with cell survival induced by c-IAP-2 mediated anti-apoptosis[35]. Among the genes affected by NF-κB activation, HNRPDL and EMK1 were identified in the current microarray analysis and were confirmed by RT-PCR to be suppressed by NF-κB inhibition. HNRPDL is reported to be a member of the family of heterogeneous nuclear ribonucleoproteins (hnRNPs) that function in mRNA biogenesis and mRNA metabolism[73]. EMK (ELKL motif kinase) belongs to a small family of serine/threonine protein kinases involved in the control of cell polarity, microtubule stability, and cancer[74].

ERK signaling is activated by *H pylori* infection and leads to the expression of some oncogenes, such as *c fos* and cyclin-D1[75,76]. The upregulated genes under ERK-signaling activation included VCL and VASP, which are involved in integrin-mediated cell adhesion. Jawhari *et al*., reported that E-cadherin contributes to the development and progression of the neoplastic phenotype in gastric carcinoma[77]. Kuroda *et al*., reported that the activation of Rho-Ras signaling induces the dissociation of cell-cell adhesion and it is associated with the cell migration and metastasis of carcinoma cells[78]. Recently, Cottet *et al*., identified that *H pylori*-induced Rho-Ras signaling proteins[79].

In conclusion, we characterized the gene expression induced by *H pylori* using cDNA microarray, and we determined the contribution of *cag*PAI-coding type IV secretion system and NF-κB/ERK signaling pathways on the most part of the gene expression induced by *H pylori*. In the future, we should elucidate how the NF-κB and/or ERK contribute to the development of gastric inflammation *in vivo* and characterize the gastric mucosal gene expression in human beings which may help us to understand the gastric pathogenesis induced by *H pylori* infection.

ACKNOWLEDGMENTS

We thank Mitsuko Tsubouchi for her excellent technical assistance.

REFERENCES

1 **Marshall BJ**, Warren JR. Unidentified curved bacilli in the stomach of patients with gastritis and peptic ulceration. *Lancet* 1984; **1**: 1311-1315
2 Schistosomes, liver flukes and *Helicobacter pylori*. IARC Working Group on the Evaluation of Carcinogenic Risks to Humans. Lyon, 7-14 June 1994. *IARC Monogr Eval Carcinog Risks Hum* 1994; **61**: 1-241
3 **Parsonnet J**, Friedman GD, Vandersteen DP, Chang Y, Vogelman JH, Orentreich N, Sibley RK. *Helicobacter pylori* infection and the risk of gastric carcinoma. *N Engl J Med* 1991; **325**: 1127-1131
4 **Nomura A**, Stemmermann GN, Chyou PH, Kato I, Perez-Perez GI, Blaser MJ. *Helicobacter pylori* infection and gastric carcinoma among Japanese Americans in Hawaii. *N Engl J Med* 1991; **325**: 1132-1136
5 **Graham DY**, Lew GM, Klein PD, Evans DG, Evans DJ Jr, Saeed ZA, Malaty HM. Effect of treatment of *Helicobacter pylori* infection on the long-term recurrence of gastric or duodenal ulcer. A randomized, controlled study. *Ann Intern Med* 1992; **116**: 705-708
6 **Wotherspoon AC**, Doglioni C, Diss TC, Pan L, Moschini A, de Boni M, Isaacson PG. Regression of primary low-grade B-cell gastric lymphoma of mucosa-associated lymphoid tissue type after eradication of *Helicobacter pylori*. *Lancet* 1993; **342**: 575-577
7 **Forbes GM**, Glaser ME, Cullen DJ, Warren JR, Christiansen KJ, Marshall BJ, Collins BJ. Duodenal ulcer treated with *Helicobacter pylori* eradication: seven-year follow-up. *Lancet* 1994; **343**: 258-260
8 **Sung JJ**, Lin SR, Ching JY, Zhou LY, To KF, Wang RT, Leung WK, Ng EK, Lau JY, Lee YT, Yeung CK, Chao W, Chung SC. Atrophy and intestinal metaplasia one year after cure of *H pylori* infection: a prospective, randomized study. *Gastroenterology* 2000; **119**: 7-14
9 **Uemura N**, Okamoto S, Yamamoto S, Matsumura N, Yamaguchi S, Yamakido M, Taniyama K, Sasaki N, Schlemper RJ. *Helicobacter pylori* infection and the development of gastric cancer. *N Engl J Med* 2001; **345**: 784-789
10 **Peek RM Jr**, Blaser MJ. *Helicobacter pylori* and gastrointestinal tract adenocarcinomas. *Nat Rev Cancer* 2002; **2**: 28-37
11 **Backert S**, Ziska E, Brinkmann V, Zimny-Arndt U, Fauconnier A, Jungblut PR, Naumann M, Meyer TF. Translocation of the *Helicobacter pylori* CagA protein in gastric epithelial cells by a type IV secretion apparatus. *Cell Microbiol* 2000; **2**: 155-164
12 **Odenbreit S**, Puls J, Sedlmaier B, Gerland E, Fischer W, Haas R. Translocation of *Helicobacter pylori* CagA into gastric epithelial cells by type IV secretion. *Science* 2000; **287**: 1497-1500
13 **Segal ED**, Cha J, Lo J, Falkow S, Tompkins LS. Altered states: involvement of phosphorylated CagA in the induction of host cellular growth changes by *Helicobacter pylori*. *Proc Natl Acad Sci USA* 1999; **96**: 14559-14564
14 **Stein M**, Rappuoli R, Covacci A. Tyrosine phosphorylation of the *Helicobacter pylori* CagA antigen after cag-driven host cell translocation. *Proc Natl Acad Sci USA* 2000; **97**: 1263-1268
15 **Asahi M**, Azuma T, Ito S, Ito Y, Suto H, Nagai Y, Tsubokawa M, Tohyama Y, Maeda S, Omata M, Suzuki T, Sasakawa C. *Helicobacter pylori* CagA protein can be tyrosine phosphorylated in gastric epithelial cells. *J Exp Med* 2000; **191**: 593-602
16 **Viala J**, Chaput C, Boneca IG, Cardona A, Girardin SE, Moran AP, Athman R, Memet S, Huerre MR, Coyle AJ, DiStefano PS, Sansonetti PJ, Labigne A, Bertin J, Philpott DJ, Ferrero RL. Nod1 responds to peptidoglycan delivered by the *Helicobacter pylori* cag pathogenicity island. *Nat Immunol* 2004; **5**: 1166-1174
17 **Mimuro H**, Suzuki T, Tanaka J, Asahi M, Haas R, Sasakawa C. Grb2 is a key mediator of *helicobacter pylori* CagA protein activities. *Molecular Cell* 2002; **10**: 745-755
18 **Higashi H**, Tsutsumi R, Muto S, Sugiyama T, Azuma T, Asaka M, Hatakeyama M. SHP-2 tyrosine phosphatase as an intracellular target of *Helicobacter pylori* CagA protein. *Science* 2002; **295**: 683-686
19 **Churin Y**, Al-Ghoul L, Kepp O, Meyer TF, Birchmeier W, Naumann M. *Helicobacter pylori* CagA protein targets the c-Met receptor and enhances the motogenic response. *J Cell Biol* 2003; **161**: 249-255
20 **Amieva MR**, Vogelmann R, Covacci A, Tompkins LS, Nelson WJ, Falkow S. Disruption of the epithelial apical-junctional complex by *Helicobacter pylori* CagA. *Science* 2003; **300**: 1430-1434
21 **Peek RM Jr**, Moss SF, Tham KT, Perez-Perez GI, Wang S, Miller GG, Atherton JC, Holt PR, Blaser MJ. *Helicobacter pylori* cagA+strains and dissociation of gastric epithelial cell proliferation from apoptosis. *J Natl Cancer Inst* 1997; **89**: 863-868
22 **Argent RH**, Kidd M, Owen RJ, Thomas RJ, Limb MC, Atherton JC. Determinants and consequences of different levels of CagA phosphorylation for clinical isolates of *Helicobacter pylori*. *Gastroenterology* 2004; **127**: 514-523
23 **Keates S**, Hitti YS, Upton M, Kelly CP. *Helicobacter pylori* infection activates NF-kappa B in gastric epithelial cells. *Gastroenterology* 1997; **113**: 1099-1109
24 **Sharma SA**, Tummuru MK, Blaser MJ, Kerr LD. Activation of IL-8 gene expression by *Helicobacter pylori* is regulated by transcription factor nuclear factor-kappa B in gastric epithelial cells. *J Immunol* 1998; **160**: 2401-2407
25 **Aihara M**, Tsuchimoto D, Takizawa H, Azuma A, Wakebe H, Ohmoto Y, Imagawa K, Kikuchi M, Mukaida N, Matsushima K. Mechanisms involved in *Helicobacter pylori*-induced interleukin-8 production by a gastric cancer cell line, MKN45. *Infect Immun* 1997; **65**: 3218-3224
26 **Meyer-ter-Vehn T**, Covacci A, Kist M, Pahl HL. *Helicobacter pylori* activates mitogen-activated protein kinase cascades and induces expression of the proto-oncogenes c-fos and c-jun. *J Biol Chem* 2000; **275**: 16064-16072
27 **Barnes PJ**, Karin M. Nuclear factor-kappaB: a pivotal transcription factor in chronic inflammatory diseases. *N Engl J Med* 1997; **336**: 1066-1071
28 **Baeuerle PA**. IkappaB-NF-kappaB structures: at the interface of inflammation control. *Cell* 1998; **95**: 729-731
29 **Ghosh S**, May MJ, Kopp EB. NF-kappa B and Rel proteins: evolutionarily conserved mediators of immune responses. *Annu Rev Immunol* 1998; **16**: 225-260
30 **Sha WC**. Regulation of immune responses by NF-kappa B/Rel transcription factor. *J Exp Med* 1998; **187**: 143-146
31 **Neurath MF**, Becker C, Barbulescu K. Role of NF-kappaB in immune and inflammatory responses in the gut. *Gut* 1998; **43**: 856-860
32 **Munzenmaier A**, Lange C, Glocker E, Covacci A, Moran A, Bereswill S, Baeuerle PA, Kist M, Pahl HL. A secreted/shed product of *Helicobacter pylori* activates transcription factor nuclear factor-kappa B. *J Immunol* 1997; **159**: 6140-6147
33 **Eckmann L**, Smith JR, Housley MP, Dwinell MB, Kagnoff MF. Analysis by high density cDNA arrays of altered gene expression in human intestinal epithelial cells in response to infection with the invasive enteric bacteria Salmonella. *J Biol Chem* 2000; **275**: 14084-14094
34 **Noach LA**, Bosma NB, Jansen J, Hoek FJ, van Deventer SJ, Tytgat GN. Mucosal tumor necrosis factor-alpha, interleukin-1 beta, and interleukin-8 production in patients with *Helicobacter pylori* infection. *Scand J Gastroenterol* 1994; **29**: 425-429
35 **Yanai A**, Hirata Y, Mitsuno Y, Maeda S, Shibata W, Akanuma M, Yoshida H, Kawabe T, Omata M. *Helicobacter pylori* induces antiapoptosis through buclear factor-kappaB activation. *J Infect Dis* 2003; **188**: 1741-1751
36 **Keates S**, Keates AC, Warny M, Peek RM Jr, Murray PG, Kelly CP. Differential activation of mitogen-activated protein kinases in AGS gastric epithelial cells by cag+ and cag- *Helicobacter pylori*. *J Immunol* 1998; **66**: 5552-5559

37 **Hirata Y**, Maeda S, Mitsuno Y, Tateishi K, Yanai A, Akanuma M, Yoshida H, Kawabe T, Shiratori Y, Omata M. *Helicobacter pylori* CagA protein activates serum response element-driven transcription independently of tyrosine phosphorylation. *Gastroenterology* 2002; **123**: 1962-1971

38 **Mitsuno Y**, Maeda S, Yoshida H, Hirata Y, Ogura K, Akanuma M, Kawabe T, Shiratori Y, Omata M. *Helicobacter pylori* activates the proto-oncogene c-fos through SRE transactivation. *Biochem Biophys Res Commun* 2002; **291**: 868-874

39 **Han J**, Lee JD, Bibbs L, Ulevitch RJ. A MAP kinase targeted by endotoxin and hyperosmolarity in mammalian cells. *Science* 1994; **265**: 808-811

40 **Kyriakis JM**, Banerjee P, Nikolakaki E, Dai T, Rubie EA, Ahmad MF, Avruch J, Woodgett JR. The stress-activated protein kinase subfamily of c-Jun kinases. *Nature* 1994; **369**: 156-160

41 **Lee JC**, Laydon JT, McDonnell PC, Gallagher TF, Kumar S, Green D, McNulty D, Blumenthal MJ, Heys JR, Landvatter SW. A protein kinase involved in the regulation of inflammatory cytokine biosynthesis. *Nature* 1994; **372**: 739-746

42 **Schena M**, Shalon D, Davis RW, Brown PO. Quantitative monitoring of gene expression patterns with a complementary DNA microarray. *Science* 1995; **270**: 467-470

43 **Schena M**, Shalon D, Heller R, Chai A, Brown PO, Davis RW. Parallel human genome analysis: microarray-based expression monitoring of 1000 genes. *Proc Natl Acad Sci USA* 1996; **93**: 10614-10619

44 **Maeda S**, Otsuka M, Hirata Y, Mitsuno Y, Yoshida H, Shiratori Y, Masuho Y, Muramatsu M, Seki N, Omata M. cDNA microarray analysis of *Helicobacter pylori*-mediated alteration of gene expression in gastric cancer cells. *Biochem Biophys Res Commun* 2001; **284**: 443-449

45 **Cox JM**, Clayton CL, Tomita T, Wallace DM, Robinson PA, Crabtree JE. cDNA array analysis of cag pathogenicity island-associated *Helicobacter pylori* epithelial cell response genes. *Infect Immun* 2001; **69**: 6970-6980

46 **Guillemin K**, Salama NR, Tompkins LS, Falkow S. Cag pathogenicity island-specific responses of gastric epithelial cells to *Helicobacter pylori* infection. *Proc Natl Acad Sci USA* 2002; **99**: 15136-15141

47 **Bach S,** Makristathis A, Rotter M, Hirschl AM. Gene expression profiling in AGS cells stimulated with *Helicobacter pylori* isogenic strains (cagA positive or cagA negative). *Infect Immun* 2002; **70**: 988-992

48 **Lim JW**, Kim H, Kim KH. Cell adhesion-related gene expression by *Helicobacter pylori* in gastric epithelial AGS cells. *Int J Biochem Cell Biol* 2003; **35**: 1284-1296

49 **Sepulveda AR**, Tao H, Carloni E, Sepulveda J, Graham DY, Peterson LE. Screening of gene expression profiles in gastric epithelial cells induced by *Helicobacter pylori* using microarray analysis. *Aliment Pharmacol Ther* 2002; **16**(Suppl 2): 145-157

50 **Wang HT**, Li ZH, Yuan JP, Zhao W, Shi XD, Tong SQ, Guo XK. Effect of *Helicobacter pylori* VacA on gene expression of gastric cancer cells. *World J Gastroenterol* 2004; **10**: 109-113

51 **Yuan JP**, Li T, Li ZH, Yang GZ, Hu BY, Shi XD, Shi TL, Tong SQ, Guo XK. mRNA expression profiling reveals a role of *Helicobacter pylori* vacuolating toxin in escaping host defense. *World J Gastroenterol* 2004; **10**: 1528-1532

52 **Wen S**, Felley CP, Bouzourene H, Reimers M, Michetti P, Pan-Hammarstrom Q. Inflammatory gene profiles in gastric mucosa during *Helicobacter pylori* infection in humans. *J Immunol* 2004; **172**: 2595-2606

53 **Mills JC**, Syder AJ, Hong CV, Guruge JL, Raaii F, Gordon JI. A molecular profile of the mouse gastric parietal cell with and without exposure to *Helicobacter pylori*. *Proc Natl Acad Sci USA* 2001; **98**: 13687-13692

54 **Mueller A**, O'Rourke J, Grimm J, Guillemin K, Dixon MF, Lee A, Falkow S. Distinct gene expression profiles characterize the histopathological stages of disease in Helicobacter-induced mucosa-associated lymphoid tissue lymphoma. *Proc Natl Acad Sci USA* 2003; **100**: 1292-1297

55 **Ogura K**, Maeda S, Nakao M, Watanabe T, Tada M, Kyutoku T, Yoshida H, Shiratori Y, Omata M. Virulence factors of *Helicobacter pylori* responsible for gastric diseases in Mongolian gerbil. *J Exp Med* 2000; **192**: 1601-1610

56 **Maeda S**, Yoshida H, Ogura K, Mitsuno Y, Hirata Y, Yamaji Y, Akanuma M, Shiratori Y, Omata M. *H pylori* activates NF-kappaB through a signaling pathway involving IkappaB kinases, NF-kappaB-inducing kinase, TRAF2, and TRAF6 in gastric cancer cells. *Gastroenterology* 2000; **119**: 97-108

57 **Maeda S**, Akanuma M, Mitsuno Y, Hirata Y, Ogura K, Yoshida H, Shiratori Y, Omata M. Distinct mechanism of *Helicobacter pylori*-mediated NF-kappa B activation between gastric cancer cells and monocytic cells. *J Biol Chem* 2001; **276**: 44856-44864

58 **Dudley DT**, Pang L, Decker SJ, Bridges AJ, Saltiel AR. A synthetic inhibitor of the mitogen-activated protein kinase cascade. *Proc Natl Acad Sci USA* 1995; **92**: 7686-7689

59 **Otsuka M**, Kato M, Yoshikawa T, Chen H, Brown EJ, Masuho Y, Omata M, Seki N. Differential expression of the L-plastin gene in human colorectal cancer progression and metastasis. *Biochem Biophys Res Commun* 2001; **289**: 876-881

60 **Otsuka M**, Aizaki H, Kato N, Suzuki T, Miyamura T, Omata M, Seki N. Differential cellular gene expression induced by hepatitis B and C viruses. *Biochem Biophys Res Commun* 2003; **300**: 443-447

61 **Mori M**, Shimada H, Gunji Y, Matsubara H, Hayashi H, Nimura Y, Kato M, Takiguchi M, Ochiai T, Seki N. S100A11 gene identified by in-house cDNA microarray as an accurate predictor of lymph node metastases of gastric cancer. *Oncology Reports* 2004; **11**: 1287-1293

62 **Eisen MB**, Spellman PT, Brown PO, Botstein D. Cluster analysis and display of genome-wide expression patterns. *Proc Natl Acad Sci USA* 1998; **95**: 14863-14868

63 **Draghici S**, Khatri P, Bhavsar P, Shah A, Krawetz SA, Tainsky MA. Onto-Tools, the toolkit of the modern biologist: Onto-Express, Onto-Compare, Onto-Design and Onto-Translate. *Nucleic Acids Res* 2002; **79**: 3775-3781

64 **Khatri P**, Draghici S, Ostermeier GC, Krawetz SA. Profiling gene expression using onto-express. *Genomics* 2002; **79**: 266-270

65 **Draghici S**, Khatri P, Martins RP, Ostermeier GC, Krawetz SA. Global functional profiling of gene expression. *Genomics* 2003; **81**: 98-104

66 **Yang YL**, Xu B, Song YG, Zhang WD. Overexpression of c-fos in *Helicobacter pylori*-induced gastric precancerosis of Mongolian gerbil. *World J Gastroenterol* 2003; **9**: 521-524

67 **Yang H**, Jeffrey PD, Miller J, Kinnucan E, Sun Y, Thoma NH, Zheng N, Chen PL, Lee WH, Pavletich NP. BRCA2 function in DNA binding and recombination from a BRCA2-DSS1-ssDNA structure. *Science* 2002; **297**: 1837-1848

68 **Churin Y**, Kardalinou E, Meyer TF, Naumann M. Pathogenicity island-dependent activation of Rho GTPases Rac1 and Cdc42 in *Helicobacter pylori* infection. *Mol Microbiol* 2001; **40**: 815-823

69 **Hotchin NA**, Cover TL, Akhtar N. Cell vacuolation induced by the VacA cytotoxin of *Helicobacter pylori* is regulated by the Rac1 GTPase. *J Biol Chem* 2000; **275**: 14009-14012

70 **van Belzen N**, Dinjens WN, Diesveld MP, Groen NA, van der Made AC, Nozawa Y, Vlietstra R, Trapman J, Bosman FT. A novel gene which is up-regulated during colon epithelial cell differentiation and down-regulated in colorectal neoplasms. *Lab Invest* 1997; **77**: 85-92

71 **Crabtree JE**, Xiang Z, Lindley IJ, Tompkins DS, Rappuoli R, Covacci A. Induction of interleukin-8 secretion from gastric epithelial cells by a cagA negative isogenic mutant of *Helicobacter pylori*. *J Clin Pathol* 1995; **48**: 967-969

72 **Sharma SA**, Tummuru MK, Miller GG, Blaser MJ. Interleukin-8 response of gastric epithelial cell lines to *Helicobacter pylori* stimulation *in vitro*. *Infect Immun* 1995; **63**: 1681-1687

73 **Tsuchiya N**, Kamei D, Takano A, Matsui T, Yamada M. Cloning and characterization of a cDNA encoding a novel hetero-

geneous nuclear ribonucleoprotein-like protein and its expression in myeloid leukemia cells. *J Biochem* 1998; **123**: 499-507

74 **Espinosa L**, Navarro E. Human serine/threonine protein kinase EMK1: genomic structure and cDNA cloning of isoforms produced by alternative splicing. *Cytogenet Cell Genet* 1998; **81**: 278-282

75 **Hirata Y**, Maeda S, Mitsuno Y, Akanuma M, Yamaji Y, Ogura K, Yoshida H, Shiratori Y, Omata M. *Helicobacter pylori* activates the cyclin D1 gene through mitogen-activated protein kinase pathway in gastric cancer cells. *Infect Immun* 2001; **69**: 3965-3971

76 **Mitsuno Y**, Yoshida H, Maeda S, Ogura K, Hirata Y, Kawabe T, Shiratori Y, Omata M. *Helicobacter pylori* induced transactivation of SRE and AP-1 through the ERK signalling pathway in gastric cancer cells. *Gut* 2001; **49**: 18-22

77 **Jawhari AU**, Noda M, Farthing MJ, Pignatelli M. Abnormal expression and function of the E-cadherin-catenin complex in gastric carcinoma cell lines. *Br J Cancer* 1999; **80**: 322-330

78 **Kuroda S**, Fukata M, Nakagawa M, Fujii K, Nakamura T, Ookubo T, Izawa I, Nagase T, Nomura N, Tani H, Shoji I, Matsuura Y, Yonehara S, Kaibuchi K. Role of IQGAP1, a target of the small GTPases Cdc42 and Rac1, in regulation of E-cadherin- mediated cell-cell adhesion. *Science* 1998; **281**: 832-835

79 **Cottet S**, Corthesy-Theulaz I, Spertini F, Corthesy B. Microaerophilic conditions permit to mimic in vitro events occurring during in vivo *Helicobacter pylori* infection and to identify Rho/Ras-associated proteins in cellular signaling. *J Biol Chem* 2002; **277**: 33978-33986

Science Editor Guo SY **Language Editor** Elsevier HK

PO Box 2345, Beijing 100023, China
www.wjgnet.com
wjg@wjgnet.com

ELSEVIER

World J Gastroenterol 2005;11(39):6144-6151
World Journal of Gastroenterology ISSN 1007-9327
© 2005 The WJG Press and Elsevier Inc. All rights reserved.

• *BASIC RESEARCH* •

Endothelin-1 stimulates contraction and migration of rat pancreatic stellate cells

Atsushi Masamune, Masahiro Satoh, Kazuhiro Kikuta, Noriaki Suzuki, Kennichi Satoh, Tooru Shimosegawa

Atsushi Masamune, Masahiro Satoh, Kazuhiro Kikuta, Noriaki Suzuki, Kennichi Satoh, Tooru Shimosegawa, Division of Gastroenterology, Tohoku University Graduate School of Medicine, Sendai, Japan
Supported by Grant-in-Aid for Encouragement of Young Scientists from Japan Society for the Promotion of Science, No. 16590572 (to AM.), by Pancreas Research Foundation of Japan, No. 01-01 (to AM.), by the Kanae Foundation for Life and Socio-Medical Science (to AM), and by the Uehara Memorial Foundation (to AM)
Correspondence to: Dr. Atsushi Masamune, Division of Gastroenterology, Tohoku University Graduate School of Medicine, 1-1 Seiryo-machi, Aoba-ku, Sendai 980-8574, Japan. amasamune@int3.med.tohoku.ac.jp
Telephone: +81-22-717-7171 Fax: +81-22-717-7177
Received: 2004-12-19 Accepted: 2005-02-18

Abstract

AIM: To examine the ability of ET-1 to affect the cell functions of PSCs and the underlying molecular mechanisms.

METHODS: PSCs were isolated from the pancreas of male Wistar rats after perfusion with collagenase, and cells between passages two and five were used. Expression of ET-1 and ET receptors was assessed by reverse transcription-PCR and immunostaining. Phosphorylation of myosin regulatory light chain (MLC), extracellular-signal regulated kinase (ERK), and Akt was examined by Western blotting. Contraction of PSCs was assessed on hydrated collagen lattices. Cell migration was examined using modified Boyden chambers. Cell proliferation was assessed by measuring the incorporation of 5-bromo-2'-deoxyuridine.

RESULTS: Culture-activated PSCs expressed ET_A and ET_B receptors, and ET-1. ET-1 induced phosphorylation of MLC and ERK, but not Akt. ET-1 induced contraction and migration, but did not alter proliferation of PSCs. ET-1-induced contraction was inhibited by an ET_A receptor antagonist BQ-123 and an ET_B receptor antagonist BQ-788, whereas migration was inhibited by BQ-788 but not by BQ-123. A Rho kinase inhibitor Y-27632 abolished both contraction and migration.

CONCLUSION: ET-1 induced contraction and migration of PSCs through ET receptors and activation of Rho-Rho kinase. ET_A and ET_B receptors play different roles in the regulation of these cellular functions in response to ET-1.

© 2005 The WJG Press and Elsevier Inc. All rights reserved.

Key words: Pancreatitis; Pancreatic fibrosis; Pancreatic stellate cells; Endothelin-1; Rho kinase

Masamune A, Satoh M, Kikuta K, Suzuki N, Satoh K, Shimosegawa T. Endothelin-1 stimulates contraction and migration of rat pancreatic stellate cells. *World J Gastroenterol* 2005; 11(39): 6144-6151
http://www.wjgnet.com/1007-9327/11/6144.asp

INTRODUCTION

In 1998, star-shaped cells in the pancreas, namely pancreatic stellate cells (PSCs), were identified and characterized[1,2]. In normal pancreas, stellate cells are quiescent and can be identified by the presence of vitamin A-containing lipid droplets in the cytoplasm. In response to pancreatic injury or inflammation, they are transformed ("activated") from their quiescent phenotype into myofibroblast-like cells, which actively proliferate, express the cytoskeletal protein α-smooth muscle actin, and produce extracellular matrix components. Many of the morphological and metabolic changes associated with the activation of PSCs in animal models of fibrosis also occur when these cells are grown in serum-containing medium in culture on plastic. There is accumulating evidence that activated PSCs play a pivotal role in the development of pancreatic fibrosis[1-4]. In addition, PSCs may participate in the pathogenesis of acute pancreatitis[3,5]. The activation of signal transduction pathways such as p38 mitogen-activated protein (MAP) kinase[6], Rho-Rho kinase[7], and c-Jun N-terminal kinase[8] is likely to play a role in PSC activation. But intracellular signal transduction pathways in PSCs remain largely unknown.

Endothelin-1 (ET-1), which acts through G-protein coupled ET_A and ET_B receptors, was initially described as a potent endothelial cell-derived vasoconstrictor isolated from the culture medium of porcine aortic endothelial cells[9]. Subsequent studies have shown that ET-1 is produced by a variety of cells and exhibits several biological activities such as vasoconstriction, regulation of peptide secretion, migration, and positive or negative effects on cell growth[10,11]. ET-1 has been implicated in the pathogenesis of cardiovascular, pulmonary, renal, and developmental disorders[11]. In addition, ET-1 plays a key role in the development of portal hypertension and hepatic fibrosis through its effects on hepatic stellate cells[12,13]. ET-1 has been shown to stimulate contraction via ET_A receptor[14], and inhibit proliferation via ET_B receptor[15] in hepatic stellate cells. But, the roles of ET-1 and ET receptors in the regulation of cell functions of PSCs remain largely unknown. In this study, we examined

the ability of ET-1 to affect the cell functions of PSCs and the underlying molecular mechanisms. We here report that ET-1 stimulated contraction and migration, but not proliferation, of PSCs through ET receptors and Rho-Rho kinase pathway.

MATERIALS AND METHODS

Materials

ET-1 was purchased from Peptide Institute (Osaka, Japan). Collagenase P was obtained from Roche Diagnostics (Mannheim, Germany). Rat recombinant platelet-derived growth factor (PDGF)-BB was purchased from R&D Systems (Minneapolis, MN). Rhodamine-labeled phalloidin was purchased from Molecular Probes (Eugene, OR). BQ-123, BQ-788, and U0126 were purchased from Calbiochem (La Jolla, CA). Y-27632 was a generous gift from Mitsubishi Pharma Co. (Osaka, Japan). Rabbit antibodies against extracellular-signal regulated kinase (ERK; phosphorylated and total), Akt (phosphorylated at Ser^{473} and total), and myosin regulatory light chain II (MLC; phosphorylated at Ser^{19} and total) were purchased from Cell Technologies, Inc. (Beverly, MA). Rabbit antibody against glyceraldehyde-3-phosphate dehydrogenase (GAPDH) was obtained from Trevigen (Gaithersburg, MD). All other reagents were purchased from Sigma-Aldrich (St. Louis, MO) unless specifically described.

Cell culture

All animal procedures were performed in accordance with the National Institutes of Health Animal Care and Use Guidelines. Rat PSCs were prepared from the pancreas tissues of male Wistar rats (Japan SLC Inc., Hamamatsu, Japan) weighing 200-250 g using the Nycodenz solution (Nycomed Pharma, Oslo, Norway) after perfusion with 0.3 g/L collagenase P as previously described[16]. The cells were resuspended in Ham's F-12 medium containing 100 mL/L heat-inactivated fetal bovine serum (MP Biomedicals, Irvine, CA), penicillin sodium, and streptomycin sulfate. Cell purity was always more than 90% as assessed by a typical star-like configuration and by detecting vitamin A autofluorescence. All experiments were performed using cells between passages two and five. We incubated PSCs in serum-free medium for 24 h before the addition of experimental reagents. For some experiments, BQ-123, BQ-788, U0126, or Y-27632 were added 30 min prior to the ET-1 treatment.

Reverse transcription-PCR

Total RNA was isolated using RNeasy total RNA preparation kit (Qiagen, Chatsworth, CA). Total RNA was reverse-transcribed, and the resultant cDNA was subjected to PCR as previously reported[17]. Specific primer sets were as follows (listed 5'-3'; forward and reverse, respectively). ET-1 precursor (preproET-1): TTGCTCCTGCTCCTC-CTTGAG and GGTCTTGATGCTGTTGCTGATG; ET_A: CGTCTTCTGCTTGGTTGTCA and TGGTTCT-GCTCCTGGTTCTT; ET_B CAAGACAGTATTCTGC CTGG and CAAGCAGGATTGCTTCTCCT. They were amplified using 30 cycles at 94 ℃ (for 1 min), at 50 ℃ (for 1 min), and at 72 ℃ (for 1 min). The products of PCR were separated by 15 g/L agarose gel electrophoresis and visualized under ultraviolet light after staining with ethidium bromide. The expected sizes of the PCR products were 382 bp for preproET-1, 321 bp for ET_A receptor, and 297 bp for ET_B receptor.

Immunostaining

PSCs were grown directly on slides, serum-starved for 24 h, and immunostaining for ET-1 was performed using a streptavidin-biotin peroxidase complex detection kit (Histofine Kit; Nichirei, Tokyo, Japan) as previously described[18]. Briefly, cells were fixed with 1 000 mL/L methanol at -20 ℃, and then endogenous peroxidase activity was blocked by incubation with hydrogen peroxide in methanol. After immersion in normal rabbit serum, the slides were incubated with mouse anti-ET-1 antibody (at 1:200 dilution) at 4 ℃ overnight. The slides were incubated with biotinylated anti-mouse immunoglobulin antibody, followed by peroxidase-conjugated streptavidin. Finally, color was developed by incubating the slides for several minutes with diaminobenzidine (Dojindo, Kumamoto, Japan). The expression of ET_A and ET_B was examined in a similar manner.

Western blotting

The level of activated, phosphorylated ERK was determined by Western blotting as previously described[19]. Cells were lysed in sodium dodecyl sulfate buffer. Cellular proteins (approximately 100 μg) were fractionated on a 100 g/L sodium dodecyl sulfate-polyacrylamide gel. They were transferred to a nitrocellulose membrane (Bio-Rad, Hercules, CA), and the membrane was incubated overnight at 4 ℃ with rabbit anti-phosphospecific ERK antibody. After incubation with peroxidase-conjugated goat anti-rabbit immunoglobulin G antibody for 1 h, proteins were visualized using an ECL kit (Amersham Biosciences, UK). The levels of total ERK, Akt (phosphorylated and total), and MLC (phosphorylated and total) were determined in a similar manner.

Fluorescence microscopy

Stress fibers were stained with rhodamine-labeled phalloidin as previously described[20]. After fixation with 40 g/L paraformaldehyde for 5 min, PSCs were permeablized with 1.5 mL/L Triton X-100 in PBS for 5 min. Cells were then incubated for 2 h at room temperature in a dark place with rhodamine-labeled phalloidin in blocking buffer (10 g/L bovine serum albumin in PBS). Cells were then washed thrice with PBS for 10 min each, and coverslipped with Fluoromount (Vector Laboratories, Burlingame, CA). Cells were observed with a Leica fluorescence microscope. Images were captured with a Leica QFISH system (Wetzlar, Germany).

Collagen gel contraction assay

Contraction of PSCs on collagen lattices was examined in six-well flat-bottom tissue culture plates (Becton Dickinson, Bedford, MA) as previously described[21]. Culture vessels were preincubated with PBS containing 10 g/L bovine serum albumin for 2 h at 37 ℃, washed, and air-dried. The gel mixture consisted of eight parts Vitrogen-100 (Collagen Corp., Palo Alto, CA), one part 10×minimal essential medium,

and one part 0.2 mol/L HEPES, pH 9.0, which resulted in a final collagen concentration of 2.4 g/L. It was prepared at 4 ℃, added to the culture vessel, and incubated at 37 ℃ for 2 h to allow gelation. PSCs were trypsinized, resuspended in serum-free medium (at 1×10^9 cells/L), plated on top of the gels (1 mL/well), and allowed to attach for 2 h. The collagen lattices were detached from the plate by gentle circumferential dislodgement using a fine needle, and ET-1 (at 100 nmol/L) was added to elicit contraction. After 24-h incubation, we measured the diameter of the collagen lattices, and calculated the "% of the original diameter (= 35 mm)". In addition, cell-free collagen lattices were incubated with 100 nmol/L ET-1 or serum-free medium alone.

Cell migration assay

Cell migration was assessed as previously described[16]. Serum-starved PSCs were trypsinized, and resuspended at the concentration of 3×10^8 cells/L in serum-free medium containing 10 g/L bovine serum albumin. For the assay, we used modified Boyden chambers with 8-μm pore filters (Iwaki Glass Co. Ltd., Funabashi, Japan) coated with rat-tail type I collagen. ET-1 was added to the lower chamber, and 250 μL of cell suspension was added to the upper chamber. The chambers were then incubated at 37 ℃ for 24 h. At the end of the incubation, the cell suspension in the upper chamber was aspirated, and the upper part of the filter was cleaned with cotton plugs. The cells migrated to the underside of the filter were stained with Difquick (Sysmex, Kobe, Japan), viewed, and counted at 200× magnification.

Cell proliferation assay

Serum-starved PSCs (approximately 80% density) were treated with ET-1 in the presence or absence of 100 mL/L fetal bovine serum or PDGF-BB (at 25 μg/L). Cell proliferation was assessed using a commercial kit (Cell proliferation ELISA, BrdU; Roche Diagnostics) according to the manufacturer's instruction. This is a colorimetric immunoassay based on the measurement of 5-bromo-2'-deoxyuridine (BrdU) incorporation during DNA synthesis. After 24-h incubation with experimental reagents, cells were labeled with BrdU for 3 h at 37 ℃. Cells were fixed, and incubated with peroxidase-conjugated anti-BrdU antibody. Then the peroxidase substrate 3,3',5,5'-tetramethylbenzidine was added, and BrdU incorporation was quantitated by $A_{370\text{-}492}$.

Statistical analysis

The results were expressed as mean±SD. Luminograms and autoradiograms are representative of at least three experiments. Differences between the groups were evaluated by ANOVA, followed by Fisher's test for post hoc analysis. A P value less than 0.05 was considered statistically significant.

RESULTS

Activated PSCs expressed ET-1 and ET receptors

We first examined whether culture-activated PSCs expressed ET-1 and ET receptors. ET-1 is a product of the gene coding for a large precursor protein (i.e. preproET-1)[9]. Culture-activated PSCs expressed ET_A and ET_B receptors, and ET-1, as assessed by reverse transcription-PCR and immunostaining (Figure 1).

ET-1 induced phosphorylation of ERK and MLC, but not Akt

In an attempt to elucidate the effect of ET-1 on cell functions of PSCs, we examined whether ET-1 activated intracellular signaling pathways. We examined the activation of ERK, Akt, and MLC, all of which are implicated in ET-1-induced cellular contraction and/or migration[22-24]. PSCs were treated with ET-1 at 100 nmol/L, and the activation of the signaling pathways by Western blotting using anti-phosphospecific antibodies. We chose this ET-1 concentration because previous studies have shown that ET-1 acts on ET receptors in a dose-dependent manner and ET-1 at this concentration effectively elicited effects in a variety of cell types[14,15,25,26]. PDGF-BB induced phosphorylation of ERK, Akt, and MLC whereas ET-1 induced phosphorylation of ERK and MLC but not Akt (Figure 2).

Y-27632 decreased stress fiber formation and MLC phosphorylation

It has been shown that RhoA, acting through its downstream effector Rho kinase, stimulates MLC phosphorylation, stress fiber formation, and contractile force generation[27,28]. The fact that ET-1 induced phosphorylation of MLC prompted us to examine the effect of Y-27632, a specific Rho kinase inhibitor[29], on the phosphorylation of MLC and stress fiber formation. Y-27632 decreased phosphorylation of MLC in a dose-dependent manner (Figure 3A). When cells were treated with Y-27632 at 25 μmol/L for 24 h, disassembly of stress fibers was observed (Figures 3B and 3C). In these experiments, Y-27632 up to 25 μmol/L did not affect the cell viability during the incubation as assessed by trypan blue exclusion test (data not shown). In addition, the effects of Y-27632 were reversible within 48 h after the removal of Y-27632 (Figures 3A and 3D). However, when PSCs were treated with Y-27632 at 50 μmol/L, cytotoxic effects were observed during the incubation (data not shown).

ET-1 induced contraction of PSCs

We examined whether ET-1 induced contraction of PSCs using collagen lattices. With no stellate cells, the size of the collagen lattices did not change in response to ET-1 (data not shown). When PSCs were plated on the lattices, and incubated with serum-free medium alone for 24 h, there was a slight reduction in the diameter of the lattices to 89±3% of their original size (Figure 4A). By incubation with 100 nmol/L ET-1, the diameter of the lattices decreased to 54±8% (Figure 4B). ET-1-induced contraction of PSCs was inhibited by an ET_A receptor antagonist BQ-123[30], an ET_B receptor antagonist BQ-788[31]. Y-27632 abolished ET-1-induced contraction, whereas a MAP kinase inhibitor U0126[32] was ineffective.

ET-1 induced migration, but did not alter proliferation of PSCs

ET-1 induced migration of PSCs, which was inhibited by BQ-788, Y-27632, and U0126, but not BQ-123 (Figure 5).

Previous studies have shown that ET-1 showed positive or negative effects on cell growth[15,25,26]. In agreement with the previous study[16], PDGF-BB and 100 mL/L fetal bovine serum increased proliferation of PSCs (Figure 6). ET-1 did not affect basal proliferation or proliferation in response to PDGF or serum.

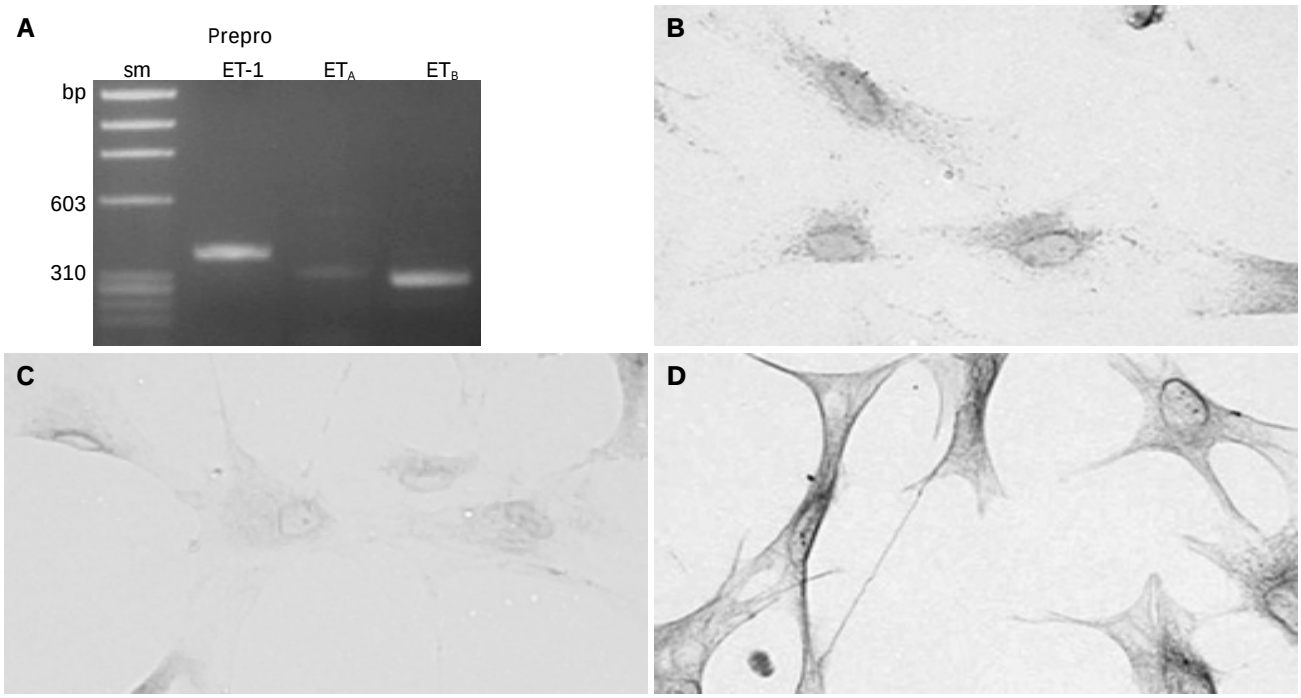


Figure 1 Culture-activated PSCs expressed ET and ET receptors. A: Total RNA was prepared from culture-activated, serum-starved PSCs. The expression of preproET-1, ET_A receptor and ET_B receptor was examined by reverse transcription-PCR. The expected sizes of the PCR products were 382 bp for preproET-1, 321 bp for ET_A receptor, and 297 bp for ET_B receptor. sm: size marker (ϕX174 *Hae*III digest). bp: bp; B-D: Serum-starved PSCs were grown directly on slides. Immunostaining for ET-1 (panel B), ET_A receptor (panel C), and ET_B receptor (panel D) was performed using a streptavidin-biotin peroxidase complex detection kit. Original magnification: ×20 objective.

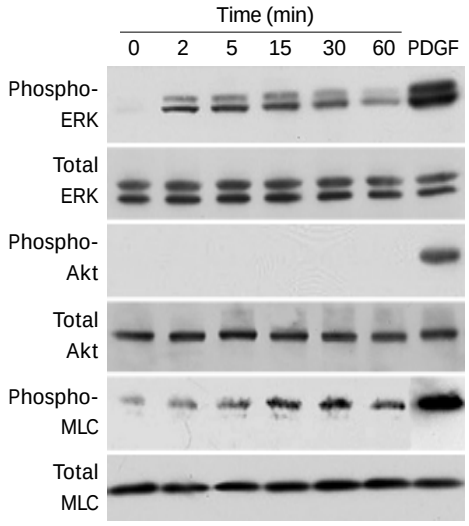


Figure 2 ET-1 induced phosphorylation of ERK and MLC, but not Akt. PSCs were treated with ET-1 (at 100 nmol/L) for the indicated time. Total cell lysates (approximately 100 μg) were prepared, and the levels of phosphorylated ERK, Akt, and MLC were determined by Western blotting. As positive controls, total cell lysates were prepared from PSCs treated with PDGF-BB (at 25 μg/L) for 5 min, and Western blotting was performed in a similar manner. Levels of total ERK, Akt, and MLC were also determined.

DISCUSSION

There is accumulating evidence that activated PSCs play a pivotal role in the pathogenesis of pancreatic fibrosis and inflammation[1-5]. We here showed that culture-activated PSCs expressed ET_A and ET_B receptors, and ET-1. ET-1 stimulated contraction and migration of PSCs, suggesting autocrine and paracrine mechanisms of ET-1-regulated cellular functions of PSCs. ET-1-induced contraction was inhibited by ET_A and ET_B receptor antagonists whereas ET-1-induced migration was inhibited by ET_B receptor antagonist but not by ET_A receptor antagonist. Thus, ET_A and ET_B receptors play different roles in the regulation of these cellular functions in response to ET-1.

Cellular migration and contraction are complex processes involving dynamic changes in the actin-myosin cytoskeleton, including generation of contractile forces[33]. It has been shown that contractile force is powered by myosin, which is activated by phosphorylation of MLC[33]. Phosphorylation of MLC is regulated by the balance of two enzymatic activities, i.e., MLC kinase(s) and myosin phosphatase. For example, MLC is phosphorylated by MLC kinase in a Ca^{2+}/calmodulin-dependent manner in smooth muscle cells[34]. RhoA, acting through its downstream effector Rho kinase, stimulates MLC phosphorylation and consequently contractile force generation through the inhibition of myosin phosphatase[27,28]. Activated Rho kinase promotes the contraction of isolated stress fibers and generates a long-lasting tensile activity by the maintained inhibition of myosin phosphatase[35]. On the other hand, contractile force generation by certain non-muscle cell types including fibroblasts may occur independently of myosin phosphorylation[36,37]. To clarify the role of myosin in ET-1-induced contraction and migration of PSCs, we examined the effect of ET-1 on the phosphorylation of MLC. We here showed that ET-1 induced the phosphorylation of MLC, supporting a role of myosin in contractile force generation in PSCs. In addition, an inhibitor of Rho kinase

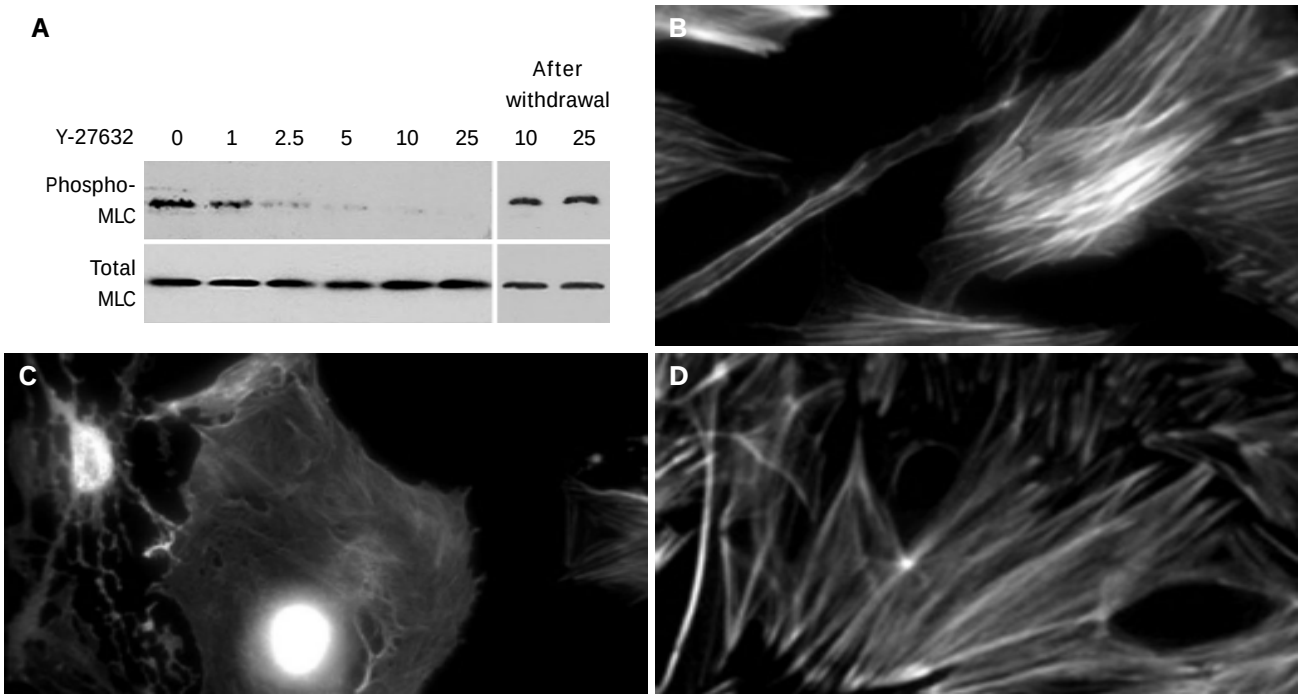


Figure 3 Y-27632 decreased stress fiber formation. A: PSCs were treated with ET-1 (at 100 nmol/L) in the presence of Y-27632 at the indicated concentrations (at μmol/L) for 30 min. Total cell lysates (approximately 100 μg) were prepared, and the levels of phosphorylated and total MLC were determined by Western blotting. In parallel experiments, Y-27632 was withdrawn after 30-min incubation, and replaced with 10% FBS. After 48-h incubation with 10% FBS, total cell lysates were prepared, and the levels of phosphorylated and total MLC were determined by Western blotting; B-D: PSCs were incubated with ET-1 (at 100 nmol/L) in the absence (B) or presence (C) of Y-27632 (at 25 μmol/L) for 24 h, and stained with rhodamine-labeled phalloidin. In parallel experiments, Y-27632 was withdrawn and replaced with 10% FBS. After 48-h incubation with 10% FBS, PSCs were stained with rhodamine-labeled phalloidin (D). Original magnification: ×60 objective.

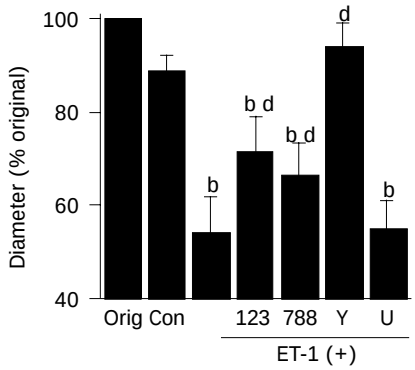


Figure 4 ET-1 induced contraction of PSCs. PSCs were plated on the surface of collagen lattices prepared in each well of a six-well plate and incubated for 2 h to allow adherence. The collagen lattices were then detached from the plate by gentle circumferential dislodgment. Serum-starved PSCs were left untreated ("Con") or were treated with ET-1 (at 100 nmol/L) in the absence or presence of BQ-123 ("123" at 10 μmol/L), BQ-788 ("788" at 10 μmol/L), Y-27632 ("Y" at 25 μmol/L), or U0126 ("U" at 5 μmol/L). Lattices were then detached from the plate, and incubated in serum-free medium (control, "Con") with or without 100 nmol/L ET-1. After 24-h incubation, we measured the diameter of the collagen lattices, and calculated the "% of the original diameter ("Orig" = 35 mm)". Data are shown as mean±SD (% of the original diameter, n = 8). ^{b}P<0.01 *vs* control (serum-free medium only), ^{d}P<0.01 *vs* ET-1 treatment only.

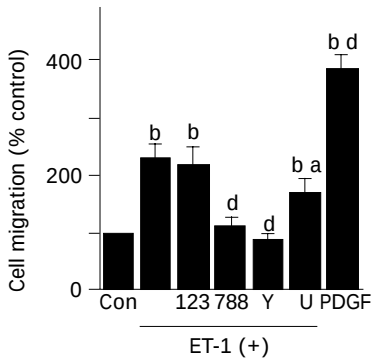


Figure 5 ET-1 induced migration of PSCs. Cell migration was assessed using modified Boyden chambers with 8-μm pore filters. Serum-starved PSCs were left untreated ("Con") or were treated with ET-1 (at 100 nmol/L) in the lower chamber in the absence or presence of BQ-123 ("123" at 10 μmol/L), BQ-788 ("788" at 10 μmol/L), Y-27632 ("Y" at 25 μmol/L), or U0126 ("U" at 5 μmol/L). After 24-h incubation, the cells migrated to the underside of the filter were stained, and counted under a light microscopy. As positive controls, cells were treated with PDGF-BB (at 25 μg/L) in the lower chamber, and cell migration was assessed in a similar manner. Data are shown as mean±SD (% of the control, n = 6). ^{b}P<0.01 *vs* control (serum-free medium only), ^{a}P<0.05, ^{d}P<0.01 *vs* ET-1 treatment only.

Y-27632 abolished the phosphorylation of MLC, stress fiber formation, contraction, and migration. These results agree with the idea that force generation by the myofibroblasts depends on the isometric contraction of stress fibers containing α-smooth muscle actin, and is mediated through Rho-Rho kinase[38]. Indeed, myosin mediates contractile force generation by hepatic stellate cells in response to ET-1[24]. We have previously shown that PDGF-BB induced migration of PSCs through the activation of phosphatidylinositol 3-kinase/Akt pathway[16]. Unlike PDGF-BB, ET-1 did not activate Akt but did induce migration of PSCs, excluding a role of phosphatidylinositol 3-kinase/Akt pathway in ET-

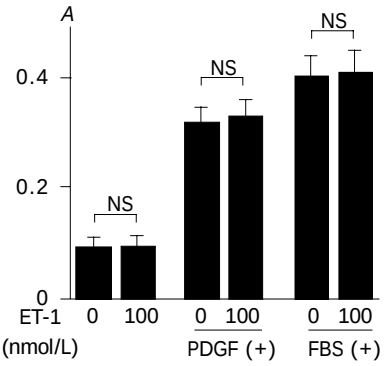


Figure 6 ET-1 did not alter basal or inducible proliferation of PSCs. Serum-starved PSCs were treated with ET-1 at 0 or 100 nmol/L in the absence or presence of PDGF-BB (at 25 μg/L) or 100 mL/L fetal bovine serum ("FBS"). After 24-h incubation, DNA synthesis was assessed by BrdU incorporation enzyme-linked immunosorbent assay. Data are shown as mean±SD (n = 6). NS: not significant, *A*: optical density.

1-mediated migration.

In this study, ET-1 induced contraction of PSCs through both ET_A and ET_B receptors as assessed by the contraction of collagen lattices. This is in agreement with the previous study showing that both ET_A and ET_B receptors play an important role in contraction of colonic myofibroblast cells[26], but disagrees with hepatic stellate cells where ET-1 induced contraction is through ET_A receptor[14]. Investigation of cellular contraction using collagen lattices (gels) was introduced by Bell *et al*.[39], and has been validated as a model of study of cellular contraction in a variety of cell types. Fibroblasts seeded on top of type I collagen gels bind and organize underlying collagen fibrils, both in close proximity and at a distance from cells[40]. After such reorganization, lattices are converted into a dense mass with the morphological appearance of dermal scar. Kawada *et al*.[41], reported a morphological study of ET-1-induced contraction of hepatic stellate cells on hydrated collagen gels. They demonstrated that contracted form of the stellate cells was morphologically characterized by the retraction of dendritic processes and the bending of the extended cell bodies that enfold the underlying collagen matrix. Because the cell body and processes are both closely attached to the collagen fibers, their contraction generates effective forces for the contraction of collagen gels.

ET-1 did not alter the proliferation of PSCs. The effect of ET-1 on growth and the underlying mechanisms depend on cell type. For example, ET-1 promotes the proliferation of human pulmonary artery smooth muscle cells through ET_A and ET_B receptors[25]. ET-1 did not affect the proliferation of human colonic myofibroblast cells[26]. In human hepatic stellate cells, ET-1 has been shown to inhibit the serum-induced proliferation through ET_B receptor, whereas ET-1 did not induce proliferation by itself[15]. Of note, Pinzani *et al*.[14], reported that ET-1 induced proliferation of early-passaged human hepatic stellate cells (passages 1 and 2), but the effect was less evident at a later stage of culture. This phenomenon is attributable at least in part to the progressive shift from a relative predominance of ET_A receptor to ET_B receptor during culture[14]. Because the effects of ET-1 on cell growth might be mediated by distinct ET receptors, the ratio between ET_A and ET_B receptors in the cells might constitute an additional factor that could affect the sensitivity of cells to the growth regulatory effects of ET-1. We and others have shown that ERK is a key mediator of PDGF-BB-induced mitogenic signals in PSCs[16,42]. In spite of the ability to activate ERK, ET-1 failed to alter the proliferation, suggesting that activation of ERK is required but not sufficient for the proliferation of PSCs. This is also in the case of stimulation by ethanol, acetaldehyde, and 4-hydroxy-2,3-nonenal in PSCs[43], and in agreement with the concept that activation of ERK, although necessary, may not be sufficient to justify the mitogenic properties of an agonist[44].

Klonowski-Stumpe *et al*.[45], reported that activated PSCs expressed ET_A receptor and ET-1, and that ET-1 increased cytosolic Ca^{2+} concentration[45]. Exogenous ET-1 did not induce contraction, and, even in the absence of exogenous addition of ET-1, PSCs reduced the area of hydrated collagen lattices to 75% of the original value within 6 h, which was significantly attenuated by BQ-123, but not by another ET_B receptor antagonist IRL-1 038. The reason for discrepancy of the results between our study and theirs remain unknown, but the different experimental systems (e.g., different cell passages, different ET-1 concentrations, different ET_B receptor antagonist, and different serum-starvation condition) employed may be one explanation. As the ET_A receptor antagonist inhibited basal contraction of PSCs in their study, the endogenous ET-1 from PSCs or ET-1 that remained in the culture supernatant appeared to be responsible for the basal contraction of PSCs. In addition to ET_A receptor, we here have shown for the first time that activated PSCs express ET_B receptor, and that exogenously added ET-1 induces migration of PSCs.

It has been accepted that hepatic stellate cell contraction in response to ET-1 plays an important role in the regulation of sinusoidal blood flow, and in the development of portal hypertension and hepatic fibrosis[12,13]. ET-1 is markedly overexpressed in different cellular elements in cirrhotic liver tissue, particularly in sinusoidal endothelial cells and activated hepatic stellate cells located in the sinusoids of the regenerating nodules at the edge of fibrous septa[16]. On the other hand, the pathophysiological implication of ET-1-induced contraction of PSCs remains obscure. Although PSCs are located predominantly in the periacinar regions in normal pancreas[1,2], perivascular and periductal localization has been also reported[46]. Ikejiri[46] showed that vitamin A-storing cells (now recognized as PSCs) were perivascularly localized in the pancreas of rats fed with vitamin A. Perivascular PSCs might participate in the regulation of blood flow and the development of microvascular ischemia during pancreatitis through ET-1 production[47]. Izumi *et al*.[48], reported that PSCs were found in the pancreatic duct wall of normal pancreas, and that the amount of such cells was excessively increased in patients with focal pancreatitis. They assumed that circular contraction of the ductal wall by proliferating PSCs might induce the stenosis of the main pancreatic duct and block the efflux of pancreatic juice from branch pancreatic ducts at the stenotic portion, leading to localized acinar atrophy and fibrosis[48]. In addition, PSCs might participate in control of the intraductal pressure, epithelial

cell reconstitution, and duct remodeling during the healing of ductal injury. Along this line, it is now well accepted that the contractile activity of myofibroblasts is responsible for connective tissue remodeling during wound healing[38]. Obviously, further studies are necessary to clarify the pathop-hysiological relevances of ET-1-mediated cell functions of PSCs.

ACKNOWLEDGMENTS

The authors thank Dr. Kenzo Kaneko for fluorescence microscopy, and Mitsubishi Pharma Co. for Y-27632.

REFERENCES

1 **Apte MV,** Haber PS, Applegate TL, Norton ID, McCaughan GW, Korsten MA, Pirola RC, Wilson JS. Periacinar stellate shaped cells in rat pancreas: identification, isolation and culture. *Gut* 1998; **43**: 128-133
2 **Bachem MG,** Schneider E, Gross H, Weidenbach H, Schmidt RM, Menke A, Siech M, Beger H, Grunert A, Adler G. Identification, culture, and characterization of pancreatic stellate cells in rats and humans. *Gastroenterology* 1998; **115**: 421-432
3 **Haber PS,** Keogh GW, Apte MV, Moran CS, Stewart NL, Crawford DH, Pirola RC, McCaughan GW, Ramm GA, Wilson JS. Activation of pancreatic stellate cells in human and experimental pancreatic fibrosis. *Am J Pathol* 1999; **155**: 1087-1095
4 **Masamune A,** Kikuta K, Satoh M, Sakai Y, Satoh A, Shimosegawa T. Ligands of peroxisome proliferator-activated receptor-gamma block activation of pancreatic stellate cells. *J Biol Chem* 2002; **277**: 141-147
5 **Masamune A,** Sakai Y, Kikuta K, Satoh M, Satoh A, Shimosegawa T. Activated rat pancreatic stellate cells express intercellular adhesion molecule-1 (ICAM-1) *in vitro*. *Pancreas* 2002; **25**: 78-85
6 **Masamune A,** Satoh M, Kikuta K, Sakai Y, Satoh A, Shimosegawa T. Inhibition of p38 mitogen-activated protein kinase blocks activation of rat pancreatic stellate cells. *J Pharmacol Exp Ther* 2003; **304**: 8-14
7 **Masamune A,** Kikuta K, Satoh M, Satoh K, Shimosegawa T. Rho kinase inhibitors block activation of pancreatic stellate cells. *Br J Pharmacol* 2003; **140**: 1292-1302
8 **Masamune A,** Kikuta K, Masamune A, Kikuta K, Suzuki N, Satoh M, Satoh K, Shimosegawa T. A c-Jun NH2-terminal kinase inhibitor SP600125 (anthra[1,9-cd]pyrazole-6 (2H)-one) blocks activation of pancreatic stellate cells. *J Pharmacol Exp Ther* 2004; **310**: 520-527
9 **Yanagisawa M,** Kurihara H, Kimura S, Tomobe Y, Kobayashi M, Mitsui Y, Yazaki Y, Goto K, Masaki T. A novel potent vasoconstrictor peptide produced by vascular endothelial cells. *Nature* 1988; **332**: 411-415
10 **Sakurai T,** Yanagisawa M, Masaki T. Molecular characterization of endothelin receptors. *Trends Pharmacol Sci* 1992; **13**: 103-108
11 **Levin ER.** Endothelins. *N Engl J Med* 1995; **333**: 356-363
12 **Friedman SL.** Molecular regulation of hepatic fibrosis, an integrated cellular response to tissue injury. *J Biol Chem* 2000; **275**: 2247-2250
13 **Rockey DC,** Chung JJ. Endothelin antagonism in experimental hepatic fibrosis. Implications for endothelin in the pathogenesis of wound healing. *J Clin Invest* 1996; **98**: 1381-1388
14 **Pinzani M,** Milani S, De Franco R, Grappone C, Caligiuri A, Gentilini A, Tosti-Guerra C, Maggi M, Failli P, Ruocco C, Gentilini P. Endothelin 1 is overexpressed in human cirrhotic liver and exerts multiple effects on activated hepatic stellate cells. *Gastroenterology* 1996; **110**: 534-538
15 **Mallat A,** Fouassier L, Preaux AM, Gal CS, Raufaste D, Rosenbaum J, Dhumeaux D, Jouneaux C, Mavier P, Lotersztajn S. Growth inhibitory properties of endothelin-1 in human hepatic myofibroblastic Ito cells. *J Clin Invest* 1995; **96**: 42-49
16 **Masamune A,** Kikuta K, Satoh M, Kume K, Shimosegawa T. Differential roles of signaling pathways for proliferation and migration of rat pancreatic stellate cells. *Tohoku J Exp Med* 2003; **199**: 69-84
17 **Wendel-Wellner M,** Noll T, Konig P, Schmeck J, Koch T, Kummer W. Cellular localization of the endothelin receptor subtypes ET_A and ET_B in the rat heart and their differential expression in coronary arteries, veins, and capillaries. *Histochem Cell Biol* 2002; **118**: 361-369
18 **Masamune A,** Satoh M, Kikuta K, Suzuki N, Shimosegawa T. Establishment and characterization of a rat pancreatic stellate cell line by spontaneous immortalization. *World J Gastroenterol* 2003; **9**: 2751-2758
19 **Masamune A,** Satoh K, Sakai Y, Yoshida M, Satoh A, Shimosegawa T. Ligands of peroxisome proliferator-activated receptor-gamma induce apoptosis in AR42J cells. *Pancreas* 2002; **24**: 130-138
20 **Kaneko K,** Satoh K, Masamune A, Satoh A, Shimosegawa T. Myosin light chain kinase inhibitors can block invasion and adhesion of human pancreatic cancer cell lines. *Pancreas* 2002; **24**: 34-41
21 **Rocky DC,** Housset CN, Friedman SL. Activation-dependent contractility of rat hepatic lipocytes in culture and *in vivo*. *J Clin Invest* 1993; **92**: 1795-1804
22 **Ishihata A,** Tasaki K, Katano Y. Involvement of p44/42 mitogen-activated protein kinases in regulating angiotensin II- and endothelin-1-induced contraction of rat thoracic aorta. *Eur J Pharmacol* 2002; **445**: 247-256
23 **Shi-Wen X,** Chen Y, Denton CP, Eastwood M, Renzoni EA, Bou-Gharios G, Pearson JD, Dashwood M, du Bois RM, Black CM, Leask A, Abraham DJ. Endothelin-1 promotes myofibroblast induction through the ETA receptor via a rac/phosphoinositide 3-kinase/Akt-dependent pathway and is essential for the enhanced contractile phenotype of fibrotic fibroblasts. *Mol Biol Cell* 2004; **15**: 2707-2719
24 **Saab S,** Tam SP, Tran BN, Melton AC, Tangkijvanich P, Wong H, Yee HF Jr. Myosin mediates contractile force generation by hepatic stellate cells in response to endothelin-1. *J Biomed Sci* 2002; **9**: 607-612
25 **Davie N,** Haleen SJ, Upton PD, Polak JM, Yacoub MH, Morrell NW, Wharton J. ETA and ETB receptors modulate the proliferation of human pulmonary artery smooth muscle cells. *Am J Respir Crit Care Med* 2002; **165**: 398-405
26 **Kernochan LE,** Tran BN, Tangkijvanich P, Melton AC, Tam SP, Yee HF Jr. Endothelin-1 stimulates human colonic myofibroblast contraction and migration. *Gut* 2002; **50**: 65-70
27 **Kimura K,** Ito M, Amano M, Chihara K, Fukata Y, Nakafuku M, Yamamori B, Feng J, Nakano T, Okawa K, Iwamatsu A, Kaibuchi K. Regulation of myosin phosphatase by Rho and Rho-associated kinase (Rho-kinase). *Science* 1996; **273**: 245-248
28 **Somlyo AP,** Somlyo AV. Signal transduction by G-proteins, rho-kinase and protein phosphatase to smooth muscle and non-muscle myosin II. *J Physiol* 2000; **522**: 177-185
29 **Uehata M,** Ishizaki T, Satoh H, Ono T, Kawahara T, Morishita T, Tamakawa H, Yamagami K, Inui J, Maekawa M, Narumiya S. Calcium sensitization of smooth muscle mediated by a Rho-associated protein kinase in hypertension. *Nature* 1997; **389**: 990-994
30 **Ihara M,** Noguchi K, Saeki T, Fukuroda T, Tsuchida S, Kimura S, Fukami T, Ishikawa K, Nishikibe M, Yano M. Biological profiles of highly potent novel endothelin antagonists selective for the ETA receptor. *Life Sci* 1992; **50**: 247-255
31 **Ishikawa K,** Ihara M, Noguchi K, Mase T, Mino N, Saeki T, Fukuroda T, Fukami T, Ozaki S, Nagase T, Nishikibr M, Yano M. Biochemical and pharmacological profile of a potent and selective endothelin B-receptor antagonist, BQ-788. *Proc Natl Acad Sci USA* 1994; **91**: 4892-4896
32 **Favata MF,** Horiuchi KY, Manos EJ, Daulerio AJ, Stradley DA, Feeser WS, Van Dyk DE, Pitts WJ, Earl RA, Hobbs F, Copeland RA, Magolda RL, Scherle PA, Trzaskos JM. Identification of a novel inhibitor of mitogen-activated protein kinase kinase. *J Biol Chem* 1998; **273**: 18623-18632

33 **Lauffenburger DA,** Horwitz AF. Cell migration: A physically integrated molecular process. *Cell* 1996; **84**: 359-369
34 **Somlyo AP,** Somlyo AV. Signal transduction and regulation in smooth muscle. *Nature* 1994; **372**: 231-236
35 **Katoh K,** Kano Y, Amano M, Onishi H, Kaibuchi K, Fujiwara K. Rho-kinase-mediated contraction of isolated stress fibers. *J Cell Biol* 2001; **153**: 569-584
36 **Obara K,** Nikcevic G, Pestic L, Nowak G, Lorimer DD, Guerriero V Jr, Elson EL, Paul RJ, de Lanerolle P. Fibroblast contractility without an increase in basal myosin light chain phosphorylation in wild type cells and cells expressing the catalytic domain of myosin light chain kinase. *J Biol Chem* 1995; **270**: 18734-18737
37 **Skuta G,** Ho CH, Grinnell F. Increased myosin light chain phosphorylation is not required for growth factor stimulation of collagen matrix contraction. *J Biol Chem* 1999; **274**: 30163-30168
38 **Hinz B,** Gabbiani G. Mechanisms of force generation and transmission by myofibroblasts. *Curr Opin Biotechnol* 2003; **14**: 538-546
39 **Bell E,** Ivarsson B, Merrill C. Production of a tissue-like structure by contraction of collagen lattices by human fibroblasts of different proliferative potential *in vitro*. *Proc Natl Acad Sci USA* 1979; **76**: 1274-1278
40 **Guidry C,** Grinnell F. Contraction of hydrated collagen gels by fibroblasts: evidence for two mechanisms by which collagen fibrils are stabilized. *Coll Relat Res* 1987; **6**: 515-529
41 **Kawada N,** Harada K, Ikeda K, Kaneda K. Morphological study of endothelin-1-induced contraction of cultured hepatic stellate cells on hydrated collagen gels. *Cell Tissue Res* 1996; **286**: 477-486
42 **Jaster R,** Sparmann G, Emmrich J, Liebe S. Extracellular signal regulated kinases are key mediators of mitogenic signals in rat pancreatic stellate cells. *Gut* 2002; **51**: 579-584
43 **Masamune A,** Kikuta K, Satoh M, Satoh A, Shimosegawa T. Alcohol activates activator protein-1 and mitogen-activated protein kinases in rat pancreatic stellate cells. *J Pharmacol Exp Ther* 2002; **302**: 36-42
44 **Blenis J.** Signal transduction via the MAP kinases: proceed at your own RSK. *Proc Natl Acad Sci USA* 1993; **90**: 5889-5892
45 **Klonowski-Stumpe H,** Reinehr R, Fischer R, Warskulat U, Luthen R, Haussinger D. Production and effects of endothelin-1 in rat pancreatic stellate cells. *Pancreas* 2003; **27**: 67-74
46 **Ikejiri N.** The vitamin A-storing cells in the human and rat pancreas. *Kurume Med J* 1990; **37**: 67-81
47 **Kakugawa Y,** Paraskevas S, Metrakos P, Giaid A, Qi SJ, Duguid WP, Rosenberg L. Alterations in pancreatic microcirculation and expression of endothelin-1 in a model of chronic pancreatitis. *Pancreas* 1996; **13**: 89-95
48 **Izumi M,** Suda K, Torii A, Inadama E. Pancreatic ductal myofibroblasts. Proliferative patterns in various pathologic situations. *Virchows Arch* 2001; **438**: 442-450

Science Editor Guo SY **Language Editor** Elsevier HK

PO Box 2345, Beijing 100023, China
www.wjgnet.com
wjg@wjgnet.com

ELSEVIER

World J Gastroenterol 2005;11(39):6152-6158
World Journal of Gastroenterology ISSN 1007-9327
© 2005 The WJG Press and Elsevier Inc. All rights reserved.

• *BASIC RESEARCH* •

Identification of *anrF* gene, a homology of *admM* of andrimid biosynthetic gene cluster related to the antagonistic activity of *Enterobacter cloacae* B8

Xu-Ping Yu, Jun-Li Zhu, Xue-Ping Yao, Shi-Cheng He, Hai-Ning Huang, Wei-Liang Chen, Yong-Hao Hu, De-Bao Li

Xu-Ping Yu, Jun-Li Zhu, Xue-Ping Yao, Shi-Cheng He, Veterinary Medicine Department, Animal Science College, Zhejiang University, Hangzhou 310029, Zhejiang Province, China
Xu-Ping Yu, Hai-Ning Huang, Wei-Liang Chen, De-Bao Li, Institute of Biotechnology, Zhejiang University, Hangzhou 310029, Zhejiang Province, China
Jun-Li Zhu, College of Food Science, Biotechnology and Environmental Engineering, Zhejiang Gongshang University, Hangzhou 310035, Zhejiang Province, China
Xue-Ping Yao, Yong-Hao Hu, Veterinary Medicine Department, Animal Science College, Gansu Agricultural University, Lanzhou 730070, Gansu Province, China
Supported by the National Natural Science Foundation of China, No. 39870034; the National High Technology Research and Development Program of China, the 863 Program, No. 104-04-01-01; and the Major Project of Science and Technology Development of Zhejiang Province, No. 021102529
Co-first-authors: Xu-Ping Yu and Jun-Li Zhu
Co-correspondents: Xu-Ping Yu and De-Bao Li
Correspondence to: Dr. Xu-Ping Yu, Veterinary Medicine Department, Animal Science College, Zhejiang University, Hangzhou 310029, Zhejiang Province, China. xpyu@zju.edu.cn
Telephone: +86-571-86971096 Fax: +86-571-86971096
Received: 2005-01-24 Accepted: 2005-04-11

Abstract

AIM: To identify the gene (s) related to the antagonistic activity of *Enterobacter cloacae* B8 and to elucidate its antagonistic mechanism.

METHODS: Transposon-mediated mutagenesis and tagging method and cassette PCR-based chromosomal walking method were adopted to isolate the mutant strain (s) of B8 that lost the antagonistic activity and to clone DNA fragments around Tn5 insertion site. Sequence compiling and open reading frame (ORF) finding were done with DNAStar program and homologous sequence and conserved domain searches were performed with BlastN or BlastP programs at www.ncbi.nlm.nih.gov. To verify the gene involved in the antagonistic activity, complementation of a full-length clone of the *anrF* gene to the mutant B8F strain was used.

RESULTS: A 3 321 bp contig around the Tn5 insertion site was obtained and an ORF of 2 634 bp in length designated as *anrF* gene encoding for a 877 aa polyketide synthase-like protein was identified. It had a homology of 83% at the nucleotide level and 79% ID/87% SIM at the protein level, to the *admM* gene of *Pantoea agglomerans* andrimid biosynthetic gene cluster (AY192157). The Tn5 was inserted at 2 420 bp of the gene corresponding to the COG3319 (the thioesterase domain of type I polyketide synthase) coding region on B8F. The antagonistic activity against *Xanthomonas oryzae pv. oryzae* was resumed with complementation of the full-length *anrF* gene to the mutant B8F.

CONCLUSION: The *anrF* gene obtained is related to the antagonistic activity of B8, and the antagonistic substances produced by B8 are andrimid and/or its analogs.

© 2005 The WJG Press and Elsevier Inc. All rights reserved.

Key words: *Enterobacter cloacae* B8; Antagonistic mechanism; *anrF* gene; Andrimid biosynthetic gene cluster

Yu XP, Zhu JL, Yao XP, He SC, Huang HN, Chen WL, Hu YH, Li DB. Identification of *anrF* gene, a homology of *admM* of andrimid biosynthetic gene cluster related to the antagonistic activity of *Enterobacter cloacae* B8. *World J Gastroenterol* 2005; 11(39): 6152-6158
http://www.wjgnet.com/1007-9327/11/6152.asp

INTRODUCTION

Enterobacter cloacae strain B8 isolated from rice leaves was first recognized as an antagonistic bacterium of *Xanthomonas oryzae pv. oryzae*[1]. Its biological characteristics, antagonistic activity, and substances have been reported[2,3]. Satisfactory results have been obtained on anti-rice bacterial leaf brilliant in net house and in field[4]. Additionally, *E. cloacae* B8 is also antagonistic to many other plant bacterial pathogens such as *Pseudomonas*, *Agrobacterium*[3]. It has been reported that substances purified from *E. cloacae* B8 inhibit human (animal) bacterial pathogens such as MRSA[5,6].

Few but an *E. cloacae* strain EcCT-501R3 was reported to have antagonistic activity, which inhibits *Pythium ultimum* sporangium germination[7,8]. A competitive exclusion mechanism, competitive utilization of long-chain fatty acids of seed exudates, has been discovered and verified with transposon-mediated mutagenesis and tagging[9]. Previous researches on *E. cloacae* B8, however, showed that it produces antagonistic substances and differs from EcCT-501R3[1,3].

To elucidate the antagonistic mechanism of *E. cloacae* B8, transposon tagging[9-12] strategy was employed to clone DNA fragment related to its antagonistic activity. After a DNA fragment was cloned, cassette PCR-based chromosomal

walking[13-15] was used to get the flanked unknown DNA. We have previously reported the cloning and analysis of an antagonistic-related DNA fragment[16,17] and the verification of loss of antagonistic activity of mutant strains, by Southern blotting analysis, as a result of the insertion of a single copy of Tn5[18]. Here, we report the cloning and identification of the full-length *anrF* gene and the verification of its participation in the antagonism of B8.

MATERIALS AND METHODS

Bacterial strains, plasmids and chemicals

E. cloacae B8 (rif^r) is the antagonistic bacterium isolated from rice leaves in our laboratory[3,19]. *X. oryzae pv. oryzae* strain Xcom3104 (rif^r kan^r) was used as an indicator bacterium of antagonistic activity. The suicide plasmid pZJ25 (cm^r kan^r mob::Tn5) and its host *E.coli* S17-1 (thi pro $hsdR^-$ $hsdM^+$ recA RP4)[20] were gifts from Professor Jin-Sheng Wang of Nanjing Agricultural University, China. The cloning vector pBluescript SK+ (pBS) and its host *E. coli* DH5a were purchased from Stratagene. pFastBac^{TM}HTA was purchased from Invitrogen. pMD18-T vector was a product of Takara. Restriction enzymes, T4 DNA ligase, CIAP, *Taq* DNA polymerase, dNTPs, DNA marker DL2000, marker 3 kb, PCR product purification kit, etc., were supplied by Promega, Takara, Sangon and/or Zeheng. Oligonucleotides and primers used in this research were synthesized in Bioasia Biotech.

Transposon-mediated mutagenesis

The transfer of suicide plasmid pZJ25 from *E. coli* host S17-1 (donor) to *E. cloacae* B8 (receptor, rif^r) was mediated with conjugation[21]. Tranposonated B8 clones (rif^r kan^r cm^s) were selected on plates with rifampicin and kanamycin. The antagonistic characteristics were then checked using Xcom 3104 (rif^r kan^r) as an indicator[19].

Cloning of F fragment from B8F with tagging method

Genomic DNA of B8F, an antagonistic mutant strain of B8, was isolated, cut with *Bam*HI and ligated to *Bam*HI cut and dephosphorylated pBS. Recombinant clones were selected on plates with both kanamycin and ampicillin. Only one DNA fragment on the left of the insertion site was obtained with this step, as *Bam*HI cut Tn5 into two fragments and the intact Kan^r gene was in the 2.7 kb left fragment. The F fragment was a DNA fragment on the left of inserted Tn5 on B8F genome (Figure 1).

Cloning of DNA on the right of insertion site with chromosomal walking

Two sets of cassettes and primers were adopted in our chromosomal walking experiments. The *Pst*I cassette and its related CP primer were synthesized as previously described[12]. The *Sau*3AI cassette and its related CS primer and FS2, F1815 and F2000, the specific primers corresponding to known sequences, were newly designed and synthesized. They were as follows:

*Pst*I cassette:
5' HO-AGATTCGGTGCGTGCTTGACTGCA-OH 3'
3' HO-TCTAAGCCACGCACGAACTG-OH 5'
*Sau*3AI cassette:
5' HO-CTGTGGTGGTTCCGATGTATG-OH 3'
3' HO-ACCACCAAGGCTACATACCTAG-OH 5'
Cassette primers:
CP primer: AGATTCGGTGCGTGCTTGAC
CS primer: CTGTGGTGGTTCCGATGTAT
Specific primers:
FS2: GTTTACTGGCCAGTTATTGTTG
F1815: CCACAGAACGTCTTGTCAT
F2000: CGGAATGAAGAGGGTAAGG

Genomic DNA was extracted from B8 and partially digested with *Sau*3AI or completely digested with *Pst*I. DNA of 2-10 kb in length was recovered from gel and ligated to *Sau*3AI or *Pst*I cassette to construct cassette genomic libraries. Related cassette primer (CS or CP) and specific primer were used to amplify target DNA of unknown region from the libraries. The PCR conditions were as follows: pre-denaturation for 5 min at 94 ℃, and denaturation at 94 ℃ for 30 s, annealing at 52 ℃ for 60 s and extension at 72 ℃ for 5 min for 30 cycles, and a final extension at 72 ℃ for 10 min. Three rounds of PCR-based chromosomal walking, using *Pst*I and *Sau*3AI cassettes and related primers by turns, were performed to cover the full length of *anrF* gene (Figure 1).The full-length *anrF* gene was shown on the top (gray single line). The direction of the gene (narrow horizontal arrow, at right) and the Tn5 insertion site (thick vertical arrow) were marked. The long double line underneath stood for the F contig obtained in this research. The dark part on

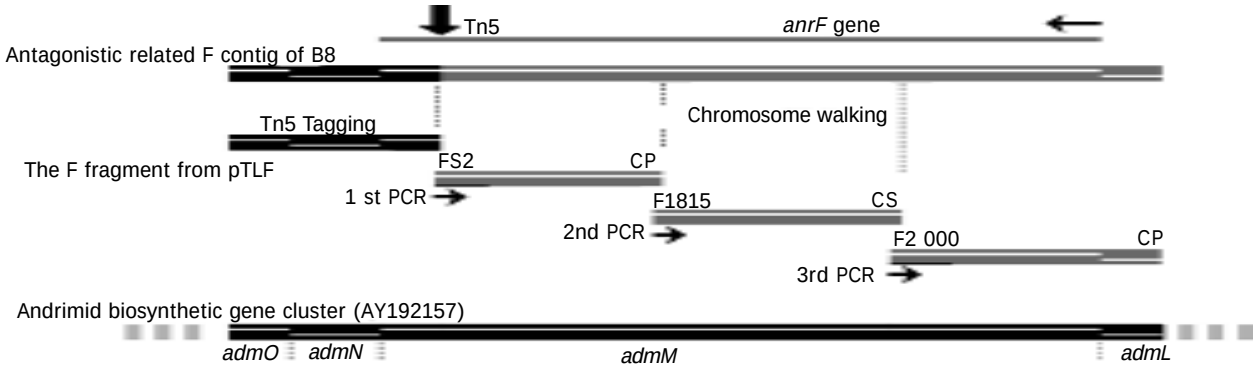


Figure 1 Framework of the cloning of full-length *anrF* gene with transposon tagging and chromosome walking.

the left of Tn5 insertion site (the F fragment) was obtained with transposon tagging. The gray part on the right was obtained with chromosomal walking. The four separate lines below were four steps (one tagging and three rounds of PCR) to get the contig. Primers were marked on top of the three gray lines. The black double line at the bottom showed the corresponding genes of *P. agglomerans* andrimid biosynthetic gene cluster (AY192157).

DNA sequencing and data analysis

The F fragment was sequenced, after subcloning of pTLF from M13 universal primer and P1 primer (CATGGAAG-TCAGATCCTGGA), a primer designed according to the sequence of the left edge of Tn5. PCR products of chromosomal walking were cloned into T-vector and sequenced using M13 universal primer. The DNA sequencing was done in Bioasia Biotech, Shanghai. DNA sequences obtained were edited, compiled, translated, and compared using DNAStar program. Homologous sequence and putative-conserved domain searches were done with BlastN and/or tBlastX and/or BlastP program at www.ncbi.nlm.nih.gov.

Continuity analysis of anrF gene in original B8 and its mutant B8F strain

Two primers were designed to amplify the full-length *anrF* gene. The upstream primer F21 (TTTTGTTGATGGAA-AGTCGCA) was located 144-126 bp up of the start codon. The downstream primer F2600 (CACCCAGCTGA-TGAAGTAAT) was located on opposite strand 73-56 bp down of the stop codon. The DNA fragments between the primers in the genomes of B8 and B8F were about 2 851 bp and 8.3 kb respectively. Genomic DNA of B8 or B8F was used as template. After 30 cycles of amplification, 6 μL of PCR products were applied to agarose gel electrophoresis to check the amplification. The amplified products were cloned and sequenced.

Verification of anrF gene participation in antagonism of B8

The full-length *anrF* gene amplified from B8 was cloned into pMD18-T vector and the resulting recombinant plasmid was designated as pMD-F. Gentamicin-resistance gene (*Gen*^{r}) was amplified with two primers (acc1-up: CGTGGAAACG-GATGAAG, acc1-down: ACCTGGCGGCGTTGTGACA) from pFastBac^{TM}HTA and cloned into pMD18-T too. The resulting recombinant plasmid was designated as pMD-G. The *Gen*^{r} gene was recovered from pMD-G with *Hin*dIII and *Bam*HI double cut and filled with klenow and inserted into *Xba*I cut and klenow filled pMD-F. The target plasmid with *Gen*^{r} and the full-length *anrF* gene was designated as pMD-FG.

Mutant *E. cloacae* B8F was cultured to an A_{600} about 0.6 in LB medium, and washed thrice in cold glycerol buffer. Plasmid pMD-FG was transformed into B8F with electroporation. The transformed bacteria were screened on plates with both ampicillin and gentamicin and verified by PCR amplification of *anrF* and *Gen*^{r} genes. The pMD-FG transformed strains were then inoculated on Wakimoto agar and cultured at 30 ℃ for 48 h, the resume of antagonistic characteristics was checked with the indication of *X. oryzae pv. oryzae* strain Xcom3104.

RESULTS

Transposon-mediated mutagenesis

The suicide plasmid pZJ25 was transferred into *E. cloacae* B8 by conjugation with the help of donor *E. coli* S17-1. The conjugation and transposition ratio was about 5×10^{-6}. A total of 1 500 transposed colonies (Rif^r Kan^r Cm^s) were obtained and two antagonistic mutant strains, one of which was designated as B8F, were selected.

Cloning of F fragment from B8F with tagging method

A recombinant plasmid designated as pTLF, a plasmid with intact *Kan*^{r} gene of Tn5 and a DNA fragment on the left of the insertion site (designated as F fragment), was isolated. The pTLF had two foreign *Bam*HI fragments, one of which was about 3.5 kb in length and contained the target F fragment and a fragment of Tn5 (with the *Kan*^{r} gene, about 2.7 kb in length). After subcloning, the 735 bp sequence of the F fragment was obtained with M13 universal sequencing primer and P1 primer.

Cloning of DNA fragments on the right of Tn5 insertion site with chromosomal walking

Only one DNA fragment on the left of insertion site was obtained with transposon tagging method. In order to know the full-length gene interrupted by Tn5 insertion, cassette PCR-based chromosomal walking method was adopted to clone DNA fragments on the right of insertion site. The framework of the cloning of the full-length *anrF* gene with transposon tagging and chromosomal walking was shown (Figure 1). With the use of specific primers (FS2, F1815, or F2000) and cassette primers (CP or CS) by turns, DNA fragments of unknown region were amplified from related cassette (*Pst*I or *Sau*3AI) libraries. The PCR products from three different rounds of chromosomal walking were obtained (Figure 2). They were about 1.2 kb in *Pst*I library (1st walking), about 950 bp in *Sau*3AI library (2nd walking), and about 900 bp in *Pst*I library (3rd walking), respectively. The total sequence obtained with chromosomal walking was 2 586 bp.

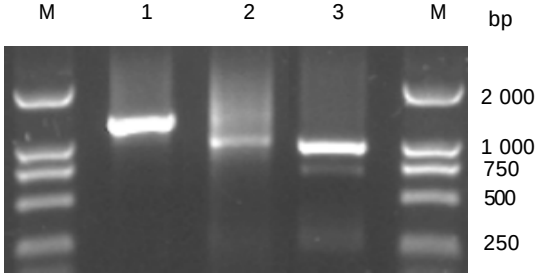


Figure 2 PCR products from three rounds of chromosomal walking. 1: PCR products, 1 209 bp in size, amplified from B8/*Pst*I-cassette library with FS2 and CP primers; 2: PCR products, 962 bp in size, amplified from B8/*Sau*3AI cassette library with F1815 and CS; 3: PCR products, mainly 900 bp in size, amplified from B8/*Pst*I cassette library with F2000 and CP; M: marker DL2000.

Sequence analysis of full-length anrF gene

A contig of 3 321 bp in length was obtained by transposon tagging and three rounds of chromosomal walking. Four ORFs, two complete and two partial were identified. One ORF, 2 634 bp in length, disrupted by the insertion of Tn5

in B8F was designated as *anrF* gene (accession no. AY633625) encoding for a 877 aa polyketide synthase-like protein. The Tn5 insertion site was at 2 420 bp of the *anrF* gene, and was at 214 bp before the stop codon.

BlastN search showed that the nucleotide sequence of *anrF* gene had a homology of 83% to that of *admM* gene of *P. agglomerans* andrimid biosynthetic gene cluster (AY192157). The alignment of *anrF* and *admM* genes is shown in Figure 3.

BlastP search showed that the deduced amino acid sequence encoded by the *anrF* gene was homologous to AdmM (79%

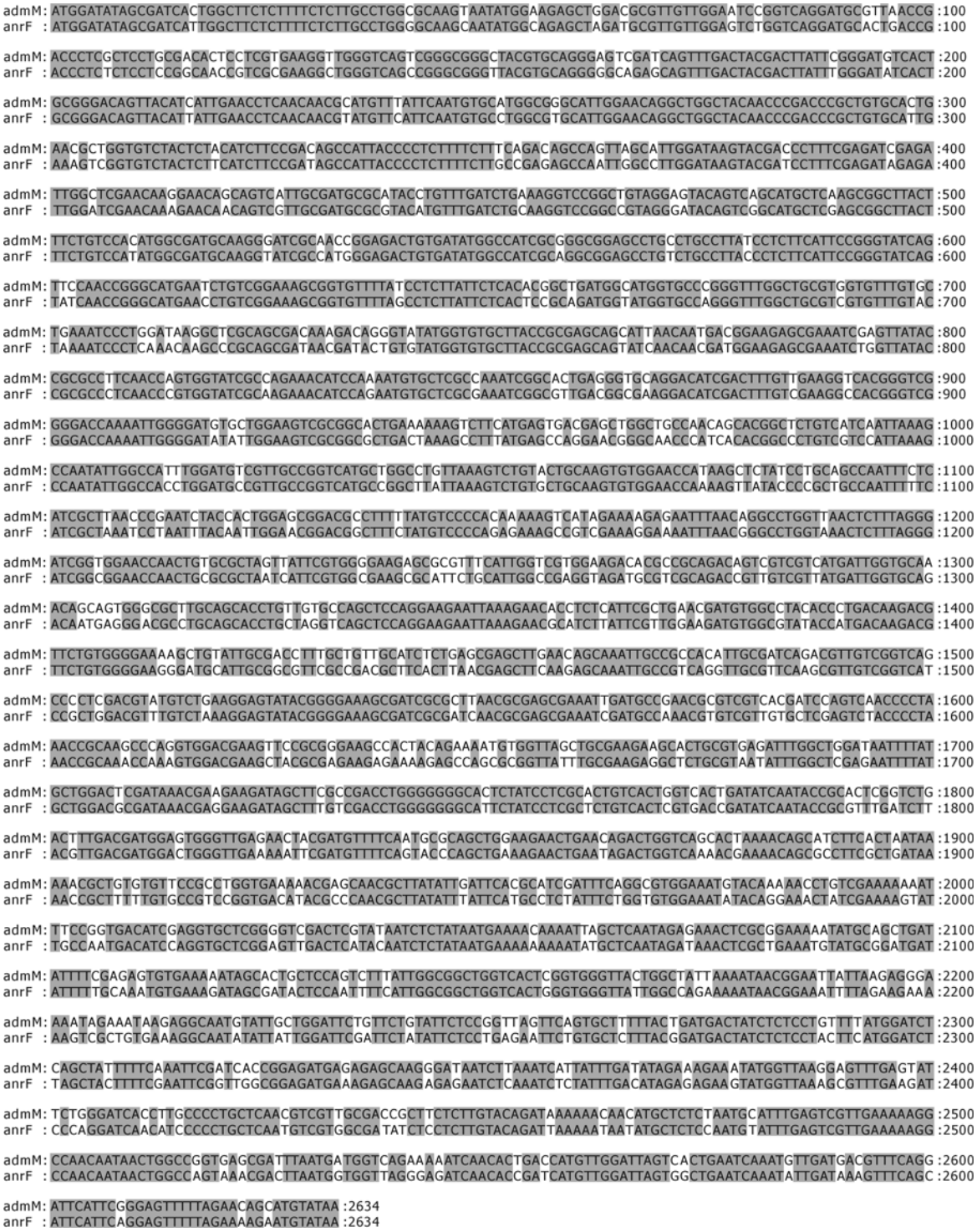


Figure 3 Alignment of nucleotide sequences of *anrF* gene and *admM* gene of *P. agglomerans* andrimid biosynthetic gene cluster (AY192157). The names of the genes are typed at the left and the number of nucleotides is at the right. The identical nucleotides between two genes are marked with gray background.

ID/87% SIM) and many other proteins of polyketide/non-ribosomal peptide synthetase or polyketide synthase (type I) modules (about 28-38% ID/45-58% SIM). Conserved domain search showed that the N-terminal of the protein (about 1-410 aa) encoded for a polyketide synthase module (COG3321) or animal-type fatty-acid synthase (KOG1202) or ketoacyl synthase (pfam00109 and pfam02801) or 3-oxoacyl-(acyl-carrier-protein) synthase (FabB or COG0304, and KOG1394)-like domain. The middle sequence (about 550-610 aa) encoded for a phosphopantetheine attachment site (pfam00550)-like domain. The C terminal (about 640-877 aa) encoded for a thioesterase of type I polyketide synthase (COG3319, pfam00975, and COG3208)-like domain, which was disrupted by the insertion of Tn5 in B8F.

Continuity analysis of anrF gene in original B8 and its mutant B8F strain

With F21 and F2600 as primers, no band was amplified in the reaction mixture using B8F genomic DNA as template, while a PCR product 2.8 kb in length, as expected, was observed in that of B8 (Figure 4). The 2.8 kb PCR product of B8 was further cloned and sequenced. The sequence result conformed the continuity of the *anrF* gene in B8.

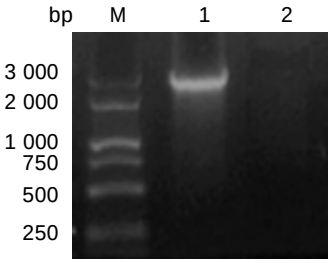


Figure 4 PCR amplification of full-length *anrF* gene. 1: PCR products amplified from B8; 2: PCR products amplified from B8F; M: marker 3 kb.

Verification of anrF gene participation in antagonism of B8

The pMD-FG, a plasmid with the full-length *anrF* and *Gen*^{r} genes, was constructed and transformed into the mutant *E. cloacae* B8F. The antagonistic activity of pMD-FG transformed B8F against *X. oryzae pv. oryzae* was then resumed, though the antagonistic ring was a little bit small and ambiguous (Figure 5).

DISCUSSION

E. cloacae B8 is an antagonistic bacterium isolated from rice leaves, using *X. oryzae pv. oryzae* Xcom3104 as an indicator[1]. It has a strong antagonistic activity against *X. oryzae pv. oryzae* and satisfactory results have been obtained on anti-rice bacterial leaf brilliant in net house and in field[4]. Further researches showed that *E. cloacae* B8 and its antagonistic substances are also antagonistic to many other plant bacterial pathogens such as *Pseudomonas*, *Agrobacterium*[3], and human (animal) bacterial pathogens such as MRSA[5,6]. *E. cloacae* B8 and its antagonistic substances can be potentially used for the control of the rice bacterial leaf brilliant and many other bacterial diseases of plants, animals and humans.

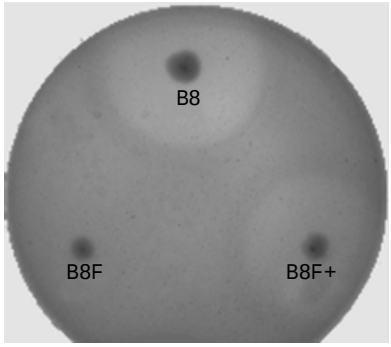


Figure 5 Antagonistic activity of B8, B8F and B8F/pMD-FG. B8F+: pMD-FG transformed B8F.

It was reported that *E. cloacae* EcCT-501R3 has an antagonistic activity[7,8]. Two antagonistic-related genes for linoleic acid utilization, *fadB* and *fadL*, have been cloned using transposon-mediated mutagenesis and tagging. Further researches have verified that *E. cloacae* EcCT-501R3 inhibits *Pythium ultimum* sporangium germination by a competitive exclusion mechanism, the competitive utilization of long-chain fatty acids of seed exudates[9].

Our previous work, however, showed that B8 has an antagonistic mechanism different from what has been reported[1,3]. To elucidate the antagonistic mechanism and to clarify the antagonistic substances of *E. cloacae* B8, transposon tagging strategy[9-12] was employed to clone genes related to its antagonistic activity. With suicide plasmid pZJ25 carrying Tn5, two antagonistic mutant strains, one of which was named B8F, were selected. Tagging with *Kan*^{r} gene of Tn5, the F fragment on the left of Tn5 insertion site was cloned in pTLF. Then, cassette PCR[13-15]-based chromosomal walking was applied to the amplification of unknown DNA fragments on the right of Tn5 insertion site. A contig of 3 321 bp in length was obtained after three rounds of chromosomal walking together with the F fragment from transposon tagging. One complete ORF of 2 634 bp in length, disrupted by the Tn5 insertion in B8F, was identified in the contig. It encoded for a 877 aa polyketide synthase-like protein and was designated as *anrF* gene. The Tn5 insertion site was at 2 420 bp of the *anrF* gene, and was at 214 bp before the stop codon, suggesting that the loss of antagonistic activity of mutant strain B8F was a result of the knock-out of *anrF* gene by Tn5.

To confirm this theory, the continuity of the *anrF* gene in the original B8 and its mutant B8F strains was checked. The complete *anrF* gene 2.8 kb in length was amplified from the B8 genome. The sequence result further confirmed the continuity of *anrF* gene in the original B8. The length of the DNA fragment between the primers in the genome of B8F was about 8.3 kb. However, no band was amplified from B8F. As the parameters set for amplification were suitable for amplification fragments 2.8 kb or less in length but not for fragments up to 8.3 kb.

In addition, plasmid pMD-FG with full-length *anrF* and *Gen*^{r} genes was constructed. After pMD-FG was transformed into B8F, a mutant strain of B8 knocked out by Tn5-mediated mutagenesis, the antagonistic

characteristics were resumed, indicating that the *anrF* gene participated in the production of the antagonistic activity of B8.

BlastN search showed that the nucleotide sequence of the *anrF* gene had a homology of 83% to that of the *admM* gene of *P. agglomerans* andrimid biosynthetic gene cluster (AY192157). BlastP search showed the deduced amino acid sequence encoded by the *anrF* gene was homologous to the AdmM (79% ID/87% SIM) and many other proteins of polyketide synthase/non-ribosomal peptide synthetase (about 28-38% ID/45-58% SIM). Domain search showed that the N-terminal of the protein encoded for a polyketide synthase module (COG3321) or animal-type fatty-acid synthase (KOG1202)-like domain. The middle sequence encoded for a phosphopantetheine attachment site (pfam00550)-like domain. And the C terminal encoded for a thioesterase of type I polyketide synthase (COG3319)-like domain, which was disrupted by the insertion of Tn5. It was this insertion that led to the loss of antagonistic activity of B8F, suggesting that the protein encoded by *anrF* gene is a polyketide synthase similar to AdmM of *P. agglomerans*, and that the antagonistic substances produced by B8 are andrimid and/or analogs of andrimid. This result is consistent with our early observations[1,3].

Andrimid and its analogs are antibiotic substances of the polyketide (pyrrolidinedione) family[22]. Only three different strains of bacteria, other than B8, have been reported to produce these substances so far. Frenenhagen *et al.*[23], first reported the identification of andrimid, a new peptide antibiotic produced by an intracellular bacterial symbiont isolated from a brown planthopper. It has been reported that andrimid exhibits a moderate activity against *Bacillus sp.* and a very good activity against *X. campestris*, an early name of the pathogen of bacterial blight in rice plants[23]. Needham *et al.*[24], reported that andrimid and Moiramides A-C are produced in culture by a marine isolate of *Pseudomonas fluorescens*. Singh *et al.*[25], further showed that andrimid secreted from this strain exhibits antibacterial activity against both Gram-positive and Gram-negative bacteria. Oclarit *et al.*[26], found that anti-*Bacillus* peptide antibiotic, an andrimid in the marine sponge, *Hyatella* species, is produced by an associated *Vibrio* species bacterium. Freiberg *et al.*[22], reported that andrimid and its analogs act as selective inhibitors of bacterial acetyl-CoA carboxylase.

However, no genes related to the production of andrimid are published so far, except for the andrimid biosynthetic gene cluster of *P. agglomerans* (AY192157). The complete genome of AY192157 is 28 485 bp in length and encodes for 21 genes, from *admA*, *admB* to *admU*. The *anrF* gene cloned in this research has a homology of 83% to *admM*. Furthermore, the arrangement and the sequences of other ORFs or non-coding regions around the *anrF* gene have shown that the F contig obtained in this research is an equivalent of a part of AY192157 (data not shown). *P. agglomerans* (formerly *Erwinia herbicola*) is a closely related but nonpathogenic bacterium of *E. amylovora*[27]. It usually accompanies *E. amylovora* in the wild and produces a family of antibiotics[28-30] to inhibit fire blight, a devastating disease of rosaceous plants such as apple and pear caused by the latter bacterium. *E. cloacae* B8 has been isolated from rice leaves as an antagonistic bacterium of *X. oryzae pv. oryzae*. However, both *E. cloacae* and *P. agglomerans* are members of the *Enterobacteriacea* family. Whether this is the reason why the *anrF* and *admM* genes have a high similarity, or whether the equivalents of andrimid biosynthetic genes are similar or identical in bacteria other than *Enterobacteriacea* family, including *Pseudomonas* and *Vibrio* remains to be studied.

REFERENCES

1 **Chen WL**, Ge WX, Li DB. A study on *Enterobacter cloacae* B8, *Bacillus subtillus* B826 and their antagonistic substance to *Xanthomonas campestris pv. oryzae*. *Zhejiang Nongye Daxue Xuebao* 1990; **16**(Suppl 2): 61-67

2 **Xu YP**, Zang RC, Chen WL, Lou YC. Promoting plant growth and IAA analysis of *Enterobacter cloacae* B8 fermentation liquid. *Zhejiang Daxue Xuebao* 2001; **27**: 282-284

3 **Chen WL**. Antagonistic substances produced by bacterial strains to *Xanthomonas oryzae pv. oryzae*. Ph. D. thesis. *Zhejiang Unviersity* 2001: 59-66

4 **Chen WL**, Xu P, Gong FH, Li DB. Study on coloninzation of *Enterobacter cloacae* B8x on rice leaves and its control of rice bacterial leaf blight (*Xanthomonas oryzae pv. oryzae*). *Nongye Shengwujishu Xuebao* 1994; **2**: 61-66

5 **Zhang R**, Chen WL, Zhu BR. The antagonistic activities of the extract of *Enterobacter clocae* B8 to methicillin-resistant *Staphylococcus aureus*. *Zhonghua Weishengwuxue He Mianyixue Zazhi* 2003; **23**: 172

6 **Ya-Ping J**, Wei-Liang C, Rong Z, Bai-Rong Z. The biological activity of antibacterial substance produced by *Enterobacter cloacae* B8. *Rinsho Biseibutshu Jinsoku Shindan Kenkyukai Shi* 2003; **13**: 115-120

7 **van Dijk K**, Nelson EB. Inactivation of seed exudates stimulants of *Pythium ultimum* sporangium germination by biocontrol strain of *Enterobacter cloacae* and other seed-associated bacteria. *Soil Biol Biochem* 1998; **29**: 351-355

8 **Kageyama K**, Nelson EB. Differential inactivation of seed exudate stimulation of *Pythium ultimum* sporangium germination by *Enterobacter cloacae* influences biological control efficacy on different plant species. *Appl Environ Microbiol* 2003; **69**: 1114-1120

9 **van Dijk K**, Nelson EB. Fatty acid competition as a mechanism by which *Enterobacter cloacae* suppresses *pythium ultimum* sporangium germination and damping-off. *Appl Environ Microbiol* 2000; **66**: 5340-5347

10 **Wei JF**, Zhang SG, Ma YC. Transposon Tn5-induced INA$^-$ Mutants in INA$^+$ Bacteria. *Yunan Nongye Daxue Xuebao* 2002; **17**: 1-4

11 **Mills D**. Transposon mutagenisis and its potential for studying virulence genes in plant pathogens. *Ann Rev Phytopathol* 1985; **23**: 297-320

12 **Kumar A**, des Etages SA, Coelho PS, Roeder GS, Snyder M. High-throughput methods for the large-scale analysis of gene function by transposon tagging. *Methods Enzymol* 2000; **328**: 550-574

13 **Kilstrup M**, Kristiansen KN. Rapid genome walking: a simplified oligo-cassette mediated polymerase chain reaction using a single genome-specific primer. *Nucleic Acids Res* 2000; **28**: E55-58

14 **Riley J**, Butler R, Ogilvie D, Finniear R, Jenner D, Powell S, Anand R, Smith JC, Markkham AF. A novel rapid method for the isolation of terminal sequences from yeast artificial chromosome (YAC) clones. *Nucleic Acids Res* 1990; **18**: 2887-2890

15 **Zhang Z**, Gurr SJ. Walking into the unknown: a 'step down' PCR-based technique leading to the direct sequence analysis of flanking genomic DNA. *Gene* 2000; **253**: 145-150

16 **Yu XP**, Zhu JL, Yao XP, He SC, Huang HN, Chen WL, Li DB.

Cloning and analysis of the antagonistic related genes of *Enterobacter cloacae* B8. *Chin Sci Bull* 2004; **49**: 1370-1375
17 **Yu XP**, Zhu JL, Yao XP, He SC, Huang HN, Chen WL, Li DB. Cloning and analysis of the antagonistic related genes of *Enterobacter cloacae* B8. *Kexue Tongbao* 2004; **49**: 1139-1144
18 **Huang HN**, Yu XP, Gong HF, Xu P, Chen WL, Li DB. Cloning and detecting of the antagonistic related genes of *Enterobacter cloacae* B8 with transposon tagging method. *Zhejiang Daxue Xuebao* 2005, in press
19 **Xu P**, Chen WL, Zhu WG, Li DB. A drug resisitant mutant of antagonistic bacterium *Eterobacter cloacae* B8. *Zhejiang Nongye Daxue Xuebao* 1992; **18**: 115-119
20 **Li P**, Long JY, Huang YC, Zhang Y, Wang JS. The avrXa3, a new member of avrBs3 family isolated from *Xanthomonas oryzae pv. oryzae* is an avirulent gene of double function. *Ziran Kexue Jinzhan* 2004; **14**: 767-781
21 **Wang JS**, He CY, Ye HY. Tn5-induced virulence gene mutants and their biochemical properties of *Xanthomonas campestris pv. oryzae*. *Zhiwu Bingli Xuebao* 1992; **22**: 217-223
22 **Freiberg C**, Brunner NA, Schiffer G, Lampe T, Pohlmann J, Brands M, Raabe M, Habich D, Ziegelbauer K. Identification and characterization of the first class of potent bacterial acetyl-CoA carboxylase inhibitors with antibacterial activity. *J Biol Chem* 2004; **279**: 26066-26073
23 **Frenenhagen A**, Tamura SY, Kenny PTM, Komura H, Naya Y, Nakanishi K. Andrimid, a new peptide antibiotic produced by an intracellular bacterial symbiont isolated from a brown planthopper. *J Am Chem Soc* 1987; **109**: 4409-4411
24 **Needham J**, Kelly MT, Ishige M, Andersen RJ. Andrimid and moiramides A-C, metabolites produced in culture by a marine isolate of the bacterium *Pseudomonas fluorescens*: structure elucidation and biosynthesis. *J Org Chem* 1994; **59**: 2058-2063
25 **Singh MP**, Mroczenski-Wildey MJ, Steinberg DA, Andersen RJ, Maiese WM, Greenstein M. Biological activity and mechanistic studies of andrimid. *J Antibiot* 1997; **50**: 270-273
26 **Oclarit JM**, Okada H, Ohta S, Kaminura K, Yamaoka Y, Iizuka T, Miyashiro S, Ikegami S. Anti-bacillus substance in the marine sponge, *Hyatella* species, produced by an associated *Vibrio* species bacterium. *Microbios* 1994; **78**: 7-16
27 **Gavini F**, Mergaert J, Beji A, Mielcarek C, Izard D, Kersters K, de Ley J. Transfer of *Enterobacter agglomerans* (Beijerinck 1988) Ewing and Fife 1972 to *Pantoea* gen. nov. as *Pantoea agglomerans* comb. nov. and description of *Pantoea dispersa* sp. nov. *Int J Syst Bacteriol* 1989; **39**: 337-345
28 **Wright SA**, Zumoff CH, Schneider L, Beer SV. *Pantoea agglomerans* strain EH318 produces two antibiotics that inhibit *Erwinia amylovora in vitro*. *Appl Environ Microbiol* 2001; **67**: 284-292
29 **Giddens SR**, Houliston GJ, Mahanty HK. The influence of antibiotic production and pre-emptive colonization on the population dynamics of *Pantoea agglomerans* (*Erwinia herbicola*) Eh1087 and *Erwinia amylovora* in planta. *Environ Microbiol* 2003; **5**: 1016-1021
30 **Wodzinski RS**, Paulin JP. Frequency and diversity of antibiotic production by putative *Erwinia herbicola* strains. *J Appl Bacteriol* 1994; **76**: 603-607

Science Editor Wang XL and Guo SY **Language Editor** Elsevier HK

PO Box 2345, Beijing 100023, China
www.wjgnet.com
wjg@wjgnet.com

ELSEVIER

World J Gastroenterol 2005;11(39):6159-6164
World Journal of Gastroenterology ISSN 1007-9327
© 2005 The WJG Press and Elsevier Inc. All rights reserved.

• *BASIC RESEARCH* •

Receptor-binding domain of SARS-Cov spike protein: Soluble expression in *E.coli*, purification and functional characterization

Jing Chen, Lin Miao, Jia-Ming Li, Yan-Ying Li, Qing-Yu Zhu, Chang-Lin Zhou, Hong-Qing Fang, Hui-Peng Chen

Jing Chen, Lin Miao, Yan-Ying Li, Hong-Qing Fang, Hui-Peng Chen, Institute of Biotechnology, Academy of Military Medical Science, Beijing 100071, China
Jing Chen, Chang-Lin Zhou, The Pharmaceutical University of China, Nanjing 210009, Jiangsu Province, China
Jia-Ming Li, Qing-Yu Zhu, Institute of Microbiology and Epidemiology, Academy of Military Medical Sciences, Beijing 100071, China
Co-Correspondence: Hui-Peng Chen
Correspondence to: Hong-Qing Fang, Institute of Biotechnology, Academy of Military Medical Science, 20 Dongda Street, Fengtai District, Beijing 100071, China. fanghongqing@yahoo.com.cn
Telephone: +86-10-66948824
Received: 2005-03-22 Accepted: 2005-04-11

Abstract

AIM: To find a soluble and functional recombinant receptor-binding domain of severe acute respiratory syndrome-associated coronavirus (SARS-Cov), and to analyze its receptor binding ability.

METHODS: Three fusion tags (glutathione *S*-transferase, GST; thioredoxin, Trx; maltose-binding protein, MBP), which preferably contributes to increasing solubility and to facilitating the proper folding of heteroprotein, were used to acquire the soluble and functional expression of RBD protein in *Escherichia coli* (BL21(DE3) and Rosetta-gamiB (DE3) strains). The receptor binding ability of the purified soluble RBD protein was then detected by ELISA and flow cytometry assay.

RESULTS: RBD of SARS-Cov spike protein was expressed as inclusion body when fused as TrxA tag form in both BL21 (DE3) and Rosetta-gamiB (DE3) under many different cultures and induction conditions. And there was no visible expression band on SDS-PAGE when RBD was expressed as MBP tagged form. Only GST tagged RBD was soluble expressed in BL21(DE3), and the protein was purified by ÄKTA Prime Chromatography system. The ELISA data showed that GST•RBD antigen had positive reaction with anti-RBD mouse monoclonal antibody 1A5. Further flow cytometry assay demonstrated the high efficiency of RBD's binding ability to ACE2 (angiotensin-converting enzyme 2) positive Vero E6 cell. And ACE2 was proved as a cellular receptor that meditated an initial-affinity interaction with SARS-Cov spike protein. The geometrical mean of GST and GST•RBD binding to Vero E6 cells were 77.08 and 352.73 respectively.

CONCLUSION: In this paper, we get sufficient soluble N terminal GST tagged RBD protein expressed in *E.coli* BL21 (DE3); data from ELISA and flow cytometry assay demonstrate that the recombinant protein is functional and binding to ACE2 positive Vero E6 cell efficiently. And the recombinant RBD derived from *E.coli* can be used to developing subunit vaccine to block S protein binding with receptor and to neutralizing SARS-Cov infection.

© 2005 The WJG Press and Elsevier Inc. All rights reserved.

Key words: Receptor-binding domain; SARS-Cov; Spike protein expression; *E.coli*

Chen J, Miao L, Li JM, Li YY, Zhu QY, Zhou CL, Fang HQ, Chen HP. Receptor-binding domain of SARS-Cov Spike protein: Soluble expression in *E.coli*, purification and functional characterization. *World J Gastroenterol* 2005; 11(39): 6159-6164

http://www.wjgnet.com/1007-9327/11/6159.asp

INTRODUCTION

Severe acute respiratory syndrome (SARS), a newly emerging infectious disease, is caused by a SARS-associated coronavirus (SARS-Cov)[1,2]. SARS-Cov can infect African green monkey kidney cells (Vero E6) and cause a similar disease in *Cynomolgus macaques* (*Macaca fascicularis*)[3,4]. The SARS viral genome comprises approximately 30 000 nucleotides, which are organized into approximately 13-15 open reading frames (ORFs), taking into consideration only those exceeding 50 amino acids in translational capacity[5,6]. Sequence comparison with corresponding ORFs of other known coronaviruses reveals a similar pattern of gene organization typical of coronaviruses[7]. SARS-Cov contains a single-strand plus-sense RNA genome about 30 kb in length and has a 5'-cap structure and a 3'-polyadenylation tract. And the genomic organization is typical of coronaviruses, having five major ORFs that encode the replicase polyproteins: the spike (S), envelope (E), and membrane (M) glycoproteins. The full-length genome sequence of SARS-Cov has been elucidated within few weeks after the identification of this novel pathogen[8-10].

When coronavirus enters the cells, the 50-region of viral genome is translated into a large poly-peptide that is cleaved by viral-encoded proteases to release RNA-dependent RNA polymerase and adenosine triphosphatase/helicase. These proteins, in turn, are responsible for replicating the viral genome as well as generating nested transcripts that are used in the synthesis of viral proteins. Viral membrane proteins, including S and M, are inserted into the endoplasmic reticulum (ER), while RNA genome assembles with the N

protein. This RNA-protein complex then associates with M proteins and buds into the lumen of the ER. The virus particles then migrate through the Golgi complex and exist in the cells by exocytosis[6,11]. The first step *in viral* infection is the binding of viral proteins to certain cellular receptors. So far, the S protein of coronavirus is considered as the site of viral attachment to the host cells. It has been shown that a cellular metallopeptidase, angiotensin-converting enzyme 2 (ACE2), could bind to S1 domain of SARS-Cov' S protein and support viral replication[12]. And a 193-amino-acid fragment of the S protein (residues 318-510) is a receptor binding domain (RBD) of SARS-Cov S protein[13]. Here we reported the soluble expression, purification, and functional characterization of RBD expressed in *Escherichia coli*.

MATERIALS AND METHODS

Materials

E.coli DH5α competent cells, *E.coli* BL21(DE3) competent cells, *E.coli* Rosetta-gamiB (DE3) competent cells, pET22b, TrxATag (Thioredoxin) expression vector pET32a were products of Novagen Inc. The genotype of Rosetta-gamiB (DE3): △*ara-leu 7697* △*lacX74* △*phoAPvuII pho*R *araD139 ahpC gale galK rspL* F'[*lac*+(*lacIq*)*pro*] *gor522*::Tn*10* (TcR) *trxB*:: kan (DE3) pRARE (CmR). GSTag (glutathione *S*-transferase) expression vector pGEX-4t-2 was purchased from Invitrogen Inc. Chromatography media Q Sepharose Fast Flow, Q Sepharose High Performance, Butyl Sepharose Fast Flow, Superdex 75, goat anti-GST polyclone antibody were purchased from Amersham Inc. FITC-labeled rabbit anti-goat IgG, goat anti-mouse IgG conjugated with HRP were products of Beijing Xin Jing Ke Biotechnology Co., Ltd. The primers with restriction enzyme sites *Bam*HI and *Xho*I to amplify RBD gene were synthesized by Beijing Bioasia Inc. pET-S plasmid containing the full length gene of S protein of SRAS-Cov (isolate BJ01, GenBank accession number AY278488) was kindly provided by Beijing Hua Da Gene Research Center. Anti-RBD of S protein mouse monoclonal antibody 1A5 was provided by the Institute of Microbiology and Epidemiology, Academy of Military Medical Sciences. pET-MBP was constructed by inserting maltose-binding protein (MBP) gene derived from *E.coli* JM109 strain into pET22b between *nde*I and *Bam*HI restriction enzyme sites, conserved by the Institute of Biotechnology, Academy of Military Medical Sciences.

Plasmids construction and engineering bacteria

A pair of primers was used in PCR reaction to amplify RBD gene (N terminal 318-510 amino acid fragments) of S protein from pET-S plasmid (EC1: 5'-CGGGATCCGACG-ATGACGATAAGAATATTACAAACTTGTGTCCT-3', EC2: 5'-CCG CTCGAGTTAAACCGTGGCCGGT-GGATTTAA-3'). The amplified RBD gene fragment was purified on a 10 g/L low-melting agarose gel, utilizing the PCR purification system (Q Biogene Inc.) The purified PCR products were directly ligated into expression vector pET32a, pETGEX-4t-2, and pET-MBP respectively. The progress of vector construction follows the example of pET32-RBD according to the clone strategy from TaKaRa Biotechnology Co., Ltd. (Figure 1). After transformation of the *E.coli* strain DH5α competent cells, the clone was selected on ampicillin containing (100 mg/L) plates for mini-preparation and insert evaluation was by enzyme digestion and DNA sequencing. Bacterial transformation for expressing RBD was carried out by incubating bacterial strain BL21(DE3) (Novagen) with pET32-RBD, pGEX-RBD, and pET-MBP-RBD plasmid DNAs on ice for 30 min and heat-shock treatment for 90 s as per the manufacturer's instruction, so did transforming pET32-RBD into bacterial strain Rosetta-gamiB(DE3) (Novagen) but ampicillin (100 mg/L), chloramphenicol (34 mg/L), kanamycin (12 mg/L), tetracycline (12.5 mg/L) selection. Hence expression of four engineering bacteria was performed (Table 1).

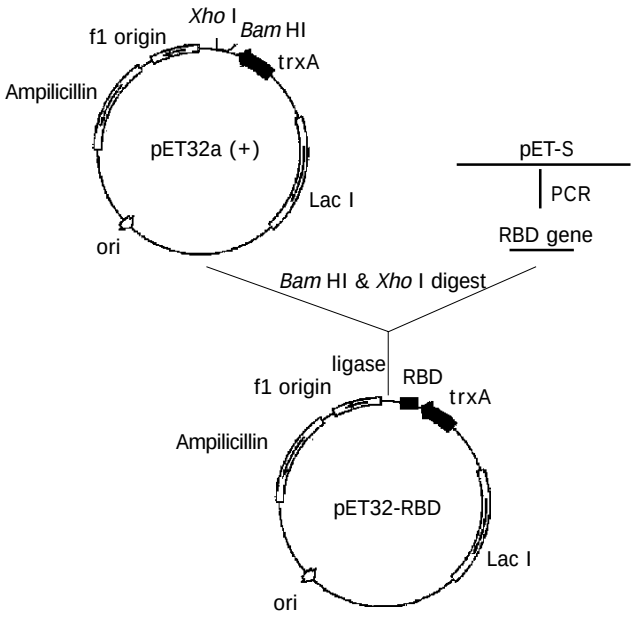


Figure 1 Schematic illustration of the constructs of expression vector pET32-RBD.

Optimization of protein expression and solubility analysis in E.coli

Each single colony on the LB plate was inoculated into

Table 1 Construction of recombinant plasmid and expression of engineering bacterium

Engineering bacterium	Recombinant plasmid	Expression host (*E.coli* strain)	Expression vector used	Fusion tag
E.coli BL-TB	pET32-RBD	BL21(DE3)	pET32a	TrxA·tag S·tag
E.coli R-TB	pET32-RBD	Rosetta-gamiB(DE3)	pET32a	TrxA·tag S·tag
E.coli BL-GB	pGEX-RBD	BL21(DE3)	pGEX-4t-2	GST·tag
E.coli BL-MB	pET-MBP-RBD	BL21(DE3)	pET-MBP	MBP·tag

5 mL of LB broth containing 100 μg/mL ampicillin (chloramphenicol (34 mg/L), kanamycin (12 mg/L), tetracycline (12.5 mg/L) additional for *E.coli* R-TB) and incubated overnight at 37 ℃ in a bacterial shaker. One hundred microliters of fresh engineering bacterium preparation was added to 20 mL of antibiotic containing LB broth. The bacteria were induced with 0.25-5 mmol/L IPTG when the optical density of the bacteria reached between 0.5 and 0.6 $A_{600\ nm}$, then shaked for an additional 1-8 h in a bacterial shaker at 20 or 37 ℃. One milliliter of the bacteria was taken out at 2, 4, 6, and 8 h, centrifuged, and lysed. Four microliters of cell lysate, after centrifuging the soluble and insoluble fragments, was electrophoresed on a 150 g/L SDS-PAGE for evaluation of protein expression. The expression of engineering bacteria derived from BL21(DE3) also performed by FML medium which is enriched in LB broth (7 g/L K_2HPO_4, 3 g/L NaH_2PO_4, 0.5 g/L $MgSO_4$, 2 g/L glucose, 2 mmol/L lactose) and target protein was induced by lactose. The protein expression has been evaluated after being cultured 9 h later as the same way.

Purification of the recombinant RBD protein

The *E.coli* BL-GB pellet from the 1 L culture was washed with 20 mmol/L Tris-HCl, pH 7.4, 5 mmol/L sodium EDTA, and 200 g/L sucrose. The pellet was resuspended with sonication buffer (20 mmol/L Tris-HCl, pH 8.0, 5 mmol/L EDTA) at the ratio of 1:40. The suspension was sonicated for lysing cells cooled in ice between sonication pulses. The lysate was centrifuged at 12 000 *g* for 30 min at 4 ℃ to separate out the debris. Then supernatant containing the recombinant RBD protein was purified by ÄKTA Prime Chromatography system using Q Sepharose FastFlow, Q Sepharose High Performance, Butyl Sepharose FastFlow, Superdex 75 gel exclusion Columns (Amersham-Pharmacia) respectively. The purified protein which conserved in 1×PBS was electrophoresed on a 150 g/L SDS-PAGE gel and stained with Coomassie blue. The gel was destained with 70 mL/L acetic acid and 50 mL/L methanol. The protein appeared to be induced quite well and purified to single band entities, demonstrating high purity of the protein products. The protein migrated at approximately 48 ku as expected.

ELISA

Purified GST·RBD protein was blocked to Maxisorp ELISA plate in 1×PBS at 1 μg/well. Anti-RBD of SARS-Cov spike protein mouse monoclonal antibody 1A5, then goat anti-mouse IgG conjugated with HRP was incubated with different ratios of dilution in each well at 37 ℃ for 2 h. Wells were washed with buffer then $A_{450\ nm}$ was measured.

Flow cytometry assay

A Becton Dickinson FACSCalibur cytofluorometer, which was in the Institute of Biotechnology, Academy of Military Medical Sciences, was used for flow cytometry. SARS-Cov susceptible Vero E6 cell was cultured in 12-well plate (5×10^6 cells/well). Cells were incubated at 37 ℃ for 3 h with 0.4 mg/mL purified GST protein and GST·RBD protein respectively, then washed thrice with fluorescence-activated cell sorting (FACS) buffer (PBS containing 20 g/L bovine serum)[14-16]. After being trypsinized, the cells were washed thrice with FACS buffer and then centrifuged at 2 000 r/min for 4 min in a 1.5 mL eppendorf tube for collecting cells. The prime antibody goat anti-GST polyclone antibody diluted in PBS containing 50 g/L bovine serum albumin at the ratio 1:2 000 were adsorbed to 5×10^6 cells in suspension for 1 h at room temperature. Then the secondary antibody was also adsorbed. Control, which was negative, was Vero E6 cells alone.

RESULTS

Soluble expression of recombinant RBD protein

TrxA tagged RBD protein expressed in two engineering bacteria (*E.coli* BL-TB and R-TB) were inclusion bodies. Under various cultures and induction conditions, *E.coli* BL-TB expressed RBD protein as inclusion body, including reduced IPTG induction concentration, shortened induction time and lowered induction temperature (data not shown). *E.coli* R-TB yielded high target protein expression, with level approaching approximately 40% of the total cellular protein but inclusion body. Especially, bacterial strain Rosetta-gamiB carries the thioredoxin reductase (*TrxB*) and glutathione reductase (*gor*) mutations which have the potential to enhance disulfide bond formation and ultimately solubility and activity, meanwhile it carries pRare plasmid which directs the rare tRNA genes synthesis that can enhance the expression of target protein. But the predominance of Rosetta-gamiB (DE3) for protein soluble expression was not clear. Maybe the overexpression of heteroprotein greatly counteract the helpfulness of host's *TrxB* and *gor* double mutations to the proper folding of the protein . Or the nature RBD folding form does not depend upon the disulfide bond formed by two cysteines (Figure 2A).

There was no visible expression in *E.coli* BL-MB in which RBD was MBP fused according to SDS-PAGE analysis. Some secondary structure might emerge at the upstream of ribosome binding domain of cloned gene in the pET-MBP-RBD. Or there was very little protein expressed and needed detection by Western blot. Among all four engineering bacteria, only *E.coli* BL-GB expressed soluble RBD protein GST tagged, and its expressional capacity was greater in FML medium than in LB broth. The protein migrated on SDS-GAGE at approximately 48 ku as expected (Figure 2B). So engineering bacterium BL-GB was selected to generate recombinant GST·RBD for further research (Figure 2C).

ELISA

Data from ELISA showed that the purified GST·RBD antigen had positive reaction with anti RBD mouse monoclonal antibody 1A5. Test result primarily indicated that the recombinant protein was by nature a three-dimensional structure (Figure 3).

Flow cytometry assay

To better detect the receptor binding ability of GST·RBD and then prove it was of dimensional structure and functional, flow cytometric analysis was performed (Figure 4). Because Vero E6 cell is SARS-Cov susceptible, the functional recombinant RBD should bind to ACE2 existing at the cell membrane of Vero E6 cell, after prime antibody and fluorescence-

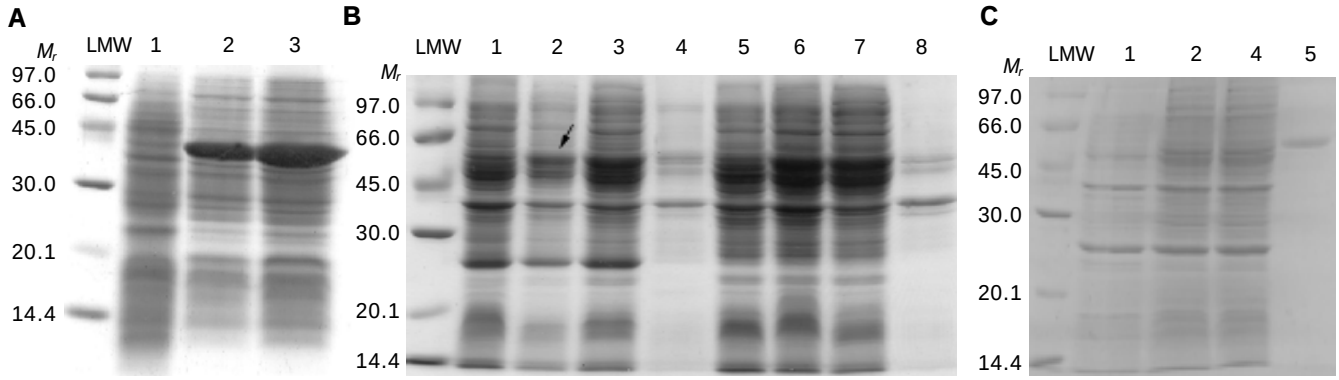


Figure 2 A: RBD expressed in *E.coli* R-TB as inclusion body form. LMW: protein low molecule weight marker (Amersham-Pharmacia); lane 1: *E.coli* BL21(DE3) negative control; lane 2: *E.coli* R-TB 5 mmol/L IPTG induced 4 h later; lane 3: *E.coli* R-TB 5 mmol/L IPTG induced 6 h later; B: *E.coli* BL-GB and BL-MB expression and solubility analysis. LMW: protein low molecule weight marker (Amersham-Pharmacia); lane 1: *E.coli* BL21(DE3) negative control; lane 2: *E.coli* BL-GB in FML medium; lane 3: soluble fraction; lane 4: insoluble fraction; lane 5: *E.coli* BL21(DE3) negative control; lane 6: *E.coli* BL-MB induced at 5 mmol/L IPTG 6 h later; lane 7: soluble fraction; lane 8: insoluble fraction; C: The purified recombinant RBD protein expressed in *E.coli* BL-GB. LMW: protein low molecule weight marker (Amersham-Pharmacia); lane 1: *E.coli* BL21(DE3) negative control; lane 2: IPTG induced *E.coli* BL-GB; lane 2: soluble fraction; lane 4: purified RBD protein.

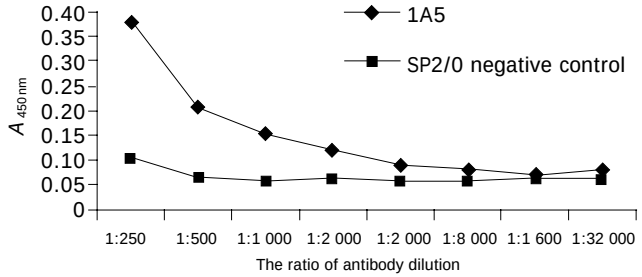


Figure 3 ELISA of GST·RBD antigen.

labeled secondary antibody was absorbed, it can be subjected to flow cytometry assay. Another negative control was set (Vero E6 cells with purified GST protein) to exclude the interference of GST tag and antibodies binding to cells. It has been seen that GST·RBD bound Vero E6 cells effectively. It also proved that the binding progress was decided by three-dimensional structure attachment because no side chain glycosylation was formed when heteroprotein expressed in *E.coli*.

DISCUSSION

During the pandemic outbreak of SARS in 2002/2003, despite the lack of effective and specific therapy, most SARS patients survived after the acute illness, and neutralizing antibodies were detectable in the sera of convalescent SARS patients[17,18]. Many researchers devoted themselves into developing anti SARS-Cov drugs. Currently, one candidate vaccine using inactivated SARS-Cov is in a phase I clinical trial in China. Although the inactivated SARS-Cov may be effective in protecting animals from challenge by the virus, its efficacy in human is unclear. There has been a serious safety concern since some antigens in the virions may elicit antibodies that did not neutralize, but rather infected. Some viral proteins may induce harmful immune and inflammatory response, a potential cause of SARS pathogenesis[19]. Now a number of vaccine candidates are of preclinical study, including inactivated vaccines, DNA vaccines, and attenuated viruses encoding SARS-Cov S protein[20-23]. Especially, vaccine blocking SARS-Cov entry into susceptible cell is a good way to fight against the virus[24].

The S proteins of coronaviruses are large type I membrane glycoprotein projections from viral envelope[25]. S proteins are responsible for both binding to receptors on host cells and for membrane fusion[11,12]. S proteins also contain important virus-neutralizing epitopes that elicit neutralizing

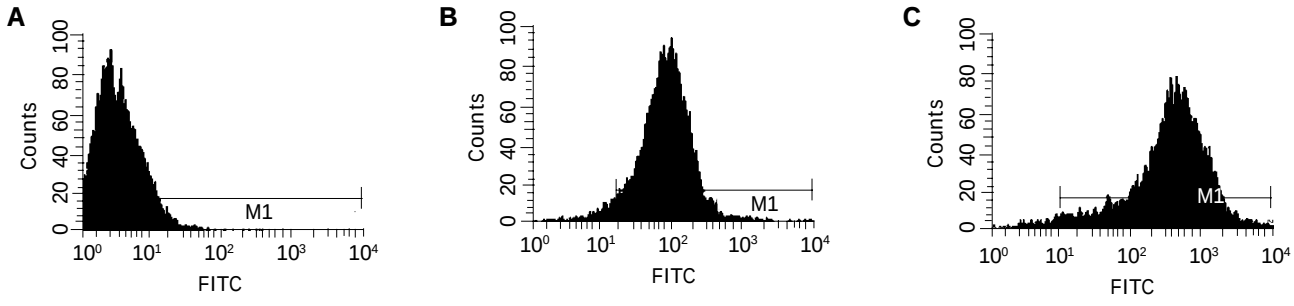


Figure 4 Cell binding test preformed by flow cytometry assay. A: Vero E6 cells alone, geometrical mean 3.3; B: Vero E6 cells+GST protein+two antibodies, geometrical mean 77.08; C: Vero E6 cells+GST·RBD+two antibodies, geometrical mean 352.73.

antibody in the host species. Furthermore, mutations in this gene dramatically affect the virulence, pathogenesis, and host cell tropism. The S1 domain of all characterized coronaviruses, including that of SARS-Cov, meditated an initial-affinity interaction with a cellular receptor[26-28]. In respect of that mutations in S protein' gene dramatically affect the virulence, pathogenesis, and host cell tropism, at the same time S proteins also contain important virus-neutralizing epitopes that elicit neutralizing antibody in the host species, so much work about antigenicity and receptor-binding ability of full length or fragments were done to discover the potent neutralization of SARS-Cov infection[29-32]. It has been proved that a cellular metallopeptidase, ACE2, could bind to S1 domain of SARS-Cov S protein and support viral replication[20]. Recent reports showed that a 193-amino-acid fragment of the S protein (residues 318-510) bound ACE2 more efficiently than did the full S1 domain and should be RBD of S protein of SARS-Cov, and rabbit antisera directed against RBD (cell expressed) were effective in binding to RBD on the S1 domain of SARS-Cov S protein and blocking RBD binding to soluble and cell-expressed ACE2. These data confirmed that the RBD of S protein has the potential to be developed as a subunit vaccine since it induces highly potent antibodies to block S protein binding to ACE2 and to neutralize SARS-Cov infection and has lower level of risk comparing with inactivated viruses. In these researches, the RBD protein was all expressed in mammalian cells and still in research pipeline.

These results suggested that RBD of S protein is a good candidate for vaccine because neutralizing antibodies are directed against S protein. Moreover, RBD of S protein is also a good target for antiviral therapies because blockade of binding of S protein to cellular receptor can prevent virus entry.

To research the receptor-binding ability of RBD, we chose *E.coli* as an expression host to get recombinant protein. According to the database from Internet there is 88.2% possibility of the recombinant RBD expressed in *E.coli* as inclusion body (www.biotech.ou.edu), at the same time, the gene of RBD contains lots of codon rarely used in *E.coli*, the expressional capacity should be little. In order to acquire soluble and functional recombinant protein, different fusion vectors, *E.coli* strain, culture, and induction conditions were considered. In this paper we adopted three fusion tags (GST, TrxA, MBP) which preferably contributes to increasing solubility and to the proper folding of heteroprotein when expressed in *E.coli*. At the same time we chose two *E.coli* strains: BL21 (DE3) and Rosetta-gamiB(DE3). Unexpectedly, TrxA tagged RBD protein expressed in Rosetta-gamiB(DE3) was inclusion body still, nature RBD folding form might not depend upon the disulfide bond formed by two cysteines. At last we got soluble expressed recombinant RBD protein as GST fusion form.

The recombinant GST·RBD protein was purified, and then proved positive reaction with anti RBD of S protein monoclonal antibody by ELISA and to have effective binding ability to ACE2 positive Vero E6 cell by flow cytometry assay. After removing the fusion tag, the recombinant protein can be directly used to develop subunit vaccine for blocking S protein binding with receptor and to neutralize SARS-Cov infection.

REFERENCES

1 **Lee N**, Hui D, Wu A, Chan P, Cameron P, Joynt GM, Ahuja A, Yung MY, Leung CB, To KF, Lui SF, Szeto CC, Chung S, Sung JJY. A major outbreak of severe acute respiratory syndrome in Hong Kong. *N Engl J Med* 2003; **348**: 1986-1994

2 **Peiris JS**, Lai ST, Poon LL, Guan Y, Yam LY, Lim W, Nicholls J, Yee WK, Yan WW, Cheung MT, Cheng VC, Chan KH, Tsang DN, Yung RW, Ng TK, Yuen KY. SARS study group. Coronavirus as a possible cause of severe acute respiratory syndrome. *Lancet* 2003, **361**: 1319-1325

3 **Fouchier RA**, Kuiken T, Schutten M, van Amerongen G, van Doornum GJ, van de Hoogen BG, Peiris M, Lim W, Stöhr K, Osterhaus AD. Aetiology: Koch's postulates fulfilled for SARS virus. *Nature* 2003; **423**: 240

4 **Ksiazek TG**, Erdman D, Goldsmith CS, Zaki SR, Peret T, Emery S, Tong S, Urbani C, Comer JA, Lim W, Rollin PE, Dowell SF, Ling AE, Humphrey CD, Shieh WJ, Guarner J, Paddock CD, Rota P, Fields B, DeRisi J, Yang JY, Cox N, Hughes JM, LeDuc JW, Bellini WJ, Anderson LJ. SARS Working Group. A novel coronavirus associated with severe acute respiratory syndrome. *N Engl J Med* 2003; **348**: 1953-1966

5 **Rota PA**, Oberste MS, Monroe SS, Nix WA, Campagnoli R, Icenogle JP, Penaranda S, Bankamp B, Maher K, Chen MH, Tong S, Tamin A, Lowe L, Frace M, DeRisi JL, Chen Q, Wang D, Erdman DD, Peret TC, Burns C, Ksiazek TG, Rollin PE, Sanchez A, Liffick S, Holloway B, Limor J, McCaustland K, Olsen-Rasmussen M, Fouchier R, Gunther S, Osterhaus AD, Drosten C, Pallansch MA, Anderson LJ, Bellini WJ. Characterization of a novel coronavirus associated with severe acute respiratory syndrome. *Science* 2003; **300**: 1394-1399

6 **Marra MA**, Jones SJ, Astell CR, Holt RA, Brooks-Wilson A, Butterfield YS, Khattra J, Asano JK, Barber SA, Chan SY, Cloutier A, Coughlin SM, Freeman D, Girn N, Griffith OL, Leach SR, Mayo M, McDonald H, Montgomery SB, Pandoh PK, Petrescu AS, Robertson AG, Schein JE, Siddiqui A, Smailus DE, Stott JM, Yang GS, Plummer F, Andonov A, Artsob H, Bastien N, Bernard K, Booth TF, Bowness D, Czub M, Drebot M, Fernando L, Flick R, Garbutt M, Gray M, Grolla A, Jones S, Feldmann H, Meyers A, Kabani A, Li Y, Normand S, Stroher U, Tipples GA, Tyler S, Vogrig R, Ward D, Watson B, Brunham RC, Krajden M, Petric M, Skowronski DM, Upton C, Roper RL. The Genome sequence of the SARS-associated coronavirus. *Science* 2003; **300**: 1399-1404

7 **Drosten C**, Günther S, Preiser W, Van der Werf S, Brodt HR, Becker S, Rabenau H, Panning M, Kolesnikova L, Fouchier RAM, Berger A, Burguière AM, Cinatl J, Eickmann M, Escriou N, Grywna K, Kramme S, Manuguerra JC, Müller S, Rickerts V, Stürmer M, Vieth S, Klenk HD, Osterhaus ADME, Schmitz H, Doerr HW. Identification of a Novel Coronavirus in patients with Severe Acute Respiratory Syndrome. *N Engl J Med* 2003; **348**: 1967-1976

8 **Holmes KV**. SARS-Associated Coronavirus. *N Engl J Med* 2003; **348**: 1948-1951

9 **Tsui SK**, Chim SS, Lo YM. Chinese university of Hong Kong molecular SARS Research Group. Coronavirus genomic-sequence variations and the epidemiology of the severe acute respiratory syndrome. *N Engl J Med* 2003; **349**: 187-188

10 **Ying W**, Hao Y, Zhang Y, Peng W, Qin E, Cai Y, Wei K, Wang J, Chang G, Sun W, Dai S, Li X, Zhu Y, Li J, Wu S, Guo L, Dai J, Wang J, Wan P, Chen T, Du C, Li D, Wan J, Kuai X, Li W, Shi R, Wei H, Cao C, Yu M, Liu H, Dong F, Wang D, Zhang X, Qian X, Zhu Q, He F. Proteomic analysis on structural proteins of Severe Acute Respiratory Syndrome coronavirus. *Proteomics* 2004; **4**: 492-504

11 **Simmons G**, Reeves JD, Rennekamp AJ, Amberg SM, Piefer AJ, Bates P. Characterization of severe acute respiratory syndrome-associated coronavirus (SARS-CoV) spike glycoprotein-mediated viral entry. *Proc Natl Acad Sci USA* 2004; **101**: 4240-4245

12 **Li W**, Moore MJ, Vasilieva N, Sui J, Wong SK, Berne MA, Somasundaran M, Sullivan JL, Luzuriaga K, Greenough TC, Choe H, Farzan M. Angiotensin- converting enzyme 2 is a functional receptor for the SARS coronavirus. *Nature* 2003; **426**: 450-454

13 **Wong SK**, Li W, Moore MJ, Choe H, Farzan M. A 193-amino-acid fragment of the SARS coronavirus S protein efficiently binds angiotensin- converting enzyme 2. *J Biol Chem* 2004; **279**: 3197-3201
14 **Jeffers SA**, Tusell SM, Gillim-Ross L, Hemmila EM, Achenbach JE, Babcock GJ, Thomas WD Jr, Thackray LB, Young MD, Mason RJ, Ambrosino DM, Wentworth DE, DeMartini JC, Holmes KV. CD209L (L-SIGN) is a receptor for severe acute respiratory syndrome coronavirus. *Proc Natl Acad Sci USA* 2004; **101**: 15748-15753
15 **Wang P**, Chen J, Zheng A, Nie Y, Shi X, Wang W, Wang G, Luo M, Liu H, Tan L, Song X, Wang Z, Yin X, Qu X, Wang X, Qing T, Ding M, Deng H. Expression cloning of functional receptor used by SARS coronavirus. *Biochem Biophys Res Commun* 2004; **315**: 439-444
16 **Chang MS**, Lu YT, Ho ST, Wu CC, Wei TY, Chen CJ, Hsu YT, Chu PC, Chen CH, Chu JM, Jan YL, Hung CC, Fan CC, Yanga YC. Antibody detection of SARS-CoV spike and nucleocapsid protein. *Biochem Biophys Res Commun* 2004; **314**: 931-936
17 **Zheng BJ**, Guan Y, Wong KH, Zhou J, Wong KL, Young BW, Lu LW, Lee SS. SARS-related virus predating SARS outbreak, Hong Kong. *Emerg Infec Dis* 2004; **10**: 176-178
18 **Nie QH**, Luo XD, Zhang JZ, Su Q. Current status of severe acute respiratory syndrome in China. *World J Gastroenterol* 2003; **9**: 1635-1645
19 **He Y**, Zhou Y, Liu S, Kou Z, Li W, Farzan M, Jiang S. Receptor-binding domain of SARS-CoV spike protein induces highly potent neutralizing antibodies: implication for developing subunit vaccine. *Biochem Biophys Res Commun* 2004; **324**: 773-781
20 **Zeng F**, Chow KY, Hon CC, Law KM, Yip CW, Chan KH, Peiris JS, Leung FC. Characterization of humoral responses in mice immunized with plasmid DNAs encoding SARS-CoV spike gene fragments. *Biochem Biophys Res Commun* 2004; **315**: 1134-1139
21 **Gao W**, Tamin A, Soloff A, D'Aiuto L, Nwanegbo E, Robbins PD, Bellini WJ, Barratt-Boyes S, Gambotto A. Effects of a SARS-associated coronavirus vaccine in monkeys. *Lancet* 2003; **362**: 1895-1896
22 **Sui J**, Li W, Murakami A, Tamin A, Matthews LJ, Wong SK, Moore MJ, Tallarico AS, Olurinde M, Choe H, Anderson LJ, Bellini WJ, Farzan M, Marasco WA. Potent neutralization of severe acute respiratory syndrome (SARS) coronavirus by a human mAb to S1 protein that blocks receptor association. *Proc Natl Acad Sci USA* 2004**; 101**: 2536-2541
23 **Bisht H**, Roberts A, Vogel L, Bukreyev A, Collins PL, Murphy BR, Subbarao K, Moss B. Severe acute respiratory syndrome coronavirus spike protein expressed by attenuated vaccinia virus protectively immunizes mice. *Proc Natl Acad Sci USA* 2004; **101**: 6641-6646
24 **Yang ZY**, Kong WP, Huang Y, Roberts A, Murphy BR, Subbarao K, Nabel GJ. A DNA vaccine induces SARS coronavirus neutralization and protective immunity in mice. *Nature* 2004; **428**: 561-564
25 **Ho Y**, Lin PH, Liu CY, Lee SP, Chao YC. Assembly of human severe acute respiratory syndrome coronavirus-like particles. *Biochem Biophys Res Commu* 2004; **318**: 833-838
26 **Liu S**, Xiao G, Chen Y, He Y, Niu J, Escalante CR, Xiong H, Farmar J, Debnath AK, Tien P, Jiang S. Interaction between heptad repeat 1 and 2 regions in spike protein of SARS-associated coronavirus: implications for virus fusogenic mechanism and identification of fusion inhibitors. *Lancet* 2004; **363**: 938-947
27 **Bosch BJ**, Martina BE, Van der Zee R, Lepault J, Haijema BJ, Versluis C, Heck AJ, Groot R, Osterhaus AD, Rottier PJ. Severe acute respiratory syndrome coronavirus (SARS-CoV) infection inhibition using spike protein heptad repeat-derived peptides. *Proc Natl Acad Sci USA* 2004; **101**: 8455-8460
28 **Spiga O**, Bernini A, Ciutti A, Chiellini S, Menciassi N, Finetti F, Causarono V, Anselmi F, Prischi F, Niccolaia N. Molecular modelling of S1 and S2 subunits of SARS coronavirus spike glycoprotein. *Biochem Biophys Res Commun* 2003; **310**: 78-83
29 **Ho TY**, Wu SL, Cheng SE, Wei YC, Huang SP, Hsiangc CY. Antigenicity and receptor-binding ability of recombinant SARS coronavirus spike protein. *Biochem Biophy Res Commun* 2004; **313**: 938-947
30 **Xiao X**, Chakraborti S, Dimitrov AS, Gramatikoff K, Dimitrov DS. The SARS-CoV S glycoprotein: expression and functional characterization. *Biochem Biophys Res Commun* 2003; **312**: 1159-1164
31 **Huang LR**, Chiu CM, Yeh SH, Huang WH, Hsueh PR, Yang WZ, Yang JY, Su IJ, Chang SC, Chen PJ. Evaluation of antibody responses against SARS coronaviral nucleocapsid or spike proteins by immunoblotting or ELISA. *J Med Viro* 2004; **73**: 338-346

Science Editor Guo SY **Language Editor** Elsevier HK

PO Box 2345, Beijing 100023, China
www.wjgnet.com
wjg@wjgnet.com

ELSEVIER

World J Gastroenterol 2005;11(39):6165-6169
World Journal of Gastroenterology ISSN 1007-9327
© 2005 The WJG Press and Elsevier Inc. All rights reserved.

• *BRIEF REPORTS* •

Effects of *Saccharomyces boulardii* on fecal short-chain fatty acids and microflora in patients on long-term total enteral nutrition

Stéphane M Schneider, Fernand Girard-Pipau, Jérôme Filippi, Xavier Hébuterne, Dominique Moyse, Gustavo Calle Hinojosa, Anne Pompei, Patrick Rampal

Stéphane M Schneider, Jérôme Filippi, Xavier Hébuterne, Gustavo Calle Hinojosa, Patrick Rampal, Department of Hepato-Gastroenterology and Clinical Nutrition, Archet University Hospital, Nice, France
Fernand Girard-Pipau, Anne Pompei, Bacteriology Laboratory, Archet University Hospital, Nice, France
Dominique Moyse, Biostatistician, Paris, France
Gustavo Calle Hinojosa, Patrick Rampal, Department of Hepato-Gastroenterology, Princess Grace Hospital, Monte-Carlo, Monaco
Supported by a research grant from Laboratoires Biocodex, Montrouge, France, EU
Correspondence to: Dr. Stéphane M Schneider, Department of Gastroenterology and Clinical Nutrition, Archet University Hospital, BP 3079, F-06202 Nice Cedex 3, France. stephane.schneider@unice.fr
Telephone: +33-4-92-03-61-68 Fax: +33-4-92-03-65-75
Received: 2005-01-12 Accepted: 2005-06-02

Abstract

AIM: To assess the effects of *Sb* on fecal flora and short-chain fatty acids (SCFA) in patients on long-term TEN.

METHODS: Ten patients (3 females, 7 males, 59±5.5 years), on TEN for a median of 13 mo (1-125), and 15 healthy volunteers (4 females, 11 males, 32±2.0 years) received *Sb* (0.5 g bid PO) for 6 d. Two stool samples were taken before, on the last 2 d and 9-10 d after treatment, for SCFA measurement and for culture and bacterial identification. Values (mean±SE) were compared using sign tests and ANOVA.

RESULTS: Fecal butyrate levels were lower in patients (10.1±2.9 mmol/kg) than in controls (19.2±3.9, $P = 0.02$). Treatment with *Sb* increased total fecal SCFA levels in patients (150.2±27.2 *vs* 107.5±18.2 mmol/kg, $P = 0.02$) but not in controls (129.0±28.6 *vs* 113.0±15.2 mmol/kg, NS). At the end of treatment with *Sb*, patients had higher fecal butyrate (16.0±4.4 *vs* 10.1 [2.9] mmol/kg, $P = 0.004$). Total SCFAs remained high 9 d after treatment was discontinued. Before the treatment, the anaerobe to aerobe ratio was lower in patients compared to controls (2.4±2.3 *vs* 69.8±1.8, $P = 0.003$). There were no significant changes in the fecal flora of TEN patients.

CONCLUSION: *Sb*-induced increase of fecal SCFA concentrations (especially butyrate) may explain the preventive effects of this yeast on TEN-induced diarrhea.

© 2005 The WJG Press and Elsevier Inc. All rights reserved.

Key words: Enteral nutrition; Diarrhea; *Saccharomyces boulardii*; Short-chain fatty acids; Intestinal microbiota

Schneider SM, Girard-Pipau F, Filippi J, Hébuterne X, Moyse D, Hinojosa GC, Pompei A, Rampal P. Effects of *Saccharomyces boulardii* on fecal short-chain fatty acids and microflora in patients on long-term total enteral nutrition. *World J Gastroenterol* 2005; 11(39): 6165-6169
http://www.wjgnet.com/1007-9327/11/6165.asp

INTRODUCTION

Diarrhea is the most frequent complication of enteral tube feeding, with an incidence as high as 63%[1]. Its consequences range from discomfort to life-threatening acidosis, increased morbidity and mortality, and higher financial costs for health providers[2]. One of the causes of diarrhea in tube-fed patients may be the consequences on colonic trophicity of a deficiency in luminal short-chain fatty acids (SCFAs). We have reported a major imbalance (namely a drop in the number of fecal anaerobic bacteria and an increase in the number of aerobic bacteria) in patients on long-term total enteral nutrition (TEN)[3]. The modifications of the intestinal microflora induced by a fiber-free polymeric enteral diet can be compared to those induced by broad-spectrum antibiotics such as ceftriaxone[4,5]. These effects may be synergic[6] and explain why antibiotics are a risk factor for enteral nutrition-induced diarrhea[7,8] and why enteral nutrition is a risk factor for antibiotic-induced diarrhea[9] and *Clostridium difficile* infection[10]. SCFAs, one of the most important by-products of anaerobes in the colon, are the main fuel for the colonocyte and they are involved in water and electrolyte absorption by the colonic mucosa. They have been shown to reverse fluid secretion in the ascending colon during enteral feeding[11], and may represent the link between diarrhea and the intestinal microflora during enteral nutrition.

Saccharomyces boulardii (*Sb*) is a probiotic yeast that has been successfully used for years in the prevention of antibiotic-associated diarrhea[12]. *Sb* has been proven to prevent the relapse of *Clostridium difficile* infection[13], and seems effective in preventing relapses in patients with Crohn's disease[14]. Three randomized controlled studies have reported its efficacy in the prevention of diarrhea in TEN patients from intensive care units, with a reduction in the number of patient-days with diarrhea by 25-83%[15-17]. However, these studies did not address the mechanisms of action of the probiotic. We therefore designed a prospective study to assess the effects of *Sb* on fecal SCFAs and intestinal microflora in TEN patients. Healthy volunteers (HVO) were

used as controls.

MATERIALS AND METHODS

Subjects

The TEN group consisted of 10 patients (3 females and 7 males), mean age 59±5.5 years (mean±SE), who had been on TEN for a median of 13 mo (range: 1-125 mo). The indication for TEN was dysphagia in six patients (three head and neck tumors, two strokes, and one resected neurinoma); three patients had upper gastro-intestinal surgery, and one patient had low oral intake due to severe depression. Two patients were receiving proton pump inhibitors. A commercially available polymeric diet, fiber-, lactose-, and gluten-free, with a concentration of 1.33 kcal/mL (Sondalis HP®, Nestlé Clinical Nutrition, Noisiel, France) was used to provide 20% protein (50% from casein and 50% from soy protein), 45% carbohydrate (maltodextrin), and 31% fat (24% from corn oil, 22% from colza oil, and 47% as medium-chain triglycerides). Nutrition was given through gastrostomy ($n = 7$), jejunostomy ($n = 2$), or naso-gastric ($n = 1$) tubes. Enteral nutrition was total, but patients who could drink water or tea were allowed to do so. Fifteen HVO (4 females and 11 males), mean age 32±2.0 years ($P<0.05$ *vs* TEN patients) were also studied. All HVO consumed a regular Western diet, and none of them had a history of gastrointestinal disease. At the time of the study, all experimental and normal subjects were in a stable condition, and none had diarrhea. Energy provided by the diet was covering their maintenance needs as calculated using the Harris and Benedict formulas, and the enteral feeds were stable throughout the study. No subject had undergone colectomy, and none had taken antibiotics or laxatives for at least 2 wk prior to the study. All subjects gave their written informed consent and the study was performed according to the Declaration of Helsinki and approved by the regional Ethics Committee.

Study design

Five hundred milligrams b.i.d. of *Sb* as lyophilized powder, provided by Laboratoires Biocodex (Montrouge, France), were administered orally (HVO) or via the feeding tube (TEN patients) for six consecutive days. Two fecal samples were collected at 1-d intervals from all subjects on the 2 d before treatment, on the last 2 d of treatment, and 9 and 10 d after treatment was discontinued. Antibiotic or laxative use during the study was an exclusion criterion.

Stool analysis

Stool samples were taken immediately after production, and analyzed within 2 h. SCFAs were studied as follows[18]: an aliquot of 200 mg of feces was weighed. This was suspended in sterile distilled water (1.6 mL) and hexanoic acid (0.2 mL) was added. 50% aqueous H_2SO_4 (0.4 mL) and diethyl ether (2 mL) were then added. The sample was mixed for 45 min with an orbital shaker, and centrifuged for 5 min at 3 000 r/min at room temperature. Anhydrous $CaCl_2$ was then added in order to remove residual water, and 2 μL of the extract was injected in the gas-liquid chromatograph (Hewlett-Packard 5890 Series II with a flame ionization detector). The standard solution was as follows: acetic, propionic, isobutyric, butyric, isovaleric, valeric, isocaproic, caproic, and hexanoic acids (10 meq/L each); it was assayed before each stool sample was analyzed. Sensitivity was 1 mmol. 500 mg of feces was taken from the center of the stool, weighed and submitted to serial dilutions up to 10^{-8} in BHI broth. Then, 0.1 mL of each dilution was spread on a range of selective and non-selective media. Whenever necessary, the media were pre-reduced to allow anaerobic growth. Media inoculated and incubated at 37 ℃ in aerobiosis were as follows: trypticase agar, Columbia agar supplemented with sheep blood, Columbia agar supplemented with nalidixic acid and colistin, and Drigalski medium (equivalent to Mac Conkey medium) at dilutions 10^{-2}, 10^{-4}, and 10^{-6}[19]. For anaerobic bacteria, media inoculated were as follows: Columbia agar supplemented with sheep blood spread with the dilutions 10^{-2}, 10^{-4}, and 10^{-8}, Columbia blood agar supplemented with kanamycin and vancomycin, *Bifidobacterium* agar, and *Bacteroides* agar (dilutions 10^{-2}, 10^{-4}, and 10^{-7}), rifampicin agar (10^{-1} and 10^{-7}), and CCFA (for isolation of *Clostridium difficile*), MRS agar (for isolation of lactobacilli), *Veillonella* agar, and crystal violet agar, all spread with dilutions 10^{-1} and 10^{-5}[19]. The differences between dilutions for each medium were based on the differences between the concentrations of concerned bacteria[20]. After 24-48 h of incubation in an anaerobic cabinet, the number of colonies of each colony type growing on each of the media used were counted. The absence of growth under 50 mL/L carbon dioxide was verified for anaerobic strains. Routine identification was performed with standard methods, then with microstrips (API 20 Enterobacteries or ID 32 Anaerobies, BioMerieux, Marcy L'Etoile, France). The ratio between anaerobes and aerobes was calculated as a marker of microbial imbalance[3,21].

Statistical analysis

Results are expressed as mean±SE. All fecal bacterial counts (colony-forming units [CFU] per gram of wet feces) were transformed to logarithms ($\log_{10}$ CFU) for statistical analysis. Values were compared at baseline using a non-parametric method. Comparisons within groups used a sign test; differences *vs* baseline are presented with distribution-free confidence intervals.

A two-way ANOVA was performed for quantitative parameters for exploratory purposes. The model included group (TEN or HVO), period of time (before, during or after treatment) and interaction group*period of time; all two by two differences between adjusted means were calculated and tested using *t*-tests. No adjustment was performed in this exploratory context. For SFCA assessments, two values were considered in the model at each time. Statistics were performed on SAS software from SAS Institute (Cary, NC, USA). Differences were considered as statistically significant for P lower than 0.05. A pilot study that reported a 40% increase of total SCFA concentration after treatment with *Sb* allowed us to calculate a number needed to treat ten subjects per group.

RESULTS

Fecal short-chain fatty acids

Acetate, propionate, and butyrate values are represented in Table 1. For all three main SCFAs, no significant change,

either during or after treatment, was observed in HVO. In TEN patients, butyrate concentrations were increased significantly (about 60%) during treatment. SCFA values 9 d after discontinuing *Sb* were not significantly different from baseline. The sum of all SCFAs was increased significantly in TEN patients under treatment, with an average increase of 42.8 mmol/kg (95%CI: 0.0-55.2, $P = 0.02$) during treatment and an average increase of 51.8 mmol/kg (95%CI: 14.4-110.6, $P = 0.02$) after treatment (Figure 1). There were no changes in HVO. Minor SCFAs did not change in either group.

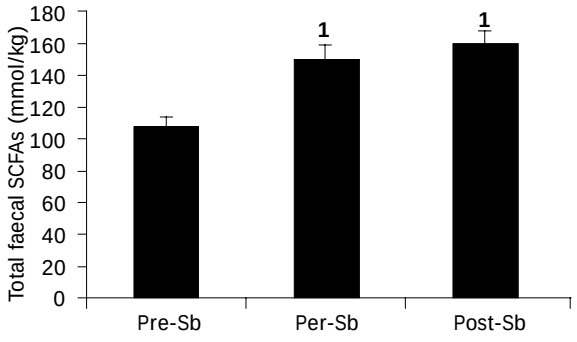


Figure 1 Fecal SCFAs in TEN patients. SCFA: short-chain fatty acids; *Sb*: *Saccharomyces boulardii*; [1]$P = 0.02$ *vs* pre-treatment values.

ANOVA showed an overall increase for acetate and SCFA sum after treatment on change from baseline values; significant interactions were noticed for propionate due to the increase in the TEN group opposed to a decrease in the HVO group, and for butyrate corresponding to differences in after-treatment concentrations higher in the HVO group in spite of higher baseline values in this group.

Fecal flora

Before treatment, there were significant differences in the fecal flora between HVO and TEN patients, as the latter had higher counts of aerobic bacteria and a lower anaerobes/aerobes ratio (Table 2). Among aerobes, the number of enterococci was higher in TEN patients (7.42±0.64 log CFU/g) than in HVO (6.1±0.46 log CFU/g, $P = 0.02$). Among anaerobes, peptostreptococci and *Bifidobacterium* spp., present in HVO, were absent in TEN patients. *Clostridium difficile* was not identified in any subject. There were no significant changes in the numbers of colony forming units of individual species or groups of bacteria in TEN patients during treatment with *Sb*, or after treatment. The only change observed in HVO was a decrease of Gram-positive anaerobes from 8.6±0.3 log CFU/g to 6.8±0.8 during treatment ($P = 0.035$).

Table 2 Fecal bacterial populations in TEN patients and HVO

		Before treatment concentration	During treatment concentration	After treatment concentration
Total bacteria	TEN	9.64 (0.31)	9.31 (0.41)	9.54 (0.36)
(log CFU/g)	HVO	9.53 (0.16)	9.56 (0.21)	9.20 (0.19)
Anaerobes	TEN	8.25 (1.01)	7.72 (0.76)	8.63 (0.62)
(log CFU/g)	HVO	9.47 (0.16)	8.73 (0.45)	8.97 (0.25)
Aerobes	TEN	8.84 (0.26)	8.83 (0.34)	8.71 (0.32)
(log CFU/g)	HVO	7.63 (0.22)	7.63 (0.24)	7.61 (0.26)
Anaerobes/				
aerobes ratio	TEN	2.42 (2.28)	0.51 (2.23)	2.89 (2.43)
	HVO	69.81 (1.81)	60.13 (2.47)	23.02 (2.01)

Mean (SE). TEN, total enteral nutrition; HVO, healthy volunteers. No significant difference.

Tolerance

There were no significant changes in the number of bowel movements and the consistency of stools during or after treatment in either HVO or TEN patients (data not shown). No fever or fungemia was reported. The only adverse effect attributed to *Sb* was a case of mild diarrhea in one patient which resolved without discontinuation of treatment.

Table 1 Fecal SCFAs in TEN patients and HVO

		Before treatment concentration (SEM)	During treatment			After treatment		
			Concentration (SEM)	Difference with pre-treatment value (95%CI)	P^1	Concentration (SEM)	Difference with pre-treatment value (95%CI)	P^1
Acetate	TEN	69.9 (12.3)	97.9 (25.2)	28.0 -6.1; 36.2	0.18	110.3 (24.1)	40.4 14.4; 71.4	0.02
	HVO	71.3 (10.3)	98.4 (29.8)	27.1 -13.1; 35.6	0.79	111.5 (17.5)	40.2 -7.0; 116.0	0.42
Propionate	TEN	20.9 (3.7)	26.2 (3.8)	5.3 -0.2; 12.6	0.18	26.0 (3.4)	5.1 -3.3; 14.3	0.18
	HVO	22.9 (3.0)	18.4 (2.4)	-4.5 -11.8; 4.5	0.30	23.0 (2.7)	0.1 -3.1; 6.9	0.12
Butyrate	TEN	10.1 (2.9)	16.0 (4.4)	5.8 0.1; 12.3	0.004	12.9 (2.5)	2.7 -3.9; 12.3	0.51
	HVO	19.2 (3.9)	16.4 (3.3)	-2.7 -9.7 ; 5.6	0.61	23.3 (3.1)	4.1 -1.4 ; 16.3	0.12

Values in mmol/kg of wet feces: mean (SE); TEN: total enteral nutrition, HVO: healthy volunteers. [1]Probability of sign test.

DISCUSSION

This study shows that both the fecal concentration of butyric acid and the anaerobe/aerobe ratio were lower in patients at high risk for diarrhea due to TEN than in HVO. Despite great inter-individual variations, treatment with *Sb* increased total SCFAs and butyrate fecal concentrations in TEN patients with a long-lasting increase of total SCFA concentrations when treatment was discontinued. Treatment with *Sb* did not affect the fecal flora in TEN patients, while it decreased Gram-positive anaerobes in HVO.

Sb is known to interact with the intestinal flora. Yeast proteins have been shown to neutralize cholera toxin[22] and to repress *Clostridium difficile* toxins A and B[23]; *Sb* also has an antagonistic effect on the growth of pathogenic micro-organisms in the intestine[24]. In our study, increased SCFA concentrations might explain the reported prevention by *Sb* of TEN-induced diarrhea by an increased water and electrolyte absorption and by a reduction in colonic pH, even though it was not measured in the stool samples from our subjects. A lower pH inhibits the growth of *Clostridium difficile*[25,26], a bacteria that can be acquired in up to 15% of hospitalized EN patients[10]. A viable mixed culture of *Lactobacillus acidophilus* and *Lactobacillus bulgaricus* (1 g t.i.d.) failed to prevent diarrhea in hospital inpatients receiving EN in a randomized controlled study[27]. Unlike *Sb*, lactobacilli taken orally do not increase SCFA fecal levels[28,29], which might explain these negative results. Prebiotics can also increase SCFAs in the colon; in a recently published study, administration for 2 wk of a soluble dietary fiber (galactomannans) in 20 elderly inpatients receiving EN was shown to decrease the water content of the feces and the frequency of daily bowel movements[30]. These results were associated with an increase of fecal SCFA levels, significant for total SCFAs, acetic and propionic acids. Although we confirmed the 40% increase in total SCFAs in the pilot phase of the study that was used to determine the number of subjects, a high variability prevented some important differences from reaching statistical significance. This variability did not seem to be time- or diet-dependent, as it was comparable in volunteers on a free diet and in patients who were on a stable controlled diet. *Sb* recovery in the stools after chronic administration is known to reach a plateau by the 3rd d and to disappear 5 d after treatment is discontinued[31]. The persistence of the effects on total SCFA concentrations 9-10 d after *Sb* discontinuation is suggestive of a prolonged action of the yeast and may indicate that daily treatment may not be necessary to sustain its effects on fecal SCFA concentrations.

known to be associated with a decrease of fecal anaerobes[35]; however, age does not influence fecal SCFA levels[36]; (2) Bacterial concentrations are known to differ depending on the intestinal segment in which samples are taken; nevertheless, analysis of feces is the most feasible technique and provides an accurate information on the intestinal microflora[37]; (3) Analysis of samples rather than 24 h-stools certainly deprives us of some information as TEN is known to modify the volume of daily stools. However, stool collection is often difficult in bed-ridden patients, especially those with neurological disorders. This is the main reason why we chose to perform this study in patients without diarrhea; (4) The correlation between SCFAs and bacterial counts in feces is reportedly poor[38]; (5) Lastly a standard bacterial count, however thorough, may miss some information. Molecular techniques[39] may help progressing in this field.

There is growing evidence regarding the health benefits of probiotics. In EN patients; besides prevention of diarrhea, a recent study reports less post-operative infections in patients receiving EN supplemented with fiber and *Lactobacillus plantarum* 299 than in those receiving parenteral nutrition of fiber-free TEN[40].

In conclusion, this study suggests one possible mechanism of action of the probiotic yeast *Sb*, especially for its preventive effects in enteral nutrition-induced diarrhea. It also supports its use, especially in patients who have other risk factors, such as antibiotic intake.

ACKNOWLEDGMENTS

The authors wish to thank Dr. Christine Alquier and Dr. Marie-Emmanuelle Le Guern for their invaluable help with study design and data handling, and Dr. Philippe Marteau and Dr. Ian Janssen for their advice.

REFERENCES

1 **Bliss DZ**, Guenter PA, Settle RG. Defining and reporting diarrhea in tube-fed patients - what a mess! *Am J Clin Nutr* 1992; **55**: 753-759
2 **Adam S**, Batson S. A study of problems associated with the delivery of enteral feed in critically ill patients in five ICUs in the UK. *Intensive Care Med* 1997; **23**: 261-266
3 **Schneider SM**, Le Gall P, Girard-Pipau F, Piche T, Pompei A, Nano JL. Total artificial nutrition is associated with major changes in the fecal flora. *Eur J Nutr* 2000; **39**: 248-255
4 **Welling GW**, Meijer-Severs GJ, Helmus G, van Santen E, Tonk RH, de Vries-Hospers HG. The effect of ceftriaxone on the anaerobic bacterial flora and the bacterial enzymatic activity in the intestinal tract. *Infection* 1991; **19**: 313-316
5 **Meijer-Severs GJ**, Van Santen E, Meijer BC. Short-chain fatty acid and organic acid concentrations in feces of healthy human volunteers and their correlations with anaerobe cultural counts during systemic ceftriaxone administration. *Scand J Gastroenterol* 1990; **25**: 698-704
6 **Hébuterne X**, Schneider SM. Impact of enteral nutrition on gastrointestinal functions. *Clin Nutr* 2001; **20**(Suppl 2): 57-61
7 **Keohane PP**, Attrill H, Love M, Frost P, Silk DB. Relation between osmolality of diet and gastrointestinal side effects in enteral nutrition. *Br Med J* 1984; **288**: 678-680
8 **Guenter PA**, Settle RG, Perlmutter S, Marino PL, DeSimone GA, Rolandelli RH. Tube feeding-related diarrhea in acutely ill patients. *J Parenter Enteral Nutr* 1991; **15**: 277-280
9 **Surawicz CM**, Elmer GW, Speelman P, McFarland LV, Chinn J, van Belle G. Prevention of antibiotic-associated diarrhea by *Saccharomyces boulardii*: a prospective study. *Gastroenterology* 1989; **96**: 981-988
10 **Bliss DZ**, Johnson S, Savik K, Clabots CR, Willard K, Gerding DN. Acquisition of *Clostridium difficile* and *Clostridium difficile*-associated diarrhea in hospitalized patients receiving tube feeding. *Ann Intern Med* 1998; **129**: 1012-1019
11 **Bowling TE**, Raimundo AH, Grimble GK, Silk DB. Reversal by short-chain fatty acids of colonic fluid secretion induced by enteral feeding. *Lancet* 1993; **342**: 1266-1268
12 **D'Souza AL**, Rajkumar C, Cooke J, Bulpitt CJ. Probiotics in prevention of antibiotic-associated diarrhea: meta-analysis. *BMJ* 2002; **324**: 1361-1366
13 **McFarland LV**, Surawicz CM, Greenberg RN, Fekety R, Elmer GW, Moyer KA, Melcher SA, Bowen KE, Cox JL, Noorani Z. A

randomized placebo-controlled trial of *Saccharomyces boulardii* in combination with standard antibiotics for *Clostridium difficile* disease. *JAMA* 1994; **271**: 1913-1918
14 **Guslandi M**, Mezzi G, Sorghi M, Testoni PA. *Saccharomyces boulardii* in maintenance treatment of Crohn's disease. *Dig Dis Sci* 2000; **45**: 1462-1464
15 **Bleichner G**, Bléhaut H, Mentec H, Moyse D. *Saccharomyces boulardii* prevents diarrhea in critically ill tube-fed patients. A multicenter, randomized, double-blind placebo-controlled trial. *Intensive Care Med* 1997; **23**: 517-523
16 **Schlotterer M**, Bernasconi P, Lebreton F, Wassermann D. Intérêt de *Saccharomyces boulardii* dans la tolérance digestive de la nutrition entérale à débit continu chez le brûlé. *Nutr Clin Metabol* 1987; **1**: 31-34
17 **Tempé JD**, Steidel AL, Bléhaut H, Hasselmann M, Lutun P, Maurier F. Prévention par *Saccharomyces boulardii* des diarrhées de l'alimentation entérale à débit continu. *Sem Hop Paris* 1983; **59**: 1409-1412
18 **Holdeman LV**, Cato EP, Moore WEC. Anaerobe laboratory manual, anaerobe laboratory. 4th edn ed. *Blacksburg VA Virginia Polytechnic Institute and State University* 1977
19 **Phillips E**, Nash P. Culture media. In: Lennette EH, Balows A, Hausler Jr WJ, Shadomy HJ, editors. Manual of Clinical Microbiology. 4th edition ed. *Washington DC American Society for Microbiology* 1985: 1051-1092
20 **Drasar BS**, Roberts AK. Methods for the study of anaerobic microflora. In: Levett PN, editor. Anaerobic microbiology. A practical approach. *Oxford Oxford University Press* 1991: 183-200
21 **Ruseler-van Embden JG**, Schouten WR, van Lieshout LM. Pouchitis: result of microbial imbalance? *Gut* 1994; **35**: 658-664
22 **Czerucka D**, Roux I, Rampal P. *Saccharomyces boulardii* inhibits secretagogue-mediated adenosine 3',5'- cyclic monophosphate induction in intestinal cells. *Gastroenterology* 1994; **106**: 65-72
23 **Castagliuolo I**, Riegler MF, Valenick L, LaMont JT, Pothoulakis C. *Saccharomyces boulardii* protease inhibits the effects of *Clostridium difficile* toxins A and B in human colonic mucosa. *Infect Immun* 1999; **67**: 302-307
24 **Ducluzeau R**, Bensaada M. Effet comparé de l'administration unique ou en continu de *Saccharomyces boulardii* sur l'établissement de diverses souches de *Candida* dans le tractus digestif de souris gnotoxéniques. *Ann Microbiol* 1982; **118B**: 491-501
25 **Rolfe RD**. Role of volatile fatty acids in colonization resistance to *Clostridium difficile*. *Infect Immun* 1984; **45**: 185-191
26 **Wang X**, Gibson GR. Effects of the *in vitro* fermentation of oligofructose and inulin by bacteria growing in the human large intestine. *J Appl Bacteriol* 1993; **75**: 373-380
27 **Heimburger DC**, Sockwell DG, Geels WJ. Diarrhea with enteral feeding: prospective reappraisal of putative causes. *Nutrition* 1994; **10**: 392-396
28 **Hove H**, Nordgaard-Andersen I, Mortensen PB. Effect of lactic acid bacteria on the intestinal production of lactate and short-chain fatty acids, and the absorption of lactose. *Am J Clin Nutr* 1994; **59**: 74-79
29 **Fukuda M**, Kanauchi O, Araki Y, Andoh A, Mitsuyama K, Takagi K. Prebiotic treatment of experimental colitis with germinated barley foodstuff: a comparison with probiotic or antibiotic treatment. *Int J Mol Med* 2002; **9**: 65-70
30 **Nakao M**, Ogura Y, Satake S, Ito I, Iguchi A, Takagi K. Usefulness of soluble dietary fiber for the treatment of diarrhea during enteral nutrition in elderly patients. *Nutrition* 2002; **18**: 35-39
31 **Bléhaut H**, Massot J, Elmer GW, Levy RH. Disposition kinetics of *Saccharomyces boulardii* in man and rat. *Biopharm Drug Dispos* 1989; **10**: 353-364
32 **Wells CL**, Maddaus MA, Reynolds CM, Jechorek RP, Simmons RL. Role of anaerobic flora in the translocation of aerobic and facultatively anaerobic intestinal bacteria. *Infect Immun* 1987; **55**: 2689-2694
33 **Cummings JH**, Macfarlane GT. Role of intestinal bacteria in nutrient metabolism. *Clin Nutr* 1997; **16**: 3-11
34 **Zimmaro DM**, Rolandelli RH, Koruda MJ, Settle RG, Stein TP, Rombeau JL. Isotonic tube feeding formula induces liquid stool in normal subjects: reversal by pectin. *J Parenter Enteral Nutr* 1989; **13**: 117-123
35 **Hopkins M**, Sharp R, Macfarlane G. Age and disease-related changes in intestinal bacterial populations assessed by cell culture, 16S-rRNA abundance, and community cellular fatty acid profiles. *Gut* 2001; **48**: 198-205
36 **Weaver GA**, Krause JA, Miller TL, Wolin MJ. Short chain fatty acid distributions of enema samples from a sigmoidoscopy population: an association of high acetate and low butyrate ratios with adenomatous polyps and colon cancer. *Gut* 1988; **29**: 1539-1543
37 **Whelan K**, Judd PA, Preedy VR, Taylor MA. Enteral feeding: the effect on faecal output, the faecal microflora and SCFA concentrations. *Proc Nutr Soc* 2004; **63**: 105-113
38 **Meijer-Severs GJ**, van Santen E. Short-chain fatty acid and organic acid concentrations in feces of 10 human volunteers and their correlation with anaerobe cultural counts over a 15-mo period. *Scand J Gastroenterol* 1989; **24**: 1276-1280
39 **Harmsen HJ**, Gibson GR, Elfferich P, Raangs GC, Wildeboer-Veloo AC, Argaiz A. Comparison of viable cell counts and fluorescence in situ hybridization using specific rRNA-based probes for the quantification of human fecal bacteria. *FEMS Microbiol Lett* 2000; **183**: 125-129
40 **Rayes N**, Hansen S, Seehofer D, Muller AR, Serke S, Bengmark S. Early enteral supply of fiber and Lactobacilli versus conventional nutrition: a controlled trial in patients with major abdominal surgery. *Nutrition* 2002; **18**: 609-615

Science Editor Guo SY **Language Editor** Elsevier HK

PO Box 2345, Beijing 100023, China
www.wjgnet.com
wjg@wjgnet.com

ELSEVIER

World J Gastroenterol 2005;11(39):6170-6175
World Journal of Gastroenterology ISSN 1007-9327
© 2005 The WJG Press and Elsevier Inc. All rights reserved.

• *BRIEF REPORTS* •

Prevalence of cholelithiasis in patients with chronic inflammatory bowel disease

Wolfgang Kratzer, Mark M Haenle, Richard A Mason, Christian von Tirpitz, Volker Kaechele

Wolfgang Kratzer, Mark M Haenle, Richard A Mason, Christian von Tirpitz, Volker Kaechele, Department of Internal Medicine I, University Hospital Ulm, Robert-Koch-Str. 8, D-89081 Ulm, Germany
Correspondence to: PD Dr. med. Wolfgang Kratzer, University Hospital Ulm, Department of Internal Medicine I, Robert-Koch-Str. 8, 89081 Ulm, Germany. wolfgang.kratzer@medizin.uni-ulm.de
Telephone: +49-731-500-2-4538 Fax: +49-731-500-2-4867
Received: 2004-10-22 Accepted: 2005-01-05

Abstract

AIM: To investigate the effect of chronic inflammatory bowel disease (CIBD) specific risk factors for cholecystolithiasis, as duration and involvement pattern of the disease and prior surgery in patients with Crohn's disease (CD) and ulcerative colitis (UC).

METHODS: A total of 222 patients with CD (135 females, 87 males; average age, 35.8±11.8 years; range 17-81 years) and 88 patients with UC (39 females, 49 males; average age, 37.2±13.6 years; range 16-81 years) underwent clinical and ultrasound examinations. Besides age, sex and degree of obesity, patients' CIBD specific parameters, including duration and extent of disease and prior operations were documented and evaluated statistically using logistic regression.

RESULTS: The overall prevalence of gallbladder stone disease in patients with CD was 13% (n = 30). Only age could be shown to be an independent risk factor (P = 0.014). Compared to a collective representative for the general population in the same geographic region, the prevalence of cholecystolithiasis was higher in all corresponding age groups. Patients with UC showed an overall prevalence of gallbladder stone disease of only 4.6%.

CONCLUSION: Only age but not disease-specific factors such as duration and extent of disease, and prior surgery are independent risk factors for the development of cholecystolithiasis in patients with CIBD.

© 2005 The WJG Press and Elsevier Inc. All rights reserved.

Key words: Crohn's disease, Ulcerative colitis, Gallstone disease, Ultrasonography, Ultrasound

Kratzer W, Haenle MM, Mason RA, von Tirpitz C, Kaechele V. Prevalence of cholelithiasis in patients with chronic inflammatory bowel disease. *World J Gastroenterol* 2005; 11(39): 6170-6175

http://www.wjgnet.com/1007-9327/11/6170.asp

INTRODUCTION

Besides the other extraintestinal complications[1], there is an increased rate of cholecystolithiasis in patients suffering from chronic inflammatory bowel disease (CIBD)[2-5]. The findings reported for ulcerative colitis (UC) are contradictory[6,7]. In the case of Crohn's disease (CD), the reports published to date are also inconsistent with regard to disease-specific factors, such as the duration of the disease[3,5,7,8], prior surgery (bowel resection)[2-4,7,8] and the pattern of disease involvement[2-6]. However, the incidence rate of gallbladder stone disease in patients with CIBD is often twice as high as in the general population, though the reason for this difference has yet to be satisfactorily explained[2-4].

In the majority of European and North American studies of the prevalence of cholecystolithiasis, there is a preponderance of cholesterol gallstones in the general population. The main identifiable risk factors for developing gallbladder stones include female sex, obesity and increasing age. In Asians, who show a high proportion of pigment gallstones, this predominance of females over males is not seen[9,10].

The pathophysiological explanation for the increased prevalence of gallbladder stones in patients with CD refers to the reduced absorption of bile acids in individuals with extensive involvement of the terminal ileum or following ileal resection[6,8]. The absolute number of bowel resections, the length of resected bowel and postoperative hypomotility of the gallbladder with subsequent formation of sludge and later, stones are currently under discussion as major risk factors for the higher prevalence of cholecystolithiasis in patients with CIBD[2-5].

The present study was to evaluate the importance of both the classical cholecystolithiasis risk factors, such as age, female sex and obesity and the effect of disease-specific parameters such as duration of the disease, pattern of involvement and prior surgery on the prevalence of gallbladder stones in patients with CD and UC.

MATERIALS AND METHODS

Patients

A total of 310 patients with CIBD presenting consecutive to our departmental section on Crohn's disease and ulcerative colitis over a period of approximately one year were screened for inclusion in the present study. The present study was conducted prospectively in accordance with the

principles of the Helsinki Declaration and approved by the Ethics Commission of the Medical Faculty.

Inclusion criteria included histologically confirmed CIBD and no history of cholecystolithiasis prior to first diagnosis of CIBD. Included in the study population were 222 patients with CD (135 females, 87 males; average age, 35.8±11.8 years; range 17-81 years) and 88 patients with UC (39 females, 49 males; average age, 37.2±13.6 years; range 16-81 years). The average period since the first diagnosis was 8.9±7.5 years (range: 0-34 years) in the group with CD and 6.8±5.8 years (range: 0-29 years) in the UC collective.

Risk factors

Besides the classical risk factors (age, female sex, obesity), disease-specific parameters such as time elapsed since the first diagnosis, pattern of disease involvement and prior surgical bowel resection in patients with CIBD were studied. Patients were subdivided into four age groups: ⩽30 years, 31-40 years, 41-50 years and 51 years and above.

For evaluation of obesity, patients were divided into three groups on the basis of their body-mass index (BMI):

Females:		Males:	
Ideal weight:	BMI < 21 kg/m²	Ideal weight:	BMI < 22 kg/m²
Normal weight:	BMI 21 -25 kg/m²	Normal weight:	BMI 22 -26 kg/m²
Overweight:	BMI > 25 kg/m²	Overweight:	BMI > 26 kg/m²

In order to study the effects of the duration of the disease (expressed as time elapsed since the first diagnosis with histological confirmation to the time of examination in the present study), patients were divided into four groups: up to 5 years, 6-10 years, 11-15 years and greater than 15 years. With regard to the parameter extent/pattern of disease, we differentiated in the CD group between patients who underwent or did not undergo surgical bowel resection. The group of patients who underwent resection was further subdivided into those who underwent ileocaecal resection and those who had undergone colectomy we did not further differentiate between partial and total colectomy (Figure 1). Type and number of bowel resections were obtained from the patient's chart. Patients with UC were divided into three subgroups: patients with no active disease, patients with disease involvement up to the left colic flexure, and patients with disease extending beyond the left colic flexure (Figure 2). Because only a few patients in the UC collective underwent either partial or total colectomy, a further differentiation between subcollectives with or without history of prior surgery was not done.

Examination

Patients presented in the morning for ultrasound examination in a fasting state.

The criteria for the diagnosis of cholecystolithiasis were defined as follows: one or more echogenic structures in the gallbladder with dorsal shadow; one or more echogenic structures in the gallbladder without dorsal shadow, which by means of multiplanar visualization or attempted mobilization could be differentiated with certainty from a gallbladder septum, Heister's valve or gallbladder polyps; a structure with significant echogenicity and dorsal shadow in the area of the gallbladder,

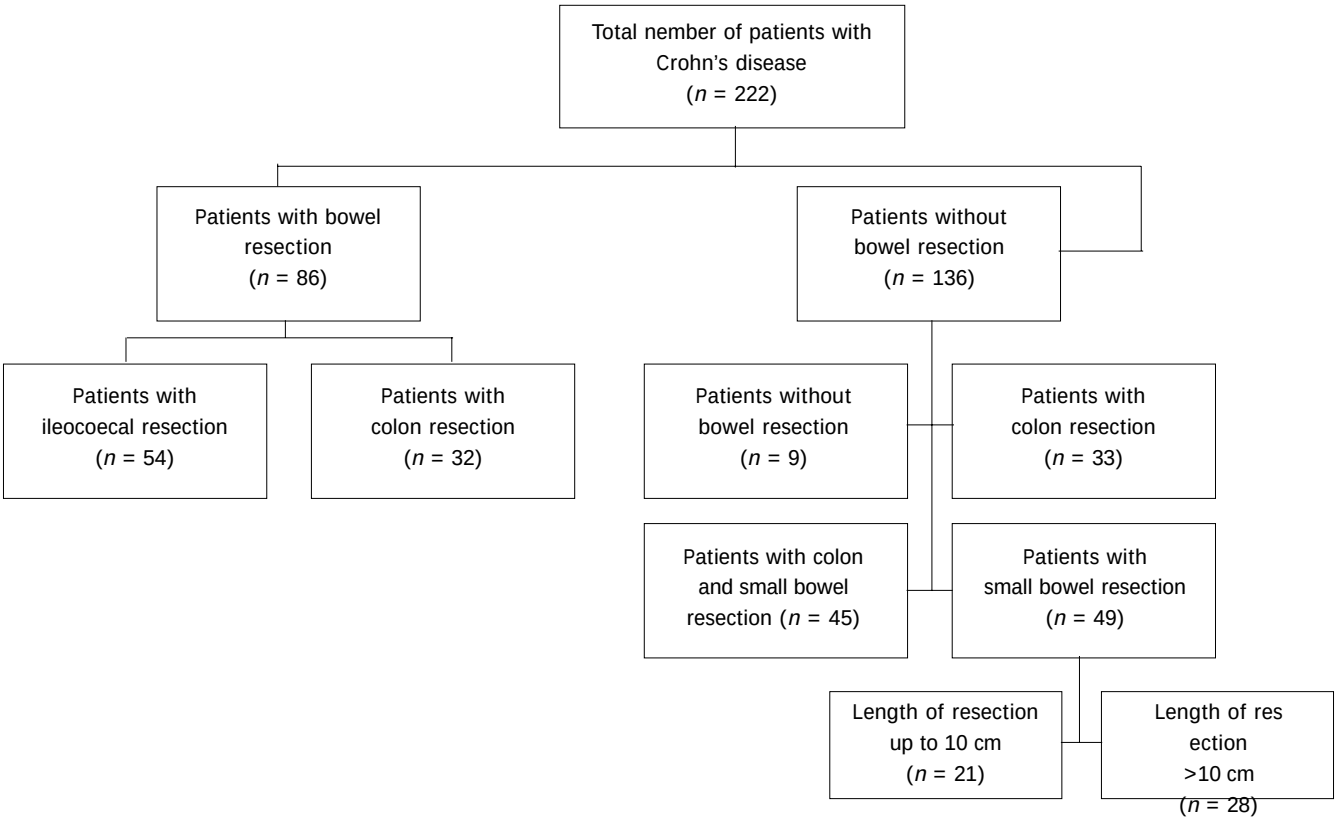


Figure 1 Pattern of involvement and bowel resections in patients with Crohn's disease.

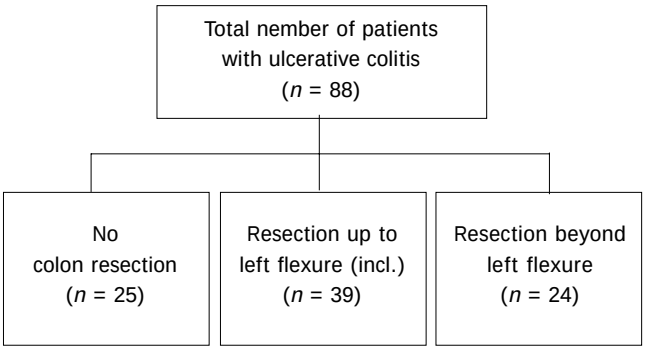


Figure 2 Pattern of involvement and bowel resections in patients with ulcerative colitis.

whose lumen was not definitely visualized; one or more echogenic structures in the gallbladder with or without dorsal shadow in the biliary tract; and no visualized gallbladder lumen in patients with history of prior cholecystectomy and corresponding incision(s) in the right upper abdominal quadrant.

Ultrasound examinations were performed using either the Ultramark 4 Plus or Ultramark 9 HDI with the 3.5- and 5.0-MHz transducer heads (ATL, Bothell, Washington, USA). Examination of the upper abdomen was conducted using the 3.5-MHz transducer head, while examination of the bowel was performed using the 5.0-MHz head. Ultrasound examinations were performed exclusively by two physicians experienced in diagnostic ultrasound of the abdomen. One-time visualization of concrements in the gallbladder based on the above criteria led to the patient's classification as suffering from cholecystolithiasis.

Evaluation of the pattern of disease involvement in the bowel was performed on the basis of sonographic criteria considering thickening of the intestinal wall. Wall thickness greater than 3 mm was considered pathologic. Bowel resection and time elapsed since the first diagnosis were established from the patient's history and chart.

Statistical treatment of the data

All data were first evaluated descriptively. For quantitative parameters, either mean with standard deviation or median with minimum and maximum was documented. While for qualitative parameters, relative and absolute frequencies were calculated.

The evaluation for prevalence in the subgroups and their confidence intervals was performed using a logistic regression model[11]. This model reproduces the influence of potential risk factors (independent variables) for the occurrence of a disease (dichotomous target parameter: here, cholecystolithiasis: yes/no). The importance of the potential risk factor was determined by the likelihood ratio test. By multiple application, several influence parameters could be simultaneously tested in one model and their respective influences were adjusted with regard to the other variables. The respective odds ratios, 95% confidence intervals and *P*-values served to quantify the change in risk of developing cholecystolithiasis due to the given factor. *P*-values between 0.05 and 0.1 were considered to represent trends or tendencies, while $P<0.05$ was considered statistically significant and the factor was classified as a "risk". The classical risk factors such as age, sex and BMI were included in the evaluation. Statistical calculation was performed using the SAS statistics software program (Institute Inc., Cary, NC).

RESULTS

Crohn's Disease

Patients with existing cholecystolithiasis and those with prior cholecystectomy were treated as a single group. Examination revealed gallbladder stones in 18 of the 222 patients with CD, while the other 12 underwent prior cholecystectomy, yielding a gallbladder stone prevalence of 13.5% ($n = 30$). The group of patients ⩽30 years of age numbered 101 subjects, representing nearly half of the collective. In these patients, gallbladder stone prevalence stood at 8% ($n = 8$). Prevalence of gallbladder stone disease increased with advancing age. The highest prevalence was found in the group of patients aged ⩾51 years, and stood at 37% in 10 of 27 subjects. No sex-specific differences were observed (Table 1).

Due to disease-specific implications, overweight patients with CD were rare. Thus, 45% of patients belonged to class I ($n = 100$), 37% to class II ($n = 83$) and only 18% to class III ($n = 39$). Assignment of patients to the various weight classes yielded a gallbladder stone prevalence of 14% ($n = 14$) for class I, 11% ($n = 9$) for class II and 13% ($n = 7$) for class III (Table 2).

Another parameter studied was the duration of CIBD. In the group of patients in whom elapsed time since the first diagnosis was 1-5 years, prevalence was the lowest. While in the other groups, the prevalence stood at 12%, 9%, and 28%, respectively (Table 2).

Isolated disease involvement affecting only the small bowel was observed in 49 patients. Isolated disease involvement affecting only the colon was seen in 33 patients, while the remaining 45 patients suffered from disease involving both the small bowel and colon. Patients who underwent surgical treatment were counted as a separate subgroup. The subgroup of patients with isolated disease affecting either the small intestine or colon only showed prevalence of 6%, each.

Table 1 Prevalence of cholecystolithiasis in relation to age and sex in Crohn's disease patients

Age(yr)	Males		Females		Total	
	n	prevalence (%)	*n*	prevalence (%)	*n*	prevalence (%)
⩽30	39	3	62	11	101	8
31-40	20	10	41	12	61	11
41-50	14	14	19	16	33	15
51⩾	14	36	13	38	27	37
Total	87	11	135	15	222	13.5

Table 2 Prevalence of cholecystolithiasis in relation to BMI, disease duration, pattern of involvement and bowel resections in Crohn's disease patients

BMI-classes	Patients (*n*)	Prevalence (%)
Ideal weight (males:< 22; females:< 21)	100	14
Normal weight (males: 22-26; females: 21-25)	97	11
Overweight (males: > 26; females: > 25)	26	13
Total	222	13.5
Disease duration in years		
1-5 yr	86	8
6-10 yr	57	12
11-15 yr	32	9
16-34 yr	47	28
Total	222	13.5
Pattern of disease involvement or prior surgery		
No visualized involvement	9	22
Isolated to small bowel	49	6
Isolated to colon	33	6
Both small bowel and colon involved	45	13
Ileocaecal-/ileal resection	54	22
Partial or total colectomy	32	16
Total	222	13.5

Patients with disease affecting both the small and large bowel, gallbladder stone prevalence stood at 13% (Table 2).

Evaluating for length of affected bowel segments, prevalence of gallbladder stones in a group of 21 patients with segment length up to 10 cm stood at 5% (n = 1) and at 7% in 28 patients with segment length exceeding of 10 cm (n = 2).

Eighty-six of all the patients in the CD group, underwent surgical bowel resection. Fifty-four patients underwent ileocaecal and/or ileum resection, while four other patients underwent ileotransversostomy or ileoascendostomy in addition to ileocaecal resection. Seventeen patients had a history of right hemicolectomy, while the other 10 underwent segmental colectomy. Only one patient underwent total colectomy. The groups with ileocaecal resection and ileum resection were combined in the univariate statistical analysis and compared to the group with colon resections.

In the group of patients who underwent partial resection of the small bowel, prevalence of gallbladder stone disease stood at 22% (12 of 54) and at 16% (5 of 32) in the colectomized group.

A logistic regression model considering patients' age, sex and BMI identified only age as a risk factor for developing gallbladder stone disease. No correlation with the prevalence of gallbladder stones was observed for the parameters such as sex, BMI, disease pattern, duration of the disease and prior intestinal resections (Table 3).

Ulcerative Colitis

Criteria used in the evaluation of the collective of patients with UC corresponded to those applied to CD patients. The overall prevalence of gallbladder stones in the UC group was lower than the comparable prevalence in the CD group. In the smaller subcollective of the UC group, gallbladder stones were observed only in female subjects. Using the same BMI-based weight classes applied to the CD collective, the following distribution according to weight was found in the UC group: 42% (n = 37), ideal weight; 34% (n = 30), normal weight; and 24% (n = 21), overweight. In the group of UC patients at ideal body weight, 5% (n = 2) had gallbladder stones, compared to 7% (n = 2) in those at normal weight and in none of the 21 overweight patients

Table 3 Risk factors for gallbladder stone disease at multiple logistic regression in patients with Crohn's disease

Risk factors	Odds ratio (OR)	95% CI	*P*
Age (yr)	1.048	1.010-1.089	[1]0.0143
Female Sex	1.732	0.704-4.263	0.2321
BMI (kg/m²)	0.937	0.822-1.069	0.3357
Duration of disease	1.045	0.983-1.111	0.1627
Pattern of involvement / bowel resections	0.236	0.025-4.611	0.4970

[1]statistically significant.

Univariate analysis yielded a gallbladder stone prevalence of 2% in patients who had elapsed 1-5 years since the first diagnosis of UC, 10% in the 6-10 year group and 6% in the 11-15 year group. In the group of patients who had passed 16-34 years since the first diagnosis, no disease was complicated by the development of cholecystolithiasis.

In 39 patients, disease did not extend the left colic flexure, while areas of bowel involvement beyond the left colic flexure were observed in 24 patients. Failure to visualize thickening of the intestinal at the time of examination was documented in 25 patients. Prevalence of gallbladder stone disease stood at 3% (n = 1) in patients with disease not extending the left colic flexure, but in 12.5% (n = 3) in those with disease involvement beyond the left colic flexure. We did not find evidence of gallbladder stone disease in any of the patients without documented bowel wall thickening at the time of examination. Unlike the group of patients with CD, the number of patients in the UC group with a history of prior bowel resections was too small for meaningful statistical analysis.

Because of the small number of gallstones (n = 4) identified in the UC group, no subgroup analyses were conducted.

DISCUSSION

The prevalence of gallbladder stones in patients with Crohn's disease in our collective was 13.5%, which is almost twice as high as that (7-8%) for age-matched groups of the general population in the same geographic area[12]. Comparable findings have also been reported from Italy and Sweden[2-4]. On the other hand, patients with ulcerative colitis have a prevalence of 4.6% and are not more frequently affected by cholecystolithiasis. Only Lorusso *et al.*[6], and Jones *et al.*[13], have reported that the prevalence of cholecystolithiasis is higher in UC patients than in the general population. Recent prospective sonographic surveys of larger CD and UC populations have studied the prevalence of cholecystolithiasis in these groups in comparison to a general population and used a multivariate logistic regression model to estimate the relative risk associated with the respective parameters[2-6].

Many, mostly earlier studies are unsuitable for comparison because of selection bias in the reference group, non-correspondence of the survey period or survey in another geographic region[14-17]. Other researchers have not drawn a comparison[7,18].

In the group of patients with CD, the prevalence increased with age from 8% in the group of subjects under 30 years of age to 37% in the 51-and-over age group. The multivariate analysis identified only age as an independent risk factor (OR: 1.048; CI: 1.010-1.089; $P = 0.0143$). It was reported that the prevalence of gallbladder stone increases in higher age groups[5,6] . In our own collective of patients with UC, we were not able to identify any correlation between advancing age and increased prevalence of cholecystolithiasis.

In our initial evaluation, sex was also identified as a univariate risk factor in CD and UC patients, though this did not hold true when the multiple logistic regression model was applied. The actual influence of female sex as a risk factor in the etiology of gallbladder stones is controversial[2,3,6,7,14]. Because of the small number of subjects in most studies, the results should be interpreted with caution.

Multiple analysis failed to demonstrate an increased prevalence of cholecystolithiasis in relation to the degree of obesity in either the CD ($P = 0.3357$) or UC ($P = 0.8397$) groups in our population. Most studies, especially the newer ones, have not included BMI as a risk factor in studies of UC patients[14-16,19]. Lorusso *et al*.[6], and Schölmerich *et al*.[7], have also failed to identify evidence supporting patients' degree of obesity as an independent risk factor contributing to the development of cholecystolithiasis.

Univariate analysis of disease duration suggested a correlation between the increasing length of time elapsed since the first diagnosis of CIBD and the prevalence of gallbladder stone disease. This was not confirmed by multiple logistic regression analysis ($P = 0.1627$) as it has been previously[2,3]. Findings in the literature are contradictory[17,20,21]. Reasons for the divergent findings are to be sought in the characteristics of the disease and in individual disease history of patients. In order to arrive at a relevant and objective evaluation of disease duration as an independent risk factor contributing to increased prevalence of cholecystolithiasis, analysis must include other factors, such as inflammatory activity, pattern of disease involvement, number and type of bowel resections, number and duration of remission phases, as well as type and success of other therapeutic measures. Because of the small number of cases in this subgroup, further statistical evaluation of these influence parameters was not meaningful. Gallstone prevalence was at 22% in patients with partial resection of the small bowel ($n = 12$) and 16% in the group that underwent resection of the colon ($n = 12$). Partial resection of the small bowel could not be identified as an independent risk factor in the multivariate analysis ($P = 0.4970$). Our data contradict those of previous[2,3]. A possible reason for the failure to identify the extent and number of bowel resections as independent risk factors at multivariate analysis may be the smaller number of patients in our collective who underwent ileocecal resection.

Because a separate evaluation of pattern of disease involvement and bowel resection is difficult, we defined these as a single parameter in our multiple logistic regression. The retrospective evaluation of surgical findings further limits the strength of our results. Multiple analysis failed to reveal any correlation between cholecystolithiasis, pattern of disease involvement and prior surgical bowel resection in CD patients ($P = 0.4970$). Earlier radiologic studies have shown an increase in gallbladder stone prevalence in relation to the length of resected bowel segments[4,8,9,16,18]. The disadvantages of these studies, however, refer primarily to the absence of multivariate analysis and a small number of subjects.

Studies showed that the bile acid pool reduces in patients with Crohn's disease[22]. Lapidus *et al*.[23,24], showed that the risk for pigment gallstones increases in patients with ileocoecal resections accompanied with manifestly elevated bilirubin and deoxycholic acid fractions in the bile suggesting that an increased risk for cholesterol gallstones in these patients does not exist.

Recently published data show that patients with Crohn's disease after colectomy or patients with small bowel Crohn's disease have an increased risk for cholesterol stones, and that patients with ileitis are prone to develop mixed, pigment-rich gallstones[25]. These changes after colectomy have not been detected in patients with ulcerative colitis[26].

In conclusion, the findings of the present study have identified only "age" as an independent risk factor for increased prevalence of gallbladder stones. Neither disease duration, pattern of disease involvement nor number or total length of resected bowel segments appear to be risk factors contributing to the development of gallbladder stones in these patients. Prospective multicenter studies should be conducted to assess all potential risk factors including therapy intervals between disease flares, phases of parenteral nutrition and prospective documentation of surgical data.

REFERENCES

1 **Lakatos L**, Pandur T, David G, Balogh Z, Kuronya P, Tollas A, Lakatos PL. Association of extraintestinal manifestations of inflammatory bowel disease in a province of western Hungary with disease phenotype: Results of a 25-year follow-up study. *World J Gastroenterol* 2003; **9**: 2300-2307

2 **Bargiggia S**, Maconi G, Elli M, Molteni P, Ardizzone S. Sonographic prevalence of liver steatosis and biliary tract stones in patients with inflammatory bowel disease: study of 511 subjects at a single center. *J Clin Gastroenterol* 2003; **36**: 417-420

3 **Fraquelli M**, Losco A, Visentin S, Cesana BM, Pometta R, Colli A. Gallstone disease and related risk factors in patients with Crohn disease: analysis of 330 consecutive cases. *Arch Intern Med* 2001; **8**: 2201-2204

4 **Lapidus A**, Bangstad M, Astrom M, Muhrbeck O. The prevalence of gallstone disease in a defined cohort of patients with Crohn's disease. *Am J Gastroenterol* 1999; **94**: 1261-1266

5 **Hutchinson R**, Tyrrell PN, Kumar D, Dunn JA, Li JK, Allan RN. Pathogenesis of gall stones in Crohn's disease: an alternative explanation. *Gut* 1994; **35**: 94-97

6 **Lorusso D**, Leo S, Mossa A, Misciagna G, Guerra V. Cholelithiasis in inflammatory bowel disease. A case-control study. *Dis Colon Rectum* 1990; **33**: 791-794

7 **Schölmerich J**, Braun G, Volk BA, Spamer C, Hoppe-Seyler P, Gerok W. Detection of extraintestinal and intestinal abnormalities in inflammatory bowel disease by ultrasound. *Dig Surg* 1987; **4**: 82-87

8 **Kangas E**, Lehmusto P, Matikainen M. Gallstones in Crohn's

disease. *Hepatogastroenterology* 1990; **37**: 83-84
9 **Brett M**, Barker DJ. The world distribution of gallstones. *Int J Epidemiol* 1976; **5**: 335-341
10 **Kratzer W**, Mason RA, Kachele V. Prevalence of gallstones in sonographic surveys worldwide. *J Clin Ultrasound* 1999; **27**: 1-7
11 **Hosmer DW Jr**, Lemeshow S. Applied logistic regression. *New York Wiley* 1989
12 **Kratzer W**, Kron M, Hay B, Pfeiffer MM, Kachele V. Prevalence of cholecystolithiasis in South Germany-an ultrasound study of 2 498 persons of a rural population. *Z Gastroenterol* 1999; **37**: 1157-1162
13 **Jones MR**, Gregory D, Evans KT, Rhodes J. The prevalence of gallbladder disease in patients with ileostomy. *Clin Radiol* 1976; **27**: 561-562
14 **Kurchin A**, Ray JE, Bluth EI, Merritt CR, Gathright JB, Pehrsson BF. Cholelithiasis in ileostomy patients. *Dis Colon Rectum* 1984; **27**: 585-588
15 **Baker AL**, Kaplan MM, Norton RA, Patterson JF. Gallstones in inflammatory bowel disease. *Am J Dig Dis* 1974; **19**: 109-112
16 **Hill GL**, Mair WS, Goligher JC. Gallstones after ileostomy and ilealresection. *Gut* 1975; **16**: 932-936
17 **Heaton KW**, Read AE. Gall stones in patients with disorders of the terminal ileum and disturbed bile salt metabolism. *Br Med J* 1969; **3**: 494-496
18 **Andersson H**, Bosaeus I, Fasth S, Hellberg R, Hulten L. Cholelithiasis and urolithiasis in Crohn's disease. *Scand J Gastroenterol* 1987; **22**: 253-256
19 **Bluth EI**. Ultrasound evaluation of small bowel abnormalities. *Am J Gastroenterol* 1983; **78**: 788-793
20 **Heaton KW**. Disturbances of bile acid metabolism in intestinal disease. *Clin Gastroenterol* 1977; **6**: 69-89
21 **Marks JW**, Conley DR, Capretta TL, Bonorris GG, Chung A, Coyne MJ. Gallstone prevalence and biliary lipid composition in inflammatory bowel disease. *Am J Dig Dis* 1977; **22**: 1097-1100
22 **Vantrappen G**, Ghoos Y, Rutgeerts P, Janssens J. Bile acid studies in uncomplicated Crohn's disease. *Gut* 1977; **18**: 730-735
23 **Lapidus A**, Einarsson K. Effects of ileal resection on biliary lipids and bile acid composition in patients with Crohn's disease. *Gut* 1991; **32**: 1488-1491
24 **Lapidus A**, Einarsson C. Bile composition in patients with ileal resection due to Crohn's disease. *Inflamm Bowel Dis* 1998; **4**: 89-94
25 **Pereira SP**, Bain IM, Kumar D, Dowling RH. Bile composition in inflammatory bowel disease: ileal disease and colectomy, but not colitis, induce lithogenic bile. *Aliment Pharmacol Ther* 2003; **17**: 923-933
26 **Akerlund JE**, Einarsson C. Effects of colectomy on bile composition, cholesterol saturation and cholesterol crystal formation in humans. *Int J Colorectal Dis* 2000; **15**: 248-252

Science Editor Wang XL and Guo SY **Language Editor** Elsevier HK

PO Box 2345, Beijing 100023, China
www.wjgnet.com
wjg@wjgnet.com

ELSEVIER

World J Gastroenterol 2005;11(39):6176-6181
World Journal of Gastroenterology ISSN 1007-9327
© 2005 The WJG Press and Elsevier Inc. All rights reserved.

• *BRIEF REPORTS* •

Quantitative evaluation of long-term liver repopulation and the reconstitution of bile ductules after hepatocellular transplantation

Yun-Wen Zheng, Nobuhiro Ohkohchi, Hideki Taniguchi

Yun-Wen Zheng, Hideki Taniguchi, Department of Regenerative Medicine, Graduate School of Medical Science, Yokohama City University, Yokohama 236-0004, Japan
Nobuhiro Ohkohchi, Yun-Wen Zheng, Department of Surgery, Institute of Clinical Medicine, University of Tsukuba, Tsukuba 305-8575, Japan
Hideki Taniguchi, Research Unit for Organ Regeneration, Center for Developmental Biology, RIKEN, Kobe 650-0047, Japan
Supported by the National Project for Realization of 'Regenerative Medicine' and Grants-in-Aid (14207046, 12557096) for Scientific Research from the Ministry of Education, Culture, Sports, Science and Technology, Japan and a grant from MITSUBISHI Foundation
Correspondence to: Professor Hideki Taniguchi, MD, PhD, Department of Regenerative Medicine, Graduate School of Medical Science, Yokohama City University, Fukuura 3-9, Kanazawa-Ku, Yokohama 236-0004, Japan. rtanigu@med.yokohama-cu.ac.jp
Telephone: +81-45-787-8963 Fax: +81-45-787-8963
Received: 2004-12-22 Accepted: 2005-03-21

Abstract

AIM: The treatment of liver disease is severely limited by a shortage of donor livers. In trying to address this growing problem, hepatocellular transplantation (HTx) has received much attention as an alternative to whole organ transplant. However, the expansion of transplanted cells is at low level, and the reconstitution of functional liver tissue is limited by this cellular property. We set up an animal model to better understand cell dose effect and the kinetics of liver repopulation following HTx.

METHODS: Dipeptidyl peptidase IV (DPPIV)-deficient rats treated with retrorsine and subjected to partial hepatectomy were infused with DPPIV-positive hepatocytes. Rats were injected with varying numbers of donor hepatocytes down to 100 cells low, and liver repopulation was examined at different time points up to 20 mo long. Repopulation was assessed by computer-aided quantitative detection.

RESULTS: Transplanted hepatocytes underwent multiple rounds of proliferation and stably repopulated the injured livers after 20 mo and at all cell doses. Transplanted cells divided 14 times within the 3-mo time period following infusion, and the liver repopulation reached a plateau between 3 and 20 mo. Approximately 90% replacement occurred. Donor-derived cells also reconstituted the bile ductules of the recipients.

CONCLUSION: The ability of transplanted hepatocytes to fully reconstitute injured livers strongly supports further investigation into the clinical potential of HTx. Additionally, the observation that transplanted hepatocytes also form components of the biliary system suggests that these cells may have bi-potential property of the stem cells.

© 2005 The WJG Press and Elsevier Inc. All rights reserved.

Key words: Hepatocellular transplantation; Hepatic stem cell; Kinetics; Cell dose; Long-term repopulation; Bile ductules; Quantification; *In vivo*; Therapeutic potential

Zheng YW, Ohkohchi N, Taniguchi H. Quantitative evaluation of long-term liver repopulation and the reconstitution of bile ductules after hepatocellular transplantation. *World J Gastroenterol* 2005; 11(39): 6176-6181
http://www.wjgnet.com/1007-9327/11/6176.asp

INTRODUCTION

In patients with end-stage liver disease, liver transplantation is the only effective treatment, but this is limited by the shortage of potential organs. Cell transplantation (Tx) has the potential to overcome this shortage as well as the high cost and morbidity associated with the whole organ transplant. Isolated hepatocellular transplantation (HTx) was investigated several decades ago as one of the earliest forms of cell transplantation[1] and has come to the stage of clinical therapies in recent years[2,3]. However, transplanted hepatocytes do not seem to proliferate well and reconstitution of liver function is not sufficient in the models used thus far[3,4]. Endogenous hepatocytes greatly outnumbered the transplanted cells and it is conceivable that, if both populations respond equally well to proliferative stimuli, donor cells would never achieve sufficient numbers[5]. Some models allowing for the selective proliferation of transplanted cells have made progress in addressing this problem[6-9]. Disruption of the proliferative capacity of endogenous hepatocytes followed by transplantation is an alternative strategy to achieve these goals. Retrorsine[7,10] or irradiation[9] has been used to inhibit the proliferation of endogenous hepatocytes and allow transplanted hepatocytes to fully repopulate the liver, making the clinical application of HTx more feasible. Application of the prospective therapy may become a reality if answers to the following questions are obtained. How long can donor-derived hepatocytes continue to repopulate the damaged recipient liver? What is the relationship between repopulation efficiency and cell dose of HTx? Will transplanted hepatocytes be able to repopulate other tissues in addition to the liver parenchyma? Moreover, the capability of long-term tissue repopulation[5] should also be addressed in the animal model, with a longer post-transplant period than the life span of liver cells.

We used dipeptidyl peptidase IV (DPPIV) as a genetic marker of transplanted cells in rats treated with retrorsine and subjected to partial hepatectomy (PH). Retrorsine, a DNA-alkylating agent that disrupts cell-cycle progression in hepatocytes, prevented the recipient hepatocytes from proliferating, and, following PH, only transplanted cells proliferated and repopulated the liver[7]. Using this model, we addressed the above questions and discussed the prospects of HTx in clinical application, and also the heterogeneity and the stem cell property of hepatocytes.

MATERIALS AND METHODS

Animals

Male Fischer 344 DPPIV wild-type ($DPPIV^+$) rats used as hepatocyte donors for Tx were purchased from SLC of Japan and female Fischer 344/DuCrj DPPIV-deficient ($DPPIV^-$) recipient rats were purchased from Charles River of Japan. Animals were maintained in daily 12-h cycles of alternating light and darkness. All studies were conducted under protocols approved by the Laboratory Animal Resource Center of University of Tsukuba, Japan.

Retrorsine treatment and partial hepatectomy

Recipients, 4-wk-old Fischer 344 rats, were treated with retrorsine similar to previous descriptions with some modifications[7,11]. Briefly, a retrorsine (Sigma) working solution was prepared in acidified saline with 1 mol/L HCl; this was neutralized with 1 N NaOH and adjusted to a final concentration of 6 mg/mL. The animals received two intraperitoneal injections with 30 mg/kg body weight 2 wk apart. Donor cells were infused either 1 mo or 2 wk following retrorsine treatment. All recipients were subjected to two-thirds surgical PH.

Cell isolation and transplantation

Parenchymal hepatocytes were isolated from normal adult rats (8-10-wk old) using a standard two-step collagenase perfusion method described by Seglen[12]. After perfusion, the cells were centrifuged at 50 g for 1 min and filtered with a nylon mesh to remove aggregated cells and residual tissue. Cell viability was between 80% and 90% as determined by trypan blue dye exclusion. Limiting dilution of the freshly isolated cells was performed from 2×10^6, 1×10^6, 1×10^5, 1×10^4, and 1×10^3 to 1×10^2. Hepatocytes in 0.2 mL Dulbecco's modified Eagle's medium were infused through the portal vein. Two to three animals were used for each time point, and experiments were repeated at least twice. After 1-3 mo, and up to 20 mo following Tx, animals were killed and the livers were sampled.

Histochemical staining

DPPIV histochemical staining was performed as described[7,13]. Sampled rat livers were embedded in optimum cutting temperature compound, frozen in liquid nitrogen and stored at -80 ℃. DPPIV activity was visualized in tissues fixed with chloroform–acetone (1:1, v/v) for 10 min, followed by incubation with glycyl-L-proline-4-methoxy-2-naphthyl-amide (Sigma) substrate for 30 min at room temperature. The counterstaining was performed with hematoxylin.

Quantitative detection

DPPIV-positive areas were captured by Photograb-2500, v1.0 (Fujifilm) through a Nikon Eclipse E800 microscope and analyzed by computer program, WinROOF v3.2 (Mitani Corp.).

To determine the number of hepatocytes per repopulated colony, we considered a colony as a large sphere and a single hepatocyte as a small sphere. If the average radius of one colony in cross-sectional analysis on slide is expressed as R, the overall volume of the colony is $2\pi R^3\sqrt{1.5}$. The number of hepatocytes estimated per colony sphere was calculated by $\text{volume}_{\text{colony-sphere}}/\text{volume}_{\text{hepatocyte}}$. Cell division during Tx for a colony sphere was calculated by $\log_{10}(1.5(R/r)^3\sqrt{1.5})/\log_{10}2$ ($r\approx10$ μm, radius of one hepatocyte).

RESULTS

Kinetics of liver repopulation

The canaliculi enzyme DPPIV is highly expressed in epithelial cells (including hepatocytes) of many organs in rats except in one substrain of inbred Fischer rats. It is a stable and easily distinguishable marker for use in enzyme histochemistry in models of HTx[7,14]. After transplantation, DPPIV-positive cells constituted 14.8±4.2%, 50.7±13.9% and 70.4±9.0% of the total hepatocyte number at 1, 2, and, 3 mo of follow-up, respectively (Figures 1A-C). Twenty months after transplantation, a repopulation rate as high as 95% was observed, with an average rate of 89.8±4.7% (Figure 1D). Histochemical analysis also clearly showed that donor cells proliferated and expanded through recipient liver tissue (Figure 2A and Table 1), and, at the latest time point, occupied nearly the full volume of the recipient liver (Figure

Table 1 Effect of transplant cell dose and time on the efficiency of liver repopulation *in vivo* after HTx

Time of Tx (mo)	Kinetics of repopulation				Effect of cell dose on repopulation				
	1	2	3	20	3	3	3	3	3
Infused cell number Post Tx	2×10^6	2×10^6	2×10^6	1×10^6	1×10^6	1×10^5	1×10^4	1×10^3	1×10^2
Liver repopulation (%)	14.8±4.2	50.7±13.9	70.4±9.0	89.8±4.7	51.0±4.7	28.9±7.2	13.8±15.0	1.1±1.2	0.6±0.6
Colony number/mm^2	5.48±1.10	5.1±1.40	NA	NA	2.64±0.16	0.91±0.05	0.37±0.39	0.09±0.07	0.01±0.01
Diameter of colony (μm)	149.4±110.5	280.1±219.4	NA	NA	425.2±278.8	376.7±64.8	476.5±54.5	354.5±108.9	698.7±39.2
Number of animals	6	6	3	4	3	3	4	4	4
Area examined (mm^2)	365.0	402.0	66.6	2386.5	77.6	284.1	464.8	458.0	470.5

Donor cells were derived from $DPPIV^+$ rats. Recipients were DPPIV-deficient rats treated with retrorsine and two-thirds PH; $DPPIV^+$ cells were visualized by their enzymatic activity after histochemical staining of cryostat sections. The characteristics of repopulation, colony number and colony diameter were analyzed based on $DPPIV^+$ cells. Computer-aided area analysis was used for quantitative detection of repopulation. All of the data presented as mean±SD from three to six individuals in two or three independent experiments. HTx: hepatocellular transplantation; Tx: transplantation; NA: not applicable.

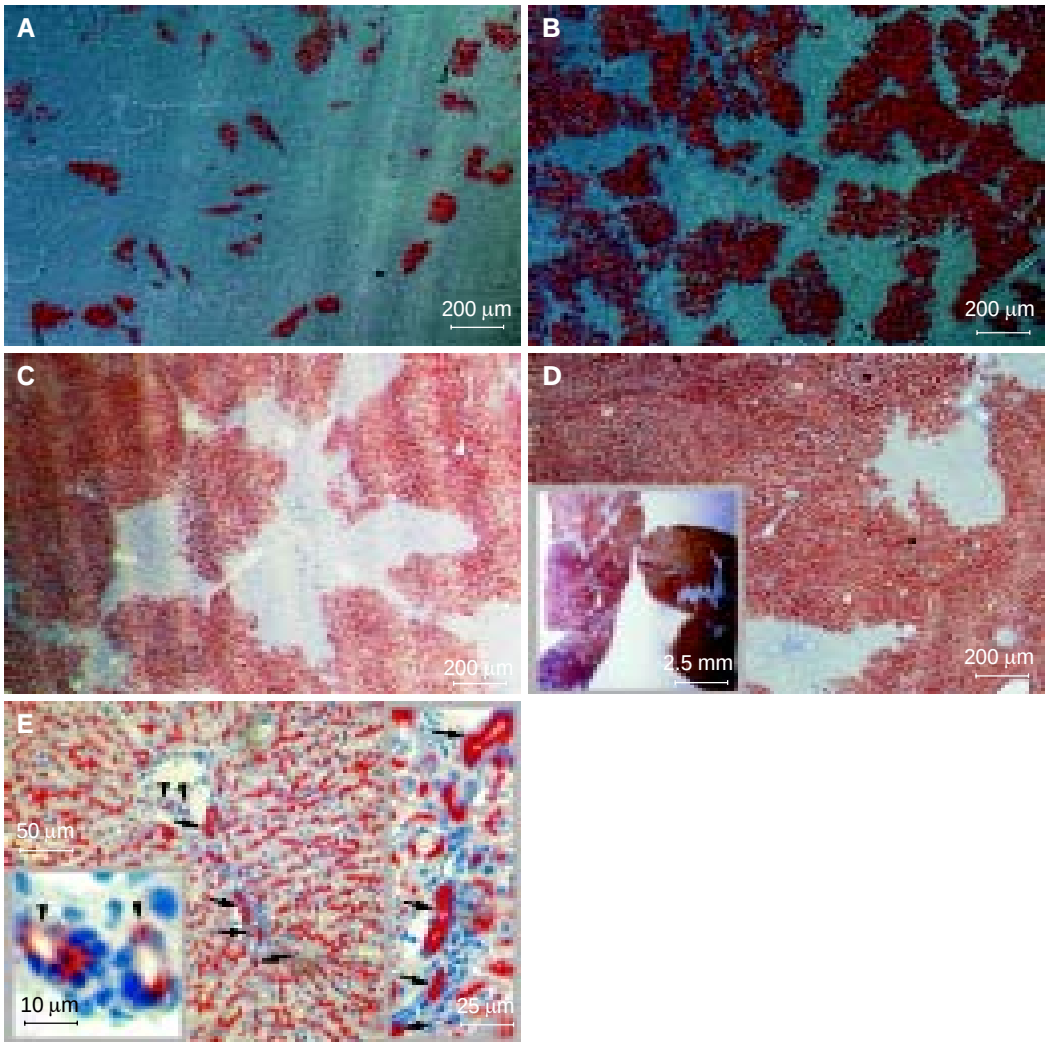


Figure 1 Long-term liver repopulation 1-20 mo after hepatocellular Tx and hepatic epithelial reconstitution from donor hepatocytes. Recipient DPPIV-deficient Fischer rats were treated with retrorsine and subjected to two-thirds PH. DPPIV-positive donor hepatocytes were infused through the portal vein. 2×10^6 donor cells per recipient in A-C and 1×10^6 in D and E. Cryostat sections show DPPIV-positive cells as red-brown after histochemical staining. Data presented as mean±SD from three to six individuals in two or three independent experiments. Tx: transplantation; DPPIV: dipeptidyl peptidase IV. A: 1-mo repopulation: 14.8±4.2%; polarization contrast image; B: 2-mo repopulation: 50.7±13.9%; polarization contrast image; C: 3-mo repopulation: 70.4±9.0% with hematoxylin counterstaining; D: 20-mo repopulation: 89.8±4.7% with hematoxylin counterstaining. The inset box displays the cross-sections of hepatic lobes under stereomicroscopy and E: DPPIV-positive cells not only were expressed in parenchyma but also were found in Hering's canal-like structures (arrow) and interlobular bile duct-like structure (arrowhead) in recipient liver; hematoxylin counterstaining.

1D, inset). Between 3 and 20 mo, the repopulation rate increased by only 20%, suggesting that the phenomena had reached a plateau. Using a similar model, Laconi *et al.*[15], observed a repopulation rate of 81% at 8 mo in female recipients; this is consistent with our results.

The lobular architecture and overall histological appearance of the livers were normal following HTx, and hepatocyte morphology, hepatic plate structure, and the appearance of cells lining the sinuses were normal compared to untreated livers (data not shown). Despite extensive hepatocyte proliferation and the appearance of "nodules" of transplanted cells, no tumors were observed in the liver up to 20 mo after Tx. Additionally, the survival of all four recipients up to 20 mo indicates that no abnormalities incompatible with life develop following transplant.

Colony size and cell replication

Colony size analyses more clearly defined the magnitude of transplanted cell proliferation in recipient animals. Table 1 presents the characteristics and distribution of donor cells following transplantation with varied cell numbers and at different time points after Tx. $DPPIV^+$ colonies expanded linearly between 1 and 3 mo after Tx from 150 to 425 μm in diameter (Figure 2B). The area of recipient livers occupied by donor cells similarly increased over 3 mo.

Hepatocytes are thought to be symmetric, 8 or 12-sided cells[16], but, in order to simplify calculations, we considered a hepatocyte as a sphere and assumed that one colony arose from one hepatocyte. Additionally, we made the assumption that repopulated colonies assumed a grossly spherical shape, and the number of cells occupying these colonies could be calculated by comparing the volume of one cell with the volume of a colony. Based on these assumptions and analyses, transplanted hepatocytes underwent about nine rounds of cell replication after the 1st mo and another three and two rounds in 2nd and 3rd mo, respectively. Donor cell

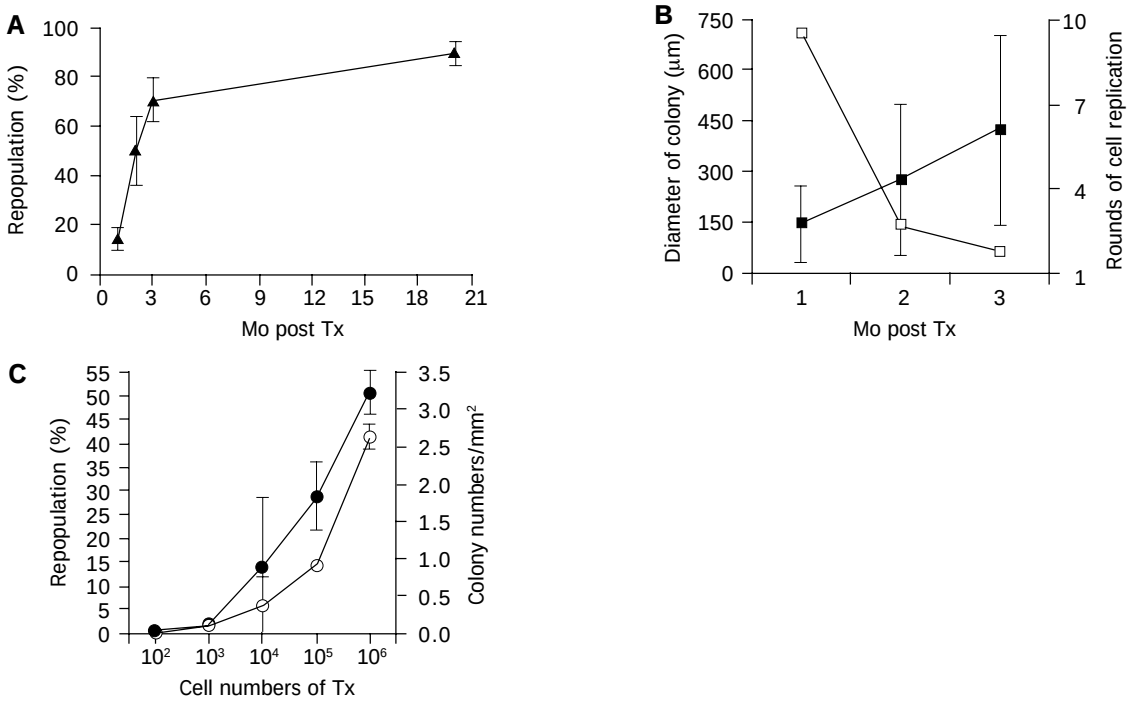


Figure 2 Repopulation kinetics of hepatocellular Tx. DPPIV$^+$ donor hepatocytes were isolated and infused into DPPIV-deficient rats through the portal vein. The visualized DPPIV$^+$ cells in recipient were processed by a computer-aided analysis. Data are presented as mean±SD from three to six individuals in two or three independent experiments. Tx: transplantation; DPPIV: dipeptidyl peptidase IV. A: Kinetics of liver repopulation. Transplanted cell numbers into 1-3 mo and 20 mo were 2×10^6 and 1×10^6, respectively. The repopulation rate increased dramatically over 3 mo and reached a plateau at 20 mo; B: Kinetics of colony size and cell replication. Transplanted cell numbers into 1-2 mo and 3 mo were 2×10^6 and 1×10^6, respectively. The estimation technique of cell replication rounds is explained in Results. The average colony size from donor hepatocytes in the 3 mo after Tx are filled squares and the estimated number of rounds of cell replication are open squares and C: Cell-dose effect on liver repopulation and colony numbers. All samples collected at 3 mo after Tx and the repopulation rate (filled circles) and colony numbers (open circles) showed a similar trend.

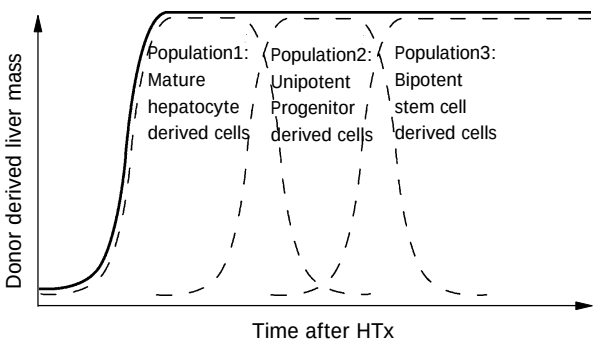


Figure 3 Schematic diagram of long-term repopulation after HTx. Different cell populations may be required for different phases of liver regeneration/repopulation. The solid lines express the repopulation of donor-derived cells in the liver and the broken lines are the repopulation from the possible contributors. This assumes a heterogeneous population of transplanted hepatocytes. HTx: hepatocellular transplantation.

division was high only in the 1st mo, and it dramatically decreased over the following period (Figure 2B), but replication never stopped although it slowed down to very low level.

Effect of cell dose on liver repopulation

The ability of different numbers of transplanted cells to repopulate the liver is unknown, despite the importance of this information for stem cell biology and the clinical application of HTx. As seen in Table 1 and Figure 2C, transplantation of 10^2-10^6 led to liver repopulation rates from 0.6% up to 51% 3 mo after transplant, and the repopulated colonies reached 0.01-2.64/mm^2 in recipient livers. Effective repopulation occurred even in the 100-cell group. Therefore, liver repopulation for no more than 3 mo does not seem to depend on an infrequent cell fraction, but hepatocytes in general are able to form colonies following transplantation.

DPPIV-positive cholangiocytes in recipient livers

DPPIV is expressed in both hepatocytes and bile duct epithelial cells, in a characteristic bile canalicular distribution and a diffuse cytoplasmic pattern, respectively[7,17,18]. Twenty months after transplant with one million hepatocytes, interlobular bile duct-like cells and Hering's canal-like cells also expressed the donor-derived genetic marker, DPPIV (Figure 1E). To our knowledge, this is the first report of bile duct differentiation of transplanted hepatocytes. This finding contrasts with the widely accepted view that hepatocytes are uni-potential following transplant[19].

DISCUSSION

In contrast to fully differentiated cells in adult mammalian tissues, hepatocytes possess an enormous proliferative capacity and are capable of replacing the entire liver mass under some circumstances. In the normal resting liver, the hepatocyte turnover rate at any given time is about 1 in 20 000-40 000 cells, and normal liver tissue is replaced over the course of 1 year[20]. If transplanted hepatocytes did not undergo cell

division or the division did not last for a sufficient duration of time, few donor cells would have remained at the 20-mo time point. However, recipient livers were almost exclusively comprised of donor cells at 20 mo after transplant (Figure 1D, inset). The tissue renewal by donor-derived hepatocytes occurs multiple times in the recipient liver in more than 1-year long-term repopulation. The present findings demonstrate that the 'long-term tissue repopulation' characteristics defined for stem cells[5] are expressed by adult hepatocytes as well. The present study markedly differs from previous reports[7,14,15] in having the post-transplantation period longer than the life span of liver cells, and it also takes into account the cell-dose effect. The extremely long period of observation was necessary because it facilitated analysis of cell kinetics of long-lived cells to trace the transplanted cells and to show whether they possess the stem cell properties or not.

To differentiate and colonize, a wide range of tissues to reconstitute them *in vivo* is another important property of stem cells. In the present study, bi-potential capability of donor-derived cells displayed an interesting aspect of tissue reconstitution. Hepatocytes are thought to be "functional" or "committed" progenitors[19], but 20 mo after transplant, cholangiocytes (interlobular bile duct-like cells and Hering's canal-like cells) expressed the donor cell marker (Figure 1E). It indicates that the bi-potential stem cells, however, existed in donor-derived cells. We had not previously observed donor-derived cholangiocytes in other no longer than 6-mo old Tx groups. Why is the regeneration of biliary system so rare to be observed? One possible answer is that a minor proportion of donor-derived bi-potential cells spend a long time to differentiate and competitively reconstitute the system in the recipient. The low frequent appearance may predict and represent an important inherent nature of hepatic stem cells.

Hepatocytes may be capable of only one or two rounds of cell division when responding to cell loss under normal physiological conditions[21,22], but we observed at least 14 rounds of replication in the 3-mo time period following transplantation. Various physiological needs may stimulate a variety of responses from different populations of hepatocytes. It is possible that the transplanted cells were not a homogenous population of hepatocytes. This could explain the ability of the donor cells to proliferate to a greater extent than previously thought as well as the generation of cholangiocytes. Indeed, adult hepatocytes exhibit heterogeneous proliferative potential *in vitro*[23]. The potential complexity of the liver cells populations is outlined in Figure 3. Liver tissue may be comprised of a large number of mature hepatocytes that rapidly respond to physiological cell loss and tissue injury (population 1) for a short time, a small number of uni-potential progenitors that rapidly replicate in response to liver injury for a limited time period (population 2), and rare bi-potential stem cells capable of self-renewal that slowly respond to severe liver injury for a long time (population 3). Further studies with some other approaches, such as, flow-cytometric cell sorting and *in vitro* colony assay[24,25] are clearly needed to investigate this hypothesis.

While the biological phenomena underlying our observations are not very clear, the therapeutic potential of hepatocyte transplant is very clear. A small number of transplanted cells efficiently and stably repopulated injured rat livers. With the expansion of waiting lists for orthotopic liver transplant growing, the availability of donor cells makes HTx even more attractive. Among the potential applications of HTx, supply metabolic support in acute or chronic liver failure and definitive treatment of inherited metabolic disorders are included. At the very least, HTx could be used as a bridge therapy to prolong the lives and function of patients awaiting transplants. It is reasonable to assume that mechanism that controls regeneration may be fairly similar among various species, and the knowledge obtained from researches of liver regeneration in the animal model is applicable to the human liver. Our study may be a guide for initial investigations of HTx in human. For example, in our animal model, the cell infusion ratio of donor cells to recipient liver cells was about 1/200 ($2\times10^6/4\times10^8$), and we achieved 50% and 70% repopulation rates 2 and 3 mo after Tx. Human liver tissue is thought to weigh 1 500 *g* with 2.5×10^{11} parenchymal cells. Extrapolating from our data, approximately 1.25×10^9 cells would be used for human HTx, and if 10% of isolated hepatocytes could be collected from a liver (2.5×10^{10}cells), a single liver could be used for 20 HTx. The low cost, high preservability and availability of sources could make HTx an extremely promising treatment for end-stage liver disease.

Taken together, the long-term repopulation potential, high replacement rate and full tissue reconstitution following HTx in our model further strengthens the therapeutic potential of this technique. Additionally, our observations raise interesting possibilities as to the composition and proliferation of hepatocyte populations as well as the hepatic stem cell nature.

ACKNOWLEDGMENTS

Authors thank Dr. Mei Gu, Dr. Pei Gan, Dr. Hirotoshi Miyoshi, Dr. Kennichi Yanagi and Dr. Chika Miyoshi for expert technical assistances on liver perfusion and surgical operation.

REFERENCES

1 **Matas AJ,** Sutherland DE, Steffes MW, Mauer SM, Sowe A, Simmons RL, Najarian JS. Hepatocellular transplantation for metabolic deficiencies: decrease of plasms bilirubin in Gunn rats. *Science* 1976; **192**: 892-894

2 **Grossman M,** Raper SE, Kozarsky K, Stein EA, Engelhardt JF, Muller D, Lupien PJ, Wilson JM. Successful *ex vivo* gene therapy directed to liver in a patient with familial hypercholesterolaemia. *Nat Genet* 1994; **6**: 335-341

3 **Fox IJ,** Chowdhury JR, Kaufman SS, Goertzen TC, Chowdhury NR, Warkentin PI, Dorko K, Sauter BV, Strom SC. Treatment of the Crigler-Najjar syndrome type I with hepatocyte transplantation. *N Engl J Med* 1998; **338**: 1422-1426

4 **Grossman M,** Rader DJ, Muller DW, Kolansky DM, Kozarsky K, Clark BJ 3rd, Stein EA, Lupien PJ, Brewer HB Jr, Raper SE, Wilson JM. A pilot study of *ex vivo* gene therapy for homozygous familial hypercholesterolaemia. *Nat Med* 1995; **1**: 1148-1154

5 **Shafritz DA,** Dabeva MD. Liver stem cells and model systems for liver repopulation. *J Hepatol* 2002; **36**: 552-564

6 **Rhim JA,** Sandgren EP, Degen JL, Palmiter RD, Brinster RL. Replacement of diseased mouse liver by hepatic cell transplantation. *Science* 1994; **263**: 1149-1152

7 **Laconi E,** Oren R, Mukhopadhyay DK, Hurston E, Laconi S, Pani P, Dabeva MD, Shafritz DA. Long-term, near-total liver replacement by transplantation of isolated hepatocytes in rats treated with retrorsine. *Am J Pathol* 1998; **153**: 319-329

8 **Overturf K,** Al-Dhalimy M, Tanguay R, Brantly M, Ou CN, Finegold M, Grompe M. Hepatocytes corrected by gene therapy are selected *in vivo* in a murine model of hereditary tyrosinaemia type I. *Nat Genet* 1996; **12**: 266-273

9 **Guha C,** Sharma A, Gupta S, Alfieri A, Gorla GR, Gagandeep S, Sokhi R, Roy-Chowdhury N, Tanaka KE, Vikram B, Roy-Chowdhury J. Amelioration of radiation-induced liver damage in partially hepatectomized rats by hepatocyte transplantation. *Cancer Res* 1999; **59**: 5871-5874

10 **Gordon GJ,** Coleman WB, Grisham JW. Bax-mediated apoptosis in the livers of rats after partial hepatectomy in the retrorsine model of hepatocellular injury. *Hepatology* 2000; **32**: 312-320

11 **Gordon GJ,** Coleman WB, Grisham JW. Temporal analysis of hepatocyte differentiation by small hepatocyte-like progenitor cells during liver regeneration in retrorsine-exposed rats. *Am J Pathol* 2000; **157**: 771-786

12 **Seglen PO.** Preparation of isolated rat liver cells. *Methods Cell Biol* 1976; **13**: 29-83

13 **Lojda Z,** Gossrau R, Schiebler TH. Peptidase. In: Enzyme Histochemistry: A laboratory manual. *Berlin Springer Verlag* 1979: 199-203

14 **Coleman WB,** McCullough KD, Esch GL, Faris RA, Hixson DC, Smith GJ, Grisham JW. Evaluation of the differentiation potential of WB-F344 rat liver epithelial stem-like cells *in vivo*. Differentiation to hepatocytes after transplantation into dipeptidylpeptidase-IV-deficient rat liver. *Am J Pathol* 1997; **151**: 353-359

15 **Laconi S,** Pillai S, Porcu PP, Shafritz DA, Pani P, Laconi E. Massive liver replacement by transplanted hepatocytes in the absence of exogenous growth stimuli in rats treated with retrorsine. *Am J Pathol* 2001; **158**: 771-777

16 **Elias H,** Sherrick JC. Morphology of the liver. *New York Academic Press* 1969: 5-74

17 **Hubbard AL,** Bartles JR, Braiterman LT. Identification of rat hepatocyte plasma membrane proteins using monoclonal antibodies. *J Cell Biol* 1985; **100**: 1115-1125

18 **Walborg EF Jr,** Tsuchida S, Weeden DS, Thomas MW, Barrick A, McEntire KD, Allison JP, Hixson DC. Identification of dipeptidyl peptidase IV as a protein shared by the plasma membrane of hepatocytes and liver biomatrix. *Exp Cell Res* 1985; **158**: 509-518

19 **Zheng YW,** Taniguchi H. Diversity of hepatic stem cells in the fetal and adult liver. *Semin Liver Dis* 2003; **23**: 337-348

20 **Zimmermann A.** Liver regeneration: the emergence of new pathways. *Med Sci Monit* 2002; **8**: RA53-63

21 **Sell S.** Heterogeneity and plasticity of hepatocyte lineage cells. *Hepatology* 2001; **33**: 738-750

22 **Magami Y,** Azuma T, Inokuchi H, Kokuno S, Moriyasu F, Kawai K, Hattori T. Cell proliferation and renewal of normal hepatocytes and bile duct cells in adult mouse liver. *Liver* 2002; **22**: 419-425

23 **Tateno C,** Takai-Kajihara K, Yamasaki C, Sato H, Yoshizato K. Heterogeneity of growth potential of adult rat hepatocytes *in vitro*. *Hepatology* 2000; **31**: 65-74

24 **Suzuki A,** Zheng YW, Kondo R, Kusakabe M, Takada Y, Fukao K, Nakauchi H, Taniguchi H. Flow-cytometric separation and enrichment of hepatic progenitor cells in the developing mouse liver. *Hepatology* 2000; **32**: 1230-1239

25 **Suzuki A,** Zheng YW, Kaneko S, Onodera M, Fukao K, Nakauchi H, Taniguchi H. Clonal identification and characterization of self-renewing pluripotent stem cells in the developing liver. *J Cell Biol* 2002; **156**: 173-184

Science Editor Guo SY **Language Editor** Elsevier HK

PO Box 2345, Beijing 100023, China
www.wjgnet.com
wjg@wjgnet.com

ELSEVIER

World J Gastroenterol 2005;11(39):6182-6187
World Journal of Gastroenterology ISSN 1007-9327
© 2005 The WJG Press and Elsevier Inc. All rights reserved.

• *BRIEF REPORTS* •

Serum leptin levels and insulin resistance are associated with gallstone disease in overweight subjects

Nahum Méndez-Sánchez, Luisa B Bermejo-Martínez, Yolanda Viñals, Norberto C Chavez-Tapia, Irina Vander Graff, Guadalupe Ponciano-Rodríguez, Martha H Ramos, Misael Uribe

Nahum Méndez-Sánchez, Yolanda Viñals, Norberto C Chavez-Tapia, Irina Vander Graff, Martha H Ramos, Misael Uribe, Departments of Biomedical Research and Gastroenterology and Liver Unit, Medica Sur Clinic and Foundation, Mexico City, Mexico
Luisa B Bermejo-Martínez,Clinical Research Center, National Institute of Perinatology. Mexico City, Mexico
Guadalupe Ponciano-Rodríguez,Faculty of Medicine, National Autonomous University of Mexico (UNAM). Mexico City, Mexico
Supported by the National Council of Science and Technology of Mexico (CONACYT) and The Ministry of Health (SSA), Mexico project No. M0059-M9602 (NM-S and MU)
Correspondence to: Nahum Méndez-Sánchez, MD, PhD, Departments of Biomedical Research, Gastroenterology and Liver Unit, Medica Sur Clinic and Foundation, Puente de Piedra 150, Col. Toriello Guerra, Mexico City, Mexico. nmendez@medicasur.org.mx
Telephone: +52-55-5606-6222-4215 Fax: +52-55-5666-4031
Received: 2005-01-05 Accepted: 2005-06-02

Abstract

AIM: To establish an association between the serum leptin levels and the development of gallstone disease (GD).

METHODS: We carried out a non-matched case-controlled study in a university hospital in Mexico City. Two hundred and eighty-seven subjects were included: 97 cases with gallstones and 190 controls. Body mass index (BMI), fasting plasma leptin, insulin, serum lipid, and lipoprotein levels were measured. Insulin resistance was calculated by homeostasis model assessment (HOMA-IR). Unconditional logistic regression analysis (univariate and multivariate) stratified by BMI was used to calculate the risk of GD.

RESULTS: The multivariate conditional regression analysis revealed a model for those patients with BMI <30. The selected variables in the model were HOMA-IR index with OR = 1.31, P = 0.02 and leptin higher than median with OR = 2.11, P = 0.05. In the stratum of BMI ⩾30, we did not find a useful model.

CONCLUSION: We concluded that insulin resistance and the development of GD appears to be associated with serum leptin levels in subjects with overweight, but not in obese subjects with similar metabolic profiles.

© 2005 The WJG Press and Elsevier Inc. All rights reserved.
Key words: Obesity; Leptin; Gallstones; Cholesterol; Insulin resistance

Méndez-Sánchez N, Bermejo-Martínez LB, Viñals Y, Chavez-Tapia NC, Graff IV, Ponciano-Rodríguez G, Ramos MH, Uribe M. Serum leptin levels and insulin resistance are associated with gallstone disease in overweight subjects. *World J Gastroenterol* 2005; 11(39): 6182-6187
http://www.wjgnet.com/1007-9327/11/6182.asp

INTRODUCTION

The prevalence of obesity has been increasing progressively worldwide, and is closely associated with the increased morbidity caused by several of the most common diseases in the Western world, including diabetes, hypertension, cardiovascular disease, cancer, and gallstone disease (GD)[1]. Obesity is one of the main risk factors for cholesterol gallstone formation and has been associated with the supersaturation of bile with cholesterol as a result of the increased hepatic secretion of this sterol[2-5].

On the other hand, leptin, the product of the *ob* gene, is an adipose-tissue-derived hormone considered to regulate the limitation of food intake and increased energy expenditure, and thus adiposity[6]. These findings are similar in human beings mainly failure to produce adequate amounts of leptin, or resistance to its central action, which may result in the development of obesity[7].

To identify a link between leptin and the effects of obesity on gallstone formation, Duggirala *et al*.[8], in a previous study explored the role of leptin as an indicator of adiposity and its relation to GD in a Mexican-American population. They reported that leptin levels correlated significantly with the incidence of GD in both sexes, especially in women. Ruhl and Everhart[9] evaluated the possibility that serum leptin levels are better predictors of GD than the body mass index (BMI). They found that leptin concentrations were associated with GD in both sexes (P<0.001), but this association disappeared after controlling BMI and waist-to-hip circumference in both women (P = 0.29) and men (P = 0.65). They concluded that serum leptin concentrations are not better predictors of GD than anthropometry.

Mendez-Sanchez *et al*.[10], demonstrated a significant and positive correlation between plasma leptin levels and biliary cholesterol saturation in a group of obese subjects. This correlation emerged following a modest degree of weight loss. We believe that one additional mechanism with obesity and high risk for GD is serum leptin level and insulin resistance. The aim of the present study was to find whether there is an association between serum leptin levels and the development of GD.

MATERIALS AND METHODS

Populations and sample

This study was carried out at the check-up unit of the Diagnostic Clinic at the Medica Sur Clinic and Foundation. This hospital provides care mainly for middle- and high-income individuals from Mexico City and other metropolitan Mexican areas. The study was approved by the Human Subjects Committee at The Medica Sur Clinic and Foundation as conforming to the ethical guidelines of the 1975 Declaration of Helsinki, and written informed consent was obtained from all participants before entry. A total of 287 subjects were included in this study: 97 cases with gallstones (42 women and 55 men) and 190 controls (79 women and 111 men). Ages were similar in both groups (52.9±11.8 and 52.7±11.7 years). GD cases and controls were a series of consecutive asymptomatic subjects who were referred to the unit by their companies as an annual requirement, but not for symptomatic disease. Abdominal ultrasound was performed on all subjects using a Sonoline Elegra instrument (Siemens Medical System, Germany) with a 3.5 MHz transducer. Ultrasound diagnosis of GD was assessed by the presence of strong intraluminal echoes that were gravity-dependent or attenuated ultrasound transmission (acoustic shadowing). At the completion of each patient's participation in the study, all ultrasonographic studies were evaluated by the same radiologist. No discrepancies were found between the results of the first and second evaluations ($\kappa = 0.93$).

Physical examination

Body weight was measured, in light clothing and without shoes, to the nearest 0.10 kg. Height was measured to the nearest 0.5 cm. BMI was calculated as weight in kilograms divided by height in square meters.

Analytical techniques

Plasma leptin levels were determined by radioimmunoassay using a human leptin RIA kit (Linco Research, St. Charles, MO, USA). Both the intra- and inter-assay coefficients of variation were less than 5%. Insulin levels were measured using an immunoenzymometric assay (MEIA; Abbott Diagnostics), with inter- and intra-assay coefficients of variation less than 3%. Plasma glucose in the fasting state was measured in duplicate with an automated analyzer. The coefficient of variation for a single determination was 1.5%. Cholesterol, HDL-cholesterol, and triglycerides were measured by enzymatic colorimetric methods, using CHOL, HDL-C plus (second generation) and TG assays (Roche Diagnostics Co., Indianapolis, IN, USA). Low-density lipoprotein (LDL) cholesterol concentrations were calculated using the Friedewald formula[11]. Non-HDL cholesterol was calculated as total cholesterol minus HDL cholesterol, as surrogate in cases where LDL cholesterol was inaccurate[12]. Insulin resistance was calculated by means of the homeostasis model assessment (HOMA-IR). HOMA-IR = [fasting insulin (μU/mL) ·fasting glucose (mmol/L)]/22.5, high index of insulin resistance a value >2.5[13].

Statistical analysis

We examined the relationship between anthropometric measures and serum leptin and concentrations by first comparing means of these variables in persons with and without GD. To further study these relations while controlling the effects of covariates related to GD, we used logistic regression for the univariated and multivariated analysis stratifying by BMI (EGRET: Epidemiological Graphics, Estimation, and Testing Package v 1.02.10. Cytel Software Corporation, USA, 1997). Multivariate analyses excluded persons with missing values for any factor were included in the model. The comparison of single frequencies and crossing variables, χ^2 test, *F* exact test, and Mann-Whitney U, and clustering by using SPSS/PC 10.0 program (Chicago, IL, USA, 1999). $P<0.05$ was considered to indicate statistical significance.

RESULTS

We collected information from 97 cases and 190 matched controls (control/patient ratio of 1.96). Cases and their respective controls did not differ in age or lipid values (Table 1). Patients and controls tended to differ in BMI values (28.2 *vs* 27, $P = 0.12$). The index for resistance to insulin (HOMA-IR) was higher among patients than controls (2.9 *vs* 2.4, $P = 0.04$, Table 1).

We stratified subjects according to overweight or obesity, with a BMI value of 30 as the cut-off point, according to World Health Organization[14]. We observed a statistically

Table 1 Comparison of variables between cases and controls

Variable	Cases *n* = 97					Controls *n* = 190					*P*[1]
	Mean	SD	Median	Min	Max	Mean	SD	Median	Min	Max	
Age (yr)	52.1	12.1	51.0	19.0	85.0	50.5	11.7	50.0	18.0	85.0	0.25
BMI (kg/m^2)	28.2	5.5	27.7	18.6	54.9	27.0	3.9	26.9	19.0	40.1	0.12
Leptin (ng/mL)	18.2	44.7	10.2	1.9	431.0	11.0	6.5	9.5	1.3	40.7	0.11
Insulin (μU/mL)	11.1	7.4	9.1	1.8	35.7	9.4	6.3	7.6	2.0	43.7	0.07
T-chol (mmol/L)	5.43	1.09	5.46	2.48	8.38	5.38	1.03	5.4	3.36	9.44	0.95
LDL (mmol/L)	3.44	0.85	3.36	1.11	5.61	3.49	0.85	3.41	1.60	6.13	0.73
HDL (mmol/L)	1.19	0.36	1.14	0.47	2.72	1.22	0.36	1.14	0.52	2.56	0.42
NHDL (mmol/L)	4.27	1.03	4.34	1.78	7.34	4.27	0.98	4.24	2.40	8.53	0.90
TGC (mmol/L)	1.89	1.15	1.70	0.43	6.78	1.71	0.96	1.46	0.06	7.38	0.18
HOMA-IR	2.9	2.2	2.3	0.4	11.7	2.4	1.8	1.8	0.4	13.2	0.04

[1]Mann-Whitney *U* test. BMI, body mass index; T-chol, total cholesterol; LDL, low-density cholesterol; HDL, high-density cholesterol; NHDL, non-HDL cholesterol; TGC, triglycerides.

significant difference in rate between cases and controls according to the tercile distribution in those patients who were not obese (34.7% *vs* 22.9%, $P = 0.04$, Table 2). In the same stratum (BMI<30), cases had a higher prevalence of insulin resistance, according to HOMA-IR, than controls, with borderline statistical significance (40.3% *vs* 27.5%, $P = 0.07$, Table 2). In a multivariate model, adjusted for BMI and insulin levels did not change the association related with leptin levels (data not shown). In the stratum of obese patients (BMI≥30), we observed no statistical differences between control and patient variables, except for hypertriglyceridemia, which had a higher incidence among cases than among controls.

Because of the matched design of the investigation, we analyzed the data under conditional logistic regression analyses. With univariate conditional logistic regression, we observed a higher probability of GD in those patients with BMI <30 according to HOMA-IR index value (OR = 1.33; 95%CI 1.06-1.68, $P = 0.02$) and to both leptin levels (by median or tercile distribution with an OR=2.25; 95%CI 1.08-4.69, $P = 0.03$ and OR = 1.67; 95%CI 1.03-2.69, $P = 0.04$, respectively; Table 3). In the stratum of obese patients, we identified a lower probability of GD associated with high levels of leptin, with both median and tercile distributions (OR = 0.12; 95%CI 0.01-1.0, $P = 0.05$ and OR = 0.14; 95%CI 0.02-0.98, $P = 0.05$, respectively; Table 3). Other variables were not significantly associated.

Multivariate conditional regression analysis (92 cases and 188 controls) identified a correlation for those patients with BMI <30. The selected variables in the model were HOMA-IR with OR = 1.31; 95%CI 1.04-1.66, $P = 0.02$ and

Table 2 Comparison of variables between cases and controls, stratified by BMI

Variable	BMI <30				P^1	BMI ≥30				P^1
	Cases $n = 72$		Controls $n = 153$			Cases $n = 25$		Controls $n = 37$		
	No	%	No	%		No	%	No	%	
Gender (male)	42	58.3	89	58.2	1.0	13	52.0	22	59.5	0.61
Age >50 yr	38	52.8	69	45.1	0.32	13	52.0	21	56.8	0.80
Leptin ≥9.78 ng/mL	37	51.4	61	39.9	0.11	16	64.0	30	81.1	0.15
Leptin					0.04[2]					0.25[2]
$Tercile_1$<7.67 ng/mL	22	30.6	64	41.8		5	20.0	4	10.8	
$Tercile_2$7.6–12.4 ng/mL	25	34.7	54		35.3		7	28.0	9	24.3
$Tercile_3$>12.4 ng/mL	25	34.7	35	22.9		13	52.0	24	64.9	
Insulin≥20 μU/mL	9	12.5	0	0	<0.0001	4	16.0	12	32.4	0.24
HOMA-IR (>2.5)	29	40.3	42	27.5	0.07	15	60.0	24	64.9	0.79
T-chol≥6.21 mmol/L	19	26.4	45	29.4	0.75	6	24.0	6	16.2	0.52
LDL≥4.14 mmol/L[3]	19	27.1	40	26.7	1.0	5	21.7	7	18.9	1.0
HDL<1.03 mmol/L	27	37.5	50	32.7	0.55	8	32.0	13	35.1	1.0
NHDL ≥4.91 mmol/L	20	27.8	43	28.1	1.0	5	20.0	7	18.9	1.0
TGC ≥1.70 mmol/L	32	44.4	62	40.5	0.66	17	68.0	14	37.8	0.04

[1]*F* exact test. [2]χ^2 for linear trend. [3]Five missing values for cases and 2 for controls. BMI, body mass index; T-chol, total cholesterol; LDL, low-density cholesterol; HDL, high density cholesterol; NHDL, non-HDL cholesterol; TGC, triglycerides.

Table 3 Univariated analysis of conditional logistic regression, stratified by BMI

Variable	BMI <30			BMI ≥30		
	OR	95%CI	*P*	OR	95%CI	*P*
Age (yr)	1.20	0.97–1.49	0.09	0.93	0.68–1.26	0.62
Leptin (ng/mL)	1.06	0.99–1.13	0.09	0.91	0.81–1.03	0.15
Insulin (μU/mL)	1.09	1.02–1.16	0.01	0.94	0.86–1.03	0.17
HOMA-IR	1.33	1.06–1.68	0.02	0.85	0.61–1.17	0.32
T-chol (mmol/L)	1.0	0.99–1.00	0.32	1.02	0.99–1.05	0.27
LDL (mmol/L)	1.0	0.99–1.01	0.51	1.01	0.98–1.05	0.39
HDL (mmol/L)	0.99	0.97–1.01	0.44	1.02	0.95–1.09	0.66
NHDL (mmol/L)	1.0	0.99–1.01	0.44	1.02	0.99–1.05	0.30
TGC (mmol/L)	1.0	1.0–1.0	0.86	1.0	1.0–1.01	0.30
Leptin ≥9.78 ng/mL	2.25	1.08–4.69	0.03	0.12	0.01–1.0	0.05
Leptin terciles (ng/mL)	1.67	1.03–2.69	0.04	0.14	0.02–0.98	0.05
Insulin ≥20 μU/mL		Non convergence		0.47	0.12–1.88	0.29
HOMA-IR >2.5	1.46	0.75–2.83	0.27	0.44	0.11–1.84	0.26
T-chol ≥6.21 mmol/L	0.86	0.42–1.74	0.67	3.88	0.38–39.5	0.25
LDL ≥4.14 mmol/L	1.06	0.55–2.04	0.87	1.50	0.36–6.30	0.58
HDL <1.03 mmol/L	1.26	0.66–2.41	0.49		Non convergence	
NHDL ≥4.91mmol/L	1.07	0.54–2.13	0.84	0.78	0.07–8.88	0.84
TGC ≥1.7 mmol/L	1.09	0.60–1.99	0.77	3.03	0.76–12.1	0.12

OR, odds ratio; 95%CI, 95% confidence intervals; BMI, body mass index; T-chol, total cholesterol; LDL, low-density cholesterol; HDL, high density cholesterol; NHDL, non-HDL cholesterol; TGC, triglycerides.

leptin levels higher than the median value, with OR = 2.11; 95%CI 0.99-4.53, $P = 0.05$ (Table 4). In the stratum with BMI ⩾30, we did not identify any useful correlation.

Table 4 Multivariated analysis of conditional logistic regression, stratified by BMI

Variables	BMI <30			BMI ⩾30		
	OR	95%CI	*P*	OR	95%CI	*P*
HOMA-IR	1.31	1.04–1.66	0.02	No model founded		
Leptin ⩾9.78 ng/mL	2.11	0.99–4.53	0.05			

OR, odds ratio; 95%CI, 95% confidence intervals.

DISCUSSION

This study was designed to examine the role of serum leptin levels as a risk factor for developing GD. We observed that plasma leptin levels and the HOMA-IR are highly associated in the group of subjects with BMI <30, because they increase the probability of GD, but that the same plasma leptin levels are associated with a lower probability of GD in the group of subjects with BMI >30.

How can we explain these findings? Bile is the route by which cholesterol is eliminated from the body, and reverse cholesterol transport is the metabolic pathway by which cholesterol is moved from peripheral tissues to the liver for biliary secretion[15,16]. Van Patten *et al.*[17], reported that obesity in leptin-receptor-defective Zucker (*fa/fa*) rats is associated with decreased biliary cholesterol secretion due to the uncoupling of cholesterol and phospholipid from bile-salt secretion. High-dose leptin partially normalized cholesterol secretion in these obese rats without altering lipid composition, implying that both the chronic effects of obesity and a relative resistance to leptin contributed to the impaired biliary cholesterol elimination. From these data, it is clear that leptin plays a role in the elimination of cholesterol from the body.

In the present study, the question arises: Why is BMI important in the association between serum leptin levels and GD, especially in subjects with BMI <30. It has been suggested that in human obesity, leptin levels adapt to changes in energy balance. During fasting[17] or weight loss[18], leptin concentrations decrease, whereas they increase during overfeeding or weight gain. Obese human beings have high leptin concentrations[18]. Leptin mRNA expression in fat cells correlates significantly with body fat mass[18]. Hyperleptinemia is thought to be indicative of "leptin resistance", and may play a role in the pathogenesis of obesity[18,19]. We believe that leptin levels are important risk factors for GD, before "leptin resistance" is apparent, i.e., when the leptin levels are not as high as those observed in obese subjects. In accordance with this hypothesis, Hyogo *et al.*[20], showed that weight loss in chow-fed C57BL/6J *ob/ob* mice induced by chronic intraperitoneal administration of high-dose leptin (10 μg/g per d) is associated with cholesterol gallstone formation.

A 25% reduction in body weight over a 28-d period was sufficient to produce cholesterol crystals and gallstones in the gallbladder bile of all lithogenic-diet-fed mice treated with low-dose leptin. Nevertheless, neither cholesterol crystals nor stones were observed in any chow-fed mouse. These findings indicate that, whereas leptin replacement is required for cholesterol cholelithiasis in *ob/ob* mice, a lithogenic diet accelerates this process[21].

The other variable associated with GD in the present study was the HOMA-IR. Recently, we have found a strong relationship between GD and metabolic syndrome, of which the cardinal feature is hyperinsulinemia[22]. In fact, hyperinsulinemia has been proposed as a risk factor for GD, and some studies support this hypothesis. For example, Scragg *et al.*[23], found that mean fasting insulin levels to be higher in patients of both sexes with GD, independent of age and triglyceride levels. Laakso *et al.*[24], also found that subjects with GD had significantly higher levels of insulin than controls. Haffner *et al.*[25], in the San Antonio Heart Study, observed increasing hyperinsulinemia and a high incidence of GD in both Mexican-Americans and non-Hispanic whites. In Mexico, Gonzalez Villalpando *et al.*[26], found higher fasting insulin levels in women with GD than in controls, but no such relationship was observed in men. Ruhl and Everhart[27], in an well-presented study, have confirmed this association of GD with higher fasting serum insulin and C-peptide levels in women. The association was independent of fasting glucose levels and other covariates related to GD.

Increasing cholesterol saturation of the bile and decreasing gallbladder motility are two possible mechanisms by which insulin plays a role in gallstone formation. At present, these are considered very important in the pathogenesis of gallstones. It has also been suggested that high concentrations of insulin increase the activity of 3-hydroxy-3-methylglutaryl coenzyme A reductase[28,29], the rate-limiting enzyme in hepatic synthesis of new cholesterol, or by activating LDL receptors, resulting in greater hepatic uptake of LDL cholesterol[30]. By inhibiting basal and cholecystokinin-stimulated gallbladder motility, insulin might also increase the risk of developing gallstones through an effect on motility[31].

There are several unresolved issues concerning the biological effects of leptin and its relationship to GD about the importance of motility[32], secretion or both. Tran *et al.*[33,34], included other factors in the link between obesity and gallstone formation, particularly an impaired response to neurotransmitters (mainly neuropeptide Y). The present work shows that there is probably a threshold to the biological activity of leptin, and the differences between our experimental groups indicate that leptin has a "lithogenic effect" in selected overweight subjects. Wauters *et al.*[35], analyzed how polymorphisms in the leptin-receptor gene influence fat topography and levels of abdominal fat in human beings, providing further evidence for the wide response spectrum to several grades of obesity and several grades of leptin-resistance. Similar data on the effects of leptin on lipid metabolism demonstrate differences between sexes and grades of obesity[36], including evidence for the independent effects of leptin on lipid metabolism[37]. These complex data were observed in both healthy subjects and disease models[38,39]. Recently, it was observed that besides fat mass and gender, which are the main determinants of leptin levels in type 2 diabetic and healthy subjects, insulin

secretion and the degree of insulin resistance also contribute significantly to leptin levels[40]. In the present study, there were more insulin-resistant subjects in the BMI >30 group, and these data indicate a correspondence between greater obesity, higher resistance, and a lack of biological effects (in this case GD). This study contribute to show one side of a wide clinical response of a metabolic disturbance, in subjects with similar grade of insulin resistance, but different phenotype (BMI) we observe an unexpected response of leptin effect. However, this is only a hypothesis drawn from the data on the relationship between leptin and insulin resistance[41].

Due to the sample analyzed (mainly employees) we loose randomization effect, and could not reflect general population behavior. By otherwise a lack of metabolic difference between cases and controls (HOMA-IR), could explain contradictory data in obese group; however, this unexpected finding could represent similar leptin response even do differences in body composition.

In conclusion, the results of the present study show that, as with insulin resistance, the development of GD appears to be associated with serum leptin levels in overweight subjects.

ACKOWLEDGEMENTS

The authors thank to Dr. Antonio R. Villa for his kind assistance in the statistical analysis.

REFERENCES

1 **Mantzoros CS.** The role of leptin in human obesity and disease: a review of current evidence. *Ann Intern Med* 1999; **130**: 671-680
2 **Mabee TM,** Meyer P, DenBesten L, Mason EE. The mechanism of increased gallstone formation in obese human subjects. *Surgery* 1976; **79**: 460-468
3 **Reuben A,** Maton PN, Murphy GM, Dowling RH. Bile lipid secretion in obese and non-obese individuals with and without gallstones. *Clin Sci* 1985; **69**: 71-79
4 **Stahlberg D,** Rudling M, Angelin B, Bjorkhem I, Forsell P, Nilsell K, Einarsson K. Hepatic cholesterol metabolism in human obesity. *Hepatology* 1997; **25**: 1447-1450
5 **Bennion LJ,** Grundy SM. Effects of obesity and caloric intake on biliary lipid metabolism in man. *J Clin Invest* 1975; **56**: 996-1011
6 **Rohner-Jeanrenaud F,** Jeanrenaud B. Obesity, leptin, and the brain. *N Engl J Med* 1996; **334**: 324-325
7 **Hickey MS,** Israel RG, Gardiner SN, Considine RV, McCammon MR, Tyndall GL, Houmard JA, Marks RH, Caro JF. Gender differences in serum leptin levels in humans. *Biochem Mol Med* 1996; **59**: 1-6
8 **Duggirala R,** Mitchell BD, Blangero J, Stern MP. Genetic determinants of variation in gallbladder disease in the Mexican-American population. *Genet Epidemiol* 1999; **16**: 191-204
9 **Ruhl CE,** Everhart JE. Relationship of serum leptin concentration and other measures of adiposity with gallbladder disease. *Hepatology* 2001; **34**: 877-883
10 **Mendez-Sanchez N,** Gonzalez V, King-Martinez AC, Sanchez H, Uribe M. Plasma leptin and the cholesterol saturation of bile are correlated in obese women after weight loss. *J Nutr* 2002; **132**: 2195-2198
11 **Friedewald WT,** Levy RI, Fredrickson DS. Estimation of the concentration of low-density lipoprotein cholesterol in plasma, without use of the preparative ultracentrifuge. *Clin Chem* 1972; **18**: 499-502
12 **Packard CJ,** Saito Y. Non-HDL cholesterol as a measure of atherosclerotic risk. *J Atheroscler Thromb* 2004; **11**: 6-14
13 **Matthews DR,** Hosker JP, Rudenski AS, Naylor BA, Treacher DF, Turner RC. Homeostasis model assessment: insulin resistance and beta-cell function from fasting plasma glucose and insulin concentrations in man. *Diabetologia* 1985; **28**: 412-419
14 Obesity : preventing and managing the global epidemic : report of a WHO consultation. Technical report series / World Health Organization, 894. 2000, Geneva: World Health Organization. 253
15 **Fredenrich A,** Bayer P. Reverse cholesterol transport, high density lipoproteins and HDL cholesterol: recent data. *Diabetes Metab* 2003; **29**: 201-205
16 **Rader DJ.** Regulation of reverse cholesterol transport and clinical implications. *Am J Cardiol* 2003; **92**: 42J-49J
17 **Van Patten S,** Ranginani N, Shefer S, Nguyen LB, Rossetti L, Cohen DE. Impaired biliary lipid secretion in obese Zucker rats: leptin promotes hepatic cholesterol clearance. *Am J Physiol Gastrointest Liver Physiol* 2001; **281**: G393-404
18 **Considine RV,** Sinha MK, Heiman ML, Kriauciunas A, Stephens TW, Nyce MR, Ohannesian JP, Marco CC, McKee LJ, Bauer TL, Caro JF. Serum immunoreactive-leptin concentrations in normal-weight and obese humans. *N Engl J Med* 1996; **334**: 292-295
19 **Maffei M,** Halaas J, Ravussin E, Pratley RE, Lee GH, Zhang Y, Fei H, Kim S, Lallone R, Ranganathan S, Kern PA, Friedman JM. Leptin levels in human and rodent: measurement of plasma leptin and ob RNA in obese and weight-reduced subjects. *Nat Med* 1995; **1**: 1155-1161
20 **Hyogo H,** Roy S, Paigen B, Cohen DE. Leptin promotes biliary cholesterol elimination during weight loss in ob/ob mice by regulating the enterohepatic circulation of bile salts. *J Biol Chem* 2002; **277**: 34117-34124
21 **Hyogo H,** Roy S, Cohen DE. Restoration of gallstone susceptibility by leptin in C57BL/6J ob/ob mice. *J Lipid Res* 2003; **44**: 1232-1240
22 **Mendez-Sanchez N,** Chavez-Tapia NC, Motola-Kuba D, Sanchez-Lara K, González V, Ponciano-Rodríguez G, Baptista H, Ramos MH, Uribe M. Metabolic syndrome as a risk factor for gallstone disease. *World J Gastroenterol* 2005; **11**: 1653-1657
23 **Scragg RK,** Calvert GD, Oliver JR. Plasma lipids and insulin in gall stone disease: a case-control study. *Br Med J* 1984; **289**: 521-525
24 **Laakso M,** Suhonen M, Julkunen R, Pyorala K. Plasma insulin, serum lipids and lipoproteins in gall stone disease in non-insulin dependent diabetic subjects: a case control study. *Gut* 1990; **31**: 344-347
25 **Haffner SM,** Diehl AK, Mitchell BD, Stern MP, Hazuda HP. Increased prevalence of clinical gallbladder disease in subjects with non-insulin-dependent diabetes mellitus. *Am J Epidemiol* 1990; **132**: 327-335
26 **Gonzalez Villalpando C,** Rivera Martinez D, Arredondo Perez B, Martinez Diaz S, Gonzalez Villalpando ME, Haffner SM, Stern MP. High prevalence of cholelithiasis in a low income Mexican population: an ultrasonographic survey. *Arch Med Res* 1997; **28**: 543-547
27 **Ruhl CE,** Everhart JE. Association of diabetes, serum insulin, and C-peptide with gallbladder disease. *Hepatology* 2000; **31**: 299-303
28 **Nepokroeff CM,** Lakshmanan MR, Ness GC, Dugan RE, Porter JW. Regulation of the diurnal rhythm of rat liver beta-hydroxy-beta-methylglutaryl coenzmye A reductase activity by insulin, glucagon, cyclic AMP and hydrocortisone. *Arch Biochem Biophys* 1974; **160**: 387-396
29 **Osborne AR,** Pollock VV, Lagor WR, Ness GC. Identification of insulin-responsive regions in the HMG-CoA reductase promoter. *Biochem Biophys Res Commun* 2004; **318**: 814-818
30 **Chait A,** Bierman EL, Albers JJ. Low-density lipoprotein receptor activity in cultured human skin fibroblasts. Mechanism of insulin-induced stimulation. *J Clin Invest* 1979; **64**: 1309-1319
31 **Gielkens HA,** Lam WF, Coenraad M, Frolich M, van Oostayen JA, Lamers CB, Masclee AA. Effect of insulin on basal and

cholecystokinin-stimulated gallbladder motility in humans. *J Hepatol* 1998; **28**: 595-602

32 **Goldblatt MI,** Swartz-Basile DA, Svatek CL, Nakeeb A, Pitt HA. Decreased gallbladder response in leptin-deficient obese mice. *J Gastrointest Surg* 2002; **6**: 438-442

33 **Tran KQ,** Goldblatt MI, Swartz-Basile DA, Svatek C, Nakeeb A, Pitt HA. Diabetes and hyperlipidemia correlate with gallbladder contractility in leptin-related murine obesity. *J Gastrointest Surg* 2003; **7**: 857-862

34 **Tran KQ,** Swartz-Basile DA, Nakeeb A, Pitt HA. Gallbladder motility in agouti-yellow and leptin-resistant obese mice. *J Surg Res* 2003; **113**: 56-61

35 **Wauters M,** Mertens I, Chagnon M, Rankinen T, Considine RV, Chagnon YC, Van Gaal LF, Bouchard C. Polymorphisms in the leptin receptor gene, body composition and fat distribution in overweight and obese women. *Int J Obes Relat Metab Disord* 2001; **25**: 714-720

36 **Tungtrongchitr R,** Pongpaew P, Phonrat B, Tribunyatkul S, Viroonudomphol D, Supawan V, Jintaridhi P, Lertchavanakul A, Vudhivai N, Schelp FP. Serum leptin and lipid profiles in Thai obese and overweight subjects. *Int J Vitam Nutr Res* 2001; **71**: 74-81

37 **Marinari GM,** Scopinaro N, Adami GF. Leptin and HDL-cholesterol in non-diabetic normotensive subjects. *Obes Surg* 2001; **11**: 252-253

38 **Remsberg KE,** Talbott EO, Zborowski JV, Evans RW, McHugh-Pemu K. Evidence for competing effects of body mass, hyperinsulinemia, insulin resistance, and androgens on leptin levels among lean, overweight, and obese women with polycystic ovary syndrome. *Fertil Steril* 2002; **78**: 479-486

39 **Silha JV,** Krsek M, Hana V, Marek J, Jezkova J, Weiss V, Murphy LJ. Perturbations in adiponectin, leptin and resistin levels in acromegaly: lack of correlation with insulin resistance. *Clin Endocrinol* 2003; **58**: 736-742

40 **Wauters M,** Considine RV, Yudkin JS, Peiffer F, De Leeuw I, Van Gaal LF. Leptin levels in type 2 diabetes: associations with measures of insulin resistance and insulin secretion. *Horm Metab Res* 2003; **35**: 92-96

41 **Ceddia RB,** Koistinen HA, Zierath JR, Sweeney G. Analysis of paradoxical observations on the association between leptin and insulin resistance. *Faseb J* 2002; **16**: 1163-1176

Science Editor Guo SY **Language Editor** Elsevier HK

PO Box 2345, Beijing 100023, China
www.wjgnet.com
wjg@wjgnet.com

ELSEVIER

World J Gastroenterol 2005;11(39):6188-6192
World Journal of Gastroenterology ISSN 1007-9327
© 2005 The WJG Press and Elsevier Inc. All rights reserved.

• *BRIEF REPORTS* •

Treatment of genotype 2 and 3 chronic hepatitis C virus-infected patients

Perdita Wietzke-Braun, Volker Meier, Katrin Neubauer-Saile, Sabine Mihm, Giuliano Ramadori

Perdita Wietzke-Braun, Volker Meier, Katrin Neubauer-Saile, Sabine Mihm, Giuliano Ramadori, Abteilung für Gastroenterologie und Endokrinologie, Georg-August-Universität, Göttingen, Germany
Correspondence to: Professor Dr. Giuliano. Ramadori, Abteilung für Gastroenterologie und Endokrinologie, Georg-August-Universität, Robert-Koch-Strasse 40, 37075 Göttingen, Germany. gramado@med.uni-goettingen.de
Telephone: +49-551-39-6301 Fax: +49-551-39-8596
Received: 2004-12-30 Accepted: 2005-03-21

Abstract

AIM: Before pegylated interferon alpha (IFN) was introduced for the therapy of chronic hepatitis C virus (HCV)-induced hepatitis, conventional thrice weekly IFN therapy was supplemented by ribavirin. Also, at that time, higher and more frequent doses of IFN were expected to be more effective than the standard regimen of 3 MU thrice weekly. As ribavirin significantly increases side effects and negatively influences the quality of life particularly in young patients, we started a prospective non-randomized study with a daily IFN-2a monotherapy as an initial treatment for chronic hepatitis C.

METHODS: Forty-six consecutive chronic HCV-infected patients received 3 MU IFN-2a per day as an initial treatment. Patients with genotype 2 or 3 (n = 12) were treated for 24 wk, and patients with genotypes other than 2 or 3 (n = 34) for 48 wk. Treatment outcome was followed up for 48 wk after the end of treatment (EOT). Virological response was defined as the absence of detectable serum HCV-RNA. Patients without virological response at 12 wk after the start of treatment received low-dose ribavirin (10 mg(kg • d)) additionally.

RESULTS: During treatment, three genotype 3 patients were excluded from the study due to incompliance. The remaining patients (n = 9) infected with genotype 2 or 3 showed an initial virological response rate of 100%. Six patients (66.7%) were still found to be virus-free at the end of follow-up period. In these patients, initial virological response was evident already after 2 wk of treatment. In contrast, initial virological response occurred first after 4 wk of treatment in the three patients who relapsed (33.3%). In comparison, patients infected with genotypes other than 2 or 3 (n = 34) showed an initial virological response rate of only 23.5% (n = 8), and even in combination with ribavirin a sustained virological response (SVR) rate of only 11.8% (n = 4) could be achieved.

CONCLUSION: In chronic HCV-infected patients with genotype 2 or 3, a SVR can be expected after 24 wk of daily dose IFN-2a treatment without ribavirin, if initial virological response develops early. This finding is worth to be confirmed in a prospective randomized study with pegylated IFN.

© 2005 The WJG Press and Elsevier Inc. All rights reserved.

Key words: Chronic hepatitis C virus infection; Genotype 2 and 3; Alpha interferon; Daily dose interferon therapy

Wietzke-Braun P, Meier V, Neubauer-Saile K, Mihm S, Ramadori G. Treatment of genotype 2 and 3 chronic hepatitis C virus-infected patients. *World J Gastroenterol* 2005; 11 (39): 6188-6192
http://www.wjgnet.com/1007-9327/11/6188.asp

INTRODUCTION

The hepatitis C virus (HCV) is the most common infectious agent associated with post-transfusion and community-acquired non-A-non-B hepatitis as well as cryptogenic cirrhosis[1,2]. Most of the patients with acute HCV infection will develop chronic liver disease[2]. In studies with 10-20 years of follow-up, cirrhosis secondary to chronic HCV infection develops in 20-30%[2,3] and is the most common indication for liver transplantation worldwide[4]. Also, patients with HCV-associated cirrhosis have an increased risk for the development of hepatocellular carcinoma, which is estimated to be between 1% and 4% per year [5].

Even before the discovery of HCV, introduction of interferon alpha (IFN) for the treatment of non-A-non-B hepatitis was an outstanding revolution in antiviral therapy in 1986[6]. Initial therapeutic regimen consisted of 3 MU IFN thrice weekly (TIW) for 6 mo. The response rate at the end of treatment (EOT) resulted in 29-32%[7,8], but the sustained virological response (SVR) rate was only about 6-18%[7-10]. Apart from extending the duration of IFN monotherapy to 12 or 18 mo, higher doses of IFN TIW failed to significantly increase virologic response rates at EOT and SVR rates (range 13-20%) in most studies[7,11,12]. Combination of IFN 3 MU TIW and ribavirin 1 000-1 200 mg/d for 6 mo was shown to increase the response rate at EOT up to 53-57% and SVR rates up to 31-35%[7,12]. With the combination of IFN 3 MU TIW and ribavirin 1 000-1 200 mg/d for 12 mo, the response rates at EOT of 50-54% and SVR rates of 38-47% could be obtained[7,12-14]. However, ribavirin can increase side effects (e.g., hemolysis and renal dysfunction) and has been shown to have teratogenic

and/or embryocidal effects[15]. Many HCV-infected patients are either women at child bearing age or fertile men. Thus, addition of ribavirin to IFN should be avoided when possible. One of the reasons for marginal response to IFN is its short half-life of approximately 8 h[16], which leads to wide fluctuations in IFN plasma concentrations during treatment. Among patients treated with IFN TIW, an intermittent increase in viral load can be observed on treatment-free days[17]. Daily dose IFN therapy might sustain more stable IFN plasma concentrations, thus maintaining a better antiviral effect on HCV. Viral kinetic studies suggest that higher and more frequent doses of IFN may improve the initial response rate and may be more effective in HCV clearance[18,19]. Therefore, we evaluated the efficacy, safety, and tolerability of initial daily IFN monotherapy in naive patients with chronic HCV-infection. This monocentric non-randomized study was started before pegylated IFN was introduced into the market.

MATERIALS AND METHODS

Selection of patients

Patients who were 18 years or older, with compensated chronic HCV infection, not previously treated with IFN or ribavirin were eligible for the study. Eligible patients had persistent elevations of serum alanine aminotransferase (ALT) and/or aspartate aminotransferase (AST) activities for at least 6 mo before the start of treatment, a positive third-generation anti-HCV test using an immunoblot procedure (CHIRON RIBA HCV 3.0 SIA, Ortho Diagnostic Systems Inc., Raritan, USA), and positive serum HCV RNA by reverse transcriptase-polymerase chain reaction (RT-PCR). Patients with decompensated liver disease, serum elevated alpha-fetoprotein concentration, previous organ transplantation, severe cardiac or chronic pulmonary disease, neoplastic disease, seizure disease, hemoglobinopathies, poorly controlled diabetes, severe retinopathy, autoimmune disorders, thyroid gland alterations, active alcohol or injection drug abuse, history of major psychiatric disease, pregnancy, unwillingness to practice contraception, significant anemia (hemoglobin <120 g/L), leukocytopenia (<3 000/μL) or thrombocytopenia (<50 000/μL) were not included. Active hepatitis A virus, human immunodeficiency virus, hepatitis B virus, cytomegalovirus or Ebstein-Barr virus infections were excluded by conventional laboratory tests. Findings consistent with a diagnosis of chronic hepatitis C were shown on liver biopsy during the preceding year, as determined by a single pathologist. The study was approved by the local ethics committee and conformed to the ethical guidelines of the 1975 Declaration of Helsinki. Informed consent was obtained from all treated patients.

Detection of serum HCV-specific RNA by RT-PCR

RNA was extracted from serum samples (140 μL) using the QIAamp Viral RNA Kit (Qiagen, Hilden, Germany) according to the manufacturer's protocol. One-fifth of the extracted material from serum was subjected to a nested RT-PCR procedure essentially as described[20].

Quantification of serum HCV-specific RNA

The amount of serum HCV-RNA was determined by using the AmpliSensor System according to the instruction of the manufacturer (AmpliSensor System, BAG, Lich, Germany).

Determination of HCV genotypes

HCV genotyping was performed using the Innolipa HCV II line probe assay (Innogenetics, Ghent, Belgium).

Treatment

Patients received subcutaneously 3 MU IFN-2a (Roferon-A, F.Hoffmann-La Roche, Basel, Switzerland) daily. Patients with genotype 2 or 3 were treated for 24 wk, and patients with genotypes other than 2 or 3 for 48 wk. Follow-up period was 48 wk after EOT. Virological response was defined as non-detectability of serum HCV-RNA. Patients who had no virological response after 12 wk of treatment received ribavirin (10 mg/kg BW/day) additionally as described previously[21].

Monitoring

All patients were assessed in an outpatient setting for safety, tolerance, and efficacy at the end of weeks 2, 4, 6, 8, and every further 4th wk during treatment. When treatment was completed, patients were assessed at wk 4, 12, and 24, 36 and 48. Clinical examination, total blood cell counts and routine biochemical tests were conducted at that time. Serum was analyzed for the presence of HCV-RNA by RT-PCR before treatment, and at wk 2, 4, 12, 24, 36, and 48 during treatment for patients treated for 48 weeks and at wk 2, 4, 12, and 24 for patients treated 24 wk. During follow-up period, serum was tested for the presence of HCV-RNA at wk 4, 12, 24, 36 and 48.

RESULTS

Characteristics of the patients

Forty-six consecutive chronic HCV-infected patients (16 female, 30 male, mean age 42 years, ranging from 21 to 67 years) were enrolled. The cause for HCV transmission could be identified as blood transfusions in 17.4% (n = 8) and injection drug use in 39.1% (n = 18). Twenty patients (43.5%) had other or unknown transmission of HCV infection. Before treatment, AST levels were elevated with a mean of 27.9 U/L ranging from 12 to 67 U/L, ALT levels with a mean of 51.5 U/L ranging from 16 to 142 U/L, and gamma glutamyl transpeptidase (gamma-GT) levels with a mean of 34.5 U/L ranging from 5 to 288 U/L. HCV genotypes were classified in 12 patients (26%) as 1a, in 20 (43.5%) as 1b, in 1 (2.2%) as 1a and 1b, in 1 (2.2%) as 2a and 2c, in 4 (8.7%) as 3a, in one (2.2%) as 3a and 3c, in 6 (13%) as 3c, and in 1 (2.2%) as 5a. Before treatment, the mean serum HCV-RNA level was 4.87×10^5 copies/mL ranging from 1×10^3 to 6.5×10^6 (SD 1.02×10^6). Patients showed histological diagnosis of mild chronic hepatitis (39.1%, n = 18), moderate chronic hepatitis (37%, n = 17), severe chronic hepatitis (8.7%, n = 4), cirrhosis (8.7%, n = 4), or unknown histology in 6.5% (n = 3). All patients received daily dose IFN-2a therapy as initial treatment.

Outcome of patients with genotype 2 or 3

Patients with genotype 2 or 3 (n = 12) showed an initial

virological response rate of 100% under daily dose IFN-2a treatment. During treatment, however, three genotype 3 patients were excluded from the study due to incompliance. Thus, at that time (two patients after 4 wk and one patient after 12 wk of treatment) the drop outs were virological responders. All patients who completed therapy (n = 9) had a complete biochemical and virological response at the end of 24-wk treatment. During follow-up, after EOT three of nine patients (33.3%) developed a relapse. In these patients, initial virological response first occurred after 4 wk of treatment. The remaining six patients (66.7%) sustainingly eradicated the virus, i.e. serum viral RNA was non-detectable for at least a 48-wk period after EOT. Data of treatment response and follow-up are shown in Figure 1.

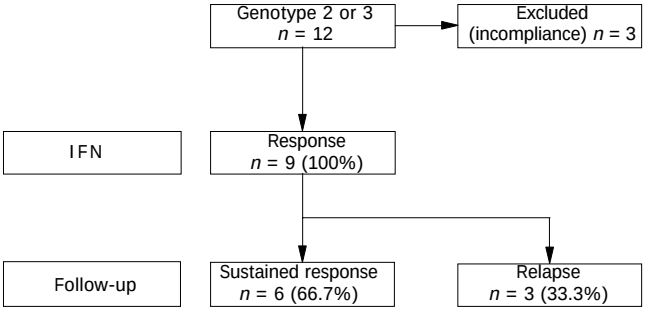


Figure 1 Outcome of 12 HCV-infected patients with genotype 2 or 3 after *the* end of treatment and follow-up. Abbreviations: EOT (end of treatment), IFN (interferon al*pha*).

Outcome of patients with genotypes other than 2 or 3

Patients with genotypes other than 2 or 3 (n = 34) showed an initial virological response rate of 23.5% (8/34) under daily dose IFN-2a treatment. These 8/34 patients (23.5%) were still virological responders at the end of 48 wk daily dose IFN-2a treatment. Two of thirty-four patients (5.9%) stopped IFN therapy due to alopecia (n = 1) and loss of weight (n = 1). During follow-up, five patients (14.7%) who had eliminated the virus at EOT relapsed, and three (8.8%) had a SVR, 48 weeks after EOT.

Twenty-four of thirty-four patients (70.6%) failed to develop an initial virological response under IFN-2a monotherapy and were treated with ribavirin (10 mg/kg BW/day) in combination as described previously[22]. Ten patients (29.4%) showed a response and 13 (38.2%) a non-response at the end of 48-wk treatment. One patient (2.9%) stopped combination therapy due to hemolysis. During follow-up, 9 (26.5%) patients with a response at EOT relapsed and only one (2.9%) patient showed a SVR, 48 weeks after EOT.

Overall outcome

During treatment, three patients with genotype 3 had to be excluded from the study due to incompliance. At the completion of 24- and 48-wk treatment, 27 of 43 patients (62.8%) showed a virological response and 13 of 43 patients (30.2%) showed a virological non-response. In 3 of 43 patients (7%), treatment was discontinued due to alopecia (n = 1) and loss of weight (n = 1) under IFN-2a monotherapy, and due to hemolysis (n = 1) under combination therapy. Forty-eight weeks after the end of 24- and 48-wk treatment, 17 of 27 patients with a response at the end of 24- and 48-wk treatment relapsed (63%). In summary, the overall SVR rate was 23.3% (10 of 43 patients) 48 wk after EOT.

Side effects

Beside the 3/43 (7%) drop outs, daily dose IFN-2a therapy (3 MU) was well tolerated. Monitoring of side effects by questioning and clinical examination revealed flu-like symptoms (e.g. pyrexia, myalgia and rigors) in one quart of cases. Mild leukocytopenia (minimum 1 800/μL) and thrombocytopenia (minimum 70 000/μL in a patient without cirrhosis and 59 000/μL in a patient with cirrhosis) was generally seen.

Side effects of additional ribavirin therapy were thyroid gland alterations (two patients with hypothyroidism and one with hyperthyroidism) and loss of weight (n = 1). Beside the one drop out due to hemolysis (minimum hemoglobin 86 g/L), decrease in hemoglobin was generally seen to a minimum of 98 g/L. There was no need of transfusion or drug dose reduction. All side effects were completely reversible within 1 mo after EOT.

DISCUSSION

In chronic HCV-infected patients, SVR rates range from 6-15% after a 6-mo course of IFN TIW to 13-25% after 12 mo of therapy[11]. One of the reasons for marginal response to IFN is its short half-life of approximately 8 h[16], which leads to wide fluctuations in the plasma concentrations of the drug during treatment period. Among patients treated with IFN TIW, an intermittent increase in viral load can be observed on treatment-free days[17]. In this prospective monocentric non-randomized study, we report our experience on 46 consecutive chronic HCV-infected patients who received 3 MU IFN-2a daily as initial regimen. Patients with genotype 2 or 3 were treated for 24 wk, and patients with genotypes other than 2 and 3 for 48 wk. Three patients with genotype 3 were excluded from the study due to incompliance. At the end of 24-wk treatment, 17/43 (39.5%) of our patients including 9/9 (100%) with genotype 2 or 3 and 8/34 (23.5%) with genotypes other than 2 or 3 eliminated the virus below the limit of detectability. In comparison, IFN 3 MU TIW for 24 wk resulted in virological response rates of 29-32% at EOT[7,8]. The rate of complete responders (23.5%) was unchanged after 48 wk of treatment in our patients with genotypes other than 2 or 3. IFN 3 MU TIW for 48 wk can induce virological response at EOT in 24-33%[7,12] of patients including different genotypes. Also, a dose of IFN 6 MIU TIW for 12 wk followed by IFN 3 MIU TIW for the remaining 36 wk resulted in a complete response rate of 25% at EOT in patients including different genotypes[22].

SVR, 48 wk after EOT resulted in 6/9 (66.7%) of our patients with genotype 2 or 3 after 24 wk 3 MU IFN daily therapy and 3/34 (8.8%) with genotypes other than 2 or 3

after 48 wk 3 MU IFN daily therapy. Compared to our results, IFN 3 MU TIW for 24 wk resulted in SVR in 2% of patients with genotype 1 and in 16% with other genotypes[7]. IFN 3 MU TIW for 48 wk resulted in SVR in 7% of patients with genotype 1 and in 29% with other genotypes[7]. In the trial of Poynard *et al.*[12], a SVR after IFN 3 MU TIW for 48 wk was observed in 33% of patients with genotype 2 and 3 and in 11% with genotype 1, 4, 5, and 6.

Combination of IFN 3 MU TIW with ribavirin at a dosage of 1 000-1 200 mg/d for 24 wk is able to induce response rates at EOT in 53-57%[7,12]. SVR was observed in 18% of patients with genotype 1, 4, 5, or 6[12] and in 16% of patients with genotype 1[7]. Our results are difficult to compare with these results, because we added ribavirin in a lower dose (10 mg/kg BW/day) after 12 wk of daily dose IFN-2a therapy in patients with genotype other than 2 or 3 who were virological non-responders at that time. However, addition of low-dose ribavirin (10 mg/kg BW/day) is able to induce a response at 48-wk EOT in 10/24 (41.7%) initial virological non-responders to a daily dose IFN-2a monotherapy. But SVR 48 wk after EOT is low (1/10 patients), because relapse occurred in the other 9 patients. Therefore, for patients with genotypes other than 2 or 3, this regimen appears not to be sufficient. They need a combination therapy from the beginning on for a longer time or in higher dose.

Nowadays, data on pegylated IFN for treatment of HCV-infected patients are available in the literature[13,14,22]. Interestingly, pegylated IFN-2a monotherapy at a dosage of 180 μg once a week for 48 wk can induce SVR rates of 45% in patients with genotype 2 and 3[22]. Compared to these results, daily dose IFN 3 MU for 24 wk is able to induce 66.7% SVR rates in patients with genotype 2 and 3. These patients with a SVR 48 wk after EOT showed an initial virological response already after 2 wk daily dose IFN-2a monotherapy, whereas patients who relapsed after EOT showed the initial virological response first after 4 wk daily dose IFN-2a treatment. Thus, avoidance of ribavirin in a subgroup of patients with genotype 2 and 3 who showed an initial virological response early after 2 wk of IFN treatment might prevent drug associated adverse events and potential teratogenic effect in patients at child bearing age[15]. This is of particular interest, because the majority of treated patients in our study had a mean age of 42 years and 41-44 years in studies using IFN TIW monotherapy, pegylated IFN monotherapy, and combination with ribavirin[7,12-14,22]. During and 6 mo after the administration of ribavirin, at least two forms of effective contraception are advised[15]. An additional economic fact is the increased cost of ribavirin treatment in HCV patients.

Side effects are comparable with those reported for 3-6 MU TIW IFN therapy[7,12,22]. None of our patients needed dose modification due to adverse event or laboratory abnormality, but in 7% of our patients IFN therapy was discontinued due to alopecia (n = 1) and loss of weight (n = 1), and ribavirin associated hemolysis (n = 1). For comparison of our results, meta-analysis of individual patient data from European centers revealed approximately 10% withdrawal of patients during treatment[23]. In studies with 3-6 MU IFN TIW, discontinuation from therapy ranges from 10% to 14% of patients[7,12,22]. Daily dose IFN therapy does not increase the discontinuation rate in comparison to TIW IFN therapy.

In conclusion, the use of daily dose IFN-2a 3 MU for HCV-infected patients is safe and well tolerated, but is able to induce only similar SVR rates 48 wk after EOT compared to IFN TIW for patients with genotypes other than 2 or 3. Addition of low-dose ribavirin after 12 wk daily dose IFN-2a monotherapy in virological non-responders at that time can increase the initial response at EOT, but relapse rate is high during follow-up. However, in patients with genotype 2 or 3, SVR rates of 66.7% can be achieved (48 wk after EOT with 3 MU IFN-2a monotherapy daily for 24 wk). Thus, our regimen appears to be at least as effective as pegylated IFN-2a for 48 wk[22]. Noteworthy is the finding that the development of a SVR seems to be related to the time of the initial virological response. In all cases, an early initial virological response after 2 wk of IFN treatment was followed by a SVR after 24 wk daily IFN monotherapy without ribavirin. A later initial virological response after 4 wk was associated with a relapse after EOT. In accordance with our results, Bekkering *et al.*[24], retreated 11 non-responders to previous TIW IFN therapy with daily dose IFN and found that all three sustained responders (genotype 3 in two cases and genotype 1a in one case) had undetectable plasma HCV RNA at d 14.

Recently, promising results in patients with genotype 2 and 3 treated with pegylated IFN and ribavirin combination therapy have been published[25,26]. Cornberg *et al.*[25], reduced the duration of combination therapy with standard weight-based dose of ribavirin (1 000-1 200 mg/d) from 48- to 24-wk treatment in patients with genotype 2 and 3. This regimen resulted in a SVR of approximately 85%[25]. In March 2004, Hadziyannis *et al.*[26], published the results of 1 311 patients treated with different regimens of short- and long-term pegylated IFN-2a (24 or 48 wk) in combination with low-dose ribavirin (800 mg/d) or standard weight-based dose of ribavirin (1 000 or 1 200 mg/d). Patients with genotype 2 or 3 were shown to be adequately treated with low-dose ribavirin in combination with pegylated IFN-2a for 24 wk[26]. Furthermore, our data suggest that there is a subgroup of patients with genotype 2 or 3 that can clear the virus with IFN-2a alone. As a result of the introduction of pegylated IFN, daily dosing of IFN has become outdated and in patients with genotype 2 or 3 HCV-infection pegylated IFN should be used as primary treatment for 24 wk with secondary addition of low-dose ribavirin (after 2 wk) only in case of failure of initial virological response 2 wk after initiation of therapy.

REFERENCES

1 **Choo QL,** Kuo G, Weiner AJ, Overby LR, Bradley DW, Houghton M. Isolation of a cDNA clone derived from bloodborne non-A, non-B viral hepatitis genome. *Science* 1989; **244**: 359-362

2 **Hoofnagle JH.** Course and Outcome of hepatitis C. *Hepatology* 2002; **36**: S21-S29

3 **Cohen J.** The Scientific Challenge of Hepatitis C. *Science* 1999; **285**: 26-30

4 **Wietzke-Braun P,** Braun F, Sattler B, Ramadori G, Ringe B. Initial steroid-free immunosuppression after liver transplantation in recipients with hepatitis C virus related cirrhosis. *World J Gastroenterol* 2004; **10**: 2213-2217

5 **Di Bisceglie AM.** Hepatitis C and Hepatocellular Carcinoma. *Hepatology* 1997; **26**: 34S-38S

6 **Hoofnagle JH,** Mullen KD, Jones DB, Rustgi VK, Di Bisceglie A, Hellahan C, Park Y, Meschievitz C, Jones EA. Treatment of chronic non-A, non-B hepatitis with recombinant human alpha interferon: a preliminary report. *N Engl J Med* 1986; **315**: 1575-1578

7 **McHutchison JG,** Gordon S, Schiff ER, Shiffman ML, Lee WM, Rustgi VK, Goodman Z, Ling MH, Cort S, Albrecht JK. Interferon alfa-2b alone or in combination with ribavirin as initial treatment for chronic hepatitis C. *N Engl J Med* 1998; **339**: 1485-1492

8 **Lai MY,** Kao JH, Yang PM, Wang JT, Chen PJ, Chan KW, Chu JS, Chen DS. Long term efficacy of ribavirin plus interferon alfa in the treatment of chronic hepatitis C. *Gastroenterology* 1996; **111**: 1307-1312

9 **Chemello L,** Cavalletto L, Bernardinello E, Guido M, Pontisso P, Alberti A. The effect of interferon alfa and ribavirin combination therapy in naive patients with chronic hepatitis C. *J Hepatology* 1995; **23**: 8-12

10 **Reichard O,** Norkrans G, Fryden A, Braconier JH, Sonnerborg A, Weiland O. Randomized, double-blind, placebo-controlled trial of interferon alpha-2b with and without ribavirin for chronic hepatitis C. *Lancet* 1998; **351**: 83-87

11 **Poynard T,** Leroy V, Cohard M, Thevenot T, Mathurin P, Opolon P, Zarski PJ. Meta-analysis of interferon randomized trials in the treatment of viral hepatitis C: effects of dose and duration. *Hepatology* 1996; **24**: 778-789

12 **Poynard T,** Marcellin P, Lee SS, Niederau C, Minuk GS, Ideo G, Bain V, Heathcote J, Zeuzem S, Trepo C, Albrecht J. Randomized trial of interferon alpha2b plus ribavirin for 48 wk or for 24 wk versus interferon alpha2b plus placebo for 48 wk for treatment of chronic infection with hepatitis C virus. *Lancet* 1998; **352**: 1426-1432

13 **Manns MP,** McHutchison JG, Gordon SC, Rustgi VK, Shiffman M, Reindollar R, Goodman ZD, Konry K, Ling M, Albrecht JK. Peginterferon alfa-2b plus ribavirin compared with interferon alfa-2b plus ribavirin for initial treatment of chronic hepatitis C: a randomised trial. *Lancet* 2001; **358**: 958-965

14 **Fried MW,** Shiffman ML, Reddy KR, Smith C, Marinos G, Goncales FL Jr, Haussinger D, Diago M, Carosi G, Dhumeaux D, Craxi A, Lin A, Hoffman J, Yu J. Peginterferon alfa-2a plus ribavirin for chronic hepatitis C virus infection. *N Engl J Med* 2002; **347**: 975-982

15 **Keating GM,** Curran MP. Peginterferon-α-2a (40 kD) plus ribavirin. A review of its use in the management of chronic hepatitis C. *Drugs* 2003; **63**: 1-29

16 **Wills RJ.** Clinical pharmacokinetics of interferons. *Clin Pharmacokinet* 1990; **19**: 390-399

17 **Lam NP,** Neumann AU, Gretch DR, Wiley TE, Perelson AS, Layden TJ. Dose-dependent acute clearance of hepatitis C genotype 1 virus with interferon alfa. *Hepatology* 1997; **26**: 226-231

18 **Neumann AU,** Lam NP, Dahari H, Gretch DR, Wiley TE, Layden TJ, Perelson AS. Hepatitis C viral dynamics *in vivo* and the antiviral efficacy of interferon alfa therapy. *Science* 1998; **282**: 103-107

19 **Zeuzem S,** Schmidt JM, Lee JH, von Wagner M, Teuber G, Roth WK. Hepatitis C virus dynamics *in vivo*: effect of ribavirin and interferon alfa on viral turnover. *Hepatology* 1998; **29**: 245-252

20 **Mihm S,** Hartmann H, Fayyazi A, Ramadori G. Preferential virological response to interferon-alpha 2a in patients with chronic hepatitis C infected by virus genotype 3a and exhibiting a low gamma-GT/ALT ratio. *Dig Dis Sci* 1996; **41**: 1256-1264

21 **Wietzke-Braun P,** Meier V, Braun F, Ramadori G. Combination of ‚low-dose' ribavirin and interferon alfa-2a therapy followed by interferon alfa-2a monotherapy in chronic HCV-infected non-responders and relapsers after interferon alfa-2a monotherapy. *World J Gastroenterol* 2001; **7**: 222-227

22 **Zeuzem S,** Feinman SV, Rasenack J, Heathcote EJ, Lai MY, Gane E, O'Grady J, Reichen J, Diago M, Lin A, Hoffman J, Brunda MJ. Peginterferon alfa-2a in patients with chronic hepatitis C. *N Engl J Med* 2000; **343**: 1666-1672

23 **Schalm SW,** Hansen BE, Chemello L, Bellobuono A, Brouwer JT, Weiland O, Cavalletto L, Schvarcz R, Ideo G, Alberti A. Ribavirin enhances the efficacy but not the adverse effects of interferon in chronic hepatitis C. *J Hepatol* 1997; **26**: 961-966

24 **Bekkering FC,** Brouwer JT, Leroux-Roels G, van Vlierberghe H, Elewaut A, Schalm SW. Ultrarapid hepatitis C virus clearance by daily high-dose interferon in non-responders to standard therapy. *J Hepatol* 1998; **28**: 960-964

25 **Cornberg M,** Hüppe D, Wiegand J, Felten G, Wedemeyer H, Manns MP. Treatment of chronic Hepatitis C with Peg-Interferon alpha-2b and ribavirin: 24 wk of therapy are sufficient for HCV genotype 2 and 3. *Z Gastroenterol* 2003; **41**: 517-522

26 **Hadziyannis SJ,** Sette H, Morgan TR, Balan V, Diago M, Marcellin P, Ramadori G, Bodenheimer H Jr, Bernstein D, Rizzetto M, Zeuzem S, Pockros PJ, Lin A, Ackrill AM. Peginterferon alpha-2a and ribavirin combination therapy in chronic hepatitis C: a randomized study of treatment duration and ribavirin dose. *Ann Intern Med* 2004; **140**: 346-355

Science Editor Guo SY **Language Editor** Elsevier HK

PO Box 2345, Beijing 100023, China
www.wjgnet.com
wjg@wjgnet.com

ELSEVIER

World J Gastroenterol 2005;11(39):6193-6196
World Journal of Gastroenterology ISSN 1007-9327
© 2005 The WJG Press and Elsevier Inc. All rights reserved.

• *BRIEF REPORTS* •

Quantitative analysis of plasma HBV DNA for early evaluation of the response to transcatheter arterial embolization for HBV-related hepatocellular carcinoma

Ying-Wen Su, Yu-Wen Huang, Sheng-Hsuan Chen, Chin-Yuan Tzen

Ying-Wen Su, Division of Hematology-Oncology, Department of Internal Medicine, Mackay Memorial Hospital, Taipei, Taiwan, China
Yu-Wen Huang, Department of Medical Research, Mackay Memorial Hospital, Taipei, Taiwan, China
Sheng-Hsuan Chen, Department of Gastroenterology, Taipei Medical University Hospital, Taipei, Taiwan, China
Chin-Yuan Tzen, Department of Medical Research, Department of Pathology, Mackay Memorial Hospital, Taipei, Taiwan, China
Supported by the grant NSC91-2314-B-195-026 from National Science Council, Taiwan, China
Co-first-authors: Ying-Wen Su
Correspondence to: Dr. Chin-Yuan Tzen, MD, PhD, Department of Pathology, Mackay Memorial Hospital, 45 Minsheng Road, Tamshui, Taipei, Taiwan, China. jeffrey@ms2.mmh.org.tw
Telephone: +886-2-28094661-2491 Fax: +886-2-28093385
Received: 2005-03-24 Accepted: 2005-06-02

Abstract

AIM: To assesse changes in plasma HBV DNA after TAE in HBV-related HCC and correlate the levels with the pattern of lipiodol accumulation on CT.

METHODS: Between April and June 2001, 14 patients with HBV-associated HCC who underwent TAE for inoperable or recurrent tumor were studied. Levels of plasma HBV DNA were measured by real-time quantitative PCR daily for five consecutive days after TAE. More than twofold elevation of circulating HBV DNA was considered as a definite elevation. Abdominal CT was performed 1-2 mo after TAE for the measurement of lipiodol retention.

RESULTS: Circulating HBV DNA in 10 out of 13 patients was elevated after TAE, except for one patient whose plasma HBV DNA was undetectable before and after TAE. In group I patients (n = 6), the HBV DNA elevation persisted for more than 2 d, while in group II (n = 7), the HBV DNA elevation only appeared for 1 d or did not reach a definite elevation. There were no significant differences in age or tumor size between the two groups. Patients in group I had significantly better lipiodol retention (79.31±28.79%) on subsequent abdominal CT than group II (18.43±10.61%) (P = 0.02).

CONCLUSION: Patients with durable HBV DNA elevation for more than 2 d correlated with good lipiodol retention measured 1 mo later, while others associated with poor lipiodol retention. Thus, circulating HBV DNA may be an early indicator of the success or failure of TAE.

Key words: Hepatocellular carcinoma; Transcatheter arterial embolization; HBV DNA

Su YW, Huang YW, Chen SH, Tzen CY. Quantitative analysis of plasma HBV DNA for early evaluation of the response to transcatheter arterial embolization for HBV-related hepatocellular carcinoma. *World J Gastroenterol* 2005; 11 (39): 6193-6196

http://www.wjgnet.com/1007-9327/11/6193.asp

INTRODUCTION

In patients with advanced hepatocellular carcinoma (HCC), transcatheter arterial embolization (TAE) has been widely used in Asian countries[1,2]. After TAE, tumor necrosis appears to be complete by 2 d[3]. Circulating plasma DNA is increased after traumatic injury and has been postulated as a prognostic marker for such condition[4]. We wondered if there were other circulating markers that would allow an earlier assessment of response to treatment. Although HCC lacks universal oncogene, HBV is closely linked to HCC. Integrated HBV fragments are frequently detected in the tumors of patients with positive hepatitis B surface antigen (HBsAg)[5]. We therefore studied patients with HBV-related HCC to determine how their circulating plasma and HBV DNA changed after TAE and how those measurements correlated with lipiodol retention on computed tomography (CT).

MATERIALS AND METHODS

Patients

HBsAg-positive patients with advanced HCC between April and June 2001 at the Mackay Memorial Hospital, Taipei, Taiwan were considered for enrollment. Only those who had inoperable tumors that were also not suitable for percutaneous ethanol injection were included. Diagnosis of HCC was made by cytology or by elevated α-fetoprotein (AFP) and typical imaging results (CT and celiac angiography). Patients with contraindications for TAE (such as uncorrectable bleeding disorder, severe thrombocytopenia [platelet count <50 000], a history of radiocontrast allergy, Child's grade C liver cirrhosis, elevated serum creatinine [>2.0 mg/dL], or tumor thrombus in the main portal trunk) were excluded. All patients studied gave informed consent. Patients who could not complete five consecutive days of study were excluded from the final analysis.

TAE through selective hepatic arterial catheterization

was performed via a femoral artery by radiologists at Mackay Memorial Hospital. Under fluoroscopic guidance, 3-10 mL of iodized oil (Laboratoire Guerbet, France) was injected slowly followed by gelatin-sponge pieces (Gelfoam, Johnson and Johnson Med Ltd) and 1 g of cephazolin. Gelfoam was used to activate intravascular thrombosis and cephazolin was used to prevent bacterial infection. After embolization, angiography was performed to determine the extent of vascular occlusion and to assess blood flow in other arteries. After the procedure, patients received intravenous hydration, antiemetic medication, and acetaminophen for pain control. They were discharged from the hospital when oral intake was adequate.

Blood tests and follow-up studies

Blood samples for HBV DNA were taken before TAE and after the procedure every 18-24 h for five consecutive days. Liver function was evaluated before and at 1 wk and 1 mo after TAE to assess the degree of toxicity. Enhanced CT scans of the abdomen using a 10-mm thick slice were performed on a GE HiSpeed scanner (GE Medical Systems) 1-2 mo after TAE. The tumor volume and volume of tumor retaining lipiodol were calculated with GE HiSpeed CT/i system software by reconstructing and viewing the data on a GE Advantage Windows Workstation. The morphologic therapeutic response was assessed by calculation of lipiodol-retaining tumor volume as a percentage whole tumor volume: Percentage of lipiodol retention = (lipiodol-retained lesion volume)/(whole tumor volume)×100%.

Real-time quantitative PCR for HBV DNA

Real-time quantitative PCR analysis was performed on an ABI Prism 7700 Sequence detection system (PE Applied Biosystems) by using SYBR green I as a double-strand DNA-specific binding dye. Briefly, DNA was extracted from a 400 μL plasma sample by using a QIAamp Blood kit (Qiagen Ltd) according to the manufacturer's instruction. The primers for HBV DNA were 184F 5'-GGA CCC CTG CTC GTG TTA CA-3' and 273R 5'-GAG AGA AGT CCA CCM CGA GTC TAG A-3' according to Pas *et al*.[6]. A product of 89 bp from a region of the HBV pre-S gene was amplified. The region was chosen because the pre-S to S open reading frame is generally conserved whereas the core gene is frequently deleted and the X ORF is often truncated[7]. Each reaction mixture contained 5 μL of 10× SYBR Green PCR buffer, 25 mmol/L $MgCl_2$, 200 nmol/L of each deoxynucleoside triphosphate (dATP, dCTP, dTTP, and dGTP), Taq Gold DNA polymerase 0.25 μL, AmpErase uracil *N*-glycosylase (UNG) 0.5 μL, 100 nmol/L of forward and reverse primers and 5 μL of the DNA extract from the plasma sample. The final volume of each PCR reaction mixture was 50 μL. Each sample was assayed in triplicate. Multiple negative water blanks were included in each run as a negative control. Thermal cycling was performed under the following conditions: stage I: at 50 ℃ 2 min, during which UNG could inactivate possible contaminating amplicons, and at 95 ℃ for 10 min, to allow Taq Gold polymerase to activate and inactivate the UNG; stage II: 40 cycles at 95 ℃ for 15 s and 60 ℃ for 1 min, and then stage III: 95 ℃ for 15 s, followed by 60 ℃ for 2 min. After real-time PCR, the amplified products were gradually heated to 95 ℃ for about 20 min. The instrument automatically measured the changing level of fluorescence continuously. This analysis gave the melting temperature. HBV standards were prepared from the serum of two patients with recently reactivated hepatitis B. Amplified PCR products were cloned into pGEM®-T easy vector (Promega Co.) and transformed into JM 109 competent cells. Plasmid DNA was isolated using a plasmid DNA miniprep system (Viogene, USA). Plasmid preparations were quantified spectrophotometrically and standards were prepared by serial dilution from 4×10^1 to 4×10^8 copies/mL.

Data analysis

After amplification, data were captured onto a Macintosh computer, analysis was done with Sequence Detection software (PE Applied Biosystems). Data were collected at the annealing step (60 ℃) of every cycle, and the threshold cycle (Ct) for each sample was calculated by determining the point at which the fluorescence exceeded the threshold limit. A standard curve was calculated automatically by plotting the Ct values against standards of known concentration and calculation of the linear regression line of this curve. Calculation of the correlation coefficient (r^2) was done for each run, using a minimal value of 0.95. Sample copy numbers were calculated by interpolation of the experimentally determined standard curve. In this study, the percent coefficient of variation (%CV) of threshold cycle was 1.25% (range: 0-4.73%) for HBV DNA, similar to that of a previous report 19.

Changes in plasma HBV DNA and statistical analysis

Patient's plasma HBV DNA with twofold elevation was considered as a definite elevation. We classified the changes in plasma HBV DNA into two groups. Group I patients had an elevated HBV DNA level post-TAE for more than 2 d. In group II patients, the HBV DNA elevation only appeared for 1 d or did not reach the definite elevation before d 5. Data were reported as the mean±SD. Clinical characteristics and lipiodol retention of the two groups were compared by using Student *t* test and Fisher test. A P value <0.05 was considered statistically significant.

RESULTS

Fourteen HBsAg seropositive patients with HCC (12 men and 2 women) were studied. The average age was 62 years, ranging between 39 and 81 years. Thirteen had Child Class A and one had Child Class B cirrhosis. Five patients received TAE for the first time and the others were being treated again for recurrent disease. The post-embolization symptoms (fever, abdominal pain, and vomiting) in all patients were mild and subsided within one week. Liver function recovered completely in all patients within one week, and no subsequent liver dysfunction was noted over the course of the study.

Plasma HBV DNA changes after TAE

Except for one patient with undetectable plasma HBV DNA before and after TAE, 10 out of 13 patients had increased plasma HBV DNA after embolization. Six patients had HBV DNA rising for more than 2 d (group I). Among seven

patients in group II, three patients did not reach definite HBV elevation and the other four had temporal HBV DNA elevation within 3 d after TAE. The mean diameter of the embolized tumor in group I was 5.92±3.98 and 5.00±2.20 cm in group II, a non-significant difference (P = 0.61). The lipiodol retention in the embolized tumors in group I was 79.31±28.79% and in group II, 18.43±10.61%, a statistically significant difference (P = 0.02). No significant differences were observed between the two groups regarding age or tumor size (Table 1).

Table 1 Basic characteristics before TAE and lipiodol retention percentage after TAE of group I and group II patients

	Group I (n = 6)	Group II (n = 7)	P
Age, yr (range)	57.6 (39-79)	65.6 (38-81)	0.34
Gender (male/female)	6/0	5/2	-
Pretreatment AFP (ng/mL)	707±1 536	3 024±5 307	0.32
Tumor size (cm)	5.92±3.98	5.00±2.20	0.61
Disease status at entry			-
For the first time TAE (n)	3	2	
For recurrence (n)	3	5	
Lipiodol retention (%)	79.31±28.79	18.43±10.61	0.02[a]

n: patient number. Statistical data are expressed as mean±SD. [a]P<0.05, with statistical significance.

DISCUSSION

Our study showed a significant correlation between durable elevation of plasma HBV DNA concentration after TAE and lipiodol retention one month later. Group I patients with an persistently elevated HBV DNA level apparently sustained more tumor damage after TAE as evidenced by good lipiodol retention, while group II patients with temporary or no elevation in HBV DNA probably had unsuccessful TAE, as indicated by poor lipiodol retention.

The anticancer effects caused by TAE are due to selective blockade of the tumor blood supply. Integrated HBV DNA can be detected in both tumor and nontumor liver tissues of HBV carriers[8]; so the immediate elevation of plasma HBV DNA after TAE might come from damages to the two parts of the same arterial territory. Both integrated HBV DNA and non-integrated episomal HBV DNA are included. Although it has been recently published that HBV may be reactivated by transarterial chemoembolization (TACE), the reported time to reactivation after the last TACE was more than 25 d[9]. In our study, none of our patients had persistently abnormal or deteriorating liver dysfunction after TAE, suggesting that HBV reactivation was not likely to occur within the short period.

With gelfoam embolization, it can produce temporary or permanent occlusion of the targeted artery[10]. From our results, plasma HBV DNA elevated within short-term follow-ups in 10 out of 13 patients. They can be considered as consequences of ischemic injury to liver although the effects may be temporary or persistent. Persistence of HBV DNA in our patients indicates that the occlusion of tumor feeding artery by TAE was complete. It correlated with good lipiodol retention, a factor known to predict a good response. Among patients without persistent elevation of circulating DNA (group II), they tend to have less successful TAE, which may be due to technical or tumor factors (such as incomplete arterial occlusion, presence of collateral blood supply, or tumors with resistance to reperfusion injury)[11-15]. In such patients, other treatment modalities should be considered early to achieve better tumor control.

Monitoring the outcome of TAE is important because it is an important prognostic factor influencing management decisions, such as retreating, incorporation of various non-surgical procedures (e.g., percutaneous ethanol injection, intra-arterial chemotherapy, or local ablation techniques), or deciding to withhold further anti-tumor therapy[16]. In order to evaluate response to TAE, clinicians commonly use tumor regression, AFP levels, and the degree of lipiodol accumulation on CT. All these methods have limitations. Tumor regression is seldom recognized before 4 wks after TAE, and some tumors fail to shrink despite complete necrosis found on pathology of resected lesions[17,18]. Although a good correlation has been found between histologically proven tumor necrosis and reduction in AFP, this correlation has only been demonstrated in patients with a pre-TAE AFP level $\geqslant$200 ng/mL[19]. This marker is therefore of little use in patients who do not have markedly elevated AFP before TAE. The degree of lipiodol retention also correlates well with the degree of necrosis[18]. Compact lipiodol uptake has also been correlated with a better chance of survival than less compact uptake, indicating its usefulness as a post treatment prognostic marker. However, the need to wait 4 wk after treatment for the agent to be cleared from the uninvolved hepatic parenchyma[20] limits its usefulness. In some cases, hepatic washout is particularly slow, making interpretation of the CT image difficult[21].

Recent data indicate that human plasma DNA possesses a short half-life in the circulation[22]. The rapid kinetics suggests that circulating DNA analysis may be useful in monitoring clinical progress. One potential limitation of its clinical application is that serial blood sampling after TAE may be inconvenient for patients. If, as implied by this preliminary study, circulating plasma DNA persistently correlates with lipiodol retention, it may prove to be a useful tool for early evaluation of the response to TAE. If further studies support our findings, circulating levels of HBV DNA after TAE may be an early indicator for which patients require additional treatment.

REFERENCES

1 **Liu CL**, Fan ST. Nonresectional therapies for hepatocellular carcinoma. *Am J Surg* 1997; **173**: 358-365
2 **Acunas B**, Rozanes I. Hepatocellular carcinoma: treatment with transcatheter arterial chemoembolization. *Eur J Radiol* 1999; **32**: 86-89
3 **Yoshida T**, Sakon M, Umeshita K, Kanai T, Miyamoto A, Takeda T, Gotoh M, Nakamura H, Wakasa K, Monden M. Appraisal of transarterial immunoembolization for hepatocellular carcinoma: a clinicopathologic study. *J Clin Gastroenterol* 2001; **32**: 59-65
4 **Lo YM**, Rainer TH, Chan LY, Hjelm NM, Cocks RA. Plasma DNA as a prognostic marker in trauma patients. *Clin Chem* 2000; **46**: 319-323
5 **Lai MY**, Chen DS, Chen PJ, Lee SC, Sheu JC, Huang GT, Wei TC, Lee CS, Yu SC, Hsu HC. Status of hepatitis B virus DNA

in hepatocellular carcinoma: a study based on paired tumor and nontumor liver tissues. *J Med Virol* 1988; **25**: 249-258

6 **Pas SD**, Fries E, De Man RA, Osterhaus AD, Niesters HG. Development of a quantitative real-time detection assay for hepatitis B virus DNA and comparison with two commercial assays. *J Clin Microbiol* 2000; **38**: 2897-2901

7 **Brechot C**. Pathogenesis of hepatitis B virus-related hepatocellular carcinoma: old and new paradigms. *Gastroenterology* 2004; **127**(5 Suppl 1): S56-S61

8 **Shafritz DA**, Shouval D, Sherman HI, Hadziyannis SJ, Kew MC. Integration of hepatitis B virus DNA into the genome of liver cells in chronic liver disease and hepatocellular carcinoma. Studies in percutaneous liver biopsies and post-mortem tissue specimens. *N Engl J Med* 1981; **305**: 1067-1073

9 **Jang JW**, Choi JY, Bae SH, Kim CW, Yoon SK, Cho SH, Yang JM, Ahn BM, Lee CD, LeeYS, Chung KW, Sun HS. Transarterial chemo-lipiodolization can reactivate hepatitis B virus replication in patients with hepatocellular carcinoma. *J Hepatol* 2004; **41**: 427-435

10 **Huang MS**, Lin Q, Jiang ZB, Zhu KS, Guan SH, Li ZR, Shan H. Comparison of long-term effects between intra-arterially delivered ethanol and Gelfoam for the treatment of severe arterioportal shunt in patients with hepatocellular carcinoma. *World J Gastroenterol* 2004; **10**: 825-829

11 **Liou TC**, Shih SC, Kao CR, Chou SY, Lin SC, Wang HY. Pulmonary metastasis of hepatocellular carcinoma associated with transarterial chemoembolization. *J Hepatol* **23**: 563-568

12 **Savastano S**, Miotto D, Casarrubea G, Teso S, Chiesura-Corona M, Feltrin GP. Transcatheter arterial chemoembolization for hepatocellular carcinoma in patients with Child's grade A or B cirrhosis: a multivariate analysis of prognostic factors. *J Clin Gastroenterol* 1999; **28**: 334-340

13 **Sonomura T**, Yamada R, Kishi K, Nishida N, Yang RJ, Sato M. Dependency of tissue necrosis on gelatin sponge particle size after canine hepatic artery embolization. *Cardiovasc Intervent Radiol* 1997; **20**: 50-53

14 **Yamakado K**, Nakatsuka A, Tanaka N, Matsumura K, Takase K, Takeda K. Long-term follow-up arterial chemoembolization combined with transportal ethanol injection used to treat hepatocellular carcinoma. *J Vasc Interv Radiol* 1999; **10**: 641-647

15 **Selzner M**, Rudiger HA, Selzner N, Thomas DW, Clavien PA. Transgenic mice overexpressing human Bcl-2 are resistant to hepatic ischemia and reperfusion. *J Hepatol* 2002; **36**: 218-225

16 **Catalano O**, Esposito M, Lobianco R, Cusati B, Altei F, Siani A. Hepatocellular carcinoma treated with chemoembolization: assessment with contrast-enhanced doppler ultrasonography. *Cardiovasc Intervent Radiol* 1999; **22**: 486-492

17 **Solomon B**, Soulen MC, Baum RA, Haskal ZJ, Shlansky-Goldberg RD, Cope C. Chemoembolization of hepatocellular carcinoma with cisplatin, doxorubicin, mitomycin-C, ethiodol, and polyvinyl alcohol: prospective evaluation of response and survival in a U.S. population. *J Vasc Interv Radiol* 1999; **10**: 793-798

18 **Takayasu K**, Arii S, Matsuo N, Yoshikawa M, Ryu M, Takasaki K, Sato M, Yamanaka N, Shimamura Y, Ohto M. Comparison of CT findings with resected specimens after chemoembolization with iodized oil for hepatocellular carcinoma. *Am J Roentgenol* 2000; **175**: 699-704

19 **Okusaka T**, Okada S, Ueno H, Ikeda M, Yoshimori M, Shimada K, Yamamoto J, Kosuge T, Yamasaki S, Iwata R, Furukawa H, Moriyama N, Sakamoto M, Hirohashi S. Evaluation of the therapeutic effect of transcatheter arterial embolization for hepatocellular carcinoma. *Oncology* 2000; **58**: 293-299

20 **Choi BI**, Kim HC, Han JK, Park JH, Kim YI, Kim ST, Lee HS, Kim CY, Han MC. Therapeutic effect of transcatheter oily chemoembolization therapy for encapsulated nodular hepatocellular carcinoma: CT and pathologic findings. *Radiology* 1992; **182**: 709-713

21 **Lencioni R**, Pinto F, Armillotta N, Di Giulio M, Gaeta P, Di Candio G, Marchi S, Bartolozzi C. Intrahepatic metastatic nodules of hepatocellular carcinoma detected at lipiodol-CT: imaging-pathologic correlation. *Abdom Imaging* 1997; **22**: 253-258

22 **Lo YM**, Zhang J, Leung TN, Lau TK, Chang AM, Hjelm NM. Rapid clearance of fetal DNA from maternal plasma. *Am J Hum Genet* 1999; **64**: 218-224

Science Editor Guo SY **Language Editor** Elsevier HK

PO Box 2345, Beijing 100023, China
www.wjgnet.com
wjg@wjgnet.com

ELSEVIER

World J Gastroenterol 2005;11(39):6197-6201
World Journal of Gastroenterology ISSN 1007-9327
© 2005 The WJG Press and Elsevier Inc. All rights reserved.

• *BRIEF REPORTS* •

Glutamine-supplemented total parenteral nutrition attenuates plasma interleukin-6 in surgical patients with lower disease severity

Ming-Tsan Lin, Sung-Pao Kung, Sung-Ling Yeh, Koung-Yi Liaw, Ming-Yang Wang, Ming-Liang Kuo, Po-Houng Lee, Wei-Jao Chen

Ming-Tsan Lin, Department of Surgery and Primary Care Medicine, National Taiwan University Hospital and National Taiwan University College of Medicine, Taipei, Taiwan, China
Sung-Pao Kung, Department of Surgery, School of Medicine, National Yang-Ming University, Taipei, Taiwan, China
Sung-Ling Yeh, Institute of Nutrition and Health Sciences, Taipei Medical University, Taipei, Taiwan, China
Koung-Yi Liaw, Ming-Yang Wang, Po-Houng Lee, Wei-Jao Chen, Department of Surgery, National Taiwan University Hospital and National Taiwan University College of Medicine, Taipei, Taiwan, China
Ming-Liang Kuo, Laboratory of Molecular and Cellular Toxicology, Institute of Toxicology, National Taiwan University College of Medicine, Taipei, Taiwan, China
Supported by a Research Grant from the National Science Council, Taipei, Taiwan, No. NSC91-2314-B002-245
Co-correspondents: Sung-Pao Kung
Correspondence to: Wei-Jao Chen, MD, PhD, Department of Surgery, National Taiwan University Hospital, 7 Chung-Shan S. Road, Taipei, Taiwan, China. chenwj@ha.mc.ntu.edu.tw
Telephone: +886-2-23123456-2122 Fax: +886-2-23412969
Received: 2005-02-15 Accepted: 2005-06-09

Abstract

AIM: To evaluate whether the effect of Gln dipeptide-enriched total parenteral nutrition (TPN) on postoperative cytokine alteration depended on the disease severity of surgical patients.

METHODS: Forty-eight patients with major abdominal surgery were allocated to two groups to receive isonitrogenous (0.228 g nitrogen/kg per d) and isocaloric (30 kcal/kg per d) TPN for 6 d. Control group (Conv) using conventional TPN solution received 1.5 g amino acids/kg per day, whereas the test group received 0.972 g amino acids/kg per day and 0.417 g L-alanyl-L-glutamine (Ala-Gln)/kg per day. Blood samples were collected on d 1 and d 6 postoperatively for plasma interleukin (IL)-2, IL-6, IL-8, and interferon (IFN)-γ analysis.

RESULTS: Plasma IL-2 and IFN-γ were not detectable. IL-6 concentrations were significantly lower on the 6th postoperative day in the Ala-Gln group than those in the Conv group in patients with APACHE II≤6, whereas no difference was noted in patients with APACHE II>6. There was no difference in IL-8 levels between the two groups. No difference in cumulative nitrogen balance was observed on d 2-5 after the operation between the two groups (Ala-Gln -3.2±1.6 g *vs* Conv -6.5±2.7 g). A significant inverse correlation was noted between plasma IL-6 levels and cumulative nitrogen balance postoperatively in the Ala-Gln group, whereas no such correlation was observed in the Conv group.

CONCLUSION: TPN supplemented with Gln dipeptide had no effect on plasma IL-8 levels after surgery. However, Gln supplementation had a beneficial effect on decreasing systemic IL-6 production after surgery in patients with low admission illness severity, and lower plasma IL-6 may improve nitrogen balance in patients with abdominal surgery when Gln was administered.

© 2005 The WJG Press and Elsevier Inc. All rights reserved.

Key words: Glutamine; Total parenteral nutrition; Interleukin-6; Abdominal surgery

Lin MT, Kung SP, Yeh SL, Liaw KY, Wang MY, Kuo ML, Lee PH, Chen WJ. Glutamine-supplemented total parenteral nutrition attenuates plasma interleukin-6 in surgical patients with lower disease severity. *World J Gastroenterol* 2005; 11(39): 6197-6201
http://www.wjgnet.com/1007-9327/11/6197.asp

INTRODUCTION

Glutamine (Gln) is the most abundant amino acid in plasma and in the intracellular free amino acid pool[1]. It is essential for a wide variety of physiologic process, in particular, the growth and function of immune cells including lymphocytes and macrophages[2]. Gln has traditionally been thought as a nonessential amino acid; however, previous reports have shown that Gln depletion occurs in critically injured patients. The extent and duration of Gln depletion are proportional to the severity of illness[3,4]. Laboratory and clinical data suggest that Gln is essential during certain catabolic conditions, such as burns, major surgery, and infection[5-8]. Total parenteral nutrition (TPN) is widely used in the treatment of critically ill patients. Conventional TPN solution does not contain Gln, because Gln is relatively unstable in solution during heat sterilization and long-term storage. Exogenous Gln may be required to satisfy the body's Gln requirement under stressed conditions. Previous studies have shown that TPN supplemented with Gln improved nitrogen balance, enhanced immune response and shortened hospital stay in surgical patients[9-12].

Surgery is known to impair the immune response, and may consequently increase risk of postoperative infection and sepsis[13]. The decrease in the plasma Gln

level following major surgery may contribute to the state of immunosuppression[12,14]. Studies have shown that depressed Gln concentrations were associated with reduced proliferation of lymphocyte in healthy volunteers[14], and Gln depletion may be partly responsible for T cell suppression seen in severely stressed patients[15,16]. In addition to its role in lymphocyte function, Gln may have an indirect effect to mediate a reduction in proinflammatory cytokine release. Parry-Billings *et al*.[3], demonstrated that plasma Gln level was negatively correlated with the production of interleukin (IL)-6 under major surgery. De Beaux *et al*.[17], showed that Gln-supplemented TPN significantly reduced blood mononuclear cell IL-8 release in severe acute pancreatitis patients. A previous report by our laboratory have shown that the effect of Gln administration on improving nitrogen economy was only observed in patients with low, but not high Chronic Health Evaluation (APACHE II) scores[11]. This result indicates that the effect of Gln on attenuating catabolic response may depend on the characteristics and severity of the diseases. We hypothesized that the effect of synthetic Gln supplementation on proinflammatory cytokine release was also associated with the severity of diseases. In this study, we administered a Gln-dipeptide containing TPN to patients postoperatively to investigate the effect of synthetic Gln-dipeptide on cytokine production after surgery. Also, the Gln effect on the severity of stress and cytokine production was evaluated.

MATERIALS AND METHODS

Patients

This was a randomized, double-blind, parallel multicenter clinical trial carried out in National Taiwan University Hospital and Veterans General Hospital, Taipei, Taiwan. This study was performed from August 1999 to May 2000, and was approved by the ethical committee of the two centers. Patients with major metabolic, circulatory, and renal diseases were excluded, and no emergency cases were included. Only major gastrointestinal surgery patients who needed TPN for nutritional support were enrolled. APACHE II score and Therapeutic Intervention Scoring system (TISS) were evaluated after admission[18]. Patients with APACHE II between 2-10 and TISS>10 were included. The informed consent was obtained from each patient before the experiment was performed. A total of 48 patients (28 males and 20 females, age range 40-82 years, mean 66 years) were included. These patients were randomly allocated to either a test group or a control group. The separation of patients into low and high APACHE II groups was post hoc. Since patients with APACHE II score between 2 and 10 were enrolled, we chose the midpoint 6 as the cut-off point to differentiate low- and high-disease severity in this study. Demographic for all patients is summarized in Table 1.

Feeding regimen

The two groups were isonitrogenous and isocaloric. Nitrogen intake was 0.228 g/kg body weight per ds. Caloric intake was 30 kcal/kg per ds. The nonprotein calories were given as dextrose and fat in a ratio of 70:30. Patients of the control group (Conv group, n = 23) were administered a commercially available amino acid solution (Moriamin-SN 10%, Chinese Pharmaceuticals, Taipei, Taiwan). The Conv group received 1.5 g amino acid/kg per day. Patients of the test group (L-alanyl-L-glutamine (Ala-Gln) group, n = 25) received 0.972 g amino acid/kg per day supplemented with 0.417 g/kg per ds Ala-Gln, which provide 0.28 g Gln/kg per day (Dipeptiven, Fresenius Kabi, Bad Homburg, Germany). The Gln containing solutions were prepared by the clinical pharmacist under aseptic condition and adjusted to the weight of each individual patient. The amino acids and dextrose mixture with electrolytes, vitamins, and trace elements were administered through a central venous catheter. Fat emulsion (Lipovenos 20%, Fresenius AG, Germany) was given through a separate canal in the central venous line. Half strength was administered on the 1st d, and full strength was given thereafter for the remaining days. During the experimental period, no enteral nutrition was administered. Neither the patients nor the investigator knew that the applied TPN regimens were with or without Ala-Gln.

Measurements of the plasma parameters and cumulative nitrogen balance

Routine clinical chemistry was measured before and after the surgery. The blood samples were also obtained on postoperative d 1 and on d 6 after TPN administration for analysis of plasma cytokine concentrations. Cytokines including IL-2, IL-6, IL-8, and interferon (IFN)-γ were measured using a commercially available ELISA in microtiter

Table 1 Demographic data of the patients

	Ala-Gln group			Conv group		
	All patients	APACHE ≤6	APACHE >6	All patients	APACHE ≤6	APACHE >6
Age (yr)	66.7±9.0	61.7±11.2	70.1±6.0	67.6±8.4	64.5±7.6	70.6±8.7
Weight (kg)	56.9±9.1	57.7±8.6	56.3±10.1	57.6±10.3	55.3±8.6	59.8±12.0
Height (cm)	157.8±6.4	160.4±6.7	156.0±6.1	160.1±8.3	158.8±8.0	161.3±9.0
Male/female	14/11	4/6	10/5	14/9	6/5	8/4
Diagnosis:						
Gastric Ca	18	6	12	14	6	8
Pancreas Ca	4	3	1	4	2	2
Colon Ca	1	0	1	3	2	1
Hepatoma	1	1	0	1	1	0
Duodenal Ca	0	0	0	1	0	1
Rectal Ca	1	0	1	0	0	0

plates (BioSource International, Camarillo, CA, USA). Antibody specific for human IL-2, IL-6, IL-8, and IFN-γ were coated onto the wells of microtiter stripes provided. Urine and drainage was collected throughout the study, and cumulative nitrogen balance was calculated from postoperative d 2-5 as previously described[11].

Statistics

The data are expressed as mean±SD, repeated measure analysis of variance were used to compare the treatment differences at each day, and *t*-test was used for the difference between the two groups. Pearson's correlation coefficients were used to calculate the linear relationship between plasma IL-6 and cumulative nitrogen balance of the patients. A *P* value <0.05 was considered significant.

RESULTS

Most of the patients had laboratory values within normal range at baseline and on d 6 after the operation despite the patients being administered with Conv or Ala-Gln solution (data not shown). No adverse reactions were found after the Gln-dipeptide containing solution was administered.

Plasma IL-2 and IFN-γ levels were not detectable. Plasma IL-6 concentrations were significantly lower after TPN administration for 6 d, regardless whether the patients were in Conv group or Ala-Gln group. In patients with APACHE II≤6, plasma IL-6 concentrations on the postoperative d 6 in the Ala-Gln group were significantly lower than those in the Conv group. However, there were no differences in IL-6 concentrations between the two groups after infusing TPN for 6 d in patients with APACHE II>6 (Table 2). No significant difference in plasma IL-8 concentrations were observed between the postoperative d 6 and d 1, regardless whether the patients were infused with Ala-Gln or Conv solution. Also, there were no differences in IL-8 levels between the two groups on d 6 and 1 postoperatively (Table 3).

There was no difference in cumulative nitrogen balance on days 2-5 after the operation between the two groups (Ala-Gln -3.2±1.6 g *vs* Conv -6.5±2.7 g). A significant inverse correlation was observed between plasma IL-6 levels on d 6 and cumulative nitrogen balance postoperatively in the Ala-Gln group ($P = 0.027$), whereas no such correlation was noted in the Conv group ($P = 0.919$) (Table 4).

Table 2 Plasma IL-6 concentrations on d 1 postoperatively and on d 6 after TPN administration

	Conv (pg/mL)	Ala-Gln (pg/mL)
All patients	(23)	(25)
D 1[1]	38.8±31.5	52.5±48.7
D 6	12.4±12.1[a]	7.9±5.9[a]
APACHE II≤6	(11)	(10)
D 1	31.2±21.8	37.1±35.4
D 6	11.9±10.5[a]	3.2±1.9[a,b]
APACHE II>6	(12)	(15)
D 1	45.1±41.7	59.8±53.4
D 6	12.9±14.8[a]	16.1±17.2[a]

[1]D 1 represents the data obtained after TPN administration. Figures in parentheses indicate number of patients. [a]P<0.05 *vs* d 1 after Surgery. [b]$P = 0.029$ from Conv group D 6 in APACHE II ≤ 6.

Table 3 Plasma IL-8 concentrations on d 1 postoperatively and on d 6 after TPN administration

	Conv (pg/mL)	Ala-Gln (pg/mL)
All patients	(23)	(25)
D 1[1]	18.9±8.4	37.6±46.1
D 6	28.3±22.4	64.6±62.8
APACHE II≤6	(11)	(10)
D 1	19.4±9.9	15.6±9.0
D 6	36.9±45.9	24.5±8.9
APACHE II>6	(12)	(15)
D 1	18.5±7.3	48.4±52.3
D 6	31.0±30.4	81.3±67.9

[1]D 1 represents the data obtained before TPN administration. Figures in parentheses indicate number of patients.

Table 4 Correlation between plasma IL-6 concentrations and cumulative nitrogen balance postoperatively

	r	*P*
Total patients (38)	–0.2092	0.249
Ala-Gln group (20)	–0.6608	0.027[a]
Conv group (18)	0.033	0.919

[a]P<0.05 using pearson's correlation.

DISCUSSION

In this study, we analyzed plasma IL-2, IL-6, IL-8, and IFN-γ concentrations on postoperative days, because these cytokines are involved in the response to tissue injury[19,20]. IL-2 is produced by mitogen-stimulated T lymphocyte, and was originally isolated as a T-cell growth factor. IFN-γ promotes production of proinflammatory mediator such as IL-1 and TNF-α[19,20]. IL-1β, TNF-α, and IL-6 are major mediators of inflammation and acute phase response. We only measured IL-6 levels, because TNF-α and IL-1 have rarely been detected in the plasma of injured patients[20,21]. In this study, plasma IL-2 and IFN-γ were not detectable either. It is possible that the cytokines are bioactive in biologic fluid at levels well below the range of detectability by current immunoassays[20]. The effect of Gln supplementation on plasma IL-2 and IFN-γ cannot be found in this study.

IL-8 is a chemotactic and activating factor for immune response. Previous reports had shown that plasma IL-8 concentration were much higher in patients with sepsis compared with noninfectious shock, and associated with a fatal outcome[19]. Study by De Beaux *et al*.[17], showed that Gln-supplemented TPN reduces *in vitro* blood mononuclear cell IL-8 release in acute pancreatitis. In this study, no significant differences in plasma IL-8 concentrations were observed between the postoperative d 1 and 6. Also, there were no differences in IL-8 levels between the two groups on postoperative days. This result indicated that Gln administration did not influence the changes of IL-8 in surgical patients. Since IL-8 is associated with clinical,

biochemical, and inflammatory markers of sepsis[22,23], it is compatible to the fact that patients in this study were not complicated with infection, as shown in our previous report[11].

IL-6 is a multifunctional cytokine expressed by a variety of cells. Cruickshank *et al.*[21], reported that systemic response of IL-6 to surgical trauma increased with the severity of surgical insult. Elevation of IL-6 after trauma and elective surgery has been associated with infectious morbidity as well as mortality[24]. Foex and Shelly[25] suggest that IL-6 is a sensitive marker of tissue damage after surgery. In this study, we observed that plasma IL-6 concentrations significantly reduced after TPN administration for 6 d, regardless whether the patients were in Conv group or Ala-Gln group. This result might mean that TPN formula administration attenuated the inflammatory response of the surgical insult. The result also showed that plasma IL-6 levels on postoperative d 6 in the Ala-Gln group were significantly lower than the Conv group in patients with APACHE II$\leqslant$6, but not in patients with higher APACHE II scores. This finding suggests that in patients with lower disease severity, TPN supplemented with Gln had a significant favorable effect on reducing inflammatory response postoperatively. Studies have shown that after operation and trauma, Gln deprivation is observed and the severity of Gln deprivation is proportional to the severity of diseases[3,4]. It is possible that in patients with lower APACHE II score, the demand of Gln is much less than the patients with higher score, and Gln supplementation provides adequate substrate for the function of immune system, and thus reduced the inflammatory response of the surgical insult. Palmer *et al.*[4], showed that TPN supplemented with Gln had no effect on muscle and plasma biochemical changes in critically ill patients. Since this study was a post hoc investigation, whether higher dose of Gln may have beneficial effect on reducing IL-6 concentrations in patients with higher disease severity needs to be clarified.

In this study, we observed a negative correlation between plasma IL-6 and cumulative nitrogen balance postoperatively in the Ala-Gln group, whereas such correlation was not found when data of all patients were pooled and in the Conv group. This finding may indicate that the severity of protein catabolism cannot be predicted by plasma IL-6 level, possibly because the variation of nitrogen loss and plasma IL-6 levels was wide among individual surgical patient. However, Gln administration may consistently improve nitrogen balance and reduced plasma IL-6, and thereby a negative correlation between cumulative nitrogen balance and plasma IL-6 was found. Since nitrogen balance represents a complicated net result of protein catabolism and synthesis in the body, whether Gln play roles in modulating the relationship between IL-6 and protein metabolism required further investigation.

In summary, this study showed that TPN supplemented with Gln dipeptide had no significant influence on plasma IL-8 levels after surgery. However, Gln supplementation had a beneficial effect on decreasing systemic IL-6 production after surgery in patients with low admission illness severity, and lower plasma IL-6 may improve nitrogen balance in patients with abdominal surgery when Gln was administered.

ACKNOWLEDGMENTS

The authors thank Ms. Irene Cheng and Ms. Hui-Jen Huang for their help in collecting data and blood samples. We thank Frensenius AG (Bad Homburg, Germany) for supporting and supplying Gln dipeptide.

REFERENCES

1 **Bergstrom J,** Furst P, Noree LO, Vinnars E. Intracellular free amino acid concentration in human muscle tissue. *J Appl Physiol* 1974; **36**: 693-697
2 **Smith RJ,** Willmore DW. Glutamine nutrition and requirements. *J Parenter Enter Nutr* 1990; **14**: 94S-99S
3 **Parry-Billings M,** Baigrie RJ, Lamont PM, Morris P, Newsholme EA. Effects of major and minor surgery on plasma glutamine and cytokine levels. *Arch Surg* 1992; **127**: 1237-1240
4 **Palmer TEA,** Griffiths RD, Jones C. Effect of parenteral L-glutamine on muscle in the very severely ill. *Nutrition* 1996; **12**: 316-320
5 **Willmore DW,** Shabert JK. Role of glutamine in immunologic responses. *Nutrition* 1998; **14**: 618-626
6 **De-Souza DA,** Greene LJ. Phamacological nutrition after burn injury. *J Nutr* 1998; **128**: 797-803
7 **Quan ZF,** Yang C, Li N, Li JS. Effect of glutamine on change in early postoperative intestinal permeability and its relation to systemic inflammatory response. *World J Gastroenterol* 2004; **10**: 1992-1994
8 **Li JY,** Lu Y, Hu S, Sun D, Yao YM. Preventive effect of glutamine on intestinal barrier dysfunction induced by severe trauma. *World J Gastroenterol* 2002; **8**: 168-171
9 **Jiang ZM,** Cao JD, Zhu XG, Zhao WX, Yu JC, Ma EL, Wang XR, Zhu MW, Shu H, Liu YW. The impact of alanyl-glutamine on clinical safety, nitrogen balance, intestinal permeability, and clinical outcome in postoperative patients: a randomized, double-blind, controlled study of 120 patients. *J Parenter Enter Nutr* 1999; **23**: S62-S66
10 **Morlion BJ,** Stehle P, Wachtler P, Siedhoff HP, Koller M, Konig W, Furst P, Puchstein C. Total parenteral nutrition with glutamine dipeptide after major abdominal surgery. *Ann Surg* 1998; **227**: 302-308
11 **Lin MT,** Kung SP, Yeh SL, Lin C, Lin TH, Chen KH, Liaw KY, Lee PH, Chang KJ, Chen WJ. Glutamine-supplemented total parenteral nutrition on nitrogen economy depends on severity of diseases in surgical patients. *Clin Nutr* 2002; **21**: 213-218
12 **Heberer M,** Babst R, Juretic A, Gross T, Horig H, Harder F, Spagnoli GC. Role of glutamine in the immune response in critical illness. *Nutrition* 1996; **12**: S71-S72
13 **Lennard TW,** Shenton BK, Borzotta A, Donnelly PK, White M, Gerrie LM, Proud G, Taylor RM. The influence of surgical operations on components of human immune system. *Br J Surg* 1985; **72**: 771-776
14 **Parry-Billings M,** Evans J, Calder PC, Newsholme EA. Does glutamine contribute to immunosuppression after major burns? *Lancet* 1990; **336**: 523-525
15 **Rohde T,** Maclean DA, Klarlund Pedersen B. Glutamine, lymphocyte proliferation and cytokine production. *Scand J Immunol* 1996; **44**: 648-650
16 **Yaqoob P,** Calder PC. Glutamine requirement of proliferating T lymphocytes. *Nutrition* 1997; **13**: 646-651
17 **De Beaux AC,** O'riordain MG, Ross JA, Jodozi L, Carter DC, Fearon KC. Glutamine-supplemented total parenteral nutrition reduces blood mononuclear cell interleukin-8 release in severe acute pancreatitis. *Nutrition* 1998; **14**: 261-265
18 **Dellinger EP.** Use of scoring systems to assess patients with surgical sepsis. *Surg Clin North Am* 1988; **68**: 123-145
19 **Ertel W,** Morrison MH, Wang P, Zheng F, Ayala A, Chaudry IH. The complex of cytokines in sepsis. *Ann Surg* 1991; **214**: 141-148

20 **Fong Y,** Moldawer LL, Shires GT, Lowry SF. The biologic characteristics of cytokines and their implication in surgical patients. *Surg Gynecol Obstet* 1990; **170**: 363-378
21 **Cruickshank AM,** Fraser WD, Burns HJG, Van Dame J, Shenkin A. Response of serum interkeulin-6 in patients undergoing elective surgery in varing intensity. *Clin Sci* 1990; **79**: 161-165
22 **Marty C,** Misset B, Tamion F, Fitting C, Carlet J, Cavaillon JM. Circulating interleukin-8 concentrations in patients with multiple organ failure of septic and nonseptic origin. *Crit Care Med* 1994; **22**: 673-679
23 **Baigrie RJ,** Lamont PM, Kwiatkowski D, Dallman MJ, Morris PJ. Systemic cytokine response after major surgery. *Br J Surg* 1992; **79**: 757-760
24 **Biffl WL,** Moore EE, Moore FA, Peterson VM. Interleukin-6 in the injured patient: marker of injury or mediator of inflammation? *Ann Surg* 1996; **224**: 647-664
25 **Foex BA,** Shelly MP. The cytokine response to critical illness. *J Accid Emerg Med* 1996; **13**: 154-162

Science Editor Guo SY **Language Editor** Elsevier HK

PO Box 2345, Beijing 100023, China
www.wjgnet.com
wjg@wjgnet.com

ELSEVIER

World J Gastroenterol 2005;11(39):6202-6207
World Journal of Gastroenterology ISSN 1007-9327
© 2005 The WJG Press and Elsevier Inc. All rights reserved.

• *BRIEF REPORTS* •

Expression of serine protease SNC19/matriptase and its inhibitor hepatocyte growth factor activator inhibitor type 1 in normal and malignant tissues of gastrointestinal tract

Lei Zeng, Jiang Cao, Xing Zhang

Lei Zeng, First Affiliated Hospital, College of Medicine, Zhejiang University, Hangzhou 310003, Zhejiang Province, China
Jiang Cao, Xing Zhang, Clinical Research Institute, Sir Run Run Shaw Hospital, Zhejiang University, Hangzhou 310016, Zhejiang Province, China
Supported by the National Natural Science Foundation of China, No. 30271450; the Natural Science Foundation of Zhejiang Province, No. 300466
Correspondence to: Dr. Jiang Cao, Clinical Research Institute, Sir Run Run Shaw Hospital, Zhejiang University, 3 East Qingchun Road, Hangzhou 310016, Zhejiang Province, China. caoj@zju.edu.cn
Telephone: +86-571-86006336 Fax: +86-571-86960497
Received: 2005-03-01 Accepted: 2005-04-18

Abstract

AIM: To provide the expression profile of serine protease SNC19/matriptase and its inhibitor hepatocyte growth factor activator inhibitor type 1 (HAI-1) in normal and malignant tissues of gastrointestinal tract at mRNA level for further study on their correlations with tumor progression and metastasis.

METHODS: Total RNAs were prepared from 37 samples of colorectal cancer tissues, 40 samples of gastric cancer tissues, and their adjacent normal tissues. The expression of SNC19/matriptase and HAI-1 in these samples was detected by real-time fluorescent quantitative PCR using glyceraldehyde-3-phosphate dehydrogenase as internal standard, and the clinical significance for the correlation with clinicopathological parameters was evaluated.

RESULTS: In gastric cancer tissues the expression of HAI-1 and SNC19/matriptase was significantly lower than that in the corresponding adjacent normal tissues (Z = -3.280, P = 0.006; Z = -4.651, P = 0.000). HAI-1:SNC19/matriptase ratio showed no difference between normal and malignant tissues (P>0.05). Analysis of clinicopathological parameters showed decreased expression of HAI-1 and HAI-1:SNC19/matriptase ratio associated with stage III/IV gastric tumors as compared to stage I/II ones (Z = -2.140, P = 0.031; Z = -2.155, P = 0.031), and with lymph node-positive gastric cancer tissues as compared to lymph node-negative ones (Z = -2.081, P = 0.036; Z = -2.686, P = 0.006). The expression of SNC19/matriptase had no relationship with stages and lymph node metastasis (P>0.05). The expression of HAI-1 and HAI-1:SNC19/matriptase ratio increased in well-differentiated gastric cancer tissues, but there was no statistical significance (P>0.05). The difference of SNC19/matriptase expression was not significant in gastric cancer tissues of different histological differentiation status (P>0.05). In colorectal cancer tissues, the expression of HAI-1 and SNC19/matriptase was also markedly lower than that in their adjacent normal tissues (Z = -3.100, P = 0.002; Z = -2.731, P = 0.006), whereas HAI-1:SNC19/matriptase ratio showed no difference. Decreased expression of HAI-1 was associated with increased invasive depth and lymph node metastasis, but there was no statistical significance (P>0.05). The difference of SNC19/matriptase expression and HAI-1:SNC19/matriptase ratio was not significant in different stages and different lymph node metastasis status (P>0.05). The expression of SNC19/matriptase, HAI-1 or HAI-1:SNC19/matriptase ratio showed no difference in colorectal cancer tissues of different histological differentiation status (P>0.05).

CONCLUSION: The expressions of SNC19/matriptase and its inhibitor HAI-1 are decreased in gastrointestinal cancer tissues compared to their normal counterparts, and the decreased expression of HAI-1 may correlate with invasion and lymph node metastasis. The possible mechanisms involved need to be further investigated.

© 2005 The WJG Press and Elsevier Inc. All rights reserved.

Key words: Matriptase; Hepatocyte growth factor activator inhibitor type 1; Expression; Metastasis

Zeng L, Cao J, Zhang X. Expression of serine protease SNC19/matriptase and its inhibitor hepatocyte growth factor activator inhibitor type 1 in normal and malignant tissues of gastrointestinal tract. *World J Gastroenterol* 2005; 11(39): 6202-6207
http://www.wjgnet.com/1007-9327/11/6202.asp

INTRODUCTION

Hepatocyte growth factor (HGF), also known as scatter factor (SF)[1], is a pleiotropic factor which functions as a mitogen, a morphogen, and a motogen for a variety of cells bearing Met receptor tyrosine kinase, particularly for epithelial cells and vascular endothelial cells[2-4]. To date, a significant body of evidence is accumulating in favor of the notion that HGF/SF and Met play an important role in tumorigenesis, invasiveness, differentiation and angiogenesis of tumor cells[5,6]. HGF/SF is secreted by mesenchymal cells as an inactive precursor form, which lacks biological activity. The proteolytic activation of a single-chain precursor

form to a two-chain heterodimeric active form is a critical limiting step in the HGF/SF-induced Met signaling pathway[7]. Five proteases have been supposed to be responsible for the activation of HGF/SF: hepatocyte growth factor activator (HGFA), which exhibits the most potent activity, urokinase-type plasminogen activator (uPA), tissue-type plasminogen activator, blood coagulation factor XIIa[8,9], and SNC19/matriptase[10,11]. SNC19 initially identified from subtractive hybridization screening[12], has been confirmed to be indistinguishable from serine protease matriptase, which was first found in T47-D human breast cancer cells[13]. In addition to activation of HGF/SF, SNC19/matriptase can also degrade extracellular matrix (ECM), and activate another ECM-degrading protease uPA which is involved in tumor invasion[13-15]. SNC19/matriptase contributes to ECM degradation, cellular motility, epithelial migration and turnover, tissue remodeling, and it is supposed to be involved in tumor cell invasion and metastasis[14,16].

Hepatocyte growth factor activator inhibitor type 1 (HAI-1) is a Kunitz-type serine protease inhibitor which was initially purified from the conditioned medium of a human MKN45 stomach carcinoma cell line in 1997[17]. HAI-1 can specifically inhibit serine proteases HGFA and SNC19/matriptase, and they both are activators of HGF/SF[17-19]. Although it is supposed that HAI-1 and SNC19/matriptase may be involved in tumorigenesis, progression, and metastasis[16,20-22], more evidence is needed to draw a definite conclusion. This paper presents new evidence for the expression of HAI-1 and SNC19/matriptase in normal and malignant tissues of gastrointestinal tract at mRNA level, and their correlations with tumor progression and metastasis.

MATERIALS AND METHODS

Patients and tissues

A total of 40 samples from gastric cancer patients (median age, 58.95±12.43 years; range, 29-82 years; 28 men and 12 women) and 37 samples from colorectal cancer patients (median age, 61.64±13.54 years; range, 32-89 years; 13 men and 24 women), after surgical treatment in Second Affiliated Hospital, Zhejiang University College of Medicine, were studied retrospectively. The stage of gastric cancer was classified according to UICC guidelines (1985). Dukes' stage of colorectal cancer was classified according to the diagnosis and treatment criteria for common malignancy in China (1990). Tumor location, tumor histology, and histological grade were determined by pathological examination.

Specimens and RNA preparation

Cancer tissues and their adjacent normal tissues at least 15 cm away from cancer were collected immediately after excision, snap-frozen in liquid nitrogen, and stored at -80 ℃ for RNA extraction. Total RNAs were extracted from the tissue samples by TRIzol reagent (Gibco BRL Co., USA) according to the manufacturer's instructions in 0.1% RNase-free DEPC H_2O. RNA samples were quantified by ultraviolet spectrophotometry (Hewlett-Packard Co., USA).

Primers and probes

Primers and probes used for real-time fluorescent quantitative PCR were designed with the software PrimerExpress (Applied Biosystems Inc., USA). To avoid possible amplification of contaminating genomic DNA, primers were designed, so that each PCR product covered at least one intron. The sequences of primers and probes are listed in Table 1.

Table 1 Sequences of primers and probes

Target gene (amplicon size)		Sequence (5′–3′)
HAI-1	Upstream primer	TGA GGA AGA GCA GCA GTG CC
(151 bp)	Downstream primer	GGC TAC CAC CAC CAC AAT GC
	Probe	*FAM*-CCA GCA CAG GCT CTG TGG AGA TGG C -*TAMRA*
SNC19/ matriptase	Upstream primer	GGG ACA CAC CCA GTA TGG AGG
(168 bp)	Downstream primer	CCG GAA TCA CCC TGG CAG GA
	Probe	*FAM*-TCC TGC AAA AGG GTG AGA TCC GCG -*TAMRA*
GAPDH	Upstream primer	CTT AGC ACC CCT GGC CAA G
(151 bp)	Downstream primer	GAT GTT CTG GAG AGC CCC G
	Probe	*FAM*-CAT GCC ATC ACT GCC ACC CAG AAG A -*TAMRA*

PCR standards

Plasmids containing HAI-1, SNC19/matriptase or glyceraldehyde-3-phosphate dehydrogenase (GAPDH) cDNAs were constructed and maintained in our laboratory. Purified plasmid DNAs were quantified by absorbance at 260 nm and serially diluted as PCR standards.

Real-time RT-PCR

Two micrograms of total RNA was used in a 25 μL reverse transcription reaction system containing oligo $(dT)_{15}$ and M-MLV reverse transcriptase (Promega Co., USA). For real-time PCR, the cDNA samples were brought to a final concentration of 50 mmol/L KCl, 10 mmol/L Tris-HCl (pH 9.0), 1.5 mmol/L $MgCl_2$, 0.1% Triton-X 100, 200 μmol/L dNTPs, 0.2 μmol/L each primer, 0.1 μmol/L probe, and 5 U/μL Taq DNA polymerase (Promega Co., USA). The reactions were carried out under pre-optimized conditions. Samples were amplified with a hold at 95 ℃ for 5 min, followed by 40 cycles of denaturation at 95 ℃ for 20 s, annealing at 60 ℃ for 20 s and extension at 72 ℃ for 20 s in the ABI Prism 7700 sequence detector (Perkin Elmer Co., USA). Serially diluted standard specimens with the concentration of 10^6-10^{10} copies/mL were used to plot the standard curve. No template control and no reverse transcription control were included; 2% agarose gel electrophoresis was used in optimizing procedure.

Statistical analysis

All statistical analyses were done by the SPSS 11.0 software package. Non-parametric data were analyzed with Wilcoxon, Mann-Whitney, and Kruskal-Wallis rank sum tests to evaluate the association between SNC19/matriptase and HAI-1 mRNA expression and clinicopathological parameters. $M(Q_R)$ was computed as summary statistics.

RESULTS

Real-time RT-PCR of SNC19/matriptase and HAI-1

Real-time fluorescent quantitative RT-PCR was performed to determine the expression of SNC19/matriptase and HAI-1 at mRNA level using GAPDH as internal control. Figure 1 shows the detection and plotting of the GAPDH standard curve. The PCR products were subjected to 2% agarose gel electrophoresis in optimized procedure, as shown in Figure 2. The products were specific, with anticipated sizes confirmed by DNA sequencing.

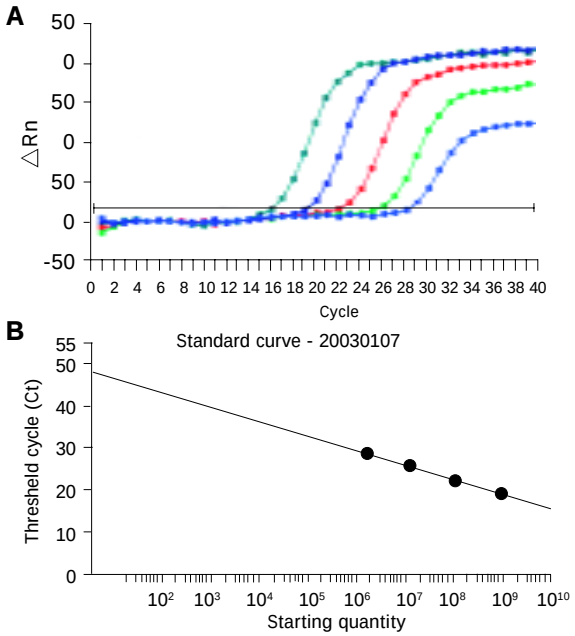


Figure 1 Representative real-time RT-PCR analysis for GAPDH mRNA copy levels. A: Amplification plots of pGEM-T Easy/GAPDH cDNA; B: standard curve plotted against pGEM-T Easy/GAPDH cDNA copy number.

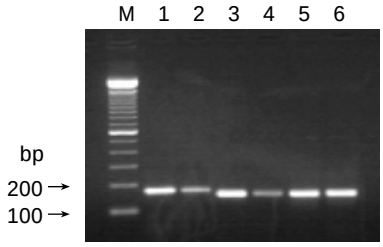


Figure 2 Expression of SNC19/matriptase and HAI-1 in gastric cancer tissue and its corresponding normal tissue (real-time RT-PCR products assay). M: Marker (100-bp DNA ladder); lanes 1 and 2: SNC19/matriptase (168 bp); lanes 3 and 4: HAI-1 (151 bp); lanes 5 and 6: GAPDH (151 bp); lanes 1, 3 and 5: gastric normal tissues; lanes 2, 4, and 6: gastric cancer tissues. Figures in brackets indicate the sizes of real-time RT-PCR products.

Expression of HAI-1 and SNC19/matriptase in normal and malignant tissues of gastrointestinal tract and correlation with clinicopathological parameters

The mRNA copy numbers of HAI-1, SNC19/matriptase and internal control GAPDH in each of normal and malignant tissues of gastrointestinal tract were detected by real-time fluorescent quantitative RT-PCR technique. The ratios of HAI-1:GAPDH and SNC19/matriptase: GAPDH were used as the relative expression level of HAI-1 and SNC19/matriptase, respectively. As shown in Table 2, the expression of HAI-1 and SNC19/matriptase in both gastric and colorectal cancer tissues was markedly lower than that in their adjacent normal tissues ($P<0.01$), while HAI-1:SNC19/matriptase ratio showed no significant difference between normal and malignant tissues of gastrointestinal tract ($P>0.05$).

The correlations between the expression of HAI-1 and SNC19/matriptase and clinicopathological parameters were evaluated (Tables 3 and 4). In gastric cancer tissues (Table 3), decreased expression of HAI-1 and HAI-1: SNC19/matriptase ratio were associated with stage III/IV cancer tissues compared to stage I/II ones ($Z = -2.140$, $P = 0.031$; $Z = -2.155$, $P = 0.031$). The expression of SNC19/matriptase had no relationship with clinical stages ($P>0.05$). The expression of HAI-1 and HAI-1:SNC19/matriptase ratio in lymph node-positive cancer tissues were lower than those in lymph node-negative ones ($Z = -2.081$, $P = 0.036$; $Z = -2.686$, $P = 0.006$). The expression of HAI-1 and HAI-1:SNC19/matriptase ratio increased in well-differentiated gastric cancer tissues, but there was no statistical significance ($P>0.05$). The differences of SNC19/matriptase were not significant in gastric cancer tissues with different histological differentiation status ($P>0.05$). In colorectal cancer tissues, the expression of HAI-1 was lower in Dukes' C/D cancer tissues than in Dukes' B ones. HAI-1 expression in lymph node-positive cancer tissues was lower than that in lymph node-negative ones. Decreased expression of HAI-1 was associated with increased invasive depth and lymph node metastasis, although there was no statistical significance ($P>0.05$). However, the differences of SNC19/matriptase expression and HAI-1:SNC19/matriptase ratio were not significant in different stages and different lymph node metastasis status ($P>0.05$). All the expression of HAI-1 and SNC19/matriptase and their ratio showed no statistical significance in different histological differentiation status ($P>0.05$). In gastrointestinal cancers, the expression of HAI-1 and SNC19/matriptase and HAI-1:SNC19/matriptase ratio showed no difference in patients of different ages, genders, location of tumors, and histological types ($P>0.05$).

Table 2 Expression of HAI-1 and SNC19/matriptase in normal and malignant tissues of gastrointestinal tract [$M(Q_R)$]

	Gastric tissues			Colorectal tissues		
	HAI-1	SNC19	HAI-1:SNC19	HAI-1	SNC19	HAI-1:SNC19
Normal tissues	0.012 (0.021)	0.010 (0.014)	1.420 (1.662)	0.014 (0.022)	0.010 (0.014)	0.971 (1.415)
Malignant tissues	0.005 (0.013)	0.004 (0.005)	1.365 (1.820)	0.009 (0.007)	0.005 (0.005)	1.520 (1.215)
Z	-3.280	-4.651	-0.121	-3.100	-2.731	-0.999
P	0.001	0.000	0.904	0.002	0.006	0.318

Table 3 Correlation between HAI-1 and SNC19/matriptase expression and clinicopathology in gastric cancer tissues [$M(Q_R)$]

	Patients	HAI-1	SNC19	HAI-1:SNC19
Age (yr)				
<40 yr	3	0.005 (0.011)	0.003 (0.002)	1.415 (1.416)
40–60 yr	17	0.005 (0.016)	0.005 (0.006)	1.680 (2.022)
>60 yr	20	0.005 (0.001)	0.003 (0.003)	0.882 (0.144)
Gender				
Men	28	0.005 (0.013)	0.004 (0.004)	1.220 (1.631)
Women	12	0.005 (0.020)	0.003 (0.005)	1.680 (1.571)
Location				
Cardia	7	0.005 (0.004)	0.003 (0.002)	1.430 (0.210)
Body	7	0.007 (0.023)	0.004 (0.005)	2.620 (2.846)
Pylorus	17	0.005 (0.015)	0.005 (0.005)	1.080 (1.631)
Unknown	9	0.005 (0.110)	0.003 (0.004)	1.220 (1.219)
Tumor histology				
Adenocarcinoma	18	0.005 (0.008)	0.004 (0.004)	1.365 (1.442)
Mucoid carcinoma	7	0.005 (0.021)	0.003 (0.008)	1.740 (1.626)
Poorly differentiated carcinoma	11	0.003 (0.016)	0.003 (0.004)	0.882 (2.377)
Unknown	4	0.005 (0.114)	0.005 (0.004)	1.555 (1.386)
N factor				
N0	12	0.017 (0.032)[a]	0.004 (0.005)	2.280 (3.148)[e]
N1/N2	28	0.004 (0.005)	0.004 (0.005)	1.080 (1.489)
UICC stage				
I/II	10	0.017 (0.020)[c]	0.004 (0.005)	2.280 (2.718)[g]
III/IV	30	0.004 (0.007)	0.003 (0.004)	1.245 (1.541)
Histological grade				
Well	3	0.011 (0.008)	0.003 (0.002)	2.870 (1.753)
Moderate	15	0.005 (0.004)	0.004 (0.004)	1.400 (1.121)
Poor	22	0.004 (0.017)	0.003 (0.007)	1.150 (0.470)

[a]P<0.05, [c]P <0.05 *vs* lymph node-positive group (N1/N2); [e]P <0.05, [g]P<0.05 *vs* stage III/IV group.

Table 4 Correlation between HAI-1 and SNC19/matriptase expression and clinicopathology in colorectal cancer tissues [$M(Q_R)$]

	Patients	HAI-1	SNC19	HAI-1:SNC19
Age (yr)				
<40 yr	3	0.004 (0.003)	0.005 (0.002)	0.778 (0.349)
40–60 yr	10	0.007 (0.102)	0.003 (0.003)	0.798 (1.096)
>60 yr	23	0.009 (0.104)	0.005 (0.005)	0.677 (0.459)
Unknown	1			
Gender				
Men	13	0.005 (0.109)	0.005 (0.006)	0.944 (0.728)
Women	24	0.009 (0.100)	0.005 (0.004)	0.667 (0.592)
Location				
Cecum/ascending colon	9	0.009 (0.101)	0.005 (0.006)	0.660 (0.482)
Transverse colon	2	0.003 (0.003)	0.002 (0.002)	0.862 (0.377)
Descending/ sigmoid colon	6	0.010 (0.004)	0.006 (0.002)	0.663 (0.715)
Rectum	19	0.005 (0.009)	0.004 (0.005)	0.778 (1.158)
Unknown	1			
Tumor histology				
Adenocarcinoma	32	0.005 (0.009)	0.004 (0.005)	0.734 (0.788)
Mucoid carcinoma	4	0.009 (0.012)	0.005 (0.004)	0.511 (0.194)
Poorly differentiated carcinoma	1			
N factor				
N0	18	0.010 (0.015)	0.005 (0.009)	1.470 (0.699)
N1/N2	19	0.007 (0.005)	0.005 (0.004)	1.480 (0.980)
Dukes' stage				
A	7	0.011 (0.015)	0.004 (0.008)	1.790 (3.860)
B	10	0.010 (0.016)	0.006 (0.015)	1.290 (1.243)
C/D	20	0.006 (0.006)	0.005 (0.005)	1.385 (0.955)
Histological grade				
Well	8	0.005 (0.010)	0.006 (0.024)	0.891 (1.482)
Moderately	24	0.009 (0.009)	0.004 (0.005)	1.485 (1.250)
Poorly	5	0.009 (0.012)	0.005 (0.005)	1.790 (1.000)

DISCUSSION

The inhibitors of serine proteases are important regulators of enzyme activities. They are classified into at least 10 families[23]. Among them, serpins (serine protease inhibitor) such as Kunitz-type inhibitors are correlated with suppression of tumor invasion[24].

Serine protease SNC19/matriptase is a newly characterized ECM-degrading protease, which may also function as an activator for HGF/SF and other proteases. HAI-1, the cognate Kunitz type inhibitor of SNC19/matriptase, was first found in the stomach carcinoma cell line. Although the expression of HAI-1 has been studied in some types of cancer, the expression profile in normal and malignant gastric tissues is still absent.

As was found in epithelial ovarian cancers that all HAI-1-positive tumors are also SNC19/matriptase positive[16], the imbalance between the protease and the inhibitor may play an important role in the development of tumors. In this study, HAI-1 and SNC19/matriptase showed a remarkable decrease in cancer tissues compared to their adjacent normal tissues in gastrointestinal tract, but the ratio of HAI-1: SNC19/matriptase showed no significant difference between normal and malignant gastrointestinal tissues. Whether the ratio is critical to tumor development or progression needs to be further investigated. Since a novel function of the integral membrane Kunitz-type inhibitor in the regulation of pericellular protease activity has been suggested, HAI-1 may act not only as an inhibitor but also as a reservoir of this enzyme on cell surface[25,26]. With this possibility and other lines of evidence, the situation in cancer may be more complicated. HAI-1 has a strong affinity for both HGFA and SNC19/matriptase to form a protease/inhibitor complex and its specific Kunitz domains are responsible for the inhibitory activity[27]. It was reported that HAI-1 may participate in the activation of SNC19/matriptase through their low-density lipoprotein receptor class A domains interacting with each other, and HAI-1-mediated activation and inhibition of SNC19/ matriptase occur in human mammary epithelial cells[28]. At the same time, HAI-1 not only inhibits the activity of SNC19/matriptase but also prevents it from being hydrolyzed by other proteases[29]. It was reported that decreased immunoreactivity of membrane-form HAI-1 and enhanced ectodomain shedding of HAI-1 are found in colorectal adenocarcinoma cells[30]. There might be a more complicated interaction between HAI-1 and SNC19/matriptase rather than simple activity inhibition. In breast cancer cells, SNC19/matriptase is detected mainly as an uncomplexed form, whereas in human milk a complex containing matriptase and HAI-1 is detectable[18]. The active form of SNC19/matriptase may release from HAI-1 fragment into extracellular milieu, thus playing a role in tumor cells as ectodomain shedding of HAI-1 enhances, which may provide SNC19/matriptase opportunities to actively down-stream biological factors.

HAI-1 expression and HAI-1: SNC19/matriptase ratio decrease in gastric cancer tissues where invasion and lymph node metastasis occur. HAI-1 may play a role in progression and metastasis of gastric cancer by inhibiting HGF. SNC19/ matriptase showed no significant difference in invasive tumors in this study. Lower ratio of HAI-1:SNC19/

matriptase in stage III/IV cancers compared to stage I/II ones may be due to the down-regulated expression of HAI-1. The expression of HAI-1 tends to increase in well-differentiated gastric cancer tissues. It was reported that the expression of HAI-1 increases as the histological grade decreases in hepatocellular carcinoma [31], and decreases in poorly differentiated breast tumors [32]. HAI-1 displays different patterns of expression in different tissues[33].

In colorectal cancer tissues, HAI-1 expression is inverse correlated tumor invasion and lymph node metastasis. In our study, the expression of HAI-1, SNC19/matriptase and their ratio did not show differences in colorectal cancer tissues with different differentiation status, but the expression of HAI-1 seemed to be related to histological grades. Further analysis regarding the patients' age, gender, location, and histological type of tumor showed no correlation with HAI-1 expression.

In conclusion, both SNC19/matriptase and HAI-1 are downregulated in gastrointestinal cancer tissues, and the underlying mechanisms need to be extensively investigated. A larger scale study both in case number and disease spectrum needs to be carried out to elucidate the exact role of SNC19/matriptase and HAI-1 in tumor development and progression.

REFERENCES

1 **Weidner KM,** Arakaki N, Hartmann G, Vandekerckhove J, Weingart S, Rieder H, Fonatsch C, Tsubouchi H, Hishida T, Daikuhara Y. Evidence for the identity of human scatter factor and human hepatocyte growth factor. *Proc Natl Acad Sci USA* 1991; **88**: 7001-7005

2 **Naldini L,** Weidner KM, Vigna E, Gaudino G, Bardelli A, Ponzetto C, Narsimhan RP, Hartmann G, Zarnegar R, Michalopoulos GK. Scatter factor and hepatocyte growth factor are indistinguishable ligands for the MET receptor. *Embo J* 1991; **10**: 2867-2878

3 **Boros P,** Miller CM. Hepatocyte growth factor: a multifunctional cytokine. *Lancet* 1995; **345**: 293-295

4 **Matsumoto K,** Nakamura T. Emerging multipotent aspects of hepatocyte growth factor. *J Biochem* 1996; **119**: 591-600

5 **Bellusci S,** Moens G, Gaudino G, Comoglio P, Nakamura T, Thiery JP, Jouanneau J. Creation of an hepatocyte growth factor/scatter factor autocrine loop in carcinoma cells induces invasive properties associated with increased tumorigenicity. *Oncogene* 1994; **9**: 1091-1099

6 **Nakamura T,** Matsumoto K, Kiritoshi A, Tano Y. Induction of hepatocyte growth factor in fibroblasts by tumor-derived factors affects invasive growth of tumor cells: *in vitro* analysis of tumor-stromal interactions. *Cancer Res* 1997; **57**: 3305-3313

7 **Gak E,** Taylor WG, Chan AM, Rubin JS. Processing of hepatocyte growth factor to the heterodimeric form is required for biological activity. *FEBS Lett* 1992; **311**: 17-21

8 **Shimomura T,** Miyazawa K, Komiyama Y, Hiraoka H, Naka D, Morimoto Y, Kitamura N. Activation of hepatocyte growth factor by two homologous proteases, blood-coagulation factor XIIa and hepatocyte growth factor activator. *Eur J Biochem* 1995; **229**: 257-261

9 **Mars WM,** Zarnegar R, Michalopoulos GK. Activation of hepatocyte growth factor by the plasminogen activators uPA and tPA. *Am J Pathol* 1993; **143**: 949-958

10 **Cao J,** Zheng S, Zheng L, Cai X, Zhang Y, Geng L, Fang Y. A novel serine protease SNC19 associated with human colorectal cancer. *Chin Med J* 2001; **114**: 726-730

11 **Lee SL,** Dickson RB, Lin CY. Activation of hepatocyte growth factor and urokinase/plasminogen activator by matriptase, an epithelial membrane serine protease. *J Biol Chem* 2000; **275**: 36720-36725

12 **Cao J,** Cai X, Zheng L, Geng L, Shi Z, Pao CC, Zheng S. Characterization of colorectal-cancer-related cDNA clones obtained by subtractive hybridization screening. *J Cancer Res Clin Oncol* 1997; **123**: 447-451

13 **Lin CY,** Anders J, Johnson M, Sang QA, Dickson RB. Molecular cloning of cDNA for matriptase, a matrix-degrading serine protease with trypsin-like activity. *J Biol Chem* 1999; **274**: 18231-18236

14 **Satomi S,** Yamasaki Y, Tsuzuki S, Hitomi Y, Iwanaga T, Fushiki T. A role for membrane-type serine protease (MT-SP1) in intestinal epithelial turnover. *Biochem Biophys Res Commun* 2001; **287**: 995-1002

15 **Mignatti P,** Rifkin DB. Biology and biochemistry of proteinases in tumor invasion. *Physiol Rev* 1993; **73**: 161-195

16 **Oberst MD,** Johnson MD, Dickson RB, Lin CY, Singh B, Stewart M, Williams A, al-Nafussi A, Smyth JF, Gabra H, Sellar GC. Expression of the serine protease matriptase and its inhibitor HAI-1 in epithelial ovarian cancer: correlation with clinical outcome and tumor clinicopathological parameters. *Clin Cancer Res* 2002; **8**: 1101-1107

17 **Shimomura T,** Denda K, Kitamura A, Kawaguchi T, Kito M, Kondo J, Kagaya S, Qin L, Takata H, Miyazawa K, Kitamura N. Hepatocyte growth factor activator inhibitor, a novel Kunitz-type serine protease inhibitor. *J Biol Chem* 1997; **272**: 6370-6376

18 **Lin CY,** Anders J, Johnson M, Dickson RB. Purification and characterization of a complex containing matriptase and a Kunitz-type serine protease inhibitor from human milk. *J Biol Chem* 1999; **274**: 18237-18242

19 **Kataoka H,** Miyata S, Uchinokura S, Itoh H. Roles of hepatocyte growth factor (HGF) activator and HGF activator inhibitor in the pericellular activation of HGF/scatter factor. *Cancer Metastasis Rev* 2003; **22**: 223-236

20 **Oberst M,** Anders J, Xie B, Singh B, Ossandon M, Johnson M, Dickson RB, Lin CY. Matriptase and HAI-1 are expressed by normal and malignant epithelial cells *in vitro* and *in vivo*. *Am J Pathol* 2001; **158**: 1301-1311

21 **Johnson MD,** Oberst MD, Lin CY, Dickson RB. Possible role of matriptase in the diagnosis of ovarian cancer. *Expert Rev Mol Diagn* 2003; **3**: 331-338

22 **Kang JY,** Dolled-Filhart M, Ocal IT, Singh B, Lin CY, Dickson RB, Rimm DL, Camp RL. Tissue microarray analysis of hepatocyte growth factor/Met pathway components reveals a role for Met, matriptase, and hepatocyte growth factor activator inhibitor 1 in the progression of node-negative breast cancer. *Cancer Res* 2003; **63**: 1101-1105

23 **Laskowski M Jr,** Kato I. Protein inhibitors of proteinases. *Annu Rev Biochem* 1980; **49**: 593-626

24 **Kobayashi H,** Shinohara H, Takeuchi K, Itoh M, Fujie M, Saitoh M, Terao T. Inhibition of the soluble and the tumor cell receptor-bound plasmin by urinary trypsin inhibitor and subsequent effects on tumor cell invasion and metastasis. *Cancer Res* 1994; **54**: 844-849

25 **Kataoka H,** Shimomura T, Kawaguchi T, Hamasuna R, Itoh H, Kitamura N, Miyazawa K, Koono M. Hepatocyte growth factor activator inhibitor type 1 is a specific cell surface binding protein of hepatocyte growth factor activator (HGFA) and regulates HGFA activity in the pericellular microenvironment. *J Biol Chem* 2000; **275**: 40453-40462

26 **Kataoka H,** Itoh H, Hamasuna R, Meng JY, Koono M. Pericellular activation of hepatocyte growth factor/scatter factor (HGF/SF) in colorectal carcinomas: roles of HGF activator (HGFA) and HGFA inhibitor type 1 (HAI-1). *Hum Cell* 2001; **14**: 83-93

27 **Denda K,** Shimomura T, Kawaguchi T, Miyazawa K, Kitamura N. Functional characterization of Kunitz domains in hepatocyte growth factor activator inhibitor type 1. *J Biol Chem* 2002; **277**: 14053-14059

28 **Lee MS,** Kiyomiya KI, Benaud C, Dickson RB, Lin CY. Simultaneous activation and HAI-1-mediated inhibition of matriptase induced at activation foci in human mammary epithelial cells. *Am J Physiol Cell Physiol* 2004; **288**: C932-C941
29 **Oberst MD,** Williams CA, Dickson RB, Johnson MD, Lin CY. The activation of matriptase requires its noncatalytic domains, serine protease domain, and its cognate inhibitor. *J Biol Chem* 2003; **278**: 26773-26779
30 **Nagaike K,** Kohama K, Uchiyama S, Tanaka H, Chijiiwa K, Itoh H, Kataoka H. Paradoxically enhanced immunoreactivity of hepatocyte growth factor activator inhibitor type 1 (HAI-1) in cancer cells at the invasion front. *Cancer Sci* 2004; **95**: 728-735
31 **Nagata K,** Hirono S, Ido A, Kataoka H, Moriuchi A, Shimomura T, Hori T, Hayashi K, Koono M, Kitamura N, Tsubouchi H. Expression of hepatocyte growth factor activator and hepatocyte growth factor activator inhibitor type 1 in human hepatocellular carcinoma. *Biochem Biophys Res Commun* 2001; **289**: 205-211
32 **Parr C,** Watkins G, Mansel RE, Jiang WG. The hepatocyte growth factor regulatory factors in human breast cancer. *Clin Cancer Res* 2004; **10**: 202-211
33 **Parr C,** Jiang WG. Expression of hepatocyte growth factor/scatter factor, its activator, inhibitors and the c-Met receptor in human cancer cells. *Int J Oncol* 2001; **19**: 857-863

Science Editor Wang XL and Guo SY **Language Editor** Elsevier HK

PO Box 2345, Beijing 100023, China
www.wjgnet.com
wjg@wjgnet.com

ELSEVIER

World J Gastroenterol 2005;11(39):6208-6211
World Journal of Gastroenterology ISSN 1007-9327
© 2005 The WJG Press and Elsevier Inc. All rights reserved.

• *BRIEF REPORTS* •

Microcirculation disturbance affects rats with acute severe pancreatitis following lung injury

Xue-Min Liu, Qing-Guang Liu, Jun Xu, Cheng-En Pan

Xue-Min Liu, Qing-Guang Liu, Jun Xu, Cheng-En Pan, Department of Hepatobiliary Surgery, Xi'an Jiaotong University First Hospital, Xi'an 710061, Shaanxi Province, China
Supported by the National Natural Science Foundation of China, No. 30371398
Correspondence to: Dr. Xue-Min Liu, Department of Hepatobiliary Surgery, Xi'an Jiaotong University First Hospital, Xi'an 710061, Shaanxi Province, China. a1090224@pub.xaonline.com
Telephone: +86-29-85324009
Received: 2004-02-28 Accepted: 2004-04-05

Abstract

AIM: To study the effects of microcirculation disturbance (MD) on rats with acute severe pancreatitis (ASP).

METHODS: We developed ASP rat models, and anatomized separately after 1, 3, 5, 7, and 9 h. We took out blood and did hemorrheologic examination and erythrocyte osmotic fragility test, checked up the water content, capillary permeability, and genetic expression of intercellular adhesion molecule-1 (ICAM-1) in lung tissues, examined the apoptosis degree of blood vessel endothelium while we tested related gene expression of Bax and Bcl-2 in lung tissues. We did the same examination in control group.

RESULTS: The viscosity of total blood and plasma, the hematocrit, and the erythrocyte osmotic fragility were all increased. Fibrinogen was decreased. The water content in lung tissues and capillary permeability were increased. Apoptosis degree of blood vessel endothelium was increased too. ICAM-1 genetic expression moved up after 1 h and reached its peak value after 9 h.

CONCLUSION: MD plays an important role in ASP following acute lung injury (ALI). The functional damage of blood vessel endothelium, the apoptosis of capillary vessel endothelium, WBC edging-concentration and the increasing of erythrocyte fragility are the main reasons of ALI.

© 2005 The WJG Press and Elsevier Inc. All rights reserved.

Key words: Microcirculation; Acute pancreatitis; Lung injury

Liu XM, Liu QG, Xu J, Pan CE. Microcirculation disturbance affects rats with acute severe pancreatitis following lung injury. *World J Gastroenterol* 2005; 11(39): 6208-6211
http://www.wjgnet.com/1007-9327/11/6208.asp

INTRODUCTION

Microcirculation change has a great effect on causing diseases and acute severe pancreatitis (ASP) process. The lung can be damaged easily[1]. About 70% of deaths are due to acute respiratory distress syndrome[2,3]. In this study, we observed the microcirculation in rats and the changes in lung. The relationship between acute lung injury (ALI) and microcirculation change in rats with ASP was studied.

MATERIALS AND METHODS

Experimental animals and grouping

Rats were provided by the Experimental Animal Center of Medical School of Xi'an Jiaotong University. Experiment group (40 rats) was injected with 4% sodium taurocholate 1 mL/kg by puncturing pancreatic duct to make ASP models. Control group (eight rats) was only turned over duodenum. Experiment group was divided into five subgroups, eight rats in each group. They were anatomized after 1, 3, 5, 7, and 9 h, respectively.

Hemorrheologic examination and erythrocyte osmotic fragility test

Blood sedimentation (BS) was done with 0.2 mL venous blood. After centrifugation, hematocrit was read. The content of fibrinogens (CB) was recorded after water bath and centrifugation. The viscosity of total blood (VTB) and plasma (VP) was checked up in another 1-2 mL venous blood. The resistance of RBC to different concentrations of hypo-osmotic saline was examined. The permeability fragility of RBC was detected.

TUNEL examination

Lung tissues were fixed and sliced. Apoptosis staining experiment was done. We observed the change of lung capillary vessel endothelium apoptosis under a light microscope. The cells with brown-blue nuclei were considered as apoptosis cells.

Lung Bcl-2 and Bax protein examination with immunohistochemical method

The cells stained brown or brown-yellow were positively stained cells. To account the positive staining, we counted four high-power fields according to the formula: positive rate = the number of positive cells/total number of cells×100%. It was determined as negative staining (-) when the positive rate was <15%, and as positive staining when the positive rate was 15-50% (+), 50-75% (++), and >75% (+++), respectively.

Lung capillary permeability

The change of lung capillary permeability was detected by injecting Evan's blue into veins. Using a 625-nm spectrophotometer, the concentration of Evan's blue represented the milligrams of the dyes per gram of wet weight lung.

Water content in lung tissue

First, we weighed the wet weight of lung tissues, and after being parched for 72 h at 70 ℃, we weighed the dry weight. The water content (%) = (wet weight-dry weight)/wet weight.

RT-PCR examination of ICAM-1

We took β-actin as an inner contrast gene. Lung RNA was isolated by TRIzol. Oligo(dT)$_{15}$ was used as a primer. The reaction conditions were at 42 ℃ for 15 min, at 99 ℃ for 5 min, at 4 ℃ for 4 min, and then we got the first chain of cDNA. PCR was done for 1 min at 94 ℃, for 1 min at 55 ℃, for 2 min at 72 ℃, 35 circles in all. Finally, it was expanded for 10 min at 72 ℃. After electrophoresis, we confirmed the quantity with a white/ultraviolet transilluminator. The expanding quantity of targeted genes/the expanding quantity of inner contrast genes expressed the quantity of detected genes.

Statistical analysis

The data were expressed as mean±SD. Kruskal-Wallis method and Mann-Whitney method were adopted to compare the two indexes.

RESULTS

Pathological observation of lung tissues

We observed the pathological change of lung tissues and found that interstitial pulmonary edema, focal and congestive pulmonary atelectasis were present at the forepart of ASP. PMNs were present in capillaries, and thrombosis was visible in capillaries (Figure 1). The changes aggravated gradually.

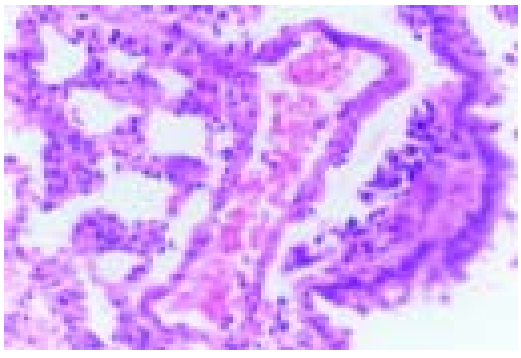


Figure 1 Interstitial pulmonary edema, infiltration of PMNs, and thrombosis in capillaries in lung, HE staining, ×20.

Apoptosis of capillary endothelium in lung

Apoptosis endothelium could be examined in lungs of control group. After the models were made, the number of apoptosis endothelial cells was increased. When we compared the number of apoptosis cells at 3 h with that at 9 h, we found that the number of apoptosis endothelial cells at 9 h was greater than that at 3 h. This trend was related to the grade of ALI.

Lung Bcl-2 and Bax protein expression

Bcl-2 and Bax protein were less expressed in normal lung tissues. After ASP models were made, we found that Bcl-2 and Bax protein expression was obvious. Bax protein expression accorded with the changes of cell apoptosis, and reached its peak in 7-9 h. Bcl-2 expression was inversely correlated with the changes of cell apoptosis, and declined gradually after 3 h (Table 1).

Table 1 Positive staining rate of Bcl-2 and Bax in each period of time (%, mean±SD, n = 8)

	1 h	3 h	5 h	7 h	9 h
Bcl-2[a]	37.3±4.3	84.6±4.3	67.4±2.1	70.3±4.2	52.3±5.3
Bax[a]	42.3±4.4	62.6±4.8	68.2±3.3	77.6±4.2	79.3±5.7

[a]P<0.05 *vs* each period of time.

ICMA-1 and RT-PCR examination

The genetic expression of intercellular adhesion molecule-1 (ICAM-1) in lung tissues was increased after 1 h and reached its peak after 9 h. The gene expressions of ICAM-1 were significantly different in each period of time (P<0.05, Figure 2).

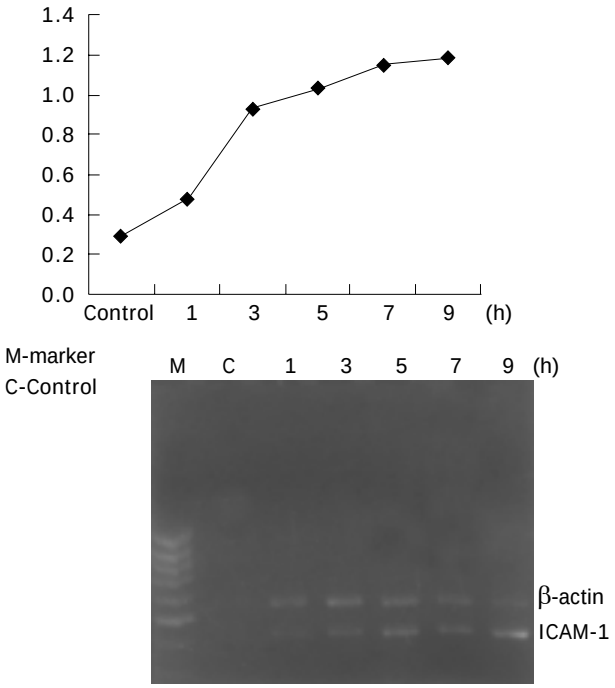


Figure 2 ICAM-1 genetic expression in different periods of time. The genetic expression of ICAM-1 in lung tissues was increased after 1 h and reached its peak after 9 h (n = 8).

Water content and capillary permeability in lung

Compared with control group, the water content and capillary permeability in lung tissues in ASP group were both increased

Table 2 Water content and capillary permeability in lung tissues in each period of time (mg/g, mean±SD, n = 8)

	Control	1 h	3 h	5 h	7 h	9 h
Water content[b]	0.69±0.03	0.72±0.02	0.74±0.02	0.75±0.02	0.76±0.02	0.77±0.03
Capillary permeability[b]	0.048±0.005	0.068±0.005	0.086±0.010	0.106±0.009	0.113±0.012	0.112±0.004

[b]P<0.01 *vs* control group.

Table 3 Hemorrheology in ASP in each period of time (mean±SD, n = 8)

	Control	1 h	3 h	5 h	7 h	9 h
High VTB (mPa·s)[b]	5.65±1.04	7.66±0.90	7.81±0.41	7.79±0.32	8.32±0.46	9.49±1.34
Low VTB (mPa·s)[b]	14.57±4.00	22.72±2.26	23.77±3.13	22.80±1.61	29.46±4.81	30.91±7.28
VP (mPa·s)[b]	3.57±0.49	5.10±0.87	4.56±1.08	5.76±0.88	6.25±1.00	8.00±1.34
BS (mm/h)[b]	9.33±0.82	0.90±0.11	0.59±0.31	0.33±0.15	0.12±0.11	0.03±0.03
Hematocrit (%)[b]	44.92±2.73	56.00±2.59	57.17±2.88	57.67±1.86	59.17±2.96	62.17±3.39
CB (g/L)[b]	452.3±29.9	145.0±45.4	142.0±14.6	88.3±20.8	67.4±17.7	51.3±19.1
Original hemolysis[b]	0.45±0.02	0.47±0.02	0.47±0.02	0.47±0.02	0.47±0.02	0.49±0.02
Complete hemolysis[b]	0.36±0.00	0.38±0.02	0.39±0.02	0.40±0.03	0.41±0.02	0.43±0.02

[b]P<0.01 *vs* control group.

obviously in each period of time (Table 2).

Hemorrheologic examination

Compared with control group, each items of hemorrheology were diverse in each period of time (Table 3).

DISCUSSION

The main characteristic of acute pancreatitis is the change in blood circulation of pancreas and the whole body[4-6]. Blood volume declined obviously in early period of ASP. Hemoperfusion could exacerbate ASP. In this experiment, sodium taurocholate was injected through the pancreatic duct to make ASP models. We observed various indexes of ASP at different time points. Significant hemorrheology changes could be observed in rats with ASP. The blood viscosity and the erythrocyte osmotic fragility were increased. The capillary permeability in lung tissues was also increased. Interstitial pulmonary and microthrombosis were found. Obvious microcirculation disturbance (MD) could be observed in lung tissues and the whole body of rats with ASP. After the models were made, the number of apoptosis endothelial cells and the genetic expression of ICAM-1 in lung tissues were significantly increased, suggesting that ASP can cause MD in many ways and plays an important role in causing and exacerbating ALI.

WBCs adhered to the blood vessel endothelium could cause inflammation[7-9]. Adhesion molecule could play an important role in adhesion process, and its expression could reflect the change of blood vessel endothelium[10-17]. After ASP models were made, ICAM-1 gene expression was increased and became easier for WBCs to adhere to blood vessel endothelium. Therefore, it made WBCs to invade the lung tissues more easily.

For vein wall permeability, blood vessel endothelium is the main barrier. In this study, the number of apoptosis cells increased and apoptosis was accorded with the increasing of lung tissues, vessel permeability and water content. We think that the increasing of apoptosis cells in lung tissues could alter the structure integrality of capillary endothelium. Because the endothelial cells could not renew rapidly by themselves, apoptosis could lead to decrease of blood vessel endothelial cell storage. This kind of change results in the increase of blood vessel endothelium gap and its permeability[18,19].

Our study found that hemorrheology changed obviously in blood of ASP rats, thus leading to more serious MD of pancreas and other organs. This is the main reason for pancreas necrosis and ARDS representation[20,21]. The primary presentations are the decline of RBC aggregation capacity, increase of VTB and VP as well as WBC edging-concentration. The later is the primal step of WBCs swimming outside of blood vessel, leading to grievous inflammation and ALI[22]. WBC edging-concentration in rats with ASP was affected not only by inflammation medium and chemotatic factor but also by other factors, such as tiny vein, blood viscosity, and RBC aggregation[23].

The erythrocyte fragility was increased after ASP presentation, and became more serious following the progress of the disease. The increase of erythrocyte fragility could reflect the defective capacity of RBC distortion. RBCs break up easily, and release adenosine diphosphate, thus causing the activation of coagulation system and disseminated intravascular coagulation, leading to the decrease of fibrinogen.

In conclusion, MD plays an important role in the process of ASP with lung injury. Ameliorating MD could not only reduce local damages in pancreas, but also protect the lung and other organs in the body. Therefore, ameliorating MD is an effective therapy in treating ASP.

REFERENCES

1 **Zhu AJ**, Shi JS, Sun XJ. Organ failure associated with severe acute pancreatitis. *World J Gastroenterol* 2003; **9**: 2570-2573
2 **Liu XM**, Pan CE, Liu QG, Wang ZF. The diagnosis and treatment of lung injury following severe acute pancreatitis. *Zhonghua Gandan Waike Zazhi* 2002; **8**: 116-117
3 **Zhao M**, Chen RF. The pathogenesis of lung injury following acute necrotizing pancreatitis. *Shijie Huaren Xiaohua Zazhi* 2001; **9**: 954-957

4 **Foitzik T**, Eibl G, Hotz B, Hotz H, Kahrau S, Kasten C, Schneider P, Buhr HJ. Persistent multiple organ microcirculatory disorders in severe acute pancreatitis: experimental findings and clinical implications. *Dig Dis Sci* 2002; **47**: 130-138
5 **Zhou ZG**, Zhang ZD, Yan LN, Shu Y, Cheng Z, Zhao JC, Lan P, Feng XM, Wang R. The feature of pancreatic microcirculatory impairment in caerulein induced acute pancreatitis. *Zhonghua Waike Zazhi* 1999; **37**: 138-140
6 **Xia SH**, Zhao XY, Guo P, Da SP. Hemocirculatory disorder in dogs with severe acute pancreatitis and intervention of platelet activating factor antagonist. *Shijie Huaren Xiaohua Zazhi* 2001; **9**: 550-554
7 **Chen H**, Li F, Cheng YF, Sun JB. Pathogenic role of neutrophils in evolution of acute pancreatitis in rats. *Shijie Huaren Xiaohua Zazhi* 2001; **9**: 776-779
8 **Gukovskaya AS**, Vaquero E, Zaninovic V, Gorelick FS, Lusis AJ, Brennan ML, Holland S, Pandol SJ. Neutrophils and NADPH oxidase mediate intrapancreatic trypsin activation in murine experimental acute pancreatitis. *Gastroenterology* 2002; **122**: 974-984
9 **Kyriakides C**, Jasleen J, Wang Y, Moore FD Jr, Ashley SW, Hechtman HB. Neutrophils, not complement, mediate the mortality of experimental hemorrhagic pancreatitis. *Pancreas* 2001; **22**: 40-46
10 **Sun W**, Zhang JD, Zhao Y, Zhao Y, Wang Q. Expression of IL-6 and integrin family cell adhesion molecules in acute necrotizing pancreatitis complicated with multiple organ injury in rats. *Shijie Huaren Xiaohua Zazhi* 2003; **11**: 753-755
11 **Shi L**, Tian FZ, Huang DR, Li X, Zhao B, Gu DY, Tang XD, Wang Y. Effect of hepatic NF-κB on ICAM-1 expression in rats with acute pancreatitis. *Shijie Huaren Xiaohua Zazhi* 2003; **11**: 1505-1507
12 **Yi Y**, Gao NR. The celluliar adhering elements and acute pancreatitis. *Shijie Huaren Xiaohua Zazhi* 2001; **9**: 70-71
13 **Lundberg AH**, Fukatsu K, Gaber L, Callicutt S, Kotb M, Wilcox H, Kudsk K, Gaber AO. Blocking pulmonary ICAM-1 expression ameliorates lung injury in established diet-induced pancreatitis. *Ann Surg* 2001; **233**: 213-220
14 **Nakae H**, Endo S, Sato N, Wakabayashi G, Inada K, Sato S. Involvement of soluble adhesion molecules in acute pancreatitis. *Eur Surg Res* 2001; **33**: 377-382
15 **Powell JJ**, Siriwardena AK, Fearon KC, Ross JA. Endothelial-derived selectins in the development of organ dysfunction in acute pancreatitis. *Crit Care Med* 2001; **29**: 567-572
16 **Telek G**, Ducroc R, Scoazec JY, Pasquier C, Feldmann G, Roze C. Differential upregulation of cellular adhesion molecules at the sites of oxidative stress in experimental acute pancreatitis. *J Surg Res* 2001; **96**: 56-67
17 **Frossard JL**, Saluja A, Bhagat L, Lee HS, Bhatia M, Hofbauer B, Steer ML. The role of intercellular adhesion molecule 1 and neutrophils in acute pancreatitis and pancreatitis-associated lung injury. *Gastroenterology* 1999; **116**: 694-701
18 **Liu XM**, Liu QG, Pan CE, Xu GF, Zhang T, Huang JY, Zhang M. Influence of apoptosis of endothelial cell on lung injury following severe acute pancreatitis in rats. *Disi Junyi Daxue Xuebao* 2003; **24**: 1677-1679
19 **Wu RQ**, Song XH, Xu YX, Meng XJ. Apoptosis of endothelial cells in alteration of microvascular permeability in lung during sepsis. *Zhonghua Waike Zazhi* 2000; **38**: 385-387
20 **Wang ZF**, Pan CE, Liu SG, Liang GG, Zhang M. The significance of hemorrheologic alternation in acute necrotizing pancreatitis. *Zhongguo Putong Waike Zazhi* 2000; **9**: 225-227
21 **Wang ZF**, Pan CE, Liang GG, Liu SG, Zhang M. The treatment of acute necrotizing pancreatitis by modifying hemorrheologic alternation. *Zhonghua Gandan Waike Zazhi* 2000; **6**: 89
22 **Zhou YK**, Wu Y. The correlation between blood rheology and multiple organic injury in acute pancreatitis. *Shijie Huaren Xiaohua Zazhi* 2000; **8**: 1055-1057
23 **Liang GG**. The study of the relationship between apparent vislosity and the aggregation of erythrocytes when the blood performs a tubular steady laminal flow with small pressure difference. *Xi'an Yike Daxue Xuebao* 2000; **21**: 259-262

Science Editor Wang XL and Li WZ **Language Editor** Elsevier HK

PO Box 2345, Beijing 100023, China
www.wjgnet.com
wjg@wjgnet.com

ELSEVIER

World J Gastroenterol 2005;11(39):6212-6215
World Journal of Gastroenterology ISSN 1007-9327
© 2005 The WJG Press and Elsevier Inc. All rights reserved.

• *BRIEF REPORTS* •

Effects of hepatitis B virus on p53 expression in hepatoma cell line SMMU-7721

Jian-Hui Qu, Ming-Hua Zhu, Jing Lin, Can-Rong Ni, Fang-Mei Li, Zhi Zhu, Guan-Zhen Yu

Jian-Hui Qu, Ming-Hua Zhu, Jing Lin, Can-Rong Ni, Fang-Mei Li, Zhi Zhu, Guan-Zhen Yu, Department of Pathology, the Second Military Medical University, Shanghai 200433, China
Supported by the National Natural Science Foundation of China, No. 30070344
Co-first-authors: Jian-Hui Qu and Ming-Hua Zhu
Correspondence to: Ming-Hua Zhu, Department of Pathology, the Second Military Medical University, Shanghai 200433, China. mhzhu2000@hotmail.com
Telephone: +86-21-25074604
Received: 2004-10-18 Accepted: 2005-03-28

Abstract

AIM: To investigate the contribution of HBV in the development of hepatocarcinoma by examining the effects of HBV on p53 function in SMMU-7721 cell line.

METHODS: Plasmid pCMVp53 was transfected or cotransfected with pCMVHBVa (wild-type HBV) or PCMVHBVb (mutation type HBV) into the hepatoma cell line SMMU-7721 by lipofectamine. Apoptosis cells were labeled with annexin V-FITC and confirmed by flow cytometry. Reporter plasmid PG13-CAT or p21-luc was cotransfected, respectively, into each group to determine the transactivation activity of p53 and its effect on p21 promoter. Western blot was performed to observe p53 expression in hepatoma cell line of each group.

RESULTS: The group transfected with pCMVp53 alone exhibited higher luciferase activity and higher apoptosis rate, otherwise, the p53 expression and reporter activity of PG13-CAT or P21-luc as well as cell apoptosis rate were obviously higher in the group cotransfected of pCMVp53 with pCMVHBVa, but not in the other cotransfected group.

CONCLUSION: Transient transfection of HBV into the SMMU-7721 cell line can enhance p53 expression and its effects on development of hepatocarcinoma.

© 2005 The WJG Press and Elsevier Inc. All rights reserved.

Key words: Hepatitis B virus; p53; p21; Hepatoma

Qu JH, Zhu MH, Lin J, Ni CR, Li FM, Zhu Z, Yu GZ. Effects of hepatitis B virus on p53 expression in hepatoma cell line SMMU-7721. *World J Gastroenterol* 2005; 11(39): 6212-6215
http://www.wjgnet.com/1007-9327/11/6212.asp

INTRODUCTION

HBV is a major etiological factor associated with hepatocarcinogenesis, but its role in the transformation process remains unknown. p53 is an important tumor suppressor and its mutation or inactivation is thought to be involved in the development of various types of cancers, including primary hepatocellular carcinoma (PHC)[1]. It has been reported that the p53 protein could bind with HBx antigen to form the complexes, which led to p53 inactivation[2,3]. Genetic alterations in the cellular genome in HBV-transfected HepG2 cells were also detected, which could indicate HBV replication[4]. In view of the intimate relationship between HBV infection and hepatoma, relationship between HBV and p53 is always a research spot. In this experiment, we observed the effect of HBV on p53 expression and activity in SMMU-7721 cell line.

MATERIALS AND METHODS

Materials

Plasmids and cell Human hepatoma cell line, SMMU-7721, was constructed in our laboratory, which can express wild type p53, but without HBV replication. The plasmids of pCMVHBVa (wild type HBV), pCMVHBVb (mutant type HBV, C-T substitution at 1 653 bp) and pCMVp53 (containing wild type p53 1.8 kb cDNA) were supplied by the Center for Human Virology of Thomas Jefferson University. PG13-CAT was kindly provided by Dr. Vogelstein, which contains 13 consecutive p53 recognition sites, making the expression of chloramphenicol acetyltransferase (CAT) regulated by p53 protein in the cells, and its inner control plasmid was pSVβ-gal (Promega, USA). p21-luc (kindly provided by Dr. Vogelstein) contains p53 binding site with p21 promoter and luciferase reporter gene. The inner control plasmid PRL-SV40 (Promega) was cotransfected into cells to eliminate the difference caused by transfection efficiency or cell counts.

Chemicals and reagents Lipofectamine™ transfection reagent was purchased from Gibco BRL (Gaithersburg, MD, USA). Dual Luciferase Assay System was purchased from Promega (USA). Annexin-V-FITC reagent was from Bender MedSystems (Vienna, Austria), CAT-ELISA kit was purchased from Roche (Mannheim, Germany). BCA protein detection kit was from Tian-Cheng Company (Shanghai, China). Protein prestained marker was provided by BioLabs (Australasia). Western blotting luminal reagent was from Santa Cruz (USA). Mouse mAb P53-DO7 was from Antibody Diagnostica Incorporation (USA). Internal control β-actin antibody was from Sigma (USA). Goat-anti-mouse horseradish peroxidase antibody and PVDF were from Hua-Mei Biological Company (Shanghai, China).

Methods

Cell culture and transient transfection with plasmid DNA SMMU-7721 cells were cultured in DMEM media supplemented with 100 mL/L fetal calf serum (FCS) and antibiotics, and incubated at 37 ℃ in a humidified atmosphere containing 50 mL/L CO_2. The experiment was divided into four groups: pCMVp53 was transfected alone or cotransfected with pCMVHBVa or pCMVHBVb into the SMMU-7721 cell; and the control group was transfected by sperm DNA. The total of 2 μg DNA was transfected into the cells in each group. DNA amount was held constant in all experiments by adjusting with sperm DNA. Plasmid DNAs were introduced into SMMU-7721 by lipofectamine™ following the manufacturer's instructions. Briefly, cells were seeded into 35-mm culture dishes for 24 h and the medium was refreshed 4 h before transfection. The DNA mixed with 12 μL of lipofectamine™ was added to each plate and incubated in serum-free medium at 37 ℃ for 6.5 h, and then the medium was replaced with RPMI containing 100 mL/L FCS. Sixty hours after transfection, cells were observed under microscope. Cells were harvested to detect the apoptotic rate by flow cytometry or p53 expression by Western blot.

CAT ELISA Cells were prepared and transfected as aforementioned. Total amount (2.0 μg) of DNAs were kept constant by adding PG13-CAT. SV40-driven β-gal internal control plasmid and the respective test plasmids were as follows: pCMVHBVa, pCMVHBVb, pCMVp53, or the control sperm DNA. Before harvesting, the cells were washed thrice with PBS and extracted following the manufacturer's instructions. β-Galactosidase activity was determined in 96-well plates. A total of 200 μL aliquot of the clear lysates was tested for CAT concentration in the CAT ELISA according to the manufacturer's instructions (Roche Molecular Biochemicals). The CAT concentration of each sample was normalized with respect to β-gal activity.

Luciferase assays Transfections were carried in triplicate. Exponentially growing cells were plated at a density of 5×10^4/well in 0.5 mL medium into 24-well plates. Cells were cultured overnight before transfection. Then 300 ng of luciferase reporter constructs were cotransfected with 300 ng of constructs expressing wild-type p53 proteins or pCMVHBVa or pCMVHBVb. Renilla luciferase expression vector (3 ng) was regarded as an internal control. DNA amount was held constant in all experiments by adjusting with sperm DNA. The cells were harvested 60 h after transfection by lysis with passive lysis buffer (Promega). Firefly and Renilla luciferase activities were assayed using Dual Luciferase Assay System (Promega) according to the manufacturer's instructions. The firefly luciferase activity was normalized to Renilla luciferase activity to compensate for variability in transfection efficiencies.

Flow cytometric analysis of apoptotic cells The cells were stained with FITC-labeled annexin V (Bender MedSystems) and propidium. FITC-labeled annexin V has been used to detect apoptotic cells because annexin binds PS exposed to the outer membrane in apoptotic cells[5-7]. Flow cytometric analysis was performed with a Becton Dickinson flow cytometer (FACScan), and the results were analyzed with the CELLQUEST program (Becton Dickinson).

Western blot analysis Cell pellets were lysed in lysis buffer containing protease inhibitors. The protein concentration of each cell lysate was determined with the BCA assay kit. Eighty micrograms of total protein was separated in a 100 g/L SDS-polyacrylamide gel and transferred to a polyvinylidene difluoride transfer membrane according to standard procedures. Western blotting using anti-p53 mouse mAb DO-7 (1:1 000 dilution) was performed. ECL internal control protein β-actin detection was performed simultaneously.

Statistical analysis

The results were expressed as mean±SD. Differences between experimental groups were evaluated by Student's *t*-test. *P* value <0.05 was considered statistically significant.

RESULTS

The promoter activity of p21 in each transient transfection group

Expression of p53 has an influence on the p21 promoter. As a control, we first tested whether wild-type p53 protein could activate transcription from a p21 promoter. Wild-type p53 triggered an increase in transcription from the p21 promoter and the luciferase values increased significantly when pCMVHBVa was cotransfected, but not in the pCMVHBVb-cotransfected group (Table 1).

Table 1 Luciferase activity in each group (mean±SD)

Groups	p21-luc
pCMVp53	1.218±0.041[a]
pCMVp53+pCMVHBVa	2.197±0.522[a,c]
pCMVp53+pCMVHBVb	0.937±0.210[e]
Control	0.764±0.274

[a]*P*<0.05 *vs* control group; [c]*P*<0.05 *vs* pCMVp53 group; [e]*P*<0.05 *vs* pCMVp53+pCMVHBVa group.

Effect of HBV on transcription activity of p53

To determine the effect of HBV on the transcriptional activities of p53, p53 plasmid was transfected transiently alone or cotransfected with HBVa or HBVb, along with the PG13-CAT reporter construct (the CAT reporter gene under the control of a p53-responsive element). Even in the group transfected with PG13-CAT plasmid alone, a weak expression of CAT enzyme (1.272±0.253) was observed, which suggested that there was an underlying transcription effect of p53 in SMMU-7721. However, in the group with pCMVp53 transfection-induced overexpression of p53, CAT activity was found to be greatly increased (3.585±0.869). Moreover, the group cotransfecting HBVa with PG13-CAT also had a significantly increased CAT activity than that of the group transfected with PG13-CAT alone (2.559±0.231), while cotransfection of HBVb had no marked influence on CAT activity of PG13-CAT (Table 2).

Western blot for p53 expression

It was found that an increase in p53 transcription activity was associated with HBV replication, then it was interesting to examine whether it was caused by the upregulation of p53 protein expression. Our results showed that p53 had a weak expression in the normal SMMU-7721 cells. However,

Table 2 CAT activity in each group

Groups	CAT activity
PG13-CAT	1.272±0.253
HBVa+PG13-CAT	2.559±0.231[a]
HBVb+PG13-CAT	1.585±0.347
pCMVp53+PG13-CAT	3.585±0.869[a]

[a]$P<0.05$ *vs* PG13-CAT group.

p53 expression was markedly increased after transfection with the pCMVp53 plasmid. Furthermore, cotransfection of pCMVp53 with pCMVHBVa showed an even higher p53 expression, while the change was not remarkable when pCMVHBVb was cotransfected with p53 (Figure 1).

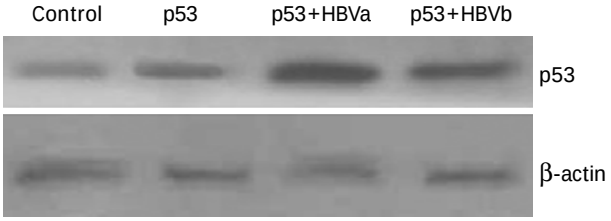


Figure 1 Western blot analysis of p53 expression in each group. Cell lysates (80 μg) were electrophoresed on SDS-PAGE gels and proteins were transferred to PVDF membranes.

Detection of apoptosis by FITC-annexin V/PI double staining

One of the important effects of p53 was its apoptosis-promoting effect. Thus, we observed the apoptosis rate which, in some sense, could indicate p53 activity. We observed that pCMVp53-transfected group had a significantly higher apoptosis rate than the control group (12.32% *vs* 6.91%). There was a much higher apoptosis rate in the pCMVp53 and pCMVHBVa cotransfected group (23.08%), but not in the pCMVp53 and pCMVHBVb cotransfected group (12.20%, Figure 2).

DISCUSSION

Although several data have suggested that the transformation process and tumorigenesis result from activation of oncogenes and inactivation of tumor suppressor genes of the DNA repair system, the question remains of what applies to PHC development. Despite the long-standing association between HBV and PHC development, the role of HBV in the transformation process is still unknown.

The long list of loci with frequent mutations associated with PHC suggests that the mechanism generating these genetic changes might be important in PHC development and needs to be identified. Mutation or inactivation of tumor suppressor gene p53 and its downstream gene p21WAF1 may have an implication in the PHC development [8]. Under normal conditions, p53 is most probably latent. Exposure of cells to p53-activating signals can lead, within a relatively short time, to a marked elevation of p53 protein.

In this experiment, HBV and p53 were transiently transfected into SMMU-7721 cell in order to investigate the apoptosis of the cells, p53 expression, and activity of p53 downstream gene-p21WAF1 promoter and the replication of HBV. Our results showed that the transfection of p53

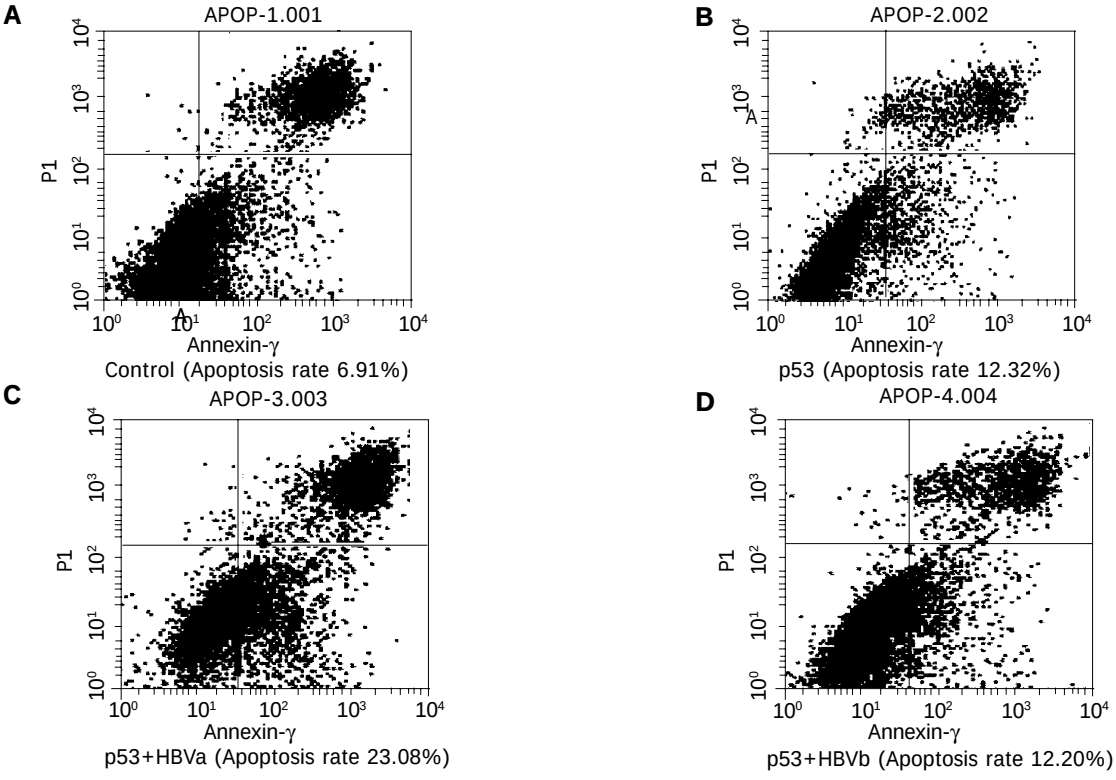


Figure 2 Flow cytometric analysis of cell apoptosis. SMMU-7721 cells were transfected with p53, p53+HBVa, p53+HBVb. The cells were stained by FITC-labeled annexin V and propidium (A-D).

alone in SMMU-7721 cells could increase p21-promoter activity and the apoptosis rate of the cells, suggesting that p53 could promote p21 transcription and contribute to the apoptosis process of the cells. While cotransfection of wild-type HBV markedly increased both p53 protein expression and its transcription activity, and simultaneously, the cell apoptosis rate was significantly increased. In contrast, cotransfection of mutant HBV did not show any effect.

As we know, wild-type p53 is usually a very labile protein, turning over with a half-life sometimes as short as few minutes[9]. On contrary, mutant p53 has a longer half-life, which makes its accumulation in cells. It is generally accepted that the accumulation of active p53 in response to stress occurs mainly through post-translational mechanism, which stabilizes the p53 and increases the ability of nucleolus location[10]. The current results showed that HBV may contribute to promote the stability and activity of p53.

Shi *et al*.[11], showed that p21 (WAF1/CIP1) expression was inversely correlated with p53 expression in hepatitis C virus (HCV)-related hepatocellular carcinomas (HCCs), but not with HBV-related HCCs and HCCs without viral infection, suggesting that different modes of p21 (WAF1/CIP1) regulation are involved in HCCs, differing from their hepatitis viral infection status, and p21 (WAF1/CIP1) expression appears to be predominantly related to altered p53 in HCV-related HCCs. Livezey *et al*.[12], analyzed the p21/Waf1 protein expression in several different kinds of cells by Western blot and indicated that p21/Waf1 protein was upregulated in cells that replicate HBV, but there was still no reasonable interpretation about this phenomenon. Since p21WAF1/CIP1 (p21) is a universal inhibitor of cyclin-dependent kinases and is regulated transcriptionally by p53, which is activated by DNA stress, its expression reflects DNA stress in chronic hepatitis. We observed the correlationship of HBV with p53 and p21, raising the possibility that HBV may have an effect on p21 expression through p53 upregulation, thereby leading to the cell apoptosis.

It has been reported that expression of p21WAF1 in the hepatic disease may be correlated with the disease progression. p21 expression has been reported to be upregulated by the stress of inflammation and fibrosis, and might be influenced by viral proteins in human chronic liver disease. Once the liver develops HCC, the p21 mRNA expression decreases to prominently low levels[13]. In hepatocarcinogenesis induced by HBV and aflatoxin B in tree shrews, the immunopositivity for p21 was found before HCC development, which suggested that p21 protein might be an early marker in the development of HCC[14]. The upregulated p21 expression may play a role as a guard to prevent hepatocytes from tumorgenicity in hepatitis.

Most of the previous reports deemed that apoptosis could not happen to the carcinogenesis cells and/or such cells had no response to the death signal, which lead to unlimited cell growth. But recent research indicates that tumor cells not only exhibited excessive proliferation, but also underwent apoptosis at rates that far exceed those in normal tissue. Proliferation and apoptosis of the tumor cells coexist at all stages and the rates of cell replication are higher than that of apoptosis, allowing a preferential net gain of pre-neoplastic cells[15]. Though HBV chronic infection is an important risk factor of HCC development, HBV-related hepatocarcinoma often happens after dozens of years of infection. In this study, we found that transient transfection of HBV induced apoptosis of SMMU-7721 cells and inactively proliferation. Thus, it is considered that there may be a balance between proliferation and apoptosis in HBV-infected hepatic cells. Hence, disruption of this balance, that is, predominance of proliferation over apoptosis, leads to tumorigenesis.

REFERENCES

1 **Harris CC**. p53: at the crossroads of molecular carcinogenesis and risk assessment. *Science* 1993; **262**: 1980-1981
2 **Zhu MH**. Department of Pathology, Fourth Military Medical University, Xi'an. *Zhonghua Yixue Zazhi* 1993; **73**: 325-328
3 **Feitelson MA**, Zhu M, Duan LX, London WT. Hepatitis B x antigen and p53 are associated *in vitro* and in liver tissues from patients with primary hepatocellular carcinoma. *Oncogene* 1993; **8**: 1109-1117
4 **Livezey KW**, Negorev D, Simon D. Hepatitis B virus-transfected Hep G2 cells demonstrate genetic alterations and de novo viral integration in cells replicating HBV. *Mutat Res* 2000; **452**: 163-178
5 **Martin SJ**, Reutelingsperger CP, McGahon AJ, Rader JA, van Schie RC, LaFace DM, Green DR. Early redistribution of plasma membrane phosphatidylserine is a general feature of apoptosis regardless of the initiating stimulus: inhibition by overexpression of Bcl-2 and Abl. *J Exp Med* 1995; **82**: 1545-1556
6 **Koopman G**, Reutelingsperger CP, Kuijten GA, Keehnen RM, Pals ST, van Oers MH. Annexin V for flow cytometric detection of phosphatidylserine expression on B cells undergoing apoptosis. *Blood* 1994; **84**: 1415-1420
7 **Vermes I**, Haanen C, Steffens-Nakken H, Reutelingsperger C. A novel assay for apoptosis. Flow cytometric detection of phosphatidylserine expression on early apoptotic cells using fluorescein labelled Annexin V. *J Immunol Methods* 1995; **184**: 39-51
8 **Hussain SP**, Hollstein MH, Harris CC. p53 tumor suppressor gene: at the crossroads of molecular carcinogenesis, molecular epidemiology, and human risk assessment. *Ann N Y Acad Sci* 2000; **919**: 79-85
9 **Rogel A**, Popliker M, Webb CG, Oren M. p53 cellular tumor antigen: analysis of mRNA levels in normal adult tissues, embryos, and tumors. *Mol Cell Biol* 1985; **5**: 2851-2855
10 **Meek DW**. Mechanisms of swithing on p53: a role for covalent modification. *Oncogene* 1999; **18**: 7666-7675
11 **Shi YZ**, Hui AM, Takayama T, Li X, Cui X, Makuuchi M. Reduced p21(WAF1/CIP1) protein expression is predominantly related to altered p53 in hepatocellular carcinomas. *Br J Cancer* 2000; **83**: 50-55
12 **Livezey KW**, Negorev D, Simon D. Hepatitis B virus-transfected Hep G2 cells demonstrate genetic alterations and de novo viral integration in cells replicating HBV. *Mutat Res* 2000; **452**: 163-178
13 **Wagayama H**, Shiraki K, Yamanaka T, Sugimoto K, Ito T, Fujikawa K, Takase K, Nakano T. P21WAF1/CTP1 expression and hepatitis virus type. *Dig Dis Sci* 2001; **46**: 2074-2079
14 **Su JJ**, Ban KC, Li Y, Qin LL, Wang HY, Yang C, Ou C, Duan XX, Lee YL, Yang RQ. Alteration of *p53* and *p21* during hepatocarcinogenesis in tree shrews. *World J Gastroenterol* 2004; **10**: 3559-3563
15 **Grasl KB**, Ruttkay NB, Mullauer L, Taper H, Huber W, Bursch W, Schulte-Hermann R. Inherent increase of apoptosis in liver tumors: implications for carcinogenesis and tumor regression. *Hepatology* 1997; **25**: 906-912

Science Editor Kumar M and Guo SY **Language Editor** Elsevier HK

PO Box 2345, Beijing 100023, China
www.wjgnet.com
wjg@wjgnet.com

ELSEVIER

World J Gastroenterol 2005;11(39):6216-6218
World Journal of Gastroenterology ISSN 1007-9327
© 2005 The WJG Press and Elsevier Inc. All rights reserved.

• *BRIEF REPORTS* •

Alterations of intestinal immune function and regulatory effects of L-arginine in experimental severe acute pancreatitis rats

Shi-Feng Qiao, Tian-Jing Lü, Jia-Bang Sun, Fei Li

Shi-Feng Qiao, Department of General Surgery, Beijing Shijitan Hospital, Beijing 100038, China
Tian-Jing Lü, Department of Immunology, Institute of Urology, Peking University, Beijing 100034, China
Jia-Bang Sun, Fei Li, Department of General Surgery, Xuanwu Hospital of Capital University of Medical Sciences, Beijing 100053, China
Correspondence to: Shi-Feng Qiao, Department of General Surgery, Beijing Shijitan Hospital, Yangfangdian District, Beijing 100038, China. qiaoshf@tom.com
Received: 2004-12-08 Accepted: 2005-01-05

Abstract

AIM: To discuss the changes of intestinal mucosal immune function in rats with experimental severe acute pancreatitis (SAP) and the regulatory effect of L-arginine.

METHODS: Male adult Wistar rats were randomly divided into pancreatitis group, sham-operation group, and L-arginine treatment group. Animals were killed at 24, 48, and 72 h after SAP models were developed and specimens were harvested. Endotoxin concentration in portal vein was determined by limulus endotoxin analysis kit. CD3+, CD4+, CD8+ T lymphocytes in intestinal mucosal lamina propria were examined by immunohistochemistry. Secretory immunoglobulin A (SIgA) in cecum feces was examined by radioimmunoassay.

RESULTS: Compared to the control group, plasma endotoxin concentration in the portal vein increased, percentage of CD3+ and CD4+ T lymphocyte subsets in the end of intestinal mucosal lamina propria reduced significantly, CD4+/CD8+ ratio decreased, and SIgA concentrations in cecum feces reduced at 24, 48, and 72 h after SAP developed. Compared to SAP group, the L-arginine treatment group had a lower level of plasma endotoxin concentration in the portal vein, a higher CD3+ and CD4+ T lymphocyte percentage in the end of intestinal mucosal lamina propria, an increased ratio of CD4+/CD8+ and a higher SIgA concentration in cecum feces.

CONCLUSION: Intestinal immune suppression occurs in the early stage of SAP rats, which may be the main reason for bacterial and endotoxin translocation. L-arginine can improve the intestinal immunity and reduce bacterial and endotoxin translocation in SAP rats.

© 2005 The WJG Press and Elsevier Inc. All rights reserved.

Key words: Acute pancreatitis; Immunity; Intestinal mucosa; L-arginine

Qiao SF, Lü TJ, Sun JB, Li F. Alterations of intestinal immune function and regulatory effects of L-arginine in experimental severe acute pancreatitis rats. *World J Gastroenterol* 2005; 11(39): 6216-6218
http://www.wjgnet.com/1007-9327/11/6216.asp

INTRODUCTION

Infection is a common and usually lethal complication during severe acute pancreatitis (SAP). In previous studies, the prevalence of infection in SAP varies between 40% and 70%, and most of the deaths of patients are related with infection. The gastrointestinal tract may be the origin of bacterial translocation during SAP, and SAP may influence the gut barrier function, leading to the occurrence of gut origin sepsis. In this study, we discussed the changes of intestinal immunity in SAP rats.

MATERIALS AND METHODS

Animals and materials

Male Wistar rats weighing 250-300 g; L-arginine (Sigma Chemical Co.); sodium taurocholate (Sigma Chemical Co.); mouse anti-rat anti-CD3, CD4, CD8 mAb (Santa Cruz Co.); SIgA radioimmunoassay kit (Institute of Atomic Energy Physics Chinese Academy of Sciences, Beijing); limulus endotoxin analysis kit (Shanghai Medical Laboratory) were used in the study.

SAP model and experimental groups

Rats were fasted for 14 h before the experiment. Animals were anesthetized by intraperitoneal injection of 10% chloral (3 mL/kg) and then SAP models were developed as previously described[1]. Under sterile conditions, a middle laparotomy was performed. The SAP rat model was developed by pumping 3% sodium taurocholate (TCA) into the pancreatic tract at a rate of 18 mL/h (1 mL/kg). Fifty-four rats were randomly divided into SAP group (n = 18), sham group (n = 18), and L-arginine treatment group (n = 18). The rats were allowed to drink 1% L-arginine water for 5 d before SAP model was developed. At 24, 48, and 72 h after the model was developed, animals from each experimental group were killed and specimens were harvested.

Analysis of serum endotoxin in portal vein by limulus methods

The serum endotoxin concentration in portal vein was assayed by chromogenic limulus analysis kit according to the manufacturer's protocol.

Immunohistochemistry

Intestinal tissue fragment (3 cm from cecum) was cut and fixed by immersing in 4% paraformaldehyde immediately. The specimens were embedded in regular paraffin wax and cut into 4-μm-thick sections. Tissue sections were deparaffinized and rehydrated in PBS. Endogenous peroxidase activity was blocked by incubation with 3% H_2O_2/PBS for 10 min. After being immersed in 1% BSA/PBS at 37 ℃ for 1 h, the sections were incubated with mouse anti-rat anti-CD3, CD4, CD8 mAb at 4 ℃ overnight. The specimens were incubated with peroxidase-conjugated goat anti-rat secondary antibody for 2 h at room temperature. Finally, the specimens were immersed in DAB for 10 min. Brown staining cells were defined as positive cells and counted in four high microscope view, the percentage of positive cells and CD4+/CD8+ ratio were calculated.

Analysis of SIgA content by radioimmunoassay methods

Cecum feces were diluted with water to double volumes. Samples were shaken at 4 ℃ overnight and then examined by SIgA radioimmunoassay test kit.

Statistical analysis

Data were analyzed by *t* test and expressed as mean±SD. $P<0.05$ was considered statistically significant.

RESULTS

Changes of serum endotoxin in portal vein of rats

Compared to the control group, plasma endotoxin concentration in the portal vein increased significantly 24, 48, and 72 h after SAP model was developed ($P<0.01$). The L-arginine treatment group had a lower level of endotoxin concentration than SAP group ($P<0.01$, Table 1).

Table 1 Changes of serum endotoxin in rat portal vein (U: Eu/mL)

Group	24 h	48 h	72 h
NS	0.041±0.011	0.039±0.007	0.042±0.015
SAP	0.157±0.024[b]	0.150±0.018[b]	0.146±0.014[b]
L-Arg	0.087±0.011[d]	0.079±0.016[d]	0.082±0.013[d]

[b]$P<0.01$ *vs* NS; [d]$P<0.01$ *vs* SAP.

Percentage of CD3+, CD4+, CD8+ T lymphocytes in intestinal mucosal lamina propria Percentage of CD3+, CD4+ T lymphocytes subsets in the end of intestinal mucosal lamina propria in SAP group reduced significantly and the CD4+/CD8+ ratio decreased. Compared to the SAP group, the L-arginine treatment group had a higher CD3+, CD4+ T lymphocyte percentage and a higher ratio of CD4+/CD8+ (Table 2).

Changes of SIgA content in cecum feces SIgA concentrations in cecum feces reduced significantly 24, 48, and 72 h after SAP was developed. SIgA concentrations in cecum feces increased in the L-arginine treatment group (Table 3).

Table 2 Percentage of CD3+, CD4+, CD8+ T lymphocytes in intestinal mucosal lamina propria (mean±SD)

Group		24 h	48 h	72 h
CD3+	NS	20.54±3.46	22.32±4.78	21.24±5.32
	SAP	11.24±3.06[b]	12.07±4.24[b]	11.07±3.16[b]
	L-Arg	14.36±2.12[c]	17.45±3.52[c]	15.42±4.18[c]
CD4+	NS	12.78±3.39	11.56±3.14	12.47±2.53
	SAP	7.23±1.46[a]	8.34±1.69[a]	9.06±2.94[a]
	L-Arg	9.85±2.51	9.22±2.75	9.42±2.72
CD8+	NS	9.69±1.65	8.89±1.95	9.41±2.57
	SAP	9.73±2.75	9.12±2.47	8.12±3.59
	L-Arg	8.72±2.63	9.05±3.95	7.87±1.79
CD4+/CD8+	NS	1.32	1.30	1.35
	SAP	0.74	0.91	0.96
	L-Arg	1.13	1.02	1.07

[a]$P<0.05$ *vs* NS; [b]$P<0.01$ *vs* NS; [c]$P<0.05$ *vs* SAP.

Table 3 Changes of SIgA content in cecum feces (mean±SD, μg/mL)

Group	24 h	48 h	72 h
NS	8.70±2.69	8.52±1.84	9.24±1.73
SAP	4.75±1.07[a]	4.45±0.94[a]	4.69±1.28[a]
L-Arg	7.57±1.69[c]	7.55±1.45[c]	8.42±2.17[c]

[a]$P<0.05$ *vs* NS; [c]$P<0.05$ *vs* SAP.

DISCUSSION

SAP is a very common disease in clinical surgery. Though the diagnosis and therapy have been improved, its mortality is 10-20%. Secondary pancreatic infection and multiple organ dysfunction syndrome (MODS) are major causes of death in patients with SAP. Infection is the most common clinical syndrome at present and the morbidity in SAP patients is about 40-70%[2]. Infection is also an important factor for SAP followed by MODS[3]. Bacterial infection is devastative for the pancreas and other tissues, and increases the mortality of acute pancreatitis patients. Clinical data and animal experimental studies have shown that most bacteria-associated pancreatic and peripancreatic infection are of enteric origin[4], and the gut seems to be the principal source of the infection[5]. The gastrointestinal tract is regarded as the largest immune organ in the body containing diverse immunocytes to prevent bacterial and endotoxin translocation from indigenous gut flora. Viable enteric bacteria must pass through the intestinal mucosal barrier to extraintestinal sites, leading to gut-associated infection. During the course of SAP, gastrointestinal tract may be attacked and gut-barrier function is damaged, allowing a large amount of bacteria and endotoxin to enter into the systemic circulation, leading to bacteremia and endotoxemia that may cause more severe complications. Prevention of gut bacterial translocation is most important in avoiding extraintestinal infection and improving the prognosis of SAP patients.

SIgA plays an important role in intestinal mucosal defense and is the first line of defense on intestinal and extra-intestinal mucosal surfaces. SIgA can prevent bacterial adherence and subsequent invasion of the mucosal surface, which is considered crucial in initiating mucosal invasion and infection. SIgA deficiency results in bacterial overgrowth, adherence and translocation[6]. Our results showed that SIgA concentration in cecum feces of the SAP group reduced significantly, indicating that SIgA secretion from intestinal mucosa to the intestinal tract was decreased in SAP rats. SIgA deficiency may increase dissociative bacteria and

endotoxin concentration in the intestinal tract, and their migration through the intestinal mucosa and entry into the portal vein blood[7].

CD3 molecules are expressed on the surface of all mature T lymphocytes and can be used to measure the total number of mature T lymphocytes. In our study, the number of CD3+, CD4+ T lymphocytes in intestinal mucosal lamina propria reduced significantly in SAP rats and remained at the lower level at 72 h. The ratio of CD4+/CD8+ T lymphocytes markedly decreased, indicating that mature T lymphocytes are decreased in intestinal mucosa and immune function is suppressed in SAP rats, while CD8+ T lymphocytes do not change significantly. Because the majority of T lymphocytes in intestinal mucosal lamina propria are CD4+ T lymphocytes, change of CD8+ T lymphocytes is not the main trend[8]. Further experiments are needed to validate the results. Since the number of CD4+ T lymphocytes reduces, cytokines including IL-2, IL-4, IL-6, IL-7, IL-12, IFN-γ are secreted by CD4+ T helper (T_H) lymphocytes and the number of active effector Tc cells reduces accordingly. Thus, the intestinal immune function decreases significantly in SAP rats.

L-arginine is important for the proliferation and maturation of CD3+ T lymphocytes. Dietary arginine may increase the number of CD4+ and CD8+ T lymphocytes as well as the IgG and IgA content[9-11]. Our results have confirmed that oral supplement of L-arginine increases the number of CD3+ and CD4+ T lymphocytes as well as the ratio of CD4+/CD8+ T lymphocytes in intestinal mucosal lamina propria and SIgA concentration in cecum feces in SAP rats, suggesting that L-arginine can improve the immune responsibility of intestinal mucosa and decrease the bacterial and endotoxin translocation in SAP rats.

REFERENCES

1 **Aho HJ**, Koskensalo SM, Nevalainen TJ. Experimental pancreatitis in the rat sodiumtaurocholate-induced acute hemorrhagic pancreatitis. *Scand J Gastroenterol* 1980; **15**: 411-416

2 **Bassi C**, Mangiante G, Falconi M, Salvia R, Frigerio I, Pederzoli P. Prophylaxis for septic complications in acute necrotizing pancreatitis. *J Hepatobiliary Pancreat Surg* 2001; **8**: 211-215

3 **Isenmann R**, Rau B, Beger HG. Bacterial infection and extend of necrosis are determinants of organ failure in patients with acute necrotizing pancreatitis. *Br J Surg* 1999; **86**: 1020-1024

4 **McNaught CE**, Woodcock NP, Mitchell CJ, Rowley G, Johnstone D, MacFie J. Gastric colonisation, intestinal permeability and septic morbidity in acute pancreatitis. *Pancreatology* 2002; **2**: 463-468

5 **Samel S**, Lanig S, Lux A, Keese M, Gretz N, Nichterlein T, Sturm J, Lohr M, Post S. The gut origin of bacterial pancreatic infection during acute experimental pancreatitis in rats. *Pancreatology* 2002; **2**: 449-455

6 **Langkamp-Henken B**, Glezer JA, Kudsk KA. Immunological structure and function of the gastrointestinal tract. *Nutr Clin Pract* 1992; **7**: 100-108

7 **Qin HL**, Su ZD, Gao Q, Lin QT. Early intrajejunal nutrition: bacterial translocation and gut barrier function of severe acute pancreatitis in dogs. *Hepatobiliary Pancreat Dis Int* 2002; **1**: 150-154

8 **Gautreaux MD**, Deitch EA, Berg RD. T lymphocytes in host defense against bacterial translocation from the gastrointestinal tract. *Infect Immun* 1994; **62**: 2874-2884

9 **Ochoa JB**, Strange J, Kearney P, Gellin G, Endean E, Fitzpatrick E. Effects of L-arginine on the proliferation of T lymphocyte subpopulations. *J Parenter Enteral Nutr* 2001; **25**: 23-29

10 **Kung SP**, Wu CW, Lui WY. Arginine modulated cyclosporine-induced immune suppression in rats transplanted with gastric cancer cells. *In Vivo* 2001; **15**: 39-44

11 **Kobayashi T**, Yamamoto M, Hiroi T, McGhee J, Takeshita Y, Kiyono H. Arginine enhances induction of T helper 1 and T helper 2 cytokine synthesis by Peyer's patch alpha beta T cells and antigen-specific mucosal immune response. *Biosci Biotechnol Biochem* 1998; **62**: 2334-2340

Science Editor Wang XL and Guo SY **Language Editor** Elsevier HK

PO Box 2345, Beijing 100023, China
www.wjgnet.com
wjg@wjgnet.com

ELSEVIER

World J Gastroenterol 2005;11(39):6219-6220
World Journal of Gastroenterology ISSN 1007-9327
© 2005 The WJG Press and Elsevier Inc. All rights reserved.

• *CASE REPORT* •

Primary biliary cirrhosis after aortoiliac reconstruction surgery using a Y-graft: A case report

Tomoko Inoue, Katsuya Shiraki, Hiroyuki Fuke, Yutaka Yamanaka, Kazumi Miyashita, Keiichi Ito, Masahiro Suzuki, Kazushi Sugimoto, Kazumoto Murata, Takeshi Nakano

Tomoko Inoue, Katsuya Shiraki, Hiroyuki Fuke, Yutaka Yamanaka, Kazumi Miyashita, Keiichi Ito, Masahiro Suzuki, Kazushi Sugimoto, Kazumoto Murata, Takeshi Nakano, First Department of Internal Medicine, Mie University School of Medicine, 2-174 Edobashi, Tsu, Mie 514-8507, Japan
Correspondence to: Katsuya Shiraki, MD, PhD, First Department of Internal Medicine, Mie University School of Medicine, 2-174 Edobashi, Tsu, Mie 514-8507, Japan. katsuyas@clin.medic.mie-u.ac.jp
Telephone: +81-59-231-5015
Received: 2004-08-14 Accepted: 2004-09-30

Abstract

Primary biliary cirrhosis (PBC) is an autoimmune disease characterized by anti-mitochondrial antibodies and destruction of intra-hepatic bile ducts. Though little is known about the etiology of PBC, some reports suggest that xenobiotics and viral infections may induce PBC. We describe a case of PBC after the aortoiliac reconstruction surgery using a Y-graft.

© 2005 The WJG Press and Elsevier Inc. All rights reserved.

Key words: Gall bladder cancer; Metastasis; Metastatic cardiac tumor

Inoue T, Shiraki K, Fuke H, Yamanaka Y, Miyashita K, Ito K, Suzuki M, Sugimoto K, Murata K, Nakano T. Primary biliary cirrhosis after aortoiliac reconstruction surgery using a Y-graft: A case report. *World J Gastroenterol* 2005; 11(39): 6219-6220
http://www.wjgnet.com/1007-9327/11/6219.asp

INTRODUCTION

Primary biliary cirrhosis (PBC) is a chronic inflammatory process primarily affecting the medium-sized intra-hepatic bile ducts, leading to chronic cholestasis and often progressing to cirrhosis and liver failure, which requires liver transplantation. PBC is thought of as an autoimmune disease because it is closely associated with various immunological abnormalities, the hallmark being the presence of anti-mitochondrial antibodies in over 95% of patients.

CASE REPORT

A 61-year-old male was admitted to our hospital in September 1995 with biochemical cholestasis and abnormal liver function tests. He had taken anti-hypertensive agents (amlodipine and betaxolol) since February 1995. His blood examination sometimes presented very mild biochemical cholestasis without any symptoms. Viral hepatitis was denied, but autoantibody was not checked at that time. Earlier in March 1995, he had an abdominal aortic aneurysm and underwent aortoiliac reconstruction using a Y-graft. Ten days after the surgery, his chemistry showed marked cholestasis, including alkaline phosphatase levels 5-10 times the upper limit of normal and gamma glutamyltransferase levels 5-15 times higher than the upper limit of normal. At first, drug-induced cholestasis was suspected and he started other anti-hypertensive medications (nifedipine and imidapril). Cholestasis improved after changing these medications for a while, but it worsened in August 1995. On admission to our hospital in September 1995, he denied any preceding or on-going fever, flu-like illness, pruritus, abdominal pain, anorexia, vomiting, joint pain, dry eyes, or skin rashes. He denied previous blood transfusion, iv drug abuse, or alcohol abuse. There was no family history of liver disease or malignancy.

Physical examination revealed mild hepatomegaly, but no ascites or mass. The laboratory data showed an alkaline phosphatase level of 572 IU/L, a gamma glutamyltransferase level of 726 IU/L, an AST of 43 IU/L, an ALT of 30 IU/L, a total bilirubin of 0.5 g/dL, a direct bilirubin of 0.2 g/dL, an IgG level of 2 180, an IgM level of 384, and a total cholesterol level of 204 mg/dL. Antinuclear antibody titer was 1 280-fold beyond the upper normal limit, anti-smooth muscle antibody was 80-fold, and anti-mitochondrial antibody was 80-fold higher. A hepatitis profile for hepatitis B and C was negative. An abdominal ultrasound revealed a slightly atrophic liver with dull edge, dilated common bile duct (12 mm), and a gallbladder stone. His liver biopsy showed inflammatory destruction of the intrahepatic septal and interlobular bile ducts within the portal space, and expanded portal tracts by lymphocytes with sparse neutrophils or eosinophils, suggesting PBC (stage I by Scheuer staging) (Figure 1).

A diagnosis of asymptomatic PBC was established on the basis of cholestasis, a positive AMA, and the histological findings. The patient was started on ursodeoxycholic acid 600 mg thrice a day, with a positive response to the cholestasis.

DISCUSSION

PBC is a chronic cholestatic liver disease of unknown cause. Progressive bile duct injury from portal and periportal inflammation could result in progressive fibrosis and eventually cirrhosis. Evidence to date suggests that

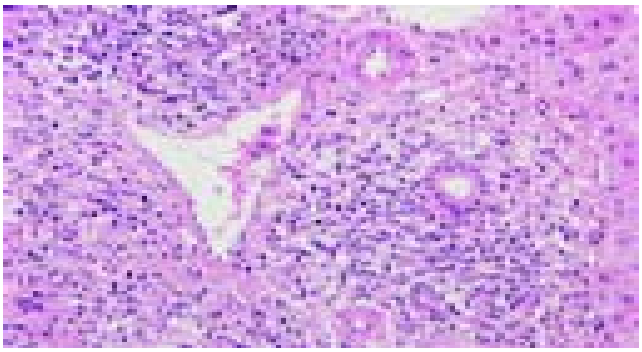


Figure 1 The liver biopsy showed inflammatory destruction of the intrahepatic septal and interlobular bile ducts within the portal space, and expanded portal tracts by lymphocytes with sparse neutrophils or eosinophils.

immunological and genetic factors might cause the disease. Evidence for an immunologic cause of PBC includes immunohistochemical data showing the presence of activated T cells in areas of bile duct destruction and the presence of highly specific autoantibodies reactive with antigens on the surface of biliary epithelial cells. Environmental factors[1] and infectious agents[2-4] also may trigger an autoimmune attack. Other reports suggest that the disease may be induced by xenobiotics and that halogenated compounds will bind to the PDC-E2 autoantigen, breaking tolerance and leading to an intense mucosal response[5]

Our patient had mild cholestasis before the operation and developed marked biochemical cholestasis after the aortoiliac reconstruction using a Y-graft. This suggests that he may have been in the very early stages of PBC before the surgery and the graft implantation might have exacerbated the autoimmune response, leading to further bile duct injury. The trigger might be the graft itself or the drugs used in the perioperative period. There is only one case report of PBC after graft replacement for abdominal aortic aneurysm[6], in which the graft itself was considered to induce the autoimmune response, resulting in liver injury. Some reports suggest that xenobiotics are metabolized in the liver, thereby increasing the potential for liver-specific alteration of proteins, and that a liver-specific autoimmune disease can be observed in some patients exposed to anesthetics[5]

We report a rare case of PBC after aortoiliac reconstruction using a Y-graft, suggesting that the graft itself or medications in the perioperative period might induce or exacerbate an autoimmune response, leading to bile duct injury. In the view of the risk to trigger onset of PBC, it becomes worthwhile to carefully evaluate past surgeries and medications carefully.

REFERENCES

1 **Parikh-Patel A,** Gold EB, Worman H, Krivy KE, Gershwin ME. Risk factors for primary biliary cirrhosis in a cohort of patients from the United States. *Hepatology* 2001; **33**: 16-21

2 **Roesler KW,** Schmider W, Kist M, Batsford S, Schiltz E, Oelke M, Tuczek A, Derrenborn T, Beringer D, Kreisei W. Identification of beta-subunit of bacterial RNA-polymerase-a non-species-specific bacterial protein-as a target of antibodies in primary biliary cirrhosis. *Dig Dis Sci* 2003; **48**: 561-569

3 **Poupon R,** Poupon RE. Retrovirus infection as a trigger for primary biliary cirrhosis? *Lancet* 2004; **363**: 260-261

4 **Xu L,** Shen Z, Guo L, Federa B, Keogh A, Joplin R, O'Donnell B, Aitken J, Carman W, Neuberger J, Mason A. Does a betaretrovirus infection trigger primary biliary cirrhosis? *Proc Natl Acad Sci USA* 2003; **100**: 8454-8459

5 **Long SA,** Water JV, Gershwin ME. Antimitochondrial antibodyies in primary biliary cirrhosis: the role of xenobiotics. *Autoimmunity Reviews* 2002; **1**: 37-42

6 **Ohmori S,** Itoh K, Kuniyoshi M, Shimizu A, Takase K, Nakano T, Tameda Y, Kosaka Y. An elder man's case of primary biliary cirrhosis with autoimmune hepatitis after the graft replacement of abdominal aortic aneurysma. *Acta Hepatol Japonica* 1999; **40**: 409-413

Science Editor Zhu LH and Guo SY **Language Editor** Elsevier HK

PO Box 2345, Beijing 100023, China
www.wjgnet.com
wjg@wjgnet.com

ELSEVIER

World J Gastroenterol 2005;11(39):6221-6224
World Journal of Gastroenterology ISSN 1007-9327
© 2005 The WJG Press and Elsevier Inc. All rights reserved.

• *CASE REPORT* •

Primary pancreatic anaplastic large cell lymphoma, ALK negative: A case report

Christos G Savopoulos, NE Tsesmeli, GD Kaiafa, AT Zantidis, MT Bobos, AI Hatzitolios, ST Papavramidis, IS Kostopoulos

Christos G Savopoulos, NE Tsesmeli, GD Kaiafa, AT Zantidis, AI Hatzitolios, 1st Medical Propedeutic Department, AHEPA Hospital, Aristotle University of Thessaloniki, St. Kyriakidi 1, Thessaloniki 54636, Greece
MT Bobos, IS Kostopoulos, Department of Pathology, Aristotle University Medical School, Thessaloniki 54006, Greece
ST Papavramidis, 3rd Department of Surgery, AHEPA Hospital, Aristotle University of Thessaloniki, St. Kyriakidi 1, Thessaloniki 54636, Greece
Correspondence to: Dr. Christos G Savopoulos, 1st Medical Propedeutic Department, AHEPA Hospital, Aristotle University of Thessaloniki, St. Kyriakidi 1, Thessaloniki 54636, Greece. chrsavop@med.auth.gr
Telephone: +30-2310-994783 Fax: +30-2310-285128
Received: 2005-04-13 Accepted: 2005-05-12

Abstract

We present the fourth case of a primary pancreatic anaplastic large cell lymphoma (ALCL), ALK-. An 80-year-old man was admitted to our clinic for further investigation of a fever of unknown origin. He noted anorexia, weight loss and fatigue. His laboratory tests showed anemia and a great elevation of ESR, LDH, and β_2 microglobulin. In CT and MRI scan, a soft tissue mass in the pancreas was observed. A repeated endoscopy after his admission revealed an ulcerated mass-like deformity of the duodenal bulb. Explorative laparotomy confirmed a diffuse spread of an unresectable malignant pancreatic mass extending to the adjacent organs. Duodenal and surgical biopsies identified an ALCL of T-cell lineage, ALK-. The patient died in the Intensive Care Unit due to hemodynamic instability. Our case is the first one indicating that primary pancreatic lymphoma should be suspected in a patient with pancreatic mass and elevated serum LDH and β_2 microglobulin.

© 2005 The WJG Press and Elsevier Inc. All rights reserved.

Key words: Anaplastic large cell lymphoma; Primary pancreatic lymphoma; Lactate dehydrogenase; β_2 microglobulin

Savopoulos CG, Tsesmeli NE, Kaiafa GD, Zantidis AT, Bobos MT, Hatzitolios AI, Papavramidis ST, Kostopoulos IS. Primary pancreatic anaplastic large cell lymphoma, ALK negative: A case report. *World J Gastroenterol* 2005; 11(39): 6221-6224
http://www.wjgnet.com/1007-9327/11/6221.asp

INTRODUCTION

Malignant tumors of the pancreas constitute about 15% of cancer patients and the most frequent of them is the adenocarcinoma of the pancreas[1]. Primary pancreatic lymphoma (PPL) is a very rare disease constituting less than 0.5% of all pancreatic malignancies and less than 2% of extranodal lymphomas[2]. Primary pancreatic anaplastic large cell lymphomas (PPALCL) are extremely rare. Only three cases of PPALCL have been reported in the literature[1,3,4]. Herein we report the fourth case of PPALCL which was diagnosed by duodenal and surgical biopsies.

CASE REPORT

An 80-year-old man, who was under evaluation of a fever of unknown origin in a Private Health Center, was admitted to our clinic for further investigation. He was complaining of an intermittent fever of 2 mo duration which stabilized during the last 3 wk. Anorexia, weight loss of about 10 kg in the last 6 mo and fatigue were also reported. Physical examination was unremarkable except for a leg edema. His hematological profile was as follows: Hct: 31%, Hb: 9.9 g/L, MCV: 92 fl, MCH: 30 pg/cell, reticulocytes: 1.6%, WBC: 10.6×10^9 cells/L (neutrophils 80% -lymphocytes 11% -monocytes 6% -eosinophils 2.5% -basophils 0.5%), PLT: 389×10^9/L, ESR: 110 mm, CRP: 13 mg/dL (normal range: 0-0.8 mg/dL). Serum biochemistry showed a great elevation of LDH: 1 880 U/L (normal range: 313-618 U/L) and hypoalbuminemia: 2.1 g/L (normal range: 3.4-4.8 g/L), with normal total proteins: 7.1 g/L (normal range: 6.6-8.7 g/L) though. Elevated b_2 microglobulin: 4.19 mg/L (normal range: 1.42-3.21 mg/L) was also found. Other biochemical, serologic and immunologic investigations were normal. Laboratory studies performed after the onset of the symptoms, with values similar to our findings, were available from the patient's file. A chest and abdominal CT scan, also available to us, had demonstrated that the uncinate process and partially the head of the pancreas were blurred (Figure 1A); enlarged peripancreatic, mesenteric, para-aortic and inferior vena cava lymph nodes were found. At that time, he had undergone a gastrointesinal endoscopy without pathologic findings. In further imaging study with MRI scan, a soft tissue mass located in the head of the pancreas and especially the uncinate process had appeared (Figure 1B). A slow flow signal of inferior vena cava had been observed due to the mass compression. After his admission in our clinic, a new endoscopy of the upper gastrointestinal tract revealed an ulcerated mass-like deformity of the duodenal bulb with a friable surface (Figure 2). Gastric and duodenal mucosal biopsy specimens were taken. Bone marrow biopsy was also performed. Glucocorticoids were administrated

as a second choice therapy after antibiotics treatment, based on FUO treatment's protocol and on the high indication of a lympho-proliferative disorder. Temporary clinical and laboratory improvement was noticed (ESR declination: 55 mm). Explorative laparotomy confirmed a diffuse spread of a malignant mass of the pancreas extending to the adjacent organs. Because of the brittle consistency and necrotic surface of the pancreatic mass, the biopsy specimen was taken from the adhesion of pancreatic surface with gastric serosa. Hematoxylin-and-eosin-stained sections of the duodenal biopsy revealed a diffuse dense infiltration of duodenal mucosa by large pleomorphic cells with abundant eosinophilic cytoplasm, ovoidal or irregular nuclei with one or prominent nucleoli (Figure 3A). Rare cells with embryo-like, horseshoe-shaped nuclei or cells with multiple nuclei resembling Reed-Sternberg cells were found. The mitotic activity was intermediate and several atypical mitoses were observed. Scanty neoplastic cells infiltrated the epithelium of intestinal glands as well as the surface epithelium. Histologic sections from the second biopsy material showed loose connective tissue with numerous dilated vessels and lymphatics, most of them having tumor cell emboli with morphology similar to the neoplastic population of the duodenal mucosa (Figure 3B). The intravascular presence of neoplastic cells was confirmed by immunohistochemistry using the endothelial cell marker CD34 (Novocastra, Newcastle, UK). Immunohistochemical stains of both biopsies showed the following tumor-cell immunophenotype: CD45+, CD45RO+, EMA+, CD43+ (DakoCytomation, Glostrup, Denmark), CD30+ (Figure 4), Muc1+, Fascin+ (Novocastra, Newcastle, UK), CD20-, CD45RA-, CAM 5.2-, Anaplastic Lymphoma Kinase (ALK)1-(DakoCytomation, Glostrup, Denmark) and CD3- (Novocastra, Newcastle, UK). Cellular phenotype and immunophenotype support

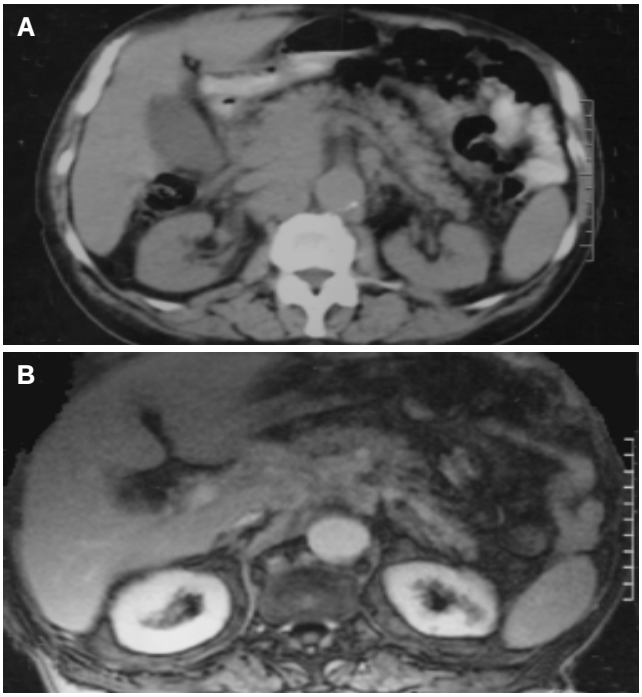


Figure 1 A: Abdominal CT scan showing the head of the pancreas and the uncinate process blurred. B: The mass in the pancreatic head and especially the uncinate process in MRI scan.

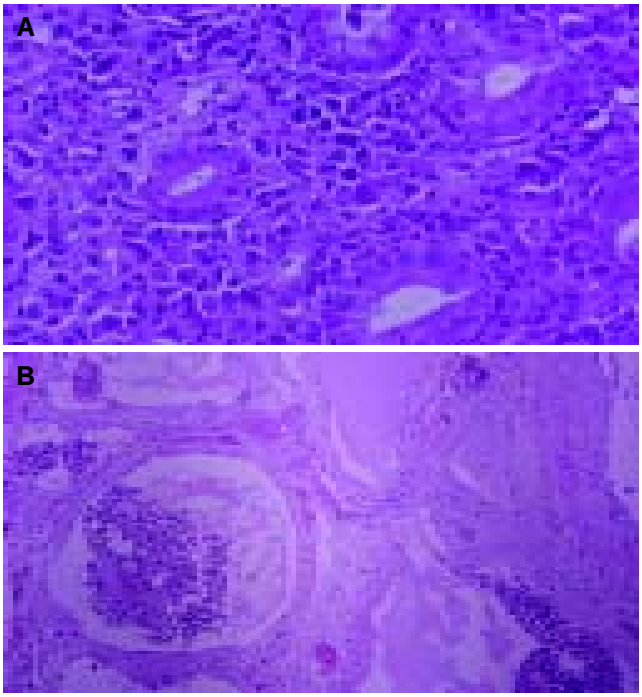


Figure 3 A: Duodenal mucosa infiltrated by polymorphous neoplastic lymphoid cells with eosinophilic cytoplasm and large nuclei. Small numbers of acute inflammatory cells are also present (hematoxylin-eosin ×400). B: Connective tissue and vascular lumens with neoplastic emboli with similar morphologic features as in the duodenal biopsy (hematoxylin-eosin ×200).

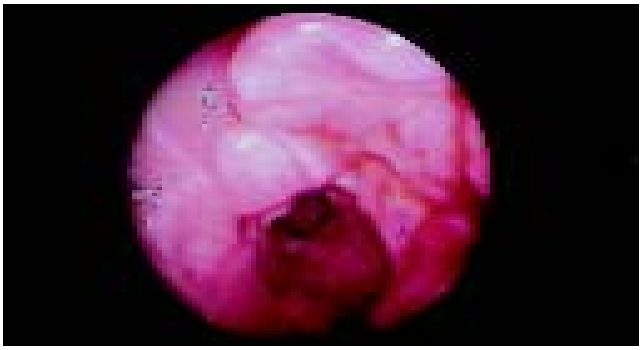


Figure 2 Endoscopic view of the ulcerated mass-like deformity of the duodenal bulb with a friable surface.

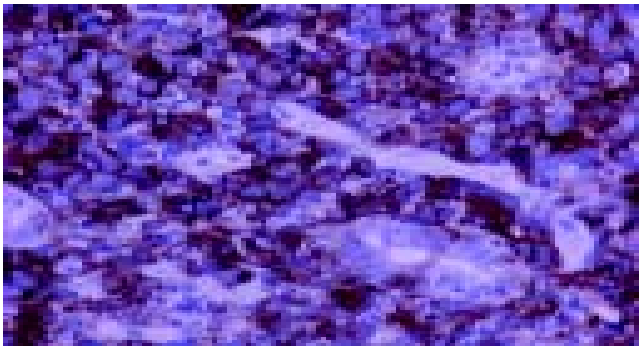


Figure 4 Strong CD30 immunohistochemical expression of lymphoma cells in the duodenal mucosa (×400).

the diagnosis of anaplastic large cell lymphoma (ALCL), of T-cell lineage, ALK negative. Fluorescent *in situ* hybridization (FISH) using LSI ALK dual color, break apart rearrangement probe (Abbott GmbH and Company, KG, Wiesbaden-Delkenheim, Germany) was performed in paraffin-embedded tissue sections from both specimens. Presence of two fused yellow signals or two adjacent (one orange and one green signals) in 200 non-overlapping tumor-cell nuclei showed lack of ALK gene rearrangement at 2p23 region. Bone marrow biopsy showed no evidence of lymphoma involvement. The patient died in the Intensive Care Unit 2 d later due to hemodynamic instability.

DISCUSSION

PPL is an extremely rare neoplasm that may be confused with the most common pancreatic adenocarcinoma. The majority of PPL reported to date in literature have been classified as B-cell type, but several cases of T-cell pancreatic lymphomas have also been described[2]. Most cases are intermediate or high grade NHL with diffuse large B-cell lymphoma being the predominant type. Presenting symptoms are nonspecific, including abdominal pain, weight loss, nausea, vomiting. Systemic-B symptoms such as fever, chills and night sweats are uncommon. Imagining techniques such as CT, percutaneous U/S and recently endoscopic U/S are the most useful procedures to evaluate the staging of pancreatic masses, although they cannot identify their neoplastic nature. A cytohistological diagnosis can be performed by U/S and CT guided techniques, endoscopy and explorative laparotomy[2]. Chemotherapy treatment with CHOP (cyclophosphamide, adriamycin, vincristine, and prednisolone) is usually administrated in patients with lymphomas[1,2]. The accurate distinction of ALCL from non-lymphoid malignancies is critical from the standpoint of patient's management because primary ALCL responds to radically different chemotherapy than adenocarcinoma[5,6].

ALCL is an uncommon type of NHL, first described by Stein *et al.*, in 1985 as a pleomorphic large cell lymphoma with strong membrane and Golgi associated CD30/Ki-1 antigen expression in a very high percentage of neoplastic lymphoid cells, with the involvement of paracortical region and sinuses of lymph nodes[7]. In the latest World Health's Organization (WHO) classification of NHLs, ALCL is a distinctive nature T-cell lymphoma subtype[5]. Clinical presentations of ALCL include a systemic form with nodal and/or extranodal involvement, primary cutaneous ALCL, HIV-related ALCL and ALCL occurring as a secondary event in patients with lymphomatoid papulosis, mycosis fungoides and rarely Hodgkin disease. The main histologic patterns accepted by WHO are the common variant, the lymphohistiocytic and the small cell variant[5]. In these lymphomas, the most frequent genetic alteration is the translocation t (2; 5) (p23; q35) between the ALK gene on chromosome 2 and the nucleophosmin (NPM) gene on chromosome 5. As a result of this translocation, the hybrid (NPM-ALK) gene promotes the production of chimeric NPM-ALK protein. The NPM-ALK fusion chimeric protein can be detected immunohistochemically using monoclonal or polyclonal antibodies, by RT-PCR and FISH[5,8]. ALK immunohistochemical expression is detected in 60-85% of ALCL cases[5]. ALK+ ALCL is most frequent in the first decades of life, shows a male predominance and often has advanced stage disease with frequent B-symptoms and extranodal involvement. It also tends to respond better to chemotherapy than ALK-systemic ALCL[5,8].

Our patient was considered to be affected by PPL according to Dawson *et al.*, clinical criteria which include: (1) the absence of superficial lymphadenopathy or enlargement of mediastinal lymph nodes on chest radiography, (2) a normal leukocyte count in peripheral blood, (3) main mass in the pancreas with lymph-nodal involvement confined to the peripancreatic region, and (4) the absence of hepatic or splenic involvement[9]. The elevated values of LDH and β_2 microglobulin in addition to the clinical characteristics of our patient, such as intermittent fever, anorexia, weight loss and fatigue, also suggested the lymphoproliferative nature of the mass. Moreover, the presence of the mass in the pancreas at imaging techniques while the duodenum was normal in the first endoscopy, proved that it originated in the pancreas and not in the duodenum which is an extremely rare location also.

Only three patients with primary pancreatic ALCL are reported in the literature. The first case described in 1997 in Japan by Maruyama *et al.*, was diagnosed by both duodenal and surgical pancreatic biopsies[3]. The second case was published in 2003 in Israel by Cohen *et al.*, and was diagnosed by operative pancreatic biopsy[1]. Chim *et al.*, recently reported the third case and they supported the diagnosis on operative mesenteric lymph node material biopsy because the tumor resection was not possible[4]. In our case a pancreaticoduodenectomy, the "Whipple procedure" was not performed, as in the case of Chim *et al.*, because of a friable tissue consistency and patient's hemodynamic instability during surgery. Therefore, the diagnosis of our PPALCL was based on the biopsy material taken from duodenal mucosa (three small pieces) and the adhesion of pancreatic surface with gastric serosa.

LDH and β_2 microglobulin are considered to be tumor markers in lymphoproliferative disorders and have an important prognostic value[10,11]. According to the textbook of Sleisenger and Fordtran's, whenever a large mass is identified in the pancreas without biliary obstruction or pain the diagnosis of pancreatic lymphoma should be contemplated, particularly in the presence of an elevated serum LDH level[12]. A high LDH level was found in our patient in contrast to the three previously reported cases of PPALCL. The LDH values were normal in the cases of Chim *et al.*, and Cohen *et al.*, and non-recorded in the case of Maruyama *et al.* In addition, an elevated β_2 microglobulin level was noticed in our case such as reported in ALCL either ALK+ or ALK-in the study of Rassidakis *et al.*[11].

After chemotherapy administration, a remission of disease for 30 mo in the case reported by Cohen *et al.*, and for 18 mo in the case reported by Maruyama *et al.*, were achieved respectively, whereas in the recently reported case by Chim *et al.*, a partial remission of 6 mo duration was noticed because the patient died of disease progression. Our patient did not receive a postoperative chemotherapy because unfortunately he died 2 d after the explorative

Table 1 Clinical and pathologic data of primary pancreatic ALCL reported cases in chronological order

	Maruyama *et al*.[3]	Cohen *et al*.[1]	Chim *et al*.[4]	Present study
A/G	46/F	22/M	27/F	80/M
Clinical symptoms	Back pain, anorexia	Upper abdominal pain, upper GI bleeding	Upper abdominal pain, weight loss	FUO, anorexia, weight loss, fatigue
Physical examination	Icteric conjunctivae, flat and soft abdomen with mild tenderness	Pallor, epigastric mass	Epigastric mass	Leg edema
Radiological findings	CT: mass in pancreatic head, ERP: without pathologic changes in MPD	CT: mass in pancreatic head	CT: mass in pancreatic head	CT: mass in pancreatic head and uncinate process, MRI: CT findings+IVC compression
Endoscopy	Submucosal protrusion with erosion of the second portion of the duodenum	Duodenal bleeding near to Vater's papilla	Bleeding ulceration of the first portion of the duodenum	Ulcerated mass-like deformity of the duodenal bulb
Laboratory findings	ALT, AST, ALP, total, and direct bilirubin elevated, serum amylase decreased, LDH: ND	Peripheral eosinophilia, LDH: in normal range	LDH: in normal range	LDH: elevated, β_2 microglobulin: elevated
Surgical operation	Whipple's	Whipple's	Not performed	Not performed
Pathologic (IHC) findings	CD30+, CD45+, CD45RO+, EMA-, ALK:ND	CD30+, CD45RO+, CD3+, EMA+, ALK-	CD30+, CD45–, CD45RO+, ALK:ND	CD30+, CD45+, CD45RO+, EMA+, CD3-, ALK-
Treatment	MACOP-P	CHOP	CHOP	Glucocorticoids (symptomatic)
Follow up	NED at 18 mo	NED at 30 mo	6 mo, died of disease progression	Died due to hemodynamic instability 2 d after explorative laparotomy

A/G: age/gender, ALK: anaplastic lymphoma kinase, ALP: alkaline phosphatase, ALT: alanine aminotransferase, AST: aspartate aminotransferase, CHOP: chemotherapy regimen consisting of cyclophosphamide, adriamycin, vincristine and prednisolone, EMA: epithelial membrane antigen, ERP: endoscopic retrograde pancreatography, F: female, FUO: fever of unknown origin, GI: gastrointestinal, IHC: immunohistochemistry, IVC: inferior vena cava, LDH: lactate dehydrogenase, M: male, MACOP-P: chemotherapy regimen consisting of methotrexate, adriamycin, cyclophosphamide, vincristine, prednisolone and peplomycin, MPD: main pancreatic duct, ND: no data available, NED: no evidence of disease.

laparotomy.

The clinical information, laboratory and pathologic findings of the present case and the previously reported ones, are summarized in Table 1.

In conclusion, our case - added to the three published cases - is the fourth one of primary pancreatic ALCL, ALK-. From the clinical point of view, since most clinicians do not consider PPL in the differential diagnosis of a pancreatic mass, our case indicates that PPL should be suspected in a patient with pancreatic mass and elevated serum markers, particularly LDH and β_2 microglobulin. Biopsy specimens' results from either the mass or the adjacent infiltrated organs, such as the duodenum in our case, confirm the diagnosis and identify the lymphoma. Thus, an earlier diagnosis leads to an appropriate and timeable treatment and finally, a better prognosis.

REFERENCES

1 **Cohen Y**, Libster D, Amir G, Hiller N, Da'as N, Ben Yehuda D, Polliack A. Primary ALK positive anaplastic large cell lymphoma of the pancreas. *Leuk Lymphoma* 2003; **44**: 205-207

2 **Arcari A**, Anselmi E, Bernuzzi P, Berte R, Lazzaro A, Moroni CF, Trabacchi E, Valisa D, Vercelli A, Cavanna L. Primary pancreatic lymphoma. Report of five cases. *Haematologica* 2005; **90**: ECR09

3 **Maruyama H**, Nakatsuji N, Sugihara S, Atsumi M, Shimamoto K, Hayashi K, Tsutsumi M, Konishi Y. Anaplastic Ki-1-positive large cell lymphoma of the pancreas: a case report and review of the literature. *Jpn J Clin Oncol* 1997; **27**: 51-57

4 **Chim CS**, Ho J, Ooi GC, Choy C, Liang R. Primary anaplastic large cell lymphoma of the pancreas. *Leuk Lymphoma* 2005; **46**: 457-459

5 **Delsol G**, Ralfkiaer E, Stein H, Wright D, Jaffe ES. Anaplastic large cell lymphoma. In: Jaffe ES, Harris NL, Stein H, Vardiman JW, eds. Pathology & Genetics. Tumors of Haematopoetic and Lymphoid Tissues. *Lyon IARC Press* 2001: 230-235

6 **Yoshikawa I**, Murata I, Tanaka Y, Kanagawa K, Tabaru A, Itoh H, Otsuki M. Primary CD30 (Ki-1)-positive anaplastic large cell lymphoma of the duodenum. *Dig Dis Sci* 1996; **41**: 2343-2347

7 **Stein H**, Mason DY, Gerdes J, O'Connor N, Wainscoat J, Pallesen G, Gatter K, Falini B, Delsol G, Lemke H. The expression of the Hodgkin's disease associated antigen Ki-1 in reactive and neoplastic lymphoid tissue: evidence that Reed-Sternberg cells and histiocytic malignancies are derived from activated lymphoid cells. *Blood* 1985; **66**: 848-858

8 **Greer JP**, Kinney MC, Loughran TP Jr. T Cell and NK cell lymphoproliferative disorders. *Hematology* 2001; **72**: 259-281

9 **Dawson IM**, Cornes JS, Morson BC. Primary malignant lymphoid tumours of the intestinal Tract: Report of 37 cases with a study of factors influencing prognosis. *Br J Surg* 1961; **49**: 80-89

10 **Cooper D**. Tumor Markers. In: Goldman L, Ausiello D, eds. Cecil Textbook of Medicine, 22nd edition. *Philadelphia SAUNDERS* 2004: 1131-1134

11 **Rassidakis GZ**, Goy A, Medeiros JL, Jiang Y, Thomaides A, Remache Y, Cabanillas F, Sarris AH, Gilles F. Prognostic significance of Muc-1 expression in systemic anaplastic large cell lymphoma. *Clin Cancer Res* 2003; **9**: 2213-2220

12 **Fernandez-del Castillo C**, Jimenez RE. Pancreatic cancer, cystic pancreatic neoplasms, and other nonendocrine pancreatic tumors. In: Sleisenger & Fordtran's, eds. Gastrointestinal and Liver Disease, 7th edition. *Philadelphia SAUNDERS* 2002: 970-987

Science Editor Guo SY **Language Editor** Elsevier HK

PO Box 2345, Beijing 100023, China
www.wjgnet.com
wjg@wjgnet.com

ELSEVIER

World J Gastroenterol 2005;11(39):6225-6227
World Journal of Gastroenterology ISSN 1007-9327
© 2005 The WJG Press and Elsevier Inc. All rights reserved.

• *CASE REPORT* •

Adenosquamous carcinoma arising within a retrorectal tailgut cyst: Report of a case

Zoran Krivokapic, Ivan Dimitrijevic, Goran Barisic, Velimir Markovic, Miodrag Krstic

Zoran Krivokapic, Ivan Dimitrijevic, Goran Barisic, Velimir Markovic, Miodrag Krstic, Institute for Digestive Diseases, Clinical Center of Serbia, Belgrade, Serbia and Montenegro
Correspondence to: Zoran Krivokapic, MD, FRCS, First Surgical Clinic, Koste Todorovica 6, Belgrade 11000, Serbia and Montenegro. scpy@beotel.yu
Telephone: +381-11-3031-830 Fax: +381-11-3031-830
Received: 2005-03-07 Accepted: 2005-04-02

Abstract

Retrorectal, developmental tail gut cysts, include dermoid cysts, rectal duplication cysts and retrorectal cyst-hamartomas. Retrorectal cyst-hamartomas (RCH) are derived from remnants of the tail gut, the most caudal part of the embryonic hind gut, which normally involutes by the 8th wk of embryonic development (3-8 mm stage). They have specific radiological and histopathological features that distinguish them from other similar formations (dermoid cysts, enteric duplication cysts and teratomas). We report a patient with adenosquamous carcinoma arising within RCH, who underwent complete resection of the cyst through anterior laparotomy, and reached complete (recurrence-free for 14 mo, so far) functional recovery. The cyst was incidentally discovered during hysterectomy 12 years ago. Diagnostic, therapeutic and histopathological aspects of this rare case are discussed. The mentioned period between diagnosis and surgical treatment suggests that RCH, given enough time, can develop malignant degeneration, and should be resected at the time of diagnosis.

© 2005 The WJG Press and Elsevier Inc. All rights reserved.

Key words: Tailgut cyst; Malignant transformation

Krivokapic Z, Dimitrijevic I, Barisic G, Markovic V, Krstic M. Adenosquamous carcinoma arising within a retrorectal tailgut cyst: Report of a case. *World J Gastroenterol* 2005; 11 (39): 6225-6227
http://www.wjgnet.com/1007-9327/11/6225.asp

CASE REPORT

The report was about a 47-year-old woman with a family history, where both her mother and daughter underwent surgery for presacral cysts in other institutions. Both of these cysts were benign in nature. The patient also had a positive history of obstructional bronchitis. The presacral cyst was discovered 11 years ago during hysterectomy because of myomatous uterus. Physical examination showed a fistulous opening on the perianal skin near posterior commissure with no apparent communication with the cyst. Proctoscopic examination showed posterior extrinsic compression of the rectum. Aside from these findings, there were no other abnormalities. Laboratory studies showed anemia and hypoproteinemia (RBC 2, 40×10E12/L; HGB 79 g/L; total proteins 45 g/L). Abdominal ultrasound showed no abnormalities. Transrectal ultrasound showed the tailgut cyst posterior to and causing deformity of rectal wall. The scan identifies five layers of the rectal wall of which the outer hypoechoic layer represents the muscularis propria (Figure 1). There was no radiological evidence of extrapelvic disease. After preoperative immunological testing, because of hypersensitivity to a number of drugs, she underwent complete resection of the mass through anterior laparotomy. The cystic mass was loosely connected to the lower sacrum through fibrous attachments. Communication with the opening was not established. After removal of the intact cyst, the opening on perianal skin was sutured. The patient soon reached a complete functional recovery.

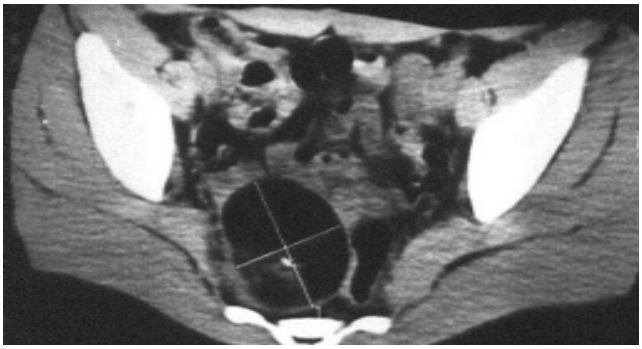


Figure 1 CT scan of the pelvis showing solitary cystic, retrorectal tumor.

PATHOLOGIC FINDINGS

Gross examination revealed irregularly shaped ovoid multiloculated cystic formation measuring 85 mm in greatest diameter (Figure 2). On cut surface, there was a large dominant cyst surrounded by number of small irregular cysts with diameter up to 15 mm, all of them showing mucopurulent content. Microscopically, a wide range of epithelial covering were represented, commonly found in gastrointestinal tract, focally eroded or displaced by respiratory-type epithelium in some areas. Ulcerated areas were surrounded with strong histiocyte infiltrate.



Figure 2 Showing irregularly shaped ovoid formation measuring 85 mm in greatest diameter.

Malignant alteration of the cyst was presented as ill-defined nodular thickening (7 mm), histologically presenting adenosquamous carcinoma, mostly well-differentiated adenocarcinoma admixed with foci of squamous differentiation or poorly differentiated areas and clear resection margins (Figures 3A and B).

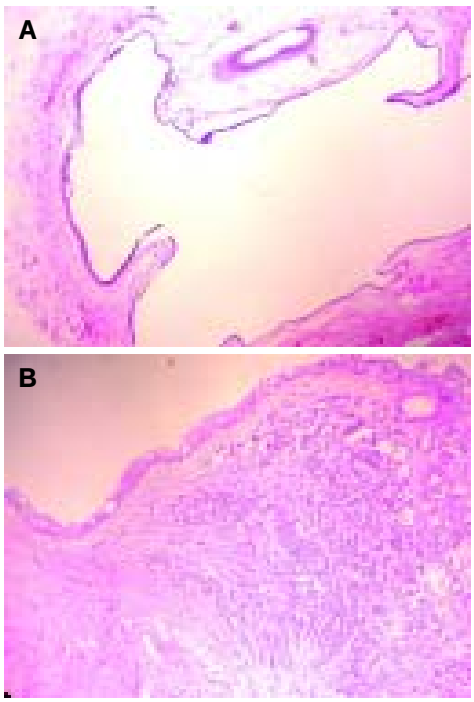


Figure 3 A and B Showing malignant alteration of the cyst histologically presenting adenosquamous carcinoma, mostly well differentiated adenocarcinoma admixed with foci of squamous differentiation or poorly differentiated areas and clear resection margins.

DISCUSSION

Retrorectal cyst-hamartomas (RCH) are reasonably rare, and they are always localized within the retrorectal space, which is bordered by rectum anteriorly, posteriorly by the sacrum, superiorly by the peritoneal reflection, inferiorly by the levator ani and coccygeus muscle, and laterally by the ureters and iliac vessels[1].

They can be found in all age groups including infancy, but they are more commonly reported in middle-aged females, and as mentioned, they are thought to arise from postnatal primitive gut remnants[2,3].

The clinical presentation of the cyst is non-specific, and it is most frequently related to a compressive effect of a growing mass within the pelvis (e.g. rectal fullness, urinary frequency, change in stool caliber, rectal bleeding)[4].

Around 50% of the cysts are discovered incidentally on routine physical examination[1]. Symptoms due to infection are also possible, and fistulous communication with the rectum or with the perianal skin can develop, often after inappropriate surgery. Recurring retrorectal abscess or recidivant perianal fistula can in fact be the infected tail gut cyst[1].

Plain radiography may show a soft tissue mass without destruction of the bone. Irigography can only confirm extramural compression of the rectum[1]. Computed tomography (CT) shows a well marginated retrorectal mass with CT numbers varying from water to soft tissue density.

Transrectal ultrasound is used to asses rectal and perirectal masses[1]. Its good sides are that it is simple, accurate and inexpensive. A diagnostic biopsy for cystic masses is not advised[4]. It may fail to confirm potential malignant diagnosis, and it carries a significant hazard of spillage of malignant cells, or may lead to the infection of the cyst.

Malignant transformation of RCH is very rare. Prasad *et al*.[5], identified 10 cases of malignancy in the literature. The outcome of the treatment of these malignancies varies from case to case. The most important factors for the prognosis are the time of the diagnosis, radicality of surgical resection and histopathological diagnosis; much better prognosis is with neuroendocrine cases, than with adenocarcinomas.

Complete excision of the cyst along with the margin of normal tissue followed by careful examination of the specimen is recommended. Anterior approach, as mentioned, was used in this case. Posterior approach is used for resection of the cyst localized below the level of S4, higher lesions are addressed through anterior approach, and smaller lesions can be reached through transvaginal approach. Combined anterior and posterior pelvic approach is advised by some authors[4] in cases of malignant transformation of the cyst.

Although this case demonstrates how malignant cyst can be successfully removed, with complete functional and oncological recovery, other experiences[4] show rapid and diffuse systemic failure and it is strongly recommended to aggressively address all RCHs as early as identifiable. For the same reason, adjuvant chemotherapy should be considered in some cases at least. Other interesting aspect of this case is the possible hereditary component, which certainly needs additional investigation.

REFERENCES

1 **Hutton KAR,** Benson EA. Case Report: Tailgut Cyst-Assesment with Transrectal Ultrasound. *Clin Radiol* 1992; **45**: 288-289
2 **Hjermstad BM,** Helwing EB. Tailgut cysts: report of 53 cases. *Am J Clin Pathol* 1988; **89**: 139-147
3 **Mourra N,** Caplin S, Parc R, Flejou JF. Presacral Neuroendo-

crine carcinoma Developed in a Tailgut Cyst: report of a case. *Dis Colon Rectum* 2003; **46**: 411-413
4 **Schwarz RE,** Lyda M, Lew M, Paz IB. A carcinoembryonic antigen-secreting adenocarcinoma arising within a retrorectal tailgut cyst: clinicopathological consideratinos. *Am J Gastroenterol* 2000; **95**: 1344-1347
5 **Prasad AR,** Amin MB, Randolph TL, Lee CS, Ma CK. Retrorectal cyst-hamartoma. Report of 5 cases with malignancy arising in 2. *Arch Pathol Lab Med* 2000; **124**: 725-729
6 **Bohm B,** Milsom JW, Fazio VW, Lavery IC, Church JM, Oakley JR. Our approach to the management of congenital presacral tumors in adults. *Int J Colorectal Dis* 1993; **8**: 134-138
7 **Madanes AE,** Kennison RD, Mitchhell G Jr. Removal of a presacral tumor via a Schuchatdt incision. *Obstet Gynecol* 1981; **57**: 945-965
8 **Freirer DT,** Stanley JC, Tompson NW. Retrorectal tumors in adults. *Surg Gynec Obstet* 1971; 681-686
9 **Abel ME,** Nelson R, Prasad ML, Pearl RK, Orsay CP, Abcarian H. Parasacrococcygeal approach for the resection of retrorectal developmental cysts. *Dis Colon Rectum* 1985; **28**: 855-858
10 **Spencer RJ,** Jackman RJ. Surgical management of precoccygeal cysts. *Surg Gynec Obstet* 1962; 449-452

Science Editor Guo SY **Language Editor** Elsevier HK

PO Box 2345, Beijing 100023, China
www.wjgnet.com
wjg@wjgnet.com

ELSEVIER

World J Gastroenterol 2005;11(39):6228-6231
World Journal of Gastroenterology ISSN 1007-9327
© 2005 The WJG Press and Elsevier Inc. All rights reserved.

• *CASE REPORT* •

Agenesis of the gallbladder: A dangerously misdiagnosed malformation

Nicolas Peloponissios, Michel Gillet, René Cavin, Nermin Halkic

Nicolas Peloponissios, Michel Gillet, Nermin Halkic, Department of Surgery, Centre Hospitalier Universitaire Vaudois, Lausanne 1011, Switzerland
René Cavin, Department of Surgery, Centre Hospitalier de la Riviera, Montreux 1820, Switzerland
Correspondence to: Dr. Nermin Halkic, Department of Surgery/ CHUV/BH 15, Lausanne 1011,
Switzerland. nermin.halkic@chuv.hospvd.ch
Telephone: +41-21-314-22-48 Fax: +41-27-314-23-60
Received: 2003-08-02 Accepted: 2004-04-29

Abstract

Isolated agenesis of the gallbladder is a rare anomaly, often asymptomatic. However, one patient out of four presented with right upper abdominal pain, nausea, and fatty food intolerance. The condition is frequently mistaken with an excluded or sclero-atrophic gallbladder, regardless of the imaging modality used. Consequently, AG often leads to unnecessary and potentially dangerous laparoscopic surgery as described in a few case reports over the last 10 years. The aim of this study is to clarify the diagnostic and therapeutic approach of this unusual pathology. Two cases seen in our institutions were retrospectively reviewed, together with a review of the American and European literature. During laparoscopy, the absence of normal anatomical structures and the impossibility of pulling on the gallbladder to expose and dissect the triangle of Callot increases the risk of iatrogenic injury to biliary or portal structures. Depending on the experiment of the surgeon in laparoscopic procedure, this has to be taken into account to decide a conversion to laparotomy. A high index of suspicion is necessary when interpreting the radiological images. In case of doubt, a MRI-cholangiography is mandatory. Because of possible inherited transmission, relatives with a history of biliary symptoms should be investigated.

© 2005 The WJG Press and Elsevier Inc. All rights reserved.

Key words: Gallbladder; Laparoscopy; Pathology

Peloponissios N, Gillet M, Cavin R, Halkic N. Agenesis of the gallbladder: A dangerously misdiagnosed malformation. *World J Gastroenterol* 2005; 11(39): 6228-6231
http://www.wjgnet.com/1007-9327/11/6228.asp

INTRODUCTION

In animals, the absence of a gallbladder has been a subject of research since the Aristotelian era[1]. Present in 1/6 of cases of biliary atresia[2], the isolated absence of the gallbladder and cystic duct is rare. Patients become symptomatic in 23% of cases[3,4], and agenesis of the gallbladder (AG) will almost always be misinterpreted as cholecystitis with cystic duct obstruction or as a sclero-atrophic gallbladder, therefore leading to unnecessary surgery. Reported for the first time in human beings by Bergman in 1702[5], it has since been described several times in case reports. During laparoscopic surgery, it represents a pitfall for the surgeon[6,7]: the biliary or portal structures can easily be injured during dissection as one searches for a gallbladder that does not exist. The absence of normal anatomical structures and the inability to pull on the gallbladder to dissect the triangle of Callot represent a risk of iatrogenic injury.

This review is based on a Medline and PubMed search from 1960 to 2003. Keywords used were agenesis of the gallbladder, absence of gallbladder, congenital syndromes, ultrasound, cholangiography, hepatobiliary scintigraphy, endoscopic retrograde cholangiopancreatography, magnetic resonance cholangiography, biliary dyskinesia, postcholecystectomy syndrome, laparoscopic surgery. Relevant literature was selected from the abstracts and cross-references of the retrieved literature were used to complete the search.

Between 1992 and 1999, two cases of AG were reported in our two institutions (Centre Hospitalier Universitaire Vaudois and Centre Hospitalier Cantonal de Fribourg), which are briefly described.

CASE REPORT

Case one

A 34-year-old man was admitted for right upper abdominal pain and bloating after meals for the last 9 years. The ultrasonography showed a scleroatrophic gallbladder and the intravenous cholangiogram revealed a very narrow biliary tree without opacification of the gallbladder. Total bilirubin was slightly elevated, and the direct fraction was twice the normal value. Other laboratory results were within normal limits. During the laparoscopic procedure, no gallbladder could be identified. A branch of the right hepatic duct was injured. Laparoscopy was converted to a median laparotomy. Initial dissection was carried out on the vena portis thought to be an ectopic gallbladder. Neither the intraoperative cholangiogram performed through the accidentally divided segmental duct nor the surgical exploration could demonstrate a gallbladder. The segmental biliary duct was ligated and the area drained.

Case two

A 76-year-old asymptomatic man went to his physician for

a check-up. Ultrasonography revealed a tumor of the right kidney, which was confirmed by a CT scan. Both failed to identify the gallbladder, but showed an increased size of the common bile duct. A median laparotomy was decided in order to deal with both pathologies. In place of the gallbladder, a small fibrous structure (1.5 cm×1 cm) was found and excised. The intraoperative cholangiogram did not show an ectopic gallbladder. A choledocotomy with the extraction of two gallstones was realized and an abdominal right nephrectomy performed. The histopathological analysis did not demonstrate any gallbladder tissue.

DISCUSSION

AG can be observed in both children and adults, with a median age of 46 at the time of diagnosis[8]. It is almost always a fortuitous finding during abdominal surgery or at autopsy. The prevalence range is 0.007-0.13%. The incidence of this malformation is slightly lower in surgical cholecystectomy series (0.007-0.027%)[9,10] than that in autopsy reports (0.04-0.13%)[5,11-13]. The male to female ratio is equal in autopsy reports[11,14] but seems to reach the same ratio (2-3 women for 1 man) in the clinical group as other biliary tract diseases[15,16]. AG occurs in association with other malformations in 40-65% of cases[8,11,17]. It is then found above all in children[8,11,13], leading in most cases to death in the first year of life[8,13,18,19]. Two congenital syndromes with multiple anomalies including gallbladder agenesis have been described: cerebrotendinous xanthomatosis[20] and the G syndrome[18]. AG has been occasionally mentioned with trisomy 18 and the Klippel-Feil syndrome[8,21,22]. Some authors[23-25] reported this anomaly in children with congenital malformations caused by thalidomide (up to 10% in Männl's series)[24].

This anomaly is explained by an embryological disturbance occurring during the 3rd wk of gestation and concerning the caudal portion of the anterior diverticulum of the primitive gut. It is an anomaly of the development of vessels located on each side of the gallbladder bud (sinus venosus cordis, omphaloenteric, and umbilical veins)[26]. This may explain the association of this anomaly with cardiac, vascular, gastro-intestinal, and abdominal wall malformations observed in the multiple fetal anomaly group[18]. AG may be inherited, with several familial cases observed, including across two generations[4,15,19,27-29]. These series suggest a non-sex-linked heredity with variable penetration.

Patients with AG will become symptomatic in about 23% of cases[4,19,30,31]. In 1988, Bennion *et al*.[8], found 208 symptomatic cases of AG in the literature. 90.1% presented with right upper abdominal pain, 66.3% with nausea or vomiting and 37.5% with fatty food intolerance. Thirty-two percent of these patients presented with a common bile duct dilatation whereas only 27% had gallstones. In the literature, AG is associated with a dilatation of the common duct or gallstones in 25-50% of cases[15,31,32]. The symptomatology and the increased frequency of gallstones has been attributed, by some authors, to biliary dyskinesia[16,30-34] and compared by others to a postcholecystectomy syndrome[8]. According to Toouli *et al*.[35], and Meshkinpour *et al*.[36], the biliary dyskinesia may be due to a hypertonic muscular retrograde contraction of the Oddi sphincter leading to a common duct dilatation, biliary stasis and gallstone formation[35,37]. Tanaka *et al*.[38], showed in 1983 that induction of a spasm of the Oddi sphincter reproduced the same painful symptomatology as biliary dyskinesia, and was associated with increased pressure in the common bile duct. However, it does not explain why the majority of patients become asymptomatic postoperatively (94% of cases in Bennion's series)[8]. Furthermore, the presence and development of a sphincter regulating the bile flow seems to be related to the presence or absence of the gallbladder. Indeed in animals without a gallbladder, the sphincter is poorly developed[39]. According to Lindskog[40], common bile duct dilatation without stones may simply indicate that the calculi have passed. Nevertheless, when we compare the frequency of common duct stones after cholecystectomy (5%) with the frequency of stones in AG (23%), we must recognize that this condition predisposes to calculus formation. Ahlberg *et al*.[9], did not show any changes in the bile lipid composition of patients with AG. However, the small number of patients in this study does not allow any conclusions to be drawn. Similar studies were realized in postcholecystectomy patients with conflicting results due to differences in methodology and patient selection[9,41-44].

When reviewing the literature, with the exception of two cases of AG[27,33], the preoperative investigations carried out on symptomatic patients failed to demonstrate the diagnosis. Whatever the method was used, cholangiography, hepatobiliary scintigraphy, ultrasound (US) or even endoscopic retrograde cholangiopancreatography (ERCP), the diagnosis proposed was almost always cystic duct obstruction or a small contracted gallbladder[3,6,7,45-47].

Ultrasonography is actually the investigation method of choice for the diagnosis of common bile duct stones, with a sensitivity of 95-98%. Crade *et al*.[48], defined three categories of abnormal ultrasounds of the gallbladder. The only case of AG in this study came from the second category (as also seen in other numerous cases described in the literature[7,30,46,47,49]): (1) shadowy gravity-dependent opacities within the gallbladder, (2) nonvisualization of the gallbladder lumen, and (3) nonshadowy opacities within the gallbladder lumen. The accuracy of US in these three different categories is 100%, 96%, and 61%, respectively[48]. The great difficulty in visualizing a contracted gallbladder on stones is well known[48,50]. According to Hammond[51], there is always either a recognizable segment of wall or a thin rim of bile identifying the gallbladder. He bases his assertion on MacDonald's *et al*.[52], and Raptopoulos's *et al*.[53], reports, which described the WES triad (demonstration of the gallbladder wall, the echo of the stone, and the acoustic shadow) or the double arc shadow (two parallel arcuate echogenic lines separated by a thin anechoic space with distal acoustic shadowing). However, the examination conditions as well as the examiner's experience does not always permit such accurate appreciation. Shadowy opacities misdiagnosed as stones can be due to intestinal gas artefacts or to other structures in close proximity, such as a calcified hepatic lesion or a surgical clip[46,51].

The hepatobiliary scintigraphy with new ^{99m}Tc-IDA agents and quantification of function is increasingly giving results,

especially in the detection of gallbladder anomalies[54]. Nevertheless, the nonvisualization of the gallbladder remains typical of cystic duct obstruction, as well as AG[54].

ERCP has been used in addition to other diagnostic methods[6,27,33,55,56]. Again, the nonvisualization of the gallbladder was interpreted as an occlusion of the cystic duct.

Magnetic resonance cholangiography is a noninvasive and well demonstrated imaging method in the evaluation of the biliary tract[57–59]. As it does not require contrast administration to visualize the bile, it is not compromised by biliary stasis. It can then demonstrate an excluded and/or ectopic gallbladder. However, this technique is not readily available. It may not yet replace ultrasound as the gold standard of acute gallbladder imaging but it is an ideal complementary study to inconclusive sonographic studies[60].

Selective arteriography of the hepatic artery has been proposed to prove gallbladder agenesis[6,61], but remains a very invasive procedure.

Reviewing the recent literature[62-65] concerning the AG, we noticed that symptomatic patients are still unnecessarily operated. In only two cases, AG was demonstrated by nonoperative means[27,33]. It was the evocation of this disorder in the initial assessment (US and cholangiography), which led to diagnosis. An ERCP increased the suspicion and AG was confirmed in each case by repeated US and cholangioscintigraphy during follow-up in asymptomatic patients.

In conclusion, AG is an unusual anomaly, mimicking a biliary stone disease in 23% of cases. This condition must be kept in mind in the differential diagnosis of ultrasonographically undetected or scleroatrophic gallbladder. When the WES triad or double arc shadow are not present, this congenital malformation should be suspected. An ectopic location of the gallbladder should be excluded. In case of doubt a conservative approach involving repeat investigations, in asymptomatic patients or after the acute phase, will avoid unnecessary surgery.

When AG is a laparoscopical discovery, the possibility of iatrogenic injury, by dissecting the portal structures without normal anatomical landmarks, has to be taken into account to decide a conversion to laparotomy. An intraoperative cholangiography should be realized through the common duct. Intraoperative ultrasound can demonstrate an ectopic gallbladder but is not always available. The lesser omentum, the falciform ligament, and the liver must be palpated. The exploration will also include a Kocher maneuver to explore the posterior wall of the duodenum as well as the head of the pancreas. The scar tissue in the gallbladder bed and the portal area must be carefully explored.

Associated malformations need not be systematically sought in adults, but family heredity has to be taken into account. Relatives with past or repetitive biliary symptomatology should have at least an ultrasonography when asymptomatic.

REFERENCES

1 **Vanderpool D,** Klingensmith W, Oles P. Congenital absence of the gallbladder. *Am J Surg* 1964; **30**: 324-330
2 **Rabinovitch J,** Rabinovitch P, Rosenblatt P, Pines B. Rare anomalies of the gallbladder. *Ann Surg* 1958; **148**: 161-168
3 **Serour F,** Klin B, Strauss S, Vinograd I. False-positive ultrasonography in agenesis of the gallbladder: a pitfall in the laparoscopic cholecystectomy approach. *Surg Laparosc Endosc* 1993; **3**: 144-146
4 **Nadeau LA,** Cloutier WA, Konecki JT, Morin G, Taylor RW. Hereditary gallbladder agenesis: twelve cases in the same family. *J Maine Med Assoc* 1972; **63**: 1-4
5 **Latimer EO,** Mendez FL, Hage W. Congenital absence of gallbladder. Report of three cases. *Ann Surg* 1947; **126**: 229-242
6 **Cabajo CM,** Martin del Olmo JC, Blanco AJ, Atienza SR. Gallbladder and cystic duct absence. An infrequent malformation in laparoscopic surgery. *Surg Endosc* 1997; **11**: 483-484
7 **Amaral JF,** Ferland R. Agenesis of the gallbladder: laparoscopic diagnosis. *Surg Laparosc Endosc* 1993; **3**: 337-341
8 **Bennion RS,** Thompson JEJ, Tompkins RK. Agenesis of the gallbladder without extrahepatic biliary atresia [see comments]. *Arch Surg* 1988; **123**: 1257-1260
9 **Ahlberg J,** Angelin B, Einarsson K, Leijd B. Biliary lipid composition and bile acid kinetics in patients with agenesis of the gallbladder with a note on the frequency of this anomaly. *Acta Chir Scand* 1978; **482**: 15-20
10 **Ferris DO,** Glazer IM. Congenital absence of gallbladder. Four surgical cases. *Arch Surg* 1965; **91**: 359-361
11 **Monroe SE,** Ragen FJ. Congenital absence of the gallbladder. *California Medicine* 1956; **85**: 422-423
12 **Mouzas G,** Wilson AK. Congenital absence of the gall-bladder with stone in the common bile-duct. *Lancet* 1953; **1**: 628-629
13 **Tallmage GK.** Congenital absence of the gallbladder. *Arch Pathol* 1938; **26**: 1060-1062
14 **Heffernon EW,** Weber CM. Congenital absence of the gallbladder. *JAMA* 1960; **174**: 844-895
15 **Wilson JE,** Deitrick JE. Agenesis of the gallbladder: case report and familial investigation. *Surgery* 1986; **99**: 106-109
16 **Sanders GB,** Flores T, Arriola P. Congenital absence of the gallbladder and cystic duct: a review of the literature and report of a case. *Am Surg* 1968; **34**: 750-754
17 **Haughton V,** Lewicki AW. Agenesis of the gallbladder. Is preoperative diagnosis possible? *Radiology* 1973; **106**: 305-306
18 **Turkel SB,** Swanson V, Chandrasoma P. Malformations associated with congenital absence of the gall bladder. *J Med Genet* 1983; **20**: 445-449
19 **Sterchi JM,** Baine RW, Myers RT. Agenesis of the gallbladder-an inherited defect? *South Med J* 1977; **70**: 498-499
20 **Winter RB,** Baraitser M. Multiple congenital anomalies. a diagnostic compendium. First edition ed. Cambridge: *Chapman and Hall Medical* 1991: 109
21 **Gajic SI.** Gallbladder agenesis in a patient with Klippel-Feil syndrome [letter]. *Arch Pathol Lab Med* 1981; **105**: 682-683
22 **Warkany J,** Passarge E, Smith LB. Congenital malformations in autosomal trisomy syndromes. *Am J Dis Child* 1966; **112**: 502-517
23 **Schinzel A.** Phocomelia and additional anomalies in two sisters. *Hum Genet* 1990; **84**: 539-541
24 **Mannl HF.** Gallbladder agenesis. *Med Welt* 1978; **29**: 1969-1974
25 **Kreipe U.** Abnormalities of internal organs in thalidomide embryopathy. A contribution to the determination of the sensitivity phase in thalidomide administration during early pregnancy. *Arch Kinderheilkd* 1967; **176**: 33-61
26 **Blechschmidt CM.** Agenesis of the gallbladder-borderline-case of normality? *Anat Anz* 1982; **151**: 281-285
27 **Venuta A,** Laudizi L, Miceli F, Pantusa M, Laudizi Z. Agenesis of the gallbladder. Description of 2 cases in 2 siblings. *Pediatr Med Chir* 1989; **11**: 465-466
28 **Becker IW,** Mastroni PP. Congenital absence of the gallbladder with a family history. *Am Surg* 1979; **45**: 541-542
29 **Kobacker JL.** Congenital absence of the galbladder: a possible hereditary defect. *Ann Int Med* 1950; **25**: 1008-1012
30 **Jackson RJ,** McClellan D. Agenesis of the gallbladder. A cause of false-positive ultrasonography. *Am Surg* 1989; **55**: 36-40
31 **Dickinson CZ,** Powers TA, Sandler MP, Partain CL. Congenital absence of the gallbladder: another cause of false-

positive hepatobiliary image. *J Nucl Med* 1984; **25**: 70-72
32 **Langley JR,** Hull DC. Congenital absence of the gallbladder: Review of the literature and report of a new case. *Am Surg* 1974; **40**: 548-551
33 **O'Sullivan J,** O'Brien PA, MacFeely L, Whelton MJ. Congenital absence of the gallbladder and cystic duct: nonoperative diagnosis. *Am J Gastroenterol* 1987; **82**: 1190-1192
34 **Frey C,** Bizer L, Ernst C. Agenesis of the gallbladder. *Am J Surg* 1967; **114**: 917-926
35 **Toouli J,** Geenen JE, Hogan WJ, Dodds WJ, Arndorfer RC. Sphincter of Oddi motor activity: a comparison between patients with common bile duct stones and controls. *Gastroenterology* 1982; **82**: 111-117
36 **Meshkinpour H,** Mollot M, Eckerling GB, Bookman L. Bile duct dyskinesia. Clinical and manometric study. *Gastroenterology* 1984; **87**: 759-762
37 **Madden JL.** Common duct stones. Their origin and surgical management. *Surg Clin North Am* 1973; **53**: 1095-1113
38 **Tanaka M,** Ikeda S, Nakayama F. Continuous measurement of common bile duct pressure with an indwelling microtransducer catheter introduced by duodenoscopy: new diagnostic aid for postcholecystectomy dyskinesia-a preliminary report. *Gastrointest Endosc* 1983; **29**: 83-88
39 **Gilloteaux J.** Introduction to the biliary tract, the gallbladder, and gallstones. *Microsc Res Tech* 1997; **38**: 547-551
40 **Lindskog BI.** Congenital absence of the gallbladder. *Acta Chir Scand* 1973; **139**: 208-209
41 **Almond HR,** Vlahcevic ZR, Bell CCJ, Gregory DH, Swell L. Bile acid pools, kinetics and biliary lipid composition before and after cholecystectomy. *N Engl J Med* 1973; **289**: 1213-1216
42 **Pomare EW,** Heaton KW. The effect of cholecystectomy on bile salt metabolism. *Gut* 1973; **14**: 753-762
43 **Kimball A,** Pertsemlidis D, Panveliwalla D. Composition of biliary lipids and kinetics of bile acids after cholecystectomy in man. *Am J Dig Dis* 1976; **21**: 776-781
44 **Shaffer EA,** Small DM. Biliary lipid secretion in cholesterol gallstone disease. The effect of cholecystectomy and obesity. *J Clin Invest* 1977; **59**: 828-840
45 **Belli G,** D'Agostino A, Iannelli A, Rotondano G, Ceccarelli P. Isolated agenesis of the gallbladder. An intraoperative problem. *Minerva Chir* 1997; **52**: 1119-1121
46 **Kestenholz PB,** von FM, Harder F. Agenesis of the gallbladder in adults: a laparoscopic diagnosis. *Chirurg* 1997; **68**: 643-645
47 **Azmat N,** Francis KR, Mandava N, Pizzi WF. Agenesis of the gallbladder revisited laparoscopically. *Am J Gastroenterol* 1993; **88**: 1269-1270
48 **Crade M,** Taylor KJ, Rosenfield AT, de GC, Minihan P. Surgical and pathologic correlation of cholecystosonography and cholecystography. *Am J Roentgenol* 1978; **131**: 227-229
49 **Hershman MJ,** Southern SJ, Rosin RD. Gallbladder agenesis diagnosed at laparoscopy. *J R Soc Med* 1992; **85**: 702-703
50 **Vas W,** Salem S. Cholecystosonography in diagnosis of cholelithiasis-pathologic and radiographic correlation. *J Can Assoc Radiol* 1980; **31**: 116-119
51 **Hammond DI.** Unusual causes of sonographic nonvisualization or nonrecognition of the gallbladder: a review. *J Clin Ultrasound* 1988; **16**: 77-85
52 **MacDonald FR,** Cooperberg PL, Cohen MM. The WES triad-a specific sonographic sign of gallstones in the contracted gallbladder. *Gastrointest Radiol* 1981; **6**: 39-41
53 **Raptopoulos V,** D'Orsi C, Smith E, Reuter K, Moss L, Kleinman P. Dynamic cholecystosonography of the contracted gallbladder: the double- arc-shadow sign. *Am J Roentgenol* 1982; **138**: 275-278
54 **Gad MA,** Krishnamurthy GT, Glowniak JV. Identification and differentiation of congenital gallbladder abnormality by quantitative technetium-99m IDA cholescintigraphy. *J Nucl Med* 1992; **33**: 431-434
55 **Lotz G,** Stahlschmidt M. Agenesis of the gallbladder. *Chirurg* 1986; **57**: 37-39
56 **Kennard GK.** Congenital agenesis of the gallbladder. A diagnostic problem. Report of a case. *Mil Med* 1985; **150**: 283-285
57 **Chan FL,** Chan JK, Leong LL. Modern imaging in the evaluation of hepatolithiasis. *Hepatogastroenterology* 1997; **44**: 358-369
58 **Vanbeckevoort D,** Van HL, Ponette E, Marchal G, Bosmans H, De CB. Imaging of gallbladder and biliary tract before laparoscopic cholecystectomy: comparison of intravenous cholangiography and the combined use of HASTE and single-shot RARE MR imaging. *J Belge Radiol* 1997; **80**: 6-8
59 **Schuster DM,** Pedrosa MC, Robbins AH. Magnetic resonance cholangiography. *Abdom Imaging* 1995; **20**: 353-356
60 **Adusumilli S,** Siegelman ES. MR imaging of the gallbladder. Magn Reson Imaging. *Clin N Am* 2002; **10**: 165-184
61 **di Natale I.** Agenesis of the gallbladder (diagnostic considerations). Apropos of a case. *Chir Ital* 1985; **37**: 618-623
62 **Gotohda N,** Itano S, Horiki S, Endo A, Nakao A, Terada N, Tanaka N. Gallbladder agenesis with no other biliary tract abnormality: report of a case and review of the literature. *J hepatobiliary Pancreat Surg* 2000; **7**: 327-330
63 **Fisichella PM,** Di Stefano A, Di Carlo I, La Greca G, Russello D, Latteri F. Isolated agenesis of the gallbladder: report of a case. *Surg Today* 2002; **32**: 78-80
64 **Sarli L,** Violi V, Gobbi S. Laparoscopic diagnosis of gallbladder agenesis. *Surg Endosc* 2000; **14**: 373
65 **Dell'Abate P,** Iosca A, Galimberti A, Faraci R, Soliani P, Foggi E. Agenesis of the gallbladder found at laparoscopy in an adult patient with cardiac malformation. *Dig Surg* 2000; **17**: 284-286

Science Editor Zhang JZ **Language Editor** Elsevier HK

PO Box 2345, Beijing 100023, China
www.wjgnet.com
wjg@wjgnet.com

ELSEVIER

World J Gastroenterol 2005;11(39):6232-6234
World Journal of Gastroenterology ISSN 1007-9327
© 2005 The WJG Press and Elsevier Inc. All rights reserved.

• *CASE REPORT* •

Treatment of a duodenal perforation secondary to an endoscopic sphincterotomy with clips

Panagiotis Katsinelos, George Paroutoglou, Basilios Papaziogas, Athanasios Beltsis, Stavros Dimiropoulos, Konstantinos Atmatzidis

Panagiotis Katsinelos, George Paroutoglou, Athanasios Beltsis, Stavros Dimiropoulos, Department of Endoscopy and Motility Unit, "G.Gennimatas" Hospital, Ethnikis Aminis 41, 54635 Thessaloniki, Greece
Basilios Papaziogas, Konstantinos Atmatzidis, 2nd Surgical Clinic, "G.Gennimatas" Hospital, Aristotle University of Thessaloniki, Ethnikis Aminis 41, 54635 Thessaloniki, Greece
Correspondence to: Dr. Panagiotis Katsinelos, Department of Endoscopy and Motility Unit, "G.Gennimatas" Hospital, Ethnikis Aminis 41, 54635 Thessaloniki, Greece. pantso@the.forthnet.gr
Telephone: +30-2310-211221 Fax: +30-2310-210401
Received: 2004-11-29 Accepted: 2005-02-18

Abstract

Perforation is one of the most serious complications of endoscopic sphincterotomy (ES) necessitating immediate surgical intervention. We present a case of successful management of such a complication with endoclipping. A 85-year-old woman developed duodenal perforation after ES. The perforation was identified early and its closure was achieved using three metallic clips in a single session. There was no procedure-related morbidity or complications and our patient was discharged from hospital 10 d later. Endoclipping of duodenal perforation induced by ES is a safe, effective and alternative to surgery treatment.

© 2005 The WJG Press and Elsevier Inc. All rights reserved.

Key words: Endoclipping; Duodenal perforation; Endoscopic sphincterotomy

Katsinelos P, Paroutoglou G, Papaziogas B, Beltsis A, Dimiropoulos S, Atmatzidis K. Treatment of a duodenal perforation secondary to an endoscopic sphincterotomy with clips. *World J Gastroenterol* 2005; 11(39): 6232-6234
http://www.wjgnet.com/1007-9327/11/6232.asp

INTRODUCTION

The most serious complications of endoscopic sphincterotomy (ES) are pancreatitis, hemorrhage and perforation[1]. Although perforation is uncommon, occurring in less than 1% of patients undergoing ES, it is associated with high morbidity and mortality[2].

Applications of endoscopic metallic clips other than the treatment of bleeding lesions have been reported, such as sealing of iatrogenic endoscopic perforations[3].

We describe a 85-year-old woman who developed symptomatic post-ES perforation and was successfully treated by endoscopic clip placement. To our knowledge, this is the second reported case of post-ES perforation that was treated endoscopically with clip placement.

CASE REPORT

A 85-year-old woman was admitted because of recurrent episodes of abdominal pain, fever, and jaundice over a period of 1 mo. Her past medical history revealed a cholecystectomy 10 years ago, mild heart failure and hypertension. Laboratory tests showed cholestasis. US demonstrated intra- and extra-hepatic biliary dilatation. Magnetic resonance imaging cholangiography showed a large stone (diameter 18 mm) in the lower part of the common bile duct.

Endoscopic biliary sphincterotomy was performed using an electrosurgical unit with standard pull sphincterotome without the use of guidewire. The length of sphincterotomy was large, according to the size of the common bile duct stone. The extraction of the stone was impossible. We performed a successful mechanical lithotripsy and the fragments were extracted with a basket.

Twelve hours later, the patient complained of moderate pain in the upper abdomen, which diminished after analgesics administration. Physical examination disclosed fever of 37.8 ℃ but no signs of peritoneal irritation. A chest X-ray was normal. Laboratory studies revealed an elevated ESR (75 mm/h) and C-reactive protein concentration (3.62 mg/dL, normal <0.5 mg/dL). The WBC count was 11 888/μL (normal 4 000-8 000/μL) and the percentage of neutrophils was high (86%).

An abdominal CT demonstrated free retroperitoneal air and a small amount of dirty fluid around the duodenum as well as enhancement of choledochal duct with gastrografin (Figure 1).

We decided to try endoscopic repair of the duodenal perforation, after an extensive discussion about the type of therapy with her relatives, and an informed consent was signed. With a rotating colon clipping device (HX-6UR-1, Olympus), five clips were carefully placed in the upper part of sphincterotomy. Although two were misclipped, the other three were well fitted (Figure 2). A standard 0.035-inch biliary super-stiff guidewire (Jagwire, Microvasive) was then passed endoscopically and fluoroscopically into the jejunum and a nasogastric tube with the tip removed was passed into the duodenum and centered over the perforation site.

Intravenous hyperalimentation and treatment with antibiotics (ciprofloxacin 1 g/d and metronidazole 1.5 g/d)

were administered. Clinically, the patient did well and the abdominal pain that was initially present decreased, no signs of peritonitis developed and the fever subsided. Three days later, a water-soluble contrast was instilled via the nasogastric tube and on radiography no leakage of contrast was found. She began to eat 7 d after the clipping procedure and was discharged on d 10. A second abdominal CT performed 20 d later demonstrated resolution of the retroperitoneal air and inflammation.

No further problems occurred after 5 mo of follow-up.

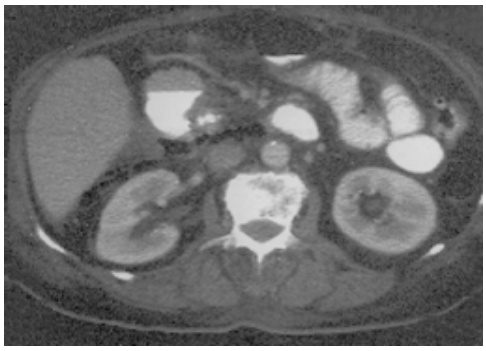


Figure 1 Free retroperitoneal air and a small amount of dirty fluid around the duodenum.

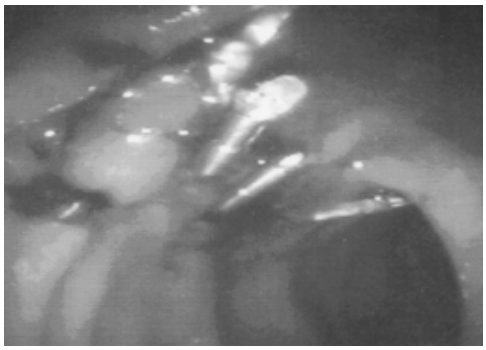


Figure 2 Three clips placed on the upper part of sphincterotomy.

DISCUSSION

The approach to management of duodenal perforation after ES is controversial. Some investigators advocate conservative management based on clinical course, while others advocate surgical repair in all cases because of the complications associated with delayed operative intervention[4-6].

Dunham *et al*.[4], have reported about the outcome after conservative treatment in seven patients when free air was recognized immediately. Two of these patients died after the development of toxic shock despite delayed surgery. In a recent prospective study by Freeman *et al*.[1], five of the eight ES perforations were severe and one resulted in death.

In recent years, endoscopic clip placement, developed as a hemostatic procedure, has been used for closure of iatrogenic perforations[3]. Binmoeller *et al*.[7], described the first successful endoscopic closure of an iatrogenic perforation by using a clip-application device in 1993. Subsequently, the use of this method in the esophagus[8,9], duodenum[10], and colon[11,12] has been described. Baron *et al*.[13], described the first case of a 39-year-old man with familial adenomatous polyposis who presented duodenal perforation after a papillectomy and ES. They identified immediately free air in the retroperitoneum and the perforation was closed by the use of a clipping device and the placement of five clips.

The decision about the treatment after an iatrogenic perforation must be made very carefully, because conservative treatment may surely be used when perforation is small and retroperitoneal, non-operative management failed but with delayed laparotomy results in greater contamination necessitating major surgery. In our patient, the perforation was small, well defined, and detected without delay, thus meeting all the criteria for a conservative approach. Therefore, we decided to try to close the perforation immediately with metallic clips. After successful endoscopic clipping, our patient recovered quickly without any complication and was discharged early from hospital. The immediate closure of the perforation prevented any further abdominal contamination and contributed to the good outcome of the patient. Although this complication could be resolved with the conservative management strategy of nasogastric suction and antibiotics, we believe that our patient with the size of the duodenal wall defect may require prolonged hospitalization and/or surgical management.

It must be emphasized that the endoclipping device has been designed for use through the end-viewing endoscope. Therefore, the deployment of clips is more difficult when a side-viewing endoscope is used and damage to the endoclipping device may occur. The deployment of the clips requires significant experience from the endoscopist when a duodenoscope is used, especially in a limited space as is the major papilla area. The placement of the clips should be made carefully on the upper part of the sphincterotomy to avoid closure of pancreatic or common bile duct orifice.

In cases of iatrogenic perforation, if the defect is closed early with metallic clips, contamination of the peritoneal cavity or retroperitoneal space can be minimized. Although the difference in outcome between conservative management and clipping is unknown, clipping therapy is more certain to prevent contamination.

In conclusion, when perforation is caused by ES, endoscopic closure using metallic clips without laparotomy might be the first choice of treatment, although it is essential to monitor the patient closely, with particular attention to signs of transition from localized to generalized peritonitis.

REFERENCES

1 **Freeman ML,** Nelson DB, Sherman S, Haber GB, Herman ME, Dorsher PJ, Dorsher PJ, Moore JP, Fennerty MB, Ryan ME, Shaw MJ, Lande JD, Pheley AM. Complications of endoscopic sphincterotomy. *N Engl J Med* 1996; **335**: 909-918

2 **Cotton PB,** Lehman G, Vennes J, Geenen JE, Russell RC, Meyers WC, Liguory C, Nickl N. Endoscopic sphincterotomy complications and their management: a attempt at consensus. *Gastrointest Endosc* 1991; **37**: 383-393

3 **Raju GS,** Gajula L. Endoclips for GI endoscopy. *Gastrointest Endosc* 2004; **59**: 267-279

4 **Dunham F,** Bourgeois N, Gelin M, Jeanmart J, Toussaint J, Cremer M. Retroperitoneal perforations following endoscopic

sphincterotomy: clinical course and management. *Endoscopy* 1982; **14**: 92-96

5 **Chung RS,** Sivak MV, Ferguson DR. Surgical decision in the management of duodenal perforation complicating endoscopic sphincterotomy. *Am J Surg* 1993; **165**: 700-703

6 **Chaudhary A,** Aranya RC. Surgery in perforation after endoscopic ephincterotomy: sonner, later, or not at al? *Ann R Coll Surg* 1996; **78**: 206-208

7 **Binmoeller KF,** Grimm H, Soehendra N. Endoscopic closure of a perforation using metallic clips after snare excision of a gastric leiomyoma. *Gastrointest Endosc* 1993; **39**: 172-174

8 **Wewalka FW,** Clodi PH, Haidinger D. Endoscopic clipping of esophageal perforation after pneumatic dilatation for achalasia. *Endoscopy* 1995; **27**: 608-611

9 **Cipolletta L,** Bianco MA, Torindano G, Marmo R, Piscopo R, Meucc C. Endoscopic clipping of perforation following pneumatic dilation of esophagojejunal anastomotic strictures. *Endoscopy* 2000; **32**: 720-722

10 **Roses LL,** Ramirez AG, Seco AL, Blanco ES, Alonso DL, Avila S, Lopez BU. Clip closure of a duodenal perforation secondary to a biliary stent. *Gastrointest Endosc* 2000; **51**: 487-489

11 **Mana F,** Vogelaere KD, Urban D. Iatrogenic perforation of the colon during diagnostic colonoscopy: endoscopic treatment with clips. *Gastrointest Endosc* 2001; **54**: 258-259

12 **Yoshikane H,** Hidano H, Sakakibara A, Ayakawa T, Mori S, Kawashima H, Goto H, Niwa Y. Endoscopic repair by clipping of iatrogenic colonic perforation. *Gastrointest Endosc* 1997; **46**: 464-466

13 **Baron TH,** Gostout CJ, Herman L. Hemoclip repair of a sphincterotomy-induced duodenal perforation. *Gastrointest Endosc* 2000; **52**: 566-568

Science Editor Wang XL and Guo SY **Language Editor** Elsevier HK

PO Box 2345, Beijing 100023, China
www.wjgnet.com
wjg@wjgnet.com

ELSEVIER

World J Gastroenterol 2005;11(39):6235-6237
World Journal of Gastroenterology ISSN 1007-9327
© 2005 The WJG Press and Elsevier Inc. All rights reserved.

• *CASE REPORT* •

Ruptured hepatoblastoma with massive internal bleeding in an adult

Hung-Yen Ke, Jia-Hui Chen, Yee-Min Jen, Jyh-Cherng Yu, Chung-Bao Hsieh, Cheng-Jueng Chen, Yao-Chi Liu, Teng-Wei Chen, De-Chuan Chan

Hung-Yen Ke, Jia-Hui Chen, Yee-Min Jen, Jyh-Cherng Yu, Chung-Bao Hsieh, Cheng-Jueng Chen, Yao-Chi Liu, Teng-Wei Chen, De-Chuan Chan, Division of General Surgery, Department of Surgery, Department of Radio-Oncology, Tri-Service General Hospital, National Defense Medical Center, Taipei, Taiwan, China
Correspondence to: Dr. De-Chuan Chan, Division of General Surgery, Tri-Service General Hospital, 325, Sec. 2, Chen-Kung Road, Neihu 114, Taipei, Taiwan, China. drkehy@yahoo.com.tw
Telephone: +886-2-8792-7191 Fax: +886-2-8792-7273
Received: 2005-04-18 Accepted: 2005-05-24

Abstract

Hepatoblastoma is the most common primary hepatic tumor of children. However, only a very few cases have been reported in adults. Most studies support treatment with chemotherapy followed by surgical resection. We present the first reported case of adult hepatoblastoma in Taiwan. A 52-year-old female suffered from sudden onset of abdominal pain and general weakness for days. Internal bleeding with hemorrhagic shock was suspected and two massive lesions in both lobes of the liver with hemoperitoneum were noted from imaging studies. Surgical resection of the larger left lobe tumor and radio-frequency ablation of the right smaller one were performed. The histopathology diagnosis was of a hepatoblastoma.

© 2005 The WJG Press and Elsevier Inc. All rights reserved.

Key words: Adult hepatoblastoma; Hepatoblastoma rupture; Internal bleeding; Hepatoblastoma; Mixed type hepatoblastoma

Ke HY, Chen JH, Jen YM, Yu JC, Hsieh CB, Chen CJ, Liu YC, Chen TW, Chan DC. Ruptured hepatoblastoma with massive internal bleeding in an adult. *World J Gastroenterol* 2005; 11(39): 6235-6237
http://www.wjgnet.com/1007-9327/11/6235.asp

INTRODUCTION

Hepatoblastoma is the most common tumor of the liver for children under the age of 2 years[1]. Reports of adult cases are extremely rare. Most of these tumors arise in the embryo during the development of the liver and contain embryonic features such as numerous mitoses. They sometimes show ribbon-like, rosette-like, or papillary formations[2]. We present the first case of adult hepatoblastoma that was reported in Taiwan.

CASE REPORT

The patient was a 52-year-old female, who suffered from abdominal discomfort and called into a regional hospital for help. Abdominal computed tomography (CT) revealed two large hepatic masses with intra-abdominal fluid accumulation. Hepatic tumor with rupture was suspected, and she was referred to our hospital for further evaluation. She had been relatively healthy in the past. There was no significant past history or family history. Laboratory studies showed the following values: AST 58 U/L; ALT 44 U/L; hemoglobin 74 g/L; platelet count 101 000/UL; hepatitis B antigen negative; anti-hepatitis B antibody positive; anti-hepatitis C antibody positive. CT scans of the abdomen (Figure 1) showed massive accumulation of intra-abdominal fluid and one large heterogeneous mass (c. 11.4 cm×18.8 cm×22 cm) with cystic and solid components in the left lobe of the liver. Another homogeneous well-enhanced lesion about 3 cm wide in segment 8 of the liver was also noted. Catheter angiography (Figure 2) showed a huge hepatic tumor with faint tumor blush in the left lobe and a 2.5 cm large hypervascular tumor in the right lobe. These were presumed to be hepatocellular carcinomas. Further intra-arterial embolization was not performed because of technical problems and lack of cooperation by the patient. We diagnosed a ruptured and bleeding hepatocellular carcinoma. Exploratory laparotomy with a left lateral hepatectomy was performed to resect the tumor. Intraoperative radio-frequency ablation (RFA) was also applied to the smaller tumor in the right lobe of the liver.

The specimen recovered consisted of an encapsulated mass measuring 22 cm×16 cm×15 cm in size with extensive necrosis and hemorrhage. Grossly, it was friable and soft in consistency (Figure 3). Microscopically, histopathology sections showed pictures of immature hepatocytic epithelial elements intermixed with prominent vessels and extramedullary hematopoiesis including all three lineages (Figure 4A). There was extensive tumor necrosis and hemorrhage. Immunohistochemical stains showed the following: vimentin positive (Figure 4B); myeloperoxidase (MPO) positive for the extramedullary hematopoietic myeloid series (Figure 4C); factor 8 positive for extramedullary hematopoietic megakaryocytes (Figure 4D); CD34 positive for vascular endothelium and hematoprogenitor cells; alpha fetoprotein negative; S100 positive. These pathology results were consistent with the diagnosis of a hepatoblastoma. The patient was discharged 10 d after the operation.



Figure 1 CT scans of the abdomen showed massive accumulation of intra-abdominal fluid and one large heterogeneous mass (c 11.4 cm×18.8 cm×22 cm) with cystic and solid components in the left lobe of the liver.

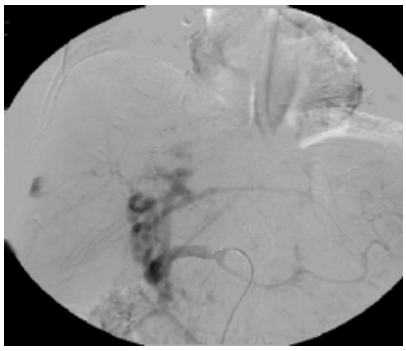


Figure 2 Catheter angiography showed a huge hepatic tumor with faint tumor blush in the left lobe and a 2.5 cm large hypervascular tumor in the right lobe. These were presumed to be hepatocellular carcinomas.



Figure 3 The specimen recovered consisted of an encapsulated mass measuring 22 cm×16 cm×15 cm in size with extensive necrosis and hemorrhage. Grossly, it was friable and soft in consistency.

DISCUSSION

Hepatoblastoma is a highly malignant tumor occurring in infants, and reports of adult cases are extremely rare. A review search in the literature revealed only 23 adult cases of hepatoblastoma including the present one. This case is also the first adult hepatoblastoma that was reported in Taiwan.

Ishank and Glunz classified hepatoblastomas into two groups in 1967: epithelial type and mixed epithelial and mesenchymal type[3]. The tumor type from this patient was distinguished from a hepatocellular carcinoma by the presence of angiodysplasia and also by the peculiar arrangement of bright and dark epithelial cells in sheets or ribbons[3-5]. This patient, therefore, had a tumor of the mixed epithelial and mesenchymal type according to this

Table 1 Summary of reported hepatoblastoma in adults

Case	Reporter	Sex/Age (yr)	Pathology type	Diagnosis	Survival time
1	Barnett[6] (1958)	M/35	Mixed	Embryonic tumor	Died 1 mo after surgery
2	Alexander[7] (1961)	F/68	Mixed	Primary mixed tumor	Postmortem
3	Ojima[8] (1964)	M/48	Mixed	Malignant mixed tumor	Postmortem
4	Kerr[5] (1966)	M/56	Mixed	Hepatic embryonic mixed tumor	Sudden death
5	Blanding[9] (1968)	M/84	Mixed	Malignant tumor	Died after biopsy
6	Cater[10] (1969)	M/78	Mixed	Hepatoblastoma	1 mo after surgery
7	Goldman[11] (1969)	F/65	Mixed	Rhabdomyosarco-hepatoma	Sudden death
8	Meyer[12] (1974)	F/19	Mixed	Hepatoblastoma	Not described
9	Ludwig[13] (1975, case 1)	F/53	Mixed	Mixed malignant tumor	Died after surgery
10	Ludwig[13] (1975, case 2)	M/40	Mixed	Mixed malignant tumor	Postmortem
11	Jameson[14] (1978)	F/51	Mixed	Hepatoblastoma	Postmortem
12	Yoshida[15] (1979)	M/60	Mixed	Hepatoblastoma	Died 2 mo after surgery
13	Honan[16] (1980)	F/27	Mixed	Mixed hepatoblastoma	Postmortem
14	Kishimoto[17] (1984)	M/60	Mixed	Malignant mixed tumor	Died 2 d after surgery
15	Kawarada[18] (1985, case 1)	M/43	Mixed	Nonhepatocytic malignant mixed tumor	Alive for 32 mo after surgery
16	Kawarada[18] (1985, case 2)	M/49	Mixed	Hepatocytic malignant mixed tumor	Postmortem
17	Sugino[2] (1989)	M/22	Epithelial	Hepatoblastoma	Died 9 mo after surgery
18	Altmann[19] (1992, case 1)	M/73	Mixed	Hepatoblastoma	Not described
19	Altmann[19] (1992, case 2)	F/35	Epithelial	Hepatoblastoma	Not described
20	Harada[20] (1995)	M/24	Mixed	Hepatoblastoma	Died 16 mo after surgery
21	Sugino[2] (1995)	F/22	Mixed	Hepatoblastoma	Alive for 38 mo after surgery
22	Ahn[1] (1997)	F/51	Mixed	Hepatoblastoma	Died 2 mo after surgery
23	Present case (2005)	F/52	Mixed	Hepatoblastoma	Alive 6 mo after surgery

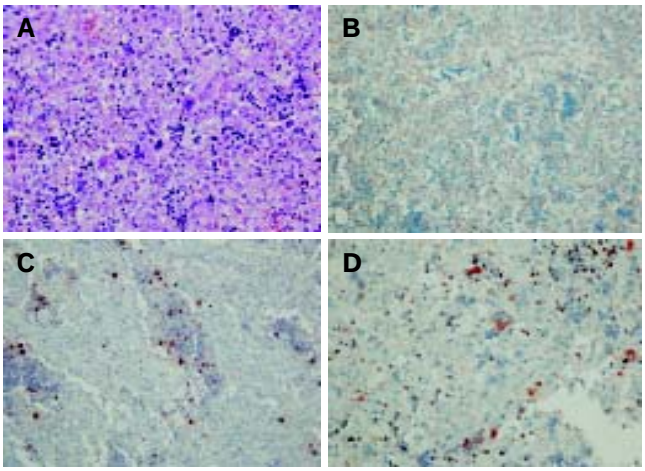


Figure 4 Immature hepatocytic epithelial elements intermixed with prominent vessels and extramedullary hematopoiesis including all three lineages (A). Vimentin positive (B); MPO positive for the extramedullary hematopoietic myeloid series (C); factor 8 positive for extramedullary hematopoietic megakaryocytes (D).

classification. Most cases in the literature are of the mixed type.

The precise mechanism to cause the tumor has been elusive; present investigations of the cytogenetic and molecular genetic aberrations in hepatoblastomas revealed involvement of chromosomal loci on 1q, 2 (or 2q), 4q, 8 (or 8q), and 20[21]. Loss of heterozygosity imprinting at locus 11p 15.5 also suggest a common genetic basis for hepatoblastoma[21]. Shin-ichi *et al*., found that abnormalities in Wnt signaling pathway seen in frequent mutation of the β-catenin gene may play a role in the genesis of hepatoblastoma[22]. They also found that the patients with hepatoblastoma with high expression of polo-like kinase 1 (PLK1) represented significantly poorer outcome[22]. Therefore, PLK1 may become a useful tool to develop new diagnostic as well as therapeutic strategies of hepatoblastoma.

Otherwise, only one of the previously reported cases was a 12-year-old boy who presented with a ruptured tumor with massive bleeding as we saw in this patient[23]. We successfully resected the larger hepatic tumor and treated the smaller one with RFA, although most adult cases of hepatoblastoma have been unresectable[4]. The clinical and pathological findings of previously reported cases and the present one are summarized in Table 1. The mean age of the 23 patients was 48.5 years and there were more males (13) than females (10). Eleven patients received surgery. Twenty one of these tumors were of the mixed type. Survival time ranged from 1 to 38 mo after surgery with a mean survival time of 9.7 mo. The prognosis for patients with this disease is very poor. Current treatments for the tumor include surgery and chemotherapy. Combination chemotherapy with adriamycin and cisplatin has been considered effective for hepatoblastoma[2]. Our patient has just been discharged and will be followed up.

REFERENCES

1 **Ahn HJ.** Mixed hepatoblastoma in an adult – A case report and literature review. *JKMS* 1997; **12**: 369–373
2 **Sugino K,** Dohi K, Matsuyama T, Asahara T, Tamamoto M. A case of hepatoblastoma occurring in an adult. *Jpn J Surg* 1989; **19**: 489–493
3 **Ishank KG,** Glunz PR. Hepatoblastoma and hepatocarcinoma in infancy and childhood: report of 47 cases. *Cancer* 1967; **20**: 396–422
4 **Inoue S,** Nagao T, Ishida Y, Wada C, Beck Y, Uchida H, Okudaira M. Successful resection of a large hepatoblastoma in a young adult: report of a case. *Surg Today* 1995; **25**: 974–977
5 **Kerr JFR.** Hepatic embryonic mixed tumor in an adult. *J Pathol Bacter* 1966; **92**: 238–240
6 **Barnett W,** Erickson E, halpert B. Embryonic tumor of the liver in an adult. *Cancer* 1958; **11**: 306-309
7 **Alexander M.** A mixed tumor of the liver in an adult. *J Pathol* 1961; **82**: 217-219
8 **Ojima MA,** Sugiyama T, Takeda T, Hazama F, Nakakuki F, Uesugi Y, Miyazaki A, Suzuki Y, Fukushima M. Six cases of rare malignant tumors of the liver. *Acta Pathol pn* 1964; **14**: 95-102
9 **Blanding J.** Mixed malignant tumors in the liver of adults. Case report and review of some features. *Arch Pathol Lab Med* 1968; **86**: 108-110
10 **Cater R.** Hepatoblastoma in an adult. *Cancer* 1969; **23**: 191-197
11 **Goldman R,** Friedman N. Rhabdomyosarcohepatoma in an adult and embryonal hepatoma in a child. *Am J Clin Pathol* 1969; **51**: 137-143
12 **Meyer P,** Livolsi V, Cornog J. Hepatoblastoma associated with oral contraceptive. *Lancet* 1974; **2**: 1387
13 **Ludwig J,** Grier MW, Hoffman HN, McGill DB. Calcified mixed alignant tumor of the liver. *Arch Pathol Lab Med* 1975; **99**: 162-166
14 **Jameson CP.** Hepatoblastoma in a middle aged South African woman. *SA Med J* 1978; **53**: 143-144
15 **Yoshida T,** Okazaki N, Yoshino M, Shimamura Y, Miyazawa N, Miyamoto K, Kishi K. A case of hepatoblastoma in adult. *Jpn J Clin Oncol* 1979; **9**: 163-168
16 **Honan RP,** Haqqani MT. Mixed hepatoblastoma in the adult: case report and review of the literature. *J Clin Pathol* 1988; **3**: 1058-1063
17 **Kishimoto Y,** Hijiya S, Nagasaki R. Malignant mixed tumor of the liver in adults. *Am J Gastroenterol* 1984; **79**: 229-235
18 **Kawarada Y,** Uehara S, Noda M, Yatani R, Mizumoto R. Nonhepatocytic malignant mixed tumor primary in the liver. *Cancer* 1985; **55**: 1790-1798
19 **Altmann HW.** Epithelial and mixed hepatoblastoma in the adult – Histological observation and general considerations. *Path Res Pract* 1992; **188**: 16-26
20 **Harada T,** Matsuo K, Kodama S, Higashihara H, Nakayama Y, Ikeda S. Adult hepatoblastoma: case report and review of the literature. *Aust New Zeal J Surg* 1995; **65**: 686-688
21 **Toshihito N,** Masanori N, Hiroyuki S, Motoaki C, Kiminobu S, Taro I, Tsugumichi K, Masahiro F, Mitsuru I, Hideo M. Cytogenetic abnormalities in hepatoblastoma: report of two new cases and review of the literature suggesting imbalance of chromosomal regions on chromosome 1, 4, and 12. *Cancer Genet Cytogenet* 2005; **156**: 8-13
22 **Yamada S,** Ohira M, Horie H, Ando K, Takayasu H, Suzuki Y, Sugano S, Hirata T, Goto T, Matsunaga T, Hiyama E, Hayashi Y, Ando H, Suita S, Kaneko M, Sasaki F, Hashizume K, Ohnuma N, Nakagawara A. Expression profiling and differential screening between hepatoblastomas and the corresponding normal livers: identification of high expression of the PLK1 oncogen as a poor-prognostic indicator of hepatoblastomas. *Oncogene* 2004; **23**: 5901-5911
23 **Toshio I,** Masahiro S, Yuki T, Toru K, Jyunichi T, Takaya M, Hiroharu T, Hisahiro N, Shinji H, Koaki O. Successful resection of a ruptured hepatoblastoma prior to chemotherapy: report of a case. *Surg Today* 2004; **34**: 710-714

Science Editor Guo SY **Language Editor** Elsevier HK

PO Box 2345, Beijing 100023, China
www.wjgnet.com
wjg@wjgnet.com

ELSEVIER

World J Gastroenterol 2005;11(39):6238
World Journal of Gastroenterology ISSN 1007-9327
© 2005 The WJG Press and Elsevier Inc. All rights reserved.

Acknowledgments to Reviewers of *World Journal of Gastroenterology*

Many reviewers have contributed their expertise and time to the peer review, a critical process to ensure the quality of *World Journal of Gastroenterology*. The editors and authors of the articles submitted to the journal are grateful to the following reviewers for evaluating the articles (including those were published and those were rejected in this issue) during the last editing period of time.

Trond Berg, Professor
Department of Molecular Biosciences, University of Oslo, PO Box 1041 Blindern, Oslo 0316, Norway

Bruno Clement, Professor
INSERM U-620, University of Rennes I, Faculty of Medicine, 2 ave. L. Bernard, Rennes 35043, France

Xue-Gong Fan, Professor
Xiangya Hospital, Changsha 410008, China

Edoardo G Giannini, Assistant Professor
Department of Internal Medicine, Gastroenterology Unit, Viale Benedetto XV, no. 6, Genoa, 16132, Italy

Hans Gregersen, Professor
The Research Administration, Aalborg Hospital, Hobrovej 42 A, Aalborg 9000, Denmark

Anna S Gukovskaya, Professor
Department of Medicine, UCLA, 11301 Wilshire Blvd, Los Angeles 91301, United States

Werner Hohenberger, Professor
Chirurgische Klinik und Poliklinik, Krankenhausstrasse 12, Erlangen D-91054, Germany

Masayoshi Ito, M.D.
Department of Endoscopy, Yotsuya Medical Cube, 5-5-27-701 Kitashinagawa, Shinagawa-ku, Tokyo 1410001, Japan

Hiroaki Itoh, M.D.
First Department of Internal Medicine, Akita University Scool of Medicine, 1-1-1, Hondou, Akita City 010-8543, Japan

Tsuneo Kitamura, Associate Professor
Department of Gastroenterology, Juntendo University Urayasu Hospital, Juntendo University School of Medicine, 2-1-1 Tomioka, Urayasu-shi, Chiba 279-0021, Japan

Zahariy Krastev, Professor
Department of Gastroneterology, Universiti Hospital "St. Ivan Rilski", #15, blvd "Acad. Ivan Geshov", Sofia 1431, Bulgaria

Shoji Kubo, M.D.
Hepato-Billiary-Pancreatic Surgery, Osaka City University Graduate School of Medicine, 1-4-3 Asahimachi, Abeno-ku, Osaka 545-8585, Japan

Fin Stolze Larsen, Associate Professor
Hepatology A-2121, Rigshospitalet Univ. Hospital of Copenhagen, Blegdamsvej 9, Copenhagen 2100, Denmark

James Neuberger, Professor
Liver Unit, Queen Elizabeth Hospital, Birmingham B15 2TH, United Kingdom

Mikio Nishioka, M.D.
Ehime Rosai Hospital, 13-27 Minami Komatsubara, Niihama 792-8550, Japan

Gustav Paumgartner, Professor
University of Munich, Klinikum Grosshadern, Marchioninistr. 15, Munich D-81377, Germany

Zhiheng Pei, Assistant Professor
Department of Pathology and Medicine, New York University School of Medicine, Department of Veterans Affairs, New York Harbor Healthcare System, 6001W, 423 East 23rd street, New York NY 10010, United States

Lun-Xiu Qin, Professor
Liver Cancer Institute and Zhongshan Hospital, Fudan University, 180 Feng Lin Road, Shanghai 200032, China

Manfred Stolte, Professor
Institute of Pathology, Klinikum Bayreuth, Preuschwitzer Str. 101, Bayreuth 95445, Germany

Michael Trauner, Professor
Medical University Graz, Auenbruggerplatz 15, Graz A-8036, Austria

Takato Ueno, Professor
Research Center for Innovative Cancer Therapy, Kurume University, 67 Asahi-machi, Kurume 830-0011, Japan

Toshio Watanabe, Associate Professor
Department of Gastroenterology, Osaka City University, Graduate School of Medicine, 1-4-3 Asahimachi, Abenoku-ku, Osaka 545-8585, Japan

Harry H-X Xia, M.D.
Department of Medicine, The University of Hong Kong, Pokfulam Road, Hong Kong, China

PO Box 2345, Beijing 100023, China
www.wjgnet.com
wjg@wjgnet.com

ELSEVIER

World J Gastroenterol 2005;11(40):6243-6248
World Journal of Gastroenterology ISSN 1007-9327
© 2005 The WJG Press and Elsevier Inc. All rights reserved.

• *GASTRIC CANCER* •

Endothelial adhesion of synchronized gastric tumor cells changes during cell cycle transit and correlates with the expression level of CD44 splice variants

Anton Oertl, Jens Castein, Tobias Engl, Wolf-Dietrich Beecken, Dietger Jonas, Richard Melamed, Roman A. Blaheta

Anton Oertl, Jens Castein, Tobias Engl, Wolf-Dietrich Beecken, Dietger Jonas, Richard Melamed, Roman A. Blaheta, Zentrum der Chirurgie, Klinik für Urologie und Kinderurologie, Johann Wolfgang Goethe-Universität, 60590 Frankfurt am Main, Germany
Supported by the "Matthias Lackas-Stiftung" and the "Gisela Stadelmann-Stiftung"
Correspondence to: Dr. Roman Blaheta, J. W. Goethe Universitätsklinik, Zentrum der Chirurgie, Klinik für Urologie und Kinderurologie, Interdisziplinäres Forschungs und Laborgebäude, Haus 25, Raum 204, Theodor-Stern-Kai 7, D-60590 Frankfurt am Main, Germany. blaheta@em.uni-frankfurt.de
Telephone: +49-69-6301-6415 Fax: +49-69-6301-7108
Received: 2005-02-24 Accepted: 2005-05-24

Abstract

AIM: To study adhesion capacity and CD44 expression of human gastric adenocarcinoma MKN45 cells at different stages of a first cell cycle.

METHODS: MKN45 cells were synchronized by aphidicolin and assayed for adhesion to an endothelial cell (HUVEC) monolayer. Surface expression of CD44 and CD44 splice variants on MKN45 cells was evaluated by flow cytometry. Functional relevance of CD44 adhesion receptors was investigated by blocking studies using anti CD44 monoclonal antibodies or by hyaluronan digestion.

RESULTS: Adhesion of MKN45 to HUVEC was increased during G2/M transit, after which adhesion returned to baseline levels with cell cycle completion. In parallel, CD44 splice variants CD44v4, CD44v5, and CD44v7 were all up-regulated on MKN45 during cell cycle progression with a maximum effect in G2/M. The function of CD44 surface receptors was assessed with specific receptor blocking monoclonal antibodies or removal of hyaluronan by digestion with hyaluronidase. Both strategies inhibited tumor cell adhesion to HUVEC by nearly 50%, which indicates that MKN45-HUVEC-interaction is CD44 dependent.

CONCLUSION: CD44 expression level is linked to the cell cycle in gastrointestinal tumor cells, which in turn leads to cell cycle dependent alterations of their adhesion behaviour to endothelium.

© 2005 The WJG Press and Elsevier Inc. All rights reserved.

Key words: Cell cycle; CD44; Adhesion; Gastrointestinal tumors

Oertl A, Castein J, Engl T, Beecken WD, Jonas D, Melamed R, Blaheta RA. Endothelial adhesion of synchronized gastric tumor cells changes during cell cycle transit and correlates with the expression level of CD44 splice variants. *World J Gastroenterol* 2005; 11(40): 6243-6248
http://www.wjgnet.com/1007-9327/11/6243.asp

INTRODUCTION

Enhanced invasive capacity and proliferative activity are among the array of functions a tumor cell must fulfil to settle as a metastasis in a distant organ. The dynamic process of tumor dissemination requires cooperative activities between the tumor cell itself and the surrounding tissue and involves several molecule classes. The CD44 transmembrane glycoproteins belong to the families of adhesion molecules and were originally thought to mediate lymphocyte homing to peripheral lymphoid tissues. It has now been recognized that CD44 molecules may also initiate metastatic spread of the tumor cells[1]. Still, the precise role of CD44 as a regulatory element of tumor growth and invasion is not clearly understood.

Several clinical studies have been carried out on patients suffering from colorectal neoplasms, but no consistent statement can be drawn about the relevance of CD44 receptors in tumor cell malignancy. Some authors hypothesize that CD44 contributes to both tumor cell proliferation and motility, whilst others do not see any logical link between CD44 expression, proliferative activity and migratory behaviour: Sumiyoshi *et al*., (28 cases) and Yue *et al*., (31 cases) reported a positive relationship between the expression of the proliferating nuclear antigen PCNA, CD44, and metastasis formation in colorectal cancer[2,3]. In contrast, no statistical correlation was found between CD44 positivity and disease free intervals in studies including a total of 113 colorectal tumor patients[4,5]. Additionally, evaluation of the characteristics of colorectal carcinoma during the metastatic process did not favour an association between CD44 expression, proliferative activity and metastatic ability of tumor cells.

Analyses of surgical specimens of 22 colorectal carcinomas revealed CD44 expression in tumors associated with proliferative areas. However, there was no apparent association between CD44 positivity and tumor stage, differentiation and progression[6]. In a further study, CD44 expression in a series of 110 colorectal carcinomas correlated well with tumor size, although extensive CD44 expression was also found in the majority of adenomas that were investigated[7]. Based on a

topographical investigation, the cellular localization of CD44 and PCNA was found to be different in colorectal tumor cells, and PCNA was present most frequently in cells lacking CD44. The authors concluded that tumors, negative for CD44, have a higher probability of replicating[8].

The conflicting results are partially caused by the retrospective nature of immunohistochemical studies. Furthermore, examination of tissue specimen does not allow unequivocable evaluation of the time-dependent dynamics of tumor-host interactions. There is no doubt that tumor dissemination and malignancy is characterized by a fine-tuned interplay between CD44 expression level, cell cycle activation and migratory capacity. However, there is still little knowledge about how these processes are linked together. To clearly assess if CD44 triggered tumor cell invasion is cell-cycle dependent, we established a cell culture system consisting of aphidicolin-synchronized human gastric adenocarcinoma MKN45 cells. CD44 surface expression was quantified, when MKN45 cells were released into S-phase, G2/M-phase and G0/G1-phase, as well as when adhering to human umbilical vein endothelial cells (HUVEC).

MATERIALS AND METHODS

Cell cultures

Endothelial cells (HUVEC) were isolated from human umbilical veins and harvested by enzymatic treatment with chymotrypsin. HUVEC were grown in Medium 199 (Biozol, Munich, Germany), 10% fetal calf serum (FCS; Gibco, Karlsruhe, Germany), 10% pooled human serum (Blood Bank of The German Red Cross, Frankfurt am Main, Germany), 20 μg/mL endothelial cell growth factor (Boehringer, Mannheim, Germany), 0.1% heparin (Roche, Basel, Switzerland), 100 ng/mL gentamicin (Gibco) and 2% 1 mol/L HEPES-buffer (Seromed, Berlin, Germany). To control the purity of HUVEC cultures, cells were stained with fluorescein isothiocyanate (FITC)- labelled monoclonal antibody against Factor VIII-associated antigen (Von Willebrand factor; clone F8/86; Dako, Hamburg, Germany) and analyzed microsc-opically, or by FACscan (Becton Dickinson, Heidelberg, Germany; FL-1H (log) channel histogram analysis; 1×10^4 cells/scan). Cell cultures with a purity >95% were serially passaged. Subcultures from passages 2-4 were selected for experimental use.

Human gastric adenocarcinoma MKN45 cells were obtained from the tumor cell bank of the Johannes Gutenberg University, Mainz, Germany, and grown in RPMI medium supplemented with 10% FCS, 100 ng/mL gentamicin and 2% 1 mol/L HEPES-buffer. To prepare the tumor cells for the invasion assays, cells were detached from the culture flasks by Accutase (PAA Laboratories).

Cell synchronization

MKN45 cells were reversibly blocked at the G1/S transition by a 24 h treatment with 5 μg/mL aphidicolin (Sigma, München, Germany). To allow S-phase progression, cells were washed extensively and replated in tumor cell culture medium in the absence of aphidicolin. Cells were sampled at successive time points to assess their position in the cell cycle, their adhesion capacity and their CD44 expression level. Non-synchronized control cell cultures were incubated in aphidicolin free culture medium. Viability of tumor cells was assessed by propidium iodide dsDNA-intercalation (facs-analysis) or by the evaluation of lactate dehydrogenase (LDH) release (Cytotoxicity Detection Kit; Roche) at 490 nm using an automatic microtiter plate reader.

Flow cytometric analysis of cell cycle status

MKN45 cells were reversibly blocked with aphidicolin and subsequently washed and replated in tumor cell culture medium in the absence of aphidicolin. Cells were sampled at successive time points and incubated with propidium iodide and RNAse (Cycle Test Plus; Becton Dickinson). DNA content and cell cycle distribution were analyzed using a Becton Dickinson FACScan flow cytometer. Cytofluorometric analysis was performed using CellQuest software (Becton Dickinson), on 10 000 cells per sample. The percentage of cells in S-phase, G2/M-phase and G0/G1-phase was determined using Modfit 2.0 software (Becton Dickinson).

Flow cytometric analysis of CD44 expression

CD44 standard and splice variant (v) expression were determined with anti human CD44 monoclonal antibodies: CD44standard, clone SFF-2; CD44v3, clone VFF-327v3; CD44v4, clone VFF-11; CD44v5, clone VFF-8; CD44v6, clone VFF-7; CD44v7, clone VFF-9; CD44v7+8, clone VFF-17; CD44v10, clone VFF-14 (all: Bender MedSystems, Eching, Germany). Primary antibodies were conjugated with fluorescein isothiocyanate (FITC). CD44 surface expression of MKN45 cells was then measured using a FACscan (Becton Dickinson; FL-1H (log) channel histogram analysis; 1×10^4 cells/scan) and expressed as mean fluorescence units (MFU). Mouse IgG1-FITC (Dianova-CBL, Hamburg, Germany) was used as an isotype control.

Adhesion of MKN45 to HUVEC monolayer

HUVEC were transferred to six-well multiplates (Falcon Primaria; Becton Dickinson). When confluency was reached, MKN45 cells (synchronized *versus* non-synchronized) were detached from the culture flasks and 0.5×10^6 cells were then added to the HUVEC monolayer for 60 min. Subsequently, non-adherent tumor cells were washed off using 37 ℃ Medium 199. The remaining cells were fixed with 1% glutaraldehyde. Adherent tumor cells were counted in five different fields of a defined size (5 mm×0.25 mm) using a phase contrast microscope (20×objective) and the mean cellular adhesion rate was calculated. Proliferative activity of tumor cells was estimated by the PicoGreen assay[9]. Cells were washed and dried at several time points (0-24 h). Cells were then digested with papain (0.125 mg protein/mL) for 20 h at 60 ℃. Thereafter, the fluorescent dye PicoGreen (MoBiTec, Goettingen, Germany), which shows high specificity for dsDNA, was added (1:200 dilution) for 10 min at 20 ℃. Fluorescence intensity was determined using a computer-controlled fluorescence reader (Cytofluor 2300 plate scanner; Millipore, Eschborn, Germany) at λ_{ex} = 485 nm and λ_{em} = 530 nm.

CD44 blocking experiments

MKN45 cells were preincubated for 60 min with anti CD44v4,

anti CD44v5 or anti CD44v7 monoclonal antibodies at 1:80 dilution. MKN45 cells were then added to HUVEC monolayer to evaluate the adhesion capacity as described above. In a second set of experiments, HUVEC were treated with hyaluronidase (Worthington, Lakewood, USA) for 60 min (1 000 U/mL, 2 500 U/mL, or 5 000 U/mL), before MKN45 cells were added. Non treated HUVEC served as the controls. Adhesion capacity of tumor cells was then analyzed as described above.

Statistical analysis

All studies were performed 3-6 times. Statistical significance was investigated by the Wilcoxon-Mann-Whitney-*U*-test. Differences were considered statistically significant at a *P* value less than 0.05.

RESULTS

Synchronization of MKN45 cells

MKN45 tumor cells were synchronized to monitor the changes in adhesion behaviour at various stages during cell cycle transit. The procedure based on treatment with aphidicolin effectively allowed us to follow cells in distinct phases of a single cell cycle prior to any cell division: in G0/G1, at the G2/M transition and in S phase.

Non-synchronized MKN45 reside in the S phase of the cell cycle (Figure 1). However, they were reversibly blocked at the G1/S transition by a 24 h treatment with 5 μg/mL aphidicolin. After extensive washing and replacement in fresh medium to allow cell cycle progression, MKN45 quickly entered S phase after 4 h and reached G2/M after 8 h. MKN accumulated in G0/G1 after 16 h (Figure 1).

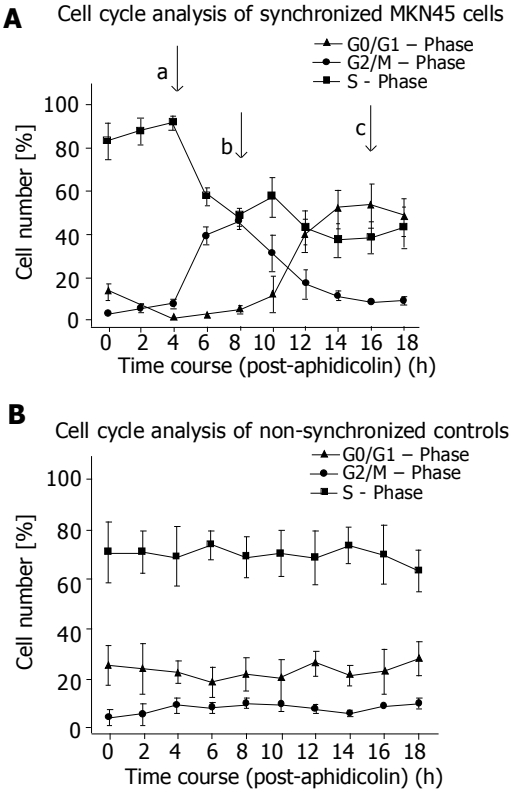


Figure 1 Facs analysis of synchronized MKN45 cells. Cell number is given in %. Non-synchronized control cells reside in the S-phase of the cell cycle. When MKN45 cells were blocked with aphidicolin and then replated in fresh medium to allow cell cycle progression, MKN45 entered S phase after 4 h (arrow a), G2/M after 8 h (arrow b) and G0/G1 after 16 h (arrow c). Mean±SD of *n* = 3 experiments (**A**,**B**).

Aphidicolin synchronization had no toxic effects on MKN45 because cell viability and adhesion events of synchronized cells to HUVEC were not diminished, compared to untreated controls.

Adhesion of synchronized MKN45 to HUVEC

Adhesion of MKN45 to HUVEC was determined at 0 h (immediately after washing out aphidicolin), 4, 8, and 16 h after the end of aphidicolin treatment. This was in accordance to the maximum accumulation of synchronized MKN45 in the S phase, G2/M phase or in G0/G1. Typically, adhesion capacity increased when cells progressed to G2/M (Figure 2; $P<0.05$). The increased number of adherent MKN45 seen after 8 h was not due to an increase in the total cell number. The PicoGreen assay, which had been carried out as well, revealed no proliferative activity of MKN45 during the experimental procedure. Furthermore, non-synchronous control cultures adhered to HUVEC uniformly at all time points.

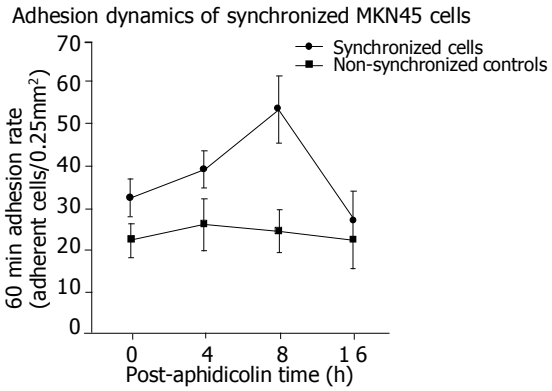


Figure 2 Adhesion capacity of synchronized MKN45 cells to HUVEC. MKN45 cells were treated for 24 h with aphidicolin. Cells were then washed and replated in fresh medium to allow cell cycle progression. Cells were sampled after 0, 4, 8 and 16 h following aphidicolin treatment (*n* = 6). A 60-min adhesion to HUVEC was determined at each time point and compared with non-synchronous cells. Mean±SD of *n* = 6 experiments.

Expression of CD44 variants on synchronized MKN45 cells

Analysis of CD44 expression in asynchronous control cultures revealed significant expression of CD44 splice variants CD44v4, CD44v5, and CD44v7. CD44 variants CD44v3, CD44v6, CD44v8, and CD44v10 were not detected (Figure 3). Therefore, subsequent studies concentrated on CD44v4, CD44v5, and CD44v7 adhesion receptors. To correlate the differences in CD44 expression level during cell cycle transit with parallel changes of MKN45 adhesion behavio, CD44 splice variants were evaluated 0, 4, 8, 12, and 16 h after the end of aphidicolin treatment. Figure 4 shows that CD44v4, CD44v5 and CD44v7 expression in synchronized cell cultures were all up-regulated during cell cycle progression with a maximum effect 8 h after the experimental onset, i. e. in G2/M ($P<0.05$). In contrast, non-synchronized MKN45

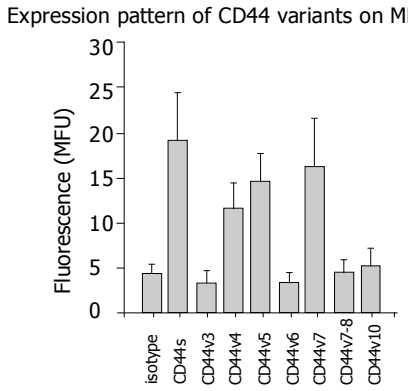


Figure 3 Facs analysis of CD44 and CD44 splice variant expression of MKN45 cells. Primary antibodies, indicated in methods, were conjugated with fluorescein isothiocyanate (FITC). CD44 surface expression of MKN45 cells was then measured using a FACscan (FL-1H (log) channel histogram analysis; 1 x10^4 cells/scan) and expressed as mean fluorescence units (MFU). Mouse IgG1-FITC was used as an isotype control. Mean±SD of n = 3 experiments.

expressed CD44 variants equally well at all time points.

Relevance of CD44 for MKN45 adhesion

To evaluate whether CD44v4, v5 and v7 receptors facilitate adhesion of MKN45 to HUVEC, tumor cells were treated with their respective monoclonal antibodies, or the CD44 ligand hyaluronan on HUVEC was removed by digestion with hyaluronidase. Pretreatment of MKN45 cells with anti CD44 monoclonal antibodies decreased adhesion to HUVEC by nearly 50%, irrespective of the CD44 splice variant used (P<0.05). In good accordance, digestion of hyaluronan on HUVEC blocked MKN45 cell attachment to HUVEC with a maximum effect at a hyaluronidase concentration of 2 500 U/mL (P<0.05; Figure 5).

DISCUSSION

CD44, an integral membrane glycoprotein expressed by many cell types, serves as the principal receptor which binds hyaluronan and might be a determinant of metastatic and invasive behaviour in carcinomas[10]. One of the basic features of carcinoma cells is their ability to generate a large number of alternatively spliced isoforms of CD44[11,12]. Although the structural characteristics of these isoforms are documented, the functional consequences of CD44 isoform expression on the biology of colon cancer cells still remains unclear.

CD44 surface analysis demonstrated that MKN45 tumor cells strongly express the CD44 splice variants CD44v4, CD44v5 and CD44v7. This is in good accordance with studies on tissue specimens revealing elevated expression of CD44v5 in human colon carcinoma cells which was associated with tumor progression and growth[13]. Mulder and coworkers observed high expression of CD44v5 in most colorectal neoplasms (83%-96%), independent of stage, which indicates that CD44v5 might be an earlier marker of colonic epithelium transformation[14,15]. Using immunohistochemical staining and Northern blotting, Harn HJ *et al.* showed that the expression of CD44 variant encoding exon v5 was up-regulated in human gastric carcinomas[16]. Most notably, CD44v5 was expressed preferentially in poorly differentiated human gastric carcinomas and metastatic lymph nodes[17].

Overexpression of CD44 variants v4 and v7 contributes to the genesis of gastric cancer as well[18,19], although limited data are available and the biological significance of the receptor modulation is not clear[20].

Based on our adhesion-blocking study using specific anti-CD44 monoclonal antibodies, we hypothesize that CD44v4, CD44v5, as well as CD44v7 receptors are important elements which regulate adhesive interactions between gastric tumor cells and the vessel wall. Results of additional experiments, in which endothelial cells were treated with hyaluronidase, further demonstrate that the interaction of CD44 molecules on MKN45 cells with hyaluronan on HUVEC is a critical factor in the adhesion process.

To address the question of whether CD44 expression is linked to the cell cycle, the CD44 splicing isoforms CD44v4, CD44v5 and CD44v7 were evaluated on synchronized MKN45 tumor cells. Intriguingly, CD44 variants increased after cells were released from arrest, showing maximal expression 8 h after the experimental onset. At the same time point, cells passed through G2/M. Therefore, these experiments clearly indicate that CD44 receptor expression "follows" the proliferative

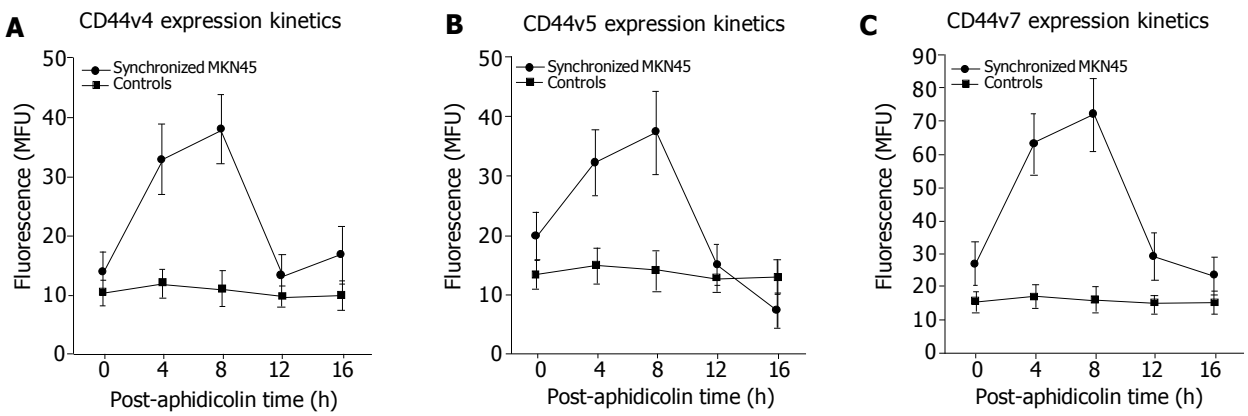


Figure 4 Expression of CD44v4(**A**), CD44v5(**B**) and CD44v7(**C**) on MKN45 cells during cell cycle transit. Synchronized MKN45 cells were labeled with anti-CD44v4, anti-CD44v5 or anti-CD44v7 at indicated time points. Non-synchronized cells served as controls. Fluorescence intensity was measured using a FACscan (FL-1H (log) channel histogram analysis; 1 x10^4 cells/scan) and expressed as mean fluorescence units (MFU). Mean±SD of n = 6 experiments.

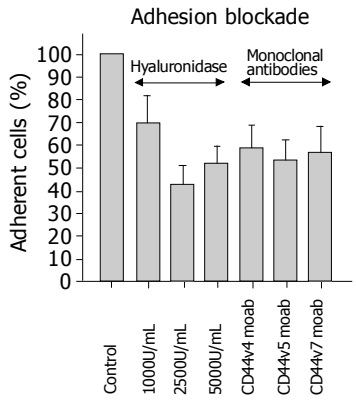


Figure 5 MKN45 cells were preincubated for 60 min with anti CD44v4, anti CD44v5 or anti CD44v7 monoclonal antibodies at 1:80 dilution. MKN45 cells were then added to HUVEC monolayer to evaluate the adhesion capacity (right part of Figure 5). In a second set of experiments, HUVEC were treated with hyaluronidase for 60 min (1 000, 2 500, or 5 000 U/mL), before MKN45 cells were added (left part of Figure 5). Non treated HUVEC served as the 100% control. Mean±SD of n = 6 experiments.

activity of tumor cells with an enhanced expression level in G2/M, and subsequent repression in G0/G1 and S.

This is the first report demonstrating a link between cell cycle and CD44 expression in gastric carcinoma cells. However, data derived from other tumor entities support our findings. CD44 ligation with an anti-CD44 monoclonal antibody inhibited the proliferation of human acute myeloid leukemia cells. The effects of anti-CD44 on myeloid cells were associated with specific disruption of cell cycle events and induction of G0/G1 arrest[21]. Experimentally induced proliferation blockade of malignant rhabdoid tumors led to an accumulation in G0/G1, which was accompanied by CD44 down-regulation[22]. In a similar way, CD44 was down-modulated, when human breast cancer cells were blocked in the G1 phase[23]. Interestingly, analysis of 131 patients who underwent surgery for papillary thyroid carcinoma revealed a close relation between extrathyroidal invasion, G2M-phase fraction and CD44 expression[24].

The molecular background of the cell cycle-CD44 axis has not been evaluated in detail. Experiments on myeloid leukemia cells demonstrated that ligation of CD44 with monoclonal antibodies causes growth arrest through the down-regulation of c-Jun expression via AP-1 sites. Decreased JNK expression and a consequent decrease in c-Jun phosphorylation was also assumed to be involved in the down-regulation of the c-Jun promoter activity[21]. Nevertheless, although this is an attractive hypothesis, these events might not necessarily occur in our culture system. Several authors describe progressive changes of the p53 protein and the anti-apoptotic protein bcl-2 in carcinomas, with an inverse relationship between p53, bcl-2 and CD44 expression[7,25]. Both p53 and bcl-2, as well as their downstream targets p21, p27, and/or p130, play key roles in cell proliferation and cell cycle progression[26,27], and therefore might also contribute to CD44 modulation.

The finding that CD44 surface expression was altered during mitosis, together with the fact that CD44 receptors regulate tumor cell endothelial cell interactions, prompted us to speculate that tumor cells change their adhesive behaviour in a cell-cycle dependent manner. Indeed, the number of synchronized MKN45 binding to HUVEC drastically increased in G2/M, and dropped down to basal values in G0/G1 and S. The adhesion dynamics exactly match the cell-cycle dependent expression course of CD44 variants v4, v5, and v7. Based on this, we conclude that CD44 expression level, cell cycle activation and migratory capacity of gastric tumor cells are linked together, with the most aggressive behaviour of tumors in the G2/M phase.

From a clinical viewpoint, therapeutic modulation of the tumor cell cycle might alter the sensitivity of these cells to anti-tumoral compounds and, consequently, might enhance the efficacy of the current treatment protocols.

ACKNOWLEDGMENTS

We would like to thank Karen Nelson for critically reading the manuscript.

REFERENCES

1 **Jothy S**. CD44 and its partners in metastasis. *Clin Exp Metastasis* 2003; **20**: 195-201
2 **Sumiyoshi Y**, Yamashita Y, Maekawa T, Sakai N, Shirakusa T, Kikuchi M. Expression of CD44, vascular endothelial growth factor, and proliferating cell nuclear antigen in severe venous invasional colorectal cancer and its relationship to liver metastasis. *Surg Today* 2000; **30**: 323-327
3 **Yue SQ**, Yang YL, Dou KF, Li KZ. Expression of PCNA and CD44mRNA in colorectal cancer with venous invasion and its relationship to liver metastasis. *World J Gastroenterol* 2003; **9**: 2863-2865
4 **Jungling B**, Menges M, Goebel R, Wittig BM, Weg-Remers S, Pistorius G, Schilling M, Bauer M, Konig J, Zeitz M, Stallmach A. Expression of CD44v6 has no prognostic value in patients with colorectal cancer. *Z Gastroenterol* 2002; **40**: 229-233
5 **Indinnimeo M**, Cicchini C, Giarnieri E, Stazi A, Mingazzini PL, Stipa V. Evaluation of CD44 variant 6 expression and clinicopathological factors in pulmonary metastases from colon carcinoma. *Oncol Rep* 2003; **10**: 1875-1877
6 **Abbasi AM**, Chester KA, Talbot IC, Macpherson AS, Boxer G, Forbes A, Malcolm AD, Begent RH. CD44 is associated with proliferation in normal and neoplastic human colorectal epithelial cells. *Eur J Cancer* 1993; **29A**: 1995-2002
7 **Ioachim E**, Goussia A, Agnantis NJ. Glycoprotein CD44 expression in colorectal neoplasms. An immuno-histochemical study including correlation with cathepsin D, extracellular matrix components, p53, Rb, bcl-2, c-erbB-2, EGFR and proliferation indices. *Virchows Arch* 1999; **434**: 45-50
8 **Furuta K**, Zahurak M, Yang XL, Rosada C, Goodman SN, August JT, Hamilton SR. Relationship between CD44 expression and cell proliferation in epithelium and stroma of colorectal neoplasms. *Am J Pathol* 1996; **149**: 1147-1155
9 **Blaheta RA**, Kronenberger B, Woitaschek D, Weber S, Scholz M, Schuldes H, Encke A, Markus BH. Development of an ultrasensitive *in vitro* assay to monitor growth of primary cell cultures with reduced mitotic activity. *J Immunol Methods* 1998; **211**: 159-169
10 **Miyake K**, Underhill CB, Lesley J, Kincade PW. Hyaluronate can function as a cell adhesion molecule and CD44 participates in hyaluronate recognition. *J Exp Med* 1990; **172**: 69-75
11 **Tarin D**, Bolodeoku J, Hatfill SJ, Sugino T, Woodman AC, Yoshida K. The clinical significance of malfunction of the CD44 locus in malignancy. *J Neurooncol* 1995; **26**: 209-219
12 **Tolg C**, Hofmann M, Herrlich P, Ponta H. Splicing choice from 10 variant exons establishes CD44 variability. *Nucleic Acids Res* 1993; **21**: 1225-1229
13 **Leister I**, Manegold S, Schuler P, Alves F, Becker H, Fuzesi L,

Markus PM. Effect of laparotomy and CO(2) pneumoperitoneum on tumor growth of human colon carcinoma and expression pattern of tumor-associated proteins in the SCID mouse. *Int J Colorectal Dis* 2003; **18**: 508-513

14 **Mulder JW**, Wielenga VJ, Polak MM, van den Berg FM, Adolf GR, Herrlich P, Pals ST, Offerhaus GJ. Expression of mutant p53 protein and CD44 variant proteins in colorectal tumorigenesis. *Gut* 1995; **36**: 76-80

15 **Mulder JW**, Kruyt PM, Sewnath M, Seldenrijk CA, Weidema WF, Pals ST, Offerhaus GJ. Difference in expression of CD44 splice variants between proximal and distal adenocarcinoma of the large bowel. *Br J Surg* 1995; **82**: 1468-1470

16 **Heider KH**, Dammrich J, Skroch-Angel P, Muller-Hermelink HK, Vollmers HP, Herrlich P, Ponta H. Differential expression of CD44 splice variants in intestinal- and diffuse-type human gastric carcinomas and normal gastric mucosa. *Cancer Res* 1993; **53**: 4197-4203

17 **Harn HJ**, Ho LI, Chang JY, Wu CW, Jiang SY, Lee HS, Lee WH. Differential expression of the human metastasis adhesion molecule CD44V in normal and carcinomatous stomach mucosa of Chinese subjects. *Cancer* 1995; **75**: 1065-1071

18 **Montgomery E**, Abraham SC, Fisher C, Deasel MR, Amr SS, Sheikh SS, House M, Lilliemoe K, Choti M, Brock M, Ephron DT, Zahuruk M, Chadburn A. CD44 loss in gastric stromal tumors as a prognostic marker. *Am J Surg Pathol* 2004; **28**: 168-177

19 **Torbenson M**, Dhir R, Nangia A, Becich MJ, Kapadia SB. Prostatic carcinoma with signet ring cells: a clinicopathologic and immunohistochemical analysis of 12 cases, with review of the literature. *Mod Pathol* 1998; **11**: 552-559

20 **Tempfer C**, Losch A, Heinzl H, Hausler G, Hanzal E, Kolbl H, Breitenecker G, Kainz C. Prognostic value of immunohistochemically detected CD44 isoforms CD44v5, CD44v6 and CD44v7-8 in human breast cancer. *Eur J Cancer* 1996; **32A**: 2023-2025

21 **Zada AA**, Singh SM, Reddy VA, Elsasser A, Meisel A, Haferlach T, Tenen DG, Hiddemann W, Behre G. Downregulation of c-Jun expression and cell cycle regulatory molecules in acute myeloid leukemia cells upon CD44 ligation. *Oncogene* 2003; **22**: 2296-2308

22 **Oruetxebarria I**, Venturini F, Kekarainen T, Houweling A, Zuijderduijn LM, Mohd-Sarip A, Vries RG, Hoeben RC, Verrijzer CP. P16INK4a is required for hSNF5 chromatin remodeler-induced cellular senescence in malignant rhabdoid tumor cells. *J Biol Chem* 2004; **279**: 3807-3816

23 **Righi L**, Deaglio S, Pecchioni C, Gregorini A, Horenstein AL, Bussolati G, Sapino A, Malavasi F. Role of CD31/platelet endothelial cell adhesion molecule-1 expression in *in vitro* and *in vivo* growth and differentiation of human breast cancer cells. *Am J Pathol* 2003; **162**: 1163-1174

24 **Kurozumi K**, Nakao K, Nishida T, Nakahara M, Ogino N, Tsujimoto M. Significance of biologic aggressiveness and proliferating activity in papillary thyroid carcinoma. *World J Surg* 1998; **22**: 1237-1242

25 **Jackson PA**, Green MA, Pouli A, Hubbard R, Marks CG, Cook MG. Relation between stage, grade, proliferation, and expression of p53 and CD44 in adenomas and carcinomas of the colorectum. *J Clin Pathol* 1995; **48**: 1098-1101

26 **Vairo G**, Soos TJ, Upton TM, Zalvide J, DeCaprio JA, Ewen ME, Koff A, Adams JM. Bcl-2 retards cell cycle entry through p27(Kip1), pRB relative p130, and altered E2F regulation. *Mol Cell Biol* 2000; **20**: 4745-4753

27 **Kaul R**, Mukherjee S, Ahmed F, Bhat MK, Chhipa R, Galande S, Chattopadhyay S. Direct interaction with and activation of p53 by SMAR1 retards cell-cycle progression at G2/M phase and delays tumor growth in mice. *Int J Cancer* 2003; **103**: 606-615

Science Editor Guo SY **Language Editor** Elsevier HK

PO Box 2345, Beijing 100023, China
www.wjgnet.com
wjg@wjgnet.com

ELSEVIER

World J Gastroenterol 2005;11(40):6249-6253
World Journal of Gastroenterology ISSN 1007-9327
© 2005 The WJG Press and Elsevier Inc. All rights reserved.

Preliminary study on proteomics of gastric carcinoma and its clinical significance

Hong-Gang Qian, Jing-Shen, Hong Ma, Hua-Chong Ma, Ya-Hui Su, Chun-Yi Hao, Bao-Cai Xing, Xin-Fu Huang, Cheng-Chao Shou

Hong-Gang Qian, Jing-Shen, Hong Ma, Ya-Hui Su, Chun-Yi Hao, Bao-Cai Xing, Xin-Fu Huang, Cheng-Chao Shou, Peking University School of Clinical Oncology and Beijing Cancer Hospital, Beijing 100036, China
Hua-Chong Ma, Beijing Chaoyang Hospital, Beijing 10020, China
Supported by the Major State Basic Research Development Program of China (973 Program), No. 20004CB518702
Correspondence to: Dr. Hong-gang Qian, Department of Surgery, Peking University School of Clinical Oncology and Beijing Cancer Hospital, 52 Fucheng lu, Haidian District, Beijing 100036, China. qianhg@sohu.com
Telephone: +86-10-88121122-2099 Fax: +86-10-88141293
Received: 2005-03-21 Accepted: 2005-04-18

Abstract

AIM: To explore the preliminary identification of serum protein pattern models that may be novel potential biomarkers in the detection of gastric cancer.

METHODS: A total of 130 serum samples, including 70 from patients with gastric cancer and 60 from healthy adults, were detected by surface-enhanced laser desorption and ionization time-of-flight mass spectrometry (SELDI-TOF-MS). The data of spectra were analyzed by Biomarker Patterns Software (BPS). Thirty serum samples of gastric cancer patients and 30 serum samples of healthy adults were grouped into the training group to build models, and the other 70 samples were used to test and evaluate the models. The samples of the test group were judged only with their peaks' height and were separated into cancer group or healthy control group by BPS automatically and the judgments were checked with the histopathologic diagnosis of the samples.

RESULTS: Sixteen mass peaks were found to be potential biomarkers with a significant level of $P<0.01$. Among them, nine mass peaks showed increased expression in patients with gastric cancer. Analyzed by BPS, two peaks were chosen to build the model for gastric cancer detection. The sensitivity, specificity, and accuracy of the model were 90%, 36/40, 86.7%, 26/30, and 88.6%, 62/70, respectively, which were greatly higher than those of clinically used serum biomarkers CEA (carcinoembryonic antigen), CA19-9 and CA72-4. Stage I/II gastric cancer samples of the test group were all judged correctly.

CONCLUSION: The novel biomarkers in serum and the established model could be potentially used in the detection of gastric cancer. However, large-scale studies should be carried on to further explore the clinical impact on the model.

© 2005 The WJG Press and Elsevier Inc. All rights reserved.

Key words: SELDI-TOF-MS; Serum; Gastric cancer

Qian HG, Shen J, Ma H, Ma HC, Su YH, Hao CY, Xing BC, Huang XF, Shou CC. Preliminary study on proteomics of gastric carcinoma and its clinical significance. *World J Gastroenterol* 2005; 11(40): 6249-6253
http://www.wjgnet.com/1007-9327/11/6249.asp

INTRODUCTION

Gastric cancer is the second leading cause of cancer death in the world and is predicted still to be one of the leading causes of all deaths in the near future[1,2]. Almost 40% of gastric cancer cases occur in China, where it is the most common cancer. According to WHO IARC (International Agency for Research on Cancer) database and Globocan 2002 database, about 393 000 cases are diagnosed with gastric cancer in China, and of these about 308 000 have died. However, few specific tumor markers with high sensitivity could be useful in the diagnosis of gastric cancer. The sensitivity of existing serum biomarkers carcinoembryonic antigen (CEA), CA19-9 or CA72-4 is only about 40%[3-6].

Proteomic technologies, especially the surface-enhanced laser desorption/ionization time-of-flight mass spectrometry (SELDI-TOF-MS) technology, are providing the tools needed to discover and identify the disease-associating biomarkers[7-10]. Ciphergen Biosystems has developed the ProteinChip technology coupled with SELDI-TOF-MS to facilitate protein profiling of complex biological mixtures[11-14]. In SELDI-TOF-MS analysis, a nitrogen laser desorbs the protein/energy-absorbing molecule mixture from the array surface, enabling the detection of the proteins captured by the array[15,16]. It has been reported recently that the promising SELDI-TOF-MS technology could be used for the diagnosis of cancer by analyzing the protein markers in serum[17,18]. Moreover, the SELDI-TOF-MS technology could be used to analyze other kinds of sample, such as nipple aspirate fluid, urine,

serum-free conditioned medium of cell culture, *etc*.[19-21].

In this study, not only 16 peaks were identified as the potential biomarkers with a significant level of $P<0.01$, but also a model of two markers combination was established, which can be used in the detection of gastric cancer. In the double-blind test, this model was evaluated. The sensitivity, specificity, and accuracy are much better than those of any other biomarker used clinically.

MATERIALS AND METHODS

Serum samples

A total of 130 serum specimens from 60 healthy adults and 70 patients with gastric cancer were obtained from Tissue Bank of Beijing Cancer Hospital and Beijing Chaoyang Hospital in 2002-2003. All patients of gastric cancer were confirmed histopathologically. Serum samples of gastric cancer had been collected from patients preoperatively and without chemotherapy. The median age of the patients with gastric cancer was 64 years (range, 32-81 years), and the median age of the control group was 52 years (range, 15-84 years). The TNM staging of 70 patients with gastric cancer are shown in Table 1. All samples were obtained with the consent of the patient and Institutional Review Board approval.

Table 1 Samples of control and gastric cancer staged by TNM classification

	Training group	Test group	Total
Gastric cancer	30	40	70
Stage I	6	6	
Stage II	4	5	
Stage III	12	16	
Stage IV	8	13	
Control	30	30	60
Total	60	70	130

Preparation of serum samples for SELDI analysis

All samples were stored at -80 °C until use. WCX2 (Weak Cation Exchange) chips and software were provided by Ciphergen Biosystems (Fremont, CA, USA). The array spots of WCX2 chips were preactivated with binding buffer (100 mmol/L sodium acetate, pH 4.5) at room temperature for 5 min in a humidifying chamber with gently shaking, and repeated once. Each serum sample was first diluted 1:2 with 1% DTT U9 (DTT: dithiothreitol; U9: 9 mol/L urea, 2% Chaps, 50 mmol/L Tris-HCl, pH 9.0), and then diluted 1:12 in binding buffer. One hundred microliters of each diluted sample was spotted onto preactivated WCX2 protein array chips and incubated in a humidfiying chamber for 1 h at room temperature. The chips were washed twice with binding buffer and once with HPLC H_2O, air-dried, then sequentially treated by 0.5 μL 100% saturated sinapinic acid (3,5-dimethoxy-4-hydroxycinnamic acid) solution twice. The sinapinic acid solution was 50% acetonitrile and 0.5% trifluoroacetic acid. The chips were analyzed by the Ciphergen ProteinChip Reader (model PBSII). All reagents were provided by Sigma Co.

Ciphergen ProteinChip SELDI-TOF-MS analysis

The mass spectra of proteins were generated by using 112 laser shots at a laser intensity of 175-180.The optimized detection size range was between 3 000 and 10 000 u, with a high mass to 100 000 u. The laser was focused at by optimization center. The starting detector sensitivity was set at 9, and the mass deflector was set to 800 u.

Statistical analysis

The data were analyzed with Ciphergen ProteinChip Software version 3.1.1 (Ciphergen Biosystems). For comparison, the mass peaks of test group (n=70) were normalized to that of all 60 training samples using one peak as common calibrate before analysis. The Biomarker Wizard application (Ciphergen Biosystems) was used to automatically detect mass peaks to cluster. Peak labeling was completed by using first-pass 7 S/N, minimum peak threshold 30% of all, second-pass 3 S/N, with 0.3% of the cluster mass window, and estimated peaks were added. The cluster data was analyzed by using Biomarker Patterns™ Software (BPS) 4.0.1 (Ciphergen Biosystems).

RESULTS

By using Biomarker Wizard application, more than 100 mass peaks were identified in the samples of the training group, and 16 qualified mass peaks were identified with a significant level of $P<0.01$ (Table 2). Nine mass peaks, 7 567, 15 117, 15 326, 15 847, 7 934, 4 524, 8 052, 6 982, 4 714 u, showed increased expression in patients with gastric cancer. The other seven mass peaks, 5 252, 2 675, 5 546, 5 340, 4 177, 3 995, 3 245 u, showed decreased expression in patients with gastric cancer. A representative pseudogel view of specific candidate gastric cancer tumor markers and a stacked trace view of candidate markers from diseased *vs* control individuals are shown in Figure 1.

All clusters were exported to BPS 4.0.1 and analyzed.

Table 2 Mass peaks found in the model group

M/Z	*P*	Mean-cancer	Mean-control
7 567	0.0000000037	9.92	2.14
15 117	0.0000001024	10.14	1.69
15 326	0.0000002675	2.57	0.60
15 847	0.0000286434	7.08	2.32
5 252	0.0000742542	1.59	4.24
2 675	0.0006036111	1.16	2.29
5 546	0.0008794540	2.09	3.97
7 934	0.0012685350	8.04	3.25
4 524	0.0013355919	2.63	1.66
5 340	0.0013355919	14.90	27.46
8 052	0.0016378394	3.80	1.86
4 177	0.0022105930	2.80	6.73
3 995	0.0052019227	1.35	1.97
6 982	0.0074510883	2.78	1.78
4 714	0.0088747087	3.10	2.08
3 245	0.0096738522	1.49	2.26

The model was generated by using Gini method with favor-even-splits 0. The v-fold cross-validation was set to 11, while the other options remained as defaults. The relative cost of the model tree is 0.200, shown in Figure 2. Two peaks, 7 567 and 5 252 u, were chosen to make the model tree. And the judgment of cancer or healthy control was made according to the rules of the model tree (data not shown). The double-blind test group samples were normalized to the training group using the same procedure and the same parameters. Seventy test samples were judged only with their peaks' height of the two mass ranges and were separated into cancer group or healthy control group by BPS automatically. The judgments were checked with the histopathologic diagnosis of the test samples. The results demonstrated that the sensitivity, specificity, and accuracy were 90% (95% confidence interval 76.9-96.0%), 86.7% (70.3-94.7%), and 88.6% (79.0-94.1%), respectively, shown in Table 3.

Table 3 Statistical summary of the model (by BPS)

Group	Sensitivity (%)	Specificity (%)	Accuracy (%)
Training	96.7	96.7	96.7
Test	90.0	86.7	88.6

DISCUSSION

Recent advances in genomics and proteomics hold great potential for diagnostic, prognostic, and therapeutic applications[22-24]. They help to discover new therapeutic target, design rational individual drug and obtain early-detection biomarkers[25-28]. Proteomic analysis to identify biomarkers has been reported for the detections of several kinds of cancer, such as pancreatic cancer, ovarian cancer, renal cancer, *etc.*[29-32]. However, to our best knowledge gastric cancer has not found potential biomarkers, which can be used for detection as yet. Although the serum tumor-related antigen, such as CEA, CA72-4 and CA19-9 have been examined as routine in some clinics, their sensitivity and specificity for gastric cancer were too low to be used alone for diagnosis, which limited their diagnostic value. SELDI-TOF-MS technology provides a better and easier tool to identify cancers with barely 3 μL serum.

In this study, we found a novel panel of biomarkers and a model built with them. The sensitivity, specificity, and accuracy of the model in test group were 90%, 86.7%, and 88.6%, respectively, which are greatly higher than those of CEA , CA72-4 and CA19-9 whose molecular weight are more than 100 000 u. This made it possible that the model can be used as biomarkers in the detection for gastric cancer.

The four miss-judged (false negative) test samples of the gastric cancer group were obtained from patients with poorly differentiated tumor, and in stage III or IV, are shown in Table 4. Stage I/II gastric cancer samples of the test group were all judged correctly. It suggested that the model can also be used for early detection, not only for advanced gastric cancer. In the test group, 14 gastric cancer samples obtained from patients were with poorly differentiated tumor. The miss-judged samples may reflect the biological heterogeneity of tumor, which leads the change in serum proteins and influences the judgment. In the test group, 3 of 17 female patients of gastric cancer

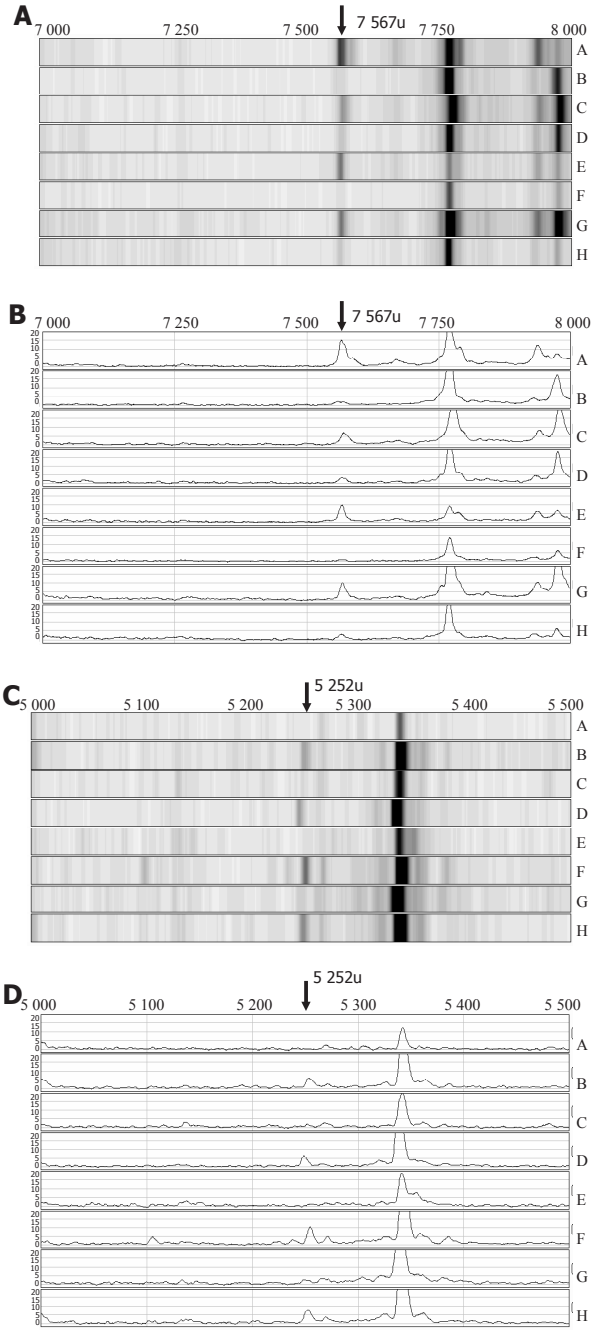
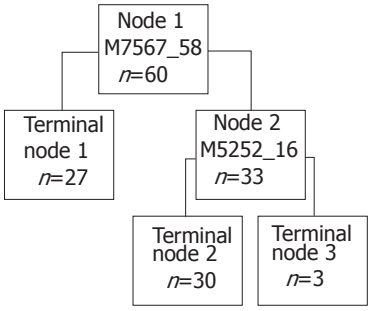


Figure 1 Detection of differentially expressed gastric cancer-associated serum proteins within a WCX2 chip. The arrows direct to the potential cancer markers detected in the mass spectra, 7 567 u (**A**, **B**) and 5 252 u (**C**, **D**), which were significantly different in gastric cancer samples compared with healthy controls. A, C, E and G were gastric cancer samples and the others were controls. **A** and **C:** A stacked trace view of candidate markers from diseased *vs* control individuals. **B** and **D:** A representative pseudogel view of SELDI-TOF-MS analysis of serum samples.

A



B

Tree Sequence

Tree number	Terminal nodes	Resubstitution relative cost	Cross-Validated relative cost	Complexity
1	5	0.300 ± 0.091	0.000	0.000
2	3	0.200 ± 0.077	0.067	0.017
3	2	0.200 ± 0.077	0.167	0.050
4	1	1.000 ± 0.000	1.000	0.417

Figure 2 Model tree established by BPS using the training group and relative cost. **A:** Two peaks, 7 567 and 5 252 u, were chosen to make the model tree. n represents the number of the samples that belong to the node; **B:** The relative cost of the model tree is 0.200.

Table 4 Status of the miss-judged test samples

Sex	Age (yr)	Differentiation of tumorgy	TNM	Stage
1 Female	32	Poor	T4N1M1	IV
2 Male	58	Poor, partially with signet ring cell	T3N2M0	III
3 Female	63	Poor	T4N2M1	IV
4 Female	50	Poor, partially with signet ring cell	T4N1M0	III

and 2 of 10 female healthy adults were miss-judged. Therefore, the sensitivities of the female group and the male group are 82.4% and 95.7%, and the specificities are 80% and 90%, respectively. However, the sensitivities had no statistical difference between sexes (P=0.394), neither did the specificities (P=0.407). Large-scale studies should be carried on to further explore the clinical impact on the model.

Although the model was composed of two peaks, 7 567 u had the highest importance score (data not shown), and can contribute to the model independently with cross-validated relative cost 0.200, as shown in Figure 2B. The peak was significantly higher in the gastric cancer group than in the control group. Therefore, it is more important. We now have focused on the purification and identification of it by using tandem mass spectrometry. If antibodies against the specific proteins are available, we will perform ELISA or immunohistochemistry to further verify the biomarker and make the cancer detection cheaper and easier. Besides, more samples are needed to confirmthat this peak is a specific biomarker of gastric cancer, not of other types of cancer.

REFERENCES

1 **Pisani P,** Parkin DM, Bray F, Ferlay J. Estimates of the worldwide mortality from 25 cancers in 1990. *Int J Cancer* 1999; **83:** 18-29
2 **Murray CJ,** Lopez AD. Alternative projections of mortality and disability by cause 1990-2020: Global Burden of Disease Study. *Lancet* 1997; **349:** 1498-1504
3 **Gaspar MJ,** Arribas I, Coca MC, Díez-Alonso M. Prognostic value of carcinoembryonic antigen, CA 19-9 and CA 72-4 in gastric carcinoma. *Tumour Biol* 2001; **22:** 318-322
4 **Marrelli D,** Roviello F, De Stefano A, Farnetani M, Garosi L, Messano A, Pinto E. Prognostic significance of CEA, CA 19-9 and CA 72-4 preoperative serum levels in gastric carcinoma. *Oncology* 1999; **57:** 55-62
5 **Carpelan-Holmström M,** Louhimo J, Stenman UH, Alfthan H, Haglund C. CEA, CA 19-9 and CA 72-4 improve the diagnostic accuracy in gastrointestinal cancers. *Anticancer Res* 2002; **22:** 2311-2316
6 **Takahashi Y,** Takeuchi T, Sakamoto J, Touge T, Mai M, Ohkura H, Kodaira S, Okajima K, Nakazato H. The usefulness of CEA and/or CA19-9 in monitoring for recurrence in gastric cancer patients: a prospective clinical study. *Gastric Cancer* 2003; **6:** 142-145
7 **Issaq HJ,** Conrads TP, Prieto DA, Tirumalai R, Veenstra TD. SELDI-TOF MS for diagnostic proteomics. *Anal Chem* 2003; **75:** 148A-155A
8 **Wiesner A.** Detection of tumor markers with ProteinChip technology. *Curr Pharm Biotechnol* 2004; **5:** 45-67
9 **Tang N,** Tornatore P, Weinberger SR. Current developments in SELDI affinity technology. *Mass Spectrom Rev* 2004; **23:** 34-44
10 **Shiwa M,** Nishimura Y, Wakatabe R, Fukawa A, Arikuni H, Ota H, Kato Y, Yamori T. Rapid discovery and identification of a tissue-specific tumor biomarker from 39 human cancer cell lines using the SELDI ProteinChip platform. *Biochem Biophys Res Commun* 2003; **309:** 18-25
11 **Caputo E,** Moharram R, Martin BM. Methods for on-chip protein analysis. *Anal Biochem* 2003; **321:** 116-124
12 **Weinberger SR,** Dalmasso EA, Fung ET. Current achievements using ProteinChip Array technology. *Curr Opin Chem Biol* 2002; **6:** 86-91
13 **Fung ET,** Thulasiraman V, Weinberger SR, Dalmasso EA. Protein biochips for differential profiling. *Curr Opin Biotechnol* 2001; **12:** 65-69
14 **Issaq HJ,** Veenstra TD, Conrads TP, Felschow D. The SELDI-TOF MS approach to proteomics: protein profiling and biomarker identification. *Biochem Biophys Res Commun* 2002; **292:** 587-592
15 **Kozak KR,** Amneus MW, Pusey SM, Su F, Luong MN, Luong SA, Reddy ST, Farias-Eisner R. Identification of biomarkers for ovarian cancer using strong anion-exchange ProteinChips: potential use in diagnosis and prognosis. *Proc Natl Acad Sci USA* 2003; **100:** 12343-12348
16 **Petricoin EF,** Liotta LA. SELDI-TOF-based serum proteomic pattern diagnostics for early detection of cancer. *Curr Opin Biotechnol* 2004; **15:** 24-30
17 **Cazares LH,** Adam BL, Ward MD, Nasim S, Schellhammer PF, Semmes OJ, Wright GL. Normal, benign, preneoplastic, and malignant prostate cells have distinct protein expression profiles resolved by surface enhanced laser desorption/ionization mass spectrometry. *Clin Cancer Res* 2002; **8:** 2541-2552
18 **Li J,** Zhang Z, Rosenzweig J, Wang YY, Chan DW. Proteomics and bioinformatics approaches for identification of serum biomarkers to detect breast cancer. *Clin Chem* 2002; **48:** 1296-1304
19 **Coombes KR,** Fritsche HA, Clarke C, Chen JN, Baggerly KA, Morris JS, Xiao LC, Hung MC, Kuerer HM. Quality control and peak finding for proteomics data collected from nipple aspirate fluid by surface-enhanced laser desorption and ionization. *Clin Chem* 2003; **49:** 1615-1623
20 **Schaub S,** Wilkins J, Weiler T, Sangster K, Rush D, Nickerson P. Urine protein profiling with surface-enhanced laser-

desorption/ionization time-of-flight mass spectrometry. *Kidney Int* 2004; **65:** 323-332

21 **Sasaki K,** Sato K, Akiyama Y, Yanagihara K, Oka M, Yamaguchi K. Peptidomics-based approach reveals the secretion of the 29-residue COOH-terminal fragment of the putative tumor suppressor protein DMBT1 from pancreatic adenocarcinoma cell lines. *Cancer Res* 2002; **62:** 4894-4898

22 **Cho WC,** Yip TT, Yip C, Yip V, Thulasiraman V, Ngan RK, Yip TT, Lau WH, Au JS, Law SC, Cheng WW, Ma VW, Lim CK. Identification of serum amyloid a protein as a potentially useful biomarker to monitor relapse of nasopharyngeal cancer by serum proteomic profiling. *Clin Cancer Res* 2004; **10:** 43-52

23 **Espina V,** Dettloff KA, Cowherd S, Petricoin EF, Liotta LA. Use of proteomic analysis to monitor responses to biological therapies. *Expert Opin Biol Ther* 2004; **4:** 83-93

24 **Srinivas PR,** Kramer BS, Srivastava S. Trends in biomarker research for cancer detection. *Lancet Oncol* 2001; **2:** 698-704

25 **Chambers G,** Lawrie L, Cash P, Murray GI. Proteomics: a new approach to the study of disease. *J Pathol* 2000; **192:** 280-288

26 **Hobbs SK,** Shi G, Homer R, Harsh G, Atlas SW, Bednarski MD. Magnetic resonance image-guided proteomics of human glioblastoma multiforme. *J Magn Reson Imaging* 2003; **18:** 530-536

27 **Sauter ER,** Zhu W, Fan XJ, Wassell RP, Chervoneva I, Du Bois GC. Proteomic analysis of nipple aspirate fluid to detect biologic markers of breast cancer. *Br J Cancer* 2002; **86:** 1440-1443

28 **Zhukov TA,** Johanson RA, Cantor AB, Clark RA, Tockman MS. Discovery of distinct protein profiles specific for lung tumors and pre-malignant lung lesions by SELDI mass spectrometry. *Lung Cancer* 2003; **40:** 267-279

29 **Koopmann J,** Zhang Z, White N, Rosenzweig J, Fedarko N, Jagannath S, Canto MI, Yeo CJ, Chan DW, Goggins M. Serum diagnosis of pancreatic adenocarcinoma using surface-enhanced laser desorption and ionization mass spectrometry. *Clin Cancer Res* 2004; **10:** 860-868

30 **Bandera CA,** Ye B, Mok SC. New technologies for the identification of markers for early detection of ovarian cancer. *Curr Opin Obstet Gynecol* 2003; **15:** 51-55

31 **Rogers MA,** Clarke P, Noble J, Munro NP, Paul A, Selby PJ, Banks RE. Proteomic profiling of urinary proteins in renal cancer by surface enhanced laser desorption ionization and neural-network analysis: identification of key issues affecting potential clinical utility. *Cancer Res* 2003; **63:** 6971-6983

32 **Fels LM,** Buschmann T, Meuer J, Reymond MA, Lamer S, Röcken C, Ebert MP. Proteome analysis for the identification of tumor-associated biomarkers in gastrointestinal cancer. *Dig Dis* 2003; **21:** 292-298

Science Editor Wang XL and Guo SY **Language Editor** Elsevier HK

PO Box 2345, Beijing 100023, China
www.wjgnet.com
wjg@wjgnet.com

ELSEVIER

World J Gastroenterol 2005;11(40):6254-6257
World Journal of Gastroenterology ISSN 1007-9327
© 2005 The WJG Press and Elsevier Inc. All rights reserved.

• *GASTRIC CANCER* •

Capsaicin-induced cell death in a human gastric adenocarcinoma cell line

Yi-Ching Lo, Yuan-Chieh Yang, I-Chen Wu, Fu-Chen Kuo, Chi-Ming Liu, Hao-Wei Wang, Chao-Hung Kuo, Jeng-Yi Wu, Deng-Chyang Wu

Yi-Ching Lo, Chi-Ming Liu, Hao-Wei Wang, Department and Graduate Institute of Pharmacology, Kaohsiung Medical University, Kaohsiung City, Taiwan, China
Yuan-Chieh Yang, Department of Clinical Pathology, Kaohsiung Medical University Hospital, Kaohsiung City, Taiwan, China
I-Chen Wu, Chao-Hung Kuo, Jeng-Yi Wu, Deng-Chyang Wu, Division of Gastroenterology, Department of Internal Medicine, Kaohsiung Medical University Hospital. Kaohsiung City, Taiwan, China
Fu-Chen Kuo, Department of Gynecology and Obstetrics, E-DA Hospital, I-Shou University, Kaohsiung, Taiwan, China
Supported by Grants from the National Science Council of the ROC, No. NSC 89-2314-B-037-073 and NSC-89-2315-B-037-004
Correspondence to: Dr. Deng-Chyang Wu, Chief of Gastroenterology, Kaohsiung Medical University Hospital, 100 Zih-You 1st Road Kaohsiung City, 807 Taiwan, China. dechwu@yahoo.com
Telephone: +886-7-3121101-7451 Fax: +886-7-3135612
Received: 2004-12-23 Accepted: 2005-02-18

Abstract

AIM: Capsaicin, a pungent ingredient found in red pepper, has long been used in spices, food additives, and drugs. Cell death induced by the binding of capsaicin was examined in a human gastric adenocarcinoma cell line (AGS cells).

METHODS: By using XTT-based cytotoxicity assay, flow cytometry using the TUNEL method, and quantitation of DNA fragmentation, both cell death and DNA fragmentation were detected in AGS cells treated with capsaicin. By using Western blotting methods, capsaicin reduced the expression of Bcl-2, the antiapoptotic protein, in AGS cells in a concentration-dependent manner.

RESULTS: After incubation of AGS cells with capsaicin for 24 h, cell viability decreased significantly in a dose-dependent manner. After incubation of AGS cells with capsaicin for 24 h, apoptotic bodies also significantly increased, and were again correlated with the dose of capsaicin. When the concentration of capsaicin was 1 mmol/L, the amount of DNA fragments also increased. Similar results were also in the lower traces.

CONCLUSION: These results suggest that capsaicin-induced cell death might be via a Bcl-2 sensitive apoptotic pathway. Therefore, capsaicin might induce protection from gastric cancer.

© 2005 The WJG Press and Elsevier Inc. All rights reserved.

Key words: Capsaicin; Human gastric adenocarcinoma; Apoptosis; Bcl-2

Lo YC, Yang YC, Wu IC, Kuo FC, Liu CM, Wang HW, Kuo CH, Wu JY, Wu DC. Capsaicin-induced cell death in a human gastric adenocarcinoma cell line. *World J Gastroenterol* 2005; 11(40): 6254-6257
http://www.wjgnet.com/1007-9327/11/6254.asp

INTRODUCTION

Carcinoma of the stomach is currently the leading cause of cancer-related death among the Chinese. The two most likely factors for such a high incidence of stomach cancer has been thought to be either *Helicobacter pylori*[1] or diet. Capsaicin (8-methyl-N-vanillyl-6-nonenamide), the main ingredient of hot chili peppers, has long been used in spices, food additives, and drugs[2]. Capsaicin has been shown to protect the gastric mucosa of animals and humans against various kinds of damage[3-6]. It is generally considered that capsaicin's effect results from the activation of sensory afferent neurons in the stomach, and is mediated by various physiological functions, such as mucosal blood flow[7-10], mucus secretion[11], and bicarbonate secretions[12]. Vanilloid receptor subtype 1 (VR1), a receptor responsible for capsaicin action, has been cloned[13] and demonstrated to be located in both neural and non-neural cells[14]. VR1 has also been found to be expressed peripherally in gastric mucosal epithelial cells, playing a role in cell protection[15]. Recently, a series of studies have demonstrated that capsaicin inhibits mutagenicity and DNA binding of some chemical carcinogens, possibly by suppressing their metabolic activation[16-18]. With cells in culture, capsaicin-inhibited proliferation of HeLa, ovarian carcinoma, and mammary adenocarcinoma by decreasing NADH oxidase activity[19]. Capsaicin can also alter the expression of tumor forming-related genes by mediating the overexpression of *p53* and/or *c-myc* genes in a Korean stomach cancer cell line[20]. Capsaicin was found to induce apoptosis in T cells by increasing the reactive oxygen species and by a subsequent mitochondrial transmembrane potential[21]. In this report, we have examined the underlying mechanism by which capsaicin induces apoptotic cell death in a human gastric adenocarcinoma cell line (AGS).

MATERIALS AND METHODS

Cell line

A human gastric adenocarcinoma cell line (AGS) was

obtained from American Type Culture Collection. The cells were maintained in RPMI 1640 medium (Life Technologies, Inc., Melbourne, Australia) supplemented with 10% heat-inactivated fetal bovine serum with penicillin (100 U/mL) and streptomycin (100 μg/mL). Cultures in 75- or 25-mL culture flasks were incubated at 37 ℃ in a humidified gas mixture containing 50 mL/L CO_2 balanced with air.

XTT-based cytotoxicity assay

Unlabeled AGS cells (1×10^4/well) were distributed on to a 96-well flat-bottomed plate. Appropriate numbers of cells were added, resulting in triplicate wells, and a final volume of 100 μL of RPMI medium with 10% bovine serum was obtained. After incubation of AGS cells for 24 h, the medium was then replaced with serum-free RPMI medium containing capsaicin (0.05 μmol/L-10 mmol/L) at 37 ℃ for 24 h. The quantity of viable cell was determined using a cell proliferation ELISA kit from Boehringer Mannheim (No. 1465015), according to the recommendations of the supplier. Each sample was tested in triplicate.

Detection of apoptotic cells by flow cytometry using TUNEL method

For demonstration of apoptosis, TUNEL assay was performed with an *in situ* cell death detection kit (POD, Boehringer Mannheim) according to the manufacturer's recommendations. After incubation of AGS cells for 24 h, cells were analyzed by Epics Elite ESP flow cytometer. Apoptosis was analyzed using the Wincycle Software (Coulter). Adherent cells were harvested and stained in hypotonic fluorochrome solution (propidium iodide 50 μg/mL in sodium citrate plus 0.1% Triton X-100, Sigma). Apoptotic nuclei were identified as a subgenomic DNA peak and were distinguished from cell debris on the basis of both forward light scatter and fluorescence of propidium iodide.

Quantitation of DNA fragmentation

Apoptosis was also evaluated with a cell death ELISA kit (Boehringer Mannheim, Indianapolis, IN, USA) which utilizes a monoclonal antibody against histone to detect DNA fragments in the cytosolic fraction of lysed cells. Cells treated with or without capsaicin were harvested and lysed according to the manufacturer's instructions. The samples were transferred into 96-well dishes coated with a mouse monoclonal antibody against histone. After incubation and washing, anti-DNA-peroxidase was added to the wells. The reaction was developed with the substrate supplied by the manufacturer and the absorbance of the wells was read at 410 nm. The ratio of the absorbance of the treated cells to the untreated cells was calculated as an enrichment factor, which provides a qualitative assessment of apoptosis. Each sample was tested in triplicate.

Western blotting

After incubation of AGS cells for 24 h, about 10^7 cells were washed in PBS and solubilized buffer (50 mmol/L Tris-HCl pH 7.4, 125 mmol/L NaCl, 0.1% NP-40, 5 mmol/L NaF, 1 mmol/L PMSF, 1 ng/mL leupeptin, 10 ng/mL soybean trypsin inhibitor, 1 ng/mL aprotinin, 10 ng/mL N-tosyl-L-phenylalanyl chloromethyl ketone) for 60 min on ice. Lysates were centrifuged at 2 500 *g* for 5 min. Protein concentration was determined by means of the Bradford protein assay (BioRad Lab., Richmond, CA, USA) using bovine serum albumin as the standard. Thirty micrograms of protein was resolved by electrophoresis on 10% polyacrylamide gels, electrotransferred to a polyvinylidene difluoride filter (Millipore, Bedford, MA, USA), and then blotted with mouse monoclonal antibody for Bcl-2 (1∶500 dilution). Blots were developed with peroxidase-labeled anti-mouse IgG (1∶400 dilution) using a Lumi-Light Plus Western Blotting Kit (Boehringer Mannheim).

Statistical analysis

All values in the text and figures are expressed as mean±SE. Statistical differences were evaluated by Student's *t*-test in unpaired samples, by paired *t*-test in paired samples, or by Wilcoxon's sum of ranks test. When evaluating multiple values, the Bonferroni correction was used. Probability values less than 0.05 were considered to be significant in all experiments. Analysis of the data and plotting of the figures were done with the aid of software (SigmaStat and SigmaPlot, Version 5.0, Jandel, USA; PHARM/PCS, Version 4.2, MCS, USA) run on an IBM PC-AT computer. Protein blot images were captured by an Imaging Densitometer with the aid of software (Bio-ID, V.97 software for Windows 95, Vilber Laurmat, France). Comparisons were made only between averaged values of bands within the same gel.

RESULTS

Based on the XTT assay, DNA fragmentation and flow cytometric analysis, induction of apoptosis by capsaicin was reconfirmed in stomach tumor cell line AGS. In this study, after incubation of AGS cells with capsaicin for 24 h, cell viability decreased significantly in a dose-dependent manner (Figure 1A). This reduction in cell viability induced by treatment with capsaicin was ascribed to apoptotic DNA fragmentation, and the amounts of fragmented DNA were also dependent on the dose of capsaicin (Figure 1B). After incubation of AGS cells with capsaicin for 24 h, apoptotic bodies also significantly increased, and were again correlated with the dose of capsaicin. The upper traces of Figure 2 show capsaicin-induced, concentration-dependent positive TUNEL staining. When the concentration of capsaicin was 1 mmol/L, the amount of DNA fragments also increased. Similar results were also in the lower traces of Figure 2, where apoptotic bodies increased due to the application of capsaicin. Figure 3 shows that the expression of Bcl-2, the antiapoptotic protein, was significantly reduced in AGS cells by capsaicin in a concentration-dependent manner.

DISCUSSION

Apoptosis, or programmed cell death, is a natural form of cell death controlled by a constitutively expressed machinery that induces condensation of the nucleoplasm and cytoplasm, blebbing of cytoplasmic membranes, and fragmentation of the cell into apoptotic bodies that are rapidly recognized and eliminated by adjacent cells[22-24]. Induction of apoptosis by the vanilloid compound capsaicin has been reported in several studies. Vanilloid compounds

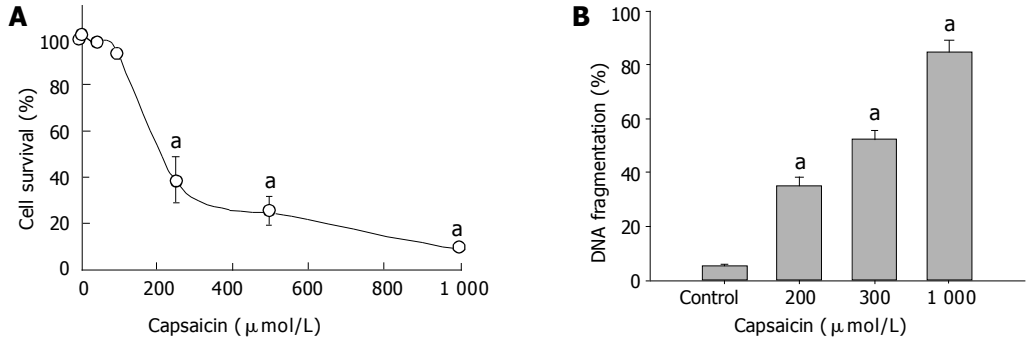


Figure 1 **A:** Effect of capsaicin on cell survival in the cultured gastric cancer cell line, AGS. Survival was analyzed by a cell proliferation ELISA kit from Boehringer Mannheim. The results are the mean±SE of three experiments. $^{a}P<0.05$ *vs* solvent control; **B**: Effect of capsaicin on the amount of DNA fragmentation in the cultured gastric cancer cell line, AGS. The amount of fragmented DNA produced was determined with an ELISA kit from Boehringer Mannheim. The results are the mean±SEM of three experiments. $^{a}P<0.05$ *vs* solvent control.

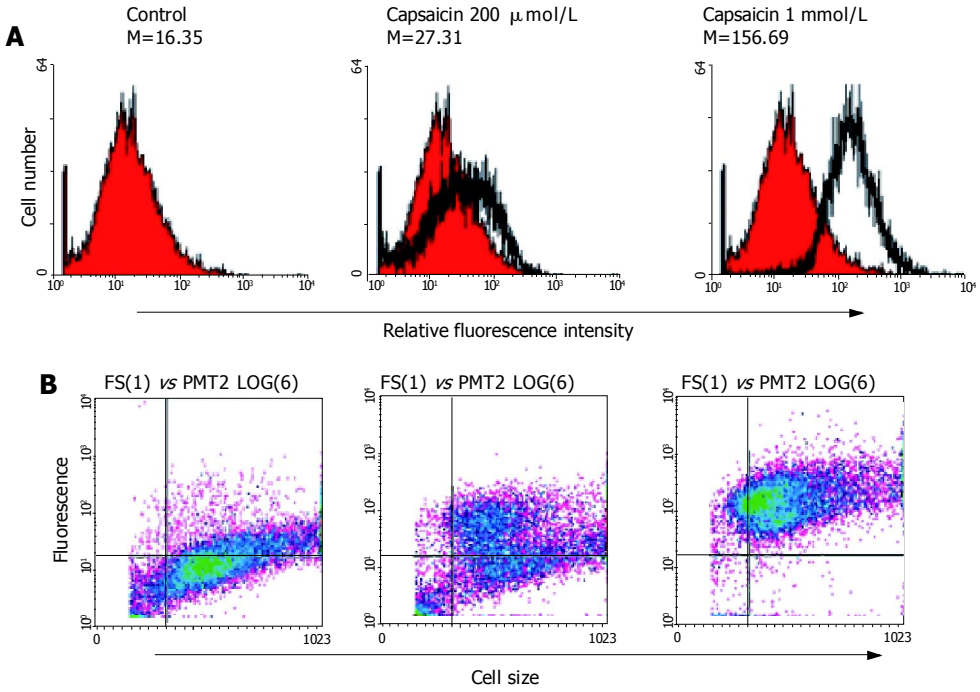


Figure 2 Flow cytometry analysis for capsaicin-induced apoptosis in AGS gastric carcinoma cells (**A**,**B**).

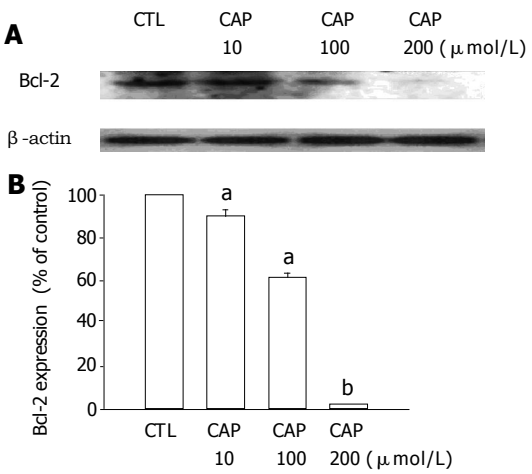


Figure 3 Effect of capsaicin (CAP) on the expression of Bcl-2 in AGS cells. Each bar represents means±SE of three experiments(**A**,**B**). $^{a}P<0.05$, $^{b}P<0.01$ *vs* solvent control (CTL).

are quinone analogs that inhibit the NADH-plasma membrane electron transport system and induce apoptosis in transformed cells[21]. Capsaicin (3.5-10 μmol/L) induces apoptotic cell death in an *in vitro* Korean stomach tumor cell (SNU-1), which may possibly be mediated by overexpression of *p53* and/or *c-myc* genes, but not by overexpression of those of *c-erb*B-2, *c-jun* and *bcl*-2 genes[20], based on XTT assay, DNA fragmentation and flow cytometric analysis. In our study, induction of apoptosis by capsaicin was reconfirmed in another stomach tumor cell line, AGS. In this study, cell viability significantly decreased in a dose-dependent manner after incubation of AGS cells with capsaicin for 24 h. This reduction in cell viability induced by treatment with capsaicin was ascribed to apoptotic DNA fragmentation, and the amounts of fragmented DNA were also dependent on the dose of capsaicin. After incubation of AGS cells with capsaicin for 24 h, apoptotic bodies increased significantly in a dose-dependent manner.

We examined the role of Bcl-2 in capsaicin-induced cell death. In this study, the expression of Bcl-2, the antiapoptotic protein, was significantly reduced by capsaicin. Savill J *et al*.[25] were the first to report that *bcl*-2 can prolong cell survival. Recently, the *bcl-2* gene has emerged as a critical regulator of programmed cell death in a variety of physiological and pathological contexts[26]. Bcl-2 has also been reported to regulate transmembrane calcium fluxes[27,28]. It is of interest to note that when AGS cells were exposed to higher doses (10-200 μmol/L) of capsaicin, the expression of Bcl-2 protein was reduced, which differs from findings reported by Kim *et al*.[20], and suggests that vanilloid compound-induced cell death might be via a Bcl-2 sensitive apoptotic pathway in the AGS cells.

In conclusion, capsaicin reduced the expression of Bcl-2 in a concentration-dependent manner in AGS cells, which suggests that Bcl-2 may play an important role in capsaicin-induced apoptosis.

REFERENCES

1 **Marchetti M,** Arico B, Burroni D, Figura N, Rappuoli R, Ghiara P. Development of a mouse model of *Helicobacter pylori* infection that mimics human disease. *Science* 1995; **267**: 1655-1658

2 **Cordell GA,** Araujo OE. Capsaicin: identification, nomenclature, and pharmacotherapy. *Ann Pharmacother* 1993; **27**: 330-336

3 **Szolcsanyi J,** Bartho L. Impaired defense mechanism to peptic ulcer in the capsaicin-desensitized rat. In: Mozsik G, Hannien O, Javor T, editors. Gastrointestinal defense mechanisms. Oxford, Budapest: Pergamon Press and Akademiai Kiado; 1981. p. 39-51. Mozsik G HO, Javor T, editor. Oxford: Budapest: Pergamon Press and Akademiai Kiado,1981.p.39-51; 1981. p. 39-51

4 **Holzer P,** Sametz W. Gastric mucosal protection against ulcerogenic factors in the rat mediated by capsaicin-sensitive afferent neurons. *Gastroenterology* 1986; **91**: 975-981

5 **Holzer P,** Lippe IT. Stimulation of afferent nerve endings by intragastric capsaicin protects against ethanol-induced damage of gastric mucosa. *Neuroscience* 1988; **27**: 981-987

6 **Yeoh KG,** Kang JY, Yap I, Guan R, Tan CC, Wee A, Teng CH. Chili protects against aspirin-induced gastroduodenal mucosal injury in humans. *Dig Dis Sci* 1995; **40**: 580-583

7 **Holzer P,** Pabst MA, Lippe IT, Peskar BM, Peskar BA, Livingston EH, Guth PH. Afferent nerve-mediated protection against deep mucosal damage in the rat stomach. *Gastroenterology* 1990; **98**: 838-848

8 **Holzer P,** Livingston EH, Saria A, Guth PH. Sensory neurons mediate protective vasodilatation in rat gastric mucosa. *Am J Physiol* 1991; **260**: G363-G370

9 **Lippe IT,** Pabst MA, Holzer P. Intragastric capsaicin enhances rat gastric acid elimination and mucosal blood flow by afferent nerve stimulation. *Br J Pharmacol* 1989; **96**: 91-100

10 **Matsumoto J,** Takeuchi K, Okabe S. Characterization of gastric mucosal blood flow response induced by intragastric capsaicin in rats. *Jpn J Pharmacol* 1991; **57**: 205-213

11 **Kang JY,** Teng CH, Wee A, Chen FC. Effect of capsaicin and chilli on ethanol induced gastric mucosal injury in the rat. *Gut* 1995; **36**: 664-669

12 **Takeuchi K,** Ueshima K, Matsumoto J, Okabe S. Role of capsaicin-sensitive sensory nerves in acid-induced bicarbonate secretion in rat stomach. *Dig Dis Sci* 1992; **37**: 737-743

13 **Caterina MJ,** Schumacher MA, Tominaga M, Rosen TA, Levine JD, Julius D. The capsaicin receptor: a heat-activated ion channel in the pain pathway. *Nature* 1997; **389**: 816-824

14 **Gunthorpe MJ,** Benham CD, Randall A, Davis JB. The diversity in the vanilloid (TRPV) receptor family of ion channels. *Trends Pharmacol Sci* 2002; **23**: 183-191

15 **Kato S,** Aihara E, Nakamura A, Xin H, Matsui H, Kohama K, Takeuchi K. Expression of vanilloid receptors in rat gastric epithelial cells: role in cellular protection. *Biochem Pharmacol* 2003; **66**: 1115-1121

16 **Teel RW.** Effects of capsaicin on rat liver S9-mediated metabolism and DNA binding of aflatoxin. *Nutr Cancer* 1991; **15**: 27-32

17 **Zhang Z,** Hamilton SM, Stewart C, Strother A, Teel RW. Inhibition of liver microsomal cytochrome P450 activity and metabolism of the tobacco-specific nitrosamine NNK by capsaicin and ellagic acid. *Anticancer Res* 1993; **13**: 2341-2346

18 **Teel RW.** Effects of different inducers of cytochrome P450 on the mutagenesis of the tobacco-specific nitrosamine 4-(methylnitrosamino)- 1-(3-pyridyl)-1-butanone (NNK) in Salmonella typhimurium TA1535. *Anticancer Res* 1992; **12**: 1287-1290

19 **Morre DJ,** Chueh PJ, Morre DM. Capsaicin inhibits preferentially the NADH oxidase and growth of transformed cells in culture. *Proc Natl Acad Sci USA* 1995; **92**: 1831-1835

20 **Kim JD,** Kim JM, Pyo JO, Kim SY, Kim BS, Yu R, Han IS. Capsaicin can alter the expression of tumor forming-related genes which might be followed by induction of apoptosis of a Korean stomach cancer cell line, SNU-1. *Cancer Lett* 1997; **120**: 235-241

21 **Macho A,** Blazquez MV, Navas P, Munoz E. Induction of apoptosis by vanilloid compounds does not require de novo gene transcription and activator protein 1 activity. *Cell Growth Differ* 1998; **9**: 277-286

22 **Suzuki YJ,** Forman HJ, Sevanian A. Oxidants as stimulators of signal transduction. *Free Radic Biol Med* 1997; **22**: 269-285

23 **Willmott NJ,** Choudhury Q, Flower RJ. Functional importance of the dihydropyridine-sensitive, yet voltage-insensitive store-operated Ca2+ influx of U937 cells. *FEBS Lett* 1996; **394**: 159-164

24 **Kerr JF,** Wyllie AH, Currie AR. Apoptosis: a basic biological phenomenon with wide-ranging implications in tissue kinetics. *Br J Cancer* 1972; **26**: 239-257

25 **Savill J,** Fadok V, Henson P, Haslett C. Phagocyte recognition of cells undergoing apoptosis. *Immunol Today* 1993; **14**: 131-136

26 **Weil M,** Jacobson MD, Coles HS, Davies TJ, Gardner RL, Raff KD, Raff MC. Constitutive expression of the machinery for programmed cell death. *J Cell Biol* 1996; **133**: 1053-1059

27 **Vaux DL,** Cory S, Adams JM. Bcl-2 gene promotes haemopoietic cell survival and cooperates with c-myc to immortalize pre-B cells. *Nature* 1988; **335**: 440-442

28 **Reed JC.** Bcl-2 and the regulation of programmed cell death. *J Cell Biol* 1994; **124**: 1-6

Science Editor Guo SY **Language Editor** Elsevier HK

PO Box 2345, Beijing 100023, China
www.wjgnet.com
wjg@wjgnet.com

ELSEVIER

World J Gastroenterol 2005;11(40):6258-6261
World Journal of Gastroenterology ISSN 1007-9327
© 2005 The WJG Press and Elsevier Inc. All rights reserved.

• *LIVER CANCER* •

Augmentation of tumor necrosis factor family-induced apoptosis by E3330 in human hepatocellular carcinoma cell lines via inhibition of NFκB

Yukiko Saitou, Katsuya Shiraki, Takenari Yamanaka, Kazumi Miyashita, Tomoko Inoue, Yutaka Yamanaka, Yumi Yamaguchi, Naoyuki Enokimura, Norihiko Yamamoto, Keiichi Itou, Kazushi Sugimoto, Takeshi Nakano

Yukiko Saitou, Katsuya Shiraki, Takenari Yamanaka, Kazumi Miyashita, Tomoko Inoue, Yutaka Yamanaka, Yumi Yamaguchi, Naoyuki Enokimura, Norihiko Yamamoto, Keiichi Itou, Kazushi Sugimoto, Takeshi Nakano, First Department of Internal Medicine, Mie University School of Medicine, Tsu, Mie 514-8507, Japan
Correspondence to: Katsuya Shiraki, MD, PhD, Assistant Professor, First Department of Internal Medicine, Mie University School of Medicine, 2-174 Edobashi, Tsu, Mie 514-8507, Japan. katsuyas@clin.medic.mie-u.ac.jp
Telephone: +81-59-231-5015 Fax: +81-59-231-5201
Received: 2004-08-26 Accepted: 2004-10-07

Abstract

AIM: To investigate the reduction of cell viability in human hepatocellular carcinoma (HCC) cell lines induced by inhibition of nuclear factor κB (NFκB).

METHODS: HLE, SKHep1, and HepG2 were incubated and E3330 was used to compare the stimulation of some chemotherapeutic drugs with that of TNF family, Fas ligand, TNFα and TNF-related apoptosis-inducing ligand (TRAIL) at the point of the reduction of cell viability by inhibiting NFκB.

RESULTS: E3330 decreased NFκB levels in HLE cells stimulated by TNF and TRAIL. The cytotoxicity of the combination of TRAIL, TNFα, Fas ligand, and E3330 increased synergistically in a dose-dependent manner compared to either E3330 alone in all HCC cell lines by MTT assay. However, the combination of some chemotherapeutic drugs and E3330 did not decrease the cell viability.

CONCLUSION: Inhibition of NFκB sensitizes human HCC cell lines to TNF-mediated apoptosis including TRAIL, and TRAIL-based tumor therapy might be a powerful potential therapeutic tool in the treatment of human HCC.

© 2005 The WJG Press and Elsevier Inc. All rights reserved.

Key words: E3330; NFκB inhibitor; Cytotoxicity; TRAIL; TNFα; Fas ligand; Doxorubicin; Camptotecin

Saitou Y, Shiraki K, Yamanaka T, Miyashita K, Inoue T, Yamanaka Y, Yamaguchi Y, Enokimura N, Yamamoto N, Itou K, Sugimoto K, Nakano T. Augmentation of tumor necrosis factor family-induced apoptosis by E3330 in human hepatocellular carcinoma cell lines via inhibition of NFκB. *World J Gastroenterol* 2005; 11(40): 6258-6261
http://www.wjgnet.com/1007-9327/11/6258.asp

INTRODUCTION

The process of apoptosis is fundamental in the developmental and homeostatic maintenance of complex biological systems[1,2]. Dysregulation or failure of normal apoptotic mechanisms contributes to the transformation of cells and provides a growth advantage to cancer cells[3]. TNF family members, such as TNFα and Fas ligand, play an important role in determining cell death or survival in a variety of human cells and transformed cells[2,4]. However, the potential use of systemically administered TNFα and Fas ligand is limited by their acute cytotoxic effects on normal tissues *in vivo*, thereby limiting their widespread use in the treatment of cancer[5,6]. In contrast, TNF-related apoptosis-inducing ligand (TRAIL) is able to kill a wide spectrum of tumor cells, and appears to be nontoxic to most normal cells[7].

Nuclear factor κB (NFκB) is an essential survival factor in many physiological conditions, such as embryonic liver development and liver regeneration[8]. In liver neoplasm, NFκB plays an important role in the resistance to TNF cytotoxicity and functional pathways including TNF receptor-associated factor 2[9].

Compound E3330 has a therapeutic effect in murine models of endotoxin-mediated hepatitis and in rats with galactosamine-induced hepatitis, presumably as a result of E3330 inhibition of TNFα generation[10,11]. E3330 inhibits NFκB DNA binding, most probably via an interaction with a nuclear factor that activates NFκB activity[12].

Previously we have demonstrated that incubation with TRAIL induces NFκB activation in hepatocellular carcinoma (HCC) cell lines, and the cells show strong resistance to TRAIL-induced apoptosis[13-17]. Therefore, we have investigated the reduction of cell viability induced by inhibition of NFκB using E3330 and some chemo-therapeutic drugs or TNF family members, especially TRAIL.

MATERIALS AND METHODS

Reagents

E3330, a quinone derivative ((2E)-3-[5-(2,3-dimethoxy-6-methyl-1,4-benzoquinoyl)]-2-propenoic acid), was a gift from

Eisai Co., Ltd. E3330 could inhibit LPS-induced TNFα generation in human monocytes[18]. TNF-family members, TRAIL, TNFα, Fas ligand were obtained from MBL, Nagoya, Japan. Chemotherapeutic agents doxorubicin and camptotecin were obtained from Sigma.

HCC cell lines

The HLE cell line was purchased from the Health Science Research Resources Bank (Osaka, Japan). HepG2 and SKHep1 cells were purchased from American Type Culture Collection (Rockville, MD, USA). Cells were cultured in Dulbecco's modified Eagle's medium (Dainippon Pharmaceutical Co., Ltd., Osaka, Japan) at 37 ℃. All media were supplemented with 1% penicillin/streptomycin (GIBCO BRL) and 10% heat-inactivated fetal calf serum (GIBCO BRL).

NFκB luciferase reporter gene assay

The pNFκB-Luc vector (Mercury Pathway Profiling System) and the pCMV-IkBa vector were obtained from Clontech (San Diego, CA, USA). Human HCC cells (2×10^5) were grown in six-well plates in triplicate the day before transfection. Cells were transfected using FuGENE 6 (Boehringer Mannheim) and incubated for 18 h at 37 ℃. The medium was removed and cells were incubated in complete media for 24 h. Cells were stimulated with 20 ng/mL TRAIL (R&D Systems, Nagoya, Japan), 100 U/mL TNFα (Genzyme-Techne, Cambridge, MA, USA) for 24 h. Luciferase activity was determined from cell extracts using a luciferase assay system (Promega) and a luminometer (Berthold Analytical Instruments, Nashua, NH, USA). The results were presented as the fold induction above the luciferase activity found in cells without stimulation.

Detection of apoptosis

To assess the viability of human HCC cell lines, 3-(4,5-dimethylthiazol-2-yl)-2,5-diphenyl tetrazolium bromide (MTT) assay was performed. The cells ware plated at a density of 5×10^3 cells/well in 96-well microtiter plates and each plate was incubated for 24 h at 37 ℃ in 50 mL/L CO_2. HCC cell lines were treated with E3330 for 12 h and then with TRAIL (20 ng/mL), TNFα (100 U/mL), Fas ligand (500 ng/mL), doxorubicin (0.1 μg/mL) and/or camptotecin (0.1 μg/mL) for another 12 h. The live-cell count was assayed using a cell titer 96 assay kit (Promega, Madison, WI, USA) according to the manufacturer's instructions. The absorbance of each sample was measured at 570 nm with a microtiter plate reader (Bio-Rad Laboratories, Hercules, CA, USA).

RESULTS

NFκB activation was induced by TNFα, TRAIL and E3330 in HLE cells. Because all human HCC cell lines showed strong resistance to TNFα- and TRAIL-mediated apoptosis, we investigated NFκB levels by NFκB luciferase reporter gene assay 12 h after NFκB inhibitor (E3330) application in HLE cell line. E3330 decreased NFκB levels in a dose-dependent manner in HLE cells stimulated by TNFα and TRAIL (Figure 1).

The cell viability was decreased by the combination of TRAIL, TNFα, Fas ligand, and E3330 in HCC cell lines. The effect of E3330 on apoptosis induced by TRAIL, TNFα and Fas ligand was examined because E3330 was shown to inhibit the activity of NFκB. We incubated human HCC cell lines with E3330 for 12 h, then combined E3330 with TNFα (100 U/mL), Fas ligand (500 ng/mL), or TRAIL (20 ng/mL), and examined the cell viability after 12 h by MTT assay. The cytotoxicity of the combination of TRAIL, TNFα, Fas ligand and E3330 increased synergistically in a dose-dependent manner compared to E3330 alone in all HCC cell lines (Figure 2).

Next, we investigated the cell viability of HCC cell lines inhibited by both chemotherapeutic agents and E3330. We incubated human HCC cell lines with E3330 for 12 h, then combined E3330 with doxorubicin (0.1 mg/mL) or camptotecin (0.1 mg/mL) for an additional 12 h and examined the cell viability after 12 h by MTT assay. Interestingly, doxorubicin and camptotecin had little effect on the reduction of cell viability in all HCC cell lines though they were used in combination with E3330 (Figure 2).

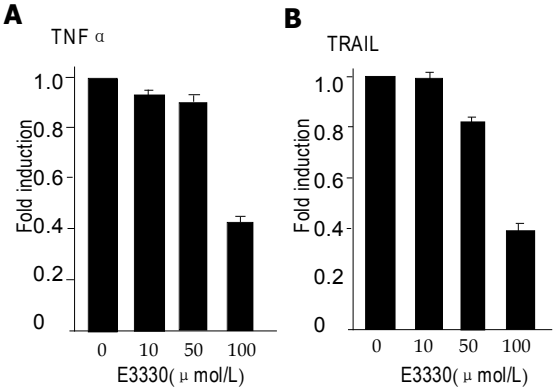


Figure 1 TRAIL-induced NFκB activation in HLE cells (**A**,**B**).

DISCUSSION

TRAIL can induce apoptosis by interaction with two receptors, TRAIL-R1 (DR4) and TRAIL-R2 (DR5)[19-24]. These receptors have a death domain that mediates cellular apoptosis. Two other receptors, known as TRAIL-R3 and TRAIL-R4, inhibit apoptosis by acting as decoy receptors because they do not contain the cytoplasmic death domain. These decoy receptors are highly expressed in normal tissues, but have a substantially lower expression in malignant cells[21-26].

However, it is of interest to determine at which level HCC cells inhibit TRAIL-induced death signaling in HCC cells. NFκB is a key mediator in the inhibition of apoptotic responses and NFκB activation has been shown to increase the antiapoptotic threshold of cells and tissues exposed to cytotoxic cytokines such as TNF by suppressing the initiation of caspase-8 activation[27]. On the other hand, NFκB has many wide-ranging effects that are controlled by a complex regulatory network of inhibitors and coactivators[28-30]. Given the intimate connection between host defense reactions and NFκB, this transcription factor and its associated regulators

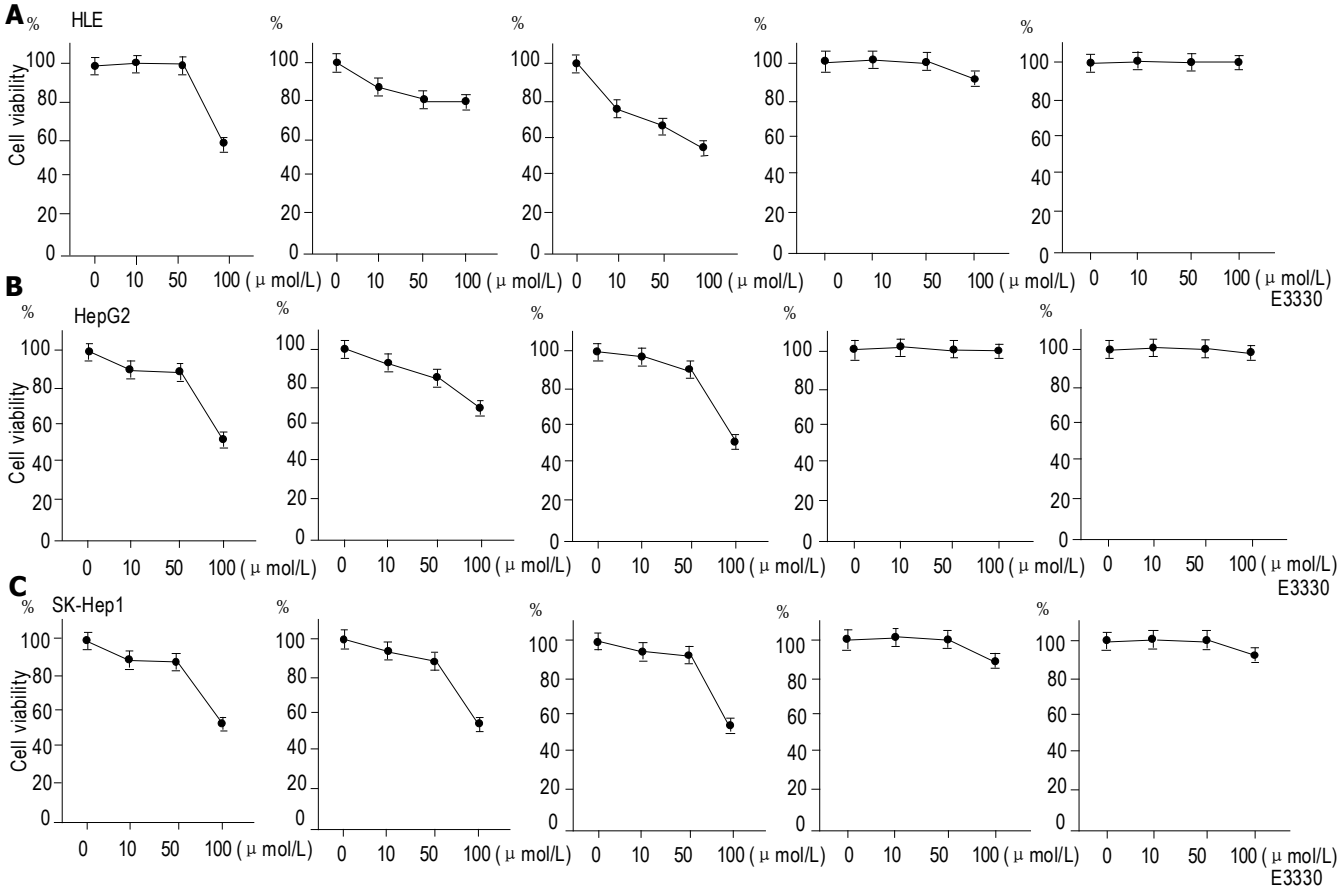


Figure 2 Proliferation of HLE (**A**), HepG2 (**B**), SK-Hep1 (**C**) cells induced by TNFα (1), Fas ligand (2), TRAIL (3), doxorubicin (4), and camptotecin (5).

could provide attractive targets for therapeutic intervention in a number of diseases or pathologic conditions. In this line, a number of anti-NFκB drugs have already been developed[12].

In the current report, E3330 inhibits NFκB DNA binding, most probably via an interaction with a nuclear factor that activates NFκB activity[12]. We studied E3330-inhibited NFκB activity in HCC cell line and found that E3330 decreased NFκB levels in a dose-dependent manner at HLE cells stimulated by TNFα and TRAIL.

NFκB may inhibit the apoptosis induced by TNF family members such as TRAIL, TNFα, Fas ligand. Our results indicate that the inhibition of NFκB could increase cytotoxicity in combination with TNF family members such as TRAIL, TNFα and Fas ligand in HCC cell lines, while E3330 could inhibit NFκB in a dose-dependent manner. Thus, we believe that inhibition of NFκB could augment the cellular apoptosis induced by TNF family members.

Within the TNF family members, the receptor/ligand pair Fas/Fas ligand has been noted to play an important role in the apoptosis of hepatocytes. In contrast to Fas/Fas ligand, TRAIL is able to kill a broad spectrum of tumor cells, but appears to be nontoxic to most normal cells[7]. We demonstrated that inhibition of NFκB sensitized human HCC cell lines to TNF-mediated apoptosis, suggesting that TRAIL-based tumor therapy in combination with anti-NFκB agents might be a powerful potential therapeutic tool in the treatment of human HCC.

REFERENCES

1 **Steller H.** Mechanisms and genes of cellular suicide. *Science* 1995; **267**: 1445-1449
2 **Nagata S.** Apoptosis by death factor. *Cell* 1997; **88**: 355-365
3 **Thompson CB.** Apoptosis in the pathogenesis and treatment of disease. *Science* 1995; **267**: 1456-1462
4 **Schulze-Osthoff K,** Ferrari D, Los M, Wesselborg S, Peter ME. Apoptosis signaling by death receptors. *Eur J Biochem* 1998; **254**: 439-459
5 **Havell EA,** Fiers W, North RJ. The antitumor function of tumor necrosis factor (TNF), I. Therapeutic action of TNF against an established murine sarcoma is indirect, immunologically dependent, and limited by severe toxicity. *J Exp Med* 1998; **167**: 1067-1085
6 **Ogasawara J,** Watanabe-Fukunaga R, Adachi M, Matsuzawa A, Kasugai T, Kitamura Y, Itoh N, Suda T, Nagata S. Lethal effect of the anti-Fas antibody in mice. *Nature* 1993; **364**: 806-809
7 **Mundt B,** Kuhnel F, Zender L, Paul Y, Tillmann H, Trautwein C, Manns MP, Kubicka S. Involvement of TRAIL and its receptors in viral hepatitis. *FASEB J* 2003; **17**: 94-96
8 **Kuhnel F,** Zender L, Paul Y, Tietze MK, Trautwein C, Manns M, Kubicka S. NFkappaB mediates apoptosis through transcriptional activation of Fas (CD95) in adenoviral hepatitis. *J Biol Chem* 2000; **275**: 6421-6427
9 **Natoli G,** Costanzo A, Guido F, Moretti F, Bernardo A, Burgio VL, Agresti C, Levrero M. Nuclear factor kB-independent cytoprotective pathways originating at tumor necrosis factor receptor-associated factor 2. *J Biol Chem* 1998; **273**: 31262-31272
10 **Nagakawa J,** Hirota K, Hishinuma I, Miyamoto K, Sonoda J, Yamanaka T, Katayama K, Yamatsu I. Protective effect of E3330, a novel quinone derivative, in galactosamine-induced

hepatitis in rats. *J Pharmacol Exp Ther* 1993; **264**: 496-500
11 **Nagakawa J,** Hishinuma I, Miyamoto K, Hirota K, Abe S, Yamanaka T, Katayama K, Yamatsu I. Protective effects of (2E)-3-[5-(2,3-dimethoxy-6-methyl-1,4- benzoquinoyl)]-2-nonyl-2-propenoic acid on endotoxin-mediated hepatitis in mice. *J Pharmacol Exp Ther* 1992; **262**: 145-150
12 **Hiramoto M,** Shimizu N, Sugimoto K, Tang J, Kawakami Y, Ito M, Aizawa S, Tanaka H, Makino I, Handa H. Nuclear targeted suppression of NF-kappa B activity by the novel quinine derivative E3330. *J Immunol* 1998; **160**: 810-819
13 **Okano H,** Shiraki K, Inoue H, Kawakita T, Yamanaka T, Deguchi M, Sugimoto K, Sakai T, Ohmori S, Fujikawa K, Murata K, Nakano T. Cellular FLICE/caspase-8-inhibitory protein as a principal regulator of cell death and survival in human hepatocellular carcinoma. *Lab Invest* 2003; **83**: 1033-1043
14 **Ito T,** Shiraki K, Sugimoto K, Yamanaka T, Fujikawa K, Ito M, Takase K, Moriyama M, Kawano H, Hayashida M, Nakano T, Suzuki A. Survivin promotes cell proliferation in human hepatocellular carcinoma. *Hepatology* 2000; **31**: 1080-1085
15 **Suzuki A,** Hayashida M, Kawano H, Sugimoto K, Nakano T, Shiraki K. Hepatocyte growth factor promotes cell survival from fas-mediated cell death in hepatocellular carcinoma cells via Akt activation and Fas-death-inducing signaling complex suppression. *Hepatology* 2000; **32**: 796-802
16 **Shiraki K,** Tsuji N, Shioda T, Isselbacher KJ, Takahashi H. Expression of Fas ligand in liver metastases of human colonic adenocarcinomas. *Proc Natl Acad Sci USA* 1997; **94**: 6420-6425
17 **Yamanaka T,** Shiraki K, Sugimoto K, Ito T, Fujikawa K, Ito M, Takase K, Moriyama M, Nakano T, Suzuki A. Chemotherapeutic agents augment TRAIL-induced apoptosis in human hepatocellular carcinoma cell lines. *Hepatology* 2000; **32**: 482-490
18 **Miyamoto K,** Nagakawa J, Hishinuma I, Hirota K, Yasuda M, Yamanaka T, Katayama K, Yamatsu I. Suppressive effects of E3330, a novel quinone derivative, on tumor necrosis factor-alpha generation from monocytes and macrophages. *Agents Actions* 1992; **37**: 297-304
19 **Pan G,** O'Rourke K, Chinnaiyan AM, Gentz R, Ebner R, Ni J, Dixit VM. The receptor for the cytotoxic ligand TRAIL. *Science* 1997; **276**: 111-113
20 **Schneider P,** Thome M, Burns K, Bodmer JL, Hofmann K, Kataoka T, Holler N, Tschopp J. TRAIL receptors 1 (DR4) and 2 (DR5) signal FADD-dependent apoptosis and activate NF-kappaB. *Immunity* 1997; **7**: 831-836
21 **Schneider P,** Bodmer JL, Thome M, Hofmann K, Holler N, Tschopp J. Characterization of two receptors for TRAIL. *FEBS Lett* 1997; **416**: 329-334
22 **MacFarlane M,** Ahmad M, Srinivasula SM, Fernandes-Alnemri T, Cohen GM, Alnemri ES. Identification and molecular cloning of two novel receptors for the cytotoxic ligand TRAIL. *J Biol Chem* 1997; **272**: 25417-25420
23 **Pan G,** Ni J, Wei YF, Yu G, Gentz R, Dixit VM. An antagonist decoy receptor and a death domain-containing receptor for TRAIL. *Science* 1997; **277**: 815-818
24 **Sheridan JP,** Marsters SA, Pitti RM, Gurney A, Skubatch M, Baldwin D, Ramakrishnan L, Gray CL, Baker K, Wood WI, Goddard AD, Godowski P, Ashkenazi A. Control of TRAIL-induced apoptosis by a family of signaling and decoy receptors. *Science* 1997; **277**: 818-821
25 **Pan G,** Ni J, Yu G, Wei YF, Dixit VM. TRUNDD, a new member of the TRAIL eceptor family that antagonizes TRAIL signalling. *FEBS Lett* 1998; **424**: 41-45
26 **Degli-Esposti MA,** Dougall WC, Smolak PJ, Waugh JY, Smith CA, Goodwin RG. The novel receptor TRAIL-R4 induces NF-kappaB and protects against TRAIL-mediated apoptosis, yet retains an incomplete death domain. *Immunity* 1997; **7**: 813-820
27 **Wang CY,** Mayo MW, Korneluk RG, Goeddel DV, Baldwin AS. NF-kappaB antiapoptosis: induction of TRAF1 and TRAF2 and c-IAP1 and c-IAP2 to suppress caspase-8 activation. *Science* 1998; **281**: 1680-1683
28 **Grilli M,** Chiu JJ, Lenardo MJ. NF-kappa B and Rel: participants in a multiform transcriptional regulatory system. *Int Rev Cytol* 1993; **143**: 1-62
29 **Baeuerle PA,** Henkel T. Function and activation of NF-kappa B in the immune system. *Annu Rev Immunol* 1994; **12**: 141-179
30 **Siebenlist U,** Franzoso G, Brown K. Structure, regulation and function of NF-kappa B. *Annu Rev Cell Biol* 1994; **10**: 405-455

Science Editor Wang XL and Guo SY **Language Editor** Elsevier HK

PO Box 2345, Beijing 100023, China
www.wjgnet.com
wjg@wjgnet.com

ELSEVIER

World J Gastroenterol 2005;11(40):6262-6268
World Journal of Gastroenterology ISSN 1007-9327
© 2005 The WJG Press and Elsevier Inc. All rights reserved.

Classification tool for the systematic histological assessment of hepatocellular carcinoma, macroregenerative nodules, and dysplastic nodules in cirrhotic liver

A Quaglia, MA Jutand, A Dhillon, A Godfrey, R Togni, P Bioulac-Sage, C Balabaud, M Winnock, AP Dhillon

A Quaglia, A Dhillon, A Godfrey, AP Dhillon, Department of Histopathology, Royal Free and University College Medical School, Pond Street, London NW3 2QG, United Kingdom
R Togni, Department of Histopathology, Ospedale Santa Chiara, Largo Medaglie d'Oro 9, Trento 38100, Italy
P Bioulac-Sage, C Balabaud, Lab pathology, INSERM E9917, Université Victor Ségalen, 146 rue Léo Saignat, Bordeaux 33076, France
M Winnock, MA Jutand, INSERM U593, Université Victor Ségalen, 146 rue Léo Saignat, Bordeaux 33076, France
Correspondence to: Dr. A Quaglia, Department of Histopathology, Royal Free Hospital, Pond Street, London NW3 2QG,
United Kingdom. alberto.quaglia@kingsch.nhs.uk
Telephone: +44-20-7830-2227 Fax: +44-20-7435-3289
Received: 2005-01-26 Accepted: 2005-05-24

Abstract

AIM: To design a classification tool for the histological assessment of hepatocellular carcinoma (HCC), dysplastic nodules (DN), and macroregenerative nodules (MRN) in cirrhotic liver.

METHODS: Two hundred and twelve hepatocellular nodules (106 HCC; 74 MRN; 32 DN) were assessed systematically, quantitatively, and semiquantitatively as appropriate for 10 histological features that have been described as helpful in distinguishing small HCC, DN, and MRN in cirrhotic livers. The data were analyzed by multiple correspondence analysis (MCA).

RESULTS: MCA distributed HCC, DN, and MRN as defined by traditional histological evaluation as well as the individual histological variables, in a "malignancy scale". Based on the MCA data representation, we created a classification tool, which categorizes an individual nodular lesion as MRN, DN, or HCC based on the balance of all histological features (i.e., vascular invasion, capsular invasion, tumor necrosis, tumor heterogeneity, reticulin loss, capillarization of sinusoids, trabecular thickness, nuclear atypia, and mitotic activity). The classification tool classified most (83%) of a validation set of 47 nodules in the same way as the routine histological assessment. No discrepancies were present for DN and MRN between the routine histological assignment and the classification tool. Of 25 HCC assigned by routine assessment in the validation set, 8 were assigned to the DN category by the classification tool.

CONCLUSION: We have designed a classification tool for the histological assessment of HCC and its putative precursors in cirrhotic liver. Application of this tool systematically records histological features of diagnostic importance in the evaluation of small HCC.

© 2005 The WJG Press and Elsevier Inc. All rights reserved.

Key words: Hepatocellular carcinoma; Cirrhosis; Multiple correspondence analysis; Large regenerative nodule; Dysplastic nodule

Quaglia A, Jutand MA, Dhillon A, Godfrey A, Togni R, Bioulac-Sage P, Balabaud C, Winnock M, Dhillon AP. Classification tool for the systematic histological assessment of hepatocellular carcinoma, macroregenerative nodules, and dysplastic nodules in cirrhotic liver. World J Gastroenterol 2005; 11(40): 6262-6268
http://www.wjgnet.com/1007-9327/11/6262.asp

INTRODUCTION

The current histological classification of hepatocellular carcinoma (HCC) and its putative precursor nodular lesions is controversial and unsatisfactory, particularly with small lesions of 1-2 cm in diameter. Most of the histological criteria for the evaluation of early HCC and its putative precursors have not been validated properly, and the diagnosis of these lesions still depends largely on subjective interpretation of histological features, which are rarely recorded either in routine diagnostic practice or in the published literature.

The aim of this study was to derive a classification tool based on individual histological features that enable the distinction between HCC, dysplastic nodules (DN), and macroregenerative nodules (MRN) in cirrhotic liver. The design of this classification tool was based on the correspondence between the routine histological classification of liver cell nodules and the classification of the same liver cell nodules by a systematic analysis of the individual histological features that may contribute towards the subjective diagnostic assignment. Lesion size was considered specifically in addition because this aspect is currently the most important item that determines the management of HCC in cirrhotic patients according to the recent Barcelona guidelines[1].

MATERIALS AND METHODS

Dataset for construction of the classification tool

Two hundred and twelve liver hepatocellular nodules were retrieved from the files of the Department of Histopathology of the Royal Free Hospital using the Liver Tumor Database of the Royal Free Liver Pathology Unit. These nodules had been isolated during the routine diagnostic pathological examination of the cirrhotic livers, which were removed from 321 consecutive liver transplant patients who received liver transplantation at the Royal Free Hospital between 1996 and 2001 for various etiologies. Sixty-eight of these patients (59 males, 26 HCV, 19 HBV, 10 cryptogenic cirrhosis, 6 alcoholic liver disease, 3 alcoholic liver disease and HCV, 2 HCV and HBV, 1 Wilson's disease, 1 primary biliary cirrhosis) were found to have HCC in the explanted liver, and/or DN and/or MRN, and livers of these patients constitute our study group. For each nodule, a hematoxylin and eosin (H&E)-stained section was performed as part of the routine histological assessment, as well as a silver impregnation for reticulin fibers using the Gordon and Sweets' method and an immunohistochemical staining for CD34 and smooth muscle actin (SMA).

Histological assessment

The overall assessment was performed assigning each liver cell nodule to one of the three groups: HCC; DN; or MRN by "traditional" subjective diagnostic assessment (APD), using the histological criteria defined by Ferrell *et al*[2], and the International Working Party[3]. The systematic scoring procedure (AQ) was conducted separately from the overall assignment, in order to eliminate bias.

Histological features used to construct the classification tool

The following histological features were chosen for the systematic histological assessment of each lesion: nodule size, nodule heterogeneity, reticulin loss, trabecular thickness, capillarization, number of solitary arterioles, cellular atypia and mitotic activity, necrosis, vascular invasion, and capsular invasion.

These features were chosen because they are currently considered by many liver pathologists as the most useful histological criteria in the histological assessment of hepatocellular lesions, as it appears from published work on this subject[4-8]. Each lesion was reviewed with systematic documentation of these individual features, and a semiquantitative score was given to reticulin loss, capillarization, and cellular atypia (Table 1), as described below.

Size The evolution from cirrhotic liver to MRN, DN, and HCC is usually accompanied by an increase in nodule size. In other words, the greater the size of the lesion, the greater the likelihood that it is a dysplastic nodule or HCC[2-4,7,9,10]. Size was determined macroscopically as maximum diameter of the lesion and expressed in millimeters.

Reticulin loss This has been traditionally considered to be a diagnostic feature of HCC. The following scale was used: grade 0 was given when the reticulin stroma was preserved; grade 1-5 was defined by the number of liver cells included between residual strands of silver-staining reticulin, with grade 1 when liver plates were 3-cell thick; and subsequent 1-cell increments up to grade 5 when liver plates were 7-cell thick or more.

Trabecular thickness This means, the number of liver cells composing a hepatocyte plate and may be considered as a corollary of reticulin loss (see above). In overt HCC, hepatocyte plates tend to be thicker than normal[3,11]. Trabecular thickness was assessed using H&E staining and graded as number of liver cells composing a trabecular plate.

Arterialization and capillarization Number of solitary arterioles[12-14] and capillarization[15] are related to the changes of vascular supply in the evolution of HCC from precursor nodular lesions including acquisition of a predominantly arterial vascular supply and of a diffuse pattern of expression of CD34 by sinusoidal endothelium.

Capillarization was graded as 0 when marginal (i.e., staining only septal endothelium and endothelium of limiting plate of the nodule); Patchy (grades 1-2) when non-confluent patches (grade 1 = in one-third of the nodule; grade 2 in at least two-thirds of the nodule) showing diffuse CD34 immunostaining were seen; incomplete (grade 3) when confluent areas showing diffuse CD34 immunostaining were seen, occupying approximately two-thirds of the nodule; diffuse incomplete (grade 4)

Table 1 Scheme for the systematic assessment of histological features in liver cell nodules in cirrhotic livers

Feature	Modality of assessment					
Nodule maximum diameter	Measurement in millimeter					
Solitary arterioles	Average of individual arteries ×100 (medium power field, MPF) fields					
Mitotic activity	Number of mitoses per 10 ×400 (10 high power fields, 10 HPF) fields					
Trabecular thickness	Number of liver cells forming trabecular (LCT) width					
Vascular invasion	Present/absent					
Capsular invasion	Present/absent					
Necrosis[2]	Present/absent					
Nodule heterogeneity[1]	Present/absent					
Reticulin loss[3]	None	Grade 1	Grade 2	Grade 3	Grade 4	Grade 5
Capillarization (CD34)[3]	None	Grade 1	Grade 2	Grade 3	Grade 4	Grade 5
Cellular atypia[3]	None	Grade 1	Grade 2	Grade 3	Grade 4	Grade 5

[1]Phenotypically recognizable "clonal" changes e.g. clear cell change, fatty change, microacinar structures; [2]excluding post-treatment necrosis; [3]see text pages 5-6.

when diffuse CD34 staining was seen in the whole nodule apart from scattered CD34-ve patches; diffuse (grade 5) when the entire nodule stained for CD34.

Solitary arterioles: these were counted as average of unpaired arteries detected in 10 medium (100×) power fields, on H&E sections[14].

Cellular atypia and mitotic activity The International Working Party included both cellular atypia and mitotic activity in morphological diagnostic criteria of HCC[3]. Cellular atypia was graded as mild (grades 1-2), moderate or severe (grades 4-5) depending on the similarity in terms of features, such as nuclear contour, hyperchromatism, and nuclear cytoplasmic ratio, when compared to background cirrhotic liver[8] with mild atypia described as minimal difference (and grade 1 or 2 depending on the extent of the changes within the nodule, grade 1 in 1/3 of the surface examined; grade 2 in 2-3/3 of the surface examined), severe atypia as prominent nuclear changes with marked pleomorphism and severe hyperchromatism (and grade 4 or 5 depending on the extent of the changes within the nodule, grade 1 in 1/3 of the surface examined; grade 2 in 2-3/3 of the surface examined), and moderate atypia as intermediate changes.

Mitotic activity was graded as shown in Table 1, counting the number of mitoses in 10 high (400×) power fields[3].

Heterogeneity This term describes the morphological changes seen in a hepatocellular lesion and presumably related to the clonal evolution seen in the development of HCC. This is evident morphologically, for example, as a "nodule in nodule pattern" and consists of areas with one or more morphological changes distinct from the parent nodule and often with compression of the parent nodule suggesting an increased growth rate. These morphological changes include small cell change, microacinar change, clear cell change, fatty change, groups of Mallory body or fibrinogen containing cells, and loss or accumulation of iron or bile compared to the background liver[3,4].

Tumor necrosis usually occurs when cell growth exceeds the vascular supply and is usually seen in tumors at a relatively advanced biological stage. Necrosis was considered to be diagnostically relevant only when it was "spontaneous" in the absence of previous history of pre-transplantation local treatment (e.g., trans-arterial chemoembolization, percutaneous ethanol injection, *etc.*).

Invasion Vascular invasion was considered as invasion of vascular structures identified histologically. Capsular invasion was recorded when there was invasion of perinodular dense fibrous tissue[5,8,16].

For each nodule, H&E-stained section was performed as part of the routine histological assessment, as well as a silver impregnation for reticulin fibers using the Gordon and Sweets' method and an immunohistochemical staining for CD34 and SMA.

Dataset for validation of the classification tool

The classification tool (Table 3) was tested prospectively on a subsequent separate set of hepatocellular nodules identified in 11 consecutive liver explants with 47 distinct nodular liver cell lesions removed at transplantation in the year 2002. The test set of nodules consisted of 25 HCC (mean size, 19.4 mm; SD, 14 mm), 9 DN (mean size, 10.7 mm; SD, 3 mm), and 13 MRN (mean size, 7.7 mm; SD, 2.2 mm).

Statistical analysis

The individual histological features described above were analyzed by multiple correspondence analysis (MCA). MCA is an exploratory technique[17] allowing the synthesis, description, and graphic analysis of large contingency tables. The results provide information that is similar in nature to those produced by factor analysis techniques, and they allow one to explore the structure of categorical variables included in the table. No tests of statistical significance are applied to the results and the main goal is to produce a "simplified" representation of the data.

In the present work, MCA was used in two ways: (1) To see whether this method could reliably categorize HCC, DN, and MRN using the individual histological features described above, and how this analysis compared to the overall (routine) histological assessment. MCA produces a graphic representation of the data in the form of a horizontal line, which represents a "malignancy" scale and shows how each nodule is placed in a "malignancy" scale. In theory, malignant nodules are placed at one end of the scale and benign nodules are placed at the opposite end of the scale, with equivocal nodules in between. Each variable has a certain value in an axis, and the « position » in the chart represents the composite point of different planes (features) for a given nodule; (2) To see if this method could rank the individual histological features in order to assess the relative contribution of each individual histological observation in the assignment of a liver cell nodule to one of the three categories (HCC, DN, and MRN), so that the histological features could be incorporated into a classification tool to distinguish HCC from DN from MRN.

RESULTS

Multiple correspondence analysis

An exploratory set of 212 hepatocellular nodules (106 HCC mean size 18.8 mm, SD 13 mm; 74 MRN mean size 10 mm, SD 3.2 mm; 32 DN mean size 12.4 mm, SD 5.5 mm, as per routine histological assessment) were analyzed histologically. Figure 2 shows how MCA redistributes these nodules. The horizontal line represents a "malignancy" scale. In other words, the projection of every dot towards the horizontal line (e.g., three dotted lines in chart) shows how each nodule is placed in a "malignancy" scale. HCC are placed in the left-hand side of the chart, whereas MRN are placed towards the other end. Each variable has a certain value in an axis, and the « position » in the chart represents the resulting point of different planes for a given nodule. Size (Figure 1) does not allow a reliable classification of nodules. In other words, HCC can be of all sizes, and although large nodules are usually HCC, small nodules may also be HCC. Conversely, MRN and DN can be of considerable size (up to 21 and 24 mm, respectively, in our series).

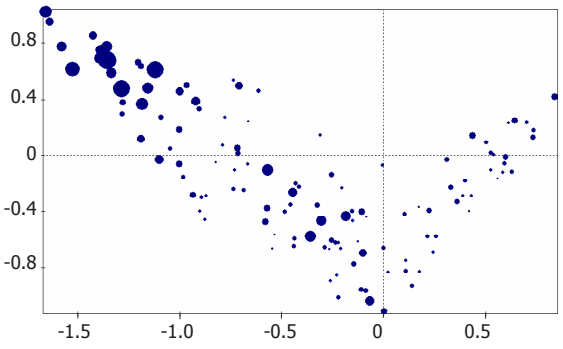


Figure 1 MCA of exploratory set of 212 hepatocellular nodules in cirrhotic livers. The relative lesion size of the hepatocellular nodules is depicted as blue dots. The diameter of the dots varies according to the size of the nodule observed. Size does not seem to allow a classification of nodules, in other words, HCC can be of all sizes, and large nodules are usually HCC. However, small nodules are not necessarily MRN or DN.

Figure 2B shows how the individual variables (e.g., capsular invasion, vascular invasion, etc.) relate to each other, and how they are distributed along the "malignancy scale". As in Figure 2A, the horizontal line represents a "scale of malignancy". The projection of each group of values in the horizontal axis shows that the variables form a continuum, with capsular invasion being the "most" malignant feature, and absence of heterogeneity the "least" malignant feature. Table 2 shows how the groups of values depicted in Figure 2B are distributed in the three types of nodular lesions.

These data were used to create a classification tool for the assessment of these nodular lesions.

Construction of the classification tool

The values shown in Figure 2 and Table 2 can be distributed into six main groups, depending on their proportional representation in the three categories HCC, DN, and MRN, as follows:

Group 1 (capsular invasion, vascular invasion). Features present exclusively in HCC 44 (41.5%) and 27 (25.5%), respectively, by definition.

Group 2 (necrosis present, mitosis present, capillarization = 5, cellular atypia = 3-5, reticulin loss = 4-5, trabecular thickness>4). Features present, in 16-52.8% (mean 36%) of HCC but not present in MRN or DN.

Group 3 (solitary arterioles ⩾1, heterogeneity present, capillarization = 4, reticulin loss = 1-3, trabecular thickness = 4). Features present in 21.7-94.3 (mean = 47%) HCC, 3-72% (mean = 37%) DN and 0-14% (mean = 20%) MRN.

Group 4 (capsular invasion not present, vascular invasion not present, necrosis not present, mitosis not

Table 2 MCA of the values of the histological variables in the three categories (HCC, MRN, and DN) in the exploratory set of 212 hepatocellular nodules in cirrhotic livers

Position	Feature	Grade	HCC number (total 106)	%	DN number (total 32)	%	MRN number (total 74)	%
1	Vascular invasion	Present	27	25.5	0	0	0	0
2	Necrosis	Present	17	16	0	0	0	0
3	Capsular invasion	Present	44	41.5	0	0	0	0
4	Cellular atypia	4-5	30	28.3	0	0	0	0
5	Trabecular thickness	>4	35	33	1	3	0	0
6	Mitosis	Any	50	47.2	0	0	0	0
7	Reticulin loss	4-5	47	44.3	0	0	0	0
8	Capillarization	5	56	52.8	0	0	0	0
9	Cellular atypia	3	38	35.8	0	0	0	0
10	Solitary arterioles	>2	23	21.7	1	3	1	1
11	Trabecular thickness	4	27	25.5	3	9	0	0
12	Capillarization	4	27	25.5	1	3	0	0
13	Solitary arterioles	2	37	34.9	5	15	1	1
14	Heterogeneity	Present	100	94.3	23	72	5	7
15	Reticulin loss	1-3	56	52.8	9	28	2	3
16	Solitary arterioles	1	33	31.1	7	22	10	14
17	Capillarization	3	19	17.9	8	25	2	3
18	Trabecular thickness	<4	44	41.5	27	84	72	97
19	Cellular atypia	1-2	37	34.9	12	38	16	22
20	Necrosis	Not present	89	84	32	100	74	100
21	Vascular invasion	Not present	79	74.5	32	100	74	100
22	Capsular invasion	Not present	62	58.5	32	100	74	100
23	Mitosis	Not present	56	52.8	32	100	74	100
24	Solitary arterioles	<1	13	12.3	19	59	62	84
25	Capillarization	0–2	4	3.8	23	72	72	97
26	Cellular atypia	0	1	0.9	20	63	58	78
27	Heterogeneity	Not present	6	5.7	9	28	69	93
28	Reticulin loss	0	3	2.8	23	72	72	97

Position = This means the position of each variable in "malignancy scale" as shown in Figure 2, i.e. position number 1 = left side of the chart (higher "degree of malignancy") and position 28 = right side of the chart (lower degree of malignancy).

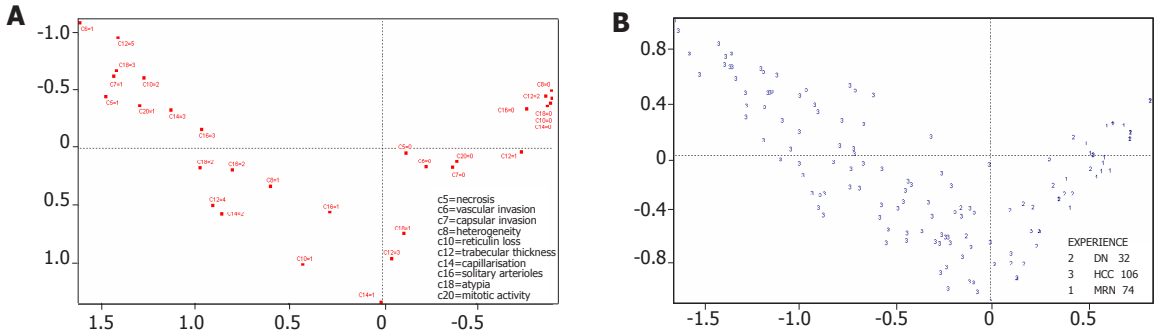


Figure 2 **A**: MCA of exploratory set of 212 hepatocellular nodules in cirrhotic livers; **B**: Distribution of histological variables in the exploratory set of 212 hepatocellular nodules. This chart shows how MCA redistributes the different types of nodules (i.e. HCC, DN, and MRN as assigned by routine histological evaluation), taking into consideration all variables of the scoring system except size. Each variable has a certain value in an axis, and the « position » in the chart represents the resulting point of different planes for a given nodule. Please note that the total number of « nodules » shown does not equal 212 because there is a certain degree of overlapping among observations and there is a lack of resolution in the chart.

present). Features present in 100% MRN and DN, and in 53-84% (mean 67%) of HCC.

Group 5 (capillarization = 3, cellular atypia = 1-2). Features present in 25-38% (mean = 31%) DN, 17.9-34.9% (mean = 26%) HCC and 3-22% (mean = 12%) MRN.

Group 6 (solitary arterioles<1, heterogeneity not present, capillarization = 0-2, reticulin loss = 0, trabecular thickness<4). Features present in 78-97% (mean = 91%) MRN, 59-72% (mean = 63%) DN and 0.9-41.5 (mean = 11%) HCC.

These six groups can be organized into a three column table as shown in Table 3. This table constitutes the classification tool.

The histological features of a given nodule are assessed individually and then allocated to the classification tool.

Table 3 Classification tool for hepatocellular lesions in cirrhotic liver. Assess each individual histological feature (as per Table 1) and go to Table 4a

3a HCC *vs* DN/MRN

Column 1	Column 2
HCC	DN or MRN
	Vascular invasion not present
	Capsular invasion not present
Necrosis present	Necrosis not present
Mitosis present	Mitosis not present
Capillarization score 4 or 5	Capillarization Score 0, 1, 2 or 3
Cellular atypia score 3, 4, or 5	Cellular atypia score 0, 1, or 2
Reticulin loss score 1, 2, 3, 4, or 5	Reticulin loss score 0
Trabecular thickness>3	Trabecular thickness<4
Solitary arterioles ⩾1	Solitary arterioles<1
Heterogeneity present	Heterogeneity absent

If the given lesion is not HCC according to this table, Table 3b provides guidance regarding the assignment of DN *vs* MRN.

3b DN *vs* MRN. The nodule is DN, if the number of features in the "DN, column 3" is higher than the number of the features in the "MRN, column 4" and vice versa. In case of an even balance, the nodule is regarded as DN

Column 3	Column 4
DN	MRN
Capillarization score 3, 4, or 5	Capillarization score 0, 1, or 2
Cellular atypia score 1, 2, 3, 4, or 5	Cellular atypia score 0
Reticulin loss score 1, 2, 3, 4, or 5	Reticulin loss score 0
Trabecular thickness >3	Trabecular thickness <4
Solitary arterioles ⩾1	Solitary arterioles <1
Heterogeneity present	Heterogeneity absent
Necrosis present	
Mitosis present	

HCC, hepatocellular carcinoma; DN, dysplastic nodule; MRN, macroregenerative nodule.

Validation of the classification tool

This classification tool, when tested prospectively on the separate set of liver cell nodules described above gave the following results: out of 47 nodules, 39 (83%) were classified in the same way as the routine histological assessment. All 13 MRN and all 9 DN, as defined by routine histological assessment were considered as such by the classification tool. Of the 25 HCC, as defined by routine histological assessment, 8 were considered as DN by the classification tool (Table 4).

Table 4 Performance of the classification tool on a second validation set of liver cell nodules in cirrhotic livers

			Histological assessment using the classification tool		
		HCC	DN	MRN	*Total*
Routine Histologica Diagnosis	HCC 25	17	8	0	25
	lDN 9	0	9	0	9
	MRN 13	0	0	13	13
	Total	17	17	13	*Total*

DISCUSSION

Despite the consensus document published by the International Working Party[3], the terminology used in the literature is still confusing, particularly due to the use of different classifications and different histological criteria by different centers[6]. In fact, the bulk of the relevant literature offers few clues about which precise observations allocated any particular lesion (however, named) into the given categorical assignment. In this work, we have investigated how those individual histological features considered in the literature will be helpful in the histological assessment of small hepatocellular

nodular lesions in cirrhosis that can be used to create a classification tool for the evaluation of these nodules. Application of the classification tool documents systematically the individual histological features that contribute to the categorical assignment of MRN, DN, and HCC.

MCA is a descriptive technique, which identifies the best factor representing a set of data. In the present analysis, the horizontal factor, which could be called "malignancy" is the most important one in representing the dataset. The nodular lesions of the present study can be imagined as a "cluster" of dots in space, and the distance between two points depends on the plane (axis of assessment, or histological features) used to look at them. For example, if the horizontal axis is used to look at two lesions, and the projections of these lesions are close together on that axis, these lesions may be considered to be at a similar degree of malignancy. The same lesions on another plane may be very far apart from each other.

MCA distributes the 212 lesions assessed by the components of the histological assessment placing HCC at the left and MRN at the right of the "malignancy" scale, and DN in the middle, although some "misclassifications" are present, with overlap between different categories (Figure 2A), i.e. between HCC and DN and DN and MRN. This is not unexpected, as this analysis represents the nodular lesions as a continuum in a "malignancy" scale. Moreover (Figure 2A), one could also imagine different degrees of malignancy within the HCC subgroup.

When tested on a second set of nodules, the classification tool classified the large majority of all nodules (83%) in the same way as the routine histological assessment. No discrepancies were noted for DN and MRN between the routine diagnosis and the assignment by the classification tool. Eight of twenty-five HCC (32% of HCC, 17% of all nodules, as defined by routine histological assessment) were assigned to the DN category by the classification tool, which is not surprising given the well-recognized difficulties in separating these two categories[3]. The reason for this discrepancy is obscure, and underlines the need for correlation with other modalities of investigation, such as molecular data and clinical follow-up, which may be informative to validate the histological criteria[3] (and this will be the subject of further work). Overall, the classification tool seems to correspond reasonably well to the routine histological assessment.

The classification tool has several advantages. Firstly, the idea of including all important histological features in the evaluation, systematically ensures that the final assignment does not rest on a single feature subjectively or selected group of features, but on the balance of all components. This classification tool is based on a systematic collection of histological data and can be integrated in a database. Once all the fields required for the completion of the classification tool have been entered, a computer can easily run the classification tool and return the result. As more data become available[18], and as additional informative histological features of HCC (such as stromal invasion) are characterized[16,19,20], the accumulated information can be used to improve and refine the classification tool.

In conclusion, we have designed a classification tool for the histological assessment of HCC and its putative precursor nodular lesions in cirrhotic liver. The classification tool is based on a systematic and balanced assessment of 10 histological features.

REFERENCES

1 **Bruix J,** Sherman M, Llovet JM, Beaugrand M, Lencioni R, Burroughs AK, Christensen E, Pagliaro L, Colombo M, Rodés J. Clinical management of hepatocellular carcinoma. Conclusions of the Barcelona-2000 EASL Conference. *J Hepatol* 2001; **35**: 421-430

2 **Ferrell LD,** Crawford JM, Dhillon AP, Scheuer PJ, Nakanuma Y. Proposal for standardized criteria for the diagnosis of benign, borderline, and malignant hepatocellular lesions arising in chronic advanced liver disease. *Am J Surg Pathol* 1993; **17**: 1113-1123

3 Anonymous, International Working Party. Terminology of nodular hepatocellular lesions. *Hepatology* 1995; **22**: 983-993

4 **Theise ND.** Macroregenerative (dysplastic) nodules and hepatocarcinogenesis: theoretical and clinical considerations. *Semin Liver Dis* 1995; **15**: 360-371

5 **Quaglia AP,** Bhattacharjya S, Dhillon A. Limitations of the histopathological diagnosis and prognostic assessment of hepatocellular carcinoma. *Histopathology* 2001; **38**: 167-174

6 **Kojiro M.** Premalignant lesions of hepatocellular carcinoma: pathologic viewpoint. *J Hepatobiliary Pancreat Surg* 2000; **7**: 535-541

7 **Bhattacharya S,** Davidson B, Dhillon AP. Blood supply of early hepatocellular carcinoma. *Semin Liver Dis* 1995; **15**: 390-401

8 **Lauwers GY,** Terris B, Balis UJ, Batts KP, Regimbeau JM, Chang Y, Graeme-Cook F, Yamabe H, Ikai I, Cleary KR, Fujita S, Flejou JF, Zukerberg LR, Nagorney DM, Belghiti J, Yamaoka Y, Vauthey JN. International Cooperative Study Group on Hepatocellular carcinoma. Prognostic histologic indicators of curatively resected hepatocellular carcinomas: a multi-institutional analysis of 425 patients with definition of a histologic prognostic index. *Am J Surg Pathol* 2002; **26**: 25-34

9 **Furuya K,** Nakamura M, Yamamoto Y, Togei K, Otsuka H. Macroregenerative nodule of the liver. A clinicopathologic study of 345 autopsy cases of chronic liver disease. *Cancer* 1988; **61**: 99-105

10 **Kondo F,** Ebara M, Sugiura N, Wada K, Kita K, Hirooka N, Nagato Y, Kondo Y, Ohto M, Okuda K. Histological features and clinical course of large regenerative nodules: evaluation of their precancerous potentiality. *Hepatology* 1990; **12**: 592-598

11 **Scheuer P,** Lefkowitch J. Liver Biopsy Interpretation. 6th ed. London, Edimburgh, New York, Philadelphia, St Louis, Sidney, Toronto: *W.B. Saunders* 2000: 191-227

12 **Himeno H,** Enzan H, Saibara T, Onishi S, Yamamoto Y. Hitherto unrecognized arterioles within hepatocellular carcinoma. *J Pathol* 1994; **174**: 217-222

13 **Nakashima Y,** Nakashima O, Hsia CC, Kojiro M, Tabor E. Vascularization of small hepatocellular carcinomas: correlation with differentiation. *Liver* 1999; **19**: 12-18

14 **Kutami R,** Nakashima Y, Nakashima O, Shiota K, Kojiro M. Pathomorphologic study on the mechanism of fatty change in small hepatocellular carcinoma of humans. *J Hepatol* 2000; **33**: 282-289

15 **Dhillon AP,** Colombari R, Savage K, Scheuer PJ. An immunohistochemical study of the blood vessels within primary hepatocellular tumours. *Liver* 1992; **12**: 311-318

16 **Kondo F,** Kondo Y, Nagato Y, Tomizawa M, Wada K. Interstitial tumour cell invasion in small hepatocellular carcinoma. Evaluation in microscopic and low magnification views. *J Gastroenterol Hepatol* 1994; **9**: 604-612

17 **Lebart L,** Morineau A, Piron M. Statistique exploratoire multidimensionnelle. Analyse en composantes principales. 2nd ed. *Paris, France: Dunod* 1997: 32-66

18 **Selaru FM,** Xu Y, Yin J, Zou T, Liu TC, Mori Y, Abraham JM, Sato F, Wang S, Twigg C, Olaru A, Shustova V, Leytin A, Hytiroglou P, Shibata D, Harpaz N, Meltzer SJ. Artificial neural networks distinguish among subtypes of neoplastic colorectal lesions. *Gastroenterology* 2002; **122**: 606-613

19 **Miyao Y,** Ozaki D, Nagao T, Kondo Y. Interstitial invasion of well-differentiated hepatocellular carcinoma and subsequent tumor growth. *Pathol Int* 1999; **49**: 208-213

20 **Tomizawa M,** Kondo F, Kondo Y. Growth patterns and interstitial invasion of small hepatocellular carcinoma. *Pathol Int* 1995; **45**: 352-358

Science Editor Guo SY **Language Editor** Elsevier HK

PO Box 2345, Beijing 100023, China
www.wjgnet.com
wjg@wjgnet.com

ELSEVIER

World J Gastroenterol 2005;11(40):6269-6276
World Journal of Gastroenterology ISSN 1007-9327
© 2005 The WJG Press and Elsevier Inc. All rights reserved.

Mechanism of metastasis by membrane type 1-matrix metalloproteinase in hepatocellular carcinoma

Ying-Chi Ip, Siu-Tim Cheung, Ka-Ling Leung, Sheung-Tat Fan

Ying-Chi Ip, Siu-Tim Cheung, Ka-Ling Leung, Sheung-Tat Fan, Centre for the Study of Liver Disease and Department of Surgery, The University of Hong Kong, Pokfulam, Hong Kong, China
Supported by the Seed Funding Program of the University of Hong Kong
Correspondence to: Dr. Siu -Tim Cheung, Department of Surgery, The University of Hong Kong, L9-55, Faculty of Medicine Building, 21 Sassoon Road, Hong Kong, China. stcheung@hkucc.hku.hk
Telephone: +852-28199651 Fax: +852-28184407
Received: 2005-03-17 Accepted: 2005-04-09

Abstract

AIM: To investigate the precise role of membrane type 1-matrix metalloproteinase (MT1-MMP) in hepatocellular carcinoma (HCC) metastasis.

METHODS: Human HCC cells Hep3B with overexpression of MT1-MMP were established by stable transfection, and compared with control cells carrying the empty vector. Cells were examined *in vivo* for their differences in the metastatic ability of athymic nude mice, and analyzed *in vitro* for their differences in invasion ability by invasion chamber coated with Matrigel, adhesion towards collagen I and migration through culture chamber. Cell proliferation and apoptosis in adherent and suspension status were evaluated by MTT and flow cytometry analysis.

RESULTS: We found that overexpression of MT1-MMP could increase intrahepatic metastasis in nude mice with orthotopic implantation of HCC cells (incidence of 100% [MT1-MMP transfectants] *vs* 40% [vector control transfectants], $P<0.05$). MT1-MMP could also enhance cell invasion through Matrigel (107.7 *vs* 39.3 cells/field, $P<0.001$), adhesion towards matrix (0.30 *vs* 0.12 absorbance unit at 540 nm, $P<0.001$), cell migration (89.3 *vs* 39.0 cells/field, $P<0.001$), and cell proliferation (24.3 *vs* 40.5 h/doubling, $P<0.001$). We also observed that MT1-MMP supported cell survival (71.4% *vs* 23.9%, $P<0.001$) with reduced apoptosis (43.7% *vs* 51.0%, $P<0.05$) in an attachment-free environment.

CONCLUSION: MT1-MMP overexpression could enhance metastasis. In addition to its active role in matrix degradation during tumor invasion, MT1-MMP enhances tumor cell survival upon challenge of detachment, which is important during metastasis when cells enter the circulation.

© 2005 The WJG Press and Elsevier Inc. All rights reserved.

Key words: MT1-MMP/MMP14; Liver cancer; Invasion; Metastasis

Ip YC, Cheung ST, Leung KL, Fan ST. Mechanism of metastasis by membrane type 1-matrix metalloproteinase in hepatocellular carcinoma. *World J Gastroenterol* 2005; 11(40): 6269-6276 http://www.wjgnet.com/1007-9327/11/6269.asp

INTRODUCTION

Membrane type 1-matrix metalloproteinase (MT1-MMP or MMP14) is the well-characterized transmembrane MMP. It triggers the activation cascade of other pro-MMPs via the activation of pro-MMP2[1] and pro-MMP13[2] resulting in the cleavage of a complex array of extracellular matrix proteins. MT1-MMP itself also aids in maintaining the homeostasis of extracellular matrix by regulating the turnover of types I-III collagens, fibronectin, vitronectin, laminin, fibrin, and proteoglycan[3,4] for tissue remodeling and development. MT1-MMP knock-out mice show inadequate collagen turnover resulting in dwarfism, osteopenia, arthritis, connective tissue abnormalities, and early postnatal death[5]. In addition, MT1-MMP deficiency causes impaired endochondral ossification and angiogenesis[6].

MT1-MMP is involved in the progression of different malignancies[7], and localizes in invadopodia of invading tumor cells tethering extracellular matrix breakdown at invasive front[8,9]. Numerous studies support its role in cancer dissemination by demonstrating that MT1-MMP alters cell behaviors through proteolysis[10-13]. All these point out that MT1-MMP is a versatile enzyme that contributes to invasion and metastasis through numerous mechanisms[14].

Our recent study has revealed upregulation of MT1-MMP specifically in hepatocellular carcinoma (HCC) tissues with venous invasion ($P<0.001$)[15]. HCC is a hypervascular tumor, in which venous invasion is common and an important risk factor for tumor metastasis. Earlier studies of MT1-MMP focused on its increased expression in invasive HCC[16-20], association with extracellular matrix remodeling[21], poor prognosis[19], and induction of its expression by HBV X protein[22]. In this study, we demonstrated a novel role of MT1-MMP in metastasis, where cell survival in an attachment-deprived condition was maintained with reduced apoptosis. The current data indicate that MT1-MMP plays an important role in supporting cell survival when cells enter the circulation during metastasis, in addition to its prominent role in matrix degradation during tumor invasion.

MATERIALS AND METHODS

Construction of plasmid

Full-length human MT1-MMP cDNA was PCR-amplified

using the first-stranded cDNA reverse-transcribed from total RNA of normal liver according to the published sequence (GenBank accession number NM 004995) using specific primers (forward primer: 5'-GAGAT ATCAT GTCTC CCGCC CCAAG A-3'; reverse primer: 5'-CCTCT AGACA CCTGC TGCCA CTG-3') under the conditions: at 94 ℃ for 10 min; at 94 ℃ for 1 min, at 60 ℃ for 1 min, at 68 ℃ for 1 min for 30 cycles by Platinum® *Taq* DNA polymerase high fidelity (Invitrogen, Carlsbad, CA, USA). Expression construct was made by cloning the PCR product into a mammalian expression vector, pcDNA3.0 (Invitrogen).

Cell culture and transfections

Human HCC cell line Hep3B purchased from the American Type Culture Collection (ATCC, Rockville, MD, USA) was cultured in DMEM supplemented with 100 mL/L fetal bovine serum (FBS), 2 mmol/L L-glutamine, 100 U/mL penicillin, and 100 μg/mL streptomycin. Constructs were transfected using the LipofectAMINE reagent (Invitrogen) according to the protocol suggested by the manufacturer. Stable transfectants were selected in DMEM complete medium with 400 μg/mL Geneticin (USB, Cleveland, OH, USA) for 3 wk. Hep3B cells stably transfected with empty pcDNA3.0 vector were used as control for all the experiments, in comparison with the MT1-MMP transfectants. Expression levels of MT1-MMP in transfectants were compared by semi-quantitative RT-PCR and Western blotting.

Intrahepatic tumor model

Male BALB/c *nu/nu* (nude) mice were obtained from the Charles River Laboratories (Wilmington, MA, USA) and the study protocol was approved by the Committee on the Use of Live Animals in Teaching and Research of the University of Hong Kong. Hepatic tumor was generated by slow intrahepatic injection of 2×10^6 cells into the left liver lobe of a 7-wk-old mouse during laparotomy. Ten mice were injected for each transfectant and were killed 60 d after the operation. After macroscopic examination and measurement, livers, hearts, spleens, lungs, kidneys, and pancreas were harvested. Intrahepatic metastasis was defined macroscopically as nodules that were clearly distinguishable from primary tumors by naked eyes or microscopically as clusters of tumor cells with α-fetoprotein (AFP) expression confirmed by immunohistochemistry and hematoxylin and eosin staining on paralleled sections.

MT1-MMP RNA expression quantitation

MT1-MMP RNA expression level was assessed by semi-quantitative RT-PCR using MT1-MMP specific primers (forward primer as described above; reverse primer: 5'-AATGC TCGAG CCCCA GGGCA-3') and control 18S rRNA (forward primer: 5'-CTCTT AGCTG AGTGT CCCGC-3' and reverse primer: 5'-CTGAT CGTCT TCGAA CCTCC-3'). PCR for MT1-MMP and 18S rRNA was first performed for 20-32 and 10-32 cycles, respectively. The PCR product was electrophoresed in agarose gel and the intensity was quantified by densitometric scanning using a gel-imaging system and UVP GelWorks ID Intermediate version 3.01 (Ultra Violet Products Ltd, Cambridge, UK). The number of cycles at linear increase of PCR product was chosen for comparison. The relative MT1-MMP RNA level was determined as the MT1-MMP intensity normalized by the 18S rRNA intensity of respective samples.

Immunohistochemistry

For immunohistochemical staining, AFP polyclonal antibody (DAKO, Carpinteria, CA, USA) and Ki67 mAb (BD PharMingen, San Diego, CA, USA) were used at 1:3 000 and 1:100, respectively. Paraffin-embedded tissues were cut into 4-μm-thick sections, dewaxed, rehydrated in graded ethanol and antigen retrieved by boiling for 10 min in a citrate buffer, pH 6.0. Endogenous peroxidase activity was quenched by DAKO peroxidase block, followed by 30-min incubation with primary antibody. After being washed with PBS, localization of protein was detected using the DAKO Envision™+System. The tissue sections were counterstained with hematoxylin.

Protein extraction and Western blotting

Total protein was extracted with urea buffer (9 mol/L urea, 50 mmol/L Tris-Cl, pH 7.5) in the presence of Complete™ protease inhibitor cocktail (Roche, Mannheim, Germany). Twenty micrograms of total protein was analyzed with 2 μg/mL MT1-MMP polyclonal antibody (AGI, Sunnyvale, CA, USA).

Immunoreactive bands were visualized with the Enhanced Chemiluminescence Western Blotting Detection Kit (Amersham Biosciences, Buckinghamshire, UK). β-actin antibody (Santa Cruz Biotechnology, Santa Cruz, CA, USA) served as loading control. The reactive bands in the exposed films were quantified by densitometric scanning as described above. The relative amount of MT1-MMP level for the active form (62 ku) and the total MT1-MMP (summation of pro-form, 64 ku; active form, 62 ku; and cleaved forms, 20-43 ku) were calculated, respectively, after normalization by the actin reactive band.

Cell proliferation

Three thousand cells per well were seeded at the start of the experiment. Cell proliferation was assessed using conversion of 3-[4,5-dimethylthiazol-2-yl]-2,5-diphenyltetrazolium bromide (MTT, Sigma-Aldrich, St. Louis, MO, USA) to formazan product at 24-h intervals. Briefly, 0.5 mg/mL MTT was added to the well for 4 h and terminated by adding 100 μL of 0.1 mol/L HCl/isopropanol. Absorbance was measured at 540 nm. Cell proliferation was also assessed by counting the total cell number. Briefly, 30 000 cells/well were seeded at the start of the experiment. The cells were trypsinized and counted at 24-h intervals for 5 d by the trypan blue exclusion method. The doubling time of the cells was assessed at the linear phase of the growth curve.

In vitro invasion assay

Fifty thousand cells were seeded in 500 μL DMEM in the upper compartment of the BD BioCoat™ Matrigel™ Invasion Chamber (Becton Dickinson, Bedford, MA, USA). The lower compartment was filled with 500 μL of DMEM/10% FBS. After 24 h, cells on the undersurface of the filters were fixed, stained with hematoxylin and eosin, and counted under a microscope at a magnification of ×200

for 10 random fields.

Cell attachment assay

Fifty thousand cells were seeded in 100 μL DMEM/10% FBS in collagen I-coated plates for 1 h. After extensive washes, adherent cells were fixed and stained with crystal violet in 10% ethanol. Following washing with PBS, the incorporated dye was extracted with a 1:1 mixture of 100 mmol/L sodium phosphate, pH 4.5 and 50% ethanol. Absorbance was read at 540 nm.

Cell migration assay

Fifty thousand cells were re-suspended in 0.5 mL DMEM and loaded into cell culture insert. The lower chamber was filled with 0.5 mL DMEM/10% FBS. After 24 h, cells at the membrane's undersurface were fixed, stained, and counted at a magnification of ×200 for four microscopic fields.

Anoikis assay

Three million cells were held in suspension in poly-HEMA (Sigma-Aldrich)-coated petri dishes. At indicated time points, the cells were collected, centrifuged, and washed once in PBS. Cell clumps were dispersed by a 5-min treatment of 500 μL 0.5 mmol/L EDTA, followed by an addition of 9.5 mL DMEM/10% FBS. Then, 100 μL cells was seeded and the ability to convert MTT to formazan product was examined as described above for 3 h. The percentage of absorbance value divided by the absorbance value at 0 h after background correction was presented. Cells at indicated time points were also stained with propidium iodide for 15 min followed by an analysis using the flow cytometer (Becton Dickinson).

Statistical analysis

Each data point represented results from at least three independent experiments performed in duplicate and was presented as mean±SD. Comparison between groups was made with the Student's *t*-test and considered statistically significant if the *P* value was less than 0.05. Statistical analysis was carried out using the statistical software (SPSS version 9.0 for Windows; SPSS, Chicago, IL, USA).

RESULTS

Establishment of stable MT1-MMP overexpression transfectant

To examine the biological function of MT1-MMP, we first established a stable Hep3B transfectant that overexpressed MT1-MMP. Semi-quantitative RT-PCR (Figure 1A) confirmed that the MT1-MMP RNA transcript level in overexpressing transfectants increased by 2.9-fold compared to vector control transfectants, whereas the Western blot analysis (Figure 1B) showed that in MT1-MMP transfectants there was an 1.5-fold increase of active MT1-MMP and 2.0-fold increase of total reactive forms of MT1-MMP protein compared to the vector control. The higher levels of the 43 and 20 ku MT1-MMP, which are cleavage products generated by active MMP2, indirectly evidenced the increased active MMP2 generated by MT1-MMP in overexpression transfectants compared to the vector control[23,24].

MT1-MMP increased metastasis and tumorigenicity

The stable transfectants were inoculated into the left liver lobe of the athymic nude mice to study the effect on metastasis (Figure 2). The intrahepatic tumors grew within the liver and the tumor nodules were physically close to each other. Physical separation of tumor and non-tumor liver tissues by detailed dissection for weight and volume measurement became infeasible, because this would ruin the subsequent histological analysis for tumor margin assessment of these nodules. Hence, the size was presented as the greatest dimension measured reflecting the weight and volume of the tumor mass. In 60 d, MT1-MMP overexpression resulted in a higher incidence of xenograft formation and a larger primary tumor (incidence of 80% and size of 2.0±1.3 cm), as compared to the control group (incidence of 50% and size of 0.8±0.5 cm; Table 1), supporting its role in enhancing tumorigenicity and

Table 1 Summary of *in vivo* tumorigenicity assay

	Primary tumor		Metastasis
	Incidence	Size (cm)	tumor
MT1-MMP	8/10	2.0±1.3	8/8
Vector control	5/10	0.8±0.5	2/5

MT1-MMP overexpression resulted in significantly larger primary tumor and frequent metastasis.

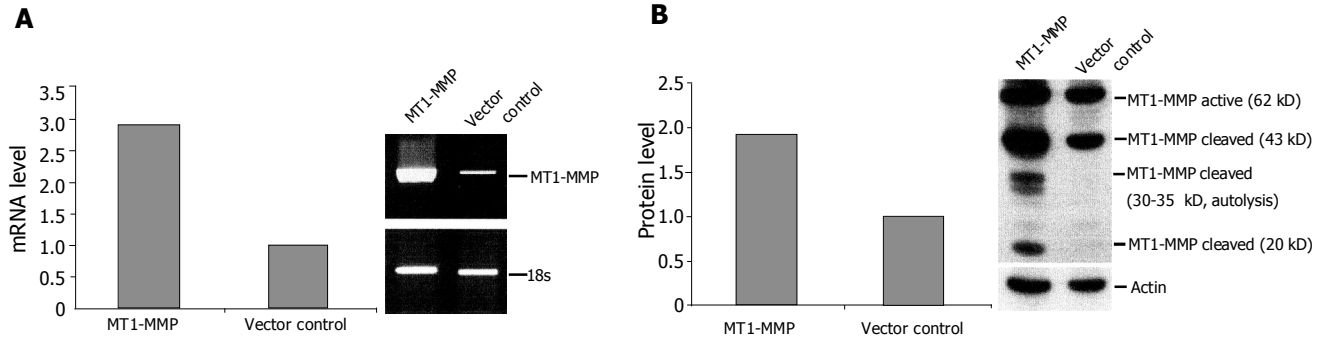


Figure 1 Establishment of stable MT1-MMP transfectants. **A**: RNA transcript levels were compared in linear phases by semi-quantitative RT-PCR after normalization with 18S level; **B**: protein expression levels were compared by Western blotting analysis after normalization with actin level.

growth. The possibility of tumor implantation into the portal vein during the experiment was excluded, because portal vein injection resulted in multiple liver tumors (data not shown).

In the non-injection liver lobes, a higher incidence of variably sized tumor nodules was found in the MT1-MMP transfected group (Figure 2). Microscopic metastasis was further confirmed by AFP staining, as Hep3B cells expressed AFP but not the normal mouse hepatocytes. The microscopic metastases were counted by the presence of clusters of AFP-positive cells, as the clinical significance of single solitary AFP-positive tumor cells was unknown. In general, more intrahepatic metastases were found in the MT1-MMP transfected group than in the vector control group (100% and 40%, respectively; Table 1). No AFP-producing cell was found in kidneys, lungs, spleens, hearts, and pancreas.

MT1-MMP enhanced tumor dissemination and growth

Enhanced metastasis *in vivo* further prompted us to look

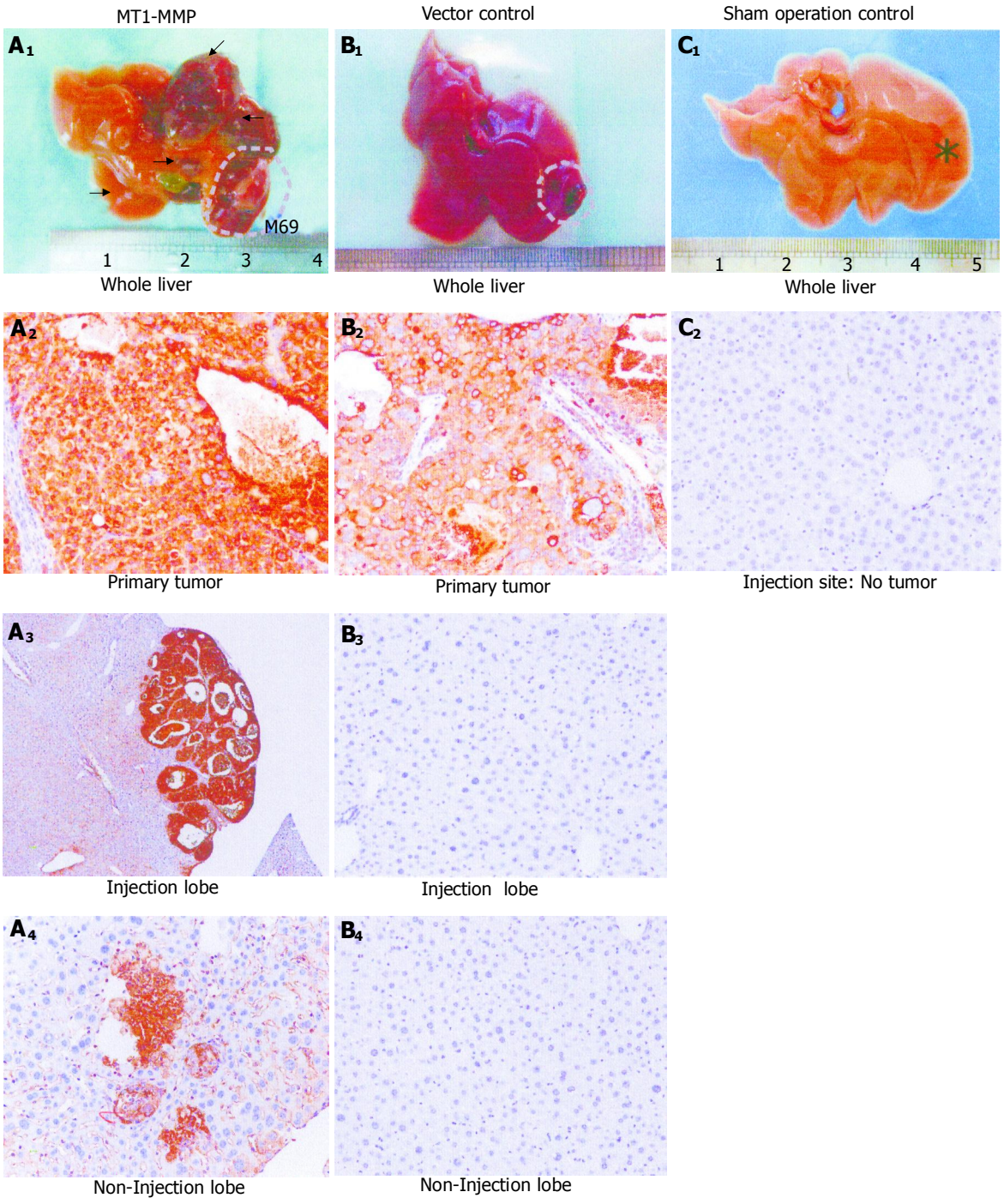


Figure 2 Tumorigenicity and metastasis *in vivo* enhanced by MT1-MMP. A_{1-4}: Large primary tumor nodule with prominent metastases produced by MT1-MMP overexpression; B_{1-4}: Small primary tumor nodule and rare metastasis produced by vector control transfectants; C_{1-2}: Tumor-free control liver injected with saline. Primary tumors, metastases, and injection site were indicated by dotted lines, arrows, and an asterisk, respectively. Sections from all tissues collected were then subjected to AFP staining.

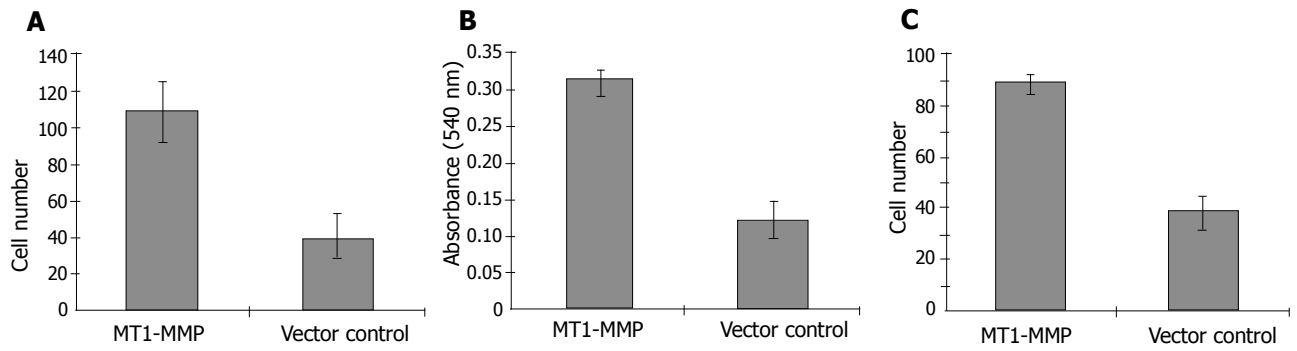


Figure 3 Cell invasion, adhesion efficiency, and cell motility *in vitro* enhanced by MT1-MMP. **A**: Cell invasive ability in standard Boyden chamber; **B**: Adhesion efficiency on collagen I; **C**: Directional migration ability by cell motility assay.

into the sequential steps of metastasis by *in vitro* assays. In a standard Boyden chamber assay, MT1-MMP transfectants significantly increased the number of cells that invaded through Matrigel-coated filters by 174.0% (107.7±15.5 and 39.3±12.1 cells/field, respectively; $P<0.001$; Figure 3A). Furthermore, 150% more MT1-MMP transfectants adhered onto collagen I compared to the control within a fixed time (0.3±0.02 and 0.12±0.03 absorbance unit at 540 nm, respectively; $P<0.001$; Figure 3B). When the transfectants were plated into plain transwells without a Matrigel layer, increased MT1-MMP enhanced cell migration by 129.0% (89.3±6.7 and 39.0±2.3 cells/field, respectively; $P<0.001$; Figure 3C). Collectively, increased MT1-MMP facilitated cells in suspension to arrest onto collagen I (cell attachment to matrix during metastasis at the secondary site), enhanced their directional cell motility and thereby promoted invasion through matrix. This was particularly important during extravasation.

Increase in tumor size *in vivo* led us to examine the cell proliferation rate. Intense Ki67 staining was observed in MT1-MMP xenografts (Figure 4A) indicating MT1-MMP enhanced growth *in vivo*. Cell proliferation of transfectants in culture was monitored by the assessment of mitochondrial activity in MTT assay (Figure 4B) and counting the total cell number (Figure 4C) at 24-h intervals over 5 d, and both assay methods demonstrated that MT1-MMP promoted cell proliferation *in vitro*. The doubling time of MT1-MMP overexpressing transfectants and control transfectants was 24.3 and 40.5 h, respectively. Taken together, MT1-MMP increased cell proliferation *in vivo* and *in vitro*.

MT1-MMP reduced anoikis

Adherent cells undergo apoptosis shortly after loss of cell-substratum adhesion, a phenomenon known as

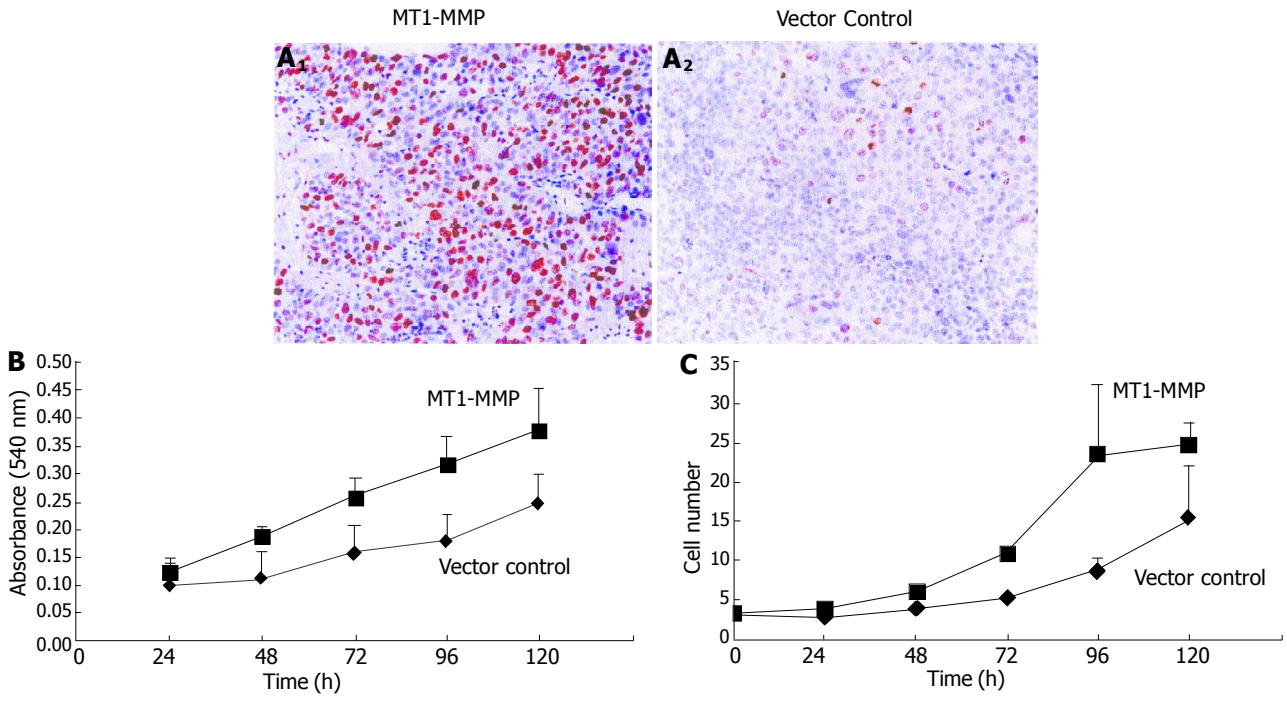


Figure 4 Cell proliferation *in vivo* and *in vitro* enhanced by MT1-MMP. A_{1-2}: Primary tumors in athymic nude mice examined by Ki67 staining; **B**: Cells examined by MTT assay; **C**: Cell number counted at regular time intervals.

"anoikis". Cell viability under attachment-deprived conditions is critical after the cells enter the circulation during the process of metastasis. To examine the cell viability under attachment-deprived conditions, the transfectants were prepared as single cell suspension, challenged by anoikis by plating out in attachment-deprived dishes and examined by MTT assay (Figure 5). As reflected by the conversion of MTT to its substrate, MT1-MMP transfectants maintained a higher metabolism than the vector control during the 24 h detachment. By 24 h in an attachment-free environment, MT1-MMP transfectants maintained 71.4% metabolic activity, whereas the metabolic activity of control transfectants declined to only 23.9%.

To evaluate if the MT1-MMP level plays a role in anoikis, the two transfectants at 0 and 24 h after detachment were subjected to propidium iodide staining and then analyzed by the flow cytometer. Difference in detachment-induced death was observed between the MT1-MMP and vector control transfectants at 24 h (43.7±2.0% *vs* 51.0±4.1%, respectively; $P<0.05$). In summary, MT1-MMP enhanced cell survival with reduced apoptosis upon detachment challenge.

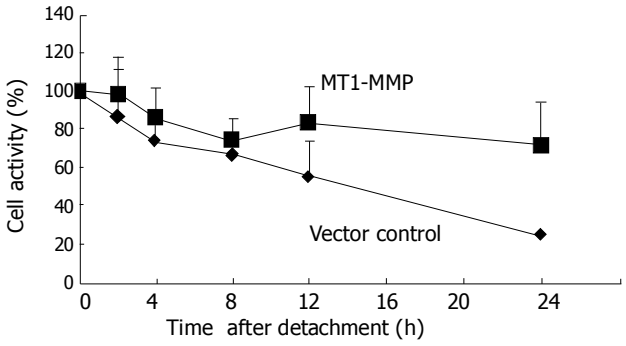


Figure 5 MT1-MMP delayed anoikis. The cell metabolic activity of two transfectants after detachment was compared.

DISCUSSION

MT1-MMP is crucial in HCC progression[15,17,20-22]. Here, we have demonstrated that MT1-MMP protected tumor cells from anoikis, in addition to its classical roles in tumor invasion to pave way for tumor cells to migrate in circulation for distal metastasis after crossing the extracellular matrix and basement membrane. Such a finding is important because even when large number of tumor cells enter the circulation successfully, only a small percentage of tumor cells can actually metastasize due to "metastastic inefficiency"[25-28], the failure to establish metastasis. Only if tumor cells have sustained survival in circulation, the attachment-deprived environment, there would be successful metastasis. Thus, the protection from anoikis contributed by MT1-MMP in the first 24 h upon detachment is of paramount importance during HCC invasion and metastasis.

Increased intrahepatic metastasis by MT1-MMP was observed in the spontaneous metastasis assay performed *in vivo*. *In vitro,* MT1-MMP was also shown to enhance invasion through matrix, adhesion to collagen I and in directional cell migration. Collagen I is the most abundant extracellular matrix component in liver, especially in cirrhotic liver. Enhanced cell attachment to collagen I was observed in the MT1-MMP transfectants in suspension status. Thus, MT1-MMP could also facilitate cell attachment at a new site for metastasis, aside from its leading role in matrix degradation and enhanced cell migration ability for cell invasion to take place to leave the primary site.

Apoptosis is the "rate-determining" step subsequent to the cells entering the circulation. Others have reported that inhibition of apoptosis in the first 24 h could already enhance lung metastasis[25,29,30]. In the current study, MT1-MMP expression conferred a survival advantage in the attachment-deprived environment. Notably, MT1-MMP expression also contributed to evasion of apoptosis in suspension status, although the percentage difference was not enormous but statistically significant. The significant gain in survival advantage but marginal improvement in evasion of apoptosis by MT1-MMP overexpression during suspension status could be due to a number of reasons. The remaining viable control cells became dormant (or less active in converting MTT to a formazan product) in adverse conditions, whereas the viable MT1-MMP transfectant was able to withstand the stress and maintained the cell metabolism. Therefore, even when a similar proportion of cells died, a considerable difference in cell metabolism between two transfectants was observed. The higher cell metabolism of MT1-MMP transfectants in suspension culture also suggests that MT1-MMP may still underpin proliferation and, therefore, promotes the selection for a population of cells that are more tumorigenic and resistant to anoikis. Although other factors like immune attack and mechanical shear force from circulation were not taken into account in our experimental settings, cell survival upon detachment could definitely enhance metastatic potential. Further, experiments on proliferation and apoptosis are needed to confirm if proliferation occurs during suspension.

Potential mechanisms exist for the contribution of MT1-MMP to survival advantage during cell suspension status. Indirect links might be mediated through its enzymatic activity. MT1-MMP may alter processing of proteins and thus overrides the apoptotic stimuli during the challenge of detachment. For instance, MT1-MMP modulation of integrin processing and downstream regulation of FAK signaling pathways[31] are related to apoptotic pathways. During osteoblast transdifferentiation, MT1-MMP activates latent transforming growth factor-β and maintains osteoblast survival[32,33]. In support of this view, MMP1 degradation of type I collagen has been shown to expose new cryptic domains that bind to the αvβ3 integrin and trigger survival signals in melanoma cells[34]. On the other hand, MT1-MMP might directly link to various pathways[12,31,35,36] leading to distinct biological outcome in a number of recent studies[36-38]. The localization of MT1-MMP in clathrin-coated pits[39,40] and caveolae[41-44], which are rich in signaling molecules[45], also raises the possibility of direct activation of signal transduction pathways by MT1-MMP. Therefore, it is conceivable that MT1-MMP can contribute to the activation

of intracellular pathways.

From therapeutic perspectives, total elimination of MMP protease function by inhibitors is impossible and would cause a number of side effects. Nevertheless, the MMP-related subject is promising in the field of tumor detection, prognosis, prevention, and therapeutic purposes in defined situations[46,47]. Our findings have a direct impact on cancer therapy because molecular understanding of the biological activities mediated by proteases provides exciting opportunities for specific interventions in pathways critical for tumor progression.

In conclusion, MT1-MMP promotes HCC tumorigenicity and intrahepatic metastasis with increased tumor growth and invasion ability. More importantly, increased MT1-MMP expression reveals survival advantage and protects HCC cells from apoptosis in the first 24 h in the attachment-free condition. These results strengthen the emerging opinion that the role of MT1-MMP does not only confine to matrix degradation, but also extends to alteration of cell behaviors including survival advantage in the attachment-deprived environment.

ACKNOWLEDGMENTS

The authors thank the members of the Division of Hepatobiliary and Pancreatic Surgery of the University of Hong Kong. The authors also thank Doug Ross of Applied Genomics for providing us with the MT1-MMP antibody.

REFERENCES

1 **Sato H,** Takino T, Okada Y, Cao J, Shinagawa A, Yamamoto E, Seiki M. A matrix metalloproteinase expressed on the surface of invasive tumour cells. *Nature* 1994; **370**: 61-65
2 **Knauper V,** Lopez-Otin C, Smith B, Knight G, Murphy G. Biochemical characterization of human collagenase-3. *J Biol Chem* 1996; **271**: 1544-1550
3 **d'Ortho MP,** Will H, Atkinson S, Butler G, Messent A, Gavrilovic J, Smith B, Timpl R, Zardi L, Murphy G. Membrane-type matrix metalloproteinases 1 and 2 exhibit broad-spectrum proteolytic capacities comparable to many matrix metalloproteinases. *Eur J Biochem* 1997; **250**: 751-757
4 **Ohuchi E,** Imai K, Fujii Y, Sato H, Seiki M, Okada Y. Membrane type 1 matrix metalloproteinase digests interstitial collagens and other extracellular matrix macromolecules. *J Biol Chem* 1997; **272**: 2446-2451
5 **Holmbeck K,** Bianco P, Caterina J, Yamada S, Kromer M, Kuznetsov SA, Mankani M, Robey PG, Poole AR, Pidoux I, Ward JM, Birkedal-Hansen H. MT1-MMP-deficient mice develop dwarfism, osteopenia, arthritis, and connective tissue disease due to inadequate collagen turnover. *Cell* 1999; **99**: 81-92
6 **Zhou Z,** Apte SS, Soininen R, Cao R, Baaklini GY, Rauser RW, Wang J, Cao Y, Tryggvason K. Impaired endochondral ossification and angiogenesis in mice deficient in membrane-type matrix metalloproteinase I. *Proc Natl Acad Sci USA* 2000; **97**: 4052-4057
7 **Yana I,** Seiki M. MT-MMPs play pivotal roles in cancer dissemination. *Clin Exp Metastasis* 2002; **19**: 209-215
8 **Nakahara H,** Howard L, Thompson EW, Sato H, Seiki M, Yeh Y, Chen WT. Transmembrane/cytoplasmic domain-mediated membrane type 1-matrix metalloprotease docking to invadopodia is required for cell invasion. *Proc Natl Acad Sci USA* 1997; **94**: 7959-7964
9 **Nabeshima K,** Inoue T, Shimao Y, Okada Y, Itoh Y, Seiki M, Koono M. Front-cell-specific expression of membrane-type 1 matrix metalloproteinase and gelatinase A during cohort migration of colon carcinoma cells induced by hepatocyte growth factor/scatter factor. *Cancer Res* 2000; **60**: 3364-3369
10 **Nakamura H,** Suenaga N, Taniwaki K, Matsuki H, Yonezawa K, Fujii M, Okada Y, Seiki M. Constitutive and induced CD44 shedding by ADAM-like proteases and membrane-type 1 matrix metalloproteinase. *Cancer Res* 2004; **64**: 876-882
11 **Sounni NE,** Devy L, Hajitou A, Frankenne F, Munaut C, Gilles C, Deroanne C, Thompson EW, Foidart JM, Noel A. MT1-MMP expression promotes tumor growth and angiogenesis through an up-regulation of vascular endothelial growth factor expression. *Faseb J* 2002; **16**: 555-564
12 **Sounni NE,** Roghi C, Chabottaux V, Janssen M, Munaut C, Maquoi E, Galvez BG, Gilles C, Frankenne F, Murphy G, Foidart JM, Noel A. Up-regulation of vascular endothelial growth factor-A by active membrane-type 1 matrix metalloproteinase through activation of Src-tyrosine kinases. *J Biol Chem* 2004; **279**: 13564-13574
13 **Takino T,** Koshikawa N, Miyamori H, Tanaka M, Sasaki T, Okada Y, Seiki M, Sato H. Cleavage of metastasis suppressor gene product KiSS-1 protein/metastin by matrix metalloproteinases. *Oncogene* 2003; **22**: 4617-4626
14 **Egeblad M,** Werb Z. New functions for the matrix metalloproteinases in cancer progression. *Nat Rev Cancer* 2002; **2**: 161-174
15 **Chen X,** Cheung ST, So S, Fan ST, Barry C, Higgins J, Lai KM, Ji J, Dudoit S, Ng IO, Van De Rijn M, Botstein D, Brown PO. Gene expression patterns in human liver cancers. *Mol Biol Cell* 2002; **13**: 1929-1939
16 **Harada T,** Arii S, Mise M, Imamura T, Higashitsuji H, Furutani M, Niwano M, Ishigami S, Fukumoto M, Seiki M, Sato H, Imamura M. Membrane-type matrix metalloproteinase-1(MT1-MTP) gene is overexpressed in highly invasive hepatocellular carcinomas. *J Hepatol* 1998; **28**: 231-239
17 **Ishii Y,** Nakasato Y, Kobayashi S, Yamazaki Y, Aoki T. A study on angiogenesis-related matrix metalloproteinase networks in primary hepatocellular carcinoma. *J Exp Clin Cancer Res* 2003; **22**: 461-470
18 **Kaneyoshi T,** Nakatsukasa H, Higashi T, Fujiwara K, Naito I, Nouso K, Kariyama K, Kobayashi Y, Uemura M, Nakamura SI, Iwasaki Y, Tsuji T. Actual invasive potential of human hepatocellular carcinoma revealed by *in situ* gelatin zymography. *Clin Cancer Res* 2001; **7**: 4027-4032
19 **Maatta M,** Soini Y, Liakka A, Autio-Harmainen H. Differential expression of matrix metalloproteinase (MMP)-2, MMP-9, and membrane type 1-MMP in hepatocellular and pancreatic adenocarcinoma: implications for tumor progression and clinical prognosis. *Clin Cancer Res* 2000; **6**: 2726-2734
20 **McKenna GJ,** Chen Y, Smith RM, Meneghetti A, Ong C, McMaster R, Scudamore CH, Chung SW. A role for matrix metalloproteinases and tumor host interaction in hepatocellular carcinomas. *Am J Surg* 2002; **183**: 588-594
21 **Theret N,** Musso O, Turlin B, Lotrian D, Bioulac-Sage P, Campion JP, Boudjema K, Clement B. Increased extracellular matrix remodeling is associated with tumor progression in human hepatocellular carcinomas. *Hepatology* 2001; **34**: 82-88
22 **Lara-Pezzi E,** Gomez-Gaviro MV, Galvez BG, Mira E, Iniguez MA, Fresno M, Martinez AC, Arroyo AG, Lopez-Cabrera M. The hepatitis B virus X protein promotes tumor cell invasion by inducing membrane-type matrix metalloproteinase-1 and cyclooxygenase-2 expression. *J Clin Invest* 2002; **110**: 1831-1838
23 **Lehti K,** Lohi J, Valtanen H, Keski-Oja J. Proteolytic processing of membrane-type-1 matrix metalloproteinase is associated with gelatinase A activation at the cell surface. *Biochem J* 1998; **334**(Pt 2): 345-353
24 **Stanton H,** Gavrilovic J, Atkinson SJ, d'Ortho MP, Yamada KM, Zardi L, Murphy G. The activation of ProMMP-2 (gelatinase A) by HT1080 fibrosarcoma cells is promoted by culture on a fibronectin substrate and is concomitant with an increase in processing of MT1-MMP (MMP-14) to a 45 kDa

form. *J Cell Sci* 1998; **111**(Pt 18): 2789-2798
25 **Fidler IJ,** `Nicolson GL. Fate of recirculating B16 melanoma metastatic variant cells in parabiotic syngeneic recipients. *J Natl Cancer Inst* 1977; **58**: 1867-1872
26 **Koop S,** Schmidt EE, MacDonald IC, Morris VL, Khokha R, Grattan M, Leone J, Chambers AF, Groom AC. Independence of metastatic ability and extravasation: metastatic ras-transformed and control fibroblasts extravasate equally well. *Proc Natl Acad Sci USA* 1996; **93**: 11080-11084
27 **Weiss L.** Metastatic inefficiency. *Adv Cancer Res* 1990; **54**: 159-211
28 **Yu Q,** Toole BP, Stamenkovic I. Induction of apoptosis of metastatic mammary carcinoma cells *in vivo* by disruption of tumor cell surface CD44 function. *J Exp Med* 1997; **186**: 1985-1996
29 **Fidler IJ.** Critical factors in the biology of human cancer metastasis: twenty-eighth G.H.A. Clowes memorial award lecture. *Cancer Res* 1990; **50**: 6130-6138
30 **Wong CW,** Lee A, Shientag L, Yu J, Dong Y, Kao G, Al-Mehdi AB, Bernhard EJ, Muschel RJ. Apoptosis: an early event in metastatic inefficiency. *Cancer Res* 2001; **61**: 333-338
31 **Baciu PC,** Suleiman EA, Deryugina EI, Strongin AY. Membrane type-1 matrix metalloproteinase (MT1-MMP) processing of pro-alphav integrin regulates cross-talk between alphavbeta3 and alpha2beta1 integrins in breast carcinoma cells. *Exp Cell Res* 2003; **291**: 167-175
32 **Karsdal MA,** Andersen TA, Bonewald L, Christiansen C. Matrix metalloproteinases (MMPs) safeguard osteoblasts from apoptosis during transdifferentiation into osteocytes: MT1-MMP maintains osteocyte viability. *DNA Cell Biol* 2004; **23**: 155-165
33 **Karsdal MA,** Larsen L, Engsig MT, Lou H, Ferreras M, Lochter A, Delaisse JM, Foged NT. Matrix metalloproteinase-dependent activation of latent transforming growth factor-beta controls the conversion of osteoblasts into osteocytes by blocking osteoblast apoptosis. *J Biol Chem* 2002; **277**: 44061-44067
34 **Montgomery AM,** Reisfeld RA, Cheresh DA. Integrin alpha v beta 3 rescues melanoma cells from apoptosis in three-dimensional dermal collagen. *Proc Natl Acad Sci USA* 1994; **91**: 8856-8860
35 **Takino T,** Miyamori H, Watanabe Y, Yoshioka K, Seiki M, Sato H. Membrane type 1 matrix metalloproteinase regulates collagen-dependent mitogen-activated protein/extracellular signal-related kinase activation and cell migration. *Cancer Res* 2004; **64**: 1044-1049
36 **Deryugina EI,** Ratnikov BI, Postnova TI, Rozanov DV, Strongin AY. Processing of integrin alpha(v) subunit by membrane type 1 matrix metalloproteinase stimulates migration of breast carcinoma cells on vitronectin and enhances tyrosine phosphorylation of focal adhesion kinase. *J Biol Chem* 2002; **277**: 9749-9756
37 **Ratnikov BI,** Rozanov DV, Postnova TI, Baciu PG, Zhang H, DiScipio RG, Chestukhina GG, Smith JW, Deryugina EI, Strongin AY. An alternative processing of integrin alpha(v) subunit in tumor cells by membrane type-1 matrix metalloproteinase. *J Biol Chem* 2002; **277**: 7377-7385
38 **Deryugina EI,** Soroceanu L, Strongin AY. Up-regulation of vascular endothelial growth factor by membrane-type 1 matrix metalloproteinase stimulates human glioma xenograft growth and angiogenesis. *Cancer Res* 2002; **62**: 580-588
39 **Jiang A,** Lehti K, Wang X, Weiss SJ, Keski-Oja J, Pei D. Regulation of membrane-type matrix metalloproteinase 1 activity by dynamin-mediated endocytosis. *Proc Natl Acad Sci USA* 2001; **98**: 13693-13698
40 **Uekita T,** Itoh Y, Yana I, Ohno H, Seiki M. Cytoplasmic tail-dependent internalization of membrane-type 1 matrix metalloproteinase is important for its invasion-promoting activity. *J Cell Biol* 2001; **155**: 1345-1356
41 **Annabi B,** Lachambre M, Bousquet-Gagnon N, Page M, Gingras D, Beliveau R. Localization of membrane-type 1 matrix metalloproteinase in caveolae membrane domains. *Biochem J* 2001; **353**: 547-553
42 **Hotary KB,** Allen ED, Brooks PC, Datta NS, Long MW, Weiss SJ. Membrane type I matrix metalloproteinase usurps tumor growth control imposed by the three-dimensional extracellular matrix. *Cell* 2003; **114**: 33-45
43 **Galvez BG,** Matias-Roman S, Yanez-Mo M, Vicente-Manzanares M, Sanchez-Madrid F, Arroyo AG. Caveolae are a novel pathway for membrane-type 1 matrix metalloproteinase traffic in human endothelial cells. *Mol Biol Cell* 2004; **15**: 678-687
44 **Labrecque L,** Nyalendo C, Langlois S, Durocher Y, Roghi C, Murphy G, Gingras D, Beliveau R. Src-mediated tyrosine phosphorylation of caveolin-1 induces its association with membrane type 1 matrix metalloproteinase. *J Biol Chem* 2004; **279**: 52132-52140
45 **Carver LA,** Schnitzer JE. Caveolae: mining little caves for new cancer targets. *Nat Rev Cancer* 2003; **3**: 571-581
46 **Matrisian LM,** Sledge GW, Mohla S. Extracellular proteolysis and cancer: meeting summary and future directions. *Cancer Res* 2003; **63**: 6105-6109
47 **Zucker S,** Cao J, Chen WT. Critical appraisal of the use of matrix metalloproteinase inhibitors in cancer treatment. *Oncogene* 2000; **19**: 6642-6650

Science Editor Wang XL and Guo SY **Language Editor** Elsevier HK

PO Box 2345, Beijing 100023, China
www.wjgnet.com
wjg@wjgnet.com

ELSEVIER

World J Gastroenterol 2005;11(40):6277-6280
World Journal of Gastroenterology ISSN 1007-9327
© 2005 The WJG Press and Elsevier Inc. All rights reserved.

Percutaneous ethanol injection, radiofrequency and their combination in treatment of hepatocellular carcinoma

Bao-Ming Luo, Yan-Ling Wen, Hai-Yun Yang, Hui Zhi, Xiao-Yun Xiao, Bing Ou, Jing-Sheng Pan, Jian-Hong Ma

Bao-Ming Luo, Yan-Ling Wen, Hai-Yun Yang, Hui Zhi, Xiao-Yun Xiao, Bing Ou, Jing-Sheng Pan, Jian-Hong Ma, Department of Ultrasound, the Second Affiliated Hospital, Sun Yat-sen University, 107 Yanjiangxi Rd, Guangzhou 510120, Guangdong Province, China
Supported by the Natural Science Foundation of Guangdong province of China No.31710 and the Medical Research Foundation of the Bureau of Health of Guangdong Province of China No.A2003203
Co-first-authors: Bao-Ming Luo and Yan-Ling Wen
Correspondence to: Dr. Yan-Ling Wen, Department of Ultrasound, the Second Affiliated Hospital, Sun Yet-Sen University, 107 Yanjiangxi Rd, Guangzhou 510120, Guangdong Province, China. yanlingwen20@hotmail.com
Telephone: +86-20-81332516
Received: 2005-07-05 Accepted: 2005-07-15

Abstract

AIM: To evaluate the therapeutic effect and the indication of percutaneous ethanol injection (PEI), radiofrequency ablation (RFA) and their combination in treatment of hepatocellular carcinoma (HCC).

METHODS: Two hundred and fifty-five patients with HCC received treatment of PEI, RFA or their combination. Group1 (< 3 cm in diameter, *n*=85) was treated with PEI, group2 (< 3 cm in diameter, *n*=153) with RFA. Group3 (>3 cm in diameter, *n*=86) was divided into two groups. Group 3a (*n*=34) was treated with RFA, while group 3b (*n*=52) was treated with RFA for 2 wk after transcatheter arterial chemoembolization or PEI. Contrast-enhanced sonography was performed for 61 patients before and after RFA. Liver function and serum alpha-fetoprotein (AFP) were measured for all patients. Changes of the lesions on ultrasound and contrast-enhanced CT/MRI were evaluated for assessing the therapeutic responses. The 1-, 2-, 3- and 5-year survival rates were recorded after treatment.

RESULTS: In group 1, the complete necrosis rate of lesions after 1 mo was 77.6% (66/85). The level of AFP declined conspicuously after 1 mo. The 1-, 2-, 3- and 5-year survival rate after treatment was 80.0% (52/65), 60.4% (32/53), 52.5% (21/40) and 33.3% (7/21), respectively. In group 2, the complete necrosis rate of lesions after 1 moh was 92.2% (141/153). The level of AFP decreased conspicuously after 1 mo. The 1-, 2-, 3- and 5-year survival rate after treatment was 94.6% (88/93), 73.2% (52/71), 63.5% (33/52) and 46.4% (13/28), respectively. In group 3a, the complete necrosis rate of lesions after 1 mo was 23.5% (8/34). AFP dropped down to the normal level in only one patient after 1 mo. The 1-, 2- and 3-year survival rate after treatment was 47.6% (10/21), 42.9% (6/14) and 27.3% (3/11), respectively. Only one patient was still alive after 5 years. In group 3b, the complete necrosis rate of lesions after 1 mo was 57.7% (30/52). The level of AFP decreased after 1 mo. The 1-, 2-, 3- and 5-year survival rate after treatment was 68.6% (24/35), 46.2% (12/26), 36.8% (7/19) and 27.3% (3/11), respectively.

CONCLUSION: The therapeutic effect of RFA on small HCC is better than that of PEI. Small HCC is the optimal indication of RFA. For recurrent HCC (diameter>3 cm), the combined treatment of RFA and PEI/ACE should be used.

© 2005 The WJG Press and Elsevier Inc. All rights reserved.

Key words: Hepatocellular carcinoma; Radiofrequency ablation; Percutaneous ethanol injection; Embolism; Therapeutic effect

Luo BM, Wen YL, Yang HY, Zhi H, Xiao XY, Ou B, Pan JS, Ma JH. Percutaneous ethanol injection, radiofrequency and their combination in treatment of hepatocellular carcinoma. *World J Gastroenterol* 2005; 11(40): 6277-6280
http://www.wjgnet.com/1007-9327/11/6277.asp

INTRODUCTION

With the advance in surgical techniques, surgical resection in combination with intervention therapy for hepatocellular carcinoma (HCC) has been developed. This combined treatment has improved the survival rate of HCC patients. However, most HCC patients lose the chance of resection because they are in advanced stage of the disease when they see a doctor. Furthermore, some HCCs are multicenter in origin. All these factors lead to a high recurrence after resection[1-4]. Though patients with recurrent tumor can undergo re-resection, most of them do not endure it because of poor liver function[5] or poor quality of life after surgery. Therefore, non-surgical partial ablative treatments, such as transcatheter arterial chemoembolization (TACE), PEI, RFA and microwave ablation, are commonly used for HCC. These methods have their own advantages and limitations. It is worth discussing how to choose a suitable method according to the different situation of patients to achieve the best therapeutic effect. This study aimed to compare the therapeutic effects of different treatments.

MATERIALS AND METHODS

Materials

From August 1999 to May 2005, 255 patients with HCC received the treatment of PEI, RFA or their combination. There were 187 men and 68 women. Their age ranged from 31 to 72 years, Two hundred and eleven of the 255 patients had liver cirrhosis due to hepatitis B (n=206) or alcoholic hepatitis (n=5). Their liver function was Child A in 36, Child B in 208 and Child C in 11.

In group 1, 71 patients were treated with PEI. The diameter of the lesions ranged 1.32~2.91 cm (2.21±1.48 cm). In group 2, 118 patients were treated with RFA. The diameter of the lesions ranged 1.07~2.96 cm (2.39±1.57 cm). In group 3, 24 patients were treated with RFA (group 3a). The diameter of the lesions ranged 3.09~6.18 cm (4.86±2.24 cm). The remaining 42 patients underwent RFA after TACE or PEI. The diameter of the lesions ranged 3.56~7.21 cm (5.44±2.87 cm). The level of alanine aminotransferase in each patient before and two weeks after treatment was measured. AFP level and imaging changes on B-mode sonography, color Doppler flow imaging (CDFI) and contrast-enhanced CT/MR were also evaluated. Contrast-enhanced ultrasound (CEUS) was performed in 61 patients before and after RFA. The 1-, 2-, 3- and 5-year survival rates were recorded. If hypervascularity was observed in the lesions by imaging techniques, TACE or PEI was given followed by FRA within one week. On the contrary, if the lesions were hypovascular, RFA was performed. In the patients with partial necrosis of the lesions, RFA or PEI was done again in the remaining part.

Criteria

The criteria for the therapeutic effect were based on the imagings. Complete necrosis: no enhancement of the lesion on contrast-enhanced CT/MR 1 mo after treatment and no blood flow on CDFI or CEUS with enhanced echo of the whole lesions; partial necrosis: partial enhancement of the lesion on contrast-enhanced CT/MR 1 month after treatment and blood flow signals of the lesion on CDFI or CEUS with partial or no enhancement of the echo in the whole lesion. The 1-, 2-, 3- and 5-year survival rates after treatments were recorded.

Machines

A cool tip RF system (Radionics, UAS) was used in the study. The cooling liquid used was 0 °C pure water. The puncture was guided by Esaote Technos MPX (Esaote SpA, Italy) or ALOKA SSD-2000 (Aloka Co., Japan) sonographic unit.

Statistical analysis

Statistical analysis was done using the SPSS 11.0. Homogeneity test of variance was performed before statistical analysis. Medians were used to describe the data in non-normal distribution. The data in normal distribution were expressed as mean±SD. T-test was used to analyze the difference between the two groups. Paired t-test was used to detect the difference before and after treatment. Analysis of variance and paired Snk-q test were used to detect the differences among the groups. P<0.05 was considered statistically significant.

RESULTS

In group 1, a total of 268 times of PEI were performed with guidance of ultrasound in 71 patients with HCC (mean, 3.2 times/lesion). Eleven lesions received PEI once, 15 lesions PEI twice, 19 lesions PEI thrice, 30 lesions PEI 4 times and 10 lesions PEI 5 times. The complete necrosis rate 1 mo after the treatment was 77.6% (66/85). The AFP level before treatment ranged 11.8 - 4102 μg/mL (median, 192.6 μg/mL) and was higher than 25μg/mL in 48 of the patients and dropped below 25 μg/mL 1 mo after the treatment in 31 of them. But the AFP level was even higher than before in 4 patients. The AFP level after treatment ranged 2.8~2313 μg/mL (median, 17.7 μg/mL). The 1-, 2-, 3- and 5-year survival rate after treatment was 80.0% (52/65), 60.4% (32/53), 52.5% (21/40) and 33.3% (7/21), respectively (Figure 1).

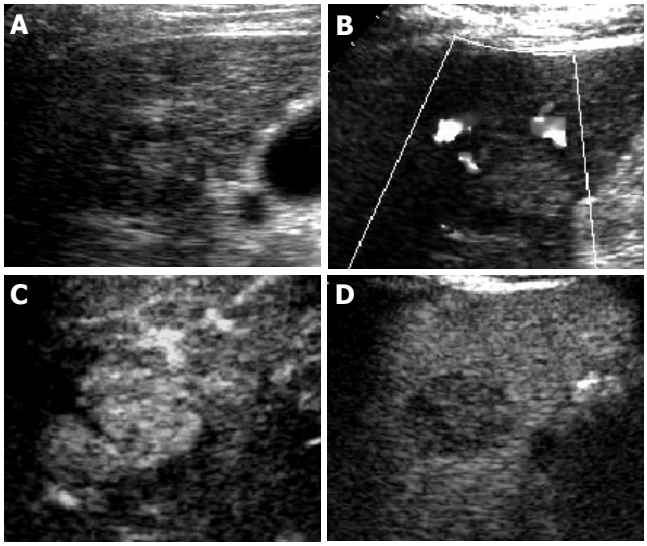


Figure 1 Typical HCC in contrast-enhanced sonography of hypervascular HCC before RFA. **A:** Hypoechoic lesion in the right lobe of the liver on B-mode sonography; **B:** Blood signals of the lesion on CDFI; **C:** Intratumoral enhancement in the early arterial phase of contrast-enhanced sonography; **D:** Hypoechoic lesion compared to the peripheral liver tissue in the late phase.

In group 2, 118 patients received RFA 199 times (mean, 1.3 times/lesion). Ninety-five lesions received RFA once, 35 lesions RFA twice and 13 lesions RFA thrice. The complete necrosis rate 1 mo after treatment was 92.2% (141/153). The level of AFP (2.8~31.3 μg/mL, median 18.5 μg/mL) decreased 1 mo after treatment in 74 patients. The 1-, 2-, 3- and 5-year survival rate was 94.6% (88/93), 73.2% (52/71), 63.5% (33/52) and 46.4% (13/28), respectively (Figure 2).

In group 3a, 24 patients received RFA 91 times (mean,

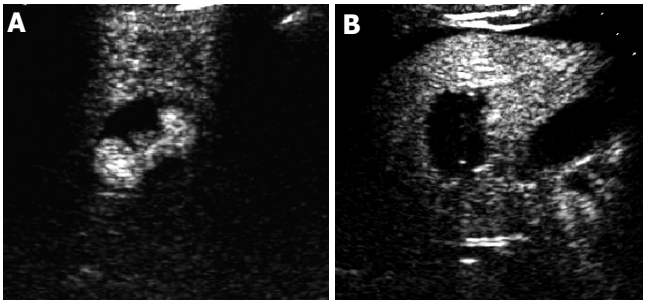


Figure 2 HCC after RFA. **A:** Incomplete necrosis of the lesion in the early arterial phase of contrast-enhanced sonography; **B:** Complete necrosis of the lesion after further RFA.

2.7 times/lesion). Four lesions received RFA once, 10 lesions RFA twice, 13 lesions RFA thrice, 7 lesions RFA 4 times. The complete necrosis rate 1 mo after treatment was 23.5% (8/34). Before treatment, the level of AFP ranged 5.8 - 11 246 μg/mL (median, 417.3 μg/mL). One month after treatment, the level of AFP ranged 12.8~13 513 μg/mL (median, 412.2 μg/mL). The level of AFP dropped below 25 μg/mL in only 1 patient. The 1-, 2-, 3-year survival rate was 47.6% (10/21), 42.9% (6/14) and 27.3% (3/11), respectively. Only one patient was alive after 5 years (Figure 3).

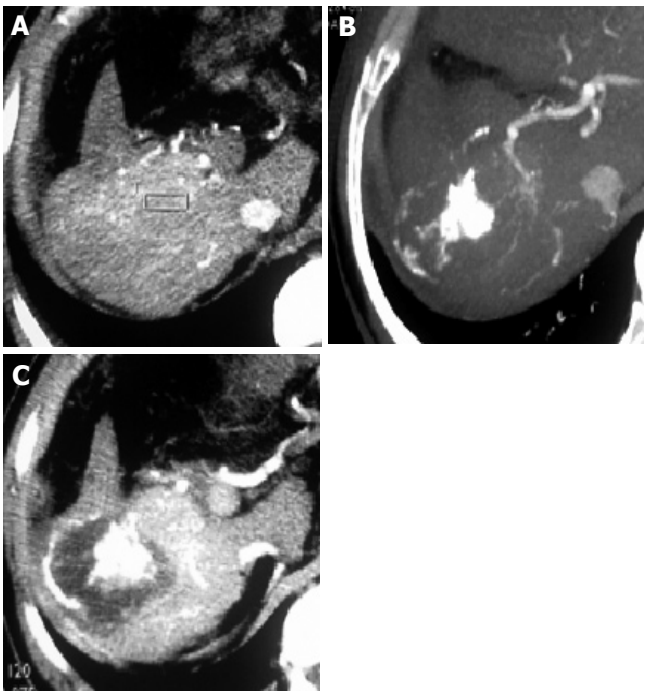


Figure 3 HCC treated with TACE and RFA. **A:** Enhancement of the recurrent HCC after resection in the early arterial phase; **B:** After TACE, lesion restrained with iodine (red arrow) and an un-embolized feeding artery (yellow arrow) in the arterial phase; **C:** After RFA, no enhancement in the lesion in the early arterial phase (red arrow) and enhancement in the inner part of the lesion (yellow arrows) indicating incomplete necrosis.

In group 3b, 42 patients received RFA 110 times (mean, 2.1 times/lesion) after TACE or PEI. Fourteen lesions received RFA once, 23 lesions RFA twice, 10 lesions RFA thrice, 5 lesions RFA 4 times. The complete necrosis rate 1 mo after treatment was 57.7% (30/52). Before treatment, the level of AFP ranged 4.7 - 10 247 μg/mL (median, 423.9 μg/mL). One month after treatment, the level of AFP ranged 5.7~8912 μg/mL (median, 17.7 μg/mL). The 1-, 2-, 3- and 5-year survival rate was 68.6% (24/35), 46.2% (12/26), 36.8% (7/19) and 27.3% (3/11), respectively (Figure 4).

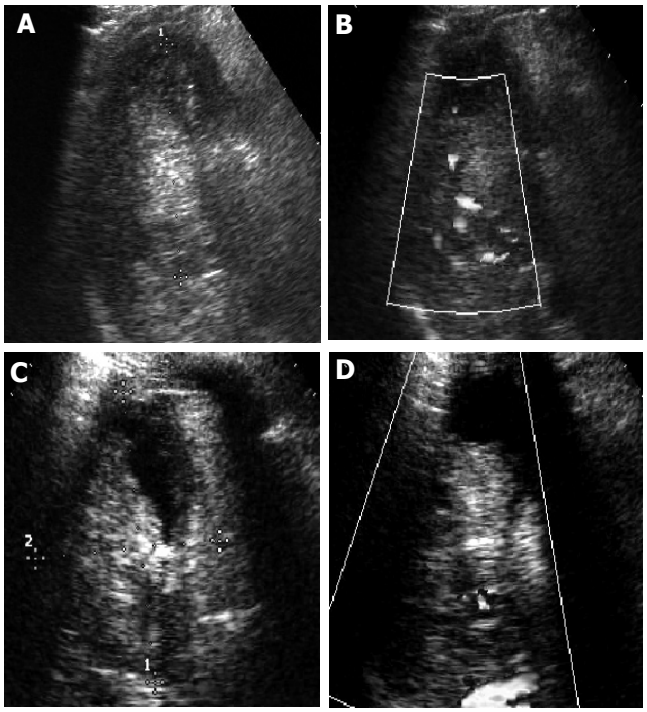


Figure 4 Recurrent HCC treated with TACE and RFA. **A:** hyperechoic lesion on B-mode image; **B:** Color blood signals on CDFI; **C:** Irregular echo-free area in the lesion on B-mode image after combined treatment, indicating partial colliquation of the necrotic tumor; **D:** Color blood signals inside the tumor on CDFI, suggesting incomplete treatment.

There was no significant difference in the levels of ALT before and after RFA. Two weeks after treatment, the level of ALT (73±38 IU) in group 1 was higher than that (32±23 IU) before treatment ($P<0.05$). There was no significant difference in the level of ALT (36±25 IU) 4 wk after treatment compared to that before treatment ($P>0.05$).

DISCUSSION

PEI has become a new interventional method for HCC, and better therapeutic effect has been achieved[6, 7]. However, because of the repetitive injection and the inhomogeneous diffusion of ethanol within the tumor, it is difficult to achieve complete necrosis of some large inhomogeneous

tumors. In addition, the treatment is often suspended because of unendurable pain. Furthermore, PEI decreases the immune function of patients and leads to severe impairment of liver function because of the damage to peripheral liver tissue caused by diffusion of ethanol. In patients with liver cirrhosis before treatment, the curative dose of ethanol may elicit severe complications such as hemorrhage of the congestive ducts or liver failure [8]. RFA is a local chemotherapy and kills tumor cells more completely with less influence on the peripheral liver tissue. This study showed that the complete necrosis rate of lesions and the 1-, 2-, 3- and 5-year survival rates of patients receiving PEI were significantly lower than those of patients receiving RFA. The lower therapeutic effect, worse complications and severer pain of PEI compared to RFA suggest that it is better to choose RFA for treatment of small HCC.

Furthermore, the complete necrosis rate of lesions in group 2 one month after the treatment was 92.2% (141/153). The level of AFP in this group decreased conspicuously. The 1-, 2-, 3- and 5-year survival rates after treatment (94.6%, 73.2%, 63.5%, and 46.4%, respectively) were significantly higher than those of in groups 3a and 3b, suggesting that the therapeutic effect of RFA is good, which is comparable to that of surgical resection.

However, even RFA has better therapeutic effect of HCC with fewer side effects[9-12], it is difficult to obtain complete coagulation in large HCC. One of the limitations of RFA is the small volume of treatment because of the heat from the pole is quickly decreased when it is transmitted in tumor tissue. When the electrode is used, the largest-treated area is about 3 cm in diameter, resulting in more times of RFA and worse therapeutic effect[13] in large tumors. In this study, even more times of ablation were performed in group 3a, the complete necrosis rate was lower than that in group 2. The residual tumor in the treated area maybe one of the most important reasons.

Many different methods have been used to obtain a larger treated area of RFA. TACE is one of the most commonly used non-surgical methods for HCC. It can acquire good therapeutic effect in enveloped small HCC[14]. But for HCCs without envelope or the envelope has been invaded, even small HCC can not be completely necrotized by TACE[15]. However, TACE can reduce the blood supply for the tumor[16]. In group 3b, TACE was performed before RFA in 23 patients (27 lesions), while PEI was performed before RFA in 19 patients (25 lesions). The complete necrosis rate after 1 mo was 57.7% (30/52) in group 3b, significantly higher than that in group 3a (23.5%, 8/34) ($P<0.05$). Therefore, when the tumor is larger than 3 cm in diameter, combined treatment of RFA with TACE or PEI is suggested in order to improve the therapeutic effect.

In conclusion, RFA is one of the optimal choices of treatment for small HCC and combined treatment is suggested for larger HCC.

REFERENCES

1 **Poon RT,** Fan ST, Ng IO, Lo CM, Liu CL, Wong J. Different risk factors and prognosis for early and late intrahepatic recurrence after resection of hepatocellular carcinoma. *Cancer* 2000; **89:** 500-507

2 **Tang ZY,** Yu YQ, Zhou XD, Ma ZC, Wu ZQ. Progress and prospects in hepatocellular carcinoma surgery. *Ann Chir* 1998; **52:** 558-563

3 **Figueras J,** Jaurrieta E, Valls C, Ramos E, Serrano T, Rafecas A, Fabregat J, Torras J. Resection or transplantation for hepatocellular carcinoma in cirrhotic patients: outcomes based on indicated treatment strategy. *J Am Coll Surg* 2000; **190:** 580-587

4 **Belghiti J,** Hiramatsu K, Benoist S, Massault P, Sauvanet A, Farges O. Seven hundred forty-seven hepatectomies in the 1990s: an update to evaluate the actual risk of liver resection. *J Am Coll Surg* 2000; **191:** 38-46

5 **Tang ZY.** Treatment of hepatocellular carcinoma. *Digestion* 1998; **59:** 556-562

6 **Livraghi T,** Giorgio A, Marin G, Salmi A, de Sio I, Bolondi L, Pompili M, Brunello F, Lazzaroni S, Torzilli G. Hepatocellular carcinoma and cirrhosis in 746 patients: long-term results of percutaneous ethanol injection. *Radiology* 1995; 197: 101 –108

7 **Shiina S,** Tagawa K, Niwa Y, Unuma T, Komatsu Y, Yoshiura K, Hamada E, Takahashi M, Shiratori Y, Terano A. Percutaneous ethanol injection therapy for hepatocellular carcinoma: results in 146 patients. *AJR* 1993; **160:** 1023-1028

8 **Livraghi T.** Percutaneous ethanol injection in the treatment of hepatocellular carcinoma in cirrhosis. *Hepatogastroenterology* 2001; **48:** 20-24

9 **Lin SM,** Lin CJ, Lin CC, Hsu CW, Chen YC. Radiofrequency ablation improves prognosis compared with ethanol injection for hepatocellular carcinoma < or =4 cm. *Gastroenterology* 2004; **127:** 1714-1723

10 **Livraghi T**, Goldberg SN, Lazzaroni S, Meloni F, Ierace T, Solbiati L, Gazelle GS. Hepatocellular carcinoma: radio-frequency ablation of medium and large lesions. *Radiology* 2000; **214:** 761-768

11 **Solbiati L,** Goldberg SN, Ierace T, Livraghi T, Meloni F, Dellanoce M, Sironi S, Gazelle GS. Hepatic metastases: percutaneous radio-frequency ablation with cooled-tip electrodes. *Radiology* 1997; **205:** 367-373

12 **Francica G,** Marone G. Ultrasound-guided percutaneous treatment of hepatocellular carcinoma by radiofrequency hyperthermia with a 'cooled-tip needle': a preliminary clinical experience. *Eur J Ultrasound* 1999; **9:** 145-153

13 **Rossi S,** Garbagnati F, Lencioni R, Allgaier HP, Marchianò A, Fornari F, Quaretti P, Tolla GD, Ambrosi C, Mazzaferro V, Blum HE, Bartolozzi C. Percutaneous radio-frequency thermal ablation of nonresectable hepatocellular carcinoma after occlusion of blood supply. *Radiology* 2000; **217:** 119-126

14 **Choi BI,** Kim HC, Han JK, Park JH, Kim YI, Kim ST, Lee HS, Kim CY, Han MC. Therapeutic effect of transcatheter oily chemoembolization therapy for encapsulated nodular hepatocellular carcinoma: CT and pathologic findings. *Radiology* 1992; **182:** 709-713

15 **Kuroda C,** Sakurai M, Monden M, Marukawa T, Hosoki T, Tokunaga K, Wakasa K, Okamura J, Kozuka T. Limitation of transcatheter arterial chemoembolization using iodized oil for small hepatocellular carcinoma. A study in resected cases. *Cancer* 1991; **67:** 81-86

16 **Cheng HY,** Shou Y, Wang X, Xu AM, Chen D, Jia YC. Adjustment of lipiodol dose according to tumor blood supply during transcatheter arterial chemoembolization for large hepatocellular carcinoma by multidetector helical CT. *World J Gastroenterol* 2004; **10:** 2753-2755

Science Editor Wang XL and Guo SY **Language Editor** Elsevier HK

PO Box 2345, Beijing 100023, China
www.wjgnet.com
wjg@wjgnet.com

ELSEVIER

World J Gastroenterol 2005;11(40):6281-6287
World Journal of Gastroenterology ISSN 1007-9327
© 2005 The WJG Press and Elsevier Inc. All rights reserved.

• *LIVER CANCER* •

Overexpression of cyclooxygenase-2 in human HepG2, Bel-7402 and SMMC-7721 hepatoma cell lines and mechanism of cyclooxygenase-2 selective inhibitor celecoxib-induced cell growth inhibition and apoptosis

Ning-Bo Liu, Tao Peng, Chao Pan, Yu-Yu Yao, Bo Shen, Jing Leng

Ning-Bo Liu, Tao Peng, Bo Shen, Jing Leng, Laboratory of Reproductive Medicine, Department of Pathology, Nanjing Medical University, Nanjing 210029, Jiangsu Province, China
Chao Pan, Yu-Yu Yao, Atherosclerosis Research Center, Nanjing Medical University, Nanjing 210029, Jiangsu Province, China
Supported by Medical Science Research Foundation of Jiangsu Health Bureau Grant Z200314 (to JL) and Medical Science Research Foundation of Nanjing Medical University Grant NY1999023 (to NBL) and CX2003012 (to JL)
Correspondence to: Dr. Jing Leng, Laboratory of Reproductive Medicine, Department of Pathology, Nanjing Medical University, Nanjing 210029, Jiangsu Province, China. lengjing@njmu.edu.cn
Telephone: +86-25-86862685 Fax: +86-25-86862685
Received: 2004-11-15 Accepted: 2004-12-03

Abstract

AIM: To investigate the cyclooxygenase-2 (COX-2) expression level in human HepG2, Bel-7402 and SMMC-7721 hepatoma cell lines and the molecular mechanism of COX-2 selective inhibitor celecoxib-induced cell growth inhibition and cell apoptosis.

METHODS: Hepatoma cells were cultured and treated with celecoxib. Cell *in situ* hybridization (ISH) and immunocytochemistry were used to detect COX-2 mRNA and protein expression. Proliferating cell nuclear antigen and phosphorylated Akt were also detected by immunocytochemistry assay. Cell growth rates were assessed by 3-(4, 5-dimethylthiazol-2-yl-2, 5-diphenyltetrazolium (MTT) bromide colorimetric assay. Celecoxib-induced cell apoptosis was measured by terminal deoxynucleotidyl transferase-mediated dUTP nick end labeling (TUNEL) and flow cytometry (FCM). The phosphorylated Akt and activated fragments of caspase-9, caspase-3 were examined by Western blotting analysis.

RESULTS: Increased COX-2 mRNA and protein expression were detected in all three hepatoma cell lines. Celecoxib could significantly inhibit cell growth and the inhibitory effect was in a dose- and time-dependent manner evidenced by MTT assays and morphological changes. The apoptotic index measured by TUNEL increased correspondingly with the increased concentration of celecoxib and the reaction time. With 50 μmol/L celecoxib treatment for 24 h, the apoptotic index of HepG2, BEL-7402 and SMMC-7721 cells was 25.01±3.08%, 26.40±3.05%, and 30.60±2.89%, respectively. Western blotting analysis showed remarkable activation of caspase-9, caspase-3 and dephosphorylation of Akt (Thr^{308}). Immunocytochemistry also showed the reduction of PCNA expression and phosphorylation Akt (Thr^{308}) after treatment with celecoxib.

CONCLUSION: COX-2 mRNA and protein overexpression in HepG2, Bel-7402 and SMMC-7721 cell lines correlate with the increased cell growth rate. Celecoxib can inhibit proliferation and induce apoptosis of hepatoma cell strains in a dose- and time-dependent manner.

© 2005 The WJG Press and Elsevier Inc. All rights reserved.

Key words: Apoptosis; Akt; Celecoxib; Caspase; Cell proliferation; COX-2; HCC; PCNA

Liu NB, Peng T, Pan C, Yao YY, Shen B, Leng J. Overexpression of cyclooxygenase-2 in human HepG2, Bel-7402 and SMMC-7721 hepatoma cell lines and mechanism of cyclooxygenase-2 selective inhibitor celecoxib-induced cell growth inhibition and apoptosis. *World J Gastroenterol* 2005; 11(40): 6281-6287
http://www.wjgnet.com/1007-9327/11/6281.asp

INTRODUCTION

Cyclooxygenase (COX), known as a PGs synthase, catalyzes the metabolism of arachidonic acid to PGs and thromboxanes, and has three isoforms: COX-1, COX-2 and COX-3[1]. COX-1 is a constitutively expressed enzyme found in most tissues and remains unaltered in cancer. COX-2 is expressed at sites of inflammation, which has led to the speculation that its inhibition could provide all the benefits of current non-steroidal anti-inflammatory drugs (NSAIDs) but without their major side effects on the gastrointestinal system[2,3] (which are due to the inhibition of COX-1). New NSAIDs, which are selective inhibitors of COX-2, can exert therapeutic efficacy without toxic effects due to the inhibition of COX-1. Celecoxib, a selective COX-2 inhibitor approved by US FDA, has been shown preclinically and clinically to have efficacy comparable to that of NSAIDs on relief of pain and inflammation in osteoarthritis.

Recently, COX-2 has been suggested to be associated with carcinogenesis and high expression of COX-2 has been

found in many cancers[4-6] such as colorectal cancer, prostatic cancer, breast cancer and gastric cancer. Although selective COX-2 inhibitors could reduce the growth of various cancer cell lines[7-9] and display anti-tumor effect by sensitizing cancer cells to apoptosis[10-12], it is unknown whether COX-2 contributes to the malignant growth and whether inhibition of COX-2 function modifies the malignant potential of tumors.

In hepatocarcinoma (HCC), the expression pattern of COX-2 protein is well correlated with the differentiation grade, suggesting that abnormal COX-2 expression plays an important role in hepatocarcinogenesis[13]. However, the exact anti-tumor mechanisms are not well known. Leng *et al*.[8] have proved that COX-2 could promote HCC cell growth and selective COX-2 inhibitor celecoxib could mediate cell apoptosis in HepG2 and Hep3B cell lines. In this article, we investigate the expression pattern of COX-2 on HepG2 and two other human HCC cell lines, BEL-7402 and SMMC-7721 and evaluate the efficacy of selective COX-2 inhibitor celecoxib in order to understand the potential role of COX-2 in promoting HCC cell growth and to provide theoretical evidence for searching a new agent for the treatment of HCC.

MATERIALS AND METHODS

Materials

Human HepG2, BEL-7402 and SMMC-7721 hepatoma cell lines were obtained from The Committee of Type Culture Collection of Chinese Academy of Sciences (Shanghai, China). RMPI1640, DMEM and MEM culture medium were purchased from Gibco BRL. Fetal bovine serum (FBS) was provided by Sijiqing Biological Engineering Material (Hangzhou, China). Rabbit anti-COX-2 was from Cayman. Mouse anti-caspase3 was from Boster Biological Technology (Wuhan, China). Rabbit anti-caspase9, anti-actin, rabbit anti-phospho-Akt/PKB (Thr^{308}), sheep anti-rabbit, sheep anti-mouse secondary antibody, Western blotting luminol reagent were purchased from Santa Cruz. *In situ* cell death detection kit (TUNEL) and sensitive *in situ* hybridization detection kit were purchased from Roche. Rainbow molecular weight markers were from Amersham. 3-(4, 5-Dimethylthiazol-2-yl)-2, 5-diphenyltetrazolium bromide (MTT) was provided by Amersco. Celecoxib was provided by Scenry Chemical (Hefei, China).

Cell lines and culture conditions

SMMC-7721 cell line was cultured in DMEM supplemented with 100 mL/L heat-inactivated FBS and 100 U/mL penicillin/streptomycin. Bel-7402 cell line was cultured in RPMI 1640 supplemented with 100 mL/L heat-inactivated FBS and 100 U/mL penicillin/streptomycin. HepG2 cell line was cultured in MEM supplemented with 100 mL/L heat-inactivated FBS, 100 U/mL penicillin/streptomycin and 1% nonessential amino acid. All cells were grown in 50 mL/ L CO_2 humidified atmosphere at 37 ℃.

Morphological changes

Celecoxib-treated cells and control were digested by trypsin, washed with phosphate-buffered saline (PBS) and centrifuged at 1 500 r/min for 5 min. After the cells were mixed with glycerine and egg white, the mixtures were fixed in alcohol for 30 min. Then the mass was embedded and fabricated to paraffin section with H&E staining. Morphological changes were observed under light and inverted microscopes.

In situ hybridization (ISH) assays

The digoxigenin-labeled COX-2 oligonucleotide probe for ISH was prepared with the sequence 5'-TGATATCA-TCTAGTCCGGAGCGGGAAG-3'(TaKaRa Bio). ISH was performed according to the instructions of the enhanced sensitive ISH detection kit. Briefly, the sections were deparaffinized with xylene, dehydrated with graded ethanol and embryos were incubated in 1 mL of 20 μg/mL proteinase K for 20 min. Re-fix embryos were incubated for 10 min in 4% formaldehyde. Then all were removed and 20 μL pre-hybridization solution was added for 2 h. Solution was removed and replaced with 20 μL hybridization solution to hybridize overnight at 37 ℃. After these, embryos were washed twice in 2× SSC and 0.01× at 37 ℃ SSC for 5 min each, replaced with anti-digoxygenin-alkaline phosphatase antibody and 40 μL AP-coupled antibodies at 37 ℃ for 1 h. The last wash was replaced with AP reaction buffer and the reaction was terminated when it became dark.

Westen blotting

Celecoxib-treated three cell lines and control were lysed by 4 g/L trypsin containing 0.2 g/L EDTA, then collected after being washed twice with cold PBS. Total protein extract from cells was prepared using cell lysis buffer [50 mmol/L Tris-HCL (pH 8.0), 150 mmol/L NaCl, 1%Triton X-100, 100 μg/mL PMSF, 1 μg/mL aprotinin]. The extract (40 ug) was electrotransferred to nitrocellulose membrane. The membranes were blocked with 5% nonfat dry milk in TBST (10 mmol/L Tris-HCL, pH 8.0, 100 mmol/L NaCl, and 0.05% Tween-20) for 1 h at room temperature and then incubated with appropriate primary antibody overnight at 4 ℃, followed by incubation with horseradish peroxidase-conjugated secondary antibody at 1∶2 000 dilution for 1 h at room temperature. The polyclonal anti-COX-2 and anti-actin were used at 1∶1 000 dilution. The polyclonal anti-caspase-3, anti-caspase-9, anti-phospho-Akt/PKB were used at 1∶400 dilution. The immunoblots were visualized by enhanced chemiluminescence.

Immunocytochemical assays

Briefly, the sections were subjected to immunostaining using an ultrasensitive streptavidin–peroxidase technique (DAKO). Endogenous peroxidases were blocked by incubating with 5 mL/L H_2O_2 for 30 min at room temperature. The sections were subsequently treated for 10 min with Triton X-100, and incubated for 30 min at 37 ℃ with normal non-immune serum before overnight incubation at 4 ℃ with specific antibody at a dilution of 1∶200. The sections were then treated with biotin-conjugated second antibody before streptavidin-peroxidase was added. For color reaction, diaminobenzidine (DAB) was used. If the positive signals were present, the cytoplasm or the nuclei were stained brown. For negative control, the antibody was replaced by PBS.

Cell growth assays (MTT assays)

The number of viable cells was determined by MTT assays. Each cell sample was plated at a density of 10 000 cells/well in 96-well cluster dishes before treatment. On the same day, the medium was changed and celecoxib was added in concentrations and analyzed at indicated time points. After addition of MTT solution (10/100 μL medium) in each well, the cells were incubated at 37 ℃ for 4 h, and then 100 μL DMSO was added to dissolve the dark blue crystals. The absorbance was measured in an ELISA plate reader with a test wavelength of 570 nm.

Cell cycle analysis by FCM

Celecoxib-treated cells were fixed with 700 mL/L alcohol for 15 min at 4 ℃, and then stained with propidium iodide (PI, Sigma, USA). The red fluorescence of DNA-bound PI in individual cells was measured at 488 nm with a FACSCalibur (Becton Dickinson, USA) and the results were analyzed using CELL QuestV1.22 software.

Apoptosis detection (TUNEL assay)

The apoptotic cells were identified by the terminal deoxynucleotidyl transferase-mediated dUTP nick end labeling (TUNEL) assay according to the manufacturer's instructions. The cells were counterstained with royal blue. In each experiment, 400 cells were examined using four high-power fields each (magnification×400). The experiments were performed at least twice independently.

Image analysis

The results of TUNEL and immunocytochemistry were analyzed in a blinded fashion by image analysis system (RXA_2, Leica) using *Qwin* software. The apoptosis index (AI) was determined by observing more than 400 nuclei for each sample.

Statistical analysis

Statistical significance was assessed by the nonparametric ANOVA test with SPSS 10.0 software and $P<0.05$ was considered statistically significant.

RESULTS

COX-2 expression in hepatoma cell lines

ISH, Western blotting and immunocytochemical staining were performed on HepG2, Bel-7402 and SMMC-7721 cell lines. Significant mRNA and protein of COX-2 were detected in all test cell lines. A representative Western blotting showed that the COX-2 expression level of the HCC cell lines in sequence was SMC-7721>BEL-7402>HepG2 (Figure 1). COX-2 protein was located in the cytoplasm of the cells shown by immunocytochemical staining. No staining was observed in the negative control slide.

Growth inhibitory effect of celecoxib

The effects of celecoxib on the cell viability were determined by MTT assay. Cells became sparse, round and detached from the dishes when treated with 6.25, 12.50, 25.00, 50.00, and 100.00 μmol/L concentrations of celecoxib for 24 h (Figure 2), and resulted in 11.9%, 23.9%, 43.8%, 62.4% and 72.7% cell growth reduction, respectively, in HepG2 cells (Figure 3).

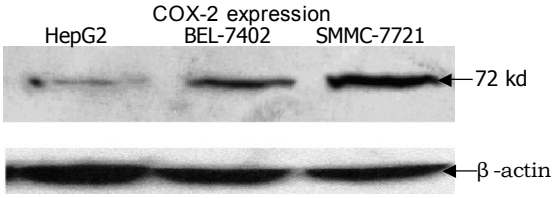


Figure 1 Expression of COX-2 in HepG2, BEL-7402 and SMMC-7721 HCC cell lines shown by Western blotting.

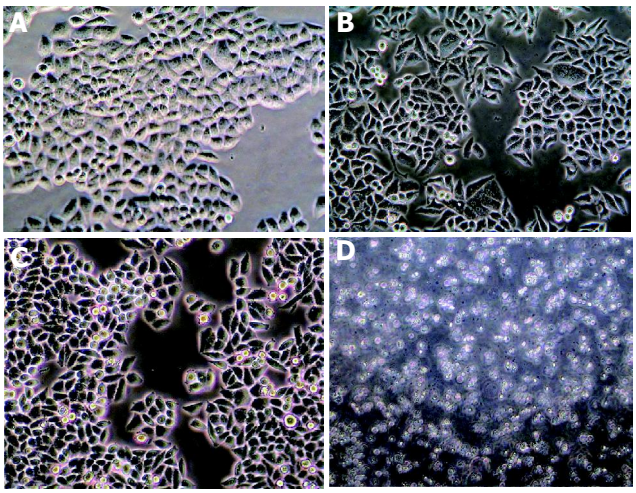


Figure 2 Growth inhibitory effect of celecoxib on SMMC-7721 cell lines. **A**: Normal control; **B**: 25.00 μmol/L celecoxib for 6 h; **C**: 25.00 μmol/L celecoxib for 24 h; **D**: 50.00 μmol/L celecoxib for 48 h. (Original magnification, ×200).

Down-regulation of PCNA expression in celecoxib-treated hepatoma cells

The effects of celecoxib on PCNA expression in cultured HCC cells were assessed by immunocytochemical staining. PCNA-positive cells were more abundant in control cells than in celecoxib-treated cells (Figure 4).

Human HCC cell apoptosis induced by celecoxib

Morphologic changes were evident in the three cell lines after treatment with celecoxib for 24 h. Progressive cytoplasmic shrinkage and nuclear condensation (the typical morphologic signs of apoptosis under light microscope) could be observed. To further make sure of these apoptotic morphologic changes, TUNEL staining was performed. As shown in Figure 5, celecoxib induced HepG2 cell apoptosis in a dose-dependent manner, the percentage of TUNEL-positive cells increased from 2.80±0.84% to 25.01±3.08% after treatment with 6.25 or 50 μmol/L celecoxib for 24 h, respectively. Celecoxib-treated BEL-7402 and SMMC-7721 cell lines showed the same results.

Results of FCM also showed apoptosis induced by celecoxib in SMMC-7721 cell lines. A subdiploid (subG1) peak was observed after being treated with 6.25, 12.

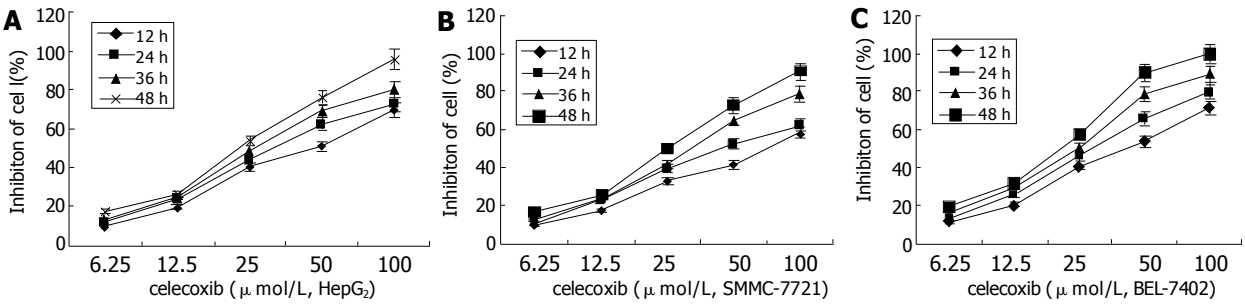


Figure 3 Growth inhibitory effects of celecoxib on HepG2 (**A**), SMMC-7721 (**B**) and BEL-7402 (**C**) HCC cells.

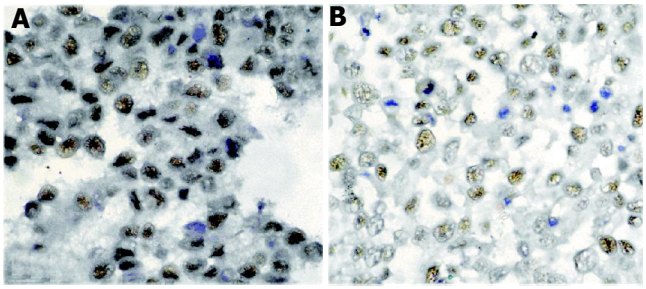


Figure 4 Immunocytochemical staining of PCNA in HepG2 cells in the presence or absence of celecoxib. **A**: normal control; **B**: 25.00 μmol/L celecoxib for 24 h.

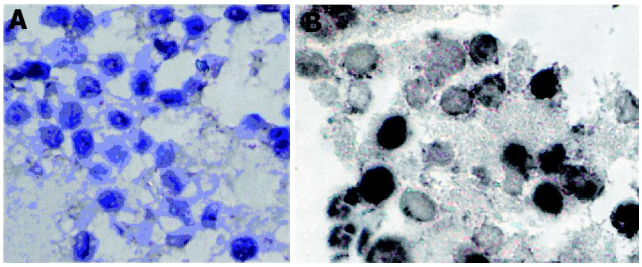


Figure 5 Cell apoptosis induced by celecoxib. **A**: Normal control; **B**: Apoptosis of BEL-7402 cell assessed by TUNEL.

50, 25.00 and 50.00 μmol/L celecoxib for 24 h, and the apoptosis rate was 4.84%, 16.10%, 22.80% and 33.80%, respectively, compared to 0.81% in normal control (Table 1).

Caspase-9 and caspase-3 activated by celecoxib

Western blotting analysis revealed that celecoxib induced activation of caspase-9 and caspase-3 (Figure 9). Activation of caspase-3 was reflected by a decrease in the 32-kd precursor and a concomitant increase in the 20-kd cleaved band. Activation of caspase-9 was reflected by conversion of the 47-kd precursor to the active 35- and 37-ku proteolytic cleavage products. The activation level of caspase-9 and caspase-3 was in a dose- and time-dependent manner to the celecoxib treatment (Figure 6).

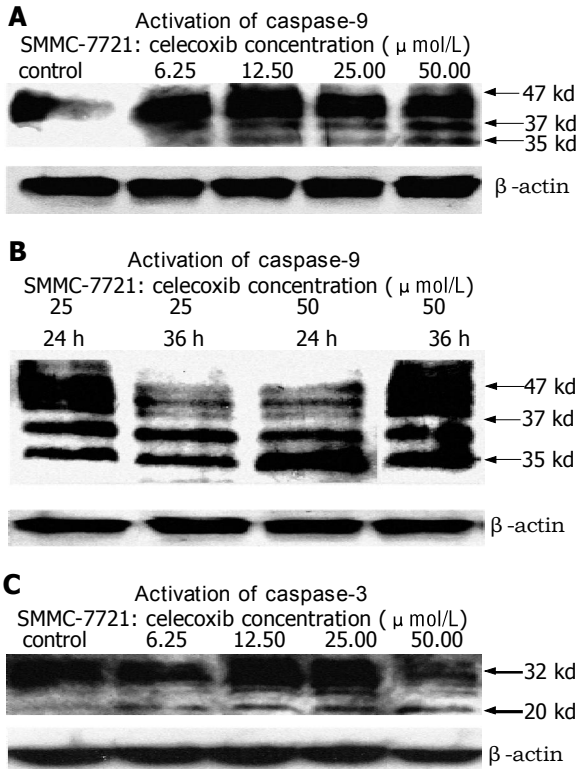


Figure 6 Activation of caspase-9 and caspase-3 after treatment with celecoxib. **A:** Activation of caspase-9 after being treated with celecoxib for 12 h; **B:** Activation of caspase-9 after being treated with different concentrations of celecoxib for different time; **C:** Activation of caspase-3 after being treated with celecoxib for 12 h.

Phosphorylation of Akt reduced by celecoxib

Table 1 AI induced by celecoxib (mean±SD)

Cell line	Control	6.25	12.5	25	50
BEL- 7402	0.60±0.89	3.40±1.14	7.60±2.41	15.20±3.49	26.40±3.05
SMMC-7721	1.20±0.84	4.20±1.48	9.80±2.59	19.60±3.36	30.60±2.89
HepG2	1.00±1.00	2.80±0.84[a]	5.40±1.52	15.00±1.58	25.01±3.08

[a]$P<0.05$ *vs* control

To evaluate the effect of celecoxib on Akt/PKB activity, HepG2, BEL-7402 and SMMC-7721 cells were treated with celecoxib for 4, 12 or 24 h, and phosphorylation at Thr^{308} was examined by specific phospho-Akt antibody. Western blotting analysis showed that celecoxib significantly reduced Akt/PKB phosphorylation (Figure 7). Immunocy-tochemistry assay also displayed dephosphorylation of Akt Thr^{308} (Figure 8) in a dose- and time-dependent manner when analyzed with Leica-*Qwin* computer image analysis system. The results are shown in Figure 9.

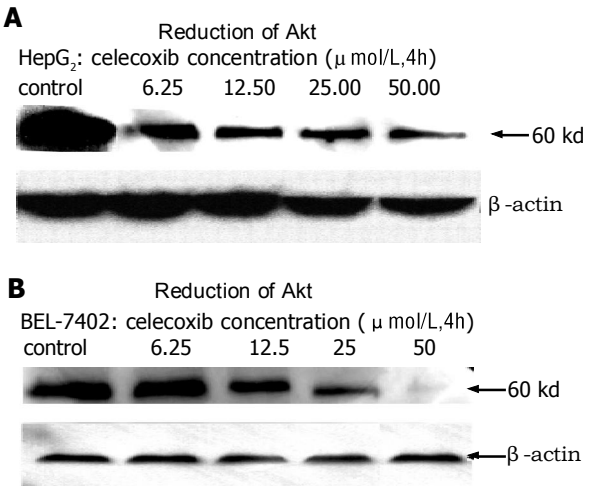


Figure 7 Dephosphorylation of Akt/PKB after treatment with celecoxib for 4 h. **A**: HepG2 cell line; **B**: BEL-7402 cell line.

DISCUSSION

COX-2, an isoform of cyclooxygenase, is inducible by a variety of factors including cytokines, growth factors, and tumor promoters[2,3]. It was reported that COX-2 expression increases in many human cancers including HCC[13]. The mechanism leading to COX-2 overexpression in HCC is still unknown. It was demonstrated that overexpression of COX-2 increases cell survival by inhibiting cell apoptosis and stimulating angiogenesis, and enhancing cellular adhesion to the matrix proteins[14,15]. In this article, we have observed a high expression of COX-2 mRNA and protein in human HepG2, Bel-7402 and SMMC-7721 hepatoma cell lines. These results suggest that studies are warranted to determine the role of COX-2 in hepatocarcinogenesis. Furthermore, we have shown that celecoxib, a selective COX-2 inhibitor, could strongly suppress cell proliferation.

Morphologic changes and results obtained by MTT assay support the suggestion that celecoxib down-regulates cell growth activity. It was reported that COX-2 inhibitors may have antineoplastic effects during the early stages of hepatocarcinogenesis[16].

PCNA is an essential protein found in proliferating eukaryotic cells, and plays a crucial role in DNA replication, repair, and control of cell proliferation[17,18]. This protein is involved in the synthesis of both leading and lagging DNA strands, providing an anchorage site and increasing the processivity of DNA polδ and DNA polε, which is the basis of PCNA serving as a DNA synthesis marker for evaluating cell proliferation[19,20]. Therefore, overexpression of COX-2 may be mitogenic in HCC cells through up-regulation of PCNA expression. Selective COX-2 inhibitor celecoxib can block the activity of COX-2 and down-regulate PCNA expression, thus causing cell growth inhibition.

Apoptosis plays a central role in tumor development and lack or failure of apoptosis leads to the development of many tumors including hepatocarcinoma[21,22]. Thus, induction of apoptosis of tumor cells is an effective approach to delay the tumor progress. In this study, we found that celecoxib could induce the characteristic features of apoptosis including morphological changes, TUNEL-positivity, FCM and caspase-9/3 activation of the three tested HCC cell lines.

There are at least two extrinsic and intrinsic broad pathways that lead to apoptosis[23-25]. The "extrinsic" pathway begins with the binding of Fas ligand (FasL or CD95L) to the Fas receptor (CD95) and results in recruiting FADD and pro-caspase-8 to the complex. Concentration of pro-caspase-8 results in its autocatalysis and activation. Activated caspase-8 cleaves pro-caspase-3, which then undergoes autocatalysis to form active caspase-3, a principle effector caspase of apoptosis. The "intrinsic" apoptosis pathway always begins with mitochondrial damage and results in release of cytochrome C from damaged mitochondria. In cytosol or on the surface of mitochondria, cytochrome C is bound to the protein Apaf-1 (apoptotic protease activating factor) which then activates an initiator caspase, caspase-9, then activates caspase-3[26,27]. Caspase families play an important role in apoptosis signaling pathway. They are present in the cytoplasm in normal condition as inactive pro-enzymes, most of which are activated by proteolytic cleavage when undergoing apoptosis[28,29]. Both caspase-8 and caspase-9 can activate the effector caspase, caspase-3, by proteolytic cleavage and subsequent processes result in the nuclear DNA fragmentation and formation of apoptotic bodies, indicating that activation of caspase-3 is a central event in the process of apoptosis.

In this article, Western blotting analysis revealed that celecoxib induced the activation of caspase-9 and caspase-3. Activation of caspase-9 is reflected by conversion of the 47-kd inactive precursor to the active 35-kd and 37-kd proteolytic cleavage products. Activation of caspase-3 is indicated by a decrease of the 32-kd precursor accompanied with a concomitant increase in the 20-kd cleaved band. Leng *et al*.[8], reported that celecoxib-treated HepG2 cells significantly release cytochrome C in the cytosol. Thus we propose the hypothesis that celecoxib allows the release of cytochrome C from mitochondria and activates caspase-9 and caspase-3 in sequence and finally induces apoptosis of HCC cells.

Our works have also shown that celecoxib down-regulates the phosphorylation of Akt/PKB at Thr^{308} in a dose- and time-dependent manner. Akt/PKB[30,31], the major downstream effector of PI3-kinase, is a Ser/Thr

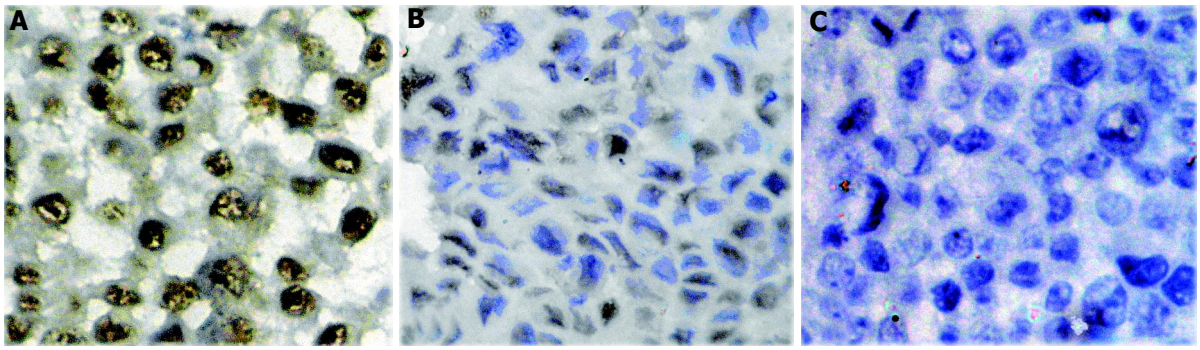


Figure 8 Down-regulation of phosphorylation of Akt Thr308 after treated with celecoxib. **A:** Normal control; **B:** SMMC-7721 cell line; (**C**): Negative control.

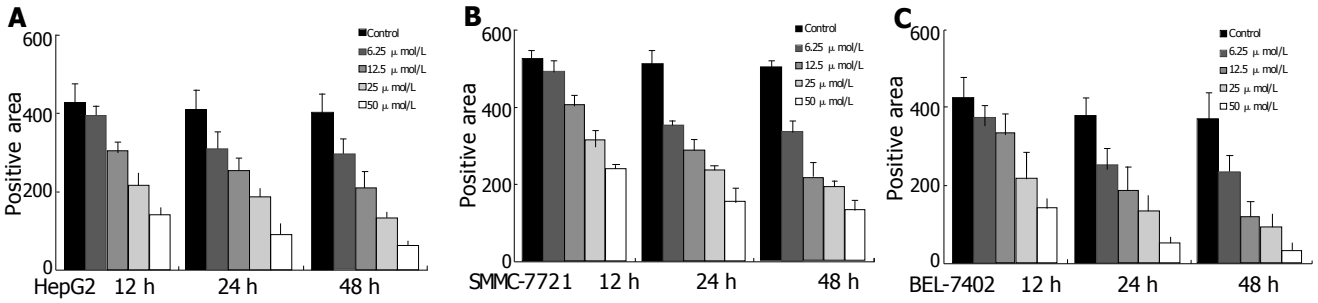


Figure 9 Dose- and time-dependent effects of reduced phosphorylation of Akt (Thr^{308}) on HepG2 cell (**A**), SMMC-7721 cell (**B**), BEL-7402 cell (**C**).

protein kinase that exerts a crucial role in the regulation of several cellular signaling pathways. Akt/PKB is a regulator of cell survival and apoptosis, and its activation can protect a variety of cells against apoptosis. Akt/PKB is phosphorylated at two regulatory sites, Thr^{308} and Ser^{473}, essential for its activation. Activated Akt/PKB can phosphorylate BAD, IκB kinase, glycogen synthase kinase-3β, and forkhead transcription factors[32,33], leading to their inactivation and cell survival. Interestingly, it was reported that caspase-9 activity is regulated by phosphorylation[34]. Akt phosphorylates pro-caspase-9 at Ser^{196} and inhibits proteolytic processing of pro-caspase-9.

Celecoxib blocks the activation of Akt, thereby attenuating the activity of a major anti-apoptotic pathway and inducing cell apoptosis. It remains unclear how celecoxib affects Akt phosphorylation because it does not affect PI3-kinase activity directly[35]. Other potential consequences of COX-2 inhibition, such as modulation of the RAS-signaling pathway, p53 expression, and other members of the BCL-2 family, such as MCL-1[36,37], activation of the sphingomyelin-ceramide pathway, and interference with the NF-κB[38] need to be investigated in future.

In conclusion, COX-2 is overexpressed in human HepG2, BEL-7402 and SMMC-7721 hepatoma cells and may play a key role in tumor cell proliferation and carcinogenesis. Selective COX-2 inhibitor celecoxib can suppress the growth of HCC cells by inhibiting cell growth and inducing cell apoptosis. The mechanism of apoptosis induced by celecoxib is due to activation of the caspase cascade, which is correlated with phosphorylation of Akt/PKB. These results suggest that selective COX-2 inhibitor offers potential as an effective chemotherapeutic and chemopreventive strategy against human liver cancer.

REFERENCES

1 **Chandrasekharan NV,** Dai H, Roos KL, Evanson NK, Tomsik J, Elton TS, Simmons DL. COX-3, a cyclooxygenase-1 variant inhibited by acetaminophen and other analgesic/antipyretic drugs: cloning, structure, and expression. *Proc Natl Acad Sci USA* 2002; **99**: 13926-13931

2 **Zhang F,** Warskulat U, Wettstein M, Schreiber R, Henninger HP, Decker K, Haussinger D. Hyperosmolarity stimulates prostaglandin synthesis and cyclooxygenase-2 expression in activated rat liver macrophages. *Biochem J* 1995; **312**(Pt 1): 135-143

3 **Feng L,** Xia Y, Yoshimura T, Wilson CB. Modulation of neutrophil influx in glomerulonephritis in the rat with anti-macrophage inflammatory protein-2 (MIP-2) antibody. *J Clin Invest* 1995; **95**: 1009-1017

4 **Hussain T,** Gupta S, Mukhtar H. Cyclooxygenase-2 and prostate carcinogenesis. *Cancer Lett* 2003; **191**: 125-135

5 **Peng JP,** Su CY, Chang HC, Chai CY, Hung WC. Overexpression of cyclo-oxygenase-2 in squamous cell carcinoma of the hypopharynx. *Hum Patho1* 2002; **33**: 100-104

6 **Sheng H,** Shao J, Morrow JD, Beauchamp RD, DuBois RN. Modulation of apoptosis and Bcl-2 expression by prostaglandin E2 in human colon cancer cells. *Cancer Res* 1998; **58**: 362-366

7 **Vogiagis D,** Brown W, Glare EM, O'Brien PE. Rat colorectal tumours treated with a range of non-steroidal anti-inflammatory drugs show altered cyclooxygenase-2 and cyclooxygenase-1 splice variant mRNA expression levels. *Carcinogenesis* 2001; **22**: 869-874

8 **Leng J,** Han C, Demetris AJ, Michalopoulos GK, Wu T. Cyclooxygenase-2 promotes hepatocellular carcinoma cell growth through Akt activation: evidence for Akt inhibition in celecoxib-induced apoptosis. *Hepatology* 2003; **38**: 756-768

9 **Kinoshita T,** Takahashi Y, Sakashita T, Inoue H, Tanabe T,

Yoshimoto T. Growth stimulation and induction of epidermal growth factor receptor by overexpression of cyclooxygenases 1 and 2 in human colon carcinoma cells. *Biochem Biophys Acta* 1999; **1438**: 120-130

10 **Johnsen JI,** Lindskog M, Ponthan F, Pettersen I, Elfman L, Orrego A, Sveinbjornsson B, Kogner P. Cyclooxygenase-2 is expressed in neuroblastoma, and nonsteroidal anti-inflammatory drugs induce apoptosis and inhibit tumor growth *in vivo*. *Cancer Res* 2004; **64**: 7210-7215

11 **Jacoby RF,** Seibert K, Cole CE, Kelloff G, Lubet RA. The cyclooxygenase-2inhibitor celecoxib is a potent preventive and therapeutic agent in the min mouse model of adenomatous polyposis. *Cancer Res* 2000; **60**: 5040-5044

12 **Kanayama N,** Terao T. Plasma fibronectin receptor levels during pregnancy complicated by preeclampsia and abruptio placentae. *Gynecol Obstet Invest* 1992; **33**: 147-152

13 **Bae SH,** Jung ES, Park YM, Kim BS, Kim BK, Kim DG, Ryu WS. Expression of cyclooxygenase-2 (COX-2) in hepatocellular carcinoma and growth inhibition of hepatoma cell lines by a COX-2 inhibitor, NS-398. *Clin Cancer Res* 2001; **7**: 1410-1418

14 **Masunaga R,** Kohno H, Dhar DK, Ohno S, Shibakita M, Kinugasa S, Yoshimura H, Tachibana M, Kubota H, Nagasue N. Cyclooxygenase-2 expression correlates with tumor neovascularization and prognosis in human colorectal carcinoma patients. *Clin Cancer Re*s 2000; **6**: 4064-4068

15 **Fujiwaki R,** Iida K, Kanasaki H, Ozaki T, Hata K, Miyazaki K. Cyclooxygenase-2 expression in endometrial cancer: correlation with microvessel count and expression of vascular endothelial growth factor and thymidine phosphorylase. *Hum Pathol* 2002; **33**: 213 -219

16 **Denda A,** Kitayama W, Murata A, Kishida H, Sasaki Y, Kusuoka O, Tsujiuchi T, Tsutsumi M, Nakae D, Takagi H, Konishi Y. Increased expression of cyclooxygenase-2 protein during rat hepatocarcinogenesis caused by a choline-deficient, L-amino acid-defined diet and chemopreventive efficacy of a specific inhibitor, nimesulide. *Carcinogenesis* 2002; **23**: 245-256

17 **Zheleva DI,** Zhelev NZ, Fischer PM, Duff SV, Warbrick E, Blake DG, Lane DP. A quantitative study of the *in vitro* binding of the C-terminal domain of p21 to PCNA: affinity, stoichiometry, and thermodynamics. *Biochemistry* 2000; **39**: 7388-7397

18 **Kelman Z.** PCNA: structure, functions and interactions. *Oncogene* 1997; **14**: 629-640

19 **Kurki P,** Vanderlaan M, Dolbeare F, Gray J, Tan EM. Expression of proliferating cell nuclear antigen (PCNA)/cyclin during the cell cycle. *Exp Cell Res* 1986; **166**: 209-219

20 **Robbins BA,** de la Vega D, Ogata K, Tan EM, Nakamura RM. Immunohistochemical detection of proliferating cell nuclear antigen in solid human malignancies. *Arch Pathol Lab Med* 1987; **111**: 841-845

21 **Kerr JF,** Wyllie AH, Currie AR. Apoptosis: a basic biological phenomenon with wide-ranging implications in tissue kinetics. *Br J Cancer* 1972; **26**: 239-257

22 **Evan G,** Littlewood T. A matter of life and cell death. *Science* 1998; **281**: 1317-1322

23 **Yang J,** Liu X, Bhalla K, Kim CN, Ibrado AM, Cai J, Peng TI, Jones DP, Wang X. Prevention of apoptosis by Bcl-2: release of cytochrome c from mitochondria blocked. *Science* 1997; **275**: 1129-1132

24 **Li P,** Nijhawan D, Budihardjo I, Srinivasula SM, Ahmad M, Alnemri ES, Wang X. Cytochrome c and dATP-dependent formation of Apaf-1/caspase-9 complex initiates an apoptotic protease cascade. *Cell* 1997; **91**: 479-489

25 **Bossy-Wetzel E,** Newmeyer DD, Green DR. Mitochondrial cytochrome c release in apoptosis occurs upstream of DEVD-specific caspase activation and independently of mitochondrial transmembrane depolarization. *EMBO J* 1998; **17**: 37-49

26 **Liu X,** Kim CN, Yang J, Jemmerson R, Wang X. Induction of apoptotic program in cell-free extracts: requirement for dATP and cytochrome c. *Cell* 1996; **86**: 147-157

27 **Zou H,** Henzel WJ, Liu X, Lutschg A, Wang X. Apaf-1, a human protein homologous to C. elegans CED-4, participates in cytochrome c-dependent activation of caspase-3. *Cell* 1997; **90**: 405-413

28 **Sakai T,** Liu L, Teng X, Mukai-Sakai R, Shimada H, Kaji R, Mitani T, Matsumoto M, Toida K, Ishimura K, Shishido Y, Mak TW, Fukui K. Nucling recruits Apaf-1/pro-caspase-9 complex for the induction of stress-induced apoptosis. *J Biol Chem* 2004; **279**: 41131-41140

29 **Arnoult D,** Gaume B, Karbowski M, Sharpe JC, Cecconi F, Youle RJ. Mitochondrial release of AIF and EndoG requires caspase activation downstream of Bax/Bak-mediated permeabilization. *EMBO J* 2003; **22**: 4385-4399

30 **Dudek H,** Datta SR, Franke TF, Birnbaum MJ, Yao R, Cooper GM, Segal RA, Kaplan DR, Greenberg ME. Regulation of neuronal survival by the serine-threonine protein kinase Akt. *Science* 1997; **275**: 661-665

31 **Franke TF,** Kaplan DR, Cantley LC. PI3K: downstream AKTion blocks apoptosis. *Cell* 1997; **88**: 435-437

32 **Fang X,** Yu S, Eder A, Mao M, Bast RC, Boyd D, Mills GB. Regulation of BAD phosphorylation at serine 112 by the Ras-mitogen-activated protein kinase pathway. *Oncogene* 1999; **18**: 6635-6640

33 **Rena G,** Prescott AR, Guo S, Cohen P, Unterman TG. Roles of the forkhead in rhabdomyosarcoma (FKHR) phosphorylation sites in regulating 14-3-3 binding, transactivation and nuclear targetting. *Biochem J* 2001; **354**(Pt 3): 605-612

34 **Cardone MH,** Roy N, Stennicke HR, Salvesen GS, Franke TF, Stanbridge E, Frisch S, Reed JC. Regulation of cell death protease caspase-9 by phosphorylation. *Science* 1998; **282**: 1318-1320

35 **Zhou H,** Summers SA, Birnbaum MJ, Pittman RN. Inhibition of Akt Kinase by cell-permeable ceramide and its implications for ceramide-induced apoptosis. *J Biol Chem* 1998; **273**: 16568–16575

36 **Hsu AL,** Ching TT, Wang DS, Song X, Rangnekar VM, Chen CS. The cyclooxygenase-2 inhibitor celecoxib induces apoptosis by blocking Akt activation in human prostate cancer cells independently of Bcl-2. *J Biol Chem* 2000; **275**: 11397-11403

37 **Lin MT,** Lee RC, Yang PC, Ho FM, Kuo ML. Cyclooxygenase-2 inducing Mcl-1-dependent survival mechanism in human lung adenocarcinoma CL1.0 cells. Involvement of phosphatidylinositol 3-k inase/Akt pathway. *J Biol Chem* 2001; **276**: 48997-49002

38 **Lee JY,** Ye J, Gao Z, Youn HS, Lee WH, Zhao L, Sizemore N, Hwang DH. Reciprocal modulation of Toll-like receptor-4 signaling pathways involving MyD88 and phosphatidylinositol 3-kinase/AKT by saturated and polyunsaturated fatty acids. *J Biol Chem* 2003; **278**: 37041-37051

Science Editor Wang XL and Guo SY **Language Editor** Elsevier HK

PO Box 2345, Beijing 100023, China
www.wjgnet.com
wjg@wjgnet.com

ELSEVIER

World J Gastroenterol 2005;11(40):6288-6294
World Journal of Gastroenterology ISSN 1007-9327
© 2005 The WJG Press and Elsevier Inc. All rights reserved.

• *COLORECTAL CANCER* •

Avidin-biotin system pretargeting radioimmunoimaging and radioimmunotherapy and its application in mouse model of human colon carcinoma

Gui-Ping Li, Hui Zhang, Cheng-Mo Zhu, Jian Zhang, Xu-Feng Jiang

Gui-Ping Li, Hui Zhang, Department of Nuclear Medicine, Nanfang Hospital, Southern Medical University, Guangzhou 510515, Guangdong Province, China
Cheng-Mo Zhu, Jian Zhang, Xu-Feng Jiang, Department of Nuclear Medicine, Ruijin Hospital, Shanghai Second Medical University, Shanghai 200025, China
Correspondence to: Gui-Ping Li, MD, Department of Nuclear Medicine, Nanfang Hospital, Southern Medical University, Guangzhou 510515, Guangdong Province, China. ligp@fimmu.com
Telephone: +86-20-61642129 Fax: +86-20-61642121
Received: 2004-10-09 Accepted: 2004-12-21

Abstract

AIM: To evaluate the multi-step pretargeting radioimmunoimaging (RII) and radioimmunotherapy (RIT) in nude mice bearing human colon carcinoma with avidin-biotin system labeled with ^{153}Sm.

METHODS: Two- and three-step strategies for avidin-biotin system pretargeting techniques were established. In a three-step procedure, human colon carcinoma bearing nude mice were first injected with biotinylated monoclonal antibody (McAb-Bt) followed by cold avidin (Av) 48 h later and then ^{153}Sm-DB_2 24 h thereafter; whereas the two-step procedure consisted of injection of ^{153}Sm-SA 48 h after pretargeting with biotinylated anti-CEA monoclonal antibody (CEA McAb-Bt). SPECT imaging and biodistribution were performed at 4, 24, 48, or 72 h after injection of ^{153}Sm-labeled compounds. Five groups of nude mice subcutaneously grafted with human colon carcinoma were treated 3 d after grafting. One group received the injection with 100 μg CEA McAb-Bt followed by cold avidin (80 μg) after 2 d and 11.1 MBq ^{153}Sm-DB_2 after 1 d. Four control groups were treated respectively with 11.1 MBq ^{153}Sm-CEA McAb, 11.1 MBq ^{153}Sm-nmIgG, 11.1 MBq ^{153}Sm-DB_2, 100 μL normal saline. Toxicity was evaluated by changes of leukocyte count, and the efficacy by variation in tumor volume. Histological analyses of tumors were performed.

RESULTS: The three-step procedure allowed faster blood clearance and yielded higher tumor blood ratios (5.76 at 4 h and 12.94 at 24 h) of the ^{153}Sm-DB_2. The tumor was clearly visualized at 4 h in γ-imaging after the injection of ^{153}Sm-DB_2, while a significant accumulation of ^{153}Sm-SA in the tumor was observed only 24 h after the injection and tumor blood ratios at 4 and 24 h were 1.00 and 2.03, respectively, in the two-step procedure. Pretargeting RIT and ^{153}Sm-CEA McAb had a strong tumor-inhibiting effect. The tumor inhibitory rate was 80.67% and 78.44%, respectively, five weeks after therapy. Histopathological evidence also indicated radioactive damage in tumor tissues as necrosis of tumor cells, while in the other organs such as liver and kidney no radioactive damage was observed. Leukocyte counts showed significant decrease after treatment in groups of ^{153}Sm-CEA McAb and ^{153}Sm-nmIgG.

CONCLUSION: The two kinds of pretargeting strategies can elevate the target-to-nontarget ratio, decrease the blood background and shorten the imaging time compared to ^{153}Sm-CEA McAb. Three-step pretargeting RIT is as efficient as ^{153}Sm-CEA McAb, but markedly less toxic. This study provides experimental evidence for the clinical application of pretargeting RII and RIT.

© 2005 The WJG Press and Elsevier Inc. All rights reserved.

Key words: Radioimmunoimaging; Radioimmunotherapy; Avidin-biotin; Colon carcinoma

Li GP, Zhang H, Zhu CM, Zhang J, Jiang XF. Avidin-biotin system pretargeting radioimmunoimaging and radioimmunotherapy and its application in mouse model of human colon carcinoma. *World J Gastroenterol* 2005; 11(40): 6288-6294
http://www.wjgnet.com/1007-9327/11/6288.asp

INTRODUCTION

Radioimmunoimaging (RII) and radioimmunotherapy (RIT) are nowadays popular research realms in tumor nuclear medicine[1,2]. Various groups have investigated the concept of tumor pretargeting based on the avidin-biotin system[3-6], exploiting the high specificity and strong affinity (Ka = 10^{-15} mol/L) of avidin (or streptavidin, SA) for biotin, so as to accelerate the elimination of tumor-unbound labeled antibodies from blood and enhance the tumor-to-nontumor (T/NT) ratio. Two-step procedures were thus designed[7]. Paganelli *et al*.[8], have further explored the potential of the avidin-biotin system by devising a three-step procedure, based on the administration of a cold biotinylated antibody, followed by an excess of cold avidin and finally by a radiolabeled biotin derivative. Currently, the pretargeting technique based on avidin-biotin system is widely applied to RII and radioimmunoguided surgery (RIGS) for tumor[9-11]. Avidin-biotin pretargeting RIT is also utilized to treat various tumors and has achieved promising clinical results[12-15].

Samarium-153 (^{153}Sm) is a nuclide that can be produced in high yield and has a high specific activity. It is a β-emitter [E_{max} = 640 (30%), 710 (50%), and 810 (20%) keV] with a half-life ($T_{1/2}$) of 1.95 d and 2.5-mm peak path length in tissue and also emits a 103 keV γ-ray that is suitable for γ-camera detection. It possesses excellent property in nuclear physics and chemistry for diagnosis and therapy. Dosimetry estimates can therefore be made by quantification of γ-camera data. Compared to ^{131}I, ^{153}Sm can result in minimal cross irradiation of normal organs and minimal radiation exposure to medical personnel and is a very attractive radioisotope for RII and RIT[16].

We, in this investigation, established the labeling method of SA and biotin with ^{153}Sm, and then the two- and three-step pretargeting RII and three-step RIT were adopted in nude mice bearing human colon carcinoma. The biodistribution and the SPECT imaging were observed and the feasibility of this three-step pretargeting RIT in tumor treatment was also explored.

MATERIALS AND METHODS

Biotinylation of anti-CEA McAb

mAb against carcinoembryonic antigen (anti-CEA McAb) and normal mouse IgG (nmIgG) were prepared by Shanghai Institute of Immunology. BNSH/dimethyl sulfoxide (DMSO) solution was added into bicarbonate buffer solution containing CEA McAb (1 g/L) at a ratio of 15-50∶1. The mixture was gently stirred at room temperature for 2 h and finally purified by Sephadex G50 chromatography. Indirect ELISA was performed to assess the activity of biotin, and the purity of biotinylated antibody was determined by SDS-PAGE.

Conjugation of anti-CEA McAb or nmIgG with DTPA

Coupling of cyclic anhydride DTPA (cDTPAa) to anti-CEA McAb or nmIgG was carried out as previously described[19]. Briefly, cDTPAa was suspended in chloroform (1 g/L). An aliquot containing cDTPAa at a molar ratio of 20∶1 DTPA: IgG was added to an acid-washed vial and evaporated to dryness under a stream of high-purity dry nitrogen. Anti-CEA McAb or nmIgG (200 μg) was added, the vial was vortexed for 1 min, and then allowed to stand at room temperature for 15-20 min. Acetic acid was added to the mixture to stop the reaction. Separation of the DTPA-CEA McAb or nmIgG conjugate from free DTPA was achieved by Sephadex G50 chromatography. Immunoreactivity of the DTPA-CEA McAb conjugate was assessed using indirect ELISA.

Radiolabeling of anti-CEA McAb, nmIgG, or SA

$^{153}SmCl_3$ was supplied by Isotopes Center of China Atomic Energy Institute. SA was purchased from Sigma Chemical Co. (St. Louis, MO, USA). $^{153}SmCl_3$ at a dose of approximately 40 MBq (with specific activity of 22.2 GBq/mL) was mixed with purified CEA McAb, nmIgG, or SA-DTPA conjugate (0.1 mL) and incubated at room temperature for 20 min. Paper chromatography was carried out, using Xinhua No.1 filter paper (30% ammonium nitrate-treated) as the supporter and the mixture of tributyl phosphate, butanone, and acetic ether (at a proportion of 4∶10∶3) as the developing agent, to determine the labeling efficiency and radiochemical purity. Immunoreactivity of the labeled McAb was tested using indirect ELISA.

Radiolabeling of DB_2

Diethylenetriaminepentaacetic acid *d,ω-bis*(biocytinamide) (DB_2; Sigma Chemical Co., St. Louis, MO, USA) was labeled with ^{153}Sm as follows. $^{153}SmCl_3$ (37 MBq) was added into 10 μL DB_2 solution (2 g/L) for reaction at room temperature for 20 min. Thin-layer chromatography was employed to determine the labeling efficiency and radiochemical purity, using 85% methanol as the developing agent. ^{153}Sm-DB_2 had a specific activity of 37 MBq/mL, with a binding capacity to 80% biotin agarose beads.

Nude mouse models bearing human colon carcinoma

Balb/c nu/nu mice (female, 20 g) were xenografted subcutaneously in the thigh with 5×10^6 LoVo cells. Tumor growing to approximately 1 cm in diameter was cut into tiny pieces, which were suspended in normal saline, aspirated and injected (approximately 0.2 mL) subcutaneously into the forelimb of nude mice (4- to 5-wk old). The wounds healed in 12 h. When the tumor grew to a volume of 0.5-1.0 cm^3, the mice were used for the subsequent study of pretargeting RII and biodistribution. Therapeutic study was initiated on the 3rd d following tumor inoculation.

Pretargeting radioimmunoimaging and biodistribution studies

Fifty nude mice bearing human colon carcinoma were randomly divided into five groups (three-step group, two-step group, directly labeling group, ^{153}Sm-DB_2 group, and ^{153}Sm-SA group), with 10 in each group. In three-step group, the mice were subjected to injections via the tail vein with 100 μg McAb-Bt, then with 30 μg avidin 48 h later, followed by intra-peritoneal (ip) injection of 3.7 MBq (20 μg) ^{153}Sm-DB_2. In two-step group, the mice were injected with 100 μg McAb-Bt followed by ip injection of 3.7 MBq (15 μg) ^{153}Sm-SA 48 h later. In directly labeling group, only ^{153}Sm-DTPA-CEA McAb (3.7 MBq, 20 μg) was administrated via ip injection 72 h after the initiation of the experiment. In ^{153}Sm-DB_2 group, the mice received only ip injection of ^{153}Sm-DB_2 (3.7 MBq, 20 μg). In ^{153}Sm-SA group, the mice received only ip injection of ^{153}Sm-SA (3.7 MBq, 15 μg). Static plane imaging with Siemens ZLC3700 SPECT was performed on the mice of each group at 4, 24, 48, and 72 h, respectively, after the injections. The mice were killed at each time point following the imaging, their organs were isolated and weighed, and the radioactivity counts were determined. The percentage of injected dose per gram of tissue (% ID/g) and T/NT ratio were calculated.

Pretargeting radioimmunotherapy studies

Grouping of the mice Twenty-five tumor-bearing mice were randomly divided into A-E groups (five in each group). The mice in group A received three-step treatment, consisting of injections via the tail vein with 100 μg McAb-Bt, 80 μg Av 48 h later and 11.1 MBq (100 μL) ^{153}Sm-DB_2 ip injection after another 24 h. Groups B-D were therapeutic control groups, which were given ^{153}Sm-CEA McAb, ^{153}Sm-nmIgG, and ^{153}Sm-DB_2, respectively, at a dose of 11.1 MBq (100 μL). As nontherapeutic control, mice in group E were only given

100 μL of normal saline by ip injection.

Observation of tumor inhibiting effect The length (*a*) and width (*b*) of tumor mass were measured double-blindly with a sliding caliper once a week for 5 wk. Tumor volume (*V*) was calculated according to the formula: $V = (1/6)\pi ab^2$. The inhibition rate (IR) of tumor growth was calculated according to the formula: IR = [(mean tumor volume of nontherapeutic control-mean tumor volume of therapeutic group)/(mean tumor volume of nontherapeutic control)]×100%.

Histological examination Pathological examination was also performed on these mice at the end of the treatment. The mice were killed. Their organs were isolated, weighed, and fixed in a 40 g/L formaldehyde solution, embedded in paraffin, cut into 4-μm-thick sections and then stained with hematoxylin and eosin (HE) for microscopic observation.

Observation of radiation toxicity Toxicity was evaluated by the change of the peripheral WBC counts. The number of WBC of all animals was determined on the day of injection and then once a week for 5 wk consecutively.

Statistical analysis

Data were expressed as mean±SD and analyzed by Student's *t*-test. $P<0.05$ was considered statistically significant.

RESULTS

Quality control of labeled compounds

In the preparation of McAb-Bt, it was found that one molecule of antibody could conjugate with three molecules of biotin on average at the biotin/McAb molar ratio of 20∶1. The resultant McAb-Bt possessed better capability of SA-binding and immunoreactivity. The optimal coupling condition of the McAb and DTPA was as follows: McAb to cDTPAa molar rate of 1∶20, pH value of 7-8, and an antibody concentration at 20 mg/mL. The labeling efficiency of ^{153}Sm-CEA McAb was 56-60%, radiochemical purity was over 95% and immunoreactivity was about 50%. The labeling efficiency of ^{153}Sm-DB_2 exceeded 80%, and radiochemical purity was over 95% after binding to SA. The labeling efficiency of ^{153}Sm-SA was over 95% and radiochemical purity was over 98%.

Biodistribution in tumor-bearing nude mice during multi-step pretargeting

The percent of ID/g and T/NT ratio in various organs at different time points during three- and two-step pretargeting are listed in Tables 1 and 2, respectively.

As shown in Tables 1 and 2, tumor uptake (% ID/g) was 1.78% and 1.36% in three-step pretargeting group, 4 and 24 h after the injection, and 1.35% and 2.10% in two-step pretargeting group. The tumor/blood ratio at the same time point was 5.76 and 12.94 in three-step pretargeting group, and only 1.00 and 2.03 in two-step pretargeting group. In directly labeling group, the tumor uptake (% ID/g) reached as high as 1.42% 48 h after the injection, but the level of blood background activity was also high (1.01%ID/g). The tumor uptake (% ID/g) and the ratios of tumor to other organs were all lower in ^{153}Sm-DB_2 and ^{153}Sm-SA groups.

Pretargeting radioimmunoimaging

In the three-step procedure, higher radioactive uptake in the implanted tumor was observed 4 h after the injection, and better tumor display and higher T/NT ratio were also obtained at 24 h because the level of blood background activity was markedly reduced. In the two-step procedure, radioactivity accumulation in the tumor could be visualized at 24 and 48 h. However, higher radioactive uptake was observed in the liver, spleen, and kidney. In the group of directly labeled McAb with ^{153}Sm, radioactive uptake at the site of tumor implantation occurred 72 h after the injection; while in ^{153}Sm-DB_2 and ^{153}Sm-SA groups, no significant radioactivity uptake in tumor was observed.

Observation of tumor inhibiting effect

In the 1st wk of treatment, the tumor volume showed little difference among the groups; while in the 2nd wk slower tumor growth rate in groups A and B was observed, indicating tumor inhibition. Till the 5th wk, the tumor volume was obviously smaller in groups A and B than in nontherapeutic control group (Figure 1), and the difference was statistically

Table 1 Biodistribution of drugs in tumor-bearing nude mice during multi-step pretargeting (% ID/g, mean±SD)

Group	*n*	h	Organs						
			Tumor	Liver	Spleen	Kidney	Bone	Lung	Blood
Three-step pretargeting	3	4	1.78±0.11	1.40±0.16	1.60±0.48	4.60±2.22	0.67±0.27	0.27±0.10	0.33±0.09
		24	1.36±0.17	0.92±0.09	0.78±0.12	5.50±1.55	0.58±0.14	0.43±0.26	0.12±0.06
		48	0.94±0.08	0.66±0.12	0.61±0.03	1.30±0.48	0.36±0.02	0.17±0.02	0.08±0.02
Two-step pretargeting	3	4	1.35±0.22	3.05±0.07	2.31±0.55	3.37±0.15	0.64±0.12	0.50±0.03	1.41±0.45
		24	2.10±0.16	2.02±0.30	1.82±0.19	4.56±0.42	0.33±0.04	0.37±0.03	1.05±0.13
		48	1.24±0.01	1.26±0.01	1.26±0.01	2.30±0.12	0.26±0.01	0.27±0.02	0.96±0.07
Directly labeling McAb	3	4	0.54±0.17	2.01±0.20	1.86±0.21	3.21±0.55	0.94±0.17	0.50±0.10	2.08±0.18
		24	0.99±0.16	1.53±0.10	1.00±0.12	2.42±0.24	0.61±0.01	0.44±0.11	1.29±0.48
		48	1.42±0.05	1.34±0.04	0.77±0.07	1.27±0.07	0.54±0.07	0.34±0.03	1.01±0.13
^{153}Sm-DB_2	3	4	0.21±0.01	1.07±0.10	1.14±0.10	5.76±0.68	0.38±0.04	0.37±0.10	0.22±0.05
		24	0.12±0.02	0.83±0.03	0.78±0.08	3.44±0.24	0.24±0.03	0.22±0.04	0.12±0.01
		48	0.10±0.01	0.62±0.11	0.53±0.02	2.60±0.84	0.14±0.04	0.18±0.05	0.10±0.02
^{153}Sm-SA	3	4	0.32±0.01	2.95±0.87	2.27±0.46	3.79±0.48	0.40±0.05	0.36±0.12	0.94±0.08
		24	0.22±0.03	1.89±0.01	1.82±0.17	2.72±0.10	0.22±0.01	0.33±0.07	0.85±0.11
		48	0.19±0.03	1.53±0.16	1.38±0.13	1.03±0.08	0.11±0.01	0.20±0.04	0.59±0.05

Table 2 T/NT ratio in tumor-bearing nude mice during multi-step pretargeting (mean±SD)

Group	*n*	h	Organs					
			Liver	Spleen	Kidney	Bone	Lung	Blood
Three-step	3	4	1.28±0.18	1.21±0.51	0.46±0.23	2.93±1.05	7.12±2.64	5.76±1.64
pretargeting		24	1.47±0.11	1.76±0.12	0.27±0.08	2.39±0.27	4.06±2.47	12.94±5.05
		48	1.44±0.27	1.53±0.07	0.81±0.40	2.64±0.41	5.65±1.32	11.19±1.80
Two-step	3	4	0.44±0.08	0.60±0.10	0.40±0.08	2.18±0.60	2.71±0.60	1.00±0.22
pretargeting		24	1.05±0.15	1.16±0.07	0.46±0.08	6.48±1.30	5.78±0.82	2.03±0.37
		48	0.98±0.01	0.98±0.01	0.54±0.02	4.77±0.15	4.66±0.22	1.30±0.08
Directly	3	4	0.27±0.12	0.30±0.12	0.17±0.07	0.73±0.36	1.06±0.16	0.26±0.08
labeling McAb		24	0.65±0.11	1.01±0.23	0.41±0.09	1.62±0.27	2.31±0.57	0.85±0.37
		48	1.07±0.02	1.87±0.20	1.14±0.13	2.71±0.49	4.20±0.44	1.42±0.13
^{153}Sm-DB_2	3	4	0.20±0.01	0.19±0.02	0.04±0.01	0.56±0.04	0.61±0.15	1.01±0.22
		24	0.14±0.02	0.15±0.04	0.03±0.01	0.50±0.14	0.55±0.18	0.95±0.14
		48	0.17±0.03	0.20±0.01	0.04±0.01	0.75±0.21	0.59±0.17	1.04±0.19
^{153}Sm-SA	3	4	0.11±0.04	0.14±0.03	0.08±0.01	0.80±0.07	0.93±0.22	0.34±0.04
		24	0.12±0.01	0.12±0.02	0.08±0.01	1.02±0.10	0.70±0.24	0.26±0.07
		48	0.13±0.03	0.14±0.02	0.19±0.04	1.77±0.34	1.01±0.30	0.33±0.02

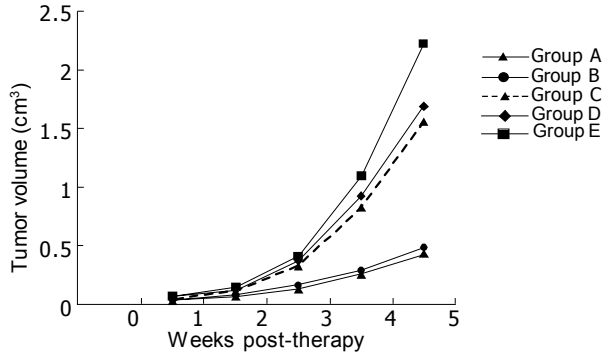


Figure 1 Transplant tumor growth curves.

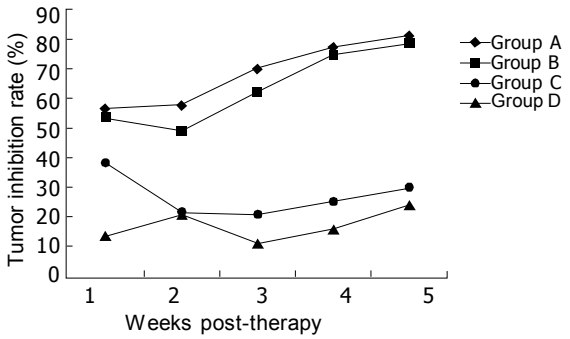


Figure 2 Curves of growth inhibition rate of transplant tumors.

significant (P<0.01). It was also noted that the tumor volume was smaller in groups C and D than in group E, and the difference was also statistically significant (P<0.01). If the tumor inhibition rate in nontherapeutic control group was considered as zero, the tumor inhibition rate 5 wk post-therapy was as high as 80.67% and 78.44% in groups A and B, much higher than that in groups C and D (Figure 2). In the latter two groups, the tumor inhibition rate was only 29.78% and 23.99%, and no significant difference existed between them. However, significant difference existed between the former two and the latter two groups (P<0.01).

Histopathological evidence also showed that the tumor cell nuclei were pyknotic, karyoclastic, and autolytic in three-step pretargeting RIT and ^{153}Sm-CEA McAb groups, which were not seen in the other controls (Figure 3). In the non-treated group, tumor tissue was characterized by the absence of necrosis, and took on typical forms of carcinoma cells (Figure 3).

Observation of side effects

Compared to non-treatment group, the number of peripheral blood WBC in treatment groups decreased after injection of 11.1 MBq of ^{153}Sm to some degree (Figure 4). However, WBC counts showed significant decrease after treatment in ^{153}Sm-CEA McAb and ^{153}Sm-nmIgG groups, and WBC recovery was also slower in both groups. Microscopic observation revealed no obvious tissue radiation damage in organs such as heart, liver, spleen, lungs, and brain in all nude mice at the end of the treatment.

DISCUSSION

Radiolabeled McAb specific for tumor-associated antigens is used for diagnosis and therapy of malignant tumors[1,2]. However, the blood clearance of antibodies is slow and T/NT ratio of radioactivity in the current system is not high. In order to increase the amount of radioactivity bound to cancer cells, a new approach in cancer therapy called pretargeting has been used. The pretargeting approach can be carried out as a two-step or as a three-step procedure. The two-step procedure is based on the administration of SA-antibody conjugate followed by radioactive biotin or biotinylated antibody is injected followed by radioactive SA[4,18]. In the three-step procedure, biotinylated antibody is injected followed by an excess of avidin/SA and then radioactive biotin is injected[4,19]. In both the methods, the radioactivity of tumor cells is increased[14,20]. Using pretargeting technique of avidin-biotin system, high T/NT ratios have been reported, not only in animal experiments, but also in clinical trials. The avidin-biotin system is also used to reduce the background radioactivity of directly labeled antibody as well as RIGS[9,21]. The success of the approach is due, in part, to the extremely high binding affinity of

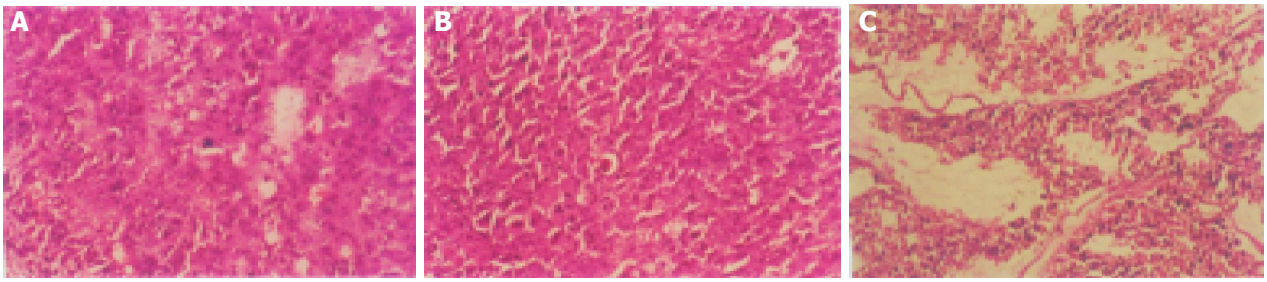


Figure 3 HE staining of tumor tissues in nude mice bearing human colon carcinoma after receiving three-step pretargeting RIT (**A**), ^{153}Sm-CEA McAb RIT (**B**) and normal saline (**C**).

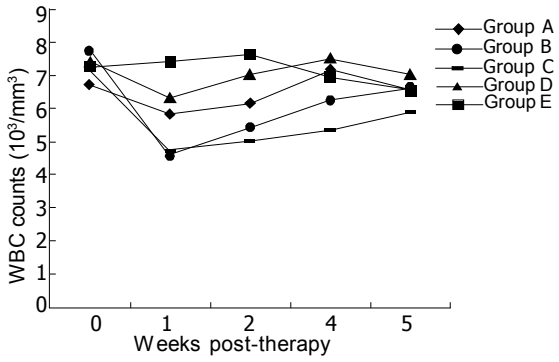


Figure 4 WBC counts after injection of drugs.

biotin to avidin/SA, which provides a high tumor targeting efficiency and a long retention at the tumor site. Further, the small size of biotin and its derivatives provides rapid renal clearance of radiolabeled biotin, eliminating much of the irradiation of nontarget tissues. In the present study, the two-step procedure applied consists of injection of radiolabeled SA after pretargeting with biotinylated antibody. The three-step procedure described in our study is as follows. First, tumor pretargeting was done by biotinylated anti-tumor McAbs. Second, when the uptake of McAbs in tumor cells reached its maximum within 24-48 h postinjection, circulating biotinylated McAbs were quickly (5-10 min) removed from the blood by the liver following the administration of avidin as a clearing agent. Finally, postlabeling of the tumor was done by a fast-clearing radioactive biotin and its derivatives. Since one molecule of McAb is capable of binding multiple molecules of biotin, the reaction of avidin with biotin and its derivatives is amplified. One molecule of avidin can bind to four molecules of biotin, and then further amplification of the reaction takes place. In other words, three-step pretargeting technique, like an amplifier, may result in an amplification of signals at the tumor target sites. Meanwhile, transchelating time of radioactive metal *in vivo* is shortened, and consequently normal tissue uptake of the antibody is reduced and antibody immunoreactivity is preserved unlike directly radiolabeled antibodies, which result in the loss of antibody immunoreactivity due to autoradiolysis and enzyme treatment.

Studies using ^{90}Y-biotin have been successful[14,22]. Biotin has also been labeled with several chelated radionuclides for cancer therapy such as ^{99m}Tc, ^{188}Re, ^{166}Ho, and ^{211}At[23-26]. ^{153}Sm is a radiolanthanide, which has not yet been widely used, but possesses nuclear characteristics suitable for RIT. It can be produced in reactors by enriched samarium (^{152}Sm) through the (n, γ) reaction. This enables the production of ^{153}Sm at low cost. As far as we know, studies of labeling antibodies and biotin with ^{153}Sm are very few[27]. It has been recognized that the cation $^{153}Sm^{3+}$ has good chelating capabilities with polyaminopolycarboxylic acids, such as EDTA or DTPA. In our study, we chose DTPA as the intermediate chelating agent, which can be linked to the antibodies or SA via bicyclic anhydride (cDTPAa). The main purpose of our investigation was to establish the labeling method of McAb and SA as well as biotin with ^{153}Sm and to evaluate the pretargeting RII and RIT in nude mice bearing human colon carcinoma with SA-biotin system labeled with ^{153}Sm. In the three-step procedure, the tumor was clearly visualized at 4 h in γ-imaging and at the same time point tumor blood pool ratio was 5.76, which was significantly higher than that of control groups. In the two-step procedure, a significant accumulation of ^{153}Sm-SA in the tumor was observed only 24 h after injection. The tumor blood ratios at 4 and 24 h were 1.00 and 2.03, respectively. However, the higher radioactive accumulation was also observed in the liver, spleen, and kidney. This deposition may result from complex formation of biotinylated antibodies with radiolabeled SA in circulation. In addition, in molecule of SA there exists three-peptide amino acid sequences (Arg-Thy-Asp), which may bind to the surface of many types of cells[28]. The advantages of pretargeting technique lie in that it is safe and simple, biotinylation of antibody and other reagents are easily prepared. Since the clearance of radiolabeled biotin or SA from normal tissue is much more rapid than that of directly radiolabeled antibody because of its small molecular weight, background radioactivity levels are drastically reduced, and the high T/NT ratio can be reached shortly after injection of the radiolabel[3,15,29]. Our preliminary studies also showed that compared to directly labeled McAb with ^{153}Sm, multi-step pretargeting could efficiently decrease the blood background levels, elevate the T/NT ratio, shorten the imaging time and improve the quality of imaging. Earlier and better images of tumor can be obtained using these methods, especially the three-step procedure.

RIT has shown disappointing results in bulky, solid tumors, probably due to the low specific accretion of radiolabeled antibody in the tumor target as compared to normal tissues[30]. Tumors have intrinsic characteristics

that unfavorably affect localization and intratumoral distribution of McAbs: heterogeneous expression of the antigen, relatively poor tumor vasculature, elevated interstitial pressure and tumor necrosis. Previous investigations have shown that tumor uptake and radiation doses are inversely correlated with tumor size [31,32]. Therefore, RIT may be a viable option, especially for small-volume and minimal residual tumors. ^{153}Sm emits β-rays with intermediate or low energy, which can effectively kill microtumors. In view of these considerations, our RIT experiment was devised to initiate on the 3rd d following tumor inoculation. The results showed that pretargeting RIT and ^{153}Sm-CEA McAb had a strong tumor inhibition effect. The tumor inhibitory rate was 80.67% and 78.44%, 5 wk after therapy. Histopathological evidence also indicated radioactive damage as necrosis of the tumor, which was not seen in the other controls. RIT and pretargeting RIT may be more effective for early stage carcinoma. The reason may be related to lower quantity of tumor cells in early stage, less heterogeneity in tumor antigen expression and greater sensitivity to radiation. In addition, there was, to certain degrees, tumor inhibitory effect in groups of ^{153}Sm-nmIgG and ^{153}Sm-DB_2 with a tumor inhibitory rate of 29.78% and 23.99%, respectively, 5 wk after therapy. This may result from unspecific radiation effect. Because ^{153}Sm-nmIgG and ^{153}Sm-DB_2 cannot bind specifically with anti-CEA McAb, effective localization in tumor cells *in vivo* would not take place, thus this unspecific radiation effect is limited.

In three-step pretargeting RIT, ^{153}Sm-DB_2 at a single dose of 11.1 MBq/100 μL produced potent tumor-inhibiting effect, and no significant bone marrow toxicity was observed as evidenced by milder decrease of WBC counts. However, in ^{153}Sm-CEA McAb and ^{153}Sm-nmIgG groups, WBC counts significantly decreased, and WBC recovery was also slower than that in three-step pretargeting RIT, indicating that the hemopoietic function of bone marrow might be affected. When ^{153}Sm-CEA McAb and ^{153}Sm-nmIgG enter into blood circulation, its slower blood clearance may result in high background radioactivity levels and cause more radiation-related damage to normal tissues or organs. The rapid clearance of ^{153}Sm-DB_2 from blood may drastically reduce background radioactivity levels. Consequently, radiation exposure to normal tissues especially bone marrow is decreased.

In conclusion, pretargeted RIT with ^{153}Sm-DB_2 has higher anti-tumor efficacy but lower toxicity than ^{153}Sm-CEA McAb. It may serve as an adjuvant therapy for tumor, particularly for small tumor or micrometastatic disease and residual cancer cells in surgical tumor resection areas. Therefore, it is of good prospect in clinical application.

REFERENCES

1 **Bian HJ**, Chen ZN, Deng JL. Direct technetium-99m labeling of anti-hepatoma monoclonal antibody fragment: a radioimmunoconjugate for hepatocellular carcinoma imaging. *World J Gastroenterol* 2000; **6**: 348-352

2 **Goldenberg DM**. Targeted therapy of cancer with radiolabeled antibodies. *J Nucl Med* 2002; **43**: 693-713

3 **Zhang M**, Zhang Z, Garmestani K, Schultz J, Axworthy DB, Goldman CK, Brechbiel MW, Carrasquillo JA, Waldmann TA. Pretarget radiotherapy with an anti-CD25 antibody-streptavidin fusion protein was effective in therapy of leukemia/lymphoma xenografts. *Proc Natl Acad Sci USA* 2003; **100**: 1891-1895

4 **Hnatowich DJ**, Virzi F, Rusckowski M. Investigations of avidin and biotin for imaging applications. *J Nucl Med* 1987; **28**: 1294-1302

5 **Paganelli G**, Malcovati M, Fazio F. Monoclonal antibody pretargetting techniques for tumour localization: the avidin-biotin system International Workshop on Techniques for Amplification of Tumour Targetting. *Nucl Med Commun* 1991; **12**: 211-234

6 **Yao Z**, Zhang M, Kobayashi H, Sakahara H, Nakada I, Yamashina J, Konishi J. Improved targeting of radiolabeled streptavidin in tumors pretargeted with biotinylated monoclonal antibodies through an avidin chase. *J Nucl Med* 1995; **26**: 837-841

7 **Paganelli G**, Belloni C, Magnani P, Zito F, Pasini A, Sassi I, Meroni M, Mariani M, Vignali M, Siccardi AG, Fazio F. Two-step tumour targeting in ovarian cancer patients using biotinylated monoclonal antibodies and radioactive streptavidin. *Eur J Nucl Med* 1992; **19**: 322-329

8 **Paganelli G**, Magnani P, Zito F, Villa E, Sudati F, Lopalco L, Rossetti C, Malcovati M, Chiolerio F, Seccamani E. Three-step monoclonal antibody tumor targeting in carcinoembryonic antigen-positive patients. *Cancer Res* 1991; **51**: 5960-5966

9 **Paganelli G**, Stella M, Zito F, Magnani P, De-Nardi P, Mangili F, Baratti D, Veglia F, Di-Carlo V, Siccardi AG. Radioimmunoguided surgery using iodine-125-labeled biotinylated monoclonal antibodies and cold avidin. *J Nucl Med* 1994; **35**: 1970-1975

10 **Lewis MR**, Wang M, Axworthy DB, Theodore LJ, Mallet RW, Fritzberg AR, Welch MJ, Anderson CJ. *In vivo* evaluation of pretargeted ^{64}Cu for tumor imaging and therapy. *J Nucl Med* 2003; **44**: 1284-1292

11 **Modorati G**, Brancato R, Paganelli G, Magnani P, Pavoni R, Fazio F. Immunoscintigraphy with three step monoclonal pretargeting technique in diagnosis of uveal melanoma: preliminary results. *Br J Ophthalmol* 1994; **78**: 19-23

12 **Boerman OC**, van Schaijk FG, Oyen WJ, Corstens FH. Pretargeted radioimmunotherapy of cancer: progress step by step. *J Nucl Med* 2003; **44**: 400-411

13 **Axworthy DB**, Reno JM, Hylarides MD, Mallett RW, Theodore LJ, Gustavson LM, Su F, Hobson LJ, Beaumier PL, Fritzberg AR. Cure of human carcinoma xenografts by a single dose of pretargeted yttrium-90 with negligible toxicity. *Proc Natl Acad Sci USA* 2000; **97**: 1802-1807

14 **Grana C**, Chinol M, Robertson C, Mazzetta C, Bartolomei M, De Cicco C, Fiorenza M, Gatti M, Caliceti P, Paganelli G. Pretargeted adjuvant radioimmunotherapy with yttrium-90-biotin in malignant glioma patients: a pilot study. *Br J Cancer* 2002; **86**: 207-212

15 **Paganelli G**, Chinol M. Radioimmunotherapy: is avidin-biotin pretargeting the preferred choice among pretargeting methods? *Eur J Nucl Med Mol Imaging* 2003; **30**: 773-776

16 **Boniface GR**, Izard ME, Walker KZ, McKay DR, Sorby PJ, Turner JH, Morris JG. Labeling of monoclonal antibodies with ^{153}Sm for combined radioimmunoscintigraphy and radioimmunotherapy. *J Nucl Med* 1989; **30**: 683-691

17 **Hnatowich DJ**, Childs RL, Lanteigne D, Najafi A. The preparation of DTPA-coupled antibodies radiolabeled with metallic radionuclides: an improved method. *J Immunol Methods* 1983; **65**: 147-157

18 **Paganelli G**, Pervez S, Siccardi AG, Rowlinson G, Deleide G, Chiolerio F, Malcovati M, Scassellati GA, Epenetos AA. Intraperitoneal radio-localization of tumors pretargeted by biotinylated monoclonal antibodies. *Int J Cancer* 1990; **45**: 1184-1189

19 **Magnani P**, Paganelli G, Modorati G, Zito F, Songini C, Sudati F, Koch P, Maecke HR, Brancato R, Siccardi AG, Fazio F. Quantitative comparison of direct antibody labeling and tumor pretargeting in uveal melanoma. *J Nucl Med* 1996; **37**:

967-971

20 **Hamblett KJ**, Kegley BB, Hamlin DK, Chyan MK, Hyre DE, Press OW, Wilbur DS, Stayton PS. A streptavidin-biotin binding system that minimizes blocking by endogenous biotin. *Bioconjug Chem* 2002; **13**: 588-598

21 **Kobayashi H**, Sakahara H, Hosono M, Yao Z, Toyama S, Endo K, Konishi J. Improved clearance of radiolabeled biotinylated monoclonal antibody following the infusion of avidin as a "chase" without decreased accumulation in the target tumor. *J Nucl Med* 1994; **35**: 1677-1684

22 **Knox SJ**, Goris ML, Tempero M, Weiden PL, Gentner L, Breitz H, Adams GP, Axworthy D, Gaffigan S, Bryan K, Fisher DR, Colcher D, Horak ID, Weiner LM. Phase II trial of yttrium-90-DOTA-biotin pretargeted by NR-LU-10 antibody/streptavidin in patients with metastatic colon cancer. *Clin Cancer Res* 2000; **6**: 406-414

23 **Correa-Gonzalez L**, Arteaga de Murphy C, Ferro-Flores G, Pedraza-Lopez M, Murphy-Stack E, Mino-Leon D, Perez-Villasenor G, Diaz-Torres Y, Munoz-Olvera R. Uptake of ^{153}Sm-DTPA-bis-biotin and ^{99m}Tc-DTPA-bis-biotin in rat as-30D-hepatoma cells. *Nucl Med Biol* 2003; **30**: 135-140

24 **Lindegren S**, Karlsson B, Jacobsson L, Andersson H, Hultborn R, Skarnemark G. ^{211}At-labeled and biotinylated effector molecules for pretargeted radioimmunotherapy using poly-L- and poly-D-Lysine as multicarriers. *Clin Cancer Res* 2003; **9** (10Pt 2): 3873S-3879S

25 **Ferro-Flores G**, Arteaga de Murphy C, Pedraza-Lopez M, Monroy-Guzman F, Melendez-Alafort L, Tendilla JI, Jimenez-Varela R. Labeling of biotin with ^{166}Dy/^{166}Ho as a stable *in vivo* generator system. *Int J Pharm* 2003; **255**: 129-138

26 **Ferro-Flores G**, Pimentel-Gonzalez G, Gonzalez-Zavala MA, Arteaga de Murphy C, Melendez Alafort L, Tendilla JI, Croft BY. Preparation, biodistribution, and dosimetry of ^{188}Re-labeled McAb ior ceal and its F(ab')$_2$ fragments by avidin-biotin strategy. *Nucl Med Biol* 1999; **26**: 57-62

27 **Kraeber-Bodere F**, Mishra A, Thedrez P, Faivre-Chauvet A, Bardies M, Imai S Le, Boterff J, Chatal JF. Pharmacokinetics and biodistribution of samarium-153-labeled OC125 antibody coupled to CITCDTPA in a xenograft model of ovarian cancer. *Eur J Nucl Med* 1996; **23**: 560-567

28 **Rosebrough SF**, Hartley DF. Biochemical modification of streptavidin and avidin: *in vitro* and *in vivo* analysis. *J Nucl Med* 1996; **37**: 1380-1384

29 **Kassis AI**, Jones PL, Matalka KZ, Adelstein SJ. Antibody-dependent signal amplification in tumor xenografts after pretreatment with biotinylated monoclonal antibody and avidin or Streptavidin. *J Nucl Med* 1996; **37**: 343-352

30 **Behr TM**, Goldenberg DM, Becker WS. Radioimmunotherapy of solid tumors: a review "of mice and men." *Hybridoma* 1997; **16**: 101-107

31 **Behr TM**, Sharkey RM, Juweid ME, Dunn RM, Ying Z, Zhang CH, Siegel JA, Goldenberg DM. Variables influencing tumor dosimetry in radioimmunotherapy of CEA-expressing cancers with anti-CEA and antimucin monoclonal antibodies. *J Nucl Med* 1997; **38**: 409-418

32 **Behr TM**, Liersch T, Greiner-Bechert L, Griesinger F, Behe M, Markus PM, Gratz S, Angerstein C, Brittinger G, Becker H, Goldenberg DM, Becker W. Radioimmunotherapy of small-volume disease of metastatic colorectal cancer. *Cancer* 2002; **94**: 1373-1381

Science Editor Wang XL, Zhu LH and Guo SY **Language Editor** Elsevier HK

PO Box 2345, Beijing 100023, China
www.wjgnet.com
wjg@wjgnet.com

ELSEVIER

World J Gastroenterol 2005;11(40):6295-6304
World Journal of Gastroenterology ISSN 1007-9327
© 2005 The WJG Press and Elsevier Inc. All rights reserved.

Classifying genotype F of hepatitis B virus into F1 and F2 subtypes

Hideaki Kato, Kei Fujiwara, Robert G. Gish, Hiroshi Sakugawa, Hiroshi Yoshizawa, Fuminaka Sugauchi, Etsuro Orito, Ryuzo Ueda, Yasuhito Tanaka, Takanobu Kato, Yuzo Miyakawa, Masashi Mizokami

Hideaki Kato, Kei Fujiwara, Fuminaka Sugauchi, Etsuro Orito, Ryuzo Ueda, Department of Internal Medicine and Molecular Science, Nagoya City University Graduate School of Medical Sciences, Nagoya, Japan
Yasuhito Tanaka, Takanobu Kato, Masashi Mizokami, Department of Clinical Molecular Informative Medicine, Nagoya City University Graduate School of Medical Sciences, Nagoya, Japan
Robert G. Gish, Hepatology and Gastroenterology, California Pacific Medical Center, CA, United States
Hiroshi Sakugawa, First Department of Medicine, University Hospital, Faculty of Medicine, University of the Ryukyus, Okinawa, Japan
Hiroshi Yoshizawa, Department of Epidemiology and Control of Infectious Diseases, Hiroshima University Graduate School of Biomedical Sciences, Hiroshima, Japan
Yuzo Miyakawa, Miyakawa Memorial Research Foundation, Tokyo, Japan
Correspondence to: Prof. Masashi Mizokami, Department of Clinical Molecular Informative Medicine, Nagoya City University Graduate School of Medical Sciences, Nagoya 467-8601, Japan. mizokami@med.nagoya-cu.ac.jp
Telephone: +81-52-853-8292 Fax: +81-52-842-0021
Received: 2004-11-08 Accepted:2004-12-23

Abstract

AIM: To explore the propriety of providing hepatitis B virus (HBV) genotypes F and H with two distinct genotypes.

METHODS: Eleven HBV isolates of genotype F (HBV/F) were recovered from patients living in San Francisco, Japan, Panama, and Venezuela, and their full-length sequences were determined. Phylogenetic analysis was carried out among them along with HBV isolates previously reported.

RESULTS: Seven of them clustered with reported HBV/F isolates in the phylogenetic tree constructed on the entire genomic sequence. The remaining four flocked on another branch along with three HBV isolates formerly reported as genotype H. These seven HBV isolates, including the four in this study and the three reported, had a sequence divergence of 7.3-9.5% from the other HBV/F isolates, and differed by >13.7% from HBV isolates of the other six genotypes (A-E and G). Based on a marked genomic divergence, falling just short of >8% separating the seven genotypes, these seven HBV/F isolates were classified into F2 subtype and the former seven into F1 subtype provisionally. In a pairwise comparison of the S-gene sequences among the 7 HBV/F2 isolates and against 47 HBV/F1 isolates as well as 136 representing the other six genotypes (A-E and G), two clusters separated by distinct genetic distances emerged.

CONCLUSION: Based on these analyses, classifying HBV/F isolates into two subtypes (F1 and F2) would be more appropriate than providing them with two distinct genotypes (F and H).

© 2005 The WJG Press and Elsevier Inc. All rights reserved.

Key words: Genotypes; Hepatitis B virus; Phylogenetic analysis; Subtypes

Kato H, Fujiwara K, Gish RG, Sakugawa H, Yoshizawa H, Sugauchi F, Orito E, Ueda R, Tanaka Y, Kato T, Miyakawa Y, Mizokami M. Classifying genotype F of hepatitis B virus into F1 and F2 subtypes. *World J Gastroenterol* 2005; 11(40): 6295-6304

http://www.wjgnet.com/1007-9327/11/6295.asp

INTRODUCTION

Seven genotypes of hepatitis B virus (HBV) have been differentiated by a sequence divergence in the entire genome >8%, and they are named by capital alphabet letters from A to G[1-3]. Among the seven genotypes of HBV, F is the most divergent from the other six and separated from them by >14% in the full-length sequence. Recently, an eighth genotype was proposed for HBV isolates from Central America based on a sequence divergence from those of the seven genotypes (A-G) barely exceeding 8%[4].

An attempt was made in the present study to evaluate the independence of genotype H from the others by systematic phylogenetic analysis on the entire nucleotide sequences and their open reading frames of 25 HBV isolates of genotype F (HBV/F) or H, including the 11 from patients with acute or chronic hepatitis B from San Francisco, Japan, Panama, and Venezuela that were determined anew.

Because of a mediocre sequence divergence, a little short of clearing the >8% difference separating the seven HBV genotypes (A-G), taken along with their relationship in phylogenetical analysis, the two clades of HBV/F isolates would better be classified into two subtypes of genotype F, and they were provisionally assigned the designations F1 and F2. A possibility is proposed for distinguishing F1 and F2 subtypes by combining serotypes of the preS2-region product[5-7], for the determination of HBV genotypes, and subtypes of hepatitis B surface antigen (HBsAg).

MATERIALS AND METHODS

Patients

Of the patients with acute or chronic hepatitis B who were

Table 1 Demographic characteristics and liver diseases of the 11 patients from whom HBV isolates of genotype F were recovered

HBV strains	Accession number	Age (yr)	Gender	Ethnicity	Clinical diagnosis
USF10	AB059659	46	Female	Caucasian	Liver cirrhosis
USF1122	AB064315	46	Male	Hispanic	Liver cirrhosis
USF1778	AB059660	44	Male	Hispanic	Liver cirrhosis
USF2065	AB059661	47	Male	Hispanic	Acute hepatitis
USF2573	AB064316	67	Male	Hispanic	Liver cirrhosis
JPF1130	AB086397	43	Male	Asian	Chronic hepatitis
JPNTAKA	AB116654	NA	Male	Asian	NA
VENEZ2	AB116549	35	Male	Hispanic	Acute hepatitis
VENEZ4	AB116550	35	Male	Hispanic	Acute hepatitis
PANAM5	AB116551	NA	NA	NA	NA
PANAM6	AB116552	NA	NA	NA	NA

NA: not available.

taken care of in Gastroenterology Division of California Medical Center in San Francisco, Ryukyu University Hospital in Okinawa, Japan and National Hospitals in Panama and Venezuela, 11 were found to be infected with HBV/F. Demographic characteristics and liver diseases of the 11 patients are shown in Table 1. Their sera were tested for HBV markers, and HBV/F isolates in them were sequenced over the entire genome. The study design was approved by Ethics Committees of the institutions, and an informed consent was obtained from each patient.

Determination of the seven HBV genotypes (A-G) by preS2 serotypes

The seven major genotypes of HBV, i.e., A, B, C, D, E, F and G, were determined by ELISA with commercial kits (HBV Genotype EIA, Institute of Immunology, Tokyo, Japan) which distinguishes serotypes of the product of the preS2 region that are specific for each genotype[5-7]. It involves monoclonal antibodies directed to five preS2 epitopes designated *b*, *k*, *m*, *s* and *u*, respectively. Since the expression of preS2 epitopes are influenced by HBV genotypes, the combination thereof can define genotypes serologically; the epitope *b* is expressed regardless of HBV genotypes and guarantees the presence of preS2 product in the test serum. Thus, a serotype *bsu* is specific for genotype A, *bm* for B, *bks* for C and *bk* for F. Although genotypes D and E have the same serotype (*bksu*), they are differentiated by distinct behavior in the binding with another monoclonal antibody against the epitope *g* immobilized on a solid support. HBsAg of genotype E binds with immobilized anti-*g*, so that it is sandwiched between antibody to the common determinant *a* of HBsAg labeled with horseradish peroxidase, while HBsAg of genotype D is not. Although HBsAg of genotype G has a preS2 serotype for D, *bksu(g)*, it has HBsAg subtype of *adw* unlike *ayw* in almost all HBsAg samples of genotype D. Thus, genotype G can be detected serologically by the combination of preS2 serotype *bksu(g)* and HBsAg subtype *adw*.

Determination of the full-length sequences of six HBV/F isolates

Nine sets of primers used in this study are shown in

Table 2 Primers used for PCR and sequencing

Primer[1]	Polarity	Sequence (5′–3′)	Positions (nt)
HBV/Ff1	Sense	GGG TCA CCA TAT TCT TGG GAA	2 814–2 834
HBV/Fr1	Antisense	CGT TGC CGA GCA ACG GGG TAA AGG	1 163–1 140
HBV/Ff2	Sense	GTT TCT CCT GGC TCA GTT TA	660–679
HBV/Fr2	Antisense	AAA AAG TTG CAT GGT GCT GG	1 825–1 806
HBV/Ff3	Sense	ACG TCG CAT GGA GAC CAC CG	1 601–1 620
HBV/Fr3	Antisense	GAA CTG GAG CCA CCA GCA GG	75–56
HBV/Ff4	Sense	CCT CCT GCT TCC ACC AAT CG	3 124–3 143
HBV/Fr4	Antisense	AGA TGA GGC ATA GCA GCA GGA TG	431–409
HBV/Ff5	Sense	GTC TAG ACT CGT GGT GGA CTT CTC	246–269
HBV/Fr5	Antisense	AAG CCA GAC AGT GGG GGA AAG C	730–709
HBV/Ff6	Sense	CTC GCC AAC TTA CAA GGC CTT T	1 098–1 119
HBV/Fr6	Antisense	GAT TCA GCG CCG ACG GGA CGT A	1 447–1 426
HBV/Ff7	Sense	CTC TGC CGA TCC ATA CTG CGG AA	1 256–1 278
HBV/Fr7	Antisense	TGA GAT CTT CTG CGA CGC GGC	2 431–2 410
HBV/Ff8	Sense	TCA GGC AAG CTA TTT TGT GCT GG	2 064–2 086
HBV/Fr8	Antisense	TGT TCA CAT TTG TGT ATC AAA T	2 587–2 565
HBV/Ff9	Sense	GCC GCG TCG CAG AAG ATC TCA A	2 410–2 431
HBV/Fr9	Antisense	AAA ATG AGG CGC TAT GTG TGG ATT	2 811–2 788

[1]The first three pairs of primers (HBV/Ff1 to HBV/Fr3) were used for PCR and sequencing, while the remaining six pairs (HBV/Ff4 to HBV/Fr9) for sequencing only.

Table 2. The genomes of 11 HBV/F isolates were sequenced through 3 overlapping fragments; they were amplified by PCR with 3 sets of primers (HBV/Ff1-HBV/Fr1, HBV/Ff2-HBV/Fr2 and HBV/Ff3-HBV/Fr3). AmpliTaq Gold was activated at 96 ℃ for 9 min, and PCR was performed for 40 cycles (96 ℃ for 1 min; 55 ℃ for 1 min; 72 ℃ for 1.5 min [5 min in the last cycle]). The three nucleotide fragments were sequenced directly by the dideoxy method with use of the BigDye Terminator cycle sequencing kit in a fluorescent 3100 DNA sequencer (Applied Biosystems, Foster City, CA, USA) using the remaining six sets of primers along with the three primer sets used for PCR (Table 2).

Molecular evolutionary analyses

The number of nucleotide substitutions per site was estimated by the 6-parameter method[8], and phylogenetic trees were constructed by the neighbor-joining method[9] based on the numbers of substitutions. To confirm the credibility of phylogenetic analyses, bootstrap resampling tests were carried out 1 000 times[10]. Evolutionary distances between nucleotide sequences of the S gene were calculated in accordance with the HCV Database. These analyses were conducted with use of the ODEN program of the National Institute of Genetics (Mishima, Japan)[11]. Frequency distribution analysis was performed with the StatView J-4.5 program.

RESULTS

Eleven HBV/F isolates

Eleven patients with HBV-associated liver disease were found to be infected with HBV/F by ELISA with monoclonal antibodies against preS2 epitopes[5-7]. Table 1 shows demographics and liver disease of the 11 patients from whom HBV/F strains were recovered. Four of them had liver cirrhosis, three had acute hepatitis and one presented with chronic hepatitis; diagnosis of liver disease was not available for the remaining three. They included six Hispanics, two Asians and one Caucasian.

The entire nucleotide sequences of the 11 HBV/F isolates designated USF2573 (accession no. AB064316), USF10 (AB059659), USF1122 (AB064315), USF1778 (AB058660), USF2065 (AB059661), JPF1130 (AB086397), JPNTAKA (AB116654), PAMAN5 (AB116549), PANAM6 (AB116550), VENEZ2 (AB116551) and VENEZ4 (AB116552) have been deposited in the international DDBJ/GenBank/EMBL database. They were subjected to phylogenetic analyses over the entire genome and within the open reading frames among themselves and against 59 HBV isolates of the 7 genotypes (A-G) for which the full-length sequences are known (Figure 1).

Eleven HBV/F and three HBV/H isolates with known entire genomic sequences were recruited from the literature[2,12,13]. One (USF2573) of the five San Franciscan HBV/F isolates, two from Japan (JPF1130 and JPNTAKA), two from Panama (PANAM5 and PANAM6) and two from Venezuela (VENEZ2 and VENEZ4) clustered with the 11 reported HBV/F isolates in phylogenetic trees (Figures 1A-D). The remaining four (USF10, USF1122, USF1778 and USF2065) flocked on a separate branch along with two isolates from Nicaragua and one from Los Angeles, that have been classified into genotype H[4].

Classifying genotype F of HBV into F1 and F2 subtypes

The four strains (USF10, USF1122, USF1778 and USF2065) as well as three reported (LAS2523 [accession no. AY090460], 1853Nic [AY090454], 2928Nic [AY090457]) were compared among one another and against the seven isolates each representative of genotype F (AB064316 [USF2573 isolate]) and the other six genotypes (AB064314 for genotype A, D23678 for B, S75184 for C, D23681 for D, X75657 for E and AF160501 for G) over the full-length sequence and regions thereof (Table 3). In the comparison of the full-length sequence, the seven isolates were similar among themselves in $\geqslant$96.3%, and to the representative HBV/F isolate in $\geqslant$91.0%. They were, however, similar to any representatives of the other six genotypes in only $\leqslant$86.5%.

Table 4 compares homology in the entire nucleotide sequence among the 11 HBV/F isolates examined in this

Table 3 Sequence homology of seven HBV/F2 isolates among themselves and to seven HBV isolates representative of HBV/F1 as well as the other genotypes (A, B, C, D, E, and G)

Genomic regions	Homology within seven HBV/F2 isolates and that of HBV/F2 to seven representative of HBV/F1 as well as genotypes A, B, C, D, E, and G[1]							
	F2	F1	A	B	C	D	E	G
Full genome	97.5	91.6	86.0	85.9	85.7	85.7	86.1	84.5
	(96.3–99.2)	(91.0–92.1)	(85.4–86.5)	(85.5–86.2)	(85.2–86.0)	(85.1–86.3)	(85.6–86.4)	(84.1–84.8)
PreS1 region	98.1	90.0	77.3	75.7	78.9	79.3	81.4	80.6
	(97.2–99.4)	(89.1–90.5)	(76.8–78.2)	(75.1–76.5)	(77.9–80.1)	(78.3–80.2)	(80.7–82.0)	(80.4–81.1)
PreS2 region	97.4	90.9	82.9	79.2	82.6	81.2	83.3	81.3
	(92.7–100)	(86.1–92.7)	(78.0–84.2)	(75.8–80.6)	(79.4–83.6)	(77.6–82.4)	(79.4–84.2)	(77.0–83.0)
S gene	99.4	96.4	92.2	92.6	91.3	92.7	92.6	92.8
	(98.7–99.9)	(95.9–96.8)	(91.8–92.5)	(92.5–92.8)	(91.0–91.6)	(92.4–93.0)	(92.2–92.8)	(92.4–93.0)
C gene	95.8	91.9	84.8	87.3	86.6	84.9	85.8	87.2
	(90.9–100)	(88.8–93.5)	(83.0–85.8)	(85.1–88.6)	(84.8–87.5)	(82.8–86.6)	(84.1–86.8)	(84.9–88.2)
P gene	97.9	91.7	86.2	85.8	86.3	86.1	86.5	86.1
	(96.6–99.1)	(90.9–92.0)	(85.7–86.6)	(85.4–86.0)	(86.1–86.6)	(85.5–86.4)	(86.2–86.8)	(85.7–86.4)
X gene	97.1	91.1	87.7	88.7	85.4	89.2	88.3	84.2
	(94.2–99.8)	(89.3–92.3)	(86.5–88.7)	(86.8–90.1)	(84.7–86.8)	(88.0–90.2)	(87.1–89.5)	(85.0–83.7)

[1]The seven representatives of each genotype were: F1 (AB064316 [USF2573 isolate]), A (AB064314), B (D23678), C (S75184), D (D23681), E (X75657) and G (AF160501).

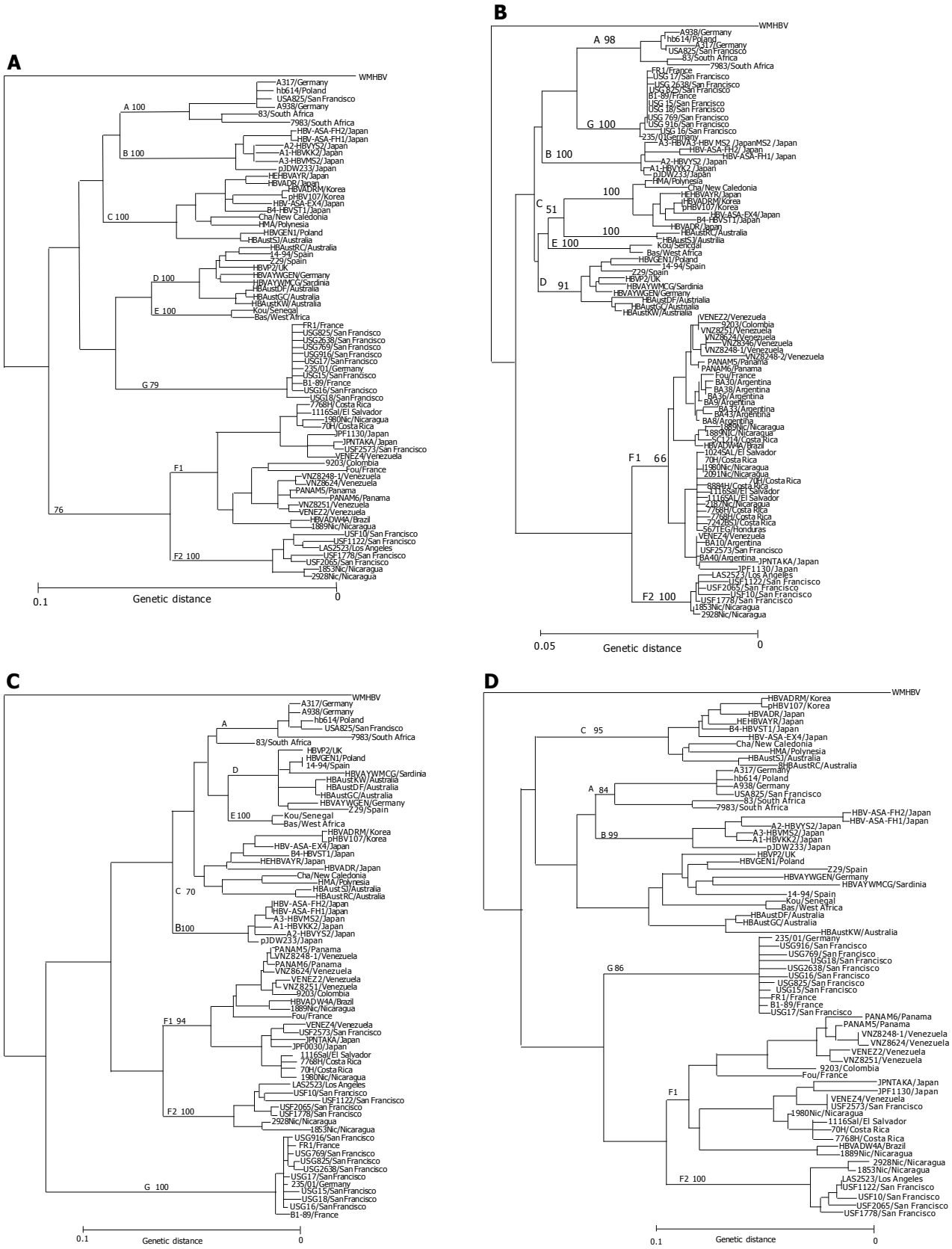


Figure 1 Phylogenetic trees constructed by HBV isolates of the major seven genotypes (A-G) on the full-genome (**A**), S gene (**B**), X gene (**C**) and core gene (**D**). Each tree includes 11 HBV/F isolates identified in this study as well as 59 HBV isolates retrieved from Database, and an additional 22 HBV/F isolates (shown as boldface) joined in the phylogenetic tree of the S region. Confidence values calculated by bootstrap analysis are indicated as a suffix to each genotype.

study and the 13 reported. The sequence divergence among the 7 isolates (USF10, USF1122, USF1778, USF2065, LAS2523, 1853Nic and 2928Nic) and the 10 reported[2,4,12,13] as well as the 7 (USF2573, JPF1130, JPNTAKA, PANAM5, PANAM6, VENEZ2 and VENEZ4) in this study exceeded 7.3%, which fell a little short of clearing a sequence divergence >8% distinguishing the 7 genotypes of HBV[1-3]. It would be appropriate, therefore, to classify the seven isolates into subtypes of genotype F. Thus, F1 subtype (HBV/F1) was assigned to the 11 reported HBV/F isolates and the 7 in this study (USF2573, JPF1130, JPNTAKA, PANAM5, PANAM6, VENEZ2 and VENEZ4) (Figure 1), while F2 subtype (HBV/F2) was consigned to the 7 isolates, 4 from San Francisco (USF10, USF1122, USF1778 and USF2065), 1 from Los Angeles (LAS2523) and 2 from Nicaragua (1853Nic and 2928Nic), all of which were examined in the present study.

Three HBV/F2 isolates examined in this study (USF10, USF1778 and USF2065) had the identical genomic length of 3 215 bp as the original three HBV/F isolates including X69798[12], X75658[2] and AB036905 [13]. The remaining one HBV/F2 isolate (USF1122) had a shorter length of 3 206 bp due to a deletion of 9 bp in the preS2 region. They all possessed 226 amino acids (aa) coded for by the S gene, 29 aa by the preC region, 183 aa by the C gene, 843 aa by the polymerase (P) gene (840 aa for USF1122) and 154 aa by the X gene. The subtype of HBsAg was deduced to be *adw4* in all HBV/F isolates by the expression of Lys^{122}, Leu^{127}, and Lys^{160} [14]. The YMDD motif that is prone to mutation during the lamivudine therapy was identified over aa 549-552 (aa 546-549 in USF1122) with methionine at position 550 (547 in USF1122).

Distribution of genetic distance within the S-gene sequence

Figure 2 illustrates genetic distance in the S-gene sequences of 47 HBV/F1 isolates, 7 HBV/F2 isolates and 136 HBV isolates of the other 6 genotypes (A-E and G). When all of them were compared two-by-two, they clustered into two heaps that were not separated clearly (Figure 2A). The heap with the mean genetic distance of 0.017 represented divergence of HBV isolates among the same genotype (intra-genotype), and that with the mean distance of 0.073 represented divergence between any two HBV isolates of distinct genotypes (inter-genotype). In Figure 2B, the 7 HBV/F2 and 47 HBV/F1 were compared among themselves (F1 *vs* F1 or F2 *vs* F2), each other (F1 *vs* F2) and against the other genotypes. In this two-by-two comparison, the genetic distance was distributed in two clusters of different orders. The genetic distance among 47 HBV/F1 isolates as well as the 7 HBV/F2 isolates stayed within the intra-genotype heap, and that of HBV/F1 as well as HBV/F2 against other genotypes stood within the inter-genotype heap. Notably, the genetic distance between HBV/F1 and HBV/F2 isolates clustered within the heap of intra-genotype. These distinct hierarchical orders of sequence divergence indicated that HBV/F2 would be closer to HBV/F1 than to any HBV isolates of the other six genotypes (A-E and G). Genetic distance in the S-gene sequences of 22 HBV/E isolates, 16 HBV/D isolates and 158 isolates of the other HBV genotypes is shown in the right half of Figure 2B. The genetic distance within HBV/D and HBV/E stayed within the intra-genotype heap, and that of those against the other genotypes as well as that between HBV/D and HBV/E isolates were kept within the inter-genotype heap.

Genotype- or subtype-specific nucleotide substitutions

When all the nucleotide sequences of 68 HBV isolates including 7 HBV/F2 isolates were compared, nucleotide substitutions specific for HBV/F2 were identified at 8 positions (A^{22}, T^{1467}, C^{1552}, G^{1754}, T^{2495}, C^{2628}, C^{3121}, and A^{3129}) (Table 5). Genotype- or subtype-specific nucleotide substitutions clustered within the P gene, and they were unique to each genotype except for genotype A as well as two subtypes of genotype F. Thus, C^{2606} was specific for genotype B, A^{2596} for C, C^{2579}/C^{2634} for D, T^{2603}/C^{2636} for E, C^{2558}/C^{2660} for G, T^{2622} for F1, and C^{2628} for F2.

Genotype- or subtype-specific amino acid substitutions

Substitutions specific for HBV/F2 were identified at the amino acid level within each open reading frame except for the preS2 region. Eight unique amino acid residues were identified within the polymerase (Gln^{92}, Ser^{267}, Thr^{272}, Thr^{275}, Glu^{282}, Thr^{308}, Thr^{313}, and Pro^{823}), four in X (Trp^{32}, Ala^{60}, Pro^{102} and Leu^{127}), two in preS1 (Ala^{8} and Pro^{90}), two in HBsAg (Val^{44} and Pro^{45}) and one in core region (Ala^{157}). Six of the eight (75%) unique amino acid residues identified in the polymerase region were found within the spacer region.

Serotypes of the preS2-region product determined by ELISA

Figure 3 illustrates amino acid sequences of the preS2-region product with reference to the expression of preS2 epitopes detected by four monoclonal antibodies named *b*, *f*, *k*, and *s*[5]. The preS2 epitope *b*, which is common to HBV isolates of any genotypes and borne by a tetramer with the sequence of LYFP[5], was not fully conserved in two of the seven HBV/F2 isolates despite the detection of epitope *b* in their preS2-region products; it was present in all 13 HBV/F1 isolates. The seven HBV/F1 isolates (USF2573, JPF1130, JPNTAKA, PANAM5, PANAM6, VENEZ2, and VENEZ4) had the *bkf* serotype that was compatible with the preS2 serotype assigned to genotype F[5]. Although serotypes of the six reported HBV/F1 isolates were unknown, they all shared the amino acid sequence for the expression of *k* and *f* epitopes; their combination is characteristic of the preS2 serotype (*bkf*) for genotype F[5].

Unlike the 13 HBV/F1 isolates, all the 7 HBV/F2 isolates possessed G as amino acid 19, and therefore, would bind to the monoclonal antibody against *s*[5], for the expression of *bksf* serotype. Thus, the expression of preS2 epitope *s* would be able to differentiate between F2 and F1 subtypes. Taking the other genotypes into consideration, the combination of preS2 serotype of *bksf* with HBsAg serotype *adw* would be specific for HBV/F2, since that with HBsAg serotype *adr* occurs in HBV isolates of genotype C[5,6]. Hence, HBV/F2 can be serologically differentiated

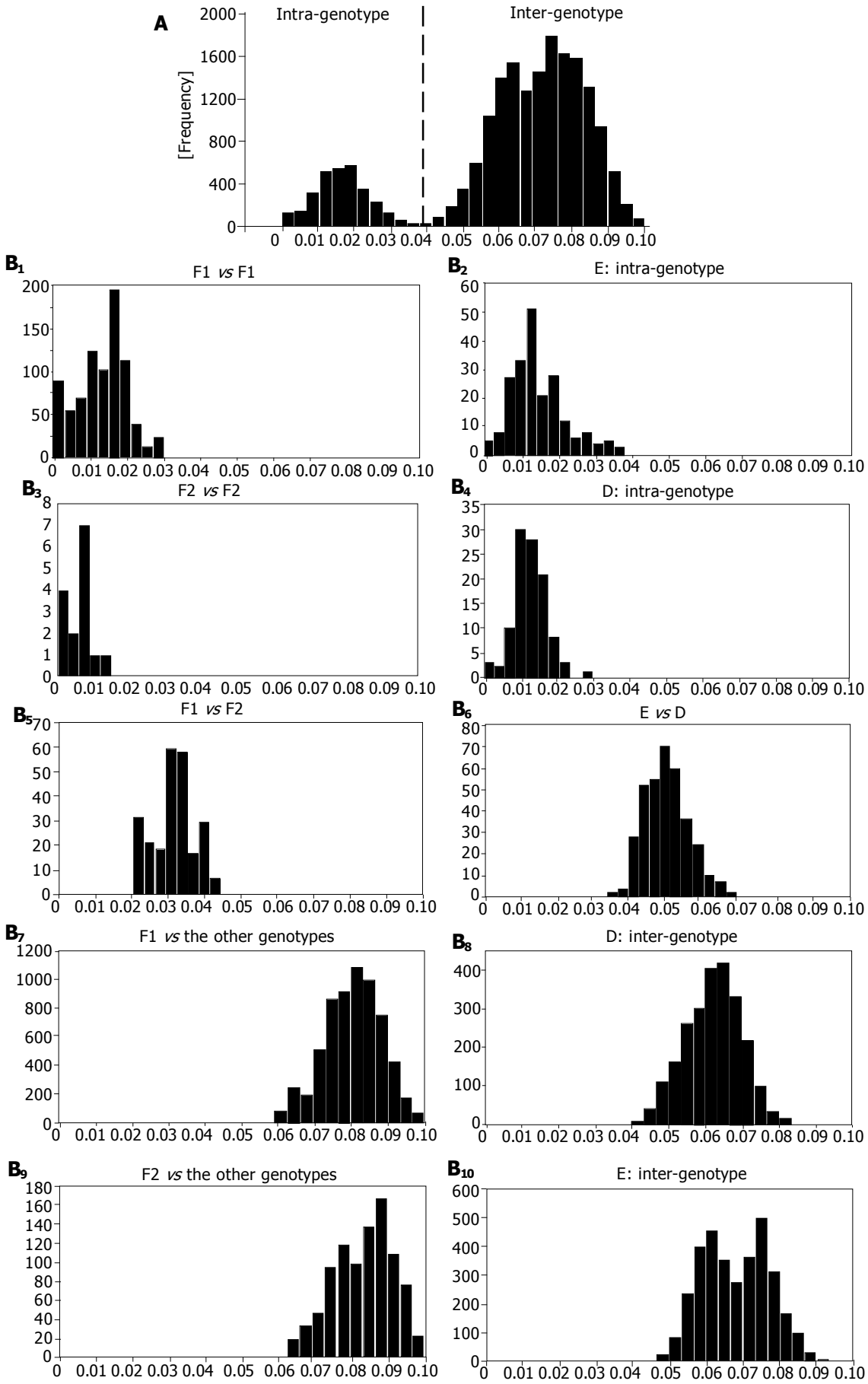


Figure 2 Pair-wise comparison of S-gene sequences. Distribution of genetic distance among HBV isolates of all genotypes (**A**) and that of HBV/F1, HBV/F2, HBV/D, HBV/E, each other and among themselves ($\mathbf{B}_{1\text{-}10}$). Joined in comparison were seven HBV/F2 isolates, 47 HBV/F1 isolates and 136 HBV isolates of the other genotypes. X-axis and y-axis indicate genetic distance and frequency, respectively.

from HBV/F1 as well as the other six genotypes (A-E and G).

DISCUSSION

Of the seven HBV genotypes (A-G), which are defined by a sequence divergence >8% in the entire genomic sequence, F is unique in that it is the remotest (>15%) from the other six genotypes (A-E and G)[2,12,13]. The origin of HBV/F is proposed in the New World, because it is frequent in Central and South America; F is the major HBV genotype in Venezuela and Argentina[15-19]. A remote genetic distance of genotype F from the other six genotypes mirrors the relationship between HBV of woolly monkeys in the New World and HBV species of major apes (orangutans, gibbons, gorillas, and chimpanzees) in the Old World (reviewed in Ref.[20]). Furthermore, human HBV of genotype F is closer to HBV of woolly monkeys than those of the other six genotypes (A-E and G). Combined, these lines of evidence would point to the co-evolution of human HBV of genotype F and HBV of woolly monkeys in the New World since the distant past, as well as their distinction, respectively, from those of the other six HBV genotypes and HBV species of great apes in the Old World.

Originally, four HBV genotypes (A-D) were proposed by sequence divergence in the entire genome >8%[1]. The four genotypes were followed by three others (E-G) defined by the same criterion[2,3]. In the present study, 11 HBV/F isolates were recovered from patients in San Francisco, Japan, Panama and Venezuela, and they were found to cluster into two groups of four (USF10, USF1122, USF1778 and USF2065) and 7 isolates (USF2573, JPF1130, JPNTAKA, PANAM5, PANAM6, VENEZ2, and VENEZ4) in the phylogenetical analysis on the full-length sequence. The 7 HBV/F isolates in 1 group nested on the same branch as reported 11 HBV/F isolates[2,4,12,13], and the remaining 4 flocked on the same branch as 3 isolates reported under the classification of genotype H [4]. The two groups of HBV isolates differed in the full-length sequence by only >7.3% (range: 9.5-7.3; mean: 8.4±0.6%) (IV).

The observed sequence difference of the seven HBV/F isolates, four in this study (USF10, USF1122, USF1778, and USF2065) and three reported (LAS2523, 1853Nic, and 2928Nic), from the others fell in short of clearing >8% separating the seven HBV genotypes, although two of them (USF10 and USF1122) cleared this margin. It has to be pointed out that the >8% distance was set arbitrarily in

Table 4 Homology in the entire nucleotide sequence of the seven HBV/F2 isolates to HBV/F1 isolates and among themselves

	F2 subtype (this study)				F2 subtype (reported)			F1 subtype (this study)						
	USF10	USF1122	USF1778	USF2065	1853Nic	2928Nic	LAS2523	USF2573	JPF1130	JPNTAKA	PANAM5	PANAM6	VENEZ2	VENEZ4
HBV/F1 isolates (reported)														
AB036905	**91.7**	**91.9**	92.3	92.6	92.3	92.7	92.5	94.6	94.1	93.6	99.2	97.9	99.0	94.7
AB036910	**91.7**	**91.9**	92.3	92.7	92.2	92.6	92.6	94.7	94.1	93.6	99.2	98.0	99.5	94.8
AB036920	**91.7**	**91.9**	92.2	92.5	92.2	92.7	92.5	94.6	94.0	93.6	99.1	97.8	98.8	94.7
X69798	**91.1**	**91.4**	**91.9**	92.2	**91.6**	92.1	92.2	94.3	93.9	93.6	96.2	95.2	96.1	94.5
X75659	**90.5**	**90.7**	**91.2**	**91.6**	**91.0**	**91.4**	**91.4**	93.6	92.9	92.6	95.4	94.3	95.5	93.7
X75663	**91.0**	**91.2**	**91.8**	92.2	**91.7**	92.1	**91.9**	94.0	93.3	92.8	97.2	96.0	97.6	94.1
AY090455	**91.0**	**91.1**	**91.5**	**91.9**	**91.4**	**91.9**	**91.9**	94.2	93.8	93.4	96.0	94.9	95.8	94.3
AY090458	**90.8**	**90.9**	**91.5**	92.0	**91.6**	**91.9**	**91.6**	97.9	97.3	96.9	94.9	93.8	94.9	98.1
AY090459	**90.8**	**90.8**	**91.5**	**91.9**	**91.6**	**91.9**	**91.5**	98.2	97.5	97.2	95.0	93.9	94.9	98.3
AY090461	**90.9**	**91.0**	**91.6**	92.0	**91.6**	**91.9**	**91.7**	98.1	97.5	97.1	95.0	93.9	94.8	98.3
HBV/F1 isolates (this study)														
USF2573	**91.0**	**91.1**	**91.6**	92.0	**91.8**	92.1	**91.8**	–	98.5	97.9	94.8	93.7	94.7	99.6
JPF1130	**90.7**	**90.6**	**91.3**	**91.5**	**91.3**	**91.6**	**91.3**	98.5	–	97.8	94.3	93.4	94.2	98.4
JPNTAKA	**90.5**	**90.5**	**91.1**	**91.3**	**91.0**	**91.3**	**91.1**	97.9	97.8	–	93.9	92.9	93.7	97.9
PANAM5	**91.9**	92.0	92.4	92.8	92.3	92.8	92.7	94.8	94.3	93.9	–	98.6	99.2	95.0
PANAM6	**91.1**	**91.2**	**91.7**	**91.7**	**91.4**	**91.9**	**91.7**	93.7	93.4	92.9	98.6	–	98.0	93.8
VENEZ2	**91.8**	**92.1**	92.5	92.8	92.3	92.8	92.7	94.7	94.2	93.7	99.2	98.0	–	94.9
VENEZ4	**91.1**	**91.2**	**91.7**	92.1	**91.9**	92.2	92.0	99.6	98.4	97.9	95.0	93.8	94.9	–
F2 isolates (this study)														
USF10	–	97.0	96.9	97.2	96.3	96.6	97.9	**91.0**	**90.7**	**90.5**	**91.9**	**91.1**	**91.8**	**91.1**
USF1122	97.0	–	97.1	97.6	96.5	96.9	98.2	**91.1**	**90.7**	**90.5**	92.0	**91.2**	92.1	**91.2**
USF1778	96.9	97.1	–	98.6	97.2	97.4	98.0	**91.6**	**91.3**	**91.1**	92.4	**91.7**	92.5	**91.7**
USF2065	97.2	97.6	98.6	–	97.6	97.8	98.4	92.0	**91.5**	**91.3**	92.8	**91.7**	92.8	92.1
F2 isolates (reported)														
1853Nic	96.3	96.5	97.2	97.6	–	99.2	97.5	**91.8**	**91.3**	**91.0**	92.3	**91.4**	92.3	**91.9**
2928Nic	96.6	96.9	97.4	97.8	99.2	–	97.7	92.1	**91.6**	**91.3**	92.8	**91.9**	92.8	92.2
LAS2523	97.9	98.2	98.0	98.4	97.5	97.7	–	**91.8**	**91.3**	**91.1**	92.7	**91.7**	92.7	92.0

Values less than 92, clearing genotype difference, are shown in boldface.

Table 5 Genotype- or subtype-specific nucleotides

HBV isolates	Genotype /subtype	Nucleotide positions																
		P gene																
		22	1 467	1 552	1 754	2 495	2 558	2 579	2 596	2 603	2 606	2 622	2 628	2 634	2 636	2 660	3 121	3 129
X70185	A	T	G	T	T	G	T	T	T	C	T	A	A	A	A	T	A	T
D00329	B	–	–	–	–	–	–	–	–	A	**C**	–	–	–	–	–	G	–
D50520	C	–	–	–	–	A	–	–	**A**	–	–	–	–	–	–	–	G	–
D23681	D	–	–	–	–	–	A	**C**	–	–	A	–	–	**C**	–	–	G	G
X75657	E	–	–	–	–	–	–	–	–	**T**	–	–	–	–	**C**	–	G	G
AB056515	G	–	–	–	C	–	**C**	A	–	–	–	–	–	–	–	**C**	G	G
X68798	F1	–	–	–	–	–	–	–	–	–	A	**T**	–	–	–	–	G	G
X75658	F1	–	–	–	C	–	–	A	–	–	A	**T**	–	–	–	–	G	G
X75663	F1	–	–	–	C	–	–	A	–	–	G	**T**	–	–	–	–	G	G
AB036905	F1	–	–	–	C	–	–	A	–	–	G	**T**	–	–	–	–	G	G
AB036910	F1	–	–	–	C	–	–	A	–	–	G	**T**	–	–	–	–	G	G
AB036920	F1	–	–	–	C	–	–	A	–	–	G	**T**	–	–	–	–	G	G
USF2573	F1	–	–	–	–	–	–	A	–	G	–	**T**	–	–	–	–	G	G
JPF1130	F1	–	–	–	–	–	–	A	–	–	–	**T**	–	–	–	–	G	G
JPNTAKA	F1	–	–	–	–	–	–	A	–	–	–	**T**	–	–	–	–	G	G
PANAM5	F1	–	–	–	C	–	–	A	–	–	G	**T**	–	–	–	–	G	G
PANAM6	F1	–	–	–	C	–	–	A	–	–	G	**T**	–	–	–	–	G	G
VENEZ2	F1	–	–	–	C	–	–	A	–	–	G	**T**	–	–	–	–	G	G
VENEZ4	F1	–	–	–	T	A	–	A	–	–	–	**T**	–	–	–	–	G	G
USF10	F2	**A**	**T**	**C**	**G**	**T**	–	A	–	–	A	–	**C**	–	–	–	**C**	**A**
USF1122	F2	**A**	**T**	**C**	**G**	**T**	–	A	–	–	A	–	**C**	–	–	–	**C**	**A**
USF1778	F2	**A**	**T**	**C**	**G**	**T**	–	A	–	–	A	–	**C**	–	–	–	**C**	**A**
USF2065	F2	**A**	**T**	**C**	**G**	**T**	–	A	–	–	A	–	**C**	–	–	–	**C**	**A**
AY090454	F2	**A**	**T**	**C**	**G**	**T**	–	A	–	–	A	G	**C**	–	–	–	**C**	**A**
AY090457	F2	**A**	**T**	**C**	**G**	**T**	–	A	–	–	A	G	**C**	–	–	–	**C**	**A**
AY090460	F2	**A**	**T**	**C**	**G**	**T**	–	A	–	–	A	–	**C**	–	–	-	**C**	**A**

Genotype- or subtype-specific nucleotides are shown in boldface, and a dash (–) indicates the nucleotide identical to that of X70185.

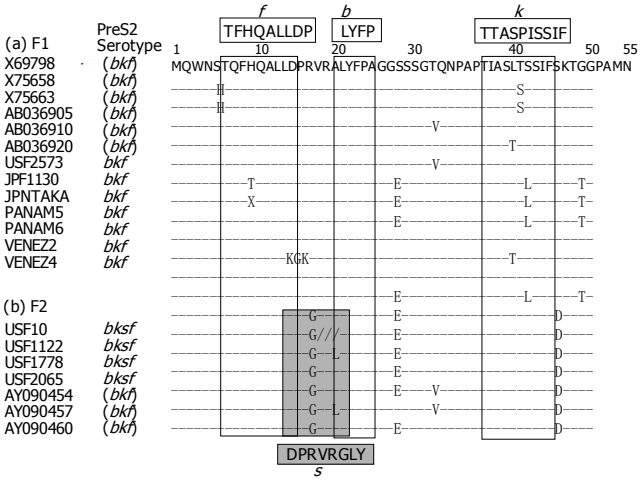


Figure 3 Amino acid sequences of the product of preS2 region of HBV/F isolates. Sequences are shown for the 13 HBV/F isolates of F1 subtype and the 7 of F2 subtype. Epitopes recognized by monoclonal antibodies, used for ELISA for the determination of serotypes[5,6], are shown above and below the nucleotide sequences in columns.

1988 when only a score of HBV isolates with the entire sequence known were available, and before genotype F came along[1]. Although the criterion has helped distinguishing the seven HBV genotypes, it may not be "the gold standard" in genotyping and would need to be modified as new developments arise.

In 1993, Simmonds and his colleagues performed an elegant analysis of HCV isolates by two-by-two comparison of a partial sequence of 222 bp[21]. They found them distribute in three clusters, thereby attesting to the three distinct orders of sequence divergence. They considered a cluster with the shortest evolutionary distance would represent isolate variation, another with a middle distance intra-subtypic variation and the other with the longest distance intra-typic variation. Based on their analysis, they constructed a hierarchical system to classify HCV into six types named by Arabic numbers, each of which breaks down into respective subtypes designated by lower-case alphabet letters. Their classification straightened out a big turmoil created by various nomenclature systems, and has become the standard of HCV genotypes.

The entire sequences of the seven HBV isolates including four in this study (USF10, USF1122, USF1778, and USF2065) and three reported (LAS2523, 1853Nic, and 2928Nic), differing by >7.3% from the other HBV/F isolates[2,12,13], were subjected to the classification method of Simmonds *et al.*[21], within the S-gene sequence (Figure 3). Just like HCV isolates, two clusters with different degrees of genetic distance (intra- and inter-genotypic heap) emerged in the comparison of S-gene sequences of the seven HBV isolates among themselves and against representatives of the seven HBV genotypes (A-G) (Figure 2B). Although the seven HBV isolates were separated from the other HBV/F isolates, they were closer to them than to any HBV isolates of the other six genotypes (A-E and G) in the S-gene sequence.

Bowyer and Sim[22] found ranges of genetic distance among isolates, subtypes and genotypes overlap in the S-gene sequence, thereby preventing distinction between them. In support of their findings, no clear differentiation between isolates and subtypes was observed in pairwise comparison of the S-gene sequence, while genotypes were clearly distinguished from isolates and subtypes (Figure 2A). When looking from HBV/F1 isolates, the genetic distance to HBV/F2 distributed within the intra-genotype range. Hence, it would be justified to classify the four isolates from San Francisco (USF10, USF1122, USF1778, and USF2065) and three reported (LAS2523, 1853Nic, and 2928Nic) into distinct subtypes rather than different genotypes.

On the basis of these analyses, and in hope of avoiding future confusion created by logging into an ever expanding alphabet list of HBV genotypes, four HBV isolates from San Francisco (USF10, USF1122, USF1778, and USF2065) and three reported (LAS2523, 1853Nic, and 2928Nic) would better be classified into subtypes of genotype F, rather than given an independent genotype. Accordingly, the seven variants of HBV/F (USF10, USF1122, USF1778, USF2065, LAS2523, 1853Nic, and 2928Nic) were classified into F2 subtype, while the former HBV/F isolates and the one from San Francisco (USF2573), two from Japan (JPF1130 and JPNTAKA), two from Panama (PANAM5 and PANAM6) and two from Venezuela (VENEZ2 and VENEZ4) into F1 subtype, provisionally. Mbayed *et al.*, have reported four clusters of HBV/F isolates by comparison of S-gene sequences[18,19]. F1 subtype covers Clusters I, II and IV, while F2 subtype corresponds to Cluster III in their classification. As the entire genomic sequences of HBV isolates accumulate, there may be HBV/F isolates that are closer to F1 and F2 than to any of the other six genotypes (A-E and G). They will be assigned F3 and F4 subtypes in the chronological order of sequence determination.

There is a possibility for distinguishing between F1 and F2 subtypes by serological means[5,6]. HBV/F2 isolates expressed a preS2 serotype of *bksf*, in contrast to that of *bkf* in HBV/F1 isolates. The combination of preS2 serotype of *bksf* with HBsAg serotype *adw* appears specific for HBV/F2, distinguishing it from HBV/F1 and the other six genotypes (A-E and G). Serological differentiation of HBV/F2 from HBV/F1 would facilitate their detection in epidemiological and clinical settings. It will allow easy evaluation of F1 and F2 subtypes for different virological virulence and disease-inducing capacity which have been reported for HBV genotypes[23-25].

In classifying microbes, one is tempted to be either a *lumper* who wants to put groups together in a simplified system or a *splitter* who likes to break down a clade into many. In classifying HBV genotypes, one may need to lump or split them as required, taking into considerations virological phylogeny and clinical relevance of each genotype or subtype[26,27]. For instance, there are two subtypes of genotype B, one of which has the recombination with genotype C in the precore region and core gene, while the other does not have it[28]. Because these two subtypes of genotype B influence the response to lamivudine in patients with chronic hepatitis B, they are clinically useful[29]. Our proposal for two subtypes of HBV genotype F based on phylogenetic analysis would be preferred to classifying them into genotypes F and H[4]. The method for serologically distinguishing between subtypes F1 and F2 would facilitate the evaluation of their differences, some of which may turn out to be clinically relevant.

ACKNOWLEDGMENTS

Dr. Masashi Mizokami was granted by Ministry of Health, Labour and Welfare of Japan (H13-kaken-2).

REFERENCES

1 **Okamoto H,** Tsuda F, Sakugawa H, Sastrosoewignjo RI, Imai M, Miyakawa Y, Mayumi M. Typing hepatitis B virus by homology in nucleotide sequence, comparison of surface antigen subtypes. *J Gen Virol* 1988; **69**: 2575–2583

2 **Norder H,** Courouce AM, Magnius LO. Complete genomes, phylogenetic relatedness, and structural proteins of six strains of the hepatitis B virus, four of which represent two new genotypes. *Virology* 1994; **198**: 489–503

3 **Stuyver L,** De Gendt S, Van Geyt C, Zoulim F, Fried M, Schinazi RF, Rossau R. A new genotype of hepatitis B virus: complete genome and phylogenetic relatedness. *J Gen Virol* 2000; **81**: 67–74

4 **Arauz-Ruiz P,** Norder H, Robertson BH, Magnius LO. Genotype H, a new Amerindian genotype of hepatitis B virus revealed in Central America. *J Gen Virol* 2002; **83**: 2059-2073

5 **Usuda S,** Okamoto H, Iwanari H, Baba K, Tsuda F, Miyakawa Y, Mayumi M. Serological detection of hepatitis B virus genotypes by ELISA with monoclonal antibodies to type-specific epitopes in the preS2-region product. *J Virol Methods* 1999; **80**: 97–112

6 **Usuda S,** Okamoto H, Tanaka T, Kidd-Ljunggren K, Holland PV, Miyakawa Y, Mayumi M. Differentiation of hepatitis B virus genotypes D and E by ELISA using monoclonal antibodies to epitopes on the preS2-region product. *J Virol Methods* 2000; **87**: 81–89

7 **Kato H,** Orito E, Sugauchi F, Ueda R, Gish RG, Usuda S, Miyakawa Y, Mizokami M. Determination of hepatitis B virus genotype G by polymerase chain reaction with hemi-nested primers. *J Virol Methods* 2001; **98**: 153–159

8 **Gojobori T,** Ishii K, Nei, M. Estimation of average number of nucleotide substitutions when the rate of substitution varies with nucleotide. *J Mol Evol* 1982; **18**: 414–423

9 **Saitou N,** Nei M. The neighbor-joining method: a new method for reconstructing phylogenetic trees. *Mol Biol Evol* 1987; **4**: 406–425

10 **Felsenstein J.** Confidence limits on phylogenesis, an approach using the bootstrap. *Evolution* 1985; **39**: 783–791

11 **Ina Y.** ODEN: a program package for molecular evolutionary analysis and database search of DNA and amino acid sequences. *Comput Appl Biosci* 1994; **10**: 11–12

12 **Naumann H,** Schaefer S, Yoshida CF, Gaspar AM, Repp R, Gerlich WH: Identification of a new hepatitis B virus (HBV) genotype from Brazil that expresses HBV surface antigen subtype adw4. *J Gen Virol* 1993; **74**: 1627–1632

13 **Nakano T,** Lu L, Hu X, Mizokami M, Orito E, Shapiro C, Hadler S, Robertson B: Characterization of hepatitis B virus genotypes among Yucpa Indians in Venezuela. *J Gen Virol* 2001; **82**: 359–365

14 **Okamoto H,** Imai M, Tsuda F, Tanaka T, Miyakawa Y, Mayumi M: Point mutation in the S gene of hepatitis B virus for a d/y or w/r subtypic change in two blood donors carrying a surface antigen of compound subtype adyr or adwr. *J Virol* 1987; **61**: 3030–3034

15 **Arauz-Ruiz P,** Norder H, Visona KA, Magnius LO: Genotype F prevails in HBV infected patients of hispanic origin in Central America and may carry the precore stop mutant. *J Med Virol* 1997; **51**: 305–312

16 **Arauz-Ruiz P,** Norder H, Visona KA, Magnius LO: Molecular epidemiology of hepatitis B virus in Central America reflected in the genetic variability of the small S gene. *J Infect Dis* 1997; **176**: 851–858
17 **Blitz L,** Pujol FH, Swenson PD, Porto L, Atencio R, Araujo M, Costa L, Monsalve DC, Torres JR, Fields HA, Lambert S, Van Geyt C, Norder H, Magnius LO, Echevarria JM, Stuyver L: Antigenic diversity of hepatitis B virus strains of genotype F in Amerindians and other population groups from Venezuela. *J Clin Microbiol* 19981; **36**: 648–651
18 **Mbayed VA,** Lopez JL, Telenta PF, Palacios G, Badia I, Ferro A, Galoppo C, Campos R: Distribution of hepatitis B virus genotypes in two different pediatric populations from Argentina. *J Clin Microbiol* 1998; **36**: 3362–3365
19 **Mbayed VA,** Barbini L, Lopez JL, Campos RH: Phylogenetic analysis of the hepatitis B virus (HBV) genotype F including Argentine isolates. *Arch Virol* 2001; **146**: 1803–1810
20 **Robertson BH,** Margolis HS. Primate hepatitis B viruses – genetic diversity, geography and evolution. *Rev Med Virol* 2002; **12**: 133–141
21 **Simmonds P,** Holmes EC, Cha TA, Chan SW, McOmish F, Irvine B, Beall E, Yap PL, Kolberg J, Urdea MS. Classification of hepatitis C virus into six major genotypes and a series of subtypes by phylogenetic analysis of the NS-5 region. *J Gen Virol* 1993; **74**: 2391–2399
22 **Bowyer SM,** Sim JG. Relationships within and between genotypes of hepatitis B virus at points across the genome, footprints of recombination in certain isolates. *J Gen Virol* 2000; **81**: 379–392
23 **Mayerat PC,** Mantegani A, Frei C. Does hepatitis B virus (HBV) genotype influence the clinical outcome of HBV infection? *J Viral Hepatitis* 1999; **6**: 299–304
24 **Kao JH,** Chen PJ, Lai MY, Chen DS. Hepatitis B genotypes correlate with clinical outcomes in patients with chronic hepatitis B. *Gastroenterology* 2000; **118**: 554–559
25 **Orito E,** Mizokami M, Sakugawa H, Michitaka K, Ishikawa K, Ichida T, Okanoue T, Yotsuyanagi H, Iino S. A case-control study for clinical and molecular biological differences between hepatitis B viruses of genotypes B and C. Japan HBV Genotype Research Group. *Hepatology* 2001; **33**: 218–223
26 **Miyakawa Y,** Mizokami M. Classifying hepatitis B virus genotypes. *Intervirology* 2003; **46**: 329-338
27 **Sugauchi F,** Orito E, Ichida T, Kato H, Sakugawa H, Kakumu S, Ishida T, Chutaputti A, Lai CL, Gish RG, Ueda R, Miyakawa Y, Mizokami M. Epidemiologic and virologic characteristics of hepatitis B virus genotype B having the recombination with genotype C. *Gastroenterology* 2003; **124**: 925-932
28 **Sugauchi F,** Orito E, Ichida T, Kato H, Sakugawa H, Kakumu S, Ishida T, Chutaputti A, Lai CL, Ueda R, Miyakawa Y, Mizokami M. Hepatitis B virus of genotype B with or without recombination with genotype C over the precore region plus the core gene. *J Virol* 2002; **76**: 5985-5992
29 **Akuta N,** Suzuki F, Kobayashi M, Tsubota A, Suzuki Y, Hosaka T, Someya T, Kobayashi M, Saitoh S, Arase Y, Ikeda K, Kumada H. The influence of hepatitis B virus genotype on the development of lamivudine resistance during long-term treatment. *J Hepatol* 2003; **38**: 315-321

Science Editor Guo SY **Language Editor** Elsevier HK

PO Box 2345, Beijing 100023, China
www.wjgnet.com
wjg@wjgnet.com

ELSEVIER

World J Gastroenterol 2005;11(40):6305-6311
World Journal of Gastroenterology ISSN 1007-9327
© 2005 The WJG Press and Elsevier Inc. All rights reserved.

Interleukin-17 levels in *Helicobacter pylori*-infected gastric mucosa and pathologic sequelae of colonization

Tomokazu Mizuno, Takafumi Ando, Kazuo Nobata, Tomoyuki Tsuzuki, Osamu Maeda, Osamu Watanabe, Masaaki Minami, Kenji Ina, Kazuo Kusugami, Richard M. Peek, Hidemi Goto

Tomokazu Mizuno, Takafumi Ando, Masaaki Minami, Osamu Watanabe, Kazuo Nobata, Tomoyuki Tsuzuki, Osamu Maeda, Kenji Ina, Kazuo Kusugami, Hidemi Goto, Department of Gastroenterology, Nagoya University Graduate School of Medicine, Nagoya, Japan
Richard M. Peek, Division of Gastroenterology, Departments of Medicine and Cancer Biology, Vanderbilt University School of Medicine, Nashville, Tennessee, United States
Correspondence to: Dr. Takafumi Ando, Department of Gastroenterology, Nagoya University Graduate School of Medicine, 65 Tsurumai-cho, Showa-ku, Nagoya 466-8550, Japan. takafumia-gi@umin.ac.jp
Telephone: +81-52-7442144 Fax: +81-52-7442175
Received: 2004-12-30 Accepted: 2005-02-18

Abstract

AIM: To determine the role of interleukin (IL)-17 in gastric ulcerogenesis.

METHODS: Thirty-six gastric ulcer (GU) patients and 29 non-ulcer (NU) patients were enrolled in this study. Mucosal biopsy samples were obtained from the gastric antrum and GU site during endoscopy. Samples were used in *in situ* stimulation for 48 h in the presence of 10 μg/mL phytohemagglutinin-P (PHA), histological examination, and *Helicobacter pylori* (*H pylori*) culture. IL-17 and IL-8 protein levels in culture supernatants were assayed by ELISA. IL-17 mRNA expression was analyzed by reverse transcriptase-polymerase chain reaction (RT-PCR). *H pylori cagA* and *vacA* status was assessed by reverse hybridization using a line probe assay (LiPA). IL-8 levels in culture supernatants were assayed after AGS cells were co-cultured with *H pylori* strain 26 695 or recombinant human (rh) IL-17.

RESULTS: All 36 GU patients and 15 of 29 NU patients were found to be *H pylori*-positive, while 14 NU patients were *H pylori*-negative. All 51 *H pylori* strains from both GU and NU patients were *cagA*- and *vacA*s1/m1-positive. Antral mucosal tissues from *H pylori*-positive patients contained significantly (*H pylori*-positive NU patients: median 467 pg/mg/protein, range 53-2 499; *H pylori*-negative NU patients: median 104 pg/mg/protein, range 16-312, $P<0.0005$) higher levels of IL-17 than those from uninfected patients. IL-17 levels at the ulcer site were significantly (ulcer site: median 1 356 pg/mg/protein, range 121-1 3730; antrum: median 761 pg/mg/protein, range 24-7 620, $P<0.005$) higher than those at distant sites in the antrum. Biopsies from *H pylori*-positive GU and NU patients showed IL-17 mRNA expression in all samples whereas those from the antrum of the *H pylori*-negative controls showed no detectable expression. A significant correlation was seen between IL-17 and IL-8 levels at each biopsy site (ulcer: $r = 0.62$, $P<0.0001$; antrum: $r = 0.61$, $P<0.0001$) in GU patients. RhIL-17 and *H pylori* strain 26 695 each stimulated IL-8 production from AGS cells.

CONCLUSION: IL-17 may play an important role in the inflammatory response to *H pylori* colonization, and may ultimately influence the outcome of *H pylori*-associated diseases that arise within the context of gastritis.

© 2005 The WJG Press and Elsevier Inc. All rights reserved.

Key words: *Helicobacter pylori*; Gastric ulcer; Histological gastritis; Interleukin-17; Interleukin-8

Mizuno T, Ando T, Nobata K, Tsuzuki T, Maeda O, Watanabe O, Minami M, Ina K, Kusugami K, Peek RM, Goto H. Interleukin-17 levels in *Helicobacter pylori*-infected gastric mucosa and pathologic sequelae of colonization. *World J Gastroenterol* 2005; 11(40): 6305-6311
http://www.wjgnet.com/1007-9327/11/6305.asp

INTRODUCTION

Helicobacter pylori (*H pylori*), a microaerophilic, Gram-negative bacterium that selectively colonizes the human stomach, is the major cause of chronic active gastritis and peptic ulcer disease[1-3]. In *H pylori* infection, neutrophils are present within epithelial glands and the underlying lamina propria, and an increase in chronic inflammatory cells such as lymphocytes, macrophages, eosinophils, and plasma cells is also found in the lamina propria[4-8]. Recent studies have shown that *H pylori* produces various cytokines that are related to neutrophil or mononuclear cell accumulation, such as interleukin-β (IL-1β), interferon (IFN)-γ, IL-6, IL-8, tumor necrosis factor (TNF)-α and MIP-1α[7-10]. Among these cytokines, IL-8, the major human PMN chemoattractant, plays an important role in *H pylori*-associated acute inflammatory responses[7,8,11]. IL-8 mRNA has been detected in the vast majority of antral biopsy tissues from *H pylori*-positive patients[8], indicating that *H pylori*-infected gastric mucosa is an active site of IL-8 synthesis. It was reported that IL-8 activity increases at ulcer sites[12], a finding which may be important to gastric ulcerogenesis.

IL-17, originally identified as cytotoxic T lymphocyte-associated antigen 8 (CTLA-8)[13], is a proinflammatory cytokine derived mainly from activated T cells[14-16]. A number of recently discovered related molecules form a family of

cytokines, the IL-17 family, and have been designated as IL-17A-F, with the prototype member being IL-17A[13,17-22]. IL-17A is produced exclusively by $CD4^+$ activated T cells[13,23], and more specifically by $CD4^+CD45RO^+$ memory T cells[18,24]. The human IL-17A gene product is a protein of 155 amino acids with a molecular weight of 20-30 ku which is secreted as a disulfide-linked homodimer of a 30-35-ku glycoprotein[25,26]. IL-17 stimulates IL-8 release by gastric epithelial cells and facilitates the chemotaxis of neutrophils through an IL-8-dependent mechanism, and contributes to the enhancement of IL-8 levels in *H pylori*-colonized gastric mucosa[27].

Recently, several *H pylori* genes related to an increased risk of disease have been identified[28]. The cytotoxin-associated gene (*cagA*) is a marker for the *cag* island, the presence of which is associated with a more severe clinical outcome[29-32]. *vacA* encodes a protein that induces vacuoles in epithelial cells[33]. *vacA* is present in all *H pylori* strains and contains at least two variable regions[34]. The s-region (encoding the signal peptide) exists as a s1 (including s1a, s1b, and s1c) or a s2 allelic type[35], while the m-region (middle) occurs as a m1 or a m2 allelic type. It was reported that *vacA*s1/m1 *H pylori* strains are more strongly associated with disease than *cagA*-negative *vacA*s2/m2 strains[36,37]. The evaluation of these genes is therefore an essential part of any investigation into the association between *H pylori* infection and pathogenesis.

In view of evidence that the eradication of *H pylori* reduces the risk of peptic ulcer recurrence[38] and ameliorates associated gastric inflammatory changes and chemokine production in the background gastric mucosa[7,8], clarification of the pathogenesis of *H pylori*-positive peptic ulcer disease requires an understanding of the host inflammatory response to this pathogen. We hypothesized that IL-17 secreted at the ulcer site might play a role in ulcerogenesis through the mucosal damage caused by the emigration and activation of various inflammatory effector cells together with IL-8. In the present study, we examined the secretion of IL-17 and expression of IL-17 mRNA using biopsy specimens from the ulcer site in 36 gastric ulcer (GU) patients with *H pylori* infection, and compared results to the severity of gastritis and IL-8 levels.

MATERIALS AND METHODS

Study groups and mucosal biopsy samples

Mucosal biopsy samples were obtained from the gastric antrum and ulcer site in 36 patients with GU, 15 with *H pylori* infection but without ulcers and 14 without either *H pylori* infection or ulcers whose conditions were diagnosed during upper gastroduodenal endoscopic examination in Nagoya University Hospital from October 2001 to January 2002 (Table 1). Thirteen patients had an active open ulcer and 23 had ulcer scaring. None of the patients took non-steroidal anti-inflammatory drugs, antibiotics or bismuth compounds during the preceding 3 mo. Six antral specimens were taken from adjacent areas of endoscopically intact mucosa in the GU and control patients, with one for bacterial culture, and rapid urease test (CLO test; Delta West, Bentley, Australia) and histological examination, and three for *in vitro* organ cultures for IL-17 and IL-8 measurement. Four additional specimens were taken from the margin of the open ulcer or the center of the ulcer scar in GU patients, one for histological examination and three for IL-17 and IL-8 measurement. All samples were obtained under informed consent in accordance with the Helsinki Declaration. *H pylori* infection was confirmed by positive results in at least two of four diagnostic methods, namely bacterial culture, rapid urease test, [^{13}C]-urea breath test and identification of the organism on tissue sections (Giemsa stain). The absence of infection was defined by a negative result in all the four tests.

Table 1 Characteristics of study groups (mean±SD)

	Patients (*n*)	Sex (male/female)	Age (yr)
GU	36	27/9	57.8±8.4
H pylori-positive			
Open ulcer	13	12/1	56.5±9.5
Ulcer scar	23	15/8	58.5±7.8
NU	29	17/12	47.1±15.6
H pylori-positive	15	10/5	49.8±18.9
H pylori-negative	14	7/7	44.1±11.0
Total	65	44/21	53.0±13.2

Organ culture

Mucosal biopsy tissues were weighed and cultured in a 50 mL/L CO_2 incubator for 48 h on a culture insert (Falcon, Oxnard, CA, USA) placed over polystyrene plates (Falcon) containing RPMI 1640 (Life Technologies, Inc., Rockville, MD, USA) medium with 5% heat-inactivated fetal calf serum, 15 mmol/L HEPES buffer, 100 U/mL of penicillin-G, and 100 μg/mL of streptomycin (culture medium) under the conditions of 10 μg/mL of phytohemagglutinin-P (PHA; Sigma Chemical Co., St. Louis, MO, USA). At the end of the culture period the supernatants were collected and kept at -70 ℃ until assayed for IL-17 and IL-8 levels. Total protein in biopsy homogenates was assayed by a modification of the Lowry method.

Histology

In accordance with the updated Sydney system[6], activity (neutrophil infiltration), inflammation (mononuclear cell infiltration), glandular atrophy and intestinal metaplasia and *H pylori* density were assessed on a four-grade scale of 0, 1, 2, and 3 (corresponding to none, mild, moderate, and severe in the Sydney system) using tissue sections stained with hematoxylin-eosin and those stained with Giemsa. In addition, the numbers of neutrophils and mononuclear cells infiltrating the lamina propria were counted in five high-power fields (×200 magnification). Respective numbers were classified into four grades of 0, 1, 2, and 3. All histologic evaluations were conducted without the knowledge of *H pylori* status or experimental results.

Cell cultures

AGS human gastric epithelial cells (American Type Culture Collection CRL 1739) were grown in RPMI 1640 supplemented with 10% fetal bovine serum (FBS) and

gentamicin 20 μg/mL in an atmosphere of 50 mL/L CO_2 at 37 ℃. For coculture experiments, *H pylori* was grown in brucella broth with 5% FBS for 48 h. Cells were harvested by centrifugation (2 000 r/min) and resuspended in antibiotic-free RPMI 1640 with 10% FBS to yield a final concentration of 10^9 CFU/mL. *H pylori* was added to AGS cells at a bacteria/cell ratio of 1 000:1 for the IL-8 assay. Experiments were performed in antibiotic-free medium with 10% FBS using T-150 flasks (Corning Costar, Cambridge, MS, USA) or 6-well polypropylene tissue culture plates (Becton Dickinson, Franklin Lakes, NJ, USA).

IL-17 and IL-8 assay

IL-17 and IL-8 protein levels in culture supernatants were assayed in duplicate using ELISA kits specific for IL-17 (R&D Systems, Minneapolis, MN, USA) and IL-8 (Biosource International, Camarillo, CA, USA) according to the manufacturer's instructions. In these assays, the lower limits of detection were 15 pg/mL for IL-17 and <5.0 pg/mL for IL-8. The amount of IL-17 and IL-8 in the organ cultures was expressed relative to protein content in the homogenate of biopsy tissues (IL-17, pg/mg protein; IL-8, ng/mg protein).

Extraction of RNA and RT-PCR amplification for human IL-17 mRNA

RNA was extracted from freshly obtained biopsy tissue by the acid guanidinium thiocyanate-phenol-chloroform method[41]. As a positive control, RNA was also extracted from peripheral blood mononuclear cells (PBMC) stimulated with PHA for 3 h. Two micrograms of extracted RNA was reverse-transcribed into first-stand complementary DNA (cDNA) at 42 ℃ for 1 h using 0.5 μL of Rous-associated virus 2 reverse-transcriptase (Takara Biomedicals, Ohtsu, Japan) and 0.1 μmol/L of oligo d(T) (Amersham Pharmacia Biotech, UK) in a 50-μL reaction mixture. Twenty-five microliters of cDNA from samples was amplified with 0.2 μmol/L of the sense and anti-sense primers for β-actin or IL-17 in a 100 μL reaction mixture containing 0.5 μL of Taq polymerase (Promega Corporation, Madison, WI, USA) for 35 cycles of denaturation at 94 ℃ for 1 min, annealing at 55 ℃ for 1 min, and extension at 72 ℃ for 2 min in a DNA thermal cycler (Perkin Elmer Cetus, Norwalk, CO, USA). PCR primers were as follows: β-actin, 5'-GTG GGG CGC CCC AGG CAC CA-3' and 5'-CTC CTT AAT GTC ACG CAG GAT TTC-3'[42], and IL-17, 5'-AGA GAT ATC CCT CTG TG ATC-3' and 5'-TAC CCC AAA GTT ATC TCA -3'[43]. Negative controls for PCR amplification were prepared by omitting the cDNA sample from the reaction mixture. The amplified products were subjected to electrophoresis in an 1.5% agarose gel containing ethidium bromide and visualized by UV transillumination.

Assessment of H pylori cagA and vacA status

A chloroform-phenol extraction method was used to obtain DNA from the *H pylori* isolates as previously described[44]. *cagA* and *vacA* status was assessed by reverse hybridization using a line probe assay (LiPA)[45].

Statistical analysis

Statistical analysis was performed using the Mann-Whitney *U* and paired tests and linear regression analysis. The results were expressed as mean±SD. $P<0.05$ was considered statistically significant.

RESULTS

Mucosal IL-17 and IL-8 levels

Mucosal IL-17 (Figure 1A) and IL-8 (Figure 1B) levels were determined using *in vitro* organ cultures of mucosal tissues taken from the gastric antrum and ulcer site of 36 patients with GU and from the gastric antrum of 29 patients with non-ulcer (NU) under PHA stimulation. Among the 36 GU patients, the ulcer was located in the corpus in 27 and in the antrum in 9. Culture supernatants contained measurable levels of IL-17 and IL-8 in both *H pylori*-positive and -negative subjects. IL-17 levels were significantly higher in antral mucosal tissues from GU (median 761 pg/mg protein, range 24-7 620: $P<0.0001$) and *H pylori*-positive NU patients (median 467 pg/mg protein, range 53-2 499: $P<0.0005$) than in those from *H pylori*-negative NU patients (median 104 pg/mg protein, range 16-312). There was no significant difference in IL-17 levels in the supernatants of antral gastric tissue between GU and *H pylori*-positive NU patients. Levels were significantly higher in mucosal tissues from the ulcer site of GU patients (median 1 356, range 121-13 730) than in those from the antrum of any patient group, including GU patients themselves (median 466, range 24-7620: $P<0.05$, Figure 1A). IL-8 levels were significantly higher in mucosal tissues of the antrum from GU (median 30 ng/mg protein, range 3-261: $P<0.0001$) and *H pylori*-positive NU patients (median 38 ng/mg protein, range 7-107: $P<0.0005$)

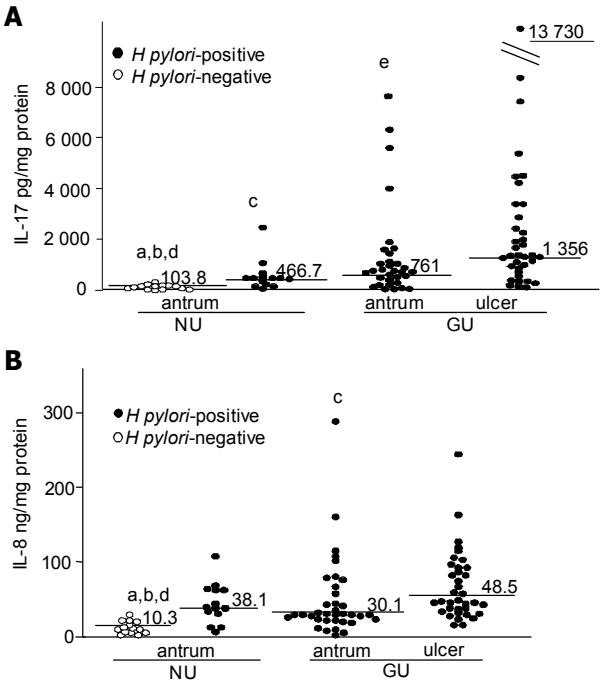


Figure 1 Levels of IL-17 (**A**) and IL-8 (**B**) secreted in organ cultures of biopsies from *H pylori*-positive (closed circle) and -negative (open circle) patients. The bar indicates the median value for each group. **A**: [a]$P<0.0005$ a *vs* b, [b]$P<0.0001$ a *vs* c, [c]$P<0.0005$ b *vs* c, [d]$P<0.0001$ a *vs* d, [e]$P<0.0005$ c *vs* d; **B**: [a]$P<0.0005$ a *vs* b, [b]$P<0.0001$ a *vs* c, [c]$P<0.0005$ a *vs* d, [d]$P<0.0001$ a *vs* d (NS:not significant).

than in those from *H pylori*-negative NU patients (median 10 ng/mg protein, range 1-22). There was no significant difference in IL-8 levels in the supernatant of gastric tissue from the antrum between GU and *H pylori*-positive NU patients. Levels were also significantly higher in mucosal tissues of the ulcer site of GU patients (median 49, range 15-164) than in those from the antrum of any patient group, including GU patients themselves (median 30, range 1-161: $P<0.05$, Figure 1B). There was a significant relationship between IL-17 and IL-8 levels in both antrum ($r = 0.61$, $P<0.0001$, Figure 2A) and ulcer site ($r = 0.62$, $P<0.001$, Figure 2B). With regard to ulcer stage in GU patients, there was no significant difference in IL-17 and IL-8 levels between samples from open ulcers (Figure 3A) and ulcer scars (Figure 3B).

Cytokine levels and histological findings

The association between cytokine levels and histological findings was investigated by comparing levels of IL-17 and IL-8 secretion *in vitro* with the severity of gastritis (activity, inflammation, atrophy, and metaplasia). A significant association was identified between IL-17 and IL-8 levels and the histological degree of activity and inflammation, but IL-17 and IL-8 levels were not associated with the degree of glandular atrophy or intestinal metaplasia (data not shown). The association was further investigated by quantifying the number of infiltrating neutrophils and mononuclear cells. In the antrum, IL-17 showed a stronger association ($r = 0.55$, $P<0.0001$) with the number of infiltrating mononuclear cells than IL-8 ($r = 0.45$, $P<0.0005$), whereas IL-17 ($r = 0.51$, $P<0.0001$) and IL-8 ($r = 0.54$, $P<0.0001$) showed a similarly strong association with the number of neutrophils. At the ulcer site, IL-17 had a stronger correlation with mononuclear cells (IL-17: $r = 0.64$, $P<0.0001$; IL-8: $r = 0.38$, $P = 0.012$, Figures 4A and B) and neutrophils (IL-17: $r = 0.74$, $P<0.0001$; IL-8: $r = 0.44$, $P = 0.078$) than IL-8 (Figures 4C and D).

IL-17 mRNA expression

The potential of gastric mucosa to synthesize IL-17 was studied by RT-PCR analysis using biopsy specimens from the ulcer sites and antrum of 5 *H pylori*-positive GU patients, and from the antrum of 5 *H pylori*-positive and 5 *H pylori*-negative NU patients. Consistent with the enhanced activity of IL-17 identified in organ cultures, all fresh biopsy specimens from the ulcer sites and antrum of *H pylori*-positive GU or NU patients had detectable IL-17 mRNA expression (IL-17: GU patients; ulcer sites 5/5, antrum 5/5, NU patients; antrum 5/5) (Figure 5). In contrast, IL-17 transcripts were not detected in any of the 5 *H pylori*-negative NU patients.

Effect of IL-17 on IL-8 production in AGS cells

To further investigate the role of IL-17 in the induction of IL-8 in gastric mucosa, we tested the effect of recombinant human (rh) IL-17 on the secretion of IL-8 by AGS cells (Figure 6). Stimulation of AGS cells cultured with graded doses of rhIL-17 at 1, 10 or 100 ng/mL for 24 h was followed by a dose-dependent increase in IL-8 secretion as measured by ELISA compared to unstimulated cell culture

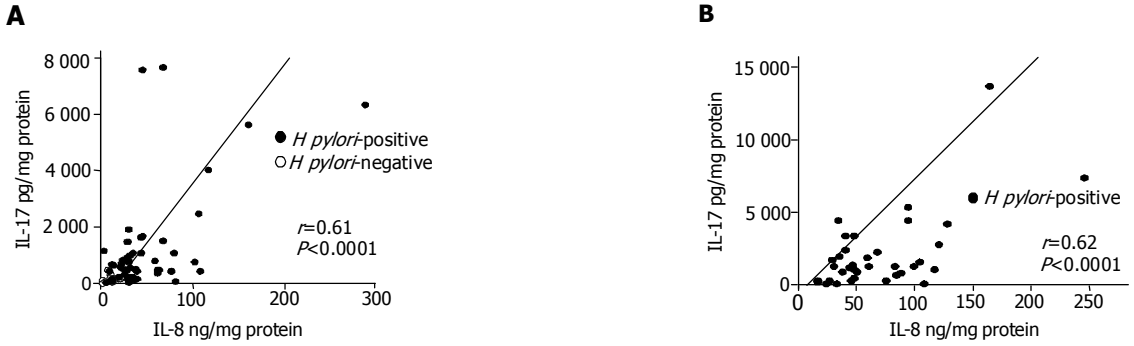


Figure 2 Relationship between IL-17 and IL-8 levels in biopsy culture supernatants from antrum (**A**) and ulcer site (**B**). The bar indicates the median value for each group.

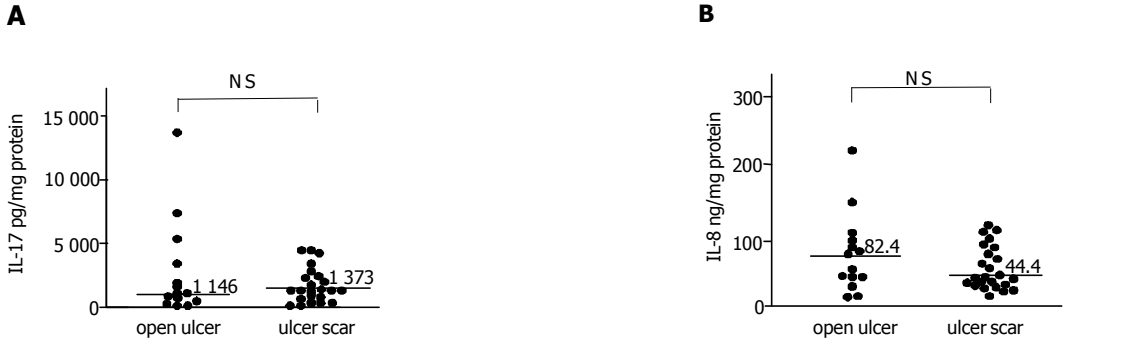


Figure 3 IL-17 (**A**) and IL-8 (**B**) levels in biopsy culture supernatants of GU patients according to ulcer stage.

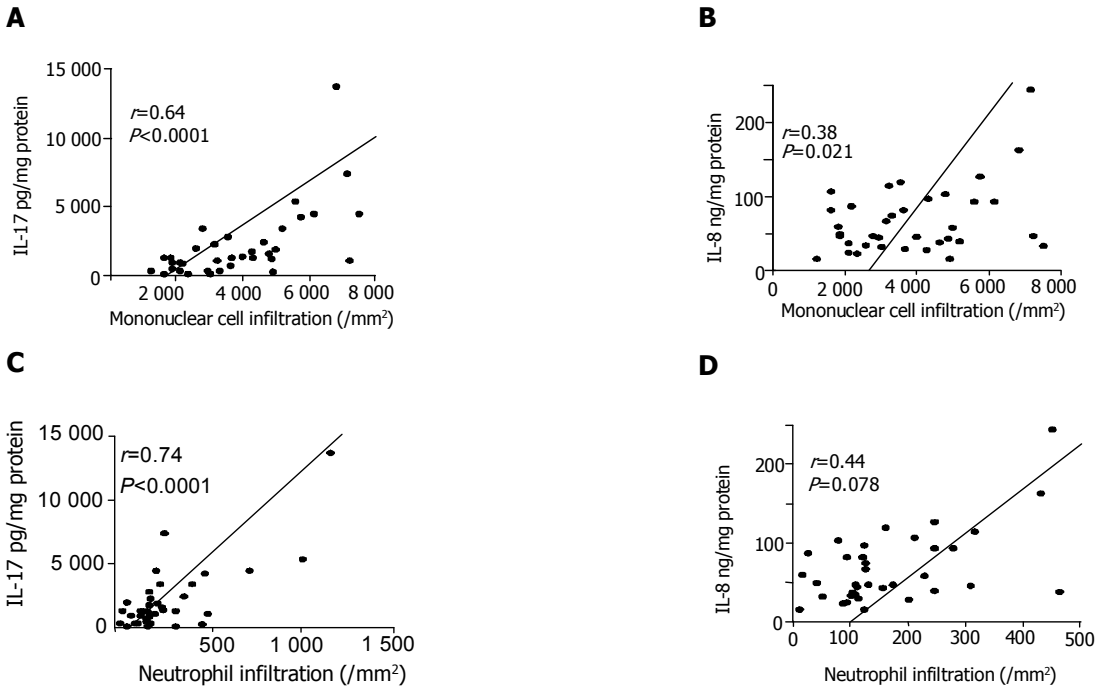


Figure 4 Relationship between IL-17 (**A** and **C**) or IL-8 (**B** and **D**) levels and mononuclear cell infiltration or neutrophil infiltration at ulcer sites.

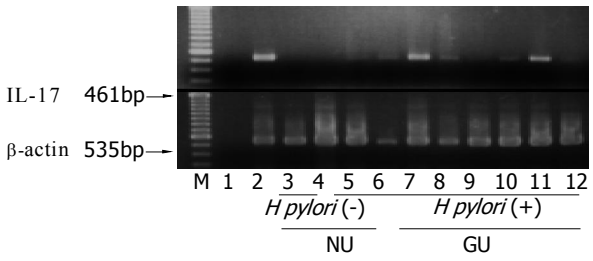


Figure 5 RT-PCR analysis of IL-17 and β-actin mRNA. M: 100-bp ladder marker; lane 1: negative (no cDNA sample); lane 2: positive control (PBMC stimulated by PHA for 3 h); lanes 3 and 4: antral biopsies from *H pylori*-negative NU patients with endoscopically normal mucosa; lanes 5 and 6: antral biopsies from *H pylori*-positive NU patients with gastritis; lanes 7, 9, and 11: antral biopsies from *H pylori*-positive GU patients; lanes 8, 10, and 12: mucosal biopsies from the ulcer site of *H pylori*-positive GU patients.

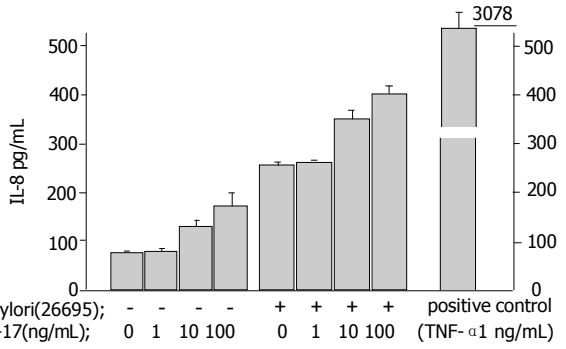


Figure 6 IL-8 levels in culture supernatants of AGS cells co-cultured with graded doses of rhIL-17, *H pylori* strain 26 695, or both.

supernatants. The addition of *H pylori* strain 26 695 to the cell culture at any concentration of rhIL-17 produced a further increase in IL-8 production.

Assessment of H pylori cagA and vacA status

Determination of genotype of *H pylori* strains isolated from GU and NU patients by LiPA confirmed that all 51 strains (GU, n = 36; NU, n = 15) were *cagA*-positive *vacA*s1/m1 (Table 2). Most strains were *vacA* subtype s1c, while the rest were *vacA* s1a. Thus, GU and NU patients had a similar *cagA* and *vacA*s1/m1 status.

DISCUSSION

On the basis of previous findings that IL-8 production increases at the ulcer site in patients with GU[12] and that IL-17 has the ability to stimulate IL-8 production in both epithelial cells[27] and fibroblasts[22], we investigated the production of IL-17 at ulcer and exogenous NU sites in GU patients. Among 36 GU patients, the ulcer was located in the corpus in 27 and in the antrum in 9. In preliminary studies to determine the site of biopsy for IL-17 measurement, IL-17 production in the antrum, corpus, and ulcer site was compared in 10 patients (5 GU and 5 gastritis). Because specimens from the corpus and the antrum showed no significant difference in IL-17 production (data not shown), specimens for comparison to the ulcer site were limited to the antrum to reduce the number of gastric biopsies. Our results show that IL-17 and IL-8 activities in organ cultures of biopsy specimens from the antrum are substantially higher in *H pylori*-positive patients than in *H pylori* -negative patients, and that among *H pylori*-infected GU patients, the gastric mucosa at the ulcer sites contains significantly more IL-17 and IL-8 than the mucosa of the antrum.

Further, IL-17 and IL-8 levels were significantly correlated with the number of infiltrating mononuclear cells

Table 2 *H pylori cagA* and *vacA* gene status

		cagA status		*vacA* status					
				Signal region				Middle region	
	n	Positive	Negative	s1a	s1b	s1c	s2	m1	m2
GU	36	36	0	5	0	31	0	36	0
NU	15	15	0	2	0	13	0	15	0
Total	51	51	0	7	0	44	0	51	0

and neutrophils at both antral and ulcer sites, suggesting that IL-17 and IL-8 generated locally within the gastric mucosa, may be relevant to the background histological gastritis caused by *H pylori* infection. IL-17 and IL-8 levels in the antrum showed significant associations with the number of infiltrating mononuclear cells and neutrophils. At the ulcer site, however, IL-17 had a stronger correlation with mononuclear cells and neutrophils than IL-8, and a stronger correlation with neutrophils than with mononuclear cells. IL-17 and IL-8 have been reported to cause neutrophil recruitment[44], and neutrophils are known to cause damage to tissues they infiltrate[27]. On the basis of these results, we hypothesize that, together with IL-8, IL-17 might contribute to ulcerogenesis in GU patients as a result of its induction of neutrophil recruitment at the ulcer site.

When IL-17 and IL-8 levels in gastric mucosa at the ulcer site were compared between GU patients in the active stage and those in the healed stage, no significant difference was seen. Moreover, comparison of infiltrating neutrophils and mononuclear cells at ulcer site between ulcer stages showed no significant difference in IL-17 and IL-8 levels (data not shown). These results suggest that immunological background might not differ by GU stage, but might rather be fundamentally the same, regardless of stage.

Another important finding is the significant correlation between IL-17 and IL-8 levels at both the antrum and ulcer site. As this indicates a likely association between IL-17 and IL-8, we subsequently examined the effect of IL-17 as well as *H pylori* on IL-8 production by AGS cells. Co-culture of AGS cells with *H pylori* strain 26 695, in the presence or absence of rhIL-17, showed that both *H pylori* strain 26 695 and rhIL-17 stimulated IL-8 production from AGS cells.

Consistent with the increased secretion of IL-17 protein in organ cultures, biopsies from *H pylori*-positive GU and NU patients contained mRNA for this cytokine in all samples tested, but no expression in samples from the antrum of *H pylori*-negative controls. We previously reported that IL-8 mRNA expression is often detected in gastric biopsy tissues from *H pylori*-positive patients, but rarely in those from *H pylori*-negative controls[7], indicating that gastric mucosa is an active site for the synthesis of both IL-17 and IL-8 in *H pylori*-infected GU patients. Considering that IL-17 and IL-8 induce exocytosis and a respiratory burst in neutrophils[46], we hypothesize that locally secreted IL-17 and IL-8 are biologically active key chemotactic factors for the recruitment and activation of neutrophils, particularly at ulcer sites in *H pylori*-infected GU patients. We additionally speculate that enhanced synthesis and secretion of IL-17 and IL-8 may contribute to ulcerogenesis in *H pylori*-infected patients.

In conclusion, IL-17 and IL-8 may play an important role in the inflammatory response to *H pylori* colonization, and may ultimately influence the outcome of *H pylori*-associated diseases arising within the context of gastritis. Further studies are necessary to determine the mechanisms of this elevation in mucosal IL-17 and IL-8 activity in *H pylori* infection.

REFERENCES

1 **Marshall BJ,** Warren JR. Unidentified curved bacilli in the stomach of patients with gastritis and peptic ulceration. *Lancet* 1984; **1**: 1311-1315

2 **Graham DY,** Malaty HM, Evans DG, Evans DJ, Klein PD, Adam E. Epidemiology of *Helicobacter pylori* in an asymptomatic population in the United States. Effect of age, race, and socioeconomic status. *Gastroenterology* 1991; **100**: 1495-1501

3 **Blaser MJ.** Hypothesis: the changing relationships of *Helicobacter pylori* and humans: implications for health and disease. *J Infect Dis* 1999; **179**: 1523-1530

4 **Crabtree JE,** Taylor JD, Wyatt JI, Heatley RV, Shallcross TM, Tompkins DS, Rathbone BJ. Mucosal IgA recognition of *Helicobactor pylori* 120 KDa protein, peptic ulceration and gastric pathology. *Lancet* 1991; **338**: 332-335

5 **Dixon MF.** Pathophysiology of *Helicobacter pylori* infection. *Scand J Gastroenterology* 1994; **201**: 7-10

6 **Dixon MF,** Genta RM, Yardley JH, Correa P. Participants in the international workshop on the histopathology of gastritis, houston classification, grading of gastritis. The updated sydney system. *Am J Surg Pathol* 1996; **20**: 1161-1181

7 **Ando T,** Kusugami K, Ohsuga M, Shinoda M, Sakakibara M, Saito H, Fukatsu A, Ichiyma S, Ohta M. Interleukin-8 activity correlates with histological severity in *Helicobacter pylori*-associated antral gastritis. *Am J Gastroenterol* 1996; **91**: 1150-1156

8 **Ando T,** Kusugami K, Ohsuga M, Ina K, Shinoda M, Konagaya T, Sakai T, Imada A, Kasuga N, Nada T, Ichiyama S, Blaser MJ. Differential normalization of mucosal interleukin-8 and interleukin-6 activity after *Helicobacter pylori* eradication. *Infect Immun* 1998; **66**: 42-47

9 **Yamaoka Y,** Kita M, Kodama T, Sawai N, Takahashi T, Kashima K, Imanishi J. Chemokines in the gastric mucosa in *Helicobacter pylori* infection. *Gut* 1998; **42**: 609-617

10 **Kusugami K,** Ando T, Imada A, Ina K, Ohsuga M, Simizu T, Sakai T, Konagaya T, Kaneko H. Mucosal macrophage inflammatory protein-1 alpha activity in *Helicobacter pylori* infection. *J Gastroenterol Hepatol* 1999; **14**: 20-26

11 **Crabtree JE.** Role of cytokines in pathogenesis of *Helicobacter pylori*-induced mucosal damage. *Dig Dis Sci* 1998; **43**: 46S-55S

12 **Shimizu T,** Kusugami K, Ina K, Imada A, Nishio Y, Hosokawa T, Ohsuga M, Shimada M, Noshiro M, Kaneko H, Ando T. *Helicobacter pylori*-associated gastric ulcer exhibits enhanced mucosal chemokine activity at the ulcer site. *Digestion* 2000; **62**: 87-94

13 **Rouvier E,** Luciani MF, Mattei MG, Denizot F, Golstein P. CTLA-8, cloned from an activated T cell, bearing AU-rich messenger RNA instability sequences, and homologous to a

herpesvirus saimiri gene. *J Immunol* 1993; **150**: 5445-5456
14 **Chabaud M,** Durand JM, Buchs N, Fossiez F, Page G, Frappart L, Miossec P. Human interleukin-17: A T cell-derived proinflammatory cytokine produced by the rheumatoid synovium. *Arthritis Rheum* 1999; **42**: 963-970
15 **Aarvak T,** Chabaud M, Kallberg E, Miossec P, Natvig JB. Change in the Th1/Th2 phenotype of memory T-cell clones from rheumatoid arthritis synovium. *Scand J Immunol* 1999; **50**: 1-9
16 **Chabaud M,** Aarvak T, Garnero P, Natvig JB, Miossec P. Potential contribution of IL-17-producing Th(1)cells to defective repair activity in joint inflammation: partial correction with Th(2)-promoting conditions. *Cytokine* 2001; **13**: 113-118
17 **Spriggs MK.** Interleukin-17 and its receptor. *J Clin Immunol* 1997; **17**: 366-369
18 **Shin HC,** Benbernou N, Fekkar H, Esnault S, Guenounou M. Regulation of IL-17, IFN-gamma and IL-10 in human CD8 (+) T cells by cyclic AMP-dependent signal transduction pathway. *Cytokine* 1998; **10**: 841-850
19 **Moseley TA,** Haudenschild DR, Rose L, Reddi AH. Interleukin-17 family and IL-17 receptors. *Cytokine Growth Factor Rev* 2003; **14**: 155-174
20 **Witowski J,** Ksiazek K, Jorres A. Interleukin-17: a mediator of inflammatory responses. *Cell Mol Life Sci* 2004; **61**: 567-579
21 **Huang SH,** Frydas S, Kempuraj D, Barbacane RC, Grilli A, Boucher W, Letourneau R, Madhappan B, Papadopoulou N, Verna N, De Lutiis MA, Iezzi T, Riccioni G, Theoharides TC, Conti P. Interleukin-17 and the interleukin-17 family member network. *Allergy Asthma Proc* 2004; **25**: 17-21
22 **Hwang SY,** Kim JY, Kim KW, Park MK, Moon Y, Kim WU, Kim HY. IL-17 induces production of IL-6 and IL-8 in rheumatoid arthritis synovial fibroblasts via NF-kappaB- and PI3-kinase/Akt-dependent pathways. *Arthritis Res Ther* 2004; **6**: R120-R128
23 **Yao Z,** Painter SL, Fanslow WC, Ulrich D, Macduff BM, Spriggs MK. Armitage RJ. Human IL-17: a novel cytokine derived from T cells. *J Immunol* 1995; **155**: 5483-5486
24 **Kennedy J,** Rossi DL, Zurawski SM, Vega F, Kastelein RA, Wagner JL, Hannum CH, Zlotnik A. Mouse IL-17: a cytokine preferentially expressed by alpha beta TCR + CD4-CD8-T cells. *J Interferon Cytokine Res* 1996; **16**: 611-617
25 **Fossiez F,** Djossou O, Chomarat P, Flores-Romo L, Ait-Yahia S, Maat C, Pin JJ, Garrone P, Garcia E, Saeland S, Blanchard D, Gaillard C, Das Mahapatra B, Rouvier E, Golstein P, Banchereau J, Lebecque S. T cell interleukin-17 induces stromal cells to produce proinflammatory and hematopoietic cytokines. *J Exp Med* 1996; **183**: 2593-2603
26 **Fossiez F,** Banchereau J, Murray R, Van Kooten C, Garrone P, Lebecque S. Interleukin-17. *Int Rev Immunol* 1998; **16**: 541-551
27 **Luzza F,** Parrello T, Monteleone G, Sebkova L, Romano M, Zarrilli R, Imeneo M, Pallone F. Up-regulation of IL-17 is associated with bioactive IL-8 expression in *Helicobacter pylori*-infected human gastric mucosa. *J Immunol* 2000; **165**: 5332-5337
28 **Mobley HL.** Defining *Helicobacter pylori* as a pathogen: strain heterogeneity and virulence. *Am J Med* 1996; **100**: 2S-9S
29 **Tummuru MK,** Cover TL, Blaser MJ. Cloning and expression of a high-molecular-mass major antigen of *Helicobacter pylori*: evidence of linkage to cytotoxin production. *Infect Immun* 1993; **61**: 1799-1809
30 **Covacci A,** Censini S, Bugnoli M, Petracca R, Burroni D, Macchia G, Massone A, Papini E, Xiang Z, Figura N, Rappuoli R. Molecular characterization of the 128-kDa immunodominant antigen of *Helicobacter pylori* associated with cytotoxicity and duodenal ulcer. *Proc Natl Acad Sci USA* 1993; **90**: 5791-5795
31 **Blaser MJ,** Perez-Perez GI, Kleanthous H, Cover TL, Peek RM, Chyou PH, Stemmermann GN, Nomura A. Infection with *Helicobacter pylori* strains possessing *cagA* is associated with an increased risk of developing adenocarcinoma of the stomach. *Cancer Res* 1995; **55**: 2111-2115
32 **Odenbreit S,** Puls J, Sedlmaier B, Gerland E, Fischer W, Haas R. Translocation of *Helicobacter pylori* CagA into gastric epithelial cells by type IV secretion. *Science* 2000; **287**: 1497-1500
33 **Cover TL,** Tummuru MK, Cao P, Thompson SA, Blaser MJ. Divergence of genetic sequences for the vacuolating cytotoxin among *Helicobacter pylori* strains. *J Biol Chem* 1994; **269**: 10566-10573
34 **Telford JL,** Ghiara P, Dell'Orco M, Comanducci M, Burroni D, Bugnoli M, Tecce MF, Censini S, Covacci A, Xiang Z. Gene structure of the *Helicobacter pylori* cytotoxin and evidence of its key role in gastric disease. *J Exp Med* 1994; **179**: 1653-1658
35 **Atherton JC,** Cao P, Peek RM, Tummuru MK, Blaser MJ, Cover TL. Mosaicism in vacuolating cytotoxin alleles of *Helicobacter pylori*. Association of specific vacA types with cytotoxin production and peptic ulceration. *J Biol Chem* 1995; **270**: 17771-17777
36 **Atherton JC.** The clinical relevance of strain types of *Helicobacter pylori*. *Gut* 1997; **40**: 701-703
37 **van Doorn LJ,** Figueiredo C, Sanna R, Plaisier A, Schneeberger P, de Boer W, Quint W. Clinical relevance of the *cagA*, *vacA*, and *iceA* status of *Helicobacter pylori*. *Gastroenterology* 1998; **115**: 58-66
38 **Ford AC,** Delaney BC, Forman D, Moayyedi P. Eradication therapy in *Helicobacter pylori*-positive peptic ulcer disease: systematic review and economic analysis. *Am J Gastroenterol* 2004; **99**: 1833-1855
39 **Chomczynski P,** Sacchi N. Single-step method of RNA isolation by acid guanidinium thiocyanate-phenol-chloroform extraction. *Anal Biochem* 1987; **162**: 156-159
40 **Yamamura M,** Uyemura K, Deans RJ, Weinberg K, Rea TH, Bloom BR, Modlin RL. Defining protective response to pathogens: cytokine profiles in leprosy lesions. *Science* 1991; **254**: 277-279
41 **Fujino S,** Andoh A, Banba S, Ogawa A, Hata K, Araki Y, Bamba T, Fujiyama Y. Increased expression of interleukin 17 in inflammatory bowel disease. *Gut* 2003; **52**: 65-70
42 **Wilson K.** 1995; Preparation of genomic DNA from bacteria, p. 2.4.1-2.4.5. *In* F. Ausubel M, Brent R, Kingston RE, Moore DD, Seidman JG, Smith JA, and Struhl (ed.) K, Current protocols in molecular biology, vol. 1. John Wiley & Sons, Inc., New York, N.Y.
43 **van Doorn LJ,** Figueiredo C, Rossau R, Jannes G, van Asbroek M, Sousa JC, Carneiro F, Quint WG. Typing of *Helicobacter pylori vacA* gene and detection of *cagA* gene by PCR and reverse hybridization. *J Clin Microbiol* 1998; **36**: 1271-1276
44 **Laan M,** Cui ZH, Hoshino H, Lotvall J, Sjostrand M, Gruenert DC, Skoogh BE, Linden A. Neutrophil recruitment by human IL-17 via C-X-C chemokine release in the airways. *J Immunol* 1999; **162**: 2347-2352
45 **Witowski J,** Pawlaczyk K, Breborowicz A, Scheuren A, Kuzlan-Pawlaczyk M, Wisniewska J, Polubinska A, Freiss H, Gahl GM, Frei U, Jorres A. IL-17 stimulates intraperitoneal neutrophil infiltration through the release of Groa chemokine from mesothelial cells. *J Immunol* 2000; **165**: 5814-5821
46 **Prause O,** Laan M, Lotvall J, Linden A. Pharmacological modulation of interleukin-17-induced GCP-2-, GRO-alpha- and interleukin-8 release in human bronchial epithelial cells. *Eur J Pharmacol* 2003; **462**: 193-198

Science Editor Wang XL and Guo SY **Language Editor** Elsevier HK

PO Box 2345, Beijing 100023, China
www.wjgnet.com
wjg@wjgnet.com

ELSEVIER

World J Gastroenterol 2005;11(40):6312-6321
World Journal of Gastroenterology ISSN 1007-9327
© 2005 The WJG Press and Elsevier Inc. All rights reserved.

• *BASIC RESEARCH* •

Expression of matrix metalloproteinases and tissue inhibitor metalloproteinases increases in X-irradiated rat ileum despite the disappearance of CD8a T cells

Carine Strup-Perrot, Marie-Catherine Vozenin-Brotons, Marie Vandamme, Christine Linard, Denis Mathé

Carine Strup-Perrot, Marie-Catherine Vozenin-Brotons, Marie Vandamme, Christine Linard, Laboratoire d'étude des pathologies Radio-induites, SRBE/DRPH, Institut de Radioprotection et de Sûreté Nucléaire, Fontenay-aux-Roses 92262, France
Marie-Catherine Vozenin-Brotons, Denis Mathé, Laboratoire UPRES EA 27-10 'Radiosensibilité des tumeurs et tissus sains', Institut Gustave Roussy/Institut de Radioprotection et de Sûreté Nucléaire, Villejuif Cedex 94805, France
Correspondence to: Carine Strup-Perrot, Laboratoire d'étude des pathologies Radio-induites, SRBE/DRPH, Institut de Radioprotection et de Sûreté Nucléaire, Fontenay-aux-Roses 92262, France. carine.strup@irsn.fr
Telephone: +33-1-58357760
Received: 2004-10-12 Accepted: 2004-12-23

Abstract

AIM: To investigate their expression and activity in the rat ileum after exposure to ionizing radiation along with that of the cellular effectors and molecular mediators involved in the regulation of MMPs.

METHODS: Rats were exposed to a single 10-Gy dose of X-rays delivered to the abdomen. A combination of methods, such as zymography, immunohistochemistry and real time reverse transcriptase-polymerase chain reaction, were used to localize and quantify MMPs and the molecules involved in MMP activating and inhibitory pathways (plasmin/plasminogen, TIMPs), CD8+, as well as inflammatory (interleukin (IL)-1β, IL-8, tumor necrosis factor-α, TNF-α) and fibrogenic mediators (transforming growth factor-β1-3) within ileal tissue at 1, 3, and 7 d after irradiation.

RESULTS: A marked increase in MMP-2 and -14 mRNA and protein levels associated with an increased activity of MMP-2 was observed in irradiated ileal tissue. MMP-2 and -14 expression was mainly observed in inflammatory, epithelial, and mesenchymal cells, whereas a slight increase in MMP-3 expression was detected in the few infiltrating macrophages at d 1 after irradiation. Conversely, MMP-1, -7, and -9 mRNA levels were not found to be affected by abdominal irradiation. Irradiation was found to induce disappearance of CD8+ cells. Furthermore, we have observed that TNF-α and IL-1β protein levels increased 6 h after irradiation, whereas those of IL-8 only increased after 3 d and was concomitant with neutrophil infiltration. In addition, the expressions of molecules involved in MMP activating and inhibitory pathways (urokinase-type plasminogen activator and tissue-type plasminogen activator; TIMP-1, TIMP-2, and plasminogen activator-inhibitor-1) were found to be increased after abdominal irradiation.

CONCLUSION: This study showed that abdominal irradiation induces an acute remodeling of the ileum associated with an increased expression of MMPs and TIMPs that do not involve CD8+ T cells but involve mesenchymal and epithelial cells, although to a lesser extent, and probably even soluble inflammatory and fibrogenic mediators.

© 2005 The WJG Press and Elsevier Inc. All rights reserved.

Key words: Matrix metalloproteinases; Irradiation; Ileum; T cells; Cytokines

Strup-Perrot C, Vozenin-Brotons MC, Vandamme M, Linard C, Mathé D. Expression of matrix metalloproteinases and tissue inhibitor metalloproteinases increases in X-irradiated rat ileum despite the disappearance of CD8a T cells. *World J Gastroenterol* 2005; 11(40): 6312-6321
http://www.wjgnet.com/1007-9327/11/6312.asp

INTRODUCTION

Acute intestinal toxicity may occur in response to therapeutic or accidental exposure to ionizing radiation. At the histopathological level, it is characterized by a decrease in the depth of the intestinal crypts and the height of the villi. It is associated with basement membrane degradation, and ultimately leads to mucosal barrier breakdown and ulceration. Classical radiation-induced toxicity symptoms include diarrhea, malabsorption, and protein losing enteropathy[1]. Depending on the delivered dose of radiation, a restoration phase involving desquamation and re-epithelialization may occur. This requires extracellular matrix (ECM) remodeling, a process in which proteases and especially matrix metalloproteinases (MMPs) play an essential role[2], and which is associated with the overexpression of inflammatory and fibrogenic cytokines, such as interleukin-1β (IL-1β), tumor necrosis factor-α (TNF-α) and transforming growth factor-β (TGF-β)[3,4].

Cell adhesion, migration, proliferation, and differentiation are required for complete wound healing and rely on interactions between cells and the ECM. Normal wound–ECM interactions are therefore essential to wound healing. The rate, quality/effectiveness, and organization of this process are determined

by a dynamic balance between overall matrix synthesis, deposition, and degradation. Disruption of this balance likely induces abnormal matrix degradation or accumulation. MMPs are a large family of zinc-dependent matrix degrading enzymes, involved in the fine tuning of ECM homeostasis. MMPs are classified, based on their substrate specificity and structural features, into six categories: gelatinases (MMP-2 and -9), stromelysins (MMP-3, -10, and -11), elastases (MMP-12), collagenases (MMP-1, -8, -13, and -18), matrilysins (MMP-7 and -26) and membrane-type MMPs (MMP-14, -15, -16, and -17)[2]. The primary regulatory mechanism of MMP activity occurs at the transcriptional level and consists of a variety of extracellular signals involving cytokines, growth factors, and cell–matrix interactions[5,6]. MMPs are then secreted as zymogens, which require prior proteolytic activation. *In vivo* activation of pro-MMPs is mainly mediated through the plasminogen–plasmin system, but MMPs themselves may also be involved. The third level of regulation is ensured by the physiological inhibitors of MMPs, which include tissue inhibitors of metalloproteinases (TIMPs). Four subtypes of TIMPs (TIMP 1-4) have been identified so far[7]. TIMP-1 inhibits several MMPs, while TIMP-2 seems to specifically inhibit MMP-2.

Overexpression of MMPs has been known to occur in both physiological and pathological conditions and to involve tissue restoration and/or destruction. Many studies reported that the alteration of ECM remodeling and MMP/TIMP expression occur in inflammatory bowel diseases[8-12]. Furthermore, some studies showed that T cells play a central role in the activation of MMPs in inflammatory bowel diseases[13,14]. However, few studies have examined the role of MMPs in radiation-induced gastrointestinal disorders. After intraoperative irradiation, Seifert *et al.*[15], observed a prolonged gelatinolytic activity in rat colonic anastomoses. Two clinical studies conducted in patients reported controversial data. Hovdenak *et al.*[16], observed increased MMP-2 and MMP-9 expression after irradiation, while Kumar *et al.*[17], did not. In this study, we aimed at confirming that observations made on gelatinases also applied to other types of MMPs. We investigated the expression of MMPs after abdominal X-irradiation and their activating and inhibitory systems (i.e., plasminogen/plasmin and TIMP-1 and -2). We simultaneously investigated the stimulatory signals and focused on the expression of pro-inflammatory (TNF-α, IL-1β) and fibrogenic cytokines (TGF-β) in the ileum after irradiation. Finally, we investigated the involvement of CD8a+T cells in MMP activation after irradiation. The results presented in this study show that irradiation induces a moderate inflammatory state, a significantly increased expression of MMP-2, MMP-14, TIMP-1, and TIMP-2, and the disappearance of CD8a+T cells.

MATERIALS AND METHODS

Animals and irradiation conditions

Experiments were performed using male Wistar rats (Janvier, Le Genest Saint Isle, France), weighing initially between 225 and 250 g. Prior to irradiation, rats were anesthetized by groups of six with 2.5% isoflurane, administered at a rate of 0.4 L/min (Abbott, Rungis, France). A protective lead screen (5 mm thick) was placed over each animal to cover them from the top of the head to 1 cm below the ribs. The given dose was 10 Gy at a rate of 0.62 Gy/min (Phillips, 250 MeV, 0.2-mm Cu filter). Sham-irradiated rats were placed within the apparatus and anesthetized, but were not exposed to X-rays. Animals were weighed and food intake was measured 10 d before exposure to radiation and daily during the week following irradiation. All experiments were conducted according to the French regulations on animal experimentation (Ministry of Agriculture, Act No. 87-848, October 19, 1987).

Tissue collection

One, three, and seven days after irradiation, rats were anesthetized with 2.5% isoflurane and the terminal ileum was removed before euthanasia (sodium pentobarbitone, 100 mg/kg, ip; Sanofi, La Ballastière, France) and rinsed with sterile physiological saline. The ileum was cut into three equal pieces immediately after resection: The tissue samples were formalin-fixed for histology, frozen in liquid nitrogen, and crushed into powder for RNA and protein extraction.

Histology

Samples were fixed in 40 g/L formaldehyde (Carlo Erba, Rueil Malmaison, France) for 3 d at room temperature. They were then dehydrated, paraffin-embedded, and cut into 4-μm-thick sections. Slides were stained with hematoxylin, eosin, and saffron for histological analysis.

Immunostaining

MMP and TIMP antibodies were purchased from Chemicon (Euromedex, Mundolshiem, France) and used as follows: anti-MMP-1 (41-1E5, 1:15 000), anti-MMP-2 (42-5D11, 1:200), anti-MMP-3 (SL-1 IIIC4, 1:200), anti-MMP-7 (ID-2, 1:300), anti-MMP-14 (113-5B7, 1:500), anti-TIMP-1 (102B1, 1:50), and anti-TIMP-2 (67-4H11, 1:1 000). The anti-myeloperoxidase antibody was from Novocastra (Tébu, Le Perray en Yvelines, France; NCL MYELOp, 1:300) and the anti-CD8a antibody was from Cedarlane (Tébu; CL004AP, 1:600).

Following deparaffinization and rehydration, endogenous peroxidase activity was inhibited with 30 mL/L hydrogen peroxide in PBS. In order to detect MMP-3, MMP-7, and CD8a epitopes, sections were placed in 0.01 mol/L hot citrate buffer (pH 6.0). The protein block serum-free blocking solution (Dako, Trappes, France) was used to inhibit non-specific staining. Primary antibodies were diluted in antibody diluent (Dako). Antibodies against MMP-1, MMP-2, and TIMP-1 were detected using the LSAB2-HRP system (Dako), whereas antibodies against CD8a, MMP-3, MMP-7, MMP-14, and TIMP-2 were detected using the StrepABC-HRP system (Dako) for myeloperoxidase. Immunostaining was performed using the Vector NovaRED substrate kit for peroxidase (Biovalley, Conches, France, for Vector Laboratories, USA). Sections were counterstained with differentiated Mayer's Hemalum (Merck for VWR, Fontenay-sous-bois, France). Slides were rinsed between each stage with Tris HCl-NaCl-Tween (50 mmol/L, 0.3 mol/L, 1 g/L). Control staining, without the primary antibody and using an irrelevant mouse IgG, was performed concomitantly with each immunostaining to ensure staining specificity. A semiquantitative analysis of MMP-2, MMP-3, MMP-14,

TIMP-1, and TIMP-2 expression was performed. Mean staining intensity scores, which reflected staining intensity in the epithelium, lamina propria, submucosa, blood vessels, and muscularis propria, were attributed. The following scoring system was used: no staining (-); weak staining intensity (+); moderate staining intensity (++); strong staining intensity (+++); and very strong staining intensity (++++).

Gelatin zymography

Crushed tissue samples were homogenized in 50 mmol/L Tris-HCl buffer (pH 7.6) containing 150 mmol/L NaCl, 10 mmol/L $CaCl_2$, 10 g/L Triton X-100, and protease inhibitors (Sigma-reverse Aldrich, St. Quentin Fallavier, France). Protein concentration was determined using the Lowry method.

Zymography was performed as previously described[18]. Briefly, samples (4 μg protein) and MMP-2/9 standards (CC073 Chemicon, Euromedex, Mundolsheim, France) were separated by electrophoresis on 80 g/L SDS-polyacrylamide gels copolymerized with 1 g/L gelatin (Type A from porcine skin; Sigma-Aldrich, St. Quentin Fallavier, France). Gels were washed in 25 g/L Triton X-100, incubated in a buffer containing 50 mmol/L Tris–HCl (pH 7.8), 5 mmol/L $CaCl_2 \cdot 2H_2O$, 50 mmol/L NaCl, 0.1 g/L Brij 35, and 0.2 g/L NaN_3 at 37 ℃, stained with 5 g/L Coomassie blue in 250 mL/L isopropanol/100 mL/L acetic acid, and destained in a 100 mL/L methanol/100 mL/L acetic acid solution. Gelatinolytic bands appeared as clear zones against the blue background. Gelatinases were identified by their molecular weight and after inhibition using 20 mmol/L EDTA or 1 mmol/L *o*-phenanthroline. Densitometric analyses were performed using an imaging workstation (Biocom, Les Ulis, France) interfaced with the Phoretix image analysis software (Nonlinear Dynamics, Newcastle upon Tyne, UK).

RNA extraction and quantitative RT-PCR

Total RNA was extracted from crushed tissue samples by homogenization in 4 mol/L guanidine isothiocyanate, purified using the method of Chomczynski and Sacchi and quantified by spectrophotometry (A_{260}/A_{280}). RNA was treated with RNase-free DNase (0.5 U/μL) to remove contaminating genomic DNA. RNA integrity was assessed by denaturing agarose-gel electrophoresis and staining with ethidium bromide.

Real-time reverse transcriptase-polymerase chain reaction (RT-PCR) was used to quantify the levels of MMP-2, -9, -14, TIMP-1, -2, plasminogen, urokinase-type plasminogen activator (u-PA), tissue-type plasminogen activator (t-PA), plasminogen activator-inhibitor-1 (PAI-1), IL-8, TGF-β1, TGF-β2, and TGF-β3 RNA transcripts as previously described[19]. Primers were generated with the Primer Express software (Applied Biosystems, Courtaboeuf, France) and purchased from Invitrogen (Cergy-Pontoise, France): MMP-2 5'-ACCGTCGCCCATCATCAA-3' (forward), 5'-CCTTCAGCACAAAGAGGTTGC-3' (reverse); MMP-9 5'-TGTCCAGACCAAGGGTACAGC-3' (forward), 5'-GAAGAATGATCTAAGCCCAGCG-3' (reverse); MMP-14 5'-GAGGGTCATGAGAAGCAGGC-3' (forward), 5'-TCAAAGGGTGTGCTGTCGC-3' (reverse); TIMP-1 5'-AGAAGGGCTACCAGAGCGATC-3' (forward), 5'-ATCGAGACCCCAAGGTATTGC-3' (reverse); TIMP-2 5'-CTACATCTCCTCCCCGGATGA-3' (forward), 5'-GGTGCCCATTGATGCTCTTC-3' (reverse); plasminogen 5'-CTGAGTATCTAAACAACAGAGTCAAATCC-3' (forward), 5'-TCGAAGCAAACCAGAGGTCC-3' (reverse); PAI-1 5'-ATGGCTCAGAACAACAAGTTCAAC-3' (forward), 5'-CAGTTCCAGGATGTCGTACTCG-3' (reverse); t-PA 5'-GACGTGAAGCCCTGGTGC-3' (forward), 5'-CAAGCCGGCGTGCTG-3' (reverse); u-PA 5'-GTTTGAGGTGGAGCAGCTCAT-3' (forward), 5'-GCTATGTCATTATGGAAGGCCAG-3' (reverse); TNF-α 5'-ATCCGAGATGTGGAACTGGC-3' (forward), 5'-CGATCACCCCGAAGTTCAGTA-3' (reverse); TGF-β1 5'-AGTCCCAAACGTCGAGGTGA-3' (forward), 5'-CCATGAGGAGCAGGAAGGG-3' (reverse); TGF-β2 5'-TGCTGAGAACCTTTTTGCTCC-3' (forward), 5'-GTCGAGGGTGCTGCAGGTA-3' (reverse); TGF-β3 5'-CAAGCAGCGCTACATAGGTGG-3' (forward), 5'-CAGTGACATCGAAGGACAGCC-3' (reverse); IL-8 5'-GACTGTTGTGGCCCGTGAG-3' (forward), 5'-CCGTCAAGCTCTGGATGTTCT-3' (reverse), and IL-1β 5'-CAACAAAAATGCCTCGTGC-3' (forward), 5'-TGCTGATGTACCAGTTGGG-3' (reverse).

Cytokine immunoassays

Crushed tissue was weighed and homogenized in 10 mmol/L phosphate buffer (pH 7.4) supplemented with protease inhibitors, such as 2 mmol/L PMSF, 10 μg/mL pepstatin A, 1 μg/mL aprotinin, 10 μg/mL leupeptin, and 0.5 mg/mL EDTA (Sigma-Aldrich, St. Quentin Fallavier, France). Protein concentration was measured using a modified version of the Bradford method (Bio-Rad Laboratories, Marne-la-Coquette, France). Concentration of IL-1β and TNF-α was determined by ELISA (R&D Systems, Minneapolis, MN, USA). All data were expressed in picogram per milligram of protein.

Statistical analysis

Each real-time RT-PCR and cytokine immunoassay were done in six animals and results were expressed as mean±SE. The ANOVA and Student-Newman-Keuls test were used to determine whether the difference between the values obtained with the control group and the irradiated group was statistically significant. P value <0.05 was considered statistically significant.

RESULTS

Abdominal X-irradiation (10-Gy) induced the inhibition of food intake and decrease in body weight. Diarrhea was observed between d 3 and 5 after irradiation.

Alteration of structure of ileal tissue by a single 10-Gy dose of X-rays

Histopathological changes after irradiation are shown in Figure 1. No significant histological changes were seen 24 h after irradiation, whereas a marked alteration of the intestinal mucosa was observed 3 d after irradiation. A significant decrease in the thickness of the mucosa (-15%, P<0.01), the sloughing of epithelial cells at the top of the villi, associated

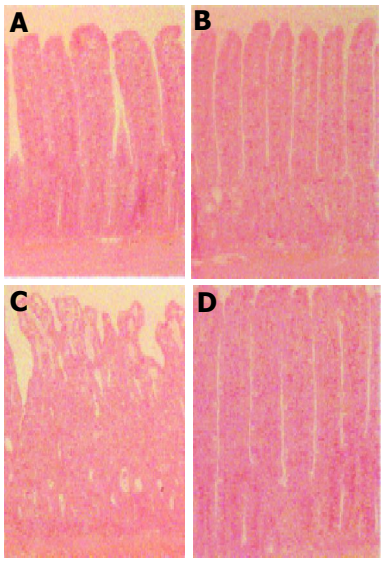


Figure 1 Histopathological study in ilea after X-irradiation with a single dose of 10 Gy. Ileal structure before (**A**) and one (**B**), three (**C**) and seven (**D**) days after abdominal X-irradiation. Magnification x100.

with an atrophy of the villi, dilation of the crypts, and absence of mucus secretion were observed. Muscle layers, on the other hand, appeared normal. Seven days after irradiation, the ileal epithelium seemed to be regenerated. We observed a significant increase in the thickness of the mucosa of irradiated mice compared to controls (+14%, $P<0.01$), with an increase in the number of epithelial cells located in the villi. Some crypts were still dilated at this time.

Increase in the expression and activity of gelatinase A by a single 10-Gy dose of X-rays

Gelatin zymography allowed the detection of both active and pro-forms of gelatinases (Figure 2A). Equal amounts of pro- (72 ku) and active (62 ku) MMP-2 were detected in control ileal tissues (Figure 2B). The pro-MMP-2 band significantly increased from d 1-7 (×3.8 on d 1; ×5.0 on d 3; ×4.0 on d 7, all $P<0.01$) after irradiation. Induction of active MMP-2 peaked on d 1 (×2.9, $P<0.01$) and was still higher than control values on d 3 (×1.5, $P<0.05$) and 7 (×1.8, $P<0.01$). We observed a weak gelatinolytic band with a molecular weight, which corresponded to that of pro-MMP-9, but as it was not inhibited by EDTA, it could not be attributed to MMP-9. The high molecular weight bands (125 and 200-220 ku) were, on the other hand, completely inhibited by EDTA and phenanthroline. These gelatinolytic activities, which might have MMP-9 dimers or an MMP-9-lipocalin complex, were equivalent on d 1 and 7 after irradiation, but weaker on d 3 (Figure 2B).

Irradiation-induced transcriptional activation of MMP-2 was confirmed by real-time RT-PCR. MMP-9 mRNA levels, however, were not significantly altered (Figure 2C). Since MMP-14 is involved in the activation of MMP-2, we studied the alterations in MMP-14 mRNA levels. We found that MMP-14 was induced 3 and 7 d after irradiation (Figure 2C).

Tissue localization of gelatinase A and other MMPs after X-irradiation with a single dose of 10 Gy

Immunohistochemistry was used to investigate the cell

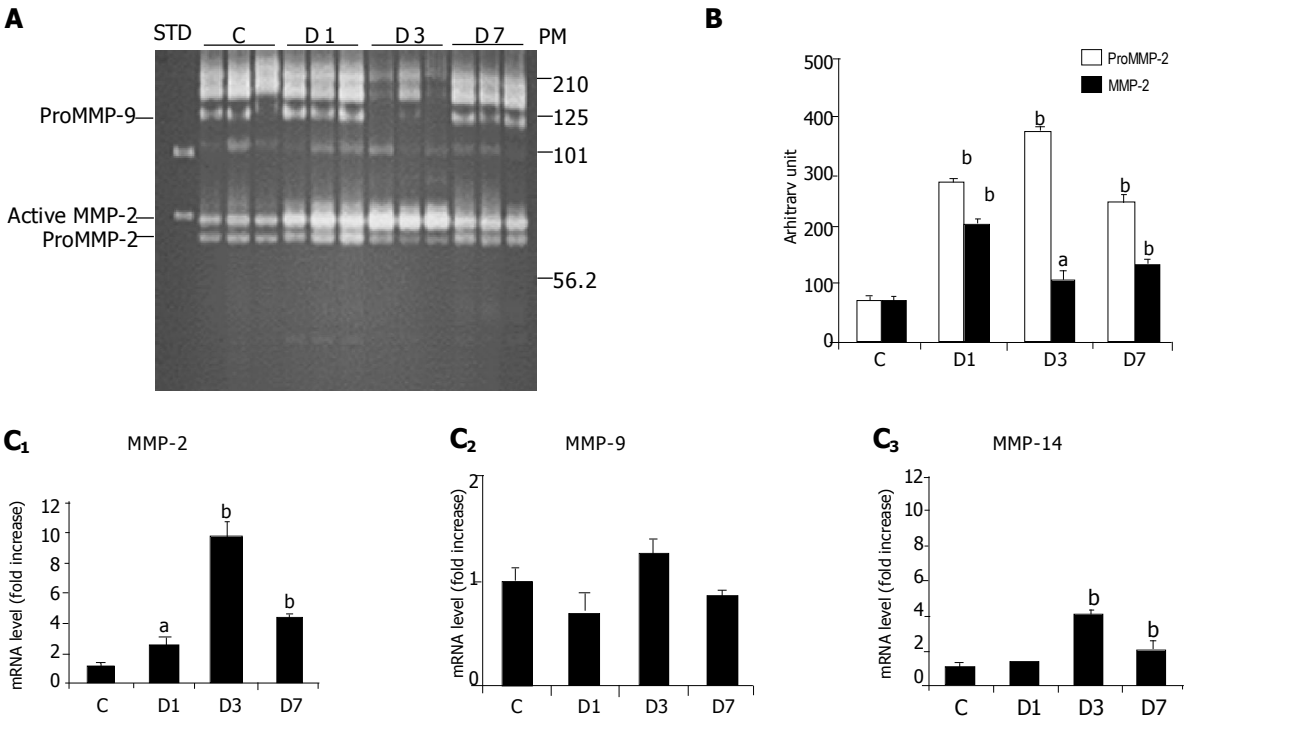
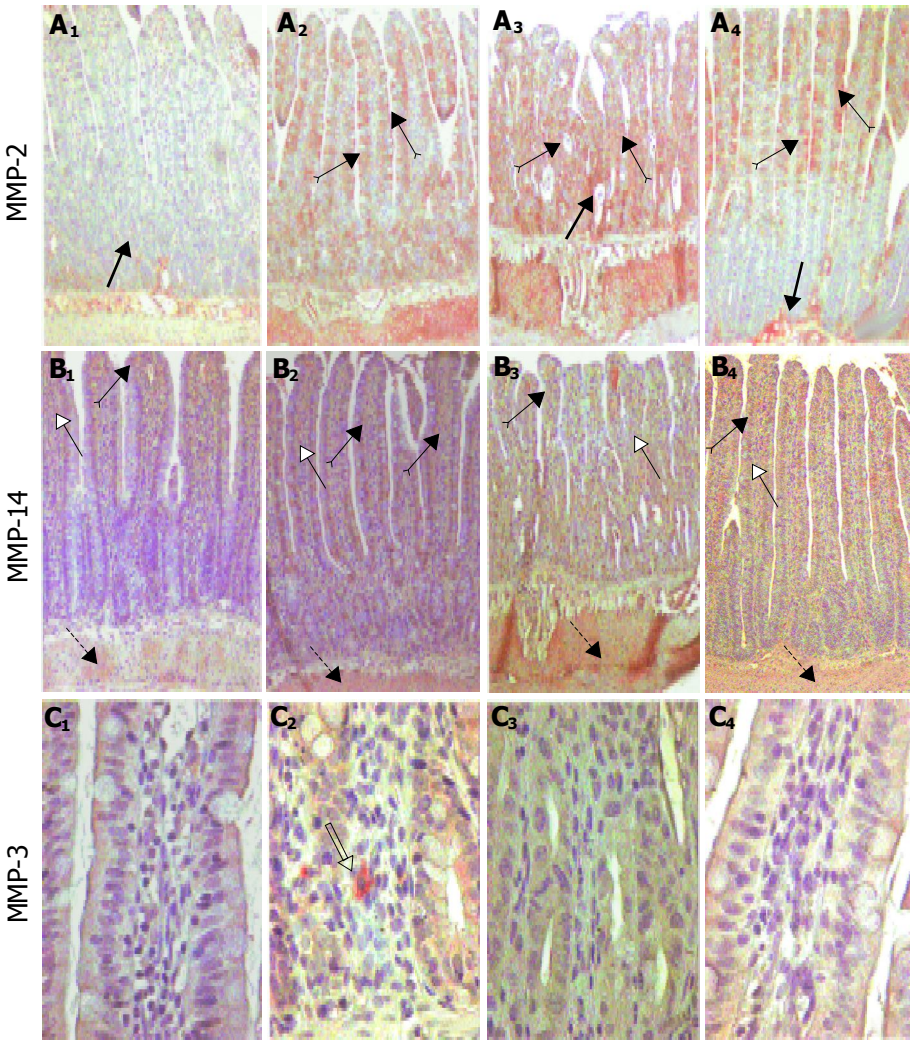


Figure 2 Gelatinases activities in ilea after X-irradiation with a single dose of 10 Gy. **A:** Study of gelatinases activities by zymography. Lane STD shows MMP-2 and MMP-9 standards, lane 2-4, 5-7; 8-10; 11-13 shows gelatinase activities in ilea from control rats (C) and one (D1), three (D3) and seven (D7) days after X-irradiation respectively; **B:** Densitometric analysis of zymography. Results are mean±SE, significantly different from controls: $^{a}P<0.05$, $^{b}P<0.01$ *vs others*. **C_{1-3}:** Analysis of MMP-2, MMP-9 and MMP-14 gene expression. mRNA levels were measured by real time RT-PCR in control ilea from control rats (C) or one (D1), three (D3) and seven (D7) days after X-irradiation respectively. Results are mean±SE, significantly different from controls: $^{a}P<0.05$, $^{b}P<0.01$ *vs others*.

types that expressed gelatinase after irradiation. A weak MMP-2 staining restricted to the pericryptal sheath myofibroblasts, inflammatory cells, and smooth muscle cells was observed in the control ileal tissues (Figures 3A and B). A significant transmural increase in MMP-2 staining was, however, found on d 1 after irradiation in smooth muscle and epithelial cells, and on d 3 in smooth muscle cells, epithelial cells of the villi, and in pericryptal sheath myofibroblasts. MMP-2 staining decreased on d 7.

In control samples, MMP-14 staining was observed in epithelial cells at the top of the villi, inflammatory cells in the lamina propria, and smooth muscle cells. As for mRNA, in irradiated samples, MMP-14 staining was unchanged on d 1, but had increased on d 3 and had spread to the whole tissue. On d 7, however, MMP-14 staining in irradiated and control samples was equivalent except in epithelial cells at the top of the villi, which exhibited weak MMP-14 staining (Figures 3A and B).



Neutrophil polynuclear
Large mononuclear macrophage-like cell
Epithelial cell
Myofibroblast
Muscular cell
Lamina propria cell

D

	C	D 1	D 3	D 7
MMP-1	+	+	+	+
MMP-2	+	+++	++++	+/++
MMP-3	-	+	-	-
MMP-7	+++	+++	+++	+++
MMP-14	+	+/++	++/+++	++/+

Figure 3 Tissue localization of gelatinase A and other MMPs in ilea after X-irradiation with a single dose of 10 Gy. **A_2:** MMP-2, MMP-14 and MMP-3 immunostaining. In control ilea, MMP-2 staining was observed in the pericryptal myofibroblast sheath, inflammatory cells and smooth muscle cells (A_1, x100). On day one and three (A_2; A_3, x100), increased MMP-2 staining was found in all of the layer of the bowel particularly in smooth muscle cells and in epithelial cells. On day seven (A_4, x100) MMP-2 staining was weaker and found in smooth muscle cells, epithelial cells of the villus only and pericryptal myofibroblast sheath. In control ilea, MMP-14 staining was observed in the inflammatory cells of the lamina propria, smooth muscle cells and some epithelial cells of the top of the villi (B_1, x100). No significant modification in MMP-14 staining was found in irradiated ilea on day one (B_2; x100), whereas on day three MMP-14 staining spread to the whole tissue (B_3, x100). On day seven (B_4, x100), MMP-14 staining return to control level except in the epithelial cells of the top of the villus. In control ilea, no MMP-3 staining was observed (C_1, x400), but a staining was observed in mononuclear infiltrated cells day one after X-irradiation (C_2, x400); **D:** MMPs immunostaining scoring. (-) represent no staining, (+) weak staining, (++) moderate staining, (+++) important and (++++) strong staining.

Furthermore, we focused on the expression and immunolocalization of MMP-1, -3, and -7. MMP-1 and -7 were found to be expressed in control ileal tissue, and no changes were observed after irradiation (Figure 3B). MMP-3 was not detected in control samples, but staining was observed at d 1 in some infiltrating mononuclear cells, which were morphologically similar to macrophages (Figures 3A and B).

Disappearance of CD8+T lymphocytes from the ileum after X-irradiation with a single dose of 10 Gy

To investigate whether T cells could be involved in MMP activation after X-irradiation, a subset of peripheral T cells, the majority of natural killer (NK) cells, and granular intraepithelial leukocytes of the small intestine were stained with an antibody directed against an antigen present on the surface of thymocytes. This antigen is the rat homolog of the human CD8. Figure 4 shows that X-irradiation of the abdomen with a dose of 10 Gy caused a marked decrease in the number of CD8+ cells as early as 1 d after exposure, which was also observed on d 3 and 7.

Increase in the number of polynuclear neutrophils and expression of inflammatory and fibrogenic factors after irradiation with a single dose of 10 Gy

Neutrophil infiltration after abdominal X-irradiation was quantified based on myeloperoxidase staining. While we observed a slight increase in myeloperoxidase staining at d 1 and 3 after irradiation, the number of positive cells returned to control values at d 7 (Figure 5A).

Pro-inflammatory cytokines and fibrogenic growth factors are potent inducers of MMPs expression and activity. Thus, expressions of TNF-α, IL-1β, IL-8, and TGF-β1, -2, and -3 were assessed after X-irradiation. Tissue concentration of pro-inflammatory cytokines TNF-α and IL-1β significantly increased 6 h after irradiation (2.3-fold and 2.3-fold, respectively, $P<0.01$) as shown in Figure 5B. This early increase was followed by an increase in IL-8 at d 3 (6.4-fold, $P<0.01$) as shown in Figure 5B.

TGF-β1 and -3 mRNA levels increased 3 d after irradiation (2.5-fold and 1.5-fold, respectively, $P<0.01$). Furthermore, an increase in TGF-β1 and -3 mRNA levels was also seen on d 7 (2.8-fold, $P<0.01$; and 1.6-fold, $P<0.05$, respectively). TGF-β2 mRNA level, on the other hand, increased at d 1 and remained significantly high thereafter (2.1-fold on d 1, 3.2-fold on d 3, and 1.8 fold on d 7, all $P<0.01$) as shown in Figure 5C.

Expression of MMP activating factors after X-irradiation with a single dose of 10 Gy

Because the plasminogen system is known to regulate MMP activation, we investigated variations in the mRNA levels of plasminogen, t-PA, u-PA, and PAI-1 after irradiation (Figure 6). Irradiation induced a significant decrease in plasminogen mRNA level on d 7, and a marked increase in u-PA (6.1-fold, $P<0.01$), t-PA (21-fold, $P<0.01$), and PAI-1 (19-fold, $P<0.01$) on d 3, which was also observed on d 7.

Expression of gelatinase inhibitors after X-irradiation with a single dose of 10 Gy

We investigated TIMP-1 and -2 expression, i.e., intensity and localization, in the sections of X-irradiated rat ileum. In control ileal tissue, a moderate TIMP-1 staining was observed in only a few epithelial cells, in inflammatory cells in the lamina propria, and in smooth muscle cells (Figure 7A). TIMP-1 staining increased in all of the layers of the bowel 1 d after irradiation; the most intense staining was observed in epithelial cells. Staining intensity peaked on d 3 after irradiation (Figure 7A). TIMP-1 expression pattern after irradiation was confirmed by the analysis of mRNA level (Figure 7A).

A weak TIMP-2 staining was observed in control ileal tissues (Figure 7B). A slight increase in TIMP-2 staining intensity was observed in epithelial, inflammatory, and smooth muscle cells 1 d after irradiation and could still be observed on d 3 and 7 (Figure 7B). This increase in TIMP-2 mRNA level only reached significance 3 d after irradiation (fourfold increase, $P<0.01$, Figure 7B).

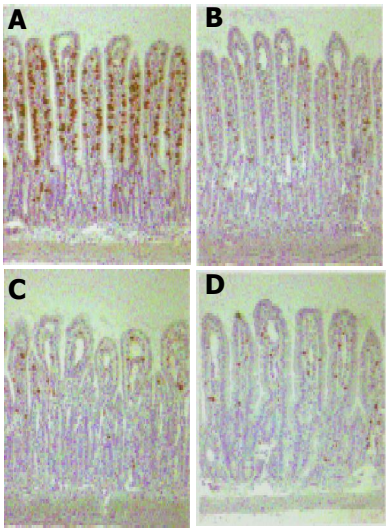


Figure 4 CD8a positive T cells after X-irradiation with a single dose of 10 Gy. Immunostaining for CD8a positive cells in control ilea (**A**) and one (**B**), three (**C**) and seven (**D**) days after X-irradiation. Magnification x100.

DISCUSSION

In this study, we have shown that abdominal X-irradiation with a dose of 10 Gy simultaneously enhances synthesis and activity of MMP-2 and -14. This enhancement is concomitant with an induction of pro-inflammatory cytokines, fibrogenic growth factors, and plasminogen system, which suggests that a complex interplay of factors actually controls radiation-induced activation of MMPs in the intestine. Inhibitory pathways are simultaneously activated as the expression of TIMP-1 and -2 increases, which is suggestive of an irradiation-induced alteration of ECM remodeling. Finally, we observed a decrease in the number of T cells after abdominal irradiation. Our data on radiation-induced induction of gelatinase are in agreement with a previous report by Seifert *et al*.[15], who observed a prolonged gelatinolytic activity in rat colonic anastomoses after intraoperative irradiation. Our results concerning the absence of T cells during radiation-induced ECM remodeling, however, markedly differ from those obtained in models of inflammatory bowel diseases. Our study shows that T lymphocytes are not directly involved in

radiation-induced mucosal injuries, suggesting that radiation-induced mucosal breakdown may be promoted by specific cellular pathways and specific molecular signals, which have been investigated further in this study.

Direct evidence of an important T cell-mediated process in the pathogenesis of mucosal lesions has been shown in *in vivo* and *ex vivo* models, in which T cells are activated by pokeweed mitogen or anti-CD3 and IL-12 in explants of human fetal intestine[13]. In these models, a severe tissue injury occurs following a massive increase in MMP synthesis (mainly MMP-3 and -9). De Winter *et al*.[22], provided evidence of a cross-talk between lymphocytes and epithelial cells *in vivo*. This cross-talk is mediated through cytokines that are locally produced by epithelial cells, which regulate immune responses in the intestine. Using the MRC OX8 antibody, specific for T cytotoxic/suppressor cells, granular intraepithelial leukocytes, and NK cells[23], we sought to determine whether T cells were present in the ileal wall. We observed that CD8+ staining completely disappeared 24 h after irradiation, possibly due to radiation-induced apoptosis. Specific target cells are activated after abdominal irradiation, and neutrophils, epithelial, and mesenchymal cells are responsible for the increased expression of MMPs.

Molecular mediators potentially involved in this radiation-induced enhancement of MMP expression were therefore investigated. We focused on the pro-inflammatory cytokines IL-1β and TNF-α as they are seemingly the mediators that are most frequently reported to be involved in bowel inflammatory diseases[24]. In agreement with a previous study[4], levels of IL-β1 and TNF-α increased as soon as 6 h after irradiation, and were returned to control values on d 1, 3, and 7 after irradiation (data not shown). The early increase in IL-β1 and TNF-α may be due to radiation-induced mast-cell degranulation[25]. This increase likely promotes IL-8 induction, leading to leukocyte recruitment and granulocyte infiltration. The radiation-induced inflammatory status, however, appeared to be moderate (twofold increase in TNF-α and IL-β1 protein levels)[4] in comparison to what was reported in Crohn's disease by Louis *et al*.[11], (10- and 8-fold increase, respectively). This weak inflammatory status may account for the weak MMP-3 stimulation observed in the irradiated ileum. This hypothesis is supported by Mengshol *et al*.[26], who reported that high levels of pro-inflammatory cytokines are required to stimulate MMP-3 secretion by subepithelial

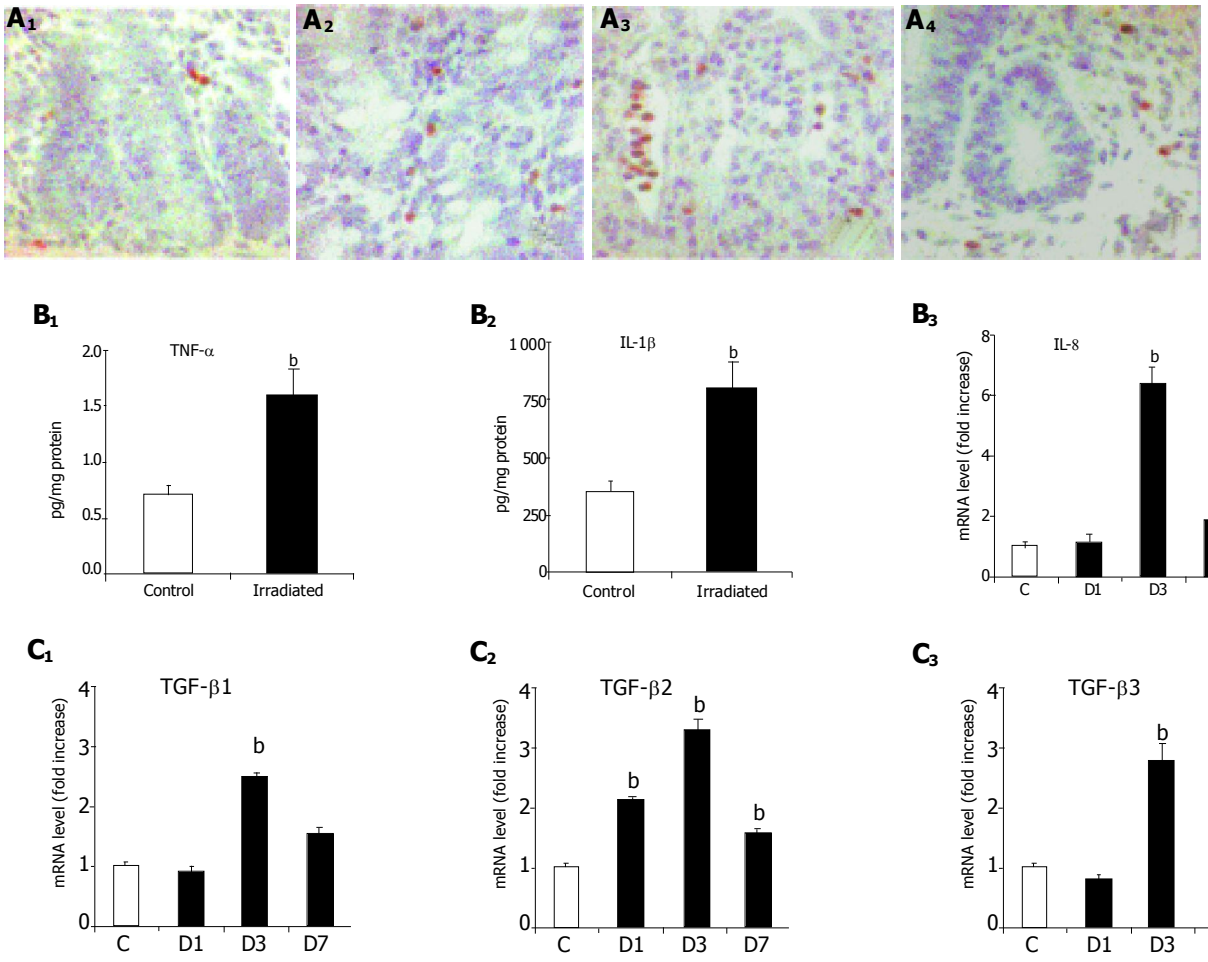


Figure 5 Radiation-induced inflammation. **A:** Myeloperoxidase positive cells in X-irradiated ilea. Immunostaining for myeloperoxidase positive cells in control ilea (A_1) and one (A_2), three (A_3) and seven (A_4) days after X-irradiation respectively. Magnification x 400; **B_{1-3}:** Concentration of TNF-α and IL-1β six hours, and IL-8 mRNA level one to seven days, after X-irradiation with a single dose of 10 Gy. Results are mean±SE, significantly different from controls: $^aP<0.05$, $^bP<0.01$ *vs* others; **C_{1-3}:** TGF-β1, β2 and β3 mRNA level after X-irradiation with a single dose of 10 Gy. Gene expression of TGF-β1, TGF-β2 and TGF-β3, was determined by real-time RT-PCR in control ilea (C) one (D1), three (D3) and seven (D7) days after X-irradiation respectively. Results are mean±SE, significantly different from controls: $^aP<0.05$, $^bP<0.01$ *vs* others.

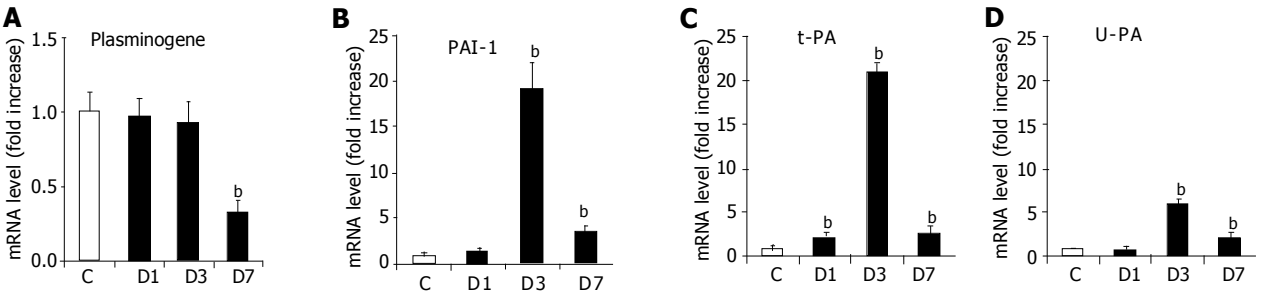


Figure 6 Plasminogen, U-PA, t-PA and PAI-1 mRNA level after X-irradiation with a single dose of 10 Gy. Gene expressions of plasminogen, U-PA, t-PA and PAI-1 were determined by real-time RT-PCR measured in control ilea (**C**) and one (D1), three (D3) and seven days (D7) after X-irradiation. Results are mean±SE, significantly different from controls: [a]*P*<0.05, [b]*P*<0.01 *vs* others (**A-D**).

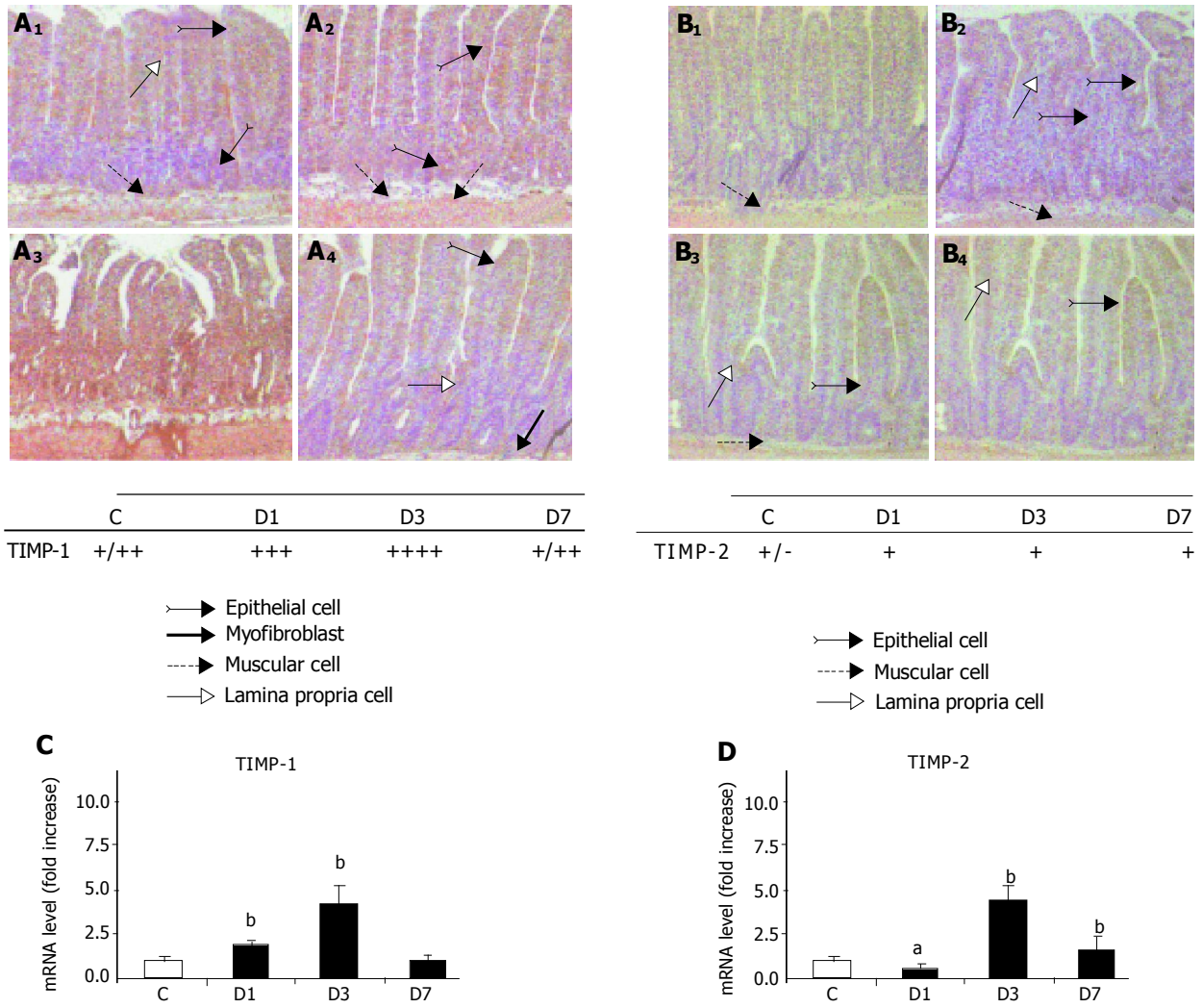


Figure 7 TIMP expression after X-irradiation with a single dose of 10 Gy. **A:** In control ilea, TIMP-1 staining was observed in the inflammatory cells of the lamina propria, smooth muscle cells and some rare epithelial cells of the crypt and of the top of the villus (A_1, x100). On day one (A_2, x100), TIMP-1 staining was found in all layers of the bowel and particularly in epithelial cells and in smooth muscle cells . On day three (A_3, x100), the staining spread to the whole tissue. On day seven (A_4, x100), TIMP-1 staining was found in smooth muscle cells, epithelial cells of the villus only , in pericryptal myofibroblast sheath and in inflammatory cells of the lamina propria. Gene expression of TIMP-1, determined by real-time RT-PCR was measured in control ilea (**C**) one (D1), three (D3) and seven (D7) days after X-irradiation respectively. Results are mean±SE, significantly different from controls: [a]*P*<0.05, [b]*P*<0.01. **B:** In control ilea, weak TIMP-2 staining was observed in smooth muscle cells (B_1, x100). On day one (B_2, x100) and day three (B_3, x100) after X-irradiation, a slight TIMP-2 increase was found in smooth muscle cells, in epithelial cells and in inflammatory cells of the lamina propria. On day seven (B_4, x100),(**C,D**) TIMP-2 staining was observed in epithelial cells on the top of the villus, inflammatory cells of the lamina propria. Gene expression of TIMP-2, determined by real-time RT-PCR was measured in control ilea (**C**) one (D1), three (D3) and seven (D7) days after X-irradiation respectively. Results are mean±SE, significantly different from controls: [a]*P*<0.05, [b]*P*<0.01 *vs* others.

myofibroblasts *in vitro*. Fibrogenic growth factors, such as TGF-β, are also involved in the regulation of cell proliferation, inflammation, immune response, and ECM deposition, which are important parts of the healing process [27,28]. Furthermore, previous studies have suggested that all three TGF-β isoforms are overexpressed during the early phase of radiation-induced injury, while TGF-β1 appears to be predominant in the late phase[29,30]. In this study, we observed an early peak of TGF-β2 induction at d 1, while the other two isoforms (TGF-β1 and TGF-β3) were overexpressed after 3 d, at the onset of the restoration phase. We also observed that induction of MMP-2 mRNA synthesis was concomitant with that of the two TGF-β isoforms. The modulation of MMP-2 expression by TGF-β has already been reported in other models[31,32], and the present results likewise support the hypothesis that the TGF-β family is involved in the regulation of MMP-2 expression after radiation-induced injury.

We investigated the plasminogen-plasmin system, an another activating pathway that is known to regulate MMP activity[2]. This system is a key regulator of fibrinolysis and ECM degradation[33]. Generation of plasmin from plasminogen is regulated by complex interactions between various activators and inhibitors. Classically, plasminogen is known to be activated by u-PA and t-PA. In this study, both u-PA and t-PA were found to be overexpressed 1 d after irradiation, suggesting that the plasmin system is acutely activated after abdominal irradiation. These results are in accordance with the previous reports[34-36] that showed an increase in the fibrinolytic activity in the intestinal mucosa after irradiation. At d 3 and 7, however, the increased expressions of u-PA and t-PA were associated to an increased expression of the inhibitor PAI-1, which may limit plasminogen activation.

Furthermore, we studied the expression of TIMP-1 and TIMP-2, the physiological inhibitors of MMPs. The involvement of TIMPs in inflammatory bowel diseases is still controversial. Heuschkel *et al*.[10], have shown that MMP-3 is overexpressed while TIMP-1 is not. von Lampe *et al*.[37], observed an increase in the level of TIMP-1 mRNA and no modification of the level of TIMP-2 mRNA, suggesting a net increase in the proteolytic activity in inflamed mucosa. Our observations seem consistent with these data obtained in human beings. Induction of TIMP-1 was observed after 1, 3, and 7 d of irradiation, whereas an upregulation of TIMP-2 was seen on d 3 after irradiation. MMP induction rates, however, significantly exceeded TIMP-1 induction. TIMP-2 has been reported to have a bimodal function and to promote activation of MMP-2 when associated with molecules, such as pro-MMP-2 and MMP-14, into large molecular complexes[38]. In this case, synthesis of MMP-14 seems to be the major rate-limiting factor of MMP-2 activation[39]. In this study, expression of both MMP-14 and TIMP-2 was increased after irradiation. Furthermore, MMP-14/TIMP-2 and MMP-2/TIMP-2 mRNA ratios suggested that activation of pro-MMP-2 must have occurred, since a marked increase in the level of active MMP-2 was observed at d 1 after exposure.

In conclusion, the molecular cascades induced by ionizing radiation are complex and are likely to involve more molecules than those studied here. These observations, however, bring new insights on radiation-induced ECM remodeling in the intestine. The fact that CD8a+ cells disappear after abdominal irradiation suggests that specific cellular effectors are involved in radiation-induced activation of MMPs.

REFERENCES

1 **Becciolini A**, Balzi M, Potten CS. Radiation effects on proliferation and differentiation in the rat small intestine In. Potten CS, Hendry JH, eds. Radiation and Gut. *Amsterdam: Elsevier* 1995: 85-143
2 **Sternlicht MD**, Werb Z. How matrix metalloproteinases regulate cell behavior. *Annu Rev Cell Dev Biol* 2001; **17**: 463-516
3 **Burger A**, Loffler H, Bamberg M, Rodemann HP. Molecular and cellular basis of radiation fibrosis. *Int J Radiat Biol* 1998; **73**: 401-408
4 **Linard C**, Ropenga A, Vozenin-Brotons MC, Chapel A, Mathe D. Abdominal irradiation increases inflammatory cytokine expression and activates NF-kappaB in rat ileal muscularis layer. *Am J Physiol Gastrointest Liver Physiol* 2003; **285**: G556-G565
5 **Nagase H**, Woessner JF. Matrix metalloproteinases. *J Biol Chem* 1999; **274**: 21491-21494
6 **Pender SL**, Salmela MT, Monteleone G, Schnapp D, McKenzie C, Spencer J, Fong S, Saarialho-Kere U, MacDonald TT. Ligation of alpha4ss1 integrin on human intestinal mucosal mesenchymal cells selectively Up-regulates membrane type-1 matrix metalloproteinase and confers a migratory phenotype. *Am J Pathol* 2000; **157**: 1955-1962
7 **Baker AH**, Edwards DR, Murphy G. Metalloproteinase inhibitors: biological actions and therapeutic opportunities. *J Cell Sci* 2002; **115**: 3719-3727
8 **Bailey CJ**, Hembry RM, Alexander A, Irving MH, Grant ME, Shuttleworth CA. Distribution of the matrix metalloproteinases stromelysin, gelatinases A and B, and collagenase in Crohn's disease and normal intestine. *J Clin Pathol* 1994; **47**: 113-116
9 **Baugh MD**, Perry MJ, Hollander AP, Davies DR, Cross SS, Lobo AJ, Taylor CJ, Evans GS. Matrix metalloproteinase levels are elevated in inflammatory bowel disease. *Gastroenterology* 1999; **117**: 814-822
10 **Heuschkel RB**, MacDonald TT, Monteleone G, Bajaj-Elliott M, Smith JA, Pender SL. Imbalance of stromelysin-1 and TIMP-1 in the mucosal lesions of children with inflammatory bowel disease. *Gut* 2000; **47**: 57-62
11 **Louis E**, Ribbens C, Godon A, Franchimont D, De Groote D, Hardy N, Boniver J, Belaiche J, Malaise M. Increased production of matrix metalloproteinase-3 and tissue inhibitor of metalloproteinase-1 by inflamed mucosa in inflammatory bowel disease. *Clin Exp Immunol* 2000; **120**: 241-246
12 **Saarialho-Kere UK**, Vaalamo M, Puolakkainen P, Airola K, Parks WC, Karjalainen-Lindsberg ML. Enhanced expression of matrilysin, collagenase, and stromelysin-1 in gastrointestinal ulcers. *Am J Pathol* 1996; **148**: 519-526
13 **Salmela MT**, MacDonald TT, Black D, Irvine B, Zhuma T, Saarialho-Kere U, Pender SL. Upregulation of matrix metalloproteinases in a model of T cell mediated tissue injury in the gut: analysis by gene array and *in situ* hybridisation. *Gut* 2002; **51**: 540-547
14 **Pender SL**, Tickle SP, Docherty AJ, Howie D, Wathen NC, MacDonald TT. A major role for matrix metalloproteinases in T cell injury in the gut. *J Immunol* 1997; **158**: 1582-1590
15 **Seifert WF**, Wobbes T, Hoogenhout J, de Man BM, Hendriks T. Intra-operative irradiation prolongs the presence of matrix metalloproteinase activity in large bowel anastomoses of the rat. *Radiat Res* 1997; **147**: 354-361
16 **Hovdenak N**, Wang J, Sung CC, Kelly T, Fajardo LF, Hauer-Jensen M. Clinical significance of increased gelatinolytic activity in the rectal mucosa during external beam radiation

therapy of prostate cancer. *Int J Radiat Oncol Biol Phys* 2002; **53**: 919-927
17 **Kumar A**, Collins HM, Scholefield JH, Watson SA. Increased type-IV collagenase (MMP-2 and MMP-9) activity following preoperative radiotherapy in rectal cancer. *Br J Cancer* 2000; **82**: 960-965
18 **Kleiner DE**, Stetler-Stevenson WG. Quantitative zymography: detection of picogram quantities of gelatinases. *Anal Biochem* 1994; **218**: 325-329
19 **Strup-Perrot C**, Mathe D, Linard C, Violot D, Milliat F, Francois A, Bourhis J, Vozenin-Brotons MC. Global gene expression profiles reveal an increase in mRNA levels of collagens, MMPs and TIMPs in late radiation enteritis. *Am J Physiol Gastrointest Liver Physiol* 2004; **287**: G875-G885
20 **MacDonald TT**, Spencer J. Evidence that activated mucosal T cells play a role in the pathogenesis of enteropathy in human small intestine. *J Exp Med* 1988; **167**: 1341-1349
21 **Pender SL**, Lionetti P, Murch SH, Wathan N, MacDonald TT. Proteolytic degradation of intestinal mucosal extracellular matrix after lamina propria T cell activation. *Gut* 1996; **39**: 284-290
22 **De Winter H**, Elewaut D, Turovskaya O, Huflejt M, Shimeld C, Hagenbaugh A, Binder S, Takahashi I, Kronenberg M, Cheroutre H. Regulation of mucosal immune responses by recombinant interleukin 10 produced by intestinal epithelial cells in mice. *Gastroenterology* 2002; **122**: 1829-1841
23 **Lyscom N**, Brueton MJ. Intraepithelial, lamina propria and Peyer's patch lymphocytes of the rat small intestine: isolation and characterization in terms of immunoglobulin markers and receptors for monoclonal antibodies. *Immunology* 1982; **45**: 775-783
24 **Schuppan D**, Hahn EG. MMPs in the gut: inflammation hits the matrix. *Gut* 2000; **47**: 12-14
25 **MacNaughton WK**, Leach KE, Prud'homme-Lalonde L, Ho W, Sharkey KA. Ionizing radiation reduces neurally evoked electrolyte transport in rat ileum through a mast cell-dependent mechanism. *Gastroenterology* 1994; **106**: 324-335
26 **Mengshol JA**, Vincenti MP, Coon CI, Barchowsky A, Brinckerhoff CE. Interleukin-1 induction of collagenase 3 (matrix metalloproteinase 13) gene expression in chondrocytes requires p38, c-Jun N-terminal kinase, and nuclear factor kappaB: differential regulation of collagenase 1 and collagenase 3. *Arthritis Rheum* 2000; **43**: 801-811
27 **Dignass AU**, Podolsky DK. Cytokine modulation of intestinal epithelial cell restitution: central role of transforming growth factor beta. *Gastroenterology* 1993; **105**: 1323-1332
28 **Beck PL**, Rosenberg IM, Xavier RJ, Koh T, Wong JF, Podolsky DK. Transforming growth factor-beta mediates intestinal healing and susceptibility to injury *in vitro* and *in vivo* through epithelial cells. *Am J Pathol* 2003; **162**: 597-608
29 **Ruifrok AC**, Mason KA, Lozano G, Thames HD. Spatial and temporal patterns of expression of epidermal growth factor, transforming growth factor alpha and transforming growth factor beta 1-3 and their receptors in mouse jejunum after radiation treatment. *Radiat Res* 1997; **147**: 1-12
30 **Wang J**, Zheng H, Sung CC, Richter KK, Hauer-Jensen M. Cellular sources of transforming growth factor-beta isoforms in early and chronic radiation enteropathy. *Am J Pathol* 1998; **153**: 1531-1540
31 **Edwards DR**, Murphy G, Reynolds JJ, Whitham SE, Docherty AJ, Angel P, Heath JK. Transforming growth factor beta modulates the expression of collagenase and metalloproteinase inhibitor. *Embo J* 1987; **6**: 1899-1904
32 **Overall CM**, Wrana JL, Sodek J. Transcriptional and post-transcriptional regulation of 72-kDa gelatinase/type IV collagenase by transforming growth factor-beta 1 in human fibroblasts. Comparisons with collagenase and tissue inhibitor of matrix metalloproteinase gene expression. *J Biol Chem* 1991; **266**: 14064-14071
33 **Vassalli JD**, Sappino AP, Belin D. The plasminogen activator/plasmin system. *J Clin Invest* 1991; **88**: 1067-1072
34 **Rao JS**, Rayford A, Yamamoto M, Ang KK, Tofilon P, Sawaya R. Modulation of fibrinolysis by ionizing radiation. *J Neurooncol* 1994; **22**: 161-171
35 **Boothman DA**, Wang M, Lee SW. Induction of tissue-type plasminogen activator by ionizing radiation in human malignant melanoma cells. *Cancer Res* 1991; **51**: 5587-5595
36 **Sawaya R**, Rayford A, Kono S, Ang KK, Feng Y, Stephens LC, Rao JS. Elevated levels of plasminogen activators in the pathogenesis of delayed radiation damage in rat cervical spinal cord *in vivo*. *Radiat Res* 1994; **138**: 386-391
37 **von Lampe B**, Barthel B, Coupland SE, Riecken EO, Rosewicz S. Differential expression of matrix metalloproteinases and their tissue inhibitors in colon mucosa of patients with inflammatory bowel disease. *Gut* 2000; **47**: 63-73
38 **Wang Z**, Juttermann R, Soloway PD. TIMP-2 is required for efficient activation of proMMP-2 *in vivo*. *J Biol Chem* 2000; **275**: 26411-26415
39 **Werb Z**. ECM and cell surface proteolysis: regulating cellular ecology. *Cell* 1997; **91**: 439-442

Science Editor Kumar M and Guo SY **Language Editor** Elsevier HK

PO Box 2345, Beijing 100023, China
www.wjgnet.com
wjg@wjgnet.com

ELSEVIER

World J Gastroenterol 2005;11(40):6322-6329
World Journal of Gastroenterology ISSN 1007-9327
© 2005 The WJG Press and Elsevier Inc. All rights reserved.

• *BASIC RESEARCH* •

Pioglitazone, a specific ligand of peroxisome proliferator-activated receptor-gamma, protects pancreas against acute cerulein-induced pancreatitis

Peter C Konturek, Artur Dembinski, Zygmunt Warzecha, Grzegorz Burnat, Piotr Ceranowicz, Eckhart G Hahn, Marcin Dembinski, Romana Tomaszewska, Stanislaw J Konturek

Peter C Konturek, Grzegorz Burnat, Eckhart G Hahn, First Department of Medicine, University Erlangen-Nürnberg, Germany
Artur Dembinski, Zygmunt Warzecha, Piotr Ceranowicz, Marcin Dembinski, Stanislaw J Konturek, Department of Physiology, Jagiellonian University Medical College, Cracow, Poland
Romana Tomaszewska, Department of Pathology, Jagiellonian University Medical College, Cracow, Poland
Correspondence to: Peter C Konturek, First Department of Medicine, University Erlangen-Nürnberg, Erlangen, Germany. peter.konturek@med1. imed.uni-erlangen.de
Telephone: +49-9131-8535211 Fax: +49-9131-8535212
Received: 2005-01-12 Accepted: 2005-04-30

Abstract

AIM: To determine the effect of pioglitazone, a specific peroxisome proliferator-activated receptor-γ (PPARγ) ligand, on the development of acute pancreatitis (AP) and on the expression of heat shock protein 70 (HSP70) in the pancreas.

METHODS: AP was induced in rats by subcutaneous infusion of cerulein for 5 h. Pancreatic blood flow was measured by laser Doppler flowmetry. Plasma lipase activity, interleukin-1β (IL-1β) and IL-10 were determined. Pancreatic weight and histology were evaluated and pancreatic DNA synthesis and blood flow as well as pancreatic mRNA for IL-1β and HSP70 were assessed in rats treated with pioglitazone alone or in combination with cerulein.

RESULTS: Pioglitazone administered (10-100 mg/kg i.g.) 30 min before cerulein, attenuated dose-dependently the pancreatic tissue damage in cerulein-induced pancreatitis (CIP) as demonstrated by the improvement of pancreatic histology, reduction in plasma lipase activity, plasma concentration of pro-inflammatory IL-1β and its gene expression in the pancreas and attenuation of the pancreatitis-evoked fall in pancreatic blood flow. CIP increased pancreatic HSP70 mRNA and protein expression in the pancreas and this effect was enhanced by pioglitazone treatment.

CONCLUSION: Pioglitazone attenuates CIP and the beneficial effect of this pioglitazone is multifactorial probably due to its anti-inflammatory activities, to the suppression of IL-1β and to the overexpression of HSP70. PPARγ ligands could represent a new therapeutic option in the treatment of AP.

© 2005 The WJG Press and Elsevier Inc. All rights reserved.

Key words: Cerulein-induced pancreatitis; PPARγ ligand; Heat shock protein 70

Konturek PC, Dembinski A, Warzecha Z, Burnat G, Ceranowicz P, Hahn EG, Dembinski M, Tomaszewska R, Konturek SJ. Pioglitazone, a specific ligand of peroxisome proliferator-activated receptor-gamma, protects pancreas against acute cerulein-induced pancreatitis. *World J Gastroenterol* 2005; 11(40): 6322-6329
http://www.wjgnet.com/1007-9327/11/6322.asp

INTRODUCTION

Acute pancreatitis (AP) is associated with high morbidity and mortality. Approximately 25% of patients develop severe inflammation with pancreatic and peripancreatic fat necrosis that requires intensive care. AP is a multifactorial disease associated with the release of digestive enzymes to the pancreatic interstitium and to the systemic circulation as well as with the increased cytokine production and release, which can ultimately lead to deleterious local and systemic effects[1].

In general, the pathomechanism of AP is still poorly understood. Recently, the modulatory role of peroxisome proliferator-activated receptors (PPARs) has been proposed in the inflammatory response of different organs[2]. The PPAR family consists of at least three different isoforms; PPARα, PPARδ, and PPARγ[3]. PPARγ is predominantly detected in adipose tissue, but it is also expressed in other tissues, including pancreatic tissue. When activated by a specific ligand, PPARs heterodimerize with retinoid X receptor and then bind to peroxisome proliferator response element leading to the change in the transcription of target genes involved in lipid metabolism, glucose homeostasis, cell proliferation and differentiation, and inflammatory response. PPARs are activated by natural ligands such as fatty acids, eicosanoids, oxidized fatty acids, and by pharmacological compounds such as glitazones. Pioglitazone is a member of glitazones and it has been clinically used to increase the sensitivity to insulin[4].

Several reports have demonstrated an anti-inflammatory action of the specific ligands of PPARγ. Activators of

PPARγ inhibit the generation of pro-inflammatory cytokines such as interleukin-1β (IL-1β), tumor necrosis factor-α (TNF-α) and interleukin-6[5] and this effect seems to be dependent on the inhibition of nuclear factor-κB (NFκB) pathway[6].

Heat shock-proteins (HSPs) are a group of cytoprotective proteins that help to maintain the metabolic and structural integrity of cells. HSPs are produced in many cell types in response to a variety of stresses, including heat, free radicals, and toxins[7]. HSPs are highly conserved proteins and play essential functions in protein folding, transport, translocation, degradation, and assembly[8]. In the pancreas, HSPs have been shown to provide the protection against cerulein- and arginine-induced pancreatitis[9,10]. HSP70 (also referred as HSP72 or inducible HSP70) is perhaps the most well-studied member of HSPs. However, it is not known whether PPARγ ligands interact with HSP70 and what is the biological consequence of this potential interaction.

The aim of the present study was: (1) to determine the effect of pioglitazone, a specific PPARγ ligand, on the development of acute cerulein-induced pancreatitis (CIP); (2) to assess the effect of treatment with pioglitazone on pancreatic expression of HSP70; and (3) to evaluate the effect of pre-treatment with pioglitazone on pancreatic synthesis and plasma level of IL-1β.

MATERIALS AND METHODS

Experimental model of pancreatitis

Studies were performed on male Wistar rats weighing 150-200 g, in accordance with the experimental protocol approved by the Committee for Research and Animal Ethics of Jagiellonian University College of Medicine, Cracow, Poland. Animals were housed in cages under standard conditions, on a commercial pellet chow, at room temperature with a 12-h light-dark cycle. Prior to the start of experiments, rats were deprived of food, while drinking water was available *ad libitum*. AP was induced by cerulein that was diluted in saline and infused subcutaneously (s.c.) for 5 h at a dose 10 μg/kg/h as described earlier[11].

To study the effect of pioglitazone on the development of AP, the rats were divided into following groups: (1) rats infused with 0.9% vehicle saline s.c. for 5 h (control); (2) rats infused with 0.9% saline s.c. for 5 h and pretreated with pioglitazone (10-100 mg/kg i.g., 30 min before saline infusion); (3) rats infused with cerulein (10 μg/kg/h) s.c. for 5 h; and (4) rats infused with cerulein (10 μg/kg/h) s.c. for 5 h and pretreated with pioglitazone (10-100 mg/kg i.g., 30 min before cerulein infusion). Animals were anesthetized and killed after 5 h of saline or cerulein infusion. This particular dose of pioglitazone 50 mg/kg was used because, in our previous studies, similar dose was highly effective in speeding up of the healing rate of gastric ulcer[12].

Determination of pancreatic blood flow

Following the infusion of saline or cerulein, animals were anesthetized with ketamine (50 mg/kg i.p., Bioketan, Biowet, Gorzów, Poland) and the abdomen was opened. The pancreas was exposed for the measurement of the blood flow by laser Doppler flowmeter, using PeriFlux 4001 Master monitor (Perimed AB, Järfälla, Sweden) as described previously[13]. The pancreatic blood flow was presented as percent change from the value obtained in rats infused with saline.

Determination of plasma lipase, IL-1β, and IL-10 concentration

Immediately after the measurement of pancreatic blood flow, the abdominal aorta was exposed and blood was taken for the determination of plasma lipase activity, and plasma IL-1β and IL-10 concentrations as described before[14].

Plasma lipase activity was determined with a Kodak Ectachem DT II System analyzer (Eastman Kodak Company, Rochester, NY, USA). The values of plasma lipase activity were expressed as units per liter.

The values of plasma IL-1β and IL-10 were measured in duplicate, using the Biosource Cytoscreen rat IL-1β and IL-10 kit based on a solid phase sandwich ELISA (BioSource International Inc., Camarillo, CA, USA) according to the manufacturer's instructions. Concentrations were expressed as picogram per milliliter.

Histological examination

After the collection of blood samples, the pancreas was dissected out and divided into samples for analysis of pancreatic mRNA, pancreatic protein, measurement of pancreatic DNA synthesis, and histological examination. Samples of pancreatic tissue for histological examination were fixed in 40 g/L formaldehyde and stained with hematoxylin and eosin. The histologic grading of edema was made using a scale ranging from 0 to 3; 0 = no edema, 1 = interlobular edema, 2 = interlobular edema and moderate intralobular edema, and 3 = interlobular edema and severe intralobular edema. Leukocytic infiltration was graded from 0 (absent) to 3 for maximal alterations (diffuse infiltration in the entire pancreatic gland). Grading of vacuolization was based on the appropriate percentage of cell involved; 0 = absent, 1 = less than 25%, 2 = 25-50%, and 3 = more than 50%.

Determination of pancreatic DNA synthesis

The rate of DNA synthesis in samples of pancreatic tissue was determined as described previously[15]. Briefly, the minced pancreatic tissue was incubated at 37 ℃ for 45 min in 2 mL of medium containing 8 μCi/mL of [^{3}H]thymidine ([6-^{3}H]thymidine, 20-30 Ci/mmoL; Institute for Research, Production and Application of Radioisotopes, Prague, Czech Republic). DNA concentration was determined by the Giles and Myers[16] procedure. The incorporation of mL [^{3}H] thymidine into DNA was determined by counting 0.5 mL DNA-containing supernatant in a liquid scintillation system. DNA synthesis was expressed as [^{3}H]thymidine disintegrations per minute per microgram DNA.

Determination of pancreatic mRNA for IL-1β and HSP70

Samples of pancreatic tissue for reverse transcriptase-polymerase chain reaction (RT-PCR) were snap-frozen in liquid nitrogen, and then stored at -80 ℃ until the time of RNA extraction. Total RNA was extracted from the pancreatic samples using the extraction kit from Stratagene (Heidelberg, Germany). Following precipitation, RNA was

resuspended in RNAse-free water and its concentration was estimated by absorbance at 260 nm wavelength. RNA samples were stored at -80 ℃ until analysis.

Single stranded cDNA was generated from 5 μg of total cellular RNA using Moloney murine leukemia virus reverse transcriptase (Stratagene, Heidelberg, Germany) and oligo-(dT)-primers (Stratagene, Heidelberg, Germany) in accordance with the procedure described by our group previously[17]. The resultant cDNA (2 μL) was amplified in 50 μL reaction volume containing 2 U Taq polymerase, dNTP (200 μmol/L each), 1.5 mmol/L $MgCl_2$, 5 μL 10× PCR buffer (100 mmol/L KCl, 20 mmol/L Tris-HCl, pH 8.3) and specific primers used at a final concentration of 1 mmol/L (all reagents were obtained from Takara, Shiga, Japan). The reaction mixture was amplified in a DNA thermal cycler (Perkin-Elmer-Cetus, Norwalk, CT, USA) and the incubation and thermal cycling conditions were as follows: denaturation at 94 ℃ for 1 min, annealing at 60 ℃ for 45 s and extension at 72 ℃ for 2 min. The number of cycles was 28 for GAPDH, 30 for HSP70, and 33 for IL-1β. The nucleotide sequence of the primers for GAPDH, IL-1β, and HSP70 were based on the sequences of the published cDNAs as described previously[18,19]. The primer sequence for IL-1β was: sense 5'-GCT ACC TAT GTC TTG CCC GT-3'; antisense 5'-GAC CAT TGC TGT TTC CTA GG-3'. Primer pair for IL-1β produced a 543-bp product according to the cDNA sequence. The primer sequence for HSP70 was: sense 5'-GTG AAG ATC TGC GTC TGC TTG-3'; antisense 5'-TTTGACAACAGG CTGGTG AAC C-5'. The expected length of the product was 590 bp. GAPDH primers were same as previously published by our group[17]. All primers were synthesized by GIBCO BRL/Life Technologies (Eggenstein, Germany). PCR products were detected by electrophoresis on a 1.5% agarose gel containing ethidium bromide. Location of a predicted product was confirmed by using 100-bp ladder (Takara, Shiga, Japan) as a standard size marker.

Protein extraction and analysis of pancreatic HSP70 expression by Western blot analysis

Shock frozen tissue from rat pancreas was homogenized in a lysis buffer (100 mmol/L Tris-HCl, pH 7.4, 15% glycerol, 2 mmol/L EDTA, 2% SDS, 100 mmol/L DDT) by the addition of 1:20 dilution of aprotinin and 1:50 dilution of 100 mmol/L PMSF. Insoluble material was removed by centrifugation at 12 000 *g* for 15 min. Approximately 50 μg of total protein extracts were loaded on SDS-polyacrylamide gels and run 40 mA, followed by transfer on nitrocellulose membrane (Protran, Schleicher & Schuell, Germany) by electroblotting. Three percent of BSA (Sigma-Aldrich, Germany) in TBS/Tween-20 buffer (137 mmol/L NaCl, 20 mmol/L Tris-HCl, pH 7.4, 0.1% Tween-20) was used to block filters for at least 1 h at room temperature. Specific primary antibody against HSP70 (mouse monoclonal, 1:200 dilution; Stressgen Biotechnologies Corp., Canada), or β-actin (mouse monoclonal, dilution 1:5 000; Sigma-Aldrich, Germany) was added to the membrane, followed by an anti-mouse-IgG HRP conjugated secondary antibody (dilution 1:20 000; Promega, USA) dissolved in 1% non-fat milk in TBS-Tween-20 buffer. Incubation of primary antibody was followed by washing thrice with TBS-Tween-20 buffer for 10 min. Incubation of the secondary antibody was followed by five washes for 10 min. Immunocomplexes were detected by the SuperSignal West Pico Chemiluminescent Kit (Pierce, USA). Thereafter, the developed membrane was exposed to an X-ray film (Kodak, Wiesbaden, Germany). Comparison between different treatment groups was made by determining the examined protein/β-actin ratio of the immunoreactive area by densitometry as described elsewhere[18].

Statistical analysis

Comparison of the difference between the mean values of various groups of experiments was made by analysis of variance and the Student's *t*-test for unpaired data. A difference with a *P* value of less than 0.05 was considered statistically significant. Results are expressed as mean±SE.

RESULTS

Effects of pioglitazone on the development of cerulein-induced pancreatitis and pancreatic blood flow

Four criteria were used to confirm the AP in rats infused with cerulein at a total dose of 50 μg/kg (10 μg/kg/h s.c. ×5 h): macroscopic and microscopic signs of AP, pancreatic edema leading to the increase in pancreatic weight and the rise in serum lipase activities. All these criteria were fulfilled in all rats treated with cerulein.

After the infusion of cerulein, the pancreas was enlarged with a visible collection of edematous fluid and the pancreatic mass was almost doubled (Figure 1). At light microscopic level, profound interlobular and intralobular edema, vacuolization of acinar cells, and moderate perivascular and scare diffuse leukocyte infiltration were observed. In rats pretreated with pioglitazone before the start of cerulein infusion, the inflammatory changes in the pancreas were significantly less pronounced when compared to changes observed in rats treated with cerulein alone (Figure 2 and Table 1). Treatment with pioglitazone alone had no effect on morphological features of the pancreas.

Plasma lipase activity in control, saline-infused rats, reached 57.0±6.0 U/L. In rats infused with cerulein, plasma lipase activity was almost increased eightfold, compared to the level obtained from control rats infused with saline. In rats pretreated with pioglitazone before cerulein, a significant and dose-dependent reduction in plasma lipase activity was

Table 1 Histology findings in the pancreas after treatment with various doses of pioglitazone alone or in combination with cerulein infused s.c. to induce pancreatitis

	Edema	Leukocyte infiltration	Vacuolization of acinar cells
Control	0	0	0
Pioglitazone 10 mg/kg	0	0	0
Pioglitazone 20 mg/kg	0	0	0
Pioglitazone 50 mg/kg	0	0	0
Pioglitazone 100 mg/kg	0	0	0
Cerulein	2/3	2	2/3
Pioglitazone 10 mg/kg+cerulein	2/3	1/2	2
Pioglitazone 20 mg/kg+cerulein	2	1	0.5
Pioglitazone 50 mg/kg+cerulein	1/2	0/1	1
Pioglitazone 100 mg/kg+cerulein	1	1	1

Table 2 Pancreatic DNA synthesis, pancreatic blood flow, plasma lipase activity, and the levels of IL-1β and IL-10 in rats treated with various doses of pioglitazone alone or in combination with cerulein infused s.c. to induce pancreatitis

	Pancreatic DNA synthesis (dpm/μg DNA)	Pancreatic blood flow (% of control)	Plasma lipase activity (U/L)	Plasma IL-1β (pg/mL)	Plasma IL-10 (pg/mL)
Control	58.8±1.6	100±2.0	57.0±6.0	70.3±4.2	67.0±5.0
Pioglitazone 10 mg/kg	61.3±1.9	98.9±1.7	62.3±5.6	69.7±3.9	66.9±4.1
Pioglitazone 20 mg/kg	60.9±2.2	99.6±2.1	59.2±6.7	74.2±5.5	72.7±5.1
Pioglitazone 50 mg/kg	61.6±1.1	101.5±1.7	60.5±4.5	68.2±4.9	73.0±3.0
Pioglitazone 100 mg/kg	57.4±2.1	97.6±2.4	71.8±6.9	76.8±5.4	71.9±5.1
Cerulein	33.8±1.4[a]	60.9±2.5[a]	400.3±10.6[a]	212.0±8.6[a]	79.2±3.5
Pioglitazone 10 mg/kg+cerulein	37.6±2.8[a]	66.2±2.1[a]	372.1±12.1[a]	198.4±5.7[a]	73.1±3.8
Pioglitazone 20 mg/kg+cerulein	41.6±1.7[a,c]	69.3±1.5[a,c]	322.4±9.6[a,c]	153.2±6.2[a,c]	81.6±7.2
Pioglitazone 50 mg/kg+cerulein	45.9±1.7[a,c]	79.2±2.2[a,c]	288.3±18.0[a,c]	131.3±7.2[a,c]	75.1±3.0
Pioglitazone 100 mg/kg+cerulein	39.6±2.3[a]	65.1±2.3[a]	269.3±13.9[a]	129.3±6.9[a]	64.6±3.2

[a]*P*<0.05 *vs* control, [c]*P*<0.05 *vs* cerulein alone.

found (Figure 3 and Table 2).

In saline-infused control rats, total pancreatic DNA synthesis reached 58.8±1.6 dpm/μg DNA (Figure 4). Treatment with pioglitazone alone did not affect pancreatic DNA synthesis in animals infused with saline. The induction of AP by cerulein was associated with a significant fall in DNA synthesis in the pancreas for about 44%. This effect was partly, but significantly reversed by the treatment with pioglitazone.

Pancreatic blood flow measured in rats with CIP was reduced by about 40% as compared to the control group (Figure 5). Treatment with pioglitazone did not affect pancreatic blood flow in animals infused with vehicle saline. In contrast, in rats given a cerulein infusion, pretreatment with pioglitazone was associated with a significant reverse in the cerulein-induced fall in the pancreatic blood flow.

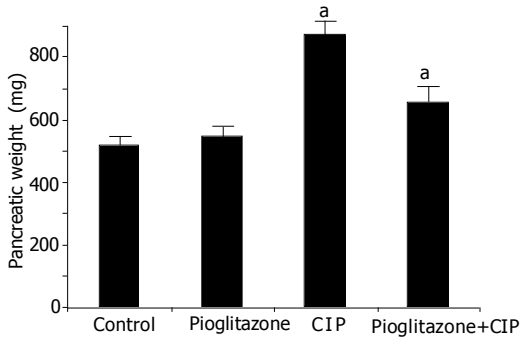


Figure 1 Pancreatic weight in rats with or without CIP pretreated with saline or pioglitazone at a dose 50 mg/kg. Mean±SE of eight rats in each experimental group. Asterisk indicates a significant change as compared to the value in rats infused with saline. Cross indicates a significant change as compared to rats with CIP alone. [a]*P*<0.05 *vs* CIP alone.

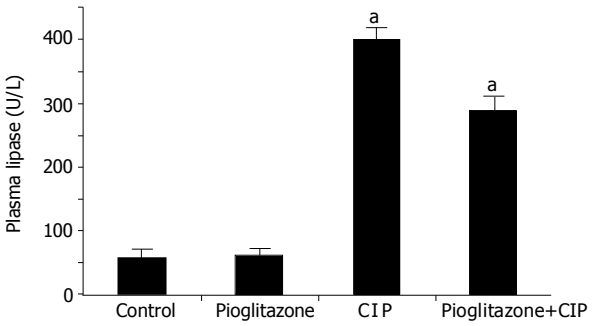


Figure 3 Plasma lipase activity in rats with or without CIP and pretreated with saline or pioglitazone at a dose 50 mg/kg. Mean±SE of eight rats in each experimental group. Asterisk indicates a significant change as compared to the value in rats infused with saline. Cross indicates a significant change as compared to rats with CIP alone. [a]*P*<0.05 *vs* CIP alone.

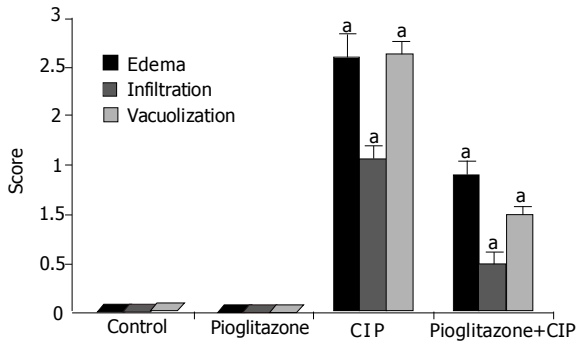


Figure 2 Histological changes (edema, infiltration, and vacuolization) observed in rats with or without CIP and pretreated with saline or pioglitazone at a dose 50 mg/kg. Mean±SE of eight rats in each experimental group. Asterisk indicates a significant change as compared to the value in rats infused with saline. Cross indicates a significant change as compared to rats with CIP alone. [a]*P*<0.05 *vs* CIP alone.

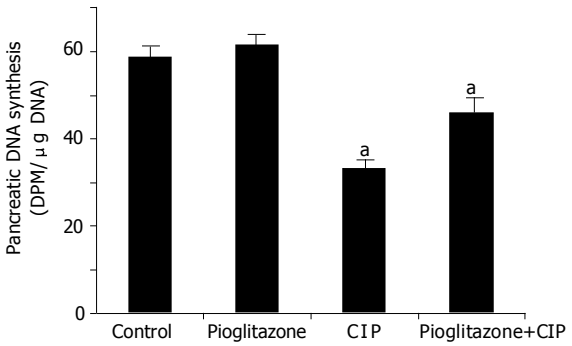


Figure 4 Pancreatic DNA synthesis in rats with or without CIP and pretreated with saline or pioglitazone at a dose 50 mg/kg. Mean±SE of eight rats in each experimental group. Asterisk indicates a significant change as compared to the value in rats infused with saline. Cross indicates a significant change as compared to rats with CIP alone. [a]*P*<0.05 *vs* CIP alone.

The measurement of plasma level of IL-10 showed no significant changes in rats with CIP or treated with pioglitazone as compared to control group (Figure 6). In contrast, IL-1β was significantly increased in rats with CIP. Pretreatment with pioglitazone did not significantly affect plasma IL-1β concentration in rats infused with saline, but pretreatment with pioglitazone caused a significant and dose-dependent reduction in plasma level of this important pro-inflammatory cytokine in animals with CIP.

In tissue samples taken from control pancreas without CIP, a weak but detectable signal for IL-β1 mRNA was observed (Figure 7). The expression of GAPDH was well preserved in all the samples. After the induction of CIP, a significant increase in IL-1β mRNA was found. This effect was strongly attenuated in rats pretreated with pioglitazone.

The analysis of mRNA expression of HSP70 showed a detectable signal of HSP70 in the samples of the pancreas obtained from control group (Figure 8). After the induction of CIP, a strong upregulation of mRNA for HSP70 was observed. Interestingly, the treatment with pioglitazone caused a further increase in mRNA expression for HSP70.

At the protein level, similar results were observed; a weak signal for HSP70 in control pancreas, a significant increase of the signal in CIP, and a further increase in HSP70 expression in rats with CIP pretreated with pioglitazone (Figure 9).

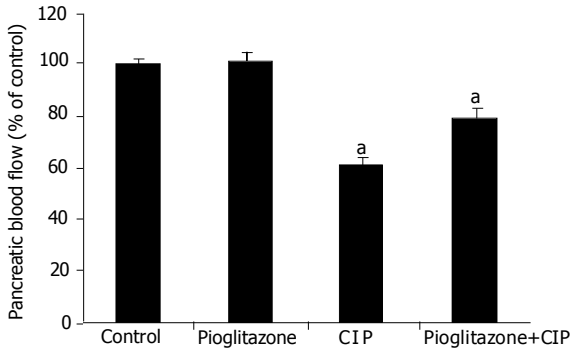


Figure 5 Pancreatic blood flow in rats with or without CIP and pretreated with saline or pioglitazone at a dose 50 mg/kg. Mean±SE of eight rats in each experimental group. Asterisk indicates a significant change as compared to the value in rats infused with saline. Cross indicates a significant change as compared to rats with CIP alone.[a]*P*<0.05 *vs* CIP alone.

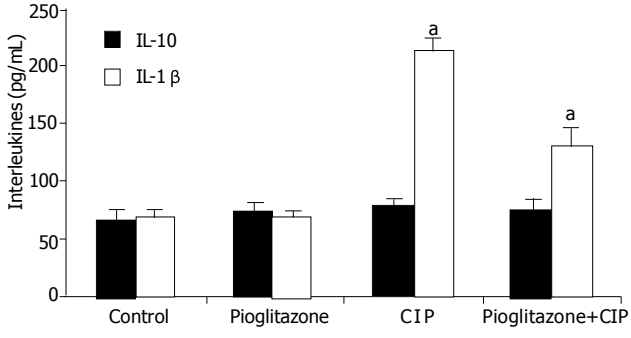


Figure 6 Plasma IL-1β and IL-10 levels in rats with or without CIP and pretreated with saline or pioglitazone at a dose 50 mg/kg. Mean±SE of eight rats in each experimental group. Asterisk indicates a significant change as compared to the value in rats infused with saline. Cross indicates a significant change as compared to rats with CIP alone.[a]*P*<0.05 *vs* CIP alone.

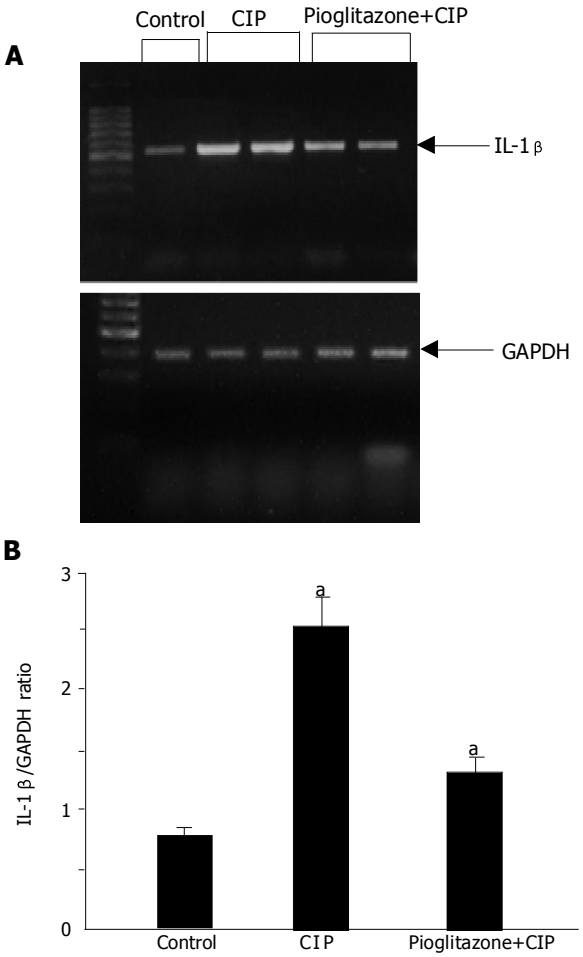


Figure 7 Expression of IL-1β mRNA and densitometric analysis of IL-1β mRNA expression (IL-1β/GAPDH ratio) in rats infused with saline without pancreatitis (control), rats with CIP and rats with CIP pretreated with pioglitazone. (**A**,**B**) Asterisk indicates a significant change as compared to the value in rats infused with saline. Cross indicates a significant change as compared to rats with CIP alone.[a]*P*<0.05 *vs* CIP alone.

DISCUSSION

We have reported in this study that the pre-treatment of rats with pioglitazone, a specific PPARγ ligand, significantly and dose-dependently attenuated the development of CIP. This result is in accordance with the earlier report that natural PPARγ ligand, 15d-PGJ2, reduced the severity of CIP[19]. The mechanisms underlying the protective effect of pioglitazone on the CIP remain unclear. First of all, the beneficial effect of pioglitazone on the pancreas subjected to acute injury by cerulein over-stimulation could be due to its local and systemic anti-inflammatory properties. Previous reports indicated that PPARγ agonists exhibit anti-inflammatory effects both in *in vitro* and *in vivo* studies[5,19]. This anti-inflammatory effect seems to be related to multiple mechanisms. Ricote *et al.*[20], demonstrated that PPARγ ligands inhibit macrophage activation and inflammatory cytokine production. Our previous studies showed that pioglitazone reduces acute and chronic gastric mucosal lesions due to the inhibition of TNF-α and IL-1β expression[12]. Furthermore, Meier *et al.*[21], showed that PPARγ ligands exert anti-inflammatory activity by inducing the production

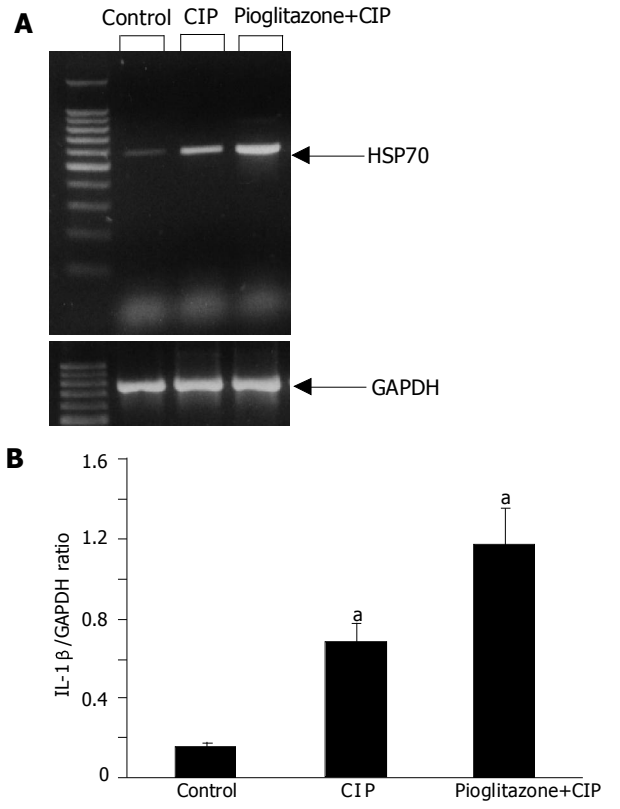


Figure 8 Expression of HSP70 mRNA and densitometric analysis of HSP70 mRNA expression (HSP70/GAPDH ratio) in rats infused with saline without pancreatitis (control), rats with CIP and rats with CIP pretreated with pioglitazone. (**A**,**B**) Asterisk indicates a significant change as compared to the value in rats infused with saline. Cross indicates a significant change as compared to rats with CIP alone.[a]*P*<0.05 *vs* CIP alone.

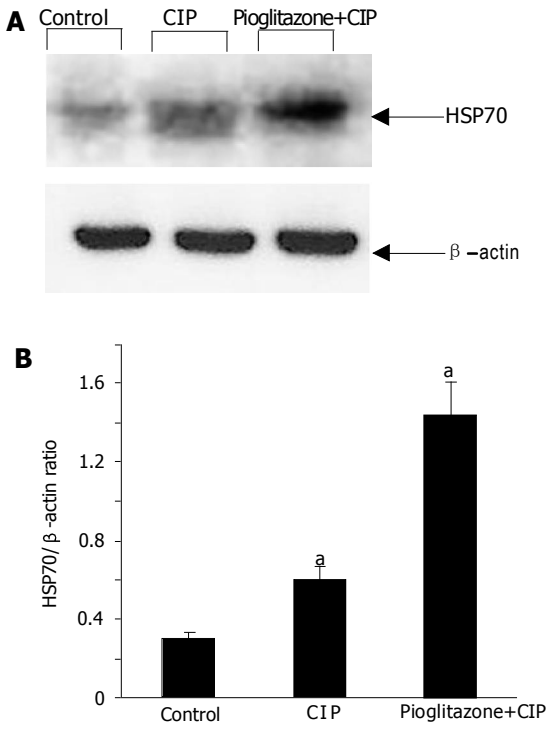


Figure 9 Expression of HSP70 protein and densitometric analysis of HSP70 protein expression (HSP70/β-actin ratio) in rats infused with saline without pancreatitis (control), rats with CIP and rats with CIP pretreated with pioglitazone. (A,B) Asterisk indicates a significant change as compared to the value in rats infused with saline. Cross indicates a significant change as compared to rats with CIP alone.[a]*P*<0.05 *vs* CIP alone.

of IL-1 receptor antagonist. One of the important mechanisms by which pioglitazone inhibits the inflammatory reaction is the reduction in activation of the transcription factor, NFκB, by the IκB-dependent mechanism[19]. Moreover, Imamoto *et al*.[22], found that pioglitazone exerts a strong inhibitory effect on the expression of adhesion molecule VCAM-1 on neutrophils and endothelial cells, thus reducing the leukocyte recruitment in the inflamed tissue. There is also clinical evidence for the anti-inflammatory effects of glitazones. Haffner *et al*.[23], reported that treatment of type 2 diabetes mellitus patients with rosiglitazone resulted in a reduction of serum concentration of C-reactive protein and WBCs count. All these reports underline the importance of PPARγ ligands in the modulation of inflammatory reaction in different organs, particularly in reducing the cerulein-induced oxidative stress in pancreatic tissue[24].

Our present study confirms and extends previous findings[25-27] by showing that inflammatory infiltration of pancreatic tissue caused by CIP is accompanied by a significant increase in pancreatic mRNA expression of IL-1β and increased release of this cytokine in rats infused for 5 h with supramaximal dose of cerulein. The new finding of our present study is that pretreatment with pioglitazone at a dose of 50 mg/kg significantly suppresses the gene expression and plasma level of IL-1β, as well as reduces leukocyte infiltration of pancreatic tissue in the course of CIP. This observation indicates that pioglitazone, a specific PPARγ ligand, is a powerful modulator of inflammatory response.

In contrast to IL-1β, IL-10 is found to be a major anti-inflammatory cytokine[28]. It reduces activation of macrophages and inhibits the production of reactive oxygen species and pro-inflammatory cytokines[28]. Van Laethem *et al*.[29], showed that administration of IL-10 before and during the induction of AP decreases the severity of this pancreatitis. Also, administration of some growth factor such as hepatocyte growth factor[30] or insulin-like growth factor-1[13] increases a plasma level of IL-10 and inhibits the development of AP. In our present study, we did not observe any alteration in plasma IL-10 concentration after the development of acute CIP or pretreatment with pioglitazone at various doses. This result suggests that the anti-inflammatory action of pioglitazone does not depend upon the release of IL-10.

The most important finding of this study is the observation that pioglitazone increased significantly the expression of HSP70. HSPs are highly conserved cytoprotective proteins that have essential functions in protein folding, transport, degradation, and assembly. HSPs are classified into six major families (small HSP, HSP40, HSP60, HSP70, HSP90, and HSP100) depending on their molecular weight[7]. HSP70 is the best studied member of HSPs family. Previous studies demonstrated that both thermal and non-thermal stress protects against CIP and prevents trypsinogen activation in the pancreas and this effect is mediated by HSP70[31]. The potential protective mechanisms of HSPs on pancreas

include: stabilization and refolding of damaged proteins, resistance of the cells to apoptosis or necrosis, decrease in the level of pro-inflammatory cytokines and antioxidant effects and interference with intra-acinar zymogen activation[7,31-33]. Our results are in accordance with the previous studies showing an increase of HSP70 at mRNA and protein level after induction of CIP. The major finding is, however, the observation of the further increase in HSP70 expression in rats pretreated with pioglitazone. This indicates that the protective effects of pioglitazone could be mediated, at least in part, through increased HSP expression. This issue needs to be clarified in further studies, especially in *in vitro* studies.

Administration of pioglitazone alone did not affect pancreatic DNA synthesis. Induction of AP by cerulein caused a reduction in the pancreatic DNA synthesis, that is in agreement with our previous observation[34], and may be considered as an index of pancreatic damage. In rats with the induction of pancreatitis by cerulein, the pretreatment with pioglitazone attenuated the pancreatitis-evoked fall in pancreatic DNA synthesis. This observation is an additional evidence of protective effect of pioglitazone against pancreatic damage in CIP.

It is well known that the development of AP is associated with the reduction in pancreatic blood flow[35-37], whereas vasodilatation and the improvement of pancreatic blood flow reduces the development of AP[37]. Our results are in accordance with these observations. Administration of cerulein induced acute edematous pancreatitis and reduced the pancreatic blood flow. Pretreatment with pioglitazone partly reversed cerulein-induced fall in pancreatic blood flow, suggesting that the improvement of pancreatic microcirculation might contribute to the protective effect of pioglitazone administration. The mechanism of vascular effects of pioglitazone administration is unclear. Pioglitazone given alone without cerulein infusion had no effect on pancreatic blood flow. This observation indicates that pioglitazone acts indirectly on pancreatic blood flow, probably by the reduction of cerulein-induced pancreatic edema and reduction of leukocyte activation.

The fact that pioglitazone strongly inhibits the inflammatory reaction in CIP, suggests that this compound may offer a new treatment opportunity, especially in the prophylaxis of pancreatitis in human beings. This issue should be studied in the prospective protocol in human beings. Moreover, the protective effect of pioglitazone should be checked in other acute and chronic experimental models of pancreatitis.

In summary, our study provides evidence that pioglitazone, a specific PPARγ ligand, ameliorates significantly the pancreatic damage associated with the CIP confirmed by the improvement of pancreas histology and the reduction in plasma lipase activity. Treatment with pioglitazone significantly inhibited the production and release of IL-1β and enhanced the expression of pancreatic HSP70. These observations indicate that the treatment with pioglitazone may offer a new therapeutic option in the treatment or prophylaxis of pancreatitis.

REFERENCES

1 **Kingsnorth A.** Role of cytokines and their inhibitors in acute pancreatitis. *Gut* 1997; **40**: 1-4

2 **Chinetti G,** Fruchart JC, Staels B. Peroxisome proliferator-activated receptors and inflammation: from basic science to clinical applications. *Int J Obes Relat Metab Disord* 2003; **27** (Suppl 3): S41-45

3 **Mangelsdorf DJ,** Thummel C, Beato M, Herrlich P, Schutz G, Umesono K, Blumberg B, Kastner P, Mark M, Chambon P, Evans RM. The nuclear receptor superfamily: the second decade. *Cell* 1995; **83**: 835-839

4 **Berger J,** Moller DE. The mechanisms of action of PPARs. *Annu Rev Med* 2002; **53**: 409-435

5 **Jiang C,** Ting AT, Seed B. PPAR-gamma agonists inhibit production of monocyte inflammatory cytokines. *Nature* 1998; **391**: 82-86

6 **Su CG,** Wen X, Bailey ST, Jiang W, Rangwala SM, Keilbaugh SA, Flanigan A, Murthy S, Lazar MA, Wu GD. A novel therapy for colitis utilizing PPAR-gamma ligands to inhibit the epithelial inflammatory response. *J Clin Invest* 1999; **104**: 383-389

7 **Rakonczay Z,** Takacs T, Boros I, Lonovics J. Heat shock proteins and the pancreas. *J Cell Physiol* 2003; **195**: 383-391

8 **Parcellier A,** Gurbuxani S, Schmitt E, Solary E, Garrido C. Heat shock proteins, cellular chaperones that modulate mitochondrial cell death pathways. *Biochem Biophys Res Commun* 2003; **304**: 505-512

9 **Wagner AC,** Weber H, Jonas L, Nizze H, Strowski M, Fiedler F, Printz H, Steffen H, Goke B. Hyperthermia induces heat shock protein expression and protection against caerulein-induced pancreatitis in rats. *Gastroenterology* 1996; **111**: 1333-1342

10 **Tashiro M,** Ernst SA, Edwards J, Williams JA. Hyperthermia induces multiple pancreatic heat shock proteins and protects against subsequent arginine-induced acute pancreatitis in rats. *Digestion* 2002; **65**: 118-126

11 **Konturek PC,** Jaworek J, Maniatoglou A, Bonior J, Meixner H, Konturek SJ, Hahn EG. Leptin modulates the inflammatory response in acute pancreatitis. *Digestion* 2002; **65**: 149-160

12 **Konturek PC,** Brzozowski T, Kania T, Konturek SJ, Kwiecien S, Pajdo R, Hahn EG. Pioglitazone, a specific ligand of peroxisome proliferator-activated receptor-gamma, accelerates gastric ulcer healing in rats. *Eur J Pharmacol* 2003; **38**: 468-476

13 **Konturek SJ,** Szlachcic A, Dembinski A, Warzecha Z, Jaworek J, Stachura J. Nitric oxide in pancreatic secretion and hormone-induced pancreatitis in rats. *Int J Pancreatol* 1994; **15**: 19-28

14 **Warzecha Z,** Dembinski A, Ceranowicz P, Konturek SJ, Tomaszewska R, Stachura J, Konturek PC. IGF-1 stimulates production of interleukin-10 and inhibits development of caerulein-induced pancreatitis. *J Physiol Pharmacol* 2003; **54**: 575-590

15 **Warzecha Z,** Dembinski A, Konturek PC, Ceranowicz P, Konturek SJ. Epidermal growth factor protects against pancreatic damage in cerulein-induced pancreatitis. *Digestion* 1999; **60**: 314-323

16 **Giles KW,** Myers A. An improvement diphenylamine method for the estimation of deoxyribonucleic acid. *Nature* 1965; **206**: 93

17 **Warzecha Z,** Dembinski A, Ceranowicz P, Konturek S, Tomaszewska R, Stachura J, Nakamura T, Konturek PC. Inhibition of cyclooxygenase-2 reduces the protective effect of hepatocyte growth factor in experimental pancreatitis. *Eur J Pharmacol* 2004; **486**: 107-119

18 **Konturek PC,** Brzozowski T, Kania J, Konturek SJ, Hahn EG. Nitric oxide-releasing aspirin protects gastric mucosa against ethanol damage in rats with functional ablation of sensory nerves. *Inflamm Res* 2003; **52**: 359-365

19 **Hashimoto K,** Ethridge RT, Saito H, Rajaraman S, Evers BM. The PPARgamma ligand, 15d-PGJ2, attenuates the severity of cerulein-induced acute pancreatitis. *Pancreas* 2003; **27**: 58-66

20 **Ricote M,** Li AC, Willson TM, Kelly CJ, Glass CK. The peroxisome proliferator-activated receptor-gamma is a negative regulator of macrophage activation. *Nature* 1998; **391**: 79-82

21 **Meier CA,** Chicheportiche R, Juge-Aubry CE, Dreyer MG, Dayer JM. Regulation of the interleukin-1 receptor antagonist in THP-1 cells by ligands of the peroxisome proliferator-acti-

vate receptor gamma. *Cytokine* 2002; **18**: 320-328
22 **Imamoto E,** Yoshida N, Uchiyama K, Kuroda M, Kokura S, Ichikawa H, Naito Y, Tanigawa T, Yoshikawa T. Inhibitory effect of pioglitazone on expression of adhesion molecules on neutrophils and endothelial cells. *Biofactors* 2004; **20**: 37-47
23 **Haffner SM,** Greenberg AS, Weston WM, Chen H, Williams K, Freed MI. Effect of rosiglitazone treatment on nontraditional markers of cardiovascular disease in patients with type 2 diabetes mellitus. *Circulation* 2002; **106**: 679-684
24 **Fu K,** Sarras MP, De Lisle RC, Andrews GK. Expression of oxidative stress-responsive genes and cytokine genes during caerulein-induced acute pancreatitis. *Am J Physiol* 1997; **273**: G696-G705
25 **Norman JG,** Fink GW, Denham W. Tissue-specific cytokine production during experimental acute pancreatitis. A probable mechanism for distant organ dysfunction. *Dig Dis Sci* 1997; **42**: 1783-1788
26 **Warzecha Z,** Dembinski A, Ceranowicz P. Calcitonin gene-related peptide can attenuate or augment pancreatic damage in caerulein-induced pancreatitis in rats. *J Physiol Pharmacol* 1999; **50**: 49-62
27 **Moore KW,** O'Garra A, de Waal Malefyt R, Vieira P, Mosmann TR. Interleukin-10. *Annu Rev Immunol* 1993; **11**: 165-190
28 **de Waal Malefyt R,** Abrams J, Bennett B, Figdor CG, de Vries JE. Interleukin-10 (IL-10) inhibits cytokine synthesis by human monocytes: an autoregulatory role of IL-10 produced by monocytes. *J Exp Med* 1991; **174**: 1209-1220
29 **Van Laethem JL,** Marchant A, Delvaux A, Goldman M, Robberecht P, Velu T, Deviere J. Interleukin 10 prevents necrosis in murine experimental acute pancreatitis. *Gastroenterology* 1995; **108**: 1917-1922
30 **Warzecha Z,** Dembinski A, Konturek PC, Ceranowicz P, Dembinski M, Stachura J, Konturek SJ. Hepatocyte growth factor attenuates pancreatic damage in caerulein-induced pancreatitis. *Eur J Pharmacol* 2001; **430**: 113-121
31 **Frossard JL,** Bhagat L, Lee HS, Hietaranta AJ, Singh VP, Song AM, Steer ML, Saluja AK. Both thermal and non-thermal stress protect against caerulein induced pancreatitis and prevent trypsinogen activation in the pancreas. *Gut* 2002; **50**: 78-83
32 **Takayama S,** Reed JC, Homma S. Heat-shock proteins as regulators of apoptosis. *Oncogene* 2003; **22**: 9041-9047
33 **Bhagat L,** Singh VP, Hietaranta AJ, Agrawal S, Steer ML, Saluja AK. Heat shock protein 70 prevents secretagogue-induced cell injury in the pancreas by preventing intracellular trypsinogen activation. *J Clin Invest* 2000; **106**: 81-89
34 **Dembinski A,** Warzecha Z, Konturek PC, Ceranowicz P, Konturek SJ, Tomaszewska R, Stachura J. Adaptation of pancreas to repeated caerulein-induced pancreatitis in rats. *J Physiol Pharmacol* 1996; **47**: 455-467
35 **Menger MD,** Plusczyk T, Vollmar B. Microcirculatory derangements in acute pancreatitis. *J Hepatobiliary Pancreat Surg* 2001; **8**: 187-194
36 **Zhou ZG,** Chen YD, Sun W, Chen Z. Pancreatic microcirculatory impairment in experimental acute pancreatitis in rats. *World J Gastroenterol* 2002; **8**: 933-936
37 **Warzecha Z,** Dembinski A, Ceranowicz P, Konturek PC, Stachura J, Konturek SJ, Niemiec J. Protective effect of calcitonin gene-related peptide against caerulein-induced pancreatitis in rats. *J Physiol Pharmacol* 1997; **48**: 775-787

Science Editor Guo SY **Language Editor** Elsevier HK

PO Box 2345, Beijing 100023, China
www.wjgnet.com
wjg@wjgnet.com

ELSEVIER

World J Gastroenterol 2005;11(40):6330-6337
World Journal of Gastroenterology ISSN 1007-9327
© 2005 The WJG Press and Elsevier Inc. All rights reserved.

• *BASIC RESEARCH* •

Distinct immune response induced by peptidoglycan derived from *Lactobacillus sp*

Jin Sun, Yong-Hui Shi, Guo-Wei Le, Xi-Yi Ma

Yong-Hui Shi, Guo-Wei Le, the Key Laboratory of Food Science and Security, Ministry of Education, Southern Yangtze University, Wuxi 214036, Jiangsu Province, China
Jin Sun, Yong-Hui Shi, Guo-Wei Le, Xi-Yi Ma, Institute of Food Nutrition and Safety, School of Food Science and Technology, Southern Yangtze University, Wuxi 214036, Jiangsu Province, China
Supported by the PhD Programs Foundation of Ministry of Education of China, No. 20040295005
Correspondence to: Professor Yong-Hui Shi, Institute of Food Nutrition and Safety, School of Food Science and Technology, Southern Yangtze University, 170 Huihe Road, Wuxi 214036, Jiangsu Province, China. yhshi@sytu.edu.cn
Telephone: +86-510-5869236 Fax: +86-510-5869236
Received: 2004-11-28 Accepted: 2005-01-03

Abstract

AIM: To analyze the distinct immune responses induced by *Lactobacillus* peptidoglycan (PG).

METHODS: BALB/c mice were intraperitoneally injected with PG once a day for three consecutive days. Peritoneal macrophage and splenocyte mRNA was extracted and the gene expression profile was studied using high-density oligonucleotide microarrays. Inhibitory effects of *Lactobacillus* PG on colon tumor tissue were studied *in vitro* and *in vivo*.

RESULTS: The gene expression profiles revealed that the TLR-NF-κB and Jak-STAT signaling pathways were highly activated. An inflammatory phenotype was induced when peritoneal macrophages were initially exposed to *Lactobacillus* PG and switched to a more complex phenotype when BALB/c mice were treated with three doses of *Lactobacillus* PG. A protective physiological inflammatory response was induced after three consecutive days of PG treatment. It was tending toward Th1 dominant immune response. *Lactobacillus* PG also appeared to induce a significant *in vivo* anti-colon tumor effect.

CONCLUSION: *Lactobacillus* PG is responsible for certain immune responses induced by *Lactobacilli*. Anti-tumor effects of *Lactobacilli* are likely to attribute to the activation of macrophages by PG expressed on the bacterial cell surface.

© 2005 The WJG Press and Elsevier Inc. All rights reserved.

Key words: *Lactobacillus* peptidoglycan; Gene expression; Immune response

Sun J, Shi YH, Le GW, Ma XY. Distinct immune response induced by peptidoglycan derived from *Lactobacillus sp.* *World J Gastroenterol* 2005; 11(40): 6330-6337
http://www.wjgnet.com/1007-9327/11/6330.asp

INTRODUCTION

Lactobacilli have been shown to affect selected aspects of immune function that may involve one or several components of the humoral, cellular or nonspecific immunity[1]. These functions suggest that the potential use of *Lactobacilli* in foodstuffs or medicines can prevent infection of pathogenic bacteria[2] or induction of cancer[3-5]. It is not known entirely, however, how *Lactobacilli* affect the immune system and exert these immunostimulative effects. It has been suggested that *Lactobacilli* activate innate immunity response and mediate a protective inflammatory response in the gut. The first defense mechanism in inflammation is innate immunity and involves epithelial barrier, phagocytes and release of cell-derived inflammatory mediators (i.e. cytokines). Innate immunity activates rapidly after exposure of the host to inflammatory stimuli. It has been found that pathogenic microbes express highly conserved molecular structures called pathogen-associated molecular patterns (PAMPs)[6]. PAMPs include microbial cell wall components such as lipopolysaccharide (LPS), lipoteichoic acid and peptidoglycan (PG)[7]. Active innate immune cells express pattern-recognition receptors (PRRs) which are capable of recognizing common features of PAMPs. Toll-like receptors (TLRs) are important PRRs involved in the activation of pro-inflammatory reactions[6]. TLR2 is an important TLR member that recognizes PG. Binding of bacteria or bacterial products (i.e. PG) to TLRs leads to activation of intracellular signaling cascades, resulting in the activation of transcription factors, including nuclear factor κB (NF-κB), which regulates a wide variety of innate immunity responses. Activation of NF-κB has been found to induce the expression of several inflammatory mediators such as pro-inflammatory cytokines and cell adhesion proteins[8]. These factors acting alone, sequentially, or in combination, stimulate and amplify the inflammatory response. Recent studies indicate that, in addition to pathogenic microbes and their products, immune responses can be primed or activated by non-pathogenic commensal bacteria, including the probiotics such as *Lactobacillus* and *Bifidobacteria* species[1]. Probiotics share distinct commensal-associated molecular patterns (CAMPs)[9], which enhance epithelial barrier function in the gut, activate NF-κB and cytokine production in monocytes/macrophages and natural killer (NK) cells and induce phagocytic activity in neutrophils[10].

Rakoff-Nahoum *et al.*[11], demonstrated that the beneficial effects of commensal bacteria or probiotics are due to recognition of their surface molecules by TLRs. This recognition triggers TLRs to regulate genes that foster homeostasis of the intestinal epithelium. It also confers a protective effect on these cells and induces tissue repair. Elucidating the interaction between host and probiotic cell surface molecules is the key to this protective effect. However, there are few reports on systematic investigation of host cell responses to CAMPs from various probiotic strains. In an earlier study[12], we found that *Lactobacillus* PG, a type of CAMP, enhances immune surveillance in mice. To delineate this response in a more comprehensive way, we undertook a genome-wide analysis of the immune response to *Lactobacillus* PG. The results reveal that the transcription of most genes participating in the immune response is modulated after PG treatment. Many of these genes are involved in the activation of TLR-NF-κB and Jak-STAT signaling pathways. Activation of these signaling pathways is likely to invoke pro-helper T type-1 immune/cell-mediated immune response (Th1/CMI). Due to this induced response, anti-colon tumor effects of *Lactobacillus* PG were also studied and the results suggest that *Lactobacillus* PG can be used as a potential mediator in cancer immunotherapy.

MATERIALS AND METHODS

Preparation of peptidoglycan

A livestock feces derived *Lactobacillus* strain, *Lactobacillus* sp., was used. The strains were maintained at -80 ℃ as 15% glycerol stocks and subcultured in MRS broth or on MRS agar plates at 37 ℃. *Lactobacillus* PG was prepared as previously described[13] with minor modifications. Briefly, *Lactobacillus sp.* was grown in MRS liquid medium for 48 h at 37 ℃ without shaking. The culture was quickly chilled in an ice bath and the bacteria were harvested by centrifugation (2 000 r/min, 10 min, 4 ℃) and washed several times with water. The cells were placed in a boiling water bath for 20 min before they were broken by sonication. The suspension was centrifuged at 1 000 r/min for 15 min to sediment unbroken bacteria and the supernatant containing the cell walls was decanted. After the centrifugation at 10 000×*g* for 10 min, the pelleted cell walls were incubated in 2% sodium dodecyl sulfate for 30 min at 60 ℃. After being washed four times with water and twice with dehydrated alcohol, covalently bound proteins were digested with 0.02% trypsin in 0.1 mol/L Tris-HCl buffer (pH 7.5) for 20 h at 37 ℃. The walls were washed several times with water and lyophilized, resuspended in 10% trichloroacetic acid and stirred for 20 min at 60 ℃. PG was concentrated by centrifugation (10 000×*g*, 20 min) and washed extensively with water. All reagents used were sterile, and disposable plasticware or glassware baked at 180 ℃ was used to avoid contamination with endotoxin.

PG administration and preparation of macrophages and splenic lymphocytes

Three groups of BALB/c mice (three per group) were injected ip with either 0.5 mL of PBS (control) or PG (25 mg/kg weight in 0.5 mL PBS) once a day for one day or three consecutive days. Mice were killed after administration of PG. Peritoneal macrophages and splenic lymphocytes were isolated and mixed together (1×10^7 cells each) for each treatment and stored at -70 ℃ in 2 mL TRIzol reagent for future use.

Analysis of gene expression by high-density oligonucleotide arrays

Gene expression analysis was performed using the Affymetrix MOE430A GeneChip system according to the manufacturer's instructions (Protocol for Eukaryotic Sample and Array Processing in http://www.Affymetrix.com). Briefly, total RNA was isolated using the RNeasy Mini Kit from QIAGEN. Double-stranded cDNA was synthesized using 0.2 μg poly (A)-RNA. Biotin-labeled cRNA was synthesized using the BioArray high-yield RNA transcript-labeling kit (Enzo Biochem) and equal amounts of fragmented RNA (30 μg) were hybridized to each array. The arrays were washed using the EukGW2 protocol on the GeneChip Fluidics Station 400 series and scanned using the GeneArray scanner.

Colon tumor inhibition by peptidoglycan

In order to determine *in vitro* inhibition of colon tumors by PG, CT26 colon tumor cells were collected in log phase, treated with 0.25% trypase, washed twice, and resuspended to 5×10^4 cells/mL in RPMI 1640 medium. The cell suspension (0.1 mL), and 0.1 mL of RPMI 1640 medium, with or without PG (100 μg/mL or 2 000 μg/mL), were added to each well of 40-well flat plates. After incubation for 48 h at 37 ℃ in a humidified atmosphere containing 50 mL/L CO_2 and 95% air, the cell supernatant was discarded and 100 μg methyl thiazolyl tetrazolium was added to each well. After another 4-6 h incubation, the suspension was centrifuged at 162 r/min at 4 ℃ for 5 min, the supernatant was discarded, and 100 μL dimethyl sulfoxide was added before A_{192} was determined.

To determine inhibition of colon tumors by PG *in vivo*, 30 BALB/c mice were inoculated with 0.2 mL CT26 cells (5×10^4 cells/mL) into the wall of left posterior limb and randomly allocated to three groups averagely. Mice were then administered ip with 0.5 mL physiologic saline, 0.1 or 0.5 mg PG in 0.5 mL physiologic saline, once in 2 d for 16 d. On d 17, tumor tissue and spleen were removed and stored at -80 ℃ for measurement of tumor weight, spleen weight, and analysis of tumor DNA by agarose gel electrophoresis.

Statistical analysis

The gene expression data were normalized and further processed using GeneChip analysis Microarray Suite 5.0 (Affymetrix) and Data Mining Tool Version 2.0 (Affymetrix). The GeneChip software performed statistical analysis of array data and generated signal intensity values representing the relative expression levels of each gene on the array. A comparison analysis was performed that directly compared probe pairs from one GeneChip to another. The signal log ratio (SLR) was used to estimate the change in expression level for a transcript between baseline and an experiment

array. This change was expressed as the $\log_2$ ratio. The fold change was calculated from the log ratio formula as follows: fold change = $2^{\text{single log ratio}}$ (if single log ratio $\geqslant 0$) or $(-1)\times 2^{-\text{single log ratio}}$ (if single log ratio<0). Therefore, a $\log_2$ ratio of 1 has a fold change of 2.

For annotation of genes, known or putative gene functions were ascertained from gene ontology (GO) classifications (provided at http://www.NetAffx.com). Probe sets can be found at http://www.NetAffx.com that provides oligonucleotide sequences of the probes and links to UniGene and other descriptive information. Pathways in KEGG (http://www.genome.ad.jp/kegg/) were analyzed to provide speculation on the possible biological pathways activated by PG, as suggested by the GeneChip data.

Inhibitions of colon tumors were analyzed using the SAS program. The statistical significance of the differences between group means was calculated by Student's two-tailed *t*-test for two groups, by single factor ANOVA, or by Tukey's test for three or more groups.

RESULTS

Global view of differentially expressed genes

To study the interaction between host cells and *Lactobacilli*, BALB/c mice were injected ip with PG derived from *Lactobacillus sp.* once a day for three consecutive days, and peritoneal macrophage and splenic lymphocyte mRNA was harvested. These mRNA samples were hybridized to oligonucleotide arrays containing 22 690 oligonucleotide probe sets (MOE430A GeneChip), each representing an expressed gene. The general information of gene expression is presented in Figure 1. Changes in gene expression were generally more marked after mice were treated once (e.g., expression of 5 085 genes was changed) than after three administrations during which only 3 995 genes were differentially regulated. When mice were treated once, a rapid and widespread response was triggered resulting in substantial changes in 3 332 genes (SLR was more than 1) and the total number of upregulated genes (1 762) was less than the number of genes whose expression was suppressed (3 323). When treated thrice, however, a slow but more specific response was induced resulting in transcriptional changes of 857 genes (SLR was more than 1) (Figure 1A). The total number of upregulated genes (1 846) was similar to that of genes whose expression was suppressed (2 149). Of the 3 332 or 857 genes (absolute values of SLR were more than 1) in two different stimulating procedures, at least 125 upregulated and 191 downregulated genes of the mouse genome were mobilized in response to one or three times of stimuli (Figure 1B). Of these PG-responsive genes, 86 upregulated genes and 128 downregulated genes encoded proteins with known biological functions. These genes were divided into 10 functional categories (Figure 2) as defined by the Gene Ontology Consortium (http://www.geneontology.org/). The three categories of response to stress, signal transduction, and metabolism, accounted for 59% of the PG-responsive genes. Genes playing a role in defense and immunity (response to stress) or signal transduction comprised 44% of the PG-induced genes but only 14% of the downregulated genes. In contrast, genes with functions in intermediary metabolism made up 42% of the genes whose expression was suppressed by PG, but only 9% of the induced genes.

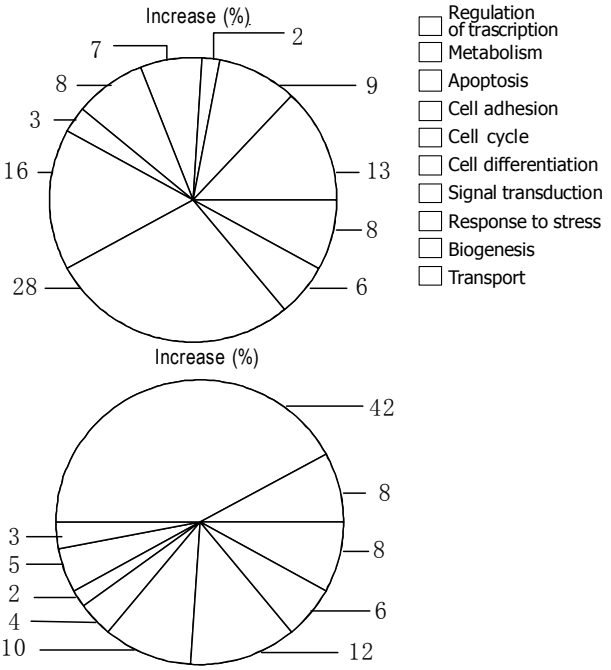


Figure 2 Functional profiles of expression changed by PG derived from *Lactobacillus sp.* in peritoneal macrophages and splenic lymphocytes.

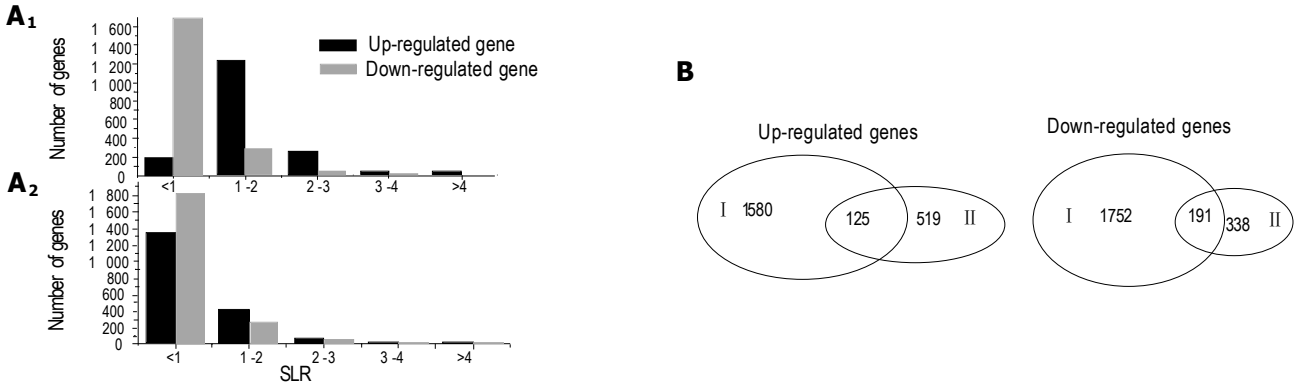


Figure 1 General information of gene expression change. **A**: Distribution of induced (black bars) and repressed genes (gray bars) based on their LSR; **B**: All induced and repressed genes with absolute value of LSR more than 1 after one and three doses of PG treatment and their intersection. I: One dose of PG treatment. II: Three doses of PG treatment.

Effects of peptidoglycan on genes involved in NF-κB pathway

At least 361 and 57 stress response genes responded to PG when mice were treated once or thrice (absolute value of SLR was more than or equaled to 1). Expressions of 17 genes encoding important proteins that participate in TLR-NF-κB pathway were regulated in different patterns after both treatments. According to the pathways defined at the KEGG database, a possibly regulated branch of TLR-NF-κB signaling pathway is shown in Figure 3A. TLR2 could mediate response to PG and cell wall components of Gram-positive bacteria[14]. Gene expression profile indicated that expression of TLR2 was only upregulated significantly after mice were treated with PG thrice. According to the findings of Anderson[15], the strong expression of TLR2 would present in antigen presenting cells such as peritoneal macrophages. Different expressions of TLR2 in different treatments revealed that, in certain tissues, expression of certain TLR was different according to the time or frequency of cell interaction with particular probiotic CAMPs.

Several intracellular signal transduction pathways were activated when TLRs reacted with microbial products. The most prominent and best characterized of these is the NF-κB signaling pathway[16]. Expressions of downstream genes of TLR signal were analyzed. Results revealed that only certain branches of NF-κB pathway were impacted by PG stimulation. Specifically, expression of toll-interleukin 1 receptor domain containing adaptor protein decreased after both PG treatments, suggesting that the cytoplasmic domain of TLRs was modified, affecting recruitment of myeloid differentiation primary response gene 88 (MyD88). Expression of thymoma viral proto-oncogene 1 (Akt1) was suppressed after a single PG dose. Expression of interleukin-1 receptor-associated kinase 1 (Trak1) was activated after a single PG stimulation. Expressions of Tnf receptor-associated factor 6 (Traf6) NF-κB1 and NF-κB2 were only induced after chronic stimulation. Furthermore, expression of mitogen-activated protein kinase 14 (P38) was upregulated after PG treatment.

It was demonstrated that once activated, Irak released from the receptor, and bound to and activated Traf6[17]. In that study, increased expression of Irak was linked to the activation of Traf6. We postulate that the expression of Traf6 was induced during the later time of Irak stimulation. Akt1 is another important protein, which can directly phosphorylate inhibitor of kappaB kinase α (IKKa) and mitogen-activated protein kinase kinase 6 (MKK6), leading to the activation of both Jun amino-terminal kinase (JNK)/p38 and NF-κB signaling pathways[18]. After single administration of PG, Akt1 expression decreased, indicating that in early period of stimulation Traf6 was a primary mediator of Ikk phosphorylation and led to nuclear transferring of NF-κB. In three-dose stimulation, however, both TRAF6 and Akt1 took part in nuclear transport of NF-κB. Perhaps the differential expression of Traf6 and Akt1 could lead to differential expression of products of NF-κB signaling pathway. Many components of the NF-κB pathway were stimulated only after the mice were treated thrice with PG. This finding could imply that constitutively expressed proteins comprising the NF-κB pathway were sufficient for early defense responses. Additional proteins might undergo degradation after initial PG stimulation. A series of genes encoding proteins of ubiquitin-proteasome proteolytic pathway were activated as shown in Table 2. Products of these genes could mediate destruction of NF-κB pathway memberships. Tollip is a negative regulatory molecule in TLR signaling[19]. In the present study, expression of Tollip was downregulated after acute injection of PG and the expression was resumed after mice received chronic PG treatment.

Some genes encoding products of NF-κB pathway were upregulated (e.g., IL-1, IL-6, CD80, CD86) after PG treatment. IL-12 was only upregulated after acute PG treatment. It was reported that tumor necrosis factor (TNF) and IL-2 are molecules induced by some pathogens or probiotics exposed to macrophages[16]. Our previous study suggested that PG could cause production of TNF in macrophages of cyclophosphamide-treated mice whose immune system was inhibited[12]. In the present study, TNF gene expression was only upregulated when mice were treated chronically with PG. IL-2 expression, however, was not similarly induced. Therefore, expression of these molecules could be differentially regulated in healthy individuals compared to immune-compromised individuals. Because the expression of several cytokines such as interleukin-2 (IL-2), interferon-γ (IFN-γ), TNF-α and IL-3, as well as several growth factors, have been shown to be regulated by stabilization/destabilization of mRNA[20], and IL-2 expression was not significantly affected by PG treatment in this study. IL-2 mRNA might go degradation, and was beneficial for the control of host immune response. After PG treatment, no change in iNOS (also named as NOS2 encoding a protein responsible for induced production of nitrogen monoxidum) mRNA levels was found. Although basic production of nitrogen monoxidum (NO) was beneficial for host to regulate defense response, too much NO induced a severe inflammatory response that might lead to tissue damage[21]. *Lactobacillus* PG did not induce NO production, implying that inflammatory response induced by *Lactobacillus* was solely for enhancement of host immune surveillance.

Possible macrophage phenotype induced by PG

On the basis of macrophage gene expression patterns, Stoy[22] has functionally classified macrophages into various phenotypes. External triggers, acting via cell membrane receptors (e.g., TLR2), and activation of the NF-κB-dependent intracellular signaling pathway in macrophages, might be the most important determinants leading to the pro-inflammatory phenotype. NF-κB could increase the release of cytokines (e.g., TNF-α, IL-1, IL-6, IL-12 and interferons), as well as amyloid A, adhesion molecules (e.g., Vcam-1 and Icam-1)[23], chemokines, major histocompatibility complex (MHC) class I and II molecules[24] from macrophages and a variety of other mammalian cell types. PG-induced proteins related to pro-inflammatory response and ant-inflammatory response are listed in Table 1. The innate response induced by *Lactobacillus* PG, reinforced over a limited period of time (one dose), sustained an elevation of IL-1 expression, increased IL-1 receptor type 2 mRNA

Table 1 Relationship between *Lactobacillus* PG-induced expression of proteins and pro-inflammatory and anti-inflammatory response

Probe set	Gene symbol	SLR		Probe set	Gene symbol	SLR	
		I	II			I	II
1450788_at	Amyloid A1	NC	1.1	1419282_at	Ccl12	–2.1	NC
1449326_x_at	Amyloid A2	–2.1	1.8	1420380_at	Ccl2	–4	NC
1450826_a_at	Amyloid A3	–2.4	NC	1417925_at	Ccl22	–1.2	0.5
1448162_at	Vcam1	2	1.6	1450488_at	Ccl24	–3.2	NC
1448862_at	Icam2	1.5	1.7	1421228_at	Ccl7	–4.3	0.6
1422930_at	Icam4	1.8	NC	1419684_at	Ccl8	–2.5	–1.3
1435290_x_at	H2-Aa	2	0.6	1417936_at	Ccl9	–1.6	NC
1451721_a_at	H2-Ab1	1.7	0.6	1419209_at	Cxcl1	NC	2.6
1422527_at	H2-DMa	1.4	0.6	1418930_at	Cxcl10	NC	3.6
1419744_at	H2-DMb1	1.6	0.6	1419697_at	Cxcl11	NC	4.5
1422891_at	H2-Ea	2.1	0.6	1417851_at	Cxcl13	NC	2.9
1417025_at	H2-Eb1	1.6	0.6	1449984_at	Cxcl2	NC	1.1
1419297_at	H2-Oa	2.4	NC	1418652_at	Cxcl9	NC	2.1
1418536_at	H2-Q7	1.3	0.7	1418480_at	Cxcl7	NC	–1.9
1449875_s_at	H2-T10	1.6	0.7	1418457_at	Cxcl14	–6.9	–1.3
1449556_at	H2-T23	1.2	0.7	1449195_s_at	Cxcl16	–1.1	NC
1422160_at	H2-T24	NC	0.6	1448995_at	Cxcl4	–1.5	NC
1452544_x_at	H2-K	NC	0.5	1419600_at	Defb4	–1.2	NC
1450534_x_at	H2-Q1	NC	0.5	1420653_at	Tgfb1	–2.2	0.6
1417314_at	H2-Bf	NC	1	1417455_at	Tgfb3	–2.5	NC
1426324_at	H2-D1	NC	1.1	1425947_at	Ifng	NC	0.9
1419413_at	Ccl17	1.5	1.7	1450330_at	Il10	NC	1.4
1419426_s_at	Ccl21a	3.8	NC	1418219_at	Il15	NC	3.5
1419561_at	Ccl3	2.6	1.9	1417268_at	Cd14	1.2	NC
1421578_at	Ccl4	2.5	2.4	1419532_at	Il1r2	1.2	NC

Probe set: probe used in Affymetrix GeneChip. NC: change in gene expression is not significant. Minus SLR: gene expression is downregulated. I: One dose of PG treatment. II: Three doses of PG treatment.

Table 2 Genes related to ubiquitin-dependent protein catabolism

Probe set	Gene symbol	SLR (I)	SLR (II)
1417172_at	Ubce8	2.7	NC
1422462_at	2700084L22Rik	1.7	NC
1452058_a_at	Rnf11	1.6	NC
1426404_a_at	Rnf11	1.1	NC
1454802_x_at	Arih2	1.1	1.1
1450696_at	Psmb9	1.3	NC
1422962_a_at	Psmb8	1	NC
1452402_at	Uchl3	1.5	NC
1449855_s_at	Uchl3	1.4	NC
1423107_at	Ube2b	1.1	NC
1454036_a_at	Usp15	1.2	NC
1450037_at	Usp9x	NC	1
1418191_at	Usp18	NC	2.1
1448420_a_at	Fbxl12	NC	1

Probe set: probe used in Affymetrix GeneChip. NC: change in gene expression is not significant. Minus SLR: gene expression is down-regulated. I: One dose of PG treatment. II: Three doses of PG treatment.

and induced (three doses) expression of PRRs, such as TLR2.

Serum amyloid (A1 and A2), intercellular adhesion molecules (Vcam1 and Icam2) increased after PG treatment. Icam4 was only induced after acute treatment. The majority of class II MHC genes were induced during the early period of stimulation with PG (SLR>1). Expressions of H2-T24, H2-K, H2-Q1 were induced during the later time period of stimulation with PG. H2-D1 and H2-b1, however, were induced after PG treatments. Eleven of C-C family chemotactic factors were inconsistently induced or suppressed after either treatment. Expressions of seven C-X-C chemotactic factors were induced consistently after chronic PG treatment. These induced proteins, in addition to the pro-inflammatory cytokines (Figure 3A), were produced by activated macrophages and maintained the activated state. Upregulated expression of IL-12 and class II MHC genes mediated the initiation of the adaptive immune response of *Lactobacillus* PG by $CD4^+$ T cells (Th cells). Studies have demonstrated adjuvant-like activity of *Lactobacillus*[27], and factors induced by *Lactobacillus* PG in this study contributed to the enhancement of immune surveillance PG. Compared to one dose of PG treatment, a greater number of inflammatory genes were upregulated after three doses of PG treatment. Anti-inflammatory cytokines, such as TGF, were also upregulated during chronic PG treatment. This complex cytokine profile could lead to differential activation of helper T cells. Consequently, activated macrophages displayed an inflammatory phenotype, which switched to a complex phenotype induced by both inflammatory and anti-inflammatory factors. This differential response revealed the plasticity of macrophages when they were affected by *Lactobacillus* PG.

Immune processes underlying PG-mediated pro-Th1 signaling

One of the important signaling pathways induced by cytokines was involved in Janus tyrosine kinases (Jak kinases), signal transducers and activators of transcription (STAT proteins). At least 30 genes relating to T-cell proliferation and differentiation were observed to undergo significant alterations in expression after treatment. The Jak-STAT pathway was coordinately upregulated (Figure 3B), especially

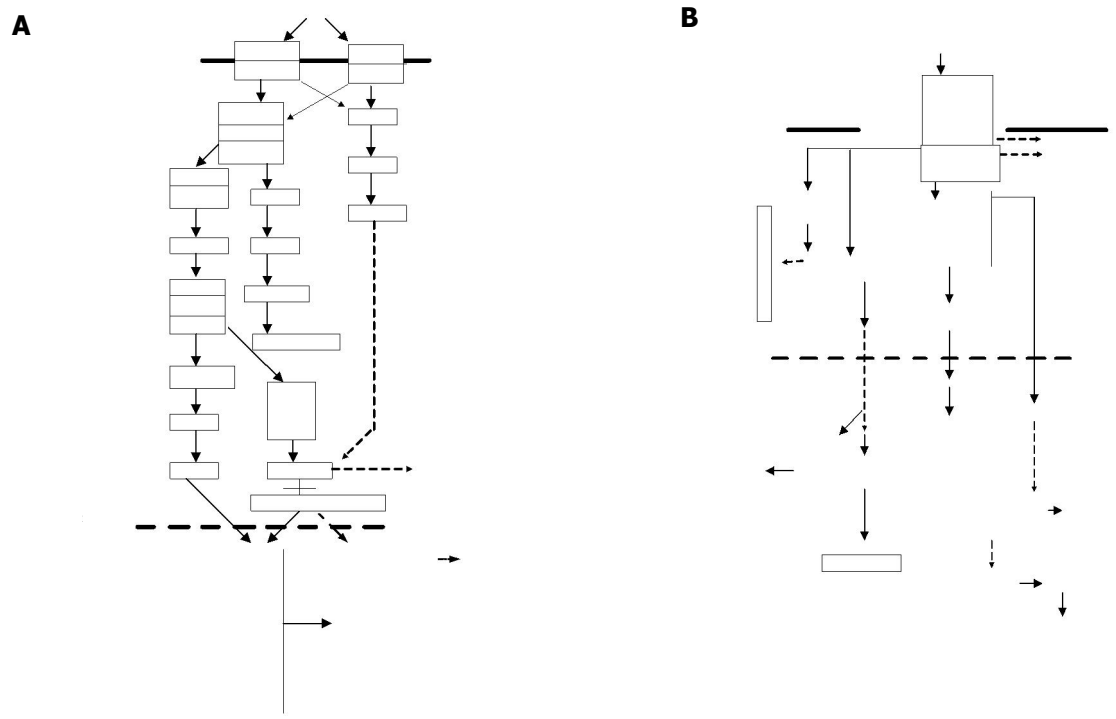


Figure 3 Functional mapping of genes to pathways for products of pro-inflammatory cytokines (**A**) and IFN-γ and T-cell proliferation (**B**).

after consecutive PG treatment. After PG treatment, IL-2 receptor and proto-oncogene (Myb and Myc) were upregulated, essential for T-cell proliferation. This finding is coincident with those from our previous study[12] in which proliferation of splenic lymphocytes was stimulated after single injection (ip) of *Lactobacillus* PG. Experimental evidence indicates that pro-Th1 immunoregulation is dependent on the ability of *Lactobacillus* to promote interferon production[26], which in turn drives the production of pro-interferon monokines (principally IL-12 and IL-18). One dose PG treatment greatly induced expression of IL-12 and Stat4 (SLR was 1.9 and 2.6 respectively). Furthermore, expression of CD3 was also upregulated stimulating naive $CD4^+$ T cell differentiated into type 1 helper T cells. It has been demonstrated that differentiation of T cells occurs 48-72 h after stimulation[27]. In this experiment, upregulated expression of IFN-γ was observed after chronic PG treatment (about 72 h), suggesting the polarization of naive $CD4^+$ T cells toward Th1 cells and the activation of the IL-12/IFN-axis. After either treatment, the gene encoding IL-18 receptor was also upregulated and served to maintain the development of CMI/Th1 response. Many downstream proteins involved in cytokine/cytokine receptor interaction within the Jak-STAT pathway were strongly activated after chronic PG treatment (Figure 3B). The major genes affected were Jak, Stat, cytokine inducible SH2-containing protein (cish), and pim-1 oncogene (Pim), suggesting that only certain branches of Jak-STAT pathway are activated. It should also be noted that continuous stimulation of mice with PG induced production of IL-10 and its receptor, likely to protect host from damage by CMI response. On the other hand, both Stat1 and Stat3 are activated by IL-6, IL-10[28,29], which may lead to proliferation or differentiation of macrophages or lymphocytes via activation of the Jak-STAT pathway.

Colon tumor suppression by Lactobacillus PG

Microarray analysis indicated that peritoneal macrophages were activated by *Lactobacillus* PG. We studied whether activation of macrophages could induce tumoricidal activity against CT26 colon cancer cells. Results indicated that there was a dose-dependent inhibition of CT26 colon cancer development in mice treated with PG ($P<0.01$) (Figure 4B). The inhibition ratio of high PG dose was 54.2%. A DNA ladder appeared in the apoptosis analysis (Figure 5), indicating that cancer apoptosis was induced by PG. On the other hand, cancer cell line growth *in vitro* following PG treatment showed no direct inhibitory effect (Figure 4A), suggesting that PG-induced immune responses might be primarily responsible for these anti-tumor effects.

DISCUSSION

A recent study has shown that cytokine production by cells of the immune system can be altered by *Lactobacillus* strain[1]. In the present study, immune response induced by *Lactobacillus* PG agreed with results induced by these *Lactobacillus* strains, indicating that *Lactobacillus* PG is responsible for certain immune responses induced by this type of important probiotic organism. *Lactobacillus* PG, as a distinct CAMP, could modulate the production of cytokines and other immunoregulatory factors of macrophages. Through these factors, macrophages play a pivotal immunoregulatory role in the Th1 and Th2 cell balance. In the present study, one dose of PG induced a temperate inflammatory reaction, and three doses of PG enhanced antigen presentation and T-cell differentiation. One dose of *Lactobacillus* PG induced the expression of IL-12 and

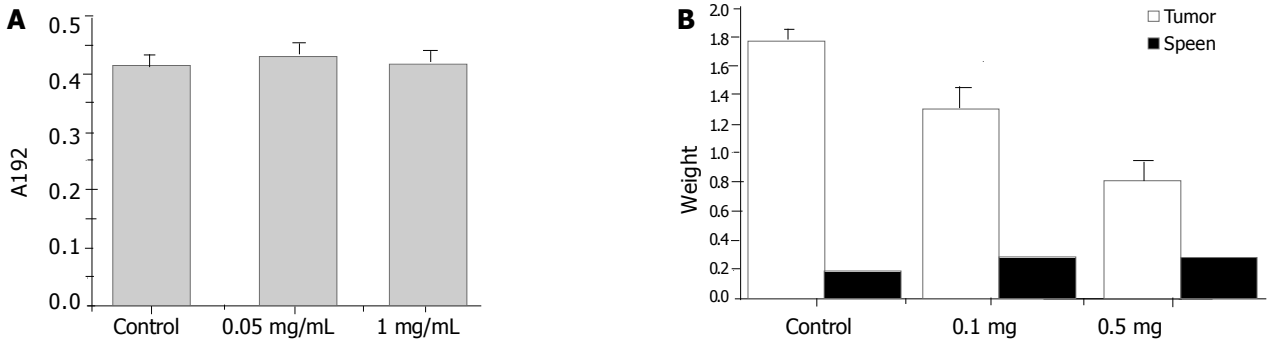


Figure 4 *In vitro* (**A**) and *in vivo* (**B**) inhibitory effects of PG on growth of CT26. Values are mean±SD.

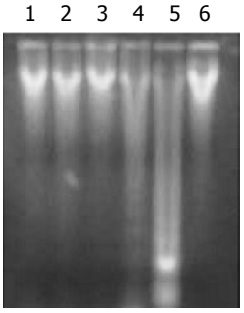


Figure 5 DNA of inoculated colon tumor in 2% agarose gel. Lane 1-3 and 6: control; lane 4: tumor-inoculated mice treated with low doses of PG; lane 5: tumor-inoculated mice treated with high doses of PG.

three doses of PG increased the expression of IFN-γ, suggesting that the induced immune response may develop toward Th1 immune response (CMI response). CMI response is important for tumor inhibition. The present study demonstrated that *Lactobacillus* PG could inhibit CT26 colon cancer development *in vivo*, which was mediated by increased CMI.

Enhanced phagocytic activity, NK cell activity, T- and B-cell function, and antigen-specific antibody responses are likely to result in an increased resistance to tumor incidence. All these types of tumoricidal activity require macrophage activation[30]. Interaction between PAMPs and cell surface PRRs induce macrophage activation[31]. Macrophages are important antigen-presenting cells that present throughout the gastrointestinal tract. Macrophages under lamina propria may be targets for modulation by gut microbes, including ingested probiotics. It has been found that foreign *Lactobacillus murinus* and cell fragments can penetrate the gut wall by translocation through the epithelial layer or through Peyer's patches[31]. Indigenous intestinal bacteria including *Lactobacilli* are also able to cross the intestinal mucous layer and can survive in the spleen or in other organs for many days where they stimulate phagocytic activity. It is possible that physiologically translocated *Lactobacilli* carry PG or other CAMPs to macrophages in gut or other sites and can induce the production of modulatory molecules.

An important finding revealed by gene expression assay is that different doses of PG induce different cytokine profiles. In the present study, expression of Traf6 and Tollip was changed by different doses of *Lactobacillus* PG, suggesting that expression of cytokine is regulated by activation or inhibition of Traf6 or Tollip expression. Zhang and Ghosh[19] reported that overexpression of Tollip causes interaction with TLR2 and TLR4 and inhibits TLR signaling, indicating that Tollip plays a negative regulatory role in TLR signaling. These findings imply that *Lactobacillus* PG can modulate the activating state of TLR signaling partly, although it may change the expression of inhibitory molecules. On the other hand, in mammals, Traf proteins are key components in various NF-κB activating pathways and overexpression of Traf2 or Traf6 activates NF-κB[32]. Traf6 knockout mice exhibit defects in IL-1 and LPS-induced NF-κB activation[33]. In the present study, three doses of *Lactobacillus* PG-induced high activation of TLR-NFκB signaling might be a result of increased expression of TRAF6.

Although used widely, different strains of *Lactobacillus* can induce increased systemic or mucosal immune response at different levels of stimulation, and the stimulation is also dose-dependent[27]. Maassen *et al*.[34], have also found that the growth phase of orally administered individual *Lactobacillus* strains can differentially affect antigen-specific antibody subclasses IgG1 and IgG2a. This differential antibody response is likely due to growth phase-dependent differences in bacterial cell compositions[31]. In the present study, we found that different doses of *Lactobacillus* PG led to different immune responses, suggesting that difference in CAMPs compositions and amount of CAMPs reaching to macrophages influences immune stimulatory effect of *Lactobacilli*.

In conclusion, the *Lactobacillus* PG-induced response is dominant in Th1, and a stimulatory effect is dose-independent. *Lactobacillus* PG influences the expression of signaling regulatory molecules modulating the cytokine profile and activation of lymphocytes. Pro-Th1 immune signals generated by probiotic *Lactobacilli* at the gut mucosal interface (and in some cases at other mucosal sites) can stimulate systemic CMI responses relating to cancer immunotherapy[35].

REFERENCES

1 **Erickson KL,** Hubbard NE. Probiotic immunomodulation in health and disease. *J Nutri* 2000; **130**: 403S-409S
2 **Reid G,** Burton J. Use of Lactobacillus to prevent infection by

pathogenic bacteria. *Microbes Infect* 2002; **4**: 319-324
3 **Rafter JJ.** The role of lactic acid bacteria in colon cancer prevention. *Scand J Gastroenterol* 1995; **30**: 497–502
4 **Bolognani F,** Rumney CJ, Pool-Zobel BL, Rowland IR. Effect of lactobacilli, bifidobacteria and inulin on the formation of aberrant crypt foci in rats. *Eur J Nutr* 2001; **40**: 293–300
5 **Wollowski I,** Ji ST, Bakalinsky AT, Neudecker C, Pool-Zobel BL. Bacteria used for the production of yogurt inactivate carcinogens and prevent DNA damage in the colon of rats. *J Nutr* 1999; **129**: 77–82
6 **Poltorak A,** He X, Smirnova I, Liu MY, Van Huffel C, Du X, Birdwell D, Alejos E, Silva M, Galanos C, Freudenberg M, Ricciardi-Castagnoli P, Layton B, Beutler B. Defective LPS signaling in C3H/HeJ and C57BL/10ScCr mice: mutations in Tlr4 gene. *Science* 1998; **282**: 2085-2088
7 **Astarie-Dequeker C,** N'Diaye EN, Le Cavec V, Rittig MG, Prandi J, Maridonneau-Parini I. The mannose receptor mediates uptake of pathogenic and nonpathogenic *mycobacteria* and bypasses bactericidal responses in human macrophages. *Infect Immun* 1999; **67**: 469-477
8 **Baeuerle PA,** Baltimore D. I dappa B: a specific inhibitor of the NF-kappa B transcription factor. *Scinence* 1988; **242**: 540-546
9 **Cario E,** Brown D, McKee M, Lynch-Devaney K, Gerken G, Podolsky DK. Commensal-associated molecular patterns induce selective Toll-like receptor-trafficking from apical membrane to cytoplasmic compartments in polarized intestinal epithelium. *Am J Pathol* 2002; **160**: 165-173
10 **Madsen K,** Cornish A, Soper P, Mckaigney C, Jijon H, Yachimec C, Doyle J, Jewell L, De Simone C. Probiotic bacteria enhance murine and human intestinal epithelial barrier function. *Gastroenterology* 2001; **121**: 580-591
11 **Rakoff-Nahoum S,** Paglino J, Eslami-Varzaneh F, Edberg S, Medzhitov R. Recognition of commensal microflora by Toll-Like receptors is required for intestinal homeostasis. *Cell* 2004; **118**: 229-241
12 **Ma XY,** Le GW, Shi YH. Studies on the colon tumor inhibition and its mechanisms of peptidoglycan derived from Lactobacillus. *Zhongguo Yingyang Xuebao* 2003; **26**: 467-470
13 **Beranova-Giorgianni S,** Desiderio DM, Pabst MJ. Structure of biologically active muramyl peptides from peptidoglycan of Streptococcum Sanguis. *J Mass Spectrom* 1998; **33**: 1182-1191
14 **Takeuchi O,** Hoshino K, Kawai T, Sanjo H, Takada H, Ogawa T, Takeda K,Adira S. Differential roles of TLR2 and TLR4 in recognition of gram-negative and gram-positive bacterial cell wall components. *Immunity* 1999; **11**: 443–451
15 **Anderson KV.** Toll signaling pathways in the innate immune response. *Curr Opin Immunol* 2000; **12**: 13–19
16 **Hamann L,** El-Samalouti V, Ulmer AJ, Flad HD, Rietschel ET. Components of gut bacteria as immunomodulators. Int. *J Food Microbio* 1998; **41**: 141-154
17 **Cao Z,** Xiong J, Takeuchi M, Kurama T, Goeddel DV. TRAF6 is a signal transducer for interleukin-1. *Nature* 1996; **383**: 443-446
18 **Wang C,** Deng L, Hong M, Akkaraju, GR, Inoue J, Chen ZJ. TAK1 is an ubiquitin-dependent kinase of MKK and IKK. *Nature* 2001; **412**: 346-351
19 **Zhang G,** Ghosh S. Negative regulation of Toll-like receptormediated signaling by Tollip. *J Biol Chem* 2002; **277**: 7059–7065
20 **Zubiaga AM,** Belasco JG, Greenberg ME. The nonamer UUAUUAUU is the key AU-rich sequence motif that mediates mRNA degradation. *Mol Cell Biol* 1995; **15**: 2219-2230
21 **Rachmilewitz D,** Stamler JS, Bachwich D, Karmeli F, Ackerman Z, Poolsky DK. Enhanced colonic metric oxide generation and nitric wide synthase activity inulcerative colitis and Crohn's disease. *Gut* 1995; **36**: 718-723
22 **Stoy N.** Macrophage biology and pathobiology in the evolution of immune responses: a functional analysis. *Pathobiology* 2001; **69**: 179-211
23 **Ruetten H,** Thiemermann C, Perrctti M. Upregulation of ICAM-1 expression on J774.2 macrophages by endotoxin involves activation of NF-kappaB but not protein tyrosine kinase: comparison to induction of iNOS. *Mediators Inflamm* 1999; **8**: 77-84
24 **Pruett SB,** Zheng Q, Fan R, Matthews K, Schwab C. Acute exposure to ethanol affects Toll-like receptor signaling and subsequent responses: an overview of recent studies. *Alcohol* 2004; **33**: 235-239
25 **Pedigon G,** Alvarez S, Rachid M, Aguero G, Gobbato N. Immune system stimulation by probiotic. *Dairy Sci* 1995; **78**: 1597-1606
26 **Kato I,** Tanaka K, Yokokura T. Lactic acid bacterium potently induces the production of interleukin-12 and interferon-gamma by mouse splenocytes. *Int J Immunopharmacol* 1999; **21**: 121–131
27 **Xin TJ,** Zhang L. Basic and clinic of Th genus cell polarization colony.1sted. *Beijing: Junshi Yixue Kexue Chubanshe* 2002: 25
28 **Darnell JE,** Kerr IM, Stark GR. Jak-STAT pathways and transcriptional activation in response to IFNs and other extracellular signaling proteins. *Science* 1994; **264**: 1415-1421
29 **Takeda K,** Clausen BE, Kaisho T, Tsujimura T, Terada N, Forster I, Akira S. Enhanced Th1 activity and development of chronic enterocolitis in mice devoid of Stat3 in macro-phages and neutrophils. *Immunity* 1999; **10**: 39-49
30 **Gordon S.** Alternative activation of macrophages. *Nat Rev Immunol* 2003; **3**: 23-35
31 **Link-Amste H,** Rochat F, Saudan KY, Mignot O, Aeschlimann JM. Modulation of a specific humoral immuneresponse and changes in intestinal flora mediated through fermented milk intake. *FEMS Immunol Med Microbiol* 1994; **10**: 55-63
32 **Arch RH,** Gedrich RW, Thompson CB. Tumor necrosis factor receptor-associated factors (TRAFs): a family of adapter proteins that regulates life and death. *Genes Dev* 1998; **12**: 2821-2830
33 **Lomaga MA,** Yeh WC, Sarosi I, Duncan GS, Furlonger C, Ho A, Morony S, Capparelli C, Van G, Kaufman S, van der Heiden A, Itie A, Wakeham A, Khoo W, Sasaki T, Cao Z, Penninger JM, Paige CJ, Lacey DL, Dunstan CR, Boyle WJ, Goeddel DV, Mak TW. TRAF6 deficiency results in osteopetrosis and defective interleukin-1, CD40, and LPS signaling. *Genes Dev* 1999; **13**: 1015-1024
34 **Maassen CB,** Boersma WJ, van Holten-Neelen C, Claassen E, Laman JD. Growth phase of orally administered Lactobacillus strains differentially affects IgG1/IgG2a ratio for soluble antigens: implications for vaccine development. *Vaccine* 2003; **21**: 2751-2757
35 **Cross ML.** Immunoregulation by probiotic lactobacilli: pro-Th1 signals and their relevance to human health. *Clinical Applied Immunol Reviews* 2002; **3**: 115–125

Science Editor Wang XL and Guo SY **Language Editor** Elsevier HK

PO Box 2345, Beijing 100023, China
www.wjgnet.com
wjg@wjgnet.com

ELSEVIER

World J Gastroenterol 2005;11(40):6338-6347
World Journal of Gastroenterology ISSN 1007-9327
© 2005 The WJG Press and Elsevier Inc. All rights reserved.

• *CLINICAL RESEARCH* •

Characterization of colonic dendritic cells in normal and colitic mice

Sheena M Cruickshank, Nicholas R English, Peter J Felsburg, Simon R Carding

Sheena M Cruickshank, Simon R Carding, Institute of Molecular and Cellular Biology, University of Leeds, Leeds LS2 9JT, United Kingdom
Nicholas R English, Antigen Presentation Research Group, Faculty of Medicine, Imperial College, Northwick Park and St Mark's Campus, Harrow HAI 3UJ, United Kingdom
Peter J Felsburg, Department of Clinical Science, University of Pennsylvania, Philadelphia, PA 1904, United States
Supported by the National Institutes of Health (RO1 AI41562 and PO1 RR12211) to SRC and PJF
Correspondence to: Professor SimonR Carding, School of Biochemistry and Microbiology, University of Leeds, Leeds LS2 9JT, United Kingdom. s.r.carding@leeds.ac.uk
Telephone: +44-113-343-1404 Fax: +44-113-343-1421
Received: 2004-09-13 Accepted: 2004-12-23

Abstract

AIM: Recent studies demonstrating the direct involvement of dendritic cells (DC) in the activation of pathogenic T cells in animal models of inflammatory bowel disease identify DC as important antigen presenting cells in the colon. However, very little is known about the properties of colonic DC.

METHODS: Using immunohistochemistry, electron microscopy and flow cytometry we have characterized and compared colonic DC in the colon of healthy animals and interleukin-2-deficient ($IL2^{-/-}$) mice that develop colitis.

RESULTS: In the healthy colon, DC resided within the lamina propria and in close association with the basement membrane of colonic villi. Type 1 myeloid ($CD11c^+$, $CD11b^+$, $B220^-$, $CD8\alpha^-$) DC made up the largest (40-45%) population and all DC expressed low levels of CD80, CD86, and CD40, and had high endocytic activity consistent with an immature phenotype. In colitic $IL2^{-/-}$ mice, colonic DC numbers increased four- to five-fold and were localized within the epithelial layer and within aggregates of T and B cells. They were also many more DC in mesenteric lymph nodes (MLN). The majority (>85%) of DC in the colon and MLN of $IL2^{-/-}$ mice were type 1 myeloid, and expressed high levels of MHC class II, CD80, CD86, CD40, DEC 205, and CCR5 molecules and were of low endocytic activity consistent with mature DC.

CONCLUSION: These findings demonstrate striking changes in the number, distribution and phenotype of DC in the inflamed colon. Their intimate association with lymphocytes in the colon and draining lymph nodes suggest that they may contribute directly to the ongoing inflammation in the colon.

© 2005 The WJG Press and Elsevier Inc. All rights reserved.

Key words: Colonic dendritic cells; Interleukin 2; Colitis

Cruickshank SM, English NR, Felsburg PJ, Carding SR. Characterization of colonic dendritic cells in normal and colitic mice. *World J Gastroenterol* 2005; 11(40): 6338-6347
http://www.wjgnet.com/1007-9327/11/6338.asp

INTRODUCTION

There is increasing evidence that inflammatory bowel disease (IBD) is the result of dysregulated immune and T cell responses to the intestinal bacterial microflora resulting in chronic intestinal inflammation[1,2]. However, it is not clear how antigen is taken up and processed in the colon. In the small intestine antigen uptake is believed to occur via specialized epithelial cells, or M cells, located in Peyer's patches[3]. Peyer's patches represent a relatively small area of the small intestine and no equivalent to the M cell has yet been described in the colon resulting in the speculation as to whether cells such as epithelial cells and lamina propria (LP) dendritic cells (DC) may contribute to antigen uptake and presentation. However, little is known about the nature of antigen presentation in the colon.

It is likely that DC play a pivotal role in both the initiation and regulation of immune responses in the intestinal tract. Our recent studies, using the interleukin 2-deficient ($IL2^{-/-}$) mouse model of ulcerative colitis (UC), demonstrated the direct involvement of colonic DC in the activation of pathogenic T cells[4]. Both colitis as well as spontaneous bone loss in these animals were caused by increased production of the TNF family member, receptor activator of NFκB ligand (RANKL) by activated $CD4^+$ T cells. Modulation of the interaction of RANKL with its receptor RANK by the administration of osteoprotegerin, a soluble decoy receptor for RANKL, resulted in reduced intestinal inflammation and ablation of colonic DC. However, a detailed analysis of the phenotype and function of these cells in the murine colon in healthy and inflamed tissue is lacking.

DC derived from murine Peyer's patches have been extensively characterized and comprise at least three populations: (1) MAC-1^+ (CD11b) myeloid DC in the subepithelial dome; (2) CD8α lymphoid DC in the interfollicular T cell regions and: (3) $CD11b^-$ $CD8\alpha^-$ in both areas[5,6]. In contrast, little is known about the phenotype of colonic DC. DC from human colonic biopsies of normal and inflamed colon have been described as a heterogenous population of immature cells[7]. In contrast, preliminary

analyses of DC from normal and colitic mice have suggested that DC are immature in the normal colon but mature in the diseased colon[3,8].

The observation that DC are key to the development of colitis in IL2$^{-/-}$ model[3] makes it important to elucidate their phenotype and function to gain a greater understanding of their role in driving immune responses within the colon. In the current study, we have used immunohistochemistry, electron microscopy and flow cytometry to characterize and compare the DC present in colonic tissue from healthy and inflamed murine colon. This study represents the first attempt to characterize colonic DC in the IL2$^{-/-}$ model of UC.

MATERIALS AND METHODS

Materials

Animals C57BL/6 and C57BL/6-IL2$^{-/-}$ transgenic mice were purchased from Jackson Laboratory (Bar Harbor, ME) and housed under specific pathogen free conditions at the University of Leeds. IL2$^{-/-}$ mice were obtained from heterozygote matings and were identified by PCR analysis of tail DNA samples[2]. Mice were killed at 7-8 wk of age. Sentinel mice were routinely screened for common mouse pathogens and none were detected.

Methods

Immunohistochemistry Colonic tissue from the distal, mid, and proximal colons of C57BL/6- IL2$^{-/-}$ mice and age-matched littermate controls were snap frozen in OCT medium. Sections (6 μm) were fixed in cold acetone and stained for cell-specific markers using the tyramide amplification method (Perkin Elmer, Berkshire) as described previously[6]. Sections were stained with antibodies to F4/80, CD11c, MAC-1, CD4, B220, (all supplied by Becton Dickinson, Cowley, Oxford), and cytokeratin (Sigma, Poole, Dorset) and then counterstained with 4'-6-diamidino-2-phenolinodole dihydrochloride (DAPI) to visualize cell nuclei. Slides were mounted with Mowiol and analyzed with a Zeiss Axioplan u.v. microscope.

Cell isolation Colonic LP cells were isolated as described previously[4]. Briefly, colons were opened longitudinally, washed, and finely minced. LP cells were released from the tissue by incubation for 2 h under gentle agitation at 37 ℃ with collagenase I (4 mg/mL) in RPMI containing 10% FBS. The resultant cells were washed, resuspended in a 40% solution of Percoll (Amersham, Buckinghamshire) and gently layered onto a 60% Percoll gradient (400 g, 30 min). The cells were collected at the gradient interface, washed and prepared for analyses by flow cytometry or electron microscopy as described below. Mesenteric lymph node (MLN) cells were excised from C57BL/6 and C57BL/6- IL2$^{-/-}$ mice and homogenized to obtain a suspension of mononuclear cells.

Flow cytometry MLN and colonic LP cells were analyzed by flow cytometry on a FACScan flow cytometer using CELLQuest software (Becton Dickinson). Cells were stained with fluorochrome and/or biotin conjugated antibodies to CD45, B7.1 (CD80), B7.2 (CD86), CD40, CD8α, CD4, B220 (CD45R), GR-1, F4/80, MAC-1 (CD11b), I-A/I-E, CD11c, CCR5 (Becton Dickinson), DEC205 (Serotec Ltd, Oxford) and streptavidin conjugated to Alexa Fluor 633 (Molecular Probes, OR, USA). Isotype-matched antibodies of irrelevant specificity were used to determine the level of non-specific staining and frequency of cells stained with test antibodies.

Electron microscopy CD11c$^+$ LP cells from C57BL/-IL2$^{-/-}$ and C57BL/6 littermate controls were enriched by negative immunomagnetic selection to deplete the cell preparation of T (CD3$^+$) and B (CD19$^+$) cells prior to preparing the samples for electron microscopy. Between 1-5×10^5 cells were fixed in 0.1 mol/L sodium phosphate buffer, pH 7.4 containing 3% glutaraldehyde for at least 12 h at 4 ℃. After washing in sodium phosphate buffer, the cells were embedded as a pellet in low gelling temperature agarose (Sigma). The pellet was washed thoroughly and post-fixed for 1 h in 1% osmium tetroxide, washed and left overnight in dH_2O prior to being stained for 2-4 h in 2% uranyl acetate. After washing in dH_2O, the cells were dehydrated using an acetone gradient, embedded in araldite resin prior to curing for 18 h at 65 ℃. Ultrathin sections (100 nm thick) were cut on a Reichert-Jung Ultracut E microtome and collected on a 200 mesh copper grid. After staining with Reynold's lead citrate, the grid was carbon coated and visualized using a JEOL 1200 EX electron microscope. All samples analyzed by electron microscopy were also analyzed by flow cytometry to confirm the presence of DC in the cell samples.

Endocytosis assay Endocytic activity was assessed by measuring the uptake of FITC-dextran (Sigma). Freshly isolated MLN and LP cell preparations (2×10^5 cells/mL) from C57BL/6 and C57BL/6-IL2$^{-/-}$ mice were incubated at 37 ℃ with FITC-DX (1 mg/mL, Sigma) for 1 h. Control samples were incubated at 4 ℃. Incubation was stopped by washing in ice-cold PBS, stained with antibodies to CD11c or F4/80 as described above, fixed in 1% paraformaldehyde and permeabilized in 0.1% saponin and analyzed by flow cytometry as described above. Results are expressed as the proportion of cells (F4/80$^+$ or CD11c$^+$) which have specifically taken up the FITC-DX minus the background staining (cells incubated at 4 ℃).

Statistical analysis

Data are presented as mean±SE. Statistical significance was evaluated using a Mann-Whitney test.

RESULTS

Distribution of colonic DC is altered in the inflamed colon

A comparative analysis of the localization and type of DC and macrophages within the colons of normal (7 wk old C57BL/6) and colitic (7 wk old C57BL/6-IL2$^{-/-}$) mice was carried out using a three fluorochrome immunohistochemical procedure. The relatively few CD11c$^+$ DC present in the normal colon (Figure 1C) were mostly found within the LP and in close association with the basement membranes of the colonic villi (Figure 1C). Similarly, F4/80$^+$ macrophages were also found located within the LP and basement membrane of the normal colon (Figure 1A). F4/80$^+$ macrophages outnumbered CD11c$^+$ DC in the normal, healthy colon.

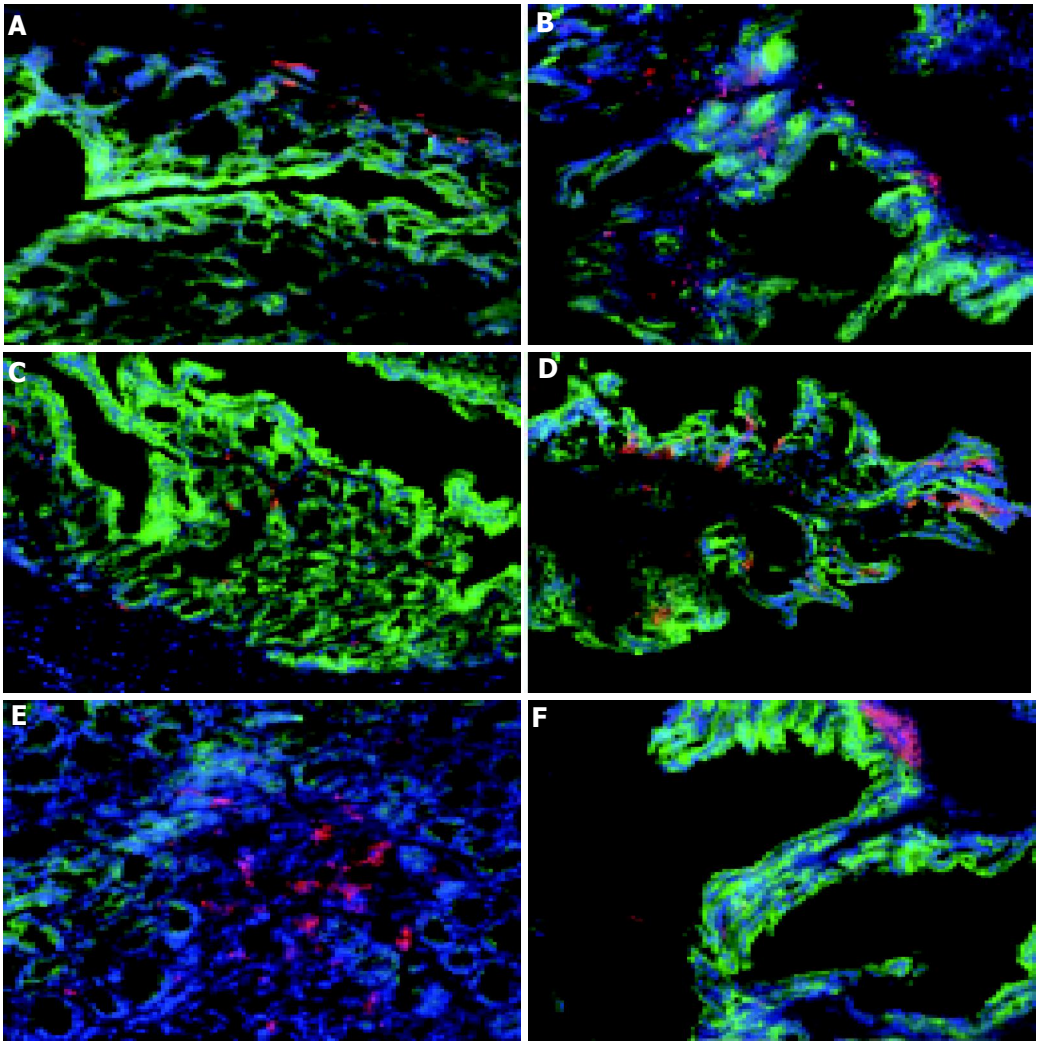


Figure 1 Distribution of macrophages and DC in normal and colitic colon. Sections of cryopreserved colon from normal C57BL/6 (**A, C,** and **E**) and colitic C57BL/6-IL2$^{-/-}$ mice (**B, D,** and **F**) were labeled with F4/80 and Cy-3 to identify macrophages (**A** and **B**), CD11c and Cy-3 to identify DC (**C**-**F**) and cytokeratin-FITC to identify epithelial cells (**A**-**F**) and counterstained with DAPI. Although there were increased numbers of macrophages in colitic animals, their distribution was unaltered (**A** and **B**). The number of DC was increased in the inflamed colon and their distribution was altered with DC being found in close proximity to the epithelium (**C** and **D**). Aggregates of CD11c$^+$ DC were also observed at the base of villi of both normal and colitic colons (**E** and **F**). Magnification, ×160. Tissue was analyzed from the colons of 5 C57BL/6-IL2$^{-/-}$ and 4 C57BL/6 animals.

In contrast, there were changes in both the number and distribution of F4/80$^+$ macrophages and CD11c$^+$ DC in the colon of colitic IL2$^{-/-}$ mice. C57BL/6-IL-2$^{-/-}$ mice spontaneously develop a progressive form of intestinal inflammation that is restricted to the colon and histopathologically resembles human UC[9], and has been shown to be triggered by commensal gut bacteria[9,10]. There were more macrophages (82.5±40.2 compared with 106.1±27.1 per field of view) and colonic DC (52.5±5.2 compared with 80.2±16.1 per field of view) in the inflamed colons of IL2$^{-/-}$ mice compared to the normal healthy colon (Figures 1B and D). Furthermore, the distribution of colonic CD11c$^+$ DC was altered in colitic animals with the majority of DC found in close association with the luminal surface, adjacent to the colonic epithelia (Figure 1D). This suggests that in colitic animals, colonic DC are mobile and migrate to the epithelial layer perhaps in response to epithelial derived signals or microbial antigens from the gut lumen. Of note, in the inflamed colon was the accumulation of CD11c$^+$ in aggregates, or lymphoid follicle like structures, at the base of crypts beneath the epithelial layer (Figure 1F). Although, similar clusters of colonic DC were also found in the colons of normal animals (Figure 1E), they were less well organized and much rarer.

To ascertain if colonic DC were restricted to specific parts of the colon, sections of the distal, mid, and proximal colon of both normal and colitic animals were analyzed. CD11c$^+$ cells were detected throughout the entire colon (Figures 2D-F) in both normal and colitic animals. Of note, a greater proportion of the aggregates of CD11c$^+$ were observed in the mid and distal areas compared to the proximal area of the colon in IL2$^{-/-}$ mice. The number of DC aggregates varied from mouse to mouse with 2-4 being observed in the sections of tissue from IL2$^{-/-}$ mice.

The phenotype of colonic DC was determined by immunolabeling with antibodies specific for MAC-1 (CD11b) and B220. The majority of CD11c$^+$ cells co-expressed MAC-1$^+$ (Figures 2A-C) consistent with them being myeloid DC. A small proportion (approximately 5%) of the colonic CD11c$^+$ cells within the lymphoid aggregates of IL2$^{-/-}$ animals co-

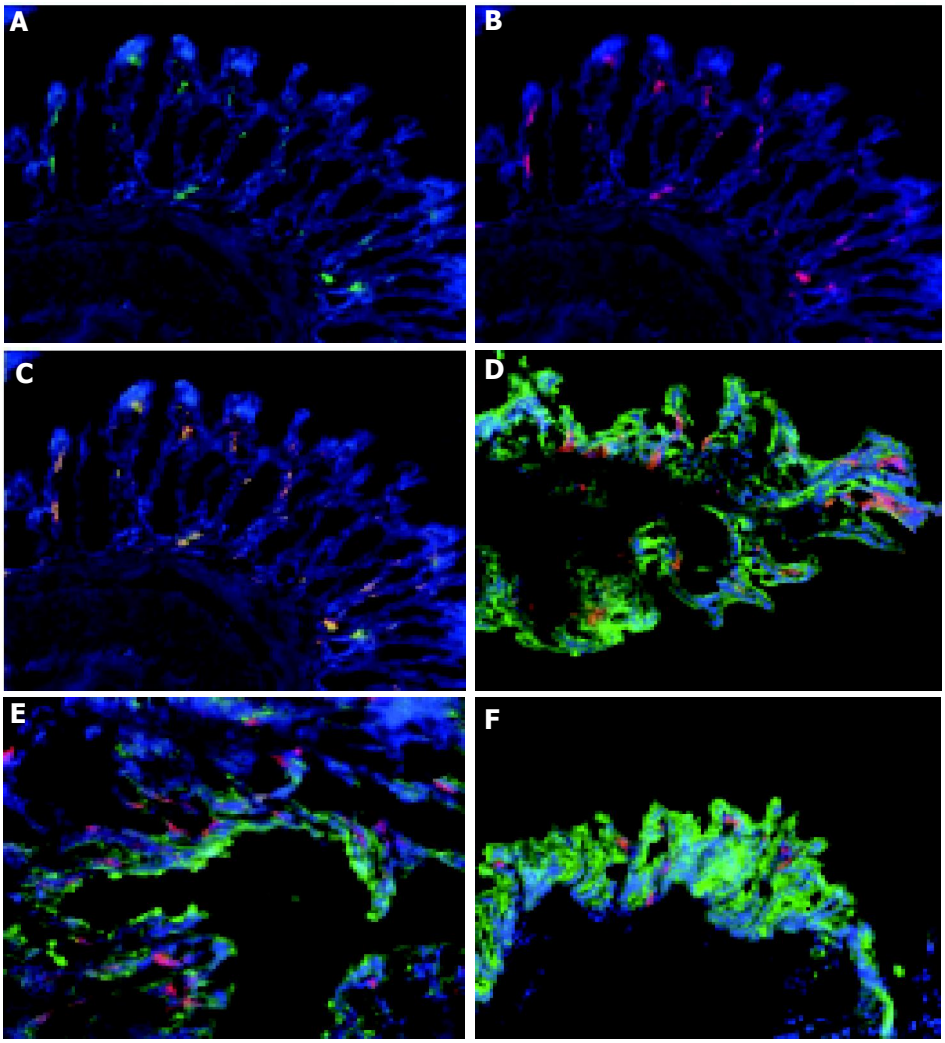


Figure 2 Colonic DC are myeloid DC which are distributed throughout the colon. Frozen sections of normal colon were stained with MAC-1 and FITC (**A**), CD11c and Cy3 (**B**) and counterstained with DAPI. The overlay of the combined images (**C**) shows that CD11c and MAC-1 co-localized (yellow) consistent with these cells being MAC-1$^+$, CD11c$^+$ myeloid DC. Tissue from the proximal (**D**), mid (**E**), and distal (**F**) colon of normal animals were immunolabeled with CD11c-Cy.3 to identify DC, cytokeratin-FITC to identify epithelial cells and counterstained with DAPI. DC were distributed throughout the colon. Magnification, ×160. Tissue was analyzed from the colons of 5 C57BL/6-IL2$^{-/-}$ and 4 C57BL/6 animals.

expressed B220 (see below, Figures 3G-I) suggesting that they may be plasmacytoid DC. The majority of CD11c$^+$ cells in the lymphoid aggregates were MAC-1$^+$ myeloid DC (data not shown).

The distribution of CD11c$^+$ cells in lymphoid aggregates within the colons (Figure 3) of colitic animals was analyzed next. These follicular-like structures were found at the base of crypts, with up to four being found per section with the exact number varying between individual mice. In IL2$^{-/-}$ mice these follicular structures were comprised of tightly packed groups of CD11c$^+$ cells which were particularly evident at the margins of these follicular structures (Figures 1F and 3). The cellular composition of these follicle-like structures was determined by immunolabeling with antibodies specific for B220 and CD4. Whereas, CD11c$^+$ cells were primarily localized to the outer edges of the structures, B220$^+$ B cells and CD4$^+$ T cells were found in the centre (Figure 3). There was also evidence of co-localization of CD4 and CD11c antibody staining (Figures 3A-C) indicating that either some CD11c$^+$ cells were also CD4$^+$, as described in the small intestine[11] and colon[8], or that some CD11c$^+$ cells are in intimate contact with CD4 T cells. Such close contact of CD11c$^+$ cells with CD4$^+$ T cells would suggest that local activation of T cells may be occurring within these sites. Although the majority of CD4$^+$ cells were found in the follicular structures, smaller numbers of positive cells were also seen in the LP of the villi and in blood vessels. B220$^+$ B cells were almost entirely restricted to the lymphoid follicle-like structures (Figures 3D-F). A small proportion of B220$^+$ cells co-localized with CD11c$^+$ cells within the lymphoid follicle (Figures 3G-I), which may represent plasmacytoid DC. CD11c$^+$, B220$^+$ cells were found primarily at the interface of the B220$^+$ cells in the centre of the lymphoid follicle and CD11c$^+$ cells at the aggregate margin.

The identity and type of DC present in the colons of normal C57BL/6 and colitic C57BL/6 IL2$^{-/-}$ mice was confirmed by electron microscopy (Figure 4). Of the total cells analyzed from C57BL/6 mice, DC represented approximately 2-4% of the cells counted. DC have been classified into three types by electron microscopy[12,13]. Type 1 DC are small, irregularly shaped cells with small cell surface

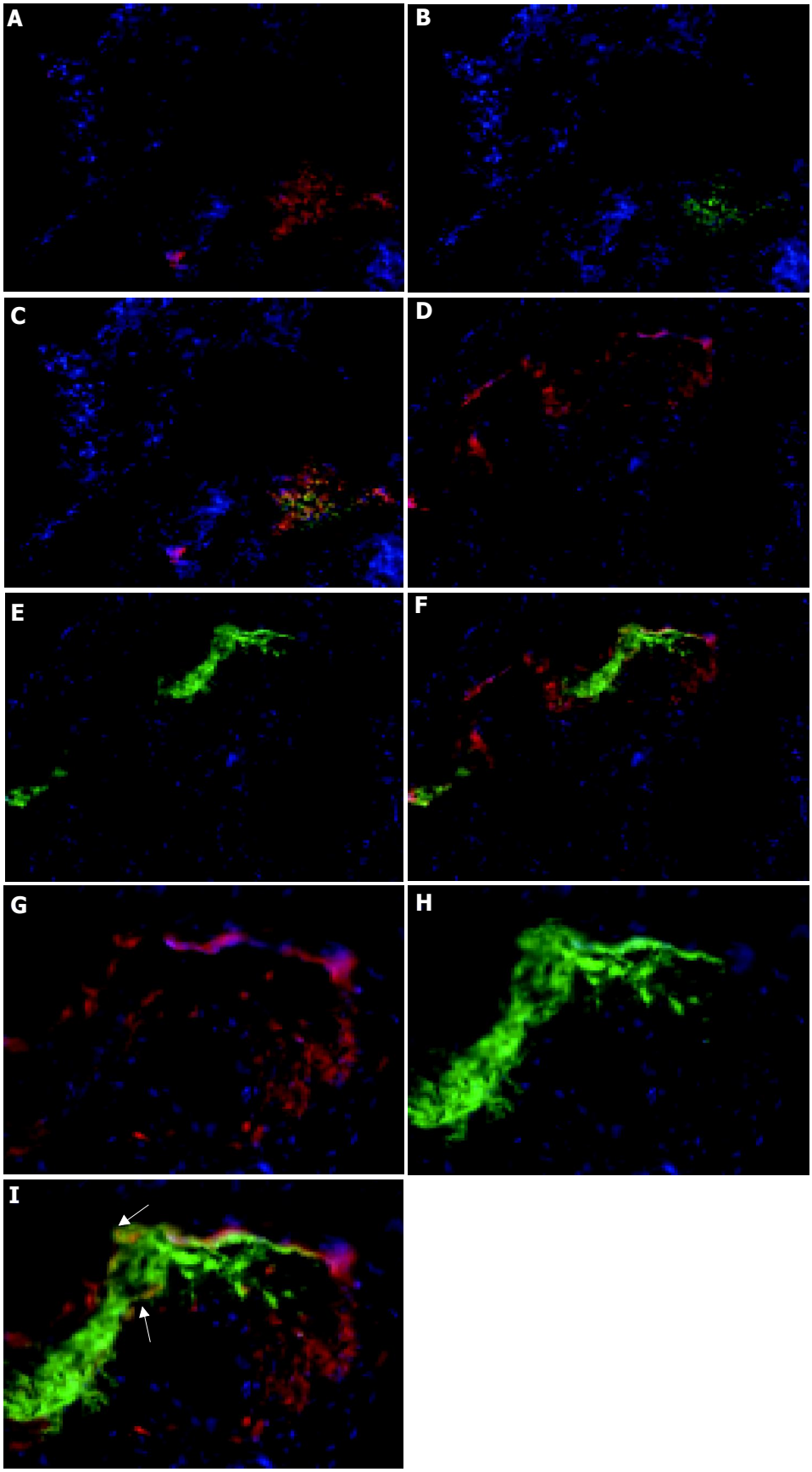


Figure 3 Lymphoid follicles in the colon. Colon sections were immunolabeled with CD11c and Cy3 to identify DC (red, **A, C, D, F, G,** and **I**), CD4 and FITC to identify Th cells (**B** and **C**) and B220 and FITC to identify B cells (**E, F, H,** and **I**) and counterstained with DAPI. Magnification, ×160. The bottom panel shows that there are $B220^{+}$ $CD11c^{+}$ cells (yellow) within the lymphoid follicles of colitic mice (magnification, ×400). The dual stained cells have been arrowed to indicate their localization. Tissue was analyzed from the colons of 5 C57BL/6-$IL2^{-/-}$ and 4 C57BL/6 animals.

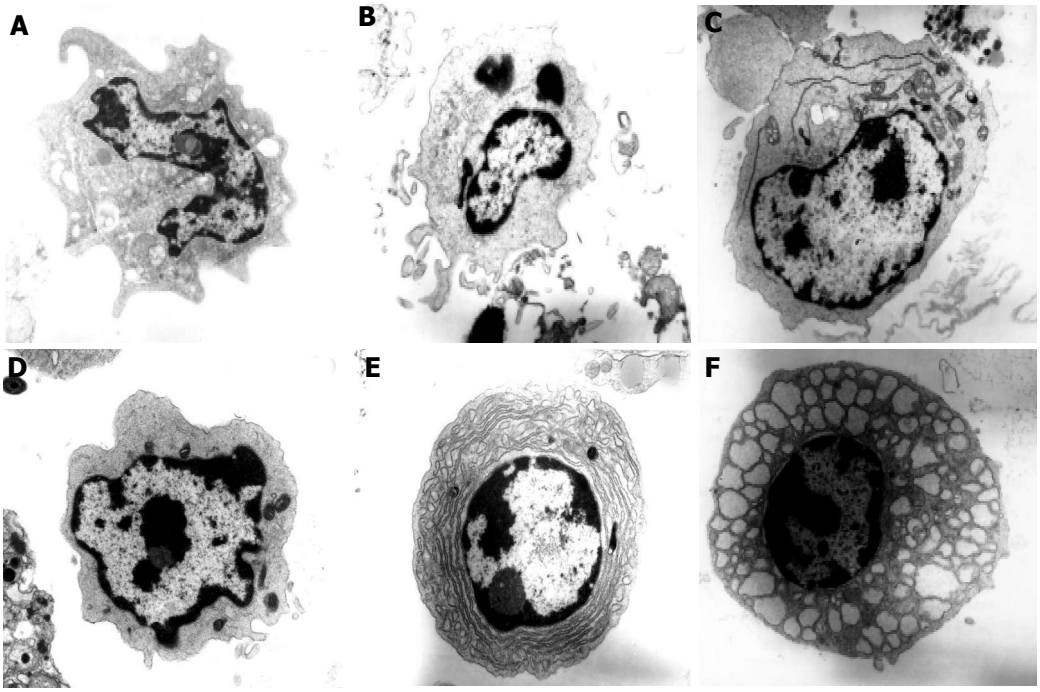


Figure 4 Electron micrographs of colonic DC from normal and colitic mice. Electron micrographs of cells from the colonic LP of normal C57BL/6 and colitic C57BL/6-IL2$^{-/-}$ mice showing (**A**) dendritic cell type 1 (myeloid DC) from a C57BL/6 mouse (×17 250), (**B**) dendritic cell type 1-2 from C57BL/6-IL2$^{-/-}$ mouse (×17 250), (**C**) dendritic cell type 2 (plasmacytoid DC) from C57BL/6-IL2$^{-/-}$ mouse (×13 800) with prominent RER, (**D**) dendritic cell type 1 (myeloid DC) from C57BL/6-IL2$^{-/-}$ mouse (×23 000), (**E**) plasma cell from C57BL/6-IL2$^{-/-}$ mouse (×17 250) and (**F**) Mott cell from C57BL/6-IL2$^{-/-}$ mouse (×17 250). Tissue was analyzed from the colons of 3 C57BL/6-IL2$^{-/-}$ and 3 C57BL/6 animals.

projections and heterochromatic nuclei with the chromatin found in a thick band at the nuclear margin and also in small condensed areas. Type 2 DC are larger than type 1 cells and have fewer projections and a euchromatic nucleus with disaggregated chromatin which is also found as a thin band at the nuclear margin. DC especially type 2 DC can have a prominent rough endoplasmic reticulum. Some cells appear to have features of both types 1 and 2 DC and have been termed type 1-2. Type 3 DC have a veiled appearance and euchromatic nuclei.

Colonic DC from normal C57BL/6 mice were mostly Type 1 (Figure 4A) with approximately 1% representing type 3 DC. However, some DC type 1 can have long projections making them appear similar to type 3 DC so this small subset of cells may in fact represent DC type 1. In comparison with normal colonic DC, many more colonic DC were identified in IL2$^{-/-}$ mice (13% compared with 2%) confirming our immunohistochemical findings. Colonic DC in the IL2$^{-/-}$ mice were comprised of type 1 DC (7-9%), type 1-2 (2%) and type 2 (2-3%, Figures 4B-D). Some of the DC (Figure 4C) had a prominent rough endoplasmic reticulum characteristic of plasmacytoid DC [14]. This would appear to confirm our immunohistochemical finding that there are small numbers of B220$^+$ CD11c$^+$ plasmacytoid DC within the colonic mucosa of IL2$^{-/-}$ mice. No type 3 DC were detected in the IL2$^{-/-}$ sample. Of the type 1 DC, half had undeveloped cytoplasm and may therefore represent a more immature population. Overall, these results confirm and extend our immunohistochemical findings that the majority of CD11c$^+$ DC detected by immunohistochemistry were CD11b$^+$ myeloid DC.

The presence of B220$^+$ B cells within the lymphoid follicular structures in the colons of IL2$^{-/-}$ mice was also confirmed by electron microscopy. Plasma cells represented approximately 10% of cells counted (Figure 4E) in the IL2$^{-/-}$ sample. The majority of plasm a cells detected had a dilated rough endoplasmic reticulum with vacuoles containing protein (Russell bodies). These are known as Mott cells and make more immunoglobulins than they are able to secrete[15]. The presence of plasma cells within the colonic lymphoid follicles suggests that the follicles are functional and that lymphocyte activation may occur locally within the colon, contributing to the chronic inflammation seen in these animals.

Phenotype of colonic DC from healthy and inflamed colonic tissue

The phenotype of DC was further analyzed by flow cytometry. There was approximately a five fold increase in the number of colonic DC in colitic animals with colonic CD11c$^+$ DC representing $3.0\pm1.3\times10^5$ of the total cells in IL2$^{-/-}$ mice compared with $6.0\pm1.4\times10^4$ cells in normal colons. These numbers were calculated by evaluating the CD45$^+$ CD11c$^+$ cells as a proportion of the absolute cell numbers and were generated from four different age- and sex-matched pairs of mice. These results confirm the increase in numbers of colonic DC in colitic mice seen by both electron microscopy and immunohistochemistry.

Expression of co-stimulatory molecules (CD40, CD80, and CD86) on CD11c$^+$ cells was compared on DC from C57BL/6 and C57BL/6-IL2$^{-/-}$ mice. Cell surface expression

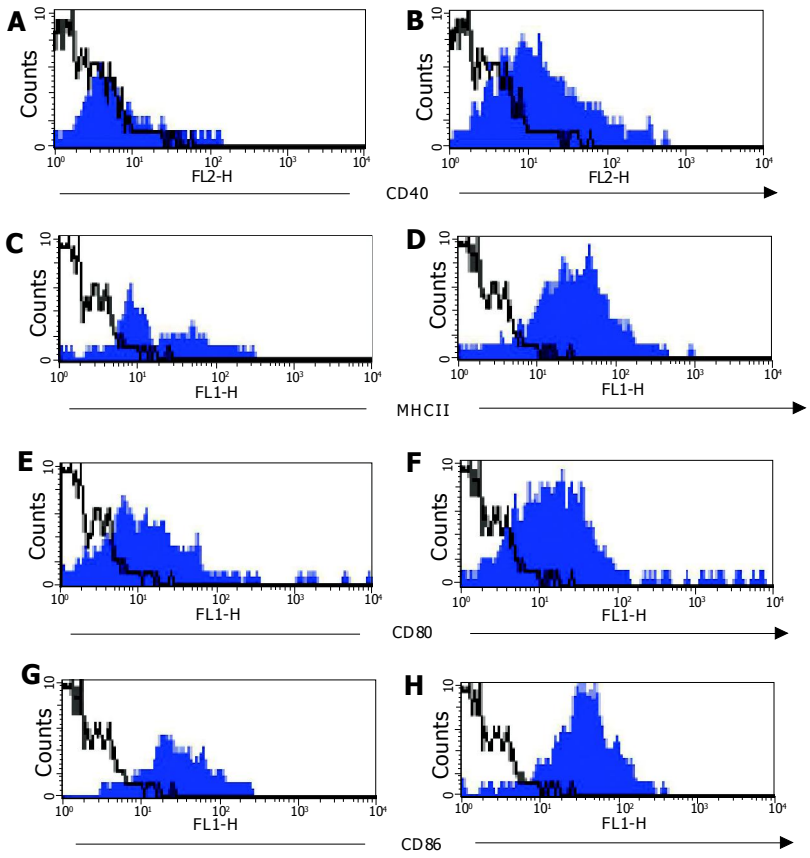


Figure 5 Co-stimulatory molecule expression on colonic LP DC. Expression of CD40 (**A+B**), MHCII (**C+D**), CD80 (**D+E**), and CD86 (**G+H**) was analyzed on CD11c$^+$ colonic LP DC from normal C57BL/6 (filled histogram left hand panel) and C57BL/6-IL2$^{-/-}$ (filled histogram right hand panel) mice by flow cytometry. Isotype control staining is represented by the open histograms with a dotted line. Data shown is a representative experiment from a total of six independent experiments.

of MHCII and CD40 was low, and CD80 and CD86 was low to moderate on CD11c$^+$ cells derived from normal colons (Figure 5). In contrast, expression of CD40, MHCII, CD80, and CD86 were all higher on DC derived from colitic animals (Figure 5). Furthermore, DC from colitic animals also expressed high levels of DEC205 (data not shown). CD11c$^+$ cells from both C57BL/6 and C57BL/6-IL2$^{-/-}$ mice all expressed high levels of the chemokine receptor CCR5 (data not shown).

The myeloid phenotype of the majority of colonic DC was also confirmed by flow cytometry with CD11c$^+$ cells being uniformly MAC-1$^+$ and CD8α. A small proportion of CD11c$^+$ DC were B220$^+$ confirming the immunohistochemical observations that there were small numbers of plasmacytoid DC present in the colons of colitic animals.

Phenotype of DC from mesenteric lymph nodes of healthy and colitic mice

In parallel to analyzing DC from the colonic LP, MLN cells were analyzed from normal and colitic animals. There were many more DC in the MLN of colitic C57BL/6-IL2$^{-/-}$ ($3.0\pm0.9\times10^5$) compared with normal C57BL/6 ($9.7\pm2\times10^4$) mice. MLN DC expressed high levels of MHCII and CD86, and moderate levels of CD40 and CD80. Furthermore, MLN DC from both C57BL/6 and C57BL/6-IL2$^{-/-}$ animals all expressed the marker DEC205. It was interesting to note that in the MLN of IL2$^{-/-}$ animals, there was an enrichment of DC populations, which expressed lower levels of MHCII (Figure 6B) and CD86 (Figure 6D). In normal mice, myeloid DC represented approximately 40-45% of DC detected in the MLN whereas in IL2$^{-/-}$, they represented up to 87% of the total DC detected. As for LP DC, all MLN DC expressed CCR5.

Endocytic activity of colonic DC

That colonic DC from normal C57BL/6 and colitic C57BL/6-IL2$^{-/-}$ animals are immature and mature, respectively, was confirmed by analyzing their endocytic activity (Figure 7). Colonic DC from normal animals were significantly more endocytically active ($P<0.001$) compared with DC from colitic animals (Figure 7A) consistent with their immature and mature status, respectively. Compared to DC, colonic macrophages were more endocytically active and took up a greater proportion of the FITC-dextran (Figure 7B). Macrophages from colitic animals endocytosed slightly more FITC-dextran than those from normal C57BL/6 animals although this was not statistically significant. Contaminating epithelial cells present in the colonic LP cell preparations all demonstrated endocytic activity. Consistent with MLN DC being mature cells, they had low endocytic activity (data not shown).

DISCUSSION

This study represents the first to attempt to quantify and characterize colonic DC in the normal, healthy colon and

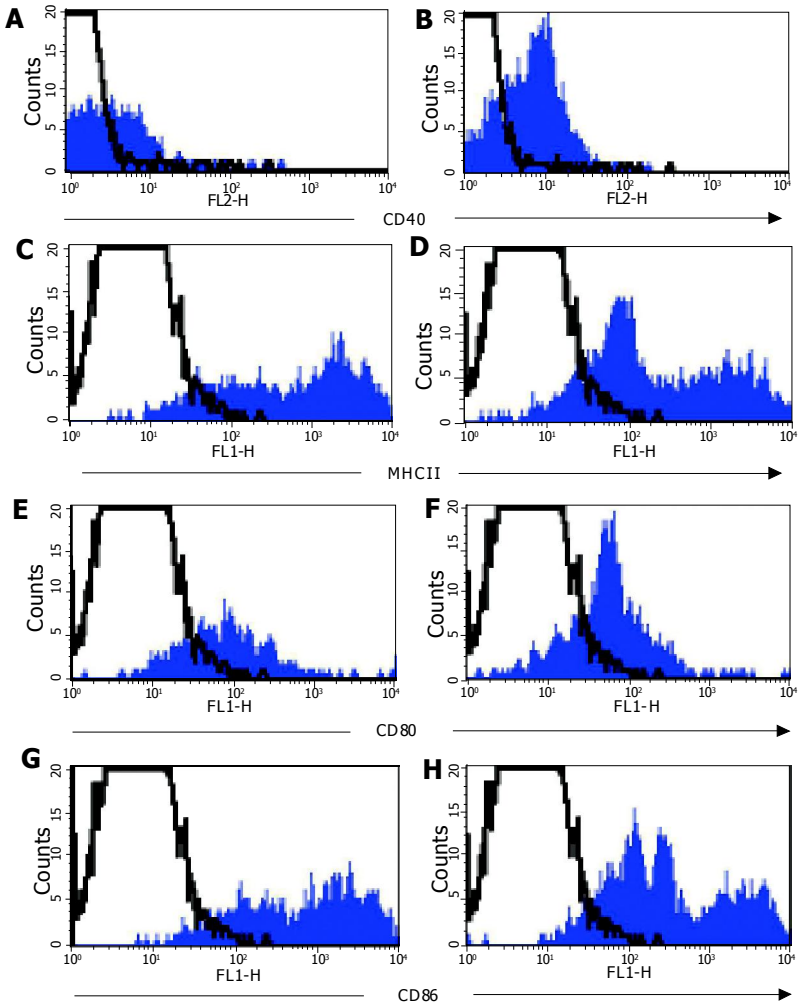


Figure 6 Co-stimulatory molecule expression on MLN DC. Expression of CD40 (**A+B**), MHCII (**C+D**), CD80 (**D+E**) and CD86 (**G+H**) was analyzed on CD11c$^+$ MLN DC from normal C57BL/6 (filled histograms left hand panel) and C57BL/6-IL2$^{-/-}$ (filled histograms right hand panel) mice by flow cytometry. Isotype control staining is represented by the open histograms with a dotted line. Data shown is a representative experiment from a total of six independent experiments.

in the colon of colitic mice. We have shown that DC in the normal colon are primarily myeloid of an immature phenotype with high endocytic activity. In contrast, colitic animal, colonic DC are mature and poor at taking up antigen. Furthermore, the redistribution and migration of DC in C57BL/6-IL2$^{-/-}$ mice and the accumulation of DC, B and T cells within lymphoid follicle-like structures suggests that activation of lymphocytes may occur locally within the colon.

There is a profound increase in the number of DC present in the inflamed colon as shown by three independent approaches. This contrasts, however, with a previous study that attempted to quantify DC in colonic biopsies from normal, UC and Crohn's patients in which it was not possible to identify any differences in the number of DC in the normal *vs* diseased colon[16]. In using, a murine model of colitis, it was possible to enumerate DC throughout the entire colon including cells within the lymphoid follicles in which many of the DC appeared to reside. By their very nature, biopsy samples may not be representative of the distribution of different cell types throughout the colon and may exclude some or all of these cells. Alternatively, these different findings may simply reflect species-specific differences.

Colonic DC are primarily myeloid DC with a small proportion of plasmacytoid DC present in the inflamed colon. This contrasts with a previous study using *rag-1*$^{-/-}$ mice transfused with CD4 T cells to induce intestinal inflammation in which CD8α CD11c$^+$ lymphoid DC were detected in the colon, which expanded two- to three-fold during inflammation[8]. This apparent difference may reflect differences in the properties of colonic DC in lymphocyte-replete *vs* lymphocyte-deficient mice, and different genetic backgrounds[17]. Alternatively, since some plasmacytoid DC have been reported to co-express CD8α the expanded population seen in CD4 T cell-transfused *rag-1*$^{-/-}$ mice may also represent an expansion of resident plasmacytoid DC which we have identified here. Although expression of the GR-1 antigen has been used to identify plasmacytoid DC in somestrains of mice[17], it was not possible to attempt this analysis here since plasmacytoid DC in C57BL/6 mice do not express GR-1.

The significance of different DC populations in normal and colitic colons is not clear. Plasmacytoid DC are associated with inflammatory responses and can secrete cytokines such as IFNα and IFNβ in response to viruses or bacterial antigens (CpG-DNA)[17,18]. Their role as APC *in vivo*, however,

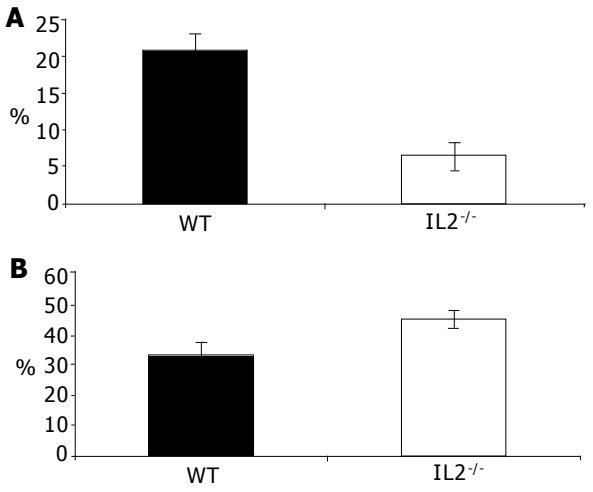


Figure 7 Increased endocytic activity by colonic DC from WT mice. Endocytic uptake of colonic lamina propria cells was measured by incubating colonic LP cells with FITC-dextran and antibodies to identify $CD11c^+$ DC (**A**) and $F4/80^+$ macrophages (**B**) from normal C57BL/6 (WT) and colitic C57BL/6-$IL2^{-/-}$ ($IL2^{-/-}$) mice. DC from colitic $IL2^{-/-}$ mice took up less FITC-dextran than their WT counterparts ($P<0.001$) consistent with them being mature DC. In contrast, colonic macrophages from $IL2^{-/-}$ mice took up more antigen than their WT counterparts although this was not significant (**B**). Results are from three independent experiments.

remains controversial with evidence of their involvement in the induction of tolerance[18-20]. Interestingly, they have also been associated with human plasma cell differentiation[21] and our observation that they localize to lymphoid follicles suggests that they may also be involved in plasma cell differentiation in the mouse. Myeloid DC may be important in promoting T regulatory/tolerogenic responses. Peyer's patch myeloid DC preferentially produce IL-10 in response to *S. aureus* and prime T cells to synthesize IL4 and IL-10 whereas lymphoid and $CD8\alpha^-CD11b^-$ DC primed IFNγ production by T cells [11]. However, our findings that myeloid DC are present in lymphoid follicle structures in the colon and comprise the major DC population in colitic animals suggests that they may promote local immunogenic or pathogenic rather than tolerogenic responses. Their ability to promote Th2 CD4 T cell responses[11] may be important for B cell class switching and contribute to the activation of the plasma cells observed in the lymphoid follicles of colitic $IL2^{-/-}$ mice. It is important to note, however, that DC from the colon and small intestine may not possess the same functional properties. For example, it has been shown that treatment of mice with RANKL promotes tolerogenic T cell responses in the small intestine[22] whereas excessive RANKL in the colon drives colonic inflammation by promoting DC maturation and survival[23, 24]. Furthermore, the nature of the signals that promote DC maturation can have a significant impact on the resultant immune response. Signaling through different toll-like receptors (TLR) generates distinct biological responses and differential expression of TLR by different DC subsets enables them to respond to distinct microbial structures in a specific manner[25,26]. Therefore, ligation of pattern recognition receptors by different bacteria may promote different types of T cell responses, including tolerogenic responses, and differences in small intestine and colonic DC function may therefore be due to different environmental influences[22,27,28]. For example, the interaction of DC with other cell types in the colon may be of significance, since colonic epithelial cells (CEC) can suppress T-cell activation even in the presence of professional APC[29]. Thus, the interactions of different cell types in the colon and the influence of the cell environment may have profound effects on the immune response generated.

The localization of colonic DC was altered in colitis. DC in $IL2^{-/-}$ animals were found adjacent to the colonic epithelium and may therefore access the lumen. This is not the case in normal animals, in which the colonic DC were found exclusively within the LP. DC have been reported as forming tight junctions with epithelial cells[30] enabling them to sample luminal antigens. However, our observation that, DC in the normal colon although capable of endocytosis are excluded from the epithelial layer, suggests that colonic DC may not normally sample luminal antigens in healthy mice. By contrast, in colitic mice DC are well positioned to take up luminal antigen although as mature cells they had low endocytic activity. Interestingly, we also found that CEC are strongly endocytic which may support the hypothesis that they are the primary cells involved in sampling luminal antigens within the colon. Based on this assumption we would propose that DC interact directly with CEC. Indeed, we have found that colonic DC express CCR5 and CEC secrete a variety of chemokines including ligands for CCR5 (MCP-1, MIP1α, and MIP1β) in response to different bacterial stimuli and may therefore play a role in attracting DC to the epithelial layer[31].

The number of $CD11c^+$ DC in the MLN of colitic mice was increased compared to normal mice and a population of $MHCII^{int}$, $CD86^{int}$ DC were expanded in the MLN, corresponding to the phenotype of mature LP DC which suggested that some colonic LP DC may have migrated from the colonic mucosa to the MLN. In addition to T-cell activation occurring within the MLN, there may also be local activation of lymphocytes within the colon as we found organized aggregates of DC at the base of the crypts in the inflamed colon, which primarily comprised DC, B cells, and T cells. The presence of plasma cells including Mott cells, which were identified by electron microscopy, in the colonic LP of $IL2^{-/-}$ animals adds weight to this hypothesis. Of note, similar aggregates of DC, B, and T cells have been described in human UC[32]. The formation of lymphoid aggregates may also contribute significantly to the pathology of IBD as DC which mature in inflamed tissue and fail to migrate to the lymph nodes are thought to act as nucleation sites to organize lymphoid structures which can sustain chronic inflammation[33].

In conclusion, we have characterized the phenotype of colonic DC in normal mice and mice with colitis. There is a dramatic increase in DC numbers within the colonic LP of the inflamed colon which have an altered phenotype and localization. Furthermore, we have described the formation of lymphoid aggregates which may contribute directly to the ongoing inflammation. Further study of these cells may

be informative in understanding the etiology of colitis and persistence of chronic inflammation.

REFERENCES

1 **Duchmann R,** Kaiser I, Hermann E, Mayet W, Ewe K, and Meyer zum Buschenfelde KH. Tolerance exists towards resident intestinal flora but is broken in active inflammatory bowel disease (IBD). *Clin Exp Immunol* 1995; **102**: 448-455

2 **Contractor NV,** Bassiri H, Reya T, Park AY, Baumgart DC, Wasik MA, Emerson SG, Carding SR. Lymphoid hyperplasia, autoimmunity, and compromised intestinal intraepithelial lymphocyte development in colitis-free gnotobiotic IL-2-deficient mice. *J Immunol* 1998; **160**: 385-394

3 **Garside P,** Mowat AM. Oral tolerance. *Semin Immunol* 2001; **13**: 177-185

4 **Ashcroft AJ,** Cruickshank SM, Croucher PI, Perry MJ, Rollinson S, Lippitt JM, Child JA, Dunstan C, Felsburg PJ, Morgan GJ, Carding SR. Colonic dendritic cells, colitis and T cell mediated bone destruction are regulated by RANK/RANK LIGAND interactions. *Immunity* 2003; **19**: 849-861

5 **Kelsall BL,** Stuber E, Neurath M, Strober W. Interleukin-12 production by dendritic cells. The role of CD40-CD40L interactions in Th1 T-cell responses. *Ann New York Acad Sci* 1996; **795**: 116-126

6 **Iwasaki A,** Kelsall BL. Localization of distinct Peyer's patch dendritic cell subsets and their recruitment by chemokines macrophage inflammatory protein (MIP)-3alpha, MIP-3beta, and secondary lymphoid organ chemokine. *J Exp Med* 2000; **191**: 1381-1394

7 **Bell SJ,** Rigby R, English N, Mann SD, Knight SC, Kamm MA, Stagg AJ. Migration and maturation of human colonic dendritic cells. *J Immunol* 2001; **166**: 4958-4967

8 **Krajina T,** Leithauser F, Moller P, Trobonjaca Z, Reimann J. Colonic lamina propria dendritic cells in mice with CD4+ T cell-induced colitis. *Eur J Immunol* 2003; **33**: 1073-1083

9 **Sadlack B,** Merz H, Schorle H, Schimpl A, Feller AC, Horak I. Ulcerative colitis-like disease in mice with a disrupted interleukin-2 gene. *Cell* 1993; **75**: 253-261

10 **Contractor NV,**Bassiri H,Reya T,Park AY,Baumgart DC, Wasik MA.Emerson SG,Carding SR.Lymphoid hyperplasia, autoimmunity and compromised intestinal intraepithelial lymphocyte development in colitis-free gnotobiotic IL2-deficient mice. *J Immunol* 1998; **160**: 385-394

11 **Iwasaki A,** Kelsall BL. Unique functions of CD11b+, CD8 alpha+, and double-negative Peyer's patch dendritic cells. *J Immunol* 2001; **166**: 4884-4890

12 **Patterson S,** Gross J, Bedford P, Knight SC. Morphology and phenotype of dendritic cells from peripheral blood and their productive and non-productive infection with human immunodeficiency virus type 1. *Immunol* 1991; **72**: 361-367

13 **Robinson SP,** Patterson S, English N, Davies D, Knight SC, Reid CD. Human peripheral blood contains two distinct lineages of dendritic cells. *Eur J Immunol* 1999; **29**: 2769-2778

14 **Cavanagh LL,** Von Andrian UH. Travellers in many guises: The origins and destinations of dendritic cells. *Immunol Cell Biol* 2002; **80**: 448-462

15 **Jiang Y,** Hirose S, Hamano Y, Kodera S, Tsurui H, Abe M, Terashima K, Ishikawa S, Shirai T. Mapping of a gene for the increased susceptibility of B1 cells to Mott cell formation in murine autoimmune disease. *J Immunol* 1997; **158**: 992-997

16 **Turley SJ,** Inaba K, Garrett WS, Ebersold M, Unternaehrer J, Steinman RM, Mellman I. Transport of peptide-MHC class II complexes in developing dendritic cells. *Science* 2000; **288**: 522-527

17 **Hochrein H,** O'Keeffe M, Wagner H. Human and mouse plasmacytoid dendritic cells. *Hum Immunol* 2002; **63**: 1103-1110

18 **Kelsall BL,** Biron CA, Sharma O, Kaye PM. Dendritic cells at the host-pathogen interface. *Nat Immunol* 2002; **3**: 699-702

19 **Wakkach A,** Fournier N, Brun V, Breittmayer JP, Cottrez F, Groux H. Characterization of dendritic cells that induce tolerance and T regulatory 1 cell differentiation *in vivo*. *Immunity* 2003; **18**: 605-617

20 **Bilsborough J,** George TC, Norment A, Viney JL. Mucosal CD8alpha+ DC, with a plasmacytoid phenotype, induce differentiation and support function of T cells with regulatory properties. *Immunology* 2003; **108**: 481-492

21 **Jego G,** Palucka AK, Blanck JP, Chalouni C, Pascual V, Banchereau J. Plasmacytoid dendritic cells induce plasma cell differentiation through type I interferon and interleukin 6. *Immunity* 2003; **19**: 225-234

22 **Williamson E,** Bilsborough JM, Viney JL. Regulation of mucosal dendritic cell function by receptor activator of NF-kappa B (RANK)/RANK ligand interactions: impact on tolerance induction. *J Immunol* 2002; **169**: 3606-3612

23 **Yoneyama H,** Narumi S, Zhang Y, Murai M, Baggiolini M, Lanzavecchia A, Ichida T, Asakura H, Matsushima K. Pivotal role of dendritic cell-derived CXCL10 in the retention of T helper cell 1 lymphocytes in secondary lymph nodes. *J Exp Med* 2002; **195**: 1257-1266

24 **Josien R,** Li HL, Ingulli E, Sarma S, Wong BR, Vologodskaia M, Steinman RM, Choi Y. TRANCE, a tumor necrosis factor family member, enhances the longevity and adjuvant properties of dendritic cells *in vivo*. *J Exp Med* 2000; **191**: 495-502

25 **Kadowaki N,** Ho S, Antonenko S, Malefyt RW, Kastelein RA, Bazan F, Liu YJ. Subsets of human dendritic cell precursors express different toll-like receptors and respond to different microbial antigens. *J Exp Med* 2001; **194**: 863-869

26 **Stagg AJ,** Hart AL, Knight SC, Kamm MA. The dendritic cell: its role in intestinal inflammation and relationship with gut bacteria. *Gut* 2003; **52**: 1522-1529

27 **Re F,** Strominger JL. Toll-like receptor 2 (TLR2) and TLR4 differentially activate human dendritic cells. *J Biol Chem* 2001; **276**: 37692-37699

28 **Kapsenberg ML.** Dendritic-cell control of pathogen-driven T-cell polarization. *Nat Rev Immunol* 2003; **3**: 984-993

29 **Cruickshank SM,** McVay LD, Baumgart DC, Felsburg PJ, Carding SR. Colonic Epithelial cell-mediated suppression of CD4 T cell activation. *Gut* 2004; **53**: 678-684

30 **Rescigno M,** Rotta G, Valzasina B, Ricciardi-Castagnoli P. Dendritic cells shuttle microbes across gut epithelial monolayers. *Immunobiology* 2001; **204**: 572-581

31 **Lan JG,** Cruickshank SM, Singh JC, Farrar M, Lodge JP, Carding SR.Differential cytokine response of primary colonic epithelial cells to commensal bacteria. *World J Gastreoententerology* 2005; **11;** 3375-3383

32 **Yeung MM,** Melgar S, Baranov V, Öberg Å, Danielsson Å, Hammarström S, Hammarström ML. Characterisation of mucosal lymphoid aggregates in ulcerative colitis: immune cell phenotype and TcR-gd expression. *Gut* 2000; **47**: 215-227

33 **Sallusto F,** Lanzavecchia A. Mobilizing dendritic cells for tolerance, priming, and chronic inflammation. *J Exp Med* 1999; **189**: 611-614

Science Editor Guo SY **Language Editor** Elsevier HK

PO Box 2345, Beijing 100023, China
www.wjgnet.com
wjg@wjgnet.com

ELSEVIER

World J Gastroenterol 2005;11(40):6348-6353
World Journal of Gastroenterology ISSN 1007-9327
© 2005 The WJG Press and Elsevier Inc. All rights reserved.

• *CLINICAL RESEARCH* •

Hemodynamic and morphologic changes of peripheral hepatic vasculature in cirrhotic liver disease: A preliminary study using contrast-enhanced coded phase inversion harmonic ultrasonography

Rong-Qin Zheng, Bo Zhang, Masatoshi Kudo, Yasuhiro Sakaguchi

Rong-Qin Zheng, Bo Zhang, Department of Ultrasound, the Third Affiliated Hospital, Sun Yat-Sen University, Guangzhou 510630, Guangdong Province, China
Masatoshi Kudo, Yasuhiro Sakaguchi, Department of Gastroenterology and Hepatology, Kinki University School of Medicine, Osaka-Sayama, Japan
Correspondence to: Dr. Rong-Qin Zheng, Department of Ultrasound, the Third Affiliated Hospital, Sun Yat-Sen University, Guangzhou 510630, Guangdong Province, China. ultrasoundzh@sohu.com
Telephone: +86-20-88348792 Fax: +86-20-87536401
Received: 2005-02-24 Accepted: 2005-07-29

Abstract

AIM: To provide the useful information for the diagnosis of liver cirrhosis by observing the morphology of peripheral hepatic vessels and the hemodynamics of microbubble arrival time in these vessels.

METHODS: Twenty-one subjects including 5 normal volunteers and 16 patients (liver cirrhosis, n=10; chronic hepatitis, n=6) were studied by contrast-enhanced coded phase inversion harmonic sonography (GE LOGIQ 9 series) using a 6-8 MHz convex-arrayed wide-band transducer. The images of peripheral hepatic artery, portal and hepatic vein were observed in real-time for about 2 min after intravenous injection of Levovist. The time when microbubbles appeared in the peripheral vessels (microbubble arrival time) was also recorded. The morphologic changes of peripheral hepatic vasculature were classified as marked, slight, and no changes based on the regularity in caliber, course, ramification, and the delineation of vessels compared to normal subjects.

RESULTS: The microbubble arrival time at peripheral artery, portal, and hepatic vein was shorter in cirrhotic patients than in chronic hepatitis patients and normal subjects. The marked, slight and no morphologic changes of peripheral hepatic vasculature found in 5 (5/6, 83.3%), 1 (1/6, 16.7%), and 0 (0/6, 0%) liver cirrhosis patients, respectively, and in 1 (1/10, 10%), 6 (6/10, 60%), and 3 (3/10, 30%) chronic hepatitis patients, respectively. There was a significant difference between the two groups (P<0.001).

CONCLUSION: Evaluation of the hemodynamics and morphology of peripheral hepatic vasculature by contrast-enhanced coded pulse inversion harmonic sonography can provide useful information for the diagnosis of liver cirrhosis.

© 2005 The WJG Press and Elsevier Inc. All rights reserved.

Key words: Contrast medium; Sonography; Liver cirrhosis; Hemodynamics

Zheng RQ, Zhang B, Kudo M, Sakaguchi Y. Hemodynamic and morphologic changes of peripheral hepatic vasculature in cirrhotic liver disease: A preliminary study using contrast-enhanced coded phase inversion harmonic ultrasonography. *World J Gastroenterol* 2005; 11(40): 6348-6353
http://www.wjgnet.com/1007-9327/11/6348.asp

INTRODUCTION

Ultrasonography (US) is widely used for the purpose of screening for liver tumors. However, it has a limited value for the diagnosis of liver cirrhosis due to its low sensitivity and specificity[1].

With the advent of ultrasound contrast agent and associated ultrasonic technologies, drastic improvements have been achieved in the diagnosis and treatment of hepatic tumors[2]. However, application of contrast-enhanced US in the evaluation of diffused liver diseases is rare. Recently, using spectral Doppler US with time-intensity analysis software to measure the arrival time of microbubble agent, Levovist, in hepatic vein, Albrecht *et al*.[3] found a much earlier onset of microbubble enhancement in cirrhotic patients than in normal controls or non-cirrhotic patients, and stressed that this method is a sensitive non-invasive test for liver cirrhosis. However, this technique is based on the Doppler US that has limitations in detecting slow blood signals in small vessels. Furthermore, it is not easy to perform continuous spectral Doppler tracing.

Microbubble-specific technologies, such as phase/pulse inversion harmonic imaging (PIHI) and coded harmonic angio, can display microbubble signals in blood vessels on a gray-scale background in real time[4]. Theoretically,

microbubble arrival time can be measured using such gray-scale harmonic imaging techniques by direct visualization of microbubble enhancement in hepatic vessels, that is both hemodynamics and morphology of hepatic vessels can be evaluated simultaneously. Bang *et al*.[5] recently used the pulse inversion imaging technique to assess the arrival time of microbubbles in hepatic vein and compared it with the spectral Doppler tracing method[3]. They noticed that there is no significant difference between these two methods.

On the assumption that the evaluation of hepatic vascular morphology when observing the hemodynamics of microbubble arrival time in hepatic vessels may provide more information for the diagnosis of liver cirrhosis, we conducted a study to observe the morphology of and microbubble arrival time in peripheral hepatic vessels in patients with liver cirrhosis and chronic hepatitis using contrast-enhanced coded harmonic angio mode, which is a real-time vascular imaging technique that combines PIHI with coded technology. The purpose of this preliminary study was to evaluate whether it is possible to provide useful information for the diagnosis of liver cirrhosis by observing the morphology and hemodynamics of hepatic vessels using contrast-enhanced coded harmonic angio technique.

MATERIALS AND METHODS

Patients

This study consisted of 5 normal volunteers (4 men and 1 woman; age range 28-38 years, mean age 31 years) and 16 patients (12 men and 4 women; age range 18-73 years, mean age 54 years). Among the 16 patients, 10 had chronic hepatitis (hepatitis C, n=7; hepatitis B, n=3), 6 had liver cirrhosis (hepatitis C-related cirrhosis, n=3; hepatitis B-related cirrhosis, n=3). In addition, 4 patients (3 with cirrhosis and 1 with chronic hepatitis) were accompanied with hepatocellular carcinoma (HCC) with 1 (n=3) or 2 (n=1) nodules (less than 4 cm in diameter) in the right (n=3) or left (n=1) liver lobe. The diagnosis of chronic hepatitis (n=9) and liver cirrhosis (n=1) was made by histology in 10 patients. Other patients were diagnosed on the basis of clinical, biochemical and imaging findings on US (n=6), CT (n=5), MRI (n=3) and/or angiography (n=2). Normal subjects had no history or clinical signs of liver diseases. The Institutional Ethics Board of our university approved the study protocol and informed consent was obtained from all subjects.

Methods

In this study, we used Levovist (Schering, AG, Berlin, Germany) as a contrast agent, an intravenous microbubble agent consisting of 99.9% D-galactose and 0.1% palmitic acid. In brief, 2.5 g Levovist suspension at a concentration of 400mg/mL was prepared according to the manufacturer's introductions. The suspension was injected via a 21- gauge cannula placed in the antecubital vein at a speed of 1 mL/s, and followed by a 10 mL normal saline flush.

Contrast-enhanced US study was carried out using GE LOGIQ 9 series (General Electric Medical System, Milwaukee, WI). A M7C convex-arrayed wide-band transducer with a frequency of 6-8 MHz was used. All subjects were fasted for at least 5 h before examination. Before contrast-enhanced study, fundamental B-mode imaging was performed to screen for any local lesions. Patients who had multiple (more than two nodules) and large (larger than 4 cm in diameter) nodules of solid occupying lesions were excluded in this study. The scanning section was selected at the right liver lobe through an intercostal approach. A non-tumor section was chosen to avoid the interference of the tumor for patients with HCC. Color Doppler imaging was also performed before the contrast study to ascertain the location and course of different liver vessels (especially the portal and hepatic vein) for the reference of identifying these vessels on contrast-enhanced images.

Contrast-enhanced US was then studied using coded harmonic angio mode with the mechanical index (MI) of 0.4-0.5, dynamic range of 72 decibels, main gain of 35-40 G and frame rate of 6-7 Hz. The scanning depth was maintained within 6-8 cm from the body surface. Single focus point was set at 1-2 cm beneath the liver surface. After the administration of Levovist, an inner time-meter was switched on. All the subjects were asked to breathe gently during examination. Real-time scanning with no background display was used to observe the vessel images of hepatic vasculature from the level equal to the origin of the third order branches of portal vein (segment level) to the liver surface, for about 2 min after injection. Simultaneously, the time when microbubbles appeared in the hepatic artery, portal and hepatic vein (microbubble arrival time) in the area described above was measured.

Real-time data were recorded on S-VHS videotapes and stored in the cine memory of the machine, which could load more than 2 000 frames of images (about 5 min in real time), and then saved to the hard disk for later review. After the examination, the dynamic contrast-enhanced images were replayed in the cine loop derived from the hard disk frame and series pictures were printed in the time sequence for later analysis.

Data analysis

Contrast-enhanced US studies were performed by the same operator using the same protocol in order to minimize the variations from the operators and condition settings. Another two authors reviewed the series pictures and evaluated the results without any knowledge of the subjects' clinical data.

Referring to the evaluation method used in hepatic venography[6] and transhepatic portography[7], the morphologic changes of peripheral hepatic vasculature in patients with chronic liver disease were classified as marked, slight and no changes based on the regularity in caliber, course, ramification, and the delineation of vessels compared to normal subjects.

The peripheral vascular morphologic changes were compared among different groups using chi-square test, while the microbubble arrival time at different hepatic vessels was compared using Mann-Whitney test. $P<0.05$ was considered statistically significant.

RESULTS

The peripheral artery could not be seen on coded harmonic angio mode before contrast, while the relative large portal and hepatic veins could be visualized during respiration (Figure 1A). After injection of contrast medium, microbubbles in the peripheral hepatic artery were displayed as small bright dots (Figure 1B). When enhanced by the contrast medium, the portal and hepatic vein became more echogenic than they were on pre-contrast images (Figure 2). In some subjects, the microbubble arrival time at different vessels could not be measured because of inadequate section showing no target

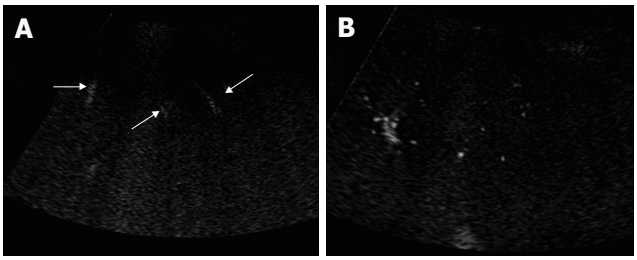


Figure 1 Pre-contrast image in a 32-year-old normal control (**A**) and contrast-enhanced US image in a 64-year-old cirrhotic patient (**B**).

vessels, or interference with deep breath of the subjects.

In the normal subjects, microbubbles appeared in the peripheral hepatic artery in about 16-28 s after Levovist injection. Arterial vessels were thin and regular in the early arterial phase in which only intraheaptic arterial vessels were visualized on contrast-enhanced images (Figure 3A). Portal venous vessels were enhanced by microbubbles in about 28-39 s, and then hepatic venous vessels were stained in about 35-71 s. In the vascular phase, intrahepatic portal and hepatic veins were visualized on contrast-enhanced images, peripheral hepatic vessels were regular in caliber, course and ramification, tapering smoothly as they run to the periphery (Figures 3B and 3C). When the vessel images on contrast-enhanced US were evaluated by another two authors blindly, all the normal subjects were regarded to having no abnormal morphologic changes.

The microbubble arrival times at peripheral artery, portal and hepatic vein were shorter in cirrhotic patients than in chronic hepatitis patients and normal subjects. However, it showed statistical significant differences only in hepatic venous arrival time ($P<0.05$) (Table 1). Whereas, there were no significant differences in arrival times at different vessels between chronic hepatitis patients and normal controls (Table 1). Markedly morphologic changes of peripheral hepatic vessels including poor delineation

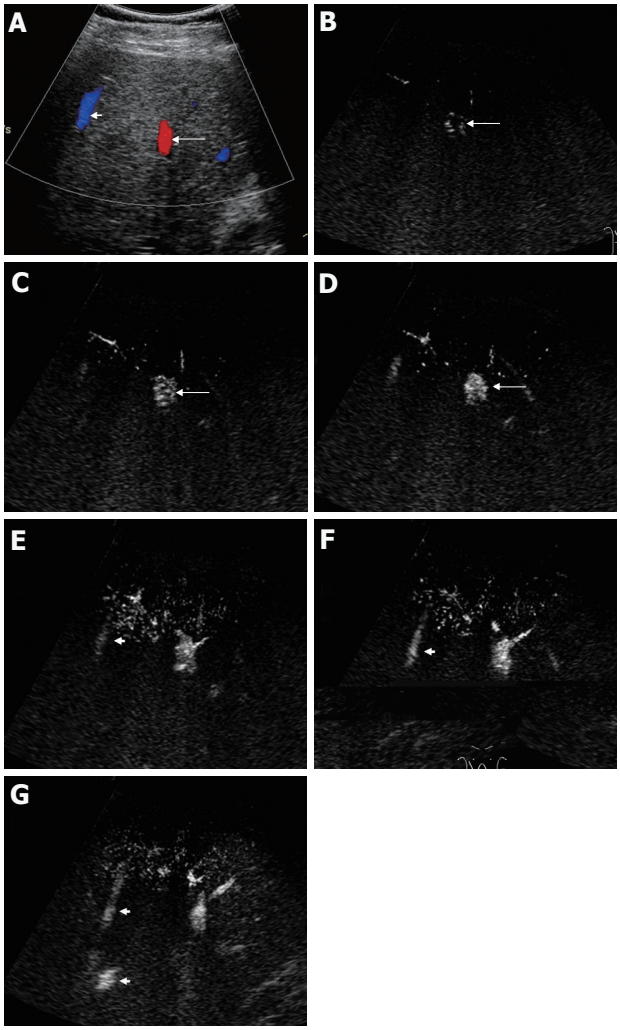


Figure 2 Contrast-enhanced US images in a 32-year-old normal control. **A:** Before contrast, color Doppler US was performed to show the location and course of the portal vein (arrow) and hepatic vein (arrowhead); **B:** In the early arterial phase, the portal vein was not enhanced, while the parallel running artery was displayed by microbubble enhancement (arrow); **C:** Twenty-eight seconds after injection of Levovist, bright dots of microbubbles began to fill in the portal vein (arrow); **D:** Four seconds later, the portal vein was obviously enhanced by microbubbles (arrow); **E:** Before microbubbles arrived, the hepatic vein (arrowhead) was mildly echogenic; **F** and **G:** Thirty-seven seconds after injection of contrast medium, the hepatic vein (arrowhead) became more echogenic (**F**) than it was on **E**, indicating enhancement by microbubbles, and 4 s later the proximal part of hepatic vein was also clearly seen (arrowheads) (**G**).

of vessels, irregularity in caliber, course, and ramification without tapering of vessels (Figure 4A), or visualization of abnormal structures such as ring-like vessels (Figure 4B), were found in 5 of the 6 cirrhotic patients (5/6, 83.3%) Slight morphologic changes were identified in one cirrhotic patient (1/6, 16.7%). Marked, slight and no morphologic changes were found in 1 (1/10, 10%), 6 (6/10, 60%), and 3 (3/10, 30%) chronic hepatitis patients, respectively ($P<0.001$, Table 2). If marked morphologic changes of peripheral hepatic vessels were taken as a criterion for the diagnosis of liver cirrhosis, the diagnostic sensitivity and specificity were 83.3% and 93.3%, respectively.

The microbubble arrival time at hepatic vein was shorter in cirrhotic patients who had marked morphologic

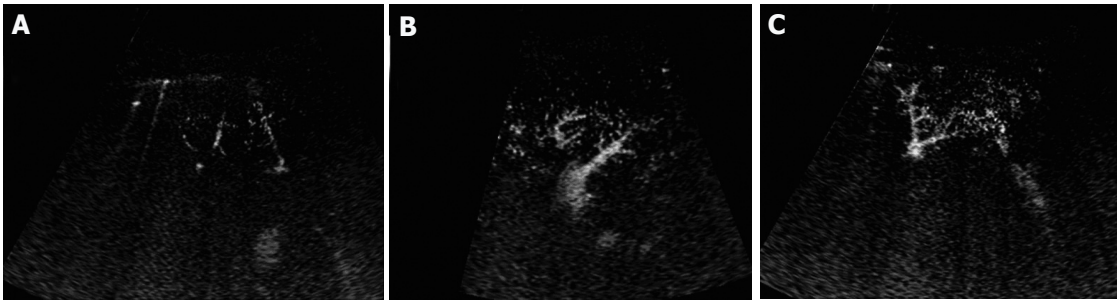


Figure 3 Contrast-enhanced US images in normal controls. **A:** In the early arterial phase, only the peripheral arteries were displayed, they were thin and regular; **B** and **C:** In the vascular phase of contrast-enhanced US, the peripheral portal vein (**B**) and hepatic vein (**C**) were portrayed as regular in caliber, course, and ramification, tapering smoothly as they run to the liver surface.

Table 1 Microbubble arrival time at hepatic vessels (mean±SD)

	Artery (*n*)	Portal vein (*n*)	Hepatic vein (*n*)
Cirrhosis	16.4±5.3 (5)	21.3±6.7 (3)	21.3±7.7 (3)
Chronic hepatitis	23.5±9.1 (8)	35.1±19.4 (8)	44.3±20.8 (7)
Normal control	20.3±5.4 (4)	31.3±6.7 (3)	45.5±17.1 (4)
*P*1	0.537	0.077	0.046
*P*2	0.185	0.26	0.03

P 1: Comparison between cirrhosis and normal control. *P* 2: Comparison between cirrhosis and chronic hepatitis.

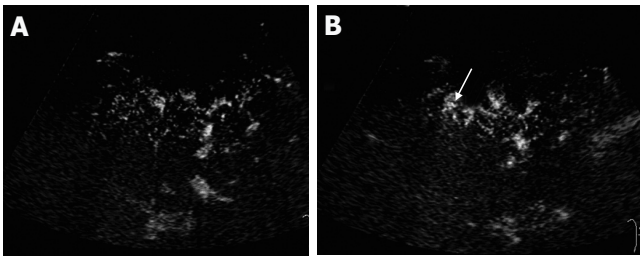


Figure 4 Contrast-enhanced US images in cirrhotic patients. **A** and **B:** On contrast-enhanced US images, the peripheral vessels had poor delineation and were irregular (**A**). There was no tapering of the vessels. Small branches of the vessels were rarely seen (**A**), while abnormal ring-like structure (**B**, arrow) was displayed.

changes than in those who had slight morphologic changes of peripheral hepatic vasculature (16-25 s *vs* 37 s). In one of the cirrhotic patients without HCC, the arterial arrival time was short (11 s). During the early arterial phase, one distal portal vein branch was enhanced by microbubbles (14 s) prior to the enhancement of proximal portal vein and other branches at the same level (Figure 5A). An adjacent peripheral hepatic vein was also stained (16 s) (Figures 5B and 5C). A small intrahepatic arterioportal shunt was suspected. Unfortunately, the patient did not undergo hepatic angiography.

DISCUSSION

In liver cirrhosis, circulatory changes play an important role in the progression of regenerative nodular formation and extensive stromal fibrosis and vice versa[8]. Microscopically, these circulatory changes in the liver, such as capillarization

Table 2 Abnormal morphologic changes of peripheral hepatic vasculature on contrast-enhanced US

	Marked (%)	Slight (%)	None (%)	Total
Cirrhosis	5 (83.3)	1 (16.7)	0	6
Chronic hepatitis	1 (10)	6 (60)	3 (30)	10
Normal control	0	0	5 (100)	5

^{b}P<0.001 *vs* cirrhosis, chronic hepatitis and normal control.

of sinusoids, arterialization, and intrahepatic shunts[9-11], can be observed by microcirculation evaluation methods such as microvascular casts[8], color gelatin injection postmortem[11]. Macroscopically, circulatory morphological changes in liver cirrhosis can be demonstrated by different angiographic techniques, such as hepatic angiography, arterial portography or transhepatic portography and hepatic venography[7]. However, angiographic techniques are invasive and cannot be used routinely. Color and power Doppler ultrasonography can also be used in the evaluation of hepatic vasculature. However, they can not achieve satisfactory results due to their limitations in detecting slow blood flow signals in fine vessels.

Contrast-enhanced code harmonic angio is an advanced microbubble-specific technique that combines PIHI with coded technology, which amplifies the wide-bind signals from microbubbles and suppresses signals from the tissue[2,4]. It provides the possibility to assess the morphology of hepatic vessels in real time under physiological conditions. In this study, the morphology of peripheral hepatic vasculature was clearly demonstrated by a high frequency probe, which has high resolution in showing superficial structures. Compared to normal subject, marked morphologic changes including poor delineation of vessels, irregularity in caliber, course, and ramification without tapering of the vessels, or visualization of abnormal structures, were portrayed in most cirrhotic patients (83.3%), while few of chronic hepatitis patients (10%) and none of normal subjects had marked morphologic changes of peripheral hepatic vasculature, suggesting that it has a relatively high sensitivity and specificity for the diagnosis of liver cirrhosis. The results indicate that contrast-enhanced code harmonic angio can recognize the differences in peripheral vasculature between cirrhotic and non-cirrhotic subjects,

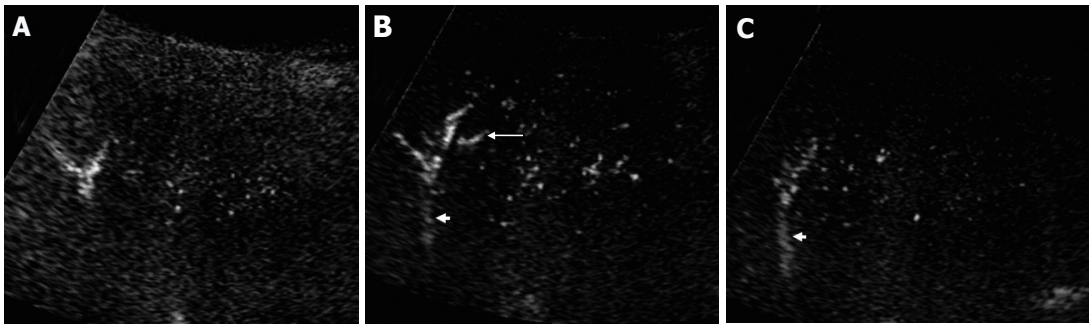


Figure 5 Contrast-enhanced US images in a 64-year-old cirrhotic patient. **A:** In the early arterial phase 14 s after Levovist injection, a "Y"-shaped distal portal venous branch was enhanced by microbubbles (arrow), while the proximal portal vein and other portal venous branches at the same level were not seen; **B** and **C:** An adjacent hepatic venous branch was enhanced by contrast medium at 16 s after injection of Levovist (arrows).

and might provide useful information for the diagnosis of cirrhosis.

In addition, evaluation of peripheral hepatic vasculature might facilitate the differential diagnosis of pseudotumors caused by intrahepatic arterioportal shunt, which is not rare in liver cirrhosis especially in peripheral area of the liver[7,12,13]. It was reported that these pseudolesions mimic hypervascular tumors on hepatic imaging and bring about problems of differential diagnosis in cirrhotic patients especially when they are round or nodular in shape[12,13]. Usually, intrahepatic arterioportal shunts are confirmed by hepatic angiography. However, when the arterioportal shunt-induced pseudolesion is small (less than 1 cm in diameter), it can hardly be visualized on hepatic angiogram because of the limited spatial resolution and overlapping of liver parenchyma[13]. In this situation, contrast-enhanced US may show the small intrahepatic arterioportal shunt in peripheral area of the liver. Theoretically, when distal portal venous branches are enhanced earlier in the early arterial phase before microbubbles arrive at the proximal branches, an intrahepatic arterioportal shunt can be diagnosed by hepatic angiography. In addition, the abnormal ring-like structures on contrast-enhanced US images in some cirrhotic patients might also indicate small intrahepatic shunts or abnormal anastomoses in artery, portal or hepatic vein. Unfortunately, this assumption was not confirmed in this study because we did not perform any prospective angiography. Further investigations are needed to validate the possibility.

Compared to angiography, contrast-enhanced coded harmonic angio imaging has several advantages in showing morphologic changes of peripheral vessels. First, it is non-invasive. Second, peripheral vessels including hepatic artery, portal and hepatic vein, can be seen. Third, the kinetics of microbubble contrast agent in peripheral hepatic vessels can be evaluated simultaneously. However, it has some disadvantages. The morphologies of different hepatic vessels displayed on contrast-enhanced US are not so clear compared to angiography because of overlapping of different vessels. In addition, the visual fields on contrast-enhanced US cannot display the whole vascular tree.

We could also assessed the microbubble arrival time at different peripheral vessels in some subjects using contrast-enhanced coded harmonic angio mode. The results showed that hepatic venous arrival time was shorter in cirrhotic patients than in other subjects, which is in accordance with those observed by Albrecht *et al*.[3] Furthermore, the venous arrival time was shorter in cirrhotic patients who had marked morphological changes of peripheral hepatic vasculature, indicating that hemodynamic changes in liver cirrhosis are due to the morphologic changes of hepatic circulation. We also noticed that not only the hepatic venous arrival time, but also the arterial and portal venous arrival time were shorter in cirrhotic patients than in chronic hepatitis patients and normal controls, though there was no statistically significant difference, suggesting that both intrahepatic and extrahepatic hemodynamic changes such as pulmonary arteriovenous shunt and systemic hyperdynamic circulatory state may occur in liver cirrhosis[3], which might contribute to the early arrival of microbubbles in hepatic artery and portal vein.

Except for the evaluation of hemodynamics changes in chronic liver disease, assessing microbubble arrival time at different hepatic vessels might help to study the time phases on contrast-enhanced US images, which is important in the diagnosis and differential diagnosis of liver tumors.

There are several limitations in this preliminary study. First, the number of patients with liver cirrhosis was not large enough. Second, angiography examinations were not prospectively studied, lacking of data to validate the findings on contrast-enhanced the United States. Third, the microbubble arrival time was not available in some subjects because of several interfering factors. Furthermore, we did not use the time-intensity analyzing software to measure the microbubble arrival time, the accuracy was certainly not very high. However, the results obtained in our study and other studies[5] are not significantly different from those obtained using time-intensity analyzing software[3].

In conclusion, contrast-enhanced coded pulse inversion harmonic imaging can evaluate the hemodynamics and morphology of peripheral hepatic vasculature and provide useful information for the diagnosis of liver cirrhosis.

REFERENCES

1 **Sanford NL,** Walsh P, Matis C, Baddeley H, Powell LW. Is ultrasonography useful in the assessment of diffuse parenchymal liver disease? *Gastroenterology* 1985; **89:** 186-191

2 **Ding H,** Kudo M, Onda H, Suetomi Y, Minami Y, Maekawa K. Contrast-enhanced subtraction harmonic sonography for evaluating treatment response in patients with hepatocellular carcinoma. *AJR* 2001; **176:** 661-666

3 **Albrecht T,** Blomley MJ, Cosgrove DO, Taylor-Robinson SD, Jayaram V, Eckersley R, Urbank A, Butler-Barnes J, Patel N. Non-invasive diagnosis of hepatic cirrhosis by transit-time analysis of an ultrasound contrast agent. *Lancet* 1999; **353:** 1579-1583

4 **Kudo M.** Imaging blood flow characteristics of hepatocellular carcinoma. *Oncology* 2002; **62(suppl):** 48-56

5 **Bang N,** Nielsen MB, Rasmussen AN, Osterhammel PA, Pedersen JF. Hepatic vein transit time of an ultrasound contrast agent: simplified procedure using pulse inversion imaging. *Br J Radiol* 2001; **74:** 752-755

6 **Futagawa S,** Fukazawa M, Musha H, Isomatsu T, Koyama K, Ito T, Horisawa M, Nakayama S, Sugiura M, Kameda H, Okuda K. Hepatic venography in noncirrhotic idiopathic portal hypertension. Comparison with cirrhosis of the liver. *Radiology* 1981; **141:** 303-309

7 **Okuda K,** Takayasu K, Matsutani S. Angiography in portal hypertension. *Gastroenterol Clin North Am* 1992; **21:** 61-83

8 **Haratake J,** Hisaoka M, Yamamoto O, Horie A. Morphological changes of hepatic microcirculation in experimental rat cirrhosis: a scanning electron microscopic study. *Hepatology* 1991; **13:** 952-956

9 **Villeneuve JP,** Dagenais M, Huet PM, Roy A, Lapointe R, Marleau D. The hepatic microcirculation in the isolated perfused human liver. *Hepatology* 1996; **23:** 24-31

10 **Zoli M,** Magalotti D, Bianchi G, Ghigi G, Orlandini C, Grimaldi M, Marchesini G, Pisi E. Functional hepatic flow and Doppler-assessed total hepatic flow in control subjects and in patients with cirrhosis. *J Hepatol* 1995; **23:** 129-134

11 **Popper H,** Elias H, Petty DE. Vascular pattern of the cirrhotic liver. *Am J Clin Pathol* 1952; **22:** 717-729

12 **Yu JS,** Kim KW, Sung KB, Lee JT, Yoo HS. Small arterial-portal venous shunts: a cause of pseudolesions at hepatic imaging. *Radiology* 1997; **203:** 737-742

13 **Kim TK,** Choi BI, Han JK, Chung JW, Park JH, Han MC. Nontumorous arterioportal shunt mimicking hypervascular tumor in cirrhotic liver: two-phase spiral CT findings. *Radiology* 1998; **208:** 597-603

Science Editor Wang XL and Guo SY **Language Editor** Elsevier HK

PO Box 2345, Beijing 100023, China
www.wjgnet.com
wjg@wjgnet.com

ELSEVIER

World J Gastroenterol 2005;11(40):6354-6359
World Journal of Gastroenterology ISSN 1007-9327
© 2005 The WJG Press and Elsevier Inc. All rights reserved.

•*CLINICAL RESEARCH* •

Imaging findings of biliary hamartomas

Rong-Qin Zheng, Bo Zhang, Masatoshi Kudo, Hirokazu Onda, Tatsuo Inoue

Rong-Qin Zheng, Bo Zhang, Department of Ultrasound, the Third Affiliated Hospital, Sun Yat-sen University, Shipai, Guangzhou 510630, Guangdong Province, China
Masatoshi Kudo, Hirokazu Onda, Tatsuo Inoue, Gastroenterology and Hepatology, Kinki University School of Medicine, Osaka-Sayama, Japan
Correspondence to: Dr Rong-Qin Zheng, Department of Ultrasound, the Third Affiliated Hospital, Sun Yat-sen University, Shipai, Guangzhou 510630, Guangdong Province, China. ultrasoundzh@sohu.com
Telephone: +86-20-88348792 Fax: +86-20-87536401
Received: 2005-02-24 Accepted: 2005-04-02

Abstract

AIM: To evaluate the imaging findings of biliary hamartomas (von Meyenburg complexes, VMCs) and discuss the differential diagnosis with other related diseases.

METHODS: Imaging findings of biliary hamartomas on ultrasonography (US), computed tomography (CT), magnetic resonance imaging (MRI), MR cholangiopancreatography (MRCP)and hepatobiliary scintigraphy were retrospectively analyzed in six patients.

RESULTS: On ultrasound images, five of the six cases showed multiple small hyper- and hypo-echoic lesions with comet-tail echoes, especially when magnified by US with the usage of zoom function. In all the six cases, multiple tiny hypodense lesions less than 10 mm in diameter were revealed as scattered throughout the liver with no enhancement on CT. These tiny lesions were demonstrated to be hyper- and hypo-intensity on T2- and TI-weighed images, respectively, in three patients who underwent MRI examinations. MRCP was performed in two patients, and clearly showed multiple tiny irregular- and round-shaped hyper-intensity lesions. MRCP and hepatobiliary scintigraphy showed normal appearances of intra- and extra-hepatic bile ducts in two and one patients, respectively.

CONCLUSION: Imaging modalities are useful in the diagnosis and differential diagnosis of VMCs. A correct diagnosis might be obtained when typical imaging findings are present even without a histological confirmation.

© 2005 The WJG Press and Elsevier Inc. All rightsreserved.

Key words: Biliary hamartomas; Ultrasonography; CT; MRI; MR cholangiopancreatography

Zheng RQ, Zhang B, Kudo M, Onda H, Inoue H. Imaging findings of biliary hamartomas. *World J Gastroenterol* 2005; 13(40); 6354-6359
http://www.wjgnet.com/1007-9327/11/6354.asp

INTRODUCTION

Biliary hamartomas also called as von Meyenburg complexes (VMCs) are benign liver malformations that histologically contain cystic dilated bile ducts within 10 mm in diameter surrounded by abundant fibrous stroma[1,2]. They are usually uncovered by autopsy as an incidental finding. Detecting by imaging modalities is thought to be uneasy because of their asymptomatic nature and small size[3]. To our knowledge, except for a few case reports, there are only two imaging studies on VMCs with small series of cases that have been published in the literature so far[1,3]. Although VMCs are rare, they are easily confused with metastatic diseases of the liver on imaging[4]. Therefore, discerning the imaging characteristics of VMCs is desirable for the differential diagnosis, and thus reducing the needs for invasive methods such as biopsy or laparotomy[5].

Herein, we retrospectively analyze the imaging findings of VMCs on ultrasonography (US), computed tomography (CT), magnetic resonance imaging (MRI), MR cholangiopancreatography (MRCP), and hepatobiliary scintigraphy in six patients, and discuss the differential diagnosis with other related diseases.

MATERIALS AND METHODS

Materials

There were four men and two women with ages ranging from 29 to 72 years (mean, 54 years). Hepatic lesions were found incidentally when the patients underwent routine physical checkup by US (n=2), screening for liver metastasis of a known ovary carcinoma by US and CT (n=1), and abdominal US examinations for Hashimoto disease associated with abnormal liver function tests (n=1), as well as diabetes (n=2). All imaging studies including US, CT, and MRI were performed in three patients. Among them, additional MRCP was performed in two patients; hepatobiliary scintigraphy was carried out in another patient. Both US and CT scans were available in another three patients. Three- to ten-time follow-up US and/or CT examinations were obtained in all the six patients for over a period of 7–100 months. Histologic

confirmation was acquired in three patients.

Methods

US examinations were performed by using GE LOGIQ 700 EXPERT series and LOGIQ 500 MD series (GE Medical System, Milwaukee, WI, USA), Toshiba Powervision 8000 (Toshiba Medical System) with convex probes at the frequency of 3.0–4.4 MHz. A helical CT system (Toshiba X-vigor) was used for CT scans. The section thickness was 7 mm with no interslice gap. Both plain and enhanced CT scans were carried out in five patients. For enhanced CT, a total of 100 mL of Iopamiron (Iopamidol, Nihon Schering) was intravenously injected with the iodine concentration of 370 mg/mL. MRI was performed by using a 1.5 T MR unit (VISART HYPER, Toshiba) with 160 × 256 matrix. SE T1- and T2-weighed images were acquired by using 500/15 ms (TR/TE) and 3 000/80 ms (TR/TE), respectively, with two excitations. Slice thickness was set to 8 mm, and interslice gap of 1 mm. Fast SE MRCP was performed with 6 000/250 ms (TR/TE), and 4–8 mm slice thickness. Hepatobiliary scintigraphy was carried out by using 99mTC-N-pyridoxy 1-5-methyl tryptophan (99mTC-PMT).

RESULTS

Multiple hepatic lesions were scattered throughout both the right and left liver lobes in five patients, distributed predominantly in the right liver lobe in one case. Of the five patients with scattered distribution of the lesions, apparent location of the lesions in the subcapsular areas was observed in four cases. The lesion size measured within 10 mm in five cases. In another case, most of the lesions were less than 10 mm in diameter; in addition, four to five typical cysts with round or oval shape in the right liver measuring from 11 to 25 mm were noted in one case. Multiple right renal cysts (3 in number and 10-20 mm in diameter) together with one cyst (10 mm in diameter) in the left kidney were detected in one case.

On US images, five cases showed multiple small hyper- and hypo-echoic lesions with comet-tail echoes (Figure 1A). Liver echo textures were heterogeneous. When zoom function was used, some small hyper-echoic dot-like lesions were showed to be tiny cystic lesions with distal acoustic enhancement (comet-tail echoes) (Figures 2A and 3A). One case was revealed as multiple hypo-echoic lesions. In five cases, three- to ten-time follow-up US examinations were performed for 19-100 mo, and no remarkable changes were found.

On plain CT, multiple hypodense lesions with irregular and round shape were observed in six cases (Figures 1B and 3B). After intravenous administration of contrast medium, all the lesions showed no enhancement in either the periphery or the center areas, and the delineation of all the lesions became more conspicuous than on plain CT (Figures 1C and 3C). Three- to six-time follow-up CT scans performed for 7-84 months in three patients revealed no obvious changes of the lesions when compared with the findings on the first time CT images.

MRI was performed in three cases. Multiple small hepatic lesions were demonstrated to be of low signal intensity on T1-weighed images and high signal intensity on T2-weighed images (Figures 1D, 3D, and E). After gadolinium administration was performed in one case, no enhancement was noted on T1-weighed images (Figure 1E). In two cases, MRCP clearly portrayed numerous

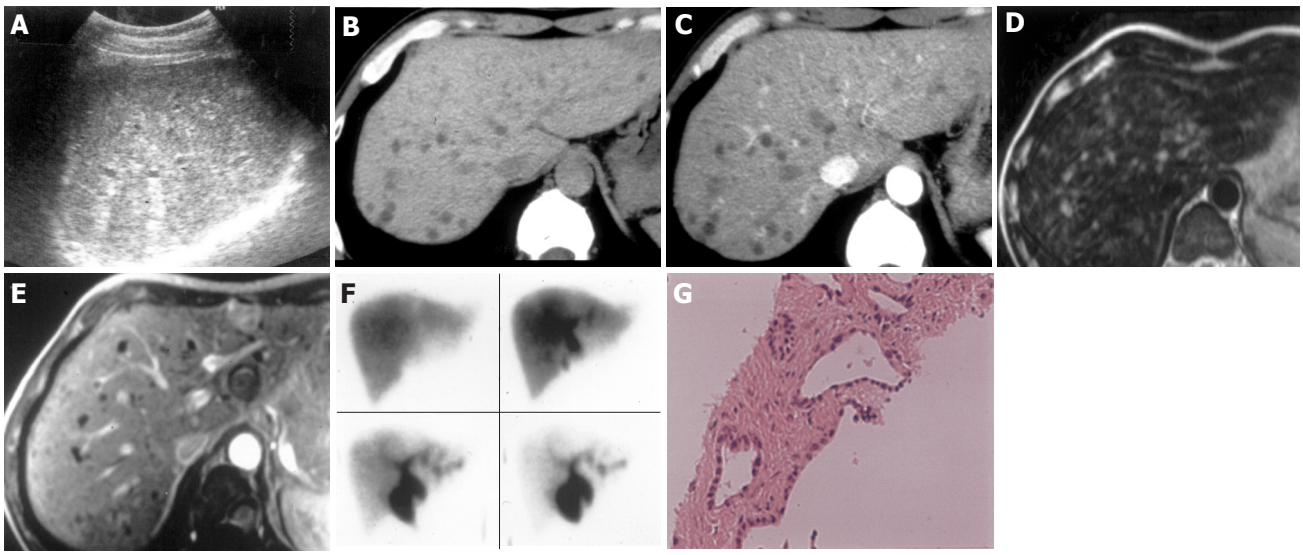


Figure 1 A 51-year-old man with VMCs. **A:** B-mode US showed multiple small hyper- and hypoechoic lesions less than 10 mm in diameter with multiple comet-tail echoes; **B:** On plain CT, multiple small hypodense lesions scattered in the whole liver especially in the subcapsular area of posterior segment of the right liver lobe; **C:** On enhanced CT, the small lesions became well delineated when compared with that on plain CT. No enhancements were noted in these lesions; **D:** T2-weighed image revealed multiple small lesions with high signal intensity; **E:** After gadolinium administration on T1-weighed image, hypo-intensity of the lesions was clearly shown without contrast medium enhancement; **F:** Hepatobiliary scintigraphy by using 99mTC-PMT showed normal appearances of biliary system without pooling areas; **G:** On histology, multiple irregularly dilated bile ducts lined by a single layer of cubic epithelium were shown.

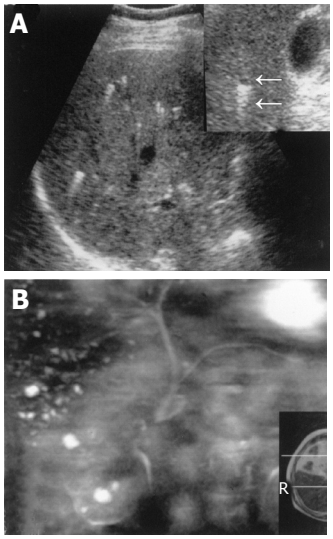


Figure 2 A 72-year-old man with VMCs. **A:** On B-mode US, multiple small hyperechoic lesions were shown, while hypo-echoic lesions were not evident on the conventional scanning plan. However, with the use of zoom function, the hypoechoic lesion with comet-tail echo was clearly shown (arrows); **B:** On MR cholangiopancreatography, multiple small hyper-intensity lesions were revealed except for the demonstration of normal intrahepatic and extrahepatic bile ducts. In addition, several small cysts in the right kidney were also shown.

tiny irregular-shaped and few round-shaped small hyperintense nodules (Figures 2B and 3F). The lesions were displayed more distinctly and in more numbers on MRCP than on CT and MRI (Figure 3). Intra- and extra-hepatic bile ducts were normal (Figures 2B and 3F). Hepatobiliary scintigraphy performed in one case showed no obvious pooling in the liver, which was found in Caroli's disease. The biliary system excreting function of radioisotope was normal (Figure 1F).

US guided liver biopsy was performed in three cases. On histology, multiple dilated bile ducts lined by a single layer of cubic epithelium (Figure 1G) were revealed in two cases, and the diagnosis of VMCs was confirmed. The patient with ovary carcinoma underwent operations twice for hysterectomy plus ovariotomy, and secondary omentectomy, respectively. During the operation, liver metastasis was suspected by the palpation of the liver surface. However, US and CT displayed multiple small typical cystic lesions without any changes on three-time follow-up CT scans performed for over 7 mo period. US guided liver biopsy was performed without demonstrating any malignant cells, although VMC findings were also not found. Liver metastases were not considered according to imaging findings. VMCs were thought to be the most possible diagnosis. The patient died from severe complications after secondary omentectomy later.

The details of the six cases with VMCs are summarized in Table 1.

DISCUSSION

VMCs are considered as congenital bile duct malformations due to the failure of embryonic involution[2,4,6]. Macroscopically, the lesions present as gray-white to gray-yellow or black nodules mostly uniform in size measuring less than 5 mm, some up to 10 mm in diameter[3,7,8]. They are usually scattered throughout both of the liver lobes, especially in the subcapsular region of the liver[8]. Microscopically, VMCs are generally well defined, irregular or round in shape, consisting of a variable number of dilated, tortuous or branching bile ducts that were lined by a single layer of cuboidal cells and embedded in a fibrocollagenous stroma[4,8,9]. The lumina of these dilated bile ducts sometimes contain bile-stained granular or amorphous materials[4,8]. Some VMCs contain sclerotic arteries, however, most of them are not associated with vascular proliferation, and some are even devoid

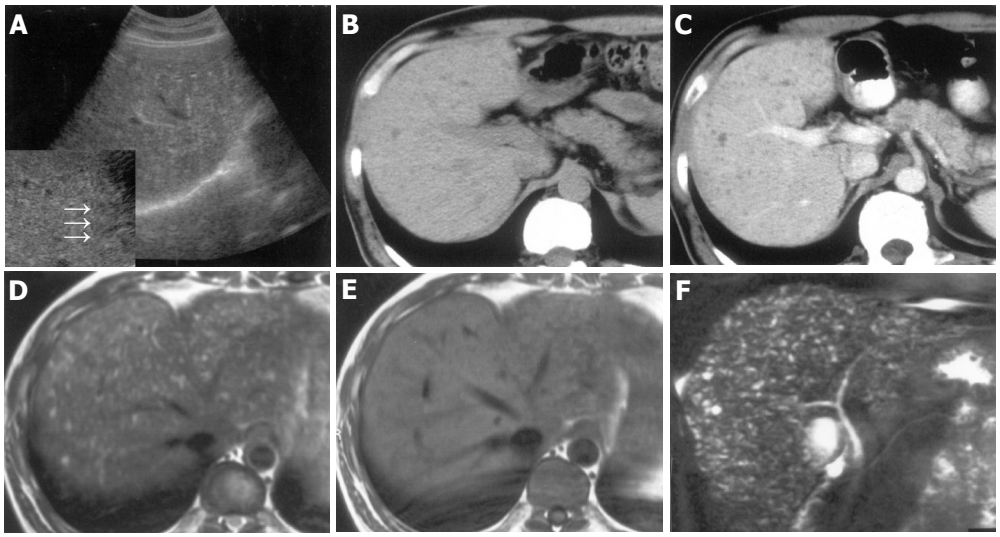


Figure 3 A 44-year-old man with VMCs. **A:** B-mode US scan with routine depth showed a vague image of multiple small hyper- and hypoechoic lesions. When magnified by using zoom function, the tiny hypoechoic lesion and the comet-tail echo were clearly seen (arrows); **B,C:** Multiple tiny hypodense lesions were displayed more conspicuously on enhanced CT (**C**) than on plain CT (**B**), and no enhancements were found in the lesions (**C**); **D,E:** the lesions.

Table 1 Details of six patients

No	Sex/age (yr)	Clinical Background	Imaging findings										Histological diagnosis
			Size (mm)	Number	Distribution	US	CT		MRI		MRCP/ scintigraphy	Associated findings	Follow-up. (time: month)	
							Attenuation	enhancement	T1	T2				
1	M/51	No symptoms	<10	Multiple	Scattered, whole liver	Hyper- and hypoechoic, with comet-tail echoes	Low	No	Hypo-intensit y	Hyper-intensity	Normal bile ducts	No	US for 52 mo, no change	VMCs
2	F/61	Ovary carcinoma	most lesions <10, several cysts 11-25	Multiple	Scattered, whole liver	Hyper- and hypoechoic, with comet-tail echoes	Low	No				Hepatic cysts	CT for 7 mo, no change	No
3	F/68	Hashimoto disease with liver damage	<10	Multiple	Scattered, whole liver	Hypoechoic	Low	No				No	US/CT for 19–48 mo, no change	
4	M/72	No symptoms	<10	Multiple	Predominant in the right lobe	Hyper- and hypoechoic, with comet-tail echoes	Low	No	Hypo-intensity	Hyper-intensity	Hyperintensity, normal bile ducts(MRCP)	Right and left renal cysts	US/C T for 27–84 mo, no change	
5	M/44	Diabetes	<10	Multiple	Scattered, whole liver	Hyper- and hypoechoic, with comet-tail echoes	Low	No	Hypo-intensity	Hyper-intensity	Hyperintensity, normal bile ducts (MRCP)	No	US for 25 mo, no change	VMCs
6	M/29	Diabetes	<10	Multiple	Scattered, whole liver	Hyper- and hypoechoic, with comet-tail echoes	Low	No				No	US for 100 mo, no change	

AUPBD: anomalous union of the pancreatic and biliary ducts.

of vessels[4,8]. The incidence of VMCs was estimated at 0.69-5.6% in autopsy series[8,10], and 0.6% in needle biopsy series[9]. In some cases, association with polycystic liver and kidney diseases, simple liver cysts or pancreatic cysts were reported in the literature[2-4,6,7,10]. Although VMCs are generally considered to be benign liver lesions without clinical manifestations, less frequent association with malignant transformation was also described[11,12]. However, the most important clinical significance is that VMCs are easily misdiagnosed as multiple liver metastases on imaging[2,6,13,14] or even on gross examination[8].

Imaging manifestations of VMCs are various[2-6,14-17] and have not been well illustrated yet. US findings have been described as hypoechoic, hyperechoic or mixed heterogenic echoic structures[6,7,13-15]. These variations might reflect the histologic features of VMCs including dilated bile ducts and fibrocollagenous stroma. Luo *et al*[3] described the sign of multiple comet-tail echoes, and speculated that it might be the specific US finding of VMCs. However, this sign was observed only in one case of their study. In our series, multiple small comet-tail echoes appeared in all but one case. It manifested as posterior echo enhancement of the lesions, which might be due to the cystic feature of dilated bile duct and therefore resulted in good transmission of the sound beam. Especially when magnified by US, some small hyperechoic lesions were actually found to be tiny cystic lesions with comet-tail echoes. This evidence strongly suggests that the sign of multiple small comet-tail echoes is a unique US feature of VMCs, which have diagnostic value.

On plain CT images, almost all VMCs that had been reported were demonstrated to be multiple small hypodense lesions[1-5,7,13,14,16,17]. While on enhanced CT images, although homogeneous enhancement of the lesions was noted in two case reports[2,17], no enhancement of the lesions was observed in most of the reported cases after intravenous administration of contrast medium[1,3–5,13,14,16], as in our series. This phenomenon might correlate to the poor vascularity of VMCs described on histology[4].

On MRI, VMCs, including our series, were revealed as hypo-intense on T1-weighed images and hyper-intense on T2-weighed images when compared with surrounding liver parenchyma[3,5,7,17–19]. Recently, MRCP has been considered to be highly sensitive in depicting intra- and extrahepatic bile duct anomalies and cystic lesions of the liver as well as their relationship with bile duct system[5,20], which is superior to the sensitivity of CT[20]. In the two cases of our study, MRCP displayed the VMC lesions more clearly than CT and MRI concerning both the lesion number and shape. As for the superior sensitivity of MRCP, this may be partially due to the relatively large slice thickness used in CT and MRI scans in our study, resulting in overlooking of lesions smaller than the slice thickness. In addition, the poor MR imaging quality in our study also accounts for one of the reasons.

Some authors claimed that imaging findings of VMCs were not specific and liver biopsy was needed for a definitive diagnosis[1,4]. However, with the use of advanced imaging modalities and long-term imaging follow-up, some authors pointed out that it might be possible to make a correct diagnosis of VMCs by imaging[4,5]. This view is supported by our studies. When typical imaging findings appear, such as multiple small comet-tail echoes on US, multiple tiny hypodense lesions scattered throughout the liver with no enhancement on CT, and cystic appearance with normal extra- and intrahepatic bile duct on MRI and MRCP, a diagnosis of VMCs can be considered. Liver biopsy may have limitations such

as sample errors and performance difficulties due to the very small size of the VMCs, which was reflected by the fact that the reported incidence (0.6%)[9] of VMCs in a series of needle biopsy was relatively lower than that of autopsy (0.69–5.6%)[8,10]. Therefore, long-term follow-up by imaging examinations may have the same important significance in the diagnosis of VMCs. Although histological confirmation was obtained in only three cases in our series, typical imaging findings and relative long-time imaging follow-up that showed identical findings are strongly suggestive of VMCs. However, the case number in our series is small. Further observations on large series are still needed to clarify our stand.

The spectrum of differential diagnosis of VMCs is fairly wide. However, the most important one is liver metastasis especially in patients with extrahepatic malignant tumors. Usually, multiple small metastases are ill defined on plain CT, and show various degrees of enhancement (such as rim enhancement) after intravenous administration of contrast medium. However, for difficult patients, final exclusion of metastatic lesions should still depend on liver biopsy or follow-up imaging studies. Diffuse primary hepatocellular carcinoma usually occurs in cirrhotic patients, and is seldom revealed to be a cystic lesion on US and CT. Simple hepatic cysts are variable in number, size, and location, and usually round in shape[3]. As VMCs may coexist with simple hepatic cysts or polycystic liver and kidney diseases[2-4,6,7,10], sometimes it is difficult to make a definitive differentiation especially from polycystic liver disease on imaging. We are likely to approve simple hepatic cysts, when the lesions are larger than 10 mm in diameter and round in shape, as in one case of our series, since most VMCs were reported to be less than 10 mm in diameter[1-5]. Peribiliary cysts are multiple small cystic dilatations of the intrahepatic extramural peribiliary glands[21] and should also be included in the differential diagnoses of VMCs. However, they are located exclusively in the hepatic hilum and along the larger portal tract[21], which is different from the scattered distribution of VMCs. In addition, some peribiliary cysts were reported to be gradually increasing in size and number[20], which has never been described in VMCs. Microabscesses of the liver can be differentiated from VMCs by means of clinical and radiological data, such as having a history of immuosuppression, symptoms of fever and epigastralgia, multiple round or loculated hypodense lesions on CT[4,16,22], and "target" appearance on US[22]. Furthermore, intrahepatic bile duct anomalies such as dilated bile ducts and Caroli's disease can be readily distinguished from VMCs by imaging, especially when MRCP is performed for this purpose[5], as MRCP offers optimal visualization of the spatial relationship between hepatic lesions and intrahepatic bile ducts[5,20]. Besides, biliary scintigraphy also facilitates the differentiation.

In conclusion, imaging modalities are useful in the diagnosis and differential diagnosis of VMCs. Imaging findings, such as multiple small comet-tail echoes on US, multiple tiny hypodense lesions scattered throughout the liver with no enhancement on CT, and cystic nature with normal extra- and intrahepatic bile duct on MRI and MRCP, can be considered as typical or highly suggestive manifestations of VMCs. A correct diagnosis might be obtained when typical imaging findings are present even without a histological confirmation. However, in patients with extrahepatic malignant tumors, follow-up imaging examinations or liver biopsy are needed.

REFERENCES

1 **Lev-Toaff AS,** Bach AM, Wechsler RJ, Hilpert PL, Gatalica Z, Rubin R. The radiologic and pathologic spectrum of biliary hamartomas. *AJR Am J Roentgenol* 1995; **165:** 309-313

2 **Wei SC, Huang GT,** Chen CH, Sheu JC, Tsang YM, Hsu HC, Chen DS. Bile duct hamartomas. A report of two cases. *J Clin Gastroenterol* 1997; **25:** 608-611

3 **Luo TY, Itai Y,** Eguchi N, Kurosaki Y, Onaya H, Ahmadi Y, Niitsu M, Tsunoda HS. Von Meyenburg complexes of the liver: imaging findings. *J Comput Assist Tomogr* 1998; **22:** 372-378

4 **Cooke JC,** Cooke DA. The appearances of multiple biliary hamartomas of the liver (von Meyenberg complexes) on computed tomography. *Clin Radiol* 1987; **38:** 101-102

5 **Mortelé B,** Mortelé K, Seynaeve P, Vandevelde D, Kunnen M, Ros PR. Hepatic bile duct hamartomas (von Meyenburg Complexes): MR and MR cholangiography findings. *J Comput Assist Tomogr* 2002; **26:** 438-443

6 **Saló J,** Bru C, Vilella A, Ginès P, Gilabert R, Castells A, Bruguera M, Rodés J. Bile-duct hamartomas presenting as multiple focal lesions on hepatic ultrasonography. *Am J Gastroenterol* 1992; **87:** 221-223

7 **Gallego JC,** Suarez I, Soler R. Multiple bile duct hamartomas: US, CT, and MR findings. A case report. *Acta Radiol* 1995; **36:** 273-275

8 **Chung EB.** Multiple bile-duct hamartomas. *Cancer* 1970; **26: 287-296**

9 **Thommesen N.** Biliary hamartomas (von Meyenburg complexes) in liver needle biopsies. *Acta Pathol Microbiol Scand [A]* 1978; **86:** 93-99

10 **Redston MS,** Wanless IR. The hepatic von Meyenburg complex: prevalence and association with hepatic and renal cysts among 2843 autopsies [corrected]. *Mod Pathol* 1996; **9:** 233-237

11 **Hasebe T,** Sakamoto M, Mukai K, Kawano N, Konishi M, Ryu M, Fukamachi S, Hirohashi S. Cholangiocarcinoma arising in bile duct adenoma with focal area of bile duct hamartoma. *Virchows Arch* 1995; **426:** 209-213

12 **Papadogiannakis N,** Gad A, Sjöstedt S, Tour R, Thörne A, Seensalu R. Adenocarcinoid of the liver arising within an area of hamartoma with predominant bile duct component. *J Clin Gastroenterol* 1996; **23:** 145-151

13 **Eisenberg D,** Hurwitz L, Yu AC. CT and sonography of multiple bile-duct hamartomas simulating malignant liver disease (case report). *AJR Am J Roentgenol* 1986; **147:** 279-280

14 **Iha H,** Nakashima Y, Fukukura Y, Tanaka M, Wada Y, Takazawa T, Nakashima O, Kojiro M. Biliary hamartomas simulating multiple hepatic metastasis on imaging findings. *Kurume Med J* 1996; **43:** 231-235

15 **Tan A,** Shen JF, Hecht AH. Sonogram of multiple bile duct hamartomas. *J Clin Ultrasound* 1989; **17:** 667-669

16 **Sada PN,** Ramakrishna B. Computed tomography of von Meyenburg complex simulating micro-abscesses. *Australas Radiol* 1994; **38:** 225-226

17 **Martinoli C,** Cittadini G Jr, Rollandi GA, Conzi R. Case

report: imaging of bile duct hamartomas. *Clin Radiol* 1992; **45:** 203-205
18 **Slone HW,** Bennett WF, Bova JG. MR findings of multiple biliary hamartomas. *AJR Am J Roentgenol* 1993; **161:** 581-583
19 **Maher MM,** Dervan P, Keogh B, Murray JG. Bile duct hamartomas (von Meyenburg complexes): value of MR imaging in diagnosis. *Abdom Imaging* 1999; **24:** 171-173
20 **Kudo M.** Hepatic peribiliary cysts: clinically harmless disease with potential risk due to gradual increase in size and number. J Gastroenterol 2001; **36:** 286-288
21 **Nakanuma Y,** Sasaki M, Terada T, Harada K. Intrahepatic peribiliary glands of humans. II. Pathological spectrum. *J Gastroenterol Hepatol* 1994; **9:** 80-86
22 **Callen PW,** Filly RA, Marcus FS. Ultrasonography and computed tomography in the evaluation of hepatic microabscesses in the immunosuppressed patient. *Radiology* 1980; **136:** 433-434

Science Editor Ma JY and Guo SY **Language Editor** Elsevier HK

PO Box 2345, Beijing 100023, China
www.wjgnet.com
wjg@wjgnet.com

ELSEVIER

World J Gastroenterol 2005;11(40):6360-6365
World Journal of Gastroenterology ISSN 1007-9327
© 2005 The WJG Press and Elsevier Inc. All rights reserved.

• *CLINICAL RESEARCH* •

Distinction between short-segment Barrett's esophageal and cardiac intestinal metaplasia

Gui-Sheng Liu, Jun Gong, Peng Cheng, Jun Zhang, Ying Chang, Lei Qiang

Gui-Sheng Liu, Jun Gong, Peng Cheng, Jun Zhang, Ying Chang, Department of Gastroenterology, the Second Hospital of Xi'an Jiaotong University, Xi'an 710004, Shaanxi Province, China
Lei Qiang, Department of Pathology, the Second Hospital of Xi' an Jiaotong University, Xi'an 710004, Shaanxi Province, China
Supported by the grant from Clinical Key Project of the Healthy Congress, No. 20012130
Co-first-authors: Gui-Sheng Liu and Jun Gong
Co-correspondent: Gui-Sheng Liu
Correspondence to: Dr. Jun Gong, Department of Gastroenterology, the Second Hospital of Xi'an Jiaotong University, Xi'an 710004, Shaanxi Province, China. gongxiaoyishan@sina.com
Telephone: +86-29-88083495
Received: 2004-11-23 Accepted: 2005-03-16

Abstract

AIM: To investigate the roles of mucin histochemistry, cytokeratin 7/20 (CK7/20) immunoreactivity, clinical characteristics and endoscopy to distinguish short-segment Barrett's esophageal (SSBE) from cardiac intestinal metaplasia (CIM).

METHODS: High iron diamine/Alcian blue (HID/AB) mucin-histochemical staining and immunohistochemical staining were used to classify intestinal metaplasia (IM) and to determine CK7/20 immunoreactivity pattern in SSBE and CIM, respectively, and these results were compared with endoscopical diagnosis and the positive rate of gastroesophageal reflux disease (GERD) symptoms and *H pylori* infection. Long-segment Barrett' s esophageal and IM of gastric antrum were designed as control.

RESULTS: The prevalence of type III IM was significantly higher in SSBE than in CIM (63.33% *vs* 23.08%, $P<0.005$). The CK7/20 immunoreactivity in SSBE showed mainly Barrett's pattern (76.66%), and the GERD symptoms in most cases which showed Barrett' s pattern were positive, whereas *H pylori* infection was negative. However, the CK7/20 immunoreactivity in CIM was gastric pattern preponderantly (61.54%), but there were 23.08% cases that showed Barrett's pattern. *H pylori* infection in all cases which showed gastric pattern was significantly higher than those which showed Barrett' s pattern (63.83% *vs* 19.30%, $P<0.005$), whereas the GERD symptoms in gastric pattern were significantly lower than that in Barrett's pattern (21.28% *vs* 85.96%, $P<0.005$).

CONCLUSION: Distinction of SSBE from CIM should not be based on a single method; however, the combination of clinical characteristics, histology, mucin histochemistry, CK7/20 immunoreactivity, and endoscopic biopsy should be applied. Type III IM, presence of GERD symptoms, and Barrett's CK7/20 immunoreactivity pattern may support the diagnosis of SSBE, whereas non-type III IM, positive H pylori infection, and gastric CK7/20 immunoreactivity pattern may imply CIM.

© 2005 The WJG Press and Elsevier Inc. All rights reserved.

Key words: Short-segment Barrett's esophageal; Cardiac intestinal metaplasia; Cytokeratin 7/20 immunoreactivity

Liu GS, Gong J, Cheng P, Zhang J, Chang Y, Qiang L. Distinction between short-segment Barrett's esophageal and cardiac intestinal metaplasia. *World J Gastroenterol* 2005; 11(40): 6360-6365
http://www.wjgnet.com/1007-9327/11/6360.asp

INTRODUCTION

The incidence of adenocarcinoma at the distal esophagus and gastric cardia has been increasing rapidly for more than two decades in the Western world, but the adenocarcinoma of distal stomach is decreasing gradually. This phenomenon has so far not been satisfactorily explained. These gastroesophageal junction (GEJ) carcinomas appear to arise from intestinal metaplasia (IM) foci that develop either in the distal esophagus or in the proximal stomach (gastric cardia). Some studies indicate that short-segment Barrett's esophageal (SSBE) and cardiac intestinal metaplasia (CIM) are precancerous conditions of the adenocarcinoma at GEJ[1,2]. However, the potential carcinogenesis, and the roles in the development of adenocarcinoma at GEJ are probably the differences between them[3]. Some studies have shown that the risk of malignancy is substantially higher for IM in the SSBE than CIM[4], and medical societies, therefore, have recommended endoscopic cancer surveillance routinely for patients with SSBE, but not for patients with CIM[5]. A recent study has shown that biopsy specimens taken from the GEJ frequently show specialized IM, even in patients who have no esophageal symptoms and a normal-

appearing distal esophagus[6,7]. Therefore, it is necessary to distinguish SSBE from CIM. However, there are not precise criteria in endoscopy and histology, and reliable methods in distinguishing SSBE from CIM have not yet been established[8]. Ormsby *et al*[9] once observed a specific pattern of immunoreactivity for cytokeratin 7 and 20 (CK7/20), defined as Barrett's CK7/20 pattern, which seemed to be distinctive for Barrett's esophageal, but this method has been disputed by others[10,11].

In this study, we used high iron diamine/Alcian blue (HID/AB) mucin-histochemical methods and CK7/20 immunoreactivity, combined with clinical characteristics and endoscopic appearances, to diagnose SSBE and CIM strictly, and long-segment Barrett's esophageal (LSBE) and intestinal metaplasia of gastric antrum (GA-IM) were designed as control. We aimed to investigate the roles of these methods in distinguishing SSBE from CIM.

MATERIALS AND METHODS

Patients

The study group consisted of 118 patients who underwent endoscopies because of a variety of upper gastrointestinal complains. All patients were required to record complete clinical, histological, and endoscopic data.

Clinical data included age, gender, complains, and symptoms of gastroesophageal reflux disease (GERD), which included heartburn, reflux acid, and regurgitation. The diagnostic criteria of GERD were as follows: there were at least twice of aforementioned symptoms within 1 week, and persisted at least 6 months, and all symptoms could be relieved significantly with H2 receptor blocker or proton pump inhibitor.

Histological data required presence of IM, which was proved with hematoxylin–eosin (HE) staining, and excluded dysplasia or adenocarcinoma.

Endoscopic data included precise biopsy location, precise site of squamocolumnar junction (SCJ) and GEJ, and presence or absence of hiatus hernia.

The patients who were classified into four groups according to histological and endoscopic data are as follows:

LSBE with IM: Twenty-eight patients with IM in LSBE, which was defined as 3 cm or more of columnar mucosa in the esophagus. Biopsies were taken from reddish island-like or long tongue-like columnar mucosa in distal esophagus.

SSBE with IM: Thirty patients with IM in SSBE, which was defined endoscopically as tongues less than 3 cm in length above GEJ with its resemblance to small intestine having well-formed microvilli, and biopsies were taken from red, velvet-like columnar mucosa in distal esophagus.

CIM: Twenty-six patients with SCJ coincided precisely with GEJ, and biopsies were obtained within 2 cm below GEJ.

GA-IM: Thirty-four patients who underwent biopsies from gastric antrum.

On the other hand, eight normal distal esophagus mucosa and cardiac mucosa were selected as normal controls, which were defined as such by the combination of a normal endoscopic appearance of the mucosa and the absence of acute or chronic inflammation, IM, and dysplasia or adenocarcinoma.

HID/AB mucin-histochemical staining

Each endoscopic biopsy was sliced into three sections with a thickness of 4-5 μm to carryout histological examination. Biopsies with IM were stained with HID/AB to identify neutral mucins, sialomucins, and sulfomucins. Briefly, slides were immersed into HID solution for more than 18-24 h (includes 6–8 h in warm-box at 60 °C). Slides were then stained with 10 g/L Alcian blue solution (pH 2.5) for 30 min. Finally, the slides were stained with 10 g/L neutral red solution for 2 min.

Immunohistochemical staining for CK7/20

Slides were deparaffinized and rehydrated through graded alcohols. Antigen retrieval was performed by using citrate buffer in a microwave, both for CK7 and CK20 at 92-96 °C. Slides were incubated in 30 mL/L hydrogen peroxide/methanol for 20 min to block nonspecific background staining due to endogenous peroxidase. Using the standard streptavidin–biotin–peroxidase complex (ABC) method, the slides were incubated with primary antibodies CK7 (1:50 dilution) and CK20 (1:30 dilution). The slides were further incubated for 30 min in a secondary antibody solution. Diaminobenzidine served as the chromogen. The slides were counterstained with hematoxylin. The samples of breast carcinoma and colon carcinoma were used as positive controls for CK7 and CK20, respectively. Negative controls were produced with the same tumor samples and staining methods by omitting the primary antibodies.

Giemsa staining

Giemsa staining was used to assess *H pylori* infection.

Histological diagnostic criteria

Classification of IM IM was classified into three subtypes as previously described by El-Zimaity *et al*[12]: complete type (type I); incomplete small intestinal type (type II); and incomplete colonic type (type III). Type I: non-secretory absorptive cells and sialomucin-secreting goblet cells. Type II: few absorptive cells, columnar cells secreting neutral and acid sialomucin, and goblet cells secreting mainly sialomucin but occasionally sulfomucin. Type III: columnar cells secreting predominantly sulfomucin and goblet cells secreting sialomucin or sulfomucin. The HID/AB method stains sialomucins blue and sulfomucin brown (Figure 1). Normal colonic mucosa served as a positive control for this stain. Type I was classified as complete IM, and type II and III were grouped into incomplete IM.

CK7/20 immunoreactivity staining pattern

Three types of CK7/20-staining patterns were recognized in areas of IM, similar to those described by Ormsby *et al*[9]. Barrett's CK7/20 pattern was defined as staining of both superficial and deep metaplastic epithelium for CK7, and staining of the superficial epithelium for CK20 (Figures

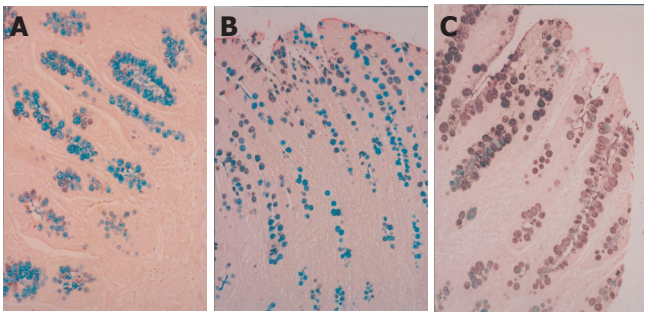


Figure 1 Classifications of IM(HID-AB). **A:** Complete type (Type Ⅰ, ×100); **B**: Incomplete small intestinal type (Type Ⅱ, ×100); **C**: Incomplete colonic type (Type Ⅲ, ×200)

2A and B). Gastric CK7/20 pattern that depended on the histochemical type of IM are as follows: complete IM was characterized by absence of CK7 immunostaining and strong diffuse CK20 immunostaining (Figures 2C and D), whereas incomplete IM was characterized by weak patchy CK7 staining and moderate patchy CK20 immunostaining. All the patterns that did not belong to Barrett's or gastric pattern were defined as other patterns.

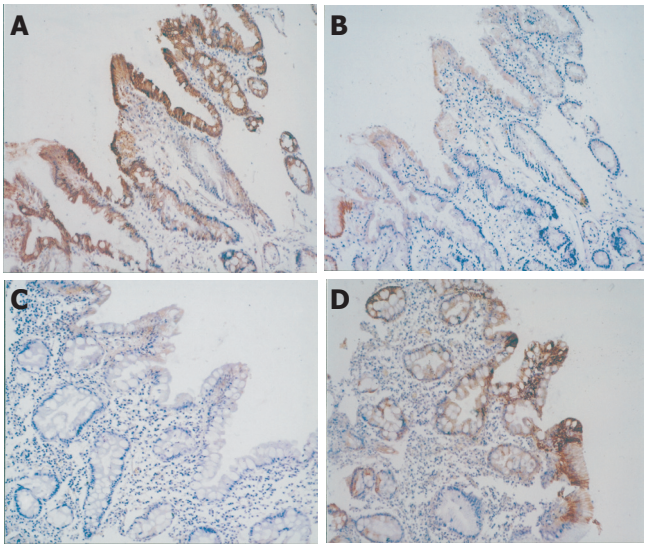


Figure 2 Barrett's(**A**,**B**) and gastric(**C**,**D**) CK7/20 immunoreactivity staining pattern (SABC). **A**: CK7: Strong staining of both superficial and deep metaplastic epithelium (×200); **B**: CK20: Weak staining of the superficial epithelium (×200);**C**: Absent immunostaining of both superficial and deep metaplastic epithelium (×400); **D**: CK20: Strong diffuse immunostaining (×400).

Statistical analysis

Using software SPSS 10.0 for Windows, statistical analyses were performed. The comparison of prevalence at different sites was performed using $\chi 2$ test. A P value <0.05 was considered statistically significant.

RESULTS

HID/AB mucin-histochemical staining

The classifications of IM at different sites are shown in Table 1.

Table 1 Phenotype of IM at different sites

Site of IM	*n*	subtype of IM		
		type I (%)	type II (%)	type III (%)
LSBE	28	3(10.71)	4(14.29)	21(75.00)[a,c]
SSBE	30	7(23.33)	4(13.33)	19(63.33)[a,b]
CIM	26	11(42.31)	9(34.62)	6(23.08)
GA-IM	34	18(52.94)	10(29.41)	6(17.65)

[a]P<0.005 *vs* GA-IM; [b]P<0.01, [c]P<0.005 *vs* CIM

The prevalence of type III IM in SSBE was 63.33%, similar to LSBE (75.00%), but significantly higher than CIM (23.08%) and GA-IM (17.65%, P<0.005). However, there was no statistical difference between CIM and GA-IM. On the contrary, the preponderant subtype of IM in CIM and GA-IM were type I and type II. These results indicated that the LSBE and SSBE mainly contained type III subtypes of IM, whereas there were low incidence of type III in CIM and GA-IM.

CK7/20 immunoreactivity staining

The CK7/20 immunoreactivity patterns at different sites are shown in Table 2.

Table 2 CK7/20 immumoreactivity pattern of IM at defferent site

Site of IM	*n*	Barrett's CK7/20 pattern	Gastric CK7/20 pattern	
LSBE	28	22(78.57%)[a]	4(14.29%)[a]	2(7.14%)
SSBE	30	22(73.33%)[a]	4(13.33%)[a]	4(13.33%)
CIM	26	7(26.92%)	15(57.69%)	4(15.38%)
GA-IM	34	6(17.65%)	24(70.59)	4(11.76%)

[a]P< 0.005 *vs* CIM

There were significant differences in CK7/20 immunoreactivity staining among LSBE, SSBE, CIM, and GA-IM (P<0.005). The CK7/20 immunoreactivity pattern in SSBE was mainly Barrett's pattern (73.33%), similar to LSBE (78.57%). On the contrary, the preponderant CK7/20 immunoreactivity pattern in CIM was gastric pattern (57.69%), similar to GA-IM (70.59%), but there were still 26.92% cases in CIM, which showed Barrett' s pattern. These results implied that although there was a significant difference in CK7/20 immunoreactivity pattern between SSBE and CIM, there were also several cases, which did not belong to either Barrett's pattern or gastric pattern. Therefore, CK7/20 immunoreactivity pattern alone could not distinguish all SSBE and CIM reliably. No difference in CK7/20 immunoreactivity pattern was observed between types II and III IM at any site. However, all cases with type I IM were stained with gastric CK7/20 immunoreactivity pattern.

Relationship between CK7/20 immunoreactivity pattern and symptoms of GERD and H pylori infection (Table 3)

Comparing the differences between the expression of CK7/20 immunoreactivity pattern and the positive prevalence of GERD and *H pylori* infection at different sites of IM, comprehensively, we observed that the

positive prevalence of GERD in the cases with Barrett's CK7/20 pattern was significantly higher than those with gastric CK7/20 pattern. On the contrary, the positive prevalence of *H pylori* infection in the cases with gastric CK7/20 pattern was significantly higher than those with Barrett's CK7/20 pattern. Furthermore, the symptoms of GERD in the cases with LSBE and SSBE that showed Barrett's pattern were all positive, whereas the *H pylori* infection in 60% (6/10) cases that showed gastric pattern was positive. H pylori infection in all the cases that showed gastric pattern in CIM was positive, and accompanied with chronic atrophic gastritis, whereas the symptoms of GERD in six cases with Barrett's pattern were all positive. These results implied that LSBE and SSBE were probably associated with GERD, whereas CIM was mainly associated with *H pylori* infection, but the CK7/20 immunoreactivity pattern showing Barrett's pattern in CIM was probably associated with GERD. Furthermore, these results suggested that the CK7/20 immunoreactivity pattern could be used to distinguish CIM caused by GERD from that was caused by *H pylori* infection.

Table 3 Relationships betweeen CK7/20 immunoreactivity patterns and symptoms of GERD and *H pylori* infection

	Barett's CK7/20 pattern(=57)(%)	Gastric CK7/20 pattern (=47) (%)	Other pattern (=14)(%)
Symptoms of GERD	49(85.96)[a]	10(21.28)	3(21.43)
H pylori infection	11(19.30)[a]	30(63.83)	4(28.57)

[a]$P<0.005$ *vs* Gastric CK / 20 pattern

DISCUSSION

IM may develop in GEJ in patients either with SSBE or carditis, which is defined as CIM. Distinction between these two entities is important, since the etiology and risk of developing adenocarcinoma are different[13,14]. SSBE is believed to be caused by GERD, and associated with an increased risk of esophageal adenocarcinoma, similar to LSBE[15-17], whereas the etiology and clinical importance of CIM are unclear. Therefore, it is necessary to distinguish them from each other. However, because there are not precise criteria used to diagnose SSBE and CIM in histology, as well as in endoscopy, it is not so easy to distinguish them precisely.

The best criterion for the distinction between SSBE and CIM is the precise knowledge that the biopsy specimens are from the esophagus or the stomach, but because of the effects of the anatomic variation of GEJ and SCJ, inflammation and hiatus hernia, this is not always possible in endoscopy. In histological morphology, there is also no significant difference between SSBE and CIM. Although few scholars have reported that the areas adjacent to CIM show normal foveolar epithelium, whereas those of Barrett's epithelium contain pre-goblet cells that can be stained positive by Alcian blue method[18], these characteristics do not exist in all biopsy specimens. Therefore, it is not reliable to distinguish SSBE from CIM histologically. HID/AB staining have also been used to distinguish SSBE from CIM. IM at GEJ (or ultra-short-segment Barrett's esophagus) has been more frequently found to express sulfomucins, which is defined as type III in classification of IM, and to involve the surface glandular epithelium than CIM[19,20]. Piazuelo *et al*[21] also found that the area covered with incomplete type of IM and the proportion of sulfomucins were significantly higher in the esophagus compared to the stomach. In our study, we found that the prevalence of type III IM in SSBE was 63.33%, similar to LSBE, but significantly higher than CIM (23.08%). Therefore, we think that the HID/AB method could be used to distinguish SSBE from CIM initially, based on the different expressions of neutral mucins, sialomucins, and sulfomucins.

Cytokeratins (CK) are a family of at least 20 structural proteins found in the cytoskeletons of epithelial cells. Certain epithelia exhibit characteristic patterns of CK expression depending on the type, location, and differentiation of the epithelium. CK7, essentially, is not expressed in normal epithelium of the gastrointestinal tract, whereas CK20 is expressed in intestinal epithelium, gastric foveolar epithelium, and endocrine cells in the upper portions of the pyloric glands[22]. Ormsby *et al*[9] observed a pattern of immunoreactivity for CK7 and CK20 that seemed to be distinctive for Barrett's esophagus, which was defined as staining of the superficial epithelium for CK20 and staining of both superficial and deep metaplastic epithelium for CK7. This so-called "Barrett' s CK7/20 pattern" was found in 100% esophageal biopsy specimens from LSBE, but none of the specimens of IM were from the stomach. Ormsby *et al*[23] later found that this Barrett's CK7/20 pattern was present in 82% of patients with SSBE. Studies by Sarbia *et al*[24], Glickman *et al*[20] and Jovanovic *et al*[25] confirmed findings of Ormsby *et al*[9] in 90.3%, 91%, and 94% of their cases with LSBE, respectively. However, some other studies did not support the findings of Ormsby *et al*[9]. In addition, Mohammed *et al*[10] and by El-Zimaity *et al*[11] demonstrated that the proposed Barrett's CK7/20 pattern was observed only in 54% and 39% of patients with LSBE, respectively. Differences in patient populations and endoscopic biopsy techniques may have contributed to the discrepancies among these studies, especially, the sites of the biopsies. Previous anatomic and endoscopic studies have shown the gastric cardia to be a small structure varying from about 0 to 10 mm in length (mean length 3 mm) beneath the GEJ[26], but there are no agreement on the precise distal extent of the cardia[5]. In our study, we have defined the distal extent of the cardia as less than 2 cm beneath the GEJ, which is accepted by most scholars at present, and applied an anterograde approach to obtain biopsies by avoiding biopsy across the SCJ, aiming to eliminate biopsy error to most extent. On the other hand, we compared the results of SSBE and CIM with LSBE and GA-IM. The results indicated that 73.33% of SSBE showed Barrett's CK7/20 immunoreactivity pattern, which was similar to LSBE; whereas 57.69% of CIM showed gastric CK7/20 pattern, which was similar to GA-IM. These results implied that CK7/20 immunoreactivity pattern could be

used to distinguish most of SSBE from CIM. However, there were a large number of cases, which belonged to neither Barrett's pattern nor gastric pattern, since they showed some controversial results; therefore, we have simply based our study on the CK7/20 immunoreactivity pattern, and could not distinguish all SSBE from CIM.

The etiology and pathogenesis of SSBE and CIM are unclear until recently. Recent data have suggested the cause of SSBE, like that of LSBE, is probably related to chronic GERD, and not to *H pylori* infection[14,27,28]. However, the cause of CIM is still controversial. Schnell *et al*[29] suggest GERD as a probable cause, whereas Dulai *et al*[30] have found an association with *H pylori* infection. Few scholars even think that CIM has dual etiologies: gastroesophageal reflux in some and *H pylori* infection in others[31,32]. A recent report has described findings in biopsies of the cardia that are said to distinguish between gastroesophageal reflux and *H pylori* as the etiology[33]. On the basis of these findings, some scholars have proposed that the CK7/20 immunoreactivity patterns with gastroesophageal reflux symptoms and the status of the remainder of the gastric mucosa, including *H pylori* infection, can distinguish IM caused by GERD from that caused by *H pylori* infection. Balaji *et al*[31] found that there were two different patterns of CK7/20 staining in patients with CIM, which support the concept of dual etiologies for CIM. A Barrett's staining pattern was associated with objective evidence of gastroesophageal reflux and the absence of *H pylori*, suggesting that CK7/20 immunostaining is useful to determine the likely etiology of CIM. Couvelard *et al*[34] also found that the Barrett's type CK7/20 pattern was related to a high frequency of gastroesophageal reflux symptoms and normal endoscopic appearance of the stomach, but the gastric type CK7/20 pattern was linked to high frequency of *H pylori* infection, antral inflammation with atrophy and IM. In the present study, we found that the symptoms of GERD were all positive in some cases of LSBE and SSBE, which showed the Barrett's type CK7/20 pattern, whereas in other cases that showed gastric CK7/20 pattern, the symptoms of GERD were all negative, but *H pylori* infection was positive conversely. In contrast, in the CIM cases that showed gastric type CK7/20 pattern, *H pylori* infection was all positive, and the symptoms of GERD were mostly negative, whereas in other cases which showed Barrett' s type, the symptoms of GERD were all positive. These results indicate partly that the CK7/20 immunoreactivity patterns, combined with gastroesophageal reflux symptoms and statuses of *H pylori* infection, could imply the probable cause of SSBE and CIM, and even help to distinguish from each other. However, although GERD symptoms were significantly more common among the patients with IM showing a Barrett's CK7/20 pattern, Couvelard *et al*[34] also found that most of those patients (57%) had no symptoms of GERD. Conversely, although H pylori infection was found significantly more often in gastric biopsy specimens from patients with IM showing a gastric CK7/20 pattern, 34% of those patients had no demonstrable *H pylori* infection. Our findings are also in agreement with the above results. Thus, the concept that CK7/20 immunoreactivity patterns can distinguish IM caused by GERD from that caused by *H pylori* infection is appealing, and further investigations are needed to resolve this dispute.

Therefore, on the basis of our results, we conclude that the distinction of SSBE from CIM should not be based on a single method or factor or characteristic, but the combination of clinical characteristics, histological results, mucin-histochemistry, CK7/20 immunoreactivity, and especially precise endoscopic biopsy. Type III IM, presence of GERD symptoms and Barrett's CK7/20 immunoreactivity pattern may support the diagnosis of SSBE, whereas non-type III IM, presence of *H pylori* infection and gastric CK7/20 immunoreactivity pattern may support the diagnosis of CIM.

ACKNOWLEDGMENT

We thank Professor Wei Ding, Department of Pathology, the First Affiliated Hospital, Medical College of Zhejiang University, for gifting us the reagent of HID/AB.

REFERENCES

1 **Ruol A,** Parenti A, Zaninotto G, Merigliano S, Costantini M, Cagol M, Alfieri R, Bonavina L, Peracchia A, Ancona E. Intestinal metaplasia is the probable common precursor of adenocarcinoma in Barrett esophagus and adenocarcinoma of the gastric cardia. *Cancer* 2000; **88:** 2520-2528

2 **Cameron AJ,** Souto EO, Smyrk TC. Small adenocarcinomas of the esophagogastric junction: association with intestinal metaplasia and dysplasia. *Am J Gastroenterol* 2002; **97:** 1375-1380

3 **Goldblum JR.** The significance and etiology of intestinal metaplasia of the esophagogastric junction. *Ann Diagn Pathol* 2002; **6:** 67-73

4 **Sharma P,** Weston AP, Morales T, Topalovski M, Mayo MS, Sampliner RE. Relative risk of dysplasia for patients with intestinal metaplasia in the distal oesophagus and in the gastric cardia. *Gut* 2000; **46:** 9-13

5 **Spechler SJ.** The role of gastric carditis in metaplasia and neoplasia at the gastroesophageal junction. *Gastroenterology* 1999; **117:** 218-228

6 **Law S,** Lam KY, Chu KM, Wong J. Specialized intestinal metaplasia and carditis at the gastroesophageal junction in Chinese patients undergoing endoscopy. *Am J Gastroenterol* 2002; **97:** 1924-1929

7 **Hirota WK,** Loughney TM, Lazas DJ, Maydonovitch CL, Rholl V, Wong RK. Specialized intestinal metaplasia, dysplasia, and cancer of the esophagus and esophagogastric junction: Prevalence and clinical data. *Gastroenterology* 1999; **116:** 277 -285

8 **Morales CP,** Spechler SJ. Intestinal metaplasia at the gastroesophageal junction: Barrett's, bacteria, and biomarkers. *Am J Gastroenterol* 2003; **98:** 759-762

9 **Ormsby AH,** Goldblum JR, Rice TW, Richter JE, Falk GW, Vaezi MF, Gramlich TL. Cytokeratin subsets can reliably distinguish Barrett's esophagus from intestinal metaplasia of the stomach. *Hum Pathol* 1999; **30:** 288-294

10 **Mohammed IA,** Streutker CJ, Riddell RH. Utilization of cytokeratins 7 and 20 does not differentiate between Barrett's esophagus and gastric cardiac intestinal metaplasia Mod Pathol 2002; **15:** 611 616

11 **El-Zimaity HM, Graham DY**. Cytokeratin subsets for distinguishing Barrett's esophagus from intestinal metaplasia in the cardia using endoscopic biopsy specimens *Am J Gastroenterol* 2001; **96:** 1378 1382

12 **El-Zimaity HM,** Ramchatesingh J, Saeed MA, Graham DY. Gastric intestinal metaplasia: subtypes and natural history. *J Clin Pathol* 2001; **54:** 679-683
13 **Wang LD,** Zheng S, Zheng ZY, Casson AG. Primary adenocarcinomas of esophagus, esophagogastric junction and gastric cardia: in special reference to China. *World J Gastroenterol* 2003; **9:** 1156-1164
14 **Goldblum JR,** Vicari JJ, Falk GW, Rice TW, Peek RM, Easley K, Richter JE. Inflammation and intestinal metaplasia of the gastric cardia: the role of gastroesophageal reflux and *H. pylori* infection *Gastroenterology* 1998; **114:** 633-639
15 **Haggitt RC.** Barrett's esophagus, dysplasia, and adenocarcinoma. *Hum Pathol* 1994; **25:** 982-993
16 **Blot WJ,** Devesa SS, Fraumeni JF. Continuing climb in rates of esophageal adenocarcinoma: an update. JAMA 1993; 270:1320
17 **Haggitt RC.** Adenocarcinoma in Barrett's esophagus: a new epidemic? *Hum Pathol* 1992; **23:** 475 476
18 **Mueller J,** Werner M, Stolte M. Barrett's esophagus: histopathologic definitions and diagnostic criteria. *World J Surg* 2004; **28:** 148-154
19 **Hackelsberger A,** Günther T, Schultze V, Manes G, Dominguez-Muñoz JE, Roessner A, Malfertheiner P. Intestinal metaplasia at the gastro-oesophageal junction: Helicobacter pylori gastritis or gastro-oesophageal reflux disease? *Gut* 1998; **43:** 17-21
20 **Glickman JN,** Wang H, Das KM, Goyal RK, Spechler SJ, Antonioli D, Odze RD. Phenotype of Barrett's esophagus and intestinal metaplasia of the distal esophagus and gastroesophageal junction: an immunohistochemical study of cytokeratins 7 and 20, Das-1 and 45 MI. *Am J Surg Pathol* 2001; **25:** 87 94
21 **Piazuelo MB,** Haque S, Delgado A, Du JX, Rodriguez F, Correa P. Phenotypic differences between esophageal and gastric intestinal metaplasia. *Modern Pathology* 2004; **17:** 62-74
22 **Kurtkaya-Yapicier O,** Gencosmanoglu R, Avsar E. The utility of cytokeratins 7 and 20 (CK7/20) immunohistochemistry in the distinction of short-segment Barrett esophagus from gastric intestinal metaplasia: Is it reliable? *BMC Clin Pathol* 2003; **3:** 5
23 **Ormsby AH,** Vaezi MF, Richter JE, Goldblum JR, Rice TW, Falk GW, & Gramlich TL. Cytokeratin immunoreactivity patterns in the diagnosis of short-segment Barrett's esophagus. *Gastroenterology* 2000; **119:** 683 690
24 **Sarbia M,** Donner A, Franke C, Gabbert HE. Distinction between intestinal metaplasia in the cardia and in Barrett's esophagus: the role of histology and immunohistochemistry. *Hum Pathol* 2004; **35:** 371-376
25 **Jovanovic I,** Tzardi M, Mouzas IA, Micev M, Pesko P, Milosavljevic T, Zois M, Sganzos M, Delides G, Kanavaros P. Changing pattern of cytokeratin 7 and 20 expression from normal epithelium to intestinal metaplasia of the gastric mucosa and gastroesophageal junction, *Histol Histopathol* 2002; **17:** 445 454
26 **Takubo K,** Mafune K, Tanaka Y, Sasajima K. Pathology of the cardia. *Nihon Geka Gakkai Zasshi* 1998; **99:** 547-551
27 **Goldblum JR.** Inflammation and intestinal metaplasia of the gastric cardia: Helicobacter pylori, gastroesophageal reflux disease, or both. *Dig Dis* 2000; **18:** 14-19
28 **Csendes A,** Smok G, Quiroz J, Burdiles P, Rojas J, Castro C, Henríquez A. Clinical, endoscopic, and functional studies in 408 patients with Barrett's esophagus, compared to 174 cases of intestinal metaplasia of the cardia. *Am J Gastroenterol* 2002; **97:** 554-560
29 **Schnell TG,** Sontag SJ, Chejfec G, Aranha G, Metz A, O'Connell S, Seidel UJ, Sonnenberg A. Long-term nonsurgical management of Barrett's esophagus with high-grade dysplasia. *Gastroenterology* 2001; **120:** 1607-1619
30 **Dulai GS,** Guha S, Kahn KL, Gornbein J, Weinstein WM. Preoperative prevalence of Barrett's esophagus in esophageal adenocarcinoma: A systematic review. *Gastroenterology* 2002; **122:** 26-33
31 **Balaji NS,** DeMeester SR, Wickramasinghe KS, Hagen JA, Peters JH, DeMeester TR. Etiology of intestinal metaplasia at the gastroesophageal junction. *Surg Endosc* 2003; **17:** 43-48
32 **DeMeester SR,** Wickramasinghe KS, Lord RV, Friedman A, Balaji NS, Chandrasoma PT, Hagen JA, Peters JH, DeMeester TR. Cytokeratin and DAS-1 immunostaining reveal similarities among cardiac mucosa, CIM, and Barrett's esophagus. *Am J Gastroenterol* 2002; **97:** 2514-2523
33 **Griffel LH,** Amenta PS, Das KM. Use of a novel monoclonal antibody in diagnosis of Barrett s esophagus. *Dig Dis Sci* 2000; **45:** 40-48
34 **Couvelard A,** Cauvin JM, Goldfain D, Rotenberg A, Robaszkiewicz M, Fléjou JF. Cytokeratin immunoreactivity of intestinal metaplasia at normal oesophagogastric junction indicates its aetiology. *Gut* 2001; **49:** 761 766

Science Editor Kumar M and Guo SY **Language Editor** Elsevier HK

PO Box 2345, Beijing 100023, China
www.wjgnet.com
wjg@wjgnet.com

ELSEVIER

World J Gastroenterol 2005;11(40):6366-6372
World Journal of Gastroenterology ISSN 1007-9327
© 2005 The WJG Press and Elsevier Inc. All rights reserved.

• *BRIEF REPORTS* •

Helicobacter pylori vacA s1a and s1b alleles from clinical isolates from different regions of Chile show a distinct geographic distribution

MI Díaz, A Valdivia, P Martínez, JL Palacios, P Harris, J Novales, E Garrido, D Valderrama, C Shilling, A Kirberg, E Hebel, J Fierro, R Bravo, F Siegel, G Leon, G Klapp, A Venegas

MI Díaz, A Valdivia, P Martínez, JL Palacios, A Venegas, Departamento de Genética Molecular y Microbiología. Pontificia Universidad Católica de Chile. Santiago, Chile
P Harris, Departamento de Pediatría, Unidad de Gastroenterología, Facultad de Medicina, Pontificia Universidad Católica de Chile. Santiago Chile
J Novales, E Garrido, Centro de Diagnóstico Terapéutico Los Angeles, Servicio Salud Bio-Bio. Los Angeles, Chile
D Valderrama, Unidad de Gastroenterología, Hospital Valparaíso, Valparaíso, Chile
C Shilling, Anatomía Patológica, Hospital San Martín de Quillota, Quillota, Chile
A Kirberg, Centro de Endoscopía Quirúrgica, Hospital de Iquique. Iquique, Chile
E Hebel, J Fierro, Departamento de Pediatría, Universidad de La Frontera, Temuco, Chile
R Bravo, Hospital Base de Linares, Linares, Chile
F Siegel, Hospital Regional de Valdivia, Valdivia Chile
G. León, Instituto de Bioquímica, Universidad Austral de Chile, Valdivia, Chile
G. Klapp, Hospital Regional de Punta Arenas, Chile
Supported by FONDECYT, Comisión Nacional Científica y Tecnológica, Chile No.1000730 No.1030894 and No. 1000734 from and NIH No.DK54495
Correspondence to: Venegas A, Departamento de Genética Molecular y Microbiología. Pontificia Universidad Católica de Chile. Alameda 340, Santiago Chile. avenegas@genes.bio.puc.cl
Telephone: +56-2-686-2661 Fax: +56-2-222-2810
Received: 2005-04-01 Accepted: 2005-04-09

Abstract

AIM: To establish the most common *vacA* alleles in *Helicobacter pylori* (*H pylori*) strains isolated from Chilean patients and its relationship with gastritis and gastroduodenal ulcers.

METHODS: Two hundred and forty five *H pylori* clinical isolates were obtained from 79 biopsies from Chilean infected patients suffering from gastrointestinal diseases. An average of 2-3 strains per patient was isolated and the *vacA* genotype was analyzed by PCR and 3% agarose electrophoresis. Some genotypes were checked by DNA sequencing.

RESULTS: The most prevalent *vacA* genotype in Chilean patients was s1b m1 (76%), followed by s1a m1 (21%). In contrast, the s2 m2 genotype was scarcely represented (3%). The s1b m1 genotype was found most frequently linked to gastropathies ($P<0.05$) rather than ulcers. Ulcers were found more commonly in male and older patients. Curiously, patients living in cities located North and far South of Santiago, the capital and largest Chilean city, carried almost exclusively strains with the s1b m1 genotype. In contrast, patients from Santiago and cities located South of Santiago carried strains with either one or both s1a m1 and s1b m1 genotypes. Regarding the s2 m2 genotype, comparison with GenBank sequences revealed that Chilean s2 sequence was identical to those of Australian, American, and Colombian strains but quite different from those of Alaska and India.

CONCLUSION: Differences in geographic distribution of the s and m *vacA* alleles in Chile and a relationship of s1b m1 genotype with gastritis were found. Sequence data in part support a hispanic origin for the *vacA* genotype. Asymmetric distribution of genotypes s1b m1 and s2 m2 recedes *H Pylori* strain distribution in Spain and Portugal.

© 2005 The WJG Press and Elsevier Inc. All rights reserved.

Key words: *H pylori; vacA* alleles; Chilean isolates; s1; s2; m1 and m2 sequences

Díaz MI, Valdivia A, Martínez P, Palacios JL, Harris, P, Novales J, Garrido E, Valderrama D, Shilling C, Kirberg A, Hebel E, Fierro J, Bravo R, Siegel F, Leon G, Klapp G, Venegas A. *Helicobacter pylori vacA* s1a and s1b alleles from clinical isolates from different regions of Chile show a distinct geographic distribution. *World J Gastroenterol* 2005; 11(40): 6366-6372
http://www.wjgnet.com/1007-9327/11/6366.asp

INTRODUCTION

Helicobacter pylori (*H pylori*) is a curved Gram-negative bacterium frequently present in the human stomach. Once the host has been colonized, this microorganism persists for years or decades[1]. This microorganism has a worldwide distribution and its prevalence increases with age[2], and is a major etiological agent in the development of peptic ulcer and gastric cancer[3,4]. Several potential virulence factors have been suggested to play a role in the pathogenesis caused by this microorganism. The most studied *H pylori* virulence factors are CagA and VacA. The first one, called the cytotoxin associated antigen[5] is one of the proteins encoded by the pathogenicity island, a unique genomic fragment containing about thirty genes and some of them encode the machinery required for the secretion of the CagA protein. Strains carrying a functional *cagA* gene have been associated with a variety of clinical outcomes[5].

VacA is a vacuolating cytotoxin which induces cytoplasmic

vacuolation in a variety of mammalian cell lines *in vitro*[6]. It is responsible for the gastric epithelial damage and causes mucosal ulceration when administered intragastrically to mice[7]. Recently, the VacA cytotoxin has been described as a permease that promotes urea diffusion across the epithelia[8] providing an additional source of nutrients to sustain *H pylori* growth *in vivo*. It has been recently reported that the cytotoxin is able to induce apoptosis in epithelial cells as well as a specific inhibition of the immune response[9,10]. Different allelic variants in the *vacA* sequence in two regions of the gene have been described: the s allele located in the region encoding the N-terminal signal region which may occurs as the alleles s1- (s1a or s1b) or s2 type, and the m allele located at the middle of the *vacA* gene, which is present as m1 or m2 type[11]. The variable structure resulting of different arrangements of these alleles in the gene has been related to the differences in the level of cytotoxin production and to distinct clinical outcomes of the *H pylori* infection[12-14].

In Chile, a country with one of the higher mortality rates of gastric cancer, gastroduodenal diseases are common causes of medical consultations[15]. Serological studies have indicated that over 70% of asymptomatic adults older than 35 years old are infected by *H pylori*[16]. Our previous studies[17] have revealed that 83% of Chilean infected patients from Santiago have antibodies against VacA or CagA virulence factors determined by Western blot using purified recombinant proteins and by ELISA tests based on the detection of CagA and VacA antibodies[17].

Few studies have been carried out on strains from the South Cone and in particular from Chilean patients[18]. Recent data from *H pylori* strains from Argentina have revealed that most of the *vacA* alleles are s1b m1[19]. Reports about the characterization of strains isolated from Brazilian children indicated that s1 allele is associated with the presence of peptic ulcer[20] and genotype *cagA*+*vacA* s1b m1 is the most frequent in Brazilian adults with non-mixed infections[21]. Recent studies done with strains from 63 patients from the central area in Santiago, Chile, found that s1m1 is also the most common allele associated to ulcer patients[22].

Since information in Latin American countries is rather scarce, the present study adds new pieces of information in this respect and it has been focused on the distribution of *vacA* alleles of *H pylori* strains obtained from infected patients along this country (more than 5 000 kilometers long) to identify, as a preliminary study, the most frequent *vacA* alleles in this population and their relationship with different pathologies.

MATERIALS AND METHODS

Strains, growth and collection of clinical specimens

E. coli DH5α was used as a host for cloning experiments. *Campylobacter yeyuni* VPI H840 (ATCC 29428), kindly provided by Dr. H. Fernández (Universidad Austral de Chile) was used as DNA source of a negative *vacA* genotype control. Strains 26695 (ATCC 700392), 60190 (ATCC 49503), T×30a (ATCC 51932), NCTC 11637 (ATCC 43504) and J99 (ATCC 700824) were used as well characterized *vacA* alleles sources.

H pylori clinical strains were isolated from human gastric biopsies obtained from each patient who underwent upper gastrointestinal endoscopy for medical indication. Patients were recruited from different hospitals and clinics from 10 Chilean cities. Biopsies were transported to Santiago as frozen samples in dry ice and immediately after arrival suspended in PBS (500 μL), manually grinded and plated on *Brucella* agar plates. This medium contained 5% fresh horse blood, 5 mg vancomycin, 2.5 mg cefsulodin, 2.5 mg trimethoprime lactate, 2.5 mg amphotericin B, and 1.5 g agar per 100 mL of medium. Colonies were grown for three to four days under microaerophilic conditions using the microaerophilic system envelopes with palladium catalyst. Two or three specimens per biopsy were obtained and a total of 245 isolates were characterized.

Patients

Seventy- nine consent patients who gave informed consent including 35 males and 44 females aged between 3 and 79 years old with symptoms warranted upper gastrointestinal endoscopies. Twenty- two patients from Iquique (IQ), 1 from La Calera (LC), 3 from Quillota (QU), 6 from Valparaíso (VA), 12 from Santiago (SA), 5 from Linares (LI), 6 from Los Angeles (LA), 2 from Temuco (TE), 8 from Valdivia (VD) and 14 from Punta Arenas (PA) were analyzed in this study.

Criteria for enrollment included nocturnal or burning abdominal pain, chronic vomiting, hematemesis or history of recurrent abdominal pain plus a first degree relative with an endoscopically proven diagnosis of peptic ulcer disease. Exclusion criteria included hemodynamically unstable patients and recent antibiotic therapy, antisecretory drugs or bismuth compounds in the last 4 wk. Signed informed consent forms by the patients or their parents in the case of minors were obtained. The institutional Review Board of the local participating institutions reviewed and approved the study.

Endoscopy, histology and criteria of H pylori infection

The endoscopic findings in the esophagus, stomach and duodenum were described in a standardized protocol. The macroscopic appearance was recorded according to the presence of nodularity, erosion or ulceration. Diagnosis of gastritis and duodenitis were done on histological basis. Gastropathy was diagnosed when abnormalities such as erosions or nodularity were observed. Ulcer was diagnosed when either a circumscribed break in the gastroduodenal mucosa that measured at least 5 mm in diameter or a scar was observed. Two biopsies were obtained from the distal antrum of each patient to determine *H pylori* status. One of the biopsies was used for rapid urease test (Hepy test, BiosChile).

Serial sections of formalin-fixed and embedded in paraffin gastric tissue from the second antrum biopsy of each patient were stained either with Warthin-Starry silver or H&E stain and examined for the presence of *H pylori* and associated pathology for pathologists who were unaware of the results of other tests. Bacteria were defined as *H pylori* on the basis of size, spiral morphology, and tissue location. A subject was considered colonized by *H pylori* when both invasive diagnostic techniques (rapid urease test and *H pylori* staining) were positive. A patient was considered negative for *H pylori* when both invasive diagnostic tests were negative. We confirmed this assignment in most of the cases by isolation of colonies which gave positive for urease, catalase, and peroxidase enzyme tests.

Isolation of H pylori chromosomal DNA

DNA was obtained by using the method described by Owen

and Bickley[28], with CTAB (Cetyltrimethylammonium bromide) as the detergent for cell lysis. Briefly, single colonies were grown in plates as described above. Cells coming from half a plate were collected and transferred to an Eppendorf tube using a sterile loop and processed as described[23].

PCR reactions, primers, cloning and sequencing

Reactions were done according to the conditions established by Atherton *et al*.[11,12]. Cloning of s1a, s1b, s2, m1, m2 PCR fragments from some isolates were done by ligation into the pGEM-T vector (Promega) and electroporation into *E. coli* DH5α cells which were plated on Luria agar plates containing ampicillin 50 μg/mL. Some cloned PCR fragments were sequenced by using ABI Prism-3 100 genetic analyzer (Applied Biosystems).

Study groups and statistical analysis

H pylori infected patients were assigned to one of three groups according to their endoscopical or histological findings as follows: Chronic Active Gastritis group (CG) included patients with normal or non-specific endoscopic findings, plus chronic gastritis by histology; Gastropathy Group (GG) included patients with significant endoscopic abnormalities (nodularity, polyps or erosions but not ulcers) and chronic gastritis by histology; and Peptic Ulcer Disease group (PUD) included patients with gastric or duodenal ulcer at endoscopy and chronic gastritis by histology.

To asses whether the presence or absence of ulcers in infected patients could be related with the gender, age, or allele type, cross tabulation and χ^2 test were performed using the Minitab release 12 program (State College, PA, USA). A P value < 0.05 was considered significant. The s2 m2 strains were not included in this analysis due to its low frequency (3%).

Accession numbers

The GenBank accession numbers of sequences used in this study were: Sant4, # AY167579; Sant50, #AY167580; Sant51, #AY167581; Sant52, #AY167582; Oroan10, #AY168871; Oroan15, #AY168872; Sant53, #AY167583; 95-54, #U95971; 90, #AF2201191; 87-203, #U05677; V-296, #ABO57273; CHCTX-1, #AF479032; LA-12, #AY840127; CHN5027ass, #AF050379.1; IQ-61, #AY858851; QU-61, #AY858850; QU-31 #AY858849; AR-312, #AY185131; AR-710, #AY185128; SA-64, #AY839241; USA2781, # ABO572201; SS-1, #AY049006; NA2010, #AB057202.1; NA1986, #AB077199.1; India 3, #AF217727.1; Alaska5, #AB057171.1; Alaska20, #AB057186.1; Alaska08, #AB057174.1; Alaska03, #AB057169.1; Alaska04, #AB057170.1; India27, #AF217733.1.

RESULTS

Detection of the m1 and m2 alleles in Chilean H pylori strains

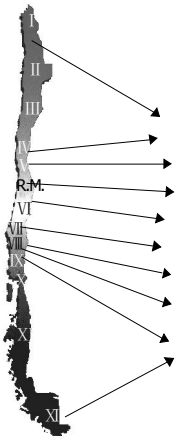
Seventy nine biopsies from *H pylori* infected patients living at 10 Chilean cities were used as a source to isolate 245 *H pylori* colonies. Amplification of the m2 *vacA* allele was obtained for two patients from Iquique and one from Santiago. Among the 245 studied strains, 97% of them harbored the m1 allele and 3% the m2 allele. Hybrids corresponding to m1/m2 alleles or non-typable alleles were not detected.

Detection of the s1 and s2 alleles in Chilean H pylori strains

Most of the strains carried the s1 allele (97%). The 72.1% of these was s1b and 24.1% was s1a. A summary of these results according to the strain origin (city) and the s and m alleles is displayed in Figure 1.

Identification of the m1 and m2 alleles of Chilean strains by DNA sequencing

Strain CHCTX-1 and LA-12 were utilized to amplify the m1 *vacA* allele. The PCR fragments were cloned in the pGEM-T vector and then sequenced. The results are shown in Figure 2A. After the alignment of the amino acid sequences with those available at in the GenBank, we found that the Chilean m1 sequences were similar to the Indian m1 deposited sequences. Seven strains out of 245 isolates presented the genotype s2m2. A further characterization



City	Patient number	CG	GG	PUD	Strains with alleles		
					S1am1	S1bm1	s2m2
Iquique	22*	18	2	2	-	56	4
La Calera	1	1	-	-	-	3	-
Quillota	3	3	-	-	-	6	-
Valparaíso	6	2	-	4	-	18	-
Santiago	12*	4	2	6	27	6	3
Linares	5	3	-	2	6	7	-
Los Angeles	6	5	1	-	15	-	-
Temuco	2	2	-	-	-	2	-
Valdivia	8	3		5	13	9	
Punta Arenas	14	12	2			70	
Totals	79	53	7	19	61	177	7

Figure 1 Chilean map and strain distribution according to the *vacA* alleles. Map of Chile including the location of the cities where biopsies were taken. The corresponding *vacA* alleles, as well as the number of strains and patients are displayed (*). Two patients, one from Iquique and the other from Santiago, had mixed infections. Chronic Active Gastritis (CG), Gastropathy Group (GG), Peptic Ulcer Disease (PUD). Total amount of strains = 245.

A

```
                 10                  20                  30                  40                  50                  60
                  .                   .                   .                   .                   .                   .
G Q N A V M D Y S Q F S N L T I Q G D F I N N Q G T I N Y L V R G G K V A T L N V G N A A A M M F N N D I D S A T G F Y
* * * * * * * * * * A F Q F * * * * * * * * * * * * * * * * * * * * * * * * * * A * * * * * * * * D * * * * * * * * * *
* * * * * * * * * * * * * * * * * * * * T * * * * * * * * * * * * * Q * * * * * * * * * * * * L * * * N V * * * * * * *
* * * * * * * * * * * * * * * * * * * * T * * * * * * * * * * * * * Q * * * * * * * * * * * * L * * * N V * * * * * * *

         70                  80                  90                  97
          .                   .                   .                   .
K P L I K I N S A Q D L I K N T E H V L L K A K I I G Y G N V S T G T N G       CHCTX-1           (Chile)
* * * * * * * * * * * * * * * * * * * * * * * * * * * * * * * * * * * * *       LA-12             (Chile)
Q * * M * * * * * * * * * * * K * * * * * * * * * * * * * * * * A * * * S       Sant4,50,51,52    (India)
Q * * M * * * * * * * * * * * K * * * * * * * * * * * * * * G * A * * * S       Oroan10,15, Sant53 (India)
```

B

```
         10        20        30        40        50        60
          .         .         .         .         .         .
GAPGNIAGKTGLMFNNLTLNSNASMDYGKDLDLTIQGHFTNNQGTMNLFVQDGRVATLNA      SA-64      (Chile)
*S**********************************************************      95-54      (Italy)
****Y*******************************************************      90         (India)
**********************************S*********S***************      97-203     (USA)
*PQ*SPW*TAK**S*****GP**Q***SQFSNV****D*******I*YL*RG*NIE**SV      V-296      (Taiwan)

         70        80        90        100       110       117
          .         .         .         .         .         .
GHQASMIFNNLVDSATGFYKPLIKINNAQNLTKNKEHVLVKARNIDYNLVGVQGASY      SA-64    (Chile)
*********************************************************      95-54    (Italy)
**********V**********************************************      90       (India)
*****************************************G***************      97-203   (USA)
*NA*V*S***DI**************S**A*I*******L**KI*G*ENASLGTN*I      V-296    (Taiwan)
```

C

```
         10        20        30        40        50        60 62
          .         .         .         .         .         . .
SITPQQSHAAFFTTVIIPAIVGGIATGTAVGTVSGLLSWGLKQAEEANKTPDKPDKVWRIQA      CHCTX        (CHILE)
*IT**Q********************************************************      LA-12        (Chile)
*****K*******************S*A*********G************************      CHN3295b     (Chn)
SAIPQESHAAFFTTVIIPAIVGGIATGTAVGTVSGLLSWGLKQAEEANKTPDKPDKVWRIQA      IQ-61        (Chile)
**************************************************************      QU-31        (Chile)
**************************************************************      QU-61        (Chile)
*IT**Q*********************A**********************************      AR-312,710   (Arg)
```

D

```
         10        20        30        40        50        60    66
          .         .         .         .         .         .     .
ANTPNDPIHSESRAFFTTVIIPAIVGGIATGAAVGTVSGLLSWGLKQAEQANKAPDKPDKVWRIQA      SA-64       ◆
****************************************************************K*      NA1995      ●
*****************************************************T************      Alaska  20
***************************L*************************T************      Alaska  08
**********************************E******G*******E***T****E*****K*      Alaska  03
**********************************E******G*******E***T****E*****K*      India   27
***************************L***T**E******G*******E***T****E*****K*      Alaska  04
```

Figure 2 Alignment of s and m alleles as *vacA* amino acid partial sequences. **A:** Alignment of amino acid sequences corresponding to the amplified m1 *vacA* allele of Chilean strains CH-CTX1 and LA-12 with other representative m1 Indian sequences obtained from the GenBank; **B:** Alignment of amino acid sequences corresponding to the amplified m2 *vacA* allele and other representative m2 sequences obtained from the GenBank. The m2 allele from strain SA-64 was amplified using primers VA4F and VA4R and both strands were sequenced. The oligonucleotide sequence was translated (126 amino acids) and compared with other representative m2 allele sequences. These m2 sequences were obtained from GenBanK and corresponded to strains 95-54 from Italy, India 90, 97-203 from USA and V-296 from Taiwan; **C:** Alignment of amino acid sequences corresponding to Chilean strains having the s1a allele (CH-CTX1 and LA-12) and comparison with a s1a sequences from China. Sequences of Chilean s1b strains (IQ-61, QU-31 and QU-61) and comparison with other s1b sequences obtained from the GenBank from Argentinean strains AR-312 and AR-710; **D:** Alignment and comparison of amino acid sequences corresponding to the s2 sequence of the Chilean strain SA-64 and other sequences obtained from the GenBank of strains isolated in different locations. Sequences of the s2 *vacA* allele from different strains were aligned starting from amino acid position 30 in the *vacA* precursor sequence and the segment was fit with the ends defined by the Atherton primers for amplification of the s2 allele. ◆ Includes identical s2 sequences for strains: SA-64 from Chile, USA2781 from Arizona, USA, SS-1 from Australia, NA2010 and NA1986 from Colombia. ●Represents identical s2 sequences from strains NA1995, NA1992 and NA1685 from Colombia, India 3 and Alaska 5 from USA. Accession numbers are displayed in Materials and methods.

of the m2 *vacA* allele was done on strain SA-64 by DNA sequencing the amplified cloned fragment. Comparison of this m2 allele sequence (Figure 2B) with other m2 sequences taken from the GenBank revealed almost identical amino acid sequences (one amino acid difference) with the m2 sequence of the Italian strain 95-54. Conversely, we found 45% amino acid identity for the SA-64 m2 sequence when compared to the Taiwanese strain V 296 as displayed in Figure 2B. These findings put the Chilean strain SA-64 closer to the strains that share a common ancestor from hispanic origin and far from those strains isolated from Asiatic patients.

Sequences of the s2 and s1 alleles of Chilean strains

Strains CHCTX-1 and LA-12 were used as DNA source for amplification and sequencing of the s1a alleles, strains IQ-61, QU-31 and QU-61 for sequencing s1b allele (Figure. 2C), and strain SA-64 for sequencing the s2 allele (Figure. 2D). Comparison with other s1a, s1b, and s2 sequences available at the GenBank are displayed in Figures 2C and D. It was found that the s2 allele sequence from Chilean strain SA-64 was identical to those reported for American (USA2781), Australian (SS-1) and Colombian (NA2010) strains but far away from those of Alaskian (Alaska 4) and Indian (India 27) strains (in a segment of 66 amino acids there were 8 and 6 amino acid differences, respectively).

Correlation of vacA *alleles and patient gastric diseases*

The s1bm1 allele combination was more common in patients with chronic gastritis without ulcers and other endoscopic findings ($P<0.05$). The s1am1 has a homogeneous distribution among patients with chronic gastritis, gastrophaties or peptic ulcer diseases (Figure 3A). Figure 3B shows patient gender and disease occurrence. There was not significant difference between males and females regarding different clinical outcomes (Figure 3B). There was an age dependent increase in the frequency of peptic ulcer disease and an age dependent decrease in the frequency of chronic gastritis, without reaching statistical significance (Figure 3C).

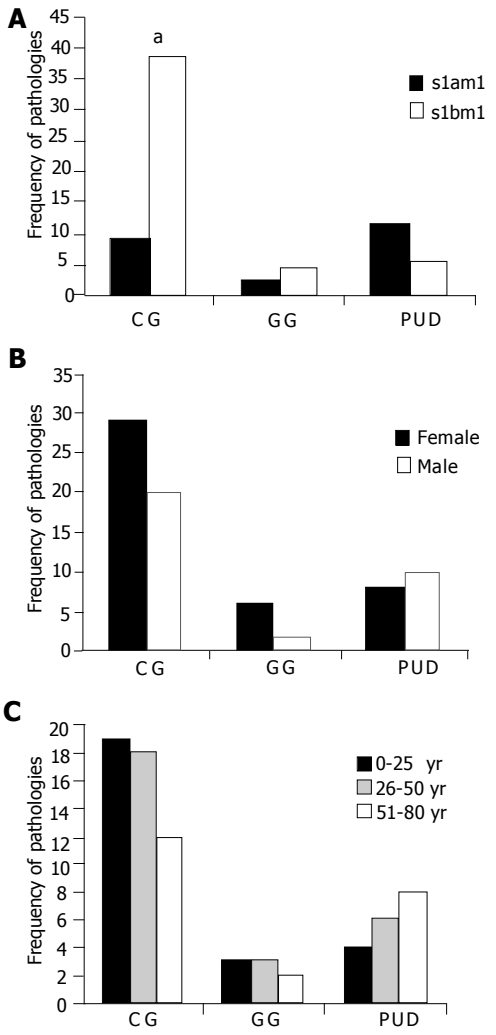


Figure 3 Analysis of gastropathies outcome frequencies respect to *VacA*. genotype, gender and patient age; **A:** Relationship between pathologies and alleles. Minitab Release 12 PA.USA and χ^2 test for categorical variables was used ($P<0.05$). $P<0.05$ was considered significant. The s2m2 allele was excluded of the statistics test due a low frequency (3%); **B:** Relationship between gastropathies and gender. F: female, M: male. A total of 43 females and 32 males were studied ($P>0.5$), four patients carrying strains with s2 m2 allele were excluded from this study; **C:** Relationship between gastropathies and patient age ($P>0.5$).

DISCUSSION

A variety of structural and functional characteristic of the *H pylori* virulence factors have been used for strain genotyping, since they define a particular genotype which can be associated with an increased risk of peptic ulcer in human beings. Among these, genes of virulence factors such as *cagA*, *vacA*, *hpaA, iceA and babA* have been used before for classification purposes[24]. However one of the most extensively studied has been the *vacA* cytotoxin genotypes. This gene has a mosaic-like structure which is very uncommon in bacterial cytotoxins. Moreover, it is also unique for *H pylori* because the VacA polypeptide precursor promotes its own secretion. A similar auto-promoted mechanism has been observed for IgA proteases secreted by *Neisseria gonorrhoeae* and *Haemophilus influenzae*[25,26]. Some *vacA* gene regions have been used for genotyping and to evaluate the relationship between some *vacA* allele and a particular disease caused by *H pylori*[22].

We have studied 245 *H pylori* Chilean strains collected from patients belonging to different cities along the country. Most of the samples were collected from patients living at the central valley and some from the North and South regions as displayed in Figure 1. It should be noted that to the North of Chile is located the Atacama desert, one of the driest places in the world and this region do not support the development of cities. On the other hand, Southern Chile is under-populated because vast areas are preserved as ecological native resources and inhabited zones are rather minimal. Northern Chile also includes indigenous population. We included in the group of patients living in IQ, some strains isolated from native descendants from ancestral *Aimara* population. Curiously, all strains isolated from these patients had s1bm1 genotype. Also, a "*Mapuche*" native from Valdivia city (Southern Chile) presented the same genotype. A *Mapuche* autochthonous is considered a descendant of native Chileans before Hispanic colonization. Further analyses will be required to establish if the *vacA* genotype and other virulence markers

within the autochthonous population remain homogeneous.

The analysis of the signal sequence s region showed that barely 3% of the isolated strains exhibited the s2 allele (just 7 out of 245 strains) and 97.1% was classified as s1 type. Therefore, most of the strains were classified either as s1a or s1b alleles. The analysis of the medium region ("m" alleles) revealed that only 3% was m2 type, which was always associated to the s2 allele. Considering simultaneously both "s" and "m" alleles, 72% of all characterized strains was s1b m1 and 25.1% was s1a m1. These results are quite different from those reported by Martínez *et al*.[27], in particular to the frequency of the s2 and m2 alleles for one Chilean city Concepción, not included in our study. They found a higher proportion (44%) of this genotype in 34 infected patients and, considering each allele independently, 32% was s2 and 58% was m2 in an extended study for this city with 50 patients. Compared to our data, this could be an overestimation of the s2m2 genotype, since the screened patients were all recruited from a single city. In addition, they used in some cases a different set of primers to detect the m2 allele, based on a 6 bp difference in fragment length (m1 = 116 bp; m2 = 122 bp) which is difficult to distinguish even in a 3% agarose gel. Moreover, their results were not confirmed by DNA sequencing of the amplified alleles. In any case, our data support the idea of a putative hispanic origin for the Latin American strains, considering that the preferred s1bm1 allele distribution was also detected in the strains from patients from Spain and Portugal, as reported by van Doorn *et al*.[28]. In addition, it is noticeable that the allele s2 m2 that we described for 7 Chilean strains has not frequently been described in other South American countries yet. Also, the s2 and m2 alleles occur in the lowest proportion in Spain and Portugal[28]. The s2 m2 Chilean allele seemed to be interesting to sequence since, as mentioned, it represents a local uncommon *vacA* genotype. The m2 allele cloned from strain SA-64 was sequenced. The amino acid sequence revealed a closer similarity to the m2 allele of strain 95-54 isolated from an Italian patient (one aminoacid difference). A feasible explanation for the low occurrence of this genotype could be that this allele may confer a disadvantage for natural *in vivo* selection of the strain such as a lower VacA activity, a feature proposed by some authors[11,29]. Alternatively, it may have resulted from a recombination event that actually occurs at very low frequency. The latter argument is sustained in part by the finding that some patients infected with multiple *H pylori* strains allow the exchange of bacterial DNA along the course of the disease[30,31].

Results of *H pylori* strain typing based on *vacA* allele done in other countries indicate that differences between m1 and m2 strains raise diversity in the level of cytotoxin activity. However, at present it is not clear if differences between s1 and s2 phenotypes also affect the level of cytotoxin expression by a reduction in the amount of exported cytotoxin. One hypothesis strongly proposes that S2 type allele containing a different signal sequence exports a cytotoxin precursor through the inner membrane in a less efficient way[13]. On the other hand, it has been demonstrated that when a short oligonucleotide extension encoding 12 amino acids (as part of the s2 allele) is transferred to a *vacA* gene displaying the s1 genotype. This completely abolishes the vacuolating activity but has no effect on VacA cytotoxin production[11,29].

A strong correlation between the severity of the clinical diagnosis and *vacA* genotype has been proposed by several authors. For instance, in South African patients, the allele s1m1 is associated to ulcer disease[32] and in other cases to gastric cancer, as described for German patients[33]. The s2 allele has also been associated with the lack of peptic ulcer[11]. Indeed, in the present analysis those strains whose s2 and m2 alleles were sequenced and reported here were isolated from patients suffering from mild gastritis and corresponded to supposedly less aggressive genotypes. However, one patient had a mixed infection carrying, in addition to the genotype s2m2, other strains with the s1am1 and s1bm1 genotypes. It remains to be established if the strains with genotype s2m2 are actually producing a VacA protein with attenuated cytotoxic properties.

We have reported here that most of the patients carrying the s1b m1 VacA allele suffered chronic gastritis (females mainly) and this genotype was preponderant in patients living in cities located to the north of Santiago. The s1am1 genotype was most frequently associated to isolates from patients suffering from ulcers (mild male predominance). Patients from Santiago and cities located south of Santiago (Central Chile) carried strains with either one or both s1am1 and s1bm1 genotypes. It should be noted that Santiago, as the Chilean capital city, attracts immigrants not only from the neighboring countries but also from Asian countries, and in a lesser extent, natives from Northern and Southern cities searching for jobs, a fact that may explain a mixed allele distribution found in strains isolated from patients living in Santiago.

Finally, this study supports the fact that *H pylori* is actually one of the microorganisms with the highest genetic variability and this feature may complicate genotyping[34]. The genomic variability is so high that some researchers consider *H pylori* as a *quasi* strain[34]. Also, in some cases, mutations in other genetic loci may be responsible for the generation of unexpected and more virulent strains.

ACKNOWLEDGMENTS

We gratefully acknowledge Emily Miller, from New York University, USA, for reading the manuscript and helpful suggestions.

REFERENCES

1 **Blaser MJ**. *Helicobacter pylori* and the pathogenesis of gastroduodenal inflammation. *J Infect Dis* 1990; **161**: 626-633

2 **Graham DY**, Klein PD, Opekun AR, Boutton TW. Effect of age on the frequency of active *Campylobacter pylori* infection diagnosed by the [^{13}C]-urea breath test in normal subjects and patients with peptic ulcer disease. *J Infect Dis* 1988; **157**: 777-780

3 **Blaser MJ**. *Helicobacter pylori*: its role in disease. *Clin Infect Dis* 1992; **15**: 386-391

4 **Cover TL**, Blaser MJ. *Helicobacter pylori* infection, a paradigm for chronic mucosal inflammation: pathogenesis and implications for eradication and prevention. *Adv Intern Med* 1996; **41**: 85-117

5 **Censini S**, Lange C, Xiang Z, Crabtree JE, Ghiara P, Borodovsky M, Rappuoli R, Covacci A. Cag, a pathogenicity island of *Helicobacter pylori*, encodes type I-specific and disease-associ-

ated virulence factors. *Proc Natl Acad Sci USA* 1996; **93**: 14648-14653
6 **Leunk RD**, Johnson PT, David BC, Kraft WG, Morgan DR. Cytotoxic activity in broth-culture filtrates of *Campylobacter pylori*. *J Med Microbiol* 1988; **26**: 93-99
7 **Sundrud MS**, Torres VJ, Unutmaz D, Cover TL. Inhibition of primary human T cell proliferation by *Helicobacter pylori* vacuolating toxin (VacA) is independent of VacA effects on IL-2 secretion. *Proc Natl Acad Sci USA* 2004; **101**: 7727-7732
8 **Tombola F**, Morbiato L, Del Giudice G, Rappuoli R, Zoratti M, Papini E. The *Helicobacter pylori* VacA toxin is a urea permease that promotes urea diffusion across epithelia. *J Clin Invest* 2001; **108**: 929-937
9 **Fischer W**, Gebert B, Haas R. Novel activities of the *Helicobacter pylori* vacuolating cytotoxin: from epithelial cells towards the immune system. *Int J Med Microbiol* 2004; **293**: 539-547
10 **Willhite DC**, Blanke SR. *Helicobacter pylori* vacuolating cytotoxin enters cells, localizes to the mitochondria, and induces mitochondrial membrane changes correlated to toxin channel activity. *Cell Microbiol* 2004; **6**: 143-154
11 **Atherton JC**, Cao P, Peek RM Jr, Tummuru MKR, Blaser MJ, Cover LT. Mosaicism in vacuolating cytotoxin alleles of *Helicobacter pylori*: association of specific vacA types with cytotoxin production and peptic ulceration. *J Biol Chem* 1995; **270**: 17771-17777
12 **Atherton JC**, Peek RM, Tham KT, Cover TL, Blaser MJ. Clinical and pathological importance of heterogeneity in vacA, the vacuolating cytotoxin gene of *Helicobacter pylori*. *Gastroenterology* 1997; **112**: 92-99
13 **McClain MS**, Cao P, Iwamoto H, Vinion-Dubiel AD, Szabo G, Shao Z, Cover TL. A 12-amino-acid segment, present in type s2 but not type s1 *Helicobacter pylori* VacA proteins, abolishes cytotoxin activity and alters membrane channel formation. *J Bacteriol* 2001; **183**: 6499-6508
14 **Telford JL**, Ghiara P, Dell'Orco M, Comanducci M, Burroni D, Bugnoli M, Tecce MF, Censini S, Covacci A, Xiang Z. Gene structure of the *Helicobacter pylori* cytotoxin and evidence of its key role in gastric disease. *J Exp Med* 1994; **179**: 1653-1658
15 **Duarte I**, Ohmke J, Ciani S, Villaroel L. Patrones de carcinoma en gastrectomías de adultos chilenos: estudio multivariado en un país de alto riesgo. *Gastr Latinoam* 2001; **12**: 12-18
16 **Medina E**. Las enfermedades digestivas en Chile: panorama epidemiológico. *Rev Med Chile* 1998; **116**: 282-288
17 **Opazo P**, Müller I, Rollan A, Valenzuela P, Yudelevich A, García-de la Guarda R, Urra S, Venegas A. Serological response to *Helicobacter pylori* recombinant antigens in Chilean infected patients with duodenal ulcer, non-ulcer dispepsia and gastric cancer. *APMIS* 1999; **107**: 1069-1078
18 **Müller I**, Medina-Selby A, Palacios JL, Martínez P, Opazo P, Bruce E, Mancilla M, Valenzuela P, Yudelevich A, Venegas A. Cloning and comparison of ten gene sequences of a Chilean *H pylori* strain with other *H pylori* strains revealed higher variability for VacA and CagA virulence factors. *Biol Res* 2002; **35**: 67-84
19 **Catalano M**, Matteo M, Barbolla RE, Jiménez Vega DE, Crespo O, Leanza AG, Toppor J, Antelo P. *Helicobacter pylori vacA* genotypes, *cagA* status and *ure A-B* polymorphism in isolates recovered from an Argentinean population. *Diagn Microbiol Infect Dis* 2001; **41**: 205-210
20 **De Gusmao VR**, Nogileira Mendes E, De Magalhaes Queiroz DM, Aguiar Rocha G, Camargos Rocha AM, Ramadan Ashour AA, Teles Canalho AS. VacA genotypes in *Helicobacter pylori* strains isolated from children with and without duodenal ulcer in Brazil. *J Clin Microbiol* 2000; **38**: 2853-2857
21 **Ashour AA**, Magalhaes PP, Mendes EN, Collares GB, de Gusmao VR, Queiroz DM, Nogueira AM, Rocha GA, de Oliveira CA. Distribution of vacA genotypes in *Helicobacter pylori* strains isolated from Brazilian adult patients with gastritis, duodenal ulcer or gastric carcinoma. *FEMS Immunol Med Microbiol* 2002; **33**: 173-178
22 **Faúndez G**, Troncoso M, Figueroa G. CagA and vacA in strains of *Helicobacter pylori* from ulcer and non-ulcerative dispepsia patients. *BMC Gastroenterol* 2002; **2**: 20
23 **Owen RJ**, Bickley J. Insolation of *H pylori* genomic DNA and restriction analysis In: Clayton CL, Mobley HLT. Methods in Molecular Medicine: *Helicobacter pylori* protocols, Tolowa, N J, Humana Press 1997: 81-88
24 **Hocker M**, Hohenberg P. *Helicobacter pylori* virulence factors-one part of a big picture. *Lancet* 2003; **362**: 1231-1233
25 **Schmitt W**, Haas R. Genetic analysis of the *Helicobacter pylori* vacuolating cytotoxin: structural similarities with the IgA protease type of exported protein. *Mol Microbiol* 1994; **12**: 307-319
26 **Veiga E**, Sugawara E, Nikaido H, de Lorenzo V, Fernández LA. Export of autotransported proteins proceeds through an oligomeric ring shaped by C-terminal domains. *EMBO J* 2002; **21**: 2122-2131
27 **Martínez A**, González C, Kawaguchi F, Montoya R, Corvalán A, Madariaga J, Roa J, García A, Salgado F, Solar H, Palma M. *Helicobacter pylori*: *cagA* status and *vacA* genotyping in Chile. Detection of a s2/m1 strain. *Rev Med Chil* 2001; **129**: 1147-1153
28 **Van Doorn LJ**, Figueiredo C, Megraud F, Pena S, Midolo P, Magalhaes DM, Carneiro F, Vanderborght B, Pegado Mda GF, Sanna R, de Boer W, Schneeberger PM, Correa P, Ng EKW, Atherthon J, Blazer MJ, Quint WG. Geographic distribution of *vacA* allelic types of *Helicobacter pylori*. *Gastroenterology* 1999; **116**: 823-830
29 **Letley DP**, Atherthon JC. Natural diversity in the N-terminus of the mature vacuolating cytotoxin of *Helicobacter pylori* determines cytotoxin activity. *J Bacteriol* 2000; **182**: 3278-3280
30 **Kersulyte D**, Chalkauskas H, Berg DE. Emergence of recombinant strains of *Helicobacter pylori* during human infection. *Mol Microbiol* 1999; **31**: 31-43
31 **Marshall DG**, Dundon WG, Beesley SM, Smith CJ. *Helicobacter pylori*- a conundrum of genetic diversity. *Microbiology* 1998; **144**: 2925-2939
32 **Kidd M**, Lastovica AJ, Atherton JC, Louw JA. Heterogeneity in the *Helicobacter pylori vacA* and *cagA* genes: association with gastroduodenal disease in South Africa? *Gut* 1999; **45**: 499-502
33 **Mielke S**, Kirsch C, Agha-Amiri K, Gunther T, Lehn N, Malfertheiner P, Stolte M, Ehninger G, Bayerdorffer E. The *Helicobacter pylori vacA* s1, m1 genotype and *cagA* is associated with gastric carcinoma in Germany. *Int J Cancer* 2000; **87**: 322-327
34 **Covacci A**, Rappuoli R. *Helicobacter pylori*: molecular evolution of a bacterial quasi-species. *Curr Opin Micro*biol 1998; **1**: 96-102

Science Editor Guo SY **Language Editor** Elsevier HK

PO Box 2345, Beijing 100023, China
www.wjgnet.com
wjg@wjgnet.com

ELSEVIER

World J Gastroenterol 2005;11(40):6373-6380
World Journal of Gastroenterology ISSN 1007-9327
© 2005 The WJG Press and Elsevier Inc. All rights reserved.

• *BRIEF REPORTS* •

Effects of glucocorticoids on the growth and chemosensitivity of carcinoma cells are heterogeneous and require high concentration of functional glucocorticoid receptors

Yen-Shen Lu, Huang-Chun Lien, Pei-Yen Yeh, Kun-Huei Yeh, Min-Liang Kuo, Sung-Hsin Kuo, Ann-Lii Cheng

Yen-Shen Lu, Sung-Hsin Kuo, Min-Liang Kuo, Department of Oncology, National Taiwan University Hospital, Graduate Institute of Clinical Medicine, National Taiwan University College of Medicine, Taipei, Taiwan, China
Huang-Chun Lien, Departments of Pathology, National Taiwan University Hospital, Taipei, Taiwan, China
Pei-Yen Yeh, Department of Oncology, National Taiwan University Hospital, Taipei, Taiwan
Kun-Huei Yeh, Department of Oncology, and Departments of Internal Medicine, National Taiwan University Hospital, Departments of Internal Medicine and Medical Research, Far Eastern Memorial Hospital, Taipei, Taiwan, China
Ann-Lii Cheng, Department of Oncology, and Department of Internal Medicine, National Taiwan University Hospital, Taipei, Taiwan, China
Supported by grants from the National Science Council No.NSC 93-2314-B-002-006, Taiwan, and grants from National Taiwan University Hospital 91-N006
Correspondence to: Ann-Lii Cheng, Department of Oncology, and Department of Internal Medicine, National Taiwan University Hospital, No. 7, Chung-Shan South Road, Taipei 10016, Taiwan, China. andrew@ha.mc.ntu.edu.tw
Telephone: +886-2-23123456-7251 Fax: +886-2-23711174
Received: 2005-02-15 Accepted: 2005-04-18

Abstract

AIM: To determine how glucocorticoids (GCs) may affect the growth and chemosensitivity of common carcinoma cells.

METHODS: The effect of dexamethasone (DEX) on growth and chemosensitivity was assessed in 14 carcinoma cell lines. The function of GC receptors (GR) was assessed by MMTV reporter assay. Overexpression of GR was done by *in vitro* transfection and expression of a GR-expressing vector. Immunohistochemical stain of tissues and cells were done by PA1-511A, an anti-GR monoclonal antibody.

RESULTS: DEX inhibited cell growth of four (MCF-7, MCF-7/MXR1, MCF-7/TPT300, and HeLa), increased cisplatin cytotoxicity of one (SiHa), and decreased cisplatin cytotoxicity of two (H460 and Hep3B) cell lines. The GR content of the seven cell lines affected by DEX was significantly higher than those of the seven cell lines unaffected by DEX ($5.2\pm2.5\times10^4$ sites/cell *vs* $1.3\pm1.4\times10^4$ sites/cell, $P = 0.005$). Only two DEX-unresponsive cell lines (NPC-TW01 and NPC-TW04) contained high GR amounts in the range ($1.9\text{-}8.1\times10^4$ sites/cell) of the seven DEX-responsive cell lines. The GR function of NPC-TW01 and NPC-TW04, however, was found to be impaired. The importance of high cellular amount of GR in mediating DEX susceptibility of the cells was further exemplified by GR dose-dependent drug resistance to cisplatin of AGS, a cell line with low GR content and was unaffected by DEX before transfection of GR-expressing vector. Immunohistochemical studies of human cancer tissues showed that 5 of the 45 (11.1%) breast cancer and 43 of the 85 (50.6%) non-small cell lung cancer had high GR contents at the ranges of the GC-responsive carcinoma cell lines.

CONCLUSION: The growth and chemosensitivity of human carcinomas with high GR contents may be affected by GC. However, in light of the heterogeneous and even contradictive effects of GC on these cells, routine examination of GR contents of human carcinoma tissues may not be clinically useful until other markers that help predict the ultimate effect of GC on individual patients are identified.

© 2005 The WJG Press and Elsevier Inc. All rights reserved.

Key words: Glucocorticoids; Glucocorticoid receptor; Carcinoma; Cell growth; Chemosensitivity; Drug resistance

Lu YS, Lien HC, Yeh PY, Yeh KH, Kuo ML, Kuo SH, Cheng AL. Effects of glucocorticoids on the growth and chemosensitivity of carcinoma cells are heterogeneous and require high concentration of functional glucocorticoid receptors. *World J Gastroenterol* 2005; 11(40): 6373-6380
http://www.wjgnet.com/1007-9327/11/6373.asp

INTRODUCTION

Although glucocorticoids (GCs) are effective in inducing apoptosis via uncharacterized pathways in many hematological malignancies[1], they are generally thought to be ineffective in the treatment of non-hematological solid tumors. However, in the treatment of patients with solid tumors, co-administration of GC with anti-cancer drugs is a common clinical practice to prevent drug-induced allergic reaction or nausea/vomiting. Although GC receptors (GRs) are ubiquitous in cancer cells and have been linked to signal transduction pathways pertinent to their growth, defense, and apoptosis[2-4], little is known regarding the effects of GC on the growth and chemosensitivity of common human carcinomas. Several studies have shown diverse effects of GC on chemosensitivity in non-hematological neoplastic cells. GC has been reported to inhibit cell growth[5-7] and affect

the chemosensitivity[8-12] in some sarcoma and carcinoma cell lines. Further, the pretreatment with dexamethasone (DEX) may increase antitumor activity of carboplatin and gemcitabine in tumor xenografts due to increased intra cancer cell drug accumulation was also reported[13]. More comprehensive study is needed to clarify the role of GC on chemosensitivity of non-hematological neoplastic cells. In the present study, we examined the effects of DEX on the chemosensitivity of 14 carcinoma cell lines. We found that GC exerted a GR-related differential effect on the growth or chemosensitivity of half of carcinoma cells. Further, we have demonstrated that a substantial portion of human carcinomas do contain high GR contents and, therefore, the tumor response to chemotherapy may be affected by the co-administered GC.

MATERIALS AND METHODS

Cell culture and chemicals

SiHa, HeLa, Caski (human cervical carcinoma), H460 (human lung carcinoma), Hep3B, Huh 7 (human hepatocellular carcinoma), and MCF-7 (human breast cancer) were obtained from the American Type Culture Collection (Rockville, MD, USA). MCF-7/MXR1 and MCF-7/TPT300 cells were derived from MCF-7 cells by selection for growth in increasing the concentrations of mitoxantrone or topotecan, respectively. MCF-7/MXR1 cells were gifts from Dr. Kenneth Cowan (National Cancer Institute, USA). MCF-7/TPT300 cells were selected as previously described[14]. NPC-TW01 and NPC-TW04 (nasopharyngeal cancer) were obtained as previously described[15,16]. They were maintained in Dulbecco's modified Eagle's medium supplemented with 2 mmol/L glutamine, 100 U/mL penicillin, and 100 μg/mL streptomycin (Sigma Chemical Co., St. Louis, MO, USA), and 10% heat-inactivated fetal bovine serum (Life Technologies, Inc., Gaithersburg, MD, USA). AGS, N87, and SNU1 cells (human gastric cancer) were obtained from the American Type Culture Collection (Rockville, MD, USA) and maintained in RPMI 1640 (Sigma Chemical Co.) supplemented with 2 mmol/L glutamine, 10% fetal bovine serum, 100 U/mL penicillin, and 100 μg/mL streptomycin. Cisplatin was obtained from Pharmacia-Upjohn (Kalamazoo, MI, USA). DEX was purchased from Sigma Chemical Co., and [^{3}H] DEX (specific activity 35-50 Ci/mmol) was from Blossom Biotechnologies Inc. (Blossom, TX, USA).

Cytotoxicity assay

The *in vitro* growth inhibitory effects of the drugs in 14 carcinoma cell lines were determined by the MTT assay as previously described with slight modification[17]. Briefly, cells were plated in 96-well plates at 5×10^3 cells/well. After overnight incubation, various concentrations of drugs were added in triplicate samples to each culture. Cells were exposed to drugs continuously. After 3-4 d of culture, when cells in drug-free wells reached 90% confluency, 50 μL of 2.5 mg/mL MTT (Sigma Chemical Co.) in PBS was added to each well, followed by incubation for 4 h at 37 ℃. The formazan crystals were dissolved in DMSO. The absorbance was determined with an ELISA reader at 540 nm. Absorbance values were normalized to the values obtained for the vehicle-treated cells to determine the percentage of surviving cells. Each assay was performed in triplicate.

Measurement of GR content of cancer cell lines by [^{3}H]-labeled ligand binding assay

The GR content was measured by a whole-cell binding assay as previously described with minor modification[18]. Briefly, cells with 90% confluency were subcultured and allowed to grow overnight, and then trypsinized and suspended in a culture medium containing 10% fetal bovine serum (pH 7.2) to a density of $1\text{-}10\times10^6$ cells/mL. Cells were exposed to various concentrations of [^{3}H] DEX from 1 to 100 nmol/L in the presence or absence of 10 μmol/L unlabeled DEX, followed by incubation for 1 h at 37 °C, and harvested by centrifugation at 1 200 r/min for 1 min. Cells were then washed thrice in 3.0 mL of Hank's balanced salt solution and finally suspended in 1.6 mL of the same solution. A 0.2-mL aliquot of this suspension was used for the determination of cell number, and 1.0 mL was assayed for radioactivity by a liquid scintillation counter. The presence of at least 200-fold excess of unlabeled DEX effectively competed out all of the binding of [^{3}H] DEX to specific GR. The binding of [^{3}H] DEX to specific GR was represented as the difference in disintegrations per minute per cell between those samples incubated with [^{3}H] DEX alone and those with at least 200-fold excess of unlabeled DEX. Using the specific activity of [^{3}H] DEX, the number of receptors per cell was calculated, assuming that each receptor binds to one DEX molecule.

Examination of endogenous GR function by MMTV reporter assay

The human GR-expressing plasmid, pS-hGR, and the luciferase reporter plasmid, MMTV reporter plasmid were gifts from Prof. Chawnshang Chang (George H Whipple Laboratory for Cancer Research, University of Rochester, Rochester, NY, USA). The MMTV reporter plasmid contains the 1.4-kb MMTV LTR which encompasses the natural GRE sequences[19]. MCF-7, TW01, and TW02 cells were either transiently transfected with MMTV reporter plasmid cells, or co-transfected with MMTV reporter plasmid and pS-hGR (in a ratio of 5∶1) by Lipofectamine 2000 (Life Technologies, Inc. [GIBCO BRL], Gaithersburg, MD, USA) according to the manufacturer's protocol. Forty-eight hours after transfection, 1×10^5 transfected cells were stimulated with 1 μmol/L DEX and incubated for an additional 6 h. Reporter gene activity was determined with the Luciferase Reporter Assay System (Packard, the Netherlands).

Transfection of GR-expressing vector into cancer cell lines with low GR content

AGS cells were transfected with the pS-hGR by Lipofectamine 2000 (Life Technologies, Inc. [GIBCO BRL], Gaithersburg, MD, USA) according to the manufacturer's protocol. The stable clones were selected by 400 μg/mL hygromycin for 20 d. Single cell clones were obtained by limiting dilution of the hygromycin-resistant cells. The success of transfection was verified by Western blot analysis of GR and β-actin using rabbit polyclonal antibodies purchased from Santa Cruz Biotechnology (Santa Cruz, CA, USA) with signals

visualized by an enhanced chemiluminescence kit followed by exposure to X-ray films. The GR number in different clones of transfected cells was measured by [^{3}H]-labeled ligand binding assay.

GR immunohistochemistry study in cell lines and human cancer tissue samples

The GR immunocytochemistry study was performed in the 14 carcinoma cell lines. Cells with 90% confluency were subcultured and allowed to grow overnight, then were harvested and centrifuged at 400 r/min for 1 min. The cell pellets were fixed in 4% buffered formalin and embedded in paraffin.

Eighty-five human non-small cell lung cancer and 45 breast cancer tissue specimens which had been fixed in 4% buffered formalin and embedded in paraffin were used for immunohistochemistry study. Use of these tissue materials had followed the regulation of the research ethical committee of the National Taiwan University Hospital.

Five micrometers of paraffin-embedded cell block sections prepared on coated slides (DAKO Ltd.) were dewaxed and rehydrated, and endogenous peroxidase activity was blocked by incubation with 3% H_2O_2-methanol solution for 10 min. Heat retrieval was used for antigen retrieval. Endogenous biotin was blocked by normal goat serum (DAKO Ltd). Slides were then incubated with anti-GR antibody (PA1-510A, 511A and 512, Affinity BioReagents, Golden, CO, USA). The DAKO Envision system (Copenhagen, Denmark) was used to further avoid endogenous biotin contamination. Sites of bound peroxidase were visualized using liquid 3',5'-diaminobenzidine (DAKO, Glostrup, Denmark) and counterstained with hematoxylin. Under this staining condition, only the carcinoma cells with high (>10 000 sites/cell) GR content were positively stained. Tumor tissue samples were considered to be having high GR expression, when more than 20% of tumor cells were positively stained.

Statistical analysis

Independent *t* test was used to assess the correlation of GR content with the effect of DEX.

RESULTS

DEX affects either growth or chemosensitivity in 7 of the 14 carcinoma cell lines

DEX (0.01-1.0 μmol/L) inhibited cell growth in MCF-7, MCF-7/MXR1, MCF-7/TPT300, and HeLa cells (Figure 1A). However, DEX alone, up to 20 μmol/L, had no effect on the growth in the other 10 cell lines, including AGS, N87, SNU1, SiHa, Caski, Hep3B, Huh 7, TW01, TW04, and H460 (representative data shown in Figure 1A). The latter 10 carcinoma cell lines were further tested for the effect of GC on the chemosensitivity of carcinoma cells toward cisplatin. Pretreatment of SiHa cells with 1 μmol/L DEX for 3 h decreased the IC_{50} of cisplatin from 18.6±1.9 to 9.7±2.0 mmol/L (Figure 1B). This cytotoxicity-enhancing effect could be observed even when the concentration of DEX was as low as 1 nmol/L (data not shown). In contrast, DEX slightly increased cisplatin resistance in H460 and Hep3B cells (Figures 1C and D). DEX had no effect on the chemosensitivity of AGS, N87, SNU1, Huh-7, Caski, NPC-TW01, and NPC-TW04 cells (representative data shown in Figure 1E).

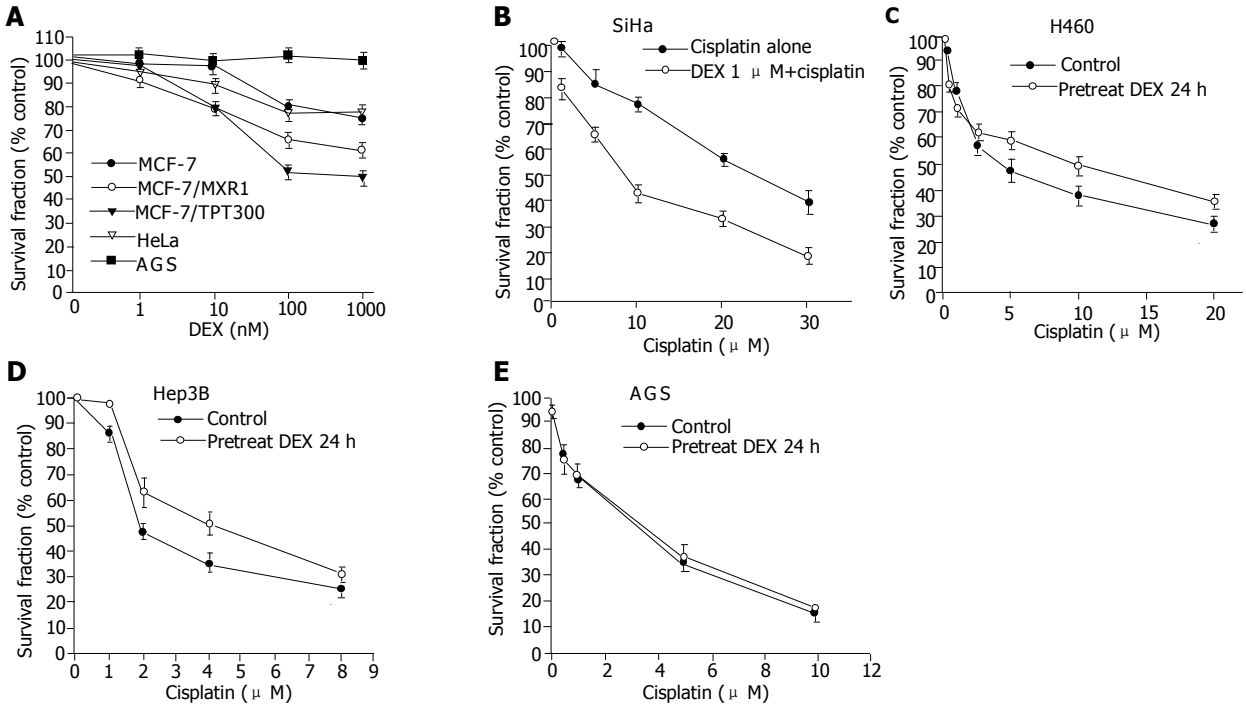


Figure 1 Effect of DEX on the growth and chemosensitivity in carcinoma cell lines. Cell numbers were measured by MTT assay and were plotted as a percentage of the control (cells not exposed to drugs); **A:** Growth of MCF-7, MCF-7/MXR1, MCF-7/TPT300, and HeLa cells were suppressed by DEX. Data of AGS represent the other 10 cell lines, growth of which was not affected by DEX; **B:** SiHa cells pretreated with DEX for 3 h were more sensitive to cisplatin; **C** and **D:** Pretreatment with DEX 1 μmol/L for 24 h diminished cisplatin cytotoxicity in H460 cells and Hep3B cells; **E:** Data of AGS represent the seven cell lines (AGS, N87, Caski, Hut 7, SNU1, NPC-TW01, and NPC-TW04), of which cytotoxicity of cisplatin was not affected by DEX. All values represent mean±SD of six separate wells.

Effects of GC correlate well with GR content of the cells

The GR contents of these 14 cell lines are listed in Table 1. The GR contents of the seven cell lines affected by DEX were significantly higher than those of the other seven cell lines unaffected by DEX ($5.2\pm2.5\times10^4$ sites/cell *vs* $1.3\pm1.4\times10^4$ sites/cell, $P = 0.005$) suggesting GR is one of the pivotal mediators of the effect of DEX on carcinoma cell. The GR content of human lymphocytes, the internal control for these experiments, was tested parallel and was within the reported range (2 500-5 400 sites/cell)[20].

GC-unresponsive GR-rich carcinoma cells have dysfunctional GR

As shown in Table 1, DEX had no effect on NPC-TW01 and NPC-TW04, two cell lines with GR content as high as that of the seven GC-responsive cell lines. The function of the GR in these two cell lines was further examined. As shown in Figure 2, MCF-7 cells contained endogenous DEX-responsive GR, while NPC-TW01 and NPC-TW04 cells did not. Further, when NPC-TW01 and NPC-TW04 cells were co-transfected with MMTV reporter plasmid and pS-GR, which contains functional human GR gene, the response to DEX were restored (Figure 2). These data strongly suggested that the function of endogenous GR of NPC-TW01 and NPC-TW04 cells was probably impaired.

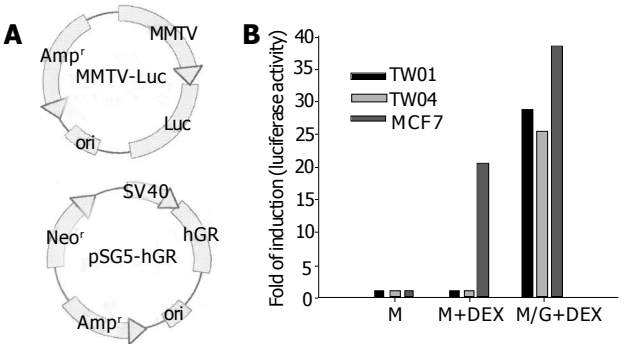


Figure 2 Functional assay of the GR in NPC-TW01 and NPC-TW04 cells. NPC-TW01, NPC-TW04, and MCF-7 cells were transiently transfected with MMTV reporter plasmid (lanes M and M+DEX) or co-transfected with MMTV reporter plasmid and pS-hGR (lane M/G+DEX). The cells were then treated with 1 μmol/L DEX for 6 h (lanes M+DEX and M/G+DEX). Then the luciferase activity was assayed and represented in terms of folds of the induction activity of the control (lane M). All values represent mean±SD of three experiments(**A**,**B**).

Expression of GR in GR low-expressing cells increases their responsiveness to DEX

To further examine whether the GR content is pivotal in mediating the susceptibility to DEX in carcinoma cell, pS-hGR was transfected into AGS cells, a GR low-expressing cell line. The GR content in empty vector-transfected AGS cells, and pooled stably pS-hGR-transfected AGS cells were 5.2×10^3 and 1.42×10^4/cell, respectively. The GR contents of clone 1, 2, and 3 were 1.54×10^4, 1.32×10^4, and 5.8×10^3/cell, respectively. Treatment of DEX alone had no effect on cell growth in these cells (data not shown). However, as shown in Figure 3, pS-hGR transfected AGS cells that expressed high GR content became susceptible to the effect of DEX with increasing drug resistance toward cisplatin. The cells that express higher GR content (pooled cells, clones 1 and 2) were more resistant toward cisplatin, while cells with lower GR content (empty vector and clone 3) remained non-susceptible to DEX treatment.

Tumor tissues of common human carcinomas may express high level of GR

GR expression was examined by immunohistochemical stain in the carcinoma cell lines (Figure 4A), and tumor tissue samples of human breast cancer and human non-small cell lung cancer (Figure 4B). Positive GR immunoreactivity (representing high GR content) was observed in 5 of the 45 tumor samples (11.1%) of breast cancer and 43 of the 85 tumor samples (51%) of non-small cell lung cancer patients.

DISCUSSION

This study has demonstrated that GC affects either growth or chemosensitivity in a substantial portion of carcinoma cells. Since GC is commonly co-administered with anticancer drugs such as taxanes and platinums, how GC alters the effect of chemotherapy may have to be taken into consideration in clinical practice. As shown in this study, it may not be difficult to identify those carcinoma patients of whom tumor response is going to be affected by GC, since only cells with high GR content are affected. However, how GC will actually

Table 1 Correlation of GR content with the effect of DEX in carcinoma cells

Cells	Origin	Effect of DEX	GR (sites/cell)
MCF7	Breast	Growth inhibition	6.37×10^4
MCF7/TPT300	Breast	Growth inhibition	7.43×10^4
MCF7/MXR1	Breast	Growth inhibition	5.9×10^4
HeLa	Uterine cervix	Growth inhibition	1.94×10^4
SiHa	Uterine cervix	Increased sensitivity toward cisplatin	8.1×10^4
H460	Lung	Increased resistance toward cisplatin	2.1×10^4
Hep3B	Liver	Increased resistance toward cisplatin	4.3×10^4
NPC-TW01	Nasopharyngeal	Noeffect	4.2×10^4
NPC-TW04	Nasopharyngeal	Noeffect	2.0×10^4
Caski	Uterine cervix	Noeffect	7.2×10^3
Huh7	Liver	Noeffect	7.9×10^3
AGS	Stomach	Noeffect	5.7×10^3
N87	Stomach	Noeffect	5.0×10^3
SNU1	Stomach	Noeffect	1.97×10^3

DEX: dexamethasone; GR: glucocorticoid receptor.

affect the growth of tumors of these cancer patients remains uncertain since the effects of GC, as disclosed in this study, are extremely diverse and even contradictory.

A direct correlation between GR content of the cells and the magnitude of physiologic response to GC has been reported in hematologic malignancies[21]. The sensitivity of many lymphoid cell lines to GC-induced growth arrest and apoptosis is directly proportional to intracellular receptor content[22-24]. Several studies also identified a correlation between reduced GR expression and a poor treatment response as well as poor prognosis in patients with acute lymphocytic leukemia, suggesting that reduced GR expression could lead to clinical GC resistance[22,25-27]. Our study demonstrated that the susceptibility to the effect of DEX on cell growth or chemosensitivity in carcinoma cells also correlate well with the level of GR content. However, the GR contents of the GC-responsive carcinoma cells are almost 10 times higher than that of lymphoid cells[27-29], suggesting that the cellular contexts or the signal transduction pathways for the interaction of GC and GR are probably different between epithelial and lymphoid malignant cells.

In this study, the only two cell lines, NPC-TW01 and NPC-TW04, which have relatively high GR content but not susceptible to the growth regulatory effect of DEX, were found to have non-functional endogenous GR. Previous studies on both human and mouse cell lines have shown that somatic mutation in the GR gene is the principal mechanism for *in vitro* acquisition of GC resistance[28-30]. However, we failed to detect GR gene mutations in NPC-TW01 and NPC-TW04 (data not shown). Beside the GR number and GR gene mutations, the phosphorylation status of GR has also been reported to be correlated with GR resistance[31]. The expression level of GR co-regulators was also important to normal GR function[32]. Therefore, there should be other mechanisms associated with the malfunction of GR in these two cell lines.

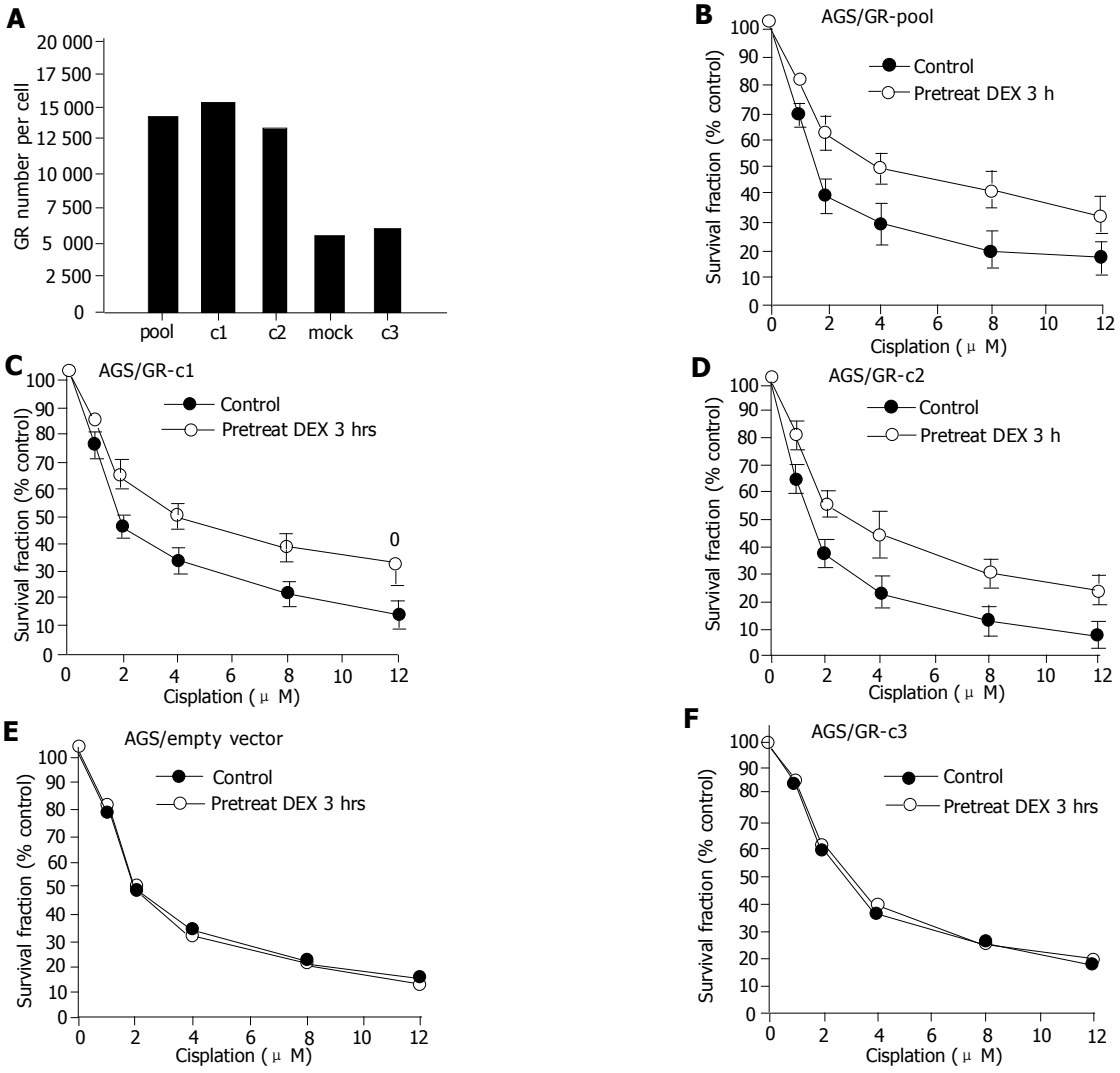


Figure 3 Increased drug resistance to cisplatin in pS-hGR-transfected AGS. AGS cells were transfected with pS-hGR and MTT assay were performed. **A:** GR number measured by [^{3}H]-labeled ligand binding assay. Pool: AGS/GR-pool; AGS cells transfected with pS-hGR, pooled cells. c1: AGS/GR-c1; AGS cells transfected with pS-hGR, single cell cloned, clone 1. c2: AGS/GR-c2; AGS cells transfected with pS-hGR, single cell cloned, clone 2. Mock: AGS/empty vector; AGS cells transfected with empty vector. c3: AGS/GR-c3; AGS cells transfected with pS-hGR, single cell cloned, clone 3; **B-D:** Pretreatment with DEX 1 μmol/L for 3 h diminished cisplatin cytotoxicity in AGS/GR-pool, AGS/GR-c1, and AGS/GR-c2 cells; **E** and **F:** Pretreatment with DEX 1 μmol/L for 3 h had no effect on the cisplatin cytotoxicity in AGS/empty vector cells and AGS/GR-c3. All values represent mean±SD of six separate wells.

Activated GR may activate or suppress gene expression through interaction with respective positive or negative *cis*-acting regulatory elements in the promoters regions[33,34]. Activated GR can also regulate the expression of GC responsive genes indirectly through protein-protein interactions with other transcription factors such as NF-κB and AP-1[35-37]. Inactivation of NF-κB or AP-1 has been shown to alter the vulnerability of cancer cells to several cytotoxic agents[38,39]. Our preliminary data have indicated that suppression of NF-κB by GC is one of the major mechanisms of increasing cisplatin sensitivity in SiHa cell[40]. Some studies have demonstrated variable potential other mechanisms of GC related growth arrest in non-hematologic cancer cells that included upregulation of p21Cip1[7], p57 Kip2[8], and inhibition of ERK/MAPK kinase pathway[9], and mechanisms of GC related chemosensitivity alteration include induction of GC-inducible protein kinase-1 (SGK-1) and mitogen-activated protein kinase phosphatase-1 (MKP-1)[14], and modulation of bcl-x expression[11]. However, it remains difficult to explain the diverse and even contradictive effect of GC on GR-rich carcinoma cells. The possibilities that the specific presence of certain co-regulators of GR in different carcinoma cells may dictate the ultimate effect

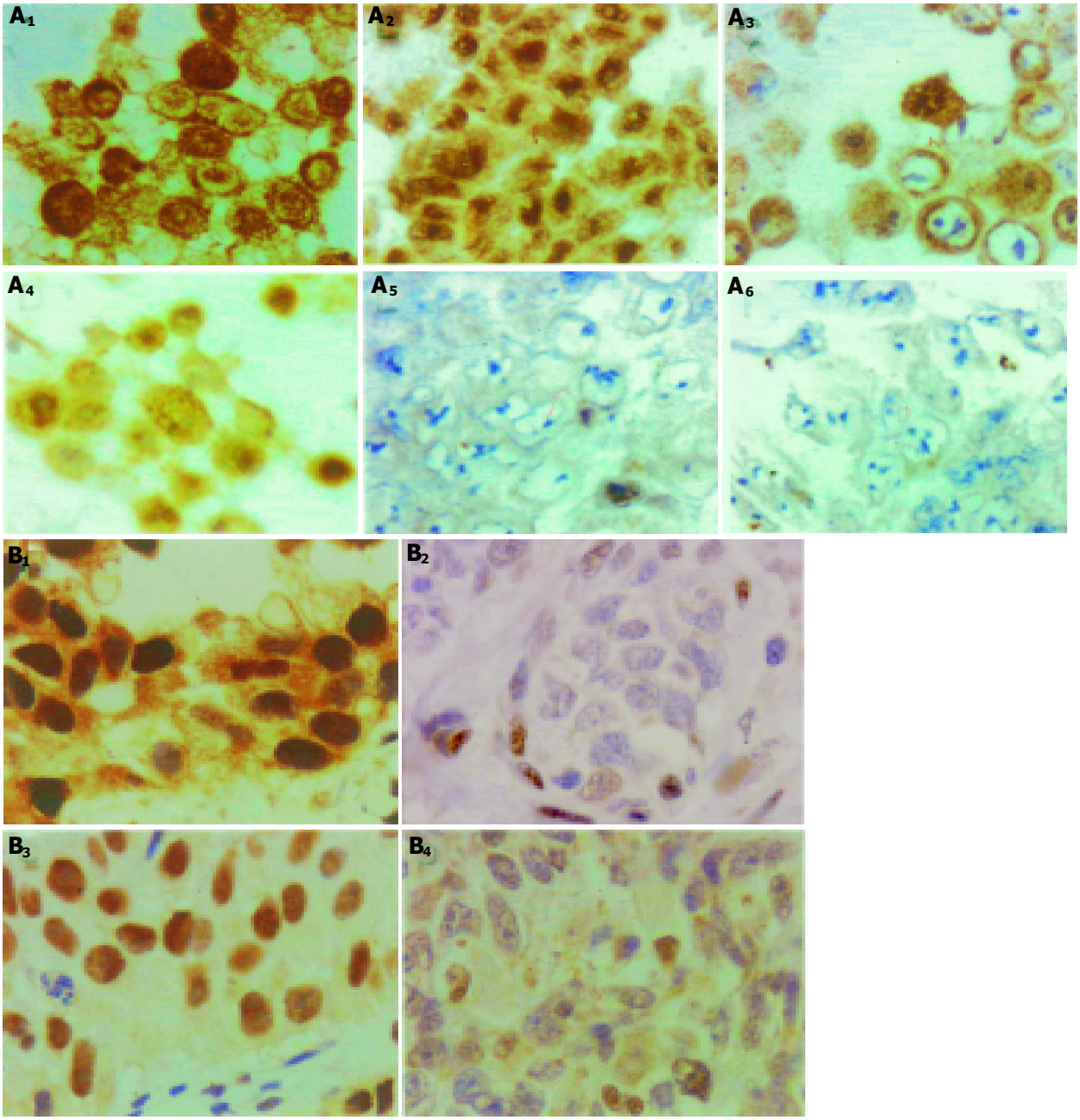


Figure 4 A: Immunocytochemical stain for GR expression in representing carcinoma cell lines. (A_1) and (A_2): SiHa cells, which had GR content about 8.1×10^4/cell according to ligand binding assay; (A_3) and (A_4): HeLa cells, with GR content about 1.97×10^4/cell; (A_5) and (A_6): N87 cells, with GR content about 5.0×10^3/cell. (A_2), (A_4), and (A_5): cells treated with DEX for 3 h before harvest. In (A_1) and (A_3), the GR immunoreactivity localized in cytoplasm. After DEX treatment, the immunoreactive GR translocalized to nuclei (A_2) and (A_4). The low GR content cancer cells N87 showed negligible immunoreactivity. **B:** Immunohistochemical stain for GR expression in human carcinoma tumor tissue samples. Non-small cell lung cancer tumor samples, with high GR expression (B_1), and low GR expression (B_2). Breast cancer tumor samples, with high GR expression (B_3), and low GR expression (B_4).

of GC needs to be clarified.

The [^{3}H] labeled DEX ligand binding assay has been the standard method to measure the GR content in cell lines and *in vivo* human leukemia samples. The GR amount measured by [^{3}H] labeled DEX ligand binding assay is expressed as GR number per cell. However, this method is hard to apply to solid tumor tissue samples, since it is difficult to quantify the cell number in tissue samples. There were other methods to detect the expression of GR in the *in vivo* solid tumor samples, including cytosol DCC-competitive (dextran-coated charcoal) protein binding assay[41,42], and RT-PCR[43]. These methods all use tissue homogenizer and the results were normalized by the total protein or RNA amount. Therefore, the result was the average of the GR content of the whole tissue sample, which includes the cancer cells as well as the stroma cells and adjacent normal tissues component. Besides, the cytosol DCC-competitive protein binding assay required fresh frozen tissue which limited its applicability. In this study, we have shown an ideal staining condition by which only cancer cells with high GR content were stained positively (Figure 4). We have also demonstrated that a substantial portion of common human carcinoma do express high level of GR, and therefore are potentially susceptible to the growth and chemosensitivity-regulatory effect of GC.

Clinically, the serum concentration of DEX was found to be around 0.12 μmol/L, lasting for 1-3 h, after a single oral dose of 7.5 mg of DEX[44]. However, the serum concentration of DEX may reach 2 μmol/L after a single intravenous infusion of 80-100 mg of DEX[45]. Since the administration of relatively high-dose DEX, at the range of 10-50 mg/d, or its equivalents, has been widely used for the prevention of cisplatin-induced nausea/vomiting and taxanes-induced allergic reactions, the possible effect of GC on the chemosensitivity of some cancer patients needs to be seriously considered.

In summary, the results of this study suggest that GC exerts a GR-dependent effect on the growth or chemosensitivity in a substantial portion of carcinoma cells. The clinical relevance and the cellular mechanisms that dictate the disparate effects of GC need to be further clarified.

REFERENCES

1 **Frankfurt O,** Rosen ST. Mechanisms of glucocorticoid-induced apoptosis in hematologic malignancies: updates. *Curr Opin Oncol* 2004; **16:** 553-563
2 **Wright AP,** Zilliacus J, McEwan IJ, Dahlman-Wright K, Almlof T, Carlstedt-Duke J, Gustafsson JA. Structure and function of the glucocorticoid receptor. *J Steroid Biochem Mol Biol* 1993; **47:** 11-19
3 **Schwartzman RA**, Cidlowski JA. Glucocorticoid-induced apoptosis of lymphoid cells. *Int Arch Allergy Immunol* 1994; **105:** 347-354
4 **McEwan IJ,** Wright AP, Gustafsson JA. Mechanism of gene expression by the glucocorticoid receptor: role of protein-protein interactions. *Bioessays* 1997; **19:** 153-160
5 **Rogatsky I,** Trowbridge JM, Garabedian MJ. Glucocorticoid receptor-mediated cell cycle arrest is achieved through distinct cell-specific transcriptional regulatory mechanisms. *Mol Cell Biol* 1997; **17:** 3181-3193
6 **Samuelsson MK,** Pazirandeh A, Davani B, Okret S. p57Kip2, a glucocorticoid-induced inhibitor of cell cycle progression in HeLa cells. *Mol Endocrinol* 1999; **13:** 1811-1822
7 **Greenberg AK,** Hu J, Basu S, Hay J, Reibman J, Yie TA, Tchou-Wong KM, Rom WN, Lee TC. Glucocorticoids inhibit lung cancer cell growth through both the extracellular signal-related kinase pathway and cell cycle regulators. *Am J Res Cell & Mol Biol* 2002; **27:** 320-328
8 **Wolff JE,** Denecke J, Jurgens H. Dexamethasone induces partial resistance to cisplatinum in C6 glioma cells. *AntiCancer Res* 1996; **16:** 805-809
9 **Chang TC,** Hung MW, Jiang SY, Chu JT, Chu LL, Tsai LC. Dexamethasone suppresses apoptosis in a human gastric cancer cell line through modulation of bcl-x gene expression *FEBS Lett* 1997; **415:** 11-15
10 **Naumann U,** Durka S, Weller M. Dexamethasone-mediated protection from drug cytotoxicity: association with p21 WAF1/CIP1 protein accumulation? *Oncogene* 1998; **17:** 1567-1575
11 **Benckhuijsen C,** Osman AM, Hillebrand MJ, Smets LA. Glucocorticoid effect on melphalan cytotoxicity, cell-cycle position, cell size, and [3H]uridine incorporation in one of three human melanoma cell lines. *Cancer Res* 1987; **47:** 4814-4820
12 **Wu W,** Chaudhuri S, Brickley DR, Pang D, Karrison T, Conzen SD. Microarray analysis reveals glucocorticoid-regulated survival genes that are associated with inhibition of apoptosis in breast epithelial cells. *Cancer Res* 2004; **64:** 1757-1764
13 **Wang H,** Li M, Rinehart JJ, Zhang R. Pretreatment with dexamethasone increases antitumor activity of carboplatin and gemcitabine in mice bearing human cancer xenografts: in vivo activity, pharmacokinetics, and clinical implications for cancer chemotherapy. *Clin Cancer Res* 2004; **10:** 1633-1644
14 **Yang CH,** Schneider E, Kuo ML, Volk EL, Rocchi E, Chen YC. BCRP/MXR/ABCP expression in topotecan-resistant human breast carcinoma cells. *Biochem. Pharmacol* 2000; **60:** 831-837
15 **Lin CT,** Wong CI, Chan WY, Tzung KW, Ho JK, Hsu MM, Chuang SM. Establishment and characterization of two nasopharyngeal carcinoma cell lines. *Lab Investig* 1990; **62:** 713-724
16 **Lin CT,** Chan WY, Chen W, Huang HM, Wu HC, Hsu MM, Chuang SM, Wang CC. Characterization of seven newly established nasopharyngeal carcinoma cell lines. *Lab Invest* 1993; **68:** 716-727
17 **Carmichael J,** DeGraff WG, Gazdar AF, Minna JD, Mitchell JB. Evaluation of a tetrazolium-based semiautomated colorimetric assay: assessment of chemosensitivity testing. *Cancer Res* 1987; **47:** 936-942
18 **Harmon JM,** Thompson EB. Isolation and characterization of dexamethasone-resistant mutants from human lymphoid cell line CEM-C7. *Mol Cell Biol* 1981; **1:** 512-521
19 **Scheidereit C,** Geisse S, Westphal HM, Beato M. The glucocorticoid receptor binds to defined nucleotide sequences near the promoter of mouse mammary tumour virus. *Nature* 1983; **304:** 749-752
20 **Lippman ME,** Yarbro GK, Leventhal BG. Clinical implications of glucocorticoid receptors in human leukemia. *Cancer Res* 1978; **38:** 4251-4256
21 **Vanderbilt JN,** Miesfeld R, Maler BA, Yamamoto KR. Intracellular receptor concentration limits glucocorticoid-dependent enhancer activity. *Mol Endocrinol* 1987; **1:** 68-74
22 **Gehring U,** Mugele K, Ulrich J. Cellular receptor levels and glucocorticoid responsiveness of lymphoma cells. *Mol Cell Endocrinol* 1984; **36:** 107-113
23 **Bourgeois S,** Newby RF. Diploid and haploid states of the glucocorticoid receptor gene of mouse lymphoid cell lines. *Cell* 1977; **11:** 423-430
24 **Chapman MS,** Askew DJ, Kuscuoglu U, Miesfeld RL. Transcriptional control of steroid-regulated apoptosis in murine thymoma cells. *Mol Endocrinol* 1996; **10:** 967-978
25 **Bloomfield CD,** Smith KA, Peterson BA, Munck A. Glucocorticoid receptors in adult acute lymphoblastic leukemia. *Cancer Res* 1981; **41:** 4857-4860
26 **Pui CH,** Dahl GV, Rivera G, Murphy SB, Costlow ME. The relationship of blast cell glucocorticoid receptor levels to response to single-agent steroid trial and remission response in children with acute lymphoblastic leukemia. *Leuk Res* 1984; **8:** 579-585

27 **Pui CH,** Costlow ME. Sequential studies of lymphoblast glucocorticoid receptor levels at diagnosis and relapse in childhood leukemia: an update. *Leuk Res* 1986; **10:** 227-229
28 **Wells RJ,** Mascaro K, Young PC, Cleary RE, Bachner RL. Glucocorticoid receptors in the lymphoblasts of patients with glucocorticoid-resistant childhood acute lymphoblastic leukemia. *Am J Pediatr Hematol Oncol* 1981; **3:** 259-264
29 **Powers JH,** Hillmann AG, Tang DC, Harmon JM. Cloning and expression of mutant glucocorticoid receptors from glucocorticoid-sensitive and glucocorticoid-resistant human leukemic cells. *Cancer Res* 1993; **53:** 4059–4065
30 **Ashraf J,** Thompson EB. Identification of the activation-labile gene: a single point mutation in the human glucocorticoid receptor presents as two distinct receptor phenotypes. *Mol Endocrinol* 1993; **7:** 631–642
31 **Buttgereit F,** Saag KG, Cutolo M, da Silva JA, Bijlsma JW. The molecular basis for the effectiveness, toxicity, and resistance to glucocorticoids: focus on the treatment of rheumatoid arthritis. *Scand J Rheumatol* 2005; **34**: 14-21
32 **McKenna NJ,** Lanz RB, O'malley BW. Nuclear receptor coregulators: cellular and molecular biology. *Endocr Reviews* 1999; **20:** 321-344
33 **Beato M,** Chavez S, Truss M. Transcriptional regulation by steroid hormones. *Steroids* 1996; **61:** 240–251
34 **Reichardt HM,** Schutz G. Glucocorticoid signaling–multiple variations of a common theme. *Mol Cell Endocrinol* 1998; **146:** 1-6
35 **McEwan IJ,** Wright APH, Gustafsson JÅ. Mechanism of gene expression by the glucocorticoid receptor: role of protein-protein interactions. *Bioessays* 1997; **19:** 153-160
36 **Dumont A,** Hehner SP, Schmitz ML, Gustafsson JÅ, Liden J, Okret S, van der Saag PT, Wissink S, van der Burg B, Herrlich P, Haegeman G, De Bosscher K, Fiers W. Cross-talk between steroids and NF-k: what language? *Trends Biochem. Sci* 1998; **23:** 233-235
37 **Gottlicher M,** Heck S, Herrlich P. Transcriptional cross-talk, the second mode of steroid hormone receptor action. *J Mol Med* 1998; **76:** 480-489
38 **Van Antwerp DJ,** Martin SJ, Kafri T, Green DR, Verma IM. Suppression of TNF-alpha-induced apoptosis by NF-kappa B. *Science* 1996; **274:** 787-789
39 **Wang CY,** Mayo MW, Baldwin AS. TNF-alpha and cancer therapy-induced apoptosis: potentiation by inhibition of NF-κB. *Science* 1996; **274:** 784-787
40 **Chuang SE,** Yeh PY, Lu YS, Lai GM, Liao CM, Gao M, Cheng AL. Basal levels and patterns of anticancer drug-induced activation of nuclear factor-kappaB (NF-kappaB), and its attenuation by tamoxifen, dexamethasone, and curcumin in carcinoma cells. *Biochem Pharmacol* 2002; **63:** 1709-1716
41 **Allegra JC,** Lippman ME, Thompson EB, Simon R, Barlock A, Green L, Huff KK, Do HM, Aitken SC. Distribution, frequency, and quantitative analysis of estrogen, progesterone, androgen, and glucocorticoid receptors in human breast cancer. *Cancer Res* 1979; **39:** 1447-1454
42 **Liu SH,** Otal-Brun M, Webb TE. Glucocorticoid receptors in human tumors. *Cancer Lett* 1980; **10:** 269-275
43 **Smith RA,** Lea RA, Curran JE, Weinstein SR, Griffiths LR Expression of glucocorticoid and progesterone nuclear receptor genes in archival breast cancer tissue. *Breast Cancer Res* 2003; **5:** R9-12
44 **Weijtens O,** Schoemaker RC, Cohen AF, Romijn FP, Lentjes EG, van Rooij J, van Meurs JC. Dexamethasone concentration in vitreous and serum after oral administration. *Am J Ophthalmol* 1998; **125:** 673-679
45 **Brady ME,** Sartiano GP, Rosenblum SL, Zaglama NE, Bauguess CT. The pharmacokinetics of single high doses of dexamethasone in cancer patients. *Eur J Clin Pharmacol* 1987; **32:** 593-596

Science Editor Guo SY **Language Editor** Elsevier HK

PO Box 2345, Beijing 100023, China
www.wjgnet.com
wjg@wjgnet.com

ELSEVIER

World J Gastroenterol 2005;11(40):6381-6384
World Journal of Gastroenterology ISSN 1007-9327
© 2005 The WJG Press and Elsevier Inc. All rights reserved.

• *BRIEF REPORTS* •

Apoptosis induced by nucleosides in the human hepatoma HepG2

Suh-Ching Yang, Che-Lin Chiu, Chi-Chang Huang, Jiun-Rong Chen

Suh-Ching Yang, Che-Lin Chiu, Chi-Chang Huang, Jiun-Rong Chen, School of Nutrition and Health Sciences, College of Public Health and Nutrition, Taipei Medical University, Taipei, Taiwan, China
Co-first-authors: Suh-Ching Yang and Che-Lin Chiu
Co-correspondents: Suh-Ching Yang
Correspondence to: Dr. Jiun-Rong Chen, School of Nutrition and Health Sciences, College of Public Health and Nutrition, Taipei Medical University, 250 Wu-Hsing Street, Taipei 110, Taiwan, China. sokei@tmu.edu.tw
Telephone: +886-2-2736-1661-6551-121
Received: 2005-03-14 Accepted: 2005-04-02

Abstract

AIM: To investigate the apoptotic effects of nucleosides on the human hepatoma HepG2.

METHODS: The nucleosides included inosine (I), cytidine (C), uridine (U), thymidine (T), adenosine (A), and guanosine (G). Cells were incubated by the mediums with or without nucleosides at 37 ℃ in a 50 mL/L CO_2 humidified atmosphere.

RESULTS: It was found that the cell viabilities were significantly decreased, when cells were treated with 30 mmol/L I, 30 mmol/L C, 30 mmol/L U, 30 mmol/L T, 0.5 mmol/L A, and 0.5 mmol/L G after 12 h incubation ($P<0.05$). About the apoptotic phenomenon, the cell percentages of sub-G_1 cells were significantly increased in the mediums containing nucleosides such as C, U, T, A, and G ($P<0.05$). Furthermore, the caspase-3 activity was increased, when the cells were incubated with T ($P<0.05$). The protein expressions of p53 and p21 showed no difference in each group. To investigate the mechanism of apoptosis induced by nucleosides, it was found that the contents of soluble Fas ligand contents were increased in HepG2 cells following I, U, T, and A treatment ($P<0.05$). But, TNF-α and cytochrome *c* were undetectable.

CONCLUSION: Thymidine may induce the apoptosis in HepG2, but the effective dosages and reactive time must be investigated in the future study. However, the apoptosis-inducing abilities of other nucleosides were still unclear in this study.

© 2005 The WJG Press and Elsevier Inc. All rights reserved.

Key words: Apoptosis; Nucleoside; HepG2

Yang SC, Chiu CL, Huang CC, Chen JR. Apoptosis induced by nucleosides in the human hepatoma HepG2. *World J Gastroenterol* 2005; 11(40):6381-6384

http://www.wjgnet.com/1007-9327/11/6381.asp

INTRODUCTION

According to the statistics tabulated by the Department of Health, Taiwan in 2003, cancer is the first leading cause of death in Taiwan. Among the various cancers, the morbidity of hepatoma is the highest in Taiwanese. The great medical expenses covering not only drugs but also in providing nutritional supplements for treating or preventing the liver diseases and hepatoma are the heavy burdens of Taiwanese. Food-derived inducers of apoptosis may be significant as exogenous anti-tumor substances in the control of malignant cell proliferation despite little understanding about their molecular and cellular basis of action. Many healthy foods that are rich in nucleosides have anti-carcinogenic effects, such as the hot water extract of chlorella[1–3]. Current evidence suggests that nucleosides induce cell death by apoptosis[4-6]. Nucleosides that act as signaling molecules are well documented and are mostly released from cells, when cells are under stress, such as anoxia or injury[7-9]. In addition, it has been presumed that a vast majority of tumor promoters are potent inhibitors of apoptosis, and cancer cells did not produce apoptosis-inducing nucleosides[10]. However, little is known about the signaling or the biochemical mechanisms of nucleosides-mediated cell death.

Thus, the purpose of this study was to investigate the apoptosis-inducing ability and the molecular mechanisms of nucleosides in human hepatoma HepG2.

MATERIALS AND METHODS

Cell culture and treatment

The human hepatoblastoma cell line, HepG2 (HB-8065), was obtained from the American Type Culture Collection. Cells were cultured in MEM supplemented with 5% FBS. Cells were grown in a humidified incubator under 50 mL/L CO_2 at 37 ℃ and medium was changed every 2 d. When the cell status was stable after several passages, the experiments started. Cells were seeded in 100-mm dishes at a density of 1×10^6 cells/well. They were incubated with defined concentrations of nucleosides for 12 h. The cells and media were collected and analyzed after incubation. The nucleosides included inosine (I), cytidine (C), uridine (U), thymidine (T), adenosine (A), and guanosine(G).

Cell viability assay

The cell viability was determined using CellTiter^{R}96 Aqueous One Solution Cell Proliferation Assay (Promega, Madison,

WI, USA). The assay is an MTT-based method, which measures the ability of metabolically active cells to convert tetrazolium salt into a cleavage product and its absorbance is recorded at 490 nm[11].

Flow cytometric analysis

Cells were harvested by 0.25% trypsin release, washed twice with PBS, permeated with 75% ethanol, treated with 3 μL RNase A and finally stained with 1 mL propidium iodide (40 μg/mL final concentration). Distribution of cell-cycle phases with different DNA contents was determined using FACScan flow cytometer (Becton Dickenson, San Jose, CA, USA). Cells that were less intensely stained than G_1 cells (sub-G_1 cells) in flow cytometric histograms were considered as apoptotic cells.

Caspase-3 activity and soluble Fas ligand content

After treatment for 12 h, cells were collected and lysed with 50 μL cell lysis buffer. Then, the cell lysate was centrifuged and the supernatants were retained to determine the caspase-3 activity with Caspase-3/CPP32 Colorimetric Kit (Biosource International, Camarillo, CA, USA). Furthermore, the soluble Fas ligand contents (sFas-L) in the medium were detected with Human sFas Ligand ELISA kit (Biosource International).

Protein extraction and Western blot assay

Cell proteins were extracted from cells in a buffer containing 50 mmol/L Tris-HCl, pH 7.5, 150 mmol/L NaCl, 1% Nonidet P-40, 0.5% sodium deoxycholate, 4% protease inhibitors, and 1% phosphatase inhibitors. The cell lysate was rotated at 4 ℃ for 30 min, centrifuged at 10 000 r/min for 10 min and the precipitates were discarded. Protein contents were determined by the DC Bio-Rad protein assay kit using bovine serum albumin as a standard. The cell proteins were added to an equal volume of 2× sample buffer containing 0.125 mol/L Trizma base, 4% sodium dodecyl sulfate (SDS), 20% glycerol and 10% 2-mercaptoethanol and boiled during 3 min at 100 ℃. Then, proteins (100 μg) were separated by 12% SDS-polyacrylamide gels and transferred onto polyvinylidene difluoride membranes (Schleicher & Schuell BioScience, Keene, NH, USA), which was then incubated with primary antibody, such as p53 mouse monoclonal IgG_2a (Santa Cruz Biotechnology, Santa Cruz, CA, USA) and F-5 mouse monoclonal IgG_2b (Santa Cruz Biotechnology). HRP-conjugated goat anti-mouse IgG (Santa Cruz Biotechnology) was used as a secondary antibody. The immunoreactive bands were washed four times in PBS-T (PBS in 0.2% Tween 20), dried and exposed to Kodak film. The relative intensity of the bands was analyzed by densitometry.

Statistical analysis

All data are expressed as the mean±SD. One-way analysis of variance and Fisher's least significant difference test were used to compare the differences of means using the SAS software (v.6.12, SAS Institute, Cary, NC, USA). Statistical significance was assigned at the 0.05 level.

RESULTS

Cell viability assay

The cell viabilities were significantly decreased when cells were treated with defined concentrations of nucleosides after 12-h incubation (Table 1). The most effective dosages were 30 mmol/L for I, C, U, and T, 0.5 mmol/L for A and G. Thus, these effective concentrations were used in later experiments.

Flow cytometric analysis

Figure 1 is the example of flow cytometer graph from all results in each group. The quantity of various phase percentages is shown in Table 2. About the apoptotic phenomenon, the cell percentages of sub-G_1 phase were significantly increased in the media containing nucleosides such as C, U, T, A, and G (Table 2). In particular, thymidine induced the highest cell percentages of sub-G_1 phase among the nucleosides. The cell-cycle progression of I, A, and G groups was similar to that of control group. Moreover, C and U treatments caused an increase in the cell numbers in the G_0/G_1 phase of the cell cycle. Certainly, the cell numbers of S phase in C and U groups were significantly decreased.

Caspase-3 activity and soluble Fas ligand content

Caspase-3 activity was increased when the cells were incubated with T (Table 2). To investigate the mechanism of apoptosis induced by nucleosides, it was found that the contents of sFas-L contents were increased in HepG2 cells following I, U, T, and A treatment (Table 2). But, TNF-α and cytochrome *c* were undetectable (data not shown).

Western blot assay

HepG2 is the wild type hepatoma with p53 gene. The expressions of p53 and p21 showed no difference in each group (Figure 1). The densitometric result was also unchanged (Figure 2).

Table 1 Effects of nucleosides on HepG2 cell viability by MTS assay[1]

Treatment	Inosine (%)	Cytidine (%)	Uridine (%)	Thymidine (%)	Adenosine(%)	Guanosine(%)
0 mmol/L	103.9±3.5[a]	101.8±1.6[a]	103.5±3.5[a]	102.2±1.9[a]	101.3±1.2[a]	103.1±2.7[a]
7.5 mmol/L	94.0±1.2[a]	92.0±3.8[a]	100.6±6.6[a]	101.5±5.1[a]		
15 mmol/L	69.5±1.8[a]	75.6±1.7[a]	99.1±2.8[a]	99.0±0.3[a]		
30 mmol/L	67.7±0.7[a]	61.4±5.9[a]	86.1±1.3[a]	84.5±3.2[a]		
0.1 mmol/L					93.0±5.2[a]	86.3±3.5[a]
0.3 mmol/L					80.9±2.0[a]	89.4±2.1[a]
0.5 mmol/L					78.4±1.8[a]	86.3±3.3[a]

[1] Cells were incubated with different treatments for 12 h. Cell viability was measured with MTS assay kits. Values are expressed as the mean±SD of six independent experiments. [a]$P<0.05$ *vs* 0 mmol/L.

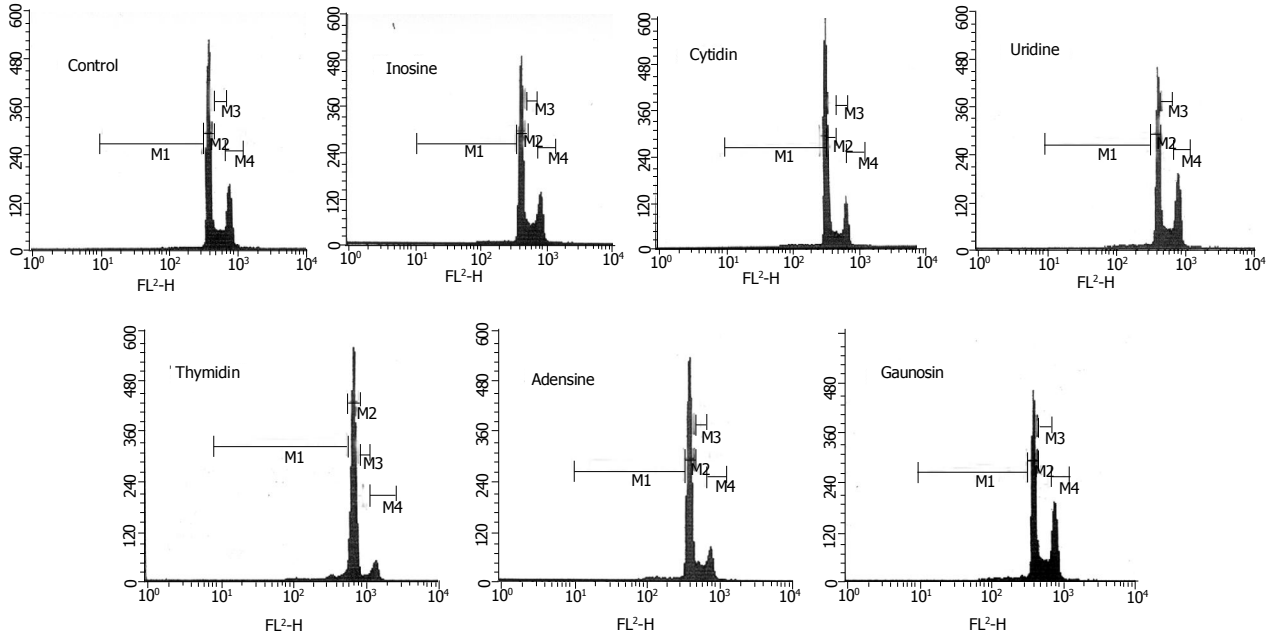


Figure 1 Effects of nucleosides on the cell cycle progression of HepG2 cells. HepG2 cells untreated (control) or treated with nucleosides were stained with propidium iodide and analyzed using a flow cytometer. The contents of inosine, cytidine, uridine, and thymidine in mediums were 30 mmol/L, respectively. And, the contents of adenosine and guanosine were 0.5 mmol/L. This experiment was repeated thrice and obtained similar results were obtained. Figure 1 was the example from all results in each group. M1, M2, M3, and M4 represented Sub G1, G0/G1, S, and G2/M phases, respectively (A-G).

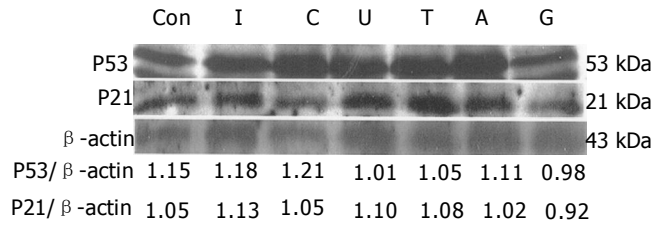


Figure 2 Effects of nucleosides on the p53 and p21 protein expressions in HepG2 cells. One hundred μg of cytosolic proteins were separated by SDS-PAGE, and P53, P21, and β-actin protein were detected, respectively. This experiment was repeated thrice and similar results obtained.

DISCUSSION

The cytotoxicity of nucleosides at defined concentrations in human hepatoma HepG2 cells was proved in this study. However, it has been reported that 1 mmol/L I, C, U, and T did not inhibit the proliferation of HL-60 and Caco-2 cells[12]. In addition, the inhibition effects were observed after 1 mmol/L A and G treatment[12]. Thus, it was speculated that the different cell type of tumor might lead to completely opposite influences.

The cell percentages of sub-G_1 phase were increased after C, U, T, A, and G treatment. However, the variation of sub-G_1 phase in C, U, A, and G groups was weaker than other apoptosis-related researches[13,14]. More apoptotic indicators or treatment dosages of nucleosides must be investigated further.

Thymidine increased the caspase-3 activity in HepG2 cells. Moreover, the sFas-L was also increased when cells were cultured with thymidine. However, these effects were not extremely obvious. These results indicated that thymidine might have the potential to induce the apoptosis, but the effective dosage and reactive time must be investigated further.

The cell percentages of sub-G_1 phase and caspase-3 activities were still unchanged despite sFas contents were higher after inosine and uridine treatments. Similarly, cytidine did not increase the caspsase-3 activity and sFas-L contents,

Table 2 Effects of nucleosides on the cell cycle progression, caspas-3 activity and sFas-L content in HepG2 cells[1]

Treatment	Control	Inosine	Cytidine	Uridine	Thymidine	Adenosine	Gaunosine
SubG1 (%)	2.6±0.8[a]	3.2±0.3[a]	6.9±0.2[a]	6.5±1.5[a]	26.8±2.3[a]	9.6±1.5[a]	5.7±1.2[a]
G0/G1(%)	67.7±1.1[a]	69.2±0.1[a]	74.1±1.3[a]	84.8±2.6[a]	54.4±1.8[a]	64.8±1.4[a]	68.0±1.9[a]
S (%)	15.7±0.0[a]	18.8±0.3[a]	8.5±0.2[a]	3.1±0.3[a]	12.0±0.2[a]	10.6±0.4[a]	17.3±0.7[a]
G2/M (%)	14.0±1.9[a]	8.8±0.1[a]	10.5±1.0[a]	5.7±0.8[a]	6.8±0.8[a]	15.0±0.9[a]	9.0±1.3[a]
Caspase-3 (%)[2]	100±0[a]	101±5[a]	97±6[a]	98±5[a]	148±2[a]	104±4[a]	100±3[a]
sFas-L (pg/mL)	0.11±0.01[a]	0.14±0.01[a]	0.08±0.03[a]	0.15±0.03[a]	0.17±0.02[a]	0.15±0.07[a]	0.10±0.03[a]

[1]Cells were treated with or without nucleosides for 12 h. The contents of inosine, cytidine, uridine, and thymidine in the mediums were 30 mmol/L, respectively, and, the contents of adenosine and guanosine were 0.5 mmol/L. Values are expressed as the mean±SD of four independent experiments. [a]$P<0.05$ *vs* others.
[2]Caspase-3 activity was shown as percentage to compare with control group.

but raised the cell percentages of sub-G_1 phase. Insufficient data indicated the apoptosis-inducing action of inosine, uridine, and cytidine. There are two possibilities, which can explain these results. One is that the apoptosis induced by inosine, uridine, and cytidine might occur later than 12-h incubation. The other is that the cell death induced by inosine, uridine, and cytidine, which showed in MTS assays, was necrosis not apoptosis. Besides, the cell cycle progressions of uridine and cytidine were different from those of other nucleosides. It was observed that uridine and cytidine induced G_0/G_1 phase arrest in HepG2 cells. This effect may be associated with the growth inhibitory action of uridine and cytidine.

Chow *et al*. indicated that adenosine induced apoptosis of HL-60 cells by activating the G protein and increasing the cytosolic Ca^{2+} concentration when adenosine combined with its receptors, P1[15,16]. Moreover, guanosine appears to improve the release of adenosine from cell, and induce cell death via the action of adenosine[17]. But, in this study, the apoptotic-related signals, such as sFas-L content and caspase-3 activity, were not altered in cells after adenosine and guanosine treatments. Thus, the treatment concentration and time point must be reconsidered.

The tumor suppressor p53 is the most commonly mutated gene in human cancers. Cells can respond to the activation of the tumor-suppressor protein p53 by undergoing apoptosis[18,19]. Active p53 is able to stimulate the transcription of a variety of genes including p21, which is a universal inhibitor of the cyclin-dependent kinases (CDK)[20-22]. There were few researches that investigated the relationships between the p53 and nucleosides. In this study, it was found that nucleotides did not alter the expression of p53 and p21 after 12-h incubation with cells.

In conclusion, thymidine might have the potential to induce the apoptosis; however, the apoptosis-induced abilities of other nucleosides were still unclear in this study. It is necessary to recheck the dosage and time of treatment and measure more apoptotic indicators, such as DNA fragmentation and morphological analysis.

REFERENCES

1 **Tanaka K,** Konishi F, Himeno K, Taniguchi K, Nomoto K. Augmentation of antitumor resistance by a strain of unicellular green algae, *Chlorella vulgaris*. *Cancer Immunol Immunother* 1984; **17**: 90-94

2 **Tanaka K,** Tomita Y, Tsuruta M, Konishi F, Okuda M, Himeno K, Nomoto K. Oral administration of *Chlorella vulgaris* augments concomitant antitumor immunity. *Immunopharmacol Immunotoxicol* 1990; **12**: 277-291

3 **Noda K,** Ohno N, Tanaka K, Kamiya N, Okuda M, Yadomae T, Nomoto K, Shoyama Y. A water-soluble antitumor glycoprotein from *chlorella vulgaris*. *Planta Med* 1996; **62**: 423-426

4 **Van Buren CT,** Rudolph F. Dietary nucleotides: a conditional requirement. *Nutrition* 1997; **13**: 470-472

5 **Chow SC,** Kass GE, Orrenius S. Purines and their roles in apoptosis. *Neuropharmacology* 1997; **36**: 1149-1156

6 **Ockner RK.** Apoptosis and liver diseases: recent concepts of mechanism and significance. *J Gastroenterol Hepatol* 2001; **16**: 248-260

7 **Collis MG,** Hourani SM. Adenosine receptor subtypes. *Trends Pharmacol Sci* 1993; **14**: 360-366

8 **Fishman P,** Bar-Yehuda S, Ohana G, Pathak S, Wasserman L, Barer F, Multani AS. Adenosine acts as an inhibitor of lymphoma cell growth: a major role for the A3 adenosine receptor. *Eur J Cancer* 2000; **36**: 1452-1458

9 **Wu JM,** Lin JS, Xie N, Liang KH. Inhibition of hepatitis B virus by a novel L-nucleoside, beta-L-D4A and related analogues. *World J Gastroenterol* 2003; **9**: 1840-1843

10 **Wright SC,** Zhong J, Larrick JW. Inhibition of apoptosis as a mechanism of tumor promotion. *FASEB J* 1994; **8**: 654-660

11 **Kwon KB,** Kim EK, Lim JG, Jeong ES, Shin BC, Jeon YS, Kim KS, Seo EA, Ryu DG. Molecular mechanisms of apoptosis induced by Scorpio water extract in human hepatoma HepG2 cells. *World J Gastroenterol* 2005; **11**: 943-947

12 **Meisel H,** Günther S, Martin D, Schlimme E. Apoptosis induced by modified ribonucleosides in human cell culture systems. *FEBS Lett* 1998; **433**: 265-268

13 **Gali-Muhtasib HU,** Abou Kheir WG, Kheir LA, Darwiche N, Crooks PA. Molecular pathway for thymoquinone-induced cell-cycle arrest and apoptosis in neoplastic keratinocytes. *Anticancer Drugs* 2004; **15**: 389-399

14 **Kluck RM,** Bossy-Wetzel E, Green DR, Newmeyer DD. The release of cytochrome c from mitochondria: a primary site for Bcl-2 regulation of apoptosis. *Science* 1997; **275**: 1132-1136

15 **Chow SC,** Kass GEN, Orrenius S. Purines and their roles in apoptosis. *Neuropharmacology* 1997; **36**: 1149-1156

16 **Schrier SM,** Tilburg EWV, Meulen HVD, Ijzerman AP, Mulder GJ, Nagelkerke. Extracellular adenosine-induced apoptosis in mouse neuroblastoma cells studies on involvement of adenosine receptors and adenosine uptake. *Biochem Pharmacol* 2001; **61**: 417-425

17 **Soussi T.** The p53 tumour suppressor gene: a model for molecular epidemiology of human cancer. *Mol Med Today* 1996; **2**: 32-37

18 **Miyashita T,** Krajewski S, Krajewska M, Wang HG, Lin HK, Liebermann DA, Hoffman B, Reed JC. Tumor suppressor p53 is a regulator of bcl-2 and bax gene expression in vitro and *in vivo*. *Oncogene* 1994; **9**: 1799-1805

19 **Selvakumaran M,** Lin HK, Miyashita T, Wang HG, Krajewski S, Reed JC, Hoffman B, Liebermann D. Immediate early up-regulation of bax expression by p53 but not TGF β 1:a paradigm for distinct apoptotic pathways. *Oncogene* 1994; **9**: 1791-1798

20 **Kagawa S,** Fujiwara T, Hizuta A, Yasuda T, Zhang WW, Roth JA, Tanaka N. p53 expression overcomes p21WAF1/CIP1-mediated G1 arrest and induces apoptosis in human cancer cells. *Oncogene* 1997; **15**: 1903-1909

21 **Vogelstein B,** Kinzler KW. p53 function and dysfunction. *Cell* 1992; **70**: 523-526

22 **Wagner AJ,** Kokontis JM, Hay N. Myc-mediated apoptosis requires wild-type p53 in a manner independent of cell cycle arrest and the ability of p53 to induce p21 waf/cipl. *Gene Dev* 1994; **8**: 2817-2830

Science Editor Guo SY **Language Editor** Elsevier HK

PO Box 2345, Beijing 100023, China
www.wjgnet.com
wjg@wjgnet.com

ELSEVIER

World J Gastroenterol 2005;11(40):6385-6388
World Journal of Gastroenterology ISSN 1007-9327
© 2005 The WJG Press and Elsevier Inc. All rights reserved.

• *BRIEF REPORTS* •

Effect of a nitric oxide synthase inhibitor NG-nitro-L-arginine methyl ester on invasion of human colorectal cancer cell line SL-174T

Li-Bo Yu, Xin-Shu Dong, Wen-Zhou Sun, Dong-Lu Zhao, Yue Yang

Li-Bo Yu, Xin-Shu Dong, Wen-Zhou Sun, Department of General Surgery, the Affiliated Tumor Hospital of Harbin Medical University, Harbin 150040, Heilongjiang Province, China
Dong-Lu Zhao, Yue Yang, Cancer Research Institute of Harbin Medical University, Harbin 150040, Heilongjiang Province, China
Correspondence to: Li-Bo Yu, Department of General Surgery, the Tumor Hospital Affiliated Harbin Medical University, Harbin 150040, Heilongjiang Province, China
Telephone: +86-451-86677581-2142
Received: 2004-11-16 Accepted: 2005-02-18

Abstract

AIM: To investigate the effect and mechanism of action of the nitric oxide synthase (NOS) inhibitor NG-nitro-L-arginine methyl ester (L-NAME) on invasion and metastasis of human colorectal cancer cell line SL-174T.

METHODS: Human colorectal cancer cell line SL-174T was cultured and treated separately with four different dosages of L-NAME for 72 h. Nitric oxide (NO) production was measured with Griess reagent. The effect of L-NAME on invasion and migration of SL-174T cells were evaluated by using Transwell chambers attached with polycarbonate filters and reconstituted basement membrane (Matrigel). RT-PCR was performed to determine the mRNA levels of matrix metalloproteinase-2 (MMP-2) and tissue inhibitor metalloproteinase-2 (TIMP-2).

RESULTS: L-NAME could significantly inhibit NO production of SL-174T in a dose-dependent manner. After being treated for 72 h with 0.2, 0.4, 0.8, and 1.0 mmol/L L-NAME, respectively, the ability of the L-NAME treated SL-174T cells to invade the reconstituted basement membrane decreased significantly (t = 8.056, P<0.05; t = 14.467, P<0.01; t = 27.785, P<0.01; and t = 29.405, P<0.01, respectively) and the inhibition rates were 10.29%, 19.62%, 34.08%, and 42.23%, respectively. Moreover, L-NAME could inhibit migration of SL-174T cells, and the inhibition rates were 20.76%, 24.95%, 39.43%, and 46. 85% for L-NAME at 0.2, 0.4, 0.8, and 1.0 mmol/L, respectively (t = 15.116, P<0.01). In addition, after treatment with L-NAME, expression of MMP-2 mRNA was significantly decreased (t = 71.238, P<0.01) and that of TIMP-2 mRNA was markedly increased (t = -13.020, P<0.01).

CONCLUSION: L-NAME exerts anti-invasive and anti-metastatic effects on SL-174T cell line via downregulating MMP-2 mRNA expression and upregulating TIMP-2 mRNA expression.

© 2005 The WJG Press and Elsevier Inc. All rights reserved.

Key words: Nitric oxide synthase inhibitor; Colorectal cancer; Invasion

Yu LB, Dong XS, Sun WZ, Zhao DL, Yang Y. Effect of a nitric oxide synthase inhibitor NG-nitro-L-arginine methyl ester on invasion of human colorectal cancer cell line SL-174T. *World J Gastroenterol* 2005; 11(40): 6385-6388
http://www.wjgnet.com/1007-9327/11/6385.asp

INTRODUCTION

Colorectal cancer is one of the leading causes of cancer deaths in men and women, and more effective and potent agents for chemotherapy of colorectal cancer are urgently needed. A number of *in vitro* and *in vivo* investigations have indicated the possible involvement of nitric oxide (NO) in promoting tumor carcinogenesis, migration, invasiveness, and angiogenesis. NO is produced from L-arginine, catalyzed by three isoforms of nitric oxide synthases (NOS): (1) calmodulin- and Ca^{2+}-dependent endothelial NOS (eNOS); (2) neuronal NOS (nNOS); and (3) calmodulin- and Ca^{2+}-independent endothelial NOS (iNOS)[1]. An NOS inhibitor NG-nitro-L-arginine methyl ester (L-NAME) has been reported to exert anticancer effects against human head and neck cancer and mammary tumor *in vitro*[2,3]. However, the effects of this agent against colorectal cancer remain to be determined. In the present study, we, therefore, examined the anticancer effects and mechanisms of L-NAME in highly metastatic colorectal cancer cell line SL-174T.

MATERIALS AND METHODS

Cell line and treatment

The human colorectal cancer cell line SL-174T was purchased from Cancer Research Institute of Harbin Medical University and maintained in RPMI 1640 medium (Gibco/BRL), supplemented with 100 mL/L heat-inactivated fetal calf serum (Gibco) and 10 g/L penicillin-streptomycin solution (10 000 U/mL). The cells were incubated in plastic tissue culture flasks (Falcon) at 37 ℃ in a humidified atmosphere containing 50 mL/L CO_2 in air. In the experiments designed to block NO synthesis, L-NAME (Sigma) was added to the medium at various concentrations (0.2, 0.4, 0.8, and 1.0 mmol/L).

NO production assay

Using a microplate assay with Griess reagent, NO production was determined by measuring nitrite accumulation in culture supernatants. After the cells were treated with different

concentrations of L-NAME (0.2, 0.4, 0.8, and 1.0 mmol/L) for 72 h, NOS activity was assessed by measuring nitrite production following the manufacturer's instructions. Cell supernatants (1 000 μL) were mixed with 1 000 μL of the Griess reagent. After 10-min incubation at room temperature, the absorbency was read at 540 nm on a spectrophotometer.

Tumor cell invasion and migration assays

The ability of cells to migrate through control (migration) or invade through Matrigel-coated filters (invasion) was measured in a Transwell chamber (Costar). Eight-micron Transwell filters, which were coated with or without 5 μg Matrigel (Becton Dickinson) and 5 μg fibroblast (Promega), were placed in the lower chamber as a chemoattractant. Then SL-174T cells, treated with different concentrations of L-NAME for 72 h, were added into the upper room and incubated for additional 4 h at 37 ℃ in a humidified atmosphere containing 50 mL/L CO_2 in air. The cells that had not penetrated the filter were wiped out with cotton swabs, and the cells that had migrated to the lower surface of the filter were examined using bright field microscopy, and photographed. The values for invasion were determined as the average number of migrated cells bound per microscopic field over four fields per assay and expressed as average values for triplicate experiments.

Detection of MMP-2 mRNA and TIMP-2 mRNA expression

After the cells were treated with different concentrations of L-NAME (0.2, 0.4, 0.8, and 1.0 mmol/L) for 72 h, total RNA was extracted from SL-174T cells with the TRIzol reagent (Gibco/BRL, Life Technologies Inc.) according to the manufacturer's instructions. The primers were designed using Primer Premier 5 software. The primers used for PCR amplification of matrix metalloproteinase-2 (MMP-2) were 5'-TCTTCAAGGACCGGTTCATTTG-3' (sense) and 5'-GATGCTTCCAAACTTCACGCTC-3' (antisense), 500 bp long. The primers used for PCR amplification of tissue inhibitor metalloproteinase-2 (TIMP-2) were 5'-ACC TGGATGCCGTCGTGGAC-3' (sense) and 5'-TGTGGCAGCACCAGGGCAGC-3' (antisense), 376 bp long. The primers used for β-actin PCR amplification were 5'-TACATGGCTGGGGTGTTG AA-3' (sense) and 5'-AAGAGAGGCATCCTCACCCT-3' (antisense), 218 bp long. PCR primers were synthesized by Biology Engineering Corporation of Shanghai. Ten-microliter aliquots of the PCR product were loaded on 20 g/L polyacrylamide gel. Absorbency ratios of MMP-2 and TIMP-2 to control β-actin mRNA expression were considered as expression indices of the former two genes and used for semi-quantitation.

Statistical analysis

SAS for Windows 6.12 was used to solve the data. The data were mean value of at least three different experiments and expressed as mean±SD. The LSD-*t* test and Dunnett's *t* test were used to compare the data. $P<0.05$ was considered statistically significant.

RESULTS

Effect of L-NAME on NO production

NO production was significantly decreased after the treatment with different dilutions of L-NAME. We observed significant differences in NO levels between control group and treatment groups (Table 1).

Table 1 Effect of different concentrations of L-NAME on NO production by SL-174T cells (mean±SD)

Concentration mmol/L	No. of experiments	NO (μmol/L) 72 h
Control	3	147.80±0.78[b]
0.2	3	135.66±0.45
0.4	3	95.73±0.23
0.8	3	59.80±0.65
1.0	3	56.43±0.64

[b]$P<0.01$, *vs* control.

Influence of L-NAME on invasion and migration of SL-174T cells

Compared with the control group, SL-174T cells treated with different concentrations of L-NAME for 72 h had decreasing tendency for invasion and the inhibition rates were 10.29%, 19.62%, 34.08%, and 42.23% for L-NAME at 0.2 mmol/L ($P<0.05$), 0.4, 0.8, and 1.0 mmol/L ($P<0.01$), respectively. In addition, L-NAME could markedly inhibit SL-174T cells migration, and the inhibition rates were 20.76%, 24.95%, 39.43%, and 46.85% for L-NAME at 0.2, 0.4, 0.8, and 1.0 mmol/L ($P<0.01$), respectively (Figures 1 and 2A-D).

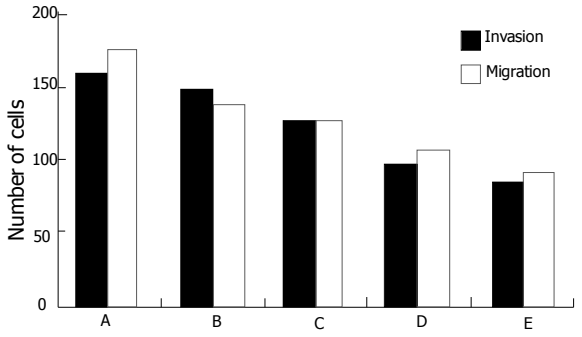


Figure 1 SL-174T treated with different concentrations of L-NAME. **A:** Control; **B:** 0.2 mmol/L; **C:** 0.4 mmol/L; **D:** 0.8 mmol/L; **E:** 1.0 mmol/L. Data are represented as mean±SD of triplicate determinations.

Expression of MMP-2 mRNA and TIMP-2 mRNA

After the treatment with L-NAME for 72 h, expression of MMP-2 mRNA and TIMP-2 in SL-174T cells is shown in Figures 3A and B. The expression of MMP-2 mRNA was significantly decreased in the treatment groups as compared to the control ($P<0.05$). On the contrary, the expression of TIMP-2 mRNA was significantly higher in the treatment groups as compared to the control ($P<0.05$).

DISCUSSION

NO has dual action on tumor growth that may be dependent on local concentrations, type of tumor, and susceptibility of tumor cells to NO. Over production of endogenous

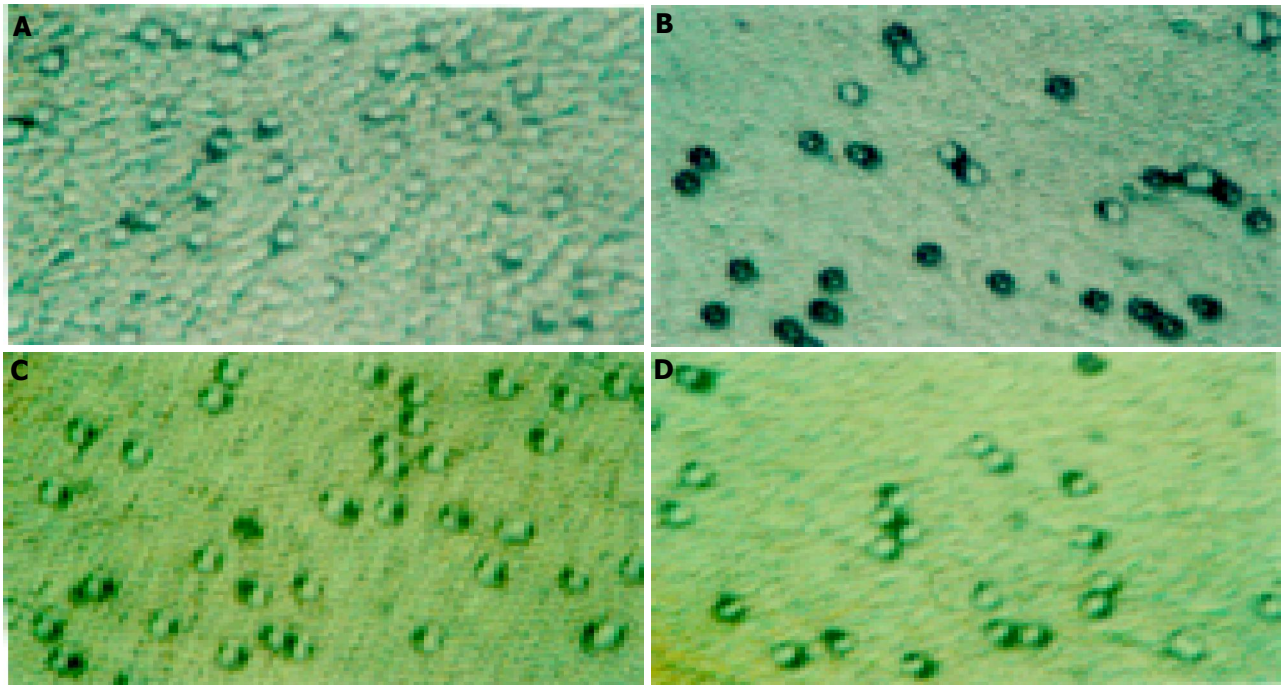


Figure 2 Invasion and migration of different groups of SL-174T cells (×200). **A**: Invasion of control group cells; **B**: 0.8 mmol/L L-NAME invasion group; **C**: migration of control group; **D**: 0.8 mmol/L L-NAME migration group.

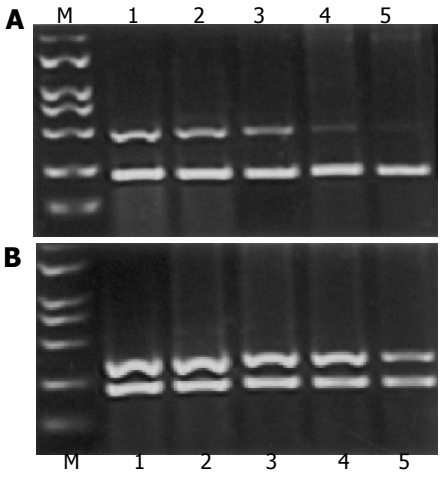


Figure 3 **A:** Expression of MMP-2 mRNA in SL-174T cells treated with different concentrations of L-NAME. M: Marker; lane 1: control; lanes 2-5: SL-174T cells treated with 0.2, 0.4, 0.8, and 1.0 mmol/L of L-NAME, respectively. The experiments were carried out in triplicate. Data are expressed as mean±SD; **B**: Expression of TIMP-2 mRNA in SL-174T cells treated with different concentrations of L-NAME. M: Marker; lane 1: control; lanes 2-5: SL-174T cells treated with 0.2, 0.4, 0.8, and 1.0 mmol/L of L-NAME, respectively. The experiments were carried out in triplicate. Data are expressed as mean±SD.

NO would cause tumor toxicity, induce cell apoptosis, and prevent tumor angiogenesis. NO level produced in tumor microenvironment usually was up to two orders of magnitude lower than that associated with NO-dependent tumor apoptosis. Endogenous NO produced by blood vessel endothelial cells and tumor cells plays an important role in supplying tumor blood and maintaining tumor growth, also in dilating blood vessel and increasing angiogenesis[4,5]. NO can dilate arteriola, decrease leukocyte-endothelial interactions, and enhance vascular permeability in solid tumor. Much scientific research has focused on the role of NO in tumor progression; although two apparently conflicting views exist, overall an overwhelming amount of clinical and experimental evidence supports a positive association between NO production and tumor progression. The level of NOS protein and/or activity in the tumor has been shown to be positively correlated with the degree of malignancy for tumors of the human reproductive tract[6], breast[7,8], central nervous system[5], lung cancer[10], and prostate carcinomas[11]. Several studies have shown an increase of iNOS expression in colorectal cancer tissue when compared to normal mucosa and its extent correlates with tumor metastasis[12,13]. A specific cause-effect relationship between the upregulation of the iNOS gene and colon cancer has been recently demonstrated by Ahn and Oshima[14]. It has been demonstrated that tumors derived from human colon adenocarcinoma cells engineered to generate NO continuously (iNOS-19) are significantly more vascularized and more invasive than the wide controls.

This study clearly demonstrated that human colorectal cancer cell line SL-174T exhibited a strong ability to invade Matrigel and the NOS inhibitor L-NAME markedly decreased the invasion and migration. We explored the mediators of the NO-stimulated invasion, which lead to essential steps as migration and matrix degradation. MMPs and TIMPs have the ability to modulate the structure of the extracellular matrix (ECM), and changes of their expression level or activation of MMPs weaken the integrity of the ECM, which is a prerequisite for invasion and metastasis. Our study demonstrated that NOS inhibitor L-NAME reduced invasive and migratory capacities of cell line SL-174T by downregulation of MMP-2 mRNA and upregulation of TIMP-2 mRNA expression. Further work needs to demonstrate a corresponding shift in the activities

of the enzyme and its inhibitors at the protein level. Additional mechanisms underlying NO-mediated stimulation of cellular invasiveness may exist. For example, NO has been shown to upregulate urokinase-type plasminogen activator (uPA) in endothelial cells of post-capillary venules during NO-mediated stimulation of angiogenesis[15]. Since uPA converts plasminogen to plasmin, which can activate numerous MMPs, this may represent another pathway of NO-mediated stimulation of matrix degradation.

In conclusion, the NOS inhibitor L-NAME can reduce invasive and migratory capacities of SL-174T cell line via downregulating MMP-2 mRNA expression and upregulating TIMP-2 mRNA expression. Thus, NOS inhibitors may prove to be important components of combination therapy protocols in human tumors, including colorectal cancer.

REFERENCES

1 **Geller DA,** Billiar TR. Molecular biology of nitric oxide synthases. *Cancer Metastasis Rev* 1998; **17**: 7-23
2 **Gallo O,** Masini E, Morbidelli L, Franchi A, Fini-Storchi I, Vergari WA, Ziche M. Role of nitric oxide in angiogenesis and tumor progression in head and neck cancer. *J Natl Cancer Inst* 1998; **90**: 587-596
3 **Jadeski LC,** Lala PK. Nitric oxide synthase inhibition by N^G-nitro-L-arginine methyl ester inhibits tumor-induced angiogenesis in mammary tumors. *Am J Pathol* 1999; **155**: 1381-1390
4 **Moncada S,** Palmer RM, Higgs EA. Nitric oxide: physiology, pathophysiology, and pharmacology. *Pharmacol Rev* 1991; **43**: 109–142
5 **Fukumura D,** Jain RK. Role of nitric oxide in angiogenesis and microcirculation in tumors. *Cancer Metastasis Rev* 1998; **17**: 77-89
6 **Thomsen LL,** Lawton FG, Knowles RG, Beesley JE, Riveros-Moreno V, Moncada S. Nitric oxide synthase activity in human gynecological cancer. *Cancer Res* 1994; **54**: 1352-1354
7 **Thomsen LL,** Miles DW, Happerfield L, Bobrow LG, Knowles RG, Moncada S. Nitric oxide synthase activity in human breast cancer. *Br J Cancer* 1995; **72**: 41-44
8 **Duenas-Gonzalez A,** Isales CM, del Mar Abad-Hernandez M, Gonzalez-Sarmiento R, Sangueza O, Rodriguez-Commes J. Expression of inducible nitric oxide synthase in breast cancer correlates with metastatic disease. *Mod Pathol* 1997; **10**: 645-649
9 **Cobbs CS,** Brenman JE, Aldape KD, Bredt DS, Israel MA. Expression of nitric oxide synthase in human central nervous system tumors. *Cancer Res* 1995; **55**: 727-730
10 **Fujimoto H,** Ando Y, Yamashita T, Terazaki H, Tanaka Y, Sasaki J, Matsumoto M, Suga M, Ando M. Nitric oxide synthase activity in human lung cancer. *Jpn J Cancer Res* 1997; **88**: 1190-1198
11 **Klotz T,** Bloch W, Volberg C, Engelmann U, Addicks K. Selective expression of inducible nitric oxide synthase in human prostate carcinoma. *Cancer* 1998; **82**: 1897-1903
12 **Kojima M,** Morisaki T, Tsukahara Y, Uchiyama A, Matsunari Y, Mibu R, Tanaka M. Nitric oxide synthase expression and nitric oxide production in human colon carcinoma tissue. *J Surg Oncol* 1999; **70**: 222-229
13 **Lagares-Garcia JA,** Moore RA, Collier B, Heggere M, Diaz F, Qian F. Nitric oxide synthase as a marker in colorectal carcinoma. *Am Surg* 2001; **67**: 709-713
14 **Ahn B,** Ohshima H. Suppression of intestinal polyposis in $Apc^{(Min/+)}$ mice by inhibiting nitric oxide production. *Cancer Res* 2001; **61**: 8357-8360
15 **Ziche M,** Morbidelli L, Masini E, Amerini S, Granger HJ, Maggi CA, Geppetti P, Ledda F. Nitric oxide mediates angiogenesis *in vivo* and endothelial cell growth and migration *in vitro* promoted by substance P. *J Clin Invest* 1994; **94**: 2036-2044

Science Editor Kumar M and Guo SY **Language Editor** Elsevier HK

PO Box 2345, Beijing 100023, China
www.wjgnet.com
wjg@wjgnet.com

ELSEVIER

World J Gastroenterol 2005;11(40):6389-6394
World Journal of Gastroenterology ISSN 1007-9327
© 2005 The WJG Press and Elsevier Inc. All rights reserved.

• *BRIEF REPORTS* •

Construction of prokaryotic expression system of TGF-β1 epitope gene and identification of recombinant fusion protein immunity

Yong-Hong Guo, Zhi-Ming Hao, Jin-Yan Luo, Jun-Hong Wang

Yong-Hong Guo, Jin-Yan Luo, Jun-Hong Wang, The Second Affiliated Hospital of Xi'an Jiaotong University, Xi'an710004, Shannxi Province, China
Zhi-Ming Hao, The Post Doctor Xijing Hospital of Fourth Military Medical University, Xi'an 710004, Shannxi Province, China
Supported by the JRC Research Fund
Correspondence to: Dr. Yong-Hong Guo, Department of Infectious Diseases, the Second Affiliated Hospital, Xi'an Jiaotong University, Xi'an 710004, China. xiaoqing9759@sina.com
Telephone: +86-029-87679274; 13891866147
Received: 2005-03-10 Accepted: 2005-04-12

Abstract

AIM: To insert the constructed TGF-β1 epitope gene into the el loop of C-terminus of truncated hepatitis B core antigen to increase TGF-β1 antigenicity in its prokaryotic expression system and to identify immunity of the expressed recombinant protein in order to exploit the possibility for obtaining anti- TGF-β1 vaccine.

METHODS: The TGF-β1 encoding epitope gene (the mature TGF-β1 from 78-109 amino acid residues, TGF-β_1^{32}) was amplified by polymerase chain reaction from the recombinant pGEM-7z/ TGF-β_1^{32} vector. The HBcAg gene fragments (encoding HBcAg from 1-71 and 89-144 amino acid residues) were amplified from PYTA1-HBcAg vector. The recombinant vector pGEMEX-1 was used to insert HBcAg1-71, TGF-β_1^{32} and HBcAg89-144 into restrictive endonuclease enzyme and ligated with T_4 ligase. The fusion gene fragments HBcAg1-71-TGF-β_1^{32}-HBcAg89-144 were recloned to pET28a(+) and the DNA sequence was confirmed by the dideoxy chain termination method. The recombinant vector pET28a (+)/CTC was transformed and expressed in *E. coli* BL21 (DE3) under induction of IPTG. After purification with Ni^{+2}-NTA agarose resins, the antigenicity of purified protein was detected by ELISA and Western blot and visualized under electron microscope.

RESULTS: Enzyme digestion analysis and sequencing showed that TGF-β1 epitope gene was inserted into the el loop of C-terminus of truncated hepatitis B core antigen. SDS-PAGE analysis showed that relative molecular mass (Mr) of the expressed product by pET28a (+)/CTC was Mr 24 600.The output of the target recombinant protein was approximately 34.8% of the total bacterial protein, mainly presented in the form of inclusion body. Western blotting and ELISA demonstrated that the fusion protein could combine with anti-TGF-β1 polyclonal IgG but not with anti-HBcAg. The purity of protein was about 90 % and the protein was in the form of self-assembling particles visualized under electron microscope. This fusion protein had good anti-TGF-β1 antigenicity and could be used as anti-TGF-β1 vaccine.

CONCLUSION: A recombinant prokaryotic expression system with high expression efficiency of the target TGF-β1 epitope gene was successfully established. The fusion protein is in the form of self-assembling particles and HBcAg can increase the antigenicity of TGF-β1. The expressed TGF-β1 epitope gene shows good immunogenicity and antigenicity.

© 2005 The WJG Press and Elsevier Inc. All rights reserved.

Key words: Prokaryotic expression system; TGF-β1 epitope; Immunogenicity; Antigenicity

Guo YH, Hao ZM, Luo JY, Wang JH. Construction of prokaryotic expression system of TGF-β1 epitope gene and identification of recombinant fusion protein immunity. *World J Gastroenterol* 2005; 11(40): 6389-6394
http://www.wjgnet.com/1007-9327/11/6389.asp

INTRODUCTION

Liver fibrosis is commonly resulted from diverse liver injuries. Liver fibrosis can be reversed while liver cirrhosis is irreversible[1]. However, no efficient therapy is available at present for this disease[2]. Searching for a new therapy seems very important. Transforming growth factor (TGF-β), especially TGF-β1, plays a pivotal role in the fibrogenesis of liver fibrosis and cirrhosis. TGF-β1, a major cytokine, can regulate the production, degradation, and accumulation of ECM[3-6]. Over expression or activation of TGF-β1 for a prolonged period of time after tissue damage may induce a fibrosis proliferating response and deposition of ECM, resulting in fibrosis in vital organs[7-9]. Inhibition of TGF-β1 can prevent progression of liver fibrosis and enhance hepatocyte regeneration. Blockage of TGF-β1 may have therapeutic effects on liver fibrosis[10-14].

Anti-cytokine vaccination is a safe and effective pathway to blockage hepatic lesions as long as high antibody levels

are maintained[15]. It is difficult to induce high titer antibody since TGF-β_1 is a self-protein and B cells are immune silence. Fusion peptide epitope-encoded sequences of HBcAg can enhance TGF-β_1 immunogenicity, because HBcAg components help T-cells, and the fusion proteins retain the polymeric or the particulate nature of HBcAg[16].

In this paper, fusion protein sequences carrying the TGF-β_1 epitope inserted into the el loop of C-terminus of truncated HBcAg were expressed in *E.coli BL21*. The fusion protein can form particles. HBcAg has the potential to increase the TGF-β_1 antigenicity and immunogenicity. Our results indicate that the fusion protein can be used as an effective anti-TGF-β_1 vaccine.

MATERIALS AND METHODS

Materials

Recombinant vector pGEM-7z/TGF-β_1^{32} (TGF-β_1^{32} is the encoding gene of mature TGF-β_1 79-108 amino acid residues)[17] and vector pET28a (+) were provided by Dr Zhi-Ming Hao (Novagen). Top10 and *E.coli BL21*strains were provided by Xi'an Huaguang Biology Company. Plasmid pYTA1-HBcAg was constructed by Institute of Virology of Chinese Academy of Preventive Medicine. Rabbit anti-human TGF-β_1-IgG was purchased from Santa Cruz. Restriction endonuclease enzymes (*Eco*RI, *Hind* III, *Bam*HI, *Xho*l),TagDNA polymerase and T_4 DNA ligase were purchased from Huamei Company and TaKaLa Company. dNTP and isopropyl-β -D-thiogalactopyranoside (IPTG) were obtained from Sigma and oligonucleotide primers were obtained from Shanghai Shenggong Company.

Cloning of target genes

The encoding genes of TGF-β_1 epitope (mature TGF-β_1 amino acid residues from 79-108) and HBcAg were cloned from amino acid residues 1-71 and 89 - 144.

Oligonucleotide primers were designed to amplify the encoding genes based on GenBank TGF-β_1^{32} was cloned from the recombinant plasmid pGEM-7z/ TGF-β_1^{32} as the PCR fragment template. The primers have a Xhol site incorporated into the 5' end and a BamHI site at the 3' end and their sequences are as follows (5'-3'): CC CTC GAG TGC GTG CCG CAG GCG CTG (forward) and CC GGA TCC GCA GGA GCG CAC GAT CAT (reverse). HBcAg gene was amplified by PCR from the vector pYTA1-HBcAg as the template (constructed by Institute of Virology, Chinese Academy of Preventive Medicine).The primers of $HBcAg_{(1-71)}$ have a EcoR Ⅰ site incorporated into the 5' end and a Xhol site at the 3' end and their sequences are as follows (5'-3'): GGAATTCAT GATTACGCCAAGCTTGGCTGCAGAGTTCCATATG (forward) and CCCTCGAGTCCACCCCAGGTAGCT AGAGTC (reverse) .The primers of $HBcAg_{(89-144)}$ have a BamH Ⅰ site incorporated into the 5' end and a *Hind*Ⅲ site at the 3' end and their sequences are as follows (5'-3'): CGGATCCGGTGGAGTCAACAACACTAATATGGG C (forward) and CCAAGCTTCCGCGGAAGTGTTGA TAGGAT (reverse). Total volume per PCR was 100 mL containing 2.5 mol/L each dNTP, 250 nmol/L each of the 2 primers, 15 mol/L $MgCl_2$, 3.0U Taq-plus polymerase, 100 ng DNA template and 1×PCR buffer. The PCR consisted of 30 cycles of denaturation at 94 °C for 60 s, annealing at 52 °C for 30 s, and extension at 72 °C for 30 s. The products were visualized on 10 g/L agarose gel under UV light, pre-stained with ethidium bromide. The PCR products were digested respectively using *Eco*R/*Xho*l , *Xho*I/*Bam*HI, *Bam*H Ⅰ/*Hind*Ⅲ. After digestion with the restriction endonuclease enzymes simultaneously, the expected sizes of target amplification fragments $HBcAg_{1-71}$, TGF-β_1^{32} and $HBcAg_{89-144}$ was 268, 96 and 177 bp, respectively.

Construction of recombinant prokaryotic expression vector

The PCR products were digested respectively using *Eco*R Ⅰ/*Xho*l, *Xho*I /*Bam*HI, *Bam*H Ⅰ/*Hind*Ⅲ and ligated into the cloning vector pGEM-Teasy. The resulting fragments were cloned into the vector pGEMEX-1. The purified products were cloned into the compatible sites of the vector pGEMEX-1 (Promega, USA) using T4 DNA ligase at a molar ratio of 4:1 at 4 °C overnight. The recombinant plasmid clones pGEMEX-1/ $HBcAg_{1-71}$- TGF-β_1^{32}-$HBcAg_{89-144}$ [$HBcAg_{1-71}$-TGF-β_1^{32}-$HBcAg_{89-144}$ (CTC)] were sequenced using the dideoxy chain termination method. After digestion with the restriction endonuclease enzymes *Eco*RI and *Hind*Ⅲ simultaneously, the fusion gene fragments CTC were cloned into the compatible sites of the prokaryotic expression vector pET-28a(+), downstream of the 6-His tag to facilitate the protein purification using T4 DNA ligase at a molar ratio of 4:1 at 4 °C overnight. The recombinant vector pET28a(+)/ CTC was selected and identified by enzyme digestion and sequencing. IPTG at the dose of 1.0 mmol/L could efficiently induce pET28a/CTC in *E.coli BL21(DE3)* to express the fusion gene composed of 606 base pairs and encode objective polypeptides of 201 amino acid residues(Figure 1).

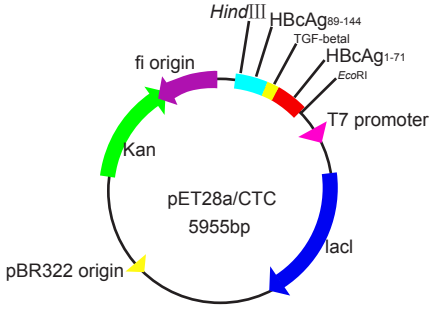


Figure 1 Schematic construction of plasmid pET28a(+)/CTC.

Extraction and expression of recombinant plasmids

The single bacterial colony (Top10/pET28a(+)/CTC) was picked and incubated in 2 mL LB containing 100 g/L of Kanamycin, at 300 r/min overnight at 37 °C, then recombinant plasmids were extracted according to the manufacturer's instructions and identified by PCR and restriction endonuclease enzyme digestion. *E.coli BL21 (DE3)* strains containing recombinant plasmids were grown until mid-log phase (optical density at 600 nm=0.5-1.0), and then induced to express recombinant fusion protein by adding 1 mmoL/L IPTG for 8 h. Bacteria were harvested by centrifugation at 12 000 *g* for 2 min, resuspended in protein-buffer and seethed for 5 min. Total protein was electrophoresed on 150 g/L SDS-PAGE gel and stained with Coomassie. The rate of recombinant fusion protein to total protein was deduced by Image Master Band Leader 3.0 software.

Purification of pET28a(+)/CTC fusion protein

Due to C end of the recombinant fusion antigen with six histidines, Ni^{2+}-NTA agarose resin was used to purify the recombinant fusion antigen. Briefly, 500 ml of cultivated bacterial suspension was prepared, centrifuged, resuspended with the buffer liquid (50 mmoL/L phosphate, 300 mmoL/L NaCl, pH 7.0), and sonicated by ultrasonic wave with the energy of 600 W for 30 min, and ultracentrifuged for 15 min at 10 000 *g* at 4°C. The sonicated recombinant fusion antigen was purified by Ni^{2+}-NTA agarose resin with abluent (50 mmoL/L phosphate, 300 mmoL/L NaCl, 20 mmoL/L imidazole, pH 7.80) and lavation (50 mmoL/L phosphate, 300 mmoL/L NaCl, 250 mmoL/L imidazole, pH 7.80) respectively, and quantified. pET28a(+)/HBc-TGF-β_1^{32} fusion protein was expressed and purified by SDS-15% PAGE. In contrast with the induced product of pET-28a(+) (negative control), a recombinant protein with expected molecular weight of 24.6X103Da was expressed in *E. coli BL21 (DE3)* as shown by SDS-PAGE.

Immunoblotting analysis of recombinant fusion protein

ELISA The expressed fusion protein was stabilized as antigen at the coated concentration (1:100, 1:200, 1:400, 1:800, 1:1600 dilution) with CBS buffer overnight at 4 °C, and blocked with 100 g/L bovine serum albumin (BSA) for 1 h at room temperature, incubated with the anti-TGF-β_1 antibody and HBc antibody as the first antibody respectively for 2 h at room temperature. After a washing, the proteins were detected by incubating in HRP-goat anti-rabbit IgG antibody(1:1000 dilution) (Zhongshan, Beijing) and anti-human IgG (Xi'an Huagguang) as the second antibody respectively for 1 h at room temperature. The first antibodies were replaced by PBS and used as negative control. The result of ELISA for the sample was considered as positive if the A value at 490 nm (A_{490}) was over the mean plus 2.1 SD of the negative samples.

Western blot

After bacteria BL21/pET-28a(+)/CTC were incubated by adding of 1 mmol./L IPTG for 8 h, 1 ml of cultivated medium was ultracentrifuged, resuspended in protein-buffer and seethed for 5 min. Total protein was electrophoresed on 150 g/L SDS-PAGE gel, and then the proteins of SDS-PAGE-separated (150 g/L acrylamide) were transferred to 0.45 mm pore size PVDF membrane. Following a 30-min washing in tris-saline blotting buffer, antigen-impregated PVDF strips were incubated with anti-TGF-β_1 antibody and anti-HBc antibody respectively for 2 h at room temperature. After a washing, the proteins were detected by incubating the strips in alkaline phosphatase-conjugated goat anti-rabbit IgG antibody and anti-human IgG respectively for 1 h at room temperature.

RESULTS

Sequence analysis of recombinant vectors nucleotide and open reading frame (ORF)

The recombinant vectors pGEMEX-1/ CTC and pET28a(+)/CTC were identified by restriction enzyme digestion in 10 g/L agarose gel electrophoresis. The recombinant vector clones were sequenced using dideoxy chain termination method. The inserted 6xHis- $HBcAg_{1-71}$-TGF-β_1^{32}-$HBcAg_{89-144}$ had the correct open reading frame in the expression vector and correctly sequenced DNA. The nucleotide sequence of the fusion genes was analyzed. Recombinant vector pET-28a(+)/CTC was digested by bi-enzyme digestion with *Hind*III,*Eco*RI, then digestive products were visualized on 10 g/L agarose gel (Figure 2). The amplified fused $HBcAg_{1-71}$-TGF-β_1^{32}-$HBcAg_{89-144}$ DNA fragments were confirmed by restriction enzyme digestion and contained the objective gene.

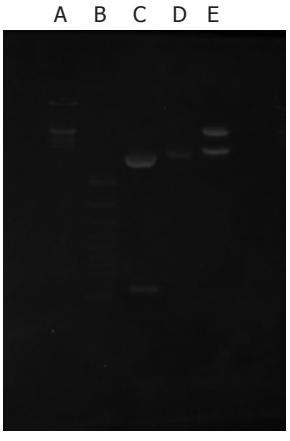


Figure 2 Recombinant vector pET28a/CTC identified by restriction enzyme digestion. Lane A: 200 bp DNA ladder; lane B: λDNA/ *Hind* IIIMarkers; lane C: *Eco*RI+*Hind* III enzyme digestion(546 bp+3.9 kb); lane D: vector pET28a as negative control; lane E: *Eco*RI+*Hind* III enzyme digestion pET28a

Analysis of recombinant fusion protein

Total protein was electrophoresed on 150 g/L SDS-PAGE gel and stained with Coomassie. Its molecular mass was Mr 24 600 as demonstrated by 150 g/L SDS-PAGE gel analysis. The fusion protein was about 34.8 % of total cellular protein. After purification by Ni^{2+}-NTA agarose

resin columniation, the purity of recombinant fusion protein was about 90% (Figure 3).

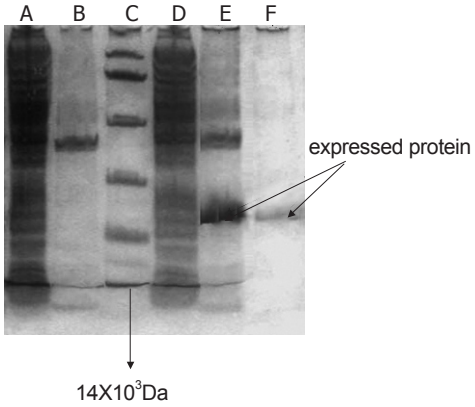


Figure 3 Expressed and purified pET28a/CTC fusion protein by 150 g.l-1 SDS –PAGE in combination with Coomassie blue staining. Lane A: Bacterial protein expressed in the supermatant fraction of pET-28a(+) vector after induction with IPTG; lane B: Bacterial protein expressed in the precipitation of lysate of fraction of pET-28a(+) vector after induction with IPTG; lane C: Standard protein low-molecular-mass marker (Mr 97.4, 66.2, 43.0, 31.0, 20.1, and 14KD); lane D: Bacterial protein expressed in the supernatant fraction of the vector pET-28a(+)/CTC after induction with IPTG; lane E: Bacterial protein expressed in the precipitation of lysate of fraction of the vector pET-28a(+)/ CTC after induction with IPTG; lane F: Purity of recombinant fusion protein.

Antigenicity of recombinant fusion protein

The antigen-impregated PVDF strips of *BL21*/pET32a(+)/CTC were recognized by anti-TGF-β_1 antibody, showing brown strips corresponding to the site of the recombinant fusion protein. They could not be recognized by HBc antibody, showing no brown strips corresponding to the site of the fusion protein (Figure 4).

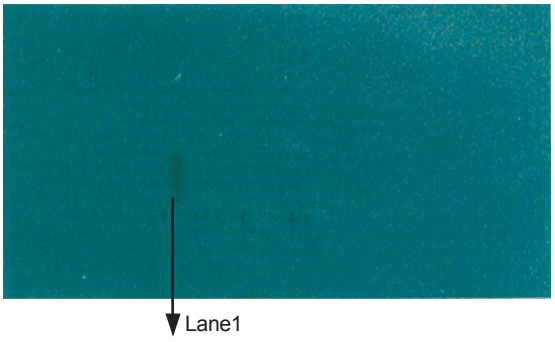


Figure 4 Antigenic analysis of the expression of recombinant vector by Western blot. Lane 1: BL21/pET28a(+)/CTC.

Antigenicity of fusion protein displayed in ELISA

Staining was positive in the fusion protein and negative in the negative controls. The expressed fusion protein did not react with anti-HBc polyAb and mAb. The expressed protein reacted with anti-TGF-β_1 antibody.

Electron microscopy

The expressed proteins by the constructs formed core particles observed under electron microscope, which were bigger than HBcAg core particles (Figure 5).

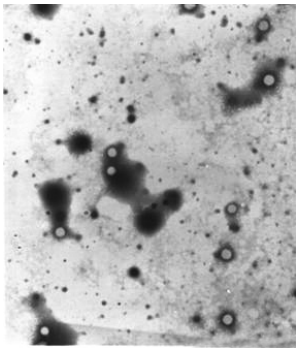


Figure 5 Electron microscopy of the core-like particles formed in fusion protein.

DISCUSSION

Anti-cytokine vaccination is a safe and effective therapy[19]. Imbalance in cytokine production or cytokine receptor expression and /or dysregulation of cytokine production provides the basis for generating pathological disorders. Cytokine production by effector cells (induced by activation but controlled by negative feedback regulation) does not accumulate in the extracellular compartment under physiologic conditions. The anti-cytokine therapeutic vaccine is to raise antibody levels over the background levels of natural antibodies while enhancing their affinity and neutralizing activity block the accumulation of overproduced cytokines, thereby inhibiting its pathogenic effects. In contrast, the neutralizing Abs do not interfere with cytokine production in normal tissues. Since it has no side effects in normal tissues, high-affinity Abs can be induced safely and effectively.

The TGF-β_1 is chosen as an antifibrosis vaccine because it is a key cytokine in hepatic fibrosis and blockade of TGF-β_1 prevents liver fibrosis. It is difficult to induce high titer antibody since TGF-β_1 is a self-protein. T cells undergo a thymic-negative clonal selection against self-cytokines though anti-cytokine B cells still exist. HBcAg is an attractive candidate for induction of cytokine foreign epitopes because the HBcAg component helps T-cells and the fusion proteins retain the polymeric or the particulate nature of HBcAg. HBcAg behaves as highly immunogenic TI and TD antigens[18,19]. In recent years epitopes of various origin have been inserted into the core antigen of hepatitis B virus (HBV) allowing formation of chimeric HBV core particles. Chimeric core particles carrying the protein can induce protective immunity.

The high immunogenicity of HBcAg depends both on its structure with repetitive spikes on the surface to induce TI responses and on the efficient presentation of HBcAg by B cells to induce TD responses[20]. Fusion

of peptide epitope sequences to HBcAg can enhance their immunogenicity. Virus-like particles generated by the heterologous expression of virus structural proteins are able to potentiate the immunogenicity of foreign epitopes presented on their surface. Several foreign epitopes from hepatitis B virus, Papillomavirus, Plasmodium falciparum and hantavirus[21-24] have been introduced successfully into HBcAg capsids, and immunogenicity of the new epitopes has been demonstrated.

Foreign epitope sequence of varying length was inserted into HBcAg in various protein regions, including the N-,C-termini and some internal sites including immunodominant el loop without loss of the self-assembly properties of HBcAg[25].It has been demonstrated that the loop in the main determinant of the core antigen is the most promising insertion site from the immunological point of view. Epitopes inserted there possess higher antigenicity and immunogenicity than anywhere. But not all chimeric proteins are able to be particulated. The ability of chimeric HBcAg to self-assemble is most likely to depend on the physical and chemical properties of the amino acid residues forming the inserted foreign peptide.

The fusion of sequences carryies the epitope of the TGF- β_1 (mature encode zone amino acids 78-109)[26] to the el loop of C-terminus of truncated HBcAg, produced in *E. coli. BL21 (DE3)*. The expressed fusion protein is in the form of self-assembling particles observed under electron microscope. The results demonstrate that recombinant fusion protein has a good anti-TGF- β_1 antigenicity. Mr 24 600 recombinant fusion protein has HBcAg characteristics and possesses TGF- β_1 antigen specialty. The fusion proteins carrying the TGF- β_1 antigen-dominant fragment induce antibodies that react effectively with native TGF- β_1, suggesting that the recombinant fusion protein can be used as a true vaccine candidate. In the present study, recombinant plasmid was constructed and expressed in *BL21(DE3)* to explore the possibility for obtaining a vaccine conferring protection against liver fibrosis. We are going to use it in the hepatic fibrosis model as an anti-fibrosis vaccine. Further study is needed to detect its anti-fibrosis effect as a therapeutic vaccine.

ACKNOWLEDGMENTS

This work was supported by Mr.Yang Guangxiao and Wang Quanying of the Xi'an Huaguang Biologic Company.

REFERENCES

1 **Wang JY,** Guo JS, Yang CQ. Expression of exogenous rat collagenase in vitro and in a rat model of liver fibrosis. *World J Gastroenterol* 2002; **8:** 901-907
2 **Murphy F,** Arthur M, Iredale J. Developing strategies for liver fibrosis treatment. *Expert Opin Investig Drugs* 2002; **11:** 1575-1585
3 **Nakamura T,** Sakata R, Ueno T, Sata M, Ueno H. Inhibition of transforming growth factor beta prevents progression of liver fibrosis and enhances hepatocyte regeneration in dimethylnitrosamine-treated rats. *Hepatology* 2000; **32:** 247-255
4 **Dooley S,** Delvoux B, Lahme B, Mangasser-Stephan K, Gressner AM. Modulation of transforming growth factor beta response and signaling during transdifferentiation of rat hepatic stellate cells to myofibroblasts. *Hepatology* 2000; **31:** 1094-1106
5 **Si XH,** Yang LJ. Extraction and purification of TGFbeta and its effect on the induction of apoptosis of hepatocytes. *World J Gastroenterol* 2001; **7:** 527-531
6 **Moustakas A,** Pardali K, Gaal A, Heldin CH. Mechanisms of TGF-beta signaling in regulation of cell growth and differentiation. *Immunol Lett* 2002; **82:** 85-91
7 **Sporn MB,** Roberts AB. Transforming growth factor-beta: recent progress and new challenges. *J Cell Biol* 1992; **119:** 1017-1021
8 **Friedman SL.** Seminars in medicine of the Beth Israel Hospital, Boston: The cellular basis of hepatic fibrosis -- Mechanisms and Treatment Strategies. *N Engl J Med* 1993; **328:** 1828-1835
9 **Border WA & Noble NA.** Mechanisms of Disease: Transforming Growth Factor ß in Tissue Fibrosis. *N Engl J Med* 1994; **331:** 1286-1292
10 **Komesli S,** Vivien D, Dutartre P. Chimeric extracellular domain type II transforming growth factor (TGF)-β receptor fused to the Fc region of human immunoglobulin as a TGF-β antagonist. *Eur J Biochem* 1998; **254:** 505-513
11 **Qi Z,** Atsuchi N, Ooshima A, Takeshita A, Ueno H. Blockade of type β transforming growth factor signaling prevents liver fibrosis and dysfunction in the rat. *Proc Natl Acad Sci USA* 1999; **96:** 2345-2349
12 **Nakamura T,** Sakata R, Ueno T, Sata M and Ueno H: Inhibition of transforming growth factor β prevents progression of liver fibrosis and enhances hepatocyte regeneration in dimethylnitrosamine-treated rats. *Hepatology* 2000; **32:** 247-255
13 **Arias M,** Lahme B, Van de Leur E, Gressner AM, Weiskirchen R. Adenoviral delivery of an antisense RNA complementary to the 3′ coding sequence of transforming growth factor-β_1 inhibits fibrogenic activities of hepatic stellate cells. *Cell Growth Differ* 2002; **13:** 265- 273
14 **Ueno H,** Sakamoto T, Nakamura T, Qi Z, Astuchi N, Takeshita A, Shimizu K, Ohashi H. A soluble transforming growth factor beta receptor expressed in muscle prevents liver fibrogenesis. *Hum Gene Ther* 2000; **11:** 33-42
15 **Zagury D,** Burny A, Gallo RC. Toward a new generation of vaccines: the anti-cytokine therapeutic vaccines. *PNAS* 2001; **98:** 8024-8029
16 **Schödel F,** Peterson D, Hughes J, Milich D. Hepatitis B virus core particles as a vaccine carrier moiety. *Int Rev Immunol* 1994; **11:** 153-165
17 **Zhiming Hao,** Jinyan Luo, Quanying Wang, Guangxiao Yang, Prokaryotic expression of TGFβ_1(78 - 109)-HBV core fusion protein. *Xi'an Jiaotong Daxue Xuebao (Medical Sciences)* 2003; **24:** 105-108
18 **Milich DR,** Peterson DL, Zheng J, Hughes JL, Wirtz R, Schödel F. The hepatitis nucleocapsid as a vaccine carrier moiety. *Ann N Y Acad Sci* 1995; **754:** 187-201
19 **Milich DR,** McLachlan A. The nucleocapsid of hepatitis B virus is both a T cell-independent and a T cell-dependent antigen. *Science* 1986; **234:** 1398-1401
20 **Milich DR,** Chen M, Schödel F, Peterson DL, Jones JE. Hughes JL. Role of B cells in antigen presentation of the hepatitis B core. Proc. Natl. *Acad Sci USA* 1997; **94:** 14648-14653
21 **Borisova G,** Arya B, Dislers A, Borschukova O, Tsibinogin V, Skrastina D, Eldarov MA, Pumpens P, Skryabin KG, Grens E. Hybrid hepatitis B virus nucleocapsid bearing an immunodominant region from hepatitis B virus surface antigen. *J Virol* 1993; **67:** 3696–3701
22 **Tindle RW,** Herd K,Londoño P, Fernando GJ, Chatfield SN, Malcolm K, Dougan G. Chimeric hepatitis B core antigen particles containing B and Th-epitopes of human papillomavirus type 16 E7 protein induce specific antibody and T-helper responses in immunised mice. *Virology* 1994; **200:** 547-557
23 **Schödel F,** Wirtz R, Peterson D, Hughes J, Warren R, Sadoff J,

Milich D. Immunity to malaria elicited by hybrid hepatitis B virus core particles carrying circumsporozoite protein epitopes. *J Exp Med* 1994; **180:** 1037-1046

24 **Ulrich R,** Koletzki D, Lachmann S, Lundkvist A, Zankl A, Kazaks A, Kurth A, Gelderblom HR, Borisova G, Meisel H, Krüger DH. New chimaeric hepatitis B virus core particles carrying hantavirus (serotype Puumala) epitopes: immunogenicity and protection against virus challenge. *J Biotechnol* 1999; **73:** 141-153

25 **Pumpens P,** Borisova GP, Crowther RA, Grens E. Hepatitis B virus core particles as epitope carriers. *Intervirology* 1995; **38:** 63-74

26 **Tahara N,** Yasumitsu H, Umeda M. Synthetic peptide-generated monoclonal antibodies to transforming growth factor-beta 1. *Hybridoma* 1993; **12:** 441-453

Science Editor Wang XL and Guo SY **Language Editor** Elsevier HK

PO Box 2345, Beijing 100023, China
www.wjgnet.com
wjg@wjgnet.com

ELSEVIER

World J Gastroenterol 2005;11(40):6395-6401
World Journal of Gastroenterology ISSN 1007-9327
© 2005 The WJG Press and Elsevier Inc. All rights reserved.

• *BRIEF REPORTS* •

Treatment efficacy of radiofrequency ablation of 338 patients with hepatic malignant tumor and the relevant complications

Min-Hua Chen, Wei Yang, Kun Yan, Wen Gao, Ying Dai, Yan-Bin Wang, Xiao-Peng Zhang, Shan-Shan Yin

Min-Hua Chen, Wei Yang, Kun Yan, Wen Gao, Ying Dai, Yan-Bin Wang, Xiao-Peng Zhang, Shan-Shan Yin, Department of Ultrasound, Peking University School of Oncology, 52 Fu-cheng Rd, Haidian District, Beijing 100036, China
Correspondence to: Min-Hua Chen, Department of Ultrasound, Peking University School of Oncology, 52 Fu-cheng Rd, Haidian District, Beijing 100036, China. minhuachen@vip.sina.com
Telephone: +86-10-88121122-2299 Fax: +86-10-88140655
Received: 2004-12-31 Accepted: 2005-03-24

Abstract

AIM: To investigate the treatment efficacy of radiofrequency ablation (RFA) of hepatic malignant tumor and the relevant complications.

METHODS: A total of 338 patients with 763 hepatic tumors underwent ultrasound-guided RFA (565 procedures). There were 204 cases of hepatic cellular carcinoma (HCC) with 430 tumors, the mean largest diameter was 4.0 cm. Of them, 48 patients (23.5%) were in stages I-II (UICC Systems) and 156 (76.5%) in stages III-IV There were 134 cases of metastatic liver carcinoma (MLC), with 333 metastases in the liver, the mean diameter was 4.1 cm, the liver metastases of 96 patients (71.6%) came from gastrointestinal tract. Ninety-three percent of the 338 patients were treated using the relatively standard protocol. Crucial attention must be paid to monitor the abnormal changes in ultrasound images as well as the vital signs of the patients to find the possible hemorrhage and peripheral structures injury in time. The tumors were considered as ablated completely, if no viability was found on enhanced CT within 24 h or at 1 mo after RFA. These patients were followed up for 3-57 mo.

RESULTS: The ablation success rate was 93.3% (401/430 tumors) for HCC and was 96.7% (322/333 tumors) for MLC. The local recurrence rate for HCC and MLC was 7.9% (34/430 tumors) and 10.5% (35/333 tumors), respectively. A total of 137 patients (40.5%) underwent 2-11 times of repeated ablations because of tumor recurrence or metastasis. The 1st, 2nd, and 3rd year survival rate was 84.6%, 66.6%, and 63.1%, respectively; the survival rate from 48 patients of I-II stage HCC was 93.7%, 80.4%, and 80.4%, respectively. The major complication rate in this study was 2.5% (14 of 565 procedures), which consisted of 5 hemorrhages, 1 colon perforation, 5 injuries of adjacent structures, 2 bile leakages, and 1 skin burn.

CONCLUSION: RFA, as a minimally invasive local treatment, has become an effective and relatively safe alternative for the patients of hepatic malignant tumor, even of advanced liver tumor, tumor recurrence, and liver metastases. Knowledge about possible complications and their control may increase the treatment efficacy and help to promote the use of RFA technique.

© 2005 The WJG Press and Elsevier Inc. All rights reserved.

Key words: Radiofrequency ablation; Liver neoplasms; Survival; Complication; Ultrasonography

Chen MH, Yang W, Yan K, Gao W, Dai Y, Wang YB, Zhang XP, Yin SS. Treatment efficacy of radiofrequency ablation of 338 patients with hepatic malignant tumor and the relevant complications. *World J Gastroenterol* 2005; 11(40): 6395-6401

http://www.wjgnet.com/1007-9327/11/6395.asp

INTRODUCTION

The treatment efficacy of radiofrequency ablation (RFA) of liver tumors has been confirmed by sufficient quantity of clinical results[1-4]. With the improvement in both equipments and treatment skills, RFA has gradually been developed in China to treat large tumors[5,6], and provided an efficient alternative for the tumors which were difficult to manage with conventional treatments. With the wide adoption of the RFA technique, the complications increased accordingly, which drew a very important clinical attention. Large tumor and advanced tumor were commonly seen in China. Taking into consideration the characteristics of the tumors of our contrary study, this research aimed to summarize the treatment efficacy of RFA in 338 malignant liver tumors and explore the effective measures for complications.

MATERIALS AND METHODS

Patients

From 1999 to 2004, 338 patients with 763 hepatic tumors underwent 565 US-guided percutaneous RFA. All patients were diagnosed by biopsy at least on one lesion. Two hundred and forty-four patients were men (mean age, 59.1 years; age range, 24-87 years) and 94 were women (mean age, 58.6 years; age range, 32-86 years). Two hundred and four were hepatic cellular carcinoma (HCC) patients (430 tumors), with mean diameter of 4.0 cm (range, 1.2-10.8 cm). Of these 204 HCC patients, 96, 95, and 13 had Child-Pugh class A, B, and C cirrhosis, respectively. According to the UICC-TNM staging system, 48 patients (23.5%) were

in stages I-II, 156 were in stages III-IV. In the 204 HCC patients, 29 were given palliative treatment because of large size, unclear tumor border, invasion to the surrounding anatomical structure or multi-tumor occurrence. One hundred and thirty-four patients (333 tumors) had metastatic liver carcinomas (MLCs) with mean diameter of 4.1 cm (range, 1.0-10.0 cm). The primary tumors were from gastric and colorectal tract (n = 96, 71.6%), breast cancer (n = 16), lung cancer (n = 10), pancreatic cancer (n = 5), other organs (n = 7), respectively. Nine of them were given palliative treatment because of large size or multi-tumors. Eleven patients were found to have extrahepatic metastases when the first RFA was performed. The tumors larger than 3.5 cm, accounted for 61.8% (209/338 patients) in this study. There were 51 patients (15.1%) with 54 tumors adjacent to the gastrointestinal tract and 46 patients (13.9%) with 51 tumors adjacent to the gallbladder in this group.

Equipment

The RF system used in this study was a 460-kHz generator (Model 1500; RITA Medical System, Mountain View, CA, USA) that is capable of delivering a maximum power of 150 W through a 14-G electrode. The electrode contained nine hook-shaped prongs that could be deployed from the cannula, when the cannula was inserted into the surface of the tumor. The high-frequency electric current was passed through the deployed prongs to the tumor tissue, causing the vibration and friction of ions in the tissue, resulting in the temperatures of up to 100 ℃, which produced a sphere-like coagulation area of 2.0-5.0 cm in diameter. The time to produce a 5-cm ablation sphere was about 20 min. If multiple-overlapping ablations were required to ablate large tumors, much more time was needed.

Methods

Ninety-three percent of the patients were treated using the established protocol. The ablation area should cover the tumor and at least 0.5-1.0 cm of the surrounding tissue, and the margin should even be more than 1 cm when the tumor border was unclear. The treatment protocol was decided according to the ablation range. The ablation number and relevant placement mode should be decided, if the ablation range was greater than 4.5 cm in diameter[6]. For example, a regular tetrahedron overlapping mode with 4 ablations should be used, if the ablation range was 5.1-5.3 cm; the regular three- to six-sided prism overlapping mode with 5-8 ablations should be adopted, if the ablation range was 5.4-6.6 cm; the three segment overlapping ablation mode with 12 ablations was needed, if the ablation range was 6.7-7.5 cm. Furthermore, the sequence of the ablations and the skill of electrode placement were also crucial[7].

During the ablation process, real-time ultrasound scan was performed to monitor the electrode placement and the ablation, and post-ablation ultrasound was performed to find the potential complications so that the corresponding measures could be carried out in time[8].

Anesthesia

All patients underwent percutaneous RFA under general anesthesia or conscious sedation. Conscious sedation was induced with intravenous administration of 2.5-5.0 mg of midazolam (Roche; Basel, Switzerland) and 50-100 μg of fentanyl (Fentaini; Renfu, Yichang, China). Local infiltration anesthesia was induced by 5-15 mL of 1% lidocaine (Liduokayin; Yimin, Beijing, China). When tumors were adjacent to the diaphragm or the liver surface, an intravenous bolus of propofol (Diprivan; Zeneca, Macclesfield, UK, 1-2 mg/kg) and fentanyl (50-100 μg) was given to enhance anesthesia in combination with local anesthesia.

Assessment of therapeutic efficacy

For irregular tumors larger than 5 cm and near the gastrointestinal tract, enhanced CT within 24 h after the treatment was used to detect any residual viable tissue that would require a second RFA and to observe possible complications. To evaluate the tumor response to RFA therapy, contrast-enhanced CT was performed 1 mo post-ablation and the complete ablation of the tumor was considered to be achieved if the scans revealed: (1) the ablation zone was beyond the tumor borders, (2) the margin of the ablation zone was clear and smooth, and (3) no contrast enhancement was detected within or around the tumor. Subsequently, the patients were monitored regularly for intrahepatic recurrence in the outpatient clinic by a follow-up protocol including serum α-fetoprotein (AFP), abdominal US and enhanced CT every 2-3 mo for the first year, and then AFP every 2-3 mo, abdominal US and enhanced CT every 4-6 mo after the first year. Suspected intrahepatic recurrence was confirmed by percutaneous fine needle biopsy. Local recurrence was defined as tumor recurrence within or at the periphery of the ablated lesion in the follow-up CT scan. Distant intrahepatic recurrence referred to a new tumor that appeared in the liver separated from the ablated area. Patients were followed-up for 3-57 mo, follow-up rate was 91.4% (309 patients).

Statistical analysis

Cumulative survival rate of each group was calculated using the Kaplan-Meier method and compared by log-rank test. The level of significance was set at 0.05 for all tests. SPSS statistical analysis software (SPSS, Chicago, IL, USA) was used.

RESULTS

Therapeutic efficacy

The ablation success rate after the first RFA based on the CT findings were: HCC 93.3% (401/430 tumors), MLC 96.7% (322/333 tumors), the results are detailed in Table 1.

11.2% (38/338 cases) of the patients in this study had tumor residue, of which 31 cases (81.6%) were those with tumors larger than 3.5 cm; success rate for patients with tumors larger than 3.5 cm was 85.2% (178/209 cases, Figure 1). For tumor adjacent to bowel or gallbladder, the ablation success rates were 83.3% (45/54 tumors) and 86.3% (44/51 tumors), respectively. Local tumor recurrence was found in 34 of HCC patients (7.9%), 35 of MLC patients (10.5%), respectively, after the follow-up of 3-57 mo. 40.5% of patients received additional 2-11 RFA treatments because of the metastases or recurrence. The overall survival

Table 1 Therapeutic results of 338 patients after radio-frequency ablation

Tumor type	No. of patients	No. of tumors	Tumor size[1] (cm)	No. of tumors completely ablated[2] (%)	No. of local recurrence (%)
HCC	204	430	4.0 (1.2-10.8)	401 (93.3)	34 (7.9)
MLC	134	333	4.1 (1.0-10)	322 (96.7)	35 (10.5)
Total	338	763	4.1 (1.0-10.8)	723 (94.8)	69 (9.0)

[1]The largest average diameter of the tumors. [2]The ablation was considered a success, if the 1 mo CT scan showed no contrast enhancement detected within or around the tumor.

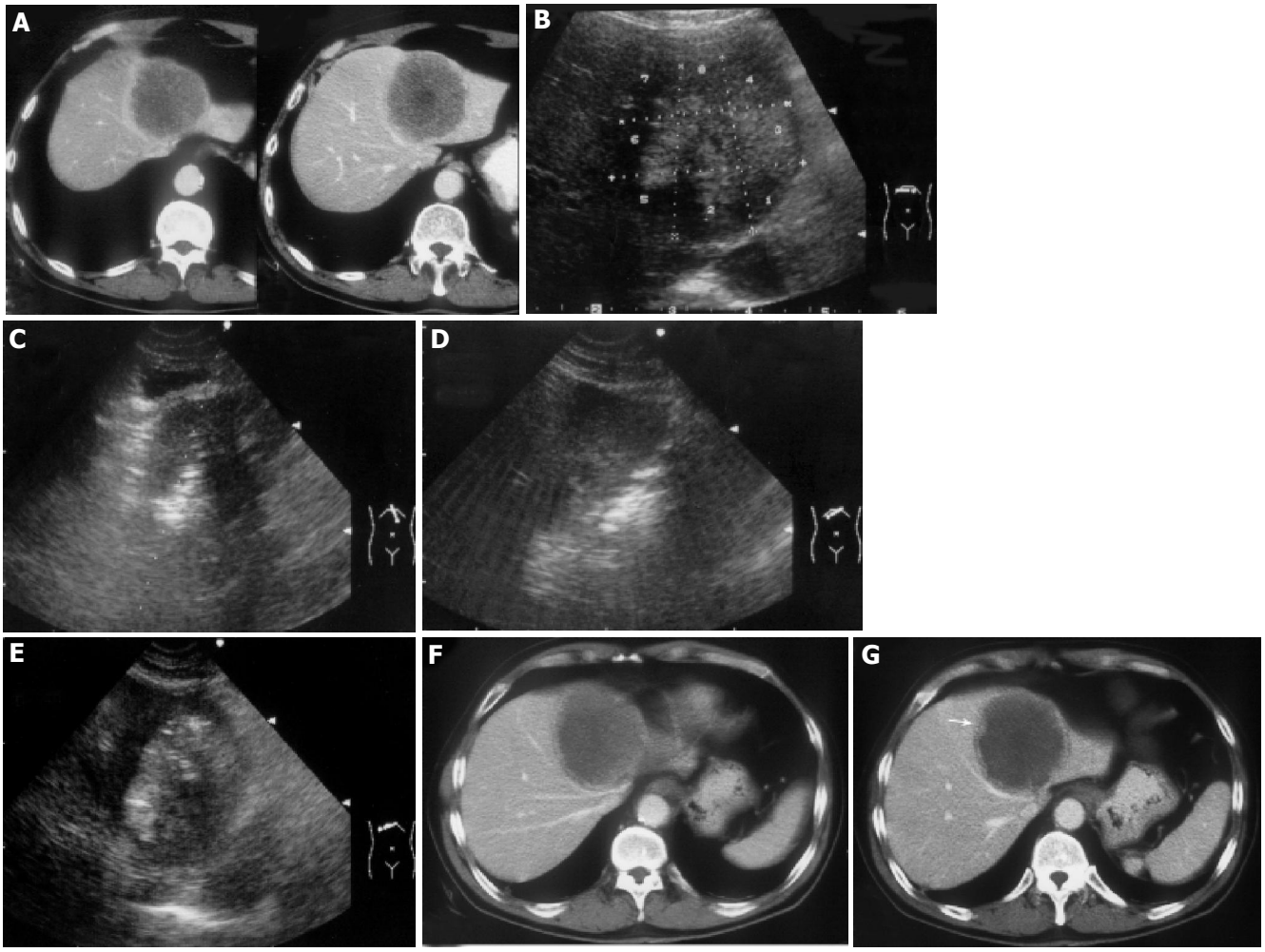


Figure 1 A 55-year-old man developed liver metastasis from colon cancer. **A:** Enhanced transverse CT scans obtained before treatment showed a spherical tumor invading into the diaphragm; **B:** The ablation protocol was designed and eight target sites were determined in this section. The tumor area near the heart and stomach were ablated first. **C:** The fourth ablation was conducted; **D:** The fifth ablation was conducted; **E:** The ablation was finished and the tumor area was presented as hyperechoic; **F:** Enhanced transverse CT scans obtained 1 d after the treatment showed that most of the tumor was coagulated and necrosis; **G:** Enhanced transverse CT scans obtained 1 d after the treatment showed slight enhancement (↑) on the lower margin of the tumor. The patient received the second treatment and achieved complete ablation.

rate of 300 patients with malignant liver tumor after RFA is shown in Table 2.

The overall survival rate was higher in HCC group than in MLC group (P<0.001), so was the survival rate in HCC group of stages III-IV than in MLC group (P<0.05); and the survival rate in HCC group of stages I-II than in HCC group of stages III-IV (P<0.001).

Complications

The occurrence rate of major complications was 2.5% (14/565 RFA procedures), including hemorrhage (n = 5, Figure 2), bile leakage (n = 2), colon perforation (n = 1), stricture of bile duct (n = 2), cholecystitis (n = 1), hemothorax (n = 2), skin burn (n = 1), minor complications consisted of bellyache, shoulder pain, breath-related right-superior bellyache, fever after RFA, transient hepatic dysfunction, etc.

DISCUSSION

All the therapeutic alternatives commonly used to treat HCC or MLC have limitations. In the recent decade, US-guided percutaneous ethanol injection (PEI) as a local therapy for

Table 2 The comparison of survival rates of 300 patients with malignant liver tumor after RFA

Tumor type	Survival rate		
	1 yr	2 yr	3 yr
MLC (n = 125)	75.3	50.2	25.1
HCC (n = 175)[b]	84.6	66.6	63.1
Stages I–II (n = 48)[b,d]	93.7	80.4	80.4
Stages III–IV (n = 127)[a]	81.3	61.7	57.2
Total (n = 300)	80.6	60.1	50.4

[a]P<0.05, [b]P<0.01 *vs* MLC; [d]P<0.01 *vs* HCC of stages III–IV , P<0.01.

hepatic tumors has gradually been replaced by intraoperative or percutaneous RFA[2,9,10], which was considered by many as superior to other existing locoregional therapies such as PEI, TACE, and microwave ablation[9,11,12]. However, the efficacy of RFA was reduced by its high recurrence rate and relevant complications, especially in the treatment of large tumors or special location tumors. Livraghi *et al*.[13], reported complications of RFA in 2 320 patients with focal liver cancer treated by a collaborative group in Italy, and demonstrated that bleeding and gastrointestinal perforation were the most common major complications which might lead to death. Thus, studies on the treatment protocol of RFA to increase its efficacy and the preventive measures of the relevant complications have become a major issue.

RFA skills

Generally, a single ablation of 5 cm in diameter could successfully destroy a liver tumor smaller than 3.5 cm plus the "safety margin" of 0.5-1.0 cm. Patients with tumors larger than 3.5 cm accounted for 61.8% (207/335 cases) of the whole population in this study. With the help of the correct electrode placement, the operation skills and the established protocol, we got a response rate of 85.2% (178/209 cases), indicating that the protocol could be used to guide the RFA of large liver tumors[7]. However, this mathematic protocol was not always easy to perform in practice because of some factors, such as deviation of needle placement or failure of full deployment of prongs, due to rigid texture of the tumor or hepatic parenchyma, limitation of puncture angle, or insufficient safe margin due to being adjacent to major structures. For treating tumors with undesirable locations such as being adjacent to diaphragm, gallbladder, and gastrointestinal tract, etc. an individualized protocol was required. Some adjunctive measures or combination treatment of multiple modalities were also adopted to deal with particular features of the tumors[7,14].

Regarding the tumors being adjacent to diaphragm, gallbladder, gastrointestinal tract, the puncture direction of the electrode should be vertical to the organs and the cannular should be lifted a little, while the prongs had been deployed, besides multiple-overlapping ablations of 2-3 cm should be performed to ablate the risky area of tumor. If necessary, enhanced CT was performed within 24 h to detect residual tumor and decided if additional ablations were required. For the tumors adjacent to the colon, most part of the tumor which was near to the center of the liver should be ablated first, stage II resection should be adopted 2-4 wk later. Combination treatments including the TACE or obstruction of the liver arteries prior RFA should be adopted, if the tumor had abound blood supply; anyway, combination treatments were very important to improve the therapeutic efficacy[15].

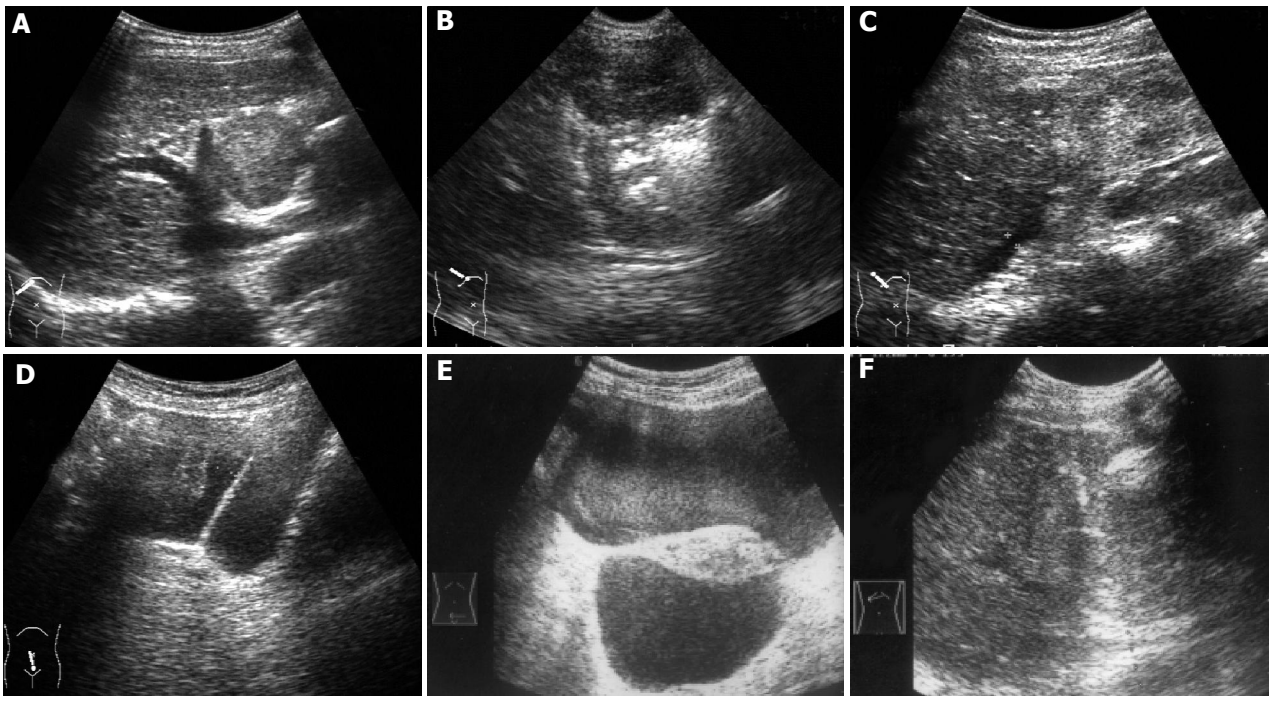


Figure 2 A 72-year-old woman developed intrahepatic recurrence 2 years after hepatic resection for HCC. **A:** US scan before treatment showed a large tumor protruding from the liver surface; **B:** US guided ablation was conducted; **C:** US scan immediately obtained after treatment showed little fluid under the liver. **D:** Five minutes later, US scan showed accumulative fluid in pelvic cavity; **E:** Nine hours later, US scan showed a great deal of hemorrhage in pelvic cavity. **F:** Ten hours later, US guided ablation of bleeding site was performed.

Analysis of therapeutic efficacy

There are many factors that can affect the therapeutic efficacy of RFA. The most important factor is the size of the tumor. Sufficient data confirmed that RFA could successfully ablate the small liver tumors. The ablation success rate of the initial RFA in this study was 94.8% (723/763 tumors). Of the 40 incompletely ablated tumors, 33 (82.5%) were larger than 3.5 cm. The ablation success rate of RFA on MLC patients reached 96.7% (322/333 tumors). It was considered that the MLC tumor was more sensitive to heat energy due to less blood supply[16]. Furthermore, in our study, most MLCs were treated with extended ablation margin as there were enough liver function reserve and surrounding liver tissue, thus contributing to a satisfactory short-term outcome of MLC in this study. In this study, six patients were found to have 1-3 MLC as well as primary stomach or colon cancer. The primary cancer had been successfully resected before RFA. Therefore, as an adjuvant therapy to the surgical resection, RFA could increase the opportunity of surgical resection of those patients with advanced liver tumor. Although additional RFA had been performed due to the new metastases in the liver after RFA, four of six patients had survived beyond 2-3 years. Although most of the HCC patients in our study were in stages III-IV, the 1-, 2- and 3- year survival rates after RFA was 84.6%, 66.6%, 63.1%, respectively, and 93.7%, 80.4%, 80.4% for HCC patients of stages I-II. These results indicated that RFA could have a similar efficacy compared with surgery resection as long as the tumors were completely ablated. However, the long-term efficacy of MLC post RFA was no good, the survival rate of 2nd, 3rd year was lower than that of HCC. Solbiati *et al*.[3], reported that the average survival of MLC patients after RFA was 35.4 mo, which was higher than that of ours. It might be explained by the reason that most MLC patients in our study had large sized tumor, multi-tumor or extrahepatic metastases.

Another major factor to affect the efficacy was the undesirable location of the tumor, such as being adjacent to hepatic hilum, diaphragm, gastrointestinal tract or invasion to large vessels, or intruding outward from the liver surface, and RFA on those tumors may more likely induce tumor residue or complications.

The management of complications

More complications about RFA have been reported as more patients have been treated, despite that RFA is a minimally invasive technique[13,17]. The major complication rate in this study was 2.5% (14/565 procedures), which consisted of mechanical and thermal injuries. It is very important to find the auspice symptoms in time and adopt appropriate management.

Two of the five cases of hemorrhage occurred during the RFA treatment. One was due to liver capsule laceration when the electrode was deployed to treat a 1-cm metastatic liver tumor near the liver surface but unfortunately was pushed deep forward, and the anechoic area of hemorrhage in front of the liver enlarged to 1-3 cm in thickness in 2 min. The other case with metastatic tumor from rectum cancer was the result of stabbing subcapsular arterial-venous shunt by the RFA electrode and the anechoic area of hemorrhage increased to 2.5 cm in thickness. The above two cases of hemorrhage were stopped by using RFA at the bleeding sites without moving and the tumors were ablated successfully at the same time. The other three cases of hemorrhage were all HCC with liver cirrhosis. One hemorrhage occurred in a small HCC patient and was controlled by ablating the bleeding site. The other two occurred in patients with large liver tumors located near the liver surface and deteriorated coagulation functions. The hemorrhage was caused by the increased abdominal pressure due to cough or sudden position change at half or 4 h after the RFA treatment. The bleeding was controlled by hemostatics intravenously and local oppression and in one case whose bleeding amount was large that the patient even received blood transfusion of 800 mL.

Colon perforation occurred in one case in our early practice. The patient with HCC located in segment VI received two sessions of RFA procedure and a new 4-cm tumor near the colon hepatic flexure was found 1 year later. Contrast enhanced US demonstrated rich blood flow within the tumor, which was adhered to the colon. Overlooking this phenomenon, the tumor was ablated aggressively. Colon perforation occurred 1 wk later and the patient underwent surgical operation. In retrospect, we reckoned that the perforation might have been avoided if an individualized treatment protocol had been adopted with greater care as follows: (A) the patients were placed in the right anterior oblique position, so that the transverse colon and intestines would migrate to the left, away from the liver. (B) During the ablation, the patients were instructed to make repeated abdominal breaths to keep the bowels moving and to avoid continual hyperthermia in the bowel wall. (C) After the ablation, the patient needs to fast for 24 h and then has semi-fluid diets for 2 d. If the patient complains about right upper abdominal pain or has thickened bowel wall demonstrated by US or CT examination 24-48 h after the treatment, ask the patient to fast longer and receive infusion and other conservative treatment. In our later series of 51 patients with liver tumors near the bowels and 3 mo later, 8 (15.7%) patients demonstrated bowel adhesion but no colon perforation occurred.

Other adjacent structure injury occurred in eight cases. One patient with gallbladder stone developed cholecystitis and recovered after antibiotic administration. For tumors near the gallbladder, RFA might lead to a series of syndromes caused by parasympathetic stimulation with decreased heart rate and pain in stomach or pericardial area. Of the 46 cases with tumors near the gallbladder, 38 (82.6%) complained of pain in stomach and pericardial area, 17 (36.9%) had decreased heart rate with the lowest being 27 per min. Enhancing anesthesia and injecting of atropine of 0.25-1.0 mg could control these disorders. Two patients with slightly dilated bile duct due to tumor invasion had jaundice and obviously dilated bile duct after the RFA. Both recovered after percutaneous transhepatic biliary drainage.

Diaphragm injury occurred in two cases. One with bloody pleural infusion was given hemostatics and drainage of pleural cavity. The other with large amount of pleural effusion and thickened diaphragm recovered after draining out pink effusion fluid.

Two cases of biliary leakage occurred in patients with metastatic tumors from pancreatic cancer within 1 wk after RFA. The tumors were located near the liver surface with the size of 3.5 and 4.5 cm. One of them recovered after 2-3 mo of percutaneous drainage but the other did not till death.

Skin burn occurred in one case. The patient had large scars in the abdominal wall due to previous operation for purulent cholecystitis. It was difficult to avoid the scar area when we inserted the RFA electrode to treat a 5-cm tumor in segment IV. The outer insulate coat of the electrode melted during the RFA and led to skin burn of the scarred area. Thus it was essential to avoid the scar while inserting the electrode.

Besides these major complications, other patients complained about some mild complications, such as fever and bellyache. The temperature could reach about 37.8-38.5 ℃, and lasted about several days to two weeks. If the temperature was too high or lasted too long, a blood test should be taken in time and relevant treatments should be adopted. The anesthetic drugs used during the RFA process could cause vomiting and nausea. The symptoms of bellyache post-RFA could be relieved within 3-7 d without any drugs; however, little acesodyne was occasionally needed. But if the tumor was close to the diaphragm, the RFA could induce an ache on the right shoulder; besides, if the intercostals nerve, peritoneum, or abdominal wall were injured, a transient breath-related pain could happen, and sometimes acesodyne was needed.

Some patients experienced transient liver dysfunction 2 wk post RFA; Western or Chinese medicines to protect liver function should be adopted to facilitate the general health and liver function.

Advantages and problems in the RFA of liver tumors

It was easy and feasible to perform RFA on liver tumors. Most RFA could be administered with local anesthesia and acesodynes on outpatient, and the rest of the patients could be discharged after 1-2 d of observation. The RITA electrode in our practice was satisfying, and the information about temperatures at the needle tip helped to control the RFA area. Another advantage was RFA could be performed repeatedly on the condition of subsequent metastases or tumor recurrence. The quality of patient life and the immune status was good after RFA treatment. One patient's with HCC was repeatedly treated 11 times and 21 tumors in total were ablated successfully, the patient has survived for more than 4 years. Another patient with liver metastases from stomach sarcoma was treated seven times and 11 metastases in total were treated, the patient has survived for 27 mo. The obvious advantage was that the whole cost of RFA was less expensive than other treatment options; RFA was minimally invasive and relatively safe, most patients experienced body weight increase, improvement of appetite and general health without serious liver dysfunction after RFA. There were seven cases who had mild to severe ascites before RFA, the ascites of two patients disappeared and that of three decreased significantly after RFA, further supporting the advantages of RFA in its minimal invasiveness and good efficacy.

Most of the liver tumor patients in China were at the very late stages when they were diagnosed, and large tumors were commonly seen. In order to develop the RFA technique effectively, we should pay enough attention to the standard protocol and the operation skill. Combination treatments may help to improve the therapeutic efficacy, including hepatic artery embolization or infusion before RFA, combined resection and RFA[15,18] and subsequent stage II surgical resection after RFA. These options will no doubt improve the therapeutic level of liver tumors.

RFA, as a minimally invasive local treatment of liver tumors, was an effective and relatively safe alternative for the advanced liver tumor patients, tumor recurrence, liver metastases which were unresectable or difficult to treat with traditional therapies. The complications usually occurred during or shortly after RFA, so we should follow them up closely to find the possible hemorrhage or periphery structures injury in time; as long as the precautious measures are taken and effective managements are carried out, the serious complication rate would be reduced to the least, so that the final goal of improvement of general health and long-term survival time could be reached.

REFERENCES

1 **Curley SA**, Izzo F, Delrio P, Ellis LM, Granchi J, Vallone P, Fiore F, Pignata S, Daniele B, Cremona F. Radiofrequency ablation of unresectable primary and metastatic hepatic malignancies: results in 123 patients. *Annals of Surgery* 1999; **230**: 1-8

2 **Gazelle GS**, Goldberg SN, Solbiati L, Livraghi T. Tumor ablation with radio- frequency energy. *Radiology* 2000; **217**: 633-646

3 **Solbiati L**, Livraghi T, Goldberg SN, Ierace T, Meloni F, Dellanoce M, Cova L, Halpern EF, Gazelle GS. Percutaneous radio-frequency ablation of hepatic metastases from colorectal cancer: long-term results in 117 patients. *Radiology* 2001; **221**: 159-166

4 **Livraghi T**, Goldberg SN, Lazzaroni S, Meloni F, Ierace T, Solbiati L, Gazelle GS. Hepatocellular carcinoma: radio-frequency ablation of medium and large lesions. *Radiology* 2000; **214**:761-768

5 **Chen MH**, Liu JB, Yan K, Wu JY, Huo L, Yang RJ, Zhang XP, Huang XF. Ultrasound-guided radiofrequency ablation of malignant hepatic tumors. *Chin J Ultrasonogr* 2001; **10**: 404-407

6 **Cai ZH**, Chen T, Chen Q, Wang T, Shi L. The ultrasound-guided method for radio-frequency ablation to treat large hepatocelluar carcinoma. *Chin J Ultrasonogr* 2001; **10**: 408-409

7 **Chen MH**, Yang W, Yan K, Zou MW, Solbiati L, Liu JB, Dai Y. Large liver tumors: protocol for radiofrequency ablation and its clinical application in 110 patients--mathematic model, overlapping mode, and electrode placement process. Radiology. *Radiology* 2004; **232**: 260-271

8 **Chen MH**, Yan K, Wu JY, Yang W, Dai Y, Song YP, Huang XF. Ultrasound-guided radiofrequency ablation for the treatment of 131 patients with malignant hepatic tumors. *Chin J Gen Surg* 2002; **17**: 520-522

9 **Livraghi T**, Goldberg SN, Lazzaroni S, Meloni F, Solbiati L, Gazelle GS. Small hepatocellular carcinoma: treatment with radio-frequency ablation versus ethanol injection. *Radiology* 1999; **210**: 655-661

10 **Lin SM,** Lin CJ, Lin CC, Hsu CW, Chen YC. Radiofrequency ablation improves prognosis compared with ethanol injection for hepatocellular carcinoma < or =4 cm. *Gastroenterology* 2004; **127**:

1714-1723

11 **Livraghi T**. Radiofrequency ablation, PEIT, and TACE for hepatocellular carcinoma. *J Hepatobiliary Pancreat Surg*2003; **10**: 67-76

12 **Shibata T**, Iimuro Y, Yamamoto Y, Maetani Y, Ametani F, Itoh K, Konishi J. Small hepatocellular carcinoma: comparison of radio-frequency ablation and percutaneous microwave coagulation therapy. *Radiology* 2002; **223**: 331-337

13 **Livraghi T**, Solbiati L, Meloni MF, Gazelle GS, Halpern EF, Goldberg SN. Treatment of focal liver tumors with percutaneous radio-frequency ablation: complications encountered in a multicenter study. *Radiology* 2003; **226**: 441-451

14 **Dodd GD**, Frank MS, Aribandi M, Chopra S, Chintapalli KN. Radiofrequency thermal ablation: computer analysis of the size of the thermal injury created by overlapping ablations. *AJR Am J Roentgenol* 2001; **177**: 777-782

15 **Buscarini L**, Buscarini E, Di Stasi M, Quaretti P, Zangrandi A. Percutaneous radiofrequency thermal ablation combined with transcatheter arterial embolization in the treatment of large hepatocellular carcinoma. *Ultraschall Med* 1999; **20**: 47-53

16 **Wu JY**, Chen MH, Yan K, Zhang H, Wang HY, Huo L, Yang W, Song YP. Ultrasound-guided radiofrequency ablation in the treatment of liver metastases. *J Peking University* 2001; **33**: 449-451

17 **Curley SA**, Marra P, Beaty K, Ellis LM, Vauthey JN, Abdalla EK, Scaife C, Raut C, Wolff R, Choi H, Loyer E, Vallone P, Fiore F, Scordino F, De Rosa V, Orlando R, Pignata S, Daniele B, Izzo F. Early and late complications after radiofrequency ablation of malignant liver tumors in 608 patients. *Ann Surg* 2004; **239**: 450-458

18 **Pawlik TM**, Izzo F, Cohen DS, Morris JS, Curley SA. Combined resection and radiofrequency ablation for advanced hepatic malignancies: results in 172 patients. *Auu Surg Oncol* 2003; **10**: 1059-1069

Science Editor Guo SY **Language Editor** Elsevier HK

PO Box 2345, Beijing 100023, China
www.wjgnet.com
wjg@wjgnet.com

ELSEVIER

World J Gastroenterol 2005;11(40):6402
World Journal of Gastroenterology ISSN 1007-9327
© 2005 The WJG Press and Elsevier Inc. All rights reserved.

Acknowledgments to Reviewers of *World Journal of Gastroenterology*

Many reviewers have contributed their expertise and time to the peer review, a critical process to ensure the quality of *World Journal of Gastroenterology*. The editors and authors of the articles submitted to the journal are grateful to the following reviewers for evaluating the articles (including those were published and those were rejected in this issue) during the last editing period of time.

Charles Paul Balabaud, Professor
Service d'hepatologie, Hospital Saint André, 1 Rue Jean Burguet, Bordeaux 33075, France

Xue-Gong Fan, Professor
Department of Infectious Diseases, Xiangya Hospital, Central South University, Changsha 410008, Hunan Province, China

Hans Gregersen, Professor
The Research Administration, Aalborg Hospital, Hobrovej 42 A, Aalborg 9000, Denmark

Anna S Gukovskaya, Professor
VA Greater Los Angeles Health Care System ,University of California, Los Angeles, 11301 Wilshire Blvd, Los Angeles 91301, United States

Werner Hohenberger, Professor
Chirurgische Klinik und Poliklinik, Krankenhausstrasse 12, ErlangenD-91054, Germany

Masayoshi Ito, MD
Department of Endoscopy, Yotsuya Medical Cube, 5-5-27-701 Kitashinagawa, Shinagawa-ku, Tokyo 1410001, Japan

Hiroaki Itoh, MD
First Department of Internal Medicine, Akita University Scool of Medicine,1-1-1,Hondou, Akita City 010-8543, Japan

Tsuneo Kitamura, Associate Professor
Department of Gastroenterology, Juntendo University Urayasu Hospital, Juntendo University School of Medicine, 2-1-1 Tomioka, Urayasu-shi, Chiba 279-0021, Japan

Zahariy Krastev, Professor
Department of Gastroneterology, Universiti Hospital "St. Ivan Rilski",#15, blvd "Acad. Ivan Geshov", Sofia 1431, Bulgaria

Shoji Kubo, MD
Hepato-Billiary-Pancreatic Surgery, Osaka City University Graduate School of Medicine, 1-4-3 Asahimachi, Abeno-ku, Osaka 545-8585, Japan

Fin Stolze Larsen, Associate Professor
Hepatology A-2121, Rigshospitalet University Hospital of Copenhagen, Blegdamsvej 9, Copenhagen 2100, Denmark

James Neuberger, Professor
Liver Unit, Queen Elizabeth Hospital, Birmingham B15 2TH, United Kingdom

Gustav Paumgartner, Professor
University of Munich, Klinikum Grosshadern, Marchioninistr. 15, Munich, D-81377, Germany

Zhiheng Pei, Assistant Professor
Department of Pathology and Medicine, New York University School of Medicine, Department of Veterans Affairs, New York Harbor Healthcare System, 6001W, 423 East 23rd street, New York NY 10010, United States

Lun-Xiu Qin, Professor
Liver Cancer Institute and Zhongshan Hospital, Fudan University, 180 Feng Lin Road, Shanghai 200032, China

Claudio Romano, Dr, Assistant professor
Department of Pediatrics, University of Messina, Italy

Manfred Stolte, Professor
Institute of Pathology, Klinikum Bayreuth, Preuschwitzer Str. 101, Bayreuth 95445, Germany

Michael Trauner, Professor
Medical University Graz, Auenbruggerplatz 15, Graz A-8036, Austria

Takashi Yao, MD
Department of Anatomic Pathology, Graduate School of Medical Science, Kyushu University, 3-1-1, Maidashi, Higashi-ku, Fukuoka 812-8582, Japan

Arthur Zimmermann, Professor
Director, Institute of Pathology of the University, Berne, Switzerland, Murtenstrasse 31, 3010 Berne, Switzerland

PO Box 2345, Beijing 100023, China
www.wjgnet.com
wjg@wjgnet.com

ELSEVIER

World J Gastroenterol 2005;11(40):6406
World Journal of Gastroenterology ISSN 1007-9327
© 2005 The WJG Press and Elsevier Inc. All rights reserved.

World Journal of Gastroenterology standard of quantities and units

Number	Nonstandard	Standard	Notice
1	4 days	4 d	In figures, tables and numerical narration
2	4 days	four days	In text narration
3	day	d	After Arabic numerals
4	Four d	Four days	At the beginning of a sentence
5	2 hours	2 h	After Arabic numerals
6	2 hs	2 h	After Arabic numerals
7	hr, hrs,	h	After Arabic numerals
8	10 seconds	10 s	After Arabic numerals
9	10 year	10 years	In text narration
10	Ten yr	Ten years	At the beginning of a sentence
11	0,1,2 years	0,1,2 yr	In figures and tables
12	0,1,2 year	0,1,2 yr	In figures and tables
13	4 weeks	4 wk	
14	Four wk	Four weeks	At the beginning of a sentence
15	2 months	2 mo	In figures and tables
16	Two mo	Two months	At the beginning of a sentence
17	10 minutes	10 min	
18	Ten min	Ten minutes	At the beginning of a sentence
19	50% (*V/V*)	500 mL/L	
20	50% (m/*V*)	500 g/L	
21	1 M	1 mol/L	
22	10 μM	10 μmol/L	
23	1N HCl	1 mol/L HCl	
24	1N H_2SO_4	0.5 mol/L H_2SO_4	
25	4rd edition	4^{th} edition	
26	15 year experience	15- year experience	
27	18.5 kDa	18.5 ku,18 500u or M_r18 500	
28	25 $g.kg^{-1}/d^{-1}$	25 g/(kg·d) or 25 g/kg per day	
29	6900	6 900	
30	1000 rpm	1 000 r/min	
31	sec	s	After Arabic numerals
32	1 pg $\cdot L^{-1}$	1 pg/L	
33	10 kilograms	10 kg	
34	13 000 rpm	13 000 *g*	High speed; *g* should be in italic and suitable conversion.
35	1000 *g*	1 000 r/min	Low speed. *g* cannot be used.
36	Gene bank	GenBank	International classified genetic materials collection bank
37	Ten L	Ten liters	At the beginning of a sentence
38	Ten mL	Ten milliliters	At the beginning of a sentence
39	umol	μmol	
40	30 sec	30 s	
41	1 g/dl	10 g/L	10-fold conversion
42	OD_{260}	A_{260}	"OD" has been abandoned.
43	One g/L	One microgram per liter	At the beginning of a sentence
44	*A*260 nm	A_{260}nm	*A* should be in italic.
	$^bP<0.05$	$^aP<0.05$	In Table, no note is needed if there is no significance in statistics: $^aP<0.05$, $^bP<0.01$ (no note if $P>0.05$). If there is a second set of *P* value in the same table, $^cP<0.05$ and $^dP<0.01$ are used for a third set: $^eP<0.05$, $^fP<0.01$.
45	**F*=9.87, §*F*=25.9, #*F*=67.4	^1F=9.87,^2F=25.9, ^3F=67.4	Notices in or under a table
46	KM	km	kilometer
47	CM	cm	centimeter
48	MM	mm	millimeter
49	Kg, KG	kg	kilogram
50	Gm, gr	g	gram
51	nt	N	newton
52	l	L	liter
53	db	dB	decibel
54	rpm	r/min	rotation per minute
55	bq	Bq	becquerel, a unit symbol
56	amp	A	ampere
57	coul	C	coulomb
58	HZ	Hz	
59	w	W	watt
60	KPa	kPa	kilo-pascal
61	p	Pa	pascal
62	ev	EV	volt (electronic unit)
63	Jonle	J	joule
64	J/mmol	kJ/mol	kilojoule per mole
65	10×10×10cm^3	10 cm×10 cm×10 cm	
66	N·km	KN·m	moment
67	$\bar{x}\pm s$	mean±SD	In figures, tables or text narration
68	Mean±SEM	mean±SE	In figures, tables or text narration
69	*im*	im	intramuscular injection
70	*iv*	iv	intravenous injection
71	Wang et al	Wang *et al.*	
72	EcoRI	*Eco*RI	*Eco* in italic and RI in positive. Restriction endonuclease has its prescript form of writing.
73	Ecoli	*E.coli*	Bacteria and other biologic terms have their specific expression.
74	Hp	*H pylori*	
75	Iga	*Iga*	writing form of genes
76	*igA*	IgA	writing form of proteins
77	-70 kDa	~70 ku	